CURRENT PROTOCOLS IN TOXICOLOGY

EDITED BY

LUCIO G. COSTA
ERNEST HODGSON
DAWID A. LAWRENCE
DONALD J. REED
WILLIAM F. GREENLEE

Current Protocols in Toxicology

ISBN: 0-471-24106-7

Last time updated: September 2005

Current Protocols in Toxicology is a "best-practices" collection of lab protocols for accurate, efficient assessments of toxicity in whole organisms, organs and tissues, cells, and biochemical pathways. Continuously updated since its initial publication in May 1999, this quarterly-updated two-volume set...
- provides the latest models and methods from molecular biology, cell biology, biochemistry, and genetics, plus sophisticated toxicological procedures from leading laboratories.
- offers expert guidelines for evaluating the effects of substances on human physiology and metabolism.
- provides valuable reference information in three appendices, including stock solutions and equipment, commonly used techniques, and using information.

Edited by: Lucio G. Costa (University of Washington); Ernest Hodgson (North Carolina State University); David A. Lawrence (Wadsworth Center); Terence R. Ozolins (Pfizer, Inc.); Donald J. Reed (Oregon State University); William F. Greenlee, Advisory Editor (CIIT);
Past Editor-in-Chief: Mahin Maines; Past Editors: I. Glenn Sipes, Shigeru Sassa

Series Editor: Kathy Morgan

Editors

FOREWORD

Toxicological research is driven by the need to understand and assess the human and ecological risks of exposure to chemicals and other toxicants as well as by interest in using toxic agents to elucidate basic biological and pathobiological processes. The level of research activity in this field is higher, the rate of change in knowledge more rapid, and interest in applying scientific information to societally important issues is greater than ever before. These are exciting and challenging times to be working in toxicology. The ongoing ferment builds on the extraordinary advances being made in the understanding of biological systems at the molecular level. This fundamental knowledge provides the opportunity for greatly enhanced insight into how chemicals and other stressors may damage biological structures and processes, influence the rate of biological repair, and lead to reversible or irreversible diseases or to a return to health.

Society increasingly calls on the scientific community for the knowledge needed both to reevaluate the health hazards of existing products and technologies and to evaluate the prospective hazards of new ones. Such information is used to develop guidelines and regulations designed to ensure that these new products and technologies do not harm people or the environment.

Acquiring sound, reproducible scientific data that can be integrated with existing information to advance the knowledge of toxicants and living systems requires rigorous adherence to the scientific method. This means intelligent, thoughtful individuals identifying important needs, formulating testable hypotheses, designing experiments to test them, meticulously conducting these experiments, carefully reviewing and interpreting data, and ultimately presenting this information to scientific peers, including publishing it in the peer-reviewed literature. *Current Protocols in Toxicology* is a clear and well-documented compendium of the most important methods in the field—proven approaches developed by leading researchers—for the benefit of other experimentalists, from students to seasoned investigators. Since toxicology by its nature is multidisciplinary, other titles in the Current Protocols series may also provide relevant methods. Although review of the literature cited for each procedure can give added insight into the underlying theory and breadth of applications, the protocols have been carefully designed to provide clear, step-by-step descriptions that can easily be followed even by the relatively inexperienced.

Regular updates to *Current Protocols in Toxicology* manual will help ensure an awareness of changes in previously documented methods and of methods newly developed. Use of these protocols will avoid unnecessary duplication of effort in development and validation when the methods are applied without modification, and will speed up the development of more refined methods that will further advance the field of toxicology and, in turn, may have a place in future updates.

Roger O. McClellan
Chemical Industry Institute of Toxicology
Research Triangle Park, North Carolina

Contributed by Roger O. McClellan
Current Protocols in Toxicology (1999)

PREFACE

The span of research in toxicology has been expanding and diversifying precipitously in recent years. One cause for this is the ongoing increase in industrial activity and in the generation of toxic compounds that then find their way into the environment. Another is the intensifying public awareness of the health effects of chemical exposure. The expansion of the field can be observed by attending any major scientific event dedicated to toxicology—such as the annual meetings of the Society of Toxicology, whose attendance has tripled in the course of the 1990s.

Examining the meeting program for one of these events provides a very good feel for the broad scope of toxicology. For those who have attended such meetings periodically over the past few years, the dynamic nature of the field and its explosive growth is obvious: there is simply more in-depth research going on every year. This is in contrast to toxicology's early years, when the field was dominated by research involving gross assessment of organisms' responses to toxic chemicals. More recent times have witnessed the emergence of applications of state-of-the-art technology to the study of toxicity responses in organisms and living cells, along with phenomenal advancement in molecular and biochemical techniques, which increasingly are finding their way into toxicology research laboratories. A growing number of presentations at toxicology meetings constitute bridges between basic toxicology research and approaches to improving human health and environmental quality. It is this changing and expanding face of toxicology and its methodologies that represented the greatest challenge in assembling *Current Protocols in Toxicology*. We have attempted to include those methods that are presently central to modern toxicology and that we expect will remain valuable tomorrow. Like the field of toxicology, with its quarterly supplements this book will continue to expand in scope, to include more topics and methods as the field advances.

Because toxicological questions may be addressed using methods deriving from a wide variety of disciplines, other titles in the Current Protocols series may also provide methods that can be applied in your research. Molecular biology techniques, in particular, are integral to toxicological investigation. Such techniques are included where appropriate within units in this book; however, where these protocols are located may not be readily apparent from the table of contents. To help you find them, Table A.3A.1 in *APPENDIX 3A* provides a listing of specific techniques and where they can be found, either in this book or in related Current Protocols manuals. In addition, protocols for a number of basic techniques will be added to *APPENDIX 3* in future supplements.

Although mastery of the techniques in this manual will enable readers to pursue research in toxicology, the manual is not intended to be a substitute for graduate-level courses or a comprehensive textbook in the field. An inevitable hazard of manual writing is that protocols may become obsolete as the field expands and new techniques are developed. To safeguard this manual from inexorable obsolescence (and perhaps pleasantly surprise the users of the manual!), we provide quarterly supplements to provide protocols that utilize new innovations and technologies in the field. The updatable formats—looseleaf binder, CD-ROM, Intranet, and online Internet—easily accommodate the addition of this new material.

Contributed by Mahin D. Maines, Lucio G. Costa, Donald J. Reed, Shigeru Sassa, and I. Glenn Sipes
Current Protocols in Toxicology (1999) iii-vi

HOW TO USE THIS MANUAL

Format and Organization

This publication is available in both looseleaf and CD-ROM format. For looseleaf purchasers, a binder is provided to accommodate the growth of the manual via the quarterly update service. This format allows easy insertion of new pages, units, and chapters that are added. The index and table of contents are updated with each supplement. CD-ROM purchasers receive a completely new disc every quarter and should dispose of their outdated discs. The material covered in the two versions is identical.

Subjects in this manual are organized by chapters, and protocols are contained in units. Protocol units, which constitute the bulk of the book, generally describe a method and include one or more protocols with listings of materials, steps and annotations, recipes for unique reagents and solutions, and commentaries on the "hows" and "whys" of the method. Other units present more general information in the form of explanatory text with no protocols. Overview units contain theoretical discussions that lay the foundation for subsequent protocols. Other discussion units present more general information.

Page numbering in the looseleaf version reflects the modular arrangement by unit; for example, page 1.2.3 refers to Chapter 1 (Toxicological Models), *UNIT 1.2* (Statistical Methods in Toxicology), page 3 of that particular unit.

Many reagents and procedures are employed repeatedly throughout the manual. Instead of duplicating this information, cross-references among units are used and recipes for common reagents are supplied in *APPENDIX 2A*. Cross-referencing helps to ensure that lengthy and complex protocols are not overburdened with steps describing auxiliary procedures needed to prepare raw materials and analyze results.

Introductory and Explanatory Information

Because this publication is first and foremost a compilation of laboratory techniques in toxicology, we have included explanatory information where required to help readers gain an intuitive grasp of the procedures. Some chapters begin with special overview units that describe the state of the art of the topic matter and provide a context for the procedures that follow. Chapter and unit introductions describe how the protocols that follow connect to one another, and annotations to the actual protocol steps describe what is happening as a procedure is carried out. Finally, the Commentary that closes each protocol unit describes background information regarding the historical and theoretical development of the method, as well as alternative approaches, critical parameters, troubleshooting guidelines, anticipated results, and time considerations. All units contain cited references and many indicate key references to inform users of particularly useful background reading, original descriptions, or applications of a technique.

Protocols

Many units in the manual contain groups of protocols, each presented with a series of steps. One or more *basic* protocols are presented first in each unit and generally cover the recommended or most universally applicable approaches. *Alternate* protocols are provided where different equipment or reagents can be employed to achieve similar ends, where the starting material requires a variation in approach, or where requirements for the end product differ from those in the basic protocol. *Support* protocols describe additional steps that are required to perform the basic or alternate protocols; these steps are separated from the core protocol because they might be applicable to other uses in the manual, or because they are performed in a time frame separate from the basic protocol steps.

Reagents and Solutions

Reagents required for a protocol are itemized in the materials list before the procedure begins. Many are common stock solutions, others are commonly used buffers or media, while others are solutions unique to a particular protocol. Recipes for the latter solutions are provided in each unit, following the protocols (and before the commentary) under the heading Reagents and Solutions. It is important to note that the *names* of some of these special solutions might be similar from unit to unit (e.g., electrophoresis buffer) while the *recipes* differ; thus, make certain that reagents are prepared from the proper recipes. On the other hand, recipes for commonly used stock solutions and buffers are provided once in *APPENDIX 2A*. These universal recipes are cross-referenced parenthetically in the materials lists rather than repeated with every usage.

Commercial Suppliers

Throughout the manual, we have recommended commercial suppliers of chemicals, biological materials, and equipment. In some cases, the noted brand has been found to be of superior quality or it is the only suitable product available in the marketplace. In other cases, the experience of the author of that protocol is limited to that brand. In the latter situation, recommendations are offered as an aid to the novice in obtaining the tools of the trade. Experienced investigators are therefore encouraged to experiment with substituting their own favorite brands.

Addresses, phone numbers, and facsimile numbers of all suppliers mentioned in this manual are provided in the *SUPPLIERS APPENDIX*.

Safety Considerations

Anyone carrying out these protocols may encounter the following hazardous or potentially hazardous materials: (1) radioactive substances, (2) toxic chemicals and carcinogenic or teratogenic reagents, and (3) pathogenic and infectious biological agents. Check the guidelines of your particular institution with regard to use and disposal of these hazardous materials. Although cautionary statements are included in the appropriate units, we emphasize that users must proceed with the prudence and precaution associated with good laboratory practice, and that all materials must be used in strict accordance with local and national regulations.

Animal Handling

Many protocols call for use of live animals (usually rats or mice) for experiments. Prior to conducting any laboratory procedures with live subjects, the experimental approach must be submitted in writing to the appropriate Institutional Animal Care and Use Committee (IACUC) or must conform to appropriate governmental regulations regarding the care and use of laboratory animals. Written approval from the IACUC (or equivalent) committee is absolutely required prior to undertaking any live-animal studies. Some specific animal care and handling guidelines are provided in the protocols where live subjects are used, but check with your IACUC or governmental guidelines to obtain more extensive information.

Reader Response

Most of the protocols included in this manual are used routinely in the authors' laboratories. These protocols work for them; to make them work for you they have annotated critical steps and included critical parameters and troubleshooting guides in the commentaries to most units. However, the successful evolution of this manual depends upon readers' observations and suggestions. Consequently, a self-mailing reader-response

survey can be found at the back of the manual (and is included with each supplement); we encourage readers to send in their comments.

ACKNOWLEDGMENTS

This manual is the product of dedicated efforts by many of our scientific colleagues who are acknowledged in each unit and by the hard work by the Current Protocols editorial staff at John Wiley and Sons. We are extremely grateful for the critical contributions by Kathy Morgan (Series Editor), who kept the editors and the contributors on track and played a key role in bringing the entire project to completion, and by Gwen Crooks and Virginia Chanda, who provided developmental support in the early stages of the project. Other skilled members of the Current Protocols staff who contributed to the project include Joseph White, Kathy Wisch, Michael Gates, Demetra Kagdis, Alice Ro, Scott Holmes, Tom Cannon, and Alda Trabucchi. The extensive copyediting required to produce an accurate protocols manual was ably handled by Rebecca Barr, Allen Ranz, Elizabeth Harkins, Ben Gutman, Karen Hopkin, Monte Kendrick, Caroline Lee, Candace Levy, and Cathy Lundmark, and electronic illustrations were prepared by Gae Xavier Studios.

Mahin D. Maines, Lucio G. Costa, Donald J. Reed,
Shigeru Sassa, and I. Glenn Sipes

CHAPTER 1
Toxicological Models

INTRODUCTION

This chapter illustrates a variety of general models and approaches that can be used in toxicological studies. As such, it is considerably broader and more diverse than other chapters in *Current Protocols in Toxicology*, presenting a broad group of methodological approaches, in vivo models, and in vitro systems. As well as established toxicological protocols, the chapter will cover both traditional and novel methods developed in other disciplines that have potential application to toxicology.

UNIT 1.1 examines the role of nonhuman primates as animal models in toxicology research. While not used extensively, for certain obvious reasons (such as cost and the necessity for special facilities), their similarity animals to humans makes nonhuman primates invaluable in certain aspects of toxicology. The unit discusses several areas of investigation (including reproductive toxicology, neurobehavioral toxicology, and immunotoxicology) where studies in nonhuman primates have provided important data relating to understanding mechanisms of toxicity and setting safe levels of exposure to toxicants.

Because the end-points of toxicity used in in vivo or in vitro studies are so diverse, use of the appropriate statistical approach is of the utmost importance. *UNIT 1.2* reviews statistical methods in toxicology, with an emphasis on the approaches that should be used with different toxicological tests.

The ability to generate transgenic animals, most often mice, that overexpress or lack a certain protein (such as an enzyme or receptor) has been one of the major achievements in life science research over the past several years. The availability of transgenic animals allows a much better understanding of the physiological functions of proteins of interest and of their potential role in chemical toxicity. *UNIT 1.3* discusses strategies and applications of transgenic animals in toxicology, as well as methods currently used to generate transgenic mice.

DNA microarrays, also known as DNA "chips," allow detection of expression of RNA for thousands of genes that can be modified by toxic chemicals. In addition, they can be used to detect DNA sequence polymorphisms, thus providing a powerful method to assess genetic variations. An overview of the technologies of DNA microarrays and their applications to toxicology is presented in *UNIT 1.4*.

UNIT 1.5 describes a series of methods for the preparation and use of fish-derived cell lines for cytotoxicity testing of environmental contaminants. Another interesting model system for toxicity testing is represented by sea urchin embryos and larvae. The model, described in *UNIT 1.6*, appears to be particularly promising for studies of the effects of developmental neurotoxicants.

UNIT 1.7 describes yet another rather novel test system—the zebrafish—which has potential for a number of applications.

Contributed by Lucio G. Costa
Current Protocols in Toxicology (2003) 1.0.1-1.0.2

Two important in vivo models for studying Parkinson's disease are discussed in *UNIT 1.8*; they utilize treatments with MPTP in mice and non-human primates and with 6-OHDA in rats.

Upcoming units will discuss in vitro methods to assess toxicity and genotoxicity in mammalian cells among other topics.

Lucio G. Costa

Nonhuman Primates as Animal Models for Toxicology Research

The use of nonhuman primates in biomedical research has a long and distinguished history (Bennett et al., 1995). An integral part of this history is biomedical research in the area of toxicology. The purpose of this unit is to present an overview of the use of nonhuman primate models in toxicological research. The unit is organized into five sections. The first section provides an overview of the extensive work with nonhuman primate models in the areas of reproductive toxicology and teratology (birth defects). The second section focuses on neurotoxicology research, including a brief discussion of nonhuman primate models for Parkinson's disease and methanol-induced ocular toxicity. This section also offers an overview of studies that used infant nonhuman primate models to investigate the neurobehavioral toxicology of early exposure to environmental pollutants (lead, methylmercury, polychlorobiphenyls) and drugs of abuse (ethanol, cocaine). Section three focuses on immunotoxicology. Recent studies that used nonhuman primate models to examine the effects of polychlorobiphenyls (PCBs) and early ethanol exposure are provided as examples. The fourth section discusses research in respiratory or lung toxicology and highlights the use of nonhuman primate models in studies of inhaled particles. The final section provides an overview of the use of nonhuman primate models for research in chemical carcinogenesis. This section also discusses long-term National Cancer Institute studies that used nonhuman primates in tumor-incidence research. More recent uses of nonhuman primates in studies of the role of diet in the development of cancer are also presented. The unit closes with a few comments on other important uses of nonhuman primates in toxicological research.

Although this unit describes the numerous contributions of nonhuman primate models in toxicology, it is important to keep in mind that the majority of toxicology research is conducted using rodent animal models. Rodents have more diverse behavioral repertoires, are less expensive to purchase (thus allowing larger sample sizes), and are easier to care for than nonhuman primates. Rodents also develop quickly, so adult physical stature and sexual maturity are reached in months instead of years.

Mazue and Richez (1982) delineated the benefits and problems associated with using nonhuman primates in toxicological research. Issues such as phylogenetic proximity and physiologic, metabolic, and behavioral similarity were listed as benefits, whereas supply, small sample sizes, the potential for disease transmission to humans, and cost were listed as problems. In addition to the above, the ethical use and treatment of nonhuman primates is an issue of great importance in toxicology research. Although the ethical issues are not specific to nonhuman primate research or research in toxicology (Dennis, 1997), researchers in toxicology must weigh these issues—such as why nonhuman primates are necessary in the investigation of toxic effects and how many animals are required to define potential toxicity—carefully when the use of nonhuman primates is considered.

The nonhuman primates most frequently used in toxicology are members of the *Macaca* genus and include the crab-eating macaque (*M. fascicularis*), the rhesus macaque (*M. mulatta*), and the pig-tailed macaque (*M. nemestrina*). Less widely used are the baboon, squirrel monkey, and chimpanzee. The specific requirements for housing and maintenance of these animals are described in the congressional Animal Welfare Act (AWA). (To obtain a copy of the AWA, call the USDA at 916-857-6205.) Administered by the US Department of Agriculture (USDA), this act covers all warm-blooded animals, with the exception of rats, mice, and birds. The US Public Health Service (USPHS) requires that all institutions supported by the National Institutes of Health (NIH) meet or exceed the regulations published in the AWA. Briefly, the minimum space (cage size) that must be provided to nonhuman primates is based on the animal's weight, except for brachiating species (those that rely on an overhead arm swing for locomotion) and the great apes (i.e., chimpanzees, orangutans, and gorillas). The AWA contains a table for calculating appropriate cage size. Animals are typically fed twice a day to support natural foraging behavior and to minimize the potential of clinical disorders, such as bloating. Purina High Fiber Monkey Chow (#5049) provides all the basic nutritional requirements, although diets are typically supplemented with vegetables and

Contributed by Thomas M. Burbacher and Kimberly S. Grant
Current Protocols in Toxicology (1999) 1.1.1-1.1.9

fruits, such as grapes, apples, green peppers, cherry tomatoes, onions, potatoes, and yams. Water is typically available ad libitum. Recently, the AWA was amended to include environmental enrichment programs for nonhuman primates and dogs. Environmental enrichment for primates typically includes regular opportunities for social contact for grooming and play, chew toys, at least one perch in each cage, food treats, positive interaction with a caregiver or another familiar person, and daily visual and auditory contact with at least one animal of the same or a compatible species.

When working with nonhuman primates, all laboratory personnel must follow special precautions for minimizing the transmission of zoonoses. These precautions include, but are not limited to, gloves, protective eyewear, shoe covers, and laboratory coats. Many of these steps have been adopted in response to the potential lethal nature of the herpes B virus. Because small research facilities find it difficult to meet all the necessary requirements, most nonhuman primate research in the United States is carried out at one of the seven NIH-sponsored Regional Primate Research Centers (*www.ncrr.nih.gov/compmed/cmrprc.htm*).

REPRODUCTIVE TOXICOLOGY AND TERATOLOGY

Reproductive Toxicology

The value of the nonhuman primate model in reproductive toxicology is largely based on similarities of the hypothalamic-pituitary-ovarian-uterine axis in monkeys and humans. The general reproductive parameters shared between many nonhuman primates and humans include the plasma hormone patterns that support menstruation, the length of the menstrual cycle, the onset of chorionic gonadotropin secretion, placental structure, and length of gestation (Hendrickx and Cukierski, 1987). Macaque menstrual cycles are typically 28 days long with 3 to 5 days of actual menses, closely matching the human menstrual cycle. Conception rates vary among species and laboratories, ranging from 25% to 50% after a single mating. In addition, similarities in embryonic and fetal development are evident, beginning with the timing and length of organogenesis. As in humans, successful reproduction in primates requires a fertilized oocyte to implant in the endometrial lining of the uterus and complex hormonal interactions to successfully maintain the pregnancy. Once conception has taken place, both humans and macaques show similar early pregnancy plasma hormone patterns. Organogenesis begins on day 21 in the macaque and day 18 in the human, ending on day 50 in the macaque and day 60 in the human. Although human placentas are monodiscoid (single lobed) and macaque placentas are bidiscoid (double lobed), placental function is virtually identical. The gestation of a full-term infant macaque ranges from 165 to 175 days (23 to 25 weeks), whereas human gestation is, on the average, ~280 days (40 weeks).

Ovarian function and pregnancy are generally well understood in many nonhuman primate species and thus provide an opportunity to examine the relationship between toxicant exposure and reproductive dysfunction (e.g., alterations in menses and fertility). Studies can be designed to evaluate changes in the production of steroids after toxicant exposure and the role these changes may play in adverse reproductive outcomes. In addition to more immediate outcome measures, such as menses, ovulation, and pregnancy, reproductive processes at the opposite end of the reproductive continuum, such as menopause, can also be examined in lifespan studies (Sakai and Hodgen, 1988).

Within the context of reproductive toxicology, Sakai and Hodgen (1988) pointed out the importance of minimally invasive experimental procedures. Examples of such procedures are the collection of blood during the menstrual cycle for analysis of gonadotropin and steroid concentrations, the collection of urine for analysis of steroids and pregnancy gonadotropins, and minor surgical procedures (e.g., laparoscopy and laparotomy). Behavioral methods have also been developed to minimize the handling and subsequent stress of adult female monkeys used for reproductive toxicology studies. Monkeys can be trained to present their perineum to human observers so menstrual bleeding can be detected, and early pregnancies can be reliably palpated by 3 to 4 weeks postconception (Burbacher et al., 1988).

Various macaque species have been used as models in studies investigating the reproductive effects of exposure to environmental pollutants (lead, methylmercury) and of drug abuse (ethanol, cocaine). Procedures for evaluating the characteristics of the menstrual cycle (length, hormone status), breeding status (number of timed matings to conception, conception rate, live-birth delivery rate), and offspring viability (gestation length, birth size, perinatal mortality) are typically included in these studies. Results indicated that lead exposure suppresses circulating levels of luteinizing hormone (LH),

follicle-stimulating hormone (FSH), and 17-β-estradiol (E_2) during the menstrual cycle in crab-eating macaques (*M. fascicularis*). The length of the menstrual cycle, the length of menses, and the circulating levels of progesterone were unaffected (Foster, 1992). Chronic methylmercury exposure was associated with a decrease in the number of live-born offspring in crab-eating macaques, but the menstrual cycle and menses lengths were again unaffected (Burbacher et al., 1988). Reproductive effects associated with ethanol exposure in pig-tailed macaques (*M. nemestrina*) also included a significant decrease in the number of live-born offspring (Clarren and Astley, 1992). This effect was primarily the result of an increase in the number of abortions. A study of the effects of maternal cocaine exposure in rhesus monkeys (*M. mulatta*) did not reveal significant effects on reproductive parameters (Morris et al., 1996a). The number of females investigated in this study (n = 3/group) may, however, have been too small to detect such effects.

Teratology

One of the most important uses of nonhuman primate models has been in research aimed at identifying toxicants that cause birth defects. Compared to adults, embryos and fetuses exhibit an increased sensitivity to the structural and functional effects of many chemical compounds. Studies designed specifically to address the risk of birth defects are required to evaluate the health risks from exposure to certain environmental compounds or drugs. For drugs that are likely to be taken by pregnant women and for a widespread environmental pollutant, such as lead or methylmercury, studies using nonhuman primate models may be appropriate.

The antinausea drug thalidomide provides a good example of the importance of using nonhuman primate models in teratology research. Limb malformations documented in infants born to women who used this drug during pregnancy were not observed in routine teratology tests using rodent models. Parallel effects were observed in nonhuman primates, including timing (sensitive period), type of malformation (limb defects), and the dose required to produce the teratogenic response (Hendrickx, 1973). The thalidomide episode established nonhuman primates as an important animal model for specific malformation syndromes seen in human infants. However, as Hendrickx and Binkerd (1990) noted, although nonhuman primates provided an excellent model for the effects of thalidomide, this was not the case for the developmental effects after exposure to the rubella virus in early pregnancy. In a study evaluating fifteen known human teratogens, rodent models predicted a human teratogenic response ~70% of the time, but nonhuman primate models predicted such a response only ~50% of the time (Schardein et al., 1985). Although several factors may account for this—e.g., metabolic differences and the small sample size typical in nonhuman primate work—it is prudent to note that nonhuman primates do not always mimic humans in their teratogenic responses.

Nonhuman primate models have been used in a wide range of studies aimed at assessing the safety of pharmaceutical agents, environmental pollutants, physical agents (e.g., X-rays), and drugs of abuse as well as the effects of infectious diseases. Hendrickx and Binkerd (1990) provided a comprehensive listing of the compounds that have been tested using nonhuman primate models and the corresponding indices of toxicity in the offspring (e.g., fetal death, structural malformations, growth retardation, and functional deficits). In addition to thalidomide, nonhuman primate models are particularly well recognized for helping elucidate the dysmorphology associated with prenatal exposure to vitamin A and its derivatives (retinoids), the anticonvulsant valproic acid, and triamcinolone acetonide (a synthetic glucocorticoid). Nonhuman primate models have also played a contributory role in defining the genital malformations associated with diethylstilbestrol.

NEUROTOXICOLOGY

One of the best known nonhuman primate models in neurotoxicity is the 1-methyl-4-phenyl-1,2,3,6-tetrahydropyridine (MPTP)–treated monkey (Kaakkola and Teravainen, 1990; Bezard et al., 1997). The neurotoxic effects after exposure to MPTP in human and nonhuman primates resemble those associated with Parkinson's disease: i.e., hypokinesia, rigidity, resting tremor, stooping posture, dysphagia, depletion of striatal dopamine, and loss of cells in the substantia nigra. Response to drug therapy (e.g., levodopa) is also similar in humans and nonhuman primates exhibiting these symptoms. Studies using neural grafts in MPTP-treated monkeys reported a reduction in parkinsonism. Studies using MPTP-treated monkeys will continue to provide important information regarding the pathophysiology and neurochemical effects associated with Parkinson's disease. Studies of potential innovative or

long-term drug therapies will also continue to use this animal model.

Another excellent example of an important nonhuman primate model is ocular toxicity caused by methanol exposure. Methanol (methyl alcohol or wood alcohol) poisonings have been reported since the turn of the 20th century and are characterized by severe metabolic acidosis; ocular toxicity; and, in the most serious cases, coma and death. Early studies using nonhuman primate models indicated that formate (formic acid), a metabolite of methanol, was responsible for the toxicity associated with methanol intake. Human and nonhuman primates display similar effects from high-dose methanol exposure, owing to their limited capacity, compared with rodents, to metabolize formate to carbon dioxide (Black et al., 1985). Elevated formate concentrations are believed to cause the optic disc edema and optic nerve lesions associated with methanol poisoning. As is the case with MPTP exposure and induction of a parkinsonian-like condition, treatment with formate in the monkey induces the optic nerve toxicity commonly associated with human methanol poisoning. Use of this animal model has aided the development of treatment strategies designed to mitigate the severe and frequently permanent consequences of acute high-dose methanol intake.

Neurobehavioral Toxicology

The highly evolved behavioral repertoire of nonhuman primates makes them excellent subjects for investigations of the functional effects of neurotoxicants. The nonhuman primate model is especially useful in studies of developmental exposures and effects, because monkeys, like humans, have relatively long periods of gestation, infancy, and adolescence. Studies can investigate possible critical periods in development for neurotoxicant effects. Special testing procedures are available for infant nonhuman primates that target milestones in cognitive and sensory development and physical growth.

Macaque and human infants share certain limitations and abilities, particularly during the first months of life. The emergence of reflexes like sucking, rooting, grasping, clasping, and righting can be evaluated as early as postnatal day 1. Infant rhesus macaques (*M. mulatta*) developmentally exposed to lead exhibit lower muscle tonus and increased agitation on tests of neonatal reflexes and behavioral organization compared to controls (Levin et al., 1988).

Early cognition can be studied in monkeys during the first months of life using procedures identical to those used to evaluate human infants. Tests of object permanence are generally believed to measure coordinated reaching responses and spatial memory. Studies of in utero exposure to methylmercury in crab-eating macaques (*M. fascicularis*) indicated a delay in object permanence development. On average, infant crab-eating macaques exposed in utero to methylmercury exhibited object permanence a full month after controls (90 versus 60 days; Burbacher et al., 1990a).

Visual recognition memory can be measured in both humans and monkey infants using a test in which novel visual stimuli are paired with familiar stimuli; looking times to each are recorded (Fagan, 1990). Visual preferences for novel stimuli are considered evidence for recognition memory because some aspects of the familiar stimuli must be retained in memory for the novelty response to occur. Deficits in visual recognition memory have been found in a number of monkey groups at high risk for poor developmental outcome, including those exposed to known human teratogens (methylmercury, ethanol; Burbacher et al., 1990a). Studies with human infants also reported reduced visual recognition scores in infants prenatally exposed to PCBs (Jacobson et al., 1985).

The development of primate social behavior appears relatively sensitive to neurotoxicant exposure. Infants exposed in utero to methylmercury exhibited reduced levels of social play and spent more time engaged in passive, nonsocial behaviors (Burbacher et al., 1990b). Infant monkeys fed lead acetate daily from birth to 1 year of age demonstrated disrupted social development, resulting in decreased levels of social play and increased levels of fear and self-stimulation (Laughlin et al., 1991). These effects persisted after dosing was terminated. Infants exposed in utero to 2,3,7,8-tetrachlorodibenzo-*p*-dioxin (TCDD) initiated more play, retreated less frequently, and were displaced less often from preferred positions in the playroom (Schantz et al., 1992). TCDD-exposed monkeys also displayed increased levels of self-directed behaviors.

Several learning and memory assessments have been developed for older infant, juvenile, and adult nonhuman primates. Tests have been designed to study both spatial and nonspatial memory, using simple and complex learning paradigms—e.g., discrimination, alternation, reversal, and concept learning (matching and nonmatching to sample). Computer-controlled

presentation of test stimuli allows the opportunity to test both monkeys and children on identical measures of cognition. Studies using these procedures have also been used to investigate the effects of in utero cocaine exposure on learning in rhesus monkeys (Morris et al., 1996b). Rice and associates have had one of the most productive neurobehavioral toxicology programs using nonhuman primate models to study caffeine, lead, PCBs, and methylmercury. Results from their research program described learning deficits on several test procedures in monkeys exposed to lead during development (Rice, 1996). The performance of the lead-exposed monkeys was characterized by an inability to attend to relevant cues and to keep pace with changing environmental contingencies. These effects are similar to those observed in children exposed to lead (e.g., attention deficits).

The assessment of sensory functioning is a frequently overlooked area in neurobehavioral toxicology studies. Sensory tests not only are valuable tools in evaluating toxicant-related brain injury but also provide a measure of neurotoxicity that is relatively unencumbered by psychological variables, such as learning ability. Vision is probably the best studied of all sensory systems and is certainly the dominant sense in both human and nonhuman primates. Tests of this nature typically involve assessment of visual acuity and contrast sensitivity and are based on a signal-detection paradigm. Monkeys exposed to chronic low levels of methylmercury from birth exhibited impaired spatial vision relative to controls under conditions of both high and low luminance (Rice and Gilbert, 1982). Studies indicate that in utero exposure to methylmercury also impairs spatial vision in adulthood (Burbacher et al., 1999). Auditory and somatosensory functioning were also evaluated using the signal-detection paradigm. Auditory detection thresholds were studied in monkeys who were exposed to methylmercury during their first 7 years of life (Rice and Gilbert, 1992). Results showed a selective high-frequency hearing loss in treated animals. Somatosensory function was also evaluated in monkeys exposed to methylmercury or lead (Rice and Gilbert, 1995). Animals exposed to methylmercury demonstrated elevated vibration detection thresholds on this procedure, whereas results from the lead-treated monkeys were somewhat equivocal.

IMMUNOTOXICOLOGY

Studies of the anatomy and function of the immune system of nonhuman primates reported many similarities to that of humans (Bleavins and de la Iglesia, 1995). Using monoclonal antibodies raised against human antigens, researchers noted extensive cross-reactivities in several nonhuman primate species, including macaques (Tryphonas et al., 1996). For example, a study by Ozwara et al. (1997) examined the reactivity of 161 antihuman monoclonal antibodies in chimpanzees, rhesus macaques, and squirrel monkeys. Antibodies directed against T cell surface antigens and against cytokine receptors were examined for their reactivity with peripheral blood mononuclear cells. The results of the study indicated that 38 of 161 monoclonal antibodies reacted in all three nonhuman primate species; 112 monoclonal antibodies reacted in one or two of the species. Chimpanzees showed the highest cross-reactivity (65%), followed by rhesus macaques (45%) and squirrel monkeys (42%). Tryphomas et al. (1996) reported extensive cross-reactivities with antihuman monoclonal antibodies in *M. fascicularis* infants. An important finding in this study was the reported sex differences in the levels of CD4 monoclonal antibodies and for the CD4/CD8 ratio (females > males), a sex difference similar to that observed in humans. Bleavins and de la Iglesia (1995) reported the results of a study aimed at developing a delayed-type hypersensitivity procedure using crab-eating macaques (*M. fascicularis*). Delayed-type hypersensitivity was measured using the human multitest cell-mediated immunity (CMI) skin test, which includes seven antigens. Responses to the skin tests paralleled those observed in humans. The authors proposed the use of this delayed-type hypersensitivity procedure in *M. fascicularis* for preclinical safety testing.

A number of sensitive methods are available for evaluating the effects of compounds on the immune systems of humans and animals. In a series of articles, Luster et al. (1993) described a screening battery for evaluating the potential immunotoxicity of compounds in mice. Five parameters were included in the battery (immunopathology, humoral-mediated immunity, CMI, nonspecific immunity, and host resistance challenge) in a two-tier approach. Studies using nonhuman primate models of immune system toxicity have included assessments of these parameters. For example, Tryphomas (1995) published a series of reports describing the effects of PCB exposure on the immune system of adult rhesus macaques. The results of the study indicated that low-level chronic (55 months) exposure to PCBs (Aroclor 1254) was

associated with changes in several immunological parameters in the rhesus macaque (Table 1.1.1). These changes were most likely the result of altered T cell and/or macrophage function.

Pig-tailed macaques (*M. nemestrina*) have been used to study the immune effects associated with fetal alcohol exposure (Grossmann et al., 1993). Monkeys exposed to ethanol in utero were more susceptible to disease and exhibited reduced T lymphocyte proliferation and lower titers to tetanus toxoid than did nonexposed controls. The reduction in T cell proliferation was consistent with reports from studies of children with fetal alcohol syndrome (FAS) and rodent models of prenatal alcohol exposure. The authors noted that several of the effects seemed sex dependent and cautioned investigators about the need to control for sex in nonhuman primate studies of immune system effects.

RESPIRATORY TOXICOLOGY

Reports of cross-species comparisons of the anatomy and physiology of the respiratory system and the rates of deposition, clearance, and retention of inhaled particles have described many similarities between nonhuman primates and humans (Snipes, 1989, 1996; Nikula et al., 1997). For example, humans and nonhuman primates clear particles from the alveolar region more slowly, have larger alveoli and alveolar ducts, and have more complex acini than do rodents. Nonhuman primate models have been used extensively in studies of dust-induced pulmonary lesions (Snipes, 1996). In rats, chronic inhalation of poorly soluble dusts causes "lung overload," which can result in altered pulmonary clearance and pulmonary fibrosis. Humans and nonhuman primates exhibit a different pattern of dust accumulation in the lungs after chronic exposure. Whereas rats show fast pulmonary clearance of dust and retain dust predominantly in macrophages within the alveoli, human and nonhuman primates exhibit a slower pulmonary clearance of dust and retain dust burdens in the pulmonary interstitium. The rat pattern of dust accumulation may be related to the increased susceptibility of this animal to alterations in pulmonary clearance after chronic dust exposure compared to nonhuman primates. The rodent animal model may not

Table 1.1.1 Immunological Parameters Assessed in PCB-Exposed Rhesus Monkeys[a,b]

Parameter	Result[c]
Cell-mediated immunity	
Lymphocyte proliferation	D
Host-resistance challenge	
Pneumococcus titers	N
Nonspecific immunity	
Serum complement (CH_{50})	I
Natural killer cells	I
Serum thymosin	I
Monocyte activation	D
Total interferon	I[d]
Interleukin	D
Tumor necrosis factor	N
Humoral-mediated immunity	
CD2, CD4, CD8, CD20	N[e]
IgM and IgG titers	D

[a]Summarized from Tryphonas (1995).

[b]Serum hydrocortisone levels were normal in all exposure groups.

[c]I = increased, N = normal, D = decreased.

[d]Significant increase in low and high groups; significant decrease in moderate group.

[e]Significant decrease in percent of total T lymphocytes (CD2).

provide data relevant to the risk of pulmonary disease after chronic dust exposure in humans.

In addition to dust particles, respiratory effects have been described in nonhuman primate models after exposure to diesel exhaust (Nikula et al., 1997), ozone (Dimitriadis, 1993), marijuana smoke (Flifeil et al., 1991), and different forms of beryllium (Haley et al., 1994).

CLINICAL CARCINOGENESIS

In 1961, the National Cancer Institute began a program aimed at examining the susceptibility of nonhuman primates to chemicals that were known to cause tumors in rodents. Since then, the long-term carcinogenic activity of several therapeutic agents, food additives and compounds, environmental contaminants, N-nitroso compounds, and model rodent carcinogens have been evaluated. In addition, valuable data have been collected regarding the incidence of spontaneous tumors in several nonhuman primate species. Thorgeirsson et al. (1994) reported that the spontaneous tumor rate over a 32-year period for 181 rhesus monkeys was 2.8% for malignant tumors and 3.9% for benign tumors. For 130 crab-eating macaques and 62 African green monkeys, the corresponding rates were 1.5% and 0.8% and 8% and 0%, respectively.

Continuous dosing studies with the artificial sweeteners (cyclamate or saccharin) over a 22-year period provided no evidence of carcinogenic effects. Fungal food contaminants such as aflatoxin B1 and sterigmatocystin, however, were found to be potent hepatocarcinogens. 2-Amino-3-methylimidazo[4,5-*f*]quinoline (IQ), an imidazole heterocyclic amine (HCA) present in cooked meat, was also found to be a potent hepatocarcinogen, inducing malignant liver tumors in 65% of monkeys tested during a 7-year dosing period. Snyderwine et al. (1997) reported that IQ is activated in monkeys via N-hydroxylation carried out by cytochrome P-450 CYP3A4 and/or CYP2C9/10. Human hepatic microsomes have been shown to have a greater capacity to activate HCAs compared to rodents and nonhuman primates. Current estimates of the daily intake of HCAs are on the order of 1 to 20 mg/person. Based on animal data, the estimates of the cancer risk to humans associated with this intake of HCAs are 10^{-3} to 10^{-4}.

Nonhuman primate models have also been used to examine the uptake and metabolic characteristics of suspected carcinogens when different susceptibilities are observed in rodent models. For example, studies indicated that mice are much more sensitive than rats to the carcinogenic effects of 1,3-butadiene and benzene (Henderson, 1996a,b). Studies using crab-eating macaques reported a low uptake of 1,3-butadiene after inhalation exposure. Concentrations of butadiene metabolites in the blood were 5 to 50 times lower in monkeys than in mice and 4 to 14 times lower than in rats. Studies of benzene also reported species differences in metabolism after inhalation exposure. Mice metabolize a greater fraction of a given dose of benzene than do rats and nonhuman primates. Mice also exhibit higher urinary concentrations of hydroquinone and its conjugates. Both rats and mice metabolize a higher fraction of benzene to ring-breakage metabolites than do nonhuman primates, as indicated by the levels of muconic acid in urine. Ring-breakage metabolites and hydroquinone have both been implicated in benzene carcinogenesis.

SUMMARY

This unit describes several important uses of nonhuman primate models in toxicological research. The examples provided are by no means exhaustive. Nonhuman primates continue to be used in studies of drug metabolism and of the toxicokinetics of environmental pollutants. Monkeys are also likely to be used more as new biotechnology products are discovered. In all of these areas of research, monkeys represent a unique resource, given the close evolutionary history they share with humans. The decision to use nonhuman primate models should always be made after careful consideration of all other alternatives. When nonhuman primate models are deemed necessary, researchers bear a special responsibility to ensure that procedures to minimize pain and discomfort are used and that proper environmental enrichment programs are in place (Bloomsmith et al., 1991).

LITERATURE CITED

Bennett, B.T., Abee, C.R., and Hendrickson, R. 1995. Nonhuman Primates in Biomedical Research: Biology and Management. American College of Laboratory Animal Medicine Series. Academic Press, San Diego.

Bezard, E., Imbert, C., Deloire, X., Bioulac, B., and Gross, C.E. 1997. A chronic MPTP model reproducing the slow evolution of Parkinson's disease: Evolution of motor symptoms in the monkey. *Brain Res.* 766:107-112.

Black, K.A., Eells, J.T., Noker, P.E., Hawtrey, C.A., and Tephly, T.R. 1985. Role of tetrahydrofolate in the species differences in methanol toxicity. *Proc. Natl. Acad. Sci. U.S.A.* 82:3854-3858.

Bleavins, M.R. and de la Iglesia, F.A. 1995. Cynomolgus monkeys (*Macaca fascicularis*) in preclinical immune function safety testing: Development of a delayed-type hypersensitivity procedure. *Toxicology* 95:103-112.

Bloomsmith, M.A., Brent, L.Y., and Schapiro, S.J. 1991. Guidelines for developing and managing an environmental enrichment program for nonhuman primates. *Lab. Anim. Sci.* 41:372-377.

Burbacher, T.M., Mohamed, M., and Mottet, N.K. 1988. Methylmercury effects on reproduction and offspring size at birth. *Reprod. Toxicol.* 1:267-278.

Burbacher, T., Gunderson, V., Grant-Webster, K., and Mottet, N.K. 1990a. Methods for assessing neurobehavioral development during infancy in primates. *In* Advances in Neurobehavioral Toxicology: Applications in Occupational and Environmental Health (B. Johnson, ed.) pp. 449-454. Lewis, Chelsea, Mich.

Burbacher, T., Sackett, G., and Mottet, N.K. 1990b. Methylmercury effects on the social behavior of *Macaca fascicularis* infants. *Neurotoxicol. Teratol.* 12:65-71.

Burbacher, T.M., Grant, K.S., Gilbert, S.G., and Rice, D.C. 1999. The effects of methylmercury exposure on visual and auditory functions in nonhuman primates. *Toxicologist* 48:362.

Clarren, S.K. and Astley, S.J. 1992. Pregnancy outcomes after oral administration of ethanol during gestation in the pig-tailed macaque: Comparing early gestational exposure to full gestational exposure. *Teratology* 45:1-9.

Dennis, J.U. 1997. Morally relevant differences between animals and human beings justifying the use of animals in biomedical research. *J. Am. Vet. Med. Assoc.* 210:612-618.

Dimitriadis, V.K. 1993. Tracheal epithelium of bonnet monkey (*Macaca radiaca*) and its response to ambient levels of ozone. A cytochemical study. *J. Submicrosc. Cytol. Pathol.* 25:53-61.

Fagan, J.F. 1990. The paired-comparison paradigm and infant intelligence. *Ann. N.Y. Acad. Sci.* 608:337-364.

Flifeil, S.E.G., Beals, T.F., Tashkin, D.P., Paule, M.G., Scallet, A.C., Ali, S.F., Bailey, J.R., and Slikker, W. 1991. Marijuana exposure and pulmonary alterations in primates. *Pharmacol. Biochem. Behav.* 40:637-642.

Foster, W.G. 1992. Reproductive toxicity of chronic lead exposure in the female cynomolgus monkey. *Reprod. Toxicol.* 6:123-131.

Grossman, A., Astley, S.J., Liggitt, H.D., Clarren, S.K., Shiota, F., Kennedy, B., Thouless, M.E., and Maggio-Price, L. 1993. Immune function in offspring of nonhuman primates (*Macaca nemestrina*) exposed weekly to 1.8 g/kg ethanol during pregnancy: Preliminary observations. *Alcohol Clin. Exp. Res.* 17:822-827.

Haley, P.J., Pavia, K.F., Swafford, D.S., Davila, D.R., Hoover, M.D., and Finch, G.L. 1994. The comparative pulmonary toxicity of beryllium metal and beryllium oxide in cynomolgus monkeys. *Immunopharmacol. Immunotoxicol.* 16:627-644.

Henderson, R.F. 1996a. Species differences in metabolism of 1,3-butadiene. *In* Advances in Experimental Medicine and Biology, Vol. 387: Biological Reactive Intermediates V (R. Snyder, J.J. Kocsis, I.G. Sipes, G.F. Kalf, D.J. Jollow, H. Greim, T.J. Monks, and C.M. Witmer, eds.) pp. 371-376. Plenum Press, New York.

Henderson, RF. 1996b. Species differences in metabolism of benzene. *Environ. Health Perspect.* 104(Suppl 6):1173-1175.

Hendrickx, A.G. 1973. The sensitive period and malformation syndrome produced by thalidomide in the crab-eating (*Macaca fascicularis*) monkey. *J. Med. Primatol.* 2:267-276.

Hendrickx, A.G. and Binkerd, P.E. 1990. Nonhuman primates and teratological research. *J. Med. Primatol.* 19:81-108.

Hendrickx, A.G. and Cukierski, M.A. 1987. Reproductive and developmental toxicology in nonhuman primates. *In* Progress in Clinical and Biological Research, Vol. 235: Preclinical Safety of Biotechnology Products Intended for Human Use (C.E. Graham, ed.) pp. 73-88. Alan R. Liss, New York.

Jacobson, S., Fein, G., Jacobson, J., Schwartz, P., and Dowler, J. 1985. The effect of intrauterine PCB exposure on visual recognition memory. *Child Dev.* 56:853-860.

Kaakkola, S. and Teravainen, H. 1990. Animal models of parkinsonism. *Pharmacol. Toxicol.* 67:95-100.

Laughlin, N., Bushnell, P., and Bowman, R. 1991. Lead exposure and diet: differential effects on social development in the rhesus monkey. *Neurotoxicol. Teratol.* 13:429-440.

Leary, R. 1958. Analysis of serial discrimination by monkeys. *J. Comp. Physiol. Psychol.* 51:82-86.

Levin, E., Schneider, M., Ferguson, S., Schantz, S., and Bowman, R. 1988. Behavioral effects of developmental lead exposure in rhesus monkeys. *Dev. Psychobiol.* 21:371-382.

Luster, M.I., Portier, C., Pait, D.G., Rosenthal, G.J., Germolec, D.R., Corsini, E., Blaylock, B.L., Pollock, P., Kouchi, Y., Craig, W., White, K.L., Munson, A.E., and Comment, C.E. 1993. Risk assessment in immunotoxicology II. Relationships between immune and host resistance tests. *Fund. Appl. Toxicol.* 21:71-82.

Mazue, G. and Richez, P. 1982. Problems in utilizing monkeys in toxicology. *In* Animals in Toxicological Research (I. Bartoseck, A. Guaitani, and E. Pacei, eds.) pp. 147-163. Raven Press, New York.

Morris, P., Binienda, Z., Gillam, M.P., Harkey, M.R., Zhou, C., Henderson, G.L., and Paule, M.G. 1996a. The effect of chronic cocaine exposure during pregnancy on maternal and infant outcomes in the rhesus monkey. *Neurotoxicol. Teratol.* 18:147-154.

Morris, P., Gillam, M.P., Allen, R.R., and Paule, M.G. 1996b. The effect of chronic cocaine exposure during pregnancy on the acquisition of operant behaviors by rhesus monkey offspring. *Neurotoxicol. Teratol.* 18:155-166.

Nikula, K.J., Avila, K.J., Griffith, W.C., and Mauderly, J.L. 1997. Sites of particle retention and lung tissue responses to chronically inhaled diesel exhaust and coal dust in rats and cynomolgus monkeys. *Environ. Health Perspect.* 105(Suppl. 5):1231-1234.

Ozwara, H., Niphuis, H., Buijs, L., Jonker, M., Heeney, J.L., Bambra, C.S., Thomas, A.W., and Langermans, J.A.M. 1997. Flow cytometric analysis on reactivity of human T lymphocyte–specific and cytokine-receptor-specific antibodies with peripheral blood mononuclear cells of chimpanzee (*Pan troglodytes*), rhesus macaque (*Macaca mulatta*), and squirrel monkey (*Saimiri sciureus*). *J. Med. Primatol.* 26:164-171.

Rice, D. and Gilbert, S. 1982. Early chronic low-level methylmercury poisoning in monkeys impairs spatial vision. *Science* 216:759-761.

Rice, D. and Gilbert, S. 1992. Exposure to methylmercury from birth to adulthood impairs high-frequency hearing in monkeys. *Toxicol. Appl. Pharmacol.* 115:6-10.

Rice, D. and Gilbert, S. 1995. Effects of developmental methylmercury exposure or lifetime lead exposure on vibration sensitivity function in monkeys. *Toxicol. Appl. Pharmacol.* 134:161-169.

Rice, D.C. 1996. Behavioral effects of lead: Commonalities between experimental and epidemiologic data. *Environ. Health Perspect.* 104(Suppl. 2):337-351.

Sakai, C.N. and Hodgen, G.D. 1988. Use of primate folliculagenesis models in understanding human reproductive biology and applicability to toxicology. *Reprod. Toxicol.* 1:207-221.

Schantz, S., Ferguson, S., and Bowman, R. 1992. Effects of 2,3,7,8-tetrachlorodibenzo-*p*-dioxin on behavior of monkeys in peer groups. *Neurotoxicol. Teratol.* 14:433-446.

Schardein, J.L., Schwartz, B.A., and Kenel, M.F. 1985. Species sensitivities and prediction of teratogenic potential. *Environ. Health Perspect.* 61:55-67.

Snipes, M.B. 1989. Long-term retention and clearance of particles inhaled by mammalian species. *CRC Crit. Rev. Toxicol.* 20:175-211.

Snipes, M.B. 1996. Current information on lung overload in nonrodent mammals: Contrast with rats. *Inhal. Toxicol.* 8(Suppl.):91-109.

Snyderwine, E.G., Turesky, R.J., Turteltaub, K.W., Davis, C.D., Sadrieh, N., Schut, H.A.J., Nagao, M., Sugimura, T., Thorgeirsson, U.P., Adamson, R.H., and Thorgeirsson, S.S. 1997. Metabolism of food-derived heterocyclic amines in nonhuman primates. *Mutat. Res.* 376:203-210.

Thorgeirsson, U.P., Dalgard, D.W., Reeves, J., and Adamson, R.H. 1994. Tumor incidence in a chemical carcinogenesis study of nonhuman primates. *Reg. Toxicol. Pharmacol.* 19:130-151.

Tryphomas, H. 1995. The use of nonhuman primates in the study of PCB immunomodulation. *Hum. Exp. Toxicol.* 14:107-110.

Tryphomas, H., Lacroix, F., Hayward, S., Izaguirre, C., Parenteau, M., and Fournier, J. 1996. Cell surface marker evaluation of infant *Macaca* monkey leukocytes in peripheral whole blood using simultaneous dual-color immunophenotypic analysis. *J. Med. Primatol.* 25:89-105.

Contributed by Thomas M. Burbacher and Kimberly S. Grant
University of Washington
Seattle, Washington

The authors would like to thank Noelle Liberato for her dedicated assistance. The preparation of this manuscript was supported by NIH grants ES06673 and ES03745.

Statistical Approaches to the Design of Toxicology Studies

Statistical methods provide an essential tool set for use across the field of toxicology. These methods may serve to perform any combination of three possible tasks. The most familiar is hypothesis testing—i.e., determining if two (or more) groups of data differ from each other at a predetermined level of confidence. The second function involves the construction and use of models, which is most commonly linear regression or the derivation of some form of correlation coefficient. Model fitting allows researchers to relate one variable (typically a treatment, or **independent**, variable) with other variables (usually one or more effects of **dependent** variables). The third function, reduction of dimensionality, is less commonly used than the first two and includes methods for reducing the number of variables in a system while only minimally reducing the amount of information, therefore making a problem easier to visualize and understand. Examples of such techniques are factor analysis and cluster analysis. A subset of the third function, discussed under Descriptive Statistics, is the reduction of raw data to single expressions of central tendency and variability (such as the mean and standard deviation). There is also a special subset (data transformation, which includes such things as the conversion of numbers to log or probit values) that is part of both the second and third functions of statistics. Figures 1.2.1, 1.2.2, 1.2.3, and 1.2.4 present a series of decision trees for selecting individual statistical techniques within the framework of the classification of methodologies.

This unit presents an overview of statistics. Gad (1998) presents a much more extensive discussion. Salsburg (1986) and Krewski and Franklin (1991) have also published works devoted to the field of statistical analysis in toxicology; and although these are more narrow in scope, they provide useful insights.

DESCRIPTIVE STATISTICS

Descriptive statistics is a fundamental starting place, used to convey the general nature of any set of collected data. The statistics describing any single group of data have two components. One of these describes the location of the data, and the other gives a measure of the dispersion of the data in and about this location. A fact that is often overlooked is that the choice of what parameters are used to convey these pieces of information implies a particular nature for the distribution of the data.

Most commonly, for example, location is described by giving the (arithmetic) mean, and dispersion is described by giving the standard

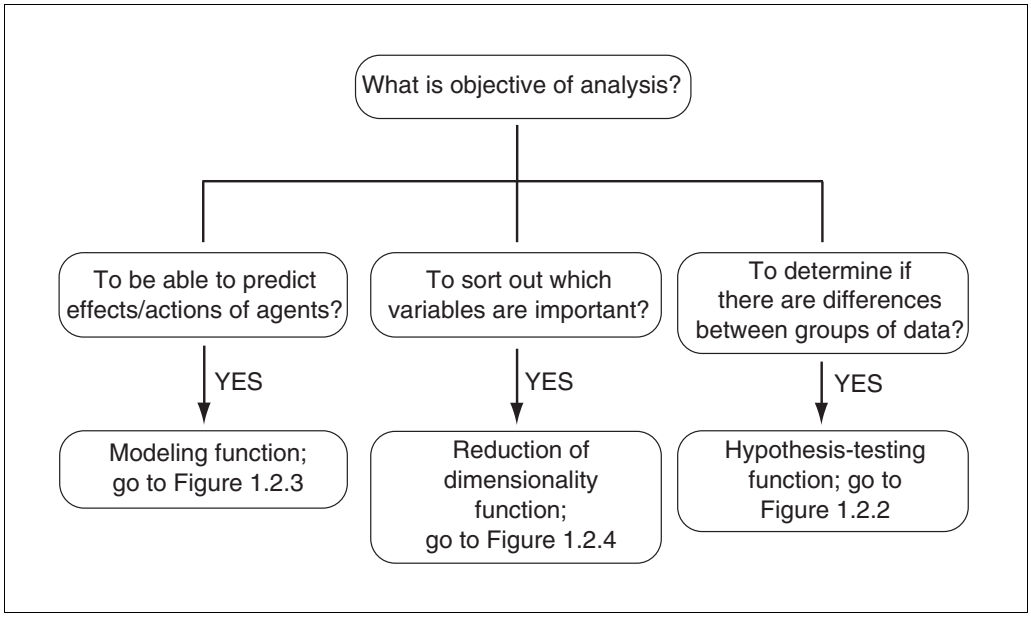

Figure 1.2.1 Overall decision tree for selecting statistical procedures. See Gad (1998) for an explanation of the statistical methods.

Contributed by Shayne C. Gad
Current Protocols in Toxicology (1999) 1.2.1-1.2.18

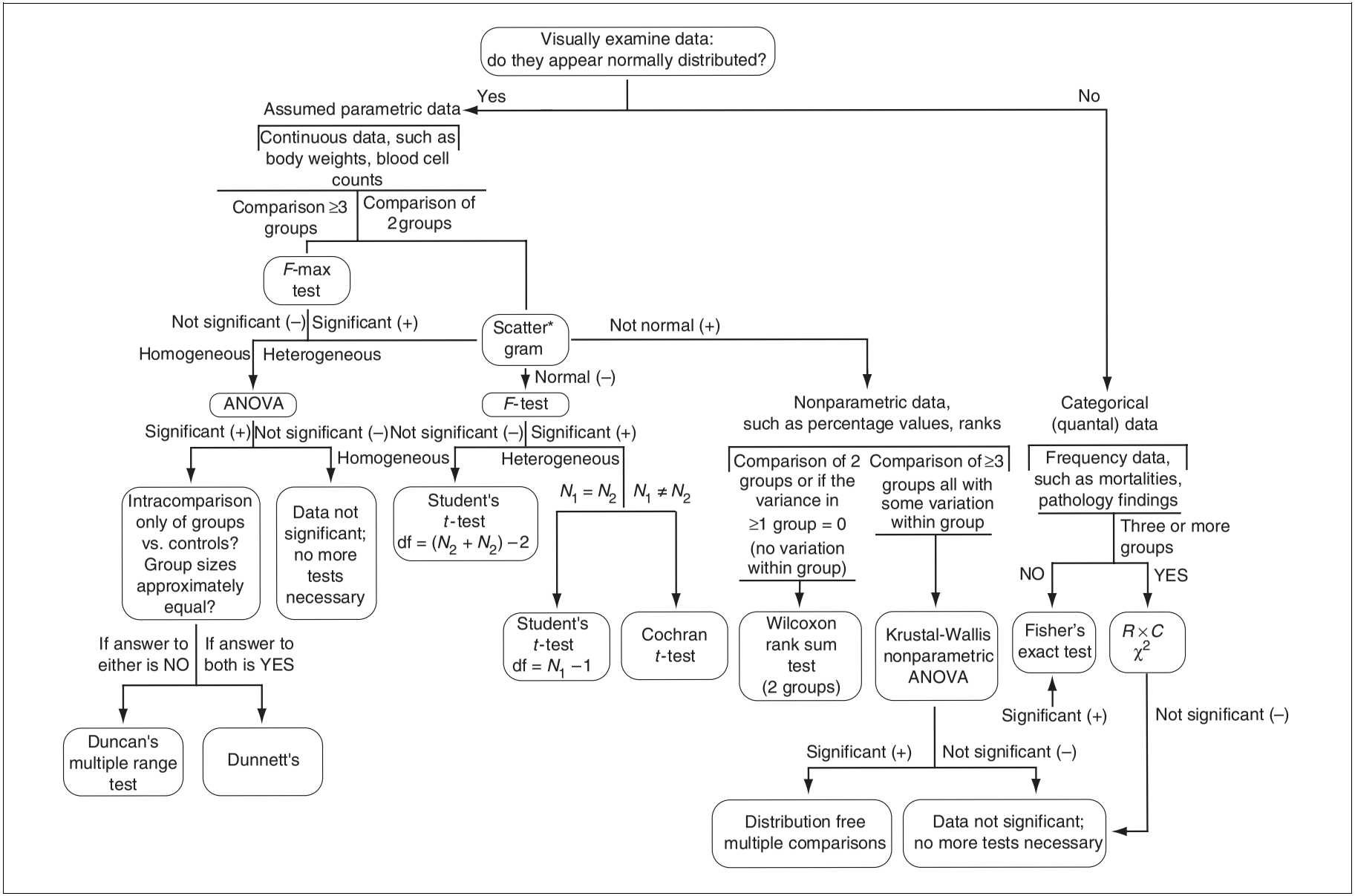

Figure 1.2.2 Decision tree for selecting hypothesis-testing procedure. *, if plot does not clearly demonstrate lack of normality, exact test may be employed; +, if continuous data, Kolmongorox-Smirnov test may be used; –, if discontinuous data, χ^2 goodness-of-fit test may be used. See Gad (1998) for an explanation of the statistical methods.

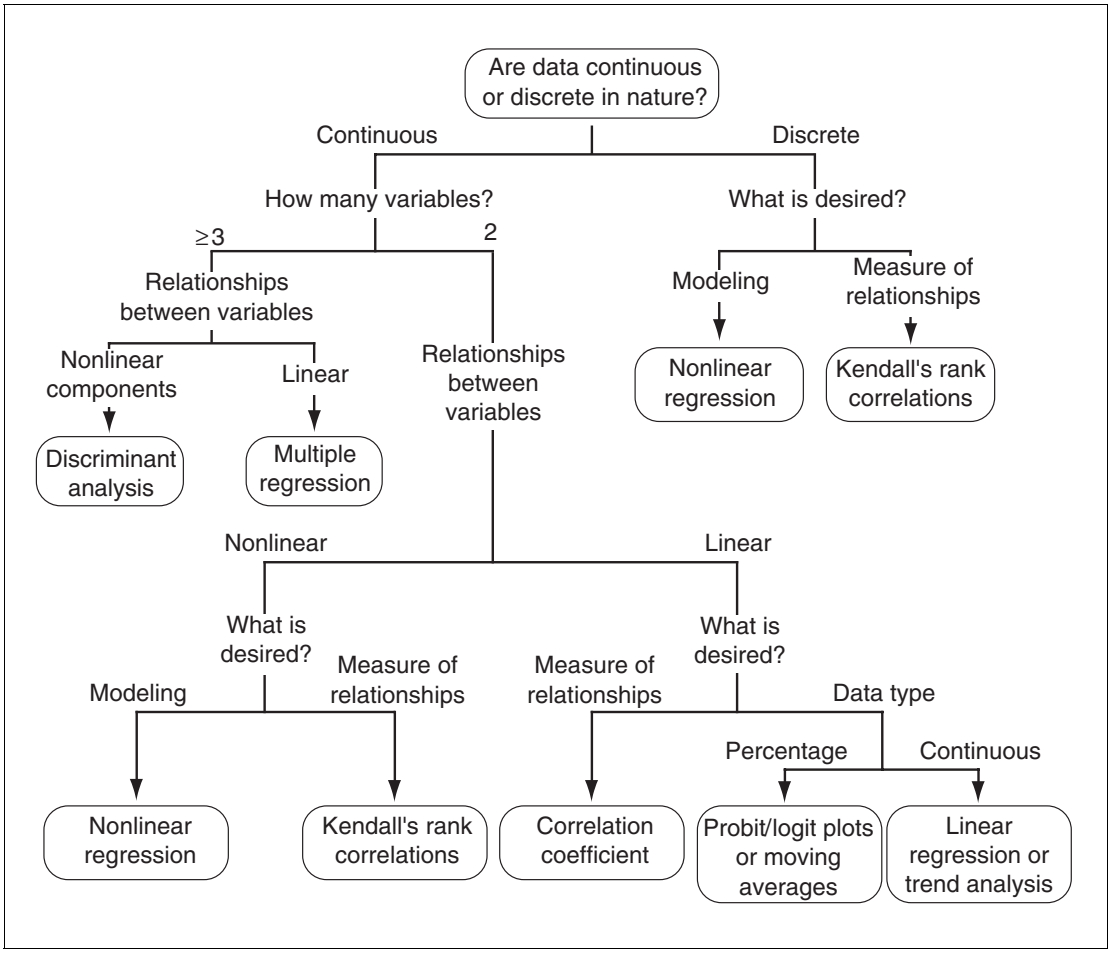

Figure 1.2.3 Decision tree for selecting modeling procedures. See Gad (1998) for an explanation of the statistical methods.

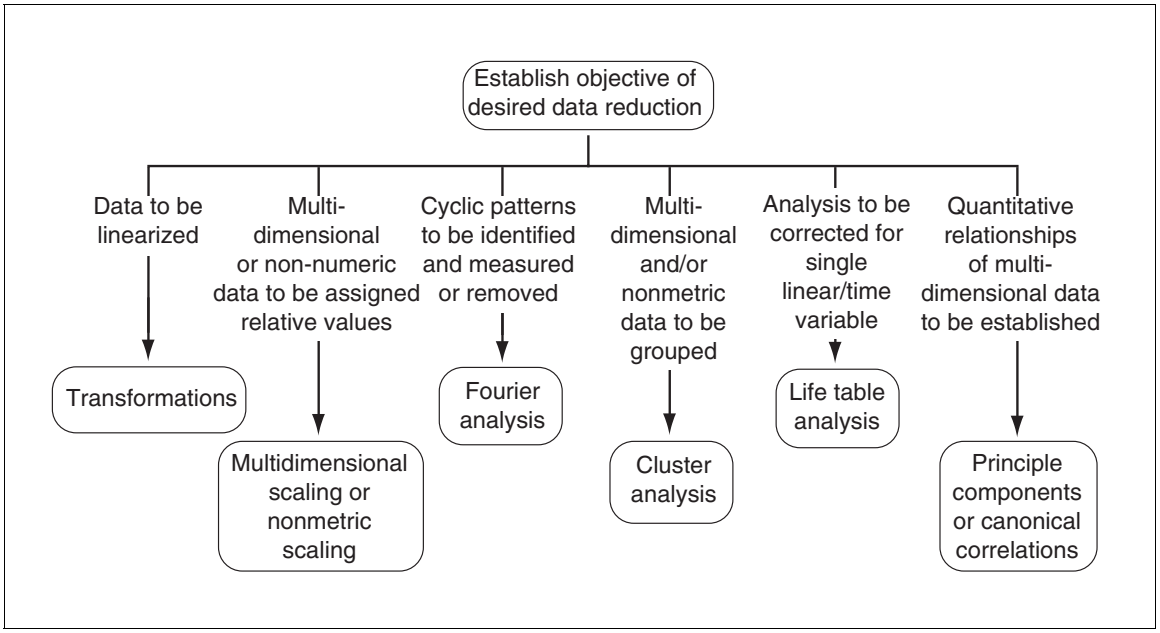

Figure 1.2.4 Decision tree for selecting reduction of dimensionality procedures. See Gad (1998) for an explanation of the statistical methods.

deviation (SD) or the standard error of the mean (SEM). For continuous variables, the character of a sample (x) may be described using the measures of central tendency and dispersion with which researchers are generally most familiar: the mean, denoted by the symbol $\overline{X}$ and also called the arithmetic average, is calculated by adding up all the values in a group then dividing by N (or n), the number of data points in a group. The SD is denoted by the symbol s for samples and σ for populations; in the former case it is calculated as

$$s = \sqrt{\frac{\sum x^2 - \frac{\left(\Sigma \overline{X}\right)^2}{N}}{N-1}}$$

where X is the individual datum. If the total number of data in the group is N, then the SEM is calculated as

$$\text{SEM} = \frac{SD}{\sqrt{N}}$$

The use of these parameters (the mean with either the SD or SEM) to describe a group implies, however, that there is reason to believe that the data being summarized are from a population that is at least approximately normally distributed. If this is not the case, then the researcher should instead use a set of terms that do not have such a rigid underpinning: commonly, the median for location and the semiquartile distance for dispersion.

When all the numbers in a group are arranged in a ranked order (i.e., from smallest to largest), the **median** is the middle value. If there is an odd number of values in a group, then the middle value is obvious (e.g., in the case of 13 values, the seventh largest is the median). When the number of values in the sample is even, the median is calculated as the midpoint between the (N/2)th and the ([N/2] + 1)th number. For example, the series of numbers 7, 12, 13, 19, the median value would be the midpoint between 12 and 13, which is 12.5.

EXPERIMENTAL DESIGN

A priori selection of statistical methodology (as opposed to the post hoc, or after the fact, approach) is as significant a portion of the process of protocol development and experimental design as any other and can measurably enhance the value of the study. The prior selection of statistical methodology is essential for the effective detailing of other parts of the protocol, such as the number of animals per group and the sampling intervals for body weight. To make such a selection, the toxicologist must have both an in-depth knowledge of the area of investigation and an understanding of the general principles of experimental design, because the analysis of any set of data is dictated to a large extent by the manner in which the data are obtained.

The four statistical principles of experimental design are replication, randomization, concurrent ("local") control, and balance.

Replication. Any treatment must be applied to more than one experimental unit (animal, plate of cells, etc.) to allow an estimate of the variability of the unit. This provides more accuracy in the measurement of a response than can be obtained from a single observation, because underlying experimental errors tend to cancel each other out. It also supplies an estimate of the experimental error derived from the variability among all the measurements taken (**replicates**).

Randomization. This is practiced to ensure that every treatment will have its fair share of extreme high and extreme low values and allows the toxicologist to proceed as if the assumption of "independence" were valid. That is, there is no avoidable/known systematic bias in how one obtains data.

Concurrent control. Comparisons between treatments should be made, to the maximum extent possible, between experimental units from the same group. That is, animals used as a **control** group should come from the same source and lot as the test-group animals. And, except for the treatment being evaluated, test and control samples should be maintained and handled in exactly the same manner.

Balance. If the effect of several different factors is being evaluated simultaneously, the experiment should be laid out in such a way that the contributions of the different factors can be separately distinguished and estimated.

The goal of all these principles is good statistical efficiency and the economizing of resources. Montgomery (1997) provides a comprehensive review of the area of experimental design.

The first precise or calculable aspect of experimental design encountered is determining sufficient test- and control-group sizes to allow one to have an adequate level of confidence in the results of a study (i.e., in the ability of the study design with the statistical tests used to detect a true difference, or effect, when it is present). The statistical test contributes a level of power to such a detection. The **power** of a

statistical test is the probability that a test results in rejection of the null hypothesis, H_0, when some other hypothesis, H, is valid. This is termed the power of the test "with respect to the (alternative) hypothesis H."

If there is a set of possible alternative hypotheses, the power, regarded as a function of H, is termed the **power function** of the test. When the alternatives are indexed by a single parameter Π, simple graphical presentation is possible. If the parameter is a vector Π, one can visualize a **power surface**.

If the power function is denoted by $\vartheta(\Pi)$ and H_0 specifies $\Pi = \Pi_0$, then the value of $\vartheta(\Pi)$—the probability of rejecting H_0 when it is in fact valid—is the significance level. A test's power is greatest when the probability of a type II error, or the probability of having a false-negative result (whereas a type I error refers to a false-positive result), is the least. Specified powers can be calculated for tests in any specific or general situation.

Some general rules to keep in mind are

1. The more stringent the significance level, the greater the necessary sample size. More subjects are needed for a 1% level test than for a 5% level test.

2. Two-tailed tests require larger sample sizes than do one-tailed tests. Assessing two directions at the same time requires a greater investment in resources.

3. The smaller the critical effect size, the larger the necessary sample size. Subtle effects require greater efforts (i.e., larger sample sizes).

4. Any difference can be significant if the sample size is large enough.

5. The larger the power required, the larger the necessary sample size. Greater protection from failure requires greater effort (more precision or larger sample size). The smaller the sample size, the smaller the power—i.e., the greater the chance of failure.

6. The requirements and means of calculating necessary sample size depends on the desired (or practical) comparative sizes of test and control groups.

This number (N), or the necessary sample size, can be calculated by using the following formula:

$$N = \frac{(t_1 + t_2)^2}{d^2} s^2$$

where t_1 is the one-tailed t-value with $N - 1$ degrees of freedom (df) corresponding to the desired confidence level; t_2 is the one-tailed t-value with $N - 1$ df corresponding to the probability that the sample size will be adequate to achieve the desired precision; s is the sample standard deviation, typically derived from historical data and calculated as follows (with υ being the variable of interest):

$$s = \sqrt{\frac{1}{N-1}\sum(\upsilon_1 - \upsilon_2)^2}$$

and d is the acceptable range of variation in the variable of interest. This calculation is illustrated in Example 1.

Example 1

In a subchronic dermal study in rabbits, the principal point of concern is the extent to which the compound causes oxidative damage to erythrocytes. To quantitate this, the laboratory will measure the numbers of reticulocytes in the blood. What then would be an adequate sample size to allow the question at hand to be addressed with reasonable certitude?

To determine this, use the one-tailed t-value for an infinite number of degrees of freedom at the 95% confidence level (i.e., $P \leq 0.05$). A set of t-tables shows this number to be 1.645. From prior experience, it is known that the usual values for reticulocytes in rabbit blood are from 0.5 to 1.9 $\times 10^6$/ml. The acceptable range of variation, zero, is therefore equal to the span of this range, or 1.4 (d). Likewise, an examination of the control data from previous rabbit studies shows that the sample standard deviation is 0.825 (s). When all these numbers are inserted into the equation for sample size (presented above), the required sample size (N) is calculated to be

$$= \frac{(1.645 + 1.645)^2}{(1.4)^2}(0.825)^2$$

$$= \frac{10.824}{1.96}(0.825)^2$$

$$= 4.556$$

In other words, in this case, in which there is little natural variability, measuring the reticulocyte counts of groups of only five animals each should be sufficient.

A good approximation can be generated by substituting t-values for an infinite number of degrees of freedom.

OUTLIERS AND ROUNDING OF NUMBERS

Outliers are extreme (high or low) values that are widely divergent from the main body

of a group of data and from what is the common experience. They may arise from an instrument (such as a balance) being faulty, they may be caused by the seemingly natural urge of some animals to frustrate research, or they may be indicative of a "real" value. Outlying values can be detected by visual inspection of the data; by use of a scattergram (discussed later); or (if the data set is small enough, which is usually the case in toxicology) by a large increase in the parameter estimating the dispersion of data, such as the standard deviation.

When it is possible to solidly tie one of the above error-producing processes (such as a balance being faulty) to an outlier, it can be safely deleted from consideration. But if it is not possible to positively attribute such a cause to an outlier (even if the researcher has strong suspicions), the problem is much more complicated, for then such a value may be one of several other things. It could be a result of a particular cause that is the grounds for the entire study—i.e., the very "effect" that is being sought—or it could be because of the collection of legitimate effects that constitute sample error. As will be discussed later (see Characteristics of Screens) and as is now becoming more widely appreciated, in animal studies outliers can be an indication of a biologically significant effect that is not yet statistically significant. Variance inflation can result from such outliers and can be used to detect them. Outliers, in fact, by increasing the variability within a sample, decrease the sensitivity of the statistical tests and may actually preclude a statistically significant result.

Alternatively, the outlier may be the result of an unobserved technician error. In this case the data point should be rejected—excluded from consideration with the rest of the data. Identifying legitimate cases (based on technical—i.e., actual technique-based measurement—error) for rejection from statistical analysis is the most complicated aspect of outlier issues.

When the number of digits in a number is to be reduced (because of limitations of space or to reflect the extent of significance of a number), it is necessary to round it off. Failure to have a rule for performing this operation can lead to both confusion and embarrassment for a facility (during such times as study audits). One common rule follows.

A digit to be rounded is not changed if it is followed by a digit <5—the digits following it are simply dropped off (**truncated**). If the number is followed by a digit >5 or by a 5 followed by other nonzero digits, it is increased to the next highest number. When the digit to be rounded is followed by 5 alone or 5 followed by zeros, it is unchanged if it is even but increased by one if it is odd. Examples of this rule for a case in which the numbers must be reduced to 3 digits follows:

1374 becomes 137
1376 becomes 138
13852 becomes 139.

The rationale behind this procedure is that over a period of time the results should even out, because as many digits will be increased as are decreased.

METHODS

The brevity of this unit enforces a focus on applications at the expense of methodology. In addition to Gad (1998), the reader is urged to consult Sheskin (1997) for detailed presentations and considerations of actual statistical methodologies.

Randomization

Randomization is the act of assigning a number of items (e.g., plates of bacteria or test animals) to groups in such a manner that there is an equal chance for any one item to end up in any one group. This is a control against any possible unconscious bias in assignment of subjects to test groups. One variation on this is what is called a **censored randomization**, which ensures that the groups are equivalent in some aspect after the assignment process is complete. The most common example of a censored randomization is one in which it is ensured that the body weights of the test animals in each group are not significantly different from those in the other groups. This is done by examining weights by analysis of variance after group assignment, then rerandomizing if there is a significant difference at some nominal level, such as $P \leq 0.10$. The process is repeated until there is no difference. A second valuation is stratified (or blocked) randomization, by which members of subclasses (such as litter mates) are assigned to different groups.

There are several alternatives for actually performing the randomization process. The three most commonly employed are card assignment, use of a random number table, and use of a computerized algorithm.

In the card-based method, individual identification numbers for items (e.g., plates or animals) are placed on separate index cards. These cards are then shuffled and placed one at a time in succession into piles corresponding to

the required number of test groups. The results are the random group assignment.

The random number table method requires that one assign unique numbers to the test subjects and have access to a random number table. For example, one may simply set up a table with a column for each group to which subjects are to be assigned. Start from the head of any one column of numbers in the random number table (each time the table is used, a new starting point should be used). If there are fewer than 100 test subjects, use only the last two digits of each random number in the table. If there are more than 99 but less than 1000, use only the last three digits. To generate group assignments, read down a column of the table, one number at a time. As you come across digits that correspond to a subject number, assign that subject to a group (enter its identifying number in a column), proceeding from left to right and filling one row at a time. After an animal is assigned to a group, any duplication of its unique number is ignored. Use as many successive columns of random numbers as needed to complete the process.

The third (and now most common) method is to use a random-number generator that is built into a calculator or computer program. Instructions for the use of such programs are provided by the manufacturer or developer.

One is also occasionally required to evaluate whether a series of numbers (such as an assignment of animals to test groups) is random. This requires the use of a randomization test, of which there are a large variety. The χ^2 test (described later), can be used to evaluate the goodness of fit to a random assignment. If the result is not critical, a simple sign test will work. For the sign test, first determine the middle value in the numbers being checked for randomness. Then go through a list of the numbers assigned to each group, scoring each as a "+" (greater than the middle number) or "–" (less than the middle number). The number of pluses and minuses in each group should be approximately equal.

APPLICATIONS

Median Lethalities

The data required to calculate the median lethality (LD_{50}) or the median effective dose (ED_{50}) include several dosage (or exposure) levels, the number of animals dosed, and the number that died. If the purpose is only to establish the median effective dose in a range-finding test, then testing four or five animals per dose level, using Thompson's method of moving averages, is the most efficient methodology and will give a sufficiently accurate solution. With two dose levels, if the ratio between the high and low dose is ≤2, even total and no mortality at those two dose levels will yield an acceptable, accurate median lethal dose, although a partial mortality is desirable. If, however, the purpose is to estimate a number of toxicity levels (LD_{10}, LD_{90}) and to establish the slope of the dose/lethality curve more precisely, it is common to use at least 10 animals per dosage level and to employ the log/probit regression technique. Note that in the equation $Y_i = a + bx_i$, b is the slope of the regression line and that the method already allows one to calculate 95% confidence intervals about any point in this line. Tests of significance between two or more such sets of data (i.e., slopes of mortality curves) may readily be done by the *t*-type test (discussed earlier) at any one set of points, such as the LD_{50} values of two curves. The confidence interval at any one point will be different from the interval at other points and must be calculated separately. In addition, the nature of the probit transform is such that toward the extremes—LD_{10} and LD_{90}, for example—the confidence intervals will "balloon," i.e., become very wide. Because the slope of the fitted line in these assays has a large uncertainty in relation to the uncertainty of the LD_{50} itself (the midpoint of the distribution), much caution must be used with calculated LD_x values other than LD_{50} values.

Body and Organ Weights

Body weight and the weights of selected organs are among the sets of data normally collected in studies for which animals are repeatedly dosed with (or exposed to) a chemical. Body weight is frequently the most sensitive parameter for indicating an adverse effect. How to best analyze this and in what form to analyze the organ weight data (as absolute weights, weight changes, or percentages of body weight) have been the subjects of a number of articles (Weil and Gad, 1980). The author's experience has been that the following procedures are appropriate if the sample sizes are sufficient (≥10). With smaller sample sizes, the normality of the data becomes increasingly uncertain and nonparametric methods, such as that of Kruskal-Wallis, may be more appropriate (Zar, 1974).

1. Organ weights as percentages of total body weights are calculated.

2. Body weights are analyzed either as weights or as changes in body weight. Even if

Table 1.2.1 Association of Changes in Biochemical Parameters with Actions at Particular Target Organs

Parameter 1	Organ system								Comments
	Blood	Heart	Lung	Kidney	Liver	Bone	Intestine	Pancreas	
Albumin	—	—	—	Dec.	Dec.	—	—	—	Produced by liver; very significant reductions require extensive liver damage
ALP	—	—	—	—	Inc.	Inc.	Inc.	—	Elevations usually associated with cholestasis; bone alkaline phosphatase tends to be higher in young animals
Total bilirubin	Inc.	—	—	—	Inc.	—	—	—	Elevations usually associated with cholestasis owing to obstruction or hepatopathy
BUN	—	—	—	Inc.	Dec.	—	—	—	Estimates blood filtering capacity of the kidneys; does not become significantly elevated until kidney function is reduced 60% to 75%
Calcium	—	—	—	Inc.	—	—	—	—	Can be life-threatening and result in sudden death
Cholinesterase	—	—	—	Inc.	Dec.	—	—	—	Found in plasma, brain, and RBC
CPK	—	Inc.	—	—	—	—	—	—	Most often elevated as a result of skeletal muscle damage but can also be produced by cardiac muscle damage; can be more sensitive than histopathology
Creatinine	—	—	—	Inc.	—	—	—	—	Also estimates blood-filtering capacity of kidney, as does BUN, but is more specific

continued

the groups were randomized properly at the beginning of a study (no group significantly different in mean body weight from any other group, and all animals in all groups within two standard deviations of the overall mean body weight), there is an advantage to using the computationally slightly more cumbersome changes in body weight.

3. Bartlett's test is performed on each set of data to ensure that the variances of the sets are homogeneous.

4. As appropriate, the sequence of analysis outlined in the decision trees (see Figs. 1.2.1, 1.2.2, 1.2.3, and 1.2.4) is followed.

Clinical Pathology

A number of clinical chemistry and hematology parameters are now assessed in the blood and urine collected from animals in chronic toxicity studies. In the past (and still, in some places), the accepted practice has been to evaluate these data using univariant-parametric methods (primarily *t*-tests and/or analysis of variance, ANOVA); however, it can be shown that this is not the best approach on a number of grounds.

First, such biochemical and blood cell parameters are rarely independent of each other, and interest is not often focused on just one parameter. Rather, there are batteries of parameters associated with toxic actions at particular target organs. For example, increases in creatine phosphokinase, α-hydroxybutyrate dehydrogenase, and lactate dehydrogenase occurring together strongly indicate myocardial damage. In such cases, the interest is not in a significant increase in just one of these, but in all three. Table 1.2.1 gives a short summary of the association of various clinical chemistry parameters with known target organ toxicities. Similarly, changes in serum electrolytes (sodium, potassium, and calcium) interact with each other; a decrease in one is frequently tied to an increase in one of the others. Loeb and Quimby (1989) provide an excellent source of detailed understanding of the meaning and de-

Table 1.2.1 Association of Changes in Biochemical Parameters with Actions at Particular Target Organs, continued

Parameter 1	Organ system								Comments
	Blood	Heart	Lung	Kidney	Liver	Bone	Intestine	Pancreas	
Glucose	—	—	—	—	—	—	—	Inc.	Alterations other than those associated with stress are uncommon and reflect an effect on the pancreatic islets or anorexia
GGT	—	—	—	—	Inc.	—	—	—	Elevated in cholestasis; a microsomal enzyme, the levels of which often increase in response to microsomal enzyme induction
HBDH	—	Inc.	—	—	Inc.	—	—	—	—
LDH	—	Inc.	Inc.	Inc.	Inc.	—	—	—	Increases usually the result of skeletal muscle, cardiac muscle, and liver damage; not very specific
Total protein	—	—	—	Dec.	Dec.	—	—	—	Absolute alterations are usually associated with decreased production (liver) or increased loss (kidney); can see increases in cases of muscle "wasting" (catabolism)
SGOT	—	Inc.	—	Inc.	Inc.	—	—	Inc.	Present in skeletal muscle and heart; most commonly associated with damage to these structures
SGPT	—	—	—	—	Inc.	—	—	—	Elevations usually associated with hepatic damage or disease
SDH	—	—	—	—	Inc. or Dec.	—	—	—	Liver enzyme; can be quite sensitive but is fairly unstable; samples should be processed as soon as possible

Abbreviations: Inc., increase of chemistry values; Dec., decrease in chemistry values; ALP, alkaline phosphatase; BUN, blood urea nitrogen; RBC, red blood cells; CPK, creatinine phosphokinase; GGT, gamma glutamyl transferase; HBDH, hydroxybutyric dehydrogenase; LDH, lactic dehydrogenase; SGOT, serum glutamic oxaloacetic transaminase (also called aspartate aminotransferase; AST); SGPT, serum glutamic pyruvic transaminase (also called alanine amino transferase; ALT); SDH, sorbitol dehydrogenase.

tails of laboratory animal clinical chemistries. Furthermore, for some parameters—owing to their biological background or the measurement method—the data are frequently either not normally distributed (particularly because of being markedly skewed) or not continuous. This can be seen in some of the reference data for experimental animals in Weil (1982). Both normality (a normal distribution) and continuous data are underlying assumptions in the parametric statistical techniques most commonly used and described in this unit.

Finally, it should always be kept in mind that it is rare for a change in any single parameter to be biologically significant. Rather, because parameters are so interrelated, patterns of changes in parameters should be expected and analyzed.

Incidence of Histopathologic Lesion

In recent years, there has been as increasing emphasis on histopathologic examination of many tissues collected from animals in subchronic and chronic toxicity studies. Although it is not true that only those lesions that occur at a statistically significant increased rate in treated/exposed animals are of concern (because there are cases in which a lesion may be of such a rare type that the occurrence of only one or a few such treated animals raises a flag), it is true that, in most cases, a statistical evaluation is the only way to determine if what is seen in treated animals is significantly worse than what is seen in control animals. And although cancer is not the only concern, among the possible classes of lesion it is the one that is of greatest interest.

Typically, comparison of incidences of any one type of lesion between controls and treated animals are made using χ^2 or Fisher's exact test with a modification of the denominators. Too often, experimenters exclude from consideration all those animals (in both groups) that died before the first animals were found with a tumor at that site.

Two major controversial questions are involved in such comparisons: should they be based on one-tailed or two-tailed distribution, and what are the effects and implications of multiple comparisons?

The one- versus two-tailed distribution controversy revolves around the question of which hypothesis is being properly tested in a study such as a chronic carcinogenicity study. Is the tumor incidence different between the control and treated groups? In such cases, the hypothesis is bidirectional and therefore a two-tailed distribution is being tested against. Or is the question whether the tumor incidence is greater in the treated group than in the control group? In the latter case, the hypothesis is unidirectional, and only the right-hand tail of the distribution is under consideration. The implications of the answer to this question are more than theoretical; significance is much greater (exactly double, in fact) in the one-tailed case than in the two-tailed. For example, a set of data analyzed by Fisher's exact test, which would have a two-tailed P level of 0.098 and a one-tailed level of 0.049, would be flagged as significantly different.

The multiple comparisons problem is a much more lively one. In chronic studies, the lesion/tumor incidence on each of a number of tissues, for each sex and species, is tested, and each result is flagged if it exceeds the fiducial limit of $P \geq 0.05$.

The point to ponder here is the meaning of "$P \geq 0.05$." This is the level of the probability of making a type I error (incorrectly concluding that there is an effect when, in fact, there is not). It is necessary to accept the fact that there is a 5% chance of producing a false positive from this study. The tradeoff is a much lower chance (typically 1%) of a type II error (i.e., of passing as safe a compound that is not safe). These two error levels are connected; to achieve a lower type II level inflates the type I level. The problem in this case is that making a large number of such comparisons involves repeatedly taking the chance of "finding" a false-positive result. The set of lesions and/or tumor comparisons described above may number >70 tests for significance in a single study, which will result in a large inflation of false-positive findings.

The extent of this inflated false-positive rate (and what can best be done to reduce its effects) has been discussed and estimated with a great degree of variability. Salsburg (1977) estimated that the typical National Cancer Institute (NCI)–type cancer bioassay has a probability of type I error of between 20% and 50%. Fears et al. (1977), however, estimated it as being between 6% and 24%. Without some form of correction factor, the false-positive rate of a series of multiple tests can be calculated as being equal to $1 - 0.95^N$, where N is the number of tests and the selected alpha level (type I error rate) is 0.05.

What, then, is a proper use of such results? Or, conversely, how can the researcher control for such an inflated error rate? There are statistical methods available for dealing with this multiple comparisons problem. One is the use of Bonferroni inequalities to correct for successive multiple comparisons (Wilks, 1962). These methods have the drawback that there is some accompanying loss of power, expressed as an inability to identify true positives properly.

A second approach is to use the information in a more mature decision-making process. First, the historical control incidence rates (such as are given for the B6C3FI mouse and Fischer-344 rats in Fears et al., 1977) should be considered; some background incidences are so high that these tissues are null and void for making decisions. Second, one should not look for just a single significant incidence in a tissue but rather for a trend. For example, the following percentages of a liver tumor incidence were found for the female rats of a study: (a) control, 3%; (b) 10 mg/kg, 6%; (c) 50 mg/kg, 17%; and (d) 250 mg/kg, 54%. In this study only the incidence at the 250-mg/kg level might be statistically significant; however, the trend through the levels suggests a dose response. Looking for such a trend is an essential step in a scientific assessment of the results; and one of the available trend analysis techniques should be used.

Reproductive Toxicology

Reproductive implications of the toxic effects of chemicals have become increasingly important. Along with other types of studies that are closely related (such as teratogenesis and dominant lethal mutagenesis), reproduction studies are now common companions to chronic toxicity studies.

One point that must be keep in mind with all the reproduction-related studies is the nature of the appropriate sampling unit. Put another way: What is the appropriate *N* in such a study—the number of individual pups or the number of litters (or pregnant females)? Fortunately, it is now fairly well accepted that the first case (using the number of offspring as the *N*) is inappropriate (Weil, 1970). The real effects in such studies are actually occurring in the female that receives the dosage or exposure to the chemical or that is mated to a male that received a dosage or exposure. What happens to her, and to the development of the litter she is carrying, is biologically independent of what happens to every other female/litter in the study. This cannot be said for each offspring in each litter; the death of, or other change in, one member of a litter can and will be related to what happens to every other member in numerous fashions. Or the effect on all the offspring might be similar for all those from one female and different or lacking in another.

As defined by Oser and Oser (1956), there are four primary variables of interest in a reproduction study. First, there is the fertility index, which may be defined as the percentage of attempted matings (i.e., each female housed with a male) that resulted in pregnancy; pregnancy is determined by a method such as the presence of implantation sites in the female. Second, there is the gestation index, which is defined as the percentage of mated females, as evidenced by a dropped vaginal plug or a positive vaginal smear, that deliver viable litters (i.e., litters with at least one live pup). Two related variables that may also be studied are the mean number of pups born per litter and the percentage of total pups per litter that are stillborn. Third, there is the viability index, which is defined as the percentage of offspring born that survive at least 4 days after birth. Finally, there is the lactation index, which is the percentage of those animals per litter alive at 4 days that survive to weaning. In rats and mice, this is classically taken to be 21 days after birth. An additional variable that may reasonably be included in such a study is the mean weight gain per pup per litter.

Given that *N* is at least 10 (proper sample size is discussed in Developmental Toxicology), it is possible to test each of these variables for significance using a method such as the Wilcoxon-Mann-Whitney *U* test, or the Kruskal-Wallis nonparametric ANOVA. If *N* <10, the central limit theorem cannot be expected to be operative, and the Wilcoxon sum or ranks (for two groups) or the Kruskal-Wallis nonparametric ANOVA (for three or more groups) should be used to compare groups.

Developmental Toxicology

When the primary concern of a reproductive/developmental study is the occurrence of birth defects or deformations (terata, either structural or functional) in the offspring of exposed animals, the study is one of developmental toxicology. In the analysis of the data from such a study, several points must be considered.

First is sample size. Earlier in this unit the general concerns of this topic were reviewed and a method to estimate a sufficient sample size was presented. The difficulties with applying these methods here revolve around two points: selecting a sufficient level of sensitivity for detecting an effect and factoring in how many animals will be removed from the study (without contributing a datum) by either not becoming pregnant or not surviving to a sufficiently late stage of pregnancy. Experience generally dictates that one should attempt to have 20 pregnant animals per study group if a pilot study has provided some confidence that the pregnant test animals will survive the dose levels selected. Again, it is essential to recognize that the litter, not the fetus, is the basic independent variable.

A more basic consideration, as alluded to in the section on reproduction, is that as more animals are used, the mean of means (each variable will be such in a mathematical sense) will approach normality in its distribution. At sample size of 10 or greater, the approximation of normality is such that an aparametric test (such as a *t*-test or ANOVA) may be used to evaluate results. At sample sizes <10, a nonparametric test (Wilcoxon rank-sum or Kruskal-Wallis nonparametric ANOVA) is more appropriate. One nonparametric method that is widely used is the Wilcoxon-Mann-Whitney *U* test.

Diet and Chamber Analyses

In a feeding study, desired doses of a material are delivered to animals by mixing the material with their diet. Similarly, in an inhalation study, the material is mixed with the air the test animals breathe.

In both cases, the medium (feed or atmosphere) must be sampled and the samples analyzed to determine what levels or concentrations of material were actually present and to ensure that the test material is homogeneously

distributed. Having an accurate picture of these delivered concentrations, and how they varied over the course of time, is essential on a number of grounds:

1. The regulatory agencies and sound scientific practice require that analyzed diet and atmosphere levels be ≥10% of the target level.

2. Marked peak concentrations could, owing to the overloading of metabolic and repair systems, result in extreme acute effects that would add to apparent results in a chronic study that are not truly indicative of the chronic low-level effects of the compound, but rather of periods of metabolic and physiologic overload. Such results could be misinterpreted if the true exposure/diet were not known.

Sample strategies are not just a matter of numbers (for the statistical aspects) but of geometry—so that the contents of a container or the entire atmosphere in a chamber is truly sampled—and of time, in accordance with the stability of the test compound. The samples must be both randomly collected and *representative* of the entire mass of what is being characterized. In the special case of sampling and characterizing the physical properties of aerosols in an inhalation study, some special considerations and terminology apply. Because of the physiologic characteristics of the respiration of humans and of test animals, the concern is very largely limited to particles or droplets that are of a respirable size. Unfortunately, "respirable size" is a somewhat complexly defined characteristic, based on aerodynamic diameter, density, and physiologic characteristics. A second misfortune is that, although particles with an aerodynamic diameter of <10 μm are generally agreed to be respirable in humans (i.e., they can be drawn down to the deep portions of the lungs), in the rat this characteristic is more realistically limited to particles <3 μm in aerodynamic diameter. The one favorable factor is that there are now available a selection of instruments that accurately (and relatively easily) collect and measure aerodynamically sized particles or droplets. These measurements provide data for concentrations in a defined volume of gas, which can be expressed as either a number concentration or a mass concentration (the latter being more common). Such measurements generate categorical data—concentrations are measured in each of a series of aerodynamic size groups (such as >100 μm, 100 to 25 μm, 25 to 10 μm, 10 to 3 μm). The appropriate descriptive statistics for this class of data are the geometric mean and its standard deviation. These aspects, and the statistical interpretation of the data that are finally collected, should be considered carefully after consultation with appropriate experts. Typically, it then becomes a matter of calculating measures of central tendency and dispersion statistics, and identifying the values that are beyond acceptable limits (Bliss, 1965).

Mutagenesis

Since the early 1960s a wide variety of tests for mutagenicity have been developed and brought into use. These tests provide a quicker and cheaper (although less conclusive) way of predicting whether a material of interest is a mutagen, and possibly a carcinogen, than do longer-term whole-animal studies.

How to analyze the results of this multitude of tests—e.g., Ames (*UNIT 3.1*), DNA repair, micronucleus, host mediated, cell transformation, sister chromatid exchange, and *Drosophila*—is a new and extremely important question. Some workers in the field have held that test results can simply be judged to be positive or not positive on the basis of whether they achieve a particular degree of increase in the incidence of mutations in the test organism. Such quantitations of potency are complicated by the fact that the phenomenon is nonlinear. Although low doses of most mutagens produce a linear response curve, the curve will flatten out (and even turn into a declining curve) with increasing doses, because higher doses take the target systems into levels of acute toxicity.

Several concerns that differ from those previously discussed need to be examined, because the concern has now shifted from how a multicellular organism acts in response to one of a number of complex actions to how a mutational event is expressed, most frequently by a single cell. Given that it is possible to handle large numbers of experimental units in systems that use small test organisms, it is possible to detect both weak and strong mutagens.

What are the background mutation level and the variability in the technique? As any good genetic or general toxicologist will acknowledge, matched concurrent control groups are essential. Fortunately, with these test systems large *N*'s are readily attainable.

Instrumentation and Technique Factors

Most if not all toxicology studies depend on at least some instrumentation. Very frequently overlooked here (and, indeed, in most research) is that instrumentation, by its operating characteristics and limitations, goes a long way toward

determining the nature of the data it generates. An activity monitor measures motor activity in discrete segments. If it is a jiggle-cage type monitor, the segments are constricted so that only a distinctly limited number of counts can be achieved in a given period of time and then only if they are of the appropriate magnitude. Likewise, technique can readily determine the nature of the data. When measuring response to pain, for example, the technician could record it as a quantal measure (present or absent), as a rank score (on a scale of 1 to 5 from decreased to increased responsiveness, with 3 being normal), or as scalar data (by using an analgesia meter, which determines how much pressure or heat is required to evoke a response).

Study Design Factors

Study design is probably the most widely recognized of the factors that influence the type of data generated. Number of animals used, frequency of measures, and length of observation period are three obvious design factors that are readily under the control of the researcher and that directly help determine the nature of the data.

SCREENING STUDIES

Perhaps the major set of activities in toxicology is screening for the presence of an effect. Screening for nervous system, immune system, and other involvement, in particular for the effects of chemicals, has been a long-standing enterprise that has taken on new importance with both the advent of the Toxic Substance Control Act (TSCA) and the growing concern over new chemicals, drugs, and food additives coming to market with significant human exposure (Zbinden et al., 1984). Perhaps ironically, despite this level of awareness and activity, screening tests have not to any great extent undergone standardization or validation, and the relationships between the observed systemic effects and underlying causes remain largely unknown. The result is less information on more structures but an overall increase in the efficiency with which compounds of concern are discovered (assuming that truly active compounds are entering at a steady rate).

It should be noted that the methods described here are better suited to analyzing screening data when the interest is truly in detecting the absence of an effect with little chance of false negatives. Anderson et al. (1980) should be consulted for a more thorough discussion of considerations involved in cases in which the desire is to have few false positives (i.e., when the direction of the hypothesis test has been reversed).

The design of each assay and the choice of the activity criterion should, therefore, be adjusted, bearing in mind the relative costs of retaining false positives and rejecting false negatives. Decreasing the group sizes in the early assays reduces the chance of obtaining significance at any particular level (such as 5%) so that the activity criterion must be relaxed, in a statistical sense, to allow more compounds through. At some stage, however, it becomes too expensive to continue screening many false positives; and the criteria must be tightened up accordingly. Where the criteria are set depends on the acceptable noise levels in a screening system.

Screening systems may be approached by one of at least three different formats: single stage, sequential, and tier. For the purposes of this discussion, only the single-stage case is considered in depth, although the other forms are described.

Characteristics of Screens

The basic assumptions underlying screening are that a compound is either active or inactive and that the proportion of actives can be estimated from past experience. After testing, a compound is classified as positive or negative. It is then possible to design the assay to optimize the following characteristics: **sensitivity**, the ratio of true positives to total actives; **specificity**, the ratio of true negatives to total inactives; **positive accuracy**, the ratio of true to observed positives; **negative accuracy**, the ratio of true to observed negatives; **capacity**, the number of compounds evaluated per unit time, and **reproducibility**, the ability to have operational characteristics replicated.

An advantage of testing more compounds is that it gives the opportunity to average activity evidence over structural classes or to study quantitative structure-activity relationships (QSARs). QSARs can be used to predict the composite activities of new compounds and thus reduce the chance of actual testing on compounds of interest passing through the system.

Screens may thus truly be considered the biologic equivalent of exploratory data analysis (EDA). EDA methods, in fact, provide a number of useful possibilities for less rigid and yet quite effective approaches to the statistical analysis of the data from screens, and are one of the alternative approaches presented here.

Such screens are almost always focused on detecting a single end point of effect (e.g., mutagenicity, lethality, neurotoxicity, developmental toxicity) and have a particular set of operating characteristics in common.

1. A large number of compounds must be evaluated; therefore, ease and speed of performance (which may also be considered efficiency) are major desirable characteristics.

2. The screen must be very sensitive in its detection of potential effective agents. An absolute minimum of effective agents should escape detection—i.e., there should be very few false negatives (in other words, the type II error rate, or beta level, should be low). Stated another way, the signal gain should be significantly elevated.

3. It is desirable that the number of false positives be small (i.e., that there be a low type I error rate, or alpha level). The exact level selected depends on test characteristics and what kind of separation of screened compounds is desired. Less than 0.10 is usually inappropriate for a screen, however.

4. Items 1 to 3 are all to some degree contradictory, requiring the researchers involved to agree on a set of compromises. These typically start with acceptance of a relatively high noise level (0.10 or more).

5. In an effort to better serve item 1, such screens are frequently performed in batteries, so that multiple end points are measured in the same operation. In addition, such measurements may be repeated over a period of time in each model as a means of supporting item 2.

NEW APPROACHES TO STATISTICAL ANALYSIS

Trend Analysis

A variation on the theme of regression testing that has gained popularity in toxicology over the last 15 years is trend analysis. In the broadest sense, this is determining whether a sequence of observations taken over a period of time (e.g., the cumulative proportions of a group of animals that have tumors of a particular sort) exhibit some sort of pattern of change: an increase (upward trend) or decrease (downward trend). There are a number of tests that can be used to evaluate data to determine if a trend exists. The most popular test in toxicology is currently the one presented by Tarone (1975), because it is the one used by the NCI in the analysis of carcinogenicity data. A simple but efficient alternative is the Cox and Stuart test (1955), which is a modification of the sign test. For each point at which there is a measure (e.g., the incidence of animals observed with tumors), a pair of observations is formed, one from each of the groups being compared. In a traditional NCI bioassay, this would mean pairing control with low dose and low dose with control (to explore a dose-related trend) or each time period observation in a dose group (except the first) with its predecessor (to evaluate a time-related trend). When the second observation in a pair exceeds the first observation, record a plus sign for that pair. When the first observation is greater than the second, record a minus sign for that pair. A preponderance of plus signs suggests a downward trend, whereas an excess of minus signs suggests an upward trend. A formal test of the hypothesis at a preselected confidence level can then be performed.

Expressed more formally, first (having defined what trend is to be tested for) match pairs as $(X_1 + X_{1+c}), (X_2, X_{2+c}), \ldots, (X_{n'-c}, X_{n-})$, where $c = n'/2$ when n' is even and $c = (n' + \frac{1}{2})$ when n' is odd (where n' is the number of observations in a set). The hypothesis is then tested by comparing the resulting number of excess positive or negative signs against a sign test table (Beyer, 1976).

It is possible, of course, to combine a number of observations to actively test for a set of trends, such as the existence of a trend of increasing difference between two groups of animals over a period of time. This is demonstrated in Example 2.

Example 2

A chronic feeding study in rats is set up to test, in the second year of the study, the hypothesis that there is a dose-responsive increase in tumor incidence over time associated with receiving the test compound. A Cox-Stuart test for trend to address this question is used. All groups start the second year with an equal number of animals. The data are presented in Table 1.2.2.

Control Charts

The control-chart approach (Montgomery, 1985), commonly used in clinical laboratories for quality control, used as a form of screening offers some desirable characteristics. By keeping records of cumulative results during the development of the screen methodology, for example, the researcher can make an initial estimate of the variability (such as standard deviation) of each assay, which is available when full-scale use of the screen starts. The

initial estimates can then be revised as more data are generated (i.e., as familiarity with the screen increases).

The example below shows the usefulness of control charts for control measurements in a screening procedure. The example test for screening potential muscle strength–suppressive agents measures reduction of grip strength by test compounds compared to a control treatment. A control chart was established to monitor the performance of the control agent to establish the mean and variability of the control and to ensure that the results of the control for a given experiment are within reasonable limits (a validation of the assay procedure). The average grip strengths and the average range of a series of experiments are presented in Tables 1.2.3 and 1.2.4; Example 3 shows the construction and use of the resulting control chart.

As in control charts for quality control, the mean and average range of the assay were determined from previous experiments. In this

Table 1.2.2 Data for Example 2

Month of study	Control		Low dose			High dose		
	Total X animals with tumors	Change $[X_{A-B}]$	Total Y animals with tumors	Change $[Y_{A-B}]$	Compared with control $(Y - X)$	Total Z animals with tumors	Change $[Z_{A-B}]$	Compared with control $(Z - X)$
12(A)	1	NA	0	NA	NA	5	NA	NA
13(B)	1	0	0	0	0	7	2	(+)2
14(C)	3	2	1	1	(−)1	11	4	(+)2
15(D)	3	0	1	0	0	11	0	0
16(E)	4	1	1	0	(−)1	13	2	(+)1
17(F)	5	1	3	2	(+)1	14	1	0
18(G)	5	0	3	0	0	15	1	(+)1
19(H)	5	0	5	2	(+)2	18	3	(3)
20(I)	6	1	6	1	0	19	1	0
21(J)	8	2	7	1	(−)1	22	3	(+)1
22(K)	12	4	9	2	(−)2	26	4	0
23(L)	14	2	12	3	(+)1	28	2	0
24(M)	18	4	17	5	(+)1	31	3	(−)1
Sum of signs[a]								
+					4+			6+
−					4−			1−
$N = 12$					$Y - X = 0$ (no trend)			$Z - X = 5$

[a]Reference to a sign table is not necessary for the low dose comparison (where there is no trend) but clearly shows the high dose to be significant at the $P \leq 0.05$ level.

Table 1.2.3 Average Grip Strengths and Ranges for Screening Procedures

Test number	Mean	Range	Test number	Mean	Range
1	380	40	11	280	120
2	430	30	12	410	100
3	340	30	13	400	220
4	480	60	14	340	50
5	380	240	15	370	40
6	450	40	16	430	140
7	490	50	17	370	60
8	320	90	18	450	80
9	480	50	19	320	70
10	340	80	21	420	130

example, the screen had been run 20 times previous to the data shown. The initial data showed a mean grip strength of 400 g and a mean range R of 90 g. These values were used for the control chart. The size of the subgroups is 5. The action limits for the $\overline{X}$ and range charts were calculated as follows:

$$\overline{X} \pm 0.58R = 400 \pm 0.58 \times 90$$
$$= 348 - 452$$
$$= (X \text{ chart})$$

$$2.11R = 2.11 \times 90$$
$$= 190, \text{ the upper limit for the range}$$

Note that the range limit actually established a limit for the variability of the data, that it is in fact a "detector" for the presence of outliers (extreme values). This data set in a control-chart format is shown in Figure 1.2.5.

Such charts may also be constructed and used for proportion or count types of data. Charts constructed for the range of control data can be used as rapid and efficient tools for

Table 1.2.4 Values for Determining Upper and Lower Limits for Mean (X) and Range Charts

Sample size of subgroup (N)	A: factor for X chart	Range chart factors lower limit (DL)	
2	1.88	0	3.27
3	1.02	0	2.57
4	0.73	0	2.28
5	0.58	0	2.11
6	0.48	10	2.00
7	0.42	0.08	1.92
8	0.37	0.14	1.86
9	0.34	0.18	1.82
10	0.31	0.22	1.78
20	0.18	0.41	1.59

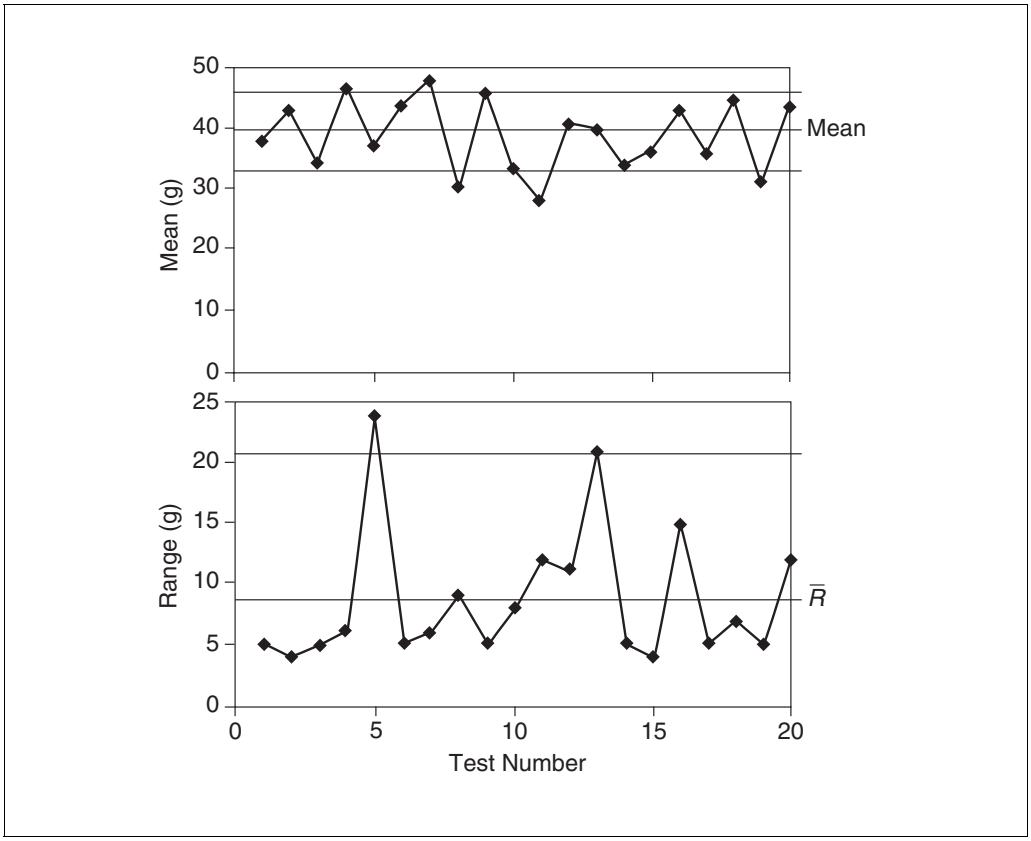

Figure 1.2.5 Example of control chart used to prescreen (i.e., explore and identify influential) data from a portion of a functional observational battery.

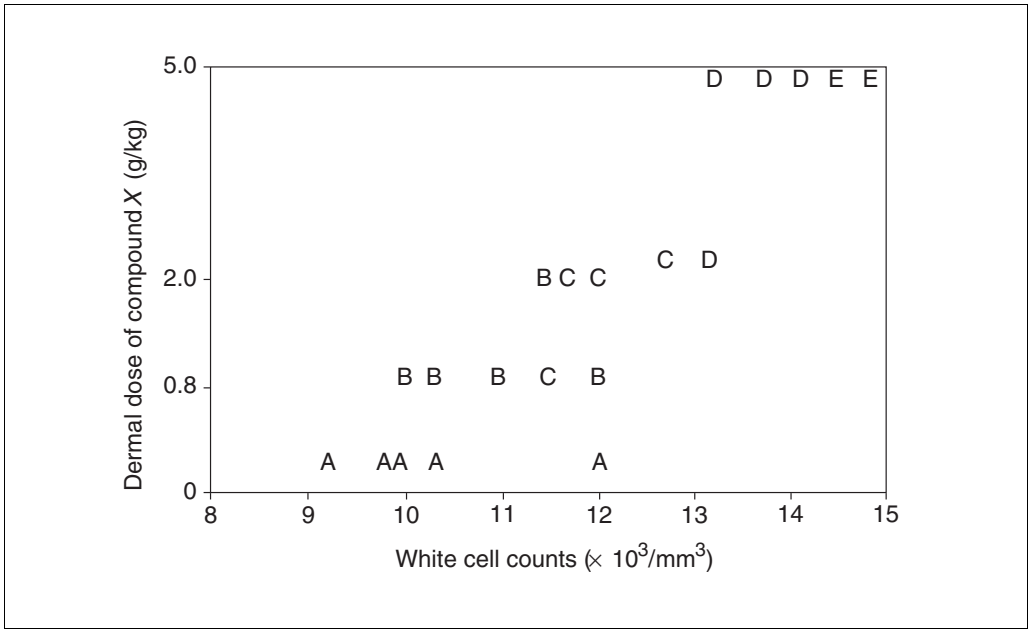

Figure 1.2.6 Effective two-dimensional visual display of three-dimensional data. A correlative plot of a rabbit dermal study with white blood cell counts.

detecting effects in groups being assessed for that same screen end point.

Graphical Methods

The use of innovative visual displays of data as a means of both analysis and communication of relationships has been developed extensively since the 1980s. These methods should be of particular interest to practicing toxicologists, because detecting, understanding, and communicating relationships in more than two dimensions is a constant challenge. Figure 1.2.6 provides one simple example of such an approach.

The reader's attention is particularly directed to the work of Tufte (1997) as an excellent source for this field.

LITERATURE CITED

Anderson, S., Auquier, A., Hauck, W.W., et al. 1980. Statistical Methods for Comparative Studies. John Wiley & Sons, N.Y.

Beyer, W.H. 1976. Handbook of Tables for Probability and Statistics. pp. 269-378, 409-413. Chemical Rubber Company, Cleveland, Ohio.

Bliss, C.I. 1965. Statistical relations in fertilizer inspection. *Bulletin*, p. 674. Connecticut Agricultural Experiment Station, New Haven, Conn.

Cox, D.R. and Stuart, A. 1955. Some quick tests for trend in location and dispersion. *Biometrics* 42:80-95.

Fears, T.R., Tarone, R.E., and Chu, K.C. 1977. False-positive and false-negative rates for carcinogenicity screens. *Cancer Res.* 27:1941-1945.

Gad, S.C. 1998. Statistics and Experimental Design for Toxicologists, 3rd ed. CRC Press, Boca Raton, Fla.

Krewski, D. and Franklin, C. 1991. Statistics in Toxicology. Gordon and Breach Science Publishers, N.Y.

Loeb, W.F. and Quimby, F.W. 1989. The Clinical Chemistry of Laboratory Animals. Pergamon Press, Elmsford, N.Y.

Montgomery, D.C. 1985. Introduction to Statistical Quality Control. John Wiley & Sons, N.Y.

Montgomery, D.C. 1997. Design and Analysis of Experiments, 4th ed. John Wiley & Sons, N.Y.

Oser, B.L. and Oser, M. 1956. Nutritional studies on rats on diets containing high levels of partial ester emulsifiers. II. Reproduction and lactation. *J. Nutr.* 60:429.

Salsburg, D.S. 1977. Use of statistics when examining life time studies in rodents to detect carcinogenicity. *J. Toxicol. Environ. Health* 3:611-628.

Salsburg, D.S. 1986. Statistics for Toxicologists. Marcel Dekker, N.Y.

Sheskin, D.J. 1997. Handbook of Parametric and Nonparametric Statistical Methods. CRC Press, Boca Raton, Fla.

Tarone, R.E. 1975. Tests for trend in life table analysis. *Biometrika* 62:679-682.

Tufte, E.R. 1997. Visual Explanations. Graphic Press, Cheshire, Conn.

Weil, C.S. 1970. Selection of the valid number of sampling units and a consideration of their combination in toxicological studies involving reproduction, teratogenesis or carcinogenesis. *Food Cosmet. Toxicol.* 8:177-182.

Weil, C.S. 1982. Statistical analysis and normality of selected hematologic and clinical chemistry measurements used in toxicologic studies. *Arch. Toxicol.* (Suppl.) 5:237-253.

Weil, C.S. and Gad, S.C. 1980. Applications of methods of statistical analysis to efficient repeated-dose toxicologic tests. 2. Methods for analysis of body, liver, and kidney weight data. *Toxicol. Appl. Pharmacol.* 52:214-226.

Wilks, S.S. 1962. Mathematical Statistics. pp. 290-291. John Wiley & Sons, N.Y.

Zar, J.H. 1974. Biostatistical Analysis. p. 50. Prentice-Hall, Englewood Cliffs, N.J.

Zbinden, G., Elsner, J., and Boelsterli, U.A. 1984. Toxicological screening. *Regul. Toxicol. Pharmacol.* 4:275-286.

Contributed by Shayne C. Gad
Gad Consulting Services
Raleigh, North Carolina

Transgenic Animals in Toxicology

STRATEGIES AND APPLICATIONS

A transgenic (Tg) animal is defined as an animal in which genetic material has been experimentally introduced into, or deleted from, the germ cells. The altered DNA need not be genetically active, but should be heritable. Tg mice can be generated to express two distinct generalized phenotypes, gain of function and loss of function. Gain of function is usually associated with an overexpressing, randomly integrated transgene. Loss of function is created by targeting the deletion of a specific gene using embryonic stem (ES) cell technology. However, randomly integrated transgenes can result in functional inactivity of a gene product, and, vice versa, transgenes can be targeted for overexpression using ES cell technology (see discussion of Production of Tg Mice by Gene Targeting). Tg mice are a unique tool for understanding how interactions between individual genes and the environment affect human health. Tg animal models in the area of toxicology can be useful for a number of applications, including mutagenesis, carcinogenesis, risk assessment, and stress response (see Table 1.3.1). Transgenic technology is rapidly evolving, and future developments will allow scientists the opportunity to address difficult questions in toxicology where no specific targets have been identified. It must be remembered that animal systems are not passive, and along with technical advancements intensive studies must be undertaken to understand how specific gene expression is controlled.

Understanding toxic mechanisms is difficult because of the complexity of animal systems, and extrapolation between species is generally speculative. The anticipated promise of transgenic technology is to provide sets of Tg animals with individual but related characteristics, using human genes, and subject them to standard toxicology protocols. The end result will be a delineation of the relationship between biochemical and metabolic pathways and chemical toxicity. Several Tg mouse models have been developed and characterized for mutagenesis and carcinogenesis testing. The mutagenesis systems in Tg mice incorporate well understood bacterial genes into the murine genome. Genes from chemically treated mice are then extracted and tested for mutagenic effect in simple bacterial assays. Two systems that are gradually gaining acceptance are commercially available and use a bacteriophage lambda shuttle vector from the *E coli* β-galactosidase *lac*Z gene (Tinwell et al., 1994; Douglas et al., 1997). The Hazelton Mutamouse (Hazelton Research) and the Stratagene Big Blue systems use the structural *lac*Z gene and repressor *lac*I gene, respectively. The two systems use similar testing procedures. Briefly, Tg mice are exposed to a mutagen for a period of time and then euthanized. DNA is then isolated from various organs and treated with a commercial lambda packaging system. The resultant bacteriophages are plated on an appropriate bacterial *E. coli* background, and mutants are counted according to their ability to express β-galactosidase. This enzyme is easily detected in bacteriophage plaques using an indicator dye, 5-bromo-4-chloro-3-indolyl-β-D-galactoside (Xgal), which produces a blue color on the plate.

Tg mice used in chemical carcinogenesis assays carry an activated oncogene, or lack a tumor-suppressor gene, which can result in increased sensitivity to tumor development (Brown et al., 1995). The concept in this case is based on the increased probability of a cell accumulating the full complement of events required for malignancy if an oncogene has already been activated, or if the lack of suppressor gene allows it to become activated. A number of Tg mice carrying activated oncogenes have been reported and studied, as shown in Table 1.3.1. Expression of the oncogene is usually determined by the type of promoter/enhancer sequence associated with the transgene, thus making it possible to target specific organs or tissues. For example, the *TG:AC* Tg mouse exhibits the unique phenotype of chemical papillogenesis, which provides a model for identifying potential carcinogens (Spaulding et al., 1993).

The *p53* tumor-suppressor gene knockout mouse is an example of a Tg mouse that has more broad-spectrum utility in determining compound-induced carcinogenesis (Donehower et al., 1992). The *p53* gene has been shown to control the entry of damaged cells into specific stages of the cell cycle and appears to be an essential component of the pathway by which malignancies develop in several tissues. Homozygous *p53* knockout mice, which lack the *p53* gene on both alleles, develop a high incidence of predominantly hematopoietic tu-

Contributed by Warren C. Ladiges and Carol B. Ware

Current Protocols in Toxicology (1999) 1.3.1-1.3.26

Table 1.3.1 Examples of Transgenic Mouse Models in Toxicology

Gene	Promoter/ null mutation	Phenotype	Reference
*Lac*Z	Lambda phage	β-Galactosidase reporter	Gossen et al., 1989
*Lac*I	Lambda phage	β-Galactosidase reporter	Kohler et al., 1991
Myc+H-*Ras*	MMTV	Mammary adenocarcinoma	Sinn et al., 1987
Ah	Knockout	Dioxin toxicity, infertility	Fernandez-Salguero et al., 1995
TGFα GF	MMTV	Mammmary hyperplasia and adenocarcinoma	Matsui et al., 1990
Myc	Eμ	B cell lymphoma	Adams et al., 1985
H-*Ras*	Albumin	Enlarged liver	Sandgren et al., 1989
Rag-2	Knockout	T and B cell deficiency	Shinkai et al., 1992
Myc	Albumin	Hepatic dysplasia	Sandgren et al., 1989
TGFα	Metallothionein	Hepatocellular carcinoma	Jhappan et al., 1990
p53	Knockout	Lymphoma, hemangiosarcoma	Donehower et al., 1992
H-*Ras*	Keratin	Skin papillomas	Bailleul et al., 1990
pim-1	Eμ	T cell lymphomagenesis	Breuer et al., 1991
TG:AC	Fetal globin	Skin tumorigenesis	Spaulding et al., 1993
Cyp1a2	Knockout	Neonatal lethality	Pineau et al., 1995

Abbreviations: MMTV, mouse mammary tumor virus; Eμ, immunoglobulin; Ah, aryl hydrocarbon; Cyp, cytochrome P-450.

mors within the first 6 months of life, and thus are of no value for potential carcinogenic evaluations. However, the *p53* heterozygotes, which lack the *p53* gene on one allele, remain tumor-free for up to 1 year, but the mutation renders the mice more sensitive to the effects of at least some carcinogens. Studies have shown that *p53* heterozygotes exposed to dimethylnitrosamine have an increased sensitivity to the induction of hemangiosarcomas (Harvey et al., 1993). Kemp et al. (1993) showed that *p53* heterozygotes had an earlier onset and increased frequency of malignancy than the wild-type background strain when both groups were exposed to chemical carcinogens.

The application of transgenic technology has provided important information on the roles of various enzyme systems in the developing organism. For example, the cytochrome P-450 enzyme system is involved in metabolic oxidation of a number of endogenous and exogenous materials, including fatty acids, steroids, drugs, and environmental toxicants. The system has been well characterized in adults but little is known about its role during development. Tg knockout mice have been generated for cytochrome P-450 1a2 and shown to express a neonatal lethal phenotype (Pineau et al., 1995). However, another Tg knockout line for cytochrome P-450 1a2 did not have developmental abnormalities, but exhibited deficient drug metabolism (Liang et al., 1996). A second example of the value of transgenic technology in developmental biology is the homeobox gene system, which influences embryonic development by determining the order of expression of various regulators of embryonic development. A number of laboratories have developed Tg knockout mice that lack expression of specific *Hox* genes, thus allowing identification of the associated area required for development (developmental domain). These Tg mouse studies may be useful in defining functional periods of toxic exposure during gestation.

A collective family of genes, which produces stress proteins in response to toxic exposure, comprises a generalized repair system for protecting cells from a wide variety of nongenotoxic environmental exposures. Heavy metals, pesticides, and other reagents, including free radicals, induce stress proteins (Hightower, 1991). Elucidation of the genes in this family could lead to the generation of new Tg models capable of screening for toxic agents. For example, Tg nematodes were generated by inserting a *lac*Z reporter gene fused to a heat-shock protein gene (Stringham et al., 1992). When the organism was subjected to stress, heat-shock proteins were induced. Tg mice carrying a stress-inducible gene associated with a common reporter gene could provide an easily detectable and sensitive biological assay for toxicological exposure.

Techniques used to generate Tg mice have frequently been described in the literature. The remainder of this unit provides an overview of commonly accepted procedures for producing overexpression, point mutation, and null

Table 1.3.2 Comparison of Steps for Generating Overexpression and Gene-Targeted Transgenic Mice

Step	Pronuclear transgenesis (overexpression)	Gene targeting
1	Prepare construct	Prepare construct
2	Select mouse strain as embryo donor	Transfect ES cells, clone, and analyze
3	Microinject DNA into pronuclei	Microinject targeted ES cells into blastocysts
4	Transfer embryo to oviduct	Transfer embryo to uterus
5	Test pups for transgene DNA	Identify male chimeras by coat color
6	Breed positive mice	Breed chimeric mice
7	Test pups for DNA expression	Test pups for targeted mutation
8	Expand colony	Expand colony

ES, embryonic stem cells.

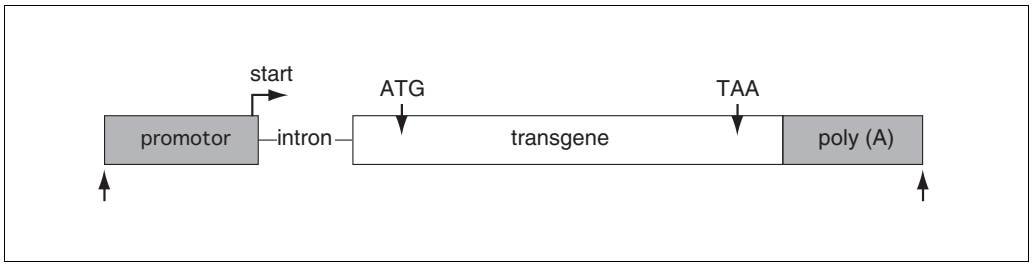

Figure 1.3.1 An example of a construct design for random integration via pronuclear microinjection. The transcription start site is depicted as an arrow rising from the promoter point right. The initiation (ATG) and stop (TAA) codons are represented by arrows pointing into the transgene. The two arrows pointing upward represent the restriction sites used to remove the bacterial plasmid sequences. The polyadenylation site is designated as poly(A).

(knockout) Tg mice. Transgenic technology consists of two basic avenues: pronuclear microinjection of one-cell embryos, and blastocyst microinjection (or aggregation) of gene-targeted ES cells with the formation of chimeras. A flow chart comparing the steps involved in both procedures is presented in Table 1.3.2. This unit focuses exclusively on the mouse. The rat is used extensively in toxicology studies, but unfortunately the understanding of preimplantation embryology and transgenesis lags behind that of the mouse. However, several recent articles have been published on generation of Tg rats (Sullivan and Ouhibi, 1995; Charreau et al., 1996).

DNA CONSTRUCT CONSIDERATIONS

Constructs for Overexpression Tg Mice

Construct design for producing overexpression Tg mice is fairly straightforward. The construct should contain a functional promoter, initiation codon (ATG), and polyadenylation site (Fig. 1.3.1). The 3′ poly(A) site, consisting of a polyadenylation signal, cleavage site, and cleavage binding factor, ensures that mRNA will be correctly processed to produce a polyadenylated transcript. Transgenes are constructed to consist of a full-length cDNA or genomic DNA for a specific gene fused to the enhancer/promoter sequence. Entire genes, containing endogenous introns, exons, and the 5′-flanking promoter sequences, have been used. However, the larger the DNA fragment, the lower the efficiency of producing Tg mice. The use of intact genes also does not allow the flexibility of promoter choice and external temporal control of transgene expression. Many vectors used in cloning can interfere with expression of the transgene. Consequently, unique restriction sites at the 5′ and 3′ ends of the transgene should be available to remove plasmid sequences. Sequencing of junction fragments to confirm that the transgene contains all the elements in the correct orientation, as well as testing for expression in a tissue culture system, are useful steps to ensure that the best possible conditions are available for transgene integration. Transgenes should be constructed to be easily identified subsequent to integration. It is important that a screening scheme to detect DNA in potential founder mice be devised before starting pronuclear microinjections.

PCR is the most frequently used method for analyzing transgene integration, although both Southern and dot blot analyses are often used.

The choice of promoter depends on the target tissue of interest, or the desire to direct the ubiquitous expression of a transgene. There is limited information on promoters that can focus the expression of genes to a broad array of tissues. The chick β-actin promoter has broad-spectrum activity, inducing high levels of transgenic expression in heart, muscle, lung, and brain; however, expression in liver, kidney, spleen, and intestine is low or undetectable (Oberly et al., 1993; Kagan et al., 1994). Another promoter, human cytomegalovirus (CMV), directs high expression of transgenes in a number of tissues including muscle, heart, kidney, spleen, testis, and brain, but expression is low or undetectable in liver (Furth et al., 1991). Examples of specific-tissue promoters that have been successful in Tg mice used as models in toxicology are shown in Table 1.3.1.

Inducible promoters are preferable in a number of situations in order to obtain maximum quantity of the gene product and to regulate its expression. The human metallothionein promoter is activated by heavy metals, but appears to lack desired specificity (Palmiter et al., 1983). A tetracycline-inducible system has been developed and demonstrated to be effective in several studies (Shockett and Schatz, 1996). The latter is referred to as a binary system since it requires two sets of transgenes. The expression of a specific transgene in one mouse (Tg line 2) depends on a tetracycline-sensitive transactivator transgene from another mouse (Tg line 1) for the promoter region of the transgene of interest. When offspring from a cross of the two lines are treated with tetracycline, the transactivator gene remains inactive. When the tetracycline is removed, the transactivator gene is activated and triggers the promoter and subsequent expression of the specific DNA inserted in Tg line 2. Two new binary systems that have recently been introduced are the estrogen-inducible (Braselmann et al., 1993) and ecdysone-inducible (No et al., 1996) systems. Studies to confirm their applications in Tg mice used for toxicology models are forthcoming.

Frequently, transgenes fail to be expressed, spatial or temporal patterns are not followed, or expression cannot be distinguished from endogenous gene levels. The size limitation of standard transgenic constructs, set by the cloning capacity of plasmid, phage, or cosmid vectors, may prevent the inclusion of necessary but distinct regulatory elements. Yeast artificial chromosomes (YACs) have proven to be a powerful tool in transgenic technology because they provide a means of cloning and stably maintaining DNA >1 Mb in size (Montoliu et al., 1993). YAC-borne DNA can be microinjected into one-cell embryos in an efficient manner, provided steps are taken to prevent shearing (W.C. Ladiges, unpub. observ.). The ability to introduce such large segments of DNA into laboratory mice provides the opportunity to study the functional analysis of genes too large to clone by conventional methods, and allows a practical means of evaluating regulatory activity in large clusters such as *Hox* and globin genes.

A recent approach in construct design which has extended the usefulness of randomly integrated transgenes is the creation of a dominant negative mutation so that endogenous gene function will be blocked with subsequent creation of a functional null mutation. For example, dominant negative retinoic acid receptor (RAR) transgenes have been used to generate Tg mice in order to address the effects of blocking specific functional domains of these receptors in various organ systems (Damm et al., 1993; Saitou et al., 1995). The use of dominant negative mutations requires a detailed characterization of functional domains of the protein(s) involved.

Constructs for Gene Targeting

In contrast to random integration, homologous recombination allows targeted alterations of the murine genome. These can be as defined as specifically as a point mutation or as broadly as gene function ablation (null mutation). The components of a vector destined for homologous recombination in ES cells include sequences that are homologous to the desired site of integration, a selection marker, and a plasmid backbone. There are two basic approaches: replacement and insertion vectors (Fig. 1.3.2). Subtle mutations require further selection, following vector insertion, for naturally occurring recombination events that result in the desired gene configuration. The entire process of vector insertion followed by loss of target-site sequences is termed hit and run (Fig. 1.3.3). Hasty and Bradley (1993) and Bronson and Smithies (1994) provide lucid explanations of overall vector design.

Replacement vectors are most commonly used to make null mutations. The positive selection cassette is inserted in an area of homology that ablates the ability to encode a functional RNA. Therefore, some understanding of exon correlation to protein function prior to

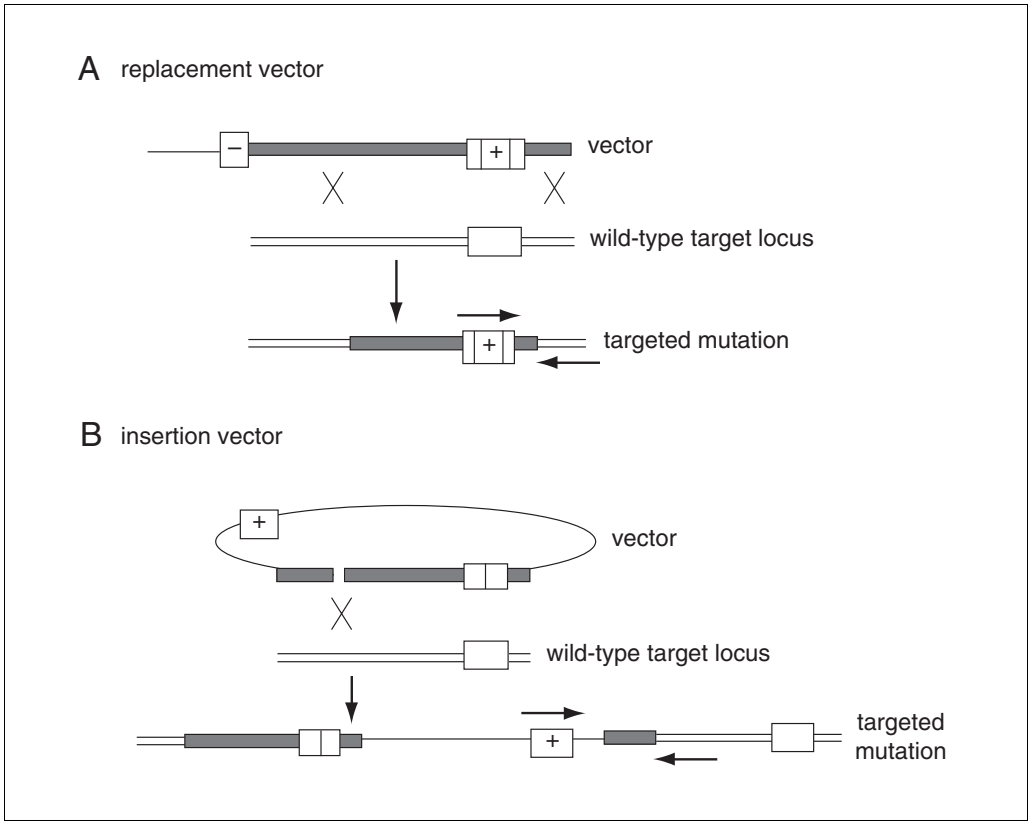

Figure 1.3.2 Replacement and insertion vector integration patterns. A thick line represents vector homology with the target locus and the thin, single line represents the plasmid backbone. The box containing a minus sign is the negative selection marker. The double line represents wild-type homology with the vector. The exon targeted for mutation is represented as an open box. Arrows pointing horizontally represent PCR primer locations. The X's are crossover points for vector integration. (**A**) The box containing a plus is the sequence homologous to the targeted exon disrupted by the positive selection marker. (**B**) The box containing a single line in the middle represents a subtle mutation engineered into the homologous sequences for the target exon. The break in the thick line on the vector represents the vector linearization site.

vector design is advantageous. Other vector considerations include the provision of a unique restriction site outside the area of homology to linearize the construct. There should be ≥5 kb of homology overall (Hasty et al., 1991a). Acentric homology such that the short arm contains 0.5 to 2 kb of homologous sequences is desired if PCR analysis of targeted events is to be pursued (Hasty and Bradley, 1993). Otherwise, Southern analysis to determine successful targeting can incorporate any length of homology on the individual 5′ and 3′ ends, with overall length of homology the primary consideration (Hasty et al., 1991a). PCR analysis requires that one primer be located outside the area of homology, while the other primer should be located within the vector, often utilizing sequences within the positive selection marker (Fig. 1.3.2A). The resulting PCR product should be short enough to allow efficient amplification (≤2 kb). Replacement recombination products may be the result of single-copy or multicopy vector insertion, thus containing the plasmid backbone. Inclusion of a negative selection marker in the vector design may eliminate these undesirable events through drug (antibiotic) selection. Diagnostic Southern blot analysis is used to verify that one set of vector sequences is integrated within the target site in the correct orientation. A unique probe which hybridizes to a sequence outside one or both regions of homology is used to detect restriction-fragment size. Often a restriction site is engineered into the vector to assist in analysis.

Insertion vectors are used to generate either subtle or null gene mutations. Targeted integration can occur more frequently by insertion than replacement (Hasty et al., 1991b). Insertion events result in duplication of the area of homology (Fig. 1.3.2B) which can lead to null mutation. A primary difference in vector requirements between insertion and replacement

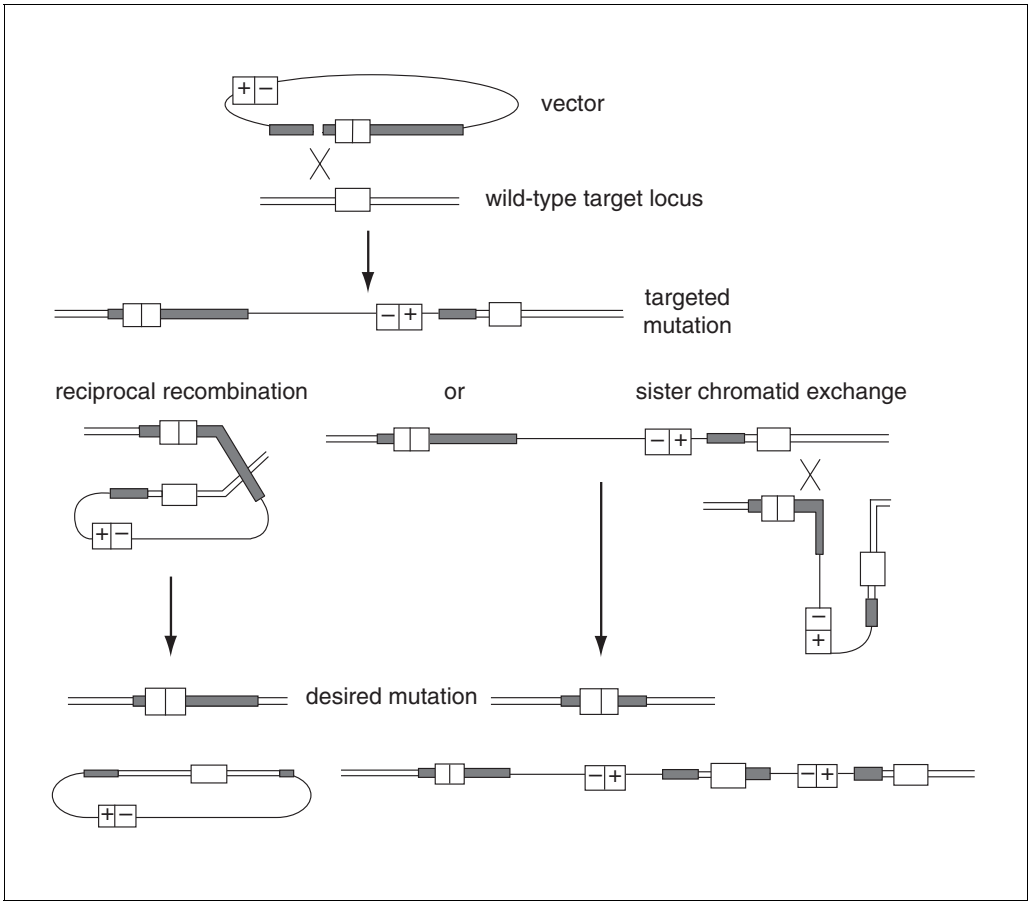

Figure 1.3.3 Hit and run vector insertion and intrachromosomal recombination patterns. The thick line represents vector homology with the target locus and the single line represents the plasmid backbone. The box containing a plus sign is the positive selection marker. The box containing a minus sign is the negative selection marker. The exon targeted for mutation is represented as an open box. The box containing a single line in the middle represents a subtle mutation engineered into the homologous sequences for the target exon. The break in the thick line on the vector represents the linearization site. The double line represents wild-type homology with the vector. The X's are the crossover points for vector integration and sister chromatid exchange. Intrachromosomal recombination of the insertion product can occur by single reciprocal recombination (left) or uneven sister chromatid exchange (right) to result in the desired targeted mutation. The diagram at the bottom shows how undesirable recombination products are lost through excision and degradation (left) or sensitivity to negative selection (right).

vectors is that location of the restriction site for vector linearization is incorporated within the area of homology rather than the plasmid backbone. The recommended level of overall homology is the same (≥5 kb). A positive selection marker can be included either within an exon or, more commonly, in the plasmid backbone, depending on the ultimate goal. Analysis of insertion events by PCR takes advantage of repair of DNA deleted from the insertion vector at the linearization site, such that one primer is within the area of repair and one within the vector, often utilizing sequences within the positive selection marker (Fig. 1.3.2B). As with replacement, the Southern analysis strategy for insertion relies on the use of an external probe.

Hit and run strategy involves the loss of vector sequences following vector insertion to generate either a subtle or a null mutation. The unwanted sequences (plasmid backbone, selection markers, and one complement of the target locus duplication) are lost through spontaneous intrachromosomal recombination (Fig. 1.3.3). Inclusion of a negative selection marker fused to the positive selection cassette is utilized to detect successful loss of sequences through recombination.

It is desirable to optimize the frequency of site-specific homologous recombination to reduce the eventual clone-analysis workload. Vectors containing homologous sequences cloned from isogenic DNA are generally more effi-

cient at targeting (Deng and Capecchi, 1992). A commonly used approach involves inclusion of a negative selection marker, such as thymidine kinase, on one end of the replacement vector. This is called positive negative selection (PNS) and allows a higher frequency of detection of targeted events by sensitizing clones,—derived by random, concatemer, or vector circle integration—to the presence of a negative selection drug (Mansour et al., 1988). A similar approach—using an antisense cassette of the positive selection marker containing a strong promoter in reverse orientation located outside the area of homology—allows positive and negative selection to occur simultaneously in response to addition of only one selection drug (Skryabin and Schmauss, 1997). Targeting frequency can be improved by driving a positive selection marker using the endogenous promoter or enhancer at the site of integration, as long as neither promoter nor enhancer is included within the area of sequence homology on the positive selection marker (Schwartzberg et al., 1990).

Temporal and cell-type-specific control of gene targeting provide a means to more accurately assess the physiological role of the gene of interest. The Cre-*lox*P system is used in gene targeting to remove vector sequences by flanking the sequences to be removed with *lox*P sites. The vector sequences are then excised using Cre recombinase (Lakso et al., 1992; Orban et al., 1992), either by in vitro exposure to Cre recombinase or in vivo by introducing a Cre recombinase transgene. The Cre-*lox*P system not only duplicates one goal of hit and run vector design by removing the selection marker, but can be utilized for tissue-specific targeted gene mutation (Gu et al., 1994) and temporal control of targeted gene mutation (Kühn et al., 1995; Feil et al., 1996). Any portion of a gene can be excised by predetermining the *lox*P site location within a vector. Through the choice of promoter to drive the Cre recombinase gene, tissue and site-specific gene alteration can be controlled. Finally, the administration of a drug to switch on Cre recombinase activity allows temporal expression of the site-specific gene alteration. Prior to Cre recombinase induction, the animal must be homozygous for the targeting event and hemizygous (heterozygous for the transgene) for Cre recombinase overexpression in order to look at temporally targeted mutations. This represents a significant investment in time prior to biological assessment of gene function. It is important to be aware that with each level of control of transgenic production, the burden on the investigator to make wise choices in experimental aim and vector design increases.

Overall, the concerns that drive vector design are: (1) size of the desired mutation; (2) exon location of the targeting event; (3) sequence homology length; (4) location of selection marker(s); (5) incorporation and location of a unique restriction site to linearize the vector; (6) PCR and/or Southern blot analysis strategy to detect and clarify targeted events; (7) whether to incorporate strategies to improve targeting frequency; and (8) whether to include refinements, such as incorporation of a reporter gene as an expression marker (see Bonnert and Nicolas, 1993; Vernet et al., 1993), or inclusion of *lox*P sites.

Overexpression of a transgene can be achieved following introduction of a vector into embryonic stem (ES) cells. This is a relatively efficient means of producing random-insertion Tg mice, and is useful when the transgene may profoundly affect development (Jaffe et al., 1992; Kitsukawa et al., 1995), when stable integration of a large piece of unrearranged DNA is needed (Jakobovits et al., 1993; Lamb et al., 1993; Strauss et al., 1993), or when a genetically defined inbred background is required in cases where a suitable ES line is available (C. Ware, unpub. observ.). This method has the added advantage that clones can be characterized for integration copy number and, depending on the promoter used, determination of the level of transgene expression before introduction into mouse embryos. Often, a selection marker that incorporates a promoter that is expressed in ES cells is included in the electroporation mix in a ratio of 1 part selection marker to 10 parts desired gene vector. Following this scheme, the gene construct is identical to that described for pronuclear injection. Otherwise, the selection marker can be incorporated directly within the vector construct. It is important to be aware that overexpression using ES cells will require the production of chimeras to introduce the mutation into the germ line. This effectively adds one generation to the time frame, relative to standard pronuclear microinjection.

MOUSE HUSBANDRY

A number of different inbred, outbred, and hybrid strains of mice have been used to produce Tg mice. F2 hybrid embryos, generated from matings between F1 hybrid mice are most commonly used for DNA microinjection. Hybrids that are commonly used include (C57BL/6XSJL)F1, (C57BL/6XC3H/He)F1, (C57BL/

6XDBA/2)F1, and (BALB/ cXC57BL/6)F1. Inbred strains, such as C57BL/6, FVB, BALB/c, and C3H are also used, but the efficiency of generating Tg mice is less than with hybrid strains. However, the problems of genetic variation between F2 animals, genetic drift in subsequent generations, and the extensive backcrossing onto an inbred background required to regain genetic definition are greatly minimized by using an inbred embryo strain. Inbred strains are routinely used as blastocyst donors to provide a constant genetic background for the production of chimeras. Outbred Swiss albino strains, such as CD1, ICR, and SW, are frequently used as embryo donors because they are relatively inexpensive. However, they do not respond to superovulation as well as hybrid strains, and their embryos develop more slowly. Table 1.3.3 provides an overview of criteria for selecting a donor mouse strain based on physiological and biological characteristics.

There may also be scientific considerations for selecting a genetically defined background strain. Historically, inbred strains have been phenotypically characterized in a wide variety of biological studies. Thus, many toxicology studies are based on data using inbred strains. The ease and efficiency of generating Tg mice using hybrid strains must be weighed against the relatively lower efficiency, but scientific validity, of generating Tg mice on defined genetic backgrounds of commonly used inbred strains.

Embryo Collection

Natural ovulation in the mouse occurs 2 to 3 hr prior to the onset of estrus, producing 10 to 12 ova, depending on the mouse strain. Figure 1.3.4 schematically shows the time course of embryos as they are released from the ovary and travel through the oviduct and into the uterus. The administration of exogenous hormones to sexually immature female mice (<5 weeks of age) is usually thought to increase the quantity of viable ova to 15 to 30 per mouse and synchronize the release of ova from females within the same group. Superovulation consists of injecting two hormones in sequence—pregnant mare's serum gonadotrophin (PMSG) followed by human chorionic gonadotrophin (hCG) 42 to 48 hr later—into 3- to 4-week-old sexually immature female mice. However, adult females as old as 9 weeks of age have been found to respond favorably to superovulation (W.C. Ladiges, unpub. observ.). PMSG contains a relatively higher ratio of follicle-stimulating hormone to luteinizing hormone than does hCG, and will increase the number of developing ova that will mature just before ovulation. On the other hand, hCG contains a relatively higher ratio of luteinizing hormone to follicle-stimulating hormone, and stimulates the synchronous ovulation of almost all of the PMSG-stimulated follicles within 6 to 8 hr following injection. Both hormones are given intraperitoneally in sterile saline at a dose of 3 to 8 IU per mouse. Inbred strains typically require lower doses (3 to 5 IU per mouse), while hybrid strains often need slightly higher doses (5 to 7 IU per mouse). In actual practice, it is acceptable to administer 5 IU per mouse, regardless of the strain. The timing of administration is also of importance, depending on the light cycle of the room where mice are housed. If a standard 6 a.m. to 6 p.m. light cycle is used, PMSG should be given later in the day, between 12 noon and 4 p.m. A specific time should be

Table 1.3.3 Suggestions for Selecting a Mouse Strain for Transgenic Manipulation

Strain	Genetic status	Superovulation[a]	Embryo quality[b]	Litter size[c]	Cost[d]
C57BL/6	Inbred	Medium	Acceptable	Average	High
FVB	Inbred	Medium	Outstanding	High	Medium
BALB/c	Inbred	Low	Acceptable	Average	High
Swiss	Outbred	Medium	Acceptable	High	Low
CD1	Outbred	High	Acceptable	High	Low
B6SJL	Hybrid	High	Acceptable	High	Medium
B6C3	Hybrid	High	Acceptable	High	Medium
B6D2	Hybrid	Low	Acceptable	Average	Medium
SWR	Inbred	High	Outstanding	Average	High

[a]In response to gonadotrophins as described in the text.

[b]Quality is defined as viable embryos with easily observable pronuclear features.

[c]Based on a litter size of 5 to 8 pups.

[d]Based on purchase costs from commercial vendors.

selected and used consistently. The authors routinely use 12 noon, so that 47 hr later hCG can be given and females placed with fertile male studs, on a one female to one male basis. The following morning, plugged females are euthanized and embryos collected for microinjection. For blastocyst collection, plugged females are held for three days and then euthanized for the collection procedure. It is advisable to use ten females for each microinjection. From this group, expect between 200 and 300 ova, and 20 to 60 blastocysts, depending on the strain and season.

Pseudopregnant Recipients

The female mouse is a spontaneously ovulating animal, with an estrus cycle of 4 to 5 days and an estrus period lasting from 9 to 20 hr. The standard procedure for generating Tg mice calls for transferring microinjected embryos into the reproductive tract of a recipient female within a few hours following microinjection. These

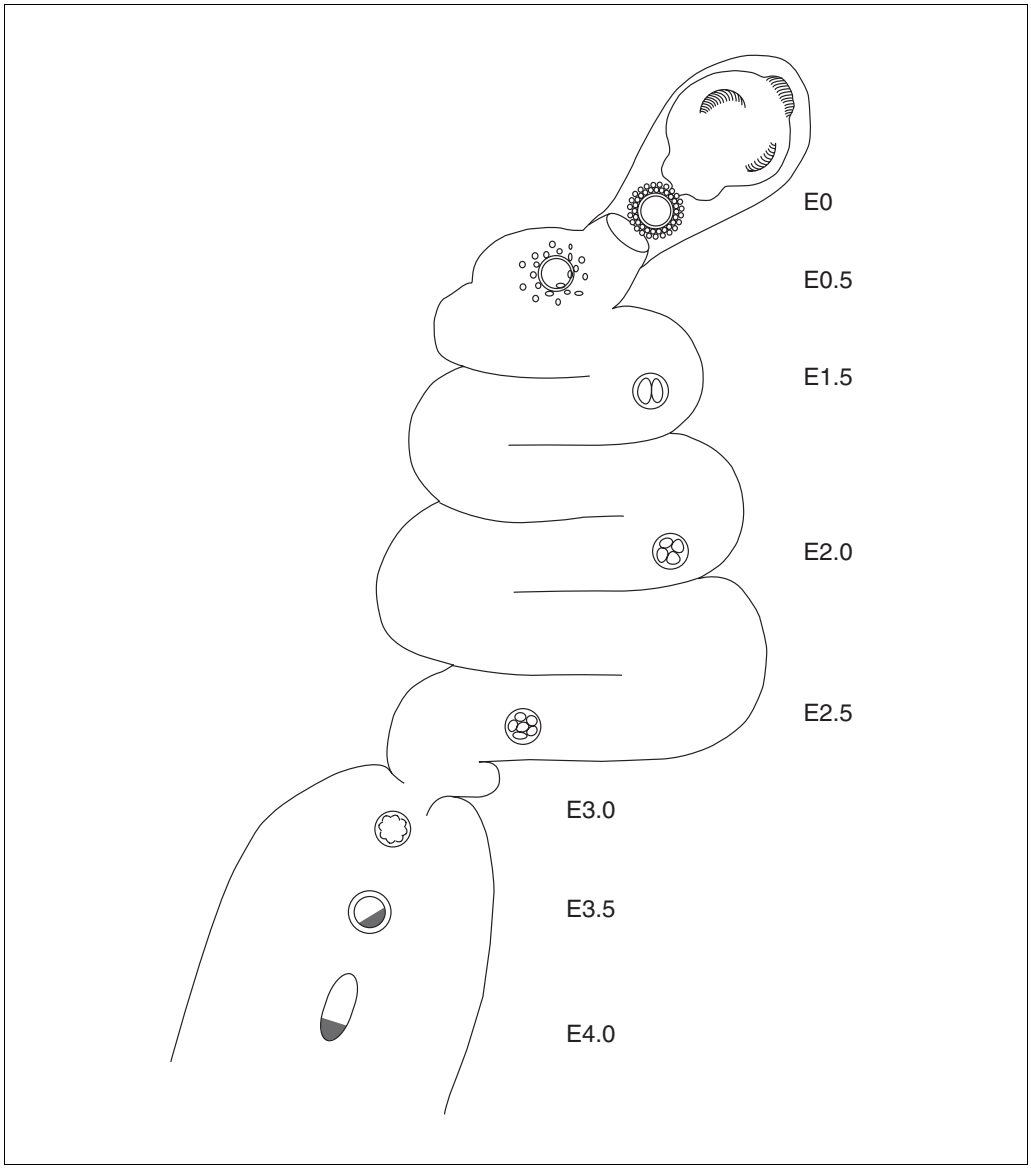

Figure 1.3.4 Diagram of the location of developing embryos within the murine reproductive tract. The days of embryonic development are designated by E followed by a number. An unfertilized one-cell oocyte (shown surrounded in cumulus oophorus) is released from an ovarian follicle on E0, when it enters the oviduct. Fertilized one-cell embryos (shown with the cumulus expanding) are collected on E0.5 for pronuclear injection. On E1.5, a two-cell embryo has formed and the cumulus has been shed. On E.2.0, this has grown to a four-cell embryo. On E2.5, eight-cell embryos (uncompacted or compacting) are still within the oviduct near the utero-tubal junction. Embryos enter the uterus by E3.0 (morula stage), become blastocysts by E3.5, and become hatched blastocyst by E4.0. Embryos for ES cell injection or aggregation can be used from E2.5 to E3.5.

recipient females must be synchronized to receive the embryos at the proper developmental time, without interference by endogenous fertilized ova. This is accomplished by the natural mating of females, generally of a reproductively vigorous outbred strain, with vasectomized males (duds) of any reproductively aggressive background, to induce pseudopregnancy. Females to be used as pseudopregnant recipients are selected for their hardiness, ability to withstand the surgical implantation procedure, and mothering ability. A common practice is to use strains expressing a different coat color than that expected for the Tg litter. Outbred CD1-type mice are routinely used, but FVB females also make good recipients under some conditions (W.C. Ladiges, unpub. observ.). The females are mated to the vasectomized males the day before DNA microinjection of embryos if they are to be transferred as one-cell embryos. If they are to be transferred as two-cell embryos, the recipient females are mated with the duds the same day as embryo microinjection. The following morning, plugged females are collected for surgical implantation. If recipients are needed for uterine transfer of ES cell–injected blastocysts, females are held for 2 days after first detection of plugs. Regardless of how the recipients will be used, approximately four times the number of females that are actually needed will have to be mated with duds, since natural mating will result in only ~25% of the females having detectable vaginal plugs (a vaginal plug is evidence of copulation). Plugged females that are not used can be placed back in the breeding rotation after a 14-day holding period. Females beyond the stage of good reproductive performance (generally 12 weeks, depending on the strain) should be culled from the recipient pool. Vasectomized males should be at least 8 weeks of age and can remain sexually active for up to 1 year, but it is advisable to replace them at ~9 months of age.

PRODUCTION OF Tg MICE BY PRONUCLEAR MICROINJECTION

DNA should be linearized before microinjection since linearized DNA is more efficiently integrated than circular DNA. DNA <10 kb in length is commonly used, since large-molecular-weight DNA becomes highly viscous, making it difficult to load and inject through the 1- to 2-μm opening of a microinjection needle. The gene unit should be cut from its plasmid vector sequences and isolated by gel electrophoresis. Purification is necessary to remove contaminants, and this is a major factor in determining successful or unsuccessful integration of the transgene. Injection buffer consists of 10 mM Tris·Cl/0.25 mM EDTA, pH 7.6. The optimum concentration for injection is 2 to 5 ng/μl (Brinster et al., 1985).

Good microinjection needles and holding pipets are essential for successful transfer of DNA into pronuclei of E0.5 embryos (see Fig. 1.3.4 for an explanation of E terminology). A detailed description of the pros and cons of micropipet size and shape and the techniques for making them have been published (DePamphilis et al., 1988; Mann and McMahon, 1993). The injection equipment consists of an inverted microscope with a movable stage and Nomarski differential interference contrast optics, micromanipulators to support the holding and injection pipets and reduce hand movements, and a vibration-free table to hold the microinjection apparatus. In addition, the flow of DNA into and out of the microinjection pipet, as well as the suction needed for the holding pipet, can easily be controlled by oil or air lines hooked up to airtight microsyringes or a micro-injector (described by Hogan et al., 1994). Before microinjection, the DNA preparation is centrifuged to sediment precipitates that may clog the injection needle. It is often necessary to remove obstructing contaminants from the construct using an ultrapure 0.45-μm spin filter. The actual technique of microinjection has been described (Gordon, 1993; see Fig 1.3.5). An experienced operator can inject between 100 and 200 embryos, in an injection chamber containing HEPES-buffered medium under oil, in 1 to 2 hr.

The standard medium for E0.5 embryo collection and pronuclear injection is M2 (available from Sigma; Quinn et al., 1982). This is buffered for use in air and is suboptimal for embryo culture of more than several hours. If embryos are to be transferred immediately after microinjection, at the one-cell stage, they can be transferred directly in M2. Often, embryos are cultured overnight in a medium buffered with bicarbonate in a 5% CO_2/air atmosphere, for transfer at the two-cell stage. A number of media have been used successfully for the culture of one-cell mouse embryos. The plethora of medium options and the continuing improvement of medium choices is due to a great body of work on various mammalian species that has been given a recent boost by the economic importance of early human embryo culture. The most commonly used medium for overnight culture of mouse embryos to the two-cell stage

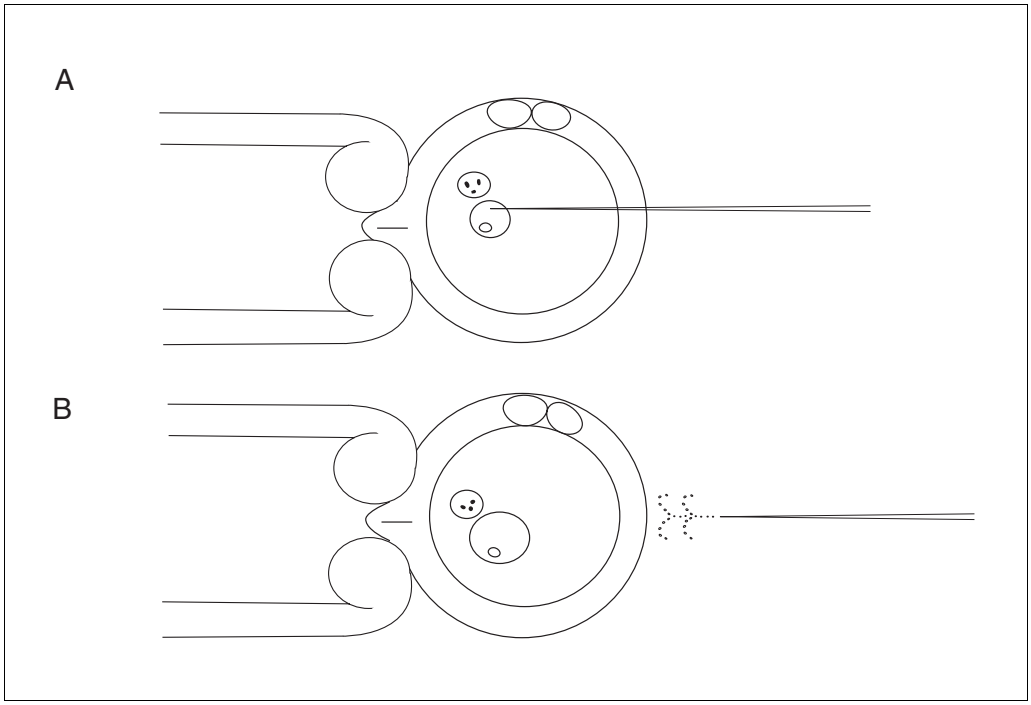

Figure 1.3.5 Pronuclear microinjection. The one-cell embryo is being held by the zona pellucida with an embryo holder on the left. The microinjection needle is on the right. Two polar bodies are in view beneath the zona pellucida. The small female pronucleus is above the male pronucleus. (**A**) The microinjection needle containing DNA has entered the male pronucleus, which will swell when DNA is injected into it. (**B**) The injected pronucleus is swollen and the microinjection needle has been withdrawn from the embryo. Note the steady flow of DNA from the needle.

is M16 (available from Sigma; Whittingham, 1971).

The surgical transfer of microinjected embryos to E0.5 pseudopregnant recipients is technically demanding but straightforward, and must be performed aseptically and rapidly, but gently. Mice are administered a general anesthetic, such as Avertin (Hogan et al., 1994) or ketamine/xylazine combination (0.35 ml per 20 g mouse mouse weight of a mixture of 1 part 20 mg/ml xylazine and 3 parts 100 mg/ml ketamine, diluted 1 to 10), which, when given intraperitoneally, generally provides quick, safe, and adequate levels of anesthesia for short periods of time. The surgical procedure is best performed under a dissecting microscope. It consists of exteriorizing one oviduct through a laparotomy incision, and placing the embryos through a puncture incision in the oviduct just anterior to the ampulla, using a glass transfer pipet (Fig. 1.3.6). An optional port of entry for the embryos is the ostium of the infundibulum. More embryos per recipient are transferred at the one-cell compared to the two-cell stage (typically 20 one-cell or 15 two-cell embryos per recipient). The aim is to have comfortably sized litters of 5 to 8 pups. Results do not differ using either stage of embryo, so the choice depends more on individual preference and laboratory schedules. An optional method yielding similar success rates is to transfer embryos to oviducts on both sides. In this case, the oviducts are exteriorized via bilateral dorsal incisions, and 4 to 12 embryos are transferred into each oviduct as already described. Following recovery from anesthesia, females should be housed no more than two per cage in relative isolation for the duration of their anticipated pregnancy.

Tail- or ear-punch biopsies are obtained from 2- to 4-week-old potential founder pups as a source of DNA for testing transgene integration. Pups are individually identified so transgene-positive animals can be retained for breeding. Approximately 1.0 to 1.5 cm of the distal tip of the tail is snipped for DNA extraction. Identification of Tg mice by PCR analysis of saliva has recently been described (Irwin et al., 1996). Cells from the oral cavity of weanling or adult mice are obtained by flushing with a small amount of sterile water using a plastic pipet tip. No surgical procedure is required and sampling can be repeated as often as needed. The DNA obtained from tissue biopsies can be analyzed by PCR, Southern blot analysis, or other hybridization techniques. PCR is rapid and efficient for detecting the presence of the transgene DNA. Southern blot analysis, while

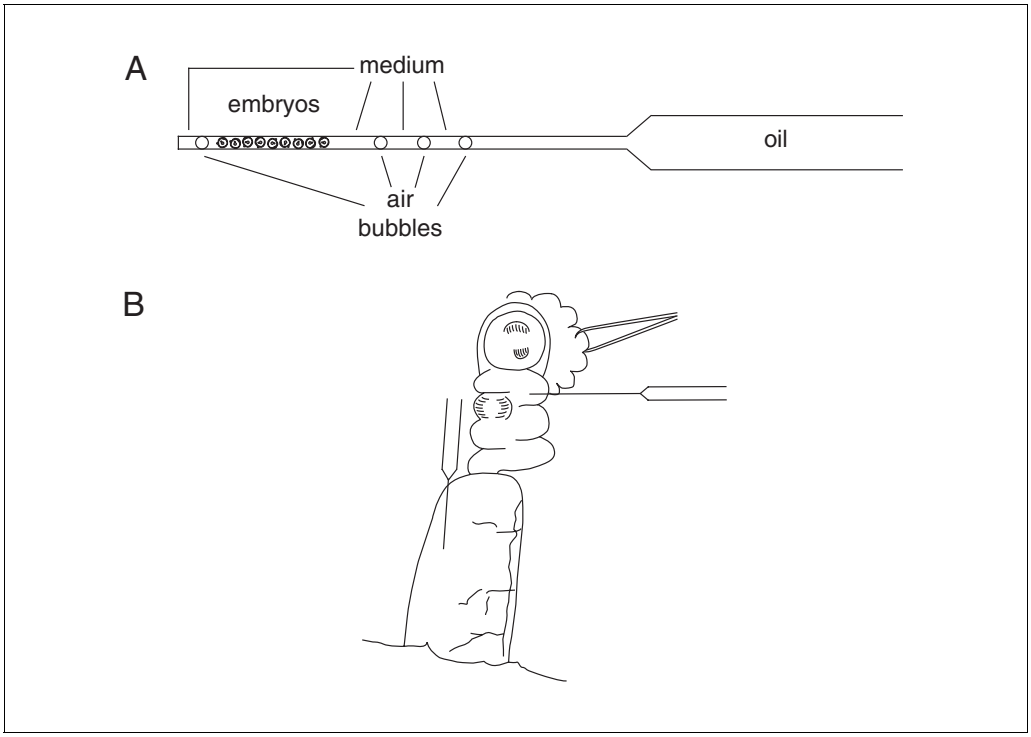

Figure 1.3.6 Embryo transfer. (**A**) Embryos are transferred with a glass pipet pulled so that the interior diameter can hold embryos in single file (~150 mm). Oil is loaded into the capillary, followed by two short columns of embryo-holding medium (M2), separated by air bubbles. Embryos are loaded in a minimum amount of medium separated by an air bubble from a tiny column of medium at the tip. (**B**) Transfer into the oviduct or uterus. For oviductal transfer (on the right), the ovary and oviduct are exteriorized under a dissecting microscope to place the ampulla in view. A 30-G needle is used to make a small opening in the oviduct just anterior to the ampulla on the infundibulum side. The tip of the transfer pipet is inserted into the opening and the embryos are transferred into the oviduct. Visualization of the first air bubble in the oviduct is evidence that the tip of the pipet is in the oviduct, while visualization of the second air bubble confirms that embryos were placed in the oviduct and the pipet can then be withdrawn. For uterine transfer (on the left), the tip of the uterus is exteriorized and held in place using the ovarian fat pad. The ovary is checked for corpora lutea. The uterine wall is punctured into the lumen with a 25-G needle, while avoiding capillaries. The transfer capillary is inserted into the puncture and embryos expelled using the air bubbles as markers so that oil is not placed in the uterus.

technically more cumbersome, will provide an estimate of transgene copy number, and is used by many to confirm PCR results. Once potential founders are identified, they are raised to sexual maturity and mated to non-Tg mice of the desired background strain. The offspring are tested for transmission of the transgene using the same assay as used for the parents. Mice that test positive for expression of the transgene can then be legitimately designated as founders for that specific line.

Interpretation of transgene expression can at times be a daunting task. The integration site can have a major influence on expression because a transgene may be incorporated into a "silent" region of the genome, so expression of the transgene will not be detected, or detected only at very low levels. Of more concern is whether active integration of the transgene disturbs the expression of endogenous host genes, resulting in an inadvertent phenotype. Therefore, it is essential to demonstrate that overexpression of a transgene is responsible for a specific phenotype by observing at least two and preferably three Tg lines from different founders. Evidence that the phenotype was due to the overexpression of the transgene in question would be conclusive if similar phenotypes were observed in separate founder lines.

There are several patterns of transgene transmission in founder mice. Most founders will transmit their transgene to 50% of their offspring. If 30% or less of the offspring are positive for the transgene, the founder is probably mosaic. Founder mice with 80% or more positive offspring may have more than one integration site. Southern blotting will help verify insertion sites. Offspring of founders

should transmit the transgene in a Mendelian fashion. However, loss of the transgene in subsequent generations has been observed (Gorden, 1993). The goals of breeding the founder mice are: (1) to observe the inheritance and expression patterns of Tg lines through several generations; (2) to expand the colony to provide mice for experimental study; and (3) to produce transgene homozygosity for comparison with the heterozygous state.

Mice can be mated when they are sexually mature, at 6 to 8 weeks of age. Tg founders are mated to the inbred strain of choice, but one of the most commonly used strains is C57BL/6. It takes six generations of mating onto the C57BL/6 background to obtain at least 99% of the Tg background as C57BL/6. It will then be possible to control for the influence of genetic background on gene expression by comparing Tg mice with normal C57BL/6 mice. Sexually mature female mice cycle every 3 to 4 days and have a gestation time of 19 to 21 days, so pups should be born within a month of breeder setup. If no pups are produced within 1 month, mice caged with a potential Tg founder should be replaced. It is possible that Tg founders may be infertile as a result of Tg expression or other unknown causes.

The production of homozygous Tg lines entails additional analysis to identify the first homozygotes. This is done by Southern blotting and genetic testing (Gorden, 1993). A potential homozygous Tg mouse is mated to several naive mice, and if all offspring are DNA-positive (assuming a minimum of 14 offspring tested), there is reasonable assurance the founder is homozygous. Additional test breeding will be necessary to ensure that homozygosity is maintained. There is also the risk that Tg expansion of a homozygous Tg line may result in a phenotype unassociated with the transgene, since ~10% of transgene integration events interrupt an endogenous gene involved in normal development. If homozygosity provides no scientific advantages, Tg lines should be maintained in the hemizygous (heterozygous for the transgene) state—i.e., in which the transgene is on only one chromosome.

PRODUCTION OF Tg MICE BY GENE TARGETING

Embryonic Stem Cell Culture

ES cell lines are derived from the inner cell mass of mouse embryos at embryonic day 3.5 (E3.5, where E0.5 is the day of plug; Fig. 1.3.4). ES cells can give rise to teratocarcinomas and teratomas when placed in an extrauterine site within a host mouse. They are not contact-inhibited in vitro and are able to grow in suspension, which are hallmarks of transformed cells. Thus, they form an interesting link between tumor formation and normal development. The aim of successful ES cell culture is to retain developmental capability so that when the cells are reintroduced into an embryo host, they can participate in development of an individual to make a chimera, i.e., an animal comprising cells from both the host embryo and the ES cells. Under most circumstances, it is desirable that among the tissue contributions, ES cells participate in the germ-cell lineage and thus transmit genetic changes introduced into ES cells into the germ line of chimeras. The doubling time (18 to 24 hr) of ES cells and the ability to retain germ-line potential (totipotency) in culture allow rare, induced genetic mutation events to be detected and the cells containing the desired mutation to be clonally grown and analyzed for reintroduction into embryos.

ES cells in culture have a remarkable ability to differentiate. Growth factors that interact with the leukemia inhibitory factor receptor (LIFR) subunit suppress ES-cell differentiation (Gearing et al., 1991; Rose et al., 1994; Pennica et al., 1995). Because ES cells are not contact-inhibited and lack the architectural elements that facilitate movement on a tissue culture plate, they tend to pile up as they divide (Fig. 1.3.7A). If cells are trapped within a cell cluster and lose direct exposure to growth factors bound to the feeder layer and/or in soluble form in the medium, the internal cells of the cluster influence the outer layer to differentiate into endoderm cells, which then gain contact inhibition and grow in a characteristic fashion (Fig. 1.3.7B and C). ES cell culture to eventually generate mutations in the germ line is primarily an effort to keep the cells in small, undifferentiated colonies, and so requires frequent passage accompanied by thorough dispersion of colonies using trypsin-EDTA. Passaging the cells every 2 days at three densities is useful for routine maintenance. Ideally, the culture medium should be changed daily. In general, ES cells thrive best in the presence of other ES cells, but are extremely fragile under pH conditions fluctuating too far from 7.2. Consequently, successful maintenance is a balance between keeping the cell density high enough without overly acidifying the medium by crowding. It is better to err on the side of lighter cell density as acid (yellow) medium can destroy the ES culture germ line potential overnight.

Isolation of ES lines from various murine strains has met with varying success

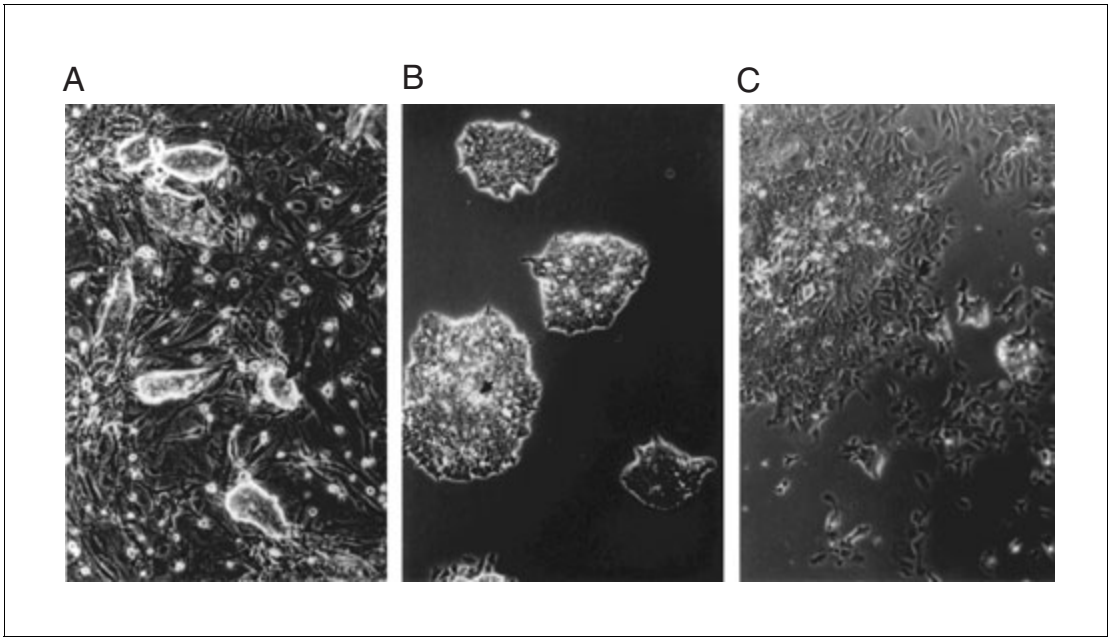

Figure 1.3.7 ES cells growing in vitro. (**A**) Small colonies of ES cells growing on a fibroblast feeder. The large arrow points toward an undifferentiated colony. Note the bright edge indicating that the colony is mounding as the cells divide. The small arrow points toward a flattened colony. Normal cultures contain both colony morphologies. Whether a flattened morphology is an indicator of early differentiation has not been determined. When passaging ES cells for injection into embryos, the aim is to have approximately three-fold more colonies of either morphology within this size range per unit area on the day of injection. (**B**) Undifferentiated ES cells growing for 4 days in the absence of a feeder, with added LIF. The arrow points to an area of vacuole formation that indicates stress due to crowding. (**C**) Differentiating ES cells growing for 4 days in the absence of a feeder layer,without added LIF. The arrow points to the leading edge of an ES colony that has differentiated into endoderm. Note the presence of cells that remain undifferentiated.

(Doetschmann et al., 1985; Ledermann and Bürki, 1991; Roche et al., 1995). If it is important to have specific strain backgrounds other than 129, it may be most effective to chose an ES line of that particular strain, if available. ES cell culture conditions have become fairly standardized; however, it is beneficial to obtain and follow the culture conditions used to isolate and establish the ES line. Lines that are transferred between laboratories,such as R1 (Nagy et al., 1993) and D3 (Doetschmann et al., 1985), are coming into common use, as are the culture conditions to maintain them. Abbondanzo et al. (1993) and Wurst and Joyner (1993) provide excellent protocols for ES culture techniques.

ES cells are routinely grown on a gelatinized plate in medium supplemented with 10^3 U/ml leukemia inhibitory factor (LIF) and/or on a growth-inactivated feeder layer plated on a gelatinized plate. When ES cells were first derived, they were grown on fibroblast feeder layers (Evans and Kaufman, 1981; Martin, 1981). Subsequently, it was determined that LIF suppresses differentiation in ES cells and that fibroblast feeder cells commonly used to support ES cells make LIF (Smith et al., 1988; Williams et al., 1988). However, all fibroblast feeders are not equal in their ability to maintain undifferentiated cultures (Suemori and Nakatsuji, 1987) nor is LIF alone as a medium supplement as good as a fibroblast feeder layer in maintaining an undifferentiated culture (Nichols et al., 1990). Consequently, it is recommended that a feeder layer be used for ES growth and that the feeder layer be derived from mid-gestation mouse fetuses (primary murine embryonic fibroblasts or PMEFs) and carried as a nonestablished line for only eight passages. PMEFs can be successfully frozen; therefore, low-passage PMEFs can be stockpiled. The use of feeders in conjunction with positive selection drugs requires that the feeder cells contain a gene that confers resistance to selection. This can be accomplished by deriving PMEFs from pregnancies in transgenic mice carrying the selection marker. If selection-resistant PMEFs are unavailable, some ES lines can endure culture in the absence of feeders on a gelatinized plate in medium supplemented with LIF for the time it takes to select resistant clones.

PMEFs, either proliferating or growth-arrested, as well as ES cells, are routinely held in liquid nitrogen frozen storage using standard tissue culture protocols. Bulk freezing of ES parent stocks is recommended because ES cells can drift rapidly in culture. A routine of thawing a new batch of parent cells prior to vector introduction helps to keep the transgenic lines at as low a passage number as possible. Following DNA transfection, ES cells should be stored frozen for the duration of analysis so that the cells destined for injection into embryos for chimera production are at as low a passage number as possible Figure 1.3.8 illustrates the passaging routine.

Abnormal variants continue to arise even under the best of culture conditions and are especially problematic if the ES culture has become contaminated by mycoplasma. Unfortunately, variants that no longer retain germ-

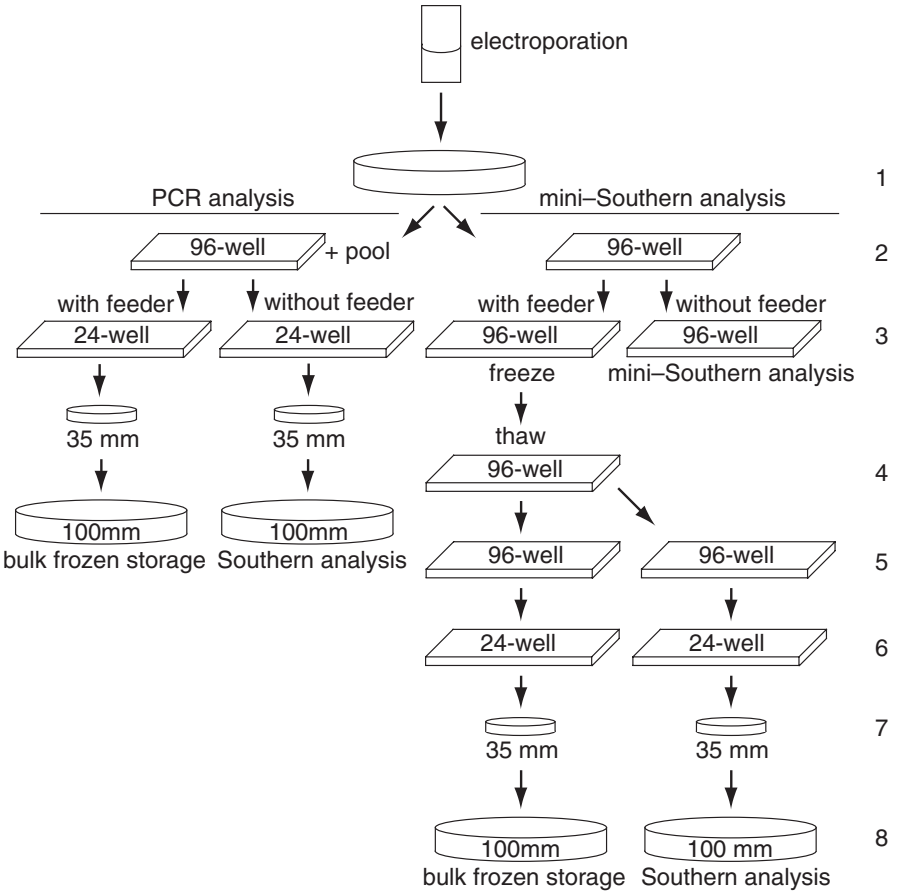

Figure 1.3.8 Comparison of number of passages of ES cells required following PCR versus Southern analysis of targeted events. Beginning with electroporation, represented by the rectangle in the upper center, passage numbers, on the right, are shown. During passage 1 the cells are grown clonally in the presence of selection drug(s). Picking colonies for growth in individual wells on a 96-well plate is passage 2. Half of each colony is pooled with other colonies for PCR analysis, represented on the left, while the entire colony goes into the well for mini-Southern analysis, represented on the right. Further divergence between culture methods occurs upon handling passage 3 plates. In the case of PCR analysis, on the left, the cells are passaged onto individual wells of a 24-well plate containing a feeder layer for eventual frozen storage of positive clones at passage 5 and without a feeder layer for Southern analysis of positive clones, also at passage 5. Mini-Southern analysis (on the right) requires freezing of the cells on the passage-3 96-well plate, while the sister plate is used for mini–Southern analysis. When successfully targeted colonies are identified, those colonies are thawed and passaged for bulk frozen storage and standard Southern analysis, as with the PCR scheme on the left. These represent ideal passage conditions. One passage should be added if initial isolated colony growth (passage 2) is poor.

line potential are not readily obvious by gross phenotype. Karyotypic analysis for chromosome number, or more finely by G or C banding (e.g., Abbondanzo et al., 1993), is helpful in analyzing colony drift and clonal loss of germ-line potential. Parent ES cell cultures that have drifted from the norm can be rescued by cloning.

Homologous recombination vectors are commonly transfected into ES cells via electroporation. The vector stock should be at a concentration of ~1 mg/ml, linearized (Ramirez-Solis et al., 1993), and free of toxic contaminants such as ethanol, ethidium bromide, and excess salt. ES cells, passaged 1 day prior to electroporation, should be growing densely in small colonies. Reports of the number of cells and amount of vector used for electroporation vary. Median amounts are 2×10^7 ES cells in PBS (without Ca^{2+} and Mg^{2+}) containing 25 µg vector. Electroporater settings vary from unit to unit. A short, high-voltage electrical pulse is applied to the ES-vector mixture. Pores form in the ES cell membrane that allow entry of the vector. Ideally, an immediate upshot of successful electroporation is 50% killing of the ES cells, as assessed by the trypan blue exclusion test of cell viability. This is a useful method to predetermine effective electroporater settings. DNA can also be injected directly into the nucleus by monolayer microinjection (Zimmer and Gruss, 1989). Although homologous recombination is efficient enough following microinjection so that no selection marker is required, the technique requires expertise and expensive equipment and is not commonly reported.

Following electroporation, the cells are plated either directly onto gelatinized plates in medium containing LIF or onto selection-resistant feeders. Reported cell densities vary; however, the aim is to plate the cells sparsely enough so that overgrowth prior to selection taking effect does not occur, and so that the cells are not plated so sparsely as to be wasteful of medium. Positive selection drugs, such as neomycin, vary in effectiveness from batch to batch and should be tested for complete killing of parent ES cells prior to use for selection of integration. One day after electroporation, the selection drug or drugs are added to the plates. Negative selection with ganciclovir may be responsible for lowered germ-line potential of resulting clones, so it is present for only 4 days, while the positive selection drug is present for the duration of selection, or 7 to 12 days. Cultures require frequent fluid changes prior to and during the death of nonresistant cells.

When colonies of resistant cells can be detected they are picked and dispersed. Colonies destined for PCR analysis are divided in half between cells designated for further culture on a feeder (individual wells on a 96-well plate) and pools with a few other clones to be immediately analyzed by PCR (Fig. 1.3.8). Colonies destined for initial analysis by mini–Southern blot analysis (Ramirez-Solis et al., 1992, 1993) are placed individually in one well of a 96-well plate. At this point, the aim is to grow the cells sufficiently to complete analysis by PCR, and to do this rapidly enough to passage only candidate clones for further analysis and bulk frozen storage. Alternatively, if analysis is by a mini-Southern approach, the aim is to grow only enough cells for frozen storage so as to be able to retrieve interesting clones during analysis. Again, it is important to freeze the cells at sufficient density and at the lowest passage number possible for successful thawing and chimera production. See Ramirez-Solis et al. (1993) and Wurst and Joyner (1993) for standard electroporation and selection protocols.

Production of Chimeras

Early mouse embryos are able to incorporate ES cells into the inner cell mass, which allows functional contribution of the introduced cells to all tissues of the resulting pup. Because there is no intracellular mixing of genetic material between host embryo and ES cell, the resulting mice are chimeras. The entire effort of ES cell culture in regard to production of transgenic mice is to maintain the potential of ES cells to participate in the murine germ line so that induced genetic alterations will be inherited. Consequently, it is important to verify that ES culture conditions are sufficient to achieve this, by directly testing parental ES cell lines prior to genetic manipulation for germ-line potential.

The most frequently used ES lines are male (XY) for several reasons. Male ES cells contribute functional gametes to a male host embryo, resulting in a gamete mix derived from ES cells and host embryo. Female ES lines tend to lose one X chromosome upon culture to become XO. The female ES cells containing an XO or XX chromosome complement are viable in the resulting germ line of female host embryos; thus only female chimeras will transmit the ES genotype (Robertson, 1986). A strong male ES contribution can switch the phenotype of a female embryo to male. When this happens, the host embryo can no longer contribute cells to the germ line, and resulting functional gametes are completely ES derived (Robertson,

1986). Thus, a good male ES line will skew the offspring sex ratio to predominately male. However, this also means that many of the phenotypic males may be sterile due to incomplete sex conversion. Some male ES lines do not skew the sex ratio of resulting chimeras and can transmit through a female chimera, presumably due to partial or total loss of the Y chromosome, resulting in XO ES cells (Kuehn et al., 1987). Establishment of a mutation proceeds more quickly through founder male chimeras; however, it can proceed through female chimeras when the ES line is an XO or XX female.

ES cells should be passaged 1 to 2 days prior to injection, at different densities to ensure that on the day of injection there will be one plate that is seeded relatively densely with small colonies (Fig. 1.3.7A). Cells from plates older than 2 days do not trypsinize well, resulting in poorly dispersed ES cell aggregates containing cells that have begun to differentiate.

Sparse plates result in a high feeder-to-ES cell ratio, making ES cell selection under the microscope tedious. Feeder cells can be partially removed by preplating; however, this technique can increase the incidence of cell aggregates. Disaggregated ES cells are resuspended in injection medium and held at 4°C until use.

Choice of host mouse strain will depend on the strain origin of the ES cells. Initial studies on interstrain chimeras (Mintz, 1965, 1969) were suggestive as to useful, commonly available strain mixtures for successful chimerism. Most ES lines are derived from various substrains of 129 and contribute efficiently within C57BL/6 host embryos. ES cells from the 129 strain can carry white, chinchilla, or black agouti coat colors. All potential 129 coat colors contrast sufficiently with black to identify extent of coat chimerism. C57BL/6 ES cells contribute well within white BALB/c host embryos. ES cells, particularly of 129 origin, can be so efficient at populating the C57BL/6 host embryo that there has been no need to identify a more suitable host. Optimization of embryo host strain for non-129 ES lines remains to be elucidated.

Chimera production can be divided into three basic tasks: embryo production, microinjection (or aggregation), and transfer. Superovulation of immature females for embryo production is identical to methods used to obtain pronuclear-stage embryos. The use of naturally mated adult females results in lower numbers, but higher quality embryos. See Hogan et al. (1994) for a natural mating protocol. Flow in the murine reproductive system is unidirectional, so that nothing can flow retrograde from the uterus into the oviduct. Embryo recovery method is determined by the stage and method chosen to place ES cells into the embryo. Eight-cell (E2.5) embryos are collected from within the oviduct at the utero-tubal junction (Fig. 1.3.9A) while morulae and blastocysts (E3.5) are collected from the uterus (Fig. 1.3.9B). See Nagy and Rossant (1993) for eight-cell embryo collection methods; see Papaioannou and Johnson (1993) for blastocyst collection methods.

There is no consensus on the best medium for either embryo holding, injection, or culture.

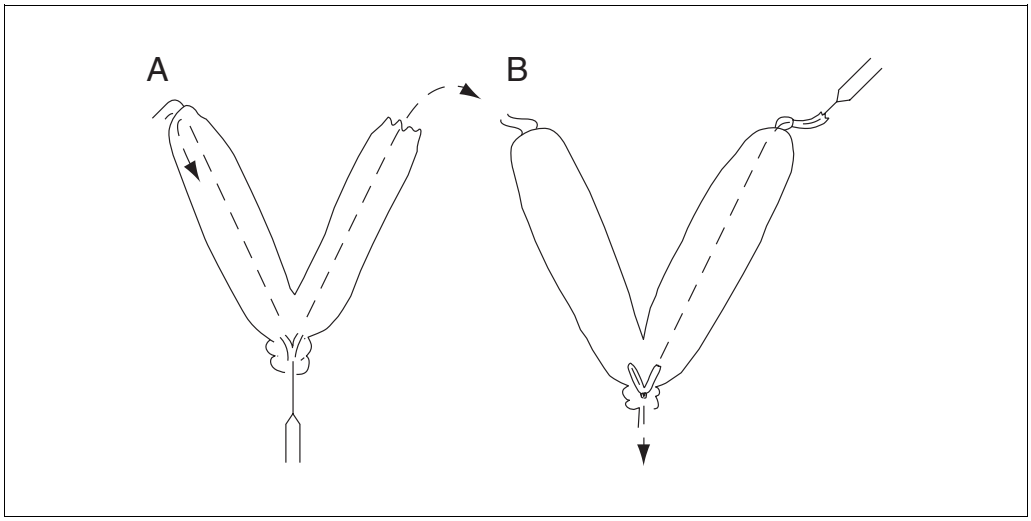

Figure 1.3.9 Direction of uterine flush. (**A**) Retrograde flush requires that the tip of the uterine horn be removed so that flush medium can flow out. (**B**) Flush through the oviduct through the utero-tubal junction allows flush collection through the cervix.

Medium for holding embryos in an air atmosphere needs to be buffered for air, using either a phosphate buffer or a bicarbonate-buffered medium containing HEPES. Culture requirements for mouse embryos from the eight-cell stage onward are less demanding than for earlier stages. However, limiting metabolic activity by reducing the temperature below 37°C and limiting time under substandard culture conditions are aims when working with morula and blastocyst stages. With this in mind, embryos can be successfully flushed, held, injected, and transfered in M2 medium (Quinn et al., 1982). Other medium options are described by Hogan et al. (1994), Stewart (1993), and Papaioannou and Johnson (1993).

Microinjection is the most common route for placing ES cells into embryos. Eight-cell (E2.5) to blastocyst (E3.5) stages can be used for microinjection, while embryo aggregation relies on the use of precompacted eight-cell embryos. Micromanipulation equipment is similar to that described for pronuclear injection. However, microscope optics need not be as refined nor as powerful because the cell interior does not need to be visualized, as is the case for pronuclear injection. Therefore, phase contrast at 100× magnification is sufficient to select healthy looking ES cells with clear, round morphology, and to determine the location of trophoblast cell junctions. Insertion of the injection needle at the junction between trophoblast cells will allow successful entry into the blastocoel without occlusion of the needle tip with cytoplasm, which could occur as a result of cell lysis (Fig. 1.3.10). Because phase contrast is sufficient to visualize the microinjection process, the injection chamber can be plastic. The lid of a 35-or 100-mm petri dish is sufficient to contain the injection droplets covered in oil. Use of a cooled chamber is optional. Holding ES cells at 4°C until they are placed in the injection chamber increases the time they can be held in suspension for injection. ES cells aggregate into unworkable clumps after 30 to 60 min at room temperature. Cells in the chamber need to be replaced with cooled cells when the existing cells become difficult to aspirate.

Microinjection of ES cells into embryos using micromanipulation requires the use of two specific tools, an embryo holder and an injection needle (Fig. 1.3.10). These require the use of specialized equipment to pull and bend the capillary tubing and generate the required tips. Embryo holders are the same as those used for pronuclear injection. Control of pressure on the injection needle ought to be fine enough to allow slow, easy ES cell aspiration and expulsion. Cleaning the interior of the needle using acid or sonication is useful to improve flow. The forces required for DNA microinjection may make the injection apparatus used for pronuclear injection too insensitive for ES cell injection. This is easily remedied by using a larger-diameter oil line. Fluorinert (Sigma) as a buffer between the oil in the line and the injection medium helps to increase control. ES cells are injected into the space between the uncompacted eight-cell embryo and the zona pellucida, into the center of a compacted eight-cell embryo or morula or into the blastocoel of a blastocyst, whether unhatched or hatched. The most difficult stage to inject is the hatched blastocyst, because trophoblast junctions are extremely tight while the embryo is difficult to hold firmly without a zona pellucida to prevent inadvertent collapse of the blastocyst. Glass pipets used for moving embryos from dish to dish are similar to the embryo transfer pipet and are made without using specialized instruments. See Papaioannou and Johnson (1993) and Stewart (1993) for overall manipulation setups and injection protocols. Another method of ES cell introduction into embryos is via aggregation to eight-cell embryos. This avoids the use of expensive toolmaking and microinjection equipment and can be as successful as microinjection (Nagy and Rossant, 1993).

Embryos can be transferred into either the oviduct or uterine lumen of E2.5 pseudopregnant recipients (Fig. 1.3.6). Suitable recipient mice are obtained as described for transfer of pronuclear-injected embryos. Uterine transfer is convenient due to its simplicity, but care should be taken to avoid introducing blood into the lumen or causing uterine contractions through rough handling. Pups are born ~18 days after transfer. Detection of chimerism is possible as early as 3 days later, but cannot be quantified until hair grows in, 5 to 7 days after birth. See Papaioannou and Johnson (1993) and Stewart (1993) for embryo-transfer techniques.

Extent of ES coat color contribution is used as a measure of potential germ-line contribution. However, coat color is not directly correlated with the germ-cell lineage in that the extent of chimerism in all tissues within the chimeric pup may not be uniform (Lallemand and Brulet, 1990; C.B. Ware, unpub. observ.).

A rule of thumb is to use only male chimeras where ≥50% of the coat color is from the ES contribution for testing germ line transmission of the induced mutation. This rule can be bent under circumstances where strong male chime-

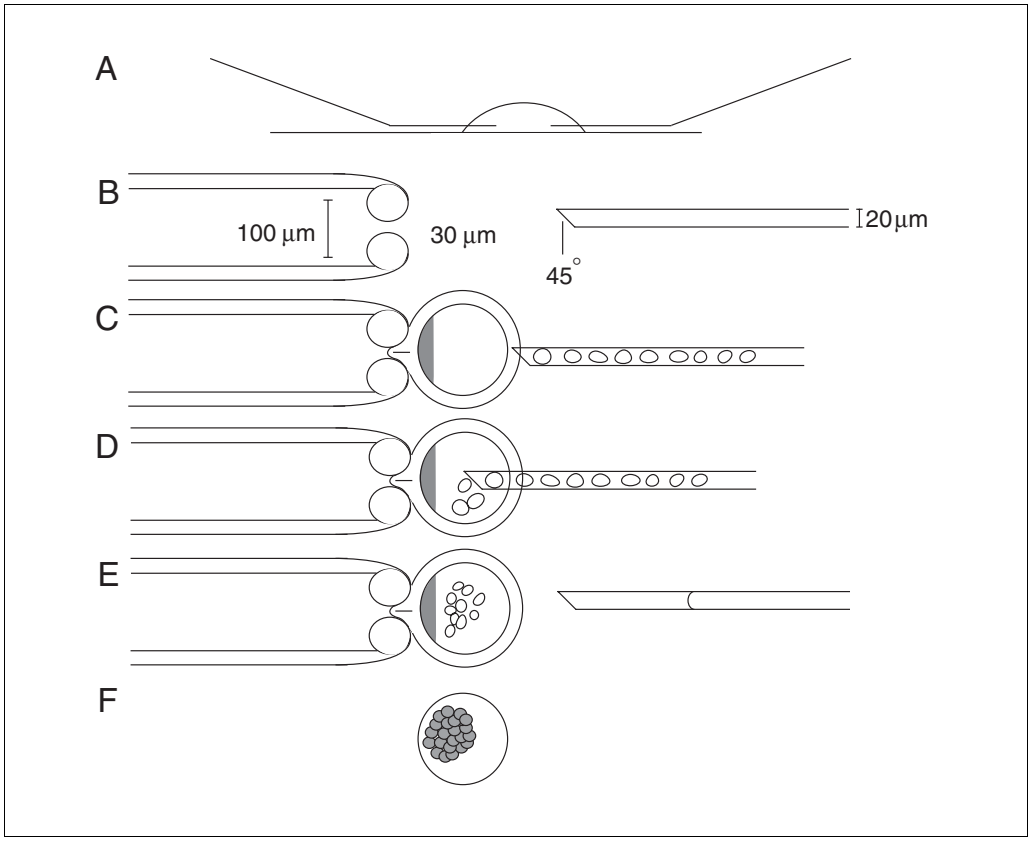

Figure 1.3.10 Embryo microinjection of ES cells. (**A**) Side view of the injection-droplet arrangement. Embryos and ES cells are placed in the droplet, which is overlaid with mineral oil. The two injection tools enter from opposite sides of the droplet and have an elbow bend that allows the tools to rest almost parallel with the plate bottom. (**B**) Tools used for injection. An embryo holder (left) should be about the size of an embryo, including zona pellucida, 80 to 100 µm, with an opening of 25 to 50 µm. Sizing is determined by individual preference. The injection needle is on the right. It has an internal diameter equivalent to the diameter of an ES cell (~18 to 20 µm). The tip has a 45° bevel and is sharpened. The orientation of the bevel when looking under the microscope is such that the tip is either on the bottom or on the top of the bevel (as shown). (**C**) The embryo is held with the holder. The inner cell mass is represented by a darkened semicircle on the left of the embryo. The injection needle is filled with ES cells and is approaching a trophoblast cell junction. (**D**) The needle is pushed through the cell junction and 10 to 15 cells dropped within the blastocoel. (**E**) The injection needle is withdrawn. A meniscus is seen between the medium and Fluorinert. (**F**) The embryo collapses around the ES cells.

ras are rare and the low frequency of targeted mutation events does not allow testing of alternate clones.

The genetic background of the 129 mouse strain is questionable (Threadgill et al., 1997). Chimeras generated from a 129 ES background are usually mated onto a better characterized strain with superior breeding performance. If kept on a 129 background, coat color frequently will not indicate germ line transmission, so offspring would have to be genotyped for the targeted mutation. Many mutations have been successfully analyzed on several generations of an F2 background. For example, test mating of chimeras is often accomplished with C57BL/6 females. The resulting black offspring are derived only from the host embryo background. Black agouti offspring are derived from ES cell contribution, due to coat color genetics of all the ES 129 substrains. These pups are further tested, using tail or ear biopsies, to determine whether the wild-type or the targeted allele was transmitted. Pups determined to be heterozygous (+/–) for the mutation are retained for breeding. At this point, a decision must be made whether to breed closer to an inbred background and/or to breed to homozygosity. In this example, mating the +/–animal to wild-type C57BL/6 will bring the resulting pups closer to C57BL/6 at a rate of 50% C57BL/6 contribution per generation. Each generation must be genotyped and only +/–animals must be bred

to C57BL/6. Three generations of crosses to C57BL/6, including the initial chimera mating, will bring the line to 87.5% C57BL/6. Seven to eight generations and more than 1.5 years later, the line is >99% C57BL/6, though drifted somewhat from C57BL/6 (Green, 1966). It is particularly unfortunate that genes in proximity to the targeted mutation are the least likely to be brought onto the C57BL/6 background. Once the line is predominantly C57BL/6, brother-sister matings will be the most rapid way to bring loci linked with the induced mutation to homozygosity (Green, 1966).

Breeding directly to homozygosity means +/– brother to +/– sister mating of offspring from chimera matings. If the chimera was not mated to a female of the ES strain, the background will be a random mix of ES cell and maternal strain backgrounds. Consequently, controls cannot be considered identical, nor might the resulting phenotype be as consistent among individuals as desired. In this situation, within-litter controls are the best available; however, independent wild-type or +/–brother-sister matings of the same generation can serve as useful controls. Depending on the target mutation, this may not be critical for successful biological analysis. However, the importance of having a genetically defined background for analysis may not be apparent during conceptualization of experimental design. Relevant to previously existing data, use of ES cells that are derived from an inbred background, such as C57BL/6, can overcome these difficulties (Fig. 1.3.11 and Fig. 1.3.12).

Tissue biopsy is usually taken from the tail as described for overexpression transgenics (see Production of Tg Mice by Pronuclear Microinjection). Frequently, the various targeted mutation genotypes can be easily identified using PCR for the positive selection marker in combination with primers to amplify the wild-type gene. Less tissue is required for PCR, so ear-biopsy tissue is sufficient for analysis. DNA extraction and analysis follow standard protocols. If PCR analysis is efficient, it may be convenient to use a quick DNA extraction, without cleaning away contaminating protein. It is advisable to look at the mutation in +/– pups from chimera matings using the same restriction digests used when selecting ES clones for chimera production, followed by Southern analysis. This will verify that no confounding rearrangements have occurred when the mutation passed through the chimera germ line.

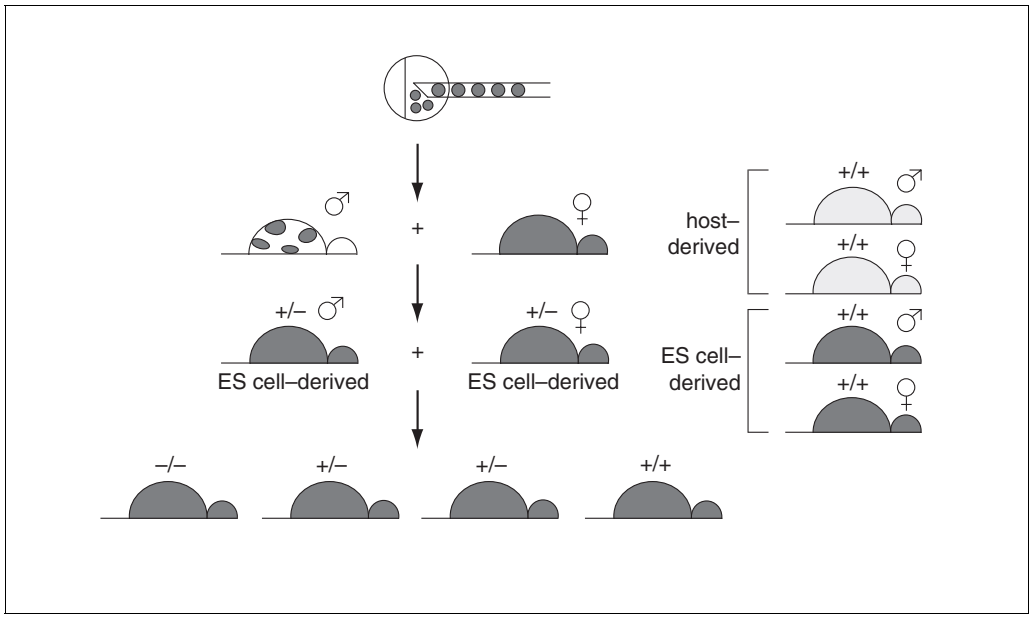

Figure 1.3.11 Breeding scheme to derive homozygous mutant animals from injection of targeted C57BL/6 ES cells into Balb/c blastocysts. The diagram at the top represents a BALB/c embryo being injected with C57BL/6 ES cells. The strain coat colors are represented by a white inner cell mass and black ES cells. The injected embryo results in a chimeric male (spotted animal on the left). It is mated with a C57BL/6 wild-type female. Paternal inheritance of the offspring is from either the host embryo (light gray animals, F1 between C57BL/6 ×BALB/c, on the right) or from the ES cells (inbred C57BL/6 animals). ES cell contribution is either from the wild-type allele (+/+, black animals on the right) or the targeted allele (+/–, black animals on the left). Heterozygous brother-sister matings result in inbred C57BL/6 homozygous targeted (–/–), +/–targeted and +/+ animals.

Figure 1.3.12 C57BL/6 ES ×BALB/c embryo chimeric mouse mated with wild-type BALB/c female, with their offspring. Pups are all derived solely by germ-line transmission of the C57BL/6 ES genome from the father. Consequently, all the pups have a brown coat color (C57Bl/6 from the chimeric father and BALB/c from the mother). If the targeted mutation is transmitted in a Mendelian fashion, half of these pups carry the targeted allele (+/–). Had the host embryo contributed to the germ line of the chimera, pups would be white (BALB/c from the chimeric father and BALB/c from the mother).

The resulting phenotype of targeted mutations is unpredictable, and may lead to developmental lethality. In this case, if +/– animals are viable and fertile, the mutation can be carried in this state and the offspring of +/– matings can used for phenotype analysis. Study of +/– animals prior to mutation-induced death is required if the mutation is dominant lethal or if the +/– animals are infertile. If the gene is critical in the heterozygous state for gamete or vital-system function, chimeras and in vitro differentiation may be the only route for phenotype analysis. See Papaioannou and Johnson (1993) for a description of animal husbandry.

COLONY MANAGEMENT

An ideal record-keeping system should allow the recording of data of all activities within the breeding colony, including individually identifying each mouse and its ancestry, breeders set up and pups born, and experimental phenotypes unique to each mouse. All mice born within a Tg colony should be individually identified. Ear tags are commonly used because they are relatively permanent, inexpensive, and easy to apply starting at 3 weeks of age. Other methods include toe and ear clipping and tattoo application. All data for lines within a Tg colony should be recorded so that phenotype patterns can be accurately evaluated on a retrospective basis. Records should be maintained in a format that allows for rapid and clear determination of the relationships between colony components. This can be done by simple hand entry of data into a breeding notebook, or by more elaborate maintenance on a computer spreadsheet. The authors use a standard Excel spreadsheet to maintain a Master List of every mouse that is ear tagged. Ear tag numbers consist of a two-digit letter code and a numerical code of up to four digits. The Master List contains birth date, transgene name, generation, line, sex, parents, phenotype and genotype, and information about the specific project. A pedigree should be established for each founder mouse that is mated. Customized cage cards can be printed for breeder cages to provide a summary of the breeding activity for each cage. Customized weaning cards can be used to record the line and ear tag numbers so weanlings can be readily located and tracked. A separate spreadsheet file should be used for breeding records, containing birthdates of litters, number of pups born and weaned per litter, ear tag numbers for pups, breeder setup date, breeder retirement date, strain, generation, line, and comments. Computer software packages specifically for mouse colony record keeping have been developed and are commercially available (Silver, 1993).

Because it requires a considerable effort to generate a Tg line, it is prudent to be sensitive to the health status of the mice and also of the environment where they are housed. Many researchers opt to maintain Tg lines in specific-pathogen-free housing facilities where the mice and the environment are diligently monitored for mouse pathogens. It generally costs more to maintain mice under these conditions, but complicating disease factors and loss of a Tg line will be greatly minimized. This is particularly appropriate where underlying disease states compromise biological analysis, or where analysis requires investigation in an uninfected background. Another way to help in the preservation of infection-free lines is to store embryos under cryopreservation in liquid nitrogen.

A registry of Tg strains and their characteristics is essential to prevent duplication of existing strains, to promote comparison among related strains, and to maintain valuable Tg models. The Oak Ridge National Laboratory (Oak Ridge, Tennessee) has developed a database for cataloging Tg animals, referred to as TBASE, which is currently administered by the Jackson Laboratory. To this end, an acceptable standardized nomenclature for Tg animals is necessary. Tg nomenclature must incorporate information related to both the methods used to produce Tg mice and the diversity of genetic elements that are inserted into their germ line. The actual format has been standardized (Standard Nomenclature for Transgenic Animals, 1992) and starts with the symbol "Tg" followed by a letter code for the mode of trangenesis where "N" stands for nonhomologous recombination by pronuclear microinjection or electroporation, "H" stands for homologous recombination, usually via targeted ES cells, and "R" stands for retroviral transfection. Following the letter for the mode of transgenesis is a set of parentheses enclosing relevant information about the transgene, which generally should not exceed eight characters. Finally, letter codes designating the laboratory of origin complete the nomenclature designed for Tg mice. Designation of the founder strain precedes the nomenclature if the background strain is maintained throughout the breeding. An example of a typical lineage nomenclature would be designated as follows: FVB-TgN(pkrGe)551Wcl, where FVB stands for the inbred strain, N for pronuclear microinjection, pkrGe for a genomic clone of the PKR gene, and 551Wcl for the Tg founder mouse number 551 in the laboratory of Warren C. Ladiges.

LITERATURE CITED

Abbondanzo, S.J., Gadi, I., and Stewart, C.L. 1993. Derivation of embryonic stem cell lines. *Methods Enzymol.* 225:803-823.

Adams, J.M., Harris, A.W., Pinkert, C.A., Corcoran, L.M., Alexander, W.S., Cory, S., Palmiter, R.D., and Brinster, R.L. 1985. The *c-myc* oncogene driven by immunoglobulin promoters enhances lymphoid malignancy in transgenic mice. *Nature* 313:533-538.

Bailleul, B., Surani, M.A., White, S., Barton, S., Brown, K., Blessing, M., Jorcano, J., and Balmain, A. 1990. Skin hyperkeratosis and papilloma formation in transgenic mice expressing a *ras* oncogene from a suprabasal keratin promoter. *Cell* 62:697-708.

Bonnert, C. amd Nicolas. J-F. 1993. Application of *Lac*Z gene fusions to postimplantation development. *Methods Enzymol.* 225:451-469.

Braselmann, S., Granniger, P., and Busslinger, M. 1993. A selective transcriptional induction system for mammalian cells based on Gal4-estrogen receptor fusion proteins. *Proc. Natl. Acad. Sci. U.S.A.* 90:1657-1661.

Breuer, M., Wientjens, E., Verbeek, S., Slebos, R., and Berns, A. 1991. Carcinogen-induced lymphomagenesis in pim-1 transgenic mice: Dose dependence and involvement of *myc* and *ras*. *Cancer Res.* 51:958-963.

Brinster R.L., Chen, H.Y., Trumbaur, M.E., Yagle, M.K., and Palmiter, R.D. 1985. Factors affecting the efficiency of introducing foreign DNA into mice by microinjecting eggs. *Proc. Natl. Acad. Sci. U.S.A.* 82:4438-4442.

Bronson, S.K. and Smithies, O. 1994. Altering mice by homologous recombination using embryonic stem cells. *J. Biol. Chem.* 269:27155-27158.

Brown, K., Burns, P.A., and Balmain, A. 1995. Transgenic approaches to understanding the mechanisms of chemical carcinogenesis in mouse skin. *Toxicol. Lett.* 82/83:123-130.

Charreau, B., Tesson, L., Soulillou, J-P., and Anegon, I. 1996. Transgenesis in rats: Technical aspects and models. *Transgenic Res.* 5:223-234.

Damm, K., Heyman, R.A., Umesono, K., and Evans, R.M. 1993. Functional inhibition of retinoic acid response by dominant negative retinoic acid receptor mutants. *Proc. Natl. Acad. Sci. U.S.A.* 90:2889-2893.

Deng, C. and Capecchi, M.R. 1992. Reexamination of gene targeting frequency as a function of the extent of homology between the targeting vector and the target locus. *Mol. Cell. Biol.* 12:3365-3371.

DePamphilis, M.L., Herman, S.A., Martinez-Salas, E., Chalifour, L.E.., Wirak, D.O., Cupo, D.Y., and Miranda, M. 1988. Microinjecting DNA into mouse ova to study DNA replication and gene expression and to produce transgenic animals. *BioTechniques* 6:662-680.

Doetschmann, T.C., Eistetter, H., Katz, M., Schmidt, W., and Kemler, R. 1985. The in vivo development of blastocyst-derived embryonic stem cell lines: Formation of visceral yolk sac, blood islands and myocardium. *J. Embryol. Exp. Morph.* 87:27-45.

Donehower, L.A., Harvey, M., Slagle, B.L., McArthur, M.J., Montgomery, C.A., Butel, J.S., and Bradley, A. 1992. Mice deficient for p53 are developmentally normal but susceptible to spontaneous tumors. *Nature* 356:215-221.

Douglas, G.R., Gingerich, J.D., Soper, L.M., and Jiao, J. 1997. Toward an understanding of the use of transgenic mice for the detection of gene mutations in germ cells. *Mutat. Res.* 388:197-212.

Evans, M.J. and Kaufman, M.H. 1981. Establishment in culture of pluripotential cells from mouse embryos. *Nature* 292:154-156.

Feil, R., Brocard, J., Mascrez, M., LeMeur, M., Metzger, D., and Chambon, P. 1996. Ligand-activated site-specific recombination in mice. *Proc. Natl. Acad. Sci. U.S.A.* 93:10887-10890.

Fernandez-Salguero, P., Pineau, T., Hilbert, D.M., McPhail, T., Lee, S.S., Kimura, S., Nebert, D.W., Rudikoff, S., Ward, J.M., and Gonzalez, F. 1995. Immune system impairment and hepatic fibrosis in mice lacking the dioxin-binding Ah receptor. *Science* 268:722-726.

Furth, P.A., Hennighausen. L., Baker, C., Beatty, B., and Woychick, R. 1991. The variability in activity of the universally expressed human cytomegalovirus immediate early gene enhancer/promoter in transgenic mice. *Nucl. Acids Res.* 19:6205-6208.

Gearing, D.P., Thut, C.J., VandenBos, T., Gimpel, S.D., Delaney, P.B., King, J., Price, V., Cosman, D., and Beckmann, M.P. 1991. Leukemia inhibitory factor receptor is structurally related to the IL-6 signal transducer, gp130. *EMBO J.* 10:2839-2848.

Gorden, J.C. 1993. Production of transgenic mice. *Methods Enzymol.* 225:747-770.

Gossen, J.A., de Leeuw, W.J., Tan, C.H., Zwarthoff, E.C., Berends, F., Lohman, P.H., Knook, D.L., and Vijg, J. 1989. Efficient rescue of integrated shuttle vectors from transgenic mice: A model for studying mutations in vivo. *Proc. Natl. Acad. Sci. U.S.A.* 86:7971-7985.

Green, E.L. 1966. Breeding systems. *In* Biology of the Laboratory Mouse, 2nd ed. (E.L. Green, ed.) pp. 11-22. McGraw-Hill, New York.

Gu, H., Marth, J.D., Orban, P.C., Mossmann, H., and Rajewsky, K. 1994. Deletion of a DNA polymerase b gene segment in T cells using cell type-specific gene targeting. *Science* 265:103-106.

Harvey, M., McArthur, M.J., Montgomery, C.A, Butel, J.S., Bradley, A., and Donehower, L.A. 1993. Spontaneous and carcinogen-induced tumorigenesis in p53-deficient mice. *Nature Genet.* 5:225-229.

Hasty, P. and Bradley, A. 1993. Gene targeting vectors for mammalian cells. *In* Gene Targeting: A Practical Approach (A.L. Joyner, ed.) pp. 1-31. IRL Press, Oxford.

Hasty, P., Rivera-Pérez, J., and Bradley, A. 1991a. The length of homology required for gene targeting in embryonic stem cells. *Mol. Cell. Biol.* 11:5586-5591.

Hasty, P., Rivera-Pérez, J., Chang, C., and Bradley, A. 1991b. Target frequency and integration pattern for insertion and replacement vectors in embryonic stem cells. *Mol. Cell. Biol.* 11:4509-4517.

Hightower, L.E. 1991. Heat shock, stress proteins, chaperones, and proteotoxicity. *Cell* 66:191-197.

Hogan, B., Beddington, R., Costantini, F., and Lacy, E. 1994. Manipulating the Mouse Embryo: A Laboratory Manual. 2nd ed. Cold Spring Harbor Laboratory Press, Cold Spring Harbor, N.Y.

Irwin, M.H., Moffatt, R.J., and Pinkert, C.A. 1996. Identification of transgenic mice by PCR analysis of saliva. *Nature Biotechnol.* 14:1146-1148.

Jaffe, L., Robertson, E.J., and Bikoff, E.K. 1992. Developmental failure of chimeric embryos expressing high levels of H-2Dd transplantation antigens. *Proc. Natl. Acad. Sci. U.S.A.* 89:5927-5931.

Jakobovits, A., Moore, A.L., Green, L.L., Vergara, G.J., Maynard-Currie, C.E., Austin, H.A., and Klapholz, S. 1993. Germ-line transmission and expression of a human-derived yeast artificial chromosome. *Nature* 362:255-258.

Jhappan, C., Stahle, C., Harkins, R., Fausto, N., Smith, G.H., and Merlino, G.T. 1990. TGFα overexpression in transgenic mice induces liver neoplasia and abnormal development of the mammary gland and pancreas. *Cell* 61:1137-1146.

Kagan, D., Platt, J., and Byrne, G.W. 1994. Expression of complement regulatory factors using heterologous promoters in transgenic mice. *Transplant. Proc.* 26:1242.

Kemp. C.J., Donehower, L.A., Bradley, A., and Balmain, A. 1993. Reduction of p53 gene dosage does not increase initiation or promotion but enhances malignant progression of chemically induced skin tumors. *Cell* 74:813-822.

Kitsukawa, T., Shimono, A., Kawakami, A., Kondoh, H., and Fujisawa, H. 1995. Overexpression of a membrane protein, neuropilin, in chimeric mice causes anomalies in the cardiovascular system, nervous system and limbs. *Development* 121:4309-4318.

Kohler, S.W., Provost, G.S., Kieck, A., Kretz, P.L., Bullock, W.O., Sorge, J.A., Putman, D.A., and Short, J.M. 1991. Spectra of spontaneous and mutagen-induced mutations in the *lac*I gene in transgenic mice. *Proc. Natl. Acad. Sci. U.S.A.* 88:7958-7962.

Kühn, R., Schwenk, F., Aguet, M., and Rajewsky, K. 1995. Inducible gene targeting in mice. *Science* 269:1427-1429.

Kuehn, M.R., Bradley, A., Robertson, E.J., and Evans, M.J. 1987. A potential animal model for Lesch-Nyhan syndrome through introduction of HPRT mutations into mice. *Nature* 326:295-298.

Lakso, M., Sauer, B., Mosinger, B., Jr., Lee, E.J., Manning, R.W., Yu, S.-H., Mulder, K.L., and Westphal, H. 1992. Targeted oncogene activation by site-specific recombination in transgenic mice. *Proc. Natl. Acad. Sci. U.S.A.* 89:6232-6236.

Lallemand, Y. and Brulet, P. 1990. An in situ assessment of the routes and extents of colonization of the mouse embryo by embryonic stem cells and their descendants. *Development* 110:1241-1248.

Lamb, B.T., Sisodia, S.S., Lawler, A.M., Slunt, H.H., Kitt, C.A., Kearns, W.G., Pearson, P.L., Price, D.L., and Gearhart, J.D. 1993. Introduction and expression of the 400 kilobase amyloid precursor protein gene in transgenic mice. *Nature Genet.* 5:22-30 (erratum *Nature Genet.* 5:312).

Ledermann, B. and Bürki, K. 1991. Establishment of a germ-line competent C57BL/6 embryonic stem cell line. *Exp. Cell Res.* 197:254-258.

Liang, H.C., Li, H., McKinnon, R.A., Duffy, J.J., Potter, S.S., Puga, A., and Nebert, D.W. 1996. Cyp1a (–/–) null mutant mice develop normally but show deficient drug metabolism. *Proc. Natl. Acad. Sci. U.S.A.* 93:1671-1676.

Mann, J.R. and McMahon, A.P. 1993. Factors influencing frequency production of transgenic mice. *Methods Enzymol* 225:771-793.

Mansour, S.L., Thomas, K.R, and Capecchi, M.R. 1988. Disruption of the proto-oncogene *int-2* in mouse embryo-derived stem cells: Ageneral strategy for targeting mutations to non-selectable genes. *Nature* 336:348-352.

Martin, G.R. 1981. Isolation of a pluripotent cell line from early mouse embryos cultured in medium conditioned by teratocarcinoma stem cells. *Proc. Natl. Acad. Sci. U.S.A.* 78:7634-7638.

Matsui, Y., Halter, S.A., Holt, J.T., Hogan, B.L., and Coffey, R. 1990. Development of mammary hyperplasia and neoplasia in MMTV-TGF α transgenic mice. *Cell* 61:1147-1155.

Mintz, B. 1965. Experimental genetic mosaicism in the mouse. *In* Ciba Foundation Symposium on Preimplantation Stages of Pregnancy (G.E.W. Wolstenholme and M. O'Connor, eds.) pp. 194-207. Little, Brown, Boston.

Mintz, B. 1969. Developmental mechanisms found in allophenic mice with sex chromosomal and pigmentary mosaicism. *Birth Defects* 5:11-22.

Montoliu, L., Schedl, A., Kelsey, G., Lichter, P., Larin, Z., Lehrach, H., and Schutz, G. 1993. Generation of transgenic mice with artificial chromosomes. *Cold Spring Harbor Symp. Quant. Biol.* 58:55-62.

Nagy, A. and Rossant, J. 1993. Production of completely ES cell-derived fetuses. *In* Gene Targeting: A Practical Approach (A.L. Joyner, ed.) pp. 147-179. IRL Press, Oxford.

Nagy, A., Rossant, J., Nagy, R., Abramov-Newerly, W., and Roder, J.C. 1993. Derivation of completely cell culture–derived mice from early-passage embryonic stem cells. *Proc. Natl. Acad. Sci. U.S.A.* 90:8424-8428.

Nichols, J., Evans, E.P., and Smith A.G. 1990. Establishment of germ-line-competent embryonic stem (ES) cells using differentiation inhibiting activity. *Development* 110:1341-1348.

No, D., Yao, T.P., and Evans, R.M. 1996. Ecdysone-inducible gene expression in mammalian cells and transgenic mice. *Proc. Natl. Acad. Sci. U.S.A.* 93:3346-3351.

Oberly, T.D., Cousin, D.B., Cihla, H.P., Oberly, L.W., El-Sayyed, N., and Ho, Y.S. 1993. Immunolocalization of manganese superoxide dismutase in normal and transgenic mice expressing the human enzyme. *Histochem. J.* 25:267-279.

Orban, P.C., Chui, D., and Marth, J.D. 1992. Tissue- and site-specific DNA recombination in transgenic mice. *Proc. Natl. Acad. Sci. U.S.A.* 89:6861-6865.

Palmiter, R. Norstedt, G., Gelinas, R.E., Hammer, R.E., and Brinster, R.L. 1983. Metallothionein-human GH fusion genes stimulate growth of mice. *Science* 222:809-814.

Papaioannou, V. and Johnson, R. 1993. Production of chimeras and genetically defined offspring from targeted ES cells. *In* Gene Targeting: A Practical Approach (A.L. Joyner, ed.) pp. 107-146. IRL Press, Oxford.

Pennica, D., Shaw, K.J., Swanson, T.A., Moore, M.W., Shelton, D.L., Zioncheck, K.A., Rosenthal, A., Taga, T., Paoni, N.F., and Wood, W.I. 1995. Cardiotrophin-1: Biological activities and binding to the leukemia inhibitory factor receptor/gp130 signaling complex. *J. Biol. Chem.* 270:10915-10922.

Pineau, T., Fernandez-Salguero, P., Lee, S., McPhail, T., Ward, J.M., and Gonzalez, F.J. 1995. Neonatal lethality associated with respiratory distress in mice lacking cytochrome p450 1a2. *Proc. Natl. Acad. Sci. U.S.A.* 92:5134-5138.

Quinn, P., Barros, C., and Whittingham, D.G. 1982. Preservation of hamster oocytes to assay the fertilizing capacity of human spermatozoa. *J. Reprod. Fertil.* 66:161-168.

Ramirez-Solis. R., Rivera-Pérez, J., Wallace, J.D., Wims, M., Zheng, H., and Bradley, A. 1992. Genomic DNA microextraction: A method to screen numerous samples. *Anal. Biochem.* 201:331-335.

Ramirez-Solis. R., Davis, A.C., and Bradley, A. 1993. Gene targeting in embryonic stem cells. *Methods Enzymol.* 225:855-878.

Robertson, E.J. 1986. Pluripotential stem cell lines as a route into the mouse germ line. *Trends Genet.* 2:9-13.

Roche, M.L., Stock, J.L., Byrum, R., Koller, B.H., and McNeish, J.D. 1995. A new embryonic stem cell line from DBA/lacJ mice allows genetic modification in a murine model of human inflammation. *Exp. Cell Res.* 221:520-525.

Rose, T.M., Weiford, D.M., Gunderson, N.L., and Bruce, A.G. 1994. Oncostatin M (OSM) inhibits the differentiation of pluripotent embryonic stem cells in vitro. *Cytokine* 5:48-54.

Saitou, M., Sugal, S., Tnaka, T., Shomouche, K., Fuchs, E., Narumiya, S., and Kakizuka, A. 1995. Inhibition of skin development by targeted expression of a dominant negative retinoic acid receptor. *Nature* 374:159-162.

Sandgren, E.P., Quaife, C.J., Pinkert, C.A., Palmiter, R.D., and Brinster, R.L. 1989. Oncogene-induced liver neoplasia in transgenic mice. *Oncogene* 4:715-724.

Schwartzberg, P.L., Robertson, E.J., and Goff, S.P. 1990. Target gene disruption of the endogenous *c-abl* locus by homologous recombination with DNA encoding a selectable fusion protein. *Proc. Natl. Acad. Sci. U.S.A.* 87:3210-3214.

Shinkai, Y., Rathbun, G., Lam, K.P., Oltz, E.M., Mendesohn, M., Carron, J., Datta, M., Young, F., Stall, A.M., and Alt, F.W. 1992. RAG-2-deficient mice lack mature lymphocytes owing to inability to initiate V(D)J rearrangement. *Cell* 6:68-71.

Shockett, P.E. and Schatz, D.G. 1996. Diverse strategies for tetracycline-regulated inducible gene expression. *Proc. Natl. Acad. Sci. U.S.A.* 93:5173-5176.

Silver, L.M. 1993. Record keeping and database analysis of breeding colonies. *Methods Enzymol.* 225:3-15.

Sinn, E., Muller, W., Pattengale, P., Tepler, I., Wallace, R., and Leder, P. 1987. Coexpression of MMTV/v-Ha-ras and MMTV/c-myc genes in transgenic mice: Synergistic action of oncogenes in vivo. *Cell* 49:465-475.

Skryabin, B.V. and Schmauss, C. 1997. Enhanced selection for homologous-recombinant embryonic stem cell clones with a neomycin phosphotransferase gene in antisense orientation. *Transgenic Res.* 6:27-35.

Smith, A.G., Heath, J.K., Donaldson, D.D., Wong, G.G., Moreau, J., Stahl, M., and Rogers, D. 1988. Inhibition of pluripotential embryonic stem cell differentiation by purified polypeptides. *Nature* 336:688-690.

Spaulding, J.W., Momma, J., Elwell, M.R., and Tennant, R.W. 1993. Chemically-induced skin carcinogenesis in a transgenic mouse line (TG.AC) carrying a *V-Ha-ras* gene. *Carcinogenesis* 14:1335-1341.

Standard Nomenclature for Transgenic Animals. 1997. *ILAR News* 34:45-52.

Stewart, C.L. 1993. Production of chimeras between embryonic stem cells and embryos. *Methods Enzymol.* 225:823-855.

Strauss, S., Dausman, J., Beard, C., Johnson, C., Lawrence, J.B., and Jaenisch, R. 1993. Germ line transmission of a yeast artificial chromosome spanning the murine a_1(l) collagen locus. *Nature* 259:1904-1907.

Stringham, E.G., Dixon, D.K., Jones, D., and Candido, E.P. 1992. Temporal and spatial expression patterns of the small heat shock (hsp 16) genes in transgenic *Caenorhabditis elegans*. *Mol. Biol. Cell.* 3:221-233.

Suemori, H. and Nakatsuji, N. 1987. Establishment of the embryo-derived stem (ES) cell lines from mouse blastocysts: Effects of the feeder cell layer. *Dev. Growth Differ.* 29:133-139.

Sullivan, N, and Ouhibi, N. 1995. Preimplantation rat embryology: Chimeric and transgenic strategies. *In* Strategies in Transgenic Animal Science (G.M. Monastersky and J.M. Robl, eds.) pp. 37-55. American Society for Microbiology, Washington D.C.

Threadgill, D.W., Lee, D., Martin, A., Nadeau, J.H., and Magnuson, T. 1997. Geneology of the 129 inbred strains: 129/SvJ is a contaminated inbred strain. *Mammal. Genome* 8:390-393.

Tinwell, H., Lefevre, P.A., and Ashby, A. 1994. Response of the Muta Mouse *lacZ/galE* transgenic mutation assay to DMN: Comparisons with the corresponding Big Blue (*lacI*) responses. *Mutat. Res.* 307:169-173.

Vernet, M., Bonnert, C., Briand, P., and Nicolas, J-F. 1993. Application of *Lac*Z gene fusions to preimplantation development. *Methods Enzymol.* 225:434-451.

Whittingham, D.G. 1971. Culture of mouse ova. *J. Reprod. Fertil.* 14 (suppl.):7-21.

Williams, R.L., Hilton, D.J., Pease, S., Willson, T.A., Stewart, C.L., Gearing, D.P., Wagner, E.F., Metcalf, E.F., Nicola, N.A., and Gough, N.M. 1988. Myeloid leukemia inhibitory factor maintains the developmental potential of embryonic stem cells. *Nature* 336:684-687.

Wurst, W. and Joyner, A. L. 1993. Production of targeted embryonic stem cell clones. *In* Gene Targeting: A Practical Approach (A.L. Joyner, ed.) pp. 33-61. IRL Press, Oxford.

Zimmer, A. and Gruss, P. 1989. Production of chimaeric mice containing embryonic stem (ES) cells carrying a homeobox Hox 1.1 allele mutated by homologous recombination. *Nature* 338:150-153.

KEY REFERENCES

Davisson, M.T. 1994. Rules and guidelines for genetic nomenclature in mice. *Mouse Genome* 92(2):1-32.

Explains the details in providing Tg animals with a standard nomenclature and provides resources available for assistance.

Hogan et al., 1994. See above.

Classic handbook for overall mouse embryo techniques.

Joyner, A.L. 1993. Gene Targeting: A Practical Approach. IRL Press, Oxford.

Focuses on the protocols required for gene targeting by homologous recombination.

Wassarman, P.M. and DePamphilis, M.L. (eds.) 1993. Guide to techniques in mouse development. Parts X and XI. *Methods Enzymol.* vol. 225.

Overall presentation of transgenic techniques.

INTERNET RESOURCES

http://tbase.jax.org/docs/tb.html

Web site for accessing TBASE, the transgenic/targeted mutation database administered by The Jackson Laboratory.

http://www.lists.ic.ac.uk/hypermail/transgenic-list

Web site to pick up past messages from the transgenic list discussion, which is an informal discussion on all aspects of transgenics.

http://www.med.umich.edu/tamc

The transgenic web site at the University of Michigan, which contains access to a wide array of other websites of use in the pursuit of transgenics.

majordomo@ic.ac.uk

E-mail address to join the transgenics list discussion group. Message must include: subscribe transgenic-list<name><e-mail address>.

lsilver@molbiol.princeton.edu

E-mail address for Dr. Lee Silver, to obtain information on the mouse colony management software Animal House Manager, which is a software package for keeping track of mouse breeding colonies.

http://www.informatics.jax.org/

The Mouse Genome Informatics Web site at The Jackson Laboratory, which contains information on mouse genetic markers, molecular segments, phenotypes, comparative mapping data, experimental mapping data, and graphical displays for genetic, physical, and cytogenetic maps.

Contributed by Warren C. Ladiges and Carol B. Ware
University of Washington
Seattle, Washington

DNA Microarrays: An Overview of Technologies and Applications to Toxicology

AIMS AND OBJECTIVES

The Genome Project and the technological innovations that it spawned have dramatically altered the future course of all biological research, including toxicology. The GenBank database already harbors billions of base pairs of DNA sequences derived from millions of individual sequence entries (*http://www.ncbi.nlm.nih.gov/Genbank/index.html*). The first complete genomic sequence to be completed almost 5 years ago was that of *Heamophilus influenzae.* Since then, the genomes of more than two dozen additional organisms have been completed and made available to the research community (*http://www.ncbi.nlm.nih.gov/Entrez/Genome/org.html*). Continued improvement in high throughput DNA sequence technology has made it possible to complete the reference human genome sequence by the year 2001, several years ahead of schedule. Exploiting the enormous potential of genome-wide sequence information will require the development of a battery of new tools for high throughput and highly parallel molecular analyses and commensurate bioinformatics tools to analyze data sets of unprecedented depth and complexity.

An increasing number of molecular techniques continue to be developed for high throughput analyses of gene expression and genetic polymorphisms. Included among these methodologies are automated DNA sequencing, serial analysis of gene expression (Velculescu et al., 1995), denaturing high performance liquid chromatography (Underhill et al., 1996), differential display (Liang and Pardee, 1992), high-density filter hybridization (Zhao et al., 1995), and highly sensitive mutation assays coupled with iterative sample repooling strategies (Zarbl et al., 1998). While each of these approaches has advantages and limitations, none possess the versatility or potential of DNA microarrays, also known as DNA "chips". The unprecedented capacity of chips for highly parallel detection of RNA expression and/or DNA variation at the genomic level suggests that microarrays will play a major role in functional genomics, the study of how genome-wide genetic variation and patterns of gene expression interact to produce complex biological responses.

The response of cells or organisms to toxic stimuli is an example of such a complex response, which ranges all the way from the induction of a specific xenobiotic metabolizing enzyme to the induction of cellular suicide or apoptosis. Except in the case where a toxicant induces immediate cellular destruction, toxicants invariably induce an altered pattern of gene expression in exposed cells. Moreover, it is now well understood that polymorphisms in genes comprising the toxic response pathways can have a major effect on toxicity, while also effecting the pattern of gene expression in cells with the variant genotypes. The availability of DNA sequence data and DNA microarray technologies provides toxicologists with the unique opportunity to study these complex cellular responses to environmental toxicants or stimuli on a genomic scale, simultaneously observing effects on all cellular components and the effect of genetic polymorphisms. This combination of genomics and toxicology has been deemed toxicogenomics (Nuwaysir et al., 1999) and is expected to impact all areas of environmental research. The purpose of this unit is to provide an overview of the currently available, state-of-the-art DNA microarray technologies. Specific protocols are not presented because they are evolving at a very rapid pace and some remain proprietary. Instead, potential applications to the science of toxicology are discussed with emphasis on present limitations and potential pitfalls associated with use of these technologies, and whenever applicable suggest possible mitigating experimental approaches.

DEVELOPMENT OF DNA "CHIPS": A QUANTUM LEAP IN MOLECULAR DETECTION TECHNOLOGY

Oligonucleotide Arrays

Allele-specific oligonucleotide (ASO) hybridization for detection of specific DNA sequence changes was developed in the early 1980s (Conner et al., 1983). The availability of ASO technology prompted several groups to independently propose the use of oligonucleotide hybridization on a large scale as a method for sequencing DNA. The first strategy proposed involved the arraying of individual sequences of interest (targets) onto membrane filters, which would then be sequentially hybridized with a large number of individual oli-

Contributed by Helmut Zarbl
Current Protocols in Toxicology (2001) 1.4.1-1.4.16

gonucleotide probes (Drmanac et al., 1989). Since each labeled target molecule hybridizes specifically to its complementary oligonucleotide probe, this approach allows for highly parallel extraction of sequence information from a single hybridization. If many thousands of clones were arrayed on a single membrane, ASO hybridization with even a single oligonucleotide could yield hundreds of base pairs of sequence information. However, this strategy required the synthesis of a large number of oligonucleotide probes, each of which would then be individually labeled and sequentially hybridized to each array.

The alternative approach was to array a large number of oligonucleotide probes on a solid support, and then hybridize the array with labeled DNA (target) from the cells of interest (Fodor et al., 1991; Khrapko et al., 1991; Southern et al., 1992). Several methodologies, including micro-injection of synthesized oligomers into patches of activated polyacrylamide (Khrapko et al., 1991) and the coupling of synthesized oligomers to surface-modified glass or polypropylene, were independently developed in a number of laboratories (Maskos and Southern, 1993; Matson et al., 1995). However, arraying a large number of individual oligonucleotides to a solid support represents a formidable technical challenge as the number of probes increases. The limitations imposed by arraying individual probes could only be overcome by in situ synthesis of the individual oligonucleotides at spatially addressable sites on the solid support. The latter approach requires the precise and sequential delivery of chemical reagents to individual positions on the solid support. These prerequisites were satisfied by using "masks" that allow the sequential protection and deprotection of specific areas of the surface from reaction synthetic reagents (Fodor et al., 1991; Southern et al., 1992). By using combinatorial methods of chemical synthesis and sequential masking of the reactive surface, it is possible to synthesize large numbers of oligonucleotide sequences using a limited number of nucleotide coupling reactions. Given that there are 4 possible nucleotides at any position in an oligonucleotide, the number of sequences that can be generated increases as a function of 4^n, where n is the length of the sequence. It is theoretically possible to synthesize 4^n sequences using n coupling reactions.

Among the procedures developed for in situ synthesis of oligonucleotides is the use of channels formed by sealing the surface with a chemical mask, guiding the precursor molecules to the appropriate areas on the surface (Southern et al., 1992). Channel plates can apply the reagents in strips with a resolution of 1 cm. An alternative approach being developed is the use of modified inkjet printer heads to, in effect, spray the reagents onto a designated address on the surface (Marshall and Hodgson, 1998). In this technology, the "masks" are defined by the two-dimensional displacement of the printer head. Using the inkjet technology, reagents can be applied with a much higher spatial precision, making it possible to synthesize thousands of oligonucleotides per cm^2. The inkjet technology has the further advantage of flexibility, in that the pattern of reagents applied to the surface can be easily adapted to a new application.

The most sophisticated technology for the synthesis of oligonucleotide arrays is an adaptation of the photolithography methods that are used by the semiconductor industry to produce computer chips (Fodor et al., 1991). A comprehensive description of the technology for production of these arrays can be viewed at the Affymetrix website (*http://www.Affymetrix.com/technology/index.html*). The key innovation that made this approach feasible was the development of novel nucleotide precursors with protecting groups that can be cleaved by exposure to light of a specific wavelength. These precursors make it possible to deprotect specific regions of the chip by shining high-intensity light through openings in a light-impermeable, chromium mask. As a result, only regions of the surface not protected by the mask are chemically reactive to the next nucleotide precursor washed across the entire surface of the chip. By using a series of masks, it is possible to synthesize any nucleotide sequence at a given site on the chip. With this technology, it is presently possible to produce high-density arrays comprised of tiles or addresses that are 20 to 50 μm^2 in size, each consisting of a specific oligonucleotide sequence ≥25 nucleotides in length. It is therefore possible to synthesize 65,536 separate probes using 50-μm^2 tiles, or as many as 409,605 different probes using 20-μm^2 tiles, on a single 1.28-cm^2 chip. The density of the probe on each tile is between 10^7 and 10^8 molecules.

Oligonucleotide arrays represent a momentous leap forward in the capacity to analyze DNA sequences present in biological specimens. Microarrays are useful in a variety of DNA sequence-based assays including but not limited to the detection of single nucleotide polymorphisms (SNPs), loss of heterozygosity (LOH), constitutive and somatic allelotyping, genetic linkage analysis, mRNA expression

analysis, gene mapping, and methylation mapping.

cDNA Microarrays

The simplest expression arrays consist of individual cDNA clones spotted onto nitrocellulose or nylon filters. These arrays are then hybridized sequentially or in parallel with different radioactively labeled target cDNAs, and data is collected by phosphoimager analysis (Drmanac and Drmanac, 1999). Filters with thousands of arrayed human or murine genes and the requisite analysis software are available from several commercial suppliers (see Internet Resources for Web addresses of commercial suppliers).

A limitation of these spotted arrays remains the variability in the amount of probe that is applied to each spot, which increases the variance in the data and limits the sensitivity in comparing results among experiments. A second limitation derives from the use of radioactively labeled target cDNA. Scattering of the signal resulting from radioactive decay of the radionucleides and the tendency of filters to warp during experimental manipulation limits the density at which probes can be arrayed and still retain the ability to resolve individual signals. The former limitation can be mitigated with ^{33}P-labeled hybridization probes.

A significant step forward resulted from the availability of methods for generating fluorescently labeled target DNA (Schena et al., 1995; Shalon et al., 1996). When combined with confocal imaging of the fluorescence signal emitted following hybridization with labeled target, these approaches provide a significant increase in the performance of parallel assays. Detection by fluorescence does not suffer from the spatial restraints encountered using radioactive probes. However, the inherent fluorescence of nitrocellulose and nylon filters spurred the development of novel solid supports on which to array the cDNAs. Techniques for automated transfer of cDNAs by spotting onto derivatized glass supports were pioneered by Pat Brown and his colleagues and the complete plans for the inexpensive assembly of the robotic arrayer are available at the following website: *http://cmgm.stanford.edu/pbrown/mguide/index.html.* Robotic arrayers are also commercially available from numerous suppliers in a range of prices. The lower costs of hardware and chips make cDNA microarrays more attractive and accessible to most researchers than the commercially fabricated oligonucleotide arrays. Nonetheless, it is important to remember that cDNA arrays still require the production, purification, and handling of the individual cDNAs to be spotted onto the matrix. Typically, the cDNA clones or genomic DNAs of interest are obtained and amplified using the polymerase chain reaction (PCR). The advantage of using clones from cDNA libraries is that one pair of vector primers can be used to amplify coding sequences from all of the clones, whereas multiple primer pairs are required for each exon to be amplified from genomic DNA. In either case, the amplifications are performed in a multi-well format that can be automated (Fig. 1.4.1). The amplified probes, which should ideally be between 500 and 2500 nucleotides in length, are then arrayed onto the matrix with or without further purification. Printing chips with more than a few hundred probes will therefore require a substantial investment of effort and resources to produce and amplify the individual cDNAs.

Microarrays can then be used to compare expression levels of each represented gene under two sets of experimental conditions, such as before and after exposure to toxicants. Messenger RNA is extracted from the cell types and cDNA is produced by reverse transcription in the presence of a different fluorescence-labeled dNTP precursors for each mRNA, typically Cye3-dUTP for the reference sample and Cye5-dUTP for the test sample. The labeled cDNAs are then co-hybridized to the microarray such that each target molecule will form a stable duplex with its corresponding probe on the array. The amount of each labeled target molecule hybridized to the probe spot is a function of how much of each target was present in each cell type. Each spot on the array is then scanned for fluorescence at the optimal wavelength for the Cye3 and Cye5 fluors using lasers, or high-intensity light and monochromatic filters as in the case of Array Worx Scanner shown (Applied Precision). Expression data for each gene represented on the array is expressed as a ratio of flurescence intensities normalized to the reference sample (i.e., Cye3/Cye5). Shown in the figure is an array with the entire set of yeast genes printed and hybridized in the facility at the Fred Hutchinson Cancer Research Center. If the expression of a gene is unchanged, the ratio will remain close to unity (yellow color on computer-generated false image). Any significant deviation from unity indicates either an increase (>1, image becomes more red) or a decrease (<1, image becomes more green) in the level of expression between the test and the reference sample, and the magnitude of the

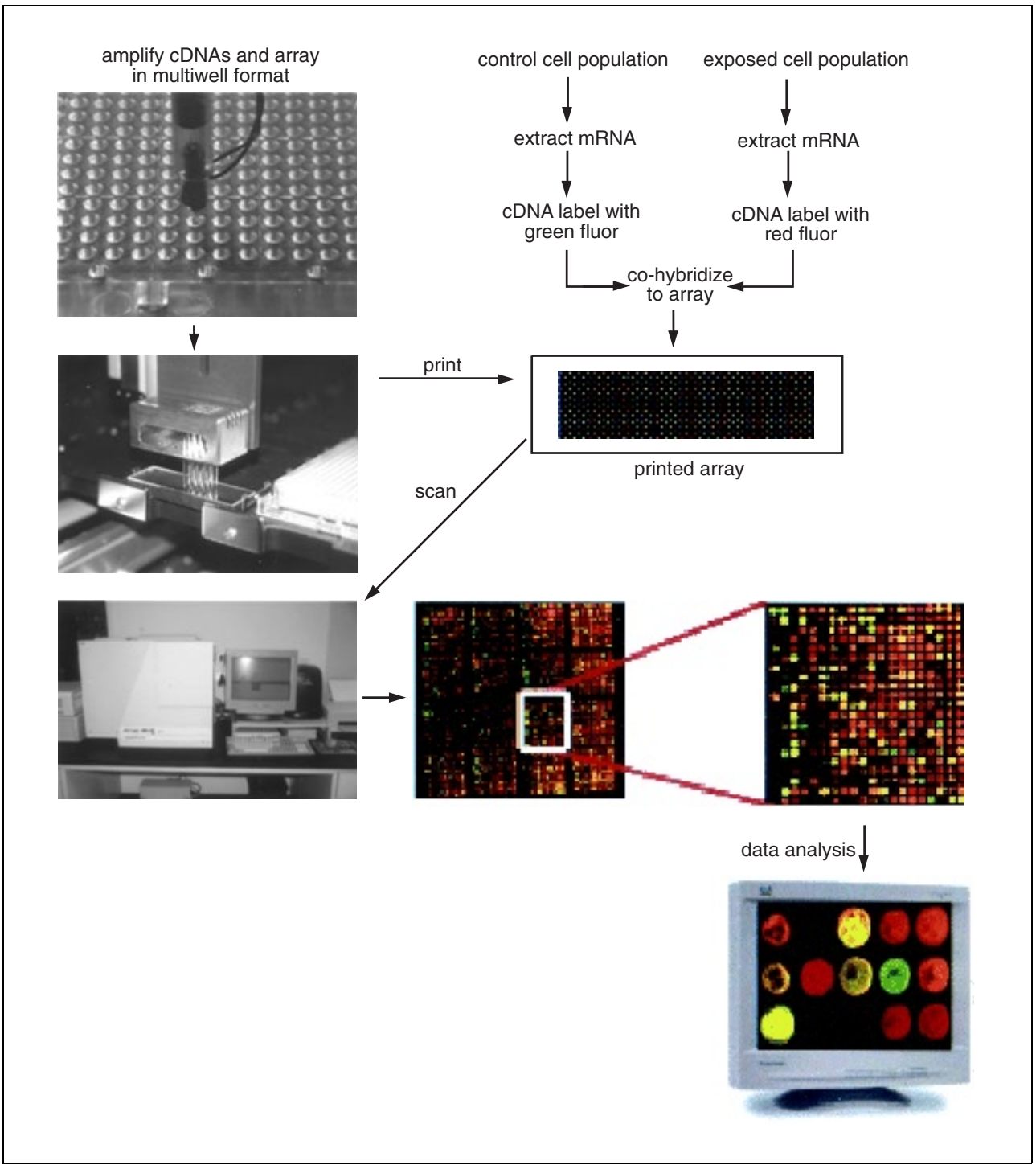

Figure 1.4.1 Expression analysis using cDNA microarrays. To produce cDNA microarrays, individual cDNA clones are amplified by PCR and arrayed in a multiwell format with or without purification. The upper left panel shows samples being arrayed with a piezoceramic fluid dispensing system (Engineering Arts). The multiwell plates with cDNA clones are then placed on a robotic printer such as the Gene Machines system shown in the second panel. The software that drives the robot is used to assign each clone to a specific address on the surface of a polylysine-coated or chemically derivatized microscope slide. Spotting of individual clones is accomplished using a series of pins or quills that are dipped into each well to take up a sufficient volume of the cDNA solution to spot or print each clone onto all of the slides. Printing is accomplished by rapid displacement of the robot head and the microscope stage using precision micromanipulation technologies. After each round of printing, the pins are washed and the process repeated until all clones have been printed on each slide to produce a microarray. *This black and white facsimile of the figure is intended only as a placeholder; for full-color version of figure go to http://www.currentprotocols.com/colorfigures*

change is indicative of the fold difference in the expression levels. Fluorescence intensity data are collected in the form of a spread sheet, which is merged with a database that contains the identity of the gene at each position on the array. The complete set of specific alterations defines the expression signature for the given experimental condition relative to the reference condition (e.g., a toxicant signature for a given exposure condition). Expression signatures can be compared using a variety of statistical and visual tools. Data from multiple experiments can also be compared using appropriate "data mining" software.

Most available methods utilize finely machined pins or quills to mechanically spot the probes onto polylysine-coated or chemically derivatized microscope slides. The pins, which function much like a fountain pen, are dipped into individual wells of multi-well plates, and a sufficient volume of probe is retained to spot multiple slides at the same relative position. The pins are then washed and dried, and the next cDNA probe is printed onto all of the slides. Most high-speed robots using a multiple-pin format can print 100 or so slides with thousands of probes each in a single day. The density of spots is defined by the size and quality of the pins, by the arrangements of the pins within the robotic head, and by the software used to drive the robotics. Currently, it is possible to print >18,000 cDNA clones onto a single microscope slide.

ANALYSIS OF GENE EXPRESSION PATTERNS USING NUCLEIC ACID ARRAYS

The fundamental determinant of cell growth, differentiation, and phenotype is the pattern of gene expression. The amounts of each gene expressed in a cell at any given time are a function of the genetic and epigenetic constitution of the cell, and how the cells integrate responses to environmental stimuli. The pattern of gene expression, thus, provides a signature of the cell's physiological state. By hybridizing arrays (the probe) with labeled cDNA or in vitro transcribed cRNA from cells (the target) one can simultaneously compare the levels of thousands of mRNAs between cells under different exposure conditions. The ability to detect and understand the meaning of these altered patterns of gene expression may lead to a better understanding of the biochemical mechanisms and hence, predictions of cellular responses associated with exposure to toxicants.

Analysis of gene expression patterns can be performed using either printed cDNA arrays (Fig. 1.4.1) or oligonucleotide arrays (Fig. 1.4.2). Typically, hybridizations to a single cDNA microarray require 5 µg of labeled cDNA. Production of such quantities of labeled cDNA using methods that do not involve amplification typically requires 50 to 200 µg of total RNA or 2 to 5 µg of poly(A)$^+$ RNA. To prepare cDNA or cRNA targets for hydridization and fluorescently labeled nucleotides that can be directly incorporated into the cDNA by reverse transcriptase. Typically, Cy3-dUTP and Cy5-dUTP are used to label target RNA from each of the two cell types being compared for expression profiles (De Risi et al., 1997). A more efficient labeling protocol involves the incorporation of amino-allyl derivatives of dNTPs, followed by chemical coupling of amino-allyl groups by reaction with NHS-esters of Cy3 or Cy5 (*http://cmgm.stanford.edu/pbrown/protocols/aadUTPCoupling Procedure.htm*). In either labeling protocol, the amount of label associated with each target mRNA is a function of the amount of each in the cell from which the mRNA was extracted. The differentially labeled targets are then co-hybridized to the array under conditions that allow each target mRNA to hybridize with its corresponding probe. Hence, the ratio Cy3 to Cy5 of fluorescence associated with each probe is a measure of the fold change in the level of expression of each gene represented on the probe array (Fig. 1.4.1).

However, for most experiments involving clinical specimens, the amounts of tissue available for mRNA extraction will be limiting. Thus, a number of techniques have been developed to amplify the starting poly(A)$^+$ RNA or the cDNA (Lockhart et al., 1996; Phillips and Eberwine, 1996; Trenkle et al., 1998). Many of these increase detection by orders of magnitude and are now widely used in experiments involving human samples (Lockhart and Winzler, 2000; Wang et al., 2000). In the author's experience, most of these allow one to generate enough labeled target from 5 µg of total mRNA. Wang et al. (2000) recently reported a method of amplification that combined antisense RNA amplification with the strand-switching effect (Clontech). The latter protocol may be applicable when using significantly smaller quantities of target mRNA.

In contrast to oligonucleotide arrays that are hybridized to a single target, cDNA microarrays require the co-hybridization of each target cDNA or cRNA to a reference sample. The latter

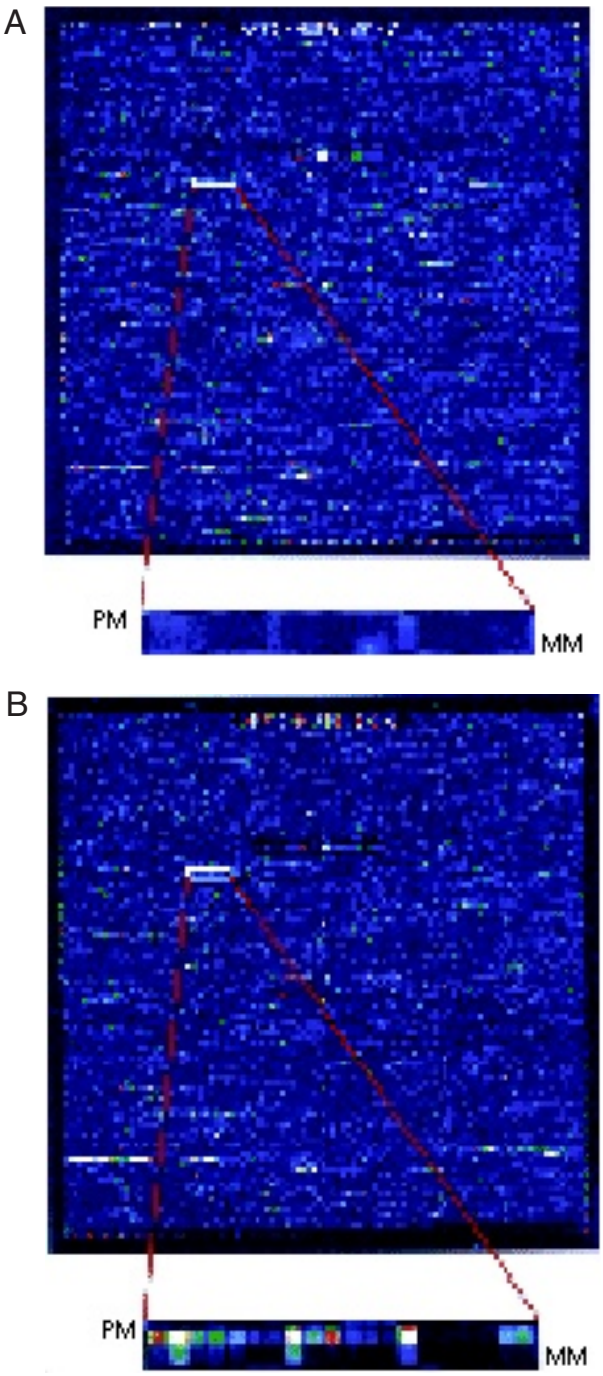

Figure 1.4.2 Expression analysis using oligonucleotide arrays. The figure shows expression patterns for (**A**) normal human squamous epithelial cells and (**B**) chronically exposed cells (M.T. Barrett, K.Y. Yueng, P.L. Blount, R.C. Sullivan, H. Zarbl, J. Delrow, and B.J. Reid, unpub. observ.) using oligonucleotide GeneChip Expression arrays produced by light-directed chemical synthesis (Affymetrix). Each array comprises tens of thousands of probes that interrogate the expression levels of ~1700 genes. Messenger RNA extracted from each cell type is reverse transcribed into cDNA and is subjected to linear amplification by in vitro transcription in the presence of biotinylated oligonucleotides. The amplified cRNA targets from each cell are hybridized to a separate microarray. The amount of each target sequence hybridized to a probe is quantified by binding of strepavidin phycoerythrin, excitation with laser light, and collection of fluorescence intensity data using a Hewlett-Packard scanner. *This black and white facsimile of the figure is intended only as a placeholder; for full-color version of figure go to http://www.currentprotocols.com/colorfigures*

can consist of target generated from a cell line or tissue to which all experimental samples are then compared. For example, one could compare bronchioepithelium from smokers to normal lung epithelium or a bronchioepithelial cell line. There are several disadvantages to using such reference samples. A tissue sample is not a renewable resource and the variability in gene expression profiles among tissue samples from different donors is subject to variability due to differences in genotype and environmental exposures. These limitations can be partially mitigated by preparing large cultures of a cell line under reproducible growth conditions. However, any given cell line will only express a limited number of genes. For example, genes induced during malignant progression of initiated cells may not be expressed at detectable levels in the normal cells. Thus, in half of the replicate experiments the denominator in Cy3:Cy5 fluorescence ratio will be zero (background), and vice versa, thereby complicating statistical analyses of the data. A more type-useful reference mRNA, initially proposed by Perou et al. (2000) and now available commercially (Stratagene), is comprised of mRNAs pooled from ≥10 cell lines representing different tissue types. Such a reference set is a renewable resource that expresses the majority of the genes detectable on the probe array at levels that are statistically significantly above background. In addition to the benefits alluded to above, use of a common reference allows the standardization of the data and permits all samples to be compared to one another relative to the reference set.

A significant limitation of chips produced by mechanical spotting is the variability in the volume of probe solution and hence the amount of probe deposited in each spot. The volume deposited is affected by surface characteristics, speed of the robot, time and pressure of the pin on the slide surface, viscosity, and other factors. Even when comparable volumes are deposited, evaporation from the pins or the sample wells during the printing process can change the concentration of the probes on the pin or in the wells. Although evaporation of the probe solution can be minimized by increased humidity in the printing area, the amount of probe deposited can still vary several-fold among spots. Thus, a variety of alternative technologies such as inkjet printers and piezoelectric dispensers, are being evaluated in a number of laboratories including the author's own.

Variability on printed arrays can, to a large extent, be overcome by simultaneously hybridizing a given array with the target cDNA from the two cell types or states being compared, each of which is labeled with a different fluorescent molecule. The relative amount of a specific mRNA expressed in the two cells can then be determined by measuring the amount of fluorescence from each fluor. For molecules with similar emission spectra but different absorption spectra, one can use different wavelengths of incident light. For molecules with different emission spectra but similar absorption spectra, one can use a single source of incident light and monochromatic filters to measure fluorescence at individual wavelengths. A variety of array scanners with different capabilities are commercially available and usually include software for spot detection and identification, data capture, and quantitative analysis. Once fluorescence intensity data are collected, they can be expressed as a ratio, such that the relative signals from each spot are internally controlled for variance in probe density on the array. By expressing the data as ratios, it is possible to compare relative changes in expression among arrays despite a high level of inter-array variability. To further reduce variance within the data, the same probe can be replicated on a single array or the same hybridization repeated, usually with reversal of the dyes used to label the target cDNA. Nonetheless, variance remains the significant consideration when comparing the expression of low-abundance genes, which generate weak fluorescence signals, such that even the ratios of intensities are subject to large fluctuations.

Another limitation of cDNA arrays is that it may not be possible to discern signals that are generated by the cross hybridization of a labeled target sequence derived from one member of a gene family with the probe for another family member. The latter limitation could in theory be addressed using shorter oligonucleotide probes for each transcript and by selecting probes from regions of the cDNA where gene family members show little sequence identity. Despite these limitations, the relatively lower cost and the flexibility to alter the probes on the chips makes cDNA arrays the preferred method in most research settings.

The use of arrays produced by chemical synthesis of oligonucleotide probes directly on a solid support to monitor gene expression patterns at the transcriptional level (Lockhart et al., 1996) has several advantages over printed arrays. First and foremost is that the amount of each probe synthesized on the chip surface using photolithographic techniques is highly repro-

ducible (Fodor et al., 1991, 1993). This reproducibility allows for direct comparison of expression data obtained among chips. In practice, this means the target nucleic acid from each cell studied is hybridized to a separate chip, an important consideration when multiple comparisons are to be made using samples with limited cell numbers.

Another advantage is that the higher probe density makes it possible to include multiple probes representing different regions of each transcript. The GeneChip Expression analysis system produced by Affymetrix is comprised of a set of four chips that collectively can compare the levels of up to ~40,000 separate human transcripts. The design of the arrays is such that the level of each transcript is interrogated by at least ten separate perfectly matched probes (PM). In addition, a probe with a mismatched base (MM) relative to each PM probe is included on the chip. By comparing the amount of hybridization between the PM and the MM probes, it is possible to differentiate signal from noise and to distinguish among signals from hybridization with transcripts from gene family members (Fig. 1.4.2). Real signals will show preferentail hybridization to the PM probes with little hybridization to the MM probes, while noise will be comparable among both probe sets. GeneChip Software applies statistical parameters to compare the fold change in expression of all genes for a given test sample relative to the baseline sample (e.g., untreated controls). On the two panels the PM and MM hybridization signals for the probes representing a single gene are highlighted and magnified as an example of the data that are obtained using this type of microarray (computer generated images). These arrays can reproducibly detect changes in mRNA levels that are as low as two- to three-fold. Moreover, the fluorescent signal generated by hybridization with the fluorescent target yields linear data over four orders of magnitude. These parameters endow the high-density microarrays with an unprecedented level of sensitivity and specificity. Studies indicate that the arrays can detect transcripts that are present at a frequency of 1:300,000 in the mRNA of the target cells.

To monitor gene expression using the GeneChip Expression arrays, mRNA extracted from cells is reverse transcribed using a primer comprised of a T7 polymerase start site at its 5′-end and an oligo dT sequence at its 3′-end. Following second-strand synthesis, the purified double-stranded cDNA is used as a template for in vitro transcription using T7 polymerase. Biotinylated ribonucleotides are incorporated into the cRNA during the in vitro transcription reaction. After purification and fragmentation to an optimal size, the labeled target cRNA is hybridized to the appropriate DNA chips. In order to yield high-quality data, the hybridization requires ~10 μg of labeled, in vitro transcribed cRNA. Typically, this amount of labeled target cRNA can be generated when starting with as little as 0.1 μg of poly(A)$^+$ mRNA, or $\geq 5 \times 10^5$ cells. Following hybridization, the target molecules are stained with strepavidin-phycoerythrin or fluorescently labeled antibodies using proprietary protocols. Fluorescence associated with each tile is then analyzed using a Hewlett-Packard Gene Array Scanner. Since the amount of each target cRNA molecule synthesized depends on the original number of mRNA molecules present in the poly(A)$^+$ mRNA preparation, the signal emitted by each tile should reflect the relative amounts of each target mRNA. Fluorescence intensity data are collected automatically by the GeneChip software and an image of the probe array is displayed in real time (Fig. 1.4.2). Following the image acquisition, the software algorithms compute the average fluorescence intensity for each PM and MM probe. Statistical analyses are then used to estimate fold changes in the expression of each gene in a test sample relative to the levels in a baseline array, such as untreated control cells in a toxicology experiment.

APPLICATION OF DNA CHIP TECHNOLOGY TO DETECT DNA SEQUENCE POLYMORPHISMS (SNPs)

Another important advantage of oligonucleotide arrays is the possibility of performing DNA sequencing by allele-specific hybridization. While the primary result of a toxic exposure is an altered pattern of gene expression, the ultimate biological effect of the toxicant is also dependent on the genotype of the exposed cell. Thus, genetic polymorphisms within key toxic response genes may abrogate the potential benefit of altered gene expression in the exposed cell.

A method for sequencing based on hybridization with an arrayed set of all possible oligonucleotides of a fixed size was proposed first in 1991 (Khrapko et al., 1991). The capacity for highly parallel, in situ synthesis of high-density oligonucleotide arrays has made this approach practical. Using the combinatorial approach and series of appropriate chromium masks, it is possible to synthesize all possible octomers (4^8 = 65,536) using as few as 32 rounds of synthesis

on a single chip with 50-μm^2 tiles, a level of resolution which has already been reduced to practice. Similarly, the set of all of the ~10^{12} possible 20-mers, or a subset thereof could be synthesized in just 80 nucleotide coupling reactions. Although such an approach is feasible, it is not practical for sequencing since analysis of the data would be complex and multiple rounds of hybridization would be required to obtain complete sequence information.

Oligonucleotide arrays can, however, be used for high throughput resequencing of genes in multiple individuals. The simplest format of the high-density DNA arrays for use in DNA resequencing is the so-called 4*L* tiled array (Chee et al., 1996). In this format, the complete set of overlapping oligonucleotides of a given length (usually 25-mers) that comprise the complete sequence of interest are synthesized on a chip. Also included are the sets of overlapping probes representing all possible single base pair substitutions at each position in the sequence interrogated by the array. Thus, all possible sequences can be interrogated by 4*L* oligonucleotides, where *L* is the number of bases in the target sequence. When the labeled target DNA is hybridized to the array, labeled DNA fragments will hybridize most efficiently with the oligonucleotides to which the sequence is perfectly complementary. By the same token, the target will show reduced hybridization with probes that contain a single base mismatch. By comparing the strength of the hybridization among the set of four probes that define each position, it is possible to directly read the sequence of the target DNA from the fluorescence image. Since each probe will have its own T_m, the maximal fluorescence intensity observed when the target hybridizes with its complementary probe can vary over four orders of magnitude. However, since comparisons are only made among the four probes that interrogate the given oligomer, these differences have no effect on the analysis of the data. The 4*L* array is the basis of the sequencing GeneChips, including those designed to sequence portions of the BRCA1 tumor suppressor gene, the p53 tumor suppressor gene, and the HIV viral genome (Hacia, 1999).

Using a variation on the sequencing chip design, it is possible to simultaneously detect the presence of multiple alleles that differ by a single nucleotide (SNPs; Chee et al., 1996; Wang et al., 1998). For all polymorphic sites, a series of 5 columns of probes is used to interrogate the sequence of the polymorphic base and 2 bases on either side (Fig. 1.4.3). The columns are comprised of a set of four different oligonucleotide probes (4*L*) that collectively detect all 4 possible nucleotides at each position within the 5 bp. In such an analysis, the presence of an allelic variant in the target DNA will result in a characteristic pattern of hybridization. The mutant target will show reduced hybridization with the wild-type probe and strong hybridization with the probe that carries the corresponding base substitution. The variant target DNA will also form one or more mismatches when it hybridizes to the probes that interrogate flanking sequences (Chee et al., 1996). This characteristic footprint of reduced hybridization with sequences flanking the variant specific probe provides further evidence for the presence of a variant sequence in the target DNA. Furthermore, when more than one allele is present in the target DNA, two or more tiles within a given set of four probes will show intense hybridization relative to that seen with a reference wild-type probe. This approach can be used not only to detect allelic variants of a given sequence among individuals, but it can be used also to design arrays for use in genetic linkage studies and to detect allelic losses that occur during tumor progression.

For SNP detection, genomic DNA is extracted and a region of several hundred base pairs flanking each polymorphic site is amplified by multiplexed PCR. After verifying that each region of interest was amplified, the PCR products are fragmented to a size optimal for hybridization and 3′-end labeled using fluoresceinated deoxyribonucleosides and a terminal transferase enzyme. Following hybridization and scanning, the data are analyzed by appropriate software and genotypes are assigned to each sample. The ability to detect SNPs is presently the sole dominion of oligonucleotide arrays, although the author's laboratory is developing a method that will allow simultaneous genotyping and expression analysis on printed cDNA arrays.

Potential Uses for Microarrays in Toxicology

Toxicant signatures

A central tenet of toxicology is that, with the possible exception of acute cell necrosis, every toxic exposure leads to an alteration in the pattern of gene expression. This altered pattern of gene expression reflects the cell's attempt to cope with the toxic insult and can range from induction of xenobiotic metabolism to the extreme of cell suicide or apoptosis. While numer-

ous studies have looked at changes in the expression of a limited number of genes thought to play a role in these adaptive responses, the power of array technology is the ability to obtain a comprehensive survey of thousands of genes simultaneously. This global analysis of gene expression affords researchers the ability to discern specific patterns or signatures of expression that are associated with particular classes of toxicants. These signatures are likely to include classes of genes not previously implicated in response to specific toxic insults (Jelinsky and Samson, 1999). As such the applications of array technologies to toxicology will undoubtedly enhance understanding of the cellular response to toxicants, which should by

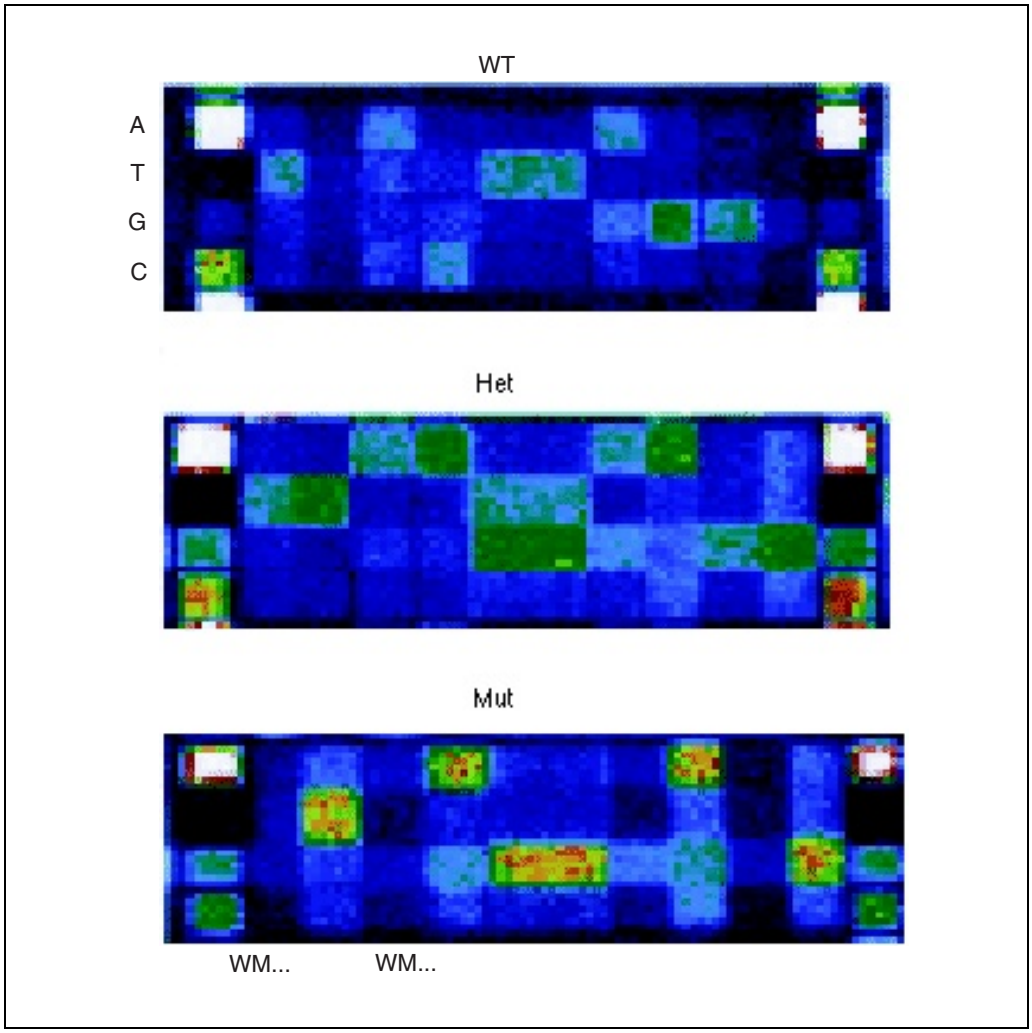

Figure 1.4.3 Detection of single nucleotide polymorphisms (SNPs) using oligonucleotide arrays. This is an example of the data obtained for individuals that are wild-type homozygous (WT), heterozygous (Het), or mutant homozygous (Mut) for a specific allele of the P450 cyp 2D16 gene. Experiments were performed using the GeneChip P450 oligonucleotide arrays produced by light-directed chemical synthesis (Affymetrix). For each polymorphic site, there is a series of five columns of probes that interrogate the polymorphic base and 2 bases on either side. Columns from left to right interrogate sequences at position –2 to +2 relative to the site interrogated and alternate from left to right between wild-type (W) and mutant (M) probes. The columns are each comprised of four probes (4*L*) that collectively detect all 4 possible nucleotides at each position within the 5-bp sequence. The presence of wild-type and mutant alleles is determined by the pattern of hybridization with probes that detect wild-type and/or mutant targets. For SNP detection, genomic DNA is extracted and a region of several hundred base pairs flanking each polymorphic site is amplified by multiplexed PCR. After verification that each region of interest was amplified, the PCR products are fragmented to a size optimal for hybridization and 3′-end labeled using fluoresceinated deoxyribonucleosides and terminal transferase enzyme. Following hybridization and scanning, the data are analyzed by appropriate software and genotypes are assigned to each sample. *This black and white facsimile of the figure is intended only as a placeholder; for full-color version of figure go to http://www.currentprotocols.com/colorfigures*

inference also provide insight into the mechanism of toxicity. For example, agents that induce genes involved in DNA repair almost certainly must be directly or indirectly genotoxic to the cell.

There is significant evidence to suggest that specific toxic exposures will produce discernible expression signatures. Studies in yeast and mammalian cells have demonstrated that a reproducible subset of genes will show altered expression in response to specific conditions such as anoxia, nutrient deprivation, exposure to alkylating agents, and chemotherapeutic agents (DeRisi et al., 1997; Iyer et al., 1999; Jelinsky and Samson, 1999). It is therefore reasonable to hypothesize that toxicant signatures will exist for individual classes of toxicants such as polycyclic aromatic hydrocarbons (PAH), alkylating agents, ionizing radiation, and neurotoxicants. Moreover the individual signatures will almost certainly reflect underlying mechanisms of toxicity such as oxidative stress, DNA damage, inhibition of oxidative phosphorylation, and disruption of cell membrane potentials (Marton et al., 1998; Norman et al., 1999). Since many toxicants will have multiple mechanisms of action, the signature will also reflect this complexity of mechanisms. As an example, the signature of PAHs will almost certainly include genes involved in their xenobiotic metabolism and genes that are involved in the response to oxidative stress. Also, the ability of gene expression signatures to provide insight into the underlying mechanisms would make it possible to predict the mechanism of toxicity of unknown compounds. For example, if the expression signature of an unknown compound includes a set of genes that are common to other inducers of peroxisome proliferation, then the unknown can be tentatively assigned to this class of toxicants.

Another exciting application of array technology is the possibility of defining thresholds of exposure below which there is no biological effect. In toxicology, a wide variety of biological tests are used to assess the toxicity of given compounds or exposures. In vivo animal models such as the rodent bioassays and carcinogenicity tests remain the standard in the field. These animal model systems are increasingly replaced or supplemented with an ever-increasing number of in vitro assays, such as the Ames test (*UNIT 3.1*), human cell mutation assays (*UNIT 3.3*), cell transformation assays (*UNIT 3.4*), assays for sister chromosome exchange, unscheduled DNA synthesis (*UNIT 3.7*), and micronuclei (*UNIT 3.5*). While each of these tests has its strengths and limitations, they all measure complex biological endpoints that are many steps removed from the initial exposure. Arguably, altered gene expression is the earliest measurable biological endpoint in response to a given exposure. Moreover, the signatures for doses of toxicant that do not have any biological effect are likely to be distinct from the signatures of doses that induce cellular stress and adaptation. Signatures at even higher doses will reflect more acute cellular responses such as apoptosis. Application of array technology to toxicology testing could, thus, make it possible to define biologically meaningful toxicity thresholds. The classical NOEL (no observable effect levels) is established by tests whose endpoints (e.g., mutation, transformation, unscheduled DNA synthesis) rely on the integration of complex responses at the level of the cell and in some cases at the level of the organism (teratology). By contrast, toxicant signatures measure the earliest cellular responses and provide information on the nature of the cellular response. In addition, toxicant signatures should reveal if the effects of multiple nontoxic doses are cumulative at the level of gene expression, the earliest cellular response. The ability to obtain and compare toxicant signatures of many different compounds, at different doses, and as complex mixtures is expected to herald a new chapter in toxicology research.

Factors affecting toxicant signatures

Although the application of microarray technology will have an enormous impact on the understanding of mechanisms underlying toxicity, it is important to realize that the toxicant signatures obtained will be highly sensitive to the assays' conditions and methodologies. The data obtained will be affected by numerous factors ranging from the composition of the array to the source of the target nucleic acid.

Microarrays used to define toxicant signatures can include probes from all available genes or can be designed using the subset of genes already shown or suspected to be involved in the toxic response (some housekeeping genes are included as controls). The latter type of array is exemplified by the Tox-Chips being designed by researchers at the N.I.E.H.S. (Nuwaysir et al., 1999). These arrays will detected 325 transcripts that were elevated and 76 that were decreased after exposure. Eighteen of the novel inducible additional genes were elevated to higher levels than the previously studied genes. Significantly, the data also allowed these researchers to conclude that alkylating agents activated a

previously unsuspected program of gene expression to eliminate and replace adducted proteins. Neither the novel genes nor the protein replacement pathways would have been detected if the chip contained a subset of all yeast genes, and this underscores the need to develop comprehensive signatures for toxicants. Of course comprehensive screens are not yet possible for human cells. At present, the GeneChip Expression array from Affymetrix can simultaneously examine ~40,000 transcripts *(http://www.affymetrix.com)*, and printed arrays are quickly approaching that number. It is likely that the entire gene set for humans will be arrayed within the next several years. While the cost of comprehensive screens remains a major hindrance, it would seem prudent to make screens as comprehensive as possible to derive toxicant signatures. Lower cost arrays with subsets of genes could then be designed and used for routine screening of compounds for functionally relevant signatures.

Other important considerations when using microarrays to study responses to toxicants are the experimental parameters. The expression pattern detected by a single array represents a snapshot of the cellular response in time and physiological state. As already discussed above, the response of a cell to a given exposure will be a function of the toxicant dose. However, the response at the mRNA level will also vary as a function of time after exposure. Experience in yeast experiments clearly demonstrates that the induction or repression of genes follow predictable temporal patterns, which may fall into clusters for sets of genes that define affected biochemical pathways (DeRisi et al., 1997). Moreover, the kinetics of the response could depend on dose. It is, therefore, important to examine toxicant signatures under a variety of experimental settings. Even when all experiments are carefully controlled, there will always be minor variations in conditions due to operator handling, small differences in cell density, temperature, and anoxia, each of which will contribute to the observed expression pattern in a given experiment. The impact of the interexperiment variation can be minimized either by performing replicate assays, or by pooling mRNA samples from multiple experiments prior to analysis on arrays. In the former, outliers could be eliminated statistically; while in the latter, the spuriously elevated or decreased mRNAs would be averaged with levels in other experiments. Finally the choice of cell type will affect the observed signatures. It is likely that the response at the level of gene expression will vary among cell types, since many toxicants are known to be highly tissue specific.

Application to animal models used in toxicology testing

Despite an increased emphasis on developing alternatives, animal testing persists as the mainstay of toxicology testing. Even though new in vitro methods and models systems continue to be developed and evaluated, there are, as of yet, few viable alternatives for complex biological response testing such as neurotoxicity, immunotoxicity, reproductive and developmental toxicity, carcinogenesis, and teratology. However, animal testing remains both controversial and problematic. In addition to the requirement for a large number of animals and the associated costs, these assays often require years to complete. More significantly, the results obtained cannot always be easily extrapolated to humans due to interspecies variations and the fact that the doses used are often not relevant to human exposures. The addition of microarray technologies to the arsenal of toxicology tests could significantly impact the need for animal testing. Toxicant signatures could be used to assign compounds with unknown biological activities to specific functional groups before animal testing, thereby eliminating the need for expensive global testing and simplifying cross-species extrapolations. For example, a compound that has the expression signature of a neurotoxicant without elements of genotoxicity may not require assessment via the expensive and dubious rodent cancer bioassay.

The sensitivity of gene expression patterns to low levels of toxic exposures could also make it possible to assess toxicity at dose rates more relevant to human experience. Moreover, the assay endpoint, gene expression patterns, will be altered within hours of exposure. Results can therefore be obtained and analyzed in days instead of years, while using fewer animals. In addition, expression signatures based on an underlying mechanism may simplify the results obtained with complex mixtures or environmental samples.

Although the potential advantages of combining microarray technology with animal testing are readily appreciated, there are also potential pitfalls and sources of error. If toxicant signatures are to be used to exempt unknown compounds from animal bioassays, then care must be taken to establish that the model system will permit extrapolation to human exposures. Gene expression signatures, which should be also obtained for a variety of species, organs,

and cell type can present numerous challenges. While expression signatures can be readily obtained in vitro using cell lines, the same may not be true for organs or tissues comprised of multiple cell types. A toxicant signature derived for a whole organ may belie the effect on a specific cell type or cells at specific states of differentiation within the organ (i.e., stem cells). For example, looking at the toxicant signature of a compound on the whole brain may fail to detect the effect a specific center in the brain comprised of few cells, since the resulting toxicant gene expression signature would be diluted by the vast excess of unaffected cells. Likewise, toxic effects on limited numbers of stem cells in an organ might not be detected in signatures of whole organs, even though they could have dire consequences. It may be essential to examine signatures for specific cell types in tissues and organ. Such an approach will require significant effort to develop protocols for cell enrichment, such as cell sorting and immunoaffinity separations. Even if enrichment can be achieved, it must be demonstrated that the processes of organ/tissue disruption and cell purification do not, in and of themselves, alter the pattern of gene expression in ways that will mask the intended observation.

Finally, if the cells are present in limited numbers, the amount of mRNA available may be insufficient to perform an assay on the microarrays. In this case, the cells from numerous animals may need to be pooled for each assay. Alternatively, the mRNA from individual animals would have to be amplified prior to labeling of the target. In this case care must be taken to ensure that the method of amplification does not distort the pattern of expression by preferential amplification of some targets. Exponential amplification, such as occurs during PCR, is thus inappropriate. Alternatives, such as the production of cDNA libraries from single cells, are being evaluated for this purpose.

In summary, the use of array technology in toxicology testing has enormous potential for reducing costs and efforts associated with animal testing. Since the assay endpoint is based on underlying mechanisms, the toxicant signatures obtained may simplify cross-species extrapolations, allow for assessment of doses more relevant to human exposures, and more readily permit evaluation of complex mixtures. Nonetheless, the potential for missing effects on specific cell types or differentiation states within tissues and organs warrants caution and careful design of test parameters.

Applications to exposure monitoring

The exquisite sensitivity of expression signatures could also find numerous applications in monitoring environmental exposures. Since gene expression is affected seconds to hours after exposures, toxicant signatures are most appropriate as biomarkers of recent or chronic exposures. Microarrays are thus expected to provide highly sensitive and specific toxicity data in occupational settings or in patients given specific therapeutic compounds or treatments, where a cell sample can be obtained from the same individual before and after exposure. Since gene expression patterns provide mechanistic underpinning of the response, the data obtained should provide an effective dosimeter of biological consequences to an exposed individual in the face of genetic variations in sensitivity. However, care must be taken that the cells available for these assays (e.g., blood, buccal scrapes) are appropriate surrogates for cells that are the targets of toxicity. Moreover, expression profiles will be affected by a wide range of exposures, including diet, lifestyle, other medication, nonoccupational sources, etc.; it will therefore be important to minimize the effects of these confounding factors. As discussed above, the effects of spurious alterations in gene expression can be minimized by sample pooling, but pooling may not be appropriate for defining individual exposure. The alternative is to compare multiple samples from many exposed individuals to define the toxicant-specific signature. This "mining" of data will require the establishment of large databases and the appropriate bioinformatics tools to extract commonality of patterns across individual arrays (Bassett et al., 1999).

Gene expression may also prove to be an effective tool in environment exposures. As an early response biomarker, toxicant signatures could be used to monitor biological effect of environmental accidents on invertebrate and vertebrate indicator species. By comparing patterns in the same species from areas with known or suspected exposures to those without exposure, it may also be possible to monitor the effects of long-term exposures to low doses of compounds. Expression signatures may also prove effective in detecting the effects of compounds such as endocrine disruptors, whose biological effects are difficult to monitor using traditional biomarkers.

Applications to toxicogenetics

A major issue in toxicology testing is the difficulty in understanding and predicting indi-

vidual variation in toxicant sensitivity. Toxicogenetics seeks to establish the genetic basis for these variations. A great deal of research has already identified numerous genetic polymorphisms in genes comprising biochemical pathways important for resistance to toxicants (e.g., xenobiotic metabolism and DNA repair). In some cases, a specific polymorphism has been linked to a specific phenotype of chemical susceptibility. However, sensitivity to more complex effects of toxic exposure, such as cancer and birth defects, may depend on the integrated effects of numerous polymorphisms. As a result, most attempts to find an association between genetic polymorphisms in xenobiotic metabolizing genes and cancer risk have found only minimal and often conflicting effects, and even meta-analyses of the data can yield inconclusive results (Taioli, 1999). Clearly, the ability to perform highly parallel genotyping at multiple alleles will be required to define the effects of genes showing high population prevalence but low phenotypic penetrance. DNA sequencing by allele-specific hybridization on oligonucleotide arrays has the capacity to make highly parallel analysis of single nucleotide polymorphisms (SNPs) a reality (Wang et al., 1998). From a small number of cells from an individual, it is possible to obtain genotypes at thousands of alleles.

Widespread application of this technology is still limited by the number of SNP sequenced and by the high cost of designing and producing oligonucleotide arrays. The concerted effort for SNP detection by both academic and commercial enterprises should deal with the former, while the development of alternative technologies such as the inkjet oligonucleotide synthesizers should address the latter limitation. Another limitation affecting high-throughput genotyping on arrays is the need to amplify and label each individual allele or target prior to analysis on an array. Multiplexing of PCR reactions can minimize the number of amplification reactions, but it still requires considerable effort in development and intensive quality control during implementation. Low cost, high-throughput genotyping on arrays will not really be feasible until technologies are developed to eliminate the need for target amplification prior to hybridization to the probes on the array. A final limitation of SNP detection is the fact that SNP detection is based on allele-specific hybridization. The problem arises from the fact that all of the hybridizations on a probe array are occurring at the same condition of salt, temperature, etc. Therefore, it is important to select probe sequences such that all allele-specific hybridizations will have the appropriate specificity for allelic discrimination under the given experimental condition. As the number of probes on the array increases, the possibility of finding conditions at which all probes show sufficient allele discrimination becomes more difficult. For these reasons, the author's laboratory is developing methods of SNP analysis on cDNA arrays that are independent of hybridization conditions. The latter approach also holds the promise of obtaining expression signatures and genotypes from the same array experiment.

While toxicant signatures should, in theory, include the effects of genetic variability and predict individual susceptibility, SNPs have the advantage that they can be detected without exposure and in a very small number of readily available cells. In addition, SNPs can be used for linkage analysis, disease association studies, and loss of heterozygosity studies to define other disease genes. The application of microarray technology promises to dramatically enhance understanding of variability in response to toxicants.

COMPUTATIONAL BIOLOGY

The previous section outlined available microarray technologies, their application to toxicogenomics and toxicogenetics, as well as their limitations. Implicit in the above discussion was the assumption that adequate computational and bioinformatics tools would be available for analysis of the unprecedented size and complexity of the data these studies would generate. The development of these tools remains a formidable challenge and may prove to be the rate-limiting step in the implementation of these exciting new methodologies to toxicology. A number of programs for statistical evaluation of data have already been developed in both academic (Ermolaeva et al., 1998; Bassett et al., 1999) and commercial settings. The computer software required falls into several categories. The first type deals with capture and statistical analysis of the data and may include the ability to compare expression levels between two cell types or conditions. This type of analysis software is usually provided with array scanners or can be obtained from academic investigators. Continued development in this statistical analysis software remains an area of active research. The second area for software development is for analysis of data across experimental conditions. For example, an investigator may want to find sets of genes that show common temporal pro-

files of altered expression after an exposure. Similarly, genes could be clustered on the basis of function categories, dose response, and biochemical pathways. This type of analysis typically makes use of clustering algorithms. A discussion of these methods is beyond the scope of this unit, and the reader is referred to the Key References for additional information.

The third and vastly more complex area for software development is for analysis of data across all experiments. For example, an investigator may wish to find patterns of gene expression common to all individuals that are sensitive to a complex mixture of toxicants. Such a pattern might be used to predict the risk of individuals to that exposure. This type of analysis exemplifies the complexity and issues associated with the use of array technology in any setting, including toxicology. In addition to having adequate computing power and appropriate software for the required comparisons, one also needs to have publicly accessible databases containing the information gathered by many laboratories. The databases must also be annotated with experimental parameters to facilitate comparisons. The software used must allow for exchange of information among different laboratories and different computer platforms. Moreover, the software must be compatible with data generated by different microarray platforms. It might also be important to combine expression data with genotype data.

The successful application of array technology to toxicogenetics and toxicogenomics will require continued technology development, the establishment of public databases with accepted standards for data annotation, and the development of powerful new statistical and bioinformatics tools. Clearly, many promises and challenges lie ahead.

LITERATURE CITED

Bassett, D.E. Jr., Eisen, M.B., and Boguski, M.S. 1999. Gene expression informatics—it's all in your mine. *Nature Genet.* 21:51-55.

Chee, M., Yang, R., Hubbell, E., Berno, A., Huang, X.C., Stern, D., Winkler, J., Lockhart, D.J., Morris, M.S., and Fodor, S.P. 1996. Accessing genetic information with high-density DNA arrays. *Science* 274:610-614.

Conner, B.J., Reyes, A.A., Morin, C., Itakura, K., Teplitz, R.L., and Wallace, R.B. 1983. Detection of sickle cell beta S-globin allele by hybridization with synthetic oligonucleotides. *Proc. Natl. Acad. Sci. U.S.A.* 80:278-282.

DeRisi, J.L., Iyer, V.R., and Brown, P.O. 1997. Exploring the metabolic and genetic control of gene expression on a genomic scale. *Science* 278:680-686.

Drmanac, R. and Drmanac, S. 1999. cDNA screening by array hybridization. *Methods Enzymol.* 303:165-178.

Drmanac, R., Labat, I., Brukner, I., and Crkvenjakov, R. 1989. Sequencing of megabase plus DNA by hybridization: Theory of the method. *Genomics* 4:114-128.

Ermolaeva, O., Rastogi, M., Pruitt, K.D., Schuler, G.D., Bittner, M.L., Chen, Y., Simon, R., Meltzer, P., Trent, J.M., and Boguski, M.S. 1998. Data management and analysis for gene expression arrays. *Nature Genet.* 20:19-23.

Fodor, S.P., Read, J.L., Pirrung, M.C., Stryer, L., Lu, A.T., and Solas, D. 1991. Light-directed, spatially addressable parallel chemical synthesis. *Science* 251:767-773.

Fodor, S.P., Rava, R.P., Huang, X.C., Pease, A.C., Holmes, C.P., and Adams, C.L. 1993. Multiplexed biochemical assays with biological chips. *Nature* 364:555-556.

Hacia, J.G. 1999. Resequencing and mutational analysis using oligonucleotide microarrays. *Nature Genet.* 21:42-47.

Iyer, V.R., Eisen, M.B., Ross, D.T., Schuler, G., Moore, T., Lee, J.C.F., Trent, J.M., Staudt, L.M., Hudson, J., Jr., Boguski, M.S., Lashkari, D., Shalon, D., Botstein, D., and Brown, P.O. 1999. The transcriptional program in the response of human fibroblasts to serum [see comments]. *Science* 283:83-87.

Jelinsky, S.A. and Samson, L.D. 1999. Global response of *Saccharomyces cerevisiae* to an alkylating agent. *Proc. Natl. Acad. Sci. U.S.A.* 96:1486-1491.

Khrapko, K.R., Lysov Yu, P., Khorlin, A.A., Ivanov, I.B., Yershov, G.M., Vasilenko, S.K., Florentiev, V.L., and Mirzabekov, A.D. 1991. A method for DNA sequencing by hybridization with oligonucleotide matrix. *DNA Sequence* 1:375-388.

Liang, P. and Pardee, A.B. 1992. Differential display of eukaryotic messenger RNA by means of the polymerase chain reaction [see comments]. *Science* 257:967-971.

Lockhart, D.A and Winzler, E.A. 2000. Genomics, genes expression and DNA arrays. *Nature* 405:827-836.

Lockhart, D.J., Dong, H., Byrne, M.C., Follettie, M.T., Gallo, M.V., Chee, M.S., Mittmann, M., Wang, C., Kobayashi, M., Horton, H., and Brown, E.L. 1996. Expression monitoring by hybridization to high-density oligonucleotide arrays [see comments]. *Nature Biotechnol.* 14:1675-1680.

Marshall, A. and Hodgson, J. 1998. DNA chips: An array of possibilities. *Nature Biotechnol.* 16:27-31.

Marton, M.J., DeRisi, J.L., Bennett, H.A., Iyer, V.R., Meyer, M.R., Roberts, C.J., Stoughton, R., Burchard, J., Slade, D., Dai, H., Bassett, D.E., Jr., Hartwell, L.H., Brown, P.O., and Friend, S.H. 1998. Drug target validation and identification of secondary drug target effects using DNA microarrays [see comments]. *Nat. Med.* 4:1293-1301.

Maskos, U. and Southern, E.M. 1993. A study of oligonucleotide reassociation using large arrays of oligonucleotides synthesised on a glass support. *Nucl. Acids Res.* 21:4663-4669.

Matson, R.S., Rampal, J., Pentoney, S.L., Jr., Anderson, P.D., and Coassin, P. 1995. Biopolymer synthesis on polypropylene supports: Oligonucleotide arrays. *Anal. Biochem.* 224:110-116.

Norman, T.C., Smith, D.L., Sorger, P.K., Drees, B.L., O'Rourke, S.M., Hughes, T.R., Roberts, C.J., Friend, S.H., Fields, S., and Murray, A.W. 1999. Genetic selection of peptide inhibitors of biological pathways. *Science* 285:591-595.

Nuwaysir, E.F., Bittner, M., Trent, J., Barrett, J.C., and Afshari, C.A. 1999. Microarrays and toxicology: The advent of toxicogenomics. *Mol. Carcinog.* 24:153-159.

Perou, C.M., Sorlie, T., Eisen, M.B., Van de Rijn, M., Jeffrey, S.S., Rees, C.A., Pollack, J.R., Ross, D.T., Johnson, H., Akslen, L.A., Pluge, O., Pergamenschikov, A., Williams, C., Zhu, S.X., Lonning, P.E., Borrensen-Dale, A.L., Brown, P.O., and Botstein, D. 2000. Molecular portraits of human breast tumors. *Nature* 406:747-752.

Phillips, J. and Eberwine, J.H. 1996. Antisense RNA amplification: A linear amplification method for analyzing the mRNA population from single living cells. *Methods* 10:283-288.

Schena, M., Shalon, D., Davis, R.W., and Brown, P.O. 1995. Quantitative monitoring of gene expression patterns with a complementary DNA microarray [see comments]. *Science* 270:467-470.

Shalon, D., Smith, S.J., and Brown, P.O. 1996. A DNA microarray system for analyzing complex DNA samples using two-color fluorescent probe hybridization. *Genome Res.* 6:639-645.

Southern, E.M., Maskos, U., and Elder, J.K. 1992. Analyzing and comparing nucleic acid sequences by hybridization to arrays of oligonucleotides: Evaluation using experimental models. *Genomics* 13:1008-1017.

Taioli, E. 1999. International collaborative study on genetic susceptibility to environmental carcinogens. *Cancer Epidemiol. Biomarkers Prev.* 8:727-728.

Trenkle, T., Welsh, J., Jung, B., Mathieu-Daude, F., and McCellandm, M. 1998. Non-stoichiometric reduced complexity probes for cDNA arrays. *Nucl. Acids Res.* 26:3883-3891.

Underhill, P.A., Jin, L., Zemans, R., Oefner, P.J., and Cavalli-Sforza, L.L. 1996. A pre-Columbian Y chromosome-specific transition and its implications for human evolutionary history. *Proc. Natl. Acad. Sci. U.S.A.* 93:196-200.

Velculescu, V.E., Zhang, L., Vogelstein, B., and Kinzler, K.W. 1995. Serial analysis of gene expression [see comments]. *Science* 270:484-487.

Wang, D.G., Fan, J.B., Siao, C.J., Berno, A., Young, P., Sapolsky, R., Ghandour, G., Perkins, N., Winchester, E., Spencer, J., Kruglyak, L., Stein, L., Hsie, L., Topaloglou, T., Hubbell, E., Robinson, E., Mittmann, M., Morris, M.S., Shen, N., Kilburn, D., Rioux, J., Nusbaum, C., Rozen, S., Hudson, T.J., and Lander, E.S. 1998. Large-scale identification, mapping, and genotyping of single-nucleotide polymorphisms in the human genome. *Science* 280:1077-1082.

Wang, E., Miller, L.D., Ohnmacht, G.A., Liu, E.T., and Marincola, M. 2000. High-fidelity mRNA amplification for gene profiling. *Nature Biotechnol.* 18:457-459.

Zarbl, H., Aragaki, C., and Zhao, L.P. 1998. An efficient protocol for rare mutation genotyping in a large population. *Genet. Testing* 2:315-321.

Zhao, N., Hashida, H., Takahashi, N., Misumi, Y., and Sakaki, Y. 1995. High-density cDNA filter analysis: A novel approach for large-scale, quantitative analysis of gene expression. *Gene* 156:207-213.

KEY REFERENCES

Supplement to volume 21 of *Nature Genet.* (1999) The Chipping Forecast.

This supplement consists of fourteen comprehensive articles written by the leaders in the field of microarray technologies. The reviews provide detailed descriptions of all aspects of array technologies, including the chemistry and interactions occurring in the array surface, reviews of different technologies and applications, how to build and run an array facility, detailed protocols for hybridization, specific research applications, and overviews of data management and statistical analysis, including cluster analysis and data exploration.

INTERNET RESOURCES

http://www.ncbi.nlm.nih.gov/Genbank/index.html

A public database of all DNA sequence entries.

http://www.ncbi.nlm.nih.gov/Entrez/Genome/org.html

A public database of all completed genomic sequences.

http://www.affymetrix.com/technology

A commercial Web site provided by Affymetrix of Santa Clara, California. The site provides detailed descriptions of chip production using photolithography and includes video of the process. Complete description of products, publications, etc. are also provided at this site.

http://cmgm.stanford.edu/pbrown/mguide/index.htm

Web page provided by the laboratory of Patrick O. Brown at Stanford University. Provides detailed information on building a robotic arrayer and using cDNA arrays for expression analysis.

Contributed by Helmut Zarbl
N.I.E.H.S./University of Washington Center for Ecogenetics and Environmental Health and Fred Hutchinson Cancer Research Center
Seattle, Washington

The Use of Fish-Derived Cell Lines for Investigation of Environmental Contaminants

Fish-derived cell lines are being used for at least three basic purposes in the investigation of environmental contaminants. One is in ascertaining the mechanisms by which contaminants exert their toxicity; a second is in determining the relative toxicity of different chemical contaminants; and a third application is in evaluating the toxicity of environmental samples. These three goals are interrelated, as toxic mechanisms give insight into the basis of toxicity rankings and allow the risk of untested compounds and of environmental samples to be estimated. The endpoints that are used in these studies can be specific or general. A specific response evaluates a particular function, which might be expressed by only certain fish-derived cell lines and is caused by just some classes of chemical contaminants. General responses assess fundamental cellular activities, which would be expressed by all fish cell lines and caused by a wide range of contaminants.

In this unit, three assays for assessing a change in cell viability, a general response, are described. Each assay is done on cells in microwell cultures and uses a different fluorescent indicator dye, but the results are quantified in arbitrary fluorescent units (FU) with a common instrument—a fluorescent plate reader (O'Connor et al., 1991; Schirmer et al., 1997). Cell viability is compared in toxicant-treated cultures by expressing their FU as a percentage of the FU for control cultures. The use of these assays is illustrated with some members of an important class of environmental contaminants, the polycyclic aromatic hydrocarbons (PAHs), which can act as toxicants and as phototoxicants (Schirmer et al., 1998a,b).

This unit describes a protocol on how to culture fish cell lines, which provide a continuous supply of cells. These cells are used to initiate microwell cultures for exposure to environmental toxicants in the dark and in the presence of UV radiation, and cell viability is assessed using the fluorescent indicator dye alamar blue (see Basic Protocol). Cell viability is also assessed using other fluorescent indicator dyes, such as CFDA-AM to assess membrane integrity (see Alternate Protocol 1) and neutral red to assess lysosomal activity (see Alternate Protocol 2).

EVALUATION OF TOXICITY IN FISH-DERIVED CELL LINES USING ALAMAR BLUE TO ASSESS METABOLIC ACTIVITY

BASIC PROTOCOL

This protocol describes the routine maintenance of salmonid cell lines, although very similar procedures could likely be used for cell lines from other groups of fish. Approximately 30 different fish cell lines are available in total from the American Type Culture Collection (ATCC) and the European Collection of Animal Cell Cultures (ECACC), although many more have been described in the literature. The rainbow trout gill cell line, RTgill-W1, which is available from ATCC as CRL-2523, is used as an example in this protocol for growing fish cells.

This protocol outlines the steps for setting up confluent monolayers of cultures of fish-derived, RTgill-W1 cell lines in 48- and 96-well microwell plates (6-, 12-, 24-, and 384-well plates are also available), which will then be exposed to toxicants in the presence or absence of UV irradiation. This allows the detection of directly cytotoxic compounds, or those that need the presence of UV irradiation to become toxic, in which case the compound is called photocytotoxic (Schirmer et al., 1998a,b). Upon termination of the experiment, cell viability as measured by metabolic activity is assessed by using the fluorescent indicator dye alamar blue. Other fluorescent dyes are used to assess membrane

Contributed by Vivian R. Dayeh, Niels C. Bols, Kristin Schirmer, and Lucy E.J. Lee
Current Protocols in Toxicology (2003) 1.5.1-1.5.17

integrity (CDFA-AM; see Alternate Protocol 1) and lysosomal activity (neutral red; see Alternate Protocol 2).

Alamar blue is a commercial preparation of the dye resazurin (O'Brien et al., 2000) and is increasingly being used in pharmacology to screen for compounds toxic to mammalian cells (Evans et al., 2001). Resazurin, which is not fluorescent, becomes fluorescent upon reduction by living cells.

Materials

70% ethanol solution
Confluent culture of RTgill-W1 cells (CRL-2523, ATCC) in a 75-cm^2 flask
0.53 mM versene (EDTA; Life Technologies) diluted 1:5000 (1× 0.2 g tetrasodium EDTA/liter in PBS)
Trypsin solution (see recipe)
Leibovitz's (L-15) complete medium containing FBS (see recipe)
Test compounds (toxicants) in dimethyl sulfoxide (DMSO), stock solutions
DMSO
L-15/ex solution (see recipe)
Alamar blue (Immunocorp)

Laminar flow hood, either horizontal or vertical
Inverted phase-contrast microscope
Vacuum aspirator
15-ml centrifuge tubes, sterile
Hemacytometer
48- or 96-well tissue-culture treated microwell plate
75 cm^2 tissue culture flask
Incubator (see Critical Parameters and Troubleshooting)
Catch basin (a plastic container at least slightly larger than the size of the microwell plate)
Positive displacement digital micropipet (e.g., Nichiryo model 800)
Glass pipet tips for digital micropipet (Nichiryo)
Parafilm
Radiation exposure chamber containing UV-A and/or UV-B fluorescent lamps (Southern N.E. Ultraviolet) and a fan
Spectroradiometer (e.g., InstaSpec II photodiode array spectroradiometer, Oriel)
Transformer to modulate UV intensity
Fluorometric microwell plate reader

NOTE: All solutions and equipment coming into contact with cells must be sterile, and aseptic technique should be used accordingly. Work >6-in. from the front of the vertical laminar flow hood, as the sterile zone begins there.

Prepare fish-derived cell cultures

1. Turn on the laminar flow hood, and wipe all surfaces with 70% ethanol solution.
2. Examine the confluent culture of RTgill-W1 cell flask under an inverted phase-contrast microscope.

   Note the general appearance of the culture, checking for inadvertent microbial contamination or unexpected rounding and detachment of the fish-derived cells. Cultures to be passaged should appear normal and confluent (i.e., covering the bottom of the flask completely) or close to confluence.

3. Under the laminar flow hood, aspirate the old medium and add 1.5 ml of 0.53 mM versene to the flask. Swirl it around gently, leave for 1 min, and aspirate it off.

4. Add 1 ml versene and 1 ml trypsin solution to the flask, replace the cap, and observe under the inverted phase-contrast microscope. Do not leave the cells in trypsin for >5 min as cellular digestion and cell death may ensue.

   The cells will begin to detach from the culture surface in ~1 to 3 min. Older cultures that have not been passaged for a long period of time are difficult to detach. Ideally, the cells will detach individually, and form a single-cell suspension.

5. Add 3 ml Leibovitz's complete medium containing FBS to the flask. Pipet the medium up and down, directing the stream towards the bottom of the flask, to make sure that all cells are dislodged and resuspended in the medium.

   Trypsin inhibitors in FBS stop the action of the trypsin.

6. Transfer the cell suspension to a sterile 15-ml centrifuge tube and centrifuge 5 min at 200 × *g*, room temperature, in a tabletop centrifuge.

7. Aspirate the supernatant from the 15-ml centrifuge tube, being careful not to aspirate the cell pellet. Leave a small amount of supernatant (0.25 ml) over the cell pellet. Flick the centrifuge tube to resuspend the cells in the small volume of medium.

Plate cells to maintain cell line

8a. Add 10 ml fresh medium to the centrifuge tube and transfer 5 ml to each of two 75 cm^2 tissue culture flasks. Add 5 ml medium to each flask.

9a. Examine flasks using a phase-contrast microscope. Note whether cells have detached as single cells or as clumps and whether the suspension has been distributed equally between the two flasks.

10a. Allow the cells to grow at 18° to 22°C. When the cultures are confluent (7 to 10 days), split 1:3 or harvest to use for an experiment.

Plate cells in microwell plates

8b. Add 4 ml Leibovitz's complete medium containing FBS. Determine the cell density using a hemacytometer (*APPENDIX 3B*). Using fresh medium, adjust cell density to 1×10^5 cells/ml if using 48-well plates and to 1.5×10^5 cells/ml if using 96-well plates.

9b. If using a 48-well tissue-culture microwell plate, add 5×10^4 RTgill-W1 cells in 500 µl of Leibovitz's complete medium to 40 wells of a 48-well tissue-culture microwell plate. Use the remaining eight wells as blanks by adding Leibovitz's complete medium alone. If using a 96-well tissue-culture microwell plate, add 3×10^4 RTgill-W1 cells in 200 µl of Leibovitz's complete medium to 84 wells of a 96-well tissue culture plate. Use the remaining twelve wells as blanks by adding Leibovitz's complete medium alone.

10b. Allow the cells to grow for 3 to 4 days in the dark at 18° to 22°C to form a confluent cell monolayer for the 48-well plates and for 2 to 3 days for the 96-well plates.

   Growing cells over a 2- to 4-day period allows for a more consistent cell density and better adherence of cells than newly initiated, dense cultures.

Expose fish-derived cell lines to putative toxicants

11. Turn on the laminar flow hood, and wipe all surfaces with 70% ethanol solution.

12. Examine the plated microwell plate under the inverted phase-contrast microscope.

    Note the general appearance of the cell culture, making sure that the bottom of the wells contain a confluent monolayer and inadvertent microbial contamination is absent.

13. Make serial dilutions (working solutions) from test compound stock solutions in carrier solution (e.g., DMSO).

    If the carrier solution is an organic solvent, prepare working solutions such that the concentrations are at least 200 times the final concentrations desired in the culture wells.

    Serial dilutions are necessary to ensure that the solvent is diluted sufficiently in the culture medium in the wells in order minimize interference due to the solvent with cell viability and/or toxicant uptake. For more water-soluble compounds, a dilution series can be prepared directly in culture medium. However, many organic toxicants, including PAHs, will require the use of an organic carrier solvent.

14. Remove growth medium from plates by inverting over a catch basin. Drain plates further for a few seconds on a small stack of paper towels.

15. Rinse each culture well with 500 µl L-15/ex solution if using 48-well plates or 200 µl L-15/ex solution if using 96-well plates. Remove this rinsing medium by inverting over a catch basin. Drain plates further for a few seconds on a small stack of paper towels. Then add 500 µl L-15/ex solution to each well if using 48-well plates or 200 µl L-15/ex solution if using 96-well plates.

16. Expose cells to the test compound in a vertical laminar flow hood. For example, if working solutions were prepared in DMSO at 200 times the final concentration required, pipet 2.5 µl test compound to each well containing 500 µl/well L-15/ex solution in 48-well plates using a positive displacement digital micropipet. If using a 96-well plate, pipet 1.0 µl test compound dissolved in DMSO to each well containing 200 µl/well L-15/ex solution.

    Because cells in L-15/ex solution are particularly sensitive to DMSO, tilt the plates before adding the test compound to increase the volume of medium above the cells as a protective layer. Dispense the 2.5 µl or 1 µl test compound above the level of the medium, and then touch the droplet to the surface of the medium to aid in dispersion. In addition, reduce the light level in the flow hood to avoid irradiation of cells in the presence of the toxicant.

17. In a 48-well plate, dose six wells (five wells with confluent cell monolayers and one well without cells to serve as a blank) for each of seven concentrations of compounds and the DMSO control. In a 96-well plate, dose eight wells (seven wells with confluent cell monolayers and one without cells to serve as a blank) for each of twelve concentrations of compounds and the DMSO control. Wrap plates in Parafilm to prevent evaporation during the exposure period.

    The use of plate sealing foils, which are commercially available, e.g., Nunc or Greiner, is recommended in order to minimize well-to-well transfer and losses due to evaporation of more volatile toxicants.

For exposure of fish-derived cells to toxicants in the dark

18a. For exposures in the dark, incubate plates up to 48 hr at 18°to 22°C.

19a. If not specifically desired (see below), avoid exposure of the plates to light.

    Although L-15/ex is unlikely to be affected by irradiation, many toxicants may be altered chemically.

20a. At the end of the dark exposure, remove plates from the incubator and continue with the cytotoxicity assay for assessing metabolic activity with the fluorescent dye alamar blue, proceed to step 23 (for membrane integrity assessment, use CDFA-AM, see Alternate Protocol 1; or for lysosomal activity assessment, use neutral red, see Alternate Protocol 2).

For exposure of fish-derived cells to toxicants in the presence of irradiation

18b. Turn on the lamps of the radiation exposure chamber at least 15 min prior to use in order to allow lamps to warm up and emit a stable radiation.

The radiation chamber should contain at least two fixtures to hold lamps, e.g., one UV-A and one UV-B fluorescent lamp, and it should be shielded from any radiation outside the chamber. Ideally, lamps should be linked to a transformer in order to allow for easy manipulation of the radiation output.

19b. Place the appropriate unit of the spectroradiometer into the radiation exposure chamber in order to perform UV radiation measurements as described in the user manual of the spectroradiometer.

Ensure that the appropriate unit of the spectroradiometer is positioned the same distance from the UV lamps as the culture plate would be. Also, place the lid of the culture plate on top of the unit to measure the amount of UV irradiation passing through the lid of the plate.

20b. Using the transformer, adjust UV intensities as desired.

For example, a 10:1 ratio of UV-A to UV-B may be desirable in order to mimic the ratio of these two UV components in nature. If no transformer is available, radiation intensity may be adjusted by varying the distance between the exposure tray and the lamps but this method is somewhat cumbersome.

21b. Once the radiation exposure chamber has been set up, place tissue culture plates into the chamber in an atmosphere of air for the required exposure period. Place a second tissue culture plate into the chamber at the same time but protected from radiation.

This second plate serves as the dark control.

22b. At the end of the UV exposure, remove plates from the chamber and proceed with the cytotoxicity assay for assessing metabolic activity using alamar blue, proceed to step 23 (for membrane integrity using CDFA-AM, see Alternate Protocol 1; or for lysosomal activity using neutral red, see Alternate Protocol 2).

Assess metabolic activity using alamar blue

23. Prepare a 5% (v/v) working solution of alamar blue in L-15/ex solution.

Alamar blue is purchased as a ready-to-use solution in quantities of 25 ml and 100 ml. When stored in the dark at 2° to 8°C and kept aseptically, alamar blue can be used for at least 1 year.

24. Remove exposure medium from plates by inverting over a catch basin. Drain plates further for a few seconds on a small stack of paper towels.

25. Add 100 to 150 µl of 5% alamar blue working solution to each well of a 48-well plate, or 50 to 100 µl per well to a 96-well plate.

The general rule is to at least cover the growth surface of the wells although some plate readers may require slightly larger volumes for accurate readings.

26. Incubate the plates in the dark at 18° to 22°C for 30 min.

Although longer incubation times are also possible, the yield of fluorescent units from alamar blue can decline if the incubation period is too long (O'Brien et al., 2000).

27. Measure alamar blue on the fluorometric plate reader at excitation and emission wavelengths of 530 and 590 nm, respectively.

ALTERNATE PROTOCOL 1

EVALUATION OF TOXICITY IN FISH-DERIVED CELL LINES USING CFDA-AM TO ASSESS MEMBRANE INTEGRITY

Although esterase substrates have been used as a measure of cell membrane integrity since the 1960s (Rotman and Papermaster, 1966), 5-carboxyfluorescein diacetate acetoxymethyl ester (CFDA-AM) is an example of one developed to improve this application (Haugland, 1996). CFDA-AM diffuses into cells rapidly and is converted by non-specific esterases of living cells from a nonpolar, nonfluorescent dye into a polar, fluorescent dye, 5-carboxyfluorescein (CF), which diffuses out of cells slowly. In this protocol, fish cells in microwell cultures are exposed for a period of time to a putative toxicant, and after removal of the putative toxicant, CFDA-AM is added and the capacity of the cells to produce CF is measured.

Additional Materials *(also see Basic Protocol)*

4 mM 5-carboxyfluorescein diacetate acetoxymethyl ester (CFDA-AM, see recipe)
RTgill-W1 cells in a 48-well or 96-well plate exposed to toxicants (see Basic Protocol, steps 1 to 22)

1. Prepare a working solution of 4 µM CFDA-AM by diluting the 4 mM CFDA-AM stock solution 1:1000 in L-15/ex solution.
2. Remove exposure medium from RTgill-W1 cells in a 48-well or 96-well plate exposed to toxicants by inverting over a catch basin. Drain plates further for a few seconds on a small stack of paper towels.
3. Add 100 to 150 µl of 4 µM CFDA-AM working solution to each well of a 48-well plate or 50 to 100 µl of 4 µM CFDA-AM working solution to each well of a 96-well plate and incubate the plate in the dark for 30 to 120 min at 18°to 22°C.
4. Measure CF fluorescence on the fluorometric plate reader at respective excitation and emission wavelengths of 485 and 530 nm.

Alamar blue (see Basic Protocol, steps 23 to 27) and CFDA-AM can be added together to perform the two assays in a single step (Schirmer et al., 1997) because the fluorescent products of the two indicator dyes can be detected at different emission wavelengths without interfering with each other. The advantage of doing so is the conservation of material and time as fluorescent readings are taken on the same culture wells. Thus, in order to perform the two assays together, add the appropriate amount of alamar blue to make a 5% (v/v) working solution in L-15/ex solution and then dilute the CFDA-AM stock solution (4 mM in DMSO) 1:1000 in that same volume of L-15/ex solution. Proceed with the incubation period as described above in step 3.

Inasmuch as alamar blue and CFDA-AM do not affect the viability of cells, fluorescent dyes can be removed after fluorescent measurement and replaced by culture medium to allow the cells to recover for a period of time after which the indicator dyes can be re-applied.

ALTERNATE PROTOCOL 2

EVALUATION OF TOXICITY IN FISH-DERIVED CELL LINES USING NEUTRAL RED TO ASSESS LYSOSOMAL ACTIVITY

Although first used to evaluate cell viability in virology, neutral red (NR) has been utilized most intensively in in vitro toxicology. The principle is that viable cells accumulate NR (3-amino-7-dimethylamino-2-methylphenazine hydrochloride) in lysosomes (Borenfreund and Puerner, 1984). NR can be applied before or after the exposure of cell cultures to toxicants, so that the measured endpoint represents either the release or uptake of the dye (Borenfreund and Puerner, 1984; Reader et al., 1990). Measurements can be done either spectrophotometrically (Borenfreund and Puerner, 1984) or fluorometrically (Essig-Marcello and van Buskirk, 1990). In this protocol, the use of NR after the exposure of fish cells to toxicants and the fluorometric measurement of any subsequent changes in NR uptake are described.

Additional Materials *(also see Basic Protocol)*

Neutral red stock solution (see recipe)
RTgill-W1 cells in a 48-well or 96-well plate exposed to toxicants (see Basic Protocol, steps 1 to 22)
Neutral red fixative solution (see recipe)
Neutral red extraction solution (see recipe)
Orbital shaker

1. Prepare a working solution of 33 µg/ml neutral red by diluting the neutral red stock solution 1:100 in L-15/ex solution.
2. Remove exposure medium from RTgill-W1 cells in a 48-well or 96-well plate exposed to toxicants by inverting over a catch basin. Drain plates further for a few seconds on a small stack of paper towels.
3. Add 100 to 150 µl of 33 µg/ml neutral red working solution to each well of a 48-well plate or 50 to 100 µl of 33 µg/ml working solution to each well of a 96-well plate and incubate the plate in the dark for 60 min at 18°to 22°C.
4. Remove the neutral red working solution by inverting over a catch basin and drain a few seconds on a small stack of paper towels.

   It is critical to remove all the neutral red working solution from each well, especially in a 96-well plate.

5. Rinse wells once with 100 µl/well of neutral red fixative solution.

   The rinsing step removes any excess neutral red that has not been localized in lysosomes.

6. Add 100 µl/well of neutral red extraction solution to solubilize the lysosomal neutral red. Place plates on an orbital shaker and shake at ~40 rpm for 10 min.
7. Measure neutral red fluorescence on the fluorometric plate reader at excitation and emission wavelengths of 530 and 645 nm, respectively.

   In the interest of conserving material and for performing cell viability assays on the same set of cells, the neutral red assay can be performed on the same plate previously used to assess alamar blue (see Basic Protocol) and/or CFDA-AM fluorescence (see Alternate Protocol 1). After termination of the alamar blue and CFDA-AM exposures, remove the dye solution(s) and start by adding neutral red as described above. However, inasmuch as the neutral red assay will terminate the cell culture because cells will be fixed, a separate plate needs to be used if the alamar blue/CFDA-AM plates are to be used to study recovery.

REAGENTS AND SOLUTIONS

Use Milli-Q-purified water or equivalent in all recipes and protocol steps. For common stock solutions, see ***APPENDIX 2E****; for suppliers, see* ***SUPPLIERS APPENDIX****.*

CFDA-AM stock solution, 4 mM

Dissolve the 5-mg vial of CFDA-AM (Molecular Probes) in 2.35 ml of sterile anhydrous DMSO (final concentration 4 mM) in a laminar flow hood. Dispense into sterile 1.5-ml microcentrifuge tubes in 50-µl aliquots to prevent degradation from thawing and refreezing. Wrap each microcentrifuge tube in aluminum foil to prevent light degradation. Store dessicated up to 1 year at −20°C to avoid ester hydrolysis due to moisture.

L-15/ex solution

Development of this modified medium is outlined in Schirmer et al. (1997) and is based on the constituents of basal medium, L-15 (Leibovitz, 1963). Make up all components from cell-culture grade reagents (Sigma) and prepare in cell-culture grade, distilled water.

Salt solution A: In 600 ml water, dissolve: 80 g NaCl, 4.0 g KCl, 2.0 g $MgSO_4$, 2.0 g $MgCl_2$

Salt solution B: In 100 ml water, dissolve: 1.4 g $CaCl_2$

Salt solution C: In 300 ml water, dissolve: 1.9 g Na_2HPO_4, 0.6 g KH_2PO_4

Autoclave each solution separately and store up to 1 year at room temperature.

Sodium pyruvate solution: In 100 ml of water, dissolve 5.5 g sodium pyruvate. Filter sterilize through a 0.2-µm filter, dispense in 5.7-ml aliquots, and store up to 1 year at −20°C.

Galactose solution: In 100 ml of water, dissolve 9.0 g galactose. Filter sterilize through a 0.2-µm filter, dispense in 5.7-ml aliquots, and store up to 1 year at −20°C.

To prepare L-15/ex solution:

To 500 ml of sterile cell culture-grade, distilled water, add aseptically:
34.0 ml salt solution A
5.7 ml salt solution B
17.0 ml salt solution C
5.7 ml sodium pyruvate solution
5.7 ml galactose solution
Store L-15/ex solution up to 1 year at room temperature

Leibovitz's L-15 complete medium containing FBS

To 500 ml of Leibovitz's L-15 medium (Sigma), aseptically add 50 ml fetal bovine serum (FBS; Sigma). Final FBS concentration in culture medium is 8.9%, which is usually referred to as 10%. Aseptically add 10 ml of penicillin/streptomycin (100 IU/ml penicillin, 100 µg/ml streptomycin; Sigma). Store up to 1 year at 4°C.

Neutral red extraction solution

Prepare 1% (v/v) acetic acid and 50% (v/v) ethanol in deionized, distilled water. Store for up to 1 year at room temperature in the dark.

Neutral red fixative solution

Prepare 0.5% (v/v) formaldehyde and 1% (w/v) $CaCl_2$ in deionized, distilled water. Store for up to 1 year at room temperature in the dark.

Neutral red stock solution

Dissolve 3.3 mg of neutral red powder (Sigma) per milliliter of Dulbecco's PBS (D-PBS; Sigma or Life Technologies) in an amber vial. Store for up to 1 year at 4°C.

Alternatively, neutral red stock solution can be purchased dissolved in D-PBS at a concentration of 3.3 mg/ml (Sigma).

Trypsin solution

Dissolve 100 mg trypsin (Sigma) in 10 ml of Ca^{2+}- and Mg^{2+}-free Hank's balanced salt solution (Sigma) to make a trypsin stock solution. Dispense 0.5 ml of this solution into 9.5 ml of Ca^{2+}- and Mg^{2+}-free Hank's balanced salt solution. Store for up to 1 year at −20°C.

COMMENTARY

Background Information

The many in vitro toxicology tests can be divided into two types: general (basal) cytotoxicity tests and tests of differentiated cell function (Flint, 1990). The general type consists of tests that measure cytotoxic phenomena only, e.g., the inhibition of cell proliferation. One premise of this approach is that all toxic phenomena are fundamentally related to an impairment of some aspect of cellular activity in vivo. Therefore, toxicity in vivo should be expected if the test agent is bioavailable to a target tissue at concentrations that are observed to impair cell viability in vitro. A potential weakness of this approach is the observation that rather than being a general phenomenon of all tissues, toxicity in vivo is often limited to a small group of organs and cells within these organs. Thus, specific toxic effects might occur at concentrations well below those causing general cytotoxicity. The second class of in vitro tests attempts to overcome this weakness by monitoring a cellular function specific for the differentiated state of the cultured cell. From a risk assessment point of view, the tests for differentiated cell functions are usually more valuable (Flint, 1990). To date, general cytotoxicity tests mostly have been used in fish toxicology and are described in this unit.

Many general cytotoxicity tests have been described. They measure impairment of cellular activities by potentially toxic treatments. However, since their first introduction, assays of cytotoxicity and/or cell viability have been criticized as to their meaning and have aroused debate as to which assay is most appropriate (Schrek, 1965; Shaw, 1994). Cytotoxicity assays that monitor reproductive capacity have been described as being the most comprehensive because they integrate the soundness of the entire cellular machinery (Shaw, 1994). However, proliferation assays are not ideal for all purposes. They usually reveal little about the specific cellular events that lead to impaired proliferation and can miss subtle, transitory effects. They give little insight into the potential short-term impact of an effect on cells to the integrity of an organ or tissue. Also, colony formation and proliferation rates are impractical endpoints with most fish cell lines because the cells grow slowly. As an alternative to proliferative endpoints, assays of cell viability and cell injury can be performed (Shaw, 1994), such as the ones described here.

Although numerous assays of cell viability have been developed, those that utilize fluorometric indicator dyes are perhaps best. First, more and more dyes are becoming commercially available to evaluate distinct cellular parameters. Second, the development of fluorometric multiwell plate readers has made the use of fluorometric dyes easy and rapid, such as for the assays in this unit. The microwells conserve material resources by reducing the number of cells needed and increasing the number of replicates. The plate readers have the potential for high interlaboratory reproducibility and can be coupled to computers in order to manage data quickly and easily.

Critical Parameters and Troubleshooting

Temperature

The choice of temperature for growth, exposure, and assay of fish cell cultures is flexible and can be dictated by practical considerations or by scientific objectives. This is because fish cells can be grown over a wide temperature range, e.g., from 5° to 25°C for salmonid cells (Bols et al., 1992). The medium used in this unit is based on Leibovitz's L-15, which does not need a 5% CO_2 atmosphere in order for the pH to be buffered (Leibovitz, 1963). As a result, the "incubator" for fish cell cultures in CO_2-independent media, such as L-15, can be a desk drawer at room temperature, or a temperature-regulated chamber, such as a conventional incubator or a refrigerator. For all the protocols that are described in this unit with salmonid cells, temperatures from 18° to 22°C give consistent results, and fluctuations within this range have little or no effect on the outcome.

Toxicant preparation

The acts of dissolving compounds and of adding them to cell cultures can be the source of several problems. Unfortunately, these are difficulties that cannot really be solved, but are important to consider when interpreting results. The problems are most severe for hydrophobic environmental contaminants, such as the PAHs. Several alternative strategies for toxicant delivery have to be considered. One is whether or not to use carrier solutions to dissolve the compounds. The second is whether or not to completely remove the medium that was used to initiate the cell cultures from the microwells and to replace it with an equivalent volume of

toxicant solution. For compounds that are going to be presented without the use of a carrier, there is usually no choice, the original medium has to be replaced with the toxicant solution. Except for extremely water-soluble compounds, the highest doses in dose-response curves cannot be achieved by adding small aliquots of a concentrated solution. By contrast, high concentrations of hydrophobic compounds can be achieved in carrier solutions, allowing them to be added to cultures in small aliquots. Potential problems with carriers, exposure media, and presentation strategies for toxicants are further discussed below.

Carriers such as dimethylsulfoxide (DMSO) have nearly always been used to dissolve environmental contaminants for toxicity testing, but they potentially can influence the results. For example, fluoranthene that was dissolved in L-15/ex solution with DMSO was slightly more photocytotoxic to RTgill-W1 cells than fluoranthene dissolved in L-15/ex solution without DMSO (Schirmer et al., 1997). Differences can also be found between carriers. DDT in DMSO was more cytotoxic to tilapia brain cells than DDT in acetone (Parkinson and Agius, 1987). The induction of 7-ethoxyresorufin o-deethylase (EROD) activity in RTL-W1 cells was better after exposure to 2,3,7,8-tetrachlorodibenzo-*p*-dioxin (TCDD) in DMSO than in isooctane (Clemons et al., 1994). Also, the carrier could influence the induction potency of some compounds (Yu et al., 1997).

Exposure medium

The medium in which cells are incubated during exposure to environmental contaminants is another variable that can influence results. An extremely simple one is used in this unit, which contains salts, galactose, and pyruvate at specified concentrations in the basal medium, Leibovitz's L-15 (Leibovitz, 1963), which is termed L-15 exposure or L-15/ex (Schirmer et al., 1997). L-15/ex has several advantages. For photocytotoxicity studies, the absence of vitamins and aromatic amino acids prevents the inadvertent generation of toxicants from these compounds during the UV treatment. L-15/ex is also advantageous for detecting toxicants that cause cytotoxicity through the generation of reactive oxygen species (ROS). This is because expression of their toxicity should be aided by the absence in L-15/ex of most antioxidants. The one exception might be the presence of pyruvate. For mammalian cells, pyruvate is part of an antioxidant defense (O'Donnell-Tormey et al., 1987). A limitation of L-15/ex is that exposure times are restricted to several days, as ultimately nutrient deprivation will cause cell death. The short exposure times mean that toxicants acting by inducing particular cellular processes, such as xenobiotic metabolism, and causing accumulative damage might be missed. Yet, RTgill-W1 cells survive in L-15/ex for at least 100 hr (Schirmer et al., 1997). Although addition of fetal bovine serum (FBS) to the medium extends the life of cell cultures, the antioxidants of FBS prevents the detection of fluoranthene photocytotoxicity (Schirmer et al., 1997). Also, FBS can alter the bioavailability of toxicants (Schirmer et al., 1997; Hestermann et al., 2000).

Dosing strategies

One strategy for presenting toxicants to cells is to completely remove the medium that was used to initiate the cell cultures from the microwells and add an equivalent volume of solution with the toxicant under study. Both steps present difficulties. The medium removal step has two problems. First, removal must be done quickly without damaging cells, which can be done by aspirating off the medium. But, this sometimes causes cell death. Death usually appears within minutes of aspiration and occurs in large patches over the culture surface. Routinely examining cultures with an inverted phase-contrast microscope shortly after aspiration easily identifies this problem. Alternatively, the medium can be removed by inverting the plate over a catch basin and blotting with a paper towel. This is the recommended medium removal technique because the cells are not subjected to the same force as aspiration may involve. Second, complete removal of the initiating medium over the cell cultures has the potential to change the physiology of cell cultures. An example of this is the rapid induction of 7-ethoxyresorufin o-deethylase (EROD) activity upon the removal of medium from cultures of the rainbow trout liver cell line, RTL-W1 (Segner et al., 2000). For short-term exposures (as described in this unit), this should not be a problem. Replacing the medium with toxicant solution is problematic for hydrophobic compounds. A concentrated solution of toxicant in a carrier such as DMSO must be serially diluted in an aqueous solution to prepare concentrations for dose-response curves. Hydrophobic compounds have a tendency to stick to the walls of containers and pipets used to prepare these solutions. Thus, the final toxicant concentrations that the cultures receive can be

lower than the concentrations apparently added. The problem cannot be solved by simply measuring the concentrations through analytical chemistry methods, for this approach also requires the use of containers and pipets that can lead to an underestimation of final concentrations.

The second presentation strategy is to use micropipets to add small volumes (≤10 µl) of the toxicant in carrier solvent to the medium over the cells in microwells. Dosing in this manner must be done very carefully with carriers, such as DMSO. The small volume of DMSO sometimes falls as a blob directly onto the cells, immediately killing them. Again, examining cultures with an inverted phase-contrast microscope easily identifies this problem. As mentioned, the difficulty can be avoided by keeping the pipet tip close to the medium surface and allowing the surface tension to disperse the DMSO rapidly and evenly through the culture. This second presentation strategy has at least two advantages. Changing the medium is avoided, which also avoids any possible changes in the cells caused by this act. Final culture concentrations are closer to the apparent toxicant concentration that is added. In extreme cases, a compound might appear to be toxic with this dosing method, but not by the method of preparing the toxicant in exposure medium and using this solution to replace the growth medium of cell cultures. If the results of the two different dosing strategies are profoundly different, they should be reported as such, as this will aid others in replicating the results in any future studies and will stress the subtlety of the cytotoxicant's actions.

UV irradiation

For the concurrent exposure of cultures to environmental contaminants and UV light, the radiation exposures can be expressed in different ways, sometimes causing confusion. The most important distinction is between energy units, which refer to the wave-like character of radiation, and quantum units, which reflect the corpuscular character. The conversion from energy content to photon content is defined by Planck's equation. Fluence rates are used to refer to the quantity of radiation per area per time. Thus, Wm^{-2} and Jm^{-2} sec^{-1} are expressions of energy fluence rates, whereas $moles_{(photons)}m^{-2}sec^{-1}$ is an expression of photon fluence rates. In contrast to the fluence rates, the total amount of radiation received by the cells can be expressed as fluence, that is quantity per area. Thus, the energy fluence (Jm^{-2}= $Wm^{-2}sec$) or the photon fluence ($mol_{(photons)}m^{-2}$) can be calculated by multiplying the fluence rate by the time of irradiation (in seconds). For example, a photon fluence rate of UV-B at 313 nm of 1.4 $\mu mol(m^{-2})sec^{-1}$, which has been shown to be environmentally relevant (Oris and Giesy, 1987), is equivalent to an energy fluence rate at that wavelength of 53 μWcm^{-2}(or 53 $\mu Jcm^{-2}sec^{-1}$). If irradiation is performed for 2 hr, the energy fluence that the cells are exposed to is 0.4 $Wcm^{-2}sec$ (or 0.4 Jcm^{-2}).

Inasmuch as UV radiation exposure decreases with increasing distance from the UV source, it is important to measure UV radiation at the position at which culture plates will be placed. In order to account for absorption of UV radiation by culture plate lids, place a lid between the UV source and the radiation measurement device. The irradiation of cells in the presence of tissue culture plate lids is highly recommended for two reasons. First, the lids ensure sterility during the illumination process. Second, the plate lids absorb any radiation below a wavelength of 290 nm, a filtering process which, under natural conditions, is carried out by a stratospheric ozone (Schirmer et al., 1997).

While measurements of UV irradiance should be done frequently to ensure that UV intensities of the fluorescent lamps are as required, initial measurements should confirm that the culture medium covering the cells does not detrimentally affect UV penetration. To study this, a lid-covered tissue culture plate with and without culture medium should be placed between the UV source and the spectroradiometer and the values compared. If measurements are the same, it can be concluded that the culture medium used has no discernible effect on UV penetration. In contrast, lower UV intensities measured in the presence of culture medium indicate that cells obtain less UV radiation than anticipated. For example, the authors found that UV intensities were not significantly affected upon passage through a 4.7 mm path of L-15/ex medium, which equals 500 µl L-15/ex medium in a 48-well tissue culture plate. In contrast, the same passage of UV in the presence of 10% FBS led to a reduction of UV readings of 27% for UV-B and 9% for UV-A (Schirmer et al., 1997). Another factor to consider is temperature. In the presence of a small fan and a distance of the tissue culture plates from the UV lamps of at least 15 cm, the authors did not find temperature to rise in the tissue culture medium within 2 hr of UV-irradiation at a photon fluence rate of 10 µmol m^{-2}

sec^{-1}UV-A and 1 μmol $m^{-2}sec^{-1}$UV-B (Schirmer et al., 1998b). However, longer exposures or higher UV intensity may potentially lead to an increase in temperature.

Toxicant removal

Termination of toxicant exposures prior to the addition of the fluorescent indicator dyes to cell cultures must be done carefully and consistently. Inverting plates over a catch basin is recommend over aspiration. Removal must be done rapidly but without damaging cells. Viewing control cultures with an inverted phase-contrast microscope will identify any problems. Of course, at this stage, the loss of cells from toxicant-treated cultures can be expected.

Fluorescent microwell plate readers

A number of manufacturers (e.g., Molecular Devices, Applied Biosystems) make fluorescent plate readers, and likewise, microwell plates are produced by several companies (e.g., Falcon, Costar, Nunc). Although all fluorescent plate readers are likely suitable, the crucial issue is to make sure the microwell plate correctly matches the plate reader. Under most circumstances, only the appropriate settings need to be chosen, as the plate readers have been designed to accept most plates from various manufacturers. However, sometimes the dimensions for a particular microwell plate must be obtained from the manufacturer and entered into the plate reader.

As mentioned earlier, the minimum volume of fluorescent indicator dyes needed for accurate measurement might vary for different microwell plate readers. Thus, initial experiments should determine the most suitable volume.

Anticipated Results

Data analysis: Calculation of EC_{50}

The raw fluorescent units resulting from the cell viability assays are used to evaluate the toxicity of the chemical being tested. Cell viability is expressed as a percent of non-toxicant exposed cells (% of control). For each concentration of toxicant, there is one well that contains no cells (no cell control). Both the well with no cells and the wells with cells are exposed to the toxicant. Prior to calculating percent of control, subtract the fluorescent units (FU) for wells without cells from the experimental (ex) and control (con) values with cells. To calculate the cell viability (% of control) use the following formula:

$$\%\ \text{of control} = (FU_{\text{ex cells}} - FU_{\text{ex no cells}}) \times 100/(\text{average}\ [FU_{\text{con}} - FU_{\text{con no cells}}])$$

Data for each well of each concentration are expressed as a percent of control. Then, the average and standard deviation for each concentration are calculated. These values are used to calculate the EC_{50} for the toxicant.

Dose-response data typically follow a sigmoidal relationship and can be analyzed by nonlinear regression in most graphing software such as SigmaPlot (Jandel Scientific). The data is fitted to the four-parameter logistic function for continuous response data. The logistic function is:

$$y(d) = Y_{\min} + (Y_{\max} - Y_{\min})\backslash\{1 + \exp[-g(\ln(d) - \ln(EC50))]\}^{-1}$$

where $y(d)$ is the % cell viability at the dose d, $Y_{\min}$ is the minimum percent cell viability, $Y_{\max}$is the maximum percent cell viability, $g$is a slope parameter, $EC_{50}$is the dose that produces 50% of cell viability.

Inasmuch as cell viability data are expressed on a 0% to 100% basis, the four-parameter equation is simplified to a two-parameter equation because $Y_{\max}$ and $Y_{\min}$ are constants of 100% and 0%, respectively:

$$y(d) = 0\% + (100\% - 0\%)\ \{1 + \exp[-g(\ln(d) - \ln(EC_{50}))]\}^{-1}$$

Interpretation of results

With each fluorescent indicator dye (alamar blue, CFDA-AM, and NR), a reduction in fluorescent unit readings in experimentally treated cultures relative to the readings in control cultures indicates cytotoxicity or a loss of cell viability. The use of multiple dyes has the potential of revealing the mechanism(s) behind the cytotoxicity. However, the results and the interpretation can be straightforward or complicated, depending on the toxicant under study. Both a simple (Fig. 1.5.1) and a complex example (Fig. 1.5.2) are presented.

When the dose-response curves for the three indicator dyes are identical or very similar for cell cultures after short exposures to toxicants, e.g., illustrated in Figure 1.5.1 for 1,4-dimethyl naphthalene, this indicates that the toxic mechanism is general membrane damage, which includes impairment of organelle membranes, such as those for mitochondria and lysosomes, as well as the plasma membrane. Because this loss of cell viability occurs quickly, it has come to be known as direct cytotoxicity to indicate that cellular metabolism of the toxicant is unlikely to be involved

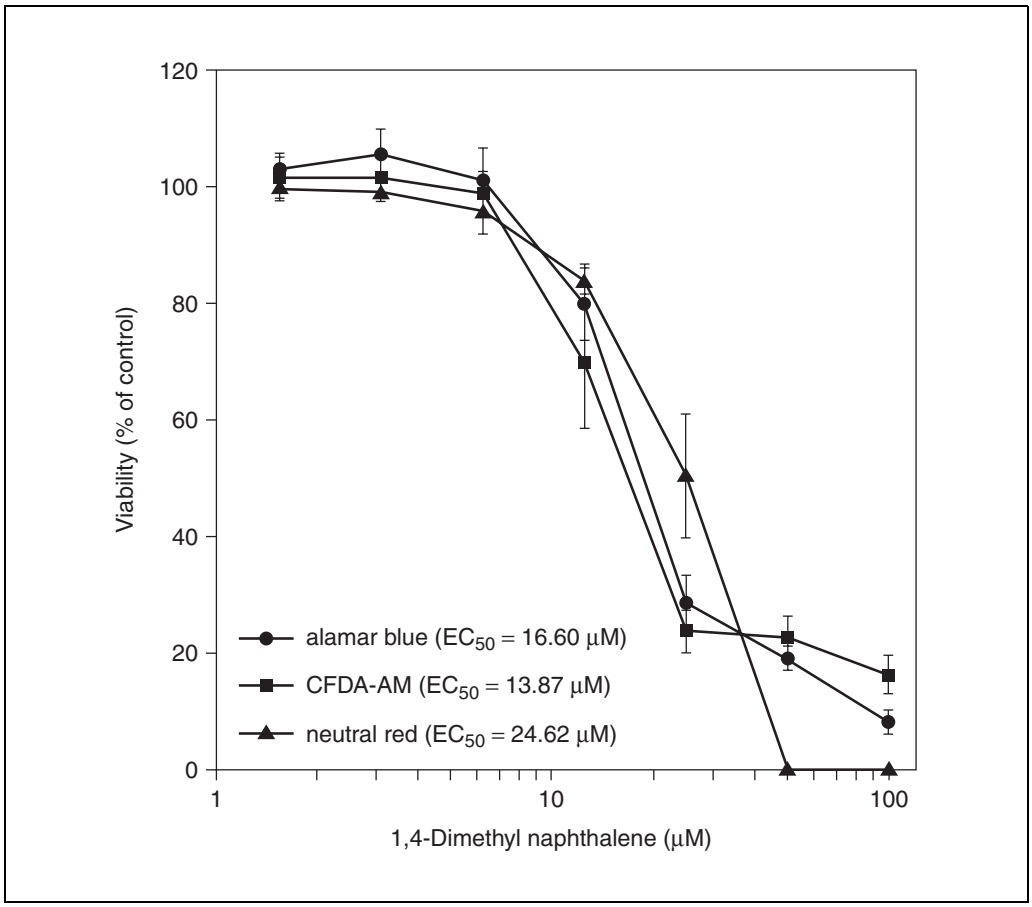

Figure 1.5.1 Effect of 1,4-dimethyl naphthalene on viability of RTgill-W1 cultures. After the cultures had been exposed for 2 hr, cell viability was assessed with alamar blue (circles), CFDA-AM (squares), and neutral red (triangles). Results were expressed as a percentage of the readings in control wells exposed to L-15/ex solution with DMSO.

(Schirmer et al., 1998a). The terms ultra-fast cell death, or less preferably, necrosis, have been suggested for cell death that occurs quickly in mammalian cell cultures in response to strong stimuli (Blagosklonny, 2000). Ultra-fast cell death appears before the activation of caspase, which is a characteristic of apoptosis (Blagosklonny, 2000). For mammalian cells, Blagosklonny (2000) has suggested that a time frame for the development of a decline in cell viability can be used to distinguish ultra-fast cell death (2 to 16 hr), apoptosis (16 to 36 hr), and slow cell death (>36 hr). As cellular phenomena take longer to develop in fish cells being grown at 18° to 22°C than in mammalian cells at 37°C, the time frame for these in fish cell lines might be increased considerably.

Alternatively, the dose-response curves with the different indicator dyes can be unlike one another. Several examples already have appeared in the literature. One combination of outcomes is a decline in cell viability as measured with alamar blue being accompanied by little or no change in cell viability as measured with CFDA-AM. Such results have been seen with benzo[a]pyrene (BaP) and 6, 12-BaP quinone (Schirmer et al., 2000). As the reduction of alamar blue to a fluorescent product is now thought to indicate cellular metabolism rather than specifically mitochondrial activity (O'Brien et al., 2000), the results are interpreted as indicating that these compounds impair metabolism without impacting plasma membrane integrity. Another outcome combination is that of a greater decline in cell viability as measured with neutral red than in the cell viability monitored with alamar blue and CFDA-AM. This was seen in studies on the photocytoxicity of acenaphthylene, acenaphthene, phenanthrene, fluoranthene, pyrene, anthracene, and benzo[g,h,i]perylene (Schirmer et al., 1998b) . The interpretation of these results is that specific lysosomal damage has occurred immediately after concurrent exposure to these com-

pounds and UV radiation, with little or no impairment of plasma membranes and cellular metabolism.

The CFDA-AM assay appears to monitor impairment to plasma membranes, but Figure 1.5.2A illustrates a perplexing outcome. A decline in fluorescent readings occurs at lower concentrations of 2-ethyl phenanthrene with CFDA-AM than with alamar blue, resulting in a lower EC_{50} for this toxicant. If the CFDA-AM measures membrane integrity, then cellular metabolism evaluated with alamar blue would not be expected to continue with little or no impairment while the integrity of the plasma membrane has been lost. An explanation can be advanced for this apparent anomaly. When carried out as described here, a decrease in fluorescent readings with CFDA-AM actually measures a decline in the total esterase activity within a microwell cell culture. The decrease in esterase activity with toxicant treatment could be achieved in two general ways: the loss of plasma membrane integrity and/or specific inhibitory actions on cellular esterases. In turn, the loss of plasma membrane integrity could decrease culture esterase activity in two slightly different ways. The first of these would be the complete or partial lysis of the cells upon toxicant exposure so that the esterases are released into the medium and lost when the medium is removed and replaced with the CFDA-AM solution. Another possible cause for the diminution of esterase activity is a change in plasma membrane integrity so that cytoplasmic constituents are lost to the medium but the esterases remain contained within the cells, which are still attached to the surface of the microwells. This change in the cytoplasmic milieu would be less able to support maximal esterase activity. Alternatively, the toxicant treatment could leave membrane integrity unimpaired but specifically interfere with cellular esterases, causing activity to decline. Examples of this would be a toxicant interfering with the uptake of the substrate, CFDA-AM, across the plasma membrane or inhibiting the catalytic activity of the esterases. The results in Figure 1.5.2A in which increasing 2-ethyl phenanthrene concentrations cause a more precipitous decline in CFDA-AM readings than in alamar blue readings are likely an example of a toxicant impairing esterase activity rather than the plasma membrane.

Additional information into mechanisms of toxicity can be obtained by applying the indicator dyes both immediately after terminating toxicant exposure and later after a period of potential recovery. The assays with alamar blue and CFDA-AM are non-toxic and can be applied on the same microwell cultures for both time points. For the NR assay, which requires cultures to be extracted, separate microwell cultures must be used. Differences between dose-response curves immediately and 24 hr after toxicant exposures have been found, suggesting impairments at specific cellular sites and the capacity of cells to repair them. For example, alamar blue readings decreased immediately after the end of exposures to BaP and 6, 12 BaP quinone, but recovered 24 hr later (Schirmer et al., 2000). As the CFDA-AM readings showed no changes, these results suggested that short exposures to these compounds transitorily disrupted cellular metabolism, although continuous exposure would ultimately lead to cell death. By contrast, a comparison of Figures 1.5.2A and 1.5.2B suggests that a 2-hr exposure to high concentrations of 2-ethyl phenanthrene initiates a process leading to irreparable cellular damage that is expressed as a loss of cell viability 24 hr later. As the development of this cytotoxicity occurs quickly, and for most of the time in the absence of significant amounts of test compound in the medium, the cytotoxicity is unlikely to be due to the generation of toxic metabolites by cell metabolism during the recovery period. Instead, during the 2-hr exposure period, 2-ethyl phenanthrene likely partitions into cell membranes, and in cultures with high concentrations, reaches levels that begins disrupting the plasma membrane. As a membrane-bound toxicant would not be easily removed upon termination of toxicant exposure, the process of plasma membrane impairment would continue during the recovery period, leading to cell death.

The above discussion illustrates some of the complexities that might be anticipated. Likely, all the possible scenarios for cellular responses to toxicants as measured with these three indi-

Figure 1.5.2 *(at right)* Effect of 2-ethyl phenanthrene on viability of RTgill-W1 cultures. After the cultures had been exposed for 2 hr (**A**), cell viability was assessed with alamar blue (circles), and CFDA-AM (squares). The exposure medium was replaced with complete medium and the cells were incubated for an additional 24 hr (**B**), after which viability was reassessed with alamar blue (hexagons) and CFDA-AM (diamonds). Results were expressed as a percentage of the readings in control wells exposed to medium with DMSO.

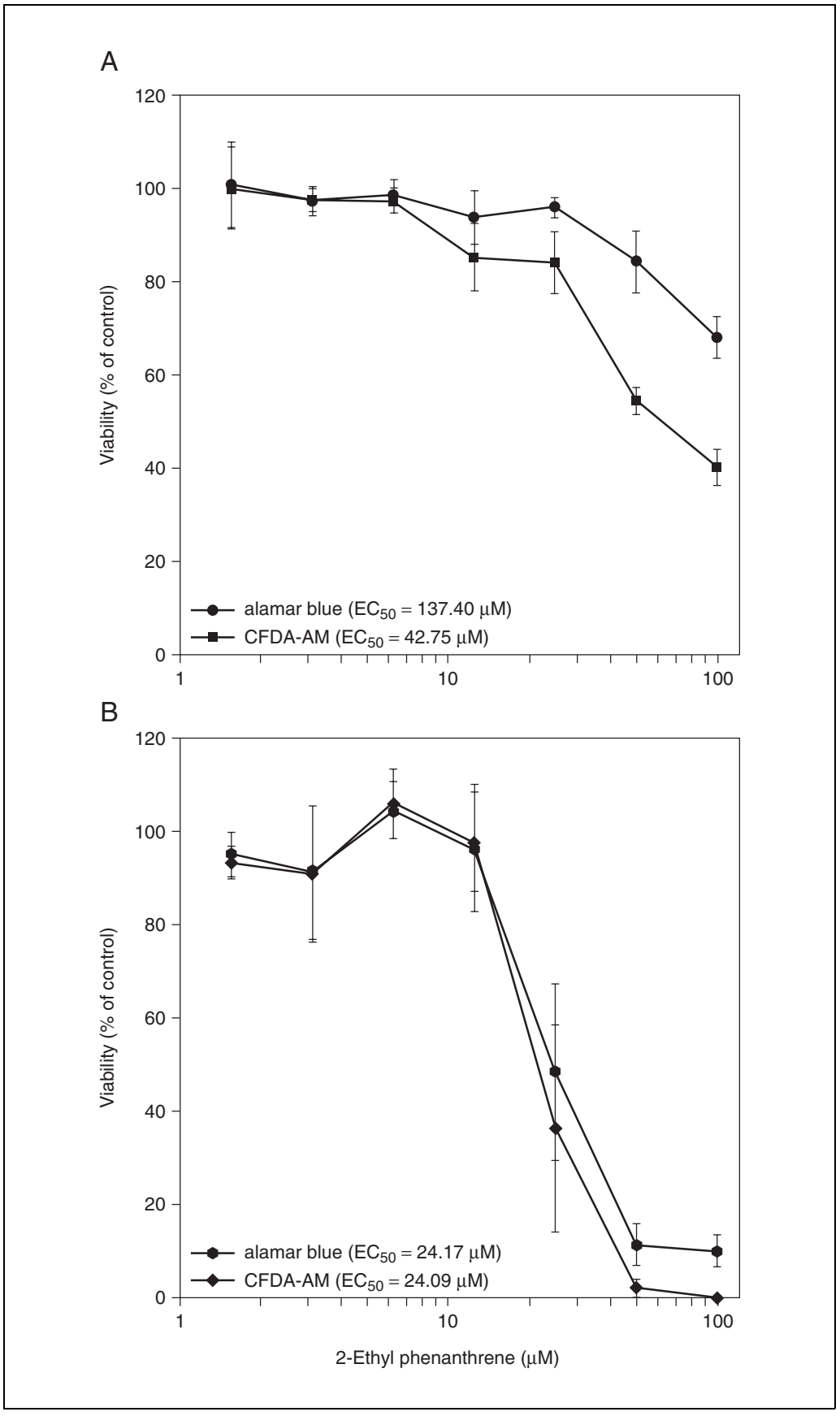
A
120
100
80
60
40
20
0
Viability (% of control)
alamar blue (EC50 = 137.40 μM)
CFDA-AM (EC50 = 42.75 μM)
1
10
100
B
120
100
80
60
40
20
0
Viability (% of control)
alamar blue (EC50 = 24.17 μM)
CFDA-AM (EC50 = 24.09 μM)
1
10
100
2-Ethyl phenanthrene (μM)

cator dyes have yet to be described. Several additional complicated scenarios will likely be revealed only by examining more compounds with these indicator dyes. For example, under some circumstances, neutral red readings might increase (Zhang et al., 1990). Overall, the methods described in this unit allow the rapid and inexpensive screening of toxicants for fish cells and at the same time give potential insight into their mechanism(s) of toxicity. In the future, understanding better the cellular function(s) being monitored with each indicator dye will improve their utility in identifying toxicity mechanisms.

Time Considerations

One must consider the time to culture the fish-derived cell lines in preparation for exposure to the toxicants. The time between subculturing of the stock culture is between 7 and 10 days if a 1 to 3 split is used routinely. Once the flask is confluent, the cells are transferred to a microwell culture plate allowing the cells to attach and become a confluent monolayer on the bottom of each well, which will take ~2 to 3 days depending on the use of 48-well or 96-well plates. The time for exposure to a toxicant can vary. Commonly, 2-hr exposures are done with toxicants that are believed to act through a necrotic process of ultra-fast cell death. Longer exposures, commonly 24- or 48-hr exposures, can be done to test toxicants that do not have a response within 2 hr. In terms of the cytotoxicity assays, all three assays can be done using one microplate. Thus, in <2 hr, results for metabolic activity, membrane function, and lysosomal activity can be assessed.

Literature Cited

Blagosklonny, M.V. 2000. Cell death beyond apoptosis. *Leukemia* 14:1502-1508.

Bols, N.C., Mosser, D.D., and Steels, G.B. 1992. Temperature studies and recent advances with fish cells in vitro. *Comp. Biochem. Physiol.* 103A:1-14.

Borenfreund, E. and Puerner, J.A. 1984. A simple quantitative procedure using monolayer cultures for cytotoxicity assays. *J. Tissue Cult. Methods* 9:7-12.

Clemons, J.H, van den Heuvel, M.R., Stegeman, J.J., Dixon, D.G., and Bols, N.C. 1994. A comparison of toxic equivalent factors for selected dioxin and furan congeners derived using fish and mammalian liver cell lines. *Can. J. Fish. Aquat. Sci.* 51:1577-1584.

Essig-Marcello, J.S., and van Buskirk, R.G. 1990. A double-label in situ cytotoxicity assay using the fluorescent probes neutral red and BCECF-AM. *In Vitro Toxicol.* 3:219-227.

Evans, S.M., Casartelli, A., Herreros, E., Minnick, D.T., Day, C., George, E., and Westmoreland, C. 2001. Development of a high throughput in vitro toxicity screen predictive of high acute in vivo toxic potential. *Toxicol. In Vitro* 15:579-584.

Flint, O.P. 1990. In vitro toxicity testing: Purpose, validation and strategy. *Altern. Lab. Anim.*18:11-18.

Haugland, R.P. 1996. Handbook of Fluorescent Probes and Research Chemicals. pp. 365-398, 549. Molecular Probes, Inc., Eugene, Oregon.

Hestermann, E.V., Stegemann, J.J., and Hahn, M.E. 2000. Serum alters the uptake and relative potencies of halogenated aromatic hydrocarbons in cell culture bioassays. *Toxicol. Sci.* 53:316-325.

Leibovitz, A. 1963. The growth and maintenance of tissue-cell cultures in free gas exchange with the atmosphere. *American J. Hygiene* 78:173-180.

O'Brien, J., Wilson, I., Orton, T., and Pognan, F. 2000. Investigation of the alamar blue (resazurin) fluorescent dye for the assessment of mammalian cell cytotoxicity. *Eur. J. Biochem.* 267:5421-5426.

O'Connor, S., McNamara, L., Swerdin, M., and Van Buskirk, R.G. 1991. Multifluorescent assays reveal mechanisms underlying cytotoxicity- phase I CFTA compounds. *In Vitro Toxicol.* 4:197-207.

O'Donnell-Tormey, J., Nathan, C.F., Lanks, K., DeBoer, C.J., and de la Harpe, J. 1987. Secretion of pyruvate. An antioxidant defense of mammalian cells. *J. Exp. Med.*165:500-514.

Oris, J.T, and Giesy, J.P. 1987. The photo-induced toxicity of polycyclic aromatic hydrocarbons to larvae of the fathead minnow (*Pimephales promelas*). *Chemosphere* 16:1395-1404.

Parkinson, C., and Agius, C. 1987. The effects of solvents on the toxicity of DDT to fish cells. *Arch. Toxicol.* Suppl. 11:240-242.

Reader, S.J., Blackwell, V., O'Hara, R., Clothier, R.H., Griffin, G., and Balls, M. 1990. Neutral red release from pre-loaded cells as an in vitro approach to testing for eye irritancy potential. *Toxicol. In Vitro* 4:264-266.

Rotman, B. and Papermaster, B.W. 1966. Membrane properties of living mammalian cells as studied by enzymatic hydrolysis of fluorogenic esters. *Proc. Natl Acad. Sci. U.S.A.* 55:134-141.

Schirmer, K., Chan, A.G.J., Greenberg, B.M., Dixon, D.G., and Bols, N.C. 1997. Methodology for demonstrating and measuring the photocytotoxicity of fluoranthene to fish cells in culture. *Toxicol. In Vitro* 11:107-119.

Schirmer, K., Greenberg, B., Dixon, D.G., and Bols, N.C. 1998a. Ability of 16 priority PAHs to be directly cytotoxic to a cell line from the rainbow trout gill. *Toxicology* 127:129-141.

Schirmer, K., Chan, A.G.J., Greenberg, B.M., Dixon, D.G., and Bols, N.C. 1998b. Ability of 16 priority PAHs to be photocytotoxic to a cell line from the rainbow trout gill. *Toxicology* 127:143-155.

Schirmer, K., Chan, A.G.J., and Bols, N.C. 2000. Transitory metabolic disruption and cytotoxicity

elicited by benzo[a]pyrene in two cell lines from rainbow trout liver. *J. Biochem. Mol. Toxicol.*14:262-276.

Schrek, R. 1965. In vitro methods for measuring viability and vitality of lymphocytes exposed to 45°, 47°C and 50°C. *Cryobiology* 3:322-328.

Segner, H., Behrens, A., Joyce, E.M., Schirmer, K., and Bols, N.C. 2000. Transient induction of 7-ethoxyresorufin-o-deethylase (EROD) activity by medium change in the rainbow trout liver cell line, RTL-W1. *Mar. Environ. Res*. 50:489-493.

Shaw, A.J. 1994. Defining cell viability and cytotoxicity. *A.T.L.A.* 22:124-126.

Yu, K.O., Fisher, J.W., Burton, G.A., and Tillitt, D.E. 1997. Carrier effects of dosing the H4IIE cells with 3,3′,4,4′-tetrachlorobiphenyl (PCB 77) in dimethyl sulfoxide or isooctane. *Chemosphere* 35:895-904.

Zhang, S.Z., Lipsky, M.M., Trump, B.F., and Hsu, I.C. 1990. Neutral red (NR) assay for cell viability and xenobiotic-induced cytotoxicity in primary cultures of human and rat hepatocytes. *Cell Biol. Toxicol*. 6:210-234.

Key References

Bols, N.C. and Lee, L.E.J. 1994. Cell lines: Availability, propagation and isolation. *In* Biochemistry and Molecular Biology of Fishes, vol. 3. (P.W. Hochachka and T.P. Mommsen, eds.) pp. 145-159. Elsevier Science, Amsterdam.

An overview of protocols for obtaining and growing fish cell lines.

Ganassin, R.C., Schirmer, K., and Bols, N.C. 2000. Cell and tissue culture. *In* The Laboratory Fish (G.K. Ostrander, ed.) pp. 631-651. Academic Press, San Diego.

Gives technical protocols for using fish cell lines in toxicology.

Babich, H. and Borenfreund, E. 1991. Cytotoxicity and genotoxicity assays with cultured fish cells: A review. *Toxicol. In Vitro* 5:91-100.

Bols, N.C., Whyte, J.J., Clemons, J.H., Tom, D.J., van den Heuvel, M.R., and Dixon, D.G. 1997. Use of liver cell lines to develop toxic equivalency factors and to derive toxic equivalent concentrations in environmental samples. *In* Ecotoxicology: Responses, Biomarkers and Risk Assessment (J.T. Zelikoff, ed.) pp. 329-350. SOS Publications, Fair Haven, NJ.

Fent, K. 2001. Fish cell lines as versatile tools in ecotoxicology: Assessment of cytotoxicity, cytochrome P4501A induction potential and estrogenic activity of chemicals and environmental samples. *Toxicol. In Vitro*15:477-488.

Segner, H. 1998. Fish cell lines as a tool in aquatic toxicology. *In* Fish Ecotoxicology (T. Braunbeck, D.E. Hinton, and B. Streit, eds.) pp. 1-38. Birkauser-Verlag, Basel.

These four articles provide a broad overview on use of fish cell lines in toxicology and ecotoxicology.

Contributed by Vivian R. Dayeh and Niels C. Bols
University of Waterloo
Waterloo, Canada

Kristin Schirmer
UFZ-Centre for Environmental Research
Leipzig, Germany

Lucy E.J. Lee
Wilfrid Laurier University
Waterloo, Canada

Sea Urchin Embryos and Larvae as Biosensors for Neurotoxicants

Functionally active neurotransmitter substances and neurotransmitter receptors are found in early embryos of all vertebrate and invertebrate species studied (reviewed in Buznikov et al., 1996, 2001a). These preneuronal neurotransmitter systems have been studied in detail in sea urchin embryos and larvae, where they play critical roles in morphogenesis. Because neurotransmitter molecules in sea urchin embryos may recapitulate the trophic functions that they exert in mammalian nervous system development, these invertebrates have been used as biosensors for many different neuroactive substances, including pharmaceutical compounds and pesticides (Buznikov, 1990; Falugi, 1993; Buznikov et al., 1997b, 1998, 2001a,b).

The normal features of sea urchin development are well characterized, as are typical developmental malformations caused by a variety of neuroactive compounds (reviewed in Buznikov, 1990; Buznikov et al., 2001b). Therefore, the developmental effects of new pharmaceutical compounds or suspected neurotoxicants can be compared with those previously observed for compounds possessing defined pharmacological, biochemical, or molecular characteristics. In addition, the developmental dynamics of responses can provide clues to the mechanisms underlying teratogenic alterations.

A major advantage of this animal model is the ability to test for developmental defects caused by neuroactive compounds in large, homogeneous populations of staged embryos or larvae (Basic Protocols 1 to 4). The uniform phenotypic response of entire populations allows for the rapid determination of dose-response characteristics of test compounds and the identification of critical periods of vulnerability (Buznikov et al., 2001b). The relative ease and low cost of carrying out these experiments are additional advantages. Basic Protocol 5 and Alternate Protocols 1 to 3 describe methods for analyzing neurotoxicants that affect the cholinergic and serotonergic neurotransmitter systems.

Sea urchins thus provide an inexpensive high-throughput system for determining developmental actions and dose-response characteristics of pharmacologic agents or environmental neurotoxicants in both applied and basic biologic contexts.

MAINTAINING AND HANDLING ADULT SEA URCHINS

BASIC PROTOCOL 1

Adult *Lytechinus variegatus* sea urchins are available from Duke University Marine Laboratory and from private suppliers. *Strongylocentrotus droebachiensis* sea urchins can be collected by trawling or using SCUBA. Both species should be maintained at 0° to 4°C during transportation. They can then be kept on their normal food (seaweed) in aquaria with continuously flowing natural sea water (NSW) or circulating and filtered artificial sea water (ASW; see recipe), which is also available commercially (e.g., Instant Ocean; Aquarium Systems), up to a salinity of 3.30% at the appropriate temperature for that species (8° to 10°C, *S. droebachiensis;* 20° to 22°C, *L. variegatus*). Calcium-free artificial sea water (CFASW; see recipe) is used for some experiments. If seaweed is unavailable, artificial food can be used (see Internet Resources).

NOTE: Adult sea urchins can start to spawn spontaneously or because of unfavorable conditions (such as a sharp increase in temperature). The spawning of a single specimen can evoke spawning of many adults in an aquarium, making the entire group unusable. The first sign of spontaneous spawning is the typical appearance of turbidity in the water of the aquarium. It is necessary to rinse all animals quickly with deionized water and to transfer them to another aquarium with fresh ASW (or filtered NSW). Washing with deionized water is also helpful after long-distance transportation of animals.

Contributed by Gennady A. Buznikov, Theodore A. Slotkin, and Jean M. Lauder

Current Protocols in Toxicology (2003) 1.6.1-1.6.24

BASIC PROTOCOL 2

HARVESTING SEA URCHIN GAMETES

Injection of 0.55 mM KCl is used both to determine sex and ripeness of gametes and to harvest gametes. KCl (~0.2 to 0.5 ml) is injected using a 1-ml syringe with a 22-G needle via the peristome wall or through one of the gonopores of an adult sea urchin. After injection, a ripe urchin will begin to release gametes (white sperm or yellowish eggs; other sea urchin species can have eggs of a different color) through the gonopores. Males releasing sperm are inverted with the aboral side (i.e., the upper or gonopores side) down over a Petri dish in order to collect dry sperm. Dry sperm are collected in microcentrifuge tubes and can be stored at 2° to 4°C for 2 to 3 days. Ripe females are inverted over a 50-ml glass beaker containing artificial sea water (ASW; see recipe) for 10 to 15 min with the gonopores contacting the ASW surface. The egg suspension is then filtered via a nylon net for cleaning and elimination of jelly coats. After filtration, eggs are washed twice in ASW and resuspended. Depending on the species, eggs should be fertilized immediately (*L. variegatus*) or the egg suspension can be stored for 12 to 24 hr at 2° to 4°C (*S. droebachiensis*). Adult animals can be returned to aquaria with adequate seaweed or other food and may become ripe again after 3 to 4 weeks. Animals that have undergone gamete collection should be kept in separate aquaria from ripe adults.

NOTE: It is possible to obtain up to 3 to 4 ml packed eggs, embryos, or larvae from one female of *L. variegatus* or up to 10 to 20 ml from *S. droebachiensis*. If a large volume of material is necessary, the eggs from several females must be combined. It is better, however, to work with fully homogenous material, using for corresponding experiments other sea urchin species such as *S. franciscanus* (North Pacific) or *Echinus esculentus* (North Atlantic), which each produce up to 50 to 100 ml of packed eggs from one female. For some experiments, *S. purpuratus* is recommended, as was used for the sea urchin genome project (Cameron et al., 2000).

BASIC PROTOCOL 3

FERTILIZING AND INCUBATING SEA URCHIN EGGS

Fertilization and the incubation of fertilized eggs should be carried out under optimal temperature conditions (as for adult animals of a given species). One drop (~20 µl) of dry sperm (see Basic Protocol 2) is diluted in 5 ml ASW and is mixed with eggs (0.1 to 0.2 ml sperm per 100 ml dense egg suspension; see Basic Protocol 2). After 1 to 2 min, the suspension is diluted 10- to 20-fold with ASW (see recipe), and after the eggs settle, the ASW is changed. This washing is repeated two to three times. Embryos are incubated in ASW with continuous gentle agitation using a Nutator (Fisher) or small electromotor (~60 rpm). The optimal density of embryos or larvae in this suspension should not exceed 10,000 to 40,000 specimens/ml. Sea urchins will develop under such conditions up to the larval stage mid-pluteus 2 (i.e., the onset of active feeding).

BASIC PROTOCOL 4

EMBRYONIC AND LARVAL DEVELOPMENT OF SEA URCHINS

Normal development of sea urchins has been described in many monographs, papers, and web sites (Harvey, 1956; Stephens, 1972; Czihak, 1975; also see Internet Resources). Here the authors present the original table of the stages of sea urchin development as published by Buznikov and Podmarev (1990), with some modifications (Table 1.6.1; Figs. 1.6.1-1.6.3). In Table 1.6.2, the authors present a schedule of development for both *S. droebachiensis* and *L. variegatus*, including a method of staging embryos in dimensionless units (first described by Dettlaff and Dettlaff, 1961). This allows direct developmental comparisons to be made across sea urchin species.

The first external sign of successful fertilization (see Basic Protocol 3) is the separation of the so-called fertilization envelope from the egg surface and the formation of the

Table 1.6.1 Brief Description of the Main Developmental Stages of Sea Urchins

Stage	Diagnostic features of stages	Images
0	Unfertilized egg; no fertilization envelope	Fig. 1.6.1A
1a	Fertilized egg; fertilization envelope formed; no hyaline layer	Fig. 1.6.1B
1b	Fertilized egg; hyaline layer formed	Fig. 1.6.1C
2a	The pronuclei are fused[a]	Fig. 1.6.1D
2b	Narrow streak; prophase of first cleavage division	
2c	Wide streak; metaphase-anaphase of first cleavage division	
3	2 cells (blastomeres)	Fig. 1.6.1E
4	4 cells (blastomeres)	Fig. 1.6.1F
5	8 cells (blastomeres)	Fig. 1.6.1G
6	16 cells (blastomeres); first asynchronous cleavage division with formation of 4 macro-, 8 meso-, and 4 micromeres	Fig. 1.6.1H
7	32 cells; micromeres are visible among other blastomeres	Fig. 1.6.1I
8	Early blastula 1 (~128-256 cells)	Fig. 1.6.2A
9	Early blastula 2; blastomeres have lost their spheroid form partly from the side of blastocoele	Fig. 1.6.2B
10	Midblastula 1; blastomeres have lost their spheroid form fully	Fig. 1.6.2C
11	Midblastula 2; the start of ciliary beating and hatching; last embryonic and first larval stage	Fig. 1.6.2D
12	Late (mesenchyme) blastula 1; blastula wall at the vegetal pole somewhat flattened; first cells of primary mesenchyme into blastocoele	Fig. 1.6.2E
13	Late (mesenchyme) blastula 2; the cluster of primary mesenchyme cells near the flattened vegetal side of the blastocoele	Fig. 1.6.2F
14	Early gastrula 1; onset of blastopore formation	Fig. 1.6.2G
15	Early gastrula 2; onset of archenteron formation	Fig. 1.6.2H
16	Mid-gastrula 1; archenteron reaches the center of blastocoele; onset of secondary mesenchymal cell formation	Fig. 1.6.2I
17	Mid-gastrula 2; archenteron reaches almost definitive size; no oral contact yet	Fig. 1.6.3A
18	Late gastrula 1; contact of archenteron with the larval wall in the region of future mouth (oral contact); first signs of bilateral symmetry	Fig. 1.6.3B
19	Late gastrula 2; bilaterally symmetric larva with flattened animal wall; appearance of 2 symmetrical spiculae of larval skeleton	Fig. 1.6.3C
20	Prism 1; larva assumes the characteristic angular form; first signs of differentiation of digestive tract	Fig. 1.6.3D
21	Prism 2; digestive tract consists of weakly delineated esophagus, stomach, and intestine; developed larval skeleton	Fig. 1.6.3E
22	Early pluteus 1; small rudiment of the first pair of arms	Fig. 1.6.3F
23	Early pluteus 2; first pair of arms and stomach enlarge	Fig. 1.6.3G
24	Early pluteus 3; small, not divided rudiment of second pair of arms appears; the color of larval suspension changes sharply because of chromatophore development	Fig. 1.6.3H
25	Midpluteus 1; the second pair of arms starts to differentiate	Fig. 1.6.3I

[a]The fusion of the male and female pronuclei (formation of diploid nucleus) is visible in the eggs with very transparent cytoplasm (*Lytechinus variegatus* or *L. pictus*, for instance). If the cytoplasm is not too transparent (*Strongylocentrotus droebachiensis, S. intermedius*) or has strong pigmentation (*S. purpuratus, Arbacia punctulata*), it is easier to determine stages 2b and 2c (see Buznikov and Podmarev, 1990).

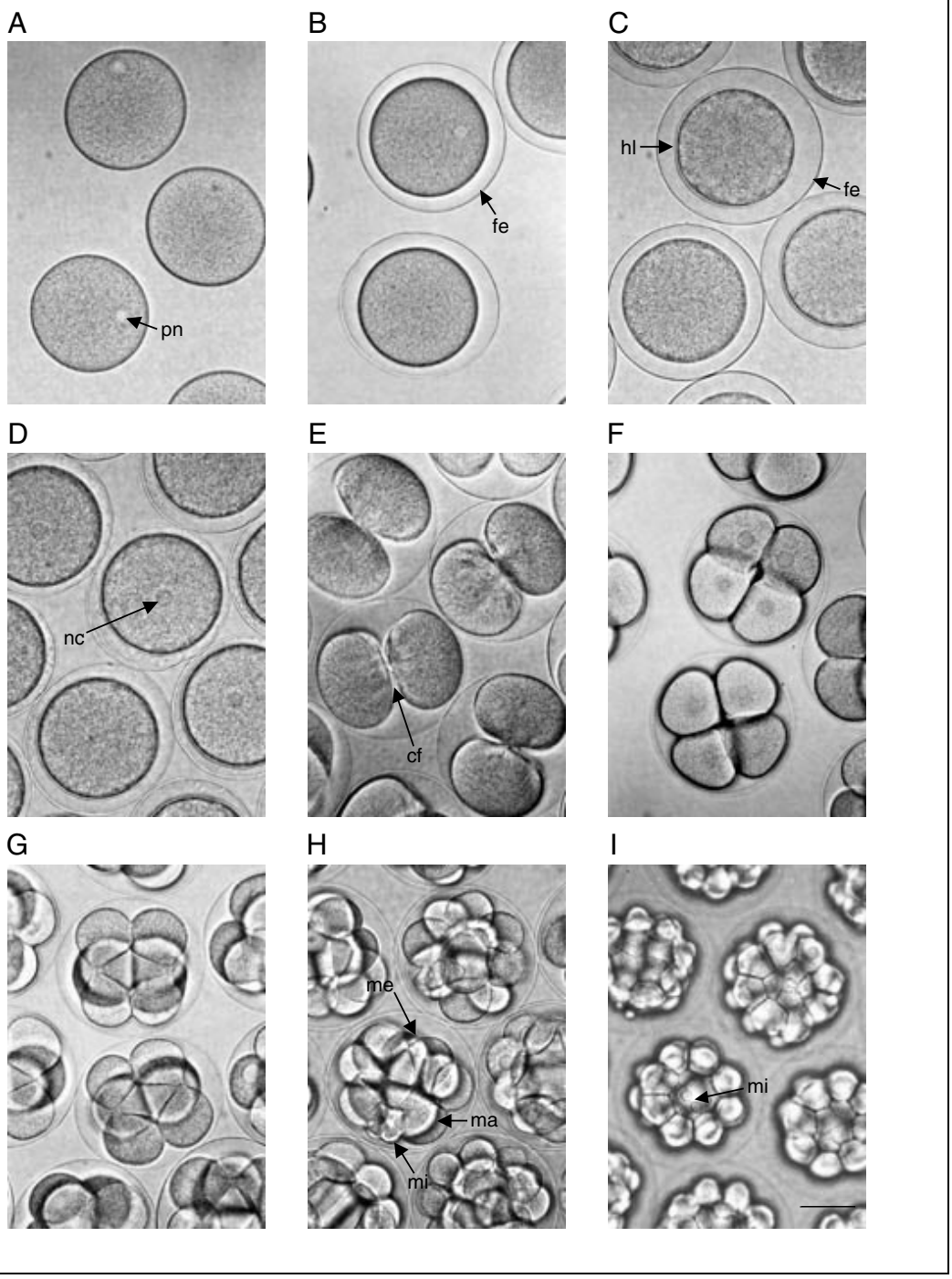

Figure 1.6.1 Developmental stages of the sea urchin *L. variegatus*: (**A**) stage 0, (**B**) stage 1a, (**C**) stage 1b, (**D**) stage 2a, (**E**) stage 3, (**F**) stage 4, (**G**) stage 5, (**H**) stage 6, and (**I**) stage 7. Abbreviations: cf, cleavage furrow; fe, fertilization envelope; hl, hyaline layer; ma, macromeres; me, mesomeres; mi, micromeres; nc, nucleus; pn, pronucleus. Scale bar, 50 μm.

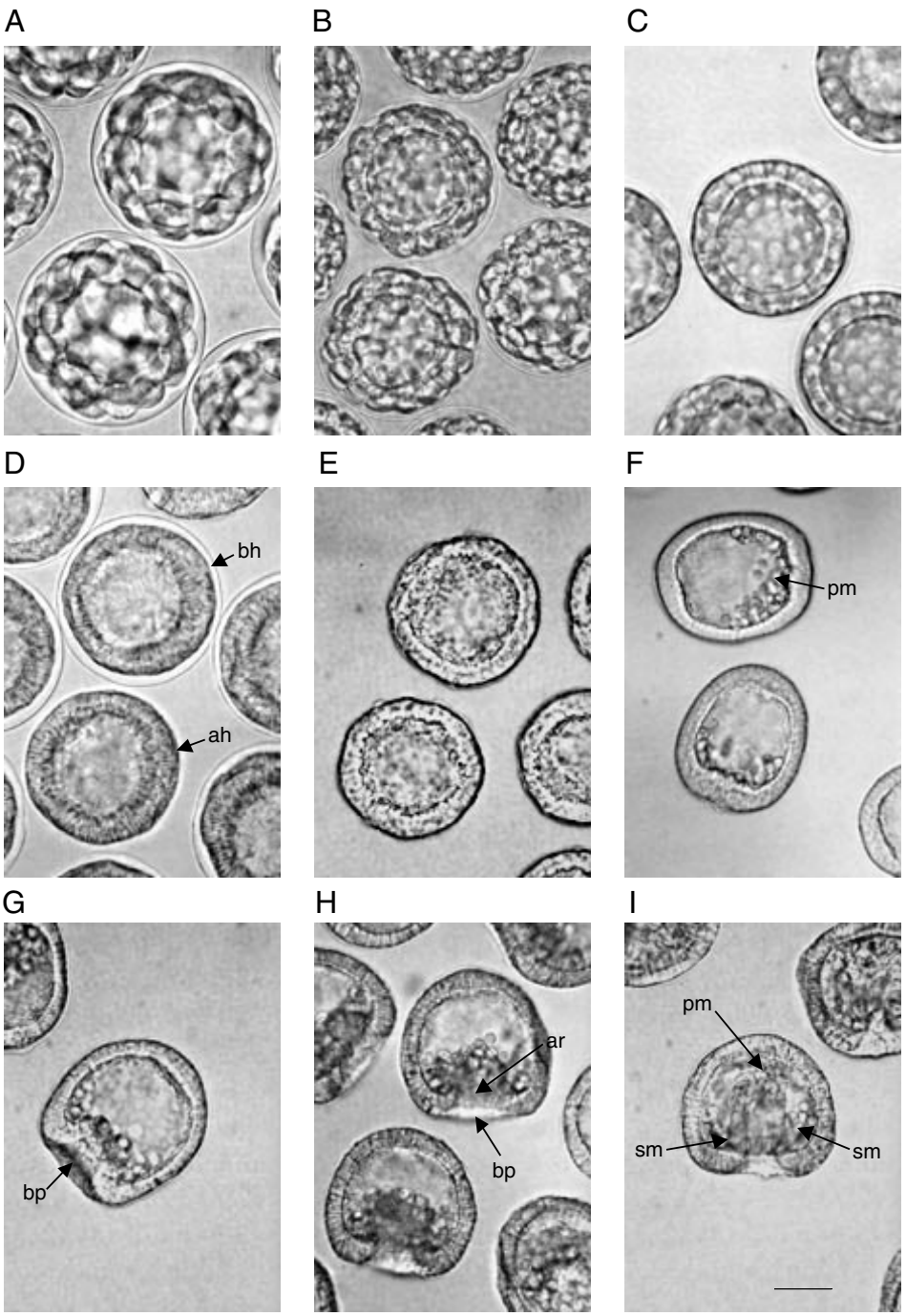

Figure 1.6.2 Developmental stages of the sea urchin *L. variegatus*: (**A**) stage 8, (**B**) stage 9, (**C**) stage 10, (**D**) stage 11, (**E**) stage 12, (**F**) stage 13, (**G**) stage 14, (**H**) stage 15, and (**I**) stage 16. Abbreviations: ah, after hatching; ar, archenteron; bh, before hatching; bp, blastopore; pm, primary mesenchyme; sm, secondary mesenchyme. Scale bar, 50 μm.

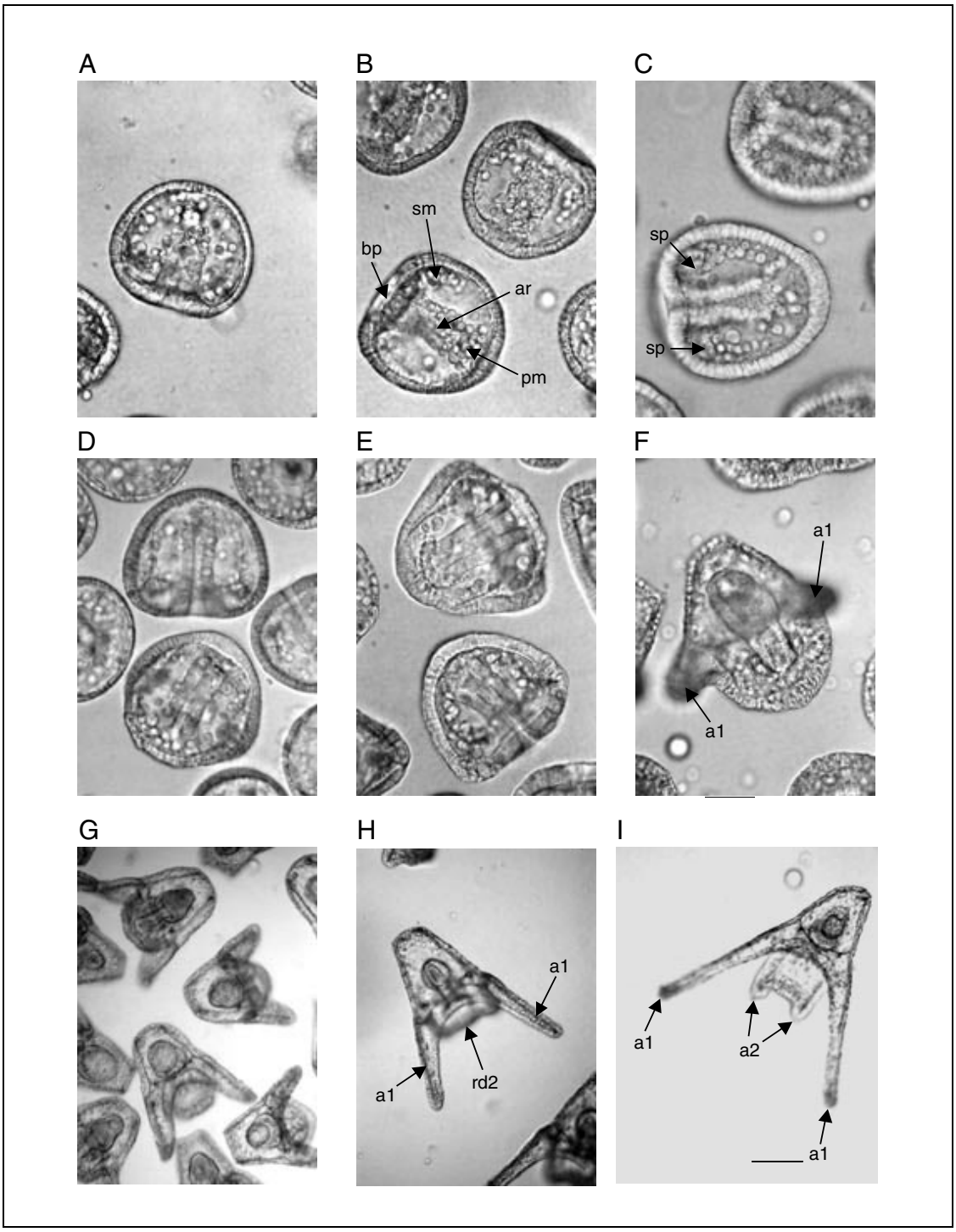

Figure 1.6.3 Developmental stages of the sea urchin *L. variegatus*: (**A**) stage 17, (**B**) stage 18, (**C**) stage 19, (**D**) stage 20, (**E**) stage 21, (**F**) stage 22, (**G**) stage 23, (**H**) stage 24, and (**I**) stage 25. Abbreviations: a1, first pair of arms; a2, second pair of arms; ar, archenteron; bp, blastopore; pm, primary mesenchyme; rd2, rudiment of second pair of arms; sm, secondary mesenchyme. Scale bars, 50 μm (A-F) and 100 μm (G-I).

Table 1.6.2 Time Schedule of Sea Urchin Development

Stage	Age (time after fertilization)			
	S. droebachiensis, 8°C		*L. variegatus*, 21°C	
	Days.hours.minutes	Dimensionless units (τ_0)[a]	Days.hours.minutes	Dimensionless units (τ_0)[a]
1a	00.00.05	NA	00.00.02	NA
1b	00.01.15	NA	00.00.15	NA
2a	ND	ND	0.00.30—00.00.40	~1.0
2b	00.01.50	0.9	ND	ND
2c	00.02.10	1.1	ND	ND
3	00.03.10	1.6	00.01.10	2.0
4	00.05.10	2.6	00.01.45	3.0
5	00.07.00	3.5	00.02.20	4.0
6	00.08.40	4.3	00.02.52	4.9
7	00.11.00	5.5	00.03.27	5.9
8	00.14.00.	7.0	00.04.06	7.0
9	00.17.40	8.8	00.05.15	9.0
10	01.00.00	12.0	00.07.00	12.0
11	01.06.00	15.0	00.09.00	15.0
12	01.11.00	17.5	00.10.16	17.6
13	01.15.00	19.5	00.11.05	19.0
14	01.21.00	22.5	00.12.43	21.8
15	02.03.30	25.75	00.14.50	25.0
16	02.12.00	30.0	00.16.28	28.2
17	02.16.00	32.0	00.17.30	30.0
18	02.19.30	33.75	00.18.40	32.00
19	03.00.00	36.0	00.19.55	34.2
20	03.04.00	38.0	00.22.57	38.2
21	03.20.00	46.0	01.01.40	44.0
22	04.00.00	48.0	01.03.25	47.0
23	04.13.00	54.5	01.07.37	54.2
24	05.00.00	60	01.11.35	61
25	07.00.00	84	02.01.00	84
26	12.00.00	144	ND	ND

[a]One dimensionless unit (τ_0; Dettlaff and Dettlaff, 1961) is equal to the duration of the second cell cycle after fertilization for a given species and temperature of incubation (in this case 2 hr 00 min for *S. droebachiensis*, 8°C and 35 min for *L.variegatus*, 21°C). NA, not applicable; ND, not determined.

perivitelline space. This process begins on the surface of the egg at the point of sperm entry and spreads over the entire surface. Separation of the fertilization envelope is completed at stage 1a (Table 1.6.2 and Fig. 1.6.1). The number of successfully fertilized eggs must be 98% to 100%. Otherwise, the original quality of the eggs or sperm, composition of the ASW, or fertilization procedure is likely to be at fault, and the batch of eggs must be discarded. Also, the percent of polyspermic eggs should not be more than 0.2% to 0.5%. Usual signs of polyspermy are formation of multinuclear, uncleaved eggs or precocious and nonregular cleavage divisions, most often with simultaneous formation of three blastomeres.

Spontaneous malformations arising immediately after the midblastula stage (i.e., before or during gastrulation) are signs of larvae that are of poor quality, ASW that has not been properly made, hypoxia, or other problems. The most common malformations are exogastrulation, total inhibition of gastrulation (with embryos remaining as blastulae, often with multilayer walls), and underdevelopment of the archenteron during gastrulation.

Dimensionless units of sea urchin development

Theoretically, embryos and larvae of all sea urchin species can be used for testing of neurochemicals. However, some species (*Arbacia lixula* and possibly *A. punctulata*) are much more sensitive than other species to certain neurotransmitter receptor antagonists (and are therefore not discussed in our protocols). All information about sea urchin development is applicable not only to *S. droebachiensis* and *L. variegatus* but also to other sea urchin species that are grown at optimal temperatures, if dimensionless units of development are calculated (Dettlaff and Dettlaff, 1961). This is done by determining the duration of the second cell cycle (cleavage division) for the optimal temperature for that species and using this value as a dimensionless (biological) unit (τ_0) for the conversion of the time schedule of development (Table 1.6.2). Using this method, the authors have found that the age of embryos and larvae from several different sea urchin species, when expressed in dimensionless units, is practically the same for a given stage of development. For example, for *S. droebachiensis* and *L. variegatus*, mid-blastula 2 stage (stage 11) occurs at 15 τ_0, early gastrula 1 stage (stage 14) occurs at 22 to 23 τ_0, and late gastrula 2 stage (stage 19) occurs at 34 to 36 τ_0.

PROTOCOLS FOR TESTING NEUROTOXICANTS

The following set of protocols uses sea urchin embryos or larvae to test the effects of various classes of neurotoxicants. They also incorporate methods for assessing potential rescue compounds.

CAUTION: All of the compounds used in these assays, but especially chlorpyrifos (cpf), nicotine, D-tubocurarine, and phorbol-12-myristate-13-acetate (PMA), are toxic and should be handled with caution. Avoid inhalation and dermal exposure. Dispose of waste materials in an appropriate approved manner.

BASIC PROTOCOL 5

Testing of Chlorpyrifos on Sea Urchin Embryos and Larvae

Chlorpyrifos (*O*,*O*-diethyl *O*-3,5,6-trichloro-2-pyridyl phosphorothioate; cpf) is one of the most widely used organophosphate pesticides. It can be an environmental pollutant because of its stability and persistence. Cpf acts as a developmental toxin in embryos and larvae of sea urchins and similarly has adverse effects on mammalian neurodevelopment (Slotkin, 1999; Buznikov et al., 2001b). Its specific actions depend on the stage of development, which corresponds to the expression of particular genes of the embryonic genome, and the consequent participation of acetylcholine as a trophic modulator. The sea urchin model system is suitable for both detailed investigations of stage-dependent actions of cpf and the isolation of its underlying mechanisms (e.g., intracellular signaling cascades), as well as the search for compounds capable of rescuing the developmental phenotype. The cpf protocol also provides a method for step-by-step testing of developmental effects of other neurochemicals and suspected environmental neurotoxicants.

Materials

Sea urchin embryos and larvae, stages 1a or 1b, 3 or 4, 10, 11, 13 (Tables 1.6.1 and 1.6.2; Figs. 1.6.1 and 1.6.2; see Basic Protocol 4)

ASW (see recipe) or commercially available artificial sea water (e.g., Instant Ocean; Aquarium Systems)

20 mM chlorpyrifos (cpf; Chem Service) in 100% (v/v) methanol, store up to 1 to 2 weeks at −20°C

Potential rescue compound, such as the polyenoic fatty acid derivatives (see recipe) dimethylaminoethyl arachidonate (AA-DMAE) and dimethylaminoethyl docosahexaenoate (DHA-DMAE), or other substance of interest

Digital imaging system, including microscope (e.g., Leica), digital color videocamera (e.g., Spot RT; Diagnostic Instruments), and computer with appropriate software

12- or 24-well tissue culture plates

1. Prepare a homogeneous suspension of ~1000 sea urchin embryos or larvae/ml ASW and determine their quality and stage of development using a digital imaging system.

   Alternatively, filtered natural sea water (NSW) can be used to prepare the suspension of embryos or larvae.

2. Place 200 or 100 µl suspension into each well of a 12- or 24-well tissue culture plate, respectively, and add ASW to a final volume of 2 or 1 ml.

   The suspension must be mixed continuously prior to plating, otherwise the final density of specimens (which should be ~100 specimens/ml) will differ between wells, and the effects of test compounds will be variable. The sensitivity of embryos or larvae to cpf, as well as to other neurotransmitter-related substances, decreases sharply when the density is too high (≥250 to 500 specimens/ml).

   For each test compound concentration to be tested, one to three wells of specimens should be prepared. Sufficient wells should also be prepared for controls (step 4).

3. Dilute 20 mM cpf in ASW to the necessary concentrations. Prepare dilutions of a potential rescue compound or other substance in ASW.

   Standard cpf concentrations are 50, 100, 200, and 400 µM. Higher or lower concentrations may be needed depending on the goals of the experiment. Useful concentrations for potential rescue compounds or other substances must be determined empirically; 200 or 400 µM is generally an appropriate starting point.

   Other substances may be used in the assay that can strengthen the effects of cpf or that may prove to have no effect.

4. Transfer 0.2 ml or 0.1 ml dilute neurotoxicant solution (with and without the potential rescue compound or other substance) to the appropriate wells of the 12- or 24-well plate, respectively. Carefully agitate the plates to distribute the neurotoxicant and incubate at the appropriate temperature.

   To reveal possible side effects, the following controls should be included: ASW with the corresponding concentration of methanol (i.e., the vehicle for cpf), ASW with the corresponding concentration of vehicle for the rescue compound, and rescue compound without cpf. If undesirable effects of the vehicles or rescue compound are found, concentrations should be adjusted and re-examined.

   L. variegatus embryos and larvae are incubated at room temperature; S. droebachiensis embryos and larvae are incubated at 8° to 10°C.

   Further shaking or agitation of the multiwell plate during the experiment is not necessary.

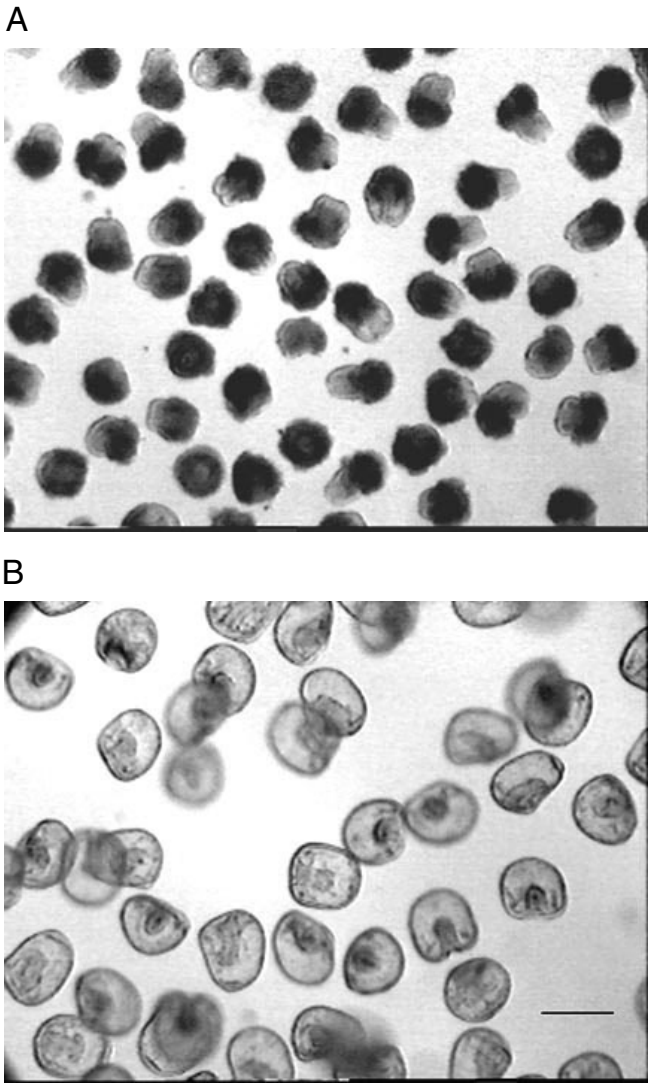

Figure 1.6.4 Effects of chlorpyrifos (cpf) introduced at stage 11 (25 hr 30 min after fertilization, 10°C or 30 hr 00 min, 8°C) on development of the sea urchin, *S. droebachiensis*. (**A**) Mushroom-like (defect III) larvae after exposure to 20 μM cpf. (**B**) Practically normal (defect 0) larvae (stage 20) after exposure to 0.5 μM cpf. They are similar to controls, but with a small retardation in development. Imaging was done 62 hr after fertilization (10°C). Scale bar, 200 μm. Modified from Buznikov et al., 2001b.

5. View and record the development of treated and control embryos and/or larvae using the digital imaging system at appropriate time intervals. Collect images until the treated embryos or larvae display maximal abnormal phenotypes or control larvae reach the mid-pluteus 1 stage.

   L. variegatus should be viewed 2 to 4 hr after the neurotoxicant has been added; S. droebachiensis should be viewed after 4 to 8 hr. Embryos and larvae should then be viewed at 2- to 4-hr intervals (or longer) until the end of the experiment.

   Each well should be imaged at low (40×) magnification; only after this should representative specimens be selected for imaging at higher magnifications (100 or 200×). Otherwise, the final results may be biased.

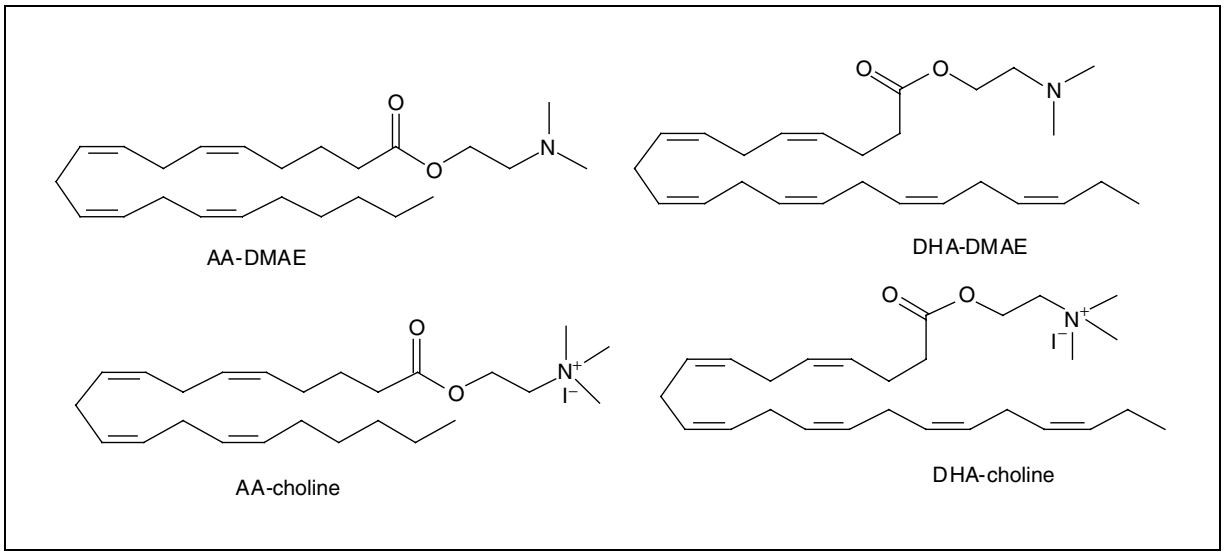

Figure 1.6.5 Structure of the choline and dimethylaminoethyl esters of polyenoic fatty acid. Abbreviations: AA-choline, arachidonoylcholine; AA-DMAE, dimethylaminoethyl arachidonate; DHA-choline, docosahexaenoylcholine; DHA-DMAE, dimethylaminoethyl docosahexaenoate.

For routine work, cpf concentrations that produce a given phenotype for 100% of treated embryos or larvae in experimental wells should be used (Fig. 1.6.5).

6. Compare images of treated and control embryos and/or larvae (Figs. 1.6.1-1.6.4; Table 1.6.1). Determine from which developmental stage cpf started to disturb development. Characterize malformations and protective actions, if any, of the rescue compound.

   The recorded images must be comparable. If it is necessary to digitize many different variants simultaneously, development can be stopped by adding a few drops of 1% (v/v) formaldehyde in ASW to the wells.

Testing of L-Nicotine on Sea Urchin Embryos and Larvae

ALTERNATE PROTOCOL 1

L-nicotine, the addictive substance in tobacco, acts as a cholinergic neurotoxicant affecting mammalian brain development (Slotkin, 1998, 1999) and similarly affects morphogenesis in sea urchin larvae (Buznikov et al., 1998, 2001c). The comparison of its action with the effects of chlorpyrifos (cpf) is interesting and demonstrates some additional peculiarities of the biosensor under consideration. This action presumably occurs through activation of nicotinic acetylcholine receptors, nAChRs (Falugi, 1993; Buznikov et al., 1997b; Ivonnet and Chambers, 1997). The sensitivity of sea urchin embryos and larvae to L-nicotine is moderate but may be enhanced or altered by manipulating intracellular signaling cascades downstream from nAChR activation, with such compounds as phorbol 12-myristate 13-acetate (PMA), a protein kinase C activator. The search for compounds capable of rescuing the developmental phenotype after L-nicotine treatment is similar to that used for cpf, although the spectrum of effects for L-nicotine is not identical for the two compounds, which probably reflects noncholinergic effects of cpf that are not shared by nicotine, a direct cholinergic agonist (Slotkin, 1998, 1999). Experiments with L-nicotine provide some additional information related to nAChRs of sea urchin embryos and larvae and, therefore, the role of preneuronal and/or non-neuronal cholinergic systems in regulating events of early development.

Additional Materials *(also see Basic Protocol 5)*

20 mM L-nicotine bitartrate in 100% (v/v) methanol, store in dark up to 1 to 2 weeks at 4°C

Potential rescue compound, such as:

20 mM D-tubocurarine chloride (Sigma), store up to 1 week at −20°C

20 mM imechine (Latoxan), store up to 1 to 2 weeks at 4°C

20 mM QX-222 (Astra Pharmaceuticals), store up to 1 to 2 weeks at 4°C

20 mM 1-(5-isoquinolinesulfonyl)-2-methylpiperazine) (H-7; Sigma), store for several days at −20°C

CFASW (see recipe)

2 mM PMA (see recipe)

1. Set up sea urchin embryos or larvae in appropriate tissue culture plates as described (see Basic Protocol 5, steps 1 and 2).

2. Dilute 20 mM L-nicotine and a potential rescue compound in CFASW or ASW. Prepare a 0.01 to 0.2 µM PMA solution (Buznikov et al., 1998) in CFASW or ASW.

   Standard L-nicotine concentrations are 500, 1000, and 2000 µM. Higher or lower concentrations may be needed depending on the goals of the experiment. Nicotine solutions should be stored in the refrigerator with aluminum foil around the bottle, because the compound is subject to oxidation that is promoted by light and heat. Useful concentrations for potential rescue compounds or other substances must be determined empirically; 200 or 400 µM is generally an appropriate starting point.

   Other substances may be used in the assay that can strengthen the effects of nicotine or that may prove to have no effect.

   Phorbol 12-myristate 13-acetate (PMA), an activator of protein kinase C, enhances and alters the developmental effects of L-nicotine. Cleaving sea urchin embryos completely or partly lose their sensitivity to L-nicotine with PMA when incubated in CFASW (Buznikov et al., 1997b, 1998).

   When CFASW is used as the incubation medium, the eggs must be fertilized in ASW, as usual, and washed with CFASW three to four times before their transfer to CFASW. Such incubation is possible during cleavage divisions and blastulation only; it disturbs later development.

3. Expose the specimens to L-nicotine (with and without PMA) and the potential rescue compound and analyze the effects as described (see Basic Protocol 5, steps 4 to 6).

   When the embryos or larvae are treated with the mixture L-nicotine in the presence of PMA, developmental malformations occur and reach a maximum very quickly. Therefore, viewing and digitization must be started earlier (1 to 2 hr after compound exposure for L. variegatus or 2 to 4 hr for S. droebachiensis) and must be carried out more often (every 1 to 2 hr up to the end of the experiment).

ALTERNATE PROTOCOL 2

Testing of Arachidonoylcholine and Docosahexaenoylcholine on Sea Urchin Embryos and Larvae

Arachidonoylcholine (AA-choline) and docosahexaenoylcholine (DHA-choline; Fig. 1.6.5) act on embryonic and larval development of sea urchins as lipophilic agonists of nAChRs (i.e., they can penetrate cells to stimulate intracellular receptors). In addition, they have a noncholinergic component of teratogenic activity that may reflect actions on intracellular signaling cascades rather than on the nAChRs themselves (Bezuglov et al., 2001).

Additional Materials *(also see Basic Protocol 5)*

Polyenoic fatty acid derivatives (see recipe), including:
Arachidonoylcholine (AA-choline)
Docosahexaenoylcholine (DHA-choline)

1. Set up sea urchin embryos or larvae in appropriate tissue culture plates as described (see Basic Protocol 5, steps 1 and 2).
2. Dilute AA-choline and DHA-choline and a potential rescue compound (e.g., AA-DMAE and DHA-DMAE) in CFASW or ASW.

   Standard AA-choline and DHA-choline concentrations are 50, 100, 200, and 400 μM. Higher or lower concentrations may be needed depending on the goals of the experiment.

   The polyenoic fatty acid derivatives dimethylaminoethyl arachidonate (AA-DMAE) and dimethylaminoethyl docosahexaenoate (DHA-DMAE) rescue the effects of AA-choline. Useful concentrations for potential rescue compounds must be determined empirically; 200 or 400 μM is generally an appropriate starting point.

   Cleaving sea urchin embryos completely or partly lose their sensitivity to AA-choline and DHA-choline when incubated in CFASW. When CFASW is used as the incubation medium, the eggs must be fertilized in ASW, as usual, and washed with CFASW three to four times before their transfer to CFASW. Such incubation is possible during cleavage divisions and blastulation only; it disturbs later development.
3. Expose the specimens to AA-choline and DHA-choline and the potential rescue compound and analyze the effects as described (see Basic Protocol 5, steps 4 to 6).

Testing of Ritanserin on Sea Urchin Embryos and Larvae

ALTERNATE PROTOCOL 3

Acetylcholine is by no means the only neurotransmitter that modulates development of sea urchin embryos and larvae. For instance, the biogenic amines (serotonin [5-HT] and catecholamines) all play critical roles in proper morphogenesis (Buznikov, 1990; Buznikov et al., 2001a). Accordingly, the sea urchin model system is suitable for testing and studying different neurochemicals, including many ligands for biogenic amine receptors (Buznikov, 1990). Ritanserin, a pan-5-HT_2 receptor antagonist, was selected for this protocol because of its ability to cause very typical and reproducible concentration-dependent malformations.

Additional Materials *(also see Basic Protocol 5)*

20 mM ritanserin (Sigma) in methanol, store up to 2 days at 20°C
20 mM serotonin hydrochloride (5-HT), store in dark up to 24 hr at 4°C
Polyenoic fatty acid derivatives (see recipe), such as the following serotonin agonists:
Serotonamide of arachidonic acid (arachidonoyl serotonin; AA-5-HT)
Serotonamide of docosahexaenoic acid (DHA-5-HT)
Serotonamide of eicosapentaenoic acid (EPA-5-HT)

1. Set up sea urchin embryos or larvae in appropriate tissue culture plates as described (see Basic Protocol 5, steps 1 and 2).
2. Dilute 20 mM ritanserin in ASW. Prepare 400-μM solutions of 5-HT and other serotonin agonists in ASW.

   Standard ritanserin concentrations are 25, 50, 100, and 200 μM. Higher or lower concentrations may be needed depending on the goals of the experiment.

   In this experiment, serotonin agonists function to rescue ritanserin's effects.
3. Expose the specimens to ritanserin (with and without serotonin agonists) and analyze the effects as described (see Basic Protocol 5, steps 4 to 6).

REAGENTS AND SOLUTIONS

Use distilled or deionized water or equivalent in all recipes and protocol steps. For common stock solutions, see ***APPENDIX 2A****; for suppliers, see* ***SUPPLIERS APPENDIX****.*

Artificial sea water (ASW)

To 0.3 to 0.4 liter H_2O add:
26.05 g NaCl (445 mM final)
5 g $MgCl_2 \cdot 6H_2O$ (24.6 mM final)
4.46 g $MgSO_4 \cdot 7H_2O$ (18.1 mM final)
0.67 g KCl (9.2 mM final)
0.198 g $NaHCO_3$ (2.36 mM final)
1.27 g $CaCl_2$ (11.5 mM final)
Add H_2O to 1 liter
Adjust pH to 7.5 with 1 N NaOH
Store indefinitely at room temperature

There are other ASW recipes, but the authors have used this composition for many years with good results. The authors use ASW for fertilization and incubation of fertilized eggs, embryos, and larvae, whereas Instant Ocean (Aquarium Systems) is routinely used to maintain adults in aquaria.

Depending on the sea urchin species that is used, the ASW should be prewarmed or precooled if necessary.

A second method for preparing ASW from stock solutions follows. Stock solutions can be stored indefinitely at room temperature. The pH adjustment and storage conditions are as described above.

Stock solutions	*For 1 liter ASW*
776 g/liter $MgCl_2 \cdot 6H_2O$	6.5 ml
446 g/liter $MgSO_4 \cdot 7H_2O$	10 ml
276 g/liter KCl	5 ml
39.7 g/liter $NaHCO_3$	5 ml
285.2 g/liter $CaCl_2$	5 ml
	26.05 g NaCl

Calcium-free artificial sea water (CFASW)

Dissolve 380.1 mg ethylene glycol bis(β-aminoethylether)-*N*,*N*,*N′*,*N′*-tetraacetic acid (EGTA) in 12.5 ml distilled or deionized water (1 mM final) and add this solution to 300 to 400 ml water. Dissolve 26.05 g NaCl (445 mM final) in this mixture. Add stock solution volumes for remaining compounds except $CaCl_2$ as described for ASW (see recipe). Add water to 1 liter. Adjust the pH to 7.5 with 1 N HCl. Store indefinitely at room temperature.

There are other CFASW recipes in which the elimination of $CaCl_2$ is compensated for by a corresponding increase in the concentration of magnesium salts.

Depending on the sea urchin species that is used, the CFASW should be prewarmed or precooled if necessary.

Phorbol 12-myristate 13-acetate (PMA), 2 mM

Add 0.81 ml dimethyl sulfoxide or 100% (v/v) ethanol to 1 mg PMA and vortex. Store protected from light up to 1 to 2 months at −20°C.

Polyenoic fatty acid derivatives

These compounds are synthesized by V.V. Bezuglov and his collaborators at the Laboratory of Oxylipins, Shemyakin-Ovchinnikov Institute of Bioorganic Chemistry, Russian Academy of Sciences (117997, Moscow, Russia) as solutions in 100% (v/v) ethanol (10, 20, or 50 mg/ml [w/v]). Store up to 1 to 2 years protected from

continued

light in ampules under argon at −20°C. If the solutions are not colorless and transparent, they are degraded. Make fresh intermediate solutions in ASW (see recipe) or CFASW (see recipe) daily. Arachidonyl serotonin (AA-5-HT) is now commercially available from Cayman Chemical.

COMMENTARY

Background Information

Sea urchin embryos and larvae can be used as cost-effective biosensors for rapid, high-throughput screening of environmental neurotoxicants and other neurodevelopmental disruptors as well as heavy metals, detergents, metabolic poisons, cytotoxic and tumorigenic compounds, and disruptors of the cytoskeleton (Dinnel et al., 1989; Buznikov et al., 1997a; Bottger and McClintock, 2001). They can be used to study the mechanisms underlying the effects of these compounds as well as critical periods of vulnerability (reviewed in Buznikov, 1990). Stage-dependent morphological malformations evoked by given doses of a test compound can be contrasted with the known effects of previously studied compounds targeting specific neurotransmitter systems, thereby providing a comparative framework for prospective identification of parallel, vulnerable pathways in the developing mammalian nervous system. The investigation of corresponding substances that provide protection or rescue from adverse effects is equally important for two reasons. First, this information can be useful to corroborate conclusions about specific mechanisms, receptors, or signaling pathways involved in the adverse developmental effects. Second, it can indicate directions for potential therapeutic interventions that might avoid adverse effects after exposure or provide guidance for strategies that can reverse the effects so as to normalize developmental parameters. In addition, identification of the effects of neurotoxicants on defined receptor or signaling targets can also be used to identify the processes underlying neurotrophic control of embryonic development, which may then be translated to study equivalent neurotrophic processes in the mammalian brain. In that way, studies in sea urchins can point the way to acquiring new information about mammalian brain development as well as its vulnerability to neurotoxicants.

Experiments with chlorpyrifos (cpf), L-nicotine, arachidonoylcholine (AA-choline), docosahexaenoylcholine (DHA-choline), and ritanserin provide good examples of studies of the effects of different neurotoxicants (including those with an environmental context) using the sea urchin model. These studies demonstrate that cpf and nicotine, when introduced immediately after fertilization, and even at high concentrations (≤200 μM), do not disturb early embryonic development (blastulation; see Anticipated Results and Fig. 1.6.7). Later, from the midblastula 1 to early gastrula 1 stages (Figs. 1.6.4, 1.6.6, and 1.6.8; stages 10 to 14 of Table 1.6.1), cpf at 1 to 40 μM or L-nicotine at 50 to 200 μM causes dose-dependent developmental malformations. In the case of cpf, many cells of different origin (up to ~90% of all embryonic cells) are apparently transformed into an abnormal phenotype and accumulate in the blastocoel. (These disruptions occur with no accompanying increase in cell proliferation.) These transformed cells are extruded from the blastocoel at the animal pole and form an extralarval cluster. In the case of L-nicotine, cells are extruded from the blastocoel at the vegetal pole (i.e., in the opposite direction; Fig. 1.6.8). It is remarkable that moderate concentrations of cpf (2.5 to 5.0 μM) do not evoke the extrusion of transformed cells but can cause outward growth of the primary gut or archenteron (known as exogastrulation) at later stages. In some cases, formation of the extralarval cluster of transformed cells is also followed by exogastrulation (i.e., the normal oriented cell movements towards the animal pole can be changed into movements in the opposite direction; Fig. 1.6.6).

The sensitivity of larvae to cpf decreases during gastrulation and the first postgastrulation stages of development. Although the late developmental dynamics of sensitivity to L-nicotine have not yet been studied, it is clear that the period of maximal sensitivity for both cpf and L-nicotine extends from the end of blastulation to the beginning of gastrulation. This period corresponds to the so-called midblastula transition (MBT) when genomic activity changes significantly (Buznikov et al., 2001b).

Lipophilic cholinergic receptor ligands (AA-choline, DHA-choline) also disturb cleavage divisions (as indicated by formation of multinuclear one-cell embryos followed by cell

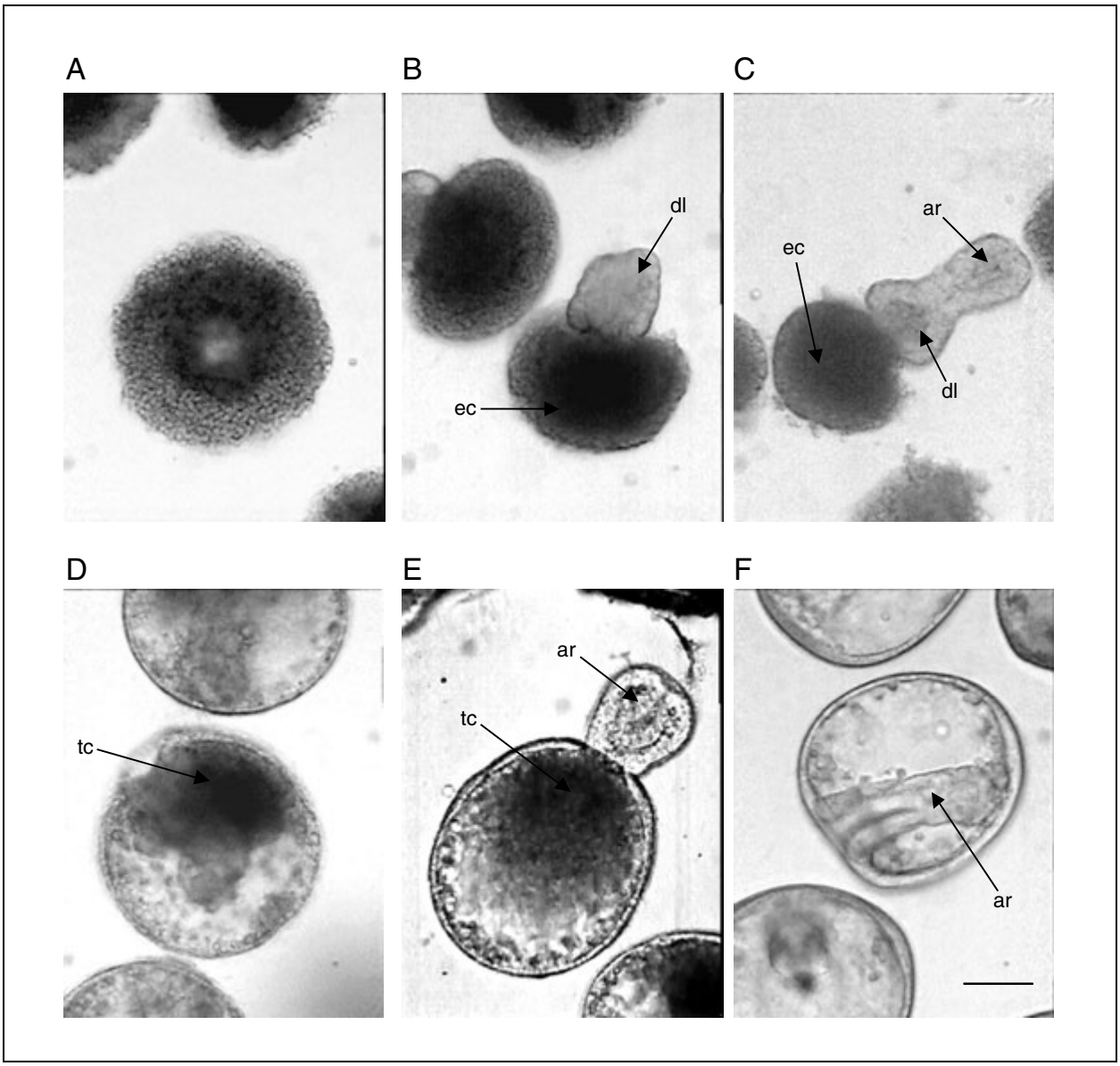

Figure 1.6.6 Effects of chlorpyrifos (cpf) introduced at stage 11 (25 hr 30 min after fertilization, 10°C) on the development of the sea urchin, *S. droebachiensis*. (**A**) Extruded, transformed (pigmented) cells cover the entire surface of larvae (defect IV) after exposure to 40 μM cpf. (**B**) Transformed cells (>50% of all larval cells) form an extralarval cluster (defect III, first phase) after exposure to 20 μM cpf. (**C**) Exogastrulation (defect II, second phase) after exposure to 40 μM cpf. (**D**) Transformed cells accumulate in the blastocoel without extruding (defect I) after exposure to 5 μM cpf. (**E**) Exogastrulation (defect I, second phase) after exposure to 5 μM cpf. (**F**) At stage 19, larvae appear normal after exposure to 40 μM cpf with 40 μM dimethylaminoethyl arachidonate (AA-DMAE). Imaging was done 62 hr after fertilization (A,B,D,F) or 10 hr later (C,E). Abbreviations: dl, dwarf larva; ec, extralarval cell cluster; tr, transformed (pigmented) cells. Scale bar, 50 μm.

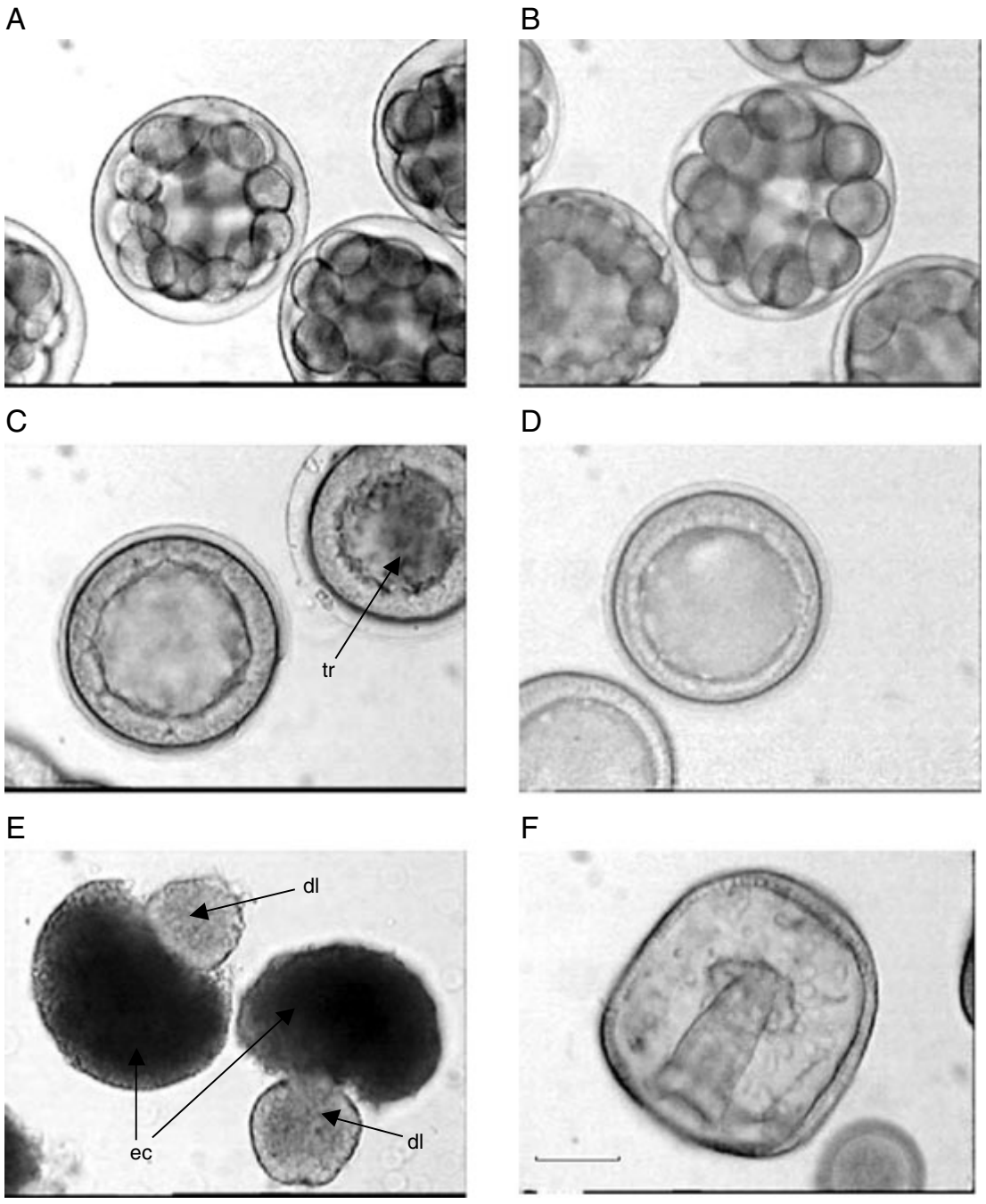

Figure 1.6.7 Effects of chlorpyrifos (cpf) introduced at stage 1b (30 min after fertilization, 10°C) on the development of the sea urchin, *S. droebachiensis*. (**A**) Exposure to 160 μM cpf. (**B**) Control stage 8 (8 hr 45 min after fertilization) specimen. (**C**) Exposure to 40 μM cpf. (**D**) Control stage 10 (22 hr 25 min after fertilization) specimen. (**E**) Mushroom-like larvae after exposure to 40 μM cpf. (**F**) Control stage 20 (64 hr 30 min after fertilization) specimen. Abbreviations: dl, dwarf larva; ec, extralarval cell cluster; tr, transformed (pigmented) cells. Scale bar, 50 μm. Modified from Buznikov et al., 2001b.

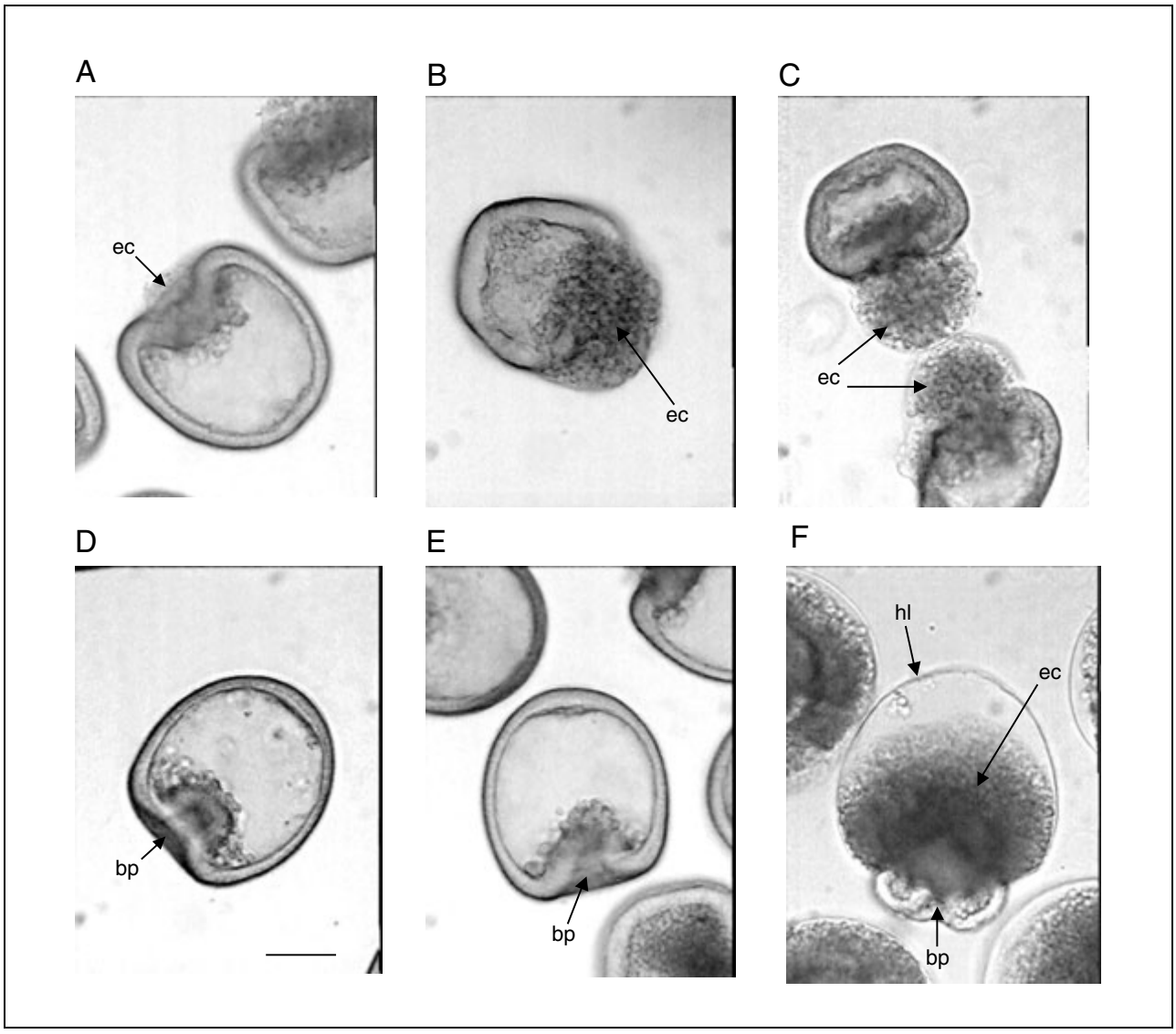

Figure 1.6.8 Effect of L-nicotine introduced at stage 12 (35 hr after fertilization, 8°C) on development of the sea urchin, *S. droebachiensis. (***A**-**C**) Development of extralarval cell cluster near the vegetal pole of larvae after exposure to 200 μM L-nicotine. Imaging was done (A) 47, (B) 51, and (C) 60 hr after fertilization. (**D**) Normal larva at stage 15 (51 hr after fertilization) after exposure to 200 μM L-nicotine and 50 μM imechine. (**E**) Nearly normal larva at stage 15 after exposure to 200 μM L-nicotine and 40 μM dimethylaminoethyl docosahexaenoate (DHA-DMAE). (**F**) Extralarval cell cluster near the animal pole of a larva 60 hr after fertilization following exposure to 50 μM L-nicotine and 0.2 μM phorbol 12-myristate 13-acetate (PMA). Abbreviations: bp, blastopore; ec, extralarval cell cluster; hl, hyaline layer (enfoliated). Scale bar, 50 μm.

lysis; Fig. 1.6.9), but, like nicotine and cpf, the period of maximal sensitivity is the MBT. When these lipophilic choline derivatives are introduced during the MBT, they, like cpf, evoke extrusion of transformed cells and formation of extralarval cell clusters at the animal pole (Fig. 1.6.9).

In keeping with the fact that it acts on a different neurotransmitter, ritanserin, an antagonist of 5-HT_2 receptors, has very different pharmacological characteristics and does not evoke extrusion of transformed cells. Instead, it causes the formation of a multilayered embryonic or larval wall (Fig. 1.6.10). The period of maximal sensitivity to ritanserin does, however, coincide with the MBT, reflecting the fact that different neuromodulators participate together in assembly of the embryo at a critical developmental period.

Developmental malformations evoked by cholinergic ligands can be prevented by antagonists of nicotinic acetylcholine receptors (nAChRs) but not by atropine, an antagonist of muscarinic cholinergic receptors. The most effective antidotes for L-nicotine are D-tubocurarine, imechine, QX-222, and some

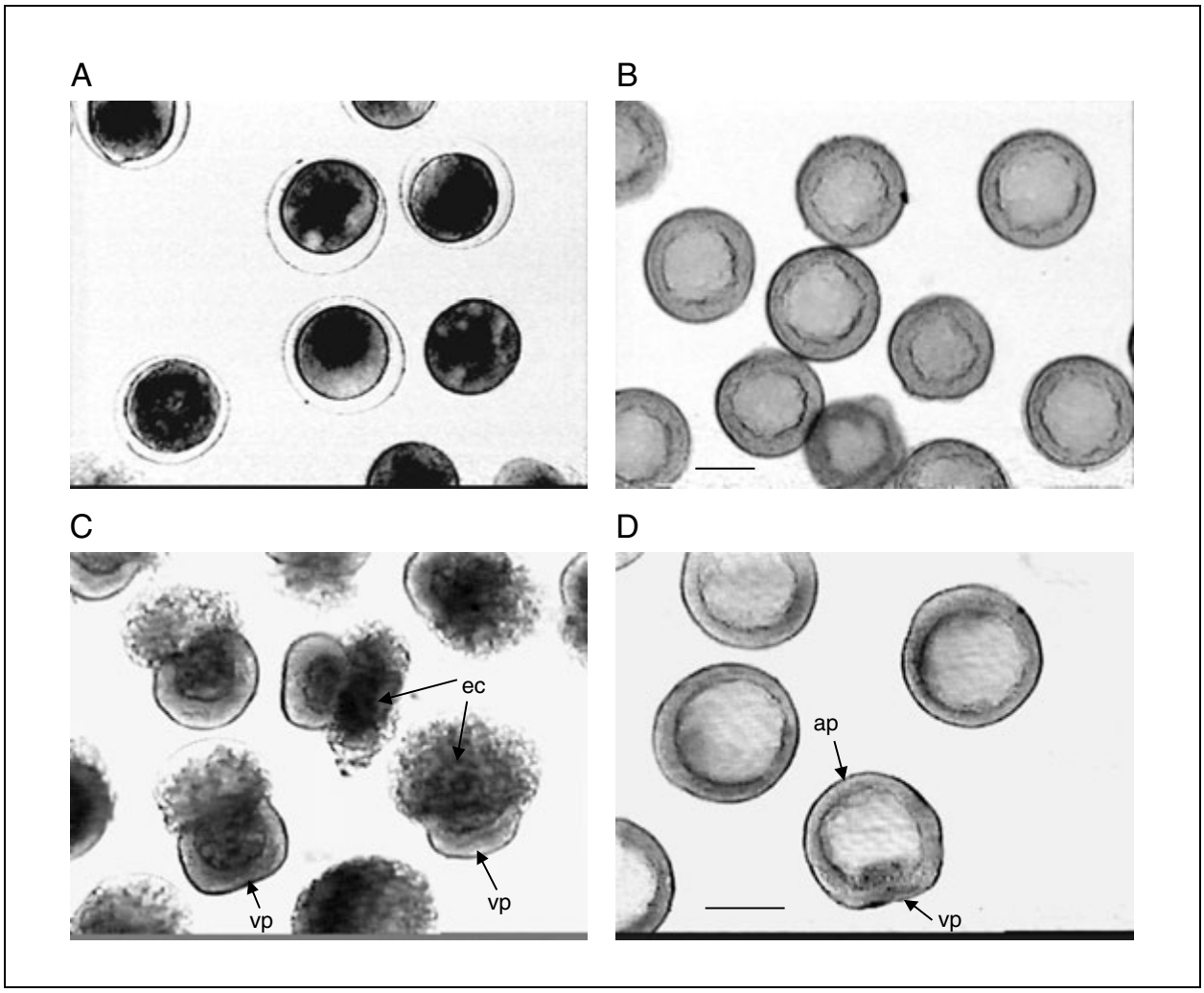

Figure 1.6.9 Effects of 40 μM arachidonoylcholine (AA-choline) on development of the sea urchin, *S. droebachiensis* and protective action of 40 μM dimethylaminoethyl arachidonate (AA-DMAE). (**A**) AA-choline produces one-cell multinuclear embryos, which are beginning to undergo cell lysis. (**B**) AA-choline with AA-DMAE produces normal hatched larvae (stage 11). (**C**) AA-choline produces typical mushroom-like larvae at later stages. (**D**) AA-choline with AA-DMAE produces normal larvae (stages 12 to 13). Substances were introduced at stage 1b (15 min after fertilization; A, B) or at stage 10 (28 hr after fertilization; C,D). Specimens were imaged 3 hr (A) or 27 hr (B) later or 40 hr after fertilization (C,D). Abbreviations: ap, animal pole; ec, extralarval cell cluster; vp, vegetal pole. Scale bars, 50 μm.

other competitive and noncompetitive drugs, especially hydrophilic (quaternary and bisquaternary) compounds. Lipophilic nAChR antagonists such as dimethylaminoethyl arachidonate (AA-DMAE) and dimethylaminoethyl docosahexaenoate (DHA-DMAE) are less effective or ineffective (Buznikov et al., 2001c). Quite the opposite situation exists for cpf and AA-choline, for which AA-DMAE or DHA-DMAE provides full protection (Fig. 1.6.9), compared with only partial or even insignificant protection by hydrophilic nAChR antagonists.

None of the cholinergic antagonists tested prevents the developmental malformations evoked by ritanserin, which acts on 5-HT_2 receptors. All rescue compounds for ritanserin are 5-HT receptor agonists, especially very lipophilic compounds such as serotonamide of arachidonic acid (AA-5-HT), serotonamide of docosahexaenoic acid (DHA-5-HT), and serotonamide of eicosapentaenoic acid (EPA-5-HT; Fig. 1.6.11), which completely rescue the ritanserin phenotype. 5-HT itself (which is hydrophilic) provides only partial protection, however, and the very hydrophilic compound *N,N,N*-trimethylserotonin iodide (5-HTQ) does not protect at all (Fig. 1.6.10). This suggests that putative intracellular 5-HT receptors (or more precisely, functional equivalents of 5-HT receptors) are the targets for all of the substances that rescue the ritanserin phenotype (and apparently for endogenous 5-HT also).

Neurotransmitter receptors ultimately affect gene expression, and hence cell replication and

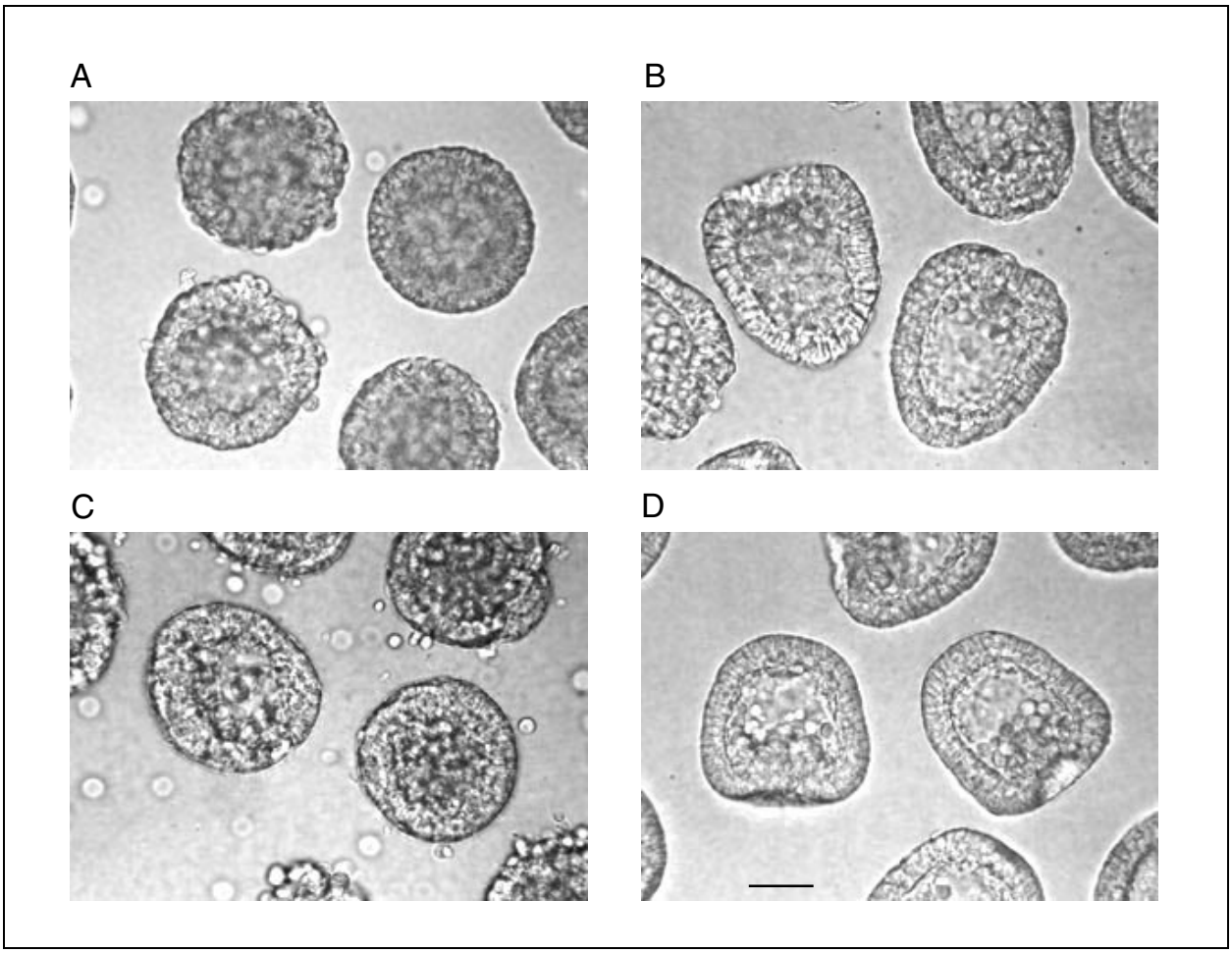

Figure 1.6.10 Effect of ritanserin introduced at stage 11 (9 hr 15 min after fertilization, 21°C) on development of the sea urchin, *L. variegatus*. (**A**) Exposure to 10 μM ritanserin produces blastulae with multilayered cell walls. (**B**) Exposure to 10 μM ritanserin with 40 μM serotonamide of arachidonic acid (AA-5-HT) produces almost normal larvae at stage 15. (**C**) Exposure to 10 μM ritanserin with 40 μM *N,N,N*-trimethylserotonin iodide (5-HTQ) provides no protection. (**D**) Control larvae, stage 15. Imaging was done 15 hr after fertilization. Scale bar, 50 μm.

differentiation, by stimulating or inhibiting the activity of intracellular signaling pathways. Phorbol 12-myristate 13-acetate (PMA; 0.01 to 0.2 μM), an activator of protein kinase C, when introduced together with L-nicotine during the MBT, enhances and alters the reaction of sea urchin larvae to nicotine. The relative number of transformed cells increases sharply, and they are extruded at the animal pole (Fig. 1.6.8) rather than the vegetal pole. In the presence of PMA, cleaving embryos become sensitive to L-nicotine (as seen by the formation of multinuclear one-cell embryos and their quick lysis). The developmental effects of L-nicotine with PMA are very similar to the those of AA-choline, not just morphologically but also pharmacologically (as shown by the complete protective action of AA-DMAE and DHA-DMAE and the incomplete or insignificant protection by D-tubocurarine, imechine, or QX-222). These malformations can be prevented or reduced by 1-(5-isoquinolinesulfonyl)-2-methylpiperazine) (H-7), whereas similar effects of cpf are potentiated by this protein kinase C inhibitor. HA-1004, an inhibitor of protein kinase A, does not affect the sensitivity to any cholinergic neurotoxicants studied. In addition, cleaving sea urchin embryos completely or partly lose their sensitivity to both L-nicotine with PMA and AA-choline when incubated in calcium-free artificial sea water (CFASW). These results provide cogent examples of how the sea urchin model can be used to dissect the intracellular events underlying the mechanisms by which neurotoxicants perturb development. The obvious next step is to pursue the parallel signaling events in the mammalian brain so as to determine if they too reflect actions on these signaling intermediates.

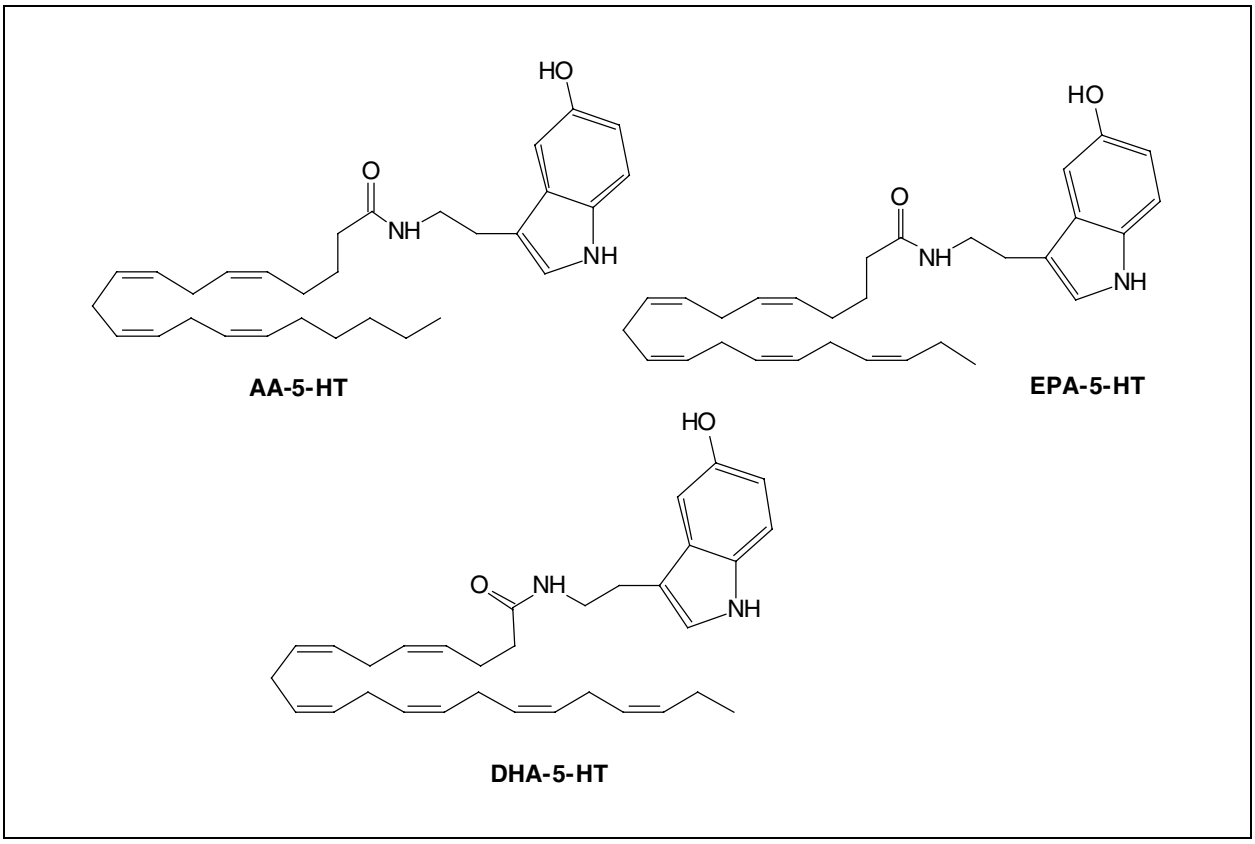

Figure 1.6.11 Structure of serotonamides of polyenoic fatty acid. Abbreviations: AA-5-HT, serotonamide of arachidonic acid; DHA-5-HT, serotonamide of docosahexanoic acid; EPA-5-HT, serotonamide of eicosapentanoic acid.

As another example of how this model helps to explore mechanisms of developmental toxicity, the authors have evaluated the effects of chlorpyrifos-oxon (a metabolite of cpf known to be the active inhibitor of cholinesterase). Unlike cpf itself, cpf-oxon does not perturb sea urchin development (Buznikov et al., 2001b). Therefore, the developmental effects of cpf are not associated with inhibition of cholinesterase activity, and the underlying cholinergic component reflects the actions of cpf itself directed towards nAChRs and their associated signaling pathways. In contrast to the ease with which these conclusions were reached with the sea urchin model, comparable mechanistic conclusions in mammalian models would require extensive evaluations of placental transfer, maternal effects, and systemic toxicity of cpf-oxon, all of which are avoided with the invertebrate model.

Based on these studies, the authors hypothesize that cpf, AA-choline, and DHA-choline have dual (cholinergic and noncholinergic) actions on sea urchin development. In other words, they can act as agonists of nAChRs coupled to L-type Ca^{2+} channels together with signal transduction cascades involving PKC and intracellular Ca^{2+}. Such actions are consistent with the dual effects of cpf on mammalian central nervous system (CNS) development (Slotkin, 1999). nAChRs located at the cell surface are already present at the one-cell stage of sea urchin development and during blastulation (Buznikov et al., 1997b, 1998; Ivonnet and Chambers, 1997); they can be available to some cholinergic ligands that evoke malformations during cleavage divisions (e.g., lipophilic cholines and L-nicotine with PMA). The typical changes in morphogenetic cell movements that occur during the MBT, however, appear to be coincident with rapid changes in expression or function of nAChRs that take place immediately prior to gastrulation. Judging by these morphological and pharmacological data, it appears that cholinergic neurotoxicants may disturb genomic regulatory signals mediated by endogenous acetylcholine during the MBT. Other regulatory signals may be mediated by endogenous 5-HT acting on 5-HT_2 receptors, which are disturbed by ritanserin (Buznikov et al., 2001a). Future studies to test this hypothesis should be very informative.

Invertebrate models such as sea urchin embryos and larvae may ultimately provide us with tools for rapid, high-throughput screening of neurotoxicants that affect mammalian brain development. They may also provide a framework for characterizing the cellular events underlying the neuroteratogenesis of a wide variety of compounds and environmental agents that converge on neurotrophic signals or their downstream signaling cascades. There are, of course, limitations to this model. The sea urchin, like culture-based models, cannot elucidate the importance of maternal-fetal pharmacokinetics and metabolism in determining the concentration of neuroteratogens that reach the fetus. Accordingly, the thresholds necessary to elicit effects in sea urchins cannot provide an absolute guide to the appropriate calculation of exposure limits for regulatory purposes, although they can be used for physiologically based pharmacokinetic models that provide a measure of exposure level of the fetal mammalian brain. On the other hand, the sensitivity of sea urchin embryos and larvae seen with the compounds used in these protocols is quite comparable to that of in vitro mammalian models, such as whole embryos, neuronal cell lines, or CNS cultures (Slotkin, 1999). The authors' results indicate the potential utility of this model system (or of similar invertebrate model systems) to screen compounds for potential neuroteratogenic activity in a comparative manner and to assist in the identification of heretofore unsuspected cellular targets underlying neuroteratogenesis.

Critical Parameters and Troubleshooting

There are three main critical parameters of experiments with sea urchin embryos. (1) The specimens in the embryo suspensions must be maintained at an optimal density. (2) The optimal temperature for the particular species must be constantly maintained. (3) The eggs, embryos, and larvae must be protected from mechanical injuries, evaporation of water from wells of culture plates, and direct bright light. These are the main reasons that embryos or larvae are of an unsatisfactory quality. Sometimes specimens develop relatively normally up to the beginning of gastrulation, but then their subsequent development can be disturbed. If the relative number of abnormal larvae is 5% to 10% or more in controls, then the experiment needs to be aborted. It is then necessary to assess which conditions (e.g., transportation and maintenance of adult sea urchins) contributed to the disturbances.

Developmental dynamics are one of the main peculiarities of developing embryos as biosensors. Some neurotoxicants tested on sea urchin embryos inhibit, disturb, or block cleavage divisions, whereas others start to evoke developmental malformations at the midblastula stage or later. It is possible to determine the critical periods of vulnerability for different neurotoxicants and to use this information for subsequent analysis of results. Therefore, the timing of experiments is a critical parameter that is worth special attention.

Anticipated Results

Cpf (40 μM or greater) added at stages 10 to 12 should evoke the maximal effect (Buznikov et al., 2001b; defect IV), where ~90% of embryonic or larval cells are transformed, extruded from the blastocoel at the animal pole, and are observed to cover the surface of the larvae (Fig. 1.6.6A). Lower cpf concentrations (20 to 30 μM) should produce an effect that is strong but less than maximal (defect III), where 50% to 75% of all extruded embryonic or larval cells form a mushroom-like cap (Fig. 1.6.6B). Defects III and IV are incompatible with further development. Cpf at 10 to 15 μM should produce a moderate effect (defect II), where the extralarval cap includes ~20% to 40% of larval cells (Fig. 1.6.6C) and can be lost, resulting in dwarf larvae that are motile but incapable of further normal development. Defect II is often accompanied by exogastrulation. Cpf at 2.5 to 5 μM should evoke the accumulation of transformed cells in the vegetal half of the blastocoel followed by exogastrulation, but not the extrusion of transformed cells (Fig. 1.6.6D,E and Buznikov et al., 2001b; defect I). These exogastrulated larvae can develop as far as stages 20 to 22. Cpf at 0.5 to 1 μM should not disturb development up to at least stage 25 (Fig. 1.6.4). If cpf is introduced at the one-cell stage or during the first cleavage divisions, embryos should develop quite normally up to stage 10 to 11. In this case, typical developmental malformations may become noticeable when control larvae begin gastrulation (Fig. 1.6.7).

AA-choline and DHA-choline (10 to 40 μM) or L-nicotine (25 to 100 μM) with PMA (0.05 to 0.2 μM) added at the one-cell stage evoke the formation of multinuclear embryos followed by rapid cell lysis (Fig. 1.6.9). If the embryos are incubated in CFASW, they are

more or less insensitive to these effects. The same substances added at stages 10 to 12 should evoke malformations (Fig. 1.6.8) very similar to those caused by cpf. In the case of choline derivatives, the dependence of developmental malformations on the concentration of ligand is clear: 20 to 40 μM AA-choline or DHA-choline produces maximal effects, whereas 2.5 to 5 μM are near-threshold concentrations.

All developmental malformations described above can be fully prevented by lipophilic cholinergic compounds (e.g., 40 μM AA-DMAE or DHA-DMAE) introduced simultaneously with cpf or 1 to 2 hr earlier (Fig. 1.6.6F). Nonlipophilic cholinergic compounds such as D-tubocurarine, imechine, or QX-222, however, only partially protect against cpf.

L-nicotine alone (50 to 100 μM and even 200 μM) should not disturb the cleavage divisions but evokes the extrusion of cells near the vegetal pole of larvae during gastrulation (Fig. 1.6.8). This effect is prevented by different nonlipophilic nAChR antagonists (D-tubocurarine, imechine, QX-222) but not by atropine; the protective action of lipophilic cholines is incomplete or even insignificant.

Ritanserin (2.5 to 10 μM), added during the MBT, blocks gastrulation and evokes the formation of additional cell layers in the larval wall. AA-5-HT, DHA-5-HT, or EPA-5-HT used in equimolar or higher concentrations completely prevents this typical malformation, whereas the protective action of 5-HT is incomplete but observable. 5-HTQ provides no protection against ritanserin.

Time Considerations

If cpf, lipophilic choline, or ritanserin are introduced at stage 10 (24 hr after fertilization for *S. droebachiensis*, 8°C or 7 hr after fertilization for *L. variegatus*, 21°C), anomalies become evident by 20 hr or 5 to 6 hr later, respectively, with maximal effects occurring after the next 8 to 10 hr (*S. droebachiensis*) or 2 to 3 hr (*L. variegatus*).

Literature Cited

Bezuglov, V.V., Zinchenko, G.N., Nikitina, L.A., and Buznikov, G.A. 2001. Arachidonoylcholine and *N*,*N*-dimethylaminoethyl arachidonate are new cholinergic compounds. *Bioorg. Khim.* 27:227-230.

Bottger, S.A. and McClintock, J.B. 2001. The effects of organic and inorganic phosphates on fertilization and early development in the sea urchin *Lytechinus variegatus* (Echinodermata: Echinoidea). *Comp. Biochem. Physiol. C Toxicol. Pharmacol.* 129:307-315.

Buznikov, G.A. 1990. Neurotransmitters in Embryogenesis. Harwood Academic Publishers, Chur, Switzerland.

Buznikov, G.A. and Podmarev, V.I. 1990. The sea urchins *Strongylocentrotus droebachiensis, S. nudus*, and *S. intermedius*. *In* Animal Species for Developmental Studies, Vol. 1. Invertebrates (T.A. Dettlaff and S.G. Vassetzky, eds.) pp. 253-285. Plenum, New York and London.

Buznikov, G.A., Shmukler, Y.B., and Lauder, J.M. 1996. From oocyte to neuron: Do neurotransmitters function in the same way throughout development? *Cell. Mol. Neurobiol.* 16:533-559.

Buznikov, G.A., Jokanovic, M., Kovacevic, N., and Rakic, L.J. 1997a. Sea urchin embryos and larvae as biosensors for screening and detailed study of pharmacologically active substances. *Arch. Toxicol. Kinet. Xenobiot. Metab.* 5:393-400.

Buznikov, G.A., Koikov, L.N., Shmukler, Y.B., and Whitaker, M.J. 1997b. Nicotine antagonists (piperidines and quinuclidines) reduce the susceptibility of early sea urchin embryos to agents evoking calcium shock. *Gen. Pharmacol.* 29:49-53.

Buznikov, G.A., Marshak, T.L., Malchenko, L.A., Nikitina, L.A., Shmukler, Y.B., Buznikov, A.G., Rakic, L.J., and Whitaker, M.J. 1998. Serotonin and acetylcholine modulate the sensitivity of early sea urchin embryos to protein kinase C activators. *Comp. Biochem. Physiol. A* 120:457-462.

Buznikov, G.A., Lambert H.W., and Lauder, J.M. 2001a. Serotonin and serotonin-like substances as regulators of early embryogenesis and morphogenesis. *Cell Tissue Res.* 305:177-186.

Buznikov, G.A., Nikitina, L.A., Bezuglov, V.V., Lauder, J.M., Padilla, S., and Slotkin, T.A. 2001b. An invertebrate model of the developmental neurotoxicity of insecticides: Effects of chlorpyrifos and dieldrin in sea urchin embryos and larvae. *Environ. Health Persp.* 109:651-661.

Buznikov, G.A., Bezuglov, V.V., Nikitina, L.A., Slotkin, T.A., and Lauder, J.M. 2001c. Cholinergic regulation of sea urchin embryonic and larval development. *Ross. Fiziol. Zh. Im. I. M. Sechenova* 87:1548-1556.

Cameron, R.A., Mahairas, G., Rast, J.P., Martinez, P., Biondi, T.R., Swartzell, S., Wallace, J.C., Poutska, A.J., Livingston, B.T., Wray, G.A., Ettensohn, C.A., Lehrach, H., Britten, R.J., Davidson, E.H., and Hood, L. 2000. A sea urchin genome project: Sequence scan, virtual map, and additional resources. *Proc. Natl. Acad. Sci. U.S.A.* 97:9514-9518.

Czihak, G. (ed.) 1975. The Sea Urchin Embryo: Biochemistry and Morphogenesis. Springer, New York.

Dettlaff, T.A. and Dettlaff, A.A. 1961. On relative dimensionless characteristics of development duration in embryology. *Arch. Biol.* 72:1-16.

Dinnel, P.A., Link, J.M., Stober, Q.J., Letourneau, M.W., and Roberts, W.F. 1989. Comparative sen-

sitivity of sea urchin sperm bioassay to metals and pesticides. *Arch. Environ. Contam. Toxicol.* 18:748-755.

Falugi, C. 1993. Localization and possible role of molecules associated with the cholinergic system during "non-nervous" developmental events. *Eur. J. Histochem*. 37:287-294.

Harvey, E.B. 1956. The American Arbacia and Other Sea Urchins. Princeton University Press, Princeton, N.J.

Ivonnet, P.I. and Chambers, P.L., 1997. Nicotinic acetylcholine receptors of neuronal type occur in plasma membrane of sea urchin eggs. *Zygote* 5:277-287.

Slotkin, T.A. 1998. Fetal nicotine or cocaine exposure: Which one is worse? *J. Pharmacol. Exp. Ther.* 285:931-945.

Slotkin, T.A. 1999. Developmental cholinotoxicants: Nicotine and chlorpyrifos. *Environ. Health Persp.* 10(Suppl. 1):71-80.

Stephens, R.E. 1972. Studies on the development of the sea urchin *Strongylocentrotus droebachiensis*. I. Ecology and normal development. *Biol. Bull.* 142:132-144.

Internet Resources

http://www.stanford.edu/group/Urchin

Describes all procedures related to maintaining adult sea urchins and obtaining and handling sea urchin embryos and larvae.

Contributed by Gennady A. Buznikov
N.K. Koltzov Institute of Developmental Biology
Moscow, Russia

Theodore A. Slotkin
Duke University Medical Center
Durham, North Carolina

Jean M. Lauder
University of North Carolina School of Medicine
Chapel Hill, North Carolina

Zebrafish: An Animal Model for Toxicological Studies

During the last century, teleosts (bony fish) have been widely used as sentinels for assessing environmental hazards including aquatic pollutants. Species used for assessing environmental toxicity include small fish such as fathead minnow, medaka, and zebrafish, as well as large fish such as trout, salmon, and catfish. The underlying biology of environmental toxicity in teleosts has been extensively studied and well described. Molecular biology and genetics have recently been used to elucidate the underlying mechanisms of toxicity in zebrafish and medaka and to predict effects in mammals. The versatile zebrafish is now incorporated in biopharmaceutical programs for elucidating human disease and for preclinical drug discovery and screening.

ZEBRAFISH AS AN ANIMAL MODEL

Zebrafish (*Danio rerio*), a member of the Cyprinidae family, originate in South Asia. Zebrafish prefer warm water, but they thrive in many environments. Zebrafish have been used as a model organism for biological research since the 1930s. The zebrafish embryo has been extensively studied and described (Kimmel et al., 1995) since then and has become a popular model for developmental biology, toxicology, and recently for drug discovery (Peterson et al., 2000; Parng et al., 2002a). In addition, embryogenesis has been investigated using several large-scale genetic screens (Driever et al., 1996; Haffter et al., 1996). The model is now well established in many areas of biological research.

Zebrafish are easy to breed and inexpensive to maintain. Adult fish grow to 4 to 5 cm long, and reach sexual maturity in 3 to 4 months. In addition, each female can lay 200 to 300 eggs per week. Zebrafish embryos develop rapidly; embryogenesis is complete five days after fertilization. Because the embryo is transparent, morphological structures and internal organs, including brain, eyes, heart, liver, and kidney can be easily visualized using light microscopy, without the need for surgery. Organ-specific and overall developmental toxicity can be assessed visually or quantified using dyes. Enzyme induction and gene expression can also be easily monitored. In addition, many intracellular biomarkers, such as glutathione, reactive oxygen species, and protein and DNA-adduct formation can be studied in the whole animal.

Because of its small size, a single embryo can be maintained in fluid volumes as small as 100 µl for the first six days of development and can be raised in individual wells of microtiter plates. Zebrafish embryos are remarkably permeable. Small molecules added directly to the fish water easily diffuse into the embryos, simplifying drug dispensing and assay processing (Peterson et al., 2000; Parng et al., 2002a). Large or lipophilic molecules can be injected into several hundred embryos in one hour. Because the embryo develops rapidly, compound screening can be completed in a few days. These features make the zebrafish a unique vertebrate model for high-throughput chemical screening, which is useful for preclinical drug discovery and toxicological evaluation (Fishman, 2001; Table 1.7.1).

ZEBRAFISH DEVELOPMENTAL AND GENETIC STUDIES

Developmental and genetic studies using whole animals have typically been performed with invertebrates, including fruit fly and nematode. However, these animal models are not closely related to humans and lack many vertebrate organs, hence their use for predicting human toxicity is limited. Zebrafish are more closely related to humans and share many biological traits, genes, developmental processes, anatomy, physiology, and behavior.

The size of the zebrafish genome is ~50% of the mouse genome (Matthews, 2001). In addition, there is extensive synteny between zebrafish and mammalian genomes, and zebrafish genes are ~75% homologous to human genes on average (Barbazuk et al., 2000). Zebrafish orthologs for some genes that are known to play key roles in human diseases have been identified, and results from large-scale mutant screens have demonstrated that mutations in some of these zebrafish orthologs display phenotypes similar to those present in human diseases (Dooley and Zon, 2000; Ward and Lieschke, 2002).

Developmental Stages

Compared with other vertebrates, the embryonic development of zebrafish is rapid. Cell

Contributed by Chaojie Zhang, Catherine Willett, and Trisha Fremgen
Current Protocols in Toxicology (2003) 1.7.1-1.7.18

Table 1.7.1 Zebrafish as an Animal Model for Toxicity

Advantages	Disadvantages
Ease of maintenance	Use for toxicity testing not standardized by regulatory agencies in the U.S.
Large number of offspring: ~200 eggs per female every two weeks	Physiology less well characterized than mammals
Rapid embryogenesis (6 days)	
Rapid generation cycle (2–3 months)	
Well characterized developmental stages	
Transparent embryo: internal organs can be visualized during embryogenesis	
Embryos are permeable to small molecules, and large or lipophilic molecules can be microinjected	
Embryos can be directly used to monitor water, soil, and waste water samples	
Small test sample size required per animal	
Genetics are well studied with many mutants available and easy to generate	
Genomic sequence is nearly complete with many genes cloned	
Transgenic reporter and disease lines available and easy to generate	
Methods and guidelines for toxicity studies established in Europe	

division begins shortly after fertilization, and by 6 hr post fertilization (hpf) gastrulation has begun (Fig. 1.7.1). The body plan is established within the first 20 hpf; by 24 hpf the heart is beating and there is a rudimentary circulatory loop (Stainier and Fishman, 1994). Hatching from the chorion occurs at ~72 hpf, and the hatching rate is usually >80% (Creaser, 1934; Hisaoka and Firlit, 1960). By 96 hpf, the animal can swim and eat, although it still receives nourishment from the yolk. The majority of zebrafish morphogenesis is completed during this time; a marker for this stage is protrusion of the lower jaw and inflation of the swim bladder. By 120 hpf (5 days), all the internal organs, including heart, liver, kidney, and pancreas are fully developed and functioning. The stages of early development have been carefully described, and these stages are considered the standard for developmental biologists (Kimmel et al., 1990). The staging described by Kimmel was performed at 28°C, and this temperature is consistently used in developmental studies; however, much of the toxicity literature describes experiments performed at 26°C. Since development of the exothermic zebrafish embryo is affected by small changes in temperature, it is important to consider experimental temperature when comparing results.

Mutagenic Screens

In the late 1970s, George Streisinger at the University of Oregon recognized that zebrafish embryos have many advantages that make them superior to *C. elegans* and *Drosophila* for developmental and genetic studies (Streisinger et al., 1981). Dr. Streisinger used X rays to generate chromosomal abnormalities and developed a technique for producing homozygous diploid fish that made it possible to detect rare recessive mutations and to produce large clones of genetically identical fish. Streisinger's colleagues at the University of Oregon continued to lay the foundations for establishing zebrafish as a model for developmental genetics. Normal development has been described in considerable detail, and a number of mutations that affect embryogenesis have been described (Kimmel et al., 1995).

In the late 1980s, based on the work performed by Streisinger and his colleagues, several developmental biologists recognized that zebrafish would be an extremely useful verte-

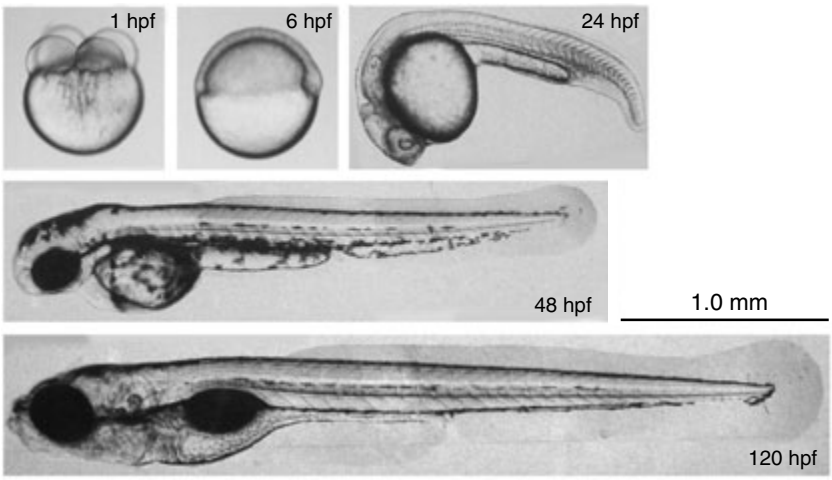

Figure 1.7.1 Zebrafish development occurs rapidly. By 1 hpf (top left), two cell divisions have occurred. Gastrulation begins at 6 hpf (top center). By 24 hpf (top right), the organ primordia have been laid down and the brain has significantly developed. The heart is beating and a rudimentary circulatory loop through the main body axis has been established. By 48 hpf (middle panel), pigment has begun to form; the body axis has elongated. By 120 hpf (bottom panel), organ morphogenesis is complete and most organs are functioning. The swim bladder has inflated and the embryo can swim and eat on its own. At this point the embryo is considered a larva.

brate for extensive genetic studies. Beginning in 1992, large-scale screens for mutations affecting embryonic development were conducted by Nüsslein-Volhard's and Driever's groups in Germany and Boston, respectively (Driever et al., 1996; Haffter et al., 1996). These experiments resulted in the identification and characterization of a large number of mutants affecting many aspects of embryonic development, and the results were jointly published in a dedicated volume of *Development* (1996, vol. 123). Since then, cell lineage, embryonic axis formation, nervous system development, heart and muscle formation, and differential regulation of gene expression have been extensively studied at various stages of development in wild-type and mutant embryos (Stainier et al., 1993; Driever et al., 1994; Lee et al., 1994; Mullins et al., 1994; Strahle and Blader, 1994; Driever, 1995; Solnica-Krezel et al., 1995; Wilson et al., 1995; Lele and Krone, 1996).

Many mutated genes have been cloned, which was an arduous process since chemical mutagenesis used in the screens typically results in point mutations (Talbot and Schier, 1999). Several cloned genes are orthologs of mammalian genes and these mutations result in similar phenotypes as those in humans. Thus, zebrafish is potentially a predictive model for human disease (Dooley and Zon, 2000; Ward and Lieschke, 2002).

In the mid-1990's, a genetic screen was performed by insertional mutagenesis (Golling et al., 2002). Since this mutagenic process is laborious compared to chemical mutagenesis, this screen yielded fewer mutants, but the mutated genes are tagged by insertions so they can be easily cloned. Several mutants were found in known genes, and several novel genes were identified (Golling et al., 2002). At least one of the mutants resembles a mutation that causes kidney disease in humans (Sun and Hopkins, 2001). Ongoing research into the development and genetics of zebrafish will further strengthen the utility of zebrafish as a model organism for biological studies, including toxicity.

Gene Inactivation by RNA Interference

Gene replacements and targeted deletions are not yet feasible in zebrafish; however, it is possible to remove a specific gene product by interfering with translation, a method called RNA interference (RNAi). In zebrafish, a type of RNAi using synthesized oligomers called morpholinos has been successfully used to knockdown expression of a number of genes (Nasevicius and Ekker, 2000; and references in *Genesis*, 2001, 30:89-200). RNAi knockdown can be used to: (1) identify the function of novel genes, (2) identify possible candidate genes when cloning a gene by position, or (3) inves-

tigate whether a gene cloned by homology is a functional ortholog of a mammalian gene.

Transgenic Reporter Lines

Transgenic fish are a powerful tool for studying gene regulation and expression, disease mechanisms and progression, and drug efficacy and toxicity. Transgenic lines can be created that express a visible marker, such as green fluorescent protein (GFP), under the regulation of specific promoters. These lines can serve as reporters to detect changes in expression of the marked gene and can serve as sentinels to detect the presence of bioactive compounds. The procedure for generating transgenic zebrafish is well established (Stuart et al., 1988, 1990; Westerfield et al., 1992; Lin et al., 1994). The use of live reporter gene markers such as GFP simplifies the screening for progeny that carry the transgene. Recently, high germline transmission rates (nearly 50%) were achieved by attaching DNA to nuclear localization signal peptides or by coinjecting I-*Sce*I meganuclease (Liang et al., 2000; Thermes et al., 2002).

Transgenic lines using organ-specific promoters expressing GFP have been created for vessels, kidney, blood, central nervous system, and lymphocytes (Jessen et al., 1999; Goldman et al., 2001; Huang et al., 2001). These lines have been used to study gene regulation, organ development, and the effect of mutations and drugs on development.

Several transgenic lines have been developed to assess toxicity. A line expressing GFP from the heat shock protein 70 promoter is currently used to study organ toxicity of heavy metals (Blechinger et al., 2002). Transgenic lines have been created that combine several response elements, such as those for aromatic hydrocarbons, electrophiles, metals, estrogen, and retinoic acid, driving the expression of luciferase or GFP, for use as sentinels of aquatic pollution (Carvan et al., 2000; Kinoshita et al., 2000). Another transgenic line has been developed for screening estrogenic activity (Legler et al., 2002; Schreurs et al., 2002). Advantages of these lines include the ability to distinguish aquatic pollutants using living biosensors and to elucidate toxicity response to various toxins in whole animals.

TOXICOLOGICAL STUDIES

Starting in the 1950s, zebrafish have been used to test the toxicity of synthetic chemicals and natural products (Battle and Hisaoka, 1952; Hisaoka and Hopper, 1953, 1957; Hisaoka, 1955). The toxic effects of some metals (e.g., zinc, selenium, mercury, and copper) and some organic solvents (e.g., phenol, aniline, and cyclohexane) were also assessed in zebrafish (Vitozzi and De Angelis, 1991). Because of the convenience and low cost of maintaining and handling zebrafish, subsequent studies in all areas of toxicology were performed in order to understand the adverse effects of chemicals and to predict results in humans. In experiments performed using zebrafish, lethality and malformation (during embryonic development) were used as general parameters for assessing toxicity. These studies demonstrated that zebrafish are amenable to chemical screens and exhibit good dose responsiveness to toxicity. In addition, the zebrafish embryo may have a predictive value similar to mammalian teratogenicity and toxicity assays (Van Leeuwen et al., 1990; Ensenbach and Nagel, 1995). However, since few compounds were tested, and effects on individual tissues and organs were not assessed, more studies are needed to further validate the correlation between the zebrafish and mammalian toxicity tests.

Ecotoxicological Studies

Ecotoxicological studies are performed to detect, manage, and monitor the presence of environmental pollutants in water, soil, and waste. Assays using zebrafish have been developed to directly monitor water, soil, and wastewater quality (Ruoppa and Nakari, 1988). Zebrafish have also been used to assess risks, predict hazards associated with petroleum products and by-products, and evaluate working conditions in the petrochemical and mining industries (Vitozzi and De Angelis, 1991; Lele and Krone, 1996). In addition, pesticides, polychlorinated biphenyls (PCBs), dioxin, and some of their derivatives have been studied in zebrafish embryos (Burkhardt-Holm et al., 1999; Wiegand et al., 2000, 2001; Anderson, 2001; Andreasen et al., 2002).

Because zebrafish develop rapidly, many toxicological endpoints can be evaluated a few days after fertilization. According to Schulte and Nagel (1994), toxicological endpoints at 72 hpf fall into two major groups. Type I endpoints are used for general morphological evaluation of development and include egg coagulation, embryo gastrulation, somite formation, tail extension, heart function, spontaneous movement, and hatching frequency. Type II endpoints are more detailed and include quantification of number of somites, blood circula-

tion, eye development, spontaneous movement at 24 hpf, cardiac function measured by heart rate, otolith development, melanocyte development, skeletal malformation, and delayed hatching (Zhu and Shi, 2002).

In Europe, zebrafish are widely accepted as an assay system for ecotoxicological studies. A number of recent guidelines from the Organisation of Economic Co-operation and Development (OECD; Guidelines 203, 210, and 212; OECD, 1992a,c, 1998) recommend zebrafish for aquatic toxicity testing. Different guidelines recommend using zebrafish at various stages, such as egg- and sac-fry-stage fish, early-life-stage fish, and juvenile fish. When testing a compound for acute toxicity (lethality), Guideline 203 (Fish Acute Toxicity Test; OECD, 1992a) recommends that medium lethal concentration (LC_{50}) be obtained using zebrafish 2.0 ± 1.0 cm long (i.e., 2- to 3-month-old juvenile to adult fish), using an incubation time of 96 hr. Guideline 210 (Fish, early-life stage toxicity test; OECD, 1992c) suggests the use of early life stage fish, from 4 hpf to day 16, for chemical testing. Briefly, 4-hpf embryos are exposed to a chemical, usually under flow-through conditions, until all the fish are free swimming and feeding exogenously. Observation continues until day 16. Lethal and sublethal effects on parameters such as growth are assessed and compared with controls. Since larval and early fry stages are the most sensitive stages for assessing developmental effects of xenobiotics, OECD Guideline 212 (Fish, short-term toxicity test on embryo and sac-fry stages; OECD, 1998) focuses on developmental toxicity in the early fish, from shortly after fertilization to 5 days post-hatching. Each guideline includes a detailed discussion of the principle of the test, a description of the method, procedures, and formats for data reporting and analysis.

Zebrafish embryos have been used to assess the toxicity of heavy metals, organic pesticides, and organic reagents (Vitozzi and De Angelis, 1991; Zhu and Shi, 2002). The no-observed-effect level (NOEL) and lowest-observed-effect level (LOEL) were determined after treatment with copper, mercury, lead, nickel, chromium, zinc, and cobalt for 16 days, starting at 4 hpf. Treatment effects included delayed hatching and developmental toxicity (Zhu and Shi, 2002). Organic pesticides, such as astrazine, malathion, carbaryl, urea, and lindane have been tested and the LC_{50} values were reported (Dave, 1987; Gorge and Napel, 1990; Dave and Xiu, 1991; Groth et al., 1993; Schulte and Nagel, 1994; Zhu and Shi, 2002). The LC_{50} of 40 organic-solvent reagents were assessed after incubating for 48 or 96 hr (Zhu and Shi, 2002). Zebrafish-derived cell lines are also used for these purposes. Toxicity studies with polychlorinated dioxin compounds, biphenyl, and antifouling compounds have also been reported (Henry, 2000; Okamura, 2002).

Results from these experiments showed that the zebrafish embryo is sensitive to environmental toxins and is a reliable and convenient model for toxicity testing. Furthermore, zebrafish can be used to monitor and elucidate the toxicological mechanisms underlying embryo development and to identify organs targeted by specific compounds.

Endocrine Disruption

There is increasing awareness that both man-made and naturally occurring chemicals may mimic or interfere with the endocrine processes in humans. Such substances have been termed endocrine disruptors (EDCs). A range of synthetic chemicals and some natural compounds have been reported to mimic estrogen effects in aquatic organisms (Pelissero and Sumpter, 1992; Sumpter and Jobling, 1995; Harries et al., 1996). Currently, there is a great demand for new assay methods, predictive endpoints, and reliable animal models for endocrine disruption testing and assessment (EDTA). EDCs interfere with homeostasis by interacting with receptors for endogenous hormones, or they can exert effects in a receptor-independent manner. Estrogens and their analogs, such as 17-β-estrodiol (E2) and 17-α-ethinylestradiol (EE2), are the most potent EDCs identified so far.

OECD recommends the use of several fish species for monitoring estrogens and estrogen analogs (OECD, 1992b,c, 2000). According to these Guidelines, teleosts such as fathead minnow, zebrafish, and medaka are the most promising models. Although fathead minnow, zebrafish, and medaka are all small fish and have similar generation cycles (3 to 4 months), zebrafish has several inherent advantages for EDTA studies, including a unique process of sexual development that differs from either the fathead minnow or medaka. Sex determination in zebrafish is not genetically determined: sex ratios are dependent on population density and food availability during development. In addition, gonadal development in zebrafish passes through a stage of juvenile hermaphroditism (Takahashi, 1977; Chan and Yenung, 1983). This means that short-term exposure may affect the genetic regulation of both female and male

Table 1.7.2 Comparison of Toxicity in Zebrafish and Mammalian Models[a]

Compound	Zebrafish		Mammalian models		
	LC_{50}/log LC_{50} (mg/liter)	Target organs	LC_{50}/log LC_{50} (mg/kg)	Model (dose route)	Target organs
Acetaminophen	252/2.4	Liver	500/2.69	Mouse (i.p.)	Liver, kidney, gastrointestinal
Aspirin	100.9/2.0	Gastrointestinal, teratogenic, kidney, muscle	167/2.22	Mouse (i.p.)	Gastrointestinal, kidney, ureter, cardiovascular, muscle
Caffeine	108/2.03	Behavioral, neuronal	127/2.1	Mouse (i.p.)	Behavioral, neuronal
Col-3	1.0/0	Teratogenic, liver, Gastrointestinal	75/1.87	Rat (oral)	Gastrointestinal, kidney, liver, bone marrow[b]
Cyclophosphamide	650/2.8	Developmental, liver	315/2.5	Mouse (oral)	Teratogenic, liver
Cyclosporin A	69/1.83	Teratogenic, liver, cardiovascular, kidney	170/2.23	Mouse (i.v.)	Kidney, ureter, bladder
Dexamethasone	324/2.51	Liver, gastrointestinal, kidney	410/2.61	Mouse (i.p.)	Liver, heart, kidney, gastrointestinal
DCA	72/1.85	Teratogenic, liver, kidney	1500/3.17	Rat (oral)	Liver, kidney, cardiovascular
Didemnin B	6.2/0.79	Developmental	4.0/0.6	Mouse (i.v.)	Kidney
DNT	23/1.4	Teratogenic, liver	268/2.4	Rat (oral)	Teratogenic, carcinogenic, liver, reproductive
Doxorubicin	30.3/1.51	Teratogenic, liver, cardiovascular, kidney	21/1.35	Mouse (i.v.)	Liver, cardiovascular
Ecteinascidin	0.42	Teratogenic, kidney	—	—	—
Ethanol	11,180/4.0	Teratogenic, neuronal, craniofacial	7,000/3.8	Rat (oral)	Liver, teratogenic, neuronal, craniofacial
Epirubicin	16.3/1.2	Cardiac, hemorrhage	16/1.2	Mouse (i.v.)	Carcinogenic, mutagenic, cardiac
Flavopiridol	2.2/0.34	Teratogenic, liver, gastrointestinal	3/0.48	Rat (oral[c])	Teratogenic, liver, gastrointestinal, spleen, bone marrow (Arneson et al., 1995)
5-FU	3.3/0.52	Liver, kidney	18.9/1.2	Rabbit (oral)	Reproductive, liver, kidney
Fujisawa peptide	30/1.48	Teratogenic, heart, kidney	5.1/0.7	Rat (i.v.)	Lung, heart

continued

Table 1.7.2 Comparison of Toxicity in Zebrafish and Mammalian Models[a], continued

Compound	Zebrafish		Mammalian models		
	LC_{50}/log LC_{50} (mg/liter)	Target organs	LC_{50}/log LC_{50} (mg/kg)	Model (dose route)	Target organs
Geldanamycin	3.13/0.49	Liver	1.0/0	Mouse (i.p.)	Liver
Ibuprofen	5.56/0.74	Liver, kidney	495/2.69	Mouse (i.p.)	Kidney
Methotrexate	454/2.6	Gastrointestinal, liver, kidney, teratogenic	180/2.3	Rat (oral)	Gastrointestinal, liver, teratogenic
Naproxen	13.2/1.12	Liver, gastrointestinal	435/2.63	Mouse (i.v.)	Gastrointestinal
Phenylurea dithiocarbamate	1.5	Teratogenic, liver	Unknown	—	Liver
PCBs	10/1	Liver, gastrointestinal	8000/3.9	Rat (i.v.)	Liver
Staurosporine	0.012/–1.92	Liver, kidney	Unknown	—	Unknown
SU5416	1.0/0	Teratogenic, liver, cardiovascular	Unknown	—	Unknown
Tacrine	11.13/1.04	Teratogenic, liver	20/1.3	Mouse (i.p.)	Liver
TCDD	0.98/–0.015	Cardiovascular, liver, kidney, teratogenic, growth inhibition, neuronal	0.114/–0.94	Rat (oral)	Cardiovascular, liver, kidney, teratogenic, neuronal
Trithiophene	2.7/0.43	Liver, muscle	110/2.04	Rat (i.p.)	Liver
Vinblastine sulfate	90.9/1.96	Liver, gastrointestinal, developmental	3.05/2.48	Rat (oral)	Mutagenic, bone marrow, depression, liver, developmental

[a]Abbreviations: DCA, dichloroacetic acid; DNT, 2,4-dinitrotoluene; 5-FU, 5-fluorouracil; PCBs, polychlorinated biphenyls.

[b]See Page et al. (1998).

[c]Maximum tolerance dose.

development, resulting in a change of sex or sexual characteristics. However, sexual differentiation in medaka begins before hatching in females and at ~13 days post hatching in males (Kime and Nash, 1999). Gonad development in the fathead minnow is less well characterized. Moreover, the sex ratio has been well characterized for zebrafish under specific conditions (Fenske et al., 1999), but it is not known for either fathead minnow or medaka. Therefore, use of zebrafish for EDTA studies may produce more accurate and predictive results than other species. Furthermore, due to the small size of zebrafish compared to larger species such as rainbow trout, zebrafish assays can substantially reduce the cost, time, and space required for testing.

It has been reported that treatment with estrogen or its analogs changed the sex ratio of the siblings of exposed female zebrafish, caused necrosis in testes, and induced over-expression of vitellogenin protein (VTG; Kime, 1998; Olsson et al., 1999). VTG is an egg yolk protein synthesized in the liver and excreted into blood in the female fish. Estrogen is believed to regulate the expression of VTG. Due to the low concentration of circulating estrogen in male and juvenile fish, their blood levels of VTG are usually low. An increase in VTG in nonfemale fish indicates the presence of EDCs. Therefore, monitoring the blood levels of VTG in male fish has become a reliable endpoint for EDTA studies (Sumpter and Jobling, 1995).

Whole-fish homogenate is used in EDTA tests because it is difficult to obtain enough blood from zebrafish. Using a zebrafish-specific anti-VTG antibody, VTG at concentrations as low as 40 ng/g fish can be detected by ELISA. Other approaches include immunohistochemical studies, RT-PCR to detect VTG mRNA, histological analysis of gonad development, reproduction rates, and reproductive strength of the following generation. For histological examination after chemical exposure, the gonad is removed and sectioned. Sections are fixed on a slide and examined under a light microscope for any morphological change or necrosis. Studies related to reproduction include the ability to lay eggs, the fertilization rate, and the fertility of the subsequent generation.

It has been reported that EDCs caused developmental arrest of eggs from exposed females (Kime and Nash, 1999; Olsson et al., 1999). PCBs and their metabolites, di-2-ethylhexyl phthalate, 2,3,7,8-tetrachlorodibenzo-p-dioxin (TCDD), and toxaphene have been tested on zebrafish (Holm et al., 1995; Orn et al., 1998; Olsson et al., 1999). It has been proposed that TCDD exerts its antiestrogenic effect by binding to the Ah-receptor, rather than by interfering with the estrogen receptor. Although the mechanism of action is not fully known, TCDD has been shown to reduce egg number and cause abnormality in offspring of mature females that ingested TCDD (Wannemacher et al., 1992; Fahraus-Van Ree and Payne, 1997; Gillesby and Zacharewski, 1998). However, which signal transduction pathway is involved in toxicity of PCBs is controversial. PCBs, like TCDD, have been reported to bind to the Ah-receptor (Cook et al., 1997). In contrast, PCB 104 was capable of mimicking the effect of E2 by inducing ER mRNA (Billsson et al., 1998). Since the mechanisms of endocrine disruption are quite complicated, additional research is needed in this area.

TOXICITY TESTING OF THERAPEUTICS: A COMPREHENSIVE APPROACH USING ZEBRAFISH

The authors have recently developed a family of assays in which chemical toxicity can be rapidly assessed in zebrafish. These methods include acute toxicity testing, target organ toxicity, developmental toxicity and teratogenicity, and an assay for apoptosis.

Using 30 chemicals which were commercially available or provided by the National Cancer Institute (NCI), the authors demonstrated the feasibility of using zebrafish embryos to study toxicity response by assessing LC_{50}, developmental teratogenicity, and specific organ toxicity (Table 1.7.2). The data show good correlation with LC_{50} values in other mammalian models (Fig. 1.7.2). In addition, as expected, >90% of the compounds showed specific tissue, organ, and behavioral toxicity. These results suggest that zebrafish is an excellent model organism for drug toxicity testing.

LC_{50} results showed that a few of the compounds (trithiophene, naproxen, ibuprofen, Col-3, DCA, PCBs, and 2,4-DNT) were more toxic in zebrafish than in mammals, perhaps because testing in zebrafish was performed on embryos, a developmental system, while the comparative mammalian toxicity was obtained using adult animals. The finding that a subset of compounds is more toxic in zebrafish than in mice or rats suggests that zebrafish may be a more sensitive model for chemical toxicity.

Zebrafish embryos exhibit responses to xenobiotic chemicals similar to those in mammals, including induction of xenobiotic enzymes and generation of oxidative stress (Wiegand et al., 2000; Dong et al., 2001). In addition to developmental defects (see below), changes in gene expression can be used for toxicogenomic studies. Although zebrafish orthologs of many genes involved in human toxicity have been identified (Table 1.7.3), expression of the cytochrome gene CYP 1A1, the first cytochrome gene cloned and characterized, is examined in most zebrafish toxicity studies. CYP 1A1 has been shown to be up-regulated in a zebrafish liver cell line treated with TCDD and β-naphthoflavone (BNF; Miranda et al., 1993). Additionally, CYP 1A1 has been shown to be functionally active in embryos in late gastrula stage, and its expression can be induced by TCDD or hexachlorobenzene (HCB; Mizell and Roming, 1997).

Recent studies designed to assess effects of several drugs on toxicity response demonstrate that CYP 1A1 expression was up-regulated in zebrafish embryos treated with 10 μM tacrine and 50 μM phenytoin, and down-regulated with 10 μM ibuprofen and 100 μM doxorubicin (Fig. 1.7.3). These results suggest that, similar to mammalian models (Sinz and Woolf, 1997; Nakamura et al., 2000), CYP P450 in zebrafish is responsive to drug treatment (Parng et al., 2002b; Semino et al., 2002). Expression of several genes has been examined in response to a number of drugs (Parng et al., 2002b; Semino et al., 2002), and currently DNA arrays are

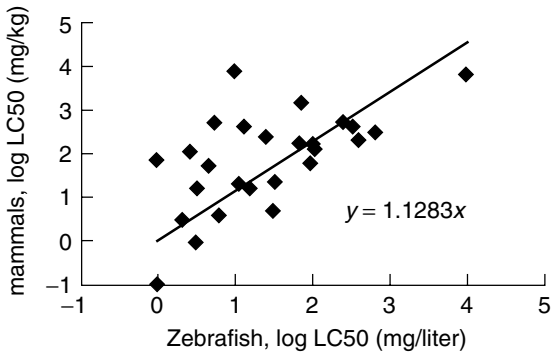

Figure 1.7.2 Comparative LC_{50} values. LC_{50} values obtained with zebrafish (expressed as mg/liter in Table 1.7.2) are compared with the corresponding LD_{50} values (mg/lg) obtained with mammals, in logarithmic scale. A graphic representation of the data was developed; the line represents the best fit between the two sets of values (slope = 1.13). LD_{50} values for mammals were obtained from the NIH TOXNET database, NCI, and others.

Table 1.7.3 Examples of Zebrafish Homologs of Mammalian Toxicity Related Genes

Gene	GenBank no.[a]	Gene	GenBank no.[a]
Apoptosis		*Stress response*	
Bad	AF231017	Egr1	U12895
Bax	AF231015	Heat shock factor 1a	AF159134
Bcl-L	AAK81706	Heat shock factor 1b	AF159135
Caspase 3	AB047003	Max	L11711
Casp8	AF273220	MDM2	AF010255
Mcl 1b	AF441284	Mix1	AAA19324
Mcl-1A	AF302805	*c*-Myc	L11710
Survivin 2	AY057058	Nueronal nitric oxide synthase	AF219519
TRAIL-like protein	AF250041	P53	NM_131327
TNF	AF250042	*Xenobiotic*	
Cell cycle		AhR1	NM_131028
CDK5	AF203736	AhR2	NM_131264
Cyclin B1	NM_131513	Catalase	AAF89686
Cyclin D1	NM_131025	COX-1	AY028584
Cyclin E	NM_130995	COX-2	AY028585
Proliferation		CYP 1A1	AF210727
CBP/p300	AF359242	CYP 2E1	AA605954
IGF-1	AF268051	CYP 2A6	AI545376
IGF-2	AF194333	CYP 3A4	BF717373
STAT3	AJ005693	ERalpha	AB037185
Neurotrophin-7	AF055906	ERβ1	AJ414566
Ngr1	AF036149	ERβ2	AJ414567
NurD	AF036148	Glutathione-*S*-transferase	NM_131734
Pax-6	X63183	Pyruvate carboxylase	NM_131550
PDGF	AF200951		
WT-1	AY028627		

[a]See *http://www.psc.edu/general/software/packages/genbank/genbank.html*.

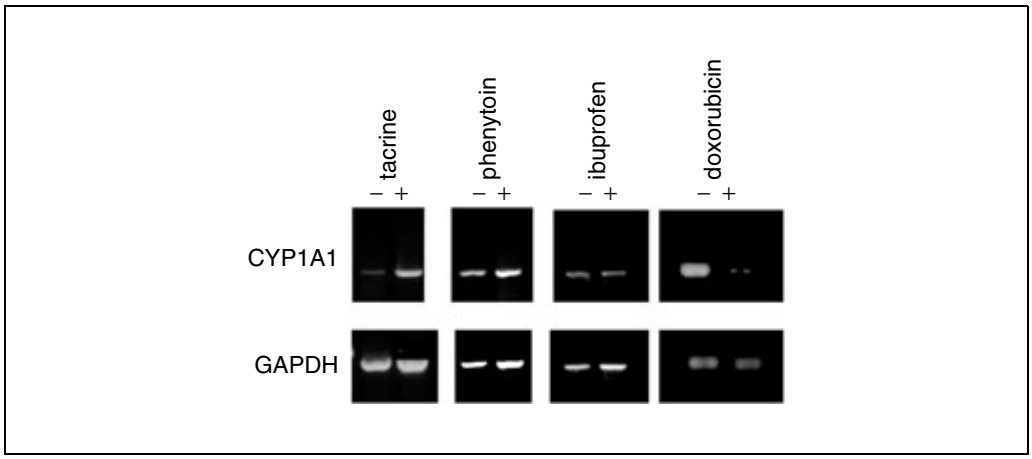

Figure 1.7.3 CYP 1A1 expression in zebrafish embryos. Zebrafish embryos (96 hpf) were treated with 0.1% DMSO (–) or 10 μM tacrine, 50 μM phenytoin, 10 μM ibuprofen, or 10 μM doxorubicin (+) for 4 hr. RNAs were isolated, and RT-PCR was used to analyze expression of both CYP 1A1 and GAPDH, a housekeeping gene. CYP 1A1 was up-regulated by tacrine and phenytoin treatment and down-regulated by ibuprofen and doxorubicin treatment.

being generated to assess patterns of gene expression and toxicity (by Phylonix, MWG Biotech, and Oakridge National Labs). Although these results suggest that P450 metabolism in zebrafish may be similar to that in mammals, the function of P450 in zebrafish has not been directly studied.

ORGAN TOXICITY

Organ toxicity studies include examining liver, gastrointestinal (GI), and kidney morphologies. Liver and GI toxicity is assessed using a staining method that relies on the presence of biotinylated proteins in the liver and gut: biotin is visualized by the application of streptavidin-peroxidase followed by a chromogenic substrate for peroxidase to specifically visualize the liver and intestine after drug treatment (Fig. 1.7.4A). The data showed that treating a 24-hpf zebrafish embryo with 100 μM dexamethasone for 5 days caused a dramatic reduction in liver size. Kidney toxicity is assessed by staining with an antibody against the mouse sodium/potassium ATPase (Fig. 1.7.4B). Antibody staining outlines the pronephric duct (black arrows) and the newly developed nephron (white arrow) at 48 hpf. Treating embryos for 24 hr with 5 μM brefeldin A had little effect on the pronephric duct, but completely inhibited nephron development.

Using the same methods described above, organ toxicity was quantified by staining with soluble substrate. The intensity of the resulting colorimetric product is proportional to the size of the organ. In addition to quantifying the toxic response, this method can be automated to process a large number of animals using a microplate reader. The results show that dexamethasone (from 1 to 100 μM) reduced liver and GI size in 144-hpf zebrafish embryos in a dose dependent manner (Fig. 1.7.5).

A functional assay for fatty acid metabolism in the gut has also been developed (Farber et al., 2001). This assay relies on the change in the fluorescence of phospholipase A2 after cleavage in the gut and can be used to identify chemicals that alter lipid metabolism.

Developmental toxicity in zebrafish embryos has been assessed after treatment with valproic acid (VPA), an anticonvulsant drug, and twelve other related substances (Herrmann, 1993). It was shown that VPA and the twelve other compounds cause retardation, developmental arrest, and malformation, including edema, brain deformation, shortened and bent tail, and bipartite axiation of the posterior trunk. These findings show that results with zebrafish embryos are similar to those observed in hydroids and in mammalian embryo culture systems. Furthermore, zebrafish development is highly synchronous and the developmental stages can be accurately determined, making zebrafish embryos a suitable model for drug toxicity testing. The authors have developed a detailed system to assess developmental toxicity in response to chemicals and therapeutics treatment (see below).

Developmental Toxicity and Teratogenicity

Developmental toxicity is a major aspect of environmental pollutants and a significant

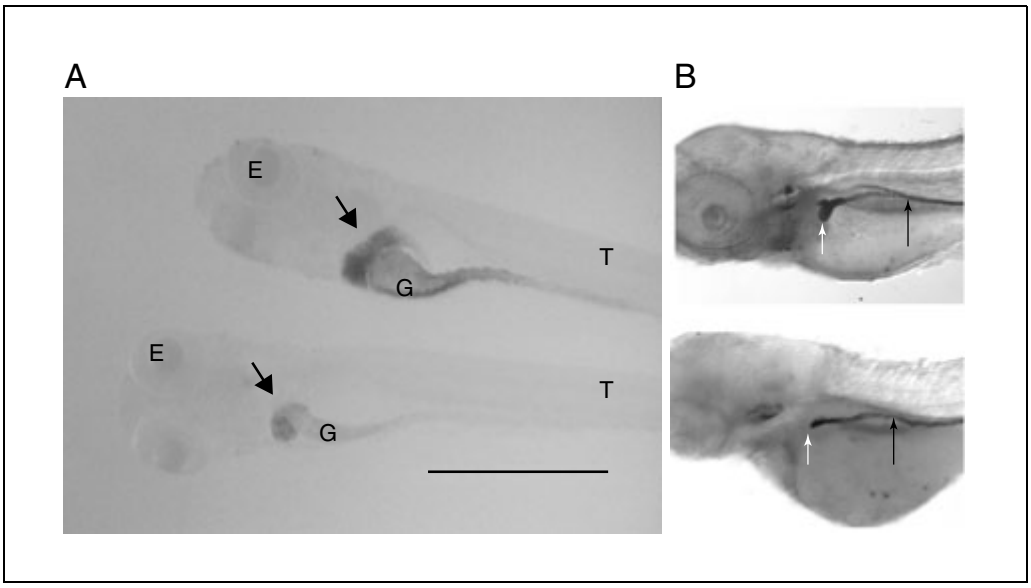

Figure 1.7.4 Visual assessment of liver and kidney organ toxicity. (**A**) Zebrafish embryos (24 hpf) treated for 5 days were used to determine the effects of dexamethasone on liver toxicity. The embryos were fixed with paraformaldehyde, incubated with streptavidin-peroxidase, and stained with a chromogenic dye to specifically label biotinylated enzymes in the liver and gut. Arrows indicate the position of the liver. Top, untreated embryo; bottom, embryo treated with 100 μM dexamethasone for 5 days. E, eye; G, gastrointestine; T, tail. Scale bar = 1 mm. (**B**) Zebrafish embryos (48 hpf) were fixed with methanol and formalin and stained with a mouse antibody against sodium/potassium ATPase. Black arrow indicates the position of the pronephric duct; white arrow indicates the nephron. Top, untreated embryo; bottom, embryo treated with 5 μM brefeldin A for 24 hr.

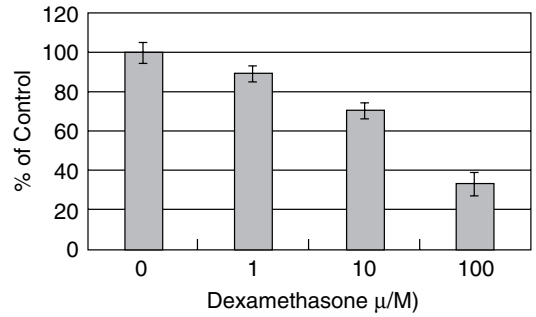

Figure 1.7.5 Quantification of liver toxicity after dexamethasone treatment: generation of dose response. Larva 144 hpf show a dose response to 1 to 100 μM dexamethasone on liver size detected and quantified by peroxidase and stained with a soluble dye. Ten zebrafish were analyzed for each concentration. The absorbance was detected at 405 nm. Values are expressed as a percentage of control (% Control) ± standard deviation.

problem with numerous pharmaceutical agents. Several mammalian models are typically used for developmental toxicity studies, including rat and mouse whole-embryo, organ, and tissue cultures (Chatot et al., 1980; Cicurel and Schmid, 1988). However, mammalian whole-embryo cultures are complicated: embryos must be explanted with the visceral yolk sac and ectoplacental cone intact for culture, and the embryo culture time is limited to 48 hr (Bechter et al., 1991). Partly due to the embryonic attributes described above, zebrafish is a much simpler model system for assessing toxicity.

The frog embryo teratogenesis assay-*Xenopus* (FETAX) is well established for evaluating developmental toxicity (Van Leeuwen et al., 1990; Dawson, 1991; Fort et al.,

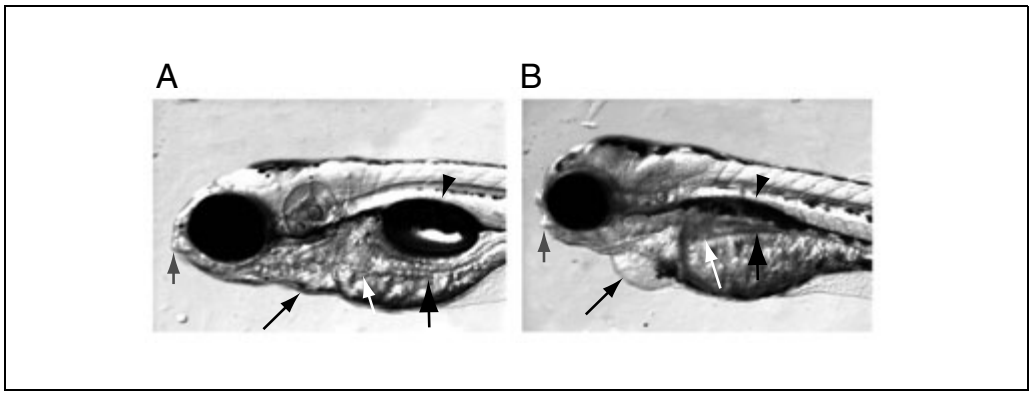

Figure 1.7.6 Morphological characteristics for developmental index assessment. Comparison of zebrafish (120 hpf) untreated (**A**) and treated (**B**) with 5 μM brefeldin A. Treated zebrafish shows heart edema (black arrow), necrotic liver (white arrow), undeveloped intestine (large arrow), underdeveloped jaw (gray arrow), and lack of swim bladder (arrowhead).

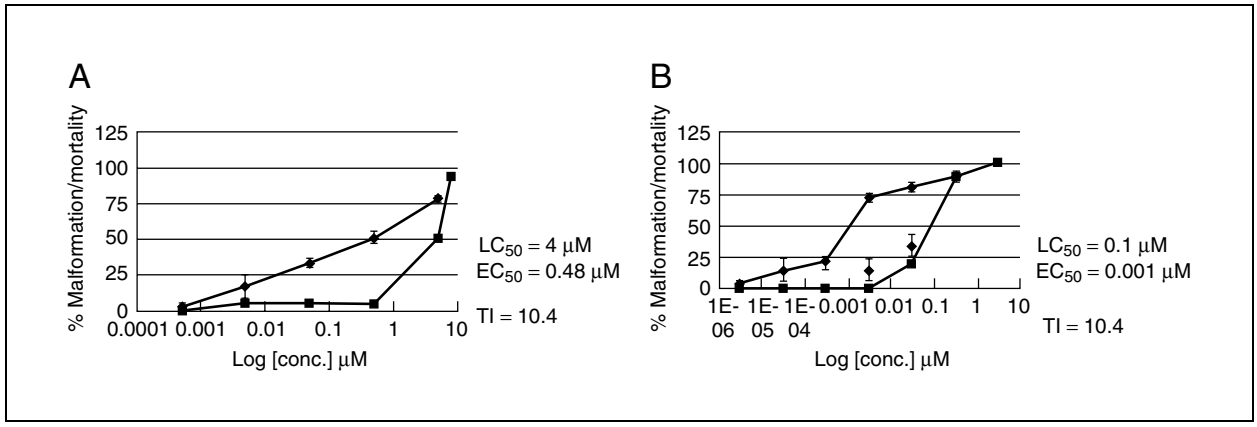

Figure 1.7.7 Dose-response curves for developmental toxicity of flavopiridol (A) and TCDD (B). Developmental malformation (diamonds) and mortality (squares) are shown.

1991; Stringer and Blankememyer, 1993). However, it appears that the frog is not responsive to halogenated aromatic hydrocarbons (HAHs), such as 2,3,7,8-tetrachlorodibenzo-*p*-dioxin (TCDD; Beck and Powell, 2002), a major class of environmental toxins. Another complication of FETAX is that many compounds require activation by metabolic liver enzymes; since toxicity is evaluated before the embryonic frog liver develops, FETAX assessment of some compounds must be done in the presence of liver extract (Fort et al., 1991, 1998). Furthermore, since frog embryos are not transparent, it is difficult to inspect effects on internal organs.

The authors have developed a scoring system for evaluating developmental toxicity using zebrafish embryos. The scoring system consists of 20 toxicological endpoints, including heart shape, swim bladder inflation, jaw development, body edema, hemorrhage, several aspects of organ malformation, and necrosis (Fig. 1.7.6). The authors determine the mortality (LC_{50}), malformation (EC_{50}), no-observed-effect level for malformation (NOEL), and teratogenic index (TI) by generating dose-response curves for mortality and developmental malformation.

The authors have assessed the effects of eight chemicals, including environmental contaminants and common drugs, and more studies are ongoing. The results are shown in Fig. 1.7.7 and Table 1.7.4. Treatment by semistatic emersion (compounds replenished daily) was initiated at 24 hpf (day 1) and terminated at 120 hpf (day 5). Mortality was monitored each day and used to obtain the dose-response curve to establish the LC_{50} value—i.e, the percentage lethality was plotted against the concentration to obtain the concentration that caused 50% lethality (LC_{50}). To obtain the dose-response curve for malformation, the developmental score was plotted against the concentrations for each compound. The concentration that caused

Table 1.7.4 Comparison of Chemical Teratogenicity[a,b]

Chemicals	Zebrafish TI	Zebrafish LC_{50} (mg/liter)	FETAX (TI)	LC_{50} or MTD in other species	Teratogenicity in mammals
Col-3	3	1.0	75 mg/kg	Rat (oral)	Mouse, rat
2,4-DNT	1.7	23	24.3 mg/liter	96-hpf fathead minnow	Mouse, rat, rabbit
Epirubicin	0.75	16.3	16 mg/kg	Mouse (i.v.)	—
Flavopiridol	10.4	2.2	3 mg/kg (MTD)	Rat (oral)	Mouse, rat, hamster
Methotrexate	18.2	454[b]	504 mg/liter	FETAX	Mouse, rat, hamster
Staurosporine	1.0	0.012	Unknown	—	—
SU 5416	4.3	1.0	Unknown	—	Unknown
TCDD	100	0.98	0.81 mg/kg	*Streptopelia rioria* (oral)	Mouse, rat, rabbit

[a]Abbreviations: DNT, 2,4-dinitrotoluene; FETAX, frog embryo teratogenesis assay-*Xenopus*; MTD, maximum tolerated dose; TCDD, 2,3,7,8,-tetrachlorodibenzo-*p*-dioxin.

[b]FETAX TI value 19.3. See Bantle (1995).

50% malformation is defined as the medium effective concentration (EC_{50}). The teratogenic index (TI) is defined as the ratio of LC_{50}/ EC_{50}. The test compound is considered teratogenic if the TI value is >1.5 (Bantle et al., 1989, 1990; Bantle, 1995). Dose-response curves for EC_{50} and LC_{50} for flavopiridol (a cyclin-dependent kinase inhibitor used as an experimental anticancer compound), and TCDD, are shown in Figure 1.7.7. Developmental toxicity of the eight compounds was studied using the scoring system and compared with data for other species (Table 1.7.4). Although the authors have only assessed eight compounds to date, the data strongly suggest that zebrafish embryo is a suitable model for studying developmental toxicity and teratogenicity.

TOXICITY-RELATED CELL DEATH

Cell death often occurs in response to exposure to toxic compounds. General cell death, or necrosis, is easily scored in the developing embryo by localized opacity within an organ (Fig. 1.7.6). Apoptosis, or programmed cell death, is a mechanism of ridding the organism of unwanted or damaged cells and is involved in organ toxicity of many classes of compounds. The pathways and mechanisms of apoptosis in zebrafish appear to be similar to those in mammals. For example, specific caspase inhibitors have been shown to inhibit DNA fragmentation in zebrafish embryos, similar to mammals (Inohara and Nunez, 2000). Prevention of apoptosis in zebrafish embryos using caspase inhibitors has also been reported (Chan and Yager, 1998). Homologs of many genes in the apoptotic pathway in zebrafish have been identified and cloned, including nine Bcl-2 family genes (Mcl-1a, Mcl-1b, BLP1, Bcl-xl, Bax, Bad, Nip3, Nip3L, NR13), and seven caspase member genes (caspase 2, 3, 4, 6, 8, 9, 13; Parng et al., 2002a). Other apoptosis-related genes identified in zebrafish include four IAPs (inhibitor of apoptosis), four death receptor genes, ten apoptosis related kinases, and other related transcriptional genes and molecules (Ikegami et al., 1997). Therefore, zebrafish is a promising animal model for studying apoptosis mechanisms and gene regulation in response to environmental toxins and for evaluating the potential toxicity of therapeutics.

To detect apoptotic cells in live embryos, the authors developed apoptosis assays that rely on fluorescent reagents, including acridine orange and caspase substrates. Apoptotic cells are stained with fluorescent dyes that are easily detected in vivo with an epifluorescent microscope. In developing zebrafish embryos, naturally occurring apoptosis is consistently detected in the dorsal neural tube, hatching glands, retina, lens, cornea, inner ear, and olfactory organs (Bader et al., 1982; Yabu et al., 2001; Parng et al., 2002a); therefore, reagents that alter this developmental apoptosis pattern can be effectively screened in transparent embryos and the target organs or cells of pro-apoptotic reagents can be identified. As shown in Figure 1.7.8, increased apoptosis can be visualized in the liver of neomycin-treated embryos. In addition, these assays can be adapted for quantitative microtiter plate analysis using the same approach described for organ toxicity screens.

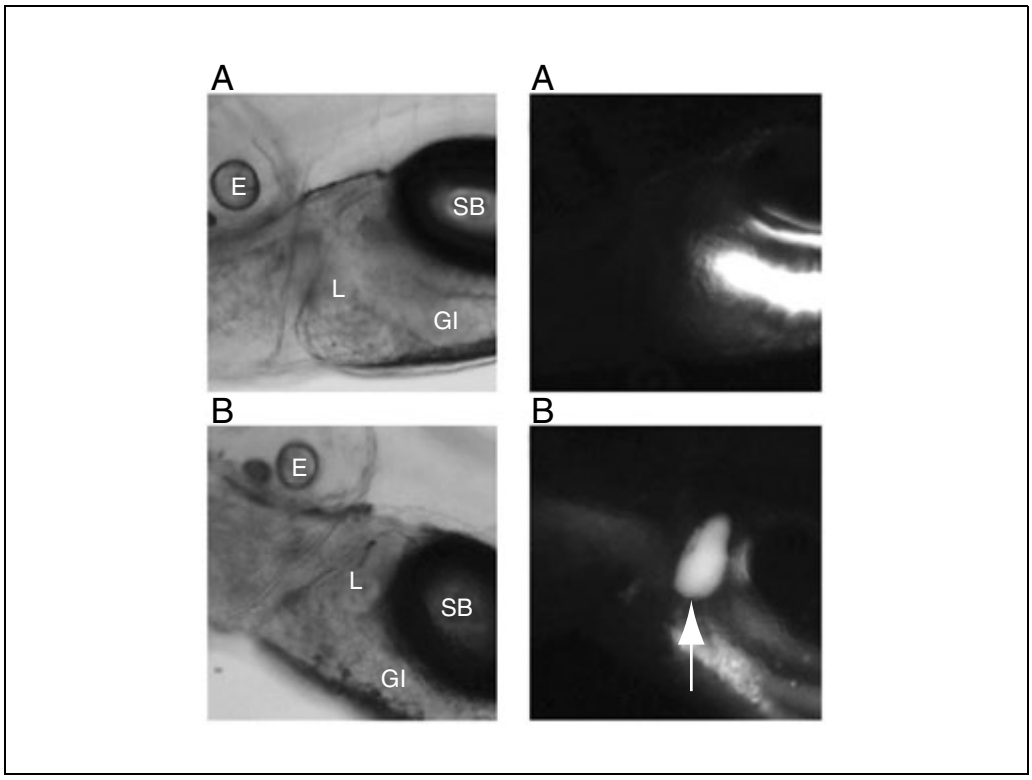

Figure 1.7.8 Neomycin-induced liver apoptosis in zebrafish. Zebrafish embryos (96 hpf) were stained with acridine orange. (**A**) Untreated zebrafish. (**B**) Zebrafish treated with 2.5 μg/ml neomycin for 24 hr. Left panels show light micrographs and right panels, fluorescent micrographs. Neomycin induced apoptosis in the liver (arrow in lower right panel). Intestine (GI) is fluorescent in both treated and untreated zebrafish due to ingestion of dye. Abbreviations: L, liver; E, ear; SB, swim bladder.

SUMMARY

Zebrafish is a unique animal model for assessing toxicity. It is a vertebrate that completes morphogenesis in 120 hpf, and embryos are transparent and develop ex utero. Since zebrafish has become a popular model for geneticists and developmental biologists, information about all aspects of zebrafish biology is rapidly accumulating. In addition, for decades zebrafish has been used to evaluate environmental toxicity, and formal protocols have been established by the OECD. Exploratory research for evaluating toxicity using many classes of compounds, from environmental toxins to therapeutics, shows that, in general, responses in zebrafish are similar to those in mammals. All of these factors indicate that this model organism will become a valuable tool for assessing environmental toxicity and for predicting drug toxicity.

LITERATURE CITED

Anderson, P.L., Berg, A.H., Bjerselius, R., Norrgren, L., Olsen, H., Olsson, P.E., Orn, S., and Tysklind, M. 2001. Bioaccumulation of selected PCBs in zebrafish, three-spined stickleback, and arctic char after three different routes of exposure. *Arch. Environ. Contam. Toxicol.* 40:519-530.

Andreasen, E.A., Spitsbergen, J.M., Tanguay, R.L., Stegeman, J.J., Heideman, W., and Peterson, R.E. 2002. Tissue-specific expression of AHR2, ARNT2, and CYP1A in zebrafish embryos and larvae: Effects of developmental stage and 2,3,7,8-tetrachlorodibenzo-p-dioxin exposure. *Toxicol. Sci.* 68:403-419.

Bader, D., Masaki, T., and Fisherman, D.A. 1982. Immunochemical analysis of myosin heavy chain during avian myogenesis in vivo and in vitro. *J. Cell Biol.* 95:763-770.

Bantle, J.A. 1995. FETAX: A developmental toxicity assay using frog embryos. *In* Fundamentals of Aquatic Toxicology: Effects, Environmental Fates, and Risk Assessment (G.M. Rand, ed.) pp. 207-230. Taylor & Francis, Philadelphia.

Bantle, J.A., Fort, D.J., and James, B.L. 1989. Identification of developmental toxicants using the frog embryo teratogenesis assay-Xenopus (FETAX). *Hydrobiology* 188/189:577-585.

Bantle, J.A., Dumont, J.N., Finch, R.A., DeYoung, D.J., and Bush, S.J. 1990. Further evaluation of FETAX: Evaluation of the developmental toxicity of five known mammalian teratogens and non-teratogens. *Drug Chem. Toxicol.* 13:267-282.

Barbazuk, W.B., Korf, I., Kadavi, C., Heyen, J., Tate, S., Wun, E., Bedell, J.A., McPherson, J.D., and Johnson, S.L. 2000. The syntenic relationship of the zebrafish and human genomes. *Genome Res.* 10:1351-1358.

Battle, H.I. and Hisaoka, K.K. 1952. Effects of ethyl carbamate (urethan) on the early development of the zebrafish (*Brachydanio rerio*). *Cancer Res.* 12:334-340.

Bechter, R., Terlouw, G., Lee, Q., and Juchau, M. 1991. Effects of QA 208-199 and its metabolite 209-668 on embryonic development in vitro after microfiltration into the exocoelomic space or into the amniotic cavity of cultured rat conceptuses. *Teratogen. Carcinogen. Mutagen.* 11:185-194.

Beck, C. and Powell, W. 2002. Cloning and evolutionary analysis of two cDNAs encoding aryl hydrocarbon receptors (AHRs) in Xenopus laevis, in, Kenyon College, Gambier, OH 43022.

Billsson, K., Westerlund, L., Tysklind, M., and Olsson, P.E. 1998. Developmental disturbances caused by polychlorinated biphenyls in zebrafish (*Brachydanio rerio*). *Marine Environ. Res.* 46:461-464.

Blechinger, S.R., Warren, J.T., Kuwada, J.Y., and Krone, P.H. 2002. Developmental toxicology of cadmium in living embryos of a stable transgenic zebrafish line. *Environ. Health Perspect.* 110:1041-1046.

Burkhardt-Holm, P., Oulmi, Y., Schroeder, A., Storch, V., and Braunbeck, T. 1999. Toxicity of 4-chloroaniline in early stages of zebrafish (*Danio rerio*): II. Cytopathology and regeneration of liver and gills after prolonged exposure to waterborne 4-chloroaniline. *Arch. Environ. Contam. Toxicol.* 37:85-102.

Carvan, M.J., Dalton, T.P., Stuart, G.W., and Nebert, D.W. 2000. Trangenic zebrafish as sentinels for aquatic pollution. *Ann. N.Y. Acad. Sci.* 919:133-147.

Chan, S.T.H. and Yenung, W.S.B. (eds.) 1983. Sex Control and Sex Reversal in Fish Under Natural Conditions. Academic Press, New York.

Chan, D.W. and Yager, T.D. 1998. Preparation and imaging of nuclear spreads from cells of the zebrafish embryos: Evidence for large degradation intermediates in apoptosis. *Chromosoma* 107:39-60.

Chatot, C., Klein, N.W, Piatek, J., and Pierro, L.J. 1980. Successful culture of rat embryos on human serum: Use in the detection of teratogens. *Science* 207:1471-1473.

Cicurel, L. and Schmid, B. 1988. Postimplantation embryo culture for the assessment of the teratogenic potential and potency of compounds. *Experientia* 44:833-840.

Cook, P., Zabel, E., and Peterson, R. 1997. The TCDD toxicity equivalence approach for characterizing risks for early life-stage mortality in trout. *In* Chemically Induced Alternations in Functional Development and Reproduction of Fishes: Proceeding from a Session at the 1995 Wingspread Conference (R. Rolland, M. Gilbertson, and R. Peterson, eds.) pp 9-27. SETAC Press, Pensacola, Fl.

Creaser, C.W. 1934. The technic of handling the zebrafish (*Brychyanio rerio*) for the production of eggs which are favourable for embryological research and are available at any specified time throughout the year. *Copeia* 4:159-161.

Dave, G. 1987. Ring test of an embryo-larval toxicity test with zebrafish (*B. rerio*) using chromium and zinc as toxicants. *Environ. Toxicol. Chem.* 6:61-71.

Dave, G. and Xiu, R.Q. 1991. Toxicity of mercury, copper, nickel, and cobalt to embryo and larva of zebrafish (*B. rerio*). *Arch. Environ. Contamination Toxicol.* 21:126-134.

Dawson, D. 1991. Additive incidence of development malformation for Xenopus embryos exposed to a mixture of ten aliphatic carboxylic acids. *Teratology* 44:531-546.

Dong, W., Teraoka, H., Kondo, S., and Hiraga, T. 2001. 2,3,7,8-tetrachlorodibenzo-*p*-dioxin induces apoptosis in the dorsal midbrain of zebrafish embryos by activation of arylhydrocarbon receptor. *Neurosci. Lett.* 303:169-172.

Dooley, K. and Zon, L.I. 2000. Zebrafish: A model system for the study of human disease. *Curr. Opin. Genet. Dev.* 10:252-256.

Driever, W. 1995. Axis formation in zebrafish. *Curr. Opin. Genet. Dev.* 5:610-618.

Driever, W., Semple, D., Schier, A., and Solnica-Krezel, L. 1994. Zebrafish: Genetic tools for studying vertebrate development. *Trends Genet.* 10:152-159.

Driever, W., Solnica-Krezel, L., Schier, A.F., Neuhauss, S.C.F., Malicki, J., Stemple, D.L., Stainier, D.Y.R., Zwartkruis, F., Abdelilah, S., Rangini, Z., Belak, J., and Boggs, C. 1996. A genetic screen for mutations affecting embryogenesis in zebrafish. *Development* 123:37-46.

Ensenbach, U. and Nagel, R. 1995. Toxicity of complex chemical mixtures, acute and long-term effects on different life stages of zebrafish (*Brachydanio rerio*). *Ecotoxic. Environ. Saf.* 30:151-157.

Fahraus-Van Ree, G.E. and Payne, J.F. 1997. Effect of toxaphene on reproduction of fish. *Chemosphere* 34:855-867.

Farber, S.A., Pack, M., Ho, S.-Y., Johnson, I.D., Wagner, D.S., Dosch, R., Mullins, M.C., Hendrickson, H.S., Hendrickson, E.K., and Halpern, M.E. 2001. Genetic analysis of digestive physiology using fluorescent phospholipid reporters. *Science* 292:1385-1388.

Fenske, M., Maack, G., Ensenbach, U., and Segner, H. 1999. Assessment of estrogenic effects in the zebrafish, *Danio rerio*. *In* 6th International Symposium on Reproductive Physiology of Fish. July 4-9, 1999. Bergen, Norway.

Fishman, M.C. 2001. Zebrafish—the canonical vertebrate. *Science* 294:1290-1291.

Fort, D.J., Rayburn, J.R., DeYoung, D.J., and Bantle, J.A. 1991. Developmental toxicity testing with frog embryo teratogenesis assay-Xenopus (FETAX): Efficacy of aroclor 1245–induced exogenous metabolic activation system. *Drug Chem. Toxicol.* 14:143-160.

Fort, D., Stover, E.L., Propst, T., Faulkner, B.C, Vollmuth, T., and Murray, F. 1998. Evaluation of the developmental toxicity of caffeine and caffeine metabolites using the frog embryo teratogenesis assay -Xenopus (FETAX). *Food Chem. Toxicol.* 36:591-600.

Gillesby, B.E. and Zacharewski, T.R. 1998. Exoestrogens: Mechanisms of action and strategies for identification and assessment. *Environ. Toxicol. Chem.* 17:3-14.

Goldman, D., Hankin, M., Li, Z., Dai, X., and Ding, J. 2001. Transgenic zebrafish for studying nervous system development and regeneration. *Transgenic Res.* 10:21-33.

Golling, G., Amsterdam, A., Sun, Z., Antonelli, M., Maldonado, E., Chen, W., Burgess, S., Haldi, M., Artzt, K., Farrington, S.M., Lin, S., Nissen, R., and Hopkins, N. 2002. Insertional mutagenesis in zebrafish rapidly identifies genes essential for early vertebrate development. *Nat. Genet.* 31:135-140.

Gorge, G. and Napel, R. 1990. Toxicity of lindane, atrazine, and deltamethrin to early life stages of zebrafish (*B. rerio*). *Ecotoxicol. Environ. Saf.* 20:246-255.

Groth, G., Schreeb, K., and Herdt, V. 1993. Toxicity studies in fertilized zebrafish eggs treated with *N*-methylamine, *N*,*N*-demethylamine, 2-aminoethanol, aniline, isopropylamine, *N*-methylaniline, *N*,*N*-demethylaniline, quinone, chloroacetaldehyde, or cyclohexanol. *Bull. Environ. Contam. Toxicol.* 50:878-882.

Haffter, P., Granato, M., Brand, M., Mullins, M.C., Hammerschmidt, M., Kane, D.A., Odenthal, J., van Eeden, F.J.M., Jiang, Y.-J., Heisenberg, C.-P., Kelsh, R.N., Furutani-Seiki, M., Vogelsang, E., Beuchle, D., Schach, U., Fabian, C., and Nusslein-Volhard, C. 1996. The identification of genes with unique and essential functions in the development of zebrafish, *Danio rerio*. *Development* 123:1-36.

Harries, J.E., Sheahan, D.A., Jobling, S., Matthiessen, P., Neall, P., Routledge, E.J., Rycroft, R., Sumpter, J.P., and Tylor, T. 1996. A survey of estrogenic activity in United Kingdom inland waters. *Environ. Toxicol. Chem.* 11:1993-2002.

Henry, T.R., Nesbit, D.J., Heideman, W., and Peterson, R.E. 2000. Relative potencies of polychlorinated dibenzo-*p*-dioxin, bibenzofuran, and biphenyl congeners to induce cytochrome p4501A mRNA in a zebrafish liver cell line. *Environ. Toxicol. Chem.* 20:1053-1058.

Herrmann, K. 1993. Effects of the anticonvulsant drug valproic acid and related substances on the early development of the zebrafish (*Brachydanio rerio*). *Toxicol. In Vitro* 7:41-54.

Hisaoka, K.K. 1955. The response of the zebrafish embryo to the action of 2-acetylaminofluorene. *Anat. Rec.* 122:418.

Hisaoka, K.K. and Hopper, A.F. 1953. The effects of certain nucleic acid inhibitors on the development of the zebrafish. *Anat. Rec.* 117:520.

Hisaoka, K.K. and Hopper, A.F. 1957. Some effects of barbituric and diethylbarbituric acid on the development of the zebrafish, *Brachydanio rerio*. *Anat. Rec.* 129:297-308.

Hisaoka, K.K. and Firlit, C.F. 1960. Further studies on the embryonic development of the zebrafish, *Brachydanio rerio* (Hamilton-Buchanan). *J. Morphol.* 107:205-225.

Holm, G., Hallden, T., and Norrgren, L. 1995. Reproductive effects of di-2-ethylhexyl phthalate (DEHP) on zebrafish (*Brachydanio rerio*). *Mar. Environ. Res.* 33:357.

Huang, H., Voigelm, S.S., Liu, N., Melton, D.A., and Lin, S. 2001. Analysis of pancreatic development in living transgenic zebrafish embryos. *Mol. Cell. Endocrin.* 177:117-124.

Ikegami, R., Zhang, J., Rivera-Bennetts, A.K., and Yager, T.D. 1997. Activation of the metaphase checkpoint and an apoptosis programme in the early zebrafish embryo, by treatment with the spindle-destabilising agent nocodazole. *Zygote* 5:329-350.

Inohara, N. and Nunez, G. 2000. Genes with homology to mammalian apoptosis regulators identified in zebrafish. *Cell Death Differ.* 7:509-510.

Jessen, J., Willett, C.E., and Lin, S. 1999. Artificial chromosome transgenesis reveals long-distance negative regulation of *rag1* in zebrafish. *Nat. Genet.* 23:15-16.

Kime, D.E. 1998. Introduction to fish reproduction. *In* Endocrine Disruption in Fish (D.E. Kime, ed.) pp. 83-107. Kluwers Academic Press, Boston.

Kime, D.E. and Nash, J.P. 1999. Gamete viability as an indicator of reproductive endocrine disruption in fish. *Sci. Total Environ.* 233:123-129.

Kimmel, C.B., Warga, R.M., and Schilling, T.F. 1990. Origin and organization of the zebrafish fate map. *Development* 108:581-594.

Kimmel, C.B., Ballard, W.W., Kimmel, S.R., Ullmann, B., and Schilling, T.F. 1995. Stages of embryonic development of the zebrafish. *Dev. Dynamics* 203:253-310.

Kinoshita, M., Tanaka, M., and Yamashita, M. 2000. Development of transgenic fish strain and promoter analysis. *Tanpakushitsu Kakusan Koso* 45:2954-2961.

Lee, R.K., Stainier, D.Y.R., Weinstein, B.M., and Fishman, M.C. 1994. Cardiovascular development in the zebrafish. *Development* 120:3361-3366.

Legler, J., Zeinstra, L.M., Schuitemaker, F., Lanser, P.H., Bogerd, J., Brouwer, A., Vethaak, A.D., De Voogt, P., Murk, A.J., and Van der Burg, B. 2002. Comparison of in vivo and in vitro reporter gene assays for short-term screening of estrogenic activity. *Environ. Sci. Technol.* 36:4410-4415.

Lele, Z., and Krone, P.H. 1996. The zebrafish as a model system in developmental, toxicological and transgenic research. *Biotechnol. Adv.* 14:57-72.

Liang, M.R., Alestrom, P., and Collas, P. 2000. Glowing zebrafish: Integration, transmission, and expression of a single luciferase transgene promoted by noncovalent DNA-nuclear trans-

port peptide complexes. *Mol. Reprod. Dev.* 55:8-13.

Lin, C.H., Yang, S., and Hopkins, N. 1994. LacZ expression in germline transgenic zebrafish can be detected in living embryos. *Devel. Biol.* 161:77-83.

Matthews, D.J. 2001. From model animal to animal model: Synergy between model organism genetics and high-throughput drug discovery. *Curr. Drug Discovery*, November, pp. 19-22.

Miranda, C.L., Collodi, P., Zhao, X., Barnes, D.W., and Buhler, D.R. 1993. Regulation of cytochrome p450 expression in a novel liver cell line from zebrafish (*Brachydanio rerio*). *Arch. Biochem. Biophys.* 305:320-327.

Mizell, M. and Roming, E.S. 1997. The aquatic vertebrate embryo as a sentinel for toxins: Zebrafish embryo dechorionation and perivitelline space microinjection. *Int. J. Devel. Biol.* 41:411-423.

Mullins, M.C., Hammerschmidt, M., Haffter, P., and Nusslein-Volhard, C. 1994. Large-scale mutagenesis in the zebrafish: In search of genes controlling development in a vertebrate. *Curr. Biol.* 4:189-202.

Nakamura, T., Okada, K., Nagata, K., and Yamzoe, Y. 2000. Intestinal cytochrome P450 and response to rifampicin in rabbits. *Japanese J. Pharm.* 82:232-239.

Nasevicius, A. and Ekker, S.C. 2000. Effective targeted gene "knockdown" in zebrafish. *Nature Genet.* 26:216-220.

OECD. 1992a. Guideline 203: Guidelines for testing of chemicals: Fish, aquatic toxicity test, adopted: 17.07.92. Organisation for Economic Co-operation and Development, Paris.

OECD. 1992b. Guideline 204: Guidelines for testing of chemicals: Fish, prolonged toxicity test: 14-day study. Organisation for Economic Co-operation and Development, Paris.

OECD. 1992c. Guideline 210: Guidelines for testing of chemicals: Fish, early-life stage toxicity test, adopted: 17.07.92. Organisation for Economic Co-operation and Development, Paris.

OECD. 1998. Guideline 212: Guidelines for testing of chemicals: Fish, short-term toxicity on embryo and sac-fry stages, adopted 21.09.98. Organisation for Economic Co-operation and Development, Paris.

OECD. 2000. Guideline 215: Guidelines for testing of chemicals: Fish, juvenile growth test, adopted: 21.01.2000. Organisation for Economic Co-operation and Development, Paris.

Okamura, H., Wantanbe, T., Aoyama, I., and Hasobe, M. 2002. Toxicity evaluation of new antifouling compounds using suspension-cultured fish cells. *Chemosphere* 46:945-951.

Olsson, P.E., Westerlund, L., Teh, S., Billsson, K., Berg, H., and Tysklind, M. 1999. Effects of maternal exposure to estrogen and PCB on different life stages of zebrafish (*Danio rerio*). *AMBIO* 28:100-106.

Orn, S., Andersson, P., Forlin, L., Tysklind, M., and Norrgren, L. 1998. The impact on reproduction of an orally administrated mixture of selected PCBs in zebrafish (*Danio rerio*). *Arch. Environ. Contam. Toxicol.* 35:52-57.

Page, J.G., Rogers, T.S., Fulton, R.B., Thompson, C.R., Hill, D.L., Smith, A.C., and Tomaszewski, J.E. 1998. Toxicity of COL-3 to rats and monkeys. *Proc. Am. Assoc. Cancer Res.* 39:596.

Parng, C., Seng, W.L., Semino, C., and McGrath, P. 2002a. Zebrafish: A preclinical model for drug screening. *Assay Drug Dev. Technol.* 1:41-48.

Parng, C., Semino, C., Zhang, C., and McGrath, P. 2002b. Gene expression profiling in zebrafish after drug treatment. *Toxicologist* 66:LB75.

Pelissero, C., and Sumpter, J.P. 1992. Steroids and "steroids-like" substances in fish diets. *Aquaculture* 107:283-301.

Peterson, R.T., Link, B.A., Dowling, J.E., and Schreiber, S.L. 2000. Small molecule developmental screens reveal the logic and timing of vertebrate development. *Proc. Natl. Acad. Sci. U.S.A.* 97:12965-12969.

Ruoppa, M. and Nakari, T. 1988. The effects of pulp and paper industry waste water on the fertilized eggs and alevins of zebrafish and on the physiology of rainbow trout. *Water Sci. Technol.* 20:201-202.

Schreurs, R., Lanser, P., Seinen, W., and Van der Burg, B. 2002. Estrogenic activity of UV filters determined by an in vitro reporter gene assay and an in vivo transgenic zebrafish assay. *Arch. Toxicol.* 76:257-261.

Schulte, C. and Nagel, R. 1994. Test acute toxicity in the embryo of zebrafish, *Brachydanio rerio*, as an alternative to the acute fish test: Preliminary results. *Altern. Lab. Anim.* 22:12-19.

Semino, C., Zhang, C., Parng, C., and McGrath, P. 2002. Zebrafish as an animal model to assess drug toxicity. *Toxicologist* 66:LB59.

Sinz, M.W. and Woolf, T.F. 1997. Characterization of the induction of rat microsomal cytochrome P450 by tacrine. *Biochem. Pharmacol.* 54:425-427.

Solnica-Krezel, L., Stemple, D.L., and Driever, W. 1995. Transparent things: Cell fates and cell movements during early embryogenesis of zebrafish. *BioEssays* 17:931-939.

Stainier, D.Y.R. and Fishman, M.C. 1994. The zebrafish as a model system of cardiovascular development. *Trends Cardiovasc. Med.* 4:117-121.

Stainier, D.Y.R., Lee, R.K., and Fishman, M.C. 1993. Cardiovascular development in the zebrafish. *Development* 119:31-40.

Strahle, U. and Blader, P. 1994. Early neurogenesis in the zebrafish embryos. *FASEB J.* 8:692-698.

Streisinger, G., Walker, C., Dower, N., Knauber, D., and Singer, F. 1981. Production of clones of homozygous diploid zebra fish (*Brachydanio rerio*). *Nature* 291:293-296.

Stringer, B. and Blankememyer, J. 1993. Rapid measurement of toxicity using electrochromic

dyes and frog embryos. *Bull. Environ. Contam. Toxicol.* 51:557-563.

Stuart, G.W., McMurray, J.V., and Westerfield, M. 1988. Replication, integration and stable germline transmission of foreign sequences injected into early zebrafish embryos. *Development* 103:403-412.

Stuart, G.W., Vielkind, J.R., McMurray, J.V., and Westerfield, M. 1990. Stable lines of transgenic zebrafish exhibit reproducible patterns of transgene expression. *Development* 109:577-584.

Sumpter, J.P. and Jobling, S. 1995. Vitellogenesis as a biomarker for estrogenic contamination of the aquatic environment. *Environ. Health Perspect.* 103:173-178.

Sun, Z. and Hopkins, N. 2001. vhnf1, the MODY5 and familial GCKD-associated gene, regulates regional specification of the zebrafish gut, pronephros, and hindbrain. *Genes Dev.* 15:3217-3229.

Takahashi, H. 1977. Juvenile hermaphroditism in the zebrafish (*Brachydanio rerio*). *Bull. Faculty of Fisheries Hokkaido University* 28:57-65.

Talbot, W.S. and Schier, A.F. 1999. Positional cloning of mutated zebrafish genes. *In* The Zebrafish: Genetics and Genomics (H.W.III Detrich, M. Westerfield, and L. Zon, eds.) pp 260-286, Academic Press, San Diego.

Thermes, V., Grabher, C., Ristoratore, F., Bourrat, F., Choulika, A., Wittbrodt, J., and Joly, J. 2002. I-*Sce*l meganuclease mediates highly efficient transgenesis in fish. *Mech. Dev.* 118:91.

Van Leeuwen, C.J., Grootellar, E.M., and Niebeek, G. 1990. Fish embryos as teratogenicity screens: A comparison of embryotoxicity between fish and birds. *Ecotoxicol. Environ. Saf.* 20:42-52.

Vitozzi, L. and De Angelis, G. 1991. A critical review of comparative acute toxicity data on freshwater fish. *Aquatic Toxicol.* 19:167-204.

Wannemacher, R., Rebstock, A., Kulzer, E., Schrenk, D., and Bock, K. 1992. Effects of 2,3,7,8-tetrachlorodibenzo-*p*-dioxin on reproduction and oogenesis in zebrafish. *Chemosphere* 24:1361-1368.

Ward, A.C. and Lieschke, G.J. 2002. The zebrafish as a model system for human disease. *Frontiers Biosci.* 7:d827-d833.

Westerfield, M., Wegner, J., Jegalian, B.G., DeRobertis, E.M., and Puschel, A.W. 1992. Specific activation of mammalian Hox promoters in mosaic transgenic zebrafish. *Genes Dev.* 6:591-598.

Wiegand, C., Pflugmacher, S., Giese, M., Frank, H., and Steinberg, C. 2000. Uptake, toxicity, and effects on detoxication enzymes of atrazine and trifluoroacetate in embryos of zebrafish. *Ecotoxicol. Environ. Saf.* 45:122-131.

Wiegand, C., Krause, E., Steinberg, C., Pflugmacher, S. 2001. Toxicokinetics of atrazine in embryos of the zebrafish. *Ecotoxicol. Environ. Saf.* 49:199-205.

Wilson, E.T., Cretekos, C.J., and Helde, K.A. 1995. Cell mixing during epiboly in the zebrafish embryo. *Dev. Genet.* 17:6-15.

Yabu, T., Kishi, S., Okazaki, T., and Yamashita, M. 2001. Characterization of zebrafish caspase-3 and induction of apoptosis through ceramide generation in fish fathead minnow tailbud cells and zebrafish embryo. *Biochem. J.* 360:39-47.

Zhu, L. and Shi, S.J. 2002. Utilization of embryo development technique of zebrafish to evaluate toxicity on various chemicals. *Ying Yong Sheng Tai Xue Bao* 13:252-254.

Contributed by Chaojie Zhang and Catherine Willett
Phylonix Pharmaceuticals
Cambridge, Massachusetts

Trisha Fremgen
Northeastern University
Boston, Massachusetts

Preclinical Models of Parkinson's Disease

Parkinson's disease (PD) is a neurodegenerative disorder in which pigmented midbrain neurons progressively die producing a dopamine (DA) deficit in the striatum, which manifests as an akinetic movement disorder. Experimentally induced striatal DA depletion in animals is a valid model of parkinsonism (Schultz, 1982). The capacity of certain substances to damage catecholaminergic neurons has been used extensively to produce DA deficiency in animals (Ungerstedt, 1971a,b; Burns et al., 1983; Annett et al., 1992). This unit describes methods for inducing parkinsonism in nonhuman primates and rodents using the neurotoxins 1-methyl-4-phenyl-1,2,3,6-tetrahydropyridine (MPTP; Basic Protocols 1 and 4 and Alternate Protocol 1) and 6-hydroxydopamine (6-OHDA; Basic Protocols 2 and 3). Additionally, procedures for evaluating the animals are presented (Support Protocols 1 to 4). Other models are briefly reviewed in the Commentary.

STRATEGIC PLANNING

Model Selection: Species

Rodent models of PD are good anatomical and biochemical models of the disease. However, they are not good functional models because the behavioral syndrome only superficially resembles some aspects of idiopathic PD, and the progressive nature of the disease is not reproduced. The complex behavioral repertoire of monkeys provides greater scope for determining the extent of functional recovery.

In nonhuman primates, administration of MPTP can induce a stable parkinsonian syndrome that is remarkably similar to the idiopathic disease (Burns et al., 1983). All primates are susceptible to MPTP toxicity. However, marmosets show considerable motor recovery despite biochemical and histological evidence for extensive damage, so that in the chronic stage only mild akinesia and incoordination of movement remain. The choice of species for specific experiments depends on the cost, availability of the animals, the type of study proposed (some species, like squirrel monkeys, are difficult to train), and the size of the brain required (for certain neuroimaging studies, such as positron emission tomography or PET scanning, the large brain of baboons is preferable). All results and specifications concerning doses and behavior in this unit refer to macaques (Rhesus and Cynomolgus) in the MPTP models and marmosets for the 6-OHDA lesions.

As in primates, MPTP and 6-OHDA are the most common toxicants used to induce DA depletion in rodents. Rats are the most commonly used experimental rodents, but they are rather insensitive to MPTP, requiring high doses and, with most strains, intracerebral administration of 1-methyl-4-phenyl-pyridinium (MPP^+; the toxic metabolite of MPTP). So far, 6-OHDA lesioning continues to be the most popular parkinsonian model in rats.

Lesion

Different lesions yield appropriate animal models to evaluate different therapeutic strategies, such as DA replacement (cell-mediated or pharmacological), neuroprotection, and neuroregeneration, as well as physiopathological mechanisms of neurodegeneration. Complete DA lesions in experimental animals are considered, at least in a neuropathological sense, analogous to end-stage PD. Data obtained from studies using this type of model are useful for the evaluation of therapeutic strategies aimed at DA replacement, as the DA-mediated positive effects will not be complicated by the potential response of remaining host DA neurons. On the other hand, experimental PD models sparing some DA terminals are analogous to less severe stages of the disease and are appropriate for investigating the potential benefit of regenerative approaches (e.g., the use of trophic

Contributed by Krys S. Bankiewicz, Rosario Sanchez-Pernaute, Yoshitsugu Oiwa, Malgorzata Kohutnicka, Alex Cummins, and Jamie Eberling

Current Protocols in Toxicology (2003) 1.8.1-1.8.31

factors) that require the presence of some residual DA neurons. In the context of tissue transplantation, the relative contributions of DA replacement or graft-induced trophic responses of a particular procedure are probably best addressed when efficacy is compared in both types of model.

Toxin

MPTP

The capacity of MPTP to induce persistent parkinsonism in humans (Davis et al., 1979) and in nonhuman primates (Burns et al., 1983) provides the opportunity to investigate both therapeutic approaches and possible pathogenic mechanisms of PD in primate models. Three models can be induced in primates by MPTP administration: (1) the unilateral model, induced by internal carotid artery (ICA) administration; (2) the bilateral model, induced by systemic (i.v., i.m., or s.c.) administration; and (3) the combined overlesioned or bilateral asymmetric model, induced by unilateral ICA plus i.v. administration. Basic Protocol 1 describes procedures for both ICA and systemic administration.

Mice exhibit characteristic neuropathological and biochemical signs of DA system damage following systemic administration of MPTP (Basic Protocol 4). Loss of tyrosine hydroxylase (TH)–positive neurons is seen in the substantia nigra pars compacta (SNc) and decreased levels of DA and its metabolites are observed in the striatum. These changes are accompanied by akinesia-depressed spontaneous motor activity (Heikkila et al., 1985; Hallman et al., 1985; Donnan et al., 1987; Sundstrom et al., 1990). Rats are very resistant to MPTP; to produce significant DA damage, the toxic metabolite MPP^+ has to be directly administered into the CNS.

6-OHDA

6-Hydroxydopamine has been used extensively to produce parkinsonism in rodents; however, few studies in primates have used this toxin (Schultz, 1982; Annett et al., 1992), most likely because it requires intracerebral administration. Basic Protocols 2 and 3 describe the respective procedures for stereotactic administration of this toxin in primates and rats.

NOTE: All protocols using live animals must first be reviewed and approved by an Institutional Animal Care and Use Committee (IACUC) and must follow officially approved procedures for the care and use of laboratory animals.

BASIC PROTOCOL 1

COMBINED ICA AND INTRAVENOUS ADMINISTRATION OF MPTP: THE OVERLESIONED (BILATERAL ASYMMETRIC) PRIMATE MODEL

In both humans and nonhuman primates, administration of MPTP produces a stable parkinsonian syndrome (Burns et al., 1983). MPP^+ is the toxic metabolite of MPTP (Nicklas et al., 1985), and conversion of MPTP to MPP^+ is mediated by monoamine oxidase B (MAO-B). MPP^+ accumulates selectively in neurons possessing a DA uptake system (Javitch et al., 1985) and is further concentrated in mitochondria. The basis of the toxic effects of MPP^+ is only partially understood; retrograde axonal transport, melanin binding, and damage to the mitochondrial respiratory system (Nicklas et al., 1985) have been implicated in the pathogenesis of injury to DA neurons. Replacement of DA with L-3,4-dihydroxyphenylalanine (L-DOPA) is the most common therapeutic approach in PD, and thus far the most efficacious. L-DOPA response is a diagnostic criterion and staging tool in PD and, as such, it is included in this unit with other outcome measures for parkinsonian primates. Evaluation of the response of MPTP-lesioned nonhuman primates to L-DOPA is also useful for validating the sensitivity of the specific neurobehavioral measures used to assess the effect of novel therapies and to compare the relative efficacy of such therapies, taking into account both positive and adverse effects. Moreover, the direct effect of different therapies on the response to L-DOPA can be investigated.

Materials

Sterile saline: 0.9% (w/v) NaCl
10-mg vial of 1-methyl-4-phenyl-1,2,3,6-tetrahydropyridine HCl (MPTP·HCl; Sigma)
Adult macaques (Rhesus and Cynomolgus; Sierra Biomedical or Charles River)
Ketamine/xylazine
Isoflurane
Betadine
70% (v/v) ethanol
0.1 M HCl
Peroxide

10- and 60-ml sterile syringes
10- or 30-ml sterile vial
Animal balance (accurate to 0.1 g)
Intravenous (i.v.) extension set
Electric shaver
Alcohol pads
22-G i.v. catheter
Tracheal tube
Surgical table
Absorbant blue benchpads
Stretch gauze and cotton swabs
Sterile surgical tools: scalpel, large forceps, delicate curved forceps, scissors, needle holders, retractors, mosquito hemostats
27-G sterile needle
Infusion pump (fitted for a 60-ml syringe)
3-0 Vicryl with needle
Plastic, transparent millimeter-scale ruler
22-G angiocatheter
Heated water pad
Drapes
2/0 silk suture
Towel clamps

CAUTION: The most hazardous operations in conducting MPTP animal experiments are the preparation, handling, and injection of concentrated solutions of MPTP. Always use a chemical hood and skin protection (gloves, Tyvex laboratory coat) and mask. Any spilled MPTP should be degraded by spraying with 0.1 N HCl, while excess solution should be mixed 1:1 with 6 M H_2SO_4 and degraded by adding 4.7 mg potassium permanganate per 100 ml. The concentration of MPTP in the solution used for ICA administration is very low (0.03 to 0.07 mg/ml) and therefore quite safe. However, solutions for i.v. administration (even small volumes) are much more concentrated, and additional caution must be taken.

NOTE: Animals should be adults and should interact well with the investigators so clinical evaluation can be performed.

Prepare MPTP solution

1. Fit a 10-ml sterile syringe with a 20- or 23-G needle and fill with sterile saline.
2. Infuse 1 ml sterile saline into a sterile vial containing 10 mg MPTP·HCl. Aspirate the 1-ml solution back into the syringe to complete the 10-ml volume (final 1 mg/ml MPTP).
3. Transfer the entire 10-ml MPTP solution into a sterile 10- or 30-ml vial.

4. Weigh the animal (within 0.1 g) and determine the total dose, adjusting for the HCl group using a 1.2× conversion factor.

   Particular caution should be exercised when calculating the dose for intracarotid administration. MPTP is toxic during the infusion (i.e., first pass effect) only because it undergoes peripheral conversion to MPP^+, which cannot cross the blood brain barrier. For this route of administration, MPTP should be calculated according to brain size, which tends to be constant over wide body weight ranges, instead of per body weight. The latter can give the false impression that older (heavier) animals are more susceptible to MPTP, when in fact they are receiving larger doses for similar brain sizes. As a general guideline, 2 to 2.5 mg can be used for small (3 to 5 kg) animals, 3 to 3.5 mg for a 6- to 10-kg monkey, and 4 mg for large (>10 kg) animals.

5. Fill a sterile 60-ml syringe with 2 to 4 ml MPTP solution (2 to 4 mg MPTP). Fill the rest of the syringe with sterile saline and attach an i.v. extension set.

   The final concentration in the syringe is 2 to 4 mg/60 ml (0.033 to 0.067 mg/ml MPTP).

Prepare the animal

6. Anesthetize a macaque monkey with ketamine (10 mg/kg) and xylazine (1 mg/kg) in the home cage. Transfer to the procedure room.
7. Shave the calves and neck region of the animal using an electric shaver. Palpate the calf muscle and identify the saphenous vein.
8. Clean the skin with an alcohol pad. Using a 22-G i.v. catheter, cannulate the vessel and flush with saline.
9. Intubate the animal with a 3.5- to 5-mm (inside diameter) tracheal tube, according to the size of the animal.
10. Transfer the animal to a surgery room, place it on a surgical table with absorbant blue benchpads, and a heated water pad at 37°C. Maintain isoflurane anesthesia at 1.5% with an oxygen flow of ~0.3 liters/min.
11. Hyperextend the head on the surgical table by placing stretch gauze through the canines and applying gentle retraction. Secure the head in position by tying the gauze to the surgery table.
12. Cover the animal completely with a series of sterile drapes. Cut out an opening in the drape for the neck incision and secure drapes with towel clamps. Scrub the surgery site with Betadine followed by 70% ethanol.
13. Make a midline incision through the skin of the neck with a sterile scalpel.
14. Using blunt dissection technique, locate and open the carotid sheath, exposing the common carotid artery, internal jugular vein, and vagus nerve (Fig. 1.8.1). Isolate the common carotid artery below the carotid bifurcation.
15. Locate the superior thyroid artery and the external carotid artery and temporarily clamp the vessels using mosquito hemostats.

    Typically, both superior thyroid and external carotid arteries form a very short branch medially to the carotid bifurcation. Hemostats should be clamped on this branch, if possible. Another alternative is to clamp both the thyroid superior and external carotid (below the external maxillary branch) arteries using single hemostats distal to the carotid bifurcation. Use only mosquito hemostats with an adjusted clipping mechanism formed by bending handles inside.

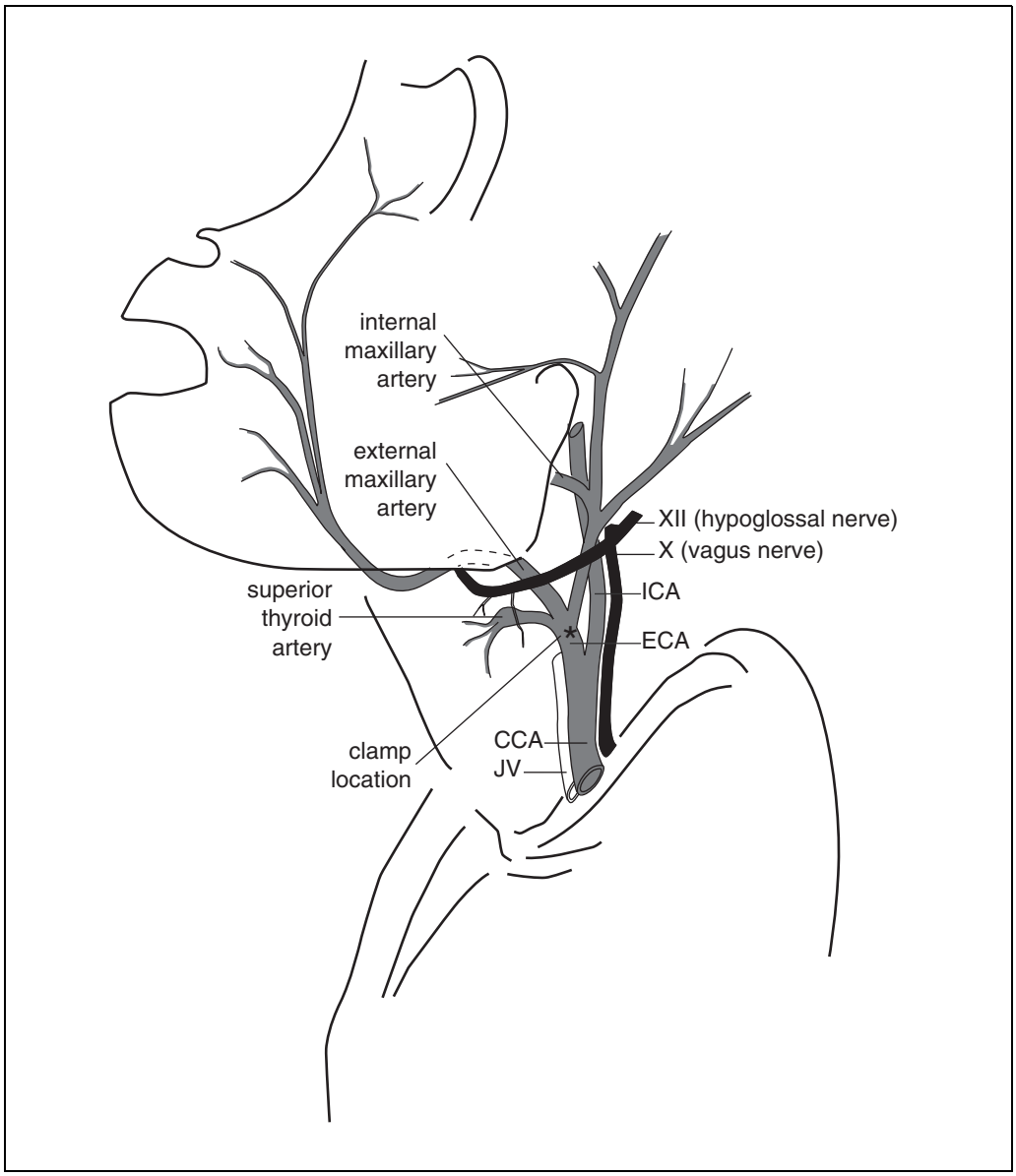

Figure 1.8.1 ICA dissection. The common carotid artery (CCA) at the level of the bifurcation showing the internal carotid artery (ICA), the X and XII cranial nerves, the external carotid artery (ECA), and its first branches: the superior thyroid artery and the external maxillary artery. An asterisk marks the recommended location of the vascular clamp, in the ECA proximal to the superior thyroid artery origin. JV, jugular vein.

16. Attach a 27-G needle to the i.v. extension tubing and drain all the air from the needle by activating an infusion pump for several seconds. Drain all excess MPTP onto a sponge soaked with 0.1 M HCl solution.

Perform ICA infusion

17. Insert the 27-G needle (with attached extension set and 60-ml MPTP syringe) into the internal carotid artery in a direction retrograde to the direction of blood flow.

18. Program the infusion pump to deliver 4 ml/min and infuse the entire volume from the syringe (2 to 4 mg MPTP).

19. Remove the vascular clamps (or mosquito hemostat) from the superior thyroid and external carotid arteries. Withdraw the needle from the common carotid artery and apply pressure for 5 min (until bleeding has stopped).

20. Clean the wound with peroxide, close the incision site at the neck with 3-0 Vicryl, and clean the sutured area.

21. Monitor the recovery of the animal and return it to the animal room. Record ipsilateral pupil mydriasis (dilation) by measuring the diameter of both pupils with a plastic transparent millimeter-scale ruler.

    In most cases, ipsilateral pupil mydriasis of 3 to 5 mm follows ICA infusion of MPTP solution. Absence of mydriasis does not indicate that lesion has not been successful, but its presence is a good indicator of unilateral damage.

    CAUTION: *Whenever possible, keep the animals in a quarantine room for 48 to 72 hr. Animal excreta may contain considerable amounts of unmetabolized MPTP; thus, precautions should be taken to minimize skin contact with animal fur and excreta and to avoid inhalation of bedding dust from MPTP-treated animals. As a general precaution, 0.1 N HCl solution should be used to spray the bedding in monkey cages during the first 48 hr after MPTP administration, and the cages should then be washed with an acidic solution. This ensures that any free MPTP is converted to its nontoxic form (for safety concerns see Yang et al., 1988).*

22. House animals for 2 weeks before i.v. administration.

Administer systemic (i.v.) MPTP

23. Weigh the animal (within 0.1 g) and determine the total dose of MPTP required, adjusting for the HCl group using a 1.2× conversion factor.

    For i.v. administration, the recommended dose is 0.3 mg/kg body weight.

24. Anesthetize the animal with ketamine (10 mg/kg) and xylazine (1 mg/kg) in the home cage. Transfer the monkey to the procedure room.

25. Shave the calves using an electric shaver. Palpate the calf muscle and identify the saphenous vein. Clean the vein with an alcohol pad.

26. Using a 22-G angiocatheter, cannulate the vessel and flush with sterile saline.

27. Fill a sterile 3- to 6-ml syringe with the appropriate volume of 1 mg/ml MPTP solution (0.3 ml/kg or 0.3 mg/kg) and infuse the MPTP into the vein over 3 min.

28. Flush the line with 3 ml sterile saline.

29. Remove the needle and apply pressure to the saphenous vein until bleeding stops.

    All safety guidelines described for ICA administration should be followed (see annotation to step 21).

Evaluate motor behavior

30. One week after i.v. administration of MPTP, assess the syndrome using a motor rating scale for primates (Table 1.8.1) based on the unified Parkinson's disease rating scale (UPDRS). Monitor response to L-DOPA (see Support Protocol 1) and activity (see Support Protocol 2).

Table 1.8.1 Rating Scale for Parkinsonian Primates[a]

Parameter	Score	Degree
Tremor (right arm/left arm)[b]	0	Absent
	1	Occasional or barely detectable (normal for aged), occurring while active
	2	Frequent or easily detectable, occurring while active or at rest
	3	Continuous or intense, occurring while active and at rest
Freezing	0	Absent
	1	Occasional episodes of short duration (<5 sec)
	2	Occasional episodes of moderate duration (6 to 10 sec)
	3	Frequent episodes or episodes of long duration (>10 sec)
Locomotion	0	Uses all four limbs smoothly and symmetrically
	1	Walks slowly (normal for aged), noticeable limp
	2	Walks very slowly and with effort, may drag limb or refuse to bear weight
	3	Unable to ambulate
Fine motor skills (right arm/left arm)[b]	0	Normal function: able to grasp/retrieve small objects, aims accurately, independent use
	1	Reduced ability in grasping/retrieving small objects, independent use, may have reduced aim
	2	Able to grasp small objects rarely, only with assistance, or with great difficulty
	3	Unable to grasp/retrieve small objects
Bradykinesia (right arm/left arm)[b]	0	Quick, precise movements
	1	Mild slowing of movements (normal for aged)
	2	Slow deliberate movements with marked impairment initiating movements
	3	No movements
Hypokinesia	0	Moves freely, alert, responsive
	1	Reduced activity (normal for aged), moves less frequently (without provocation)
	2	Minimal activity, moves with provocation, may have reduced facial expression
	3	Akinetic (essentially no movements)
Balance	0	Requires no assistance for maintaining posture
	1	Requires assistance for standing
	2	Requires assistance for walking, or falls
	3	Face down, or unable to maintain posture
Posture	0	Normal posture, stands erect
	1	Reduced posture (normal for aged), stands with feet apart, knees flexed
	2	Stooped posture, hunched, legs bent
	3	Unable to maintain posture, recumbent
Startle response	0	Immediate, robust response to provocation
	1	Slightly diminished or delayed response, open mouth threat
	2	Minimal response or longer delay, without open mouth threat
	3	No response to provocation
Gross motor skills (right arm/left arm)[b]	0	Normal function, able to grasp/retrieve large objects accurately
	1	Reduced ability/frequency of grasping/retrieving large objects
	2	Great difficulty in grasping/retrieving large objects, rarely used
	3	Unable to grasp/retrieve large objects

[a]According to mean scores in the scale, animals are classified into five stages. Stage 0: A maximum of 5 points is considered normal according to the authors' results in healthy animals. Stage 1: Total of 5-12 points; hemiparkinsonian monkeys do not show axial impairment. Stage 2: Total 12-20 points; mild to moderate bilateral symptoms. Stage 3: Total 21-30 points; moderate to severe bilateral symptoms, but without major systemic consequence. Stage 4: Total >30 points; severely damaged and can be difficult to manage due to feeding difficulties and complications of akinesia; may require DA replacement.

[b]Score each arm separately and add the total.

ALTERNATE PROTOCOL 1

SYSTEMIC MPTP LESION IN PRIMATES

The principal advantage of this approach is that the behavioral syndrome closely resembles that of Parkinson's disease in humans. The main drawbacks are that it takes a long time to produce animals with stable and uniform lesions and, if the lesion is too extensive, it produces a considerable mortality. Total dose is not predetermined, but will depend on the highly variable response of each animal to the toxin. Therefore, careful clinical evaluation is mandatory throughout the lesion progression. The toxic effect is cumulative.

Additional Materials (also see Basic Protocol 1)

3-ml syringes equipped with 26-G needles
Cage with back-squeezing mechanism

1. Prepare MPTP as described (see Basic Protocol 1, steps 1 to 3).
2. Weigh the animal and determine the appropriate dose (0.33 to 1 mg/kg), adjusting for the HCl group with a 1.2× conversion factor.
3. Fill a sterile syringe with the appropriate volume of MPTP solution.
4. With the monkey in a cage with a back-squeezing mechanism, squeeze the back of the cage to hold the animal and inject the MPTP intramuscularly or subcutaneously into the thigh or arm. For better results, inject twice a week.

   Follow safety guidelines described for ICA administration (see Basic Protocol 1, step 21).

   If the animal shows general symptoms such as feeding difficulty or profound akinesia, stop the injections and reevaluate the motor syndrome (see Table 1.8.1) 2 to 4 weeks later.
5. Assess the syndrome as described (see Basic Protocol 1, step 30).

BASIC PROTOCOL 2

UNILATERAL 6-OHDA LESION IN PRIMATES

6-OHDA uses the catecholamine uptake system to enter catecholamine neurons and kill the cells through oxidative mechanisms. Unilateral injection of 6-OHDA into the medial forebrain bundle of marmosets produces a severe loss of tyrosine hydroxylase-immunoreactive neurons in the ipsilateral SNc and DA depletion of >90% in the dorsal striatum, accumbens, and frontal cortex ipsilateral to the lesion (Annett et al., 1992). Levels of 5-hydroxytryptamine and noradrenaline (NA) are also decreased, but previous administration of NA uptake blockers (e.g., desipramine) limits the non-DA damage. The animals show ipsilateral spontaneous rotation, contralateral apomorphine-induced rotation, reduced spontaneous activity, contralateral sensorimotor neglect, and ipsilateral hand preference with variable impairment of hand skill (Annett et al., 1992). Persistent deficits are observed in animals with >95% DA depletion.

Materials

Sterile saline: 0.9% (w/v) NaCl
Adult marmosets (Sierra Biomedical or Charles River)
Ketamine/xylazine
Isoflurane
Betadine
70% (v/v) ethanol
4 mg/ml 6-hydroxydopamine (6-OHDA), HBr (Sigma) in 0.01% (w/v) ascorbate/0.9% (w/v) NaCl (protect from light)

Stereotaxic frame/tower (David Kopf Instruments)
Manipulator arm
Spinal needle

5-ml syringes
Intravenous (i.v.) line with 3-way stopcock
22-G angiocatheter
Animal balance
Electric razor
Alcohol pads
Surgical tape
Tracheal tube
Isoflurane inhalation chamber
Sterile drapes, gauze, and rubber bands
Towel clamps
Tissue forceps
Scissors
Electric cauterizer
Water heating pad
Dremel drill with carbide bur excavating tip
10-µl Hamilton syringes and needle
3-0 Vicryl
2-0 silk sutures

NOTE: Animals should be adults and should interact well with the investigators so clinical evaluation can be performed.

Calibrate stereotactic frame

1. Fix the settings on the ear bars of a stereotactic frame so the bars are ~1 mm apart.
2. Fit the manipulator arm with a 20-G spinal needle and position it on the stereotactic frame. Ensure that the mark readings on both ear bars are identical.
3. Advance the spinal needle into the space between the ear bars. Adjust the position of the needle along the anterior/posterior (A/P) scale to correlate with the plane of the ear bars.

Prepare animal

4. Flush an i.v. line with sterile saline using a 5-ml syringe, then prime a 22-G angiocatheter and 3-way stopcock with saline.
5. In the animal room, weigh a marmoset and anesthetize with 10 mg/kg ketamine/1 mg/kg xylazine. Transfer animal to the surgery room.
6. Shave the calves, arms, and head for surgical and intravenous access using an electric razor.
7. Palpate the calf muscle or flex and extend the ankle to visualize the saphenous vein. Clean the shaved area with an alcohol pad.
8. Insert the 22-G angiocatheter into the saphenous vein and flush with saline to ensure patency.
9. Attach the 3-way stopcock with i.v. line to the catheter and start a slow saline drip (1 ml/min) to maintain patency of the vessel. Secure the i.v. line onto the calf muscle using surgical tape.
10. Intubate the animal with an appropriate size tracheal tube and maintain on isoflurane anesthesia by inhalation.

Position animal in stereotactic frame

11. Place the animal in the stereotactic frame and tighten the right ear bar to the frame. Elevate the animal's head and insert the right ear bar into the ear canal.
12. Position the left ear bar in the animal's left ear. Ensure that the animal's eyes are parallel to the front plane of the frame.
13. Center the animal's head such that the same setting for both ear bars is achieved. Position the eye bars in the inferior border of the orbits. Set the incisor bar and readjust the eyebars to the inferior orbital rim. Fix the incisor bar at an adequate height.
14. Clean the entire surface of the cranium by scrubbing in an outward circular motion with Betadine scrub followed by 70% ethanol. Spray the stereotactic frame with 70% ethanol. Use sterile gloves for cranium preparation.
15. Cover the animal completely with a heating pad and then cover it with a series of sterile drapes. Cut out an opening in the drape for the craniotomy and secure drapes with towel clamps.

Administer 6-OHDA

16. Determine the target skin incision site using the baseline A/P coordinates as a guideline. Make a small sagittal incision through the skin and fascia using an electric cauterizer.
17. Using sterile gauze, retract the skin and fascia to expose the cranial surface. Secure the skin in place with towel clamps.
18. Cover a Dremel drill with sterile drapes and fix in place with sterile rubber bands. Use a carbide bur excavating tip and make a burr hole that exposes the dura.
19. Position the spinal needle over the first target site and manually advance the needle to the surface of the cranium. For marmosets, use the following coordinates with reference to stereotactic zero (Annett et al., 1992), with all five injection sites at A/P +6.5:

    one lateral (3 µl): lateral (L) ±3.2, ventral (V) 7.5
    two central (2 µl each): L ±2.2, V 6.5 and V 7
    two medial (2 µl each): L ±1.2, V 6 and V 7.

20. Insert the needle at the first target site, then touch the electric cauterizer to the needle and withdraw manually.
21. Place a 10-µl Hamilton syringe on the arm holder and infuse the selected volume of 4 mg/ml 6-OHDA at a rate of 0.5 µl/min. Leave the syringe in place for 5 min to avoid overflow.
22. Repeat steps 19 to 21 at the remaining four injection sites.
23. Suture the fascia with sterile 3-0 Vicryl. Close the incision site by subcutaneous suturing of the skin with 2-0 silk sutures. Clean and dry the incision site with sterile gauze and spray with Betadine.

Evaluate motor behavior

24. Evaluate nigral damage in vivo and post mortem using the methods described for the MPTP model (see Support Protocol 1 and Support Protocol 2). Also evaluate rotational behavior (see Support Protocol 3).

EVALUATION OF CHANGES IN MOTOR BEHAVIOR IN RESPONSE TO L-DOPA

Once the animals show a stable deficit (typically ~6 weeks), it is possible to evaluate the changes in motor behavior following an intramuscular injection of L-DOPA methyl ester (M-L-DOPA) with a peripheral inhibitor of L-aromatic amino acid decarboxylase. Dosing with Sinemet preparation does not provide predictable results due to inadequate control of intake and stomach content. M-L-DOPA injection should be used to ensure adequate brain delivery, as estimation of the effective dose is highly inaccurate with oral administration. Local complications are not observed using intramuscular (i.m.) injection.

The effect of L-DOPA can be evaluated using the activity or motor tasks shown in Table 1.8.1. For each animal, the response to saline injection should be used as control.

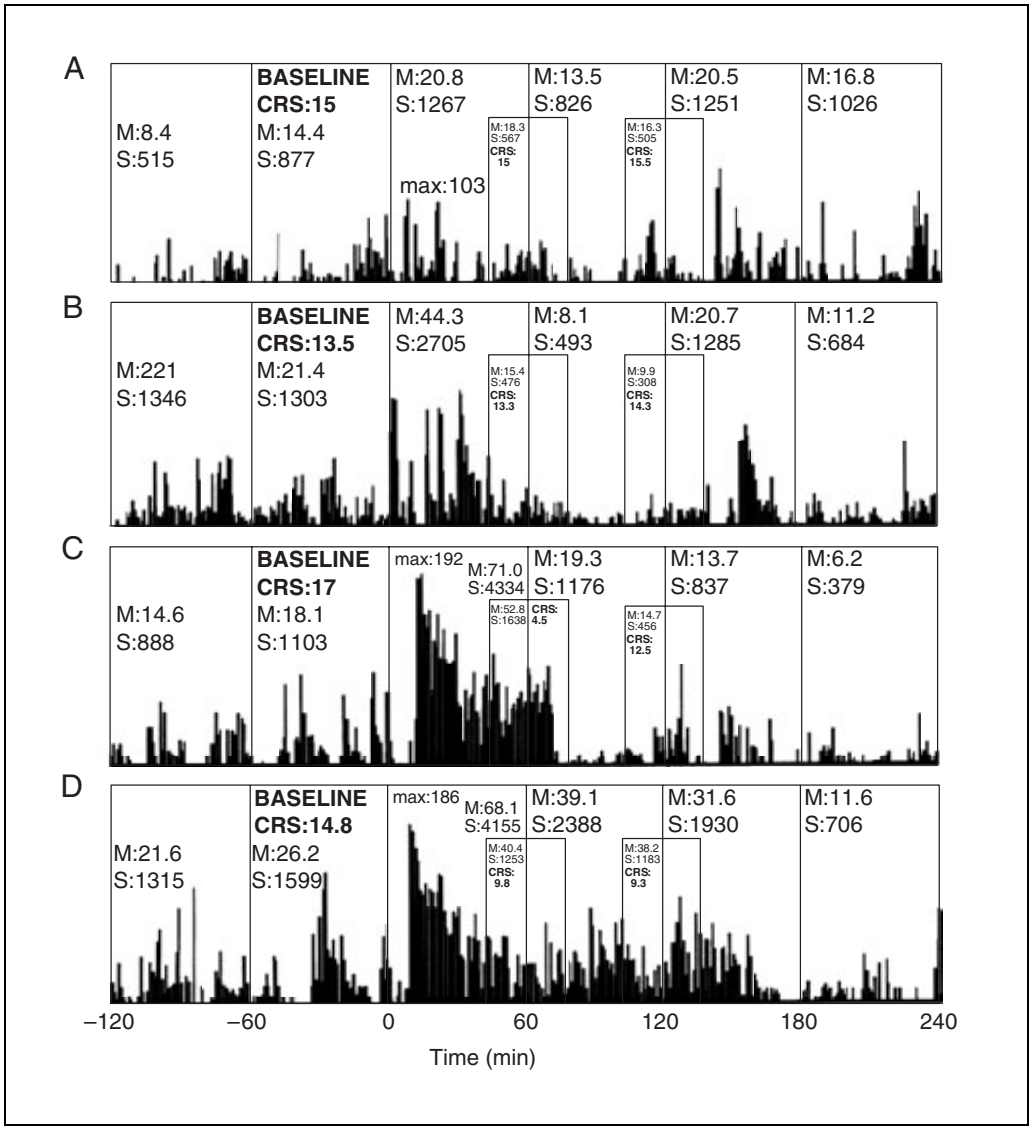

Figure 1.8.2 Activity and clinical rating scale (CRS) outcome of administration of increasing doses of M-L-DOPA in an overlesioned monkey. The drug was administered at time zero and activity is shown from 120 min before to 240 min following administration of (**A**) 5 mg, (**B**) 10 mg, (**C**) 20 mg, and (**D**) 40 mg M-L-DOPA. Mean and raw activity data for each segment is shown along with clinical score. During this experiment a shorter version of the scale was used; therefore, clinical score values are smaller than would be recorded using the scale as shown in Table 1.8.1. Increase of drug-induced activity is associated with clinical improvement in a dose-responsive manner. In panels, M, mean counts; S, sum of counts.

Materials

Lesioned animal (see Basic Protocol 1, Alternate Protocol 1, and Basic Protocol 2)
L-3,4-Dihydroxyphenylalanine methyl ester (M-L-DOPA; Sigma)
Benserazide (Sigma)
Sterile saline: 0.9% (w/v) NaCl

Cage with back-squeezing mechanism
3-ml syringes
26- to 30-G needles

1. Prepare the total dose of M-L-DOPA and add benserazide at a 1:10 benserazide/M-L-DOPA ratio. Mix and dilute in 1 to 2 ml sterile saline.

   Appropriate doses might vary for different stages and between species, but typical doses are 5 to 50 mg/kg.

2. With a lesioned monkey in a cage with a back-squeezing mechanism, squeeze the cage and inject i.m. into the thigh of the animal using a 3-ml syringe with a 26- to 30-G needle.

   It is advisable to keep the monkeys in cages with back-squeezing mechanisms so they can easily be held for i.m. injections, removal of monitors, or other quick procedures.

3. Rate the response according to the parameters described in Table 1.8.1. Evaluate the response 45 to 60 min after injection and at later time points when duration of the response is relevant.

   It is useful to videotape the animals, particularly when they display abnormal movements that might be difficult to categorize. Figure 1.8.2 shows typical results of the procedure.

SUPPORT PROTOCOL 2

MONITORING ACTIVITY TO ASSESS MPTP-TREATED MONKEYS

Whole-body activity measurement is a useful indicator of DA lesion in MPTP-treated monkeys and correlates with the global motor score (Fig. 1.8.3). This objective measure approximates akinesia, which is most pronounced in animals with moderate to severe lesions. The baseline motor activity is reduced and the normal pattern disappears after the MPTP lesion. An example of the striking MPTP effect on activity is shown in Figure 1.8.4. The personal activity monitors (PAM) contain a biaxial piezoelectric sensor that is calibrated to detect threshold activities $>0.024 \times g$ acceleration. Sensitivity and epoch length is programmable. The acceleration signal is sampled and digitally integrated to quantify all activity under the signal curve. The information is converted to a reference scale of data counts or acceleration units (G). The PAM monitor can be inserted into a vest that the animal wears during testing or into a collar around the neck. Activity data are normally acquired over four to five days that should include a weekend.

Materials

Lesioned animal (see Basic Protocol 1, Alternate Protocol 1, and Basic Protocol 2)
Ketamine/xylazine

Personal activity monitors (PAM; ActiTrac, Individual Monitoring Systems)
PAM connector cable
Computer
Nylon cable ties
Vetwrap
Nylon collars/vest

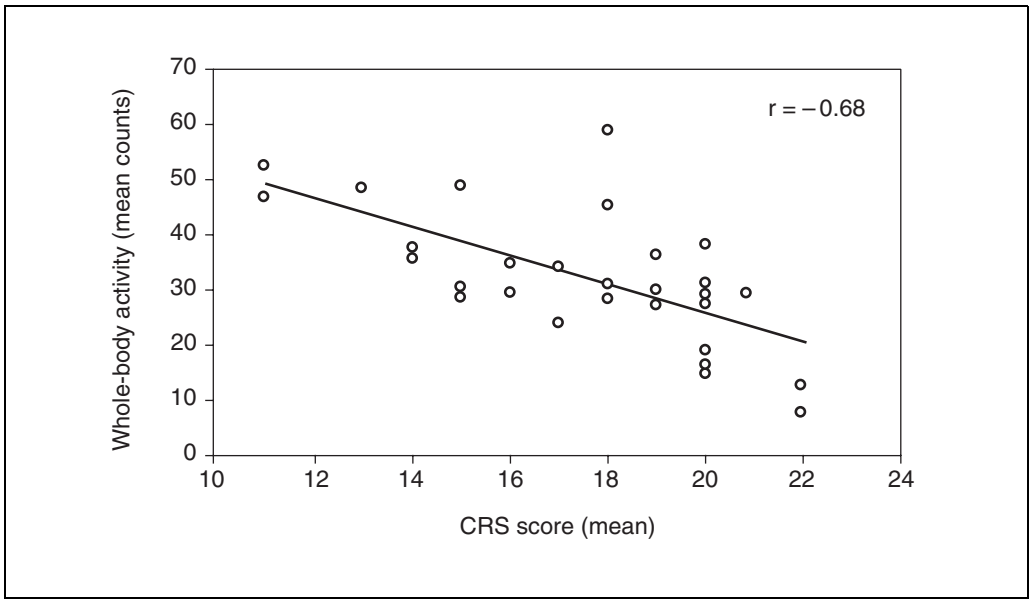

Figure 1.8.3 Correlation between clinical rating scale and whole-body activity in overlesioned hemiparkinsonian monkeys. Increased parkinsonian disability correlates well with a decrease in whole-body activity. Data from 28 overlesioned monkeys in stages 1, 2, and 3 are shown.

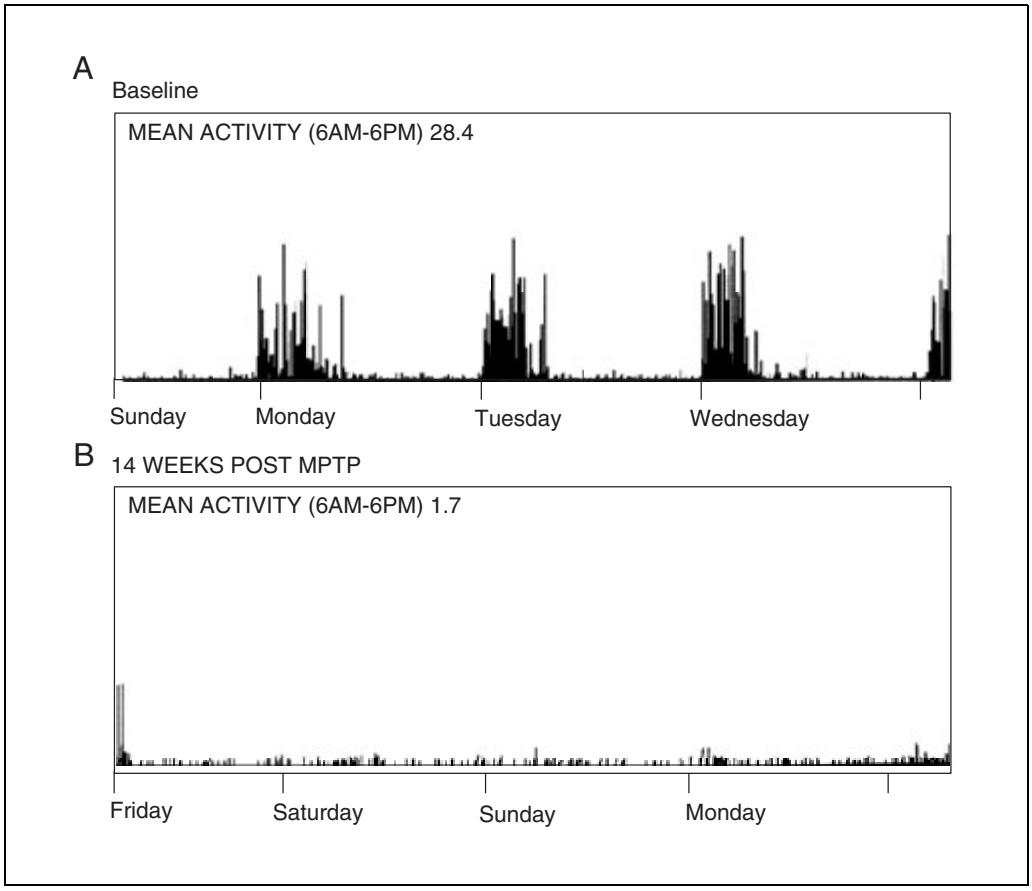

Figure 1.8.4 Whole-body activity measured by activity monitors (**A**) before and (**B**) 14 weeks after MPTP administration. Activity was recorded over 3 days.

1. Connect a PAM to a computer. Check that the battery level for the PAM is >5.25 volts, and program the sensitivity, epoch length, and start time and date. Enter the animal and test data.

   ActiTrac has a battery life of 4 years and memory allows up to 62 days of continuous recording. An epoch time of 1 min provides adequate information for time periods >60 min; to detect short-lived changes, use 30 sec.

2. Place the PAM in a horizontal position such that the PAM label faces outward. Secure the PAM to the collar using nylon cable ties. Wrap the monitor and cable ties with Vetwrap.
3. Anesthetize a lesioned animal in its home cage with 7 mg/kg ketamine and 1 mg/kg xylazine.
4. Place a nylon collar around the animal's neck and then wrap the buckle with Vetwrap.
5. Record the animal's identification number, the date and time, and the PAM identification number.
6. Begin activity data acquisition 60 min after administration of anesthesia.

   As long as data analysis is done comparing similar time periods (excluding setup and removal), the exact delay between anesthesia and activity monitoring is not critical.

7. Anesthetize the animal as in step 3 and remove the PAM.
8. Connect the PAM to the interface and download information to a data file.
9. Extract 12-hr segments (e.g., 6:00 am to 6:00 pm) and summarize them in a table (Fig. 1.8.4).

   Depending upon the study, activity is normally evaluated at the following time points: prelesion baseline, postlesion baseline, and postexperimental treatment. Mean and total counts can be used to compare animals but, as there is considerable variability between subjects, it is better to compare relative values (e.g., percentage with respect to baseline).

SUPPORT PROTOCOL 3

ROTATIONAL BEHAVIOR AS A MEASURE OF UNILATERAL NIGROSTRIATAL LESIONS

In animals with a unilateral DA lesion (see Basic Protocol 2), there is an imbalance of motor activity such that they usually display spontaneous turning toward the side of the lesion. Administration of indirect DA agonists (e.g., DA-releasing drugs such as D-amphetamine) increases the imbalance and the ipsilateral rotation. Administration of direct DA agonists (e.g., apomorphine) evokes contralateral turning, which is considered to be the result of denervation hypersensitivity of DA receptors in the lesioned side. Rotational behavior in response to DA agonists grossly correlates with the severity of the lesion (it is, in fact, better correlated with asymmetry indices). Quantification of the rotational response can be accomplished in monkeys by videotaping the animals and counting the turns, and in rats by using specific devices called rotometers (Ungerstedt, 1971a,b).

Suggested compounds and doses include 0.5 to 5 mg/kg D-amphetamine sulfate (Sigma) in saline and 0.025 to 0.25 mg/kg apomorphine·HCl (Sigma) in saline. Avoid amphetamine whenever possible, particularly if tests have to be repeated, as it might increase the mortality rate. For either compound, use the lower end of the range for primates (primates are susceptible to compound effects), the higher end for rats.

6-OHDA LESIONS IN RATS

In rats, several models can be induced by unilateral intracerebral stereotactic injection of 6-OHDA into different brain structures. Bilateral application of 6-OHDA is rarely used because of high mortality due to diencephalic damage (adipsia and aphagia); hence, only unilateral models are discussed here.

Complete DA lesion can be induced by unilateral injection of 6-OHDA in the medial forebrain bundle or in the SNc (Ungerstedt and Arbuthnott, 1970; Ungerstedt, 1971a). These animals demonstrate a characteristic asymmetric motor behavior in response to antiparkinsonian drugs (Ungerstedt, 1971b) that enables distinction between drugs with predominantly DA receptor agonist activity from those with predominantly DA-releasing activity. Systemic administration of L-DOPA or direct DA receptor agonists leads to contralateral rotation (towards the undamaged side), while administration of DA-releasing substances (amphetamine, amantadine) leads to ipsilateral rotation (in the direction of the damaged side). This model is also useful in studies of DA replacement therapy and neuroprotection factors.

Partial lesion models are induced by injection of 6-OHDA in the medial forebrain bundle (MFB) or SNc in smaller doses that leave a number of DA neurons intact (Zigmond and Strickler, 1989). These are useful models for the study of pathophysiological mechanisms and neuroregeneration.

The *selective A-9 lesion model* can be induced by injection of 6-OHDA in the SNc, leaving the ventral tegmental area (VTA or A-10 region) neurons intact (Perese et al., 1989; Thomas et al., 1994), thus reproducing the selective vulnerability of DA neurons in the SNc observed in idiopathic PD. This model is useful to study the contribution by other DA areas to the restoration of the nigrostriatal pathway and the differential effects of protective and repair mechanisms on different DA nuclei.

The *striatal lesion model* is induced by injections of 6-OHDA into the striatum, causing progressive retrograde degenerative changes of the corresponding DA neurons in the SNc (Sauer and Oertel, 1994; Lee et al., 1996). This is a useful model for pathophysiological, neuroregenerative, and neuroprotective studies.

Materials

Sprague-Dawley rats, 200 to 250 g
Isoflurane
Betadine
70% (w/v) ethanol
4 mg/ml 6-hydroxydopamine (6-OHDA, HBr; Sigma) in 0.01% (w/v) ascorbate/saline (protect from light)
Sterile saline: 0.9% (w/v) NaCl

Animal balance (accurate to 0.1 g)
Isoflurane inhalation chamber
Electric razor
Stereotactic frame
Scalpel
Tissue forceps
Scissors
10-µl Hamilton syringes and needles
Dental drill
Sutures or staples

Prepare animal

1. Weigh a Sprague-Dawley rat (within 0.1 g) and place in an isoflurane chamber until deeply anesthetized.
2. Position the animal in a stereotactic frame and fix the plastic tube connected to the anesthesia machine to the nose of the animal using surgical tape (make sure that the snout bar does not collapse the tube). Maintain isoflurane at ~1.5% with an oxygen flow of 2 to 3 liters/min.

   Alternative anesthetics such as ketamine/xylazine or chloral hydrate may also be used.
3. Shave the head with an electric razor. Clean the skin with Betadine and 70% ethanol.
4. Perform a midline incision with a scalpel and identify the bregma at the intersection of the coronal and the sagittal sutures.

Administer 6-OHDA

5. Fill a 10-µl Hamilton syringe with the appropriate 6-OHDA solution. Attach syringe to the holder on the stereotactic frame. Adjust 6-OHDA solutions according to the region of injection:

   For medial forebrain bundle lesion: 2 µg/µl 6-OHDA in saline containing 0.1% (w/v) ascorbic acid
   For SNc lesion: 4 µg/µl 6-OHDA in saline containing 0.02% (w/v) ascorbic acid
   For striatal lesion: 0.4 µg/µl 6-OHDA in saline containing 0.1% (w/v) ascorbic acid
   For A-9 selective lesion: 2 µg/µl 6-OHDA in saline containing 0.02% (w/v) ascorbic acid.
6. Calculate the stereotactic coordinates for injection (Paxinos and Watson, 1986). Some examples of possible injection sites include:

   For medial forebrain bundle lesion: Anteroposterior (A/P) −2.2 mm, mediolateral (M/L) 1.5 mm with reference to bregma; ventrodorsal (V/D) −8.0 mm with reference to dura
   For SNc: A/P −5.4 mm, M/L 2.2 mm with reference to bregma, V/D −7.5 mm with reference to dura
   For striatal lesion: A/P +0.5 mm, M/L 2.8 mm with reference to bregma, V/D −4.5 mm with reference to dura
   For A-9 selective lesion:
   1st lesion: A/P +3.5 mm, M/L 1.9 mm, V/D −7.1 mm with reference to lambda and dura with needle bevel directed rostrally
   2nd lesion: A/P +3.5 mm, M/L 2.3 mm, V/D −6.8 mm with reference to lambda and dura.
7. Adjust the incisor bar in the animal until the heights of lambda and bregma skull points are equal.
8. Drill a burr hole at the target site using a dental drill.
9. Lower the needle of the Hamilton syringe through the dura down to the selected depth and start injection at a rate of 0.5 to 1 µl/min. Adjust volumes (and doses) of 6-OHDA according to the region of injection:

   For medial forebrain bundle lesion: 4 µl solution (8 µg 6-OHDA)
   For SNc lesion: 2 µl solution (8 µg 6-OHDA)
   For striatal lesion: 20 µl solution (8 µg 6-OHDA)
   For A-9 selective lesion: 2 µl solution (4 µg 6-OHDA).

10. Leave the needle in place for 5 min and withdraw slowly (1 mm/min).
11. Close scalp margins with sutures or staples. Remove the animal from the stereotactic frame and place it in its home cage. Put food on the floor of the cage and monitor the animal's weight for 3 days after surgery. Supplement the diet (e.g., with fruit) if there is >10% weight loss.

Evaluate behavior

12. Evaluate rotational behavior (see Support Protocol 3).

MPTP LESION IN MICE

BASIC PROTOCOL 4

This model is induced by systemic administration of MPTP, which causes transient impairment of DA system function in these animals. It is a simple and useful model for studies on the pathophysiology of neurodegenerative processes as well as the effects of neurotrophic and neuroprotective agents.

Many different protocols have been used with various doses, routes of administration, and species. An example of the model induced by intraperitoneal administration of MPTP to C57Black mice, using four injections of 10 mg/kg (total 40 mg/kg), is described (Ricaurte et al., 1987).

Materials

C57Black mouse, age 8 to 12 months
1-Methyl-4-phenyl-1,2,3,6-tetrahydropyridine HCl (MPTP·HCl; Sigma)
Isotonic saline

Animal balance (accurate to 0.1 g)
1-ml syringe equipped with 26-G needle

1. Weigh a C57Black mouse (within 0.1 g).
2. Prepare a 1 mg/ml MPTP solution in isotonic saline.
3. Fill a 1-ml syringe, equipped with a 26-G needle, with MPTP solution to provide a dose of 10 mg/kg (e.g., 0.4 ml for 40-g mouse).
4. Hold mouse in dorsal recumbency with left leg immobilized. Insert the needle in the lateral aspect of the lower left abdominal quadrant through the skin and musculature, and immediately lift the needle against the abdominal wall and inject the solution.
5. Repeat the injection three times at 1-hr intervals.
6. Observe animals for any changes in general locomotion, stooped posture and piloerection (see Support Protocol 4).

MONITORING ACTIVITY IN MPTP-TREATED MICE

SUPPORT PROTOCOL 4

Open-field locomotor activity can be measured to evaluate the toxic effect of MPTP in mice and correlates with the content of dopamine in the striatum and nucleus accumbens (Leroux-Nicollet and Costentin, 1986). However, MPTP induces an acute increase in activity in some mouse strains, as the predominant effect in the early stage is inhibition of DA reuptake by MPTP. This effect can be blocked with neuroleptics. In C57 Bl/6 mice, MPTP produces a decrease in baseline activity (~60% in albino and 40% in black mice) that is prevented by administration of monoamine oxidase inhibitors. Amphetamine induces an increase in locomotor activity in normal animals that is absent in MPTP-lesioned animals. Apomorphine induces a decrease in locomotor activity that is not significantly different between normal and MPTP-injected animals.

Measurement of locomotor activity can range from simple observation to sophisticated automated procedures. In general, these instruments use an array of infrared photobeams and reveal the activity of the animal by the number and pattern of beam interruptions. The Digiscan Animal Activity Monitor (Omnitech Electronics) consists basically of a Plexiglas cage with infrared monitoring sensors at determined distances. A Digiscan analyzer collects data and transmits them to a computer for storage and further use. Several variables can be recorded, such as horizontal activity, movement time, total distance, average speed, average distance per horizontal movement, and number of movements.

Materials

MPTP-lesioned mouse (see Basic Protocol 4)
Dexamphetamine sulfate
Saline: 0.9% (w/v) NaCl

Automated open-field instrument (e.g., Digiscan Animal Activity Monitor; Omnitech Electronics)
1-ml syringe with 26- to 30-G needle

1. Place an MPTP-lesioned mouse in a Digiscan cage and record activity for the selected period of time.

   It is mandatory to perform pre-exposure habituation to get a reliable baseline.

2. Prepare dexamphetamine sulfate at 0.5 mg/ml in saline and place in a 1-ml syringe with a 26- to 30-G needle.
3. Weigh mouse and inject intraperitoneally at 1.5 mg/kg.
4. Place the animal in the Digiscan cage and record data for ≥30 min.

   It is important to perform all experiments at the same time of day as activity varies with circadian cycles.

COMMENTARY

Background Information

Evaluation of DA deficit in primates

Many different methods have been used to rate motor impairment induced in primates by MPTP and 6-OHDA. Rotational behavior and reach-and-grasp timed tasks are usually employed to quantify motor deficits in unilateral models. Marked delay in initiating movements on the side contralateral to ICA MPTP administration manifests clinically as "neglect" but, unlike cortical neglect, the animals respond when stimuli are maintained long enough, showing that the apparent inattention is really a profound hypokinesia. In these animals, this characteristic parkinsonian sign can be measured independently.

In most studies in which the functional capabilities of unilaterally lesioned monkeys have been examined, there are obvious deficits in gross motor behavior evident upon direct observation or detected by the use of automated monitoring devices or measurement of voluntary reaching movements. However, these measures provide little information about the cognitive abilities of the animal. Delayed responses and delayed alternation tests, which are measures sensitive to disruption of the frontostriatal system, are altered in monkeys treated with MPTP. These changes occur in monkeys with measurable motor deficits and also in animals treated chronically with low doses of MPTP that retain normal motor function by clinical assessment (Schneider and Kovelowski, 1990).

Neuroimaging techniques such as positron emission tomography (PET), single photon emission tomography (SPECT), and functional magnetic resonance imaging (MRI) are powerful methods that allow in vivo evaluation of DA function in parkinsonian monkeys. However, selecting the most appropriate approach depends largely on available resources. PET and the DA metabolism tracer [^{18}F]-6-fluoro-L-DOPA (FDOPA) have been used extensively to evaluate DA function in the striatum of normal

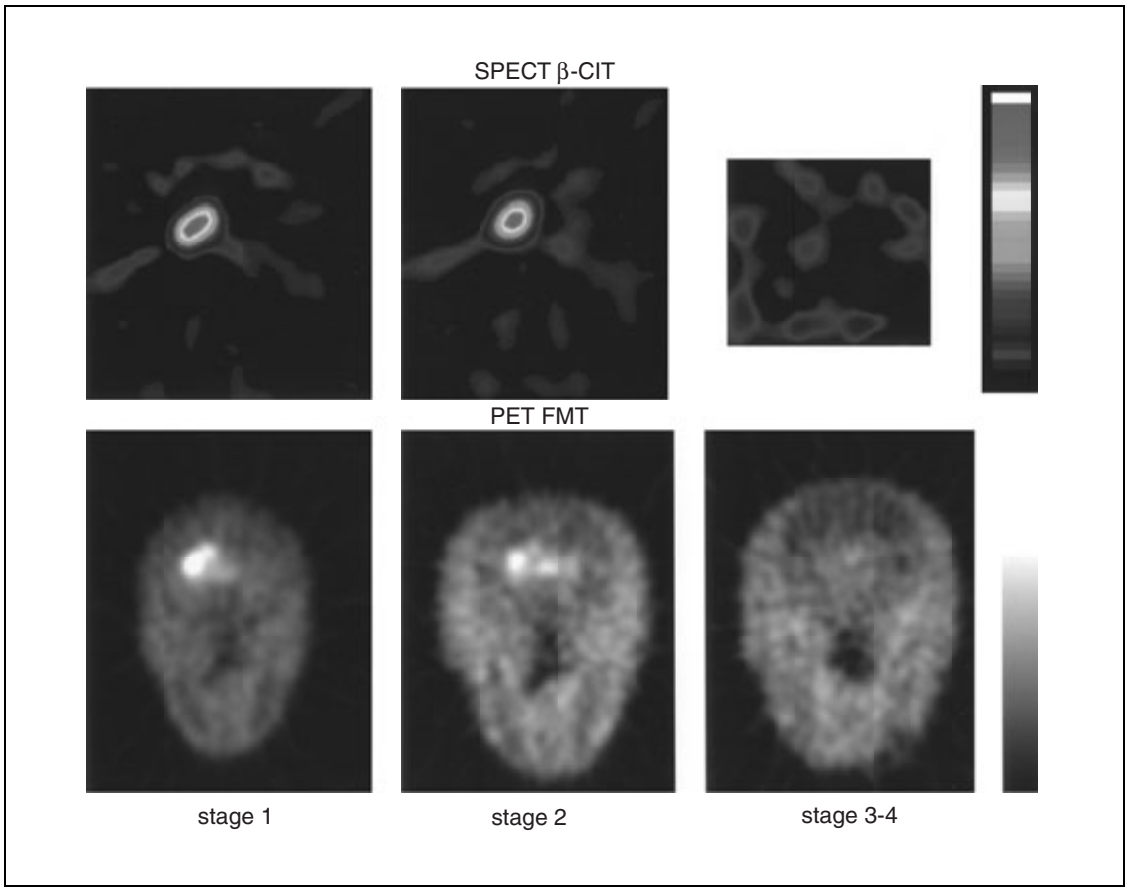

Figure 1.8.5 Neuroimaging representation of mild (stage 1), moderate (stage 2), and severe (stage 3-4) MPTP-induced DA lesion in overlesioned monkeys. Note that the side ipsilateral to the intracarotid infusion of MPTP is severely depleted at all stages. The contralateral side shows a progressive DA depletion on both (top row) SPECT β-CIT [2β-carbomethoxy-3β-(4-iodophenyl)tropane, a cocaine analogue with a high affinity for the dopamine transporter] and (bottom row) PET FMT images as the animals display more severe signs of PD. *This black-and-white facsimile of the figure is intended only as a placeholder; for full-color version of figure go to http://www.interscience.wiley.com/c_p/colorfigures.htm.*

and MPTP-treated monkeys (Doudet et al., 1989; Pate et al., 1993) but not in midbrain structures due to limitations in both tomograph resolution and quantification of FDOPA metabolism. The use of the DA tracer [^{18}F]-6-fluoro-L-*m*-tyrosine (FMT; Melega et al., 1989) provides a high level of image contrast and a high signal-to-noise ratio, reflecting its more restricted metabolism in both peripheral and central tissues, and permitting the evaluation of DA activity in the SNc and striatum (Eberling et al., 1997, 1998; Jordan et al., 1997). For examples of SPECT and PET images, see Figure 1.8.5, Figure 1.8.6, and Figure 1.8.7.

^{123}Iodine-2β-carbomethoxy-3β-(4-iodoph enyl) tropane ([^{123}I]β-CIT) has been used to measure DA transporter activity in both human and nonhuman primates using SPECT (Laruelle et al., 1993). Although [^{123}I]β-CIT has high affinity for both DA and serotonin transporters, the high density of DA transporters in the striatum makes striatal tracer uptake a relatively specific indicator of striatal DA transporter density (Laruelle et al., 1993). Postmortem studies have shown a reduction in DA transporter density in the striatum of PD patients that parallels the loss of DA, and SPECT [^{123}I]β-CIT studies have shown a reduction in striatal DA transporters in PD and an association between clinical signs and striatal uptake of [^{123}I]β-CIT. Discussing detailed neuroimaging methods is beyond the scope of this unit, but as shown in Figure 1.8.5, both PET and SPECT can be used successfully to determine the severity of a lesion in monkey striatum following MPTP administration.

ICA MPTP administration as a model of active degeneration of the nigrostriatal DA pathway

An interesting approach to study neuroprotection in MPTP-treated monkeys is based on

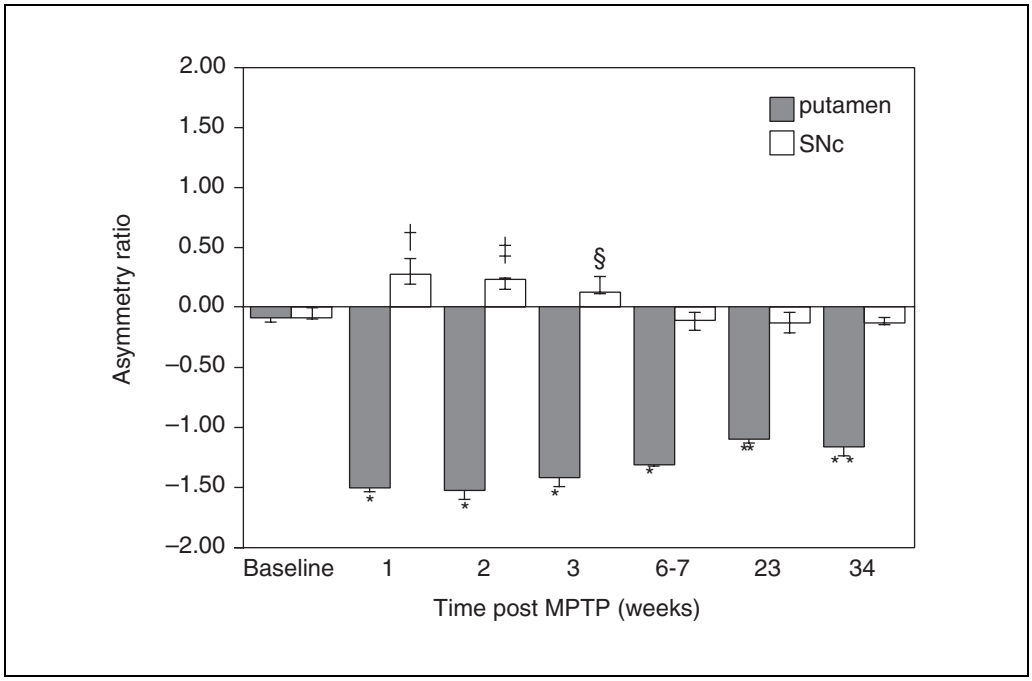

Figure 1.8.6 Following ICA administration of MPTP, DA terminals degenerate first, followed by degeneration of DA neurons in the SNc 5 weeks later. During the time period between MPTP administration and DA cell death in the SNc there is a transient upregulation of activity in the SNc that can be measured by PET. This upregulation represents the time course of cell death and can be used as an indicator of DA cell degeneration. Asymmetry ratios were constructed to evaluate differences in FMT accumulation between ipsilateral (the side of ICA MPTP infusion) and contralateral sides at eight different time points. Asymmetry ratios for the putamen and SNc were calculated as the K_i value for the ipsilateral side minus the K_i value for the contralateral side divided by the mean of the two K_i. A negative asymmetry ratio indicates that K_i was lower on the ipsilateral side, while positive ratios indicate higher K_i values on the ipsilateral side. $^*p < 0.0001$ significantly less than baseline; $\dagger p = 0.001$, $\ddagger p = 0.002$, and $\S p = 0.04$ significantly greater than baseline; $^{**}p < 0.05$) significantly greater than 1 week, 2 weeks, 3 weeks.

the finding that following ICA MPTP administration, MPP^+ is sequestered in both DA terminals and cell bodies as a result of its selective uptake by the DA transporter system. This initiates molecular changes that ultimately result in neuronal degeneration, most likely by compromising mitochondrial function. Within the first few weeks following MPTP administration, DA levels are profoundly decreased in the striatum with little or no morphological changes in the nigral cell bodies. MPTP-induced nigrostriatal degeneration begins almost immediately in the striatal terminals and results in cell body degeneration within 4 to 6 weeks (Fig. 1.8.7 and Fig. 1.8.8). The difference in the time course of degeneration in the striatum and SNc suggests that the primary mechanism of toxicity in the terminals is MPP^+, while cell body degeneration may result from both retrograde degeneration and retrograde transport of MPP^+ from the striatum (Javitch et al., 1985; Herkenham et al., 1991). Importantly, although the time course of degeneration is clearly accelerated, the MPTP model includes the key elements of idiopathic PD, including selective and progressive degeneration of the nigrostriatal DA pathway (Fig. 1.8.7). The use of FMT, along with higher resolution PET tomographs, allows direct longitudinal evaluation of DA activity in the SNc as well as in the striatum (Eberling et al., 1997; Fig. 1.8.6). Following ICA infusion of MPTP, activity of DA neurons is upregulated during degeneration of the DA pathway, which is completed within 5 weeks.

This pattern of MPTP-induced degeneration can be used to study neuroprotection. Following ICA administration of MPTP, >95% of TH-immunoreactive cells in the SNc will degenerate within 4 to 5 weeks. There is very little, if any, between-animal variation in TH-positive cell degeneration in the SNc following the successful ICA infusion of MPTP. Active neuroprotective agents should be able to protect DA neurons following ICA administration of MPTP. Such neuroprotection might be demon-

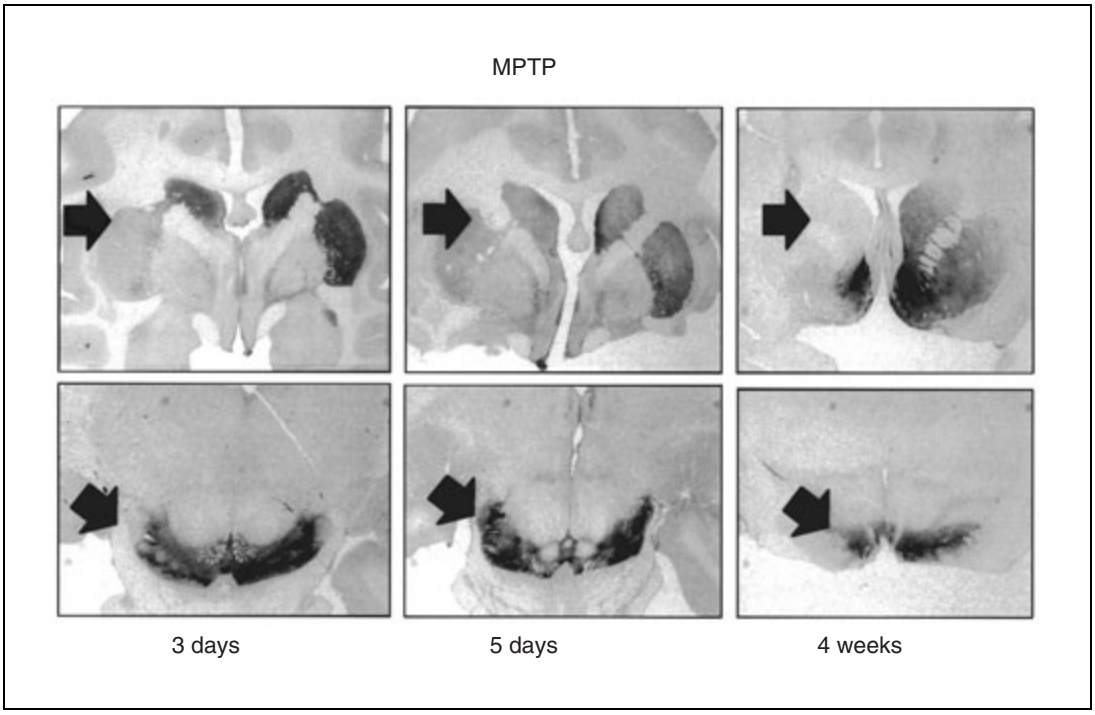

Figure 1.8.7 Low-power photomicrography showing tyrosine hydroxylase immunoreactivity in the striatum and SNc in monkeys at 3 days, 5 days, and 4 weeks following unilateral intracarotid infusion of MPTP. Terminals in the striatum degenerate first, shortly after MPTP administration, while DA cell bodies are not affected (note lack of TH staining in the striatum but not in SNc at 3 and 5 days). It takes 4 to 6 weeks for DA cells in the SNc to degenerate.

strated by preventing upregulation and/or extending survival of DA cells in the SNc on the side of MPTP infusion during the first 3 to 4 weeks following MPTP infusion.

Other models of PD in primates

Isoquinolines. For some time now there has been an active search for endogenous compounds that act like MPTP. Isoquinoline (IQ) derivatives such as tetrahydroisoquinoline (TIQ), 1-benzyl-TIQ, and (*R*)-1,2-dimethyl-5,6-dihydroxy-TIQ[(*R*)-*N*-methyl-salsolinol)] are DA-derived alkaloids that have shown potential neurotoxicity (Nagatsu and Yoshida, 1988). TIQs, like MPTP, may be activated via N-methylation by *N*-methyltransferase and via oxidation by MAO. TIQs as well as MPP^+ inhibit complex I of the electron transport system in mitochondria, thereby reducing ATP formation and producing oxygen radicals. Although the properties of TIQs are similar to those of MPTP, the neurotoxicity is weaker. Chronic administration produces parkinsonism in primates with decreased DA, biopterin, and tyrosine hydroxylase activity (Nagatsu and Yoshida, 1988). Long-term neurotoxic effects of IQs remain to be further examined in primates.

Aged monkeys. DA cells are lost during the normal course of aging at a rate of ~5% per decade in monkeys (Fearnley and Lees, 1991). Rhesus monkeys that are over 22 years of age display many Parkinson-like changes that appear to be age-related. Some, but not all, hypokinetic aged monkeys respond to L-DOPA administration as shown in Figure 1.8.9. In a recent study, motor deficits in aged monkeys were shown to correlate with decreased DA markers (Emborg et al., 1998). However, because decreased locomotion of aged monkeys can also be attributed to factors that are not DA-mediated, the response to L-DOPA might be used as a selection marker for animals that show DA-mediated hypokinesia. More work needs to be done to fully characterize aged monkeys as a potential model of PD.

Other models of PD in mice

Weaver mutant. This is a genetically induced model of cerebellum atrophy accompanied by brain DA deficiency due to abnormal development and additional degeneration of the striatal DA system. The adult weaver mutant develops striatal DA deficiency related to a reduction in the number of DA neurons in the SNc (A-9). The neuropathological and biochemical

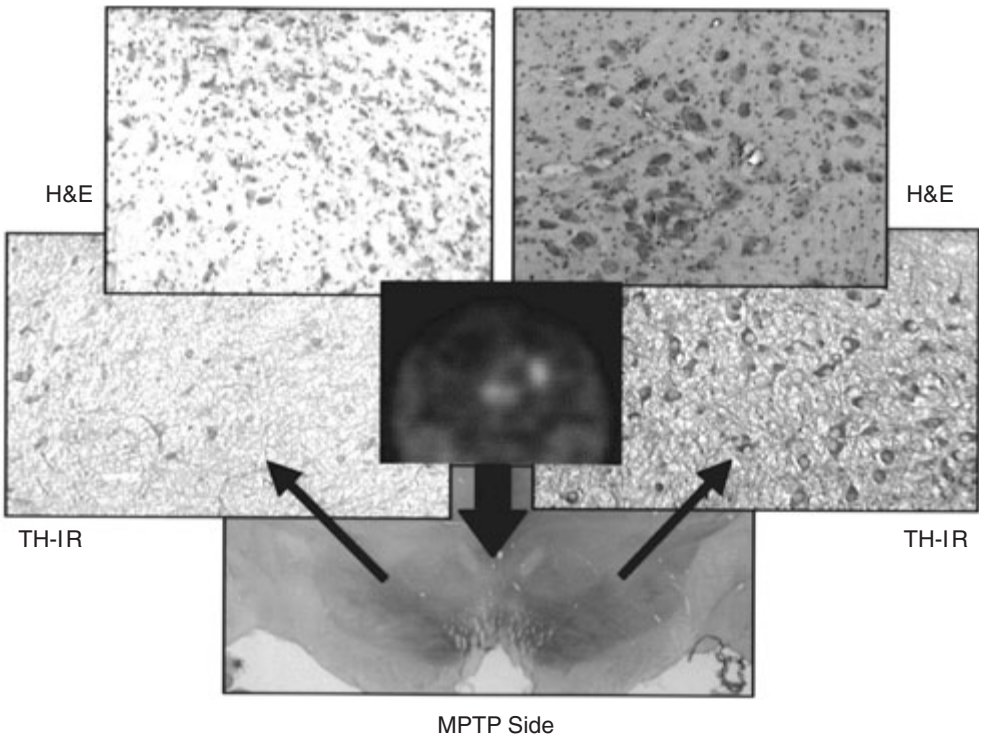

Figure 1.8.8 Three weeks following ICA administration of MPTP, this animal showed clear signs of unilateral deficit. Upon PET examination, activity in the SNC was still elevated while the signal from the putamen was absent. The animal was sacrificed one day after PET, and degenerating but still TH-positive neurons were present in the SNc. No TH staining was detected in the putamen. Abbreviations: H&E, hematoxylin and eosin staining; TH-IR, tyrosine hydroxylase immunoreactivity.

changes manifest as ataxia and fine tremor (Schmidt et al., 1982). This is a convenient model for studying potential DA trophic effects.

Homozygous weaver animals of the C57Black strain are obtained by breeding heterozygote pairs. At ~2 weeks of age, homozygous weaver animals are recognized behaviorally by poor righting response, ataxia, hypotonia, and tremor, and anatomopathologically by visible atrophy of the cerebellum.

DA-deficient mouse model. This model is created by inactivation of the TH gene resulting in an inability to synthesize DA. These mice show no TH immunoreactivity in midbrain DA neurons and their terminals have extremely low DA concentrations. Behaviorally they manifest hypoactivity, adipsia, and aphagia leading to negative growth rate and death by 4 weeks of age. L-DOPA reverses the behavioral changes, and continuous administration can lead to a nearly normal growth rate. These animals have normal development of DA midbrain neurons and nigrostriatal projections. The model is useful for DA replacement and pharmacological studies.

Critical Parameters and Troubleshooting

MPTP primate models

Handling MPTP. The experimenter should always use a chemical hood and skin protection (gloves, laboratory coat) and mask. Any spilled MPTP or excess solution should be degraded by potassium permanganate (see cautionary note in Basic Protocol 1). In case of exposure, MAO-B inhibitors block the conversion to MPP^+, thus preventing the toxic effects.

ICA administration. Selective injection in the ICA minimizes contralateral involvement. For this route, the dose should be calculated according to brain size, which is fairly stable for a wide range of body weights. In macaques there appears to be no direct correlation between the severity of the parkinsonian lesion and the dose of MPTP or the weight and age of the animal. Some monkeys are more suscepti-

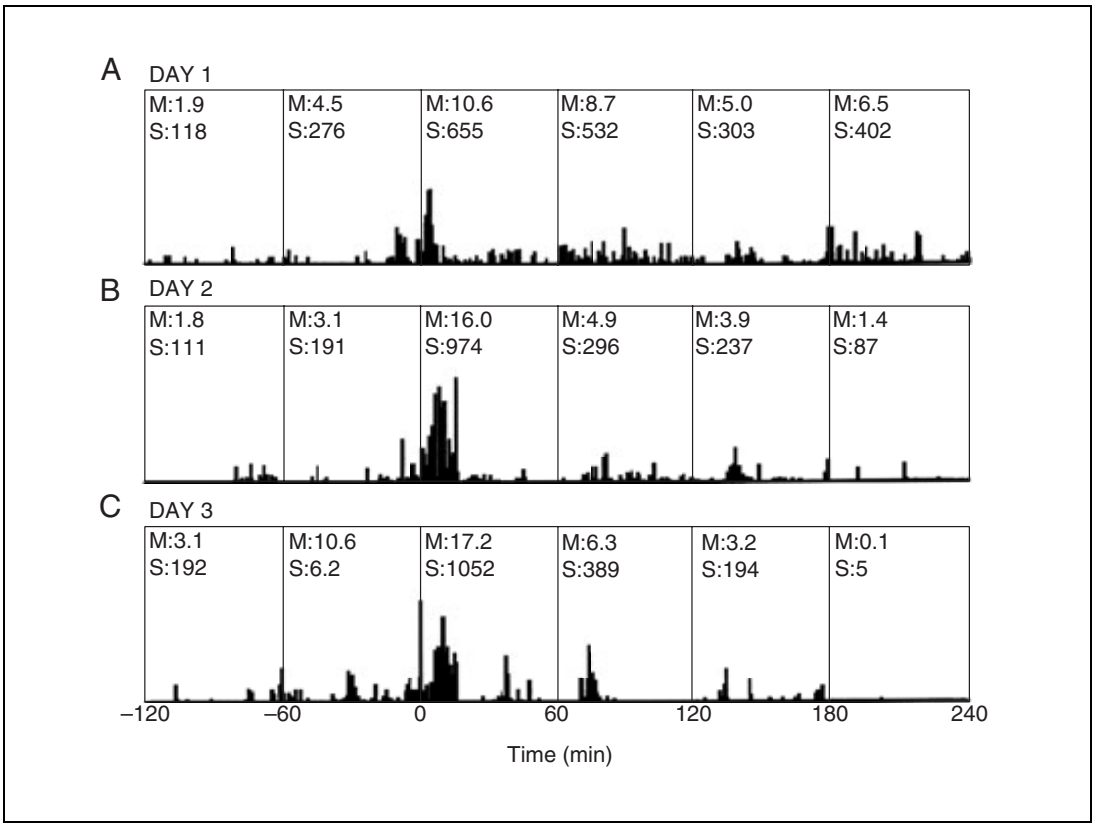

Figure 1.8.9 Activity tracing in a 24-year-old female rhesus monkey over 3 days. This animal displayed an increase of body activity 5 to 10 min following intramuscular administration of 30 mg/kg M-L-DOPA with benserazide. Only some of the hypokinetic monkeys examined showed an increase in activity in response to M-L-DOPA, suggesting that hypokinetic features in aged animals are not always due to decreased DA levels in the striatum. M, mean counts; S, sum of counts.

ble to MPTP than others and, in general, old females are more prone to MPTP toxicity than young males. The choice of anesthetics is also relevant, as the widely used ketamine inhibits DA uptake and can thus decrease MPTP toxicity by inhibiting MPP^+ uptake into the DA cells.

Acute stage. Administration of MPTP produces mydriasis, piloerection, tachycardia, and tachypnea lasting 5 to 15 min. Repeated injections produce involuntary facial (perioral) movements, facial grimacing, retrocollis, and dystonic flexion of the extremities lasting 10 to 30 min. Intake of food and water should be carefully monitored in the acute phase; some animals might require tube feeding and L-DOPA support. In the first 48 hr following ICA administration of MPTP, the animal might present partial motor seizures with occasional secondary generalization; this should be adequately treated with diazepam at 0.5 mg/kg. The degree of motor impairment is quite variable at acute stages. The severity of the motor signs increases over the first 2 weeks. This phase, which can be life threatening in severely affected animals, is followed by a period of partial improvement during the following 4 to 6 weeks, probably related to functional recovery of non-DA neurons and/or compensatory mechanisms within the nigrostriatal system. In these first weeks, dystonic posturing is frequently observed in severely lesioned animals in addition to akinesia, dyskinesia, and occasionally oculogyric crises.

L-DOPA response. Dyskinesias occur in several primate species after MPTP and chronic L-DOPA therapy (Schneider, 1989), as in the majority of patients with chronic PD who are treated with L-DOPA. In general, dyskinesias develop more rapidly in MPTP-induced parkinsonism—both in humans and nonhuman primates—than in patients with idiopathic PD, but it is exceptional when this complication appears with an acute challenge. It is nevertheless advisable to avoid the use of high doses producing significant dyskinesias as this might invalidate the test.

Model. The overlesioned bilateral model has several advantages over other models. It is a practical model in which animals are very seldom affected by MPTP to the extent that they

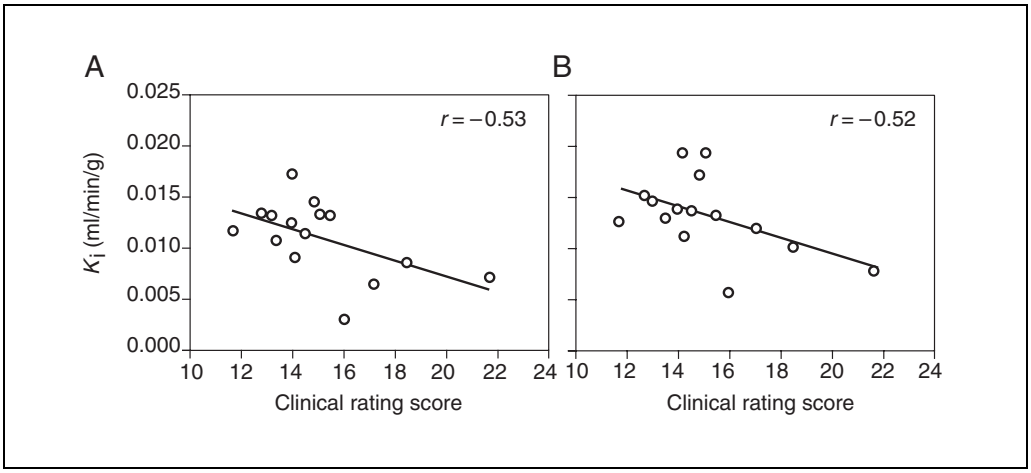

Figure 1.8.10 Relationship between K_i values for the (**A**) caudate and (**B**) putamen, and clinical rating scores for stage 2 and 3 monkeys. Monkeys with more severe clinical signs showed lower K_i values in both regions.

cannot take care of themselves. The success rate of the model is very high. Typically 80% to 90% of animals that are enrolled into the project are considered good study subjects, and the mortality rate is very low (e.g., <4%). Scientifically, this model is particularly useful because it enables approximation to several stages of PD. Monkeys defined as stage 1 and 2 are good for studies of mild stages of PD, while stage 3 animals represent a more advanced stage of the idiopathic disease. In this model, the clinical stage correlates well with biochemical markers (PET/DA punch analysis; Figs. 1.8.10, 1.8.11, and 1.8.12; Eberling et al., 1998) and with midbrain DA cell counts (Fig. 1.8.13; Oiwa et al., 2003). It is thus possible to predict the degree of the lesion on the side contralateral to ICA MPTP administration based on the clinical rating. In addition, two different types of therapeutic approaches can be addressed in the over-lesioned model:

Neuroprotection. Agents that might protect DA cells from further MPTP toxicity can be studied using monkeys in stages 1 and 2. If such agents are indeed neuroprotective, further i.v. administration will induce stage 3 parkinsonism only in a placebo control group. This is more clinically relevant than administration of a neuroprotective agent to normal animals prior to MPTP administration, because in a clinical situation neuroprotection might be used in patients with subclinical and /or mild parkinsonism.

Recovery. Therapeutic strategies aimed at improving the function of remaining DA innervation can be studied in stage 3 monkeys, as DA is only partially depleted on the side contralateral to the ICA infusion. If such an approach works, treated animals will move from stage 3 to stage 1 or 2.

6-OHDA administration in primates

6-OHDA administration in marmosets produces a persistent motor impairment in animals with extensive lesions (>97% DA depletion). In general the probability of spontaneous behavioral recovery depends on the extent of DA depletion. However, animals with a similar degree of DA denervation show different recovery profiles in behavioral tests, probably resulting from regional anatomical variation in DA content. Thus, it is necessary to obtain data from a group of animals to control for spontaneous recovery. Rotation in response to apomorphine is fairly stable over time and correlates with other motor scores. Amphetamine induces rotation, but does not increase motor activity and does not correlate with other measures.

6-OHDA rat model

The 6-OHDA rat model is rather simple and reliable, although the rotational response must be tested to select rats with severe lesions (>99% DA depletion) for use in long-term experiments. This means that it is necessary to lesion a large number of animals to produce enough well-lesioned animals. High doses (>40 μg) have a considerable mortality rate (e.g., 3% to 5%), as do bilateral lesions. The volume of the infusion is relevant, as diffusion depends directly on volume. For medial forebrain bundle (MFB) lesions, small volumes are recommended to keep the lesion limited; for striatal infusion, large volumes are necessary to cover the whole nucleus.

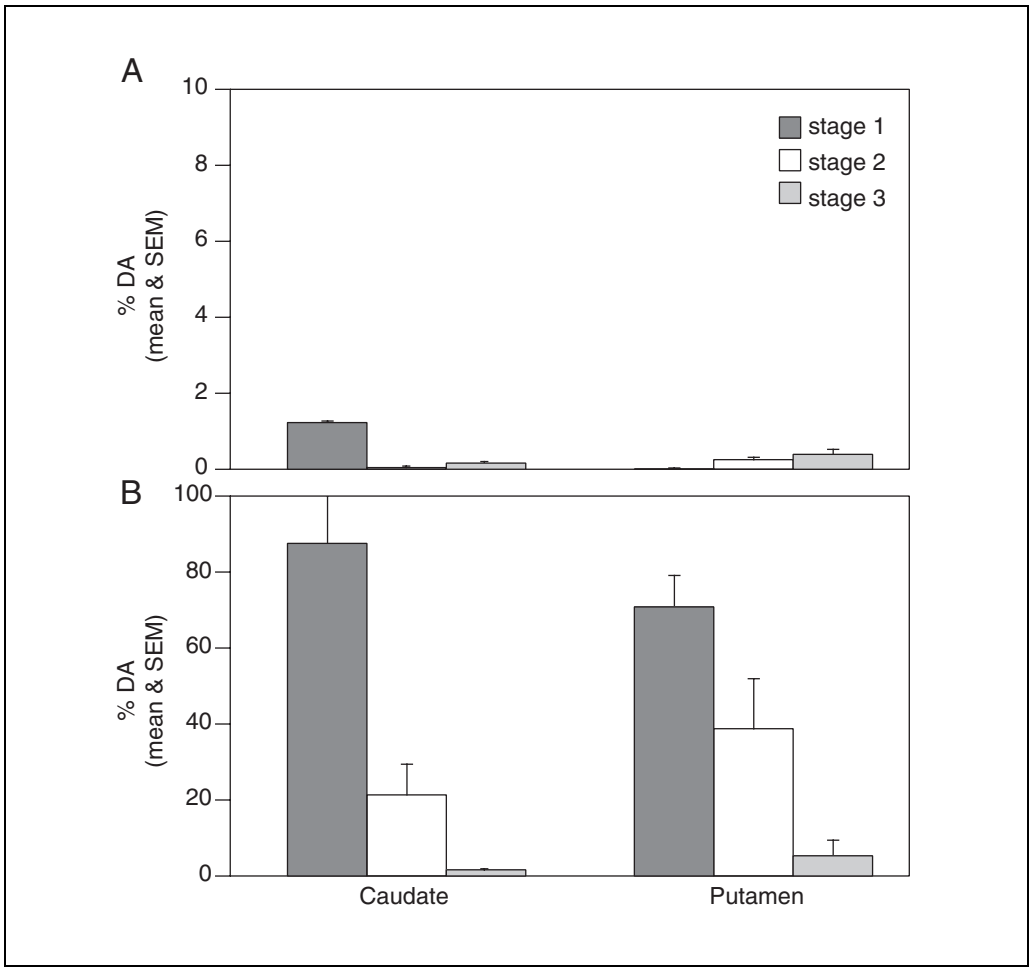

Figure 1.8.11 Tissue concentration of DA in the caudate nucleus and putamen in parkinsonian monkeys at stages 1 ($n = 3$), 2 ($n = 7$), and 3 ($n = 5$) shown as a percentage of (**A**) ipsilateral striatum and (**B**) contralateral striatum tissue concentration in normal ($n = 4$) monkeys.

MPTP administration in mice

Systemic MPTP administration in mice causes damage to the nigrostriatal rather than mesolimbic terminal areas (Donnan et al., 1987). The severity and duration of this specific damage depends on total dose, administration regimen (multiple injections are more effective than single), route of administration (subcutaneous is the most effective), strain (C57Black strain is the most sensitive), and age (older animals are more sensitive; Heikkila and Sonsalla, 1987; Date et al., 1990). The neurotoxic effect of MPTP can be augmented by coadministration of diethyldithiocarbamate, acetylaldehyde, or ethanol. Recovery of behavioral, neuropathological, and biochemical changes is observed after a variable period of time, most frequently over a period of months depending on the dose of MPTP and cotreatment regimen (Hallman et al., 1985; Donnan et al., 1987).

Anticipated Results

Motor behavior

Primates. Unilateral administration of MPTP and 6-OHDA is attended by persistent contralateral motor impairment; both upper and lower limbs show the characteristic parkinsonian signs of bradykinesia, rigidity, cogwheeling, and tremor. Spontaneous locomotor activity usually consists of continuous circling towards the lesioned side. Treatment with L-DOPA/carbidopa or the directly acting mixed D1 and D2 receptor agonist apomorphine alleviates motor deficits and reverses the direction of turning (Bankiewicz et al., 1986). The apomorphine-induced turning response in a direction away from the lesioned side is very stable over time (for ≥5 years) and can also be quantified. Assessment of drug-induced turning response and function of the contralateral arm can be used for evaluation of new experimental therapeutic strategies.

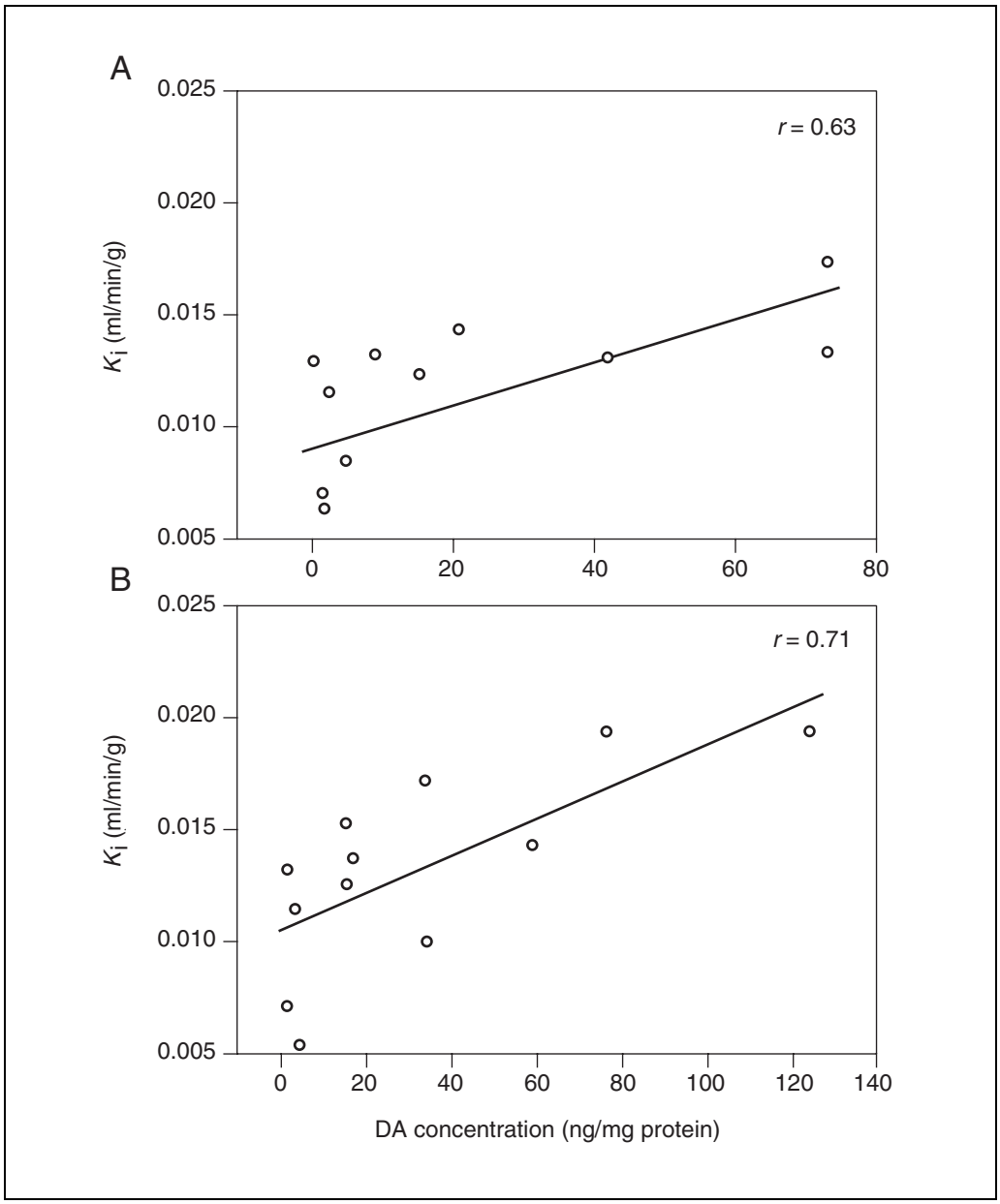

Figure 1.8.12 Correlation between levels of DA as measured by PET and HPLC in stage 2 and 3 overlesioned hemiparkinsonian monkeys in (**A**) caudate and (**B**) putamen.

Systemic and overlesioned models using MPTP produce a bilateral parkinsonian syndrome displaying axial signs, such as stooped posture and impaired balance. In these animals evaluation can be made using a specific scale similar to the UPDRS, such as the one shown in Table 1.8.1. Figure 1.8.2 shows the effect of increasing doses of L-DOPA on motor activity and scores in a stable parkinsonian primate.

Rodents. In rats, turning behavior is the easiest way to assess the degree of DA denervation. Apomorphine induces contralateral rotation in animals with >90% striatal DA depletion. In animals with partial lesions, apomorphine does not induce significant turning but amphetamine induces ipsilateral rotation demonstrating an asymmetry in DA content. In mice, a decrease of spontaneous locomotor activity and an increase in response to amphetamine can be observed.

In vivo neurochemical changes

CSF. After unilateral administration of MPTP in monkeys, the level of monoamine metabolites in cerebrospinal fluid (CSF) initially drops. However, after 3 months, only the levels of homovanillic acid remain low (Burns et al., 1983). In hemiparkinsonian monkeys, the initial decrement in CSF monoamine metabolites and DA levels is >60%; three weeks after

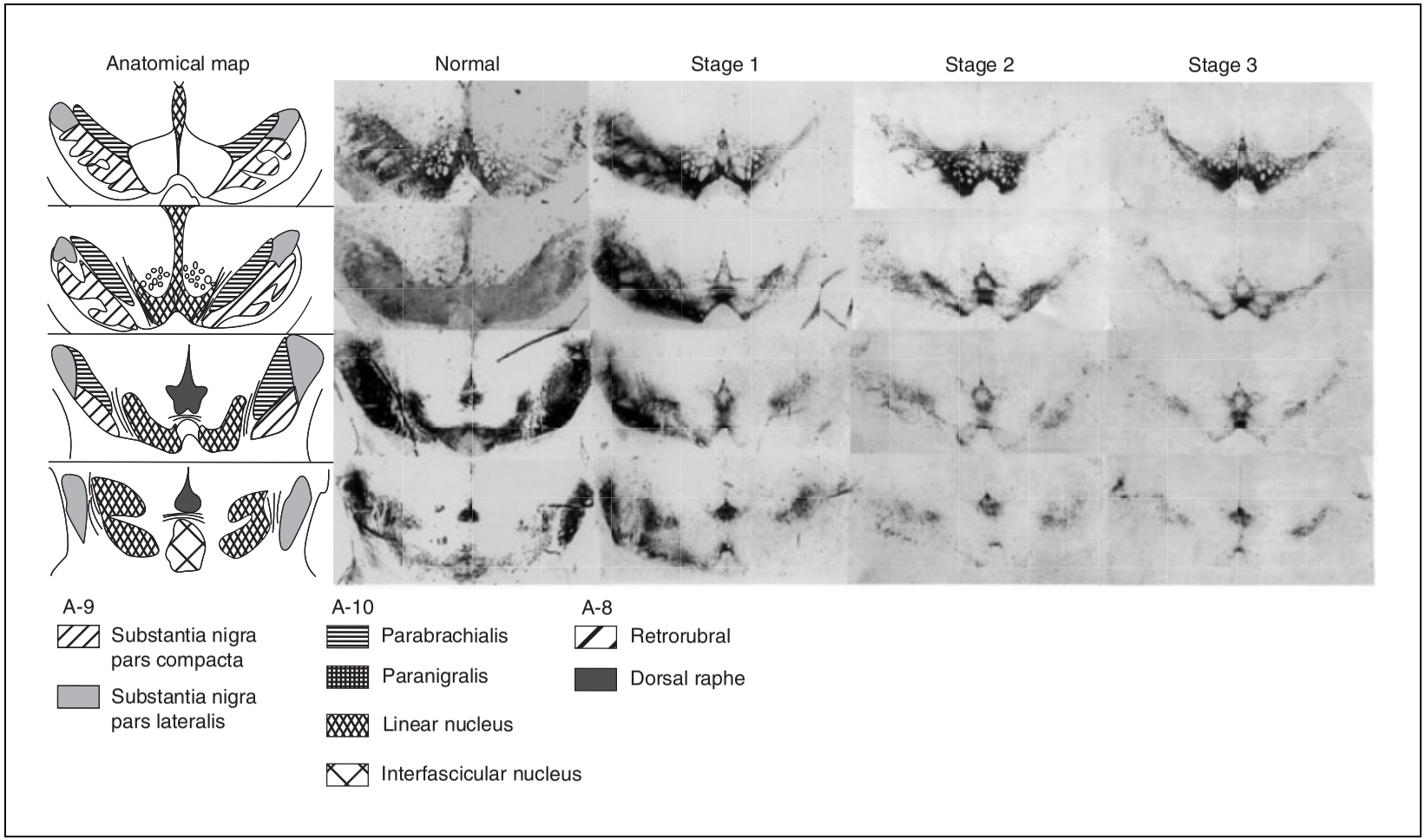

Figure 1.8.13 Anatomical representation of midbrain DA structures in normal and stage 1, 2, and 3 overlesioned hemiparkinsonian monkeys. In stage 1, DA cells in the SNc (A-9 region) are severely depleted while the contralateral side shows no significant cell death in this region. Note that TH-positive cells in the SNc are further depleted in stage 2 and 3 monkeys, which corresponds to progressive parkinsonian signs that are seen in these monkeys. Regions of the ventral tegmental area are partially spared at all stages.

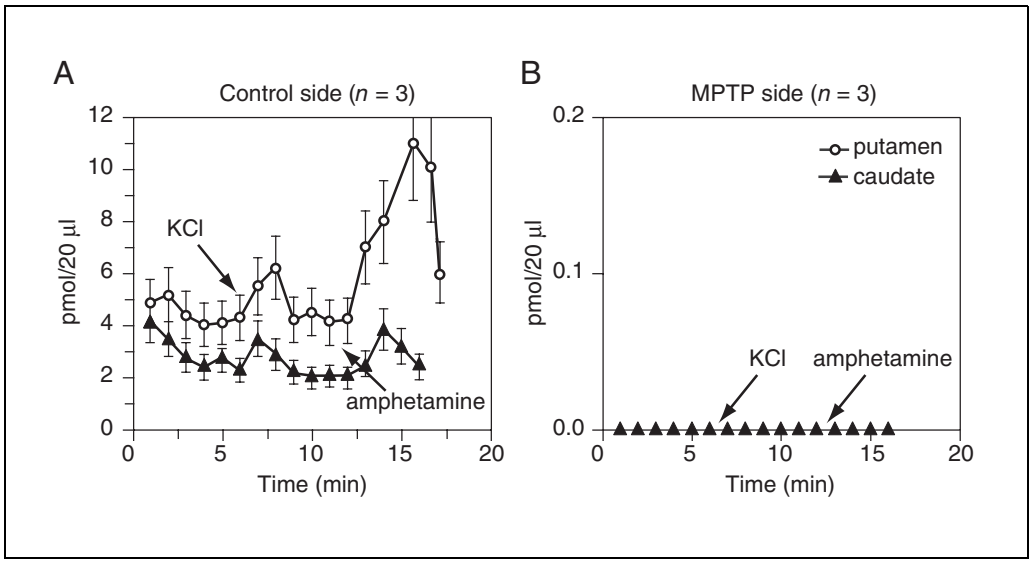

Figure 1.8.14 Results of in vivo microdialysis of three hemiparkinsonian (stage 1) monkeys. Samples were collected over 20 min from the caudate and putamen on both sides of the brain and were analyzed for levels of DA. Extracellular levels of DA were detected only on the control side (**A**), with putamen showing higher levels of DA than caudate nucleus. KCl and amphetamine induced DA release only on the control side, suggesting complete DA lesion on MPTP-treated side (**B**).

the lesion they are decreased by only 40% to 50% (Bankiewicz et al., 1990).

Microdialysis. Extracellular fluid (ECF) levels of catecholamines in brain tissue can be examined in vivo by microdialysis (Fig. 1.8.14). Using a small probe (27-G), it is possible to measure the regional distribution and concentration of DA and its metabolites in brain ECF (Wang et al., 1990). With this technique it is also possible to examine the relationship between changes in levels of different neurotransmitters in brain ECF. Methodology for performing microdialysis experiments in MPTP-treated monkeys is described elsewhere (Wang et al., 1990).

Postmortem analyses

Parkinson's disease is characterized by loss of DA neurons in the SNc leading to DA depletion in the striatum. Consequently, evaluation of nigral cell loss and striatal DA deficiency are the main post mortem outcome measures for all of these models.

Immunohistochemistry. The distribution of neuronal damage within the SNc in the MPTP-treated animal model (see Basic Protocol 1) is also of interest because histological changes in this region are exhibited in a specific pattern in PD. MPTP is selectively toxic, affecting mostly the nigrostriatal DA system while leaving the mesolimbic system relatively intact. The midline population of DA cells in the midbrain (ventral tegmental area, paranigralis nucleus, and paraventricular area), the parabrachial nucleus, and parts of nucleus lateralis are affected by MPTP (German et al., 1988). Furthermore, the damage closely resembles the histological findings in PD. TH immunoreactivity in DA midbrain nuclei and anatomic schemes of each level are shown in Figure 1.8.12 for different stages.

MPTP-treated monkeys in stage 1 (hemiparkinsonian) show a dramatic loss of DA cells (>95%) in the SNc on the MPTP-lesioned side, whereas animals at stage 2 and 3 display further loss of DA neurons on the contralateral side as they become more parkinsonian (Fig. 1.8.13). This pattern follows changes observed by neuroimaging (Figs. 1.8.5 and 1.8.6) and biochemical techniques (Fig. 1.8.11).

The decrease of TH immunoreactivity in the SNc (cell bodies) and striatum (projections) is observed in all models described here. However, it is transient in mice and, in partial lesions, a significant recovery can be observed over time.

Unilateral injection of 6-OHDA in marmosets (see Basic Protocol 2) produces a decrease in TH immunoreactivity in the SNc of 90% to 97% on the contralateral side (Annett et al., 1992).

In rats treated with 6-OHDA (see Basic Protocol 3), loss of TH-positive nigral cells depends on the type of lesion. Lesions of the

MFB and SNc at high doses should achieve a complete nigral depletion. Partial lesions should respect VTA and the medial ventral tier. Striatal lesions cause a cell loss in the ipsilateral SNc that is correlated with the dose and volume of the striatal injection.

Neurochemical changes. MPTP administration (see Basic Protocol 1) causes a profound reduction in striatal DA with no clear differences between caudate and putamen levels. After ICA MPTP administration, DA is almost completely absent in the caudate and putamen on the lesioned side. The difference in DA concentration between the normal and the MPTP-treated side is >96% (Fig. 1.8.11). This represents almost total DA denervation of the caudate and putamen on the MPTP-lesioned side. However, greater concentrations of DA are found in areas that receive innervation from remaining DA cells in the ventral tegmental area (e.g., nucleus accumbens septi, area olfactoria, septum pellucidum). In the model that combines ICA and i.v. MPTP administration, DA depletion on the side contralateral to ICA administration is much less severe than on the side of ICA administration and correlates with the severity of parkinsonian signs. DA concentration, as measured by postmortem striatal punches (Fig. 1.8.11), correlates well with in vivo PET measurements of DA activity (Fig. 1.8.12).

In marmosets lesioned with 6-OHDA (see Basic Protocol 2), the reduction of DA in the ipsilateral striatum is usually >97% (Annett et al., 1992). In rats lesioned with 6-OHDA (see Basic Protocol 3) and showing a robust rotational response to apomorphine, DA levels are decreased by >99% in the contralateral striatum.

Time Considerations

For Basic Protocol 1, ICA injection takes 30 to 60 min and i.v. injection takes 15 min. To obtain overlesioned animals, a 2-week waiting period is required between ICA and i.v. administration. It is then necessary to wait 6 to 8 weeks (acute stage and spontaneous recovery) to establish a stable parkinsonian syndrome. Clinical rating takes <10 min but is variable depending on the familiarity and cooperation of the animals. The L-DOPA test requires 5 min preparation and 60 to 120 min observation. Activity monitors require 5 min to put on and remove collars (vests take slightly longer), after which it is necessary to record for several days to account for normal variation in baseline activity.

For Basic Protocol 2, the stereotactic procedure takes 40 to 60 min and it is advisable to wait 6 to 8 weeks to ensure stable animals.

For Basic Protocol 3, the whole procedure should take 30 to 40 min, in which the infusion rate is the time-limiting factor. For long-term experiments it is necessary to test the rotational response to apomorphine/amphetamine 3 to 6 weeks later and to select only rats with a complete lesion (>99% DA depletion). These animals show a stable deficit with consistent drug-induced rotational behavior over time appropriate for such studies.

Basic Protocol 4 is a very simple and quick procedure as animals can be used right away but only for a short period of time. Animals show minimal or no behavioral symptoms after weeks to months.

Literature Cited

Annett, L.E., Rogers, D.C., Hernandez, T.D., and Dunnett, T.B. 1992. Behavioral analysis of unilateral monamine depletions in the marmoset. *Brain* 115:825-856.

Bankiewicz, K.S., Oldfield, E.H., Chiueh, C.C., Doppman, J.L., Jacobowitz, D.M., and Kopin, I.J. 1986. Hemiparkinsonism in monkeys after unilateral internal carotid artery infusion of 1-methyl-4-phenyl-1,2,3,6-tetrahydropyridine (MPTP). *Life Sci.* 39:7-16.

Burns, R.S., Chiueh, C.C., Markey, S.P., Ebert, M.H., Jacobowitz, D.M., and Kopin, I.J. 1983. A primate model of parkinsonism: Selective destruction of dopaminergic neurons in the pars compacta of the substantia nigra by *N*-methyl-4-phenyl-1,2,3,6-tetrahydropyridine. *Proc. Natl. Acad. Sci. U.S.A.* 890:4546-4550.

Date, I., Felten, D.L., and Felten, S.Y. 1990. Long term effect of MPTP in the mouse brain in relation to aging: Neurochemical and immunocytochemical analysis. *Brain Res.* 519:266-272.

Davis, G.C., Williams, A.C., Markey, S.P., Ebert, M.N., Caine, E.D., Reichert, C.M., and Kopin, I.J. 1979. Chronic parkinsonism secondary to intravenous injection of meperidine analogs. *Psychiatry Res.* 1:249-254.

Donnan, G.A., Kaczmarczyk, S.J., Mckenzie, J.S., Rowe, P.J., Kalnins, R.M., and Mendelsohn, F.A. 1987. Regional and temporal effects of 1-methyl-4-phenyl-1,2,3,6-tetrahydropyridine on dopamine uptake sites in mouse brain. *J. Neurol. Sci.* 81:261-271.

Doudet, D.J., Miyake, H., Finn, R.T., Mclellan, C.A., Aigner, T.G., Wan, R.Q., Adams, H.R., and Cohen, R.M. 1989. 6-^{18}F-L-Dopa imaging of the dopamine neostriatal system in normal and clinically normal MPTP-treated rhesus monkeys. *Exp. Brain Res.* 78:69-80.

Eberling, J.L., Bankiewicz, K.S., Jordan, S., Vanbrocklin, H.F., and Jagust, W.J. 1997. Pet studies of functional compensation in a primate model

of Parkinson's disease. *NeuroReport* 8:2727-2733.

Eberling, J.L., Jagust, W.J., Taylor, S., Bringas, J., Pivirotto, P., Vanbrocklin, H.F., and Bankiewicz, K.S. 1998. A novel MPTP primate model of Parkinson's disease: Neurochemical and clinical changes. *Brain Res.* 805:259-262.

Emborg, M.E., Ma, S.Y., Mufson, E.J., Levey, A.I., Taylor, M.D., Brown, W.D., Holden, J.E., and Kordower, J.H. 1998. Age-related declines in nigral neuronal function correlate with motor impairments in rhesus monkeys. *J. Comp. Neurol.* 401:253-265.

Fearnley, J.M. and Lees, A.J. 1991. Aging and Parkinson's disease: Substantia nigra regional selectivity. *Brain* 114:2283-2301.

German, D.C., Dubach, M., Askari, S., Speciale, S.G., and Bowden, D.M. 1988. 1-Methyl-4-phenyl-1,2,3,6-tetrahydropyridine-induced parkinsonian syndrome in *Macaca fascicularis:* Which midbrain dopaminergic neurons are lost? *Neuroscience* 24:161-174.

Hallman, H., Lange, J., Olson, L., Strömberg, I., and Johnsson, G. 1985. Neurochemical and histochemical characterization of neurotoxic effects of 1-methyl-4-phenyl-1,2,3,6-tetrahydropyridine on brain catecholamine neurons in the mouse. *J. Neurochem.* 44:117-127.

Heikkila, R.E. and Sonsalla, P.K. 1987. The use of the MPTP-treated mouse as an animal model of Parkinsonism. *Can. J. Neurol. Sci.* 14:436-440.

Heikkila, R.E., Hess, A., and Duvoisin, R.C. 1985. Dopaminergic neurotoxicity of 1-methyl-4-phenyl-1,2,3,6-tetrahydropyridine (MPTP) in the mouse: Relationships between monoamine oxidase, MPTP metabolism and neurotoxicity. *Life Sci.* 36:231-236.

Herkenham, M., Little, M.D., Bankiewicz, K., Yang, S.-C., Markey, S.P., and Johannessen, J.N. 1991. Selective retention of MPP^+ within the monoaminergic systems of the primate brain following MPTP administration: An in vivo autoradiographic study. *Neuroscience* 40:133-158.

Javitch, J.A., D'amato, R.J., Strittmatter, S.M., and Snyder, S.H. 1985. Parkinsonism-inducing neurotoxin N-methyl-4-phenyl-1,2,3,6-tetrahydropyridine: Uptake of the metabolite N-methyl-4-phenylpyridine by dopamine neurons explains selective toxicity. *Proc. Natl. Acad. Sci. U.S.A.* 82:2173-2177.

Jordan, S., Eberling, J.L., Bankiewicz, K.S., Rosenberg, D., Coxson, P.G., Vanbrocklin, H.F., O'Neil, J.P., and Emborg, M.E. 1997. 6-(^{18}F)Fluoro-L-*m*-tyrosine: Metabolism, PET kinetics and MPTP lesion in primates. *Brain Res.* 750:264-276.

Laruelle, M., Baldwin, R.M., Malison, R.T., Zea-Ponce, Y., Zoghbi, S.S., al-Tikriti, M.S., Sybirska, E.H., Zimmermann, R.C., Wisniewski, G., Neumeyer, J.L., et al. 1993. SPECT imaging of dopamine and serotonin transporters with [^{123}I]β-CIT: Pharmacological characterization of brain uptake in nonhuman primates. *Synapse* 13:295-309.

Lee, C.S., Sauer, H., and Bjorklund, A. 1996. Dopaminergic neuronal degeneration and motor impairments following axon terminal lesion by intrastriatal 6-hydroxydopamine in the rat. *Neuroscience* 72:641-653.

Leroux-Nicollet, I. and Costentin, J. 1986. Acute locomotor effects of MPTP in mice and relationships with dopaminergic systems. *In* MPTP: A Neurotoxin Producing a Parkinsonian Syndrome (S.P. Markey, N. Castagnoli, A.J. Trevor, and I.J. Kopin, eds.) pp. 419-424. Academic Press.

Melega, W.P., Perlmutter, M.M., Luxen, A., Nissenson, C.H., Grafton, S.T., Huang, S.C., Phelps, M.E., and Barrio, J.R. 1989. 4-(^{18}F)Fluoro-L-*m*-tyrosine: An L-3,4-dihydroxyphenylalanine analog for probing presynaptic dopaminergic function with positron emission tomography. *J. Neurochem.* 53:311-314.

Nagatsu, T. and Yoshida, M. 1988. An endogenous substance of the brain, tetrahydroisoquinoline, produces parkinsonism in primates with decreased dopamine, tyrosine hydroxylase and diopterin in the nigrostriatal regions. *Neurosci. Lett.* 87:178-182.

Nicklas, W.J., Vyas, R.E., and Heikkila, R.E. 1985. Inhibition of NADH-linked oxidation in brain mitochondria by 1-methyl-4-phenyl-pyridine, a metabolite of the neurotoxin 1-methyl-4-phenyl-1,2,5,6-tetrahydropyridine. *Life Sci.* 36:2503-2508.

Oiwa, Y., Eberling, J.L., Nagy, D., Pivirotto, P., Emborg, M.E., and Bankiewicz, K.S. 2003. Overlesioned hemiparkinsonian nonhuman primate model: Correlation between clinical, neurochemical and histochemical changes. *Front Biosci.* 8:A155-A166.

Pate, B.D., Kawamata, T., Yamada, T., Mcgeer, E.G., Hewitt, K.A., Snow, B.J., Ruth, T.J., and Calne, D.B. 1993. Correlation of striatal fluorodopa uptake in the MPTP monkey with dopaminergic indices. *Ann. Neurol.* 34:331-338.

Paxinos, G. and Watson, C. 1986. The Rat Brain in Stereotaxic Coordinates. Academic Press, New York.

Perese, D.A., Ulman, J., Viola, J., Ewing, S.E., and Bankiewicz, K.S. 1989. A 6-hydroxydopamine-induced selective parkinsonian rat model. *Brain Res.* 494:285-293.

Ricaurte, G.A., Irwin, I., Forno, L.S., DeLanney, L.E., Langston, E., and Langston, J.W. 1987. Aging and 1-methyl-4-phenyl-1,2,3,6-tetrahydropyridine-induced degeneration of dopaminergic neurons in the substantia nigra. *Brain Res.* 403:43-51.

Sauer, H.W. and Oertel, H. 1994. Progressive degeneration of nigrostriatal dopamine neurons following intrastriatal terminal lesions with 6-hydroxydopamine—A combined retrograde tracing and immunocytochemical study in the rat. *Neuroscience* 59:401-415.

Schmidt, M.J., Sawyer, B.D., Perry, K.W., Fuller, R.W., Foreman, M.M., and Ghetti, B. 1982. Dopamine deficiency in the weaver mutant mouse. *J. Neurosci.* 2:376-380.

Schneider, J.S. 1989. Levodopa-induced dyskinesias in parkinsonian monkeys: Relationship to extent of nigrostriatal damage. *Pharmacol. Biochem. Behav.* 34:193-196.

Schneider, J.S. and Kovelowski, C.J. 1990. Chronic exposure to low doses of MPTP. I. Cognitive deficits in motor asymptomatic monkeys. *Brain Res.* 519:122-128.

Schultz, W. 1982. Depletion of dopamine in the striatum as an experimental model of parkinsonism: Direct effects and adaptive mechanisms. *Prog. Microbiol.* 18:121-166.

Sundstrom, E., Fredriksson, A., and Archer, T. 1990. Chronic neurochemical and behavioral changes in MPTP-lesioned C56BL/6 mice: A model for Parkinson's disease. *Brain Res.* 528:181-188.

Thomas, J., Wang, J., Takubo, H., Sheng, J.G., Dejesus, S., and Bankiewicz, K.S. 1994. A 6-hydroxydopamine-induced selective parkinsonian rat model: Further biochemical and behavioral characterization. *Exp. Neurol.* 126:159-167.

Ungerstedt, U. 1971a. Striatal dopamine release after amphetamine or nerve degeneration revealed by rotational behaviour. *Acta Physiol. Scand. Suppl.* 367:51-68.

Ungerstedt, U. 1971b. Postsynaptic supersensitivity after 6-hydroxydopamine induced degeneration of the nigrostriatal dopamine system. *Acta Physiol. Scand. Suppl.* 367:69-93.

Ungerstedt, U. and Arbuthnott, G.W. 1970. Quantitative recording of rotational behavior in rats after 6-hydroxydopamine lesions of the nigrostriatal dopamine system. *Brain Res.* 24:485-493.

Wang, J., Skirboll, S., Aigner, T.G., Saunders, R.C., Hsiao, J. and Bankiewicz, K.S. 1990. Methodology of microdialysis of neostriatum in hemiparkinsonian nonhuman primates. *Exp. Neur.* 110:181-186.

Yang, S.C., Markey, S.P., Bankiewicz, K.S., London, W.T., and Lunn, G. 1988. Recommended safe practices for using the neurotoxin MPTP in animal experiments. *Lab. Anim. Sci.* 38:563-567.

Zigmond, M.J. and Strickler, E.M. 1989. Animal models of parkinsonism using selective neurotoxins: Clinical and basic implications. *Int. Rev. Neurosci.* 31:1-79.

Contributed by Krys S. Bankiewicz
University of California San Francisco
San Francisco, California

Rosario Sanchez-Pernaute
McLean Hospital and Harvard Medical School
Boston, Massachusetts

Yoshitsugu Oiwa
Wakayama Medical University
Wakayama, Japan

Malgorzata Kohutnicka
Institute of Psychiatry and Neurology
Warsaw, Poland

Alex Cummins
National Institute of Mental Health
Bethesda, Maryland

Jamie Eberling
University of California Davis
Davis, California

CHAPTER 2
Assessment of Cell Toxicity

INTRODUCTION

Environmental agents that are injurious to cells trigger a spectrum of responses that can range from cell death to adaptation, repair, and proliferation. Cell death, in turn, can take the form of apoptosis—a programmed form of cell death that requires gene expression—or necrosis. A host of environmental agents have been implicated in toxic cell injury, among them free radicals (nitrogen, oxygen, and carbon derivatives), which are known to interact with cellular constituents including membrane lipids and chromagen materials.

There are various ways of evaluating cellular toxicity and cell death, and a number of different indices for assessing cellular response to toxic stimulus or injury. *UNIT 2.1* outlines the current understanding of what constitutes cell toxicity and how it should be defined. *UNIT 2.2* presents a number of methods that can be used to discriminate between the apoptotic and necrotic modes of cell death. Because many of the distinguishing criteria are not specific to one mode, more than one method should be used to make the determination. It is now known that the mitochondrial function is changed in apoptosis. *UNIT 2.10* provides protocols for assessment of various aspects of mitochondrial function. *UNIT 2.3* describes immunochemical methods for detecting the covalent binding of chemicals to proteins as a means to investigate the interactions of potentially cytotoxic chemicals with cellular constituents. *UNIT 2.4* describes methods for detecting lipid peroxides, free radicals formed by the interaction of oxygen derivatives with membrane proteins. Oxygen free radicals have been implicated in both apoptosis and necrosis.

UNIT 2.5 provides protocols for measuring intracellular free Ca^{2+} using fluorescence spectroscopy or digital imaging microscopy. Changes in cellular Ca^{2+} homeostasis are intimately linked to cell death, with the cascade of events that they set in motion culminating in cellular necrosis and/or apoptosis. In addition, intracellular calcium is used in signaling and as a second messenger.

UNIT 2.6 provides protocols that can be used to detect cytotoxicity, which is operationally defined as the effect toxicants have on cell growth, metabolic functions, or viability. The protocols permit detection of physiological and/or morphological changes that may have occurred as a consequence of toxicant exposure. Sixteen protocols are provided to detect cytotoxicity in vitro. These protocols can be used to screen chemicals efficiently and economically before testing in animals.

UNIT 2.7 describes in situ hybridization for analyzing specific cellular mRNA in frozen and cryostat-sectioned tissues. The method combines cell and molecular biology techniques for detection and localization of specific nucleic acid sequences within individual cell or tissue preparations. Many protocols have been developed for different types of in situ hybridization. This unit includes methods using either radiolabeled or digoxigenin-labeled probes.

Contributed by Mahin D. Maines
Current Protocols in Toxicology (2004) 2.0.1-2.0.2

UNIT 2.8 presents a basic insight into the theoretical and practical possibilities and limitations of confocal microscopy. It also provides practical guidelines for the novice user of the technique. The method makes it possible to view a very thin optical plane in a specimen by excluding light from planes above and below the focal plane. Although there are several different types of confocal microscopes developed for specialized purposes, this unit concentrates on confocal scanning laser microscopy (CSLM).

The heat shock family of proteins (HSP) rapidly responds to chemical and environmental insults. The HSP70 family of proteins comprises a major family of stress-responsive proteins that have in common various functions in cellular defense mechanisms. *UNIT 2.9* provides procedures that allow measurement of response of different isotypes of the HSP70 family at the transcription and translation levels.

Mahin D. Maines

Current Concepts in Cell Toxicity

Toxicology is sometimes defined as the study of the adverse or harsh effects of toxic agents on living cells, tissues, or whole organisms. The term "toxic agent" is generally used to refer to both naturally occurring toxic substances (toxins) and to harmful products or byproducts (toxicants) generated from human activities, which may have diverse effects on living cells. These agents can be subclassified in various ways—for example, according to their target organ (e.g., liver, kidney, or reproductive organs), industrial use (e.g., food additives or pesticides), source (e.g., animal or plant toxins), and effects (e.g., cancer or liver injury). When a cell is exposed to toxic agents, it will undergo certain molecular or biochemical transformations. The biotransformations or alterations caused by the cell's exposure to harmful products is generally referred to as cell toxication or cell toxicity. On the other hand, the biotransformations or cellular alterations that lead to the elimination of toxicants or the prevention of toxic metabolite formation from these compounds are called "cell detoxification."

Cell toxicity can have reversible (short-lived or repairable) effects, or affect the cell irreversibly, leading to mutations, malignant transformation, or cell death. The final outcome of being in contact with toxic agents depends mainly on the nature of the toxic substance, the dose applied, and the exposure time. At low doses or short exposure times, small quantities of the toxic agent will come in contact with the cell and be delivered into its cytosol. This may lead to toxicity resulting from the mere presence of the agent in the cell, or the agent may interact with an array of target molecules. Such toxicity initiates a series of events leading to minor and potentially reversible injuries. These events can cause a temporary halt in some of the cellular functions. Similarly, the presence of toxic agents or cellular injuries caused by them may activate the cell's defenses—detoxification or repair mechanisms—to enable it to withstand such harsh environments and to repair the injuries that have been inflicted upon the cell. The cell's defense mechanisms involve rapid production or activation of specific molecules—examples of which are heat-shock proteins (HSPs), metallothioneins (MTs), superoxide dismutases (SODs), and catalase—which enable the cell to withstand or tolerate selective toxic agents. A number of xenobiotics (e.g., carbon monoxide, heavy-metal ions, and strong acids and bases) are directly toxic, whereas the toxicity of the others is largely due to production of metabolites. The mechanism of detoxification includes glutathione, cytochrome P-450, Cu, Zn-SOD, and Mn-SOD.

However, at high doses or prolonged exposure times, the toxic agents cause irreversible cellular damage, to the extent that the rate of toxication exceeds that of detoxification, leading to a general cellular dysfunction and cell death. This unit attempts to define cell toxicity that leads to cellular demise, with a strong emphasis on cell death via both apoptosis and necrosis, by summarizing some of the more recent developments in cellular, molecular, and biochemical studies of the events that govern the induction and execution of cell death.

CELL DEATH

Toxic cell death can occur via two processes, which are fundamentally different in their nature and biological significance (Kerr et al., 1972). These are termed necrosis and apoptosis and their features are summarized in Table 2.1.1.

Necrosis, or "accidental" cell death, was the classic model and was thought to be the universal mode of cell death until apoptosis was identified in 1972 as a separate mode of cell death. In general, necrosis is considered to be a passive process (Trump and Ginn, 1969) that is usually caused by extreme trauma or injury to the cell (Kerr et al., 1972). In tissues, necrosis is often seen as a lesion or patch consisting of many disintegrated cells. Typically, necrosis involves irreversible changes within the nuclei (such as karyolysis), loss of cytoplasmic structure, dysfunction in various organelles (especially mitochondria), and, finally, cytolysis as a result of high-amplitude swelling. The release of the dying cell's contents into the extracellular space can cause further injury or even death of neighboring cells, and may result in inflammation or infiltration of proinflammatory cells into the lesion, leading to further tissue damage (Haslett, 1992).

The first references to a different type of cell death came from developmental studies. The concept of a programmed physiological cell death in developmental biology or embryology refers to the type of cell death that occurs at

Contributed by Afshin Samali, Boris Zhivotovsky, and Sten Orrenius

Current Protocols in Toxicology (1999) 2.1.1-2.1.16

Table 2.1.1 Features of Apoptosis and Necrosis

Characteristics	Apoptosis	Necrosis
Stimuli	Physiological or pathological	Pathological (injury)
Occurrence	Single cells	Groups of cells
Reversibility	Limited	Limited
Cellular level		
Cell shape	Shrinkage and formation of apoptotic bodies	Swelling and later disintegration
Adhesion between cells	Lost (early)	Lost (late)
Phagocytosis by other cells	Present	Absent
Exudative inflammation	Absent	Present
Cellular organelles		
Membranes	Blebbing	Blebbing proir to lysis
Cytoplasm	Late-stage swelling	Very early swelling
Mitochondrial permeability transition	Present	Present
Nucleus	Convolution of nuclear outline and breakdown (karyorrexis)	Disappearance (karyolysis)
Biochemical level		
Gene activation	Present[a]	Absent[a]
Requirement for protein synthesis	Present[a]	Absent[a]
Lysosomal enzyme release	Absent	Present
Activation of non-lysosomal enzymes	Present	Present
Activation of caspases	Present	Absent
Cleavage of specific proteins	Present	—[a]
Changes in cytoskeleton	Present	Present
Level of ATP required	High	Low
Bcl-2 protection	Present	Present
Nuclear chromatin	Compaction in uniformly dense masses	Clumping not sharply defined
DNA breakdown	HMW and internucleosomal	Randomized
RNA degradation	Present	—[a]
Phosphatidylserine exposure	Present	Absent

[a]This feature is not a universal event or there are conflicting reports.

specific times during the development of the organism. Glucksmann (1951) clearly emphasized the existence of this phenomenon for the first time. This was followed by a surge of interest in 1960s (for a review see Lockshin, 1981). In the 1970s, histochemical studies of lysosomal changes in hepatic ischemia provided direct evidence for the existence of two distinct types of cell death (Kerr, 1971; Kerr et al., 1972). It was observed that rounded masses that developed in dead hepatic tissue contained cells that were morphologically different from those found in necrosis. These differences initially caused some confusion: the process was mistaken for a variation of necrosis and was called "shrinkage necrosis" (Kerr, 1971). The following year, Kerr, Wyllie, and Currie proposed the term "apoptosis" to describe the distinct morphological changes associated with this form of cell death (Kerr et al., 1972). Nowadays, apoptosis commonly refers to the process of cell death leading to the appearance of the morphological changes, rather than to the morphological characteristics themselves, which set this form of cell death apart from necrosis.

Apoptosis has been described as a form of cellular suicide, since death appears to result from induction of active processes within the cell itself. Typically, apoptosis involves margi-

nation and condensation of nuclear chromatin (pyknosis), cytoplasmic shrinkage, membrane blebbing, nuclear fragmentation, and finally, formation of apoptotic bodies.

A cell that is dying, whether by apoptosis or necrosis, undergoes rapid changes which are reflected in its structure, morphology, and biochemistry. These are generally a result of various enzymes activated through elaborate signaling pathways. Since the first description of apoptosis in 1972, there has been a surge of interest in the study of apoptosis, and very little attention has been given to necrosis. This lack of parallel study of the two processes is also reflected in the degree of detail provided here describing apoptosis and necrosis.

STRUCTURAL CHANGES DURING CELL DEATH

Considerable biochemical changes occur within the apoptotic cell, which facilitate neat packaging and removal of apoptotic bodies by neighboring cells. However, as described above, necrosis is accompanied by high-amplitude cell swelling. Modifications in the cytoskeleton and cytoplasmic membrane are required for both shrinkage and swelling to occur. During apoptosis, this results in the loss of cell-cell contact, untethering of the plasma membrane, and rapid blebbing or zeiosis (Saunderson, 1982). Similarly, necrotic cells undergo membrane blebbing, but in contrast to apoptosis, the tracts of contiguous dying necrotic cells collapse without loss of contact with neighboring cells. This results in clumps of necrotic cells rather than single cells.

Tissue transglutaminase, a Ca^{2+}-dependent protein-glutamine γ-glutamyltransferase, is induced and activated in liver hyperplasia and in glucocorticoid-treated thymocytes (Fesus et al., 1987). This enzyme cross-links cytokeratin, a component of the cytoskeleton, through ε-(γ-glutamyl) lysine bonds. During apoptosis there is a significant increase in transglutaminase mRNA, as well as the the protein itself, its enzyme activity, and protein-bound (γ-glutamyl) lysine (Fesus et al., 1987). It is thought that transglutaminase activity may stabilize apoptotic cells and inhibit membrane leakage during the early stages of the process by forming a shell around the cell. Transglutaminase activity, however, does not appear to change during necrosis. For example, it was recently reported that ethanol-induced cytotoxicity in astroglial cells was due to necrotic cell death, and that it occurred in the absence of any change in transglutaminase activity (Holownia et al., 1997).

A critical part of apoptosis, in contrast to necrosis, is the efficient recognition and removal of the apoptotic cells by phagocytes (Fadok et al., 1992). This involves the rearrangement and biochemical alteration of the plasma membrane in the dying cell. There are a number of different changes that occur in the plasma membrane of apoptotic cells. One such change results in the alteration of carbohydrates on the plasma membrane, which helps preferential binding of macrophages to apoptotic cells (Duvall et al., 1985). Recognition of apoptotic cells by macrophages can also be mediated via the vitronectin receptor (CD36; Savill et al., 1990). The loss of membrane phospholipid asymmetry in the membrane of cells undergoing apoptosis is yet another significant change leading to the externalization of phosphatidylserine at the surface of the cell, thereby enabling cell recognition by macrophages (Fadok et al., 1992). Development of fluorescently labeled annexin V, which binds specifically to phosphatidylserine residues, enables detection of this externalization in apoptotic cells (Koopman et al., 1994). However, under in vitro culture conditions, where phagocytic cells are absent, apoptotic cells and their fragments lyse in a process very similar to that observed in necrosis. This phenomenon is termed secondary necrosis or post-apoptotic necrosis. Despite such systematic changes in the plasma membranes of apoptotic cells, there are no reports of any changes in the composition of the plasma membranes of necrotic cells. Necrotic cells do not undergo phagocytosis by other cells, and the spillage of their cellular contents through plasma membrane disruption into the extracellular milieu induces cellular inflammatory responses.

Cell-volume changes are another feature of cell death. Interestingly, the cell volume changes during apoptosis and necrosis go in different directions. Apoptotic cell shrinkage, which leads to a loss of 30% to 50% of the cell volume (Saunderson, 1982), is due to budding of the endoplasmic reticulum. Vesicles thus generated migrate and fuse to the plasma membrane, releasing their contents into the extracellular region. This process requires energy (ATP), since water is moved against the osmotic gradient (Saunderson, 1982). Mitochondria, which are postulated to remain structurally and functionally intact during apoptosis, provide the necessary energy. In contrast, during necrosis the cell loses control of ion flux, resulting in a reduction in concentration gradients of Na^+, K^+, Ca^{2+}, and Mg^{2+}, as well as changes in

osmotic pressure. This, in turn, leads to uptake of water, giving rise to high-amplitude swelling of the cell and its organelles. This process is energy-independent and does not require a large amount of ATP.

MACROMOLECULAR DEGRADATION DURING CELL DEATH

Cell death is associated with activation or increase in the activity of lipases, nucleases, and different classes of proteases. In apoptosis there is an efficient and neat packaging of the cell contents into apoptotic bodies. This requires the rearrangement and breakdown of lipids, proteins, and nucleic acids. Another possible reason for efficient degradation of macromolecules in apoptotic cells prior to their phagocytosis is that contents from dead cells are thus prevented from entering the phagocyte or the neighboring cells and causing the same injuries that may have cost the dying cell its life. Which enzymes and substrates are activated depends on the induction stimuli and/or the cell type. In necrosis, the types of enzymes activated appear to be different, with very little overlap, if any, with the apoptotic enzymes. These enzymes are largely lysosomal acidic enzymes with less specific substrates than the apoptotic enzymes. However, these necrotic enzymes are thought to be activated in late apoptosis and in the absence of phagocytosis, when the cells undergo secondary necrosis. Thus, there is a similarity between the features of necrotic cells and those of apoptotic cells undergoing secondary necrosis. The major macromolecules and the mode of their degradation during apoptosis and necrosis are discussed below.

DNA Degradation

Three patterns of DNA degradation are already known to occur during apoptosis. One or more of these may occur during the progression of apoptosis in a single cell (for review see Zhivotovsky et al., 1994). These are: single-strand nicks (Gorczyca et al., 1992), chromatin cleavage with the formation of large (50- to 200-kbp) fragments (Brown et al., 1993; Zhivotovsky et al., 1994), and finally formation of nucleosome-size fragments of 180 to 200 bp, which produce the ladder pattern that has long been accepted as a biochemical hallmark of apoptosis (Wyllie, 1980).

One or more nuclear endonucleases have been suggested as being responsible for these patterns of DNA fragmentation, since isolated nuclei can be induced to produce the same pattern. A number of endonucleases have been identified in different cell systems, with different ion requirements for their activity (for review see Zhivotovsky et al., 1994). For example, the endonuclease in thymocytes is Ca^{2+}/Mg^{2+}-dependent, whereas the endonuclease operating in HL-60 cells appears to function independently of these ions (Fernandes and Cotter, 1993). Endonuclease activity in cells undergoing apoptosis can be regulated by proto-oncogenes and tumor-suppressor genes, such as *c-myc*, Ha-*ras*, *bcl-2*, and *p53*, as shown by analysis of genetic control of susceptibility to apoptosis (Arends et al., 1993). The apoptotic endonuclease or endonucleases cleave DNA at the exposed linker regions, and it has been suggested that these nucleases are topologically constrained rather than sequence constrained. Results obtained from cloning and sequencing DNA fragments from apoptotic cells show that the nuclease has no preference for specific DNA sequences or for the type of DNA to cleave. This randomness may be functionally important, and reflects the known properties of the endonucleases. The finding that apoptotic endonucleases are constitutive enzymes and that their activity can be modulated by different signals in cells undergoing apoptosis underlines the important role of nucleases in both physiological and pathophysiological processes. Although the role of intracellular endonucleases is not yet understood, one may speculate that a major function is to maintain genomic stability. Unfortunately, both purpose and mechanisms of DNA fragmentation in apoptotic cells are still unclear. Such fragmentation could serve to destroy the genetic information of unwanted cells and thus act as an irreversible step in the process. On the other hand, it may be simply a mid-to-late event that reflects ion redistribution and subsequent chromatin hypersensitivity to endonuclease(s) present in apoptotic cells. Alternatively, it may facilitate cleavage of DNA before uptake of apoptotic bodies during phagocytosis. Whatever the reason, it is still important to understand the mechanisms of this intriguing step of apoptosis.

As compared to apoptosis, at least two patterns of DNA degradation are recognized as occurring during necrosis. The first is the formation of both single- and double-strand DNA breaks. The second is randomized chromatin fragmentation. It is unclear if there is a link between these two steps of chromatin disintegration, although the probability for that is

rather high. DNA fragments isolated from necrotic cells contain 5′-OH and 3′-PO_4 end groups. Among different endonucleases isolated and characterized up to now, only one is able to produce such DNA fragments—i.e., DNase II, which is localized in lysosomes. This makes sense, since the activation of lysosomal enzymes has been observed in necrotic cells. Several publications have implicated the involvement of DNase II in apoptosis as well; however a critical role for this enzyme in apoptosis appears improbable in view of at least two considerations. First, DNase II is a lysosomal enzyme and lysosomes are intact until very late stages of apoptosis. Second, DNA fragments isolated from apoptotic cells contain 3′-OH end groups, not 3′-PO_4 groups as in necrotic cells. The search for enzymes responsible for cleaving of chromatin during necrosis is still in progress in many laboratories.

RNA Degradation

Changes in ribosomal counts occurring in response to cell injury have been known for a number of years. This phenomenon may be a result of the release of ribosomes from the endoplasmic reticulum at particular stages leading to necrosis (for review see Bowen, 1981). A detailed analysis of the role of ribosomes in the pathogenesis of liver-cell necrosis was conducted by Bernelli-Zazzera (1975). He showed that ischemia resulted in a decrease in the number of ribosomes, and that stripped rough endoplasmic reticulum from ischemic cells bound fewer added ribosomes than did the reticulum from normal cells. We have concluded that there is a "loosened relationship" between endoplasmic reticulum membranes and ribosomes in ischemic livers. However, it is unknown how specific these changes are for necrosis and what relationship they bear to this type of cell death.

There are also a number of reports that RNA, as well as DNA, is susceptible to cleavage during apoptosis. The changes in ribosomal RNA (rRNA) during apoptosis are best studied. rRNA consists of conserved and divergent (or variable) domains numbered from D1 to D12 (for review see Houge and Doskeland, 1996). The cleavage of rRNA during apoptosis selectively affects the two largest divergent domains, D2 and D8, in the large 28S rRNA molecule of the 60S ribosomal subunit, while the 18S rRNA molecule in the 40S ribosomal subunit remains unaffected (Houge et al., 1993). However, the pattern of rRNA cleavage occurring during apoptosis cannot be reproduced in necrotic cells or when exposing cell lysates to random RNase activity, suggesting that it is specific to apoptotic cells.

Recently it was demonstrated that rRNA and DNA cleavages can occur independently in apoptotic cells (Samali et al., 1997). In other words, the previously observed correlation is likely to be coincidental. The absence of apoptotic rRNA cleavage in some cell types suggests that this phenomenon is tightly regulated and unrelated to DNA fragmentation. Therefore it appears that the pattern of fragmentation seen during apoptosis is not part of a scheme for general macromolecular disintegration and degradation, but rather a trait present in only some cell types.

Protein Degradation

The prerequisite for proteolysis in apoptosis is well documented. Several proteolytic activities were implicated in both the induction and execution steps of cell killing (for review see Zhivotovsky et al., 1997). Early evidence of a role for proteases in apoptosis came from studies on granule proteases (granzymes/fragmentins). These investigations identified granzymes involved in the exocytosis pathway of lymphocyte-mediated cytotoxicity, which are responsible for the lethal damage inflicted by these cells upon target cells (Shi et al., 1992). More recently, a family of aspartic acid–specific cysteine proteases have been discovered in mammalian cells, which share homology with the *Caenorhabditis elegans* death gene, *ced-3* (Yuan et al., 1993). The newly adopted nomenclature for these enzymes, caspases, refers to the aspartic acid–specific cysteine protease activity specific to this family (Alnemri et al., 1996). At least thirteen of these proteases have now been purified and their genes cloned (for review see Zhivotovsky et al., 1997). The activation of the caspase family of proteases has been detected in numerous tissues and cell types and may function as a common pathway through which apoptotic mechanisms operate. Some procaspases, following translation, become autocatalytically cleaved at specific P1 aspartic acid residues, thereby generating a tetrameric cysteine protease holoenzyme that recognizes a characteristic cleavage motif (WXXD, DEXD, or XEXD) in target proteins (Nicholson and Thornberry, 1997). The effects of caspases in apoptosis appear to be accomplished by the cleavage of numerous proteins located in the cytoskeleton, cytoplasm, and nucleus, although the significance of these cleavages to the cell-death process is still unclear.

There have been a large number of reports on caspase involvement in apoptosis; however, there is yet very little evidence for the involvement of this family of proteases in necrosis. Recent work from our own group has shown that menadione-induced necrosis of hepatoma cells is independent of caspase activation (A. Samali et al, 1999). Furthermore, Tomaselli and co-workers (Armstrong et al., 1997) observed the activation of caspase 3 (CPP32/apopain) in cerebellar granule neurons undergoing apoptosis but not necrosis. These results appear to be in line with the work carried out in our laboratory which have shown that after the acute, necrotic death of cerebellar granule neurons exposed to glutamate, the remaining neurons undergo a delayed, apoptotic death (Ankarcrona et al., 1995). However, we did not detect any caspase activation during the "necrotic" step of our experimental model (M. Ankarcrona, B. Zhivotovsky, S. Orrenius, and P. Nicotera, unpub. observ.).

Apart from the caspase family of proteases, a number of other proteolytic enzymes are also implicated in cell death. Studies from our laboratory have suggested the involvement of Ca^{2+}-dependent proteolytic activity in oxidant injury in the liver (Nicotera et al., 1986). Although the substrates for this protease activity during cell injury remain largely unidentified, it appears that cytoskeletal and membrane-integral proteins may be a major target for this proteolytic event during chemical toxicity (Mirabelli et al., 1989). Calpain, another Ca^{2+}-dependent neutral protease and member of the papain family of cysteine proteases, degrades a number of key cellular proteins including proto-oncogenes, steroid-hormone receptors, protein kinases, and cytoskeletal proteins (Croal and DeMartino, 1991, Vanags et al., 1996). Calpain, one of the degradative nonlysosomal proteases, is also implicated in necrosis (Arai et al., 1990). Enhanced calpain activity has been observed in anoxic hepatocytes and neurons. Moreover, inhibition of calpain by acidosis, calpain protease inhibitors, and glycine delays anoxic injury. Precise mechanisms responsible for the stimulation of calpain activity during either necrosis or apoptosis are still unclear. More recently, it has been shown that hepatocellular carcinoma cells resist necrosis during anoxia by preventing phospholipase-mediated calpain activation (Arora et al., 1996). However, it is unknown whether sustained calpain activity promotes necrosis as a "deathase" by degrading key cytoskeletal proteins such as spectrin or by acting as a "signaling protease." Therefore, a better understanding of the protein substrates cleaved in necrosis will be required before the role of calpains in necrosis can be elucidated.

Another example of noncaspase proteases that may be involved in apoptosis is seen in the plasminogen activator system, which is a major proteolytic complex responsible for the breakdown of the extracellular matrix. Expression of the plasminogen activator inhibitor type 2 (PAI-2) in HeLa cells, which do not synthesize PAI-2, protects them from tumor-necrosis factor– (TNF-) induced apoptosis (Dickinson et al., 1995). Interestingly PAI-2 has a high degree of structural similarity to crmA, which inhibits interleukin 1β–converting enzyme– (ICE)–induced apoptosis (Dickinson et al., 1995). PAI-2 itself is not spared during apoptosis, and it loses its activity after cleavage by other proteases (Jensen et al., 1994). There are no reports about the involvement of this protease in necrosis.

An alternative protease system, which is thought to play a role in cell death, is that of proteasomes. The contribution of proteasomal activity during apoptosis has primarily been evaluated by using inhibitors. There are several observations that show inhibition of proteasomal activity by "specific" peptide inhibitors either fails to prevent receptor-mediated apoptosis (B. Zhivotovsky, D.H. Burgess, I. Ares-Pörn, and S. Orrenius, unpub. observ.) or drives cells into apoptosis (Shinohara et al., 1996). Currently there is no evidence that these enzymes activate caspases. Thus, a conclusive role for this enzymatic system in apoptosis remains to be elucidated. The interaction between other enzyme activities, either proximal or distal to the cleavage and activation of the procaspases, and their role in apoptosis, is the subject of rapidly evolving research.

The lytic nature of lysosomal enzymes and their release by various experimental procedures suggested long ago that they might be responsible for cell necrosis in damaged cells and tissues (for review see Bowen, 1981). DeDuve had already in the 1960s developed the concept of the lysosome as a "suicide bag" (deDuve, 1963). This hypothesis states that particle-bound acid hydrolase can be released into the surrounding cytoplasm under appropriate conditions and bring about the cell's ultimate destruction. Such a response might occur during cellular injury, but lysosomes in fact are relatively stable organelles, which fragment and release their contents after cell death rather than before. Much attention was paid to acid hydrolases in the earlier publications. Hydro-

lases, however, were later shown to occur in association with the Golgi and/or Golgi–endoplasmic reticulum lysosomes, endoplasmic reticulum extracisternal spaces, and plasma membranes (for review see Bowen, 1981). In reference to inflammatory cells, it has been shown that acid hydrolases are directly transferred from the endoplasmic reticulum into foci of cytoplasmic degeneration (Van Lancker, 1975). It was later concluded that when cells die, areas of the cytoplasm become segregated for autolysis, and that these areas are supplied with hydrolases, either from primary lysosomes or directly from the endoplasmic reticulum. Furthermore, an accumulation of free acid phosphatases around ribosomes in the extracisternal space of the endoplasmic reticulum has been linked to this type of cell death (for review see Bowen, 1981). This early extracisternal buildup appears as a prelude to cell autolysis. On the other hand, histochemical studies showed that the liberation of acid phosphatases and esterases was not an early change (Kerr et al., 1972), and the authors of that study suggested that the release of lysosomal enzymes is not responsible for the initiation of necrotic cell death, but rather accompanies this type of death. There is no evidence for preferable degradation of any proteins by lysosomal proteases during necrosis. Thus, in contrast to apoptosis, the involvement of both lysosomal and nonlysosomal protease activities in necrosis was documented. However, the precise role of these protease activities in either induction or execution of necrosis, as well as the specific cleavage of cellular proteins, remain to be elucidated.

CELLULAR SIGNALING DURING CELL DEATH

Signal transduction is thought to play a key role in the onset of both apoptosis and necrosis, and this may be mediated by an increase in intracellular Ca^{2+} levels, protein kinase C (PKC), cyclic adenosine monophosphate/protein kinase A (cAMP/PKA), or phosphatases. It has been demonstrated that glucocorticoid-induced cell death involves Ca^{2+} influx in lymphocytes and that this type of cell death can be mimicked using calcium ionophores (Kaiser and Edelman, 1978). Based on these observations it appears that intracellular Ca^{2+} levels may initiate a death signal, probably through the activation of Ca^{2+}-dependent enzymes (proteases, phospholipases, and endonucleases) in this system. The evidence for a role of Ca^{2+} in necrotic cell killing is particularly strong in the central nervous system. Ca^{2+} appears to mediate the neurotoxicity of cyanide, such heavy metals as lead and mercury, and organotin compounds (for review see Nicotera and Orrenius, 1996). Furthermore, intracellular Ca^{2+} overload, resulting from excessive stimulation of excitatory amino acid receptors and enhanced Ca^{2+} influx through membrane channels, appears to play an important role in ischemic brain damage. Much recent research has focused on glutamate-induced excitotoxicity and its contribution to brain damage in various diseases (Choi, 1992; Ankarcrona et al., 1995). The calcium ion plays a critical role in this process, and intracellular Ca^{2+} overload appears to mediate the lethal effect of *N*-methyl-D-aspartate (NMDA) receptor overactivation. This mechanism is responsible not only for the brain damage induced by certain neurotoxins, but also for excitotoxicity, which is strongly implicated in neuronal death following insults such as ischemia and trauma. Thus, NMDA receptor antagonist not only blocks Ca^{2+} influx and neuronal death elicited by glutamate or NMDA in vitro, but can also reduce the volume of infarction produced by focal ischemia in vivo. As discussed above, glutamate can trigger the onset of both apoptosis and necrosis in cerebellar granule cells (Ankarcrona et al., 1995). Radical scavengers and agents that inhibit the generation of nitric oxide by nitric oxide synthase were ineffective in preventing cell death in this system, whereas NMDA receptor/channel blockers prevented both necrosis and apoptosis in glutamate-treated cerebellar granule cells. These data suggest that Ca^{2+} overload–mediated NMDA-receptor-operated channels are sufficient to induce either necrosis or apoptosis in cerebellar granule neurons in vivo. It is clear that intracellular Ca^{2+} overload is an important factor in various in vitro models, and results from clinical studies appear to support this hypothesis. The Ca^{2+} overload seems to result from increased Ca^{2+} influx through both receptor-operated and L-type Ca^{2+} channels, as indicated by the neuroprotective effects of glutamate-receptor antagonists and L-type channel blockers. Various Ca^{2+}-dependent degradative processes have been found to contribute to Ca^{2+}-mediated necrotic cell killing in in vitro studies, and, although their relative contribution is unclear, it appears that perturbation of cytoskeletal organization, impairment of mitochondrial function, and/or activation of certain proteases may be of particular importance. For example, it has been proposed that activation of phospholipase A2 by a sustained increase in

cytosolic calcium plays an important role in necrotic cell killing. Support for this hypothesis comes from several observations that necrosis in the liver and heart caused by ischemia, as well as in hepatocellular carcinoma cells in anoxic condition, is prevented by inhibitors of this enzyme or by the inhibition of calpain activation (for review see Nicotera and Orrenius, 1996). Thus, it is likely that the calcium ion may play a determinant role in the necrotic killing process.

One of the classic signaling pathways is that of PKC, which is a multifunctional serine/threonine kinase that utilizes diacylglycerol as a second messenger (Nishizuka, 1984). Twelve different isoforms of PKC have been identified to date and are classified according to their calcium dependence and phorbol ester binding activity (for review see Lavin et al., 1996). There are some reports as to the involvement of PKC in apoptosis. For example, it has been reported that treatment of mouse thymocytes with phorbol esters, which activate PKC, induces apoptosis (Kizaki et al., 1989). Similarly, apoptosis induced by the calcium ionophore A23187 can be inhibited by the PKC inhibitor H7. However, most of the evidence to date indicates that PKC activation inhibits apoptosis (McConkey et al., 1996). This paradox may be explained by the large number of isoforms, which may be differentially regulated during apoptosis (Forbes et al., 1992).

Similarly, the role of protein phosphatases during apoptosis is not clear. There are some reports that a number of cell lines react to okadaic acid by undergoing apoptosis (Boe et al., 1991), while there are other reports that the inhibition of protein phosphatase activity blocks apoptosis in some other cell lines (Baxter and Lavin, 1992). From these reports it appears that protein activation/modification, through reversible protein phosphorylation by kinases and protein phosphatases rather than by de novo protein synthesis, may play a more central role in the regulation of apoptosis in some cells.

Receptor-mediated killing involves activation of a cascade of signaling events leading to activation of caspases. For example, apoptosis induced by ligation of the CD95 (Fas/Apo-1) receptor results in association of several cytotoxicity-dependent Apo-1-associated proteins (CAPs; Trauth et al., 1989). The aggregated receptor, together with the CAP proteins (1 to 4) form the death-inducing signaling complex or DISC. DISC formation upon engagement of the receptor is essential for CD95-induced apoptosis. CAP1/2 were identified as the serine phosphorylated Fas-associated death domain (FADD) and CAP3/4 as Fas-like (FLICE) or caspase-8, pro-enzyme and activated enzyme (for review see Wallach, 1997).

ROLE OF MITOCHONDRIA DURING CELL DEATH

Work from several laboratories has indicated that mitochondrial damage may be a common event in the development of cell injury caused by various toxic agents (Nicotera and Orrenius, 1996). It was postulated that mitochondrial damage is initially manifested by a decrease in the mitochondrial membrane potential followed by ATP depletion (Zamzami et al., 1995). During necrosis, these changes occur irreversibly and usually lead to disruption of the mitochondrial structure. These changes set necrosis aside from apoptosis, during which mitochondrial structure remains morphologically intact. Mitochondria have nevertheless been implicated in apoptosis ever since the discovery that the Bcl-2 protein localizes to the outer mitochondrial membrane (Hockenbery et al., 1990). Moreover, by using different cell-free systems, it has been shown that nuclear apoptosis depends on the presence of ATP (Lazebnik et al., 1993; Newmeyer et al., 1994; Kass et al., 1996). It has been demonstrated that cytochrome *c* can induce cleavage and activation of procaspase 3 in cytochrome *c*–minus cytoplasmic extracts (Liu et al., 1996). It has also been shown that cytochrome *c* is released from the mitochondrial intermembrane space into the cytosol by cells undergoing apoptosis. In this case cytochrome *c* release is not preceded by changes in mitochondrial membrane potential (Kluck et al., 1997).

Two groups have presented evidence that a high ATP level is required during the apoptotic process and suggested that the level of intracellular ATP determines whether a cell will die by apoptosis or necrosis (Nicotera and Leist, 1997; Tsugimoto, 1997). During exposure to glutamate, both mitochondrial membrane potential and ATP levels decline in many neurons (Ankarcrona et al., 1995). In neurons with irreversibly dissipated mitochondrial potentials, necrosis rapidly ensued. The surviving population recovered both mitochondrial membrane potential and energy levels and subsequently underwent delayed apoptosis. It was postulated that the loss of energy and the onset of rapid necrosis simply prevents the activation of the default apoptotic program. This postulate was supported by the observation that treatment of

cerebellar granule cells with a combination of glutamate and the irreversible mitochondrial uncoupler carbonyl cyanide *m*-chlorophenylhydrazone (CCCP) resulted in necrosis for most of the neuronal population, rather than in the delayed apoptosis observed with glutamate alone.

There is abundant evidence for an ATP requirement in several apoptosis models, although the critical ATP-dependent steps in the process have not been characterized in detail. They are likely to be linked to both the signaling and the execution phases of apoptosis. It was suggested (Tsugimoto, 1997) that the caspase protease cascade is regulated by ATP-dependent reactions and that the protease cascade might not proceed in an autonomous fashion. In addition, it has been shown (Yasuhara et al., 1997) that the active nuclear transport mechanism, which requires ATP hydrolysis, is involved in the apoptotic changes of the nuclei. It is likely that an another ATP-dependent step or steps downstream from caspase activation is important for perpetuation of the apoptotic process. This fact could explain the previously published data on the ATP requirement for induction of nuclear apoptosis, induced by different cytoplasmic extracts (Lazebnik et al., 1993; Newmeyer et al., 1994; Kass et al., 1996). Thus, it is not surprising that the depletion of cellular ATP blocks various events in apoptosis. The question that remains to be answered is whether, and how, ATP depletion redirects the death process towards necrosis when cells have been triggered with apoptotic stimuli, such as anti-CD95 antibodies. In addition to the possible requirement of ATP for caspase activation, redirection could also be explained by an unknown mechanism, which shortens the survival time of cells that would eventually die by necrosis resulting from energy deprivation.

The next important question that remains to be resolved is an apparent contradiction between, on the one hand, the obligatory induction of the mitochondrial permeability transition associated with a cessation of mitochondrial ATP synthesis, and, on the other hand, a need for maintenance of the intracellular ATP level during development of apoptosis, which may take many hours or days. In addition, hyperproduction of reactive oxygen species (ROS) results from the loss of mitochondrial membrane potential, yet the cell needs to maintain a reducing environment for optimal caspase activity. These controversies could be resolved if the proposed apoptosis-induced changes were restricted to a small subset of mitochondria in the cell. Maintenance of the energy level required by cells to undergo apoptosis could occur solely by glycolysis. This would be consistent with the observation by Jacobson et al. (1993) that cells lacking mitochondrial DNA and a functional respiratory chain can still undergo apoptosis. It is very likely that the mitochondrial permeability transition associated with a cessation of mitochondrial ATP plays an important role in necrotic cell death, whereas leakage of cytochrome *c* from morphologically intact mitochondria via a yet unknown and more selective pathway than outer-membrane rupture following permeability transition–induced mitochondrial swelling plays an important role in apoptotic cell death.

GENETIC MODULATION OF APOPTOTIC CELL DEATH

In recent years, enough evidence has been gathered to suggest a role for the protein products of a number of oncogenes and tumor-suppressor genes, as well as stress proteins and acute phase proteins, in the modulation cell death. These can be grouped into genes whose products are positive or negative regulators of cell death. The genes with a key role in the modulation of cell death and their effects on both apoptosis and necrosis are reviewed below.

c-myc

The *c-myc* proto-oncogene is a short-lived nuclear protein and a member of a family closely related genes that also include *v-myc*, *n-myc*, and *b-myc*. The *Myc* family plays a key role in the regulation of cell proliferation (for review see Ryan and Brinie, 1996). It has been demonstrated that *c-myc* is capable of driving apoptosis (Evan et al., 1992). For instance, when T cell hybridomas were stimulated through their CD3/T cell receptor, they rapidly underwent apoptosis that could be blocked using an antisense oligonucleotide to *c-myc* mRNA. Furthermore, in fibroblasts, *c-myc* overexpression can induce apoptosis (Evan et al., 1992). The decision to proliferate or die in cells overexpressing *c-myc* seems to depend on the presence or absence of extracellular survival factors.

p53

The p53 protein is the product of a tumor-suppressor gene whose loss of function occurs in over half of all human tumors, thus implicating p53 inactivation in tumorigenesis. Nevertheless, the main functions of p53 appear to be in mediating the cellular response to DNA dam-

age and maintaining genomic stability (Kastan et al., 1991). Many forms of genotoxic stress induce a rapid increase in p53 protein levels, through both stabilization of the protein (Kastan et al., 1991) and an increase in p53 mRNA levels (Sun et al., 1995). p53 induces growth suppression by regulating cell-cycle arrest and/or inducing apoptosis. Reintroduction and overexpression of wild-type p53 in cells that have lost endogenous p53 function may induce apoptosis (Yonish-Rouach et al., 1991). In this regard, p53 is shown to be required for both irradiation-induced G1 arrest and apoptosis in several cell systems (Lowe et al., 1993). Induction of growth arrest by p53 has been shown to be transcription activation–dependent and appears to involve induction of *p21* (*Waf1/Cip/sdi1*) and growth arrest and DNA damage-inducible gene 45 (*Gadd45*). For review see Yonish-Rouach (1996).

Although transcriptional activation appears to be involved in the induction of growth arrest, little is known about the possible downstream elements in this apoptotic pathway. p53 has been shown to induce apoptosis in the presence of transcriptional activation, in which case p53 may induce expression of Bax (Miyashita and Reed, 1995) and/or CD95 (Owen-Schaub et al., 1995). However, recent reports suggest that transcriptional activation is not essential for the induction and progression of p53-induced apoptosis (for review see Yonish-Rouach, 1996).

Bcl-2 family

This is a family of genes in which many members hold key positions in the apoptotic machinery. The proteins in this family share at least two highly conserved regions, which have been referred to as *Bcl-2* homology 1 and 2 (BH1 and BH2) domains (Oltvai et al., 1993). *Bcl-2* was the first member of this family to be identified in follicular B cell lymphomas (Bakhshi et al., 1985). Several other family members, which were discovered later, may function to inhibit apoptosis, including *Bcl-2*, *Bcl-x_L*, *Bcl-W*, *Bfl-1*, *A1*, and *MCL-1*, while others function to accelerate the rate of apoptosis once it has been induced, including *Bax*, *Bcl-x_s*, *Bag*, *Bik*, *Bim*, *Bak*, *Bar*, and *Bad*.

Bcl-2 protein is localized to the mitochondria, endoplasmic reticulum, and nuclear membrane (Hockenbery et al., 1990). Bcl-2 appears to have antioxidant properties, as it can inhibit apoptosis induced by reactive oxygen species (Hockenbery et al., 1993). However, it has also been demonstrated that Bcl-2 can inhibit cell death under conditions that preclude the formation of reactive oxygen species (Jackobson et al., 1993). Therefore, the ability of Bcl-2 to protect against the damaging effects of free radicals does not appear to completely account for the suppression of cell death by Bcl-2.

Bax is more ubiquitously expressed than Bcl-2 (Krajewski et al., 1994). The *bax* gene promoter contains four p53-binding sites, and it has been shown that the levels of its protein can be up-regulated by p53 (Miyashita and Reed, 1995). It is suggested that the ability of Bcl-2 to suppress apoptosis depends on the relative proportion of Bcl-2 homodimers and Bcl-2/Bax. In addition to Bcl-2, Bax can also heterodimerize with other Bcl-2-related proteins, including Bcl-x_L, Bcl-x_S, MCL-1, and A1, as shown by the yeast two-hybrid assay (for review see Reed, 1997). These reports suggest that Bcl-2 family members function in part through protein-protein interactions, and that susceptibility to apoptosis is determined by multiple competing dimerizations in which Bax is a common partner. However, the ultimate mechanism by which members of this family may induce or suppress apoptosis is not understood.

It has been shown recently that overexpression of Bcl-2 can also inhibit necrosis at least in neuronal cells when induced by such diverse stimuli as viruses, hypoxia, oxidative stress, or exposure to toxicants (Lezoulac'h et al., 1996; Shimizu et al., 1996). Whether this effect is cell-specific remains unclear. The mechanism of action of Bcl-2 in cells undergoing necrosis may simply involve antioxidant activity. The second possibility is that Bcl-2 prevents the consequences of mitochondrial dysfunction (collapse of the mitochondrial transmembrane potential, uncoupling of the respiratory chain, hyperproduction of superoxide anions, disruption of mitochondrial biogenesis, outflow of matrix calcium and glutathione, and release of soluble intermembrane proteins), all of which can lead to a bioenergetic catastrophe culminating in the disruption of plasma membrane integrity which is specific for necrosis (Kroemer, 1997). However, more work should be done to justify this hypothesis and to understand the mechanism of Bcl-2-induced protection from necrosis.

Ras

Members of the Ras family of proteins play an essential role in the control of normal cell growth and may induce transformation. Certain evidence has led a number of groups to advocate that Ras, in addition to inducing transformation, can also prevent cell death. Overex-

pression of the *ras* gene is shown to inhibit apoptosis in a number of cases (Wyllie et al., 1987; Arends et al., 1993). Ras appears to be a focal point for the convergence of many signaling pathways, especially during receptor/ligand interaction, such as epidermal growth factor (EGF), fibroblast growth factor (FGF) and nerve growth factor (NGF), T cell receptor–CD3 (TCR-CD3), and CD95. The question as to which protein downstream of the pathway is the key effector of the anti-apoptotic signal through Ras is unclear, but it may involve the activation of MAP kinase or phosphotidylinositol 3 kinase or both.

Stress Proteins

The stress proteins are a set of evolutionarily conserved proteins that are synthesized or activated in response to stress (for review see Lindquist and Craig, 1988). The main function of these proteins is to afford protection to cells in times of stress. When the stress element is removed, these cells continue to function normally and the levels drop back to the normal. Heat-shock proteins (HSPs), a subgroup of stress proteins, were first demonstrated to be induced as a response to elevated temperatures.

There is strong evidence suggesting that the induction of HSPs coincides with the acquisition of tolerance to higher doses of stress, which may otherwise be lethal to the cell. In this regard, it was demonstrated that a mild heat shock induces the rapid synthesis of a number of HSPs (Jaattela et al., 1992; Mosser and Martin, 1992) and that heat-shocked or thermotolerant cells demonstrated a greater degree of resistance to environmental stress (Jaattela et al., 1992), probably by resisting apoptosis (Samali and Cotter, 1996). Furthermore, it was demonstrated that thermotolerant or HSP-overexpressing cells are more resistant to cell death induced by hyperthermia or growth-factor withdrawal (Mailhos et al., 1993). This may suggest a possible role for HSPs in the resistance mechanism. Furthermore, HSPs are also implicated in drug resistance (McClean and Hill, 1992), and heat-shocked or HSP-overexpressing cells become more resistant to the cytotoxic effects of some anticancer drugs (Oesterreich et al., 1993) that are otherwise capable of inducing both apoptosis and necrosis (Martin et al., 1990).

CONCLUSIONS

Cell toxicity leading to cell death may occur via apoptosis or necrosis. The mode of cell death depends on the nature of the toxic agent, but in extreme situations the final outcome is cell disruption and disintegration. In other words, necrosis is the acute type of cell death or the cellular response to extreme toxic injury. During necrosis, chromatin adopts a highly flocculated form, and the DNA from these cells is digested randomly to give a smear when analyzed by agarose gel electrophoresis. The main feature of necrosis is an increase in cell volume. The rapid increase in cell volume results in membrane rupture and cell lysis (for review see Trump and Berezesky, 1995).

After two decades of research and development in the field of cell death, it is now universally accepted that apoptosis is an essential strategy for maintaining dynamic balance and equilibrium of living systems, and is observed to occur as a normal mechanism in development and homeostasis, as well as an altruistic mode of toxic cell death. Classification of cell death is now based on morphological and biochemical criteria, their circumstantial occurrence, or a combination of both. Although morphological characterization of apoptosis and the features distinguishing it from necrosis have been well documented, progress in our understanding of the mechanisms underlying the process has been quite slow.

There is now much evidence that classic apoptosis and necrosis represent only definitive endpoints for these two processes. However, both types of cell death can occur either simultaneously or sequentially in the same cell suspension or tissues depending on type and/or dose of toxic insult. This suggests that some early biochemical and morphological events might be similar or even identical in both types of cell death. If this is the case, different downstream events might be important in determining whether the cell will undergo apoptosis or necrosis. It could also be that after intensive toxic treatment, the cellular apoptotic machinery becomes suppressed, after which necrosis would predominate. The events summarized in Table 2.1.1 can be observed at different levels of cellular organization. Thus, both physiological or pathological stimuli can induce apoptosis, but only pathological injury leads to necrosis. Apoptosis, in contrast to necrosis, occurs in individual cells in an asynchronous fashion without damaging neighboring cells. Both processes can be protected by certain inhibitors before a point of no return is reached. Once the cascade of caspase proteolytic activities becomes active, apoptosis cannot be completely reversed. The point of no return during necrosis remains to be elucidated. Neverthe-

less, cells can be rescued from necrosis as well as from apoptosis.

Cellular shrinkage is a hallmark of apoptosis and is seen in many if not all cell types that undergo this type of death. Cell-volume regulation is a complex phenomenon, involving the homeostasis of intracellular ions such as chloride, sodium, and potassium. As the most abundant intracellular ion, K^+ has been implicated in several of the regulatory mechanisms governing cell volume, including regulatory volume decrease. It has been shown that intracellular K^+ content decreases in cells undergoing apoptosis induced either with etoposide or dexamethasone (Barbiero et al., 1995). Work in the authors' laboratory has shown a potential link between glutathione (GSH) efflux and apoptotic cell shrinkage (Nobel, 1997). Inhibitors of apoptotic GSH efflux were able to inhibit cell shrinkage in thymocytes induced to undergo apoptosis by etoposide without affecting DNA fragmentation. Moreover, the GSH efflux was accompanied by K^+ efflux in Jurkat cells treated with anti-CD95 antibody. The K^+ efflux was not blocked either by the inhibitor of GSH efflux or by any known inhibitors of K^+ channels and cotransporters tested. Concomitant with apoptotic K^+ efflux, significant inhibition of Na^+/K^+-ATPase activity was observed. Inhibition of this enzyme by ouabain caused a K^+ efflux of similar magnitude to that induced by anti-CD95 antibody, and it potentiated CD95-mediated cell shrinkage. This suggested that with Na^+/K^+-ATPase activation, K^+ and GSH effluxes facilitated apoptotic cell shrinkage, which was followed by the formation of apoptotic bodies. In contrast, necrotic cells showed extensive swelling, which resulted in subsequent disintegration of cells.

Apoptotic cells lose adhesion at the very early stages, while necrotic cells stay adherent together until very late stages. As mentioned before, individual apoptotic cells can be efficiently recognized either by neighboring cells or professional macrophages and can be removed by phagocytosis. This step of the apoptotic process involves rearrangements of and dramatic changes in the plasma membrane. Removal of the dead-cell fragments before their plasma membranes are lysed has important implications for other cells within the tissues. It is assumed that apoptosis occurs without inflammation. Lysis of plasma membranes in necrotic cells seems to precede the removal of these remnants, and exudative inflammation is a common event during necrosis.

The significance of apoptosis is based on the fact that apoptotic cells tend to be "environmentally friendly" and package their contents into membrane-bound vesicles ready for ingestion by phagocytic cells, without releasing their contents into the intercellular matrix. Hence there is no inflammatory response. Apoptosis is also an altruistic cell death, in that damaged or injured cells commit suicide to allow the neighboring cells to continue to proliferate without being affected by the death of the neighbor. In addition, sacrifice of individual abnormal cells benefits the whole organism.

Most if not all mechanisms leading to cell death involve molecular damage that is potentially reversible by cellular repair mechanisms. Therefore, if the repair mechanisms operate effectively, they may prevent cell death. It could be that in cells undergoing apoptosis, the cell-repair machinery is repressed by specific signals, which program cells to die. On the other hand, in cells undergoing necrosis this machinery might be directly suppressed by extremely strong insult (high doses of toxicants or irradiation). Since apoptosis is a gene-directed process and many genes are involved in the regulation of this multistage action, the repression of repair processes can also be regulated on this level. There is no evidence for expression of any specific genes during necrosis, which is why it is difficult to discuss the possible requirement of gene regulation for necrotic cell death. Thus, it seems that classic necrosis is a passive process. An inhibition of the activity of a number of gene products involved in apoptosis can switch the death pathway from apoptosis to necrosis. Also rapid changes in the cellular ATP levels, discussed above, and an imbalance in the ratio of nitric oxide and superoxide, can switch the form of cell death. The search on both molecular and biochemical levels for mechanisms of apoptosis and necrosis, along with attempts to understand the differences/similarities between these two types of cellular response to toxicants, are currently the hottest topics in biological research.

LITERATURE CITED

Alnemri, E.S., Livingston, D.J., Nicholson, D.W., Salvesen, G., Thornberry, N.A., Wong, W.W., and Yuan, J. 1996. Human ICE/CED-3 protease nomenclature. *Cell* 87:171.

Ankarcrona, M., Dypbukt, J.M., Bonfoco, E., Zhivotovsky, B., Orrenius, S., Lipton, S.A., and Nicotera, P. 1995. Glutamate-induced neuronal death: A succession of necrosis or apoptosis depending on mitochondrial function. *Neuron* 15:961-973.

Arai, A., Kessler, M., Lee, K., and Lynch, G. 1990. Calpain inhibitors improve the recovery of synaptic transmission from hypoxia in hippocampal slices. *Brain Res.* 532:63-68.

Arends, M.J., McGregor, A.H., Toft, N.J., Brown, E.J.H., and Wyllie, A.H. 1993. Susceptibility to apoptosis is differentially regulated by c-*myc* and Ha-*ras* oncogenes and is associated with endonuclease availability. *Br. J. Cancer* 68:1127-1133.

Armstrong, R.C., Aja, T.J., Hoang, K.D., Gaur, S., Bai, X., Alnemri, E., Litwack, G., Karanewsky, D.S., Fritz, L.C., and Tomaselli, K.J. 1997. Activation of the CED-3/ICE-related protease CPP32 in cerebellar granule neurons undergoing apoptosis, but not necrosis. *J. Neurosci.* 17:553-562.

Arora, A.S., de Groen, P.C., Croal, D.E., Emori, Y., and Gores, G.J. 1996. Hepatocellular carcinoma cells resist necrosis during anoxia by preventing phospholipase-mediated calpain activation. *J.Cell. Physiol.* 167:434-442.

Bakhshi, A., Jensen, J.P., Goldman, P., Wright, J.J., McBride, O.W., Epstein. A.L., and Korsmeyer, S.J. 1985. Cloning the chromosomal breakpoint of t(14;18) human lymphomas: clustering around JH on chromosome 14 and near a transcriptional unit on 18. *Cell* 41:899-906.

Barbiero, G., Duranti, F., Bonelli, G., Amenta, J.S., and Baccino, F.M. 1995. Intracellular ionic variations in the apoptotic death of lymphoid cells by inhibitors of cell cycle progression. *Exp. Cell Res.* 217:410-418.

Baxter, G.D. and Lavin M.F. 1992. Specific protein phosphorylation in apoptosis induced by ionizing radiation and heat shock in human lymphoid tumor lines. *J. Immunol.* 148:1949-1954.

Bernelli-Zazzera, A. 1975. Ribosomes in dying liver cells. *In* Pathogenesis and Mechanisms of Liver Cell Necrosis (D. Keppler, ed.) pp.103-111. MTP Press, Lancaster.

Boe, R., Gjertsen, B.T., Vintermyr, O.K., Houge, G., Lanotte, M., and Doskeland, S.O. 1991. The protein phosphatase inhibitor okadaic acid induces morphological changes typical of apoptosis in mammalian cells. *Exp. Cell Res.* 195:237-246.

Bowen, I.D. 1981. Techniques for demonstrating cell death. *In* Cell Death in Biology and Physiology (I.D. Bowen and R.A. Lockshin, eds.) pp. 379-444. Chapman & Hall, New York.

Brown, D.G., Sun, X.M., and Cohen, G.M. 1993. Dexamethasone-induced apoptosis involves cleavage of DNA to large fragments prior to internucleosomal fragmentation. *J. Biol. Chem.* 268:3037-3039.

Choi, D.W. 1992. Bench to bedside: The glutamate connection. *Science* 258:241-243.

Croal, D.E. and DeMartino, G.N. 1991. Calcium-activated neutral protease (calpain) system: Structure, function and regulation. *Physiol. Rev.* 71:813-847.

deDuve, C. 1963. The lysosome concept. *In* Lysosomes (A.V.S. deReuck and M.P. Cameron, eds.) pp.101-118. Churchill Livingston, London.

Dickinson, J.L., Bates, E.J., Ferrante, A., and Antalis, T.M. 1995. Plasminogen activator inhibitor type 2 inhibits tumor necrosis factor alpha–induced apoptosis. Evidence for an alternate biological function. *J. Biol. Chem.* 270:27894-27904.

Duvall, E., Wyllie, A.H., and Morris, R.G. 1985. Macrophage recognition of cells undergoing cell death (apoptosis). *Immunology* 56:351-358.

Evan, G.I., Wyllie, A.H., Gilbert, C.S., Littlewood, T.D., Hartmut, L., Brooks, M., Waters, C.M., Penn, L.Z., and Hancock, D. 1992. Induction of apoptosis in fibroblasts by c-myc protein. *Cell* 69:119-128.

Fadok, V.A., Voelker, D.R., Campbell, P.A., Cohen, J.J., Bratton, D.L., and Henson, P.M. 1992. Exposure of phosphatidylserine on the surface of apoptotic lymphocytes triggers specific recognition and removal by macrophages. *J. Immunol.* 148:2207-2216.

Fernandes, R.S. and Cotter, T.G. 1993. Activation of calcium and magnesium independent endonuclease in human leukemic cell apoptosis. *Cancer Res.* 13:1235-1260.

Fesus L., Thomazy, V., and Falus, A. 1987. Induction and activation of tissue transglutaminase during programmed cell death. *FEBS Lett.* 224:104-108.

Forbes, I.J., Zalewski, P.D., Gianniakis, C., and Cowled, P.A. 1992. Induction of apoptosis in chronic lymphocytic leukaemia cells and its prevention by phorbol esters. *Exp. Cell Res.* 198:367-372.

Glucksmann, A. 1951. Cell death is normal vertebrate ontology. *Biol. Rev.* 26:59-86.

Gorczyca, W., Bruno, S., Darzynkiewicz, R.J., Gong, J., and Darzynkiewicz, Z. 1992. DNA strand breaks occurring during apoptosis: Their early detection by terminal deoxynucleotide transferase and nick translation assays and prevention by serine protease inhibitors. *Int. J. Oncol.* 1:639-648.

Haslett, C. 1992. Resolution of acute inflammation and the role of apoptosis in tissue fate of granulocytes. *Clin. Sci.* 83:639-648.

Hockenbery, D.M., Nunez, G, Milliman, C., Schreiber, R.D., and Korsmeyer, S.J. 1990. Bcl-2 in inner mitochondrial membrane protein that blocks programmed cell death. *Nature* 348:334-336.

Hockenbery, D.M., Oltvai, Z.N., Yin, X.M., Milliman, C.L., and Korsmeyer, S.J. 1993. Bcl-2 functions in an antioxidant pathway to prevent apoptosis. *Cell* 75:241-251.

Holownia, A., Ledig, M., and Menez, J.F. 1997. Ethanol-induced cell death in cultured rat astroglia. *Neurotoxicol. Teratol.* 19:141-146.

Houge, G. and Doskeland, S.O. 1996. Divergance towards a dead end? Cleavage of a the divergant domain of ribosomal RNA in apoptosis. *Experientia* 52:963-967.

Houge, G., Doskeland, S.O., Boe, R., and Lanotte, M. 1993. Selective cleavage of 28S rRNA vari-

able regions V3 and V13 in myeloid leukemia cell apoptosis. *FEBS Lett.* 315:16-20.

Jaattela, M., Wissing, D., Bauer, P., and Li, G.C. 1992. Major heat shock protein hsp70 protects tumor cells from tumor necrosis factor cytotoxicity. *EMBO J.* 11:3507-3512.

Jacobson, M.D., Burne, J.F., King, M.P., Miyashita, T., Reed, J.C., and Raff, M.C. 1993. Bcl-2 blocks apoptosis in cells lacking mitochondrial DNA. *Nature* 361:365-369.

Jensen, P.H., Cressey, L.I., Gjertsen, B.T., Madsen, P., Mellgren, G., Hokland, P., Gliemann, J., Doskeland, S.O., Lanotte, M., and Vintermyr, O.K. 1994. Cleaved intracellular plasminogen activator inhibitor 2 in human myeloleukaemia cells is a marker of apoptosis. *Br. J. Cancer* 70:834-840.

Kaiser, N. and Edelman, I.S. 1978. Further studies on the role of calcium in glutocorticoid-induced lympholysis. *Endocrinology* 103:936-942.

Kass, G.E.N., Eriksson, J.E., Weis, M., Orrenius, S., and Chow, S.C. 1996. Chromatin condensation during apoptosis requires ATP. *Biochem. J.* 318:749-752.

Kastan, M.B., Onyekwere, O., Sidransky, D., Vogelstein, B., and Craig, R.W. 1991. Participation of p53 protein in the cellular response to DNA damage. *Cancer Res.* 51:6304-6311.

Kerr, J.F.R. 1971. Shrinkage necrosis: A distinct mode of cellular death. *J. Pathol.* 105:13-20.

Kerr, J.F.R., Wyllie, A.H., and Currie, A.R. 1972. Apoptosis: A basic biological phenomenon with wide ranging implications in tissue kinetics. *Br. J. Cancer* 26:239-257.

Kizaki, H., Tadakuma, T., Odaka, C., Maramatsu, J., and Isimura, Y. 1989. Activation of suicide process of thymocytes through DNA fragmentation by calcium ionophores and phorbol esters. *J. Immunol.* 143:1790-1794.

Kluck, R.M., Bossy-Wetzel, E., Green, D.R., and Newmeyer, D.D. 1997. The release of cytochrome *c* from mitochondria: A primary site for Bcl-2 regulation of apoptosis. *Science* 275:1132-1136.

Koopman, G., Reutelingsperger, C.P.M., Kuijten, G.A.M., Keehnen, R.M.J., Pals, S.T., and van Oers, M.H.J. 1994. Annexin V for flow cytometric detection of phosphatidylserine expression on B cells undergoing apoptosis. *Blood* 84:1415-1420.

Krajewski, S., Krajewska, M., Shabaik, A., and Reed, J.C. 1994. Immunohistochemical determination of in vivo distribution of bax, a dominant inhibitor of bcl-2. *Am. J. Pathol.* 145:1323-1336.

Kroemer, G. 1997. Mitochondrial implication in apoptosis: Towards an endosymbiont hypothesis of apoptosis evolution. *Cell Death Differ.* 4:443-456.

Lavin, M.F., Watters, D., and Song, Q. 1996. Role of protein kinase activity in apoptosis. *Experientia* 52:979-994.

Lazebnik, Y.A., Cole, S., Cooke, C.A., Nelson, W.G., and Earnshaw, W.C. 1993. Nuclear events of apoptosis in vitro in cell-free mitotic extracts: A model system for analysis of the active phase of apoptosis. *J. Cell Biol.* 123:7-22.

Lezoulac'h, F., Rupprecht, R., Holsboer, F., and Behl, C. 1996. *Bcl-2* prevents hippocampal cell death induced by the neuroleptic drug haloperidol. *Brain Res.* 738:176-179.

Lindquist, S. and Craig, E.A. 1988. The heat shock proteins. *Annu. Rev. Genet.* 22:631-677.

Liu, X., Kim, N.C., Yang, J., Jemmerson, R., and Wang, X. 1996. Induction of apoptotic program in cell-free extracts: Requirement for dATP and cytochrome *c*. *Cell* 86:147-157.

Lockshin, R.A. 1981. Cell death in metamorphosis. *In* Cell Death in Biology and Physiology (I.D. Bowen and R.A. Lockshin, eds.) pp. 79-121. Chapman & Hall, New York.

Lowe, S.W., Schmitt, E.M., Smith, S.W., Osborne, B.A., and Jacks, T. 1993. p53 is required for radiation-induced apoptosis in mouse thymocytes. *Nature* 362:847-849.

Mailhos C., Howard, M.K., and Latchman, D.S. 1993. Heat shock protects neuronal cells from programmed cell death by apoptosis. *Neuroscience* 55:621-627.

Martin, S.J., Lennon, S.V., Bonham, A.M., and Cotter, A.M. 1990. Induction of apoptosis (programmed cell death) in human leukemic HL-60 cells by inhibition of RNA or protein synthesis. *J. Immunol.* 145:1859-1867.

McClean, S. and Hill, B.T. 1992. An overview of membrane, cytosolic and nuclear proteins associated with the expression of resistance to multiple drugs in vitro. *Biochem. Biophys. Acta* 1114:107-127.

McConkey, D.J., Zhivotovsky, B., and Orrenius, S. 1996. Apoptosis: molecular mechanisms and biomedical implications. *Mol. Aspects Med.* 17:1-110.

Mirabelli, F., Salis, A., Vairetti, M., Bellomo, G., Thor, H., and Orrenius, S. 1989. Cytoskeletal alterations in human platelets exposed to oxidative stress are mediated by oxidative and Ca^{2+}-dependent mechanisms. *Arch. Biochem. Biophys.* 270:478-488.

Miyashita, T. and Reed, J.C. 1995. Tumor suppressor p53 is a direct transcriptional activator of the human *bax* gene. *Cell* 80:293-299.

Mosser, D.D. and Martin, L.H. 1992. Induced thermotolerance to apoptosis in a human T lymphocyte cell line. *J. Cell. Physiol.* 151:561-570.

Newmeyer, D.D., Farston, D.M., and Reed, J.C. 1994. Cell-free apoptosis in Xenopus egg extracts: Inhibition by Bcl-2 and requirement for an organelle fraction enriched in mitochondria. *Cell* 79:353-364.

Nicholson, D.W. and Thornberry, N.A. 1997. Caspases: Killer proteases. *Trends Biochem. Sci.* 22:299-306.

Nicotera, P. and Leist, M. 1997. Energy supply and the shape of cell death in neurones and lymphoid cells. *Cell Death Differ.* 4:435-442.

Nicotera, P. and Orrenius, S. 1996. Calcium ions in necrotic and apoptotic cell death. *In* Neurodegeneration and Neuroprotection in Parkinson's Disease and Other Neurodegenerative Disorders (C.W. Olanow, P. Jenner, and M. Youssim, eds.) pp. 143-158. Academic Press, London.

Nicotera, P., Hartzell, P., Davis, G., and Orrenius, S. 1986. The formation of plasma membrane blebs in hepatocytes exposed to agents that increased cytosolic Ca^{2+} is mediated by the activation of a non-lysosomal proteolytic system. *FEBS Lett.* 209:139-144.

Nishizuka, Y. 1984. The role of PKC in cell surface signal transduction and tumour promotion. *Nature* 308:693- 698.

Nobel, S. 1997. Thiol redox state in apoptosis: Physiological and toxicant modulation. Ph.D. Thesis, Karolinska Institutet, Stockholm.

Oesterreich, S., Weng, C., Qiu, M., Hilsenbeck, S.G., Osborne, C.K., and Fuqua, S.A.W. 1993. The small heat shock protein hsp27 is correlated with growth and drug resistance in human breast cancer cell lines. *Cancer Res.* 53:4443-4448.

Oltvai, Z., Milliman, C., and Korsmeyer, S.J. 1993. Bcl-2 heterodimerizes with a conserved homolog, bax, that accelerates programmed cell death. *Cell* 74:609-629.

Owen-Schaub, L.B., Zhang, W., Cusack, J.C., Angelo, L.S., Santee, S.M., Fujiwara, T., Roth, J.A., Deiseroth, A.B., Zhang, W.-W., Kruzel, E., and Radinsky, R. 1995. Wild-type human p53 and a temperature-sensitive mutant induce Fas/APO-1 expression. *Mol. Cell. Biol.* 15:3032-3040.

Reed, J.C. 1997. Double identity for proteins of the Vcl-2 family. *Nature* 387:773-776.

Ryan, K.M. and Birnie, G.D. 1996. *Myc* oncogenes: The enigmatic family. *Biochem. J.* 314:713-721.

Samali, A. and Cotter, T.G. 1996. Heat shock proteins increase resistance to apoptosis. *Exp. Cell Res.* 223:163-170.

Samali, A., Gilje, B., Doskeland, S.O., Cotter, T.G., and Houge, G. 1997. The ability to cleave 28S rRNA during apoptosis is a cell type dependent trait unrelated to DNA fragmentation. *Cell Death Differ.* 4:289-293.

Samali, A. Nordgren, H., Zhivotovsky, B., Peterson E., and Orrenius, S. 1999. A comparative study of apoptosis and necrosis in HepG2 cells. Oxidant-induced caspase activation leads to necrosis. *Biochem. Biophys. Res. Commun.* 256:6-11.

Saunderson, C.J. 1982. Morphological aspects of lymphocyte mediated cytotoxicity. *In* Mechanisms of Cell Mediated Cytotoxicity (W.R. Clark and P. Golstein, eds.) pp. 3-21. Plenum, New York.

Savill, J.S., Dransfeild, I., Hogg, N., and Haslett, C. 1990. Vetronectin receptor-mediated phagocytosis of cells undergoing apoptosis. *Nature* 343:170-173.

Shi, L., Kam, C.M., Powers, J.C., Aebersold, R., and Greenberg, A. 1992. Purification of three cytotocic lymphocyte granule serine proteases that induce apoptosis through distinct substrate and target cell interaction. *J. Exp. Med.* 176:1521-1529.

Shimizu, S., Eguchi, Y., Kamiike, W., Itoh, Y., Hasegawa, J., Yamabe, K., Otsuki, Y., Matsuda, H., and Tsujimoto, Y. 1996. Induction of apoptosis as well as necrosis by hypoxia and predominant prevention of apoptosis by *Bcl-2* and *Bcl-x_L*. *Cancer Res.* 56:2161-2166.

Shinohara, K., Tomioka, M., Nakano, H., Tone, S., Ito, H., and Kawashima, S. 1996. Apoptosis induction resulting from proteasome inhibition. *Biochem. J.* 317:385-388.

Sun, X., Shimizu, H., and Yamamoto, K. 1995. Identification of a novel p53 promoter element involved in genotoxic stress-inducible p53 gene expression. *Mol. Cell. Biol.* 15:4489-4496.

Trauth, B.C., Klas, C., Peters, A.M.J., Matzku, S., Moller, P., Falk, W., Debatin, K.-M., and Krammer, P.H. 1989. Monoclonal antibody-mediated tumor regression by induction of apoptosis. *Science* 245:301-305.

Trump, B.F. and Berezesky, I.K. 1995. Calcium-mediated cell injury and cell death. *FASEB J.* 9:219-228.

Trump, B.F. and Ginn, F.L. 1969. The pathogenesis of subcellular reaction to lethal injury. *In* Methods and Achievements in Experimental Pathology, vol. 4 (E. Bajusz and G. Jasmin, eds.) p. 1. Karger, Basel.

Tsugimoto, Y. 1997. Apoptosis and necrosis: Intracellular ATP level as a determinant for cell death modes. *Cell Death Differ.* 4:429-434.

Vanags, D.M., Pörn-Ares, M.A., Coppola, S., Burgess, D.H., and Orrenius, S. 1996. Protease involvement in fodrin cleavage and phosphatidylserine exposure in apoptosis. *J. Biol. Chem.* 271:31075-31085.

Van Lancker, J.L. 1975. Hydrolases and cellular death. *In* Pathogenesis and Mechanisms of Liver Cell Necrosis (D. Keppler, ed.) pp. 25-35. MTP Press, Lancaster.

Wallach, D. 1997. Placing death under control. *Nature* 388:123-126.

Wyllie, A.H. 1980. Glutocorticoid-induced thymocyte apoptosis is associated with endogenous endonuclease activation. *Nature* 284:555-556.

Wyllie, A.H., Rose, K.A., Morris, R.G., Steel, C.M., Forster, E., and Spandidos, D.A. 1987. Rodent fibroblast tumors expressing human *myc* and *ras* genes: Growth, metastasis and endogenous oncogene expression. *Br. J. Cancer* 56:251-259.

Yasuhara, N., Eguchi, Y.M., Tachibana, T., Imamoto, N., Yoneda, Y., and Tsugimoto, Y. 1997. Essential role of active nuclear transport in apoptosis. *Genes Cells* 2:55-64.

Yonish-Rouach, E. 1996. The p53 tumour suppressor gene: A mediator of a G1 growth arrest and of apoptosis. *Experientia* 52:933-1017.

Yonish-Rouach, E., Resnitzky, D., Lotem, J., Sachs, L., Kim-Chi, A., and Oren, M. 1991. Wild-type *p53* induces apoptosis of myeloid leukaemic cells that is inhibited by interlukin-6. *Nature* 353:345-347.

Yuan, J., Shaham, S., Ledoux, S., Ellis, H.M., and Horwitz, R.H. 1993. The *C. elegans* cell death gene *ced-3* encodes a protein similar to the mammalian interleukin-1β-converting enzyme. *Cell* 75:641-652.

Zamzami, N., Marchetti, P., Castedo, M., Decaudin, D., Macho, A., Hirsch, T., Susin, S.-A., Petit, P.X., Mignotte, B., and Kroemer, G. 1995. Sequential reduction of mitochondrial transmembrane potential and generation of reactive oxygen species in early programmed cell death. *J. Exp. Med.* 182:367-377.

Zhivotovsky, B., Wade, D., Nicotera, P., and Orrenius, S. 1994. Role of nucleases in apoptosis. *Int. Arch. Allergy Immunol.* 105:333-338.

Zhivotovsky, B., Burgess, D.H., Vanags, D.M., and Orrenius, S. 1997. Involvement of cellular proteolytic machinery in apoptosis. *Biochem. Biophys. Res. Commun.* 230:481-488.

Contributed by Afshin Samali, Boris Zhivotovsky, and Sten Orrenius
Karolinska Institutet
Stockholm, Sweden

Determination of Apoptosis and Necrosis

Cell death may occur by two mechanisms: apoptosis, or programmed cell death, and necrosis, or cell death due to injury or trauma (see *UNIT 2.1*). Both types of cell death have their own specific and distinct morphological and biochemical hallmarks. Apoptotic cells share a number of common features, such as phosphatidylserine (PS) exposure, cell shrinkage, chromatin cleavage, nuclear condensation, and formation of pyknotic bodies of condensed chromatin. Necrotic cells exhibit nuclear swelling, chromatin flocculation, loss of nuclear basophilia, breakdown of cytoplasmic structure and organelle function, and cytolysis by swelling. Cell death can be induced by a wide variety of stimuli, such as growth factor withdrawal, heat shock, cold shock, radiation, heavy metals, genotoxic drugs, and a number of biological ligands such as Fas-L and tumor necrosis factor (TNF). Most if not all of these can induce both apoptosis and necrosis in a time- and dose-dependent manner.

A variety of techniques have been developed to assess cytotoxicity in untreated and/or toxicant-treated cells, most of which are based on the loss of plasma membrane integrity. Membrane disruption can be detected based on the uptake of vital dyes (see Basic Protocol 1) or the release of cellular contents into the extracellular milieu (see Basic Protocol 5). However, during apoptosis, the cell membrane remains intact for a relatively long time, and therefore some of these assays cannot detect the early stages of apoptosis. Alternatively, assays that detect all types of cell death do not discriminate between apoptosis and necrosis. Therefore, more specific techniques have been developed to determine cell death, and the combination of several methods is required to distinguish between the two separate types. These techniques rely on specific morphological and molecular or biochemical changes associated with these two processes.

This unit describes some of the techniques most commonly used to detect cell death. Morphological assays include trypan blue exclusion (see Basic Protocol 1), differential staining (see Basic Protocol 2), Hoechst staining (see Basic Protocol 3), flow cytometry to measure cell size and DNA content (see Basic Protocol 4), and annexin V binding to detect externalized phosphatidylserine (see BAsic Protocol 5). Methods to detect chromatin cleavage include TUNEL assays for whole cells (see Basic Protocol 6) and paraffin sections (see Alternate Protocol 1), DNA fragmentation assays using whole cells (see Basic Protocol 7), assays of total genomic DNA (see Alternate Protocol 2), analysis of DNA fragmentation by agarose gel electrophoresis (see Alternate Protocol 3), phenol extraction of DNA for analysis of fragmentation (see Alternate Protocol 4), a quantitative assay for DNA fragmentation (see Basic Protocol 8), and detection of DNA fragmentation by pulsed-field gel electrophoresis (see Basic Protocol 9). Caspase activity is assessed by detecting proteolytic cleavage of fluorescent substrates (see Basic Protocol 10) or by immunodetection (see Basic Protocol 11). Protocols are also provided for Cytospin preparations from cell suspensions (see Support Protocol 1) and preparation of SDS-polycrylamide minigels (see Support Protocol 2). Table 2.2.1 describes how these assays are used to distinguish apoptotic cells from necrotic cells.

MORPHOLOGY ASSAYS

Loss of membrane integrity, which occurs late in apoptosis and relatively early in necrosis, can be detected by cellular uptake of the vital dye trypan blue (see Basic Protocol 1). Apoptosis and necrosis also can be identified morphologically based on the criteria described elsewhere (Bowen, 1980). These include cell shrinkage, nuclear condensation, and cleavage for apoptotic cells; and nuclear swelling, chromatin flocculation, and loss

Contributed by Boris Zhivotovsky, Afshin Samali, and Sten Orrenius
Current Protocols in Toxicology (1999) 2.2.1-2.2.34

Table 2.2.1 Methods for Determination of Apoptosis and Necrosis

Method	Protocol	Result for	
		Apoptosis	Necrosis
Morphological/cytological analysis			
Trypan blue staining	Basic Protocol 1	No staining (early apoptosis) Blue staining (late apoptosis)	Blue cells
Differential staining	Basic Protocol 2	Membrane blebbing, chromosome condensation and nuclear shrinkage, cytoplasmic constriction and loss of cell volume	Nuclear swelling, chromatin flocculation, membrane blebbing and disruption, appearance of cell "ghosts"
Hoechst staining	Basic Protocol 3	Increased blue fluorescence, fragmented or condensed nuclei	Blue nucleus with diffuse staining
Flow cytometry	Basic Protocol 4	Reduced forward and side scatter	Increased forward and side scatter
Annexin V binding and PI staining	Basic Protocol 5	Positive fluorescence response for annexin V binding; exclusion of PI	Positive fluorescence; uptake of PI
Assays for chromatin cleavage			
TUNEL assay	Basic Protocol 6 and Alternate Protocol 1	Detection of strand breaks	Detection of strand breaks
Whole-cell DNA fragmentation	Basic Protocol 7	DNA ladder	DNA smear
Total genomic DNA fragmentation	Alternate Protocol 2	DNA ladder	DNA smear
Simple protocol for DNA fragmentation	Alternate Protocol 3	DNA ladder	DNA smear
Phenol extraction for DNA fragmentation	Alternate Protocol 4	DNA ladder	DNA smear
Quantitative assay of DNA fragmentation	Basic Protocol 8	Increase in the percentage of fragmented DNA	Increase in the percentage of fragmented DNA
Pulsed-field detection of high-molecular-weight DNA	Basic Protocol 9	High-molecular-weight bands	DNA smear
Assays for caspase activation			
Specific substrate cleavage assay	Basic Protocol 10	Positive detection of cleaved fluorescent substrate	No changes in fluorescence detected
Immunodetection of caspase activation	Basic Protocol 11	Positive detection of cleavage products of procaspase	No cleavage products detected

of nuclear basophilia for necrotic cells. The levels of both apoptosis and necrosis in a particular cell population can be estimated from Cytospin preparations (see Support Protocol 1) stained with RAPI-DIFF (see Basic Protocol 2 Figure 2.2.1), Hoechst stain (see Basic Protocol 3), or propidium iodide (see Basic Protocol 4).

BASIC PROTOCOL 1

Measurement of Cell Death by Trypan Blue Exclusion

This common cell viability assay is based on the ability of a cell with an intact membrane to exclude the dye trypan blue. Therefore, this assay allows one to distinguish between cells with intact and disrupted membranes. Since this method does not give an indication of the mode of cell death, it should be used only in conjuction with a more informative morphological method.

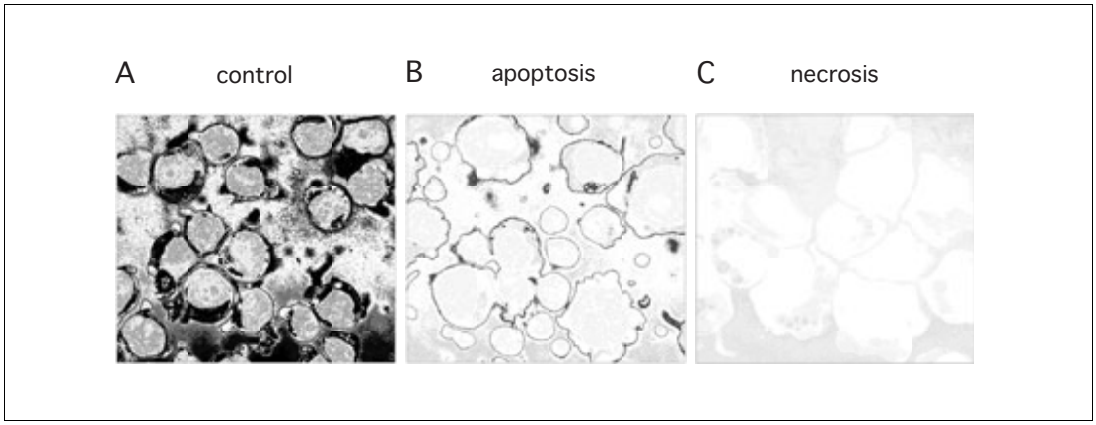

Figure 2.2.1 RAPI-DIFF staining of Cytospin preparation of HL-60 cells. Cells were treated with different concentrations of a cytotoxic drug to induce apoptosis or necrosis. (**A**) Untreated cells, (**B**) apoptotic cells, and (**C**) necrotic cells.

Materials

Cell suspension to be assessed
2× PBS tablets, pH 7.2 to 7.4 (Sigma) or 2× PBS (*APPENDIX 2A*)
0.2% (w/v) trypan blue (Sigma) in 2× PBS (store up to 1 to 2 months at 4°C)

Hemacytometer: improved Neubauer type (Karl Hecht; Baxter) or equivalent
Coverslips (e.g., Chance Propper)
Light microscope

1. Remove from the cell suspension a sample containing ~5×10^4 cells.
2. Add an equal volume of 0.2% trypan blue, mix, and incubate 1 to 2 min at room temperature to permit dye uptake.
3. Load samples onto the hemacytometer.
4. Count the total number of cells and the number of unstained cells in five of the major sections of the hemacytometer. Calculate the average number of cells per section.
5. Calculate the number of cells/ml culture medium by multiplying the average number of cells per section by the dilution factor (2 in this case) and hemacytometer index (10^4). Determine the percentage viability according to the following formula:

$$\% \text{ viability} = \frac{\text{number of unstained cells}}{\text{total number of cells}} \times 100$$

Control cells and cells in early stages of apoptosis exclude trypan blue; cells in the late stages of apoptosis and necrotic cells take up the dye and appear as blue cells.

Differential Staining of Cells

BASIC PROTOCOL 2

This staining procedure involves three steps: first cells are fixed in 100% methanol, then the nuclei are stained with an acid dye, and finally the cytoplasm is stained using a basic dye. Such three-step procedure allows differential staining and contrast between the cytoplasm and the nucleus. Apoptotic cells exhibit membrane blebbing, chromatin condensation and nuclear shrinkage, cytoplasmic constriction and loss of cell volume, and formation of apoptotic bodies. Necrotic cells undergo nuclear swelling, chromatin flocculation, cell membrane blebbing and disruption, and finally cell lysis resulting in the appearance of "ghost cells" (see Figure 2.2.1). This method can also be applied to cells growing attached to coverslips or chambered culture slides.

Materials

Cytospin preparations of cells (see Support Protocol 1)
100% methanol
Acid dye: 0.1% (w/v) eosin Y/0.1% (w/v) formaldehyde/0.4% (w/v) sodium phosphate dibasic/0.5% potassium phosphate monobasic
Basic dye: 0.4% (w/v) methylene blue–polychromed/0.4% (w/v) azure/0.4% (w/v) sodium phosphate dibasic/0.5% (w/v) monobasic potassium phosphate
DPX mountant (in solution; BDH)

Coverslips (e.g., Chance Propper)
Microscope slides (e.g., Menzel-Glaser)
Light microscope

1. Fix cells after Cytospin preparation (see Support Protocol 1) by immersing the slide ten times in 100% methanol.

   The three solutions required for this procedure are available as a kit, called RAPI-DIFF Stain kit, from Diagnostic Developments. The solutions can be stored 1 to 2 months at room temperature.

2. Stain the cell nuclei by dipping the slide in the acid dye ten times.
3. Stain the cell cytoplasm by dipping the slide in basic dye ten times.
4. Rinse the slide by dipping in distilled water, let it air dry, and mount it using DPX mountant.
5. Score the cells as normal, apoptotic, condensed and/or fragmented nuclei, or necrotic swollen cells, based on their morphological appearance under a light microscope (see *UNIT 2.1* and Fig. 2.2.1).

BASIC PROTOCOL 3

Hoechst Staining of Cells

Hoechst 33342, a bisbenzimide dye, is a cell-permeant, minor group–binding DNA stain that fluoresces bright blue upon binding to DNA. It is water soluble and relatively nontoxic. Hoechst 33342 can be excited with the UV lines of the argon-ion laser and most conventional fluorescence excitation sources, and it exhibits relatively large Stokes shifts (excitation and emission maxima ~350 and 460 nm), making it suitable for multicolor labeling experiments (Pollak and Ciancio, 1990). Cells are scored as apoptotic if they have fragmented nuclei. This method can also be applied to cells growing attached to coverslips or chambered culture slides.

Materials

Cell suspension
1× and 2× PBS, pH 7.2 to 7.4 (from Sigma 2× PBS tablets, or see *APPENDIX 2A*)
4% (w/v) paraformaldehyde (see recipe)
10 μg/ml Hoechst 33342 dye (Molecular Probes) in PBS (*APPENDIX 2A*)
50/50 (v/v) PBS/glycerol

Microscope slides (e.g., Menzel-Glaser)
Coverslips (e.g., Chance Propper)
Fluorescent microscope

Additional reagents and equipment for Cytospin preparations (see Support Protocol 1)

1. Place an aliquot of cell suspension containing $0.3–0.5 \times 10^6$ cells in a microcentrifuge tube, and centrifuge 5 min at $1000 \times g$, 4°C.

2. Remove and discard supernatant. Resuspend the dry pellet in 30 to 50 µl of 4% paraformaldehyde.
3. Spin the fixed cells onto a glass slide using a Shandon/Lipshaw Cytospin centrifuge (see Support Protocol 1). Alternatively, spread the cells onto a slide with a pipet tip, and air dry slide.
4. Stain slide with 10 µg/ml Hoechst dye.

   Hoechst 33342 dye can be diluted from 100× stock kept in the dark at 4°C.
5. Leave slide in the dark for 10 min at room temperature.
6. Rinse by dipping slide five times in distilled water, and let it air dry in the dark.
7. Mount slide with coverslip using PBS/glycerol. Monitor fluorescence with a blue filter in the fluorescence microscope, and score cells with fragmented nuclei as apoptotic.

   This method is useful for discrimination of apoptotic from nonapoptotic (untreated or necrotic) cells.

Cytospin Preparation of Cells for Analysis

SUPPORT PROTOCOL 1

Cytospin preparations can be used in many protocols for cell biology. Once slides are prepared they can be stained with variety of dyes and analyzed using light, fluorescent, and confocal microscopy, depending on the dye type. Before staining, slides can be stored up to 1 year at −20°C covered with aluminum foil. Fixed and stained slides can be stored indefinitely once mounted permanently.

Materials

Cell suspension
PBS (*APPENDIX 2A*)
Cytospin centrifuge and cups (Shandon/Lipshaw)

1. Place a sample of cell suspension containing ~0.5–1 × 10^5 cells in a microcentrifuge tube, and centrifuge 5 min at 1000 × *g*, 4°C.
2. Remove and discard supernatant. Resuspend pelleted cells in 100 µl PBS.
3. Add suspension to the Cytospin cup and slide setup, and centrifuge 2 min at 500 × *g*, 4°C.
4. Air dry the slide.

Flow Cytometric Analysis to Detect Apoptotic Cells

BASIC PROTOCOL 4

Many studies report that a reduction in cell size and buoyant density accompany apoptotic cell death (Yamada and Ohyama, 1980); thus, apoptotic cells appear smaller and more dense than their normal counterparts. These changes are accurately detected in a majority of cells by their light-scattering properties as measured by a flow cytometer (Darzynkiewicz et al., 1994; Robinson et al., 1999). The forward scatter (FSC), which indicates cell size, and the side scatter (SSC), which reveals the degree of granularity of the cell, are monitored in cells undergoing apoptosis. The DNA content profile, which is regularly used in studies of the cell cycle, indicates cells' positions in the cycle depending on their DNA content as measured by propidium iodide (PI) staining (fluorescence). Dead cells have a higher amount of subdiploid DNA which accumulates in the pre-G_1 position of cell cycle profiles. The protocol described here uses flow cytometry of fixed cells to simultaneously assess changes in cell size and granularity as well as differing DNA content.

Materials

Cell suspension
70% ethanol, ice cold
1× PBS, pH 7.2 to 7.4 (*APPENDIX 2A*)
50 µg/ml propidium iodide (Sigma) in 1× PBS (*APPENDIX 2A* for PBS; store up to 1 month at 4°C)
25 mg/ml RNase A (e.g., Sigma) in water
Flow cytometer (e.g., Becton Dickinson) and tubes

1. Place a sample of cell suspension containing ~1×10^5 cells in a microcentrifuge tube, and centrifuge 5 min at 1000 × *g*, 4°C. Remove and discard supernatant.
2. Add 1 ml ice-cold 70% ethanol dropwise while vortexing (to avoid clumping) to resuspend cells. Incubate 30 min on ice to allow cell fixation.
3. Centrifuge 5 min at 1000 × *g*, 4°C, to pellet cells.
4. Decant ethanol. Add 1 ml of 50 µg/ml propidium iodide containing 20 µl of 25 mg/ml RNase A and incubate 15 min at room temperature.
5. Set up the flow cytometer for forward scatter and side scatter (FSC and SSC) to determine cell size and granularity, together with FL-2 content for DNA (560 nm excitation, 640 nm emission; see manufacturer's instructions).

   The reduction in FSC and SSC seen in apoptotic cells is due to the decrease in cell volume and increase in cellular granularity. In necrotic cells there is an increase in both FSC and SSC, reflecting an increase cell volume and loss of cell granularity.

BASIC PROTOCOL 5

Assessment of Annexin V Binding to Detect Externalized Phosphatidylserine and Propidium Iodide Exclusion

A typical feature of apoptosis is the rearrangement and loss of plasma membrane phospholipid asymmetry as a result of externalization of phosphatidylserine (PS) from the inner leaflet of the plasma membrane to the outer leaflet. It has been demonstrated that annexin V can bind to PS in a calcium-dependent manner. This property of annexin V has made it a very useful tool for detection of apoptosis at the early stages of the process (Koopman et al., 1994), especially in conjuction with propidium iodide.

Materials

Cell suspension
PBS, pH 7.2 to 7.4 (*APPENDIX 2A*)
1 to 3 µg/ml annexin V–FITC (Bender Biosystems, Nexin Research, Roche, or Pharmingen)
HEPES buffer, pH 7.4 (see recipe)
HEPES buffer (see recipe) containing 50 µg/ml propidium iodide (e.g., Sigma)
Flow cytometer (e.g., Becton Dickinson) and tubes

1. Place a sample of cell suspension containing ~2–4 × 10^5 cells in a microcentrifuge tube, and centrifuge 5 min at 1000 × *g*, 4°C.
2. Remove and discard supernatant. Resuspend cells in 200 µl annexin V–FITC diluted 4:1 in HEPES buffer/propidium iodide. Incubate 5 min at room temperature in the dark.
3. Analyze cells by flow cytometer for both green (annexin V–FITC; FL-1, 515 nm excitation, 545 nm emission) and red (PI; FL-2, 560 nm excitation, 640 nm emission) fluorescence according to the manufacturer's instructions (see Figure 2.2.2).

   Cells that are apoptotic bind annexin V, display green fluorescence, and exclude propidium iodide. In contrast, necrotic cells with a disrupted plasma membrane display uptake of both annexin V (green fluorescence) and propidium iodide (red fluorescence; see fig 2.2.2).

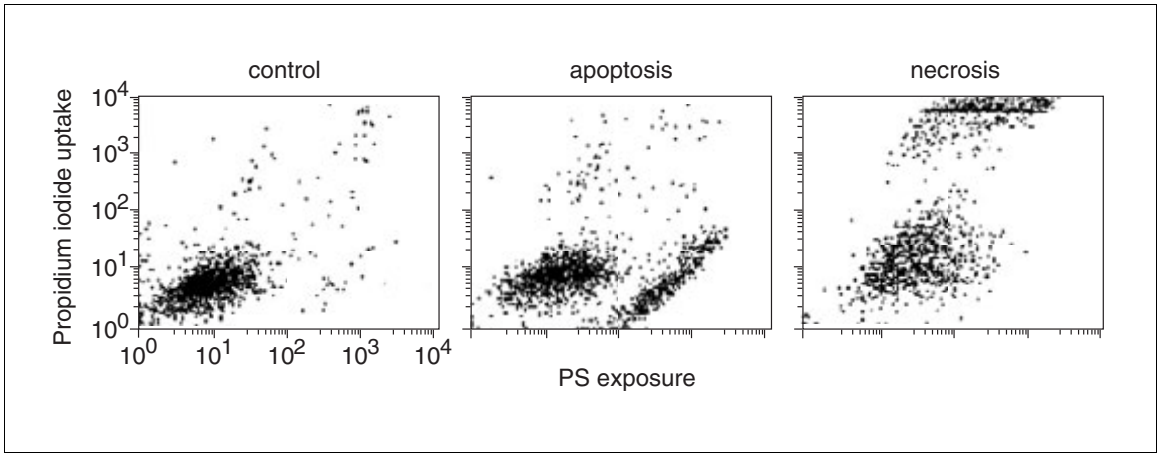

Figure 2.2.2 Flow cytometric analysis of phosphatidylserine exposure of Jurkat cells treated with different concentrations of a cytotoxic drug. Cells were double stained for annexin V and propidium iodide. Apoptotic cells are positive for annexin V only, whereas necrotic cells are positive for both annexin V and propidium iodide. (**A**) Untreated cells, (**B**) apoptotic cells, (**C**) necrotic cells. (This figure is reproduced by kind permission from Dr. M. Hampton, Institute of Environmental Medicine, Karolinska Institute, Stockholm.)

ASSAYS FOR CHROMATIN CLEAVAGE

Chromatin cleavage is a hallmark of apoptosis and involves the formation of high-molecular-weight (>50-kbp) and nucleosome-sized (200-bp) DNA fragments. The high-molecular-weight fragments can be separated by pulsed-field gel electrophoresis, and the nucleosome-sized fragments, when separated on a conventional agarose gel, demonstrate a ladder pattern. The DNA from necrotic cells, on the other hand, has a random and general cleavage pattern and produces a smear when electrophoresed on either a pulsed-field or conventional gel (see Figure 2.2.3). Prior to the formation of the cleavage products, endogenous nucleases must generate a large number of DNA strand breaks. These strand breaks in DNA can be detected by attaching biotin-conjugated nucleotides to the 3′ hydroxyl termini in a reaction catalyzed by exogenous terminal deoxynucleotidyl transferase (TdT). A number of methods can be used to identify apoptotic or necrotic DNA. All of these methods are equally successful and require the same number of cells.

TUNEL Assay for DNA Fragmentation in Cells

BASIC PROTOCOL 6

Induction of apoptosis results in the generation of single-strand DNA breaks. These can be detected using the TdT-mediated dUTP-biotin nick end-labeling (TUNEL) method (Gavrieli et al., 1992). This method requires cell fixation with cross-linking agents such as formaldehyde, which, unlike some of the alcohols (such as ethanol), prevents the extraction of degraded DNA. In other words, this fixation step prevents the loss or reduction of the cellular DNA content after the extensive washings and staining involved in this protocol. Once cells are fixed with formaldehyde, treatment with alcohols does not affect the DNA content of cells.

Materials

Cell suspension
100% methanol, –20°C
PBS, pH 7.2 to 7.4 (*APPENDIX 2A*)
1% (v/v) formaldehyde
70% ethanol, ice cold

continued

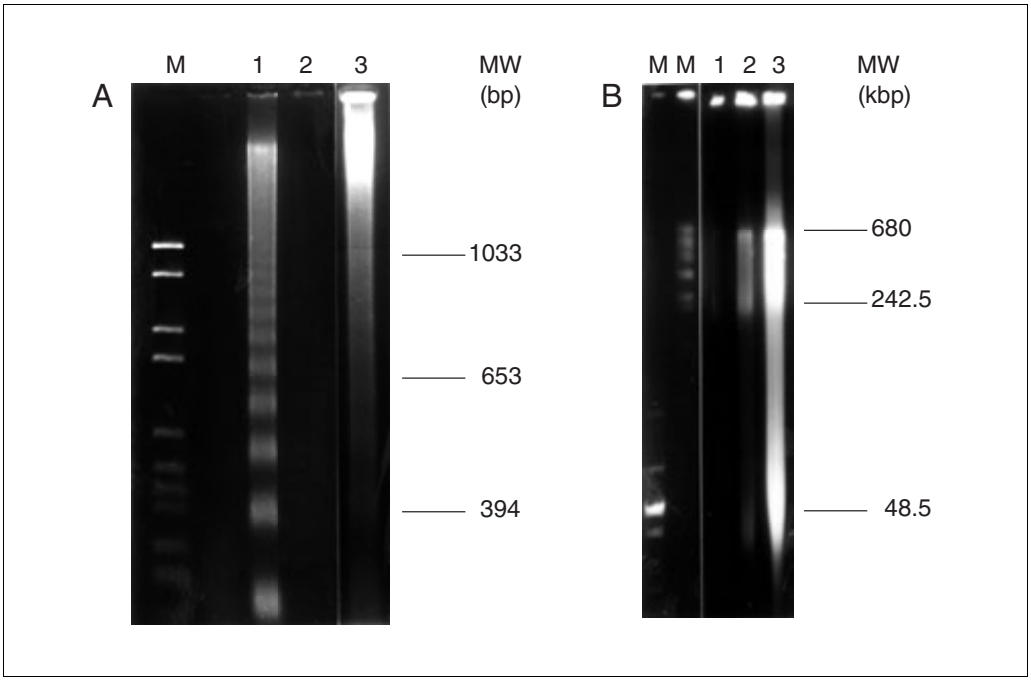

Figure 2.2.3 Gel electrophoresis of DNA from Jurkat cells treated with different concentrations of a cytotoxic drug. (**A**) Conventional gel: M, marker; lanes 1 to 3, DNA from apoptotic, untreated, and necrotic cells, respectively. The DNA ladder, when present, is a strong indicator of apoptosis. (**B**) Pulsed-field gel: MM, markers; lanes 1 to 3, DNA from untreated, apoptotic, and necrotic cells, respectively.

Terminal deoxyribonucleotidyltransferase (TdT; 25 U/µl) and 10× buffer (0.3 M Tris base/1.4 M sodium cacodylate, pH 7.2/1 mM DTT; e.g., Boehringer Mannheim)
25 mM $CoCl_2$
1 mM Bio-16-dUTP (e.g., Boehringer Mannheim)
Termination buffer: 300 mM NaCl/30 mM sodium citrate (e.g., Sigma or equivalent)
Staining buffer (e.g., Sigma; see recipe)
FACS fluid (e.g., Becton Dickinson; optional; for flow cytometry)
DPX mountant (BDH)
5 µg/ml propidium iodide in PBS (*APPENDIX 2A*)

Flow cytometer (e.g., Becton Dickinson) and tubes; *or* fluorescent microscope
Coverslips (e.g., Chance Propper)
Microscope slide (e.g., Objektträger, Menzel-Glaser)

1. Wash a sample of cell suspension containing ~10^6 cells by centrifuging 5 min at 1000 × g, 4°C, discarding supernatant, and resuspending in PBS. Transfer to microcentrifuge tube and centrifuge 5 min at 1000 × *g*, 4°C.
2. Remove and discard supernatant. Resuspend cells in 1% formaldehyde and fix for 15 min on ice.
3. Centrifuge 5 min at 1000 × *g*, 4°C. Remove and discard supernatant. Resuspend cell pellet in PBS, and repeat centrifugation. Remove and discard supernatant.
4. Resuspend cell pellet in 0.5 ml PBS and add to 5 ml ice-cold 70% ethanol.

   Cells can be stored in ethanol for several weeks at −20°C.

5. Centrifuge 5 min at 1000 × *g*, 4°C. Remove and discard ethanol. Resuspend cells in PBS, and repeat centrifugation.

6. Prepare elongation buffer (50 µl per sample):

   41.5 µl ultrapure water
   5 µl 10× TdT buffer
   2 µl 25 mM $CoCl_2$
   1 µl 1 mM Bio-16-dUTP
   0.5 µl 25 U/µl TdT enzyme.

   Add 50 µl elongation buffer to each cell pellet and resuspend. Incubate 30 min at 37°C.

   It is recommended that more than the required amount of elongation buffer be prepared; that is, multiply the total number of samples + 1 by 50 µl (the volume of the elongation buffer per sample) when calculating how much buffer to prepare. This buffer needs to be made fresh.

7. Add 5 ml PBS and centrifuge 5 min at 1000 × *g*, 4°C. Remove and discard supernatant.

   The reaction may first be stopped by incubating cells with termination buffer for 15 min at room temperature, though omission of this step does not appear to affect the results.

8. Resuspend cell pellet in 100 µl staining buffer, and incubate 30 min at room temperature.

   Again, it is recommended that extra buffer be prepared.

9. Add 2 ml PBS, resuspend cells, and centrifuge 5 min at 1000 × g, 4°C. Remove and discard supernatant. Repeat.

10. Add 1 ml of 5 µg/ml propidium iodide and incubate 30 min at room temperature in the dark.

11. Centrifuge 5 min at 1000 × g, 4°C, and remove supernatant.

12a. *For flow cytometry:* Resuspend cells in sufficient amount of PBS or FACS fluid and measure fluorescence (for FITC, 488 nm excitation, 520 ± 20 nm emission, FL-1 channel; for PI, 560 nm excitation, 640 nm emission, FL-2 or FL-3 channels).

12b. *For fluorescence microscopy:* Resuspend cells in 50 to 100 µl of PBS and spin them onto a slide as described under Cytospin preparations (see Support Protocol 1). Mount slides with DPX mountant and observe fluorescence with green and red filters under microscope.

   Cells for fluorescence microscopy can be counterstained with hematoxylin for ≤30 sec, and then rinsed with water, before microscopy.

   The number of single-strand breaks is increased during the early stages of apoptosis (increase in green fluorescence) without any change in the DNA content (measured by PI staining). With time the DNA content is decreased (red fluorescence) due to formation of apoptotic bodies, which also results in the reduction of TUNEL signal.

TUNEL Assay in Paraffin-Embedded Sections

ALTERNATE PROTOCOL 1

The TUNEL assay can also be performed on paraffin-embedded tissue sections.

Additional Materials *(also see Basic Protocol 6)*

Paraffin-embedded tissue sections on slides
4% (w/v) paraformaldehyde (see recipe) *or* 4% formaldehyde, in PBS (*APPENDIX 2A*)
96%, 90%, and 80% ethanol
Xylene
BSA (e.g., Sigma)

continued

10 mM Tris·Cl, pH 8 (*APPENDIX 2A*)
20 µg/ml proteinase K in 10 mM Tris·Cl (*APPENDIX 2A* for Tris·Cl)
3% (v/v) methanol
2% (w/v) BSA in PBS (*APPENDIX 2A* for PBS)
ExtrAvidin-peroxidase (Sigma) diluted 1/50 in PBS/1% BSA/0.5% Tween 20
3-Amino-9-ethylcarbazole (AEC)

Fluorescent microscope
Coverslips (e.g., Chance Propper)
Microscope slide (e.g., Objektträger, Menzel-Glaser)

1. Fix section in 4% paraformaldehyde or formaldehyde, then immerse in PBS.
2. Remove paraffin from sections by incubating slide 10 min at 70°C or 30 min at 58° to 60°C.
3. Rehydrate sections by sequential incubation in xylene (twice, 5 min each), 96% ethanol (twice, 3 min each), 90% ethanol (3 min), and 80% ethanol (3 min), followed by 3 min in water.

   Because paraffin traces might interfere with the enzymatic reaction in tissue sections, use of fresh solvents is recommended.
4. Treat sections with 10 mM Tris·Cl, pH 8, for 5 min, then incubate 15 min in 20 µg/ml proteinase K at room temperature. Wash slide four times in ultrapure water, 2 min each time.
5. Incubate sections in 3% methanol for 30 min at room temperature, and rinse by dipping five times in ultrapure water.
6. Prepare 100 µl per slide of elongation buffer (see Basic Protocol 6, step 6; the buffer needs to be fresh). Incubate the sections 60 min at 37°C in humid atmosphere.
7. Rinse the sections by dipping three times in ultrapure water, and incubate in termination buffer for 15 min at room temperature.
8. Place sections sequentially in PBS (5 min), 2% BSA (10 min), and PBS (5 min), all at room temperature.

   Addition of BSA prevents nonspecific binding of ExtrAvidin-peroxide.
9. Incubate the sections in ExtrAvidin-peroxidase for 15 min at room temperature.
10. Incubate the sections in 2% BSA, and wash four times in PBS.
11. Stain the sections with AEC for 30 min at 37°C, then rinse by dipping three times in ultrapure water.
12. Mount slides and observe for fluorescence.

    After mounting the covered slides can stored for many months at 4°C.

    Tissue sections, like cells, can be counterstained with hematoxylin for ≤30 sec, followed by rinsing in water.

BASIC PROTOCOL 7

Detection of DNA Fragmentation in Whole Cells

In 1976, Skalka et al. reported that the DNA in chromatin of irradiated lymphoid tissues degrades in vivo into oligonucleosome-length fragments. This observation was first linked to endonuclease activation in 1980 (Wyllie, 1980). Since then several methods have been developed to measure internucleosomal DNA fragmentation. This method was adopted from the protocol first described by Sorenson et al. (1990) and does not require DNA purification. Appearance of a DNA ladder will correspond to apoptosis, whereas a DNA smear will indicate necrosis. This also applies to all the alternate protocols in this section.

Materials

1× and 5× TBE buffer (see recipe), pH ~8.0 at room temperature (do not adjust pH)
SeaKem GTG agarose (FMC Bioproducts)
Cell suspension
50 mg/ml RNase A (see recipe)
4× DNA loading buffer: 4× TBE buffer (see recipe) containing 40% (w/v) sucrose and 0.25% (w/v) bromphenol blue (e.g., Sigma; store up to 2 to 3 weeks at 4°C)
Ultrapure agarose (Life Technologies)
10% (w/v) SDS (see recipe)
20 mg/ml proteinase K in water (store in aliquots up to 1 year at −20°C)
1× DNA loading buffer: 1× TBE buffer (see recipe) containing 10% (w/v) sucrose and 0.25% (w/v) bromphenol blue (e.g., Sigma)
DNA marker VI (pBR328 DNA cleaved with *Bgl*I and *Hin*fI; Boehringer Mannheim), 1 µl in 20 µl of 1× DNA loading buffer
TE buffer, pH 8.0: 10 mM Tris·Cl/1 mM EDTA
10 mg/ml ethidium bromide (see recipe)

Boiling water bath or microwave oven
Gel electrophoresis apparatus: GNA-100 (Amersham Pharmacia Biotech), Buffer Puffer (Owl Scientific), or equivalent
Power supply (Power-Pac 300, Bio-Rad, or equivalent)
Shaker at 4°C
MacroVue UV Transilluminator (Hoefer Scientific Instruments) or equivalent
Photoman Polaroid gel documentation system (Hoefer Scientific Instruments) or equivalent

Prepare agarose gel for electrophoresis

1. Prepare sufficient volume of 1× TBE to cast the gel and to fill the electrophoresis tank.

   It is important to use the same batch of electrophoresis buffer in both the electrophoresis tank and in the gel. Differences in pH or ionic strength can greatly affect the DNA mobility.

2. Weigh 0.9 g SeaKem agarose in a flask, and add 50 ml of 1× TBE (for GNA-100 gel electrophoresis apparatus). Heat in a boiling water bath or microwave oven until dissolved, then allow the agarose to cool to 60°C for 10 to 15 min.

   This is a standard 1.8% agarose gel. The volume should not occupy >40% of the volume of the flask.

   For the Buffer Puffer gel electrophoresis apparatus, use 2.7 g agarose and 150 ml TBE.

3. Pour gel into mold. Remove unwanted air bubbles. Place comb in the gel and allow gel to set 1 hr.

Prepare sample

4. Place a sample of cell suspension containing 4–5 × 10^5 cells in a microcentrifuge tube, and centrifuge 3 min at 1000 × *g*, 4°C.

   If necessary, the pellet may be stored up to 2 to 3 weeks in microcentrifuge tubes at −20°C before proceeding.

5. Carefully remove supernatant and resuspend pellet in 16 µl ultrapure water.

6. Add 4 µl of 50 mg/ml RNase A (final concentration 10 mg/ml), mix, and leave 20 min at room temperature.

7. Add 5 µl of 4× DNA loading buffer.

8. Using a scalpel, cut out a piece of gel between the comb and the upper edge of the gel (do not remove the comb), leaving the gel above the first one or two wells intact.

Prepare digestion gel

9. Prepare 5 ml of digestion gel by weighing 40 mg Ultrapure agarose, adding 2.75 ml ultrapure water, and stirring on a hot plate to dissolve.

   Do not use the SeaKem agarose in this step because it causes SDS to come out of solution.

   For the Buffer Puffer gel electrophoresis apparatus, prepare 10 ml of digestion gel.

10. When steam starts to rise from the flask, add 1 ml of 5× TBE and 1 ml of 10% SDS. When agarose has boiled and dissolved, take flask off the heat and allow gel to cool to 50°C.

11. Add 250 µl of 20 mg/ml proteinase K, mix gently, and pour into the gap above the main gel. Allow to cool, and remove the comb.

Set up for electrophoresis

12. Mount the gel in the electrophoresis tank, and add just enough 1× TBE buffer to cover it to a depth of 1 mm.

13. Add 1 µl DNA marker VI to 30 µl of 1× DNA loading buffer and load the marker into the well that is separated from the digestion gel. Load all other samples into the wells connected with the digestion gel.

    For the Buffer Puffer apparatus, use 2 µl DNA marker VI dissolved in 30 µl of 1× DNA loading buffer.

14. Run the gel overnight (~14 hr) at 20 V to facilitate digestion of the sample.

15. Turn the voltage up to 90 V and run for an additional 1.5 hr.

    For the Buffer Puffer apparatus, run gel 2 hr at 100 V after the initial 20-V overnight run.

Develop gel

16. Remove the gel from the tank and rinse with water.

17. Add 100 ml TE buffer and 40 µl of 50 mg/ml RNase A. Place gel on shaker for 3 to 4 hr.

18. Rinse the gel with distilled water. Add 100 ml TE buffer and 5 µl of 10 mg/ml ethidium bromide. Place gel on the shaker for 40 min.

19. Wash several times with fresh TE to remove ethidium bromide, and photograph under UV light.

ALTERNATE PROTOCOL 2

Detection of DNA Fragmentation in Total Genomic DNA

This method is a modified version of the protocol described by McGahon et al. (1995). The presence of ethidium bromide in the gel avoids later staining and destaining of the gel. Although Basic Protocol 7 and this alternate protocol are equally sensitive, the latter is less time consuming. In addition, the dry loading prevents the loss of material.

Additional Materials *(also see Basic Protocol 7)*

Lysis buffer: 2 mM EDTA/100 mM Tris·Cl, pH 8.0/0.8% (w/v) SDS (store at room temperature)

1. Place sample of cell suspension containing 4–6 × 10^5 cells in a 1.5-ml microcentrifuge tube. Centrifuge 5 min at 2000 × *g*, 4°C.
2. Remove and discard supernatant. Add 20 µl lysis buffer.
3. Add 2 µl of 50 mg/ml RNase A. Mix well by flicking the tip of the tube. Do not apply vigorous vortexing. Incubate at least 30 min at 37°C.
4. Add 10 µl of 20 mg/ml proteinase K, and incubate at least 1.5 hr at 50°C.
5. Add 8 µl of 4× DNA loading buffer.

   If necessary, after this step the samples can be stored for at least 1 week at 4°C.
6. Place 0.9 g SeaKem agarose (1.8%) in 50 ml of 1× TBE buffer in a flask (for GNA-100 gel electrophoresis apparatus). Heat in a boiling water bath or microwave oven until dissolved. Allow the agarose to cool to 60°C for 10 to 15 min. Add 3 µl of 10 mg/ml ethidium bromide.
7. Dry load the samples. Dissolve 1 µl DNA marker VI in 30 µl of 1 × DNA loading buffer and load into the gel. Apply low current (~35 mA) for 7 hr or higher current (~60 mA) for 4 hr.

   Samples are dry loaded and enough TBE buffer is added to the apparatus so it touches both sides of the gel but does not cover it. This is to ensure that the sample is not lost. After 10 min, when the samples have entered the gel, the current is stopped and more TBE is added so it covers the whole gel, and the current is then reapplied.
8. Photograph the gel under UV light.

Simple Protocol for Detection of DNA Fragments

ALTERNATE PROTOCOL 3

This simple protocol was developed in our laboratory. It is particularly useful for detection of chromatin cleavage in lymphoid cells (Zhivotovsky et al., 1995). It is also very useful for different lymphoid cells and less so for hepatocytes and epithelial cells. For these types of cells, see Alternate Protocol 4.

Additional Materials *(also see Basic Protocol 7)*

Lysis buffer, 4°C: 5 mM Tris·Cl, pH 8.0/20 mM EDTA/0.5% (v/v) Triton X-100
100% ethanol, –20°C
5 M NaCl (*APPENDIX 2A*)
RNase T1/A stock (see recipe)
Vacuum lyophilizer (e.g., Hetovac, Heto-Holten)

Prepare DNA sample

1. Place sample containing 1–2 × 10^6 cells in a microcentrifuge tube, and centrifuge 5 min at 2000 × *g*, 4°C. Resuspend pellet in 1 ml PBS and repeat centrifugation.
2. Resuspend pellet in 250 µl TE buffer, add 250 µl of 4°C lysis buffer, and vortex. Refrigerate 30 min.
3. Centrifuge sample 15 min at 15,000 × *g*, 4°C.
4. Transfer supernatant to a fresh microcentrifuge tube. Add 1 ml –20°C ethanol and 30 µl of 5 M NaCl. Mix and place in –20°C freezer overnight.
5. Centrifuge sample for 15 min at 15,000 × *g*, 4°C. Remove and discard supernatant.
6. Place precipitate in vacuum lyophilizer for 20 to 25 min.

7. Add 20 to 30 µl TE buffer and 1 µl RNase T1/A stock. Incubate 1 hr at 37°C.
8. Add 1 µl of 20 mg/ml proteinase K, and incubate an additional 1 hr at 37°C.
9. Add 8 µl of 4× DNA loading buffer.

Cast and run the gel

10. Dissolve 0.9 g SeaKem agarose in 50 ml TBE buffer (for GNA-100 gel electrophoresis apparatus) or 2.7 g SeaKem agarose in 150 ml TBE buffer (for Buffer Puffer gel electrophoresis apparatus). Heat in a boiling water bath or microwave oven until dissolved, then cool gel and pour into mold.
11. Mount the gel in the electrophoresis tank, and add just enough 1× TBE buffer to cover the gel to a depth of 1 mm.
12. Load DNA marker VI in the first well and samples in the rest of wells (see Basic Protocol 7, step 13).
13. Run the gel at 60 mA (for GNA-100) or 70 mA (for Buffer Puffer) until the bromphenol blue front is ~1 to 2 cm from the end of the gel.
14. Stain gel with ethidium bromide and photograph under UV light (see Basic Protocol 7, steps 18 to 19).

ALTERNATE PROTOCOL 4

Phenol Extraction of DNA Fragments for Agarose Gel Electrophoresis

This protocol is a modification of the classical method described by Wyllie (1980). This method requires DNA purification. Although it takes much more time tha other techniques and needs many more cells for preparation, it yields very clean, protein-free DNA fragments.

Additional Materials *(also see Basic Protocol 7)*

Lysis buffer (see Alternate Protocol 3), 4°C
100% ethanol, −20°C
5 M NaCl (*APPENDIX 2A*)
RNase T1/A stock (see recipe)
TE-saturated phenol (see recipe)
24:1 (v/v) chloroform/isoamyl alcohol (store mixture at room temperature in a fume hood)
0.5% (w/v) SDS

Prepare DNA sample

1. Place sample containing 2–5 × 10^6 cells in microcentrifuge tube, and centrifuge 5 min at 2000 × *g*, 4°C.
2. Resuspend pellet in 250 µl TE buffer, add 250 µl of 4°C lysis buffer, vortex, and refrigerate 30 min at 4°C.
3. Centrifuge sample 15 min at 15,000 × *g*, 4°C.
4. Transfer supernatant to fresh microcentrifuge tube. Add 1 ml −20°C 100% ethanol and 30 µl of 5 M NaCl. Mix and place in −20°C freezer overnight.
5. Centrifuge sample 15 min at 15,000 × *g*, 4°C. Remove and discard supernatant.
6. Add 500 µl TE buffer and 5 µl RNase T1/A stock to pellet. Incubate 30 min at 37°C.

7. Add 250 µl TE-saturated phenol and 250 µl of 24:1 chloroform/isoamyl alcohol. Vortex, and centrifuge for 2 to 3 min at 5000 × *g*, 4°C. Transfer upper layer to fresh 2-ml microcentrifuge tube.
8. Add 500 µl of TE buffer to lower layer; repeat step 7. Transfer upper layer to 2-ml microcentrifuge tube and mix with upper layer from step 7.
9. Extract the mixed samples from steps 7 and 8 with 1000 µl 24:1 chloroform/isoamyl alcohol and centrifuge again.
10. Transfer the upper layer to 1.5-ml microcentrifuge tubes, 500 µl per tube. Precipitate overnight with ethanol and NaCl as in step 4.
11. Repeat step 5.
12. Place precipitate in vacuum lyophilizer for 20 to 25 min.
13. Dissolve and mix precipitates from both microcentrifuge tubes in a total of 20 to 30 µl TE buffer/0.5% SDS. Add 5 µl of 4× DNA loading buffer.

Cast and run the gel

14. Mix a 1.8% agarose gel by dissolving 0.9 g agarose in 50 ml TBE buffer (for GNA-100 gel electrophoresis apparatus) or 2.7 agarose in 150 ml TBE buffer (for Buffer Puffer). Cool gel and pour into mold.
15. Mount the gel in the electrophoresis tank, and add just enough 1× TBE buffer to cover the gel to a depth of 1 mm.
16. Load DNA marker VI in the first well (see Basic Protocol 7, step 13) and samples in the rest of the wells.
17. Run the gel at 60 mA (for GNA-100) or 70 mA (for Buffer Puffer) until the bromphenol blue front is ~1 to 2 cm from the end of the gel.
18. Stain gel with ethidium bromide (see Basic Protocol 7, steps 18 to 19) and photograph under UV light.

Quantitative Assay of DNA Fragmentation

BASIC PROTOCOL 8

In addition to qualitative analysis by gel electrophoresis, DNA fragmentation can be quantitatively determined by using the diphenylamine reagent. This method, introduced by Burton (1956), cannot, however, discriminate between apoptotic and necrotic chromatin cleavage.

Materials

Cell suspension to be assessed
Lysis buffer (see Alternate Protocol 3), ice cold
10% (w/v) and 5% (w/v) trichloroacetic acid (TCA; keep at room temperature in dark flasks)
Diphenylamine reagent (see recipe)

10-ml conical glass tubes
Round-bottom glass tubes
Water bath, 100°C

1. Prepare cell suspension containing $1–10 \times 10^6$ cells in a 1-ml volume.
2. Transfer 0.8 ml of cell suspension to microcentrifuge tube. Add 0.7 ml ice-cold lysis buffer. Vortex, and allow lysis to proceed 15 to 30 min at 4°C.

3. Centrifuge 15 min at 15,000 × *g*, 4°C. Transfer supernatant to labeled conical glass tube.
4. Add 0.65 ml of 5% TCA to the pellet in microcentrifuge tube, and add 1.5 ml of 10% TCA to the sample in labeled glass tube.
5. Precipitate both samples overnight (≥4 hr) at 4°C.
6. Centrifuge conical tube 10 min at 2500 × *g*, room temperature.
7. Remove supernatant after centrifugation and add 0.65 ml of 5% TCA to the pellet. Prepare two blank tubes with 0.65 ml of 5% TCA to be treated the same for the remaining steps.
8. Make hole on the top of each microcentrifuge tube from step 5, and cover each conical tube with a marble.
9. Boil both sets of tubes for 15 min in 100°C water bath.
10. Cool to room temperature. Centrifuge samples 5 min at 2500 × *g*, room temperature.
11. Transfer 0.5 ml of each supernatant (from both glass and microcentrifuge tubes) to labeled, round-bottom glass tubes.
12. Add 1 ml diphenylamine reagent to each tube. Incubate ≥4 hr at 37°C with a marble covering each tube.
13. Read absorbance at 600 nm in spectrophotometer. Set zero with blanks from step 7. Express results as the percentage of DNA fragmented:

$$\%\ \text{fragmented DNA} = \frac{\text{absorbance of the supernatant}}{\text{absorbance of supernatant + pellet}} \times 100$$

BASIC PROTOCOL 9

Detection of High-Molecular-Weight Chromatin Fragments by Pulsed-Field Agarose Gel Electrophoresis

Not all forms of apoptosis are accompanied by internucleosomal DNA fragmentation (Oberhammer et al., 1993a). However, the formation of high-molecular-weight apoptotic DNA fragments of 50 to 700 kbp (see Figure 2.2.3B), which was first observed by Walker et al. (1991), has been reported to occur in all the cell types studied to date (see Background Information in Commentary).

One of the forms of pulse-field gel electrophoresis, field-inversion gel electrophoresis (FIGE), has been successfully used in several laboratories to identify high-molecular-weight DNA fragments in apoptotic cells and a smear in the same range of DNA size in necrotic cells. The authors have used both vertical and horizontal gel chambers; resolution of DNA fragments is the same. This protocol is an adaptation of an earlier method described by Anand and Southern (1990).

Materials

Cell suspension
Agarose buffer (for molds; see recipe)
SeaPlaque GTG low-melting-point agarose (FMC Bioproducts)
20 mg/ml proteinase K in water (store in aliquots up to 1 year at −20°C)
Proteinase buffer (for plugs; see recipe)
TE buffer, pH 8.0:10 mM Tris·Cl/1 mM EDTA

50 mM EDTA, pH 8.0 (*APPENDIX 2A*)
SeaKem GTG agarose (FMC Bioproducts)
5× TBE buffer (see recipe)
DNA size pulse markers: chromosomes from *Saccharomyces cerevisiae* (225 to 2200 kbp) and a mixture of λDNA *Hin*dIII fragments, λDNA, and λDNA concatemers (0.1 to 200 kbp; Sigma; supplied premade in syringe)

Gel leveling table
100-µl insert molds (Amersham Pharmacia Biotech), stored in 0.1 M HCl
12- or 24-well tissue culture plates
50°C incubator
100°C water bath or microwave oven
Pulsed-field gel electrophoresis system: vertical gel chamber with cooling elements (Protean II, Bio-Rad); horizontal gel chamber (HE 100B); power supply (PS 500 XT); and Switchback pulse controller (PC 500, Hoefer Scientific Instruments)
Thermostatic circulator Multi Temp III (Amersham Pharmacia Biotech)

Prepare sample plugs of agarose

1. Rinse insert molds extensively in distilled water and dry. Wrap Parafilm around the bottom of the molds and place them on ice to chill at least 10 min before pouring in the gel.

   Make sure to mark the sample wells with pencil or pen.

2. Place sample of cell suspension containing 1×10^6 cells in a microcentrifuge tube, and centrifuge 3 min at $2000 \times g$, 4°C. Remove and discard supernatant. Resuspend pellet in 100 µl of agarose buffer.

3. Prepare 1% low-melting-point agarose in agarose buffer, and place in a 60°C water bath until melted.

4. Add 100 µl of molten 1% agarose to the cell suspension, and mix with pipet. Immediately pipet mixture into two prechilled insert molds, 100 µl per mold.

5. Place the filled insert molds on ice for 10 to 15 min.

6. Remove Parafilm from the bottom of the insert molds, and dislodge each plug into separate well of a tissue culture plate.

   It is convenient to use 12- or 24-well tissue culture plates for this purpose.

7. Add 1 ml of proteinase buffer and 10 µl proteinase K (final concentration 0.2 mg/ml plug) to each well. Wrap Parafilm or clear tape around the plate, and incubate ≥24 hr on a shaker at 50°C.

8. Remove wrapping from plate, and remove buffer with pipet.

   If it is necessary to simultaneously analyze the low-molecular-weight DNA, it is possible to remove the DNA fragments that have leached out from the plugs during incubation with proteinase K by precipitating them from this buffer over 48 hr at −20°C. Add 0.2 volume of 10.5 M ammonium acetate and 2 volumes of cold absolute ethanol. This DNA can then be lyophilized, dissolved in 1× DNA loading buffer, and analyzed by conventional gel electrophoresis.

9. Wash each plug three times with 1 ml TE buffer, 2 hr per wash, on a shaker at 4°C.

10. Remove TE buffer, and add 1 ml of 50 mM EDTA.

    Plugs are now ready to put on a gel. To save samples for a long time, store the plugs in EDTA, in which DNA is stable for several months, at 4°C.

Prepare separating gel

11. Prepare 1% agarose (SeaKem GTG) gel in 0.5× TBE.

For horizontal gels

12a. Dissolve 2.5 g agarose in 250 ml 0.5× TBE in a boiling water bath or microwave oven. Allow the agarose to cool to 60°C for 10 to 15 min.

13a. Seal the edges of the gel platform with tape, and place platform on leveling table.

14a. Pour the gel into the mold, and remove unwanted air bubbles. Place the comb into the gel, and allow to set for 1 hr.

15a. Remove the comb very carefully so as not to break the gel. Remove tape.

For vertical gels

12b. Clamp two frosted glass plates together with 3-mm spacers in between. Seal the bottom with Parafilm to prevent leakage of warm agarose.

13b. Warm glass plates for 30 min in 50°C incubator.

14b. Melt agarose as in step 12a (1 g agarose in 100 ml 0.5× TBE), and pour into the prewarmed gel assembly to ~5 mm below top of plates. Insert comb into the gel, and allow to set for 1 hr.

15b. Remove the comb very carefully so as not to break the gel, and wash the wells with 0.5× TBE to remove partially polymerized agarose.

Load and run gel

16. Using a scalpel, cut out a 2-mm slab from one marker, and insert into first well of the gel with a spatula.

17. Repeat this procedure with the second marker.

    Make sure that the slab is flat on the bottom of the well. This applies to loading of samples as well.

18. To load sample, cut off 3 mm from sample plug, and insert it into individual well with a spatula. Repeat same procedure for all samples. Avoid introducing any air bubbles into the wells.

    Note and record the order of the samples!

19. Cement the slabs into wells with the remaining molten 1% agarose.

20. Transfer the loaded gel (either horizontal or vertical) into a precooled tank filled with 0.5× TBE.

    The buffer temperature should be 11° to 12°C at the beginning of the experiment.

21. Run the gel at a constant voltage with a suitable switcher program to achieve the desired resolution. The programs listed in Table 2.2.2 give good resolution of 50-, 300-, and 700-kbp fragments.

22. Remove gel carefully, and stain it in ethidium bromide for 1 hr (see Basic Protocol 7, step 18). Destain it in 0.5× TBE for 2 to 3 hr.

23. Visualize and photograph bands under UV light.

Table 2.2.2 Parameters for Running Pulsed-Field Agarose Gels

	Horizontal gel	Vertical gel
Running voltage[a]	170 V	200 V
Procedure	10 min: run the DNA into gel with continuous forward pulse	10 min: run the DNA into gel with continuous forward pulse
	6 hr: apply 20 sec forward time, 3:1 forward/back ratio, ramp factor 1.5[b]	2 hr: apply 12 sec forward time, 3:1 forward/back ratio, ramp factor 2[c]
	6 hr: apply 10 sec forward time, 3:1 forward/back ratio, ramp factor 2	3 hr: apply 2.4 sec forward time, 3:1 forward/back ratio, ramp factor 5.0
	12 hr: apply 0.8 sec forward time, 3:1 forward/back ratio, ramp factor 12.5	2.5 hr: apply 8.0 sec forward time, 3:1 forward/back ratio, ramp factor 3.0
Total running time	24 hr, 10 min	7 hr, 40 min

[a] Constant voltage

[b] This means that at the end of these 6 hr, the forward time should be 30 sec.

[c] This means that at the end of these 2 hr, the forward time should be 24 sec.

METHODS FOR ANALYSIS OF CASPASE PROTEOLYTIC ACTIVITY

Several proteolytic activities are implicated in apoptosis and necrosis (see *UNIT 2.1*). The activation of caspases, a family of apoptotic proteases, plays a key role in apoptosis induced by diverse stimuli. Caspases, which have been detected in numerous tissues and cell types, are synthesized as a precursor form, or proenzyme, and an apoptotic signal converts the precursor into mature enzyme. Moreover, up to now there has been no evidence concerning the involvement of caspase activities in necrosis. Therefore the detection of caspase activity in cells can be used as a discriminating criterion to distinguish apoptosis from necrosis.

All members of the caspase family of proteases share a number of amino acid residues crucial for substrate binding and catalysis. Despite their uniform requirement for an aspartate residue at the P_1 position of the substrate site, caspases can be divided into three different groups according to their substrate preferences. The first group (caspases 1, 4, and 5) has the optimal substrate cleavage sequence WEXD; the second (caspases 2, 3, and 7) preferentially cleaves targets at the DEXD motif; and the third (caspases 6, 8, and 9) has the optimal substrate cleavage sequence (L/V)EXD (Thornberry et al., 1997). The predicted caspase specificities correspond to the cleavage sites in the different intracellular caspase targets. Analysis of caspase activation is also based on the substrate specificity of the enzymes. Described here are two methods recently developed and currently used for analysis of caspase activation.

Detection of Caspase Activity by Specific Substrate Cleavage

BASIC PROTOCOL 10

This assay was adopted from the protocol first described by Thornberry (1994). Detecting proteolytic cleavage of fluorescent substrates assesses caspase activity. To determine the specificity of the assayed samples for the substrate, appropriate aldehyde-conjugated inhibitors (see Table 2.2.3 in Reagents and Solutions, below) can be added at a final concentration of 50 nM to the complete buffer containing the substrate. The resulting inhibition is biphasic: initially V_0 is equivalent to the substrate cleavage rate, and then a plateau in the rate of substrate cleavage occurs, usually within 5 to 8 min of the assay. As with all enzyme-substrate and -inhibitor interactions, the extent of inhibition is dependent on the concentration of the other components.

Materials

Cell suspension
1× PBS, pH 7.2 to 7.4 (*APPENDIX 2A*)
1× substrate buffer (SB; see recipe)
Caspase substrate and inhibitor stock solutions (see recipe)
Liquid nitrogen

96-well tissue culture plates (e.g., LabSystems)
Fluoroscan II (LabSystems)

1. Place duplicate samples containing 2–3 × 10^6 cells in microcentrifuge tubes, and centrifuge 5 min at 1000 × *g*, 4°C.
2. Remove and discard supernatant. Wash pellet with PBS, and centrifuge 5 min at 1000 × *g*, 4°C.
3. Remove and discard supernatant. Resuspend each pellet in 25 µl PBS (check pH, which should be neutral), and transfer into individual wells of a 96-well culture plate.

   The plate should be kept very cold (either by keeping it for some time at –20°C, or by having it "floating" on liquid nitrogen). If necessary, plates with cells can be stored for several days at –80°C.
4. Set up the computer control for the Fluoroscan II plate reader. Set temperature to 37°C.

   This takes about 3 to 4 min. Several computer programs are available for acquisition and data processing. The authors recommended Genesis II Windows-based microplate software (LabSystems and Life Sciences).
5. Immediately prior to use, prepare complete 1× SB by adding 1 µl of 200 mM stock solution of the substrate of interest (final concentration 50 µM) to 4 ml of 1× SB.
6. Dispense 50 µl of complete SB with substrate to each test well of cells at room temperature, and place plate immediately on the Fluoroscan II.

   The final concentration of substrate in the wells is 33.3 µM.
7. Read samples. The maximum absorption for AMC (7-amino-4-methyl coumarin) is 354 nm. Fluorometric detection for AMC cleaved from peptide is at excitation 380 nm and emission 460 nm.

BASIC PROTOCOL 11

Immunodetection of Active Caspases During Apoptosis

All caspases are expressed as proenzymes (30 to 55 kDa) that contain three domains: an NH_2-terminal domain, a large subunit (17 to 35 kDa), and a small subunit (10 to 12 kDa). Activation involves proteolytic processing between domains, followed by association of the large and small subunits to form a heterodimer. Thus, detection of large or small subunits by Western blotting can be used as a marker of caspase activation. All caspases can be described according to function as either activators or executioners of cell death. Their relative order appears to vary widely depending on the cellular background and apoptotic stimuli. Therefore, it is necessary to investigate the cleavage and activation of several caspases. Since the activation of the caspase 3–like proteases has been shown during most apoptotic process, it is reasonable to first investigate the activation of caspase 3 and then continue to look for the activation of caspases located up- and downstream (see *UNIT 2.1*). To compare the cleavage/activation of different caspases in the same samples. the membrane may be reprobed. Moreover, for densitometric analysis of results of protein degradation, the same membranes can be reprobed and stained with antibodies against marker proteins, such as glyceraldehyde-3-phosphate dehydrogenase or actin.

Materials

Cell suspension
PBS, pH 7.2 to 7.4 (*APPENDIX 2A*)
Sample buffer (see recipe)
Prestained SDS-PAGE markers, low range (e.g., Bio-Rad)
1× electrode buffer (see recipe)
4× high-salt Tris base buffer (HSB; see recipe)
High-salt Tris base buffer with Tween 20 (HSBT; see recipe)
Low-salt Tris buffer (LSB; see recipe)
Transfer buffer (see recipe)
Dry nonfat milk
BSA fraction V (e.g., Sigma)
Sodium azide
Stripping buffer (see recipe)
Primary antibodies:
  Anti–caspase 1 (Calbiochem)
  Anti–caspase 2 (Transduction Laboratories)
  Anti–caspase 3 (Pharmingen)
  Anti–caspase 6 (Research Diagnostics)
  Anti–caspase 7 (Transduction Laboratories)
  Anti–caspase 8 (Pharmingen)
  Anti–caspase 9 (Calbiochem)
  Anti–caspase 10 (Calbiochem)
Appropriate secondary antibodies for the primary antibodies listed above: peroxidase-conjugated goat anti–rabbit IgG, goat anti–mouse IgG, and mouse anti–goat IgG (Pierce)
Minigel (see Support Protocol 2)
Anti-glyceraldehyde-3-phosphate dehydrogenase (Trevigen)
Anti-actin (Sigma or Boehringer Mannheim)

ECL Western blotting detection system (Amersham Pharmacia Biotech) or equivalent
Boiling water bath
Mini-Protean II Electrophoresis Cell (Bio-Rad) or equivalent
Prot/Elec pipet tips for protein gel (Bio-Rad)
Power supply (Power-Pac 300, Bio-Rad, or equivalent)
0.45-µM nitrocellulose membranes (Sartorius AG)
Whatman 3MM filter paper
Mini Trans-Blot Transfer Cell (Bio-Rad) or equivalent
X-ray film (e.g., FujiFilm)

Additional reagents and equipment for one-dimensional SDS-PAGE, minigels (see Support Protocol 2), and immunoblotting (*UNIT 2.3*)

Prepare samples

1. Place 1×10^6 cells in a microcentrifuge tube and centrifuge 5 min at $2000 \times g$, 4°C. Resuspend pellet in 1 ml PBS, and centrifuge 2 min at $1000 \times g$, 4°C.

   Two methods may be used to extract proteins from cells for immunoblotting. Either the intact cells are resuspended directly in sample buffer, or an equal amount of proteins extracted from cells can be mixed with sample buffer. Direct resuspension of cells in sample buffer is described here.

2. Resuspend pellet in 100 µl sample buffer and incubate 4 min in boiling water bath. Let cool at room temperature.

   If samples become highly viscous as a consequence of the release of chromosomal DNA, shear the DNA either by sonication or by repeated passage through a 23-G hypodermic needle.

Set up and run gel electrophoresis

3. Release the gel holder from the casting stand (see Support Protocol 2). Assemble the inner cooling core with gels according to manufacturer's instructions, and lower them into the buffer chamber.
4. Add 300 to 350 ml of 1× electrode buffer to the bottom of the chamber so that both the bottom 1 cm of the gel and electrode are covered. Add ~120 ml of buffer to the upper buffer chamber, filling until the buffer reaches a level halfway between the short and long plates.

   Do not overfill the upper buffer chamber.
5. Remove the comb by pulling it straight up slowly and gently.
6. Load samples (20 to 30 µl) into wells under the electrode buffer with Prot/Elec Tips. Load one well with 5 µl of low-range prestained SDS-PAGE markers.
7. Attach the electrophoresis apparatus to an electric power supply. Run gel at constant 130 V in a 4° to 8°C cold room until the bromphenol blue reaches the bottom of the resolving gel (~1.5 hr).
8. After electrophoresis is complete, turn off the power supply and disconnect the electrical leads.

Immunoblot proteins

9. Remove cell lid and carefully pull inner cooling core out of lower chamber. Pour off upper buffer.
10. Remove glass plate sandwich from the inner cooling core. Push one of the spacers of the sandwich out to the side of the plates without removing it. Gently twist the spacer so the upper glass plate pulls away from the gel.
11. Mark gel orientation by cutting a right corner from bottom of gel, then immerse gel in transfer buffer.
12. Transfer the proteins from gel onto a nitrocellulose membrane by electrotransfer (see *UNIT 2.3*).

    CAUTION: *It is important to wear gloves when handling gel, filter paper, and nitrocellulose membranes.*

    The authors normally use a Mini Trans-Blot Module and Bio-Ice cooling unit, and transfer at a constant 100 V for 2 hr in a cold room.

    Control for transfer efficiency by checking transfer of prestained SDS-PAGE markers.
13. Transfer the nitrocellulose membrane into 1× HSB containing 5% dry nonfat milk, 1% BSA, and 0.05% sodium azide. Keep at least 1 hr (overnight is preferable) on a rocker in the 4° to 8°C cold room.
14. Wash membrane two times, 20 min each, in HSBT on a rocker at room temperature.
15. Put membrane into a plastic bag, and add desired primary antibody in appropriate dilution (usually 1:100 to 1:5000) in 1× HSB containing 1% BSA and 0.05% sodium azide. Incubate 1 to 2 hr on a rocker at room temperature.
16. Wash three to five times, 10 min each, with HSBT on a rocker at room temperature.
17. Add peroxidase-conjugated secondary antibody in appropriate dilution (usually 1:5,000 to 1:10,000) in 1× HSBT containing 1% BSA. Incubate for 1 hr on a rocker at room temperature.

18. Wash three times, 10 min each, with HSBT on a rocker at room temperature.
19. Wash two times, 30 min each, with LSB on a rocker at room temperature.

    No Tween 20 in this buffer!

20. Develop nitrocellulose membrane with ECL according to manufacturer's instructions.
21. Cover membrane with plastic wrap, and immediately expose to X-ray film for 30 sec to 5 min in X-ray cassette.
22. Scan the film using a densitometer, and plot graph of optical density versus concentration.

    Following ECL detection, it is possible to reprobe the nitrocellulose membrane with other antibodies against different caspases or against marker proteins such as glyceraldehyde-3-phosphate dehydrogenase or actin to either clarify the results or to obtain more information. To do this, proceed with the next steps.

    Figure 2.2.4 shows the results of a time-course study of caspase activation.

23. Submerge the membrane in stripping buffer, and incubate for 30 min at 50°C with agitation.
24. Wash the membrane with water, and repeat steps 14 to 22.

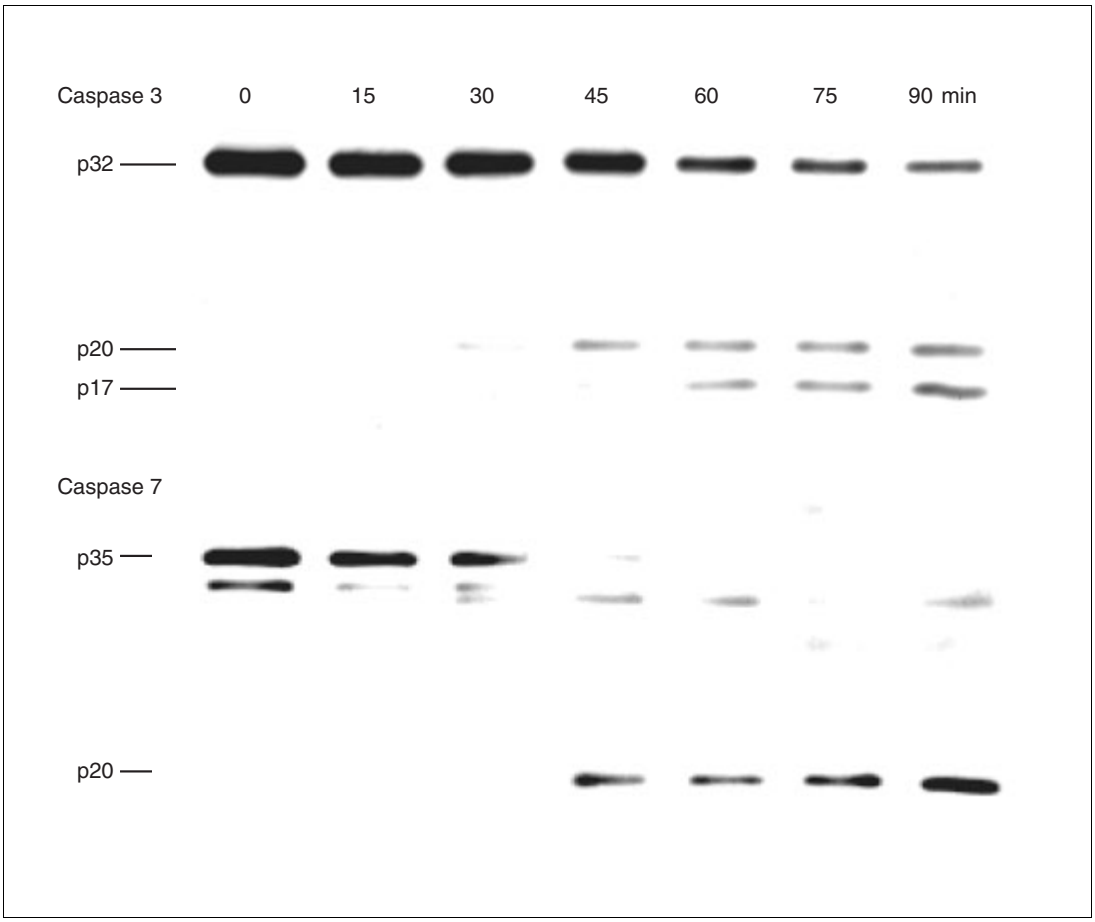

Figure 2.2.4 Time course of caspase activation in Jurkat cells treated with anti-CD95 antibodies.

SUPPORT PROTOCOL 2

Preparation of SDS-Polyacrylamide Minigels

Minigels are useful because they require shorter run times and they use smaller quantities of reagents (the latter especially helpful in immunoassays).

Materials

29% (w/v) acrylamide/1% (w/v) bisacrylamide stock (e.g., Bio-Rad)
10% (w/v) ammonium persulfate (APS; e.g., Bio-Rad): 100 mg in 1 ml water, prepared just before gel casting
1.5 M Tris·Cl, pH 8.8 (see recipe)
10% (w/v) sodium dodecyl sulfate (SDS; see recipe)
TEMED (*N*,*N*,*N*′,*N*′-tetramethylethylenediamine; e.g., Bio-Rad)
Isobutanol, water saturated
1.0 M Tris·Cl, pH 6.8 (see recipe)

Mini-Protean II Electrophoresis Cell (Bio-Rad)
Casting stand

Additional reagents and equipment for one-dimensional SDS-PAGE (see *APPENDIX 3*)

1. Assemble the glass plates for Mini-Protean II system according to the manufacturer's instructions, and check for leakage.
2. Prepare separating gel (12% gel/0.375 M Tris·Cl, pH 8.8). To make one set (two gels) for Mini-Protean II with 1.5-mm thick spacers, combine the following:

   6.7 ml H_2O
   5 ml 1.5 M Tris·Cl, pH 8.8
   200 µl 10% SDS
   8 ml 29% acrylamide/1% bisacrylamide stock
   100 µl 10% APS
   10 µl TEMED.

   Because the molecular weights of caspases vary between 30 and 55 kDa, a 12% gel is recommended.

3. Pour separating gel into the gap between the glass plates. Leave sufficient space for stacking gel to be added later (the length of the comb teeth plus 4 to 5 mm). Using a pipet, carefully overlay the gel with water-saturated isobutanol.

   The advantage of using isobutanol is that the overlay solution can be applied rapidly with a pipet and bulb with very little mixing. If water is used, the overlay must be applied carefully with a needle and syringe, using a steady, even rate of delivery to prevent mixing.

4. Allow gel to polymerize 45 to 60 min. Rinse off the overlay solution completely with distilled water.

   This is especially important with isobutanol overlays. Do not allow alcohols to remain on the gels >1 hr, or the top of the gel will dehydrate. If necessary this gel can be stored 1 to 2 days at 4°C with distilled water on top.

5. Prepare the stacking gel (4% gel/0.125 M Tris·Cl, pH 6.8). For two gels (one set), combine the following:

   7.3 ml H_2O
   1.25 ml 1.0 M Tris·Cl, pH 6.8
   100 µl 10% SDS
   1.3 ml 29% acrylamide/1% bisacrylamide stock
   50 µl 10% APS
   10 µl TEMED.

6. Pour stacking gel solution directly on top of the polymerized separating gel. Immediately insert a clean Teflon comb into the stacking gel solution, being careful to avoid trapping air bubbles. Top up with more stacking gel. Allow gel to polymerize 20 to 30 min.

The gel cannot be stored at this stage and should be used within 1 to 2 hours.

REAGENTS AND SOLUTIONS

Use Milli-Q-purified or other ultrapure water for all recipes and protocol steps. For common stock solutions, see ***APPENDIX 2****; for suppliers, see* ***SUPPLIERS APPENDIX****.*

Agarose buffer *(for molds; used in Basic Protocol 9)*

Prepare 500 ml in H_2O:
0.15 M NaCl
2 mM KH_2PO_4/KOH, pH 6.8
1 mM EGTA
5 mM $MgCl_2$
Filter sterilize through 0.2-µm filter
Store at 4°C

Caspase substrate and inhibitor stock solutions

Prepare 200 mM stock solutions of each substrate and inhibitor to be tested (see Table 2.2.3) in sterile ultrapure water. Dispense into 2-µl aliquots and store at −20°C.

Diphenylamine reagent

100 ml glacial acetic acid
1.5 g diphenylamine
1.5 ml concentrated sulfuric acid
0.5 ml 16 mg/ml acetaldehyde stock
Prepare just before use

Prepare acetaldehyde stock in ultrapure water; store in a dark flask up to 1 month at 4°C.

DTT, 1 M

Add 309 mg 1,4-dithiothreitol (DTT; Boehringer Mannheim) to 2 ml of 0.01 M sodium acetate, pH 5.2. Filter sterilize, dispense into 50-µl aliquots, and store at −20°C.

Electrode (Tris-glycine) buffer, 10×

Dissolve 90 g Tris base, 432 g glycine, and 30 g SDS in 3 liters water. Do not adjust pH with acid or base. Store up to 1 month at 4°C. If precipitation occurs, warm to 37°C before use.

For one electrophoretic run, mix 50 ml of 10× stock with 450 ml water just before electrophoresis. Concentrations in 1× buffer: 25 mM Tris, 192 mM glycine, and 0.1% SDS, pH 8.3.

Table 2.2.3 Caspase Substrates and Inhibitors

Substrate	Inhibitor	Supplier (for substrate and inhibitor)
Ac-DEVD-AMC	Ac-DEVD-CHO	Peptide Institute
Ac-VEID-AMC	Ac-VEID-CHO	Peptide Institute
Ac-IETD-AMC	Ac-IETD-CHO	Peptide Institute
Ac-WEHD-AMC	Ac-WEHD-CHO	Peptide Institute
Z-YVAD-AMC	Z-YVAD-CHO	Enzyme Systems Products
Ac-LEHD-AMC	Ac-LEHD-CHO	Enzyme Systems Products

Ethidium bromide, 10 mg/ml

Stir 10 mg/ml ethidium bromide in water on magnetic stirrer for several hours. Store up to 2 months in a dark bottle at 4°C.

HEPES buffer, pH 7.4

10 mM HEPES (*N*-hydroxyethylpiperazine-*N*-2-ethanesulfonic acid), pH 7.4 (adjusted with NaOH)
150 mM NaCl
5 mM KCl
1 mM $MgCl_2$
1.8 mM $CaCl_2$
Store up to several months at 4°C

All components may be obtained from Sigma.

HSB (high-salt Tris buffer), 4×

Dissolve 48.4 g Tris base and 233.76 g NaCl in 1.5 liters water. Adjust pH to 7.5 with 10 M HCl, and add water to 2 liters. Store up to several weeks at 4°C.

Concentrations in 1× buffer: 50 mM Tris·Cl and 500 mM NaCl, pH 7.5.

HSBT (high-salt Tris buffer with Tween)

Mix 500 ml of 4× HSB (see recipe) and 1500 ml water. Add 1 ml Tween 20 and gently mix. Store up to several weeks at 4°C.

Concentrations in 1× buffer: 50 mM Tris·Cl, 500 mM NaCl, and 0.05% Tween 20, pH 7.5.

LSB (low-salt Tris buffer)

Dissolve 12.1 g Tris base and 18 g NaCl in 1500 ml water. Adjust pH to 7.5 with 10 M HCl, and add water to 2000 ml. Store up to several weeks at 4°C.

Concentrations: 50 mM Tris·Cl and 150 mM NaCl, pH 7.5.

NP-40, 0.1% (v/v)

Add 1 µl of Nonidet P-40 (Boehringer Mannheim) to 1 ml water, vortex, and keep at 4°C.

Paraformaldehyde, 4% (w/v)

Add 8 g paraformaldehyde powder (e.g., Sigma) to 100 ml water and heat to 60°C in a fume hood. If necessary, add NaOH dropwise (one or two drops each time) to help dissolve the powder. When the solids have completely dissolved, let the solution cool to room temperature. Then add 100 ml of 2× PBS (*APPENDIX 2A*). Store at 4°C.

Because this solution cannot be kept indefinitely, it is better to prepare small volumes every week.

Phenol, TE saturated

Allow phenol to warm to room temperature, and then melt it at 68°C. Add hydroxyquinoline to a final concentration of 0.1%. Add a volume of TE buffer, pH 8.0 (10 mMTris·Cl/1 mM EDTA), equal to the volume of phenol, and vortex extensively. Allow the two phases to separate, and aspirate the upper aqueous phase. Repeat this saturation with TE buffer two to three times until volume of TE remains unchanged and the pH of the phenol phase has reached 8.0 (as measured with pH paper). Remove the aqueous phase, and add 0.1 vol fresh TE. Store up to 1 month in the dark at 4°C.

Hydroxyquinoline, a yellow antioxidant, provides a convenient way to identify the organic phase during extraction.

Proteinase buffer *(for treatment of plugs)*

Prepare 500 ml of buffer consisting of:
10 mM NaCl
10 mM Tris·Cl, pH 9.5
25 mM EDTA

Add *N*-lauroylsarcosine (Sarkosyl) to 1% final concentration and dissolve using magnetic stirrer. Check pH, and if necessary adjust to 9.5 with NaOH. Filter through 0.2-µm filter and store at 4°C.

RNase A, 50 mg/ml

Dissolve RNase A (e.g., Sigma) at a concentration of 50 mg/ml in 10 mM Tris·Cl, pH 7.5/15 mM NaCl. Heat 15 min at 50°C. Allow to cool at room temperature. Divide into aliquots and store up to several months at −20°C.

RNase T1/A stock

Mix 50 µl of 500,000 U/ml RNase T1 and 50 mg of RNase A in 5 ml of 10 mM Tris·Cl, pH 7.5/15 mM NaCl. Heat for 15 min at 50°C. Allow to cool at room temperature. Divide into aliquots and store up to several months at −20°C.

Sample buffer

625 µl 1.0 M Tris·Cl, pH 6.8 (62.5 mM final; see recipe)
2 ml glycerol (20% final)
2 ml 10% SDS (see recipe; 2% final)
0.5 ml 0.5% (w/v) bromphenol blue in H_2O (0.025 %)
0.5 ml 2-mercaptoethanol (5% final)
H_2O to 10 ml
Store up to several weeks at 4°C

This buffer is derived from Laemmli (1970).

SDS, 10% (w/v)

Dissolve 10 g of sodium dodecyl sulfate (SDS) in 90 ml of water by mixing on magnetic stirrer for several hours or by heating to 65°C to assist dissolution. Adjust the volume to 100 ml with water. Store at room temperature for up to 1 month.

Staining buffer

54.2 µl water
25 µl 20× sodium cacodylate (SSC) stock solution
20 µl blotto (25% low-fat dried milk in PBS)
0.7 µl avidin-FITC (160×)
0.1 µl Triton X-100
Store up to several weeks at 4°C

Stripping buffer

100 mM 2-mercaptoethanol
2% SDS
62.5 mM Tris·Cl, pH 6.8 (see recipe)

Add 6.25 ml of 1 M Tris·Cl, pH 6.8; 0.77 ml β-mercaptoethanol; and 20 ml 10% SDS to 73 ml water and mix. This buffer should be prepared immediately before use.

Substrate buffer (SB)

Concentrated stock:
100 mM HEPES (e.g., Boehringer Mannheim)
10% (w/v) sucrose
0.1% (w/v) CHAPS (3-[{3-cholamidopropyl}dimethylammonio]-1-propanesulfonate) (e.g., Sigma)

Do not adjust pH. Divide into aliquots and store in 40-ml Falcon tubes or equivalent. Store up to 6 months at −20°C or 2 to 3 weeks at 4°C.

1× buffer: For each 96-well plate to be processed, add 25 µl of 1 M DTT (see recipe; 5 mM final) and 5 µl of 0.1% NP-40 (see recipe; 10^{-4}% final) to 5 ml concentrated SB stock, and adjust pH to 7.25. This buffer can be kept for several hours at room temperature.

TBE (Tris/borate/EDTA) buffer, 5×

445 mM Tris base
445 mM boric acid
10 mM trisodium EDTA
Store at room temperature

All components may be obtained from Sigma. Do not adjust pH, which should be about 8.0 at room temperature. When this solution is stored for a long time, a precipitate forms. To avoid problems, discard batches that develop a precipitate.

Transfer buffer

Dissolve 22.13 g CAPS (3-cyclohexylamino-1-propanesulfonic acid) in 800 ml water. Adjust pH to 11.0 with 10 M NaOH (*APPENDIX 2A*). Add water to bring volume to 1 liter (0.1 M CAPS, pH 11.0), and store at 4°C. One hour prior to transfer, prepare the working solution. For one transfer, mix 100 ml of 0.1 M CAPS, pH 11.0; 700 ml water; and 200 ml methanol. Keep at 4°C to allow the exothermic reaction to cool down.

Tris·Cl, 1.0 M, pH 6.8

Dissolve 36.3 g of Tris base in 150 ml of water; adjust pH to 6.8 with 10 M HCl. Add water to bring volume to 300 ml, and store at room temperature for up to 1 month.

Tris·Cl, 1.5 M, pH 8.8

Dissolve 54.5 g of Tris base in 150 ml of water; adjust pH to 8.8 with 10 M HCl. Add water to bring volume to 300 ml, and store at room temperature for up to 1 month.

COMMENTARY

Background Information

A number of techniques have been developed to detect cytotoxicity and cell death in various cell types. The methods developed in the last two decades have been aimed at distinguishing between cell toxicity leading to apoptosis and that leading to necrosis. The choice of a particular method for analysis of cellular toxicity depends on the cell system; the toxin or toxicant; the expected mode of cell death; the type of information being sought; and, finally, technical limitations. There is no one single method that is satisfactory for obtaining all the information required. This is largely a result of technical and practical limitations. Therefore, to make the right interpretation of data and to draw the correct conclusions regarding the mode of cell death, a combination of some of the methods mentioned above should be used. It is recommended that a combination of at least three criteria of cell death be evaluated: cell morphology (see Basic Protocol 4), DNA fragmentation (see Assays for Chromatin Cleavage), annexin V binding (see Basic Protocol 5), and/or caspase activation (see Basic Protocols 10 and 11).

Although morphological changes are obviously secondary to biochemical alterations,

many of the published reports on cellular toxicity are based mainly on histological, cytological, and electron microscopy studies (Kerr et al., 1972; Bowen, 1980). The interpretation of histological data is based on the changes in membrane permeability. However, as mentioned in the introduction to this unit, analysis of plasma membrane integrity fails to identify cells in the early stages of apoptosis, although it can be used to identify necrotic cells in a population of interest. Alternative morphological methods draw on a mixture of optical and electron microscopy techniques. Combination of these methods allows one to distinguish between apoptotic changes—cell shrinkage, high cytoplasm density, membrane blebbing, compaction of chromatin, and formation of apoptotic bodies—and those indicative of necrosis—chromatin clumping, gross swelling of organelles, early membrane breakdown, and cell disintegration. In addition, confocal microscopy allows the combination of morphological analysis with subcellular localization of biochemical changes within damaged cells.

Other changes that accompany cell death can be used as indicators of the mode of cell death. It has been shown that phagocytosis is a response to cell death and is particularly efficient in apoptosis. Apoptotic cells can be recognized by macrophages through a number of cell surface markers. The presence of PS on the outer plasma membrane is one such marker, and it can be detected efficiently by phagocytic cells, as blockage of PS renders phagocytosis less efficient. Therefore, PS exposure can be considered a biochemical feature of apoptosis with physiological importance (Koopman et al., 1994). Annexin V has recently been utilized as a probe to monitor changes in phospholipid distribution in the plasma membrane of cells undergoing apoptosis (see Basic Protocol 5). In combination with propidium iodine, annexin V staining can reliably discriminate apoptosis from necrosis. Flow cytometry is a useful technique to examine not only changes in the plasma membrane, but also changes in cell size and granularity (see Basic Protocol 4; Darzynkiewicz et al., 1994; Robinson et al., 1999). Apoptosis is accompanied by a dramatic loss of water and consequent cell shrinkage, which can be distinguished from necrosis by a difference in light-scatter pattern. This is a rapid technique to identify apoptotic versus necrotic cells and is very widely used nowadays.

Several biochemical methods based on the detection of changes in chromatin structure have been developed. These vary from methods for detecting single-strand DNA nicks or breaks, to those for demonstrating high-molecular-weight DNA fragments, to those for showing the subsequent internucleosomal cleavage. DNA nicks can be detected using TUNEL (see Basic Protocol 6; Gavrieli et al., 1992). However, this method apparently recognizes not only nicks formed during apoptosis, but also those formed during necrosis. Thus this method should always be used in combination with other more discriminating methods.

Some other methods used for the analysis of DNA or chromatin damage appear to be better suited to discriminate between the two types of cell death. The different DNA gel electrophoresis techniques that are described here (see Basic Protocols 7 and 9; see Alternate Protocols 2, 3, and 4) can be utilized for a qualitative analysis (Wyllie, 1980; Sorenson, 1990). Although the quantitative analysis (see Basic Protocol 8) can provide limited information concerning the general cleavage of chromatin (Burton, 1956), the combination of different methods of gel electrophoresis provides more specific information concerning the type of chromatin cleavage (high-molecular-weight DNA fragments, DNA ladder, or smear). It has been shown that DNA laddering is not apparent in all apoptotic systems (Oberhammer et al., 1993a). In many types of cells, chromatin cleavage is restricted to the formation of high-molecular-weight DNA fragments (Walker et al., 1991; Oberhammer et al., 1993b). In such cases, again, the combination of two independent methods assists in drawing the correct conclusions in the study of cell death or toxicity. However, when DNA laddering occurs, it is highly indicative of apoptosis.

Activation of the caspase family of proteases has been detected in numerous cell systems and appears to function as a pathway through which apoptotic mechanisms operate (for review see Zhivotovsky et al., 1997). Upon apoptotic triggering, a hierarchy of caspases is believed to become activated in a process where more proximal caspases cleave and activate downstream caspases, giving rise to a proteolytic cascade that serves to amplify the death signal. However, not all of these caspases normally function in cell death. A recent classification divided caspases into two groups, one involved in cytokine processing (caspase 1–like proteases) and the other playing a role in cell death (Alnemri et al., 1996; Cryns and Yuan, 1998). This latter group can be further subdivided according to function as activators or executioners of cell death. Up to now there

has been no evidence concerning the involvement of caspase activities in necrosis. Therefore the detection of caspase activity in cells can be used as a discriminating criterion to distinguish apoptosis from necrosis. Caspase activity is assessed by proteolytic cleavage of flurogenic substrates (see Basic Protocol 10) or by immunodetection of protein bands corresponding to active caspases (see Basic Protocol 11).

In summary, a combination of morphological and biochemical methods is recommended to discriminate between the mode of cell death, especially if the manifestations of cell death or the stimuli used have not been previously characterized in the cell type of interest.

Critical Parameters and Troubleshooting

Morphological assays

A characteristic feature of apoptosis is that membrane integrity of the dying cell is maintained long after the process has begun. However, a reduction in membrane integrity usually occurs during the late stages of apoptosis when the cells undergo a process commonly called "secondary necrosis" or "postapoptotic necrosis." Therefore, a disadvantage of the trypan blue exclusion assay (see Basic Protocol 1) is underestimation of the level of apoptosis in a cell population.

If the cytopsin preparations are understained after a full cycle of fixation and differential staining (see Basic Protocol 2), then the procedure can be repeated a second time until the desired staining is achieved. If overstaining is the problem, preparations can be destained by immersing them in 100% methanol for up to 5 sec, followed by rinsing with water. Because membrane blebbing is a feature common to both apoptosis and necrosis, one should take care not to use this as the sole criterion for determination of the mode of cell death.

If assessing the nuclear changes in apoptotic cells is problematic, then use other conventional methods of inducing apoptosis in cells as a positive control, stain cells treated both ways with Hoechst dye (see Basic Protocol 3), and observe nuclear changes under the UV microscope. If no apoptotic changes are evident in cells, try to increase the time of incubation with apoptosis-inducing agents.

If ethanol is added too quickly to the cells for flow cytometry (see Basic Protocol 4), they may clump together, which in turn may cause blockage of the flow cytometer. Fixation of the cells in ethanol may result in dehydration and shrinkage of cells, but incubation in propidium iodide solution made in PBS rehydrates the cells. Also, if all cells dehydrate to the same extent, this should not interfere with obtaining accurate results.

Binding of annexin V to PS is Ca^{2+} dependent, and therefore the correct Ca^{2+} concentration is required for optimal binding (see Basic Protocol 5). Care should be taken when analyzing necrotic cells or cells in the late stages of apoptosis, when the cells are undergoing secondary necrosis. At this stage the plasma membrane is damaged and annexin V can enter the cell and bind to the PS in the inner leaflet of the membrane. Thus, it is possible to get false-positive results. It is therefore important to run a dye exclusion assay to confirm the results. A suitable assay would be assessment of propidium iodide (PI) exclusion, since PI cannot enter cells with intact membranes and its presence can be assessed simultaneously with annexin V binding by flow cytometry. Therefore, if a cell is positive for annexin V and negative for PI, one can conclude that apoptosis is the mode of cell death. However, if double-positive results are obtained, necrosis is implicated (see Figure 2.2.2).

Chromatin cleavage assays

The TUNEL technique (see Basic Protocol 6) is used to detect DNA strand breaks. There are rare situations when apoptosis proceeds without DNA degradation. Conversely, extensive DNA degradation may accompany necrosis. Thus, one should always use another independent assay, along with the TUNEL method, to confirm whether cells have undergone apoptosis. Costaining cells with propidium iodide or Hoechst is a very useful method to discriminate between apoptosis and necrosis in samples that have stained positively with the TUNEL technique. TUNEL-positive cells that express condensed, fragmented nuclei after staining with PI or Hoechst are apoptotic, whereas those with diffuse staining of the nuclei with PI or Hoechst are necrotic.

If a high background is present in TUNEL-treated samples, make sure that there is no DNase contamination in the test tubes or buffers. It is also possible that the number of DNA strand breaks is so large that one cannot quantify the degree of cell labeling. To eliminate this probelm, use fewer cells or decrease the incubation time.

For exogenous enzymes, such as the TdT enzyme used in TUNEL, to enter the cell, the plasma membrane has to be permeable. In

many cases, the fixation procedure is sufficient to permeabilize cells; however, sometimes an additional short incubation on ice or short (1- to 2-min) treatment with proteinase is required. To avoid loss of low-molecular-weight DNA, the permeabilized cells have to be fixed with formaldehyde before permeabilization. This fixation cross-links DNA fragments to other cellular constituents and prevents their leakage during the permeabilization step.

The procedures for assessment of DNA fragmentation in whole cells (see Basic Protocol 7) may cause the samples to become viscous and difficult to load into gel sample wells. If this is the case, dilute samples with 1× DNA loading buffer. If no detectable DNA laddering is observed in a population of cells that are known to be apoptotic, increase the number of cells used for the assay. If it is difficult to observe distinctive bands because of high background, wash gel extensively with water. If an unusual band appears in the middle of the gel in all lanes, incubate gel longer with RNase (step 17).

For analysis of fragmentation in total genomic DNA (see Alternate Protocol 2), the reagents are optimized for the stated number of cells. If larger numbers of cells are used, RNA and protein digestion will not be complete, which may interfere with electrophoresis. In addition, the procedures cause the samples to be viscous. Therefore, for minimum sheering of DNA, it is better to use pipet tips that have the ends (3 to 4 mm) cut off with a razor blade to make wide-bore tips.

If no laddering is observed in DNA phenol extracted from a population of apoptotic cells (see Alternate Protocol 4), the DNA may have been lost in the organic phase during extraction. The aqueous phase should be removed carefully during extraction to prevent DNA loss. Another possible reason for failure to detect laddering may be degradation of DNA by exogenous nucleases. All solutions must be free of nuclease contamination. If, instead of a DNA ladder, a smear appears on the gel, this indicates random and general cleavage of chromatin, indicative of necrosis (see Figure 2.2.3A, lane 3).

For quantitative assays of DNA fragmentation (see Basic Protocol 8), if absorbance of DNA in supernatant samples is below the sensitivity of detection, increase the number of cells. If all absorbance is present in the supernatant and absent from the pellet, then the pellet was mistakenly transferred together with supernatant to the labeled conical glass tubes (step 4).

There could be several reasons for large fragments not to appear on the pulsed-field electrophoresis gel (see Basic Protocol 9). If the material is still in the wells, the pulse generator power supply may not have been working properly. If some of the material is in the wells, but no sharp bands are visible and the material moved in the wrong direction, the current may not have been applied in the correct direction. If there is no material in the wells, the chromatin may have been digested by exogenous exonucleases during the preparation. If very little material is in the well, a bigger slab may have to be cut from the sample plugs. If too much material is in the lane, a smaller slab may have to be cut from the sample plugs. If thin stripes appear in any lanes in the gel, it means that either a bubble was in the well or the slab was not placed flat. Sometimes there is a leakage of buffer from the top reservoir, which may also influence the results.

Caspase assays

Release of a fluorogenic group from the peptide substrates is dependent on caspase activity and is proportional to the percentage of apoptotic cells in a cell population. In lysates of 10^6 cells, proportions of apoptotic cells of 5% to 10% can be detected by this method (see Basic Protocol 10). However, the lower limit of detection of caspase activity in cellular lysates of apoptotic cells varies with the kinetics of the apoptotic process, the percentage of apoptotic cells in a population, and the efficiency of cellular response to the apoptosis-inducing agent. If caspase activity is too low, first verify that the cells of interest are apoptotic using the morphological criteria described in this unit. Second, if cells are apoptotic, confirm that a sufficient number of cells and the right concentration of substrate are being used. If caspase activity is too high, use fewer cells.

For immunoassays of caspase activation (see Basic Protocol 11), too many bands on the film may indicate too high a concentration of primary and/or secondary antibodies. If the background of nonspecific binding of immunological probes is unacceptably high, increase the length of time washing with HSBS and LSB. If only a band corresponding to native procaspase is on the film, verify that the cells are apoptotic using other methods described in this unit. If there is no band on the film, increase duration of incubation with primary antibodies, up to 18 hr at room temperature. If a white spot on the film makes it difficult to detect the protein band of interest, a bubble may have been introduced during blotting and the whole procedure must be repeated.

If a band on the film is too strong, decrease exposure time of X-ray film to ECL-stained membrane. If gel runs too fast or too slow and poor resolution of protein occurs, decrease or increase voltage, respectively, or check buffer recipe. If no prestained markers appear on the nitrocellulose filter, check transfer buffer recipe, or reposition the location of gel towards the cathode and anode.

Anticipated Results

Morphological assays

In the trypan blue exclusion assay (see Basic Protocol 1), several thousand cells are sufficient to quantify the number of trypan blue–positive cells and to count the percentage of cells with an intact plasma membrane. Necrotic cells with rapidly disrupted membrane take up trypan blue as well.

Differential staining (see Basic Protocol 2) is one of the fastest and easiest methods for identifying dead cells. Cells are viewed under a light microscope (40× magnification), and ~300 cells are counted from separate fields of view and scored as normal, apoptotic, or necrotic based on the following morphological characteristics: membrane blebbing, chromatin condensation and nuclear shrinkage, cytoplasmic constriction and loss of cell volume, and formation of apoptotic bodies for apoptotic cells; nuclear swelling, chromatin flocculation, cell membrane blebbing and disruption, and finally cell lysis resulting in the appearance of "ghost cells" for necrotic cells (see Figure 2.2.1).

Because chromatin condensation is one of the early events of apoptosis, apoptotic cells stained with Hoechst 33342 have increased blue fluorescence compared with live cells similarly stained (see Basic Protocol 3). The intensitivity of the blue fluorescence changes with the incubation time, so that an optimal incubation time should be found for each cell system for discrimination of apoptotic cells (usually 5 to 10 min). For quantification of apoptosis, a minimum of 150 cells, from 10 to 15 fields, should be evaluated for the changes described above.

During flow cytometry analysis (see Basic Protocol 4), the cells with reduced FSC and SSC represent the apoptotic population, that is, apoptotic cells and apoptotic bodies. On the DNA content histograms, the subdiploid, pre-G_1 nonstained DNA represents the DNA from dead cells. An accumulation of subdiploid DNA content is indicative of cell death. However, if cell shrinkage is also detected, this indicates that apoptosis is the predominant mode of cell death.

The annexin V binding assay (see Basic Protocol 5) is very quick because no fixation or permeabilization of cells is required. Another advantage of this assay is the detection of apoptosis during the early stages of the death process. If a flow cytometer is not available to quantify annexin V–FITC binding during apoptosis, this assay can also be performed by directly visualizing the binding using a fluorescence microscope.

Chromatin cleavage assays

In both TUNEL protocols (see Basic Protocol 6 and Alternate Protocol 1), very little material is required for quantitative measurement of TUNEL-positive cells. Proportions of apoptotic cells as low as 10% to 15% can be detected by this method. Although the enzymatic labeling methods are time consuming (due to multiple incubation and washing steps), they are very sensitive. The method can also be applied to cryostat sections. In this case, the proteolytic pretreatment (see Alternate Protocol 1, step 4) can be shorter or even be omitted.

The whole-cell DNA fragmentation method (see Basic Protocol 7) requires only $4–5 \times 10^5$ cells. It can be used for cells growing in suspension as well as attached cells. Usually, the resolution of DNA fragmentation using this protocol is distinct and high. This method does not require DNA purification and is relatively simple and fast. Although Basic Protocol 7 and Alternate Protocol 2 are equally sensitive, the latter is less time consuming. In addition, the dry loading prevents the loss of material. Alternate Protocol 3 is particularly useful for detecting chromatin cleavage in different lymphoid cells.

Phenol extraction (see Alternate Protocol 4) is the most commonly used technique for investigating internucleosomal chromatin cleavage. Although it takes much more time than other techniques (almost $2\frac{1}{2}$ working days) and needs many more cells for preparation ($2–5 \times 10^6$ cells), it yields very clean, protein-free DNA fragments.

The quantitative assay of DNA fragmentation described (see Basic Protocol 8) is only one quantitative method for measurement of DNA fragmentation. This method is very simple, and very reproducible results can usually be obtained.

Pulsed-field gel electrophoresis can be used to detect the presence of high-molecular-

weight DNA fragments in apoptotic cells (see Basic Protocol 9). The method is very sensitive and requires 5×10^5 cells. Depending on which system is available, one can use either horizontal or vertical gel systems. If necessary, plugs can be kept for several months and run on another gel.

Caspase assays

Basic Protocol 10 is a highly sensitive, rapid, convenient, and quantitative method for in vitro determination of caspase activity. It is based on the ability of caspases to proteolytically cleave a substrate to form a free fluorescent group that can be measured fluorometrically. A number of caspase substrates conjugated to alternative fluorogenic groups are now commercially available. These include AFC (7-amino-4-trifluoromethyl coumarin), MNA (4-methoxy-2-naphthylamine), and pNA (*p*-nitroaniline). Fluorometric detection of AFC cleaved from its peptide substrate is at excitation 400 nm and emission 505 nm, and that of MNA is at excitation 340 nm and emission 425 nm. The initial rate of increase in the pNA concentration upon release from peptide can be monitored photometrically at 405 nm. Using different substrates, one can discriminate between activities of different caspases. With this method, kinetic study of enzyme activation can also be performed.

The immunological method for measuring caspase activation (see Basic Protocol 11) can be used to describe and visualize the process in apoptotic cells. The method is very sensitive, and 1×10^6 cells provide enough sample for several gels. As was mentioned above, procaspases are proteolytically cleaved to become active enzymes. With the antibodies listed in the protocol, large or small subunits (cleavable fragments) of active caspases can be detected. Appearance of these fragments can serve as an early marker of apoptosis. Crude cellular extracts can also be used to detect these fragments. This nonradioactive method does not require prelabeling of proteins.

Time Considerations

Morphology assays

The time required for preparing solutions for trypan blue exclusion is 20 to 30 min; the solutions can then be kept up to 1 to 2 months at 4°C. Trypan blue staining takes 5 min, and calculation takes 10 min.

It takes 30 min to prepare the solutions for differential staining (which can be stored 1 to 2 months at room temperature); this time is not required if the commercial kit is used. 1 hr is required to prepare and analyze samples, and 30 min to evaluate results.

It takes about 30 to 40 min to prepare solutions for Hoechst staining and 1 hr to run the test. No more than 30 min are required to evaluate results.

It takes 20 to 25 min to prepare solutions for flow cytometry, which can be stored up to 1 month. Sample preparation and analysis take 1 to 1.5 hr, and evaluation of results takes 30 min.

The whole annexin V binding test (staining and detection) takes 30 to 40 min, and evaluation of results takes another 30 to 40 min.

Chromatin cleavage assays

Approximately 3 to 4 hr are required to run TUNEL assays. The evaluation of results requires an additional 1 to 2 hr, depending on the investigator's experience.

About 1 to 2 hr are required to prepare the buffers for assessment of fragmentation in whole cells, which then can be stored for at least 1 month. Usually, gel and sample preparation, which can be done simultaneously, take 2 hr, and gel electrophoresis takes 15 to 16 hr (overnight is better). Incubation with RNase, staining, and destaining take another 6 to 7 hr. Thus, the whole experiment takes almost 1.5 days.

Analysis of fragmentation in total genomic DNA takes 1 working day.

Preparing solutions for quantitative analysis of DNA fragmentation takes 1.5 to 2 hr; however, the solutions can be stored for up to several weeks. The procedure takes 1.5 working days and 1 hr to evaluate results.

It takes about 1 week to perform the whole pulsed-field gel electrophoresis procedure. Vertical gels require a relatively shorter time (1 day less) compared with horizontal gels, with no difference in resolution.

Caspase assays

Approximately 2 hr are required to perform the whole substrate-cleavage procedure and an additional 2 hr to evaluate results.

The immunological analysis is time consuming. Only two tests (on two membranes) may be performed simultaneously. Usually, it takes several hours to prepare solutions, which can, however, be stored for months. Gel electrophoresis, blotting, and staining with antibodies take 1.5 to 2 working days, and evaluation of results takes 1 to 2 hr.

Literature Cited

Alnemri, E.S., Livingston, D.J., Nicholson, D.W., Salvesen, G., Thornberry, N.A., Wong, W.W., and Yuan, J. 1996. Human ICE/CED-3 protease nomenclature. *Cell* 87:171.

Anand, R. and Southern, E.M. 1990. Pulsed field gel electrophoresis. *In* Gel Electrophoresis of Nucleic Acid: A Practical Approach, 2nd ed. (D. Rickwood and B.D. Hames, eds.) pp. 101-123. IRL Press, Oxford.

Bowen, I.D. 1980. Techniques for demonstrating cell death. *In* Cell Death in Biology and Pathology (I.D. Bowen and R.A. Lockshin, eds.) pp. 379-444. Chapman & Hall, London–New York.

Burton, K. 1956. A study of the condition and mechanism of the diphenylamine reaction for the colorimetric estimation of deoxyribonucleic acid. *Biochem. J.* 62:315-323.

Cryns, V., and Yuan, J. 1998. Proteases to die for. *Genes Devel.* 12:1551-1570.

Darzynkiewicz, Z., Robinson, J.P., and Crisstman, H.A. (eds.) 1994. *Methods Cell Biol.*, Vols. 41 and 42 (Flow Cytometry: Part A and Part B, 2nd ed.). Academic Press, San Diego.

Gavrieli, Y., Sherman, Y., and Ben-Sasson, S.A. 1992. Identification of programmed cell death *in situ* via specific labelling of nuclear DNA fragmentation. *J. Cell Biol.* 119:493-501.

Kerr, J.F.R., Wylie, A.H., and Currie, A.R. 1972. Apoptosis: A basic biological phenomenon with wide ranging implications in tissue kinetics. *Br. J. Cancer* 26:239-257.

Koopman, G., Reutelingsperger, C.P.M., Kuijten, G.A.M., Keehnen, R.M.J., Pals, S.T., and vanOers, M.H.J. 1994. Annexin V for flow cytometric detection of phosphatidylserine expression on B-cells undergoing apoptosis. *Blood* 84:1415-1420.

Laemmli, U.K. 1970. Cleavage of structural proteins during the assembly of the head of bacteriophage T4. *Nature* 227:680-682

McGahon, A.J., Martin, S.J., Bissonnette, R.P., Mahboubi, A., Shi, Y., Mogil, R.J., Nishioka, W.K., and Green, D.R. 1995. The end of the (cell) line: Methods for the study of apoptosis in vitro. *Methods Cell Biol.* 46:153-185.

Oberhammer, F., Fritsch, G., Scmied, M., Pavelka, M., Printz, D., Purchio, T., Lassman, H., and Schulte-Hermann, R. 1993a. Condensation of the chromatin at the membrane of an apoptotic nucleus is not associated with activation of an endonuclease. *J. Cell Sci.* 104:317-326.

Oberhammer, F., Wilson, J.W., Dive, C., Morris, I.D., Hichman, J.A., Wakeling, A.E., Walker, R.A., and Sikorska, M. 1993b. Apoptotic death in epithelial cells: Cleavage of DNA to 300 and/or 50 kb fragments prior to or in the absence of internucleosomal fragmentation. *EMBO J.* 12:3679-3684.

Pollak, A. and Ciancio, G. 1990. Cell cycle phase–specific analysis of cell viability using Hoechst 33342 and propidium iodide after ethanol preservation. *Methods Cell Biol.* 33:19-24.

Robinson, J.P., Darzynkiewicz, Z., Dean, P.N., Dressler, L.G., Orfao, A., Rabinovitch, P.S., Stewart, C.S., Tanke, H.J., and Wheeless, L.L. 1999. Current Protocols in Cytometry. John Wiley & Sons, New York.

Samali, A., Nordgren, H., Zhivotovsky, B., Peterson, E., and Orrenius, S. 1999. A comparative study of apoptosis and necrosis in HepG2 cells: Oxidant-induced caspase inactivation leads to necrosis. *Biochem. Biophys. Res. Commun.* 255:6-11.

Skalka, M., Matyasova, J., and Cejkova, M. 1976. DNA in chromatin of irradiated lymphoid tissues degrades in vivo into regular fragments. *FEBS Lett.* 72:271-275.

Sorenson, C.M., Barry, M.A., and Eastman, A. 1990. Analysis of events associated with cell cycle arrest at G2 phase and cell death induced by cisplatin. *J. Natl. Cancer Inst.* 92:749-755.

Thornberry, N.A. 1994. Interleukin-1β-converting enzyme. *Methods Enzymol.* 244:615-631.

Thornberry, N.A., Rano, T., Peterson, E., Rasper, D., Timkey, T., Garcia-Calvo, M., Houtzager, V., Nordstrom, P., Roy, S., Vaillancourt, J., Chapman, K., and Nicholson, D. 1997. A combinatorial approach defines specificities of members of the caspase family and granzyme B: Functional relationships established for key mediators of apoptosis. *J. Biol. Chem.* 272:17907-17911.

Walker, P.R., Smith, C., Youdale, T., Leblamc, J., Whitfield, J.F., and Sikorska, M. 1991. Topoisomerase II–reactive chemotherapeutic drugs induce apoptosis in thymocytes. *Cancer Res.* 51:1078-1085.

Wyllie, A.H. 1980. Glucocorticoid-induced thymocyte apoptosis is associated with endogenous endonuclease activation. *Nature* 284:555-556.

Yamada, T. and Ohyama, H. 1980. Separation of the dead cell fraction from X-irradiated rat thymocyte suspension by density gradient centrifugation. *Int. J. Radiat. Biol.* 37:695-699.

Zhivotovsky, B., Gahm, A., Ankarcrona, M., Nicotera, P., and Orrenius, S. 1995. Multiple proteases are involved in thymocyte apoptosis. *Exp. Cell Res.* 221:404-412.

Zhivotovsky, B., Burgess, D.H., Vanags, D.M., and Orrenius, S. 1997. Involvement of cellular proteolytic machinery in apoptosis. *Biochem. Biophys. Res. Commun.* 230:481-488.

Contributed by Boris Zhivotovsky,
Afshin Samali,and Sten Orrenius
Karolinska Institute
Stockholm, Sweden

Detection of Covalent Binding

Earlier studies of protein covalent binding were based primarily on detection of covalently bound metabolites from radioactive xenobiotics that were administered in vivo or added to in vitro preparations. Generally, such studies involved repetitive extraction of protein suspensions to remove unbound drug or metabolites. The radioactivity that remained with the protein fraction after the extraction procedure was considered to be covalently bound. Such approaches are useful for quantifying bound metabolites in tissue homogenates or subcellular fractions and for localizing bound metabolites in tissue sections by autoradiography. However, the radiometric approach is generally not practical for studies aimed at the identification of xenobiotics bound to individual protein targets. Mechanistic research in toxicology today is not merely interested in quantification and localization of bound drug. Rather, there is increasing interest in identifying the specifically targeted proteins as a key step to clarifying the mechanistic contributions of the binding to the ensuing toxicity. To this end, immunochemical methods have been developed to detect and identify xenobiotics covalently bound to cellular proteins. Binding to individually targeted proteins as detected immunochemically has been shown to be better associated with toxicity than total covalent binding as assessed radiometrically (Beierschmitt et al., 1989).

This unit presents two protocols for the immunochemical detection of xenobiotic covalent binding to proteins. The first (see Basic Protocol 1) outlines the use of specific antibodies for detection of individual xenobiotic-protein adducts on immunoblots, and the second (see Basic Protocol 2) outlines the use of the antibodies in immunohistochemical analysis of fixed tissue sections. Support protocols are included to provide direction for the synthesis of an artificial antigen (see Support Protocol 1) and subsequent immunization (see Support Protocol 2) of a suitable host species (e.g., rabbit or goat), and for affinity purification and characterization of the antibodies in noncompetitive and competitive ELISA (see Support Protocols 3 to 7).

The details of antibody development will vary with the nature of the bound drug or metabolite, i.e., the hapten. As an example of this process, a method to elicit production of antibodies against the analgesic/antipyretic acetaminophen (*N*-acetyl-*p*-aminophenol, APAP) is described (Support Protocols 1 and 2).

The various methods described in this unit emphasize general considerations and salient features. For a more comprehensive review of the theory on individual topics, the reader is referred to additional sources (Taleporos and Ornstein, 1976; Towbin and Gordon, 1984; Tijssen, 1985; Harlow and Lane, 1988; Login and Dvorak, 1988; Ostrove, 1990; Osborn and Isenberg, 1994).

DETECTION OF COVALENT BINDING BY IMMUNOBLOTTING

BASIC PROTOCOL 1

The basic principle of immunoblotting is the use of an electrical field to transfer a complex mixture of proteins from a gel matrix to a membrane support (nitrocellulose, nylon, or PVDF) where proteins are thought to be retained by noncovalent hydrophobic interactions. Immunoblotting thus maximizes the resolving power of polyacrylamide gel electrophoresis (SDS, native, or isoelectric focusing; see *APPENDIX 3A*) to provide a discrete pattern of proteins bound to a membrane for further characterization and identification by immunodetection or protein sequencing. Two types of equipment are most widely used, and there are advantages and disadvantages to each. Wet transfer consumes ~4 liters of buffer and requires complete immersion of the gel-membrane sandwich. For semidry transfer, the sandwich is placed between absorbent paper that has been soaked in transfer

Contributed by Mary K. Bruno and Steven D. Cohen
Current Protocols in Toxicology (1999) 2.3.1-2.3.35

buffer. Wet transfer generally offers greater flexibility with respect to temperature control, voltage settings, and blotting times without buffer depletion; however, reagent consumption, cost, and experimental time are greater. The procedure described in this protocol has been employed for routine immunochemical detection of APAP-protein adducts in tissue homogenates or subcellular fractions (Bartolone et al., 1987, 1988)

The following protocol is for wet transfer of proteins from full-size (12 × 14.5–mm) 10% SDS-PAGE gels (0.75-mm thickness)—see *APPENDIX 3A* for electrophoresis protocols. It incorporates the specific instructions for use of equipment from Bio-Rad, but should be generally applicable. Modifications may be required if different equipment or a semidry blotting method are used. SDS-PAGE and steps 1 to 11 of the immunoblot protocol must be done on the same day. Incubation with primary antibody and subsequent detection of bound antibody may be done at a later time. Inclusion of prestained molecular weight protein standards during electrophoresis is recommended for orientation of the membrane during and after transfer. Gloves should be used throughout these procedures to protect the operator and to prevent contamination of gels with skin proteins.

CAUTION: If radioactivity will be used for detection, the user is required to have received institutional training in the handling of radioisotopes, and the experiment must be performed in an area designated for radioactivity use under the supervision of a licensed investigator. All steps must be carried out in accordance with the Nuclear Regulatory Commission (NRC) and institutional guidelines (also see *APPENDIX 1A*).

Materials

SDS-PAGE gel with resolved proteins
Transfer buffer (see recipe)
Methanol
Coomassie brilliant blue solution (see recipe)
Destaining solution (see recipe)
Blocking buffer (see recipe)
Primary antibody against protein-xenobiotic adduct (Support Protocol 2), affinity-purified if necessary (see Support Protocol 6)
Tris-buffered saline (TBS; see recipe) containing 0.05% (w/v) Tween 20 (store up to 1 week at room temperature)
Secondary antibody: ^{125}I-, alkaline phosphatase–, or horseradish peroxidase–conjugated IgG raised against the host animal used for production of the primary antibody
10 mg/ml nitroblue tetrazolium (prepare fresh)
25 mg/ml 5-bromo-4-chloro-3-indolyl-phosphate (BCIP) in *N*,*N*-dimethylformamide (prepare fresh)
Developing buffer (see recipe)
4-chloro-1-naphthol solution (see recipe)
30% hydrogen peroxide (store up to 1 month at 4°C)
Chemiluminescence-based detection system: e.g., ECL Kit (Amersham) or SuperSignal Kit (Pierce Chemical)

Trans-Blot apparatus (Bio-Rad) including:
  Fiber pads
  Transfer tank
  Cassette gel holder
Transfer membranes: nitrocellulose (0.2 to 0.45 μm pore size) or polyvinylidene difluoride (PVDF; 0.45 μm pore size)
23 × 33–cm and 21.5 × 21.5–cm glass baking dishes

continued

Whatman no. 1 filter paper
Platform shaker or rocker
Kodak X-Omat AR or equivalent 8 × 10–in. (20.32 × 25.4–cm) X-ray film
Lead autoradiography cassette with intensifying screen

Additional reagents and equipment for SDS-PAGE (*APPENDIX 3A*)

Transfer proteins

1. Perform SDS-PAGE (*APPENDIX 3A*), including the appropriate prestained molecular weight standards on the gel. Approximately 30 min prior to the completion of SDS-PAGE, presoak fiber pads (included with Trans-Blot apparatus) in transfer buffer in a 23 × 33–cm glass dish (e.g., a baking dish).

   Prestained molecular weight standards should always be included during gel electrophoresis to serve as a reference on the membrane. These are readily available from several commercial sources.

   The pH of the transfer buffer ranges from 8.1 to 8.3, depending on the quality of the reagents used. The inclusion of SDS in the transfer buffer facilitates complete transfer of proteins of <200 kDa molecular weight (Towbin and Gordon, 1984).

2. Cut membrane to be slightly larger than the gel—i.e., 13 × 15 cm—and cut off a small section from one corner to provide a consistent orientation marker.

3a. *For nitrocellulose membranes:* Prewet membrane in water by capillary action, then equilibrate in transfer buffer along with the fiber pads.

3b. *For PVDF membranes:* Prewet membrane in methanol for 2 to 3 sec, then rinse with distilled water for 1 to 2 min. Equilibrate in transfer buffer along with the fiber pads.

   Membranes of smaller pore size are more effective in retaining proteins of low molecular weight.

4. Cut two 14 × 16–cm pieces of Whatman no. 1 filter paper and soak in transfer buffer.

   Paper shreds easily when wet; do not soak along with the membranes.

5. Set up a separate glass baking dish containing 50 ml transfer buffer for equilibrating the gel. Following SDS-PAGE, remove gel and discard stacking gel, then cut off a small corner of the gel for orientation. Invert the gel plate, with the gel attached, into the dish containing 50 ml of transfer buffer and let the gel detach from the glass plate. Equilibrate the gel 10 to 15 min.

Assemble the transfer cassette

6. Assemble a sandwich in the cassette holder in the following sequence: a wetted fiber pad, wetted filter paper, the gel, the wetted membrane, and a second piece of wetted filter paper, aligning the cut corners of the gel and membrane during assembly.

   The polarity of transfer is from cathode (−) to anode (+). In the presence of SDS the proteins will be negatively charged and will migrate toward the positive pole (anode) and adsorb to the membrane.

7. Verify the color coding for anode (usually red) and cathode (usually black) on the equipment, and carefully orient the sandwich so that proteins will move from the gel to the membrane with the current flow.

   Transfer direction will be reversed, i.e., from anode to cathode, if the transfer buffer is of acidic rather than basic pH.

8. Roll a glass pipet over the filter paper face of the sandwich to remove any air bubbles and establish good contact between the gel and membrane.

   Good contact is important for efficient transfer.

9. Place the second fiber pad upon the filter paper to complete the sandwich, then secure the cassette assembly.

   The final sequence in the "sandwich" should be: black (cathode) face of cassette, fiber pad, filter paper, gel, membrane, filter paper, fiber pad, and red (anode) face of cassette.

10. In a 4°C cold room or refrigerated chamber, fill the transfer tank of the Trans-Blot apparatus with transfer buffer chilled to 4°C. Place the cassette assembly into the tank. Orient the cathode (black) side of the cassette toward the cathode (black). Add a magnetic stir bar.

    The membrane in the "sandwich" should be between the gel and the anode when the cassette is placed in the tank The buffer should reach to the outside bottom of the electrode holder.

11. Set up the power supply and magnetic stirrer. Before connecting the tank and power supply, remove any salts that may have built up on the electrode leads. Connect the top of the tank to the power supply, cathode to cathode, anode to anode. Electroblot 90 min at 65 V for gels containing 30 to 40 µg protein/lane.

    The temperature will rise during transfer; stirring will help to ensure uniform temperature and conductivity.

    The voltage and time of transfer can vary and may need to be determined empirically for the system being studied. Gels can be electroblotted at 30 V overnight, followed by 60 V for 1 hr. SDS should not be included in the transfer buffer if overnight blotting is used, since it will precipitate out of solution.

    The rate of protein transfer is dependent on the apparent molecular weight of the proteins. Longer transfer times are necessary for proteins of higher molecular weight (>150 kDa) or gels of higher percentage acrylamide and thickness. Decreased blotting times may be necessary for gels of lower protein load, and to prevent the loss of low-molecular-weight proteins by passage completely through the membrane. One can determine if this has occurred by adding a second membrane to the sandwich behind the first. Transfer time should be adjusted accordingly if proteins are detected on the second membrane.

Probe the membrane with antibodies

12. Disassemble the cassette. Stain blotted gel 20 min in Coomassie brilliant blue solution, then destain 1 to 2 hr in destaining solution (until most of the stain has been removed).

    If transfer was complete, only bands corresponding to higher molecular weight (>150 kDa) proteins should remain.

13. Block the membranes by incubating 1 hr at room temperature in the appropriate blocking buffer (see Reagents and Solutions for alternatives), then pour off the blocking buffer prior to adding the primary antibody.

    Nitrocellulose membranes may be allowed to dry prior to blocking and probing with antibody. PVDF membranes should be placed in blocking buffer for 15 to 60 min before drying. Alternatively, if PVDF membranes are allowed to dry without soaking in buffer, they must be prewetted again with methanol prior to blocking and probing with antibody. Drying the membranes is preferable to storing them in transfer buffer or blocking buffer overnight. Such storage in aqueous solutions will result in protein desorption, since binding to the membrane is not covalent.

Expose membrane to antibodies

14. Dilute the primary antibody (1:50 to 1:100 for affinity-purified anti-APAP antibody) in 50 ml of blocking buffer (or other volume sufficient to cover the membrane and prevent it from drying out, depending on the size of the membrane and container being used) and apply to the membrane. Incubate 3 hr at room temperature with shaking on a platform shaker.

Antibody dilutions and incubation times will vary depending on the antibody titer and the amount of antigen present. Antibodies of low avidity dissociate more rapidly from the antigen-antibody complex; therefore, lower dilutions and shorter incubation times are recommended. Antibodies of higher avidity can tolerate higher dilutions and longer incubation times (e.g., 18 to 24 hr at 4°C; Towbin and Gordon, 1984).

15. Pour off the antibody solution and wash the membrane three times, each time by immersing for 10 min in 50 to 100 ml TBS containing 0.05% Tween 20, with shaking on a platform shaker.

    The antibody solution may be reused if stored at 4°C with a preservative (e.g., 0.02% sodium azide or 0.01% merthiolate). Sodium azide inhibits horseradish peroxidase (HRP) and thus cannot be used if the secondary antibody to be used for immunodetection is conjugated with this enzyme.

16. Dilute the secondary antibody in blocking buffer and incubate the membrane for 90 min using the technique described in step 14.

    Dilution of the secondary antibody will vary depending on the type of conjugate (radiolabel or enzyme for colorimetric or chemiluminescent detection) and the commercial supplier. With anti-APAP, alkaline phosphatase and ^{125}I-conjugated secondary antibodies have been used at 1:2000 and 0.1 μCi/ml blocking solution, respectively. For chemiluminescent detection systems, e.g., ECL, follow protocols supplied by the manufacturer.

    If using a chemiluminescence system for detection, the length of the incubation with the secondary antibody may be shortened (e.g., 20 min).

17. Pour off the antibody solution and wash three times as described in step 15.

Detect bound antibody

18a. *For ^{125}I-labeled secondary antibody:* Allow membrane to dry. Enclose membrane in plastic wrap and expose to Kodak X-Omat AR film in a lead autoradiography cassette with an intensifying screen for 24 to 40 hr at −70°C. Bring the cassette to room temperature before removing and developing the film.

All manipulations involving film should be done in a darkroom. The detection limit of this method is 10 ng (Promega, 1993).

Radioactive and chemiluminescence-based detection systems have the advantage of ease of quantification. They also permit the membrane to be stripped of adsorbed antibodies and then probed again.

18b. *For alkaline phosphatase–conjugated secondary antibody:* Just before use, combine 0.5 ml of 10 mg/ml nitroblue tetrazolium and 0.5 ml of 25 mg/ml BCIP with 50 ml of developing buffer. Incubate the blotted membrane with this substrate-chromogen solution until color development of specific bands is observed. Stop the reaction by rinsing with water.

The 50 ml prepared here is sufficient volume for one full-size gel. The reaction product is an intense purple-black precipitate at the site of enzyme-conjugate binding. The background may be lavender, depending on the development time, but will revert to white upon complete drying overnight. The detection limit of this method is ~50 to 100 pg (Hoefer, 1994; Promega, 1993).

18c. *For horseradish peroxidase–conjugated secondary antibody:* Just before use, add 20 μl of 30% hydrogen peroxide to 48 ml 4-chloro-1-naphthol solution. Incubate the blotted membrane with this substrate-chromogen solution until color development of specific bands is observed. Stop the reaction by rinsing with water.

The reaction product is a brown-black precipitate at the site of enzyme-conjugate binding. The color intensity tends to fade with time and thus does not provide a good permanent record. The detection limit for this method is 1 ng (according to Promega technical applications guide).

18d. *For enzyme-linked secondary antibodies, using chemiluminescence:* Follow instructions supplied by the manufacturer of the chemiluminescence detection kit being used. For example, after washing the membrane (step 17), incubate 1 min with the mixed ECL detection reagents when using the Amersham ECL system. Drain off excess solution, then cover the membrane with plastic wrap, remove air bubbles, and place in autoradiography film cassette with the protein side facing toward the film. Expose film for optimal time required for visualization of bands, then develop film.

It is best to perform these steps in the darkroom, turning the lights off when exposing and developing film. Work as quickly as possible following the addition of the detection solution. For a given batch of antibody used under standardized conditions, the time of film exposure that gives the greatest signal-to-noise ratio will remain fairly constant. This must be determined empirically when assay conditions and reagents are changed. For anti-APAP, film-exposure times typically range between 2 and 10 min. Because of the stability and sensitivity of the reagents, the same membrane may be exposed sequentially to new film for varied lengths of time. This allows for optimization of signal detection of adducts on the film. The intensity of the signal is maximal between 1 and 5 min, with a half-life of decay of 1 hr. The limit of detection is as low as 1 pg of antigen.

Radioactive and chemiluminescence-based detection systems have the advantage of ease of quantification. They also permit the membrane to be stripped of adsorbed antibodies and then probed again.

BASIC PROTOCOL 2

DETECTION OF COVALENT BINDING BY IMMUNOHISTOCHEMISTRY

Immunohistochemistry has become increasingly important diagnostic and experimental techniques to determine the intracellular localization of a particular antigen. Methods of tissue preparation are versatile and often empirically determined based upon the tissue type and antigen-antibody interaction. Similarly, morphological examination of tissue sections can utilize light, fluorescence, or electron microscopy. The method described below localizes APAP-protein adducts in tissue sections prepared by microwave fixation and processed for immunohistochemistry (Emeigh Hart et al., 1995)

Kits other than the AS/AP kit used here, which incorporate enzyme-based detection (alkaline phosphatase or peroxidase) in combination with streptavidin/avidin and biotin interactions offer greater sensitivity and are highly recommended over the traditional enzyme-based detection systems. Such kits are available from BioGenex and Vector Laboratories.

Materials

Tissue sections (1 mm thickness) containing protein-xenobiotic adducts
0.9% NaCl (*APPENDIX 2A*)
50%, 95%, and 100% ethanol
Xylene
Tris-buffered saline (TBS; see recipe)
0.5% pepsin in 0.1 N HCl (prepare fresh), prewarmed to 37°C
Nonimmune serum from species in which secondary antibody was raised
Primary antibody: anti-APAP (see Support Protocol 2), affinity purified (see Support Protocol 6)
TBS (see recipe) containing 0.5% bovine serum albumin (BSA)
AS/AP Universal Rabbit Detection System (Bio-Can Scientific; or equivalent detection system employing alkaline phosphatase–conjugated anti-rabbit secondary antibody)

continued

Double-strength (2×) Gill's hematoxylin (see recipe or purchase from Polyscientific)
Ammonium hydroxide
Aqueous mounting medium (CrystalMount from BioMedia or equivalent)

Coverslips
Tissue-processing cassettes
Microwave oven with temperature probe
Programmable automated tissue processor (e.g., Model LX-120, Innovative Medical Systems)
Equipment for paraffin embedding and sectioning (e.g., dedicated histology laboratory)
Vacuum desiccator
Poly-L-lysine-coated glass microscope slides (see recipe)
60°C and 80°C drying ovens
Coplin jars
Glass staining pan with metal slide rack

Fix tissue

1. Trim tissue samples to 1 mm thickness and place into plastic tissue-processing cassettes.

   Tissue samples >1 to 2 mm in any dimension may be damaged by conductive heat during microwave fixation. Also, in such sections, chemical fixatives will penetrate too slowly for proper fixation.

2. Place up to five cassettes into a beaker containing 150 ml of 0.9% NaCl and insert into a microwave oven equipped with a temperature probe.

   Samples must be immersed in the buffer or buffered fixative to prevent dessication and loss of antigenicity during microwave irradiation. If samples are instead contained in individual vials, a beaker containing 300 to 400 ml water must also be placed in the microwave oven. Irradiating a small sample volume without the additional water load will lead to overheating of the samples. The water load will improve the reproducibility of microwave fixation conditions (Login and Dvorak, 1988).

3. Place the temperature probe into the beaker and microwave 5 min at 60°C.

   The time and temperature for microwave fixation may be varied as appropriate and should be optimized for tissue type, antibody, chamber design, and power output of the microwave oven.

   Samples immersed in a fixative rather than a saline solution will require much shorter microwave irradiation (e.g., seconds).

4. Transfer cassettes quickly to a beaker containing 10 vol of 50% (v/v) ethanol per vol tissue.

   Rapid replacement of the hot fixing buffer with the ethanol solution is necessary to prevent overfixation. Samples may be stored in 50% ethanol until further processing is initiated. Duration of storage without loss of antigenicity and architecture may vary and should be determined experimentally.

Process samples for histology

5. Dehydrate tissues using a programmable automated tissue processor, omitting the alcohol-formalin step. Embed tissues in paraffin and store in a vacuum dessicator until ready to section.

   These operations will normally be performed in a dedicated histology laboratory.

6. Cut 5-μm sections. Mount sections on poly-L-lysine coated glass microscope slides by warming in a drying oven set at 60°C for 30 min.

   Proper adhesion of sections to slides requires: (1) clean slides, (2) contact of the entire section with the glass surface, and (3) thorough drying. Coating with positively charged poly-L-lysine will prevent detachment of the negatively charged tissue sections. This is necessary if the sections will be subsequently treated with proteases. Tissue sections with folds and wrinkles will not have good contact with the slide surface and will adhere poorly.

7. Rehydrate and deparaffinize tissue sections by immersing sequentially, 5 min each, in Coplin jars containing the following solutions:

   Xylene
   Xylene1
   100% ethanol
   100% ethanol
   95% ethanol
   95% ethanol
   70% ethanol.

8. Transfer the slides to a staining rack and rinse with running tap water in a staining pan for 5 min.

   The position of the tissue section can be marked with a diamond pen or water-repellent marker. If peroxidase-antiperoxidase will be used for immunodetection, treat slides with 3% hydrogen peroxide for 15 min after the water rinse to quench endogenous peroxidase activity. Slides are then washed with tap water after the peroxide quench. Metal staining racks should not be used to support slides during hydrogen peroxide staining.

9. Immerse slides in TBS for 5 min.

Treat slides with pepsin

10. Incubate slides 15 min at 37°C in prewarmed 0.1 N HCl containing 0.5% pepsin.

    This treatment promotes the accessibility of epitopes for antibody recognition. Avoid metal racks and containers during the digestion step.

11. Rinse slides in running tap water for 5 min, then immerse slides in TBS for 5 min. Blot slides to remove most liquid, leaving the tissue section moist.

    This will prevent further protease digestion.

Block tissue

12. Place slides in incubation tray with the tissue section facing upward. Block the tissue by covering the section with nonimmune serum (diluted 1:50), collected from the same species used to produce the secondary antibody, then incubating 30 min at room temperature.

    Use sufficient volume to cover the tissue section. Pretreatment with nonimmune serum will reduce the nonspecific binding of the subsequently applied antibodies.

Incubate in primary antibody

13. Remove blocking serum from the slide by shaking and replace with affinity-purified anti-APAP antibody diluted 1:10 in TBS containing 0.5% BSA. Use sufficient volume to cover the tissue section. Allow antibody to bind for 18 to 21 hr at 4°C.

    A dilution series is recommended to establish the appropriate concentration of primary antibody. Most polyclonal antibodies can be diluted 1:20 to 1:100; affinity-purified antibodies may be used in the range of 5 to 20 μg/ml. Incubation of slides in a humidified atmosphere will prevent dehydration.

    Also include the appropriate controls (see Critical Parameters and Troubleshooting).

14. Wash slides three times with TBS in Coplin jars, each time for 5 min with shaking.

Separate jars must be used for slides incubated with different immunoreactants, to prevent cross-contamination. Tween 20 (0.05% w/v) may be included in the wash steps.

Incubate with enzyme-conjugated secondary antibody

15. Blot slides dry and lay flat in a staining tray. Place 2 to 4 drops of alkaline phosphatase–conjugated secondary antibody, provided with the AS/AP Universal Rabbit Detection System from Bio-Can Scientific, on the tissue section and incubate 30 min at room temperature. Wash slides as in step 14

If a kit is not used, the concentration of secondary antibody may be determined experimentally. Typical dilutions range between 1:50 and 1:150. Peroxidase-conjugated secondary antibody may be used instead of alkaline phosphatase.

Visualize staining

16. Blot slides and return to staining tray. Incubate with the chromogenic substrate supplied with the AS/AP kit for 20 min or until color development is visible.

17. Rinse slides thoroughly in running water for 5 min. Counterstain by immersing for 3 min in double-strength (2×) Gill's hematoxylin, then rinse thoroughly in running water for 5 min and blot dry.

It is advisable to purchase prepared staining solutions (e.g., from Polyscientific) as commercial preparations give more uniform results. Conditions for storage (usually room temperature) and expiration dates are provided on the label. Also note that some histology laboratories favor Mayer's hematoxylin over Gill's formulation, due to the blue staining of the nucleus and the contrast provided when used with other staining protocols.

18. Dip slides 10 times in dilute ammonium hydroxide (6 to 8 drops ammonium hydroxide in 300 ml water). Rinse thoroughly in running tap water.

Slides will turn blue.

19. Place 3 to 4 drops of aqueous mounting medium (e.g., CrystalMount) over each tissue section. Tip slides as required to coat each section uniformly with a thin film.

Avoid the use of organic solvents which may solubilize some chromogens.

20. Place slides on a metal tray and incubate in oven 15 min at 80°C. Add coverslips after cooling.

Slides may be examined under the microscope at this step. Compare slides from experimental groups to those from positive and negative controls that were run through the process simultaneously (see Commentary). For photography, permanently mount cover slips with Permount (Fisher).

PREPARATION OF APAP ANTIGEN

SUPPORT PROTOCOL 1

This method involves the use of a linker molecule (*p*-aminobenzoic acid, PABA) between the hapten (acetaminophen, also called *N*-acetyl-*p*-aminophenol or APAP is used as the example here) and the carrier protein, keyhole limpet hemocyanin (KLH). Since the 3 and 5 positions of the aromatic ring of APAP have been identified as sites for protein-adduct formation, the coupling chemistries were selected to retain the natural binding conformation. Construction of the antigen requires a three-step procedure (Fig. 2.3.1) which involves (1) diazotization of the amino group of PABA, (2) conjugation of the diazonium cation of PABA to APAP at the nucleophilic 3 or 5 positions of the APAP ring, and (3) coupling of the hapten-conjugate (APAP-PABA) to the carrier protein KLH by the mixed anhydride method, where an amide bond is introduced between the carboxyl

group of PABA and the free amino groups on KLH (Bartolone et al., 1988). Radiometric methods are used to monitor formation of the hapten conjugate and to determine epitope density.

CAUTION: If radioactivity will be used for detection, the user is required to have received institutional training in the handling of radioisotopes, and the experiment must be performed in an area designated for radioactivity use under the supervision of a licensed investigator. All steps must be carried out in accordance with the Nuclear Regulatory Commission (NRC) and institutional guidelines (also see *APPENDIX 1A*).

NOTE: All aqueous solutions should be made in water of high purity (i.e., double-distilled, or deionized using Milli-Q or equivalent filtration system).

Materials

p-aminobenzoic acid (PABA)
0.1 N HCl, 4°C
1% (v/v) sodium nitrite

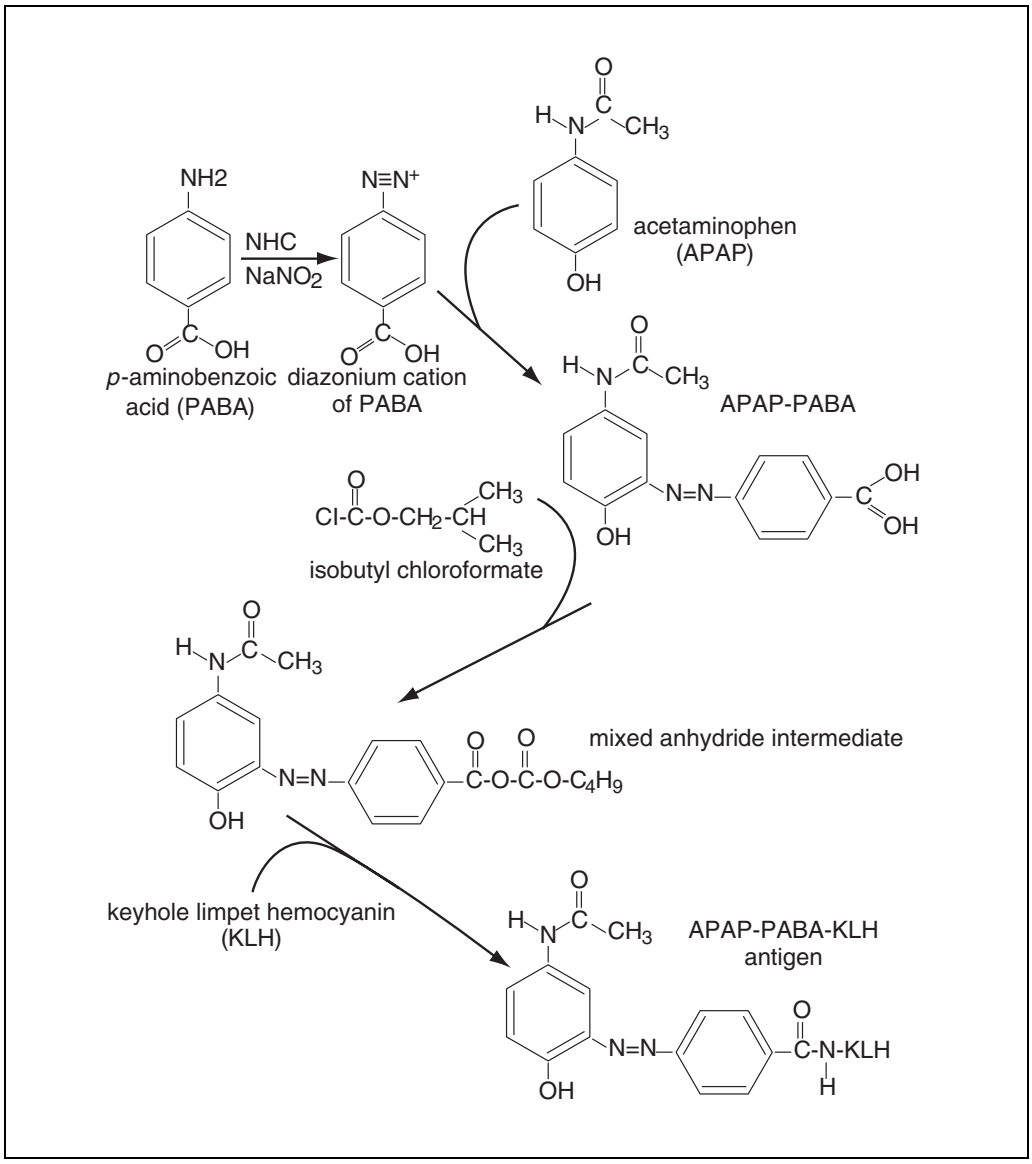

Figure 2.3.1 Synthetic scheme for formation of acetaminophen (APAP) antigen.

Source of starch (e.g., 1% starch solution, starch paper, or slice of potato) saturated with freshly prepared 50 mM potassium iodide
Acetaminophen (APAP; Sigma; minimum purity, 99%)
0.5 M carbonate/bicarbonate buffer, pH 9.0 (see recipe)
^{3}[H]acetaminophen ([^{3}H]APAP; 15.5 Ci/mmol, uniformly labeled; must be custom-synthesized)
1.0 N and 0.1 N NaOH
N,*N*-dimethylformamide
Keyhole limpet hemocyanin (KLH)
Isobutyl chloroformate (Aldrich)
Phosphate-buffered saline (PBS), pH 7.0 to 7.2 (see recipe)
6 N perchloric acid
50 mg/ml bovine serum albumin (BSA; store up to 24 hr at 4°C)
80% methanol containing 5 mM unlabeled APAP, ice-cold
Nitrogen source
Tissue solubilizer (e.g., Solvable from NEN Life Science or Amplify from Amersham; optional)

Acetone/dry ice or ethanol/dry ice bath
Lyophilizer
6000 to 8000 MWCO dialysis tubing (pretreated; see recipe) and dialysis clamps

Diazotize p-aminobenzoic acid (PABA)

1. Dissolve 4 mmol (548 mg) of PABA in 100 ml 0.1 N HCl at 4°C.

   This is best done with stirring in a large, e.g., 250-ml, beaker.

2. Add 1% (v/v) sodium nitrite solution dropwise with stirring until a yellow-green color appears. Test for completeness of the titration by placing the solution dropwise onto a source of starch, e.g., a slice of potato saturated with freshly made 50 mM KI solution, and observing for the appearance of a blue-black color which should form on the potato in ~1 min. Allow the solution to stir for an additional 15 min and retest. If starch test remains positive, proceed to step 3. If the starch test is negative, add more sodium nitrite solution, avoiding large excesses, and retest. Repeat as required.

   PABA is converted to the diazonium ion in the presence of nitrous acid. When diazotization approaches completion, the excess free nitrous acid can be detected by a positive starch test whereupon iodide is oxidized to iodine yielding a blue-black color in the presence of starch. Alternative sources of starch include 1% starch plus 50 mM potassium iodide or starch paper saturated with 50 mM potassium iodide. Free nitrous acid should remain detectable 15 min after the last addition of sodium nitrite, as determined by a positive starch reaction. Since the reaction between PABA and sodium nitrite is stoichiometric, this offers a test for completion of diazotization (Nisonoff, 1967). The reaction should consume ~27 ml of sodium nitrite solution.

Derivatize APAP to diazotized PABA

3. Dissolve 4 mmol (600 mg) of APAP in 20 ml 0.5 M carbonate/bicarbonate buffer, pH 9.0, with heating at 50° to 55°C. Add 5 µCi ^{3}[H]APAP to determine epitope density (see step 15).

   Prepare the solution just before use to avoid problems with overheating or crystallization upon cooling. APAP has limited solubility at this concentration (200 mM), and thus it is necessary to heat to 50° to 55°C. At pH 9.0, the solution of APAP will be pink.

4. Using a Pasteur pipet, slowly add the APAP solution to the diazotized PABA from step 2.

   As the solution approaches neutral pH, the yellow-green solution of PABA will turn red.

5. Quickly adjust the pH to 9.5 with 1.0 N NaOH.

   The color will deepen to a dark red. It is critical for successful derivatization that the pH not decrease below 9.0.

6. Stir the solution at 4°C, periodically checking the pH.
7. Shell freeze in an acetone/dry ice bath or ethanol/dry ice bath, then lyophilize to dryness.

   Lyophilization may take 24 to 36 hr.The product should be a fine powder. It is critical that no water be present for the subsequent steps.

Conjugate APAP-PABA to KLH

8. Set up an ice-water bath in a well-ventilated hood. Maintain temperature at 10°C.

   CAUTION: *The following reaction is exothermic. Combine reagents slowly. Take appropriate safety precautions and use chemical-resistant latex gloves.*

9. Dissolve the lyophilized APAP-PABA powder in 9.0 ml *N*,*N*-dimethylformamide and cool to 10°C.
10. Dissolve 50 mg KLH in 50 ml of 50 mM carbonate/bicarbonate buffer, pH 9.0.

    KLH dissolves slowly.

11. Add 260 µl isobutyl chloroformate to the solubilized APAP-PABA from step 9 and stir for 30 min at 10°C.

    IMPORTANT NOTE: *It is essential to avoid water. The reaction of isobutyl chloroformate with the carboxyl group of PABA-APAP to form the mixed anhydride is water-sensitive. It is also advisable to conduct the reaction in an environment with low atmospheric humidity. Anhydrides can be rapidly hydrolyzed. If water is present, competition between the acylation and hydrolysis will reduce product yield.*

12. Slowly add the KLH solution prepared in step 10 to the acid anhydride of PABA-APAP formed in step 11. Stir for 4 hr while maintaining the temperature at 10°C throughout the reaction.
13. Dialyze the antigen 2 days against PBS, pH 7.0 to 7.2, at 4°C, with at least 5 changes of buffer, using pretreated 6000 to 8000 MWCO dialysis tubing.

    The dialysate color will decrease in intensity with repeated changes of buffer.

14. Remove two 1.0-ml aliquots for determination of epitope density (see steps 15 to 21) and place in 1.5-ml microcentrifuge tubes. Divide the remaining antigen solution into 1-ml aliquots and store at −70°C.

    Antigen may be stored for several months at this temperature. Alternatively it may be stored up to 2 weeks at 4°C. The amount of protein adduct used for immunization can be determined by any protein assay presently used in the laboratory—e.g., Lowry or Bradford.

Determine epitope density

15. In each of the two 1.0-ml aliquots taken from the antigen solution (step 14), acid-precipitate the protein with 0.2 ml of 6 N perchloric acid and add 100 µl of 50 mg/ml BSA. Let stand on ice for 10 min, then microcentrifuge 5 min at 14,000 × *g*, 4°C.

    The BSA is added as a carrier protein to prevent loss of ^{3}[H]APAP-KLH.

16. Remove supernatants and discard. Resuspend pellets by vortexing in 1.0 ml ice-cold 80% methanol containing 5 mM unlabeled APAP.
17. Add 30 µl of 1.0 N NaOH to the methanol solution/resuspended pellet and confirm that the pH is alkaline with pH paper.

    This step is necessary since BSA is soluble in acidic methanol. The methanol washes remove residual APAP that is not covalently bound to KLH.

18. Let stand on ice 10 min, and microcentrifuge 5 min at 14,000 × *g*, 4°C. Repeat methanol wash (removal of supernatants followed by addition of methanol/APAP and microcentrifugation) twice more.
19. Evaporate the residual methanol solution remaining in the pellet under nitrogen.
20. Solubilize the pellet in 0.2 ml of 0.1 N NaOH or a commercially available tissue solubilizer.
21. Determine the amount of ^{3}[H]APAP associated with KLH by liquid scintillation spectrometry.

Due to the multisubunit structure and size heterogeneity of KLH, epitope density is best expressed as nmol APAP bound per μg KLH protein. The following is a sample calculation.

Starting material: 4 mmol APAP and 5 μCi [^{3}H]APAP.

Reaction volume: 9.0 ml (step 9) + 50 ml (step 10) containing 50 mg KLH

Sample volume: 1.0 ml

Specific activity of [^{3}H]APAP: 11.0 × 10^{6} dpm/4 mmol APAP = 2730 dpm/μmol

1 ml sample volume would contain 847 μg KLH with a measured amount (x) of [^{3}H]APAP. The number of μmol APAP bound per μg KLH is determined as follows:

x/2730 (specific activity of [^{3}H]APAP)/847 μg KLH.

IMMUNIZATION AND SERUM COLLECTION TO PREPARE ANTI-APAP POLYCLONAL ANTIBODIES

SUPPORT PROTOCOL 2

Historically, immunization of female New Zealand rabbits has been done with the synthetic antigen (see, e.g., Support Protocol 1) and Freund's adjuvant. Freund's adjuvant results in the formation of granulomas and ulcers at the sites of injection. Alternative adjuvants that are less injurious are now widely available and should be used in accordance with the protocols supplied by the manufacturers (Adjuvax from Alpha-Beta Technology; Hunter's Titermax from CytRx; and RAS from RIBI Immunochemical Research). Two or more rabbits should be immunized with the hapten conjugate prepared in Support Protocol 1, since not all animals will respond equally to the antigen. New Zealand rabbits that are outbred and commonly used for antibody production exhibit varied response to APAP-PABA-KLH. All personnel should receive prior instruction regarding the care and handling of laboratory animals.

NOTE: All protocols using live animals must first be reviewed and approved by an Institutional Animal Care and Use Committee (IACUC) or must conform to governmental regulations regarding the care and use of laboratory animals.

Materials

Female New Zealand white rabbits (3.5 to 4.5 kg)
APAP-PABA-KLH conjugate (see Support Protocol 1)
Adjuvant (Adjuvax from Alpha-Beta Technology, Hunter's Titermax from CytRx, or RAS from RIBI Immunochemical Research)

20- and 22-G needles
15- and 30-ml Corex glass centrifuge tubes
Refrigerated centrifuge
0.5-ml glass syringes

Additional reagents and equipment for detection of anti-APAP antibodies by ELISA (see Support Protocol 4)

Collect preimmune serum

1. One to two weeks prior to immunization, collect 5 to 10 ml of blood from unimmunized rabbit by inserting a 20-G needle into the central vein of the ear and gently holding it in place while allowing blood to drain from the open end of the needle directly into a 15-ml Corex tube.

   This will serve as the source of preimmune serum, which will be used to determine the specificity of antibody production and to detect any innate immune cross-reactivity with proteins that lack the antigenic adduct.

   Blood collection is facilitated by wrapping the rabbit in a towel, exposing only the head and ears. Heat generated from a lamp is recommended for keeping the ear warm to ensure adequate blood circulation. Shave a localized area of the ear. Palpation, rather than the use of chemical irritants (i.e., xylene), should be used to dilate the blood vessel. Donovan and Brown (1995) describe the procedure for collection of blood from the auricular vein of the rabbit.

2. Allow blood to clot at room temperature.

   The clot will retract from the wall of the tube. This can be facilitated by rolling a glass rod or similar device around the inside of the tube.

3. Centrifuge 10 min at 10,000 × *g*, 4°C. Carefully remove the serum, retain a 1-ml aliquot for initial screening, and store the remainder in 1-ml aliquots at −70°C.

Immunize rabbits

4. In a 1.5-ml microcentrifuge tube, mix 1 part APAP-PABA-KLH (containing 400 µg of the conjugate) with 1 part adjuvant.

   Antigen concentrations can range from 50 to 1000 µg/ml for rabbits.

5. Vortex 5 to 10 min to emulsify, then inject the immunogen preparation into the rabbit at multiple sites using a 0.5-ml glass syringe and 22-G needle.

   Plastic syringes are not recommended as they may swell on contact with the adjuvant. Avoid trapping air in the syringe or needle.

   The volume for injection varies with the site. A typical immunization protocol may include intramuscular injections of 0.3 to 0.5 ml into each hind leg along with two subcutaneous injections (0.1 to 0.25 ml each) at sites along the lower back.

6. Give booster injections 3 to 4 weeks after the initial immunization. Use the same formulation procedure as in step 4, but add only 200 µg antigen.

Collect and test antiserum

7. At a point 10 to 14 days after the booster injection, collect 5 ml of blood and process into serum as in steps 1 to 3. Test serum for the presence of anti-APAP antibodies by ELISA (see Support Protocol 4).

   If ELISA testing of this initial blood sample indicates the presence of specific antibodies, 20 to 25 ml should be drawn during subsequent blood collections. If no antibodies are detected, the rabbit may be given a second booster and the serum retested. If antibodies are not detected at this time, immunization of that particular rabbit should be discontinued. Peak levels of antibody are usually achieved 10 to 14 days following the booster injection and persist for 2 to 4 weeks. Subsequent booster injections may be given as needed, but should not be more frequent than every 4 to 6 weeks.

   A recommended frequency for blood collection is at 4-month intervals, at which ~30 to 40 ml of blood is withdrawn.

PREPARATION OF NAPQI-PROTEIN ADDUCTS AS COATING ANTIGEN FOR ELISA

N-acetyl-*p*-benzoquinoneimine (NAPQI)-protein adducts are used to coat the wells of the plate for the ELISA that will be used to test for antibody specificity (see Support Protocol 4). Antibodies elicited in response to conjugated haptens may be directed against the hapten, the carrier protein, and the linker molecule. To determine whether the antibodies produced following hapten-conjugate immunization can specifically recognize APAP, it is important that ELISA be performed (see Support Protocol 4) using a coating antigen that contains neither the linker, PABA, nor the carrier protein, KLH. Both BSA and aldolase which have been reacted with the APAP electrophile, NAPQI, have been used successfully as coating antigens. The unmodified protein serves as a negative control in the ELISA.

This protocol describes the method of Dahlin and Nelson (1982) and Streeter et al. (1984). APAP is converted to NAPQI and allowed to bind to BSA.

Materials

Acetonitrile
Sodium sulfate, anhydrous
Acetaminophen (APAP; Sigma; minimum purity 99%)
[^{3}H]acetaminophen ([^{3}H]APAP; 15.5 Ci/mmol; must be custom-synthesized)
Silver (I) oxide
Bovine serum albumin (BSA) or aldolase
Phosphate-buffered saline (PBS), pH 7.4 (see recipe)
10 mg/ml BSA in PBS (see recipe for PBS)
1 N perchloric acid
80% methanol, ice-cold
50 mM carbonate/bicarbonate buffer, pH 9.6 (see recipe)

5- to 7-ml glass screw-cap vials
6000 to 8000 MWCO dialysis tubing (pretreated; see recipe) and dialysis clamps

Synthesize NAPQI

1. Add the following ingredients sequentially to 625 µl acetonitrile in a 5- to 7-ml glass vial while stirring with a micro stir-bar:

   5 mg (35 µmol) anhydrous sodium sulfate
   5 mg (33 µmol) APAP
   13.2 µCi [^{3}H]APAP
   10 mg (43 µmol) silver (I) oxide.

   Anhydrous sodium sulfate is used to dry organic solvents. Silver oxide is a catalyst in the reaction and is not soluble. Sufficient radioactivity is included to facilitate quantitation of the amount of NAPQI bound to protein using an aliquot of the protein reaction as described below.

2. Stir 15 to 30 min at room temperature.

   The acetonitrile solution will change from colorless to pale yellow.

3. Transfer the reaction to a 1.5-ml microcentrifuge tube. Microcentrifuge 1 min at 14,000 × *g*, room temperature, to bring down the silver oxide precipitate.

4. Transfer the supernatant to a clean tube.

React with BSA or aldolase

5. Solubilize 10 mg BSA or aldolase in 10 ml PBS, pH 7.4

   BSA is available as a crystalline powder; aldolase is supplied as a suspension in ammonium sulfate solution and must be dialyzed against PBS to remove the salt.

6. Divide the BSA or aldolase solution into 2-ml aliquots in 7-ml glass screw cap vials. Add the appropriate volume of NAPQI solution (from step 4) to give molar ratios of NAPQI/protein of 25:1, 50:1, and 100:1 in the reaction mixture, assuming 100% conversion of APAP to NAPQI. Prepare additional vials as controls containing the unmodified protein and the unmodified protein plus the maximum volume of acetonitrile used in generating the protein adducts.

   The reaction of NAPQI with purified proteins in vitro must be carefully monitored to avoid artifactually high binding ratios of NAPQI to protein. Cysteine residues are the primary sites on proteins that react with NAPQI. BSA (66 kDa) has one free -SH residue; therefore the optimal binding of NAPQI to BSA should approximate a 1:1 molar ratio. A ratio in excess may indicate nonspecific binding or polymerization of NAPQI. Aldolase, a tetrameric protein of 160 kDa, may offer greater flexibility as a coating antigen, with 12 and 24 -SH groups available under nondenaturing and denaturing conditions, respectively.

7. React for 30 min at room temperature with shaking.

   Longer reaction times may result in decomposition of NAPQI.

8. Dialyze overnight against 2.0 liters of PBS to remove unincorporated isotope ([^{3}H]APAP), using pretreated 6000 to 8000 MWCO dialysis tubing. Following dialysis, remove two 100-µl aliquots and proceed to step 9. Store remaining volume of adduct solution at 4°C.

   It is recommended that the protein adducts, especially aldolase adducts, not be stored for >1 week. Protein denaturation may contribute to decreased sensitivity and greater variability in ELISA.

Determine amount of [^{3}H]APAP bound to the protein

9. Precipitate each of the 100-µl aliquots of [^{3}H]APAP-protein adducts (from step 8) with 1.0 ml of 1 N perchloric acid, then add 50 µl of 50 mg/ml BSA to each aliquot as a cold carrier.

   The carrier is added to prevent losses of the small amount of radioactive protein.

10. Let stand on ice for 10 min, then centrifuge 5 min at 14,000 × *g*, 4°C.

11. Remove supernatants and discard. Resuspend pellets by vortexing in 1.0 ml ice-cold 80% methanol. Add 30 µl of 1.0 N NaOH to the resuspended pellet and confirm that the pH is alkaline with pH paper. Repeat the methanol washes twice more using the technique described in Support Protocol 1, step 18.

    The step for ensuring basic pH is necessary since BSA is soluble in acidic methanol.

12. Determine the amount of bound [^{3}H]APAP (see Support Protocol 1, steps 19 to 21).

13. Calculate the nanomoles of NAPQI bound to the protein by dividing the ^{3}H dpm obtained in step 12 by the specific activity of APAP used in step 1—i.e., 0.4 µCi/µmol.

14. Calculate nanomol of NAPQI bound per nanomol protein in the aliquot sampled.

    100 µl of 1 mg/ml BSA is equivalent to 1.5 nmol BSA.

Dilute NAPQI adducts for ELISA

15. Dilute the protein adducts and corresponding controls in 50 mM carbonate/bicarbonate buffer, pH 9.6, to give 2 μg/ml. Use 100 ng (50 μl) for coating quadruplicate wells of a microtiter plate (see Support Protocol 4).

    To coat each well of the plate, 100 ng of protein adduct in 50 μl of 50 mM carbonate/bicarbonate buffer, pH 9.6, is used. From step 5, the starting concentration of protein (BSA or aldolase) is 1 mg/ml. Therefore, to obtain the desired concentration for coating, dilute the 1 mg/ml protein-adduct solution 1:10 by adding 100 μl of the protein adduct to 900 μl buffer (the volume of NAPQI solution added to the reaction with protein is <100 μl and is ignored in this calculation). Further dilute the protein adduct solution (now 100 μg/ml) 1:50 by taking 20 μl and adding to 980 μl buffer. This will give the 2 μg/ml solution used for coating the wells of the microtiter plate. Volumes can be proportionally scaled up to accommodate the number of samples being tested.

    For BSA, coat with the adduct that best approximates the 1:1 molar ratio (see step 6). With aldolase adducts, test two or more molar ratios to identify one that most conveniently facilitates detection of antibody binding on ELISA (e.g., linear kinetics with optimum color development within a convenient time frame).

DETECTION OF ANTI-APAP ANTIBODY BY NONCOMPETITIVE ENZYME-LINKED IMMUNOSORBENT ASSAY (ELISA)

SUPPORT PROTOCOL 4

The basic principle of enzyme immunoassays takes advantage of the specificity and high affinity of the antibody for its corresponding antigen. Detection of the interaction is achieved by enzymatic coupling and amplification to yield a chromogenic product. The reactions are done on a solid support, which greatly facilitates the separation of bound and free molecules. Generally, 96-well polysytrene or polyvinyl chloride (PVC) microtiter plates are used. Permutations of the assay vary according to whether the antigen or antibody is immobilized within the wells (the solid support). The assays may also be designed to be competitive or noncompetitive in nature, to permit quantification and characterization of either antigen or antibody. The application described in this protocol uses a noncompetitive ELISA to screen for the production and determination of the titer of APAP antibodies.

Materials

Coating antigen: 2 mg/ml NAPQI-protein adduct solution (see Support Protocol 3) *and* unmodified control protein solution (see Support Protocol 3, step 6)
PBST (see recipe)
1% (w/v) BSA *or* 0.2% to 0.5% (w/v) gelatin in 50 mM carbonate/bicarbonate buffer, pH 9.6 (see recipe)
Immune and preimmune rabbit serum to be assayed for anti-APAP antibodies (see Support Protocol 2)
Phosphate-buffered saline (PBS; see recipe)
Horseradish peroxidase (HRP)–conjugated anti-rabbit IgG (or IgG made against other host animal used in primary antibody production)
2,2′-azino-di-(3-ethylbenzthiazoline) sulfonic acid (ABTS)
50 mM sodium citrate, pH 4.0 (see recipe)
30% hydrogen peroxide (store up to 1 month at 4°C)
37 mM sodium cyanide (optional)

96-well flat-bottom polystyrene or polyvinyl chloride (PVC) microtiter plates
Multichannel pipettor
Microtiter plate reader with variable-wavelength filters

Coat and block the wells

1. In alternating rows of a 96-well polystyrene or polyvinyl chloride (PVC) microtiter plate, place 100 ng NAPQI-protein adduct (coating antigen) in 50 µl (i.e., 50 µl of 2 µg/ml solution) using a multichannel pipettor. Place equivalent amount of the unmodified control protein in the remaining wells.

   Antibodies elicited in response to conjugated haptens may be directed against the hapten, the carrier protein, and the linker molecule. To determine whether the antibodies produced following hapten-conjugate immunization can specifically recognize APAP, it is important that the coating antigen contain neither the linker, PABA, nor the carrier protein, KLH. Both BSA and aldolase which have been reacted with the APAP electrophile, NAPQI (Support Protocol 3), have been used successfully as coating antigens. The unmodified protein serves as a negative control in the assay.

   Coating buffers used for solubilizing and diluting the antigen include 50 mM carbonate, pH 9.6, 10 mM Tris·Cl (pH 8.5)/100 mM NaCl, or 10 mM sodium phosphate, (pH 7.2)/100 mM NaCl. Carbonate buffer is commonly used (see Support Protocol 3, step 15). The presence of detergents should be avoided during coating, since they compete with the protein for binding to the solid phase and prevent the formation of the desired hydrophobic interactions (Tijssen, 1985).

2. Incubate the plate in a humidified atmosphere at 37°C for 1 hr or at 4°C overnight to coat wells.

   Important variables for adsorption of protein to the wells are time, temperature, and concentration. Incubation time may be decreased by increasing temperature or antigen concentration.

3. Empty the contents of the plate by inversion and tap dry over paper towels on the benchtop. Wash the wells five times with PBST.

   The use of polyoxyethylene sorbitan (Tween 20) in the PBST wash solution reduces nonspecific adsorption and minimizes formation of new hydrophobic interactions between the solid support and the primary and secondary antibodies without significant disruption of bonds already formed between the coating antigen and plastic surface (Engvall, 1980).

4. Block wells by adding 100 µl of 1% BSA or 0.2% to 0.5% (w/v) gelatin in carbonate/bicarbonate buffer to each well and incubating 1 hr at room temperature.

5. Empty plate and wash five times with PBST (step 3).

   Blocking prevents direct adsorption of antibody to the plastic if all sites have not been saturated, and thus decreases nonspecific binding. If comparison of ELISAs run with or without this blocking step reveal no differences, steps 4 and 5 may be omitted from the routine protocol.

Incubate with primary and secondary antibodies

6. Serially dilute the rabbit antiserum from 1:4 to 1:1024 in PBS. Add 20 µl of each dilution to the designated well and incubate 3 hr at 37°C.

7. Empty plate and wash five times with PBST (step 3).

8. Dilute horseradish peroxidase (HRP)–conjugated goat anti–rabbit IgG 1:1000 in PBST. Add 50 µl to each well and incubate 1 hr at 37°C.

   Alkaline phosphatase–conjugated secondary antibody may be used in place of HRP-conjugated antibody, although the latter is more frequently used.

   Dilution of the secondary antibody may vary with its commercial source. Recommended dilutions are often supplied with the technical data sheets that accompany the product. Otherwise, optimal dilutions need to be determined empirically.

Detect bound antibodies

9. Turn on the microtiter plate reader and allow to warm up for 10 to 15 min or in accordance with manufacturer's instructions.
10. Empty plate and wash five times with PBST (step 3).
11. Dissolve 6.6 mg ABTS in 10 ml 50 mM sodium citrate, pH 4.0. Add 40 µl of 30% hydrogen peroxide (H_2O_2).

    This solution should be made up just before use. H_2O_2 is both a substrate and inhibitor of HRP and therefore the concentration range in which it can be used is limited (Tijssen, 1985). ABTS is a both a chromogen (absorbance at 415 nm) and hydrogen donor in the reaction catalyzed by peroxidase where cleavage of H_2O_2 is coupled to oxidation of the hydrogen donor (Engvall, 1980). Other chromogens/hydrogen donors include 5-aminosalicylic acid, o-dianisidine, o-toluidine, o-phenylenediamine, and tetramethylbenzidine (TMB).

    CAUTION: *ABTS should be handled with care because of its potential mutagenic properties. Check the MSDS for more information.*

12. Add 60 µl of the substrate-chromogen solution to each well. Determine the change in absorbance at 415 nm over the period between 4 and 7 min following addition.

    CAUTION: *NaCN is poisonous and care is advised in handling.*

    Oxidation of ABTS during the reaction will result in the formation of a greenish-blue color.

    Alternatively, endpoint determinations can be obtained by stopping color development with 0.2 vol of 37 mM NaCN. Color development should be linear throughout the interval selected (prior to the endpoint), and this may need to be determined empirically. For example, the 4- to 7-min interval selected for the kinetic reaction was based on the linearity of the reaction. Addition of NaCN results in enzyme inactivation without affecting the color produced, and is therefore advantageous over HCl, H_2SO_4, or NaOH as a stopping reagent. Lowering the pH nonspecifically increases color development, and raising the pH nonspecifically decreases it (Engvall, 1980).

Analyze data

13. Plot the difference in absorbance values between NAPQI-modified and unmodified protein as a function of antibody dilution, beginning with the lowest antibody concentration (highest dilution).

    If rate rather than endpoint measurements are used, plot the rate of change in absorbance as a function of antibody dilution. A sigmoidal curve should be obtained. A leveling off at either end of the curve is due to the fact that either the antigen or antibody is rate-limiting. A direct relationship between the absorbance and the amount of antibody is indicated by a linear response within a range of antibody concentration. This denotes the working concentration range for the antibody. Some background absorbance will be observed with the unmodified protein and whole serum; however, the specificity of antibody recognition for APAP is indicated by a 2-fold or greater difference in absorbance between the NAPQI-conjugated versus unconjugated protein. Upon affinity purification of the antibody, the background will be significantly reduced and the difference between conjugated and nonconjugated coating antigen maximized.

CHARACTERIZATION OF APAP ANTIBODY BY COMPETITIVE ELISA

SUPPORT PROTOCOL 5

A competitive ELISA is also used in the presence of compounds structurally related to APAP to determine the epitopes recognized by the antibody. The compounds *p*-aminophenol and BSA-NAPQI, as well as APAP and its dimethylated analogs, 2,6-dimethylacetaminophen and 3,5-dimethylacetaminophen, are used as competitors for antibody reactivity against BSA-NAPQI coated onto microtiter wells. Similar structures or stereospecificites to the xenobiotic to which an antibody has been newly constructed would be the basis for selection of potential competitors.

Additional Materials *(also see Support Protocol 4)*

Competitors: e.g., *p*-aminophenol, BSA-NAPQI, APAP, 2,6-dimethylacetaminophen, or 3,5-dimethylacetaminophen

1. Coat wells of microtiter plate with protein-adduct or unmodified protein, then block and wash wells (see Support Protocol 4, steps 1 to 5).
2. Prepare serial dilutions of competitor to give 0.12 to 500 µg/ml in PBS.

   The concentration of competitor per well should span a broad range (i.e., 0 to 10^5). Either units of weight/well (i.e., 1 to 100,000 ng/well) or moles/well (i.e., 1 to 100,000 pmol/well) may be used. Units of moles would be more accurate when the molecular weights of the competitors differ significantly from the compound against which they are tested. It is important that the concentration of the competing compound be in excess relative to the amount of adduct present as the coating antigen.

3. Dilute the antibody in PBST (also see Support Protocol 4, step 6).

   The antibody concentration should be rate-limiting and the final dilution of the antibody (antibody plus competing compound) should fall within the linear portion of the antibody titration curve (as determined by noncompetitve ELISA as in Support Protocol 4).

4. Combine equal volumes of diluted competitor and diluted antibody. Add 20 µl of the mixture per well and incubate plate 3 hr at 37°C.
5. Empty plate and wash five times with PBST (see Support Protocol 4, step 3).
6. Add HRP–conjugated secondary antibody to wells and incubate, then incubate plate with substrate-chromogen solution (see Support Protocol 4, steps 8 to 12).
7. Calculate the percentage inhibition by determining HRP activity in the presence and absence of the competitors.

SUPPORT PROTOCOL 6

CONSTRUCTION OF APAP AFFINITY COLUMN

The principle of affinity chromatography is based on the specific and reversible interactions between two molecules, one of which has been immobilized to a chromatographic matrix. The interactions involved in such binding are noncovalent in chemical nature and are likely to include hydrogen bonding, electrostatic forces, and van der Waals forces. Affinity purification of polyclonal anti-APAP antibody decreases the nonspecific binding in immunoblotting and immunohistochemistry. Epoxy-activated Sepharose was selected for its ability to couple ligands containing hydroxyl, amino, or thiol groups to the free epoxide groups on the oxirane spacer arm, resulting in the formation of ether, alkylamine, or thioether linkages, respectively. With APAP as the ligand, the hydroxyl group is coupled to the matrix to form a stable ether linkage. The long spacer arm is also advantageous in promoting interaction between bound APAP and its specific antibodies. This protocol is an adaptation of that provided by Amersham Pharmacia Biotech, the supplier of the epoxy-activated Sepharose.

Materials

Epoxy-activated Sepharose 6B (Amersham Pharmacia Biotech)
0.1 M NaOH, pH ~11.8
Acetaminophen (APAP; Sigma; minimum purity, 99%)
0.1 M sodium borate, pH 8.0 (see recipe), containing 0.5 M NaCl
0.1 M sodium acetate, pH 4.0 (see recipe)
1 M ethanolamine, pH 9.0 (see recipe)
Phosphate-buffered saline (PBS), pH 7.4 (see recipe)

0.04% (w/v) sodium azide in PBS (see recipe for PBS)

Sintered-glass funnels (coarse or medium) and filter flasks
50-ml conical plastic centrifuge tubes with caps
Platform shaker (e.g., Nutator from Becton Dickinson Primary Care Diagnostics)
1.0 × 10.0–cm glass column (e.g., Econo-Column from Bio-Rad or Kontes-Flex column from Kontes Glass) and 2-way stopcock valve

Couple APAP to epoxy-activated Sepharose

1. Add 2.5 g epoxy-activated Sepharose 6B to 10 ml water and allow gel to swell for 15 to 30 min.

   1.0 gram of dry powder swells to ~3 ml of gel.

2. Transfer gel to a sintered-glass funnel and wash with 500 ml water by adding 50 to 100 ml at a time, allowing the funnel to drain without allowing the Sepharose to dry out, then applying more water.

   This will remove the manufacturer's additives. A coarse sintered-glass funnel is preferable; washes can be done by gravity flow rather than under a vacuum aspirator. If washes are done under vacuum, do not allow the Sepharose to dry out.

3. After the final wash, remove as much water as possible but be careful to keep the Sepharose moist. Wash with 25 ml of 0.1 M NaOH, then allow to drain well. Transfer to a 50-ml plastic-capped centrifuge tube or similar vessel.

4. Solubilize 62 mg (0.4 mmol) APAP in 15 ml of 0.1 M NaOH (pH ~11.8) and add to the Sepharose from step 3. Place tube containing suspension on a platform shaker and allow the coupling reaction to run overnight at room temperature.

   The ratio of binding buffer (containing ligand) to gel matrix is ~2 to 1. A magnetic stirrer should not be used since it can damage the Sepharose matrix. The amount of ligand is determined from the oxirane (epoxy) group concentration of the Sepharose, which will vary from batch to batch. For example, for an epoxy group concentration of 19 to 40 µmol per ml of drained gel and assuming a 1:1 coupling ratio, this would require between 140 to 300 µmol of APAP for ~7.5 ml of gel. The efficiency of coupling is experimentally determined from the difference in absorbance at 250 nm of the APAP solution (in 0.1 M NaOH) just prior to and directly after the coupling reaction when the Sepharose has settled.

   Coupling to Sepharose oxirane groups occurs in the pH range of 9 to 13. Optimal reaction with the hydroxyl group on APAP is conducted at pH 11 to 13. Carbonate or borate buffers are preferred; at the higher pH range, dilute solutions of NaOH may be used. Tris or other nucleophilic reagents should be avoided since these will couple to the oxirane groups. The temperature for coupling can be in the range of 20° to 40°C with a reaction time of 16 hr most frequently used (Pharmacia). However, the reaction time may vary with the stabilities of the epoxy-activated Sepharose and ligand to be immobilized under the conditions of the coupling reaction. For further information, see Critical Parameters and Troubleshooting.

5. Place coupled Sepharose in a sintered-glass funnel and remove excess ligand by successive washes with the following:

   100 ml 0.1 M NaOH
   200 ml distilled H_2O
   100 ml 0.1 M sodium borate, pH 8.0, containing 0.5 M NaCl
   100 ml 0.1 M sodium acetate, pH 4.0.

6. Transfer the washed coupled Sepharose to a 50-ml capped plastic tube. Block any unreacted oxirane groups by incubating gel for 4 hr at at room temperature with ~40 to 50 ml of 1 M ethanolamine, pH 9.0 with shaking on a platform shaker.

   At this pH, the oxirane groups interact with the amino groups of ethanolamine.

7. Wash gel with 200 ml distilled water and preequilibrate by washing twice with 100 ml PBS, pH 7.4.
8. Transfer gel to a filter flask and allow to settle (the gel should occupy ~70% of the total volume). Remove excess volume to obtain a slurry consistency and degas under vacuum just prior to packing the column.

Pack the column

9. Attach a stopcock valve to a 1.0 × 10.0–cm column and turn valve to the closed position.
10. To prevent entrapment of air in the bottom of the column, add 2 to 3 ml of PBS to the empty column and allow to partially drain. Close valve when ~1.0 ml remains.
11. Pour degassed gel slurry (step 8) along the wall of the column to minimize introduction of air bubbles.
12. Fill the remainder of the column with PBS and connect with buffer reservoir; allow the gel to settle.
13. Open stopcock and establish flow. Continue equilibration of column with 200 ml PBS under gravity flow.

    After equilibration, typical flow rates are ~ 0.2 ml/min.

14. Store column at 4°C with 0.04% (w/v) sodium azide in PBS as a preservative.

    The column has been found to be stable for ≥2 years under these conditions.

15. Before purification of APAP antisera, bring the column to room temperature and wash with 300 to 500 ml PBS overnight to remove azide.

SUPPORT PROTOCOL 7

AFFINITY PURIFICATION OF APAP ANTISERUM

Affinity purification of antiserum reduces the background in immunodetection protocols. In this protocol, ammonium sulfate–precipitated and dialyzed anti-APAP antiserum is passed over a column with antigen (APAP) coupled to the Epoxy-activated Sepharose solid support. Specific antibody is eluted with a solution of unbound antigen and dialyzed to remove the antigen.

This procedure has been performed with up to 8 ml of serum. Due to the cost of the Epoxy-activated Separose, and the time involved in the preparation of the column, it is recommended that the column size not be increased but rather that the column be reused as often as needed. With proper care, the column is stable for at least 1 year.

Materials

Antiserum to APAP (see Support Protocol 2)
Saturated ammonium sulfate (SAS; see recipe)
2.0 N NaOH
Phosphate-buffered saline (PBS; see recipe)
1% (w/v) barium chloride
APAP affinity column (see Support Protocol 6)
Acetaminophen (APAP; Sigma; minimum purity, 99%)
0.04% (w/v) sodium azide in PBS (see recipe for PBS)

15-ml Corex glass centrifuge tubes
Refrigerated centrifuge

8,000 to 10,000 MWCO dialysis tubing (pretreated; see recipe) and clamps
Fraction collector
Spectrophotometer

Precipitate antibody with ammonium sulfate

1. Thaw 4 ml serum from a single rabbit and precipitate the IgG fraction by adding 2.4 ml saturated $(NH_4)_2SO_4$ solution (SAS) dropwise while stirring at room temperature.

   The IgG is precipitated at 38% $(NH_4)_2SO_4$. Do not combine batches of serum from different rabbits.

2. Adjust the pH to 7.4 with 2.0 N NaOH if necessary. Stir at room temperature for 30 min.
3. Transfer the mixture to a 15-ml Corex glass centrifuge tube and let stand on ice for 30 min.
4. Centrifuge 10 min at 10,000 × *g*, 4°C.
5. Discard the supernatant. Resuspend the pellet in 4 ml PBS and precipitate with 1.8 ml SAS, to give a final concentration of 31% $(NH_4)_2SO_4$. Let stand on ice for 30 min and repeat step 4.

   This step removes serum albumin.

6. Discard the supernatant and resuspend the pellet in 2.0 ml PBS. Transfer the resuspended protein pellet to pretreated dialysis tubing with a Pasteur pipet.
7. Dialyze overnight at 4°C against 2.0 liters of PBS to remove $(NH_4)_2SO_4$.
8. Test dialysate for removal of sulfate ions by adding an equal volume of 1% barium chloride to a 1.0-ml aliquot of dialysate. If a precipitate is observed, then replace dialysis solution with fresh PBS and continue dialysis until the test for sulfate is negative.

   If sulfate is present, barium sulfate will precipitate out of solution, giving a cloudy, milky appearance.

Affinity purify antibody

9. Close the stopcock at the base of the affinity column and remove residual PBS from above the column bed.
10. Apply the dialyzed protein solution to the column bed and open the stopcock to allow the solution to enter the column. Close the stopcock and allow the antibodies to adsorb to the APAP ligand on the column for 15 to 30 min.
11. Fill the remaining portion of the column with PBS and connect to a buffer reservoir.
12. Open the stopcock and collect 1.0-ml fractions.
13. Measure absorbance at 280 nm to monitor the elution of serum proteins not retained by the column.

    Anti-APAP antibodies are retained by the column.

14. Dissolve 25 mg of APAP in 5 ml PBS.
15. When the absorbance of fractions collected in step 13 returns to baseline, disconnect the buffer reservoir. Remove PBS from above the column bed. Add the solution prepared in step 14 to elute anti-APAP antibodies.
16. Resume fraction collection and continue to monitor absorbance at 280 nm.

    Due to the high concentration of APAP in the eluate, the absorbance will again rise above baseline since APAP also absorbs at 280 nm.

17. Pool fractions, beginning with the first fraction that showed absorbance over the baseline value.

The total pooled fraction volume is usually 5 to 7 ml, or ~2.5 to 3.5 times the volume of dialyzed protein applied.

If fractions are collected until the absorbance again returns to baseline, this could result in dilution of the antibody.

Dialyze the antibody

18. Transfer pooled fractions into dialysis tubing and dialyze against 2.0 liters PBS at 4°C.

19. Change dialysate daily for 10 to 14 days until the presence of APAP in the dialysate is no longer detectable at 250 nm.

The process of dialysis is driven by differences in the concentration of solutes on either side of the membrane. A decrease in the solute concentration in the buffer solution is achieved by changing the dialysis buffer. Extensive dialysis is required at this step, not only to remove excess free APAP in the eluate, but also to remove APAP that was specifically bound to the antibody as it was displaced from the Sepharose column. Failure to dissociate this bound APAP will result in a blocked (inhibited) antibody that will not recognize adducts in subsequent immunoassays.

20. Store the affinity-purified antibody in 1.0-ml aliquots up to 3 months at −20°C.

Reequilibrate the column

21. Treat the affinity column following purification of the antibody as follows.

a. Wash the column overnight with 500 ml PBS.
b. Continue to wash the column with 0.04% sodium azide in PBS for 2 hr.
c. Store column with 0.04% azide at 4°C.

With proper care, the column is stable for at least 1 year.

REAGENTS AND SOLUTIONS

*Use Milli-Q purified water or equivalent in all recipes and protocol steps. For common stock solutions, see **APPENDIX 2A**; for suppliers, see **SUPPLIERS APPENDIX**.*

Blocking buffer

Suitable blocking buffers include the following:
3% to 5% (w/v) nonfat milk in Tris-buffered saline (TBS; see recipe)
3% (w/v) bovine serum albumin (BSA) in TBS
3% to 5% fish gelatin (e.g., Sigma) in TBS

With anti-APAP, nonfat milk in TBS was found to be the least effective blocking agent.

Carbonate/bicarbonate buffer, 50 mM, pH 9.6 (for ELISA)

Stock solutions:
0.2 M sodium carbonate (21.2 g anhydrous Na_2CO_3/liter)
0.2 M sodium bicarbonate (16.8 g $NaHCO_3$/liter)

Combine 16 ml of 0.2 M sodium carbonate and 34 ml of 0.2 M sodium bicarbonate and dilute to 200 ml. Verify that pH is 9.6; adjust if necessary with 1 N NaOH or 1 N NaCl.

Carbonate/bicarbonate buffer, 0.5 M, pH 9.0 (for antigen construction)

0.55 g Na_2CO_3 (anhydrous)
8.00 g $NaHCO_3$
Adjust volume to 200 ml
Verify that pH is 9.0; adjust with concentrated NaOH or HCl if necessary

4-Chloro-1-naphthol solution

Dissolve 5 mg of 4-chloro-1-naphthol in 8 ml methanol. Add 40 ml Tris-buffered saline (TBS; see recipe). Prepare fresh. Immediately before use, add 20 µl of 30% H_2O_2.

Coomassie brilliant blue solution

Dissolve 0.5 g Coomassie brilliant blue in 125 ml methanol. Adjust volume to 250 ml with double-distilled water, then add 17.5 ml glacial acetic acid.

Destaining solution (25% methanol/7% acetic acid)

Mix 250 ml methanol and 70 ml glacial acetic acid, then adjust volume to 1 liter with double-distilled water.

Developing buffer

100 mM 2-amino-2-methyl-1,3-propanediol
1 mM magnesium sulfate
1 mM levamisole
Adjust pH to 9.6 using concentrated HCl
Store up to 4 months at room temperature

Ethanolamine, 1 M, pH 9.0

Prepare a 1 M solution by diluting 6.1 ml of liquid ethanolamine (density = 1.01 g/ml; mol. wt. = 61.08) to 100 ml. Adjust pH with HCl.

Gill's hematoxylin, 2×

Mix the following in the order indicated:
730 ml double-distilled water
250 ml ethylene glycol
4.0 g anhydrous hematoxylin
0.4 g potassium iodate
70.4 g aluminum sulfate
20 ml glacial acetic acid
Stir 1 hr at room temperature

Recipe from Sheehan and Hrapchak (1980). It is advisable to purchase prepared staining solutions (e.g., from Polyscientific) as commercial preparations give more uniform results. Conditions for storage (usually room temperature) and expiration dates are provided on the label. Also note that some histology laboratories favor Mayer's hematoxylin over Gill's formulation, due to the blue staining of the nucleus and the contrast provided when used with other staining protocols.

PBST

Stock solutions:
0.2 M monobasic sodium phosphate (13.9 g $NaH_2PO_4 \cdot H_2O$/500 ml)
0.2 M dibasic sodium phosphate (26.8 g $Na_2HPO_4 \cdot 7H_2O$/500 ml)

Combine 19 ml of 0.2 M monobasic sodium phosphate and 81 ml of 0.2 M dibasic sodium phosphate. Dilute to 400 ml to obtain 50 mM sodium phosphate, pH 7.4. Add NaCl to 0.8% (w/v) and Tween 20 (polyethoxyethylene sorbitan) to 0.05% (w/v). Store up to 1 week at room temperature.

Phosphate-buffered saline (PBS)

20× stock solution:
80 g NaCl
2.0 g KCl
11.5 g $Na_2HPO_4 \cdot 7H_2O$

continued

2.0 g KH_2PO_4
H_2O to 500 ml
Store up to 1 month at room temperature

Prepare 1× working solution by diluting 1 part 20× stock with 19 parts H_2O. pH should be 7.0 to 7.2; adjust to desired pH if necessary with 1 N NaOH or 1 N HCl.

Pretreated dialysis tubing

Using gloves to avoid contamination, cut dialysis tubing to slightly longer than that needed to accommodate the volume to be dialyzed, so as to allow for an increase in volume during dialysis and for closure of both ends with dialysis clamps.

As dry dialysis tubing may be contaminated with heavy metals and sulfur-containing compounds, pretreat by placing in a beaker containing 100 mM sodium bicarbonate ($NaHCO_3$)/10 mM EDTA, pH 7.0 (Pohl, 1990). Bring the solution to a boil. Allow to cool and rinse well with distilled H_2O.

Poly-L-lysine coated slides

Prepare poly-L-lysine stock solution by dissolving 1.0 g poly-L-lysine in 100 ml double-distilled water. Store in 100-µl aliquots at –20°C. Clean glass slides with ethanol before coating. Dilute stock poly-L-lysine 1:10 in distilled water (0.1% final). Place 5 µl of diluted poly-L-lysine onto each slide and streak the solution evenly over the entire surface using another glass slide. Dry the coated slides at room temperature before use.

Saturated ammonium sulfate (SAS)

Dissolve 7.67 g $(NH_4)_2SO_4$ in 10 ml distilled water in small increments with stirring under mild heat, allowing each increment of the salt to dissolve before adding more. Prepare fresh.

Sodium acetate, 0.1 M, pH 4.0

Stock solutions:
0.2 M acetic acid (dilute 5.77 ml glacial acetic acid to 500 ml)
0.2 M sodium acetate (13.6 g $NaC_2H_3O_2 \cdot 3H_2O$/500 ml)

Combine 41 ml of 0.2 M acetic acid with 9 ml sodium acetate and dilute to 100 ml. Verify that pH is 4.0; adjust if necessary with 1 N HCl or 1 N NaOH.

Sodium borate, 0.1 M, pH 8.0/0.5 M NaCl

Stock solutions:
0.2 M boric acid (6.2 g/500 ml)
0.05 M borax (sodium tetraborate decahydrate; 9.52 g/500 ml)

Combine 50 ml of 0.2 M boric acid with 4.9 ml 0.05 M borax and dilute to 100 ml. Add 2.9 g NaCl. Verify that pH is 8.0; adjust if necessary with 1 N HCl or 1 N NaOH.

Sodium citrate, 50 mM, pH 4.0

Stock solutions:
0.1 M citric acid (2.10 g/100 ml)
0.1 M sodium citrate (2.94 g $Na_3C_6H_5O_7 \cdot H_2O$ in 100 ml)

Combine 33 ml of 0.1 M citric acid and 17 ml of 0.1 M sodium citrate and dilute to 100 ml. Verify that pH is 4.0; adjust if necessary with 1 N HCl or 1 N NaOH.

Transfer buffer

25 mM Tris·Cl, pH 8.1 to 8.3 (*APPENDIX 2A*)
192 mM glycine
20% (v/v) methanol
0.05% (w/v) sodium dodecyl sulfate (SDS)
Store up to 2 weeks at room temperature

continued

The acceptable pH range for transfer buffer is 8.1 to 8.3 and the pH should not be adjusted once the buffer has been prepared.

Tris-buffered saline (TBS)

25 to 50 mM Tris·Cl, pH 7.5 (*APPENDIX 2A*)
0.9% (w/v) NaCl (*APPENDIX 2A*)
Store up to 2 weeks at room temperature

COMMENTARY

Background Information

The biotransformation of many chemically dissimilar xenobiotics can generate highly reactive intermediates that interact with and covalently bind to proteins. Covalent binding of reactive intermediates to proteins has been associated with both the development of target-organ toxicity and immune-mediated hypersensitivity reactions (Cohen and Khairallah, 1997; Pumford and Halmes, 1997). The relationship between covalent binding and the development of target-organ toxicity was first proposed in the early 1970s (Brodie et al., 1971). Initial studies that relied on radioisotopic methods for detection of the protein adducts were limiting with respect to cost, availability, and more importantly, the ability to identify the target proteins. The development of immunochemical methods as an alternative approach (Bartolone et al., 1987, 1988; Roberts et al., 1987) has gained widespread acceptance and greatly facilitated the task of identifying the protein adducts (Cohen et al., 1997), and this has been especially noteworthy for recent research on APAP toxicity (Cohen and Khairallah, 1997).

The support protocols described in this unit outline specific methods for construction of the hapten conjugate and characterization of polyclonal antibodies to acetaminophen. For other xenobiotics, selection of coupling chemistry for antigen construction and affinity chromatography will require modification of the existing protocols to accommodate the chemistry of the compound under investigation. Moreover, an understanding of the bioactivation, metabolism, and detoxification pathways is essential to predict the interaction between the putative reactive intermediate and proteins for design of the appropriate immunogen. This is a critical and complicating factor for compounds that are converted to multiple intermediates, not all of which bind to proteins. As examples, selected methods used to generate antibodies against other xenobiotics are briefly summarized.

Acetaminophen (APAP)

In addition to the method described in this unit, antibodies to APAP have also been obtained by two independent approaches (Roberts et al., 1987; Matthews et al., 1996). Bioactivation of APAP to the reactive electrophile, *N*-acetyl-*p*-benzoquinoneimine (NAPQI; Miner and Kissinger, 1979; Corcoran et al., 1980; Dahlin et al., 1984) results in covalent binding primarily to protein sulfhydryl residues (Streeter et al., 1984; Hoffman et al., 1985). To compare detection of APAP specifically bound to cysteine residues versus total binding, carboxyl groups were introduced into the APAP molecule to generate either *N*-acetylcystein-*S*-yl-APAP or 4-acetamidobenzoic acid, respectively. Carbodiimide was then used to couple the carboxyl group of modified APAP to amino groups on KLH. The resulting antisera specifically detected the 3-(cystein-*S*-yl) linkage or arylacetamide epitopes of APAP protein adducts, respectively. Anti-3-(cystein-*S*-yl)-APAP was affinity purified using sulfhydryl cellulose derivatized with NAPQI and eluted from the affinity matrix with excess APAP (Pumford et al., 1990). Comparison of immunoblots probed with these antisera to those generated by the method described in this unit yield a similar pattern of protein adducts (Matthews et al., 1996; Bartolone et al., 1987, 1988) despite differences in the antigenic determinants recognized by each of the antibodies.

Halothane

Sera from halothane hepatitis patients exhibited immune reactivity with liver microsomes from humans and animals that had been exposed to halothane. Binding of the trifluoroacetyl chloride metabolites of halothane to hepatic proteins was implicated in this process when it was demonstrated that the sera also reacted with trifluoroacetylated rabbit serum albumin (TFA-RSA). TFA-RSA was synthesized from *S*-ethyl trifluorothiolacetate and RSA and used to immunize rabbits. Immunoblot analysis of microsomes from rats and humans treated with halothane using the resulting antibody indicated that the protein fractions that had reacted with the patients' serum antibodies also reacted with the TFA-RSA antibodies (Pohl, 1993).

Carboxylate drugs (clofibric acid, diflunisal, valproic acid, and zomepirac)

Most drugs containing a carboxylic acid functional group are conjugated to glucuronic acid to form reactive acyl glucuronide metabolites. Antibodies were raised against each of the carboxylate drugs by coupling to KLH with *N*-hydroxysulfosuccinimide (sulfo-NHS) and 1-cyclohexyl-3-(2-morpholinoethyl)carbodiimide metho-*p*-toluenesulfonate (Bailey and Dickinson, 1996). Inclusion of sulfo-NHS improves the efficiency of coupling and forms more stable intermediates in aqueous environments at acidic and neutral pH. Antisera were used in immunoblotting protocols without prior affinity purification.

Diclofenac

Binding of diclofenac to proteins is believed to occur via an acyl glucuronide intermediate. Antisera against diclofenac-protein adducts have been obtained by several laboratories, all of which used a two-step reaction involving the carbodiimide EDC (1-ethyl-3-[3-dimethyaminopropyl]carbodiimide hydrochloride) as a cross-linking agent to conjugate diclofenac to KLH (Pumford et al., 1993; Kretz-Rommel and Boelsterli, 1994; Gil et al., 1995; Wade et al., 1997). Diclofenac antisera were used in immunoblot applications without purification. Despite the use of the same coupling chemistry, differences were reported between laboratories with respect to the major protein adducts detected.

3-methylindole (3-MI)

Metabolism of 3-MI produces a reactive electrophilic intermediate, 3-methyleneindolenine, which alkylates cysteine residues on proteins (Ruangyuttikarn et al., 1992). Antigen was constructed by base-catalyzed dehydration of indole-3-carbinol to form 3-methyleneindolenine. Interaction with the carrier protein metallothionein proceeded by a Michael-type thiolate addition. The antiserum demonstrated high selectivity for the thioether adducts of 3-methyleneindolenine and was used in ELISA without further purification for comparison of organ and species reactivity (Kaster and Yost, 1997).

Sulfamethoxazole (SMX)

N-hydroxylation of SMX yields an hydroxylamine intermediate which can be acetylated or oxidized to nitroso and nitro metabolites. The nitroso metabolite is the putative species involved in covalent binding. Antigen was constructed by diazotization of SMX followed by conjugation to KLH at neutral pH. Antiserum was used in immunoblotting without further purification and detected protein adducts generated in vitro but not in vivo (Cribb et al., 1996).

Trichloroethylene (TRI)

Metabolism of TRI is expected to yield dichloroacetyl chloride as one of several reactive intermediates. Antibodies were raised against dichloroacetylated protein adducts by reacting dichloroacetic anhydride directly with the protein carrier KLH (Halmes et al., 1996). Antiserum was purified on an affinity column that had been constructed by activation of dichloroacetic acid with EDC, followed by coupling to a suspension of diaminodipropylamine immobilized agarose. Antibodies were eluted from the column at low pH (0.2 M glycine, pH 2.6) and immediately neutralized with 1 M Tris·Cl, pH 8.0.

Critical Parameters and Troubleshooting

Immunoblotting

Success with the technique is dependent on the optimization of three basic components: protein transfer, antibody binding, and detection method. The objective of optimal transfer is to obtain complete and quantitative migration of proteins out of the gel and onto the membrane. Factors that influence protein mobility and affect binding to the membrane include (1) buffer composition, (2) the presence or absence of methanol and SDS, (3) the properties of the gel itself (i.e., the percentage cross-linking and thickness), and (4) the membrane.

The buffer system should be one that has low conductivity but maintains buffering capacity. Tris-glycine buffer, pH 8.1 to 8.3, containing 10% to 20% methanol (Towbin et al., 1979) is perhaps the most commonly used for transfer of most proteins to nitrocellulose or PVDF membranes. However, since the net charge on a protein molecule determines its migration, proteins with pI equivalent to the pH of the buffer will not migrate. Transfer buffers of higher or lower pH may be required for such proteins. Different buffer systems have also been developed to increase the transfer efficiency of high-molecular-weight proteins (Bolt and Mahoney, 1997).

The inclusion of methanol and/or SDS in the transfer buffer can influence both protein transfer and binding steps. Methanol minimizes swelling of the gel during electroblotting and enhances the hydrophobic interactions be-

tween the proteins and membrane (Towbin and Gordon, 1984). Methanol is especially important for protein binding to nitrocellulose, which is less hydrophobic than PVDF. However, for proteins resolved by SDS-PAGE, methanol can strip some of the SDS from the protein, especially those of higher molecular weight (>100 kDa), resulting in protein precipitation within the gel. Addition of a low concentration of SDS (0.01% to 0.1%) to the transfer buffer can improve the efficiency of transfer, but this may vary with the properties of the membrane. PVDF will tolerate higher concentrations of SDS, whereas the detergent can reduce protein binding to nitrocellulose.

Successful transfer of proteins is also dependent on gel thickness and the percentage acrylamide and cross-linker used. Lower percentages result in more rapid and efficient transfer. For most SDS-PAGE applications, a 10% resolving gel containing 2.7% to 3.4% cross-linker with 0.5 to 0.75 mm thickness will be adequate.

Membranes can bind protein noncovalently (nitrocellulose, nylon, PVDF) or covalently (activated papers). Nitrocellulose and PVDF are the most frequently used. PVDF is more hydrophobic than nitrocellulose and offers several advantages including its ease of handling, tolerance to SDS, lower susceptibility to protein loss by desorption during the subsequent incubation steps for immunodetection, and lower background staining with ^{125}I. However, the protein-binding capacity of PVDF is less than that of nitrocellulose (100 μg/cm^2) and more stringent blocking conditions are required prior to probing with antibody.

The efficiency of transfer can be determined by staining the membrane for total protein prior to immunodetection. Ponceau S is both rapid and reversible but not very sensitive (2 μg detection limit; Harlow and Lane, 1988). India ink staining is sensitive (80 ng), permanent, and generally does not interfere with the antigen-antibody reaction (Glenney, 1986). India ink cannot be used with enzyme-based detection methods because it does not provide sufficient background contrast to the colored reaction products.

It is important to keep in mind that each antigen-antibody interaction is unique, and that much success associated with immunoassays is derived from the performance of preliminary experiments aimed at optimizing conditions. The problems that may be encountered in immunoblotting can be quite extensive, and a comprehensive discussion of them is not possible here. Some of these have been addressed as they arise at specific steps in the protocol. The detection sensitivity of immunoblotting is determined by the antibody specificity. Thus, two types of problems generally occur: (1) little or no binding of the antibody to the antigen, and (2) high background (nonspecific) staining. Poor antibody-antigen interactions may be due to low titer of antibody, and this may be evidenced by nonspecific staining of multiple protein bands. Prescreening of immune serum or affinity-purified antibody against an antibody standard by ELISA or immunoblot test strips, respectively, should permit selection of the best available batches of antibody or serum to eliminate this problem. In some cases, binding to specific target antigens will be diminished if the antibody is adsorbed by one or more components of the blocking solution. Comparison of different blocking solutions will identify the problem. Alternatively, the antibody may not recognize the antigen in its denatured form following SDS-PAGE. This can be verified with dot blots using native and denatured cell extracts and can sometimes be overcome by increasing the blocking time to permit renaturation of the proteins. Transfer conditions also may contribute to poor antigen-antibody reactions. Failure to maintain good contact between the membrane and gel during electroblotting, or precipitation of proteins in the gel as a result of high methanol concentrations, result in poor transfer and thus lowers the concentration of antigen present on the membrane. In addition, extended blotting times may result in protein loss as a result of migration completely through the membrane. Staining the gel and/or membrane with a protein stain following transfer will determine if these are contributing factors.

Two types of background staining problems are often encountered: (1) a general diffuse staining, or (2) nondiffuse, apparently specific staining of nonantigen proteins. Diffuse staining may result from insufficient blocking or nonspecific interaction of the primary or secondary antibodies with the blocking buffer. This is easily remedied by increasing blocking times or changing the blocking buffer. In some cases greater dilution of the primary or secondary antibodies may also alleviate the problem. Troubleshooting experiments in which the incubation with the primary antibody is omitted or in which different dilutions of the secondary antibody are tested in the presence of a fixed concentration of primary antibody will determine if the secondary antibody alone is contributing to the background-staining problem. Al-

ternatively, the primary antibody may be contributing to the nonspecific background. This is often observed with whole serum of low titer where the relative titers of specific and nonimmune IgG determine the signal-to-noise ratio. In such instances, affinity purification of the antibody may significantly reduce the nonspecific staining. Nondiffuse background appears as distinctly stained protein bands that do not contain the specific antigen of interest. This is most likely attributable to antibody cross-reactivity with the nonantigen. Thus, it is important to include proteins from untreated tissue or cells (negative control) along with tissues or cells known to contain covalently bound xenobiotic adducts (positive control). Any immunostaining of proteins in the negative control samples must be considered as background. Affinity purification of the antibody may also reduce this type of background binding.

Immunohistochemistry

A number of factors contribute to the success of immunohistochemical techniques, but common and most critical to all is the preservation of tissue ultrastructure without destruction of antigenic determinants. This, in turn, is dependent on the choice of methods for tissue preparation, fixation, embedding and dehydration.

During tissue preparation, tissues undergo rapid decomposition once removed from the animal. To minimize tissue/cell damage and decrease metabolic activity, thereby preserving normal ultrastructure, fixation of samples should occur as rapidly as possible, usually within 15 min following excision. The volume of the tissue sample is also critically important to ensure rapid fixation. Tissue blocks between 1 and 10 mm in at least one dimension are recommended to facilitate penetration of the fixative.

Optimal fixation should (1) minimize changes to cellular morphology, (2) result in minimal denaturation of the antigen, (3) retain the antigen in its normal pattern of cellular distribution and localization, and (4) minimize diffusion of endogenous soluble components but allow penetration of the antibody for reaction with antigen. Different tissues may fix at different rates depending on their physical characteristics. Fixation methods that work well for one tissue may not be directly transferable to another. Overfixation may cause the masking or destruction of antigens whereas underfixation may result in incomplete immobilization.

Tissues can be fixed by chemical or physical agents. Organic-solvent or precipitant fixatives, such as 100% methanol or acetone, typically require immersion of the specimen in the solvent for 15 min at −20°C and subsequent washing in buffer to return the pH to neutrality. Such fixatives, although relatively mild, are more susceptible to diffusion artifacts. Cross-linking fixatives (e.g., formaldehyde and glutaraldehyde) are excellent for preserving ultrastructure but frequently destroy antigenicity, although this may be dependent on the concentration and the antigen itself. Microwave fixation has become increasingly popular for its ability to retain both ultrastructure and antigenicity (Moran et al., 1988; Login and Dvorak, 1988, 1994). It has also been used to unmask antigens that previously had no or low immunoreactivity following conventional aldehyde fixation (Login and Dvorak, 1994). Microwave irradiation of tissues at 40° to 55°C for <50 sec is commonly used. The specimen may be immersed in either saline or a buffered aldehyde solution. However, the concentration of aldehyde is very critical for retention of morphology and antigenicity. Modified Karnovsky's fixative (0.05% v/v glutaraldehyde/2% v/v formaldehyde/0.1 M sodium cacodylate, pH 7.4/0.025% v/v calcium chloride) has been used successfully (Login and Dvorak, 1988).

Dehydration in graded solvents (i.e., ethanol) is a necessary step prior to embedding and sectioning the tissue, despite its potential for causing structural damage. Embedding medium (i.e., paraffin) facilitates the handling and sectioning of the tissue sample by providing a uniform support to stabilize it against deformation generated by the pressure of the cutting knife blade. Tissue sections of ≤5 μm in thickness are difficult to obtain with unembedded tissue. Some antibody-antigen reactions may not be compatible with fixation and embedding procedures, and in such cases frozen or cryostat sections would offer a suitable alternative.

High-resolution immmunohistochemical detection of covalent adducts generally requires optimization of both the tissue fixation and immunodetection methods. For a given antibody-antigen reaction, different fixation methods should be compared to identify a method that optimizes the preservation of both morphology and antigenicity. Also, inadequate rinsing of tissue sections or failure to restore the pH to neutral following fixation can both contribute to poor results. Reagent quality is also important. Formaldehyde-based fixatives

should be prepared from depolymerized paraformaldehyde, since commercial formaldehyde contains stabilizers and methanol that may interfere with tissue fixation (Osborn, 1994). The pH of fixation should be maintained at 7.4, since the process occurs more slowly at lower pH and may lead to artifacts.

As with other immunochemical procedures, immunohistochemistry is subject to difficulties related to nonspecific staining or high background staining. These can result from inappropriate dilutions of the primary or secondary antibodies, residual peroxidase or alkaline phosphatase activity in the tissue section, poor washing of the sections, and use of inappropriate substrate concentrations during the detection step. Quenching of residual peroxidase activity is described in step 8 of Basic Protocol 2. Problems may arise if the concentration of hydrogen peroxide used in this step falls outside of its optimal range (0.003% to 0.01% is recommended). This can be further complicated by the instability of hydrogen peroxide during storage, which may make determination of its actual concentration difficult. Residual alkaline phosphatase activity in tissue sections may be inhibited by 1 mM levamisole. This inhibitor is ineffective against the intestinal form of the enzyme, which is conjugated to the secondary antibody as the detection enzyme (Tijssen, 1985).

Proper interpretation of immunohistochemical data requires concomitant analysis of the appropriate controls. Tissue sections processed for immunohistochemistry should, where possible, include both a positive (antigen present) and negative (antigen absent) control on each slide. For antibodies raised against drug-protein adducts, this involves using tissues from drug- and vehicle-treated animals, respectively. Comparison of replicate slides should include (1) the standard incubation with primary and secondary antibodies, (2) preadsorption of primary antibody with purified drug-protein adduct or the drug itself followed by the standard incubation with the preadsorbed primary and secondary antibodies, (3) replacement of the primary antibody with preimmune serum followed by incubation with secondary antibody, and (4) incubation in the presence of secondary antibody alone. Replicates 2, 3, and 4 provide the negative controls necessary to evaluate specificity of the primary antibody and to detect any nonspecific binding.

Preparation of APAP antigen

Haptens are small compounds that are not immunogenic themselves, but which, when coupled to larger protein molecules, can elicit production of antibodies. Because of their small size, haptens can provide the epitopes for binding to recognition sites on the B cell surface, but fail to provide appropriate sites for binding to class II proteins and T cell receptors (Harlow and Lane, 1988). Conjugation of the hapten with a protein carrier provides these other important sites. All three interactions are necessary to elicit the immune response. A brief summary of factors to consider in the selection of methods for hapten conjugation is presented, but for more comprehensive information the reader is referred to other texts (Tijssen, 1985; Harlow and Lane, 1988).

Bovine serum albumin (BSA), keyhole limpet hemocyanin (KLH), and ovalbumin are the most commonly used carrier proteins (Harlow and Lane, 1988); however, the choice of coupling chemistry can vary with each hapten and the reactive sites on the protein to be modified. The latter include carboxyl, α- and ε-amino, imidazole, phenolic, and sulfhydryl groups. The reaction chemistries of protein-modifying reagents can be broadly classified into three groups (Tijssen, 1985). The first group, acylating reactions, which activate the carboxyl group on haptens for conjugation with amino groups on proteins, are the most commonly used. Haptens that lack the carboxyl moiety may require the introduction of such a group. Examples of acylating reagents include acetic or mixed anhydride and *N*-hydroxysuccinimide esters. The second group, alkylating reactions, can be used to modify sulfhydryl or amino groups; maleimides are suitable reagents for this reaction. Finally, electrophilic agents, such as diazonium salts, are useful for the modification of amino or hydroxyl groups. Direct conjugation of hydroxyl groups is generally not possible. Redox reactions are also not used for conjugation.

The use of a spacer or linker molecule between the hapten and carrier protein may be advantageous. Antibodies generated against a hapten coupled to a spacer molecule are generally directed toward the portion of the hapten farthest removed from the protein linkage, thereby improving specificity and recognition of the hapten (Tijssen, 1985). However, if a spacer molecule is used, appropriate controls are needed to determine that the linker molecule itself has not elicited antibody production. Linkers may also provide a means to select and

optimize the coupling chemistry if specific reactive groups on the hapten are either absent or to be maintained intact, or if steric hindrance must be avoided.

Optimization of the number of hapten groups per carrier-protein molecule is important for immunization. Optimal coupling ratios have been reported to range between 1 mole hapten per 50 amino acid residues (Harlow and Lane, 1988) and 10 to 20 moles hapten per mole protein (Tijssen, 1985). The reader is also cautioned against conjugating too many hapten molecules per carrier, as this may lead to immune tolerance.

Immunization

Since a number of factors may contribute to antibody variability, the following guidelines are recommended to assure consistency and reproducibility of the antibody in various immunoassays. It is important to immunize more than one animal, since not all animals will respond equally to the hapten conjugate. Serum collected from each animal should be screened by ELISA to determine titer. For anti-APAP, the serum should be able to be diluted up to 200-fold in the ELISA in order to give specificity and low background in immunoblot and immunohistochemistry. This may vary for other hapten conjugates. Once a suitable antibody has been produced, aliquots should be retained as "standards" for comparison in ELISA and immunoblots with subsequent batches of serum. It is necessary to record and label serum with bleed dates and rabbit ID. The greater the similarity between antibodies from different rabbits, the greater confidence one will have in the results.

ELISA

Immobilization of the antigen (or antibody) to the plastic surface occurs by passive adsorption. Binding is noncovalent and is generally attributed to hydrophobic interactions between nonpolar groups of the protein and the plastic support (Engvall, 1980). Important variables for protein adsorption are concentration, ratio of surface area to volume, binding capacity of the support, and time and temperature of the reaction. For most soluble proteins, 100 µl of a 1 to 10 µg/ml solution is recommended for coating the wells, with the optimal concentration determined by the binding capacity of the solid support. For example, PVC has a binding capacity of 100 ng/well (Harlow and Lane, 1988). At higher protein concentrations, leaching of antigen may occur or result in multiple protein-protein interactions (Tijssen, 1985).

Competitive ELISA assays are based on bimolecular interaction similar to that described for affinity chromatography (see below). The molecules may either be identical or different, but possess structural features similar to the epitope on the immobilized antigen. When present in solution with the antibody, a competition is established between the molecule and the bound antigen for binding to the antibody. Decreased antibody binding to the immobilized antigen results in decreased binding of the enzyme-conjugated secondary antibody and is reflected by a decrease in absorbance. The concentration of the test molecule is varied while those of the immobilized antigen and the antibody are constant. The sensitivity of the assay is dependent on the concentration of antibody as being rate-limiting but within the linear portion of the antibody dilution curve.

Affinity column

Important factors to consider for the purification of xenobiotic antibodies are choice of ligand, chromatographic support, and methods used to desorb the purified antibody from the matrix in an active form. Ligands should possess chemically modifiable groups for attachment to the support and once coupled should retain specific binding affinity for the antibody to be purified. Selection of the type of chromatographic matrix is dependent on the most suitable coupling chemistry between the ligand and support. Also important are the length and type of spacer arm on the support. The spacer arm should increase the availability of the ligand binding site to the antibody. For example, when ligands of low molecular weight are used to purify samples of higher molecular weight (as described for APAP and its corresponding antibody), a long spacer arm is preferred, to limit steric hindrance and promote accessibility. Matrices that are "activated" (e.g., epoxy-activated Sepharose) are ready for use in that they require no further modification prior to ligand coupling. Desorption of the antibody from the matrix in an active form is most easily accomplished by increasing the concentration of ligand in the elution buffer relative to that bound to the matrix. Displacement results from a concentration-dependent competition between the eluant and the immobilized ligand for the bound antibody. This method was used in the purification of the APAP antibody in Support Protocol 7. Alternatively, changes in ionic

strength or pH of the elution buffer may also release bound antibody.

The amount of chromatographic matrix to use is dependent on its binding capacity; however, in general, it is recommended that two to three times the gel binding capacity be used (Ostrove, 1990). Accordingly, the concentration of ligand should be in excess of the total binding capacity of the matrix. Following coupling, nonspecific interaction arising from unreacted sites can be significantly reduced by the addition of a blocking solution at a concentration in excess of the reactive sites on the support. Choice of the blocking agent is dependent on the chemistry of the matrix. For epoxy-activated Sepharose, 1 M ethanolamine is recommended.

As noted for anti-APAP antibody purification, the reaction time depends on the stabilities of the epoxy-activated Sepharose and ligand at the pH and temperature used for the coupling reaction. At the higher pH range, an increase in hydrolysis of the epoxide groups occurs. Higher temperatures decrease the time required for coupling. Thus both the coupling chemistry and efficiency need to be considered in defining optimal conditions.

Affinity purification

Since a number of factors may contribute to antibody variability, the following guidelines are recommended to assure consistency and reproducibility of the antibody in various immunoassays. Using an ELISA, pretest new batches of serum against standard serum prior to affinity purification. Affinity purify those batches that show the best activity in the ELISA relative to this standard. This will avoid wasting time purifying batches of serum that have little activity. Screen affinity-purified antibody using immunoblot test strips containing 20 to 30 µg of protein known to contain the adduct of interest. Control protein lacking the adduct should be used for comparison. For anti-APAP antibody, the authors use liver cytosol obtained from APAP-treated and control animals or cells. Probe the immunoblot with two or more dilutions of the antibody and detect with secondary antibody (see Basic Protocol 1). Compare results to those obtained with a previous batch of affinity-purified antibody.

The goal here is to identify a batch and dilution that gives minimal reactivity with the control protein, but which exhibits significant reactivity with the test (adducted) protein. If, as is the case with APAP, several proteins of different molecular weights are targeted, it is important that the selected antibody batch consistently detect all targets.

Anticipated Results

Appropriate design and construction of the antigen should yield antibodies of good titer, demonstrating low background and selectivity in immunoassays (ELISA and immunoblot) and immunohistochemical staining. The same antigen preparation may result in antisera of different titers as a function of the individual host animal response. Thus it is advised that at least two rabbits be immunized simultaneously for evaluation of the antigen preparation. Representative results for competitive ELISA, immunoblots, and immunohistochemistry may be found in Bartolone et al. (1988, 1989), and Emeigh Hart et al. (1995), respectively.

Time Considerations

Construction of antigen (Support Protocol 1): Three consecutive days are needed, with time allocations for the following steps: diazotization of PABA and derivatization with APAP, 2 to 4 hr; lyophilization, 24 to 36 hr; conjugation to KLH, 5 to 6 hr; dialysis of the antigen, 24 to 36 hr.

Immunization and serum collection (Support Protocol 2): Blood collection and processing of serum can be completed within 90 min; immunization requires ~30 min.

Preparation of NAPQI-protein adducts (Support Protocol 3): About 1 hr is necessary for the synthesis of NAPQI and reaction with proteins. Dialysis requires 12 to 16 hr. Approximately 2 to 3 hr is needed to determine the amount of [^{3}H]APAP associated with the protein adduct depending on the rapidity of solubilization.

ELISA (Support Protocols 4 and 5): Dilution of protein adducts and coating of microtiter plates can be completed within 1 hr; incubation after coating can either be done for either 1 hr at 37°C or overnight at 4°C depending on convenience. The remaining steps will require ~6 hr.

Affinity column preparation (Support Protocol 6): The entire procedure is completed within 24 hr with the following time allocations: matrix preparation, ~90 min; coupling, 12 to 16 hr (overnight); washing, 90 min; blocking, 4 hr; washing and equilibration, 1 hr; and packing the column, 1 hr.

Affinity purification of serum (Support Protocol 7): Two consecutive days are needed. Ammonium sulfate precipitation of serum requires ~2 hr followed by dialysis overnight.

Affinity purification can be completed within 3 to 4 hr, also followed by overnight dialysis.

Immunoblotting (Basic Protocol 1): Two days are required. SDS-PAGE and transfer are completed on the first day, requiring 6 to 8 hr for full-size gels. After the membrane is dried, subsequent incubations with antibodies and washes can be done in ~6 hr. Times for detection will vary according to the method selected; 15 to 30 min is needed for enzyme-linked detection; for ^{125}I, film exposures can range from 24 to 40 hr.

Immunohistochemistry (Basic Protocol 2): Three days are needed, two of which should be consecutive. Tissue preparation and fixation and dehydration and embedding can be completed on day 1. Subsequent steps of sectioning, rehydration and deparaffinization, protease digestion, reequilibration, and blocking each require ~1 hr. Incubation with primary antibody is for 18 to 21 hr (overnight). On day 3, washes and incubation with secondary antibody require ~1 hr and detection and mounting can be done in 90 min.

Literature Cited

Bailey, M.J. and Dickinson, R.G. 1996. Chemical and immunochemical comparison of protein adduct formation of four carboxylate drugs in rat liver and plasma. *Chem. Res. Toxicol.* 9:659-666.

Bartolone, J.B., Sparks, K., Cohen, S.D., and Khairallah, E.A. 1987. Immunochemical detection of acetaminophen-bound liver proteins. *Biochem. Pharmacol.* 36:1193-1196.

Bartolone, J.B., Birge, R.B., Sparks, K., Cohen, S.D., and Khairallah, E.A. 1988. Immunochemical analysis of acetaminophen covalent binding to proteins. *Biochem. Pharmacol.* 37:4763-4774.

Bartolone, J.B., Beierschmitt, W.P., Birge, R.B., Emeigh Hart, S.G., Wyand, S., Cohen, S.D., and Khairallah, E.A. 1989. Selective acetaminophen metabolite binding to hepatic and extrahepatic proteins: An in vivo and in vitro analysis. *Toxicol. Appl. Pharmacol.* 99:240-249.

Beierschmitt, W.P., Brady, J.T., Bartolone, J.B., Wyand, D.S., Khairallah, E.A., and Cohen, S.D. 1989. Selective protein arylation and the age dependency of acetaminophen hepatotoxicity in mice. *Toxicol. Appl. Pharmacol.* 98:517-529.

Bolt, M.W. and Mahoney, P.A. 1997. High-efficiency blotting of proteins of diverse sizes following sodium dodecyl sulfate-polyacrylamide gel electrophoresis. *Anal. Biochem*. 247:185-192.

Brodie, B.B., Reid, W.D., Cho, A.K., Sipes, G., Krishna, G., and Gillette, J.R. 1971. Possible mechanism of liver necrosis caused by aromatic organic compounds. *Proc. Natl. Acad. Sci. U.S.A.* 68:160-164.

Cohen, S.D., Pumford, N.R., Khairallah, E.A., Boekelheide, K., Pohl, L.R., and Amouzadeh, H.R. 1997. Selective protein covalent binding and target organ toxicity. *Toxicol. Appl. Pharmacol.* 143:1-12.

Cohen, S.D. and Khairallah, E.A.. 1997. Selective protein arylation and acetaminophen-induced hepatotoxicity. *Drug Metab. Rev.* 29:59-77.

Corcoran, G.B., Mitchell, J.R., Vaishnav, Y.N., and Horning, E.C. 1980. Evidence that acetaminophen and *N*-hydroxyacetaminophen form a common arylating intermediate, *N*-acetyl-*p*-benzoquinone imine. *Mol. Pharmacol.* 18:536-542.

Cribb, A.E., Nuss, C.E. Alberts, D.W., Lamphere, D.B., Grant, D.M., Grossman, S.J., and Spielberg, S.P. 1996. Covalent binding of sulfamethoxazole reactive metabolites to human and rat liver subcellular fractions assessed by immunochemical detection. *Chem. Res. Toxicol.* 9:500-507.

Dahlin, D.C. and Nelson, S.D. 1982. Synthesis, decomposition, kinetics and preliminary toxicological studies of pure *N*-acetyl-*p*-benzoquinoneimine, a proposed toxic metabolite of acetaminophen. *J. Med. Chem.* 25:885-886.

Dahlin, D.C., Miwa, G.T., Lu, A.Y.H., and Nelson, S.D. 1984. *N*-acetyl-*p*-benzoquinoneimine: A cytochrome P450–mediated oxidation product of acetaminophen. *Proc. Natl. Acad. Sci. U.S.A.* 81:1327-1333.

Donovan, J. and Brown, P. 1995. Blood collection. *In* Current Protocols in Immunology (J.E. Coligan, A.M. Kruisbeek, D.H. Margulies, E.M. Shevach, and W. Strober, eds.) pp. 1.7.1-1.7.8. John Wiley & Sons, New York.

Emeigh Hart, S.G., Cartun, R.W., Wyand, D.S., Khairallah, E.A., and Cohen, S.D. 1995. Immunohistochemical localization of acetaminophen in target tissues of the CD-1 mouse: Correspondence of covalent binding with toxicity. *Fund. Appl. Toxicol.* 24:260-274.

Engvall, E. 1980. Enzyme immunoassay ELISA and EMIT. *In* Methods in Enzymology, Vol. 70 (H. Van Vunakis and J.J. Lagone, eds.) pp. 419-439. Academic Press, New York.

Gil, M.L., Ramirez. M.M., Terencio, M.C., and Castell, J.V. 1995. Immunochemical detection of protein adducts in cultured human hepatocytes exposed to diclofenac. *Biochem. Biophys. Acta* 1272:140-146.

Glenney, J. 1986. Antibody probing of western blots which have been stained with India ink. *Anal. Biochem.* 156:315-319.

Halmes, N.C., McMillan, D.C., Oatis, J.E., and Pumford, N.R. 1996. Immunochemical detection of protein adducts in mice treated with trichloroethylene. *Chem. Res. Toxicol.* 9:451-456.

Harlow, E. and Lane, D. 1988. Antibodies: A Laboratory Manual. Cold Spring Harbor Laboratory Press, Cold Spring Harbor, N.Y.

Hoefer. 1994. Protein Electrophoresis Applications Guide. Hoefer Scientific Instruments, San Francisco, Calif.

Hoffman, K-J., Streeter, A.J., Axworthy, D.B., and Baillie, T.A. 1985. Identification of the major covalent adduct formed in vitro and in vivo between acetaminophen and mouse liver proteins. *Mol. Pharmacol.* 27:566-573.

Kaster, J. and Yost, G.S. 1997. Production and characterization of specific antibodies: Utilization to predict organ- and species-selective pneumotoxicity of 3-methylindole. *Toxicol. Appl. Pharmacol.* 143:324-337.

Kretz-Rommel, A. and Boelsterli, U.A. 1994. Selective protein adducts to membrane proteins in cultured rat hepatocytes exposed to diclofenac: Radiochemical and immunochemical analysis. *Mol. Pharmacol.* 45:237-244.

Login, G.R. and Dvorak, A.M. 1988. Microwave fixation provides excellent preservation of tissue, cells and antigens for light and electron microscopy. *Histochem. J.* 20:373-387.

Login, G.R. and Dvorak, A.M. 1994. Methods of microwave fixation for microscopy: A review of research and clinical applications, 1970-1992. *Prog. Histochem. Cytochem.* 27:1-127.

Matthews, A.M., Roberts, D.W., Hinson, J.A., and Pumford, N.R. 1996. Acetaminophen-induced hepatotoxicity: Analysis of total covalent binding vs. specific binding to cysteine. *Drug Metab. Disposition* 24:1192-1196.

Miner, D.J. and Kissinger, P.T. 1979. Evidence for the involvement of *N*-acetyl-*p*-benzoquinoneimine in acetaminophen metabolism. *Biochem. Pharmacol.* 28:3285-3290.

Moran, R.A., Nelson, F., Jagirdar, J., and Paronetto, F. 1988. Application of microwave irradiation to immunohistochemistry: Preservation of antigens of the extracellular matrix. *Stain Technol.* 63:263-269.

Nisonoff, A. 1967. Coupling of diazonium compounds to proteins. *In* Methods in Immunology and Immunochemistry, Vol. 1 (C.A. Williams and M.W. Chase, eds.) pp. 120-126. Academic Press, New York.

Osborn, M. 1994. Immunofluorescence microscopy of cultured cells. *In* Cell Biology: A Laboratory Handbook, Vol. 2 (J.E. Celis, ed.) pp. 347-354. Academic Press, New York.

Osborn, M. and Isenberg, S. 1994. Immunocytochemistry of frozen and of paraffin tissue sections. *In* Cell Biology: A Laboratory Handbook, Vol. 2 (J.E. Celis, ed.) pp. 361-367. Academic Press, New York.

Ostrove, S. 1990. Affinity chromatography: General methods. *In* Methods in Enzymology, Vol. 182 (M.P. Deutscher, ed.) pp. 357-371. Academic Press, New York.

Pohl, T. 1990. Concentration of proteins and removal of solutes. *In* Methods in Enzymology, Vol. 182 (M.P. Deutscher, ed.) pp. 68-83. Academic Press, New York.

Pohl, L.R. 1993. An immunochemical approach of identifying and characterizing protein targets of toxic reactive metabolites. *Chem. Res. Toxicol.* 6:786-793.

Promega. 1993. Protein Guide: Tips and Techniques, part number AP003. Promega Corporation, Madison, Wis.

Pumford, N.R. and Halmes, N.C. 1997. Protein targets of xenobiotic reactive intermediates. *Annu. Rev. Pharmacol. Toxicol.* 37:91-117.

Pumford, N.R., Hinson, J.A., Benson, R.W., and Roberts, D.W. 1990. Immunoblot analysis of protein containing 3-(cystein-*S*-yl)acetaminophen adducts in serum and subcellular liver fractions from acetaminophen-treated mice. *Toxicol. Appl. Pharmacol.* 104:521-532.

Pumford, N.R., Myers, T.G., Davila, J.C., Highet, R.J., and Pohl, L.R. 1993. Immunochemical detection of liver protein adducts of the nonsteroidal antiinflammatory drug diclofenac. *Chem. Res. Toxicol.* 6:147-150.

Roberts, D.W., Pumford, N.R., Potter, D.W., Benson, R.W., and Hinson, J.A. 1987. A sensitive immunochemical assay for acetaminophen-protein adducts. *J. Pharmacol. Exp. Ther.* 241:527-533.

Ruangyuttikarn, W., Skiles, G.L., and Yost, G.S. 1992. Identification of a cysteinyl adduct of oxidized 3-methylindole from goat lung and human liver microsomal proteins. *Chem. Res. Toxicol.* 5:713-719.

Sheehan, D.C. and Hrapchak, B. 1980. Theory and Practice of Histotechnology. Batelle Press, Columbus, Ohio.

Streeter, A.J., Dahlin, D.C., Nelson, S.D., and Baillie, T.A. 1984. The covalent binding of acetaminophen to protein: Evidence for cysteine residues as major sites of arylation in vitro. *Chem. Biol. Interactions* 48:349-366.

Taleporos, P. and Ornstein, L. 1976. Preparation of tissue for light microscopic study with labeled antibody. *In* Methods in Immunology and Immunochemistry, Vol. V (C.A.Williams and M.W. Chase, eds.) pp. 375-424. Academic Press, New York.

Tijssen, P. 1985. Practice and theory of enzyme immunoassays. *In* Laboratory Techniques in Biochemistry and Molecular Biology, Vol. 15 (R.H. Burdon and P.H. van Knippenberg, eds.) pp. 279-384 and 449-504. Elsevier/North Holland, Amsterdam.

Towbin, H. and Gordon, J. 1984. Immunoblotting and dot immunobinding: Current status and outlook. *J. Immunol. Methods* 72:313-340.

Towbin, H., Staehelin, T., and Gordon, J. 1979. Electrophoretic transfer of proteins from polyacrylamide gels to nitrocellulose sheets: Procedure and some applications. *Proc. Natl. Acad. Sci. U.S.A.* 76:4350-4354.

Wade, L.T., Kenna, J.G., and Caldwell, J. 1997. Immunochemical identification of mouse hepatic protein adducts derived from the nonsteroidal anti-inflammatory drugs diclofenac, sulindac, and ibuprofen. *Chem. Res. Toxicol.* 10:546-555.

Contributed by Mary K. Bruno and
Steven D. Cohen
University of Connecticut
Storrs, Connecticut

Measurement of Lipid Peroxidation

There is currently considerable interest in what is termed "oxidative stress," or the oxidation of biological macromolecules, with an emphasis on its involvement in various diseases and toxicities and on methods to limit either its occurrence or effects. This unit describes traditional methods to measure the extent or rate of lipid peroxidation—assays for conjugated dienes (see Basic Protocol 1), lipid hydroperoxides (see Basic Protocol 2), the polyunsaturated lipid breakdown product malondialdehyde (see Basic Protocol 3), and hemolysis (see Basic Protocol 4)—along with some discussion of alternative methods that have been published (see Background Information).

ASSAY FOR CONJUGATED DIENES

BASIC PROTOCOL 1

Evidence for lipid peroxidation, or the rate of initiation of the process, can be determined by assays for the formation of conjugated dienes, which arise from the rearrangement of double bonds on the polyunsaturated fatty acid (PUFA) side chain (Rao and Recknagel, 1968; Buege and Aust, 1978; Pryor and Castle, 1984; Recknagel and Glende, 1984). These conjugated dienes exhibit an absorbance maximum at 233 nm. However, partially peroxidized lipids, biological materials, and extracted contaminants tend to have overlapping absorbance at 233 nm, which may limit the applicability and sensitivity of this assay when using biological samples. To account for absorbance due to partially peroxidized lipids, difference spectra obtained from 230 to 235 nm between the partially peroxidized lipids and an equivalent amount of nonperoxidized lipids can be used. Because of the overlapping absorbance of many biochemicals, this assay is best suited for use as a measure of lipid peroxidation in in vitro lipid peroxidation systems containing purified lipid; however, the conjugated diene assay may be used to analyze biological samples provided that the lipid fraction is first partially purified by Folch extraction (see Support Protocol 1; Folch et al., 1957; Bligh and Dyer, 1959).

Materials

Aqueous lipid suspension (see recipe)
Argon-purged 2:1 (v/v) chloroform/methanol (see recipe)
Argon
Cyclohexane
45°C water bath

1. To aqueous lipid suspension add 5 vol of argon-purged 2:1 (v/v) chloroform/methanol. Mix thoroughly, and centrifuge 10 min at $1000 \times g$, 4°C, to separate the aqueous and organic layers.
2. Remove the upper aqueous layer by suction or pipetting and recover the chloroform layer, which contains the lipid. Evaporate the chloroform to dryness with a constant flow of argon and maintain at 45°C in a water bath.
3. Resuspend the lipid residue in 1.5 ml cyclohexane and determine the absorbance at 233 nm versus a cyclohexane blank.
4. Calculate the approximate concentration of conjugated dienes using the extinction coefficient of 2.52×10^4 M^{-1} cm^{-1}.

It is advisable to obtain absorption spectra to assess the possibility of interference due to end absorbance of nonperoxidized lipid and other contaminants.

Contributed by Christopher A. Reilly and Steven D. Aust
Current Protocols in Toxicology (1999) 2.4.1-2.4.13

ASSAY FOR LIPID HYDROPEROXIDES

Lipid hydroperoxides formed during the peroxidation of polyunsaturated fatty acids can be measured using the iodometric assay. The assay is based on the ability of lipid hydroperoxides to oxidize I^-, ultimately generating the triiodide anion, which absorbs at 353 nm. This process is represented by the following reactions.

$$2H^+ + ROOH + 2I^- \rightarrow ROH + H_2O + I_2$$
$$I_2 + I^- \rightleftharpoons I_3^-$$

Under the conditions described, lipid hydroperoxides are selectively assayed and endoperoxides—which ultimately give rise to malondialdehyde—are excluded (Buege and Aust, 1978). Although using isopropyl alcohol as the reaction solvent can reduce the unwanted oxidation of iodide, the acetic acid/chloroform mixture described below is preferable since it promotes the reaction of iodide with hydroperoxides (Mair and Hall, 1971). Oxidation can be prevented by maintaining anaerobic conditions and purging the solutions with argon (Mair and Hall, 1971; Buege and Aust, 1978). In addition, cadmium is added as a complexing agent for unreacted iodide to prevent the iodide from becoming oxidized during quantification (Buege and Aust, 1978; Pryor and Castle, 1984). The amount of hydroperoxide present at a given time will depend upon the rate of initiation as well as the rate of decomposition by heme proteins, iron, and other transition metals. This procedure is useful for the analysis of lipid peroxidation both in vitro and in vivo; however, its use in vivo may be limited since lipid hydroperoxides are readily metabolized. In addition, the data may be altered during the assay, since lipid hydroperoxides are prone to reduction by transition metal contaminants in vitro.

Materials

Aqueous lipid suspension (see recipe)
1 mM EDTA
3:2 (v/v) acetic acid/chloroform (see recipe)
1.2 g/ml potassium iodide in argon-purged H_2O (prepare immediately before use and keep on ice protected from light)
0.5% (w/v) cadmium acetate in argon-purged H_2O (prepare fresh)
2:1 (v/v) chloroform/methanol (see recipe)
Argon
Cumene hydroperoxide or *t*-butyl hydroperoxide
45°C water bath

Additional reagents and equipment for extraction and recovery of lipids (see Basic Protocol 1)

NOTE: It is essential to minimize the exposure of solutions containing iodide to oxygen.

1. Add 1 mM EDTA (or other water-soluble iron chelator; e.g., DETAPA or PDTA) to aqueous lipid suspension. Also prepare a blank without lipid, and process in parallel in the steps that follow.
2. Extract and recover the lipids as described for the conjugated diene assay (see Basic Protocol 1, steps 1 to 2).
3. While maintaining the dried sample under a stream of argon, add 1 ml of 3:2 acetic acid/chloroform to tube to resuspend the lipid residue, immediately followed by 0.05 ml of 1.2 g/ml potassium iodide. Quickly cap the vial and mix thoroughly.
4. Incubate 5 min in the dark at room temperature.

5. Add 3.0 ml of 0.5% cadmium acetate. Mix thoroughly and centrifuge 10 min at 1000 × *g*, room temperature.
6. Determine the absorbance of the upper aqueous phase at 353 nm versus that of the extracted blank (containing all components except lipid).
7. Determine absorbance for a series of dilutions of cumene hydroperoxide or *t*-butyl hydroperoxide (approximately five increments between 0 and 150 nmol hydroperoxide/sample) and use the values to construct a standard curve of absorbance versus concentration. Estimate the concentration of lipid hydroperoxide in the sample based on the standard curve.

   The extinction coefficient for cumene hydroperoxide as a standard is 1.73×10^4 M^{-1} cm^{-1} (Buege and Aust, 1978).

MEASUREMENT OF MALONDIALDEHYDE

BASIC PROTOCOL 3

Malondialdehyde (MDA) is a product of lipid peroxidation that appears to be produced in relatively constant proportion from the breakdown of polyunsaturated fatty acids. Quantification of MDA is therefore a good indicator of lipid peroxidation, particularly in vitro (Aust, 1994). Quantification of MDA is done by reaction with thiobarbituric acid (TBA) and measurement of the pink chromophore produced. This method may be used for the analysis of MDA in vivo; however, it is limited by the interference of endogenous biochemicals that react with TBA and give rise to products that exhibit absorption spectra similar to that of the TBA-MDA adduct.

Materials

Aqueous lipid suspension (see recipe)
4× TBA/TCA/HCl reagent (see recipe)
2% (w/v) butylated hydroxytoluene (BHT) in ethanol (store protected from light up to 1 month at room temperature)
1,1,3,3-Tetramethoxypropane (optional)
Boiling water bath
Spectrophotometer or spectrofluorometer

1. Prepare 1× working solution of TBA/TCA/HCl reagent by diluting the stock solution 4-fold in water. While stirring the solution with a magnetic stir bar, add BHT to a final concentration of 0.03%.

   This solution must be prepared daily and continually stirred.

2. Combine the aqueous lipid suspension and blank (without lipid) with the TBA/TCA/HCl reagent at a reagent/sample ratio of 2:1 (v/v). Mix thoroughly, and place the samples in a boiling water bath for 15 min.
3. Allow the samples to cool to room temperature and then centrifuge 10 min at 1000 × *g*, room temperature.
4. Determine the absorbance of the solution at 535 nm against the blank that contains all reagents except lipid.

   It is also advisable to obtain an absorption spectrum to ensure that the compound detected is TBA-MDA adduct; only the TBA-MDA adduct absorbs maximally at 535 nm.

5. Calculate the concentration of MDA using the extinction coefficient of 1.56×10^5 M^{-1} cm^{-1} (Wills, 1969), or by preparing a standard curve between 0 and 50 nmol MDA/sample using 1,1,3,3-tetramethoxypropane as the standard.

   The TBA-MDA adduct may also be quantified using fluorescence emission at 553 nm upon excitation at 532 nm.

BASIC PROTOCOL 4

RED BLOOD CELL LYSIS

Peroxidation of erythrocyte membrane lipids dramatically increases their susceptibility to hemolysis. As such, the lysis of red blood cells (hemolysis), or their sensitivity to hemolysis, can be used as an estimate of lipid peroxidation or as an index of oxidative stress (Pfeifer and McCay, 1971). This method is written for use with in vitro lipid peroxidation systems; however, it may be adopted for use in vivo by comparing the sensitivity of erythrocytes obtained from treated and control animals to lysis induced by decreasing ionic strength (Hogan, 1990).

Materials

Erythrocytes (see recipe)
0.9% NaCl, pH 6.8 to 7.5 (*APPENDIX 2A*; sterile filter and store up to 1 week at 4°C)

1. Incubate the components of the lipid oxidation system being investigated at 37°C with 10% (v/v) packed erythrocytes prepared in 0.9% NaCl, pH 6.8 to 7.5, or another suitable buffer (e.g., 0.1 M Tris·Cl, pH 6.8 to 7.5). Prepare a standard with the other samples by resuspending an identical amount of erythrocytes in water (this represents 100% lysis).
2. After a specific incubation time, terminate the reactions by centrifuging the samples 10 min at 10,000 × *g*, 4°C, to pellet the remaining erythrocytes and erythrocyte ghosts.
3. Measure the absorbance of the supernatant at 545 nm (hemoglobin absorbance peak) versus a water blank and the standard. Express the values as percent hemolysis, determined by the ratio of the absorbance of the sample to that of the standard.

SUPPORT PROTOCOL 1

ANAEROBIC EXTRACTION OF LIPID

The initial purification of lipid involves the selective extraction of hydrophobic lipid from other water-soluble macromolecules (Folch et al., 1957). The inclusion of specific mineral salts in the subsequent wash steps serves to increase the ionic nature of the aqueous phase, which increases the yield of lipid. In order to minimize the oxidation of lipid during the extraction, all steps should be performed at 4°C under argon, unless otherwise stated.

Materials

Tissue to be extracted (e.g. Pel-Freez Biologicals, or live animal)
Argon gas
2:1 (v/v) chloroform/methanol (see recipe)
Aqueous Folch salt (see recipe)

Erlenmeyer and vacuum flasks
Separatory funnel
Rotary evaporator
Water bath

1. Homogenize ~1 to 3 g tissue in a minimal volume (e.g., 4 vol) of argon-purged water at 4°C, then extract with 300 ml of 2:1 chloroform/methanol by stirring 5 to 10 min in an Erlenmeyer flask on ice under a constant stream of argon.

   Approximately 50 ml homogenization solution (e.g., water) should be a sufficient volume, however, volumes up to 500 ml can be extracted with 300 ml solvent. In general, the homogenization solution should be at least four times the tissue weight.

2. Remove insoluble material by filtration using a Buchner funnel (lined with glass wool or cheese cloth) and vacuum flask. Transfer the chloroform/methanol/water solution to a separatory funnel and purge with argon 10 to 15 min.
3. Add 0.2 vol argon-purged aqueous Folch salt, mix, and allow phases to separate.
4. Aspirate off the top, aqueous phase and any precipitate at the interface. Purge the air space of the funnel with argon.
5. Add 0.4 vol argon-purged modified Folch salt, mix, and allow phases to separate.
6. Repeat steps 4 and 5, except do not remove the upper aqueous phase obtained from the second wash.
7. Collect the lower organic phase into a 1000-ml round-bottom flask.
8. Evaporate the chloroform/methanol to dryness using a vacuum evaporator equipped with a water bath maintained at 50°C.
9. Resuspend the lipid residue in 5 to 10 ml of 2:1 chloroform/methanol, and purge with argon.
10. Store the lipid under argon as 1- to 3-ml aliquots at −20°C in foil-wrapped, screw-capped culture tubes. The lipid can be stored for several months under these conditions.
11. Determine the phosphorus content of lipid samples (see Support Protocol 2).

COLORIMETRIC QUANTITATION OF PHOSPHORUS

SUPPORT PROTOCOL 2

The basis of this assay is the reduction of phosphomolybidic acid by 1-amino-2-naphthol-4-sulfonic acid in the presence of sulfite to yield a blue color (Bartlett, 1958). Total phosphate is quantitated by hydrolysis of organic phosphate esters in the presence of 10 N H_2SO_4 and high temperature. Although a variety of methods can be used to quantitate lipid, the phosphorus assay is a convenient method to estimate the concentration of phospholipid.

Materials

2:1 (v/v) chloroform/methanol (see recipe)
Stock lipid (see Support Protocol 1)
1 mM phosphoric acid or 1 mM monobasic sodium phosphate
10 N H_2SO_4
30% (v/v) H_2O_2
0.22% (w/v) ammonium molybdate
Fiske-Subbarow reagent (see recipe)

18 × 150–mm test tubes
Glass marbles
Boiling-water bath
Oven heated to 150°C
Spectrophotometer

1. In 18 × 150 mm test tubes place 50 to 500 µl aliquots of a 1:100 dilution of stock lipid in 2:1 chloroform/methanol. Bring volume up to 0.5 ml with distilled water.
2. Prepare a standard curve with 1 mM phosphoric acid or 1 mM monobasic sodium phosphate. Pipet 0, 50, 100, 150, 200, 250, and 300 µl stock phosphate into separate labeled test tubes and bring the volume up to 0.5 ml with distilled water.

A typical curve should range from 0 to 300 nmol phosphorus.

3. Add 0.5 ml 10 N H_2SO_4 to each tube, cover with a glass marble, and heat 3 hr at 150°C.
4. Remove the tubes from the oven and allow to cool. Add 20 µl of 30% H_2O_2 to each tube and cover.
5. Heat tubes an additional 1.5 hr at 150°C.
6. Add 4.6 ml of 0.22% ammonium molybdate. Mix thoroughly.
7. Add 0.2 ml of Fiske-Subbarow reagent, mix, and heat in a 100°C water bath for 7 to 10 min. Cool to room temperature.
8. Determine the absorbance of samples at 660 nm using a spectrophotometer.
9. Quantitate the amount of phosphorus in the lipid samples from a standard curve of absorbance versus phosphorus concentration.

REAGENTS AND SOLUTIONS

*Use Milli-Q-purified water or equivalent in all recipes and protocol steps. For common stock solutions, see **APPENDIX 2A**; for suppliers, see **SUPPLIERS APPENDIX**.*

Acetic acid/chloroform, 3:2

Working at <4°C, combine 3 vol glacial acetic acid with 2 vol chloroform. Purge with argon for 15 min. Seal in a glass container and allow the solution to reach room temperature prior to use. Store up to 1 month at 4°C.

Mixing must be done at <4°C to prevent unequal evaporation of the components.

Aqueous Folch salt

0.04 g $CaCl_2$
0.034 g $MgCl_2$
0.58 g NaCl
100 ml H_2O
Store up to several months at 4°C

Be sure to account for water weight when weighing mineral salts.

Aqueous lipid suspension

Prechill sonicator probe in an ice-water bath. Place ~10 µmol of lipid phosphorus (stored as a stock solution in 2:1 chloroform/methanol; see Support Protocol 1) into a thin-walled plastic tube and evaporate the solvent under a constant stream of argon. Add 1 ml of argon-purged assay solution (e.g., 50 mM NaCl) and cap the tube with a rubber stopper under a stream of argon. Keeping the lipid sample in an ice-water bath, sonicate it ~5 min using a sonication current of ~10 amps. Determine the concentration of lipid phosphorus present as a suspension (see Support Protocol 2).

Sonication is be performed anaerobically to minimize lipid oxidation.

Chloroform/methanol, 2:1

Combine 2 vol chloroform with 1 vol methanol. Purge with argon for 15 min at 0°C prior to use. Store indefinitely at 4°C.

Erythrocytes

Collect whole blood in sterile containers containing 10% (w/v) heparin as an anticoagulant. Centrifuge 10 min at 10,000 × *g*, 4°C, to isolate red blood cells. Remove the supernatant and the whitish buffy coat with a pipet. Wash the red cells three times as follows: resuspend in 0.9% (w/v) NaCl, pH 6.8 to 7.5 (*APPENDIX 2A*), and then centrifuge 10 min at 10,000 × *g*, 4°C. Store under argon at 4°C (can be stored for several days before becoming too fragile to use).

Fiske-Subbarow reagent

Combine 0.5 g 1-amino-2-naphthol-4-sulfonic acid, 30 g sodium bisulfite, and 1 g sodium sulfite as a dry mixture. Add 0.158 g of this mixture per milliliter of H_2O to make a saturated solution. Stir and filter. Prepare this solution immediately before use. Protect from light.

Modified Folch salt

Combine chloroform, methanol, and aqueous Folch salt in a 3:48:47 ratio. Store in a glass screw-cap container up to several months at 4°C.

TBA/TCA/HCl reagent, 4×

150 g trichloroacetic acid (15% final)
500 ml H_2O
20.8 ml concentrated HCl (0.2 N final)
3.7 g thiobarbituric acid (0.37% final)
H_2O to 1 liter
Heat to 70°C
Store up to several months at room temperature
Discard reagent if a precipitate forms

Heating helps dissolve the TBA.

COMMENTARY

Background Information

Oxidation of biomolecules by mechanisms other than "normal" oxidative metabolism can potentially be detrimental. Oxidation of DNA, for example, may be involved in carcinogenesis and other diseases. Oxidation of protein has also been proposed to be involved in disease, as well as in the aging process. DNA and protein oxidation are relatively new subjects of research into oxidative stress in comparison to lipid oxidation and its role in diseases and toxicities, for which extensive and long-established literature exists.

Because lipid oxidation (generally referred to as lipid peroxidation since lipid peroxides are intermediates in the process) has been linked to a variety of toxicities and pathological conditions, accurate methods for quantifying this process both in vitro and in vivo are needed. Unfortunately, the transient nature of the intermediates and products of lipid peroxidation, as well as the potential for interference by other endogenous compounds, makes the accurate quantification of lipid peroxidation in vivo extremely difficult. As a result, the study of lipid peroxidation, in many instances, is performed using in vitro model systems. In vitro lipid peroxidation systems overcome many of the difficulties associated with the study of lipid peroxidation in vivo; however, results obtained with such systems may not necessarily reflect the susceptibility and/or capacity of a tissue to undergo lipid peroxidation in vivo. The key difference is due primarily to the removal of factors that can either promote or prevent the initiation or termination of lipid oxidation in vivo (i.e., the type of lipid, antioxidant systems, transition metals). As such, the development of assays suitable for the analysis of lipid peroxidation both in vitro and in vivo is presently a priority. This unit describes the basic procedures and improvements for several assays that are frequently used to assay for lipid peroxidation and the advantages and disadvantages of each assay under different conditions.

Lipid peroxidation was most likely first recognized because of the unique susceptibility of PUFA to oxidation. This may be due to the vulnerability of lipid side chains to hydrogen abstraction from their methylene carbon(s) (LH). These methylene hydrogens have relatively low bond energy, resulting in a predisposition to abstraction. In addition, the resulting lipid radical (L·) undergoes structural rearrangement to the conjugated diene, whose relative stability helps to drive the initial oxidation reactions. The lipid radical also readily reacts with molecular oxygen to generate a lipid peroxyl radical (LOO·). Lipid peroxyl radicals can be reduced to generate lipid hydroperoxides (LOOH) by abstraction of an additional hydrogen from another PUFA side chain to continue the peroxidation process. This is termed propagation. In addition, lipid, lipid alkoxyl, and lipid peroxyl radicals may also be reduced by lipophilic antioxidants such

as vitamin E (α-tocopherol), which limits, and therefore terminates, propagation of lipid peroxidation. However, lipid hydroperoxides are also very reactive, particularly with reduced transition metals and hemoproteins. For example, lipid hydroperoxides will react with hemoglobin to produce lipid alkoxyl radicals (LO·), which can also propagate lipid peroxidation.

Systems used to study lipid peroxidation in vitro generally consist of transition metals, such as iron, and either a reductant or an oxidant of the metal, depending upon the metal's oxidation state. Ascorbic acid has been used extensively as a reductant of ADP-chelated ferric iron in a reaction that results in the initiation of lipid peroxidation (Miller and Aust, 1988). The maximum rate of lipid peroxidation was observed when a 1:1 molar ratio of ferric iron/ascorbic acid was used. Likewise, when H_2O_2 was used as an oxidant of ADP-chelated ferrous iron, the maximum rate of lipid peroxidation was observed when the concentration of H_2O_2 was enough to generate a 1:1 ratio of Fe(II):Fe(III) (Minotti and Aust, 1986). The rate of lipid peroxidation did not correlate with the rate of hydroxyl radical generation, indicating that the ·OH radical was probably not responsible for the initiation of lipid peroxidation. The authors proposed that the formation of a Fe(III)-O_2-Fe(II) complex was essential for the initiation of lipid peroxidation, and the rate was ultimately dependent upon the relative concentrations of ferric and ferrous iron (Minotti and Aust, 1986; Miller and Aust, 1988). However, the formation of this complex is debated, because the requirement for dioxygen in the complex cannot be proven since oxygen is required for lipid peroxidation.

Because free iron is capable of catalyzing a variety of deleterious reactions in the presence of oxygen, the probability that high concentrations of free iron exist in vivo is small. Although the existence of a low-molecular-weight chelated pool of iron has been proposed, attempts to isolate this form of iron have thus far been futile. In vivo, iron is primarily found complexed with proteins; ferritin is responsible for the storage of iron in vivo, and represents the single most concentrated pool of iron in cells. To more closely model the source of iron within cells, redox-cycling xenobiotics capable of mobilizing iron from ferritin, such as the bipyridyl herbicides paraquat and diquat (Saito et al., 1985; Thomas and Aust, 1986a) and the anthracycline antibiotics daunomycin and adriamycin (Thomas and Aust, 1986b; Li, 1991), were used to mobilize iron from ferritin and to initiate lipid peroxidation. The toxicity of these chemicals has been attributed to reduction by NADPH-cytochrome P-450 reductase and subsequent redox cycling with dioxygen (Bus et al., 1974; Bachur et al., 1979). In addition it has been shown that iron chelators such as Desferal mitigate the toxic effects of these substances, indicating a role for iron in the toxicity (Herman and Ferrans, 1983; Kohen and Chevion, 1985). It has been shown in vivo that diquat causes a decrease in the amount of iron associated with ferritin isolated from the livers of treated animals (Reif et al., 1988). In addition, exposure to paraquat and adriamycin causes an increase in lipid peroxidation in vivo (Bus et al., 1974; Goodman and Hochstein, 1977). Redox cycling of adriamycin and paraquat in vitro efficiently reduced and mobilized ferrous iron from ferritin and ultimately provided the iron complex needed to initiate lipid peroxidation (Saito et al., 1985; Thomas and Aust, 1986a,b; Li, 1991). The rate of ferritin-dependent lipid peroxidation was affected by the rate of iron release, the type and concentration of iron chelator(s) present, and the concentration of ferrous iron oxidants; increasing the rate and extent of ferrous iron oxidation, by treatment with chelators or H_2O_2, decreased the rate of lipid peroxidation by affecting the formation and maintenance of the needed 1:1 Fe(II)/Fe(III) ratio. These studies suggest that a plausible mechanism of toxicity for redox-cycling xenobiotics is mobilization of iron from ferritin and the subsequent initiation of lipid peroxidation.

Assays for lipid peroxidation (i.e., using conjugated dienes, hydroperoxides, and MDA as substrates) have been reported in the literature for many years. Although these assays have limitations, they are still valid for measuring lipid peroxidation in many situations (Slater, 1984). In addition, several useful improvements have been developed to enhance the specificity and applicability of these assays.

The oldest, simplest, and least time-consuming lipid oxidation assay methodology is the TBA test for MDA (Bird and Draper, 1984). MDA results from the decomposition of lipid endoperoxides during lipid peroxidation and/or during the assay, both catalyzed at least in part by transition metals. The TBA test can also be used to estimate the concentration of lipid hydroperoxides. This is achieved by comparing the amount of TBA-MDA adduct

formed in the presence and absence of an antioxidant (0.03% BHT); BHT inhibits the formation of MDA during the assay due to hydroperoxide-dependent lipid peroxidation, initiated by transition metal-dependent decomposition of lipid hydroperoxides (Wills, 1964; Aust, 1994). The assay of MDA using the TBA test is not specific for MDA but rather detects a variety of lipid breakdown products (Halliwell and Gutteridge, 1984). As a result, the data are frequently expressed in terms of thiobarbituric acid–reactive substances (TBARS). Fortunately, the TBA-MDA adduct exhibits a rather unique absorbance maximum at 535 nm, as well as a fluorescence emission at 553 nm upon excitation at 532 nm (Halliwell and Gutteridge, 1984). For this reason, the TBA test is exceptionally useful for in vitro studies of lipid peroxidation, where purified lipid is tested. As such, the TBA test is not particularly well suited for the analysis of MDA in vivo since the oxidation products of several endogenous compounds (e.g., sucrose, ascorbate, and deoxyribose) tend to react with TBA to give rise to adducts that exhibit an absorbance spectrum similar to, and may in fact be, MDA. In addition, MDA is readily metabolized by microsomal aldehyde dehydrogenases, and thus has a very short half-life in vivo (Halliwell and Gutteridge, 1984). For these reasons, the TBA test for MDA is not always appropriate for analysis of MDA in vivo. However, if specific measurement of MDA is desired, several sensitive methods for detecting the TBA adduct of MDA have been developed using high-performance liquid chromatography (HPLC; Esterbauer et al., 1984; Young and Trimble, 1991; Li and Chow, 1994; Londero and Lo Greco, 1996). In general, analysis of MDA using HPLC requires the extraction of the TBA-MDA adduct with isobutyl alcohol, followed by separation using HPLC, and then detection of the TBA-MDA adduct using UV-absorption or fluorescence-emission spectroscopy. In addition, very sensitive methods utilizing gas chromatography–mass spectrometry (GC-MS) have been developed to assay for MDA (Yeo et al., 1994). HPLC and GC-MS methods are very sensitive and more selective; however, they are considerably more time consuming because of sample processing.

Another popular method used to assay for the oxidation of PUFA is monitoring the formation of lipid hydroperoxides. Direct measurement of lipid hydroperoxides has several advantages over the TBA test in that it measures only lipid hydroperoxides, can give information relative to the rate of initiation of lipid peroxidation, is independent of the type of fatty acids constituting the lipid membrane, and is specific for the oxidation of lipid. A simple method for estimating hydroperoxide formation is by monitoring the decrease in dissolved oxygen concentration during lipid peroxidation using an oxygraph equipped with a Clark-type electrode (Halliwell and Gutteridge, 1984). Alternatively, the susceptibility of hydroperoxides to redox reactions may be exploited to quantify the amount of lipid hydroperoxide present. A common method of this type used to assay for lipid hydroperoxides is the iodometric assay (Mair and Hall, 1971; Buege and Aust, 1978; Pryor and Castle, 1984; Recknagel and Glende, 1984). The crux of the iodometric assay is the formation of the triiodide anion upon oxidation of iodide by lipid hydroperoxides. The specificity of this assay for lipid hydroperoxides is achieved by first performing a Folch extraction for lipids (see Support Protocol 1; Folch et al., 1957) with chloroform/methanol (2:1); extracting the lipid removes potential endogenous oxidants of iodide, including H_2O_2 (Wills, 1969; Buege and Aust, 1978). When performing the iodometric assay, it is absolutely essential to minimize the exposure of solutions containing iodide to oxygen; exposure to oxygen will promote the oxidation of iodide and give rise to high background concentrations of I^{3-} (Pryor and Castle, 1984). In addition, to minimize decomposition of the hydroperoxides during this assay, it is advisable to include a water-soluble iron chelator (e.g., EDTA or desferrioxamine) to minimize the coextraction of iron (Buege and Aust, 1978). In the absence of an effective iron chelator, the iron will associate and extract with the lipid, ultimately interfering with the analysis.

A second method for analyzing lipid hydroperoxides utilizes hemoglobin to catalyze the oxidation of methylene blue derivatives (Yagi et al., 1996). In this assay, lipid hydroperoxides oxidize hemoglobin, which in turn catalyzes the oxidation of methylene blue. The oxidized product of methylene blue can be quantified spectrophotometrically at its absorbance maximum. In addition, HPLC and GC-MS methods for the analysis of specific lipid hydroperoxides or their reaction products have been developed (Van Kuijk et al., 1985a,b; Yamamoto et al., 1986; Tokumaru et al., 1995).

The assay of lipid hydroperoxides is a sensitive index of lipid peroxidation both in vitro and in vivo. However, the in vivo assay may

be limited by the short half-life of lipid hydroperoxides, which results from metabolism by a variety of enzymes including glutathione peroxidase and prostaglandin synthase. In fact, several methods have been developed to quantify lipid hydroperoxides using glutathione peroxidase or another peroxidase (Heath and Tappel, 1976; Marshall et al., 1984). Enzyme-based assays for lipid hydroperoxides are quite sensitive and in some cases selective for the type of hydroperoxide; however, they are quite arduous.

Another method to directly measure the rate of initiation of lipid peroxidation is to assay for the formation of conjugated dienes resulting from rearrangement of lipid radicals. Detection of conjugated dienes can serve as a sensitive method for assaying lipid peroxidation both in vitro and in vivo. Folch extracts of biological samples and of pure lipid used within in vitro lipid peroxidation systems can be analyzed for changes in absorbance at 233 nm. This method is quite simple and can be used for a variety of sample types (Buege and Aust, 1978). It has, for example, been used by Rao and Recknagel (1968) to show changes in the concentrations of conjugated diene in rat liver following the exposure of test animals to carbon tetrachloride (a potent hepatotoxin that manifests its toxicity, in part, as lipid peroxidation).

Lysis of red blood cells is also a good index for lipid peroxidation and oxidative stress (Pfeifer and McCay, 1971). Although erythrocyte lysis may not be directly proportional to the peroxidation of membrane lipids, measurement of erythrocyte lysis can provide an estimate of oxidative damage that involves lipid peroxidation. In addition, the fragility of the erythrocyte membrane can be assessed by a simple modification of the hemolysis assay in order to obtain information on the extent of oxidative damage to the membrane; lipid peroxidation leads to an increase in membrane fragility and decreased fluidity, thus increasing the sensitivity of erythrocytes to osmotic lysis (Pfeifer and McCay, 1971; Hogan, 1990). The hemolysis assay is by far the simplest method to assay oxidative damage to membranes and may be used in concert with the other methods discussed within this unit to characterize the peroxidation of lipid membranes under a specific set of conditions. In addition, the hemolysis assay can be adopted for use with animals; comparing the hemolysis of erythrocytes isolated from both treated and control animals can serve as an index of oxidative damage to lipid membranes in vivo (Hogan, 1990).

When planning experiments that utilize lipid peroxidation as a measure of oxidative stress, it is essential to use a method of analysis that will generate the information the experiments are designed to provide. It is also advisable to fully understand the mechanisms of the reaction used to oxidize the lipid so that the data obtained from the experiments in vivo can be appropriately interpreted. For simple in vitro experiments designed to elucidate the effects of a specific chemical on lipids, all of the assays discussed in this unit are suitable, differing only in the ease of the procedure and the point in the peroxidation process being monitored. Unfortunately, there is no perfect assay for studying lipid peroxidation in vivo; however, several modifications of the assays discussed have permitted their use as an index of lipid oxidation in vivo. For example, the TBA test has been used on biological samples to accurately quantitate MDA by altering the experimental conditions such that interfering substances are not detected and/or do not react with TBA. Using this procedure, samples are first exposed to potassium iodide to reduce any lipid hydroperoxides present, and then reacted with TBA at 60°C. The TBA-MDA adduct is extracted into isobutyl alcohol, separated by HPLC, and detected using fluorescence-emission spectroscopy. This modified TBA test allows more specific and accurate determination of MDA in biological samples (Li and Chow, 1994). Although the procedures discussed in this unit are directed towards the study of lipid peroxidation in vitro, analysis of extracted biological samples by identical procedures permit their use in the study of lipid peroxidation in vivo.

Critical Parameters

The most crucial aspect of any lipid peroxidation study is careful selection of an appropriate assay that can fulfill the objectives of the experiment. A second important issue is the need to fully understand the assay. For example, lipid hydroperoxides are extremely labile, and thus susceptible to decomposition both in vivo and in vitro; assaying for lipid hydroperoxide is not advisable when metals such as iron are used to initiate lipid peroxidation. When transition metals are used to initiate lipid peroxidation, extreme care must be taken to remove and/or minimize the presence of transition metal contaminants in reagents used in the analysis procedure (Buege and Aust, 1978). It

is also important to remove contaminating transition metals to prevent the misinterpretation of results. A common method for removing transition-metal contaminants from solutions is chromatography over Chelex 100 resin (Bio-Rad). When buffers that chelate metals (e.g., acetate, Tris, phosphate) are used, it may be necessary to extract the metals using iron chelators such as phenanthroline dissolved in amyl alcohol. This extraction is necessary because the buffers have a higher binding affinity for certain metals than does Chelex; therefore, buffers and salts undergo ligand-exchange reactions with the metals complexed with the resin, ultimately removing the metals from the resin.

It is absolutely necessary to be cognizant of the probability that transition metal contaminants are present in the preparations of almost all chemicals and reagents, and that substantial amounts of metal contaminants may be introduced by common laboratory instruments and supplies such as syringes and glassware (Buettner, 1990; Buettner and Jurkiewicz, 1996). It is a popular misconception that chemicals such as ascorbic acid, cysteine, and hydroquinones autoxidize or undergo direct one- or two-electron transfer reactions with dioxygen to generate O_2^- and H_2O_2, respectively. The direct reaction of dioxygen with singlet molecules such as ascorbate is, in some instances, thermodynamically favorable. However, due to the spin restriction associated with the reaction of singlet molecules with triplet molecules (such as dioxygen) as a result of the ground electronic character of dioxygen, this reaction is kinetically inhibited ($<10^{-5}\ M^{-1}\ s^{-1}$) and requires a transition metal catalyst, such as iron (Miller et al., 1990). Ferric iron is reduced to ferrous iron by a variety of chemicals, and ferrous iron can catalyze the sequential one-electron reduction of dioxygen in the Haber-Weiss reactions. Thus, transition metals play a multifaceted role in the oxidation of chemicals; transition metals can serve as a primary oxidant, or as a means of altering the ground-electronic character of dioxygen such that oxygen radicals are generated and the reaction between singlet molecules and oxygen can occur. The resulting redox cycle between the metal, oxygen, and chemical continues until all the available reductant is oxidized. A good test for iron contamination in solutions is described by Buettner (1990). This method is based on the oxidation of ascorbic acid by metal-contaminated reagents. Ascorbate oxidation can be monitored spectrophotometrically as a decrease in absorbance at 265 nm or by electron-spin resonance (ESR) spectroscopy to measure the formation of the ascorbyl radical. It is always advisable to assess the possibility of iron contamination in reagents used to study lipid peroxidation, because it will undoubtedly affect the quality and interpretation of the data (Buege and Aust, 1978; Aust, 1994).

An additional precaution to prevent unwanted lipid oxidation is to limit exposure to light and maintain anaerobic conditions as much as possible in handling the lipid. To eliminate oxygen, argon should be continually blown over the top of solutions containing lipid. Argon is generally preferred over nitrogen since it is slightly heavier than air and tends to remain layered over the top of the solution during transfer steps. This procedure is extremely important during the extraction of lipids and subsequent evaporation of solvents where iron contaminants may be present.

Anticipated Results

The results obtained from in vitro lipid peroxidation experiments will vary, depending primarily upon the experimental conditions used to oxidize the lipid, the method used to measure peroxidation, and the type of fatty acid used. However, the results obtained for a given set of experiments can be extremely precise provided consistent technique is used to execute the particular procedure. When enough research is done prior to performing the assays and the proper controls are included, excellent results can be obtained with little difficulty. In general, the extent of lipid peroxidation observed during in vitro lipid peroxidation studies will be significantly greater, with less variation in the data, than is seen when studying lipid peroxidation in vivo. Inherent differences in metabolism of the products being assayed, individual differences in susceptibility to oxidative damage, and differences in the concentrations of endogenous compounds that can potentially interfere with the assay all contribute to the higher percentage error of in vivo studies. Nonetheless, data obtained from experiments in vivo are generally sufficiently meaningful to allow basic conclusions to be drawn regarding the oxidative processes that occur under a given set of conditions.

Time Considerations

The time required to complete a lipid peroxidation experiment will vary with the assay and the experimental conditions. In general,

however, the following amounts of time should be allotted for the respective assay: assay for conjugated dienes: 1 to 1.5 hr; assay for lipid hydroperoxides: 1 to 2 hr; measurement of malondialdehyde (MDA): 0.5 to 1 hr; red cell lysis: 0.5 to 1 hr.

Literature Cited

Aust, S.D. 1994. Thiobarbituric acid assay reactants. *In* Methods in Toxicology, Vol. 1B. In Vitro Toxicity Indicators (C.A. Tyson and J.M. Frazier, eds.) pp. 367-376. Academic Press, San Diego.

Bachur, N.R., Gordon, S.L., Gee, M.V., and Kon, A. 1979. NADPH-cytochrome P-450 reductase activation of quinone anticancer agents to free radicals. *Proc. Natl. Acad. Sci. U.S.A.* 76:954-957.

Bartlett, G.R. 1958. Phosphorus assay in column chromatography. *J. Biol. Chem.* 234:466-468.

Bird, R.P. and Draper, H.H. 1984. Comparative studies on different methods of malonaldehyde determination. *Methods Enzymol.* 105:299-304.

Bligh, E.C. and Dyer, W.J. 1959. A rapid method for total lipid extraction and purification. *Can. J. Biochem. Physiol.* 37:911-917.

Buege, J.A. and Aust, S.D. 1978. Lipid peroxidation. *Methods Enzymol.* 51:302-310.

Buettner, G.R. 1990. Ascorbate oxidation: UV absorbance of ascorbate and ESR spectroscopy of the ascorbyl radical as assays for iron. *Free Rad. Res. Commun.* 10:5-9.

Buettner, G.R. and Jurkiewicz, B.A. 1996. Catalytic metals, ascorbate and free radicals: Combinations to avoid. *Radiat. Res.* 145:532-541.

Bus, J.S., Aust, S.D., and Gibson, J.E. 1974. Superoxide- and singlet oxygen-catalyzed lipid peroxidation as a possible mechanism for paraquat (methyl viologen) toxicity. *Biochem. Biophys. Res. Commun.* 58:749-755.

Esterbauer, H., Lang, J., Zadravec, S., and Slater, T.F. 1984. Detection of malonaldehyde by high-performance liquid chromatography. *Methods Enzymol.* 105:319-328.

Folch, J., Lees, M., and Sloane Stanley, G.H. 1957. A simple method for the isolation of total lipids from animal tissues. *J. Biol. Chem.* 226:497-509.

Goodman, J. and Hochstein, P. 1977. Generation of free radicals and lipid peroxidation by redox cycling of adriamycin and daunomycin. *Biochem. Biophys. Res. Commun.* 77:797-803.

Halliwell, B. and Gutteridge, J.M.C. 1984. Free Radicals in Biology and Medicine, 2nd ed. Oxford University Press, New York.

Heath, R.L. and Tappel, A.L. 1976. A new sensitive assay for the measurement of hydroperoxides. *Anal. Biochem.* 76:184-191.

Herman, H.E. and Ferrans, V.J. 1983. ICRF-187 reduction of chronic daunomycin and doxorubicin cardiac toxicity in rabbits, beagle dogs and miniature pigs. *Drugs Exp. Clin. Res.* 9:483-490.

Hogan, G.R. 1990. Peripheral erythrocyte levels, hemolysis and three vanadium compounds. *Experientia* 46:444-446.

Kohen, R. and Chevion, M. 1985. Paraquat toxicity is enhanced by iron and reduced by desferrioxamine in laboratory mice. *Biochem. Pharmacol.* 34:1841-1843.

Li, J. 1991. Iron Release from Rat Liver Ferritin and Lipid Peroxidation by Adriamycin. M.S. Thesis. Utah State University, Logan, Utah.

Li, X.-Y. and Chow, C.K. 1994. An improved method for the measurement of malondialdehyde in biological samples. *Lipids* 29:73-75.

Londero, D. and Lo Greco, P. 1996. Automated high-performance liquid chromatography separation with spectrofluorometric detection of a malondialdehyde–thiobarbituric acid adduct in plasma. *J. Chromatogr.* 729:207-210.

Mair, R.D. and Hall, R.T. 1971. Determination of organic peroxides by physical, chemical, and colorometric methods. *In* Organic Peroxides, Vol. 2 (D. Swern, ed.) pp. 535-635. John Wiley & Sons, New York.

Marshall, P.J., Warso, M.A., and Lands, W.E. 1984. Selective microdetermination of lipid hydroperoxides. *Anal. Biochem.* 145:192-199.

Miller, D.M. and Aust, S.D. 1988. Studies of ascorbate-dependent, iron-catalyzed lipid peroxidation. *Arch. Biochem. Biophys.* 271:113-119.

Miller, D.M., Buettner, G.R., and Aust, S.D. 1990. Transition metals as catalysts of "autoxidation" reactions. *Free Rad. Biol. Med.* 8:95-108.

Minotti, G. and Aust, S.D. 1986. The requirement for iron(III) in the initiation of lipid peroxidation by iron(II) and hydrogen peroxide. *J. Biol. Chem.* 262:1098-1004.

Pfeifer, P.M. and McCay, P.B. 1971. Reduced triphosphopyridine nucleotide oxidase-catalyzed alterations of membrane phospholipids. *J. Biol. Chem.* 246:6401-6408.

Pryor, W.A. and Castle, L. 1984. Chemical methods for the detection of lipid hydroperoxides. *Methods Enzymol.* 105:293-298.

Rao, K.S. and Recknagel, R.O. 1968. Early onset of lipid peroxidation in rat liver after carbon tetrachloride administration. *Exp. Mol. Pathol.* 9:271-278.

Recknagel, R.O. and Glende, E.A., Jr. 1984. Spectrophotometric detection of lipid conjugated dienes. *Methods Enzymol.* 105:331-336.

Reif, D.W., Beales, I.L.P., Thomas, C.E., and Aust, S.D. 1988. Effects of diquat on the distribution of iron in rat liver. *Toxicol. Appl. Pharmacol.* 93:506-510.

Saito, M.E., Thomas, C.E., and Aust, S.D. 1985. Paraquat and ferritin-dependent lipid peroxidation. *J. Free Rad. Biol. Med.* 1:179-185.

Slater, T.F. 1984. Overview of methods used for detection of lipid peroxidation. *Methods Enzymol.* 105:283-292.

Thomas, C.E. and Aust, S.D. 1986a. Reductive release of iron from ferritin by paraquat and related bipyridyls. *J. Biol. Chem.* 261:13064-13070.

Thomas, C.E. and Aust, S.D. 1986b. Release of iron from ferritin by cardiotoxic anthracycline antibiotics. *Arch. Biochem. Biophys.* 248:684-689.

Tokumaru, S., Tsukamoto, I., Iguchi, H., and Kojo, S. 1995. Specific and sensitive determination of lipid hydroperoxides with chemical derivatization into 1-naphthyldiphenylphosphine oxide and high-performance lipid chromatography. *Anal. Chem. Acta* 307:97-102.

Van Kuijk, F.J.G.M., Thomas, D.W., Stephens, R.J., and Dratz, E.A. 1985a. Gas chromatography–mass spectrometry method for the determination of phospholipid peroxides. I: Transesterification to form methyl esters. *J. Free Rad. Biol. Med.* 1:215-225.

Van Kuijk, F.J.G.M., Thomas, D.W., Stephens, R.J., and Dratz, E.A. 1985b. Gas chromatography–mass spectrometry method for the determination of phospholipid peroxides. II: Transesterification to form pentafluorobenzyl esters and detection with picogram sensitivity. *J. Free Rad. Biol. Med.* 1:387-393.

Wills, E.D. 1964. The effect of inorganic iron in the thiobarbituric acid method for the determination of lipid peroxides. *Biochim. Biophys. Acta* 84:475-477.

Wills, E.D. 1969. Lipid peroxide formation in microsomes. Relationship of hydroxylation to lipid peroxide formation. *Biochem. J.* 113:333-341.

Yagi, K., Komura, S., Kayahara, N., Totano, T., and Ohishi, N. 1996. A simple assay for lipid hydroperoxides in serum or plasma. *J. Clin. Biochem. Nutr.* 20:181-193.

Yamamoto, Y., Brodsky, M.H., Baker, J.C., and Ames, B.N. 1986. Detection and characterization of lipid hydroperoxides at picomole levels by high performance-liquid chromatography. *Anal. Biochem.* 160:7-13.

Yeo, H.C., Helbock, H.J., Chyu, D.W., and Ames, B.N. 1994. Assay of malondialdehyde in biological fluids by gas chromatography–mass spectrometry. *Anal. Biochem.* 220:391-396.

Young, I.S. and Trimble, E.R. 1991. Measurement of malondialdehyde in plasma by high-performance liquid chromatography with fluorometric detection. *Ann. Clin. Biochem.* 28:504-508.

Contributed by Christopher A. Reilly and Steven D. Aust
Utah State University
Logan, Utah

Measurements of Intracellular Free Calcium Concentration in Biological Systems

Calcium is a very closely regulated ion in both serum and interstitial fluid and within the cytosol of every type of cell. Ion-specific electrodes and dyes whose absorbance spectra change upon binding calcium have allowed accurate measurement of serum and interstitial free calcium concentration ($[Ca^{2+}]$) for years; however, it is only recently, with the advent of calcium-specific fluorescent probes, that rapid, accurate measurement of intracellular free Ca^{2+} concentration has been possible. The sensitivity of the fluorescence technique permits measurement with amounts of probe small enough to avoid most problems with probe toxicity, while K_d's for calcium binding (down to hundreds of nanomolar) permit accurate measurement of intracellular $[Ca^{2+}]$. Techniques that permit these probes to be loaded into the cell in a membrane-permeable form with conversion to a membrane-impermeable, Ca^{2+}-sensitive form by the action of intracellular enzymes permit convenient loading and use of these new probes.

Intracellular $[Ca^{2+}]$ measurements are performed today using several approaches, most of which make use of fluorescent probes: (1) measurements on suspensions of cells using fluorescence spectroscopy (see Basic Protocol 1); (2) measurements on plated cells using single-cell photometry or ratio detection by means of fluorescence digital imaging microscopy (FDIM; see Basic Protocol 2) or confocal microscopy with digital imaging capability; (3) measurements using flow cytometry techniques; and (4) measurements using the bioluminescent peptide aequorin. Measurements on suspensions of cells using fluorescence spectroscopy and measurements on plated cells using FDIM are the most commonly used approaches to measurements of intracellular $[Ca^{2+}]$, in part because confocal microscopy and flow cytometry require special and expensive equipment. For this reason, and because many of the techniques used to obtain measurements of $[Ca^{2+}]$ with a confocal microscope or single-cell photometry are similar to those used with FDIM, these techniques will not be discussed separately. The focus here will be on these more commonly used approaches.

This unit contains protocols for spectroscopic measurement using ratiometric (see Basic Protocol 1) or nonratiometric probes (see Alternate Protocol) as well as FDIM using ratiometric (see Basic Protocol 2) and nonratiometric probes. In addition there are protocols for determination of K_d in suspension (see Support Protocol 1) and plated cells (see Support Protocol 2).

CAUTION: Material safety data sheets (MSDSs) can be obtained from the vendor or via the Internet at *http://siri.org/msds/index.html* for hazardous chemicals. Chemicals dissolved in DMSO, which aids in the absorption of solutes directly through the skin, are especially hazardous.

STRATEGIC PLANNING

The first choice is that of the fluorescent probe to be used. Some Ca^{2+} probes change their excitation or emission spectra upon binding Ca^{2+}, while others change their extinction coefficient or quantum yield (number of photons emitted to number of photons absorbed). Those that change their spectra are referred to as "ratiometric probes." Ratiometric probes have significant advantages over nonratiometric probes in measurement of intracellular $[Ca^{2+}]$ and should be used unless there are technical reasons (to be discussed below) for using a nonratiometric probe. A good discussion of the properties of the various probes is contained in Kao (1994).

Contributed by Karlene K. Gunter and Thomas E. Gunter
Current Protocols in Toxicology (1999) 2.5.1-2.5.52

Table 2.5.1 Properties of Various Ratiometric Ca^{2+} Fluorescent Indicators[a]

Indicator	Low-Ca^{2+} Properties			High-Ca^{2+} Properties			Approx. K_d (nm)[b]
	Ex. (nm)	$\varepsilon \times 10^{-3}$ ($cm^{-1}M^{-1}$)	Em. (nm)	Ex. (nm)	$\varepsilon \times 10^{-3}$ ($cm^{-1}M^{-1}$)	Em. (nm)	
Bis-fura	366	49	511	338	59	504	525
Fura-2[c]	363	28	512	335	34	505	224
Fura-PE3[c]	364	28	508	335	34	490	204
Fura red[d]	472	29	657	436	41	637	224
Indo-1[e]	346	33	475	330	33	401	250

[a]This information was obtained from Molecular Probes and Texas Fluorescence Laboratories (TEFLABS). Abbreviations: Ex., peak excitation; ε, extinction coefficient; Em., peak emission in aqueous media.

[b]Approx. K_d is given in the presence of 1 mM Mg^{2+}, since experiments depend upon the K_d inside cells, which contain Mg^{2+} close to this value.

[c]The quantum yield of the low-Ca form is ~0.25; that of the high-Ca form is ~0.46.

[d]The fluorescence quantum yield of Fura red is low, ~0.013 in Ca^{2+}-free solution.

[e]The quantum yield of the low-Ca form is ~0.38; that of the high-Ca form is about ~0.56.

Table 2.5.2 Properties of Various Non-ratiometric Ca^{2+} Fluorescent Indicators[a]

Indicator	Low-Ca^{2+} Properties			High Ca^{2+} Properties			Approx. K_d (nM)[b]
	Ex. (nm)	$\varepsilon \times 10^{-3}$ ($cm^{-1}M^{-1}$)	Em. (nm)	Ex. (nm)	$\varepsilon \times 10^{-3}$ ($cm^{-1}M^{-1}$)	Em. (nm)	
Calcium green 1[c]	506	81	531	506	82	531	190
Calcium green 2	506	95	536	503	147	536	550
Calcium orange	549	80	575	549	80	576	185
Calcium crimson	590	96	615	589	92	615	185
Fluo-3[d]	503	90	526	506	100	526	390
Oregon green 488 BAPTA-1[c]	494	76	523	494	78	523	170
Oregon green 488 BAPTA-2	494	105	523	494	140	523	580
Rhod-2	549	79	581	552	82	581	570

[a]This information was obtained from Molecular Probes and Texas Fluorescence Laboratories (TEFLABS). Abbreviations: Ex., peak excitation; ε, extinction coefficient; Em., emission in aqueous media.

[b]Approx. K_d is given in the absence of Mg^{2+}, Since the K_d inside of cells is what is really measured, and cells contain ~0.5 mM Mg^{2+}, the K_d inside of cells is likely to be much higher than this value.

[c]The fluorescence quantum yield is high, ~0.75 in high Ca^{2+} solution.

[d]The fluorescence quantum yield is ~0.18 in high Ca^{2+} solution.

The most commonly used ratiometric probes are Fura-2 and Indo-1. The primary disadvantages of these two probes are that they are excited in the ultraviolet and can suffer considerable interference from the autofluorescence of cells. Fura-2 is very resistant to photobleaching. Indo-1 has a greater tendency to partition into mitochondria (see Table 2.5.1 for a list of the properties of the useful ratiometric probes). Fura PE-3 is similar to Fura-2, except it is much more leakage-resistant and should be used if leakage of probe over the time course of an experiment is a problem. The probe bis-Fura is similar to Fura-2, except it has a much higher K_d and must be microinjected into cells before use; however, it has a high extinction coefficient and quantum yield and hence is very bright. Fura red has the advantage of being excited in the visible range but the disadvantage of having a low quantum yield. The most commonly used nonratiometric probes are Fluo-3 and Rhod-2. Fluo-3 is generally used in situations where rapid changes in calcium must be followed, since it binds calcium rapidly; however, significant binding to proteins affects its K_d. Rhod-2 is generally used when it is desired to follow calcium in mitochondria, since the majority of Rhod-2 is converted inside mitochondria because of its positive

charge in the AM form (Trollinger et al., 1997; see Table 2.5.2 for a list of the properties of the useful nonratiometric probes). Calcium green 1 and 2 and Oregon green 488 BAPTA 1 and 2 have quantum yields of 0.75 as compared to 0.18 for Fluo-3, which means that they can be less phototoxic to cells than Fluo-3 because less is needed. Calcium orange and calcium crimson, because of their excitation wavelengths, should have less interference from autofluorescence. However, calcium crimson tends to compartmentalize in some cell types.

The choice of probe depends on the available equipment, whether anything that interferes with any specific probe must be present in the experiment, in what location the $[Ca^{2+}]$ is to be measured, and the sensitivity. Ratiometric probes can give higher accuracy of $[Ca^{2+}]$ determination and are largely insensitive to variations in probe concentration. In some toxicological experiments, heavy metal ions may be present that can quench the fluorescence of some probes or that can bind to the probe and distort the spectra. These effects vary with the probe selected. Sometimes multiple probes are to be used in an experiment and the wavelengths to be used with the selected probe must not interfere with those of another probe to be used. Very often, the vendors of the fluorescent probes can give sound advice as to the best probe to choose to measure intracellular $[Ca^{2+}]$ in a given experiment.

If more than one type of instrument is available (spectrofluorometer, digital imaging microscope, single-cell ratio detection, or confocal microscope), the second choice involves what instrument to use. When one is interested in the statistical behavior of a large number of cells and how the average Ca^{2+} levels change, and when the Ca^{2+} transient behavior of the individual cells is not important, then a spectrofluorometer is the instrument of choice. A spectrofluorometer usually has simpler optics, a wide range of wavelength response, and excellent sensitivity. Disadvantages are that it requires suspended cells (which often behave differently from plated cells and from cells in vivo). In addition, it requires a larger number of cells for each sample than the plated-cell techniques, and probe leakage can cause severe errors in the measurement of internal free Ca^{2+}. When one is interested in the differential responses of a group of individual cells, the digital imaging microscope is the instrument of choice, since the individual responses of a large group of cells can be compared in the same field of view. In addition, if the cells are difficult to keep in suspension, it is still possible to get an idea of the statistical behavior of these cells by using this technique, which employs plated cells. Far fewer cells are needed for digital imaging microscopy than for fluorescence spectroscopy. Fluorescence digital imaging microscopy (FDIM) is good for following the behavior of free Ca^{2+} in the cytosol (including following Ca^{2+} transients), but unless the cell is very flat, this technique is not ideal for observing free Ca^{2+} in compartments such as mitochondria. Another common disadvantage of FDIM is a limited range of permitted intensity values (commonly 256). If one needs to follow free Ca^{2+} in compartments such as mitochondria or the nucleus, it is better to use a confocal microscope. The confocal microscope can have the same problems with limited range of intensity values as digital imaging microscopy. Its primary advantages are better resolution and its ability to produce a three-dimensional image of the cell. However, it requires higher light exposure, which increases the possibility of photodamage to the cells, and it requires the use a laser for excitation, which limits the probes that can be used. The last technique is single-cell ratio detection. This technique uses a microscope in conjunction with a photomultiplier rather than the SITS or CCD camera of digital imaging. It can be used to observe a group of plated cells in the same way that fluorescence spectroscopy observes a group of cells in suspension and it can be very sensitive. It has the advantages of the digital imaging microscope in that leakage of probe from the cell does not generally cause interference by the external probe, and it uses far fewer cells per experiment than the cuvette system uses. It can also be used to observe single cells, but is inefficient in this mode if sample additions to the plate cause

irreversible changes to all of the cells on the plate, in which case it is possible to observe only one cell per plate.

BASIC PROTOCOL 1

MEASUREMENT OF INTRACELLULAR [Ca^{2+}] USING FLUORESCENCE SPECTROSCOPY

Where sources of fluorescence (fluorophores) behave independently—i.e., do not transfer energy to or from one another—the total emission at a given wavelength, $\lambda_{m,}$ due to excitation at another wave length, λ_x, can be looked upon as the sum of the contributions from each type of fluorescent molecule present, including the specific probe or probes of interest. Under these conditions, a specific excitation and emission spectrum can be associated with each fluorescent species. Examples of fluorescent species are the Ca^{2+} probe of interest with a Ca^{2+} ion bound, the Ca^{2+} probe of interest without a Ca^{2+} ion bound, or the common endogenous fluorophore NADH. In general, if there is no energy transfer, one could attempt to analyze an experimental spectrum into its component parts where each part is due to a separate fluorescent species. This approach of separating the experimental spectrum into its component parts by curve (spectrum) fitting is the basis of the fluorescence spectroscopic analysis technique for determining [Ca^{2+}] (Gunter et al., 1988, 1990).

The same assumptions lead to the equations usually used in determining [Ca^{2+}] when fluorescent probes are used. In the following equation:

$$\left[Ca^{2+}\right] = K_d\left[\left(F - F_{min}\right)/\left(F_{max} - F\right)\right]$$

Equation 2.5.1

where F is the fluorescence emission of the sample containing the Ca^{2+} probe, at any wavelength, F_{min} is the fluorescence of the sample with no Ca^{2+} bound, and F_{max} is the fluorescence of the sample saturated with Ca^{2+}(Grynkiewicz et al., 1985). K_d is the apparent dissociation constant of the probe for Ca^{2+} within the cell. Any background contributions that do not change as [Ca^{2+}] is changed are automatically subtracted out using this equation. This equation can be used whether the Ca^{2+} probe of interest is ratiometric or not.

Another equation (Grynkiewicz et al., 1985) that can be used with ratiometric probes is:

$$\left[Ca^{2+}\right] = K_d\left[\left(R - R_{min}\right)/\left(R_{max} - R\right)\right]\left(S_f / S_b\right)$$

Equation 2.5.2

For probes that are ratiometric in excitation, S_f and S_b are the fluorescence emissions at any wavelength (λ_m) for a unit amount of the unbound probe and bound probe, respectively, where excitation is at wavelength λ_2. K_d is again the apparent dissociation constant, and R is the ratio of emission of the experimental sample at λ_m where excitation is at λ_1 to that where excitation is at λ_2. R_{max} and R_{min} are the ratios where [Ca^{2+}] is saturating and negligible, respectively. For probes that are ratiometric in emission, R should be interpreted as the ratio of emission at λ_1 to that at λ_2 where excitation is at any wavelength λ_x. R_{max} and R_{min} are the same where [Ca^{2+}] is saturating and negligible, respectively. S_f and S_b are the fluorescence emission at λ_2 for excitation at any wavelength λ_x for the unbound and bound probe, respectively. While it is not obvious from the equations, any background contributions that do not change with [Ca^{2+}] are correctly handled through this equation, without explicit subtraction, if the R, R_{max}, and R_{min}, as well as S_f and S_b, are all measured with identical background contributions present.

The operant words here are identical background contributions. If the background contributions due to autofluorescence at λ_1 and λ_2 (F_{a1} and F_{a2}) and incomplete conversion products (F_{i1} and F_{i2}) are large with respect to the minimum corrected fluorescence (sample fluorescence minus supernatant fluorescence) and there is >5% loss of internal probe over the course of the experiment, it is possible to get a 5% error in measured free [Ca^{2+}] even when the supernatant fluorescence (F_{s1} and F_{s2}) is subtracted. In addition, autofluorescence can change significantly during certain experimental protocols (Jiang and Julian, 1997); these changes must be ascertained as well as their strength relative to the internal calcium-sensitive probe. Thus, if one does not in general plan to subtract background contributions from the fluorescence measurements, one should still measure F_{a1}, F_{a2}, F_{i1}, F_{i2}, and probe leakage rate to ensure the accuracy of the results. F_{a1}, F_{a2}, and probe leakage rate are easy to measure; F_{i1} and F_{i2} are very difficult to measure, but it is possible to get an estimate of F_{i1} and F_{i2} and work to decrease their size by altering the incubation procedure. Note that the membrane-permeable form of the probe, often called the AM or acetoxymethyl ester form, should not be a problem because proper washing of the cells should reduce this form of the probe to very small values.

The following equations are pertinent:

in media of any [Ca^{2+}]

$$F_t = F_a + F_i + c_d\left[f_{hi}F_{hi} + (1 - f_{hi})F_{lo}\right] + F_s$$

Equation 2.5.3

in high [Ca^{2+}] media

$$(F_t)_{hi} = F_a + F_i + c_d F_{hi} + (F_s)_{hi}$$

Equation 2.5.4

in low Ca^{2+} media

$$(F_t)_{lo} = F_a + F_i + c_d F_{lo} + (F_s)_{lo}$$

Equation 2.5.5

where F_t is total, uncorrected fluorescence, F_s is the fluorescence of the supernatant, F_a is the autofluorescence of the cells, and F_i is the calcium-insensitive, incomplete conversion products of the probe, c_d is the μM concentration of Ca^{2+}-sensitive probe inside the cells, F_{hi} and F_{lo} are the fluorescence of 1 μM concentrations the Ca^{2+}-sensitive probe inside the cells in high- and low-Ca^{2+} forms, respectively and f_{hi} is the fraction of the Ca-sensitive probe in the high-Ca^{2+} form under any conditions. Autofluorescence is given by:

$$F_a = F_{ta} - F_{sa}$$

Equation 2.5.6

where F_{ta} is the fluorescence of cells without the probe at the same concentration as is used in the rest of the experiment in standard medium (see Reagents and Solutions), and F_{sa} is the fluorescence of the supernatant obtained when these cells are centrifuged 3 min at $200 \times g$.

It would be nice if F_i could be measured as easily as F_a, but measurement of F_i is difficult. It is best to estimate F_i and vary the incubation procedure to minimize its contribution. Accurate measurement of the parameters on the right side of Equations 2.5.1 and 2.5.2 is the essence of the most common way of determining intracellular [Ca^{2+}] by these fluorescence techniques. In general, this means at the very least subtracting F_s, and if F_a is a substantial fraction of the total fluorescence, it should be subtracted as well.

The steps of the measurements consist of: (1) choosing the fluorescent probe to use and checking its fluorescent characteristics in the system; (2) incubating the cells with a fluorescent probe; (3) setting up the instrument for initial measurements; (4) making measurements using a ratiometric probe; (5) assessing leakage problems; and (6) measuring of K_d.

IMPORTANT NOTE: Fluorescence is a very sensitive optical technique, but the price paid for high sensitivity is that the quantum yield, the absorbance or excitation, and even in some cases the spectra vary with many changes in conditions. Therefore, the key to accuracy in fluorescence measurements of free ion concentration is to make sure that the experimental spectra and all of the control experiments necessary for quantification are measured under conditions that are as similar as possible.

Materials

5 μM fluorescent probe free acid (FA) in low-Ca medium (see recipe)
5 μM FA in high-Ca medium (see recipe)
2 to 5 mM AM form of fluorescent Ca^{2+} probe (see recipe)
Standard medium (see recipe), ice cold
2×10^6 to 1×10^7 cell/ml suspension of sample cells in standard medium
1× calibration medium (see recipe)
2 × high-Ca medium (see recipe)
Detergent: e.g., *N*-octyl β-D-glucopyranoside
2× low-Ca medium (see recipe)
10 μM FA solution (see recipe)
Factor that will induce changes in [Ca^{2+}]
0.1 mM thapsigargin (see recipe)
2 mM oligomycin (see recipe)
1 mM carbonyl cyanide *m*-chlorophenyl hydrazone (CCCP) in ethanol (store indefinitely at −20°C; use caution as compound is hazardous)
1 mM ionophore (see recipe)
Experimental factors

Fluorescence spectrometer that can excite and detect in necessary wavelength ranges and has ability to constantly stir samples
Low-speed centrifuge for washing cells
Absorption cuvettes
Fluorescence cuvettes
37°C shaker bath
4°C agitator or shaker bath
Cuvette stir bars, preferably star head or X-shaped

Choose and characterize fluorescent probe

1. Choose the probe (see Strategic Planning).

   When working with a new [Ca^{2+}] probe, it is worthwhile to take spectra over the range of sensitivity of the probe. These measurements require the Ca^{2+}-sensitive form of the probe.

2. Make up mixtures of 5 μM probe free acid (FA) in high-Ca solution/5 μM FA in low-Ca solution at the following ratios: 0:100, 50:50, 60:40, 65:35, 70:30, and 100:0.

   These will result in [Ca^{2+}] of approximately the following: <1 nM, 67 nM, 198 nM, 678 nM, 5 μM and 50 μM, respectively.

3. Turn on the fluorescence spectrometer.

   When using an excitation ratiometric probe such as Fura-2, or a nonratiometric probe, start with the excitation slits set to between 1 and 2 nm in width and emission slits set to between 2 and 20 nm. When using Indo-1, set the excitation slits between 2 and 20 nm and the emission slits to between 1 and 2 nm in width. The actual slit widths to be used will depend upon the sensitivity of the system.

   CAUTION: *Make sure the bandwidth for excitation does not overlap the bandwidth for emission. If they overlap, the light scattering peak may be intense and might damage the detector. For a slit that is only used to attenuate the incident light, start with it partially closed in order to protect the photomultiplier tube.*

4. Add 3 ml of either the 0:100 or 100:0 solution from step 2 to a cuvette, choosing the solution which is expected to have the most intense emission. Turn on stirring.

   Always use stirring while obtaining cell fluorescence in a cuvette.

5. With emission set to the value suggested in Table 2.5.1 or Table 2.5.2, scan excitation, then set excitation at the peak excitation value and scan emission. Set the emission at the peak emission value, and then, while monitoring fluorescence, slowly open the protective slit while decreasing the emission slits (excitation slits for Indo-1) until the protective slit is wide open and the emission slits (excitation slits for Indo-1) are open just enough to obtain a maximum signal.

   For example, for Fura-2, use the 100% high-Ca solution for this step.

6a. *For all probes except ratiometric emission probes such as Indo-1:* With emission set at its peak value and all slits remaining fixed, scan excitation. Replace the above solution in turn with each of the high-Ca/low-Ca mixtures (prepared as in step 2) and scan them.

6b. *For ratiometric emission probes such as Indo-1:* With excitation set at its peak value and all slits remaining fixed, scan emission. Replace the above solution in turn with each of the high-Ca/low-Ca mixtures (prepared in step 2) and scan them.

7. Plot all these spectra on the same graph to give the characteristic spectra to be expected from the chosen Ca^{2+}-sensitive probe in the system and an idea of the slit widths that may be needed for use in the experiments.

   These spectra will give an approximate indication of R_{max} and R_{min} and also the approximate location of the probe's isosbestic point, λ_i, for the system. The wavelengths to be used for a ratiometric probe are usually chosen to make the sensitivity range as large as possible, which means making the ratio of R_{max}/R_{min} as large as possible. For Fura-2 and its analogs, these wavelengths are 340 nm and 380 nm with emission at 505 to 510 nm. For Indo-1 these wavelengths are 405 nm and 480 nm with excitation at approximately 350 nm. These wavelength pairs should only be used if the minimum fluorescence is never very close to background; if it is, the wavelength for which the signal is too close to background will have to be modified to increase its intensity, even if this means a loss in sensitivity. This is usually only a problem for FDIM (see Basic Protocol 2) where only a limited range of values for F are available.

   For a nonratiometric dye, these spectra will indicate the best excitation and emission wavelengths to use as well as the maximum sensitivity of the dye, F_{min}/F_{max}. Here, F_{min} equals the minimum fluorescence in the presence of low (or high) calcium and F_{max} equals the maximum fluorescence in the presence of high (or low) calcium.

If the spectrometer has dual-excitation monochromators with rapid switching between them, it is not necessary to balance the light intensity from the two monochromators. In fact it is often advantageous to purposely vary the light intensity between the two monochromators in order to increase sensitivity—i.e., provide more light at the wavelength for which F is lowest. This changes the measured values of R_{max} and R_{min} from day to day; however, the maximum range is independent of manipulations of this type and is characteristic of the probe and its condition. In order to obtain values of R_{max} and R_{min} that are independent of this variation, measured values of R, R_{max} and R_{min} should be corrected for this difference in light intensity (see Basic Protocol 1, step 11). This correction should also be applied when using dual-emission monochromators. When using a dual-excitation spectrometer, be sure to check for cross-talk between the two monochromators and eliminate it before starting to take data. A probe's maximum sensitivity varies slightly from lot to lot of commercially available probe and generally decreases with time as the probe changes chemically. In addition, these ratios are also a function of the solvent and hence will likely be different in the cytosol from what is measured here.

Incubate cells with probe

8. Dilute an aliquot of the AM form of the probe to a concentration of 2 to 20 μM in standard medium and mix well by vortexing or shaking. Immediately mix with an equal volume of sample cells in suspension to a final concentration of 1 to 10 μM probe with cells at $1–5 \times 10^6$ (do not incubate all of the cells with the permeant form of the probe because some probe-free cells are needed for autofluorescence corrections; see steps 13 and 18). Allow this mixture to incubate at 37°C in a shaker bath for between 30 min and 1 hr.

   IMPORTANT NOTE: *The final concentration of probe should be no more that 5 μM if at all possible because higher concentrations tend to result in incomplete enzymatic hydrolysis of the AM esters, accumulation of lipophilic AM esters in membrane lipids, and accumulation of formaldehyde from AM ester hydrolysis. Incubation should be done at 37°C unless it is desirable to have the probe present in intracellular organelles such as mitochondria, in which case, incubation should be carried out at 4°C for ~2 hr.*

   Approximately 10^8 cells will be needed to complete an experiment with 20 samples.

   While injection or other special techniques are sometimes used to load a cell with probe, the most common loading technique is to incubate the cells with a membrane-permeable, Ca^{2+}-insensitive form of the probe. The acetoxymethyl ester forms of Fura-2 and Indo-1 are used for this purpose. They are converted by the esterases in the cell interior to the pentacarboxylic acid (free acid; FA) form which is Ca^{2+}-sensitive and relatively membrane-impermeable. The operant word here is "relatively," since many cell types contain organic ion transporters (di Virgilio et al., 1990; Kao, 1994) and/or the P-glycoprotein multidrug transporter (Homolya et al., 1993), which extrude FA and AM esters of these probes from the cell, respectively. If such leakage is a problem for the cell type, use one of the leakage-resistant probes such as Fura PE-3 or add transport inhibitors such as probenecid or sulfinpyrazone.

9. Wash cells two to three times in ice-cold standard medium, each time by centrifuging 3 min at ~$200 \times g$, 4°C, removing the supernatant, and gently resuspending cells in standard medium to the original concentration. Resuspend the final pellet at 2×10^6 to 1×10^7 cells/ml using standard medium. Store the incubated cells at 4°C with constant agitation to prevent anoxia. Dilute 3 x 10^6 cells with standard medium to a final volume of 3 ml and centrifuge 3 min at ~200 x g at 4° C. Carefully remove the supernatant for measuring $(F_s)_1$ and $(F_s)_2$ at $t = 0$.

   Keeping the cells at 4°C also decreases the leakage of probe into the external medium and hence decreases problems associated with external probe. As long as $[Ca^{2+}]$ in the external medium is the same as that of the standard medium, a plot of (F_s) at λ_1 or λ_2 versus time gives a measure of leakage rate at 4°C.

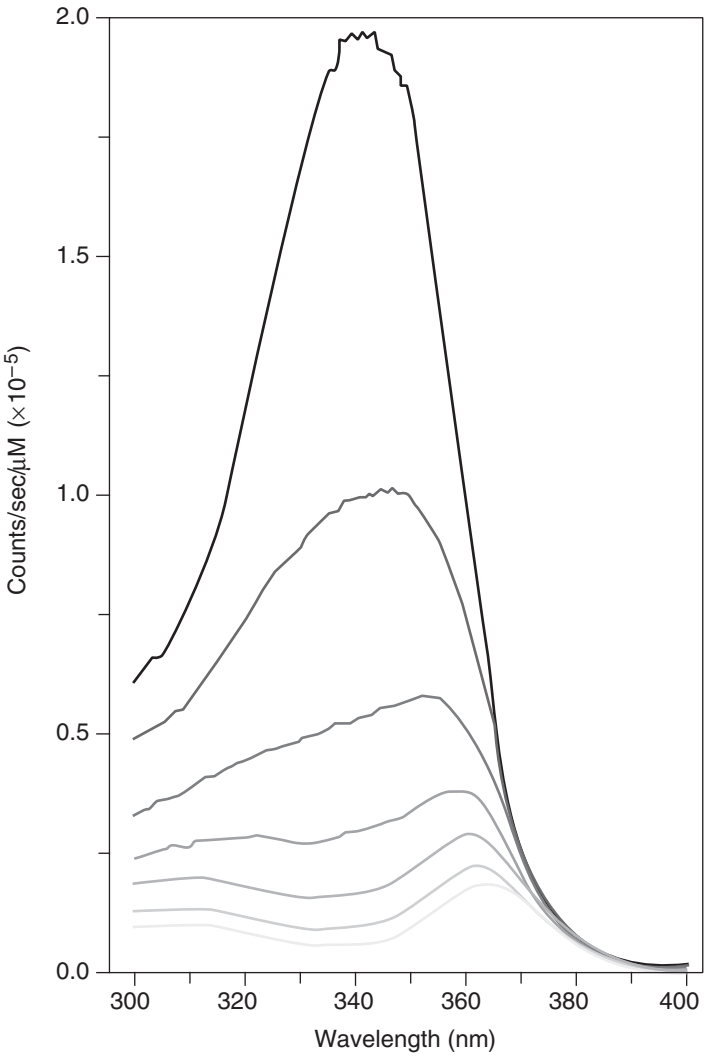

Figure 2.5.1 Inner filter effect on the Ca-bound spectra of Fura-2 FA. The curves are normalized to counts/sec/μM. As the curves decrease in height, Fura-2 FA concentrations are 3, 17.73, 45.93, 32.04, 59.43, and 72.56 μM, respectively.

Set up the instrument for initial measurements

10. Place an aliquot of incubated cells in an absorption cuvette at a concentration of 10^6 cells/ml (most instruments require a volume of 2 to 3 ml). Check the attenuation (light scattering plus absorbance) of the incident beam by the cell suspension at the excitation wavelength(s).

    IMPORTANT NOTE: *For this and all further spectrophotometric measurements, turn on stirring and temperature control for the cuvette and allow time for the sample to reach the temperature of the experiments (37°C or room temperature). From this point on it will be assumed that cells will be run at a concentration of 10^6 cells/ml in a volume of 3 ml. If this not the case, modify these instructions accordingly.*

    As a rule of thumb, the attenuation should be <0.05 absorbance units. If the turbidity (light scattering) or absorbance is too high, the intensity of the excitation beam is significantly decreased before reaching the region of the fluorescence cuvette within which fluorescence is measured (inner-filter effect; Fig. 2.5.1). Since this attenuation is a function of wavelength, it can artificially distort the spectra (or the ratios) and must be avoided. It is usually

possible to study fluorescent probes in a suspension of 10^6 cells per ml. Sensitivity can be increased by increasing the concentration of cells, but the cell concentration must not be increased to the point where inner filter effect due to the absorbance and scattering by the cells becomes a problem at any relevant wavelength.

Perform measurements

The following steps apply to all ratiometric probes except those ratiometric in emission such as Indo-1. For the latter types of probes, follow the instructions in parentheses regarding either excitation or emission.

Estimate calcium-insensitive fluorescence (F_i)

11. Wash 6.5×10^6 incubated cells three times in ice-cold 1× calibration medium, each time by centrifuging 3 min at ~200 × *g*, 4°C, removing the supernatant, and resuspending at 2×10^6 cells/ml in 3.25 ml of 1× calibration medium. Place 1.5 ml of 2× high-Ca medium in a cuvette, then add 1.5 ml of the washed cells and sufficient detergent (~0.1% to 1% w/v final concentration) such as *N*-octyl b-d-glucopyranoside to dissolve the cells. Check the intensity of fluorescence by gradually opening the protective slit as in step 5 while alternating between the two excitation (emission) wavelengths λ_1 and λ_2. If necessary, adjust the emission (excitation) slits until the total fluorescence in the presence of detergent at λ_1 $(F_{td})_{hi1}$ is ~80% of the maximum permissible fluorescence intensity. Measure total fluorescence in the presence of detergent and high calcium, $(F_{td})_{hi}$, at the wavelengths λ_1 and λ_2. Do a scan, $(S_{td})_{hi}$, of excitation (emission) including λ_1, λ_2, and the likely isosbestic point. When using dual-excitation (emission) monochromators, set both monochromators to the same wavelength (λ_1), and measure the ratio of the light between the two monochromators R_L, where $R_L = F_{mono1}/F_{mono2}$. Mono1 is the monochromator that measures λ_1 and mono2 is the monochromator that measures λ_2. Measured ratios can then be corrected for this artifact by dividing all ratios by R_L.

    R_L is generally constant during the course of a single experiment, but tends to vary between experimental sessions. Hence, it should be measured at least twice in every experimental session. Any sample containing the probe will be adequate for this measurement.

    How to choose the wavelengths, λ_1 and λ_2, was discussed in the annotation under step 7. For Fura-2 and its analogs, λ_1 is generally 340 nm and λ_2 is generally 380 nm with emission at 505 to 510 nm. For Indo-1, λ_1 is generally 405 nm and λ_2 is generally 480 nm with excitation at 350 nm.

    The estimation of F_i will be described first, since this procedure can also be used to determine the proper slits to be used for the experiment. In addition, measurement of F_i can immediately indicate whether or not the incubation procedure is adequate for the application. The goal is to identify a procedure that results in negligible F_i. This goal can usually be attained. For more details on estimating F_i, see Commentary.

    IMPORTANT NOTE: *N-octyl β-d-glucopyranoside is suggested as the best detergent because it causes few changes in the extinction coefficient or quantum yield of either the high- or low-Ca^{2+} forms of most Ca^{2+} probes. To use another detergent, check its effects on the spectra and intensity of the high or low Ca^{2+} FA forms of the probe and on the AM form of the probe.*

12. Place 1.5 ml of 2 × low-Ca medium in a cuvette, add 1.5 ml of cells washed as in step 11, and add the same amount of detergent as in step 11. Measure total fluorescence in the presence of detergent and low calcium, $(F_{td})_{lo}$, at the wavelengths λ_1 and λ_2. Do a scan, $(S_{td})_{lo}$ as in step 11.

13. Wash cells that were not exposed to the probe in 1× calibration medium as in step 11 and resuspend them in 1× calibration medium at 1×10^6 cells/ml. Place 3 ml of these cells in a cuvette and add the same amount of detergent used in steps 11 and 12.

Measure total autofluorescence in the presence of detergent, F_{ad}, at the wavelengths λ_1 and λ_2. Do a scan, S_{ad} as in step 11.

14. Place 1.5 ml of 2× high-Ca medium in a cuvette, add 1.5 ml of 2 to 10 μM FA in 1× calibration medium, and add the same amount of detergent used in step 11. Measure total fluorescence at the wavelengths λ_1 and λ_2—which is equal to $(d_c - F_{hid})$ where d_c is the concentration of Fura-2 FA in μM and F_{hid} is the fluorescence of 1 μM of the Ca-sensitive form of the probe in high-calcium medium in the presence of detergent. Do a scan, S_{hid}, as in step 11.

15. Dilute 10 μM FA solution with 1× calibration medium to create a probe concentration in the range of 2 to 10 μM. Place 1.5 ml of 2× low-Ca medium in a cuvette, add 1.5 ml of the 2 to 10 μM FA in 1× calibration medium, and add same amount of detergent used in step 11. Measure total fluorescence at the wavelengths λ_1 and λ_2—equal to $(d_c - F_{lod})$, where F_{lod} is the fluorescence of 1 μM of the Ca-sensitive form of the probe in low-Ca medium in the presence of detergent. Do a scan, S_{lod}, as in step 11.

    The actual concentration of the diluted FA added to the cuvette should be such that it is unnecessary to change the excitation or emission slits.

16. Calculate c_d using the values of $(F_{td})_{hi}$, $(F_{td})_{lo}$, F_{hid}, and F_{lod} measured at λ_1 above in steps 11, 12, 14, and and 15, respectively.

    Starting with Equation 2.5.4 and Equation 2.5.5, it is easy to see that $c_d = [(F_{td})_{hi} - (F_{td})_{lo}]/[F_{hid} - F_{lod}]$, regardless of the wavelength used to make the measurements.

17. With values for c_d, $(F_{td})_{hi}$, F_{hid}, and F_{ad} (see step 13), calculate $F_{id} = (F_{td})_{hi} - c_d F_{hid} - F_{ad}$ for each wavelength. Using the appropriate software program or a spreadsheet such as Excel, calculate $S_{id} = 0.5[(S_{td})_{hi} - (c_d/d_c)S_{hid} + (S_{td})_{lo} - (c_d/d_c)S_{lod}] - S_{ad}$. Assume that F_{id} (in the presence of detergent) approximately equals F_i (inside the cell in the absence of detergent) at each wavelength.

    IMPORTANT NOTE: *If F_i is negligible, steps 11 through this step can be skipped in future work using the same incubation protocol with the same cell type.*

Measure autofluorescence (F_a)

18. Dilute 3×10^6 cells that were not incubated with the probe to a final volume of 3 ml in standard medium and place in the cuvette. Measure total autofluorescence, F_{ta}, at the two wavelengths λ_1 and λ_2, under the same conditions that will be applied to the experimental samples. Remove this sample and centrifuge it at $200 \times g$ for 3 min. Carefully remove the supernatant and place it in the cuvette. Measure total fluorescence of the supernatant, F_{sa}, at the two wavelengths λ_1 and λ_2. Calculate $(F_a)_1 = (F_{ta})_1 - (F_{sa})_1$ and $(F_a)_2 = (F_{ta})_2 - (F_{sa})_2$.

    IMPORTANT NOTE: *If F_a is negligible, this step can be skipped in future work using the same incubation and sample protocols with the same cell type.*

Determine R_{max}, R_{min}, S_f, and S_b

19. Wash incubated cells in standard medium and resuspend at 1×10^6 cells/ml in a cuvette. Set the spectrometer to scan excitation (emission for probes that are ratiometric in emission) around the likely isosbestic point λ_i. Add some factor that will induce changes in $[Ca^{2+}]$ and immediately initiate multiple scans around λ_i until the pulse is more or less complete. Plot all of these scans on the same graph and determine λ_i.

    Factors which induce changes in $[Ca^{2+}]$ are dependent upon the cell type. Many cells when exposed to high potassium in the external medium will depolarize which results in a high calcium pulse. Most cell types respond to specific hormones. For example, chondrocytes respond to parathyroid hormone; liver cells respond to vasopressin, catecholamines, and

angiotensin; brain cells respond to almost all of the neurotransmitters. In addition, many cell types respond to thapsigargin, and muscle cells respond to caffeine.

20. Wash 6.5×10^6 incubated cells (from step 9) with 1× calibration medium and resuspend at 2×10^6 cells/ml. Place 1.5 ml of 2× high-Ca medium in a cuvette and add 1.5 ml of the cells which have just been washed.

21. When the proper temperature is reached, add 30 µl of 0.1 mM thapsigargin, 15 µl of 2 mM oligomycin, 15 µl of 1 mM CCCP, and 30 µl of 1 mM ionophore. Immediately start recording the time-based changes in fluorescence at λ_1 and λ_2 [$(F_t)_{hi1}$ and $(F_t)_{hi2}$, respectively]. As soon as these values reach an apparent steady state, record their average values and then scan excitation $(S_t)_{hi}$ (emission for probes that are ratiometric in emission). Remove the sample and immediately centrifuge it at $200 \times g$ for 3 min and save the supernatant (SN_{high}), which is taken to evaluate leakage and to correct $(F_t)_{hi1}$ and $(F_t)_{hi2}$ for spectral changes due to leakage.

    Final concentrations are 1 µM thapsigargin 10 µM oligomycin, 5 µM CCCP, and 10 µM ionophore. The CCCP is used to break down all of the cell's pH gradients. Vanadate (in the calibration medium) is used to inhibit the plasma membrane Ca^{2+} ATPase. The ionic composition of the calibration medium is used to prevent the Na^+-Ca^{2+} plasma membrane exchanger from generating a Ca^{2+} gradient. Together the ionomycin, vanadate, and ionic composition are used to equilibrate internal free Ca^{2+} with external free Ca^{2+}. Ouabain (in calibration medium) is used to inhibit the Na-K ATPase, and thapsigargin is used to empty the internal endoplasmic or sarcoplasmic reticulum stores. Oligomycin is used to prevent the mitochondria from utilizing all of the cellular ATP in an attempt to regenerate its membrane potential. The idea is to obtain the fluorescent intensities from inside the cell before cell death causes substantial loss of probe to the external medium. If too much time is allowed to elapse, probe will begin to leak out of the cell, and if the spectrum of the probe in the external medium is different from that inside the cell, these values will begin to change as soon as substantial leakage occurs.

    One of the biggest problems in calibration is accurately determining (S_f/S_b), because any variation in probe leakage will cause an error in this ratio. The amount of probe leakage can be determined by the intensity of fluorescence at the isosbestic point. However, because of association with intracellular proteins, the isosbestic point of the intracellular probe may be shifted from that in medium. To determine the intracellular isosbestic point λ_i, subject an aliquot of the cells to an agent that will induce significant changes in $[Ca^{2+}]$ (e.g., an agonist or transient depolarization with Ca^{2+} uptake through channels) and identify the wavelength at which there is no change of fluorescence intensity.

    Making sufficient ionophore available to the cells can be a real problem. Williams and coworkers (Williams and Fay, 1990) suggest that Br-A23187 may sometimes work better than ionomycin because its action is independent of pH. If there is difficulty in obtaining a substantial change in R in going from R_{min} to R_{max}, see Troubleshooting.

    When using an instrument that has two (dual excitation/emission) monochromators, $(F)_1$ or $(F)_2$ measured in the ratio mode will not necessarily be identical to the values of fluorescence taken at λ_1 and λ_2 from the excitation (emission) scan. This is because most of these machines scan either the first or second monochromator but not both. The values of $(F)_1$ or $(F)_2$ measured in the ratio mode will be used to calculate R_{max}, R_{min}, S_f and S_b. The scans will be used to correct S_f/S_b for loss of probe during calibration.

22. Repeat steps 20 and 21 using 1.5 ml of 2× low-Ca medium instead of 2× high-Ca medium.

    The resulting measurements are time scans of $(F_t)_{lo1}$ and $(F_t)_{lo2}$ at λ_1 and λ_2, respectively, and the excitation (emission for probes that are ratiometric in emission) scan $(S_t)_{lo}$. The resulting supernatant is SN_{low}.

23. For each of the supernatants (SN_{high} and SN_{low}), measure average fluorescence at λ_1 and λ_2 [$(F_s)_{hi1}$, $(F_s)_{lo1}$ and $(F_s)_{hi2}$, $(F_s)_{lo2}$, respectively] and then scan excitation (emission) of the supernatants [$(S_s)_{hi}$ and $(S_s)_{lo}$].

24. If the value of F_a found in step 18 is not negligible with respect to the internal probe fluorescence values ($F_t - F_s$) at λ_1 and λ_2 for both high and low calcium concentrations, then repeat steps 20 to 23 using 6.5×10^6 cells that were not treated with the probe—the resulting average fluorescence values will be $(F_{ta})_{hi1}$, $(F_{ta})_{hi2}$, $(F_{ta})_{lo1}$, $(F_{ta})_{lo2}$, $(F_{sa})_{hi1}$, $(F_{sa})_{hi2}$, $(F_{sa})_{lo1}$, and $(F_{sa})_{lo2}$. Use Equation 2.5.6 ($F_a = F_{ta} - F_{sa}$) to calculate $(F_a)_{hi1}$, $(F_a)_{hi2}$, $(F_a)_{lo1}$, and $(F_a)_{lo2}$. Use the appropriate software program or a spreadsheet such as Excel to calculate $(S_a)_{hi} = (S_{ta})_{hi} - (S_{sa})_{hi}$ and $(S_a)_{lo} = (S_{ta})_{lo} - (S_{sa})_{lo}$.

25. Calculate the calcium-sensitive cellular probe fluorescence, $(F) = (F_t) - (F_s) - (F_a) - (F_{id})$, for each wavelength and calcium concentration—i.e., calculate $(F)_{hi1}$, $(F)_{hi2}$, $(F)_{lo1}$, and $(F)_{lo2}$ where the values of $(F_{id})_1$ and $(F_{id})_2$ were obtained in step 17. Use the appropriate software program or a spreadsheet such as Excel to calculate the spectrum $(S)_{hi}$ and $(S)_{lo}$, where $S = S_t - S_s - S_a - S_{id}$. Compare $(S)_{hi}$ with the high-calcium spectrum found in step 7 for the high-calcium form of the probe in solution.

These two spectra should be very similar if S_{id} is small. If they are not, it is likely that either the sample did not reach a sufficiently high value of $[Ca^{2+}]_{inside}$ or that there are problems with inner filter effect. If $[Ca^{2+}]_{inside}$ approximately equals $[Ca^{2+}]_{outside}$, then $(S)_{hi}$ will look like a combination of the high- and low-calcium spectra found in step 7. If this is not the case, there probably are problems with the inner-filter effect, which is the result of having too much total dye in the viewing volume (see Troubleshooting for discussion of the impact of the inner-filter effect on spectra). Likewise, $(S)_{lo}$ should be very similar to the low-calcium spectrum found in step 7.

If $[Ca^{2+}]$ inside the cells does not approximately equal $[Ca^{2+}]_{outside}$ during these measurements, the resulting values of R_{min} and R_{max} will be incorrect and result in erroneous values of $[Ca^{2+}]$. See Support Protocol 1 for information on how to determine how bad the measured values of R_{min} and R_{max} may be and how to determine more accurate values while measuring K_d.

The assumption that F_{id} is equal to F_i will likely overestimate the value of F_i since it assumes that none of the Ca-insensitive probe was lost from the cells during the calibration procedure. Unless little or no dye was lost during calibration, this will not be true, and so it is very important that F_{id} be much less than F at λ_1 and λ_2 for both high and low calcium concentrations.

26. Calculate $R_{min} = (F)_{lo1}/(F)_{lo2}$ and $R_{max} = (F)_{hi1}/(F)_{hi2}$. Plot $(S)_{hi}$ and $(S)_{lo}$ on the same graph and calculate the constant K such that the spectrum $K - (S)_{lo}$ crosses $(S)_{hi}$ at the isosbestic point λ_i.

λ_i was found in step 19. From the result of the above calculation $(S_f/S_b) = K$—$(F)_{lo2}/(F)_{hi2}$.

If the values obtained for R_{min}, R_{max} and (S_f/S_b) from multiple measurements on the same cell type are approximately constant for the same bandpasses for λ_1 and λ_2 ,then it is probably unnecessary to measure R_{min}, R_{max} and (S_f/S_b) for every experiment as long as the bandpasses for λ_1 and λ_2 remain constant. Instead use the average values of these constants found from multiple experiments.

For dual-excitation (emission) monochromators, $R_{min} = (F)_{lo1}/(F)_{lo2}/R_L$ and $R_{max} = (F)_{hi1}/(F)_{hi2}/R_L$. R_L was found in step 11.

Measure the ratio of samples of interest

27. Start by measuring $(F_s)_1$ and $(F_s)_2$ for the $t = 0$ supernatant that was obtained in step 9. Next, add 3×10^6 incubated cells to the cuvette. Add standard medium and any other needed components for a final volume of 3 ml.

    If much time has elapsed since the cells were incubated, wash them in standard medium before adding them to the cuvette. This becomes necessary only if $(F_s)_1$ or $(F_s)_2$ represents 40% to 50% of $(F_t)_1$ or $(F_t)_2$ after correction for autofluorescence and calcium insensitive dye. Once the cells have been washed a new $t = 0$ time has been created.

    Other needed components are the experimental factors listed in Materials. In some cases, there are no such factors. For example, if the experiment involves following $[Ca^{2+}]$ as a function of time after irradiation or magnitude of irradiation, then each sample is simply suspended in standard medium and measured until a steady state value of R is obtained. On the other hand, perhaps the experiment involves determining the average $[Ca^{2+}]$ versus time for a group of cells after the addition of hormone. In this case, the experimental factor is the hormone. If the time involved in following the cells' response is large, then it will be necessary to start with a large aliquot of cells at 1 x 10^6/ml in standard medium plus the experimental factor in order to determine F_s as a function of time at 37°C or room temperature in order to correct for dye loss during the measurement.

28. Measure $(F_t)_1$ and $(F_t)_2$ and then centrifuge the sample 3 min at $200 \times g$. Record the time when the sample was centrifuged. Carefully remove the supernatant and use it to measure $(F_s)_1$ and $(F_s)_2$. Calculate $(F)_1 = (F_t)_1 - (F_s)_1 - (F_a)_1 - (F_{id})_1$, and $(F)_2 = (F_t)_2 - (F_s)_2 - (F_a)_2 - (F_{id})_2$, where $(F_{id})_1$ and $(F_{id})_2$ were measured in step 17 and $(F_a)_1$ and $(F_a)_2$ were measured in step 18, and then calculate $R = [(F)_1/(F)_2]$. $[Ca^{2+}]$ can then be calculated manually or via the appropriate software program from Equation 2.5.2, where R_{min}, R_{max}, and (S_f/S_b) were calculated in step 26. Either use an estimated K_d such as 225 nM for Fura-2, or measure it as described below for a particular cell type.

    If it was found in calculating R_{max} and R_{min} above that $(F_t)_{hi} - (F_s)_{hi}$ is much greater than $(F_a)_{hi} + (F_{id})$ and $(F_t)_{lo} - (F_s)_{lo}$ is much greater than $(F_a)_{lo} + (F_{id})$ at λ_1 and λ_2, then little error will be generated by eliminating the F_a and F_{id} terms from the sample ratio calculations. That is, instead of calculating $R = [(F_t)_1 - (F_s)_1 - (F_a)_1 - (F_{id})_1]/[(F_t)_2 - (F_s)_2 - (F_a)_2 - (F_{id})_2]$ for the samples, use $R = [(F_t)_1 - (F_s)_1]/[(F_t)_2 - (F_s)_2]$.

    For dual-excitation (emission) monochromators, $R = (F)_1/(F)_2/R_L$ and R_L was found in step 11.

ALTERNATE PROTOCOL

MEASUREMENT OF F_{MIN} AND F_{MAX} WITH NONRATIOMETRIC PROBES

Nonratiometric probes are used in a similar manner to ratiometric probes (see Basic Protocol 1) except that only fluorescent intensities and not ratios are used. That is, $[Ca^{2+}] = K_d [(F - F_{min})/(F_{max} - F)]$ where $F = F_t - F_s - F_a - F_{id}$, $F_{min} = (F)_{lo} = (F_t)_{lo} - (F_s)_{lo} - (F_a)_{lo} - F_{id}$, and $F_{max} = (F_t)_{lo} - (F_s)_{lo} - (F_a)_{lo} - F_{id}$. Clearly, the F_{id} values cancel in calculating $[Ca^{2+}]$ and so it is not necessary to attempt to measure F_{id}. Furthermore, if one can show that F_a approximately equals $(F_a)_{lo}$ and $(F_a)_{hi}$, then autofluorescence can be neglected as well even if the autofluorescence term is not small with respect to probe fluorescence. The main problem with nonratiometric dyes is leakage of dye from the cells with time. If this leakage is approximately zero over the total time course of the experiment, leakage is not a problem. On the other hand, if leakage is measurable over the course of the experiment, then F_{max}, F_{min} and each value of F must be corrected to the zero leakage case in order to obtain the correct value of $[Ca^{2+}]$. This is exactly what is done in steps 11 and 13 where k_{hi}, k_{lo} and k are calculated.

The steps used to measure calcium using nonratiometric probes are essentially the same as those for ratiometric probes except it is generally unnecessary to record wavelength

scans and all of the measurements are made at a single excitation and emission wavelength (see Basic Protocol 1, steps 1 to 7).

Measure autofluorescence (F_a)

1. Measure total autofluorescence, F_{ta}, and the autofluorescence of the supernatant, F_{sa}, as described in Basic Protocol 1, step 18. Calculate $F_a = F_{ta} - F_{sa}$.

   IMPORTANT NOTE: *If F_a is negligible, this step can be skipped in future work using the same incubation protocol and cell type.*

Determine F_{max} and F_{min}

The procedure used to measure F_{max} and F_{min} is basically the same as that used to measure R_{max} and R_{min} for ratiometric dyes. The main source of error that can occur during these measurements is the loss of probe from the cells during the course of the measurements. This fractional loss of probe can only be determined by using standards made with detergent and determining the fraction of probe that escaped into the supernatant during the course of the experiment. Each time the incubated cells are washed as a group, new standards must be made. The group of incubated should be washed as a group whenever F_2 equals 40% to 50% of F. Even so, calcium concentrations determined with nonratiometric dyes are not as accurate as those determined using ratiometric dyes.

2. Wash 1.25×10^7 incubated cells with 1× calibration medium and resuspend at 2×10^6 cells/ml. Measure the total high- and low-calcium fluorescence $(F_t)_{hi}$ and $(F_t)_{lo}$, after an apparent steady state is reached, as described in Basic Protocol 1, steps 20 to 22. Scan excitation of the high-calcium sample and save the spectrum, $(S_t)_{hi}$. Save the supernatants (SN_{high} and SN_{low}).

   SN_{high} and SN_{low} are taken to evaluate probe leakage and to correct $(F_t)_{hi}$ and $(F_t)_{lo}$ for intensity changes due to leakage.

3. Repeat Basic Protocol 1, steps 20 and 21, except along with everything else added, add enough detergent (e.g., *N*-octyl β-d-glucopyranoside) to just dissolve the cells. After a steady state is reached, measure $(F_{td})_{hi}$.

4. Repeat Basic Protocol 1, step 22, except along with everything else added, add the same concentration of detergent that was used in step 31. After a steady state is reached, measure $(F_{td})_{lo}$.

5. Measure the fluorescence of 2.75 ml of SN_{high} obtaining a good average value and save it as $(F_s)_{hi}$. Scan excitation of the high-calcium supernatant and save the spectrum, $(S_s)_{hi}$. Add the same concentration of detergent that was used in step 3. Measure fluorescence again, obtain a good average value, and save it as $(F_{sd})_{hi}$.

6. Measure the fluorescence of 2.75 ml of SN_{low} obtaining a good average value and save it as $(F_s)_{lo}$. Add the same concentration of detergent that was used in step 3. Measure fluorescence again, obtain a good average value, and save it as $(F_{sd})_{lo}$.

7. Wash the remaining incubated cells with standard medium. Add 3×10^6 cells to the cuvette then add standard medium until the final volume is 3 ml. Add the same amount of detergent that was used in step 3. After a steady state is reached, measure F_{td}.

8. If the value of F_a found in step 1 is not negligible with respect to the internal probe fluorescence values $(F_t - F_s)$ for both high and low calcium concentrations, repeat steps 2, 5, and 6. (except do not add detergent to the supernatant) using 6.5×10^6 cells that were not treated with the probe. Scan excitation (emission for probes that are ratiometric in emission) of the high-calcium sample, both total and supernatant.

The resulting spectra are $(S_{ta})_{hi}$ and $(S_{sa})_{hi}$, respectively. The resulting average fluorescence values will be $(F_{ta})_{hi}$, $(F_{ta})_{lo}$, $(F_{sa})_{hi}$, and $(F_{sa})_{lo}$. Use Equation. 2.5.6 ($F_a = F_{ta} - F_{sa}$) to calculate $(F_a)_{hi}$ and $(F_a)_{lo}$. Use the appropriate software program or a spreadsheet such as Excel to calculate $(S_a)_{hi} = (S_{ta})_{hi} - (S_{sa})_{hi}$. If F_a is approximately equal to $(F_a)_{hi}$ and $(F_a)_{lo}$, autofluorescence can be neglected in the calculations below.

9. Calculate the calcium-sensitive cellular probe fluorescence, $(F) = (F_t) - (F_s) - (F_a)$, for each calcium concentration—i.e., calculate $(F)_{hi}$ and $(F)_{lo}$ where F_t was measured in step 2, F_s was measured in steps 5 and 6, and F_a was calculated in step 9. Use the appropriate software program or a spreadsheet such as Excel to calculate the spectrum $(S)_{hi} = (S_t)_{hi} - (S_s)_{hi} - (S_a)_{hi}$, where $(S_t)_{hi}$ was measured in step 2, $(S_s)_{hi}$ was measured in step 5, and $(S_a)_{hi}$ was calculated in step 6. Compare $(S)_{hi}$ with the high-calcium spectrum found in Basic Protocol 1, step 7, for the high-calcium form of the probe in solution.

   These two spectra should be very similar. If they are very different, there are probably problems with inner-filter effect, which must be corrected (see Troubleshooting for discussion of the impact of the inner-filter effect on spectra).

10. Calculate the leakage correction factor $k_{hi} = [(F_{td})_{hi} - (F_{sd})_{hi}]/(F_{td})_{hi}$ where $(F_{td})_{hi}$ was measured in step 3 and $(F_{sd})_{hi}$ was measured in step 5. Likewise, calculate the leakage correction factor $k_{lo} = [(F_{td})_{lo} - (F_{sd})_{lo}]/(F_{td})_{lo}$ where $(F_{td})_{lo}$ was measured in step 4 and $(F_{sd})_{lo}$ was measured in step 6.

11. Calculate $F_{max} = (F)_{hi}/k_{hi}$ and $F_{min} = (F)_{lo}/k_{lo}$, where $(F)_{hi}$ and $(F)_{lo}$ were calculated in step 9.

    IMPORTANT NOTE: *$F_{max} = (F)_{hi}/k_{hi}$ and $F_{min} = (F)_{lo}/k_{lo}$ are the definition of F_{max} and F_{min}. For some nonratiometric probes, F_{min} is larger than F_{max}.*

    If $[Ca^{2+}]$ inside the cells does not approximately equal $[Ca^{2+}]_{outside}$ during these measurements, the resulting values of F_{min} and F_{max} will be incorrect and result in erroneous values of $[Ca^{2+}]$. See Support Protocol 1 for information on how to determine how bad the measured values of F_{min} and F_{max} may be and how to determine more accurate values while measuring K_d.

Measure fluorescence of samples of interest

12. Add 3×10^6 incubated cells to the cuvette. Add standard medium and any other needed components for a final volume of 3 ml.

13. Measure F_t and then centrifuge the sample 3 min at $200 \times g$. Carefully remove the supernatant and measure F_s. Add the same concentration of detergent that was used in step 3. Measure fluorescence again, obtain a good average value, and save it as F_{sd}. Calculate the correction factor $k = (F_{td} - F_{sd})/F_{td}$, where F_{td} was measured in step 7. Calculate $F = (F_t - F_a - F_s)/k$, where F_a was calculated in step 8. Then calculate $[Ca^{2+}] = K_d \cdot [(F - F_{min})/(F_{max} - F)]$, where F_{min} and F_{max} were calculated above in step 11, and either use an estimated K_d such as 390 nm for Fluo-3, or measure it below for the particular cell type under examination.

    IMPORTANT NOTE: *If the additions made to a particular sample result in changes in the free calcium in the external medium, it is necessary to make another measurement of F_{td} (step 7) for cells in this particular medium and calculate the value of k for this particular medium. Likewise, it is necessary to incubate more cells, make another measurement of F_{td} and recalculate k. In this case, this new value of F_{td} must be used to correct the previously calculated values of F_{max} and F_{min} for the new total dye concentration.*

    See Troubleshooting for assessment of leakage problems.

DETERMINATION OF K_d FOR CELLS IN SUSPENSION

The apparent K_d for Ca^{2+} binding to the probe in the cytosol of the cell is not the same as that in medium made up to mimic the cytosol. The reason is that inside the cell, the probe is subject to binding to cell components, as well as to the effects of heavy-metal ions and viscosity differences that cannot be easily mimicked by an artificial medium. Furthermore, part of the intracellular probe may be in compartments of the cell other than the cytosol. The method below assumes that the probe is located within the cytosol and discusses control experiments that can determine if probe fluorescence from mitochondria or other intracellular compartments contributes significantly to the resultant cellular fluorescence signal.

Determination of the intracellular K_d of the probe can be a difficult measurement. Many researchers begin work by assuming a K_d near that for the probe in ionic medium similar to that found in the cell cytosol and only after results have made it clear that accurate measurement of $[Ca^{2+}]$ is important, do they proceed to determine K_d in the cytosol.

For these measurements it is necessary to use combinations of EGTA and Ca^{2+} whose concentrations have been verified by analytical methods. The simplest way to do this is to purchase a calibration kit commercially, e.g., from Molecular Probes. Use a kit that allows dilutation of the Ca^{2+} concentrates into buffered solutions of any composition, so Mg, for example, can be included. These kits contain information on how to use them, but because they have been created to measure K_d in solution, not inside cells, it is necessary to use the procedure discussed below. Standards of this type are essential for measuring K_d in cells in suspension.

For purposes of discussion, the concentrated calibration kit will be assumed to contain solutions that are concentrated by a factor of 10, e.g., like the Molecular Probes Kit, which contains 100 mM K_2EGTA and 100 mM CaEGTA.

This protocol describes methods for measuring K_d for ratiometric and nonratiometric probes for cells in suspension and using either a calibration kit or prepared solutions.

IMPORTANT NOTE: Use extreme care in making dilutions because the accuracy of the calibration depends upon the accuracy of the dilutions made.

Additional Materials (also see Basic Protocol 1)

EGTA solution (see recipe for Ca^{2+} calibration standards)
CaEGTA solution (see recipe for Ca^{2+} calibration standards)
Ca solution (see recipe for Ca^{2+} calibration standards)
1 M $CaCl_2$
Cells incubated with probe (see Basic Protocol 1, step 9)

Determine K_d of a ratiometric probe for cells in suspension at 20°C

1. Make up solutions 1 through 13 using EGTA solution and CaEGTA solution in the proportions shown in Table 2.5.3.

   Table 2.5.3 shows $[Ca^{2+}]$ at 20°C for each of these solutions as well as for the EGTA solution, the CaEGTA solution, and the Ca solution.

   If the calibration is to be performed at 37°C, use Table 2.5.4 to make up solutions 1 through 13. Table 2.5.4 shows $[Ca^{2+}]$ at 37°C for each of these solutions as well as for the EGTA solution, the CaEGTA solution, and the Ca solution.

2. Wash 5.3×10^7 incubated cells with calibration medium and resuspend them in 1× calibration medium at 2.0×10^6 cells/ml.

Table 2.5.3 Composition of K_d Calibration Solutions, pH 7.20 at a Calibration Temperature of T = 20°C

Solution	Parts EGTA solution	Parts CaEGTA solution	Total Ca (mM)	Free $[Ca^{2+}]$ (nM)	$[Ca^{2+}]$ in cuvette (nM)	$[Mg^{2+}]$ in cuvette (mM)
EGTA	1	0	~.001	0.0089	0.0181	0.6952
1	11	1	1.6667	16.24	16.06	0.7128
2	7	1	2.500	25.58	25.28	0.7219
3	4	1	4.000	44.98	44.35	0.7388
4	25	10	5.7143	72.37	71.18	0.7590
5	18	10	7.1429	101.0	99.12	0.7765
6	11	10	9.5238	166.5	162.9	0.8072
7	10	14	11.6667	258.1	251.8	0.8367
8	10	22	13.750	408.2	397.2	0.8671
9	10	35	15.5556	653.2	634.0	0.8951
10	1	6	17.1429	1125	1089	0.9219
11	1	10	18.1818	1881	1817	0.9385
12	1	14	18.6667	2635	2541	0.9469
13	1	22	19.1304	4135	3974	0.9550
CaEGTA	0	1	20.000	61,460	42,030	0.9693
Ca	0	0	8.000	8.00×10^6	3.88×10^6	0.9709

Table 2.5.4 Composition of K_d Calibration Solutions, pH 7.20 at a Calibration Temperature of T = 37°C

Solution	Parts EGTA solution	Parts CaEGTA solution	Total Ca (mM)	Free $[Ca^{2+}]$ (nm)	$[Ca^{2+}]$ in cuvette (nM)	$[Mg^{2+}]$ in cuvette (mM)
EGTA	1	0	~.001	0.0068	0.0136	0.4839
1	9	1	2.000	15.15	15.14	0.5111
2	5	1	3.3333	27.43	27.36	0.5308
3	3	1	5.000	46.04	45.82	0.5574
4	2	1	6.6667	69.57	69.09	0.5865
5	13	10	8.6957	108.0	107.0	0.6259
6	10	11	10.4762	155.9	154.0	0.6645
7	1	2	13.3333	287.8	282.9	0.7362
8	1	3	15.000	436.2	427.2	0.7847
9	1	5	16.6667	735.3	717.1	0.8392
10	1	7	17.500	1036	1007	0.8690
11	1	11	18.3333	1638	1588	0.9007
12	1	17	18.8889	2540	2454	0.9230
13	1	28	19.3103	4183	4020	0.9404
CaEGTA	0	1	20.000	54,940	37,560	0.9674
Ca	0	0	8.000	8.00×10^6	3.88×10^6	0.9709

3. Place 1.50 ml of the 20 mM EGTA solution in a cuvette. Add 1.50 ml of the washed cells. When the proper temperature is reached add 30 µl of 0.1 mM thapsigargin, 15 µl of 2 mM oligomycin, 15 µl of 1 mM CCCP, and 30 µl of 1 mM ionophore to yield final concentrations of 1 µM thapsigargin 10 µM oligomycin, 5 µM CCCP and 10 µM ionophore, respectively. Immediately start recording the time-based changes in fluorescence at λ_1 and λ_2 [$(F_t)_{EGTA\lambda1}$ and $(F_t)_{EGTA\lambda2}$, respectively]. As soon as they reach an apparent steady state, record their average values. Remove the sample and immediately centrifuge it at $200 \times g$ for 3 min and save the supernatant (SN_{EGTA}).

4. Repeat step 3 for each of the EGTA/CaEGTA solutions prepared in step 1 as well as the CaEGTA solution and the Ca solution, resulting in $(F_t)_{1\lambda1}$, $(F_t)_{2\lambda1}$, ..., $(F_t)_{9\lambda1}$, $(F_t)_{CaEGTA\lambda1}$, $(F_t)_{1\lambda2}$, $(F_t)_{2\lambda2}$, ..., $(F_t)_{9\lambda2}$, $(F_t)_{CaEGTA\lambda2}$, $(F_l)_{Ca\lambda2}$, and supernatants SN_1, SN_2, ..., SN_{13}, SN_{CaEGTA}, and SN_{Ca}.

5. For each of the sixteen supernatants, carefully pipet 2.75 ml of the supernatant into the cuvette, and get a good average value of fluorescence at λ_1 and λ_2 resulting in $(F_s)_{EGTA\lambda1}$, $(F_s)_{1\lambda1}$, ..., $(F_s)_{CaEGTA\lambda1}$, $(F_s)_{Ca\lambda1,}$ $(F_s)_{EGTA\lambda2}$, $(F_s)_{1\lambda2}$, ..., $(F_s)_{CaEGTA\lambda2}$ and $(F_s)_{Ca\lambda2}$. Calculate $(F_t - F_s)$ at $_{\lambda1}$ and $_{\lambda2}$ for all of the sixteen samples. Before removing each supernatant, carefully add the same concentration of detergent used in step 11 of Basic Protocol 1 and 40 µl of 1 M $CaCl_2$. Obtain a good average value of fluorescence at λ_1 while stirring. The resulting signals are $(F_{sd})_{EGTA\lambda1}$, $(F_{sd})_{1\lambda1}$, ..., $(F_{sd})_{CaEGTA\lambda1}$, and $(F_{sd})_{Ca\lambda1}$, respectively.

   F_{sd} will be used to determine the fraction of probe lost to the supernatant during the calibration.

6. If the value of F_a found in step 18 of Basic Protocol 1 is not negligible with respect to the internal probe fluorescence values $(F_t - F_s)$ at λ_1 and λ_2 for all of the sixteen samples, then correct F for autofluorescence.

   If this is the case, $(F_a)_{hi1}$, $(F_a)_{hi2}$, $(F_a)_{lo1}$, and $(F_a)_{lo2}$ will have been measured in step 24 of Basic Protocol 1. If $(F_a)_{hi1}$ approximately equals $(F_a)_{lo1}$ and $(F_a)_{hi2}$ approximately equals $(F_a)_{lo2}$, then it can be assumed that $(F_a)_{\lambda1}$ and $(F_a)_{\lambda2}$ are the same for all of the samples. If this is not the case, it will be necessary to calculate $(F_a)_{\lambda1}$ and $(F_a)_{\lambda2}$ for all sixteen samples using the procedure detailed in step 24 of Basic Protocol 1.

7. Calculate $(F)_{x\lambda1} = (F_t)_{x\lambda1} - (F_s)_{x\lambda1} - (F_a)_{x\lambda1} - (F_{id})_{\lambda1}$ and $(F)_{x\lambda2} = (F_t)_{x\lambda2} - (F_s)_{x\lambda2} - (F_a)_{x\lambda2} - (F_{id})_{\lambda2}$ for each of the sixteen different samples, x, where F_{id} is the calcium-insensitive fluorescence found in step 17 of Basic Protocol 1.

8. Place 1.50 ml of the Ca solution in a small beaker. Add 1.50 ml of the washed cells. Add 30 µl of 0.1 mM thapsigargin, 15 µl of 2 mM oligomycin, 15 µl of 1 mM CCCP and 30 µl of 1 mM ionophore while stirring. Carefully pipet 2.75 ml of this mixture into a cuvette. Carefully add the same amount of detergent used in step 5 and 40 µl of 1 M $CaCl_2$ while stirring. Once equilibrium is reached obtain a good average value of fluorescence at λ_1. The resulting signal is $(F_{td})_{Ca\lambda1}$. Calculate the leakage correction factor $k_x = [(F_{td})_{Ca\lambda1} - (F_{sd})_{x\lambda1}]/(F_{td})_{Ca\lambda}$ 1 where $(F_{sd})_{xl1}$ was measured in step 5 for each of the sixteen standards. The results are k_{EGTA}, k_1, ..., k_{CaEGTA}, and k_{Ca}.

   The leakage correction factor corrects F to the value it would have if all of the dye were inside the cells. F_{td} will be used to determine the total probe in each sample. This correction makes it possible to accurately plot F as a function of $[Ca^{2+}]$ and to correctly calculate (S_f/S_b).

9. Once all of the proper fluorescence values have been determined, calculate the corrected fluorescence for each sample x, $F_1 = F_{x\lambda1}/k_x$, $F_{min1} = (F)_{EGTA\lambda1}/k_{EGTA} \equiv (F)_{EGTA1}$ and $F_{max1} = (F)_{Ca\lambda1}/k_{Ca} \equiv F_{Ca1}$). Using equation 2.5.1, plot log $[(F_1 - F_{min1})/(F_{max1} - F_1)]$ versus log ($[Ca^{2+}]$). Fit the linear portion of the data with the linear

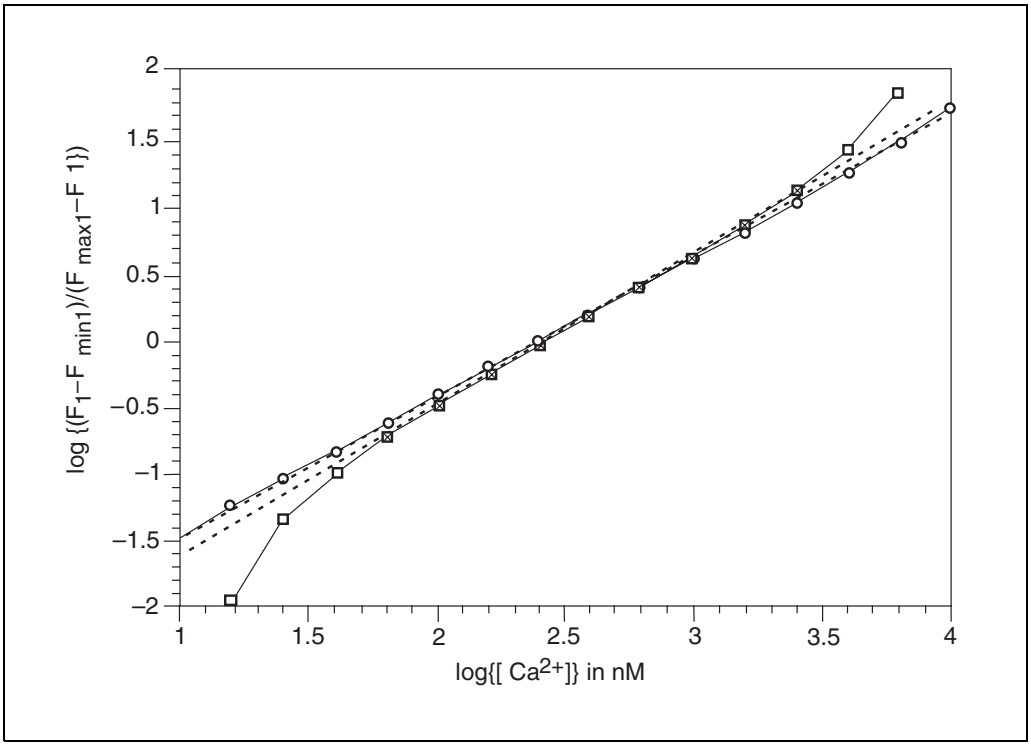

Figure 2.5.2 Sample K_d calibration curves for two different simulated calibrations. In both cases, $[Ca^{2+}]_{inside}$ does not equal $[Ca^{2+}]_{outside}$ when measuring F_{lo} and F_{hi}. In the first case (open circles), $[Ca^{2+}]_{inside}$ reached a minimum of 1 nM and a maximum of 40 μM. All of these data points can be fitted reasonably well with a straight line shown by a dotted line with the equation of the line $y = -2.5014 + 1.0408x$ with $R^2 = 0.99962$. The fact that the slope does not equal one indicates that the true value of F_{lo} and $F_{hi}$was not reached; even so, the calculated value of $K_d = 10^{2.5014/1.0408} = 253$ nM compares reasonably well to the true K_d of 258 nM. In the second case (open square), $[Ca^{2+}]_{inside}$ reached a minimum of 13 nM and a maximum of 10 μM. This data is definitely not linear and clearly indicates that the measured values of R_{min}, R_{max} and (S_f/S_b) obtained step 26 of Basic Protocol 1 will be incorrect. The X points indicate the linear portion of the data which yields a calculated value of $K_d = 10^{2.7265/1.1198} = 272$ nM, which is surprisingly close to the true value of K_d. The equation of this line is $y = -2.7265 + 1.1198x$ with $R^2 = 0.99962$.

least squares best fit line (see Fig. 2.5.2). The value of $[Ca^{2+}]$ for which $y = 0$ is a measure of the apparent K_d of the probe. If the values of F_{EGTA} and F_{Ca} are very close to their true values, the slope of the line will be one. If the values of F_{EGTA} and F_{Ca} are not close to their true values, all the data will clearly not fit a straight line, and the slope will not be one. Even when the data are poor, a reasonable approximation of the true K_d can still be found. However, in this case the use of the values of R_{max}, R_{min} and (S_f/S_b) found in step 26 of Basic Protocol 1 will lead to incorrect values of $[Ca^{2+}]$ inside the cells. Instead of using the measured values of R_{max}, R_{min} and (S_f/S_b), calculate them as follows. Using only the intermediate data points, plot fluorescence in counts/sec for both wavelengths λ_1 and λ_2 versus $[Ca^{2+}]$ and fit both sets of data with an equation of the form $F = (F_{lox} + F_{hix}/K_d[Ca^{2+}])/(1 + [Ca^{2+}]/K_d)$ where F_{lox}, F_{hix}, and K_d are unknown (see Fig. 2.5.3). If the data are very accurate, accurate values of $R_{min} = (F)_{lo1}/(F)_{lo2}$, $R_{max} = (F)_{hi1}/(F)_{hi2}$,, $(S_f/S_b) = (F)_{lo2}/(F)_{hi2}$ and K_d can be obtained from data for which $[Ca^{2+}]_{outside}$ ranges between 15 nM and 6 μM.

For dual-excitation (emission) monochromators, $R_{min} = (F)_{lo1}/(F)_{lo2}/R_L$ and $R_{max} = (F)_{hi1}/(F)_{hi2}/R_L$.where R_L was found in step 11 of Basic Protocol 1.

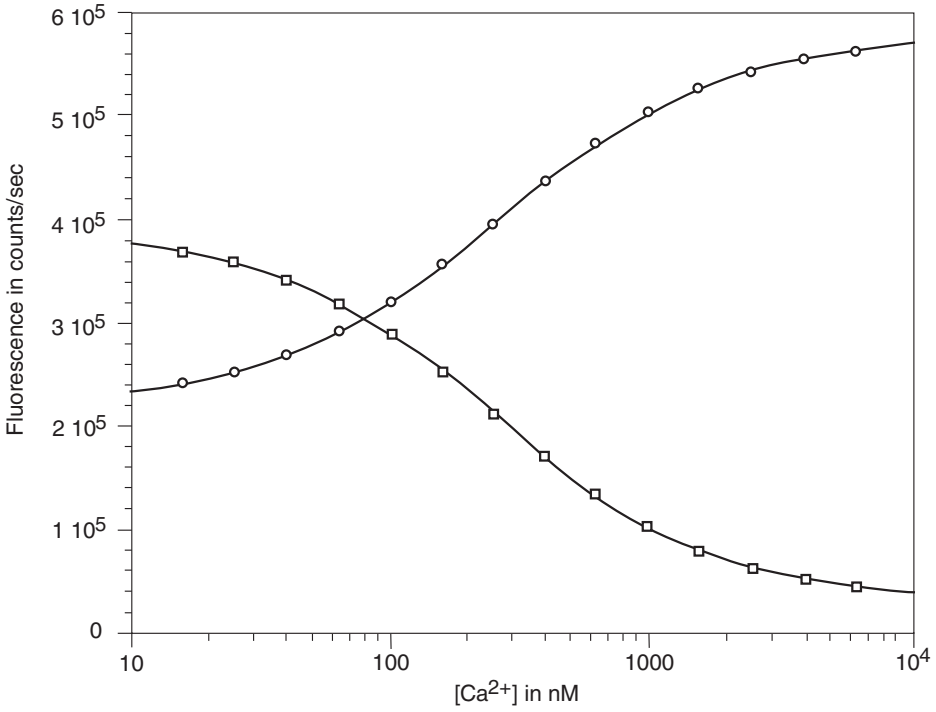

Figure 2.5.3 Alternate dye calibration technique. The open circle represents data measured for Fura-2 at a wavelength of 340 nm; the open square represents data measured for Fura-2 at a wavelength of 380 nm. Each set of data was restricted to $[Ca^{2+}]_{outside}$ ranging from approximately 15 nM to 6 μM. Each set of data was fitted by an equation of the form $F = (F_{lox} + F_{hix} \times [Ca^{2+}]/K_d)/(1 + [Ca^{2+}]/K_d)$ where F_{lox}, F_{hix} and K_d are unknown. The best fit lines are shown by the solid lines. (Most plotting programs such as KaleidaGraph permit the user to generate their own curves for fitting data.) The two calculated values of K_d can be averaged and if the data are very accurate, it is possible to calculate $R_{min} = (F)_{lo1}/(F)_{lo2}$, $R_{max} = (F)_{hi1}/(F)_{hi2}$ and $(S_f/S_b) = (F)_{lo2}/(F)_{hi2}$ very accurately.

Determine K_d of a nonratiometric probe for cells in suspension at 20°C

10. Follow steps 1 though 6 of this protocol, except record F_t values at a single wavelength only.
11. Calculate $(F)_x = (F_t)_x - (F_s)_x - (F_a)_x$ for each of the sixteen different samples x.
12. Follow steps 8 and 9 of this protocol for a single wavelength only and calculate F_{max} and F_{min}.

MEASUREMENTS OF $[Ca^{2+}]$ IN PLATED CELLS USING FLUORESCENCE DIGITAL IMAGING MICROSCOPY (FDIM)

BASIC PROTOCOL 2

For use in this protocol, cells can usually be plated on coverslips, or other systems designed for observation using microscopes, by incubating them overnight covered with complete medium. After attachment, these cells can be incubated in 1 to 5 μM concentrations of the membrane-permeable form of the probe of interest very much as described in Basic Protocol 1, and washed by simply exchanging the medium bathing the cells.

A number of commercial systems exist for viewing plated cells with an epifluorescence microscope (with excitation and emission pathways below the microscope stage). The

following will assume use of a common system in which cells are attached to a 25-mm glass coverslip mounted in a Leiden chamber; however, many current systems could be similarly described.

Note that it is not usually necessary to constantly flush the chamber with probe-free medium because the internal volume of the plated cells is very small compared to the volume of external medium and hence probe leakage cannot usually be detected.

Read the discussion at the beginning of Basic Protocol 1. According to Equation 2.5.3, $F_t = F_a + F_i + c_d [f_{hi}F_{hi} + (1 - f_{hi})F_{lo}] + F_s$. When using a cuvette-based system, F_s can be a very substantial fraction of F_t and can seldom, if ever, be ignored. On the other hand, in FDIM, F_s is basically a measurement of background and is usually used to correct for inhomogeneities of the camera/intensifier image. This background correction makes for the creation of a better mask for the images. For an intensity scale of 0 to 255, F_s should never be >3. If F_s is >3, then either probe leakage is a major problem, the standard medium contains a fluorescent component, or the compound used to help the cells adhere is fluorescent. Which of the three possibilities is causing the problem can easily be determined by checking the fluorescence of the standard medium alone and in combination with plates covered with the cell adhesive. If probe leakage is the problem, feed standard medium slowly into the chamber on one side and withdraw it by suction at the other. In this case, any probe that leaks from the cells is removed from the chamber in a short time.

F_i is not easily determined in this system. If a spectrofluorometer is available and the cells can be kept in suspension, use the procedure discussed under Basic Protocol 1 to determine the best incubation procedure to minimize F_i such that F_i is much less than $F_t - F_s$ at the detection wavelengths for any concentration of calcium. If no spectrofluorometer is available, it is still sometimes possible to determine if F_i is much less than F_t if one has a relative idea of the spectral shape of F_i. Choose a wavelength λ_i such that either $(F_i)_{\lambda i}$ is much greater than $(F_{hi})_{\lambda i}$ or $(F_i)_{\lambda i}$ is much greater than $(F_{lo})_{\lambda i}$ (see Equation. 2.5.4 and Equation 2.5.5). Next, subject the cells to either high or low calcium as is done during the calibration discussed below and measure $(F_t) - (F_s) - (F_a)$ at λ_i and see if it is much greater than expected for the Ca-sensitive form of the probe. For example, the spectrum of the Ca-insensitive form of Fura-2 (Gunter et al., 1988) is fairly similar to that of the low-calcium form and is much higher than that of the high-calcium form at 380 nm. Once everything possible is done to minimize F_i, for purposes of calculation, assume $F_i = 0$.

Because FDIM equipment permits such a limited range of intensity values, it is always important to maximize the range of intensities that the samples and standards undergo. Thus, always measure F_t first in order to determine what light intensity, excitation slits, and camera/intensifier gain should be used. Because the calibration samples represent the extremes in intensity that the samples can undergo, they should always be measured first. If, on the basis of previous samples, the value of light intensity and camera/intensifier gain are known, measure F_s first and automatically subtract F_s from F_t if the software being used has this capacity.

Because of the characteristics of the epifluorescence microscope (both excitation and emission light passing through the coverslip) and the optical frequency response of the microscope optics, there may be some distortion of the spectra and ratios of probes using near-UV wavelengths. This may alter the characteristics of the probe from those observed with a good fluorescence spectrometer, decrease the sensitivity of a probe, and change the wavelengths at which optimum sensitivity can be obtained; however; the same probes can still be used for measurement of $[Ca^{2+}]$ with modifications of the wavelengths used.

In addition, the intensity of illumination of microscope systems is usually nonuniform across the field of view. Thus, some cells receive more incident light than others.

It is important to note that when using a ratiometric probe one should always save the raw data. A ratio to observe can be calculated while data is taken, if preferred, but the raw data must be saved, not the ratio. The only exception to this rule is to automatically subtract the background from raw data if the machine has the capacity.

CAUTION: When neither viewing the cells's fluorescence nor recording an image, stop the excitation light from reaching the cells to minimize photobleaching.

Materials

Adherent cells and incubation medium
25-mm glass coverslip mounted in a Leiden chamber (Medical Systems Corp.)
1× low calcium medium (see recipe)
1× high calcium medium (see recipe)
Standard medium with cyanide (see recipe)
Fluorescence microscope with FDIM system (Photon Technology International, Inc.)
Additional reagents and equipment for fluorescence measurement of intracellular [Ca^{2+}] (see Basic Protocol 1)

Choose fluorescent probe to be used and check its fluorescent characteristics

1. Chose the fluorescent probe to be used (see Basic Protocol 1).

   To be able to calculate [Ca^{2+}], use a ratiometric probe. Except in special circumstances, it is only possible to obtain approximate values of [Ca^{2+}] with a nonratiometric probe, and the process of obtaining such information is very labor-intensive.

2. Without cells on the coverslip, turn on the equipment. Start with the excitation slits set to between 2 and 5 nm in width. Insert the proper dichroic for the probe being used. Check and adjust black level.

   For Indo-1, the equipment must have dual-emission capacity. The actual slit widths to be used depend upon the sensitivity of the system.

3. Also without cells on the coverslip, set up the equipment as follows.

   a. Add 1 ml of either the 5 μM FA in low-Ca solution or 5 μM FA in high-Ca solution. Choose the solution that is expected to have the most intense emission. For example, for Fura-2, use the high-Ca solution.

   b. Set the microscope for binocular viewing and using the white light, focus on the coverslip and then raise the focus above the coverslip using ~1.5 turns of the fine-focusing knob so as to focus well into the solution. Turn off the white light, set excitation at the peak excitation for the probe and attempt to observe the fluorescence.

   c. If there is no fluorescence, increase the intensity of the incident light but do not increase excitation band-pass much beyond 12 to 15 nm if using a ratiometric probe like Fura-2.

   d. Once fluorescence is observed (or has reached maximum band-pass for the excitation), close the shutter for the excitation light, switch the microscope to camera, turn on fast focus or its equivalent which permits observation of the coverslip in real time, and slowly open the shutter for the excitation light, making sure not to saturate the camera. If necessary, decrease the intensity of the incident light by decreasing band-pass or slits.

e. If the camera shows no image of the illuminated field of fluorescent medium, gradually increase the voltage applied to the intensifier or camera gain until a satisfactory image is observed.

Initially the maximum intensity in the image should be ~80% of the maximum possible value.

Even if there are only filters in the excitation setup, it is still necessary to determine the proper slits to use. Generally, signal can be increased by either increasing the excitation slits or by increasing the voltage applied to the intensifier or camera gain. When using an excitation ratiometric probe like Fura-2, the wider the excitation band-pass, the smaller the range of overall sensitivity to [Ca^{2+}] becomes, but increasing the voltage applied to the intensifier or camera gain increases noise, so it becomes a tradeoff between sensitivity and noise. Nonratiometric probes are less demanding, and it is usually possible to increase band-pass to increase sensitivity.

4. If the excitation setup contains a monochromator, scan excitation in order to locate the maximum excitation for the probe. When using an excitation ratiometric probe such as Fura-2, make up probe-free acid solutions in high-Ca/low-Ca solutions (see Basic Protocol 1, step 2). Obtain the excitation spectra for each one of these mixtures and plot them on the same graph. Do not change high voltage or gain while measuring these spectra.

   This usually involves creating a single large region of interest (ROI) in the field of view, choosing to record its median value, and then scanning the spectra. These are the characteristic spectra to be expected from the chosen Ca^{2+}-sensitive probe in the system. The point at which all of the spectra cross is the isosbestic point λ_t.

   IMPORTANT NOTE: *When not using the camera, turn off the high voltage or decrease gain. Furthermore, if it is necessary to observe the cells in step 6, change the microscope from camera to binocular when finished with the camera. This precaution is taken to protect the camera from being accidentally exposed to excess light intensity. In addition, when neither viewing the cells's fluorescence nor recording an image, stop the excitation light from reaching the cells to minimize photobleaching.*

5. When using dual-excitation monochromators, set both monochromators to the same wavelength (λ_1), and using one of the calcium mixtures and the ROIs from step 4, measure the median fluorescent intensity of the light between the two monochromators (F_{mono1} for the monochromator that measures λ_1 and F_{mono2} for the monochromator that measures λ_2) Measured ratios can then be corrected for this artifact by dividing all ratios by R_L, where $R_L = F_{mono1}/F_{mono2}$.

   R_L is generally constant during the course of a single experiment, but tends to vary between experimental sessions. Hence, it should be measured at least twice in every experimental session. Any sample containing the probe will be adequate for this measurement.

6. Calculate R_{max}, R_{min} and R_{max}/R_{min}.

   If R_{max}/R_{min} is much more than 20, it is necessary to adjust either λ_1 or λ_2 to increase the average intensity of the dimmest image at λ_1 or λ_2. If it is much less than that expected for the probe in question, it may be necessary to decrease the band-pass of the excitation slits. (See comments under step 7 of Basic Protocol 1 for more details.) When using an emission type of ratiometric probe, it is normally impossible to scan emission, but it is possible to calculate the median value of a large ROI for both wavelengths in high- and low-calcium media in order to calculate R_{max} and R_{min}.

Incubate cells with the probe

7. Unless the cells are already plated out, resuspend at 1×10^6 cells/ml and place 50 µl of cells in the center of a coverslip. Cover and incubate at 37°C for 2 hr to give the cells a chance to adhere, then flood with incubation medium.

If the cell type has difficulty adhering to glass, coverslips may be pretreated with an extracellular matrix material such as type I collagen or laminin.

Cells should be close to touching but without overlapping. Because the number of cells in a field of view is limited and the quality of cells can vary from plate to plate, take at least two views per plate (provided no additions to the plate cause irreversible changes in the cells) and run triplicate plates per sample. Complete calibrations can be performed on the same plate, but it often requires two or more plates. Likewise, a K_d calibration requires a minimum of two to three plates and can require as many as 20 to 40, depending on how well the cells hold up under calibration conditions. The time it takes to run these samples limits how many experimental samples can be analyzed.

8. When the cells are ready for incubation with the AM form of the probe (also see Basic Protocol 1, step 8), remove the incubation medium and replace with 0.5 ml standard medium. Add 2 to 10 μM of the AM form of the probe to 0.5 ml standard medium and mix well by vortexing or shaking and immediately add to the cells to be incubated, making sure the solution is well mixed. Allow this mixture to incubate at 37°C for 30 min to 1 hr. After incubation, rinse the cells with standard medium two to three times (see Basic Protocol 1, step 9).

   Once rinsed, these cells should be stored at room temperature or 4°C until they are used to decrease probe leakage. In the following steps, these cells will be called "incubated cells."

Make measurements using ratiometric probes

Steps 9 to 20: Perform measurements needed for calculating R_{max} and R_{min} (also see Basic Protocol 1, steps 19 to 26, for discussion on measuring R_{max}, R_{min}, S_f, and S_b).

9. Place incubated cells in the holder, rinse twice with low-Ca medium, remove all of the rinse, and then add 1.0 ml of low-Ca medium.

   IMPORTANT NOTE: *If cells cover the entire coverslip, wipe a small area free of cells for the background measurement.*

   CAUTION: *The most important step is making sure the two components are well mixed. If mixing is not complete, many or perhaps all of the cells in the field of view will not respond to changes in external [Ca^{2+}].*

10. Place the coverslip on the microscope stage, make sure the microscope is set to binocular view, and use the white light to focus on the cells. Find a likely group of cells, then turn off the white light and turn on the excitation light to examine the cells.

    The cells should be dimly visible. If not, increase the intensity of incident light if possible (see discussion about excitation band-pass in step 3 of this protocol).

    IMPORTANT NOTE: *Once the excitation band-pass to be used in an experiment is determined, do not modify it unless a new set of R_{max}, R_{min}, S_f, and S_b is determined for each change in band-pass. This is because R_{max}, R_{min}, S_f, and S_b are sensitive to band-pass. However, it is possible to modify lamp intensity, slit widths that do not change band-pass, and intensifier high voltage or camera gain without having to remeasure R_{max}, R_{min}, S_f, or S_b.*

11. Set the microscope to camera, turn on fast focus (or its equivalent), and slowly increase high voltage to the intensifier or increase camera gain until a bright image is observed at either λ_1 or λ_2. Next, vary fine focus to provide the brightest, sharpest image. Make a note of the final high voltage or gain setting.

    The brightest cell should have a maximum intensity of ~90% to 95% of the maximum permissible intensity. In the future, the expression "turn on HV/G" will mean turn on the high voltage and/or gain to the values determined in the step indicated afterwards in

parentheses. For example, "turn on HV/G (step 4). In addition, "turn off HV/G" always means" turn off the high voltage and set gain = 0."

IMPORTANT NOTE: *If it is not possible to obtain a sufficiently bright image even with high voltage or gain set to the maximum, many systems permit summing several images to increase the overall intensity of the image. This feature should only be used as a last resort because it also greatly increases noise. In addition, most intensified camera systems offer the option of averaging several images. Average as many images as are practical because averaging images reduces noise by the square root of the number of images averaged.*

12. Turn off HV/G, change the microscope to binocular, turn on the white light, and locate an area of the coverslip that has no cells in the field of view. Turn off the white light, switch the microscope to camera, turn on HV/G (step 12), and take a set of background images at λ_1 and λ_2. The resulting images are $(I_s)_{lo1}$ and $(I_s)_{lo2}$.

This region is the background for this plate and is basically a supernatant image. The primary purpose of this set of background images is to ensure that the background is not too high. If it is, determine the cause and correct the problem before continuing the measurements.

IMPORTANT NOTE: *If at any time during the course of the experiment a change is made in lamp intensity, slits not associated with band-pass, intensifier high voltage, or camera gain, take a new background for that coverslip. In general, it is best to take a background for each coverslip unless all of the backgrounds appear to be the same, in which case it is necessary only to take new backgrounds whenever a change is made in lamp intensity, slits, intensifier high voltage or camera gain.*

13. Turn off HV/G, change the microscope to binocular, turn on the white light, and locate an area of the coverslip that has discrete cells and bring them into focus. Turn off the white light, switch the microscope to camera, turn on HV/G (step 11), and turn on fast focus. Vary fine focus to provide the brightest, sharpest image, then take a set of images at λ_1 and λ_2 with backgrounds found in step 11 automatically subtracted.

If the software program cannot automatically subtract the background, the backgrounds must be subtracted manually before the images are used in any further analysis.

IMPORTANT NOTE: *If at all possible, set up an aspirator that can remove all of the liquid from the chamber without accidentally moving the coverslip. This makes it possible to make repeated measurements on exactly the same cells in exactly the same position while changing the medium between measurements. An aspirator should be set up whenever multiple changes are to be made to the same cells on a coverslip.*

14. Turn off HV/G and switch to analysis mode. If the software permits one to take the maximum of two images, take the maximum of these two images (see Fig. 2.5.4A, B, and C) and create a mask from this image, setting threshold high enough to eliminate any of the background outside of the cell but not so high as to eliminate portions of the cell (see Fig. 2.5.4D). Use the minimum of the two images to create ROIs that include only those cells whose minimum intensity image is significantly above background and whose maximum intensity image does not go off the intensity scale (see Fig. 2.5.4E).

If the software being used cannot take the maximum of two images, choose the brightest of the two images to create the mask.

The ROIs [$(ROI)_{lo}$] should be just inside of the masked cell.

15. Aspirate all of the medium from the coverslip. Add 10 µl of 0.1 mM thapsigargin, 7.5 µl of 2 mM oligomycin, 7.5 µl of 1 mM CCCP and 10 µl of 1 mM ionophore to 1.0 ml of low-Ca medium in a small tube to yield final concentrations of 1 µM thapsigargin 10 µM oligomycin, 5 µM CCCP and 10 µM ionophore, respectively.

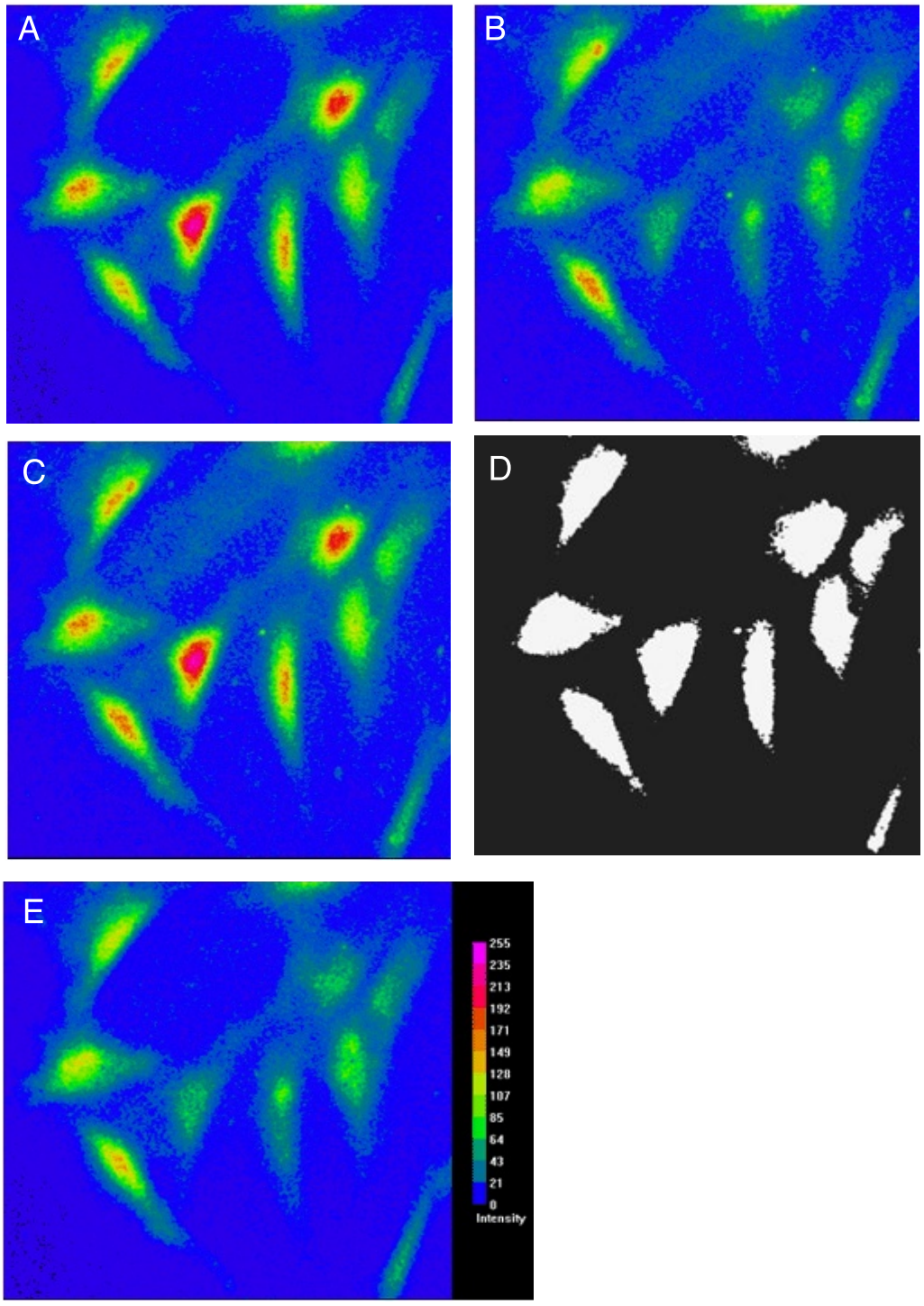

Figure 2.5.4 (**A**) Fura-2 FA 340-nm image of osteoblasts. (**B**) Fura-2 FA 380-nm image of osteoblasts. (**C**) Image created by taking the maximum of images in panel A and panel B. (**D**) Mask created by using the maximum of images in panel A and panel B and setting the threshold to an intensity of 45. (**E**) Image created by taking the minimum of images in panel A and panel B. The color scale for **A** through **D** is the same as that depicted in **E**. *This black and white facsimile of the figure is intended only as a placeholder; for full-color version of figure go to http://www.currentprotocols.com/colorfigures*

Immediately shake or vortex this mixture and then add it to the coverslip. Note the time at which this addition was made.

16. Switch back to data-acquisition mode and change the setup to record the median value of intensity inside each ROI. Turn on HV/G (step 11), take a set of images about once a minute, and plot the ROIs versus time. When the median values of most of the ROIs at both λ_1 and λ_2 reach a steady state, set the software to average the maximum number of images and save a pair of images [these are the low-calcium images $(I_t)_{lo1} - (I_s)_{lo1}$ and $(I_t)_{lo2} - (I_s)_{lo2}$]. Calculate the time it took to reach a steady state from the time the medium containing the ionophores and inhibitors was added to the coverslip (this is the minimum time required to reach low calcium inside the cell type).

    The images taken while following median values do not need to be solved.

    If too many pixels inside of the ROIs are off-scale, it may be necessary to change HV/G before saving a pair of images. In this case, turn off automatic background subtraction before taking the uncorrected low-calcium images, $(I_t)_{lo1}$ and $(I_t)_{lo2}$. If HV/G is changed, new background images, $(I_s)_{lo1}$ and $(I_s)_{lo2}$, will need to be taken and subtracted manually from the uncorrected images (see step 19).

17. If the probe is ratiometric in excitation and the equipment includes optional scanning of excitation, switch the software from time-based mode to wavelength mode, turn off automatic background subtraction, and using the ROIs, scan the entire wavelength range including λ_1 and λ_2 plus a little extra on either side. Save the resulting median values of intensity for each of the ROIs as a function of wavelength as the uncorrected low calcium spectra $(S_t)_{lo}$ inside the cells.

18. If HV/G was changed in step 16 repeat step 12 with HV/G (step 6) and the software set to average the maximum number of images to obtain the proper background images $(I_s)_{lo1}$ and $(I_s)_{lo2}$. If the probe is ratiometric in excitation, repeat step 16 on this background area using the same ROIs $[(ROI)_{lo}]$ in order to obtain the low-calcium background spectra $(S_s)_{lo}$. Turn off HV/G and switch the microscope back to binocular mode.

19. If it appears that too much probe was lost from the cells during the low-calcium calibration, place a new set of incubated cells in the holder; otherwise, use the current coverslip. Repeat steps 11 through 17 of this protocol using high-Ca medium. If the images are background corrected, the resulting images are the high-calcium images $(I_t)_{hi1} - (I_s)_{hi1}$ and $(I_t)_{hi2} - (I_s)_{hi2}$ and the ROIs $(ROI)_{hi}$. Calculate the time it took to reach a steady state from the time the medium containing the ionophores and inhibitors was added to the coverslip. This is the minimum time required to reach high calcium inside the cell type being used.

20. If the probe is ratiometric in excitation, repeat step 16. Save the resulting median values of intensity as a function of wavelength as the uncorrected high-calcium spectra $(S_t)_{hi}$ inside the cells. Repeat step 18 to obtain $(I_s)_{hi1}$ and $(I_s)_{hi2}$ [and $(S_s)_{hi}$ if the probe is ratiometric in excitation].

    IMPORTANT NOTE: *If the cells have not greatly changed relative intensities at the two different wavelengths, it is highly likely that $[Ca^{2+}]$ inside the cells is not equilibrating with external $[Ca^{2+}]$. In this case, see Troubleshooting.*

Perform measurements needed for calculating S_f and S_b for probes that are ratiometric in excitation or for systems that cannot scan excitation

Steps 21 to 22: Equipment that includes the option of scanning excitation makes it possible to measure S_f and S_b quite accurately for probes that are ratiometric in excitation. If the equipment does not include this option, then measure S_f and S_b as discussed below for

probes that are ratiometric in emission (also see Basic Protocol 1, steps 19 to 26, for discussion on measuring R_{max}, R_{min}, S_f, and S_b).

21. Place a new set of incubated cells in the holder, rinse twice with standard medium, and then add 1 ml of standard medium. Repeat steps 10 and 11 with HV/G set to the level used in step 19. Create ROIs as discussed in step 14. Switch back to data-acquisition mode and change the setup to record the median value of intensity inside of each ROI.

22. Switch the software from time-based mode to wavelength mode, turn on HV/G (step 19), and using the ROIs, scan a wavelength range centered about the isosbestic point λ_i that was found in step 4. Using a flashlight as a dim source of light in order to protect the camera (since the high voltage is on and light is reaching the camera), aspirate all of the medium, and then add 1 ml of medium containing some factor that will induce changes in $[Ca^{2+}]$ and immediately initiate multiple scans around λ_i until the pulse is more or less complete. Plot all of these scans on the same graph and determine λ_i for probe inside the cells.

    Factors which induce changes in $[Ca^{2+}]$ are dependent upon the cell type. Many cells when exposed to high potassium in the external medium will depolarize which results in a high calcium pulse. Most cell types respond to specific hormones. For example, chondrocytes respond to parathyroid hormone; liver cells respond to vasopressin, catecholamines, and angiotensin; brain cells respond to almost all of the neurotransmitters. In addition, many cell types respond to thapsigargin, and muscle cells respond to caffeine.

    Many researchers have found that both λ_i and K_d of probes inside cells can be quite different from that found in a cell-free medium (Baker et al., 1994; Brandes et al., 1993; Lipp et al., 1996).

Make measurements needed for calculating S_f and S_b for probes that are ratiometric in emission or for systems that cannot scan excitation

The major problem in accurately measuring S_f and S_b is the loss of probe from inside the cells during the course of the measurements. By repeating the low- and high-calcium calibrations on the same group of cells with λ_1 set to λ_i, the isosbestic point, it is possible to estimate dye loss between the two measurements. Since it is not possible to measure the true value of λ_i in the system, assume it is equal to the value given in the literature or that found using a spectrometer.

23. Replace the band-pass filter for λ_1 with one that will transmit λ_i. Since the same set of cells must be used for both low and high calcium measurements, set up a system that can automatically remove all of the medium from the holder. Repeat steps 9, 10, 12, and 17 except set HV/G equal to the value found that results in the brightest images at λ_2. Set the software to average the maximum number of images, wait the minimum time required to reach low calcium inside the cell type under examination, and take a set of images, which will be the uncorrected low-calcium images, $(I_t)_{loi}$ and $(I_t)_{loi2}$.

    This same set of cells must be used for the high-calcium measurements, so it is necessary to be very careful not to move the microscope stage.

24. Repeat step 15 using high-Ca medium, except use the automatic system to remove the low-Ca medium and rinses and make all additions very carefully so as to not change the field of view. Turn on HV/G and repeat step 11. Set the software to average the maximum number of images, wait the minimum time required to reach high calcium inside the cell type, and take a set of images, which will be the uncorrected high-calcium images, $(I_t)_{hii}$ and $(I_t)_{hii2}$.

25. Take a set of background images, $(I_s)_i$ and $(I_s)_{i2}$, by following the procedure of step 12 after setting HV/G (step 23) and setting the software to average the maximum number of images. If HV/G used in step 24 is different from that used in step 23, Take another set of background images, $(I_s)_{hii}$ and $(I_s)_{hii2}$, by following the procedure of step 12 after setting HV/G (step 24) and setting the software to average the maximum number of images.

If HV/G for high and low calcium measurements are the same, $(I_s)_{hii} = (I_s)_{loi}$ and $(I_s)_{hii2} = (I_s)_{loi2}$.

Measure autofluorescence (F_a)

Except for Fura red, for which autofluorescence is not a problem, the usual major source of autofluorescence for the ratiometric [Ca^{2+}] probes is NADH, whose fluorescence varies with the metabolic state of the cells. Maximum autofluorescence occurs in the presence of cyanide (5 mM); minimum autofluorescence occurs in the presence of protonophores such as CCCP (Jiang and Julian, 1997). For Fura-2 and its analogs, maximum autofluorescence will occur at λ_i or 380 nm. For Indo-1, maximum autofluorescence will occur at 480 nm. If one is unable to detect autofluorescence in the presence of 5 mM cyanide under the experimental setup, it is negligible and can be neglected. If autofluorescence cannot be neglected, make autofluorescence measurements for each value of HV/G used, as well as the corresponding background measurements. For autofluorescence and background images always set the software to average the maximum number of images.

26. Place cells that have not been incubated with the probe in the holder, rinse twice with standard medium, and then add 1 ml of standard medium. Repeat steps 9 and 10, except set HV/G to the largest value used (step 16 or 19) and observe λ_i and λ_2 for probes such as Fura-2 and 480 nm for Indo-1 If no cells can be detected in either image, replace the standard medium with standard medium containing 5 mM cyanide and repeat the measurements after 10 to 15 min. If cells still cannot be detected in either image, autofluorescence can be ignored. If autofluorescence is detected, continue with the following steps.

27. Place cells that have not been incubated with the probe in the holder. Repeat steps 9 and 10, except locate an area that contains no cells. Set the microscope to camera, turn on HV/G (step 16) and take two background images, $(I_{sa})_{lo1}$ and $(I_{sa})_{lo2}$. If steps 23 through 25 were performed, change HV/G (step 23) and take two background images, $(I_{sa})_{loil}$ and $(I_{sa})_{loi2}$. Turn off HV/G, change the microscope to binocular, turn on the white light, locate a large group of cells, and bring them into focus. Set the white light so dim you can barely seen the cells. Set the microscope to camera, turn HV/G to 0. Turn on fast focus and slowly increase HV/G and/or the intensity of light until you obtain a decent white image. Save this image as I_w and turn off white light. Change HV/G (step 17). If it is possible to automatically subtract a background image, set the backgrounds to $(I_{sa})_{lo1}$ and $(I_{sa})_{lo2}$. After the minimum time required to reach low calcium (determined in step 18), take two images of autofluorescence, $(I_a)_{lo1}$ and $(I_{sa})_{lo2}$. If steps 23 through 25 were performed, change HV/G (step 23). If it is possible to automatically subtract a background image, then set backgrounds to $(I_{sa})_{loi1}$ and $(I_{sa})_{loi2}$ and take two more images, $(I_a)_{loi1}$ and $(I_a)_{loi2}$.

Since the autofluorescence images may be very dim, the white light image can be used to help locate the cells and to create the ROIs.

28. If the software cannot subtract background automatically, manually subtract the background images from the autofluorescence images. Make a mask and create ROIs for the autofluorescence images as discussed in step 14. (If necessary, use I_w to create the ICOIs but not the mask.) Use these ROI's to measure the median values of fluorescence inside of the masked images. Calculate the average of these median

values at λ_1, λ_i, and λ_2, which will be $(F_a)_{lo1}$, $(F_a)_{lo2}$, $(F_a)_{lo1lo}$, $(F_a)_{loi1}$, and $(F_a)_{loi2}$ (see Basic Protocol 1, step 24). If the average median value $(F_a)_{lo2}$ is noticeably greater than background, measure the corresponding uncorrected low calcium autofluorescence spectra $(S_{ta})_{lo}$ at HV/G (step 17) as described in step 18 of this protocol, and then the low-calcium background spectra $(S_{sa})_{lo}$ as described in step 19. For each ROI, calculate $(S_a)_{lo} = (S_{ta})_{lo} - (S_{sa})_{lo}$ and then calculate the average spectra $[(S_a)_{lo}]_{ave}$ for HV/G (step 17). Turn off HV/G and switch the microscope back to binocular mode.

29. Repeat steps 27 and 28 with high-Ca medium instead of low-Ca medium.

This will result in $(F_a)_{hi1}$ and $(F_a)_{hi2}$ and where pertinent, $(F_a)_{hi1}$, $(F_a)_{hi2}$, and $[(S_a)_{hi}]_{ave}$.

Calculate the excitation spectra of probe inside cells for probes that are ratiometric in excitation

30. Switch to analysis and use the appropriate software program or a spreadsheet such as Excel to calculate the spectra. For each of the ROIs in $(ROI)_{lo}$ (step 17) calculate $(S)_{loj} = (S_t)_{loj} - (S_s)_{loj} - [(S_a)_{lo}]_{ave}$, where $(S_t)_{loj}$ and $(S_s)_{loj}$ were measured in steps 17 and 18 for the *j*th cell and $[(S_a)_{lo}]_{ave}$ was measured in step 28 (or is negligible). Compare these spectra with the low-calcium spectrum found in step 4 and eliminate any cells whose spectrum appears to be a combination of low- and high-calcium spectra. Using the remaining cells, calculate the average low-calcium spectrum inside the cells, $[(S)_{lo}]_{ave}$ = (sum of all of the remaining spectra $(S)_{loj}$)/(the number of cells included in the average).

If none of the spectra have approximately the correct shape, either the cells did not reach low calcium inside the cell or there are problems with inner-filter effect which must be corrected. (see Troubleshooting for discussion of the impact of the inner-filter effect on spectra).

31. In the same way, using the ROIs in $(ROI)_{hi}$ (step 19), calculate $(S)_{hij} = (S_t)_{hij} - (S_s)_{hij} - [(S_a)_{hi}]_{ave}$, where $(S_t)_{hij}$ and $(S_s)_{hij}$ were measured in step 20 for the *j*th cell and $[(S_a)_{hi}]_{ave}$ was measured in step 29 (or is negligible). Compare these spectra with the high-calcium spectrum found in step 4 and calculate the average high-calcium spectrum inside the cells, $[(S)_{hi}]_{ave}$ = (sum of all of the remaining spectra $(S)_{hij}$)/(the number of cells included in the average).

If none of the spectra have the correct shape, either the cells did not reach high calcium inside the cell or there are problems with inner-filter effect which must be corrected.

Determine R_{max}, R_{min}, S_f, and S_b

Steps 32 to 38: When taking a ratio image, most programs require setting the ratio range. If too large a range is set, the measured ratios will only cover a small part of the overall range. Since most digital imaging systems only have a limited set of intensity or ratio values, this causes a decrease in the precision to which one can measure individual ratios. Alternatively, if too small a range is set, some of the ratios may be out of range (i.e., have a ratio either larger or smaller than the set range). Some programs indicate the pixels in a ratio image that are outside the range, but others "wrap" the image around, which means that the pixels that are out of range appear to be in range, but have incorrect ratio values (see Fig. 2.5.5A). Therefore, in analyzing data, it is essential to be sure that the image never wraps around inside of cells to be used in the analysis (it does not matter if data is "wrapped" inside of cells that are not used). Below is a detailed procedure on how to avoid this problem.

32. Switch to analysis mode. Calculate $(I_{t\text{-}s})_{lo1} = (I_t)_{lo1} - (I_s)_{lo1}$ and $(I_{t\text{-}s})_{lo2} = (I_t)_{lo2} - (I_s)_{lo2}$, where $(I_t)_{lo1}$ and $(I_t)_{lo2}$ were measured in step 16 and $(I_s)_{lo1}$ and $(I_s)_{lo2}$ were measured in step 12 (or 19 if backgrounds were not automatically substracted). If the software

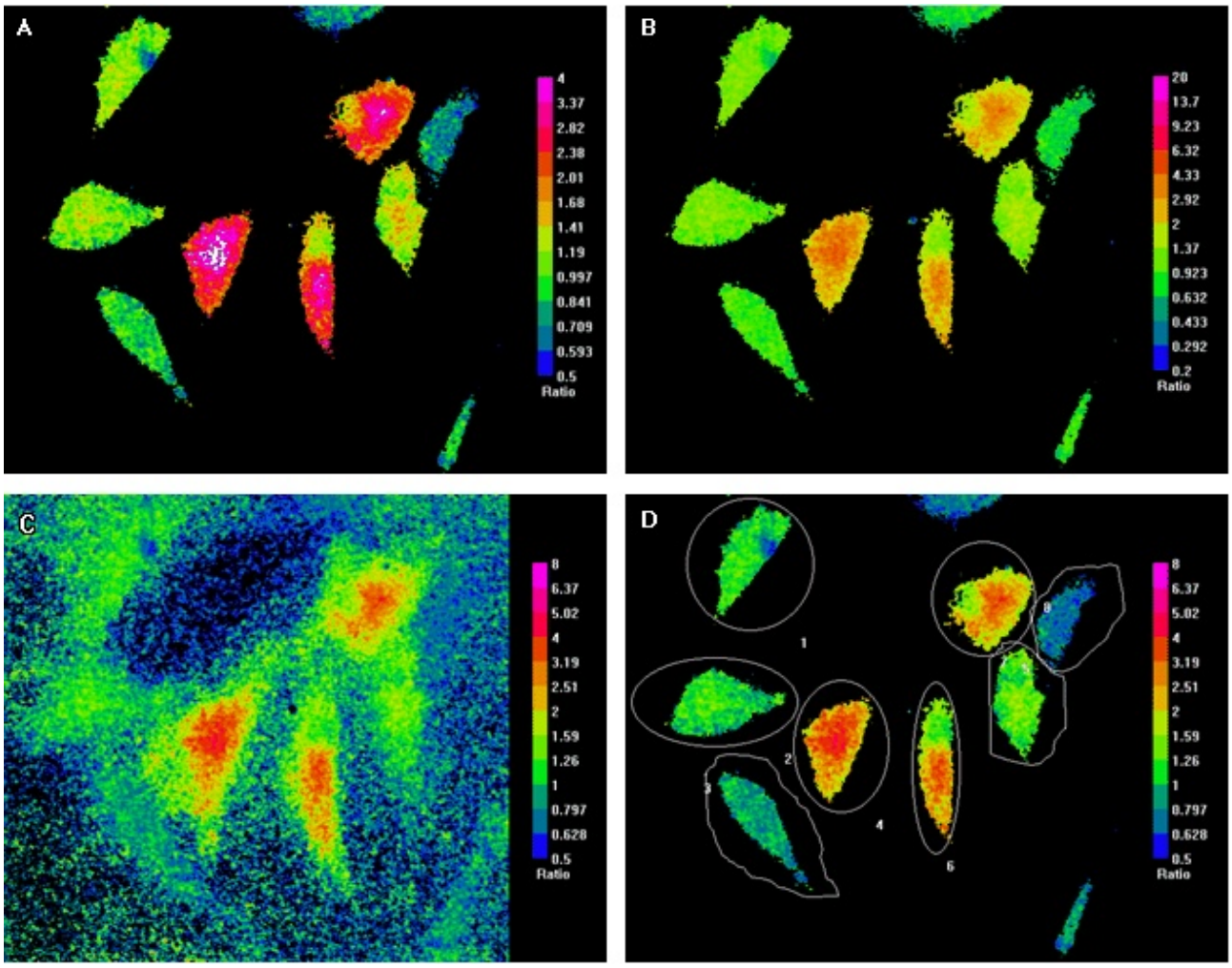

Figure 2.5.5 (**A**) Image created by taking the ratio of images in Figure 2.5.2, panels A and B, where the ratio range is too small, resulting in "wrapping" of the image. (**B**) Image created by taking the ratio of images in Figure 2.5.2, panels A and B, where the ratio range is large enough to guarantee that the image will not "wrap." (**C**) Image created by taking the ratio of images in Figure 2.5.2 panels A and B, where the ratio range is large enough to guarantee that the image will not "wrap" but small enough to easily display the differences between neighboring cells and to improve the accuracy of calculated median values. (**D**) The image in panel C of this figure with the mask applied and regions of interest drawn. These ROIs are either ellipses or free hand (software used is ImageMaster by Photon Technology International). *This black and white facsimile of the figure is intended only as a placeholder; for full-color version of figure go to http://www.currentprotocols.com/colorfigures*

permits taking the maximum of two images, take the maximum of $(I_{t\text{-}s})_{lo1}$ and $(I_{t\text{-}s})_{lo2}$. If the software cannot take the maximum of two images, choose the brightest of the two images. Use the linear profile tool to observe the linear profiles through the brightest cells and ascertain that the profile is generally bell-shaped and not too flattened across the top.

Flattening occurs when the maximum intensity for the system is reached in the raw image. A small amount of flattening in the center of the cell may be acceptable, but if large amounts of flattening occur, the data from that cell should be eliminated from the analysis.

33. Load the regions of interest $(ROI)_{lo}$ that were created in step 14 and eliminate any cells that have too much flattening (it is also possible to add any additional cells that might be bright enough to use). Use this maximum to create a mask (low-cal-mask), setting the threshold high enough to eliminate any of the background outside of the cell but not so high as to eliminate portions of the cell. If $(F_a)_{lo1}$ and $(F_a)_{lo2}$ found in step 28 are not negligible, subtract a constant equal to $(F_a)_{lo1}$ from $(I_{t\text{-}s})_{lo1}$ and subtract a constant equal to $(F_a)_{lo2}$ from $(I_{t\text{-}s})_{lo2}$—the results are $(I)_{lo1}$ and $(I)_{lo2}$, respectively.

Next, take the minimum of these two images. If the software cannot take the minimum of two images, choose the dimmest of the two images. Use the linear profile to determine that only those cells whose minimum intensity profile is significantly above zero are included. Apply the low-cal-mask; the ROI's boundaries should be just outside of the masked cells, if they are not, adjust the size of the ROIs.

This ROI will be called low-cal.roi.

CAUTION: *Suggesting that the boundaries of the ROI should be just outside of the masked cell assumes that the software does not include the masked area in any calculation of median value. If this is not the case, then be very careful in drawing the boundaries of the ROI to include as much of the cell as possible without including any area outside of the cell.*

34. Set the ratio range to be large with respect to the expected range—i.e., both higher and lower than expected (see Fig. 2.5.5B). Take the ratio $(I)_{lo1}/(I)_{lo2}$, apply low-cal-mask to the image as well as low-cal.roi and observe the result. Locate the cell or cells that are included in low-cal.roi and have the highest ratio. Use a histogram or linear profile of the cells to determine the actual maximum value of the ratio inside these cells. Set the maximum value of the ratio range, R_{hi}, slightly larger than this value. Now locate the cells or cells that are included in low-cal.roi and have the lowest ratio. Use a histogram or linear profile of these cells to determine the actual minimum value of the ratio inside these cells. Set the minimum value of the ratio range, R_{lo}, slightly smaller than this value. Change the ratio range to go from R_{lo} to R_{hi}, recalculate the ratio $(I)_{lo1}/(I)_{lo2} = I_{min}$ and apply low-cal-mask. Use low-cal.roi to measure the median value for each cell included in the ROIs (see Fig. 2.5.5C and D). Average these median values and calculate the standard deviation of the result. If any of these median values are located more than two standard deviations from the average, eliminate them from the calculation (some cells will not reach low calcium).

The final result is R_{min}. When using dual-excitation monochromators, the true value of $(R_{min})_{true} = R_{min}/R_L$ where R_L was measured in step 5.

35. Repeat steps 32 to 34 for the high-calcium images measured in step 19, the background images measured in step 20, and the median values of autofluorescence measured in step 30.

The result will be the value of R_{max} and its corresponding image I_{max}, where the ratio range for I_{max} will be quite different from that for I_{min}. When using dual-excitation monochromators, the true value of $(R_{max})_{true} = R_{max}/R_L$ where R_L was measured in step 5.

36. If the probe used is ratiometric in excitation and excitation spectra were obtained in steps 30 and 31, the ratio (S_f/S_b) is calculated as follows. Plot $[(S)_{lo}]_{ave}$ and $[(S)_{hi}]_{ave}$ on the same graph. Calculate the constant c such that $c\cdot[(S)_{lo}]_{ave}$ crosses $[(S)_{hi}]_{ave}$ at the isosbestic wavelength λ_i that was determined in step 22 and then determine the values of $[(S)_{lo}]_{ave}$ and $[(S)_{hi}]_{ave}$ at λ_2 ($[(F)_{lo2}]_{ave}$ and $[(F)_{hi2}]_{ave}$, respectively).

The ratio $(S_f/S_b) = c\cdot[(F)_{lo2}]_{ave}/[(F)_{hi2}]_{ave}$.

37. If the probe used is ratiometric in emission or it was not possible to obtain excitation spectra in steps 30 and 31, calculate the ratio (S_f/S_b) as follows. Repeat steps 23 to 24 for the low, $(I_t)_{loi}$ and $(I_t)_{loi2}$, and high, $(I_t)_{hii}$ and $(I_t)_{hii2}$, calcium images measured in steps 22 and 23, respectively.

The background images, $(I_s)_{lo1}$, $(I_s)_{lo2}$, $(I_s)_{hii}$, and $(I_s)_{hii2}$, were measured in step 25 and the median values of autofluorescence, $(F_a)_{loi}$ and $(F_a)_{loi2}$, can be obtained from step 28. The results are $(I)_{loi}$ and $(I)_{loi2}$ in low-Ca medium and $(I)_{hii}$ and $(I)_{hii2}$ in high-Ca medium, respectively.

38. Calculate $(I)_{hii}/(I)_{hii2}$ and $(I)_{loi}/(I)_{loi2}$ directly and measure the median values of these ratios, $(R)_{hij}$ and $(R)_{loj}$, respectively for the jth cell using the ROIs and mask created

in step 37. Calculate $(R)_{hij} \times (R)_{loj}$ for each cell *j* and then calculate the average value $[(R)_{hij}/(R)_{loj}]_{ave}$, for all the cells in the ROIs as well as its standard deviation. If any of these values, $(R)_{hij}/(R)_{loj}$, are located more than two standard deviations from the average, eliminate them from the calculation.

The ratio $(S_f/S_b) = [(R)_{hij}/(R)_{loj}]_{ave}$.

Measure the ratio of samples of interest

Steps 39 to 41: If it was found in step 26 that autofluorescence could not be detected under the experimental conditions, then the F_a term can be eliminated from the sample calculations. If this is not true, then autofluorescence images must be taken for every different value of HV/G and it is necessary to check to make sure that autofluorescence does not vary significantly as a result of the experimental protocol.

39. Place cells that have been incubated with the permeant form of the probe (see step 8) in the holder, rinse twice with standard medium, and then add 1 ml of standard medium. Adjust focus and HV/G as was discussed in step 12 to get a sharp, bright image. Then take a set of background images as discussed in step 13 and set the software to automatically subtract these background images or else subtract them manually later.

40. If desired, take several sets of images (at λ_1 and λ_2) of different fields of view. To study the effects of any agent on the cells, use one of the following options. Either add a concentrated solution of the agent directly to the chamber and attempt to mix it with the solution already in the chamber, remove the standard medium from the chamber and replace it with a solution of the agent under study, or use a flow cell and flow the mixture to study through the chamber. Take a series of image pairs, particularly to follow the effects of the agent on the cells with time. When the study is complete, take another set of background images to make sure that the agent added did not change the background substantially.

    IMPORTANT NOTE: *It is very difficult to add a concentrated solution to the chamber and get reproducible results for the following reasons. First, some cells may see a more concentrated solution of the agent than others, and if the response is concentration-dependent, this effect will produce errors. Second, it is difficult to get complete mixing of the agent in the chamber, especially without disturbing the field of view.*

41. Analyze these images in the same way the low-calcium images were analyzed in steps 32 to 34. If autofluorescence (F_a) is not negligible, then correct each sample image by subtracting the proper autofluorescence constant—i.e., $(F_a)_1$ or $(F_a)_2$ before calculating the ratios of the images. Calculate the ratio R_j for each chosen cell in each set of images as was discussed in steps 32 to 34 (it is not necessary to use the same ratio range for every set of images but remember the ratio range that was used to calculate each ratio image). Next, calculate $[Ca^{2+}]_j = K_d \times [(R_j - R_{min})/(R_{max} - R_j)](S_f/S_b)$ where $[Ca^{2+}]_j$ is the free calcium concentration in the *j*th cell, R_{min} was calculated in step 33, R_{max} was calculated in step 35, and (S_f/S_b) was calculated either in step 36 or 37. Either use an estimated K_d such as 225 nM for Fura-2, or measure it as described below for a particular cell type.

    When using dual-excitation monochromators, the true value of $(R_j)_{true} = R_f/R_L$ *where* R_L *was measured in step 5.*

Measurement of [Ca^{2+}] in plated cells using FDIM and nonratiometric probes

Nonratiometric probes are used in a similar way to ratiometric probes, except that only fluorescent intensities and not ratios are used—i.e., $[Ca^{2+}] = K_d \times [(F - F_{min})/(F_{max} - F)]$ where $F = F_t - F_s - F_a - F_{id}$, $F_{min} = (F)_{lo} = (F_t)_{lo} - (F_s)_{lo} - (F_a)_{lo} - F_{id}$, and $F_{max} = (F)_{hi} = (F_t)_{hi} - (F_s)_{hi} - (F_a)_{hi} - F_{id}$. Clearly, the F_{id} values cancel in calculating $[Ca^{2+}]$. In addition,

the background measurements also cancel out because all of the measurements must be carried out under identical conditions. F_a is almost certainly negligible for the currently available nonratiometric probes, because the major source of autofluorescence is NADH, which has peak excitation at 356 nm with emission at 510 nm (Jiang and Julian, 1997). Furthermore, it is easy to see that if F_a approximately equals $(F_a)_{lo}$ and $(F_a)_{hi}$, then autofluorescence can be neglected even if the autofluorescence term is not small with respect to probe fluorescence. Nonratiometric probes are fine for following changes in free calcium in a single set of cells with time, but difficult to use for accurately measuring $[Ca^{2+}]$ for different sets of cells. Leakage is a major problem with these probes when using plated cells in attempting to ascertain free calcium. To measure even approximate free calcium inside of cells using a nonratiometric probe, one must calibrate each cell in each sample at the end of the experimental procedure and hope that little leakage or bleaching of the probe occurred during the experiment, which is unlikely to be true. This process is very labor intensive and definitely not recommended. In addition, the resulting images must be corrected for nonuniformity of illumination to compare the fluorescence intensity from one cell to that of another. Such corrections are also not simple and will not be discussed here. For these reasons, the authors will not discuss how to calibrate nonratiometric probes in this system. With the exceptions noted below, the steps used to measure calcium using nonratiometric probes are essentially the same as that for ratiometric probes but it is generally unnecessary to record wavelength scans, and all of the measurements are made at a single excitation and emission wavelength (see Basic Protocol 1, steps 1 to 7).

Initial set up of the instrument

It is necessary to get an idea of the range of intensities that the probe might undergo. If the probe being used has its maximum intensity in high-calcium medium, start with high-Ca medium. If the probe being used has its maximum intensity in low-calcium medium, start with low-Ca medium. Once the cells come close to maximum intensity, adjust light intensity, band-pass, or HV/G until the brightest cell is ~90% to 95% of the maximum permissible intensity.

42. Incubate the cells in probe using the procedure described in steps 7 and 8. Follow the procedure described in steps 9, 10, and 11, using either low-Ca medium or high-Ca medium. Observe the intensity of the brightest cell. When it reaches an apparent maximum, adjust HV/G so this intensity is 90% to 95% of the maximum permissible intensity. From this point on, no adjustments should to be made to light intensity, excitation band-pass, or HV/G—to avoid having the fluorescence exceed the maximum permissible intensity.

    IMPORTANT NOTE: *As the free calcium inside of the cell equilibrates with the external free calcium, the probe's fluorescence inside the cell will increase until it reaches either $(F)_{hi}$ or $(F)_{lo}$. If one must use high-Ca medium for this step, at some point the cells will begin to die, the probe will leak out, and the dying cell's fluorescence will decrease. Attempt to adjust the high voltage or gain before this occurs. This is not usually a problem in low-Ca medium.*

Check for inner-filter effect and assess leakage

Steps 43 to 45: The inner-filter effect, which distorts the probe's spectra, will distort measurements of $[Ca^{2+}]$ (Moore et al., 1990). Therefore, it is important to check that the inner-filter effect is not a problem for the system and incubation procedure. In order to easily check for inner-filter effect, the equipment must be able to scan the excitation spectra (see Troubleshooting). Leakage is not usually a serious problem with ratiometric probes when using a microscope system, since it seldom contributes much to the supernatant background image (which is subtracted anyway), and the ratio is independent

of probe concentration. However, leakage is a very serious problem with nonratiometric probes because a change in fluorescence due to a change in [Ca^{2+}] cannot easily be distinguished from a change in fluorescence due to a change in probe concentration. Therefore, it is important to get a measure of the normal probe leakage rate from the cell type.

43. Place incubated cells in the holder, rinse twice with standard medium. Follow the procedure detailed in step 12 except set HV/G (step 42), and save a background image, I_s. Follow the procedure detailed in step 13 except set HV/G (step 42) and save an image $I_{t\text{-}s}$ or I_t. Turn off HV/G. If it is not possible to automatically subtract I_s, switch to analysis and calculate $I_{t\text{-}s} = I_t - I_s$.

44. Switch to analysis, create a mask and a set of ROIs, as described in step 14 using the image $I_{t\text{-}s}$. Switch back to acquisition, if the equipment includes optional scanning of excitation, switch the software from time-based mode to wavelength mode, turn off automatic background subtraction and using ROIs and mask, scan the excitation spectra. Save the resulting median values of intensity for each of the ROIs as the uncorrected dye spectra S_t inside the cells. Compare S_t with the spectra found in step 4.

    If many of the spectra do not have the correct shape, there are problems with inner-filter effect, which must be corrected by reducing probe concentration during incubation or reducing incubation time. If none of the spectra have the correct shape, either there are problems with inner-filter effect or with autofluorescence. (see Troubleshooting).

45. Use time-based acquisition and the ROIs and mask from step 44 and acquire median values from ROIs every minute for 20 to 30 min. Save the median values for the ROIs as a function of time. Since only cells that maintain a constant value of [Ca^{2+}] can be used to determine dye loss, eliminate cells from the ROIs whose median fluorescence (F) versus time data cannot be fit reasonably well with a straight line.

    Any change in the median value of the jth cell represents the loss of probe from the cell. Normally resting cells will not spontaneously change [Ca^{2+}]. If the machine doesn't have an automatic shutter in the excitation beam, acquire median values manually, taking care to block the excitation beam except when taking data to avoid photobleaching the dye.

Measure autofluorescence (F_a)

Do not bother to measure autofluorescence unless it appears that it is causing an apparent inner-filter effect or is large enough to cause fluctuations in F during an experimental procedure.

46. Repeat step 26 except set HV/G (step 42) and take only one image for each experimental medium.

    If autofluorescence is significant in the medium containing 5 mM cyanide, then follow steps 27 and 29 to obtain $(F_a)_{lo}$ and $(F_a)_{hi}$ repeat this measurement for any procedure that might result in significant changes in autofluorescence, in order to determine that changes detected in F are not the result of changes in F_a.

Measure the fluorescence of samples of interest

47. Place incubated cells in the holder, rinse twice with standard medium, and then add 1 ml of standard medium. Adjust focus to get a sharp, bright image. Take a background image as discussed in step 12 and set the software to automatically subtract these background images.

48. To determine the average rate of dye leakage from the cells, analyze the median values for the ROIs as a function of time found in step 45.

a. Transfer the data from the plot of F versus time found in step 45 to a spreadsheet such as Excel.

b. Average all of the data at a given time point to obtain $F_{ave}(t)$ and plot $F_{ave}(t)$ versus time.

c. Find the least squares best fit line to the plot of $F_{ave}(t)$ versus time.

The resulting slope, s_{loss}, can be used to back calculate the approximate original dye concentration in any cell. That is, if the median value of fluorescent intensity in the kth cell at time t is $(F_t)_k$, then its approximate value at t = 0 is $(F_0)_k = (F_t)_k - s_{loss}\, t$. (Note: $- s_{loss}$ is positive since s_{loss} is always negative.) This equation can be used to correct the median value of fluorescent intensity for any cell to the value it would have had if no dye loss had occurred assuming that all cells lose dye at the same rate.

49. To properly analyze the results from a time-based experiment, use step 48 to correct all of the median values of fluorescent intensity in the *k*th cell to the value they would have had if no dye loss had occurred. Plot these corrected values versus time for each cell.

Obtain approximate values of [Ca^{2+}]

If some estimate of [Ca^{2+}] is desired, the same group of cells that is used in the experiment must be used for a complete calibration. Set up a system to aspirate all of the medium from the coverslip because exactly the same group of cells must be used for the entire procedure. This must be done before the first experimental images are taken.

50. Follow the procedure described in steps 10, 12 and 13 except use the experimental medium, set HV/G (step 42) and take images at a single wavelength only. Run the experimental procedure on the group of cells (the resulting images are I_1, I_2, ..., I_{t_i}) recording the time at which each image was taken. At the end of the procedure, follow steps 16 and 17 to obtain a low-calcium image, I_{lo1}. Without changing or moving the coverslip, follow step 19 to obtain a high-calcium image, I_{hi}. Repeat steps 16 and 17 to obtain another low-calcium image, I_{lo2}. Note the time at which each of these images were saved.

The rate of dye leakage often changes during the calibration steps due to the stress caused by the additions (especially high [Ca^{2+}]) during this time. Approximate the dye loss during the calibration procedure by making a two-point plot of the fluorescence intensities of the median fluorescence intensities of the ROIs of the low Ca images and following step 48 to obtain an approximate slope of dye loss during calibration, $s_{c\text{-}loss}$.

51. Use the brightest image found in step 50 to create a mask and a set of ROIs. Use the system software to create a plot of median fluorescent intensity $(F_t)_k$ versus time for all of the data acquired in step 50 for all of the cells in the ROIs. Correct all of the data back to zero dye loss as follows. $(F_{t\ corr})_k = (F_t)_k - s_{loss}\, t$, except $(F_t)_k$ at high calcium, for which $(F_{t\ corr})_k = (F_t)_k - s_{loss}\, t_{loCa} - s_{c\text{-}loss}\,(t - t_{loCa}) = (F_{hi})_k$ where t_{loCa} is the time at which the first low-calcium image was saved. $(F_t)_k$ for the first low-calcium measurement = $(F_{lo})_k$. (Note: $- s_{loss}$ and $- s_{c\text{-}loss}$ are positive since s_{loss} and $s_{c\text{-}loss}$ are always negative.)

For any cell k in the ROIs, $[Ca^{2+}]_k \approx K_d[(F_{t\ corr})_k - (F_{lo})_k]/[(F_{hi})_k - (F_{t\ corr})_k]$.

DETERMINATION OF K_d FOR PLATED CELLS USING RATIOMETRIC PROBES

SUPPORT PROTOCOL 2

This protocol describes the method for determining the K_d for plated cells using ratiometric probes. Read the discussion in Support Protocol 1. If at all possible, measure K_d in a cell suspension rather than using plated cells because it will be more accurate.

Additional Materials (also see Basic Protocols 1 and 2)

EGTA solution (see recipe for Ca^{2+} calibration standards)
CaEGTA solution (see recipe for Ca^{2+} calibration standards)
Ca solution (see recipe for Ca^{2+} calibration standards)
1 M $CaCl_2$
Cells incubated with probe (see Basic Protocol 1, step 9)

Determine K_d of a ratiometric probe for plated cells at 20°C

1. Prepare the FDIM apparatus (see Basic Protocol 2).
2. Make up solutions 1 through 13 using EGTA solution and CaEGTA solution in the proportions shown in Table 2.5.3.

   Table 2.5.3 shows [Ca^{2+}] at 20°C for each of these solutions as well as for the EGTA solution, the CaEGTA solution, and the Ca solution.

   If the calibration is to be performed at 37°C, use Table 2.5.4 to make up solutions 1 through 13. Table 2.5.4 shows [Ca^{2+}] at 37°C for each of these solutions as well as for the EGTA solution, the CaEGTA solution, and the Ca solution.
3. Place incubated cells in the holder, rinse twice with the EGTA solution (created in step 2) and add 0.5 ml of the EGTA solution. Place another 0.5 ml of the EGTA solution in a small tube, add 10 µl of 0.1 mM thapsigargin, 7.5 µl of 2 mM oligomycin, 7.5 µl of 1 mM CCCP, and 10 µl of 1 mM ionophore to yield final concentrations of 1 µM thapsigargin, 10 µM oligomycin, 5 µM CCCP, and 10 µM ionophore, respectively. Immediately shake or vortex this mixture and then add it to the coverslip, making sure the two components are well mixed. Note the time at which this addition was made.

   IMPORTANT NOTE: *If cells cover the entire coverslip, wipe a small area free of cells for the background measurement.*
4. Place the coverslip on the microscope stage, obtain a set of background images, and set the program to automatically subtract background. Find a likely group of cells, use fast focus to provide the brightest, sharpest image, and take a set of images. Create ROIs (Basic Protocol 2, step 14) and then collect median values from the ROIs, waiting for an apparent steady state to be reached. (which should take approximately the same time it took to reach low calcium in step 15 of Basic Protocol 2). When an apparent steady state is reached, take a set of images, $(I)_{EGTA\lambda1}$ $[(I_t)_{EGTA\lambda1}]$ and $(I)_{EGTA\lambda2}$ $[(I_t)_{EGTA\lambda2}]$, respectively.

   If background was not automatically subtracted, subtract it now to obtain $(I)_{EGTA\lambda1}$ and $(I)_{EGTA\lambda2}$.
5. Repeat steps 3 and 4 for each of the solutions created in step 2, as well as for the CaEGTA solution and the Ca solution resulting in $(I_t)_{1\lambda1}$, $(I_t)_{2\lambda1}$, ..., $(I_t)_{13\lambda1}$, $(I_t)_{CaEGTA\lambda1}$, $(I_t)_{Ca\lambda1}$, $(I_t)_{1\lambda2}$, $(I_t)_{2\lambda2}$, ..., $(I_t)_{13\lambda2}$, $(I_t)_{CaEGTA\lambda2}$ and $(I_t)_{Ca\lambda2}$.

   IMPORTANT NOTE: *Be extremely careful in rinsing the chamber and in adding and removing solutions, because the same set of cells must be used for the entire procedure, and it is therefore necessary to be very careful not to move the microscope stage. Set up a system that can automatically remove all of the medium from the holder.*

   As the free calcium concentration increases, probe may begin to leak out of the cells. This is not too much of a problem for the ratiometric probes until the images become too dim to analyze properly.

   Replace the coverslip with a new one whenever necessary. For each new coverslip, take a new set of backgrounds.

6. If the values of F_a found in steps 26, 27, 28, and, and 29 of Basic Protocol 2 are not negligible with respect to the internal probe fluorescence values at λ_1 and/or λ_2 for all of the eleven samples, then correct F for autofluorescence. Measure $(I_a)_{lo1}$, $(I_a)_{lo2}$, $(I_a)_{hi1}$, and $(I_a)_{hi2}$, and calculate the average median values at λ_1, and λ_2 [these median values of intensity are $(F_a)_{lo1}$, $(F_a)_{lo2}$, $(F_a)_{hi1}$, and $(F_a)_{hi2}$].

   If $(F_a)_{hi1}$ approximately equals $(F_a)_{lo1}$ and $(F_a)_{hi2}$ approximately equals $(F_a)_{lo2}$, then it can be assumed that $(F_a)\lambda_1$ and $(F_a)\lambda_2$ are the same for all of the samples. If this is not the case, it will be necessary to calculate $(F_a)\lambda_1$ and $(F_a)\lambda_2$ for all eleven samples using the procedure detailed in steps 26 to 28 of Basic Protocol 2.

7. Create the proper masks and ROIs (see Basic Protocol 2, step 14) and eliminate any cells that are either too bright (cells whose linear profiles exhibit flattening) or too dim (cells whose linear profiles are not significantly above background) from the ROI (see Basic Protocol 2, step 32). Also, adjust the ROI to ensure that all of the ROI's boundaries are outside the masked cells.

   Each ROI should only include cells that fit the above criteria for all sixteen calibration solutions. Remember that the threshold used to create masks (if more than one mask is needed) must be identical for all masks. If the autofluorescence (see Basic Protocol 2, steps 26 to 29) is negligible, it can be ignored. Otherwise, correct each image for autofluorescence by subtracting a constant equal to $(F_a)_{j\lambda 1}$ from $(I_t)_{2\lambda 1}$ and subtracting a constant equal to $(F_a)_{j\lambda 2}$ from $(I_t)_{j\lambda 2}$ where $(F_a)_j$ is the autofluorescence found in step 6 of this protocol for the jth solution.

8. Calculate the ratio image, RI_j, for the *j*th solution using the corrected images. Set the ratio range as described in Basic Protocol 2, step 34 to the optimal value for each solution. Apply masks to these ratios and use the ROI on the masked images to collect median fluorescence ratios $(R)_{kj}$ for each cell *k* and each solution *j*, and place the results in a spreadsheet. Calculate the average value and standard deviation of $(R)_{kj}$ for the EGTA and Ca solutions. Eliminate any values that are more than two standard deviations from the averages and recalculate the average value and standard deviation.

   $(R)_{kj}\}_{ave}$ for the EGTA solution equals $R_{min;}$ $\{(R)_{kj}\}_{ave}$ for the CaEGTA solution equals R_{max}. The ratio (S_f/S_b) is calculated as in steps 33 or 36 of Basic Protocol 2.

9. Calculate the average value and standard deviation of $(R)_{kj}$ for all of the other solutions. Eliminate any values that are more than two standard deviations from the averages and recalculate the average value and standard deviation. $\{(R)_{kj}\}_{ave}$ for the jth solution equals R_j equals R as a function of $[Ca^{2+}]$. Using Equation 2.5.2, plot $\log\{[(R - R_{min})/(R_{max} - R)](S_f/S_b)\}$ versus $\log\{[Ca^{2+}]\}$. Fit the linear portion of the data with the linear least squares best fit line. The resulting graph should look just like Figure 2.5.2. The value of $[Ca^{2+}]$ for which $y = 0$ is a measure of the apparent K_d of the probe. If the values of R_{min} and R_{max} are very close to their true values, the slope of the line will be one. If the values of R_{min} and R_{max} are not close to their true values, all the data will clearly not fit a straight line and the slope will not be one. Even when the data are poor, a reasonable approximation of the true K_d can still be found. However, in this case the use of the values of R_{max}, R_{min} and (S_f/S_b) found in steps 34, 35, and 36 or 38 of Basic Protocol 2 will lead to incorrect values of $[Ca^{2+}]$ inside the cells.

10. When it is clear that values of R_{max}, R_{min} and (S_f/S_b) found in steps 34, 35 and 36 or 38 of Basic Protocol 2 are incorrect, plot R versus $[Ca^{2+}]$ using only the intermediate data points and fit the data with an equation of the form $R = \{(R_{min} + R_{max}/C\}[Ca^{2+}]/(1 + [Ca^{2+}]/C)$ where R_{min}, R_{max}, and C are unknown and $C = K_d (S_f/S_b)$ (see Fig. 2.5.3). If the data are very accurate, accurate values of R_{min}, R_{max}, and $C = K_d (S_f/S_b)$ can be obtained from data for which $[Ca^{2+}]_{outside}$ ranges between 15 nM and 6 μM for Fura-2.

For dual-excitation (emission) monochromators, $(R_{min})_{true} = R_{min}/R_L$ and $(R_{max})_{true} = R_{max}/R_L$ where R_L was found in step 5 of Basic Protocol 2.

11. Repeat steps 3 through 9 for the intermediate calcium concentrations only for the wavelength pair λ_i and λ_2, where λ_i is the isosbestic point that was determined in Basic Protocol 2, step 22. Plot the resulting R versus $[Ca^{2+}]$ and fit the data with an equation of the form $R = \{(R_a + R_b/K_d)[Ca^{2+}]\}/(1 + [Ca^{2+}]/K_d)$ where R_a, R_b and K_d are unknown. Then $(S_f/S_b) = C/K_d$.

REAGENTS AND SOLUTIONS

Use Milli-Q-purified water or equivalent for all recipes and protocol steps. To eliminate calcium contamination as much as possible, glassware should be rinsed several times in Milli-Q-purified water, dried, and stored in such a way as to eliminate dust from inside the glassware. For common stock solutions see ***APPENDIX 2A****; for suppliers, see* ***SUPPLIERS APPENDIX****.*

AM form of fluorescent Ca^{2+} probe, 2 to 5 mM

Dissolve the Ca^{2+}-insensitive, membrane-permeable form of fluorescent Ca^{2+} probe in anhydrous, reagent grade DMSO (see recipe) to a final concentration of 2 to 5 mM. Immediately split this solution into small airtight containers such as microcentrifuge tubes at 20 to 50 µl per tube. Freeze immediately and store at –20°C in the dark in a dessicator until immediately before use, because DMSO readily takes up moisture which leads to decomposition of the dye. Thaw each aliquot only once.

CAUTION: *DMSO is slightly hazardous.*

Ca^{2+} calibration standards

1. For 40 mM EGTA, carefully add 40 ml of calibrated 100 mM EGTA (see recipe) to 55 ml of 1.67× calibration medium (see recipe), adjust pH to 7.20 at the calibration temperature (either 20°C or 37°C) with 2 M KOH. Bring to a final volume of 100 ml with 1.67× calibration medium, pH 7.20 at the calibration temperature.
2. For 40 mM $CaCl_2$, carefully dilute 40 ml of calibrated 100 mM $CaCl_2$ (see recipe) to 100 ml with 1.67× calibration medium (see recipe), pH 7.20 at the calibration temperature.
3. For EGTA solution, carefully mix 1 part of 40 mM EGTA (see recipe) with 1 part 1× calibration medium (see recipe), pH 7.20 at the calibration temperature.
4. For CaEGTA solution, carefully mix 1 part of 40 mM EGTA (see recipe) with 1 part 40 mM $CaCl_2$ (see recipe), pH 7.20 at the calibration temperature.
5. For Ca solution, carefully mix 1 part of 40 mM $CaCl_2$ (see recipe) with 4 parts of 1× calibration medium (see recipe), pH 7.20 at the calibration temperature.
6. Use table 2.5.3 to create solutions 1 through 13 for calibrations at 20°C or use table 2.5.4 to create solutions 1 through 13 for calibrations at 37°C.

Calibrated $CaCl_2$, 100 mM

Purchase calibrated 100 mM $CaCl_2$ from Orion, Corning, or Molecular Probes as part of their concentrated calcium calibration kit. Carefully remove aliquots and keep tightly sealed in between removals. Store for 1 to 2 years at room temperature.

Calibrated EGTA, 100 mM

Purchase calibrated 100 mM EGTA from Molecular Probes as part of their concentrated calcium calibration kit, or make calibrated 100 mM EGTA using the technique of Moisescu and Pusch (1975) described below using ultrapure EGTA from Calbiochem or Sigma.

continued

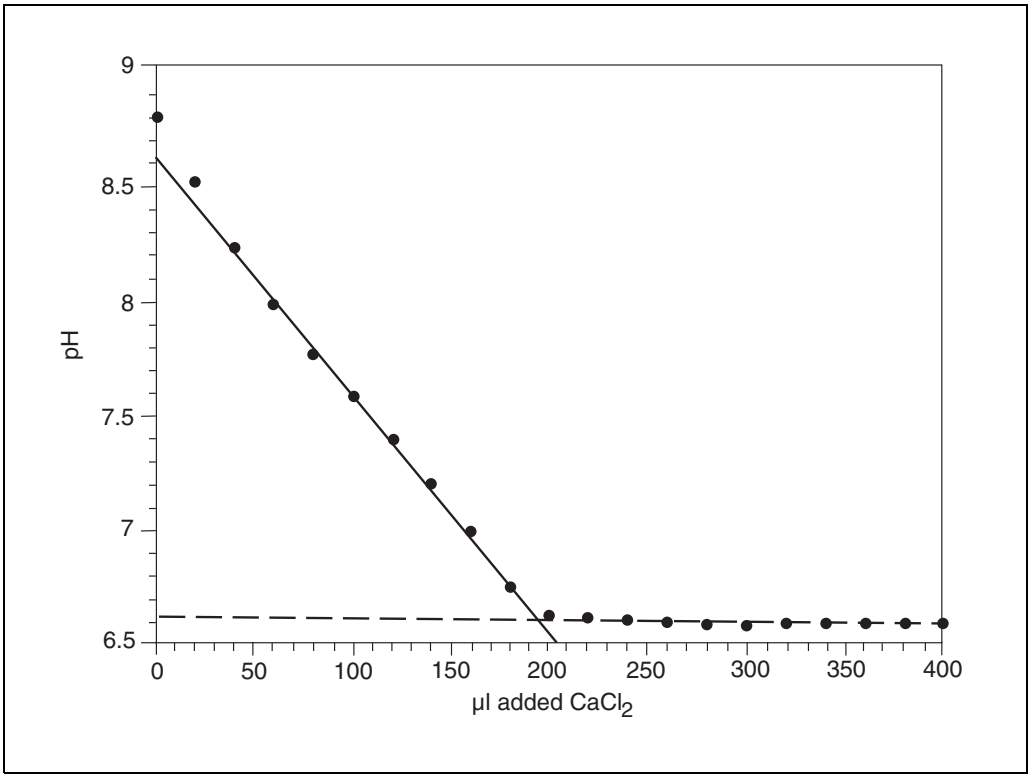

Figure 2.5.6 pH titration of EGTA. The two linear portions of the data are fitted with a linear least squares best fit straight line with the equations of the lines being $y = 8.6329 - 0.010446x$ with $R^2 = 0.99834$ and $y = 6.6286 - 0.00016818x$ with $R^2 = 0.63379$. The x value of the intercept of these two lines equals the total µmoles of EGTA in the sample.

1. Make nominal 200 mM EGTA by adding 7.608 gm of free acid ultrapure EGTA to 50 ml water alternately with 20 ml of 1 M KOH. While observing pH, add additional 1 M KOH until pH = 7.20 at room temperature. Bring to a final volume of 100 ml with water.

   The best ultrapure EGTA contains only 99+% EGTA. In addition, it can accumulate water, so this nominal 200 mM EGTA solution will be <200 mM.

2. Make 100 mM HEPES or TES by adding 2.383 gm ultrapure acid HEPES or 2.292 gm ultrapure acid TES to 80 ml water, and adjusting pH to 9.0 at room temperature with 1 M KOH. Bring to a final volume of 100 ml with water.

   Use ultrapure acid HEPES or TES from Calbiochem or Sigma. Treat glassware to eliminate calcium.

3. Make nominal 2 mM EGTA in buffer by carefully adding 1 ml of nominal 200 mM EGTA and 4 ml of 100 mM HEPES or TES to 90 ml water. Adjust pH to between 8.8 and 9.0 with 1 M KOH. Bring to a final volume of 100 ml with water.

   Starting with this solution and from this point on, the success of this technique for making 100 mM EGTA requires that all pipetting be highly accurate.

4. Titrate the EGTA by carefully pipetting 10 ml of the nominal 2 mM EGTA in buffer. Measure the pH while stirring. (Insulate the stir plate from the sample to prevent a change in temperature in the sample during this process.) Add 10 to 20 µl aliquots of 100 mM calibrated $CaCl_2$ (see recipe) and measure the pH after each addition while stirring. Plot pH versus added µl of 100 mM $CaCl_2$.

continued

The resulting graph will have a distinct V shape like that shown in Figure 2.5.6. Draw linear best fit lines through the linear portions of the data and calculate the x value of the intersection of the two lines. The µmoles of added calcium at the intercept = the µmoles of EGTA in the solution. For example, for Figure 2.5.6, the intercept occurs at 195.0 µl of added calcium which equals 19.5 µmoles calcium (= 0.195 × 100) = 19.5 µmoles EGTA in 10.195 ml. The true concentration of EGTA in this solution before dilution was 1.95 mM (= 19.5/10.0).

Thus, for this example, the true concentration of the nominal 200 mM EGTA is 195 mM for a purity of 97.5%.

5. For 100 mM calibrated EGTA, carefully dilute the nominal 200 mM EGTA whose true concentration has just been measured to 100 mM EGTA with water.

Calibration medium, 1× and 1.67×

1× medium:
130 mM KCl
15 mM NaCl
20 mM MOPS
20 mM glucose
1 mM $MgCl_2$
1 mM vanadate pentoxide (V_5O_5)
1 mM ouabain
Adjust to pH 7.2 at calibration temperature using 1 M HCl and 1 M KOH
Store up to 4 to 6 months at −20°C

1.67× medium: Prepare medium containing 1.67× all of the above components, so that when used to dilute the standards (6:4), it becomes ~1×.

Dimethylsulfoxide (DMSO), anydrous

Purchase anhydrous, reagent-grade DMSO from Aldrich or Fluka. The DMSO should be relatively fresh (<1 year old). It must be anhydrous, which means that it must be stored well sealed under argon or nitrogen and desiccated. Each time the bottle is opened, it must be flushed with argon or nitrogen before resealing

CAUTION: *DMSO is slightly hazardous.*

FA (probe free acid) in high-Ca medium, 5 µM

Add $CaCl_2$ to 1× calibration medium (see recipe) to a final concentration of 0.1 mM. Very carefully dilute this solution 1:1 with 10 µM FA solution (see recipe). Store up to 4 to 6 months in the dark at −20°C.

IMPORTANT NOTE: *It is vital that the 5 µM FA in low-Ca solution and the 5 µM FA in high-Ca solution have exactly the same amount of the FA form of fluorescent Ca^{2+} probe.*

FA (probe free acid) in low-Ca medium, 5 µM

Add EGTA to calibration medium (see recipe) to a final concentration of 0.2 mM. Very carefully dilute this solution 1:1 with 10 µM FA solution (see recipe). Store up to 4 to 6 months in the dark at −20°C.

IMPORTANT NOTE: *It is vital that the 5 µM FA in low-Ca solution and the 5 µM FA in high-Ca solution have exactly the same amount of the FA form of fluorescent Ca^{2+} probe.*

FA (probe free acid) solution, 10 µM

Stock solution: Prepare a 1 mM stock solution of the Ca-sensitive (FA) form of the fluorescent probe in water. Store up to 4 to 6 months at −20°C in the dark.

10 µM solution: Add the FA form of the fluorescent probe to a final concentration of 10 µM in 1× calibration medium (see recipe) using the 1 mM stock solution.

High-Ca medium, 2×

130 mM KCl
15 mM NaCl
20 mM MOPS
20 mM glucose
1 mM $MgCl_2$
8 mM $CaCl_2$ (or higher)
1 mM vanadate pentoxide (V_5O_5)
1 mM ouabain
Adjust pH to 7.2 at calibration temperature using 1 M HCl and 1 M KOH
Store up to 4 to 6 months at −20°C
For 1× high-Ca medium, dilute 1:1 with calibration medium (see recipe)

If one wishes to measure R_{max} within 0.5% of its true value, the amount of free calcium must be ~200 K_d of the probe in situ, or greater.

Ionophore, 1 mM

Dissolve ionomycin or dibromo A-23187 (Calbiochem) in anhydrous, reagent-grade DMSO (see recipe) to a concentration of 1 mM. Store up to one year at 4°C in the dark.

Keeping this solution anhydrous is not essential since small amounts of water cause no problems.

CAUTION: *These ionophores are hazardous.*

Low-Ca medium, 2×

130 mM KCl
15 mM NaCl
20 mM MOPS
20 mM glucose
1 mM $MgCl_2$
10 to 20 mM EGTA
1 mM vanadate pentoxide (V_5O_5)
1 mM ouabain
Adjust pH to 7.2 at calibration temperature using 1 M HCl and 1 M KOH
Store up to 4 to 6 months at −20°C
For 1× low-Ca medium, dilute 1:1 with calibration medium (see recipe)

The amount of EGTA necessary depends upon the pH of the standard medium; the more acid it is, the more EGTA is needed. The resulting free Ca^{2+} should be <1 nM when diluted 1:1 with calibration medium.

Any of the available calcium chelator programs such as MaxChelator (cpatton@leland.stanford.edu) can be used to determine how much EGTA is needed.

Oligomycin, 2 mM

Dissolve oligomycin in anhydrous, reagent-grade DMSO (see recipe) to a concentration of 2 mM. Store up to one year at −20°C in the dark.

Keeping this solution anhydrous is not essential since small amounts of water cause no problems.

CAUTION: *Oligomycin is hazardous.*

Standard medium

This is any medium that can support and nourish the cells for the time required for the experiments (min to hr), which is either nonfluorescent or minimally fluorescent. This medium should contain a buffer other than bicarbonate, since most spectrome-

continued

ters and microscopes are not set up to maintain a CO_2 atmosphere. To keep extracellular hydrolysis of AM esters to a minimum, this medium should be free of primary and secondary amines, serum (which may contain endogenous esterase activity), and phenol red.

Standard medium with cyanide

Add 5 mM potassium or sodium cyanide to standard medium (see recipe). Make this solution in the hood and handle with extreme care. Cyanide will tend to make solutions more basic.

CAUTION: *Cyanide in acid medium can generate cyanide gas which can be deadly; therefore adjust the pH of this solution with the acid form of a zwitter ion such as HEPES (1 or 2 M).*

Neutral cyanide solutions are not stable. They should be used within a day and stored in the refrigerator until use.

Thapsigargin, 0.1 mM

Dissolve thapsigargin (Calbiochem, Sigma) in anhydrous, reagent-grade DMSO (see recipe) to a final concentration of 0.1 mM. Immediately split into small airtight containers such as microcentrifuge tubes at 50 to 100 µl per tube. Freeze immediately and store at −20°C in the dark in a dessicator until immediately before use, because DMSO readily takes up moisture which leads to decomposition of thapsigargin. Thaw each aliquot only once.

CAUTION: *Thapsigargin is hazardous.*

COMMENTARY

Background Information

Ca^{2+} is a very important ion in biological systems. It is the most closely regulated ion in serum, with a free ion concentration of ~2 mM (which varies somewhat from species to species). Its concentration in the cytosol of cells is much lower (usually <100 nM) and also closely regulated. It is used as a signaling molecule or second messenger in many types of cells and during these periods of excitation can reach concentrations of >1 µM during Ca^{2+} transients or pulses.

For years, total Ca^{2+} in cells has been measured using atomic absorption spectroscopy, and free Ca^{2+} concentration ($[Ca^{2+}]$) in serum and interstitial fluid has been measured using Ca^{2+} electrodes. $[Ca^{2+}]$ inside cells has sometimes been measured in specialized laboratories using microelectrode techniques or using the bioluminescent Ca^{2+}-binding peptide aequorin, which until recently had to be injected into the cell using a micropipette. More recently the technique of choice for intracellular $[Ca^{2+}]$ measurement has been the use of Ca^{2+}-binding fluorescent indicators or probes, which can be diffused into the cell in a membrane-permeant form (usually the acetoxymethyl ester form; AM) where it is converted by intracellular esterase activity into a membrane-impermeant, Ca^{2+}-sensitive form (usually a carboxylic acid form).

The first such indicator of this type was Quin-2, which was introduced by Roger Tsien (Tsien et al., 1982). Quin-2 was followed by better probes, some of which were ratiometric such as Fura-2 and Indo-1, some of which were much brighter than Quin-2, e.g., Calcium red and Calcium green, some of which were fast binders, e.g., Fluo-3, and some of which associated with special subcellular compartments, e.g., Rhod-2. Today, many Ca^{2+} probes are available for use with either fluorescence spectroscopy, fluorescence single-cell photometry, or fluorescence digital imaging analysis.

Atomic absorption spectroscopy can only measure total Ca^{2+} in cells, and hence cannot be used to measure free Ca^{2+} concentration. Calcium-sensitive electrodes are not very sensitive below ~1 µM free calcium but can give reasonable estimates of $[Ca^{2+}]$ down to about 0.3 to 0.5 µM. Aequorin can reach lower levels of $[Ca^{2+}]$ but is difficult to calibrate accurately. On the other hand, Ca^{2+}-binding fluorescent probes can give accurate values of $[Ca^{2+}]$ down to 10 nM or less. The biggest problems with Ca^{2+}-binding fluorescent probes are the diffi-

culties in accurately measuring K_d, R_{max} (F_{max}), and R_{min} (F_{min}) inside cells (i.e., in situ), as well as the leakage of probe from cells.

Historically, K_d, R_{max} (F_{max}), R_{min} (F_{min}), and (S_f/S_b) were generally measured in vitro, and the assumption was made that these values were the same in vitro and in situ. (Many software programs used with spectrofluorometers and FDIM only describe in vitro calibrations.) That is, it was assumed that: (1) the only form of the probe inside cells is fully de-esterified, either free or bound to calcium; (2) the probe inside the cells is the only source of fluorescence; (3) the spectral properties of the probe are the same inside and outside the cell; and (4) the probe's K_d is the same inside and outside the cell (Moore et al., 1990). These assumptions are rarely true. The probe is often incompletely de-esterified (Gunter et al., 1988; Oakes et al., 1988; Moore et al., 1990; Roe et al., 1990) and leaks from inside the cells (Moore et al., 1990; Roe et al., 1990; di Virgilio et al., 1990; Kao, 1994). The probe can distribute into intracellular compartments where $[Ca^{2+}]$, K_d, R_{max} (F_{max}), R_{min} (F_{min}), and (S_f/S_b) can all be different from the cytosolic values (Gores et al., 1989; Moore et al., 1990; Roe et al. 1990; Kao, 1994) as well as from the in vitro values (Moore et al., 1990; Roe et al., 1990; Williams and Fay, 1990; Harkins et al., 1993; Baker et al., 1994; Bassani et al., 1995; Lipp et al., 1996). Exposure to intense light can damage the cell as well as bleach the probe, where the bleached probe can be fluorescent but insensitive to $[Ca^{2+}]$ in the nM or µM range (Moore et al., 1990; Roe et al., 1990). Poenie et al. (1986) found that the in situ spectra of Fura-2 were different from its in vitro spectra. They found that they could make the in situ and in vitro spectra match by increasing the viscosity of the in vitro medium, or by decreasing the in vitro R_{max} and R_{min} values by 15% and using them in Equation 2.5.2 for $[Ca^{2+}]$. This "viscosity" correction is often found as a parameter in fluorescence software to correct in vitro measurements of R_{max} and R_{min}, which can then be used to yield the proper value of $[Ca^{2+}]$ in cells. The problem with this assumption is that it has since been shown that binding of probe to cytosolic proteins is almost certainly the main source of the differences between in situ and in vitro calibrations, and (S_f/S_b) measured in situ and in vitro are not necessarily the same (Brandes et al., 1993; Harkins et al., 1993; Baker et al., 1994; Bassani et al., 1995). Baker et al. (1994) and Brandes et al. (1993) showed that K_d and (S_f/S_b) increase as protein increases, and the isosbestic point (λ_{iso}) decreases as protein increases. Baker et al. (1994) found that all of these parameters can be fit with a simple binding relationship described by $F = F_o + \Delta F_{sat} \times P/(P + P_{50})$ for a fixed concentration of probe, where F is the parameter to be fitted (K_d, (S_f/S_b), or λ_{iso}), F_o is the value of the parameter in the absence of any protein, ΔF_{sat} is the maximum change in F extrapolated to saturating protein, P is the protein concentration in the calibration media, and P_{50} is the protein concentration that causes a 50% change in F. All of the parameters are a function of the type of protein used, pH, and the relative concentrations of protein and probe. For example, they found that at pH 7.3, the K_d at saturating protein for Indo-1 was 808 ± 26 nM for frog muscle proteins and 638 ± 72 nM for rat heart proteins. Although nonratiometric probes do not have corresponding values of (S_f/S_b) and λ_{iso}, protein does cause K_d to increase and ($F_{max} - F_{min}$) to decrease (Harkins et al., 1993). Thus, to perform an in vitro calibration, ideally protein from the cell type should be included. Even then, it is necessary to vary protein concentration as above and then find the value of λ_{iso} that matches the value of λ_{iso} found in situ in order to decide upon the appropriate values of K_d and (S_f/S_b) to be used. If $[Ca^{2+}]_{in}$ cannot be forced to equal $[Ca^{2+}]_{out}$, then it is not possible to calibrate the probe in situ. Many procedures have been used to ensure that $[Ca^{2+}]_{in}$ equals $[Ca^{2+}]_{out}$ during in situ calibration. Bassani et al. (1995) exposed myocytes to caffeine in order to empty sarcoplasmic reticulum stores and then incubated the cells in low-calcium medium to remove the excess intracellular calcium. They then added the equivalent of 1 nm CCCP and 10 mM 2-deoxyglucose to achieve metabolic inhibition and to limit hypercontracture. Their calibration medium, containing 130 mM KCl, 10 mM NaCl, and the ionophore Br-A23187, was added to determine R_{max} and R_{min}. After equilibrium was apparently reached, selected cells were aggressively "poked" with a 2- to-3 µm-diameter electrode to cause external calcium to leak into the cells. If a true equilibrium had been reached, no change in fluorescence was observed. Williams and Fay (1990) mention that the main impediment to getting $[Ca^{2+}]_{in}$ to equal $[Ca^{2+}]_{out}$ during in situ calibration is the ATP-dependent Ca pump and $[Na^+]_{out}$-$[Ca^{2+}]_{in}$ exchange in the plasma membrane. The ATP-dependent Ca pump can often be inhibited by vanadate or calmodulin inhibitors such as trifluoperazine. $[Na^+]_{out}$–$[Ca^{2+}]_{in}$ exchange can be inhibited by including the Na^+-ionophore

monensin or by using medium containing 130 mM KCl and 10 to 15 mM NaCl. If the Na^+K^+-ATPase is highly active, include either a K^+-ionophore such as nigericin or a pump inhibitor such as ouabain or oligomycin, which is a potent inhibitor of many Na^+K^+-ATPases. It is seldom possible to calibrate nonratiometric probes in situ since the probe concentration must be known in order to calibrate it, and probe concentration can vary from cell to cell.

Critical Parameters

Always protect the camera or photomultiplier tube from excess light. That is, when not certain how intense the fluorescence to be detected is, use a variable aperture that can be opened slowly in the excitation beam path so that the camera/photomultiplier tube can be exposed gradually to the fluorescent light. Putting a shutter in the excitation beam path will also protect the sample from photobleaching. Photobleaching can change the spectroscopic parameters of the probe, resulting in erroneous values of $[Ca^{2+}]$ (Moore et al., 1990; Roe et al., 1990).

When preparing cells for fluorescence measurements, beware of anoxia, both during and after incubation. In addition, leakage of probe from the cells increases the difficulty of making measurements in the cuvette system for any fluorescent probe, and makes the calculation of $[Ca^{2+}]$ using FDIM for nonratiometric probes almost impossible. Leakage can be reduced by storing the cells after incubation at 4°C until use and running the experiments at room temperature if at all possible. Some cell types actively extrude either the AM form of the probe using the multidrug resistance protein (Homolya et al., 1993) or the free acid form using the organic anion transport system (Moore et al., 1990; di Virgilio et al., 1990; Kao, 1994). The first problem results in insufficient loading of the Ca-sensitive form of the probe and can often be alleviated with a monoclonal anti-MDR1 antibody, verapamil, vincristine, sodium orthovanadate or oligomycin. The second problem can result in very rapid loss of the Ca-sensitive form of the probe once it is in the cell. Probenecid and sulfinpyrazone are inhibitors of the organic anion transport system and may reduce such leakage.

Perfecting the incubation procedure to minimize autofluorescence, remaining fluorescent AM form of the probe, and the production of calcium-insensitive fluorescent forms of the probe is critical. Although large autofluorescence values can be handled, it is much simpler if autofluorescence can be ignored. If probe concentration during incubation is too high, or the incubation is too long, it is sometimes very difficult to remove all of the remaining AM form of the probe at the end of the incubation period (Homolya et al., 1993). This remaining AM form of the probe causes the same sort of problems that the other calcium-insensitive fluorescent forms of the probe do. Albumin can often be used in a rinse medium to remove extracellular AM and other calcium-insensitive fluorescent forms of the probe (Oakes et al., 1988). The calcium-insensitive fluorescence F_i can only be estimated when using fluorescence spectroscopy, and even an estimate is hard to obtain when using FDIM (Gunter et al., 1988; Moore et al., 1990; Roe et al., 1990). For fluorescence spectroscopy, the estimated value of F_i is probably correct within a factor of two, but a factor of two can be a problem unless F_i is small with respect to fluorescence from the calcium-sensitive probe at the wavelength(s) used to detect the probe. Therefore, it is well worthwhile it to spend time perfecting the incubation procedure to minimize or eliminate these problems (Gunter et al., 1988; Oakes et al., 1988; Moore et al., 1990; Roe et al., 1990; Kao, 1994).

Surprisingly, too much probe inside the system can also cause problems. If the concentration of internal dye is too large (~100 μM for Fura-2), the probe will substantially change the buffering capacity of the cell and affect the $[Ca^{2+}]$ that is being measured. If the concentration of internal dye multiplied by the thickness of the cells is greater than ~12,000 μM μm, there will almost certainly be problems with the inner-filter effect which distorts the probe's spectra (Fig. 2.5.1) and will invalidate the measurements of $[Ca^{2+}]$ (Moore et al., 1990). In addition, when interested in cytosolic $[Ca^{2+}]$, make sure that little or no probe is converted in cellular organelles. The best way to determine if probe is inside cellular organelles is to look for it with a fluorescence microscope (Gores et al., 1989; Moore et al., 1990; Roe et al., 1990; Kao, 1994; Lemasters, 1996; Trollinger et al., 1997). Fluorescence spectroscopy can be used to estimate this problem by using increasing amounts of digitonin to sequentially permeabilize cell membranes to release internal probe, but it cannot determine precisely which cellular compartment contains probe (see Troubleshooting for details).

It is important to obtain the spectra of the Ca-sensitive probe in both the bound and free forms using the same equipment that will be

used for cell experiments, because the spectral shapes are dependent upon the optics of the equipment. Once the spectra are obtained, decide which wavelengths to use if the probe is ratiometric. Usually choose the wavelength pair that provides the greatest range of sensitivity (i.e., where R_{max}/R_{min} is as large as possible; Moore et al., 1990). However, with some equipment, this range results in R_{max} or R_{min}, which is so large that either the fluorescence at one wavelength is too close to the upper limit of sensitivity or the fluorescence at the other wavelength is too close to background, in which case, one or the other of the two wavelengths should be changed.

Any time the incident light intensity or the detector sensitivity is varied, remeasure background, supernatant fluorescence, autofluorescence, and Ca-insensitive fluorescence, unless it has been demonstrated that they are negligible with respect to the Ca-sensitive signal. With a ratiometric probe, the incident light intensity or the detector sensitivity can be varied without changing R_{max}, R_{min}, or (S_f/S_b), provided the band-pass of the incident light is not changed. For a nonratiometric probe, any time there is any change in light intensity or in detector sensitivity, remeasure F_{max} and F_{min}.

When using fluorescence spectroscopy, it is absolutely essential that the supernatant signal be subtracted from the total fluorescence signal, since any Ca-sensitive probe in the supernatant will report a different $[Ca^{2+}]$ from that reported by the probe inside the cell. In addition, when interested in changes in cytosolic $[Ca^{2+}]$, make sure that no Ca-sensitive probe is sequestered in any cellular subcompartment because $[Ca^{2+}]$ in any particular subcompartment is unlikely to follow changes in cytosolic $[Ca^{2+}]$ exactly. See Troubleshooting for details on how to determine if any Ca-sensitive probe is located in organelles.

Whenever attempting to measure R_{max} (F_{max}), R_{min} (F_{min}), and (S_f/S_b) in situ, it is absolutely essential that internal $[Ca^{2+}]$ equals external $[Ca^{2+}]$. This is not necessarily easy to accomplish, and because calibration in vitro is so much simpler, many people use in vitro calibration. The main problem with in vitro calibration is that it assumes that the spectral shapes and intensities of the Ca-bound and Ca-free forms of the probe are identical in vitro and in situ. This is true only if the in vitro calibration solution has exactly the same properties as the cytosol of the cell, and this means that one must create a calibration solution that has the same properties as the cytosol of the cell and has the same concentration of probe (Baker et al., 1994). In order to reach a steady state where internal $[Ca^{2+}]$ equals external $[Ca^{2+}]$, several things must occur. First, the internal stores of calcium must be emptied and kept from refilling. Second, the electrochemical gradient for $[Ca^{2+}]$ must be set to zero. Third, the plasma membrane's Na^+/Ca^{2+} exchanger must be neutralized. Fourth, the plasma membrane ATP-dependent calcium pump must be rendered ineffective. Finally, the Na^+K^+-ATPase must be inhibited.

Caffeine can be used to empty some sarcoplasmic reticulum stores, but not all Ca-ATPases are sensitive to caffeine. However, if the cells are incubated in low-calcium medium containing 1 μM thapsigargin, the sarcoplasmic and endoplasmic reticulum calcium stores will empty within about 5 min and stay empty as long as the thapsigargin is present. The addition of a protonophore such as 5 μM CCCP will break down the mitochondrial membrane potential. This results in emptying the mitochondrial calcium stores. It has an additional benefit in that protonophores such as CCCP reduce NADH autofluorescence (Jiang and Julian, 1997), which is a major source of F_a. The addition of oligomycin is used to prevent the mitochondria from utilizing all of the cellular ATP in an attempt to regenerate its membrane potential. In addition, it is an inhibitor of many ATPases. The Na^+/Ca^{2+} exchanger can be neutralized by adding a Na^+ ionophore such as monensin and either a K^+ ionophore such as valinomycin or an inhibitor of the plasma membrane Na^+K^+-ATPase such as ouabain. Equilibration of K^+ depolarizes the plasma membrane. A simpler way to neutralize the Na^+/Ca^{2+} exchanger is to dissipate the Na^+ and K^+ gradients across the plasma membrane by using a calibration medium that contains intracellular concentrations of Na (10 to 15 mM) and K (130 to 140 mM). Because the plasma membrane Na^+K^+-ATPase will attempt to reestablish the normal Na^+ and K^+ gradients across the plasma membrane, 1 mM ouabain or a similar inhibitor must be added to inhibit it. The plasma membrane ATP–dependent calcium pump can often be inhibited by vanadate or calmodulin inhibitors such as trifluoperazine. The last necessary component is the calcium ionophore, which in conjunction with CCCP dissipates the Ca^{2+} electrochemical potential. Either ionomycin or dibromo A-23187 can be used. Making sufficient ionophore available to the cells can be a real problem. Sometimes Br-A23187 works better than ionomycin because its action is independent of pH. Ionomycin should not be used at pH values less than ~7.2 (Williams and Fay,

1990). When measuring R_{max} (F_{max}) use sufficient free calcium; the amount of calcium needed depends upon the K_d of the probe in situ. To obtain R_{max} within about 0.5% of its true value, the amount of calcium needed is ~200 times the K_d of the probe in situ. When engaged in in situ calibration with a fluorescence microscope, avoid moving the microscope stage, since the same cells must be used for the entire calibration in order to measure (S_f/S_b). Likewise do not include cells whose intensity profiles are flattened due to too intense fluorescence, or cells whose intensities are too close to background.

If it is not necessary to know the absolute value of $[Ca^{2+}]$, then it is not necessary to measure K_d in situ even if it is different from the in vitro value. If it is necessary to measure K_d in situ, be very careful to control pH, temperature, and ionic strength of the calibration solution, since EGTA is sensitive to all of these parameters. Also be very careful in dilutions to make sure of how much free calcium is employed, to calculate R_{max} (F_{max}).

If K_d in situ is measured later and found to be very different from K_d in vitro, it is very easy to correct all of the data since $[Ca^{2+}]$ is proportional to K_d. If K_d in situ equals x times K_d in vitro, then $[Ca^{2+}]_{corr} = x[Ca^{2+}]_{measured}$, where $[Ca^{2+}]_{measured}$ was calculated assuming the in vitro value of K_d.

Troubleshooting

If the cells will not attach to glass coverslips, adherence can be improved by treating the coverslips with an extracellular matrix material such as type I collagen or laminin. Rinse coverslips in ethanol, dry them, and place them in plastic petri dishes. Add 1 or 2 drops of type I collagen (1 mg/mL in 0.1% acetic acid) or laminin (0.1 mg/mL in Tris-buffered saline) and spread the drops over the coverslips. After air drying overnight, rinse the coverslips with standard medium and then add cells in the usual manner (Lemasters, 1996).

If there is difficulty in loading sufficient probe into the cells, many manufacturers recommend the use of the nonionic, low-toxicity detergent Pluronic F-127. This detergent can usually be obtained free of charge upon request of the manufacturer of the probes. Prepare a 20% (w/v) solution of this surfactant in DMSO. Gentle warming (~40°C) may assist in dissolving the detergent. This solution may be prepared in bulk and stored at room temperature. When ready to incubate the cells, add 0.5 µl of 20% Pluronic F-127 per µl of the AM form of the fluorescent probe in a small glass tube and vortex or sonicate to obtain complete mixing (Kao, 1994). Immediately before use, dilute to ~2 to 20 µM of the AM form of the fluorescent probe with standard medium and vortex. This mixture should then be added to the cell suspension or plated cells and mixed by stirring, vortexing, or pipetting. Most researchers have found that Pluronic F-127 has little effect in improving the solubility of most probes, and hence in increasing total conversion of probe. Be aware that solutions of AM esters in DMSO are unstable to hydrolysis. The presence of Pluronic F-127 may further decrease the stability of the AM ester solution, so make no more of the Pluronic F-127:AM mixture than can be used immediately.

A more likely reason for such difficulty is that the cell type either has very low esterase activity, in which case the cells should be incubated for a longer time in the cell-permeant form of the probe, or it has a very active multidrug resistance protein (Homolya et al., 1993), which can be inhibited with a monoclonal anti-MDR1 antibody, verapamil, vincristine, sodium orthovanadate, or oligomycin.

In general, it is not a good idea to incubate the cells with more than 5 µM probe in the cell-permeant form, since high concentrations of the probe can result in the uptake and conversion of the probe inside cellular organelles. High probe concentrations in the AM form also make it very difficult to remove the residual permeant probe from the cells after incubation. If it is suspected that there are problems with residual permeant probe, include 2% (w/v) albumin in the medium used to wash the cells after incubation (Oakes et al., 1988). In addition, too high a concentration of the free acid form of the probe can substantially change the Ca-buffering capacity of the cells, which will change the $[Ca^{2+}]$ that the cells will display in response to stimuli. An internal probe concentration that is <100 µM will generally not cause substantial Ca buffering (Moore et al., 1990). If the spectrum obtained for the Ca-sensitive form of the probe in situ (after subtraction of autofluorescence and the calcium-insensitive portion of the probe) does not look like some combination of the Ca-free and Ca-bound forms of the probe but looks "strange," there is likely too high a concentration of probe, which causes the inner-filter effect. Figure 2.5.1 shows the impact of the inner-filter effect on the excitation, high-calcium spectra of Fura-2 FA. Notice that as the concentration of Fura-2

increases the peak begins to flatten relative to the rest of the spectrum and eventually becomes a relative minimum. If a problem with the inner-filter effect is suspected, decrease probe concentration and/or incubation time. If a cuvette is being used, decrease the concentration of cells/ml instead. If using a tissue slice, try to decrease the thickness of the slice.

Incomplete hydrolysis of the probe is only a problem for those probes whose cell-permeant forms and partial hydrolysis forms are fluorescent. The AM forms of calcium orange, calcium crimson, Fura-2, Indo-1, and Rhod-2 are all fluorescent. The AM forms of calcium green 1 and 2, Fluo-3 and Oregon green 488 BAPTA 1 and 2 are not fluorescent. The incomplete hydrolysis of an AM fluorescent probe generally results in Ca^{2+}-insensitive fluorescence similar to that of the low Ca^{2+} form of the Ca^{2+}-sensitive probe. The presence of this incomplete hydrolysis product presents a problem only when using ratiometric probes such as Fura red, Fura-2, and Indo-1. If incomplete hydrolysis of the AM form of the probe is suspected, it can usually be detected by lysing the cells using *N*-octyl β-D-glucopyranoside (*N*-octyl glucoside), CHAPS, or CHAPSO in a high-Ca^{2+} buffer and either measuring the ratio of $(F)_{\lambda 1}/(F)_{\lambda 2}$ or scanning excitation (emission). The resulting ratio (or spectrum) should be very similar to that obtained from placing the FA form of the probe in the same high-Ca^{2+} buffer containing the same amount of detergent. Note that *N*-octyl β-D-glucopyranoside is suggested as the best detergent because it causes few changes in the extinction coefficient or quantum yield of either the high- or low-Ca^{2+} forms of most ratiometric Ca^{2+} probes, and it is not fluorescent. If another detergent is used, its effects on the high- or low-Ca^{2+} FA forms of the probe and on the AM form of the probe must be checked for intensity and spectral changes. If the accumulation of the incomplete hydrolysis products of the AM esters cannot be prevented, then it is necessary to use the spectral component curve-fitting technique of Gunter et al. (1990) to use a ratiometric probe to accurately determine intracellular free Ca^{2+}.

In general, when using a new cell line or a new probe, test to see if there is substantial conversion of probe inside cellular organelles. The most definitive way to determine the location of probe inside of a cell is to use a fluorescence microscope. If there is punctate distribution of the probe or nuclear localization, there are problems (Gores et al., 1989; Moore et al., 1990; Roe et al., 1990; Kao, 1994). One common source of such punctate fluorescence is the accumulation of probe in pinocytic or endocytic vesicles. This problem can generally be solved by prechilling the cells at 4°C for 5 to 15 min before loading at room temperature or 37°C (Roe et al., 1990). Sometimes probe distribution appears to be cytosolic (diffuse, nonlocalized) in origin but may in fact be located in organelles whose $[Ca^{2+}]$ is similar to that of the cytosol. This possibility can be verified by adding increasing concentrations of digitonin to the cells. Use 10 to 20 μM digitonin to solubilize the plasma membrane and release the cytosolic probe. The proper amount of digitonin can be determined using the titration technique of Fiskum (1985). 100 μM digitonin will release probe from lysosomes and endosomes. 0.1% Triton X-100 will release probe from mitochondria (Gores et al., 1989; Roe et al., 1990; Kao, 1994). To quantitate the results for a ratiometric probe, collect median values of fluorescence from inside the cells at the isosbestic wavelength. See the discussion about probe leakage below, for information on how to locate the isosbestic wavelength. The fraction of probe in the cytosol equals 1 − (median fluorescence after permeabilization of the plasma membrane)/(the median value of fluorescence before permeabilization). For a nonratiometric probe, any wavelength will do. In the absence of a fluorescence microscope, it is still possible to obtain similar information as follows. For a suspension of washed cells that have been incubated in the proper way with the membrane-permeable form of the probe, measure total fluorescence, supernatant fluorescence, and autofluorescence, and determine the amount of probe inside the cells. To an identical aliquot of cells, add 10 to 20 μM digitonin to permeabilize the plasma membrane but not the mitochondrial inner membrane or endoplasmic reticulum membranes. Measure total fluorescence and supernatant fluorescence and determine the amount of probe still inside the cells. From this determine the fraction of probe which is cytosolic.

Leakage of a fluorescent probe from the cells being studied is a common and serious problem in measurement of intracellular $[Ca^{2+}]$. This should be investigated during the initial work with a new probe or with a new cell line. Perhaps the simplest way to determine the amount of probe that has leaked from a suspension of cells in a given time is to spin the cells down at the end of this period and compare the

spectrum of the supernatant with that of fresh suspending medium. The spectrum of the probe that has leaked generally stands out clearly. This problem is particularly troublesome with [Ca^{+}] measurements because the [Ca^{2+}] of even "Ca^{2+}-free" medium that does not contain a Ca^{2+} buffer is in the micromolar range. While typical intracellular [Ca^{2+}] is usually 100 nM or less, any probe that leaks out of the cell will report a much higher concentration. Unless a correction is made, leakage of 10% of the probe into the medium can easily cause a 100% erroneously high result in the intracellular [Ca^{2+}] measurement. One of the advantages of using ratiometric probes is that results do not vary with the amount of probe left in the sample cells, so the usual correction for leakage of probe is simply to subtract away the signal from the external probe F_s before setting up the ratio. If F_s varies linearly with time, then in the future it will not be necessary to measure F_s for each sample. Instead, measure F_s at the beginning and end of the experiment as well as at a few intermediate points, and then calculate F_s for each sample, depending upon when it was measured and subtract the calculated value of F_s from F_t instead of having to measure it.

It is important to note that this technique of calculating F_s will only work if any additives included with the samples do not change the free calcium in the external medium.

Leakage is a much more serious problem for nonratiometric probes because F, F_{max}, and F_{min} are all proportional to c, the concentration of calcium-sensitive probe inside the cells, and hence if c changes so do they. The easiest way to handle this problem is to back-calculate F, F_{max}, and F_{min} to time $t = 0$, which is essentially what is done in steps 10 and 11 of Alternate Protocol. Once it has been determined that the loss of calcium-sensitive probe from the particular cell type is linear with time, it is only necessary to take occasional measurements of F_{sd} in order to generate a plot of k versus time. This plot can be used to calculate k for any sample as long as the time the sample was measured is known and the concentration of free calcium in the external medium is constant.

If there is substantial probe leakage, add one of the inhibitors of the organic anion transporter such as probenecid or sulfinpyrazone to the cells (di Virgilio et al., 1990). Probe leakage and its severity are easy to determine in the cuvette system, since the increase of fluorescence in the supernatant can be used to measure leakage. Probe leakage in FDIM for a nonratiometric probe is determined by measuring changes in the fluorescence from resting cells, which are unlikely to undergo spontaneous changes in [Ca^{2+}]. If there is access to a spectrofluorometer and plenty of cells, the best technique to determine probe leakage is to follow the increased fluorescence of the supernatant with time. Probe leakage is not a problem for ratiometric probes except during calibration. Prolonged high calcium is toxic to most cells and can induce the permeability transition in mitochondria which can in turn cause apoptosis. The process of apoptosis not only changes the intracellular environment drastically but can also lead to more rapid loss of probe from the cell. This type of probe loss can be most severe when measuring R_{max}. If probe loss appears to be excessive while measuring R_{max}, try adding 400 nM cyclosporin A to inhibit the permeability transition. If it is suspected that substantial probe leakage is happening during the calibration, determine the isosbestic wavelength of the probe inside the cell, because such leakage will result in an incorrect value of (S_f/S_b). This procedure is discussed in detail in both protocols.

The calibration of these probes in situ can be incorrect as a result of two things—dye leakage or not obtaining $[Ca^{2+}]_{in}$ equal to $[Ca^{2+}]_{out}$. Determining that $[Ca^{2+}]_{in}$ equals $[Ca^{2+}]_{out}$ is not simple. In general, R_{max} and R_{min} measured in situ will not be greatly different from their values measured in vitro, especially if some protein is added to the in vitro solution. (S_f/S_b) in situ can be very different from its in vitro value. If the in situ measured values of R_{max} and R_{min} are very different from their in vitro values, the sample likely did not attain $[Ca^{2+}]_{in} = [Ca^{2+}]_{out}$. In this case, try to vary the concentration of the various ionophores and inhibitors mentioned in Critical Parameters; also see the following references: Roe et al. (1990); Williams and Fay (1990); Bassani et al. (1995); Lipp et al. (1996). If there is access to an electrode setup for a fluorescence microscope, try "poking" cells with a 2- to 3-µm diameter electrode while they are in the calibration solutions and see if the fluorescent ratio for the poked cell changes as a result (Bassani et al., 1995). If the ratio does not change, $[Ca^{2+}]_{in} = [Ca^{2+}]_{out}$.

The biggest problems in calculating K_d in situ are also dye leakage during the calibration and, of course, getting $[Ca^{2+}]_{in} = [Ca^{2+}]_{out}$. As was mentioned before, correcting for dye leakage in the cuvette system is relatively easy. For

a ratiometric probe using FDIM, either calculate the spectra for each concentration of calcium and correct each spectrum so all of the spectra have the same isosbestic point, or use the isosbestic point as one of the two wavelengths and use the change of fluorescence at the isosbestic point to calculate dye loss and hence correct fluorescence at λ_2 for dye loss. The second procedure requires less time than the first but is not as accurate.

Anticipated Results

Using the techniques described in this unit should permit determination of intracellular [Ca^{2+}] with good accuracy. The sources of the largest error in determination of intracellular [Ca^{2+}] are usually error in K_d, error in R_{min}, error in (S_f/S_b), and especially error in R_{max}. Provided that the incubation procedure is chosen to give a strong cytosolic probe signal and negligible partial conversion products, and provided that leakage is negligible, absolute error is inherently limited by how far from the K_d of the probe the measured [Ca^{2+}] is, and the value of R_{max}/R_{min} of the probe. For a probe having a high R_{max}/R_{min} such as Fura-2 and a measured value of [Ca^{2+}] near the K_d, the accuracy should be within ± 5 nM under optimal conditions.

Time Considerations

Cell incubation should take no more than 1 hr. Setting up the instrument should take 30 min to 1 hr. Measuring calcium-insensitive fluorescence should take 30 min to 1 hr, and measuring autofluorescence should take 5 min to 1 hr depending upon whether it is negligible or not. Once an optimal incubation has been found, measuring calcium-insensitive fluorescence or autofluorescence will either be unnecessary or take no more than 30 min for both. A day should probably be set aside the first time for measuring R_{max} (F_{max}), R_{min} (F_{min}), S_f, and S_b in order to find out which procedure works best. Subsequently, such calibration should take no longer than 1 to 2 hr depending upon how long it takes the cell type to equilibrate $[Ca^{2+}]_{in}$ with $[Ca^{2+}]_{out}$. Measuring a sample of interest can go quite rapidly and the number of samples will determine how long it will take. Depending upon how many samples are measured, analysis can take 2 to 4 days.

Literature Cited

Baker, A.J., Brandes, R., Schreur, J.H.M., Camacho, S.A., and Weiner, M.W. 1994. Protein and acidosis alter calcium-binding and fluorescence spectra of the calcium indicator Indo-1. *Biophys. J.* 67:1646-1654.

Bassani, J.W.M., Bassani, R.A., and Bers, D.M. 1995. Calibration of Indo-1 and resting intracellular $[Ca]_i$ in intact rabbit cardiac myocytes. *Biophys. J.* 68:1453-1460.

Brandes, R., Figueredo, V.M., Camacho, S.A., Baker, A.J., and Weiner, M.W. 1993. I. Quantitation of cytosolic [Ca^{2+}] in whole perfused rat hearts using Indo-1 fluorometry. *Biophys. J.* 65:1973-1982.

di Virgilio, F., Steinberg, T.H., and Silverstein, S.C. 1990. Inhibition of Fura-2 sequestration and secretion with organic anion transport blockers. *Cell Calcium* 11:57-62.

Fiskum, G. 1985. Intracellular levels and distribution of Ca^{2+} in digitonin-permeabilized cells. *Cell Calcium* 6: 25-37.

Gores, G.J., Nieminen, A.-L., Wray, B.E., Herman, B., and Lemasters, J.J. 1989. Intracellular pH during "chemical hypoxia" in cultured rat hepatocytes. *J. Clin. Invest.* 83:386-396.

Grynkiewicz, G., Poenie, M., and Tsien, R.Y. 1985. A new generation of Ca^{2+} indicators with greatly improved fluorescence properties. *J. Biol. Chem.* 260:3440-3450.

Gunter, T.E., Restrepo, D., and Gunter, K.K. 1988. Conversion of esterified Fura-2 and Indo-1 to Ca^{2+}-sensitive forms by mitochondria. *Am. J. Physiol.* 255:c304-c310.

Gunter, T.E., Zuscik, M.J. Puzas, J.E., Gunter, K.K., and Rosier, R.N. 1990. Cytosolic free calcium concentration in avian growth plate chondrocytes. *Cell Calcium* 11:445-457.

Harkins, A.B., Kurebayashi, N., and Baylor, S. 1993. Resting myoplasmic free calcium in frog skeletal muscle fibers estimated with Fluo-3. *Biophys. J.* 65:865-881.

Homolya, L., Holló, Z., Germann, U.A., Pastan, I., Gottesman, M.M., and Sarkadi, B. 1993. Fluorescent cellular indicators are extruded by the multidrug resistance protein. *J. Biol. Chem.* 268:21493-21496.

Jiang, Y., and Julian, F.J. 1997. Pacing rate, halothane, and BDM affect Fura 2 reporting of $[Ca^{2+}]_i$ in intact rat trabeculae. *Am. J. Physiol.* 273:C2046-2056.

Kao, J.P.Y. 1994. Practical aspects of measuring [Ca^{2+}] with fluorescent indicators. *Methods Cell Biol.* 40:155-181.

Lemasters, J.J. 1996. Confocal microscopy of single living cells. *In* Fluorescence Imaging Spectroscopy and Microscopy (X.F. Wang and B. Herman, eds.) pp. 157-175. John Wiley & Sons, New York.

Lipp, P., Lüscher, C., and Niggli, E. 1996. Photolysis of caged compounds characterized by ratiometric confocal microscopy: A new approach to homogeneously control and measure the calcium concentration in cardiac myocytes. *Cell Calcium* 19:255-266.

Moisescu, D.G. and Pusch, H. 1975. A pH-metric method for the determination of the relative concentration of calcium to EGTA. *Pfluegers Arch. 355:R122.*

Moore, E.D.W., Becker, P.L., Fogarty, K.E., Williams, D.A., and Fay, F.S. 1990. Ca^{2+} imaging in single living cells: Theoretical and practical issues. *Cell Calcium* 11:157-179.

Oakes, S.G., Martin, II, W.J., Lisek, C.A., and Powis, G. 1988. Incomplete hydrolysis of the calcium precursor Fura-2 pentaacetoxymethyl ester (Fura-2 AM) by cells. *Anal. Biochem.* 169:159-166.

Poenie, M., Alderton, J. Steinhardt, R., and Tsein, R. 1986. Calcium rises abruptly and briefly throughout the cell at the onset of anaphase. *Science.* 233:886-889.

Roe, M.W., Lemasters, J.J., and Herman, B. 1990. Assessment of Fura-2 for measurements of cytosolic free calcium. *Cell Calcium* 11:63-73.

Trollinger, D.R., Cascio, W.E., and Lemasters, J.J. 1997. Selective loading of Rhod 2 into mitochondria shows mitochondrial Ca^{2+} transients during the contractile cycle in adult rabbit cardiac myocytes. *Biochem. Biophys. Res. Commun.* 236:738-742.

Tsien, R.Y., Pozzan, T., and Rink, T.J. 1982. Calcium homeostasis in intact lymphocytes: Cytosolic free calcium monitored with a new intracellular trapped fluorescent indicator. *J. Cell Biol.* 94:325-334.

Williams, D.A., and Fay, F.S. 1990. Intracellular calibration of the fluorescent calcium indicator Fura-2. *Cell Calcium* 11:75-83.

Key References

Bassani, et al., 1995. See above.

Describes how to measure K_d, R_{max}, and R_{min} inside of cells and the difficulties in so doing, including possible errors.

Kao, 1994. See above.

Excellent general reference.

McGuigan, et al., 1991.

Describes in detail how to make accurate calcium buffers.

Moore, et al., 1990. See above.

Excellent all-around reference, especially with respect to theory.

Roe, et al., 1990. See above.

Good all-around reference, especially with respect to probe loading and probe loading problems. Discusses advantages and disadvantages of in vitro and in situ calibration of probe.

Williams and Fay, 1990. See above.

Describes in detail how to choose the proper combination of ionophores for a particular cell type, including determining how much of each is needed.

Contributed by Karlene K. Gunter and Thomas E. Gunter
University of Rochester
Rochester, New York

In Vitro Methods for Detecting Cytotoxicity

The protocols provided in this unit are methods for determining cytotoxicity, a term which includes the effects toxicants can have on cell growth, metabolic functioning, or viability. These tests have value because they can provide a general indication of the sensitivity of cells to toxicants, making them appropriate for screening purposes. Although not specific indicators of the mechanisms associated with toxicant-induced effects, positive results with cytotoxicity tests indicate that physiologic or morphologic changes have occurred in exposed cells. These tests, therefore, may suggest other endpoints to be investigated to provide more specific mechanistic information about the interactions of toxicants and cells.

Cytotoxicity is generally used as an inclusive term for changes that can become irreversible and that can ultimately affect cell viability. This is true even for cytotoxicity tests that determine effects on cell growth or metabolic functioning because, with increased exposure to the toxicant, changes in growth and metabolism, too, can become irreversible and cell viability can be decreased.

This unit includes protocols for cytotoxicity determinations but does not provide protocols for culturing cells (see *APPENDIX 3B*) or protocols for exposure of cells to toxicants. These procedures vary widely both with cell type and with toxicant. Because cytotoxicity testing in vitro can be done efficiently and economically, one or more of the methods described in the sections that follow may be used to screen chemicals for the possibility they might be toxic before tests are done in animals. This screening could be followed by in vitro and/or in vivo determination of endpoint alterations more specific to the toxicant in question and/or to the organ(s) affected. The in vitro cytotoxicity tests themselves alone cannot be used independently to provide indication of hazard to man or animals.

Seventeen protocols that can be used to indicate cytotoxicity in vitro are included in this unit. They fall into three groups. First are tests primarily used to indicate the toxicant has altered cell viability. These tests are valuable for initial general screening. They can also be used in combination with endpoint assays more specific to the toxicant or target tissue to provide indication if the more specific change occurs in cells at concentrations below concentrations needed to decrease viability. This group includes: trypan blue dye uptake (see Basic Protocol 1); lactate dehydrogenase (LDH) leakage (see Basic Protocol 2 and Alternate Protocols 1 to 4); neutral red dye retention (see Basic Protocol 3 and Alternate Protocol 5); and propidium iodide (see Basic Protocol 4) or fluorescent marker (see Alternate Protocol 6) attachment to double-stranded nucleic acids.

Second, there are tests to indicate the toxicant has effects on cell growth and cell proliferation. These tests are generally more sensitive to lower concentrations of toxicants than tests affecting cell viability. These tests can also be used at concentrations of toxicant that do not necessarily cause irreversible cell damage. Therefore, they could be used to determine if recovery occurs when the cells are no longer exposed to the toxicant. This group includes: cell counts (see Basic Protocol 5); [^{3}H]thymidine uptake (see Basic Protocol 6); and cell cycle analysis with propidium iodide (see Basic Protocol 7).

Finally there are tests to indicate the toxicant has affected cellular metabolic processes. These tests may be useful to indicate if the toxicant is likely to target the cell membrane, an intracellular organelle, or a biochemical process. They can be used along with viability tests to determine concentration and time sensitivities. This group includes MTT dye conversion by mitochondria (see Basic Protocol 8); alamar blue reduction by respiring cells (see Basic Protocol 9); and fluorescent dye loss (see Basic Protocol 10) and

Contributed by Marion Ehrich and Lioudmilla Sharova

Current Protocols in Toxicology (2000) 2.6.1-2.6.27

[^{3}H]2-deoxy-D-glucose loss (see Alternate Protocol 7) from cells with compromised membranes.

The procedures for cytotoxicity included in this unit are a sampling of those available; they do not provide an all-inclusive list. The protocols do, however, include tests that differ by indicators of irreversible cell damage and by technical complexity and efficiency.

NOTE: All solutions and equipment coming into contact with cultured cells must be sterile, and aseptic techniques should be used accordingly.

NOTE: All culture incubations should be performed in a humidified 37°C, 5% CO_2 incubator unless otherwise specified.

BASIC PROTOCOL 1

TRYPAN BLUE UPTAKE TO ASSESS VIABILITY

Trypan blue uptake is commonly determined as cells are counted. This vital dye only enters dead cells (the cell membrane must be damaged before the dye can enter). Live cells exclude the dye; therefore, this procedure is used to estimate the percentage of viable cells in an incubate (also see *APPENDIX 3B*).

Materials

Cells treated with toxicant, vehicle, or 10% (v/v) Triton X-100 in suspension
Phosphate-buffered saline (PBS; see recipe), pH 7.2 to 7.4
0.1% (w/v) trypan blue (see recipe)

Hemocytometer
Phase-contrast inverted microscope
Hand counter

1. Prepare cells treated with toxicant, vehicle, or 10% (v/v) Triton X-100 in suspension.

   Cells that have attached to culture dishes need to be disassociated. This can be done by removing the medium, adding a solution of trypsin/EDTA (see recipe) for 1 to 5 min, centrifuging, and removing the trypsin solution (see APPENDIX 3B).

   Cells that are treated with 10% Triton-X100 are permeabilized and serve as a positive control.

2. Wash cells one to three times with PBS, preparing a final resuspension in an exact volume of PBS (e.g., 1.0 ml, 10.0 ml).

   The final resuspension provides the cell concentration counted on the hemocytometer.

3. Place a clean, dry hemocytometer slide on a microscope stage; apply a cover slip over the chamber so it rests equally across both overflow slots. Set the microscope to use the 10× objective and focus until the grid lines on the hemocytometer are clear.

   The hemocytometer grid has nine large squares, each with an area of 1 mm^2. The large squares are subdivided into smaller squares. (For example, each of the four corner squares contains sixteen smaller squares; see Fig. A.3B.1.) The depth of the curved chamber underneath the grid is 0.1 mm, so the volume of cell suspension under each of the nine large squares is 0.1 mm^3 or 10^{-4} ml.

4. Mix equal volumes of cell suspension and 0.1% trypan blue solution (e.g., 25 µl of each). Let the mixture stand for no longer than 3 min.

   This can be done in the well of the 96-well plate, or on any smooth hydrophobic surface (e.g., Parafilm, glass slide). Mixing can be done with a micropipet. The cell suspension/dye mixture should not stand for more than 3 min to prevent dye uptake by viable cells. Trypan blue may be used in concentrations between 0.08% and the 0.4% solution commercially available (Sigma). The cell suspension-to-dye ratio may differ from 1:1 (e.g., 1:2, 1:3, 1:4), but must be appropriately accounted for in the calculation step given below.

5. Slowly fill the hemocytometer chamber with the cell suspension/dye mixture by placing the tip of a micropipettor into the notch under the coverslip. Dispense slowly, allowing capillary action to draw the cell suspension into the chamber. Do not overfill or underfill the hemocytometer chamber.
6. Using the 10× objective of the microscope and a hand counter, count the stained (dead) and unstained (live) cells in one or more of the large squares.

   The total area counted needs to have an area of ≥1 mm^2; the total number of cells counted needs to be >100.
7. To calculate the cell concentration in the cell suspension (cells/ml), the total number of cells counted is divided by the total number of large squares counted and this number is multiplied by 2×10^4 (to account for the 0.1 mm^3, or the 10^{-4} ml volume of cells in a large square on the hemocytometer and the 2-fold dilution made when the trypan blue was added).
8. To calculate the percentage of viable cells, divide the number of viable (unstained) cells by the total number of cells counted (unstained + stained) and multiply by 100.

LACTATE DEHYDROGENASE (LDH) LEAKAGE TO ASSESS VIABILITY

BASIC PROTOCOL 2

This procedure is used as an indicator of increased membrane permeability and subsequent cell death. The increase in permeability associated with cell death causes release of the cytoplasmic enzyme, lactate dehydrogenase (LDH), which is present in mammalian cells. LDH is membrane impermeable and remains within live cells. Kits are available for LDH detection that decrease the technical complexity of this assay (Sigma).

Materials

Cells
Test compounds: toxicant, vehicle, and Triton X-100
LDH Reagent Kit (DG 1340K, Sigma) containing:
  NADH, 0.194 mmol/liter in phosphate buffer
  Phosphate buffer, 54 mmol/liter, pH 7.5
  Pyruvate, 6.48 mmol/liter in phosphate buffer

96-well microtiter plates, for cell culture
Microtiter plate spectrophotometer with wavelength at 340 nm

1. Set up a 96-well microtiter plate with 1 to 2×10^4 cells/100 µl/well or 100 µl medium/well (controls). Incubate for 18 to 48 hr to allow cells to attach and reach 60% to 80% confluency. Replace medium for adherent cells; for suspension cells, proceed directly to step 2.

   Use plates coated for cell culture. Use plates with flat-bottomed wells for attached cells and round-bottomed wells for cells in suspension.

   The plate should include wells with medium only to correct for background (e.g., serum and phenol red in medium), untreated and vehicle-treated cells (negative controls) to correct for spontaneous release of LDH, and cells treated with 10% Triton X-100 to kill all the cells (positive control) and allow estimation of the total possible LDH release.
2. Treat cells in remaining wells with test compound, using several concentrations and several time periods for incubates. Include a vehicle control.
3. To microtiter wells on a second microtiter plate, add 250 µl of NADH solution (0.194 nmol/liter NADH; 54 mmol/liter phosphate buffer, pH 7.5). For suspension cells, add 10 µl of toxicant-treated cells (>10^4 cells/ml) or control cells to these wells. For

attached cells, add 10 µl of the supernatant of toxicant-treated or control cells to the wells. Mix.

4. Initiate the reaction by adding and mixing 25 µl of a solution of 6.48 mmol/liter pyruvate.
5. Record the decrease in absorbance at 340 nm at 3 to 5 min intervals over a period of time (up to 1 hr).

   The change in absorbance needs to be determined over sufficient time to obtain a meaningful value (change of >0.1 absorbance units over the time observed).

6. After subtracting the LDH release in the negative control from the experimental incubation and the positive control, compare the rate of decrease (change in absorbance/min) to that of the positive control (10% Triton-X-100-treated cells). Express the results as change in absorbance units/min (ΔA_{340}/min).

ALTERNATE PROTOCOL 1

IN SITU LDH ASSAY TO ASSESS VIABILITY

This assay is done by initially putting 10 µl of a 7 mM (0.8 mg/ml) solution of pyruvate in PBS in the microtiter well with 1 to 2×10^4cells (attached or suspension) in 100 µl medium and initiating the reaction with 20 µl of a freshly prepared 4.5 mM (3 mg/ml) NADH solution in PBS. Also, endpoint rather than kinetic assays can be used. To do this, terminate the reaction by adding 20 µl of the LDH inhibitor oxymate [138 mM (16.6 mg/ml) oxamic acid, sodium salt, in PBS] to microtiter wells containing a 130 µl incubate of pyruvate, cells, and NADH solution. Read the absorbance at 340 nm.

ALTERNATE PROTOCOL 2

PHENYLHYDRAZINE COLORIMETRIC LDH ASSAY TO ASSESS VIABILITY

Colorimetric assays can also be used for LDH determinations. One of these procedures measures the phenylhydrazone produced when pyruvic acid not converted to lactic acid is quantified as it undergoes reaction with 2,4-dinitrophenylhydrazine. The endpoint is measured at any wavelength between 400 and 550 nm after 60 min of incubation at 37°C. This protocol can be performed using Diagnostic Kit 500 (Sigma). The choice of wavelength depends on the optional wavelength, which is determined prior to the beginning of the experiment.

ALTERNATE PROTOCOL 3

INT COLORIMETRIC LDH ASSAY TO ASSESS VIABILITY

Another colorimetric LDH assay uses the tetrazolium dye 2-*p*-iodophenyl-3-nitrophenyl tetrazolium chloride (INT), with absorbance measured at 490 nm. This can be done as an endpoint, rather than as a kinetic assay.

Materials

1 to 2×10^5 cells/ml treated with toxicant, vehicle, or 10% (v/v) Triton X-100
36 mg/ml lactate in 10 mM Tris·Cl, pH 8.5 (*APPENDIX 2B*)
INT dye (see recipe)
NAD^+ solution (see recipe)
Phosphate-buffered saline (PBS; see recipe), pH 7.2 to 7.4
16 mg/ml oxymate (oxamic acid, sodium salt) in PBS
Microtiter plate reader at 490 nm

1. Set up microtiter plate and treat cells (see Basic Protocol 2, steps 1 and 2).
2. Aliquot 100 µl of cells to each well of a microtite plate.
3. Add 20 µl freshly prepared 26 mg/ml lactate in 10 mM Tris·Cl, pH 8.5.

4. Add 20 µl 2 mg/ml INT dye.
5. Add 20 µl NAD^+ solution to each well. Incubate 20 min at room temperature.
6. After the incubation, stop the reaction by adding 20 µl of 16.6 mg/ml oxymate at specific time points <1 hr.
7. Read the absorbance at 490 nm (A_{490}).
8. Calculate the percentage of cells lysed by subtracting the change in absorbance in negative control cells from the change in absorbance in experimental cells, dividing by the total absorbance in positive control cells, and multiplying by 100.

KINETIC INT COLORIMETRIC LDH ASSAY TO ASSESS VIABILITY

ALTERNATE PROTOCOL 4

The colorimetric assay described in Alternate Protocol 3 can also be done as a kinetic assay. For this procedure, mix 100 µl of cells (10^5/ml) with 100 µl of LDH substrate (see recipe), adding the substrate mixture to each well at 3-sec intervals. Read absorbance at 490 nm at 3 to 5 min intervals.

NEUTRAL RED DYE RETENTION TO ASSESS VIABILITY

BASIC PROTOCOL 3

Neutral red is a vital dye. It is taken up and retained in viable cells that adhere to the plastic of microtiter plates. This colorimetric assay can be done in 96-well microtiter plates, meaning the assay can be conducted simultaneously on a number of incubates containing cells and various concentrations of toxicant (Babich and Borenfreund, 1992; Veronesi and Ehrich, 1993).

Materials

10^5 cells/ml cell suspension
Test compound: toxicant, vehicle, or positive control (1% w/v SDS or 1% w/v saponin)
Phosphate buffered saline (PBS; see recipe)
1% (w/v) SDS
Neutral red solution (see recipe)
Dye extractor solution (see recipe)

Flat-bottomed, 96-well microtiter plates, cell culture coated
Blotter paper (e.g., absorbent paper towels or filter paper)
Plate mixer
Microtiter plate reader, 550 nm

1. Place 2×10^4 cells (0.2 ml of 10^5 cells/ml) in wells of a flat-bottom 96-well microtiter plate. Incubate for a sufficient time to assure attachment and 60% to 80% confluency (e.g., 18 hr to 3 days).

   These plates may need specific coating (e.g., collagen or laminin) for certain cell types that do not adhere well.

2. Replace medium to include up to 1% (v/v) of toxicant, vehicle, or positive control solution/well (20 µl per total volume of 200 µl in wells). Expose cells to 1% (w/v) sodium dodecyl sulfate solution (SDS) or 1% (w/v) saponin solution as a positive control.

   The positive control is included to ensure that the assay is working and to determine the range of absorbance for the experiment.

3. Incubate cells for time previously designated in the experimental protocol (e.g., 4, 8, 12, 24, 36, 72 hr).

   Note that the neutral red assay can be done in the same microtiter plate as the incubation with toxicant provided the cells are not too confluent and the presence of the test compound(s) does not significantly decrease cell numbers. If the cells are too confluent to be a monolayer or if the cells lose adherence, replate to a uniform density before proceeding to step 5.

4. After incubation with test compounds, remove the medium from the wells by pipetting. Gently wash the cells adhering to the plate twice with 100 µl PBS. Air dry the plates to increase adherence of cells to the plate.

5. Then add 40 µl freshly prepared neutral red solution to each well and incubate the plate for 90 min at 37°C.

6. Remove the neutral red solution and gently but rapidly wash the wells 2 times with 100 µl 37°C PBS. Remove the PBS and blot dry on absorbent paper.

7. Extract the dye from the remaining cells by adding 100 µl dye extractor solution per well. Mix plate on plate mixer at room temperature for 20 min.

8. Read absorbance on the microtiter plate reader at 550 nm. Compare neutral red retention in cells exposed to toxicant and those exposed to the vehicle (which is used to provide the comparative number for 100% viable cells).

   A standard curve of neutral red may be prepared to provide results in microgram per milliliter. Plates can be reread the next day, if needed, as the neutral red in the cells is stable overnight.

ALTERNATE PROTOCOL 5

NEUTRAL RED ENDPOINT ASSAY TO ASSESS VIABILITY

This assay can be done with endpoints either in the visible range (550 nm) or as a fluorescent assay (488 nm excitation, 645 emission). First the cells are treated with toxicant, vehicle, or positive control.

For cells in suspension in test tubes rather than microtiter wells, incubate 5×10^6/ml cells with 0.036% (w/v) neutral red (prepared in commercially available Hank's balanced salt solution) at 37°C for 30 min in a humidified 37°C, 5% CO_2 incubator. Then centrifuge cells 10 min at $400 \times g$, 4°C, and wash the cell pellet twice with medium centrifuging 10 min at $400 \times g$ between washings. After washing resuspend and dilute cells in medium to 5×10^6 cells/ml. Mix 100 µl cells with 100 µl of 0.1 M acetic acid containing 1% (w/v) SDS, dilute to 1.25 ml with normal saline and read the absorbance at 540 nm or fluorescence at 645 nm with 488 nm excitation.

Alternatively, for cells in suspension, incubate 100 µl cells (1 to 2×10^5 cells/ml) with 0.1% (w/v) neutral red for 3 hr at 37°C in microtiter plates, then wash with PBS by adding 200 µl PBS to each well, mixing by pipetting, and centrifuging the plate for 10 min at 1000 rpm in a centrifuge with a plate carrier. Carefully remove the PBS. Repeat the PBS wash two to three times. Next add 1% glacial acetic acid/50% methanol to extract the dye and fix the cells. Read absorbance at 540 to 550 nm or fluorescence at 645 nm with 488 nm excitation.

PROPIDIUM IODIDE ATTACHMENT TO DOUBLE-STRANDED NUCLEIC ACIDS TO ASSESS VIABILITY

BASIC PROTOCOL 4

The fluorescent dye propidium iodide (excitation 530 nm, emission 645 nm) is excluded from living cells, but enters and combines with double-stranded nucleic acids (i.e., DNA) of dead cells. The assay for cell viability using propidium iodide attachment to double-stranded nucleic acids can be done simultaneously with determination of membrane integrity using a variety of membrane-permeant fluorescent probes (e.g., CFDA-AM, which has an excitation 485 nm and emission 530 nm) because the fluorescent spectra do not overlap (Nieminen et al., 1992).

Materials

0.5×10^5 cells/ml
Test compounds: toxicant, vehicle, and positive control
Phosphate buffered saline (PBS; see recipe)
376 µM digitonin solution
30 µM propidium iodide dye (Molecular Probes)

Flat bottomed, 96-well microtiter plates, for cell culture
Fluorescence microtiter plate reader

1. Plate cells (0.5×10^4/well) and allow to attach overnight before exposing to toxicant. Incubate with toxicant at predetermined concentrations and times. Include wells for positive and negative controls on each microtiter plate.
2. Wash plate free of medium. Add 10 µl of 376 µM digitonin solution to positive control wells. Add 100 µl propidium iodide (30 µM) to all wells.
3. Incubate plate for 30 min at 37°C.
4. Read in a microtiter plate fluorescence spectrophotometer set with excitation at 530 nm and emission at 645 nm.

   Alternatively, excite at 488 nm.

5. Compare wells exposed to test compounds and wells exposed only to vehicle (negative control) to wells exposed to digitonin (100% cell death; the positive control).

   The positive control will provide wells with the highest fluorescence.

6. Calculate per cent of viable cells as fluorescence in test wells less negative control divided by fluorescence in digitonin-treated wells less negative control, with the quotient multiplied by 100.

USING FLUORESCENT MARKERS TO ASSESS VIABILITY

ALTERNATE PROTOCOL 6

Several kits that use binding of fluorescent markers to nucleic acids as an indicator of loss of cell viability are available from Molecular Probes (Haugland, 1996). For example, the Live/Dead Assay includes calcein-AM, a membrane-permeable dye, which is cleaved by intact cells to calcein (fluoresces green) and ethidium homodimer, a membrane-impermeable dye that labels nucleic acids of membrane-compromised (nonviable) cells to produce a red fluorescence. With excitation of 488 nm, emission at 530 nm will indicate live cells and emission at 585 nm will indicate dead cells.

BASIC PROTOCOL 5

ASSAYS TO ASSESS CELL GROWTH

Cell counting is done along with determination of viability using trypan blue and is described under Basic Protocol 1. Another indicator of cytotoxicity is the loss of ability of certain cell types to extend processes (extensions >2× the length of the cell body) when exposed to agents that promote process development (e.g., retinoic acid; Abdulla and Campbell, 1993). A change in expression of specific proteins can also be an indication of cytotoxicity and forms the basis for kits manufactured by Xenometrics.

Estimation of cells counts can also be made using protein determinations, such as the Kenacid Blue dye binding method recommended by the European Fund for Replacement of Animals in Medical Experiments (FRAME; O'Hare and Atterwill, 1995).

Materials

Cells (1 to 2×10^5 cells/well) or 150 µl of 1×10^6 cells/ml, treated with toxicant, vehicle, or control in microtiter plates
Phosphate-buffered saline (PBS; see recipe), 37°C
Fixative: 1% (v/v) glacial acetic acid/50% (v/v) ethanol/49% (v/v) water
Kenacid blue dye (see recipe)
Washing solution: 10% (v/v) ethanol/5% (v/v) glacial acetic acid/85% (v/v) water
Microtiter plate reader, 577 nm

1. After cells have been exposed to toxicant, vehicle, or control solution, remove medium and rinse cells one to three times with warm PBS.
2. Add 150 µl fixative solution to each well and fix 20 min.
3. Remove fixative solution and add 150 µl freshly prepared Kenacid working solution. Shake the plate 2 to 3 hr.
4. Wash wells twice with 150 µl wash solution.
5. After last wash, fill the wells with wash solution and shake for 20 min until the dye has completely gone into solution.
6. Read absorbance at 577 nm using a well with no cells as a reference well.

   The absorbance of the reference well which contains no cells should be zero when the spectrophotometer is set at 404 nm. Absorbance of wells with cells could be read at 600 nm rather than at 577 nm.

BASIC PROTOCOL 6

[^{3}H]THYMIDINE UPTAKE TO ASSESS CELL GROWTH

This procedure can be used as an indication of cytotoxicity because toxicants can decrease the rate of cell division. The assay can also be used as an indicator of cell proliferation, as [^{3}H]thymidine incorporates into the nucleic acids of proliferating cells. This is a relatively complex, yet sensitive procedure that requires used of radiolabeled chemicals.

Materials

1 to 15×10^5 cells/ml
Serum-free chemically-defined medium (e.g., RPMI 1640 or DMEM), 37°C and ice-cold
Test compounds(s): toxicant and vehicle
20× [^{3}H]thymidine solution (see recipe)
10% (w/v) trichloroacetic acid (TCA) solution, ice-cold
0.3 N sodium hydroxide
Scintillation fluid

continued

24-well plates, coated for cell culture
Liquid scintillation counter
Radioactive waste disposal system

CAUTION: When working with radioactivity, take appropriate precautions to avoid contamination of the experimenter and surroundings. Carry out the experiment and dispose of wastes in an appropriately designated area following the guidelines provided by your local radiation safety offices (also see *APPENDIX 1A*).

CAUTION: Trichloroacetic acid is very caustic. Handle it with care.

NOTE: All incubations should be performed at 37°C using an incubator or water bath.

1. Place 1 ml cells in 24-well tissue culture plates and incubate 6 to 24 hr to allow cells to attach.

   Cells with density of 1 to 15 × 10^5/ml may be used.

2. Wash medium from wells and replace with 1 ml serum-free, chemically defined medium 24 to 48 hr before treating cells with test compounds.

   Alternatively, cells (e.g., lymphocytes) can be collected from toxicant-treated animals.

3. For in vitro exposure to toxicants, add toxicant or vehicle, 50 µl/well, to cells for the times specified in the testing protocol.

4. Add 50 µl/well sterile 20× [^{3}H]thymidine solution for the last 2 hr of incubation with the test substance. Continue to incubate at 37°C.

   For certain cell types (e.g., lymphocytes), incubation with [^{3}H]thymidine may be as long as 72 hr. When incubation is done for very short periods of time (e.g., 15 min), the concentration of [^{3}H]thymidine incubated with cells should be increased (e.g., 2.5 µCi/ml).

   Other components of nucleic acids may also be used, such as BrdU (bromo-deoxyuridine) in a relatively similar procedure. [^{3}H]leucine and [^{3}H]glycine incorporation, which are used as indicators of the rate of protein synthesis, would also be expected to provide similar results.

5. Stop the reaction by placing plates on ice. Wash cells 3 times with 1 ml of ice-cold serum-free medium, then carefully remove all medium by vacuum aspiration.

   Remember that the medium and washes are radioactive and dispose of appropriately.

6. Add 1 ml ice-cold 10% trichloroacetic acid (TCA) to each well. Leave plates on ice for 10 min to allow precipitation of DNA and protein. Remove trichloroacetic acid by aspiration.

   This aspirate may be discarded or counted for determination of unincorporated [^{3}H]thymidine.

   Rather than using the caustic TCA solution, cells may be harvested by centrifugation or harvested by using a cell harvester with fiberglass filters (the filters are subsequently placed in vials with scintillation fluid and counted).

   If cells are collected by centrifugation, wash once with warm conditioned medium (medium in which cells have been grown), and recentrifuge at low speed (e.g., centrifuge a 1- to 2-ml sample 3 min at 430 × g at 37°C in pre-warmed 12-ml glass conical centrifuge tubes). Following centrifugation, remove the supernatant, and air dry the pellet before resuspending for scintillation counting. Alternatively, the pellet may be resuspended in 0.5 ml hypertonic solution (e.g., 1.8% saline), placed on a slide for histological examination, fixed by sequential exposure for 10 min each to 5% to 7% trichloroacetic acid (at 5°C), 70% ethanol at room temperature, and 95% ethanol at room temperature, and air-dried. For example, the Kodak Emulsion slidemailer system could be used. After the cells are fixed and air-dried, the slides are covered with emulsion, exposed, developed according to the manufacturer's instructions and analyzed using a microscope.

7. Add an additional 1 ml of 10% TCA to the plates and leave on ice for an additional 5 min. Wash a third time with 10% TCA and leave on ice an additional 5 min to complete the precipitation. Remove the TCA.
8. Solubilize the precipitated protein with 0.5 ml of 0.3 N sodium hydroxide by incubating for 30 to 60 min at room temperature. Transfer 250 µl to a miniscintillation vial with 5 ml scintillation fluid and count.

Concentration and length of incubation with sodium hydroxide may be increased (e.g., to 1 N and to 24 hr) to increase digestion of the cells.

Although [^{3}H]thymidine uptake is usually the endpoint, [^{3}H]thymidine release could also be measured. With this system, incubate cells with [^{3}H]thymidine (concentration and time of incubation predetermined by protocol), wash three times, then resuspend at 4×10^4 cells/well in 24-well tissue culture plates in 1.0 ml medium. Following overnight incubation at 37°C in 5% CO_2, aspirate the medium, mix aliquots with scintillation fluid, and count. Cytotoxicity (in per cent) is calculated by comparing the radioactivity counted in the sample and control wells.

BASIC PROTOCOL 7

CELL CYCLE ANALYSIS WITH PROPIDIUM IODIDE TO ASSESS CELL GROWTH

This procedure can be used as an indicator of cytotoxicity for toxicants that affect DNA synthesis and, therefore, cause cell arrest mostly in the G1/G0 phase of the cell cycle. Some of these cells may undergo apoptosis later, whereas others may have decreased rates of cell growth and proliferation.

Propidium iodide (PI), a DNA-binding fluorochrome, is the most commonly used DNA dye for cell cycle analysis. Because it can be excited at 488 nm, it can be used on most common flow cytometers. Its stoichiometric binding to double-stranded nucleic acids allows fluorescent intensity (>620 nm) to be used as an indicator of cellular DNA content. Using propidium iodide is now a common procedure for DNA analysis (Krishan, 1975).

Materials

Toxicant-treated and control cells in suspension
Standard azide buffer (see recipe)
Vindelov's PI (see recipe)

12 × 75–mm clear polystyrene tubes
30-µm mesh (optional)
Flow cytometer

1. Harvest cells, centrifuge 5 min at 1000 × *g*, decant supernatant, and vortex pellet.
2. Resuspend cells in 1 ml standard azide buffer, count the cells, and recentrifuge 5 min at 1000 × *g*.
3. Resuspend cells in standard azide buffer so that cell concentration is 10^6/ml.
4. Transfer 1 ml of this suspension to another tube and add 0.5 ml of Vindelov's PI.
5. Let cells sit at 4°C for 5 min to 1 hr, then filter through 30-µm mesh if necessary to remove noncellular particulate material.

Filtering is optional.

6. Analyze cells by flow cytometry using 488 nm excitation, gating out doublets and clumps using pulse processing, and measuring fluorescent emission at >620 nm.

For cell proliferation determinations, the CyQUANT Cell Proliferation Assay Kit is available from Molecular Probes. Fluorescence increases when the dye binds to nucleic acids. To perform this procedure, plate cells at 10^3 to 10^4 cells per well in 200 µl medium in 96-well plates. Incubate the cells 6 to 18 hr to allow the cells to attach, replace the medium, and treat the cells with toxicant. Then remove culture medium from cells, freeze and then thaw the cells, add the reagent and cell lysis buffer provided in the kit, then measure fluorescence with 485 ± 10 nm for excitation, and 530 ± 12.5 nm emission. The manufacturer states that this method is sensitive enough to detect fluorescence in cells at a concentration as low as 50 cells/ml.

MTT DYE CONVERSION TO ASSESS METABOLIC CAPABILITY

BASIC PROTOCOL 8

This assay requires cells that are actively able to metabolize 3-(4,5-dimethylthiazol-2-yl)-2,5-diphenyl tetrazolium bromide (MTT) to an insoluble formazan precipitate. The assay is used as an indicator of mitochondrial function in live cells; however, loss of activity cannot be used to distinguish compromised cells from dead cells. As an indicator of cytotoxicity, MTT results have been reported to be comparable in sensitivity to those obtained using [^{3}H]thymidine incorporation (Mosman, 1983). The assay can be used with cultured cells or with tissues, as the colored product is solubilized and extracted from the test system. Because the dye needs to be extracted from the cells, this procedure cannot be used to provide cell counts.

Materials

5×10^4 cells/ml cell suspension
Test compound: toxicant or vehicle
Culture medium
5 mg/ml MTT in PBS (store 2 to 3 weeks at 4°C or longer at −20°C)
Dimethyl sulfoxide (DMSO), photometric grade
Sorensen's buffer (see recipe)

96-well microtiter plates, for cell culture
Aspiration system for removal of medium from cells
Micropipettor (20 to 200 µl) with sterile micropipettor tips
Microtiter plate reader

1. Plate cells at 1×10^4 cells/well by adding 200 µl of a 5×10^4 cells/ml suspension to each well of a 96-well tissue culture plate. Include control wells with medium and no cells. Incubate overnight at 37°C 5% CO_2.

   Test compounds (toxicant and vehicle) may be added before or after this incubation.

   Use plates with flat-bottomed wells for adherent cells and round-bottomed wells for suspension cells.

2. Carefully aspirate off the medium, avoiding removal of cells. If not previously incubated with toxicant, replace medium with fresh medium (200 µl) containing up to 0.1 ml of test substance. Include wells with medium without cells or test compound, medium without cells but with test compound, cells without test compound (but with test compound vehicle) as controls. Incubate at 37°C, 5% CO_2, for predetermined times (e.g., several hours, overnight, and/or for several days).

3. After incubation with test compound, carefully aspirate off medium and replace with medium and 20 to 50 µl MTT solution for a total volume of 200 µl. Incubate for 4 to 6 hr at 37°C, 5% CO_2.

4. Carefully remove the MTT-containing medium. Add 200 µl DMSO with 25 µl Sorensen's buffer per well. Mix the plate until the formazan crystals are dissolved.

Rather than DMSO, 200 µl of 0.04 N HCl in isopropanol may be used to solubilize the formazan product made from the MTT dye.

A 10% (w/v) solution of SDS in 0.01 M HCl rather than DMSO can be used to lyse the cells during an overnight incubation at 37°C.

5. Read plate on microtiter plate reader at 550 to 570 nm.

   If medium contains phenol red, readings may need to be compared to those taken at 660 nm, which is a wavelength where quenching by the medium is minimized.

6. Compare absorbance in wells containing the test substance with wells containing untreated control cells.

   Provided appropriate concentrations are used, a concentration-response curve can be constructed.

BASIC PROTOCOL 9

ALAMAR BLUE REDUCTION TO ASSESS METABOLIC CAPABILITY

This bioassay uses a water-soluble indicator of cytotoxicity, eliminating the need for the washing and fixation steps needed in other assays using vital dyes (e.g., neutral red, MTT). As dye extraction is not done, the time needed for data collection is decreased. Data may be collected as either fluorescence (excitation at 530 to 560 nm; emission at 590 nm) or absorbance at 570 or 600 nm. Either cells adhering to the plastic of microtiter plates or cells in suspension culture can be used for this assay. Since the dye is nontoxic to the cells, the same cultures can be monitored over a series of time points. This assay can be used for cell proliferation determinations as well as for cytotoxicity assays. The dye and reagents for this assay are available in a kit from Biosource International, whose technical literature states that it provides results that compare favorably with the MTT assay.

Materials

Cells in microtiter plates
Test compound: toxicant or vehicle
Alamar blue assay kit (Biosource International)
Microtiter plate reader

Additional reagents and equipment for counting cells and assessing viability using trypan blue dye (Basic Protocol 1)

1. Do preliminary experiments to establish optimal cell density and incubation time for the cells used for testing.
2. Harvest cells in log-phase growth; count and estimate viability with trypan blue (see Basic Protocol 1).
3. Plate cells using the number that provides a predetermined optimal density (e.g., 200 µl of 1×10^4 cells/ml for some cancer cell lines) and at cell numbers that provide optical densities above and below optimal. Allow cells to grow at 37°C, 5% CO_2, for sufficient time that they reach log phase (e.g., 2 to 3 days).
4. Aspirate growth medium from the wells and add 200 µl of new medium containing up to 10% volume of test compound to the wells.

   These cells should be incubated for selected periods of time with several concentrations of test compound and the plate should include some wells in which the medium contains only vehicle.

5. Aseptically add an amount of alamar blue equal to 10% of the culture volume (e.g., 20 µl in a well that will contain 200 µl total or 22 µl to a well containing 200 µl medium).

6. Return cultures to the incubator for selected incubation times (e.g., from several hours to several days).

   For all data points data can be collected immediately after the incubation or plates can be stored overnight at 4°C and read the next day. Cell proliferation can be measured once or several times over a 3- to 5-day time period. The assay should be stopped (by refrigeration at 4°C) when cells reach 80% to 90% confluence.

7. Measure fluorescence (excitation 530 to 560 nm; emission 590 nm) or absorbance (at 570 and 600 nm) in a microtiter plate reader at desired time points.

   If using absorbance, subtract the background at 600 nm from the absorbance measured at 570 nm.

   Appropriate time points should be determined by preliminary experiments analyzing the growth of the cells.

8. Calculate cytotoxicity as absorbance (or fluorescence) in treated cells over absorbance (or fluorescence) in control cells. Generate a graph that plots log concentration of test compound on the *x* axis and percent decrease in absorbance (or fluorescence) from control on the *y* axis. Compare dye reduction over time in wells containing test compound and control wells.

MEASURING FLUORESCENT DYE LOSS TO ASSESS METABOLIC CAPABILITY

BASIC PROTOCOL 10

The acetoxymethyl ester derivative of 5-carboxyfluorescein diacetate (CFDA-AM) is one of several membrane-permeant dyes available from Molecular Probes that can be used to indicate membrane integrity (Haugland, 1996). For CFDA-AM and other such dyes, membrane integrity is indicated because the product formed upon esterase-induced cleavage will not leave cells if the cell membrane is intact. The ability to leak CFDA is considered an early indicator of cell damage. This assay for cytotoxicity can be performed at the same time as the propidium iodide assay for cell viability (see Basic Protocol 4), as the spectra for fluorescence do not overlap (Nieminen et al., 1992).

Materials

Cells
Test compound: toxicant or vehicle
50 µg/ml CFDA-AM in PBS (prepared fresh)
Phosphate-buffered saline (PBS; see recipe)
Fluorescence microtiter plate reader

1. Add 0.5×10^4 cells to each well of a 96-well plate. Allow to attach overnight. Incubate with test compounds according to the experimental protocol.
2. Remove medium, wash cells with PBS, and add 100 µl of a 50 µg/ml solution of CFDA-AM.

   Other membrane-permeable dyes may be used, such as the calcein-AM that is included in the Live/Dead Viability/Cytoxicity Assay of Molecular Probes.

3. Incubate cells for 30 min in a 37°C incubator.
4. Read fluorescence using excitation at 485 nm and emission at 530 nm.

   The microtiter plate fluorescence reader should be set to a sensitivity that provides 1000 to 2000 fluorescence units per 1 to 2×10^4 cells/well.

5. Compare fluorescence in wells treated with toxicant with that of wells containing cells but no test compound or vehicle.

ALTERNATE PROTOCOL 7

USING [^{3}H]2-DEOXY-D-GLUCOSE TO ASSESS METABOLIC CAPABILITY

Another means of determining cell membrane integrity is by exposing cells to [^{3}H]2-deoxy-D-glucose, which is membrane permeable. This substrate will be converted to membrane impermeant [^{3}H]2-deoxy-D-glucose-6-phosphate within living cells, and will remain within the cells if the membrane is intact (O'Hare and Atterwill, 1995).

Materials

10^6 cells grown in 60-mm culture dishes
Test compound: toxicant or vehicle
Phosphate-buffered saline (PBS; see recipe)
0.55 µCi/ml [^{3}H]2-deoxy-D-glucose in PBS
1 mg/ml glucose in PBS
1 M NaOH
1 M HCl
Scintillation fluid

CAUTION: When working with radioactivity, take appropriate precautions to avoid contamination of the experimenter and surroundings. Carry out the experiment and dispose of wastes in an appropriately designated area following the guidelines provided by your local radiation safety offices (also see *APPENDIX 1A*).

1. Grow 10^6 cells in 60-mm culture dishes to the appropriate state of confluency.

   The appropriate state of confluency corresponds to a number estimated for each type of cell, which is determined before starting the experiment.

2. Remove the growth medium, and wash the cells twice with 5 ml PBS each wash.
3. Add 5 ml of 0.55 µCi/ml [^{3}H]2-deoxy-D-glucose in PBS. Incubate for 2 hr to load cells.
4. Remove incubation solution and wash 3 times with 5 ml PBS per wash.
5. Add 2 ml PBS containing 1 mg/ml glucose and the appropriate concentration of test compound. Incubate for predetermined times (e.g., 6, 12, and 24 hr).
6. At up to three time points during the incubation, take 50-µl samples and add the samples to 3 ml scintillation fluid.
7. At the end of the incubation, remove the medium from the cells. Add 1 ml 1 M NaOH and incubate for 30 min to dissolve the cells.
8. Add the cell lysate to 3 ml scintillation fluid.
9. Rinse the dish with 1 ml 1 M HCl and add the rinse to 3 ml scintillation fluid.
10. Count the samples, lysate, and rinse. Calculate concentration depletion of radioactivity over the time of incubation.

    The values obtained will provide a means to differentiate what remains within and what is released by the cells.

    This procedure may also be done using a patented polycarbonate perfusion block (O'Hare and Atterwill, 1995).

REAGENTS AND SOLUTIONS

Use Milli-Q-purified water or equivalent in all recipes and protocol steps. For common solutions, see ***APPENDIX 2A****; for suppliers, see* ***SUPPLIERS APPENDIX****.*

Dye extractor solution

Citrate buffer: Mix 21.01 g/liter citric acid with 200 ml 1 M NaOH. Bring volume to 1 liter with water and check that pH is 4.2. To 60 ml of this solution add 40 ml of 0.1 M HCl. Store 2 to 3 months at 4°C.

Working solution: Mix citrate buffer 1:1 (v/v) with absolute alcohol.

INT dye

Stock solution: Dissolve tetrazolium dye INT (2-*p*-iodophenyl-3-nitrophenyl tetrazolium chloride) at a final concentration of 40 mM (20 mg/ml) in DMSO to provide a stock solution that can be stored in a tightly closed bottle for 2 to 3 months at room temperature.

Working solution: Dilute the stock 1:10 (v/v) with PBS (see recipe) to prepare a 4 mM (2 mg/ml) working solution just before doing the assay.

Kenacid blue dye

0.2 g Coomassie brilliant blue R-120
125 ml ethanol
315 ml H_2O
Store for 1 to 2 months at 4°C

Kenacid Blue working solution: Add 3 ml glacial acetic acid to 22 ml Kenacid blue dye solution immediately before use.

LDH substrate

5.2×10^{-2} M L(+) lactate
6.6×10^{-4} M INT (2-*p*-iodophenyl-3-nitrophenyl tetrazolium chloride)
2.8×10^{-4} M phenazine methosulfate
1.3×10^{-3} M NAD^+
0.2 M Tris·Cl, pH 8.2 (*APPENDIX 2A*)
Prepare just before assay

NAD^+ solution

4.5 mM NAD^+ (3 mg/ml)
13.5 U/ml diaphorase
0.03% (w/v) bovine serum albumin
1.2% sucrose in PBS, pH 8.2
Prepare just before assay

Neutral red stock solution

Prepare 0.1% (w/v) neutral red in distilled water, autoclave, and acidify with 2 drops of glacial acetic acid per 100 ml. Store up to 3 months in a dark container at 4°C.

Working solution: Dilute stock solution 1:10 (v/v) with PBS (see recipe) or 1:10 with 1.8% NaCl immediately before use.

Phosphate buffered saline (PBS)

For 1 liter:
8 g NaCl (0.138 M final)
0.2 g KCl (3 mM final)
1.15 g disodium monophosphate (Na_2HPO_4; 8 mM final)
0.2 g potassium dihydrophosphate (KH_2PO_4; 2 mM final
H_2O to 1 liter

continued

Adjust pH to 7.2
Filter sterilize through a 0.4-μm filter
Store up to 3 months at 4°C

Sorenson's buffer

0.1 M glycine
0.1 M NaCl
Adjust pH to 10.5 with NaOH
Store up to 2 months at 4°C, but check pH before use

Standard azide buffer

10 gram FA Bacto buffer (Difco 2314-15-0)
10 ml of 10% (w/v) sodium azide solution
10 ml heat-inactivated fetal bovine serum (FBS)
980 ml distilled water
Adjust pH to 7.2 ± 0.05
Store in foil-wrapped bottle up to 1 month at 4°C

[^{3}H]thymidine solution, 20×

20 μl of 1 mCi/ml [^{3}H]thymidine
980 μl sterile, serum-free medium
Prepare fresh on the day of assay

For the assay 50 μl of the stock is diluted to 1000 μl with serum-free medium to give 1 μCi/ml in well.

Trypan blue, 0.1% (w/v)

Dilute 1 ml commercially available 0.4% (w/v) trypan blue solution (Sigma) with 3 ml PBS (see recipe) or balanced salt solution (Sigma). Store tightly closed up to 6 months at room temperature.

Trypan blue in concentrations of 0.08% to 0.4% (w/v) can be used to determine percentage of viable and dead cells seen on the hemocytometer. With 0.1% trypan blue the cells are not as darkly stained and are easier to visualize.

Trypsin/EDTA

To prepare 100 ml of trypsin 0.05% (w/v) with 0.02% (w/v) EDTA, add 2 ml of 10× (2.5%) trypsin (Sigma) and 0.133 ml of 15% (0.5 M) EDTA, pH 8.0, to 97.87 ml of PBS (see recipe). Keep refrigerated, but warm to 37°C before use.

A ready-made solution is available from Sigma and Life Technologies (Gibco). The trypsin solution can be kept up to 4 weeks at 4°C. If it is not used frequently, it can be stored > 1 yr frozen at −5° to −20°C.

Vindelov's propidium iodine stain (PI)

1.21 g Tris base (0.01 M final)
584 mg NaCl (10 mM final)
10 mg ribonuclease (700 U final)
50.1 mg PI (7.5×10^{-5} M final)
1.0 ml Igepal CA-630 (Sigma; 0.1% final)
1 liter H_2O
Mix until dissolved
Adjust pH to 8.0
Filter through a 0.45-μm filter
Store in foil-wrapped bottle up to 1 month at 4°C

CAUTION: *Propidium iodide is toxic and potentially carcinogenic; handle with care and label solution appropriately.*

COMMENTARY

Background Information

All of the protocols provided in this unit can be used to detect damage to cells following in vitro application of toxicants to cells. In addition, several of the procedures can also be used as in vitro determinants of cytotoxicity for cells derived from animals tested with toxicants. The endpoints are nonspecific. In other words, they can occur in many types of cells damaged under a wide variety of situations, including exposure to chemicals, anoxia, and physical agents. Cytotoxicity tests, therefore, cannot be expected to be used to define specific mechanisms of injury induced by specific toxicants. Some tests, however, can suggest a subcellular structure (e.g., the nucleus, mitochondria, membranes) affected by particular toxicants, and more specific tests could then be performed to better describe the toxicant effects (Barile, 1994; Forsby et al., 1995). Although the protocols provided in this unit have been grouped according to one of three primary endpoints (viability, cell growth, metabolic capability), all can be used to indicate dose-related toxicant-induced changes that can eventually result in cell death. For investigators hoping to use such tests to indicate toxicant-induced effects without having toxicant-induced cell death, a prudent first choice among the protocols for cytotoxicity would be among those without viability as a primary endpoint, with inclusion of concentration and time-response effects in the investigation. As an example, the investigator interested in functional disruption rather than cell death could examine concentration-related changes in metabolic capability as a more reasonable endpoint than viability (e.g., for neurotoxicants and reversible hepatotoxicants).

Concentration response is an important part of cytotoxicity determinations and should be included to provide indication of the range over which toxicant-induced cytotoxicity or response occurs. This is especially important if comparisons are to be made between irreversible effects indicative of cytotoxicity and any other, more specific, functional, biochemical, or morphological changes that occur after exposure to the toxicant. If concentrations for cytotoxicity and other alterations are similar, the toxicant-induced general cytotoxicity may contribute to the changes in all endpoints determined. If a functional change occurs at lower concentrations than cytotoxicity, the change may be reversible, and the toxicant may be having effects on more specific endpoints at concentrations lower than those that cause general cell damage. Time-response studies are also useful in cytotoxicity determinations because they, too, indicate relative sensitivities between irreversible cell damage and functional changes.

The investigator should recognize that higher concentrations or longer times of exposure may be needed for expression of some endpoints than others (e.g., loss of cell viability versus alteration of cell growth), that some toxicants may require metabolic activation before they are cytotoxic, and that it is difficult to compromise metabolic function without causing subsequent loss of viability. In fact, any of the protocols provided could be used as indicators of irreversible cell damage. Some of the protocols, however, especially those that indicate cell growth, can be used at concentrations of toxicants that are low enough for recovery to occur if the toxicant is removed.

Cytotoxicity assays can be used with cells of various tissue origin; however, the sensitivity to toxicant-induced cytotoxicity may vary with the cell type used for testing. Such differences could provide the basis for studies that determine tissue-specific sensitivities to toxicants. For example, if cells that originate in the nervous system are more sensitive than cells of other tissue origin (e.g., hepatic, kidney), it may be possible to suggest that the toxicant in question could target the nervous system. However, certain cell types used for cytotoxicity determinations (e.g., those of neoplastic origin, regardless of tissue origin) may be very hardy, and concentrations required for cytotoxic effects may or may not be physiologically relevant.

The investigator may choose an assay method based on endpoint (e.g., viability, metabolic effects), sensitivity, ease of manipulation for multiple incubates, time needed, and availability of equipment. Indications are that all procedures presented in detail in this unit, if used with sufficiently high concentrations of toxicants, may be reasonably expected to detect comparable cytotoxicity (irreversible cell damage), without indication of toxicant-specific mechanistic effects on cell function. Therefore, choice of protocol would be determined by the other factors listed above, rather than by effectiveness at detecting cytotoxicity alone. For example, if large numbers of tests are to be done, the colorimetric assays with the vital dyes neutral red, MTT, and alamar blue may be the

test systems of choice because these procedures can all be done in 96-well microtiter plates. If the investigator wishes to observe toxicant effects on the same cells over a period of time, the alamar blue procedure may be chosen. This is because, among the vital dyes, only alamar blue forms a water-soluble product; with neutral red and MTT the assay needs to be terminated to extract the colored product formed by cellular metabolic processes. Some assays can be used at lower and higher toxicant concentrations, respectively, to determine cell proliferation as well as cytotoxicity (e.g., alamar blue, MTT, propidium iodide, [^{3}H]thymidine incorporation), with the latter radiometric assay, although more complex, more sensitive than simple addition of alamar blue for this particular endpoint. The fastest and simplest method for cytotoxicity, trypan blue uptake, is too laborious for precision if large numbers of samples are to be examined for cytotoxicity. Some cytotoxicity assays are available in kit form, decreasing their technical complexity (e.g., LDH; fluorescent assays that measure attachment of markers to nucleic acids in dead cells or indicate membrane permeability; alamar blue; stress gene assays). The availability of kits as well as the detailed technical information included with such kits may make them the protocols of choice in certain situations.

For investigators initiating studies on the cytotoxic effects of toxicants, testing is best done in the cells of tissue origin relevant to the investigation. In other words, cytotoxicity testing for neurotoxicants should be done in cells of nervous system origin; cytotoxicity testing for hepatotoxicants is best done in cells of hepatic origin. Comparisons, however, should be made between sensitivities in cells of various origin if the toxicant is to be identified by its effects on a specific organ or system (e.g., a neurotoxicant or a hepatotoxicant). Dose- and time-response investigations should be included. Dose- and time-related endpoint determinations specific for the tissue in question or for the toxicant target, if known, are useful to determine if changes occur at concentrations lower than those that cause general cytotoxicity. Examples of specific endpoints are the toxicant-induced inhibition of enzymes responsible for neurotransmitter degradation in neuronal cells, toxicant-induced changes in the quantity of a protein marker for astrocytes, loss of intercellular adhesion in cells with barrier function, and alteration of extracellular markers in lymphocytes. In the absence of an endpoint that indicates a specific cellular function, comparisons of dose- and time-related changes in cell growth and proliferation assays for cytotoxicity may be made with dose- and time-related changes in viability.

Assays for cell viability

The trypan blue procedure (Basic Protocol 1) is commonly used because it not only provides indication of how many cells are alive, but also how many live cells are being used for any subsequent experiment. This quantitative test is very simple and results can be rapidly obtained. The technique requires no specific training or specialized equipment.

Measurement of LDH activity (Basic Protocol 2 and Alternate Protocols 1 to 4) is another indicator of cell viability. The enzyme activity is measured external to the cells, as it leaks from dead cells. LDH activity can be measured in the ultraviolet range (340 nm), based on the loss of NADH due to its oxidation to NAD^+ as pyruvate is converted to lactate. If a colorimetric assay is preferred, a colored phenylhydrazone produced when 2,4-dinitrophenylhydrazine is incubated with the remaining pyruvate can be measured.

LDH release can also be measured as NAD^+ is reduced when lactate is converted to pyruvate. The resultant production of NADH then reduces FAD coupled to diaphorase with subsequent transfer of $FADH_2$ electrons to the tetrazolium dye INT (2-*p*-iodophenyl-3-nitrophenyl tetrazolium chloride).

Neutral red (Basic Protocol 3 and Alternate Protocol 5) is a third assay for cell viability. Neutral red is a weakly cationic dye that is bound to anionic sites on intracytoplasmic vacuoles and granules. It accumulates in lysosomes and other intracellular vacuoles of living cells. Ability to retain this dye is lost when cell die. Neutral red needs to be extracted from the cells; to do so requires that cells be lysed. This procedure, therefore, cannot be used like trypan blue exclusion to quantitate the number of live cells taking up the dye.

Propidium iodide retention (Basic Protocol 4) is another method for determining loss of cell viability. This fluorescent dye passes through compromised cellular membranes and then intercalates between base pairs in double-stranded nucleic acids. This agent has different signals when free or bound in cells, with emission at >600 nm detecting the bound species that is formed once it passes through the compromised membranes of dead cells. Experiments by Nieminen et al. (1992) indicated that results of assays using propidium iodide for

determining cell viability correlated with the results obtained by measuring lactate dehydrogenase (LDH) release.

Assays for cell growth

The number of cells in a growing culture (Basic Protocol 5) can be decreased by exposure to toxicants. This may or may not be due to loss of viability of a certain portion of the cells. Cell numbers can be indicated directly, by counting the cells, or indirectly, by measuring protein levels, and comparing results to cultures that have not been treated with the toxicant.

Proliferating cells incorporate [^{3}H]thymidine (Basic Protocol 6) into nucleic acids, competing with unlabeled thymidine. If the toxicant inhibits cell proliferation, with or without affecting cell viability, the incorporated radioactivity will be decreased.

Like cell counting or [^{3}H]thymidine incorporation, cell cycle analysis (Basic Protocol 7) is another means for determining the effects of toxicants on cell growth and differentiation. Alterations may or may not be due to effects on cell viability. Cell cycle analysis using propidium iodide is based on the fact that DNA content is not the same during different phases of the cell cycle. It is normally diploid in G1. When cells start to synthesize new DNA in the S phase, DNA content will be greater than diploid. After DNA synthesis is completed and the cell enters the G2 phase, it has a tetraploid DNA content. During mitotic division (M phase), the DNA content comes back to normal (diploid). If the DNA is stained with a DNA-specific dye, such as propidium iodide, and the DNA content per cell is estimated by flow cytometry, the G1/S/G2 ratio can be evaluated and compared between untreated and toxicant-treated cells.

Assays for metabolic capability

Still other protocols have been included because they are reputed to indicate cytotoxicity because they measure change in the metabolic functioning of the cell. Cell functions can be compromised by toxicants, and this compromise could result in loss of viability. The MTT colorimetric assay (Basic Protocol 8) determines the ability of viable cells to convert the soluble tetrasodium salt MTT [3-(4,5-dimethylthiazol-2-yl)-2,5-diphenyl tetrazolium bromide] to an insoluble formazan precipitate. The salts initially formed can be reduced within the cell to blue-colored formazan crystals that can be visualized on a spectrophotometer. The assay is best performed on cells that have active mitochondria. It, therefore, can be used as an indication of cellular proliferation, and it is far easier to perform than [^{3}H]thymidine incorporation.

Estimation of cytotoxicity using the alamar blue technique (Basic Protocol 9) involves incorporation of an oxidation-reduction (redox) indicator that both fluoresces and changes color in response to the reduction that occurs in medium as the cells grow. Reduction occurs in the presence of $FMNH_2$, $FADH_2$, NADH, NADHPH, and cytochromes. The reduction of the dye requires that it be taken up by the cells and participate in cellular respiratory processes. The water-soluble dye is nontoxic, and growing cells, which provide a reducing environment, cause the indicator to change from a non-fluorescent to a fluorescent product.

Compromised membranes affect metabolic functioning of cells and may be used to indicate cytotoxic effects of toxicants. Membrane damage may lead to cell death. Fluorescent dye loss (Basic Protocol 10) indicates that membrane leakage is occurring. These assays make use of the fact that cells in culture contain nonspecific esterases. The basic protocol provided is based on the principle that CFDA-AM, which is able to cross cell membranes, will be hydrolyzed by intracellular esterases to CFDA, which does not cross the membrane. The CFDA will remain within the cells and fluoresce, unless membrane integrity is impaired and it leaks out. Similarly, loss of [^{3}H]2-deoxy-D-glucose from cells (Alternate Protocol 7) is also an indication of loss of membrane integrity.

Critical Parameters and Troubleshooting

These protocols alone may not provide all the information needed to obtain optimal results when in vitro methods for cytotoxicity are used. Additional details are, therefore, provided for each of the protocols in the paragraphs that follow.

When using typan dye exclusion (Basic Protocol 1) to estimate viable cell concentrations, it is important that the cell suspension be homogenous or erroneous results will be obtained as the relatively small volume counted is multiplied by the total volume of cells available. Even in the small volume of cells used for this procedure, a relatively large number of cells must be counted (>100), and some means for recording differential counts is needed, such as using a double-scale hand counter for live and dead cells or a hand counter for live cells and

pencil marks for dead cells. A decision needs to be made before starting as to how to count cells that fall on lines (i.e., count cells touching the lines at the top and left of any square but omit cells touching the lines on the bottom and right sides of the square).

Cell suspensions on which trypan blue exclusion is to be measured should be placed on the hemocytometer so they are not too concentrated or counting will be difficult. If it appears that >10% of the cells are clustered, the suspension should be redispersed by vigorous pipetting and the suspension recounted.

For trypan blue exclusion determinations, it is important not to let the cell suspension stand with the dye too long, as viable cells may then begin to take up the trypan blue. Also, trypan blue has a greater affinity for serum protein than for cellular protein; therefore, counting cells suspended in PBS is preferred to counting cells in serum-containing media.

The trypan blue uptake and cell counting procedure can be tedious if a large number of cell suspensions need to be counted. Furthermore, the hemocytometer needs to be clean and dry before counting is done. A hemocytometer that is not dry will dilute the sample and underestimate cell counts. Washing with 70% ethanol can decrease the time needed for cleaning and drying; remaining ethanol could, however, lead to underestimation of viability.

When LDH leakage (Basic Protocol 2) is used to indicate loss of cell viability, a number of cautions need to be observed in order to obtain good, reproducible results. For kinetic and endpoint assays, the negative control should produce <5% of the change in absorbance of the positive control. In addition, the positive control needs to provide a sufficiently high change in absorbance that meaningful results can be obtained. Furthermore, the reaction should be conducted under constant temperature conditions to decrease interassay variability. Since results are based on differences between control and experimental incubates, cell concentrations need to be similar. Preliminary experiments with untreated cells are useful for optimization of conditions for a particular cell type that is to be used for subsequent experiments.

Among the problems which could be encountered with the LDH assay is the possibility of a high background reading, which may be noted when LDH is present in serum-containing medium. If this occurs, decreasing the serum content of the cell culture medium to 5% (provided it does not affect cell viability) may be a reasonable alternative. Another alternative would be to grow the cells in a different type of serum and/or different medium.

Care must be taken with cell cultures, because high spontaneous release of LDH can occur in the case of suboptimal cell culture conditions (e.g., when cell density is too high or when cell damage occurs during transfer of cells or addition of medium).

Low overall absorbance values may occur during LDH determinations, especially during colorimetric assays, if substrates are degraded by light.

Neutral red uptake (Basic Protocol 3 and Alternate Protocol 5) is a technically simple method for determination of cell viability but use of this assay still requires caution. For example, neutral red solution can form crystals, especially when prepared in phosphate buffers; such crystals are unlikely to form if the solution is prepared in distilled water whether the solution is stored at 4°C or at room temperature.

If the neutral red assay is done in wells in which cells were incubated with toxicant, care must be taken when removing the medium from cells in the microtiter wells before addition of the neutral red solution. If adhering cells die, they may become less attached than control cells. Color would then be less intensive and more related to cell number than to cytotoxicity, which would be underestimated.

Plates used for the neutral red assay may be processed twelve wells at a time to ensure uniformity of adhesion.

If the cell number in incubates with toxicant is too high or if the toxicant decreases cell numbers, the cells should be replated before the neutral red assay is run.

Propidium iodide binding (Basic Protocol 4) to the DNA of dead cells is another indicator of cytotoxicity. For proper use of this protocol, optimal conditions for a particular fluorescence scanner should be determined by preliminary experiments in which both propidium iodide concentration and cell number per well are varied. Concentrations of propidium iodide >50 μM in microtiter wells are unlikely to further increase fluorescence.

The propidium iodide assay is more reproducible with cells that strongly adhere to plastic than with cells that stay in suspension.

Propidium iodide is a light-sensitive, hygroscopic powder, red to dark red in appearance. If properly stored (dry at 0° to 4°C), it will remain stable for ≥4 years. Propidium iodide dissolves readily in water at 1 mg/ml; a higher concentration (10 mg/ml) requires heating and

may contain some insolubles. Either water or PBS can be used for solubilizing propidium iodide. Solutions are stable for up to 2 years if stored at 0° to 4°C in the dark with 0.1% (w/v) sodium azide as preservative. Propidium iodide is toxic and possibly carcinogenic, so protective clothing should be worn when handling this chemical.

When cell counts (Basic Protocol 5) are used to indicate cytotoxicity, cultures that are to be used as control and cultures that are to be exposed to the toxicant need to be identical before the experiment begins. When cell number or quantity of cell protein is used as an endpoint, the culture needs to be one that continuously divides and multiplies over time. Inhibition of growth should follow a concentration response.

Because changes in cell counts or cell protein may take several days, the toxicant needs to be water soluble, relatively stable, and nonvolatile in order to remain in contact with the cells. Toxicants that need metabolic activation may not cause a response.

Cell proliferation using [^{3}H]thymidine (Basic Protocol 6) requires use of radiolabeled compounds and use of such compounds requires special precautions.

Careful pipetting of the [^{3}H]thymidine solution is needed so wells do not become contaminated. Variability increases if pipetting is not precise and if contamination occurs. Large volumes of diluted [^{3}H]thymidine should not be prepared; prepare what is needed for the experiment only.

Medium removed from the plates after the incubation with [^{3}H]thymidine is radioactive. A closed collection system that is properly labeled reduces risk.

[^{3}H]thymidine assays that use trichloroacetic acid (TCA) need to be done with extreme care because TCA is very caustic.

For cell cycle analysis (Basic Protocol 6), cell membranes need to be permeable to allow the propidium iodide to enter. This can be done by treating the cells with azide buffer or by using ethanol. The propidium iodide needs to enter and stain the DNA in all cells. Other information about propidium iodide is in the paragraphs describing Basic Protocol 4.

The propidium iodide used for cell cycle analysis binds to double-stranded nucleic acids through intercalation between base pairs, with no preference for purine or pyrimidine base pairs. It does not bind to single-stranded nucleic acids. Propidium iodide also stains double-stranded RNA and, thus, can give a wrong estimation of DNA content and placement of cells in the cell cycle. Therefore, ribonuclease treatment is critical for the staining. (The RNAase is a part of Vindelov's solution; however, further incubation of cells with 1 mg/ml ribonuclease for 5 min at room temperature may be useful in some situations. Use DNAase-free ribonuclease, or DNA damage will occur and that will interfere with the assay.)

The use of standard azide buffer is recommended for assays of phenotypic markers where there is a possibility of capping surface receptors when doing cell cycle studies. Azide prevents capping and allows an assay to be performed at room temperature (or higher, if necessary). Azide is also a microbial inhibitor.

Obtaining quality histograms from the flow cytometer during cell cycle analysis may be difficult. Each cell type may need a slightly different treatment, but saturating concentrations of propidium iodide always need to be used to be sure that all cells are stained.

The MTT assay (Basic Protocol 8), although relatively simple from a technical aspect, may differ for different cells, as each has different metabolic capability. Therefore, preliminary experiments are needed to establish the optimal cell number for each well, the duration of the experiment, the time of MTT incubation necessary in order to provide a final absorbance that can easily be measured, and conditions to provide control values sufficiently high that loss of mitochondrial function in toxicant-treated cells can be measured. (Number of cells seeded per well, for example, should be sufficient to maximize the number of cell doublings that occur over a toxicant treatment period of 2 to 5 days.) Once established, these parameters need to be kept constant over the experiments in which data are to be collected and compared.

The metabolic state of the cells will affect the outcome of MTT assays; the cells should be kept as uniform as possible. Variability among wells on a single plate can occur.

If volumes of medium differ among the wells (e.g., by >10%) during the MTT assay, absorbances will also differ. Evaporation needs to be controlled to avoid this potential cause of variability. Old medium can decrease the efficiency of the assay, causing underestimation of the metabolic capability of control cells. Absorbance can also be affected by the concentration of D-glucose in the culture medium. It can be expected to be unaffected by pH or phenol red concentrations <10 mg/ml.

Some test substances may increase mitochondrial activity; this could be a cytotoxic

effect, but would not be indicated by the lower absorbances usually expected when MTT is used to indicate cytotoxicity.

MTT does not deteriorate if kept in a light-proof container at 4°C for several weeks.

The formazan product formed from MTT needs to be completely solubilized before reading absorbance.

As with the MTT assay, optimal conditions for the alamar blue assay (Basic Protocol 9) may vary with cell line, cell density, and incubation time. Preliminary experiments are necessary to establish a cell density at a particular incubation time that provides a linear response of alamar blue reduction correlating with the cell density. Preliminary experiments should also be done to determine the incubation time that provides maximal conversion of dye added to control cells from the oxidized (blue) form to the fully reduced (red) form of the dye. Although concentration-response curves may be obtained as early as 1 hr after alamar blue is added, longer incubations are preferred to increase absorbance or fluorescent signals.

High cell numbers or extended incubation times (>24 hr) can cause loss of linearity in production of the reduced (red form) of the alamar blue dye; absorbance may not only loose its linearity, but may actually decline under these conditions. Microbes that may contaminate cultures will also reduce alamar blue.

Bovine serum concentrations up to 10% (w/v) do not interfere with the alamar blue assay, nor does the presence of phenol red in the growth medium. Phenol red, however, may increase background absorbance by as much as 0.3 optical density units. Alamar blue itself is not cytotoxic at concentrations as high as 25% with exposures for up to 20 hr.

Fluorescent dye loss (Basic Protocol 10) can also be used as an indicator of cytotoxicity. As the membrane-permeable fluorescent dye is an ester, it needs to be kept dry to avoid spontaneous hydrolysis.

[^{3}H]-2-deoxy-D-glucose retention (Alternate Protocol 7) has been used as a means for determining cell integrity. However, because the compound is radioactive, special precautions are required; thus many laboratories now prefer to use the fluorescent dyes.

Anticipated Results

In vitro methods for cytotoxicity use a variety of endpoints. For example, assessment of viability using trypan blue exclusion (Basic Protocol 1) is done by direct observation. Cell are counted by viewing them through a microscope. Live cells exclude trypan blue; dead cells do not. Control cells should be >85% viable (>85 of 100 cells counted not taking up the dye). Provided cell suspensions are homogenous and the procedure is carried out appropriately, repetitive counting of the same suspension should provide counts that do not vary by more than 20%.

LDH leakage (Basic Protocol 2 and Alternate Protocols 1 to 4) is detected spectrophotometrically. Untreated cells should retain LDH and have minimal loss over the time the assay is run; the greatest loss should be with the positive control, the Triton-X-100-treated cells. An example of results from a study that used LDH leakage is provided in Figure 2.6.1 (Song et al., 1997). In this study, LDH leakage was used as an indicator of the cytotoxic effects of MPTP (1-methyl-4-phenyl-1,2,4,6-tetrahydropyridine), an agent that induces a Parkinsonian-like syndrome in primates, and its metabolite MPP^+. With cultured cells, reproducibility among positive controls and reproducibility within negative controls should be within 20%.

The neutral red assay (Basic Protocol 3 and Alternate Protocol 5) is another spectrophotometric assay for viability. When this protocol is used, absorbance is higher when there are more live cells in a well, so values in control wells of dividing cells depend on time of incubation. The product extracted from the cells is a reddish color. As an approximate estimate, absorbances of 0.2 to 0.4 could be expected in wells containing 10^5 cells/ml. This would be ~3 µg/ml neutral red. The limit of sensitivity is estimated to be ~1000 cells/well; changes in dye retention with 2000 cells in a well have been reproducibly detected (± 20%).

With binding of propidium iodide to DNA (Basic Protocol 4), fluorescence is used as an indicator of cytotoxicity. In this protocol for cytotoxicity, untreated cells should show little fluorescence, as the dye is excluded from normal cells. The positive control cells, treated with digitonin, should show the maximal fluorescence. Propidium iodide absorbs blue-green light and fluoresces red. Reproducibility should be within ± 20%.

Cytotoxicity can also be indicated by fewer cell numbers (Basic Protocol 5) or less protein in cultures exposed to the toxicant. The decrease seen on exposure to the toxicant should follow a concentration response, with at least three points on a concentration-response curve that are significantly different from the cell number or protein in the control incubate.

Another means for detecting cytotoxicity by reduction in cell growth or proliferations is by the uptake of [^{3}H]thymidine (Basic Protocol 6). Radioactivity is dependent on the number of cells in an incubate (Fig. 2.6.2; Ahmed et al., 1994). If cytotoxicity occurs, [^{3}H]thymidine uptake should be less in treated cells than in control cells. This assay is quite sensitive, and, by increasing the time of liquid scintillation counting, discrimination among incubates can be made even if [^{3}H]thymidine incorporation is low.

Flow cytometry is used when cell cycle analysis (Basic Protocol 7) provides indication of cytotoxicity. Histograms obtained by flow cytometry allow estimation of the percentage of cells in different phases of the cell cycle. If the toxicant interferes with DNA synthesis, the

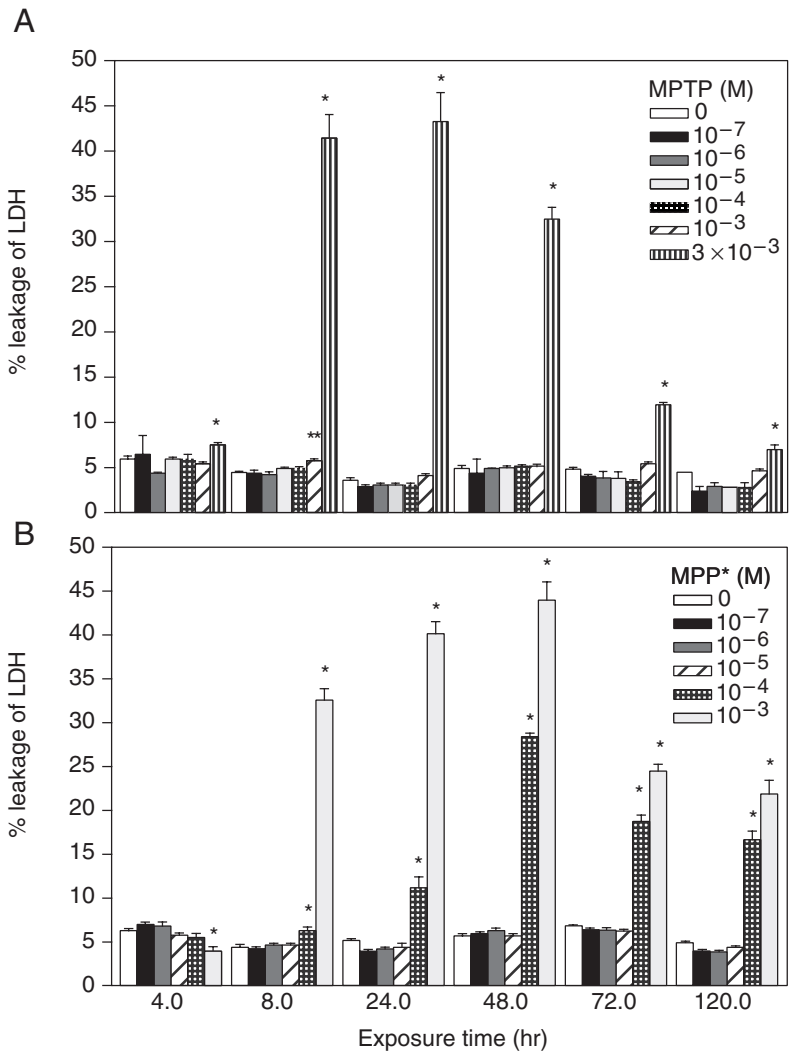

Figure 2.6.1 Effects of (**A**) MPTP and (**B**) MPP on the LDH leakage in SH-SY5Y human neuroblastoma cells. After treatment (10^{-7} to 3×10^{-3} M) for 4, 8, 24, 48, 72, 120 hr. Percent LDH leakage was determined by comparing to cells treated with Triton X-100 (100%). At the assay conditions, the LDH activity that leaked from Triton X-100-treated cells was 198.69 ± 12.81 mOK/min; the leakage of LDH from untreated cells was 4.36 ± 0.51% of the Triton X-100 treated cells. Results were averages of at least 3 individual experiments (mean ± SE). The results for MPP-treated cells are significantly different from the control ($p < 0.05$). Reprinted, with permission, from Song et al. (1997). Intox Press. (See discussion of reference for an explanation of the decrease in release of LDH after 48 hr.) Abbreviations: MPP, 1-methyl-4-phenyl-pyridine; MPTP, 1-methyl-4-phenyl-1,2,3,6-tetrahydropyridine.

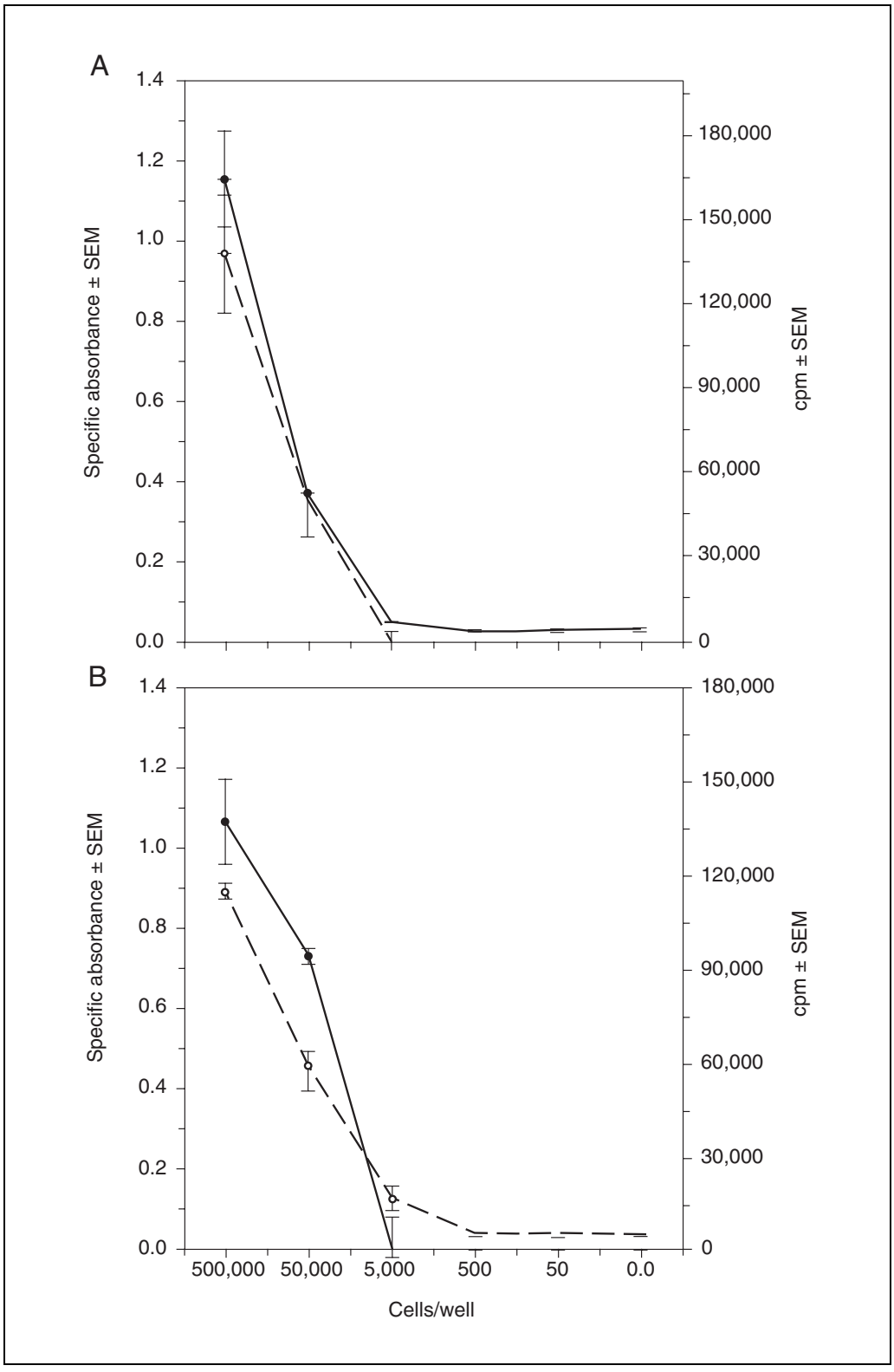

Figure 2.6.2 The spontaneous proliferation of YCD3-1 cells at indicated cell numbers per well was determined by Alamar blue (solid line) and [^{3}H]thymidine (interrupted line) assays. Alamar Blue and [^{3}H]thymidine were added 3 hr after the culture set up and proliferation determined at 24 (**A**) and 48 hr (**B**) post culture. The specific absorbance was determined by subtracting A_{600} from A_{570}. [^{3}H]thymidine incorporation data are presented as mean cpm. Reprinted, with permission, from Ahmed et al. (1994). Elsevier Science B.V.

Table 2.6.1 Effect of Various Neurotoxicants on Membrane Integrity and Viability of SH-SY5Y Human Neuroblastoma Cells[a]

Endpoint	Test chemical and concentration (M)[b]	Percent of control (±SEM) at[c]	
		4 hr	24 hr
Membrane integrity (CFDA retention)	MPTP 10^{-6}	113 (5)	100 (6)
	10^{-5}	100 (4)	88 (4)
	10^{-4}	93 (4)	89 (1)
	10^{-3}	80 (4)[d]	59 (6)[d]
	MPP^+ 10^{-6}	94 (1)	81 (6)
	10^{-5}	87 (8)	77 (1)[d]
	10^{-4}	91 (4)	69 (8)[d]
	10^{-3}	71 (9)[d]	58 (10)[d]
Viability	MPTP 10^{-6}	98 (1)	97 (1)
	10^{-5}	98 (1)	97 (1)
	10^{-4}	97 (1)	97 (1)
	10^{-3}	97 (2)	97 (1)
	MPP^+ 10^{-6}	98 (1)	97 (1)
	10^{-5}	97 (1)	97 (1)
	10^{-4}	98 (1)	97 (1)
	10^{-3}	98 (1)	98 (1)

[a]Data from Rowles et al., 1995.

[b]Abbreviations: MPP, 1-methyl-4-phenylpyridine; MPTP, 1-methyl-4-phenyl-1,2,3,6-tetrahydropyridine.

[c]Results presented as percentage of control activity, mean (SEM) of 3 to 5 replicate assays (with wells done in triplicate in each assay).

[d]Differences from control ($p < 0.05$). Values in untreated cells for retention of CFDA (indicator of membrane integrity) measured as fluorescence units = 1221 ± 115 for 1 to 2×10^{-4} cells/well (sensitivity 2 on Cytofluor fluorescence plate reader). Viability (measured with propidium iodide, verified with trypan blue) over all assays = 97% ± 1. Viability determined by binding of propidium iodide to nuclei of nonviable cells based on comparison with positive control (digitonin). Reprinted, with permission, from Rowles et al., 1995; Mary Ann Liebert, Inc., Publishers.

majority of the cells will be in the G1 phase, and a very low percentage will be in the S and G2 phases.

Metabolic capability of cells may be compromised when they are exposed to toxic substances. One method for detecting the effects of toxicants on the metabolism of cells uses MTT, which cells with intact mitochondria convert to a formazan dye which can be detected spectrophotometrically. The MTT assay (Basic Protocol 8) is rapid, versatile, quantitative, and highly reproducible, with a low intratest variation (± 15% standard deviation). Results are expressed as a percentage of control absorbance, and cell numbers per well are not quantified. Although an indicator of a cytotoxic effect on mitochondrial function, the test cannot distinguish between cells with reduced effects and those that are dead.

The alamar blue reaction (Basic Protocol 9) is a spectrophotometric or fluorescent assay that depends on the number of cells in the incubate (Fig. 2.6.2; Ahmed et al., 1994). Cytotoxicity causes cells to decrease metabolic functioning and stop growing. This will lessen the reduced environment usually present when cells are growing, and decrease the amount of fluorescent product produced. Results are comparable with other assays using vital dyes (e.g., MTT), and reproducibility should be ± 20%.

Decreased membrane integrity is indicated by fluorescent dye loss (Basic Protocol 10) in the wells of the microtiter plate that contain test compound and cells. Membrane changes can occur at time points earlier or at concentrations lower than needed for loss of cell viability, as can seen in a study with MPTP and MPP^+ (Table 2.6.1; Rowles et al., 1995). For a fluorescent dye assay, reproducibility should be ± 20%. An assay which indicates viability (e.g., propidium iodide binding, Basic Protocol 4) may be done at the same time as assays which indicate membrane compromise (Table 2.6.1; Rowles et al., 1995).

Time Considerations

The trypan blue assay (Basic Protocol 1) is probably the easiest of all protocols included

in this chapter. A cell count and viability calculation can be done in <5 min per sample.

More time is needed when LDH leakage (Basic Protocol 2 and Alternate Protocols 1 to 4) is used to indicate loss of cell viability. For this procedure, a microtiter plate which contains 96 wells would provide triplicate wells for over 20 samples and the positive and negative controls. Pipetting would take ~10 min; the plate may be stabilized by delaying the first reading of a kinetic assay for up to 7 min after initiation of the reaction. The reaction may run as long as an hour. With a microtiter plate reader, all wells can be read simultaneously; some microtiter plate readers can be programmed to do the appropriate calculations. Total time per plate would be expected to be ~2 hr.

Cell in microtiter plates previously incubated with toxicants could be processed for neutral red retention (Basic Protocol 3 and Alternate Protocol 5) in ~2.5 hr. The longest times are those needed for incubating with the dye (90 min) and the time needed for dye extraction (20 min). Over 20 samples, and positive and negative controls, could be run in triplicate on a single plate. The process can be interrupted at the air-drying step, with plates stored for several days before addition of the neutral red solution.

Propidium iodide binding to DNA of dead cells (Basic Protocol 4) can also be used to indicate toxicant effects on cell viability. For each plate processed after incubation of cells and toxicant, ~1 hr is needed.

When counting cells (Basic Protocol 5) to compare cell growth between control and toxicant-treated cells, the time at which the counting is done is dependent on the growth rate of untreated cells. Doubling time may vary from several hours to several days. The procedure itself takes little time (see Basic Protocol 1), but the time needed to determine if cytotoxic effects are occurring may take days.

After incubation for predesignated times with toxicant, [^{3}H]thymidine incorporation (Basic Protocol 6) may take from 0.25 to 24 hr. Preparation of cells for scintillation counting may take 1 to 3 hr, and scintillation counting will take additional hours.

Flow cytometric analysis for cell cycle determinations (Basic Protocol 7) may be relatively rapid (<1 hr), but time is needed for preparation and interpretation of the graphs provided. The staining procedure needed before the flow cytometry can be expected to take ~30 min. Longer incubations of cells with propidium iodide can improve results but will increase the time needed to do this assay. Incubations of cell suspensions with propidium iodide stain (at 4°C) may be overnight or even longer. To determine cytotoxicity, incubations with the toxicant may require hours to days before the staining and flow cytometry are done.

After incubation with toxicant, 4 to 6 hr are required for MTT incorporation (Basic Protocol 8). An additional hour may be required for MTT removal, dye extraction, crystal solubilization, and reading on the microtiter plate.

After incubation with toxicant, the time of the alamar blue assay (Basic Protocol 9) depends on the optimal time for incubation of dye with cells (determined by preliminary experiments). This can range from 1 to 24 hr.

Using loss of fluorescent dye (Basic Protocol 10) to determine toxicant-induced compromise of membrane integrity is a relatively straight-forward, simple procedure. After incubation of cells and toxicant ~1 hr should be sufficient to do this assay.

Literature Cited

Abdulla, E.M. and Campbell, I.C. 1993. Use of neurite outgrowth as an in vitro method of assessing neurotoxicity. *In* Markers of Neuronal Injury and Degeneration (J.N. Johansson, ed.) pp. 276-279. Ann. N.Y. Acad. Sci., 679.

Ahmed, A., Gogal, R.M., and Walsh, Y.E. 1994. A new rapid and simple non-radioactive assay to monitor and determine the proliferation of lymphocytes: An alternative to [^{3}H]thymidine incorporation assay. *J. Immunol. Methods* 170:211-224.

Babich, H. and Borenfreund, E. 1992. Neutral red assay for toxicology in vitro. *In* In Vitro Methods of Toxicology (R.R. Watson, ed.) pp. 237-251. CRC Press, Boca Raton, Fla.

Barile, F.A. 1994. Introduction to In Vitro Cytotoxicology Mechanisms and Methods. CRC Press, Boca Raton, Fla.

Forsby, A., Pilli, F., Bianchi, V., and Walum, E. 1995. Determination of critical cellular neurotoxic concentrations in human neuroblastoma (SH-SY5Y) cell cultures. *Alternatives to Lab. Animals* 23:800-811.

Haugland, R.P. 1996. Handbook of Fluorescent Probes and Research Chemicals, 6th ed. Molecular Probes, Eugene, OR.

Krishan, A. 1975. Rapid flow cytometric analysis of mammalian cell cycle by propidium iodine staining. *J. Cell Biol.* 66:188-193.

Mosman, T. 1983. Rapid colorimetric assay for cellular growth and survival: Application to proliferation and cytotoxicity assays. *J. Immunol. Methods* 65:55-63.

Nieminen, A.L., Gores, G.J., Bond, J.M., Imberti, R., Herman, B., and LeMaster, J.J. 1992. A novel

cytotoxicity screening assay using a multi-well fluorescence scanner. *Toxicol. Appl. Pharmacol.* 115:147-155.

O'Hare, S. and Atterwill, C.K. 1995. Methods in Molecular Biology 43: In Vitro Toxicity Testing Procedures. Human Press, Totowa, N.J.

Rowles, T.R., Song, X., and Ehrich, M. 1995. Identification of endpoints affected by exposure of human neuroblastoma cells to neurotoxicants at concentrations below those that affect cell viability. *In Vitro Toxicol.* 8:3-13.

Song, X., Perkins, S., Jortner, B.S., and Ehrich, M. 1997. Cytotoxic effects of MPTP on SH-SY5Y human neuroblastoma cells. *Neurotoxicology* 18:341-354.

Veronesi, B. and Ehrich, M. 1993. Differential cytotoxic sensitivity in mouse and human cell lines exposed to organophosphate insecticides. *Toxicol. Appl. Pharmacol.* 120:240-246.

Key References

Alley, M.C., Scudiero, D.A., Monks, A., Hursey, M.L., Czerwinski, M.J., Fine, D.L., Abbot, B.J., Mayo, J.G., Shoemaker, R.H., and Boyd, M.R. 1988. Feasibility of drug screening with panels of human tumor cell lines using a microculture tetrazolium assay. *Cancer Res.* 48:589-601.

This describes a microassay for MTT (Basic Protocol 8).

Application notes for the Cytofluor Fluorescent Plate Reader, Millipore Corporation, Marlborough, MA.

These notes discuss use of multiple probes for multiple endpoints in a single incubate of cells, providing excitation and emission data, that can be used when fluorescent dye loss (Basic Protocol 10) is used to indicate cytotoxicity.

Borenfreund, E., and Puerner, J.A. 1985. A simple quantitative procedure using monolayer cultures for cytotoxicity assays (HTD/NR-90). *J. Tissue Cult. Methods* 9:7-9.

This is an early paper from a laboratory with recognized expertise with the neural red assay (Basic Protocol 3 and Alternate Protocol 5).

Nieminen et al., 1992. See above.

Optimization of the procedure for measuring cell viability by propidium iodide uptake (Basic Protocol 4) is described in this reference.

Technical Information, Alamar Blue Assay, Biosource International, Camarillo, CA.

Details about the alamar blue assay system (Basic Protocol 9) and how to use it are provided.

Technical Information included with LDH Assay Kits, Sigma Chemical, St. Louis, MO.

These provide specific details for use of their kits when LDH leakage (Basic Protocol 2 and Alternate Protocols 1 to 4) is used as the indicator of loss of cell viability.

Technical Information on Trypan Blue, Sigma Chemical, St. Louis, MO.

This provides a detailed protocol, including a diagram of a hemocytometer, for the trypan blue assay (Basic Protocol 1).

Contributed Marion Ehrich and
Lioudmilla Sharova
Virginia-Maryland Regional College of
Veterinary Medicine
Blacksburg, Virginia

In Situ Hybridization Histochemistry

This unit describes in situ hybridization for analyzing specific cellular mRNA in frozen and cryostat-sectioned tissue. The localization and levels of different mRNA in the tissue of interest can be detected by using radioactive (see Basic Protocol) or nonradioactive (see Alternate Protocol) oligonucleotide probes. Support Protocols 1 and 2 describe how to prepare radioactive and nonradioactive probes. Support Protocol 3 describes the procedure for cryostat sectioning of frozen specimens.

IN SITU HYBRIDIZATION WITH RADIOACTIVE PROBES

BASIC PROTOCOL

Cryostat-sectioned, paraformaldehyde-fixed, dehydrated tissue specimens (see Support Protocol 3) are hybridized to [^{35}S]dATP-labeled oligonucleotide probes overnight, then washed, dehydrated, and exposed to X-ray film or dipped into photographic emulsion for visualization of radioactive signal. The Alternate Protocol describes hybridization with nonradioactive probes.

Materials

Hybridization buffer (see recipe)
10 mg/ml salmon testes DNA
1000 Ci/mmol [^{35}S]dATP-radiolabeled probe (see Support Protocol 1)
5 M DTT (see recipe)
Glass slide with fixed and dehydrated specimen of interest (see Support Protocol 3)
1× SSC (see recipe), 55°C
70%, 80%, 95%,and 100% ethanol
D19 X-ray film developer (Kodak)
X-ray film fixer (Kodak or equivalent)
K5 photoemulsion (Ilford)
AGFA G333 fix
Cresyl violet stock solution: 5 g cresyl violet in 1 liter H_2O
10% (v/v) acetic acid
Xylene
Mounting medium (DPX, Permount, or Petrex)

1.5-ml microcentrifuge tubes, sterile
Humidified chamber: box with tight lid and wet filter paper placed to prevent contact with slides
42°C incubator
40°C and 55°C water bath
Staining dish and slide racks
Autoradiographic ^{14}C microscale (Amersham)
Hyperfilm β-max X-ray film (Amersham)
Slide box
Black electrician's tape

CAUTION: When working with radioactivity, take appropriate precautions to avoid contamination of the experimenter and surroundings. Carry out the experiment and dispose of wastes in an appropriately designated area following the guidelines provided by your local radiation safety offices (also see *APPENDIX 1A*).

Contributed by Zaal Kokaia
Current Protocols in Toxicology (2000) 2.7.1-2.7.13

Prepare hybridization mix

1. Add the following to a sterile 1.5-ml microcentrifuge tube:

   900 µl hybridization buffer
   50 µl 10 mg/ml salmon testes DNA (final concentration 500 µg/ml)
   [^{35}S]dATP-radiolabeled probe to (1×10^7cpm/ml final) 40 µl 5 M DTT

   Adjust volume to 1 ml with hybridization buffer.

   The amount of hybridization mix should be scaled to accommodate the number of slides to be hybridized. The 1 ml of hybridization mix prepared here is for four slides.

Apply hybridization mix to sections

2. Place the glass slide with the fixed and dehydrated specimen of interest in the humidified chamber with sections upward.
3. Apply ~250 µl of hybridization mix per slide evenly distributing it over the sections. Be sure not to touch the sections with the pipet tip.
4. Cut Parafilm into pieces of size appropriate to cover the area of the slide containing the fixed specimen.
5. Place the piece of Parafilm on the slide and spread hybridization mix evenly over the sections without causing bubbles. Start on one side and gently smooth bubbles out the other.
6. Put the lid on the humidified chamber, seal it with tape, and place into the 42°C incubator for 16 to 18 hr (i.e., overnight).

Wash the sections

7. Take slides out of the humidified chamber and remove Parafilm.
8. Rinse quickly in 1× SSC, 55°C, to remove hybridization mix.
9. Place slides in the slide rack of a staining dish filled with 1× SSC, 55°C, and place the dish in a 55°C water bath.
10. Change the 1× SSC, 55°C, three times, once every 15 min.
11. For the last wash, add 1× SSC, 55°C, remove the staining dish from the 55°C water bath, and allow the solution to cool to room temperature, (~1.5 hr).
12. Wash slides twice, each time for 2 min, in water at room temperature.

Dehydrate and dry sections

13. Dip slides successively in 70%, 80%, 95%,and 100% ethanol, for 2 min in each solution.
14. Air dry the slides at room temperature.

Visualize the signal

To visualize probe by film autoradiography

15a. Place slides and autoradiographic ^{14}C microscale in an X-ray film cassette and secure their positions with tape, being careful not to cover the specimens with tape.

16a. Place X-ray film over the slides in the darkroom (the rounded corner of the film should be placed in left up corner of the cassette), close the lid of the box tightly, and expose for 1 to 21 days at 4°C.

The exposure time depends on the abundance and expression level of the gene of interest.

17a. Prepare developer by dissolving 160 g of D19 developer in 1 liter water.

Development and fixation of the film should be performed in the dark or under safelight illumination, and the temperature of the solutions should be 20° ± 5°C.

18a. Place the film in a bath filled with developer for 4 min.

19a. Rinse film in water for 10 sec and place in X-ray film fixer for no longer than 10 min.

20a. Wash film in clean running water at 20° ± 5°C for ≥5 min and air dry.

To visualize probe by emulsion autoradiography

NOTE: Dipping and developing of slides should be performed in the dark or under safe light illumination.

15b. Put a vial containing 20 ml water in the 40°C water bath. Monitor the temperature with a thermometer. When the temperature of the water in the vial reaches 40°C add 20 ml K5 photoemulsion (40 ml final volume). Mix gently every 30 min for 2 hr, avoiding bubbles.

16b. One at a time, dip slides in the vial of emulsion. Take slides out quickly and gently. Holding vertically, check that the whole surface of the slide is equally covered by the emulsion. Place the slides vertically in the slide holder and air dry them in the dark for at least 4 hr (preferably overnight).

A tube holder can be used if a slide holder is not available.

17b. Put the slides into a slide box, seal the box with black tape, and place in a refrigerator for the necessary exposure time.

The time of exposure differs from probe to probe (from 1 to 8 weeks). For old slides (3 to 4 months), exposure time should be doubled.

18b. When exposure has been completed, prepare developer by dissolving 80 g of D19 developer in 1 liter water. Place slides in the slide rack of a staining dish filled with developer for 3 min.

19b. Rinse slides for 10 sec in water and fix 10 min in AGFA G333, diluted 1:5 with water.

20b. Rinse slides with water for 10 sec, then wash them in clean running water 15 to 20 min at 20° ± 5°C and air dry.

Counterstain slides with cresyl violet and cover slip

21. Add 1.5 ml of 10% (v/v) acetic acid to 250 ml cresyl violet stock solution and filter to get rid of crystals.

22. Place developed slides in slide rack and dip them as follows:

Three times in xylene for 5 min each
Three times in 100% ethanol for 2 min each
Two times in 95% ethanol for 2 min each
Once in 70% ethanol for 2 min
Once in H_2O for 5 min
Once in cresyl violet solution prepared in step 21, for 30 sec to a few minutes
Once H_2O for 2 min
Once in 70% ethanol for 2 min

Two times in 95% ethanol for 2 min each
Three times in 100% ethanol for 2 min each
Three times in xylene for 2 min each.

CAUTION: *Xylene is a toxic solvent and all steps of counter staining and coverslipping should be carried out in a fume hood or ventilated table.*

Optimal staining time in cresyl violet varies from tissue to tissue.

23. Take slides from the xylene one by one and cover slip them directly with mounting medium.

IMPORTANT NOTE: *Avoid introducing air bubbles.*

24. Remove extra mounting medium with filter paper, place the slides flat, and let dry ≥2 days in fume hood.

ALTERNATE PROTOCOL

IN SITU HYBRIDIZATION WITH NONRADIOACTIVE PROBES

In situ hybridization can be performed not only with probes labeled with radioactivity, but also by using nonradioactive probes that allow rapid detection of hybrids without using potentially hazardous radioisotopes. Cryostat-sectioned, paraformaldehyde-fixed, dehydrated tissue specimens (Support Protocol 3) are hybridized overnight to digoxigenin (DIG)-labeled oligonucleotide probes (Support Protocol 2), and washed; hybrids are detected using antibodies and color reactions.

Materials

DIG-labeled probe (Support Protocol 2)
Hybridization buffer (see recipe)
Glass slides with fixed and dehydrated specimen
1× SSC (see recipe), 48°C
Binding buffer (see recipe), prepare fresh
Anti-DIG-alkaline phosphatase–labeled antibody (Roche Molecular Biochemicals)
Normal sheep serum
Triton X-100
Wash buffer (see recipe), prepare fresh
Color solution (see recipe)
Stop buffer (see recipe), prepare fresh
Mounting medium, aqueous (Aquamount, BDH)

Humidified chamber: box with tight lid and wet filter paper placed to prevent contact with slides
Slide racks and staining dishes
48° and 55°C water baths

Prepare hybridization mix

1. Add 2 µl DIG-labeled probe to 1 ml hybridization buffer.Vortex and keep on ice until use.

The amount of hybridization mix (in this case probe plus hybridzation buffer) should be scaled to accommodate the number of slides which are to be hybridized (prepare 1 ml hybridization mix for 4 slides).

Apply hybridization mix to the sections

2. Place the glass slide with the fixed and dehydrated specimen of interest in the humidified chamber with sections upward.

3. Apply ~250 µl hybridization mix per slide evenly distributing it over the sections. Be sure not to touch the sections with the pipet tip.
4. Cut Parafilm into pieces of size appropriate to cover the area of the slide containing the fixed specimen.
5. Place the piece of Parafilm on the slide and equally spread hybridization mix over the sections without causing bubbles.
6. Put the lid on the humidified chamber, seal it with tape, and place in a 37°C incubator for 16 to 18 hr (i.e., overnight).

Wash slides

7. Take slides out of the humidified chamber and remove Parafilm.
8. Rinse slides quickly in 100 ml of 1× SSC, 48°C, one by one, to remove hybridization mix.
9. Place slides in the slide rack of a staining dish filled with preheated 1× SSC, 48°C, and place the dish in the 48°C water bath.
10. Change 1× SSC, 48°C, three times, once every 30 min.
11. For the last wash, add 1× SSC, 48°C. Remove the staining dish from the 48°C water bath and allow the solution to cool to room temperature (~1.5 hr).
12. Wash slides twice, each time for 5 min, in binding buffer at room temperature.
13. Prepare binding buffer containing 1:500 anti-DIG-alkaline phosphatase-labeled antibody, 1% (v/v) normal sheep serum, and 0.3% (v/v) Triton X-100. Add 300 to 400 µl of this solution to each slide.
14. Incubate slides 3 hr in a humidified chamber.
15. When incubation is completed, rinse slides briefly in binding buffer.
16. Wash slides three times, each time for 10 min, in binding buffer at room temperature.
17. Rinse briefly in wash buffer.
18. Wash for 5 min in wash buffer.

Stain slides

19. Apply 150 µl color solution and incubate in the dark for 12 to 24 hr at room temperature.
20. Stop the reaction by washing slides twice, each time for 5 min, in stop buffer.
21. Wash slides twice, each time for 5 min, in water at room temperature.
22. Air dry slides overnight.
23. Coverslip sections with aqueous mounting medium (Aquamount).

    Do not use xylene-based mounting solutions. This will form crystals of color precipitate.

24. Analyze by light microscopy.

SUPPORT PROTOCOL 1

3′ LABELING OLIGONUCLEOTIDE PROBES WITH [^{35}S]dATP

Oligonucleotide probes can be end labeled with either radioactive or nonradioactive labels. In this protocol, ^{35}S labeling of oligonucleotides is described, although labeling with other isotopes (^{3}H, ^{32}P, or ^{125}I), or (nonradioactively) with biotin, can also be performed. Nonradioactive labeling (with digoxigenin) is described in Support Protocol 2. Oligonucleotides can be labeled at the 5′ end using T4 polynucleotide kinase or at the 3′ end using terminal deoxynucletidyl transferase (TdT). 3′ end labeling of oligonucleotide probes with [^{35}S]dATP is described here.

Materials

10 U/µl terminal deoxyribonucleotidyl transferase (TdT; Amersham Pharmacia Biotech)
TdT reaction buffer (supplied with TdT enzyme; also see recipe)
DEPC-treated H_2O (see recipe)
10 mCi/ml [^{35}S]dATP (1000 Ci/mmol)
Oligonucleotide to be labeled, ~50-mer
Absolute methanol (HPLC grade)
0.1 M Tris·Cl, pH 8.0 (see recipe)
20% ethanol, ice-cold
Scintillation fluid
5 M DTT (see recipe)

1.5-ml microcentrifuge tubes, sterile
NENSORB column (DuPont NEN Research Products)
10-ml syringe
Scintillation vial

CAUTION: When working with radioactivity, take appropriate precautions to avoid contamination of the experimenter and surroundings. Carry out the experiment and dispose of wastes in an appropriately designated area following the guidelines provided by your local radiation safety offices (also see *APPENDIX 1A*).

Label oligonucleotide probe

1. Place a sterile microcentrifuge tube on ice and add the following:

   2.5 µl TdT reaction buffer
   10.5 µl DEPC-treated H_2O
   7.5 µl 10 mCi/ml [^{35}S]dATP
   2 µl oligonucleotide (80 ng)
   2.5 µl TdT (25 U; keep in freezer and use a cooling block).

   Total volume should be 25 µl. If volume is less due to higher concentration of some solutions, adjust to 25 µl by adding DEPC-treated H_2O.

   Always add TdT last and never vortex.

2. Incubate tube in a 37°C water bath for 2 to 2.5 hr.

Purify labeled oligonucleotide

3. Pack the resin of a NENSORB column (one per reaction) by tapping until the column matrix is at the bottom.
4. Remove the cap and attach the column to a ring stand. Place a disposable tube under the column.

5. Add 3 ml of absolute methanol to the column directly and pass through the column with a 10-ml syringe attached to the column adapter.
6. Add 3 ml 0.1 M Tris·Cl, pH 8.0, and pass through the column with the syringe
7. Add 500 µl 0.1 M Tris·Cl, pH 8.0, to the labeled probe, mix by pipetting, and apply to the column.
8. Gently press syringe (to obtain a drop speed of 1 to 2 drops/sec) until solution has passed through the column.
9. Wash the column by forcing 1.5 ml of 0.1 M Tris·Cl, pH 8.0, through the syringe.
10. Elute the labeled oligonucleotide probe with 500 µl of 20% ice-cold ethanol, with a drop speed of 1 to 2 drops/sec.
11. Collect the first 12 to 13 drops in a sterile microcentrifuge tube.

Determine activity of probe

12. Vortex and add 2 µl from microcentrifuge tube to a small piece of filter paper and place in a scintillation vial. Add 10 ml scintillation fluid and measure radioactivity by liquid scintillation counting.

    A good probe should have at least 500,000 cpm/µl (1-2 × 10^6 cpm/ng).

13. Add 2 µl of 5 M DTT per 100 µl probe (final concentration of 10 mM) to the labeled, purified probe from step 11.
14. Store labeled, purified probe at −20°C.

3′ LABELING OF OLIGONUCLEOTIDE PROBES WITH DIGOXIGENIN

SUPPORT PROTOCOL 2

Oligonucleotide probes can be end-labeled with digoxigenin (or biotin) as an alternative to radioactive labeling techniques (Support Protocol 1). Nonradioactive in situ hybridization is much faster and safer and does not require special facilities to handle radioactive isotopes.

Materials

5× DIG labeling buffer (see recipe)
DEPC-treated H_2O (see recipe)
25 mM $CoCl_2$
1 mM DIG-dUTP (Roche Molecular Biochemicals)
Oligonucleotide
10 U/µl terminal deoxyribonucleotidyl transferase (TdT)
1.5-ml microcentrifuge tubes, sterile

1. Place a sterile microcentrifuge tube on the ice and add the following:

    5 µl 5×DIG labeling buffer
    7 µl DEPC-treated H_2O
    4 µl 25 mM $CoCl_2$
    1 µl 1 mM DIG-dUTP
    5 µl oligonucleotide (200 ng)
    3 µl TdT (30 U; keep in freezer and use a cooling block).

    Total volume should be 25 µl. If volume is 25 µl, due to a higher concentration of some solutions, bring volume to 25 µl by adding DEPC-treated water.

    Always add TdT last and never vortex.

2. Incubate tube in a 37°C water bath for 2 hr.

Use without further purification. Store at −20°C.

SUPPORT PROTOCOL 3

PREPARATION OF TISSUE

The main aim of tissue preparation is to preserve tissue morphology during in situ hybridization and at the same time create good conditions for the penetration of the probes.

Slides should be coated in order to prevent sections from falling off during different steps of hybridization and washing. Slides can be coated with either poly-L-lysine or chrome alum.

Materials

4% paraformaldehyde (see recipe)
Phosphate buffered saline (PBS; see recipe)
70%, 80%, and 90% ethanol
Poly-L-lysine or chrome alum coated slides (see recipes)

Additional materials and reagents for cryosectioning (Watkins, 1989).

Section tissue

1. Section fresh-frozen specimen on a cryostat (10- to 14-µm in thickness) and thaw mount sections on either poly-L-lysine or chrome alum–coated glass slides.
2. Dry slides at room temperature for 10 min and place at −20°C until ready for use for in situ hybridization.
3. When starting in situ hybridization take slides out of the freezer, and place them at room temperature for 10 to 15 min.

Fix and dehydrate tissue sections

4. Fix the sections 15 min in 4% paraformaldehyde.
5. Wash the sections as follows:

   Twice in PBS, each time for 10 min
   Twice in H_2O, each time for 5 min
   Twice in PBS, each time for 3 min.

6. Dehydrate sections by dipping slides in 70%, 80%,and 95% ethanol for 2 min each. Air dry the slides.

REAGENTS AND SOLUTIONS

*Use Milli-Q-purified water or equivalent for the preparation of all buffers. For common stock solutions, see **APPENDIX 2A;** for suppliers, see **SUPPLIERS APPENDIX.***

Binding buffer

Dissolve the following in 400 ml H_2O:
4.38 g NaCl
25 ml 2 M Tris (see recipe)
Adjust pH to 7.5 with 2 M HCl
Adjust volume to 500 ml with H_2O

Prepare fresh just prior use and do not autoclave.

To prepare 2 M HCl, add 16.6 ml concentrated HCl to 100 ml DEPC-treated water (see recipe).

5-Bromo-4-chloro-3-indolyl-phosphate (BCIP) solution

Dissolve 75 mg BCIP 4-toluidine salt in 1ml 100% dimethylformamide
Store up to 6 months at –20°C

Chrome alum–coated slides

Incubate slides in 100% ethanol for 5 min. Let slides dry. Heat 500 ml DEPC-treated water (see recipe) to 60°C and dissolve 2.5 g gelatin and 0.25 g chrome alum (chromium potassium sulfate). Filter solution and cool to room temperature. Dip slides once for 3 min (avoid bubbles). Air-dry slides overnight at room temperature. Store slides up to 6 months at – 20°C before using.

Color solution

Add 45 µl 75 mg/ml NBT (see recipe) and 35 µl 50 mg/ml BCIP (see recipe) to 10 ml wash buffer (see recipe). Prepare fresh.

DEPC-treated water

Add 250 µl DEPC (diethylpyrocarbonate) to 1 liter distilled water. Leave at room temperature overnight, then autoclave and store up to 6 months at 4°C.

Denhardt solution, 50×

Dissolve 1 g polyvinylpyrrolidone, 1 g BSA, and 1 g Ficoll in 77 ml DEPC-treated water (see recipe). Adjust volume to 100 ml with DEPC-treated water and filter sterilize. Divide solution into aliquots and store up to several months at –20°C.

Final concentrations are 1% (w/v) polyvinylpyrrolidone, 1% (w/v) BSA, and 1% (w/v) Ficoll.

DIG labeling buffer, 5×

1 M potassium cacodylate
0.1 M Tris·Cl, pH 6.6 (see recipe)
1.3 mg/ml bovine serum albumin
Store up to 6 months at –20°C.

Dithiothreitol (DTT), 5 M

Dissolve 7.7 g DTT in 10 ml DEPC-treated water (see recipe). Filter through a disposable 0.45-µm syringe filter Divide into aliquots and store up to 6 months at –20°C

The solution is filter sterilized because autoclaving will destroy DTT.

Hybridization buffer

Add the following to a glass dish and place on a magnetic stirrer:
50 ml deionized formamide (Sigma)
20 ml 20× SSC (see recipe)
2 ml 50× Denhardt solution (see recipe)
5 ml 20% sarkosyl (see recipe)
10 ml 0.2 M phosphate buffer, pH 7.0 (see recipe)
5 ml 11 mg/ml salmon testes DNA
10 g dextran sulfate
Adjust volume to 100 ml with 0.2 M phosphate buffer, pH 7.0 (see recipe)
Divide into aliquots and store up to 6 months at –80°C

The dextran sulfate must be added while stirring. Ensure that it has completely dissolved before adjusting the volume with phosphate buffer.

Nitroblue tetrazolium (NBT), 75 mg/ml

Dissolve 75 mg 2, 2′-di-*p*-nitrophenyl-5, 5′-diphenyl-3, 3′-(3, 3′-dimethoxy-4, 4′-diphenylene) ditetrazolium chloride (nitroblue tetrazolium, or NBT) in 1 ml 70% dimethylformamide. Store up to 6 months at −20°C.

Use dimethylformamide in glass tubes or microcentrifuge vials only (other plastics will dissolve).

Paraformaldehyde, 4% (w/v)

Dissolve 40 g paraformaldehyde in 800 ml water, adding 3 to 4 ml 5 M NaOH (10 g NaOH in 100 ml water), and heat to 60°C to dissolve. When the paraformaldehyde has been dissolved add 100 ml 10 × PBS (see recipe). Adjust the pH to 7.0 with concentrated HCl. Filter and adjust volume. Prepare fresh.

PBS, 10×

Add the following to 800 ml DEPC-treated water (see recipe):
80 g NaCl
14.4 g Na_2HPO_4
2 g KCl
2.4 g KH_2PO_4
Adjust the pH to 7.4 with concentrated HCl
Adjust volume to 1 liter with DEPC-treated H_2O
Store up to 6 months at room temperature

Phosphate buffer, 0.2 M

Dissolve 27.6 g $NaH_2PO_4 \cdot H_2O$ in 1 liter DEPC -treated water (see recipe). Dissolve 28.4 g Na_2HPO_4 in 1 liter DEPC-treated water. Mix the two solutions in a 1:3 ratio. Store up to 6 months at room temperature.

Poly-L-lysine coated slides

Incubate slides in 100% ethanol for 5 min, then allow to dry. Dissolve 25 mg poly-L-lysine in 500 ml DEPC-treated water (see recipe). Incubate slides in poly-L-lysine for 10 min. Air dry slides overnight at room temperature. Store the slides up to 6 months at −20°C before using.

Sarkosyl, 20% (w/v)

Dissolve 2 g *N*-laurylsarcosine in 10 ml DEPC-treated water (see recipe). Store 1 to 2 months at room temperature.

SSC, 20×, pH 7.0

Dissolve 175.3 g NaCl and 88.2 g sodium citrate dihydrate ($C_6H_5Na_3O_7 \cdot 2H_2O$) in 800 ml DEPC-treated water (see recipe). Adjust pH with 5 M NaOH (10 g NaOH in 100 ml DEPC-treated water), or concentrated HCl. Adjust the volume to 1 liter with DEPC-treated water. Autoclave and store up to 6 months at room temperature.

Stop buffer

Dissolve 4.38 gNaCl, 2.5 ml 2 M Tris (see recipe) and 0.186 g EDTAin 400 ml DEPC-treated water (see recipe). Adjust pH to 7.5 with 2 M HCl (16.6 ml concentrated HCl in 100 ml DEPC-treated H_2O). Adjust volume to 500 ml with DEPC-treated water.

Prepare fresh just prior use and do not autoclave.

TdT reaction buffer

500 mM sodium cacodylate, pH 7.2
10 mM $CoCl_2$
1 mM 2-mercaptoethanol
Store at −20°C

Tris·Cl, 0.1 M, pH 8.0

Dissolve 1.2 g Tris base in 80 ml DEPC-treated water (see recipe). Adjust pH to 8.0 with concentrated HCl. Adjust volume to 1 liter with DEPC-treated H_2O.

Tris, 2 M

Dissolve 24 g Tris base to 80 ml DEPC-treated water (see recipe). Adjust volume to 1 liter with DEPC-treated H_2O. Store up to 6 months at room temperature.

Wash buffer

Dissolve the following in 400 ml H_2O:
2.92 g NaCl
25 ml 2 M Tris (see recipe)
Add pH to 9.5 with 2 M HCl.
Add 5.07 g $MgCl_2 \cdot 6H_2O$ and dissolve
Adjust pH to 9.5 with 2 M HCl
Adjust volume to 500 ml with DEPC-treated H_2O

Make fresh just prior use and do not autoclave. To prepare 2 M HCl, add 16.6 ml concentrated HCl to 100 ml DEPC-treated water (see recipe).

COMMENTARY

Background Information

In situ hybridization is a powerful tool which combines anatomical and molecular biology techniques for detection and localization of specific nucleic acid sequences (usually messenger RNA) within individual cells or tissue preparations. This method is based on the formation of double-strand hybrid molecules between labeled probes and nucleotide sequences of interest by means of the hydrogen binding of complementary base pairs. High sensitivity and the possibility for precise anatomical localization of labeled mRNA make this technique valuable not only for identification of the few cells expressing a specific gene of interest, but also for quantification of changes in the synthesis of mRNA to assess the functional condition of the corresponding gene. In situ hybridization was originally developed in parallel by Pardue and Gall (1969) and John et al. (1969). Since then this technique has developed dramatically, and today it is an inevitable part of biological research. Many protocols have been developed for different types of in situ hybridization and have been published as articles or book chapters (Young, 1990; Wilkinson, 1992; Emson, 1993; Wilcox, 1993). Basically, all protocols can be divided in two main categories depending on what type of probes they describe: long DNA or RNA (e.g., complementary RNA) or short DNA (oligonucleotide) probes. The sensitivity of long probes is much higher, but if the gene of interest is highly expressed, oligonucleotide probes have several advantages: they are easy to synthesize on a DNA synthesizer, and much simpler to handle (e.g., labeling, purification, hybridization).

Probes can be labeled in two different ways: with radioactive isotope or nonradioactive marker. In general, probes labeled with radioactivity are more sensitive and give the possibility of assessing the degree of expression of a particular gene, while nonradioactive in situ hybridization is much faster, safer, and does not require special facilities to handle radioactive isotopes.

Critical Parameters and Troubleshooting

The in situ hybridization method can be subdivided in four main steps: specimen preparation (Support Protocol 3), probe labeling (Support Protocol 1 or 2), hybridization of probe to the tissue, and finally washing and detection of the probe (see Basic Protocol or Alternate Protocol). Each of these steps might be modified depending on the abundance of the target gene, type of probe, and nature of the specimen.

During all steps of in situ hybridization, it is essential to employ RNase-free conditions. Use gloves, baked glassware, sterile disposable plastic tubes, and deionized, sterile, diethylpyrocarbonate (DEPC)-treated water in all steps. Post-hybridization washes and further handling of slides do not require these precautions.

Tissue fixation for the detection of mRNAs by in situ hybridization is one of the most important steps. The main aim of tissue fixation is to preserve tissue morphology, and at the

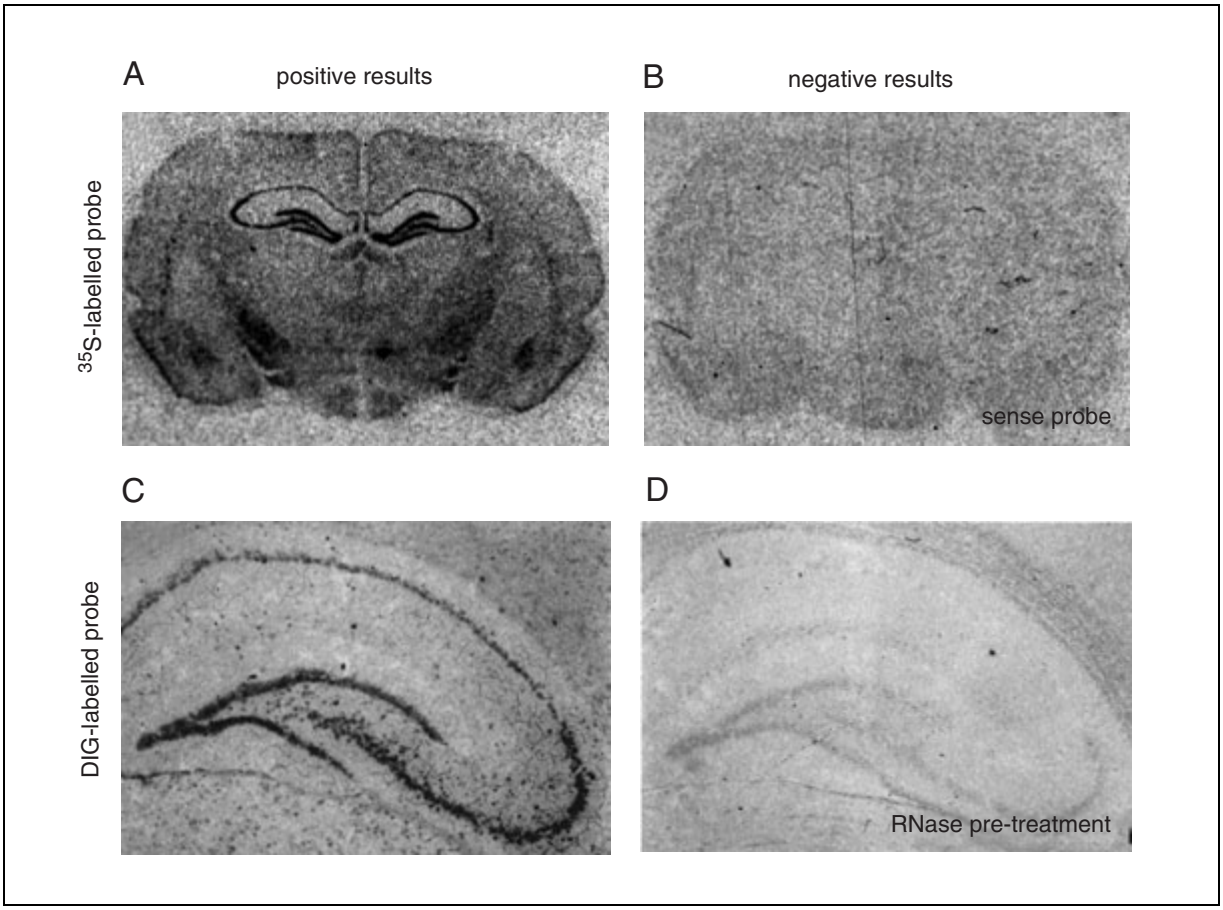

Figure 2.7.1 Expression of brain-derived neurotrophic factor mRNA in coronal sections of rat brain detected by [^{35}S]dATP and digoxigenin-labeled probes. Panels (**A**) and (**B**) represent images from X-ray film autoradiography showing a whole section hybridized to the ^{35}S-labeled antisense (A) and sense (B) probes. Panels (**C**) and (**D**) are bright-field photomicrographs of the hippocampal formation from the brain section hybridized to the digoxigenin-labeled probe without pretreatment (C) or after pretreatment with RNase (D). Note the absence of positive specific signal on (B) and (D).

same time to create conditions favorable for penetration of the probe to its target. The tissue could be fixed by transcardial perfusion with cross-linking fixative (e.g., 4% paraformaldehyde; Cassela et al., 1997), or the specimen can be frozen immediately after sacrificing the animal, and fixed after cutting sections and mounting them on the slides. Use of fresh-frozen tissue is preferable; transcardial fixation should be used only if in situ hybridization is performed in combination with immunocytochemistry. Cross-linking fixatives reduce permeability of the probes, and sometimes it becomes necessary to treat tissue (deproteinate) in order to increase signal. It is important to optimize the fixation procedure for each specific type of tissue and probe.

Use of [^{35}S]dATP or DIG-dUTP together with TdT for labeling of oligonucleotide probes gives high specific activity by adding a polymer of labeled bases (tail) to the 3′-end of oligonucleotide probe. The choice of probe label should depend on the abundance of the mRNA in the tissue. Since ^{35}S-labeled probes are more sensitive, that label is recommended for use when the expression level of the gene of interest is low or when the levels of gene expression need to be quantified. On the other hand, when the gene of interest is highly expressed or the laboratory does not have special facilities for handling radioactive isotopes, nonradioactive probes should be used.

It is very important to control for the specificity of in situ hybridization, especially when the probe is used for the first time. Use two sets of slides and hybridize them under the same conditions but use a standard, antisense probe for one set of slides and a sense probe (with opposite orientation as compared to antisense probe) for another set. This will show how specific the degree and pattern of expression of gene of interest is and will also allow assessment of the nonspecific background.

Another control is to pretreat sections with RNase (this will destroy cellular RNA) and then perform in situ hybridization. This control will reveal the nonspecific binding of the probe to tissue components (e.g., proteins, lipids) other than mRNA. Often, adding an excess (i.e., 100×) of unlabeled (cold) probe to the hybridization mix is used as a control. If the probe is detecting specific signal, this treatment will lead to the disappearance of tissue labeling. Finally, it is also advised that two or more probes be used, designed against different fragments of the gene of interest. A similar pattern of tissue labeling with different probes indicates a high level of specificity of hybridization (see Fig. 2.7.1).

Anticipated Results

Properly performed in situ hybridization will identify the location and degree of expression of the gene of interest in the tissue or defined population of cells as shown in Figure 2.7.1. Low background, reproducibility of results, and small variations in expression pattern and levels between the specimens will indicate high specificity of these results.

Time Considerations

The time required for performing an in situ hybridization experiment might vary depending on which types of probes (i.e., radioactive or nonradioactive) are used, as well as the expression levels of the gene of interest. Normally, in situ hybridization with nonradioactive probes requires 3 to 4 days. The duration of in situ hybridization with radioactive probes depends mainly on how long slides are exposed to X-ray film and/or auto radiographic emulsion. This step might last from a few days up to several weeks.

Literature Cited

Cassela, V.P., Kay, J., and Lawson, S.J. 1997. The Rat Nervous System. An Introduction to Preparatory Techniques. John Wiley & Sons, West Sussex.

Emson, P.C. 1993. In-situ hybridization as methodological tool for the neuroscientist. *Trends Neurosci*. 16:9-16.

John, H., Birnstiel, M., and Jones, K. 1969. RNA-DNA hybrids at the cytological level. *Nature* 223:582-587.

Pardue, M.L. and Gall, J.G. 1969. Molecular hybridization of radioactive DNA to the DNA of cytological preparations. *Proc. Natl. Acad. Sci. U.S.A.* 64:600-604.

Watkins, S. 1989. Cryosectioning. *In* Current Protocols in Molecular Biology (F.M. Ausubel, R. Brent, R.E. Kingston, D.D. Moore, J.G. Seidman, J.A. Smith, and K. Struhl, eds.) pp. 14.2.1-14.2.8. John Wiley & Sons, New York

Wilcox, J.N. 1993. Fundamental principles of in situ hybridization. *J. Histochem. Cytochem.* 41:1725-1733.

Wilkinson, D.G. 1992. The theory and practice of in situ hybridization. *In* In Situ Hybridization. A Practical Approach (D.G. Wilkinson ed.) pp. 1-13. Oxford University Press, New York.

Young, W.S., III. 1990. In situ hybridization histochemistry. *In* Handbook of Chemical Neuroanatomy, Vol. 8: Analysis of Neuronal Microcircuits and Synaptic Interactions (A. Björklund, T. Hökfelt, F.G. Wouterlood, and A.N. van den Pol, eds.) pp. 481-512. Elsevier Science Publishers, New York.

Contributed by Zaal Kokaia
University Hospital
Lund, Sweden

Confocal Microscopy

Confocal microscopy makes it possible to view a very thin optical plane in a specimen by excluding light from all planes above or below the focal plane. This is achieved by letting light from the focal plane pass through a small aperture, a so-called pinhole, while light from other planes in the specimen is excluded by the pinhole. By this so-called optical sectioning, sharp images of structures deep within thick sections may be obtained.

Confocal microscopy is suitable for reflecting and fluorescing specimens. It is best suited for fluorescence, since a reflecting marker largely obscures structures beneath it. The optical sectioning capacity is best realized when applied to a thick fluorescent specimen. In conventional wide-field fluorescence microscopy it would not be possible to resolve fine structures deep within such a specimen; fluorescence signals would be collected from all planes throughout the depth of the specimen, and resolution and contrast of structures in the focal plane would be lost. The optical sectioning capacity of the confocal microscope excludes fluorescence signals from planes above and below the focal plane.

Several different types of confocal microscopes have been developed for different imaging purposes with different technical solutions to the scanning procedure like stage scanning, beam scanning, tandem scanning, pinhole scanning, or slit scanning confocal microscopes (Pawley, 1995a). In this context, only the confocal laser scanning microscope will be considered, and at the end of this chapter a brief outlook on recent technical developments and their future applications will be given.

In confocal laser scanning microscopy (CLSM), the specimen is illuminated by a laser beam that scans a part of the specimen, and the fluorescence (or reflected) light is detected through the pinhole. Light passing through the pinhole is converted to a digital electronic signal, and the digital signal is passed on to a computer for storage and transformation into an image on the computer monitor. By scanning consecutive optical planes at increasing depth in the specimen, series (i.e., "stacks") of images can be collected that may be used for three-dimensional reconstruction with the computer. Moreover, by projecting all images of the consecutive optical planes onto one image plane, it is possible to view all parts of the specimen "in focus" simultaneously.

In biomedicine, CLSM is preferentially used for analysis of fluorescent specimens. By use of multiline lasers, or combinations of different types of lasers, it is possible to analyze the distribution of different fluorescent markers in the tissue. Presently, immunofluorescence is by far the predominant technique, but rapid progress is being made in the field of fluorescence in situ hybridization (FISH). The capacity to scan regions deep in the tissue obviates the necessity to use thin histological sections for high-resolution microscopy and allows the use of thick sections, or even tissue blocks, with better structural integrity than conventional histological sections. As a consequence, CLSM is the method of choice for analysis of spatial distribution of different markers, e.g., colocalization of markers in cells or cell organelles and topography of cell-cell contacts. It is beyond the scope of this unit to discuss all ways that CLSM may be used in histopathology. Instead, the information presented here is intended to give a basic insight into the theoretical and practical possibilities and limitations of the technique and to provide practical guidelines for the novice in confocal microscopy.

IMAGE CAPTURING

The focused-laser beam scans an area in the specimen, in a manner analogous to the raster scanning of a cathode ray tube (Fig. 2.8.1A). Reflected/fluorescent light from each point in this area is captured by a photon-catching device, and the intensity in each point is integrated over time illuminated by the laser (or the number of photons is counted). The signal is digitalized and transmitted to a computer. The signals from each point in the scanned area are represented as a frame, for example, 512×512 pixels.

Each pixel in the frame represents an area. The pixel size is determined by the sweep area, which depends on the magnification of the objective. In addition, an electronic zoom gives optional sweep areas for each objective. Thus, scanning a smaller area at a given frame size gives pixels representing smaller areas.

The image of the frame represents one confocal section. By scanning consecutive confocal sections at increasing depth in the specimen, it is possible to combine the different frames to

Contributed by Peter Ekström

Current Protocols in Toxicology (2000) 2.8.1-2.8.21

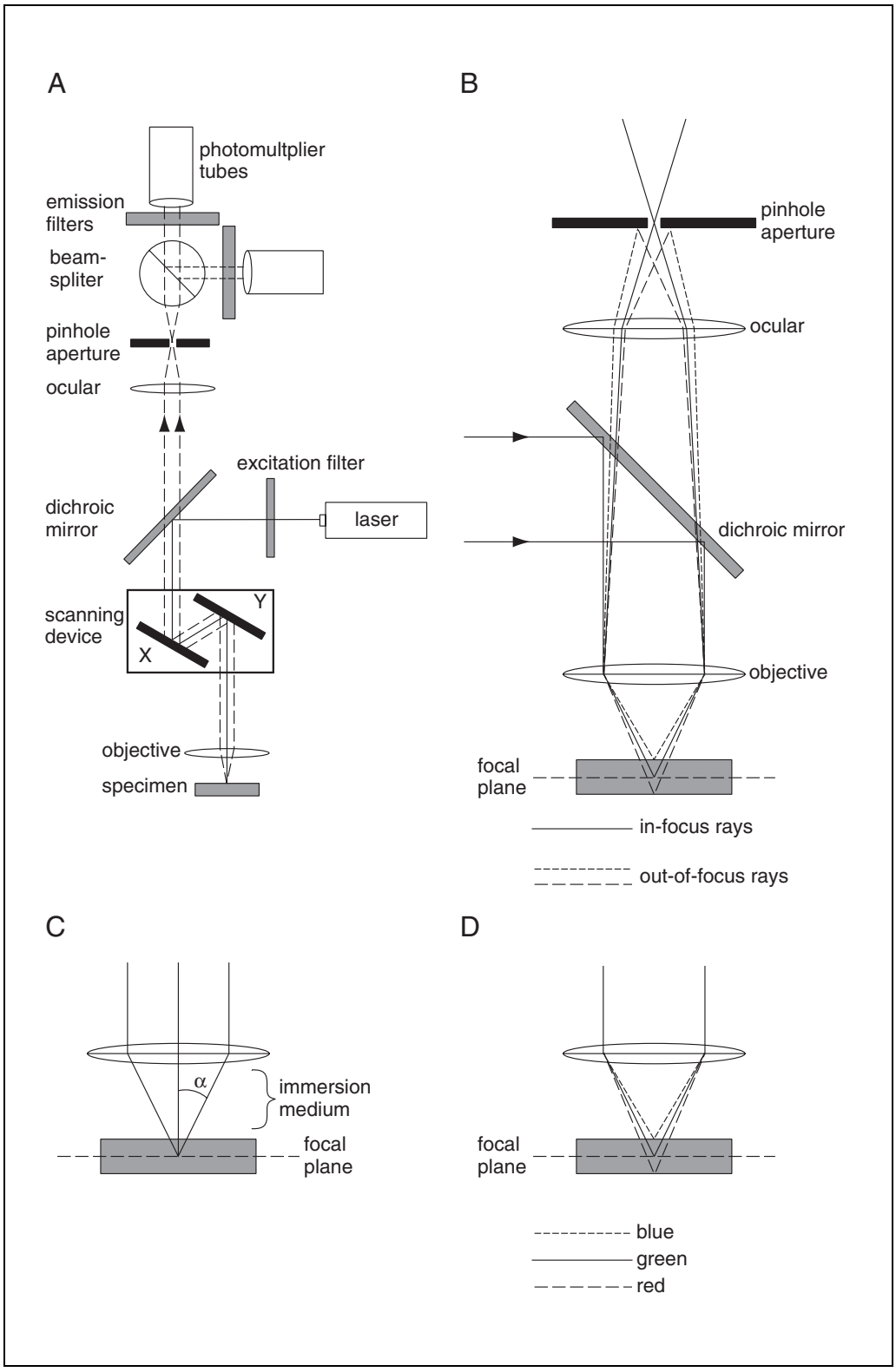

Figure 2.8.1 Legend at right.

make a three-dimensional reconstruction of the specimen. A number of consecutive confocal sections is usually called a "stack." When using stacks for three-dimensional reconstructions we deal with volume units, voxels, which represent the pixel area times the distance between the consecutive focal planes.

PRACTICAL AND THEORETICAL LIMITATIONS

To make full use of the power of confocal microscopy, it is important to appreciate its inherent limitations. The physical constraints will be briefly considered, as well as how each component of the CLSM setup contributes to the quality of the final image. For thorough analyses of these topics, the reader is referred to the Handbook of Biological Confocal Microscopy (Pawley, 1995a).

Resolution

Optical resolution depends on the numerical aperture of the objective lens, on the refractive indices of the immersion medium, coverslip, mounting medium, and specimen, as well as on the type of light used, and the wavelengths of the excitation and emission light, thus the choice of fluorescent marker. In confocal laser scanning microscopy, the small and sharply defined laser light spot for excitation, the size of the pinhole detector aperture, and the electronic system for sampling and digitalizing the fluorescent light signal, all contribute to the effective resolution.

Lateral resolution

The image of an infinitely small luminous object point is itself not infinitely small, but is in fact a circular Airy diffraction image with a central bright disk and progressively weaker concentric dark and bright rings (Fig. 2.8.1). The radius r_{Airy} of the first dark ring depends on the wavelength of the light, λ, and the numerical aperture of the objective, NA.

$$r_{\text{Airy}} = \frac{\lambda}{\text{NA}}$$

Two equally bright points of light, separated by a small distance, d, may be resolved if $d \geq r_{\text{Airy}}$. This is known as the Rayleigh criterion. Thus, the lateral resolution (x,y resolution) of point objects is defined by the least distance, x, between two objects when they still may be discerned as two objects.

$$x = K\frac{\lambda}{\text{NA}}$$

The factor K is determined by the quality of the light. The K value is higher (i.e., 1.0) for axial coherent light (i.e., laser light), and lower (i.e., <1.0) for noncoherent light (i.e., nonlaser light). Low coherence is required for bright-field and reflection microscopy, whereas high coherence is required for phase and interference microscopy. The degree of coherence is less important in fluorescence microscopy, but in fluorescence confocal laser scanning microscopy low coherence is preferred because of the lower K value, as out-of-focus defects in the

Figure 2.8.1 *(at left)* (**A**) Schematic drawing of confocal laser scanning microscope and light path. Laser light passes an excitation filter, by which the appropriate excitation wavelength is selected. The light beam is reflected by a dichroic mirror to the scanning device, into the objective, and is focused onto the specimen. The specimen is scanned line by line in a raster system. Fluorescence from the specimen travels back through the objective, via the scanning device, through the dichroic mirror to the pinhole aperture. An emission filter selects the appropriate emission wavelength range, and an ocular focuses light from the focal plane in the specimen on the small pinhole aperture. Light passing through the pinhole is captured by a photomultiplier tube. Simultaneous two-wavelength scanning requires that the dichroic mirror reflects both excitation wavelengths and lets both emission wavelengths through. Also, the two emission wavelengths passing through the pinhole are separated by a beamsplitter, and captured by two photomultipliers. (**B**) The confocal principle. The parallel light of the laser beam is focused in the specimen. Light from the focal plane is focused on the pinhole aperture, whereas light from planes above or below focus either in front of, or behind, the pinhole, thus contributing only low photon flux through the pinhole. (**C**) The numerical aperture (NA) of an objective is given by the formula NA = $\eta\sin\alpha$, where η is the refractive index of the immersion medium between the objective and the specimen, and α is half the opening angle of the objective. (**D**) Chromatic aberration. Light of different wavelengths have different focal lengths with a given lens. Unless this is corrected for (e.g., by using high-quality planapochromat lenses), scanning at different wavelengths will give incorrect optical sectioning. (Adapted from Shotton, 1995.)

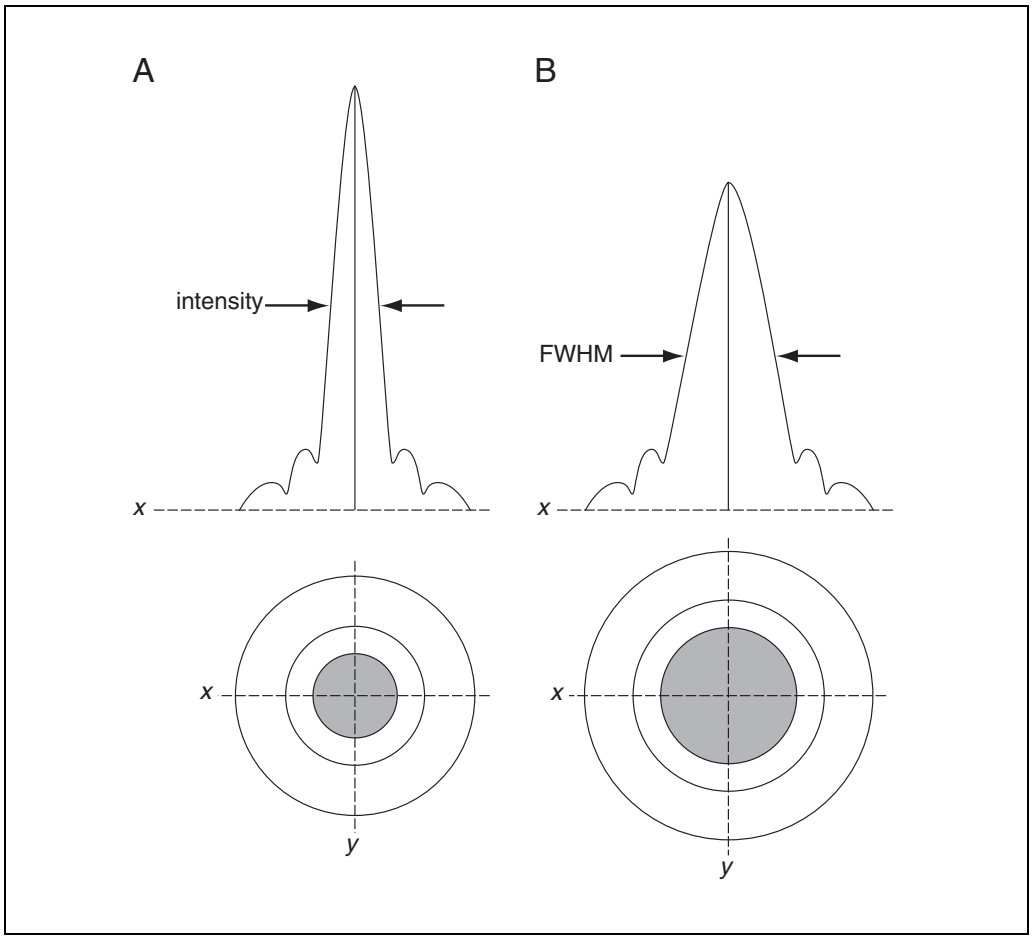

Figure 2.8.2 Intensity distribution and diffraction pattern of (**A**) laser light and (**B**) normal light. Due to a high degree of parallelism, the diameter of the diffraction-limited laser light spot is smaller than that obtained with normal light. This results in better lateral resolution with the CLSM. The full width half maximum (FWHM), i.e., the full width of the irradiance distribution at 50% irradiance, is often referred to as the optical section thickness. (Adapted from Tekola et al., 1994.)

light path may induce severe interference problems. Therefore, the coherent laser light is "scrambled" and rendered noncoherent.

In conventional optical (e.g., fluorescence) microscopy, K is set to 0.61 when the objects are two points.

$$x = 0.61\frac{\lambda}{\mathrm{NA}}$$

The intensity (irradiance) distribution in the focal point is defined by its point-spread function (PSF). In conventional fluorescence microscopy, resolution is largely determined by the PSF of the emitted (fluorescence) light. In CLSM, the laser light is focused to a confined high-intensity (diffraction-limited) light spot that illuminates a very small volume of tissue, from which light is emitted and captured by a photon-catching device. Thus, resolution depends on the PSFs of both focused laser light and emitted light.

Since laser light has a higher degree of parallelism, the diameter of the diffraction-limited laser light spot is smaller than that obtainable with nonlaser light (Fig. 2.8.2). "Scrambling" does not reduce parallelism. The restriction of illumination and detection to a very small volume gives an improvement in both lateral and axial resolution. Theoretically, in confocal microscopy the lateral resolution is 32% higher.

$$x = 0.46\frac{\lambda}{\mathrm{NA}}$$

This means that the ultimate resolution limit with the confocal microscope, using objectives with high numerical aperture (NA = 1.4), is 0.33λ.

However, this calculation is based on the assumption that an infinitely small pinhole diameter is used. In fluorescence microscopy,

light levels are often low, and the pinhole aperture has to be increased in order to obtain a strong enough signal. Thus, the theoretical improvement of lateral resolution cannot be realized, and the effective lateral resolution will approach that obtainable by conventional fluorescence microscopy. Nevertheless, illumination with a diffraction-limited light spot does contribute to a higher resolution than can be achieved with wide-field illumination. Also, due to diffraction phenomena, discussed below, lateral resolution is better with confocal microscopy, especially when viewing a focal plane deep in the tissue.

It follows that at a given (optimized) pinhole aperture size, one should always choose an objective with as high NA as possible and use short-wavelength light to achieve optimal resolution. Unfortunately, there are limitations to this strategy, as will be evident further on.

Axial (depth) resolution and optical sectioning

The axial resolution of the CLSM is determined by its optical sectioning property. The strength of the optical sectioning is the rate at which the detected intensity falls off with axial distance. It is a function of both the detector size and the object feature. Consider the situation when the object is in focus: reflected light is focused onto the pinhole and a large signal is detected. When the object is out of focus, a defocused spot is formed at the pinhole and a small signal is detected. Thus, the smaller the pinhole size, the stronger the optical sectioning (Fig. 2.8.1B).

The axial resolution can be defined as the minimum distance that the diffraction images of two points can approach each other along the z axis, yet still be seen as two. The image of a point source produced by a diffraction-limited optical system is periodic around the point of focus in the focal plane (i.e., x/y plane), and it is periodic above and below the focal plane along the z axis. The distance from the center of the three-dimensional diffraction pattern to the first axial minimum is given by:

$$z_{\min} = \frac{2\lambda\eta}{\left(\mathrm{NA}_{\mathrm{obj}}\right)^2}$$

where $z_{\min}$ is the distance in the z plane between the central maximum and the first intensity minimum, and η is the refractive index of the specimen. However, in a conventional fluorescence microscope there is no depth discrimination, and the recorded light intensity is independent of whether the object is in focus or not (i.e., one cannot see the axial minima). In confocal microscopy, due to the optical sectioning capacity, there is a dramatic drop in light intensity as the object becomes defocused (i.e., one can "see" the axial minima). The full-width-half-maximum (FWHM: the full width of the irradiance distribution at one half the maximum irradiance value; Fig. 2.8.2) of the light intensity along the z axis for reflected light confocal microscopy is given by:

$$\mathrm{FWHM} = \frac{5.6\lambda}{8\pi\eta\sin^2\left(\frac{\alpha}{2}\right)^2}$$

where α is obtained from $\mathrm{NA} = \eta\sin\alpha$ (Fig. 2.8.1C). In fluorescence confocal microscopy, the FWHM is increased by ~50%. Although this equation is not strictly correct at high numerical apertures (Wallén et al., 1992; Cogswell and Larkin, 1995), it can be seen that the axial resolution depends on the square of the NA (and thus also lateral magnification), the wavelength, and the refractive index of the specimen. Also, the size of the pinhole aperture is important, as is the optimal setting of the photon-capture device (i.e., to reduce noise).

The size of the detector pinhole aperture obviously affects the optical sectioning property. However, the strength of the sectioning is insensitive to an increase in pinhole diameter up to a certain limit, which can be estimated to the normalized pinhole radius $\upsilon_p \approx 2.5$ optical units. From the relationship between the normalized radius and real radius of the pinhole, we can calculate the actual diameter (d) of the largest pinhole with which optimal sectioning is retained.

$$\frac{M}{\mathrm{NA}} \geq \left(\frac{\pi}{2.5}\right)\frac{d}{\lambda} \quad \Leftrightarrow \quad d \leq \left(\frac{2.5}{\pi}\right)\frac{\lambda M}{\mathrm{NA}}$$

where M is the magnification of the lens system between the object and the detector. Actually, an increase in pinhole diameter will affect lateral resolution before axial resolution. To obtain true confocal lateral resolution improvement, a value of $\upsilon_p \leq 0.5$ optical units is required (Wilson, 1993).

In fluorescence confocal microscopy, axial resolution is also dependent on the β value, which in turn depends on the ratio $\lambda_{em}/\lambda_{ex} = \beta$. With increasing β value, i.e., increasing Stokes shift, the strength of the optical sectioning deteriorates. This is related to the wavelength-dependent change in the focal length of the ob-

jective lens (Fig. 2.8.1D). Without correction for this longitudinal chromatic aberration, the foci, for example, for blue and green light, will be at different depths in the specimen. As a consequence, green fluorescence emission from the focal plane defined by blue excitation light will be out of focus at the pinhole aperture (Shotton, 1995). Although objectives that are well corrected for a number of wavelengths or wavelength intervals are available, one should take great care to select the appropriate type of objective (Keller, 1995). UV-excited fluorescence, especially, requires replacement of several optical components, not only the objective (Carlsson, 1993). Also, one should attempt to operate as close to $\beta = 1$ as possible, while still being able to avoid cross-talk of fluorescent and reflected light (Wilson, 1995).

The refractive index (η) in the specimen is usually different and variable, with values between $\eta = 1.5$ for glass and immersion oil, and $\eta = 1.3$ for water. When looking into a typical biological sample, mounted in water (e.g., buffer, medium) using a high-NA oil immersion objective, the difference in refractive index creates a serious deterioration of axial resolution. When the thickness of the water layer increases from 0 to 300 μm, the optical section thickness increases by a factor of eight in fluorescence confocal microscopy (Carlsson, 1991). To obtain optimal optical sectioning it is vital that the specimen is as close to the coverslip as possible, with no intervening mounting medium (Shotton, 1995).

It is obvious that axial resolution is worse than lateral resolution. Different attempts to measure their ratio empirically, as well as theoretical calculations, have shown that axial resolution is at best 2.5 to 3 times worse than lateral resolution.

Sampling frequency

Adequate choice of sampling frequency is important not only for optimal resolution but also to ensure that no aliasing occurs. Aliasing is the introduction of false low-frequency elements by sampling at too low a frequency.

Before plunging into how optimal sampling frequency is determined, it is useful to consider some aspects of sampling theory that are important for a general understanding of how an image with optimal resolution can be generated (for more detail see Sheppard and Gu, 1992; Webb and Dorey, 1995).

First, one may consider not the size of the objects themselves, but the inverse of their size—how many objects can be seen per millimeter. By doing this, one enters the spatial frequency domain, in which the image is considered as consisting of the sum of a number of different spatial frequencies. The highest spatial frequency that can be imaged by a lens is defined by its cut-off frequency (f_c) of its optical transfer function (OTF).

$$f_c = 2\frac{\mathrm{NA}}{\lambda}$$

Resolution may be defined as the highest spatial frequency at which the image contrast is above a given value. All optical systems reduce the contrast of the low spatial frequencies (large details) less than they do higher spatial frequencies (small details), shown by the contrast transfer function (CTF) of the optical system. The CTF affects the final image, since the contrast in the image is proportional to the contrast in the object, as degraded by the CTF of the imaging system. Due to the CTF, the contrast of small features just inside the resolution limit is much lower than that of larger features.

Closely linked to the resolution of contrast is the intensity resolution of the detector. This is the capacity to resolve differences in photon flux and to transfer this into a resolvable difference in output signal. Intensity resolution can be described by the just detectable difference (jdd), which depends on Poisson statistics.

A measurement of a voltage proportional to n photons is only just detectably larger than one representing $n-\sqrt{n}$ photons, and just detectably smaller than one representing $n + \sqrt{n}$ photons. Then, jdd equals $\sqrt{n}$. It can be immediately seen from this relation that the relative magnitude of one jdd step varies with the signal intensity—i.e., the relative size of the jdd step is determined by the number of photons captured by the detector. Thus, at low photon fluxes, jdd represents a small value, but it represents a high value at high photon fluxes. This should be considered together with the relatively lower contrast of high spatial frequencies due to the CTF of the optical system.

One is usually interested in visibility, i.e., the ability of an observer to recognize two closely spaced features as being separate. Visibility depends also on the signal-to-noise ratio ($R_{S/N}$). As smaller objects have lower contrast, they require more photons to be counted in order to reduce the intrinsic noise of the background. According to the Rose criterion, to be visible, a feature that is a single pixel in size must have an intensity that differs from that of

the background by at least five times the noise level of the background.

So, what sampling frequency should be used in order not to violate the aforementioned rules concerning spatial frequencies, contrast, and visibility? According to the Nyquist criterion, the sampling frequency should be more than two times higher than the highest frequency in the data. The highest frequency in the data is determined by the size of the smallest elements in the specimen and the resolution of the optical system. The maximum frequency that can be represented using the sampling rate Δ, i.e., the Nyquist critical frequency (f_c), is as follows:

$$f_c = \frac{1}{2}\Delta$$

For nonperiodic data, the sampling rate $\Delta \geq 2.3\ f_c$. This means that, in order to preserve information that could be recorded using a given CTF, the pixels must be smaller than $1/(2.3 f_c)$. It also follows that, for a given optical system, only one pixel size (and therefore one zoom factor) matches the Nyquist criterion. For example, consider a case where the microscope resolution is 0.24 µm (e.g., at λ = 568 nm; NA = 1.4). The display is 512 × 512 pixels. The field width should be (512/2.3) × (0.24 µm) = 53.4 µm, and thus the side of each pixel 0.10 µm. For critical sampling it may be noted that the sampling distance increases with the factor √2 along the diagonal of the pixel.

It may be useful to consider the resel (R), the smallest optically resolvable entity of an object, as defined (arbitrarily) by the Rayleigh limit—the necessary separation of two self-luminous point sources such that their diffraction patterns show a detectable drop in intensity between them. "Detectable" here denotes (arbitrarily) ~20%, which means that the separation equals r_{Airy}. Thus, for conventional microscopists:

$$R = \frac{0.61\lambda}{NA}$$

In the CLSM, the confocal resel in the x/y plane is $R_{x/y} = 0.46\lambda/NA$, and in the z plane $R_z = 1.4\lambda 104\ /(NA)^2$. According to the Nyquist theorem, we need 2.3 samples for each point in a resolved pair, i.e., 2.3 pixels per resel. Therefore, we need at least a two-to-one match along a line. In a plane, we need 2 × 2 pixels per resel. When adding axial resolution we actually need 2 × 2 × 2 pixels per resel, or 8 pixels. However, we should really use 2.3 × 2.3 × 2.3 or ~12 pixels per resel in a three-dimensional volume to satisfy the Nyquist criterion. Hence, a minimum of 12 pixels is needed to resolve two separate points in space.

From the reasoning above, a few rules of thumb can be extracted:

1. For optimal lateral resolution, sample at 2.3 times the highest frequency, the side of each pixel should be 1/2.3 of the lateral resolution with the given wavelength and numerical aperture.
2. For optimal axial resolution, step size between sections can be three times the pixel width. If the specimen permits, and sampling is critical, sampling frequency can be higher to facilitate post-acquisition image processing.
3. When not working at optimal resolution of a given objective, step size axial = lateral resolution.

Signal-to-noise ratio ($R_{S/N}$) and signal-to-background ($R_{S/B}$) ratio

The term "noise" implies unwanted or nonspecific signal in the image. This signal can be derived from the specimen, the optical system, and the detector. Strictly speaking, in the CLSM, noise is any variation in the detected and digitized signal that is not associated with the specimen. The unwanted signal derived from the specimen is commonly termed background and comprises (in fluorescence CLSM) autofluorescence and specific fluorescence from other than the focal plane. In an ideal confocal microscope (i.e., with a pinhole aperture whose diameter is equal to half the width of the Airy disk), all background is rejected, and all "noise" is true noise, i.e., is derived from the optical system and/or the detector. However, in practice, a larger pinhole aperture must be used; thus, all background is not rejected. Still, with a reasonable pinhole aperture most of the background is rejected, and this is the great strength of the CLSM.

The terminology is somewhat confounded by the use of the term "background noise", which usually denotes stray light, i.e., light emanating from within the optical system. A typical example of stray light is noise emanating from autofluorescence in the cements and coatings of the optical elements of microscope systems, particularly the objective lens. Consistent with the terminology defined above, stray light, in this example, is considered noise.

The distinction between noise and background is important. Hence, signal-to-background ratio ($R_{S/B}$) is different than signal-to-noise ($R_{S/N}$). Nevertheless, both contribute to

the degradation of the image in similar ways, and both are similarly affected by some of the adjustments in the CLSM. For further discussions of $R_{S/B}$, $R_{S/N}$, and different types of noise, see Pawley (1994) and Sandison et al. (1994).

$R_{S/N}$ in the optical system

The basic limitation of the optical system is dictated by the presence of shot noise in the detected signal. Shot noise is generated by stray light and by detector noise (which will be considered below). Stray light is constant in strength throughout the image. Although it can be subtracted from the signal electronically to improve contrast, it does affect the signal-to-noise ratio ($R_{S/N}$). With a high $R_{S/N}$ (only stray light considered) the size of the pinhole has little effect on $R_{S/N}$ and may be varied within a fairly wide range. When the signal decreases in strength, the size of the pinhole becomes more critical, and for optimal performance at low $R_{S/N}$, pinhole size may only be varied within narrow limits; $R_{S/N}$ increases with both smaller and larger pinhole sizes. In practice, however, in "normal" biological specimens the $R_{S/N}$ in the optical system can be improved by decreasing the pinhole aperture size.

To minimize the impact of shot noise (regardless of its origin) on the quality of the image, it is desirable to sample at a high resolution frame (i.e., $\leq 500 \times 500$ pixels) and follow the Nyquist criterion for optimal resolution of true frequencies/objects in the sample. Moreover, sampling at a slower scan speed means that, when counting/integrating photons over a longer time per pixel, a stronger signal is achieved at each pixel and shot noise is better averaged over the image.

$R_{S/N}$ in the detector

Shot noise in the detector results from the statistical variation in the number of detected photons, which obeys a Poisson distribution. The Poisson distribution has the property that its mean is equal to its variance, and, as the noise is given by the square root of the variance, the shot noise on a signal of n_p is $\sqrt{n_p}$. Thus, the $R_{S/N}$ for this signal is:

$$n_p/\sqrt{n_p} = \sqrt{n_p}$$

The $R_{S/N}$ of the detector also depends on the quantum efficiency (Q_E) of the detector, and the sensor noise (n_n).

$$R_{S/N} = \frac{Q_E n_p}{\sqrt{\left(Q_E n_p + n_n{}^2\right)}}$$

The quantum efficiency of the detector is a measure of the proportion of photons arriving at the detector that contribute to its output signal. For any detector, the quantum efficiency is strongly dependent on the wavelength of the incoming light (Art, 1995). There are several types of sensor noise (1) subtractive noise, (2) additive noise, (3) multiplicative noise, and (4) digitization noise (Pawley, 1994).

Subtractive noise (N_1) is a measure of the photons impinging on the detector that do not contribute to the signal and thus depends on the quantum efficiency of the detector. Additive noise (N_2) includes random and periodic signals that are added to the real intensity signal. Such signals may arise either within the detector itself or be the result of stray light striking an insufficiently shielded detector. The chief source of N_2 in the photomultiplier tube (PMT) is the dark current, which is mostly caused by thermally excited photoelectrons and thus is strongly temperature-dependent; therefore, avoid heating the PMT.

Multiplicative noise (N_3) arises when some photons contribute more than others to the final recorded signal. This is because the charge amplification process in the PMT [whereby the photoelectrons (PEs) generated by captured photons generate secondary electrons (SEs) that are amplified in a number of steps] is also governed by Poisson statistics. For example, if the average number of SEs generated by a PE in the first step is 9, then one would expect that 67% of the interactions will produce between 6 and 12 SEs, whereas 33% will generate either more or fewer SEs. This process is then repeated at each amplification step. Multiplicative noise can be largely eliminated by operating the detector in the photon-counting mode. Photon-counting can be achieved with the PMT operated in pulse-counting mode. Instead of measuring the average level of output current during the time for each pixel, the individual output pulses that result from the emission of individual PEs are counted. The photon pulses are passed through a discriminator; each time the PMT output exceeds a preset threshold, one pulse is counted (Pawley, 1994, 1995b).

Digitization noise (N_4) arises because the process of digitizing the electronic signal from the detector is never perfect. The single PE-output pulses from a PMT not only vary in size, they also arrive at random time intervals. Be-

cause the analog-to-digital converter (ADC) samples the signal current in a periodic manner, it is possible for a mismatch to occur, and N_4 to be introduced.

The $R_{S/N}$ in the PMT (currently the most common detector type in commercial CLSMs) can be improved by using a sensitive low-noise PMT and by operating close to the optimal voltage of the PMT. If there is too much noise, try to reduce the PMT voltage.

The importance of choosing the correct type of photon detector cannot be overestimated. There is a wide choice of photon detectors, e.g., PMTs, cooled CCD (charge-coupled device) arrays, avalanche photodiodes, and vacuum avalanche photodiodes, which vary widely in their response properties. The quantum efficiency, responsivity, spectral response, response time, linearity, and sensor noise of the detector should be optimized for its application. In most commercial confocal laser scanning microscopes, PMTs are used as detectors, while most custom modifications include optimization of the detector(s). For a thorough description of different detector types and their usefulness in confocal microscopy, see Art (1995).

$R_{S/B}$ in the specimen

Low $R_{S/B}$ in the specimen is encountered when there is high background fluorescence, weak specific signal, or a combination of the two. There are several ways to improve $R_{S/B}$ in the image of such a specimen, but it should be remembered that the $R_{S/B}$ of this particular specimen will not be improved.

First, the pinhole size is obviously of great importance, as it rejects out-of-focus light that contributes to unwanted signal (background) in the image of the focal plane. With a small pinhole size, a confocal system behaves as a true confocal microscope, whereas with a large pinhole, the imaging capacity is identical to that of a conventional microscope. Because the signal strength in biological specimens usually precludes use of an optimal (very small) pinhole size, it is important to know what happens when one opens the pinhole aperture to get a stronger signal. Actually, increasing the size of the pinhole beyond the first minimum of the Airy disk does not increase signal strength from the focal plane appreciably. Still, increasing the size of the pinhole further does give a stronger signal, but this is because the confocal sectioning capacity is violated, and light is collected from a larger volume (i.e., a thicker optical section). This can be desirable in this case, as the optical sectioning capacity still removes a large amount of signal from the planes outside the optical section.

To improve $R_{S/B}$ further, it may be useful to first set the dark level of the detector to exclude collection of low-intensity pixels. Then, from each optical section plane, accumulate scans (add or average) at low laser intensity and optimal PMT voltage. It is also desirable in this case to scan at a high resolution frame.

In some instances, it may be desirable to operate at longer (i.e., red to far-red) wavelengths, although this compromises resolution somewhat. This may occur when one cannot circumvent the use of thick and/or highly refractive specimens, or when background fluorescence is intolerable. In such cases it may help to choose a marker molecule with longer λ_{ex} and λ_{em}, as there is generally lower background fluorescence at longer wavelengths. Moreover, long-wavelength light penetrates deeper into tissue and exhibits a lower degree of light scattering due to refraction than light of shorter wavelengths.

Optimization of $R_{S/N}$ and $R_{S/B}$

In practice, it is necessary to empirically find a good balance between pinhole size, scan speed, laser effect, and PMT voltage, for each type of specimen and labeling. After aquiring the image, the $R_{S/N}$ in the image can be further improved by image processing/filtering.

PRACTICAL GUIDELINES

Immunofluorescence

In principle, any specimen good enough for conventional immunofluorescence microscopy can be used for fluorescence CLSM. Thus, specimens can be processed and prepared in basically the same way. However, to truly benefit from the optical sectioning capacity with the highest possible resolution of the confocal microscope, attention must be given to specific steps in the protocol. The most significant difference between an immunofluorescence protocol for CLSM and one for conventional microscopy is that for CLSM it is possible to adapt the staining protocol for optimal signal; increasing background fluorescence at the same time is of little consequence, as the optical sectioning capacity eliminates most out-of-focus light.

Fixation, embedding, and sectioning

Fixation, embedding, and sectioning are performed as for conventional immunofluorescence. The choice of fixative is obviously de-

termined by its preservation of antigenicity as well as structural integrity. However, since CLSM is particularly suited for spatial analysis of fluorescent markers, it is advisable to use an aldehyde-based fixative, since alcohol-based or acetone fixation may induce shrinking and/or swelling. Commonly, the routine fixative 4% formaldehyde (freshly prepared from paraformaldehyde) in buffer is adequate, but superior tissue integrity may be achieved by the inclusion of glutaraldehyde and/or picric acid (usually 0.1% to 0.25% for both compounds).

If thick tissue sections or tissue blocks are to be processed for immunocytochemistry, it is necessary to permeabilize the tissue. Some straightforward but rather harsh methods are to subject the tissue to repeated freeze-thaw cycles, or else dehydrate it through an ascending alcohol series, rinse in xylene and then absolute alcohol, and finally rehydrate it through a descending alcohol series. As an alternative, chemical permeabilization with a detergent may be considered, e.g., Triton X-100 or saponin. Triton X-100 is an irreversible permeabilization reagent, and may be used prior to immunocytochemical processing by incubating the tissue 2 to 24 hr in 0.1% to 1.0% (v/v) Triton X-100 in incubation buffer (optimal duration and concentration have to be determined for each tissue/antibody combination). Triton X-100 may also be included in the primary antibody incubation medium (usually 0.1% to 0.25%), but it should be carefully rinsed out before incubation with fluorophore-conjugated antibodies. Saponins are less harsh to the tissue, and since saponin permeabilization is reversible, it has to be included in all incubation and rinse media. An efficient but time-consuming permeabilization method that is excellent for preservation of fine structure is to impregnate the fixed and rinsed tissue block with dimethylsulfoxide (DMSO) added dropwise to buffer, e.g., phosphate-buffered saline, to a final concentration of 25%. The tissue is then frozen in the DMSO/buffer mixture with liquid nitrogen, and permeabilized by keeping frozen at −80° for ~1 week (Brandon, 1987). We have noted that long-term storage of tissue in DMSO/buffer is possible for most antigens, but one should try it out before applying the method to critical material.

Immunofluorescence protocol

Immunofluorescence protocols basically follow a standard method (e.g., Donaldson, 1998). Even after permeabilization, tissue penetration of antibodies may be critical. Therefore it is advisable to use fluorophore-conjugated $F(ab')_2$ or Fab fragments, rather than intact IgGs.

Mounting and applying the coverslip

Critical confocal microscopy is usually performed with high-NA oil-immersion objectives. Therefore, the refractive index of the mounting medium should be as close as possible to that of the immersion medium and ideally also to that of the coverslip. For histological specimens, it is usually not necessary to use buffer or culture medium as mounting medium, and one may attempt to approach the η_{glass} of 1.5. Still, it is desirable to use a mounting medium that does not distort the tissue (e.g., by dehydration or osmotic forces). Ideally, it should also stabilize the tissue against the forces generated in the mounting medium by the placement of the coverslip and pressure changes when focusing an oil-immersion objective. The least distortion of tissue, and reasonable stabilization, is obtained with a 1:1 mixture of glycerol and PBS (Baccalao et al., 1995).

The cyanine fluorochromes (i.e., Cy2, Cy3, and Cy5) are compatible with organic solvents, and thus with mounting in nonaqueous medium, whereas the other fluorochromes require mounting in aqueous medium. It is also important to consider the necessity of including antifading compounds in the mounting medium. Antifade compounds retard photobleaching, usually by antioxidative actions. There are several commercially available mounting media, which contain antifading compounds that are more or less optimized for specific fluorochromes. An alternative is to make one's own mounting medium, including stabilizing and antifade agents. Unfortunately, most antifading agents reduce fluorescence intensity; therefore, one should initially try a mounting medium composed of a glycerol/PBS mixture without additives. If fluorescence is bright enough, and scanning can be performed without lengthy searches for suitable structures under wide-field illumination, this may prove adequate, as it has done so for the author for over 4 years. If fading is a problem, one may then first try an anti-fading agent that primarily increases fluorescence half-life, without affecting intensity too much, like DABCO (1,4-diazo-bicyclo-2,2,2)octane, 25 mg/ml in glycerol/PBS; or Citifluor (Agar, Essex, UK; ready-to-use mounting medium). If these are still not adequate, one may use an agent proven to dramatically increase fluorescence half-life, e.g., Vec-

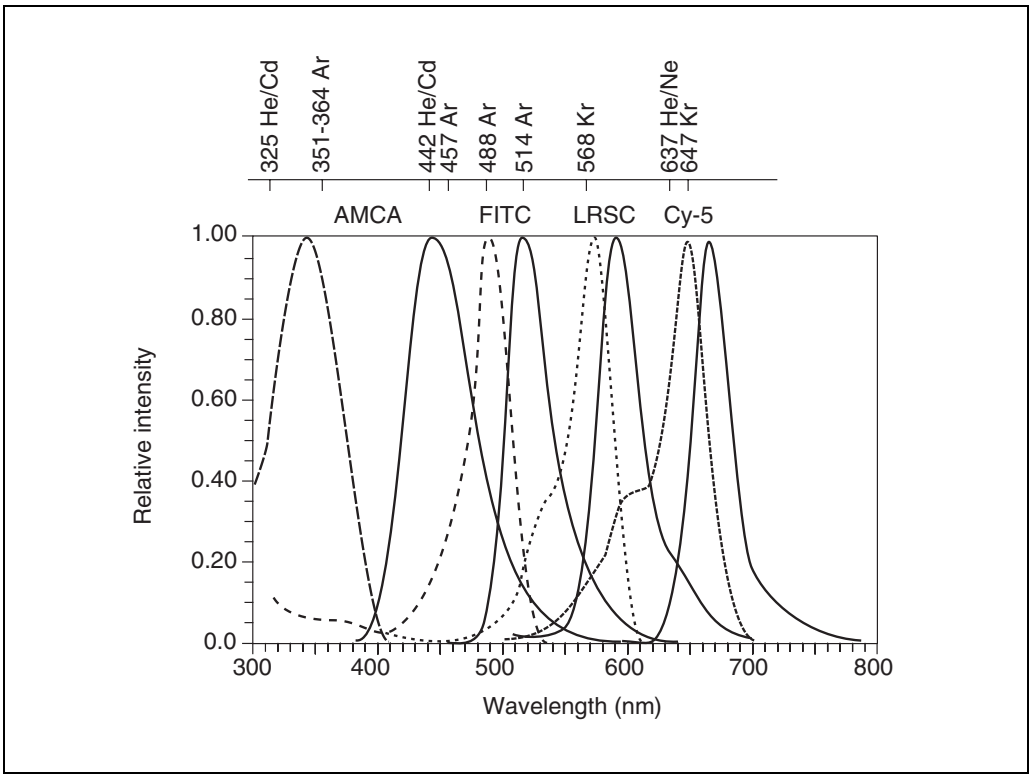

Figure 2.8.3 The excitation (dashed lines) and emission (solid lines) spectra of three fluorophores, FITC, LRSC, and Cy-5, that are excellently suited to the emission lines of the mixed gas Ar/Kr ion laser (arrows). Also, the spectra of a UV-excited fluorophore, AMCA, is included. Above, the emission lines of some commonly used laser types are shown. (Adapted from Wessendorf and Brelje, 1993 and Tsien and Waggoner, 1995.)

tashield (Vector; ready-to-use mounting medium). Other agents are in wide use, like *p*-phenylenediamine and *n*-propyl gallate, and one may refer to the more thorough discussions of different anti-fading agents by Baccalao et al. (1995) and Florijn et al. (1995).

Most microscope objective lenses are corrected for the spherical aberration generated by coverslips of a thickness of 0.17 mm. For optimal resolution, it is important to use this type of coverslip, especially for thick specimens mounted in aqueous medium. When forced to work with tissue in an aqueous medium, synthetic "Cytop" coverslips ($\eta = 1.34$) and water immersion objectives may be useful (Keller, 1995). The coverslips should be sealed around the edges, e.g., with nailpolish, to prevent dislocation and leakage of the mounting medium.

Choice of Fluorophores

Fluorescence occurs when a fluorescent molecule (i.e., fluorophore or fluorochrome) absorbs a photon of light of a particular wavelength, i.e., the excitation wavelength (λ_{ex}). The energy of this photon causes the fluorophore to enter a transient excited state; the subsequent decay from the excited state to the ground state has a characteristic delay and is accompanied by the emission of photons of a characteristic wavelength (energy; λ_{em}). The spectrum of emitted light has a longer wavelength (lower energy) range than the excitation light: $\lambda_{em} > \lambda_{ex}$. The difference $\lambda_{em} - \lambda_{ex}$ is called the Stokes shift. The Stokes shift makes it possible to separate the excitation and emission light. When choosing fluorophores for the CLSM, one has to consider the excitation wavelength, Stokes shift, quantum yield, and molar extinction coefficient of the fluorophores (Wells and Johnson, 1994).

The excitation wavelength should obviously correspond with the wavelengths available from the laser (Fig. 2.8.3). Currently, the most common lasers in CLSM are the mixed-gas argon/krypton (Ar/Kr) laser (λ: 488, 568, 647 nm), the argon ion laser (λ: 488, 514 nm; note that lines between 454 and 528 nm are also available), the argon ion UV laser (λ: usually between 334 and 364 nm; by frequency doubling down to 229 nm), and the helium/neon laser (λ: 534, 594, 612, 632 nm, infrared). As laser technology develops, more types of lasers with other useful characteristics will be available. Different types of laser light sources have

recently been discussed by Gratton and vande Ven (1995).

The Stokes shift should be sufficiently large to allow easy separation of excitation and emission light, but not so large that it may induce errors due to chromatic aberration and differential resolution properties. A small Stokes shift reduces differences in diffraction by light between the λ_{em} and λ_{ex}, but may increase noise by reflected light.

The quantum yield (Q_f) denotes the ratio of photons absorbed to photons emitted as fluorescence and is a measure of the integrated photon emission over the entire spectral band. It is generally not a function of wavelength, and the excitation spectrum of a fluorophore will thus approximate its absorbance spectrum.

The molar extinction coefficient (ε) is a measure of absorption. The product of ε and Q_f is proportional to fluorescence intensity at subsaturating excitation rates and is a practical measure of fluorescence intensity of a given compound.

Photobleaching of the fluorophore may be a serious problem in CLSM, especially when an area in the specimen is scanned repeatedly during the acquisition of a large stack of confocal sections, or in quantitative fluorescence measurements. It is a poorly understood phenomenon, but it often depends on the presence of molecular oxygen. Thus, removal of O_2 from the mounting medium and/or inclusion of protective agents like singlet oxygen quenchers may alleviate the problem (Tsien and Waggoner, 1995).

CLSM with one fluorophore—single labeling

When the CLSM should be used to study specimens labeled with one fluorophore, the choice of fluorophore is rather straightforward. Obviously, one should try to find a fluorophore with strong fluorescence (i.e., high $Q_f \times \varepsilon$ value), slow photobleaching, a reasonable Stokes shift, and optimal excitation maximum with respect to laser excitation wavelength and tissue autofluorescence (Table 2.8.1).

CLSM with multiple fluorophores—multiple labeling

Fluorophore selection should be such that each has the characteristics defined above for single labeling. Ensure that the excitation curves of the fluorophores are sufficiently well separated to be individually excited by their respective excitation wavelengths. For a CLSM with a mixed Ar/Kr ion laser, this means fluorophores with excitation maxima at or near 488, 568, and 647 nm. Then, ensure that that the emission curves are also sufficiently well separated to be distinguished by the use of proper filters. When these criteria have been fulfilled, the risk of channel crosstalk due to the choice of improper fluorophore combination is greatly reduced. Channel crosstalk occurs when one laser wavelength excites both fluorophores, or is reflected in the other channel, or when the detector and barrier filters do not distinguish the two emission wavelengths (i.e., signal "leakage").

In the author's experience, the optimal combinations of fluorophores currently used in the CLSM in immunofluorescence and fluorescence in situ hybridization (Table 2.8.1) are, when used with the Ar/Kr laser, fluorescein isothiocyanate (FITC) and lissamine rhodamine sulfonyl chloride (LRSC) for double labeling and FITC, LRSC, and Cy-5 for triple labeling (see Fig. 2.8.4A to C). However, the recently introduced Akexa Fluor 488 and 568 will probably prove powerful alternatives to FITC and LRSC, respectively. In all cases, regardless whether one or many fluorophores are to be visualized, consider the following.

First, mount specimens without antioxidants, as each compound affects the various fluorophores in different ways (Florijn et al., 1995). If photobleaching is a problem, choose an appropriate antifading compound (e.g., propyl gallate, *p*-phenylenediamine, DABCO), if possible. This should reduce photobleaching in many (but not all) cases. Because of the differential influence mentioned above, mixing may be a good idea, or commercially available anti-fade-mixtures may be purchased.

It may be advantageous to further explore the use of carbocyanine fluorophores, e.g., Cy2, Cy3, and Cy5. These are compatible with η = 1.5 mounting media, which give superior resolution and reduce the amount of available oxygen. However, dehydration may compromise structural integrity.

It is generally considered preferable to use a fluorophore with a longer excitation maximum than the laser emission line, rather than the other way around if a perfect match cannot be attained. Excitation spectra tend to quickly fall off at wavelengths longer than that of maximum excitability, whereas they tend to have a long "tail" toward shorter wavelengths (see Fig. 2.8.3; Wessendorf and Brelje, 1993).

Finally, use higher antibody concentrations than for conventional fluorescence microscopy. Background may largely be removed by confocal sectioning, and all light is needed.

Table 2.8.1 Fluorophores for CLSM[a]

Compound	λ_{ex} (nm)	λ_{em} (nm)	Laser line (nm) and type	Suitable combinations in multiple labelling
Alexa Fluor 350[b]	350	442	351, Ar UV[c]	All other listed
Alexa Fluor 488	491	515	488, Ar or Ar/Kr	Alexa Fluor 350[b], Alexa Fluor 568, Cy-5
Alexa Fluor 568	573	596	568, Kr or Ar/Kr	Alexa Fluor 350[b], Alexa Fluor 488, Cy-5
Cy-2, indodimethinecyanine	492	510	488, Ar or Ar/Kr	Cy-3, Cy-5
Cy-3, indotrimethinecyanine	554	566	568, Kr or Ar/Kr	Cy-2, Cy-5
Cy-5, indopentamethinecyanine	650	670	647, Kr or Ar/Kr; 637, He/Ne	All other listed
FITC, fluorescein isothiocyanate	492	520	488, Ar or Ar/Kr	Alexa Fluor 350[b], Alexa Fluor 568, LRSC, Texas Red, Cy-5
LRSC, lissamine rhodamine sulfonyl chloride	570	590	568, Kr or Ar/Kr	Alexa Fluor 350[b], Alexa Fluor 488, FITC, Oregon Green, Cy-5
Oregon Green 488	490	520	488, Ar or Ar/Kr	Alexa Fluor 350[b], Alexa Fluor 568, LRSC, Texas Red, Cy-5
TRITC, tetramethyl rhodamine isothiocyanate	550	570	568, Kr or Ar/Kr	Alexa Fluor 350[b], Cy-5
Texas Red	590	610-620	568, Kr or Ar/Kr	Alexa Fluor 350[b], Alexa Fluor 488, FITC, Oregon Green, Cy-2

[a]Approximate peak wavelengths for excitation and emission for a number of fluorophores often used to conjugated with antibodies in confocal laser scanning immunofluorescence. Note that the values are approximate, as they depend on type of conjugate, conjugation efficiency, pH, and type of spectrofluorometer used for determination.

[b]Alexa Fluor 350 is given as one example only of UV-excited fluorophores, since UV lasers are not commonly used in CLSM setups for analysis of multiple labeling. Fluorophores with similar properties include AMCA (aminomethylcoumarin acetate), Cascade Blue, and DAMC (diethylaminoisothiocyanatophenylmethylcoumarin).

[c]UV excitation requires special optics, that may not be optimal for longer wavelengths.

Choice of Objectives

For confocal fluorescence microscopy of histological sections, any objective that is well corrected for spherical and chromatic aberration at the relevant wavelengths will suffice, in principle. Usually, oil-immersion objectives are used because of their higher numerical aperture, but there are now several brands of high-quality objectives equipped with correction collars for different immersion media, different concentrations of solute (for water-immersion objectives), or different coverslip thickness. It is important to note, that, for UV microscopy, it is necessary to use fluorite, or glass with fluorite characteristics, for optimal performance (for in-depth discussion of different types of objective lenses, see Keller, 1995). The choice of objective is ultimately dictated by the wavelengths used, the preferred immersion medium, and the necessary working distance of the objective.

Scanning

Optimization of $R_{S/N}$ in multiple fluorescence: Single scan or sequential scan?

The factors affecting $R_{S/N}$ have been considered in an earlier section. There are, however, practical aspects concerning the actual sampling of data, i.e., the scanning procedure. It is often claimed that, when analyzing double-labeled specimens, one should strive to scan with two wavelengths and detect two fluorophores simultaneously (single scan). The single scan method, when two excitation wavelengths are used simultaneously, works well if fluorescence intensity and $R_{S/N}$ are similar for both fluorophores. This method gives the most reliable optical sectioning. The drawback of this method is that with one laser effect and two PMTs, more noise in one channel, or channel cross-talk, is likely to occur.

There is no general rule regarding the preference for single or sequential scanning. However, in the author's experience it is seldom possible to achieve optimal $R_{S/N}$ for both fluorophores with the single-scan strategy. Instead, sequential scanning with one wavelength at a time allows finer tuning of laser energy and photon detector for each fluorophore. Thus noise and channel cross-talk are reduced, and $R_{S/N}$ is appreciably better for both fluorophores. The sequential scan method is, however, much more sensitive to movement, especially stepper

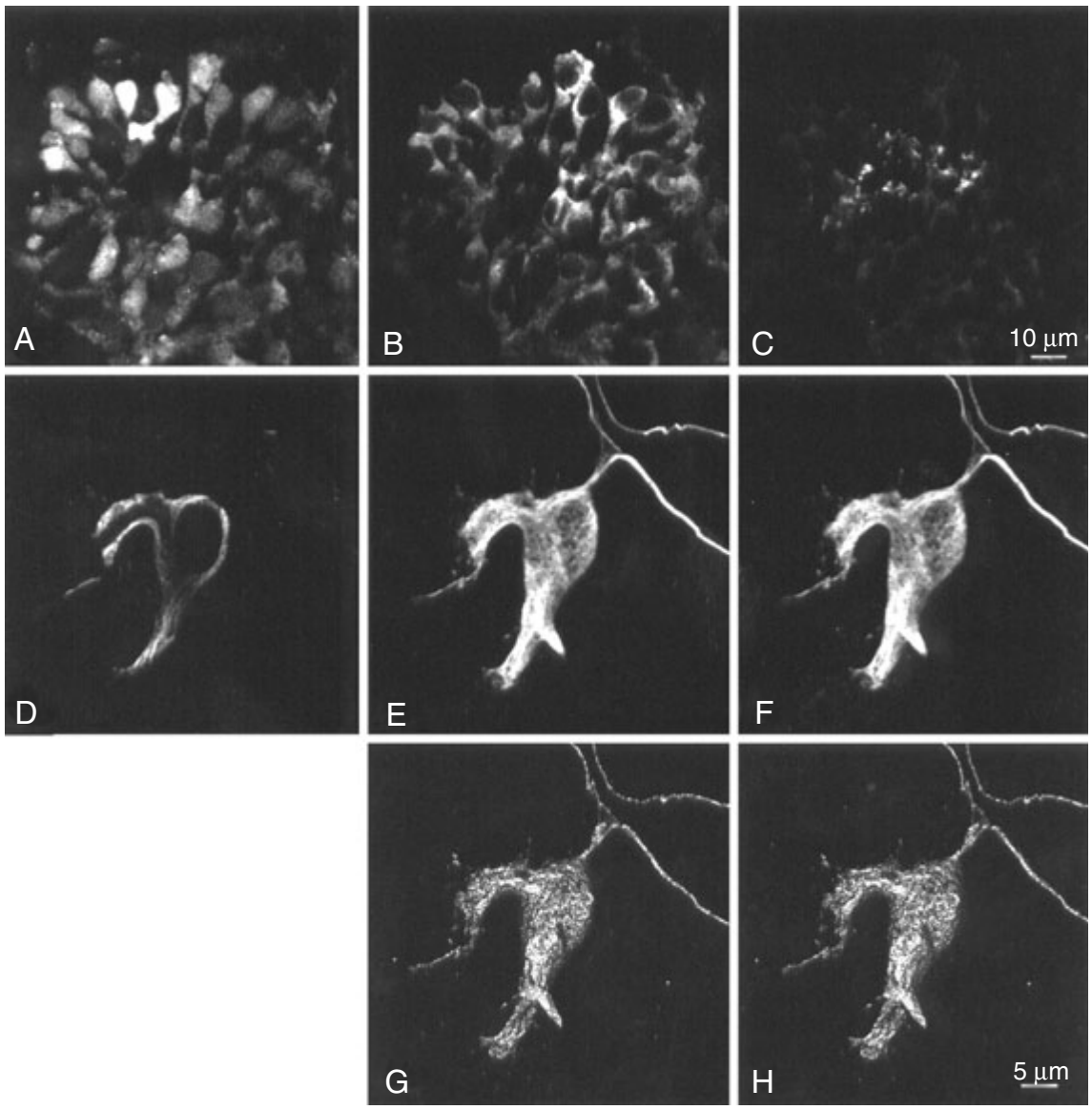

Figure 2.8.4 (**A-C**) Autofocus projections of a three-dimensional Gaussian filtered stack comprising 50 confocal sections, showing photoreceptor cells immunoreactive for serotonin (**A**, LRSC fluorescence), the phototransduction protein arrestin (**B**, FITC fluorescence), and the photopigment apoprotein opsin (**C**, Cy5 fluorescence), in the pineal organ of the salmon. The scanning was performed with a MultiProbe 2001 CLSM, using the excitation wavelengths 488 nm (B), 568 nm (A) and 647 nm of the Ar/Kr laser. (**D**) Confocal section, after three-dimensional Gaussian filtering, of a neuron that exhibits immunoreactivity for acetylated α-tubulin (mouse monoclonal clone 6-11B-1), in the salmon pineal organ. (**E-H**) Stereo pairs of (E, F) an autofocus projection, and (G, H) a surface rendering projection of 100 confocal sections of the same neuron as in (D). Scale bars represent 10 µm in A-C, and 5 µm in D-H.

drift (although modern focus-steppers are actually very reliable).

In either case, it is important to scan with a carefully adjusted laser photon flux. The photon flux should be primarily regulated by the use of NG (neutral gray) filters; usually the laser has an optimum effect range, below which irregularities in the photon flux may occur and disturb the sampling. The photon flux should be adjusted so that, at the given pinhole size and detector setting, an increase in laser power does not further increase the signal or $R_{S/N}$. This adjustment greatly reduces the risk of excitation of other fluorophores at the head or tail of their excitation curves. In some cases, it may be useful to perform repetitive scans for frame averaging or addition. It should, however, be emphasized that channel cross-talk is actually seldom a problem when using the fluorophore combinations mentioned above.

Channel cross-talk: What to do?

If channel cross-talk does occur in spite of the precautions outlined above, one must of course try to eliminate it. One way is to try to adjust laser illumination, pinhole size, and detector gain so that cross-talk is abolished (i.e., in practice, to perform the scanning at suboptimal settings). But, in the author's opinion, it is not a good idea to scan at suboptimal settings; this means losing a great part of the relevant information in the specimen. If the experiment cannot be performed again, and the data have to be collected/saved, one should try to measure the degree of cross-talk already present during the scanning procedure. This is easily done. If one has, for example, a specimen labeled with FITC and LRSC, then first select an area with only FITC label and scan it with the optimal settings for LRSC used in the "real" experiment. Then, conversely, select an area with only LRSC label and scan it with the optimal FITC settings. In this way, datasets are acquired in which one can assess the cross-talk signal levels in the two channels. This level is subtracted from each of the digital images after scanning. With luck, enough relevant information is left, but usually, it is not.

Another case of channel cross-talk, which is not related to the instrumentation and sampling, is when the fluorescent marker substances do not specifically label what they are supposed to. This possibility should also be considered, although it is outside the scope of this text to deal with labeling specificity controls. It is always necessary to determine the specificity of the labeling by the use of appropriate control specimens (Donaldson, 1998).

Image Processing and Presentation

The acquisition of images of optical sections in confocal laser scanning microscopy depends on electronic processing—digitization—of the photon flux from each point in the specimen, and the digitized signal is converted to an image by computer software. Since computer processing is an integral part of confocal laser scanning microscopy, it is necessary to briefly consider some basic principles of image processing. For a brilliant and thorough treatise on image processing, the reader is referred to *The Image Processing Handbook* (3rd ed.; Russ, 1998). Also, a recent compilation and evaluation of available image processing software is available (White, 1995).

First, it is necessary to define the goal of the experiment. Is it to visualize objects or to obtain numerical measurements of objects? Is it to achieve high-resolution images of specific elements labeled with one or more markers? Is it to perform a three-dimensional reconstruction of one or more specific elements? Is it to analyze structural relationships between objects, i.e., cell-to-cell contacts or other contacts, or "colocalization" of substances, or presence of objects within specific boundaries (e.g., *E. coli* bacteria inside epithelial cells)?

Before further analysis, data usually have to be filtered. The choice of filtering procedure depends on the goal(s) outlined above. Filters are used to reduce noice, smooth the signal, and enhance features (especially edges). By filtering, pixel intensity is adjusted by comparison with neighboring pixels' intensities within a block of pixels (a kernel). A kernel may be a two-dimensional or a three-dimensional kernel and may be of different sizes and configurations (i.e., square/cubic, rectangular, hexagonal, octogonal, "round"). Application of a two-dimensional kernel means that pixels are compared only in the plane—i.e., one confocal section—whereas with a three-dimensional kernel, pixels are compared within the confocal section and between adjacent sections. Pixel comparison is done by averaging, ranking, or a combination of averaging and ranking (so-called hybrid filters). Adequate noise suppression requires that the pixels in the image must be much smaller than the smallest important detail (remember the Nyquist criterion). Smoothing implies replacement of individual pixels that deviate strongly. Edge-definition filters are based

on comparisons of rates of change in pixel intensity.

Kernel averaging smooths the image but reduces contrast, blurs edges, and displaces boundaries. The most commonly used filters for kernel averaging are Mean filters and Gaussian filters. With a Mean filter, the central pixel of the kernel acquires the mean value of the kernel. With a Gaussian filter, the pixels are weighted according to a Gaussian distribution and the mean of the weighted pixel values is assigned to the central pixel. By changing the standard deviation of the Gaussian distribution, one can alter the weighting of pixels in the kernel. Thus, contrast reduction and blurring is much reduced compared to the Mean filter, and the Gaussian filter is the most versatile and popular averaging filter.

As previously mentioned, it is possible to use kernels of different sizes. A large kernel smooths the signal more, and is not always detrimental to preservation of fine detail, although the edges are more blurred. Also, repeated use of a small kernel is equivalent to one use of a larger kernel. Considering the blurring and displacement of edges, kernel averaging is not optimal as a preamble to quantitative analysis.

With neighborhood ranking filters, the image is less smoothed but edges are not displaced. There are several types of neighborhood ranking filters, especially for edge detection. For an overview of edge detection filters, refer to Russ (1998). The common Median filter, by which the central pixel acquires the median value of the kernel, is excellent for removal of "shot noise," i.e., isolated spikes of extreme values, as it suppresses spikes smaller than kernel width. Moreover, because the Median filter does not average or weigh pixels, and neither reduces brightness differences nor shifts boundaries, it gives minimal degradation of edges and permits repeated application without increased blurring. A Mode filter, or a Truncated Median filter, is a useful filter for assymetric distributions of pixel intensities. With the Mode filter, the central pixel acquires the value of the mode (i.e., the highest point of the distribution curve), and pixel intensities farthest from the mode are removed.

Confocal images are usually obtained as stacks of images representing consecutive confocal sections. They may be presented as single selected confocal sections, or as a mosaic layout of the sections in the series. Often, one wishes to present an overview of the scanned area by projecting all (or selected) sections onto one plane, as if one were viewing all section planes simultaneously in focus. With a so-called extended-focus projection, the intensity values of all pixels in each x,y coordinate are added along the z-axis. With a so-called autofocus projection, the maximum intensity value along each z-line is extracted from the data. The autofocus projection method produces the sharpest images, especially when performed on unfiltered images; a Median or Gaussian filter may then be applied to the resulting projected image to remove shot noise and/or smooth the image. Extended-focus projections are usually best performed on stacks that have already been filtered.

With most computer software designed for confocal microscopy, it is possible to create "sections" through the sampled volume in virtually any direction. It is also possible to view projections of the sampled volume, or parts thereof, from any direction, and thus create a series of images that simulate rotation of the volume. Moreover, it is possible to create surface simulations of the labeled elements, as well as stereo pairs. It is beyond the scope of this unit to deal with this issue in detail; Figures 2.8.4, 2.8.5, and 2.8.6 give a sample of presentation options.

The Choice: Wide-Field Microscopy or Confocal Microscopy

In some instances it is not desirable to use confocal microscopy. There are drawbacks to using confocal microscopy in comparison to wide-field (WF) microscopy, regardless of whether the image is captured on film (photomicrography) or with a cooled CCD (charge-coupled device) array camera. The most dramatic drawbacks are that the time required to achieve an image in confocal microscopy is much longer and that the sampling area per image is much smaller when sampling with reasonable confocality and optimal sampling frequency. Thus, WF microscopy is preferable when spatial information is of less value and it is possible to work with thin tissue sections (<3 μm), when large numbers of images are to be collected for analysis, and/or when large areas have to be sampled.

It is also possible to use WF microscopy for three-dimensional analysis. This requires mathematical reduction of image degradation by light from planes other than the focal plane. This process—deconvolution—may yield images comparable with those obtained by CLSM, but it may be extremely time-consuming unless appropriate computer instrumenta-

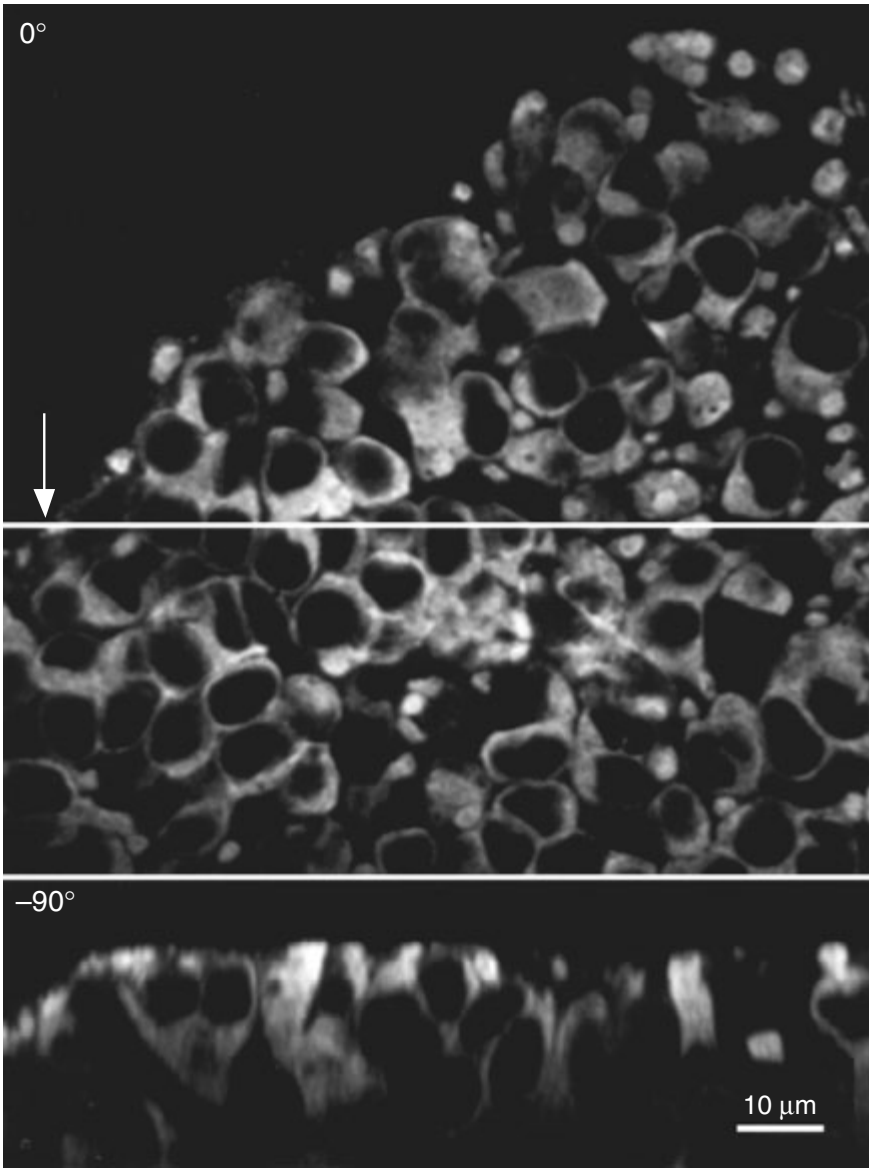

Figure 2.8.5 Confocal section (0°) of a whole-mounted salmon pineal organ, showing photosensory cells exhibiting immunoreactivity for the phototransduction protein arrestin (mouse monoclonal clone 5C6-47; courtesy of Dr. L. Donoso). The section was chosen out of a stack of 80 confocal sections. The line indicated by the arrow shows the plane of section through the stack shown below (–90°); the thickness of this digital section corresponds to a 0.5-μm-thick physical section. Note that the resolution and fluorescence intensity decreases dramatically with depth. The scanning was performed with a MultiProbe 2001 CLSM, using the excitation wavelength 488 nm (FITC fluorescence).

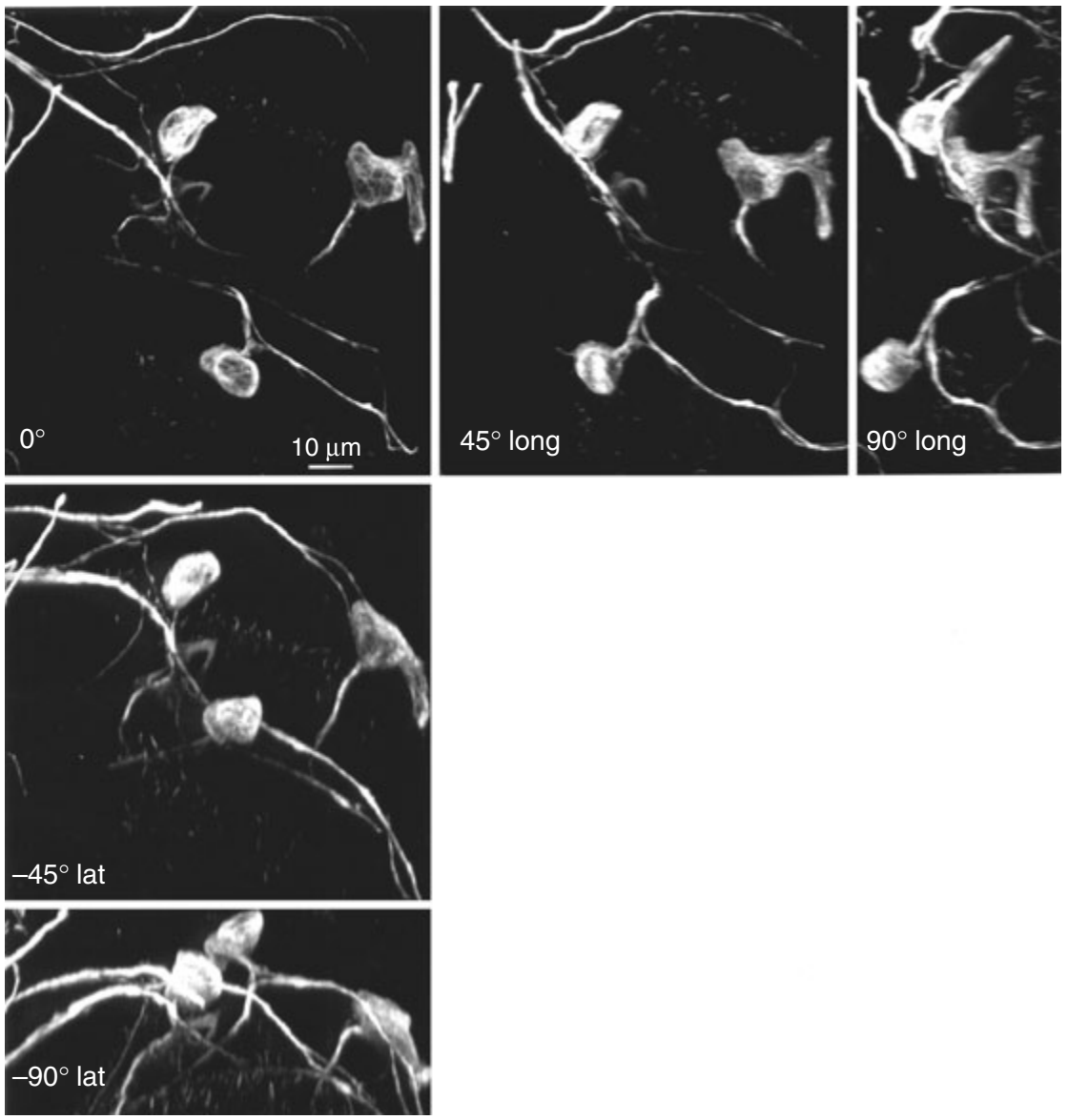

Figure 2.8.6 Autofocus projections of 125 confocal sections of a region in the salmon pineal organ that contains three neurons that exhibit immunoreactivity for acetylated α tubulin (mouse monoclonal clone 6-11B-1). Tilting the volume around the *x* axis (–45° or –90° lat.), and around the *y* axis (–45° or –90° long.) allows inspection of the volume from different angles. Presentation of such views as stereo pairs (not shown here) are of great help in determining spatial relationships between cells. When viewing the volume from a 90° angle, it is apparent that thin structures, like axons, appear broader than at 0°. This is because axial resolution is worse than lateral resolution. The scanning was performed with a MultiProbe 2001 CLSM, using the excitation wavelength 488 nm (FITC fluorescence).

tion is used (Shaw and Rawlins, 1991; Shaw, 1995).

Future Directions

There are some fairly recent developments that are of special interest in the field of confocal microscopy. One relies on the use of two-photon excitation with a tunable pulsed high-energy titanium (Ti)/sapphire laser. In two-photon excitation, two photons of longer wavelengths (λ_1 and λ_2) are simultaneously absorbed, and their combined energies excite a fluorophore that would otherwise require a single photon with a shorter wavelength $(1/\lambda_1 + 1/\lambda_2)^{-1}$. This simultaneous absorption can only take place in the plane of focus. Thus, this technique gives excellent optical sectioning even without a detector pinhole, and out-of-focus bleaching is dramatically less than in CLSM. Moreover, it is possible to use UV-excited fluorophores without special UV-laser and UV-optics (Denk et al., 1995).

Another development relies on intensity modulation of two laser beams of different wavelengths. The laser beams, which illuminate the specimen simultaneously and excite one fluorophore each, are intensity-modulated at different frequencies. The fluorescent light is divided into two wavelength regions, which are detected by two PMTs whose output signals are connected to lock-in amplifiers. Being frequency-selective, the lock-in amplifiers can distinguish the contributions to the total fluorescence signal from the two laser beams. This technique strongly reduces cross-talk between the channels (Carlsson et al., 1994).

While the intensity modulation technique relies on distinguishing the emission spectra, there is another technique that relies on the distinguishing of fluorophores by their fluorescence lifetimes. The latter technique may be used to distinguish fluorophores with overlapping emission spectra, under certain given circumstances, and may be used in parallel with "normal" confocal imaging on the same instrument (Brismar and Ulfhake, 1997).

During the quest for further improvement of the axial resolution, confocal microscopes in the 4Pi and Theta configurations have been developed. Such microscopes can also be operated in the two-photon mode (Lindek et al., 1995). Due to their complex configurations, it is not likely that they will be widely used in the analysis of histological specimens.

Typical Results

Fluorescent structures should stand out crisply against a virtually black background in a single optical section. In relatively thin (physical) sections, and with bright fluorescence, it may be possible to achieve *x*/*y* images that are of superior resolution to that possible with conventional fluorescence microscopy. This is very useful for fine-grained analysis of intracellular compartmentalization and possible colocalization of various antigens. However, the great improvement over conventional fluorescence microscopy is achieved when the fluorescence is sufficiently bright and resistant to photobleaching to allow the acquisition of large numbers of confocal sections for subsequent reconstruction of three-dimensional images. The tissue volume that may be investigated, i.e., the area and maximal depth from which images may be obtained, is determined by the characteristics of the objective lens (magnification, NA, and working distance) as well as by the match in refractive indices of the immersion and mounting media, the wavelength of light, and the scattering and refraction of light by the specimen. In optimal specimens, this would mean that it is possible to image structures at depths near the limit of the working distance; in practice, however, image quality (especially depth resolution) deteriorates with depth, the rate of deterioration being dependent on the factors above.

ACKNOWLEDGEMENTS

Supported by the Swedish Natural Science Research Council. Special thanks to Dr. Dan-Eric Nilsson for helpful discussions concerning optics.

LITERATURE CITED

Art, J. 1995. Photon detectors for confocal microscopy. *In* Handbook of Biological Confocal Microscopy, 2nd ed. (J.B. Pawley, ed.) pp. 183-196. Plenum Press, New York.

Baccalao, R., Kiai, K., and Jesaitis, L. 1995. Guiding principles of specimen preservation for confocal fluorescence microscopy. *In* Handbook of Biological Confocal Microscopy, 2nd ed. (J.B. Pawley, ed.) pp. 311-325. Plenum Press, New York.

Brandon, C. 1987. Cholinergic neurons in the rabbit retina: Dendritic branching and ultrastructural connectivity. *Brain Res.* 426:119-130.

Brismar, H. and Ulfhake, B. 1997. Fluorescence lifetime measurements in confocal microscopy of neurons labeled with multiple fluorophores. *Nature Biotechnol.* 15:373-377.

Carlsson, K. 1991. The influence of specimen refractive index, detector signal integration, and non-uniform scan speed on the imaging properties in confocal microscopy. *J. Microsc.* 163:167-178.

Carlsson, K. 1993. Utraviolet-excited fluorescence in confocal imaging. *Neuroprotocols* 2:141-149.

Carlsson, K., Åslund, N., Mossberg, K., and Philip, J. 1994. Simultaneous confocal recording of multiple fluorescent labels with improved channel separation. *J. Microsc.* 176:287-299.

Cogswell, C.J., and Larkin, K.G. 1995. The specimen illumination path and its effect on image quality. *In* Handbook of Biological Confocal Microscopy, 2nd ed. (J.B. Pawley, ed.) pp. 127-137. Plenum Press, New York.

Denk, W., Piston, D.W., and Webb, W.W. 1995. Two-photon molecular excitation in laser-scanning microscopy. *In* Handbook of Biological Confocal Microscopy, 2nd ed. (J.B. Pawley, ed.) pp. 445-458. Plenum Press, New York.

Donaldson, J. 1998. Immunofluorescent staining. *In* Current Protocols in Cell Biology (J.S. Bonifacino, M. Dasso, J.B. Harford, J. Lippincott-Schwartz, and K.M. Yamada, eds.) pp. 4.31-4.36. John Wiley & Sons, New York.

Florijn, R.J., Slats, J., Tanke, H.J., and Raap, A.K. 1995. Analysis of antifading reagents for fluorescence microscopy. *Cytometry* 19:177-182.

Gratton, E. and vande Ven, M.J. 1995. Laser sources for confocal microscopy. *In* Handbook of Biological Confocal Microscopy, 2nd ed. (J.B. Pawley, ed.) pp. 69-97. Plenum Press, New York.

Keller, H.E. 1995. Objective lenses for confocal microscopy. *In* Handbook of Biological Confocal Microscopy, 2nd ed. (J.B. Pawley, ed.) pp. 111-126. Plenum Press, New York.

Lindek, S., Stelzer, E.H.K., and Hell, S.W. 1995. Two new high-resolution confocal fluorescence microscopies (4Pi, Theta) with one- and two-photon excitation. *In* Handbook of Biological Confocal Microscopy, 2nd ed. (J.B. Pawley, ed.), pp. 417-430. Plenum Press, New York.

Pawley, J.B. 1994. Sources of noise in three-dimensional microscopical data sets. *In* Three-Dimensional Confocal Microscopy: Volume Investigation of Biological Specimens (J.K. Stevens, L.R. Mills, and J.E. Trogadis, eds.) pp. 47-94. Academic Press, San Diego.

Pawley, J.B. (ed.) 1995a. Handbook of Biological Confocal Microscopy, 2nd ed. Plenum Press, New York.

Pawley, J.B. 1995b. Fundamental limits in confocal microscopy. *In* Handbook of Biological Confocal Microscopy, 2nd ed. (J.B. Pawley, ed.) pp. 19-37. Plenum Press, New York.

Russ, J.C. 1998. The Image Processing Handbook, 3rd ed. CRC Press, Boca Raton. Fla.

Sandison, D.R., Piston, D.W. and Webb, W.W. 1994. Background rejection and optimization of signal to noise in confocal microscopy. *In* Three-Dimensional Confocal Microscopy: Volume Investigation of Biological Specimens (J.K. Stevens, L.R. Mills. and J.E. Trogadis, eds.), pp. 29-46, Academic Press, San Diego.

Shaw, P.J. 1995. Comparison of wide-field/deconvolution and confocal microscopy for imaging. *In* Handbook of Biological Confocal Microscopy, 2nd ed. (J.B. Pawley, ed.) pp. 373-387, Plenum Press, New York.

Shaw, P.J., and Rawlins, D.J. 1991. Three-dimensional fluorescence microscopy. *Prog. Biophys. Molec. Biol.*56:187-213.

Sheppard, C.J.R. and Gu, M. 1992. 3-D transfer functions in confocal scanning microscopy. *In* Visualization in Biomedical Microscopies. 3-D Imaging and Computer Applications (A. Kriete, ed.) pp. 251-282. VCH Publishers, Weinheim, Germany.

Shotton, D.M. 1995. Electronic light microscopy: Present capabilities and future prospects. *Histochem. Cell Biol.* 104:97-137.

Tekola, P., Zhu, Q., and Baak, J.P.A. 1994. Confocal laser microscopy and image processing for three-dimensional microscopy. Technical principles and an application to breast cancer. *Prog. Pathol.* 25:12-21.

Tsien, R.Y., and Waggoner, A. 1995. Fluorophores for confocal microscopy. Photophysics and photochemistry. *In* Handbook of Biological Confocal Microscopy, 2nd ed. (J.B. Pawley, ed.) pp. 267-279. Plenum Press, New York.

Wallén, P., Carlsson, K., and Mossberg, K. 1992. Confocal laser scanning microscopy as a tool for studying the 3D-morphology of nerve cells. *In* Visualization in Biomedical Microscopies. 3-D Imaging and Computer Applications (A. Kriete, ed.) pp. 109-143. VCH Publishers, Weinheim, Germany

Webb, R.H. and Dorey, C.K. 1995. The pixilated image. *In* Handbook of Biological Confocal Microscopy, 2nd ed. (J.B. Pawley, ed.) pp. 55-67. Plenum Press, New York.

Wells, S. and Johnson, I. 1994. Fluorescent labels for confocal microscopy. *In* Three-Dimensional Confocal Microscopy: Volume Investigation of Biological Specimens (J.K. Stevens, L.R. Mills, and J.E. Trogadis, eds.) pp. 101-129. Academic Press, San Diego.

Wessendorf, M.W. and Brelje, T.C. 1993. Multicolor fluorescence microscopy using the laser-scanning confocal microscope. *Neuroprotocols* 2:121-140.

White, N.S. 1995. Visualization systems for multidimensional CLSM images. *In* Handbook of Biological Confocal Microscopy, 2nd ed. (J.B. Pawley, ed.) pp. 211-254. Plenum Press, New York.

Wilson, T. 1993. Image formation in confocal microscopy. *In* Electronic Light Microscopy (D.M. Shotton, ed.) pp. 231-246. John Wiley & Sons, New York.

Wilson, T. 1995. The role of the pinhole in confocal imaging systems. *In* Handbook of Biological Confocal Microscopy, 2nd ed. (J.B. Pawley, ed.) pp. 167-182. Plenum Press, New York.

KEY REFERENCES

Inoue, S. 1997. Video Microscopy. The Fundamentals. 2nd ed. Plenum Press, New York.

Important source of information about light microscopy and video microscopy.

Kriete, A. (ed.). 1992. Visualization in Biomedical Microscopies. 3-D Imaging and Computer Applications. VCH Publishing, Weinheim, Germany.

Detailed considerations of computer-assisted image analysis in various microscopy techniques.

Matsumoto, B. (ed.). 1993. Cell Biological Applications of Confocal Microscopy. Methods in Cell Biology, Vol. 38. Academic Press, San Diego.

Useful source of practical information.

Pawley, 1995a. See above.

Excellent source of information on theoretical and technical aspects of confocal microscopy.

Russ, 1998. See above.

Excellent source of information about digital image processing.

Shotton, 1995. See above.

Concise discussion of many aspects of digital imaging in light and confocal microscopy.

Stevens, J.K., Mills, L.R., and Trogadis, J.E. (eds.). 1994. Three-Dimensional Confocal Microscopy: Volume Investigation of Biological Specimens. Academic Press, San Diego.

Covers basic theoretical considerations, gives examples of practical applications, and discusses alternative methods.

Wilson, T. (ed.). 1990. Confocal Microscopy. Academic Press, London.

Very useful source of theoretical information on confocal microscopy.

INTERNET RESOURCES

http://optics.jct.ac.il/aryeh/Spectra

Excitation/emission spectra for common fluorophores.

http://rsb.info.nih.gov/nih-image/

Use to obtain NIH Image, a powerful image analysis program for Macintosh computers developed by W. Rasband (Research Services Branch, National Institute of Mental Health, NIH).

http://www.bioimage.org/misc/companies.html

List of commercial suppliers in optical and electron microscopy.

http://corn.eng.buffalo.edu/

Links, literature, and courses.

http://www.cs.ubc.ca/spider/ladic/confocal.html

General information and links about confocal microscopy.

http://www.probes.com/

Molecular Probes, supplier of fluorescent probes and optical filters. Information about fluorescence characteristics, and numerous useful links.

Contributed by Peter Ekström
University of Lund
Lund, Sweden

Measurement of Expression of the HSP70 Protein Family

The HSP70 (heat shock protein 70) superfamily is comprised of different genes encoding proteins of molecular mass between 68 and 78 kDa, including the rodent HSP72 (inducible HSP70), HSP73 (constitutive HSP70), and the glucose-regulated proteins, GRP75 and GRP78. These proteins have the common ability to bind and hydrolyze ATP. The functions of the HSP70 family are diverse but generally involve interaction with and stabilization of unfolded and/or nascent proteins, mediating their proper folding, preventing aggregation, and facilitating transport to and across membranes (molecular chaperoning). Members of the HSP70 family are inducible by a variety of stimuli including heat shock, ischemia, toxic metals, amino acid analog, and some chemotherapeutic and anesthetic agents (see Table 2.9.1). Induction of mRNA is often observed 4 to 8 hr after the insult and can persist up to 24 hr. In contrast, induction of proteins peaks 24 to 48 hr (or later) after the stimulus. Because HSP73 mRNA and protein is constitutively present in most tissues, its induction by different stimuli is generally very small compared to that of HSP72 or the other HSP70 members.

This unit describes selected methods for the detection and quantification of the HSP70 family of proteins and mRNAs in cell culture and whole tissue—northern blot hybridization (see Basic Protocol 1), in situ hybridization with film (see Basic Protocol 2) or emulsion autoradiography (see Alternate Protocol 1), metabolic labeling and SDS-PAGE (see Basic Protocol 3), immunoblotting (see Basic Protocol 4 and Alternate Protocol 2), and immunohistochemistry (see Basic Protocol 5 and Alternate Protocols 3 and 4). This unit also contains a protocol for combining TUNEL with immunohistochemistry to detect cells that are dying and expressing stress proteins (see Alternate Protocol 5). Support protocols are included for counterstaining (see Support Protocol 1), coverslipping slides (see Support Protocol 2), Coomassie blue staining of proteins in gels (see Support Protocol 3), reversible staining of proteins on membranes (see Support Protocol 4), and preparing gelatin-coated slides (see Support Protocol 5).

NOTE: All protocols using live animals must first be reviewed and approved by an Institutional Animal Care and Use Committee (IACUC) and must follow officially approved procedures for the care and use of laboratory animals.

QUANTITATIVE DETECTION OF HSP70 FAMILY mRNA BY NORTHERN BLOT

BASIC PROTOCOL 1

Gene expression results in the production of RNA transcripts within cells. Northern blot analysis is a useful method to quantify the amount of mRNA present in tissue extracts. It is also the method of choice to determine if the oligonucleotide probe used for in situ hybridization experiments (see Basic Protocol 2) is detecting the right size transcript(s) under similar salt, formamide, and temperature conditions. Table 2.9.2 reports the sequence of common antisense oligonucleotide probes used for the detection of the HSP70 gene family in rodents. The oligonucleotide used to detect the inducible hsp70 mRNA produces two bands (hsp70 homologs) on northern blots of brain tissue samples after ischemia, heat shock, acidosis, and amphetamine treatment (Miller et al., 1991; Kinouchi et al., 1993; Narasimhan et al., 1996). In contrast, hsc70, grp75, and grp78 oligonucleotides each recognize a single transcript (Miller et al., 1991; Massa et al., 1995, 1996). The conditions described in the present protocol are adapted for the use of 30- to 45-bp long oligonucleotides.

Contributed by Marcelle Bergeron and Frank R. Sharp
Current Protocols in Toxicology (2001) 2.9.1-2.9.40

When working with RNA during northern blotting (Basic Protocol 1) or in situ hybridization (Basic Protocol 2), care should be taken to avoid contamination by RNases. It is therefore important to wear clean, powder-free disposable gloves at all time when handling all reagents and solutions. The use of RNase-free solutions (made up with DEPC-treated water, unless otherwise stated) is recommended for the preparation of all solutions before and during the hybridization steps. Because DEPC-treated water from commercial sources (e.g., from Ambion) is quite expensive. The use of low-cost, DEPC-treated water made in the lab is recommended. It is also recommended to use sterile

Table 2.9.1 Experimental Treatments That Induce the HSP70 Family in Brain Tissue

Inducer	Treatment	Species	HSP72[a]	HSP73[a]	GRP75[a]	GRP78[a]
Heat shock						
In vitro	0.5-3.0 hr incubation at 43.5°C	Primary mouse astrocytes	+	–	ND	ND
Ischemia						
Global	≥2-3 min of transient bilateral carotid artery occlusion	Gerbil	+	+	+	+
Focal	≥30 min of transient unilateral intraluminal occlusion of the middle cerebral artery	Rat	+	+	+	+
Focal	2-3 hr combined unilateral permanent carotid occlusion and concurrent 8% O_2 exposure	Rat (newborn)	+	ND	ND	ND
In vitro	3-4 hr of oxygen and glucose deprivation	Primary mouse astrocytes	+	–	ND	ND
Other inducers						
Acidosis	40 min of incubation in media at pH 5.2	Primary rat astrocytes	+	ND	ND	ND
Subarachnoid hemorrhage	Injection of 0.15 ml of lysed blood into the cisterna magna	Rat	+	ND	ND	ND
Kainic acid	10 mg/kg i.p.	Rat	+	+	ND	+
Ketamine	40-160 mg/kg i.p.	Rat	+	ND	ND	ND
MK-801	0.1-10 mg/kg i.p.	Rat	+	ND	ND	ND
Phenylcycline	5 mg/kg i.p.	Rat	+	ND	ND	ND

[a]+, induction; –, unchanged. Abbreviations: GRP, glucose-regulated protein; HSP, heat shock protein; i.p., intraperitoneal injection; ND, not determined.

Table 2.9.2 Sequence of Antisense Oligonucleotide Probes Commonly Used for Detection of HSP70 Family mRNAs in Rat Tissues

Gene	Oligonucleotide sequence	Reference	Expected band size
hsp70	5′-CGATCTCCTTCATCTTGGTCAGCACCATGG-3′	Narasimhan et al. (1996)	2.5-2.7 and 2.9 kb
hsc70	5′-ATGCCTGTGAGCTCAAACTTCCCAAGCAGG-3′	Miller et al. (1991)	2.55 kb
grp75	5′-GGTCAAATCAACCCCTGTCTCCCTCTTGAACTC-3′	Massa et al. (1995)	3.3 kb
grp78	5′-CTTCAGATCAGAAGTCTTCCAACACTTTCTG-3′	Massa et al. (1995)	2.7 kb

glassware, microcentrifuge tubes, and pipet tips. The use of RNase-free solutions is not required in post-hybridization procedures because of the resistance of RNA:RNA hybrids to RNase degradation. At this stage, the use of deionized water is adequate.

CAUTION: When working with radioactivity, take appropriate precautions to avoid contamination of the experimenter and surroundings. Carry out the experiment and dispose of wastes in an appropriately designated area following the guidelines provided by your local radiation safety officer (also see *APPENDIX 1A*).

Materials

Animals subjected to a stressful stimulus (Table 2.9.1)
Anesthesia cocktail (see recipe)
TRIzol reagent (Life Technologies; TRIzol Reagent, Sigma; or RNA STAT-60, Tel Test)
5:1 (v/v) acid phenol/chloroform solution, pH 4.7 (Ambion)
Horizontal formaldehyde/1% (w/v) agarose gel (*APPENDIX 3E*)
Nylon membrane, positively charged (e.g., Hybond, Amersham; Nytran SuPerCharge, Schleicher and Schuell; BrightStar-Plus, Ambion)
0.02% (w/v) methylene blue staining solution (see recipe)
2× and 20× SSC (see recipe)
^{32}P-labeled antisense oligonucleotide probe (Table 2.9.2) and sense control probe, (single-stranded, unlabeled oligonucleotides are obtained from Oligos Etc., or other commercial source)
Prehybridization solution (for recipe, see *APPENDIX 3E*, Basic Protocol, step 25)
50% (w/v) dextran sulfate (see recipe)
2× and 1× SSPE (see recipe)
20% (w/v) SDS

UV cross-linker (Stratagene)
Sealable bag or glass hybridization bottle
Hybridization oven or 42°C shaker water bath

Additional reagents and equipment for RNA extraction, agarose gel electrophoresis (*APPENDIX 3A*), oligonucleotide labeling (*APPENDIX 3E*), and northern blot hybridization (*APPENDIX 3E*)

NOTE: To protect from RNase contamination and fingerprint smudges, always wear clean, powder-free gloves when working RNA. Do not reuse gloves.

Prepare cell lysate

1. Subject test animal to stressful stimulus. At the appropriate time after stressful stimulus (see Table 2.9.1), anesthetize animal by intraperitoneal injection of anesthesia cocktail, excise tissue, and either freeze it promptly on powdered dry ice and store at −70°C until use or start the RNA extraction procedures immediately (see *APPENDIX 3E*).

   The speed at which the excision and processing of the tissue are performed is crucial to reduce RNA degradation.

2. Extract total RNA using TRIzol reagent and 5:1 acid phenol/chloroform (*APPENDIX 3E*).

   Isolation of mRNA using commercially available kits (such as Fastrack 2 from Invitrogen or Oligotex mRNA extraction kit from Qiagen) is highly recommended for tissue samples suspected to have a low abundance of the mRNA of interest.

Separate and immobilize RNAs on membrane

3. Size-fractionate an equal amount of total RNA or mRNA per sample (cell lysate) by electrophoresis on a horizontal formaldehyde/1% agarose gel (*APPENDIX 3E*). Use 4 to 10 μg mRNA or 20 to 40 μg total RNA per lane.

4. After separation, transfer the RNA onto a positively charged nylon membrane (*APPENDIX 3E*) using upward (Fig. A.3E.1A) or downward (Fig. A.3E.1B) capillary flow transfer.

   Make sure that the agarose gel is no more than 5 to 6 mm thick, otherwise it will reduce the transfer efficiency.

5. Cross-link RNA to the membrane in a UV cross-linker according to the manufacturer's instructions.

6. Stain the membrane with 0.02% methylene blue staining solution until the lanes become visible (~15 min). Mark the RNA marker bands on the side of the membrane with a pencil or a fluorescent pen or dye.

7. Destain with 2× SSC. Cut one corner of the membrane away to establish the orientation of the lanes.

Hybridize and detect RNA

8. Prepare and purify a [^{32}P]3′-end-labeled antisense (see Table 2.9.2) or sense oligonucleotide probe with terminal deoxynucleotidyl transferase (*APPENDIX 3E*).

   For the labeling reaction, avoid DEPC-treated water because DEPC residues may inhibit enzyme activity and decrease labeling efficiency. Use sterile water free of nuclease.

9. Transfer the membrane to a sealable bag or a glass hybridization bottle. Prehybridize the membrane in 8 ml/10 cm^2 prehybridization solution (for recipe, see *APPENDIX 3E*, Basic Protocol, step 25) for ≥2 hr, 42°C, in either a hybridization oven (for glass bottle) or submerged in a shaker water bath (for sealable bag).

10. Add 2 ml of 50% dextran sulfate to the prehybridization solution and mix well (total volume 10 ml/10 cm^2).

11. Add 10^6 to 10^7 cpm labeled probe per milliliter prehybridization solution and hybridize overnight at 42°C.

12. The next day, wash the membrane with prewarmed solutions as follows:

    2× SSPE containing 0.1% SDS for 15 min at 42°C
    2× SSPE containing 0.1% SDS for 15 min at 42°C
    1× SSPE containing 0.1% SDS for 15 min at 42°C.

13. Check the specific activity of the membrane after each wash by holding a Geiger counter 2 to 3 cm above the membrane surface. At the first sign of significantly decreased signal intensity, stop the washing procedures.

    The signal should be very intense after the first wash. With increasing wash stringency, the signal should decrease.

    If necessary, increase the temperature by 5°C after each subsequent wash as described below. If the membrane is still too radioactive after washing at 60°C, decrease the SSPE concentration to 0.5×, 0.2×, and then 0.1× SSPE. The SDS concentration remains the same (0.1%) throughout wash procedures. Increasing the temperature and decreasing the SSPE concentration provide more stringent conditions that facilitate the elimination of mismatched probe, thus decreasing non-specific background. The washes would then be:

1× SSPE containing 0.1% SDS for 15 min at 45°C
1× SSPE containing 0.1% SDS for 15 min at 50°C
1× SSPE containing 0.1% SDS for 15 min at 55°C
1× SSPE containing 0.1% SDS for 15 min at 60°C.

14. Drain the excess solution, seal the wet membrane in plastic wrap, and expose to an autoradiographic film at −70°C (*APPENDIX 3E*) for 1 to 7 days, depending on the abundance of the mRNA of interest and the specific activity of the probe.

15. Develop the film and visualize the bands.

    The probes listed in Table 2.9.2 should detect bands of the indicated sizes.

    Wet membranes can be stripped from bound radioactive oligonucleotides and reprobed with another labeled oligonucleotide (APPENDIX 3E) for direct comparison of different mRNAs on the same blot.

16. *Optional:* To account for differences in loading and mRNA concentration/integrity, strip the membrane (*APPENDIX 3E*) and reprobe with another oligonucleotide probe targeting a housekeeping gene (i.e., gene for which constitutive expression does not change with a given treatment).

    Ideally, the bands from any transcript of interest should always be normalized against a housekeeping gene like cyclophilin (5′-GAGTTGTCCACAGTCGGAGATGGTGATCTT CTTGCTGGTCTTGCC-3′; expected transcript is ~1 kb). Other housekeeping genes such as actin, GAPDH, and 18S ribosomal RNA have been used successfully.

DETECTION OF HSP70 FAMILY mRNA ON TISSUE SECTIONS BY IN SITU HYBRIDIZATION

BASIC PROTOCOL 2

Once the specificity of an oligonucleotide probe has been established by northern blot analysis (see Basic Protocol 1), in situ hybridization is used to localize specific RNA transcripts in tissue sections or cell cultures. In situ detection of mRNAs is based on concepts and procedures similar to those described for northern blotting except that it is performed directly on tissue sections. The present method is optimized for use with fresh frozen (unfixed) tissue sections. After hybridization, sections are washed, dried, and exposed directly to an autoradiographic film.

Alternatively, to obtain a better resolution at the single cell level, each radiolabeled slide can be dipped directly in photographic emulsion. Developed silver grains can be observed directly on the tissue sections (see Alternate Protocol 1).

When working with RNA during both northern blotting (Basic Protocol 1) or in situ hybridization (Basic Protocol 2), care should be taken to avoid contamination by RNases. It is therefore important to wear clean, powder-free disposable gloves at all time when handling all reagents and solutions. The use of RNase-free solutions (made up with DEPC-treated water, unless otherwise stated) is recommended for the preparation of all solutions before and during the hybridization steps. Because DEPC-treated water from commercial sources (e.g., from Ambion) is quite expensive, the use of low-cost, DEPC-treated water made in the lab is recommended. It is also recommended to use sterile glassware, microcentrifuge tubes, and pipet tips. The use of RNase-free solutions is not required in post-hybridization procedures because of the resistance of RNA:RNA hybrids to RNase degradation. At this stage, the use of deionized water is adequate.

CAUTION: When working with radioactivity, take appropriate precautions to avoid contamination of the experimenter and surroundings. Carry out the experiment and dispose of wastes in an appropriately designated area following the guidelines provided by your local radiation safety officer (also see *APPENDIX 1A*).

Materials

Animals subjected to a stressful stimulus (Table 2.9.1)
Anesthesia cocktail (see recipe)
5 M DTT (see recipe)
[^{35}S]- or [^{33}P]-labeled antisense oligonucleotide probe (Table 2.9.2) and sense control probe (single-stranded, unlabeled oligonucleotides are obtained from Oligo Etc. or other commercial source)
In situ hybridization cocktail (see recipe)
10 mg/ml heat-denatured salmon sperm DNA stock
1× SSC (see recipe), sterile, 55°C
H_2O, deionized, sterile
75%, 95%, and 100% ethanol

Dissecting instruments
Isopentane on powdered dry ice bath
Cryostat
Precoated slides with painted corners (e.g., ProbeOn or Superfrost Plus, Fisher Scientific)
Moist chamber with cover
Parafilm
Slide rack
Staining dish in a 55°C water bath
Hair dryer
Autoradiographic cassette
X-ray film (Kodak SB5 for manual processing or BioMax MR one sided emulsion for automated processor)

Additional reagents and equipment for oligonucleotide labeling (*APPENDIX 3E*)

NOTE: To protect from RNase contamination and fingerprint smudges, always wear clean, powder-free gloves when working RNA. Do not reuse gloves.

Prepare tissue

1. Subject test animals to stressful stimulus (see Table 2.9.1).
2. At the appropriate time after treatment, euthanize animals under deep anesthesia produced by an intraperitoneal injection of anesthesia cocktail. Quickly excise the tissue and freeze promptly in a bath of isopentane on powdered dry ice.

   Total sterility is not necessary at this point as long as all these steps are performed quickly.

3. Cut 14- to 20-µm sections with a cryostat and collect the slices on coated slides (e.g., ProbeOn or Superfrost Plus). Store tissue sections in a slide box at −70°C until analysis. Do not thaw and freeze again.

   The use of precoated slides is highly recommended for this step. These slides have a special coating that electrostatically adheres tissues sections to the glass without the need of special protein coating. It also reduces the slide manipulation that could introduce contaminants and RNases. Always wear gloves while manipulating the slides.

Hybridize with probe

4. Prepare and purify a [^{35}S] or [^{33}P]-3′-end-labeled antisense (see Table 2.9.2) or sense oligonucleotide probe with terminal deoxynucleotidyl transferase (*APPENDIX 3E*).
5. Just before hybridization, take the slides with specimen from the freezer and air dry for ~1 hr at room temperature.

   Always use gloves when handling the slides.

6. Determine the total amount of hybridization solution needed (~200 to 300 µl of hybridization solution for each pair of slides). Make the hybridization solution by mixing in the following order:

   12 µl 5 M DTT
   10^6 to 10^7 cpm labeled oligonucleotide probe
   In situ hybridization cocktail up to 1000 µl
   25 µl 10 mg/ml heat-denatured salmon sperm DNA stock.

   Antisense and sense oligonucleotide probes are both used with this method. Whereas the antisense probe hybridizes to the mRNA of interest, the sense probe is used to determine the level of nonspecific hybridization which should always be very minimal.

7. Pipet 200 to 300 µl radioactive hybridization solution on the surface of one slide and carefully apply another slide (face down) on top of it. Do this slowly to avoid trapping air bubbles on the slices.

   While facing each other, the tissue specimen on each slide can be incubated simultaneously in the viscous hybridization solution trapped between the two overlaying slides (Superfrost or equivalent slides have painted corners which are slightly elevated from the slide's surface, thus allowing this type of overlaying). This approach minimizes the amount of radioactive cocktail used and handled.

8. Place the slide sandwiches flat in a moist chamber containing one layer of wet paper towels at the bottom. Place a cover on the chamber and seal with Parafilm. Incubate 12 to 18 hr in an incubator-oven at 37°C.

Wash slides

9. The next day, separate the slides gently and rinse two times in 1× SSC, each time for 1 to 2 min, at room temperature.

10. Place the wet slides in a slide rack with the tissue sections all facing in the same direction.

11. Use a staining dish placed at the bottom of a 55°C water bath and immerse slides four times for 15 min in prewarmed, 55°C, 1× SSC solution (change the solution in between each 15-min wash) and a final 1× SSC wash for 1 hr at room temperature (i.e., outside the water bath).

    At this stage, the use of DEPC-water in the wash solutions is not necessary. The use of clean dishes and deionized water to make up the wash solutions is sufficient to preserve the quality of hybridization and the signal intensity.

12. Rinse 2 min in sterile water at room temperature. Dehydrate 2 min each in 75%, 95%, and 100% ethanol. Air dry the slides thoroughly using a hair dryer for ~1 hr at the lowest temperature setting.

Autoradiograph the slides

13. Once dry, tape the slides (face up) on a piece of cardboard and place at the bottom of an autoradiographic cassette.

14. In a dark room under safelight conditions, apply the emulsion side of an X-ray film directly on the radioactive slides and close the cassette tightly. Expose at room temperature for an appropriate amount of time, which depends on the abundance of the transcript in the specimen and the specific activity of the probe.

    For a medium-to-high abundance of mRNA transcript, the ^{35}S-probe signal is clearly detectable after 1 to 2 weeks exposure. ^{33}P-probes usually give stronger signal, so exposure time can be decreased.

ALTERNATE PROTOCOL 1

EMULSION AUTORADIOGRAPHY

Emulsion autoradiography coupled with counterstaining (see Support Protocol 1) allows detection of individual cells that are expressing the mRNA of interest. Individual slides are coated with an emulsion, incubated, developed, and counterstained.

Materials

NTB-2 autoradiographic emulsion (Kodak)
Slides with radioactively hybridized sections (see Basic Protocol 2, step 12)
D19 or Dektol developer and fixer (Kodak), freshly made
Milli-Q-purified water

43°C water bath
Black light-tight slide boxes
Dessicant packs (Drierite)
Dipping container
Forceps with blunt ends (optional)
Slide rack
Slide dryer (optional)
Black electrical tape
Staining dishes
Light microscope

NOTE: Use very clean glassware and reagent-grade solutions. Wear powder-free gloves for all procedures.

CAUTION: All procedures involving autoradiographic emulsion should be performed in complete darkness or under safelight conditions. The autoradiography emulsion must be refrigerated at 4°C until use. Because it is in a solid form at 4° to 10°C, the emulsion must be liquified by heating to ~45°C before use. Do not freeze or store the emulsion at room temperature to avoid high background fog and loss of detection ability.

Prepare the emulsion

1. In a darkroom under safelight conditions, place the 4-oz. (118-ml) bottle of NTB-2 autoradiographic emulsion in a water bath between 43° and 45°C. Gently swirl the emulsion bottle to speed up the liquefaction process.

   Too much agitation can result in the formation of bubbles that can interfere with the autoradiography. Liquefaction usually takes 45 to 55 min.

2. Pour the autiradiographic emulsion into a clean dipping container placed at 43°C.

3. Hold each radioactive slide at the frosted end with two fingers or with blunt-end forceps and slowly dip in the warm NTB-2 autoradiographic emulsion. Withdraw each slide slowly, drain the excess emulsion on the edge of the emulsion container, and place slide vertically against the wall or a box to air dry ≥1 hr, in complete darkness.

   Optionally, when the slides are dry to the touch (~15 min), a slide dryer may be used to accelerate the drying process.

4. Place the dried slides in a clean, black light-tight slide box containing a dessicant pack. Close the box and seal with black electrical tape, cover the entire box with foil, and store at 4°C.

   The slides should be stored in a refrigerator that contains no isotopes or organic chemicals that could react with the emulsion.

5. Expose slides two and a half to three times longer than the time generally required for direct X-ray film autoradiographic exposures.

   Several exposure times may be tested to determine optimal conditions. Because it requires long exposure periods, the dipping method is more appropriate for slides hybridized with ^{35}S-labeled probes, which have a radioactive half-life of 87 days compared with 25 days for ^{33}P-labeled probes.

Develop slides

6. Take the slide box out of the 4°C refrigerator and allow to warm up at room temperature before proceeding.
7. In the darkroom, prepare the following in separate staining dishes at room temperature:

   Freshly made D-19 developer
   Milli-Q-purified water
   Freshly made D-19 fixer
   Cold tap water.

8. In the dark, transfer the slides in a slide rack and develop as follows:

   4 min in D-19 developer
   1 min in Milli-Q-purified water (stop solution)
   5 min in D-19 fixer.

   Agitate gently during each step.

9. Rinse in gently running cold tap water for 30 min.

   It is now safe to turn on the lights.

10. Rinse briefly in Milli-Q-purified water. While still wet, scrape off the emulsion on the back of each slide with a razor blade.
11. Air dry the slides in a dust-free environment, counterstain if needed (see Support Protocol 1), and apply coverslips (see Support Protocol 2). Examine with a light microscope.

    The presence of mRNA can be visualized under a light microscope. mRNA appears as dark black spots of developed silver grains directly on the tissue specimen. Counterstaining is recommended to help identify the cellular localization of the signal.

COUNTERSTAINING WITH CRESYL VIOLET (NISSL)

SUPPORT PROTOCOL 1

Counterstaining of slides is used to permit visualization of the cellular structure of tissues.

Materials

Dry tissue specimen on slides from immunohistochemistry or in situ hybridization
Chloroform (optional)
Ether (optional)
70%, 95%, and 100% ethanol
Milli-Q-purified water
Cresyl violet staining solution (see recipe)
Glacial acetic acid

Slide racks
Glass staining dishes

NOTE: Perform all steps at room temperature, in a well-ventilated fume hood. Wear gloves at all times.

Prepare slides

1. Fill slide racks with the slides. Orient them so that the sections all face the same direction.
2. *Optional:* Immerse the slides in a glass staining dish filled with chloroform and incubate for 3 to 5 min to delipidize the tissue. Drain excess chloroform and incubate slides in ether for 3 to 5 min.

   Delipidization may be necessary in tissues with high lipid content such as the adult rat brain. For other tissues and cell cultures, it may be omitted. Try to stain a few slides first without the chloroform/ether steps to determine whether delipidization is required.

Stain sections

3. Prepare in separate glass staining dishes 70%, 95%, and 100% ethanol, Milli-Q-purified water, and Cresyl violet solution.
4. Incubate slides in 100% ethanol for 3 min. Drain excess solution and rinse slides in 95% ethanol for 3 min.
5. Drain excess solution and rinse slides in 70% ethanol for 3 min.
6. Drain excess solution and rehydrate slides in Milli-Q-purified water for 3 min.
7. Drain excess water, immerse in Cresyl violet solution and stain 5 to 10 min.
8. Drain excess staining solution and wash in water for 2 min.

Dehydrate/destain slides

9. Drain excess water and immerse in 70% ethanol. To promote the destaining process, add a few drops of glacial acetic acid in the staining dish and mix gently. Incubate 1 to 2 min.
10. Drain the excess solution and incubate in 95% ethanol 1 to 2 min.
11. Drain the excess solution and incubate in 100% ethanol 1 to 2 min.

    Each dehydration step also destains the tissue specimen. Depending on the nature and the thickness of the tissue stained, the incubation times for each ethanol/destain bath may need to be readjusted. The thinner the section, the easier it is for the Cresyl violet to penetrate the cells and the easier it is to wash the dye away in subsequent destaining steps. Very thick (>100 μm) sections may need the delipidization steps and longer destaining incubation times. Sections that show too weak staining by step 11 can be restained as follows: perform steps 10, 9, and 8, followed by steps 7 to 11.

12. Proceed with the dehydration steps and coverslip as described in Support Protocol 2.

SUPPORT PROTOCOL 2

COVERSLIPPING SPECIMENS ON SLIDES

Coverslipping specimens mounted on slides following immunohistochemistry or histological staining is a crucial step that helps preserve the stained tissue specimen and significantly increases the optical quality during light-microscope observations. It involves a brief surface rehydration of the specimens to wash off the excess salts and impurities that could interfere with the true staining signal. This is followed by successive dehydration in 75%, 95%, and 100% ethanol and clearing solutions such as xylene or Hemo-D. The specimen is then covered with a small amount of suitable water-repellant mounting medium, and a thin-glass coverslip is applied on its surface. All procedures should be performed at room temperature in a well-ventilated fume hood. Wear gloves at all times. The method described here is recommended for tissue specimen subjected to emulsion dipping after in situ hybridization (see Alternate Protocol 1), Cresyl violet

staining (see Support Protocol 1), and all chromogenic immunoreactions (see Basic Protocol 5). It is not recommended for specimen labeled with fluorescent tags (see Alternate Protocol 4).

Materials

Tissue specimens mounted and dried on slides
70%, 95%, and 100% ethanol
Clearing solution such as xylene or Hemo-D (Fisher)
Mounting medium (e.g., DePeX , BDH; Permount, Fisher; or equivalent)

Slide racks
Glass staining dishes
Forceps with blunt end
Glass coverslips, large enough to cover the tissue specimen

CAUTION: Xylene is a toxic solvent and all steps of counterstaining and coverslipping should be carried out in a fume hood or ventilated table.

Prepare slides

1. Fill slide racks with the slides to be coverslipped. Orient all slides to face in the same direction.
2. Immerse the slides in a glass staining dish filled with water and wash for 3 min.
3. Drain excess water and rinse slides in 70% ethanol for 3 min.

   Do not dry the tissue slices at anytime during the successive drainage and solution changes.
4. Drain excess solution and rinse slides in 95% ethanol for 3 min.
5. Drain excess solution and rinse slides in 100% ethanol for 3 min.
6. Drain excess solution and incubate slides in a dehydrating/clearing solution such as Hemo-D for 3 min.

   Alternatively, rinse the slides in 3:2 (v/v) xylene/ethanol for 3 min followed by two successive washes in 100% xylene for 3 min. Then follow steps 8 to 10.
7. Repeat step 6 using fresh Hemo-D.

Apply coverslip

8. With blunt-end forceps, pick one slide at a time from the clearing solution, drain briefly, and set flat on a paper towel. Immediately cover one edge of the slide with a small amount of water-repellant mounting medium and slowly apply (at a 45° angle) a thin-glass coverslip on top, being careful not to introduce any air bubbles.
9. Set slide flat on a leveled tray and air dry 1 to 2 days in a fume hood.

   Excess dried mounting medium at the edge of the slide can be scraped off gently with a clean razor blade. Wipe slides gently with 70% ethanol.
10. Store coverslipped slides in slide boxes in a cool and dry environment.

LABELING STRESS PROTEINS WITH [^{35}S]METHIONINE

BASIC PROTOCOL 3

Selective increase in the synthesis of stress proteins such as HSP70 family proteins, concomitant with a transient reduction in overall protein synthesis, is a typical response observed both in vivo and in vitro in cells exposed to a variety of insults including heat shock, ischemia, toxic metals, amino acid analogs, and some chemotherapeutic or anes-

thetic agents. This protocol introduces a rapid method to evaluate overall decreased protein synthesis and selective increases in the expression of stress proteins (Table 2.9.3), including the HSP70 family (Table 2.9.1), in cell culture at different time points after a stressful stimulus. This method depends on the incorporation of [^{35}S]methionine into cellular proteins. The ^{35}S-labeled cell lysate is then analyzed by polyacrylamide gel electrophoresis. Following staining with Coomassie blue (to verify equal loading) and drying on a filter paper, the gel is exposed to an X-ray film for subsequent band visualization (*APPENDIX 3D*). Decreased overall protein synthesis (or decreased [^{35}S]methionine incorporation into proteins) is reflected on the film emulsion as a decrease in the number and intensity of radioactive bands in each sample track. Concurrent induction of stress proteins is visualized as select bands of high intensity. In particular, the HSP70 family proteins show specific bands of molecular weights ranging from 68 to 78 kDa. Depending on the type of stressful stimulus used to treat the cells initially, some but not all stress proteins may be present and/or have increased intensity (see Table 2.9.3 for inducers). For example, hyperthermia specifically and strongly induces a band of ~72 kDa but not other bands in

Table 2.9.3 Characteristics of Some Mammalian Stress Proteins[a,b]

Stress function protein[b,c]	Major inducers	Location	Suggested function
HSP27	Heat shock, estrogen, glutamate, heavy metals, cysteamine, oxidative stress	Cytosol, nucleus	Microfilament stability
HSP32	Heat shock, hypoxia, ischemia, oxidative stress (gluthatione depletion), heme, heavy metals, UV irradiation	ER	Heme degradation
HSP34	Glucocorticosteroids	ER	Heme degradation
HSP47	Heat shock, ischemia	ER	Serine protease inhibitor, binds to collagen
HSP60	Heat shock	Mitochondria	Chaperone involved in the folding and translocation of new proteins
HSP72	Heat shock, ischemia, some anesthetic drugs, glutamate agonists, seizures, UV irradiation, acidosis	Cytosol, nucleus	Inducible HSP70, chaperone involved in folding of newly synthesized or denatured proteins, dissociates aggregates
HSP73	Ischemia, seizures	Cytosol, nucleus	Constitutive HSP70 homolog, molecular chaperone, clathrin-uncoating ATPase associated with microtubules and other cytoskeletal elements
HSP90	Heat shock, ischemia, estradiol	Cytosol, nucleus	Molecular chaperone, regulation of steroid receptors, modulation of protein synthesis
GRP75	Hypoglycemia, ischemia, calcium depletion	Mitochondria	HSP70 homolog, chaperone for newly synthesized proteins
GRP78	Hypoxia, hypoglycemia, ischemia, calcium depletion, okadaic acid	Golgi/ER	HSP70 family member, immunoglobulin heavy chain binding protein, chaperone for nascent glycoproteins
GRP94	Hypoxia, hypoglycemia, calcium depletion	Golgi/ER	Calcium binding glycoprotein
Ubiquitin	Heat shock, ischemia, pentobarbital	Cytosol, nucleus	Targets proteins for degradation

[a]For reviews, see Welch (1990, 1992), Parsell and Lindquist (1994), and Massa et al. (1996).

[b]Abbreviations: ER, endoplasmic reticulum; GRP, glucose-related protein; HSP, heat shock protein.

[c]Numbers represent the molecular weight of the protein in kilodatton.

the same molecular weight range, consistent with HSP72 being an inducible heat shock protein (Tables 2.9.1 and 2.9.3).

Although this method is simple, rapid, and relatively inexpensive, it is fairly nonspecific when it comes to discriminating between proteins of very similar molecular weight, even if optimal electrophoresis conditions are used. Therefore, the changes in expression of HSP70 family proteins should be validated by immunoblot analysis on the same cell lysate using specific antibodies against individual proteins (see Basic Protocol 4).

CAUTION: When working with radioactivity, take appropriate precautions to avoid contamination of the experimenter and surroundings. Carry out the experiment and dispose of wastes in an appropriately designated area following the guidelines provided by your local radiation safety officer (also see *APPENDIX 1A*).

Materials

Tissue culture cells in 35- to 100-mm plates
Methionine-free medium for cell culture
stressful stimulus (see Tables 2.9.1 and 2.9.3)
1000 Ci/mmol [^{35}S]methionine (Amersham Pharmacia Biotech or NEN)
Phosphate-buffered saline (PBS; *APPENDIX 2A*), ice-cold
1× SDS sample buffer (see recipe)
Protein quantitation kit (Pierce or Bio-Rad)
Bovine serum albumin (BSA) protein standards
Molecular weight markers
2-mercaptoethanol
1% (w/v) bromphenol blue (see recipe)
Water-based scintillant solution

1.5-ml microcentrifuge tubes
Cell scraper
100°C water bath
Filter-membrane spin column (optional; Amicon or Sigma)

Additional reagents and equipment for SDS-PAGE (*APPENDIX 3A*), Coomassie blue staining of gels (see Support Protocol 3), and gel drying and autoradiography (*APPENDIX 3D*)

Label cells

1. Incubate cells for 12 hr in a methionine-free medium to ensure that most of the endogenous methionine has been used up by the cells.
2. Expose cells to the stress/injury stimulus (see Tables 2.9.1 and 2.9.3).
3. At appropriate time points after the insult, add 40 µCi/ml of 1000 Ci/mmol [^{35}S]methionine directly to the medium. Incubate 2 hr at 37°C to ensure incorporation of the labeled methionine into cellular proteins.

   CAUTION: *At this point, standard radiosafety precautions should be taken for the manipulation and disposal of all radioactive solutions and plasticware.*

   Use a minimum volume of medium in the dish to minimize the volume of radioactive waste solution. Typically for this step, remove some of the incubating medium and leave a volume that is just enough to cover the cells, i.e., ~2 ml for 35-mm dish and ~4 ml for 100-mm dish. Then add the radioalabel directly to the dish. This concentration of radioactivity is fairly standard but can be adjusted depending on the level of incorporation and the desired final signal.

4. At the end of the 2-hr labeling period, pipet a small volume of the labeling medium into a microcentrifuge tube and set aside for later use. Remove the overlaying medium by aspirating through a radioactivity-approved vacuum line and rinse the cells quickly with ~2 vol ice-cold PBS to remove the unincorporated label.

Prepare lysate

5. After removing the PBS, lyse the cells directly in the dish by adding 300 to 500 µl of 1× SDS sample buffer per 100-mm dish. Use a cell scraper to detach the cells from the bottom of the dish.

6. Transfer the cell lysate into a clean microcentrifuge tube and heat 3 to 5 min in 100°C water bath. Pipet up and down several times with a 1-ml pipet tip to ensure homogeneity.

   This should help solubilize the proteins to homogeneity and inhibit all proteases. If the lysate is too viscous to be pipetted through a standard 1000-µl pipet tip, add a small volume of 1× SDS sample buffer (no more than 50 µl at a time) and mix with a pipet.

7. Microcentrifuge samples 5 min at 14,000 × *g*, room temperature. If there is cellular debris at the bottom of the tube, transfer the clear supernatant into a clean microcentrifuge tube.

   The samples (lysates) can also be clarified by centrifuging through commercially available filter-membrane spin columns adapted for use with microcentrifuge tubes.

8. Freeze samples at −70°C until further analysis.

   Since the half life of ^{35}S is ~87 days, samples can be analyzed within the next 1 to 2 weeks after collection without any significant loss of signal and sensitivity.

Prepare gel samples

9. After thawing on ice, heat samples for 1 min in a 100°C water bath.

10. Mix samples by inversion and cool to room temperature before pipetting.

    Failure to cool to ambient temperature may result in inaccurate pipetting of sample volumes.

11. Take a small aliquot of the lysate and measure the protein content in triplicate samples using a standard, commercially available protein analysis kit and BSA standards. Store the remainder of the lysate on ice.

    The use of the bicinchoninic acid protein method (Pierce) at a microscale level (4 µl of protein lysate per well) in a 96-multiwell format has proven to be very reliable and reproducible.

    If the samples already contain a dye or any substances that are incompatible with the protein assay, pipet an aliquot of an appropriate volume of protein lysates to be analyzed in a microcentrifuge tube, add 500 µl of cold 10% trichloroacetic acetic and incubate on ice for 30 min. Microcentrifuge the precipitated protein samples 10 min at 14,000 × g, 4°C. Slowly aspirate the supernatant through a <20-G needle. Then resolubilize the small protein precipitated pellet directly in an appropriate volume of protein assay reaction solution and analyze immediately. BSA standards should be treated in the same fashion.

12. Prepare samples. In separate microcentrifuge tubes, pipet an equal amount of protein for each sample. Prepare the molecular weight markers according to the manufacturer's recommendation. Bring all tubes to an equal volume by adding an appropriate amount of 1× SDS sample buffer to each tube. For each 10 µl of final protein sample, add 1 µl of 2-mercaptoethanol (final 5% v/v) and 1 µl of 1% bromphenol blue (final 0.1%). Mix well. Just before loading, heat samples for 1 min in a 100°C water bath.

Add the 2-mercaptoethanol and bromphenol blue to samples after protein determination because they interfere with the assay.

Electrophorese samples

13. Separate an equal amount of protein (20 µg) per lane by SDS-PAGE using an 8% or 10% gel (*APPENDIX 3A*), best to visualize proteins of 68 to 78 kDa.
14. After electrophoresis, stain gels with Coomassie blue to verify equal protein loading (see Support Protocol 3).
15. After drying on a filter paper, expose the gel to X-ray films overnight or longer depending on the intensity of the signal (*APPENDIX 3D*).
16. Using a scintillation counter, quantify the amount of radioactivity incorporated in total protein by adding an aliquot of the final protein lysate to a scintillation vial containing 5 to 10 ml of a water-based scintillant solution. Analyze aliquots of the original labeling medium (set aside in step 4) to verify that the initial amount of radioactivity added to each dish was equal.

COOMASSIE BLUE STAINING OF PROTEINS IN A POLYACRYLAMIDE GEL

SUPPORT PROTOCOL 3

Coomassie blue staining is based on nonspecific binding of the dye to proteins. The sensitivity of this method is 0.3 to 1.0 µg protein per track. Perform the following steps under a fume hood or in a well-ventilated room and wear gloves at all time.

Materials

SDS-PAGE gel from separation of stress proteins including the HSP70 proteins (see Basic Protocol 3, step 13)
Gel fixing solution (see recipe)
Coomassie blue staining solution (see recipe)
Gel destaining solution (see recipe)

Clean glass or plastic dishes slightly larger than the gel with lid or plastic wrap
Platform shaker
Foam sponge (optional)

1. Place the polyacrylamide gel in a clean glass or plastic dish, cover the container with a lid or plastic wrap, and incubate in gel fixing solution for 5 to 10 min at room temperature.
2. Remove the fixing solution and rinse briefly in water.
3. Remove the water, immerse the gel in Coomassie staining solution, and shake gently 4 hr to overnight at room temperature.
4. Remove staining solution and save.

   This solution can be reused many times before replacing (≤30 times).

5. Add the gel destaining solution. Shake gently for 1 hr and replace with fresh destaining solution. Continue destaining until blue bands appear against a clear background. Discard destaining solution when done.

   To accelerate the destaining process, lay a foam sponge directly on top of the gel in the destaining solution. The sponge will absorb and bind the dye by capillary action and increase transfer of the dye from the gel to the destaining solution to the sponge. Discard sponge when done.

BASIC PROTOCOL 4

QUANTITATIVE DETECTION OF HSP70 FAMILY PROTEINS BY IMMUNOBLOTTING

Immunoblotting is used to evaluate the specificity of an antibody and quantitate the amount of specific protein in tissue or cell lysates. Proteins in the lysate are separated by denaturing gel electrophoresis (*APPENDIX 3A*) and then electrotransferred onto a membrane (*UNIT 2.3*). After preincubation in a blocking solution, the membrane is probed with primary and secondary antibodies, and the protein is visualized either by chromogenic substrates or chemiluminescence (see Alternate Protocol 2).

Materials

Cell culture or animals subjected to a stressful stimulus
Phosphate-buffered saline (PBS; *APPENDIX 2A*)
1× SDS sample buffer (see recipe)
Protein quantification kit (Pierce or Bio-Rad)
Bovine serum albumin (BSA) standards
Molecular weight markers
2-mercaptoethanol
1% (w/v) bromphenol blue (see recipe)
0.2-µm mesh nitrocellulose or polyvinylidine difluoride (PVDF) membrane (Biorad, Scleicher and Schuell, NOVEX)
Immunoblot blocking solution (see recipe)
Immunoblot wash solution (see recipe)
Primary antibodies against the HSP70 protein family (see Table 2.9.4)
Secondary antibody, biotinylated or conjugated to horseradish peroxidase (Amersham Pharmacia Biotech or Vector)
0.1 M phosphate buffer, pH 7.4 (see recipe)
Standard Elite Vectastain ABC kit (Vector)
10-mg tablets of 3,3′-diaminobenzidine tetrachloride (DAB; Sigma)
30% hydrogen peroxide ≤1 to 2 months old

100°C water bath
Rotating platform shaker

Additional reagents and equipment for SDS-PAGE (*APPENDIX 3A*), transfer of proteins to membrane (*UNIT 2.3*), and Ponceau S staining (see Support Protocol 4)

Prepare sample

1a. *For cultured cells*: Rinse cells with 2 vol ice-cold PBS. Remove solution and prepare protein samples from stressed monolayer cell culture by adding 300 to 500 µl of 1× SDS sample buffer per 100-mm dish and proceed as described in Basic Protocol 3, steps 6 to 11.

1b. *For stressed animals*: Dissect fresh tissue from anesthetized stressed animals on ice, cut into small pieces and place in a microcentrifuge tube. For each 0.1 g of tissue, add ~300 to 500 µl of 1× SDS sample buffer. Heat the sample 2 to 5 min in a 100°C water bath. Dissociate the tissue by triturating through a 1000-µl pipet tip several times. Heat the sample an additional 5 min at 100°C. Triturate the sample through a 200-µl pipet tip. Clarify the lysate by microcentrifuging 5 min at 14,000 × *g*, room temperature as described in Basic Protocol 3, step 7.

The use of a micropestle adapted for microcentrifuge tubes is especially recommended for tougher tissues.

Samples can also be clarified by centrifuging through commercially available filter-membrane spin columns adapted for use with microcentrifuge tubes.

Table 2.9.4 Primary Antibodies Commonly Used to Study the HSP70 Protein Family[a]

Gene	Antibody	Molecular weight (kDa)	Suitability	Supplier
HSP72	Mouse monoclonal	72	IB, IHC	Amersham Pharmacia Biotech, StressGen
HSP73	Rat monoclonal	73	IB, IHC	StressGen
GRP75	Mouse monoclonal	75	IB, IHC	StressGen
GRP78	Rabbit polyclonal	78	IB, IHC	StressGen

[a]Abbreviations: GRP, glucose-regulated protein; HSP, heat shock protein; IB, immunoblot; IHC, immunohistochemistry. Numbers represent the molecular weight of the protein in kDa.

2. Measure the protein concentration using a protein quantitation kit and BSA standards.
3. Prepare samples. In separate microcentrifuge tubes, pipet out an equal amount of protein for each sample. Prepare the molecular weight markers according to the manufacturer's recommendation.
4. Bring all tubes to an equal volume by adding an appropriate amount of 1× SDS sample buffer to each tube. For each 10 µl of final protein sample, add 1 µl of 2-mercaptoethanol (final 5%) and 1 µl of 1% bromphenol blue (final 0.1%). Mix well. Just before loading, heat samples for 1 min in a 100°C water bath.

   Add the 2-mercaptoethanol and 1% bromphenol blue to samples after protein determination because they interfere with the assay.

Electrophorese and transfer samples

5. Separate an equal amount of protein per sample on a denaturing 8% to 10% polyacrylamide gel (*APPENDIX 3A*), to separate proteins in the 68- to 78-kDa range.

   In general and depending on the tissue and stressful stimulus, 20 to 50 µg of protein sample is sufficient to visualize the HSP70 family of proteins. In normal unstressed tissues, HSP72 is not expressed constitutively but HSP73, GRP75, and GRP78 are expressed constitutively. Following a stressful stimulus, most of these HSPs will be expressed at higher levels and will be easily detected.

6. After electrophoresis, transfer the proteins onto a 0.2-µm mesh nitrocellulose or PVDF membrane by tank transfer (*UNIT 2.3*), for 2 hr at 100 V or overnight at 15 V, 4°C.

   Alternatively, semi-dry transfer can be used. Transfer by this method should not be run for longer than 2 hr. Hydrophobic PVDF membranes have been used with success for immunoblot analysis of HSP70 proteins. However, because of its higher affinity for most proteins, nitrocellulose is the membrane of choice for the detection of HSP70 proteins. Nitrocellulose is easily wetted in water, is compatible with a variety of detection assays, and is associated with lower background.

7. To verify equal protein loading and transfer efficiency, reversibly stain the proteins on the membrane with the red water-soluble dye Ponceau S (see Support Protocol 4).

Immunodetect proteins

8. Incubate the membrane for ≥2 hr at room temperature or overnight at 4°C in freshly made immunoblot blocking solution on a rotating platform shaker.

For overnight incubation, add 1 ml of 2% (w/v) sodium azide solution (can be stored indefinitely at room temperature) to prevent bacterial growth. This amount of azide is easily removed by subsequent washes and does not interfere with subsequent reactions.

CAUTION: *Sodium azide is a neurotoxin. Use precautions when weighing powder and handling solutions.*

For monoclonal antibodies, the detergent in the incubating solutions can be omitted. The use of a monoclonal antibody on the tissues from the same species (e.g., rat monoclonal on rat tissues) may be associated with higher background depending on the tissue type. In that case, add 1% to 2% (v/v) of that species normal serum in the blocking solution to help block nonspecific sites.

9. Discard blocking solution and rinse briefly with the immunoblot wash solution.
10. Incubate the membrane for 2 hr at room temperature with the appropriate primary antibody diluted 1:1000 to 1:4000 in the wash solution on a rotating platform shaker.

    The concentration of primary antibody should be adjusted depending on the tissue, the species studied, and the level of protein expression. The appropriate concentration should be determined for each set of primary and secondary antibodies.

    Although a wide variety of antibodies against HSP72 are now commercially available, the use of the monoclonal anti-HSP72 antibody (e.g., Clone 92 from Amersham Pharmacia Biotech) is highly recommended due to its proven specificity and low background in different tissues. Antibodies against GRP75 and GRP78 proteins have not been extensively characterized and are not as widely available. The monoclonal antibodies from StressGen have been used successfully in different systems.

11. Remove the primary antibody solution and perform three 15-min washes in immunoblot wash solution.
12. Incubate the membrane for 1 to 2 hr at room temperature with the appropriate secondary antibody diluted in the immunoblot wash solution on a rotating platform shaker.

    The secondary antibody should be specific for the species in which the primary antibody was produced and should be conjugated with a suitable reporter group. The secondary antibody can be biotinylated, then incubated in an avidin-horseradish peroxidase (HRP) solution (Vectastain ABC, Vector), and visualized with a standard chromogenic method Alternatively, secondary antibodies directly conjugated to an enzyme such as horseradish peroxidase can be used for visualization by highly sensitive chemiluminescent methods (see Alternate Protocol 2).

13. Perform two 15-min washes at room temperature in immunoblot wash solution on a rotating platform shaker. Perform one wash of 15 min at room temperature in 0.1 M phosphate buffer, pH 7.4.

Visualize bound antibody

14. After incubation of the membrane with a biotinylated secondary antibody, prepare an avidin-horseradish peroxidase solution as described by the manufacturer (Standard Elite Vectastain ABC kit, Vector). In brief, mix 2 drops of reagent A with 2 drops of reagent B in 10 ml of 0.1 M phosphate buffer, pH 7.4, and let the solution react 30 min at room temperature.
15. Drain the excess wash solution and incubate the membrane in the avidin/horseradish peroxidase solution 30 min at room temperature on a rotating platform shaker.
16. Remove the solution and perform three 10-min washes in 0.1 M phosphate buffer, pH 7.4, at room temperature on a rotating platform shaker.

17. Make up the chromogen solution by dissolving a 10-mg tablet of DAB in 10 ml of 0.1 M phosphate buffer, pH 7.4. Filter through a filter paper and then add 1.67 µl of 30% hydrogen peroxide. Mix and use immediately.

    CAUTION: *DAB is a potent carcinogen and is highly toxic in both its solid and aqueous forms. Wear gloves at all time and discard all solutions and contaminated materials in accordance with the health and safety guidelines of the institution.*

18. Incubate the membrane in the DAB solution and shake gently and continuously until the bands of interest become visible (~2 to 10 min).

    DAB chromogenic visualization gives medium-dark brown bands on a light brown background. Do not prolong the incubation for too long because that could result in an unreasonably high background.

19. Stop the reaction by removing the DAB solution and washing two times for 5 min with 0.1 M phosphate buffer, pH 7.4. Air dry the membrane and store in plastic wrap at room temperature.

    Document results by taking a picture of the membrane soon after this final step because DAB signal on membranes tends to fade with time.

VISUALIZATION WITH CHEMILUMINESCENT SUBSTRATES

ALTERNATE PROTOCOL 2

Detection of low-abundance proteins in immunoblots can be achieved using chemiluminescent substrate methods, which have shown to be at least ten times more sensitive than other standard detection methods. The ECL chemiluminescent detection method (Amersham Pharmacia Biotech), described below, is quick and convenient (only one simple step), and shows high reproducibility and sensitivity. This method involves the horseradish peroxidase/hydrogen peroxide–catalyzed oxidation of luminol, which emits a blue light that can be captured on X-ray film.

Materials

Chemiluminescence horseradish peroxidase (HRP) substrate kit (e.g., ECL, Amersham Pharmacia Biotech or equivalent)
Immunoblot probed with secondary antibody directly conjugated to horseradish peroxidase (see Basic Protocol 4, step 13)
0.1 M phosphate buffer, pH 7.4 (see recipe)

50-ml conical plastic centrifuge tubes
Rotating platform shaker
X-ray film (e.g., X-Omat AR-5, Kodak)
Automatic X-ray film processor

1. In a 50-ml concial plastic centrifuge tube, mix 1 vol ECL reagent A and 1 vol ECL reagent B.

    The total volume can be adjusted depending on the size of the membrane to be analyzed. In general, 10 ml/10 cm^2 should be sufficient.

2. After the membrane has been incubated with the secondary antibody solution and washed, drain the excess wash solution. Using blunt-end forceps, transfer the membrane to a small clean container.

    The plastic lid of a small pipet tip box can be used as the clean container for minigels.

3. Add the ECL mixture and incubate the membrane at room temperature for exactly 1 min. Shake gently and continuously, making sure the membrane is always covered with the ECL solution.

4. At the end of the incubation, drain the excess ECL solution and wrap the membrane in plastic wrap. Do not dry the membrane.
5. In a dark room, expose the chemiluminescent membrane to an X-ray film for an appropriate length of time. Develop the film immediately in an automatic X-ray film processor.

   Because the ECL chemiluminescent reaction is transient and loses most of its intensity after 1 hr, expose the membrane to an X-ray film as soon as possible after incubation with the ECL reagent mixture. Several exposures are usually needed to determine the best signal-to-noise ratio. For this reason, the use of an automatic X-ray film processor for quick film development is highly recommended. In general, the time of exposure can vary from a few seconds (medium-high protein abundance) to several minutes (for low-abundance proteins).

SUPPORT PROTOCOL 4

REVERSIBLE STAINING OF TRANSFERRED PROTEIN ON MEMBRANES WITH PONCEAU S SOLUTION

To verify equal protein loading and transfer efficiency, proteins on membranes can be stained reversibly with the red water-soluble dye Ponceau S.

Materials

Membrane with transferred proteins (see Basic Protocol 4, step 6)
Ponceau S staining solution (see recipe)

1. Place the membrane in Ponceau S staining solution for 1 to 2 min at room temperature.
2. Pour out the staining solution and save.

   This solution can be reused several times.

3. Destain with deionized water for 1 to 2 min or until bands become visible against a light pink-white background.

   If using non-prestained molecular weight markers, mark the location of each standard band with a pencil or with a small cut in the membrane with a clean razor blade.

4. Completely destain the membrane for 5 to 10 min in distilled water at room temperature.

   Wet membranes can be processed directly for immunoblotting or stored at 4°C in a sealed bag for up to 1 week before analysis. Do not dry the membrane at any time.

BASIC PROTOCOL 5

DETECTION OF HSP70 FAMILY PROTEINS IN TISSUE SECTIONS BY IMMUNOHISTOCHEMISTRY

Immunohistochemistry is used to determine the cellular and regional distribution of specific proteins. This method is easily performed using tissue sections or adherent cell cultures. The method described here to detect the HSP70 protein family in tissue sections uses biotinylated secondary antibodies followed by chromogenic visualization with DAB. If the signal is weak, it can be enhanced using nickel-DAB intensification (see Alternate Protocol 3) or immunofluorescence (see Alternate Protocol 4). Fluorescence staining with two different primary antibodies—one specific for the stress protein and one specific for the cell type—and secondary antibodies conjugated with different fluorochromes (see Alternate Protocol 4) allows identification of specific cell types that are producing stress proteins. Stress-producing stimuli can be associated with cell death. TUNEL (*UNIT 2.2*) can be combined with immunofluoresence to determine the relationship between dying and stress-protein-producing cells (see Alternate Protocol 5).

Materials

Animals or cells subjected to a stressful stimulus (see Tables 2.9.1 and 2.9.3)
Anesthesia cocktail (see recipe)
0.9% (w/v) sodium chloride (saline) solution, ice cold
4% (w/v) paraformaldehyde working solution (PFA; see recipe), ice cold
30% (w/v) sucrose (see recipe)
0.1 M and 0.05 M phosphate buffer, pH 7.4 (PB; see recipe)
Immunohistochemistry peroxidase inhibiting solution (optional, see recipe)
Immunohistochemistry blocking solution (see recipe)
Primary antibodies against the HSP70 protein family (see Table 2.9.4)
Immunohistochemistry antibody dilution buffer (see recipe)
Secondary antibody conjugated to biotin
Avidin/peroxidase complex kit (e.g., ABC Standard Elite Vectastain kit, Vector)
10-mg tablets of 3,3′-diaminobenzidine tetrachloride (DAB, Sigma)
30% (v/v) hydrogen peroxide solution, stabilized, ≤1 to 2 months old (Sigma)

Vibratome or freezing microtome
Paintbrush with small, fine end
6- or 12-well tissue culture plates
Rotating platform shaker
Gelatin-coated histology slides (see Support Protocol 5)

Additional reagents and equipment for preparing gelatin-coated slides (see Support Protocol 5) and coverslipping slides (see Support Protocol 2)

Prepare tissue

1. Subject test animals to stressful stimulus (see Tables 2.9.1 and 2.9.3). At the appropriate time points after stressful stimulus, anesthetize the animal with an intraperitoneal injection of anesthesia cocktail.

2. Perfuse the whole animal through the left ventricle with cold 0.9% sodium chloride solution followed by cold 4% PFA.

3. Carefully remove the tissue of interest, post-fix in 4% PFA for no more than 1 to 4 hr, then transfer to 30% sucrose solution overnight at 4°C.

   When using the monoclonal anti-HSP72 antibody or anti-GRP-75 or anti-GRP 78 (see Table 2.9.4), it is extremely important that fixation with the aldehydes be kept to a minimum. Tissue post-fixation of >4 hr decreases or eliminates all HSP70 immunostaining when the antibody is used at a dilution of 1:2000.

   Post-fixation time will depend on the type of antigen studied and the type of tissue analyzed. The post-fixation time should always be kept to a minimum.

4. Cut 50- to 100-μm–thick sections on a vibratome or freezing microtome and distribute the slices with a small, fine-end paintbrush in a 12-well culture plate containing 2 ml of 0.1 M phosphate buffer, pH 7.4 (free-floating sections).

   Thin sections are essential for good quality immunohistochemistry as they are associated with less background than thicker sections.

   For HSP72 staining using the Amersham antibody (Clone 92, Amersham Pharmacia Biotech), the tissue should be sectioned immediately after intracardiac aldehyde perfusion or after a few hours of aldehyde post-fixation.

   A number of slices can be processed together in each of the 12 wells. If there are a large number of slices for each animal and a lot of antibody is available, 6-well tissue culture dishes can be used with 5 ml of phosphate buffer per well.

5. Wash the sections two times with 0.1 M phosphate buffer, pH 7.4, or store them in 0.1 M phosphate buffer, pH 7.4, overnight at 4°C to allow the excess PFA to diffuse out of the slices.

6. Remove the buffer solution from each well by carefully holding the slices on one side of the well with a small paintbrush or pipet tip and aspirating the solution with a vacuum line on the opposite side of the well.

Cut sections should be washed in several changes of phosphate buffer. Immunohistochemistry should be started as soon as possible after cutting.

Normally, it is important to reduce the amount of background in tissues containing a high level of endogenous peroxidases by incubating the sections in immunohistochemistry peroxidase inhibiting solution. However, in some cases, particularly for the HSP 70 family of proteins, this procedure can result in the loss of antigenicity.

Expose tissue sections to antibody

7. Incubate the sections for 2 hr at room temperature in immunohistochemistry blocking solution.

Serum or bovine serum albumin is needed to block nonspecific binding sites. Triton X-100 is a membrane detergent that improves the penetration of antibodies through tissues.

For monclonal anti-HSP 72, anti-GRP-75, and anti-GRP-78 (Table 2.9.4), the blocking solution can be simplified by omitting the nonfat dry milk solids and the whole rat serum.

8. Remove the blocking solution and wash once briefly with 0.1 M phosphate buffer, pH 7.4.

9. Remove the buffer solution and incubate the tissue sections for 12 to 24 hr at 4°C with an appropriate primary antibody (see Table 2.9.4) diluted in immunohistochemistry antibody dilution buffer.

As a negative control, incubate alternate sections from each tissue sample without the primary antibody or with preabsorbed immune serum. For each tissue, serial dilutions (1:1000, 1:2500, 1:5000, 1:10000, etc.) of primary antibody should be performed on a few slices to establish the appropriate concentration for optimal signal-to-noise ratio.

10. Remove the primary antibody solution and perform three 15-min washes in 0.1 M phosphate buffer, pH 7.4, at room temperature, on a rotating platform shaker.

11. Remove phosphate buffer wash and incubate all sections (including the negative controls) for 1.5 hr, at room temperature, with an appropriate biotinylated secondary antibody diluted 1:200 in immunohistochemistry antibody dilution buffer.

When used on rat tissues, biotinylated anti-rabbit (Vector) and anti-mouse (Amersham Pharmacia Biotech) secondary antibodies usually do not produce much of a background if diluted 1:200. When using rat tissue with an anti-rat secondary antibody, the dilution should be at least 1:300 to reduce the associated background.

12. Remove the secondary antibody solution and perform three 15-min washes in 0.1 M phosphate buffer, pH 7.4, at room temperature, on a rotating platform shaking.

Visualize bound antibody

13. Meanwhile, prepare an avidin-horseradish peroxidase solution (Standard Elite Vectastain ABC kit) by adding 2 drops of reagent A and 2 drops of reagent B to 10 ml of 0.1 M phosphate buffer, pH 7.4. Mix well and let the solution react at room temperature for ≥30 min.

14. Incubate sections in the avidin-horseradish peroxidase solution for 1.5 to 2 hr at room temperature.

15. Remove the solution and perform three 15-min washes in 0.1 M phosphate buffer, pH 7.4, at room temperature, on a rotating platform shaker.

16. Visualize the bound antibody with the DAB method. Make the DAB solution by adding a 10-mg tablet of 3,3′-diaminobenzidine tetrachloride to 50 ml of 0.1 M phosphate buffer, pH 7.4. Mix well and filter through a filter paper. Use within 30 min.

    CAUTION: *DAB is a potent carcinogen and is highly toxic in both its solid and aqueous forms. Wear gloves at all times and discard all solutions and contaminated materials in accordance with the health and safety guidelines of the institution.*

17. Incubate the tissue sections in the DAB solution for no more than 5 min (for 12-well plates, use 2 ml/well; for 6-well plates use 5 ml/well).

18. Meanwhile, prepare the hydrogen peroxide solution by adding 0.1 ml of 30% hydrogen peroxide to 10 ml of 0.1 M phosphate buffer, pH 7.4.

    Make sure the 30% hydrogen peroxide stock solution is no more than 1 to 2 months old.

19. Add 1 drop of diluted hydrogen peroxide solution for each 1 ml of DAB solution. Do this slowly, one drop at a time, on a rotating platform shaker. Incubate the tissue sections at room temperature until they turn to a light-to-medium brown color.

20. Stop the reaction by removing the DAB solution and washing twice with 0.1 M phosphate buffer, pH 7.4.

21. Mount the sections on gelatin-coated slides (see Support Protocol 5), air dry, and coverslip (see Support Protocol 2).

NICKEL-DAB INTENSIFICATION OF IMMUNOHISTOCHEMICAL SIGNALS

ALTERNATE PROTOCOL 3

Nickel intensification can be used in conjunction with the DAB method to enhance the signal of a low-abundance protein. Nickel intensification can also be followed by a second staining procedure using another primary antibody and the standard DAB method. In that case, one antigen is immunolabeled with a dark blue/black precipitate (nickel-DAB), and the second antigen is immunolabeled with a brown precipitate (standard DAB).

Additional Materials *(also see Basic Protocol 5)*

0.175 M sodium acetate, pH 6.7 (see recipe)
Nickel sulfate

1. Immunolabel tissue sections (see Basic Protocol 5, steps 1 to 14).

2. After incubation with the avidin-horseradish peroxidase solution (Vectastain ABC kit), wash the tissue slices once with 0.1 M phosphate buffer, pH 7.4, for 15 min and once with 0.175 M sodium acetate, pH 6.7, for 15 min at room temperature.

3. Prepare the substrate solution by dissolving 1.25 g of nickel sulfate and one 10-mg tablet of DAB in 50 ml of 0.175 M sodium acetate, pH 6.7. Mix well and filter the solution through filter paper. Use within 30 min.

   Because nickel ions precipitate with phosphates, the use of 0.175 M sodium acetate solution, pH 6.7, instead of phosphate buffer for regular DAB method is absolutely necessary.

4. Incubate the tissue sections in the nickel-DAB solution for no more than 5 min (for 12-well plates, use 2 ml/well; for 6-well plates, use 5 ml/well) at room temperature.

5. Meanwhile prepare the hydrogen peroxide solution by adding 0.1 ml of 30% hydrogen peroxide stock solution to 10 ml of 0.175 M sodium acetate, pH 6.7.

   Make sure the 30% hydrogen peroxide stock solution is <1 to 2 months old.

6. Add 1 drop of diluted hydrogen peroxide solution for each 1 ml of nickel-DAB solution. Do this slowly, one drop at a time, on a rotating platform shaker. Incubate the tissue sections at room temperature until they turn to a medium-purple color.

   Nickel ions coprecipitate with DAB, thus intensifying the staining. Whereas the standard DAB method results in a brown reaction product, the nickel-DAB intensification method yields a dark blue/black product. Because the nickel-DAB method can lead to unacceptably high background staining, avoid incubation times >5 to 7 min.

7. Stop the reaction by washing the tissue sections briefly in 0.175 M sodium acetate, pH 6.7, and for 15 min in 0.1 M phosphate buffer, pH 7.4.

   Prolonged incubation in 0.175 M sodium acetate, pH 6.7, should be avoided since it may result in nickel dissolution from the DAB reaction product.

8. Mount the sections on gelatin-coated slides (see Support Protocol 5), air dry, and coverslip (see Support Protocol 2).

ALTERNATE PROTOCOL 4

DOUBLE IMMUNOFLUORESCENCE STAINING FOR CELL-TYPE IDENTIFICATION

In a complex tissue, analysis of the morphology and location of a particular cell are usually not accurate enough to determine a specific cell type. Double-fluorescence immunolabeling using an antibody against cell-specific markers along with another antibody against a stress protein can be a useful method to determine in which particular cell type a stress protein is expressed. It is important to use primary antibodies of different types (made in different species) that can be recognized by two secondary antibodies also made in different host species. The two secondary antibodies have to be linked to different fluorochromes. The most common fluorescent probes used are rhodamine (emits a red signal) and fluorescein (emits a yellow/green signal). Whereas one of the secondary antibodies can be biotinylated and detected with an avidin-coupled fluorescence marker, the other secondary antibody can be directly coupled with a different fluorochrome. If the primary antibodies are made in the same species (for example, two mouse monoclonal antibodies), the stainings need to be done sequentially. The first staining should be done with the standard DAB method (see Basic Protocol 5) and the second one with fluorescence.

Additional Materials *(also see Basic Protocol 5)*

Two primary antibodies made in different species
Secondary antibodies: one conjugated to biotin, one conjugated to a fluorochrome
Avidin-conjugated fluorochrome
Fluorescence mounting medium: 3:1 (v/v) glycerol/0.1 M phosphate buffer, pH 7.4, containing 0.1% (w/v) paraphenylenediamine or Fluoromount-G (Southern Biotech) or Vectashield (Vector) or Slowfade-Light Antifade (Molecular Probes)
Light-proof box

1. Follow Basic Protocol 5, steps 1 to 9, except in step 9, substitute the primary antibody with a mixture of two primary antibodies of different types.

2. Remove the primary antibody solution and perform three 15-min washes in 0.1 M phosphate buffer, pH 7.4, at room temperature on a rotating platform shaker.

3. Remove buffer solution and incubate all sections for 2 hr at room temperature with a mixture of two appropriately conjugated secondary antibodies (one can be biotinylated and the other one can be directly conjugated to a fluorochrome) diluted in immunohistochemistry antibody dilution buffer.

   CAUTION: *All incubations involving the fluorescent probes should be performed in the dark (wrap the containers in foil) and work should be done in a dark or dim-light room.*

4. Remove the secondary antibody solution and perform three 15-min washes in 0.1 M phosphate buffer, pH 7.4, at room temperature on a rotating platform shaker.

5. Incubate, in the dark, tissue sections with an avidin-conjugated fluorochrome for 2 hr at room temperature.

   The fluorochrome linked to avidin should be different from the fluorochrome conjugated directly to the other secondary antibody used in step 3.

6. Remove the solution and perform three 15-min washes in 0.1 M phosphate buffer, pH 7.4, at room temperature, on a rotating platform shaker.

7. Mount the tissue sections on gelatin-coated slides (see Support Protocol 5) and coverslip immediately with fluorescence mounting medium.

   Do not dry the sections before coverslipping. The fluorescence mounting medium will help preserve the humidity and structure of the section and slow down fluorescence fading and photobleaching. Slides should be photographed shortly after the experiment. They can be stored horizontally in a light-proof box at 4°C or at −20°C for longer storage periods. Commercially available mounting media designed for working with fluorescent probes also provide very good results (e.g., Fluoromount-G, Southern Biotech or Vectashield, Vector or Slowfade-Light, Molecular Probes).

TUNEL STAINING OF DNA FRAGMENTATION IN COMBINATION WITH IMMUNOHISTOCHEMISTRY

ALTERNATE PROTOCOL 5

This method uses terminal deoxynucleotidyl transferase (TdT) to label the 3′-OH ends of fragmented genomic DNA in cultured cells and tissue slices (also see *UNIT 2.2*). In this assay, DNA fragments are visualized using avidin/peroxidase with nickel-DAB enhancement. Although TUNEL has been claimed to be relatively specific for apoptotic DNA fragmentation, recent studies suggest that the TUNEL method labels DNA fragmentation in both apoptotic and necrotic cells. Thus, TUNEL labeling is a marker of dying cells regardless of the mechanism. The distinction between apoptotic and necrotic cell death needs to be confirmed not only by typical morphology (chromatin condensation, cell shrinkage or swelling, cell membrane blebbing; see *UNITS 2.1 & 2.2*) and agarose gel electrophoresis analysis of genomic DNA laddering, but most importantly, by electron microscopy observation. To identify the areas of stress protein induction in relation to the areas of dying cells, the TUNEL method is used in combination with immunohistochemistry (see Basic Protocol 5 or Alternate Protocol 4).

Additional Materials *(also see Basic Protocol 5)*

0.3% (v/v) Triton X-100 in 0.1 M phosphate buffer, pH 7.4 (see recipe for buffer)
20 µg/ml proteinase K in 0.1 M phosphate buffer, pH 7.4 (see recipe for buffer; optional)
1× and 5× TdT buffer (Gibco BRL or Roche Molecular Biochemicals)
400 µM biotinylated 14-dATP (Life Technologies)
15 U/µl TdT (terminal deoxynucleotidyl transferase; Gibco BRL or Roche Molecular Biochemicals)
2× SSC (optional; see recipe)
2% (w/v) bovine serum albumin (BSA; see recipe; optional)

0.175 M sodium acetate, pH 6.7 (see recipe)
Nickel sulfate
75%, 95%, and 100% ethanol

Powdered dry ice
Cryostat
Gelatin-coated histology slides (see Support Protocol 5) or precoated slides (e.g., SuperfrostPlus or Probe-On, Fisher)
PAP pen or equivalent hydrophobic pen (ImmEdge Pen, Vector or PAP Pen, ScyTek)
Humidified chamber with lid
Coplin staining jars
Light microscope

Prepare tissue

1. Subject test animals to stress stimulus. At the appropriate time after the stimulus, euthanize animals under deep anesthesia induced by intraperitoneal injection of the anesthesia cocktail. Quickly remove the tissue of interest, freeze on powdered dry ice, and store at −70°C until analysis.

   These steps have to be performed quickly, since keeping the tissue at 20° to 37°C accelerates necrotic DNA fragmentation. To save time and prevent DNA degradation when many animals have to be dissected all at once, put the tissue in sterile saline at 4°C until all animals have been dissected, and then freeze.

2. Cut 14- to 20-µm thick sections on a cryostat and collect the slices on cold gelatin-coated or commercially precoated histology slides. Store at −70°C until analysis.

3. Prior to use, take slides from the freezer and dry at room temperature for ~10 to 20 min. Warm the slides at 40° to 55°C on a heating table to ensure better adhesion of the tissue sections to the slides. Make a circle around the sections with a hydrophophic (PAP) pen.

   This is to prevent run off of the solution to be applied in the following steps. It also saves probe, reagents, and solutions by restricting a smaller volume for incubation right over the tissue slice.

   For cell cultures grown on poly-D-lysine coated coverslips, wash the coverslip twice with cold 0.1 M phosphate buffer, pH 7.4 (see recipe), to remove the medium. Glue the dried coverslips on the surface of a microsope slide and circle with a (PAP) pen.

4. Fix the tissue sections by immersing the slides in 4% paraformaldehyde for 10 to 30 min at 4°C.

   A long fixation time may lead to low staining intensity, whereas too short a fixation time may result in a high background stain. If no proteinase K is used, fix for 10 min. If proteinase K is used, fix for 30 min. It is absolutely essential to fix the tissue onto the slide, because the steps hereafter, especially the TdT labeling step and proteinase K treatment, tend to dissolve the coating material of the slides.

5. Wash the slides in 0.3% Triton X-100 in 0.1 M phosphate buffer, pH 7.4, for 30 min at room temperature.

6. Wash two times in 0.1 M phosphate buffer, pH 7.4, for 15 min at room temperature.

7. *Optional:* Incubate the tissue sections in 20 µg/ml proteinase K for exactly 15 min at room temperature. Wash twice in 0.1 M phosphate buffer, pH 7.4, each time for 15 min at room temperature.

Do not overincubate with proteinase K if subsequent immunohistochemistry is to be performed on the same tissue section. This step is to remove all the proteins associated with genomic DNA to increase the labeling intensity. However, it significantly increases the chances of washing away the sections or cells. Furthermore, combining immunocytochemistry with TUNEL becomes very difficult if all proteins are digested by the proteinase K. Because the TUNEL staining intensity without proteinase K is usually acceptable, it is recommended that the first experiments be conducted without proteinase K treatment. If there is no TUNEL staining, proteinase K treatment may be used.

Perform TUNEL assay

8. Drain excess wash solution from the slide and preincubate in 150 to 200 µl of 5× TdT buffer/section in a humid chamber for 15 min at room temperature.

   The hydrophobic PAP pen trace should prevent this small volume of liquid from running over other areas of the slide. To avoid buffer evaporation, place slides in a humid chamber containing one layer of wet paper towels at the bottom.

9. After preincubation, drain the solution on a paper towel. To 450 µl of 1× TdT buffer, add 50 µl of 400 µM biotinylated 14-dATP (final concentration 40 µM) and 150 U TdT enzyme. Mix gently (do not vortex) and add 150 µl to 200 µl onto each tissue section. Incubate for 1 hr in a humid chamber placed in a 37°C incubator.

   Do not overincubate as it will result in nonspecific signal.

10. Wash the slides two times by immersing in 2× SSC for 15 min at room temperature in Coplin staining jars.

    SSC is used to terminate the TdT reaction.

11. Wash two times in 2% BSA for 15 min at room temperature.

    In general, washing with 0.1 M phosphate buffer, pH 7.4, is equally effective. The washes with BSA can be omitted if the background level without it is low.

12. Wash two times in 0.1 M phosphate buffer, pH 7.4, for 15 min at room temperature.

Visualize fragmented DNA

13. Meanwhile, prepare an avidin–horseradish peroxidase solution according to manufacturer's instructions (Standard Elite Vectastain ABC kit). Mix 5 µl each of reagent A and B in 500 µl of 0.1 M phosphate buffer, pH 7.4, and react at room temperature for ≥30 min.

14. Drain the excess wash solution and overlay the tissue specimens with a small volume (150 to 250 µl/slide) of avidin–horseradish peroxidase solution. Incubate for 30 min at room temperature in a humid chamber.

15. Wash two times, each time for 15 min at room temperature, by immersing slides in 0.175 M sodium acetate solution, pH 6.7, in a Coplin staining jar.

16. Prepare the substrate solution by dissolving 0.4 g of nickel sulfate and one 10-mg tablet of DAB in 40 ml of 0.175 M sodium acetate solution, pH 6.7. Mix well and filter the solution through filter paper. Just before use, add 100 µl of 30% hydrogen peroxide solution. Mix well and use immediately.

    CAUTION: *DAB is a potent carcinogen and is highly toxic both in solid and aqueous form. Wear gloves at all times and discard all contaminated solutions and materials in accordance with the health and safety guidelines of the institution.*

    Because nickel ions precipitate with phosphates, the use of 0.175 M sodium acetate solution, pH 6.7, instead of phosphate buffer as for the regular DAB method, is absolutely necessary.

17. Drain the excess wash solution from the slides and pipet a small volume of nickel-DAB solution directly on top of the tissue specimen. Monitor the staining reaction under a light microscope.

    Nickel ions coprecipitate with DAB, thus intensifying the staining. The nickel-DAB intensification method yields a dark blue/black product.

18. When the staining intensity is suitable, pour out the nickel-DAB solution and dip the slides briefly in 0.1 M phosphate buffer, pH 7.4, or 0.175 M sodium acetate solution, pH 6.7.

    Do not overincubate as it will increase background. This is especially important if immunohistochemistry is to be performed subsequently on the same section.

19. Wash the slides two times by immersing in water for 5 min at room temperature.

20. Proceed with immunohistochemistry immediately (see Basic Protocol 5 or Alternate Protocol 4).

    If desired, immunohistochemistry may be omitted.

21. Dehydrate successively in 75%, 95%, and 100% ethanol and coverslip (see Support Protocol 2).

SUPPORT PROTOCOL 5

PREPARING GELATIN-COATED SLIDES

Gelatin-coated slides improve the attachment of tissue sections to the slide surface.

Materials

Milli-Q-purified water
1% (v/v) hydrochloric acid solution
70% and 95% ethanol
Gelatin (type Bloom 275)
Chromium potassium sulfate

Slide racks
25 × 75–mm microslides with a frosted end, precleaned (Fisher)
Glass staining dishes
Whatman 3MM filter paper
Storage slide boxes

NOTE: To avoid fingerprint smudges, always wear clean, powder-free gloves when manipulating the slides. Wear safety goggles and gloves to avoid acid burn.

Wash slides

1. Fill slide racks with 25 × 75–mm microslides. Orient the slides so that they all face in the same direction. Immerse in hot soapy water for 1 hr.
2. Rinse in running tap water for 1 hr.
3. Rinse thoroughly in Milli-Q-purified water for 30 min.
4. Remove from water and drain.
5. Immerse in 1% hydrochloric acid solution for 3 min at room temperature.
6. Rinse in Milli-Q-purified water for 3 min.
7. Rinse in 70% ethanol solution for 3 min.
8. Rinse in 95% ethanol solution for 3 min.
9. Allow slides to dry before subbing.

Sub slides

10. Heat 600 ml water to 80°C. While stirring, add 3.0 g of gelatin until completely dissolved. Add 3.0 g of chromium potassium sulfate. Cool to room temperature and use immediately.
11. Filter the solution through a Whatman 3MM filter paper into a graduated cylinder.

    The final solution contains 0.5% gelatin and 0.05% chrome alum.

12. Dip the clean slides into the subbing solution for 2 min. Do this carefully to avoid air bubbles.
13. Remove slide rack from gelatin solution and drain excess solution by setting the rack tilted on its side, with the frosted sides of the slides facing downward. Air dry thoroughly or overnight before use.
14. Store the gelatin-coated slides in slide boxes at room temperature in a dry environment.

REAGENTS AND SOLUTIONS

Use Milli-Q-purified water or equivalent in all recipes and protocol steps. For common stock solutions, see ***APPENDIX 2A****; for suppliers, see* ***SUPPLIERS APPENDIX****.*

Anesthesia cocktail

200 U/kg heparin
80 mg/kg ketamine
8 mg/kg xylazine
Prepare fresh before each use.

Bovine serum albumin (BSA) solution, 2% (w/v)

2 g BSA, fraction V
100 ml 0.1 M phosphate buffer, pH 7.4 (see recipe)
Prepare fresh before use

Bromphenol blue, 1% (w/v)

0.5 g bromphenol blue
Sterile H_2O to 50 ml
Mix well and store indefinitely at room temperature

Coomassie blue staining solution

500 ml H_2O
400 ml methanol
100 ml acetic acid, glacial
1 g Coomassie blue G-250

Mix methanol and then acetic acid in water. Add the Coomassie blue and stir until dissolved. Filter through Whatman no. 1 paper. Store indefinitely at room temperature.

Cresyl violet staining solution

0.3 g Cresyl Echt Violet in 50 ml H_2O
3.48 ml acetic acid in 300 ml H_2O
5.44 g sodium acetate in 200 ml H_2O

Combine all solutions above and filter through Whatman 3MM filter paper. Store indefinitely at room temperature.

Denhardt's solution, 100×

5 g Ficoll 400
5 g polyvinylpyrrolidone
5 g bovine serum albumin, fraction V
Add sterile H_2O to 250 ml
Divide into aliquots and store frozen up to 12 months at −20°C

DEPC-treated water

0.2 ml diethyl pyrocarbonate (DEPC)
1000 ml H_2O
Shake vigorously and incubate overnight at 37°C
Autoclave the solution to inactivate traces of DEPC
Store indefinitely at room temperature

CAUTION: *DEPC is a potent carcinogen. Work in a fume hood and wear gloves at all times.*

Dextran sulfate, 50% (w/v)

Add just enough sterile water to 25 g dextran sulfate to dissolve the bulk of the solid material (the solution is extremely viscous). When the solution has set, add sterile water to 50 ml. Store at room temperature.

Dithiothreitol (DTT), 5 M

7.7 g DTT
10 ml 0.01 M sodium acetate, pH 5.2
Filter through 0.22- to 0.45-µm filter
Divide into aliquots and store frozen up to 12 months at −20°C

Gel destaining solution

70 ml acetic acid
50 ml methanol
H_2O to 1000 ml
Mix well and store indefinitely at room temperature

Gel fixing solution

400 ml methanol
70 ml acetic acid
H_2O to 1000 ml
Mix well and store indefinitely at room temperature

Immunoblot blocking solution

5 g nonfat dry milk
1 g bovine serum albumin, fraction V
0.1 ml Tween 20 (optional)
0.1 M phosphate buffer, pH 7.4 (see recipe), to 100 ml
Make fresh before each use
For overnight incubation, add 1 ml of 2% sodium azide to prevent bacterial growth.

Immunoblot wash solution

5 g bovine serum albumin, fraction V (1% w/v)
0.5 ml Tween 20 (0.1% v/v; optional)
500 ml 0.1 M phosphate buffer, pH 7.4 (see recipe)
Store up to 1 week at 4°C

Immunohistochemistry antibody dilution buffer

1 ml bovine serum albumin (BSA), fraction V
0.1 ml Triton X-100
2 ml serum from the host species used to make the secondary antibody
0.1 M phosphate buffer, pH 7.4 (see recipe), to 100 ml
Mix well, aliquot and store at −20°C

Immunohistochemistry blocking solution

5 g nonfat dry milk
1 g bovine serum albumin, fraction V
0.1 ml Triton X-100
0.5 ml rat whole serum
2 ml serum from host species used to make the secondary antibody
0.1 M phosphate buffer, pH 7.4 (see recipe), to 100 ml
Make fresh before each use

Immunohistochemistry peroxidase inhibiting solution

0.65 g sodium azide
0.2 ml 30% hydrogen peroxide solution, <1 to 2 months old
Add 0.1 M phosphate buffer, pH 7.4 (see recipe), to 100 ml
Make fresh before each use

In situ hybridization cocktail

50 ml formamide, deionized
20 ml 20× SSC (see recipe)
2 ml 100× Denhardt's solution (see recipe)
10 ml 0.2 M phosphate buffer, pH 7.0 (see recipe)
10 g dextran sulfate
5 ml 20% (w/v) *N*-lauroylsarcosine (Sarcosyl)
Mix at 37°C overnight or until the dextran crystals are dissolved
Add sterile H_2O to 100 ml
Filter through a 0.45 to 0.8-µm filter
Divide into aliquots and store up to 6 to 12 months at −20°C

Do not store for >6 to 12 months. The solution should be discarded if it is cloudy when thawed.

Methylene blue RNA staining solution, 0.02% (w/v)

2.5 g sodium acetate, anhydrous
80 ml sterile H_2O
Adjust pH to 5.5 with acetic acid
Add 0.02 g methylene blue
Add H_2O to 100 ml
Store up to 6 months at room temperature

Paraformaldehyde solution, 4% (w/v)

8% paraformaldehyde stock: Add 40 g paraformaldehyde (PFA) to 480 ml water. In a fume hood, heat to 80°C while stirring. When at 80°C, turn off the heat and add a few drops of 1 N NaOH, until the solution becomes clear. Cool to room temperature and filter through a Whatman 3MM filter paper into a 500-ml graduated cylinder. Add water to 500 ml. Store the 8% PFA stock solution up to 1 to 2 months in air-tight bottle at 4°C.

4% working solution: To use in perfusion, combine one volume of 8% PFA with an equal volume of 0.2 M phosphate buffer, pH 7.4 (stock), for a final concentration of 4% PFA in 0.1 M phosphate buffer, pH 7.4.

Phosphate buffer (pH 7.4), 0.2 M

5.24 g $NaH_2PO_4 \cdot H_2O$
23 g $Na_2H_2PO_4$
800 ml H_2O
Adjust pH to 7.4
Add H_2O to 1000 ml

Add chemicals gradually to water while stirring (the solution may need to be heated to dissolve the chemicals). Store indefinitely at room temperature.

For 0.1 M and 0.05 M phosphate buffer, dilute 0.2 M appropriately in water.

Ponceau S staining solution

2 g Ponceau S
1 ml acetic acid
H_2O to 100 ml
Mix well and store indefinitely at room temperature

SDS sample buffer, 1×

0.7 g Tris base
10 ml glycerol
2 g SDS
H_2O to 80 ml
Adjust pH to 6.8 with concentrated HCl
Add H_2O to 100 ml
Store up to 1 to 2 months at room temperature

Sodium acetate solution, pH 6.7, 0.175 M

14.4 g sodium acetate, anhydrous
900 ml H_2O
Adjust pH to 6.7 with acetic acid
Add H_2O to 1000 ml
Store up to 1 month at 4°C

SSC, 20×

175.3 g NaCl
88.2 g sodium citrate (trisodium dihydrate)
800 ml H_2O
Adjust pH to 7.0
H_2O to 1000 ml
Autoclave
Store indefinitely at room temperature

SSPE, 20×

210 g NaCl
53.6 g $Na_2HPO_4 \cdot 7\ H_2O$
7.4 g EDTA
800 ml H_2O
Adjust pH to 7.0.
H_2O to 1000 ml.
Autoclave.
Store indefinitely at room temperature

Sucrose, 30% (w/v)

Dissolve 30 g sucrose in 70 ml warm water. Add water to 100 ml. Autoclave and store up to 1 month at 4°C.

COMMENTARY

Background Information

The induction of stress proteins is a ubiquitous cellular response of most tissues and organisms to a broad variety of metabolic and environmental insults. In the last fifteen years, major classes of stress proteins have been characterized with respect to inducers, organisms, and tissues (Table 2.9.3). Many of these proteins have been associated with resistance to cellular injury, since they preserve and recover the tertiary structure and the function of various cellular protein complexes (Bergeron et al., 1996; Massa et al., 1996; Sharp et al., 1999). The HSP70 protein family has been extensively characterized. It comprises different genes, encoding proteins of molecular mass between 68 and 78 kDa. HSP72 and HSP73 act as chaperones in the nucleus and cytoplasm by preventing the formation of abnormal protein conformation. In normal cells, HSP73 is constitutively expressed whereas HSP72 is only expressed at exceedingly low levels. Following various stimuli, HSP72 expression is markedly induced compared to HSP73. In contrast, GRP75 and GRP78 are chaperone proteins within the mitochondria and the endoplasmic reticulum, respectively. The GRPs are constitutively expressed in normal cells, but both are inducible by several stimuli (Tables 2.9.1 and 2.9.3). In addition to being molecular markers of cellular stress in tissues, recent studies using heat shock or viral overexpression suggest that the induction of some HSP70s may protect against specific types of injury or pathological processes (Sharp et al., 1999).

Critical Parameters and Troubleshooting

Northern blot hybridization

The most critical element for northern blotting is the quality of the RNA extracted. It is important to excise, freeze, and/or homogenize the tissue quickly before substantial degradation occurs. It is also essential to minimize RNase contamination with the use of RNase-free chemicals, solutions, and materials, and by wearing clean powder-free gloves at all times during the experiment. Make sure to allow enough time for isopropanol precipitation and do not dry out the final RNA pellet as it will result in low RNA recovery. Because mRNA represents only a small fraction (2% to 5%) of total RNA, use mRNA extracts (instead of total RNA) when the transcript of interest is low in abundance. The use of mRNA will result in a cleaner and enhanced signal.

In general, a suitable oligonucleotide sequence for northern analysis and in situ hybridization should be ~30 to 45 bp long with a 50% to 65% GC content (Stahl et al., 1993). The oligonucleotide sequence should fall within the protein coding sequence (open reading frame). Because coding sequences show the most homology between different species, it is possible to use the same oligonucleotide for tissues obtained from different species. The specificity of the selected sequence should be verified by comparing it to known sequences in GenBank. Northern blot analysis using the antisense oligonucleotide sequences described in Table 2.9.2 shows bands of expected size in rodent tissues (Miller et al., 1991; Massa et al., 1995; Narasimhan et al., 1996).

In situ hybridization

Although in situ hybridization performed with oligonucleotides can be insensitive for rare mRNAs, it is a very useful method for mapping the mRNA expression of the HSP70 family members, because their expression can be induced several fold by various stimuli (Tables 2.9.1. and 2.9.3). The use of ^{35}S-labeled probes (instead of ^{33}P or ^{32}P) is highly recommended since it is associated with higher efficiency of grain production and less signal scattering, thus providing greater resolution. Because ^{35}S has a longer half life (87 days) than the other isotopes (14 and 25 days for ^{32}P and ^{33}P, respectively), multiple film exposures can be performed and the use of autoradiographic emulsion (which requires long exposure) becomes possible.

The experimental conditions presented here are optimized for work with short oligonucleotides (i.e., 30- to 45-mer) with a 50% to 65% guanosine-cytosine (GC) base content. This is important because a higher percentage of GC content will result in higher melting temperatures that may compromise specimen preservation. In addition, higher GC content may result in higher intramolecular probe interactions that could affect the efficiency of hybridization with the target mRNA in the tissue and lead to nonspecific pairing. Nonspecific hybridization of the probe to cellular DNA appears unlikely because the conditions described are suboptimal for DNA denaturation

in tissue specimens (Pardue, 1985). To control for the possibility that the probe might bind significantly to DNA rather than RNA in a given tissue, some slides can be treated with RNase prior to hybridization. The signal obtained from such experiments indicates the level and location of DNA hybridization in the tissue. However, the most important control experiment is to perform the in situ hybridization with the sense oligonucleotide probe of the gene of interest. The signal should be very low to undetectable. The quality of tissue sections will greatly influence the distribution and the level of transcript detected. It is important to excise the tissue quickly and freeze it in a bath of isopentane maintained at −35°C to −40°C on dry ice (~1 min). This method helps preserve the shape of the tissue and prevents quick fractures and other freezing artifacts (i.e., ice crystals in tissue) that could significantly affect sectioning and the in situ signal. While cutting sections, always keep slides at approximately −20°C on the cryostat shelf. To add a section to a slide, warm up a small area with a gloved finger, collect the slice and put the slide back on the cryostat shelf. Avoid touching the frozen sections and tissue with fingers or warm instruments. Transfer the slides to −70°C until they are assayed. It is absolutely crucial to avoid freeze-thaw-freeze cycles, which will result in rapid degradation of transcript.

Protein labeling

The protocol described in this unit has been used successfully with confluent cultures of astrocytes, NIH3T3 cells, and other mammalian cell lines. It is important to incubate the cells in a methionine-free medium ≥12 hr before metabolic labeling to ensure that most of the endogenous methionine is used up. This will favor ^{35}S-methionine incorporation and thus increase the specific activity of the proteins in the cell lysate. Because cells only incorporate a certain amount of methionine per hour (depending on their metabolic rate), using too much radioactivity will be ineffective for increasing the amount of ^{35}S-methionine incorporated. It is also more difficult to wash out the excess radioactivity, which can contribute to higher background in the cell lysates. In most normal cell systems, a 2-hr labeling period is necessary, and this time period is generally sufficient to detect a significant amount of ^{35}S-methionine incorporation into proteins. The labeling period should be optimized for a given insult and cell system. In general, longer incubations with the radioactivity will result in higher incorporation but higher background (i.e., saturated signal on autoradiograms) whereas shorter incubations may not allow enough time for incorporation and reliable detection. A 2-hr labeling period at different time points after a stressful stimulus provides a means to follow the development of a stress response (i.e., decreased overall protein synthesis with concomitant increases in specific stress proteins). This method only provides information on the overall amount of ^{35}S-methionine incorporation, which is an indirect measure of protein synthesis. In addition, this approach is nonspecific and only identifies proteins based on their apparent molecular weight. To confirm the identity of a specific protein, it is recommended that an immunoblot analysis be performed on the radioactive cell lysate.

Immunoblotting

The mouse monoclonal antibody (C-92 Clone), originally described by Welch and Suhan (1986) and now sold by Amersham Pharmacia Biotech and StressGen, produces one major band and one minor band on immunoblots in rat brain (Narasimhan et al., 1996) and only one major band in mouse brain (Bergeron et al., 1996). This antibody demonstrates a clean signal on immunoblots without the use of a detergent such as Tween 20 in the incubating solutions. Similarly, the mouse monoclonal GRP75 antibody and rabbit polyclonal GRP78 antibody both recognize a single band on immunoblots.

Because members of the HSP70 family are fairly resistant to high temperatures, protein lysates can be prepared simply and quickly by homogenizing the tissue directly in 1× SDS sample buffer followed by incubating 2 to 5 min at 100°C. For more common problems associated with SDS-PAGE and immunoblotting techniques, refer to Table 2.9.5.

Immunohistochemistry

Immunohistochemistry performed with the mouse monoclonal HSP72 antibody (Clone 92, Amersham Pharmacia Biotech or StressGen) on astrocytes transfected with the rat hsp70 gene cloned from rat brain (Longo et al., 1993) yields specific staining (Narasimhan et al., 1996). This suggests that the C-92 recognizes the protein translated from the rat hsp70 gene and confirms the identity of the gene product studied in most of the published HSP70 immunohistochemistry studies to date.

Because the HSP72 antibody (C-92 clone) is very sensitive to overfixation, the tissue should be sectioned immediately after intracardiac aldehyde perfusion or after a few hours of aldehyde postfixation. Immunohistochemistry should be started as soon as possible after cutting sections. Tissue injury can activate endogenous peroxidase activity in cells and sometimes results in false-positive signals. To control for this problem, it is essential that alternate sections be processed for immunohistochemistry without the primary antibody and/or secondary (anti-IgG) antibody. Staining present after deletion of the primary antibody suggests that the secondary antibody recognizes nonspecific sites. If this occurs, dilute the antibody further or use another source of secondary antibody. Staining that is still present after deletion of the secondary antibody (or both antibodies) may be due to activation of endogenous peroxidase activity. The common practice of quenching endogenous peroxidase activity with hydrogen peroxide cannot be used with the Amersham Pharmacia Biotech antibody because peroxide treatment attenuates staining. Similar precautions have been used successfully with the anti-GRP75 and anti-GRP78 antibodies from StressGen. For more common problems associated with immunohistochemistry techniques, refer to Table 2.9.6.

Anticipated Results

Northern blot analysis

The antisense oligonucleotide probes shown in Table 2.9.2 are derived from rat cDNAs. Therefore, northern blot analysis should reveal bands of the expected size in rodent tissues. Whereas HSP73, GRP75, and GRP78 demonstrate constitutive levels of mRNA in most normal tissues, HSP72 mRNA levels are usually not detectable. An up-regulation of all mRNAs should appear as denser bands of the same predicted sizes. Depending on the abundance of each transcript in a given tissue, 10 to 20 µg of total RNA or 2 to 10 µg of mRNA should be sufficient to detect a signal within 2 to 7 days.

In situ hybridization

RNA hybridization on tissue sections using labeled oligonucleotides should appear as an increase in regional grain density on X-ray film autoradiography with low nonspecific background signal. Although hybridization signals from ^{35}S-probes can take from a few days to weeks of film exposure for detection (depending on the abundance of the transcript), it usually shows better resolution (i.e., less signal scattering and background noise) than the higher energy ^{33}P-probes. Emulsion autoradiography should provide a better cellular resolution, especially when a light counterstaining is applied on the slide. The signal should appear as black grains over a stained cell.

Detection of [^{35}S]-labeled proteins

Lysates from labeled, unstressed cells should show a wide range of labeled proteins with bands of medium-to-high intensity. Because most stressful stimuli result in decreased overall protein synthesis, the lane on the gel corresponding to a "stressed lysate" should appear fairly clean, with very few bands of low-to-medium intensity compared to control lysates. Concomittant with decreased protein synthesis (i.e., decreased overall ^{35}S-methionine incorporation), a selective increase of stress proteins will appear in "stressed lysates" as sharp bands of different molecular weights corresponding to several of the genes shown in Table 2.9.3. Typically, 10 to 20 µg of radioactive protein lysate is sufficient to produce a medium-to-strong signal on autoradiograms after overnight exposure.

Immunoblotting

Immunoblotting should result in the detection of a single band of the appropriate size as shown in Table 2.9.4. HSP72 protein is generally not detectable in normal tissues unlike HSP73, GRP75, and GRP78, which are constitutively expressed. With the appropriate stressful stimulus, increased band density may be observed. Use caution to prevent protein degradation, which may produce multiple nonspecific bands on the blot. In certain tissues or different rodent families, the C92 antibody against HSP72 has been shown to detect one major band at 72 kDa for HSP72 and a minor band right above it corresponding to HSP73. Depending on the abundance of each protein in a given tissue, 10 to 40 µg of protein lysate will be sufficient to detect a significant signal.

Immunohistochemistry

Because GRP75 and GRP78 proteins are associated with the mitochondria and the endoplasmic reticulum, respectively, good DAB immunolabeling at the light microscopy level should result in medium-brown staining in the cytoplasmic region of cells with minimal back-

Table 2.9.5 Troubleshooting Guide for SDS-PAGE Separation and Immunoblotting

Problem	Possible cause	Solution
Dye front on the gel and bands on blot curve up at the edges (smile)	Gel is hotter in the middle than at the edges	Run gel in a cooler room or run gel at lower power. If using a tank electrophoresis system, completely submerge the gel sandwich in cool running buffer.
Distorted protein bands	Insufficient polymerization of stacking gel	Make sure the stacking gel is well polymerized before removing the comb and loading samples
	Air bubbles trapped under the comb teeth resulting in uneven polymerization of sample well	Make sure no air bubble gets trapped under the comb and rinse the sample well carefully before loading to remove traces unpolymerized acrylamide
Protein bands are fuzzy and diffuse or poorly resolved	Too much sample volume is loaded	Sample should be loaded as a tight layer in the bottom of the well. Use as small a volume as possible. Alternatively, use a thicker gel and sample well.
	Sample has diffused out in the stacking gel around the well	Start electrophoresis immediately after loading
	Sample degradation	Keep SDS protein extract on ice at all times prior to heat-denaturation. For long-term storage, keep samples at −70°C.
	Inappropriate acrylamide concentration in separating gel	Use appropriate acrylamide concentration in separating gel according to the molecular weight of the protein of interest.
Poor transfer of proteins on membrane (assessed by Ponceau staining)	Gel is too thick or gel porosity is too low	Use appropriate acrylamide concentration in separating gel according to the molecular size of the protein of interest. For the HSP70 protein family, use 8%-10% acrylamide. Load less protein on a thinner gel.
	Incorrect transfer time	Small proteins need shorter transfer time whereas larger polypeptides may require overnight transfer at low voltage, at 4°C.

continued

Table 2.9.5 Troubleshooting Guide for SDS-PAGE Separation and Immunoblotting, continued

Problem	Possible cause	Solution
	Incomplete contact of gel with the membrane	Make sure there are no air bubbles between the gel and the membrane by rolling a pipet over the wet gel-membrane sandwich
	Incorrect transfer buffer composition	High concentration of methanol in transfer buffer can interfere with the transfer of large proteins. Decrease the methanol until conditions are appropriate.
High background	Nonspecific antibody binding	Affinity purify polyclonal antibodies. If background is still high, replace primary and secondary antibody since they could be denatured.
	Antibody concentration too high	Dilute primary and/or secondary antibodies.
	Incomplete blocking	Increase blocking time and/or increase the concentration of blocking agents such as milk and serum proteins. Add 0.05%-0.1% Tween 20 in the blocking and incubation buffers.
Low or no reactivity	Tween 20 concentration too high	>0.05%-0.1% Tween 20 may elute the proteins from the membrane or may prevent the interaction of some antibodies with the specific proteins. Do not use Tween 20 or other ionic detergents in buffers unless the background is unreasonably high.
	Incorrect primary antibody	Use primary antibody that recognizes the denatured antigen.
	Incorrect incubation conditions	Increase the primary antibody concentration or increase time of incubation with the primary antibody.

ground throughout the normal tissue. Similar results should be observed with immunofluorescence. Following a stressful stimulus, an increased GRP75 and/or GRP78 expression would appear as increased cellular staining intensity and increased number of immunopositive cells, without increasing the tissue background. Because HSP72 is not constitutively expressed in most tissues, there should be no (or minimal) immunostaining found in unstressed animals, which is in contrast to constitutively expressed HSP73. In addition, because both HSP72 and HSP73 chaperone nascent or misfolded proteins in the cytoplasm and nucleus, one can expect to find increased immunostaining in these compartments following a specific stressful stimulus.

Table 2.9.6 Troubleshooting Guide for Immunohistochemical Staining

Problem	Possible cause	Solution
Chromogenic visualization		
Labeling seems specific but background is high	Nonspecific binding of primary or secondary antibody	Increase blocking time and/or increase the concentration of blocking agents such as milk (to 5%), BSA (1%-2%) or serum (to 10%-20%). Use a serum from same species as that used to make the secondary antibody.
	High activity of endogenous peroxidases (for staining with DAB reaction)	Incubate sections in peroxidase blocking solution
	Duration of DAB reaction is too long	Reduce the incubation time or dilute DAB/hydrogen peroxide solution
No labeling is seen even if a clear signal was observed on immunoblots of the same tissue	The antibody does not recognize the native form of the antigen. This occurs when the antibody is raised against denatured rather than native antigen. Because polyclonal antibodies recognize multiple epitopes of the same protein, the problem is more common with monoclonal antibodies.	Use a different antibody if possible
	Overfixation caused conformational changes of the antigen	Reduce the fixation time and cut tissue as soon as possible. Incubate sections in several washes of phosphate buffer.
	No chromogenic reaction because of the use of old hydrogen peroxide stock solution	Use fresh hydrogen peroxide stock solution (30%) of no more than 1-2 months old. Store the solution at 4°C.
Staining intensity of the tissue section is uneven	The thickness of the tissue section is uneven. This can occur when cutting extremely soft tissue (which tends to deform slightly under the movement of the blade) on a vibratome. The intensity of background staining is proportional to the relative thickness of a cut area.	For softer tissue, the use of a freezing microtome is highly recommended. Cryostat sections are useful but can be labor intensive. Alternatively, the tissue can be embedded in agarose prior to cutting on the vibratome.

continued

Table 2.9.6 Troubleshooting Guide for Immunohistochemical Staining, continued

Problem	Possible cause	Solution
	Some parts of the tissue section were not totally immersed in the incubating solutions during the procedure. This results in uneven exposure to the blocking agents, primary and secondary antibodies, or DAB reagent.	Make sure that the tissue sections are totally immersed in incubating solutions at any time.
	Some sections got stuck together during the incubations, causing uneven exposure of some tissue areas to the blocking solution, antibody, or DAB reagent	Make sure that the tissue sections are not tangled together at any time during incubations and washes. Use a small brush to seperate them.
Fluorescent visualization		
Fluorescent staining is faded	Photobleaching occured because the slides were exposed to light and/or were not kept at 4°C prior to observation	Keep slides in the dark and at 4°C at all times
Presence of fluorescence in unlabeled tissue sections	Autofluorescence often caused by aldehyde fixatives	Wash sections thoroughly in phosphate buffer, or try another fixative
Presence of fluorescence in sections incubated without the primary antibody	The concentration of the fluorescent secondary antibody is too high	Dilute the secondary antibody
	Nonspecific binding of the secondary antibody	Increase blocking time and/or increase concentration of blocking agents such as milk or serum proteins. Change the secondary antibody.
Fluorescent labeling is weak and grainy with loss of defined cellular morphology	Sections on slide have dried during the procedure or before coverslipping	Do not allow slides to dry at any time during freezing, immunocytochemistry, or before coverslipping.

Time Considerations

Northern blot analysis

Total RNA or mRNA can be isolated in 1 day. The RNA is then separated on an agarose gel and capillary transferred onto a membrane overnight. The next day, the oligonucleotide probe is radiolabeled and purified while the membrane is undergoing prehybridization. Hybridization is performed overnight. The following day, the blot is washed and then exposed to an autoradiographic film for 1 to 7 days depending on the abundance of the transcript and the specific activity of the probe.

In situ hybridization

Once frozen sections are obtained on slides (day 1), the oligonucleotide can be labeled and purified the next day. Hybridization is performed overnight. The following day, the slides are washed, dried, and exposed to an autoradiographic film for 1 to 7 days, depending on the abundance of the transcript and the specific activity of the probe.

Detection of [^{35}S]labeled proteins

The radiolabeled cell lysate is prepared and the protein concentration is determined in 1 day. Protein samples are separated and the gel stained in 1 day. The next day the gel is destained, dried, and exposed to an autoradiographic film overnight (day 3). The next morning (day 4), the film is developed and a hard copy of the result can be analyzed by densitometry on an image analyzer.

Immunoblotting

After the cell lysate has been prepared, samples can be separated by SDS-PAGE and electrotransferred to a membrane in 1 day. However, the use of larger and thicker gels can increase the time required for electrophoresis and transfer to an additional day. After overnight incubation in blocking solution, exposure of the membrane to the primary and secondary antibodies and immunoreactivity detection can be performed in 1 day.

Immunohistochemistry

Perfusion-fixation, tissue cutting, and incubation in blocking solution can be performed in 1 day. After overnight incubation with the primary antibody, sections are exposed to the secondary antibody and visualization of bound antibodies is performed on the same day. Mounting on gelatin-coated slides, drying, and coverslipping of tissue sections takes 2 days.

Literature Cited

Bergeron, M., Mivechi, N.F., Giaccia, A.M., and Giffard, R.G. 1996. Mechanism of heat shock protein 72 induction in primary cultured astrocytes after oxygen-glucose deprivation. *Neurol. Res.* 18:64-72.

Kinouchi, H., Sharp, F.R., Hill, M.P., Koistinaho J., Sagar, S.M., and Chan, P.K. 1993. Induction of 70-kDa heat shock protein and hsp70 mRNA following transient focal ischemia in the rat. *J. Cerebr. Blood Flow Metab.* 13:105-115.

Longo, F.M., Wang, P., Narasimhan, P., Zhang, J.S., Chen, J., Massa, S.M., and Sharp, F.R. 1993. cDNA cloning and expression of stress-induced rat hsp70 in normal and injured rat brain. *J. Neurosci. Res.* 36:325-335.

Massa, S.M., Longo, F.M., Zuo, J., Wang, S., Chen, J., and Sharp, F.R. 1995. Cloning of rat grp75, an hsp70-family member, and its expression in normal and ischemic brain. *J. Neurosci. Res.* 40:807-819.

Massa, S.M., Swanson, R.A., and Sharp, F.R. 1996. The stress gene response in brain. *Cerebrovasc. Brain Metab. Rev.* 8:95-158.

Miller, E.K., Raese, J.D., and Morrison-Bogorad, M. 1991. Expression of heat shock protein 70 and heat shock cognate 70 messenger RNAs in rat cortex and cerebellum after heat shock or amphetamine treatment. *J. Neurochem.* 56:2060-2071.

Narasimhan P., Swanson R.A., Sagar, S.M., and Sharp, F.R. 1996. Astrocyte survival and HSP70 heat shock protein induction following heat shock and acidosis. *Glia* 17:147-159.

Pardue, M.L. 1985. In situ hydridization. *In* Nucleic Acid Hybridization: A Practical Approach (B.D. Hanes and S.J. Higgins, eds.) pp. 179-202. IRL Press, Oxford, England.

Parsell, D.A. and Lindquist S. 1994. Heat shock proteins and stress tolerance. *In* The Biology of Heat Shock Proteins and Molecular Chaperones (R.I. Morimoto, A. Tissières, and C. Georgopoulos, eds.) pp.457-494. Cold Spring Harbor Laboratory Press, Cold Spring Harbor, N.Y.

Sharp, F.R., Massa S.M., and Swanson, R.A. 1999. Heat-shock protein protection. *Trends Neurosci*. 22:97-99.

Stahl, W.L., Eakin T.J., and Baskin, D.G. 1993. Selection of oligonucleotide probes for detection of mRNA isoforms. *J. Histochem. Cytochem.* 41:1735-1740.

Welch, W.J. 1990. The mammalian stress response: Cell physiology and biochemistry of stress proteins. *In* Stress Proteins in Biology and Medicine. (R.I. Morimoto, A. Tissières, and C. Georgopoulos, eds.) pp.223-278. Cold Spring Harbor Laboratory Press, Cold Spring Harbor, N.Y.

Welch, W.J. 1992. Mammalian stress response: Cell physiology, structure/function of stress proteins, and implications for medicine and disease. *Physiol. Rev.* 72:1063-1081.

Welch, W.J. and Suhan, J.P. 1986. Cellular and biochemical events in mammalian cells during and after recovery from physiological stress. *J. Cell. Biol.* 103:2035-2052.

Contributed by Marcelle Bergeron
Lilly Research Laboratories
Indianapolis, Indiana

Frank R. Sharp
University of Cincinnati Medical Center
Cincinnati, Ohio

Analysis of Mitochondrial Dysfunction During Cell Death

For many years mitochondria were considered only as a main energy supplier in the cell. In the middle of the 1990s it became clear that mitochondria actively participate in apoptosis, a form of cell death characterized by specific biochemical and morphological changes.

The following protocols represent basic tools widely used in estimating functional activity of mitochondria. The protocols are organized into three groups. The first group describes direct assessment of mitochondria in apoptotic cells—collection of proteins released from isolated mitochondria (see Basic Protocol 1), and from mitochondria within the cell (see Basic Protocol 2), immunoblot analysis of released proteins (see Basic Protocol 3), assessment of the mitochondrial membrane potential in apoptotic cells stained with TMRE (see Basic Protocol 4), and microscopy of apoptotic cells stained with MitoTracker Red (see Basic Protocol 5). The second group of protocols describes measurement of the mitochondrial permeability transition (MPT)—measurement of Ca^{2+} fluxes with an electrode (see Basic Protocol 6) or spectrophotometrically (see Alternate Protocol 1), measurement of the mitochondrial membrane potential with a TPP^{+} electrode (see Basic Protocol 7) or spectrophotometrically (see Alternate Protocol 2), estimation of mitochondrial swelling (see Basic Protocol 8), and measuring Ca^{2+} accumulation in permeabilized cells (see Basic Protocol 9). Support Protocols are included for the preparation of mitochondria from a number of sources—liver (see Support Protocol 1), brain (see Support Protocol 2), and cultured cells (see Support Protocol 3)—and for assessing the quality of the prepared mitochondria (see Support Protocol 4).

EVALUATION OF THE RELEASE OF PROTEINS FROM INTERMEMBRANE SPACE OF MITOCHONDRIA

The release of certain proteins from mitochondria in apoptotic cells is believed to be one of the key events in apoptosis. Therefore, estimation of the release of these proteins is important for understanding the role of mitochondria in apoptosis.

Collecting Samples of Proteins From Isolated Mitochondria

BASIC PROTOCOL 1

This method is based on the estimation of the amount of cytochrome *c* or any other protein released from the intermembrane space of mitochondria that remains in the incubation buffer after the mitochondria are removed by centrifugation. This protocol describes collecting samples of proteins released from isolated mitochondria incubated under different experimental conditions. Such experiments are very helpful in order to estimate a possible effect of certain pro-apoptotic compounds on mitochondria.

Materials

Isolated mitochondria (Support Protocols 1 to 3)
Buffer

1. Incubate mitochondria at a concentration of 1 mg protein/ml (time, conditions of incubation, and buffer to be used depend on the aim of the experiment).

   This buffer can be used for mitochondria isolated from different sources. The composition of the buffer is determined mainly by the aims of the experiment (see also Background Information, MPT-dependent release of cytochrome c). For example, estimation of the release of cytochrome c is more suitable to perform in KCl-based ionic buffer, since the

Contributed by Vladimir Gogvadze, Sten Orrenius, and Boris Zhivotovsky
Current Protocols in Toxicology (2004) 2.10.1-2.10.27

binding of cytochrome c to the inner mitochondrial membrane is significantly weaker as compared to mannitol-sucrose buffer. If the aim of the experiment is to assess MPT-independent release of cytochrome c, a calcium chelator EGTA, or cyclosporin A should be included.

2. Take a 200-µl aliquot and transfer to a microcentrifuge tube.
3. Microcentrifuge 5 min at 10,000 × *g*, 4°C.
4. Gently remove the supernatant without disturbing the pellet.
5. Resuspend the pellet in the original volume of the same buffer used for the incubation in step 1.
6. Freeze samples of supernatant (step 4) and pellet (step 5) and keep them at −20°C.

The samples are now ready for detection, e.g., of cytochrome c via immunoblotting (see Basic Protocol 3).

BASIC PROTOCOL 2

Evaluation of Cytochrome *c* Release from the Mitochondria of Apoptotic Cells

In order to analyze the release of certain proteins from mitochondria of apoptotic cells, the cellular plasma membrane should be disrupted and cytosolic fraction should be separated from membrane material. This can be achieved by preincubation of cells in a hypotonic solution that induces cell lysis.

Materials

Cells of interest (e.g., Jurkat cells, U 937, HeLa)
Apoptotic stimuli (e.g., etoposide, staurosporine)
Phosphate-buffered saline (PBS; *APPENDIX 2A*), ice-cold
S100 buffer (see recipe), ice-cold
Refrigerated low-speed centrifuge and ultracentrifuge

Additional reagents and equipment for immunoblot analysis (see Basic Protocol 3 and Gallagher et al., 1998)

1. Incubate cells with apoptotic stimuli (type, concentration, and incubation time determined by cell type).
2. Wash cells twice, each time with 5 ml of ice-cold PBS.
3. Resuspend cells at 75×10^6 cells/ml in ice-cold S100 buffer.
4. Incubate on ice for 10 to 20 min.
5. Centrifuge cells 15 min at 10,000 × *g*, 4°C.
6. Transfer supernatant to ultracentrifuge tube and ultracentrifuge 1 hr at 100,000 × *g*, 4°C.
7. Use supernatant for immunoblot analysis (see Basic Protocol 3 and Gallagher et al., 1998) with an antibody specific for cytochrome *c*.

Immunoblot Analysis of Proteins Released from the Mitochondria During Apoptosis

After separation as in Basic Protocol 1 or 2, the supernatant contains proteins released from mitochondria, while the pellet represents proteins associated with the organelles. The detection of these proteins is performed using electrophoresis with subsequent blotting and probing with specific antibodies.

Materials

Sample collected from apoptotic mitochondria (see Basic Protocol 1 or 2)
4× Laemmli's loading buffer (see recipe)
15% (w/v) SDS-PAGE gel (*APPENDIX 3F)*
5% (w/v) nonfat milk in PBS (see *APPENDIX 2A* for PBS)
Antibody specific for apoptotic protein of interest (e.g., Becton Dickinson Biosciences)
PBS (*APPENDIX 2A*) containing 2.5% (w/v) nonfat dry milk
Phosphate-buffered saline (PBS; *APPENDIX 2A*) containing 1% (w/v) bovine serum albumin and 0.01% (w/v) azide (NaN_3)
PBS (*APPENDIX 2A*) containing 15% (v/v) Tween 20
Horseradish peroxidase–conjugated secondary antibody (e.g., Pierce)
ECL Western Blotting Detection Reagents kit (Amersham Biosciences)
Additional reagents and equipment for SDS-PAGE (*APPENDIX 3F)* and electroblotting (Gallagher et al., 1998)

Perform electrophoresis

1. Mix 40 µl of sample with 12.5 µl of 4× Laemmli's loading buffer. Boil 5 min.
2. Separate the proteins on a 15% SDS-PAGE gel at 130 V (*APPENDIX 3F).*

Perform immunoblotting and detect apoptotic proteins

3. Transfer proteins to nitrocellulose membranes by electroblotting (Gallagher et al., 1998) for 2 hr at 100 V.
4. Block membranes for 1 hr with 5% nonfat milk in PBS at room temperature.
5. Probe overnight in a cold room with an antibody (diluted 1:2500 in PBS containing bovine serum albumin and 0.01% NaN_3) specific for the apoptotic protein of interest.
6. Rinse membranes for 10 min in 30 to 40 ml of PBS.
7. Rinse membranes for 15 min in 30 to 40 ml of PBS with 0.15% Tween 20.
8. Rinse membranes for 10 min in 30 to 40 ml of PBS.
9. Incubate with a horseradish peroxidase–conjugated secondary antibody (diluted 1:10,000 in PBS containing 2.5% nonfat dry milk).

Visualize bound antibodies

10. Following incubation with the secondary antibody, rinse the membranes for 10 min in 30 to 40 ml of PBS.
11. Rinse membranes for 15 min in 30 to 40 ml of PBS with 0.15% Tween 20.
12. Rinse membranes for 10 min in 30 to 40 ml of PBS.
13. Detect bound antibodies using enhanced chemiluminescence (ECL kit) according to the manufacturer's instructions.

BASIC PROTOCOL 4

Assessment of the Mitochondrial Membrane Potential in Apoptotic Cells

The mitochondrial membrane potential ($\Delta\psi$), which drives oxidative phosphorylation (Mitchell and Moyle, 1967) and which also drives mitochondrial calcium uptake, is generated by an electron-transporting chain. When electron transport ceases, for example during ischemia, the inner-membrane potential is developed at the expense of ATP hydrolysis by the mitochondrial ATP synthase. An early manifestation of apoptosis is often a decrease in the $\Delta\psi$, which is usually demonstrated using flow cytometry. The relationship between mitochondrial depolarization and apoptosis remains controversial. Some investigators consider a decrease in $\Delta\psi$ an early irreversible signal for apoptosis (Zamzami et al., 1996), while others describe it as a late event (Bossy-Wetzel et al., 1998).

Materials

Cells of interest (e.g., Jurkat cells, U 937, HeLa)
RPMI-1640 medium (Life Technologies) supplemented with 5% (v/v) heat-inactivated fetal bovine serum, 2 mM L-glutamine, penicillin (100 U/ml), and streptomycin (100 μg/ml)
25 mM TMRE stock solution: dissolve 12.8 mg tetramethylrhodamine methyl ester (TMRE; Molecular Probes) in 1 ml ethanol; store per manufacturer's instructions
HEPES buffer (see recipe)
Flow cytometer (e.g., FACS; Becton Dickinson)

1. Prepare an aliquot of 10^6 cells in RPMI-1640 medium.
2. Dilute TMRE stock solution 1:1000 with HEPES buffer (for a concentration of 25 μM).
3. Add an aliquot of the diluted (25 μM) TMRE to cells for a final concentration of 25 nM.
4. Incubate cells with TMRE 20 min at 37°C.
5. Further dilute the 25 μM TMRE 1:1000 with HEPES buffer for a final concentration of 25 nM. Centrifuge cells 5 min at 200 × *g*, room temperature, and resuspend in fresh HEPES buffer containing 25 nM TMRE.
6. Analyze membrane potential by flow cytometry according to the manufacturer's instructions for the instrument used (see Fig. 2.10.1).

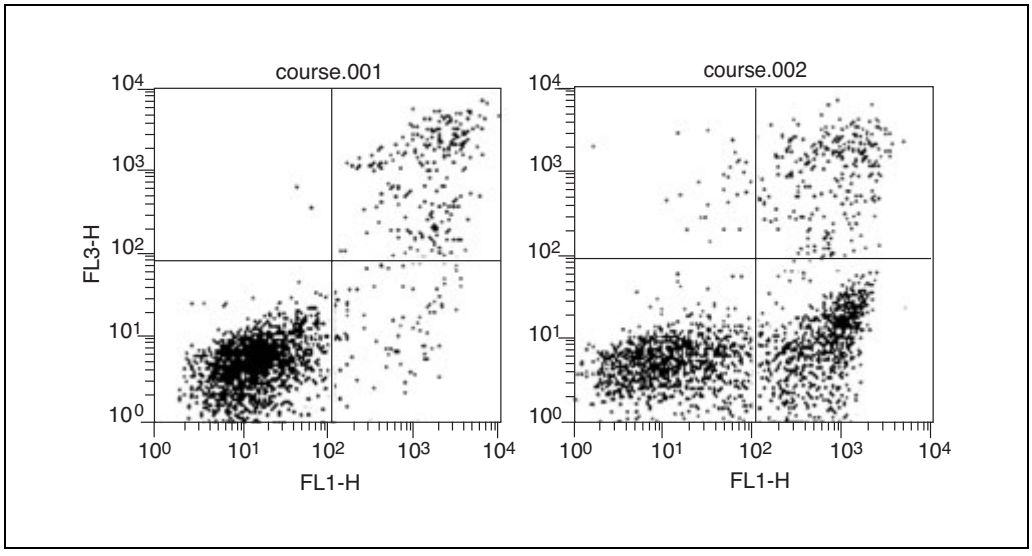

Figure 2.10.1 A typical image of FACS analysis of mitochondrial membrane potential in the cells undergoing apoptosis. Apoptosis was induced in Jurkat cells by 1 μM staurosporine and samples were analyzed 3 hr after initiation of apoptosis.

Microscopy of Apoptotic Cells Stained with MitoTracker

Fluorescent probes for mitochondria such as rhodamine 123 or tetramethylrosamine are readily sequestered by mitochondria. However, in experiments that require fixation of the organelles, these stains are easily washed out. In contrast, mitochondria-selective probes—e.g., MitoTracker Red (Molecular Probes)—are concentrated by active, energized mitochondria and retained during fixation. Once mitochondria are labeled, the cells can be fixed for further processing, for example, if cells are going to be subsequently labeled with antibody.

Materials

Cells of interest (e.g., Jurkat cells, U 937, HeLa) and appropriate culture medium
MitoTracker Red (Molecular Probes); store according the manufacturer's instructions
Dimethylsulfoxide (DMSO)
4% (w/v) paraformaldehyde in serum-free culture medium
Phosphate-buffered saline (PBS; *APPENDIX 2A*)
PBS (*APPENDIX 2A*) containing 0.2% (v/v) Triton X-100
PBS (*APPENDIX 2A*) containing 1% (v/v) fetal bovine serum (FBS)
Mounting medium: 50% (w/v) glycerol/PBS
Fluorescent or scanning confocal microscope (e.g., Bio-Rad), with 581-nm excitation filter and 644-nm emission filter

Additional reagents and equipment for cell culture (*APPENDIX 3B*)

1. Grow cells on coverslips inside a petri dish filled with the appropriate culture medium to the optimal density.

   The optimal cell density depends on the cell type.

2. Open fresh vial of MitoTracker Red and add DMSO to create a 1 mM stock. Protect from light.

3. Dilute 1 mM MitoTracker Red to final working concentration in the culture medium used to grow the cells.

   Recommended Mito Tracker Red concentration is 100 to 500 nM. Diluted MitoTracker Red can be stored up to several months at –20°C

4. When cells have reached the desired confluence, remove the medium from the dish and add the prewarmed (37°) growth medium containing MitoTracker probe. Incubate for 30 min.

5. Replace the loading solution with fresh prewarmed medium.

Fix and permeabilize cells

6. Remove the growth medium covering the cells and replace it with fresh prewarmed medium containing 4% paraformaldehyde. Incubate 15 min at 37°C.

7. Rinse cells three times, each time for 5 min with room temperature PBS.

8. Incubate fixed cells in PBS containing 0.2% Triton X-100 at room temperature for 5 min.

9. Rinse cells three times, each time for 5 min with PBS containing 1% FBS.

10. Mount coverslips on glass slides in 50% glycerol/PBS and examine under fluorescent or scanning confocal microscope with excitation at 581 nm and emission at 644 nm.

ASSESSMENT OF THE MITOCHONDRIAL PERMEABILITY TRANSITION IN ISOLATED MITOCHONDRIA

The mitochondrial permeability transition (MPT) is one of the mechanisms that can lead to the release of cytochrome *c* from mitochondria during apoptosis. MPT is a consequence of Ca^{2+} overload. Accumulation of Ca^{2+} in mitochondria is driven by the mitochondrial membrane potential supported either by mitochondrial respiration or by ATP hydrolysis. Mitochondria release Ca^{2+} when the membrane potential is dropped either by inhibitors of mitochondrial respiratory chain (if the potential is supported by oxidation of a substrate) or by inhibitors of ATPase (if the source of potential is hydrolysis of ATP).

Retention of Ca^{2+} by mitochondria stimulates processes that result in mitochondrial deterioration. Mitochondria swell and become leaky, whereupon the membrane potential drops and Ca^{2+} is released. Although Ca^{2+} is obligatory for MPT induction, the sensitivity of mitochondria to permeability transition can be enhanced by different factors. Among these factors are elevated levels of phosphate, oxidative stress, and the depletion of adenine nucleotides. When phosphate or organic peroxide is added to Ca^{2+}-loaded mitochondria, these organelles swell, membrane potential decays, and accumulated Ca^{2+} is released. All of these manifestations can be prevented by cyclosporin A (CsA), an inhibitor of pore opening. Therefore, MPT in isolated mitochondria can be assessed by monitoring either swelling, membrane potential, or the level of Ca^{2+} in the incubation buffer.

Accumulation of Ca^{2+} by mitochondria, as well as Ca^{2+} retention and release induced by different stimuli, can be monitored using a Ca^{2+}-sensitive electrode or spectrophotometrically with the Ca^{2+}-sensitive dye arsenazo III.

BASIC PROTOCOL 6

Monitoring of Ca^{2+} Fluxes Across the Inner Mitochondrial Membrane with a Ca^{2+}-Sensitive Electrode

One relatively easy method applicable to mitochondria and permeabilized cells employs a Ca^{2+}-sensitive electrode to follow the Ca^{2+}. Accumulation of Ca^{2+} by mitochondria can be followed by a decrease in the concentration of Ca^{2+} in the incubation buffer.

Materials

Incubation buffer for calcium-sensitive electrode (see recipe)
Isolated mitochondria (Support Protocol 1, 2, or 3)
2.5 mM rotenone: dissolve 1 mg rotenone (Sigma) in 1 ml ethanol; store frozen at –20°C up to 1 month
10 mM $CaCl_2$: dissolve 1.47 mg $CaCl_2 \cdot 2H_2O$ in 1 ml H_2O; store frozen at –20°C up to 1 month
0.5 M KH_2PO_4: dissolve 136.1 mg KH_2PO_4 in 2 ml H_2O and adjust pH to 7.4 with KOH; store frozen at –20°C up to 1 month

Apparatus for membrane potential measurement consisting of:
Glass (or plastic) sample chamber large enough for incubation volume, which can be warmed by being connected to a water bath and can be constantly stirred
Ca^{2+}-sensitive electrode (e.g., Orion)
pH meter as source of current
Chart recorder with variable input and chart speed
Any commercially available reference electrode for pH measurements

1. Add 2 ml of incubation buffer for calcium-sensitive electrode to the sample chamber of the measurement apparatus and set to conditions of constant stirring. Add a volume of mitochondrial suspension (which will depend on the concentration of the mitochondrial preparation) containing 2 mg of protein to the sample chamber.
2. After 30 sec, add 2 µl of 2.5 mM rotenone, for a final concentration of 2.5 µM.

   When mitochondria are energized with the complex II substrate succinate, rotenone prevents formation of oxaloacetate, an inhibitor of succinate dehydrogenase that supresses mitochondrial respiration.
3. Turn on the chart recorder.
4. After 1 min (or when stabilization has been achieved as observed by recorder trace) add 50 to 60 nmol Ca^{2+} (from 10 mM $CaCl_2$ stock) per milligram of mitochondrial protein.

   The addition of Ca^{2+} to mitochondria leads to a rapid increase in the level of this cation in the reaction buffer, followed by a return to the initial level as mitochondria accumulate the excess Ca^{2+}.
5. After 1 min, add 20 µl of 0.5 M KH_2PO_4, for a final concentration of 5 mM.

   Inorganic phosphate is a trigger for permeability transition in mitochondria loaded with calcium.
6. Follow the retention of Ca^{2+} by its release as seen from the recorder trace (see Fig. 2.10.2).

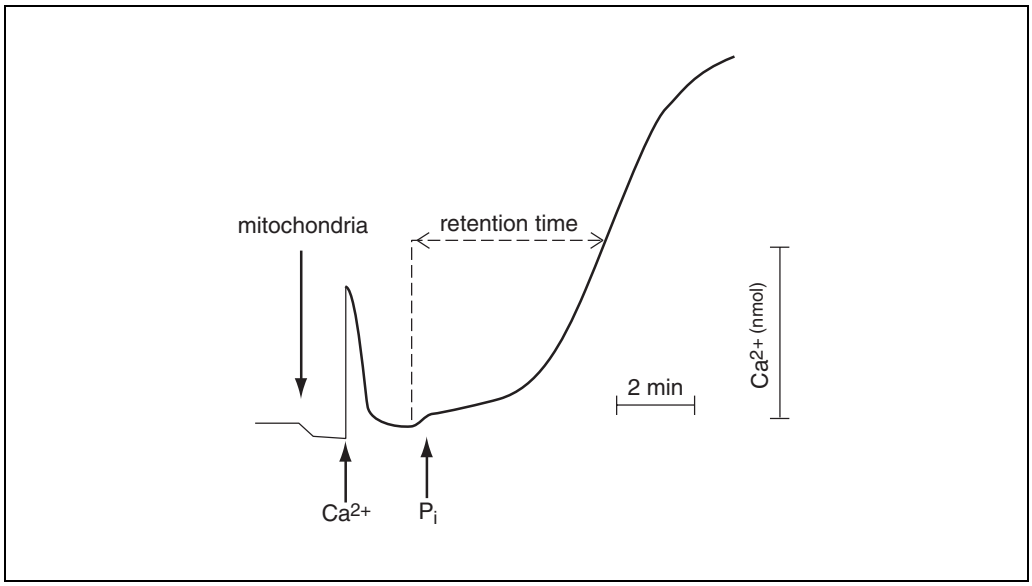

Figure 2.10.2 MPT monitored with a Ca^{2+}-sensitive electrode. Mitochondria (1 mg/ml) were incubated in KCl-based buffer. After a 1-min stabilization period, mitochondria were loaded with Ca^{2+}, and, when accumulation was complete, MPT was induced by 5 mM KH_2PO_4.

ALTERNATE PROTOCOL 1

Monitoring of Ca^{2+} Fluxes Across the Inner Mitochondrial Membrane with a Spectrophotometer

Spectrophotometric estimation of Ca^{2+} fluxes across the mitochondrial membrane should be performed using a dual-wavelength spectrophotometer, in order to avoid interference from the turbidity of mitochondrial suspension.

Additional Materials *(also see Basic Protocol 6)*

25 mM arsenazo III: dissolve 19.4 mg arsenazo III (Sigma) in 1 ml H_2O; store frozen at –20°C up to 1 month

Dual-wavelength recording spectrophotometer set at 675 versus 685 nm, with appropriate cuvettes

1. Place 2 ml of incubation buffer for calcium-sensitive electrode in a spectrophotometric cuvette and set to conditions of constant stirring. Add 2 µl of 25 mM arsenazo III, for a final concentration of 25 µM.
2. Add an aliquot of mitochondrial suspension containing 2 mg of protein, for a final concentration of 1 mg/ml.

   The volume of the mitochondrial aliquot will depend on the concentration of the mitochondrial preparation.

3. After 30 sec add 2 µl of 2.5 mM rotenone, for a final concentration of 2.5 µM.
4. After 1 min add 50 to 60 nmol Ca^{2+} (from 10 mM $CaCl_2$ stock) per mg of mitochondrial protein.

   The addition of Ca^{2+} to mitochondria leads to a rapid increase in the level of this cation in the reaction buffer, followed by a return to the initial level as mitochondria accumulate the excess Ca^{2+}.

5. After 1 min, add 20 µl of 0.5 M KH_2PO_4, for a final concentration of 5 mM.

   The retention of Ca^{2+} is followed by its release upon induction of MPT as can be seen from the recorder trace.

DETERMINATION OF MITOCHONDRIAL MEMBRANE POTENTIAL

Estimation of the mitochondrial membrane potential ($\Delta\psi$) can be performed using an electrode sensitive to the lipophilic cation tetraphenylphosphonium (TPP^+) or spectrophotometrically with a $\Delta\psi$-specific dye, safranin.

BASIC PROTOCOL 7

Measurements of Mitochondrial Membrane Potential with a TPP^+-Sensitive Electrode

Energized mitochondria rapidly accumulate TPP^+ from the incubation buffer and release this cation as $\Delta\psi$ decays. Accumulation of TPP^+ by mitochondria can be followed by a decrease in the concentration of TPP^+ in the incubation buffer.

Materials

Incubation buffer for TPP^+-sensitive electrode (see recipe)

TPP^+ stock solution: dissolve 3.75 mg tetraphenylphosphonium chloride (Aldrich) in 10 ml H_2O; store up to 1 month at room temperature

Isolated mitochondria (Support Protocol 1, 2, or 3)

2.5 mM rotenone: dissolve 1 mg rotenone (Sigma) in 1 ml ethanol; store frozen at –20°C up to 1 month

10 mM $CaCl_2$: dissolve 1.47 mg $CaCl_2 \cdot 2H_2O$ in 1 ml H_2O; store frozen at –20°C up to 1 month

0.5 M KH_2PO_4: dissolve 136.1 mg KH_2PO_4 in 2 ml H_2O and adjust pH to 7.4 with KOH; store frozen at –20°C up to 1 month

Apparatus for membrane potential measurement consisting of:

Glass (or plastic) sample chamber that can accommodate 2 ml of incubation buffer, which can be warmed by being connected to a water bath and can be constantly stirred

TPP^+ electrode (purchase from Microelectrodes, Inc. or prepare in the laboratory, Kamo et al., 1979)

pH meter as source of current

Chart recorder with variable input and chart speed

Any commercially available reference electrode

1. Place 2 ml of incubation buffer for TPP^+-sensitive electrode in the sample chamber of the measurement apparatus and set conditions to constant stirring. Add 4 µl of TPP^+ stock, for a final concentration of 2 µM TPP^+, and turn on the chart recorder.

   The recorder trace shows the basal level of TPP^+ in incubation buffer.

2. Add mitochondrial suspension to a final concentration of 1 mg/ml to the incubation buffer under conditions of constant stirring.

   The volume of the mitochondrial aliquot will depend on the concentration of mitochondrial preparation.

   Mitochondria accumulate TPP^+ according to the membrane potential so that the level of TPP^+ in the incubation buffer decreases.

3. After 30 sec add 2 µl of 2.5 mM rotenone, for a final concentration of 2.5 µM.

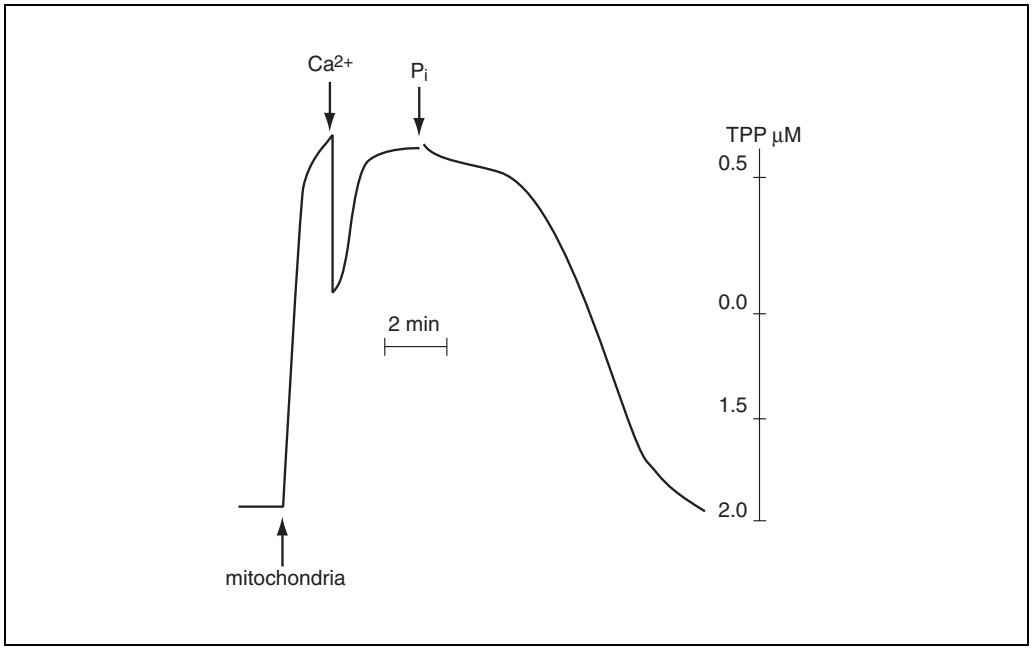

Figure 2.10.3 MPT monitored with a $\Delta\psi$-sensitive electrode. Mitochondria (1 mg/ml) were incubated in KCl-based buffer. After a 1-min stabilization period mitochondria were loaded with Ca^{2+}, and, when accumulation was complete and potential was restored, MPT was induced by 5 mM KH_2PO_4. The concentration of TPP^+ was 2 µM.

4. After 1 min, add 50 to 60 nmol Ca^{2+} (from 10 mM $CaCl_2$ stock) per milligram of mitochondrial protein.

   Upon addition of Ca^{2+}, the mitochondrial membrane potential decreases, with subsequent restoration when Ca^{2+} is accumulated.

5. After restoration of the membrane potential, add 20 µl of 0.5 M KH_2PO_4 for a final concentration of 5 mM and monitor the release of TPP^+ from mitochondria, which is indicative of the drop of the membrane potential upon induction of MPT (see Fig. 2.10.3).

   If Ca^{2+} loading is not sufficient to induce permeability transition, mitochondria will maintain membrane potential. In this case Ca^{2+} loading should be increased.

ALTERNATE PROTOCOL 2

Measurement of Mitochondrial Membrane Potential Using a Spectrophotometer

Spectrophotometric measurement of the membrane potential can be performed using safranin, a cationic dye, because of its accumulation in mitochondria and a shift in absorption spectrum that occurs when membrane potential is high. In these experiments, a dual-wavelength spectrophotometer should be used in order to avoid a contribution by the turbidity of the mitochondrial suspension to light absorption.

Additional Materials *(also see Basic Protocol 7)*

Incubation buffer for calcium-sensitive electrode (see recipe)
10 mM safranin: dissolve 3.5 mg safranin in 1 ml H_2O; store frozen at –20°C up to 1 month
Dual-wavelength recording spectrophotometer set at 511 versus 533 nm, with appropriate cuvettes

1. Place 2 ml of incubation buffer for calcium-sensitive electrode in a spectrophotometric cuvette and set to conditions of constant stirring. Add 2 µl of 10 mM safranin, for a final concentration of 10 µM.
2. Add an aliquot of mitochondrial suspension containing 2 mg of protein, for a final concentration of 1 mg/ml.

   The volume of the mitochondrial aliquot will depend on the concentration of the mitochondrial preparation.

3. After 30 sec add 2 µl of 2.5 mM rotenone, for a final concentration of 2.5 µM.
4. After 1 min add 50 to 60 nmol Ca^{2+} (from 10 mM $CaCl_2$ stock) per milligram of mitochondrial protein.

   Upon addition of Ca^{2+}, the mitochondrial membrane potential decreases, with subsequent restoration when Ca^{2+} is accumulated.

5. After restoration of the membrane potential, add 20 µl of 0.5 M KH_2PO_4, for a final concentration of 5 mM, and monitor the decrease in the membrane potential upon induction of MPT.

Estimation of Mitochondrial Swelling

One of the most reliable manifestations of mitochondrial permeability transition is swelling of the organelles. Nephelometric or turbidometric techniques have generally been used to monitor mitochondrial swelling. Mitochondrial swelling can be monitored continuously as changes in OD_{540}.

Materials

Incubation buffer for swelling (see recipe)
Isolated mitochondria (Support Protocol 1, 2, or 3)
10 mM $CaCl_2$: dissolve 1.47 mg $CaCl_2 \cdot 2H_2O$ in 1 ml H_2O; store frozen at –20°C up to 1 month
2.5 mM rotenone: dissolve 1 mg rotenone (Sigma) in 1 ml ethanol; store frozen at –20°C up to 1 month
0.5 M KH_2PO_4: dissolve 136.1 mg KH_2PO_4 in 2 ml H_2O and adjust pH to 7.4 with KOH; store frozen at –20°C up to 1 month

Spectrophotometer with 540-nm filter, or multiwavelength spectrophotometer
Chart recorder with variable input and chart speed

1. Place 2 ml of incubation buffer for swelling in a spectrophotometric cuvette and set to conditions of constant stirring. Add a volume of mitochondrial suspension (which will depend on the concentration of mitochondrial preparation) for a final concentration of 0.5 mg/ml.
2. After 30 sec, add 2 µl of 2.5 mM rotenone, for a final concentration of 2.5 µM.
3. After 1 min add 50 to 60 nmol Ca^{2+} (from 10 mM $CaCl_2$ stock) per milligram of mitochondrial protein.
4. After 1 min, add 20 µl of 0.5 M KH_2PO_4.
5. Monitor gradual decrease in OD_{540} nm due to mitochondrial swelling (see Fig. 2.10.4).

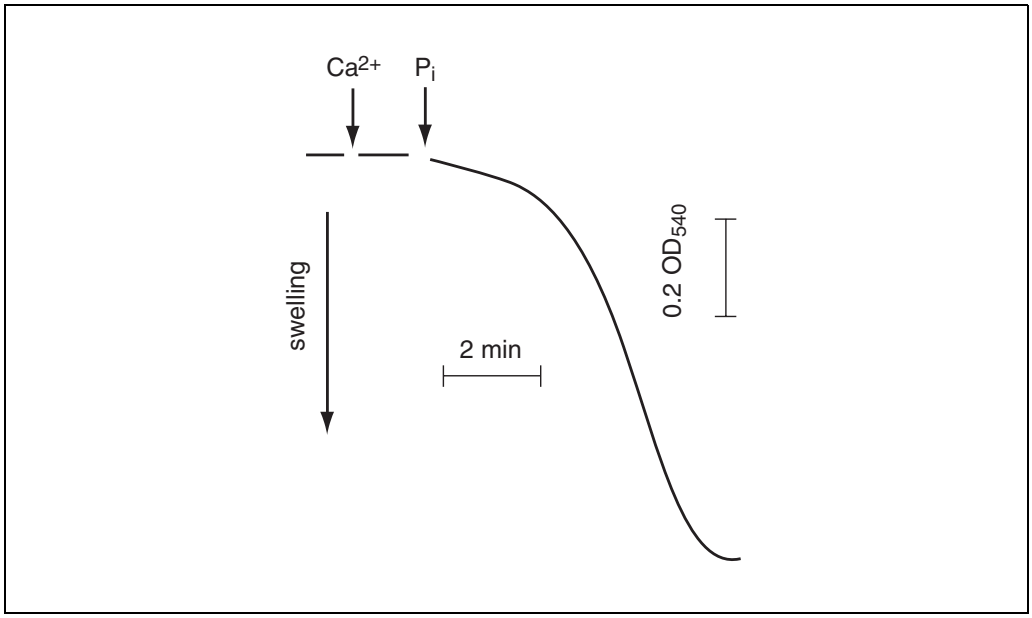

Figure 2.10.4 MPT assessed by mitochondrial swelling. Mitochondria (0.5 mg/ml) were incubated in 2 ml of KCl-based buffer. Mitochondria were loaded with Ca^{2+} and 5 mM phosphate was added. Swelling was monitored by a decrease of optical density at 540 nm.

BASIC PROTOCOL 9

Estimation of Mitochondrial Ca^{2+} Accumulation in Digitonin-Permeabilized Cells

Permeabilization of the plasma membrane allows measurement of mitochondrial activity in situ, without isolation of these organelles and the accompanying potential risk of mitochondrial damage. For the permeabilization, a steroid glycoside, digitonin, is widely used. The affinity of digitonin for cholesterol allows a selective disruption of the plasma membrane, making mitochondria accessible to specific substrates and Ca^{2+}. The concentration of digitonin must be chosen carefully and usually should not exceed 0.005% (w/v), since higher concentrations might affect the outer mitochondrial membrane barrier functions.

Permeabilization of the plasma membrane allows estimation of the main functional parameters of mitochondria, such as respiration, membrane potential, and accumulation and release of Ca^{2+}. A description of the monitoring of Ca^{2+} fluxes is given below.

Induction of MPT in apoptotic cells is thought to be one of the reasons for the decrease in $\Delta\psi$. Pore opening during apoptosis (even in a subpopulation of mitochondria) will impair the ability of the total mitochondrial population to accumulate Ca^{2+}; therefore estimation of a threshold level of Ca^{2+} loading (the Ca^{2+} capacity of mitochondria) in cells might be a criterion for changes on the mitochondrial level.

Materials

Cells of interest (Jurkat cells, U 937, HeLa)
Phosphate-buffered saline (PBS; *APPENDIX 2A*)
Incubation buffer for digitonin-permeabilized cells (see recipe)
1% (w/v) digitonin: dissolve 10 mg digitonin in 1 ml H_2O; shake vigorously before adding to cells; store up to 2 to 3 months at room temperature
2.5 mM rotenone: dissolve 1 mg rotenone (Sigma) in 1 ml ethanol; store frozen at –20°C up to 1 month
10 mM $CaCl_2$: dissolve 1.47 mg $CaCl_2 \cdot 2H_2O$ in 1 ml H_2O; store frozen at –20°C up to 1 month

Apparatus for membrane potential measurement consisting of:
Glass (or plastic) sample chamber large enough for incubation volume, which can be warmed up by being connected to a water bath and can be constantly stirred
Ca^{2+}-sensitive electrode (e.g., Orion)
pH meter as source of current
Chart recorder with variable input and chart speed
Any commercially available reference electrode for pH measurements

1. Centrifuge $3–5 \times 10^6$ cells 5 min at $200 \times g$, room temperature. Remove supernatant, resuspend cells in PBS, and centrifuge again under the same conditions.
2. Resuspend cells in 50 µl of incubation buffer for digitonin-permeabilized cells, then add the resuspended cells to 450 µl of the same buffer in sample chamber with Ca^{2+} electrode at constant stirring. Turn on the chart recorder.
3. Following a 2-min stabilization period, add 1% digitonin to a final concentration of 0.005% and 2.5 mM rotenone to a final concentration of 5 µM.
4. Load mitochondria with pulses of Ca^{2+} (20 to 25 nmol each, added from 10 mM stock) to induce MPT, which can be observed by the release of accumulated Ca^{2+} as measured by the Ca^{2+}-sensitive electrode (see Fig. 2.10.5).

The calcium capacity is calculated as a sum of the amount of Ca^{2+} in each addition.

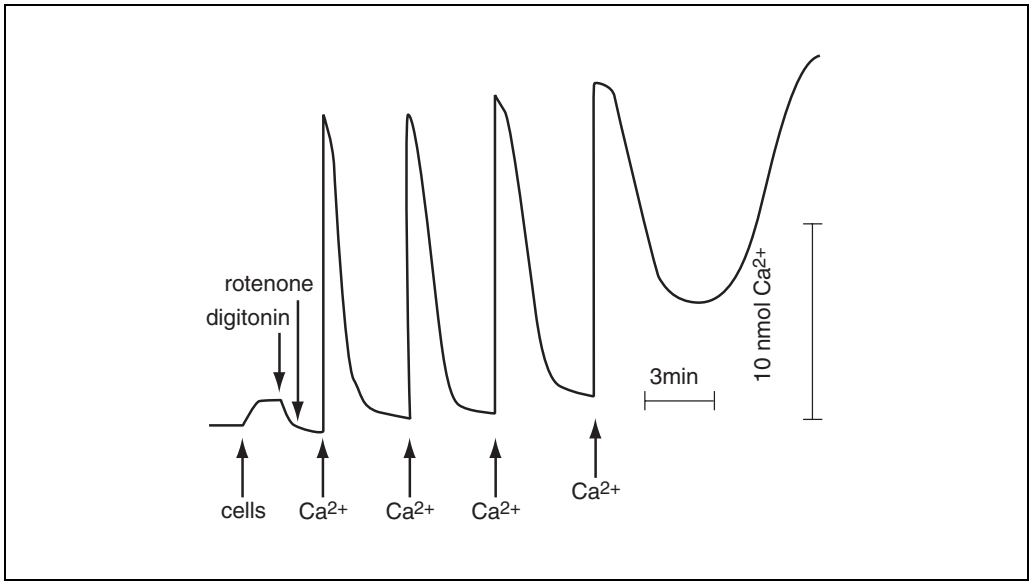

Figure 2.10.5 Estimation of mitochondrial Ca^{2+}accumulation in digitonin-permeabilized cells. Jurkat cells (2.5×10^6) were washed in PBS, resuspended in 500 µl of KCl-based buffer, and added to the incubation chamber. Following a 2-min stabilization period, cells were permeabilized with 0.005% digitonin, and 5 µM rotenone was added in order to maintain pyridine nucleotides in a reduced form. MPT was induced by sequential additions of $Ca^{2+}$and changes in the level of this cation were monitored using a Ca^{2+}-selective electrode.

ISOLATION OF MITOCHONDRIA

Experiments with isolated mitochondria are a helpful supplement to experiments on a cellular level. The former type of experiments provide better understanding of the mechanisms responsible for the mitochondrial changes in apoptotic cells. All the methods of isolation of mitochondria are based on the disruption of tissue and subsequent differential centrifugation of homogenate.

NOTE: All protocols using live animals must first be reviewed and approved by an Institutional Animal Care and Use Committee (IACUC) or must conform to governmental regulations regarding the care and use of laboratory animals.

NOTE: Mitochondria should be kept on ice at all times.

Isolation of Rat Liver Mitochondria

SUPPORT PROTOCOL 1

Isolation of liver mitochondria represents a relatively "easy" procedure giving a high yield. The liver from a 150 to 200-g rat weighs 5 to 6 g. Liver can be easily disrupted and homogenized. The most important thing is keeping the temperature not higher than 4° to 6°C.

Materials

150- to 200-g rat
Buffer A for liver (see recipe)
Buffer B: Buffer A (for liver) without EDTA

Dissecting equipment
Motor-driven glass Dounce homogenizer and tight Teflon pestle
Refrigerated centrifuge and 50-ml centrifuge tubes

Additional reagents and equipment for protein assay (*APPENDIX 3G*) and determination of the respiratory control ratio for mitochondria (Support Protocol 4)

NOTE: All operations should be done on ice, using ice-cold buffers and instruments.

Harvest the liver

1. Let the rat starve overnight.

   This step is necessary to decrease the content of fat and glycogen in the liver.

2. Sacrifice rat in accordance with institutional guidelines and the aims of the experiment.

   Donovan and Brown (1995) provide a variety of protocols for rodent euthanasia.

3. Remove liver and immerse immediately in ice-cold buffer A for liver.

4. Cut liver into pieces with scissors and wash several times by replacing the ice-cold buffer A with fresh ice-cold buffer, in order to remove as much blood as possible.

Homogenize the liver

5. Homogenize the liver in 60 ml of buffer A with 5 to 6 up-and-down strokes of the tight Teflon pestle.

   Homogenization occurs as the piston of the homogenizer rotates (driven by an electrical motor) and the pestle is slowly moved up and down five to six times, so that there are no pieces of liver big enough to be seen by eye.

6. Transfer homogenate into two cold centrifuge tubes and balance them.

7. Centrifuge the homogenate 8 min at 600 × *g*, 4°C, to remove nuclei and unbroken cells.

Isolate mitochondria

8. Discard the pellet and centrifuge supernatant 15 min at 5500 × *g*, 4°C, to form a mitochondrial pellet.

9. Remove floating fat droplets with a paper towel or piece of tissue paper.

10. Detach the pellet from the bottom of the tube with the piston of the homegenizer, add 0.2 to 0.3 ml of buffer A for liver, resuspend the pellet using the pestle, and pass mitochondria gently 3 to 4 times through the tip of a 1-ml pipet tip using automatic pipettor.

11. Dilute the mitochondrial suspension with 30 ml of buffer B, then centrifuge again as in step 9.

12. Resuspend the final mitochondrial pellet to a volume of ~1 ml in buffer B by gentle passing through a 1-ml pipet tip, then transfer into a 10-ml tube and keep on ice.

Assess the preparation

13. Determine the protein concentration using Lowry's method (or any other method available; see *APPENDIX 3G*) with bovine serum albumin as a standard.

    The protein concentration of a final suspension usually is about 90 to 100 mg/ml.

14. As a control of the mitochondrial preparation, estimate the respiratory control ratio (see Support Protocol 4). Use within 4 hr.

    Measurements can be started directly after mitochondrial isolation.

Isolation of Brain Mitochondria

Another source of mitochondria frequently used in the investigation of mitochondrial functioning (e.g., during apoptosis) is the brain. The method for isolation of brain mitochondria is similar to that for liver mitochondria (see Support Protocol 1); however, in order to get a purer preparation, a purification of homogenate with a Ficoll gradient is involved.

Materials

150- to 200-g rat
SET buffer (see recipe), ice-cold
3% and 6% (w/v) Ficoll solutions (see recipe)
MSH buffer (see recipe)

Motor-driven glass Dounce homogenizer and tight Teflon pestle
Refrigerated centrifuge and 50-ml centrifuge tubes

Additional reagents and equipment for protein assay (*APPENDIX 3G*) and determination of the respiratory control ratio for mitochondria (Support Protocol 4)

Dissect brain

1. Sacrifice rat in accordance with institutional guidelines and the aims of the experiment.
2. Open the skull with scissors, gently remove the brain, place it in ice-cold SET buffer, and chop it into pieces with scissors.
3. Wash pieces of brain several times in ice-cold SET buffer in order to remove as much blood as possible.

Homogenize brain

4. Homogenize manually chopped brain in 30 ml of SET buffer at 4°C using a Dounce homogenizer with six up-and-down strokes of the tight pestle.
5. Dilute homogenate to a final volume of 80 ml with SET buffer.
6. Place the homogenate in two cold centrifuge tubes, balance them, and centrifuge 3 min at 2000 × *g*, 4°C.
7. Decant supernatant and centrifuge again for 3 min at 2000 × *g*, 4°C.

Isolate mitochondria

8. Collect the supernatant and centrifuge 15 min at 12,000 × *g*, 4°C, to obtain a crude mitochondrial fraction.
9. Resuspend the pellet in 6 ml of ice-cold 3% Ficoll solution and layer onto 25 ml of ice-cold 6% Ficoll solution.
10. Centrifuge 10 min at 11,500 × *g*, 4°C.
11. Resuspend the final pellet in MSH buffer to a final volume of ~1 ml and keep on ice.

Assess preparation

12. Determine the protein concentration (*APPENDIX 3G).*
13. As a control of the mitochondrial preparation estimate the respiratory control ratio (see Support Protocol 4). Use within 4 hr.

Measurements can be started directly after mitochondrial isolation.

SUPPORT PROTOCOL 3

Isolation of Mitochondria from Cultured Cells

Isolation of mitochondria from cultured cells is more problematic than isolation from tissue, since it is difficult to disrupt the cell membrane without affecting the mitochondrial membrane. In order to make the plasma membrane more vulnerable, different tactics are used. The plasma membrane can be sensitized to disruption by using a buffer that contains digitonin, a steroid glycoside with a high affinity for cholesterol that selectively disrupts the cholesterol-rich plasma membrane. Another approach is based on passing cells through a needle. Both methods are followed by a differential centrifugation commonly used for preparation of mitochondria.

Materials

Tissue culture cells (e.g., Jurkat cells, U 937, HeLa; *APPENDIX 3B*)
Complete RPMI medium (*APPENDIX 3B*) or appropriate medium for cells
Buffer A for cultured cells (see recipe), ice-cold
Buffer B: Buffer A (for cultured cells) without EGTA
1% (w/v) digitonin: dissolve 10 mg digitonin in 1 ml H_2O; shake vigorously before adding to cells; store up to 2 to 3 months at room temperature
Refrigerated centrifuge and tubes

1. Take an aliquot containing 5×10^7 cells growing in culture in complete RPMI medium and centrifuge 5 min at $200 \times g$, 4°C. Remove supernatant.
2. Resuspend cells in buffer A for cultured cells. Centrifuge 4 min at $200 \times g$, 4°C.
3. Add 1% digitonin to buffer A for a final concentration of 0.01%. Resuspend cells in 5 ml of the buffer A containing 0.01% digitonin and incubate 10 min on ice.
4. Add 5 ml of ice-cold buffer A and mix well. Sediment lysed cells by centrifuging 7 min at $500 \times g$, 4°C.
5. Discard the pellet and centrifuge supernatant 15 min at $5500 \times g$, 4°C, to form a mitochondrial pellet.
6. Detach the pellet from the bottom of the centrifuge tube with a pipet tip and resuspend the pellet in 0.1 ml of buffer B using an automatic pipettor.
7. Dilute the mitochondrial suspension with 2 ml of buffer B and centrifuge again for 15 min at $5500 \times g$, 4°C.
8. Resuspend the final mitochondrial pellet in buffer B by gently passing through a pipet tip, then transfer into an microcentrifuge tube and keep on ice.

Measurements can be started directly after mitochondrial isolation.

Unfortunately, the yield from this protocol is sufficient material for an experiment but not enough to assess protein concentration and respiratory control ratio as well.

SUPPORT PROTOCOL 4

Estimation of the Quality of Isolated Mitochondria: Measuring the Respiratory Control Ratio (RCR)

One of the keystones of the chemiosmotic theory of energy transduction is impermeability of the inner mitochondrial membrane to protons. Oxidation of substrates results in extrusion of protons from the mitochondrial matrix to generate the mitochondrial membrane potential. High membrane potential suppresses further extrusion of protons and therefore inhibits respiration. Under resting conditions, the rate of respiration of mitochondria is quite low and determined by a passive leakage of protons into the matrix space.

Phosphorylation of ADP requires translocation of protons into the matrix through mitochondrial ATP synthase. This results in a decrease in membrane potential that stimulates respiration. Comparison of the rates of respiration in the resting state and during phos-

phorylation of ADP is a useful measure of the efficiency of mitochondrial functioning. The most reliable and widely used criterion of the quality of a mitochondrial preparation is the respiratory control ratio (RCR). RCR is defined as the rate of respiration in the presence of ADP (phosphorylating respiration, state 3) divided by the rate obtained following the expenditure of ADP, state 4.

Materials

Mitochondria (Support Protocol 1, 2, or 3)
Incubation buffer for testing mitochondrial quality (see recipe)
2.5 mM rotenone: dissolve 1 mg rotenone (Sigma) in 1 ml ethanol; store frozen at –20°C up to 1 month
0.5 M sodium succinate: dissolve 135 mg of sodium succinate in 1 ml of H_2O, store frozen at –20°C up to 1 month
50 mM ADP: dissolve 23 mg of ADP in 1 ml H_2O and adjust pH to 7.5 with KOH; store frozen at –20°C up to 1 month
1 mM CCCP: dissolve 0.2 mg CCCP in 1 ml ethanol and mix thoroughly; store frozen at –20°C up to 1 month
Biological oxygen monitor equipped with a Clark-type oxygen electrode (Yellow Spring Instrument Co.) or similar equipment (operate per manufacturer's instructions)
Chart recorder with variable input and chart speed
10- and 50-µl Hamilton syringes (e.g., Sigma)

1. Place 2 ml of incubation buffer for testing mitochondrial quality into the sample chamber of the oxygen monitor and set conditions to constant stirring. Add an aliquot of mitochondrial suspension (the volume of which will depend on the concentration of the mitochondrial preparation) for a final concentration of 2 mg/ml mitochondrial protein.
2. After 30 sec add 2 µl of 2.5 mM rotenone, for a final concentration of 2.5 µM.
3. Stop stirring and insert the electrode into the sample chamber. Expel all air through the slot in the plunger (slight twisting of the electrode helps to gather the bubbles at the slot) and set the chart speed.

   The desirable chart speed should be 10 to 15 mm/min.
4. After 1 min stabilization observed by recorder trace add 20 µl of 0.5 M sodium succinate, for a final concentration of 5 mM, through the slot on electrode's body with a Hamilton syringe.

   Mitochondria will now start to consume oxygen. The slope of the curve shows the rate of respiration.
5. After stabilization of respiration (~2 min) add 10 µl of 50 mM ADP.

   The rate of respiration will increase (state 3) with subsequent restoration of the initial rate of respiration (state 4) when all added ADP is phosphorylated.
6. Add 2 µl of 1 mM CCCP, for a final concentration of 1 µM.

   CCCP lowers the mitochondrial potential that stimulates oxygen consumption.
7. Calculate the rate of respiration from the recorder trace as the amount of oxygen consumed in 1 min (see Fig. 2.10.6).

   Assume that at room temperature and normal atmospheric pressure the concentration of oxygen in the incubation buffer is 250 µM.
8. Calculate the RCR by dividing the state 3 respiration rate by the state 4 respiration rate.

   Mitochondria with a respiratory control ratio above 4 are acceptable for use in the experiments.

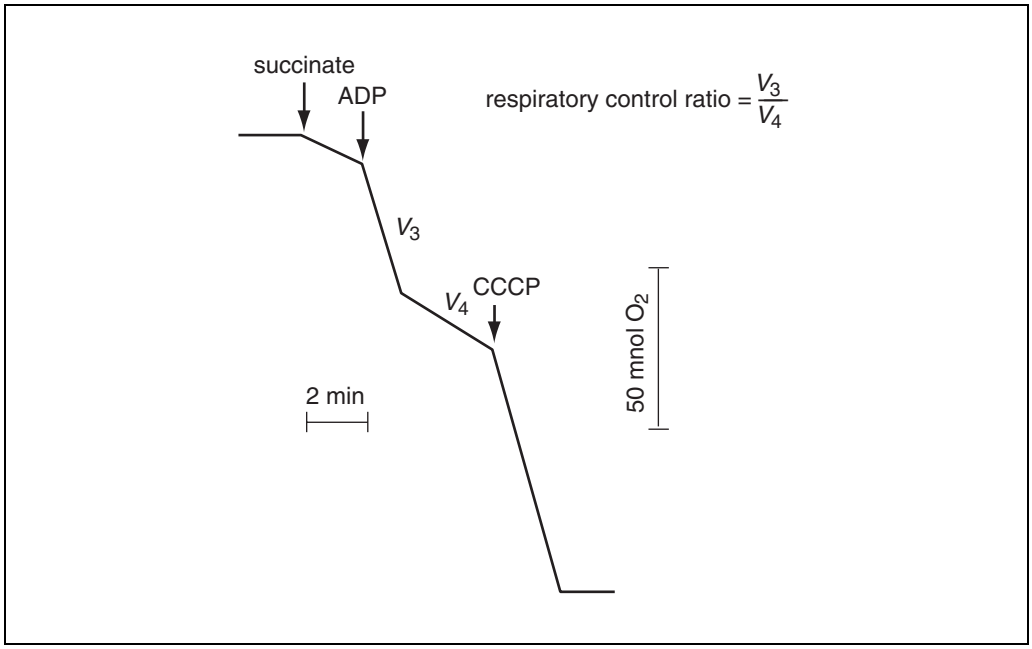

Figure 2.10.6 Estimation of mitochondrial respiration.

REAGENTS AND SOLUTIONS

*Use Milli-Q-purified water or equivalent in all recipes and protocol steps. For common stock solutions, see **APPENDIX 2A**; for suppliers, see **SUPPLIERS APPENDIX**.*

Buffer A for cultured cells

38.26 g/liter mannitol (210 mM final)
23.96 g/liter sucrose (70 mM final)
0.2g/liter $MgCl_2 \cdot 6\ H_2O$ (1 mM final)
1.2 g/liter HEPES (5 mM final)
0.38 g/liter EGTA (1 mM final)
Adjust pH to 7.5 with KOH
Store up to 3 to 4 days at 4°C

Buffer A for liver

38.26 g/liter mannitol (210 mM final)
23.96 g/liter sucrose (70 mM final)
1.2 g/liter HEPES (5 mM final)
2 ml/liter 0.5 M EDTA (1 mM final)
Adjust pH to 7.5 with KOH
Store up to 3 to 4 days at 4°C

Ficoll dilution buffer

0.25 M mannitol
60 mM sucrose
100 µM potassium EGTA
10 mM Tris·Cl, pH 7.5 (*APPENDIX 2A*)
Store up to 3 to 4 days at 4°C

Ficoll solutions, 3% and 6% (w/w)

Prepare 20% (w/v) Ficoll (Sigma) stock solution in Ficoll dilution buffer (see recipe). Store 3 to 4 days at 4°C. Before the experiment prepare 6% (v/v) and 3% (v/v) solutions by diluting 20% solution with Ficoll dilution buffer.

HEPES buffer

2.38 g/liter HEPES (10 mM final)
8.76 g/liter NaCl (150 mM final)
0.37 g/liter KCl (5 mM final)
0.2 g/liter $MgCl_2 \cdot 6H_2O$ (1 mM final)
Adjust pH to 7.4 with NaOH
Store up to 2 to 3 days at 4°C

Incubation buffer for calcium-sensitive electrode

1.11 g/100 ml KCl (150 mM final)
13.1 mg/100 ml KH_2PO_4 (1 mM final)
60 mg/100 ml Tris (5 mM final)
135 mg/100 ml sodium succinate (5 mM final)
Adjust pH to 7.4 with HCl
Store up to 2 to 3 days at 4°C

Incubation buffer for digitonin-permeabilized cells

150 mM KCl
5 mM KH_2PO_4
1 mM $MgCl_2$
5 mM sodium succinate
5 mM Tris·Cl, pH 7.4 (*APPENDIX 2A*)
Store up to 2 to 3 days at 4°C

Incubation buffer for swelling

1.11 g/100 ml KCl (150 mM final)
6.8 mg/100 ml KH_2PO_4 (0.5 mM final)
60 mg/100 ml Tris (free base; 5 mM final)
135 mg/100 ml sodium succinate (5 mM final)
Adjust pH to 7.4 with HCl
Store up to 2 to 3 days at 4°C

Incubation buffer for testing mitochondrial quality

1.11 g/100 ml KCl (150 mM final)
13.1 mg/100 ml KH_2PO_4 (1 mM final)
60 mg/100 ml Tris (free base; 5 mM final)
Adjust pH to 7.4 with HCl
Store up to 3 to 4 days at 4°C

Incubation buffer for TPP^+-sensitive electrode

1.11 g/100 ml KCl (150 mM final)
27 mg/100 ml KH_2PO_4 (2 mM final)
60 mg/100 ml Tris (free base; 5 mM final)
135 mg/100 ml sodium succinate (5 mM final)
Adjust pH to 7.4 with HCl
Store up to 2 to 3 days at 4°C

Laemmli's loading buffer, 4×

3.125 ml 1 M Tris·Cl, pH 6.8 (*APPENDIX 2A*)
4 ml glycerol
0.8 g sodium dodecyl sulfate
8 mg bromphenol blue
0.8 ml 2-mercaptoethanol
H_2O to 10 ml
Store up to several weeks at 4°C

MSH buffer

210 mM mannitol
70 mM sucrose
5 mM HEPES
Adjust pH to 7.4 with KOH
Store up to 2 to 3 days at 4°C

S100 buffer

20 mM HEPES, pH 7.5
10 mM KCl
1.5 mM $MgCl_2$
1 mM EGTA
1 mM EDTA
0.1 mM PMSF
10 mg/ml leupeptin
5 mg/ml pepstatin A
2 mg/ml aprotinin
25 mg/ml calpain I inhibitor
1 mM DTT
Store at 4°C; prepare weekly

SET buffer

8.58 g/100 ml sucrose (0.25 M final)
0.5 ml of 100 mM potassium EGTA stock solution/100 ml (0.5 mM final)
120 mg/100 ml Tris (free base; 10 mM final)
Adjust pH to 7.4 with HCl

COMMENTARY

Background Information

Mitochondrial function in apoptotic cells

Attempts to identify a common, unifying step in the apoptotic program, in response to various cytotoxic stimuli, have focused on the role of mitochondrial participation in this form of cell death (Petit et al., 1997). Specifically, the release of several proteins, normally located in the intermembrane space of mitochondria, has been observed during the early stages of apoptotic cell death (Green and Reed, 1998). Among these proteins are cytochrome *c* and other intermembrane-space proteins, including AIF (apoptosis-inducing factor), HSPs (heat shock proteins), DIABLO/Smac (direct IAP-binding protein with low pI/Second mitochondria-derived activator of caspase), AK-2 (adenylate kinase-2), several pro-caspases (Mancini et al., 1998; Köhler et al., 1999; Samali et al., 1999; Susin et al., 1999; Zhivotovsky et al., 1999; Du et al., 2000; Verhagen et al., 2000), endonuclease G, and sulfite oxidase. Although the role of many of these proteins in the apoptotic process is well characterized, the involvement of others (AK-2, sulfite oxidase) is still unclear. It is important to note that the function of the released proteins in the cytoplasm is different from their functions within mitochondria. The best-studied of these proteins is cytochrome *c*.

Cytochrome *c*, is a component of the electron transport chain that shuttles electrons between complexes III (bc1) and IV (cytochrome oxidase). Apo-cytochrome *c* is encoded by a nuclear gene, synthesized in the cytosol, and imported into the mitochondrial intermembrane space in an unfolded configuration where it receives its heme group. Covalent attachment of this heme group stimulates a conformational change, and holo-cytochrome *c* subsequently assumes its functional role as a component of the electron transport chain.

During the early phase of apoptosis, cytochrome *c* is released into the cytosol and interacts with Apaf-1 to form the apoptosome complex together with dATP and pro-caspase-9 (Li et al., 1997).

The mechanisms regulating cytochrome *c* release remain obscure. However, two distinct models for cytochrome *c* release have emerged, and these can be distinguished on the basis of whether Ca^{2+} is required for the event. In one instance, mitochondrial Ca^{2+} overload results

in opening of a pore in the inner mitochondrial membrane, with subsequent swelling and rupture of the outer membrane followed by the release of cytochrome *c* and other intermembrane space proteins (Crompton, 1999). The Ca^{2+}-independent model asserts that a more selective protein release occurs without changes in mitochondrial volume. This mechanism involves specific channels/pores in the outer mitochondrial membrane that may be opened and regulated by certain pro-apoptotic members of the Bcl-2 family of proteins, including Bax (Robertson and Orrenius, 2000). The precise manner in which Bax modulates cytochrome *c* release is controversial. In particular, the authors have reported recently that depending on the experimental conditions this protein can either act directly on mitochondria to stimulate the release of cytochrome *c* by forming a selective pore in the outer membrane, or it may facilitate opening of the permeability transition pore (Gogvadze et al., 2001). Recent evidence indicates that truncated Bid induces a conformational change in Bax that allows this protein to insert in the outer membrane, oligomerize, and stimulate cytochrome *c* release (Eskes et al., 2000).

Mitochondrial permeability transition

Energized mitochondria can take up and retain added Ca^{2+}. However this ability is not limitless. Mitochondria swell and become leaky; the membrane potential, which is the driving force for Ca^{2+} accumulation, drops, and accumulated Ca^{2+} is released. This process is called mitochondrial permeability transition (MPT). These changes are identified as a result of the opening of Ca^{2+}-dependent pore in the mitochondrial inner membrane.

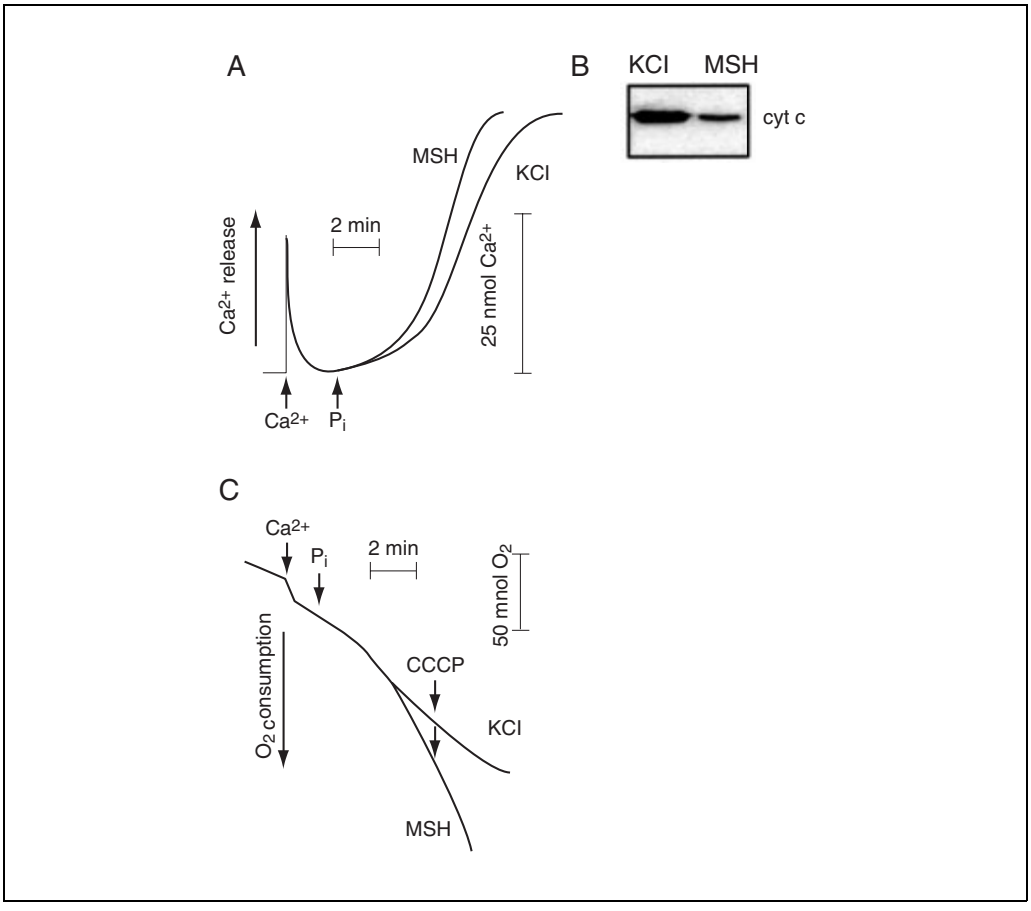

Figure 2.10.7 MPT-induced release of cytochrome *c* from mitochondria incubated in either MSH or KCl buffer. (**A**) Mitochondria were added to buffer at a concentration of 1 mg/ml. After a 2-min stabilization period, mitochondria were loaded with Ca^{2+} (50 nmol/mg protein), and MPT was induced by adding 5 mM inorganic phosphate (P_i). (**B**) Mitochondrial suspensions from (A) were centrifuged and the resulting supernatants were separated by SDS-PAGE and immunoblotted as described in Basic Protocol 3. (**C**) Mitochondrial respiration following MPT induction in either MSH or KCl buffer was analyzed as described in Support Protocol 4. The concentration of CCCP was 1 μM.

MPT-dependent release of cytochrome c

Although the kinetics of MPT are unaffected by the composition of the incubation buffer (KCl versus MSH; Fig. 2.10.7A), the amount of cytochrome *c* released is much higher when mitochondria are incubated in the physiologically more relevant KCl buffer as compared to MSH buffer. Immunoblot analysis revealed that most cytochrome *c* was present in the supernatant fraction following MPT induction in KCl buffer, whereas only partial release of cytochrome *c* was observed in MSH buffer (Fig. 2.10.7B). Further evidence of this comes from the different effects that cytochrome *c* release has on mitochondrial respiration in the two buffers (Fig. 2.10.7C). Specifically, the induction of MPT in MSH buffer resulted in a time-dependent acceleration of oxygen consumption that persisted until all oxygen was consumed. In contrast, incubation of mitochondria in KCl buffer resulted in an initial acceleration of respiration that was followed by its suppression, and no additional stimulation of oxygen consumption was observed upon the addition of the uncoupler carbonyl cyanide *m*-chlorophenylhydrazone (CCCP). Taken together, these data indicate that while MPT-induced uncoupling of mitochondria occurs in both buffers, respiration is suppressed only in KCl buffer, an effect most likely due to a loss of cytochrome *c*.

It should be taken into account that mitochondrial preparations are heterogeneous. At a given concentration of Ca^{2+}, a certain subpopulation (more susceptible) of mitochondria have undergone permeability transition at a given time, while the released Ca^{2+} is accumulated by more resistant mitochondria, which thereby in-

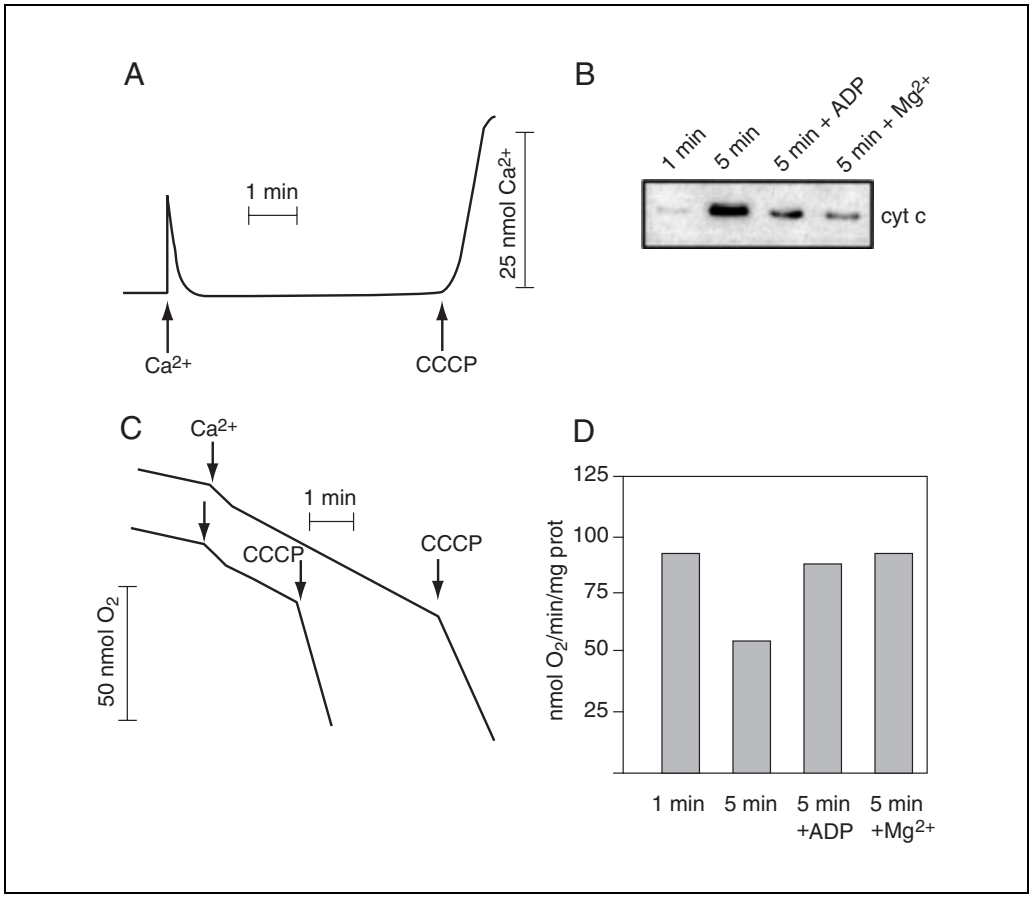

Figure 2.10.8 Ca^{2+}-induced release of cytochrome *c* from mitochondria in the absence of observable MPT. (**A**) Mitochondria (1 mg/ml) were incubated in KCl-based buffer. After a 2-min stabilization period, mitochondria were loaded with Ca^{2+} (25 nmol/mg protein) prior to the addition of 1 μM carbonyl cyanide *m*-chlorophenyl hydrazone (CCCP) at 5 min. (**B**) The amount of cytochrome *c* released from mitochondria after 1 and 5 min of Ca^{2+} retention in the presence and absence of 0.5 mM ADP or 1 mM Mg^{2+}. (**C**) Samples incubated under the same conditions as (A) were used to evaluate the rate of uncoupled respiration after 1 and 5 min. (**D**) Samples incubated under the same conditions as conditions as (B) were used to determine the effect of inhibitors of MPT on the rate of uncoupled respiration of Ca^{2+}-loaded mitochondria.

crease their load until they also undergo permeabilization (Zoratti and Szabo, 1995).

In the aforementioned protocols, cytochrome *c* release was a consequence of MPT induction, accompanied by swelling of mitochondria and rupture of the outer membrane. When Ca^{2+} loading is insufficient to induce observable manifestations of MPT, the release of cytochrome *c* can still occur despite the absence of changes characteristic of MPT.

As seen in Figure 2.10.8A, moderate Ca^{2+} loading of mitochondria did not induce MPT, and this cation was retained by mitochondria unless the uncoupler CCCP was added. The accumulation of Ca^{2+} by mitochondria in the absence of observable MPT was nevertheless sufficient to stimulate a release of cytochrome *c*, an effect that was considerably more pronounced the longer mitochondria retained the accumulated Ca^{2+}. Inhibitors of MPT, such as Mg^{2+} and ADP, suppressed this release (Fig. 2.10.8B). In addition, Ca^{2+}-loaded mitochondria exhibited controlled respiration (Fig. 2.10.8C), although increasing the Ca^{2+} retention time from 1 to 5 min prominently diminished the rate of CCCP-directed uncoupled respiration (upper trace versus versus lower trace). Inhibitors of MPT, such as Mg^{2+} and ADP, suppressed this release (Fig. 2.10.8D) and restored the rate of uncoupled respiration.

Additional evidence of cytochrome *c* release in the absence of observable MPT is presented in Figure 2.10.9A, where the sequential addition of Ca^{2+} pulses to isolated mitochondria led to a step-wise decrease in the overall optical density without the large-amplitude swelling characteristic of MPT. Meanwhile, the amount of cytochrome *c* released from mitochondria was enhanced as Ca^{2+} loading increased (Fig. 2.10.9B). This release reflected MPT induction in a subpopulation of mitochondria, which was further supported by the fact that cotreatment of isolated mitochondria with 1 μM CsA (cyclosporin A) eliminated cytochrome *c* release induced by Ca^{2+} additions ranging between 20 to 80 nmol/mg protein (data not shown). Cytochrome *c* release ultimately reached a pinnacle at 80 nmol Ca^{2+}/mg protein (Fig. 2.10.9B, lanes 6 and 7) as all mitochondria underwent MPT (Fig. 2.10.9A).

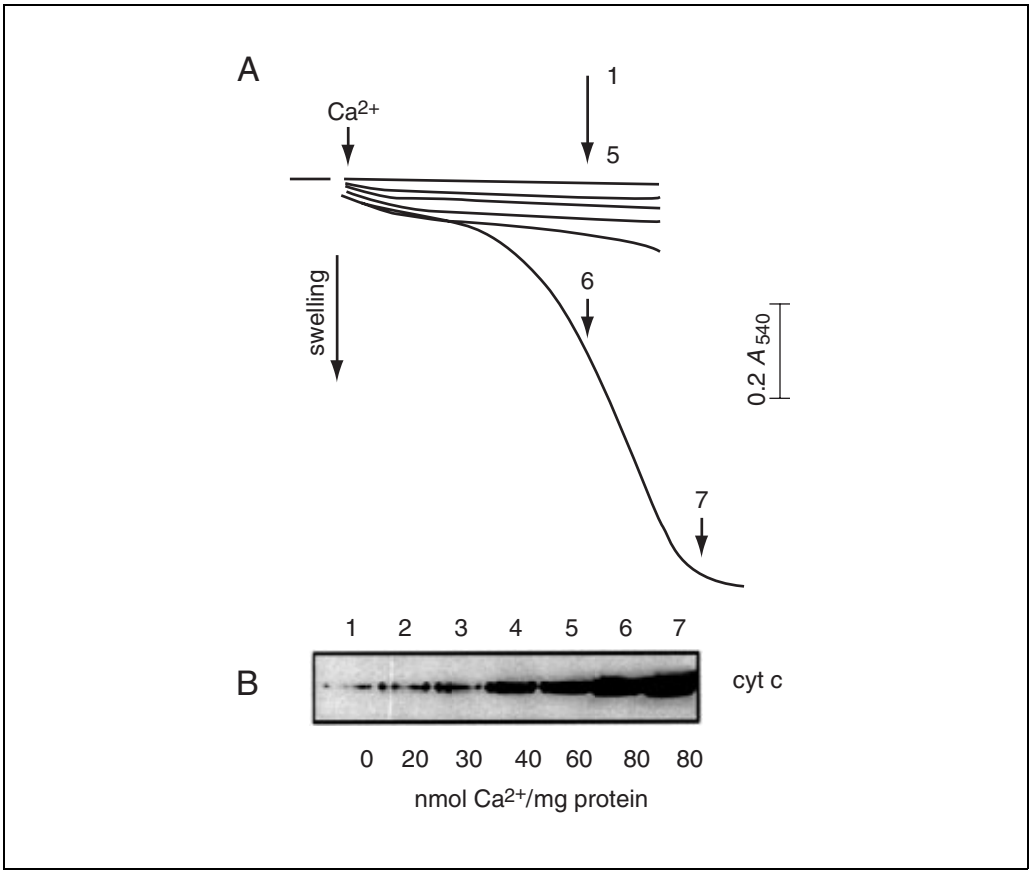

Figure 2.10.9 The effect of Ca^{2+} loading on mitochondrial swelling and the release of cytochrome *c*. Mitochondria (0.5 mg/ml) were incubated in 2 ml of KCl-based buffer. (**A**) Mitochondria were loaded sequentially with varied amounts of Ca^{2+} until MPT was induced. (**B**) Samples were taken after 5 min (lanes 1 to 6) or 8 min (lane 7) of incubation and the supernatants evaluated for cytochrome *c* content.

MPT-independent release of cytochrome c

Although it was originally believed that MPT induction was the root mechanism responsible for cytochrome *c* release in response to different cytotoxic stimuli, more recently this notion has been challenged and the precise mechanisms regulating the release of this protein are unclear. In fact, many of the early results on mechanisms of cytochrome *c* release were generated using cell-free systems wherein isolated mitochondria and nuclei were treated with different MPT pore activators, which, in turn, led to mitochondrial swelling, the release of cytochrome *c* (and other proteins), and subsequent changes in nuclear morphology that were characteristic of apoptosis. However, ample evidence from more recent studies suggests that, while MPT is likely to be a mechanism responsible for cytochrome *c* release, it is no longer regarded as *the* mechanism.

In case of MPT induction, mitochondrial swelling leads to a rupture of the outer membrane; without MPT, permeabilization can be achieved by Bcl-2 family proteins Bax or Bid that form pores in the outer membrane, leaving the inner mitochondrial membrane intact.

Discrimination between MPT-dependent and MPT-independent release of cytochrome c

While analyzing the release of cytochrome *c* from mitochondria, one should keep in mind that even without added Ca^{2+}, MPT may occur in a subpopulation of mitochondria if the trace amount of Ca^{2+} in buffers is enough to induce MPT in "susceptible" mitochondria. Therefore the release of cytochrome *c* observed in the absence of added Ca^{2+} can be mistaken for MPT-independent release of cytochrome *c*. In order to distinguish between the MPT-dependent and -independent release of cytochrome *c*, experiments should be performed in the presence of the Ca^{2+} chelator EGTA, which sequesters Ca^{2+} and therefore prevents MPT induction. Similar results can be achieved with CsA.

Critical Parameters and Troubleshooting

Collecting released proteins (Basic Protocols 1 and 2)

Separation of the mitochondria from the supernatant should be done thoroughly. Aliquots of supernatant should be taken without disturbing the pellet.

Immunoblot analysis of released proteins (Basic Protocol 3)

For immunoblot analysis, too many bands on the membrane may indicate too high a concentration of primary and/or secondary antibodies. If the background of nonspecific binding of immunological probes is unacceptably high, increase the length of the time of washing with PBS. If there is no band on the film, increase the duration of incubation with primary antibodies. If a white spot on the film makes it difficult to detect the protein band of interest, a bubble may have been introduced during blotting and the whole procedure must be repeated. If a band on the film is too strong, decrease exposure time of X-ray film to the ECL-stained membrane. If the gel runs too fast or too slow and poor resolution of protein occurs, decrease or increase voltage, respectively, or check the buffer recipe. If no prestained markers appear on the nitrocellulose filter, check the transfer buffer recipe, or reposition the location of gel towards the cathode and anode.

FACS analysis of TMRE-stained cells (Basic Protocol 4)

FACS analysis needs an appropriate gating of the cells—a selection of the population of interest, especially if the initial population is a mixture of different types of cells (for example when blood samples are analyzed).

Another critical parameter is time. The analysis of the membrane potential should be done shortly after staining of the cells. TMRE is only accumulated by mitochondria with high membrane potential and any delay in analysis may negatively affect the functional state of the mitochondria and therefore cause leakage of the dye.

Microscopy of apoptotic cells stained with MitoTracker Red (Basic Protocol 5)

To reduce potential artifacts from overloading, the concentration of dye should be kept as low as possible. However if cells are not sufficiently stained, the concentration of dye or time of incubation should be increased.

Measurement of calcium release and membrane potential (Basic Protocols 6 and 7)

The release of Ca^{2+} from mitochondria may result not from opening of the pore, but simply because of a drop of the membrane potential. This may happen, for instance, if the mitochondria consume all available oxygen. However at a mitochondrial protein concentration of 1 mg/ml

(or less), and with rapid stirring of the suspension, MPT usually occurs before the exhaustion of oxygen. If higher concentrations of mitochondrial suspension are used, possible anaerobiosis can be prevented by fine flow of oxygen blown onto the surface of the suspension.

Mitochondrial swelling (Basic Protocol 8)

Mitochondrial swelling assessed by a decrease in optical density of mitochondrial suspension represents one of the most reliable parameters of MPT induction in isolated mitochondria. However it should be kept in mind that anaerobiosis and subsequent release of accumulated Ca^{2+} due to the drop in membrane potential may prevent pore opening and terminate swelling. Anaerobiosis can be prevented by a fine flow of oxygen blown onto the surface of the suspension. On the other hand, a relatively low concentration of mitochondria (up to 1 mg/ml) should not lead to anaerobiosis.

Estimation of mitochondrial Ca^{2+} accumulation in digitonin-permeabilized cells (Basic Protocol 9)

Digitonin generally permeabilizes plasma membrane, which contains cholesterol; therefore, this detergent should be used with caution because relatively high concentrations of digitonin can affect also the outer mitochondrial membrane. The minimal concentration of digitonin that is necessary for the outer-membrane permeabilization can be detected with a Ca^{2+}-sensitive electrode. Cells do not accumulate added Ca^{2+}, since plasma membrane is permeable neither to Ca^{2+} nor to succinate, oxidation of which provides a driving force for Ca^{2+} accumulation. Upon addition of digitonin, the plasma membrane becomes permeable and the mitochondria start to accumulate Ca^{2+} from the incubation buffer.

Preparation of mitochondria (Support Protocols 1, 2, and 3)

The temperature during isolation should be kept around 4°C. Elevation of the temperature may result in activation of catabolic enzymes, in particular, mitochondrial phospholipase A_2, which leads to accumulation of free fatty acids in mitochondria. Free fatty acids are known as natural protonophores (agents that facilitate transport of protons through membrane); therefore, accumulation of fatty acids will decrease the mitochondrial membrane potential and destabilize mitochondria.

Anticipated Results

Analyzing functioning of isolated mitochondria and mitochondria in apoptotic cells: collection of released proteins and immunoblot analysis (Basic Protocols 1, 2, and 3)

Depending on the mechanisms involved in the release of cytochrome *c* or other proteins from mitochondria, the final result will be different. If the release was associated with mitochondrial swelling and the rupture of the outer membrane, most of the cytochrome *c* will be found in the supernatant after sedimentation of mitochondria. In such a situation, it would be informative also to present the data concerning changes in the content of cytochrome *c* in the pellet. Figure 2.10.10 represents a typical blot showing the release of cytochrome *c* from isolated liver mitochondria upon induction of MPT in KCl-based buffer.

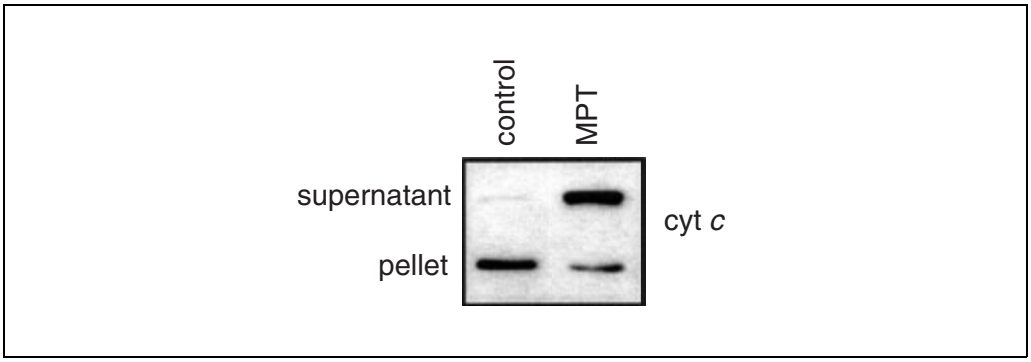

Figure 2.10.10 The release of cytochrome c from isolated rat liver mitochondria as a result of mitochondrial permeability transition (MPT). Mitochondria (1 mg/ml) were incubated in KCl-based buffer. After a 2-min stabilization period, mitochondria were loaded with Ca^{2+}, and, when accumulation was complete, MPT was induced by 5 mM KH_2PO_4. A 200-µl aliquot of mitochondrial suspension was centrifuged and the resulting supernatant and pellet were separated by SDS-PAGE and immunoblotted as described under in Basic Protocol 3. Control mitochondria were incubated for the same time but without Ca^{2+} loading.

FACS analysis of TMRE-stained cells (Basic Protocol 4)

A typical image of FACS analysis of mitochondria in the cells undergoing apoptosis is present in Figure 2.10.1. The lower left quadrant contains living cells, the lower right, apoptotic cells, and upper right, necrotic cells.

Measurement of calcium release (Basic Protocol 6)

A typical response of mitochondria to Ca^{2+} is shown in Figure 2.10.2. Addition of Ca^{2+} to isolated mitochondria results in a quick rise in the basal level of Ca^{2+} in the incubation buffer, followed by restoration of the initial level due to accumulation of Ca^{2+} in mitochondria, whereupon a new steady state is reached. After addition of phosphate, mitochondria start releasing accumulated Ca^{2+}. The lag time before the onset of MPT induction, as well as the rate of release, depend on the Ca^{2+} load. If Ca^{2+} and other conditions are held constant, the effect of phosphate on MPT induction is dose-dependent. Therefore, the opening of the pore can be modulated either by varying the Ca^{2+} concentration while keeping the concentration of phosphate constant, or by varying the concentration of phosphate.

Both methods (spectrophotometric and ion-selective electrodes) are equally sensitive, and the choice is dictated by the availability of the equipment.

Measurement of membrane potential (Basic Protocol 7)

Energized mitochondria rapidly accumulate TPP^+ from the incubation buffer and release this cation as $\Delta\psi$ decays. A typical change in mitochondrial membrane potential upon MPT induction is shown on Figure 2.10.3. As can be seen in that figure, upon induction of MPT, two distinct phases of decrease in membrane potential occur. First, a relatively slow decrease starts when an MPT-inducing agent (P_i) is added, which is followed by a second, rapid phase, which reflects the induction of MPT in the whole population of mitochondria.

Measurement of mitochondrial swelling (Basic Protocol 8)

Figure 2.10.4 shows a typical example of results from measurement of mitochondrial swelling. When mitochondria are added to incubation buffer at a concentration of 0.5 mg/ml, the initial light absorption at 540 nm is about 1.3 to 1.4. Addition of Ca^{2+} to the mitochondria, followed by inorganic phosphate, results in a time-dependent decrease in the optical density (OD) of the mitochondrial suspension.

Estimation of mitochondrial Ca^{2+} accumulation in digitonin-permeabilized cells (Basic Protocol 9)

The addition of Ca^{2+} to a permeabilized cell suspension leads to a rapid increase in the level of this cation in the reaction buffer, followed by a return to the initial level as mitochondria accumulate the excess Ca^{2+} (Fig. 2.10.5); this is an effect that can be completely abrogated by 2 μg/ml antimycin, an inhibitor of mitochondrial respiratory chain (data not shown). Mitochondria accumulate sequential additions of Ca^{2+} until MPT is induced and the accumulated Ca^{2+} is released.

Preparation of mitochondria and assessing their quality (Support Protocols 1 to 4)

Isolation of mitochondria usually takes about 60 to 75 min. For liver the yield is about 20 to 25 mg protein of mitochondria per 1 g of tissue. High concentration of the final mitochondrial preparation is a prerequisite of mitochondrial stability.

A typical respiratory response of mitochondria and the method of calculating RCR are shown in Figure 2.10.6. Addition of CCCP when added ADP is phosphorylated and state 4 respiration is stabilized allows one to determine the rate of uncoupled respiration that represents the activity of the mitochondrial respiratory chain.

Time Considerations

The time of collecting samples and preparing for immunoblotting depends on the incubation conditions as well as the experience of a researcher. Basic Protocol 1 requires 45 to 60 min, Basic Protocol 2, 2 to 2.5 hr, and Basic Protocol 3, 2 days. TMRE (Basic Protocol 4) and MitoTracker Red (Basic Protocol 5) staining takes 1 hr and 1.5 hr, respectively. Measurement of the mitochondrial permeability transition (Basic Protocols 6, 7, 8, and 9 and Alternate Protocols 1 and 2) can be completed in 5 to 20 min.

Mitochondrial preparation (Support Protocols 1, 2, and 3) takes 60 to 80 min. Assessment of respiratory control ratio takes 20 to 35 min.

Literature Cited

Bossy-Wetzel E., Newmeyer, D.D., and Green, D.R. 1998. Mitochondrial cytochrome *c* release in apoptosis occurs upstream of DEVD-specific caspase activation and independently of mitochondrial transmembrane depolarization. *EMBO J.* 17:37-49.

Crompton, M. 1999. The mitochondrial permeability transition pore and its role in cell death. *Biochem. J.* 341:233-249.

Donovan, J. and Brown, P. 1995. Euthanasia. *In* Curent Protocols in Immunology (J.E. Coligan, A.M. Kruisbeek, D.M. Margulies, E.M. Shevach, and W. Strober, eds.) pp. 1.8.1-1.8.4. John Wiley & Sons, New York.

Du, C., Fang, M., Li, Y., Li, L., and Wang, X. 2000. Smac, a mitochondrial protein that promotes cytochrome *c*-dependent caspase activation by elimination IAP inhibition. *Cell* 102:33-42.

Eskes, R., Desagher, S., Antonsson, B., and Martinou, J.C. 2000. Bid induces the oligomerization and insertion of Bax into the outer mitochondrial membrane. *Mol. Cell Biol.* 20:929-935.

Gallagher, S., Winston, S.E., Fuller, S.A., and Hurrell, J.G.R. 1998. Immunoblotting and Immunodetection. *In* Current Protocols in Cell Biology (J.S. Bonifacino, M. Dasso, J.B. Hartford, J. Lippincott-Schwartz, and K.M. Yamada, eds.) pp. 6.2.1-6.2.20. John Wiley & Sons, New York.

Gogvadze, V., Robertson, J.D., Zhibotovsky, B., and Orrenius, S. 2001. Cytochrome c release occurs via Ca^{2+}-dependent and Ca^{2+}-independent mechanisms that are regulated by Bax. *J. Biol. Chem.* 276:19066-19071.

Green, D.R. and Reed, J.C. 1998. Mitochondria and apoptosis. *Science* 281:1309-1312.

Kamo, N., Muratsugu, M., Hongoh, R., and Kobatake, Y. 1979. Membrane potential of mitochondria measured with an electrode sensitive to tetraphenyl phosphonium and relationship between proton electrochemical potential and phosphorylation potential in steady state. *J. Membr. Biol.* 49:105-121.

Köhler, C., Gahm, A., Noma, T., Nakazawa, A., Orrenius, S., and Zhivotovsky, B. 1999. Release of adenylate kinase 2 from the mitochondrial intermembrane space during apoptosis. *FEBS Lett.* 447:10-12.

Li, P., Nijhawan, D., Budihardjo, I., Srinivasula, S.M., Ahmad, M., Alnemri, E.S., and Wang, X. 1997. Cytochrome c and dATP-dependent formation of Apaf-1/caspase-9 complex initiates an apoptotic protease cascade. *Cell* 91:479-489.

Mancini, M., Nicholson, D.W., Roy, S., Thornberry, N.A., Peterson, E.P., Casciola-Rosen, L.A., and Rosen, A. 1998. The caspase-3 precursor has a cytosolic and mitochondrial distribution: Implications for apoptotic signaling. *J. Cell Biol.* 140:1485-1495.

Mitchell, P. and Moyle, J. 1967. Chemiosmotic hypothesis of oxidative phosphorylation. *Nature* 213:137-139.

Petit, P.X., Zamzami, N., Vayssiere, J.L., Mignotte, B., Kroemer, G., and Castedo, M. 1997. Implication of mitochondria in apoptosis. *Mol. Cell. Biochem.* 174:185-188.

Robertson, J.D. and Orrenius, S. 2000. Molecular mechanisms of apoptosis induced by cytotoxic chemicals. *Crit. Rev. Toxicol.* 30:609-627.

Samali, A., Cai, J., Zhivotovsky, B., Jones, D.P., and Orrenius, S. 1999. Presence of a pre-apoptotic complex of pro-caspase-3, Hsp60 and Hsp10 in the mitochondrial fraction of Jurkat cells. *EMBO J.* 19:2040-2048.

Susin, S.A., Lorenzo, H.K., Zamzami, N., Marzo, I., Brenner, C., Larochette, N., Prevost, M.C., Alzari, P.M., and Kroemer, G. 1999. Mitochondrial release of caspase-2 and-9 during the apoptotic process. *J. Exp. Med.* 189:381-394.

Verhagen, A.M., Ekert, P.G., Pakusch, M., Silke, J., Connolly, L.M., Reid, G.E., Moritz, R.L., Simpson, R.J., and Vaux, D.L. 2000. Identification of DIABLO, a mammalian protein that promotes apoptosis by binding to and antagonizing IAP proteins. *Cell* 102:43-53.

Zamzami, N., Susin, S.A., Marchetti, P., Hirsch, T., Gomez-Monterrey, I., Castedo, M., and Kroemer, G. 1996. Mitochondrial control of nuclear apoptosis. *J. Exp. Med.* 183:1533-1544.

Zhivotovsky, B., Samali, A., Gahm, A., and Orrenius, S. 1999. Caspases: Their intracellular localization and translocation during apoptosis. *Cell Death Differ.* 6:644-651.

Zoratti, M. and Szabo, I. 1995. The mitochondrial permeability transition. *Biochem. Biophys. Acta.* 121:139-176.

Contributed by Vladimir Gogvadze,
Sten Orrenius, and Boris Zhivotovsky
Institute of Environmental Medicine
Karolinska Institutet
Stockholm, Sweden

CHAPTER 3
Genetic Toxicology: Mutagenesis and Adduct Formation

INTRODUCTION

Hundreds of thousands of natural and man-made chemicals remain to be evaluated for mutagenic and carcinogenic activity. Because whole-animal studies of such activity are costly and time consuming, only a few chemicals have been tested in this fashion. A major advance in predictive toxicology was achieved when the in vitro testing procedure known as the *Salmonella* test (or Ames test, after its originator Bruce Ames) was developed to provide a sensitive and reliable method for evaluating mutagenicity (Ames, 1971; Ames et al., 1975; *UNIT 3.1*). This test has been applied quite extensively to build genotoxicity databases (Zeiger, 1997) through testing under various environmental conditions (Claxton, 1998).

The basis of the Ames test is a set of strains of *Salmonella* that each contain either a unique missense mutation or a frameshift mutation in the histidine operon. When the bacteria are treated with a chemical mutagen, some of the mutations that result will "reverse" the original mutation, restoring the cells' ability to synthesize their own histidine. Formation of such histidine-independent (his^+) revertants is evidenced by the growth of colonies on minimal agar plates with glucose. As described in *UNIT 3.1*, reversion levels in cultures treated with a putative mutagen are compared to those in untreated negative controls, with and without metabolic activation enzymes. Inclusion of positive controls (cultures treated with known mutagens) is also recommended. A desiccator assay for volatile liquids or gases and a reductive metabolism assay are also provided. Chemicals that are available only in small amounts can be assayed with a modified (Kado) microsuspension assay.

Measurement of DNA structural modifications is an important aspect of determining the consequences of chemical exposure, including exposure to reactive oxygen species that cause the formation of malondialdehyde via lipid peroxidation (*UNIT 2.4*). Assaying for malondialdehyde-DNA adducts, as described in *UNIT 3.2*, provides a true measure of the effective dose of a mutagen that can be correlated to biological changes. Although the procedures are fairly complicated and lengthy, they permit highly specific mass spectrometric quantitation of adduct with the use of a deuterated internal standard. Three protocols are included: (1) a gas chromatographic/negative chemical ionization–electron capture/mass spectrometry (GC/NCI EC/MS) assay for pyrimidopurinone (M_1G); (2) a method for HPLC quantification of nucleosides; and (3) preparation of anti-M_1G immunoaffinity gel (Sevilla et al., 1997).

Mutagenesis assays in mammalian cells complement the microbial assays in assessing genetic toxicology of potential mutagenic and carcinogenic properties of chemicals. Mammalian target genes include *hprt* (hypoxanthine-guanine phosphoribosyl transferase), *aprt* (adenine phosphoribosyltransferase), and *tk* (thymidine kinase). *UNIT 3.3* describes mutagenesis assays in the Chinese hamster V79 cell line and an analogous assay with the V79-derivative *hprt–/gpt*$^+$ G12 cell line. With the V79 cells, the toxic purine analog 6-thioguanine (6TG) is used to select *hprt* gene mutants. The G12 cell line contains an insertion of the *Escherichia coli* xanthine guanine phosphoribosyl transferase (*gpt*) gene that allows the detection of large deletions and epigenetic DNA methylation events

Contributed by Donald J. Reed
Current Protocols in Toxicology (2002) 3.0.1-3.0.4

as well as point and small intragenic mutations that can be detected in the standard V79 assays.

Cell transformation is widely used as a measure of the ability of chemical and physical agents to induce morphological changes, such as the loss of density-dependent growth regulation. Such changes include the formation of colonies with crisscrossed cells or foci of piled-up cells. Neoplastic characteristics of transformed cells resulting from exposure to carcinogens include the ability to form three-dimensional colonies in soft agar and the ability to induce tumor formation in immunosuppressed mice. Freshly isolated Syrian hamster embryo (SHE) cells, established cultured cells (mouse BALB/c-3T3), and C3H/10T1/2 cells are widely used for cell transformation assays. In *UNIT 3.4*, a basic cell transformation protocol is presented that utilizes SHE cells from pregnant Golden hamsters; secondary cell culture procedures applicable to Chinese hamster ovary (CHO) or baby hamster kidney 21 (BHK21) cells, used for an associated cytotoxicity assay, are also included. SHE cells are diploid and genetically stable, and possess the metabolic capability to bioactivate carcinogens. It should be noted that these (and indeed any) cell lines may already possess some properties characteristic of partial transformation, which will need to be considered in assessing the degree of morphological transformation caused by a putative carcinogen.

In a series of detailed steps, a number of protocols describe assays for DNA damage (*UNIT 3.5*). These protocols feature the measurement of single- and double-stranded breakage, DNA-DNA cross-links, and DNA-protein cross-links that can result from exposure to genotoxic chemicals or physical agents. Exposure to chemical and physical agents can be in vitro or in vivo. The assays for DNA damage include the "comet assay" by single-cell microgel electrophoresis (Singh, 1996) and filter elution (Kohn, 1991). K-SDS precipitation is the basis for an assay to reveal DNA-protein cross-links in cells (Zhitkovic and Costa, 1992). Other assays include measurement of repair activities such as unscheduled DNA synthesis following DNA damage. Oxidative DNA base modifications are detected by the use of exogenous bacterial repair enzymes to excise modified DNA bases.

DNA methylation has a role in mammalian development and tumorigenesis (Wolffe et al., 1999). The extent of DNA methylation can range from hypomethylation to hypermethylation, which in part may reflect the rates of methylation and demethylation. DNA methylation has even been suggested as a reversible biological signal (Ramchandani et al., 1999), and that DNA demethylase is a processive enzyme (Cervoni et al., 1999). These recent findings could be important in the analysis and interpretation of results obtained from the use of procedures described in *UNIT 3.6* on the measurement of DNA methylation. If detection of slight changes in gene methylation is desired, genomic sequencing following bisulfite-modification PCR (Clark et al., 1994) is recommended.This bisulfite mapping technique was used to determine that DNA demethylase is a processive enzyme (Cervoni et al., 1999). The first basic protocol in *UNIT 3.6* is the determination of the overall 5-methycytosine content in genomic DNA by the use of radiolabeled S-adenosylmethionine and a CpG methylase to artificially methylate DNA samples. A second basic protocol is the measurement of DNA:methyltransferase activity in the same manner as the first basic protocol but with the addition of an exogenous substrate, poly(dI-dC). Radiolabel incorporation is used as a measure of enzyme activity. A third basic protocol is based on the effect DNA methylation has on the activity of certain restriction enzymes; a measurement of gene-specific methylation. A fourth basic protocol is the measurement of deoxyribonuclease I sensitivity of active genes compared to inactive genes in chromatin with methylation causing gene inactivation by promoting chromatin condensation.

Alterations in the physical integrity of the chromosomes in toxicant-exposed cells, whether in culture, experimental animals or from humans, provides an additional experi-

mental approach to the determination of genotoxic damage. Assays for detecting chromosomal aberrations are described in *UNIT 3.7*. Visual assessment for the presence of micronuclei (Basic Protocol 1) is a measure of partial or whole chromosomes that have become separated from the main cellular nucleus. It can be used as an early marker for the identification of toxicant exposure. The state of the genome including rearrangements and translocations can be detected by Giemsa staining or trypsin/Giemsa banding (Basic Protocol 2). Fluorescent chromosome-specific painting probes are the basis for fluorescence in situ hybridization (FISH) probes that allow specificity in the evaluation of telomeric chromosomes of similar size as occurs in some mammalian species such as the mouse (Basic Protocol 3). A valuable approach to the utilization of Giemsa staining, Giemsa/trypsin banding, or FISH is the preparation of metaphase chromosome spreads on glass slides prior to staining (Support Protocol). A widely used assay, know as sister chromatid exchange, utilizes differential staining of chromatids so that each appears either dark or light after two cell cycles (Basic Protocol 4). Quantitation of toxicant-induced exchanges between sister chromatids provides the basis for genotoxic screening.

Methods for measuring DNA adducts are described in *UNIT 3.8*, Abasic Sites I: Isolation, Purification and Analysis of DNA Adducts in Intact DNA and *UNIT 3.9*, Abasic Sites II: Methods for Measurement of DNA Adducts. These two in depth units provide essential details for the analysis of DNA adducts. *UNIT 3.8* describes protocols for DNA isolation and hydrolysis for DNA adduct analyses and evaluation of abasic sites in DNA including low-temperature/antioxidant DNA isolation (Basic Protocol 1), measurement of apurinic/apyrimidinic sites (Basic protocol 2), immune slot-blot analysis of DNA adducts (Basic Protocol 3), immunohistochemical determination of DNA adducts (Basic Protocol 4) , and spectrophotometric quantification of DNA (Support Protocol).

UNIT 3.9 contains protocols for analyzing individual DNA adducts separated from the DNA backbone. Basic Protocol 1 describes HPLC methods for quantifying total guanine and Protocol 2 details similar techniques for total ribo- or deoxyribonucleosides. Other protocols describe methods to quantify individual DNA adducts with HPLC and electrochemical detection for 8-OH-dG (Basic Protocol 2), and N7-methylguanine (Basic Protocol 4). Basic Protocol 5 utilizes immunoaffinity chromatography to enrich for specific adducts that are subsequently analyzed by gas chromatography/electron capture negative chemical ionization/high resolution mass spectroscopy (GC/ECNCI/HRMS). Enzymatic DNA digestion (Support Protocol 1) preparation of immunoaffinity columns (Support Protocol 2) and determination of recovery (Support Protocol 3) are described. Other adduct purifications are described that utilize GC/ECNCI/HRMS isolation. Basic Protocol 7 utilizes liquid chromatography in combination with electrospray ionization/isotope dilution tandem mass spectrometry (LC/ESI/IDMS/MS for adduct purification and quantitation. Adduct quantification by ^{32}P postlabeling in combination with thin layer chromatography is described in Basic Protocol 8. Overall, *UNITS 3.8 & 3.9* provide a wide range of tools to determine the nature and extent of DNA modification by adduction; a critical issue in assessing the toxicology of chemicals.

LITERATURE CITED

Ames, B.N. 1971. The detection of chemical mutagens with enteric bacteria. *In* Chemical Mutagens: Principles and Methods for Their Detection, Vol. 1 (A. Hollaender, ed.) pp. 267-282. Plenum, New York.

Ames, B.N., McCann, H.J., and Yamasaki, E. 1975. Methods for detecting carcinogens and mutagens with the *Salmonella* mammalian-microsome mutagenicity test. *Mutat. Res*. 31:347-364.

Cervoni, N., Bhatacharya, S., and Szyf, M. 1999. DNA demethylase is a processive enzyme. *J. Biol. Chem.* 274:8363-8366.

Clark, S.J., Harrison, J., Paul, C.L., and Frommer, M. 1994. High sensitivity mapping of methylated cytosines. *Nucl. Acids Res.* 22:2990-2997.

Claxton, L.D. 1998. The development, validation, and analysis of *Salmonella* mutagenicity test methods for environmental situations. *In* Microscale Testing in Aquatic Toxicology. Advances, Techniques, and Practice (P.G. Wells, K. Lee, and C. Blaise, eds.) pp. 591-605. CRC Press, Boca Raton, Fla.

Kohn, K.W. 1991. Principles and practice of DNA filter elution. *Pharmacol. Ther.* 49:55-77.

Ramchandani, S., Bhatacharya, S.K., Cervoni, N., and Szyf, M. 1999. DNA methylation is a reversible biological signal. *Proc. Natl. Acad. Sci. U.S.A.* 96:6107-6112.

Sevilla, C.L., Mahle, N.H., Eliezer, N., Uzieblo, A., O'Hara, S.M., Nokubo, M., Miller, R., Rouzer, C.A., and Marnett, L.J. 1997. Development of monoclonal antibodies to the malondialdehyde-deoxyguanosine adduct, pyrimidopurinone. *Chem. Res. Toxicol.* 10:172-180.

Singh, N.P. 1996. Microgel electrophoresis of DNA from individual cells. Principles and methodology. *In* Technologies for Detection of DNA Damage and Mutations (G. Pfeifer, ed.) pp. 3-24. Plenum, New York.

Wolffe, A.P., Jones, P.L., and Wade, P.A. 1999. DNA demethylation. *Proc. Natl. Acad. Sci. U.S.A.* 96:5894-5896

Zeiger, E. 1997. Genotoxicity database. *In* Handbook of Carcinogenic Potency and Genotoxicity Databases (L.S. Gold and E. Zeiger, eds.) pp. 687-729. CRC Press, Boca Raton, Fla.

Zhitkovic, A. and Costa, M. 1992. A single sensitive assay to detect DNA-protein crosslinks in intact cells and in vivo. *Carcinogenesis* 13:1485-1489.

Donald J. Reed

The *Salmonella* (Ames) Test for Mutagenicity

The *Salmonella typhimurium*/mammalian microsome assay (Ames test) is a widely accepted short-term test for detecting chemicals that induce mutations in the DNA of organisms. This is a reverse mutation assay that employs histidine-dependent *Salmonella* bacteria with mutations at various genes in their histidine operon that render them incapable of synthesizing the amino acid histidine. When these histidine-dependent cells are grown on minimal medium agar plates containing a trace of histidine, only those cells that revert (mutate) to histidine independence (his^+) are able to form colonies. The small amount of histidine allows all the plated bacteria ($\sim 1 \times 10^8$ cells) to undergo a few cell divisions; in many cases, this growth is essential for mutagenesis to occur. The his^+ mutants are easily scored as colonies against the slight background growth of the his-dependent bacteria (bacterial lawn). The number of spontaneous mutant colonies per plate is relatively constant. However, when a mutagen is added to the plate, the number of revertant colonies is increased, usually in a dose-related manner.

Each of the basic *Salmonella* tester strains contains either a unique missense or a frameshift mutation in the histidine operon. These mutations result in a deficiency of an active enzyme or the production of an inactive enzyme in the histidine biosynthesis pathway. As a result, the cells cannot grow on minimal agar plates in the absence of histidine. A point mutation, induced by a chemical mutagen, will "reverse" the initial mutation and restore the cell's ability to synthesize its own histidine, thereby restoring its ability to grow in the absence of histidine. Such growth is evidenced by the formation of colonies (histidine revertant colonies) on minimal glucose agar plates (see Fig. 3.1.1).

Table 3.1.1 presents the genotypic characteristics of the eight most widely used *Salmonella* tester strains. Other strains that have been used for specialized testing purposes, such as for determining metabolic or genetic mechanisms, are those missing or with added nitroreductases, *O*-acetyl transferase, *N*-acetyl transferase, and glutathione-*S*-transferase (McCoy et al., 1981; Watanabe et al., 1987, 1990; Simula et al., 1993); strains to identify the specific point mutations induced (Gee et al., 1994); strains that also measure forward mutations (Ruiz-Rubio and Pueyo, 1982; Grant et al., 1992; Jurado et al., 1994); and DNA-repair proficient variants of the strains described in Table 3.1.1 (Maron and Ames, 1983).

The uniqueness of the mutation in each tester strain provides a "hot-spot" for different classes of mutagens. A chemical is considered a mutagen in the Ames test when a mutagenic response is obtained in at least one tester strain, either in the presence or absence of a metabolic activation system. There is no evidence to demonstrate that a chemical that is mutagenic in more than one strain is more potent or more mutagenic than a chemical that induces a mutation in only one strain.

There have been many test procedures developed that use histidine mutants of the *Salmonella* strains. These procedures include spot, plate, preincubation, vapor phase (chamber), and suspension tests (described by Ames et al., 1975; Maron and Ames, 1983), and other procedures such as the spiral plate assay (Houk et al., 1989, 1991) and the fluctuation test (Gatehouse and Delow, 1979). The most widely used of these procedures, which are described in this unit, are the plate test (see Basic Protocol) and preincubation test (see Alternate Protocol 1). Also described here are test procedures for highly volatile chemicals (see Alternate Protocol 2) and gases (see Alternate Protocol 3), chemicals that require reductive metabolism (see Alternate Protocol 4), and chemicals available only in

Contributed by Errol Zeiger and Kristien Mortelmans

Current Protocols in Toxicology (1999) 3.1.1-3.1.29

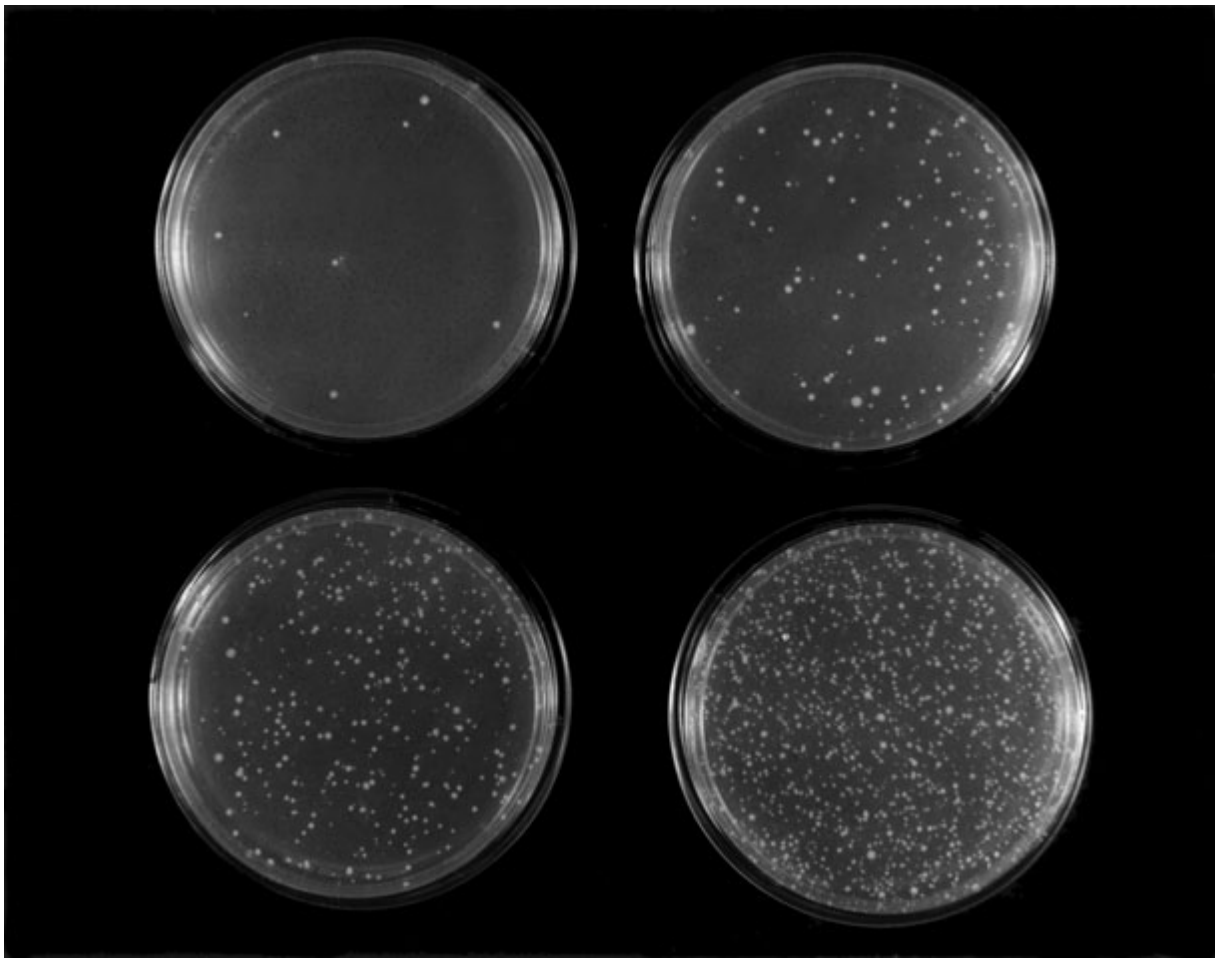

Figure 3.1.1 Petri dishes containing sodium azide–induced revertants of tester strain TA1535. The top left dish (no chemical added) shows spontaneous revertant colonies. The increase in induced revertants reflects increases in the concentration of sodium azide.

small amounts (see Alternate Protocol 5). Support protocols are included for toxicity testing to enable dose selection (see Support Protocol 1), strain maintenance and preservation (see Support Protocol 2), freezing permanent and working cultures (see Support Protocol 3), genetic analysis of strains (see Support Protocol 4), and preparation of the S-9 metabolic activation system (see Support Protocol 5).

The *Salmonella* assay is particularly well designed to detect chemically induced mutations (Ames et al., 1975). The primary impetus for its use is the high predictivity of a positive mutagenic response in *Salmonella* for rodent carcinogenicity (McCann et al., 1975; Sugimura et al., 1976; Tennant et al., 1987). The *Salmonella* test is also required or recommended by regulatory agencies prior to registration or acceptance of many chemicals, drugs, and biocides (Dearfield, et al., 1991; Kramers et al., 1991; Auletta et al., 1993; FDA, 1993; HPBGC, 1993; Kirkland, 1993; Sofuni, 1993).

ASEPTIC TECHNIQUE

The use of basic bacteriological laboratory procedures (see *APPENDIX 3*) are of utmost importance when performing the Ames assay. Aseptic procedures must be employed at all times; these include the use of sterile solutions and glassware. Contamination by bacteria or fungi will interfere with the test. Contaminated frozen permanent or working cultures of the *Salmonella* strains will render them unusable, as will contaminated

Table 3.1.1 Commonly Used *Salmonella* Tester Strains and Their Genotypes

Strain	Genotype	DNA target	Reference
TA97	*hisD6610, hisO1242* Δ(*bio chlD uvrB gal*) *rfa*, pKM101	CCCCCC	Levin et al., 1982b
TA98	*hisD3052* Δ(*bio chlD uvrB gal*) *rfa*, pKM101	CGCGCGCG	Ames et al., 1975
TA100	*hisG46* Δ(*bio chlD uvrB gal*) *rfa*, pKM101	GGG	Ames et al., 1975
TA102	*his* Δ(*G)8476*, *rfa*, pKM101, pAQ1 (*hisG428*)	TAA	Levin et al., 1982a
TA104	*hisG428* Δ(*bio chlD uvrB gal*) *rfa*, pKM101	TAA	Levin et al., 1982a
TA1535	*hisG46* Δ(*bio chlD uvrB gal*) *rfa*	GGG	Ames et al., 1975
TA1537	*hisC3076* Δ(*bio chlD uvrB gal*) *rfa*	CCCCC	Ames et al., 1975
TA1538	*hisD3052* Δ(*bio chlD uvrB gal*) *rfa*	CGCGCGCG	Ames et al., 1975

overnight cultures. Surface areas must be properly disinfected before and after use. All cultures and labware used to handle the cultures must be autoclaved before being discarded.

SAFETY CONSIDERATIONS

Because the purpose of the Ames assay is to ascertain a chemical's mutagenicity, and because of the known association of *Salmonella* mutagens with carcinogenicity, all test chemicals should be treated as potential mutagens or carcinogens, unless known to be otherwise. The positive control chemicals suggested for use consist of known rodent carcinogens and chemicals shown to be noncarcinogenic in rodent bioassays. All contaminated material (e.g., test tubes, pipets, and pipet tips) should be properly disposed of. In addition, all personnel performing the assay should wear protective clothing including safety glasses and gloves. Wearers of soft contact lenses should avoid wearing the lenses, or wear protective eye covering when performing mutagenicity testing, especially in the case of volatile chemicals. All handling of chemicals, as well as the test itself, should be performed in a chemical/biological safety hood.

Although the cell wall mutations (*gal* and *rfa*) in these *Salmonella* strains weaken their pathogenicity (Ames, 1971; Wilkinson et al., 1972), it is prudent to avoid direct contact with the cells. Gloves should be worn when handling the strains, and cultures should not be mouth-pipetted. Petri dishes and solutions containing *Salmonella* strains or colonies should not be discarded as is, but should be autoclaved or incinerated.

STANDARD PLATE INCORPORATION TEST

BASIC PROTOCOL

The standard plate incorporation assay consists of exposing the tester strain(s) to the test chemical directly on a glucose minimal agar plate (GM plate), usually in the presence and absence of a metabolic activation system. The components are first added to sterile test tubes containing 2 ml of molten top agar supplemented with limited histidine and biotin. The top agar should be maintained at a temperature between 43°C and 48°C. The contents of the tubes are mixed and poured on GM plates. After the top agar has hardened, the plates are incubated in an inverted orientation for 48 hr. Colonies are counted on all plates and the number of colonies on the test plates is compared to that on the negative solvent control plate. Figure 3.1.2 depicts the setup for performing the standard plate incorporation test.

Materials

Cultures of *Salmonella* tester strains (see Support Protocols 2 and 3)
Nutrient broth (see recipe), sterile
Glucose minimal agar plates (GM plates; 100 × 15 mm; see recipe)

continued

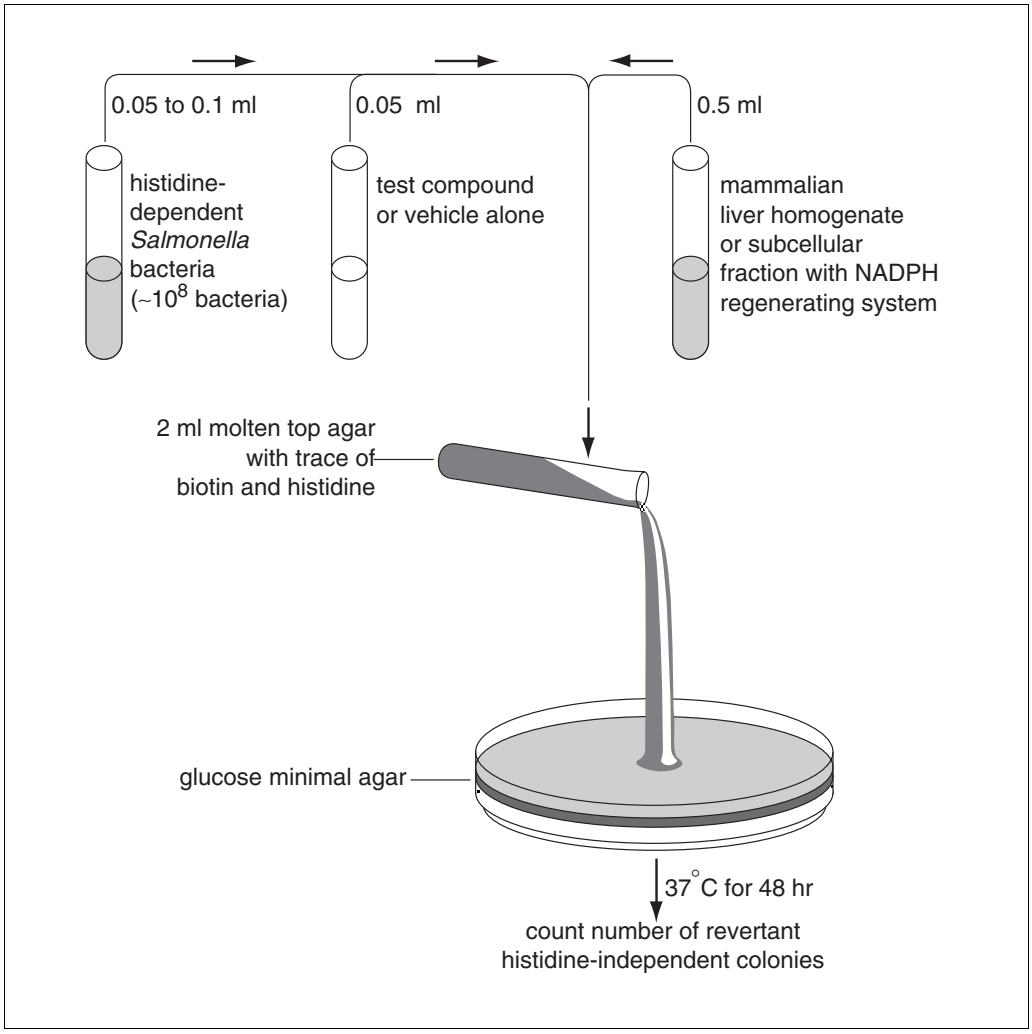

Figure 3.1.2 Standard plate incorporation assay.

Metabolic activation system (rat liver S-9 homogenate; see Support Protocol 5)
Cofactors for the S-9 mix (see recipe)
Test compound
Positive control chemicals (Table 3.1.2)
Negative control (solvent)
Top agar supplemented with biotin and limited histidine (see recipe), maintained at 43°C

37°C shaking incubator set at 100 to 120 rpm for cultivation of overnight cultures
Sterile glass test tubes (16 × 150–mm and 13 × 100–mm)
Boiling water or microwave oven to melt top agar
Oven, heating block, or water bath set at 43° to 48°C to maintain temperature of top agar
Bottle-top dispensers: 2-ml for delivering top agar and 0.5-ml for delivering buffer and S-9 mix to test tubes
Colony counter (optional)

Additional reagents and equipment for maintaining and growing bacterial stocks (*APPENDIX 3*), maintaining and growing *Salmonella* indicator strains (see Support Protocol 2), dose selection for *Salmonella* test (see Support Protocol 1), preparation of metabolic activation system for *Salmonella* test (see Support Protocol 5), and performing strain check for genetic integrity (see Support Protocol 4)

Table 3.1.2 Recommended Positive Control Chemicals and Test Concentrations[a]

Strain	Control	Chemical[b]
Without metabolic activation		
TA97	9-Aminoacridine	50 µg/plate
TA98	4-Nitro-*o*-phenylenediamine	2.5 µg/plate
TA100	Sodium azide	5 µg/plate
	Methyl methane sulfonate	250 µg/plate
TA102	Mitomycin C	0.5 µg/plate
TA104	Methyl methane sulfonate	250 µg/plate
TA1535	Sodium azide	5 µg/plate
	Methyl methane sulfonate	250 µg/plate
TA1537	9-Aminoacridine	50 µg/plate
TA1538	4-Nitro-*o*-phenylenediamine	2.5 µg/plate
With metabolic activation		
TA97	2-Aminoanthracene	1-5 µg/plate[c]
TA98	2-Aminoanthracene	1-5 µg/plate[c]
TA100	2-Aminoanthracene	1-5 µg/plate[c]
TA102	2-Aminoanthracene	5-10 µg/plate[c]
TA104	2-Aminoanthracene	5-10 µg/plate[c]
TA1535	2-Aminoanthracene	2-10 µg/plate[c]
TA1537	2-Aminoanthracene	2-10 µg/plate[c]
TA1538	2-Aminoanthracene	2-10 µg/plate[c]

[a]Other chemicals have been recommended for use as positive controls (Ames et al., 1975; Maron and Ames, 1983; Kier et al., 1986). For other strains, refer to the publications in which the strains are described.

[b]Concentrations based on 100 × 15–mm GM plates containing 20 to 25 ml agar (see Basic Protocol 1 and Reagents and Solutions).

[c]The optimum positive control concentration will depend on the source of S-9 and its concentration and must be determined empirically.

1. Inoculate *Salmonella* cultures into 16 × 150-mm sterile glass tubes containing 9 ml nutrient broth or 125-ml Ehrlenmeyer flasks containing 25 to 50 ml nutrient broth, 15 to 18 hr prior to performing the experiment. Grow overnight in a 37°C shaking incubator set to 100 to 120 rpm (see Support Protocol 2 and *APPENDIX 3*).

   The overnight culture should contain ~1–2 × 10^9 cfu/ml.

2. Label an appropriate number of GM plates and corresponding 13 × 100–mm sterile glass test tubes for each test chemical, taking into consideration that each experiment should contain a series of duplicate or triplicate plates for:

   Negative solvent control (bacteria only)
   Three or more concentrations of the test substance (diluted to at least half-log intervals), with the highest dose limited by toxicity or solubility (see Support Protocol 1)
   Positive control (see below and see Table 3.1.2).

   The positive control chemicals should be diagnostic for the unique mutation in each Salmonella strain, and a control that requires metabolic activation should be included. If a specific class of chemicals is being investigated, a positive control containing a mutagenic member of that class should be included in lieu of, or in addition to, the standard positive control chemical where ever possible.

Concurrent solvent and positive controls must be run with each trial. The positive controls and concentrations listed in Table 3.1.2 are recommended for general testing. The positive controls are designed to monitor the ability of the laboratory to obtain a positive response, to identify the tester strain, and to demonstrate the activity of the metabolic activation system. A negative control (no solvent or chemical) should be run if there is a question of the reactivity or toxicity of the solvent. Where a specific chemical class is being tested, or where the test chemical is known to be metabolized by a specific metabolic pathway, a related chemical, known to be mutagenic, should be used as the positive control. If more than one chemical is tested on the same day, only one set of positive-control chemicals need be tested. The negative solvent control is used as the base from which to determine the mutagenic activity of the test chemical.

3. Prepare metabolic activation system by mixing cofactors with S-9 at a concentration of either 5%, 10%, or 30% (v/v) of S-9 fraction. Calculate the total number of plates that will be needed and determine the volume of S-9 mix that will be needed by dividing the number of plates by 2 (since 0.5 ml of S-9 mix is added to each plate).

   Per 200 plates, a total of 100 ml of S-9 mix is needed, with the following v/v ratios of cofactors to S-9 fractions (total volume of 100 ml): for 5% S-9, 5 ml S-9 fraction/95 ml cofactors; for 10% S-9, 10 ml S-9 fraction/90 ml cofactors; for 30% S-9, 30 ml S-9 fraction/70 ml cofactors. If smaller volumes are needed, reduce the volumes of S-9 fraction and cofactors proportionally.

4. Prepare dilutions of test compound (see Support Protocol 1 for determination of dose range).

5. To the appropriately labeled sterile glass test tubes (see step 2), maintained at 43°C, add in the following order:

   2 ml of molten top agar (supplemented with 0.05 mM histidine and 0.05 mM biotin), maintained at 43°C
   0.50 ml of metabolic activation (S-9) mix or buffer
   0.05 ml of appropriate test compound dilution or control.

   Mix contents of tubes after addition of the chemical, preferably by mild vortexing, then add:

   0.05 to 0.10 ml of overnight culture of the *Salmonella* strain (from step 1).

   Mix contents of the tubes again after addition of the bacteria, preferably by mild vortexing.

6. Pour contents of each test tube onto the surface of the corresponding GM plate and gently swirl to evenly distribute the molten top agar.

7. After the top agar has hardened (2 to 3 min), invert plates and place in a 37°C incubator for 48 hr.

   If growth retardation is seen at 48 hr, as evidenced by smaller than anticipated colony sizes, the plates are incubated for an additional 12 to 24 hr.

8. Count colonies either manually or by an electronic colony counter.

   If colonies cannot be counted immediately the plates should be refrigerated. The plates can be stored in a refrigerator for up to 2 days. All plates must be removed from the incubator and be counted at the same time.

   Histidine revertant colonies on the plates can be counted by machine or "by hand." It is important that electronic counting machines be calibrated by first comparing manual counts of a few plates containing different numbers of colonies, including high numbers, with the counts obtained by the electronic counter. If an electronic colony counter is not available, a measured section of the plate can be counted by hand when there is a high

density of colonies on the plate with an even distribution across the plate. The resulting colony count can then be extrapolated to the area of the entire plate.

If an electronic counter is available, plates are machine counted, unless precipitate is present, which could interfere with the count, or the color of the test chemical on the plate could reduce the contrast between the colonies and the agar. In such instances, the colonies are hand counted.

9. Express the test results as number of revertant colonies per plate.

A strain check for genetic integrity (see Support Protocol 4) should be performed with every experiment. For this strain check it is sufficient to monitor the rfa mutation (using crystal violet) and ampicillin and tetracycline resistance using disks impregnated with the appropriate concentration of each component (Zeiger et al., 1981).

Results should be reported as the individual plate counts, or the mean and standard deviations or standard error of the mean for each dose/activation combination. The results for the solvent and positive controls should be included. Additional calculations of the "mutation index" (often defined as the fold increase over the solvent control) or of his^+ revertants/unit weight or mass, can be performed as a method for comparing the responses of a series of test substances. These latter values should not be used by themselves, because they do not represent the actual responses and can exaggerate small differences among test samples.

PLATE ASSAY WITH PREINCUBATION PROCEDURE

ALTERNATE PROTOCOL 1

This assay involves exposing the tester strains for a short period (usually 20 min) in a suspension containing the test agent, with and without metabolic activation, prior to the addition of top agar and plating. It is believed that short-lived mutagenic metabolites have a better chance of reacting with the tester strains in the small volume of the preincubation mixture, as compared to the case described in Basic Protocol 1, where the incubation mixture is plated immediately on glucose minimal agar plates (Yahagi et al., 1975; Haworth et al., 1983). In addition, the smaller preincubation volume results in a higher effective concentration of the metabolic activation system (S-9) and cofactors (also see Alternate Protocol 5).

For materials and cross-referenced procedures, see Basic Protocol.

1. Prepare bacteria, plates and test tubes, metabolic activation system, and chemicals/controls to be tested (see Basic Protocol, steps 1 to 4).
2. To the appropriately labeled sterile glass tubes, maintained at 37°C, add in the following order:

   0.50 ml of metabolic activation mix or buffer
   0.05 ml of appropriate test chemical dilution or control.

   Mix contents of tubes after addition of the chemical, preferably by mild vortexing, then add:

   0.05 to 0.10 ml of overnight culture of the *Salmonella* strain.

   Mix contents of the tubes again after addition of the bacteria, preferably by mild vortexing.
3. Incubate mixture 20 min at 37°C without shaking.

   Chemicals known or suspected to be volatile should be incubated in capped tubes.
4. Add 2 ml of molten top agar (supplemented with 0.05 mM histidine and 0.05 mM biotin), maintained at 43°C, to the incubation mixture and mix contents of each tube.

5. Pour contents of each test tube onto the surface of the corresponding GM plate and gently swirl to evenly distribute the molten top agar.
6. Incubate, count colonies, and interpret test results (see Basic Protocol, steps 7 to 9).

ALTERNATE PROTOCOL 2

DESICCATOR ASSAY FOR VOLATILE LIQUIDS

The use of a closed chamber is recommended for testing highly volatile chemicals and gases (Simmon et al., 1977; Zeiger et al., 1992). Procedures using plastic bags in lieu of desiccators have also been described (Hughes et al., 1987; Araki et al., 1994).

Figure 3.1.3 depicts a desiccator assay procedure for volatile liquids. This procedure should be used only if it is known that the test chemical will volatilize at 37°C and disperse throughout the desiccator. To aid dispersion, a magnetic stir bar is placed in the desiccator below the test chemical, and the desiccator is placed on a magnetic stir plate in the incubator. A 9-liter desiccator is recommended because it can hold up to 18 plates.

Additional Materials *(also see Basic Protocol)*

Volatile test chemical
Desiccator (9-liter) with perforated ceramic shelf
Glass petri plate (100 × 15–mm) or watch glass, sterile
Magnetic stir bar
Magnetic stirrer

1. Prepare bacteria, plates and test tubes, metabolic activation system, and chemicals/controls to be tested (see Basic Protocol, steps 1 to 4).

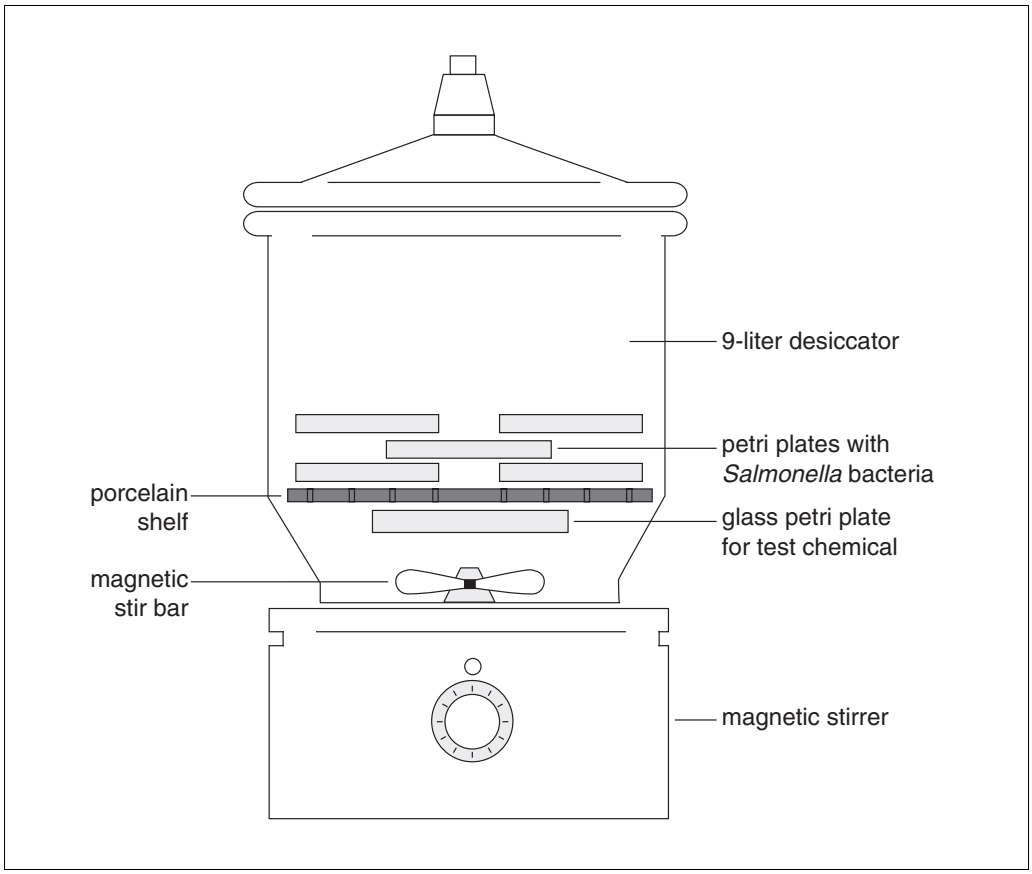

Figure 3.1.3 Desiccator assay using volatile liquids.

The plates should be labeled on their bottoms or sides because the lids will have to be removed prior to placing them in the desiccator.

The positive-control chemicals may be tested in the standard plate incorporation assay (see Basic Protocol).

2. To the appropriately labeled sterile glass tubes, maintained at 43°C, add in the following order:

   2 ml of molten top agar (supplemented with 0.05 mM histidine and 0.05 mM biotin), maintained at 43°C
   0.50 ml of metabolic activation (S-9) mix or buffer
   0.05 to 0.10 ml of overnight culture of the *Salmonella* strain.

   Mix the contents of the tubes after addition of the bacteria, preferably by mild vortexing.

3. Pour contents of each test tube onto the surface of the corresponding GM plate and gently swirl to evenly distribute the molten top agar.
4. While the top agar is hardening, remove the perforated ceramic shelf of the desiccator for attachment of a sterile bottom or top lid of a glass petri dish (or a watch glass). Attach the bottom/top lid of the dish to the shelf using a self-adhesive labeling tap in a cross configuration to support it, using sufficient tape to extend all the way to the edge of the ceramic shelf with ~1 in. remaining for taping it over the edge on the top side of the shelf.
5. Place a magnetic stir bar in the bottom of the desiccator, then replace the ceramic shelf in the desiccator.
6. With a sterile pipet, transfer a predetermined volume (see Support Protocol 1 for preliminary toxicity assay) of the liquid test chemical to the petri dish.

   For nontoxic chemicals, volumes added are typically 1, 2, 3, 4, and 5 ml per desiccator. If toxicity is observed at the lowest dose (0.5 ml) used in the preliminary assay (see Support Protocol 1), dilute the chemical 10-fold (or more if needed) in a suitable solvent. The solvent should be tested first in a desiccator for toxicity.

7. Remove the lids of the petri plates containing the *Salmonella* bacteria and S-9 mix or buffer and loosely stack the plates in an inverted position on the ceramic shelf.
8. Seal the desiccator and place on a magnetic stirrer in a 37°C incubator or warm room for 24 hr.
9. After 24 hr, place the desiccator in a chemical safety hood, remove the plates, put the lids back on, and transfer to a 37°C incubator for 24 hr.

   If growth retardation is seen after the additional 24-hr incubation, as evidenced by smaller than anticipated colony sizes, the plates are incubated for an additional 12 to 24 hr.

10. Count colonies either manually or by an electronic colony counter.

    If colonies cannot be counted immediately the plates should be refrigerated. The plates can be stored in a refrigerator for up to 2 days. All plates must be removed from the incubator and be counted at the same time.

11. Express the test results as number of revertant colonies per plate based on volume added to each desiccator—i.e., number of revertants per volume (in ml) per desiccator.

    A strain check for genetic integrity (see Support Protocol 4) should be performed with every experiment. For this strain check it is sufficient to monitor the rfa (coeffective lipopolysaccharide) mutation (using crystal violet) and ampicillin and tetracycline resistance using disks impregnated with the appropriate concentration of each component (Zeiger et al., 1981).

ALTERNATE PROTOCOL 3

DESICCATOR ASSAY FOR GASES

The use of a closed chamber is recommended for testing highly volatile chemicals and gases (Simmon et al., 1977; Zeiger et al., 1992). Procedures using plastic bags in lieu of desiccators have also been described (Hughes et al., 1987; Araki et al., 1994).

The desiccator used for testing gases is similar to that shown in Figure 3.1.3, except that it contains a stopcock for inlet of gas. To aid dispersion of the gas, a stirring bar magnet is placed in the desiccator, and the desiccator is placed on a magnetic stir plate in the incubator. A 9-liter desiccator is recommended because it can hold up to 18 plates.

Additional Materials *(see also Basic Protocol)*

Gaseous test chemical
Desiccator (9-liter) with stopcock inlet (e.g., for use as vacuum desiccator) and perforated ceramic shelf
Glass petri plate (100 × 15–mm) or watch glass, sterile
Magnetic stir bar
Polyvinyl tubing
Pressure gauge
Vacuum pump
Magnetic stirrer

1. Prepare bacteria, plates and test tubes, metabolic activation system, and chemicals/controls to be tested (see Basic Protocol, steps 1 to 4).

   The plates should be labeled on their bottoms or sides because the lids will have to be removed prior to placing them in the desiccator.

   The positive-control chemicals may be tested in the standard plate incorporation assay.

2. To the appropriately labeled sterile glass tubes, maintained at 43°C, add in the following order:

   2 ml of molten top agar (supplemented with 0.05 mM histidine and 0.05 mM biotin), maintained at 43°C
   0.50 ml metabolic activation (S-9) mix or buffer
   0.05 to 0.10 ml of overnight culture of the *Salmonella* strain.

   Mix the contents of the tubes after addition of the bacteria, preferably by mild vortexing.

3. Pour contents of each test tube onto the surface of the corresponding GM plate and gently swirl to evenly distribute the molten top agar.

4. Place a magnetic stir bar in the bottom of the desiccator and replace the ceramic shelf.

5. Remove the lids of the petri plates containing the *Salmonella* bacteria and S-9 mix or buffer and loosely stack the plates in an inverted position on the ceramic shelf.

6. Seal the desiccator and proceed with the following steps for each concentration of gas.

   a. Connect a polyvinyl tubing to a vacuum pump (or in-house vacuum) and to the stopcock of the desiccator.

      A vacuum gauge should be used to monitor the evacuation of air.

   b. Open the stopcock and partially evacuate the air from the desiccator.
   c. Close the stopcock, remove the vacuum tubing, connect the gas tubing to the stopcock, and connect the other end of the tubing to the cylinder containing the gaseous test chemical.

d. Slowly open the gas cylinder valve first, and then very slowly open the stopcock valve.

The gas will transfer to the desiccator very rapidly (within to 10 sec).

7. When atmospheric pressure is reached (after ~10 sec), close the stopcock first and then close the valve of the gas cylinder.

8. After removing the gas tubing from the desiccator stopcock, place the desiccator on a magnetic stirrer in a 37°C incubator or warm room for 24 hr.

Each laboratory performing a desiccator assay with gases should first determine how much air is removed from the desiccator at different levels of vacuum. This can be readily accomplished by using the procedure described above, but using water. The volume taken up by the agar plates should be taken into consideration when performing this procedure. The volume of water that has entered the desiccator is measured using a graduated cylinder. The procedure should be repeated for each level of vacuum that has been applied. Caution should be taken to remove no more than 50% of the air from the desiccator to prevent implosion.

9. After 24 hr, place the desiccator in a chemical safety hood, remove the plates, put the lids back on, and transfer to a 37°C incubator for 24 hr.

If growth retardation is seen after the additional 24-hr incubation, as evidenced by smaller than anticipated colony sizes, the plates are incubated for an additional 12 to 24 hr.

10. Count colonies either manually or with an electronic colony counter.

If colonies cannot be counted immediately the plates should be refrigerated. The plates can be stored in a refrigerator for up to 2 days. All plates must be removed from the incubator and be counted at the same time.

11. Express the test results as number of revertant colonies per plate based on moles of gas added to each desiccator. To calculate the moles of gas, use the formula $n = PV/RT$, where n is the number of moles, P is 1 atmosphere, V is volume in liters, R is the universal gas constant (0.0821 liter.atm/mol.°K) and T is temperature expressed in °K.

A strain check for genetic integrity (see Support Protocol 4) should be performed with every experiment. For this strain check it is sufficient to monitor the rfa mutation (using crystal violet) and ampicillin and tetracycline resistance using disks impregnated with the appropriate concentration of each component (Zeiger et al., 1981).

REDUCTIVE METABOLISM ASSAY

ALTERNATE PROTOCOL 4

This procedure is identical to that used for the preincubation assay (see Alternate Protocol 1) with the exception that a modified cofactor mix is used (Prival and Mitchell, 1982; Reid et al., 1984). This assay is recommended for testing chemicals that require reduction for their activation, such as azo dyes.

Additional Materials *(also see Basic Protocol)*

Cofactors for reductive metabolism (see recipe)
Metabolic activation system (uninduced hamster liver S-9 homogenate; see Support Protocol 5, but use hamsters and omit injection of Arochlor)
Flavin mononucleotide (FMN) solution (see recipe)

1. Prepare bacteria, plates, and test tubes (see Basic Protocol, steps 1 to 3).

2. Prepare reductive metabolic activation system by adding 30 ml of the hamster liver S-9 to 63 ml of the cofactors for reductive metabolism and keep on ice away from direct light (see Reagents and Solutions).

3. Prepare dilutions of the test compound (see Support Protocol 1 for determination of dose range).
4. Immediately before preparing the mix in step 5, add 7 ml of the flavin mononucleotide (FMN) solution to the 93 ml of the reductive metabolic activation system prepared in step 2 (also see Reagents and Solutions).
5. To the appropriately labeled sterile glass tubes, maintained at 37°C, add in the following order:

   0.50 ml of FMN-containing reductive metabolic activation mix (from step 4), or buffer
   0.05 ml of appropriate test chemical dilution or control.

   Mix contents of tubes after addition of the chemical, preferably by mild vortexing, then add:

   0.05 to 0.10 ml of overnight culture of the *Salmonella* strain.

   Mix contents of the tubes again after addition of the bacteria, preferably by mild vortexing.
6. Incubate mixture 20 min at 37°C without shaking.

   Chemicals known or suspected to be volatile should be incubated in capped tubes.
7. Add 2 ml of top agar (supplemented with 0.05 mM histidine and 0.05 mM biotin), maintained at 43°C, to the incubation mixture, and mix contents of each tube.
8. Pour contents of each test tube onto the surface of the corresponding GM plate and gently swirl to evenly distribute the molten top agar.
9. Incubate, count colonies, and interpret test results (see Basic Protocol, steps 7 to 9).

ALTERNATE PROTOCOL 5

MODIFIED (KADO) MICROSUSPENSION ASSAY

This is a highly sensitive assay for testing the mutagenicity of pure chemicals, complex mixtures, and biological samples that are available only in small amounts (Kado et al., 1983). The procedure is a slight modification of the preincubation assay (see Alternate Protocol 1) and is performed as described below.

Additional Materials *(see also Basic Protocol)*

0.1 M sodium phospate buffer, pH 7.4 (see recipe)
Centrifuge and rotor
Sterile test tubes (10 × 70–mm), with sterile caps

1. Prepare overnight cultures of bacteria, plates, and test tubes (see Basic Protocol, steps 1 to 3; but use 10 × 70–mm test tubes).

   When testing urine samples, a deconjugating enzyme system is included in the assay (Kado et al., 1983).
2. Centrifuge *Salmonella* overnight culture(s) 15 min at 9000 × *g* (8700 rpm in a Sorvall SS-34 rotor), 4°C. Wash cells twice in 0.1 M sodium phosphate buffer, pH 7.4, each time centrifuging at 9000 × *g* and removing the supernatant. Resuspend pellet in 0.1 M sodium phosphate buffer, pH 7.4, at 1/10 the original volume (10-fold concentration).
3. Prepare metabolic activation system and keep on ice.
4. Prepare dilutions of the test compound (see Support Protocol 1 for determination of dose range).

5. To the appropriately labeled 10 × 70–mm test tubes, placed in an ice bath, add in the following order:

   0.1 ml of the 10-fold concentrated overnight *Salmonella* culture from step 3.
   0.1 ml of a metabolic activation system or buffer
   0.001, 0.0025, 0.005, or 0.01 ml of test compound.

   Adjust the volume of solvent so that each tube contains the same final volume of liquid.

6. Incubate mixtures 90 min at 37°C with shaking at 120 rpm.

7. Add 2 ml molten top agar (containing 0.05 mM histidine and 0.05 mM biotin), maintained at 43°C, to each incubation mixture. Mix contents of tubes.

8. Pour contents of each tube onto the surface of the corresponding GM plate and gently swirl to evenly distribute the molten top agar.

9. Incubate, count colonies, and interpret test results (see Basic Protocol, steps 7 to 9).

TOXICITY TEST FOR DOSE SELECTION

SUPPORT PROTOCOL 1

All chemicals are tested initially in a toxicity test to determine the appropriate dose range for the mutagenicity assay. When multiple chemicals with similar properties are to be tested, it may be sufficient to perform a toxicity test on one representative chemical and use these results to estimate the dose range to be used with the other chemicals. If more than one *Salmonella* strain is to be used for the mutagenicity test, the toxicity test should be performed using strain TA100. Otherwise, the test should be performed using the strain that will be used for the definitive mutagenicity test. Alternatively, the toxicity assay can be performed using the system developed by Waleh et al. (1982).

It is sufficient to perform the test using single plates for each test chemical concentration. The experiment should contain:

1. A solvent control (bacteria only).

2. A total of 8 concentrations, in half-log intervals, of the test substance, with the highest dose limited by solubility, or by an arbitrary value (this value is usually 5000 or 10,000 μg/plate). For volatile liquids or gases that are tested in desiccators, the preliminary toxicity assay uses a high and low concentration—5 and 0.5 ml for liquids and 4.5 and 0.5 liters for gases.

3. A positive control.

4. Dose selection for the definitive test of chemicals exhibiting toxicity should include at least four nontoxic doses with only the highest dose level exhibiting toxicity. Toxic concentrations are defined as those that produce a decrease in the number of histidine independent (his^+) colonies and/or clearing in the density of the background lawn (see Critical Parameters), or absence of a background lawn, under conditions of the test.

The preliminary toxicity test is also an opportunity to determine if the test substance is soluble under the conditions of the test, if it reacts with the solvent or test medium, or if it produces other effects than might interfere with the test.

The preliminary toxicity test should be performed in the presence and absence of the metabolic activation system, using the protocol that will be used for the definitive test.

SUPPORT PROTOCOL 2

STRAIN MAINTENANCE AND PRESERVATION

All indicator strains should be kept frozen (−80°C). Upon receipt of the new strains, up to five frozen permanent cultures should be prepared from one single colony isolate that has been checked for its genotypic characteristics (*his, rfa, uvrB-bio*) and for the presence of plasmids pKM101 and pAQ1, when appropriate. These cultures should be considered the frozen permanent strains which should be accessed only for the preparation of new frozen working cultures.

Materials

Salmonella strain (Table 3.1.1): available from Dr. Bruce Ames, Biochemistry Department, University of California, Berkeley, Calif. 94720
Nutrient agar plates (see recipe)
Nutrient broth (see recipe)
Glucose minimal agar plates (GM plates; see recipe)
Enriched GM agar plates (see recipe)
Cryogenic vials

Additional reagents and equipment for growth and manipulation of bacteria (*APPENDIX 3*)

Prepare permanent cultures

1. Upon receipt of the *Salmonella* tester strain(s), streak a loopful of the culture for individual colonies (*APPENDIX 3*) on nutrient agar plates and inoculate a small inoculum in 5 ml of nutrient broth. Incubate overnight.

   The broth culture serves as a backup in case no growth is observed on the agar plate.

   In case a disk containing the strain imbedded in nutrient agar is received, first streak the disc across the surface of a nutrient agar plate, and then transfer the disc to 5 ml of nutrient broth.

2. After overnight incubation, purify three colonies by streaking a small inoculum from each colony for individual colonies on enriched GM agar plates supplemented with an excess of biotin and histidine and as needed with ampicillin (for strains carrying plasmid pKM101) and tetracycline (for strains carrying plasmid pAQ1). Incubate 1 to 2 days at 37°C.

3. After incubation, pick three colonies from the plate and inoculate preassigned locations, labeled 1, 2, and 3, on an enriched GM agar plate supplemented with the appropriate nutrients/antibiotics, which should be the same as those used in step 2.

   Label the locations on the back of the plate. These plates will serve as the master agar plates.

   For steps 2 and 3, nutrient agar plates may also be used instead of appropriately supplemented GM agar plates, however the use of minimal defined medium reduces the risk of contamination.

4. At the same time inoculate a small inoculum from each of the three colonies, individually, in 5 ml of nutrient broth.

5. After incubation at 37°C for 1 or 2 days, perform a strain check analysis (see Support Protocol 4) on each of the triplicate liquid cultures.

6. Upon completion of the strain check, select the colony from the master plate that has given the best overall results in terms of phenotypic characteristics, including the best overall spontaneous mutation induction. Inoculate a small portion from this colony in 5 ml of nutrient broth and incubate the cultures overnight at 37°C with shaking at 100 to 120 rpm.

   For "Permanent Cultures" it is usually sufficient to freeze down five 1-ml aliquots.

7. When good growth (OD_{540} between 0.1 and 0.2) is obtained, label this culture as "Permanent Culture" and freeze the cells (see Support Protocol 3), storing them in a −80°C freezer or in liquid nitrogen.

   These permanent cultures should be accessed only when new working frozen cultures are needed.

   New frozen working cultures should be prepared every 12 months with an expiration date 1 year from the time the new frozen cultures were prepared. The following steps should be followed to prepare the working cultures.

Prepare working cultures

8. Take one permanent culture from the freezer and quickly remove a small inoculum by scraping the surface of the frozen culture with a sterile loop or needle. Transfer the inoculum to 5 ml nutrient broth and incubate overnight at 37°C with shaking at 100 to 120 rpm.
9. Streak the overnight culture for individual colonies on minimal medium agar plates supplemented with an excess of biotin and histidine and as needed with ampicillin (for strains carrying plasmid pKM101) and tetracycline (for strains carrying plasmid pAQ1). Incubate 1 to 2 days at 37°C.
10. After incubation, transfer a small inoculum from each of three single, healthy-looking colonies from the plate to preassigned locations, labeled 1, 2, and 3, on a glucose minimal medium agar master plate appropriately supplemented with biotin, histidine, ampicillin and/or tetracycline (i.e., the permanent plate).

    Nutrient agar plates may be used instead of the appropriately supplemented minimal agar plates, however the use of minimal defined medium reduces the risk of contamination.

11. At the same time inoculate a small inoculum from each of the three colonies, individually, in 5 ml of nutrient broth.
12. After incubation at 37°C for 1 or 2 days, perform a strain check analysis (see Support Protocol 4) on each of the triplicate liquid cultures prepared in step 11.
13. Upon completion of the strain check, select the colony from the permanent plate that has given the best overall results in terms of phenotypic characteristics, including the best overall spontaneous mutation induction. Add a small inoculum of nutrient broth and incubate the cultures overnight at 37°C with shaking at 100 to 120 rpm.

    The number of working cultures that are prepared depends on how many times during any given year fresh cultures will be grown up overnight. Frozen working cultures are usually maintained for up to 1 year. It is not unusual for laboratories that test at least once a week to prepare at least fifty 1-ml frozen aliquots. In that case, 50 ml of nutrient broth should be inoculated with the test organism for overnight growth.

14. When good growth is obtained (OD_{540} between 0.1 and 0.2), label the cultures as "Working Cultures" and freeze the cells (see Support Protocol 3) storing them in a −80°C freezer or in liquid nitrogen.

    At the time the experiment is to be performed, carry out the remaining steps.

Propagate working cultures

15. Thaw a 1-ml frozen culture at room temperature.
16. Transfer 0.1- to 0.5-ml aliquots into volumes of nutrient broth between 10 and 50 ml, to give an initial cell density between 1×10^6 and 1×10^7 colony forming units/ml (1:100 dilution). Discard remainder of working culture.

    Frequent thawing and refreezing of the frozen cultures can result in permanent injury to the bacteria.

An alternative procedure for inoculation of the overnight cultures is to use a sterile inoculation loop to scrape a small amount of the frozen culture from the surface of the frozen culture. This procedure should be done quickly to prevent thawing of the culture.

17. Grow the cultures at 37°C for 4 hr without shaking, then with gentle shaking (100 rpm) for 11 to 14 hr.

All strains should be analyzed for their genetic integrity (see Support Protocol 4) when each experiment is performed.

SUPPORT PROTOCOL 3

FREEZING OF PERMANENT AND WORKING CULTURES

After the strain check is performed, one of the three colony isolates that gave the best overall results in terms of genetic integrity is selected from the master plate for preservation (either as frozen permanent stock cultures or as frozen working cultures). The following procedure is used for freezing down the strains.

Materials

Permanent or working culture (see Support Protocol 2, step 7 or 14), with OD_{540} between 0.1 and 0.2)
Glycerol or DMSO, sterile
2-ml cryogenic vials, sterile

1. Add sterile glycerol (or DMSO) to the culture at a final concentration of 10% (v/v). Mix thoroughly, then dispense in 1-ml aliquots in sterile 2-ml cryogenic vials.

Each 1-ml sample should contain 1–2 × 10^9 cells. Make sure that the caps of the cryogenic vials are tightly secured.

2. Quickly freeze cultures by placing on dry ice.

3. Place the frozen cultures in a −80°C freezer or in liquid nitrogen.

One ampule of the frozen overnight culture should be saved for performing a strain check (see Support Protocol 4) to ensure that the new working cultures that were frozen down have maintained their genetic integrity.

SUPPORT PROTOCOL 4

GENETIC ANALYSIS OF STRAINS

After overnight incubation the cultures are analyzed for their genetic characteristics and for the number of spontaneous revertants as follows.

Materials

Overnight culture of *Salmonella* (see Support Protocol 2, step 5 or 12)
Enriched GM agar plates (see recipe) with the following additives:
An excess of biotin (B plates)
An excess of histidine (H plates)
An excess of biotin and histidine (BH plates)
An excess of biotin and histidine, and 24 µg/ml ampicillin (BHA plates)
An excess of biotin and histidine, and 2 µg/ml tetracycline (BHT plates)
0.1% (w/v) crystal violet solution (see recipe)
Sterile filter paper disk (6-mm)

1. *Biotin dependence (bio):* Streak a loopful of the culture across one GM plate supplemented with an excess of histidine. Incubate 1 to 2 days at 37°C.

Expected result: no growth.

Because a deletion mutation stretches across the bio-uvrB region of the chromosome, it is sufficient to show that the tester strains are biotin dependent to infer that they are also

defective in the accurate DNA repair pathway due to the uvrB deletion. The presence of a deletion of the uvrB gene, rather than an inactivating point mutation, ensures that the cell will not be able to mutate back to an effective uvrB gene.

2. *Histidine dependence (his):* Streak a loopful of the culture across one GM plate supplemented with an excess of biotin. Incubate 1 to 2 days at 37°C.

   Expected result: no growth.

3. *Biotin and histidine dependence (bio, his):* Streak a loopful of the culture across one GM plate supplemented with an excess of biotin and histidine. Incubate 1 to 2 days at 37°C.

   Expected result: growth.

4. *Ampicillin resistance:* Streak a loopful of the culture across one GM plate supplemented with an excess of histidine and biotin and 24 μg/ml ampicillin. Incubate 1 to 2 days at 37°C.

   Alternatively, a sterile 6-mm filter paper disk containing 10 μg ampicillin can be placed on a streak of the strain on a glucose minimal agar plate supplemented with an excess of histidine and biotin. A strain should be included that does not carry plasmid pKM101 as a control.

   Expected result: growth of only the pKM101 strains that are ampicillin resistant. The ampicillin disks can be prepared in advance and stored aseptically in the refrigerator.

5. *Tetracycline resistance:* Streak a loopful of the culture across a GM plate supplemented with an excess of histidine and biotin and 2 μg/ml tetracycline. Incubate 1 to 2 days at 37°C.

   Alternatively, a sterile 6-mm filter paper disk containing 1 μg tetracycline can be placed on a streak of the strain on a glucose minimal agar plate supplemented with an excess of histidine and biotin. Include a strain that does not carry plasmid pAQ1 as a control.

   Expected result: growth only of the (tetracycline-resistant) pAQ1 carrying strain.

6. *Presence of rfa marker (defective lipopolysaccharide):* Streak a loopful of the culture across a glucose minimal agar plate supplemented with an excess of biotin and histidine. Place a sterile filter paper disc in the center of the streak and apply 10 μl of a 0.1% crystal violet solution. Incubate 1 to 2 days at 37°C.

   Expected result: zone of growth inhibition surrounding the disc.

   The crystal violet disks can be prepared in advance and stored aseptically at room temperature.

PREPARATION OF METABOLIC ACTIVATION SYSTEM (S-9)

SUPPORT PROTOCOL 5

The *Salmonella* strains used for these tests are not capable of performing the cytochrome-based metabolic oxidations that act in mammalian systems to metabolize chemicals to their active forms. As a result, a 9000 × *g* supernatant fraction of a rodent (usually rat) liver homogenate (referred to as S-9), in the presence of NADP and an NADPH-generating system, is added to the test to simulate mammalian metabolism. To increase the enzyme activity, the animals are usually pretreated with the mixed-function oxidase inducer Aroclor 1254. The S-9 is added to the reaction mixture along with enzymic cofactors (the S-9 mix). The metabolism of different chemicals to their mutagenic forms requires different optimum concentrations of S-9. Generally, the concentrations used range from 4% to 30% in the S-9 mix (Ames et al., 1975; Maron and Ames, 1983). In general, fewer mutagens will be "missed" by using the higher concentrations of S-9. In the absence of specific information about the optimum S-9 concentration for the chemicals to be tested, it is recommended that 10% or 30% S-9 (v/v in the cofactor mix) be

used for the initial test. The S-9 concentration can also be calculated and standardized on protein content.

The procedure described in this protocol can also be followed when animals other than rats, e.g., hamsters, are used for preparing the metabolic activation system from livers. The preparation of hamster liver S-9, required for Alternate Protocol 4, would be done via the same procedure described below, with the exception that the animals would not be treated with Aroclor or any other inducer of liver enzymes. In this case, Golden Syrian hamsters weighing ~150 g each are the species that are usually used.

The S-9 can be prepared by the testing laboratory, and aliquots frozen at −80°C. It is recommended that more than one animal be used and the homogenates pooled so as to minimize animal-to-animal variation among batches. Alternatively, a number of vendors provide S-9 preparations, along with a characterization of their enzyme activities and effectiveness with standard mutagens.

NOTE: All protocols using live animals must first be reviewed and approved by an Institutional Animal Care and Use Committee (IACUC) or must conform to governmental regulations regarding the care and use of laboratory animals.

Materials

Chemical inducer: e.g., polychlorinated biphenyl (Aroclor 1254) or phenobarbital
Corn oil
Male Sprague-Dawley rats weighing ~200 g each
0.15 M KCl

Syringes and 27-G needles
Sterile forceps and scissors
Potter-Elvehjem tissue homogenizer with loose Teflon pestle
1- or 5-ml cryogenic vials
Centrifuge with speeds up to 9000 × *g*

Induce liver enzymes

1. Dilute Aroclor 1254 in corn oil to a concentration of 200 mg/ml. Using a 27-G needle, give each animal a single intraperitoneal injection of 500 mg/kg (~0.5 ml of this mixture) 5 days before sacrifice.

   Be sure to use sterile corn oil and sterile syringes and needles.

   The solvent used, route of administration, and dose regimen will be different for different inducers. The route and regimen providing the maximum induction should be used.

2. Give the rats unrestricted access to drinking water and food until 12 hr prior to sacrifice. At that point, remove the food.

3. Stun the rat by a blow to the head and then decapitate it.

   IMPORTANT NOTE: *All subsequent steps should be performed at 0° to 4°C, using cold, sterile solutions and glassware.*

Prepare the S-9 fraction

4. Aseptically remove livers from rats and place in a preweighed beaker containing 0.15 M KCl.

   The volume of KCl should be ~1 ml/gram wet liver.

5. Weigh the beaker containing the livers and transfer to a sterile beaker containing 3 ml of 0.15 M KCl per g of wet liver (i.e., 3 vol).

6. Mince the livers with sterile scissors and homogenize using a Potter-Elvehjem homogenizer with a loose Teflon pestle.

   Other tissue homogenizers are acceptable.

7. Centrifuge homogenate 10 min at 9000 × *g*, 0° to 4°C.
8. Decant the supernatant (containing the S-9 fraction) into a sterile beaker that is kept on ice.
9. Dispense 1-ml aliquots of the S-9 fraction into sterile 1- or 5-ml cryogenic vials.

Store and test S-9 fraction

10. Quick freeze the homogenate in dry ice.
11. Store the S-9 homogenate in a −80°C freezer or in liquid nitrogen in appropriately labeled boxes.

    Typically, 1 ml of the S-9 fraction contains microsomes from ~250 mg of wet livers, with a protein concentration of ~40 mg/ml. Protein concentrations can be measured following the procedure described by Lowry et al. (1951).

12. Before being used for routine screening, test each batch of S-9 for sterility, as well as for effectiveness against the laboratory's standard positive control mutagens, or against the chemical class of interest.

REAGENTS AND SOLUTIONS

Use Milli-Q-purified water or equivalent all recipes and all protocol steps. For common stock solutions, see ***APPENDIX 2A****; for suppliers, see* ***SUPPLIERS APPENDIX.***

Ampicillin solution, 8 mg/ml

To 100 ml of deionized water add 0.8 g ampicillin. Stir on magnetic stirrer until dissolved, then filter sterilize using a 0.45-µm filter. Store up to 1 year at 4°C.

Biotin/histidine solution for top agar, 0.5 mM

In a 4-liter flask, heat 1000 ml water to near boiling. Place flask with stir bar on a magnetic stirrer. Add 0.1 g of biotin and 0.1 g of histidine and stir until dissolved. Prepare only on the day top agar (see recipe) is to be made.

If filter sterilized, the solution can be stored up to 1 year at 4°C.

Biotin solution (0.01%)

Heat 100 ml of deionized water to a boil. Add 10 mg of D-biotin. Stir on magnetic stirrer until dissolved, then filter sterilize using a 0.45-µm filter. Store up to 1 year at 4°C.

Cofactors for reductive metabolism

Thaw 63 ml of standard S-9 cofactors for the S-9 mix (see recipe) and add the following:

423 mg D-glucose-6-phosphate

142 mg nicotine adenine dinucleotide, reduced form (NADH), disodium salt

Filter sterilize through a 0.45-µm filter. Aseptically add 280 U (2.8 U/ml final) of glucose-6-phosphate dehydrogenase, then add 30 ml of liver S-9 (see Support Protocol 5). Immediately before use add 7 ml flavin mononucleotide FMN solution (see recipe). Keep on ice at all times and away from direct light.

Cofactors for the S-9 mix

Sequentially dissolve by stirring each of the following components in 200 ml of deionized H_2O:

0.3 g D-glucose-6-phosphate

0.7 g nicotinamide adenine dinucleotide phosphate (NADP)

0.4 g magnesium chloride

continued

0.5 g potassium chloride
2.5 g sodium phosphate, dibasic
0.6 g sodium phosphate, monobasic
When dissolved filter sterilize through a 0.45-µm filter

Dispense in sterile tubes in aliquots of 7, 9, and 9.5 ml for convenient use when in need of 30%, 10%, or 5% S-9, respectively, in the S-9 mix (10 ml final volume). Store up to 1 year at –20°C.

Prior to each experiment, the cofactors are thawed at room temperature before the addition of the S-9 homogenate, which should be kept on ice throughout the day.

A 10% S-9 mix contains, per 100 ml: 10 ml (10% v/v) S-9 fraction (see Support Protocol 5), 0.5 mM glucose-6-phosphate, 0.4 mM NADP, 0.8 mmol $MgCl_2$, 3.3 mM KCl, and 10 mM sodium phosphate pH 7.4. Of course, these concentrations vary when a 5% or 30% S-9 mix is used. See Support Protocol 5 for preparation of the S-9 fraction; see Basic Protocol 1, step 3, for mixture of the cofactors and the S-9 fraction.

Crystal violet solution, 0.1% (w/v)

To 100 ml of water add 0.1 g crystal violet. Mix well and store up to 1 year at room temperature in light-proof glass container.

Enriched GM agar plates

Prior to pouring GM plates (see recipe), add the following item(s) as required for Support Protocol 4 to the 2 liters of medium, and mix thoroughly:

Biotin (B) plates: Add 16 ml of 0.01% biotin solution (see recipe).

Histidine (H) plates: Add 16 ml of 0.5% L-histidine solution (see recipe).

Biotin-histidine (BH) plates: add 16 ml of 0.01% biotin (see recipe) and 16 ml of 0.5% histidine (see recipe).

Biotin-histidine-ampicillin (BHA) plates: Add 16 ml of 0.01% biotin (see recipe), 16 ml of 0.5% histidine, and 6 ml of 8 mg/ml ampicillin (see recipe; final concentration of ampicillin, 24 µg/ml).

Biotin-histidine-tetracycline (BHT) plates: Add 16 ml of 0.01% biotin (see recipe), 16 ml of 0.5% histidine (see recipe), and 0.5 ml of 8 mg/ml tetracycline solution (see recipe; final concentration of tetracycline, 2 µg/ml).

Store plates up to 1 year at 4°C

Flavin mononucleotide (FMN) solution

To 7 ml of water add 96 mg of flavin mononucleotide (FMN). Filter sterilize through a 0.45-µm filter and keep on ice while preparing the remainder of the modified cofactors (see recipe for cofactors for reductive metabolism).

Glucose minimal agar plates (GM plates)

To 1800 ml of water in a 4-liter flask add 30 g of agar. Autoclave for 30 min and let cool ~45 min to ~60°C. Add 40 ml of sterile 50× VB salts (see recipe) and swirl until salts are in solution. Add 100 ml of sterile 10% glucose (see recipe) and swirl to mix thoroughly. Dispense 20 to 25 ml in sterile, 100 × 15–mm diameter petri plates. Store plates up to 1 year at 4°C.

GM agar medium is also known as Vogel-Bonner agar medium (Vogel and Bonner, 1956). Plates can be stored in a refrigerator for several months if placed in sealed, plastic bags. Prior to use make sure the surface of the solidified agar is dry; condensate will interfere with proper adherence of the top agar. One batch (2 liters) of GM bottom agar makes ~80 plates.

The agar should never be autoclaved together with the VB salts and 10% glucose. Bottom agar made this way will not fully support the growth of the Salmonella strains due to toxicity of the free radicals in the medium produced by the autoclaving.

Glucose solution, 10%

Heat 1500 ml water in a 4-liter flask on a magnetic stirrer. Add 200 g glucose (dextrose) and stir until the mixture is clear (~5 min). Adjust final volume to 2000 ml. Dispense in 100-ml aliquots in 250-ml bottles and autoclave for 30 min. Store up to 1 year at 4°C.

Histidine solution (0.5%)

To 100 ml of deionized water add 0.5 g mg of L-histidine hydrochloride. Stir on magnetic stirrer until dissolved, then filter sterilize using a 0.45-µm filter. Store up to 1 year at 4°C.

Nutrient agar plates

Prepare nutrient broth (see recipe), then add 15 g agar per liter and heat to dissolve. Autoclave, allow mix to cool to ~60°C, then pour plates.

Nutrient broth

If using Difco nutrient broth: To 1000 ml of deionized water add 8 g of nutrient broth powder (Difco). Stir to dissolve, then dispense in Erlenmeyer flasks or test tubes. Autoclave for 20 min. Store up to 1 year at room temperature in the dark.

If using Oxoid nutrient broth #2: To 1000 ml of deionized water add 25 g of nutrient broth powder (Oxoid). Stir to dissolve, then dispense in Erlenmeyer flasks or test tubes. Autoclave for 20 min. Store up to 1 year at room temperature in the dark.

Sodium phosphate buffer, 0.1 M, pH 7.4

Per 500 ml final volume add in the following order:

60 ml 0.1 M sodium phosphate, monobasic (add 13.8 g $NaH_2PO_4 \cdot H_2O$ to 1 liter H_2O)

440 ml 0.1 M sodium phosphate, dibasic (add 14.2 g Na_2HPO_4 to 1 liter distilled H_2O)

Adjust pH, as needed, using dibasic sodium phosphate

Mix well and dispense in 100-ml aliquots

Autoclave 20 min

Store up to 1 year at 4°C

Tetracycline solution, 8 mg/ml

Prepare 100 ml of 0.02 N sodium hydroxide. Add 800 mg tetracycline and stir on magnetic stirrer until dissolved, then filter sterilize using a 0.45-µm filter. Store protected from direct light up to 1 year at 4°C.

Top agar supplemented with biotin and limited histidine

To a 4-liter flask add:

1800 ml water

12 g agar

12 g sodium chloride

Melt agar by autoclaving for 10 min. Add 200 ml of 0.5 mM biotin/histidine (see recipe). Dispense in 300-ml aliquots in 500 ml-bottles and autoclave for 30 min. Store up to 6 months at room temperature.

For preparation of smaller volumes, reduce all ingredients proportionately. Prior to use, melt the top agar in boiling water or in a microwave oven.

Vogel-Bonner (VB) salts, 50×

To 650 ml warm water, add the following components in the order indicated, making sure that each chemical is dissolved thoroughly by stirring on a magnetic stirrer before adding the next chemical (it takes ~1 hr to dissolve all ingredients):

continued

10 g magnesium sulfat e ($MgSO_4 \cdot H_2O$)
100 g citric acid, monohydrate
500 g potassium phosphate, dibasic, anhydrous (K_2HPO_4)
175 g sodium ammonium phosphate ($Na_2NH_2PO_4 \cdot 4H_2O$)
Adjust volume to 1000 ml
Dispense in 40-ml aliquots and autoclave for 30 min
Store up to 1 year at room temperature in the dark

COMMENTARY

Background Information

During the developmental stages of the Ames *Salmonella* standard plate incorporation assay, Ames and colleagues constructed or selected five genetically altered tester strains that are differentially responsive to mutagen treatment. These strains are referred to as: TA1535, TA1537, TA1538, TA98, and TA100, and are considered the standard or traditional tester strains (Ames et al., 1975; Maron and Ames, 1983). The following three genetic alterations increased the sensitivity of these tester strains significantly.

1. Elimination of the accurate DNA repair pathway by a deletion mutation through the *uvrB* gene (all strains except TA102). This deletion also includes the biotin synthesis gene (*bio*), so that the cells require biotin for growth.

2. Increased cell wall permeability through selection for phage C21-resistant bacteria (*rfa* mutation, all strains).

3. Introduction of plasmid pKM101, which enhances error-prone DNA repair (in strains TA97, TA98, TA100, TA102, and TA104).

To mimic mammalian metabolism, the microsomal fraction (S-9) from rat liver, or from other species or tissues, is incorporated into the assay procedure. In the assay, the bacteria are exposed to the test chemical in the presence and absence of the metabolic activation system.

Although the standard plate incorporation assay with the five standard tester strains and inclusion of rat liver S-9 was highly effective in detecting chemical mutagens (Ames et al., 1975), several modifications to the assay procedure (Maron and Ames, 1983) and additional mutant strains (i.e., TA97, TA102, TA104) have made the assay more versatile and enhanced its overall sensitivity.

The protocols described here are designed to determine whether a chemical is mutagenic or nonmutagenic under the specific test conditions. The amount of chemical applied to the plate or introduced into the test chamber is known, but the actual dose to which the bacteria are exposed is affected by the chemical's stability, solubility, volatility, and ability to partition between solvent and aqueous phases.

Preincubation versus standard plate incorporation assay

The preincubation assay is the assay of choice for liquid chemicals, since many of these chemicals may be volatile. For all other chemicals except highly volatile chemicals and gases, either the preincubation or the standard plate incorporation assay may be used. It may be warranted to adopt one of these two assay procedures in a laboratory for general screening purposes. The use of one assay procedure for general screening aids in getting a solid historical database for the negative, solvent, and positive controls. The other assay procedure can then be used as a backup in case equivocal or negative results are obtained in the initial experiment.

Critical Parameters

Solvents

The solvent of choice is distilled water, followed by dimethylsulfoxide (DMSO). Other useful solvents are acetone, ethyl alcohol (75%), tetrahydrofuran, dimethylformamide, and methyl ethyl ketone (MEK). If other than the standard plate assay is to be performed, the toxicity of the solvent should be determined. It is also important to determine whether the solvent will interfere with the metabolic activation system at the concentrations used (Maron et al., 1981).

Dose selection

Each chemical should be tested initially at half-log dose intervals up to a dose that elicits toxicity, or up to a dose immediately below one that was toxic in the preliminary toxicity procedure. Subsequent trials can use narrower dose increments. Chemicals that are not toxic should be tested to a maximum dose of 5 to 10 mg/plate. Chemicals that are poorly soluble should be tested up to doses defined by their solubilities. At least five doses of each chemical should be tested in triplicate, and an independent repeat

experiment performed at least one week following the initial trial. Ideally, a new stock solution of the test chemical should be made with appropriate dilutions for each repeat experiment. A maximum of 0.05 ml organic solvent should be added to each plate when delivering the test chemical.

For volatile liquid chemicals tested in 9-liter desiccators, the high dose per desiccator should be 5 ml. For gases, the high dose should be the equivalent of 4.5 liters, which is 50% of the volume of the desiccator.

Metabolic activation

A rat liver S-9 fraction is customarily used for metabolic activation, but metabolic activation systems derived from different animal species and/or organs can be used instead (Zeiger, 1985). Mammalian intestinal flora (Reid et al., 1984) can also be used. Chemicals can be tested in the presence of more than one activation system, and more than one concentration of the metabolic activation system can be used, e.g., 30% and 10% (v/v). In addition, uninduced and induced microsomal enzymes can be selected by using different inducers such as phenobarbital, β-naphthoflavone, or Aroclor 1254.

An activation system can also be used for reductive metabolism. The use of reducing agents, such as flavin mononucleotide (FMN), has been recommended for testing certain classes of chemicals in the *Salmonella* assay. The most widely publicized of these classes are those containing azo and diazo compounds (Prival and Mitchell, 1982; Reid et al., 1984). Unless reduced, such compounds usually are not mutagenic. Reduction of chemical substances can occur in mammals, including humans, by anaerobic intestinal microflora and by reductases in the intestinal wall or the liver.

Salmonella strain selection

For general screening purposes, when the potential mutagenicity of the sample is unknown, it is recommended that a tiered approach be used, starting with an initial test using strains TA98 and TA100, with and without rat liver S-9. If a positive response is obtained in one or both strains, only the positive test condition(s) needs to be repeated. If an equivocal or weak positive response is obtained in one or both of these strains, the corresponding plasmid-free parent strain(s), TA1538 and TA1535, respectively, are used to determine whether a more definitive response could be obtained. If the results with TA98 and TA100 are negative, other strains, including TA97 or TA1537, and TA1535, are used with and without S-9. If a positive response is obtained in any of these strains, a confirmation test is run.

As a general rule, a chemical is not considered nonmutagenic if it has not been tested with the four most commonly used strains, TA97 (or TA1537), TA98, TA100, and TA1535, with and without S-9 mix.

Where there is advance information about the potential mutagenicity of the chemical or chemical class, the initial testing is performed in the strain(s) considered most likely to yield a positive response. If a negative response is obtained, testing is performed in additional strains.

Strains TA102 and/or TA104 are used if it is suspected that the test chemical would cause oxidative damage (e.g., free radical production) or be a DNA cross-linking agent. Strain TA102 is the strain of choice for the latter class of chemicals, because the presence of the wild-type *uvrB* gene makes the strain more responsive to this type of damage.

Background lawn

Except for the few histidine-independent bacteria that arose during the overnight incubation (pre-existing his^+) , the 1×10^8 cells put onto each plate are histidine dependent (his^-), and are not capable of growing or forming colonies in the absence of histidine. Sufficient histidine is added to the top agar to allow all the plated cells to undergo six to eight divisions before the histidine is exhausted. This limited number of divisions makes the cells more sensitive to mutagens, and allows for the fixation of mutational lesions. In the absence of exogenous histidine, only the mutant his^+ cells continue to grow and form macroscopic colonies. The limited growth of all the plated his^- bacteria leads to a "background lawn" of cells on the plate that generally gives the plates a hazy appearance. Under a dissecting microscope (40× to 100×), this lawn can be seen to be comprised of densely packed microcolonies of cells in the absence of toxicity. However, it should be noted that the presence of a normal-appearing background lawn is not evidence of an absence of toxicity.

The density of the background lawn is used as one indicator of chemical, or other, toxicity. A sparse lawn, usually referred to as "thinning," when compared to the negative or solvent control, is a sign of chemical toxicity, especially if it is dose-related. A total absence of bacterial background lawn is evidence of a high level of toxicity. Such a toxic dose should not be used. Occasionally, numerous small colonies, re-

Table 3.1.3 Spontaneous Control Values for the *Salmonella* Tester Strains[a]

Strain	Number of revertants	
	Without S-9	With S-9
TA97	75-200	100-200
TA98	20-50	20-50
TA100	75-200	75-200
TA102	100-300	200-400
TA104	200-300	300-400
TA1535	5-20	5-20
TA1537	5-20	5-20
TA1538	5-20	5-20

[a]Values are from the authors' laboratories.

ferred to as pinpoint colonies, will be present against such a clear lawn. These pinpoint colonies consist of his^- cells that survived the toxicity. The absence of competition for histidine from the nonsurviving his^- bacteria results in more histidine being available on a per-cell basis to support the growth of the surviving his^- cells. The surviving fraction of his^- cells will undergo additional cell divisions until the excess histidine is consumed, thereby forming small his^- colonies. The histidine requirement can be checked by spotting or streaking cells from these colonies onto histidine-deficient, but biotin-containing, glucose minimal agar plates in the absence of test chemical.

Table 3.1.3 presents a range of spontaneous (solvent/negative) control values per plate for each tester strain with and without S-9.

The values presented in Table 3.1.3 are ranges found in the authors' laboratories; they should not be taken as absolute values that must be achieved by all laboratories. Each laboratory performing routine testing should develop its own control ranges. However, the values in this table do depict the range of responses that could be seen. Extreme excursions from these values should be avoided. Different S-9 sources or concentrations, or different batches of agar and media, can result in changed values. Strains TA97, TA102, and TA104 are particularly sensitive to S-9 concentration, and will show increased spontaneous values with increasing S-9 concentrations.

Data evaluation

Because testing is usually performed with more than one strain and sometimes with more than one activation condition, the data have to be evaluated for each trial (strain/activation), for the tester strain, and for the chemical. There is no generally agreed upon approach to data evaluation. The data can be evaluated using a formal statistical procedure, by means of arbitrary rules, or using subjective criteria. Statistical treatments, if used, must be relevant for the data, and recognize that the data are not always Poisson distributed. Data evaluations must be made at both the individual trial level (i.e., strain/S-9 combination) and overall chemical levels.

A chemical is designated nonmutagenic only after being tested in strains TA98, TA100, TA1535, and TA97 and/or TA1537, in the presence and absence of at least one metabolic activation system with at least one concentration of the S-9 fraction. Other S-9 concentrations can be used to clarify equivocal or weak positive responses. Additional strains may be used (e.g., TA102, TA104) if, for example, a chemical is suspected of generating oxidative DNA damage.

Blind scoring is desirable to eliminate bias in the interpretation of the results. It can be accomplished by having all chemicals coded before testing and by maintaining the code during counting of the revertant colonies and during analysis of data.

Formal statistical procedure

The data can be evaluated for a positive trend, and/or the responses at the individual dose levels can be compared against the solvent control. A statistical analysis of the data is not required; however, a number of statistical procedures and approaches recommended for the assay have been compiled and reviewed by Vollmar and Edler (1990).

Table 3.1.4 Troubleshooting Guide for Ames Test

Problem	Possible cause(s)	Solution(s)
The revertant colonies are concentrated on one half of the plate	Bottom agar solidifies on a slant, or the top agar was allowed to solidify on a slant. When the top agar is not able to spread evenly over the plate, the section with the deepest agar will have the highest number of colonies.	The plates should be on a level surface when the bottom agar is poured, and during the experiment when the top agar is added and allowed to solidify.
There is no colony growth, or relatively few cells (including pinpoint colonies) are present, and there is a clear background lawn	This is an indication of toxicity to the bacteria. If the top agar is allowed to get above 50 ° C, it is toxic to the *Salmonella* bacteria. Where there is a high level of toxicity, the majority of the plated histidine-dependent bacteria are killed, and too few survive to form a visible background lawn. The pinpoint colonies usually arise from surviving *his*$^-$ cells. Because of the death of the other cells, there is more histidine available to the survivors, and they are able to form visible colonies.	It is important to keep the top agar ideally at a temperature of 43°C, with care taken not to exceed a temperature of 48°C. There may have been too much organic solvent added to the tubes. The toxicity of the solvent should be checked, or there may be a toxic chemical contaminant in the solutions or in the tubes. Alternatively, the top agar may contain inadequate buffering capacity for the test chemical.
The positive control "doesn't work"	No response, or an inadequate response, could result from many factors, the most common being: inactive S-9 or cofactors, use of the wrong bacterial strain, omission from the tubes of a necessary component of the S-9 mix, presence of something in the tube or on the plate that was toxic to the S-9, addition of the wrong amount of chemical, omission of the positive control chemical from the tube, improper storage of the positive control chemical, reduced biological activity resulting from solution.	New positive control solutions should be prepared when a decrease in activity is observed, or the physical appearance of the solution changes. Note that positive control solutions can be prepared in advance and stored at 4°C. 2-Anthramine is light-sensitive and should be stored in a dark container. Check the identity of the bacterial strain; if it is correct, then it may be necessary to reisolate the strain to select a culture that is responsive to the chemical.
Some of the colonies on the plate look different from the majority of the colonies	Colonies of contaminating bacteria or molds often have a different color or colony morphology than the *Salmonella* strains. This can be the result of contamination in the overnight *Salmonella* culture, contaminated solutions, or contamination present in the test chemical that was not killed by the solvent.	All solutions should be tested for contamination, and controls should be included to measure possible contamination in the S-9 mix and test chemical. It is recommended that a microbiologist be consulted if contamination is suspected.

continued

Arbitrary rules. The most often used arbitrary rule is the so-called two-fold rule. Using this rule, a positive response requires a dose-response that reaches 2-fold over the solvent control. Other laboratories use what is termed a "modified" two-fold rule. In this modified rule, the strains with low spontaneous frequencies (e.g., TA98, TA1535, TA1537) are required to reach 2.5- or 3-fold above spontaneous. Some laboratories require only one dose to reach the cutoff, others require two.

Subjective criteria. The data are evaluated as described by Zeiger et al. (1992). Individual trials are judged mutagenic (+), weakly mutagenic (+w), questionable (?), or nonmutagenic (−), depending on the magnitude of the increase in his$^+$ revertants, and the shape of the dose-response. A trial is judged questionable (?) if the dose-response is considered to be insufficiently high to support a call of "+w," if only a single dose is elevated over the control, or if a weak increase is not dose-related. Distinctions between a

Table 3.1.4 Troubleshooting Guide for Ames Test, continued

Problem	Possible cause(s)	Solution(s)
The spontaneous revertant count is too low	The wrong *Salmonella* strain was used. A lower than expected spontaneous response could also indicate a toxic effect on the cells introduced during handling, or from contamination of the agar or one of the reagents.	Check the identity of the *Salmonella* strain. If necessary, reisolate strain, selecting for a culture with a spontaneous revertant value in the desired range.
	There was too little histidine added to the top agar.	Prepare fresh solutions.
The spontaneous revertant count is too high	It is possible that the initial inoculum from the frozen culture contained an unusually high number of preexisting *his*$^+$ bacteria, which would lead to a higher than expected number of preexisting mutants in the overnight culture.	Check the identity of the *Salmonella* strain. If necessary, reisolate tester strain, selecting for a culture with a spontaneous revertant value in the desired range.
	Too much histidine may have been added to the top agar, or a larger amount of the *Salmonella* culture was added to the tube (resulting in additional histidine being carried over from the culture medium).	Redo experiment.
	Plates that had been sterilized with ethylene oxide (EtO) retain and outgas the EtO even after they are received by the laboratory. EtO outgassing from the plates is mutagenic to TA100 and TA1535.	Plates not sterilized with EtO should be obtained from the supplier. Alternatively, EtO should be allowed to out-gas for a couple of days in a fume hood before the bottom agar is poured.
There is unusually heavy growth of the background lawn, along with an increase in colonies on the minimal agar	There may be free histidine in the test sample. The increased histidine on the plate with increasing concentrations of test substance will lead to increased levels of growth of the his$^-$ cells, and a concomitant increase in the number of his$^+$ revertant colonies.	Substances that contain free histidine, or that could release histidine, cannot be adequately tested in the assay. An attempt should be made to remove the histidine using an ion-exchange resin column.
The response is not reproducible	The test chemical not stable.	The chemical cannot be adequately tested using this procedure.
	The test chemical is highly volatile	Use the desiccator procedure.
	Very low (marginal) responses are often not reproducible.	Repeat the test using a narrower dose range or a different protocol.

continued

questionable response and a nonmutagenic or weakly mutagenic response, and between a weak mutagenic response and mutagenic response, are highly subjective. When using this approach, it is not necessary for a response to reach a specific fold increase over background for a trial to be judged positive. The reproducibility of the response is important in making the overall evaluation.

Troubleshooting

Table 3.1.4 presents a troubleshooting guide for the Ames test.

Anticipated Results

Using these protocols, it is possible to identify compounds that are mutagenic for *Salmonella* and that have a high probability of being carcinogenic/mutagenic in other organisms.

Time Considerations

The experimental procedure, without the 48-hr incubation, takes ~4 hr to complete for one chemical when the following matrix is used:

Four *Salmonella* tester strains
Six dose levels (including the solvent control)
Triplicate plates per dose level

Table 3.1.4 Troubleshooting Guide for Ames Test, continued

Problem	Possible cause(s)	Solution(s)
The top agar doesn't solidify properly	Gelling of the agar is retarded at acid pH.	Add additional buffering capacity to the agar, or adjust the pH of the test chemical.
	The top agar concentration was too low.	The recommended agar concentration is 0.6% (w/v).
The agar slips out of the plate	Insufficient agar was used when the bottom agar was prepared.	The wrong agar concentration may have been used. The recommended bottom agar concentration is 1.5% (w/v).
Precipitate is present on the plates	The precipitate can be of the test substance, or be formed from a reaction of the test substance with a component of the test system such as the S-9 mix. In defining a dose range for testing, at least one dose should show some precipitate.	Determine if the precipitate would interfere with the automatic colony counter; if so, these plates must be counted by hand. For consistency, all plates in the series should be counted in a similar manner. The presence of precipitate should be noted on the data sheets. Note that there are chemicals that are mutagenic only at doses at which precipitate is present (Gatehouse et al., 1994).
A colored test chemical obscures colonies or reduces contrast	Automatic colony counters require contrast differences between the colonies and the background.	The automatic colony counter will not be effective, and the colonies must be counted by hand. For consistency, all plates in the series should be counted in a similar manner.
The test chemical appears to react with the solvent or other components of the test—e.g., it may produce fumes when it is added to the solvent	The test chemical is highly reactive.	The chemical may not be testable in vitro. The products of the reaction could be tested, but the results from this testing must carry the appropriate caveats.
		If the test chemical is known or believed to react with plastics, it can be tested using glass pipets, tubes, and petri dishes.

Metabolic activation system

Positive control chemicals for each strain

Sterility check for metabolic activation, buffer, and chemical.

This time schedule also includes, inoculation of overnight cultures, melting of top agar, labeling of plates, preparation of the metabolic activation system, and dilutions of the test chemical. An additional 4 hr is required for counting the plates, which includes inspection of the background lawn, and recording and analysis of the test results. Hand counting will take longer especially if a potent mutagen is being tested. In this case quadrants of the agar plates may be counted with appropriate extrapolation to the area of the entire plate.

Media preparation, weighing of the test chemicals, and maintenance of the laboratory, including safe disposition of the chemical, is estimated to take another 4 hr. Thus, overall, the testing of one chemical may take one individual between 12 and 16 hr. Testing of multiple chemical samples on one day will reduce the time it takes to complete the testing on a per-chemical basis, since only one set of positive controls are needed, and the time to set up the experiment in the laboratory is about the same, except for labeling of plates and test tubes, which is proportional to the number of additional samples.

Literature Cited

Ames, B.N. 1971. The detection of chemical mutagens with enteric bacteria. *In* Chemical Mutagens: Principles and Methods for Their Detection, Vol. 1 (A. Hollaender, ed.) pp. 267-282. Plenum, New York.

Ames, B.N., McCann, J., and Yamasaki, E. 1975. Methods for detecting carcinogens and mutagens with the *Salmonella*/mammalian-microsome mutagenicity test. *Mutat. Res.* 31:347-364.

Araki, A., Noguchi, T., Kato, F., and Matsushima, T. 1994. Improved method for mutagenicity testing of gaseous compounds by using a gas sampling bag. *Mutat. Res.* 307:335-344.

Auletta, A.E., Dearfield, K.L., and Cimino, M.C. 1993. Mutagenicity test schemes and guidelines: U.S. EPA Office of Pollution Prevention and Toxics and Office of Pesticide Programs. *Environ. Mol. Mutagen.* 21:38-45.

Dearfield, K.L., Auletta, A.E., Cimino, M.C., and Moore, M.M. 1991. Considerations in the U.S. Environmental Protection Agency's testing approach for mutagenicity. *Mutat. Res.* 258:259-283.

FDA. 1993. Toxicological Principles for the Safety Assessment of Direct Food Additives and Color Additives Used in Food "Redbook II" [Draft]. FDA, Center for Food Safety and Applied Nutrition, Washington, D.C.

Gatehouse, D.G. and Delow, G.F. 1979. The development of a "Microtitre" fluctuation test for the detection of indirect mutagens, and its use in the evaluation of mixed enzyme induction of the liver. *Mutat. Res.* 60:239-252.

Gatehouse, D., Haworth, S., Cebula, T., Gocke, E., Kier, L., Matsushima, T., Melcion, C., Nohmi, T., Ohta, T., Venitt, S., and Zeiger, E. 1994. Recommendations for the performance of bacterial mutation assays. *Mutat. Res.* 312:217-233.

Gee, P., Maron, D.M., and Ames, B.N. 1994. Detection and classification of mutagens: A set of base-specific *Salmonella* tester strains. *Proc. Natl. Acad. Sci. U.S.A.* 91:11606-11610.

Grant, D.M., Josephy, P.D., Lord, H.L., and Morrison, L.D. 1992. *Salmonella typhimurium* strains expressing human arylamine *N*-acetyltransferases: Metabolism and mutagenic activation of aromatic amines. *Cancer Res.* 52:3961-3964.

Haworth, S., Lawlor, T., Mortelmans, K., Speck, W., and Zeiger, E. 1983. *Salmonella* mutagenicity results for 250 chemicals. *Environ. Mutagen.* 5(Suppl. 1):3-142.

HPBGC (Health Protection Branch Genotoxicity Committee Guidelines; Canada). 1993. The assessment of mutagenicity. Health Protection Branch mutagenicity guidelines. *Environ. Mol. Mutagen.* 21:15-37.

Houk, V.S., Schalkowsky, S., and Claxton, L.D. 1989. Development and validation of the spiral *Salmonella* assay: An automated approach to bacterial mutagenicity testing. *Mutat. Res.* 223:49-64.

Houk, V.S., Early, G., and Claxton, L.D. 1991. Use of the spiral *Salmonella* assay to detect the mutagenicity of complex environmental mixtures. *Environ. Mol. Mutagen.* 17:112-121.

Hughes, T.J., Simmons, D.M., Monteith, L.G., and Claxton, L.D. 1987. Vaporization technique to measure mutagenic activity of volatile organic chemicals in the Ames/*Salmonella* assay. *Environ. Mutagen.* 9:421-441.

Jurado, J., Alejandre-Duran, E., and Pueyo, C. 1994. Mutagenicity testing in *Salmonella typhimurium* strains possessing both the His reversion and Ara forward mutation systems and different levels of classical nitroreductase or *O* -acetyltransferase activities. *Environ. Mol. Mutagen.* 23:286-293.

Kado, N.Y., Langley, D., and Eisenstadt, E. 1983. A simple modification of the *Salmonella* liquid incubation assay: Increased sensitivity for detecting mutagens in human urine. *Mutat. Res.* 112:25-32.

Kier, L.D., Brusick, D.J., Auletta, A.E., Von Halle, E.S., Simmon, V.F., Brown, M.M., Dunkel, V.C., McCann, J., Mortelmans, K., Prival, M.J., Rao, T.K., and Ray, V.A. 1986. The *Salmonella typhimurium*/mammalian microsome mutagenicity assay. A report of the U.S. Environmental Protection Agency Gene-Tox Program. *Mutat. Res.* 168:67-238.

Kirkland, D.J. 1993. Genetic toxicology testing requirements: Official and unofficial views from Europe. *Environ. Mol. Mutagen.* 21:8-14.

Kramers, P.G.N., Knaap, A.G.A.C., van der Heijden, C.A., Taalman, R.D.F.M., and Mohn, G.R. 1991. Role of genotoxicity assays in the regulation of chemicals in The Netherlands: Considerations and experiences. *Mutagenesis* 6:487-493.

Levin, D.E., Yamasaki, E., and Ames, B.N. 1982a. A new *Salmonella* tester strain, TA97, for the detection of frameshift mutations: A run of cytosines as a mutational hot-spot. *Mutat. Res.* 94:315-330.

Levin, D.E., Hollstein, M., Christman, M.F., Schwiers, E.A., and Ames, B.N. 1982b. A new *Salmonella* tester strain (TA102) with AT base pairs at the site of mutation detects oxidative mutagens. *Proc. Natl. Acad. Sci. U.S.A.* 79:7445-7449.

Lowry, O.H., Rosebrough, N.J., Farr, A.L., and Randall, R.J. 1951. Protein measurement with the Folin phenol reagent. *J. Biol. Chem.* 193:265-275.

Maron, D.M. and Ames, B.N. 1983. Revised methods for the *Salmonella* mutagenicity test. *Mutat. Res.* 113:173-215.

Maron, D., Katzenellenbogen, J., and Ames, B.N. 1981. Compatibility of organic solvents with the *Salmonella*/microsome test. *Mutat. Res.* 88:343-350.

McCann, J., Choi, E., Yamasaki, E., and Ames, B.N. 1975. Detection of carcinogens in the *Salmonella*/microsome test: Assay of 300 chemicals. *Proc. Natl. Acad. Sci. U.S.A.* 72:5135-5139.

McCoy, E.C., Rosenkranz, H.S., and Mermelstein, R. 1981. Evidence for the existence of a family of bacterial nitroreductases capable of activating nitrated polycyclics to mutagens. *Environ. Mutagen.* 3:421-427.

Prival, M.J. and Mitchell, V.D. 1982. Analysis of method for testing azo dyes for mutagenic activity in *Salmonella typhimurium* in the presence of flavin mononucleotide and hamster liver S-9. *Mutat. Res.* 97:103-116.

Reid, T.M., Morton, K.C., Wang, C.Y., and King, C.M. 1984. Mutagenesis of azo dyes following metabolism by different reductive/oxidative systems. *Environ. Mutagen.* 6:247-259.

Ruiz-Rubio, M. and Pueyo, C. 1982. Double mutants with both His reversion and Ara forward mutation systems of Salmonella. *Mutat. Res.* 105:383-386.

Simmon, V.F., Kauhanen, K., and Tardiff, R.G. 1977. Mutagenic activities of chemicals identified in drinking water. *In* Progress in Genetic Toxicology (D. Scott, B.A. Bridges, and F.H. Sobels, eds.) pp 249-258. Elsevier/North-Holland, Amsterdam.

Simula, T.P., Glancey, M.J., and Wolf, C.R. 1993. Human glutathione-*S*-transferase-expressing *Salmonella typhimurium* tester strains to study the activation/detoxification of mutagenic compounds: Studies with halogenated compounds, aromatic amines and aflatoxin $_{B1}$. *Carcinogenesis* 14:1371-1376.

Sofuni, T. 1993. Japanese guidelines for mutagenicity testing. *Environ. Mol. Mutagen.* 21:2-7.

Sugimura, T., Sato, S., Nagao, M., Yahagi, T., Matsushima, T., Seino, Y., Takeuchi, M., and Kawachi, T. 1976. Overlapping of carcinogens and mutagens. *In* Fundamentals of Cancer Prevention (P.N. Magee, S. Takayama, T. Sugimura, and T. Matsushima, eds.) pp. 191-215. University Park Press, Baltimore.

Tennant, R.W., Margolin, B.H., Shelby, M.D., Zeiger, E., Haseman, J.K., Spalding, J., Caspary, W., Resnick, M., Stasiewicz, S., Anderson, B., and Minor, R. 1987. Prediction of chemical carcinogenicity in rodents from in vitro genetic toxicity assays. *Science* 236:933-941.

Vogel, H.J. and Bonner, D.M. 1956. Acetylornithinase of *E. coli*: Partial purification and some properties. *J. Biol. Chem.* 218:97-106.

Vollmar, J. and Edler, L. 1990. Tabular overview of statistical methods proposed for the analysis of Ames *Salmonella* assay data. *In* Lecture Notes in Medical Informatics, Statistical Methods in Toxicology (L. Hothorn, ed.) pp. 42-48. Springer-Verlag, Berlin.

Waleh, N.S., Rapport, S.J., and Mortelmans, K.E. 1982. Development of a toxicity test to be coupled to the Ames *Salmonella* assay and the method of construction of the required strains. *Mutat. Res.* 97:247-256.

Watanabe, M., Nohmi, T., and Ishidate, M., Jr. 1987. New tester strains of *Salmonella typhimurium* highly sensitive to mutagenic nitroarenes. *Biochem. Biophys. Res. Commun.* 147:974-979.

Watanabe, M., Ishidate, M., Jr., and Nohmi, T. 1990. Sensitive method for the detection of mutagenic nitroarenes and aromatic amines: New derivatives of *Salmonella typhimurium* tester strains possessing elevated *O*-acetyltransferase levels. *Mutat. Res.* 234:337-348.

Wilkinson, R.G., Gemski, P., Jr., and Stocker, B.A.D. 1972. Non-smooth mutants of *Salmonella typhimurium* : Differentiation by phage sensitivity and genetic mapping. *J. Gen. Microbiol.* 70:527-554.

Yahagi, T., Degawa, M., Seino, Y., Matsushima, T., Nagao, M., Sugimura, T., and Hashimoto, Y. 1975. Mutagenicity of carcinogenic azo dyes and their derivatives. *Cancer Lett.* 1:91-97.

Zeiger, E. 1985. The *Salmonella* mutagenicity assay for identification of presumptive carcinogens. *In* Handbook of Carcinogen Testing (H.A. Milman and E.K. Weisburger, eds.) pp. 83-99. Noyes Publishers, Park Ridge, N.J.

Zeiger, E., Pagano, D.A., and Robertson, I.G.C. 1981. A rapid and simple scheme for confirmation of *Salmonella* strain phenotype. *Environ. Mutagen.* 3:205-209.

Zeiger, E., Anderson, B., Haworth, S., Lawlor, T., and Mortelmans, K. 1992. *Salmonella* mutagenicity tests: V. Results from the testing of 311 chemicals. *Environ. Mol. Mutagen.* 19(Suppl. 21):1-141.

Key References

Ashby, J. and Tennant, R.W. 1991. Definitive relationships among chemical structure, carcinogenicity, and mutagenicity for 301 chemicals tested by the U.S. NTP. *Mutat. Res.* 257:229-306.

Claxton, L.D. 1998. The development, validation, and analysis of *Salmonella* mutagenicity test methods in environmental situations. *In* Microscale Testing in Aquatic Toxicology: Advances, Techniques, and Practice (P. G. Wells, K. Lee, and C. Blaise, eds.) pp. 591-605, CRC Press, Boca Raton, Fla.

Zeiger, E. 1997. Genotoxicity database. *In* Handbook of Carcinogenic Potency and Genotoxicity Databases (L.S. Gold and E. Zeiger, eds.) pp. 687-729. CRC Press, Boca Raton, Fla.

The key references will provide additional insight into how data collected from large studies are analyzed and interpreted and how such data are used to predict carcinogenicity.

Contributed by Errol Zeiger
Environmental Toxicology Program/
National Institute of Environmental Health Sciences
Research Triangle Park, North Carolina

Kristien Mortelmans
SRI International
Menlo Park, California

Measurement of a Malondialdehyde-DNA Adduct

Determination of levels of various DNA adducts has become an essential tool in modern toxicology of carcinogens. Direct measurements of DNA adduct levels, the true biologically effective dose of a mutagen, can be correlated to biological outcomes or used to probe mechanisms of adduct formation. For each adduct to be measured, there must be a specific and sensitive assay developed.

Malondialdehyde is a carcinogenic and mutagenic electrophile that is endogenously produced during the peroxidation of polyunsaturated fatty acids. Reaction of malondialdehyde (MDA) with deoxyguanosine (dG) results in the fluorescent exocyclic pyrimidopurinone M_1G (Fig. 3.2.1). This unit describes a mass spectrometric assay for M_1G. This assay is highly specific and accounts for variable loss during sample preparation and analysis, unlike other currently used assays for M_1G. This unit includes three protocols: (1) a gas chromatographic/negative chemical ionization–electron capture/mass spectrometry (GC/NCI EC/MS) assay for M_1G (see Basic Protocol); (2) preparation of anti-M_1G immunoaffinity gel (see Support Protocol 1); and (3) a method for HPLC quantification of nucleosides (see Support Protocol 2). Sample preparation includes the use of an immunoaffinity column purification step to enrich for the M_1G adduct, which improves sensitivity over previously described methods.

GC/MS ASSAY FOR PYRIMIDOPURINONE

BASIC PROTOCOL

This protocol describes a procedure used to quantify M_1G in biological tissues starting with DNA isolation, continuing with sample preparation, and concluding with a brief description of M_1G analysis by GC/NCI EC/MS. In order to determine the ratio of M_1G adducts to normal nucleosides, a known quantity of dideuterated M_1G-deoxyribose internal standard ($[^2D_2]M_1G$-dR) is added to the dissolved DNA sample, and the sample

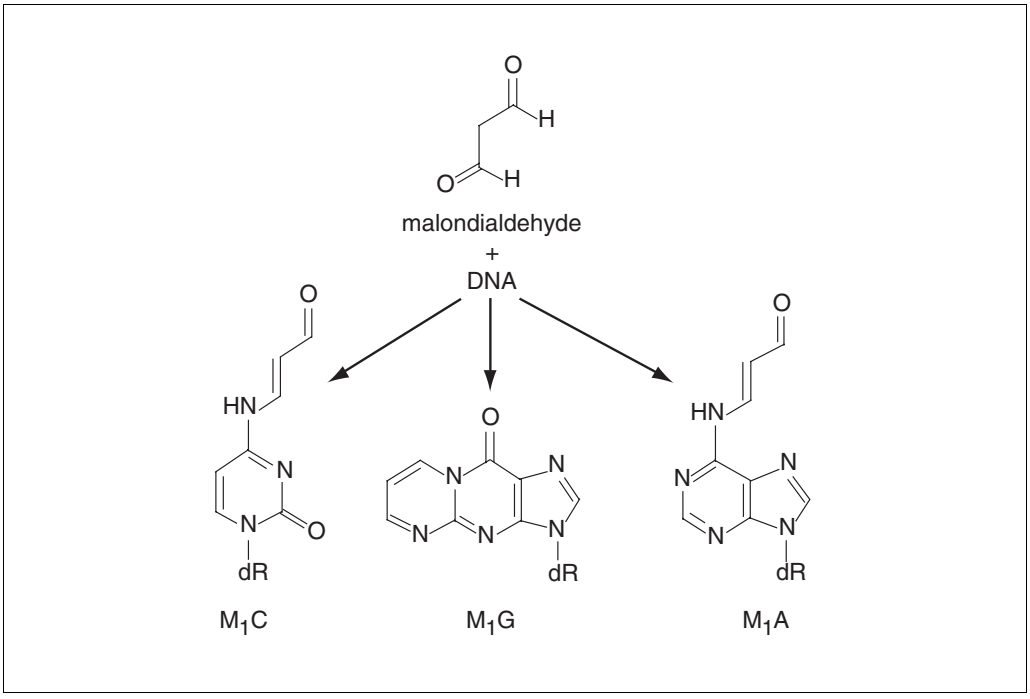

Figure 3.2.1 Structures of malondialdehyde-DNA adducts. The reaction with guanine residues yields the cyclized pyrimidopurinone M_1G.

Contributed by John P. Plastaras and Lawrence J. Marnett
Current Protocols in Toxicology (1999) 3.2.1-3.2.16

is enzymatically hydrolyzed to nucleosides. An aliquot is taken for HPLC analysis (see Support Protocol 2) to determine the total number of nucleosides. M_1G-dR is purified from the other nucleosides by immunoaffinity chromatography using Sepharose coupled to anti-M_1G monoclonal antibodies (see Support Protocol 1). The sugar is released from the nucleoside by formic acid hydrolysis to yield the M_1G base. M_1G is derivatized with pentafluorobenzyl bromide (PFB-Br), which will add a PFB group to either the N_7 or N_9 position of the base (Fig. 3.2.2). The products are subjected to solid-phase extraction with silica, and the analytes are subjected to GC/NCI EC/MS analysis.

Since the cleavage product of the internal standard, $[^2D_2]M_1G$, is two mass units heavier than M_1G, it is readily distinguished by MS (*m/z* of 188 vs. 186). By comparing the ratio of the peak area of $[^2D_2]M_1G$ to the peak area of M_1G, the quantity of M_1G in the sample before DNA hydrolysis can be determined.

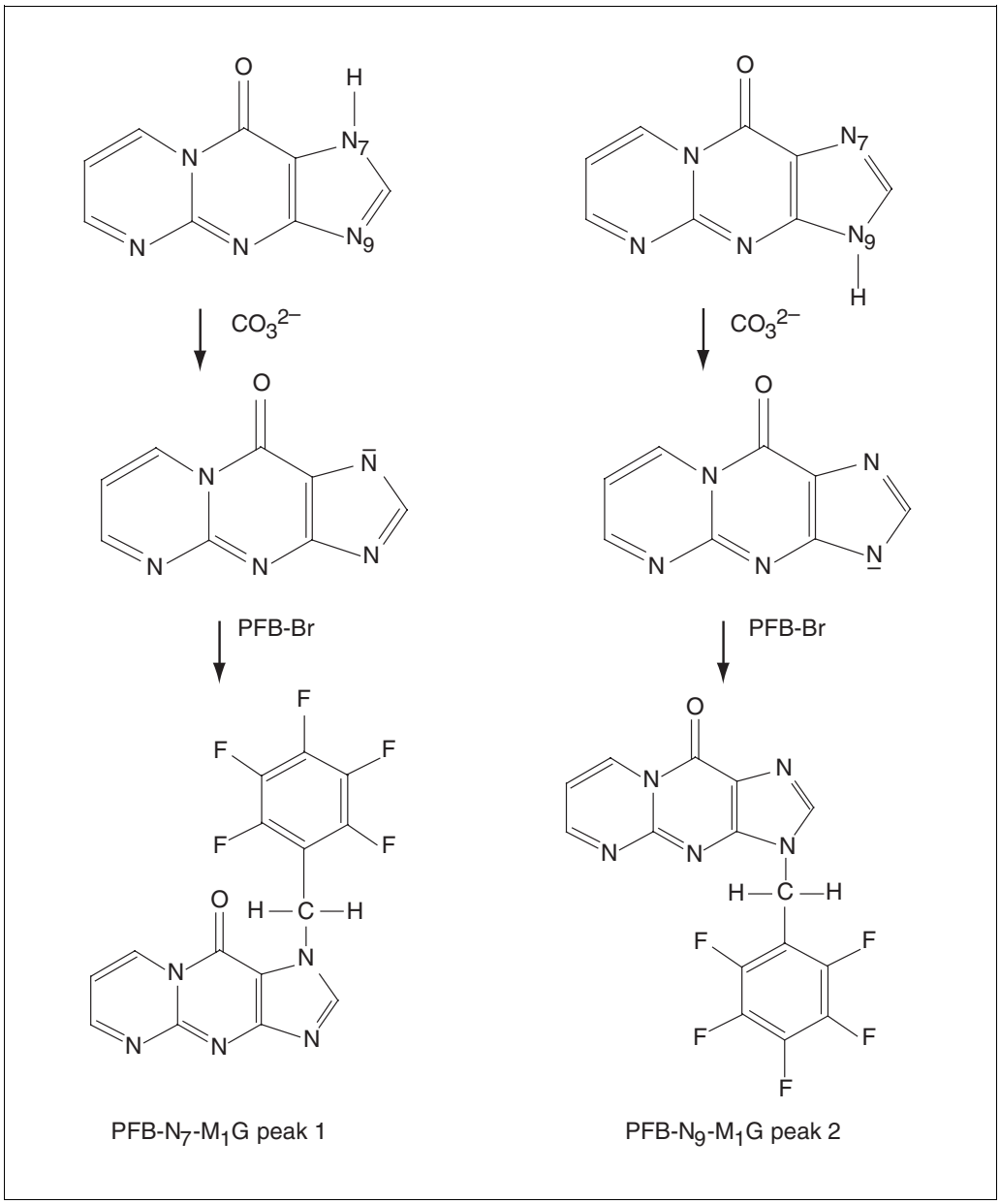

Figure 3.2.2 The M_1G base is derivatized by treatment with mild base to remove the N_7 or N_9 proton followed by reaction with pentafluorobenzyl bromide (PFB-Br) to yield two PFB-M_1G isomers. These isomers separate by gas chromatography.

NOTE: This assay takes several full days to complete, so appropriate stopping points have been mentioned in the procedure. As with any analytical method, consistency and careful attention to detail are required.

Materials

Tissue of interest
MOPS/sucrose buffer (see recipe), 4°C
2× lysis buffer (Applied Biosystems)
920 U/µl ribonuclease A (Sigma)
100,000 U/µl ribonuclease T_1 (Boehringer Mannheim)
10 to 20 U/µl proteinase K (Sigma)
Anti-oxidant MOPS buffer (see recipe)
Phenol/chloroform/water reagent (Applied Biosystems)
24:1 (v/v) chloroform/isoamyl alcohol
3 M sodium acetate (*APPENDIX 2A*)
100% and 70% (v/v) ethanol
10 mM MOPS/100 mM NaCl, pH 7.0
1.5 ng/ml [$^2D_2$]M_1G-dR standard (see Chaudhary et al., 1994b, for synthesis procedure, which is relatively straightforward)
Deoxyribonuclease (DNase) I stock solution (see recipe)
Nuclease P1 stock solution (see recipe)
25 mM $ZnCl_2$
0.4 M MOPS, pH 7.8
20 U/µl alkaline phosphatase (Sigma)
Anti-M_1G immunoaffinity gel (see Support Protocol 1)
PBS (*APPENDIX 2A*)
Nondeuterated M_1G-dR standard (see Chaudhary et al., 1994b)
Methanol
Nanopure water
Acetone
Concentrated formic acid (88% w/v)
PFB-Br derivatization solution (see recipe)
Methylene chloride
N,O-bis(Trimethylsilyl) trifluoroacetamide (BSTFA; Pierce)
Derivatized deuterated standard (see recipe)

Polytron homogenizer (Brinkmann)
Silica (Supelclean LC-Si, Supelco)
10-µl Hamilton syringe
Repeater pipetter and a range of disposable pipets
Ultrafree-Probind filters with modified PVDF membrane (Millipore)
End-over-end mixer
Solid-phase extraction vacuum manifold
6-ml glass columns with Teflon frits (Supelco)
5-ml glass conical tubes with screw caps
50-ml syringe with column attachment for positive pressure
60°C sand bath
Stills for drying solvents (see Fig. 3.2.3)
Vibrating shaker
Nitrogen evaporation chamber: N-Evap (Organomation) or equivalent
Mortar and pestle
0.5- or 1-ml glass pipet and pipet pump

Hewlett Packard MS Engine (model HP5989A) equipped with Series II Plus gas chromatograph (model HP5890), autoinjector (model 7673 GC/SFC injector), electronic pressure programming, and the negative chemical ionization option (or equivalent GC/MS equipment)
Sample vials and inserts
Vial caps
Vial cap crimper
50-µl micropipets
Micropipetter

Prepare tissue

1. If tissue is not to be processed immediately, snap freeze it by wrapping in aluminum foil and immersing in liquid nitrogen. Store at −80°C.

   The actual method used for homogenization and DNA extraction will vary depending on the tissue or cell source. This protocol has been used successfully to isolate DNA from liver, kidney, and brain for the purpose of analyzing nuclear DNA. High pH is avoided to prevent formation of the ring-opened oxopropenal form of M_1G, and MOPS buffer is used instead of Tris buffer to avoid forming a Schiff base adduct with M_1G.

2. Partially thaw tissue (~1 g/sample) and mince with a scalpel on a glass plate cooled over an ice bucket. Suspend minced tissue in cold MOPS/sucrose buffer (10 ml buffer/gram tissue).

   Avoid using Tris buffer or any other primary amine, which may react with M_1G to form a ring-opened Schiff base. MOPS buffer is a good alternative.

   Avoid pH >8.0 to prevent decomposition of the adduct.

3. Homogenize with a Polytron homogenizer on maximum setting for 20 sec, and filter through four layers of cheesecloth.

   Blood leukocytes or cells from tissue culture can be broken by suspension in MOPS/sucrose buffer followed by four freeze-thaw cycles.

Isolate nuclei

4. Centrifuge 5 min at 3000 × *g*, 4°C, to pellet nuclei. Carefully remove supernatant with pipet. Resuspend pellet in fresh MOPS/sucrose buffer (10 ml/gram tissue) and centrifuge again.

5. Remove supernatant as in step 4 and resuspend pellet in 3 ml fresh MOPS/sucrose buffer. Add 3 ml of 2× lysis buffer. Invert to mix.

Digest proteins and RNA

6. Add 400 U each per gram tissue of ribonuclease A and ribonuclease T_1. Incubate 1 hr at 37°C.

7. Add 10 mg proteinase K per gram tissue. Incubate 3 hr at 37°C.

Extract DNA

8. Add 2 ml anti-oxidant MOPS buffer. Add 8 ml phenol/chloroform/water reagent and mix thoroughly. Centrifuge 5 min at 3000 × *g*, 4°C.

9. Transfer aqueous layer to a new tube. Add 4 ml fresh anti-oxidant MOPS buffer to the organic layer, mix, and centrifuge 5 min at 3000 × *g*, 4°C.

10. Add the aqueous layer to the aqueous layer from the first extraction. Add 10 ml phenol/chloroform/water reagent to the combined aqueous layers, mix, and centrifuge for 5 min at 3000 × *g*, 4°C.

11. Transfer the aqueous layer to a new tube and add 10 ml of 24:1 (v/v) chloroform/isoamyl alcohol. Mix and centrifuge 5 min at 3000 × *g*, 4°C.

12. Transfer the aqueous layer to a new tube and add 0.1 vol of 3 M sodium acetate.

Precipitate DNA

13. Add 2 to 2.5 vol ice-cold 100% ethanol. Let the solution stand at least 2 hr at −20°C.

14. Using a glass hook, transfer DNA pellet to a microcentrifuge tube. Wash the DNA pellet twice with 70% ethanol. Allow pellet to air dry, and store at −20°C.

Resuspend DNA pellet

15. Weigh each 15-ml plastic conical tube, and transfer 1 to 2 mg dry DNA pellets to each tube. Add 2 ml of 10 mM MOPS/100 mM NaCl (pH 7.0) to each sample and let dissolve overnight on an end-over-end mixer at 4°C.

    If DNA is not completely dissolved, the sample can be treated with DNase I to finish solubilizing.

16. Vortex vigorously for 1 to 3 min to shear DNA.

17. Add 4 µl of 1.5 ng/ml [$^2D_2$]M_1G-dR standard to each sample using a dedicated 10-ml Hamilton syringe.

Digest DNA

18. Prepare fresh DNase I stock solution. Add 400 µl to each sample, and incubate 90 min in a 37°C water bath

    For running multiple samples, this addition and many of the following additions can be facilitated by using a repeater pipetter and disposable pipet.

19. Thaw an aliquot of nuclease P1 stock solution. Add 50 µl to each sample.

20. Add 100 µl of 25 mM $ZnCl_2$ to each sample. Incubate 2 hr in a 37°C water bath.

    While samples are incubating, the immunoaffinity gel may be prepared for use as in steps 22 to 25.

21. Add 1.0 ml of 0.4 M MOPS (pH 7.8) and 1.5 µl of 20 U/µl alkaline phosphatase (30 U) to each sample, and incubate 1 hr in a 37°C water bath.

    At the end of these enzymatic digestions, there will be a cloudy precipitate at bottom of each tube.

Prepare immunoaffinity gel

22. Label 15-ml conical plastic tubes. Swirl anti-M_1G immunoaffinity gel (see Support Protocol 1) and add 400 µl to each tube.

23. Add 5 ml PBS to each tube. Centrifuge 5 min at 1000 × *g*, 4°C, to pellet the gel.

24. Carefully remove and discard supernatant using a Pasteur pipet equipped with a dropper bulb.

25. Repeat steps 23 and 24. Store at 4°C until ready for use.

Recover hydrolyzed DNA

26. Dry and weigh each tube from step 21 to determine total hydrolysate volume.

    Volume is determined by subtracting the weight of the empty tube and assuming a density of 1 mg/ml. If tubes are finely graduated, the volume may be read directly.

27. Vortex samples and filter a 100-µl aliquot through a Probind filter. Store this sample at −20°C for later analysis by HPLC (see Support Protocol 2).

28. Pour DNA hydrolysate into tube with immunoaffinity gel. Wash hydrolysate tube with 3 ml PBS, then again with 2 ml PBS, each time transferring wash to tube with immunoaffinity gel. Also set up similar tubes without hydrolysate but containing a range of amounts of nondeuterated M_1G-dR (e.g., 25, 50, 100, 150, 200, and 500 pg, and possibly 1 ng).

    This will give a total volume of ~8 ml in the immunoaffinity tube.

    The nondeuterated standards are processed in parallel with the DNA tubes for the remainder of the procedure.

Purify DNA on immunoaffinity matrix

29. Cap tubes and mix on an end-over-end mixer for 30 min at room temperature.

    This incubation time can be extended without compromising results.

30. While samples are incubating, wash the 6-ml glass columns fitted with Teflon frits on a solid-phase extraction vacuum manifold attached to a side-arm faucet aspirator. Wash with at least two cycles of the following sequence: 5 ml each methanol, Nanopure water, acetone, and Nanopure water.

31. Just prior to use, wash columns with 5 ml methanol (added with glass pipet) and a final 5 ml PBS.

Pour immunoaffinity column

32. Mix the samples on an end-over-end mixer, uncap the tubes, and carefully pour the immunoaffinity gel suspension into the open column, allowing fluid to flow through.

33. Add 8 ml PBS to the immunoaffinity gel tubes. Recap, shake, and add to columns. Repeat.

34. Add 8 ml water to the immunoaffinity gel tubes. Recap, shake, and add to columns. Repeat.

Elute column

35. Add 4 ml water directly to columns. Apply vacuum to columns and allow to sit under vacuum at least 1 min until dry. Meanwhile, label 5-ml glass tubes and place in rack that fits in vacuum manifold.

36. Put rack of tubes into vacuum manifold, making sure column tips line up in tubes. With vacuum turned off, add 0.5 ml methanol with glass pipet, and wait 30 sec to allow methanol to denature IgG. Apply vacuum to elute.

    Turn off vacuum before adding each aliquot of methanol.

37. Add 0.5 ml methanol twice more to give 1.5 ml total eluent.

38. Remove columns from vacuum manifold. Either cap tubes and store at −20°C or continue with following step.

    Wash columns with water immediately to remove gel. They are difficult to clean after drying.

39. Dry samples by spinning under vacuum at ambient temperature for ~2 hr (using Speedvac evaporator). Cap and store at −20°C until ready for next step.

    Normally, no visible residue can be seen. However, when samples are dried extensively, a faint opaque residue, probably trace salt, may cloud the bottom of the tube. This will not adversely affect the results.

Acid hydrolyze base

40. Thaw samples, if stored, and set sand bath temperature to 60°C.

41. Immediately before use, add 142 µl concentrated formic acid (88% w/v) to 5 ml water to give a 2.5% (w/v) solution. Add 200 µl of 2.5% formic acid to each sample. Cap the tubes and vortex.

42. Incubate 45 min in sand bath at 60°C.

43. Immediately dry samples by spinning under vacuum at ambient temperature.

    This will take 90 min to 2 hr.

44. Cap and wrap tops of the tubes with Parafilm and freeze at −20°C, or proceed to the next step.

    IMPORTANT NOTE: *The derivatized product is sensitive to water. Therefore, this entire procedure should be performed under anhydrous conditions.*

Distill methanol

45. Set up still as illustrated in Figure 3.2.3.

46. Begin distilling 250 ml methanol and allow to reflux for 30 min to 1 hr. Heat to a low boil. In the meantime, remove samples from freezer and let warm to room temperature before removing Parafilm.

    CAUTION: *Do not allow solvent to completely evaporate.*

47. Ensure samples are dry by spinning under vacuum at ambient temperature for 15 to 20 min.

Derivatize pentafluorobenzyl-M_1G

48. Using a 0.5-ml pipet, add 0.15 ml of freshly prepared PFB-Br derivatization solution to each sample. Purge tubes with nitrogen, cap, and seal with Parafilm.

49. Vortex samples, and incubate 90 min at room temperature in a vibrating shaker.

    During this incubation, proceed with distillation of methylene chloride.

Prepare samples for chromatography

50. Evaporate samples to dryness under nitrogen in an N-Evap or similar device.

    Placing tube tips in a room temperature water bath facilitates drying. Complete dryness is indicated by appearance of a white residue; this will take ~90 min.

Distill methylene chloride

51. Set up still as illustrated in Figure 3.2.3.

52. Begin distilling 250 ml methylene chloride and allow to reflux for 30 min to 1 hr. Heat to a low boil.

    CAUTION: *Do not allow solvent to completely evaporate.*

Prepare silica columns

53. Wash 3-ml solid-phase extraction columns (tightly fitted with Teflon frits) with alternating cycles of methanol and acetone (3 ml each). Dry in oven for ~15 min at 70°C.

    These columns are reusable.

54. Place ~0.1 g silica (Supelclean LC-Si) in each column.

    This step can be done in advance and packed columns can be stored in a desiccator at room temperature.

Wash silica column

55. Set up silica columns in a tube rack over a reservoir in a fume hood.

56. Using a glass pipet, wash silica columns as follows:

Twice with 2.5 ml methanol
Twice with 2.5 ml of 20% (v/v) methanol in methylene chloride
Twice with 2.5 ml methylene chloride.

Keep columns moist with methylene chloride until samples are completely dry.

IMPORTANT NOTE: *All additions of dry organic solvents should be performed with glass pipets. Reusable pipets may be preferable because the solvent can wash the markings off disposable glass pipets, leaving flecks of ink in the samples. A syringe with column attachment may be used to improve flow rate by applying positive pressure when necessary.*

Load samples on column

57. When samples from step 50 are dry, add 1.0 ml dry methylene chloride to each.

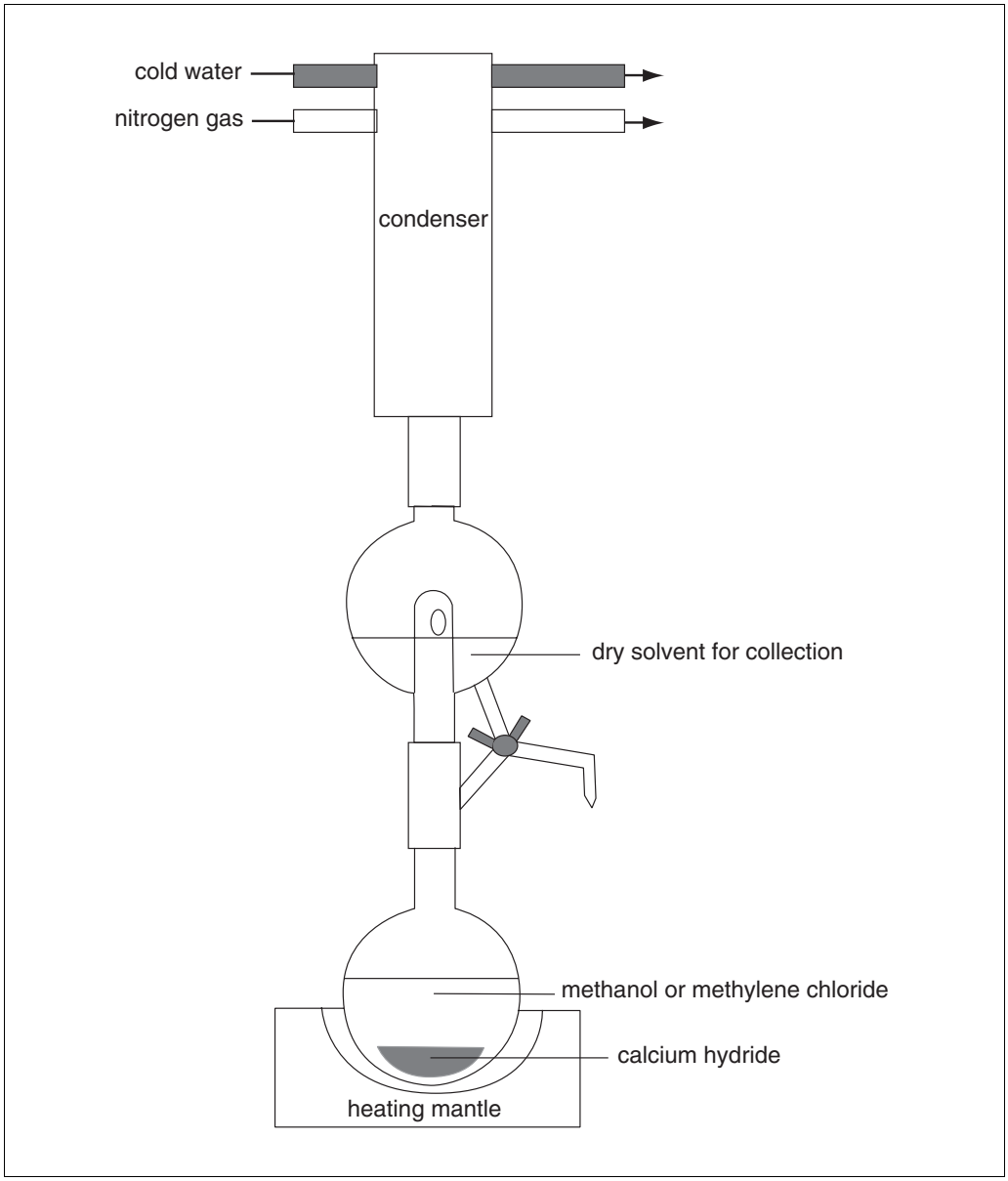

Figure 3.2.3 Distillation apparatus for drying solvents. Entire system is kept under dry nitrogen gas. Solvent is added to boiling flask with calcium hydride as a drying agent, and mantle set to keep at low boil. Dry solvent is collected in a trap equipped with drainage valve.

58. Using a Pasteur pipet, load samples onto columns carefully so as not to disturb silica bed. Leave this pipet in tube for next transfer.

59. When sample has completely entered the silica bed, add 1 ml of 1% (v/v) methanol in methylene chloride to sample tubes and transfer this wash to columns with the Pasteur pipets. Discard tubes and pipets.

60. Add 1 ml of 1% (v/v) methanol in methylene chloride directly to columns. While this is flowing, label 5-ml glass conical tubes and place them in positions in a tube rack corresponding to the columns.

61. After the wash has finished dripping, move entire rack of columns over the rack with the 5-ml glass conical tubes, being sure columns are lined up with tubes.

Elute column

62. Elute with 1 ml of 20% (v/v) methanol in methylene chloride without using positive pressure.

    Do not push any remaining liquid through with positive pressure, as this can push through some silica that will clog the gas chromatography column.

63. Evaporate samples to dryness under nitrogen. This will take ~1 hr. After samples are dry, cap the tubes, wrap in Parafilm, and store at −20°C.

    If silica columns were not sealed well, silica grains may be noticed in the sample tubes. These can clog the gas chromatography column.

Perform gas chromatography-mass spectrometry

NOTE: The following instructions work well with the Hewlett Packard MS Engine. Consult the manufacturer's instructions for other systems.

64. Use the following parameters for the gas chromatograph:

    Column: Rtx-50 (Restek) fused silica, 15 m long, 0.25 mm internal diameter
    Helium flow rate: 1.3 ml/min with a split ratio of 40:1
    Injector temperature, 280°C; transfer line temperature, 260°C
    Oven temperatures: initial 190°C, increase to 300°C at 25°C/min, maintain at 300°C or remainder of the run time (total time 10.7 min)
    Injector pressures: initial 16.0 psi, upon injection increase to 20.0 psi at 47 psi/min, hold at 20.0 psi for 0.99 min, decrease to 16 psi at 99.3 psi/min, hold at 16.0 psi for 0.25 min, increase to 30.0 psi at 3.5 psi/min, maintain at 30 psi for the remainder of the run time (total time 10.7 min)
    Splitless mode injection: volume of 2 µl.

65. Use the following parameters for the mass spectrometer:

    Negative chemical ionization with methane reagent gas at 2.6 to 3.1 Torr
    Source temperature, 270°C; quadrupole temperature, 100°C
    Selected ion monitoring at *m/z* of 186 and 188 after a 2-min solvent delay.

66. Freshly distill anhydrous methanol on day of analysis for reconstitution of samples.

67. Wash column two or three times with BSTFA prior to running samples.

68. Tune mass spectrometer to give optimum sensitivity for *m/z* of 186. Check sensitivity by injecting 2 µl of a stock solution of derivatized deuterated standard.

69. Set up data analysis to integrate peaks between 6 and 8 min for *m/z* of both 186 and 188.

    Because the PFB moiety can attach to M_1G at both the N_7 and N_9 positions, expect two peaks with retention times of between 6 and 8 min. Since the first peak (N_7) will be larger, use it for quantitation.

70. If sensitivity is adequate, reconstitute samples by adding 15 µl anhydrous methanol to each sample. Cap, vortex, and allow liquid to collect at the bottom, then transfer to sample vials using disposable micropipets. Crimp shut.

Let samples thaw before removing Parafilm

71. After injections of standard, inject pure methanol to wash injector apparatus. Make similar wash injections after every four or five samples that are analyzed.

72. Prepare a standard curve using the *m/z* 186/188 values obtained for the nondeuterated standards (see step 28). Determine the quantity of M_1G in samples by comparison to the standard curve (see Anticipated Results and Fig. 3.2.6).

SUPPORT PROTOCOL 1

PREPARATION OF ANTI-M_1G IMMUNOAFFINITY GEL

This reagent is required for the enrichment of the adducted deoxynucleoside from the sample, which will consist primarily of normal deoxynucleoside. The monoclonal anti-M_1G IgG antibody has been extensively characterized and is commercially available (Sevilla et al., 1997).

Materials

100 to 200 mg monoclonal anti-M_1G IgG antibody, protein A purified (Oxford)
CNBr-activated Sepharose 4B, freeze dried (Sigma)
1 mM HCl
Coupling buffer: 0.1 M $NaHCO_3$/0.5 M NaCl, pH 8.3
Blocking buffer: 0.1 M Tris·Cl, pH 8.0 (*APPENDIX 2A*)
Storage buffer: 0.1 M Tris·Cl/0.02% (w/v) sodium azide, pH 8.0
0.1 M sodium acetate/0.5 M NaCl, pH 4.0
200-ml glass storage bottle

Couple antibody to Sepharose

1. Swell 15 g freeze-dried CNBr-activated Sepharose 4B gel in 1 liter of 1 mM HCl. Stir for 15 min.

2. Filter with 600-ml coarse Büchner funnel. Wash with 500 ml of 1 mM HCl four times in the funnel.

When filtering liquid from the gel in this procedure, be careful not to overdry.

3. Dilute 100 to 200 mg of antibody in 90 ml coupling buffer.

4. Divide antibody solution into three 50-ml plastic tubes. Divide washed gel into these tubes using a spatula.

5. Cap and mix for 1 hr at room temperatureon an end-over-end mixer.

Block and wash coupled gel

6. Pour the contents of the coupling reaction into the Büchner funnel and filter off liquid. Turn off vacuum.

7. Add 2 vol blocking buffer directly to Büchner funnel. Let sit at room temperature for 2 hr, occasionally stirring with glass stir rod. Filter off the liquid.

8. Wash the gel with three cycles of the following:

300 ml of 0.1 M sodium acetate/0.5 M NaCl, pH 4.0
300 ml blocking buffer.

9. Wash once with 300 ml storage buffer. Filter off until almost dry.

10. Transfer the nearly dry gel with a spatula to a 200-ml bottle for storage. Add 2 vol storage buffer and store at 4°C.

The gel volume should be ~50 ml.

HPLC QUANTIFICATION OF NUCLEOSIDES

SUPPORT PROTOCOL 2

This procedure is used to determine the total number of nucleosides in DNA samples. Taken together with the amount of M_1G in a DNA sample measured in Basic Protocol, the number of adducts per number of nucleosides can be determined. This method of DNA quantification is more accurate than simply relying on UV absorbance measurements. Additionally, the success of the enzymatic hydrolysis is monitored by HPLC analysis of the hydrolysate.

Materials

DNA hydrolysate (see Basic Protocol, step 27)
Solvent A: 50 mM ammonium acetate (pH 6.2), filtered and degassed
Solvent B: acetonitrile, filtered and degassed (solvents filtered with 0.2-µm GH-Polypro membrane; Gelman)
1 mM deoxyribonucleoside mix (see recipe)

4.6 mm × 25 cm octadecylsilyl (Ultrasphere ODS) HPLC column (Beckman)
HPLC system with ultraviolet detector

1. Set up HPLC with a 4.6 mm × 25 cm octadecylsilyl (Ultrasphere ODS) HPLC column.
2. Set up elution gradient with a flow rate of 1 ml/min as follows:

   Maintain at 94% solvent A/6% solvent B for 3 min
   Increase solvent B to 12% from 3 min to 9 min
   Maintain at 12% solvent B until 12 min
   Increase solvent B to 20% from 12 min to 15 min
   Maintain at 20% solvent B until 20 min
   Increase solvent B to 50% from 20 min to 25 min
   Monitor effluent at 254 nm with UV detector, and quantitate peaks

   The elution times for the deoxyribonucleosides should be ~4 min (deoxycytidine), 6 min (deoxyguanosine), 9 min (deoxythymidine), and 11 min (deoxyadenosine)
3. Inject 20 µl of hydrolysate collected in the Basic Protocol, step 27.
4. Make serial dilutions of the 1 mM deoxyribonucleoside mix (from 0.062 mM to 1.0 mM) in water. Repeat HPLC analysis using 20-µl injections of each dilution.

   Use this standard curve to quantify nucleosides in DNA samples.
5. Determine frequency of adducts per nucleoside:

   adducts (M_1G from GC/MS assay) ÷ number of nucleosides (from HPLC)

REAGENTS AND SOLUTIONS

*Use Nanopure water or equivalent for all recipes and protocol steps. For common stock solutions, see **APPENDIX 2A**; for suppliers, see **SUPPLIERS APPENDIX**.*

Anti-oxidant MOPS buffer

Prepare 1 liter of 50 mM MOPS buffer, pH 7.8. Add 200 ml of 0.05 M butylated hydroxyanisole in ethanol. Add 4 ml of 10 mM indomethacin in ethanol. Store up to 1 month at at 4°C.

Deoxyribonucleoside mix, 1 mM each

Prepare ~10 mM solutions of each deoxynucleoside and determine actual concentrations by UV using the following extinction coefficients:

deoxycytidine (ε_{272} = 8300 $M^{-1}\cdot cm^{-1}$)
deoxyguanosine (ε_{254} = 13,600 $M^{-1}\cdot cm^{-1}$)
deoxythymidine (ε_{268} = 9700 $M^{-1}\cdot cm^{-1}$)
deoxyadenosine (ε_{260} = 14,900 $M^{-1}\cdot cm^{-1}$)

Prepare a solution containing 1 mM of all four nucleosides. Store up to 1 year at –20°C.

Derivatized deuterated standard

Derivatize 480 ng [$^2D_2$]M_1G-dR, as described in the Basic Protocol, starting with the formic acid hydrolysis step (see Basic Protocol, steps 40 to 44). Dissolve derivatized standard in 1.2 ml anhydrous methanol, vortex vigorously, and divide into 100-µl aliquots in microcentrifuge tubes. Evaporate under reduced pressure. Cap, wrap in Parafilm, and store at −20°C. On day of analysis, redissolve in 100 µl anhydrous methanol to obtain a 0.4 ng/ml solution of PFB-[$^2D_2$]M_1G (assuming 100% yield). Transfer to a sample vial and crimp shut.

Dried standards can be stored ~6 months at −20°C. The redissolved standard can be used for ~10 days if stored at −20°C between injections.

DNase I stock solution

Weigh out 0.0145 mg (1000 U) per sample of deoxyribonuclease I (lyophilized, from bovine pancreas; 68793 U/mg) and add to a 15-ml plastic conical tube (e.g., for <20 samples, use >0.29 mg). Dissolve in 10 mM MOPS/120 mM $MgCl_2$ (pH 7.0) to yield a 2.5 U/ml solution (27.5 ml buffer per mg DNase I). Mix by inversion. Prepare fresh each time.

MOPS/sucrose buffer

Dissolve 125 g of sucrose in anti-oxidant MOPS buffer (see recipe) up to a total volume of 500 ml. Store up to 1 month at 4°C.

Nuclease P1 stock solution

Add 4 ml of water to 5-mg vial of lyophilized nuclease P1 (640 U/mg; Sigma) in two separate aliquots. Transfer to a 15-ml tube. Wash vial with an additional 3 ml water and add this to the 15-ml tube. Divide into 1-ml aliquots and store at −20°C (stable >6 months).

This stock should be 5 mg nuclease P1 in 7 ml total.

PFB-Br derivatization solution

Crush a small amount of dry K_2CO_3 (kept in an oven) using a mortar and pestle. Weigh out 1 to 2 mg of crushed K_2CO_3 and add to a 5-ml glass conical tube. Add 5 ml dry methanol and vortex vigorously for 10 min. Transfer 4.75 ml of this methanol/K_2CO_3 to a 5-ml glass conical tube. Using a 0.5- or 1-ml glass pipet, add 0.25 ml of PFB-Br (Aldrich) to the methanol/K_2CO_3 to make a 5% solution. Use the same pipet to mix by pipetting up and down. Cover remaining PFB-Br with nitrogen, recap, and seal with Parafilm. Prepare fresh each time.

COMMENTARY

Background Information

Malondialdehyde (MDA) is carcinogenic in rats (Spalding, 1988) and mutagenic in bacterial and mammalian cells (Mukai and Goldstein, 1976; Basu and Marnett, 1983; Yau, 1979). It is endogenously produced from peroxidation of polyunsaturated fatty acids (Bernheim et al., 1948; Diczfalusy et al., 1977) and

has long been used as a marker of lipid peroxidation (Janero, 1990). MDA can react with DNA bases to form adducts with dA and dC, but the major product is formed with dG to yield the pyrimidopurinone nucleoside M_1G-dR (Fig. 3.2.1; Seto et al., 1983; Marnett et al., 1986). The M_1G adduct itself has been shown to be mutagenic (Fink et al., 1997). A double-stranded M13 viral vector with M_1G site-specifically incorporated was replicated in *E. coli* to study in vivo mutagenesis of M_1G (Fink et al., 1997). In these experiments M_1G partially blocked replication and had a mutation frequency of 18% when M_1G was used as template. These results show that MDA and its adducts with DNA are potential threats to genome stability and therefore justify experiments quantifying relative adduct levels.

Levels of M_1G have been measured by a variety of techniques, such as ^{32}P postlabeling (Vaca et al., 1995), HPLC/fluorescence detection (Agarwal and Draper, 1992), ELISA (Sevilla et al., 1997), and mass spectrometry (Chaudhary et al., 1994a,b). ^{32}P postlabeling and HPLC/fluorescence detection both rely on co-chromatography with synthetic standards. Measurement by ELISA relies solely on the specificity of the monoclonal antibody. In the GC/MS method described here, there is triple selectivity. First, the immunoaffinity purification step takes advantage of the monoclonal antibody's specificity for M_1G-dR and M_1G-ribose. Secondly, gas chromatography selects for the correct retention time. Finally, the mass spectrometer detects only ions of the correct molecular weight. The wide variety of DNA adducts that are being identified support the need for highly specific assays.

Another problem that potentially plagues ^{32}P postlabeling, HPLC/fluorescence detection, and ELISA is variability in sample loss during analysis. This problem is eliminated in mass spectrometric techniques by use of stable isotope dilution with $[^2D_2]M_1$G-dR (Fig. 3.2.4). At the start of an assay, DNA samples are spiked with a known amount of the stable isotope–labeled internal standard, which at the end can be differentiated by mass spectrometry. In this case, the PFB-M_1G derivative is ionized to M_1G^- (m/z = 186), and the PFB-$[^2D_2]M_1$G is ionized to $[^2D_2]M_1G^-$ (m/z = 188). The ratio of the peak areas will relate to the amount of M_1G-dR in the original sample (Fig. 3.2.5).

Because DNA adducts usually represent fewer than 1 in 10^6 normal bases, assays have to be exquisitely sensitive. Although ^{32}P postlabeling is more sensitive than the method presented here, the limit of detection with the GC/MS technique is 3 adducts per 10^8 bases in 1 mg of DNA or 100 fmol (Rouzere et al., 1997). GC/EC NCI/MS has been used to detect M_1G in human liver (90 adducts/10^8 bases; Chaudhary et al., 1994b), rat liver (50 adducts/10^8 bases; Chaudhary et al., 1994b), and human leukocytes (6 adducts/10^8 bases; Rouzer et al., 1997).

Critical Parameters

Reproducible standard curves, low background, and high signal-to-noise ratio depend on many factors in this fairly complicated assay. There are many steps and therefore many opportunities to compromise results.

The strict use of only glass after the immunoaffinity column step is imperative to keep background noise low. When organic solvents contact plastic, they can leach out trace quantities of plasticizers. These contaminants generate numerous fragments, one of which has a m/z of 186 and co-chromatographs with PFB-M_1G. Therefore, substitution of plastics in this procedure can significantly add to background noise.

One of the biggest threats to sample recovery is hydrolysis of PFB-M_1G by water. Careful

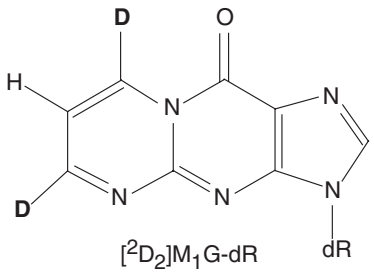

$[^2D_2]M_1$G-dR

Figure 3.2.4 Structure of stable isotope-labeled $[^2D_2]M_1$G-dR.

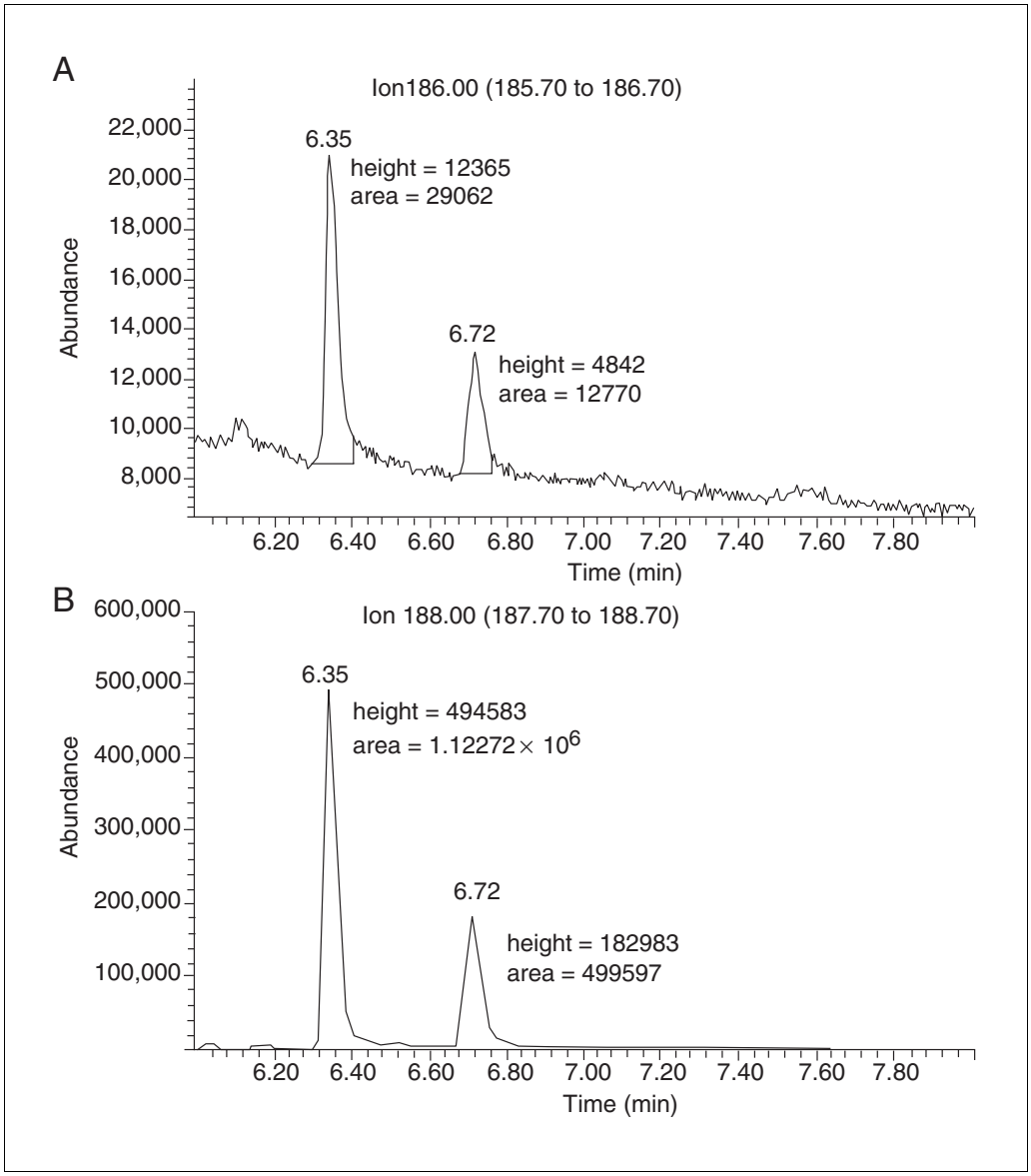

Figure 3.2.5 Selected ion monitoring at 186 for M_1G (**A**) and 188 [$^2D_2$]M_1G (**B**) during GC/MS run. Synthetic standards (340 fmol M_1G-dR and 15 pmol [$^2D_2$]M_1G-dR) were analyzed starting with the immunoaffinity gel purification step.

drying of solvents used during derivatization and solid-phase extraction is crucial in this respect. Furthermore, if samples must be stored as the PFB derivatives, they should be kept in a desiccator or covered with Parafilm.

The most critical step in maintaining high sensitivity and reproducibility is the performance of the GC/MS instrument. The authors have found that the response from stock solutions of derivatized standard varies considerably week to week. The GC interface and mass spectrometer can be very finicky, so regular maintenance is required to ensure optimum performance.

Troubleshooting

In order to ascertain the reliability and linearity of the assay, standard curves using synthetic M_1G-dR are required. If sensitivity is low or if the response is nonlinear, there are several aspects of the procedure that may require particular attention.

During the immunoaffinity step, washing with Nanopure water removes some of the bound analyte from the immunoaffinity gel. Excessive water washing should be avoided to maintain high recovery. In the derivatization step, inadequate nitrogen evaporation of the methanolic PFB-Br solution will yield unreliable results. Because columns and frits for the immunoaffinity and solid-phase extraction are

reused, they must be thoroughly washed between uses.

Poor sensitivity from the GC/MS can be the result of several potential causes. The most common problem is a dirty GC column. Clipping off the first 5 in. of the injector end often dramatically improves sensitivity, but sometimes switching to an entirely new column is warranted. Another common cause of low sensitivity is improper tuning for ions in the 180 mass range. Sensitivity is also highly dependent on the pressure of the chemical ionization

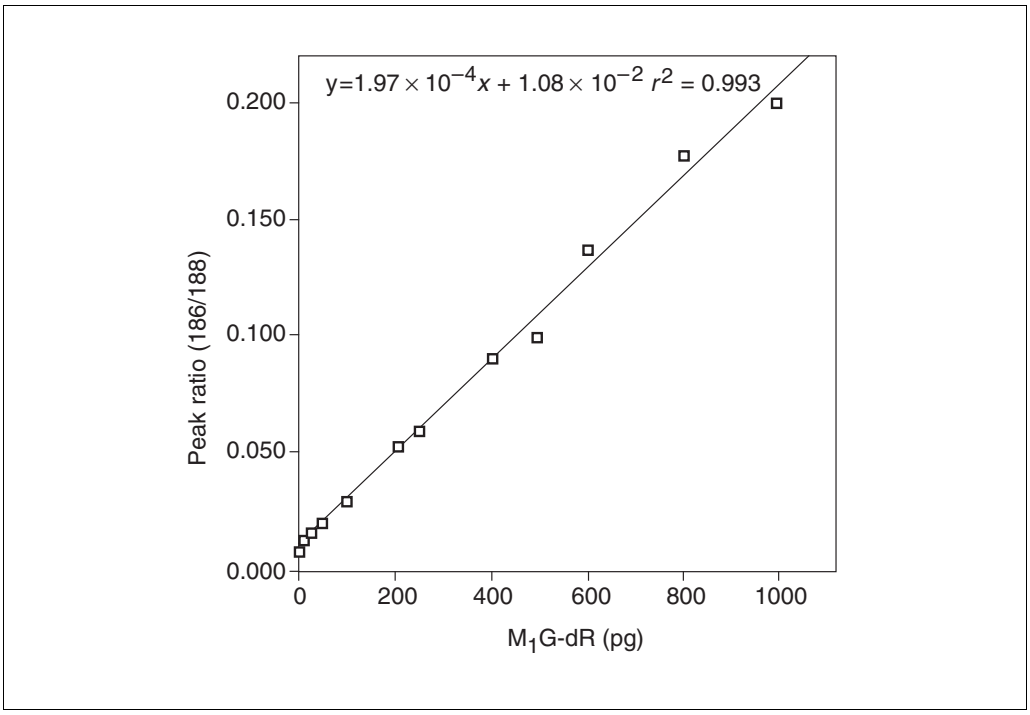

Figure 3.2.6 Standard curve generated by adding indicated amounts of M_1G-dR and a fixed amount of [$^2D_2$]M_1G-dR to immunoaffinity gel.

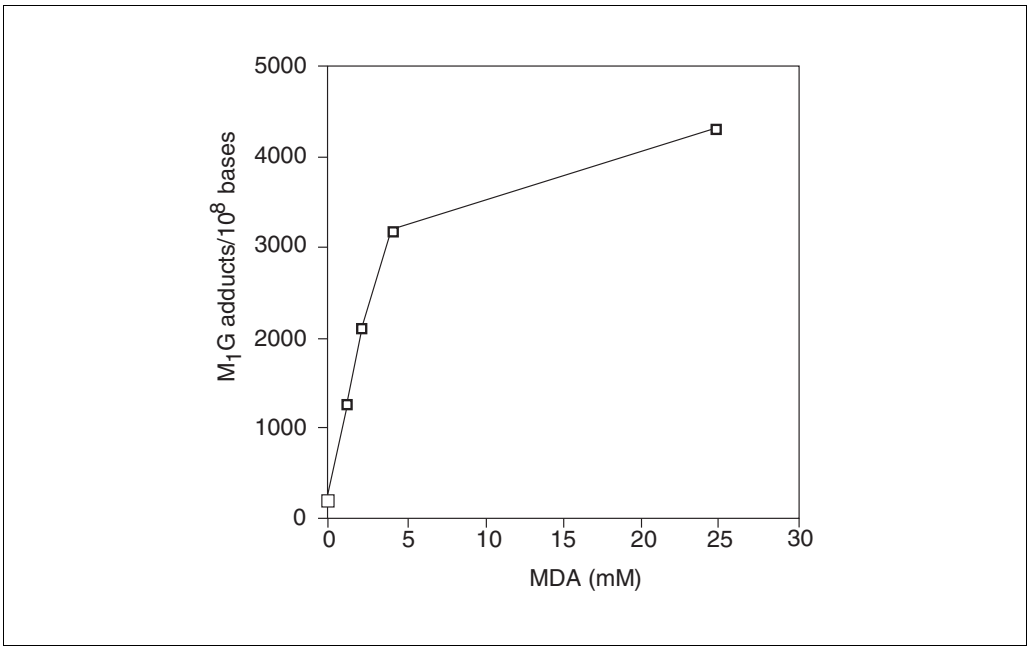

Figure 3.2.7 Calf thymus DNA was treated with indicated concentrations of malondialdehyde sodium salt and incubated at 37°C for 24 hr in 50 mM potassium phosphate buffer, pH 7.4. Adduct levels were determined by GC/MS assay and total number of bases was determined by HPLC/UV assay.

gas. Inefficient ionization can also result from a dirty or inadequately evacuated ion source. Often sensitivity improves when the instrument is allowed to equilibrate several hours to ensure thorough evacuation.

Anticipated Results

The GC/MS trace monitoring at *m/*z of 186 and 188 for an injection of 340 fmol M_1G-dR and 15 pmol [$^2D_2$]M_1G-dR taken through the derivatization procedure is shown in Fig. 3.2.5. If the signal-to-noise ratio is less than 5:1, results should be interpreted cautiously. A standard curve prepared by adding various amounts of M_1G-dR and a fixed amount of [$^2D_2$]M_1G-dR starting at the immunoaffinity step is shown in Figure 3.2.6. If calf thymus DNA is treated with various concentrations of MDA, the number of adducts per 10^8 normal bases is shown in Figure 3.2.7.

Time Considerations

Starting with isolated DNA, the overall assay takes 3 days. DNA hydrolysis and immunoaffinity column purification takes 12 to 14 hr. Formic acid hydrolysis and derivatization takes 10 to 12 hr. Setting up the instrument for the GC/MS analysis takes ~3 hr and each sample injection takes requires 12 to 15 min. Analysis of more than 24 samples in a batch becomes difficult.

Literature Cited

Agarwal, S. and Draper, H.H. 1992. Isolation of a malondialdehyde-deoxyguanosine adduct from rat liver DNA. *Free Radical Biol. Med.* 13:695-699.

Basu, A.K. and Marnett, L.J. 1983. Unequivocal demonstration that malondialdehyde is a mutagen. *Carcinogenesis* 4:331-333.

Bernheim, F., Bernheim, M.L.C., and Wilbur, K.M. 1948. The reaction between thiobarbituric acid and the oxidation products of certain lipids. *J. Biol. Chem.* 174:257-264.

Chaudhary, A.K., Nokubo, M., Marnett, L.J., and Blair, I.A. 1994a. Analysis of the malondialdehyde-2′-deoxyguanosine adduct in rat liver DNA by gas chromatography/electron capture negative chemical ionization mass spectrometry. *Biol. Mass Spectrom.* 23:457-464.

Chaudhary, A.K., Nokubo, M., Reddy, G.R., Yeola, S.N., Morrow, J.D., Blair, I.A., and Marnett, L.J. 1994b. Detection of endogenous malondialdehyde-deoxyguanosine adducts in human liver. *Science* 265:1580-1582.

Diczfalusy, U., Falardeau, P., and Hammarstrom, S. 1977. Conversion of prostaglandin endoperoxides to C17-hydroxyacids by human platelet thromboxane synthase. *FEBS Letts.* 84:271-274.

Fink, S.P., Reddy, G.R., and Marnett, L.J. 1997. Mutagenicity in *Escherichia coli* of the major DNA adduct derived from the endogenous mutagen malondialdehyde. *Proc. Natl. Acad. Sci. U.S.A.* 94:8652-8657.

Janero, D.R. 1990. Malondialdehyde and thiobarbituric acid reactivity as diagnostic indices of lipid peroxidation and peroxidative tissue injury. *Free Radical Biol. Med.* 9:515-540.

Marnett, L.J., Basu, A.K., O'Hara, S.M., Weller, P.E., Rahman, A.F.M.M., and Oliver, J.P. 1986. Reaction of malondialdehyde with guanine nucleosides: Formation of adducts containing oxadiazabicyclononene residues in the base-pairing region. *J. Am. Chem. Soc.* 108:1348-1350.

Mukai, F.H. and Goldstein, B.D. 1976. Mutagenicity of malondialdehyde, a decomposition product of peroxidized polyunsaturated fatty acids. *Science* 191:868-869.

Rouzer, C.A., Chaudhary, A.K., Nokubo, M., Ferguson, D.M., Reddy, G.R., Blair, I.A., and Marnett, L.J. 1997. Analysis of the malondialdehyde-2'-deoxyguanosine adduct, pyrimidopurinone, in human leukocyte DNA by gas chromatography/electron capture negative chemical ionization/mass spectrometry. *Chem. Res. Toxicol.* 10:181-188.

Seto, H., Okuda, T., Takesue, T., and Ikemura, T. 1983. Reaction of malondialdehyde with nucleic acid. I. Formation of fluorescent pyrimido[1,2-a]purin-10(^{3}H)-one nucleosides. *Bull. Chem. Soc. Jpn.* 56:1799-1802.

Sevilla, C.L., Mahle, N.H., Eliezer, N., Uzieblo, A., O'Hara, S.M., Nokubo, M., Miller, R., Rouzer, C.A., and Marnett, L.J. 1997. Development of monoclonal antibodies to the malondialdehyde-deoxyguanosine adduct, pyrimidopurinone. *Chem. Res. Toxicol.* 10:172-180.

Spalding, J.W. 1988. Toxicology and carcinogenesis studies of malondialdehyde sodium salt (3-hydroxy-2-propenal, sodium salt) in F344/N rats and B6C3F1 mice. *NTP Technical Report* 331:5-13.

Vaca, C.E., Fang, J-L., Mutanen, M., and Valsta, L. 1995. ^{32}P postlabeling determination of DNA adducts of malonaldehyde in humans: Total white blood cells and breast tissue. *Carcinogenesis* 16:1847-1851.

Yau, T.M. 1979. Mutagenicity and cytotoxicity of malondialdehyde in mammalian cells. *Mech. Ageing Dev.* 11:137-144.

Key References

Rouzer et al., 1997. See above.

Original publication of GC/MS assay employing immunoaffinity chromatography step as well as measurement of adduct levels in human leukocyte DNA.

Sevilla et al., 1997. See above.

Description of anti-M_1G monoclonal antibody.

Contributed by John P. Plastaras and Lawrence J. Marnett
Vanderbilt University
Nashville, Tennessee

Mutagenesis Assays in Mammalian Cells

Mutation assays using cultured mammalian cells can provide valuable information regarding the potential mutagenic and carcinogenic activities of chemicals. Due to the differences in genome organization and genetic complexity, mammalian cells are used to complement microbial assays in genetic toxicology studies (*UNIT 3.1*). A variety of mammalian target genes (e.g., *hprt, aprt, tk*) can be analyzed in several well validated assays (Aaron et al., 1994); however, one of the most commonly employed selective systems measures mutations in the *hprt* gene encoding the salvage pathway enzyme hypoxanthine-guanine phosphoribosyl transferase (HPRT). The toxic purine analog 6-thioguanine (6-TG), is used to select *hprt* gene mutants. The following protocol describes mutagenesis assays using the Chinese hamster V79 cell line, as well as an analogous assay using the V79 derivative *hgprt*$^-$/*gpt*$^+$ G12 cell line. The G12 cell line contains an insertion of the *E. coli* xanthine guanine phosphoribosyl transferase (*gpt*) gene, a functional equivalent of the mammalian *hprt* gene. The G12 assays detect large deletions and epigenetic DNA methylation events, as well as point and small intragenic mutations that can also be detected in the standard V79 assays.

MUTAGENESIS ASSAYS IN THE V79 AND DERIVED TRANSGENIC HPRT$^-$/GPT$^+$ V79 CELL LINES

BASIC PROTOCOL

In this assay, a large population of cells (V79 or G12) is exposed to the test substance for a defined period of time. After the treatment, the cells are cultured for 6 to 8 days for the depletion of residual HPRT or GPT protein and mRNA, which is referred to as the "expression period." The cells are then plated in medium containing a selective agent, 6-thioguanine (6-TG). Only cells that have inactive HPRT enzyme (V79 cells) or mutated/silenced *gpt* gene (G12 cells) will survive and give rise to 6-thioguanine–resistant colonies. For routine mutagenesis assays, use of V79 is sufficient. For test chemicals that may affect DNA methylation and lead to gene silencing, the G12 line is specifically informative because this cell line detects both mutagenic (e.g., mutations and deletions) and epigenetic (DNA methylation) changes.

NOTE: All solutions and equipment coming into contact with living cells must be sterile, and aseptic technique should be used accordingly.

NOTE: All culture incubations should be performed in a humidified 37°C, 5% CO_2 incubator unless otherwise specified.

Materials

V79 cells (ATCC CCl-93) *or* G12 cells (C. Klein, NYU School of Medicine)
F-12 medium/5% FBS (see recipe)
F-12/HAT medium (see recipe)
Physiological buffer, 37°C: Earle's balanced salt solution (EBSS; Life Technologies), phosphate-buffered saline (PBS; *APPENDIX 2A*), or HEPES-buffered saline (Life Technologies)
Substance to be tested for mutagenicity
F-12 medium/5% FBS (see recipe) containing 10 μg/ml 6-thioguanine (6-TG; freshly added)

80-cm^2 tissue culture flasks
100-mm and 60-mm tissue culture dishes

Additional reagents and equipment for toxicity assay (see Support Protocol 1) and Giemsa staining (see Support Protocol 2)

Contributed by Catherine B. Klein, Limor Broday, and Max Costa
Current Protocols in Toxicology (1999) 3.3.1-3.3.7

Grow the cells

1. Grow G12 or V79 cells in F-12 medium/5% FBS in 80-cm^2 tissue culture clasks, passaging every 3 to 5 days.

   Fresh cell cultures are initiated from frozen stocks every 6 weeks.

For G12 cells

2a. Three to four days before the mutagen treatment, seed 5×10^5 G12 cells in a 80-cm^2 tissue culture flask with 10 ml F-12/HAT medium.

   The G12 cultures are supplemented with HAT to maintain a low spontaneous mutant frequency.

3a. At least 24 hr before the mutagen treatment, remove the HAT medium (do not trypsinize the cells), wash the G12 cells with suitable 37°C physiological buffer (EBSS, PBS, HEPES-buffed saline), and feed with complete F-12 medium/5% FBS.

   The cells are removed from HAT selection one day prior to the beginning of each G12 mutagenesis experiment, and HAT is never present during mutagen treatment, or during mutant expression and selection.

For V79 cells

2b. Do not passage in F-12/HAT medium; continue growing in F-12 medium/5% FBS.

   V79 cells are not routinely pretreated with HAT, due to their inherent low spontaneous-mutant frequency.

3b. Feed V79 cells with fresh F-12/5% FBS 24 hr before mutagen treatment.

Mutagenize V79 or G12 cells with the desired test agent

4. At least 3 to 4 hr before the treatment, trypsinize the V79 or G12 cells and seed them for attachment at a density of 10^5 cells per 100-mm dish in F-12 medium/5% FBS. Use two dishes per mutagenic treatment. Incubate at 37°C for 3 to 4 hr to allow cell attachment. Establish a concurrent toxicity assay at this time (see Support Protocol 1).

   Trypsinization should be kept as short as possible (1 to 3 min at room temperature), until it is observed that the cells are detached from the vessel. Overtrypsinization will make the cells sticky.

5. After V79 or G12 cell attachment, remove the medium and gently rinse the cells with physiological buffer to remove adherent medium/serum.

   Be careful not to dislodge the weakly attached cells.

6. Add the test agent to the V79 or G12 cells in any appropriate buffer or medium, for the time and concentration determined by the preliminary toxicity assay (see Support Protocol 1).

7. At the end of the treatment, rinse the cells gently again with physiological buffer, and overlay with 10 ml fresh F-12 medium/5% FBS.

   Be careful not to aspirate agents of environmental concern into the general-use vacuum flasks. Radioactive or carcinogenic solutions must be removed to isolated containers or bottles for regulated disposal. Treatment pipets and tips must also be separated for proper disposal.

8. Allow cells to grow for 7 days ("expression period"), supplying the cells with fresh F-12/5% FBS every three days.

Select for 6-TG-resistant cells

9. Following the 7-day expression period, reseed 2×10^6 mutagenized V79 or G12 cells per treatment into F-12 medium/5% FBS containing 10 µg/ml 6-thioguanine (6-TG), at a maximum cell density of 2×10^5 cells/100-mm dish (usually 10 dishes/dose). Incubate 10 to 14 days, allowing the 6-TG-resistant mutant clones to become macroscopic. During this period, supply the cells with fresh F-12/5% FBS/6-TG every 3 to 4 days.
10. In addition, seed 300 mutagenized cells per treatment, in triplicate, in 60-mm dishes with 4 to 5 ml nonselective (plain) F-12 medium/5% FBS. Incubate these reseeding plating efficiency dishes for 1 week. Score the plates by staining with Giemsa (see Support Protocol 2) and determine the plating efficiency.

    The reseeding plating efficiency in nonselective medium (F-12) is determined for use in the mutant frequency calculations.

11. Giemsa stain (see Support Protocol 2) and score the mutant cells from the plates prepared in step 9. Alternatively, isolate individual (unstained) mutant colonies for molecular characterization of the mutations that occurred.

    If it is desirable to isolate numerous 6-TG-resistant cells for further molecular analysis, a modified cell treatment and reseeding protocol is followed to ensure that the subsequently isolated mutant colonies originated from separate populations of mutagenized parental cells. In order to collect a large number of independent mutants, 30 replicate cultures are seeded in a 6-well plate format, and each well is treated and reseeded individually (as per Klein et al., 1997). This ensures the exclusion of sibling mutants in the molecular studies.

12. Calculate mutant frequency (MF) as the total number of mutants counted on all mutation plates divided by the number of cells seeded (usually 2×10^6 cells) corrected by the reseeding plating efficiency.

TOXICITY ASSAY

SUPPORT PROTOCOL 1

Prior to mutagenicity assays toxicity/cell viability tests should be conducted. In the following assay, attached cells are exposed in situ to the test agent and then screened for clonal survival.

For reagents and equipment, see Basic Protocol.

1. Prepare V79 or G12 cells (see Basic Protocol, steps 1 to 3, a or b).
2. At least 3 to 4 hr before treatment, seed dispersed single-cell suspensions of V79 or G12 cells for attachment into labeled tissue culture dishes, three dishes per dose or control (also see Basic Protocol, step 4).

    Typical seeding densities can be 200 to 300 cells per 60-mm dish or 500 to 1000 cells per 100-mm dish. Cells can be seeded at different densities according to estimated toxicity. Always include untreated and solvent controls.

3. After cell attachment, remove the medium and gently rinse the cells with buffer to remove adherent medium/serum.
4. Add the toxicant in any appropriate buffer or medium for a given period of time, depending upon the mode and efficiency of cellular uptake.

    Short treatments in buffer are preferred, but these cannot successfully exceed 3 hr in length because the cells will detach. For studies requiring stringent pH levels during treatment, HEPES-buffered saline is preferred. For longer treatments, serum-free medium is appropriate for up to 24 hr. Initial testing is suggested to cover several orders of magnitude in dose (e.g., 10^{-4} to 10^{-7} M).

5. At the end of the treatment, rinse the cells gently again with buffer and overlay with fresh F-12 medium/5% FBS (usually 4 to 5 ml per 60-mm dish and 7 to 10 ml per 100-mm dish).

   See Basic Protocol, step 7, for disposal precautions.

6. Incubate plates at 37°C for 1 week, and stain plates with Giemsa on the seventh day (see Support Protocol 2).
7. Count the clones on all plates and average for each triplicate dose set. Determine the cloning efficiency (average number of colonies scored per number of cells seeded) and percent survival relative to the control.

SUPPORT PROTOCOL 2

GIEMSA STAINING

The V79 and V79-derived G12 cells stain very well in a one-step protocol with a working solution of 50% Giemsa/50:50 (v/v) methanol.

Materials

Plates to be stained (Basic Protocol or Support Protocol 1)
Giemsa stain (see recipe)

1. Remove medium from plates. Add ~5 ml/100-mm dish or ~3 ml/60-mm dish of Giemsa stain and wait 5 to 10 min.

   The cells are fixed by the methanol and stained simultaneously. Since the working stain solution is reutilized for several weeks, be sure that the staining solution has adequate methanol content by testing one dish in advance. If the methanol content has become inadequate, the cell clones will not be fixed to the dish and will be lost by the rinsing procedure. The working stain solution can occasionally be resupplemented with methanol (e.g., every 2 to 4 weeks) to compensate for depletion of the methanol that occurs by evaporation during use.

2. Pour the staining solution back into the bottle.

   The staining solution may be reused for 2 to 3 months, until the Giemsa stain becomes depleted. Giemsa stain depletion will become evident by lightening of the stained cell clones over several weeks of recycled stain use.

3. Rinse the stained plates gently by dipping the plates into a water-filled container. Invert the plates to dry.

REAGENTS AND SOLUTIONS

*Use Milli-Q-purified water or equivalent in all recipes and protocol steps. For common stock solutions, see **APPENDIX 2A**; for suppliers, see **SUPPLIERS APPENDIX**.*

F-12/HAT medium

F/12 medium/5% FBS (see recipe below) supplemented with:
100 µM hypoxanthine
1 µM aminopterin
100 µM thymidine
Prepare fresh as needed

F-12 medium/5% FBS

F-12 medium (Life Technologies) containing:
5% (v/v) fetal bovine serum
2 mM glutamine
1% (w/v) 10,000 U penicillin G/10,000 µg/ml streptomycin (Life Technologies)
Store up to 2 to 3 weeks at 4°C

Unsupplemented F-12 medium (i.e., without FBS, antiobiotics, and glutamine) can be stored 4 to 6 months at 4°C. Typically, FBS, antibiotics, and glutamine are added to one or more bottles of F-12 medium to make enough complete medium for use in a given week. It is useful to aliquot a 500-ml bottle of FBS into ten 50-ml aliquots that are stored frozen until use.

Giemsa stain

2 g Giemsa stain
132 ml methanol
138 ml glycerol

Keep in dark for 3 days, then filter through Whatman no. 1 filter paper and carefully pour into a new dark bottle. Store at room temperature.

COMMENTARY

Background Information

Mammalian systems for studying gene mutations include a variety of well characterized rodent cell assays to evaluate endogenous (e.g., *hprt, tk, aprt*) or transgenic gene targets in vitro and in vivo (Li et al., 1991; Aaron et al., 1994). A mammalian cell mutagenicity assay that measures the mutation rate of the *hprt* gene, which encodes the salvage-pathway enzyme hypoxanthine-guanine phosphoribosyl transferase (HPRT), is frequently employed. This enzyme catalyzes the formation of inosine or guanosine monophosphate from hypoxanthine or guanine, using 5-phosphoribosyl-1-pyrophosphate as the phosphate donor. Since the *hprt* gene is carried on the X chromosome, a single copy of the gene is present in males and expressed in females, thus greatly facilitating the detection of those cells that have an inactivating mutation in the gene (Caskey and Kruh, 1979). This allows *hprt* mutagenesis assays to also be applied to human cells. The experimental cell lines most widely used for *hprt* mutation assays are female Chinese hamster ovary (CHO) cells and male Chinese hamster lung fibroblasts (V79). After treatment of the cultured cells with a potential chemical mutagen, the cells are subcultured for 6 to 8 days so that depletion of residual HPRT protein and mRNA occurs. The cells are then plated in medium containing a selective agent, 6-thioguanine (6-TG). The HPRT enzyme forms a toxic metabolite, 6-thioguanine monophosphate from this substrate; thus only cells that have inactivated HPRT will survive and form colonies. Since a functional enzyme is not essential for DNA synthesis, 6-TG-resistant mutants may arise through base-pair substitution, frameshift mutation, or deletion in the *hprt* gene.

In order to enhance the sensitivity of this system, derivative V79 cell lines (G12 and G10) were developed (Klein and Rossman, 1990; Klein et al., 1994). These cell lines are *hprt*$^-$ mutant cell lines that contain an insertion of the functionally analogous *E. coli gpt* gene. An analogous *gpt*$^+$ transgenic cell line, CHO-AS52, has also been derived from *hprt*$^-$ CHO cells (Tindall et al., 1986; Aaron and Stankowski, 1989). The *gpt* transgenic G12 and G10 cell lines have the same phenotype (6-TG sensitivity) as the parental V79 wild-type cells and can be used to measure forward mutations yielding 6-TG resistance in the standard V79 protocol. In contrast to the mammalian *hprt* gene, the bacterial *gpt* gene target is uninterrupted by introns, and therefore is easier to examine for molecular alterations. Like the V79 *hprt* assay, the G12 and G10 assays detect a broad spectrum of gene deletions, frameshift mutations, and point mutations. However, the mutant frequency observed for the G12 and G10 cell lines is significantly higher than that at the *hprt* gene in V79 cells (Klein and Rossman, 1990; Klein et al., 1994, 1997). An added advantage of the G12 cell line is its well characterized ability to score epigenetic gene-silencing events that can occur by hypermethylation of the promotor and proximal *gpt* sequence following treatment with some test agents (Lee et al., 1995; Klein and Costa, 1997).

The V79 cells and V79-derived *gpt*$^+$ transgenic cell lines, G12 and G10, are anchorage-dependent, fetal male Chinese hamster lung fibroblast cells. The doubling time of these cell lines is between 12 to 13 hr. A stable *gpt* locus is carried at a single integration site in the Chinese hamster genome in G12 and G10 cells. The integration site is different in the G12 and G10 cell lines, and therefore the mutability of their target gene (*gpt*) is not identical. This permits the study of genome location–dependent mutagenesis from a mechanistic point of view (Kargacin et al., 1993; Klein et al., 1994, 1997; Lee et al., 1995).

The mutagenesis protocols described above are according to Klein and Rossman (1990) and

Klein at al. (1994). 6-TG-resistant mutants are isolated according to a modified replating technique published by Chang et al. (1978). Mutant frequency is expressed as 6-TG-resistant mutants per 10^6 viable cells. This is calculated by dividing the number of mutant colonies (per 10^6 cells plated) by the reseeding cloning efficiency of each treated population. The reseeding cloning efficiency is the number of colonies formed per 300 cells plated in nonselective medium.

When individual mutant clones are isolated, it is also possible to perform reversion assays using either the V79 or G12 cells (described in Stone-Wolf et al., 1985; Lee et al., 1995). Reversion assays, which detect re-expression of the previously mutated or silenced gene in HAT selection media, are especially useful for the detection of epigenetic mutations using the G12 cells.

Critical Parameters

Prior to commencing any mutagenesis assay, the toxicity of the agent must be assessed. Although several toxicity assay protocols are available, the in situ exposure of attached cells followed by clonal growth for a week is usually sufficiently informative. It is then possible to choose the experimental doses and conditions for the mutagenesis assay. The usual working doses in mammalian mutagenesis assays are chosen to yield a cell survival range of 30% to 80%.

The V79 and derived transgenic cell lines proliferate with a typical growth curve that exhibits a growth delay (lag time) after trypsinization or manipulation, followed by log phase growth for several generations and a growth plateau as the growth area becomes limited. The V79 and derived cells will, however, pack very tightly in the growth vessel and will often overgrow each other, forming sporadic foci. The cells are not sensitive to low seeding density and will eventually grow back with time from any diluted culture (even as low as a 1:20 split of a confluent flask). The cells are never trypsinized two days consecutively. Because of the regular and predictable growth of these cells, it is easy to plan ahead so that trypsinization the day before a planned experiment is avoided. It is essential that the trypsinized cells not be clumped at the time of experimental seeding, since individual single cells must be treated. V79 cells are prone to clumping under two conditions: if kept for more than a few minutes at $>10^6$ cells/ml suspension, or if made sticky by excessive trypsinization. The cells are also not sensitive to minor changes in temperature. The anchored growth of these cells is, however, sensitive to pH, atmospheric CO_2, and certain test agents, including some metals.

Anticipated Results

In the preliminary toxicity assay, the examined doses, length of treatment, and medium of treatment should include conditions ranging from the "no effect" dose level up to 10% cell viability.

If the chemical tested induced a mutagenic response, the mutation frequencies following the mutagenesis assay will be higher than the spontaneous levels. For the endogenous *hprt* gene, the spontaneous mutant frequency is ~1 $\times$ 10^{-6} surviving cells. For the V79-derived transgenic cell lines, the spontaneous mutant frequencies are 30×10^{-6} and 100×10^{-6} for G12 and G10 cells, respectively (Klein and Rossman, 1990, Klein et al., 1994). There should be an absolute increase in the number of mutants at least at some doses of the examined agent. One criterion for defining a positive mutagenic response (Cole and Arlett, 1984) is a statistically significant, reproducible dose-response curve with increases in the calculated mutant frequency per survivor of >10× the control value at one or more doses. Smaller increases in mutant frequency can be equally valid pending appropriate statistical testing (e.g., χ^2 analysis).

Time Considerations

The time required to complete one full V79 or G12 toxicity/mutagenesis assay is 4 weeks: one week for the initial toxicity assay and 3 weeks for the complete mutagenesis assay. From a practical perspective, individual concurrent experiments are initiated on a staggered weekly or biweekly schedule, if sufficient incubator space and technical support is available.

Literature Cited

Aaron, C.S. and Stankowski, L.F., Jr. 1989. Comparison of the AS52/XPRT and the CHO/HPRT assays: Evaluation of 6 drug candidates. *Mutat. Res.* 223:121-128.

Aaron, C.S., Bolcsfoldi, G., Glatt, H.R., Moore, M., Nishi, Y., Stankowski, L., Theiss, J., and Thompson, E. 1994. Mammalian cell gene mutation assays working group report. *Mutat. Res.* 312:235-239.

Caskey, C.T. and Kruh, G.D. 1979. The HPRT locus. *Cell* 16:1-9.

Chang, C.C., Castellazzi, M., Glover, T.W., and Trosko, J.E. 1978. Effects of harmon and norhar-

mon on spontaneous and ultraviolet light-induced mutagenesis in cultures Chinese hamster cells. *Cancer Res.* 38:4527-4533.

Cole, J. and Arlett, C.F. 1984. The detection of gene mutations in cultured mammalian cells. *In* Mutagenicity Testing (S. Venitt and J.M. Parry, eds.) pp. 233-273. IRL Press, Oxford.

Kargacin, B., Klein, C.B., and Costa, M. 1993. Mutagenic responses of nickel oxides and nickel sulfides in Chinese hamster V79 cell lines at the xanthine-guanine phosphoribosyl transferase locus. *Mutat. Res.* 300:63-72.

Klein, C.B. and Costa, M. 1997. DNA methylation, heterochromatin and epigenetic carcinogens. *Mutat. Res.* 386:163-180.

Klein, C.B. and Rossman, T.G. 1990. Transgenic Chinese hamster V79 cell lines which exhibit variable levels of *gpt* mutagenesis. *Environ. Mol. Mutagen.* 16:1-12.

Klein, C.B., Su, L., Rossman, T.G., and Snow, E.T. 1994. Transgenic gpt^+ V79 cell lines differ in their mutagenic response to clastogens. *Mutat. Res.* 304:217-228.

Klein, C.B., Su, L., Singh, J.T., and Snow, E.T. 1997. Characterization of gpt^- deletion mutations in transgenic Chinese hamster cell lines. *Environ. Mol. Mutagen.* 30:418-428.

Lee, Y.W., Klein, C.B., Kargacin, K., Salnikow, K., Kitahara, J., Dowjat, K., Zhitkovich, A., Christie, N.T., and Costa, M. 1995. Carcinogenic nickel silences gene expression by chromatin condensation and DNA methylation: A new model for epigenetic carcinogens. *Mol. Cell. Biol.* 15:2547-255.

Li, A.P., Aaron, C.S., Auletta, A.E., Dearfield, K.L., Riddle, J.C., Slesinski, R.S., and Stankowski, L.F., Jr. 1991. An evaluation of the roles of mammalian cell mutation assays in testing of chemical genotoxicity. *Regul. Toxicol. Pharmacol.* 14:24-40.

Stone-Wolf, D.S., Klein, C.B., and Rossman, T.G. 1985. HPRT–mutants of V79 cells that revert specifically by base pair substitution and frameshift mutations. *Environ. Mutagen.* 7:281-291.

Tindall, K.R., Stankowski, L.F., Jr., Machanoff, R., and Hsie, A.W. 1986. Analyses of mutation in pSV2gpt-transformed CHO cells. *Mutat. Res.* 160:121-131.

Contributed by Catherine B. Klein, Limor Broday, and Max Costa
New York University School of Medicine
New York, New York

Cell Transformation Assays

In vitro mammalian cell transformation assays have been widely used to test chemical and physical agents for the ability to induce morphological transformation (IARC/NCI/EPA Working Group, 1985; Kerckaert et al., 1996a). Morphologically transformed cells are characterized by the loss of density-dependent regulation of growth and the formation of colonies with crisscrossed cells or foci of piled-up cells that are not observed in untreated controls (Evans and DiPaulo, 1981). Because of the biological similarities between in vitro cell transformation and in vivo carcinogenesis, cell transformation assays are used routinely to screen chemicals for carcinogenic potential and to study the mechanisms of known carcinogens. Morphologically transformed cells are further tested for neoplastic characteristics, including the ability to form three-dimensional colonies in soft agar and/or the ability to induce tumor formation in immunosuppressed (e.g., "nude") mice (Costa, 1980).

Cell transformation assays most frequently employ freshly isolated cells from rodents, such as Syrian hamster embryos (SHE; Berwald and Sachs, 1965), or use established cultured cell lines, such as the mouse BALB/c-3T3 (Kakunaga, 1973) or C3H/10T1/2 (Reznikoff et al., 1973) cell lines. The Basic Protocol describes the establishment of primary SHE cell cultures and their use in a cell transformation assay for testing putative carcinogens. The methods are based upon those described by Costa (1980). SHE cells are diploid and genetically stable, have a finite lifespan, and are capable of metabolizing many procarcinogens to their ultimate carcinogenic form (Kerckaert et al., 1996a). They also have a low spontaneous rate of transformation. Cell lines are sometimes preferred because they are convenient and because scoring morphological transformation is often easier than with SHE cells (Rundell, 1984). However, investigators should be aware that cell lines are immortal and, as such, may already partially exhibit transformed characteristics, whereas untreated SHE cells normally do not (Costa, 1980). Guidelines regarding the use of SHE, C3H/10T1/2, and BALB/c-3T3 cells have been reviewed by Dunkel et al. (1991).

NOTE: All solutions and equipment coming into contact with living cells must be sterile, and aseptic technique should be used accordingly.

NOTE: All culture incubations should be performed in a humidified 37°C, 5% CO_2 incubator unless otherwise specified.

NOTE: All protocols using live animals must first be reviewed and approved by an Institutional Animal Care and Use Committee (IACUC) or must conform to governmental regulations regarding the care and use of laboratory animals.

Materials

Pregnant Golden Syrian hamsters
Chinese hamster ovary (CHO; ATCC)
Disinfectant solution: e.g., 2% (v/v) Orsyl
95% (v/v) ethanol
Serum-free Dulbecco's minimal essential medium (DMEM)
0.5% (w/v) trypsin solution in normal saline A
Fetal bovine serum (FBS; tested in cell culture)
Complete DMEM supplemented with 10% (v/v) FBS
Normal saline A (see recipe)
Dimethyl sulfoxide (DMSO) or glycerol
Complete DMEM supplemented with 20% (v/v) FBS
F-12 medium supplemented with 10% (v/v) FBS

Contributed by Max Costa and Jessica E. Sutherland
Current Protocols in Toxicology (1999) 3.4.1-3.4.9

Test agent
0.5% (w/v) crystal violet solution in 95% ethanol
Positive and negative control agents
Serum-free F-12 medium

Absorbant cloth, sterile
Laminar flow hood
Dissecting instruments
100-mm tissue culture plates, sterile
10-ml pipets, sterile
Freezing vials for storing cells
150-ml beakers
Inverted tissue culture microscope

Additional reagents and equipment for sacrificing animals (*APPENDIX 3*), for counting cells with a Coulter counter or hemacytometer (*APPENDIX 3*), and for trypan blue exclusion (*APPENDIX 3*)

Harvest hamster embryos

1. Obtain pregnant Golden Syrian hamsters on day 13 of gestation.

   The Syrian hamster embryo system is the preferred system because it has been claimed that these cells have a low incidence of spontaneous transformation (Trott et al., 1995).

   The 13th day of gestation is the optimal time to harvest embryos; however, cells from 12-or 14-day-old embryos can also be isolated for tissue culture.

   Pregnant hamsters can be obtained from commercial sources. Alternatively, they can be bred, but this is not recommended unless one has experience with breeding hamsters.

2. Sacrifice the hamster by CO_2 asphyxiation and immediately immerse in a disinfectant solution for a few seconds.

   Animals can be sacrificed by CO_2 asphyxiation by placing them in a glass dessicator (or large glass jar with lid) connected to a CO_2 tank by a hose or tubing.

3. Place the animal on an absorbent sterile cloth in a sterile laminar flow hood.

4. Sterilize the dissection tools by dipping them in a 150-ml beaker containing 95% ethanol and igniting the residual alcohol by passing them through a Bunsen burner flame.

5. Lay the hamster on its dorsal side and make an incision in the uterus to expose the embryonic sacs.

6. Using forceps and scissors, carefully remove the embryonic sacs and place them into a sterile 100-mm tissue culture dish.

7. Remove the embryo from each sac, and use the alive ones (as gauged by body movement) for isolation of cells.

   To prevent contamination of the cultures, remove the hamster carcass and dead embryos from the sterile area.

Isolate embryonic cells

8. Wash the embryos twice with 10 ml serum-free DMEM.

9. Transfer the embryos to a fresh 100-mm tissue culture dish containing 10 ml of 0.5% trypsin solution in normal saline A. Mince the embryos with sterile scissors.

10. Disperse into individual cells by repeatedly passing the mixture up and down through a 10-ml sterile pipet. Incubate the cells in the 0.5% trypsin solution for ~30 min.

    After this step, the embryos are reduced either to individual cells or to small clumps of cells.

11. Terminate the action of trypsin by adding 1 ml FBS.

12. Seed 5×10^6 to 1×10^7 cells in 10 ml of complete DMEM-10% FBS into 100-mm tissue culture plates.

    Cellular transformation levels can vary greatly depending upon the source and/or lot of FBS.

Establish a primary cell culture

13. Place the plates in a 37°C incubator with an atmosphere containing 5% CO_2. Incubate for 2 days.

    Cells will attach to the bottom of the plate and form a monolayer.

14. Aspirate the medium and wash cells with fresh complete DMEM-10% FBS.

15. Return plates to the incubator for 1 additional day.

    At this point, the cultures are known as primary cell cultures.

Establish a secondary cell culture

16. Wash the monolayer twice with 10 ml sterile normal saline A and disrupt the monolayer by adding 10 ml of 0.5% trypsin solution in normal saline A. Expose cells to trypsin for ~5 min. Centrifuge the cells for 10 minutes at 500*g*. Aspirate the supernatant and resuspend the cell pellet in 10 ml of fresh complete DMEM-10% FBS.

17. Replate at a density of 5×10^6 cells/100 mm plate in 10 ml complete DMEM-10% FBS. Freeze unused cells (see Step 18).

    At this point, the cells are known as secondary or second-passage cultures. Tertiary or third-passage cultures are prepared by trypsinizing cells from the secondary cultures. All subsequent trypsinization procedures are numbered by the passage giving rise to each culture.

Prepare frozen cell stocks

18. Suspend cells in 20% (v/v) DMSO or 10% (v/v) glycerol in complete DMEM-20% FBS and dispense aliquots into freezing vials. Place the freezing vials in a styrofoam holder and place in a −70°C freezer.

    This allows the cells to freeze slowly. Slow freezing yields high cell viability.

    Third- or fourth-passage cells are probably best for use in testing the carcinogenic activity of a chemical. Freezing a large batch of early passage cells is recommended so that the same batch can be used repeatedly, affording consistency in the cell transformation assay. This also prevents having to isolate cells fresh from experimental animals.

19. When frozen, transfer the vials to liquid nitrogen.

Determine cytotoxicity of test agent

20. Plate 1×10^6 CHO cells in 10 ml complete F12-10% FBS and allow to attach overnight.

The plating efficiency of primary cultures is so low that they are not optimal for determining cytotoxicity. Thus, an established cell line of hamster cells (e.g., CHO cells) should be used to obtain an approximate level of cytotoxicity of the chemical.

21. Expose these cells to the test agent using a broad range of dosages (e.g., 0.1, 0.2, 0.5, 1.0, 5, and 10 µg/ml) in order to establish an appropriate dosing regimen (i.e., low dose yields 90% to 100% plating efficiency; high dose yields 50% plating efficiency) for the cell transformation assay.

    Cells of the appropriate passage are exposed to carcinogens using one or multiple exposures. In some cases, a single 24-hr exposure will suffice, but for other agents, a longer exposure period may be necessary. The use of multiple exposures is important since the half-lives of many carcinogens are short, and multiple exposures allow the cells to be exposed to fresh carcinogens as long as possible. Long intervals of exposure are also important since this allows the cells to be exposed to the carcinogens during several rounds of proliferation. For example, in cell transformation assays with carcinogenic metals, the authors employ a 5-day exposure period with replacement of the spent medium with freshly prepared metal solution and fresh medium every 24 hr.

    If organic chemicals are tested, benzo(a)pyrene can be used as a positive control and acetone as the negative control.

22. Following treatment, remove the chemicals from the culture plates and wash cells twice with normal saline A.

    CAUTION: *The medium may contain toxic and/or carcinogenic chemicals and should be disposed of in an appropriate manner.*

23. Trypsinize the monolayer with 0.5% trypsin and count cells with a Coulter counter. Determine cell viability by trypan blue exclusion using 0.4% (w/v) trypan or hemacytometer blue solution (Life Technologies).

24. Plate 100 to 1000 cells into 100-mm tissue culture plates in 10 ml complete DMEM-10% FBS (use 6 plates per dose).

25. Incubate for 2 weeks at 37°C in 5% CO_2. Change the medium twice weekly during this period.

26. Wash the cells with normal saline A and fix in 95% ethanol for 5 min. Stain with 0.5% crystal violet solution in 95% ethanol for 5 min.

27. Wash the excess stain by holding the plate by hand and allowing water from the tap to trickle over the hand.

    The overflow will trickle onto the plate and wash away the stain, eliminating all stain not bound to the cellular material.

28. Count the number of colonies and calculate the plating efficiency. Plating efficiency = (number of colonies/number of cells plated) × 100.

    Plating efficiency refers to the percentage of cells that are initially plated that give rise to colonies. This information is used in the cell transformation assay to determine the starting number of cells to plate in order to obtain a sufficiently large number (e.g., 25-50) of surviving colonies per dish.

    It should be noted that the cytotoxicity in this particular cell line may not be exactly the same as that in SHE cells; therefore, adjustment to the dose is sometimes needed. Generally, a dose that is toxic to one hamster cell line will also be toxic to another hamster cell line.

Determine cell transformation

29. Trypsinize unexposed SHE cells (as in step 16) and neutralize the trypsin with an equal volume of fresh complete DMEM-10% FBS.

30. Seed 1000 to 5000 cells into 100-mm tissue culture plates and allow to attach for 1 or 2 days. Treat with the test compound or a positive or negative control. Use 6 dishes for each exposure level.

    Cell numbers may vary depending upon the experiment. At higher exposure levels, 5000 to 20,000 cells may be plated to counteract the low plating efficiency of these cells.

31. Place cells in a 37°C, 5% CO_2 humidified incubator for ~2 weeks or until visible colonies are formed. Replenish the medium twice weekly during this incubation period.

    Care must be taken not to shake or agitate the plates during this procedure, because this may dislodge cells from colonies. This would result in the formation of new colonies, artificially increasing or decreasing the apparent incidence of transformation by giving birth to more than one colony from one cell at risk.

32. Aspirate the medium and wash cells twice with normal saline A. Fix with 95% ethanol for 5 min.

    CAUTION: *The medium may contain potentially carcinogenic compounds and should be disposed of in an appropriate manner.*

33. Stain with 0.5% crystal violet solution in 95% ethanol for 5 min.

34. Wash off excess stain as described in step 27.

Assess the degree of morphological transformation

35. Count the number of surviving colonies in each plate and examine them for morphological transformation. Observe each colony under an inverted tissue culture microscope for cell crisscrossing and overlapping as shown in Figure 3.4.1 (normal colony) and Figures 3.4.2, 3.4.3, and 3.4.4 (transformed colonies). Circle the transformed colonies on the bottom surface of the plate with an indelible black marker. Calculate the morphological transformation frequency as the (number of transformed colonies/total number of colonies) × 100.

    At least a good portion of the colony must have cells exhibiting disorderly growth at the border as well as in the middle of the colony. Additional scoring criteria are described in detail by Dunkel et al. (1991).

    It is best that the person evaluating the plates be unaware of the specific treatment regimens employed in order to avoid bias. The evaluation of morphological transformation requires a great deal of practice, patience, and care.

REAGENTS AND SOLUTIONS

Use Milli-Q-purified water or equivalent in all recipes and protocol steps. For common stock solutions, see ***APPENDIX 2A****; for suppliers, see* ***SUPPLIERS APPENDIX****.*

Normal saline A

3.3 mM $NaHCO_3$
5 mM KCl
130 mM NaCl
5 mM glucose
Filter sterilize
Store up to 6 months at 4°C

COMMENTARY

Background Information

Since it very expensive to test a carcinogenic substance in experimental animals, it has become necessary to develop cheaper, more rapid in vitro assays to assess the potential carcinogenicity of chemicals. These assays, while useful, are somewhat limited in their ability to assess the complete carcinogenic properties of a compound. The assays can be divided into two types based on the cells used. The first type of cell transformation assay uses established cell lines that lack one or more cancer-related endpoints, and the acquisition of these various cancer-related properties are measured. For example, many cell lines do not exhibit anchorage-independent cell growth and acquire such properties following exposure to carcinogens. The second and perhaps better system uses primary cell lines. Such cells have a limited life span in culture, are not immortalized, and are

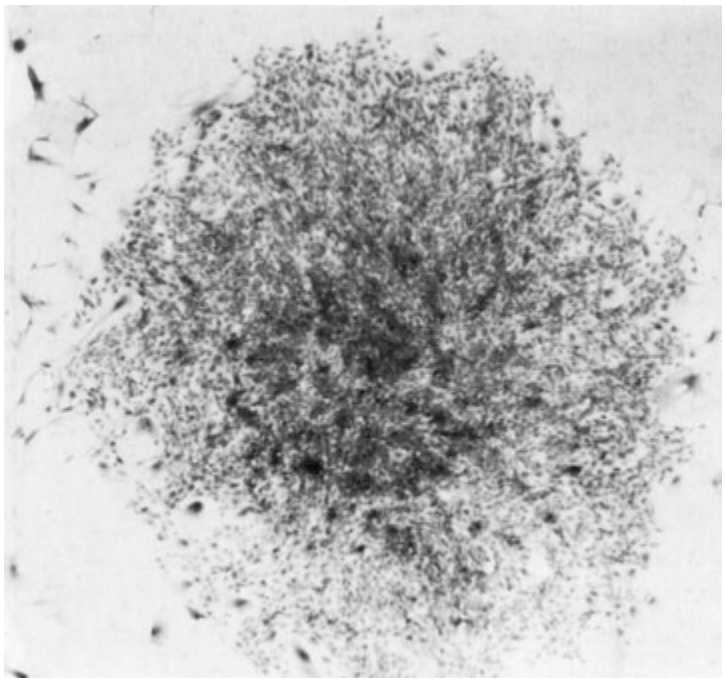

Figure 3.4.1 Normal colony of Syrian hamster embryo cells. From Costa (1980), reprinted with permission from Humana Press.

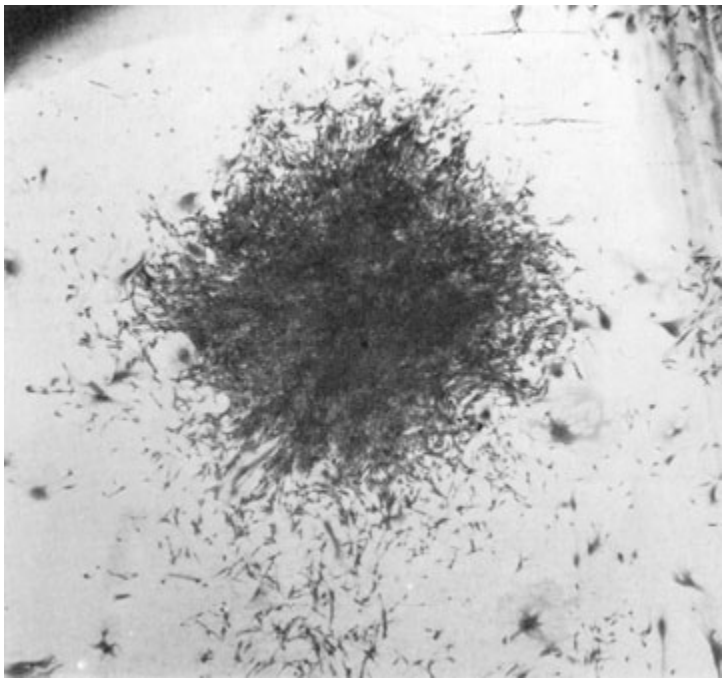

Figure 3.4.2 Ni_3S_2-transformed colony of Syrian hamster embryo cells at low magnification. From Costa (1980), reprinted with permission from Humana Press.

useful for studying the acquisition of a number of cancerous properties following exposure to carcinogens.

The most common properties that have been used to examine cell transformation of primary cultures are the pattern of growth and the morphological transformation of cells. Cells are exposed to a test substance, plated to form colonies, and the growth properties of the colonies after treatment are studied. A very dense and crisscross pattern of growth is indicative of the induction of morphological transformation.

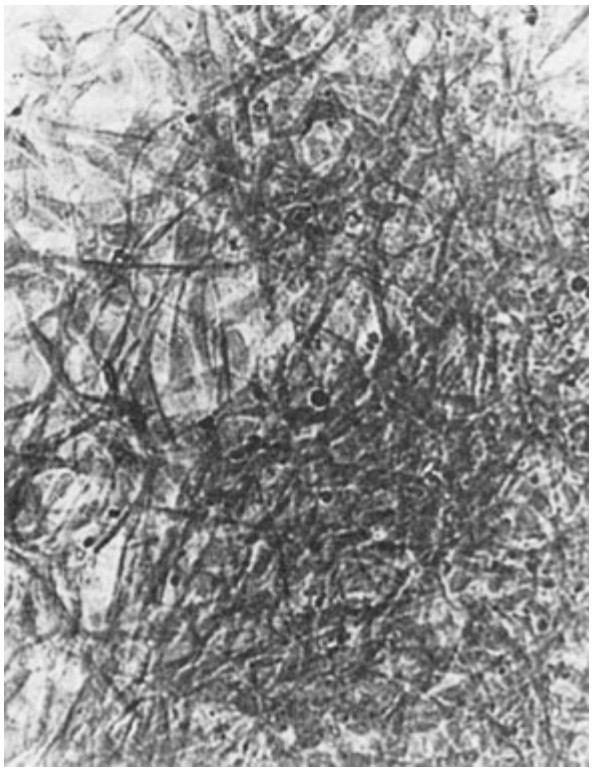

Figure 3.4.3 Higher magnification of Ni_3S_2-transformed colony of Syrian hamster embryo cells. From Costa (1980), reprinted with permission from Humana Press.

Figure 3.4.4 High magnification view of Ni_3S_2-transformed Syrian hamster embryo cells. From Costa (1980), reprinted with permission from Humana Press.

Table 3.4.1 Reported SHE Cell Morphological Transformation Frequencies for Select Chemicals

Chemical	Duration of treatment (hrs)[a]	Concentration (μg/ml)	Transformation frequency (%)	Reference
Benzo(a)pyrene	24	0	0	Berwald and Sachs (1965)
		1	2.4	
		10	4.3	
Cobalt sulfate hydrate	24	0	0.3	Kerckaert et al. (1996a)
		0.25	1.2	
		1.0	1.1	
Ethylbenzene	24	0	0.2	Kerckaert et al. (1996a)
		100	0.2	
		400	0.4	
Nickel subsulfide	96[a]	0	0.7	Costa (1980)
		1.0	5.8	
		5.0	8.9	
Sodium nitrite	24	0	0.3	Kerckaert et al. (1996a)
		500	1.7	
		750	1.5	

[a]SHE cells were exposed twice to the concentrations listed. Each exposure was with fresh medium and compound for a period of 2 days.

One can then confirm that these transformed cells are in fact tumorigenic by cloning the cells and testing them for their ability to grow in soft agar or to form tumors in nude mice; however, cells exhibiting morphological transformation usually have acquired these other cancer-related properties. Cloning and growing the cells is an additional step that is more expensive and time-consuming, but may be required to establish the carcinogenic properties of the test chemical.

Assays involving embryonic cultures plated fresh from animals have advantages over cell lines in the sense that the starting point is a cell that has not been immortalized and one can study immortalization. In contrast to established cell lines, the primary cell culture exhibits mostly normal properties.

The establishment of primary cultures from Syrian hamsters is preferred over other rodents because these have much lower rates of spontaneous immortalization. Trott et al. (1995) reported that the rates of spontaneous transformation are 10^{-5}, 10^{-6}, 10^{-6}, and less than 10^{-9} for rat, mouse, Chinese hamster, and Syrian hamster fibroblasts, respectively. In addition, SHE cells have been used extensively in carcinogenesis testing therefore data is available for a large number of test agents.

Critical Parameters

The importance of obtaining a good source of fetal bovine serum cannot be sufficiently emphasized. The authors have found that fetal bovine serum obtained from certain sources yields consistent results. Once a good batch is identified, a large number of bottles from that lot should be obtained. This assures optimal growth and consistency in the level of transformation. A different lot of fetal bovine serum may give a different level of transformation for that carcinogen. It has been reported that the serum variability problem is diminished if assays are conducted at pH 6.7 instead of the typical pH (7.1 to 7.3; Kerckaert et al., 1996b). This reduced-pH assay has also been reported to increase the frequency of morphologial transformation. A comprehensive protocol for this approach has been published by Kerckaert et al. (1996b).

Cells may be used beyond the third or fourth passage; however, splitting the cells several times ensures the elimination of many of the nonproliferating cells present in the primary cultures of mixed embryo cells. This greatly improves the evaluation of morphological transformation, since the stained plates can be easily read if nonproliferating cells and other debris are removed during the early passages. Mixed cell populations are always a problem when culturing any type of embryo-derived cell. If the cells are passaged too many times (six to seven) prior to exposure to the carcinogen, the assay does not respond as well, which may be related to the fact that the cells have a limited capacity for proliferation. Additionally,

chromosomal and/or genetic changes frequently increase with passage number and these changes could potentially impact cell transformation assays. The best results are obtained with third- or fourth-passage cells.

Anticipated Results

This assay will yield information on the toxicity and transforming capabilities of test agents and, as such, is a useful screen of potential carcinogens. A positive compound in this assay will cause morphological transformation of cells similar to that depicted in Figures 3.4.2, 3.4.3, and 3.4.4. In Table 3.4.1, some previously reported morphological transformation frequencies have been listed for a few selected chemicals.

Time Considerations

Establishment of third- or fourth-passage cell cultures takes 1.5 to 2 weeks. Exposure to the test agent and subsequent viability and transformation assays require an additional 2 to 3 weeks.

Literature Cited

Berwald, Y. and Sachs, L. 1965. In vitro transformation of normal cells to tumor cells by carcinogenic hydrocarbons. *J. Natl. Cancer Inst.* 35:641-661.

Costa, M. 1980. Metal carcinogenesis testing. Principles and in vitro methods. Humana Press, Clifton, N.J.

Dunkel, V.C., Rogers, C., Swierenga, S.H.H., Brillinger, R.L., Gilman, J.P.W., and Nestman, E.R. 1991. Recommended protocols based on a survey of current practice in genotoxicity testing laboratories: III. Cell transformation in C3H/10T1/2 mouse embryo cell, BALB/c3T3 mouse fibroblast and Syrian hamster embryo cell cultures. *Mutat. Res.* 246:285-300.

Evans, C.H. and DiPaulo, J.A. 1981. In vitro mammalian cell transformation for identification of carcinogens, cocarcinogens, and anticarcinogens. *In* Short-Term Tests for Chemical Carcinogens (H.F. Stich and R.H.C. San, eds.) pp. 306-322. Springer-Verlag, New York.

IARC/NCI/EPA Working Group. 1985. Cellular and molecular mechanisms of cell transformation and standardization of transformation assays of established cell lines for the prediction of carcinogenic chemicals: Overview and recommended protocols. *Cancer Res.* 45:2395-2399.

Kakunaga, T. 1973. A quantitative system for assay of malignant transformation by chemical carcinogens using a clone derived from BALB/3T3. *Intl. J. Cancer* 12:463-473.

Kerckaert, G.A., Brauninger, R., LeBoeuf, R.A., and Isfort, R.J. 1996a. Use of the Syrian hamster embryo cell transformation assay for carcinogenicity prediction of chemicals currently being tested by the National Toxicology Program in rodent bioassays. *Environ. Health Perspect.* 104:1075-1084.

Kerckaert, G.A., Isfort, R.J., Carr, G.J., Aardema, R.A., and LeBoeuf, R.A. 1996b. A comprehensive protocol for conducting the Syrian hamster embryo cell transformation assay at pH 6.70. *Mutat. Res.* 356:65-84.

Reznikoff, C.A., Bertram, J.S., Brankow, D.W., and Heidelberger, C. 1973. Quantitative and qualitative studies of chemical transformation of cloned C3H mouse embryo cells sensitive to postconfluence inhibition of cell division. *Cancer Res.* 33:3239-3249.

Rundell, J.O. 1984. In vitro cell transformation: An overview. *In* Carcinogenesis and Mutagenesis Testing (J.F. Douglas, ed.) pp. 39-62. Humana Press, Clifton, N.J.

Trott, D.A., Cuthbert, A.P., Overell, R.W., Russo, I., and Newbold, R.F. 1995. Mechanisms involved in the immortalization of mammalian cells by ionizing radiation and chemical carcinogens. *Carcinogenesis* 16:193-204.

Contributed by Max Costa and Jessica E. Sutherland
New York University School of Medicine
New York, New York

Assays for DNA Damage

Single- and double-strand breakage, DNA-DNA cross-links, DNA-protein cross-links, and DNA adducts are types of DNA damage that can result from exposure to genotoxic chemicals or physical agents. If not repaired, these DNA lesions are involved in teratogenesis, mutagenesis, and carcinogenesis.

Most assays detect DNA damage directly; however, damage can also be indirectly assessed by measuring DNA repair activity following the genotoxic insult. This unit describes assays that detect DNA strand breakage—e.g., by single-cell microgel electrophoresis (see Basic Protocol 1 and Alternate Protocol 1) and filter elution (see Basic Protocol 2 and Alternate Protocols 5, 6, and 7); DNA-DNA interstrand cross-links—e.g., by filter elution (see Basic Protocol 2 and Alternate Protocol 2); DNA-protein cross-links—e.g., by filter elution (see Alternate Protocol 3) or K-SDS precipitation (see Basic Protocol 3 and Alternate Protocols 8 and 9); oxidative DNA base modifications (see Alternate Protocol 4); and repair activities following DNA damage—e.g., unscheduled DNA synthesis (see Basic Protocol 4). Assays to detect DNA adduct formation can be found in *UNIT 3.2*.

These assays can be applied in vitro to cultured cells following exposure to the test agent. In addition, most of these assays can also be conducted using DNA obtained from animals or humans that were exposed to the test agent in vivo. Accordingly, some of these assays may prove valuable for ascertaining whether or not certain types of DNA damage can serve as biomarkers for assessment of human exposure to certain genotoxic agents.

DETECTION OF SINGLE-STRANDED DNA BREAKS USING THE SINGLE-CELL MICROGEL ELECTROPHORESIS ASSAY (COMET ASSAY) UNDER ALKALINE CONDITIONS

BASIC PROTOCOL 1

The single-cell microgel electrophoresis assay (SCGE or "comet assay") is a valuable tool for investigating cellular DNA damage. This assay is amenable to most cell types and thus can be used to assess DNA damage in cultured cells or in cells isolated from treated animals, including humans. Moreover, both double-strand DNA breakage (dsb) and single-strand DNA breakage (ssb) can be identified; for identification of dsb via the neutral assay, see Alternate Protocol 1. In addition, alkali-labile apurinic sites are converted to single-strand breaks at high pH and therefore can be detected in comet assays, particularly when lesion-specific repair endonucleases are used following cell lysis. This procedure describes electrophoresis of single cells following lysis in alkaline pH conditions to detect ssb. Following electrophoresis, the cells are stained with a fluorescent dye and examined microscopically. The appearance of a characteristic DNA "comet" is evidence of DNA damage. The procedures outlined here are adapted from those previously described by Singh (1996).

Materials

Cells of interest
Phosphate-buffered saline (PBS; see recipe)
Test chemical
Normal-melting-point (NMP) agarose
Low-melting-point (LMP) agarose
Alkaline lysis solution, pH 10 (see recipe), 4°C
Alkaline electrophoresis buffer (see recipe)
400 mM Tris·Cl, pH 7.4 (*APPENDIX 2A*)
20 µg/ml ethidium bromide (or other fluorescent DNA stain; e.g., propidium iodide, ethidium bromide, YOYO-1, TOTO-1)

Contributed by Jessica E. Sutherland and Max Costa
Current Protocols in Toxicology (1999) 3.5.1-3.5.36

Metal baking tray
Microscope slides, fully frosted
24 × 50–mm no. 1 coverslips
45°C water bath
200-µl pipet tips with 5 mm cut off the small end
Coplin jars or slide staining apparatus
Horizontal electrophoresis unit
Power supply capable of delivering 300 mA of current at 25 V
Fluorescence microscope with excitation and barrier filters appropriate for the selected DNA stain, and camera
Eyepiece micrometer
Digital calipers
Transparencies with mm^2 grids
Image analysis software (optional)

Prepare single-cell suspensions and treat with test chemical

1. Prepare a cell suspension at 2,000 to 200,000 cells/µl in PBS.

   Cultured cells, cells isolated from animal tissues, or lymphocytes from human blood are suitable.

2. Treat the cells with the test chemical.

   There are several approaches for treating cultured cells. The test agent can be added directly to the growth medium as long as it is freely soluble and will not form complexes with constituents of the medium. Alternatively, cells can be treated after they are embedded in agarose and mounted on the microscope slide. If embedded cells are to be treated for more than a few minutes, the agarose should contain the growth medium. McKelvey-Martin et al. (1993) reported that control lymphocytes in standard agarose (i.e., dissolved in PBS) developed comets after 1 hr of incubation time. Finally, Singh (1997) described a technique to grow human CFNF-2 fibroblasts directly on frosted slides.

   Examples of previously reported assays are provided in Table 3.5.1. In addition, Henderson et al. (1998) lists agents that have been screened with the comet assay.

   To prevent DNA repair, keep cells on ice during treatment.

Precoat slides with agarose layer (optional)

3. Warm slides (50°C) and label with pencil. Place them on a metal baking tray.

4. Prepare 3 ml of 0.5% (w/v) NMP agarose in PBS by boiling. Cool by placing into 45°C water bath. Using a cut-off pipet tip, apply 100 µl agarose to each of the (fully frosted) slides that are to be used. Gently lower a 24 × 50–mm coverslip onto the agarose, using care to avoid air bubbles. When agarose has been applied to all the

Table 3.5.1 Examples of Previously Reported Single-Cell Microgel Electrophoresis Assays

Test agent	Dose	Exposure time	Cell type	Reference
Acetaldehyde	0-100 mM	1 hr	Human peripheral lymphocytes	Singh (1996)
Dimethyl sulfate	0, 0.5 mM	10 min	Human VH10 fibroblasts	Klaude et al. (1996)
Hydrogen peroxide	0-15 mM	0.5 hr	Mouse 707 Friend erythroleukemia (FEL) cells	McCarthy et al. (1997)
Methylmethane sulfonate	0-4 mM	0.5 hr	Human HeLa (transformed epithelial) cells	Collins et al. (1997)
X-ray	0-25.6 rads	100 rads/min	Human peripheral lymphocytes	Singh (1996)

slides, place the baking tray over ice for 10 min to allow agarose to set. Remove the coverslips.

This is an optional step but pretreatment of slides lessens loss of the microgels during lysis, electrophoresis, fixation, or staining.

Embed cells in agarose, mount onto slides, and lyse cells

5. Prepare 0.5% (w/v) LMP agarose in PBS. Mix 5 µl of cell suspension in 75 µl of the 0.5% LMP agarose, maintained at 37°C.
6. Pipet 30 µl of this mixture onto a fully frosted microscope slide (optionally precoated as in step 4) and cover with a glass 24 × 50–mm coverslip.
7. Cool for 60 sec by placing the slide on a metal tray kept on ice.

   Alternatively, slides can be cooled briefly in a 4°C refrigerator.

8. Remove the coverslip and layer an additional 100 µl of 0.5% LMP agarose on top of the gel and replace the coverslip. Cool as before, and remove coverslip.
9. Place slides in a Coplin jar filled with 4°C alkaline lysis solution, pH 10, and incubate 1 hr at 4°C to lyse cells.

   IMPORTANT NOTE: *Lysis and subsequent steps should be conducted in dim light to avoid introduction of additional DNA damage.*

   Alternatively, the slides can be placed on edge in a staining rack and lowered slowly into a staining trough containing cold lysis solution.

10. (Optional) Treat slides with 1 mg/ml proteinase K in lysis solution without Triton X-100, pH 7.4, for 2 hr at 37°C.

    Alternatively, the proteinase K can be added directly to the agarose.

    This step is often performed to improve assay sensitivity.

Equilibrate slides with electrophoresis buffer and perform electrophoresis

11. Place slides onto horizontal slab of electrophoretic apparatus and carefully cover with alkaline (ssb) electrophoresis buffer. Position the slides as close as possible to the anode and close to one other. Place blank slides in empty spaces.

    The volume of buffer will depend on the size of the electrophoresis apparatus. Add enough buffer to cover gels by ~5 mm. Make sure that the gel box is horizontally level so that the volume of buffer over each slide is the same.

    Among runs, consistent temperature of the electrophoretic buffer should be maintained. A variety of temperatures (4° to 25°C) have been reported for this procedure. Sensitivity of the assay is improved at higher temperatures; however, background rates of comet formation are also increased. For this reason, Green et al. (1996) recommend a maximum temperature of 15°C.

    Singh (1997) describes a slide-holding tray that can be used for lysis and subsequent electrophoresis.

12. Allow gels to equilibrate with buffer for 20 min.

    This also allows for DNA unwinding to occur. Twenty minutes represents the minimum time for equilibration. The time may be increased to 40 min. Prolonged equilibration time (i.e., >40 min) may result in comet formation in controls (Green et al., 1996). Preelectrophoretic equilibration also ensures that the salt concentrations in the buffer and the gel will be equivalent. High salt concentrations in the gel would retard DNA migration (Fairbairn et al., 1995).

13. Begin electrophoresis using a voltage gradient of 0.4 V/cm for 60 min (usually this corresponds to 25 V). Adjust the current to 300 mA by adjusting the volume of the alkaline electrophoresis buffer.

Each experiment should be conducted at the same current. Current magnitude and electrophoresis time is highly variable among laboratories. Using the same voltage, buffer volume, and gel box should yield the same current each time.

Neutralize the alkaline buffer and stain the DNA

14. Remove slides from the alkaline electrophoresis buffer and place them in a Coplin jar (or staining trough) containing 400 mM Tris·Cl, pH 7.4, for 30 min at room temperature.

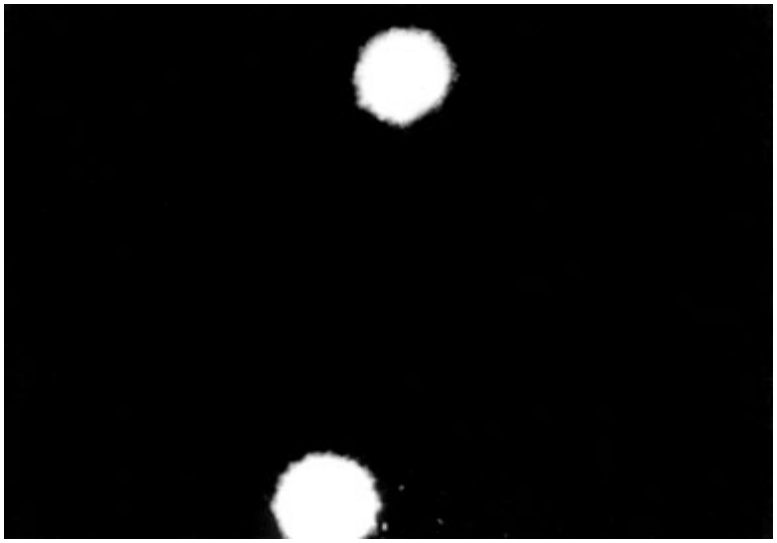

Figure 3.5.1 Untreated lymphocytes processed as controls in the comet assay. From McKelvey-Martin et al. (1993); reprinted with permission from Elsevier Science Publishers.

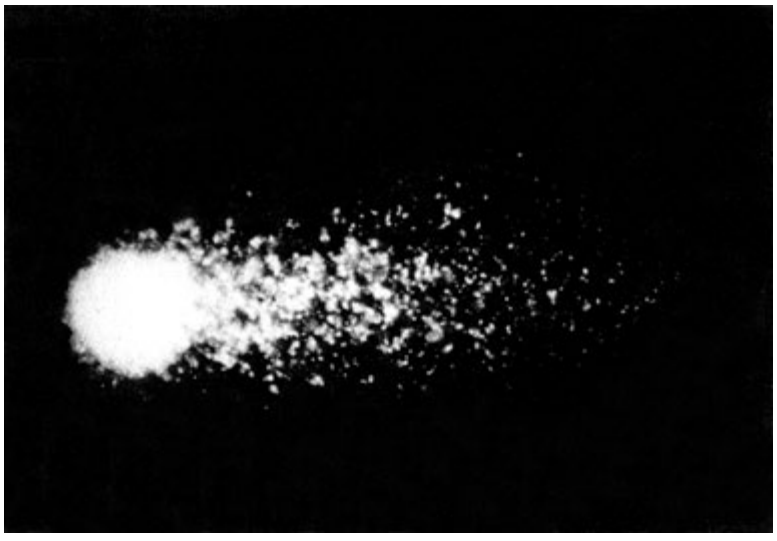

Figure 3.5.2 Human lymphocyte following treatment with 172.5 μM H_2O_2 for 1 hr at 4°C and processed in the comet assay. From McKelvey-Martin et al. (1993); reprinted with permission from Elsevier Science Publishers.

15. Transfer to fresh 400 mM Tris·Cl, pH 7.4 for additional 15 min. Repeat once.

Neutralization can also be performed by placing the slides flat on a staining tray and then rinsing with 1 ml of 400 mM Tris·Cl, pH 7.4, dropwise. This process is then repeated one more time.

16. Stain DNA with 60 µl of 20 µg/ml ethidium bromide. Cover gels with a new coverslip.

Alternatively, gels can be dehydrated and the DNA can also be fixed. To do this, immerse slides (two per Coplin jar) in absolute ethanol for 10 min at room temperature. Repeat with 70% ethanol, then dry slides at room temperature.

Other stains that have been used in comet assays are: DAPI (5 µg/ml), propidium iodide (2.5 to 5 µg/ml), TOTO-1, and YOYO-1. YOYO-1 and TOTO-1 are the most sensitive and should be used at the minimal concentration that will give good DNA staining and low background (1 to 100 µM). All of these dyes bind to nucleic acids and hence should be used with appropriate care. Continue to work in dim light to avoid photobleaching.

If desired, gels can be stored for a few days in a light-proof box. Keep moist with PBS-soaked gauze.

Examine slides with fluorescent microscope and quantitate DNA damage manually or via automated image analysis

17. Equip microscope with a filter combination appropriate for the DNA stain that was used.

For example, for ethidium bromide, an excitation filter of 515 to 560 nm and a barrier filter of 590 nm are required.

See Figure 3.5.1 and Figure 3.5.2 of control and hydrogen peroxide–treated cells, respectively, that were processed using the comet assay.

For manual quantitation

18a. Score damage empirically using a numerical rating system (0 for no damage and 4 for maximal damage). Count at least 50 comets per treatment.

19a. Measure DNA migration with an eyepiece micrometer.

20a. Use digital calipers (0 to 150 mm) to measure nuclear DNA and migrated DNA (i.e., head diameter and comet length) on negative photomicrographs.

21a. Measure comet area by placing a transparency with a mm^2 grid between a light box and a negative photomicrograph. Record the total number of squares encompassing each comet.

For quantitation by automated image analysis

18b. Quantify % head DNA, % tail DNA, tail length, comet area, and tail moment—i.e., the product of tail length and the fraction of total DNA in the tail (Olive et al., 1990)—using a computerized image analysis system.

Many other measurements are also possible with image analysis systems. Some of these are: the comet moment (Kent et al., 1995), ratio of head diameter to tail length (Olive, 1989), and ratio of overall intensities within the tail and the head (Böcker et al., 1997).

ALTERNATE PROTOCOL 1

DETECTION OF DOUBLE-STRANDED DNA BREAKS USING THE SINGLE-CELL MICROGEL ELECTROPHORESIS ASSAY UNDER NEUTRAL CONDITIONS

Neutral electrophoresis conditions allow the detection of double-strand breaks.

Additional Materials *(also see Basic Protocol 1)*

Neutral lysis solution, pH 8.3 (see recipe), *or* alkaline lysis solution, pH 10 (see recipe)
10 µg/ml RNase A in alkaline lysis solution (see recipe for the alkaline lysis solution; omit Triton X-100 and adjust pH to 7)
1 mg/ml proteinase K in alkaline lysis solution (see recipe for the alkaline lysis solution; omit Triton X-100 and adjust pH to 7)
Neutral electrophoresis buffer: 300 mM sodium acetate/100 mM Tris·Cl, pH 8.5 (see *APPENDIX 2A* for Tris·Cl)
300 mM NaOH

1. Prepare cell suspension, treat cells with test chemical, precoat slides with agarose, and embed cells in agarose (see Basic Protocol 1, steps 1 to 8).
2. Lyse cells in neutral or alkaline lysis solution at 4°C for 1 hr by placing slides in a Coplin jar filled with lysis solution.

   IMPORTANT NOTE: *Lysis and subsequent steps should be conducted in dim light to avoid introduction of additional DNA damage.*

   In an attempt to enhance migration of DNA fragments in the comet tail, many investigators have used the alkaline lysis solution followed by neutral electrophoresis when conducting neutral comet assays.

Remove RNA and protein

3. Treat slides with 10 µg/ml ribonuclease A at 37°C for 2 hr.
4. Treat slides overnight with 1 mg/ml proteinase K at 37°C in lysis solution without Triton X-100 and adjusted to pH 7.

   Alternatively, the proteinase K can be added directly to the agarose (Singh, 1997).

5. Rinse slides for 5 min with neutral electrophoresis buffer at room temperature.
6. Perform electrophoresis [see Basic Protocol 1, steps 11 and 13; substitute neutral electrophoresis buffer where alkaline electrophoresis buffer is called for and omit buffer equilibration/DNA unwinding step (Basic Protocol, step 12)].
7. Place slides in a Coplin jar (or staining trough) filled with 300 mM NaOH and incubate at room temperature for 10 min to degrade remaining RNA.
8. Neutralize NaOH, stain DNA, examine slides, and quantitate DNA damage manually or by image analysis (see Basic Protocol 1, steps 14 to 21a or 18b).

BASIC PROTOCOL 2

DETECTION OF DNA DAMAGE WITH FILTER ELUTION

Filter elution is a commonly used technique for measuring DNA stand breakage. The assay uses a filter to mechanically impede passage of long (unbroken) DNA strands during elution. Most often, this assay has been employed in alkaline conditions to measure single-strand DNA breakage (ssb). With modification, the assay has also been used to detect alkali-labile sites, DNA-protein cross-links, DNA interstrand cross-links, and double-strand DNA breakage (dsb). The assay described here is modified from the

protocol of Kohn et al. (1981) and outlines detection of single-strand DNA breakage. The alternate protocols describe modifications for the other types of DNA damage.

CAUTION: When working with radioactivity, take appropriate precautions to avoid contamination of the investigator and the surroundings. Carry out the experiment and dispose of wastes in an appropriately designated area, following the guidelines provided by your local radiation safety officer (also see *APPENDIX 1A*).

Materials

Cells of interest
[Methyl ^{3}H]thymidine (20 Ci/mmol) or [2-^{14}C]thymidine (50 mCi/mmol) for radioactive determination *or* Hoechst 33258 (bis-benzamide; for fluorometric determination)
Unlabeled thymidine
Appropriate growth medium for cells
Test compound
Phosphate-buffered saline (PBS; see recipe), ice-cold
Cell lysis solution, pH 9.7 (see recipe)
Cell lysis solution (see recipe) containing 0.5 mg/ml proteinase K
Alkaline elution solution, pH 12.3 (see recipe)
1 N HCl
0.4 N NaOH
Scintillation fluid (e.g., Ecolume, ICN Biomedicals) containing 0.7% (v/v) acetic acid
0.2 M tetrasodium EDTA, pH 10 (pH adjusted with 1 N NaOH)
1 M potassium dihydrogen phosphate
17 mM KH_2PO_4
150 µM Hoechst 33258 stock solution

Tabletop centrifuge
2.0-µm polycarbonate filter (25-mm diameter; Nucleopore, Whatman)
1-liter vacuum flask
Alkaline elution funnel apparatus (e.g., Millipore)
Aluminum foil or black paper cylinder
Multichannel peristaltic pump and suitable Tygon tubing
Fraction collector
Glass scintillation vials
60°C oven or water bath
Liquid scintillation counter or fluorometer

Additional reagents and equipment for assessing cell viability by trypan blue exclusion (*APPENDIX 3B*)

Label cells with [^{14}C] or [^{3}H]thymidine

1. Expose 10^5 cells/ml in suspension or a monolayer culture of ~10^6 cells to 0.1 µCi/ml [methyl ^{3}H]-thymidine plus 10^{-5} M unlabeled thymidine or 0.01 to 0.02 µCi/ml of [2-^{14}C]-thymidine for 24 hr. Follow with a chase period of 24 hr so that cells are uniformly labeled (i.e., not just the newly replicated DNA). Grow and label an adequate number of cells (i.e., several flasks or plates may be necessary) for the experimental protocol (see step 3).

   Radiolabeling is not required. Alternatively, DNA can be quantitated fluorometrically (see steps 15b to 22b). In this case, omit step 1. Fluorometric quantitation must be used for nonreplicating cells (e.g., peripheral lymphocytes).

2. Recover cells in suspension by centrifuging 5 min at 200 × *g*, 4°C and remove the supernatant. Or if monolayer cells are used, rinse twice with ice-cold PBS, gently scrape cells with a rubber policeman, and use a sterile pipet to transfer them into a sterile centrifuge tube. Centrifuge 5 min at 200 × *g*, 4°C and remove the supernatant. Rinse pellets with ice-cold PBS, centrifuge again, remove the supernatant and transfer an appropriate number of cells into the appropriate medium for treatment with test agent (either as suspended cells or as re-attached cells on a plate).

   If monolayer cells are used, avoid excess trypsinization or scraping as this can result in significant DNA damage.

3. Treat cells with test agent, using at least four different concentrations of the agent, a vehicle control, and a positive control, all in triplicate. Conduct cell viability tests (trypan blue exclusion; see *APPENDIX 3B*) concurrently.

   Alternatively, cells can be removed ex vivo from tissues of treated laboratory animals. Typically, nuclear suspensions are prepared and nuclei are applied to the filter. Sensitivity of the assay will depend on the degree of damage incurred by the nuclear DNA during the isolation procedure (Kohn, 1991). For biomonitoring purposes, the assay can also be applied to lymphocytes obtained from exposed and nonexposed human subjects.

Assemble and prepare filter apparatus

4. Secure the filter within the funnel apparatus and attach to a suction flask that is in turn connected to a vacuum line.

5. Add ~20 ml of ice-cold PBS to the funnel. Use a pipet to slowly add fluid while allowing air bubbles in the solution to escape. Apply a full vacuum for a few seconds to expel air from the filter. Adjust vacuum to a slow flow rate.

   Always keep enough buffer in the funnel to cover the filter, so as not to suck air into the filter. Air pockets can cause spurious elution of DNA strands.

Apply cells to filter

6. Add 0.5–2 × 10^6 cells, diluted in 20 ml ice-cold PBS, to the funnel. Continue to apply a gentle vacuum to pull the cells onto the filter.

   The number of cells to be loaded onto the filter depends upon cell size and the degree to which the cells impede the solution flow rates through the filter.

   An internal standard can be added to control for elution anomalies or variability between individual elution columns. These are cells that are labeled in a different manner than the test cells (e.g., with ^{14}C rather than ^{3}H) and that have been irradiated with X rays in order to introduce a known frequency of single-strand breaks. Elution curves of the test cells are normalized with respect to the internal standards (Kohn et al., 1981). Additionally, the frequency of single-strand breaks caused by the test agent can be calculated. The mathematical formulas are detailed by Kohn et al. (1981).

7. Just before the solution level reaches the filter, add 5 to 10 ml of additional ice-cold PBS to wash the cells. Repeat twice. During the last wash, turn off the vacuum when the fluid is ~1 cm above the filter and allow the last of the solution to flow through the filter by gravity.

8. Cover the funnel apparatus, if transparent, with foil or a black paper cylinder to shield from light.

   All subsequent steps should be performed in dim light to avoid further DNA damage.

Lyse the cells

9. Disconnect the funnel/filter apparatus from the suction flask and move to a support rack.

10. Fill the upper chamber of the filter holder with cell lysis solution, pH 9.7, by using a pipettor with a plastic tip that will fit through the filter orifice. Withdraw the tip slightly to allow for air bubbles to escape from the upper chamber. Pipet 1 ml at a time, slowly. Add a total of 5 ml of cell lysis solution. Allow the lysis solution to drip by gravity into a scintillation vial.

    Air pockets in the filter chamber may cause spurious DNA elutions.

Digest protein

11. Connect the outflow tubes to tubing leading to a peristaltic pump (with the pump turned off at this point).

12. Fill the upper chamber of the filter holder with 2 ml of cell lysis solution containing 0.5 mg/ml of proteinase K, using the procedure described above for adding the cell lysis solution. Pump through the filter at 0.035 ml/min. Turn off the pump.

    It is important to properly adjust the pump so that no retrograde flow pulsations occur. These can cause DNA breakage (Kohn, 1991).

    For the fluorometric procedure (see steps 15b to 22b, below), if DNA is to be quantitated with Hoechst 33258 fluorochrome, it is important to wash out SDS from the cell lysis solution to eliminate background fluorescence from the SDS. To accomplish this, wash the lysate with 10 ml of 0.02 M disodium EDTA buffer, pH 10, prior to the elution step (Sterzel et al., 1985).

Elute damaged DNA

13. Aspirate excess proteinase K solution from the filter funnel and add 5 ml of alkaline elution solution, pH 12.3, by slowly running the solution down the wall of the funnel. Pour an additional 30 to 40 ml of the solution into the funnel.

14. Turn on the pump at a speed of 0.035 ml per min and collect fractions into scintillation vials at 90- or 180-min intervals for 15 hr. Turn pump off.

Quantitate DNA using scintillation counting of radiolabeled DNA or fluorometry

Using radiolabeled DNA

15a. Pour off any remaining elution solution.

16a. Turn pump on to maximum speed to empty solution remaining in the line and filter holder. Collect this fraction into a scintillation vial.

17a. Turn off the pump and remove the filter. Place it in a scintillation vial containing 0.4 ml of 1 N HCl. Cap the vial and heat at 60°C in oven or water bath for 1 hr to depurinate the DNA.

18a. Add 2.5 ml of 0.4 N NaOH and shake vigorously. Allow to stand for 1 hr at room temperature. Shake again.

19a. Flush the filter holder and line tubing with 10 ml of 0.4 N NaOH by pumping at high speed. Collect into another scintillation vial. Wash again with 2.5 ml 0.4 N NaOH and count to check if all radioactivity has been removed.

20a. Add 10 ml of scintillation fluid (e.g., Ecolume, ICN Biomedicals) containing 0.7% (v/v) acetic acid to each scintillation vial.

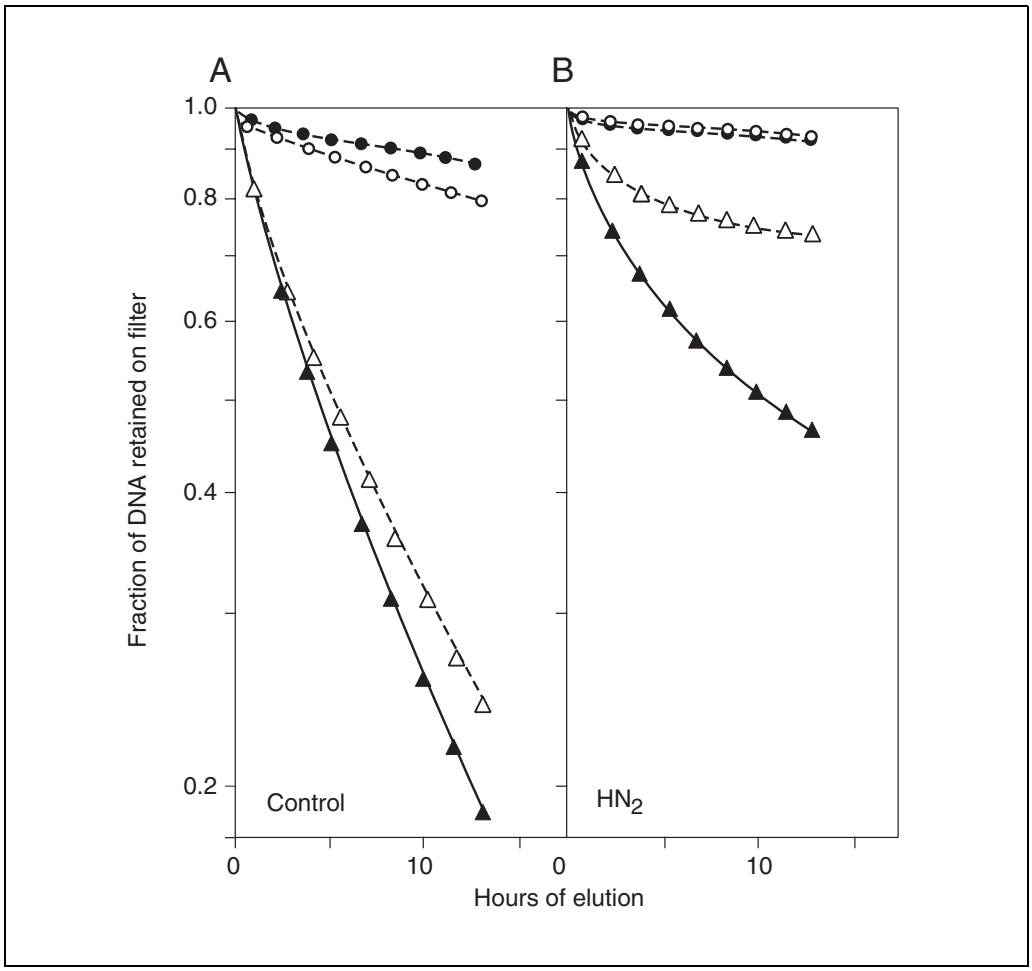

Figure 3.5.3 Protein-dependent (**A**) and protein-independent (**B**) DNA cross-linking in L 1210 cells by bis (2-chloroethyl) methyl amine (HN_2). Cells, prelabeled with [^{14}C]thymidine (20 hr) were treated with 0.1 μM HN_2 (0.5 hr). Tests were conducted with and without proteinase K and with and without 300 red of X ray. Symbols: open circles, no X ray or proteinase K; open triangle, X ray, no proteinase K; filled circle, no X ray with proteinase K; filled triangle, X ray with proteinase K. From Ewig and Kohn (1977); reprinted with permission from American Association for Cancer Research (AACR).

21a. Count the radioactivity in each of the vials containing the filters, rinse solution, and eluted fractions.

22a. Calculate results by adding the radioactivity (cpm) from the filter to the radioactivity measured in the wash of the filter holder. Add this amount to the cumulative amount of radioactivity in the fractions.

This sum will represent the total amount of labeled DNA in the assay.

23a. Plot data on a semilogarithmic plot of DNA retention [i.e., the fraction of total DNA retained on the filter (log scale)] versus elution time (arithmetic scale; see Fig. 3.5.3).

Using fluorometry (i.e., cells have not been radiolabeled; step 1 has been omitted)

15b. Wash the lysate with 10 ml of 0.02 M disodium EDTA buffer, pH 10, prior to the elution step (see step 12 above; Sterzel et al., 1985).

If DNA is to be quantitated with Hoechst 33258 fluorochrome, it is important to wash out SDS from the cell lysis solution to eliminate background fluorescence from the SDS.

16b. Conduct elution of damaged DNA (see step 13 above). Collect 3-ml fractions at rate of 30 μl/min.

17b. To recover the DNA on the membrane, transfer the membrane to a small plastic petri dish and cut into small pieces with a scalpel blade. Place the pieces in a 20-ml scintillation vial and add 5 ml of the alkaline elution solution (pH 12.3). Vortex for 1 min. Collect the wash fraction and replace with an additional 5 ml of buffer and vortex. Pool the two wash fractions.

18b. Dilute 1 ml of the pooled wash fraction with 2 ml of alkaline elution buffer.

19b. Adjust pH of each 3-ml fraction (eluant and wash fractions) to 6.8 to 7.0 by adding 175 µl of 17 mM KH_2PO_4.

20b. Add 0.8 ml 2.25 µM Hoechst 33258 dissolved in 0.15 M sodium chloride/0.015 M sodium citrate. Incubate in the dark for 30 min.

21b. Measure fluorescence with fluorometer set at an excitation wavelength of 360 nm and an emission wavelength of 450 nm.

Alternatively, DNA can be quantitated fluorometrically using an automated method. This technique requires a continuous-flow analyzer manifold with a sample carousel, proportioning pump, and fluorometer (Sterzel et al., 1985).

22b. Plot data on a semi-logarithmic plot of DNA retention [i.e., the fraction of total DNA retained on the filter (log scale) versus elution time (arithmetic scale; see Figure 3.5.3)].

DETECTION OF INTERSTRAND CROSS-LINKS

ALTERNATE PROTOCOL 2

The elution rate (see Basic Protocol 2) of broken fragments of DNA (introduced by X irradiation) is decreased if interstrand cross-links are present. After treatment with the test agent or vehicle control, irradiate cells with an X-ray dose of 300 rad at 0°C. Alternatively, hydrogen peroxide can be used as a DNA fragmenting agent (Szmigiero and Studzian, 1988). Perform alkaline elution assay as above (see Basic Protocol 2) except use a 0.8-µM polycarbonate filter (Nucleopore, Whatman). If the test agent caused interstrand linkage, a greater fraction of DNA (quantitated with radiolabeling or by fluorescence) will be retained on the filter over time as compared to the vehicle control.

DETECTION OF DNA-PROTEIN CROSS-LINKS

ALTERNATE PROTOCOL 3

After treatment with test agent as in steps 1 to 3 in Basic Protocol 2, cells are irradiated with 300 rad of X ray at 0°C to introduce DNA strand breakage. A 0.8-µm polyvinyl chloride filter (Gelman) is used instead of polycarbonate because polyvinyl chloride retains more protein. The lysis solution consists of 0.2% (w/v) sodium dodecylsarkosine/2 M NaCl/0.04 M EDTA, pH 10.0. The proteinase K treatment before alkaline elution is omitted. If the test agent has induced significant DNA-protein cross-linkage, more DNA (as quantitated by radiolabeling or fluorescence) will be retained on the filter over time as compared to the vehicle control. To better quantitate the amount of DNA-protein cross-linkage that has occurred, the results from assays conducted with and without proteinase K can be compared (see Fig. 3.5.3).

ALTERNATE PROTOCOL 4

DETECTION OF OXIDATIVE DNA BASE MODIFICATIONS

Oxidation-induced DNA lesions undergo excision repair by cellular endonucleases. This assay uses exogenous bacterial repair enzymes—e.g., 1 μg/ml foramidopyrimidine-DNA glycosylase E, 10 ng/ml endonuclease IV (Boehringer Mannheim), 30 ng/ml TY endonuclease V, 0.3 ng/ml exonuclease III—to excise modified DNA bases following cell lysis. The resulting single-stranded DNA fragments are quantified with alkaline elution (see Basic Protocol 2) and this is compared to the number of single-strand breaks detected without added repair enzymes (Pflaum et al., 1997).

ALTERNATE PROTOCOL 5

DETECTION OF DOUBLE-STRAND DNA BREAKAGE

Double-strand DNA breaks are detected with "neutral" filter elution (performed at pH 9.6). This pH is nondenaturing thus no DNA strand unwinding occurs.

Polycarbonate filters are preferred because they retain less protein than polyvinyl chloride filters. A lysis solution containing 2% (w/v) sodium dodecyl sulfate and 0.5 mg/ml proteinase K, pH 9.6, is used for 30 min (Elia et al., 1991). The eluting solution is composed of 0.05 M Tris·Cl/0.05 M glycine/0.025 M EDTA (disodium salt)/2% (w/v) sodium dodecyl sulfate. The pH of the eluting solution is adjusted to pH 9.6 with 10 N NaOH (Bradley and Kohn, 1979). DNA quantitation is conducted as above (see Basic Protocol 2) by prelabeling cells with radiolabeled thymidine or by using fluorometry.

ALTERNATE PROTOCOL 6

SIMULTANEOUS DETECTION OF DNA DOUBLE- AND SINGLE-STRAND BREAKS

Lu et al. (1996) introduced a filter-elution assay that simultaneously detected single- and double-strand DNA breaks. Double-strand breaks are estimated by measuring the DNA in the eluate following neutral cell lysis (pH 10) and proteinase K digestion. This step is followed by alkaline elution (pH 12.3) and the degree of single-strand breakage is estimated by quantitating the amount of DNA in the alkaline eluate.

ALTERNATE PROTOCOL 7

ALKALINE ELUTION USING 96-WELL PLATES

Anard et al. (1997) used the Millipore Multiscreen Assay System for alkaline elution. The system included disposable 96-well plates with hydrophobic polyvinylidenefluoride (PVDF) membranes (0.65 mm pore size) and a vacuum manifold. Eluates were collected in a standard 96-well plate placed below the vacuum manifold. The advantages of this technique included its rapidity and the fact that a large number of tests could be run in a single experiment.

BASIC PROTOCOL 3

DETECTION OF DNA-PROTEIN CROSS-LINKS BY K-SDS PRECIPITATION

This assay uses detergent and high temperatures to disrupt noncovalent DNA-protein binding. Covalent DNA-protein complexes are selectively precipitated by the addition of potassium chloride. This protocol was introduced by Zhitkovich and Costa (1992).

Materials

Culture of monolayer cells
Phosphate-buffered saline (PBS; see recipe), ice-cold
K-SDS cell lysis solution (see recipe)
4 mg/ml bovine serum albumin (BSA; molecular biology grade)
Precipitation/washing solution (see recipe)
Proteinase K solution (see recipe)
1 mg/ml Hoechst 33258 dye (freshly prepared 1:20 dilution gives A_{338} = 1.12)
20 mM Tris·Cl, pH 7.5 (*APPENDIX 2A*)
λ DNA of known concentration

3-ml syringe with 21-G needle
50° and 65°C water baths
Centrifuge with swinging-bucket rotor capable of 3300 × *g* with adapters for 1.5-ml microcentrifuge tubes (optional)
15-ml polystyrene centrifuge tubes with caps, sterile
12 × 75–mm borosilicate glass culture tubes of size appropriate for fluorometer
Centrifuge with swinging-bucket rotor capable of 1500 × *g* with adapters for 15-ml tubes
Fluorometer

Treat and lyse cells

1. Treat cultured monolayer cells with test agent or vehicle control. Scrape with a rubber policeman and wash twice with ice-cold PBS. Centrifuge at 600 × *g* for 5 min and resuspend pellet in PBS at 1–2 × 10^7 cells/ml.

   For biomonitoring purposes, this assay can be used on white blood cells or lymphocytes isolated from human blood samples (Costa et al., 1993; Taioli et al., 1995). The assay can also be applied to cells isolated from tissues of treated laboratory animals (Zhitkovich and Costa, 1992).

   Optimal density will depend on cell type. Use a cell density that yields 8 to 15 μg of total DNA per cell preparation. Starting cell densities should be the same for treated and control preparations.

2. From each plate, prepare three lysates as follows. Pipet 0.5 ml K-SDS cell lysis solution into a 1.5-ml microcentrifuge tube and then add 100 μl of cell suspension. Vortex for 5 sec at maximum speed. Spin briefly to collect lysate in bottom of tube. Freeze lysates at −70°C until analysis.

   Freeze-thawing of lysates is necessary in order to lower the background. At least 1 hr of freezing is required. Lysates can be stored frozen for at least 1 month.

3. Prepare three blank tubes as follows. To a 1.5-ml microcentrifuge tube, add 50 μl of 4 mg/ml BSA and 0.5 ml of K-SDS cell lysis solution. Vortex 5 sec at maximum speed, then microcentrifuge briefly to collect solution at bottom of tube. Freeze blanks at −70°C until analysis.

   Throughout the remaining steps of the assay, blanks and lysates should be treated in an identical manner.

Thaw lysates, shear DNA, and separate the protein-bound from the free DNA by precipitation

4. Thaw lysates in 37°C water bath and shear the DNA by passing the cell lysate four times through a 21-G needle, using a 3-ml syringe.

   Shearing of DNA assures uniform background measurements of DNA-protein cross-links. When performing this step, apply medium pressure to the syringe and avoid excess foaming of the lysate.

5. Add 0.5 ml of precipitation/washing solution. Vortex the tube at maximum speed for 5 sec, then heat in a 65°C water bath for 10 min.

   The optimal temperature of the water bath depends upon the test agent. Some DNA-protein cross-links formed by organic compounds are labile at higher temperatures (Costa et al., 1997).

6. Remove tubes from water bath and mix by inversion three times. Place on ice for 5 min to form potassium dodecyl sulfate (K-SDS) precipitates.

7. Collect the precipitate by centrifuging 6 min at 3300 × *g*, 4°C. Remove the supernatant by gently aspirating with a pipet and save in a sterile 15-ml centrifuge tube for future DNA quantitation.

   A swinging-bucket rotor is preferred for this step because it lowers background and improves the overall recovery of K-SDS precipitates. However, a fixed-angle rotor, spun at 6000 × g is satisfactory.

   Pouring off of the supernatant results in higher background during detection; hence aspiration is preferred.

Resuspend and wash the K-SDS precipitate

8. Resuspend the pellet in 1 ml of precipitation/washing solution and vortex at maximum speed for 3 sec.
9. Repeat the heating, tube inversion, and centrifugation, as described in steps 5 to 8, three times.
10. Pool the supernatants with that of step 7 above and store at 4°C.

    Final volume will be ~4 ml.

Release the protein-bound DNA from the K-SDS precipitate

11. Add 0.5 ml of proteinase K solution to the pellet.
12. Incubate the samples at 50°C for a minimum of 3 hr with occasional shaking.

    Overnight incubation is acceptable.

Reduce the SDS content of the solution by precipitation

13. Place samples on ice until precipitate forms (1 to 5 min). Add 50 µl of 4 mg/ml BSA to each tube, vortex, and place samples on ice for 30 min.
14. Centrifuge the tubes in a swinging bucket rotor 20 min at 3300 × *g*, at 4°C

    Alternatively, centrifugation may be performed for 10 min in a fixed-angle rotor at 12,000 × g, 4°C.

15. Gently aspirate 500 µl of the supernatant with a pipet, being careful not to disturb the K-SDS pellet, and transfer to a 12 × 75–mm borosilicate glass tube or to a tube or cuvette appropriate for the fluorometer.

    SDS interferes with the Hoechst 33258 assay.

Determine DNA concentrations of pooled supernatants from wash steps (total free DNA)

16. Prepare a 0.312 mg/ml solution of Hoechst 33258 dye by diluting a 1 mg/ml dye stock solution in 20 mM Tris·Cl, pH 7.5.

    Protect Hoechst dye from direct light. Perform all subsequent steps in dim light. Measure pH carefully; pH 7.5 is optimal.

17. Using a λ DNA solution of known concentration, prepare DNA standards (250, 500, 1000, 2500, 5000, and 10,000 ng/ml) in 20 mM Tris·Cl, pH 7.5.

    Choice of DNA is important. Always use standard DNA from the same source in each assay.

18. Centrifuge the tube containing the pooled supernatant 15 min at 1500 × *g* in a swinging-bucket rotor, 4°C.

    Centrifugation helps to remove residual SDS.

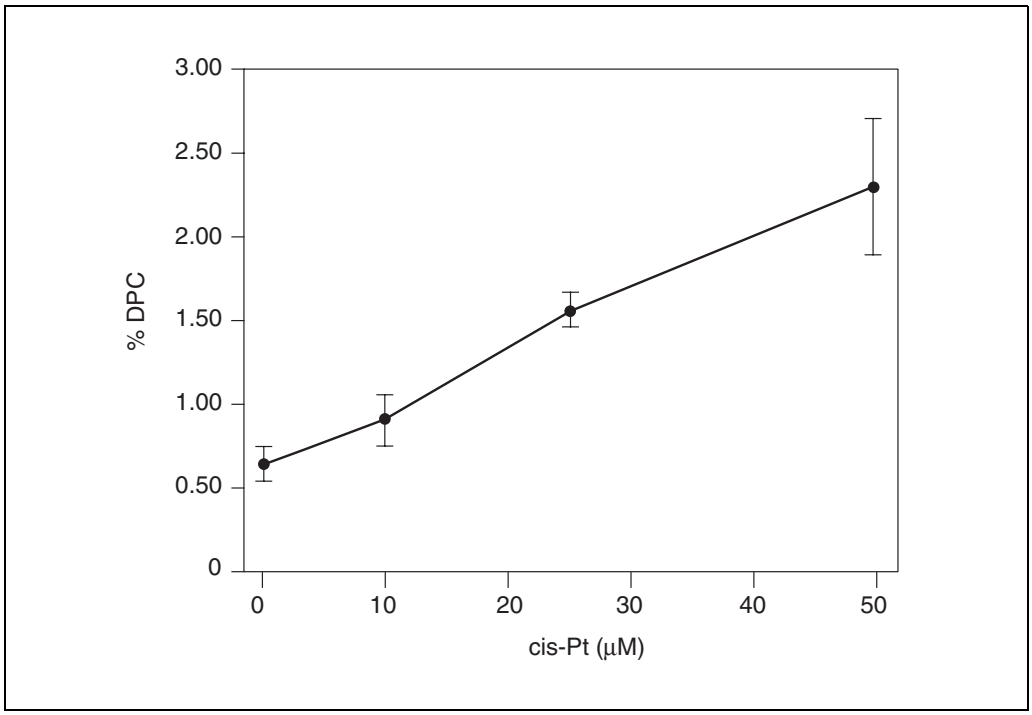

Figure 3.5.4 DNA-protein cross-links (mean ± std. dev.) induced by cis-platinum (cis-Pt; 16 hr) in EBV-transformed human Burkitt's lymphoma cells. From Costa et al. (1996). Reprinted with permission from Elsevier Science Publishers.

19. Mix (in duplicate) a 200-µl aliquot of the pooled supernatant with 0.8 ml of the Hoechst dye solution prepared in step 16. Also mix duplicate 200-µl aliquots of the BSA blanks and each of the standards with 0.8 ml of the Hoechst dye solution. Incubate 10 min in the dark.

    The final DNA concentration of the standards will be 50, 100, 200, 500, 1000, and 2000 ng/ml.

    In practice, the authors have found that it is possible to combine the pooled supernatants from all three triplicates (~12 ml) for total DNA determination. Do this only when it has been ascertained that the total amount of DNA among triplicates is similar. Perform total DNA determination in duplicate.

20. Set the excitation wavelength of the fluorometer to 365 nm and the emission wavelength to 450 to 460 nm. Read the fluorescence of the DNA standards, supernatant aliquots, and BSA blanks. Use the DNA standard curve to calculate the DNA concentration of the supernatant aliquot.

    A 96-well microtiter plate reader with appropriate filters also works well.

21. Calculate the amount of total DNA by multiplying the DNA concentration by the total volume of the pooled supernatant (~4 ml).

Determine DNA concentration in supernatant from proteinase K digest [DNA formerly cross-linked with protein (DPC)]

22. Prepare 300 ng/ml Hoechst dye in 20 mM Tris·Cl, pH 7.5.

23. Using a λ DNA solution of known concentration, prepare 100, 200, 400, 1000, 2000, and 4000 ng/ml DNA standards by diluting a 1 mg/ml stock in 20 mM Tris·Cl, pH 7.5.

24. Determine the amount of DNA formerly cross-linked to protein (DPC) by combining 0.5 ml of the supernatant from the proteinase K digestion step (step 15) with 0.5 ml

of the 300 ng/ml Hoechst fluorochrome solution. Incubate 10 min in dark. Treat blanks in an identical manner.

25. Add 0.5 ml of DNA standard to 0.5 ml of the 300 ng/ml Hoechst dye and incubate 10 min in the dark.

    The final DNA concentration of the standards will be 50, 100, 200, 500, 1000, and 2000 ng/ml.

26. Determine fluorescence, DNA concentration, and amount of cross-linked DNA as described previously for total DNA in steps 20 and 21. Correct for background fluorescence by subtracting blank measurements.

    If the standard curve is nonlinear at the high DNA concentrations or if the DPC samples exceed the highest DNA standard, repeat the DNA measurements the following day using a 250 ng/ml Hoechst dye concentration. Store the DNA samples at 4°C without light protection to quench the previously added Hoechst dye.

Calculate the DNA-protein cross-link (DPC) percentage

27. Calculate the percentage of the total DNA that was cross-linked with protein by dividing the amount of DPC DNA by the amount of total DNA and multiplying this quotient by 100.

    It is often appropriate to graphically express DPC percentage versus test agent dosage (see Fig. 3.5.4).

ALTERNATE PROTOCOL 8

USING A 96-WELL PLATE TO DETERMINE DNA CONCENTRATIONS FOR K-SDS PRECIPITATIONS

Using techniques similar to those in Basic Protocol 3, the DNA can also be quantified using Pico green dye in a 96-well plate assay.

Additional Materials *(also see Basic Protocol 3)*

Pico green (Molecular Probes)
TE buffer, pH 7.5: 10 mM Tris·Cl (*APPENDIX 2A*) containing 1 mM EDTA
1 mg/ml DNA stock solution

Polystyrene 96-well plates (Corning Costar no. 3603)
Phosphorimager or microtiter plate reader

1. Conduct the lysis, precipitation, washing, and proteinase digestion (see Basic Protocol 3, steps 1 to 15).
2. Prepare a 1:200 dilution of stock Pico green (Molecular Probes) dye in TE buffer, pH 7.5.

   Work in dim light.

   CAUTION: *Pico green is a DNA-binding agent and should be used with appropriate care.*

3. Prepare 0 to 50 ng/well λ DNA standards in 50 µl in a 96-well polystyrene plate.

   50 µl of a 1 µg/ml DNA stock solution equals 50 ng of DNA.

4. Pipet 5 µl of total DNA, or 50 µl DPC DNA or blank, into the appropriate wells of the plate.
5. Add 50 µl of Pico green dye (diluted as in step 2) to each well. Incubate at room temperature in dark for 10 min.
6. Use a phosphorimager or a microtiter plate reader to quantitate fluorescence.

   The excitation wavelength is 498 nm and the emission wavelength is 520 nm.

USING SLOT BLOTTING TO DETERMINE DNA AMOUNTS

The sensitivity of this technique for DNA-protein cross-link detection is greater than the aforementioned methods. Hence, it is useful when cell numbers are limited (1000 to 2000 cells) (Zhitkovich et al., 1998). The disadvantages are that radioactivity is used and that this method requires more time than the previously described methods.

CAUTION: When working with radioactivity, take appropriate precautions to avoid contamination of the investigator and the surroundings. Carry out the experiment and dispose of wastes in an appropriately designated area, following the guidelines provided by your local radiation safety officer (also see *APPENDIX 1A*).

Additional Materials *(also see Basic Protocol 3)*

5 M NaCl
25:24:1 (v/v/v) phenol/chloroform/isoamyl alcohol (prepared with buffered phenol; *UNIT 2.2*)
24:1 chloroform/isoamyl alcohol
DNA from test species
TE buffer, pH 8: 10 mM Tris·Cl, pH 8 (*APPENDIX 2A*) containing 1 mM EDTA
3 M NaOH
2 M ammonium acetate, pH 7
6× SSPE (see recipe for 10×)
Human Alu DNA or purified DNA from other species for use as a probe
Random priming kit (e.g., Prime-A-Gene Labeling System; Promega)
Prehybridization solution (see recipe)
2× and 0.1× SSC (see recipe for 20×)
2× SSC (see recipe for 20×) containing 1% (w/v) SDS

45° 65°, and 70°C water bath
Slot blot apparatus
UV transilluminator
Sephadex G-50 spin column
X-ray film

Additional reagents and equipment for DNA labeling with ^{32}P, purification of DNA probes, and autoradiography (*APPENDIX 3*)

1. Conduct cellular lysis, DNA shearing, K-SDS precipitation, proteinase K digestion, and removal of SDS (see Basic Protocol 3, steps 1 to 15).

   If the total cell number is <2 × 10^5 add 50 µl of BSA (2 mg BSA/ml) to the lysate, after shearing (step 4) but prior to K-SDS precipitation step (step 5).

Extract the DPC DNA

2. Transfer the supernatant from the proteinase K digestion step (0.5 ml) to a 1.5-ml microcentrifuge tube.

3. Add 25 µl of 5 M NaCl to 0.5 ml of the supernatant (200 mM NaCl, final). Add 0.5 ml of 25:24:1 phenol/chloroform/isoamyl alcohol. Do not shake. Heat 5 min at 45°C in water bath. Mix gently by inversion twice, then vortex. Micocentrifuge 5 min at maximum speed (≥10,000 rpm).

   CAUTION: *Phenol causes severe burns; use appropriate caution. Perform work in a fume hood and dispose of used phenol in a glass receptacle. Chloroform is a suspected human carcinogen.*

4. Collect aqueous (top) phase.

5. Add equal volume of 24:1 chloroform/isoamyl alcohol. Vortex. Microcentrifuge 5 min at maximum speed.
6. Collect aqueous phase.

   Final volumes from each sample should be consistent. Henceforth, this fraction will be referred to as DPC DNA.

Denature and neutralize DPC DNA and DNA standards

7. Prepare DNA standards at 2, 4, 10, 20, 40, 100, and 200 ng DNA/ml.

   The source of the DNA should match that of the test species.

8. Mix 50 µl of DPC DNA or DNA standard with 130 µl of TE buffer, pH 8, and 20 µl of 3 M NaOH.

   More DPC DNA (up to 100 µl) can be loaded if the hybridization signal is too weak. Conversely, less DPC DNA should be loaded if the signal is too strong. Final total reaction volume should always equal 200 µl.

9. Heat in 70°C water bath for 1 hr.
10. Add an equal volume (i.e., 200 µl) of 2 M ammonium acetate, pH 7.

Load samples into slot blot apparatus

11. Follow manufacturer's protocol for loading samples into slot blot apparatus.

    The authors have found that a Nytran 0.45-µm membrane (Schleicher and Schuell) works well.

12. Cross-link the DNA to the membrane with UV radiation.
13. Soak membrane in 6× SSPE 15 min at room temperature.

Make DNA probe

14. If human DNA is tested, label *Alu* DNA with ^{32}P, using a random-priming kit. For other species, label purified DNA for use as a probe. Purify the probe from the unincorporated labeled deoxynucleotide using a Sephadex G-50 spin column.

    Purification of the probe with a Sephadex G-50 spin column is required.

Hybridize probe and DPC DNA

15. Prehybridize the membrane in prehybridization solution for 2 hr at 65°C.
16. Denature probe by boiling for 10 min.
17. Keep membrane in prehybridization solution and add probe to a final concentration of 2×10^6 cpm/ml.
18. Hybridize overnight at 65°C.
19. Wash membrane with 2× SSC for 5 min at 65°C. Repeat once. Wash membrane once with 2× SSC/1% SDS for 30 min at 65°C. Wash membrane once with 0.1× SSC for 15 min at room temperature.

Quantify the amount of DPC DNA

20. Dry membrane and expose to X-ray film (autoradiography; *APPENDIX 3*).

    Exposure time will depend upon the amount of DNA on the filter and the strength of the probe.

21. Quantify the bands with densitometry.

Determine the amount of total DNA in the cell lysates

22. Remove 0.5 ml of the pooled supernatants from the wash steps (see Basic Protocol 3, step 10) and extract the DNA with phenol/chloroform as described above for DPC DNA (steps 3 to 6 in this protocol).

    In practice, the authors have found that it is possible to combine the pooled supernatants from all three triplicates (~12 ml) for total DNA determination. Do this only when it has been ascertained that the total amount of DNA among triplicates is similar. Perform total DNA determination in duplicate.

23. Mix 5 µl of purified total DNA with 175 µl of TE buffer, pH 8, and 20 µl of 3 M NaOH. Mix 50 µl of DNA standard with 130 µl of TE buffer, pH 8, and 20 µl of 3 M NaOH.

24. Heat in 70°C water bath for 1 hr.

25. Repeat steps 10 to 21, except use supernatant DNA.

26. Determine the DPC coefficient by dividing the amount of DPC DNA by the amount of total DNA. Express as a percentage.

DETECTION OF DNA REPAIR USING THE UNSCHEDULED DNA SYNTHESIS (UDS) ASSAY

BASIC PROTOCOL 4

This assay indirectly measures DNA damage by quantitating the amount of DNA synthesis that occurs in cells that are not undergoing normal S-phase DNA replication. This type of DNA synthesis has been termed "unscheduled DNA synthesis" (UDS) and is a component of DNA repair. This protocol describes how to prepare a primary hepatocyte culture and measure UDS by determining the degree of [^{3}H]thymidine incorporation into nuclear DNA following treatment with test agents. Williams (1976) was the first to describe this assay for screening xenobiotics, and it has been subsequently modified by others. This protocol is based upon that of Dean (1995).

NOTE: All protocols using live animals must first be reviewed and approved by an Institutional Animal Care and Use Committee (IACUC) or must conform to governmental regulations regarding the care and use of laboratory animals.

Materials

Male 200 to 250 g Fisher 344 rats (Charles River Laboratories, Harlan Sprague-Dawley)
General anesthetic (e.g., sodium pentobarbital)
70% and 90% (v/v) and absolute ethanol
Liver perfusion buffer 1 (see recipe)
Liver perfusion buffer 2 (see recipe)
Collagenase A
769 mM $CaCl_2$
Williams medium E-complete medium (WE-C medium; see recipe)
Williams medium E-incomplete medium (WE-I medium; see recipe)
0.4% (w/v) trypan blue stain
1 mCi/ml [^{3}H]thymidine
Phosphate-buffered saline (PBS; see recipe)
1:3 (v/v) glacial acetic acid/absolute ethanol, freshly prepared
Permount mounting medium (Fisher)
Glycerol
Kodak NTB-2 autoradiography emulsion

continued

Desiccant (e.g., silica gel or Drierite)
Kodak D19 developer
Kodak Fixer
Mayers hemalum stain (see recipe)
1% (w/v) aqueous eosin Y
Xylene

Sterile cotton surgical gauze
Dissection scissors
Suture thread
18-G and 14-G catheters
Surgical tubing ~3 mm o.d. (suitable for a peristaltic pump, e.g., high-pressure tubing with male and female Luer-Lok connectors; Harvard Apparatus)
Variable-flow peristaltic pump
6-well multi-well plates or 30-mm Petri dishes, sterile
Cheesecloth or gauze, sterile
50-ml plastic centrifuge tubes, sterile
Sterile glass beaker
Hemacytometer
Microscope with 100× objective interfaced to a colony counter
25-mm-diameter round plastic coverslips, sterile (e.g., Thermanox; Fisher)
Microscope slides
50-ml plastic graduated cylinders cut to 30-ml mark
43°C water bath
Plastic teaspoons
Light-proof slide boxes
Staining troughs
22 × 50–mm glass coverslips

Additional reagents and equipment for counting cells and assessing viability with trypan blue (*APPENDIX 3B*)

NOTE: All culture incubations should be performed in a humidified 37°C, 5% CO_2 incubator unless otherwise specified.

NOTE: All solutions and equipment coming into contact with live cells must be sterile, and aseptic technique should be used accordingly.

Anesthetize rat and perfuse the liver

1. Anesthetize rat with a dose of general anesthetic that is incompatible with recovery (e.g., 60 mg/kg sodium pentobarbital administered by intraperitoneal injection). Check reflex actions of rat (i.e., tail and toe pinch) before beginning surgery.
2. Disinfect the abdominal surface by swabbing with 70% ethanol.

   Perform perfusion as aseptically as possible.
3. Make a V-shaped incision through skin and muscle from the center of lower abdomen to the lateral aspects of the rib cage.
4. Clamp the inferior vena cava proximal to the renal vein.
5. Secure a loose ligature around the hepatic portal vein and cannulate the vein with a 18-G catheter. After the catheter is in place, remove the inner needle and tighten the ligature.

6. Cut through the diaphragm muscle and remove the ventral portion of the rib cage. Locate the superior vena cava distal to the heart and tie a loose ligature. Cannulate the vena cava with a 14-G catheter, remove the inner needle, and tighten the ligature.
7. Sterilize the surgical tubing by flushing twice with 70% ethanol, followed by sterile water. Connect the tubing to the portal vein catheter, taking care to avoid air bubbles.
8. Connect the portal vein catheter to a peristaltic pump. Connect the superior vena cava catheter to a waste line.

   It is useful to outfit the line with a three-way valve so that perfusion buffers can be switched. This way separate reservoirs for buffer 1 and buffer 2 can be used.
9. Perfuse the liver for 10 min with 400 ml of liver perfusion buffer 1 at 40 ml/min. Keep the perfusion buffer in a 37°C water bath.

   As the blood drains, the liver should turn tan in color and lobes should clear equally. If not, gently massage the liver or reposition the portal vein catheter.
10. Place 400 ml of perfusion buffer 2 in the reservoir attached to the perfusion pump. Perfuse the liver for 5 min with liver perfusion buffer 2 at 40 ml/min, until 200 ml of the buffer has been pumped. Keep the perfusion buffer 2 in a 37°C water bath.
11. While the perfusion in step 10 is in progress, dissolve 75 U (50 mg) of collagenase A in 1 ml of 769 mM $CaCl_2$, sterile filter, and add to 10 ml of liver perfusion buffer 2. Pour this solution into the remaining 200 ml of liver perfusion buffer 2 in the reservoir and perfuse the liver for ~1 min. When the dark red color of the collagenase preparation reaches the liver, move the waste line to the buffer 2 reservoir so that the solution recirculates. Reduce the flow rate of the pump to ~20 ml/min.
12. When the liver becomes spongy (10 to 15 min), stop the perfusion. Remove the liver from the body cavity and place it in a beaker containing 10 ml of the recirculated buffer 2.

Prepare primary hepatocyte culture

13. Warm WE-C medium in a 37°C water bath.

    Continue to work aseptically and prepare the primary hepatocyte culture under a laminar flow hood.
14. Move the liver to a sterile, plastic Petri dish and cut open the capsule. Gently tease out the hepatocytes with a forceps or round-tooth stainless steel comb.
15. Filter the hepatocytes through several layers of sterile cheesecloth or a four-ply layer of sterile gauze into a sterile glass beaker. Wash the residue with 120 ml of WE-C. Decant 40 ml of filtrate into three sterile 50-ml centrifuge tubes.
16. Centrifuge at 40 × *g* for 3 min at room temperature to bring down the hepatocytes. Aspirate the supernatant and resuspend the pellets in 20 ml of WE-C.
17. Centrifuge at 40 × *g* for 3 min at room temperature. Repeat the resuspension and centrifugation steps once more.
18. Combine the three pellets in 50 ml of WE-C.
19. Pipet 0.5 ml of the hepatocyte preparation into a 1.5-ml microcentrifuge tube. Add 0.5 ml of 0.4% trypan blue stain (*APPENDIX 3B*).
20. Apply 10 µl to a hemacytometer and count the viable (yellow) and non-viable (blue) cells. Calculate the viability percentage.

    Viability should be >70%.

21. Place a 25-mm sterile round plastic coverslip in each well or dish for cell attachment. Plate the hepatocytes into 6-well plates or 30-mm dishes at a density of 1.5×10^5 viable cells/ml at 3 ml of culture per well or dish. Press down gently on the coverslip. Stir cells gently to evenly distribute them over the coverslip.

    Thermanox coverslips are treated on one side for cell attachment. Be sure to place the coverslips in the correct orientation (i.e., coated-side-up) in the wells.

    Prepare three coverslips per dose, and for the negative and positive controls. Also prepare an additional three coverslips for each treatment for cell viability testing.

22. Place the plates in a 5% CO_2 incubator at 37°C. Allow cells to attach for 1.5 hr, then aspirate unattached cells and add 2 ml of 37°C WE-I medium to each of the plates or wells.

    Incubate for an additional 24 hr to allow for recovery of membrane function and cellular glutathione levels (Parton et al., 1995).

Treat hepatocyte culture with test agent and label cells with ^3H

23. Prepare test agent in appropriate solvent.

    Culture medium is appropriate for water-soluble agents unless they bind to components of the medium. Dimethy sulfoxide (DMSO) is often used for water-insoluble compounds. Solvent concentration should be ≤1% (v/v) of the growth medium to avoid cytotoxicity or induction of UDS by the solvent (Mitchell et al., 1983).

    Dosages are based upon cytotoxicity. Use the lowest cytotoxic dose (or the highest soluble concentration if nontoxic) and scale down. Test at least five concentrations, encompassing at least a 2-log range (Mitchell et al., 1983).

    2-Acetamidofluorene (2-AAF; 0.25 and 0.50 mg/ml) is frequently used as a positive control test agent.

24. Add sufficient 1 mCi/ml [^{3}H]thymidine stock solution to the medium containing the test agent to achieve a final concentration of 10 μCi/ml.

    When preparing mixtures, use normal radiochemical safety precautions.

25. Remove medium from hepatocyte cultures. Wash each cell monolayer with 2 ml of 37°C WE-I.

26. Dispense 2 ml of each test agent/[^{3}H] thymidine mixture into the corresponding plate or well. Treat the cultures designated for viability testing with the test agent only (i.e., no [^{3}H]-thymidine).

27. Incubate cultures for ≥16 hr at 37°C.

    If cytoplasmic background counts are unacceptably high, shorten the incubation period.

Assess cell viability using trypan blue exclusion test

28. From each plate or well that was designated for cell viability testing, remove 1 ml of medium. Add 1 ml of 0.4% trypan blue to the plate. Incubate for 5 min.

29. Aspirate the trypan blue/medium mixture and replace with 2 ml of PBS. Aspirate PBS to rinse plate.

30. Use an inverted microscope fitted with a graticule to view slides. Score four areas for viable (unstained) and nonviable cells (stained blue). Calculate the viability percentage for each dose and compare to the vehicle control.

    A rapid and easy alternative is the neutral red (NR) assay described by Fautz et al. (1991).

Fix cells and attach coverslips to microscope slides

31. Remove medium from wells/dishes (and dispose of radioactive waste properly). Rinse coverslips with 2 ml PBS. Add 2 ml of a freshly prepared 1:3 glacial acetic acid/absolute ethanol to each and wait 10 min. Repeat the application of the acetic acid/ethanol mixture twice more.

    Before fixation, the cells can be chased overnight with unlabeled 0.25 mM thymidine in WE-I (Hamilton and Mirsalis, 1987).

    Alternatively, one 30-min fixation step (with 1:3 glacial acetic acid/absolute ethanol) can be substituted to lessen loss of attached cells due to washing.

    Before fixation, 1% (w/v) sodium citrate can be applied to the cells to enhance swelling of the hepatocytes, which facilitates scoring of UDS (Hamilton and Mirsalis, 1987). However, Parton et al. (1995) reported that this practice ruptured large hepatocytes and contributed to high background grain counts.

32. Wash wells/dishes with distilled or deionized water four times. Retrieve the coverslips and air dry.

33. When dry, mount the coverslips (cell-side-up) onto labeled microscope slides ~1 cm from one edge, using Permount mounting medium.

34. Leave slides flat for a few hours (or overnight) in a dust-free area (e.g., plastic box with lid) until mounting medium sets.

Apply photoemulsion to slides

35. Dispense 12 ml of deionized or distilled water into 50-ml graduated cylinder cut off at the 30-ml mark. Add 0.5 ml of glycerol and place the cylinder in a 43°C water bath.

    IMPORTANT NOTE: *Perform this and all following steps in a darkroom under safelight conditions (Kodak safelight filter no. 2).*

36. Into a second cut-off cylinder, use a plastic teaspoon to transfer enough NTB-2 emulsion to reach the 20-ml mark.

    Fresh emulsion (not older than 3 months) gives the best results.

37. Place this cylinder in the 43°C water bath for 10 min to melt the emulsion. Stir occasionally with a plastic utensil, avoiding air bubbles.

38. Pour the molten emulsion into the cylinder containing the water/glycerol mixture until the 25-ml mark is reached. Return the cylinder to the water bath for 2 min and stir gently with a plastic implement. Remove air bubbles, if present, by skimming the surface with a glass microscope slide.

39. Remove emulsion from water bath. Keeping slides vertical, dip into emulsion and withdraw slowly and steadily to achieve an even coating. Hold the slides vertically for 2 sec and blot the emulsion off of the bottom of the slides.

40. Place each slide on a metal tray set on ice for 10 min to solidify emulsion.

41. Place slides in light-proof slide boxes and dry for at least 90 min at room temperature.

42. Add a dessicant (e.g., silica gel or Drierite) to each box. Seal the edges of the box with black electrical tape and wrap each box in aluminum foil. Label the box with name and date.

    A false-bottomed box containing Drierite works well. Alternatively, silica gel can be smeared on a clean microscope slide and placed at the end of the slide box.

Develop and stain exposed slides

43. Immerse each slide successively for the time indicated in staining troughs containing the following solutions:

    5 min in 1:1 (v/v) Kodak D19 developer/distilled water (19° to 21°C)
    1 min in distilled water
    5 min in 1:3 (v/v) Kodak fixer/distilled water
    10 min in tap water
    3 min in Mayer's hemalum stain (or until nuclei are pale blue)
    1 min in tap water until nuclei are pale blue
    1.5 min in 1% aqueous eosin Y
    2 min in tap water
    2 min in 70% ethanol
    2 min in 90% ethanol
    2 min in absolute ethanol
    2 min in (fresh) absolute ethanol
    3 min in xylene
    3 min in (fresh) xylene

    Other stains that have been used are methyl green Pyronin Y, or Giesma.

    Use a razor blade to scrape stain/emulsion off bottom of slides if necessary.

44. Mount coverslips onto the cell preparations using Permount mounting medium.

Score slides for UDS

45. Place the slide under a microscope. Score only morphologically normal cells. Do not score the heavily labeled S-phase cells. Do not score the same cell more than once.

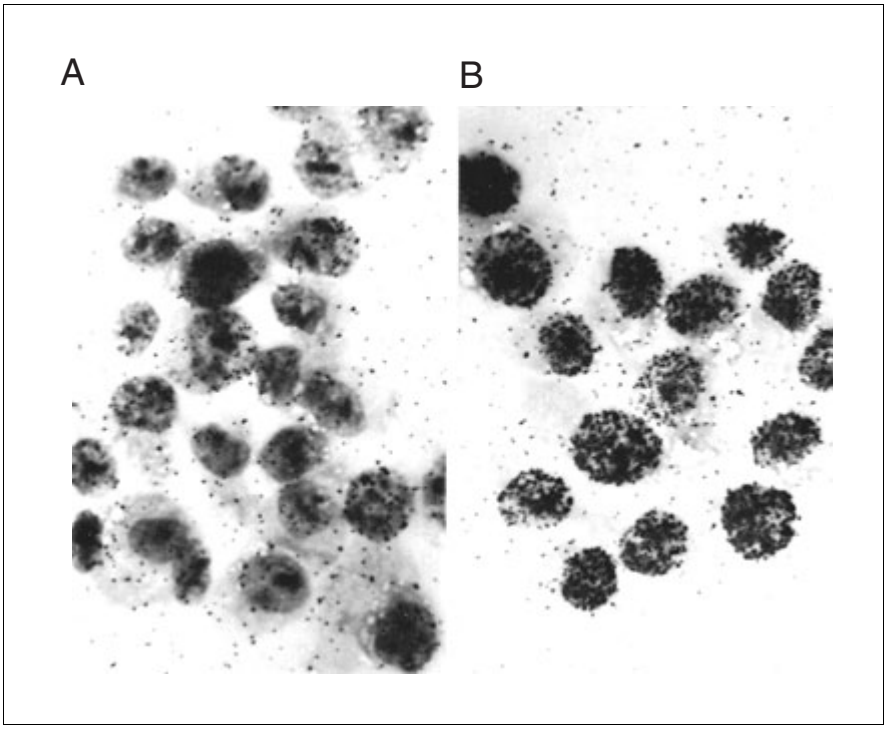

Figure 3.5.5 Unscheduled DNA synthesis (UDS) in human amnion (AV_3) cells following culture in arginine-deficient medium, treatment with 5 mM hydroxyurea (1 hr), irradiation with 254 nm ultraviolet light and exposure to [^{3}H]TdR (5 μCi/ml medium; 2 or 4 hr). (**A**) Control (unirradiated) cells pulsed for 4 hr. (**B**) Cells irradiated with 15 ergs/mm^2 and pulsed for 2 hr. From Trosko and Yager (1974); reprinted with permission from Academic Press.

Perform grain counting manually using an appropriate graticule; this is greatly facilitated by use of an automated system (e.g., a colony counter interfaced to the microscope). Count the number of grains over the nucleus and over one or more nuclear-sized areas of adjacent cytoplasm. Score 50 cells on each of the three slides for each treatment/concentration in a blind manner (see Fig 3.5.5).

Harbach et al. (1991) evaluated four different scoring methods for UDS. Hill et al. (1989) described a whole-cell counting method designed to eliminate the subjectivity of choosing the areas to be quantitated for cytoplasmic grain counts.

46. Calculate the net nuclear grain count by subtracting the mean cytoplasmic grain count from the total nuclear grain count.

REAGENTS AND SOLUTIONS

Use Milli-Q-purified water or equivalent for the preparation of all buffers. For common stock solutions, see ***APPENDIX 2A****; for suppliers, see* ***SUPPLIERS APPENDIX****.*

Alkaline electrophoresis buffer

0.1% (w/v) 8-hydroxyquinoline
10 mM disodium EDTA, pH 10
2% (v/v) dimethyl sulfoxide (DMSO)
300 mM NaOH
Store up to 3 months at room temperature

The pH of the alkaline electrophoretic buffer is highly variable (pH 9 to 13) among laboratories.

Alkaline elution solution, pH 12.3

0.1% (w/v) sodium dodecyl sulfate
20 mM tetrasodium EDTA
0.8% tetrapropylammonium hydroxide
Adjust pH to 12.3 with 20% (w/v) tetrapropylammonium hydroxide in water
Store up to 3 months at room temperature

Alkaline lysis solution, pH 10

2.5 M NaCl
100 mM disodium EDTA
10 mM Tris·Cl, pH 10
1% (v/v) Triton X-100
1% (w/v) laurylsarcosine, sodium salt (optional)
10% (v/v) dimethylsulfoxide, (add just before use; optional)
Store up to 6 months at room temperature

Cell lysis solution, pH 9.7

2% (w/v) sodium dodecyl sulfate (SDS)
0.025 M disodium EDTA
0.1 M glycine (optional)
Adjust pH to 9.7 with 1 N NaOH
Store up to 6 months at room temperature

K-SDS cell lysis solution

1% (w/v) SDS
20 mM Tris·Cl, pH 7.5 (*APPENDIX 2A*)
1 mM PMSF (add just before use)
Store up to 6 months at room temperature

Liver perfusion buffer 1

150 mM NaCl
3.73 mM $NaHCO_3$
4.84 mM Na_2HPO_4
4.97 mM KCl
1.24 mM KH_2PO_4
0.62 mM $MgSO_4$
0.62 mM $MgCl_2$
10 µg/ml phenol red
Sterile filter
Store up to 3 months at 4°C

Liver perfusion buffer 2

142 mM NaCl
24 mM $NaHCO_3$
4.37 mM KCl
1.24 mM KH_2PO_4
0.62 mM $MgSO_4$
0.62 mM $MgCl_2$
10 µg/ml phenol red
Sterile filter
Store up to 3 months at 4°C

Mayer's hemalum stain

1 g hematoxylin (dissolve with warming in 800 ml distilled H_2O)
50 g aluminum ammonium dodecahydrate (ammonium alum)
0.2 g sodium iodate
1 g citric acid
50 g chloral hydrate
H_2O to 1 liter
Store up to 6 months at room temperature

Neutral lysis solution, pH 8.3

0.5% (w/v) sodium dodecyl sulfate (SDS)
30 mM EDTA
Adjust pH to 8.3 with 1 N NaOH
Store up to 6 months at room temperature

Phosphate-buffered saline (PBS)

137 mM NaCl
2.7 mM KCl
4.3 mM $Na_2HPO_4 \cdot 7H_2O$
1.4 mM KH_2PO_4
Store up to 1 month at 4°C

Precipitation/washing solution

100 mM KCl
20 mM Tris·Cl, pH 7.5 (*APPENDIX 2A*)
Store up to 6 months at room temperature

Prehybridization solution

6× SSPE (see recipe) containing:
1% (w/v) SDS
100 µg/ml salmon sperm DNA (boiled for 10 min and added just before use)
Prepare fresh

Proteinase K solution (for Basic Protocol 3)

100 mM KCl
20 mM Tris·Cl, pH 7.5 (*APPENDIX 2A*)
10 mM EDTA
0.2 mg/ml proteinase K
Prepare fresh

SSC, 20×

3 M NaCl
0.3 M trisodium citrate·dihydrate
Store up to 6 months at room temperature

SSPE, 10×

1.8 M NaCl
100 mM NaH_2PO_4
100 mM disodium EDTA
Adjust to pH 7.4 with 1 N NaOH
Store up to 6 months at room temperature

Williams medium E-complete (WE-C)

Prepare Williams medium E-incomplete (see recipe) containing 10% fetal bovine serum. Store up to 6 months at 4°C.

Williams medium E-incomplete (WE-I)

Williams medium E (Life Technologies) containing
4 mM L-glutamine
100 µg/ml gentamycin
Store up to 6 months at 4°C.

COMMENTARY

Background Information

Microgel electrophoresis assay

Single-cell microgel electrophoresis (i.e., the comet assay; see Basic Protocol 1 and Alternate Protocol 1) is a simple, rapid, and sensitive technique for quantitating DNA strand breakage in individual cells. Cells are embedded in agarose on a microscope slide and are then permeabilized with detergent and treated with high salt to extract cellular proteins. The resulting "nucleoids" contain supercoiled DNA. If the DNA has been damaged, relaxation of the supercoiled DNA occurs, and, upon electrophoresis, the relaxed loops and broken DNA fragments will migrate toward the anode. Undamaged DNA remains trapped within the nucleoid. This creates a comet-like pattern of DNA when visualized with fluorescence microscopy.

This technique was first introduced by Ostling and Johanson (1984) who assessed DNA damage in irradiated cells. Their work was conducted at near-neutral pH. Because neutral pH does not permit much DNA strand separation, the assay was more sensitive to double rather than single DNA strand damage. Singh et al. (1988) modified the assay by using alkaline (pH 13) electrophoretic conditions, which disrupted base pairing and allowed for DNA strand separation (unwinding) and hence more sensitive detection of single-strand breakage. As a result, alkaline comet assays are sensitive to both double- and single-strand breakage, including the indirect single-strand breaks produced at alkaline-labile apurinic (AP) sites. Moreover, DNA strand breakage that occurs during DNA excision repair can be detected.

Since its introduction, numerous refinements to the assay have been published. Major adaptations have included the use of increasingly sensitive fluorescent DNA stains (Singh et al. 1994); addition of free-radical scavengers to the electrophoresis solution (Singh et al., 1994); inclusion of DNA repair enzymes (Collins et al., 1997); use of repair-deficient cell lines (Helbig and Speit, 1997) or repair inhibi-

tors; design of cell-free assays (Kasamatsu et al., 1996); and improved quantitation of DNA damage (Olive, 1989; Olive et al., 1990) via use of image analysis software (McKelvey-Martin et al., 1993).

Many other techniques exist for detecting DNA strand breakage. In the nucleoid sedimentation assay, the extent of DNA unwinding, reflecting the amount of strand breakage, is measured by the rate of sedimentation (Cook and Brazell, 1975). Sucrose sedimentation separates different sizes of DNA fragments along a sucrose gradient (McGrath and Williams, 1966). Pulsed-gel electrophoresis is based upon the assumption that intact mammalian chromosomes are too large to enter a gel. The amount of DNA that enters the gel will reflect the degree of DNA double-strand breakage (Elia et al., 1994). DNA precipitation assays rely upon the centrifugal separation of intact and broken DNA (Olive et al., 1988). Filter elution assays measure the rate of DNA elution through a filter; elution rates are proportional to the number of strand breaks (Kohn et al., 1981). In these procedures, neutral and alkaline pH conditions are employed for the detection of double- and single-strand breaks, respectively.

The comet assay has several advantages over those above. Data are collected for individual cells; therefore variability within a given cell population can be evaluated. In contrast, the other techniques only provide information regarding the average number of DNA strand breaks per cell. In addition, the comet assay requires viable cells, but because no radioactive labeling is required, cell growth is not required. Hence, the comet assay can be applied to most eukaryotic cell populations and only a few thousand cells are required. Moreover, the sensitivity of the comet assay is comparable to or greater than the sensitivity of other assays for DNA strand breakage (Olive et al., 1990; Singh et al., 1994; Singh, 1996). However, the sensitivity of the assay for detection of double-strand breaks has been questioned (Helbig and Speit, 1997).

The use of the comet assay for genotoxicity testing has increased steadily since its introduction in 1988. Henderson et al. (1998) provide a current list of agents that have been evaluated with the comet assay during genotoxicity screening. A particular strength of this assay for genotoxicity assessment is that it can be employed both in vitro and ex vivo. The latter route is especially useful because genotoxicty in a variety of target organs can be assessed. In addition to agents that directly damage DNA, other lesions such as DNA-DNA and DNA-protein cross-links can be detected using the comet assay. Pfuhler and Wolf (1996) reported that cis-platinum, mitomycin C, and formaldehyde reduced the migration of methyl methanesulfonate–damaged DNA in the comet assay, presumably because cross-linking retarded DNA migration.

A major drawback of using the comet assay for genotoxicity testing is that it lacks rigorous validation. Each investigator who has performed the assay has used a unique set of experimental conditions and scoring criteria. The effects of different protocol factors (cell type, lysis and electrophoretic conditions, and exposure times) on the overall outcome of the assay are poorly understood. Several investigators have pointed out the need for further validation in this area (Ross et al., 1995; Anderson and Plewa, 1998; Henderson et al., 1998). It is also imperative that investigators clearly detail their experimental conditions so that the results of assays can be reproduced and compared between laboratories (Ross et al., 1995).

Results from comet assays must also be cautiously interpreted both in terms of the nature of the DNA breakage that is revealed and the relationship of that damage to mutagenesis. Single-strand breakage occurs transiently during base or nucleotide excision repair. Accordingly, Collins et al. (1997) suggested that high levels of DNA strand breakage in the comet assay indicate either high damage or efficient DNA repair processes. For example, Speit et al. (1996) reported that the mutagen, benzo[a]pyrene and its reactive metabolite, (+)-anti-benzo[a] pyrene-7,8-diol 9,10-oxide were genotoxic in the comet assay, yet were only marginally mutagenic to the HPRT gene in human (MRC5CV1) cells presumably because most of the detected strand breakage represented excision repair activity.

On the other hand, the comet assay has been modified in order to exploit the process of DNA repair to reveal DNA lesions that would have gone undetected in traditional comet assays. Exogenous lesion-specific repair enzymes have been used to detect AP sites formed following DNA alkylation damage (Fortini et al., 1996), 8-0H, dG, and UV radiation-induced cyclobutane pyrimidine dimers (Collins et al., 1997). In a somewhat analogous approach, DNA repair synthesis inhibitors have been added to impede DNA ligation following excision (Gedik et al., 1992).

A final caveat to consider when interpreting comet assay results is the effect of cytotoxicity or apoptosis on the assay. DNA strand breakage occurs in necrotic and apoptotic cells. It is, therefore, important to distinguish between direct genotoxicity and DNA damage secondary to cytotoxicity or apoptosis.

Filter elution assay

The alkaline elution technique, introduced by Kohn and Ewig (1973), measures DNA single-strand breakage. Cells treated with the test agent are placed on a polycarbonate filter and lysed with detergent and proteinase. The lysate is then eluted with an alkaline buffer (pH = 12). At this pH, the double-stranded DNA molecules denature, and short broken fragments of single-stranded DNA are eluted whereas the intact longer fragments are retained on the filter. The DNA in the eluted fractions and that retained on the filter are quantified by scintillation counting if cells have been labeled prior to the experiment, or by fluorometry. To control for anomalies in the procedure, an internal standard, composed of cells labeled differently than the test cells, is often included. Most often, a defined number of single-strand breaks are introduced into the internal standard cells by X-irradiation and the elution profiles of the test cells and the standard cells are compared (Kohn et al., 1981).

The assay has been modified to detect other types of DNA damage. Interstrand linkage impedes passage of DNA through the filter. Treated and control cells are X-irradiated and then alkaline eluted. If significant interstrand linkage has been caused by the test agent, more DNA will be retained on the filter than in the control cells (Kohn, 1991).

In a similar manner, DNA-protein cross-links impede passage of DNA through a filter and can be measured using the technique described above for interstrand linkage, with the following modifications. Proteinase K digestion is omitted from the assay, and a polyvinyl chloride filter (better at retaining protein than polycarbonate) is used (Kohn, 1981). It is also instructive to run assays with and without proteinase K and compare the elution profiles.

Another lesion that can be detected with a modified alkaline elution assay is oxidative DNA base damage. These lesions are normally removed by intracellular repair endonucleases via excision repair, which results in transient single-strand breakage. To measure the formation of these damaged bases, exogenous bacterial repair enzymes are added to the assay following lysis. If the test agent has caused significant oxidative base damage, more strand breakage should result and hence less DNA should be retained on the filter compared to cells that did not undergo endonuclease treatment (Pflaum et al., 1997).

Finally, the technique has been adapted to detect primarily double-strand DNA breakage. Even though this assay is conducted at alkaline pH (9.6), it is referred to as "neutral" filter elution because this pH is nondenaturing to DNA molecules. Hence, the DNA present in the eluted fractions must have arisen from double-stranded DNA breakage (Elia et al., 1991). Bradley and Kohn (1979) first used neutral filter elution to measure double-strand breaks in mouse cells treated with X rays, bleomycin, and hydrogen peroxide (H_2O_2). Elia et al. (1991) provides a list of agents tested with the neutral elution filter method.

Advantages of the filter DNA elution are experimental reproducibility, sensitivity, and simplicity. The primary disadvantage is that populations of cells are tested, so intercell susceptibility to the test agent cannot be assessed. If the traditional method is used, only a limited number of samples can be processed effectively in one assay. Additionally, the assay is fairly time consuming.

K-SDS precipitation assay

A number of agents (e.g., γ and UV radiation, formaldehyde, cis-platinum, chromate, and nickel) induce covalent DNA-protein cross-linking (Costa, 1990). Such damage may be genotoxic if DNA replication is impaired resulting in deletions, and/or carcinogenesis if these deletions occur in tumor suppressor genes.

The K-SDS precipitation assay described here is a simple, sensitive, rapid, and inexpensive method for detecting DNA-protein cross-links. It was introduced by Muller (1983) and Liu et al. (1983) to examine DNA-topoisomerase complexes and modified by Zhitkovich and Costa (1992). SDS-resistant DNA/protein complexes form insoluble precipitates with potassium and can be separated from free DNA by low-speed centrifugation. By measurement of the free DNA in the supernatant, the total amount of DNA in the lysed cells can be quantified. The amount of DNA cross-linked to protein is determined by measuring the DNA liberated from the K-SDS/protein/DNA precipitate following proteinase K digestion. The

assay has been validated in several independent laboratories (Costa et al., 1996), and normal values of DNA-protein cross-links in lymphocytes of healthy human controls have been established (Taioli et al., 1995). The detection limit for DNA-protein cross-links is ~1 lesion per 1 to 2×10^7 bases (Zhitkovich et al., 1998).

Other approaches exist for detection of DNA-protein cross-links. Alkaline filter elution assays have been frequently used (Kohn et al., 1981). This method only indirectly measures DNA-protein cross-links by quantitating the reduction in elution rates of DNA fragments caused by cross-linkage with protein. It is also time-consuming, and a limited number of samples can be processed at one time. Another potential disadvantage is that the cell lysis conditions employed may not be sufficiently stringent to dissociate all non-covalent protein/DNA complexes (Zhitkovich and Costa, 1992). The filter-binding technique (Chiu et al., 1984) also may be impaired by insufficient stringency of lysis solutions. In addition, sensitivity is relatively low (i.e., high doses of cross-linking agents are necessary), and the biochemical nature of the interaction between the filter and the DNA/protein complexes is not well understood (Zhitkovich and Costa, 1992). Other investigators have used time-consuming ultracentrifugation to isolate DNA/protein complexes (Wedrychowski et al., 1985). It is also possible to raise antibodies against DNA/protein complexes and then use immunological assays to detect these complexes in cell lysates (Wedrychowski et al., 1985; Miller and Costa, 1989; see *UNIT 2.3*). This method is both time and labor intensive and is not generally applicable because the proteins that complex with DNA are dependent upon the test agent used, thus affecting the antigenicity of the DNA/protein complexes.

K-SDS precipitation can be used for genotoxicity testing in vitro, ex vivo, or for biomonitoring purposes in human populations. This assay has been used to measure DNA protein cross-links in leukocytes of rats and mice exposed to intraperitoneal chromate; in leukocytes of humans following chromate ingestion; in peripheral lymphocytes from cancer patients treated with cis-platinum; in residents of a chromium-contaminated area; in welders; and in chrome platers. Cultured cells exposed to chromate, cis-platinum, copper, lead, cadmium, or arsenic, or to acetaldehyde, acrolein, diepoxybutane, paraformaldehyde, 2-furaldehyde, propionaldehyde, chloroacetaldehyde, sodium arsenite, or tris(hydroxymethyl) nitromethane have also been assayed for DNA-protein cross-links with this assay (reviewed by Zhitkovich et al., 1998).

Unscheduled DNA synthesis assay

Rasmussen and Painter (1966) demonstrated that mammalian cells that were not undergoing normal S-phase DNA synthesis incorporated thymidine following ultraviolet irradiation. Accordingly, this event has been termed unscheduled DNA synthesis (UDS) and is a component of excision repair of damaged DNA. Hence, UDS assays detect DNA repair following damage by a physical or chemical agent; these assays have been used to assess the genotoxicity of a number of chemicals (Mitchell et al., 1983; Williams et al., 1989), and there are several published guidelines for genotoxicity screening (Mitchell et al., 1983; Swierenga et al., 1991; Madle et al., 1994).

There are two approaches to assessing UDS. The first is to conduct the assay solely in vitro with cultured cells. Alternatively, animals can be dosed in vivo and UDS subsequently measured in cells collected from the tissue of choice. Madle et al. (1994) provide guidelines concerning in vivo assays and a list of compounds that have been evaluated with this approach.

Hepatocytes are the cells usually chosen for in vitro UDS assays, for several reasons. These cells are easy to obtain and to culture and also retain the metabolic enzymes that activate most pro-carcinogenic and pro-mutagenic precursors into their ultimately DNA-damaging forms. Moreover, drug-metabolizing enzymes are also present; therefore, hepatocytes are an appropriate model for processes that occur in the liver in vivo. This is particularly true for males, so hepatocytes from male (particularly Fischer-344) rats have been the most frequently used in in vitro UDS assays. However, tests with females are sometimes more appropriate, depending upon the nature of the test agent. An additional advantage is that in primary hepatocyte cultures, only a small proportion of the cells undergo S-phase DNA synthesis, making the detection of UDS a relatively simple process. Recently, UDS assays have been conducted on hepatocytes obtained from human surgical samples (Brambilla and Martelli, 1995).

Other cell types are sometimes used for in vitro UDS assays, particularly when tissues other than liver are the primary targets of a chemical agent. Moreover, human liver samples are difficult to obtain, so the use of the HepG2 human liver cell line in UDS assays has

been explored (Naji-Ali et al., 1994). Results from these assays are often difficult to interpret because of several potentially confounding factors. Because S-phase cells interfere with measurement of UDS, cell division needs to be inhibited. This is accomplished by adding hydroxyurea and depleting the cultures of serum and/or arginine (Mitchell et al., 1983). In Chinese hamster V79 cells, 10 mM hydroxyurea caused DNA damage (Rueff et al., 1996). Furthermore, expression of some metabolic enzymes may be reduced in quiescent cells. Rueff et al. (1996) reported that expression of a transfected cytochrome P-450 1A2 gene in V79 Chinese hamster cells was decreased 10-fold in nonproliferating cells. This latter difficulty can be overcome by adding an exogenous metabolic activating system (e.g., liver S9 fraction; see *UNIT 3.1*) to the cultures during treatment. It should be noted, however, that the results of the assay sometimes differ depending upon the activating system used. Moreover, compounds activated by such systems may differ from those ultimately formed in vivo, and the metabolites generated exogenously may not reach the target DNA (Rueff et al., 1996).

Both autoradiography and liquid scintillation counting (LSC) have been used to quantitate the amount of [^{3}H]thymidine incorporation during UDS (Mitchell et al., 1983). Although more time-consuming than LSC, autoradiography is preferred because S-phase cells are not counted in the assay, and abnormal and dead cells can also be excluded (Madle et al., 1994). As an alternative to using radioactivity, UDS can be quantitated by measuring the incorporation of bromodeoxyuridine (BrdU) into DNA by staining with a fluorescein isothiocyanate (FITC)–tagged anti-BrdU antibody and quantitating with flow cytometry (Selden et al., 1994).

Critical Parameters

Microgel electrophoresis assay

Careful preparation of a single-cell suspension is necessary in order to avoid high background levels of comet formation. Trypsinization may cause unacceptable amounts of damage. Green et al. (1996) suggested that a "short, sharp shock" of trypsin/EDTA causes less damage than trypsin alone. In their hands, they also obtained better results with recently plated cells. Finally, they also suggested that some background damage can be ameliorated if the cells are allowed to recover on the slide for 30 to 60 min before treatment.

The type of cell used will also affect the background rates of controls. For example, human sperm cells have higher background rates of comet formation than do human lymphocytes (Anderson and Plewa, 1998). If cells are obtained ex vivo, it is also likely that background rates may vary among tissue types. Previous research with human lymphocytes has also indicated that there is inter- and intra-individual variation (Ross et al., 1995). In humans, confounding factors are age, tobacco use, physical activity, and seasonal variation (Anderson and Plewa, 1988).

McKelvey-Martin et al. (1993) recommended that a minimum genotoxicity testing protocol should include four doses of the test agent, solvent controls, and positive controls. Moreover, they suggested that each determination be made in triplicate in two independent experiments and that cell viability experiments should be conducted concurrently. For statistical purposes, comets should be chosen randomly (i.e., avoiding observer bias), and a large enough number of comets (≥50) should be scored so to provide adequate sample sizes.

The choice of scoring criterion will depend upon the equipment available to the investigator. As described previously, it is possible to numerically score damage and to measure tail length, head diameter, and total comet area without an image-analysis system. Many additional densitometric and geometric measurements of comets are attainable with image analysis, and the choice of which comet parameter best defines the degree of DNA damage is contentious (Olive et al., 1990; Kent et al., 1995; Böcker et al., 1997; McCarthy et al., 1997). The advantages of automated image analysis are that it can measure differences in fluorescence intensity (a gauge of the amount of DNA present) and that it can rapidly deliver quantitative results. It is the best method for large-scale comet analysis. On the other hand, researchers without access to such equipment can still obtain reliable results via manual methods, albeit not as rapidly (Olive et al., 1990; McCarthy et al., 1997).

The sensitivity of the assay can be adjusted by varying the lysis temperature (Ross et al., 1995), NaOH concentration in the electrophoresis buffer (Klaude et al., 1996), and the voltage, temperature, and/or duration of electrophoresis (Green et al., 1996). It is important to evaluate assay modifications in terms of whether the enhanced sensitivity outweighs increases in background comet formation in controls.

Finally, when designing experiments, it is important to remember that the amount of DNA that migrates during electrophoresis will be a function of both damage and of repair. Conducting the assay at 4°C or in the presence of repair inhibitors increases the sensitivity of detecting direct DNA strand breakage. Conversely, using exogenous endonucleases involved in excision repair increases the sensitivity of the assay for detecting DNA damage that is not due to direct inducers of DNA breakage.

Filter elution assay

When conducting filter elution, it is important not to introduce additional DNA damage because of poor technique. Following lysis, all remaining procedures should be conducted in dim light. Treatment of the cells with the test agent or X irradiation should be conducted at 0°C to prevent DNA repair. Solutions should be slowly eluted through the filter to avoid spurious DNA damage, and care should be taken to avoid air-pocket formation during all steps of the procedure.

The choice of filter and lysis conditions will determine how much protein is retained on the filter. If detection of DNA breakage is the primary goal, then deproteinizing conditions should be used. On the other hand, if the major objective is quantitation of DNA-protein cross-linkage, experimental conditions should be adjusted so that protein is retained on the filter by omitting proteinase K treatment and using polyvinyl chloride filters.

When quantifying DNA, the DNA retained on the filter should be completely hydrolyzed so as to increase the counting efficiency. All elution fractions, washes, and filters should be counted with the same counting efficiency (Elia et al., 1991).

It is also necessary to gauge the cytotoxicity of the test agent. DNA strand breakage occurs during necrotic and apoptotic cell death, and these events can confound the interpretation of results from filter elution assays (Elia et al., 1994). In other words, a genotoxic response in alkaline elution is defined as one in which DNA damage occurs at concentrations that produce low levels of immediate cytotoxicity (Elia et al., 1994).

K-SDS precipitation assay

The sensitivity and reproducibility of the K-SDS precipitation assay depends upon uniform mechanical fragmentation of DNA. Disparate precipitation of DNA/protein complexes can occur if DNA fragments vary greatly in length. Shearing of the DNA following lysis also reduces the background level of DNA/protein complexes.

Inclusion of internal standards to control for potential inter-assay variability is recommended (Zhitkovich et al., 1996). Cells designated as the internal standard should be lysed and frozen in aliquots at −70°C and assayed concurrently with the test cells.

During in vitro genotoxicity testing, it is important to assess cytotoxicity of the test agent. Many compounds have tested positive for DNA/protein cross-link formation only at cytotoxic levels (Costa et al., 1996, 1997).

Finally, some DNA-protein cross-links are thermolabile (Costa et al., 1997). The temperature of the water bath during the precipitation/washing steps may have to be adjusted accordingly.

Unscheduled DNA synthesis

It is important to monitor cell viability following hepatocyte isolation. This is most often accomplished by using the trypan blue exclusion test, which assesses membrane integrity. Depending upon the nature of the test agent, other cell-viability tests may be more appropriate. The collagenase perfusion procedure used to isolate hepatocytes can result in loss of membrane receptors and decreased activity of some membrane enzymes (Parton et al., 1995). Moreover, cytochrome P-450 activities and cellular glutathione levels may decrease during the establishment of primary hepatocyte cultures, and cell polarity is disrupted because the natural matrix is not maintained (Parton et al., 1995). Accordingly, Parton et al. (1995) reported that these potential problems could be partially alleviated by allowing a 24-hr recovery period in serum-free medium following plating and prior to treatment; they also use a collagen-fibronectin-laminin-coated matrix for hepatocyte attachment. These modifications resulted in improved sensitivity of the in vitro UDS assay.

The suitability of different scoring criteria for the UDS assay is currently a matter of debate. Many investigators have scored the results of UDS assays as positive or negative based upon a threshold value or percentage of cells undergoing repair. For example, Dean (1995) recommends scoring cells as positive for repair if their net nuclear grain counts are ≥5 and a test agent as positive if the mean net nuclear grain count is ≥5 and ≥20% of cells

were undergoing repair. Negative test agents had a mean nuclear grain count of ≤0 and <20% of the cells were in repair. Edler (1994) provided details regarding the statistical analyses of this type of data.

Madle et al. (1994) recommended that net nuclear grain values (i.e., gross nuclear grain counts minus gross cytoplasmic grain counts) should be the primary index of UDS, although gross nuclear and cytoplasmic grain counts should also be reported. Increases in net nuclear grain counts that result from decreased cytoplasmic grain counts should be cautiously interpreted because these may indicate cytotoxicity or inhibition of mitochondrial DNA synthesis. The absolute value of the net nuclear grain count can vary with the methodology used; therefore Madle et al. (1994) suggest that threshold values for distinguishing positive and negative values are unreliable indices. As an alternative, they recommended that test agents be scored as positive if they elicit a dose-dependent increase in net nuclear grain counts over at least two consecutive concentrations.

Experiments should be rejected if the positive controls are lower than the vehicle controls, if negative or solvent controls yield positive results, if cytoplasmic background grain counts are unacceptably high, or if there is low cell viability and/or poor cell attachment (Swierenga et al., 1991).

Anticipated Results

Microgel electrophoresis assay

The negative control treatments should result in no discernible comet formation (Fig. 3.5.1) If the test agent caused single or double DNA strand breaks, then comets will be visible following electrophoresis and staining (Fig. 3.5.2). The alkaline assay can detect one single-stranded break per 2×10^{10} Da of DNA (Singh et al., 1994). The neutral assay is able to detect about 200 double-stranded breaks per cell (Olive et al., 1991).

Filter elution assay

Depending upon the protocol used, this assay will yield elution profiles for single- or double-strand breaks (see Fig. 3.5.3). With modification, the influence of interstrand or DNA-protein cross-linking may also be examined. In addition, the frequency of single- or double-strand DNA breaks can be calculated if an internal standard is included. Details regarding these calculations can be obtained in Kohn et al., (1981) and Kohn (1991). Filter elution assays can detect 1 DNA lesion per 10^7 nucleotides (Kohn et al., 1981).

K-SDS precipitation assay

This assay will reveal the presence of DNA/protein cross-links in cultured cells, cells obtained ex vivo, or in lymphocytes from human subjects. Comparison of control and treated cells will indicate if the test agent induced significant levels of DNA/protein cross-links (Fig. 3.5.4). This assay can detect one adduct per $1–2 \times 10^7$ bases (Zhitkovich et al., 1998).

Unscheduled DNA synthesis assay

Treatment of primary hepatocyte cultures with a positive control agent (e.g., 2-AAF) for at least 16 hr will yield detectable UDS (Fig. 3.5.5). Note the nuclear and cytoplasmic grains and the heavily-labeled S-phase cells.

Time Considerations

Microgel electrophoresis assay

Preparation of slides, treatment of cells, and embedding takes ≤1 hr. An additional hour is required for lysis. Equilibration and electrophoresis can be completed in 1.5 hr. Neutralization, rinsing, and staining of slides requires 1 hr. The time needed for scoring of comets depends on whether or not manual or semiautomated image analysis is used. If the latter system of scoring is available, the assay can be fully completed within 8 hr. Neutral assays take longer because of additional procedural steps (e.g., an overnight incubation with proteinase K and RNase treatment).

Filter elution assay

Not counting the time required to grow the cells or treat the animals, this assay takes at least 4 days if radiolabeled cells are used. If the DNA is instead quantitated via fluorometry, allow 2 days for the assay.

K-SDS precipitation assay

The assay can be completed within 1 day. However, it is often convenient to conduct the lysis, K-SDS precipitation and wash, followed by an overnight incubation during the proteinase K digestion phase. Subsequent steps are performed the following day. An additional 1 to 2 days are required for film exposure (Alternate Protocol 9).

Unscheduled DNA synthesis assay

Not counting the time needed to house the rats, this assay takes 2 to 3 weeks to perform.

Literature Cited

Anard, D., Kirsch-Volders, M., Elhajouji, A., Belpaeme, K., and Lison, D. 1997. In vitro genotoxic effects of hard metal particles assessed by alkaline single cell electrophoresis and elution assays. *Carcinogenesis* 18:177-184.

Anderson, D. and Plewa, M.J. 1998. The international comet assay workshop. *Mutagenesis* 13:67-73.

Böcker, W., Bauch, T., Müller, W.-U., and Streffer, C. 1997. Image analysis of comet assay measurements. *Int. J. Radiat. Biol.* 72:449-460.

Bradley, M.O. and Kohn, K.W. 1979. X-ray induced DNA double-strand break production and repair in mammalian cells as measured by neutral filter elution. *Nucl. Acids Res.* 7:793-804.

Brambilla, G. and Martelli, A. 1995. Cytotoxicity, DNA fragmentation, and DNA repair synthesis in primary human hepatocytes. *In* In Vitro Testing Protocols: Methods in Molecular Biology, Vol. 43 (S. O'Hare and C.K. Atterwill, eds.) pp. 59-66. Humana Press, Totowa, N.J.

Chiu, S-M., Sokany, N.M., Friedman, L.R., and Oleinick, N.L. 1984. Differential processing of ultraviolet or ionizing radiation–induced DNA-protein cross-links in Chinese hamster cells. *Int. J. Radiat. Biol.* 46:681-690.

Collins, A.R., Dobson, V.L., Dusinska, M., Kennedy, G. and Stetina, R. 1997. The comet assay: What can it really tell us? *Mutat. Res.* 375:183-193.

Cook, P.R. and Brazell, I.A. 1975. Supercoils in human DNA. *J. Cell Sci.* 19:261-279.

Costa, M. 1990. Analysis of DNA-protein complexes induced by chemical carcinogenesis. *J. Cell. Biochem.* 44:127-135.

Costa, M., Zhitkovich, A., and Toniolo, P. 1993. DNA-protein cross-links in welders: Molecular implications. *Cancer Res.* 53:460-463.

Costa, M., Zhitkovich, A., Gargas, M., Paustenbach, D., Finley, B., Kuykendall, J., Billings, R., Carlson, T.J., Wetterhahn, K., Xu, J., Patierno, S., and Bogdanffy, M. 1996. Interlaboratory validation of new assay for DNA-protein cross-links. *Mutat. Res.* 369:13-21.

Costa, M., Zhitkovich, A., Harris, M., Paustenbach, D., and Gargas, M. 1997. DNA-protein cross-links produced by various chemicals in cultured human lymphoma cells. *J. Toxicol. Environ. Health* 50:433-449.

Dean, S. 1995. Measurement of unscheduled DNA synthesis in vitro using primary rat hepatocyte cultures. *In* In Vitro Testing Protocols: Methods in Molecular Biology, Vol. 43. (S. O'Hare and C.K. Atterwill, eds.) pp. 267-276. Humana Press, Totowa, N.J.

Edler, L. 1994. Biostatistical issues in the design and analysis of multiple or repeated genotoxicity assays. *Environ. Health Perspect.* 102 (Suppl. 1):53-59.

Elia, M.C., DeLuca, J.G., and Bradley, M.O. 1991. Significance and measurement of DNA double-strand breaks in mammalian cells. *Pharmacol. Ther.* 51:291-327.

Elia, M.C., Storer, R.D., McKelvey, T.W, Kraynak, A.R., Barnum, J.E., Harmon, L.S., DeLuca, J.G., and Nichols, W.W. 1994. Rapid DNA degradation in primary rat hepatocytes treated with diverse cytotoxic chemicals: Analysis by pulsed-field gel electrophoresis and implications for alkaline elution assays. *Environ. Mol. Mutagen.* 24:181-191.

Ewig, R.A. and Kohn, K.W. 1977. DNA damage and repair in mouse leukemia L1210 cells treated with nitrogen mustard, 1,3-bis(2-chloroethyl)-1-nitrosourea, and other nitrosoureas. *Cancer Res.* 37:2114-22.

Fairbairn, D.W., Olive, P.L., and O'Neill, K.L. 1995. The comet assay: A comprehensive review. *Mutat. Res.* 339:37-59.

Fautz, R., Husein, B., and Hechenberger, C. 1991. Application of the neutral red assay (NR assay) to monolayer cultures of primary hepatocytes: Rapid colormetric viability determination for the unscheduled DNA synthesis test (UDS). *Mutat. Res.* 253:173-179.

Fortini, P., Raspaglio, G., Falci, M., and Dogliotti, E. 1996. Analysis of DNA alkylation damage and repair in mammalian cells by the comet assay. *Mutagenesis* 11:169-175.

Gedik, C.M., Ewen, S.W.B., and Collins, A.R. 1992. Single cell gel electrophoresis applied to the analysis of UV-C damage and its repair in human cells. *Int. J. Radiat. Biol.* 62:313-320.

Green, M.H.L., Lowe, J.E., Delaney, C.A., and I.C. Green. 1996. Comet assay to detect nitric oxide–dependent DNA damage in mammalian cells. *Methods Enzymol.* 269:243-266.

Hamilton, C.M. and Mirsalis, J.C. 1987. Factors that affect the sensitivity of the in vivo-in vitro hepatocyte DNA repair assay in the male rat. *Mutat. Res.* 189:341-347.

Harbach, P.R., Rostami, H.J., Aaron, C.S., Wiser, S.K., and Grzegorczyk, C.R. 1991. Evaluation of four methods for scoring cytoplasmic grains in the in vitro unscheduled DNA synthesis (UDS) assay. *Mutat. Res.* 252:139-148.

Helbig, R. and Speit, G. 1997. DNA effects in repair-deficient V79 Chinese hamster cells studied with the comet assay. *Mutat. Res.* 377:279-286.

Henderson, L., Wolfreys, A., Fedyk, J., Bourner, C., and Windebank, S. 1998. The ability of the comet assay to discriminate between genotoxins and cytotoxins. *Mutagenesis* 13:89-94.

Hill, L.E., Yount, D.J., Garriott, M.L., Tamura, R.N., and Probst, G.S. 1989. Quantification of unscheduled DNA synthesis by a whole-cell counting method. *Mutat. Res.* 224:447-451.

Kasamatsu, T., Kohda, K., and Kawazoe, Y. 1996. Comparison of chemically induced DNA break-

age in cellular and subcellular systems using the comet assay. *Mutat. Res.* 369:1-6.

Kent, C.R.H., Eady, J.J., Ross, G.M., and Steel, G.G. 1995. The comet moment as a measure of DNA damage in the comet assay. *Int. J. Radiat. Biol.* 67:655-660.

Klaude, M., Eriksson, S., Nygren, J., and Ahnström, G. 1996. The comet assay: Mechanisms and technical considerations. *Mutat. Res.* 363:89-96.

Kohn, K.W. 1991. Principles and practice of DNA filter elution. *Pharmacol. Ther.* 49:55-77.

Kohn, K.W. and Ewig, R.A. 1973. Alkaline elution analysis, a new approach to the study of DNA single-strand interruptions in cells. *Cancer Res.* 33:1849-1853.

Kohn, K.W., Ewig, R.A.G., Erickson, L.C., and Zwelling, L.A. 1981. Measurement of strand breaks and cross-links by alkaline elution. *In* DNA Repair: A Laboratory Manual of Research Procedures (E.C. Friedberg and P.C. Hanawalt, eds.) pp. 379-401. Marcel Dekker, New York.

Liu, L.F., Rowe, T.C. Yang, L., Tewey, K.M., and Chen, G.L. 1983. Cleavage of DNA by mammalian DNA topoisomerase II. *J. Biol. Chem.* 258:15365-15370.

Lu, J., Kaeck, M.R., Jiang, C., Garcia, G., and Thompson, H.J. 1996. A filter elution assay for the simultaneous detection of DNA double- and single-strand breaks. *Anal. Biochem.* 235:227-233.

Madle, S., Dean, S.W., Andrae, U., Brambilla, G., Burlinson, B., Doolittle, D.J., Furihata, C., Hertner, T., McQueen, C.A., and Mori, H. 1994. Recommendations for the performance of UDS tests in vitro and in vivo. *Mutat. Res.* 312:263-285.

McCarthy, P.J., Sweetman, S.F., McKenna, P.G., and McKelvey-Martin, V.J. 1997. Evaluation of manual and image analysis quantification of DNA damage in the alkaline comet assay. *Mutagenesis* 12:209-214.

McGrath, R.A. and Williams, R.W. 1966. Reconstruction in vivo of irradiated *E. coli* DNA: The rejoining of broken pieces. *Nature* 212:534-535.

McKelvey-Martin,V.J., Green, M.H.L., Schmezer, P., Pool-Zobel, B.L., De Méo, M.P., and Collins, A. 1993. The single-cell gel electrophoresis assay (comet assay): A European review. *Mutat. Res.* 288:47-63.

Miller, C.A. III. and Costa, M. 1989. Immunological detection of DNA-protein complexes induced by chromate. *Carcinogenesis* 10:667-672.

Mitchell, A.D., Casciano, D.A., Meltz, M.L., Robinson, D.E., San, R.H.C., Williams, G.M., and Von Halle, E.S. 1983. Unscheduled DNA synthesis tests: A report of the U.S. Environmental Protection Agency Gene-Tox Program. *Mutat. Res.* 123:363-410.

Muller, M.T. 1983. Nucleosomes contain DNA binding proteins that resist dissociation by sodium dodecyl sulfate. *Biochem. Biophys. Res. Commun.* 114:99-106.

Naji-Ali, F., Hasspieler, B.M., Haffner, D., and Adeli, K. 1994. Human bioassays to assess environmental genotoxicity: Development of a DNA repair assay in HepG2 cells. *Clin. Biochem.* 27:441-448.

Olive, P.L. 1989. Cell proliferation as a requirement for development of the contact effect in Chinese hamster V79 spheroids. *Mutat. Res.* 117:79-92.

Olive, P.L., Chan, A.P.S., and Cu C.S. 1988. Comparison between the DNA precipitation and alkali unwinding assays for detecting DNA strand breaks and cross-links. *Cancer Res.* 48:6444-6449.

Olive, P.L., Banath, J.P., and Durand, R.E. 1990. Detection of etopside resistance by measuring DNA damage in individual Chinese hamster cells. *J. Natl. Cancer Inst.* 82:779-783.

Olive, P.L., Wlodek, D., and Banath, J.P. 1991. DNA double-strand breaks measured in individual cells subjected to gel electrophoresis. *Cancer Res.* 51:4671-4676.

Ostling, O. and Johanson, K.J. 1984. Microelectrophoretic study of radiation-induced DNA damages in individual mammalian cells. *Biochem. Biophys. Res. Commun.* 123:291-298.

Parton, J.W., Yount, D.J., and Garriott, M.L. 1995. Improved sensitivity of the unscheduled DNA synthesis assay in primary rat hepatocytes following culture in serum-free defined media. *Environ. Mol. Mutagen.* 26:147-154.

Pflaum, M., Will, O., and Epe, B. 1997. Determination of steady-state levels of oxidative DNA base modification in mammalian cells by means of repair endonucleases. *Carcinogenesis* 18:2225-2231.

Pfuhler, S. and Wolf, H.U. 1996. Detection of DNA-cross-linking agents with alkaline comet assay. *Environ. Mol. Mutagen.* 27:196-201.

Rasmussen, R.E. and Painter, R.B. 1966. Radiation-stimulated DNA synthesis in cultured mammalian cells. *J. Cell Biol.* 9:11-19.

Ross, G.M., McMillan, T.J., Wilcox, P., and Collins, A.R. 1995. The single microgel electrophoresis assay (comet assay): Technical aspects and applications: Report on the 5th L.H. Gray Trust Workshop, Institute of Cancer Research, 1994. *Mutat. Res.* 337:57-60.

Rueff, J., Chiapella, C., Chipman, J.K., Darroudi, F., Silva, I.D., Duverger-van Bogaert, M., Fonti, E., Glatt, H.R., Isern, P., Laires, A., Léonard, A., Llagostera, M., Mossesso, P., Natarajan, A.T.,Palitti, F., Rodrigues, A.S., Schinoppi, A., Turchi, G., and Werle-Schneider, G. 1996. Development and validation of alternative metabolic systems for mutagenicity testing in short-term assays. *Mutat. Res.* 353:151-176.

Selden, J.R., Dolbeare, F., Clair, J.H., Miller, J.E., McGettigan, K., DiJohn, J.A., Dysart, G.R., and DeLuca, J.G. 1994. Validation of flow cytometric in vitro DNA repair (UDS) assay in rat hepatocytes. *Mutat. Res.* 315:147-167.

Singh, N.P. 1996. Microgel electrophoresis of DNA from individual cells. Principles and methodol-

ogy. *In* Technologies for Detection of DNA Damage and Mutations. (G. Pfeifer, ed.) pp. 3-24. Plenum, New York.

Singh, N.P. 1997. Sodium ascorbate induces DNA single-strand breaks in human cells in vitro. *Mutat. Res.* 375:195-203.

Singh, N.P., McCoy, M.T., Tice, R.R., Schneider, E.L. 1988. A simple technique for quantitation of low levels of DNA damage in individual cells. *Exp. Cell Res.* 175:184-191.

Singh, N.P., Stephens, R.E., and Schneider, E.L. 1994. Modifications of alkaline microgel electrophoresis for sensitive detection of DNA damage. *Int. J. Radiat. Biol.* 66:23-28.

Speit, G., Hanelt, S., Helbig, R., Seidel, A., and Hartmann, A. 1996. Detection of DNA effects in human cells with the comet assay and their relevance for mutagenesis. *Toxicol. Lett.* 88:91-98.

Sterzel, W., Bedford, P., and Eisenbrand, G. 1985. Automated determination of DNA using the fluorochrome Hoechst 33258. *Anal. Biochem.* 147:462-467.

Stout, D.L. and Becker, F.F. 1982. Fluorometric quantitation of single-stranded DNA: A method applicable to the technique of alkaline elution. *Anal. Biochem.* 127:302-307.

Swierenga, S.H.H., Bradlaw, J.A., Brillinger, R.L., Gilman, J.P.W., Nestmann, E.R., and San, R.C. 1991. Recommended protocols based on a survey of current practice in genotoxicity testing laboratories: I. Unscheduled DNA synthesis assay in rat hepatocyte cultures. *Mutat. Res.* 246:235-253.

Szmigiero, L. and Studzian, K. 1988. H_2O_2 as a DNA fragmenting agent in the alkaline elution interstrand cross-linking and DNA-protein cross-linking assays. *Anal. Biochem.* 168:88-93.

Taioli, E., Zhitkovich, A., Toniolo, P., and Costa, M. 1995. Normal values of DNA-protein cross-links in mononuclear blood cells of a population of healthy controls. *Cancer J.* 8:76-78.

Trasko, J.E. and Yager, J.D. 1974. Method to measure physical and chemical carcinogen-induced "unscheduled DNA synthesis" in rapidly dividing eukaryotic cells. *Exp. Cell Res.* 88:47-55.

Wedrychowski, A., Ward, W.S., Schmidt, W.N., and Hnilica, L.S. 1985. Chromium-induced cross-linking of nuclear proteins and DNA. *J. Biol. Chem.* 260:7150-7155.

Williams, G.M. 1976. Carcinogen-induced DNA repair in primary rat liver cell cultures: A possible screen for chemical carcinogens. *Cancer Lett.* 1:231-236.

Williams, G.M., Mori, H., and McQueen, C.A. 1989. Structure-activity relationships in the rat hepatocyte DNA-repair test for 300 chemicals. *Mutat. Res.* 221:263-286.

Zhitkovich, A. and Costa, M. 1992. A simple, sensitive assay to detect DNA- protein crosslinks in intact cells and in vivo. *Carcinogenesis* 13:1485-1489.

Zhitkovich, A., Lukanova, A., Popov, T., Taioli, E., Cohen, H., Costa, M., and Toniolo, P. 1996. DNA-protein cross-links in peripheral lymphocytes of individuals exposed to hexavalent chromium compounds. *Biomarkers* 1:86-93.

Zhitkovich A., Voitkun, V., Kluz, T., and Costa, M. 1998. Utilization of DNA-protein cross-links as a biomarker of chromium exposure. *Environ. Health Perspect.* 106 Suppl 4:969-974.

Contributed by Jessica E. Sutherland and Max Costa
New York University School of Medicine
New York, New York

Detecting Epigenetic Changes: DNA Methylation

Epigenetic changes refer to alterations in gene expression without a change in nucleotide sequence. One of the best understood epigenetic mechanisms is DNA methylation. The protocols in this unit describe some basic methods of DNA methylation analysis: determination of the overall genomic DNA methylation levels (see Basic Protocol 1), measurement of DNA methyltransferase (Mtase) activity (see Basic Protocol 2), and determination of gene-specific methylation (see Basic Protocol 3) and chromatin condensation patterns (see Basic Protocol 4). These protocols may be used immediately after treatment with toxicant or after a suitable recovery or selection period.

DETERMINING THE OVERALL 5-METHYLCYTOSINE CONTENT IN GENOMIC DNA

BASIC PROTOCOL 1

In this protocol, which is used to detect changes in overall DNA methylation, the bacterial enzyme *Sss*I (a CpG methylase), is used to artificially methylate a DNA sample, using radioactive *S*-adenosylmethionine (SAM). Higher amounts of *S*-adenosyl-L-[methyl-^{3}H]methyl incorporation into DNA indicate lower levels of genomic DNA methylation, while less [^{3}H]methyl incorporation is indicative of higher levels of genomic DNA methylation.

Materials

Genomic DNA purified from treated and control cells
*Sss*I methylase (New England Biolabs)
60 to 85 Ci/mmol *S*-adenosyl-L-[methyl-^{3}H]methionine (Amersham Pharmacia)
15 mM nonradioactive *S*-adenosylmethionine (SAM; prepare fresh)
*Sss*I reaction buffer (see recipe or use as supplied by manufacturer)
5% (w/v) trichloroacetic acid
70% (v/v) ethanol
Scintillation cocktail

Millipore Ultrafree-MC 100,000 NMWL filter unit (polysulfone membrane)
Scintillation vials
Liquid scintillation counter

1. Combine 200 ng genomic DNA sample with 4 U *Sss*I methylase, 1.5 µM *S*-adenosyl-L-[methyl-^{3}H]methionine, and 1.5 µM nonradioactive *S*-adenosylmethionine, in *Sss*I reaction buffer (25 µl total volume). Incubate reaction mixture 4 hr at 37°C.

   It is also possible to use HpaII or HhaI methylases for comparison.

   Include control reactions without DNA and without enzyme to determine background levels.

   5-Azacytidine will decrease DNA methylation and is suitable as a positive control treatment.

2. Stop the reaction by adding 25 µl of 1 mM nonradioactive *S*-adenosylmethionine.

3. Wash the filter unit once with water and then load the reaction mixture onto the filter. Wash with 0.3 ml of 5% trichloroacetic acid and 0.3 ml of 70% ethanol.

   The unincorporated S-adenosyl-L-[methyl-^{3}H]methionine should be washed away. High background levels are a common problem in this assay, because of nonspecific binding to the filter; therefore ascertain that controls have low levels of ^{3}H incorporation. Use of the polysulfone filter unit (Ultrafree from Millipore) eliminates this problem.

Contributed by Limor Broday and Max Costa
Current Protocols in Toxicology (2000) 3.6.1-3.6.8

4. Transfer the filter unit to a scintillation vial containing 10 ml of scintillation cocktail and determine the ^3H incorporation with a liquid scintillation counter.

   Relatively higher levels of [^3H]methyl incorporation are an indication of lower levels of genomic DNA methylation, and vice versa.

5. Calculate methylation levels as dpm/ng DNA, and DNA methylation levels as percent of control.

   This protocol should detect changes in the overall level of DNA methylation.

BASIC PROTOCOL 2

MEASURING DNA: METHYLTRANSFERASE ACTIVITY ASSAY

This assay measures the methyltransferase activity in cell extracts. The assay is based upon the same principle as Basic Protocol 1, but an exogenous substrate, poly(dI-dC), is added to the reaction. The level of *S*-adenosyl-L-[methyl-^3H]methionine incorporation measured is proportional to the enzyme activity.

Materials

$\sim 1 \times 10^7$ treated and control cells to be tested
PBS (*APPENDIX 2A*)
Methyltransferase lysis buffer (see recipe)
Polydeoxyinosinic-deoxycytidylic acid [poly (dI-dC)]
60 to 85 Ci/mmol *S*-adenosyl-L-[methyl-^3H]methionine (Amerham Pharmacia)
Methyltransferase stop solution (see recipe)
1:1 (v/v) phenol/chloroform
100% ethanol, ice-cold
0.3 M NaOH
5% (w/v) trichloroacetic acid
70% ethanol
0.5 M perchloric acid
Scintillation cocktail

Syringe and 25-G needle
GF/C Whatman filter discs
Fitration unit (e.g., Millipore)
Liquid scintillation counter

Additional reagents and equipment for protein assay and phenyl/chloroform extraction/ethanol precipitation (*APPENDIX 3*).

1. Scrape 1×10^7 cells from plates with a rubber policeman, pool into 5 to 10 ml ice-cold PBS, and collect by centrifuging 10 min at $1850 \times g$, 4°C.
2. Resuspend the cells in 0.5 ml methyltransferase lysis buffer. Pass the suspension once through a 25-G needle and submit to four cycles of freeze (dry ice) and thaw (37°C).
3. Determine the protein concentration in the samples (*APPENDIX 3*).
4. Combine lysate containing 5 µg protein with 0.5 µg poly(dI-dC), 1.5 µM *S*-adenosyl-L-[methyl-^3H]methionine, and methyltransferase lysis buffer in a total volume of 20 µl. Incubate at 37°C for 2 hr.

   Also prepare control reactions lacking poly(dI-dC).

5. Stop the reaction by adding 300 µl methyltransferase stop solution and incubating 1 hr at 37°C.

   The protease incubation is necessary to obtain complete recovery of DNA, which may be complexed with protein.

6. Extract the DNA with phenol/chloroform and precipitate with 2 vol ice-cold 100% ethanol (*APPENDIX 3*).
7. Dissolve the recovered DNA in 30 µl of 0.3 M NaOH and incubate 30 min at 37°C.

   This step is done to remove any residual RNA, which might be labeled.
8. Spot the 10 µl DNA on duplicate GF/C Whatman filter discs and air dry. Transfer the filters to a filtration unit and wash the DNA five times with 10 ml of 5% trichloroacetic acid and then five times with 10 ml of 70% ethanol.
9. Transfer the dried filter to a counting vial with 0.5 ml of 0.5 M perchloric acid, and heat 1 hr at 60°C.

   The DNA is solubilized during the incubation. Perchloric acid depurinates the DNA.
10. Add 5 ml scintillation cocktail and determine the ^{3}H incorporation with a liquid scintillation counter.
11. Calculate the Mtase enzyme activity as dpm/µg of protein.

    Results are usually expressed as percent of control values (mean ± SEM).

MEASURING GENE-SPECIFIC METHYLATION: MODIFICATION-SENSITIVE RESTRICTION ENDONUCLEASES ASSAY

BASIC PROTOCOL 3

The modification-sensitive restriction endonucleases (MSREs) assay is based upon the principle that DNA methylation will affect certain restriction enzymes. As a control, comparison of digestion patterns by methylation-sensitive and methylation-insensitive isoschizomers (e.g., *Hpa*II and *Msp*I) is performed. Following digestion of the examined DNA sample, the analysis may be done by Southern blot hybridization or PCR (*APPENDIX 3*).

Materials

Genomic DNA from treated and control cells to be tested, from tissue culture cells or tissues

Methylation-insensitive restriction enzyme (with recognition sites located within the borders of the tested DNA region) and buffer

Methylation-sensitive restriction enzyme (such as the 4 cutters *HpaII* and *HaeI*, 6 cutters *EagI* and *SacII,* or 8 cutter *NotI*) and buffer

Appropriate PCR primers designed for the target region *or* appropriate probe for Southern blot hybridization analysis

Additional reagents and equipment for ethanol precipitation of DNA (*APPENDIX 3*), PCR amplification (*APPENDIX 3C*) or Southern blot hybridization (Ausubel et al., 1992), and agarose gel electrophoresis (*UNIT 2.2*)

1. *For Southern blot hybridization analysis:* Digest 10 µg genomic DNA with 5 U/µg DNA of a methylation-insensitive restriction enzyme that releases a fragment of the genomic region to be examined. Incubate 16 hr at 37°C.

   If PCR analysis is performed start this experiment at step 2, below.

   The size of the test fragment depends on the physical map of the genomic target and also on the frequency of sites and size of fragments released following digestion with the methylation-sensitive restriction enzyme.
2. Precipitate the DNA by ethanol (*APPENDIX 3*), recover pellet, and digest (again, if step 1 was carried out for Southern blotting) with 5 U/µg DNA of a cytosine methylation-sensitive restriction enzyme for an additional 16 hr at 37°C.

   When PCR is to be performed, digest a much smaller sample of DNA (0.5 µg) than that recommended in step 1.

3a. *For Southern blot hybridization analysis:* Separate the digested samples (10 μg) by electrophoresis on 1% agarose gels (*UNIT 2.2*), transfer to a nylon membrane, and hybridize according to standard procedures (Ausubel et al., 1992).

In Southern blot hybridization, the percent methylation is calculated as the intensity of the band(s) representing DNA that is not digested by the methylation-sensitive enzyme (and which is therefore methylated) relative to the combined intensity of all bands in the lane (see Background Information and Critical Parameters).

3b. *For PCR*: Use ~50 ng digested DNA per PCR reaction (*APPENDIX 3C*). Compare the PCR product to a PCR product of an uncut control DNA.

Quantitative PCR conditions should be established empirically for each gene and cell type.

Absence of the expected DNA product indicates methylation of this site. The fraction of resistant DNA equals the fraction of cells that contain this modified site (see Background Information and Critical Parameters).

BASIC PROTOCOL 4

MEASURING DEOXYRIBONUCLEASE I SENSITIVITY

This assay is based on the principle that active genes are often more prone to deoxyribonuclease I (DNase I) digestion than inactive genes in which the chromatin is much more compact and condensed, and that methylation can inactivate genes and cause this condensation. Isolated nuclei from the treated cell line are digested with different amounts of DNase I and then the specific target gene is analyzed either by PCR or Southern-blot hybridization.

Materials

Cell line to be examined, treated and control
DNase I buffer (see recipe)
DNase I
DNase I stop solution (see recipe)
1:1 (v/v) phenol/chloroform
100% ethanol, ice-cold
25° and 55°C water baths

Additional reagents and equipment for phenol/chloroform extraction and ethanol precipitation of DNA (*APPENDIX 3*), Southern blot hybridization (Ausubel et al., 1992), and PCR (*APPENDIX 3C*)

1. Isolate nuclei from the examined cell lines.
2. Resuspend 5×10^5 nuclei for each treatment in 200 µl DNase I buffer.

   All the steps should be done on ice, except where otherwise indicated.

   This amount of nuclei is appropriate for PCR analysis. For Southern blot hybridization use at least 120 times more nuclei. The volume of the reaction and amount of enzyme, should be adjusted proportionally when using higher quantities of nuclei.

3. Prepare samples with increasing amounts of DNase I (0, 0.5, 1, 2, 10 U). Incubate 30 min at 25°C.
4. Terminate the reactions by adding 200 µl DNase I stop solution to each. Incubate 4 to 20 hr at 55°C.
5. Extract the DNA with phenol/chloroform and precipitate with ethanol (*APPENDIX 3*).

6a. *For PCR:* Amplify ~50 ng of the samples using primers designed for the target region. Using quantitative PCR conditions as established empirically for each gene and cell type.

See APPENDIX 3C for PCR protocols.

6b. *For Southern blot hybridization analysis:* Digest 10 µg DNase I–digested DNA per sample with a restriction enzyme that produces fragments of the analyzed region, as done in the MSREs assay (see Basic Protocol 2, step 1).

REAGENTS AND SOLUTIONS

*Use Milli-Q-purified water or equivalent for all recipes and in all protocol steps. For common stock solutions, see **APPENDIX 2A**; for suppliers, see **SUPPLIERS APPENDIX**.*

DNase I buffer

10 mM Tris·Cl, pH 7.4 (*APPENDIX 2A*)
10 mM NaCl
3 mM $MgCl_2$
100 mM $CaCl_2$
Store up to 1 month at 4°C

DNase I stop solution

1% (w/v) SDS
0.1 M NaCl
50 mM Tris·Cl, pH 8.0 (*APPENDIX 2A*)
10 mM EDTA (*APPENDIX 2A*)
Store 1 month at 4°C
Add 1 mg/ml proteinase K just before use

Methyltransferase lysis buffer

50 mM Tris·Cl, pH 7.8 (*APPENDIX 2A*)
1 mM EDTA (*APPENDIX 2A*)
1 mM DTT
0.01% NaN_3
10% (v/v) glycerol
1% (v/v) polyoxyethylenesorbitan monooleate (closed up on Tween 80)
0.35 mM PMSF (add fresh)
100 mg/ml RNase A (add fresh)
Prepare just before use

Methyltransferase stop solution

1% (w/v) SDS
2 mM EDTA (*APPENDIX 2A*)
5% (v/v) isopropanol
125 mM NaCl
1 mg/ml proteinase K (add fresh)
0.25 mg/ml carrier DNA
Prepare fresh

SssI reaction buffer

50 mM NaCl
10 mM Tris·Cl, pH 7.9 (*APPENDIX 2A*)
10 mM $MgCl_2$
1 mM DTT
Store at −20°C

This buffer is usually supplied with the enzyme.

COMMENTARY

Background Information

Epigenetic agents heritably alter the DNA structure without altering the DNA sequence per se. DNA methylation is one of the best understood epigenetic mechanisms. DNA methylation levels of promoter regions are inversely correlated with gene expression. Increased levels of DNA methylation (hypermethylation) could potentially be a nonmutational mechanism to disrupt tumor-suppressor gene function, while reduction in DNA methylation (hypomethylation) of proto-oncogenes could facilitate their increased expression (Gonzalgo and Jones, 1997).

The first two protocols describe measurement of the overall methylation levels and DNA methyltransferase activity in the cells. The basis of the overall methylation assay is that fewer methyl groups from SAM will be transferred by *Sss*I methylase to cytosine in DNA that has relatively greater 5-methyl cytosine content, and vice versa (Wu et al., 1993). *Sss*I methylates cytosine in 5'-CpG-3' sequences, and thus it has the same recognition sequence as eukaryotic DNA methyltransferase. Since its purification (Renbaum et al., 1990), this enzyme has been widely used to artificially methylate DNA. *Sss*I has been preferred to other cytosine methylases such as *Hpa*II or *Hha*I, whose recognition sequences (CCGG and GCGC, respectively) are only a subset of all CpGs present in genomic DNA. The measurement of DNA methyltransferase activity from cell extracts is based on the same principle, but in this assay a DNA substrate is added to the reaction (Adams et al., 1991). This method is applicable to enzyme extracted from cultured cells and small pieces of tissue, where the cells have been disrupted by freeze thawing.

The remaining protocols describe gene-specific analysis of DNA methylation and chromatin condensation. The modification-sensitive restriction endonucleases (MSREs) assay uses methylation-sensitive restriction enzymes to distinguish between methylated and nonmethylated states of a specific gene or other genomic region. This is a relatively simple method for identifying modified bases at specific restriction-endonuclease sites. It requires only the map of restriction sites in the region of interest. The limitation of the method is that the methylation status can be determined only at restriction sites. Therefore, it is frequently applied as a first indication of whether or not modified bases are found in the examined genomic region.

Two techniques are used to determine the extent of DNA digestion. The first is fractionation of the digested DNA by gel electrophoresis and Southern blot hybridization (Bird and Southern, 1978). Absence of the expected DNA product indicates methylation of this site. The fraction of resistant DNA equals the fraction of cells that contain this modified site (Rein et al., 1998). As a control, comparison of digestion patterns by methylation-sensitive and methylation-insensitive isoschizomers (e.g., *HpaII* and *MspI*) is performed.

A more sensitive technique for the MSRE employs the polymerase chain reaction (PCR). After digestion, the DNA is amplified using specific primers for the genomic target. The amount of product will be proportional to the level of methylated DNA in the sites examined. However, it is necessary to calibrate the reaction conditions to achieve a linear response between input DNA and amplified product. In addition, the DNA must be completely digested. Inefficient DNA cleavage is the principle artifact of the MSRE method. Thus, small differences in methylation levels will not be detected using PCR. More sensitive methods have included quantitative PCR (Singer-Sam et al., 1990), ligation-mediated PCR (LMPCR; McGrew and Rosenthal, 1993), and genomic sequencing methods such as differential base modification by hydrazine, based on the Maxam and Gilbert sequencing reactions (Pfeifer et al., 1989), or bisulfite genomic sequencing (Clark et al., 1994). Although many alkylating agents have been identified, only a few compounds have been shown to affect CpG methylation levels directly. For example, 5-azacytidine decreased cytosine DNA methylation. It has also been shown that treatment with nickel increased methylation of a reporter gene and caused silencing (Lee et al., 1995).

Southern blot hybridization can also be used to determine the overall methylation level. The DNA is digested with methylation-sensitive restriction enzyme (e.g., a 4 cutter such as *Hpa*II), separated by electrophoresis, and hybridized with satellite sequences.

The final protocol describes a DNase I protection assay (Weintraub, 1985). Endonucleases have been widely employed to detect alterations in chromosomal states based on the accessibility of chromatin to restriction enzymes, DNase I, or micrococcal nuclease. In higher eukaryotes, heterochromatin-mediated gene silencing is accompanied by demonstra-

ble DNA hypermethylation. Methylated 5'-CpG dinucleotides within promoter regions may block transcription via the assembly of the methylated sequences into a condensed heterochromatic state (Nan et al., 1998; Bestor, 1998). In this assay, condensed, transcriptionally inactive areas will be more protected from DNase I digestion than transcriptionally active, euchromatic regions of the genome. As in the previous protocol the analysis may be done by Southern blot hybridization or by PCR.

Critical Parameters

For the determination of the overall methylation levels and methyltransferase activity, all reaction samples should be analyzed in duplicate. In addition, genomic DNA samples or cell extracts should be analyzed in triplicate. Values are obtained as dpm/ng of DNA for methylation levels or dpm/mg protein for methyltransferase activity.

Careful washing of the GF/C Whatman filter discs is crucial in Basic Protocol 2. Background problems may be overcome by washing the filters with cold SAM (1 mM) before applying the radioactive sample, adding cold SAM to the 5% TCA during the washing steps, and by using large volumes of 5% TCA. Use of the Ultrafree-MC filter unit also helps eliminate the high background levels.

In the MSREs assay (Basic Protocol 3), the use of highly purified DNA is the most critical parameter. Incomplete digestion will produce artifacts.

When performing PCR analysis for the MSREs assay or the DNase I sensitivity assay, it is always necessary to perform preliminary experiments in order to determine the appropriate conditions for quantitative PCR (e.g., amount of template DNA, number of cycles). See *APPENDIX 3C* for optimizing PCR.

Anticipated Results

In the overall methylation assay, it will be easy to distinguish between highly methylated (less ^{3}H-methyl incorporation) and nonmethylated samples (more ^{3}H-methyl incorporation), but rather difficult to elucidate differences when small changes in the genomic methylation levels have occurred. In the methyltransferase assay, higher amounts of ^{3}H-methyl incorporation into poly(dI-dC) indicate high methyltransferase activities in the tested lysates.

In the gene-specific methylation and condensation assays, highly methylated genes will yield clearly different Southern blots than controls. If PCR analysis is performed, highly methylated genes (i.e., those that are uncut by methylation-sensitive enzymes) will be amplified to a greater extent than unmethylated genes. For slight changes in gene methylation, genomic sequencing following bisulfite-modification PCR (Clark et al., 1994) is recommended.

Time Considerations

The overall methylation level protocol (see Basic Protocol 1) requires a 4-hr incubation, and ~1 hr to load, wash, and read the samples using the scintillation counter (depending on the number of samples).

The methyltransferase assay (see Basic Protocol 2) requires ~7 hr including two periods of incubation (2 hr and 1 hr), but this also depends on the number of samples examined.

For the MSREs assay (see Basic Protocol 3), 2 to 3 days are required to perform the PCR analysis if the conditions for the quantitative PCR are already established, and an additional 2 to 3 days if Southern blot hybridization is performed.

The DNase I sensitivity assay (see Basic Protocol 4), requires 1 to 2 hr of work (starting with nuclei), 4 to 20 hr incubation with the stop buffer, and 1 hr for phenol/chloroform extraction and DNA precipitation. An additional 4 to 6 hr for PCR analysis, or 2 to 3 days for Southern blot hybridization are required.

Literature Cited

Adams, R.L.P., Rinalsi, A., and Seivwright, C. 1991. Microassay for DNA methyltransferase. *J. Biochem. Biophys. Methods* 22:19-22.

Ausubel, F.M., Brent, R., Kingston, R.E., Moore, D.D., Seidman, J.G., Smith, J.A., and Struhl, K. (eds.) 1992. Short Protocols in Molecular Biology, Second Edition. John Wiley & Sons, New York.

Bestor, T.H. 1998. Methylation meets acetylation. *Nature* 393:311-312.

Bird, A.P. and Southern, E.M. 1978. Use of restriction enzymes to study eukaryotic DNA methylation: The methylation pattern in ribosomal DNA from *Xenopus laevis*. *J. Mol. Biol.* 118:27-47.

Clark, S.J., Harrison, J., Paul, C.L., and Frommer, M. 1994. High sensitivity mapping of methylated cytosines. *Nucl. Acids Res.* 22:2990-2997.

Gonzalgo, M.L. and Jones, P.A. 1997. Mutagenic and epigenetic effects of DNA methylation. *Mutat. Res*. 386:107-118.

Lee, Y.W., Klein, C.B., Kargacin, B., Salnikow, K., Kitahara, J., Dowjat, K., Zhitkovich, A., Christie, N.T., and Costa, M. 1995. Carcinogenic nickel silences gene expression by chromatin condensation and DNA methylation: A new model for

epigenetic carcinogens. *Mol. Cell Biol.* 15:2547-2557.

McGrew, M.J. and Rosenthal, N. 1993. Quantitation of genomic methylation using ligation-mediated PCR. *Biotech*. 4:722-729.

Nan, X., Ng, H-H., Johnson, C.A., Laherty, C.D., Turner, B.M., Eisenman, R.N., and Bird, A. 1998. Transcriptional repression by the methyl-CpG-binding protein MeCP2 involves a histone deacetylase complex. *Nature* 393:386-389.

Pfeifer, G.P., Steigerwald, S.D., Mueller, P.R., Wold, B., and Riggs, A.D. 1989. Genomic sequencing and methylation analysis by ligation-mediated PCR. *Science* 246:810-813.

Rein, T., Depamphilis, M.L., and Zorbas, H. 1998 Identifying 5-methylcytosine and related modifications in DNA genomes. *Nucl. Acids Res*. 26:2255-2264.

Renbaum, P., Abrahamove, D., Fainsod, A., Wilson, G.G., Rottem, S., and Razin, A. 1990. Cloning, characterization, and expression in *Escherichia coli* of the gene coding for the CpG DNA methylase from *Spiroplasma* sp. strain MQ1 (M. SssI). *Nucl. Acids Res.* 18: 1145-1152.

Singer-Sam, J., Le Bon, J.M.,Tanguay, R.L., and Riggs, A.D. 1990. A quantitative *Hpa*II-PCR assay to measure methylation of DNA from a small number of cells. *Nucl. Acids Res.* 18:687.

Weintraub, H. 1985. High-resolution mapping of S1 and DNaseI-hypersensitive sites in chromatin. *Mol. Cell Biol.* 5:1538-1539.

Wu, J., Issa, J.P., Herman, J., Bassett, D.E. Jr., Nelkin, B.D., and Baylin, S.B. 1993. Expression of an exogenous eukaryotic DNA methyltransferase gene includes transformation of N1H3T3 cells. *Proc. Natl. Acad. Sci. U.S.A.* 90:8891-8895.

Contributed by Limor Broday and Max Costa
New York University School of Medicine
New York, New York

Assays for Detecting Chromosomal Aberrations

Genotoxicity can be evaluated by studying the physical integrity of the chromosomes in toxicant-exposed cultured cells, experimental animals, or even in cells derived from humans exposed in vivo. Chromosome preparations can be initiated from any dividing cell population and can even be prepared from nondividing cells, such as peripheral blood lymphocytes, that can be stimulated by mitogens to divide for a brief period of time.

In contrast to mutagenesis assays that can identify genetic alterations related to specific gene expression, or to the identification of specific DNA base mutations by the use of molecular-biology techniques, the employment of various chromosome assays allows for direct visualization of the structural integrity of the genome. This visual assessment can be made by evaluating cells for the presence of micronuclei (see Basic Protocol 1), which are small chromatin-containing bodies containing partial or whole chromosomes that have become separated from the main cellular nucleus as a result of toxicant insult. The state of the genome can be visually observed by routine Giemsa staining or trypsin/Giemsa banding (see Basic Protocol 2) of each individual chromosome to look for any aberrations in the typical chromosome size, form, and number known for each species. Missing, misshapen, or broken chromosomes can be readily noted. Rearrangements and translocations between chromosomes can also be detected by routine Giemsa staining, or can be colorfully highlighted by the use of fluorescent chromosome-specific painting probes (see Basic Protocol 3). Toxicant-induced exchanges between sister chromatids of each chromosome can be quantitated by differentially staining the chromatids so that each appears either dark or light (see Basic Protocol 4). Overall, the visual assessment of the genome's integrity can be a useful companion to many of the other assays described in this chapter. In some cases, visible disruption of the chromosomes can signify genotoxic damage to the cell, even in the absence of detectable gene-specific mutations. Whereas the cytogenetic assays are limited by the power of visual magnification, they have the advantage of offering a broad cellular target for investigating genotoxic effects. This unit also includes a protocol for preparation of metaphase chromosome spreads (see Support Protocol).

NOTE: All solutions and equipment coming into contact with living cells must be sterile, and aseptic technique should be used accordingly.

NOTE: All culture incubations should be performed in a humidified 37°C, 5% CO_2 incubator unless otherwise specified.

MICRONUCLEUS ASSAY FOR CHROMOSOMAL ABERRATIONS

BASIC PROTOCOL 1

Micronuclei (MN) originate from acentric chromosome fragments or whole chromosomes that are not included in the main nuclei following DNA replication and nuclear division. The in vitro cytokinesis-blocked micronucleus (CBMN) technique described here uses cytochalasin B (Cyt-B), which, at appropriate concentrations, prevents cytoplasmic, but not nuclear, division. Thus, cells after one mitotic division can be recognized by their typical binucleate interphase appearance and the micronuclei can be scored in the binucleate interphase cells. The MN test is a valid tool for the detection of chromosome-damaging agents and can be used as an initial screening assay for the identification of putative carcinogenic and other environmental exposure hazards.

Contributed by Catherine B. Klein, Limor Broday, and Max Costa
Current Protocols in Toxicology (2000) 3.7.1-3.7.16

Materials

Cells to be tested, in exponential growth phase or PHA-stimulated lymphocytes
Medium and supplements appropriate for the cell line studied (*APPENDIX 3B*)
Agent to be tested for toxicity, in appropriate solvent
1 mg/ml cytochalasin B (see recipe)
Phosphate-buffered saline (PBS; *APPENDIX 2A*)
Hypotonic solution: 0.075 M KCl
80% to 100% ice-cold methanol, freshly prepared
5% (w/v) Giemsa solution (prepare fresh): dilute Giemsa stain (see recipe) 1:19 (v/v) in Sorenson's phosphate buffer, pH 6.8 (see recipe)

60-mm petri dishes
Microscope slides, –20°C

Additional reagents and equipment for culturing and trypsinizing cells (*APPENDIX 3B*), mutagenesis assays in cells (*UNIT 3.3*), and slide preparation by dropping (see Support Protocol) or cytospinning (*UNIT 2.2*)

Grow cells and treat with test agent

1. Seed 0.5 to 2 × 10^5 cells per 60-mm petri dish in 5 ml medium (four dishes are suggested for each dose of putative genotoxic agent).

   For a detailed description of mutagenicity testing, see UNIT 3.3.

2. After cell attachment, add the test agent to the dishes and incubate cells for the appropriate exposure time previously shown to yield genotoxic effects at 37°C.

   Dosage levels of the test agent are selected based on toxicity or solubility limits. If the chemical is dissolved in DMSO or other organic solvent, pure DMSO or solvent should be used as a negative control. Solvent concentration should not exceed 1%.

Inhibit cytokinesis

3. Add cytochalasin B to the cultures (from 1 mg/ml stock) to a final concentration of ~3 μg/ml. Incubate cells 24 to 72 hr at 37°C.

   This treatment blocks cytokinesis. Preliminary experiments should be performed to determine the optimal cytochalasin B concentration (0.5 to 6.0 μg/ml) and duration of exposure that yields the highest proportion of binucleated cells for each cell line tested.

Fix cells and score for micronuclei

4. Harvest the cells by washing twice with PBS and then trypsinizing (*APPENDIX 3B*).
5. Resuspend the cells in 1 ml hypotonic solution (0.075 M KCl) and incubate for 5 to 10 min in a 37°C water bath. Centrifuge 10 min at 155 × *g*, 4°C.
6. Fix the cells in freshly prepared 80% to 100% methanol for ≥90 min at 4°C.
7. Centrifuge 10 min at 155 × *g*, 4°C. Remove supernatant.
8. Repeat step 6 for 30 min and centrifuge again 10 min at 155 × *g*, 4°C.
9. Remove most of the supernatant (retain ~0.2 ml). Resuspend the cells, and spread the cell suspension on cold (–20°C) slides by dropping (see Support Protocol) or cytospinning (*UNIT 2.2*).
10. After drying, stain the slides 10 to 15 min with 5% Giemsa solution.
11. Examine the cells for micronuclei at 1000× magnification. Score the number of MN in ≥1000 binucleated cells for each independent experiment. Code and score all slides without any knowledge of the treatment condition.

The cytokinesis-blocked cells scored for MN should have two nuclei of approximately equal size. The criteria for identifying micronuclei are: (1) MN have a diameter between 1/16 and 1/3 that of either of the main nuclei; (2) MN are round or oval with the same color as the main nuclei; (3) MN are not linked to a main nuclei via a nucleoplasmic bridge; and (4) MN may sometimes overlap the boundaries of the main nuclei (Fenech, 1993). Statistical significance of MN levels can be evaluated by the T-test, and the scoring of MN can be automated (Streffer et al., 1998).

12. Calculate the mean number of micronuclei and the standard deviation in a total of three to four independent experiments.

Statistical analysis of the number of micronuclei may be done. It is also recommended that the distribution of MN among binucleate cells be determined, because the sensitivity to a particular clastogen may depend on cell-cycle status when heterogeneous cell populations are treated.

The proportion of binucleate cells should also be noted, since this can provide an index of cytotoxicity and responsiveness to the examined agent in conjunction with cytochalasin B (for an advanced statistical analysis see Johnston et al., 1997).

GIEMSA OR GIEMSA/TRYPSIN STAINING TO EVALUATE CHROMOSOME ABERRATIONS

BASIC PROTOCOL 2

From a genetic toxicology perspective, chromosome aberrations involving gains or losses of whole or partial chromosomes (aneuploidy), as well as breaks, gaps, rearrangements, translocations, ring chromosomes, dicentric chromosomes, and acentric chromosome fragments, can be analyzed in metaphase spreads of cultured mammalian cells following toxicant exposure in vitro. Chromosome aberrations can also be readily evaluated in short-term cultures of cells derived from various animal tissues (e.g., peripheral blood lymphocytes) following in vivo toxicant exposures, as well as in cell cultures of tumor-derived cells. Conventional staining or chromosome banding techniques can be used to visualize and characterize these aberrations. Staining with Giemsa will produce homogeneously stained purple chromosomes. For more enhanced visualization of chromosome rearrangements and translocations, the slides can alternatively be treated with trypsin then stained with Giemsa to produce characteristic G-banding patterns on each chromosome.

Materials

Slides containing metaphase spreads (see Support Protocol) from treated and control cells

10% (w/v) Giemsa solution (for Giemsa staining) *or* 5% (w/v) Giemsa solution (for trypsin/Giemsa staining): dilute Giemsa stain (see recipe) 1:9 (for 10%) or 1:19 (for 5%) in Sorenson's phosphate buffer, pH 6.8 (see recipe), prepare diluted stains fresh

0.05% (w/v) trypsin: dilute 2.5% (w/v) stock in PBS or other physiological saline solution

PBS (*APPENDIX 2A*) or saline solution

Permount (Fisher Scientific)

22 × 44–mm coverslips

ASA 100 color film

Stain chromosomes with Giemsa or with trypsin/Giemsa

For Giemsa staining

1a. Stain chromosomes on slides for 3 to 5 min with 10% Giemsa solution.

2a. Proceed to coverslipping (step 3).

For trypsin/Giemsa staining to produce G-banded chromosomes

1b. Incubate slides in 0.05% working solution of trypsin in PBS or other physiological saline solution, for 5 to 60 sec depending on the cell type and the age of the slides.

The duration of exposure to the trypsin should be optimized for each set of slides by evaluating the outcome of the banding process on the first test slide (faint banding will be detected even without the Giemsa staining step). If the trypsinization is insufficient, the slide can be placed into the trypsin again. Occasionally, the trypsinization step will have to be increased to 1 to 2 min. It is always better to undertrypsinize the chromosomes than to overexpose them, since the overtrypsinized situation cannot be corrected. In the case of overtrypsinization, the chromosomes will lose morphology, becoming bloated ghosts with no evident banding. Aged slides, whether air dried for ~1 week, or mechanically "aged" by placing in a drying oven for several hours, seem to yield the best G bands.

2b. Rinse slides two to three times in PBS or saline, then stain 1 to 3 min in 5% Giemsa solution.

Score chromosome aberrations (CA)

3. Coverslip slides by adding a drop of Permount to the non-frosted farthest edge of the slide. Place the edge of a 22 × 44–mm glass coverslip into the Permount at a 45° angle, then gently lower the coverslip over the viewing area of the slide letting the Permount spread evenly beneath the coverslip. Gently tease out any large bubbles and excess mounting fluid, and let the Permount dry for 15 min at room temperature.

Permounted, Giemsa-stained slides are permanently preserved, allowing for viewing at any convenient time as well as archival storage of the slides.

4. Score ≥100 well spread, intact metaphase cells for each treatment at 1000× magnification. Document representative metaphase cells (Giemsa-stained or G-banded) by routine color photography (ASA 100 film).

In addition to counting the number of chromosomes per metaphase spread, aberrant chromosomes should be classified according to standard cytogenetic definitions: chromatid gaps, chromatid breaks, chromatid deletions, chromosome gaps, chromosome breaks, chromosome deletions, acentric fragments, dicentric, rings (centric or acentric), quadriradials, and triradials. The frequency of each type of aberration should be tallied (as per Keshava et al., 1998). For banded chromosomes, translocations may also be tallied.

Mitotic index (MI), a measure of cytotoxicity, can also be calculated for each treatment by counting the number of metaphases per 1000 cells.

BASIC PROTOCOL 3

EVALUATION OF CHROMOSOME ABERRATIONS BY PAINTING WITH FLUORESCENCE IN SITU HYBRIDIZATION (FISH) PROBES

For some mammalian species such as the mouse, the karyotype consists of 40 telomeric chromosomes of similar size. This makes evaluation of complex rearrangements and translocations very difficult. The use of differently colored fluorescence in situ hybridization (FISH) probes specific for any two representative chromosomes, such as chromosomes 2 or 8 (Spruill et al., 1996), allows for rapid, accurate scoring of symmetrical and asymmetrical exchanges between painted and unpainted chromosomes. Thus, a translocation between any of the four fluorescent biotinylated chromosomes with any of the unpainted chromosomes can be easily seen as a bicolored (e.g., red/yellow) product. FISH techniques using chromosome-specific painting probes have increased the sensitivity and ease of detecting stable chromosome aberrations in both in vitro and in vivo studies in humans and other species (Tucker et al., 1995).

Materials

Chromosome-specific DNA painting probes (2 chromosomes) for the species of interest, labeled with biotin or digoxigenin (Vysis, Inc.)
Hybridization solution (see recipe)
Metaphase spreads (see Support Protocol) from test-agent-treated cells
70% (v/v) formamide/2× SSC and 50% (v/v) formamide/2× SSC (see recipe for SSC)
70%, 80%, and 100% ethanol
Rubber cement
2× SSC (see recipe)/1% (v/v) NP-40 (Ventana Medical Systems)
Sodium phosphate (PN) buffer (see recipe)
3% (w/v) powdered non-fat milk in PN buffer
5 µg/ml FITC-avidin in PN buffer
12 µg/ml biotinylated anti-avidin in PN buffer (optional)
200 µg/ml stock DAPI stain (store up to 1 year at −20°C; dilute to 0.5 µg/ml in antifade solution just before use)
200 µg/ml stock propidium iodide stain (store up to 1 year at −20°C; dilute to 1 µg/ml in antifade solution just before use)
Antifade solution (Vysis, Inc., Molecular Probes, Ventana Medical Systems)

Coplin jars
Humidified chamber (container with lid and lined with moist paper towels)
22-mm^2 coverslips
Kodak Ektachrome 400 film

1. Mix chromosome-specific biotinylated or digoxigenen-labeled probe DNA(s) with hybridization solution at 10 ng/ml in a final volume of 15 µl per slide. Denature at 70°C for 5 min and keep on ice until use.

   Human and mouse chromosome-specific fluorescent painting probes are commercially available (Vysis, Inc.). The probes are supplied in aqueous solution, or may be pre-mixed with hybridization buffer as indicated by the supplier. Alternatively, the investigator may make his own chromosome probes by PCR of microdissected chromosomes of any species (Christian et al., 1999).

2. Denature the metaphase cell slides 5 min at 70°C in 70% formamide/2× SSC, pH 7.0. Use 2 to 4 slides per test.

   CAUTION: *Care should be exercised when handling formamide and only glass Coplin jars should be used as a vessels for all formamide solutions.*

   Metaphase slides are best for FISH when well dried, either air-dried for several days, or oven-dried (1 to 2 hr at 65°C). Some FISH protocols recommend a brief protein digestion step (10% pepsin, 37°C, 10 min) prior to denaturation.

3. Dehydrate the slide(s) through a series of 5-min 70% ethanol, 80% ethanol, and 100% ethanol washes at room temperature in Coplin jars.

4. Apply 15 µl of the denatured probe/hybridization mix to the surface of each slide, cover with clean 22-mm^2 coverslip and seal edges with rubber cement. Incubate 24 to 48 hr at 37°C in a humidified chamber.

   Alternatively, Parafilm coverslips can be used in place of glass coverslips, thus eliminating the need for rubber cement. Hybridization time may vary depending on the size and sequence specificity of the fluorescent probe.

5. Remove unbound probe by rinsing the slides in three 5-min washes at 45°C of 50% formamide/2× SSC, pH 7.0, in Coplin jars.

Do not forcibly remove the coverslips after hybridization, since the chromosome spreads can easily become mechanically sheared. The coverslips will loosen and slip off into the first wash. To promote this, the slides can be very gently agitated by hand in the Coplin jar.

6. Follow with 5-min washes successively in 2× SSC at 45°C, in 2× SSC with 1% NP-40 at 45°C, and in PN buffer at room temperature.

7. Block slides 5 min with 3% powdered non-fat milk in PN buffer at room temperature.

   The blocking step will reduce the background that can result from nonspecific binding of the FITC-avidin.

8. Stain slides with 5 µg/ml FITC-avidin applied to the surface of each slide. Incubate 30 min at room temperature.

   The visualization of the fluorescent probe can be enhanced by sequential overstaining with biotinylated anti-avidin/FITC-avidin (Spruill et al., 1996).

9. Counterstain the chromosomes with 2 to 3 drops of a mixture of DAPI at 0.5 µg/ml and propidium iodide at 1 µg/ml in antifade solution. Cover the slide with a clean coverslip.

10. Visualize the fluorescent-stained chromosome under 1000× magnification using an epifluorescent photomicroscope with halogen (75-W mercury lamp) illumination.

    A DAPI filter set will allow the viewer to locate blue stained metaphases for further analysis with other UV filter sets, such as a dual red/green filter set that allows simultaneous visualization of red propidium iodide stained chromosome, contrasted with the bright yellow-green FITC stained hybridized probe regions for translocation analysis.

    FISH slides can be covered with foil or stored in any light-tight container at 4°C, for several days without fading to permit subsequent visualization at a later time.

Score chromosome aberrations (CA)

11. Score chromosome rearrangements in the equivalent of ≥200 intact metaphase cells per treatment (therefore 1000 cells, see rationale below), using the following criteria: the centromeres of all chromosomes including the four painted chromosomes must be visible, and the FITC label must be bright enough to differentiate between painted and unpainted chromosomes.

    Since chromosome painting with two chromosome-specific probes detects only a fraction of the total exchanges possible within each metaphase, five metaphase cell equivalents must be scored in order to obtain the same amount of information as obtainable from one G-banded cell (Spruill et al., 1996).

12. Document abnormal metaphases by fluorescent photomicroscopy using Kodak Ektachrome 400 film.

    Various camera set-ups can be installed for standard photomicroscopy or for digital image analysis of informative chromosome spreads. Record the position of any photographed or analyzed metaphase spread using the calibrated horizontal and vertical locators on the microscope stage.

SUPPORT PROTOCOL

PREPARATION OF METAPHASE CHROMOSOME SPREADS

Metaphase chromosome spreads are required to evaluate cells for chromosomal aberrations by Giemsa staining, Giemsa/trypsin banding, or fluorescence in situ hybridization (FISH). Cells are cultured, treated, harvested, incubated in hypotonic medium, fixed, and dropped onto glass slides to provide chromosomal spreads for staining.

Materials

Cells to be studied
Medium and supplements appropriate for the cells being studied
Agent to be tested in appropriate solvent
10 μg/ml colchicine or Colcemid
Hypotonic solution: 0.075 M KCl, 37°C
Carnoy's fixative: 3:1 (v/v) methanol/glacial acetic acid, freshly prepared (ice-cold)

60-mm petri dishes
Microscope slides, cleaned and chilled

Grow and treat cells

1. Seed 2.5×10^4 cells per 60-mm petri dish in 5 ml medium (four dishes are required for each dose of putative genotoxic agent). Incubate cells 16 to 20 hr at 37°C.

   The chemical treatment should be performed while cells are in exponential growth.

2. Add the test agent to the dishes and incubate cells at 37°C for the appropriate exposure time found previously to generate genotoxic effects.

   Dosage levels are selected based on toxicity or solubility limits. If the chemical is dissolved in DMSO or other organic solvent, pure DMSO or solvent should be used as negative control. Solvent concentration should not exceed 1%.

Harvest and fix cells

3. Before harvesting the cells, add Colcemid (from 10 μg/ml stock) to a final concentration of 0.1μg/ml. Leave the Colcemid on the cells for 1 to 2 hr.

   The duration of Colcemid exposure depends on the proportion of metaphases that are collected as determined by occasional observation under an inverted cell culture microscope. Colcemid added to actively dividing cells arrests the cells during metaphase to produce the classic chromosome morphology that is most often visualized in cytogenetic preparations. The dose and duration of Colcemid exposure should be optimized for each cell type studied. The timing of the Colcemid treatment should be kept as short as possible, since prolonged exposure to the drug will progressively shorten the metaphase chromosomes, making their evaluation more difficult.

   Colchine can be used interchangeably with Colcemid.

4. Collect the cells by trypsinization (*APPENDIX 3B*), gentle scraping, or mitotic shake-off, depending on the type of cells being used. Collect both the Colcemid-containing medium prior to trypsinization and the trypsinized cell suspension in a15-ml centrifuge tube. Centrifuge 5 min at $600 \times g$, room temperature.

   Certain mammalian cells such as those derived from Chinese hamster (V79, CHO) are amenable to mitotic shake off, thus allowing the elimination of the trypsinization step if desired.

   Retention of the medium from the Colcemid treatment will allow collection of additional metaphase cells that have become detached during the metaphase blocking step and will also facilitate inactivation of the trypsin when the trypsinized cell suspension is added to the centrifuge tube that already holds the Colcemid-containing medium.

5. Decant all but 1 ml of the supernatant, then gently resuspend the cell pellet. Add 4 ml prewarmed 0.075 M KCl hypotonic solution and incubate 5 to 10 min in a 37°C water bath.

   The optimal duration of hypotonic treatment may vary for different cell types.

   During exposure to the hypotonic salt solution, the cells expand in volume and metaphase chromosomes are distributed throughout the cytoplasm. Upon dropping the cells onto the

slides, the cells split open, thus spreading the metaphase chromosomes. This allows the examination and identification of individual chromosomes on microscopic slide preparations. Due to their fragility, hypotonically swelled cells must be handled gently to avoid cell rupture prior to fixation and slide preparation. Narrow-tipped pipets and excessive centrifugation or vortexing should be avoided.

6. Add 5 drops of ice-cold, fresh Carnoy's fixative to the 37°C cell suspension and swirl the tube gently. Collect cells from the hypotonic treatment by gently centrifuging 10 min at 200 × *g*, room temperature.

7. Aspirate the supernatant carefully with a clean glass Pasteur pipet without disrupting the loose cell pellet.

   After the hypotonic treatment and centrifugation, the cells will be clearly visible as a loose pellet. Following centrifugation, the supernatant should not be decanted by inversion, since the cell pellet is loose and in danger of being lost.

   In this and all subsequent steps, mechanical pipetting devices are usually avoided in favor of using Pasteur pipets and bulbs. This allows for more gentle handling of the cells and facilitates the dropwise additions of the fixative.

8. Add 5 ml of fresh, ice-cold Carnoy's fixative to the cell pellet in a dropwise manner.

   To avoid problems with cell clumping, the first fixation step should follow a meticulous drop-by-drop method that includes a gentle swirling of the tube in between each drop of added fixative. The fixative should be freshly prepared on the day of its use, should be iced in a −20°C freezer prior to use, and should be kept on ice during use. To reduce the evaporation of the methanol, the fixative bottle should not be left uncapped while working.

9. Refrigerate the centrifuge tubes 30 min at 4°C. Centrifuge 10 min at 300 × *g*, 4°C. Aspirate the fixative using a Pasteur pipet, as above.

   The previously visible swelled cell pellet will become significantly reduced in size during the fixation procedure. This does not indicate a loss of cells.

10. Repeat steps 8 and 9 at least two more times to ensure adequate fixation of the cells.

    After the first fixation, the dropwise addition of the Carnoy's fixative is only necessary until the cells are resuspended (first 1 ml added). The remainder of the fixative should be added slowly with gentle bubbling or swirling to mix the cells. For some cell types, fixed metaphase cells can be stored at 4°C in the final fix for several weeks or even months prior to slide preparation.

11. Centrifuge the fixed cells 10 min at 300 × *g* and decant the fixative using a pipet.

12. Add a minimal amount (0.5 to 1.5 ml) of fresh, ice-cold fixative and resuspend the cells for slide preparation.

    The amount of final fixative used for slide preparation will depend on the concentration of cells observed in each tube but should be kept to a minimum.

13. Take up a small amount (<0.5 ml) of this concentrated cell suspension into the narrow neck of a fresh Pasteur pipet, and drop 3 to 4 drops across a clean, cold microscope slide. Prepare multiple slides as permitted by the volume of the cell suspension. Air dry the slides.

    Various methods for chromosome slide preparation can be found in the literature, and individual preference should be applied. The slides for metaphase preparations can be iced/dry, iced/wet, or cold/wet. Many investigators prefer to drop the cell suspension onto the slide from a height of 1 to 2 feet to promote cell breakage. The slides can be passed over a flame, or gently blown upon to enhance metaphase spreading. Visual inspection of the first slide prepared from each tube will determine whether the cell preparation would benefit from another overnight fixation step to further weaken the cell membrane and

enhance metaphase spreading. Some cell types or staining procedures may require drying the slides on a hot plate (60°C, 2 to 5 min) or aging the slides several days at room temperature.

DETECTION OF SISTER CHROMATID EXCHANGES

BASIC PROTOCOL 4

In this assay, cells are treated with the test agent, then the thymidine analog 5-bromodeoxyuridine (BrdU) is incorporated into the DNA during two cell cycles. Metaphase chromosomes are accumulated at the second metaphase after the addition of BrdU and then stained by the 33258 Hoechst/Giemsa technique. The objective is to obtain cells containing differentially stained chromatids, in which exchanges between sister chromatids can be observed. The sister chromatid exchange (SCE) assay is a widely used assay in genotoxicity screening.

Materials

Cells to be studied
Medium and supplements appropriate for the cell line studied (*APPENDIX 3B*)
Agent to be tested
0.5 mM 5-bromodeoxyuridine (BrdU), filter sterilized, (store up to 2 to 3 weeks in the dark at −20°C)
10 μg/ml colchicine or Colcemid
Hypotonic solution: 0.075 M KCl
Carnoy's fixative 3:1 (v/v) methanol/glacial acetic acid (freshly prepared), ice-cold
2 mg/ml Hoechst 33258 in water (store several months in the dark at −20°C)
0.5× and 2× SSC (see recipe)
3% (v/v) Giemsa solution (prepare fresh): dilute Giemsa stain (see recipe) 3:97 (v/v) in Sorenson's phosphate buffer, pH 6.8 (see recipe)

60- and 100-mm petri dishes
Microscope slides, cleaned and chilled
UV light source (Philips MWL 160 W lamp)

Additional reagents and equipment for mutagenesis of cells (*UNIT 3.3*), trypsinization of cultures (*APPENDIX 3B*), and preparation of metaphase spreads (see Support Protocol)

Grow and treat cells

1. Seed ~2.5×10^4 cells per 60-mm petri dish in 5 ml medium (four dishes are suggested for each dose of putative genotoxic agent). Incubate 16 to 20 hr at 37°C.

   For a detailed description of mutagenicity testing, see UNIT 3.3. The chemical treatment should be performed while cells are in exponential growth. In addition, the initial cell number should be adjusted so that the culture will not reach confluence during the additional two cell cycles in the presence of BrdU required to perform the assay.

2. Add the test agent to the dishes and incubate cells at 37°C for any exposure time found previously to generate genotoxic effects.

   This step allows interaction of the test substance with cells before addition of BrdU. Longer exposure periods may be necessary for agents which have an effect only during DNA synthesis.

   If the chemical is dissolved in DMSO or other organic solvent, pure DMSO or solvent should be used as negative control. Solvent concentration in contact with the cells should not exceed 1%.

Incorporate BrdU into DNA

3. Wash the cells twice with PBS, and add 5 ml fresh medium containing 10 to 20 µM BrdU. Incubate cells at 37°C for the time appropriate to span two cell cycles.

   This time span differs among cell types, but may typically be 24 to 30 hr.

   The optimal concentration of BrdU varies with cell type. The final BrdU concentration should not significantly inhibit cell replication but should allow differential staining to enable scoring for SCEs. BrdU itself increases the frequency of SCE, so it is important to include a BrdU control treatment (cells that have not been treated with the test agent) in the experiment.

   All manipulation of cultures containing BrdU must be carried out in the absence of direct light because exposure to light degrades BrdU-substituted DNA.

4. Two hours before harvesting the cells, add Colcemid (from 10 µg/ml stock) to a final concentration of 0.1 µg/ml.

   Colcemid or colchicine added to mitotic cells during metaphase and anaphase disrupts spindle-fiber formation, preventing the separation of chromatids after the centromere is split.

Harvest and fix cells

5. Collect the cells by trypsinization (*APPENDIX 3B*) or gentle scraping. Centrifuge 7 min at 600 × *g*, room temperature.

6. Resuspend the cells in 1 ml hypotonic solution (0.075 M KCl) for 5 to 10 min in a 37°C water bath.

   Due to the fragility of the swollen cells, the optimal duration of hypotonic treatment may vary for different cell types.

7. Fix the cells as described for metaphase spreads (see Support Protocol, steps 6 to 10), drop the cell suspension onto clean, cold microscope slides (see Support Protocol, step 13), and air dry the slides.

   During exposure to hypotonic salt solution, the cells expand in volume and metaphase chromosomes are distributed throughout the cytoplasm. Upon dropping the cells onto the slides, the cells split open, spreading the metaphase chromosomes. This allows the examination and identification of individual chromosomes in microscopic slide preparations.

   Hypotonically swelled cells must be handled gently to avoid cell rupture prior to fixation and slide preparation. Narrow-tipped pipets should be avoided.

Stain the cells

8. Stain the slides 45 min in 50 ml of 0.5× SSC containing 50 µl of 2 mg/ml Hoechst 33258 in a Coplin jar.

9. Wash the slides 5 min in 2× SSC.

10. Immerse the slides in 5 ml of 0.5× SSC in a 100-mm tissue culture dish and expose them to UV light (Philips MWL 160-W lamp) at a distance of 10 cm for 1 hr. Do not allow the slides to dry out.

11. Incubate the slides 1 hr in fresh 0.5× SSC in a Coplin jar at 60°C and overstain 15 min with 3% Giemsa solution, pH 6.8. Add Permount and a coverslip. View at 400 to 1000× magnification.

    Differential staining of chromatids by BrdU/Giemsa (purple/white) will highlight the frequency of crossing over between the two chromatids, and thus enable scoring of SCEs.

Score for SCE

12. Count the number of SCEs in at least 50 differentially stained metaphase spreads from each treatment. Also record the number of chromosomes analyzed in each cell. Determine both the frequency of SCE per chromosome and total SCEs per cell.

    While scoring the SCEs, it is important to select an area of the slide where the metaphase chromosomes are well spread to allow screening of individual metaphase chromosomes. Each chromatid exchange is counted as a single event.

    Usually the mean and standard deviation values of the SCE per chromosome are presented for each dose (from at least three independent experiments), and are compared to the SCE values of the solvent controls, using appropriate statistical procedures.

REAGENTS AND SOLUTIONS

Use Milli-Q-purified water or equivalent in all recipes and protocol steps. For common stock solutions, see ***APPENDIX 2A****; for suppliers, see* ***SUPPLIERS APPENDIX****.*

Cytochalasin-B stock solution, 1 mg/ml

Dissolve 1 mg of cytochalasin B in 1 ml of dimethyl sulfoxide (DMSO). Store up to 2 to 3 months at −20°C.

Giemsa stain

Mix 7 g Giemsa powder with 482 ml glycerol, warm 2 hr in a 60°C water bath. Allow to cool to room temperature and add 462 ml methanol. Filter through Whatman no. 1 filter paper, store up to 6 months at room temperature in a dark glass bottle.

Some precipitation will be noted with time.

Hybridization solution

50% (v/v) formamide
2× SSC (see recipe)
10% (w/v) dextran sulfate
1.5 µl of 1µg/µl herring sperm DNA
2.0 µg species-specific COT-1 DNA (Life Technologies, Vysis, Inc.)
Store up to 6 months at −20°C in 100- to 200-µl aliquots

This solution is also commercially available from Vysis, Inc. and Ventana Medical Systems or comes supplied with the probe.

Sodium phosphate (PN) buffer for FISH

0.1 M $NaPO_4$, pH 8.0 (*APPENDIX 2A*)
0.1% (v/v) NP-40 (Ventana Medical Systems)
Store 2 to 3 months at 4°C

Sorenson's phosphate buffer

9.4 g/liter $NaHPO_4$
9.08 g/liter KH_2PO_4
Store 6 months at 4°C

2× SSC solution

0.30 M NaCl
30 mM sodium citrate
Adjust pH to 7.0 with 1 M HCl
Store 6 months at room temperature

COMMENTARY

Background Information

The micronucleus (MN) assay determines the clastogenic or chromosome-breaking effects of particular agents and examines the relative sensitivities of eukaryotic cells to such clastogens. Micronuclei are chromatin-containing bodies that represent acentric chromosomal fragments or whole chromosomes that were not incorporated into a nucleus during mitosis (Fenech, 1998). Micronuclei can be examined for the presence of a centromere by staining with anti-kinetichore antibodies. This method differentiates between whole chromosomes (with kinetichores) and acentric fragments (without kinetichores) in the micronuclei (Hermine et al., 1997).

Although the number of micronuclei within a cell is not a precise measure of chromosome breakage or gap formation (since multiple fragments may reside within a single micronucleus), it is possible to demonstrate a dose-response relationship between clastogen exposure and MN frequency, as well as a relationship between long-term survival and MN frequency.

Micronuclei assays may be conducted in vivo or in cultured cells. The in vivo assays are most often performed by counting micronuclei in immature polychromatic erythrocytes (PCE) from the bone marrow of treated mice or in peripheral blood smears (Fenech, 1998). MN remain in the cells when the nucleus is extruded during the maturation of erythroblasts.

MN assays in cultured cells have been greatly improved by the cytokinesis-block micronucleus (CBMN) technique, in which cytoplasmic division is inhibited by the fungal metabolite cytochalasin B, resulting in binucleate and multinucleate cells (Fenech and Morley, 1985; Fenech, 1993; Kirsch-Volders, 1997). In this assay, cells are exposed to the test agent and cytochalasin B is added for the last part of the culture period. Micronuclei are counted only in the binucleate cells to ensure that the cells have undergone a single nuclear division. The assay allows parallel estimation of mitotic delay (frequencies of binucleated cells), apoptosis (frequencies of condensed nuclei), chromosome breakage/chromosome loss (frequencies of micronuclei), and chromosome non-disjunction (requires FISH analysis).

For detailed analysis of chromosomal rearrangements and translocations, the production of G-bands is worthwhile. In comparison to other chromosome banding methods, such as those using fluorochromes like quinicrine, trypsin-Giemsa banding is the most convenient and reproducible and does not require the use of a fluorescent microscope. In addition, the Giemsa staining of trypsin-banded chromosomes provides a permanent record of the banding patterns, allowing historical reevaluation of slides long after the fluorescent bands would have faded. The principle behind trypsin/G-banding is that the trypsin digestion removes chromosomal proteins in distinct regions along each chromosome arm. The trypsin banding patterns are therefore characteristic for each chromosome of every species. G-banded reference karyotypes are available in the literature for virtually all species that can be used in genetic toxicology. Enlarged pitcographs of all G-banded human chromosomes are depicted in Verma and Babu (1989) with the primary nomenclature references cited therein. Various methods for optimization of G-banding procedures, as well as Q-, C-, R-banding and numerous other chromosome banding methods are also well described by Verma and Babu (1989). Only the most basic trypsin banding protocol has been included in this unit.

As an adjunct to conventional banding techniques, fluorescent in situ hybridization (FISH) has numerous research and clinical applications including but not limited to the characterization of complex structural abnormalities, chromosome enumeration using alpha-satellite probes, and gene mapping. Depending on the availability of multi-band fluorescence microscopy filters, two or three differentially colored fluorescent chromosome paints can be incorporated into these assays using a variety of fluorescent dyes. Spectral karyotyping (SKY), in which each chromosome homolog is depicted in a different color shade facilitates the identification of otherwise cryptic, complex, or very small chromosomal rearrangements (Schröck et al., 1996; Veldman et al., 1997). However, specialized costly equipment is required for SKY analyses, which may limit the routine use of this procedure in genetic toxicology studies.

Sister chromatid exchanges (SCEs) are a consequence of the interchange of replicating DNA between chromatids at apparently homologous loci. The process involves DNA breakage and reunion. A wide variety of physical and chemical mutagens induce SCEs in cultured cells and in mammals in vivo (Tucker et al., 1993). Each separate chromatid exchange

is visible cytologically after differential staining of the individual chromatids. The nature of the initial DNA damage and the mechanism of formation of SCE is still unknown; however, it appears that SCEs are produced at or near DNA replication forks. SCE frequency is increased after DNA damage by agents that inhibit or block the progression of the replication fork of a replicon (Painter, 1980). In order to screen for SCE induction, the cells are treated with the test agent, and then BrdU is added to the medium for two successive cell cycles (BrdU replaces thymidine in the newly synthesized DNA). Metaphase spreads are prepared by standard methods and the chromosomes are then stained with Hoechst 33258. This dye fluoresces at a lower intensity when bound to DNA substituted with BrdU than when bound to unsubstituted DNA. Following photosensitization which leads to degradation of highly BrdU- substituted chromatids, and staining with Giemsa, the chromatids appear differentially stained (Perry and Wolff, 1974). This process distinguishes hybrid chromosomes with one BrdU-containing strand and one darkly stained original strand from those in which both strands contain BrdU (no Giemsa stain). The sister chromatid exchanges generate the so-called "harlequin chromosomes."

Because cell lines have limited endogenous capacity for metabolic activation, it is possible to use exogenous sources of liver-derived microsomal S9 mixes (*UNIT 3.1*), when the above chromosomal aberration assays are performed (treatment of cells with S9 mix should be performed in serum-free or reduced serum medium). Alternatives to the use of S9 mixes include cocultivation, where target cells are treated in the presence of cells which are proficient for metabolic activation (Gulati et al., 1989).

Critical Parameters

The induction of chromosomal aberrations in cell culture may lead to artifacts associated with extreme culture conditions. For example, at high chemical concentrations, high osmolarity may cause apparent genotoxic effects. Highly cytotoxic doses and pH extremes may activate metabolic systems that may also be genotoxic. On the other hand, it is critical that sufficiently high doses be examined, therefore testing should be extended to doses at which some cytotoxicity is observed, as gauged by a reduction in the mitotic index (the proportion of cells in division).

A key factor in the design of cytogenetic assays in vitro is obtaining appropriate cell populations for treatment and analysis. Cells with stable, defined karyotypes, short generation times, low chromosome numbers, and large chromosomes are recommended. For this reason, Chinese hamster ovary (CHO) cells have been used extensively. Additional critical factors in cytogenetic assays are the growth conditions, controls, doses, treatment conditions, and the time intervals between treatment and the sampling of cells for analysis. In all the assays described above, it is essential that a sufficient number of cells be scored and that three to four independent experiments are performed for each toxicant dose.

While performing the MN assay, it is important to follow the criteria for scoring micronuclei as described in the protocol. Micronuclei are counted only in binucleate cells, in which two distinct nuclei are surrounded by a recognizable independent cell membrane. Only morphologically integrated cells are scored. Cells undergoing cell death, mitosis, or containing more than two nuclei, are excluded from MN scores, but included in calculations of total cell number.

By far, the most critical parameter in obtaining useful cytogenetics information from Giemsa stained, G-banded, fluorescent probe–hybridized, or SCE chromosome slides is the preparation of the metaphase spreads (also see Bangs and Donlon, 1994). These assays all require that the chromosome slides be coated with well spread non-overlapping metaphases that have not lost any chromosomes due to rough mechanical handling. A maximal number of metaphases per slide can be obtained by optimizing the Colcemid arrest timing and by not over-diluting the final cell suspension immediately prior to making the slides. During the metaphase preparations, excessive hypotonic swelling of the cells can lead to premature cell breakage, resulting in the chromosomes from many cells being mixed together in the test tube. Ideally, the swelled cells should burst at the moment of impact with the slide, allowing the chromosomes to spread out within a small radius. On the other hand, if the hypotonic treatment was insufficient, or the fixative steps did not fully weaken the cell membrane, the cells may not burst open on the slide. In this case, tightly packed poorly-stained chromosomes will be seen within ghost cells whose cytoplasm is still faintly visible. Such cells are not adequate for scoring chromosome aberrations, translocations, or SCE. Over-condensation of the chromosomes by Colcemid treatment that is too concentrated or too long will

also impact on staining and analysis in all protocols discussed above. Based on these considerations, it is essential that new investigators familiarize themselves with hands-on experience in metaphase spread preparations prior to commencing any treatment experiments. In addition, the specific parameters for Colcemid arrest, hypotonic swelling, fixation and slide preparation should also be optimized in advance for the particular cell type that will be used, since species and tissue of origin of the cells can have profound effects on these variables.

Lastly, it should be noted that the protocols specified herein are general protocols that may be standardized to include very narrow windows of timing and other processing parameters when the assays are being applied to industrial genotoxicity testing settings or when comparing data between laboratories, especially in human exposure biomarker situations (Fenech, 1998).

Anticipated Results

Clastogenic activity may be measured as an increase of MN and SCE frequencies. If the tested agent has a clastogenic potential it is expected to induce MN and SCE in a dose responsive manner. MN assays provide a measurable index of chromosome breakage or loss, but cannot replace the detailed analysis of chromosome damage obtained on Giemsa stained, banded, or FISH-painted metaphase spreads.

Baseline levels of the various cytogenetic outcomes discussed in this unit have been reported for humans and experimental animal studies for each of the specific assays discussed above. A brief review of some of those data will be presented here, with the caveat that a broad range of interpopulation, intraindividual, interlaboratory, and species differences in these values can be found in the literature. As noted above, ongoing international standardization of each of the cytogenetic assays currently used for regulatory and research purposes will undoubtedly lead to more clearly defined acceptable baseline values, test protocols, and toxicity limits for each specific assay (Kirkland, 1998). Therefore the data presented here will only serve to orient the reader to general baseline and genotoxicant exposure levels observed for some of the different cytogenetic assays that we have discussed.

With any exposure to genotoxicants, the mean MN values could increase dramatically. This was shown, for example, in a CBMN micronucleus study in which mouse liver cells were exposed to X-rays and vinblastine (Salassidis et al., 1992). Compared to the background level of MN (35/1000 cells scored) exposure of these cells to 3 Gy of X-rays induced 385 MN/1000 cells, and 0.6 μM vinblastine induced 154 MN/1000 cells. Human population studies often yield much lower values for MN frequency. As summarized recently by Fenech (1998), the CBMN assay generates mean baseline MN values of about 10 MN per 1000 binucleated (BN) cells in unexposed human lymphocytes from 20- to 45-year-old donors, with age and gender being the most important demographic variables. A large age-related variability in this value is evident, with 20 to 29 year olds showing 7.9 ± 3.3 MN/1000 BN cells, compared to 70 to 89 years olds showing 22.3 ± 7.6 MN/1000 BN cells. In contrast, variability related to different tissue culture media was not found. However, the mean MN value in the unexposed lymphocytes as determined by two independent scorers (9.2 ± 0.4 versus 11.4 ± 0.5) varied by at least 34%.

In normal human lymphocytes, the general level of chromosome aberrations is on the order of 0.5% to 1% of cells with any aberration. In a study of X-ray exposures of human lymphocytes, the frequency of cells with aberrations increased to about 26% and 72%, following 100Gy and 300Gy exposures to X-rays (Grigorova and Natarajan, 1998). In human lymphocytes, the total number of aberrant chromosomes observed in one FISH study of X-ray-induced chromosome interchanges involving chromosome 1 was even lower than the level of general aberrations, about 2.5/1000 cells scored (Boei et al., 1998). Following in vitro exposure of these cells to 3 Gy of X-rays, the level of chromosome aberrations involving rearrangements with chromosome 1 rose to near 700/1000 cells. In Chinese hamster V79 cells, background levels of SCE were reported to be about 5.5/100 cells scored, whereas the SCE levels increased to 20/100 cells following exposure to UVB light and to even higher levels of about 55/100 cells when the UVB light was combined with a topoisomerase II inhibitor (Ikushima et al., 1998).

Time Considerations

In the MN assay, the seeding of the cells and adding of the test agent will take ~9 hr (including the incubation periods). The cells are then incubated in the presence of cytochalasin B for 20 to 24 hr. Cell fixation and staining require 4 to 6 hr, and scoring of MN will take several hours, depending upon the number of inde-

pendent experiments performed and the skill of the observer. In the SCE assay, the seeding of the cells requires 1 to 2 hr and then the cells are incubated for 16 to 20 hr. The cells are then treated with the test agent for 4 hr followed by incubation with BrdU for 24 to 48 hr. Cell fixation and staining require 7 to 9 hr, and the scoring process requires an additional several hours. Following desired exposure to a genotoxicant, routine chromosome harvest and trypsin/Giemsa banding can be accomplished in a total of 6 to 8 hr; however, the banding procedure is optimal when the slides have been aged at least overnight prior to staining. FISH analysis of fluorescent painted chromosomes requires the cell exposure, then the usual 6 to 8 hr for chromosome harvest. This is followed by 2 to 4 hr for the initial prehybridization handling, 24 to 48 hr for hybridization of the painting probes, and another 2 to 4 hr of post-hybridization washing and staining. For all cytogenetic procedures, microscopic analysis of the results requires several hours to several days, depending on the number of treatments and slides to be evaluated, as well as the skill of the investigator.

Literature Cited

Bangs, C.D. and Donlon, T.A. 1994. Chromosome preparation from peripheral blood cells. *In* Current Protocols in Human Genetics (N.C. Dracopoli, J.L. Haines, B.R. Korf, D.T. Moir, C.C. Morton, C.E. Seidman, J.G. Seidman, and D.R. Smith, eds.) pp. 4.1.1-4.1.19. John Wiley & Sons, New York.

Boei, J.J.W.A., Vermeulen, S. and Natarajan, A.T. 1998. Dose-response curves for X-ray-induced interchanges and interarm interchanges in human lymphocytes using arm-specific probes for chromosome 1. *Mutat. Res.* 404:45-53.

Christian, A.T., Garcia, H.E., and Tucker, J.D. 1999. PCR in situ followed by microdissection allows whole chromosome painting probes to be made from single microdissected chromosomes. *Mammalian Genome.* 10(6):628-631.

Fenech, M. 1993. The cytokinesis-block micronucleus technique: A detailed description of the method and its application to genotoxicity studies in human populations. *Mutat. Res*. 285:35-44.

Fenech, M. and Morley, A.A. 1985. Measurement of micronuclei in lymphocytes. *Mutat. Res.* 147:29-36.

Fenech, M. 1998. Important variables that influence base-line micronucleus frequency in Cytokinesis-blocked lymphocytes- a biomarker for DNA damage in human populations. *Mutat. Res*. 404:155-165.

Grigorova, M., and Natarajan, A.T. 1998. Relative involvement of chromosome #21 in radiation induced exchange aberrations in lymphocytes of Down syndrome patients. *Mutat. Res.* 404:67-75.

Gulati, D.K., Witt, K., Anderson, B., Zeiger, E., and Shelby, M.D. 1989. Chromosome aberration and sister chromatid exchange tests in Chinese hamster ovary cells in-vitro III: Results with 27 chemicals. *Environ. Mol. Mutagen.* 13:133-193.

Hermine, T., Jones, N.J., and Parry, J.M. 1997. Comparative induction of micronuclei in repair-deficient and proficient Chinese hamster cell lines following clastogen or aneugen exposures. *Mutat. Res.* 392:151-163.

Ikushima, T., Shima, Y., and Ishii, Y. 1998. Effects of inhibitors of topisomerase II, ICRF-193 on the formation of ultraviolet-induced chromosomal aberrations. *Mutat. Res.* 404:35-38.

Johnston, P.J., Stoppard, E., and Bryant, P.E. 1997. Induction and distribution of damage in CHO-K1 and the X-ray-sensitive hamster cells line xrs5, measured by the cytochalasin-B-cytokinesis block micronucleus assay. *Mutat. Res.* 385:1-12.

Keshava, C., Keshava, N., Ong, T-M., Nath, J. 1998. Protective effect of vanillin on radiation-induced micronuclei and chromosomal aberrations in V79 Cells. *Mutat. Res.* 397:149-159.

Kirkland D. 1998. Chromosome aberration testing in genetic toxicology—past, present and future. *Mutat. Res.* 404:173-185.

Kirsch-Volders, M. (ed.) 1997. The CB in-vitro micronucleus assay in human lymphocytes. Special issue. *Mutat. Res.* 392.

Painter, R.B. 1980. A replication model for sister chromatid exchange. *Mutat. Res.* 70:337-341.

Perry, P. and Wolff, S. 1974. New Giemsa method for the differential staining of sister chromatids. *Nature* 251:156-158.

Salassidis, K., Huber, R., Zitzelberger, H., and Bauchinger, M. 1992. Centromere detection in vinblastine- and radiation-induced micronuclei of cytokinesis-blocked mouse cells by using in situ hybridization with a mouse gamma (Major) satellite DNA probe. *Environ. Mol. Mutagen*. 19:1-6.

Schröck, E., du Manoir, S., Veldman, T., Schoell, B., Wienberg, J., Ferguson-Smith, M.A., Ning, Y., Ledbetter, D.H., Bar-Am, I., Soenksen, D., Garini, Y., and Ried, T. 1996. Multicolor spectral karyotyping of human chromosomes. *Science* 273:494-497.

Spruill, M.D., Ramsey, M.J., Swiger, R.R., Nath, J., and Tucker, J.D. 1996. The persistence of aberrations in mice induced by gamma radiation as measured by chromosome painting. *Mutat. Res.* 356:135-145.

Streffer, C., Muller, W.-U., Kryscio, A., and Bocker, W. 1998. Micronuclei-biological indicator for retrospective dosimetry after exposure to ionizing radiation. *Mutat. Res.* 404:101-105.

Tucker, J.D., Auletta, A., Cimino, M.C., Dearfield, K.L., Jacobson-Kram, D., Tice, R.R., and Carrano, A.V. 1993. Sister-chromatid exchange:

Second report of the Gene-Tox program. *Mutat. Res.* 297:101-180.

Tucker J.D., Morgan, W.F., Awa, A.A., Bauchinger, M, Blakey, D., Cornforth, M.N., Littlefield, L.G., Natarajan, A.T., and Shasserre, C. 1995. PAINT: A proposed nomenclature for structural aberrations detected by whole chromosome painting. *Mutat. Res.* 347:21-24.

Veldman, T., Vignon, C., Schröck, E., Rowley, J.D., and Reid, T. 1997. Hidden chromosome abnormalities in haematological malignancies detected by multicolor spectral karyotyping. *Nature Genet.* 15:406-410.

Verma, R.S. and Babu, A. 1989. Human Chromosomes: A Manual of Basic Techniques. Pergamon Press, Elmsford, N.Y.

Contributed by Catherine B. Klein,
Limor Broday, and Max Costa
New York University School of Medicine
New York, New York

Methods for Measuring DNA Adducts and Abasic Sites I: Isolation, Purification, and Analysis of DNA Adducts in Intact DNA

The major event involved in the formation of mutations and the initiation and progression of cancer is the induction of DNA damage by reactive intermediates arising from exposure to exogenous or endogenous chemicals. Many electrophilic metabolites of chemicals covalently bind to the bases of DNA, causing specific DNA adducts. A classic reference for these interactions is the book by Singer and Grunburger (1983). More recent reviews include several chapters in Volume 12 of *Comprehensive Toxicology* (Sipes et al., 1997) and the paper by La and Swenberg (1996). In addition to these reviews that include sections on DNA adducts arising from exogenous agents, there are numerous reviews on oxidative DNA damage that arises from endogenous and exogenous sources and from lipid peroxidation (Marnett and Burcham, 1993; Chung et al., 1996).

There are several features of DNA damage that need to be understood to place the results of such research in proper perspective. The first is that different DNA adducts have different efficiencies for causing mutations. To date, the most efficient adduct reported is O^4-methylthymine, which causes a base-pair substitution ~80% of the time DNA polymerase transcribes the adduct. Other promutagenic adducts cause mutations anywhere from 1% to 20% of the time. Most of these adducts are located in the base-pairing region of the DNA, although others cause the adducted base to flip out, so that different parts of the base are involved with base-pairing. Still other DNA adducts do not appear to cause mispairing and are relatively inefficient in causing mutations. Some of these, like the N-7 alkyguanine and N-3 alkyladenine adducts, are repaired rapidly or chemically depurinated causing abasic sites. Second, DNA adducts are repaired by a variety of pathways. These repair pathways can be error prone or essentially error free. They can also be saturated (i.e., the DNA repair pathways are working at maximum speed and efficiency, but cannot keep up with the damage being done) or induced. This points out an important caveat, that the number of DNA adducts may differ in single-dose studies compared to multiple-dose studies. DNA adducts are like other toxicokinetic parameters: under conditions of continuous exposure they will reach a steady state, where the number of DNA adducts formed on a given day will equal the number that are lost from repair and depurination. Finally, it is important to remember that loss of a DNA adduct does not necessarily mean that the lesion has returned to its normal state with a correct base inserted in a normal strand of DNA. In the case of base excision repair, there are five steps including removal of the base by the glycosylase, 5′-incision of the abasic site by AP endonuclease, single nucleotide insertion by β polymerase, subsequent release of the deoxyribose fragment, and ligation of the repaired strand. If any of the steps that follow removal by glycosylase are not completed, the resulting lesion may still have genetic consequences.

This unit contains protocols for DNA isolation and hydrolysis that are suitable for the most common types of DNA adduct analyses and for the evaluation of abasic sites in DNA: low-temperature/antioxidant DNA isolation (see Basic Protocol 1), room temperature/antioxidant DNA isolation (see Alternate Protocol), measurement of apurinic/apyrimidinic sites (see Basic Protocol 2), immune slot-blot analysis of DNA adducts (see Basic Protocol 3), immunohistochemical determination of DNA adducts (see Basic Protocol 4), and spectrophotometric quantification of DNA (see Support Protocol).

Contributed by James A. Swenberg, Amy-Joan L. Ham, Kevin S. McDorman, Eric J. Morinello, Jun Nakamura, and Robert Schoonhoven

Current Protocols in Toxicology (2002) 3.8.1-3.8.18

DNA ISOLATION METHODS

The approach to DNA isolation for DNA adduct studies is generally similar to those for other endpoints. The main considerations are the purity of the DNA and the amount of DNA needed for the assay. DNA for adduct studies should be devoid of RNA and free of protein as possible. This can be accomplished through the use of RNase incubation and extensive extraction with phenol and chloroform. The amount of DNA required for measuring some DNA adducts is typically much higher than amounts required for biotechnological assays. Some of these assays require up to 300 μg DNA. Most of the DNA isolation in the authors' laboratory is done through manual extraction using phenol and chloroform.

Alternative approaches to DNA isolation involve commercially available kits that significantly reduce the amount of time involved and do not require the use of phenol or chloroform. Many DNA isolation kits are designed to produce very small amounts of DNA for molecular biology studies; however, some kits can be scaled up to produce larger amounts of DNA from cell and tissue samples. Two such kits are the Puregene system of DNA isolation (Gentra Systems) and isolation using DNAzol genomic DNA isolation reagent (Molecular Research Center).

DNA adducts are usually quantified by comparing the number of adducted bases to the total number of the same base in the DNA sample, the number of total nucleotides, or the amount of DNA. For example, when measuring N^2,3-ethenoguanine (εGua) adducts, one must first measure the amount of guanine in the sample to produce useful data (*UNIT 3.9*). One could also give the data as the number of εGua per milligram DNA or per 1×10^6 nucleotides. Before treating the isolated DNA, an aliquot (typically 10 to 20 μl) of the DNA solution should be removed for measurement of the base, nucleoside, nucleotide, or DNA content. This is typically done using an HPLC-based assay and a calibration curve (see *UNIT 3.9*).

The protocols presented in this section detail two methods of DNA isolation that are based on phenol/chloroform extraction. The main differences between the two protocols involve incubation temperatures and times. Some DNA adducts are sensitive to the effects of heat and oxidation while others are not. This variable must be determined for the adduct studied before deciding which method to use. The low-temperature/antioxidation DNA isolation method (see Basic Protocol 1), should be used if there is any question that heat may alter the assay measurement. The room-temperature/antioxidation DNA isolation method (see Alternate Protocol) can be used if it is known that heat will not alter the assay measurement. Regardless of the DNA isolation method used, the authors have found that the addition of antioxidants—i.e., 2,2,6,6-tetramethyl-1-piperidinyloxy (TEMPO) and butylated hydroxytoluene (BHT)—to the protocol has resulted in a reduction of artifactual production of oxidative DNA damage. Spectrophotometric quantification of DNA (see Support Protocol) can be used to estimate DNA content with any isolation method.

BASIC PROTOCOL 1

Low-Temperature/Antioxidation DNA Isolation

This protocol is particularly useful when dealing with assays that are sensitive to the effects of heat and oxidation (i.e., aldehyde reactive probe slot-blot assay and 8-hydroxy-2′-deoxyguanosine assay).

Materials

10 mg/ml proteinase K, nucleic acid purification grade (PE Biosystems): store powder up to 1 year at 4°C and solution up to 1 year at −20°C

1× lysis buffer/20 mM 2,2,6,6-tetramethyl-1-piperidinyloxy (lysis buffer/TEMPO; see recipe)

1× phosphate buffered saline without Ca^{2+} or Mg^{2+} (CMF-PBS; see recipe)/20 mM TEMPO

20 mg/ml butylated hydroxytoluene (BHT; Sigma-Aldrich) in isopropanol: store up to 1 month at −20°C

Tissue

70% phenol/chloroform/water (Applied Biosystems): store up to 6 months at 4°C

Sevag mixture (Applied Biosystems): store up to 6 months in a brown bottle at room temperature

2 M and 1 mM TEMPO (2,2,6,6-tetramethyl-1-piperidinyloxy; Sigma-Aldrich)

4 M NaCl: store up to 4 weeks at room temperature

100% and 70% ethanol, −20°C

30 mg/ml (~3000 Kunitz units/ml) ribonuclease A (Sigma-Aldrich)

5000 U/ml ribonuclease T_1 (Roche or Sigma-Aldrich): boil 15 min to inactivate DNases and store up to 6 months at 4°C

15- and 50-ml polypropylene centrifuge tubes

Tissue homogenizer with a glass tube and loose-fitting Teflon pestle with >0.1 to 0.15 mm tolerance

10-ml pipets

Additional reagents and equipment for determining DNA concentration (see Support Protocol)

CAUTION: TEMPO is a hazardous chemical that is corrosive, combustible, and readily absorbed through the skin. Use only in a chemical fume hood and wear suitable protection. Refer to the material safety data sheet (MSDS) for more information.

DAY 1

1. Turn on tabletop centrifuge and cool to 4°C.
2. Place stock solutions of 10 mg/ml nucleic-acid-purification-grade proteinase K, 1× lysis buffer/20 mM 2,2,6,6-tetramethyl-1-piperidinyloxy (TEMPO), and 1× phosphate buffered saline without Ca^{2+} or Mg^{2+} (CMF-PBS)/20 mM TEMPO in a bucket of ice.
3. Label microcentrifuge tubes (1 per sample), 50- (1 per sample), and 15-ml (3 per sample) polypropylene centrifuge tubes.

   CAUTION: *Use only polypropylene centrifuge tubes when working with phenol, chloroform, or other organic solvents, as polystyrene tubes will dissolve. Polypropylene tubes are usually slightly opaque, while polystyrene tubes are clear.*

Start DNA isolation

To prepare tissue/cells from fresh or frozen whole tissue

4a. Add 20 ml ice-cold CMF-PBS/20 mM TEMPO and 25 µl of 20 mg/ml butylated hydroxytoluene (BHT) in isopropanol to 1000 mg tissue in a glass homogenizer tube. Homogenize using a loose-fitting Teflon pestle, with a tolerance >0.1 to 0.15 mm. Apply as few strokes as possible.

   Typically, 5 to 10 strokes are required for complete homogenization.

5a. Transfer liquid to previously labeled 50-ml centrifuge tube and obtain a nuclear pellet by centrifuging in a tabletop centrifuge 10 min at 1500 × *g*, 4°C.

6a. Discard the supernatant and resuspend the pellet in 10 ml ice-cold lysis buffer/20 mM TEMPO.

To prepare fresh or frozen cell fractions

4b. Prepare cell fractions in microcentrifuge tubes and place on ice.

5b. Add 0.5 to 1 ml cold lysis buffer/20 mM TEMPO and 25 µl of BHT in isopropanol, and resuspend.

6b. Transfer to a labeled 15-ml centrifuge tube. Using a 10-ml pipet, add cold lysis buffer/20 mM TEMPO to reach a total volume of 4 ml.

For both tissue/cell preparations and fragments

7. Add 100 µl ice-cold proteinase K solution using a micropipet.

8. Mix by inversion for 12 to 24 hr (i.e., overnight) at 4°C.

DAY 2

9. Turn on tabletop centrifuge and cool to 4°C.

10. Place 70% phenol/chloroform/water mixture and Sevag mixture on ice at least 30 min prior to use. Add 2 M TEMPO to each to a final concentration of 20 mM (100-fold dilution of TEMPO).

    70% phenol/water/chloroform is 68% phenol/18% water/14% chloroform.

Extract DNA

11. Add 10 ml of 70% phenol/chloroform/water mixture to the sample.

    CAUTION: *Phenol is a caustic chemical and contact with skin should be avoided. Perform this step under a fume hood using only glass pipets, as chloroform/phenol will melt some plastics. Insert only the tip of the pipet into solution as the numbers and lines may be removed by the organic solvents.*

12. Mix 5 min, inverting by hand.

13. Centrifuge in a tabletop centrifuge 10 min at 1800 × *g*, 4°C.

    Centrifugation should result in the separation of the aqueous DNA (water/DNA) portion from the phenol/chloroform portion (Fig. 3.8.1).

14. Place sample tubes on ice and remove the upper phase (water/DNA layer) using a hand-held micropipettor. Transfer to a fresh labeled 15-ml centrifuge tube.

    Be sure to take the entire water/DNA layer.

15. Repeat steps 9 through 12, except reduce centrifugation time to 5 min.

16. Add 10 ml Sevag mixture (step 8) to sample.

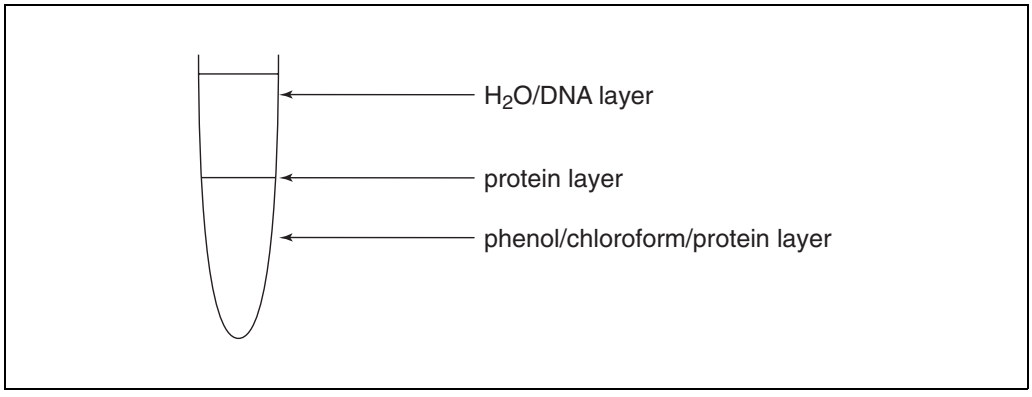

Figure 3.8.1 Centrifugation results in a distinct separation of the H_2O/DNA portion from the phenol/chloroform portion.

17. Mix 5 min, inverting by hand.
18. Centrifuge in a tabletop centrifuge 5 min at 1800 × *g*, 4°C.
19. Place sample tubes on ice and remove the upper phase (water/DNA layer) using a hand-held micropipettor. Transfer to a new, previously labeled centrifuge tube.
20. Add 750 µl of 4 M NaCl to each sample and mix by hand ten times.

    This step is useful when there is a concern about low concentrations of DNA, since salt enhances DNA precipitation. The total amount of 4 M NaCl added is 7.5% the volume water/DNA—i.e., for 3 ml, add 225 µl of 4 M NaCl (3 ml × 0.075 = 225 µl).

Precipitate DNA

21. To each sample, add 3 vol of 100% ethanol, −20°C.
22. Mix by hand and incubate the sample tubes at −80°C for 15 to 20 min.

    This step is useful for greater recovery of DNA in small samples.

23. Centrifuge sample tubes in a tabletop centrifuge 15 min at 2200 × *g*, 4°C.
24. Discard the supernatant, wash DNA pellet with 5 to 10 ml of 70% ethanol, −20°C, and mix gently.
25. Centrifuge sample tubes in a tabletop centrifuge 5 min at 1800 × *g*, 4°C.
26. Resuspend DNA in 0.75 to 3 ml CMF-PBS/20 mM TEMPO. Incubate 1 to 4 hr at 4°C.

    The amount of CMF-PBS/TEMPO will vary with DNA pellet size. Use 750 µl for a very small pellet, 1.5 ml for an average pellet, and 3 ml for a very large pellet.

Treat with RNase A

27. Add 12 µl of 30 mg/ml ribonuclease A and 12 µl of 5000 U/ml ribonuclease T_1 solutions.
28. Incubate 1 hr at 37°C, mixing continuously to generate a homogenous DNA solution.
29. *Optional:* Repeat steps 16 to 19.

    To reduce residual TEMPO and RNase, an additional Sevag extraction is useful after RNase incubation.

30. Add 1.5 ml water and 225 µl of 4 M NaCl (i.e., 7.5% total volume; see step 18) to each sample.

Precipitate DNA

31. Add 3 vol of 100% ethanol, −20°C, to each sample and invert several times by hand.
32. Using a pipet tip or spatula, transfer the DNA fiber to a new previously labeled centrifuge tube.

    The extracted DNA will appear as a white cloud or fiber structure floating in the ethanol.

33. Wash the DNA fiber with 2 to 4 ml of 70% ethanol, −20°C.
34. Centrifuge the DNA solution in a tabletop centrifuge 10 to 15 min at 1800 × *g*, 4°C.
35. Remove supernatant (ethanol) by inverting tube and allowing to dry 1 min.
36. Resuspend DNA in 1 ml of 1 mM TEMPO for 1 to 4 hr or overnight, 4°C.
37. Store resuspended DNA product up to 1 year or more at −80°C.

ALTERNATE PROTOCOL

Room Temperature/Antioxidation DNA Isolation

For many other DNA adduct assays, room temperature and heated incubations do not pose a threat to the assay measurement; therefore, an alternate shorter protocol is available. This method is used in the authors' laboratory to isolate DNA from cells or tissues prior to ethenoguanine adduct quantification. The purity of the DNA obtained by this method is not especially high, but protein contamination does not interfere with these assays. The short procedure is also thought to help minimize artifactual adduct formation.

Additional Materials *(also see Basic Protocol 1)*

Tissue or pelleted sample
1× phosphate-buffered saline without Ca^{2+} or Mg^{2+} (CMF-PBS; see recipe)
1× lysis buffer/BHT: add 1 ml of 20 mg/ml BHT (Sigma-Aldrich) in isopropanol per 450-ml bottle of 1× lysis buffer (Applied Biosystems)
RNase solution (see recipe)
70% phenol/water/chloroform containing BHT: add 1 ml of 20 mg/ml BHT in isopropanol per 450-ml bottle of 70% phenol/water/chloroform (Applied Biosystems)
Chloroform/BHT (see recipe)
3 M sodium acetate trihydrate (Mallinckrodt; *APPENDIX 2A*)
95% ethanol, −20°C
Isopropanol (Mallinckrodt)
Alumina (Sigma-Aldrich): store up to 6 months in a 60°C oven

Wheaton overhead mixer
Gel-loading tips
3-ml syringes and 22-G needles

CAUTION: Phenol is a caustic chemical and contact with skin should be avoided. Perform this step under a fume hood using only glass pipets as chloroform/phenol will melt some plastic pipets. Insert only the tip of the pipet into solution as the numbers and lines may be removed by the organic solvents.

Prepare tissue

1. Suspend tissue (typically 0.5 to 1.0 g) or pelleted cell sample in 10 ml of 1× CMF-PBS and add 25 µl of 20 mg/ml BHT in isopropanol.
2. Homogenize each sample by making 4 to 5 passes with a Wheaton overhead mixer. Transfer to a 15-ml polypropylene centrifuge tube.
3. Centrifuge the samples 10 min at 1000 × *g*, 4°C.
4. Resuspend pellet in 5 ml of 1× lysis buffer/BHT.
5. Add 40 µl RNase solution to each sample and incubate 2 hr at 37°C, mixing continuously.
6. Add 125 µl of 10 mg/ml nucleic-acid-purification-grade proteinase K solution to each sample and incubate an additional 2 hr.

Extract DNA

7. Add 5 ml 70% phenol/water/chloroform containing BHT to each sample and mix for 5 min.

   CAUTION: *Phenol is a caustic chemical and contact with skin should be avoided. Perform this step under a fume hood using only glass pipets as chloroform/phenol will melt some plastic pipets. Insert only the tip of the pipet into solution as the numbers and lines may be removed by the organic solvents.*

8. Centrifuge 10 min at 1000 × *g*, 4°C.

9. Carefully transfer the upper (aqueous) phase of each sample to a clean 15-ml centrifuge tube using a transfer pipet.
10. Repeat steps 7 through 9.
11. Add 5 ml chloroform/BHT to each sample and mix 5 min.
12. Repeat steps 8 and 9.

Precipitate DNA

13. Place samples on ice and add 0.5 ml of 3 M sodium acetate trihydrate to each sample.
14. Add 10 ml of 95% ethanol, −20°C, and mix 15 min at 4°C.
15. Centrifuge 3 min at 1000 × *g*, 4°C.
16. Pour off the supernatant and resuspend the pellet in 5 ml of 70% ethanol, −20°C.
17. Repeat the centrifugation (step 15) and discard the supernatant.
18. Remove the remaining ethanol by pipetting with gel-loading tips. Allow any residual solution to evaporate 15 min at room temperature.
19. Resuspend DNA in enough water to yield a 1 mg/ml solution (typically ~1 ml; see Support Protocol) and store overnight at 4°C.

Shear the DNA

20. Pull each sample into a 3-ml syringe though a 22-G needle until the solution flows easily and uniformly.
21. Transfer each sample to a labeled 1.7-ml microcentrifuge tube.
22. Store DNA samples up to 1 year or more at −80°C.

Spectrophotometric Quantitation of DNA

SUPPORT PROTOCOL

For each of the above isolation methods (see Basic Protocol 1 and Alternate Protocol), quantification of DNA can be performed using the following protocol.

Materials

DNA samples (see Basic Protocol 1 or Alternate Protocol)
Spectrophotometer with reference and sample slots
Quartz cuvettes with 1 cm path length

1. Prepare the spectrophotometer with reference and sample slots for photometric measurements. Set the measurement wavelength to 320 nm and press the autozero function. Correct the baseline after placing sample cuvettes filled with water in reference and sample locations. Set measurement parameters to record at 230, 260, and 280 nm.

   The 230 nm wavelength is used as a zero baseline. The 260 nm wavelength is used to quantify DNA, while both the 230 and 280 nm wavelengths are used to estimate protein contamination.

2. Make 1:20 or 1:200 dilutions of the DNA samples in water to give a final volume of 1 ml.

   Add 50 µl DNA sample to 950 µl water to make a 1:20 dilution or 1:200 dilutions if the sample size is very small.

3. For each diluted DNA sample, place the DNA sample in a quartz cuvette with 1-cm path length in the sample location. Measure the absorbance of each sample against the water reference cuvette at 260 nm and 280 nm.

   Begin with water as a sample. These measurements should be zero.

4. Calculate DNA yield:

   DNA (mg) = (A_{260}/20 mg^{-1}) × volume of DNA solution (ml) × (dilution factor)

   The dilution factor for a 1:20 dilution is 20.

   The extinction coefficient of DNA at wavelength 260 is 20 $(mg/ml)^{-1}$ cm^{-1}.

5. To estimate possible protein contamination, divide A_{260} by A_{280} and divide A_{230} by A_{260}.

   The ratio A_{260}/A_{280} should be ≥1.7; however, ratios of 1.5 and 1.6 are common. The ratio of A_{230}/A_{260} should be ≥2.3. If protein contamination is high, the DNA can be extracted again from the sample using phenol.

ANALYSIS OF DNA ADDUCTS IN INTACT DNA

Apurinic/apyrimidinic (AP) sites are base-loss lesions in nucleic acids. These lesions are introduced in DNA by spontaneous depurination and by DNA glycosylases. In addition, oxidative stress directly causes AP sites through sugar damage. It is believed that the formation of AP sites is one of the most frequent and deleterious events in genomic DNA. The AP sites need to be repaired efficiently because they introduce mutations and block DNA replication.

A sensitive assay to measure the number of AP sites in genomic DNA is essential to better understand the efficiency of base excision repair (BER). The most common AP sites (regular AP sites) are derived from simple hydrolysis of the *N*-glycosylic bond. These regular AP sites are in equilibrium with an aldehydic ring-opened form. The aldehyde-reactive probe (ARP), a specific biotin-tagged aldehydic probe, reacts with aldehydic ring-opened AP sites (Kubo et al., 1992). The number of biotin-tagged AP sites can then be determined colorimetrically by an ELISA-like assay.

BASIC PROTOCOL 2

Measurement of Apurinic/Apyrimidinic Sites

The protocol described here is a convenient and sensitive assay to measure the number of AP sites in genomic DNA by a combination of ARP and the slot-blot technique (Nakamura et al., 1998; Nakamura and Swenberg, 1999). Quantitation is based on comparisons to internal standard DNA containing known amounts of AP sites.

Materials

One primary (e.g., Dojindo) and three secondary (e.g., Dojindo or equivalent) internal DNA standards (100 and 30 AP sites/1 × 10^6 nucleotides, respectively)
Unknown DNA samples
10× PBS, pH 7.4 (see recipe)
10 mM aldehyde-reactive probe (ARP; Dojindo Molecular Technologies): store up to 1 year at −80°C
100% and 70% ethanol, −20°C
1× TE buffer, pH 7.5 (see recipe for 10×)
Calf thymus DNA (Sigma-Aldrich)
1 and 2 M ammonium acetate
5× SSC (see recipe)

Hybridization mix (see recipe)
Streptavidin-conjugated horseradish peroxidase (HRP; BioGenex Laboratories)
Washing buffer (see recipe)
ECL reagent (Amersham)

Minifold II dot/slot blotting manifold (Schleicher & Schuell)
Blotting paper (Schleicher & Schuell)
Nitrocellulose (NC) membrane—e.g., Hybond C-Super (Amersham), BA 85 (Schleicher & Schuell)
37°C environmental shaker
80°C vacuum oven
Bottle rotator
Scanning densitometer
Temperature-controlling device (e.g., thermocycler, water bath, etc.)

Additional reagents and equipment for measurement of DNA concentration (see Support Protocol)

Prepare samples

1. In a 600-µl microcentrifuge tube on ice, add ~16 µl of the following 0.5 µg/µl solutions:

   One primary standard containing 100 AP sites/1×10^6 nucleotides
   Three secondary standards containing 30 AP sites/1×10^6 nucleotides
   Unknown samples (up to 25).

   Add 15 µl of 10× PBS and adjust the volume to 135 µl with water.

2. Add 15 µl of 10 mM ARP into the tube on ice.
3. Incubate 10 min at 37°C.
4. Precipitate DNA by adding 3 vol of 100% ethanol, −20°C, and incubating 20 min at −80°C.
5. Microcentrifuge 15 min at maximum speed, 4°C.
6. Wash DNA pellet with 70% ethanol, −20°C, and microcentrifuge 5 min at maximum speed, 4°C.
7. After discarding the supernatant, add 250 µl of 1× TE buffer, pH 7.5, and mix vigorously 1 hr at room temperature by mixer, or overnight in the refrigerator.

Prepare denatured DNA solution

8. Measure DNA concentration using a spectrophotometer at 260 nm (see Support Protocol).
9. Prepare 0.5 to 1.1 µg DNA mixture in 220 µl of 1× TE buffer and ~2 ml calf thymus (blank) DNA in of 1× TE buffer at a concentration of 0.5 to 1.1 µg/220 µl.
10. Denature DNA at 100°C for 10 min.
11. During denaturation of DNA set up Minifold II dot/slot blotting manifold:
    a. Place two sheets of blotting paper on the plate of the Minifold II.
    b. Immerse blotting paper in 1 M ammonium acetate.
    c. Place one sheet of nitrocellulose (NC) membrane on the blotting paper.
    d. Immerse the NC membrane in 1 M ammonium acetate.
    e. Place the top plate on the filter and clamp.

f. Aspirate residual ammonium acetate by vacuum.

g. Add 200 µl of 1 M ammonium acetate to each slot.

h. Aspirate 1 M ammonium acetate by vacuum.

12. Transfer denatured DNA from 100°C to ice and wait ~2 min.

13. After cooling, serially dilute primary standard DNA with blank DNA containing equal concentrations (e.g., 100, 30, 10, 3, 1, 0.3, 1, and 0 AP sites/1×10^6 nucleotides).

14. Add 220 µl of 2 M ammonium acetate to the DNA solution.

Load samples

15. Load DNA onto the NC membrane in duplicate random locations using 200 µl/slot.

16. Aspirate DNA solution by vacuum.

17. Add 200 µl of 1 M ammonium acetate to each slot.

18. Aspirate ammonium acetate by vacuum.

Hybridize filter

19. Transfer the filter into 150 ml of 5× SSC and wash 15 min in a 37°C environmental shaker.

20. Bake the NC membrane 30 min in an 80°C vacuum oven.

21. Incubate the membrane 15 min with 20 ml hybridization mix in a plastic bottle at room temperature using a bottle rotator.

Visualize adducts

22. Add 2 µl streptavidin-conjugated horseradish peroxidase (HRP) and incubate the membrane 45 min at room temperature.

23. Wash the NC membrane three times with washing buffer at 37°C, 5 min each.

24. Incubate the filter 30 sec in ECL reagent at room temperature and wrap the membrane with plastic wrap.

25. Expose the NC membrane to X-ray film 30 sec to 2 min. Develop the film.

Quantify AP sites

26. After drying the X-ray film, scan the density using a scanning densitometer.

27. Using the standard curve, quantitate the number of AP sites for duplicate secondary standard samples and unknown samples.

28. Calculate the mean numbers of AP sites for triplicate secondary standard samples.

29. Calculate a factor to adjust the mean to 30 AP sites/1×10^6 nucleotides.

30. Adjust the number of AP sites for unknown samples by the same factor used for the secondary standards.

Measurement of DNA Adducts by Immuno-Slot Blot (ISB)

A number of specific antibodies against base lesions have been established to measure DNA adducts in genomic DNA (Farmer and Shuker, 1999). One of the most convenient and relatively sensitive assays to determine the number of DNA adducts is the immuno-slot blot (ISB) assay using these antibodies (Farmer and Shuker, 1999). This ISB method, which is a noncompetitive immunoassay, can quantify the number of any heat- or alkaline-stable DNA lesions. The typical detection limit of the ISB assay is 0.3 to 1 lesion/1×10^7 nucleotides. The amount of DNA needed for this assay is between 0.1 to 3 µg, making this technique suitable for determining the number of DNA lesions in the small amounts of DNA associated with epidemiological samples.

The protocol described here is a noncompetitive immunoassay used to determine the number of lesions in DNA immobilized on a nitrocellulose (NC) membrane. Quantitation of specific lesions is performed by comparing the signals of slots loaded with unknown samples to those loaded with internal standard samples.

Materials

Internal standard containing 30 DNA lesions/1×10^6 nucleotides
Unknown DNA samples
1× TE buffer, pH 7.5 (see recipe for 10×)
Calf thymus DNA (Sigma-Aldrich)
1 and 2 M ammonium acetate
5× SSC (see recipe)
Antibody blocking buffer (see recipe)
Primary antibody against specific DNA lesions (e.g., R & D Systems)
Washing buffer (see recipe)
Hybridization mix (see recipe)
Biotinylated secondary antibody (BioGenex Laboratories)
Streptavidin-conjugated HRP (BioGenex Laboratories)
ECL reagent (Amersham western kit)

37°C environmental shaker
80°C vacuum oven
Bottle rotator

Additional reagents and equipment for set up of Minifold dot/slot blotting manifold (see Basic Protocol 2, step 11)

Prepare denatured DNA samples

1. In a 600-µl centrifuge tube on ice, prepare 3 µg DNA/sample in 220 µl of 1× TE buffer, pH 7.5, containing:

   Internal standard containing 30 DNA lesions/1×10^6 nucleotides
   Unknown DNA samples (up to 30 samples).

2. Serially dilute standard DNA by a factor of ~3 using calf thymus (blank) DNA (e.g., 30, 10, 3, 1, 0.3, 0.1, 0.03, and 0 lesions/1×10^6 nucleotides).

3. Denature DNA 10 min at 100°C, and immediately place the tubes on ice.

4. During denaturation of DNA, set up Minifold II dot/slot blotting manifold (see Basic Protocol 2, step 11).

5. Add 220 µl of 2 M ammonium acetate to the DNA solution.

Load samples

6. Load DNA on the membrane in duplicate at random locations using 200 µl/slot.
7. Aspirate DNA solution by vacuum.
8. Add 200 µl of 1 M ammonium acetate to each slot.
9. Aspirate ammonium acetate by vacuum.
10. Transfer the NC membrane into 150 ml of 5× SSC and soak 15 min in a 37°C environmental shaker.
11. Bake the membrane 30 to 120 min at 80°C in a vacuum oven.
12. Incubate the NC membrane 2 hr in 20 ml blocking reagent in a plastic bottle at room temperature using a bottle rotator.

Probe membrane with antibody

13. Add the primary antibody against the specific DNA lesion and incubate the filter 2 hr at room temperature or overnight at 4°C.
14. Wash the NC membrane three times with washing buffer in a 37°C environmental shaker for 5 min each.
15. Incubate the membrane in a plastic bottle containing 20 ml hybridization mix and 10 µl biotinylated secondary antibody, using a bottle rotator for 1.5 to 2 hr at room temperature, or overnight at 4°C.
16. Wash the NC membrane three times with washing buffer 5 min at 37°C, each.

Visualize AP sites

17. Incubate the membrane 45 min at room temperature in 20 ml hybridization mix containing 2 µl streptavidin-conjugated HRP in a plastic bottle using a bottle rotator.
18. Wash the NC membrane three times with washing buffer for 5 min at 37°C, each.
19. Incubate the membrane 30 sec with ECL reagent at room temperature, and wrap the membrane in plastic wrap.
20. Expose the NC membrane to X-ray film for 30 sec to 2 min. Develop the film.
21. After drying the X-ray film, scan the density using a scanning densitometer.
22. Using the standard curve generated by peak area of slot, quantitate the number of AP sites for unknown samples.

BASIC PROTOCOL 4

Immunohistochemical Demonstration of DNA Adducts

Immunohistochemistry (IHC) is a method utilizing a primary antibody against a specific target, in this case a DNA adduct, which uses a secondary labeled antibody that can be reacted enzymatically to produce a colored or fluorescent end product which can be visualized by microscopy. The advantage of IHC is that the DNA adducts can be identified by cell type and location within the organ of interest.

Materials

Slides with tissue sections, treated and control
Xylene
100%, 95%, and 70% ethanol
1× PBS (see recipe for 10×)/1% (v/v) Tween 20

DAKO Envision Kit for HRP (Dako):
  Blocking reagent: 0.3% H_2O_2 in methanol
  Polymer-labeled secondary antibody
  DAB
  Substrate buffer
Primary antibody
Quick DAB enhancer solution (Innovex Biosciences)
Aqua Hematoxyin (Innovex Biosciences)
Permount (Fisher Scientific)

NOTE: Other manufacturers' reagents can be substituted; however, incubation times in the following procedure would have to be changed according to their directions.

NOTE: All of the following steps are performed at room temperature.

Prepare slides

1. Hydrate slides with treated and control tissue sections through three changes of xylene, three changes of 100% ethanol, two changes of 95% ethanol, and 1 change of 70% ethanol, for 4 min each.
2. Rinse the slides with two changes of water each time for 1 min.
3. Rinse slides twice with 250 µl PBS/1% (v/v) Tween 20 each time for 3 min.
4. Incubate slides 5 min in 250 µl blocking reagent from the DAKO Envision kit.
5. Repeat rinse (step 3).

Expose slides to antibody

6. Incubate slides 10 min in 250 µl diluted primary antibody.

   As most of the primary antibodies against DNA adducts are not commercially available the actual dilution factor for the primary antibody used in this step will have to be determined through a set of serial dilutions (e.g., 1:50, 1:100, 1:500, 1:1000).

7. Repeat rinse (step 3).
8. Incubate slides in 250 µl polymer-labeled secondary antibody from the Envision kit for 10 min.
9. Repeat rinse (step 3).

Visualize bound antibody

10. Add one drop DAB per milliliter substrate buffer to make working DAB solution. Incubate slides 8 min in the dark with 250 µl working DAB solution.
11. Rinse well with water.
12. Incubate slides 5 min with 250 µl DAB Enhancer solution.
13. Rinse well with water.
14. Stain with aqua hematoxylin for 25 sec and rinse with tap water.
15. Incubate 5 min in tap water.
16. Dehydrate the slides through two changes of 95% ethanol, two changes of 100% ethanol, and clear in two changes of xylene, 4 min each.
17. Coverslip the slides out of xylene using Permount to mount the coverslips.

REAGENTS AND SOLUTIONS

Use Milli-Q-purified water or equivalent in all recipes and protocol steps. For common stock solutions, see ***APPENDIX 2A****; for suppliers, see* ***SUPPLIERS APPENDIX****.*

Antibody blocking buffer

10 ml 1× TBES (see recipe) containing 0.1% (w/v) deoxycholate (DOC)
0.5% (w/v) casein
0.1% (v/v) Tween-20
Store up to 2 weeks at 4°C

Chloroform/BHT

Plug a 2.5-cm diameter column with glass wool and pour alumina to a height of 10 cm. Discard the first column volume (~50 ml) of chloroform (J.T. Baker) and collect the next 450 ml. Add 1 ml BHT stock solution (Sigma) to the chloroform and store at 4°C.

Hybridization mix

10 ml 1× TBES (see recipe) containing 0.5% (w/v) casein
0.25% (w/v) BSA
0.1% (v/v) Tween-20
Store up to 2 weeks at 4°C

Lysis buffer, 1×/2,2,6,6-tetramethyl-1-piperidinyloxy (TEMPO), 20 mM

Dilute nucleic acid–purification grade lysis buffer to 1× from a 2× stock (Applied Biosystems). Store up to the expiration date in a brown glass bottle at 4°C. Add 2 M TEMPO free-radical reagent (Sigma-Aldrich) in methanol (store up to ~1 year at −80°C) to 20 mM. Store up to 2 months at −80°C.

PBS, 10×, pH 7.4

1.37 M NaCl
2.68 mM KCl
101 mM Na_2HPO_4
17.6 mM KH_2PO_4
Adjust pH to 7.4

RNase solution

Prepare RNase solution by adding 8 µl RNase T_1 (~800 U) and 30 µl RNase A (~80 U) to 614 µl water. This is enough for 16 samples. Scale the volume up or down as needed.

SSC, 20×, 5×

For 20× solution:
3 M NaCl
0.3 M trisodium citrate
Store up to 1 month at room temperature
Dilute to 5× with H_2O
Store up to 1 month at room temperature

TBES, 10×, 1×

160 mM Tris hydrochloride
40 mM Tris base
1 M NaCl
10 mM EDTA
Dilute to 1× with H_2O
Store up to 1 month at room temperature

TE buffer, 10×

80 mM Tris hydrochloride
20 mM Tris base
10 mM EDTA
Store up to 1 month at room temperature

Washing buffer

1× TBES (see recipe) containing 4 M NaCl
0.1% (v/v) Tween-20
Store up to 1 month at room temperature

COMMENTARY

Background Information

Apurinic/apyrimidinic sites

Various DNA base adducts are produced by alkylation, deamination, and oxidation. Many of these base lesions are believed to be repaired by the base excision repair (BER) pathway. During the first process of BER, DNA glycosylase cleaves a modified DNA base at the *N*-glycosylic bond, resulting in the formation of an AP site. AP sites can also be caused spontaneously by chemical depurination of labile DNA adducts and directly by oxidative stress. Formation of apurinic/apyrimidinic (AP) sites is one of the most frequent events in chromosomal DNA under physiological conditions (Lindahl, 1993; Nakamura et al., 1998). AP sites inhibit DNA replication and result in base substitution mutations and loss of genetic integrity (Loeb and Preston, 1986).

Several methods are currently available to detect AP sites (Brent et al., 1978; Kohn et al., 1981; Weinfeld et al., 1990; Kubo et al., 1992; Maulik et al., 1999). The present unit describes one of the aldehydic reactive reagents (ARP) and a slot-blot technique to improve the sensitivity of AP site assay (see Basic Protocol 2).

Immuno-slot blots

The ISB method is a noncompetitive immunoassay, which was originally established for the quantification of ethylated base adducts such as mutagenic O^6-ethyldeoxyguanosine and O^4-ethylthymidine as described by Nehls et al. (1984). Using this technique, the number of O^6-methyldeoxyguanosine (LeDoux et al., 1996), O^2-ethylthymidine (Dragan et al., 1994), aflatoxin B1 adducts (Phillips et al., 1999), thymine glycol (Greferath and Nehls, 1997), thymine dimer (Kriste et al., 1996), and malondialdehyde-derived guanine adducts (M_1G; Leuratti et al., 1998) have been quantitated in DNA. Basically, the number of base adducts in DNA immobilized on a NC membrane are quantified colorimetrically using a combination of monoclonal antibodies specific to adducts, biotinylated secondary antibodies, avidin/streptavidin-conjugated enzymes (e.g., horseradish peroxidase or alkaline phosphatase), and suitable substrates. This assay requires a small amount of DNA and provides relatively high sensitivity. The most significant advantage of this method is its convenience. Thirty different samples are applicable in duplicate on one NC membrane and can be measured within 2 days.

Immunohistory

Immunohistochemistry uses the affinity of monoclonal and polyclonal antibodies to locate specific epitopes which can then be visualized by an enzymatic chromogenic or fluorescent reaction visualized microscopically. This technique demonstrates not only the cell type to be identified but also the location of the cell in relation to other cells within the tissues of the organ of interest.

Critical Parameters

Apurinic/apyrimidinic sites

Spontaneous depurination and oxidation during DNA extraction may artifactually introduce an increase in the number of AP sites. DNA extraction steps should be performed at ~4°C except for the RNA digestion (Nakamura and Swenberg, 1999). Antioxidant or radical trapping agents such as TEMPO should be included in the DNA extraction solution to prevent artifactual induction of AP sites by oxidative stress during DNA extraction.

Standard DNA can be prepared by incubation of DNA in a heat/acid buffer (Nakamura et al., 1998); however, the rate of depurination may vary depending on the DNA concentration. The standard DNA should be calibrated by others who routinely measure the number of AP sites.

After denaturation, the DNA sample should be loaded onto the NC membrane as quickly as possible to diminish unnecessary renaturation. In addition, the DNA should be loaded randomly and at least in duplicate to avoid reaction variation within the membrane.

The concentration of streptavidin conjugated with HRP is one of the critical parameters in this assay. Usually, lower concentrations of streptavidin conjugated with HRP work better.

Immuno-slot blots

The essential material is a specific antibody against a particular base adduct. Cross reactivity of antibodies with unmodified bases and structurally similar base adducts may introduce high background and cause inaccurate measurement of target DNA lesions. Even highly sensitive antibodies may work inefficiently. If a couple of antibodies are available, the best antibody should be selected using the ISB assay.

The ISB assay typically detects 0.3 to 1 lesion/1×10^7 nucleotides. If this detection limit is not sensitive enough to measure the target DNA lesion, it is recommended to use other methods.

The number of adducts in standard DNA has to be quantified before measuring unknown samples by the ISB assay. The ratio of modified nucleosides to either unmodified nucleosides (e.g., picomole O^6-ethyldeoxyguanosine/μmole deoxyguanosine) or to total nucleotides (e.g., O^6-ethyldeoxyguanosine/1×10^6 nucleotides) in the standard DNA is a prerequisite and has to be characterized by another method.

To quantitate the number of DNA lesions, an equal amount of DNA should be loaded on each slot including serially diluted standard DNA. The amount of DNA applicable on each slot has previously been examined (Nehls et al., 1984). Based on ^{3}H-thymidine-labeled DNA, 3 to 4 μg DNA per slot are efficiently immobilized on the NC membrane.

DNA denaturation is also essential for the immobilization of DNA onto the NC membrane. Heating at high temperature (100°C for 10 min) or incubating in an alkaline solution can achieve this immobilization. During heat denaturation, the *N*-glycosylic bonds between heat-labile base lesions and deoxyriboses are easily cleaved; therefore, the ISB assay is not suitable for the measurement of heat-labile base adducts such as *N*7-alkylguanine and *N*3-alkyladenine. In addition, these N-alkylpurine adducts are also alkaline-labile. This ISB assay may not be appropriate for the measurement of these adducts. Before measuring target adducts by this assay, the stability of the adducts under thermal or alkaline conditions should be checked.

Immunohistochemistry

Tissue fixation and trimming are two of the most important factors involved when doing IHC. Tissues should be trimmed so that they are between 2 and 3 mm thick and fixed in 10% neutral buffered formalin (NBF) for a minimum of 24 hr and a maximum of 72 hr. A change to fresh NBF should be made within the first 6 hr. The tissues should then be placed in 70% ethyl alcohol prior to paraffin processing and subsequent microtomy. During microtomy the sections should be mounted on Fisher+ slides or equivalent. After microtomy the slides should be allowed to dry overnight at room temperature. The slides should not be exposed to heat in excess of 50°C at any time prior to performing IHC. The only exception to this would be if an antigen retrieval method needed to be used.

Troubleshooting

DNA isolation

Some problems that may be encountered using these isolation protocols include lower than expected yields and/or purity. If yields are low, be sure to thoroughly homogenize the tissue and attain homogenous solutions at all incubations through gentle pipetting. If purity is low (i.e., $A_{260}/A_{280} < 1.6$), the DNA sample can be cleaned using an additional phenol extraction. Also, be sure not to aspirate the cloudy white protein layer when collecting the DNA/water portion following extraction with the 70% phenol/chloroform/water mixture. If the DNA sample is contaminated with RNA, extend the incubation time of the RNase step.

Apurinic/apyrimidinic sites

High background on the entire NC membrane may be introduced by an inappropriate membrane (e.g., different brand of NC membrane), low SSC concentration, or short incubation and baking times. Different lots of NC membranes may work differently. To improve the background problem, it is recommended to increase incubation and baking times at first. High background in the slot including blank DNA may be due to over-incubation in HRP with streptavidin. Try to reduce the concentration of HRP and incubation time. In addition, it is also important to check the temperature of the surrounding environment when incubating the NC membrane.

If the difference in the number of AP sites between groups is relatively small, it is highly recommended to react DNA in duplicate or triplicate with ARP and determine the value by using an average of the three data points.

Immuno-slot blots

The problem regarding high background in the entire NC membrane may be introduced by inappropriate membrane (e.g., different brand of NC membrane), low SSC concentration, short incubation and baking time, insufficient washing, and high antibody and enzyme concentrations. The process conditions should be optimized by using a couple of smaller sheets of the NC membrane prepared under different conditions.

If the DNA slot is not sharp and the DNA migrates from the slot area, it is recommended that the lot or brand of NC membrane be changed; however, this type of problem has rarely happened in the authors' laboratory. Once an appropriate NC membrane is found, try to stock the same lot of membranes for consistency in future studies.

The variation in the number of adducts between membranes can be avoided by using a secondary internal standard. The secondary internal standard should contain a similar level of adducts as the real samples. These standards should be loaded in duplicate or triplicate on every NC membrane and used to adjust intermembrane variation.

Immunohistochemistry

The hematoxylin solution should always be filtered (No.1 Whatman) prior to use as bacteria grow in the stock solutions. If the tissue sections are allowed to air dry at any time during the procedure, false negative or positive staining will result. Not all antibodies will work on formalin-fixed, paraffin-embedded tissue. It is sometimes necessary to use frozen sections. If the working DAB solution turns a dark brown it should not be used. Instead, discard and make fresh. It is important to note that DAB is light sensitive and the working solution should be prepared just prior to use (i.e., ~10 min). Antibody-antigen reactions are also adversely affected by exposure to light; therefore, all incubations should be done in the dark.

Anticipated Results

DNA isolation

The yield and purity using either isolation protocol will depend on the tissue used for isolation. Most parenchymal organs (liver and kidney for example) isolated using these protocols will yield ~1.5 μg DNA/milligram tissue used for isolation. Brain, lung, and other tissue will yield ~1 μg DNA/milligram tissue used for isolation. DNA purity (A_{260}/A_{280} ratios) should be between 1.5 and 1.9.

Apurinic/apyrimidinic sites

The number of endogenous AP sites are ~5 lesions/1 × 10^6 nucleotides in either HeLa S3 suspension cells (Nakamura et al., 2000) or H2E1 cells, human lymphoblastoid cells (Nakamura et al., 1998). In tissue samples, ~9 AP sites/1 × 10^6 nucleotides were detected in rat and human liver (Nakamura and Swenberg, 1999).

Immuno-slot blots

To confirm the accuracy of the ISB assay, it is recommended that the number of base adducts measured using this assay be compared to data obtained by other quantitative methods such as HPLC, LC/MS, or GC/MS.

Time Considerations

DNA isolation

The time required for low-temperature isolation is ~24 to 40 hr (including overnight incubations and DNA solubilization). Room-temperature isolation can be performed in ~8 hr (24 hr including overnight DNA solubilization). Spectrophotometric quantification can be performed in ~30 min depending on how many samples are processed.

Apurinic/apyrimidinic sites

The entire process of sample preparation and analysis for 24 unknown samples can be performed in 1 or 2 days. Sample preparation requires ~1 hr. The ARP reaction, DNA precipitation, and resuspension take ~3 hr. DNA concentration measurement and sample loading require ~2 hr. Baking and incubating the NC membrane in buffer with enzymes takes ~1.5 hr.

Immuno-slot blots

The entire process for preparing and analyzing 24 unknown samples can be performed in 2 days. Sample preparation requires ~1 hr. Denaturing and sample loading takes another 1 hr. Baking and incubating the NC membrane in buffer with antibodies or enzymes requires ~9 hr.

Immunohistochemistry

Most immunohistochemical procedures on 20 samples (slides) can be completed in 4 to 7

hr, depending on the primary and secondary antibody incubation times. Slides can usually be examined the same day.

Literature Cited

Brent, T.P., Teebor, G.W., and Duker, N.J. 1978. Lesions in alkylated DNA determined by susceptibility to alkali, apurinic endonuclease or N-glycosylase. *In* DNA Repair Mechanisms (P.C. Hanawalt, E.C. Friedberg, and C.F. Fox, eds.) pp. 19-22. Academic Press, New York.

Chung, F.L., Chen, H.J., and Nath, R.G. 1996. Lipid peroxidation as a potential endogenous source for the formation of exocyclic DNA adducts. *Carcinogenesis* 17:2105-2111.

Dragan, Y.P., Hully, J.R., Nakamura, J., Mass, M.J., Swenberg, J.A., and Pitot, H.C. 1994. Biochemical events during initiation of rat hepatocarcinogenesis. *Carcinogenesis* 15:1451-1458.

Farmer, P.B. and Shuker, D.E. 1999. What is the significance of increases in background levels of carcinogen-derived protein and DNA adducts? Some considerations for incremental risk assessment. *Mutat. Res*. 424:275-286.

Greferath, R. and Nehls, P. 1997. Monoclonal antibodies to thymidine glycol generated by different immunization techniques. *Hybridoma* 16:189-193.

Kohn, K.W., Ewig, R.A.G., Erickson, L.C., and Zwelling, L.A. 1981. Measurement of strand breaks and crosslinks in DNA by alkaline elution. *In* DNA Repair: A Laboratory Manual of Research Procedures, Vol. 1, Part B (E.C. Friedberg and P.C. Hanawalt, eds.) pp. 379-401. Marcel Dekker, New York.

Kriste, A.G., Martincigh, B.S., and Salter, L.F. 1996. A sensitive immuno technique for thymine dimer quantitation in UV-irradiated DNA. *J. Photoch. Photobio.* 93:185-192.

Kubo, K., Ide, H., Wallace, S.S., and Kow, Y.W. 1992. A novel, sensitive, and specific assay for abasic sites, the most commonly produced DNA lesion. *Biochemistry* 31:3703-3708.

La, D.K. and Swenberg, J.A. 1996. DNA adducts: Biological markers of exposure and potential applications to risk assessment. *Mutat. Res*. 365:129-146.

LeDoux, S.P., Williams, B.A., Hollensworth, B.S., Shen, C., Thomale, J., Rajewsky, M.F., Brent, T.P., and Wilson, G.L. 1996. Glial cell-specific differences in repair of O^6-methylguanine. *Cancer Res*. 56:5615-5619.

Leuratti, C., Singh, R., Lagneau, C., Farmer, P.B., Plastaras, J.P., Marnett, L.J., and Shuker, D.E. 1998. Determination of malondialdehyde-induced DNA damage in human tissues using an immunoslot blot assay. *Carcinogenesis* 19:1919-1924.

Lindahl, T. 1993. Instability and decay of the primary structure of DNA. *Nature* 362:709-715.

Loeb, L.A. and Preston, B.D. 1986. Mutagenesis by apurinic/apyrimidinic sites. *Annu. Rev. Genet*. 20:201-230.

Marnett, L.J. and Burcham, P.C. 1993. Endogenous DNA adducts: Potential and paradox. *Chem. Res. Toxicol.* 6:771-785.

Maulik, G., Botchway, S., Chakrabarti, S., Tetradis, S., Price, B., and Makrigiorgos, G.M. 1999. Novel non-isotopic detection of MutY enzyme-recognized mismatches in DNA via ultrasensitive detection of aldehydes. *Nucl. Acids Res.* 27:1316-1322.

Nakamura, J. and Swenberg, J.A. 1999. Endogenous apurinic/apyrimidinic sites in genomic DNA of mammalian tissues. *Cancer Res*. 59:2522-2526.

Nakamura, J., Walker, V.E., Upton, P.B., Chiang, S.-Y., Kow, Y.W., and Swenberg, J.A. 1998. Highly sensitive apurinic/apyrimidinic site assay can detect spontaneous and chemically induced depurination under physiological conditions. *Cancer Res*. 58:222-225.

Nakamura, J., La, D.K, and Swenberg, J.A. 2000. 5′-Nicked apurinic/apyrimidinic sites are resistant to β-elimination by β-polymerase and are persistent in human cultured cells after oxidative stress. *J. Biol. Chem.* 275:5323-5328.

Nehls, P., Adamkiewicz, J., and Rajewsky, M.F. 1984. Immuno-slot-blot: A highly sensitive immunoassay for the quantitation of carcinogen-modified nucleosides in DNA. *J. Cancer Res. Clin. Oncol*. 108:23-29.

Phillips, J.C., Davies, S., and Lake, B.G. 1999. Dose-response relationships for hepatic aflatoxin B1-DNA adduct formation in the rat in vivo and in vitro: The use of immunoslot blotting for adduct quantitation. *Teratogen. Carcinog. Mutagen*. 19:157-170.

Singer, B. and Grunburger, D. 1983. Molecular Biology of Mutagens and Carcinogens. Plenum, New York.

Sipes, I.G., McQueen, C.A., and Gandolfi, A.J. (eds.) 1997. Comprehensive Toxicology, Vol. 12, Elsevier Science, Oxford.

Weinfeld, M., Liuzzi, M., and Paterson, M.C. 1990. Response of phage T4 polynucleotide kinase toward dinucleotides containing apurinic sites: Design of a ^{32}P-postlabeling assay for apurinic sites in DNA. *Biochemistry* 29:1737-1743.

Contributed by James A. Swenberg, Amy-Joan L. Ham, Kevin S. McDorman, Eric J. Morinello, Jun Nakamura, and Robert Schoonhoven
University of North Carolina
Chapel Hill, North Carolina

Methods for Measuring DNA Adducts and Abasic Sites II: Methods for Measurement of DNA Adducts

The first unit of this series of protocols (*UNIT 3.8*) dealt with the isolation of DNA and methods for analysis that utilize intact DNA.

This unit contains protocols for analyzing individual DNA adducts separated from the DNA backbone. The first two protocols describe HPLC methods for quantifying total guanine (see Basic Protocol 1) and ribo- or deoxyribonucleosides (see Basic Protocol 2). The remaining protocols describe a variety of methods used to quantify individual DNA adducts. HPLC with electrochemical detection is used to determine 8-OH-dG (see Basic Protocol 3) and N7-methylguanine (see Basic Protocol 4). Immunoaffinity chromatography is used to enrich for specific adducts which are then analyzed using gas chromatography/electron capture negative chemical ionization/high-resolution mass spectroscopy (GC/ECNCI/HRMS; see Basic Protocol 5). Enzymatic DNA digestion (see Support Protocol 1) preparation of immunoaffinity columns (see Support Protocol 2), and determination of recovery (see Support Protocol 3) are also described. There is also a protocol for GC/ECNCI/HRMS isolation that can be used with adducts purified by other means (see Basic Protocol 6). Liquid chromatography in combination with electrospray ionization/isotope dilution tandem mass spectrometry (LC/ESI/IDMS/MS) can also be used to purify adducts for quantification (see Basic Protocol 7). Finally, ^{32}P postlabeling in combination with thin layer chromatography (TLC; see Basic Protocol 8) can be used for adduct quantification.

CAUTION: Extremely high voltage is present when a mass spectrometer is turned on from the instrument, and various components of GC and MS are at very high temperatures during operation. Operators are advised to refer to the respective instrument manuals for operation and safety (also see Critical Parameters).

NOTE: All methanol used in this unit must be HPLC grade.

MEASUREMENT OF NUCLEIC ACIDS BY HPLC

An important part of every DNA adduct analysis is to quantitate, in some way, the amount of DNA used in the assay. While spectrophotometric absorbance (*UNIT 3.8*) is useful as a reliable estimate, the most accurate method for determining DNA content is HPLC analysis of the components of DNA. In the authors' laboratories, the most common methods for DNA quantitation are the HPLC measurement of guanine (and adenine) and/or the measurement of deoxyguanosine, depending on the method of DNA hydrolysis. The choice of methodology is in the measurement of the adduct itself. If the DNA adduct is measured as a base, then guanine or the appropriate base should be measured. If the DNA adduct is measured as a nucleoside, then the measurement of the normal nucleoside must be accomplished.

HPLC Determination of Purine Bases

BASIC PROTOCOL 1

The determination of purine bases involves shearing the DNA, hydrolysis by mild acid, and heating before analysis by HPLC.

Contributed by James A. Swenberg, Amy-Joan L. Ham, Hasan Koc, David K. La, Eric J. Morinello, Brian F. Pachkowski, Asoka Ranasinghe, and Patricia B. Upton
Current Protocols in Toxicology (2002) 3.9.1-3.9.35

Materials

Hydrated DNA solution
0.1 N HCl
Mobile phase: 0.1 M ACS-grade ammonium formate (pH 2.8)/10% HPLC-grade methanol
Guanine (or adenine) standard for calibration curve

22-G needle
70°C water bath or equivalent
0.45-µm filter
HPLC system:
Isocratic HPLC pump
500-µl injection loop
10-µm × 25-cm × 0.46-cm Whatman Partisil 10 SCX analytical column
Single-wavelength UV detector set to 254 nm
Syringe and 22-G needle

Additional reagents and equipment for determination of DNA concentration by spectrophotometric absorption (*UNIT 3.8*)

1. Shear the hydrated DNA solution by pulling up and out ~5 times with a 22-G needle to ensure a homogenous solution.
2. Estimate the concentration of this solution by spectrophotometric absorption at 260 nm (where 50 µg = 1 AU; *UNIT 3.8*).
3. Dilute an aliquot of this solution with 0.1 vol of 1 N HCl.
4. Heat the acidic DNA solution 30 min in a 70°C water bath or equivalent. Place the samples on ice.

   This mild acid hydrolysis serves to effectively depurinate the DNA, releasing guanine and adenine nucleic acid bases.

5. Filter mobile phase through a 0.45-µm filter and degas by vacuum.

   Filtering and degassing helps to prevent the formation of interfering bubbles as the water and methanol mix.

6. Run mobile phase at 1.8 ml/min through the HPLC system, including a 10-µm × 25-cm × 0.46-cm Whatman Partisil 10 SCX analytical column. Equilibrate ~30 min or until the warming single-wavelength UV detector shows a stable baseline at 254 nm.
7. Set the HPLC run time as 8 min.
8. Prepare a guanine (or adenine) standard stock by dissolving a known amount in 0.1 N HCl. Dilute this stock 1:100 in 0.1 N HCl (~0.05 nmol/µl). Build a guanine standard curve by injecting and analyzing increasing amounts of dilute stock:

First injection:	5 µl (0.25 nmol standard)
Second injection:	50 µl (2.5 nmol standard)
Third injection:	100 µl (5.0 nmol standard)
Fourth injection:	200 µl (10.0 nmol standard)

   The standard curve is built by plotting the area under the guanine (or adenine) peak versus amount of guanine (or adenine) injected. The guanine standard curve is linear across a very wide range of concentrations, but be careful not to saturate the detector.

9. Inject 100 µl hydrolyzed DNA samples to be assayed for guanine (or adenine).

   The amount of sample that should be injected will depend on the estimated concentration (A_{260}; UNIT 3.8) and the dilution of the sample for mild acid hydrolysis.

10. Between injections, rinse syringe with several volumes of 100% methanol.

11. Determine the quantity of guanine by comparison of the sample peak area with the standard curve of peak area versus volume standard injected. Multiply this amount by the injection volume, divide by the dilution factor, and divide by the average amount of guanine (or adenine) in the species DNA (0.22 for rat, 0.28 for mouse, 0.20 for human and calf thymus; Fasman, 1976). Multiply by the average molecular weight of a nucleotide (320) to obtain the concentration of DNA in the sample in micrograms/milliliter.

    For a 100-µl injection of rat DNA diluted 1:10, determined to have a guanine concentration of 1.07 nmol from the standard curve, the concentration in the original sample is 156 µg/ml—i.e., 1.07 nmol × 100/1000/0.22 × 520 = 156 µg/ml.

HPLC of Ribonucleoside and Deoxynucleoside Digests

BASIC PROTOCOL 2

Following digestion of DNA to nucleosides, HPLC analysis of the digest gives a denominator to adduct analysis. This is also the way to quantify RNA contamination of the DNA solution (i.e., to give a correction factor).

Materials

Mobile phase A: 50 mM NaH_2PO_4 (pH 5.5)/10% methanol
Mobile phase B: 90% methanol
Deoxyguanosine (dGuo), deoxyadenosine (dAdo), guanosine (rGuo), and adenosine (rAdo)
50 mM NaH_2PO_4, pH 7.4 (optional)
100 mM Bis-Tris (pH 7.1)/100 mM $MgCl_2$
100 mM Tris·Cl, pH 8.5 (*APPENDIX 2A*)
Sample digest (see Support Protocol 1)

0.45-µm filter
HPLC system:
  500-µl injection loop
  5-µm × 25-cm × 0.46-cm reversed-phase column
  Single-wavelength UV detector set to 254 nm
  Isocratic HPLC pump

Set up HPLC

1. Filter mobile phases A and B through a 0.45-µm filter and degas by vacuum.

    Filtering/degassing helps to prevent the formation of interfering bubbles as the water and methanol mix.

2. Run mobile phase A at 1.8 ml/min through the HPLC system, including the 5-µm × 25-cm × 0.46-cm reversed-phase column. Equilibrate ~30 min or until the warming single-wavelength UV detector shows a stable baseline at 254 nm.

Prepare standards

3. Make 4 mM stock solutions of nucleoside standards in water—i.e., deoxyguanosine (dGuo), deoxyadenosine (dAdo), guanosine (rGuo), and adenosine (rAdo).

4. Use water or 50 mM NaH_2PO_4, pH 7.4, to dilute stock solutions of dGuo and dAdo to 0.4 mM, and stock solutions of rGuo and rAdo to 0.025 mM for use in an HPLC standard curve. Aliquot and freeze extra up to 1 year at −20°C.

5. Mix dGuo and dAdo dilutions 1:1.

    Final concentration of each is now 0.2 nmol/µl.

Table 3.9.1 Deoxyguanosine (dGuo) and Deoxyadenosine (dAdo) Standard Mixture

Standard no.	0.2 nmol/µl dAdo/dGuo mix (µl)	100 mM Bis-Tris (pH 7.1)/100 mM $MgCl_2$ (µl)	100 mM Tris·Cl, pH 8.5 (µl)	H_2O (µl)
1	20 (4 nmol)	10	3	167
2	40 (8 nmol)	10	3	147
3	80 (16 nmol)	10	3	107
4	160 (32 nmol)	10	3	27

Table 3.9.2 Guanosine (rGuo) and Adenosine (rAdo) Standard Mixture

Standard no.	0.0125 nmol/µl dAdo/dGuo mix (µl)	100 mM Bis-Tris, pH 7.1/100 mM $MgCl_2$ (µl)	100 mM Tris·Cl, pH 8.5 (µl)	Water (µl)
1	20 (0.25 nmol)	10	3	167
2	40 (0.5 nmol)	10	3	147
3	80 (1 nmol)	10	3	107
4	160 (2 nmol)	10	3	27

6. Add 100 mM Bis-Tris (pH 7.1)/100 mM $MgCl_2$ to dGuo/dAdo standards to yield approximately the same buffer concentrations as the samples (Table 3.9.1).
7. Mix the rGuo and rAdo 1:1.

   Final concentration of each is now 0.0125 nmol/µl.
8. Add 100 mM Bis-Tris (pH 7.1)/100 mM $MgCl_2$ to rGuo/rAdo standards to yield approximately the same buffer concentrations as the samples (Table 3.9.2).
9. Set the HPLC run time as 30 min with a flow rate of 1 ml/min.
10. Build a standard curve of each nucleoside by injecting and analyzing 200 µl increasing concentrations (Tables 3.9.1 and 3.9.2) and plotting the area under the peak versus the amount of standard injected.

Analyze sample

11. Inject 50 µl of each sample digest.
12. Determine quantities of dGuo/dAdo and rGuo/rAdo based on comparison with the standard curve.

QUANTIFYING DNA ADDUCTS: HPLC WITH ELECTROCHEMICAL DETECTION

Since its advent, HPLC with electrochemical detection (HPLC-ECD) has been utilized for a number of applications (Krien et al., 1992; Leung and Tsao, 1992; Achilli et al., 1993). Combining the separatory capability of HPLC with the sensitivity and selectivity of ECD makes for efficient and accurate analysis of complex samples with low analyte concentration. A popular use of HPLC-ECD is in the investigation of DNA adducts. The formation and persistence of these adducts in the genome has been linked to aging and cancer (Halliwell and Gutteridge, 1989; Swenberg et al., 1985). Quantitative analysis of

specific adducts can reveal the relationship between chemical exposure and toxicological response.

Two major types of DNA adducts analyzed by HPLC-ECD are those induced by either oxidative damage or base alkylations. Oxidative DNA damage caused by reactive oxygen species (ROS) has been associated with cancer and other degenerative diseases (Harman, 1981; Ames, 1983). The major oxidative damage product in DNA, 8-hydroxy-2′-deoxyguanosine (8-OH-dG; see Basic Protocol 3), is used as a biomarker of oxidative stress (Kasai, 1997) and in studies regarding base excision repair (BER; Nakamura et al., 2000).

The N7 position of guanine is a major site for electrophilic modification. While not promutagenic, N7-methylguanine (N7-MG) can spontaneously depurinate leaving an apurinic/apyrimidinic site (AP site) which can lead to mutagenicity. N7-MG quantification (see Basic Protocol 4) is useful in understanding the molecular dosimetry of alkylating agents (de Groot et al., 1994) and the efficiency of BER (Calléja et al., 1999).

HPLC-ECD Analysis of 8-OH-dG

BASIC PROTOCOL 3

The protocol described below for the determination of 8-OH-dG is a modification of a method described by Richter et al. (1988). Isolated DNA is subjected to enzymatic digestion to yield deoxyribonucleosides, which are then separated chromatographically and detected coulometrically.

Materials

DNA sample (see Support Protocol 1)
Mobile phase: 50 mM KH_2PO_4, (pH 5.5)/10% HPLC-grade methanol
8-OH-dG standard (see recipe)

HPLC system:
- 100-µl injection loop
- Electrochemical detector (i.e., E.S.A. Model 5600 CoulArray and Model 5040 cell with platinum target)
- 25-cm × 4.6-mm Beckman Ultrasphere (or equivalent) C_{18} column with 5-µm particle size, room temperature

37°C incubator

Additional reagents and equipment for HPLC determination of deoxyguanosine (see Basic Protocol 1)

NOTE: All water used must be distilled and deionized.

Analyze the sample

1. Set potentials of the electrochemical detector to 200, 300, 375, 450, 525, 600, 700, and 1000 mV.

   These potentials were selected in order to oxidize any interfering compounds with oxidation potentials below that of the analyte, to measure the analyte, and to oxidize any interfering compounds with oxidation potential below deoxyguanosine, which is usually monitored at 1000 mV.

2. Equilibrate the HPLC system for at least 1 hr by running mobile phase at 1 ml/min, including 25-cm × 4.6-mm C_{18} column with 5-µm particle size.

   Keep the 1 ml/min flow rate for the duration of the analysis (see Critical Parameters).

3. Run three or four standards within the likely range that 8-OH-dG will be measured.

   The standard curve for 8-OH-dG is prepared by running 3 to 4 standards within the likely range that 8-OH-dG will be measured (this can range from 10 fmol of 8-OH-dG on column

and upwards). An example of a range of standards may include 10, 30, 90, and 180 fmol 8-OH-dG on column. Using the suggested array of potentials, standards are run and 8-OH-dG is measured at 300 mV. Also see Troubleshooting.

4. Run a water blank. Make 50-µl injections at 0 and 5 min, then allow the blank to run 30 min.

   The purpose of this step is to determine if there is any standard carryover that could interfere with the analyte measurement.

5. Inject 50-µl sample into the HPLC system.

   Keep samples at storage temperature and thaw just prior to analysis.

6. Allow the sample to run at least 15 min.

   Depending on the age of the column, retention times may vary, but should be ~10 min.

7. Determine the concentration of 8-OH-dG by comparing peak areas of samples with those of a series of standards.

8. To take into account the extent of digestion, normalize the concentration of 8-OH-dG to the amount of deoxyguanosine (dG), determined by either ECD or UV detection (see Basic Protocol 2).

   The concentration of 8-OH-dG can also be normalized to the amount of DNA determined by UV analysis (UNIT 3.8).

SUPPORT PROTOCOL 1

Enzymatic DNA Digestion

The support protocol described below is used to enzymatically digest DNA to yield deoxyribonucleosides.

Materials

Digestion enzymes:
200 U/0.1ml deoxyribonuclease I (Sigma-Aldrich)
0.1 U/0.1 ml spleen phosphodiesterase (Sigma-Aldrich)
0.5 U/0.1 ml snake venom phosphodiesterase (Worthington Biochemicals)
10 U/0.1 ml alkaline phosphatase (Sigma-Aldrich)
10× digestion buffer: 400 mM Tris·Cl, pH 8.5 (*APPENDIX 2A*)/100 mM $MgCl_2$; store up to 1 month at 4°C
DNA sample

Digest DNA sample

1. Add 10 µl each digestion enzyme (i.e., deoxyribonuclease I, spleen phosphodiesterase, snake venom phosphodiesterase, and alkaline phosphatase) to 15 µl of 10× digestion buffer and keep on ice.

   The resulting 55 µl is enough for one sample of 100 µg DNA in 100 µl water.

2. Adjust the volume of isolated DNA sample (100 µg) to 100 µl with water and keep on ice.

   If the concentration of DNA is <1 mg/ml, dry the sample (i.e., in a SpeedVac; Savant) and then adjust the volume to 100 µl with water.

3. Add 55 µl digestion buffer/enzyme mixture to each sample.

4. Incubate 2 hr at 37°C.

5. Proceed to analyze immediately or store sample up to 3 months at −80°C.

HPLC-ECD Analysis of N7-Methylguanine

The protocol described below is a modified procedure for measuring the amount of N7-MG present in an exposed sample (Park and Ames, 1988a,b). Isolated DNA is heated to release labile bases (N7-MG) from the DNA backbone. The liberated bases are prepared for analysis, separated chromatographically, and detected coulometrically.

Materials

DNA sample
1 M HCl, ice cold
Mobile phase, cold: 50 mM KH_2PO_4 (pH 5.5)/2% (v/v) HPLC-grade methanol
1 M NaOH
N7-MG standards (see recipe)

HPLC system:
- 100-µl injection loop
- Electrochemical detector (E.S.A. Model 5600 CoulArray and Model 5040 cell with platinum target)
- 25 cm × 4.6–mm C_{18} column with 5-µm particle size, room temperature

100°C water bath or equivalent

NOTE: All water used must be distilled and deionized.

Prepare DNA

1. Adjust the volume of an isolated 100-µg DNA sample to 100 µl with water. Store on ice.
2. Wrap the tops of the tubes with Parafilm and subject samples to neutral thermal hydrolysis 30 min in a 100°C water bath or equivalent.

   Securing the tops of tubes is necessary, since steam generated can pop them open and contamination of the sample can occur.

3. Precipitate DNA by placing samples on ice and adding 10 µl ice-cold 1 M HCl. Vortex briefly.

   The solution should become hazy as the DNA falls out of solution.

4. Microcentrifuge 30 min at 14,000 × *g*, 4°C.

   A pellet should be observed depending on the amount of DNA used. If no pellet is visible either continue centrifugation, use a filtration device (i.e., Centricon), or proceed with preparation, keeping in mind excess DNA may clog HPLC plumbing.

5. Transfer 100 µl supernatant to a new microcentrifuge tube. Keep the new tubes on ice.
6. Add 100 µl cold mobile phase to each sample.

   This will buffer the hydrolysate solution and depending on injection volume, will allow for duplicate analysis of the sample.

7. Add 9 µl room-temperature 1 M NaOH.

   Even though alkaline conditions induce imidazole ring opening, the amount here is used to adjust the pH and does not approach the pH at which ring opening occurs (Chetsanga et al., 1981).

8. Vortex sample and either analyze immediately or store up to 6 months at −80°C.

HPLC-ECD Analysis

9. Set potentials of the HPLC system's electrochemical detector to 200, 300, 400, 500, 600, 700, 800, and 900 mV.

   The above range is a suggestion for a system with an eight-channel array detector (see Critical Parameters; also see Basic Protocol 3, step 1).

10. Equilibrate system, including 25-cm × 4.6-mm C_{18} column with 5-µm particle size, for at least 1 hr by running mobile phase at 1 ml/min. Maintain the 1 ml/min flow rate for the remainder of the analysis (see Critical Parameters).

11. Run three or four standard concentrations within the likely range that N7-MG will be measured (see Troubleshooting).

    The standard curve for N7-MG is prepared by running 3 to 4 standards within the likely range that N7-MG will be measured (this can range from 1 pmol N7-MG standard on column and upward). An example of a range of standards may include 1, 10, and 100 pmol N7-MG on column. Using the suggested array of potentials, standards are run and N7-MG is measured at 700 mV.

12. Run a water blank, making injections at 0 and 5 min. Allow the blank to run 30 min.

13. Inject 50-µl sample into HPLC system.

    Keep samples at storage temperature and thaw just prior to analysis.

14. Allow sample to run 25 min.

    Depending on the age of the column, retention times may vary but should be ~18 min.

15. Determine the concentration of N7-MG by comparing the peak areas of samples with those of a series of standards.

    Normalize the concentration of N7-MG to the amount of DNA analyzed.

BASIC PROTOCOL 5

Quantification of N^2, 3-Ethenoguanine by IA/GC/ECNCI/HRMS

The DNA adduct, N^2,3-ethenoguanine (N^2,3-εGua), is formed from a number of carcinogens, including vinyl chloride (Bartsch et al., 1994), as well as from lipid peroxidation by-products (Ham et al., 2000). The formation of this adduct occurs from the reaction of guanine with electrophiles that are produced from carcinogens as well as from endogenous sources. The method described here for the quantification of N^2,3-εGua uses immunoaffinity chromatography to purify the adduct, followed by derivatization, to increase the volatility of the adduct, and GC/ECNCI/HRMS analysis. This method is used to determine the amount of the promutagenic DNA adduct N^2,3-εGua relative to the amount of unmodified guanine bases in a sample of isolated DNA (Ham et al., 1999).

Materials

DNA sample
1 N HCl: dilute 3.3 ml concentrated HCl to 40 ml with water; store up to 6 months at room temperature
~2 fmol/ml [$^{13}C_4$,$^{15}N_2$]N^2,3-εGua internal standard
~1 fmol/ml N^2,3-εGua standard
500 mM sodium phosphate buffer, pH 7.2 (see recipe; also see *APPENDIX 2A*)
Immunoaffinity (IA) columns made with polyclonal antibodies to N^2,3-εGua (see Support Protocol 2)
5% (v/v) and 100% HPLC-grade methanol
PBS/azide (see recipe)
0.1 M formic acid

Potassium carbonate: grind to a fine powder with mortar and pestle and store at 60°C
Acetone, HPLC-grade (≥99.9%)
5% PFBBr (see recipe)
Hexane
Silica gel slurry: silica gel 60, 70-230 mesh (Fisher) in hexane
Ethyl acetate, GC/GC-MS grade
Dichloromethane, ACS or HPLC grade
5% (v/v) ethyl acetate in hexane
99.8% toluene
Helium gas
Methane gas

22-G needle
70°C water bath or heating block with H_2O in the test-tube holes
Centricon 10 concentrators
13 × 100–mm silanized, disposable, borosilicate culture tubes
5.75-in. silanized Pasteur pipets
Silanized glass wool
200-µl genomic and 100-µl gel-loading aerosol-resistant pipet tips
1.8-ml GC autosampler vials with inserts and caps
Silanized culture tubes with caps
Transfer pipets
GC-MS system:
Electron capture negative chemical ionization detector
DB-5MS 30-m × 0.32-mm × 0.1-mm film column or equivalent
Uniliner HP injection sleeve, 4.0 mm i.d. × 6.3 mm o.d. × 78.5 mm (Restek)

Additional reagents and equipment for quantifying DNA by UV spectroscopy (*UNIT 3.8*) and measurement of guanine by HPLC (see Basic Protocol 1)

NOTE: All hexane used in the protocol must be capillary GC/GC-MS grade.

Hydrolyze DNA

1. Suspend DNA sample in water and shear by passing through a 22-G needle until homogeneous. Quantify by UV spectrophotometry ($A_{260\,nm} = 20$ ml/mg cm^{-1} in water) prior to use (*UNIT 3.8*).
2. Add the following to a 1.7-ml microcentrifuge tube:

   100 ml 1 N HCl
   60 ml ~2 fmol/ml [$^{13}C_4$,$^{15}N_2$]*N*^{2},3-εGua internal standard
   Adjust to 1 ml final volume (after sample or standard is added; see step 4) with water.

3. Add 100 to 400 mg DNA (step 1) or 0, 5, 10, 25, 50, 100, and 200 ml of ~1 fmol/ml N^2,3-εGua standard to a microcentrifuge tube, cap, and mix using a vortex mixer. Incubate 30 min in a 70°C water bath or heating block with water in the test-tube holes.

   The amount of DNA required will vary depending on the anticipated amount of εGua *in the sample. Larger amounts of DNA are required for endogenous* εGua *samples, while smaller amounts can be used for carcinogen-treated samples. As little as 5 to 10 mg has been used for quantitation of in vitro samples that produce* εGua *from direct reaction.*

   During this step is a good time to cool the centrifuge rotor to 4°C if it has not been cooled already.

4. After incubation, place tubes on ice 10 min prior to hydrolysate purification.

Purify hydrolysate

5. Transfer samples and standards to sample reservoirs of Centricon 10 concentrators.

   The Centricon concentrators are used to separate the DNA backbone from the depurinated adducts and normal nucleobases.

6. Centrifuge 60 min at 5000 × *g*, 4°C.

7. Remove a 100-ml aliquot of the filtrate from each sample (not the standards) for guanine analysis (see Basic Protocol 1).

   The aliquot taken for guanine analysis will vary depending upon the amount of DNA used. For example, if 200 mg DNA is used, generally a 100-ml aliquot is taken and that aliquot is diluted 5-fold (e.g., 400 ml water is added) before guanine analysis. If small quantities of DNA are used (i.e., 5 to 10 mg), a larger aliquot may be taken and no dilution will be necessary before guanine analysis.

8. Rinse microcentrifuge tubes that contained the samples or standards with 1 ml of 500 mM sodium phosphate buffer, pH 7.2, and transfer to sample reservoirs of the same Centricon 10 concentrators. Add an additional 1 ml of 500 mM sodium phosphate buffer directly to the reservoir.

9. Centrifuge samples 75 min at 5000 × *g*, 4°C, or until only a small fraction of the retentate remains.

   The filters should be allowed to dry.

   The length of time for this centrifugation step may vary depending on the batch of Centricon filters and the amount of DNA. Generally, more DNA requires more time to complete the transfer of liquid to the filtrate reservoirs.

10. Dilute samples 2-fold with water. Check the pH of the filtrate for neutrality using pH paper.

    The pH of the filtrate should be 7.0 to 7.2 using short-range pH paper, prior to immunoaffinity chromatography. See Immunoaffinity Purification (below), for a discussion on the importance of neutrality prior to this method of chromatography.

Purify adduct

11. Precondition immunoaffinity (IA) columns made with polyclonal antibodies to N^2,3-εGua, at 4°C, by draining and sequentially adding 5 ml water, 10 ml of 100% methanol, 10 ml water, and 10 ml PBS/azide.

    Immunoaffinity columns are constructed using 500 ml polyclonal antiserum for each of four columns (see Support Protocol 2) and tested accordingly (see Support Protocol 3). The production of polyclonal antibodies for this adduct is described by Ham et al. (1999). Columns are stable for at least one year and may be reused multiple times.

12. At room temperature, transfer filtrate from Centricon filtrate reservoir to IA column.

13. Drain and wash the IA column sequentially with 5 ml PBS/azide, 5 ml water, and 10 ml of 5% methanol.

14. Elute the sample at room temperature with 3 ml of 100% methanol. Collect eluate in a 13 × 100–mm silanized, disposable, borosilicate culture tube.

    The columns and solvents were kept refrigerated during preconditioning (step 11), largely because this process takes a considerable amount of time. (It is unlikely that the columns behave differently at room temperature.) Sample application, wash, and elution (steps 12 to 14) were done at room temperature largely because it is inconvenient to apply the samples in the refrigerator. The wash solvents (i.e., PBS, water, and 5% methanol) are stored in the refrigerator and should still be cold when applied to the columns. The elution solvent (i.e.,

methanol) should be stored on the bench, and should be at room temperature when applied to the columns. In the authors' laboratory, the temperature change was not noted to induce bubble formation, but the mixing of methanol and water certainly did. It was occasionally necessary to force some solvent through the space between the frits that contained the resin when these bubbles became large enough to obstruct the flow.

15. Dry samples in a SpeedVac evaporator using low-medium heat.

16. Recondition IA columns at 4°C by sequentially adding: 5 ml 100% methanol, 5 ml water, 10 ml of 0.1 M formic acid, 10 ml water, and 10 ml PBS/azide. Store columns at 4°C in 5 ml PBS/azide.

    The recovery of the columns should be checked periodically by adding (unlabeled) analyte standard to the columns, and (labeled) internal standard to the collection tubes. New columns should be made when the calculated recovery no longer provides the required sensitivity.

Derivatize samples

17. To each dried sample tube, add a spatula tip (~25 mg) potassium carbonate, 500 µl HPLC-grade acetone, and 35 µl of 5% PFBBr. Cap and mix continuously 75 min at 50°C using a vortex mixer.

    A derivatization step is necessary to make the adduct volatile so it is suitable for gas chromatography.

18. While samples are incubating, prepare silica gel chromatography columns as follows:

    a. Plug silanized 5.75-in. Pasteur pipets with silanized glass wool.
    b. Wet plug with hexane and add silica gel slurry to a height of 1.5 to 2.0 cm.
    c. Condition columns by sequentially adding 2 ml hexane, 4 ml GC/GC-MS-grade ethyl acetate, and 6 ml hexane.

    The headspace of the column when prepared as described is ~2 ml.

19. After incubation is complete, evaporate samples to dryness using a SpeedVac evaporator without heating.

20. Resuspend the dried samples in 100 µl A.C.S.-HPLC-grade dichloromethane and transfer to silica gel columns using 200-µl genomic aerosol-resistant tips. Add an additional 100 µl dichloromethane to the sample tube to rinse and transfer the rinse to silica gel columns.

21. Wash the silica columns with 4 ml hexane and 6 ml of 5% HPLC-grade ethyl acetate in hexane.

22. Elute the samples into clean silanized culture tubes with 3 ml GC/GC-MS-grade ethyl acetate and dry in the SpeedVac evaporator using medium heat.

23. Resuspend samples in 15 to 50 µl of 99.8% toluene (depending on the anticipated amount of the adduct), vortex, and centrifuge at low speed just long enough to get toluene off the sides of the tube (i.e., to recover as much sample as possible).

24. Transfer samples to GC vial inserts with 100-µl gel-loading tips, place inserts in 1.8-ml GC autosampler vials, cap the vials, and store samples at −80°C until analysis (up to 6 months).

Perform GC/ECNCI/HRMS analysis

25. Analyze sample using GC/ECNCI/HRMS system with the following conditions:

Column:	DB-5MS 30 m × 0.32 mm × 0.1 mm film or equivalent
Injection liner:	HP 4.0 mm i.d. × 6.3 mm o.d. × 78.5 mm
Carrier gas:	Helium
Injection volume:	2 ml
Injector temperature:	290°C
Temperature program:	0.5 min at 100.0°C 20.0°C/min increase to 290°C 3 min at 290°C 50°C/min increase to 300°C 2 min at 300°C
Reagent gas:	Methane
Mode:	High-resolution, negative ion
Mass channels:	354.0413 (analyte) 360.0489 (internal standard)

These are the conditions specific to the analysis of ε*Gua by GC/ECNCI/HRMS. More detailed description of the analysis of this adduct and general considerations and troubleshooting for the analysis of DNA adducts using this technique are described below (see Basic Protocol 6).*

IMMUNOAFFINITY PURIFICATION

Because many DNA adducts are present in a very low proportion relative to unmodified bases, and because the chemical properties of adducts are often very similar to the original base, enrichment can be the biggest obstacle to quantification of adducts formed in vivo. Immunoaffinity chromatography is an approach to adduct purification that is efficient, highly selective, and less labor intensive than most traditional chromatography techniques. Here, a 1-day protocol for producing (see Support Protocol 2) and testing (see Support Protocol 3) immunoaffinity columns is described that has been successfully applied to both monoclonal and polyclonal antibodies without any requirement for antibody purification. Similar protocols have been used to quantify the vinyl chloride-induced adduct N^2,3-ethenoguanine from DNA (Ham et al., 1999), and 3-methyladenine from urine (Friesen et al., 1991).

SUPPORT PROTOCOL 2

Preparation of Immunoaffinity (IA) Columns for DNA Adduct Purification

This method is based on that originally described by Schneider et al. (1982) and later adapted by Friesen et al. (1991) for DNA adduct purification. It is designed to covalently bind an antibody raised against the adduct of interest to a Sepharose support through specific binding to Protein A.

NOTE: All procedures should be done at 4°C except when specified otherwise.

Materials

Protein A–Sepharose CL4B (Amersham Pharmacia Biotech)
100 mM Tris·Cl, pH 7.4 (*APPENDIX 2A*)
Purified antibody, hybridoma cell supernatant, or antiserum against adduct of interest
200 mM triethanolamine, pH 8.2: 13.3 ml in 500 ml (total) water; store up to 1 month at 4°C

20 mM dimethylpimelidate (DMP; Pierce Chemical) in 200 mM triethanolamine, pH 8.2, fresh
20 mM ethanolamine (Fisher Scientific) in 200 mM triethanolamine, pH 8.2
PBS/azide (see recipe)
100% HPLC-grade methanol (J.T. Baker or equivalent)

12-ml polyethylene minisorb tubes (Nunc) or 15-ml centrifuge tubes
End-over-end mixer
Four 5-ml disposable polystyrene columns with two frits each (Pierce Chemical)

1. Suspend Protein A–Sepharose CL4B by stirring with the blunt end of a Pasteur pipet. To prepare four immunoaffinity columns, transfer 1 ml of the suspension to a rinsed 12-ml polyethylene minisorb or 15-ml centrifuge tube.
2. Add 5 ml of 100 mM Tris·Cl, pH 7.4, and mix well. Centrifuge 5 min at 1000 × *g*, and discard supernatant. Repeat once.
3. Add an appropriate volume of purified antibody, hybridoma cell supernatant, or antiserum against the adduct of interest.

   Antibody is present in hybridoma cell supernatant or antiserum. The volume added is dependent on antibody concentration and may be optimized through trial-and-error. As little as 250 µl polyclonal antiserum or as much as 10 ml monoclonal hybridoma cell culture supernatant has proven adequate. Smaller volumes of purified antibody may be used depending upon antibody concentration.

4. Bring the volume to 10 ml with 200 mM Tris·Cl, pH 7.4.

   If the total volume is greater than 10 ml, do not use the full volume. Only use 10 ml or less.

5. Mix suspension end-over-end for 30 min at room temperature. Centrifuge as before (step 2) and discard supernatant.
6. Wash gel twice with 4 ml of 200 mM Tris·Cl, pH 7.4, centrifuge, and discard supernatant.
7. Wash gel twice with 4 ml of 200 mM triethanolamine, pH 8.2, centrifuge, and discard supernatant.
8. Add 10 ml of 20 mM freshly-prepared dimethylpimelidate (DMP) in 200 mM triethanolamine, pH 8.2. Mix end-over-end for 45 min at room temperature. Centrifuge and discard supernatant.
9. Add 10 ml of 20 mM ethanolamine solution and mix end-over-end for 5 min at room temperature. Centrifuge and discard supernatant.
10. Add 5 ml PBS/azide, mix, centrifuge, and discard supernatant. Repeat once.
11. Soak frits in PBS/azide for at least 1 hr, preferably overnight. Insert in the bottom of each of four disposable polystyrene columns using the blunt end of a Pasteur pipet. Plug the column.
12. Resuspend the resin in 4 ml PBS/azide and carefully transfer 1 ml to each column.
13. Rinse the tube with 4 ml PBS/azide and transfer 1 ml to each column.
14. Add 3 ml PBS/azide to each column and allow resin to settle at least 1 hr.
15. Insert a second frit into each column ~1 cm above the top of the gel bed. Remove plugs and allow columns to drain.

16. Wash columns by sequentially adding 5 ml PBS/azide, 5 ml water, 25 ml of 100% HPLC-grade methanol, 10 ml water, and 10 ml PBS/azide.

17. Cap columns and store at 4°C in PBS/azide when not in use.

    Columns can be stored indefinitely as long as the recommended storage conditions are followed.

SUPPORT PROTOCOL 3

Determination of Recovery and Adduct Purification

A crude sample is applied to the column, and a highly-purified adduct is eluted after several washes. The adduct may then be quantified by the method of choice without any need for desalting. The columns should be kept refrigerated whenever possible, but the sample application and elution steps may be done at room temperature if this is more convenient. The following procedure has been developed for the use of IA purification of the DNA adduct N^2,3-ethenoguanine (Ham et al., 1999).

Materials

IA columns (see Support Protocol 2)
5% (v/v) and 100% methanol
PBS/azide (see recipe)
Neutralized standard (e.g., ~1 fmol/ml N^2,3-εGua, pH 7.0) or sample DNA sample
0.1 M formic acid
Internal standard (optional)

Additional reagents and equipment for quantifying samples by HPLC (see Basic Protocol 1)

1. Drain IA columns and precondition by sequentially adding 5 ml water, 10 ml of 100% methanol, 10 ml water, and 10 ml PBS/azide.
2. Transfer a known amount of neutralized standard (to determine recovery) or DNA sample to column.

   The sample or standard must be loaded on an IA column at neutral pH. If pH is not neutral, the adduct will not bind to the antibody.

3. Wash the columns by adding 5 ml PBS/azide, 5 ml water, and 10 ml of 5% methanol.

   Exact washing conditions may need to be determined, depending on the stability of the antibody on the immunoaffinity column and the affinity of the IA column for contaminating substances (i.e., normal bases, nucleosides, or nucleotides).

4. Elute the sample with 3 ml of 100% methanol or mild acid (e.g., 0.1 M formic acid) at room temperature.

   The choice of eluting solvent depends upon the stability of the antibody and/or adduct and the affinity of the antibody for the IA column. Stronger affinity of the IA column for the analyte may require a stronger eluting solvent (i.e., acid). Less stable IA columns may require a milder eluting solvent (i.e., methanol).

5. If determining recovery, add a known amount of internal standard to the collection tube.
6. Dry the eluent in a rotary evaporator and quantify the standard or sample by method of choice (e.g., *UNIT 3.8*).
7. Recondition columns by adding 5 ml of 100% methanol, 5 ml water, 10 ml of 0.1 M formic acid, 10 ml water, and 10 ml PBS/azide.
8. Cap columns and store in 5 ml PBS/azide at 4°C.

QUANTIFICATION OF DNA ADDUCTS: GAS CHROMATOGRAPHY/MASS SPECTROMETRY

Various gas chromatographs made by different instrument manufacturers (e.g., Hewlett Packard, Varian Analytical Instruments, Thermoquest) interfaced with quadrupole and sector mass analyzers are typically used for quantitative GC/MS analyses. While quadrupole mass analyzers (e.g., Finnigan 70, 700, and 7000 series, HP engines, Micromass, VG Trio series) are used in low-resolution (unit-resolving-power) mass spectrometry, sectors (e.g., VG 70 series, VG AutoSpecs, and Jeol instruments) and recently time-of-flight (e.g., Micromass, Leco) analyzers are used at both unit and high-mass resolving powers. Although functional description of each GC/MS can be quite different, GC/MS quantification using isotopic dilution mass spectrometry follows basic underlying principles irrespective of the type of GC and mass analyzer used. Thus, the protocol must have guidelines for GC separation using a suitable column and temperature program, tuning and mass calibration using a reference compound, and mass measurements of the analyte and the corresponding internal standard (preferably a stable isotope of the analyte); however, one important consideration in choosing the mass spectrometer is its ability to operate under ECNCI mode because most of the bench-top MS machines may not be equipped with an ECNCI source and appropriate detector.

GC/ECNCI/HRMS Analysis of N^2, 3-ethenoguanine (εGua), 7-(hydroxyethyl) Guanine (7-HEG), and 7-(hydroxypropyl) Guanine (7-HPG) Using a VG 70-250SEQ Mass Spectrometer

BASIC PROTOCOL 6

The following protocol describes the steps that should be followed in order to analyze derivatized DNA adducts dissolved in toluene. Prior to GC/MS analysis, the biological samples are presumably cleaned and concentrated by various affinity and low-pressure chromatographic methods. Please refer to the respective methods for preparation of these samples prior to GC/ECNCI/HRMS analysis. The analyst is advised to read the paper entitled "Application of Gas Chromatography/Electron Capture Negative Chemical Ionization High-Resolution Mass Spectrometry for Analysis of DNA and Protein Adducts" by Ranasinghe et al. (1998). Although not required, basic understanding of quadrupole and sector mass spectrometers and general mass spectrometry principles can be useful for troubleshooting purposes. The method involves tuning of the MS and quantification using isotopic dilution mass spectrometry (Garland and Powell, 1981). This typically involves area measurement of two ion chromatographic peaks due to the analyte and the corresponding internal standard (IS). Note that the same method with slight modifications can be applied if the mass analysis is performed at a low (unit) resolving power (RP 1000). For example, tuning the mass spectrometer for high resolving power is not required (skip steps 5, 6, and 7 below). Also, a reference compound (PFK or FC43) is not introduced during the mass analysis (skip step 10, the needle valve is closed); therefore, no lock-mass or a check-mass is measured (skip first two rows in Tables 3.9.3, 3.9.4, and 3.9.5).

Materials

99.999% helium (Sunox)
Perflurokerosine (PFK; PCR) or perfluorotributylamine (FC43; PCR)
Sample in toluene
HP-5890 Series II gas chromatograph (GC) with appropriate column and 4.0 mm-i.d. × 6.3-mm-o.d. × 78.5-mm Restek uniliner coupled in-line to a VG 70-250SEQ mass spectrometer (Micromass UK) with EI/CI ion source and oscilloscope

1. Vent the VG 70-250SEQ mass spectrometer to atmospheric pressure. Install the ion source (EI/CI source) and the appropriate GC-column.
2. Evacuate the air and bring the mass spectrometer under vacuum and set the instrumental parameters as follows:

GC (HP-5890 Series II) conditions:	
Carrier gas:	99.999% helium, head pressure of 10 psi
Injector temperature:	290°C
Oven temperature:	200°C
Injection mode:	Direct (splitless)
Liner:	4.0-mm-i.d. × 6.3-mm-o.d. × 78.5-mm
MS conditions:	
Methane pressure:	4×10^{-5} mbar (as read by the pirani gauge)
Source temp:	250°C
Slit:	CI
CI mode:	Negative
Emission current (EC):	0.2–1 mA
Electron energy (EE):	50–150 eV
GC transfer-line temp:	300°C
Septum reservoir temp:	150°C
Septum transfer-line temp:	175°C

3. Introduce 1 µl perflurokerosine (PFK) or perfluorotributylamine (FC43) to the septum inlet.
4. Tune the mass spectrometer at a mass resolving power (RP) of 1000 for a particular ion from PFK or FC43, choosing the tuning ion closer to the monitoring masses of the analyte and the internal standard (IS). Adjust the emission current (EC), electric energy (EE), and lenses to give the highest intensity of the tuning ion displayed on the oscilloscope in the front console.
5. Close the source slit until the ion intensity is decreased to 10% of that in step 4.
6. Close the collector (analyzer) slit until the ion intensity is further decreased 50% of that in step 5.
7. Retune the mass spectrometer for the same ion at RP 10,000.

   After this tuning at RP 10,000 the peak width is 10% and the ion signal ~5% from the original signal (step 4) at RP 1000.

8. Set the instrumental parameters (Tables 3.9.3 to 3.9.5) for each adduct and calibrate the instrument using appropriate reference compound (PFK or FC43).
9. Set the multiplier voltage to 9.

   This can vary from 7 to 10 depending on the concentration of the adduct in the biological sample. The ion abundance (peak area from the ion chromatogram) should not exceed saturation level (1×10^9).

10. Adjust the needle valve until the lock mass from the reference compound is ~5 to 10 V as measured from the console (oscilloscope).
11. Finally inject 2 µl of the sample in toluene to be analyzed by GC/ECNCI/HRMS. Measure the area of the analyte and the internal standard in the ion chromatograms and calculate the concentration of the adduct using the corresponding calibration curve.

Table 3.9.3 Selected Ion Monitoring Experiment and GC Program for εGua[a]

Channel	Mass	Dwell time (msec)	Delay time (msec)
Lock (PFK)	354.9792	50	20
PFK	354.9792	20	20
εGua	354.0413	50	20
$^{13}C_4$,$^{15}N_2$ εGua (IS)	360.0489	50	20

[a]Results are for 30-m × 0.32-mm × 0.1-mm-thickness DB-5^{MS} fused silica capillary column (J & W Scientific). Column temperature program: held 30 sec at 100°C (initial), increasing 20°C/min to 290°C, held 3 min, increasing 50°C/min to 300°C, and held 2 min.

Table 3.9.4 Selected Ion Monitoring Experiment and GC Program for 7-HEG[a]

Channel	Mass	Dwell time (msec)	Delay time (msec)
Lock (FC43)	556.9695	50	20
Check (FC43)	556.9695	20	20
7-HEG	555.0515	50	20
$^{13}C_4$-7-HEG (IS)	559.0649	50	20

[a]Results are for 15-m × 0.32-mm × 0.1-mm-thickness DB-5^{MS} fused silica capillary column (J & W Scientific). Column temperature program: held 1 min at 70°C after injection, raised at 20°C/min to 290°C, and held 3 min.

Table 3.9.5 Selected Ion Monitoring Experiment and GC Program for 7-HPG[a]

Channel	Mass	Dwell time (msec)	Delay time (msec)
Lock (FC43)	575.9679	50	20
Check (FC43)	575.9679	20	20
7-HPG	569.0671	50	20
$^{13}C_4$-7-HPG (IS)	573.0807	50	20

[a]Results are for 15-m × 0.32-mm; 0.1-mm-thickness DB-5^{MS} fused silica capillary column (J & W Scientific). Column temperature program: held 1 min at 70°C after injection, raised 20°C/min to 290°C, and held 3 min.

QUANTIFYING DNA ADDUCTS: LIQUID CHROMATOGRAPHY/MASS SPECTROMETRY (LC/MS)

LC/MS methods are extremely popular for quantitation of biological compounds since they provide the specificity of a mass spectrometric method without requiring labor-intensive and time-consuming sample preparation procedures. Besides the simplified sample preparation procedures, these techniques also have the advantage of employing mild conditions; thus the possibility of sample degradation and formation of artifacts or false positives is minimized. With a continuous decrease in the cost of mass spectrometers, these powerful tools are becoming widely available for routine quantitative analysis of

biological compounds. A typical LC/MS setup uses an HPLC unit coupled to a mass spectrometer using an atmospheric pressure ionization interface—electrospray ionization and atmospheric pressure chemical ionization interfaces being the most common choices. The type of mass spectrometer to use is dictated by the need for sensitivity and specificity. Triple quadrupole mass spectrometers are the best choices since they can provide the sensitivity given by quadrupole mass analyzers and the specificity afforded through use of selected reaction monitoring as mode of detection. A mass spectrometer with single quadrupole or an ion trap mass analyzer could be sufficient, depending on the requirement.

BASIC PROTOCOL 7

Quantification of N7-Guanine Adducts by LC/ESI/IDMS/MS

The authors' laboratory has been using LC/ESI/MS/MS for quantification of mainly N7 guanine adducts (Tretyakova et al., 1998; Koc et al., 1999). Quantification of DNA adducts by LC/MS typically involves hydrolysis of DNA to cleave the adducts from DNA, enrichment of the adducts over unmodified DNA bases, desalting, and quantification by LC/MS. The enrichment step is very critical since unmodified bases may cause sensitivity loss due to signal suppression in ESI ionization. The type of enrichment method that needs to be employed depends on the method of DNA hydrolysis.

Materials

DNA sample
Isotopically labeled internal standard (e.g., $^{13}C_4$-N7-HEG)
100% methanol
SPE reversed-phase cartridge, preferably polar endcapped (e.g., ODS-AQ, Waters Chromatography or Aquasil, Keystone Scientific)
Calf thymus DNA

22-G needles
95° and ~60°C water baths
Centricon 30 filters
Autosampler vial with 250-µl insert
Mass spectrometer with electrospray ionization source and the capability to conduct selected reaction monitoring (e.g., Thermoquest TSQ 7000, Micromass Quattro II)

Perform neutral thermal hydrolysis

N7-Guanine adducts can be removed from the DNA fairly selectively by heating the DNA 30 min at 95°C, leaving most (>95%) of the unmodified bases on the DNA backbone.

1. Shear DNA sample by passing through a 22-G needle five to six times.
2. Transfer 0.1 to 1.0 mg sheared DNA into a microcentrifuge tube, spike with several hundred femtomoles isotopically labeled internal standard, and vortex.
3. Subject the solution to neutral thermal hydrolysis by incubating tubes 30 min in a 95°C water bath. Vortex the tubes two or three times during heating.
4. Cool the tubes on ice and transfer the contents of the tubes into Centricon 30 filters that have been washed with 2 ml water to remove glycerol present in these filters.
5. Centrifuge the Centricon filters at 5000 × *g*, 4°C, until all of the solution is filtered.

   The time needed to filter the sample will vary depending on the volume and DNA concentration.

6. Because some of the sample will be left on the membrane, add ~200 µl water and centrifuge again 5 min at 5000 × *g*, 4°C, to filter more of the solution.

   After the Centricon 30 filtration, DNA backbone will be left on the membrane while N7 adducts will be in the filtrate. DNA backbone can be recovered from the filter by reversing the filter, adding ~100 µl water, and centrifuging into a clean tube.

Desalt the sample

7. Run 5 ml of 100% methanol to regenerate the SPE reversed-phase cartridge. Then equilibrate with ~10 ml water.
8. Load the hydrolysate onto the reversed-phase cartridge by gravity.

   Salts present in the hydrolysate may suppress response in electrospray ionization; therefore, the salts should be removed from the sample before LC/MS analysis. This is typically done with solid-phase extraction cartridges. Alternatively, one can perform the desalting procedure on-line using column switching techniques or by simply diverting the early LC effluent to waste instead of the mass spectrometer.

9. Wash loaded cartridge three times with 1 ml water each.
10. Elute the adducts with 5 ml of 100% methanol into a clean culture tube.
11. Evaporate to dryness (i.e., remove methanol) in a SpeedVac evaporator.
12. Dissolve the contents in ~100 µl water by mild heating in a ~60°C water bath and vortexing
13. Transfer the sample into an autosampler vial with a 250-µl insert and store up to 2 years at −70°C until LC/MS analysis.

Perform LC/ESI/MS/MS analysis

14. Calibrate the mass spectrometer according to manufacturer's procedure.

    For this step, a mass spectrometer equipped with an electrospray ionization source and the capability to conduct selected reaction monitoring (SRM) experiments is used. Triple quadrupole mass spectrometers such as TSQ 7000 (Thermoquest) or Quattro II (Micromass) are most widely used for this purpose.

15. Develop an LC method on a reversed-phase column that enables separation of adducts of interest from possible interferences, mostly normal bases.
16. Using the mobile phase and flow rate used for chromatographic separation, optimize the ESI conditions (e.g., nitrogen flow rate, spray and lens voltages) for maximum sensitivity for the protonated molecular ion.
17. Optimize the collision gas pressure and collision energy to get an efficient dissociation to produce product ion (protonated guanine in this case).
18. Prepare calibration curve standards with calf thymus DNA and run them through the sample preparation procedure as if they were samples.

    A calibration curve is generated and the amount of DNA and internal standard in the calibration standards should be the same as samples.

Analyze samples

19. Prior to running a batch of samples, analyze a low-level calibration standard to make sure that sensitivity is satisfactory for the samples.
20. If satisfied with the sensitivity, inject the sample.

21. Inject standards or quality to control samples after 5 to 10 injections to monitor the instrument performance.

See Koc et al. (1999) for an example method.

QUANTIFYING DNA ADDUCTS: ^{32}P-POSTLABELING

The ^{32}P-postlabeling assay is an ultrasensitive method to detect covalently modified DNA. This technique was developed by Randerath et al. (1981) and has since undergone several refinements to enhance its sensitivity and specificity. Analysis involves enzymatic digestion of DNA to nucleotides, selective 5′-end labeling of chemically-modified nucleotides using [^{32}P]ATP, separation by TLC or HPLC to resolve DNA adducts, and detection of adducts by measuring radioactivity. ^{32}P-postlabeling has been applied to detect structurally diverse DNA adducts but is particularly useful to detect DNA modified by bulky aromatic compounds, such as polycyclic aromatic hydrocarbons (Gupta and Earley, 1988; Randerath and Randerath, 1994). Under optimal conditions, this method can achieve a level of detection as low as 1 adduct per 1×10^{10} nucleotides using 10 µg DNA.

BASIC PROTOCOL 8

^{32}P-Postlabeling Analysis of DNA Adducts

Each DNA adduct generally requires separate method development. The described method should be used as an initial approach. Different methods for adduct enrichment, as well as different chromatography conditions, may be required depending on the DNA adduct.

Materials

100% and 50% methanol
DNA sample
Hydrolysis buffer (see recipe)
0.24 U/µl micrococcal nuclease (Sigma-Aldrich): aliquot and freeze up to 1 year at −80°C
2 mg/ml spleen phosphodiesterase (Sigma-Aldrich), aliquot and freeze up to 1 year at −80°C
0.3 mM $ZnCl_2$
0.25 M sodium acetate, pH 5
5 mg/ml nuclease P1 (Sigma-Aldrich): aliquot and freeze up to 1 year at −80°C
0.5 M Tris base
Kinase buffer (see recipe)
30 U/µl polynucleotide kinase (United States Biochemical): store up to 1 year at −20°C
160 mCi/ml [γ-^{32}P]ATP (7000 Ci/mmol; ICN)
100 mM Bicine, pH 9.6
20 U/µl apyrase (Sigma-Aldrich): aliquot and freeze up to 1 year at −80°C
1 M and 1.7 M NaH_2PO_4, pH 6.0 (*APPENDIX 2A*)
5.3 M lithium formate/8.5 M urea, pH 3.5
1.2 M LiCl/0.5 M Tris·Cl (pH 8.0; *APPENDIX 2A*)/8.5 M urea
0.25 M LiCl
HPLC-grade H_2O

13 × 20–cm PEI cellulose TLC plates, flexible
5 × 20–cm Whatman 17 wick
Blow dryer
2.5-cm Whatman no. 1 filter paper wick
Phosphorescent pen

Incubator or heating block
X-ray film cassette
Darkroom
Liquid scintillation counter

CAUTION: When working with radioactivity, use appropriate precautions to avoid contamination of the experimenter and the surroundings. Carry out experiments and dispose of wastes in appropriately designated area, following the guidelines provided by the local radiation safety officer (also see *APPENDIX 1A*). All work with radioactivity must be performed using acrylic shielding and monitored using a Geiger counter.

1. Place 100% methanol, 50% methanol, and water in trays, using a sufficient volume to cover 13 × 20–cm flexible PEI cellulose TLC plates. Prepare plates by gently washing plates 5 min per solvent sequentially. Air dry TLC plates.
2. Place 5 µg DNA sample in a microcentrifuge tube and evaporate using a Speedvac evaporator. Add 4 µl water, 2 µl hydrolysis buffer, 2 µl of 0.24 U/µl micrococcal nuclease, and 2 µl of 2 mg/ml spleen phosphodiesterase. Incubate at 37°C for 3.5 hr.

   For greater amounts of DNA, adjust the amounts of enzymes appropriately.
3. Remove 2 µl of the digest.

   This aliquot will be used in step 16 for analysis of total nucleotides.
4. To the remaining DNA digest mixture, add 1.5 µl of 0.3 mM $ZnCl_2$, 3 µl of 0.25 M sodium acetate, pH 5, and 1.5 µl of 5 mg/ml nuclease P1. Incubate at 37°C for 1 hr.
5. Following completion of the nuclease P1 reaction, add 2.4 µl of 0.5 M Tris base.
6. Prepare labeling mixture by mixing 2.4 µl kinase buffer, 0.13 µl of 30 U/µl (4 U) polynucleotide kinase, 0.625 µl of 160 mCi/ml (100 µCi) [γ-^{32}P]ATP, and a volume of 100 mM Bicine, pH 9.6, sufficient to bring the total volume to 5 µl. Add 5 µl labeling mixture to each sample, and incubate at 37°C for 45 min.
7. Following completion of the labeling reaction, add 2 µl of 20 U/µl apyrase and incubate at 37°C for an additional 30 min.
8. Attach a 5 × 20–cm Whatman 17 wick along the bottom of a prewashed 13 × 20–cm TLC plate. Spot the entire incubation mixture onto the TLC plate 1.5 and 2 cm from the left and bottom edges, respectively.
9. Position the plate in the TLC tank with the wick directed outside the tank, and develop overnight in 1.0 M NaH_2PO_4, pH 6.0.
10. Cut off wick, rinse plate in a tray containing water with gentle agitation, and dry using a blow dryer.
11. Develop the plate in the opposite direction using a solution of 5.3 M lithium formate/8.5 M urea, pH 3.5, to the top of the plate.
12. Rinse the plate in water, dry using a blow dryer, and develop 90° to the previous direction in a solution of 1.2 M LiCl/0.5 M Tris·Cl/8.5 M urea, pH 8.0.
13. Rinse plate and dry using a blow dryer. Attach a 2.5-cm Whatman no. 1 filter paper wick, and develop in the same direction as the previous development in a solution of 1.7 M NaH_2PO_4, pH 6.0.
14. Dry plate using a blow dryer and mark with phophorescent pen. Expose to X-ray film in a cassette. Store at −80°C for 12 to 24 hr. Develop film.

15. Align film with the plate using marks from the phophorescent pen as guides. Mark area of plate corresponding to adduct spot, cut, and count using a liquid scintillation counter.
16. To determine the amount of normal nucleotides, dilute 2 µl digest (step 3) with 18 µl water. Prepare labeling mixture as in step 6, except use 10 µCi per sample.
17. Add 5 µl labeling mixture to 2 µl of the diluted sample and incubate 45 min at 37°C.
18. Add 1 ml water, spot 5 µl onto a TLC plate 1.5 cm from the bottom, and develop in 0.25 M LiCl.

    Several samples can be spotted on the same plate 1.5 cm apart.
19. Dry, and expose to X-ray film for 1 hr. Locate radioactive spots on origins, mark, and cut. Count using a liquid scintillation counter.
20. Determine relative adduct labeling by dividing dpm of adducted nucleotides by dpm of total nucleotides. To account for dilution, divide relative adduct labeling by 8000.

REAGENTS AND SOLUTIONS

*Use Milli-Q-purified water or equivalent for all recipes and protocol steps. For common stock solutions, see **APPENDIX 2A**; for suppliers, see **SUPPLIERS APPENDIX**.*

Hydrolysis buffer

Combine equal volumes of 200 mM sodium succinate, pH 6.0, and 100 mM $CaCl_2$. Store up to 1 month at 4°C.

Kinase buffer

Combine equal volumes of 200 mM Bicine, pH 9.6, 100 mM dithiothreitol, 10 mM spermidine, and 100 mM $MgCl_2$. Store in ~100-µl aliquots up to 1 year at −80°C.

N7-MG standards

Prepare stock solution by dissolving powder (Sigma-Aldrich) in water, adding concentrated HCl if there are problems with solubility. Make serial dilutions in water to give a range of standards between 1 and 1000 pmol/50 µl. Store up to 6 months at −80°C.

8-OH-dG standards

Prepare stock by dissolving powder (Sigma-Aldrich) in water. Make serial dilutions with water to give a range of standards between 0.005 and 1 pmol/50 µl. Store up to 6 months at −80°C.

PBS/azide

Add 500 ml 10× PBS—i.e., 10 mM phosphate buffer, pH 7.5/0.85% (w/v) NaCl (saline)—and 1 g sodium azide (0.02% w/v final) to 4500 ml water. Store up to 6 months at 4°C.

PFBBr, 5%

In a fume hood, add 25 ml 2,3,4,5,6-pentafluorobenzyl bromide (PFBBr) to 475 ml acetone for every 12 samples. Prepare fresh daily.

CAUTION: *PFBBr is a potent lachrymator; therefore, concentrated solutions should be handled only in an operating chemical fume hood. Carefully review MSDS before use.*

Sodium phosphate buffer, 500 mM, pH 7.2

Dissolve 76 g dibasic sodium phosphate in 1 liter water. Dissolve 35 g monobasic sodium phosphate in 500 ml water and add to dibasic solution until the pH is 7.2. Store up to 1 month at 4°C.

COMMENTARY

Background Information

HPLC quantification

Quantification of the DNA used for the measurement of specific adducts is necessary in order to give a common denominator. While spectrophotometric absorbance is useful as an estimate (*UNIT 3.8*), the best method for determining DNA content in samples that have been hydrolyzed by mild acid is HPLC analysis of the purines (see Basic Protocol 1). In the authors' laboratories, the most common method for the HPLC measurement of guanine (and adenine) is an adaptation of the method for the measurement of methylpurines in alklyated DNA (Lawley, 1976; Beranek et al., 1980).

Many previous papers have reported human DNA adducts based on milligram quantities of DNA, micromole quantities of guanine, or total number of nucleotides. These numbers can be equalized using the following conversion factors: 1 pmol adduct/mg DNA = 0.318 adducts/1 $\times 10^6$ nucleotides and 1 µmol guanine = 1.6 mg human DNA (Walker et al., 2000).

When measuring the amounts of DNA adducts in nucleosides, it is best to use a DNA quantification method that measures nucleosides. The method described in this unit (see Basic Protocol 2) has an advantage over the base measurement in that with this one assay, one can also measure RNA contamination in the same sample (Boucheron et al., 1987).

HPLC quantification of adducts with electrochemical detection

Many insults occur to genomic and mitochondrial DNA due to the action of exogenous or endogenous agents. The types of lesions that result from such interactions include single-strand breaks, AP sites, chromosome aberrations, and DNA adducts. The modification of DNA bases can compromise the integrity of the genetic code leading to mutation, carcinogenesis, or apoptosis. Understanding the relationship between exposure dose, adduct formation, and biological response allows for a more mechanistic approach to risk assessment (La and Swenberg, 1996).

Aerobic metabolism produces a number of reactive oxygen species (ROS) such as H_2O_2 as well as hydroxyl and superoxide radicals. The cell employs a number of defense mechanisms against ROS like superoxide dismutase and glutathione peroxidase; however, the amount of oxidants can overwhelm these anti-oxidants, thereby leading to oxidative stress. The result of such an imbalance leads to protein damage, lipid peroxidation, and DNA adduct formation. Of the oxidized bases, 8-OH-dG is the most studied. While appearing harmless, 8-OH-dG has been shown to cause misreading during DNA replication (Kuchino et al., 1987), but the primary importance of 8-OH-dG is in its use as a biomarker for oxidative stress within the genome.

Alkylation of DNA bases can cause base substitutions, AP sites, or strand breaks. Caused endogenously by S-adenosylmethionine and exogenously by agents that yield carbonium ions (*N*-nitroso compounds); these adducts have been used in studies to monitor the dosimetry of carcinogens (Bianchini and Wild, 1994; van Delft et al., 1997). Because N7-MG is repaired by DNA glycosylases, its measurement can yield information regarding the efficiency of base-excision repair.

Many DNA bases are not electrochemically active while their adducts are (Park et al., 1989). This allows for selective quantification of DNA adducts by HPLC with electrochemical detection (ECD) without the interference of normal bases (see Quantifying DNA Adducts: HPLC with Electrochemical Detection). The use of a multi-channel array detector increases this selectivity when compared to a single-potential detector. Coulometric array systems increase the resolving power by prohibiting a detected compound from interfering with analysis at subsequent electrodes. Compounds that co-elute can be differentiated on the basis of their oxidation potentials. Poor chromatographic resolution cannot be corrected with the use of a single-potential detector. The greater selectivity in array systems also allows for more sensitive detection due to the removal of interfering peaks.

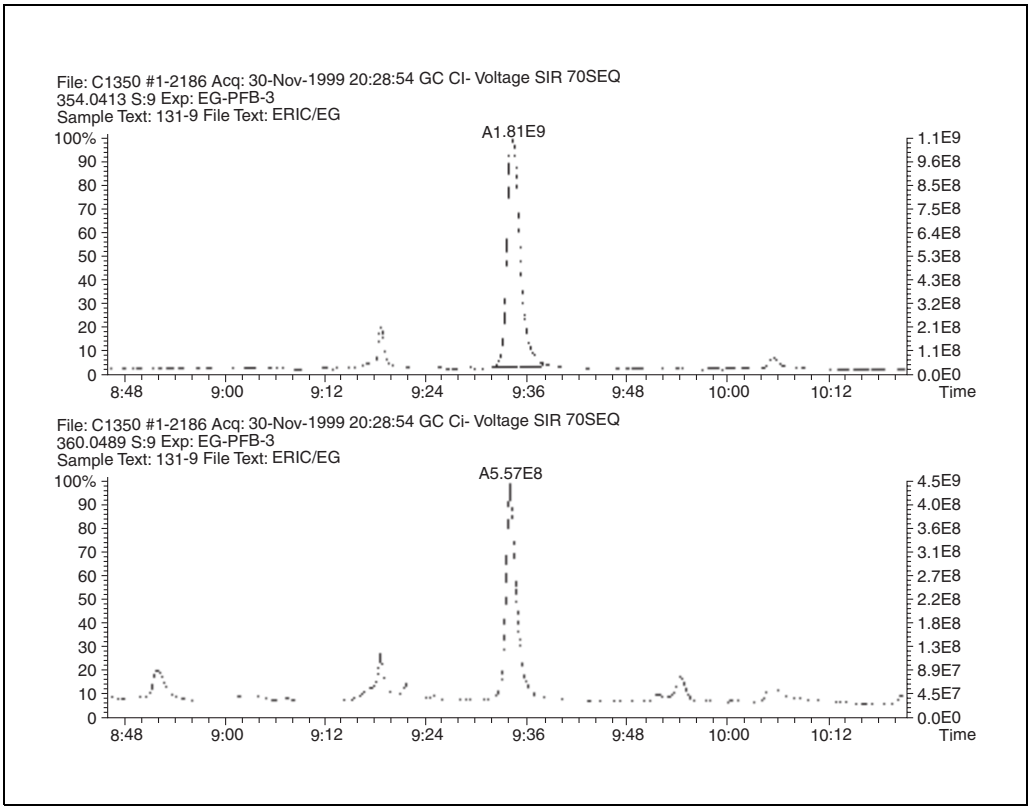

Figure 3.9.1 Detection of di-pentafluorobenzylated N^2,3-εGua (top) in rat liver DNA after exposure to vinyl chloride. The analyte is quantitated by comparison of the peak area to that of the [$^{13}C_4$, $^{15}N_2$]N^2,3-εGua internal standard (bottom).

The methods described can be used to measure other DNA adducts with little or no modification to the described protocols. A small drawback to these methods is that ECD requires total oxidation of the analyte, making sample recovery impossible.

Quantification of N^2,3-ethenoguanine

The DNA adduct N^2,3-ethenoguanine (εGua; see Fig. 3.9.1) is formed from a number of carcinogens, including vinyl chloride (VC; Bartsch et al., 1994). The formation of this adduct occurs from the reaction of guanine with electrophiles that are produced from carcinogens as well as from endogenous sources, presumably from products of lipid peroxidation (Sodum and Chung, 1988, 1989, 1991; Chen and Chung, 1994; Ham et al., 1999, 2000). In the case of VC, the highly reactive electrophile chloroethylene oxide (CEO), which is formed from the metabolic activation of vinyl chloride by cytochrome P450, alkylates DNA and forms a variety of etheno adducts, including εGua (Guengerich, 1994). The major VC-induced adduct, 7-(2′-oxoethyl)guanine, does not induce mutations in vitro (Barbin et al., 1985) and thus is not thought to play a significant role in VC-induced mutagenesis; however, the exocyclic derivatives 1,N^6-ethenoadenine, 3,N^4-ethenocytosine, N^2,3-ethenoguanine, and 1,N^2-ethenoguanine (εAde, εCyt, εGua and 1,N^2-εGua, respectively) have demonstrated miscoding potential in vitro and in vivo (Singer et al., 1987, 1991; Cheng et al., 1991; Mroczkowska and Kusmierek, 1991; Basu et al., 1993; Langouët et al., 1997, 1998). Both in vitro and in vivo studies have shown that εAde caused A to G transversions, εCyt caused C to A transversions and C to T transitions, and εGua caused G to A transitions. The results of these studies were consistent with the mutations observed in tumors from vinyl chloride–exposed humans and rats in two separate studies. In five out of six human liver angiosarcomas associated with vinyl chloride exposure, GC to AT transitions were observed at codon 13 of the c-Ki-*ras*-2 gene, consistent with either εGua or εCyt mutagenic properties (Marion et al., 1991). In another study, tumors from vinyl chloride–exposed rats showed G to A transitions, A to C transversions, and C to T transitions in N-*ras* genes, all of which are consistent with promutagenic properties of etheno adducts (Froment et al., 1994).

Although εGua is formed from VC exposure to a lesser extent than some other adducts, its greater mutagenic potential points to its possible significance in the carcinogenicity of a number of carcinogens. Fedtke et al. (1990) originally reported that εGua appeared to have a very long half-life in hepatic DNA (exceeding 30 days). It is now believed, however, that in this original report the half-life of εGua could not be calculated accurately because baseline levels of endogenous εGua were being measured rather than that of additional εGua after vinyl chloride treatment (Swenberg et al., 2000). The occurrence of DNA adducts from endogenous sources has become increasingly apparent. Most of these adducts have been postulated to occur from the reaction of DNA with products of lipid peroxidation or directly from reactive oxygen species. Chung and colleagues have shown that the related etheno adducts, 1,N^2-ethenoguanine and 1,N^6-ethenoadenine, are formed from the epoxide of the lipid peroxidation product *trans*-4-hydroxynonenal, 2,3-epoxy-4-hydroxynonenal (Sodum and Chung, 1988, 1989, 1991; Chen and Chung, 1994). Recently, the authors have also shown that εGua is formed as a result of the reaction between dGuo and 4-hydroxynonenal or ethyl linoleate under peroxidizing conditions (Ham et al., 2000). Since εGua may be formed from both endogenous and exogenous sources, it will be important to determine its formation from both sources, particularly with carcinogens that may produce εGua by both direct alkylation and by increasing lipid peroxidation. In order to study these relationships and their relevance to carcinogenicity, the authors have developed a sensitive immunoaffinity/gas chromatography/electron capture negative chemical ionization/high-resolution mass spectrometry (IA/GC/EC-NCI/HRMS) assay for the analysis of εGua (see Basic Protocol 6). This method analyzes εGua using enrichment of the adduct by IA chromatography clean up, followed by GC/EC-NCI/HRMS analysis of its pentafluorobenzyl derivative. The utility of both immunoaffinity and mass spectrometry allow for a very specific and sensitive method for this DNA adduct.

Immunoaffinity purification

Immunoaffinity chromatography is the most specific purification technique that has been applied to the routine quantitation of DNA adducts. It relies on the specific binding between an appropriate immunoglobulin and the adduct of interest. It can be used to separate species with very similar chemical and physical properties with high efficiency, even when the adducts are present at parts-per-billion concentrations relative to the parent base.

Protein A is a bacterial molecule with a high affinity for the Fc region of most immunoglobulins. When attached to a solid support, Protein A can be used to purify antibodies from biological matrices including ascites, cell culture supernatant, or serum. Once bound to Protein A, the homobifunctional imidoester cross-linker DMP is used to covalently attach the antibody to the support through amidine linkages (Hermanson, 1996). The coupling procedure is complete when ethanolamine is used to block excess imidoester functional groups (see Support Protocol 2).

^{32}P postlabeling

This assay (see Basic Protocol 8) was a major advance in the study of DNA adducts because it provided the sensitivity of radioassays, without the requirement for specific radiolabeled chemicals. It continues to be among the most sensitive methods for analyzing DNA adducts. Each adduct requires separate method development, as TLC conditions vary for different adducts. Once method development has been completed, up to 16 samples can be analyzed per assay. Analysis takes 2 days to complete, and another day is required to obtain results.

The major limitation of this assay is that it does not provide structural information about DNA adducts. In addition, adducts derived from small molecules are difficult to resolve from unmodified nucleotides and cannot be detected with great sensitivity. This method does provide high sensitivity for larger bulky aromatic compounds. The method also has particular advantage as a screening tool, since prior knowledge of adduct structure is not required. Standards of known structure can be synthesized and used as a comparison to identify DNA adducts.

Adduct enrichment is required to remove unmodified nucleotides because these nucleotides compete for phosphorylation with the modified nucleotides. This increases the amount of radioisotope required for analysis and increases the background, which decreases sensitivity. Different methods are available for enrichment. The described protocol is for the nuclease P1 method of enrichment (Reddy and Randerath, 1986). This method is based on the fact that DNA adducts are generally resistant to dephosphorylation by nuclease P1 and are

available as a substrate for polynucleotide kinase–mediated phosphorylation. By contrast, unmodified nucleotides are dephosphorylated by nuclease P1 and are not available as substrates for labeling. C-8 modified adducts, modified by aromatic amines or nitroaromatic compounds, are known to be sensitive to nuclease P1 digestion and thus would not be good candidates for analysis by this method. Other methods include HPLC enrichment and butanol extraction (Gupta, 1985; Dunn and San, 1988). HPLC enrichment involves separation of DNA adducts prior to ^{32}P-labeling. Butanol enrichment involves extractions using butanol to isolate DNA adducts from normal nucleotides. In addition, HPLC has been used to resolve DNA adducts, which provides greater reproducibility compared to TLC methods (Möller, 1993). Readers are directed to the listed references for experimental details for these methods (see Literature Cited).

Critical Parameters

HPLC quantification

DNA, after extraction (especially from tissue) and rehydration, must be sheared to give a homogenous solution to provide the most accurate pipetting. This will also ensure that the aliquot taken for guanine analysis is representative of the entire sample. The concentration of DNA can be estimated by measuring the absorbance of the solution spectrophotometrically (*UNIT 3.8*). This is only an estimation, however, and an assay (see Basic Protocol 1) must be run in order to relate the value to micromolar quantities of guanine.

Mobile phase must be made up of HPLC-grade methanol and either HPLC-grade water or distilled deionized water. Filtering and degassing is necessary to ensure the solution is free from debris and bubbles that can form when aqueous and organic solutions are mixed together. Bubbles that pass through the UV detector can appear to be peaks. Be sure to have enough mobile phase made to finish all samples and standards. If the mobile phase runs out and must be made again, rerun the standard curve and finish the remaining samples. While small changes in mobile phase rarely affect the samples, it is best to be consistent and have standards and samples run in the same mobile phase.

For guanine quantification, guanine used as the stock solution must be made well in advance of the day of assay. Guanine has limited solubility and must be prepared ahead of time to allow for dissolution. Make the stock ~3 to 5 mM in 0.1 N HCl (~3 mg/10 ml) and incubate in a 37°C environmental shaker until dissolved. Verify concentration of guanine solution by spectrophotometric measurement at 254 nm (ε_{254} = 10,000 $M^{-1}cm^{-1}$). For nucleoside quantification, make the stock solutions of standards ahead of time. Verify stock concentration spectrophotometrically and dilute in water ~1:100. Measure the absorbance of each at their absorbance maxima (λ_{max}: dGuo and rGuo, 252 nm at pH 7.0, ε = 13,700 $M^{-1}cm^{-1}$; dAdo and rAdo, 259 nm at pH 7.0, ε = 15,000 $M^{-1}cm^{-1}$). Use the Beer-Lambert equation: $A = \varepsilon bc$, where A is the absorbance at λ_{max}, b is the path length of the cuvette (typically 1 cm), and c is the concentration of the solution. This can be rearranged to $c = A/\varepsilon b$. Dilute stock solutions, aliquot, and freeze up to 1 year at −20°C.

HPLC quantification with electrochemical detection

When working with DNA-containing adducts, especially those that are heat labile, it is crucial to keep the samples on ice at all times. Care should be taken to avoid artifactual generation of 8-OH-dG when processing samples (Möller et al., 1998). If drying a DNA sample is necessary, do not completely dry the sample and add an anti-oxidant to reduce the generation of 8-OH-dG. All water used should be distilled and deionized. Reagents can be made fresh the day of sample preparation or beforehand. The potential at which the desired analyte shows the greatest response (e.g., peak area, peak height) may vary between ECD systems. To determine the optimum potential for a compound, construct a hydrodynamic voltammogram using a standard (Kissinger, 1977; Park et al., 1989).

Mobile phase should be filtered through a 0.45-µm filter and degassed. In addition to equilibrating the system for 1 hr prior to analysis, the mobile phase should be recirculated through the system overnight. This will oxidize impurities and reduce the background noise. Since samples should be kept cold until analysis, placing all the samples in an autosampler is not recommended, except if an apparatus with a refrigeration unit is available.

Quantification of N^2,3-ethenoguanine

DNA extracted from a variety of tissues, cultured cells, or other in vitro experiments can be used for this assay. Because there is evidence that the adducts may be formed from lipid peroxidation, care should be taken during DNA extraction procedures to minimized any artifac-

tual lipid peroxidation generated during extraction (see *UNIT 2.3*). The DNA should also be free from any RNA. Since the nucleobase, not the nucleoside, is being measured in the immunoaffinity assay, RNA contamination could contribute to the final εGua value making the DNA results artificially high.

Standard and internal standard solutions should be prepared in water and stored in a –80°C freezer and defrosted just prior to use. These standards are very stable and can also be stored at 4°C on a short-term basis. Check the standards for the accuracy of their concentration. As with any analytical method for quantitation, the accuracy of the standards is critical. Equally important for the quantification of this adduct is the quantification of guanine in the hydrolysate. Although the amount of DNA is quantified by UV spectrophotometry, this is only an estimate of the amount of DNA because many interferences can skew these results. Since there is no internal standard to control for the amount of guanine in the sample during work-up, it is vital that care is taken when pipetting DNA, water, internal standard, and HCl. The accuracy of the final volume of the hydrolysis mixture is important for the determination of total guanine in the sample.

The authors have also observed increases in εGua, presumably artifactual, when the pH of the mixture prior to immunoaffinity is basic (i.e., pH >8.0). Care should be taken not to allow the pH to become basic during any step of this procedure.

Derivatization efficiency may be decreased by the presence of water. Additionally, the presence of water may affect the analysis of this adduct by GC/MS. Therefore, all solvents used for derivatization, and toluene used for resuspension prior to GC/MS, should be kept as dry as possible. This can be achieved by using solvents that are relatively fresh and stored in sealed containers with desiccant when not in use. The potassium carbonate should also be kept as dry as possible, especially since it is hygroscopic. To keep the potassium carbonate as dry as possible it should be stored in an oven at 60°C.

Immunoaffinity purification

The most important aspect of developing an immunoaffinity chromatography procedure is selection of a suitable antibody. Unfortunately, this is difficult to predict and must be determined largely by trial and error. First, the antibody must have an appreciable affinity for Protein A so that it can be purified from solution and attached to the solid support. The antibody must demonstrate low affinity for unmodified bases or other potential interferences. The binding of adducts to the antibody must be strong enough to withstand the washing steps but labile enough to be eluted in a convenient solvent. Finally, because the supply of antibody is often limited and the support is expensive, the antibody should be stable enough so that the columns can be reconditioned and used many times.

It is the authors' experience that polyclonal antibodies are generally more compatible with immunoaffinity chromatography than monoclonal antibodies. They have used some polyclonal-based columns for over a year with little reduction in performance. These columns typically recover >95% of standards when new, and carryover between samples has not been observed. Due to their polyclonal nature, some interfering species may be retained by these columns, so they are best suited for use with selective quantitation techniques such as mass spectrometry. Less-specific methods of analysis, such as ^{32}P-postlabeling, may require that monoclonal antibodies be used to obtain samples of even higher purity.

It is critical that the standards or samples be applied in appropriate solutions. The pH of each sample must be near-neutral to allow binding. This is especially important when DNA is hydrolyzed in acid. In addition, the salt concentration of the sample must not be too high. Samples have been successfully neutralized in buffer to final salt concentrations of up to 250 mM.

Dimethylpimelidate (DMP) is moisture-sensitive and should be stored desiccated at 4°C. Allow the container to come to room temperature before opening and prepare the solution immediately before use. All other chemicals and materials are stable for months when refrigerated.

Extremely sensitive methods, such as GC/MS, might detect a low background amount of adduct leeching from the columns. This contamination is not due to carryover, since it is observed both in new and used columns. This release is most significant when the columns are first used, so the initial washing steps are very important. The problem may be exacerbated when using strong solvents for elution. The authors have found that this contamination with N^2,3-ethenoguanine was only detected when samples were treated with acid after immunoaffinity purification (to hydrolyze deoxynucleosides to nucleobases when using

enzymatic DNA digestion). This problem is overcome by using a DNA hydrolysis method that yields nucleobases prior to the immunoaffinity step (i.e., mild acid hydrolysis or neutral thermal hydrolysis). It is important to include appropriate blanks to ensure this does not contribute to the measurement.

Gas chromatography

Extremely high voltage (8000 V) is present when the mass spectrometer is turned on from the instrument console. Ion source access should only be attempted after turning off the instrument (push the Standby button from the console). Various components of GC and MS are at very high temperatures during operation (100° to 300°C). The operators are advised to refer to the respective instrument manuals for operation and safety information.

Liquid chromatography

If it is not done carefully, the desalting step is where most sample losses could occur; therefore, it is important to make sure SPE cartridges are equilibrated with water and samples are loaded by gravity. Particulate material could be present in the SPE eluents. Check the samples visually before injection.

Volatile buffers such as ammonium formate or acetate should be used in LC mobile phase instead of nonvolatile buffers, and the concentration of the buffers used should be kept as low as possible because they do suppress the ionization and cause a decrease in sensitivity.

Although neutral thermal hydrolysis is very specific for releasing N-7 and N-3 alkylated adducts, at least 1% to 2% unmodified Gua and Ade are released as well; therefore, the samples will still contain a high level of purine bases. Most N-7 guanine adducts elute close to unmodified Gua and Ade. To achieve a satisfactory separation between the adduct and unmodified bases, one typically needs to use a highly aqueous mobile phase. With these kinds of mobile phases, polar endcapped reversed-phase columns perform better than the conventional reversed-phase material. The authors have had good experience with Aquasil C-18 columns (Keystone Scientific) for quantification of N7-(2-hydroxyethyl)guanine.

A blank should be run after a high-level sample to ensure no carryover takes place. Most HPLC systems can rinse the needle of the injector both outside and inside after every injection. As a rule of thumb, one should avoid introducing high concentrations of the analyte of interest into the injector.

A quality control sample should be analyzed to determine whether or not the instrument has the required sensitivity and selectivity.

Troubleshooting

HPLC quantification

Table 3.9.6 provides a troubleshooting guide to problems that may be encountered during HPLC quantification of guanine, while Table 3.9.7 provides a guide for quantification of nucleosides.

HPLC quantification with electrochemical detection

Since sample preparation is simple and requires little effort, any problems that arise will most likely be from the HPLC-ECD system. Important things to monitor are the quality of the chromatograms (interfering peaks, shifts in retention time, erratic baseline) and the sensitivity of the electrochemical detector. Routine maintenance and care of the column and HPLC components will ensure accurate and reproducible chromatograms. Running standards prior to sample analysis will provide a good indication of when desired peaks will elute and the degree of response. Keeping track of the response (peak area) of the standards over a period of time will give an indication of any change in the sensitivity of the ECD. Standard degradation must also be considered and concentrations of stock solutions should be checked spectrophotometrically when preparing a series of standards. Standard degradation is retarded when they are stored at −80°C.

Quantification of N^2,3-ethenoguanine

If no peaks are seen in the GC/MS chromatogram, there are four possible problems. First, there may be a problem with the GC/MS. See Basic Protocol 6 for instructions on troubleshooting this problem. Second, the sample may have been lost during solid-phase extraction. Check all solvents and the silica gel to make sure that the correct materials were used and the columns were washed and eluted with the proper solvents. Third, derivatization may not have been efficient. Make sure all solvents are fresh and free of any water contamination. Also make sure that the samples are completely dry before staring the derivatization. If there is a lapse between the time that the samples are dried in the SpeedVac evaporator and the samples are derivatized, the samples may need to be dried again in the evaporator just to ensure the absence of water. Finally, the immunoaf-

Table 3.9.6 Troubleshooting Guide for HPLC Quantification

Problem	Possible cause	Solution
Flocculated material in guanine stock	Undissolved material	Centrifuge to pellet flocculates. Transfer supernatant to a fresh tube and measure A_{254}
Unresolved guanine and adenine peaks	Old column	Replace HPLC column
No peaks detected by UV in HPLC profile	No DNA in sample	Shear DNA and redilute for hydrolysis
	Too little DNA in sample	Use less acid (more concentrated) for hydrolysis
	No injection	Be sure sample is in injector and injector is in the proper position
Off-scale peaks	Saturation of detector	Dilute sample in 0.1N HCl and reinject

Table 3.9.7 Troubleshooting Guide to Quantification of Nucleosides by HPLC

Problem	Possible cause	Solution
Unresolved peaks	Old column	Replace HPLC column
No peaks in HPLC by UV	Not enough DNA	Concentrate DNA sample and reinject
Off-scale peaks	Saturation of detector	Dilute sample and reinject

finity columns may not be retaining the samples. If there is a peak for the internal standard, but not for the analyte, there are two possible problems, either the hydrolysis was not complete or the amount of DNA used was inadequate. Check the guanine concentrations. If guanine is present in amounts that are approximately those predicted for the amount of DNA used, then the hydrolysis was not the problem; use more DNA for analysis. If the guanine concentrations are low, the estimated value of DNA may have been miscalculated or the DNA had some contamination that interfered with its estimation by UV spectrophotometry. Again, use more DNA. If guanine is absent, then the hydrolysis was inadequate. Check the acid used for the hydrolysis for the correct concentration. Also check calculations for the volumes of water and DNA added to make sure the final concentration of acid is 0.1 N HCl.

If the amount of εGua is higher than predicted, there are several possibilities. First, check the concentration of standards, both analyte and internal, for accuracy. Also check the guanine standard and the calculation of guanine in the sample. If the guanine is miscalculated or misquantified, the results will be skewed. As discussed, there may also be artifactual generation of εGua if the samples are allowed to become too basic. Check all solutions and buffers for pH to make sure that it is not allowed to go above 8.0. Also, avoid extremes in pH and temperature after immunoaffinity. There is a contaminant that elutes from the IA columns that is converted to εGua if exposed to acid and heat (e.g., 45 min of 1% formic acid, 60°C).

Immunoaffinity purification

The recovery of standards from immunoaffinity columns should be tested before the first use and periodically afterwards. It is important to test the recovery both with the standard solution alone and with standard spiked into the sample matrix (e.g., DNA hydrolysate). When problems are encountered, it is instructive to determine under which conditions the adduct will or will not elute.

If the standard is found in the load or wash fractions, the column is not retaining the adduct. It is possible that the antibody was not bound because it has a low affinity for Protein A. This is characteristic of the IgG_1 and IgG_3 subclasses of mouse monoclonal antibodies. If this is the case, using Protein G–Sepharose or Protein A/G–Sepharose (Amersham Pharmacia Biotech) may improve binding. It is also possible that the crosslinking step was ineffective. Alternatively, the antibody may have a

relatively weak affinity for the adduct. Minimizing the number and strengths of the washing steps may increase recovery in this case.

If the standard is not found in the load, wash, or elution fractions, it is probably being bound too tightly by the antibody. It may be possible to increase the strength of the elution solvent by making it more organic, acidic, basic, or salty. It is possible that such solvents will degrade or destroy the columns, however, so extremes should be avoided whenever possible.

If recovery is high with standards alone but low when standards are spiked into samples, the antibody may have some affinity for unmodified bases. In this case, it is best to find a more specific antibody since this cross-reactivity will also increase the sample background. Alternatively, a preliminary purification step with disposable solid-phase extraction columns may help to eliminate some of the interference. It is also possible that the sample is present in an incompatible solvent (see Critical Parameters).

Some degradation of column performance over time is expected. If column recovery declines sharply, the antibody may be unstable in the solvents or its bond to the Protein A may be labile. The use of polyclonal instead of monoclonal antibodies may result in more durable columns.

Gas chromatography

GC/HRMS is a hyphenated technique, therefore the loss of the analyte signal can be caused by either GC- or MS-related problems. The first step is to isolate the problem in relation to the respective region of the instrumentation. For example, the loss of signal due to PFK tuning compound bleeding through the reservoir indicates MS problems typically resulting from the ion source due to detuning, dirty ion source, or filament deterioration. MS problems should be fixed first before attempting to fix any GC-related problems. MS problems related to the ion source can be corrected by cleaning the ion source and installing a new filament and a new heater element. GC-related problems originate mostly from a contaminated injector liner and chromatography peak broadening due to column deterioration after many sample injections. Chromatography problems can typically be fixed by cutting the column ~6 in. at the injector side and cleaning the injector liner. If the problems still persist and the sensitivity of the analyte signal from a known standard cannot be restored, the GC column should be replaced.

Instrument instability is a major concern in HRMS because the peak width of the signal is narrower (100 PPM at an RP of 10,000) compared to LRMS. The instability can be caused by several factors including mechanical vibration, electrical noise, and chemical interferences. A typical HRMS-selected ion monitoring (SIM) experiment involves monitoring the analyte ion, the corresponding labeled analog, and a reference peak originating from the calibration compound which is continuously introduced at a constant rate into the ionization chamber during HRMS analysis. While the analyte and internal standard are solely for quantitation, monitoring of the reference peak serves as a check for instrument instability and detuning of the electron capture ion source. The use of lock mass, which can be the same as the check mass, is important in HRMS because the peaks are narrow at high resolving powers. Periodically the SIM control unit may shift the acceleration voltage in order to maximize the intensity of the calibration peak which necessitates the need for the continuous lock onto the reference peak, thus keeping the instrument calibrated for each cycle of mass scanning. When large amounts of interferences are present in the ion source, the SIM control unit can misidentify an interfering peak as the reference peak and shift the accelerating voltage to a different value, causing source detuning and mass miscalibration. During each GC/MS run, any weakness or sudden disappearance of the check mass as measured (5 to 10 V) on the oscilloscope indicates instability problems. It is normal for the check mass to disappear during the first 2 min of each injection due to the solvent front. Injection of a known standard (typically a calibration standard) after every five injections of biological samples is recommended in order to test the stability of the signal.

Liquid chromatography

Table 3.9.8 is a troubleshooting guide to adduct quantification by LC/ESI/IDMS/MS.

^{32}P postlabeling

Most difficulties with the ^{32}P-postlabeling method involve improper chromatography conditions, particularly for smaller-sized DNA adducts (e.g., those derived from single aromatic ring compounds). Problems with DNA hydrolysis and labeling can be detected during analysis of normal nucleotides. For smaller DNA adducts, reducing the concentrations of the mobile phase for TLC development (see

Table 3.9.8 Troubleshooting Guide for LC/ESI/MS/MS

Problem	Possible cause	Solution
Analyte peak not detected, strong IS peak	Levels are below detection limit of the method	Either introduce more of the sample or increase sensitivity (e.g., decrease column i.d., sample preconcentration)
Both IS and AN peaks are lower than expected	Low sample recovery	Perform sample preparation more carefully to improve recovery
	Instrument sensitivity is low	Check the instrument sensitivity by running a quality control sample. If it is low, perform maintenance on the instrument to improve the sensitivity.
Sensitivity goes down after several samples	Samples contain salt or interfering compound that elutes before the analyte	Perform desalting more efficiently. Try increasing the amount of water or buffer used for rinsing in SPE.
		Divert the LC effluent to waste instead of ESI source until shortly before the analyte
		Rinse source parts with methanol or water as necessary

Basic Protocol 8, steps 11 and 12) may be required. These solutions can be diluted to 1:2 with water. If DNA adducts are not detected, other enrichment methods mentioned in the Commentary section should be explored. Initial chromatography using C-18 plates (in place of steps 8 and 9) may be particularly useful for detection of smaller DNA adducts.

Anticipated Results

HPLC quantification

The guanine standard curve should be linear. Sample peak areas should be within the range of the standard curve. The nucleoside standard curves should give linear curves. Sample peak areas should be within the range of the standard curve.

HPLC quantification with electrochemical detection

Results will vary between experiments depending on the agent used for exposure and the sample being exposed (i.e., viable cells or DNA). Samples exposed to a range of concentrations should exhibit a dose-response. Detection limits will vary among ECD systems and if any additional steps (purification) are added to the protocol.

Quantification of N^2,3-ethenoguanine

The results are calculated based on the results of a standard curve run with each experiment. The detection limits of this assay are ~3 to 5 fmol in an entire sample. This gives a good signal for an endogenous sample using 300 to 400 mg DNA, although as little as 200 mg has been used for endogenous samples. A representative GC/ECNCI/HRMS of endogenous εGua from a sample of human colonic DNA is shown in Figure 3.9.1. Table 3.9.9 shows some expected values of εGua in samples from a variety of tissues and cells.

Immunoaffinity purification

With the proper antibody, it is possible to routinely achieve recoveries of nearly 100% while obtaining a highly purified sample. There should be no detectable carryover between experiments. Since the intrinsic properties of antibodies vary greatly, these results may not be achievable in every case.

Liquid chromatography

A detection limit of 10 fmol injected amount of the N7 adducts should be easily achievable. A detection limit in terms of adducts per guanine is dependent on how much DNA is used and how much of the sample is injected. If the clean-up is efficient, an increase in DNA amount should improve the detection limit. Sample recovery should not be <60%. If it is low, it is most probably due to losses during desalting.

Table 3.9.9 εGua Content of Typical Cells

Tissue/cells	εGua (εGua/1 × 10^6 guanine)[a]
F344 rat liver—control	0.046 ± 0.028
Sprague-Dawley rat hepatocytes—control	0.035 ± 0.012
Sprague-Dawley rat brain—control	0.054 ± 0.019
Sprague-Dawley rat hepatocytes—VC exposed[b]	1.1 ± 0.6
B6C3F1 mouse liver—control	0.036 ± 0.010
Human colon—normal	0.16 ± 0.05

[a]Values expressed as mean ± standard deviation.

[b]Rats exposed to 1100 ppm vinyl chloride by inhalation 6 hr/day, 5 day/week for 4 weeks.

^{32}P postlabeling

The ^{32}P-postlabeling assay is best suited for the detection of DNA adducts arising from bulky aromatic compounds. For such DNA adducts, detection of levels as low as 1 adduct per 1 × 10^{10} nucleotides have been reported, although concentrations in the range of 1 per 1 × 10^8 to 1 × 10^9 nucleotides are more typical.

Time Considerations

HPLC quantification

Depending on the number of samples that need to be assayed, the measurement can be done in 1 day. Time must be allocated for shearing the DNA and then its dilution with HCl. As the samples are being hydrolyzed at 70°C for 30 min, the HPLC can be equilibrated and the guanine can be spectrophotometrically measured and diluted.

Because of the time involved in the enzymatic hydrolysis of the nucleoside samples and the time involved with the HPLC, this assay can take 2 days. If possible, use an autosampler and allow the HPLC to run overnight. If this is not possible, at the end of the day, run the HPLC slowly (0.2 ml/min) overnight in 100% mobile phase A. Be sure to reequilibrate the column again for 30 min in the morning at the assay flow rate. Inject one or two standards again on the second morning to verify that conditions have not changed.

HPLC quantification with electrochemical detection

The methods described allow for quick preparation and analysis for DNA adducts. The protocols require not much more than the addition of reagents and incubation periods. The preparation and analysis for the adducts described can be performed in 1 day. The preparation of 8-OH-dG samples will require at least 2 hr for enzymatic digestion while the total time for quantification, 15 min per sample, will depend on the number of samples. Sample preparation for N7-MG analysis is rapid and convenient, requiring <2 hr. The time allotment for quantitation of N7-MG, under 30 min per sample, will depend on the number of samples. Adjusting chromatographic conditions may shorten retention times, however the possibility of introducing interfering peaks becomes a risk (Park and Ames, 1988b).

Quantification of N^2,3-ethenoguanine

One and a half to 2 days are generally necessary for the preparation of samples for mass spectrometry analysis. It takes ~7 to 8 hr to hydrolyze and purify the samples by immunoaffinity (including regeneration of the immunoaffinity columns). Generally, eluent from the immunoaffinity columns can be left in the SpeedVac evaporator overnight (no heat) to dry if there is not enough time to finish this in a workday; otherwise, the samples take 2 to 3 hr to dry. Derivatization and preparation of samples takes an additional 4 to 5 hr. The sample runs on the GC/MS take ~17 min per sample so analysis time will vary.

Immunoaffinity purification

It takes ~6 hr to construct and wash a new set of columns. Approximately 4 hr are required to precondition columns, purify samples, and recondition columns. It is convenient to perform DNA hydrolysis and immunoaffinity pu-

rification in a single day, and allow the eluent to dry overnight.

Liquid chromatography

It takes ~2 days to complete LC/ESI/IDMS/MS: 1 hr for neutral thermal hydrolysis, 2 hr for filtration, 3 hr for desalting, 4 to 5 hr for evaporation to dryness, and 30 to 35 min per sample for LC/MS.

^{32}P postlabeling

It takes two full days to complete the assay. Another day is required for autoradiography and to obtain results.

Literature Cited

Achilli, G., Cellerino, G.P., Gamache, P.H., and Melzi d'Eril, G.V. 1993. Identification and determination of phenolic constituents in natural beverages and plant extracts by means of a coulometric electrode array system. *J. Chromatogr.* 632:111-117.

Ames, B.N. 1983. Dietary carcinogens and anticarcinogens. *Science* 221:1256-1264.

Barbin, A., Laib, R.J., and Bartsch, H. 1985. Lack of miscoding properties of 7-(2-oxoethyl)guanine, the major vinyl chloride-DNA adduct. *Cancer Res.* 45:2440-2444.

Bartsch, H., Barbin, A., Marion, M.J., Nair, J., and Guichard, Y. 1994. Formation, detection, and role in carcinogenesis of ethenobases in DNA. *Drug Metab. Rev.* 26:349-371.

Basu, A.K., Wood, M.L., Niedernhofer, L.J., Ramos, L.A., and Essigmann, J.M. 1993. Mutagenic and genotoxic effects of three vinyl chloride-induced DNA lesions: 1,N^6-ethenoadenine, 3,N^4-ethenocytosine, and 4-amino-5-(imidazol-2-yl)imidazole. *Biochemistry* 32:12793-12801.

Beranek, D.T., Weis, C.C., and Swenson, D.H. 1980. A comprehensive quantitative analysis of methylated and ethylated DNA using high pressure liquid chromatography. *Carcinogenesis* 1:595-606.

Bianchini, F. and Wild, C.P. 1994. 7-Methyldeoxyguanosine as a marker of exposure to environmental methylating agents. *Toxicol. Lett.* 72:175-184.

Boucheron, J.A., Richardson, F.C., Morgan, P.H., and Swenberg, J.A. 1987. Molecular dosimetry of O^4-ethyldeoxythymidine in rats continuously exposed to diethylnitrosamine. *Cancer Res.* 47:1577-1581.

Calléja, F., Jansen, J.G., Vrieling, H., Laval, F., and van Zeeland, A.A. 1999. Modulation of the toxic and mutagenic effects induced by methyl methanesulfonate in Chinese hamster ovary cells by overexpression of the rat N-alkylpurine-DNA glycosylase. *Mutat. Res.* 425:185-194.

Chen, H.J. and Chung, F.L. 1994. Formation of etheno adducts in reactions of enals via autoxidation. *Chem. Res. Toxicol.* 7:857-860.

Cheng, K.C., Preston, B.D., Cahill, D.S., Dosanjh, M.K., Singer, B., and Loeb, L.A. 1991. The vinyl chloride DNA derivative N^2,3-ethenoguanine produces G->A transitions in *Escherichia coli*. *Proc. Natl. Acad. Sci. U.S.A.* 88:9974-9978.

Chetsanga, C.J., Lozon, M., Makaroff, C., and Savage, L. 1981. Purification and characterization of *Escherichia coli* formamidopyrimidine-DNA glycosylase that excises damaged 7-methylguanine from deoxyribonucleic acid. *Biochemistry* 20:5201-5207.

de Groot, A.J.L., Jansen, J.G., van Valkenburg, C.F.M., and van Zeeland, A.A. 1994. Molecular dosimetry of 7-alkyl- and O^6-alkylguanine in DNA by electrochemical detection. *Mutat. Res.* 307:61-66.

Dunn, B.P. and San R.H.C. 1988. HPLC enrichment of hydrophobic DNA-carcinogen adducts for enhanced sensitivity of ^{32}P-postlabeling analysis. *Carcinogenesis* 9:1055-1060.

Fasman, G.D. (ed.) 1976. Handbook of Biochemistry and Molecular Biology, Third Edition, pp. 270-273. CRC Press, Cleveland.

Fedtke, N., Boucheron, J.A., Walker, V.E., and Swenberg, J.A. 1990. Vinyl chloride-induced DNA adducts. II: Formation and persistence of 7-(2′-oxoethyl)guanine and N^2,3-ethenoguanine in rat tissue DNA. *Carcinogenesis* 11:1287-1292.

Friesen, M.D., Garren, L., Prevost, V., and Shuker, D.E. 1991. Isolation of urinary 3-methyladenine using immunoaffinity columns prior to determination by low-resolution gas chromatography-mass spectrometry. *Chem. Res. Toxicol.* 4:102-106.

Froment, O., Boivin, S., Barbin, A., Bancel, B., Trepo, C., and Marion, M.J. 1994. Mutagenesis of *ras* proto-oncogenes in rat liver tumors induced by vinyl chloride. *Cancer Res.* 54:5340-5345.

Garland, W.A. and Powell, M.L. 1981. Quantitative selected ion monitoring (QSIM) of drugs and/or drug metabolites in biological matrices. *J. Chromatogr. Sci.* 19:392-434.

Guengerich, F.P. 1994. Mechanisms of formation of DNA adducts from ethylene dihalides, vinyl halides, and arylamines. *Drug Metab. Rev.* 26:47-66.

Gupta, R.C. 1985. Enhanced sensitivity of ^{32}P-postlabeling analysis of aromatic carcinogen-DNA adducts. *Cancer Res.* 5:5656-5662.

Gupta, R.C. and Earley, K. 1988. ^{32}P-adduct assay: Comparative recoveries of structurally diverse DNA adducts in the various enhancement procedures. *Carcinogenesis* 9:1687-1693.

Halliwell, B. and Gutheridge, J. 1989. Free radicals, aging, and disease. *In* Free Radicals in Biology and Medicine (B. Halliwell and J. Gutheridge, eds.) pp. 416-508. Claredon Press, Oxford.

Ham, A.J.L., Ranasinghe, A., Koc, H., and Swenberg, J.A. 2000. 4-Hydroxy-2-nonenal and ethyl linoleate form N^2,3-ethenoguanined under per-

oxidizing conditions. *Chem. Res. Toxicol.* 13:1243-1250.

Ham, A.J.L., Ranasinghe, A., Morinello, E.J., Nakamura, J., Upton, P.B., Johnson, F., and Swenberg, J.A. 1999. Immunoaffinity/gas chromatography/high resolution mass spectrometry method for the detection of N^2,3-ethenoguanine. *Chem. Res. Toxicol.* 12:1240-1246.

Harman, D. 1981. The aging process. *Proc. Natl. Acad. Sci. U.S.A.* 78:7124-7128.

Hermanson, G.T. (ed.) 1996. Homobifunctional cross-linkers. *In* Bioconjugate Techniques. pp. 187-227. Academic Press, San Diego.

Kasai, H. 1997. Analysis of a form of oxidative DNA damage, 8-hydroxy-2′-deoxyguanosine, as a marker of cellular oxidative stress during carcinogenesis. *Mutat. Res.* 387:147-163.

Kissinger, P. 1977. Amperometric and coulometric detectors for high-performance liquid chromatography. *Anal. Chem.* 49:447A-456A.

Koc, H., Tretyakova, N.Y., Walker, V., Henderson, R., Swenberg, J.A. 1999. Molecular dosimetry of N-7 guanine adduct formation in mice and rats exposed to 1,3-butadiene. *Chem. Res. Toxicol.* 12:566-574.

Krien, P.M., Margou, V., and Kermici, M. 1992. Electrochemical determination of femtomole amounts of free reduced and oxidized glutathione. *J. Chromatog.* 576:255-261.

Kuchino, Y., Mori, F., Kasai, H., Inoue, H., Iwai, S., Miura, K., Ohtsuka, E., and Nishimura, S. 1987. Misreading of DNA templates containing 8-hydroxyguanosine at the modified base and at adjacent residues. *Nature* 327:77-79.

La, D.K. and Swenberg, J.A. 1996. DNA adducts: Biological markers of exposure and potential applications to risk assessment. *Mutat. Res.* 365:129-146.

Langouët, S., Müller, M., and Guengerich, F.P. 1997. Misincorporation of dNTPs opposite 1,N^2-ethenoguanine and 5,6,7,9-tetrahydro-7-hydroxy-9-oxoimidazo[1,2-a]purine in oligonucleotides by *Escherichia coli* polymerases I exo- and II exo-, T7 polymerase exo-, human immunodeficiency virus-1 reverse transcriptase, and rat polymerase b. *Biochemistry* 36:6069-6079.

Langouët, S., Mican, A.N., Müller, M., Fink, S.P., Marnett, L.J., Muhle, S.A., and Guengerich, F.P. 1998. Misincorporation of nucleotides opposite five-membered exocyclic ring guanine derivatives by *Escherichia coli* polymerases in vitro and in vivo: 1,N^2-ethenoguanine, 5,6,7,9-tetrahydro-9-oxoimidazo[1, 2-*a*]purine, and 5,6,7,9-tetrahydro-7-hydroxy-9-oxoimidazo[1, 2-*a*]polymerases in vitro and in vivo: 1,N^2-ethenoguanine, 5,6,7,9-tetrahydro-9-oxoimidazo[1, 2-*a*]purine, and 5,6,7,9-tetrahydro-7-hydroxy-9-oxoimidazo[1, 2-*a*]. *Biochemistry* 37:5184-5193.

Lawley, P.D. 1976. Methylation of DNA by carcinogens: Some applications of chemical analytical methods. *IARC Sci. Publ.* 12:181-210.

Leung, P.Y. and Tsao, C.S. 1992. Preparation of an optimum mobile phase for the simultaneous determination of neurochemicals in mouse brain tissues by high-performance liquid chromatography with electrochemical detection. *J. Chromatog.* 576:245-254.

Marion, M.J., Froment, O., and Trepo, C. 1991. Activation of ki-*ras* gene by point mutation in human liver angiosarcoma associated with vinyl chloride exposure. *Mol. Carcinogen.* 4:450-454.

Möller, L. 1993. Optimization of an HPLC method for analyses of ^{32}P-postlabeled DNA adducts. *Carcinogenesis* 14:1343-1348.

Möller, L., Hofer, T., and Zeisig, M. 1998. Methodological considerations and factors affecting 8-hydroxy-2′-deoxyguanosine analysis. *Free Rad. Res.* 29:511-524.

Mroczkowska, M.M. and Kusmierek, J.T. 1991. Miscoding potential of N^2,3-ethenoguanine studied in an *Escherichia coli* DNA-dependent RNA polymerase *in vitro* system and possible role of this adduct in vinyl chloride-induced mutagenesis. *Mutagenesis* 6:385-390.

Nakamura, J., La, D.K., and Swenberg, J.A. 2000. 5′-Nicked apurinic/apyrimidinic sites are resistant to β-elimination by β-polymerase and are persistent in human cultured cells after oxidative stress. *J. Biol. Chem.* 275:5323-5328.

Park, J.-W. and Ames, B.N. 1988a. 7-Methylguanine adducts in DNA are normally present at high levels and increase on aging: Analysis by HPLC with electrochemical detection. *Proc. Natl. Acad. Sci. U.S.A.*. 85:7467-7470.

Park, J.-W. and Ames, B.N. 1988b. Correction. *Proc. Natl. Acad. Sci. U.S.A.*. 85:9508.

Park, J.-W., Cundy, K., and Ames, B.N. 1989. Detection of DNA adducts by high-performance liquid chromatography with electrochemical detection. *Carcinogenesis* 10:827-832.

Ranasinghe, A., Scheller, N.A., Wu, K.Y., Upton, P.B., and Swenberg, J.A. 1998. Application of gas chromatography/electron capture negative chemical ionization high-resolution mass spectrometry for analysis of DNA and protein adducts. *Chem. Res. Toxicol.* 11:520-526.

Randerath, K. and Randerath, E. 1994. ^{32}P-Postlabeling methods for DNA adduct detection: Overview and critical evaluation. *Drug Metab. Rev.* 26:67-85.

Randerath, K., Reddy, M.V., and Gupta, R.C. 1981. ^{32}P-Postlabeling test for DNA damage. *Proc. Natl. Acad. Sci. U.S.A.* 78:6126-6129.

Reddy, M.V. and Randerath, K. 1986. Nuclease P1-mediated enhancement of sensitivity of ^{32}P-postlabeling test for structurally diverse DNA adducts. *Carcinogenesis* 7:1543-1551.

Richter, C., Park, J.-W., and Ames, B.N. 1988. Normal oxidative damage to mitochondrial and nuclear DNA is extensive. *Proc. Natl. Acad. Sci. U.S.A.* 85:6465-6467.

Schneider, C., Newman, R.A., Sutherland, D.R., Asser, U., and Greaves, M.F. 1982. A one-step purification of membrane proteins using a high

efficiency immunomatrix. *J. Biol. Chem.* 257:10766-10769.

Singer, B., Spengler, S.J., Chavez, F., and Kusmierek, J.T. 1987. The vinyl chloride-derived nucleoside, N^2,3-ethenoguanosine, is a highly efficient mutagen in transcription. *Carcinogenesis* 8:745-747.

Singer, B., Kusmierek, J.T., Folkman, W., Chavez, F., and Dosanjh, M.K. 1991. Evidence for the mutagenic potential of the vinyl chloride-induced adduct, N^2,3-etheno-deoxyguanosine, using a site-directed kinetic assay. *Carcinogenesis* 12:745-747.

Sodum, R.S. and Chung, F.L. 1988. 1,N^2-ethenodeoxyguanosine as a potential marker for DNA adduct formation by *trans*-4-hydroxy-2-nonenal. *Cancer Res.* 48:320-323.

Sodum, R.S. and Chung, F.L. 1989. Structural characterization of adducts formed in the reaction of 2,3-epoxy-4-hydroxynonanal with deoxyguanosine. *Chem. Res. Toxicol.* 2:23-28.

Sodum, R.S. and Chung, F.L. 1991. Stereoselective formation of in vitro nucleic acid adducts by 2,3-epoxy-4-hydroxynonanal. *Cancer Res.* 51:137-143.

Swenberg, J.A., Bogdanffy, M.S., Hani, A., Holt, S., Kim, A., Morinello, E.J., Ranasinghe, A., Scheller, N., and Upton, P.B. 2000. Formation and repair of DNA adducts in vinyl chloride- and vinyl fluoride-induced carcinogenesis. *In* Exocyclic DNA Adducts in Mutagenesis and Carcinogenesis. IARC Scientific Publications No. 150 (B. Singer and H. Bartsch, eds.) pp. 29-43. International Agency for Research on Cancer, Lyons, France.

Swenberg, J.A., Richardson, F.C., Boucheron, J.A., and Dyroff, M.C. 1985. Relationships between DNA adduct formation and carcinogenesis. *Environ. Health Perspec.* 62:177-183.

Tretyakova, N.Y., Chiang, S.Y., Walker, V.E., and Swenberg, J.A. 1998. Quantitative analysis of 1,3-butadiene-induced DNA adducts in vivo and in vitro using liquid chromatography electrospray ionization tandem mass spectrometry. *J. Mass Spectrom.* 33:363-376.

van Delft, J.H.M., Steenwinkel, M.-J.S.T., de Groot, A.J.L., van Zeeland, A.A., Eberle-Adamkiewicz, G., Rajewsky, M.F., Thomale, J., and Baan, R.A. 1997. Determination of N7- and O^6-methylguanine in rat liver DNA and oral exposure to hydrazine by use of immunochemical and electrochemical detection methods. *Fund. Appl. Toxicol.* 35:131-137.

Walker V.E., Wu, K.-Y., Upton, P.B., Ranasinghe, A., Scheller, N., Cho,M.-H., Vergnes, J.S., Skopek, T.R., and Swenberg, J.A. 2000. Biomarkers of exposure and effect as indicators of potential carcinogenic risk arising from *in vivo* metabolism of ethylene to ethylene oxide. *Carcinogenesis* 21:1661-1669.

Contributed by James A. Swenberg, Amy-Joan L. Ham, Hasan Koc, David K. La, Eric J. Morinello, Brian F. Pachkowski, Asoka Ranasinghe, and Patricia B. Upton
University of North Carolina
Chapel Hill, North Carolina

CHAPTER 4
Techniques for Analysis of Chemical Transformation

INTRODUCTION

The mode of toxic action may be thought of as a cascade of events that starts with exposure and ends with the expression of a toxic endpoint. Events occurring during this sequence may increase the extent to which the toxic endpoint is expressed or may mitigate or even prevent toxicity. Metabolism, or biotransformation, of xenobiotics has long been known to play a key role in this process.

In general, xenobiotics enter the body because they are lipophilic. Biotransformation, which reduces lipophilicity, has been regarded as a detoxication process. However, biotransformation can lead to increased toxicity through the generation of reactive intermediates. In general, biotransformation of xenobiotics consists of two phases. In phase I, a polar group is introduced into the molecule, and in phase II this polar group serves as a center for conjugation with an endogenous metabolite. Reactions in either phase may be catalyzed by one or more of a broad array of enzymes, often referred to as xenobiotic metabolizing enzymes or XMEs. These enzymes have specific cellular locations (endoplasmic reticulum "microsomal," mitochondrial, or cytoplasmic), are usually present in multiple forms (isoforms), and have overlapping substrate specificities. XMEs are under genetic control and can be up or down regulated by both exogenous and endogenous factors. Inter-individual variation is also affected by the existence of genetic polymorphisms. Polymorphisms in coding regions of the genes for XMEs can affect expression, while polymorphisms in the coding region can cause the expression of proteins with different properties, including substrate specificity.

The anticipated format for this chapter follows; Table 4.0.1 provides indications as to which units are already included, which units are in progress, and which have yet to be initiated.

UNIT 4.1 presents a variety of classical procedures used to prepare subcellular fractions of liver and to determine the concentration of cytochrome P450 in the microsomal and mitochondrial fractions. It includes both enzymatic analysis and immunological techniques that are useful in characterizing the isoforms of cytochrome P450 present in microsomes. *UNIT 4.2* describes protocols for purifying the cytochrome P450 isoforms 2E1 and 1A2 from an *Escherichia coli* overexpression system. These isoforms are of interest to toxicologists because of their role in the bioactivation of a number of toxicants and carcinogens.

UNIT 4.3 presents a number of protocols that can be used to assess microsomal UDP-glucuronosyl transferase activity. The thin-layer chromatography procedure, based on the use of [^{14}C]UDPGA, is suitable for screening a large number of substrates simultaneously. Other procedures are described that are useful for separating glucuronides of particular classes of substrates.

UNIT 4.4 provides a general overview of high-performance liquid chromatography (HPLC) coupled to mass spectrometry (MS) as a powerful analytic tool in separation and structural characterization of metabolites of xenobiotics. This analytical system combines the

Contributed by Ernest Hodgson
Current Protocols in Toxicology (2005) 4.0.1-4.0.4

Table 4.0.1 Format of Chapter 4 in *Current Protocols in Toxicology*

Topic	Unit status
PHASE I	
Microsomal	
Cytochrome b_5/cytochrome b_5 reductase	*UNIT 4.16*
Cytochrome P450	*UNITS 4.1 & 4.2*[a]
CYP3A4	*UNIT 4.13*
FMO	*UNIT 4.9*
Cyclooxygenases	Not yet covered
Nonmicrosomal	
Alcohol dehydrogenase	In progress
Aldehyde dehydrogenase	In progress
Amine oxidases	Not yet covered
Monoamine oxidases	Not yet covered
Diamine oxidases	Not yet covered
Reductases	
Nitro reduction (probably P450)	Not yet covered
Azo reduction (probably P450)	Not yet covered
Carbonyl reductases	*UNIT 4.17*
Sulfoxide reductases	Not yet covered
Hydrolases	
Esterase/amidase enzymes	*UNITS 4.7 & 4.10* (one additional unit in progress)
Epoxide hydrolases	Not yet covered
PHASE II	
Glucuronosyl transferases	*UNIT 4.3*
Glucosyltransferases	Not yet covered
Sulfotransferases	*UNIT 4.5*
Methyltransferases	
N-Methylases	Not yet covered
O-Methylases	Not yet covered
S-Methylases	Not yet covered
Biomethylation of elements	Not yet covered
Glutathione S-transferases	Not yet covered
Mercapturic acid formation	Not yet covered
Cysteine conjugate β-lyase	Not yet covered
Acylation reactions	
Acetylases	Not yet covered
N-acetyltransferase	*UNITS 4.6 & 4.15*
N,*O*-acyltransferases	Not yet covered
Amino acid conjugation	*UNIT 4.11*
Deacetylation	Not yet covered
Phosphate conjugation	Not yet covered
Enzymes and subcellular preparations	
Induction of biotransformation enzymes	*UNIT 4.8*
Proximal tubule cells	*UNIT 4.14*
Other topics	
Detection of metabolites	*UNIT 4.4*

[a]Future units involving cytochrome P450 will focus on diagnostic and/or important substrates and inhibitors for human isoforms that metabolize xenobiotics (e.g., 1A1, 1A2, 2A6, 2B6, 2C8, 2C9, 2C19, 2D6, 2E1, 3A4).

separation power of HPLC with the sensitivity and structural characterization power of MS. The author provides information on selection and optimization of the HPLC-MS interface, discussion on the various scan modes, and a variety of examples of metabolites that have been characterized by HPLC-MS and HPLC-MS/MS.

UNIT 4.5 describes two methods for measuring aryl and alcohol sulfotransferase activity, an enzyme activity of considerable importance in both detoxication and activation of a number of xenobiotics. The first protocol is for a colorimetric method that depends upon the chloroform extraction of a paired ion formed between methylene blue and an organic sulfuric acid ester; the absorbance of the paired ion is measured at 651 nm. The second protocol is more flexible since it measures, by HPLC, adenosine 3′,5′-diphosphate (PAP), a product formed from 3′-phosphoadenosine 5′-phosphosulfate (PAPS) that is common to all sulfotransferase reactions.

UNIT 4.6 describes two methods for the measurement of the activity of arylamine *N*-acetyltransferase (NAT). This important phase II enzyme catalyzes the acetylation of aromatic amines, heterocyclic amines, and hydrazines. It may serve, depending upon the substrate and the position acetylated, as an enzyme of either detoxication or activation. The first protocol utilizes a measurement of the acetylated product, generally by HPLC, formed in the presence of a low concentration of coenzyme A maintained by a recycling system. This protocol is particularly useful for determination of kinetic constants. The Bratton-Marshall Assay measures the disappearance of an arylamine substrate.

Carboxylesterases (EC 3.1.1.1) are members of a multigene family with broad distribution in mammalian tissues, including those of humans. They hydrolyze an extensive number of exogenous and endogenous esters and amides, their importance in toxicology arising from the fact that their exogenous substrates include prodrugs, environmental contaminants (including pesticides), and carcinogens of various origins. These hydrolyses are, in the case of xenobiotics, usually detoxication reactions but, less commonly, may be activation reactions. *UNIT 4.7* describes methods for assessing carboxylesterase activity: first, a photometric method useful as a screening method; second, a highly sensitive fluorometric method; and third, an HPLC method also useful as a screening method.

The aryl hydrocarbon receptor (AhR) signal transduction pathway is of critical importance in several aspects of the mechanisms of toxic action, the mode of action of TCDD and related dioxins, and the induction of certain CYP isoforms. Several protein elements are involved in the binding of exogenous ligands followed by translocation into the nucleus, dissociation of several of these elements, and interaction of the receptor-ligand complex with DNA, thus affecting gene expression. *UNIT 4.8* is a comprehensive approach to measuring the functionality of this pathway, the importance of the unit being enhanced by the fact that the methods described measure the pathway at different points, thus providing information on how variation in different steps can affect overall function of the pathway. Basic Protocol 1 and Alternate Protocol 1 provide two different methods for measuring receptor-ligand binding. Basic Protocol 2 and Alternate Protocol 2 describe gel retardation assays for AhR-DNA binding. Basic Protocol 3 describes immunoblotting of two components, AhR and Arnt. Basic Protocol 4 is a RT-PCR method to examine mRNA for these same two components as well as that for CYP1A1 and CYP1B1 while Basic Protocol 5 utilizes yet another method, northern blotting, for measuring human CYP1A1 mRNA. Thus a broad range of the methods of contemporary molecular biology is brought to bear on a pathway with important implications for mechanistic toxicology.

UNIT 4.9 details methods for the estimation of the activity of the flavin-containing monooxygenases (FMOs). Because of the common localization of FMOs and xenobiotic-metabolizing cytochrome P450s in the endoplasmic reticulum, common cofactor requirements, and the fact that cytochrome P450 isoforms and FMOs may share common

substrates, the activity of the FMOs is often overlooked or underestimated. This problem may be important in that both P450s and FMOs are polymorphic in humans and that even with a common substrate the products may vary. *UNIT 4.9* provides procedures for measurement of FMO activity and also for the separate measurement of FMO and cytochrome P450 activities when both are present in the same preparation.

UNIT 4.10 provides methods for the identification and measurement of two types of esterase, carboxylic ester hydrolase and phosphoric triester hydrolase. The esterases, in toto, comprise an enormous group of enzymes that, because of its size and complexity, is not well understood. It is clear, however, that esterases are of critical importance in the metabolism of toxicants, including clinical drugs and agricultural chemicals, and this unit advances our ability to deal with the complexities of this important group of enzymes.

UNIT 4.11 addresses two aspects of an important pathway for the metabolism of toxicants not yet addressed in this chapter, the amino acid conjugation pathway. The enzymes addressed are carboxylic CoA ligase and acyl-CoA *N*-acetyltransferase. The coverage of the available methodology is particularly complete, and includes two basic protocols and seven alternate protocols. These protocols include radiometric and spectrophotometric methods based on different characteristics of the reactions.

UNIT 4.12 is a comprehensive method for the determination of paraoxonase I (PON1) status with information for genotyping specific polymorphic sites. Paraoxonase has been known for some time as an enzyme important in the metabolism of organophosphorus chemicals and is now known to have an important physiological function, the metabolism of oxidized lipids.

UNIT 4.13 is the first unit devoted to a single, important human CYP isoform. CYP 3A4 is quantitatively the most important CYP isoform in the human liver; it is involved in the oxidation of many drugs and xenobiotics as well as steroid hormones such as testosterone.

UNIT 4.14 is important for those who are interested in extrahepatic metabolism of xenobiotics, particularly in the function of the kidney in this regard. This unit describes several methods for the determination of toxicant biotransformations, both in subcellular fractions and in intact proximal tubule cells.

UNIT 4.15 brings this chapter into an area of increasing importance, the detection of polymorphisms in the various isoforms of xenobiotic metabolizing enzymes. This area is already critical in drug development and safety, and it is becoming of equal importance in human health risk analysis in such areas as chemical carcinogenesis. *UNIT 4.15* addresses the detection of polymorphisms in *N*-acetyltransferase-1 (NAT-1) and *N*-acetyltransferase-2 (NAT-2).

It has been known for some time that cytochrome b_5 is an absolute requirement for the cytochrome P450-dependent oxidation of some xenobiotics and is stimulatory for others. Furthermore cytochrome b_5 reductase is involved in the associated electron transfer. These effects are both substrate and P450 isoform dependent. *UNIT 4.16* is a comprehensive set of protocols to measure many aspects of the cytochrome b_5/cytochrome b_5 reductase system.

UNIT 4.17 describes comprehensive methods for the identification and measurement of different types of carbonyl reductases that are known to reduce xenobiotics, particularly in human liver.

Ernest Hodgson

Measurement of Cytochrome P-450

The majority of the forms of cytochrome P-450 in the body are located in the endoplasmic reticulum, and methods for their detection and quantification must allow for the influence of the membranes in the assays. For example, in spectrophotometric analyses, the light-scattering properties of membrane vesicles and fragments must be compensated for. The cytochromes P-450 are hemoproteins, and hemoproteins generally have extinction coefficients for their Soret peaks of ~100 $mM^{-1}cm^{-1}$. This means that one can readily detect concentrations as low as 0.1 nmol/ml spectrophotometrically, depending on the sensitivity of the spectrophotometer used.

Spectrophotometric measurements, however, will provide only quantitative information on the total pool of cytochrome P-450, and not details of its composition. In liver microsomes, for example, more than a dozen forms have been isolated; generally one or two make up the major amount, and others are present in amounts <10%. The identity of these forms can be determined by use of specific antibodies or enzyme assays with the ability to oxidize certain substrates known to be more or less specifically metabolized by one form of cytochrome P-450. All the methods of measurement have some drawbacks. For example, measurement of total cytochrome P-450 content in microsomes provides no information about the nature of the forms present. Depending on the exposure of the animals to different xenobiotics, either deliberately or serendipitously, the composition of the microsomal pool of cytochrome P-450 may vary greatly. The use of specific antibodies provides information on specific forms of cytochrome P-450 but generally will also detect denatured protein and apoprotein of the measured form, although such proteins are nonfunctional and do not form the P-450 spectrum. Substrate metabolism also has its drawbacks. Although some forms of cytochrome P-450 have high specificity toward certain substrates, almost all have very broad, overlapping substrate-metabolizing capabilities. Although one form may be capable of turning over a substrate at a rate 100 times greater than other forms, in microsomes where it is present at 1% of the total cytochrome P-450 content, it might be responsible for only half of the total observed activity. With these caveats in mind, the various methods of cytochrome P-450 measurement can be considered. For spectrophotometric analyses, the tissue preparation is merely suspended in the buffer, and the samples are subjected to difference spectroscopy in the presence or absence of carbon monoxide (see Basic Protocol 1). Although this provides a clear indication of the presence of cytochrome P-450 and allows its quantification, it is not nearly as sensitive as immunochemical analysis or substrate metabolism. The spectrophotometric analysis can be performed on microsomes, liver homogenates (see Alternate Protocol 1), or mitochondria (see Alternate Protocol 2).

Immunochemical methods (see Basic Protocol 2) take advantage of the specificity of antibodies and allow the identification of specific forms of cytochrome P-450 with a sensitivity that allows measurement in amounts as low as picomoles of cytochrome P-450. Such measurements are several orders of magnitude smaller than those possible by spectrophotometric analysis. The procedure involves immobilizing the cytochrome P-450, or antigen, on nitrocellulose and reacting it with its antibody (primary antibody). Then an alkaline phosphatase–coupled antibody (secondary antibody) to the primary antibody is bound and exposed to a substrate that forms a colored precipitate. The density of the precipitate gives a semiquantitative indication of the amount of antigen present.

Substrate metabolism, too, can give a very sensitive indication of the presence of forms of cytochrome P-450 (see Basic Protocol 3). For such measurements, small amounts of microsomes or cytochrome P-450 are added to an assay medium containing the substrate.

Contributed by John B. Schenkman and Ingela Jansson

Current Protocols in Toxicology (1999) 4.1.1-4.1.14

The cofactor NADPH is added to start the reaction; after a designated period of time, the reaction is terminated and the amount of product formed or substrate consumed is determined. Some of the highest sensitivities are obtained when fluorescent products are produced. Activities as low as picomoles per minute can be measured; but, as discussed above, precise quantification of the amounts of individual forms of cytochrome P-450 in tissues is not possible by substrate metabolism, owing to the broad, overlapping substrate specificities of the cytochromes P-450. Subcellular fractions (see Support Protocols 1 and 2) can be analyzed for the presence of cytochromes P-450 using any of these assays.

BASIC PROTOCOL 1

SPECTROPHOTOMETRIC MEASUREMENT OF CYTOCHROME P-450

This procedure takes advantage of the ability of difference spectroscopy to cancel background absorption and light scattering of membranous vesicles and fragments for the amplification and measurement of pigments at low concentrations. Hemoproteins with a sixth coordination position on the heme iron have the ability to complex with small molecules, and this is reflected in the absorption spectrum of the complex. Cytochrome b_5, which lacks a free coordination position, will not complex with carbon monoxide and, therefore, can be eliminated from interference with measurements of cytochrome P-450, which does have a reactive sixth coordination position. Because these two are the only hemoproteins present in the microsomal fraction, the assays are considerably simpler than, for example, measurements of cytochrome P-450 content in homogenates or mitochondria. In mitochondria, the presence of cytochrome oxidase, which possesses an available sixth coordination position as well as a large number of other pigments, makes spectrophotometric measurements more complicated.

Materials

Microsomal preparation containing 20 mg/ml protein (see Support Protocols 1 and 2)
0.05 M Tris·Cl, pH 7.4 (*APPENDIX 2A*)
Oxygen-free carbon monoxide in tank with two-stage valve
Dithionite: crystalline sodium hydrosulfite ($Na_2S_2O_4$)
4% (w/v) NADH in 1% $KHCO_3$ (prepared fresh daily; optional)

Spectrophotometric cuvettes with 1-cm light path for spectral analyses between 400 and 500 nm
Dual-beam UV/VIS spectrophotometer *or* spectrophotometer capable of optically or electronically producing a difference spectrum
Plastic microspatulas for stirring cuvette contents

CAUTION: When wet, dithionite will release hydrogen. It is also hygroscopic and decomposes with time. For convenience, when opening the jar for the first time, separate contents into a number of smaller vials, such as scintillation vials, 1 g into each. Tape covers with plastic electrical tape to ensure sealed jars stay dry.

1. Dilute 0.3 ml of microsomal preparation in 5.7 ml of 0.05 M Tris·Cl, pH 7.4 (to 1 mg protein/ml). Vortex gently to ensure good dispersion. Divide suspension between two spectrophotometer cuvettes.

   When liver is the source tissue, the microsomal preparation should be free of glycogen, because glycogen makes the suspension quite turbid, limiting the amount of microsomes that can be used.

2. On the spectrophotometer, record a baseline between 400 and 500 nm of equal light absorption with the suspension.

3. Slowly bubble carbon monoxide (CO) into the sample cuvette for 30 sec to allow saturation of the buffer with the gas.

   CAUTION: *This should be done in a chemical fume hood.*

   A two-stage valve is necessary to allow the very slow rate of bubbling of CO into the cuvette without foaming or displacing the microsomal suspension from the cuvette.

   The concentration of CO in the buffer will rise to 1 mM in 30 sec of slow bubbling. It is preferable to gas with CO before reduction, rather than the reverse, because bubbling will also expose the surface to oxygen. If dithionite is present, it will reduce the cytochrome P-450, which will react with the oxygen and form oxygen radicals, resulting in destruction of a portion of the cytochrome P-450. If appreciable amounts of adsorbed hemoglobin are present, a very large carbon monoxy hemoglobin peak will be seen at 420 nm.

4. Add a few crystals of dithionite to both cuvettes with a plastic microspatula, and stir gently. Wait ~1 min to ensure complete reduction, and record the spectrum. Record another spectrum after 1 to 2 min to ensure that no further change has occurred.

   If hemoglobin is adsorbed to the microsomes, the addition of dithionite to the reference cuvette will result in a large absorption peak at 445 nm in the reference cuvette. This will diminish values obtained for carbon monoxy cytochrome P-450 in the sample cuvette. To prevent this problem, when hemoglobin is present in the microsomes, bubble CO in the reference cuvette to convert it to carbon monoxy hemoglobin and do not add dithionite to that cuvette. Alternatively, add 5 μl of 4% NADH per milliliter to the reference cuvette instead of dithionite (Matsubara et al., 1982), and immediately record the difference spectrum. The NADH will reduce and cancel the absorbance of the cytochrome b_5 and will influence the measurement of the cytochrome P-450 only minimally.

   Glass spatulas may scratch the cuvette, so using plastic is advisable.

5. Calculate the concentration of cytochrome P-450 using the absorption difference between 450 and 500 nm and the equation described by Beer's law:

   $$A = \varepsilon Cl$$

   where A is the absorbance, ε is the extinction coefficient, C is the concentration, and l is the length of the light path

   Using this equation, it is possible to calculate the absorption of 0.3 nmol of P-450 in 1 ml (0.0003 mM). This is about the amount in 1 mg rat kidney microsomes suspended in 1 ml. Using cuvettes of 1-cm light path and a value for the extinction coefficient for cytochrome P-450 of 91 $mM^{-1}cm^{-1}$ (Omura and Sato, 1964), the absorbance value would be 0.027, well within the range of measurement of most spectrophotometers. If the absorbance difference of the cytochrome P-450 is known, the concentration can be calculated.

6. Determine the amount of cytochrome P-450 per milligram of microsomal protein from the concentration of cytochrome P-450 in the cuvette and the concentration of microsomal protein.

   For example, if the absorbance peak at 450 nm relative to the baseline at 500 nm is 0.12 A units, then

   $A = \varepsilon Cl$; $0.12 = 91\ mM^{-1}cm^{-1} \times C \times 1\ cm$

   $0.12 \div (91\ mM^{-1}cm^{-1} \times 1\ cm) = C$

   $C = 1.3 \times 10^{-3}$ mM cytochrome P-450, or 1.3 μM cytochrome P-450

   If a 1 mg/ml suspension of microsomes is used, then the preparation will contain 1.3 nmol of cytochrome P-450 per mg of microsomes.

ALTERNATE PROTOCOL 1

SPECTROMETRIC MEASUREMENT OF CYTOCHROME P-450 IN LIVER HOMOGENATES

The liver, with its well-developed endoplasmic reticulum, contains the highest levels of cytochrome P-450 of any of the various tissues studied. The fairly high content of cytochrome P-450 in the endoplasmic reticulum makes it possible to detect cytochrome P-450 in liver tissue by spectrophotometry. If the source of the tissue has been exposed to compounds that induce one or another form of the hemoprotein, it becomes relatively easy to monitor the cytochrome P-450. The endoplasmic reticulum cytochrome P-450 content in rat liver is more than three times higher than the content of mitochondrial cytochrome a_3 (Cinti and Schenkman, 1972). It is possible to measure this in tissue slices using specially constructed cuvettes; these are unnecessary, however, because it is easier and faster to make such measurements in the whole liver homogenate just as described for microsomes (see Basic Protocol 1). It is, however, necessary to obviate the effect of spectral overlap by mitochondrial cytochrome a_3—which in the presence of CO has an absorption peak at 420 nm, and when reduced in the absence of CO or O_2 has a peak at 445 nm. If a difference spectrum is recorded, as described in Basic Protocol 1, cytochrome oxidase in the sample cuvette will have a 420-nm peak that minimally overlaps the 450-nm cytochrome P-450 peak. In the reference cuvette, however, the dithionite-reduced cytochrome oxidase absorption peak will subtract from that of the cytochrome P-450 peak in the sample cuvette and give artificially low values. To overcome the spectral overlap, it is necessary to shift the absorption peak in the reference cuvette to a region in which it does not influence that of cytochrome P-450. This may be done by generating a cyanide complex of cytochrome oxidase (Matsubara et al., 1982) or by reducing only the mitochondrial hemoproteins in the reference cuvette by the addition of succinate in the presence of CO. All the pigments in the sample cuvette are reduced by dithionite, and the absorbance of the cytochrome oxidase complexed with CO in both cuvettes cancels.

Additional Materials *(also see Basic Protocol 1)*

Liver tissue
0.9% NaCl (*APPENDIX 2A*)
Buffered sucrose: 0.25 M sucrose/0.05 M Tris·Cl, pH 7.4 (see *APPENDIX 2A* for Tris·Cl recipe)
0.6 M sodium ascorbate (optional)
0.3 M sodium succinate in distilled water (optional)
0.6 M sodium cyanide in distilled water (optional)
Potter-Elvehjem glass homogenizer with motor-driven Teflon pestle

CAUTION: Before discarding sodium cyanide, add a few milliliters of alkali. HCN can form if the pH drops.

1. Gently perfuse the liver with 0.9% NaCl to remove blood until the liver is a pale tan.

   Perfusion is necessary because hemoglobin will absorb strongly and interfere with spectrophotometric measurements. If the animals have been treated with a cytochrome P-450–inducing agent, such as phenobarbital, the liver may be dark red to almost reddish brown after perfusion.

2. Homogenize 10 g of liver in 90 ml buffered sucrose in a Potter-Elvehjem glass homogenizer with Teflon pestle.

3. Dilute 1 ml homogenate with 9 ml of 50 mM Tris·Cl, pH 7.4. Bubble the suspension with CO for 30 sec in a fume hood. Add 3 ml gassed suspension to each of two cuvettes in the spectrophotometer.

4. Allow the cuvettes to stand 2 to 3 min to allow reduction of the mitochondrial pigment before recording a baseline of equal light absorption between 400 and 500 nm.

The mitochondrial pigments are reduced by endogenous substrates, and the reduced cytochrome oxidase–CO complex in each cuvette will cancel. Similarly, CO complexes of hemoglobin in each cuvette will cancel. If an appreciable amount of methemoglobin is present, it may cause a problem when the sample cuvette is reduced with dithionite. In that case, the addition of 15 µl of 0.6 M ascorbate (1 mM final concentration) will reduce the methemoglobin in the reference cuvette and solve the problem.

5. Add a few grains of dithionite to the sample cuvette with a plastic microspatula, and record the spectrum of the carbon monoxy cytochrome P-450.

   Another way to obtain clean carbon monoxy cytochrome P-450 spectra in homogenates without interference from hemoglobin, methemoglobin, or cytochrome oxidase is to add 5 µl of 0.6 M sodium cyanide (1 mM final concentration) and 5 µl sodium succinate (0.5 mM final concentration) to the reference cuvette (Matsubara et al., 1982). This causes reduction of the mitochondrial pigments, and the cyanide forms a complex with methemoglobin that does not overlap with the cytochrome P-450 spectrum.

6. Quantify the cytochrome P-450 (see Basic Protocol 1, steps 5 and 6).

SPECTROMETRIC MEASUREMENT OF CYTOCHROME P-450 IN MITOCHONDRIA

ALTERNATE PROTOCOL 2

Mitochondria of the adrenal gland, a steroid-synthesizing organelle, are especially high in cytochrome P-450. Measurements in bovine adrenal mitochondria have indicated levels as high as 0.6 nmol/mg protein (Cammer and Estabrook, 1967). Levels in mitochondria of other tissue, such as brain (Walther et al., 1986), are considerably lower and more difficult to measure. Procedures used must overcome interference by the mitochondrial electron transport pigments, especially cytochrome oxidase. This is easily accomplished by blocking the mitochondrial electron transport chain with cyanide.

Additional Materials *(also see Basic Protocol 1)*

Mitochondrial preparation containing 10 mg/ml protein (see Support Protocol 1, step 6)
Buffered sucrose: 0.25 M sucrose/0.05 M Tris·Cl, pH 7.4 (see *APPENDIX 2A* for Tris·Cl recipe)
0.6 M sodium cyanide in distilled water

CAUTION: Before discarding sodium cyanide, add a few milliters of alkali. HCN can form if the pH drops.

1. Dilute 1.2 ml washed mitochondria with 4.8 ml buffered sucrose (to 2 mg protein/ml). Add 10 µl of 0.6 M sodium cyanide (1 mM final concentration).
2. Gently bubble CO into the suspension for 30 sec and divide it into two cuvettes of 1 cm light path for difference spectroscopy.

   If hemoglobin is present, it will complex CO in the reference cuvette and in the sample cuvette, and the absorbances will cancel.

3. Record a baseline of equal light absorption between the cuvettes, and then add a few grains of sodium dithionite to the sample cuvette with a plastic microspatula; stir gently.
4. Allow 1 to 3 min for complete reduction of the cytochrome P-450, and record the dithionite-reduced CO difference spectrum.

   The presence of cyanide in the reference cuvette will result in reduction of the mitochondrial pigments by endogenous substrates and will prevent reducing equivalent transfer to the cytochrome P-450. If any methemoglobin is present, it will complex with the cyanide and the cyanomethemoglobin absorption peak of the reference cuvette will not interfere with the carbon monoxy cytochrome P-450 spectrum.

5. Quantify the cytochrome P-450 (see Basic Protocol 1, steps 5 and 6).

IMMUNOLOGICAL MEASUREMENT OF CYTOCHROME P-450

Cytochromes P-450 can be detected by immunoblotting, after SDS-PAGE (*APPENDIX 3*) and electroblotting (*UNIT 2.3*). Bound antibodies are detected using alkaline phosphatase–conjugated secondary antibodies.

A number of investigators will generously provide small amounts of their cytochrome P-450 and antibodies on request. Some commercial enterprises also sell forms of cytochrome P-450 and antibodies to individual forms of cytochrome P-450 (Gentest, Oxford Biomedical Research, Amersham Life Science). One can also obtain samples of human tissues, characterized with respect to cytochrome P-450 concentration and selected forms of cytochrome P-450 (International Institute for the Advancement of Medicine).

Materials

Samples for analysis
Individual forms of cytochrome P-450 as positive controls
Ponceau S solution (Sigma; dilute the solution—obtained as 2% Ponceau S in 30% TCA/30% sulfosalicylic acid—10-fold with distilled water for use)
Blocking buffer: 2.5% (w/v) BSA in PBS (with 0.1% ovalbumin, if chicken antibodies are used; *APPENDIX 2A* for PBS)
Primary antibodies: antibodies to individual forms of cytochrome P-450
Secondary antibodies: alkaline phosphatase conjugated IgG antibodies (e.g., Sigma)
Transfer buffer: 25 mM Tris base in 192 mM glycine
PBS (*APPENDIX 2A*)
5-Bromo-4-chloro-3-indolyl phosphate/nitroblue tetrazolium (BCIP/NBT) phosphatase substrate reagent (Kirkegaard & Perry; sold ready for use)
Molecular weight standards (e.g., Sigma, Amersham, Pharmacia, Biotech; 10 to 100 kDa, premixed)

Additional reagents and equipment for SDS-PAGE gel (*APPENDIX 3*) and electroblotting (*UNIT 2.3*)

Immunologically quantify individual forms of cytochrome P-450

1. Run samples (10 to 25 µg microsomes) containing cytochrome P-450 on SDS-PAGE gel (*APPENDIX 3*). To quantify the amount of a single form of the hemoprotein, interrupt electrophoresis when the bromphenol blue tracking dye has moved halfway down the lanes, and add incrementally increasing amounts (0 to 10 pmol) of that form of cytochrome P-450 in sample buffer to the individual tracks of the gel. Continue electrophoresis until the original tracking dye reaches within 1 cm of the bottom of the gel.

   For example, on a ten-track gel, assuming tracks 1 and 10 contain molecular weight standards, start additions from track 2 and add increasing amounts up to track 9.

2. Electroblot the gel onto nitrocellulose membrane (*UNIT 2.3*).
3. Rinse off the nitrocellulose membrane with transfer buffer and place in a plastic container. Add Ponceau S solution to just cover the membrane, and shake the container gently to stain all protein bands.
4. Rinse membrane with several changes of distilled water, and mark bands for the standards with a waterproof marking pen to indicate positions of the molecular-weight-marker proteins. Remove red dye by rinsing with distilled water until all red color is removed.

   Even if no protein bands are detected by Ponceau S staining, immunodetection may reveal proteins.

5. Place nitrocellulose membrane in a container with sufficient blocking buffer to cover. Shake gently for 1 hr at room temperature.

   The albumin binds to nonspecific protein-binding sites, blocking these sites so antibodies do not bind to them. This reduces background staining with the immunodetecting reagents.

Immunodetect cytochrome P-450

6. Decant blocking buffer from nitrocellulose membranes, and add primary antibody at a concentration of 1 μg IgG/ml in the same blocking buffer. Shake gently for 2 hr at room temperature.

   The antibody should be tested against the pure protein to which it has been raised to ensure that the concentration of antibody is sufficient to develop the immunoreaction color rapidly. If not, a higher concentration should be used. For some antibodies, particularly monoclonal and monospecific polyclonal antibodies, concentrations as high as 10 μg IgG/ml are sometimes needed.

7. Rinse the membrane three times by shaking with fresh blocking buffer 5 min each time.

8. Decant the last rinse, and cover the membrane with alkaline phosphatase–conjugated antibody to the species of antibodies used, diluted according to the manufacturer's specification. Shake gently 1 hr at room temperature.

   If the primary antibody to the cytochrome P-50 was raised in rabbit, then use anti–rabbit IgG–conjugated alkaline phosphatase. If the anti–cytochrome P-450 antibodies were raised in chickens, then use anti–chicken IgG–conjugated alkaline phosphatase.

9. Decant the secondary antibody from the membrane, and gently rinse nitrocellulose membrane twice 5 min with the blocking buffer, then once in PBS.

10. Develop the reaction by just covering nitrocellulose membrane with BCIP/NBT. Allow to develop 5 to 20 min, until sharp bands of intense purple color appear.

    A number of methods are available for the immunodetection, such as the use of horseradish peroxidase–conjugated second antibody and 4-chloro-1-napthol as the color-developing reagent on addition of hydrogen peroxide. The BCIP/NBT procedure is recommended because of its ease, convenience, and reproducibility. Longer development periods result in high background (pink) color levels that make visualization of low levels of protein difficult. It is better to use more primary antibody and secondary antibody in cases when low levels of protein antigen are expected.

    The BCIP/NBT solution is available as a ready-to-use reagent in the kit supplied by Kirkegaard & Perry.

11. Stop the reaction by decanting the reagent and rinsing the membrane several times with cold distilled water.

    Do not let the membranes sit too long in the reagent without rinsing, or rinse inadequately, or the background color will begin to rise, as noted.

12. Dry the nitrocellulose membrane by placing between filter papers. Place a weight on top to keep the membrane flat until dry.

13. Cover the dry nitrocellulose sheet with plastic wrap (e.g., Saran Wrap) for protection.

14. If desired, measure the density of color developed using a densitometer or by comparison with pure protein standards added to the tracks during electrophoresis for quantification.

    Match the color development of reactive bands in the immunoblot with those of the added pure proteins, which have only partially migrated and are located higher up in the tracks, to determine the amount of that form of cytochrome P-450 in the electrophoresed tissue. Individual forms of cytochrome P-450 in 10 μg of liver microsomal protein and 1 μg of pure cytochrome P-450 are readily detected by this procedure.

BASIC PROTOCOL 3

ENZYMATIC ANALYSES OF CYTOCHROME P-450 FORMS

The basic method for analysis of cytochrome P-450 forms in tissue or microsomal fraction takes advantage of an activity toward one or another substrate that is very much higher with one form of cytochrome P-450 than with other forms. This is not an absolutely accurate way of determining the presence or quantifying a specific form of cytochrome P-450 in microsomes or tissues, because the presence of a larger amount of a form with a much lower activity could still catalyze a considerable rate of metabolism of the test substrate. Nevertheless, laboratories do measure in vitro metabolism of substrates, such as 7-ethoxyresorufin O-deethylation and the 3-demethylation of caffeine as an indication of the activity of CYP1A2, the 7-hydroxylation of coumarin as an indicator of CYP2A6, the *p*-hydroxylation of aniline as an indication of CYP2E1, and the 6β-hydroxylation of testosterone as an indication of CYP3A. A general method is provided here for the assay of cytochrome P-450 enzyme activities in subcellular fractions of tissues. Various substrates may be assayed by their addition at concentrations ranging from 5 μM to 5 mM, depending on the substrate. For substrates that undergo demethylation reactions, a simple colorimetric assay may be used, based on the formation and quantification of the formaldehyde produced (Schenkman et al., 1967). Another colorimetric assay is available for the oxidation of aniline to *p*-aminophenol (Schenkman et al., 1967). Similarly, a fluorometric assay may be used for fluorescent products of 7-ethoxyresorufin O-deethylase activity (Burke et al., 1977). A very large number of drugs and chemicals are metabolized by cytochrome P-450 forms and can be quantified by gas chromatographic or HPLC analyses of metabolites formed, using the same basic assay procedure for production of metabolites—e.g., 6β-hydroxytestosterone—or consumption of substrate. Specific details are provided for measuring formaldehyde production during enzymatic N-dealkylation.

Materials

0.1 M Tris·Cl, pH 7.4 (*APPENDIX 2A*)
0.15 M $MgCl_2$
Substrates for specific forms of cytochrome P-450 (e.g., 10 mM benzphetamine·HCl)
0.15 mM glucose-6-phosphate
Glucose-6-phosphate dehydrogenase
Microsomal suspension containing 6 mg/ml protein (see Support Protocols 1 and 2)
10 mg/ml NADPH in 1% $KHCO_3$
12.5% trichloroacetic acid (TCA)
Nash reagent (see recipe)
2 mM HCHO
Water bath, 58°C

1. For each substrate to be tested, prepare the following assay medium in a 25-ml Erlenmeyer flask (3 ml total):

   1.5 ml 0.1 M Tris·Cl, pH 7.4
   0.1 ml 0.15 M $MgCl_2$
   0.3 ml substrate in distilled H_2O (e.g., 10 mM benzphetamine·HCl)
   1 U glucose-6-phosphate dehydrogenase
   0.1 ml 0.15 mM glucose-6-phosphate
   0.5 ml distilled H_2O
   0.5 ml diluted microsomal suspension (1 mg/ml final).

   An alternative to glucose-6-phosphate dehydrogenase is isocitric dehydrogenase (1 U) and 0.1 ml of 0.24 mM isocitrate. These are added to keep the NADPH in the reduced state, because the NADP formed during the monooxygenase reaction is inhibitory.

2. Place the flasks in a 37°C water bath and shake at a rate sufficient to keep the surface swirling for aeration. Wait 2 min to allow temperature equilibration.

3. Start the reaction by adding 0.1 ml of 10 mg/ml NADPH.

   The reaction is linear for at least 10 min with most substrates, and for some may be linear for up to 30 min.

4. Remove 0.4-ml aliquots at different times, and add to test tubes containing 0.1 ml of 12.5% TCA.

   CAUTION: *TCA is a very corrosive acid. Rinse promptly if any spills occur.*

   Depending on what enzyme activity will be assayed, the reaction may be stopped at different time points by removing aliquots and combining with TCA, or by extraction with organic solvent. For example, aliquots could be removed at 0.0, 0.5, 1.0, 2.0, 5.0, and 10.0 min.

   If a time course is run, the initial rate may determined. The initial rate with a substrate is often determined with microsomes from animals pretreated with different inducing agents, such as phenobarbital, and compared with initial rates obtained with microsomes of the untreated animal, because such action selectively elevates one or more forms of P-450.

5. Centrifuge tubes to precipitate the protein into a tight pellet, and add 0.4 ml of clear supernatant to 0.4 ml Nash reagent. Place tubes in a 58°C water bath for 8 min, then cool to room temperature.

6. Also prepare formaldehyde standards containing 0, 4, 8, 16, and 30 µl of 2 mM HCHO in 0.4 ml assay medium (step 1). Add 0.1 ml of 12.5% TCA and 0.5 ml Nash reagent. Heat at 58°C and cool, as in step 5.

7. Read absorbance of all standards and samples at 420 nm (yellow color) and use the values for standards to construct a standard plot of absorbance versus cytochrome P-450 concentration. Determine cytochrome P-450 concentrations of samples by comparison of their absorbance values to the standard curve.

   The formaldehyde concentration range indicated will produce an absorbance range of 0.05 to 0.5. Rat liver microsomal metabolism of substrates like benzphetamine, which are N-demethylated, will produce an amount of formaldehyde in this range within 10 min.

SUBFRACTIONATION OF DIFFERENT TISSUES FOR ANALYSIS OF CYTOCHROME P-450 CONTENT

SUPPORT PROTOCOL 1

Current methods are all modifications of the procedure for fractionation of liver by Schneider (1948). Similar methods are used for brain tissues (Walther et al., 1986), skin of newborn mice and rats (Mukhtar and Bickers, 1981), term placenta (Juchau and Smuckler, 1973), and lung tissue (Hook et al., 1972), the latter two starting with 1:3 and 1:4 homogenates, respectively. A major difference among these tissues is large amounts of contaminating hemoglobin. Alternative methods are suggested for the skin of older animals (e.g., rats; Moloney et al., 1982).

Materials

Tissue to be fractionated
0.9% NaCl (*APPENDIX 2A*), ice cold
0.25 M sucrose/10 mM Tris·Cl, pH 7.4 (*APPENDIX 2A* for Tris·Cl)
1.15% KCl/10 mM Tris·Cl, pH 7.4 (optional; see *APPENDIX 2A* for Tris·Cl recipe), ice cold
0.15 M KCl

Potter-Elvehjem glass homogenizer with motor-driven Teflon pestle (optional)
Liquid nitrogen (optional)

NOTE: Carry out all steps at 0° to 4°C.

1a. *Liver:* Remove liver from animal, then chill and carefully perfuse with ice-cold 0.9% NaCl.

1b. *Kidney:* Perfuse kidney in situ to remove blood, then remove from animal. Pierce the capsules, and squeeze the kidneys out. Split the organs, and scrape out the medullas and discarded before homogenizing the cortex.

1c. *Bovine adrenal glands:* Remove adrenals from animal. Split the organ and scrape away the medullas.

1d. *Skin of older animals:* Excise the skin, chill in ice-cold 1.15% KCl/10 mM Tris·Cl, pH 7.4, and remove the adipose and muscle layers.

2. Prepare a 1:10 homogenate in 0.25 M sucrose/10 mM Tris·Cl, pH 7.4: mince and homogenize the tissue in a Potter-Elvehjem glass homogenizer.

   The skin of older animals is too tough to homogenize. Freeze it in liquid nitrogen, grind to a fine powder, and then homogenize.

   The 10% homogenate allows for good fractionation of subcellular material without providing excessively large volumes. The tissue is easily homogenized in a glass homogenizer with a motor-driven Teflon pestle (e.g., Potter-Elvehjem) in two or three passes. Do not over-homogenize, as that can break mitochondria and decrease the efficiency of fractionation. Similarly, blade-driven blenders can fragment mitochondria. The liquid nitrogen freezing procedure is based on Moloney et al. (1982) and is very useful for subfractionating skin tissue.

3. Centrifuge the homogenate 10 min at 600 × *g* (measured at the bottom of the tube), 4°C, in a refrigerated preparative centrifuge to sediment the unbroken cells, nuclei, and cell debris.

   A layer of white lipid will float to the top of the liquid. This should be carefully removed. If yield is important, the pellet may be gently stirred in 0.2 vol sucrose/Tris·Cl, homogenized, and centrifuged again for 10 min at 600 × g. The supernatant should then be recombined with the prior supernatant fluid. This can increase the yield of microsomes by as much as 30% and will recover larger mitochondria pulled down with the debris.

4. Carefully pour the supernatant and washings into centrifuge tubes. Sediment the mitochondria from the supernatant by centrifuging 15 min at 6500 × *g*, 4°C.

   The mitochondrial pellet is dark brown in the center to beige or light tan in toward the periphery. A slight pink peripheral color is the result of lightly packed microsomes. If yield of microsomes is important, the mitochondrial fraction may be gently stirred, resuspended in 0.1 vol sucrose/Tris·Cl, and centrifuged again 10 min at 6500 × g, and the resulting supernatant added to the postmitochondrial supernatant.

5. *Optional:* If mitochondria are to be used, gently resuspend the pellets from the 6500 × *g* centrifugation and wash in half of the original volume in sucrose/Tris·Cl. Centrifuge 5 min at 15,000 × *g*, 4°C, to wash them. Repeat the wash one more time, and finally resuspend the mitochondria in the sucrose/Tris·Cl to 10 mg protein/ml. Keep on ice until use.

6. Centrifuge supernatant (from step 4) 10 min at 12,000 × *g*, 4°C, to sediment light mitochondria. Carefully decant the supernatant from the centrifuge tubes into a beaker on ice to prevent carryover of traces of mitochondria that may be lightly packed at the bottom.

   If it is important to have microsomes free of traces of mitochondria, add an additional centrifugation for 10 min at 18,000 × g. This will pellet any remaining light mitochondria, but will also sediment larger fragments of rough endoplasmic reticulum. To minimize loss of microsomes, if the brown to beige mitochondrial pellet has a significant overlaying of pink, carefully decant the supernatant. Add 5 ml sucrose/Tris·Cl to the tube, and gently swirl to recover the pink layer from the more densely packed mitochondria. Add the liquid to the supernatant fluid, and continue to the next step.

7. Centrifuge the supernatant 1 hr at 100,000 × *g* (measured at the bottom of the tube), 4°C, in a refrigerated ultracentrifuge.

   The microsomes will sediment as a pink pellet.

8. Decant the supernatant from the pellets to remove all the liquid. Add ~5 ml of 0.15 M KCl to tube.

9. Remove the microsomal pellet into the homogenizing tube with additional 0.15 M KCl to restore the volume and homogenize the pellet. Centrifuge the suspension 30 min at 100,000 × *g* to sediment the microsomal pellet.

   This step washes away traces of hemoglobin that may have been adsorbed to the microsomes. Some laboratories also buffer the KCl with 50 mM Tris·Cl, pH 7.4 (Matsubara et al., 1982). Under the pink pellet is a small translucent unpigmented pellet of glycogen. Some investigators starve the animals for 24 hr before sacrifice to remove this pellet, because glycogen will make microsomes much more turbid and spectroscopic measurements more difficult. Starvation, however, also influences the population of cytochrome P-450 in the microsomes (Favreau et al., 1987) and is best avoided. The next step makes starvation unnecessary.

10. Decant supernatant from pellets to remove all liquid. Add ~5 ml buffered sucrose to tube, and give tube a vigorous shake.

    This will cause the microsomal pellet to float free of the more tightly packed pellet of glycogen.

11. Add microsomal pellet to a chilled homogenizing vessel, and suspend in buffered sucrose to a convenient protein concentration (generally 20 mg/ml) for use (*APPENDIX 3*).

    Keep at 4°C until used, for up to 5 hr, or freeze to ≤20°C (not in frost-free freezer).

RAPID PREPARATION OF MICROSOMES

SUPPORT PROTOCOL 2

This protocol is an alternative method for preparation of microsomes, developed by Schenkman and Cinti (1978).

Additional Materials *(also see Support Protocol 1)*

80 mM $CaCl_2$

1. Homogenize tissue and prepare through 12,000 × *g* centrifugation as for subfractionation procedure (see Support Protocol 1, steps 1 to 6).

2. Determine the volume of the supernatant from the 6500 × *g* centrifugation, and add sufficient volume of 80 mM $CaCl_2$ to give a final concentration of 8 mM.

3. Allow the suspension to stand on ice for 15 min, then centrifuge 15 min at 25,000 × *g*.

   The microsomes will be a reddish opalescent pellet over a clear translucent pellet of glycogen (in fed animals).

4. Decant the supernatant fluid from the microsomal pellets, and carefully add ~5 ml of 0.15 M KCl to the tubes. Give each tube an individual, vigorous, swirling shake to float the microsomal pellet off of the glycogen pellet.

   For spectroscopy, it is important that the microsomes be free of glycogen.

5. Decant the microsomal pellets into the homogenizer and homogenize in 0.15 M KCl to a volume equivalent to the prior centrifuge tube volume.

   This procedure serves two purposes. The KCl wash removes almost all of the $CaCl_2$ and the remaining traces of hemoglobin that might be adsorbed to the microsomes.

6. Centrifuge the microsomal pellet 20 min at 25,000 × *g*.
7. Decant the supernatant. Add microsomal pellet to a chilled homogenizing vessel and suspend in buffered sucrose to 20 mg/ml for use.

Keep at 4°C until used, for up to 5 hr, or freeze to ≤20°C (not in frost-free freezer).

REAGENTS AND SOLUTIONS

Use Milli-Q-purified water or equivalent for all recipes and protocol steps. For common stock solutions, see ***APPENDIX 2A****; for suppliers, see* ***SUPPLIERS APPENDIX****.*

Nash reagent

Dissolve 150 g ammonium acetate in 900 ml distilled water and add ~3 ml glacial acetic acid to pH 6.0. Add 2 ml of colorless acetylacetone (if not colorless, redistill it), and dilute to 1 liter. Store up to 3 months at 4°C in a dark bottle.

COMMENTARY

Background Information

A very large number of forms of cytochrome P-450 exist in nature. Over 450 forms are currently on record, based on gene identification (*http://drnelson.utmem.edu/*). The various forms of cytochrome P-450 found in eukaryotic cells, from yeast to mammalian tissues, are membrane bound. In the rat >30 different forms have been identified, and estimates suggest perhaps a similar number exist in human tissues. Although spectrophotometrically these forms look alike, they differ in primary structure and catalytic activities toward different chemical substrates. The different forms of cytochrome P-450 strongly affect the physiologic, pharmacologic, and toxicologic influences of xenobiotics in the body. In recognition of this, many studies have been conducted and will continue to be carried out on the effect of the cytochrome P-450 enzymes on chemicals that enter the body.

Because cytochrome P-450 forms are hemoproteins, they have a strong absorption peak in the Soret region of the UV/VIS spectrum. Furthermore, when reduced and complexed with CO, they have an unusual strong absorption peak at 450 nm, which makes an ideal parameter for identifying and quantifying the hemoprotein. Because a large number of cytochrome P-450 forms exist in the different tissues (at least a dozen forms in liver microsomes alone) and because all have the same broad absorption peak at ~450 nm, it is not possible to discriminate among the forms and determine which form is present based on the 450-nm peak. Specific antibodies to one or another form of cytochrome P-450 in a tissue can be used for immunoquantification of that form; however, because antibodies will react with the apoproteins of the cytochrome P-450 forms, this procedure gives no indication of how much functionally active protein is present. Immunoquantification also gives no indication of the amount of other forms of cytochrome P-450 or of the total amount of cytochrome P-450 present in the tissue.

A third manner of measuring cytochrome P-450 is by enzyme activity, the measurement of the ability of the protein to metabolize a substrate. Although much has been written about the use of specific substrates of some forms of cytochrome P-450, in fact the cytochrome P-450 forms have a broad, overlapping ability to oxidize the different known substrates. One form may have a 10-fold or greater specific activity toward a substrate than does another form; but unless one knows precisely the amount of the other form present and its specific activity toward that substrate, it is not possible to determine from activity how much of a particular form of cytochrome P-450 is present in a tissue. Even antibody inhibition of substrate metabolism is not a precise measure of the amount of an enzyme present but only an indication of the possible inhibitable portion of activity in that tissue fraction attributable to the cytochrome P-450 form to which the antibody reacts. Although each of the methods discussed has drawbacks, all nevertheless have utility, depending on the information needed.

About as many different methods of subfractionating brain tissue for analysis of cytochrome P-450 forms in mitochondria and microsomes have been published as there are investigators carrying out such studies. Methods in the literature range from homogenization in 4 vol of 1.15% KCl and subfractionation as

for liver (Cohn et al., 1977; see Support Protocol 1) to homogenization in 1.15% KCl/0.02 M Tris·Cl, pH 7.4/15% glycerol/0.5 mM dithiothreitol/0.2 mM EDTA (Sasame et al., 1977) to similar preparations with sucrose concentrations ranging from 0.32 to 0.4 M. Basically, it would appear that separation of brain mitochondria and brain microsomes follows procedures similar to that of liver, and that, although cytochrome P-450 levels are considerably lower, they are readily measured in these fractions by procedures indicated in the Support Protocols.

Critical Parameters

Each of the methods discussed here has critical parameters. For example, in spectrophotometric analysis with membranous material, light scattering is a potential problem. Many spectrophotometers solve this problem by having the cuvette positioned close to the photomultiplier or detector. The farther the cuvette is from the detector, the greater the loss of light owing to scattering by the sample suspension. Turbidity of a sample increases the amount of error after additions to the cuvette, because small dilutions of a turbid sample can cause major baseline shifts if not precisely matched in the two cuvettes during difference spectroscopy. One of the major sources of turbidity in measuring liver cytochrome P-450 is glycogen. In the past, investigators would starve the animals for 24 hr before killing them. Although this did reduce glycogen levels in the liver, subsequent studies revealed that cytochrome P-450 forms present in tissue respond to starvation, some increasing in content in the microsomes and others decreasing. A better method, which does not alter the relative amounts of the different forms, is to separate the microsomes from the glycogen pellet very carefully, as described in this unit. Another potential problem, which can cause considerable confusion, involves the stability of dithionite. It is possible to detect erroneously only small amounts of cytochrome P-450, or even none, in microsomes if degraded dithionite is used. If dithionite has degraded, it will not reduce the hemoprotein or will possess only a small amount of reducing capacity. For this reason, it is important to keep the dithionite dry and periodically test its utility by its ability to reduce a known sample, for example cytochrome *c* or even a known concentration of cytochrome P-450.

In some tissues, such as brain and testes, microsomal levels of cytochrome P-450 are very low. Attempts to measure the hemoprotein level in the microsomes spectrophotometrically are often confounded by the presence of large amounts of hemoglobin adsorbed to the microsomes. It is necessary to wash away most of the hemoglobin so as not to interfere with the measurements by spectral overlap. Techniques are indicated for bypassing spectral overlap; but if too much hemoglobin is present, even these procedures are ineffectual.

In the electroblotting methods, it cannot be stressed too strongly that bubbles will interfere with the transfers. These must be carefully eliminated when preparing the transfer sandwich. Bubbles can also appear during the actual transfer if one is not careful to control the temperature of the medium. If the temperature is allowed to rise, dissolved gases will come out of solution and can collect between the polyacrylamide gel and the nitrocellulose, causing a distortion and a loss of integrity of the transfer. To prevent this, maintain the transfer temperature either by using circulating cooling water, if the transfer unit is so constructed; by running the transfer in a cold room; or by lowering the transfer voltage. In the latter case, the transfer time has to be increased.

Anticipated Results

Although some variability exists among laboratories with respect to the content of cytochrome P-450 in tissues and subcellular fractions, the variation is not that great. In general, expect to find on the order of 0.5 to 1.0 nmol of constitutive cytochrome P-450 in liver microsomes per milligram of liver microsomal protein of male rats and about twice that concentration in rabbits. Levels in female rats are generally about half those in males. The cytochrome P-450 forms are inducible by drugs and chemicals; different forms respond to exposure to different agents. Greater variability has been seen in human liver microsomes. Levels in kidney cortex microsomes generally are about half that in the liver, and much lower levels are seen in other tissues. For example, total cytochrome P-450 levels in the lung may be as low as 10% that in the liver, whereas levels in the brain are generally as low as 1% of the content in the liver, necessitating partial purification for spectral measurements.

If a specific antibody prepared against a form of cytochrome P-450 is available, it is generally possible to make measurements of that form in different tissues, even when present at picomole levels; 0.5 µg of cytochrome P-450 (10 pmol) gives a strong band in immunoblots.

Measurements of enzyme activity have a sensitivity that depends on the substrate used. For some substrates, activity is generally low but a fluorescent product is produced with an extremely high sensitivity of measurement. Of the three procedures described here, perhaps the most variable is the metabolism assay, because it requires functionally active cytochrome P-450 and functionally active NADPH–cytochrome P-450 reductase. A number of conditions of the assays will also influence the observed specific activity obtained.

Time Considerations

Spectrophotometric analyses are fairly quick, easy methods if the various buffers needed are available. Typically, the time needed is <1 hr, including zeroing of the spectrophotometer and balancing of the cuvettes spectrophotometrically. Preparation of subcellular membrane fractions could take as long as 4 or 5 hr, depending on the procedure used, the subcellular fraction desired, and the tissue examined. Immunoblotting requires ~6 hr for the various steps and intermediary handling. About 1 hr is required for the transfer of protein from the polyacrylamide gel to the nitrocellulose, followed by 1 hr for shaking the sample in blocking buffer and 2 hr for exposure to the primary antibody. Reaction with the secondary antibody takes 1 hr and development of the color up to 20 min.

The assays of metabolic activity vary with the methods used; the actual metabolism ranges from 10 to 60 min, depending on the substrate chosen. Analysis of product formed could be as short at 1 hr for the colorimetric determination of formaldehyde formed during N-demethylations to 2 or 3 hr for some of the analyses that require extractions and preparations for chromatographic measurement.

Literature Cited

Burke, M.D., Prough, R.A., and Mayer, R.T. 1977. Characteristics of a microsomal cytochrome P-448-mediated reaction. Ethoxyresorufin O-deethylation. *Drug Metab. Dispos.* 5:1-8.

Cammer, W. and Estabrook, R.W. 1967. Spectrophotometric studies of the pigments of adrenal cortex mitochondria. *Arch. Biochem. Biophys.* 122:735-747.

Cinti, D.L. and Schenkman, J.B. 1972. Hepatic organelle interaction. 1. Spectral investigation during drug biotransformation. *Mol. Pharmacol.* 8:327-338.

Cohn, J.A., Alvares, A.P., and Kappas, A. 1977. On the occurrence of cytochrome P-450 and aryl hydrocarbon hydroxylase activity in rat brain. *J. Exp. Med.* 145:1607-1611.

Favreau, L.V., Malchoff, D.M., Mole, J.E., and Schenkman, J.B. 1987. Responses to insulin by two forms of rat hepatic microsomal cytochrome P-450 that undergo major (RLM6) and minor (RLM5b) elevations in diabetes. *J. Biol. Chem.* 262:14319-14326.

Hook, G.E.R., Bend, J.R., Hoel, D., Fouts, J.R., and Gram, T.E. 1972. Preparation of lung microsomes and a comparison of the distribution of enzymes between subcellular fractions of rabbit lung and liver. *J. Pharmacol. Exp. Ther.* 182:474-490.

Juchau, M.R. and Smuckler, E.A. 1973. Subcellular localization of human placental aryl hydrocarbon hydroxylase. *Tox. Appl. Pharmacol.* 26:163-179.

Matsubara, T., Touchi, A., and Ogawa, A. 1982. Heterogenous distribution of the cytochrome P-450 monooxygenase system in rat liver lobes. *Jpn. J. Pharmacol.* 32:999-1011.

Moloney, S.J., Fromson, J.M., and Bridges, J.W. 1982. Cytochrome P-450 dependent deethylase activity in rat and hairless mouse skin microsomes. *Biochem. Pharmacol.* 31:4011-4018.

Mukhtar, H. and Bickers, D.R. 1981. Drug metabolism in skin. Comparative activity of the mixed function oxidases, epoxide hydratase, and glutathione *S*-transferase in liver and skin of the neonatal rat. *Drug Metab. Dispos.* 9:311-314.

Omura, T. and Sato, R. 1964. The carbon monoxide–binding pigment of liver microsomes. II. Solubilization, purification, and properties. *J. Biol. Chem.* 239:2379-2385.

Sasame, H.A., Ames, M.M., and Nelson, S.D. 1977. Cytochrome P-450 and NADPH cytochrome c reductase in rat brain: Formation of catechols and reactive catechol metabolites. *Biochem. Biophys. Res. Commun.* 78:919-926.

Schenkman, J.B. and Cinti, D.L. 1978. Preparation of microsomes with calcium. *Methods Enzymol.* 52:83-89.

Schenkman, J.B., Remmer, H., and Estabrook, R.W. 1967. Spectral studies of drug interaction with hepatic microsomal cytochrome. *Mol. Pharmacol.* 3:113-123.

Schneider, W.C. 1948. Intracellular distribution of enzymes III. The oxidation of octanoic acid by rat liver fractions. *J. Biol. Chem.* 176:259-266.

Walther, B., Ghersi-Egea, J.F., Minn, A., and Siest, G. 1986. Subcellular distribution of cytochrome P-450 in the brain. *Brain Res.* 375:338-344.

Contributed by John B. Schenkman and Ingela Jansson
University of Connecticut Health Center
Farmington, Connecticut

Purification of Cytochrome P-450 Enzymes

The microsomal cytochromes P-450 (P-450s) are notable as major xenobiotic-metabolizing enzymes in mammalian liver. A variety of P-450 enzymes are found in most animal tissues. P-450 2E1 is of general interest because of its role in the bioactivation of a number of potent animal carcinogens. P-450 1A2 is of interest because of its role in the oxidation of many drugs and carcinogens. In humans, P-450 1A2 is the major enzyme involved in the oxidation of caffeine and in the activation of many aryl and heterocyclic amines. Successful purification and reconstitution of the individual mammalian P-450 enzymes is useful for discriminating between their contributions when there is overlapping substrate specificity and for accurately characterizing the kinetic parameters of the individual P-450s.

Microsomal P-450s have been solubilized and at least partially purified from a variety of sources. A number of procedures have been described for purification of individual P-450s from animal tissues. The protocols described in this unit specifically describe the purification steps for isolation of microsomal P-450s 2E1 and 1A2 from an *Escherichia coli* over-expression system in which the N termini have been modified to improve expression levels. These protocols are useful for purification from other expression systems, although the yield and purity of the preparations may vary.

COLUMN CHROMATOGRAPHY FOR PURIFICATION OF RECOMBINANT HUMAN P-450 2E1

BASIC PROTOCOL 1

This protocol describes the chromatographic steps required to purify P-450 2E1 to electrophoretic homogeneity from a preparation of homogenized *E. coli* membranes over-expressing human P-450 2E1 in which the N terminus has been modified to improve expression levels (Gillam et al., 1994). Before beginning chromatographic purification, membrane-bound P-450 2E1 must be solubilized from the membranes with a detergent solution (sodium cholate and Triton N-101), and the active site stabilized by the addition of 4-methylpyrazole (4-MP), a tight-binding inhibitor of P-450 2E1. P-450 2E1 is isolated through a series of ion-exchange steps using both ionic and nonionic detergents, as well as the stabilizing ligand 4-MP, to maintain the structural integrity of the protein throughout purification. Binding and recovery at each step can easily be quantified by spectrophotometric measurement of the reduced carbon monoxide–bound P-450, observed at 450 nm (Omura and Sato, 1964; see *UNIT 4.1*). The purified protein can be stored for at least 2 years at −20°C.

NOTE: A key to success with this procedure is careful equilibration of columns before protein loading. In addition, binding is improved at lower loading rates, which can be achieved by diluting the protein or decreasing sample flow rates.

Materials

E. coli membrane preparation containing P-450 2E1 (Gillam et al., 1994)
Membrane solubilization solution for P-450 2E1 (see recipe)
Diethylaminoethyl (DEAE) Sephacel ion exchanger resin (Pharmacia Biotech)
DEAE equilibration buffer for P-450 2E1 (see recipe)
Carboxymethyl (CM) Sepharose Fast Flow ion exchanger resin (Pharmacia Biotech)
CM equilibration buffer for P-450 2E1 (see recipe)
20% (v/v) glycerol (see recipe)
0.1 to 1 M H_3PO_4

Contributed by L.C. Bell-Parikh, N.A. Hosea, M.V. Martin, and F.P. Guengerich
Current Protocols in Toxicology (1999) 4.2.1-4.2.12

50 mM CM wash buffer for P-450 2E1 (see recipe)
10 mM CM elution buffer (see recipe)
200 mM CM elution buffer (see recipe)
Hydroxylapatite (HA) Fast Flow chromatographic support (Calbiochem)
HA equilibration buffer (see recipe)
HA elution buffer (see recipe)
Post-HA dialysis buffer for P-450 2E1 (see recipe)

Empty 20- and 100-ml chromatographic columns
Empty CM Sepharose Fast Flow column
Spectrapor 12,000- to 14,000-MWCO dialysis tubing (Spectrum Medical Industries)

Additional reagents and equipment for ion exchange chromatography (*APPENDIX 3*) and for SDS-PAGE and silver staining of gels (*APPENDIX 3*)

Solubilize membranes

1. Dilute *E. coli* membrane preparation to a protein concentration of 2 mg/ml in membrane solubilization solution for P-450 2E1.

   Volumes will vary depending on the total amount of protein in the membrane preparation. For a protocol describing preparation of membranes, see Gillam et al. (1993).

Perform DEAE chromatography

2. For a bacterial membrane preparation containing ~3.5 g of total protein with a specific content of 0.4 nmol P-450/mg protein (i.e., 1400 nmol P-450), pack a 100-ml column with DEAE Sephacel resin to a volume of 75 ml (2.5 × 15 cm).

   Although CM and HA resins can be re-equilibrated and reused following protein elution, regeneration of the DEAE Sephacel column is not recommended. A freshly prepared column is highly desirable for successful purification of P-450s.

3. Equilibrate column with a minimum of 5 column volumes of DEAE equilibration buffer for P-450 2E1 at a flow rate of ~1 ml/min.

4. Remove membrane components from the solution of solubilized membranes by ultracentrifugation 60 min at $10^5 \times g$, 4°C.

   Failure to do this will result in destruction of the chromatographic bed.

5. Load solubilized membranes onto column at a flow rate of ~1 ml/min.

   P-450 2E1 elutes in the void volume. Often most, if not all, of the cytochrome P-450 (representing any denatured P-450 plus non-P-450 bacterial hemoproteins) will be removed from the sample during this step.

6. Follow the solubilized membrane preparation with at least 1 column volume of DEAE equilibration buffer to displace the P-450 in the column void volume. Collect the eluate.

Perform CM chromatography

7. Pack a CM Sepharose Fast Flow column and equilibrate with a minimum of 5 column volumes of CM equilibration buffer for P-450 2E1.

   A CM column packed to ~20 ml (1.5 × 10 cm) will typically bind up to 1000 nmol of P-450 2E1.

   It is essential that the pH of this buffer be adjusted to 6.5. At pH >6.5, P-450 2E1 will not bind well to the column. If the pH is too acidic, however, the structural integrity of the P-450 may be compromised.

8. Dilute the DEAE Sephacel void volume (step 6) 3-fold with 20% (v/v) glycerol, and adjust to pH 6.5 using dilute H_3PO_4 (0.1 to 1 M).

   The volume of the 3-fold-diluted DEAE void is substantial and it may take up to 3 days to load completely onto the CM column. Because P-450 2E1 is slightly more stable at pH 7.4 than at 6.5, dilute fractions recovered from only one DEAE column at a time. Another batch can be diluted and pH adjusted to 6.5 once the previous batch has been completely loaded onto the CM column. Alternatively, CM columns can be run in parallel if a larger preparation is done.

9. Load the protein onto the column.

   The P-450 should bind tightly to the top of the column, forming a visible brownish-red zone of binding. If the protein does not bind well, even if all of the solutions are properly adjusted to pH 6.5, decrease the flow rate of the protein solution onto the column. This may be all that is required to improve binding.

10. After the protein has completely loaded, wash the column extensively with a minimum of 5 column volumes of 50 mM CM wash buffer for P-450 2E1.

11. Elute the protein using a K^+ gradient from 10 mM to 200 mM (250 ml each of 10 mM and 200 mM CM elution buffer) at a flow rate of 1 ml/min . Collect eluate in ~5-ml fractions.

12. Analyze CM fractions by running aliquots on a 7% (w/v) acrylamide SDS-PAGE gel and visualizing proteins by silver staining (*APPENDIX 3*, Guengerich, 1994). Pool fractions that are electrophoretically homogeneous (M_r 50 kDa).

    The purified protein must be further chromatographed to remove detergent and 4-MP from the preparation.

Perform HA chromatography

13. Dialyze the pooled CM fractions ~8 to 12 hr at 4°C against three 2-liter changes of HA equilibration buffer.

    This will reduce ionic strength to permit HA binding.

14. Pack a column with HA Fast Flow chromatographic support and equilibrate with 5 column volumes HA equilibration buffer.

    A column packed to ~15 ml (1.5 × 8 cm) with HA Fast Flow will usually accommodate up to 1000 nmol of P-450 2E1.

15. Load the P-450 slowly onto the HA column at a flow rate of ≤0.5 ml/min.

    Again, the P-450 should bind tightly, forming a brownish-red zone of binding at the top of the column.

16. Wash the column extensively with HA equilibration buffer to remove Triton N-101.

    In this case, 10 or more column volumes may be required to remove the detergent completely. Detergent removal can be monitored by measuring absorbance at 280 nm. Absorbance should decrease to ≤0.01.

17. Elute the protein from the HA column using HA elution buffer.

    At this ionic strength, P-450 2E1 elutes in a very sharp band, which can easily be collected manually or by using a fraction collector.

    HA from different suppliers yields varying success at this step. Calbiochem Fast Flow HA has consistently provided the highest yield. Other preparations of HA have proven resistant to protein elution.

Dialyze protein

18. Dialyze the purified P-450 2E1 using Spectrapor 12,000- to 14,000-MWCO dialysis tubing for ~8 to 12 hr at 4°C against three successive 2-liter changes of post-HA dialysis buffer for P-450 2E1.

    This dialysis serves to decrease the concentration of potassium phosphate for long-term storage of the protein.

    When stored at 4°C, the protein is stable 1 to 2 weeks. When stored at −20°C, the preparation remains spectrally and catalytically stable ~2 years. Storage at −70°C does not significantly improve the shelf life of the purified P-450.

BASIC PROTOCOL 2

COLUMN CHROMATOGRAPHY FOR PURIFICATION OF RECOMBINANT HUMAN P-450 1A2

This protocol describes the chromatographic steps required to purify P-450 1A2 to electrophoretic homogeneity from a preparation of homogenized *E. coli* membranes over-expressing P-450 1A2 (Sandhu et al., 1994). Detergent-solubilized membranes containing P-450 1A2, stabilized by the specific inhibitor α-naphthoflavone (α-NF), are purified through a two-step chromatographic protocol. Purified P-450 1A2 can be stored for at least 2 years at −20°C.

Materials

E. coli membrane preparation containing P-450 1A2 (Sandhu et al., 1994)
Membrane solubilization solution for P-450 1A2 (see recipe)
Diethylaminoethyl (DEAE) Sephacel Fast Flow ion exchanger resin (Pharmacia Biotech)
DEAE equilibration buffer for P-450 1A2 (see recipe)
Carboxymethyl (CM) Sepharose Fast Flow ion exchanger resin (Pharmacia Biotech)
CM equilibration buffer for P-450 1A2 (see recipe)
2× dilution solution (see recipe)
50 mM CM wash buffer for P-450 1A2 (see recipe)
100 mM CM wash buffer (see recipe)
300 mM CM elution buffer (see recipe)
500 mM CM elution buffer (see recipe)
Empty 40- and 70-ml chromatographic columns
Additional reagents and solutions for ion exchange chromatography (*APPENDIX 3*) and for SDS-PAGE and silver staining of gels (*APPENDIX 3*)

Solubilize membranes

1. Dilute *E. coli* membrane preparation to a protein concentration of 2 mg/ml in membrane solubilization solution for P-450 1A2.

   For a protocol describing preparation of membranes, see Gillam et al. (1993). For further reference, see Sandhu et al. (1994).

Perform DEAE chromatography

2. Pack DEAE Sephacel resin into a column according to manufacturer's instructions to a size of 2.5 × 13 cm.
3. Equilibrate column at a flow rate of ~1 ml/min with DEAE equilibration buffer for P-450 1A2 until the pH and ionic strength of the eluate is that of the equilibration buffer.

   This usually requires 5 to 10 column volumes of buffer.

4. Remove membrane components from the solution of solubilized membranes by ultracentrifugation 60 min at $10^5 \times g$, 4°C.

   Failure to do this will result in destruction of the chromatographic bed.

5. Load solubilized membranes onto the column at a flow rate of ~1 ml/min.

6. Wash the column with 1 column volume of DEAE equilibration buffer to displace the P-450 in the column void volume. Collect the eluate.

Perform CM chromatography

7. Pack CM Sepharose resin into a column according to manufacturer's instructions to a size of 2.5 × 6 cm.

8. Equilibrate the column with CM equilibration buffer for P-450 1A2 until the pH and ionic strength of the eluate are equal to those of the equilibration buffer.

   The proper pH of the CM resin is important, because the efficiency of binding for P-450s to a CM column is sensitive to the pH of the column resin.

9. Pool the void fractions from step 6 and dilute 2-fold with 2× dilution solution to achieve a final concentration of 25 mM Tris·Cl, pH 7.4 (all other components remain at same concentration as in DEAE equilibration buffer).

10. Load the diluted P-450 sample onto the equilibrated CM column at a flow rate of ~1 ml/min.

    As the P-450 1A2 binds the CM resin, a dark brown band should appear and should not occupy >75% of the column. If overloading occurs, begin loading onto a second CM column. If the P-450 does not bind, reduce the flow rate and/or dilute the solution further before loading.

11. After the P-450 sample has completely loaded, sequentially wash column with 400 ml each of 50 mM CM wash buffer for P-450 1A2 and 100 mM CM wash buffer.

    This step will remove the α-NF and the detergent.

12. Sequentially elute the P-450 1A2 protein with 300 mM and 500 mM CM elution buffers; collect 10-ml fractions.

13. Analyze CM fractions by running aliquots on a 7% (w/v) acrylamide SDS-PAGE gel and visualizing proteins by silver staining (*APPENDIX 3*; Guengerich, 1994).

14. Pool homogeneous fractions and freeze in 1-ml aliquots at −20°C.

    For storage, the protein may be in 100, 300, or 500 mM CM elution buffer; the potassium phosphate concentration can vary between 100 mM and 500 mM, but should not be <100 mM.

REAGENTS AND SOLUTIONS

Use Milli-Q-purified water or equivalent forall recipes and protocol steps. For common stock solutions, see ***APPENDIX 2A****; for suppliers, see* ***SUPPLIERS APPENDIX****.*

For buffers containing dithiothreital (DTT), the DTT should be added immediately before use because it slowly oxidizes in solution at neutral pH. Without DTT, all buffer solutions are stable for several months at 4°C.

Carboxymethyl (CM) elution buffer, 10 mM

2.5 ml 1 M potassium phosphate, pH 7.4 (10 mM final)
2.5 ml 20% (v/v) Triton N-101 (0.2% v/v final)
50 ml glycerol (20% v/v final)
0.5 ml 100 mM sodium EDTA (see recipe; 0.2 mM final; see recipe)
40 mg DTT (1.0 mM final)
250 µl 50 mM 4-MP (50 µM final)
H_2O to 250 ml

Carboxymethyl (CM) elution buffer, 200 mM

50 ml 1 M potassium phosphate, pH 7.4 (200 mM final)
2.5 ml 20% (v/v) Triton N-101 (see recipe; 0.2% v/v final)
50 ml glycerol (20% v/v final)
0.5 ml 100 mM sodium EDTA (see recipe; 0.2 mM final)
40 mg DTT (1.0 mM final)
250 µl 50 mM 4-MP (50 µM final)
H_2O to 250 ml
Store up to several months at 4°C

Carboxymethyl (CM) elution buffer, 300 mM

300 ml 1 M potassium phosphate, pH 7.4 (300 mM final)
200 ml glycerol (20% v/v final)
2 ml 100 mM sodium EDTA (see recipe; 0.2 mM final)
160 mg DTT (1.0 mM final)
H_2O to 1 liter
Store up to several months at 4°C

Carboxymethyl (CM) elution buffer, 500 mM

500 ml 1 M potassium phosphate, pH 7.4 (500 mM final)
200 ml glycerol (20% v/v final)
2 ml 100 mM sodium EDTA (see recipe; 0.2 mM final)
160 mg DTT (1.0 mM final)
H_2O to 1 liter
Store up to several months at 4°C

Carboxymethyl (CM) equilibration buffer for P-450 2E1

10 ml 1 M sodium phosphate, pH 6.5 (20 mM final)
100 ml glycerol (20% v/v final)
1.0 ml 100 mM sodium EDTA (see recipe; 0.2 mM final)
H_2O to 500 ml
Store up to several months at 4°C

Carboxymethyl (CM) equilibration buffer for P-450 1A2

20 ml 1 M sodium phosphate, pH 7.4 (20 mM final)
200 ml glycerol (20% v/v final)
2.0 ml 100 mM sodium EDTA (see recipe; 0.2 mM final)
160 mg DTT (1.0 mM final)
6 ml 5 mM α-NF (see recipe; 30 µM final)
H_2O to 1 liter
Store up to several months at 4°C

Carboxymethyl (CM) wash buffer, 50 mM, for P-450 2E1

25 ml 1 M sodium phosphate, pH 6.5 (50 mM final)
100 ml glycerol (20% v/v final)
1.0 ml 100 mM sodium EDTA (see recipe; 0.2 mM final)
80 mg DTT (1.0 mM final)
H_2O to 500 ml
Store up to several months at 4°C

Carboxymethyl (CM) wash buffer, 50 mM, for P-450 1A2

25 ml 1 M sodium phosphate, pH 7.4 (50 mM final)
100 ml glycerol (20% v/v final)
1.0 ml 100 mM sodium EDTA (see recipe; 0.2 mM final)
80 mg DTT (1.0 mM final)
H_2O to 500 ml
Store up to several months at 4°C

Carboxymethyl (CM) wash buffer, 100 mM

100 ml 1 M sodium phosphate, pH 7.4 (100 mM final)
200 ml glycerol (20% v/v final)
2.0 ml 100 mM sodium EDTA (see recipe; 0.2 mM final)
160 mg DTT (1.0 mM final)
H_2O to 1 liter
Store up to several months at 4°C

DEAE equilibration buffer for P-450 2E1

25 ml 1 M Tris·Cl, pH 7.4 (*APPENDIX 2A*; 50 mM final)
100 ml glycerol (20% v/v final)
5.0 ml 100 mM sodium EDTA (see recipe; 1.0 mM final)
80 mg DTT (1.0 mM final)
16 ml 20% (w/v) sodium cholate (see recipe; 0.6% w/v final)
32 ml 20% (v/v) Triton N-101 (see recipe; 1.2% v/v final)
0.5 ml 50 mM 4-MP (50 μM final)
H_2O to 500 ml
Store up to several months at 4°C

DEAE equilibration buffer for P-450 1A2

25 ml 1 M Tris·Cl, pH 7.4 (*APPENDIX 2A*; 50 mM final)
100 ml glycerol (20% v/v final)
5.0 ml 100 mM sodium EDTA (see recipe; 1.0 mM final)
80 mg DTT (1.0 mM final)
16 ml 20% (w/v) sodium cholate (see recipe; 0.6% w/v final)
32 ml 20% (v/v) Triton N-101 (see recipe; 1.2% v/v final)
3 ml 5 mM α-NF (see recipe; 30 μM final)
H_2O to 500 ml
Store up to several months at 4°C

Dilution solution, 2×, for P-450 1A2

200 ml glycerol (20% v/v final)
10 ml 100 mM sodium EDTA (see recipe; 1.0 mM final)
160 mg DTT (1.0 mM final)
31.25 ml 20% (w/v) sodium cholate (see recipe; 0.625% w/v final)
62.5 ml 20% (w/v) Triton N-101 (see recipe; 1.25% w/v final)
6 ml 5 mM α-NF (see recipe; 30 μM final)
H_2O to 1 liter
Store up to several months at 4°C

Glycerol solution, 20% (v/v)

Dissolve 200 ml glycerol in ~700 ml of water with stirring. Dilute to 1 liter. Store up to several months at 4°C

Hydroxylapatite (HA) elution buffer

150 ml 1 M potassium phosphate, pH 7.4 (300 mM final)
100 ml glycerol (20% v/v final)
250 µl 100 mM sodium EDTA (see recipe; 50 µM final)
H_2O to 500 ml
Store up to several months at 4°C

Hydroxylapatite (HA) equilibration buffer

5 ml 1 M potassium phosphate, pH 7.4 (10 mM final)
100 ml glycerol (20% v/v final)
250 µl 100 mM sodium EDTA (see recipe; 50 µM final)
H_2O to 500 ml
Store up to several months at 4°C

Membrane solubilization solution for P-450 2E1

50 mM Tris·Cl buffer, pH 7.4 (*APPENDIX 2A*)
20% (v/v) glycerol
0.625% (w/v) sodium cholate (see recipe)
1.25% (v/v) Triton N-101 (see recipe)
1.0 mM sodium EDTA (see recipe for 100 mM EDTA stock)
1.0 mM DTT
50 µM 4-MP
Store up to several months at 4°C

Membrane solubilization solution for P-450 1A2

50 mM Tris·Cl buffer, pH 7.4 (*APPENDIX 2A*)
20% (v/v) glycerol
0.625% (w/v) sodium cholate (see recipe)
1.25% (v/v) Triton N-101 (see recipe)
1.0 mM sodium EDTA (see recipe for 100 mM EDTA stock)
1.0 mM DTT
30 µM α-NF (add from 5 mM α-NF stock solution; see recipe)
Store up to several months at 4°C

4-Methylpyrazole (4-MP), 50 mM

Dissolve 410 mg 4-methylpyrazole (solid, Sigma) in 100 ml acetone. Store at 4°C in sealed glass container to prevent evaporation.

α-Naphthoflavone (α-NF), 5 mM

Dissolve 64 mg α–NF (7,8-benzoflavone, FW 272.3) in 50 ml methanol. Store in a sealed amber bottle at 4°C to prevent evaporation.

Post-HA dialysis buffer

200 ml 1 M potassium phosphate, pH 7.4 (100 mM final)
1.0 ml 100 mM sodium EDTA (see recipe; 50 µM final)
400 ml glycerol (20% v/v final)
H_2O to 2 liters
Store up to several months at 4°C

Sodium cholate, 20% (w/v)

Add 100 g cholic acid (sodium salt; Sigma) to 400 ml water. Adjust to pH 6.5 with 1 M acetic acid (slowly). Adjust volume to 500 ml with water. Store at 4°C.

As acid is added to the sodium cholate mixture, precipitation will occur. Once precipitate has redissolved, continue to add more acid. Preparation of this stock solution is tedious; therefore, as a matter of convenience, it is recommended that this stock be prepared before beginning any purification steps.

Sodium EDTA, 100 mM

Add 38.0 g EDTA (tetrasodium salt) to 900 ml water. Stir until in solution (if difficult, adjust pH >8 with NaOH). Adjust pH to 7.4 with HCl. Adjust volume to 1 liter with water. Store up to several months at 4°C.

Triton N-101, 20% (w/v)

Dissolve 100 g Triton N-101 (Sigma) in water to a total volume of 500 ml. Store at 4°C.

Dissolving the detergent may be difficult; to facilitate solution the beaker containing the mixture can be stirred in an ice bucket containing warm tap water. Do not heat excessively.

COMMENTARY

Background Information

Microsomal P-450s have been solubilized and purified from a variety of sources. A number of procedures have been described for purification of individual P-450s from animal tissues (Guengerich, 1987). The choice of purification method depends on the P-450; the source of the protein; and other factors, such as whether co-purification of additional proteins is desired. Many systems have been developed for expression of various P-450s (Porter et al., 1990; Waterman and Johnson, 1991). *E. coli* has provided excellent success with high levels of expression and relatively low cost. In addition, the ease of purification is much greater than from mammalian tissues.

P-450 2E1 is of general interest because of its role in the bioactivation of a number of potent animal carcinogens. P-450 2E1 exhibits a particular difficulty in regard to purification from animal sources, because there is a high degree of interindividual variability of expression with this protein (Peter et al., 1990). The protocol in this unit specifically describes the purification steps for isolation of P-450 2E1 from an *E. coli* over-expression system in which the N terminus has been modified to improve expression levels (Gillam et al., 1994).

Other purification procedures for P-450 2E1 have been reported. Omata et al. (1994) described a method for the immunopurification of P-450 2E1 using an immunosorbent comprised of a Sepharose–monoclonal antibody conjugate. Although 10% to 20% of total microsomal P-450 can be immunopurified from rat microsomes, the specific yield of P-450 2E1 is not clear, nor is the catalytic activity following elution from the sorbent. This method, however, has the advantage that associated proteins may be co-purified. Purification using a flavodoxin affinity column has been attempted with an overall yield of ~15% (Gillam et al., 1995). The procedure reported here uses DEAE and CM ion exchange chromatography followed by binding to HA to remove detergent from the preparation. Typically, the yield of purified P-450 2E1 is 50% of the total P-450 measured in the solubilized membrane preparation. Hydrophobic chromatography has been offered as a faster alternative to CM for fractionation of proteins (Grogan et al., 1995). FPLC using an octyl-Sepharose hydrophobic column generated an electrophoretically homogeneous protein with essentially no P-420, and catalytic activities were comparable to microsomal levels. The yield was comparable to that of the procedure reported here.

P-450 1A2 is of interest because of its role in the oxidation of many drugs and carcinogens (Guengerich, 1995). In humans this P-450 is the major one involved in oxidation of caffeine and in the activation of many aryl and heterocyclic amines (Butler et al., 1989; Guengerich, 1995). Human P-450 1A2 was first purified from liver samples, but the yield and purity were problematic (Butler et al., 1989). The enzyme has been expressed in bacteria after modification of the N-terminal sequence for optimal translation (Sandhu et al., 1994). Purification was hindered by the instability of the holoprotein in the presence of detergents, but this problem was overcome by the use of the tightly bound ligand α-NF.

Other bacterial expression systems include an approach by which a fusion protein is produced with rat NADPH-P-450 reductase (Parikh and Guengerich, 1997). The fusion protein can be purified using a 2é,5é-ADP affinity column and used in catalytic assays. The catalytic activity, however, is not as high as that of purified P-450 1A2 reconstituted with reductase.

The same basic pCW vector that is used in *E. coli* can be used to express human P-450 1A2 in *Salmonella typhimurium* TA1538 (Josephy et al., 1995), and the protein can be purified using the method described here. Human P-450

1A2 has also been expressed in yeast and purified using an alternate procedure (Imaoka et al., 1996).

Modified versions of the protocols have been used to purify other human P-450 enzymes expressed in bacteria (Guengerich et al., 1996).

Critical Parameters and Troubleshooting

Sample loss during these procedures is generally not a result of the chromatography steps. During purification, P-450, in general, is most stable when bound to a column. Large sample volumes, however, prohibit rapid loading of protein onto columns. One may find that the P-450 slowly degrades in solution before it is passed over DEAE. To minimize this problem, it is important to keep all enzyme solutions and buffers at 4°C. Ideally, all chromatography is done in a refrigerated space at 4°C. Glycerol, 4-MP, and α-NF structurally stabilize the P-450 and aid in minimizing degradation. If desired, more than one column can be prepared for sample loading so that the enzyme may be more ra! pidly loaded. If materials are properly stored at 4°C, however, this is not necessary and will not substantially increase yields. This may be worthwhile in the interest of saving time.

It is useful to reiterate that an important key to success with this procedure is careful equilibration of columns before protein loading. In addition, binding is improved at lower loading rates, which can be achieved by protein dilution or by decreasing sample flow rates. Use care not to overload the columns. CM and HA columns should be no more than ~70% colored as a result of to protein binding.

Purified P-450s are not particularly soluble proteins. Glycerol (20%) is required for maintaining microsomal P-450 stability. The active site inhibitors 4-MP and α-NF should be added to all solutions, as specified, to stabilize the protein until the final purification step, when the detergent and inhibitors are removed to yield catalytically active enzymes.

Purification of P-450 2E1

For CM chromatography with P-450 2E1, pH is critical in moderating protein-binding interactions. All solutions should be adjusted to pH 6.5 for proper binding of the protein. Here again, stability may be an issue. P-450 2E1 may begin to denature at pH 6.5. To minimize protein loss, dilute and adjust the pH of the DEAE void volume in fractions. Do not prepare more enzyme solution than can be loaded within 12 hr.

In regard to the HA purification step, it should be noted that some preparations of HA bind P-450 2E1 so tightly that the purified protein is eluted with difficulty, giving rise to very poor yields. The greatest success with P-450 2E1 (but not with certain other P-450s) has been obtained with HA from Calbiochem.

Purification of P-450 1A2

One very important point regarding human P-450 1A2 is that α-NF must be present during the initial steps when detergents are added. Some other ligands have been tried but are not as effective in preventing degradation of the protein (Sandhu et al., 1994). Another point, which applies to P-450 1A2 enzymes purified from rats and rabbits as well, is that the ionic

Table 4.2.1 Typical Yields of P450 2E1 from Purification Steps

	P450 (nmol)	% yield from previous step	Total % yield
Solubilized membranes	1350	100	100
DEAE void	1200	89	89
CM-pooled fractions	700	58	52
HA-purified P450 2E1	650	93	48

Table 4.2.2 Typical Yields of P450 1A2 from Purification Steps

	P450 (nmol)	% yield from previous step	Total % yield
Solubilized membranes	684	100	100
DEAE void	470	69	69
CM-pooled fractions	210	45	31

strength of purified preparations must not be low in the absence of detergents. A safe guide is 100 mM phosphate or the equivalent ionic strength with other buffers containing NaCl, etc (e.g., Tris·Cl plus 300 mm NaCl).

Anticipated Results

Tables 4.2.1 and 4.2.2 present typical yields for the two protocols. In both cases, the resulting protein is electrophoretically homogenous.

Time Considerations

This entire purification, from solubilized membranes to purified, detergent-free P-450, takes ~1 week. Each equilibration and washing step takes ~3 hr. Equilibration of the columns can be completed in advance or overnight (be sure the columns do not run dry) to expedite the purification process. Elution of the CM column takes ~3 hr, as well. As mentioned, protein loading can take 2 or more days. Elution from the HA column may require as little as 30 min.

As with most P-450s, P-450s 2E1 and 1A2 are fairly stable at 4°C in solution. Thus loading of the P-450 sample onto all columns need not be rushed. Keep flow rates near 1 ml/min. P-450s are apparently stable for weeks when bound to CM or HA columns. It is recommended that the CM column first be washed to remove any proteins that may contribute to the degradation of the P-450 before coming to any lengthy stopping point.

Although solutions of these P-450s are somewhat stable, the unpurified protein is usually less stable in solution than when it is bound to the column. It is good practice to begin the next chromatography step within a few hours of solubilizing or eluting the protein.

After protein elution, CM and HA columns can be regenerated through extensive washing (~500 ml) with the high salt (>200 mM potassium phosphate) elution buffers. Before re-use, the columns must be re-equilibrated with the equilibration buffers described in Basic Protocols 1 and 2. In the presence of sodium EDTA, these columns can be stored for several months at 4°C.

Literature Cited

Butler, M.A., Iwasaki, M., Guengerich, F.P., and Kadlubar, F.F. 1989. Human cytochrome P-450$_{PA}$ (P-450IA2), the phenacetin O-deethylase, is primarily responsible for the hepatic 3-demethylation of caffeine and N-oxidation of carcinogenic arylamines. *Proc. Natl. Acad. Sci. U.S.A.* 86:7696-7700.

Gillam, E.M.J., Baba, T., Kim, B-R., Ohmori, S., and Guengerich, F.P. 1993. Expression of modified human cytochrome P-450 3A4 in *Escherichia coli* and purification and reconstitution of the enzyme. *Arch. Biochem. Biophys.* 305:123-131.

Gillam, E.M.J., Guo, Z., and Guengerich, F.P. 1994. Expression of modified human cytochrome P-450 2E1 in *Escherichia coli*, purification, and spectral and catalytic properties. *Arch. Biochem. Biophys.* 312:59-66.

Gillam, E.M.J., Guo, Z., Martin, M.V., Jenkins, C.M., and Guengerich, F.P. 1995. Expression of cytochrome P-450 2D6 in *Escherichia coli*, purification, and spectral and catalytic characterization. *Arch. Biochem. Biophys.* 319:540-550.

Grogan, J., Shou, M., Andrusiak, E.A., Tamura, S., Buters, J.T.M., Gonzalez, F.J., and Korzekwa, K.R. 1995. Cytochrome P-450 2A1, 2E1, and 2C9 cDNA-expression by insect cells and partial purification using hydrophobic chromatography. *Biochem. Pharmacol.* 50:1509-1515.

Guengerich, F.P. (ed.) 1987. Mammalian cytochromes P-450, Vol. 1. CRC Press, Boca Raton, Fla.

Guengerich, F.P. 1994. Analysis and characterization of enzymes. *In* Principles and Methods of Toxicology, 3rd ed. (Hayes, A.W., ed.) pp. 1259-1313. Raven Press, New York.

Guengerich, F.P. 1995. Human cytochrome P-450 enzymes. *In* Cytochrome P-450, 2nd ed. (Ortiz de Montellano, P.R., ed.) pp. 473-535. Plenum Press, New York.

Guengerich, F.P., Martin, M.V., Guo, Z., and Chun, Y.-J. 1996. Purification of functional recombinant P-450s from bacteria. *Methods Enzymol.* 272:35-44.

Imaoka, S., Yamada, T., Hiroi, T., Hayashi, K., Sakaki, T., Yabusaki, Y., and Funae, Y. 1996. Multiple forms of human P-450 expressed in *Saccharomyces cerevisiae*: Systematic characterization and comparison with those of the rat. *Biochem. Pharmacol.* 51:1041-1050.

Josephy, P.D., DeBruin, L.S., Lord, H.L., Oak, J., Evans, D.H., Guo, Z., Dong, M-S., and Guengerich, F.P. 1995. Bioactivation of aromatic amines by recombinant human cytochrome P-450 1A2 expressed in bacteria: A substitute for mammalian tissue preparations in mutagenicity testing. *Cancer Res.* 55:799-802.

Omata, Y., Robinson, R.C., Gelboin, H.V., Pincus, M.R., and Friedman, F.K. 1994. Specificity of the cytochrome P-450 interaction with cytochrome b_5. *FEBS Lett.* 346:241-245.

Omura, T. and Sato, R. 1964. The carbon monoxide-binding pigment of liver microsomes. I. Evidence for its hemoprotein nature. *J. Biol. Chem.* 239:2370-2378.

Parikh, A. and Guengerich, F.P. 1997. Expression, purification, and characterization of a catalytically active human cytochrome P-450

1A2:NADPH-cytochrome P-450 reductase fusion protein. *Protein Express. Purif.* 9:346-354.

Peter, R., Böcker, R.G., Beaune, P.H., Iwasaki, M., Guengerich, F.P., and Yang, C-S. 1990. Hydroxylation of chlorzoxazone as a specific probe for human liver cytochrome P-450 IIE1. *Chem. Res. Toxicol.* 3:566-573.

Porter, T.D., Pernecky, S.J., Larson, J.R., Fujita, V.S., and Coon, M.J. 1990. Expression of cytochrome P-450 in yeast and *Escherichia coli*. *In* Drug Metabolizing Enzymes: Genetics, Regulation and Toxicology, Proceedings of the Eighth International Symposium on Microsomes and Drug Oxidations (Stockholm, June 25-29), (M. Ingelman-Sundberg, J-Å. Gustafsson, and S. Orrenius, eds.) p. 20. Karolinska Institute, Stockholm.

Sandhu, P., Guo, Z., Baba, T., Martin, M.V., Tukey, R.H., and Guengerich, F.P. 1994. Expression of modified human cytochrome P-450 1A2 in *Escherichia coli*: Stabilization, purification, spectral characterization, and catalytic activities of the enzyme. *Arch. Biochem. Biophys.* 309:168-177.

Waterman, M.R. and Johnson, E.F. (eds.) 1991. Methods in Enzymology, Vol. 206: Cytochrome P-450. Academic Press, San Diego.

Key References

Gillam et al., 1994. See above.

Describes a high-yield expression system for P-450 2E1, as well as a procedure for isolating the P-450-containing membrane fraction from whole cells.

Sandhu et al., 1994. See above.

Describes a high-yield expression system for P-450 1A2.

Guengerich, 1995. See above.

Cites references that describe specific purification procedures for several of the major human cytochrome P-450s, reviews recombinant technology as a source of P-450s, and concisely summarizes the biological significance of major human P-450 isoforms.

Contributed by L.C. Bell-Parikh, N.A. Hosea, M.V. Martin, and F.P. Guengerich
Vanderbilt University School of Medicine
Nashville, Tennessee

Measurements of UDP-Glucuronosyltransferase (UGT) Activities

The mammalian UDP-glucuronosyltransferases (EC 2.4.1.17, UGTs) are a family of isoenzymes that catalyze the reaction of endobiotics and xenobiotics with UDP-glucuronic acid (UDPGlcUA), resulting in the formation of hydrophilic glucuronides (see Fig. 4.3.1). This pathway is an important step in the metabolism and subsequent excretion of many compounds that would otherwise have toxic effects.

The UGT enzymes are located in the endoplasmic reticulum; microsomal preparations from tissue, whole cultured cells, or membrane preparations from cultured cells are used in the glucuronidation assays. The activity of a UGT is measured as the moles of glucuronide formed during a given time period via catalysis by a standard amount of protein. The method for detecting glucuronide formation described here uses nonradioactive aglycone substrates and the radioactive cosubstrate [^{14}C]UDPGlcUA in the reaction. One of several methods is then used to separate the radioactive glucuronide from the unreacted [^{14}C]UDPGlcUA. There are no known substrates for which the glucuronidation is catalyzed by all UGT isoforms.

This unit describes three methods for measuring UGT activities. Thin-layer chromatography (TLC; see Basic Protocol 1) is a powerful screening method, and a great many substrates may be analyzed simultaneously. The Sep-Pak C18 cartridge extraction method (see Basic Protocol 2) has been specifically developed to separate opioid glucuronides from UDPGlcUA. The ethyl acetate extraction method (see Basic Protocol 3) is used for separating the glucuronides of bilirubin, steroids, and bile acids from UDPGlcUA. In each procedure, the enzyme reaction is performed using a microsome preparation from tissue (see Support Protocol 1) or cultured cells expressing cDNA for UGT (see Support Protocol 2).

CAUTION: When working with radioactivity, take appropriate precautions to avoid contamination of the investigator and the surroundings. Carry out the experiment and dispose of wastes in an appropriately designated area, following the guidelines provided by your local radiation safety officer (also see *APPENDIX 1A*).

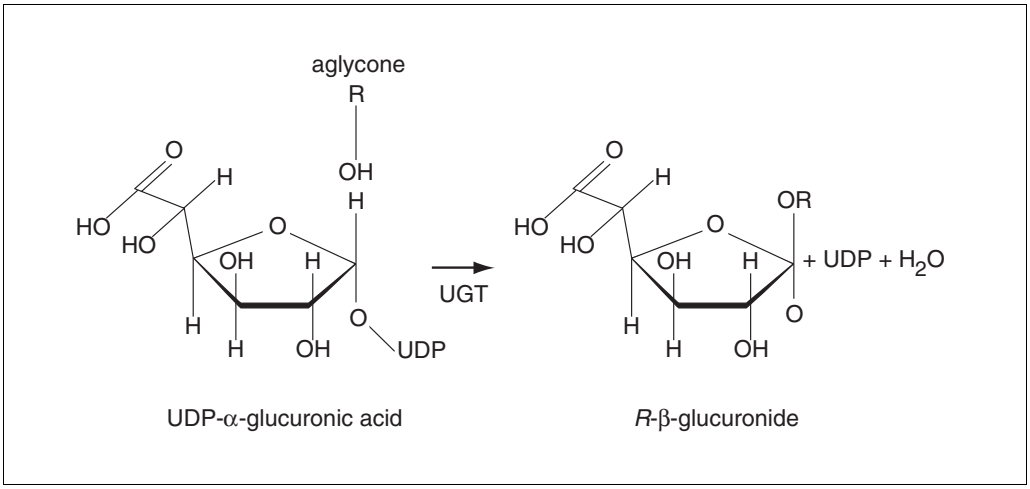

Figure 4.3.1 Glucuronidation reaction.

Contributed by Birgit L. Coffman, Gladys R. Rios, and Thomas. R. Tephly
Current Protocols in Toxicology (1999) 4.3.1-4.3.15

BASIC PROTOCOL 1

THIN-LAYER CHROMATOGRAPHY ASSAY FOR UGT ACTIVITY

This method is suitable for most substrates and is useful for screening a large number of substrates simultaneously. Its drawback is that it is very slow. It takes 1 to 4 hr to evaporate the sample to dryness and another 2 hr to apply the samples to TLC plates, although several plates can be prepared at the same time. Finally, long exposure of the X-ray film adds to the time from assay to result.

The assays for glucuronidation catalyzed by UGTs are performed using the following conditions: 50 mM Tris·Cl; 10 mM $MgCl_2$, pH 6.8 to 8.4 (aglycone dependent); 100 µg/ml phosphatidylcholine; 8.5 mM saccharolactone; 0.1 to 1 mg/ml microsomal or membrane protein; 0.1 to 5.0 mM substrate; and 2 mM [^{14}C]UDPGlcUA (specific radioactivity 1 µCi/µmol). Incubation takes place in shaker bath at 37°C for 10 min to 4 hr.

Materials

Microsomal pellet (see Support Protocol 1 or 2)
Enzyme buffer (see recipe), ice cold
Bio-Rad protein assay kit
Reaction buffer (see recipe and Table 4.3.1)
Phosphatidylcholine (see recipe)
Saccharolactone (see recipe)
Substrate solutions (see recipe and Table 4.3.1)
20 mM [^{14}C]UDPGlcUA solution (1 µCi/µmol; see recipe)
100% ethanol
1-Butanol
Acetone
Glacial acetic acid
28% (w/w) ammonium hydroxide
48% (w/w) hydrofluoric acid

3a70B counting cocktail (Research Products International) or equivalent
TLC plates: PSC plates (silica gel 60F_{254}, 20 × 20 cm, concentration zone 4 × 20 cm, 0.5 mm thickness; Merck)
TLC tanks for 20 × 20–cm plates
EN^{3}HANCE (NEN Life Science)
Kodak XAR 5 or Kodak BioMax MR film
Electronic flash (Vivitar or equivalent), dimmed by covering the emission surface with Whatman no. 3 filter paper

Table 4.3.1 Optimal Assay Conditions for Glucuronidation of Common Substrates

Substrate	Species	pH	Substrate concentration (mM)	Reaction time (min)	Basic Protocol(s)
Androsterone	Rat	8.0	0.1	10-15	1 and 3
	Human	8.4	0.1	15-30	1 and 3
Bilirubin	Rat	7.7	0.345	30-60	3
	Human	7.8	0.345	30-60	3
Codeine	Human	8.4	5	30-60	2
Morphine	Rat	8.4	5	15-30	2
	Human	8.4	5	15-30	2
Sapogenins	Human	7.5	0.1	30-120	1 and 3
Testosterone	Human	7.5	0.1	15-30	1 and 3

Carry out UGT reaction

1. Suspend the microsomal pellet in a small aliquot of ice-cold enzyme buffer using a Potter-Elvehjem homogenizer with a Teflon pestle.
2. Determine the protein concentration by the Bio-Rad protein assay and adjust the concentration to 4 to 10 mg/ml with ice-cold enzyme buffer.
3. Place incubation tubes on ice, and add the following to each tube (total volume 100 µl):

   10 µl reaction buffer (50 mM Tris·Cl/10 mM $MgCl_2$ final)
   10 µl phosphatidylcholine solution (100 µg/ml final)
   10 µl saccharolactone solution (8.5 mM final)
   1 to 10 µl aglycone substrate (0.1 to 5 mM final)
   10 to 25 µl microsomal or membrane protein (10 to 100 µg final)
   H_2O to 90 µl.

   Use round-bottomed incubation tubes, because the protein will not stay suspended in a conical microcentrifuge tube during long incubation periods.

   Include control assays with the incubations. Prepare controls without the aglycone substrate, and incubate the same time as the assays; add the aglycone after termination of the reaction (step 5). Also prepare a zero-time control by adding 200 µl of 100% ethanol before adding [^{14}C]UDPGlcUA and place the tube on ice until step 6.
4. Vortex the tubes and preincubate 5 min at 37°C.
5. Add 10 µl [^{14}C]UDPGlcUA to start the reaction; vortex the tubes, and place them in a 37°C water bath with shaking. Incubate 10 min to 4 hr.

   The optimal pH for the reaction buffer depends on the substrate used (see Table 4.3.1).

   For glucuronidation of substrates with which the reaction efficiency is very low, it may be necessary to incubate overnight to obtain measurable amounts of glucuronides.

Prepare samples for TLC

6. Stop the reaction by adding 200 µl of 100% ethanol.
7. Spin in microcentrifuge 10 min at 13,000 rpm, room temperature.
8. Transfer 200 µl of supernatant to a fresh conical 1.7-ml microcentrifuge tube.
9. Evaporate the supernatant to dryness in a spin vacuum drier (e.g., SpeedVac).

   This will take 2 to 3 hr, depending on the equipment.

Load samples on TLC plate

10. Resuspend the contents of the tube in 12 µl water to dissolve most of the formed glucuronide. Spot the 12-µl suspension in a single area, 2 cm from the lower edge in the concentration zone, in 2-µl aliquots on a TLC plate, allowing each spot to dry before making the next application.

    The spots can be dried between spottings using an air drier for 3 to 5 min at room temperature.

    Spotting one aliquot at a time ensures that the glucuronide will be concentrated in a small area, making it easier to detect small amounts.

    Up to 18 samples may be spotted on one plate as long as the samples belong to the same class.
11. Rinse the tube with 10 µl of 100% ethanol, and spot 2-µl aliquots as in step 10.
12. Add 6 µl of water to the tube, and spot 2 µl at a time onto the plate as in step 10.

13a. *For plates with glucuronides of amines and opioids (except morphine):* Prepare TLC tank with alkaline mobile phase to a height of 1 cm. Alkaline mobile-phase composition:

70 ml 1-butanol
70 ml acetone
40 ml water
20 ml 28% ammonium hydroxide.

13b. *For plates with glucuronides of all other substrates:* Prepare TLC tank with acidic mobile phase to a height of 1 cm. Acidic mobile-phase composition:

70 ml 1-butanol
70 ml acetone
40 ml water
20 ml glacial acetic acid.

14. Grease top edge of tank with vacuum grease, and replace lid to form tight seal. Equilibrate tank system 1 hr before adding plate.

Chromatograph the plate

15. Working in a fume hood, chromatograph the plate until the solvent front is ½ in. (~1.25 cm) from the top. Air dry the plate. Inspect the plate under UV light to ascertain if development was satisfactory.

CAUTION: *Steps 15 and 16 must be performed in a chemical fume hood.*

This step generally takes 2 to 4 hr. Remove the plate from the tank, and air dry the plate.

Sometimes the glucuronides streak. This may be the result of using a defective (old) TCL plate, placing the spots too close together, insufficiently drying the plates before placing them in the tank, or using the wrong solvent system.

The substrates and the solvent front are generally visible. Glucuronides generally have R_f values of 0.5 to 0.7. (R_f is the distance from the origin to the compound spot of interest divided by the distance from the origin to the solvent front; an R_f value of 0.5 means the compound spot moved halfway from the origin to the solvent front).

16. Check the plate with a hand-held Geiger counter.

If the radioactivity is detectable at the R_f of the glucuronides, a 24-hr exposure of the X-ray film is sufficient.

17. Spray the plate with EN^{3}HANCE. Air dry at least 20 min.

Visualize the products

18. Place the plate in a film cassette. Expose an X-ray film to an electronic flash at a distance of 15 in (~38 cm) from the source, and place the preflashed surface of the film against the plate. Close the cassette, and store in a −80°C freezer until sufficient exposure has been obtained.

Preflashing the film will increase the sensitivity of the film to light.

If glucuronides were not detected with the Geiger counter, an exposure time of 48 to 72 hr is necessary; for very low radioactivity an exposure time of 1 week might be necessary.

19. Develop the film either manually according to the manufacture's instructions or in an automated film developer.

Quantify radioactivity

20. Mark the positions of the radioactive spots on the TLC plate; be sure to mark the corresponding spots for the control incubations.

21. Scrape the silica gel spots off the TLC plate using a razor blade and place the gel in a scintillation vial.
22. Add 500 µl water to the vial, and vortex to break up the gel.
23. Add 500 µl of 48% hydrofluoric acid to the vial. Incubate 30 min at room temperature.
24. Add 15 ml 3a70B counting cocktail, and count the sample once it has cooled.

In this method, the radioactive glucuronide counted is two-thirds of that formed: 200 of 300 µl total reaction mixture (100 µl incubation plus 200 µl to stop the reaction).

The specific activity (picomoles glucuronide/minute/milligrams protein) is, therefore,

$$\frac{3 \times (\text{dpm}_{\text{sample}} - \text{dpm}_{\text{control}})}{2 \times (\text{dpm/pmol UDPGlcUA}) \times \text{min} \times \text{g protein}}$$

SEP-PAK ASSAY FOR UGT ACTIVITY

BASIC PROTOCOL 2

This method was developed as a fast technique for analyzing the formation of opioid glucuronides. Because many samples can be processed within a short time, it is well suited to kinetic studies. After incubation, the glucuronides can be separated from the radioactive UDPGlcUA within 10 min per twelve samples, using the manifold described here.

Materials

20 mM [^{14}C]UDPGlcUA solution (0.5 µCi/µmol; see recipe)
100% methanol
10 mM ammonium acetate (see recipe)
1 M ammonium acetate, pH 9.2 (see recipe), ice cold

13 × 100–mm glass or 75 × 12–mm polypropylene tubes
Sep-Pak C18 cartridges (Millipore)
Budget-Solve counting cocktail (Research Products International) or similar

Additional reagents and equipment for UGT reaction (see Basic Protocol 1)

1. Carry out the UGT reaction (see Basic Protocol 1, steps 1 to 5), setting up the reaction in 13 × 100–mm glass or 75 × 12–mm polypropylene tubes and using 0.5 µCi/µmol [^{14}C]UDPGlcUA solution in the reaction mixture.
2. Prepare one Sep-Pak cartridge assembly for each sample (see Fig. 4.3.2).

   It is advisable to have three flasks between the manifold and the vacuum pump. Flask 1 contains accidental radioactive overflow from the manifold. Flask 2 contains water to absorb ammonia from the ammonium acetate elutions. The water should be changed daily, according to use. Flask 3 contains a desiccant to prevent water vapor from reaching the pump.

   An inexpensive vacuum manifold can be obtained by modifying a Millipore 1225 Sampling Manifold (Millipore); see Figure 4.3.2.

3. To preequilibrate the Sep-Pak cartridges to be used for the first time, rinse the cartridges with 10 ml of 100% methanol followed by 10 ml of 10 mM ammonium acetate using vacuum aspiration. Do not allow the cartridges to become dry.

   Steps 3 to 5 are also done with vacuum aspiration.

4. Stop the reaction by adding 5 ml ice-cold 1 M ammonium acetate.
5. Rinse a Sep-Pak cartridge with 10 ml ice-cold 1 M ammonium acetate.

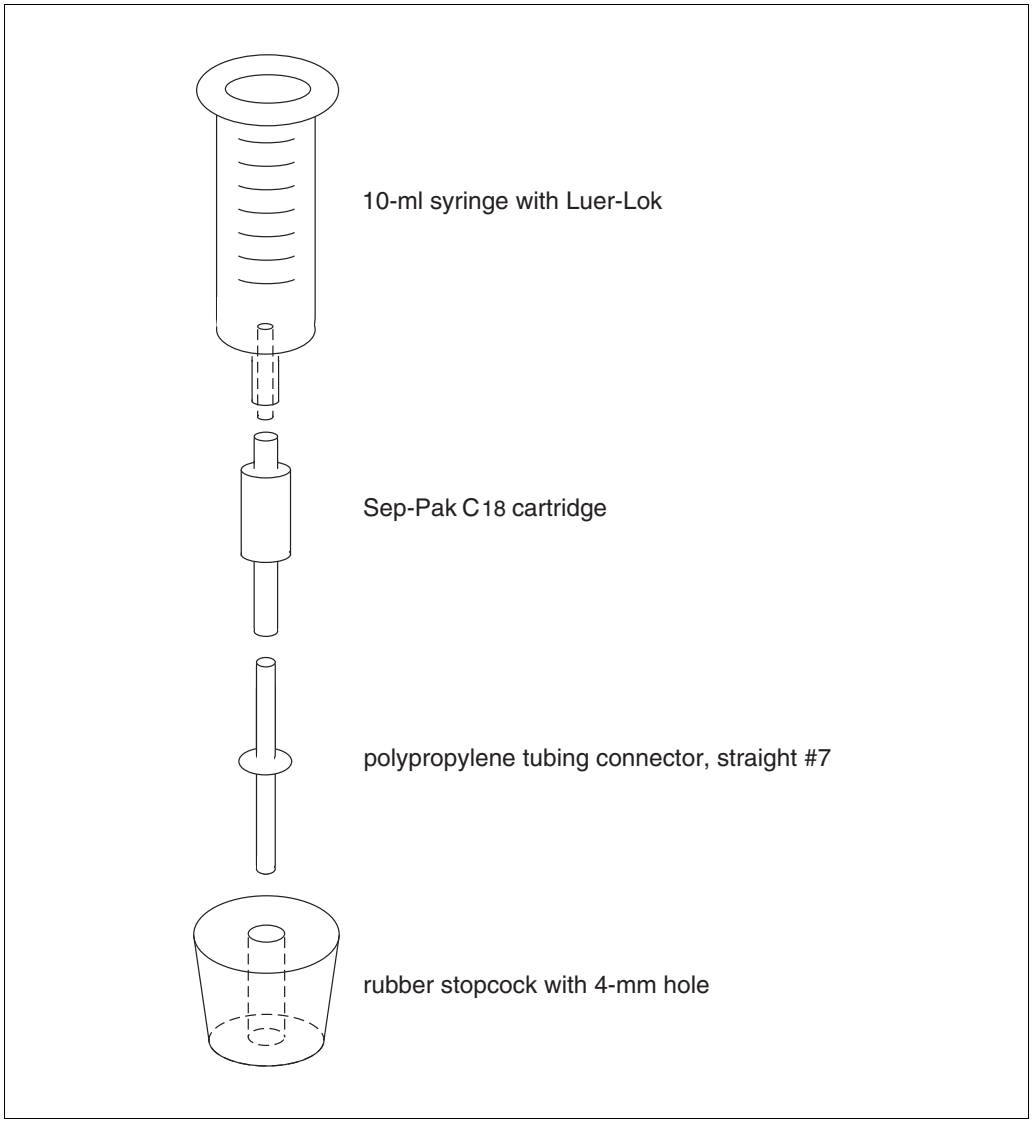

Figure 4.3.2 An assembly of a Sep-Pak cartridge and receptacle for use with the Millipore 1225 Sampling Manifold or similar manifold using stopcocks.

6. Apply the assay sample to the Sep-Pak cartridge, and rinse the reaction tube with 1 to 5 ml of 1 M ammonium acetate.
7. Wash the Sep-Pak cartridge two times with 10 ml of 10 mM ammonium acetate. Aspirate each aliquot.
8. Remove the Sep-Pak cartridge and syringe unit from the manifold, and manually elute the cartridge with 5 ml of 100% methanol directly into a scintillation vial by using the syringe plunger. Disconnect the syringe from the Sep-Pak cartridge before removing the plunger (in order not to disturb the packing of the Sep-Pak). Reassemble the cartridge unit before mounting the unit in the manifold.

   The cartridges can be regenerated with two 10-ml applications of methanol and can be reused 20 to 40 times, depending on the amount of protein that has been applied to the cartridges. When elution becomes slow and the radioactivity in the control samples doubles, the cartridges must be replaced.

9. Add 10 ml of Budget-Solve counting cocktail to the vial.

10. Count the radioactivity in the vial.

The radioactivity of the total amount of glucuronide formed is counted in this method, so the specific activity (picomoles glucuronide/minute/milligram protein) is

$$\frac{(\text{dpm}_{\text{sample}} - \text{dpm}_{\text{control}})}{(\text{dpm/pmol UDPGlcUA}) \times \text{min} \times \text{mg protein}}$$

ETHYL ACETATE EXTRACTION ASSAY FOR UGT ACTIVITY

BASIC PROTOCOL 3

This method relies on the fact that the glucuronides of bilirubin, steroids, and bile acids are more soluble in ethyl acetate than in aqueous solution at pH 2. This method is also fast: after the incubation period, it takes only ~20 min to separate the glucuronides from the [^{14}C]UDPGlcUA.

Materials

20 mM [^{14}C]UDPGlcUA solution (0.5 µCi/µmol; see recipe)
Glycine/Triton buffer (see recipe)
Water-saturated ethyl acetate
Budget-Solve counting cocktail (Research Products International) or similar

Additional reagents and equipment for UGT reaction (see Basic Protocol 1)

1. Perform the UGT enzyme reaction (see Basic Protocol, steps 1 to 5), setting up the reaction in 75 × 12-mm polypropylene tubes and using 0.5 µCi/µmol of [^{14}C]UDPGlcUA solution in the reaction mixture.
2. Stop the reaction by adding 0.1 ml glycine/Triton buffer.
3. Add 1.0 ml water-saturated ethyl acetate.
4. Shake in horizontal shaker 10 min or vortex the tube 1 min.
5. Spin 5 min in a low-speed centrifuge, room temperature.
6. Carefully pipet 0.5 ml of the organic phase (top) into a scintillation vial.

   Up to 750 µl can be removed for counting if a higher sensitivity is needed.

7. Add 10 ml of Budget-Solve counting cocktail to the vial.
8. Count the radioactivity in the vial.

   In this method, the radioactive glucuronide counted is (one-half × three-quarters) of that formed; the whole reaction is extracted with 1 ml of ethyl acetate; therefore, the specific activity (picomoles glucuronide/minute/milligram protein) is

$$\frac{2\,(\text{or } 1.33) \times (\text{dpm}_{\text{sample}} - \text{dpm}_{\text{control}})}{(\text{dpm/pmol UDPGlcUA}) \times \text{min} \times \text{mg protein}}$$

PREPARATION OF MICROSOMES FROM TISSUE

SUPPORT PROTOCOL 1

The UGTs reside in the endoplasmic reticulum anchored across the membrane. The microsomal and cell membrane preparations contain the endoplasmic reticulum and, therefore, possess an increased amount of enzyme per milligram of preparation compared with the relative amount of the enzymes in tissue snips or whole cells. This protocol is used to isolate microsomes from fresh or frozen tissue.

Materials

Organ tissue, freshly recovered or frozen tissue from a commercial source
1.15% (w/v) KCl

NOTE: Perform all steps at 4°C.

1. Weigh the tissue in grams
2. Add (4 × the weight) ml of 1.15% KCl.
3. Homogenize in a Potter-Elvehjem homogenizer using a motorized Teflon pestle.

   Be careful that the temperature of the homogenate does not rise above 4°C.
4. Centrifuge the homogenate 20 min at 9000 × *g*.
5. Carefully decant the supernatant through a layer of cotton gauze to remove fatty substances associated with tissue (especially prevalent in liver). Discard the pellet.
6. Centrifuge the supernatant in polycarbonate tubes 60 min at 100,000 × *g*. Discard the supernatant.
7. Wash the pellet by resuspending it in 4 vol of 1.15% KCl. Homogenize by hand, using a Potter-Elvehjem homogenizer.

   The homogenate can be divided into smaller tubes at this point, if desired.
8. Centrifuge the homogenate 60 min at 100,000 × *g* to sediment the pellet.
9. Decant the supernatant.
10. Overlay the pellet with at least 1 ml of 1.15% KCl, and store up to 1 year at −80°C.

SUPPORT PROTOCOL 2

PREPARATION OF MICROSOMES FROM CULTURED CELLS

This protocol is used to prepare microsomes from tissue culture cells transfected to express UGT cDNA.

Materials

Cultured cells, such as HK293, V79, or COS cells, expressing UGT after transfection with vector containing UGT cDNA
PBS (*APPENDIX 2A*)
Cell suspension buffer (see recipe)
Cell homogenate dilution buffer (see recipe)

Tissue tearer: 985-370 (Biospec Products) or equivalent
Sonifier cell disrupter: Hat system (Ultrasonic) or equivalent

NOTE: Perform all procedures at 4°C.

1. Harvest the cells and wash three times with PBS.
2. Suspend the cell pellet 1:3 (v/v) in cell suspension buffer.
3. Disrupt the cells 10 sec with a tissue tearer.
4. Dilute the homogenate 1:4 (v/v) with cell homogenate dilution buffer.
5. Sonicate three times in 10-sec bursts with a Sonifier cell disrupter, keeping the cell homogenate in a ice-water bath.
6. Homogenize by hand using a Potter-Elvehjem homogenizer with a Teflon pestle (10 strokes).

7. Centrifuge 20 min at 9000 × *g*.
8. Centrifuge the supernatant 1 hr at 100,000 × *g*.
9. Discard the supernatant.
10. Overlay the pellet with at least 1 ml of cell homogenate dilution buffer, and store up to 1 year at −80°C.

REAGENTS AND SOLUTIONS

Use Milli-Q-purified water or equivalent for all recipes and protocol steps. For common stock solutions, see ***APPENDIX 2A****; for suppliers, see* ***SUPPLIERS APPENDIX****.*

Ammonium acetate, pH 9.2, 1 M

Dissolve 308 g ammonium acetate in 4 liters water. Adjust the pH to 9.2 at 4°C with 28% (w/v) ammonium hydroxide. Store up to 1 month at 4°C.

Ammonium acetate, 10 mM

Add 20 ml of 1 M ammonium acetate, pH 9.2, to 2 liters water. Do not adjust the pH. Store up to 1 month at room temperature.

Cell homogenate dilution buffer

For 1 liter, weigh 85.6 g sucrose. Add 5 ml of 1 M HEPES, pH 7.4 (*N*-2-hydroxylthylpiperazine-*N*^{1}-2-ethanesulfonic acid; commercially prepared). Dilute to 1 liter with water; adjust the pH to 7.4 with 1 N NaOH. (Final: 0.25 M sucrose/5 mM HEPES, pH 7.4.) Store up to 1 month at 4°C.

Cell suspension buffer

Weigh 7.71 mg dithiothreitol (DTT). Add 100 ml cell homogenate dilution buffer (see recipe). (Final: 0.25 M sucrose/0.5 mM DTT/5 mM HEPES, pH 7.4.) Store up to 1 month at 4°C.

Enzyme buffer

Tris-buffered saline: Weigh 121 mg Tris·Cl and 900 mg NaCl; add water, and adjust the pH to 7.4 at 4°C with HCl. Adjust with water to a final volume of 100 ml. Store up to 1 month at 4°C.

1 M dithiothreitol (DTT): Dissolve 1.54 g DTT in 10 ml water. Store up to 2 weeks at −20°C.

Enzyme buffer: Add 5 µl of 1 M DTT to 10 ml Tris-buffered saline. Prepare just before use. (Final: 10 mM Tris-buffered saline, pH 7.4/0.5 mM DTT.)

Glycine/Triton solution

Weigh 5.25 g glycine, and dissolve in water to 90 ml. Add 1 ml Triton X-100, adjust the pH to 2 with concentrated HCl, and add water to 100 ml. (Final: 0.7 M glycine HCl, pH 2.0/1% Triton X-100.) Store up to 1 month at 4°C.

KCl, 1.15% (w/v)

Dissolve 11.5 g KCl in 1 liter water. Store up to 1 month at 4°C.

Phosphatidylcholine (1 mg/ml)

For 25 ml, weigh 25 mg L-α-phosphatidylcholine, type XVI-E from egg yolk, lyophilized powder. Add 25 ml ice-cold water, vortex, and sonicate on ice until a clear suspension is obtained. Divide into 1-ml aliquots in capped tubes, and store up to 1 year at −20°C.

Reaction buffer

For 100 ml, weigh 6.05 g Tris·Cl. Add 10 ml of 1 M $MgCl_2$ (50.8 g $MgCl_2 \cdot 6H_2O$ in 250 ml water). Add water to 100 ml and adjust the pH as needed with HCl at 37°C. (Final: 0.5 M Tris·Cl/0.1 M $MgCl_2$.) Store up to 1 month at 4°C.

Because the optimal pH for the reaction depends on the substrates used, it is convenient to prepare stock solutions of buffers with different pH values (7.0, 7.4, 7.7, 8.0, and 8.4). For a pH lower than 7.0, use 10.5 g bis-Tris instead of Tris. Although a buffer at pH 7.4 is useful for screening substrates using the TLC method, a negative result may indicate that an inappropriate pH was used. Generating an activity-versus-pH curve for unknown substrates is highly recommended.

Saccharolactone (85 mM)

For 25 ml, dissolve 408 mg saccharolactone in 25 ml water. Store in 1-ml aliquots up to 1 year at −20°C. Discard unused solution after 24 hr.

Substrate solutions

As an overall guideline, 200- to 500-µl stock solutions should be prepared in water, methanol, ethanol, DMF, or DMSO to obtain final concentrations in the incubation mixture of 0.1 to 5 mM. 1- to 50-mM solutions may be prepared in water, and 10- to 250-mM solutions in alcohol, dimethylformamide (DMF), or dimethyl sulfoxide (DMSO). The solutions should be stored at −20°C. The following solutions have generally proved convenient:

Opioids: Prepare 50-mM solutions of opium salts in water and store up to 3 months at −20°C.

Morphine: Prepare 25-mM solution of morphine sulfate in water. Store up to 1 year at −20°C.

Codeine: Prepare 100-mM solution of codeine in methanol. Store up to 2 weeks at −20°C.

Sapogenin: Prepare 10-mM solution in DMF. Store up to 2 weeks at −20°C.

Steroids: Prepare 10-mM solution in methanol. Store up to 2 weeks at −20°C.

Bilirubin: Dissolve 5 mg bilirubin in 250 µl of 0.1 N NaOH (3.4 mM bilirubin final). Add 2.25 ml of 40 mM Tris·Cl, pH 7.4, containing 30 mg/ml bovine serum albumin. Store up to 24 hr at 4°C in the dark.

The bilirubin assay should take place in the dark or shielded from light; and the tubes should be flushed with argon or nitrogen and capped before being placed in the shaker incubator.

[^{14}C]UDPGlcUA solutions (in 20 mM unlabeled UDPGlcUA)

100 mM unlabeled UDPGlcUA stock: Dissolve 315.7 mg UDPGlcUA ammonium salt in 5 ml H_2O.

20 mM [^{14}C]UDPGlcUA (1 µCi/µmol) for TLC: For 500 µl, add 400 µl of [^{14}C]UDPGlcUA (0.025 µCi/µl, 318 mCi/mmol) to 100 µl of unlabeled 100 mM UDPGlcUA.

20 mM [^{14}C]UDPGlcUA (0.5 µCi/µmol) for extractions: For 500 µl, add 200 µl [^{14}C]UDPGlcUA (0.025 µCi/µl, 318 mCi/mmol) and 200 µl H_2O to 100 µl of 100 mM unlabeled UDPGlcUA.

Store all solutions up to 1 year at −20°C.

For aglycone substrates that exhibit high activity, a lower specific activity of UDPGlcUA can be used, decreasing costs.

COMMENTARY

Background Information

Glucuronidation, the principal conjugation pathway in all vertebrate species, takes place in a wide range of tissues and accounts for most of the detoxified material in bile and urine. Conjugation with glucuronic acid confers greater polarity and water solubility on the aglycone, leading to more rapid excretion. Some generated glucuronides, however, can be pharmacologically and toxicologically relevant. For example, both the morphine-3- and -6-glucuronides have physiologic effects (Christrup, 1997), and *N*-hydroxyglucuronides from arylamines are known to initiate colon or bladder cancer in humans (Bock, 1991). The glucuronidation process is also involved in the metabolism of compounds that participate in cell growth or differentiation, such as retinoic acid and thyroid hormones (Nebert, 1991).

The glucuronidation reaction is catalyzed by a family of UGT isoenzymes. Molecular biology techniques have made it possible to identify the genes for individual mammalian UGTs and to express the UGT proteins. Thus it has been feasible to study the substrate specificities and kinetic parameters of individual UGTs (Clarke and Burchell, 1994; Burchell et al., 1995). The nomenclature for the isoenzymes is based on evolutionary divergence (Mackenzie et al., 1997).

The UGTs are membrane-bound proteins present in the liver, kidney, skin, intestine, prostate, brain, and lung; however, not all isoforms are present in all tissues. There is a great deal of overlap of substrate acceptance among the isoforms. No substrate has so far been found for which glucuronidation is catalyzed by all isoenzymes, although compounds such as 4-methylumbelliferone and *p*-nitrophenol are substrates for many of them. Therefore, using nonspecific substrates in induction and inhibition studies in tissue preparations may result in data that are difficult to interpret. The glucuronidation of some substrates is catalyzed with great efficiency by specific isoforms. These substrates are listed in Table 4.3.2 and may be used as markers for individual isoenzymes.

Earlier analytical methods made use of the spectrophotometric properties of the aglycones and their glucuronides. Herweigh and co-workers (1972) found that by diazotization of bilirubin glucuronides and solvent extraction of the products, the formation of bilirubin glucuronides could be measured spectrophotometrically. Many assay methods have used radioactive aglycones, such as *p*-nitrophenol (Frei et al., 1974), morphine (Del Villar et al., 1974), and steroids (Tukey and Tephly, 1981). Many aglycones, however, are not available in radioactive form. Lillienblum and Bock (1984) developed spectrophotofluorimetric assays for the glucuronidation of 4-methylumbelliferone, α-naphthylamine, and 4-aminobiphenyl.

The methods described in this unit are based on the use of [^{14}C]UDPGlcUA and are applicable to most substrates. The TLC method (see Basic Protocol 1) presented here was originally developed by Bansal and Gessner (1980). It has been modified to include two different resolving systems, because the glucuronides of amines and opioids (except morphine) can be separated from UDPGlcUA only in a basic solvent system. This method is excellent for screening many aglycone substrates at the same time, but relatively time-consuming.

The Sep-Pak C18 method (see Basic Protocol 2) was published by Puig and Tephly (1986). It was originally developed for detection of morphine glucuronides, but it is also applicable to other morphinan and oripavine substrates as well as tertiary amines such as imipramine. Matern et al. (1994) published a radioassay of UGT activities toward endo-

Table 4.3.2 Substrates Glucuronidated Primarily by a Single Isoenzyme

Substrate	Species	Isoenzyme
Bilirubin	Rat	rUGT1A1
Bilirubin	Human	hUGT1A1
Sapogenins	Human	hUGT1A4
Morphine	Rat	UGT2B1
Codeine (morphine)	Human	UGT2B7
Testosterone	Human	UGT2B15

genous substrates, such as hyodeoxycholic acid, bilirubin, estriol, androsterone, and testosterone, in which ethyl acetate was used as the extraction solvent. This method is given here (see Basic Protocol 3) with slight modifications to allow larger aliquots to be counted.

Finally, many HPLC methods have been developed for identifying metabolites in urine and plasma from in vivo metabolism of xenobiotics and endogenous compounds. These methods can also be used to identify and quantify glucuronides from the assays described here. Some of the methods are useful for identifying and quantifying metabolites for which the glucuronidation reaction yields several glucuronides. Svensson (1986) and Yue et al. (1990) developed a system for separating morphine-3- and -6-glucuronides, and Spivak and Yuey (1986) published a method for separating monoglucuronides and diglucuronides of bilirubin. Glucuronide formation can be quantified either by assessing peak areas or, when using radioactive UDPGlcUA, by collecting the peak volumes and quantifying the radioactivity.

These are all sensitive assays, capable of detecting activities in the range of a few picomoles per minute per milligram protein. The sensitivity depends on the specific radioactivity of the UDPGlcUA and the efficiency of catalysis of the glucuronidation reaction.

Critical Parameters and Troubleshooting

Although most UGTs are able to catalyze the reaction between UDPGlcUA and the aglycone at pH 7.4, the optimal pH may vary greatly among substrates. For example, among the opioids, the optimal pH is 8.4 for morphine and 7.0 for buprenorphine (King et al., 1997). The incubation time is also critical. For some substrates, such as testosterone and estrone, the reaction is not linear beyond 10 min. The use of optimal amounts of protein and substrates is required for linear product formation. Many substrates, especially bilirubin and morphine, exhibit product inhibition at high substrate concentrations. For these reasons, it is necessary to establish the optimal assay conditions for unknown substrates if the results are to be used for comparison with known substrates and for establishing kinetic parameters.

The K_M for UDPGlcUA is in the range of 150 to 300 μM for the UGT isozymes identified

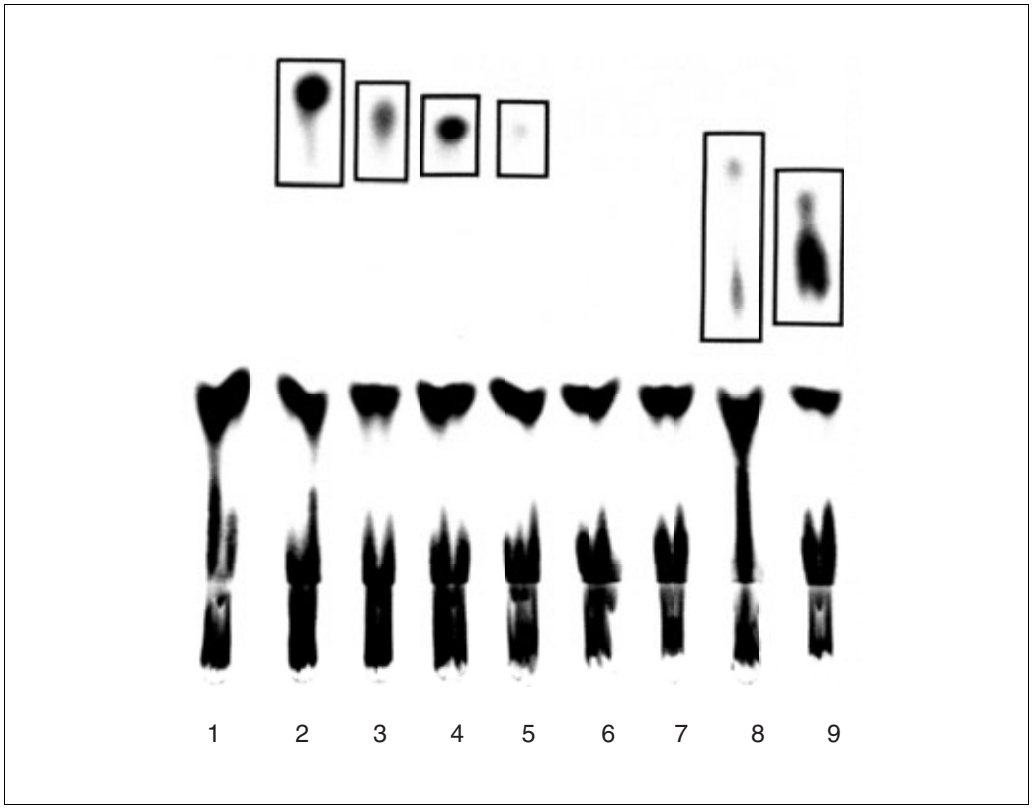

Figure 4.3.3 Autoradiogram of TLC chromatogram. The aglycones used in lanes 1 to 9 were 1, none; 2, naringenin; 3, apigenin; 4, eugenol; 5, *p*-nitrophenol; 6, hecogenin; 7, diosgenin; 8, 4-methylumbelliferone; and 9, scopoletin. The areas of the TLC plate indicated by the rectangles were scraped, and the radioactivity in the silica gel was determined as described in Basic Protocol 1.

thus far, so it is reasonable to use a concentration of 2 mM UDPGlcUA in assays. It is tempting to lower the UDPGlcUA concentration while increasing its specific radioactivity to obtain greater sensitivity; however, at concentrations that are too low, glucuronides may form so slowly that they are not detectable.

It has always been necessary to use detergents when solubilizing the UGTs in purification procedures using microsomes from tissue. Some detergents increase the UGT activity toward certain aglycones while decreasing or destroying the activity toward others. The most common detergents used are nonionic compounds, such as Brij 58, Triton X100, Emulgen 911, and digitonin or zwitterionic detergents (e.g., CHAPS and CHAPSO). For activation, very low concentrations—0.004% to 0.01% (w/v)—are used. It must be emphasized that an activity-versus-detergent-concentration curve must be established for any given substrate and detergent, before detergents are employed in assays.

When measuring very low activity, it is necessary to keep the radioactivity in the control samples as low as possible. If a radioactive spot occurs in all lanes, samples and control, of the autoradiogram of samples analyzed by Basic Protocol 1, it is an indication that the radioactive UDPGlcUA contains an impurity or that the common components of the assays have become contaminated with a compound that is a substrate for UGTs. The same conditions would cause high background counts in the assays performed using Basic Protocols 2 and 3. The [^{14}C]UDPGlcUA must have a purity >99% as measured by Sep-Pak C18 extraction (see below). If the level of impurities is too high, check with the manufacturer. Preparing new assay reagents will normally eliminate possible contaminants.

Impurity check for [^{14}C]UDPGlcUA

Remove 2 µl of [^{14}C]UDPGlcUA from the manufacturer's vial, and dilute with 5 ml ice-cold 1 M ammonium acetate, pH 9.2. Count 0.5 ml of the dilution. Apply to a Sep-Pak C18 cartridge, wash with ammonium acetate, and elute with methanol (see Basic Protocol 2, steps 6 to 11). If the counts from the methanol extraction are >0.95% of the applied counts, the [^{14}C]UDPGlcUA is not sufficiently pure.

Anticipated Results

This section gives examples of assays that were analyzed by each of the three methods described here.

Basic Protocol 1

A membrane preparation from cultured cells expressing an UGT isozyme was analyzed for activity toward naringenin, apigenin, eugenol, *p*-nitrophenol, hecogenin, diosgenin, 4-methylumbelliferone, and scopoletin. The general assay requirements are described in Basic Protocol 1. The specific conditions for this assay were pH 7.4, 50 µg 0.5 mM protein substrate, and 2 mM [^{14}C]UDPGlcUA (specific activity 1.9 dpm/pmol). The assays were incubated 60 min at 37°C, and then stopped with 200 µl of 100% ethanol. The analysis was carried out using steps 7 to 24 of Basic Protocol 1. The TLC plate was developed in an acidic system (step 13) and exposed to X-ray film for 60 hr. Figure 4.3.3 shows the developed autoradiogram. The areas on the TLC plate indicated by the rectangles were counted.

Specific activities (picomoles glucuronide/minute/milligram protein) were calculated using the following formula:

$$\frac{3 \times (\mathrm{dpm}_{\mathrm{sample}} - \mathrm{dpm}_{\mathrm{control}})}{2 \times (\mathrm{dpm/pmol\ UDPGlcUA}) \times \mathrm{min} \times \mathrm{mg\ protein}}$$

$$= \frac{3 \times (\mathrm{dpm}_{\mathrm{sample}} - \mathrm{dpm}_{\mathrm{control}})\ \mathrm{pmol}}{2 \times 1.9 \times 60 \times 0.050\ \mathrm{min} \times \mathrm{mg\ protein}}$$

$$= \frac{3.8 \times (\mathrm{dpm}_{\mathrm{sample}} - \mathrm{dpm}_{\mathrm{control}})\ \mathrm{pmol}}{\mathrm{min} \times \mathrm{mg\ protein}}$$

See Table 4.3.3 for results.

Basic Protocol 2

Microsomes prepared from rat liver were analyzed for activity toward morphine. The general assay requirements are described in Basic Protocol 2. The specific conditions for this assay were pH 8.4, 50 µg protein, 5 mM morphine, and 2 mM [^{14}C]UDPGlcUA (specific activity 107 dpm/nmol). The assays were incubated 25 min at 37°C, and then stopped with 5 ml of 1 M ammonium acetate.

The specific activity (nanomoles glucuronide/minute/milligram protein) of morphine was calculated using the following formula:

$$\frac{(\mathrm{dpm}_{\mathrm{sample}} - \mathrm{dpm}_{\mathrm{control}})}{(\mathrm{dpm/nmol\ UDPGlcUA}) \times \mathrm{min} \times \mathrm{mg\ protein}}$$

$$= \frac{(\mathrm{dpm}_{\mathrm{sample}} - \mathrm{dpm}_{\mathrm{control}})\ \mathrm{nmol}}{107 \times 25 \times 0.050\ \mathrm{min} \times \mathrm{mg\ protein}}$$

$$= \frac{0.0075 \times (\mathrm{dpm}_{\mathrm{sample}} - \mathrm{dpm}_{\mathrm{control}})\ \mathrm{nmol}}{\mathrm{min} \times \mathrm{mg\ protein}}$$

See Table 4.3.4 for results.

Table 4.3.3 Results from TLC Assay[a]

Substrate	dpm_{sample}	pmol/min/mg[b]
Apigenin	2739	689
Narengenin	6220	1605
Eugenol	3427	870
p-Nitrophenol	719	157
Hecogenin	NA	NA
Diosgenin	NA	NA
4-Methylumbelliferone	4852	1245
Scopoletin	17237	4500
No substrate	119	NA

[a]NA, not analyzed.
[b]Limit of detection was 35 pmol.

Table 4.3.4 Results from Sep-Pak Assay

Substrate	dpm_{sample}	nmol/minutes/mg[a]
Morphine	4332, 4091, 4399	31.7, 29.9, 32.2
No substrate	120, 100	—

[a]Limit of detection was 0.5 nmol.

Table 4.3.5 Results from Ethyl Acetate Extraction Assay

Substrate	dpm_{sample}	pmol/min/mg[a]
Androsterone	595, 604	285, 291
No substrate	133, 115	—

[a]Limit of detection was 35 pmol.

Basic Protocol 3

A membrane preparation from cultured cells expressing an UGT isozyme was analyzed for activity toward androsterone. The general assay requirements are described in Basic Protocol 3. The specific conditions for this assay were pH 8.4, 50 µg protein, 0.3 mM androsterone, and 2 mM [^{14}C]UDPGlcUA (specific activity 1.65 dpm/pmol). The assays were incubated 40 min at 37°C, and then stopped with 100 µl of 100% glycine/Triton solution. The analysis was carried out according to steps 3 to 8 of Basic Protocol 3. A total of 500 µl ethyl acetate was counted.

The specific activity (picomole glucuronide/minute/milligram protein) of androsterone was calculated using the following formula:

$$\frac{2 \times (dpm_{sample} - dpm_{control})}{(dpm/nmol\ UDPGlcUA) \times min \times mg\ protein}$$

$$= \frac{2 \times (dpm_{sample} - dpm_{control})\ pmol}{1.65 \times 40 \times 0.050\ min \times mg\ protein}$$

$$= \frac{0.606 \times (dpm_{sample} - dpm_{control})\ pmol}{min \times mg\ protein}$$

See Table 4.3.5 for results.

Time Considerations

For all the assays, the total time required depends in part on the duration of the reaction and the level of activity and can range from 10 min to 5 hr to overnight. TLC requires 2 to 4 hr plus 1 to 7 days for autoradiography. Sep-Pak extraction can be completed in 10 min. Ethyl acetate extraction can be completed in ~20 min.

Literature Cited

Bansal, S.K. and Gessner, T. 1980. A unified method for the assay of uridine diphosphoglucuronyltransferase activities towards various aglycones using uridine diphospho {U-^{14}C} glucuronic acid. *Anal. Biochem.* 109:321-329.

Bock, K.W. 1991. Role of UDP-glucuronosyltransferases in chemical carcinogenesis. *Crit. Rev. Biochem. Mol. Biol.* 26:129-150.

Burchell, B., Brierley, C.H., and Rance, D. 1995. Minireview. Specificity of human UDP-glucuronosyltransferases and xenobiotic glucuronidation. *Life Sci.* 57:1819-1831.

Christrup, L.L. 1997. Morphine metabolites. *Acta Anasthesiol. Scan.* 41:116-122.

Clarke, D.J. and Burchell, B. 1994. The uridine diphosphate glucuronosyltransferase multigene family: Function and regulation. *In* Handbook of Experimental Pharmacology, Vol. 112. Conjugation-Deconjugation Reactions in Drug Metabolism and Toxicity (F.C. Kauffman, ed.) pp. 3-43. Springer-Verlag, Berlin.

Del Villar, E., Sanchez, E., and Tephly, T.R. 1974. Morphine metabolism. II Studies on morphine glucuronosyltransferase activity in intestinal microsomes of rats. *Drug. Metab. Dispos.* 2:370-374.

Frei, I., Schmid, E., and Bischmeyer, H. 1974. UDP-glucuronosyltransferase. *In* Methoden der Enzymatischen Analyze (H.W. Beregmeyser, ed.) pp. 763-768. Verlag Chemie, Weinheim.

Herweigh, K.P.M., Van De Vijer, M., and Fevery, J. 1972. Assay and properties of digitonin-activated bilirubin uridine diphosphate glucuronyltransferase from rat liver. *Biochem. J.* 129:605-618.

King, C.D., Rios, G.R., Green, M.D., Mackenzie, P.I., and Tephly, T.R. 1997. Comparison of stably expressed rat UGT1.1 and UGT2B1 in the glucuronidation of opioid compounds. *Drug. Met. Dispos.* 25:251-255.

Lillienblum, W. and Bock, K.W. 1984. *N*-Glucuronide formation of carcinogenic aromatic amines in rat and human liver microsomes. *Biochem. Pharmacol.* 33:2041-2046.

Mackenzie, P.I., Owens, I.S., Burchell, B, Bock, K.W., Bairoch, A., Bélanger, A., Fournel-Gigleux, S., Green, M., Hum, D.W., Iyanagi, T., Lancet, D., Louisot, P., Magdalou, J., Roy Chowdhury, J., Ritter, J.K., Schachter, H., Tephly, T.R., Tipton, K.F., and Nebert, D.W. 1997. The UDP-glycosyltransferase gene superfamily: Recommended nomenclature update based on evolutionary divergence. *Pharmacogenetics* 7:255-269.

Matern, H., Heinemann, H., and Matern, S. 1994. Radioassay of UDP-glucuronosyltransferase activities toward endogenous substrates using labeled UDP-glucuronic acid and an organic solvent extraction procedure. *Anal. Biochem.* 219:182-188

Nebert, D.W. 1991. Proposed role of drug-metabolizing enzymes regulation of steady state levels of the ligands that effect growth, homeostasis, differentiation, and neuroendocrine function. *Mol. Endocrinol.* 5:1203-1214.

Puig, J.P. and Tephly, T.R. 1986. Isolation and purification of rat liver morphine UDP-glucuronosyltransferase. *Mol. Pharmacol.* 30:558-565.

Spivac, W. and Yuey, W. 1986. Application of a rapid and efficient H.P.L.C. method to measure bilirubin and its conjugates from native bile and in model bile systems. *Biochem. J.* 234:101-109.

Svensson, J.-O. 1986. Determination of morphine, morphine-6-glucuronide and normorphine in plasma and urine with high-performance liquid chromatography and electrochemical detection. 1986. *J. Chromatogr.* 375:174-178.

Tukey, R.H. and Tephly, T.R. 1981. Purification and properties of rabbit liver estrone and *p*-nitrophenol UDP-glucuronosyltransferase. *Arch. Biochem. Biophys.* 209:565-578.

Yue, Q., von Bahr, C., Odar-Cederlöf, I., and Säwe, J. 1990. Glucuronidation of codeine and morphine in human liver and kidney microsomes: Effect of inhibition. *Pharmacol. Toxicol.* 66:221-226.

Key References

Bansal and Gessner, 1980. See above.

Describes in detail the TLC method, which is applicable for analyzing the glucuronidation formation of many substrate samples simultaneously. A modification of this method is described in Basic Protocol 1.

Matern et al., 1994. See above.

Describes use of the extraction method to determine UGT activity toward bilirubin, steroid, and hyodeoxycholic acid. A modification of this method is described in Basic Protocol 3.

Puig and Tephly, 1986. See above.

Describes the Sep-Pak C_{18} method (Basic Protocol 2) for determining UGT activity toward opioids and amines.

Contributed by Birgit L. Coffman,
Gladys R. Rios, and Thomas. R. Tephly
University of Iowa
Iowa City, Iowa

Detection of Metabolites Using High-Performance Liquid Chromatography and Mass Spectrometry

The eventual goal of xenobiotic metabolism is to increase excretion of harmful or potentially harmful molecules. Ease of excretion is directly related to polarity of the molecule. Almost without exception, metabolites are more polar than the parent compound. The order of polarity is phase II metabolites >> phase I metabolites > parent compound (Johnston et al., 1991). This broad range of polarity between parent and metabolites translates into significant differences in chemical and physical properties including solubility, volatility, and thermal stability. The differences in these three properties between parent compound and metabolites continue to provide a challenge when attempting to identify the chemical intermediates and products (metabolites) of biotransformation reactions. Mass spectrometry (MS) is routinely used to detect, characterize, and quantify metabolites in biological samples. Yet, MS, like almost any other spectroscopic technique, suffers from the need for analytes to be pure in order to achieve high sensitivity and unambiguous structural identification. Tandem MS methods reduce the degree of purity necessary for unambiguous identification; however, problems exist when characterizing metabolites in complex mixtures by tandem MS alone. A tandem mass spectrometer can isolate and separate ions of the compounds of interest from the background by mass-to-charge ratio (*m/z*). Separation and isolation of these ions occurs in the mass analyzer after ionization, so that species that interfere with ionization are not eliminated.

Consequently, chromatographic separation must be employed prior to MS analysis of these "messy" biological samples. Gas chromatography (GC) is especially useful as a precursor to MS for resolution and separation of compounds. GC does require that the compounds being analyzed be thermally stable and volatile. Typically, metabolites are polar and tend to be both nonvolatile and thermally labile. This is especially true of phase II metabolites such as glutathione conjugates, which historically have been difficult to study due to their thermal lability and nonvolatile properties. Derivatization for gas chromatography/mass spectrometry (GC-MS) offers a partial solution; however, similar or interfering compounds present in the biological matrix can complicate or prevent derivatization and isolation of metabolites (especially phase II metabolites). Baillie and Davis (1993) summarized the situation by suggesting that MS can only make a significant contribution to studying phase II conjugation processes if a way can be found to study the conjugate intact.

High-performance liquid chromatography (HPLC) is widely used to separate and isolate metabolites. Routine detectors for liquid chromatography such as ultraviolet (UV) and refractive index (RI) often lack sensitivity and provide little structural information. When detected by these methods, metabolite identity can be deduced by cochromatography with authentic standards, if available. Obtaining authentic standards requires some prior knowledge about the identity of the metabolite. Another approach is to collect the HPLC peaks and then perform MS analysis. This approach works well but is time intensive, particularly if the sample matrix is complicated. A logical solution is to combine the separation power of HPLC with the sensitivity and structural characterization power of MS.

Although it provides a very powerful analytical concept, instrumentally the marriage of HPLC and MS has been, until recently, more of a truce than an actual joining. Numerous problems result from coupling a liquid-based high-pressure technique to a gas-phase high-vacuum technique. Chapman (1993) presents the dilemma as follows. A conventional high-vacuum pumping system of the sort found in most mass spectrometers will maintain a maximum pressure of 2.5×10^{-4} torr when faced with a vapor load of 5 to 7 ml/min. This is the approximate vapor load resulting from 5 µl/min of water or 15 µl/min of acetonitrile. HPLC separation at these flow rates can be achieved with capillary columns. However, continued operation of the mass spectrometer at pressures in the range of 10^{-4} torr would result in high background from the solvent, reduced analyte sensitivity, and greatly increased instrument maintenance. Consequently, considerable work has been done to develop an interface between the HPLC and MS that separates and

Contributed by Thomas D. McClure
Current Protocols in Toxicology (2000) 4.4.1-4.4.18

Table 4.4.1 HPLC Column Diameters and Characteristics[a]

Column type	Internal diameter	Length	Injection volume[b]	Flow rate (µl/min)	Column hardware
Conventional	3-6 mm	10-25 cm	5-20 µl	500-2000	Most widely used
Microbore	0.5-2 mm	10-100 cm	0.5-2 µl	1-50	Glass lined, staineless steel, PFTE[c]
Packed microcapillary	0.2-0.5 mm	10-50 cm	0.1 µl	0.5-2	Fused silica
Drawn packed capillaries	30-100 µm	2-20 m	0.1-1.0 µl	<0.1	Glass, loosely packed
Open tubular	5-25 µm	1-20 m	<1 nL	<0.1	Wall-coated fused silica

[a]Reprinted from Niessen and Van der Greef (1992) with permission from Marcel Dekker.

[b]Valid for isocratic conditions. The detector cell volume of a flow-through detector must be reduced to the volume quoted here as well.

[c]PFTE, teflon.

removes or reduces solvent without loss of analyte.

Within the last 20 years, several HPLC-MS interfaces have been made with varying degrees of success. This discussion will be limited to interfaces/source combinations that are currently the most widely available: atmospheric-pressure chemical ionization (APCI; Linscheid, 1992) and electrospray ionization (ESI; Whitehouse et al., 1995).

INSTRUMENTAL CONSIDERATIONS

HPLC

Chromatography is a physical separation method in which the compounds being separated are selectively distributed between two immiscible phases: a mobile phase flowing through a stationary phase bed (Niessen and Van der Greef, 1992). For HPLC, the flowing phase is a liquid solvent or solvents pumped under pressure. The stationary phase bed is a high–surface area solid material with specific physical properties. The solvent and stationary materials used are dictated by the samples/analytes and define the type of liquid chromatography. This discussion will be limited to two of the most common methods. Snyder et al. (1997) is necessary reading for the scientist developing HPLC methods for metabolite studies.

Normal- and reversed-phase HPLC

Normal-phase chromatography (NP-HPLC), also known as adsorption chromatography, uses polar functional groups (hydroxy, amino, and cyano) on the stationary phase to promote interaction with polar functional groups on analytes. The mobile phase is composed of nonpolar solvents such as hydrocarbons and chlorinated hydrocarbons. Solvent gradient programs increase in mobile phase polarity. The elution order in NP-HPLC is usually nonpolar molecules, then polar molecules, and then charged molecules.

Reversed-phase chromatography (RP-HPLC) is the opposite of NP-HPLC. The stationary phase relies on nonpolar functional groups (e.g., C_4, C_8, and C_{18} hydrocarbons, phenyl, cyanopropyl) for interaction with the nonpolar groups on the molecules being separated. The mobile phase includes varying amounts of polar organic solvents, water, and inorganic buffers. Gradient programs decrease mobile phase polarity over time. The elution order is the opposite of NP-HPLC: charged molecules, then polar molecules, and then nonpolar molecules.

Stationary phase selection

The stationary phase is packed into a cylindrical column that varies in length and inside diameter. Longer columns provide more resolving power up to an optimum. The inside diameter of the column defines the maximum flow rate through the column as shown in Table 4.4.1. HPLC flow rate is important when interfacing to a mass spectrometer. Low flow rates (nl/min) can mean less sample consumption and increased sensitivity.

The stationary phase used routinely in analytical applications consists of a solid support material ranging in particle size from 3 to 20 µm. The individual particles have pores ranging in size from 90 to 300 Å. The pores provide increased surface area; however, nonporous solid phases are also used. For different brands of columns, varying amounts of the support surface is linked to an organic bonded phase, which in turn varies the amount of interaction between the support and the analyte(s).

The most common stationary phases used in NP-HPLC are silica, alumina, and silica bonded with exposed organic functional groups

such as cyanopropyl and aminopropyl. The most common stationary phases in RP-HPLC are silica supports to which a hydrocarbon chain with four, eight, or twelve carbons is bonded. The most common RP stationary phases bonded to silica supports are listed in Figure 4.4.1.

An extensive description of stationary phases for NP- and RP-HPLC is beyond the scope of this manuscript. However, Neue (1997) has presented a comprehensive discussion on HPLC column technology with valuable chapters on column selection and maintenance.

HPLC-MS Interface and Source

Ionization of the analyte is a necessary process for detection by mass spectrometry and occurs via one of two processes: (1) solvent chemistry results in preformed ions in solution and the solvent is removed as the ions are transferred to the gas phase (via ESI), or (2) molecules are transferred to the gas phase and are then ionized. In either process, attention must be given to the gas-phase transfer process, especially if heat is used, to prevent decomposition. Often the choice between APCI and ESI involves deciding which method is best for producing ions for a given mobile phase composition and pH.

APCI

APCI is a variation on high-vacuum chemical ionization and was first described in the early 1960s (Linscheid, 1992). APCI ionizes the sample after it has been desolvated and introduced into the gas phase. The incoming solvent stream containing the analyte(s) is entrained with an inert nebulizing gas (usually nitrogen) and sprayed as a fine mist into a heated desolvation chamber at atmospheric pressure. Thermal decomposition in the desolvation chamber is minimized by using a high gas flow to keep the residence time to the minimum required for desolvation. A corona discharge is maintained at the end of the desolvation chamber from a needle held at between 1 and 5 kV. The corona discharge ionizes primarily gas-phase solvent molecules, which then ionize analyte molecules by charge transfer reactions. Once formed, the ions are accelerated through a reduced-pressure skimmer into the high-vacuum portion of the mass spectrometer for mass analysis and detection (van Baar, 1996; Hoja et al., 1997).

APCI mass spectra show little difference from their high-vacuum chemical ionization (high-vacuum CI) counterparts for the same compound. In addition, as with high-vacuum CI, the choice of the reagent gas (or HPLC solvent in the case of APCI) is an important factor in the degree of fragmentation observed in the mass spectrum. APCI spectra usually contain signals for $[M + H]^+$ or $[M - H]^-$ ions, but may be dominated by facile-fragmentation and neutral-loss ion signals. Furthermore, the mass spectra of some compounds also contain signals for $M^{+\cdot}$ or $M^{-\cdot}$ ions. Signals for ions from fragmentation of the most facile bonds are often observed.

A number of APCI source parameters can be adjusted experimentally for optimal results, as described below.

1. The HPLC mobile phase, once vaporized, becomes the CI reagent gas and should be chosen to provide chromatographic separation and promote ionization of the analyte as much as possible. Incompatibilities between ionization and chromatography can be reduced by adding ionization-enhancing materials to the mobile phase post column (i.e., volatile salt buffers such as ammonium acetate).
2. The flow rate of the mobile phase should be high enough to support chemical ionization. Typical APCI flow rates are 1 to 1.5 ml/min.
3. The temperature of the desolvation chamber should be set high enough to vaporize the HPLC solvent and analyte, but should not cause thermal decomposition.
4. The gas flow rate should be adjusted to reduce residence times in the desolvation chamber.
5. The discharge voltage should be experimentally optimized for selected analyte ions.
6. The degree of in-source fragmentation can be controlled by adjusting the accelerating potential of the newly formed ions, thus increasing or decreasing the amount and energy of collision-induced dissociation (CID) with solvent molecules.

ESI

ESI, as used for organic analysis, was first reported by Fenn and colleagues in 1984 (Yamashita and Fenn, 1984; Whitehouse et al., 1995). The liquid flow stream containing ionized analytes is pumped through a capillary in which the exit tip is held at high voltage (~4.5 kV). The liquid stream is nebulized upon exiting the capillary by nitrogen gas. The high voltage on the capillary tip attracts ions of opposite charge, so the droplets exiting the capillary are charged with the same polarity as the tip. The nebulizing gas directed around the

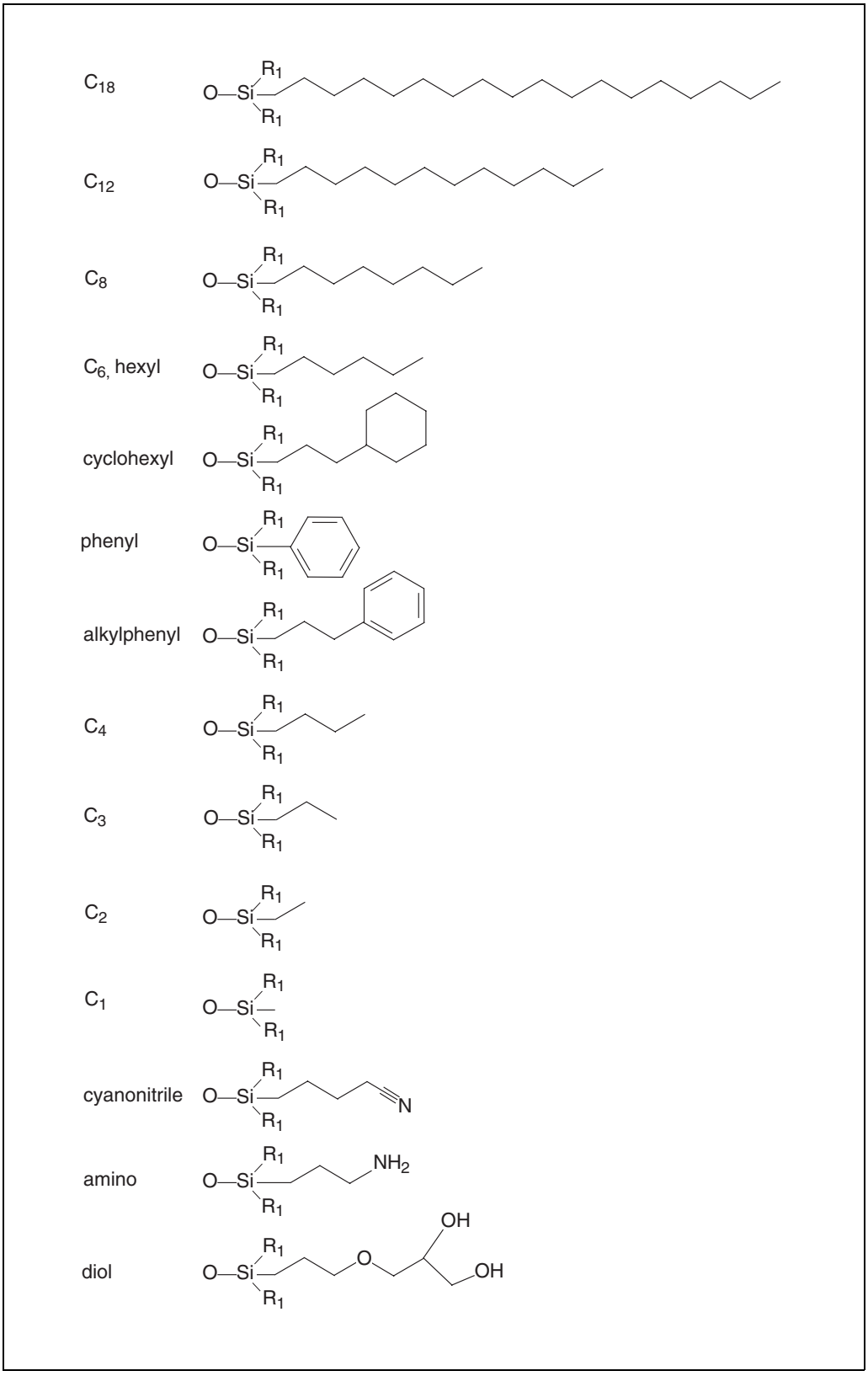

Figure 4.4.1 Bonded phases for RP-HPLC. Reprinted from Neue (1997) with permission from Wiley-VCH.

outside of the capillary helps to evaporate the neutral solvent molecules from the droplets, bringing like-charged ions closer together until coulombic repulsion destabilizes and breaks the droplets apart. This process is repeated until the gas-phase ions are desolvated. The charged particles are drawn toward a counter electrode-orifice into the mass analyzer and the remaining solvent vapor is pumped away (Linscheid, 1992; Dear et al., 1995; Hoja et al. 1997; Kebarle and Yeunghaw, 1997). The gas-phase ions may still contain a solvation layer that can be removed by gentle heating or additional gas flow.

ESI mass spectra usually contain signals for $[M + H]^+$ or $[M - H]^-$ for positive and negative experiments, respectively. Sometimes signals representing adducts with the HPLC solvent or metals (e.g., Na^+ or K^+) are observed. Some compounds will form M^+/M^- ions. Signals indicating in-source fragmentation are not usually seen in ESI spectra unless in-source CID is used. Some analyte ions support multiple charges as determined by their functional groups. ESI-MS studies of large biopolymers such as proteins, polypeptides, and oligonucleotides take advantage of this phenomenon. The molecular weight of these molecules lies outside the mass range of most mass analyzers. However, since the mass analyzer separates based upon mass-to-charge ratio (*m/z*), a sufficient number of charges on a molecule will bring the *m/z* to within the range of the mass analyzer. The ESI mass spectra of large biomolecules contain a distribution of *m/z* values corresponding to several different charge states. The multiple charge peaks in the spectrum can be mathematically deconvoluted to provide molecular weights with a high degree of accuracy.

Performance of the ESI interface is optimized by adjusting a number of parameters.

1. A mobile phase is selected that will encourage formation of ions in solution and that is compatible with the mass spectrometer. Nonvolatile buffers and salts should be eliminated from consideration, as they tend to plug the inlet to the mass analyzer and contaminate the source of conventional ESI systems. A number of instrument manufacturers are now offering ESI systems with modifications that permit the use of nonvolatile buffers without source contamination. Analyte signals can also be suppressed by ions in the sample matrix and even in the mobile phase (e.g., peptide signals are suppressed by trifluoroacetic acid in the mobile phase). Sometimes the optimum mobile phase for ESI is incompatible with optimum separation in reversed-phase chromatography. A compromise can be achieved with the use of volatile buffers that permit ion pairing (e.g., ammonium acetate). Post-column addition of mobile-phase modifiers can also be used at the expense of increased flow.

2. The flow rates into the ion source should be as low as possible, as limited by the chromatographic system, for maximum sensitivity. Flow rates range from nl/min to 1 ml/min (Gaskell, 1997).

3. The nebulizer gas flow rates should be adjusted based upon flow rate into the source. The gas flow needs to be high enough so that solvent cluster signals are eliminated but not so high that the spray current is unstable.

4. The capillary tip voltage should be set high enough to support and maintain desolvation of analyte ions without causing spray-destabilizing discharges.

5. A sheath liquid can be added to reduce the droplet surface tension and increase desolvation.

6. The degree of in-source fragmentation can be controlled by adjusting the accelerating potential of the newly formed ions, thus increasing or decreasing the amount of CID with solvent molecules.

Mass Analysis

ESI and APCI produce mass spectra that contain primarily molecular weight–related ion signals. Consequently, little structural information is revealed by these techniques. Increased fragmentation is observed by subjecting molecular weight–related ions to collision-induced dissociation (CID) in a collection of techniques termed mass spectrometry/mass spectrometry or tandem mass spectrometry (MS/MS). MS/MS is a two-dimensional technique in which one stage of mass analysis isolates the precursor ions of interest, subsequent fragmentation is induced (usually by collision with neutral gas molecules), and then a second stage of mass analysis detects the fragment or product ions (Brunnee, 1982). The type of MS/MS experiment chosen is a function of the type of information being sought and is outlined below. A graphical representation of these scan modes is presented in Figure 4.4.2.

Product ion MS/MS. Previously termed daughter-ion MS/MS, this method uses the first stage of mass analysis to select and isolate a precursor ion. The precursor ions are then fragmented via CID, and the resulting product ions are separated and detected during the second

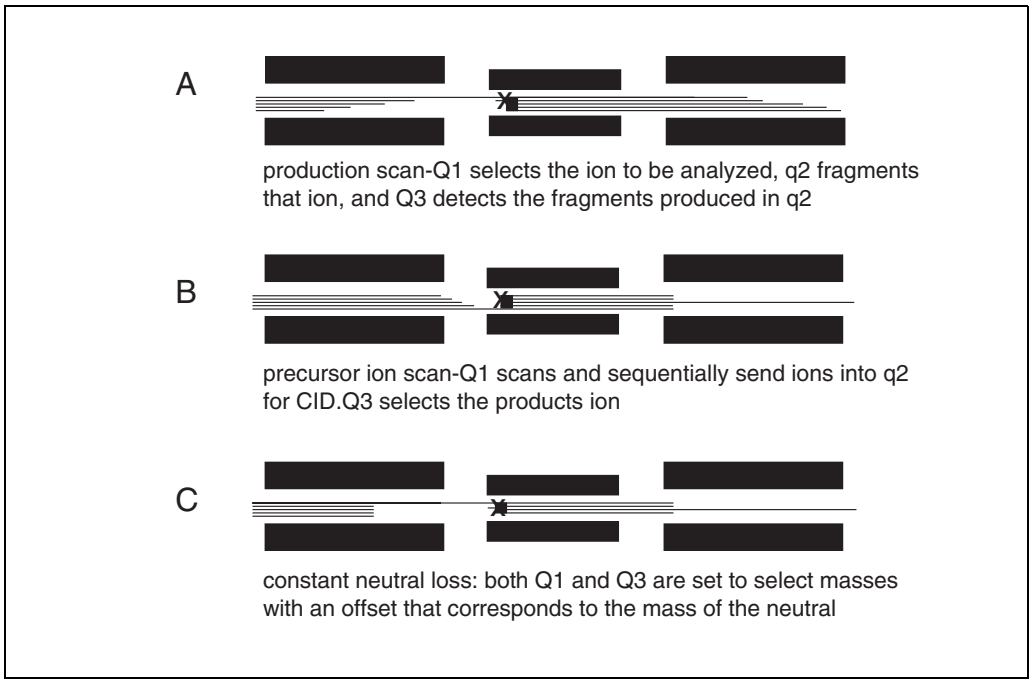

Figure 4.4.2 A graphic representation of scanning modes for (**A**) product ion, (**B**) precursor ion, and (**C**) CNL MS/MS. Q1, q2, and Q3 represent the different stages in an MS/MS experiment. These stages may be separated temporally but occur in the same device, or they may occur in three separate devices.

mass analysis stage. The resulting production spectrum contains signals for fragments directly derived from the selected precursor ion. This experiment answers the question: What are the fragments of the selected ion?

Precursor ion MS/MS. Formerly termed parent-ion MS/MS, this method separates and sequentially transmits all ions from the source during the first stage of mass analysis. These ions undergo CID fragmentation, and an ion of selected *m/z* is isolated and detected in the second stage of mass analysis. A precursor-ion mass spectrum contains signals at precursor *m/z* values for all precursor ions that fragmented to produce the selected product ion. This experiment answers the question: What ions fragment to produce ions at the selected *m/z*?

Constant neutral loss (CNL) scanning. In this MS/MS experiment, the first stage of mass analysis and the second stage of mass analysis are scanning but at a selected *m/*z offset. This offset corresponds to the mass of a lost neutral species (atom, molecule, or radical). The resulting CNL spectrum contains signals for all precursor masses that loose a selected neutral mass. This experiment answers the question: What precursor ions fragment and loose a neutral species at the offset mass?

Selected-reaction monitoring (SRM). SRM is an MS/MS scan mode using one of the three above tandem mass analysis methods. Rather than scanning one or both of the mass analyzers, both mass analyzers are held to transmit only a selected mass window. Thus, ion intensities are measured for specific MS/MS transitions. SRM has the advantage of providing increased sensitivity over scanning MS and MS/MS experiments because only one transition is monitored, and background ions generally do not have either the precursor mass or product mass being monitored. Multiple-reaction monitoring (MRM) is the same as SRM except that the mass analyzer system is stepped through more than one MS/MS transition. For example, Murphy and coworkers (Sun et al., 1996) used MRM to quantify xanomeline and its *N*-desmethyl metabolite. Low limits of quantification were reported as 0.075 ng/ml for the parent compound and 0.20 ng/ml for the *N*-desmethyl metabolite. The instrumental analysis time is 3 min per sample, allowing 130 samples plus standards to be processed in 4.4 hr (Sun et al., 1996).

In-source CID. These experiments are not true MS/MS experiments since precursor selection does not occur before induced fragmentation. The mass spectrum will contain signals for all parent and CID fragment ions in the source. However, as with the MS/MS experiments, fragmentation is increased yielding structurally significant product-ion-like spectra if only one compound is present.

COMBINED HPLC-MS METHODOLOGY

Sample Preparation for HPLC-MS Analysis

Usually some sort of sample preparation is necessary prior to HPLC-MS analysis. If an HPLC column is used (as opposed to direct introduction into the mass spectrometer), most sample matrix problems for the mass spectrometer, such as ionization suppression and coelution, are eliminated. Sample matrix–derived problems for the HPLC column usually can be reduced or eliminated by precipitation, filtration, or extraction. These preliminary preparation methods may be sufficient to allow the sample to be analyzed without HPLC separation. Introducing the sample into the mass spectrometer without a column is known as flow injection, and this method is used for uncomplicated mixtures or when MS/MS methods provide sufficient separation. Several sample extraction methods can be used.

Liquid-liquid extraction is one of the most commonly used sample preparation tools. The analytes are partitioned into a solvent that is immiscible with the sample matrix. Most importantly, the analytes must have an affinity for the extracting solvent that is not shared by the interfering substance. For example, acidic phase II metabolites (e.g., glucuronides and sulfates) can be extracted from an aqueous, salt-containing system for flow-injection MS/MS analysis. Acidic compounds are protonated to reduce polarity, causing them to partition into the organic phase while leaving the polar salts in the aqueous phase. The presence of salts in the sample may have a buffering effect that can thwart this effort. Using a strong buffer to adjust the pH eliminates this concern. Often the xenobiotic parent compound is less polar than the metabolites and will extract into the organic phase without pH adjustment. Ventura et al. (1993) extracted the phase II metabolites of mesocarb from salt-containing urine. After addition of internal standards, the samples were adjusted to alkaline pH with an ammonium chloride buffer (pH 9.5) and extracted with ethyl acetate. The ethyl acetate was evaporated and the residue dissolved in the HPLC mobile phase. The primary metabolite was identified by HPLC-MS as a sulfate conjugate of hydroxymesocarb.

Solid-phase extraction is another sample preparation technique that uses small chromatographic columns containing a limited amount of stationary phase. The column can be used to retain either the analyte or the interfering species. If the analyte is retained, the column is washed to remove all traces of the sample matrix, and the analyte is desorbed with an appropriate solvent or buffer. The packing material in these columns can be any chromatographic solid phase with particle size large enough to permit gravity flow through the column. Appropriate materials include C_{18} bound to silica (reversed phase; retains less polar compounds), alumina (normal phase; retains polar compounds), and boronate gel (retains poly-ols such as polysaccharides).

On-line solid-phase extraction, also known as column switching, is becoming popular in environments where a large number of samples are to be analyzed and sample cleanup represents much of the analysis time and effort. Two chromatographic columns are used in this technique. The first column, a trapping column, is used to separate the compounds of interest from the matrix and trap them. The trapping column is plumbed into the flow stream with multiple port valves. At the start of the analysis, the valves are configured so that the sample is introduced onto the front of the column with the effluent directed to waste. A polar aqueous mobile phase is used during this first step so that the analytes are retained and salts, proteins, and other polar interfering substances are washed through the column. At the start of the next step, the valves are switched and the HPLC mobile phase is back-flushed through the trapping column carrying the analytes to the front of the analytical column. During this step, the analytes are separated and sequentially introduced into the mass spectrometer. Zell et al. (1997) describes an analytical scheme using column switching to detect and quantify drug metabolites in plasma. Sample preparation was limited to precipitating the plasma proteins with perchloric acid, centrifuging, then neutralizing the supernatant with ammonium formate. One millilter of supernatant was injected on to the trapping column—much more than is commonly used in analytical HPLC methods. The trapping column was an LC-ABZ column (20 × 4.6–mm) and the mobile phase used to wash the trapping column was an aqueous ammonium formate buffer. The analytical column was a standard C18 column and the HPLC mobile phase used for metabolite separation was an aqueous ammonium formate/ethanol mixture. The parent compound and metabolites were detected using ESI with SRM. The analysis time from one injection to the next was 9 min. With the exception of the protein precipitation and pH adjustment, the analytical method was completely automated (Zell et al., 1997).

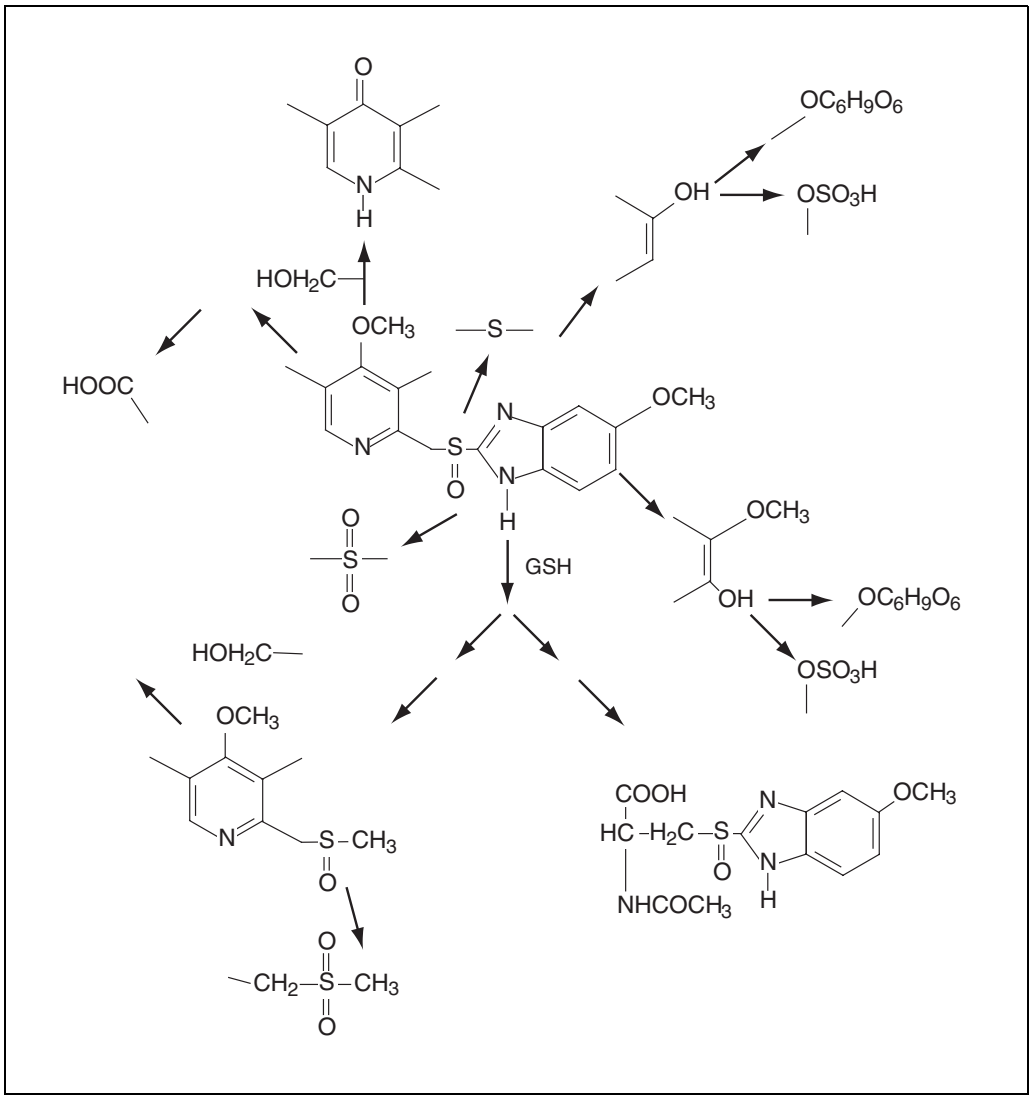

Figure 4.4.3 Metabolic pathways for omeprazole in the rat. GSH, glutathione. Reprinted from Weidolf and Covey (1992) with permission from John Wiley & Sons.

Important Considerations in Combined HPLC-MS

Mobile phase selection in an HPLC-MS method must consider more than just chromatography. For routine operation, none of the interface/source combinations tolerates the use of nonvolatile buffers, acids, bases, or salts for an extended period. Volatile buffer salts include ammonium acetate, ammonium formate, and ammonium carbonate. Acceptable volatile acids include trifluoroacetic acid, acetic acid, and formic acid. Usable volatile bases include ammonium hydroxide, N-methylmorpholine, and triethylamine. The use of high-boiling-temperature organic solvents such as dimethyl sulfoxide and dimethylformamide, which are slowly pumped away, can cause problems to the vacuum system of the mass spectrometer. Trial experiments should be conducted before these solvents are used routinely.

Short-column HPLC methods have been developed that take advantage of the extra separation possible with MS/MS systems. A short HPLC column (≤100 mm) is used to retain analytes long enough to separate them from ionization interferences in the matrix. An MS/MS scan mode (MRM or SRM for quantification) is used to provide any necessary additional separation. Short-column methods permit very rapid analysis of a large number of samples, as analysis times of 3 to 5 min are possible. Volmer et al. (1997) used a 4.0-mm-i.d. × 50-mm-length reversed-phase column and a 1-ml/min flow rate to quantify 4-quinolone antibiotics in biological samples. Ana-

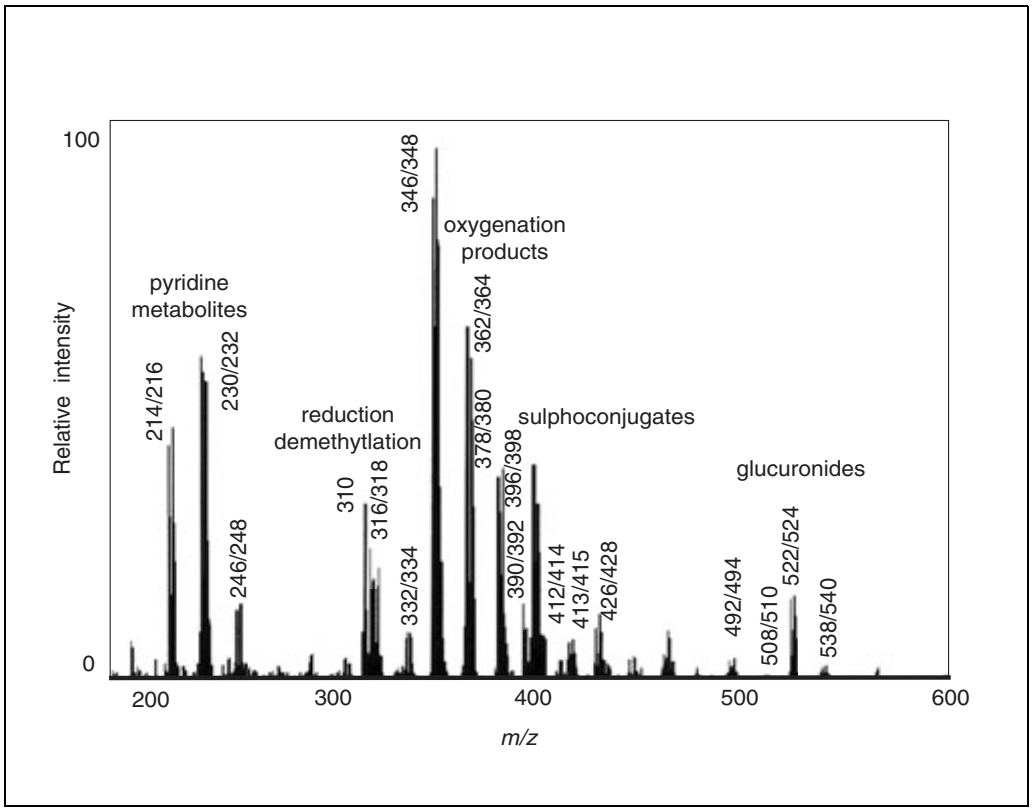

Figure 4.4.4 The metabolic mass profile of omeprazole in the rat. Reprinted from Weidolf and Covey (1992) with permission from John Wiley & Sons.

lytes in the effluent from the column were introduced into the mass spectrometer via an ESI source. The MRM scan mode was defined by the antibiotic being detected. The total analysis time was <8 min for 15 compounds. In another study, Volmer (1996) describes the use of short-column HPLC-MS/MS to study 21 sulfonamide antibiotics with analysis times of <6 min.

NP-HPLC mobile phases are nonpolar organic solvents without buffers that work well with APCI. A limitation of NP-HPLC is that analytes usually have to be extracted from aqueous biological samples.

RP-HPLC mobile phases are polar HPLC solvents that are well suited for separating polar phase II metabolites. These polar mobile phases usually contain a high water content, which works well with ESI interfaces. Beattie and Blake were able to characterize glucuronide and glutathione drug conjugates by direct injection of supernatants (from hepatocyte incubations) onto a C18 column. The mobile phase consisted of 0.1 M aqueous ammonium acetate and acetonitrile (Beattie and Blake, 1989). RP-HPLC tends to require less preparation of biological samples than does NP-HPLC, as demonstrated in the previous example.

HPLC-MS AND HPLC-MS/MS OF METABOLITES

The literature is replete with useful examples of HPLC-MS and HPLC-MS/MS techniques for detecting and characterizing phase I and phase II metabolites. Weidolf and Covey graphically demonstrate the power of HPLC-MS in the identification of the metabolites of omeprazole detected in rat urine. Figure 4.4.3 shows the pathways for the metabolism of omeprazole. Figure 4.4.4 contains a spectrum produced by summing the HPLC-ESI-MS spectra and labeling the metabolite ion signals according the their class of metabolism (Weidolf and Covey, 1992).

Phase I Metabolite Identification

Phase I metabolism adds or removes functional groups toward increased hydrophilicity and increased reactivity toward phase II conjugation. These reactions involve hydrolysis, oxidation, or reduction, and either introduce or expose the following functional groups: $–NH_2$, –OH, –SH, or –COOH. The result is only a minor increase in polarity (Parkinson, 1996). However, under the right solvent or gas-phase conditions, each of these groups will support charge. Consequently, introduction or unmask-

Table 4.4.2 Examples of HPLC-MS and HPLC-MS/MS Separation and Characterization of Phase I Metabolites[a]

Parent compound[b]	Metabolism	HPLC parameters	Ionization method	Mass analysis	Reference
Cinobufagin (Fig. 4.4.5A)	Deacetylation	C: 150 × 4.6–mm, 5-µm C18 (ODS) MP: 1:1 (v/v) acetonitrile/50 mM ammonium acetate buffer F: 0.8 ml/min	Assisted thermospray	Normal MS	Zhang et al. (1991)
Taxol (Fig. 4.4.5B)	Deacetylation, ester hydrolysis, dehydration	C: 120 × 4.6–mm, 5-µm C18 (ODS) MP: gradient of water to acetonitrile F: 1 ml/min split 250 µl/min to MS	Electrospray	Normal scan	Poon et al. (1996)
Oxodipine (Fig. 4.4.5C)	Ester hydrolysis, aromatizaton	C: 250 × 4.6–mm, 5-µm cyano bonded phase MP: 76:12:12 (v/v/v) hexane/methylene chloride/methanol F: 0.2 mL/min	Particle beam with electron ionization	Normal scan	Julien-Larose et al. (1991)
4-Nitrobiphenyl (Fig. 4.4.5D)	Ring hydroxylation, nitro-reduction, loss of nitro group	C: 250 × 4.6–mm, 5-µm C18 (ODS) MP: gradient of water to methanol F: 1 ml/min	APCI	Normal MS	Ning and Xu (1997)
(Fig. 4.4.5E)[c]	Ring hydroxylation, alkyl hydroylation	C: 150 × 4.6–mm, 5-µm C8 MP: gradient of ammonium acetate buffer (~50 mM) to acetonitrile F: 1 ml/min	APCI	Normal MS, product ion MS/MS	Taylor et al. (1994)
MPPB (Fig. 4.4.5F)	Alkyl hydroxylation	C: 150 × 4.6–mm, 5-µm C18 MP: gradient of ammonium acetate buffer (~50 mM) to acetonitrile F: 0.8 ml/min mobile phase, 0.2 ml/min matrix	Cf-FAB 3% glycerol in water added 1:4 to mobile phase; total split 1:100	Normal MS	Takahara et al. (1994)

Cortisol (Fig. 4.4.5G)	Hydroxyl oxidation to ketone, hydrogenation	C: 150 × 2–mm, 5-µm C18 MP: gradient 53:47 (v/v) 10 mM ammonium formate/methanol F: 0.080 ml/min	ESI	Normal scan, product ion scan, MRM-product transition	Dodds et al. (1997)
(Fig. 4.4.5H)[c]	N-Dealkylation	C: 250 × 4.6–mm, 5-µm phenylethyl bonded to silica MP: 4:6 (v/v) 100 mM ammonium acetate/acetonitrile F: 1 ml/min	Assisted TSP	Normal scan	Uchida et al. (1993)
(Fig. 4.4.5I)[c]	N-dealkylation, dehydration	C: 220 × 2.1–mm, 7-µm C18 MP: gradient of ammonium acetate buffer (~50 mM) to acetonitrile F: 0.2 ml/min	ESI	Normal scan, CNL scan, precursor ion scan, product ion scan	Jackson et al. (1995)
Lacidipine (Fig. 4.4.5J)	Alkyl hydroxylation, alkyl hydroxide to acid	C: 100 × 2–mm, 5-µm C18 MP: 35:10:55 (v/v/v) 50 mM ammonium acetate in water/methanol/acetonitrile F: 1.2 ml/min	Assisted thermospray	Normal scan	Rossato et al. (1992)
(Fig. 4.4.5K)[c]	Alkyl oxidation, N-dealkylation	C: 50 × 4.6–mm, 5-µm C8 MP: 90% acetonitrile/10% water/0.1% formic acid/10 mM ammonium acetate F: 1.5 ml/min	APCI	Normal scan, product ion MRM	Rossato et al. (1992)
Omeprazole (Fig. 4.4.5L)	S-methylation, S-oxidation	C: 150 × 4.6–mm, 7-µm C18 MP: gradient of 50 mM ammonium acetate in 55:45 (v/v) water/acetonitrile F: 1.0 ml/min	Unassisted TSP	Normal scan, product ion scan	Rossato et al. (1992)

[a]Abbreviations: C, column; Cf-FAB, continuous flow-fast atomic bombardment; F, flow rate; ODS, octadecyl sulfate; MP, mobile phase; TSP, thermospray.

[b]See Figure 4.4.5 for chemical structures of parent compounds.

[c]See reference for chemical identification.

ing of these groups often allows the metabolite molecule to be ionized by either APCI or ESI.

Time-consuming method development can be reduced by modifying an existing method for compounds with similar functionality. Toward this end, Table 4.4.2 and Figure 4.4.5 provide sample methodology for phase I metabolites. Some of the HPLC-MS methods listed are for ionization methods other than ESI or APCI, but none-the-less provide useful information.

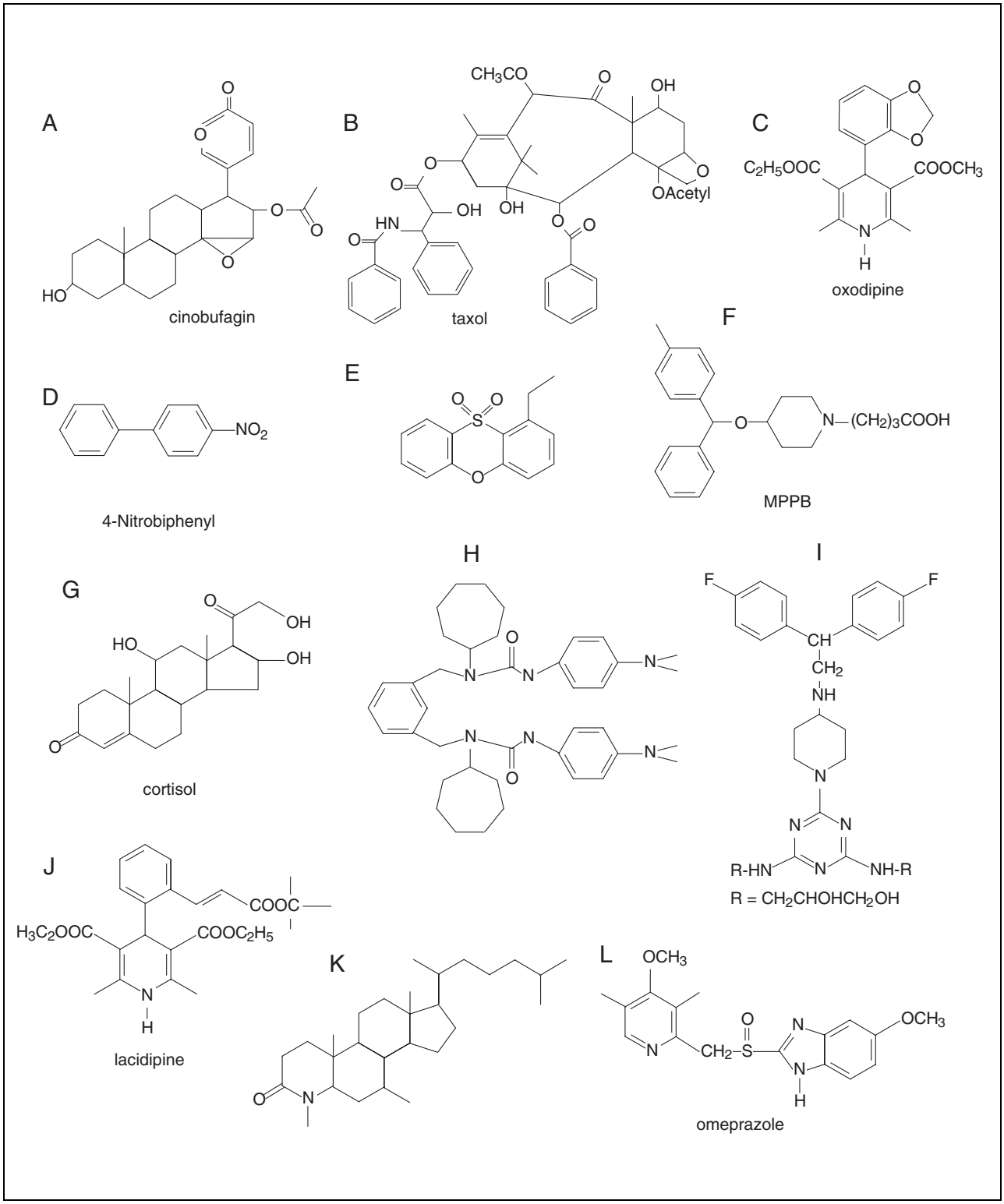

Figure 4.4.5 Parent compounds for the HPLC-MS and HPLC-MS/MS characterization of phase I metabolites shown in Table 4.4.2. See references in Table 4.4.2 for information on unnamed compounds.

Table 4.4.3 Metabolite Characteristic Fragmentation in MS/MS[a,b]

Conjugate class	Mode (+/–)	Scan
Glucuronides	(+/–)	CNL 176 Da ($-C_6H_8O_6$)
Phenolic sulfates	(+)	CNL 80 Da ($-SO_3$)
Aliphatic sulfates	(–)	Precursors of *m/z* 97 (HSO_4^-)
Sulfonates	(–)	Precursors of *m/z* 81 (HSO_3^-)
Sulfinates	(–)	CNL 64 Da ($-HSO_2$)
Aryl-GSH	(+)	CNL 275 Da ($-C_{10}H_{17}N_3O_6$)
Aliphatic-GSH	(+)	CNL 129 Da ($-C_5H_7NO_3$)
N-Acetylcysteines	(–)	CNL 129 Da ($-C_5H_7NO_3$)
Coenzyme A thioesters	(+)	Precursors of *m/z* 428 (ADP^+)
Coenzyme A thioesters	(–)	Precursors of *m/z* 339 and 357
Carnitine butyl esters	(+)	Precursors of *m/z* 103 ($C_4H_7O_3$)
Taurines (Tau)	(+)	Precursors of *m/z* 126 (Tau + H^+)
Phosphates	(–)	Precursors of *m/z* 63 (PO_3^-) and 79 (PO_3^-)

[a]Reprinted from Baillie (1994) with permission from Merck Research Laboratories.

[b]Abbreviations: ADP, adenosine diphosphate; CNL, constant neutral loss; Da, dalton (1 dalton = 1 mass unit); GSH, glutathione.

Phase II Metabolite Identification

Phase II conjugation reactions include glucuronidation, sulfation, acetylation, methylation, conjugation with glutathione (mercapturic acid synthesis), and conjugation with amino acids (such as taurine, glycine, and glutamic acid; Parkinson, 1996). In contrast with phase I metabolism, these reactions result in a large increase in polarity. Furthermore, conjugation with glutathione, glucuronic acid, and sulfate increase the thermal lability and decrease the volatility of the metabolite. Finally, these compounds tend to be easily charged in solution and can be analyzed by HPLC-ESI-MS.

In an excellent review, Baillie (1992) discusses strategies for using MS/MS to detect phase II metabolites via "metabolic mapping." One begins by precursor or CNL scanning for charged or neutral structural moieties indicative of each category of metabolite. Once an indicative charged or neutral structural element is detected, the associated precursor ion m/z is selected and a product ion scan is performed. A list of MS/MS scan and selected or offset m/z values for a number of metabolites has been compiled by Baillie (1994) and is reproduced in Table 4.4.3. As mentioned above for phase I metabolites, method development time and frustration is reduced by beginning with established methodology; methods used for a number of phase II metabolites are presented in Table 4.4.4 and Figure 4.4.6.

SUMMARY

In the last 20 years, major developments have resulted in direct coupling of analytical HPLC systems to mass spectrometers. This union, HPLC-MS and HPLC-MS/MS, has become routine even with the use of polar aqueous solvent systems and has proven to be a sensitive and structurally informative tool in the hands of the toxicologist seeking to identify xenobiotic metabolites.

FUTURE DIRECTIONS

The need for extreme sensitivity and low amounts of sample has always plagued those who work with samples of biological origin, especially metabolite samples. Developments in both HPLC and MS continue to push toward smaller sample size and lower detection limits.

Nano-flow electrospray MS, or nano-spray, is one of these developments (Wilm and Mann, 1994). The primary use of nano-spray has been to sequence peptides with exceptional sensitivity (working with amounts of peptide in the femtomole to attomole range). However, these extremes in sensitivity will apply to any electrospray-amenable compound, including xenobiotic metabolites.

Analogously, nano-scale HPLC has been described in a recent report by Chervet et al. (1996). Separations have been achieved using RP-HPLC with flow rates of 180 nl/min through 75-µm-i.d. × 150-mm-length columns packed with C_{18} stationary phase. The authors

Table 4.4.4 Examples of HPLC-MS and HPLC-MS/MS Separation and Characterization of Phase II Metabolites[a]

Parent compound[b]	Metabolism	HPLC parameters	Ionization method	Mass analysis	Reference
4-Nitrobiphenyl (Fig. 4.4.6A)	N-formylation, N-acetylation	C: 250 × 4.6–mm, 5-µm C18 (ODS) MP: gradient of water to acetonitrile F: 1 ml/min	APCI	Normal scan	Ning and Xu (1997)
Omeprazole (Fig. 4.4.6B)	Glutathione conjugation, observed *N*-acetylcysteine	C: 150 × 4.6–mm, 7-µm C18 MP: gradient - 50 mM ammonium acetate in 55:45 (v/v) water/acetonitrile F: 1 ml/min	Unassisted TSP	Normal scan, product ion scan	Weidolf et al. (1992)
Carvedilol (Fig. 4.4.6C)	Carbamate glucuronidation	C: 250 × 4.6–mm, 5-µm C18 MP: gradient of water to acetonitrile F: 1.5 ml/min	Unassisted thermospray	Normal scan, product ion scan	Schaefer et al. (1992)
Nitrophenol (Fig. 4.4.6D)	Glucuronidation, sulfation	C: flow injection MP: gradient - 1:1 (v/v) 50 mM ammonium acetate in water/methanol F: 1 ml/min	Assisted Thermospray	Normal Scan Product Ion Scan	Draper et al. (1989)
Clozapine (Fig. 4.4.6E)	Glucuronidaton, sulfation	C: 150 × 4.6–mm; 3-µm bonded cyano MP: gradient of water to 1:3 (v/v) methanol/acetonitrile F: 1.5 ml/min	Electrospray	Normal scan	Zhang et al. (1996)
PhIP (Fig. 4.4.6F)	N-Glucuronidation	C: 150 × 2.1–mm, 5-µm C18 MP: 1:1 (v/v) water/methanol with 0.1 % formic acid F: 0.2 ml/min	Electrospray	Normal scan, product ion scan, product ion MRM	Stillwell et al. (1997)

Chloroacetanilide (Fig. 4.4.6G)	Glutathione conjugation	C: 250 × 1–mm, 5-µm C18 MP: gradient (v/v) water/acetonitrile with 0.1% formic acid[c] F: 0.04 ml/min	Cf-FAB	Normal scan	Fujiwara et al. (1992)
Bambuterol (Fig. 4.4.6H)	Glutathione conjugation	C: 150 × 4.6–mm, 5-µm C18 MP: 97.5:2.5 (v/v) 50 mM ammonium acetate/acetonitrile F: 0.75 ml/min	Unassisted thermospray	Normal scan	Rashed et al. (1989)
Ceracemide (Fig. 4.4.6I)	Glutathione conjugation	C: 150 × 4.6–mm, 5-µm C18 MP: 89:11 (v/v) 50 mM ammonium acetate/acetonitrile F: 0.75 ml/min	Unassisted thermospray	Normal scan	Slatter et al. (1993)
Valproic acid (Fig. 4.4.6J)	Glutathione conjugation	C: Flow injection of collected HPLC peaks MP: 1:1 (v/v) methanol/water with 0.05% trifluoroacetic acid F: 0.05 ml/min	Electrospray	Normal scan, product ion scan	Tang and Abbott (1996)
NFA (Fig. 4.4.6K)	Glutathione conjugation	C: 150 × 1–mm, 3-µm C18 MP: gradient (v/v) water/acetonitrile with 0.05% trifluoroacetic acid[c] F: 0.050 ml/min	Electrospray	Normal scan, product ion scan, product ion MRM	Borel and Abbott (1995)
(Fig. 4.4.6L)[d]	Glutathione conjugation	C: 250 × 4.6–mm, 5-µm C18 MP: 39:61 (v/v) 0.1% aqueous TFA/0.8% methanolic glycerol F: 0.0.5 ml/min split 4:500	Cf-FAB	Normal scan	Kondo et al. (1992)

[a]Abbreviations: C, column; Cf-FAB, continuous flow-fast atom bombardment; MP, mobile phase; F, flow rate; ODS, octadecyl sulfate; TSP, thermospray.

[b]See Figure 4.4.6 for chemical structures of parent compounds.

[c]The gradient mobile phase is instrument dependent.

[d]See reference for chemical identification.

were able to show high reproducibility under gradient as well as isocratic flow conditions. Solvent use and sample consumption were low with injection volumes of ~20 nl and total analyte consumption in the 4-ng range.

A combination of nano-spray and nano-scale HPLC with a tandem mass spectrometer capable of MS^3 (MS/MS/MS) or more in a fully automated environment could conceivably provide the ultimate analytical tool. This tool would provide rapid analysis, extreme sensitivity, high resolution, and the ability to isolate xenobiotic metabolites directly from the biological matrix.

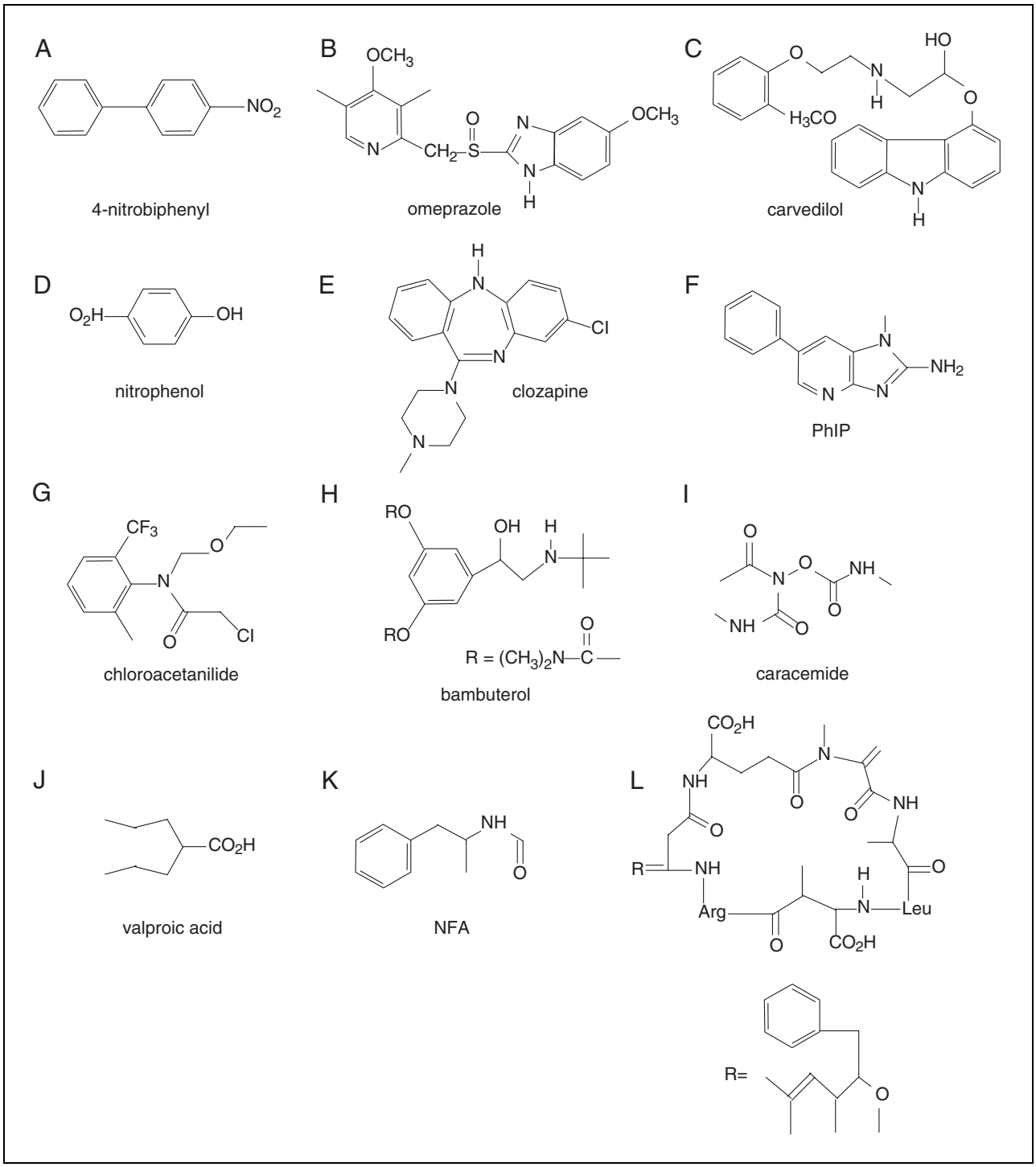

Figure 4.4.6 Parent compounds for the HPLC-MS and HPLC-MS/MS characterization of phase II metabolites shown in Table 4.4.4. See Table 4.4.4 for information on unnamed compounds.

LITERATURE CITED

Baillie, T.A. 1992. Advances in the application of mass spectrometry to studies of drug metabolism, pharmacokinetics and toxicology. *Int. J. Mass Spectrom. Ion Processes* 118-119:289-314.

Baillie, T.A. 1994. The role of LC-ionspray MS/MS in studies of drug metabolism and toxicology. *In* Proceedings, The 42nd ASMS Conference on Mass Spectrometry and Allied Topics, May 29, 1994, p. 862. American Society for Mass Spectrometry, Chicago, Ill.

Baillie, T.A. and Davis, M. 1993. Mass spectrometry in the analysis of glutathione conjugates. *Biol. Mass Spectrom.* 22:319-325.

Beattie, I.G. and Blake, T.J.A. 1989. The structural identification of drug metabolites by thermospray liquid chromatography/mass spectrometry. *Biomed. Environ. Mass Spectrom.* 18:872-877.

Borel, A.G. and Abbott, F.S. 1995. Characterization of novel isocyanate-derived metabolites of the formamide *N*-formylamphetamine with the combined use of electrospray mass spectrometry and stable isotope methodology. *Chem. Res. Toxicol.* 8:891-899.

Brunnee, C. 1982. New instrumentation in mass spectrometry. *Int. J. Mass Spectrom. Ion Phys.* 45:3-38.

Chapman, J.R. 1993. Practical Organic Mass Spectrometry: A Guide for Chemical and Biochemical Analysis, 2nd ed. John Wiley & Sons, Chichester.

Chervet, J.P., Ursem, M. and Salzmann, J.P. 1996. Instrumental requirements for nanoscale liquid chromatography. *Anal. Chem.* 68:1507-1512.

Dear, G.J., Harrelson, J.C., Jones, A.E., Johnson T.E., and Pleasance, S. 1995. Identification of urinary and biliary conjugated metabolites of the neuromuscular blocker 51W89 by liquid chromatography/mass spectrometry. *Rapid Commun. Mass Spectrom.* 9:1457-1464.

Dodds, H.M., Taylor, P.J., Cannell G.R., and Pond, S.M. 1997. A high-performance liquid chromatography-electrospray-tandem mass spectrometry analysis of cortisol and metabolites in placental perfusate. *Anal. Biochem.* 247:342-347.

Draper, W.M., Brown, F.R., Bethem, R., and Miille, M.J. 1989. Thermospray mass spectrometry and tandem mass spectrometry of polar, urinary metabolites and metabolic conjugates. *Biomed. Environ. Mass Spectrom.* 18:767-774.

Fujiwara, H., Chott, R.C., and Solsten, R.T. 1992. Utility of liquid chromatography/fast atom bombardment mass spectrometry and liquid chromatography/thermospray mass spectrometry for structure identification of metabolites of a fluorinated herbicide. *Biol. Mass Spectrom.* 21:431-440.

Gaskell, S.J. 1997. Electrospray: Principles and practice. *J. Mass Spectrom.* 32:677-687.

Hoja, H., Marquet, P., Verneuil, B., Lotfi, H., Penicaut, B., and Lachatre, G. 1997. Applications of liquid chromatography-mass spectrometry in analytical toxicology: A review. *J. Anal. Toxicol.* 21:116-126.

Jackson, P.J., Brownsill, R.D., Taylor, A.R., and Walther, B. 1995. Use of electrospray ionization and neutral loss liquid chromatography/tandem mass spectrometry in drug metabolism studies. *J. Mass Spectrom.* 30:446-451.

Johnston, J.J., Draper, W.M., and Stephens, R.D. 1991. LC-MS compatible HPLC separation for xenobiotics and their phase I and phase II metabolites: Simultaneous anion exchange and reversed-phase chromatography. *J. Chromatogr. Sci.* 29:511-516.

Julien-Larose, C., Voirin, P., Mas-Chamberlin, C., and Dufour, A. 1991. Use of particle beam liquid chromatography-electron impact mass spectrometry for structure elucidation of oxodipine and three of its metabolites. *J. Chromatogr.* 562:39-45.

Kebarle, P. and Yeunghaw, H. 1997. On the mechanism of electrospray mass spectrometry. *In* Electrospray Ionization Mass Spectrometry (R.B. Coleed, ed.) pp. 3-63. John Wiley & Sons, New York.

Kondo, F., Ikai, Y., Oka, H., Okumura, M., Ishikawa, N., Harada, K., Matsuura, K., Murata, H., and Suzuki, M. 1992. Formation, characterization, and toxicity of the glutathione and cysteine conjugates of toxic heptapeptide microcystins. *Chem. Res. Toxicol.* 5:591-596.

Linscheid, M. 1992. LC-MS for toxicological and environmental analysis: Recent developments. *Int. J. Environ. Anal. Chem.* 49:1-14.

Neue, U.D. 1997. HPLC columns, theory, technology and practice. Wiley-VCH, New York.

Niessen, W.M.A. and Van der Greef, J. 1992. Liquid Chromatography-Mass Spectrometry. Marcel Dekker, New York.

Ning, S. and Xu, X. 1997. Reductive metabolism of 4-nitrobiphenyl by rat liver fraction. *Carcinogenesis* 18:1233-1240.

Parkinson, A. 1996. Biotransformation of xenobiotics. *In* Casarett & Doull's Toxicology, Vol. 5 (C.D. Klaassen, ed.) pp. 113-186. McGraw-Hill, New York.

Poon, G.K., Bloomer, J.W., Clarke, S.E., and Maltas, J. 1996. Rapid screening of taxol metabolites in human microsomes by liquid chromatography/electrospray ionization-mass spectrometry. *Rapid Commun. Mass Spectrom.* 10:1165-1168.

Rashed, M.S., Pearson, P.G., Han, D.H., and Baillie, T.A. 1989. Application of liquid chromatography/thermospray mass spectrometry to studies on the formation of glutathione and cysteine conjugates from monomethylcarbamate metabolites of bambuterol. *Rapid Commun. Mass Spectrom.* 3:360-363.

Rossato, P., Scandola, M., Pugnaghi, F., and Grossi, P. 1992. Ether and ester glucuronic acid conjugates of lacidipine metabolites: Mass spectrometric differentiation using thermospray and particle beam techniques. *Org. Mass Spectrom.* 27:1261-1265.

Schaefer, W.H., Goalwin, A., Dixon, F., Hwang, B., Killmer, L., and Kuo, G. 1992. Structural deter-

mination of glucuronide conjugates and a carbamoyl glucuronide conjugate of carvedilol: Use of acetylation reactions as an aid to determine positions of glucuronidation. *Biol. Mass Spectrom.* 21:179-188.

Slatter, G., Davis, M.R., Deog-Hwa, H., Pearson, P.G., and Baillie, T.A. 1993. Studies on the metabolic fate of ceracemide, an experimental antitumor agent in the rat. Evidence for the release of methyl isocyanate in vivo. *Chem. Res. Toxicol.* 6:335-340.

Snyder, L., Kirkland, J.J., and Glajch, J.L. 1997. Practical HPLC Method Development, 2nd ed. John Wiley & Sons, New York.

Stillwell, W.G., Kidd, L.C., Wishnok, J.S., Tannenbaum, S.R., and Sinha, R. 1997. Urinary excretion of unmetabolized and phase II conjugates of 2-amino-1-methyl-6-phenylimidazo[4,5-b]pyridine and 2-amino-3,8-dimethylimidazo[4,5-f]quinoxaline in humans: Relationship to cytochrome P4501A2 and N-acetyltransferase activity. *Cancer Res.* 57:3457-3464.

Sun, E.L., Fennstra, K.L., Bell, F.P., Sanders, P.E., Slatter, J.G., and Ulrich, R.G. 1996. Biotransformation of lifibrol (U-83860) to mixed glyceride metabolites by rat and human hepatocytes in primary culture. *Drug Metab. Dispos.* 24:221-231.

Takahara, E., Nagata, O., Kato, H., Ohta, S., and Hirobe, M. 1994. Analysis of urinary and biliary metabolites of (+)-4-[4-(4-methylphenyl)phenylmethoxy-1-piperidinyl]butyric acid in rats by liquid chromatography-frit fast atom bombardment mass spectrometry. *J. Chromatogr.* 658:154-160.

Tang, W. and Abbott, F.S. 1996. Characterization of thiol-conjugated metabolites of 2-propylpent-4-enoic acid (4-ene VPA), a toxic metabolite of valproic acid, by electrospray tandem mass spectrometry. *J. Mass Spectrom.* 31:926-936.

Taylor, L.C.E., Johnson, R.L., St. John-Williams, L., Johnson, R., and Chang, S.Y. 1994. The use of low-energy collisionally activated dissociation negative-ion tandem mass spectrometry for the characterization of dog and human urinary metabolites of the drug BW 1370U87. *Rapid Commun. Mass Spectrom.* 8:265-273.

Uchida, T., Usui, T., Teramura, T., Watanabe, T., and Higuchi, S. 1993. Metabolic N-demethylation of 1,3-bis[[1-cycloheptyl-3-(P-dimethylaminophenyl)ureido]methyl]benzene dihydrochloride, a novel acyl-coenzyme A:cholesterol acyltransferase inhibitor. Drug Metab. Dispos. 21:524-529.

van Baar, B.L.M. 1996. Ionization methods in LC-MS and LC-MS-MS (TSP, APCI, ESP and cf-FAB). *In* Applications of LC-MS in Environmental Chemistry (D. Barceloed, ed.) pp. 71-133. Elsevier, Amsterdam.

Ventura, R., Nadal, T., Alcalde, P., and Segura, J. 1993. Determination of mesocarb metabolites by high-performance liquid chromatography with UV detection and with mass spectrometry using a particle-beam interface. *J. Chromatogr.* 647:203-210.

Volmer, D.A., 1996. Multiresidue determination of sulfonamide antibiotics in milk by short-column chromatography coupled with electrospray ionization tandem mass spectrometry. *Rapid Commun. Mass Spectrom.* 10:1615-1620.

Volmer, D.A., Mansoori, B., and Locke, S.J. 1997. Study of 4-quinolone antibiotics in biological samples by short-column liquid chromatography coupled with electrospray ionization tandem mass spectrometry. *Anal. Chem.* 69:4143-4155.

Weidolf, L. and Covey, T.R. 1992. Studies on the metabolism of omeprazole in the rat using liquid chromatography/ionspray mass spectrometry and the isotope cluster technique with [^{34}S]omeprazole. *Rapid Commun. Mass Spectrom.* 6:192-196.

Weidolf, L., Karlsson, K.E., and Nilsson, I. 1992. A metabolic route of omeprazole involving conjugation with glutathione identified in the rat. *Drug Metab. Dispos.* 20:262-267.

Whitehouse, C.M., Dreyer, R.N., Yamashita, M., and Fenn, J.B. 1995. Electrospray interface for liquid chromatographs and mass spectrometers. *Anal. Chem.* 57:675-679.

Wilm, M.S. and Mann, M. 1994. Electrospray and Taylor-Cone theory: Dole's beam of macromolecules at last. *Int. J. Mass Spectrom. Ion Processes* 136:167-180.

Yamashita, M. and Fenn, J.B. 1984. Electrospray ion source: Another variation on the free-jet theme. *J. Phys. Chem.* 88:4451-4459.

Zell, M., Husser, C., and Hopfgartner, G. 1997. Column-switching high-performance liquid chromatography combined with ion spray tandem mass spectrometry for the simultaneous determination of the platelet inhibitor Ro 44-3888 and its prodrug and precursor metabolite in plasma. *J. Mass Spectrom.* 32:23-32.

Zhang, L., Yoshida, T., Aoki, K., and Kuroiwa, Y. 1991. Metabolism of cinobufagin in rat liver microsomes. Identification of epimerized and deacetylated metabolites by liquid chromatography/mass spectrometry. *Drug Metab. Dispos.* 19:917-919.

Zhang, G.Q., McKay, G., Hubbard, J.W., and Midah, K.K. 1996. Application of electrospray mass spectrometry in the identification of intact glucuronide and sulfate conjugates of clozapine in rat. *Xenobiotica* 26:541-550.

Contributed by Thomas D. McClure
Novartis Agricultural Discovery Institute, Inc.
San Diego, California

Measurement of Aryl and Alcohol Sulfotransferase Activity

Sulfation is an important reaction in the metabolism and toxicology of a wide variety of structurally diverse drugs, carcinogens, and other xenobiotics. Whereas the sulfation of xenobiotics usually leads to decreased toxicity, there is a growing number of exceptions in which the formation of chemically reactive sulfuric acid esters is an essential step in metabolic pathways leading to toxic and/or carcinogenic responses. The enzymes that catalyze these reactions in mammals constitute a family of cytosolic sulfotransferases that transfer a sulfuryl group from 3′-phosphoadenosine 5′-phosphosulfate (PAPS) to an acceptor molecule (see Figure 4.5.1). The products of sulfation reactions are adenosine 3′,5′-diphosphate (PAP) and sulfuric acid esters (also called sulfates, sulfooxy derivatives, or sulfonoxy derivatives) or sulfamates when amines are the sulfuryl acceptor. Several previous reviews on mammalian cytosolic sulfotransferases provide background information about their importance and characteristics (Jakoby et al., 1980; Mulder and Jakoby, 1990; Weinshilboum and Otterness, 1994; Yamazoe et al., 1994; Duffel, 1997; Falany, 1997).

This unit provides two protocols for determining the activity of aryl and alcohol sulfotransferases. Basic Protocol 1 describes one of the oldest and simplest methods for rapid determination of either aryl (phenol) sulfotransferase or alcohol (hydroxysteroid) sulfotransferase activity. Originally developed for hydroxysteroid sulfotransferases (Nose and Lipmann, 1958), the method has been modified for use with phenols (Sekura et al., 1981), amines (Ramaswamy and Jakoby, 1987), and benzylic alcohols (Duffel and Janss, 1986) as sulfuryl acceptors. This procedure uses chloroform to quantitatively extract the paired ion formed between methylene blue and an organic sulfuric acid ester, either 2-naphthylsulfate or dehydroepiandrosterone sulfate. Following extraction of the paired ion, its absorbance at 651 nm is determined. Basic Protocol 2 is suitable for both aryl and alcohol sulfotransferases, and relies on HPLC determination of PAP as a product of the reaction. This method is particularly useful for molecules in which the sulfuric acid ester product is chemically reactive with nucleophiles or is otherwise unstable (Duffel et al., 1989).

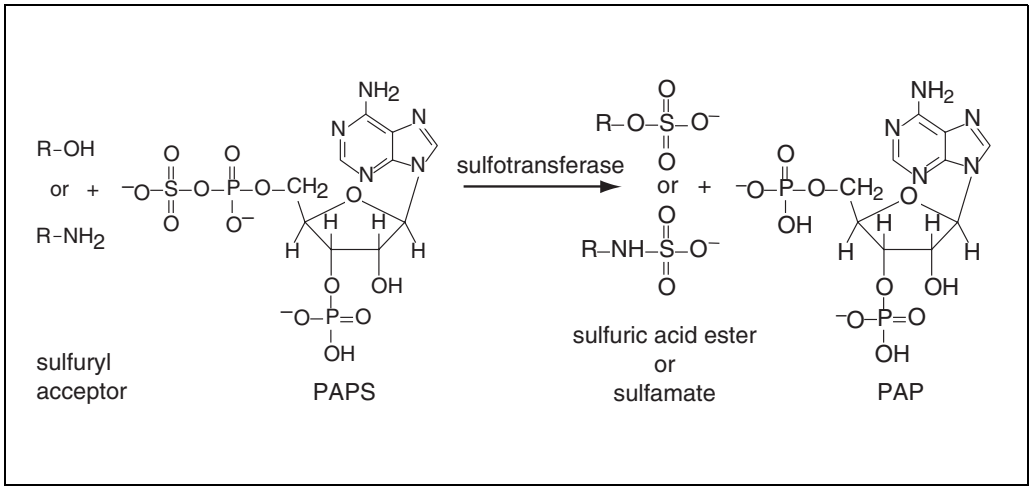

Figure 4.5.1 Reactions catalyzed by aryl and alcohol sulfotransferases. The sulfuryl acceptor is represented by either R-OH (for phenols, alcohols, *N*-hydroxy arylamines, oximes, and arylhydroxamic acids) or R-NH_2 (for amines).

Contributed by Jonathan J. Sheng, Vyas Sharma, and Michael W. Duffel
Current Protocols in Toxicology (2001) 4.5.1-4.5.9

BASIC PROTOCOL 1

METHYLENE BLUE EXTRACTION ASSAY FOR ARYL OR ALCOHOL SULFOTRANSFERASE ACTIVITY

This method utilizes PAPS as substrate and either 2-naphthol (for aryl sulfotransferase) or dehydroepiandrosterone (for alcohol sulfotransferase) as sulfuryl acceptor. It measures the aryl or alcohol sulfotransferase activities in various samples, including tissue homogenates, bacterial cell extracts for heterologous expression of mammalian sulfotransferases, intermediate fractions during purification, and homogenous proteins. This protocol is a slightly modified version of previously described methods (Nose and Lipmann, 1958; Sekura et al., 1981; Ramaswamy and Jakoby, 1987).

Materials

Reaction buffer: 41.0 g/liter sodium acetate, adjusted to pH 5.5 with acetic acid
0.1 M 2-mercaptoethanol (2-ME)
4 mM 3′-phosphoadenosine 5′-phosphosulfate (PAPS; see recipe)
10 mM 2-naphthol (recrystallized from water) in acetone (ACS reagent grade)
2.0 mM dehydroepiandrosterone (DHEA) in acetone (ACS reagent grade)
Enzyme sample of known protein concentration
Methylene blue reagent (see recipe)
Chloroform (ACS spectrophotometric grade)
Sodium sulfate (anhydrous)
13 × 100–mm glass test tubes
Spectrophotometer and quartz cuvettes

Perform sulfotransferase-catalyzed reaction

1a. *For aryl (phenol) sulfotransferase:* Place a 13 × 100–mm glass test tube on ice, and add sequentially:

200 µl reaction buffer
30 µl 0.1 M 2-mercaptoethanol
20 µl 4.0 mM PAPS
10 µl 10 mM 2-naphthol
130 µl water.

Single reactions are used for rapid analysis of fractions from chromatography in enzyme purification. Otherwise, at least three replicate reactions are performed.

1b. *For alcohol (hydroxysteroid) sulfotransferase:* Place a 13 × 100–mm glass test tube on ice, and add sequentially:

200 µl reaction buffer
30 µl 0.1 M 2-mercaptoethanol
20 µl 4.0 mM PAPS
10 µl 2.0 mM DHEA
130 µl water.

2. Set up a separate tube with the same reaction mixture as a control (incubation time = 0 min).
3. Mix on a vortex mixer, then preincubate 2 min in a 37°C water bath.
4. Add 10 µl enzyme sample to the sample tube to start the reaction, mix 1 to 2 sec on a vortex mixer, and incubate 5 to 30 min in a 37°C water bath. Meanwhile, add 10 µl enzyme to the control tube and immediately stop the reaction (step 5).

The volume of enzyme solution may be modified as necessary. The total volume should be kept constant by also changing the amount of water added to the mixture.

Extract sulfuric acid ester

5. Add 0.5 ml methylene blue reagent to stop the reaction.
6. Immediately add 2.0 ml chloroform and vortex vigorously 20 sec.
7. Centrifuge mixture 10 min at ~2000 × *g* at room temperature, to separate organic and aqueous phases.
8. Using a Pasteur pipet, transfer chloroform (lower) layer to a test tube containing 50 to 100 mg anhydrous sodium sulfate. Mix gently by hand or vortex mixer and allow sodium sulfate to settle to the bottom.

Determine specific activity

9. Carefully remove ~1.0 to 1.5 ml chloroform and measure the A_{651} with a spectrophotometer.

   The extraction of 10 nmol of 2-naphthylsulfate yields A_{651} = 0.3. This value is used in the calculation of product formed based on absorbance at 651 nm.

10. Calculate specific activity (sp. act.; nmol product/mg protein/min) using the equation:

$$\text{sp. act.} = \frac{(\text{sample } A_{651} - \text{control } A_{651}) \times (10 \text{ nmol} / 0.3 \text{ absorbance units})}{\text{mg protein} \times \text{incubation time}}$$

HPLC ASSAY FOR SULFOTRANSFERASE ACTIVITY

BASIC PROTOCOL 2

This assay was originally developed to measure sulfotransferase reactions in which sulfuric acid ester products may be chemically unstable (Duffel et al., 1989). However, the formation of PAP as the reaction product makes it applicable to many sulfotransferases and acceptor substrates, and it has been applied successfully to cytosolic fractions and bacterial cell extracts as well as purified sulfotransferases.

Materials

HPLC mobile phase (see recipe)
4.0 mM 3′-phosphoadenosine 5′-phosphosulfate (PAPS; see recipe) or 4.0 mM adenosine 3′,5′-diphosphate (PAP; see recipe)
HPLC-grade water
PAP standards (see recipe)
Reaction premix (see recipe)
Substrate solution (see recipe)
Solvent used for substrate solution
Enzyme sample of known protein concentration
HPLC-grade methanol

C18 5-µM reversed-phase HPLC column (i.d. = 4.6 mm, length = 250 mm)
High-performance liquid chromatograph (HPLC) with 20-µl sample-injection loop, uv/vis detector, and integrator
6 × 50–mm glass test tubes

Prepare HPLC for sample injection

1. About 3 hr before beginning sulfotransferase assays, equilibrate the HPLC column with HPLC mobile phase at 2.0 ml/min flow rate.
2. Make a test sample by diluting 1.5 µl of 4.0 mM PAPS or PAP in 60 µl HPLC-grade water.

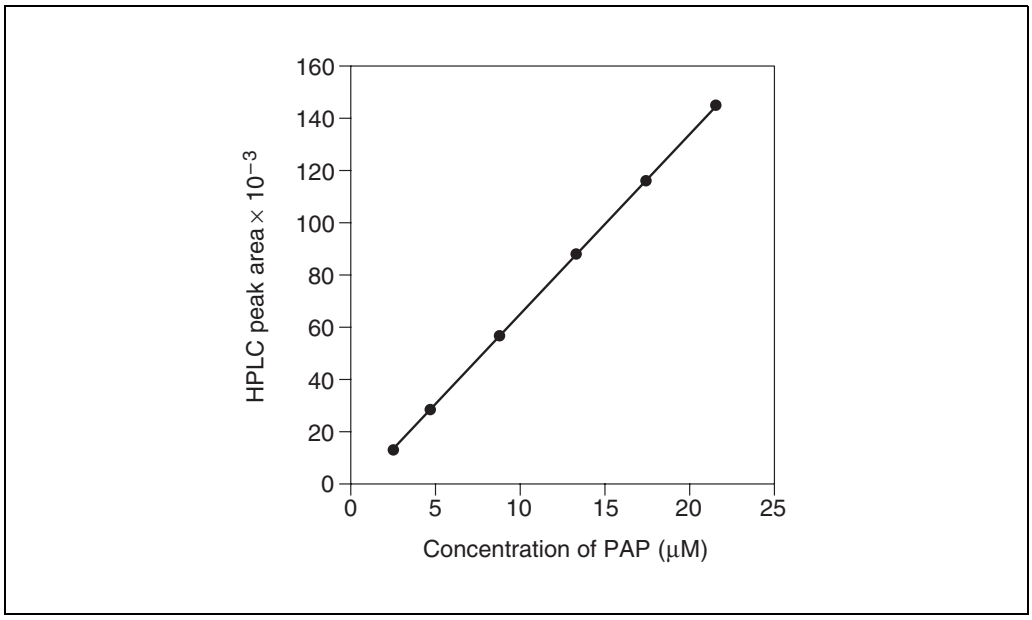

Figure 4.5.2 Representative standard curve relating the concentration of PAP to the integrated area under the corresponding HPLC peak. Peak area is in arbitrary units.

3. Completely fill the 20-µl HPLC sample-injection loop with test sample (40 to 50 µl), taking care to avoid air bubbles. Vent excess to a waste container. Maintain flow rate at 2.0 ml/min.

   The baseline absorbance should be stable, and PAP test samples should have consistent retention times.

Determine relationship between HPLC peak area and PAP concentration

4. Inject PAP standards onto the column and plot the area under the curve versus PAP concentration in µM (Figure 4.5.2).

Perform sulfotransferase-catalyzed reaction

5. Place a 6 × 50–mm glass test tube on ice and add 27.5 µl reaction premix and 1.5 µl substrate solution.
6. Prepare a control tube containing 27.5 µl reaction premix and 1.5 µl solvent used to prepare substrate solution.
7. Mix contents of each tube on a vortex mixer, then preincubate tubes 2 min at 37°C.
8. Add 1.0 µl enzyme sample to start the reaction, briefly vortex, and incubate tubes 10 min in a 37°C water bath.

   Reaction times may vary from 2 to 20 min. Use the exact time to calculate specific activity.

9. Add 30 µl HPLC-grade methanol to stop the reaction and mix vigorously on a vortex mixer. Keep tubes on ice until the HPLC analysis for PAP is completed.

Analyze by reversed-phase HPLC

10. Fill the injection loop with sample and inject onto the HPLC column. Maintain mobile phase flow rate at 2.0 ml/min.
11. Calculate the concentration of PAP formed (µM) in each tube using the standard curve. Calculate specific activity (sp. act.; nmol product/mg protein/min) as follows:

$$\text{sp. act.} = \frac{([\text{PAP}]_{\text{sample}} - [\text{PAP}]_{\text{control}}) \times 60\ \mu\text{l}}{\text{mg protein} \times \text{incubation time}}$$

The volume (60 µl) corresponds to the assay volume after dilution with methanol.

REAGENTS AND SOLUTIONS

Use glass-distilled water in all recipes and protocol steps. For common stock solutions, see ***APPENDIX 2A****; for suppliers, see* ***SUPPLIERS APPENDIX****.*

Adenosine 3′,5′-diphosphate (PAP), 4.0 mM

Purchase adenosine 3′,5′-diphosphate (PAP) as sodium salt containing 4 mol/mol sodium and 2.5 mol/mol water (formula wt. 464.2). Dissolve 25 mg PAP in 13.5 ml water. Store up to 6 months at −20°C. Keep PAP solutions at 4°C while waiting to add to reaction mixtures.

HPLC mobile phase

Dissolve 20.4 g KH_2PO_4 and 8.03 g NH_4Cl in 1760 ml HPLC-grade water. Add 340 µl *n*-octylamine, stir until it completely dissolves, and adjust to pH 5.45 with KOH. Degas solution using a trapped vacuum pump for 30 min. Add 240 ml HPLC-grade methanol and filter through a 0.45-µm membrane filter. Degas briefly. Alternatively, sparge the mobile phase with helium gas to displace air bubbles. Use at room temperature and prepare fresh daily.

The mobile phase should only be degassed briefly (3 to 5 min) after addition of methanol to avoid altering the concentration of methanol.

This mobile phase contains 75 mM potassium phosphate and 75 mM ammonium chloride. To vary salt concentrations, use different amounts of potassium phosphate and ammonium chloride as shown in Figure 4.5.3.

Methylene blue reagent

250 mg/liter methylene blue
50 g/liter anhydrous sodium sulfate
10 ml/liter sulfuric acid
Store up to 6 months at 25°C

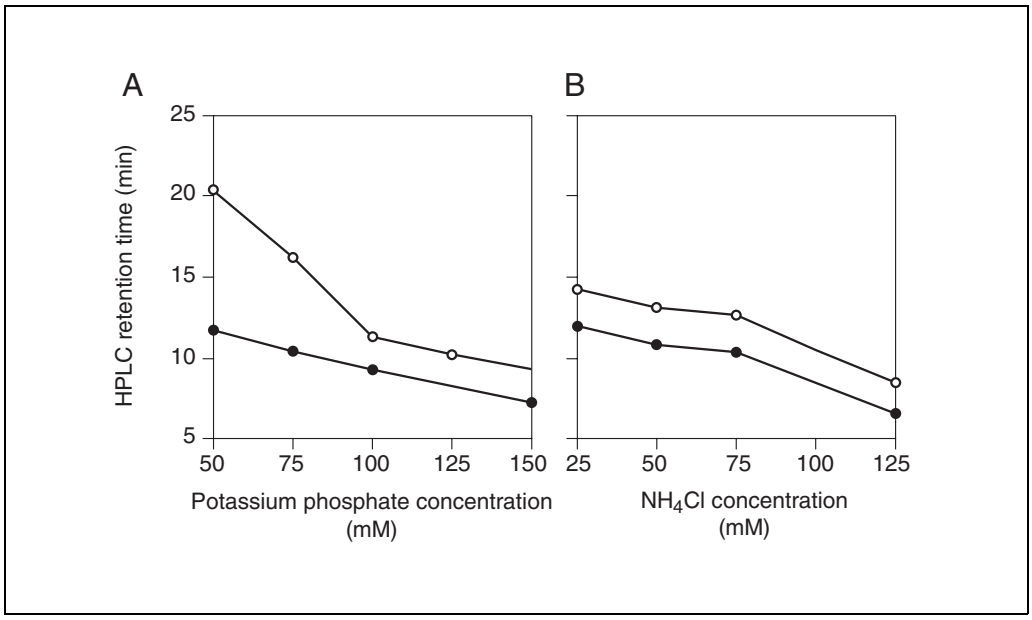

Figure 4.5.3 Effect of the concentration of potassium phosphate and the concentration of ammonium chloride on the separation of PAP (closed circles) and PAPS (open circles) by HPLC under the conditions described in Basic Protocol 2. (**A**) The effect of varied concentrations of potassium phosphate on the retention times of PAP and PAPS at 50 mM ammonium chloride. (**B**) The effect of varied concentrations of ammonium chloride on the retention times of PAP and PAPS at 75 mM potassium phosphate.

PAP standards

To six vials, add 1.2, 2.5, 5.0, 7.5, 10.0, and 12.5 µl of 4.0 mM PAP (see recipe). Add 2.0 ml water to each vial. Determine A_{259} for each standard solution, and calculate the concentration of PAP using a molar absorptivity of 15.4×10^3 at 259 nm.

3′-Phosphoadenosine 5′-phosphosulfate (PAPS), 4.0 mM

Purchase 3′-phosphoadenosine 5′-phosphosulfate (PAPS) as lithium salt containing 4 mol/mol lithium and 3 mol/mol water (formula wt. 589.1). Dissolve 25 mg PAPS in 10.6 ml water. Store up to 6 months at −20°C. Keep on ice after thawing, and refreeze the remaining stock solution.

Reaction premix

15 µl 4.0 mM PAPS (see recipe)
50 µl 1.5 M potassium phosphate, pH 7.0
25 µl 0.1 M 2-mercaptoethanol
185 µl water
Prepare just before use

The reaction premix contains all reaction components except the sulfuryl acceptor substrate and enzyme sample. This recipe makes enough for ten assays.

Substrate solution

Prepare substrate solutions in acetone, tetrahydrofuran, or acetonitrile, because most sulfuryl acceptor substrates of aryl and alcohol sulfotransferases are hydrophobic. Mix 100-µl stock solutions to give final substrate concentrations of 0.01 to 5.0 mM in the incubation mixture. In addition, be sure that the volume of acetone or acetonitrile in the enzymatic reaction does not exceed 5% of the total assay volume, and that the volume of tetrahydrofuran does not exceed 3% of the total assay volume. Prepare substrate solutions immediately before use.

COMMENTARY

Background Information

A combination of the diversity of chemicals that can serve as substrates for sulfotransferases and the many different isoforms of these enzymes has led to the development of many varied assay methods. This unit focuses on two of these methods: one that utilizes an ion-pair extraction technique with methylene blue and a second that uses HPLC to determine the substrate-dependent production of PAP.

In addition to these assays, there are various other methods available for determining the activity of aryl and alcohol sulfotransferases. Among these are procedures for direct quantitation of phenolic reactants or products by HPLC (Honkasalo and Nissinen, 1988) and fluorometric methods (Beckmann, 1991). Coupled reactions with 4-nitrophenyl sulfate have also been utilized for assay of sulfotransferases. One such assay employs an exchange reaction between 4-nitrophenyl sulfate and an acceptor phenol under conditions of limiting concentrations of PAP (Gregory and Lipmann, 1957; Duffel and Jakoby, 1981). Moreover, a coupled-enzyme assay has recently been described wherein recombinant aryl sulfotransferase IV, PAP, and 4-nitrophenyl sulfate are utilized as both a source of PAPS and an indicator of the rate of reaction for a second sulfotransferase that does not utilize phenols or phenyl sulfates as substrates (Burkart and Wong, 1999).

Several radiochemical methods are also available for the assay of sulfotransferases. A common feature of many of these procedures is the use of [^{35}S]PAPS with an unlabeled sulfuryl acceptor molecule followed by separation of the [^{35}S]labeled reaction product. Specific radiochemical assays predominantly vary by whether the radiolabeled product is separated by means of thin-layer chromatography (Sekuar et al., 1979), ecteola-cellulose chromatography (Borchardt et al., 1983), or precipitation with barium (Foldes and Meek, 1973). Radiolabeled sulfuryl acceptors such as ster-

oids (Sekura et al., 1979) and arylamines (Ramaswamy and Jakoby, 1987) have also been employed for determination of sulfotransferases. The relative merits and disadvantages of several of the radiochemical assays for sulfotransferases have been reviewed (Ramaswamy and Jakoby, 1987; Weinshilboum and Otterness, 1994).

Critical Parameters and Troubleshooting

Although the methylene blue extraction assay (Basic Protocol 1) is often preferred due to the fact that it is rapid and simple to perform, it is not as sensitive as the HPLC method (Basic Protocol 2) or the radiochemical methods that are available for assay of sulfotransferases. Troubleshooting of the methylene blue extraction assay is relatively straightforward. The assay is sensitive to the final ionic strength of the solution, because high salt concentrations increase the solubility of the methylene blue in chloroform. This effect of high salt is independent of the presence of any sulfuric acid ester. However, corrections for the effect of ionic strength on the extraction of methylene blue into chloroform are easily made either by the use of a control reaction mixture that contains all reaction components except PAPS, or by the use of a reaction mixture that contains all components but is stopped immediately after addition of the enzyme (t = 0 control). Additional compounds that might potentially interfere with the methylene blue dye-binding assay include other organic anions. For example, free fatty acids in crude cellular homogenates may interfere, but as in the case of enzyme samples with high salt concentrations, control reaction mixtures without incubation or without PAPS often provide an appropriate resolution of the problem.

For both basic protocols, it is advisable to perform preliminary experiments to determine if the enzyme is rate-limiting in the assay. The suggestions presented in these protocols for concentration of PAPS, concentration of sulfuryl acceptor, and incubation time often ensure that initial velocities are determined under conditions of saturating substrate. However, it is useful to confirm this or alter the conditions as needed.

The HPLC assay for sulfuryl acceptor–dependent formation of PAP is especially useful in cases where the sulfuric acid ester may be subject to hydrolysis, reaction with nucleophiles, or other modes of decomposition. The major difficulties that may be encountered with this assay relate either to the purity of PAPS employed in the assays or to chromatographic problems resulting from subtle changes in the resolution of the HPLC column. Commercial preparations of PAPS sometimes contain 10% to 15% PAP, and this level of contamination may prove problematic for this assay. If this is the case, purification of PAPS is readily accomplished by chromatography on DEAE-cellulose as previously described (Sekura, 1981). PAPS solutions can be stored frozen (–20°C) at a concentration of 4.0 mM in water for up to 6 months. After thawing, the stock solutions of PAPS should be kept on ice until the reaction mixtures are prepared, and the remainder of the stock solution should be refrozen as soon as possible following the sulfotransferase assays. PAPS may be stored and used in this manner until the concentration of PAP in the solution becomes >5% of the concentration of PAPS.

A final comment relevant to the HPLC assay involves optimization of the mobile phase. As the reversed-phase HPLC column is used repeatedly over the course of several weeks, the properties of the column will eventually begin to change, and thus the separation of PAP and PAPS will be altered. Compensation for this effect can be readily achieved by altering the concentration of potassium phosphate or the concentration of ammonium chloride in the elution solvent. The effects of these ions on the retention times of PAP and PAPS are seen in Figure 4.5.3, and these data can be used as a guide to altering the composition of the mobile phase as necessary to optimize the separation.

Anticipated Results

Basic Protocol 1

The catalytic activity of a preparation of recombinant rat hepatic aryl sulfotransferase (AST) IV was analyzed by the methylene blue extraction assay with 2-naphthol as substrate. The assay was conducted at pH 5.5 with 250 μM 2-naphthol as sulfuryl acceptor and 6 μg purified AST IV in a final assay volume of 0.40 ml. Enzymatic reactions were carried out at 37°C for 10 min as described in Basic Protocol 1. Absorbance at 651 nm of the chloroform extract derived from the control mixture (i.e., when all components were present, but the reaction was terminated before any incubation) was 0.038; the absorbance after 10 min incubation with AST IV was 0.325. The specific activity was calculated as follows:

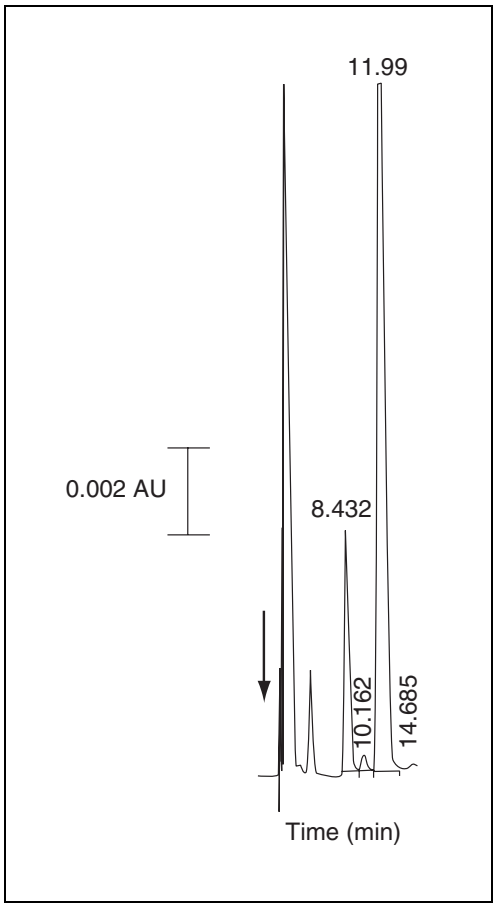

Figure 4.5.4 Representative HPLC chromatogram of the activity of 0.5 μg recombinant rat alcohol (hydroxysteroid) sulfotransferase STa as described in Basic Protocol 2. The reaction was carried out for 10 min at pH 7.0 with 50 μM DHEA as sulfuryl acceptor. The arrow in the chromatogram indicates injection of a 20-μl sample onto the HPLC column. Elution of the column was monitored at 259 nm; the chromatographic peak at 8.43 min was PAP and the peak at 11.99 min was PAPS.

$$\text{sp. act.} = \frac{(0.325 - 0.038) \times 10 \text{ nmol} / 0.3 \text{ units}}{0.006 \text{ mg protein} \times 10 \text{ min}}$$

$$= 159 \text{ nmol product/mg protein/min}$$

Basic Protocol 2

Enzymatic activity of a purified preparation of recombinant rat alcohol (hydroxysteroid) sulfotransferase STa was determined using the HPLC assay method. The assay was carried out at pH 7.0 with 50 μM DHEA as sulfuryl acceptor and 0.5 μg purified STa in a final assay volume of 30 μl. The sulfation reaction was carried out at 37°C for 10 min as described in Basic Protocol 2. The HPLC chromatogram of the reaction mixture is seen in Figure 4.5.4, with PAP eluting at 8.43 min and PAPS eluting at 11.99 min. A reaction mixture where 1.5 μl of acetone was substituted for the substrate solution served as a control assay. The concentrations of PAP in the 20 μl HPLC injection (12.2 μM sample, 10.1 μM control) were determined through the use of a standard curve relating PAP concentration to HPLC peak areas (as demonstrated in Fig. 4.5.2), and these values were used to calculate the specific activity as follows:

$$\text{sp. act.} = \frac{(12.2\,\mu\text{M} - 10.1\,\mu\text{M}) \times 60\,\mu\text{l}}{0.5 \times 10^{-3} \text{ mg protein} \times 10 \text{ min}}$$

$$= 25.2 \text{ nmol product/mg protein/min}$$

Time Considerations

The total time required for each of the two procedures will vary with the chosen incubation time. However, assuming that there is a 2-min temperature equilibration before the enzyme is added, and the sulfotransferase-catalyzed reaction is carried out for 10 min, it is possible to estimate the total time involved. For the methylene blue extraction procedure, a total time of ~40 min is required to carry out the procedure. The overall process can, however, be made more efficient by staggering the starting times for the incubation of several reaction mixtures, so that several reaction tubes are carried through the procedure simultaneously. Using the same assumptions about reaction times, the HPLC assay for PAP requires ~40 to 50 min per assay. While simultaneous reactions can also be incubated for this assay, the rate-limiting portion of the method is the HPLC separation, which typically takes 20 to 25 min per sample. Therefore in an 8-hr period, 12 to 15 samples could be assayed by the HPLC method, or ~70 to 80 samples could be analyzed by the methylene blue extraction assay.

Literature Cited

Beckmann, J.D. 1991. Continuous fluorometric assay of phenol sulfotransferase. *Anal. Biochem.* 197:408-411.

Borchardt, R.T., Baranczyk-Kuzma, A., and Pinnick, C.L. 1983. An ecteola-cellulose chromatography assay for 3′-phosphoadenosine-5′-phosphosulfate:phenol sulfotransferase. *Anal. Biochem.* 130:334-338.

Burkart, M.D. and Wong, C.H. 1999. A continuous assay for the spectrophotometric analysis of sulfotransferases using aryl sulfotransferase IV. *Anal. Biochem.* 274:131-137.

Duffel, M.W. 1997. Sulfotransferases. *In* Comprehensive Toxicology, Vol. 3: Biotransformation

(F.P. Guengerich, ed.) pp. 365-383. Elsevier Science Publishing, Oxford.

Duffel, M.W. and Jakoby, W.B. 1981. On the mechanism of aryl sulfotransferase. *J. Biol. Chem.* 256:11123-11127.

Duffel, M.W. and Janss, M.N. 1986. Aryl sulfotransferase IV catalyzed sulfation of 1-naphthalenemethanol. *In* Biological Reactive Intermediates III—Mechanisms of Action in Animal Models and Human Disease (J.J. Kocsis, D.J. Jollow, C.M. Witmer, J.O. Nelson, and R. Snyder, eds.) pp. 197:415-422. Plenum, New York.

Duffel, M.W., Binder, T.P., and Rao, S.1. 1989. Assay of purified aryl sulfotransferase suitable for reactions yielding unstable sulfuric acid esters. *Anal. Biochem.* 183:320-324.

Falany, C.N. 1997. Enzymology of human cytosolic sulfotransferases. *FASEB J.* 11:206-216.

Foldes, A. and Meek, J.L. 1973. Rat brain sulfotransferase: Partial purification and some properties. *Biochim. Biophys. Acta* 327:365-374.

Gregory, J.D. and Lipmann, F. 1957. The transfer of sulfate among phenolic compounds with 3′,5′-diphosphoadenosine as coenzyme. *J. Biol. Chem.* 229:1081-1090.

Honkasalo, T. and Nissinen, E. 1988. Determination of phenol sulfotransferase activity by high-performance liquid chromatography. *J. Chromatogr.* 424:136-140.

Jakoby, W.B., Sekura, R.D., Lyon, E.S., Marcus, C.J., and Wang, J.L. 1980. Sulfotransferases. *In* Enzymatic Basis of Detoxication, Vol. 2 (W.B. Jakoby, ed.) pp. 199-228. Academic Press, New York.

Mulder, G.J. and Jakoby, W.B. 1990. Sulfation. *In* Conjugation Reactions in Drug Metabolism (G.J. Mulder, ed.) pp. 107-161. Taylor & Francis, New York.

Nose, Y. and Lipmann, F. 1958. Separation of steroid sulfokinases. *J Biol. Chem.* 233:1348-1351.

Ramaswamy, S.G. and Jakoby, W.B. 1987. Sulfotransferase assays. *Methods Enzymol.* 143:201-207.

Sekura, R.D. 1981. Adenosine 3′-phosphate 5′-phosphosulfate. *Methods Enzymol.* 77:413-415.

Sekura, R.D., Marcus, C.J., Lyon, E.S., and Jakoby, W.B. 1979. Assay of sulfotransferases. *Anal. Biochem.* 95:82-86.

Sekura, R.D., Duffel, M.W., and Jakoby, W.B. 1981. Aryl sulfotransferases. *Methods Enzymol.* 77:197-206.

Weinshilboum, R. and Otterness, D. 1994. Sulfotransferase enzymes. *In* Handbook of Experimental Pharmacology (F.C. Kauffman, ed.) pp. 112:45-78. Springer-Verlag, Berlin.

Yamazoe, Y., Nagata, K., Ozawa S., and Kato, R. 1994. Structural similarity and diversity of sulfotransferases. *Chemico-Biol. Interact.* 92:107-117.

Contributed by Jonathan J. Sheng,
Vyas Sharma, and Michael W. Duffel
University of Iowa
Iowa City, Iowa

Measuring the Activity of Arylamine *N*-Acetyltransferase (NAT)

Arylamine *N*-acetyltransferases (NAT; EC 2.3.1.5) catalyze the acetylation of aromatic amines, heterocyclic amines, and hydrazines. The reaction can be viewed as either a detoxification or activation step depending on the substrate and the position of the acetyl group. For hydrazine derivatives, addition of an acetyl group, which is generally donated by the cofactor acetyl coenzyme A (acetyl CoA), results in the formation of a product that is less reactive than the parent. *N*-acetylation of drugs such as isoniazid (INH) results in a product that is less toxic than the parent and therapeutically inactive. *N*-acetylation of aromatic amines and heterocyclic amines is also viewed as a detoxification step. In contrast, *O*-acetylation of arylhydroxylamines or the intramolecular *N*,*O*-acetyl transfer within arylhydroxamic acids are considered to be activation steps.

NATs are cytoplasmic proteins and activities can be measured in cytosolic fractions of whole tissue or cultured cells. NAT 1 and NAT 2 have selective but overlapping substrate specificities. The three acetylation reactions, *N*-acetylation, *O*-acetylation, and *N*,*O*-acetyl transfer, are illustrated in Figure 4.6.1. All three reactions are catalyzed by the proteins designated as NAT. This unit describes methods for measuring *N*-acetylation, using either an acetyl CoA recycling system (see Basic Protocol 1) or a single concentration of acetyl CoA (see Alternate Protocol) coupled with HPLC separation of the parent aromatic amine from the acetylated product. The Bratton-Marshall method (see Basic Protocol 2) measures NAT activity by spectrophotometric monitoring of the decrease in substrate concentration over time.

CAUTION: Many aromatic amines are mutagens and carcinogens and must be handled as hazardous materials. Experimental procedures and waste disposal must follow the appropriate institutional guidelines.

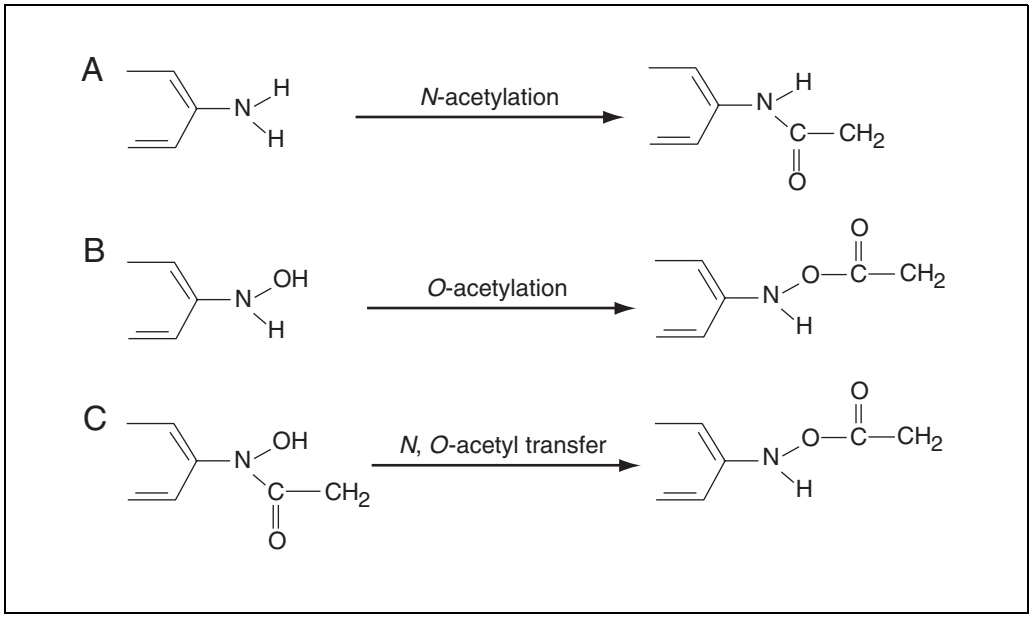

Figure 4.6.1 Reactions catalyzed by NATs. (**A**) The *N*-acetylation of an arylamine. (**B**) The *O*-acetylation of an arylhydroxylamine. (**C**) The intramolecular *N*,*O*-acetyl transfer of an arylhydroxamic acid.

Contributed by Charlene A. McQueen
Current Protocols in Toxicology (2001) 4.6.1-4.6.13

HPLC ASSAY FOR NAT ACTIVITY USING THE ACETYL CoA RECYCLING SYSTEM

The use of a recycling system to convert coenzyme A (CoA) back to acetyl coenzyme A (acetyl CoA) results in the use of acetyl CoA concentrations within a physiologic range, which is desirable when determining kinetic constants. Additionally, CoA concentrations are kept low to decrease the possibility of product inhibition of NAT by CoA. The separation and quantification of the resulting acetylated aromatic amines is most commonly done by HPLC. The major advantage is that the amount of product is measured rather than the disappearance of substrate (Basic Protocol 2); however, the conditions for the separation of product from substrate must be modified depending on the arylamine substrate.

Arylamine NAT activity is measured under the following conditions: 15 mM acetylcarnitine, 2 U carnitine acetyltransferase/µl, 2 mM EDTA, 2 mM DTT, 50 mM Tris·Cl, pH 7.5, 0.5 mM acetyl CoA, 44.4 µM arylamine substrate, and 0.5 to 2 mg/ml protein. Samples are incubated for 10 min at 37°C.

NOTE: It is advisable to do preliminary experiments to determine that assays are being performed under initial velocity conditions. This is done by varying the time of incubation and the amount of protein.

Materials

Cytosolic or S-9 fraction (see Support Protocol 1 or 2)
Pierce protein assay kit
Homogenization buffer (see recipe)
10× acetyl CoA solution 1 (22.7 mM; see recipe)
Recycling mix (RCM; see recipe)
10^{-2} M arylamine substrate (see recipe and Table 4.6.1)
~80 U/mg carnitine acetyltransferase (CAT; from pigeon breast muscle; Sigma; keep refrigerated but do not freeze, put on ice, or keep at room temperature >5 min)
Methanol, ice-cold
Solvents for mobile phase (see Tables 4.6.2, 4.6.3, and 4.6.4)

1.5-ml microcentrifuge tubes
HPLC with UV detector and column (see Tables 4.6.2, 4.6.3, and 4.6.4)

Perform NAT reaction and prepare samples for HPLC

1. Thaw a sufficient number of tubes of cytosol or S-9 for the experiment (200 µl). Keep on ice.
2. Determine the protein concentration of the cytosol or S-9 using protein assay kit. Adjust the concentration to 0.5 to 2 mg protein/50 µl with homogenization buffer.

Table 4.6.1 Commonly Used Selective Substrates[a,b]

Species	NAT1	NAT2
Human	PABA	SMZ
Mouse	INH	PABA
Rat	—	PABA
Hamster	—	PABA

[a]Grant et al., 1991; Doll and Hein, 1995; Ferguson et al., 1996; Estrada-Rogers et al., 1998.
[b]Abbreviations: INH, isoniazid; PABA, *p*-aminobenzoic acid; SMZ, sulfamethazine.

3. Thaw a sufficient number of tubes, each containing a 50-µl aliquot of 10× acetyl CoA solution 1, on ice. Prepare 1× acetyl CoA solution 1 (2.27 mM) by adding 450 µl ice-cold Milli-Q purified water to each tube. Keep on ice.
4. Add 1 µl of 10^{-2} M arylamine substrate stock solution and sufficient CAT to give ~9 U/µl RCM.

   The ratio of RCM/arylamine substrate/CAT is 97:2:1. The amount of substrate may be changed, if necessary, for determination of kinetic constants.

   There is lot-to-lot variation in CAT preparations, so it is necessary to adjust the amount used to give the desired concentration.
5. For each reaction to be performed, combine, in a 1.5-ml microcentrifuge tube, 50 µl of cytosol or S-9 protein solution (from step 2) and 20 µl of RCM/arylamine substrate/CAT (from step 4). Mix gently and incubate 1 min at 37°C.

   When the acetyl CoA solution is added in the next step, total reaction volume will be 90 µl.
6. Add 20 µl of 1× acetyl CoA solution 1 (from step 3) to each tube, gently mix, and begin timing incubation (generally 10 min) at 37°C in a water bath.
7. Stop the reaction by adding 90 µl ice-cold methanol; mix and keep on ice.
8. Microcentrifuge samples for 4 min at 14,000 × *g*, room temperature, to precipitate protein. Use 20 to 50 µl of the supernatant for HPLC analysis.

Perform HPLC analysis

9. Prepare a standard curve by injecting known amounts of an authentic standard of the acetylated product of interest (see Support Protocol 3). Plot nanograms standard (*y* axis) versus absorbance ($AUC_{product}$; *x* axis). Calculate slope and *y*-intercept by linear regression analysis.
10. Inject sample (20 to 50 µl or amount necessary for a specific instrument) onto the column and elute according to the conditions for the product being analyzed (see Tables 4.6.2, 4.6.3, and 4.6.4) at a flow rate of 1 ml mobile phase/min.
11. Calculate activity in nmol/min/mg protein by comparison of the absorbance (AUC peak area) of the product in the sample with that obtained with known amounts of authentic standard using the following formulas:

Table 4.6.2 HPLC Conditions for Sulfamethazine (SMZ)

	Method 1[a]	Method 2
Column	Microsorb-MV C18 (4.6 × 250–mm, 5 µm)	Adsorbosphere C18 (4.6 × 250–mm, 5 µm)
Mobile phase	20 mM ammonium acetate (A) and methanol (B)	18% acetonitrile in H_2O with 0.5% acetic acid
Gradient	Linear: 2% to 100% B	Isocratic
Flow rate	1 ml/min	1 ml/min
Retention (min)		
SMZ	12.0	10.8
acetyl SMZ	14.0	8.4
Absorbance wavelength (nm)	254	254

[a]Stevens et al., 1999.

Table 4.6.3 HPLC Conditions for *p*-Aminobenzoic Acid (PABA)[a]

	Method 1	Method 2
Column	Microsorb-MV C18 (4.6 × 250–mm, 5 µm)	Adsorbosphere C18 (4.6 × 250–mm, 5 µm)
Mobile phase	90% 50 mM acetic acid and 10% acetonitrile	13% acetonitrile in H_2O with 0.5% acetic acid
Gradient	Isocratic	Isocratic
Flow rate	1 ml/min	1 ml/min
Retention (min)		
PABA	7.0	6.5
acetyl PABA	13.0	8.8
Absorbance wavelength (nm)	270	270

[a]Stevens et al., 1999.

Table 4.6.4 HPLC Conditions for 2-Aminofluorene (2-AF)

	Method 1[a]	Method 2
Column	Microsorb-MV C18 (4.6 × 250–mm, 5 µm)	Versapack C18 (4.1 × 300–mm, 10 µm)
Mobile phase	20 mM ammonium acetate (A) and methanol (B)	40% acetonitrile in H_2O with 0.5% acetic acid
Gradient	Linear; 35% to 100% B	Isocratic
Flow rate	1 ml/min	2 ml/min
Retention (min)		
2-AF	20.4	2.6
2-AAF[b]	22.4	6.8
Absorbance wavelength (nm)	245	245

[a]Stevens et al., 1999.
[b]2-acetylaminofluorene.

$$\text{area under curve}_{\text{product}} \times \text{slope}_{\text{std. curve}} + y\ \text{intercept}_{\text{std. curve}} = \text{ng product/injected sample vol.}$$

$$\frac{\text{ng product} \times \text{mol. wt.}_{\text{product}} \times \text{total sample vol./injected sample vol.}}{(\text{min incubation})(\text{mg protein/sample})} = \text{nmol acetylated product/min/mg protein}$$

ALTERNATE PROTOCOL

HPLC ASSAY FOR NAT ACTIVITY USING A FIXED CONCENTRATION OF ACETYL CoA

This method uses a single concentration of acetyl CoA, which simplifies the number of components required during incubation. Arylamine NAT activity is measured under the following conditions: 2 mM EDTA, 2 mM DTT, 50 mM Tris·Cl, pH 7.5, 2.2 mM acetyl CoA, and 44.4 µM arylamine substrate.

Additional Materials *(also see Basic Protocol 1)*

1× acetyl CoA solution 2 (10^{-2} M; see recipe)
2×10^{-4} M arylamine substrate (see recipe and Table 4.6.1)

NAT reaction

1. Thaw and adjust protein concentration of cytosol or S-9 (see Basic Protocol 1, steps 1 and 2).
2. Add the following to each tube (total reaction volume 90 µl):

   50 µl cytosol or S-9 protein solution (see Basic Protocol 1, step 2)
   20 µl 2×10^{-4} M arylamine substrate solution
   20 µl 1× acetyl CoA solution 2

   Mix gently and incubate 10 min at 37°C.
3. Stop the reaction by adding 90 µl of ice-cold methanol, mixing, and keeping on ice.
4. Prepare sample and analyze by HPLC (see Basic Protocol 1, steps 8 to 11).

THE BRATTON-MARSHALL ASSAY FOR NAT ACTIVITY

BASIC PROTOCOL 2

The Bratton-Marshall assay measures the disappearance of an arylamine substrate rather than the formation of the acetylated product. The unacetylated arylamine is converted to the diazo cation by sodium nitrite, which is then reacted with *N*-1-(naphthyl)ethyl-enediamine (NED) forming a colored diazo compound with an absorbance at 540 nm. This method can potentially be utilized with any arylamine substrate of NAT. Arylamine NAT activity is measured under the following conditions: 2 mM EDTA, 2 mM DTT, 50 mM Tris·Cl, pH 7.5, 2.2 mM acetyl CoA, and 44.4 µM arylamine substrate.

Materials

Cytosolic or S-9 fraction (see Support Protocol 1 or 2)
Pierce protein assay kit
Homogenization buffer (see recipe)
1× acetyl CoA solution 2 (10^{-2} M; see recipe)
2×10^{-4} M arylamine substrate (see recipe and Table 4.6.1)
10% (w/v) trichloracetic acid (TCA; store up to 1 month at room temperature)
0.1% (w/v) sodium nitrite (prepared fresh)
0.5% (w/v) ammonium sulfamate (store up to 1 month at room temperature)
0.05% (w/v) *N*-1-(naphthyl)ethylene-diamine dihydrochloride (NED; Sigma; store up to 1 month at room temperature)
UV spectrophotometer

Perform NAT reaction

1. Thaw a sufficient number of tubes of cytosol or S-9 for the experiment (200 µl). Keep on ice.
2. Determine the protein concentration of the cytosol or S-9 using protein assay kit. Adjust the concentration to 0.5 to 2 mg protein/50 µl with homogenization buffer.
3. In a 1.5-ml microcentrifuge tube combine the following for each experimental sample or control (total volume 90 µl):

   Experimental:
   50 µl cytosol or S-9 protein solution (from step 2)
   20 µl 2×10^{-4} M arylamine substrate
   20 µl 1× acetyl CoA solution 2

   Control:
   50 µl cytosol or S-9 protein solution (from step 2)
   20 µl water
   20 µl 2×10^{-4} M arylamine substrate solution

   IMPORTANT NOTE: *Each cytosol sample needs an appropriate control tube run simultaneously with the experimental tube.*

4. Mix gently and incubate 10 min at 37°C.
5. Stop the reaction by adding 50 µl of 10% TCA and mixing.

Prepare sample

6. Add 20 µl of freshly prepared 0.1% sodium nitrite, mix, and incubate 3 min at room temperature.
7. Add 20 µl of 0.5% ammonium sulfamate, mix, and incubate at room temperature for 3 min.
8. Add 100 µl of 0.05% NED, mix, and incubate for 10 min.
9. Microcentrifuge 4 min at 14,000 × *g*, room temperature, to precipitate the protein.

Spectrophotometric analysis

10. Read each sample at 540 nm against a water blank.
11. Subtract the control from the corresponding experimental sample to determine the change in absorbance.
12. Calculate the NAT activity as follows:

$$\frac{\text{absorbance}_{\text{control}} - \text{absorbance}_{\text{exp}}}{\text{incubation time (min)}} \times \frac{1}{(\text{absorbance/ng arylamine})(\text{mol. wt.}_{\text{arylamine}})} \times \frac{1}{\text{mg/sample}} = \text{nmol/min/mg}$$

SUPPORT PROTOCOL 1

PREPARATION OF S-9 FROM TISSUE

This protocol can be used for organs or isolated cells. An S-9 fraction is generally used when only small amounts of tissue or cells are available.

Materials

Mammalian liver or cultured cells
Homogenization buffer (see recipe), ice-cold

Tissue homogenizer: Polytron (Kinematica) or equivalent
Cryovials

1. Harvest and weigh tissue. Add a volume of ice-cold homogenization buffer equal to three times the tissue weight. Homogenize using the Polytron homogenizer.

   If S-9 is being prepared from cultured cells, the medium is removed and the cells are suspended in the homogenization buffer.

2. Centrifuge 10 min at 9000 × *g*, 4°C.
3. Divide supernatant into 200- to 400-µl aliquots in cryovials and store up to 6 weeks at −80°C.

SUPPORT PROTOCOL 2

PREPARATION OF CYTOSOL

This protocol is used to prepare cytosol from mammalian liver. It can be modified for other tissues or cells by adjusting the amount of homogenization buffer.

Materials

Mammalian liver
Homogenization buffer (see recipe), ice-cold

Tissue homogenizer: Polytron (Kinematica) or equivalent
Ultracentrifuge
Cryovials

1. Harvest and weigh tissue. Add a volume of ice-cold homogenization buffer equal to three times the tissue weight. Homogenize using the Polytron homogenizer.
2. Centrifuge 10 min at 9000 × *g*, 4°C.
3. Discard pellet and ultracentrifuge supernatant 1 hr at 100,000 × *g*, 4°C.
4. Divide supernatant into 200- to 400-µl aliquots in cryovials and store up to 6 weeks at −80°C.

PREPARING A STANDARD CURVE FOR HPLC ASSAY OF NAT ACTIVITY

SUPPORT PROTOCOL 3

Known amounts of the authentic standard are used to determine absorbance (AUC peak area) at a specific wavelength.

Materials

Acetyl PABA or other acetylated arylamine of interest
DMSO (for acetyl PABA) or other appropriate solvent for acetylated arylamine
Mobile phase (see Tables 4.6.2, 4.6.3, and 4.6.4)

1. Prepare a solution of 1 mg/ml acetyl PABA in DMSO. Dilute with the mobile phase so that there are 8 to 10 tubes ranging from 0 to 10 ng/µl.
2. Inject sample into the column and elute the sample under the conditions for the appropriate arylamine (Tables 4.6.2, 4.6.3, and 4.6.4).

   For PABA, absorbance (AUC) is determined at 270 nm using reversed-phase HPLC with a C18 column and acetic acid/acetonitrile (Table 4.6.3) as the mobile phase.
3. Plot absorbance (AUC peak area; *x* axis) versus ng standard (*y* axis). Determine the slope and *y* intercept with linear regression analysis.

PREPARING A STANDARD CURVE FOR COLORIMETRIC ASSAY OF NAT ACTIVITY

SUPPORT PROTOCOL 4

Known amounts of authentic arylamine solution are used to determine the absorbance at 540 nm following diazotization with sodium nitrite and coupling with NED.

Materials

5×10^{-3} M sulfamethazine (SMZ; see recipe) or other arylamine substrate of interest
10% (w/v) trichloracetic acid (TCA; store up to 1 month at room temperature)
0.1% (w/v) sodium nitrate (prepared fresh)
0.5% (w/v) ammonium sulfamate (store up to 1 month at room temperature)
0.05% (w/v) *N*-1-(naphthyl)ethylenediamine dihydrochloride (NED; Sigma; store up to 1 month at room temperature)

1. Dilute 5×10^{-3} M SMZ 1:100 with water.
2. Pipet a series of aliquots of SMZ ranging from 0 to 450 µl, in duplicate, into separate tubes. Add water as necessary to bring the volume to 450 µl.
3. Add 250 µl of 10% TCA to each tube. Mix.
4. Add 100 µl of 0.1% sodium nitrite to each tube. Mix and wait 3 min.

   The sodium nitrate solution must be freshly prepared each day. It is also critical to allow sufficient time (3 min) for the diazotization reaction to occur.

5. Add 100 µl of 0.5% ammonium sulfamate to each tube. Mix and wait 3 min.

   It is important to wait 3 min for the reaction with the excess nitrite to occur.

6. Add 500 µl of 0.05% NED to each tube. Mix.
7. Read at 540 nm after 10 min. Do not allow more than 30 min to elapse before reading.
8. Plot the concentration of sulfamethazine (*x* axis) versus absorbance at 540 nm (*y* axis).

REAGENTS AND SOLUTIONS

Use Milli-Q purified water or equivalent in all recipes and protocol steps. For common stock solutions, see ***APPENDIX 2A****; for suppliers, see* ***SUPPLIERS APPENDIX****.*

Acetyl CoA solution 1, 10× (22.7 mM)

Weigh 9.19 mg acetyl CoA (lithium salt) add to 500 µl and water. Aliquot 50 µl into separate tubes and store at −20°C. Use within 30 days.

Acetyl CoA solution 2 (10^{-2} M)

Weigh 8.09 mg acetyl CoA and add to 1 ml water. Store at −20°C. Use within 30 days.

Arylamine substrate solutions

10^{-2} M p-aminobenzoic acid (PABA): Weigh 137 mg PABA and add 100 ml water.

2×10^{-4} M PABA: Weigh 2.74 mg PABA and add 100 ml water.

10^{-2} M sulfamethazine (SMZ): Weigh 278 mg SMZ (e.g., Sigma) and add 80 ml water. The solubility of SMZ is increased at a basic pH. Add a few drops of 0.1 M sodium hydroxide if necessary. Adjust volume to 100 ml with water.

2×10^{-4} M SMZ: Weigh 5.56 mg SMZ and dissolve as described above for 10^{-2} M.

10^{-2} M 2-aminofluorene (2-AF): Weigh 181.2 mg 2-AF (e.g., Sigma) and dissolve in 100 ml DMSO.

2×10^{-4} M 2-AF: Weigh 3.6 mg 2-AF and dissolve in 100 ml DMSO.

CAUTION: *2-AF is a carcinogen and mutagen and must be weighed, used, and disposed of following appropriate institutional procedures.*

Homogenization buffer

Prepare 1 liter of 20 mM Tris·C1, pH 7.5 (*APPENDIX 2A*). To this, add 0.15 g dithiothreitol (DTT; 1 mM final) and 0.37 g disodium ethylenediamine tetraacetate (EDTA; 1 mM final). On day of assay, add 1 ml of 50 mM phenylmethylsulfonyl fluoride (PMSF; 50 µM final) and 1 ml of 10 mM leupeptin (10 µM final).

To prepare the 50 mM PMSF stock, weigh 87 mg PMSF and add 10 ml acetonitrile. To prepare 10 mM leupeptin stock, weigh 48 mg leupeptin and add 10 ml water.

Recycling mix (RCM)

Prepare the following stock solutions:
1 M Tris hydrochloride: Weigh 78.80 g Tris hydrochloride and add 500 ml water.
100 mM dithiothreitol (DTT): Weigh 15.23 mg DTT and add 10 ml water.
100 mM EDTA: Weigh 372.24 mg disodium EDTA and add 10 ml water.

To make 50 ml RCM combine 11.25 ml of 1 M Tris hydrochloride, 4.50 ml of 100 mM DTT, and 4.50 ml of 100 mM EDTA. Bring to 40 ml with water, then add 876.5 mg acetyl-DL-carnitine (Sigma; 73.1 mM final). Adjust pH to 7.8. Bring final volume to 50 ml with water and store in 1-ml aliquots at −20°C. Use within 30 days.

The total volume of this recipe is 50 ml; final concentrations are: 225 mM Tris, 9 mM DTT, 9 mM EDTA, and 73.1 mM acetylcarnitine.

COMMENTARY

Background Information

In mammalian species, NATs are encoded by two polymorphic genes, *NAT1* and *NAT2* (see reviews by Vatsis and Weber, 1997, and Hein et al., 2000a). There is a human pseudogene, *NATP*, as well as an *NAT3* locus in the mouse. Little or no activity has been associated with the latter two genes. The acetylation of aromatic amines and hydrazines is mainly catalyzed by *NAT 1* and *NAT 2*. These genes have been isolated from mammalian species, sequenced, and expressed. A consensus nomenclature for NAT genes was first published in 1995 (Vatsis et al., 1995) and recently reviewed (Hein et al, 2000b). The Human Gene Nomenclature Committee (*http://www.gene.ucl.ac.uk/nomenclature*) has designated *NAT* as the gene symbol. A committee and web site (*http://www.louisville.edu/medschool/pharmacology/NAT.html*) is ensuring the use of the consensus nomenclature will be maintained and reviewed as necessary (Hein et al., 2000b). Rodent species also have two genes designated *NAT1* and *NAT2*, but based on substrate specificities and homologies it appears that rodent *NAT1* is comparable to human *NAT2* while rodent *NAT2* is comparable to human *NAT1* (Vatsis et al., 1995; Hein et al., 2000b).

The human *NAT* genes are both located on chromosome 8. These genes share greater than 80% nucleotide homology in the coding region (Blum et al., 1990; Hickman et al., 1994). Each gene has an intronless coding region of 870 bp (Blum et al., 1991; Vatsis et al., 1991). Allelic variants that alter enzyme activity have been reported for both human genes, with nucleotide changes representing the most common source of variation (see reviews by Vatsis and Weber, 1997, and Hein et al., 2000a). The allelic variations in *NAT 1* or *NAT 2* result in phenotypes with different activities.

NATs have a wide tissue distribution. Human NAT1 and NAT2 are found in liver as well as in extrahepatic tissue including gastrointestinal tract, urinary tissue, bladder, and lung (Windmill et al., 2000). In addition to overlapping tissue distributions, these two enzymes also share substrate specificities. While there are substrates that are selective for NAT1 or NAT2, only one specific substrate, *p*-aminobenzoylglutamate (PABAGlu), has been identified for human NAT1 and rodent NAT2 (Minchin, 1995; Ward et al., 1995). One commonly used substrate that is selective for human NAT1 is *p*-aminobenzoic acid (PABA; Grant et al., 1991). This is also used to evaluate rodent NAT2 activities (Doll and Hein, 1995; Ferguson et al., 1996; Estrada-Rogers et al., 1998). Sulfamethazine (SMZ) is a selective substrate for human NAT2 but a poor substrate for rodent NAT1. Some compounds such as the aromatic amine carcinogen 2-aminofluorene are substrates for both enzymes (Grant et al., 1991; Doll and Hein, 1995; Ferguson et al., 1996; Estrada-Rogers et al., 1998).

Acetylation is a conjugation, or phase II, reaction that may either increase or decrease toxicity of the parent compound. For hydrazines such as isoniazid or hydralazine, *N*-acetylation results in the formation of a less reactive product. A decrease in the genotoxicity of hydralazine is associated with an increase in NAT activity (Lemke and McQueen, 1995). *N*-acetylation of arylamines generally decreases toxicity. In contrast, *O*-acetylation of *N*-hydroxylamines is a major step in the activation of aromatic amines to DNA-damaging products (see review by Delclos and Kadlubar, 1997).

The enzymes that are designated as NATs catalyze the following acetylation reactions: the addition of an acetyl group to the nitrogen of an extracyclic amino or hydrazine moiety, the addition of an acetyl group to the oxygen of an *N*-hydroxylamine or the *N*,*O* intramolecular transfer of the acetyl group (Fig. 4.6.1). These activities reside in the same protein (Glowinski et al., 1980). Recombinant-expressed NATs catalyze both *N*- and *O*-acetylation reactions (Fretland et al., 1997). Since the *N*-acetyl derivatives are generally

more stable than the *O*-acetylated compounds, the former reaction is commonly measured.

The choice of methods for determination of NAT activities involves consideration of the incubation conditions and the analytical system. Initially, measurement of NAT activity for a given arylamine or hydrazine utilized a fixed concentration of acetyl CoA (Hearse and Weber, 1973). This was modified to use a system which continually regenerates acetyl CoA (Andres et al., 1985). This allows measurements at lower, more physiologic concentrations of acetyl CoA, limits inhibition of NAT by coenzyme A, and is particularly suited for determination of kinetic constants (Andres et al., 1985).

NAT activity is generally expressed as nanomole acetylated product/minute/milligram protein. Two approaches to measuring activity can be used. Since the disappearance of substrate is directly proportional to the appearance of product (Hearse and Weber, 1973), the decrease in substrate concentration may be determined. A micro-modification (Hearse and Weber, 1973) of the Bratton-Marshall method (Bratton and Marshall, 1939) involves a colorimetric determination of the parent amine. Since the method detects aromatic amines but not arylamides, the conditions for product analysis need not be altered to reflect which substrate is measured. An alternative approach for quantifying amines is based on decreasing Schiff's base formation with dimethylaminobenzaldehyde (Andres et al., 1985).

HPLC methods allow direct measurement of product formation. Although the HPLC conditions must be developed, product can be confirmed by the comigration with authentic standards and quantified by comparison to a standard curve. Conditions suitable for commonly used substrates are in Tables 4.6.2, 4.6.3, and 4.6.4. Comparable methods for these and other substrates have been reported by several laboratories.

Critical Parameters and Troubleshooting

NATs catalyze the acetylation of aromatic amines and hydrazines by a ping-pong mechanism (Fig. 4.6.2). The reaction first involves the formation of a covalent acetyl-cysteinyl NAT intermediate and CoA. The acetyl group from this intermediate is then transferred to the acceptor amine, resulting in the acetylated amine and NAT (Fig. 4.6.2; also see Weber and Cohen, 1968). The two-step process requires that the enzyme have a reactive cysteinyl thiolate (Andres et al., 1988), which in human NAT2 is Cys^{68}. Substitution at this site with Gly abolishes catalytic activity (Dupret and Grant, 1992).

Instability of NATs, particularly in highly purified preparations, is presumably caused by oxidation of sulfhydryl groups. This requires that care be taken in the handling and storage of samples. Postmortem delays in harvesting tissue increase the likelihood of enzyme degradation. Small samples of tissue or cultured cells can be frozen intact and stored for at least 1 month at −80°C. The inclusion of compounds such as DTT, PMSF, and leupeptin in the homogenization buffer are helpful in maintaining key sulfhydryl groups such as Cys^{68} in human NAT2.

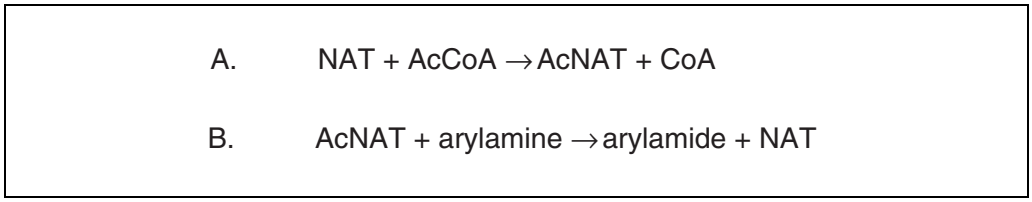

Figure 4.6.2 Mechanism of NAT catalyzed *N*-acetylation.

NAT activity can be inhibited by high concentrations of CoA. This can be minimized by using lower concentrations of acetyl CoA or the regenerating system described in Basic Protocol 1. The enzyme can also be affected by solvents such as dimethysulfoxide (DMSO). Due to the poor solubility of many aromatic amines in aqueous solutions, compounds such as 2-AF are generally dissolved in DMSO. Care should be taken to minimize the amount of DMSO in the assay. NAT activity was not inhibited by 1% DMSO, but inhibition was observed at concentrations >5% (Mattano and Weber, 1987).

Anticipated Results

Examples of the range of NAT activities calculated for human or rodent liver are illustrated in Tables 4.6.5 and 4.6.6. For human samples, cytosols were prepared from livers and analyzed for NAT activities according to Basic Protocol 1. A sample (0.5 mg protein) was incubated at 37°C for 10 min. Substrate concentration was 44.4 µM PABA or SMZ. The amount of product was determined by HPLC. Calculation of NAT activity was:

$$\frac{\text{area under curve}_{\text{sample}} \times \text{slope}_{\text{std. curve}} + \text{y intercept}_{\text{std. curve}} \times \dfrac{1}{\text{ng/nmol}} \times \dfrac{180\,\mu\text{l}}{50\,\mu\text{l}}}{(10\text{ min incubation})(0.5\text{ mg protein})} = \text{nmol product/min/mg protein}$$

The conversion from nanogram standard to nanomole requires that the molecular weight of the parent be used.

Table 4.6.5 Human Hepatic NAT Activities[a]

Sample	NAT1		NAT2	
	Alleles	PABA activity	Alleles	SMZ activity[b]
1	1*4/4	1.98	2*4/*5B	0.87
2	1*4/*10	0.64	2*5B/*5B	0.16
3	1*3/*10	1.53	2*4/*4	2.15
4	1*4/*4	0.46	2*6A/*6A	0.13
5	1*4/*4	2.76	2*4/*5B	0.87
6	1*4/*4	1.62	2*5B/*6A	0.14
7	1*10/*11	5.47	2*5C/*6A	0.11
8	1*4/*4	0.95	2*5A/*5C	0.34
9	1*4/*4	0.20	2*5B/5B	0.15

[a]Data from Stevens et al., 1999.

[b]Activities in nmole/min/mg protein.

Table 4.6.6 NAT Activity in Rodent Liver[a]

Strain/species	nmol 2-AAF[b]/min/mg protein
F-344 rat	2.93 ± 0.03
C57Bl/6J mouse	11.77 ± 0.40
A/J mouse	5.18 ± 0.96

[a]Data from Stevens et al., 2000.

[b]Abbreviations: AAF, 2-acetylaminofluorene.

Time Considerations

For NAT assays, incubations generally are <20 min. Sample preparation for HPLC takes ~5 min per sample. The HPLC run may vary, but 30 min is usually sufficient to separate product from parent. Additional time will be necessary to equilibrate the column to the initial conditions for the separation. The use of an autosampler in conjunction with the HPLC allows samples to be processed unattended.

Literature Cited

Andres, H.H., Klem, A.J., Szabo, S., and Weber, W.W. 1985. New spectrophotometric and radiochemical assays for acetyl-CoA: Arylamine *N*-acetyltransferase applicable to a variety of arylamine. *Anal. Biochem*. 145:367-375.

Andres, H.H., Klem, A.J., Schopfer, L.M., Harrison, J.K., and Weber, W.W. 1988. On the active site of liver acetyl CoA: Arylamine *N*-acetyltransferase from rapid acetylator rabbits (III/J). *J. Biol. Chem*. 263:7521-7527.

Blum, M., Grant, D., McBride, W., Heim, M., and Meyer, U.A. 1990. Human *N*-arylamine acetyltransferase genes: Isolation, chromosomal localization and functional expression. *DNA Cell Biol*. 9:193-203.

Blum, M., Demierre, A., Grant, D.M., Heim, M., and Meyer, U.A. 1991. Molecular mechanism of slow acetylation of drugs and carcinogens in humans. *Proc. Natl. Acad. Sci. U.S.A*. 88:5237-5241.

Bratton, A.C. and Marshall, E.K. 1939. A new coupling component for sulfanilamide determination. *J. Biol. Chem*. 218:537-550.

Delclos, K.B. and Kadlubar, F.F. 1997. Carcinogenic aromatic amines and amides. *In* Comprehensive Toxicology, Vol. 12 (I.G. Sipes, C.A. McQueen, and A.J. Gandolfi, eds.) pp. 141-170. Elsevier Science, Oxford.

Doll, M.A. and Hein, D.W. 1995. Cloning, sequencing and expression of *NAT1* and *NAT2* encoding genes from rapid and slow acetylator inbred rats. *Pharmacogenetics* 5:247-251.

Dupret, J.M. and Grant, D.M. 1992. Site-directed mutagenesis of recombinant human arylamine *N*-acetyltransferase expressed in *E. coli*. *J. Biol. Chem*. 267:7381-7385.

Estrada-Rogers, L., Levy, G.N., and Weber, W.W. 1998. Substrate selectivity of mouse *N*-acetyltransferases 1, 2 and 3 expressed in COS-1 cells. *Drug Metab. Dispos*. 26:502-505.

Ferguson, R.J., Doll, M.A., Rustan, T.D., and Hein, D.W. 1996. Cloning, expression and functional characterization of rapid and slow acetylator polymorphic *N*-acetyltransferase genes of the Syrian hamster. *Pharmacogenetics* 6:55-66.

Fretland, A.J., Doll, M.A., Gray, K., Feng, Y., and Hein, D.W. 1997. Cloning, sequencing and recombinant expression of *NAT1*, *NAT2* and *NAT3* derived from C3H/HeJ (rapid) and A/HeJ (slow) acetylator inbred mice: Functional characterization of the activation and detoxification of aromatic amine carcinogens. *Toxicol. Appl. Pharmacol*. 142:360-366.

Glowinski, I.B., Weber, W.W., Fysh, J.M., Vaught, J.B., and King, C.M. 1980. Evidence that arylhydroxamic acid *N*,*O*-acetyltransferase are properties of the same enzyme in rabbit liver. *J. Biol. Chem*. 255:7883-7890.

Grant, D.M., Blum, M., Beer, M., and Meyer, U.A. 1991. Monomorphic and polymorphic human arylamine *N*-acetyltransferases: A comparison of liver isozymes and expressed products of two cloned genes. *Mol. Pharmacol*. 59:184-191.

Hearse, D.J. and Weber, W.W. 1973. Multiple *N*-acetyltransferase and drug metabolism. *Biochem. J*. 132:519-526.

Hein, D.W., Doll, M.A., Fretland, A.J., Leff, M.A., Webb, S.J., Xiao, G.H., Devanaboyina, U.S., Nangju, N.A., and Feng, Y. 2000a. Molecular genetics and cancer epidemiology of the *NAT1* and *NAT2* acetylation polymorphisms. *Cancer Epidemiol. Biomark. Prev*. 9:29-42.

Hein, D.W., Grank, D.M., and Sim, E. 2000b. Update on consensus arylamine *N*-acetyltransferase gene nomenclature. *Pharmacogenetics* 10:291-292.

Hickman, D.A., Risch, A., Buckle, V., Spurr, N., Jeremiah, S.J., McCarthy, A., and Sim, E. 1994. Chromosomal localization of human genes for arylamine *N*-acetyltransferases. *Biochem. J*. 297:441-445.

Lemke, L.E. and McQueen, C.A. 1995. Acetylation and its role in the mutagenicity of the antihypertensive agent hydralazine. *Drug Metab. Dispos*. 23:559-565.

Mattano, S.S. and Weber, W.W. 1987. Kinetics of arylamine *N*-acetyltransferase in tissues from rapid and slow acetylator mice. *Carcinogenesis* 8:133-137.

Minchin, R.F. 1995. Acetylation of *p*-aminobenzoylglutamate, a folic acid catabolite, by recombinant human arylamine *N*-acetyltransferase and U937 cells. *Biochem. J*. 307:1-3.

Stevens, G.J., Payton, M., Sim, E., and McQueen, C.A. 1999. *N*-acetylation of the heterocyclic amine batracylin by human liver. *Drug Metab. Dispos*. 27:966-971.

Stevens, G.J., Burkey, J.L., and McQueen, C.A. 2000. Toxicity of the heterocyclic amine batracylin: Investigation of rodent *N*-acetyltransferase activity and potential contribution of cytochrome P450 3A. *Cell Biol. Toxicol*. 16:31-39.

Vatsis, K.P. and Weber, W.W. 1997. Acetyltransferases. *In* Comprehensive Toxicology, Vol. 3, (I.G. Sipes, C.A. McQueen, and A.J. Gandolfi, eds.) pp. 385-499. Elsevier Science, Oxford.

Vatsis, K.P., Martell, K.J., and Weber, W.W. 1991. Diverse point mutations in the human gene for polymorphic *N*-acetyltransferase. *Proc. Natl. Acad. Sci. U.S.A.* 88:6333-6337.

Vatsis, K.P., Weber, W.W., Bell, D.A., Dupret, J.M., Price-Evans, D.A., Grant, D.M., Hein, D.W., Lin, H.J., Meyer, U.A., Relling, M.V., Sim, E., Suzuki, T., and Yamazoe, Y. 1995. Nomenclature for *N*-acetyltransferases. *Pharmacogenetics* 5:1-17.

Ward, A., Summers, M.J., and Sim, E. 1995. Purification of recombinant human *N*-acetyltransferase type 1 (NAT 1) expressed in *E. coli* and characterization of its potential role in folate metabolism. *Biochem. Pharmacol*. 49:1759-1767.

Weber, W.W. and Cohen, S.N. 1968. The mechanism of isoniazid acetylation by human *N*-acetyltransferase. *Biochem. Biophys. Acta* 151:276-278.

Windmill, K.F., Gaedigk, Hall, P.D., Samaratunga, H., Grant, D.M., and McManus, M.E. 2000. Localization of *N*-acetyltransferases NAT1 and NAT2 in human tissues. *Toxicol. Sci*. 54:19-29.

Key References

Andres et al., 1985. See above.

Describes the recycling system for acetyl CoA.

Hearse and Weber, 1973. See above.

Describes the Bratton-Marshall method.

Hein et al., 2000a. See above.

Recent review of the molecular genetics and epidemiology of human NATs.

Stevens et al., 1999. See above.

Describes HPLC conditions for PABA and SMZ.

Stevens et al., 2000. See above.

Describes HPLC conditions for 2-AF.

Vatsis and Weber, 1997. See above.

Recent review of NATs.

Internet Resources

http://www.louisville.edu/medschool/pharmacology/NAT.html

Web site for NAT alleles and nomenclature.

http://www.gene.uc.ac.uk/nomenclature

Web site for Human Gene Nomenclature Committee.

Contributed by Charlene A. McQueen
University of Arizona
Tucson, Arizona

Measurement of Carboxylesterase (CES) Activities

Mammalian carboxylesterases (CES; EC 3.1.1.1) comprise a multigene family whose gene products exist in many mammalian species and humans. These enzymes efficiently catalyze the hydrolysis of a variety of ester- and amide-containing chemicals, as well as drugs (including prodrugs), to the respective free acids (Fig. 4.7.1). They are involved in detoxification or metabolic activation of various drugs, environmental toxicants, and carcinogens. CES also catalyzes the hydrolysis of endogenous compounds such as acyl-glycerol, acyl-carnitine, and acyl-CoAs. Multiple isozymes of hepatic microsomal CES exist in various animal species, and some of these isozymes are involved in the metabolic activation of certain carcinogens as well as being associated with hepatocarcinogenesis.

The CES isozymes are located on the lumen side of the endoplasmic reticulum. Microsomal preparations from tissues, whole cultured cells, or membrane preparations from cultured cells are used in hydrolysis assays. The activity of a CES is measured as the moles of respective acids or alcohol formed from substrates during a given time period via catalysis by a standard amount of protein. This unit describes three methods for measuring CES activity: (1) the photometric assay (see Basic Protocol 1), which is a simple and rapid screening method and can be used with a variety of substrates (see Alternate Protocols 1 through 3); (2) the fluorometric assay (see Basic Protocol 2), which is a high sensitivity method; and (3) the high-performance liquid chromatography (HPLC) method (see Basic Protocol 3), which is a general screening method. A great many substrates may be analyzed by these methods. In each procedure, the enzyme reaction is

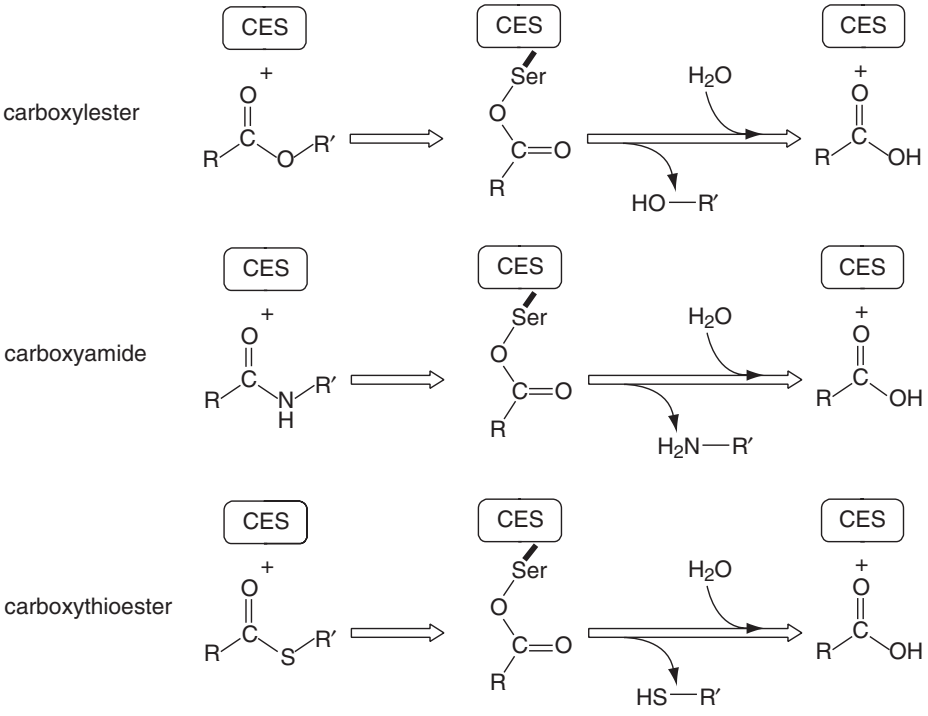

Figure 4.7.1 Reactions catalyzed by CES.

Contributed by Masakiyo Hosokawa and Tetsuo Satoh
Current Protocols in Toxicology (2001) 4.7.1-4.7.14

performed using a microsome preparation from tissue (see Support Protocol 1) or cultured cells expressing cDNA from CES isozymes (see Support Protocol 2).

BASIC PROTOCOL 1

PHOTOMETRIC ASSAY FOR CES USING *p*-NITROPHENYL ACETATE

Since this assay can be processed within 1 or 2 min, this assay system has been developed as a fast technique for analysis of hydrolysis in tissues or cultured cells. Another advantage of the assay is that all CES isozymes catalyze the hydrolysis of *p*-nitrophenyl acetate. The phenol liberated from *p*-nitrophenyl esters in basic solution is observed spectrophotometrically at 405 nm using a UV/VIS spectrophotometer with a computer.

Materials

Microsomes (see Support Protocol 1 or 2)
GET solution (see recipe), ice cold
Bio-Rad DC protein assay kit II
1 mM *p*-nitrophenyl acetate solution (see recipe for substrate solutions)
1 M Tris·Cl buffer, pH 8.0 (*APPENDIX 2A*)

5-ml Potter-Elvehjem homogenizer with Teflon pestle
5-ml test tubes
30°C water bath
1.0-ml semimicro cuvettes, 1-cm path length
UV/VIS spectrophotometer with a computer and temperature-controlled Peltier cuvette holder

1. Suspend the microsome pellet in a small aliquot of ice-cold GET solution using a 5-ml Potter-Elvehjem homogenizer with a Teflon pestle (see Support Protocol 1 or 2).
2. Determine the protein concentration using a Bio-Rad DC protein assay kit II and adjust the concentration to within the range of 0.01 to 0.5 mg/ml with ice-cold GET solution and keep on ice.
3. Transfer 0.9 ml *p*-nitrophenyl acetate solution to 5-ml test tubes and place tubes for 5 min in a 30°C water bath.
4. Add 50 µl of 1 M Tris·Cl buffer, pH 8.0, to each 5-ml test tube at room temperature.
5. Start the enzymatic reactions by adding 50 µl of 0.01 to 0.5 mg/ml microsome preparation (from step 2) to each 5-ml test tube and vortex 5 sec at maximum speed.
6. Transfer the reaction mixture to a 1.0-ml semimicro cuvettes, 1-cm path length, in a 30°C cuvette holder (temperature controlled by a peltier cell holder).
7. Monitor the release of *p*-nitrophenol using a UV/VIS spectrophotometer at 405 nm for 60 to 120 sec.

   If a recorder is used instead of a computer, record for 120 to 240 sec. The increase in absorbance is linear with time, with a difference of up to 1.0.

8. Monitor spontaneous hydrolysis in a blank, GET solution alone without addition of the microsome preparation, using a UV/VIS spectrophotometer at 405 nm.

   In this method, the molar absorbance of 16,400 liters/M(cm) as p-nitrophenol is used; therefore, the specific activity (µmol of p-nitrophenol formed/min/mg protein) is

$$\frac{(\Delta absorbance/min - \Delta blank/min) \times 1.0}{16.4 \times 0.05 \times protein\ (mg/ml)}$$

   The method for measuring the hydrolase activities towards p-nitrophenyl esters, such as p-nitrophenyl propionate, p-nitrophenyl butylate, and p-nitrophenyl valeate, are the same as that used for p-nitrophenyl acetate hydrolase activity.

PHOTOMETRIC ASSAY FOR CES USING MALATHION AND OTHER ETHYL ESTERS

Malathion hydrolysis is coupled to the reduction of *p*-iodonitrophenyl tetrazolium violet (INT) with alcohol dehydrogenase and NADH diaphorase via the following reactions:

Malathion + CES → malathion monoacid + ethanol
Ethanol + NAD + alcohol dehydrogenase → acetaldehyde + NADH
NADH + INT + diaphorase → NAD + INT (reduced form).

The absorption at 500 nm due to the reduction of INT is recorded with a UV/VIS spectrophotometer.

Additional Materials *(also see Basic Protocol 1)*

p-iodonitrophenyltetrazolium violet (INT) solution (see recipe)
72 mM NAD (see recipe)
1000 U/ml alcohol dehydrogenase
4 U/ml NAD diaphorase
60 mM malathion (see recipe for substrate solutions)

37°C water bath
2.0-ml cuvette, 1-cm path length

1. Suspend the microsome pellet in a small aliquot of ice-cold GET solution using a 5-ml Potter-Elvehjem homogenizer with a Teflon pestle (see Support Protocol 1 or 2).
2. Determine the protein concentration using a Bio-Rad DC protein assay kit II and adjust the concentration to within 0.1 to 0.5 mg/ml with ice-cold GET solution and keep on ice.
3. Transfer 1.75 ml INT solution to 5-ml test tubes and place tubes for 5 min in a 37°C water bath.
4. Add 50 µl of 72 mM NAD to each 5-ml test tube at 37°C.
5. Add 50 µl of 1000 U/ml alcohol dehydrogenase to each test tube at 37°C.
6. Add 50 µl of 4 U/ml NAD diaphorase to each test tube at 37°C.
7. Add 100 µl of 0.1 to 0.5 mg/ml microsomal preparation (from step 2) to each 5-ml test tube at 37°C.
8. Start the enzymatic reactions by adding 10 µl of 60 mM malathion to each test tube and vortex 5 sec at maximum speed.
9. Transfer the reaction mixture to 2.0-ml cuvettes, 1-cm path length, in a 37°C cuvette holder (temperature controlled by a peltier cell holder).
10. Monitor the reduction of INT for 5 to 15 min at 500 nm using a UV/VIS spectrophotometer.

    If a recorder is used instead of a computer, record for 10 to 30 min. The increase in absorbance is linear with time, a difference of up to 1.0.

11. Monitor spontaneous hydrolysis in the blank, GET solution alone without the addition of the microsome preparation, using a UV/VIS spectrophotometer at 500 nm.

    In this method, the molar absorbance of 13,750 liters/M(cm) as reduced INT is used; therefore, the specific activity (µmol of ethanol formed (INT reduced)/min/mg protein) is

$$\frac{(\Delta absorbance/min - \Delta blank/min) \times 2.01}{13.75 \times 0.1 \times protein\ (mg/ml)}$$

The method for measuring the hydrolase activity of several ethylesters, such as chlofibrate and ethyl succinate, are the same as the method used for measuring malathion hydrolase activity.

ALTERNATE PROTOCOL 2

PHOTOMETRIC ASSAY FOR CES USING BUTANILICAINE

Most CES isozymes also hydrolyze some aromatic amides. Normally, it is not possible to assay the hydrolysis of these amides by a photometric assay because the rate of cleavage of amides by CES is usually low. The photometric assay described here is more sensitive and faster than previously used methods.

Additional Materials *(also see Basic Protocol 1)*

CES assay solution (see recipe)
10 mM butanilicaine solution (see recipe for substrate solutions), prewarm to 30°C

1. Suspend the microsome pellet in a small aliquot of ice-cold GET solution using a 5-ml Potter-Elvehjem homogenizer with a Teflon pestle (see Support Protocol 1 or 2).
2. Determine the protein concentration using a Bio-Rad DC protein assay kit II and adjust the concentration to 0.1 to 1.0 mg/ml with ice-cold GET solution and keep on ice.
3. Transfer 450 µl CES assay solution to 5-ml test tubes and incubate tubes 5 min in a 30°C water bath.
4. Add 50 µl microsome preparation to each test tube at room temperature.
5. Start the enzymatic reactions by adding 500 µl of prewarmed 10 mM butanilicaine to each 5-ml test tube and vortex 5 sec at maximum speed.
6. Transfer the reaction mixture to a 1-ml semimicro cuvette, 1-cm path length, in a 30°C cell holder (temperature controlled by a peltier cuvette holder).
7. Monitor the release of produced amine using a UV/VIS spectrophotometer at 285 nm for 3 to 10 min.

If a recorder is used instead of a computer, record 6 to 20 min. The increase in absorbance is linear with time, a difference of up to 1.0.

In this case, corrections for spontaneous hydrolysis of the substrate are not necessary.

In this method, the molar absorbance of 2080 liters/M(cm) as 2-chloro-6-methylaniline is used; therefore, the specific activity (µmol of 2-chloro-6-methylaniline formed/min/mg protein) is

$$\frac{\Delta absorbance/min \times 1.0}{2.080 \times 0.05 \times protein\ (mg/ml)}$$

ALTERNATE PROTOCOL 3

PHOTOMETRIC ASSAY FOR CES USING ACYL-CoA ESTER

CES isozymes catalyze the hydrolysis of endogenous compounds such as acyl-CoA esters. Hydrolysis of acyl-CoA derivatives has been carried out by spectrophotometric methods. A convenient spectrophotometric method uses 5,5′-dithiobis-(2-nitrobenzoic acid) to detect the release of the free thiol group.

Additional Materials *(also see Basic Protocol 1)*

120 mM HEPES buffer, pH 7.4 (see recipe)
5 mM EDTA, pH 7.4 (*APPENDIX 2A*)
3 mM DTNB solution (see recipe)
400 µM long-chain acyl-CoA solution (see recipe for substrate solutions)

1. Suspend the microsomal pellet in a small aliquot of ice-cold GET solution using a 5-ml Potter-Elvehjem homogenizer with a Teflon pestle.
2. Determine the protein concentration using a Bio-Rad DC protein assay kit II and adjust the concentration to 0.01 to 0.5 mg/ml with ice-cold GET solution and keep on ice.
3. Transfer 500 µl of 120 mM HEPES buffer, pH 7.4, to 5-ml test tubes and incubate tubes for 5 min in a 30°C water bath.
4. Add 100 µl of 5 mM EDTA, pH 7.4 and 100 µl of 3 mM DTNB solution to each tube at 30°C.
5. Add 100 µl of 400 µM long-chain acyl-CoA solution to each tube at 30°C.
6. Start the enzymatic reaction by adding 100 µl microsomal preparation (from step 2) to each test tube and vortex 5 sec at maximum speed.
7. Transfer the reaction mixture to a 1-ml semimicro cuvette, 1-cm path length, in a 30°C cuvette holder (temperature controlled by peltier cell holder).
8. Monitor the release of produced 5-thio-2-nitro-benzoic acid for 1 to 2 min using a UV/VIS spectrophotometer at 412 nm.

   If a recorder is used instead of a computer, record for 2 to 4 min. The increase in absorbance is linear with time, a difference of up to 1.0.

9. Monitor spontaneous hydrolysis in a blank, GET solution alone without the addition of the microsome preparation, using a UV/VIS spectrophotometer at 412 nm.

   In this method, the molar absorbance of 13,600 liters/M(cm) CoA-SH is used; therefore, the specific activity (µmol of CoA-SH formed/min/mg protein) is

$$\frac{(\Delta absorbance/min - \Delta blank/min) \times 1.0}{13.6 \times 0.10 \times protein\ (mg/ml)}$$

FLUOROMETRIC ASSAY FOR CES USING PHENACETINE, ACETANILIDE

BASIC PROTOCOL 2

Most CES isozymes also hydrolyze some aromatic amides. Normally, it is not possible to assay the hydrolysis of these amides by a photometric assay because the rate of cleavage of amides by CES is usually low. The fluorometric assay described here is the most sensitive method for the cleavage of amides.

Materials

Microsomes (see Support Protocol 1 or 2)
GET solution (see recipe), ice cold
Bio-Rad DC protein assay kit II
250 mM Tris·Cl, pH 8.6 (*APPENDIX 2A*)
Substrate solution, e.g., 10 mM phenacetin solution or 20 mM acetanilide solution (see recipe), 30°C
1.2 M TCA solution (see recipe)
1 N NaOH

5-ml Potter-Elvehjem homogenizer with Teflon pestle
37°C water bath with shaker
Fluorometric quartz cuvette, 1-cm path length
Spectrofluorometer with a computer

Carry out CES reaction

1. Suspend the microsome pellet in a small aliquot of ice-cold GET solution using a 5-ml Potter-Elvehjem homogenizer with a Teflon pestle (see Support Protocol 1 or 2).
2. Determine the protein concentration using a Bio-Rad DC protein assay kit II and adjust the concentration to 1.0 to 10 mg/ml with ice-cold GET solution.
3. Place microcentrifuge tubes on ice and add the following to each tube:

   400 µl 250 mM Tris·Cl buffer, pH 8.6

   100 µl 1.0 to 10 mg/ml microsome preparation

   Prepare blanks with GET solution alone without the addition of microsome preparation and incubate for the same time as that for the assays. Also prepare substrate solutions without the microsome preparation; add 100 µl substrate solution after termination of the reactions (step 6).

4. Vortex tubes and pre-incubate for 5 min at 37°C.
5. Add 500 µl of prewarmed substrate solution, e.g., 10 mM phenacetin or 20 mM acetanilide solution, to start the reaction; vortex the tube and incubate for 10 to 60 min in a 37°C water bath with shaking.

Perform spectrofluorometric analysis

6. Stop the reaction by adding 500 µl of 1.2 M TCA solution.
7. Microcentrifuge for 10 min at maximum speed, 4°C.
8. Transfer 1.0 ml of the supernatant to a fresh 2-ml microcentrifuge tube.
9. Add 1.0 ml of 1 N NaOH to the tube and vortex.
10. Transfer the mixture to a fluorometric quartz cuvette.
11. Select excitation wavelengths of 282 and 305 nm for aniline and phenetidine, respectively.
12. Estimate the fluorescence using a spectrofluorometer at emission wavelengths of 348 and 372 nm for aniline and phenetidine, respectively.

    In this method, since the ratio of fluorescence between the sample and standard was used for the hydrolysis of aromatic amide, the specific activity (nmol of product formed/min/mg protein) is

$$\frac{0.1\times(\text{sample [fluorescence]} - \text{blank [fluorescence]})\times 1.0\times 1000}{(\text{standard [fluorescence]} - \text{blank [fluorescence]})\times 0.1\times \text{time (min)}\times \text{protein (mg/ml)}}$$

BASIC PROTOCOL 3

HPLC METHODS TO MEASURE CES ACTIVITY

Many HPLC methods have been developed for identifying metabolites in plasma and urine from in vivo metabolism of xenobiotics. These methods can also be used to identify and quantify metabolites of esters and amides from in vitro systems.

Materials

Microsomes (see Support Protocol 1 or 2)
GET solution (see recipe), ice cold
Bio-Rad DC protein assay kit II
120 mM HEPES buffer, pH 7.4 (see recipe)
200 µM irinotecan hydrochloride (CPT-11; see recipe for substrate solutions), 37°C
0.05 N HCl containing 200 nM CPT as an internal standard (see recipe for substrate solutions)

5-ml Potter-Elvehjem homogenizer and Teflon pestle
37°C water bath with a shaker
HPLC system consisting of model L-6000 pump (Hitachi), model L7480 FL detector (Hitachi), model AS-2000 auto-sampler (Hitachi), model D-2500 integrator (Hitachi), and a 4.6 × 150–mm YMC-Pack Ph A-402 column (YMC Co.) or equivalent.

Carry out CES reaction

1. Suspend the microsome pellet in a small aliquot of ice-cold GET solution using a 5-ml Potter-Elvehjem homogenizer with a Teflon pestle (see Support Protocol 1 or 2).

2. Determine the protein concentration using a Bio-Rad DC protein assay kit II and adjust the concentration to 0.1 to 1.0 mg/ml with ice-cold GET solution.

3. Place microcentrifuge tubes on ice and add the following to each tube:

   50 µl 120 mM HEPES buffer, pH 7.4

   50 µl 0.1 to 1.0 mg/ml microsome preparations

   Prepare blanks of GET solution alone without the addition of the microsome preparation and incubate for the same time as that of the assays.

4. Vortex tubes and preincubate for 5 min at 37°C.

5. Add 100 µl of prewarmed 200 µM irinotecan hydrochloride solution to start reaction, vortex, and place tube in a 37°C water bath with shaking. Incubate 5 to 10 min.

Analyze by HPLC

6. Stop the reaction by adding 200 µl of 0.05 N HCl containing 200 nM CPT.

7. Microcentrifuge for 10 min at maximum speed, 4°C.

8. Transfer 30 µl of supernatant to an HPLC system and analyze.

   For example, for the determination of SN-38, the mobile phase consisted of 3 mM sodium heptane sulfonic acid in 66:34 (v/v) 0.1 M potassium phosphate, pH 4.0/acetonitrile and was delivered at a flow rate of 0.8 ml/min. The fluorescence was determined using a Hitachi L7480 FL detector at an excitation wavelength of 380 nm and emission wavelength of 556 nm.

   A calibration curve is generated by the peak height ratio of SN-38/CPT.

   In this method, peak height ratio of SN38/CPT is used for the calibration curve, the specific activity (pmol of SN-38 formed/min/mg protein) is

$$\frac{SN38\,(\ pmol/ml\ ) \times 1.0}{0.1 \times time\,(min) \times protein\,(\ mg/ml\ )}$$

   This amount of SN-38 was derived from a calibration curve.

SUPPORT PROTOCOL 1

PREPARATION OF MICROSOMES FROM TISSUE

CES is located in the lumen of endoplasmic reticulum and is retained there by interaction with the KDEL receptor. The microsome preparations contain endoplasmic reticulum. This protocol is used to isolate microsomes from any of several tissues.

Materials

Organ tissue, freshly recovered or frozen
SET solution (see recipe)
GET solution (see recipe)

Potter-Elvehjem homogenizer with a motorized Teflon pestle
50-ml centrifuge tubes
30-ml ultracentrifuge tubes
Ultracentrifuge

NOTE: Perform all steps at 4°C.

1. Weigh the organ tissue in grams (~0.1 to 5 g) and add four times the weight in milliliters of SET solution.
2. Homogenize for 5 strokes in a Potter-Elvehjem homogenizer using a motorized Teflon pestle at 800 rpm.
3. Transfer the homegenate to a 50-ml centrifuge tube. Centrifuge the homogenate 20 min at 9000 × *g*, 4°C.
4. Transfer the supernatant to a 30-ml ultracentrifuge tube.

   When the tissue contains many fatty substances, filter the supernatant through a layer of cotton gauze to remove them.
5. Ultracentrifuge the supernatant 60 min at 105,000 × *g*, 4°C. Carefully discard the supernatant using a pipet.
6. Suspend the pellet in SET solution (1 g organ weight/ml) using a Potter-Elvehjem homogenizer.
7. Centrifuge the suspension for 30 min at 105,000 × *g*. Discard the supernatant.
8. Suspend pellet in GET solution (1 g organ weight/ml) using a Potter-Elvehjem homogenizer. Store for up to 1 year at −80°C

SUPPORT PROTOCOL 2

PREPARATION OF MICROSOMES FROM CULTURED CELLS

This protocol is used to prepare microsomes from tissue culture cells transfected with CES cDNA.

Materials

Cultured cells, such as V79, COS7, or HepG2 cells, expressing CES after transfection with a mammalian expression vector with CES cDNA
PBS (*APPENDIX 2A*)
SET solution (see recipe)
GET solution (see recipe)

5-ml round-bottom tubes
Sonicator with a narrow probe
Microscope
Potter-Elvehjem homogenizer with a motorized Teflon pestle
2-ml centrifuge tubes
5-ml ultracentrifuge tubes and ultracentrifuge

NOTE: Perform all procedures at 4°C.

1. Harvest the cells (1×10^8 cells) and wash with 5 ml PBS by centrifuging for 5 min at $800 \times g$, 4°C.
2. Suspend the cell pellet in 1×10^8 cells/ml SET solution. Transfer to 5-ml round-bottom tubes.
3. Sonicate with a narrow probe for 10 to 15 sec, two times, and check for lysis with a microscope.
4. Add 1×10^8 cells/ml SET solution and homogenize for 5 strokes in a Potter-Elvehjem homogenizer with a motorized Teflon pestle at 800 rpm.
5. Transfer the homogenate to a 2-ml centrifuge tube and centrifuge homogenate for 20 min at $9000 \times g$, 4°C.
6. Transfer the supernatant to a 5-ml ultracentrifuge tube and ultracentrifuge the supernatant 60 min at $105{,}000 \times g$, 4°C.
7. Carefully discard the supernatant using a pipet and suspend the pellet in 1×10^8 cells/ml GET solution using a Potter-Elvehjem homogenizer. Store for up to 1 year at −80°C

REAGENTS AND SOLUTIONS

Use Milli-Q-purified water or equivalent for the preparation of all recipes and in all protocol steps . For common stock solutions, see ***APPENDIX 2A****; for suppliers, see* ***SUPPLIERS APPENDIX****.*

CES assay solution

For 1 liter, weigh 200 g glycerol. Add 25 ml of 10% cholic acid, pH 8.0, and 220 ml of 1 M Tris·Cl buffer, pH 8.6 (*APPENDIX 2A*), and water to 1 liter. Store up to 1 month at 4°C.

DTNB solution, 3 mM

Dissolve 5.95 mg 5,5′-dithiobis-(2-nitrobenzoic acid (DTNB) in 0.5% $NaHCO_3$. Prepare just before use.

GET solution

For 100 ml, weigh 20 g glycerol. Add 0.2 ml of 0.5 M EDTA (*APPENDIX 2A*), and add 1 ml of 1 M Tris·Cl buffer, pH 7.4 (*APPENDIX 2A*). Adjust with water to a final volume of 100 ml. Store for up to 1 month at 4°C.

HEPES buffer, pH 7.4, 120 mM

Dissolve 2.86 g *N*-(2-hydroxyethyl)piperazine-*N*′-(2-ethanesulfonic acid) (HEPES) in 80 ml water. Adjust the pH to 7.4 at room temperature with 5 M NaOH (*APPENDIX 2A*). Adjust with water to a final volume of 100 ml. Store up to 1 month at 4°C.

p-Iodonitrophenyl tetrazolium violet (INT) solution

Dissolve 52.44 mg INT in 60 ml of 0.2 M Tris·Cl buffer, pH 7.5 (*APPENDIX 2A*). Adjust with water to a final volume of 105 ml. Prepare just before use.

NAD, 72 mM

Dissolve 143 mg NAD in 3 ml water. Store for up to 2 weeks at −20°C

SET solution

Add 25 ml of 1.0 M sucrose, 0.2 ml of 0.5 M EDTA (*APPENDIX 2A*), and 1 ml of 1 M Tris·Cl buffer, pH 7.4 (*APPENDIX 2A*). Adjust with water to a final volume of 100 ml. Store up to 1 month at 4°C.

Substrate solutions

p-Nitrophenyl acetate: Dissolve 18.1 mg of the ester in acetnitrile and add water to 100 ml

Malathion: Dissolve 19.82 mg in 1 ml of acetone

Clofibrate: Dissolve 14.56 mg in 1 ml of acetone

Butanilicaine hydrochloride: Dissolve 29.1 mg in 10 ml hot water

Acyl-CoA: Dissolve 2 mg of palmitoyl-CoA in 5 ml water

Phenacetine: Dissolve 17.9 mg in 10 ml hot water

Acetanilide: Dissolve 27 mg in 10 ml hot water

Phenetidine hydrochloride: Dissolve 137 mg in 1000 ml water

Aniline hydrochloride: Dissolve 130 mg in 1000 ml water

Irinotecan (CPT-11) hydrochloride: Dissolve 6.67 mg in 10 ml water

SN-38: Dissolve 6.7 mg in 10 ml methanol

Butanilicaine, N-butylaminoacetyl-2-chloro-6-methylanilide

CPT-11, 7-ethyl-10-[4-(1-piperidino)-1-piperidino]carbonyloxycamptothecin

SN-38, 7-ethyl-10-hydroxycamptothecin

Since the most of esters are spontaneously hydrolyzed in water, substrates are prepared just before use.

TCA solution, 1.2 M

Dissolve 19.608 g trichloroacetic acid (TCA) in 100 ml water. Store up to 1 month at 4°C.

COMMENTARY

Background Information

Various carboxylesterases (CES) play important roles in the hydrolytic biotransformation of a vast number of structurally diverse drugs (Satoh and Hosokawa, 1998). These enzymes are a major determinant of the pharmacokinetic behavior of most therapeutic agents containing ester or amide bonds (Heymann et al., 1981; Satoh and Hosokawa, 1998). CES activity can be influenced by interactions of a variety of compounds either directly or at the level of enzyme regulation (Mentlein et al., 1986; Hosokawa et al., 1988; Hosokawa and Satoh, 1993). Since a significant number of drugs are metabolized by CES, altering the activity of this enzyme class has important clinical implications. Drug elimination decreases and the incidence of drug-drug interactions increases when two or more drugs compete for hydrolysis by the same CES isozyme (Mentlein et al., 1980; Hosokawa et al., 1987, 1990). Exposure to environmental pollutants or lipophilic drugs can result in induction of CES activity (Hosokawa and Satoh, 1993; Hosokawa et al., 1994). Therefore, the use of drugs known to increase the microsomal expression of a particular CES increases the associated drug hydrolysis capacity in humans.

Hydrolysis is catalyzed by a family of CES isozymes. Molecular biology techniques have made it possible to identify the genes for individual mammalian CESs and to express CES proteins (Satoh and Hosokawa, 1998). Thus, it has become possible to study the substrate specificities and kinetic parameters of individual CESs. The nomenclature for the isozymes is based on evolutionary divergence (Satoh and Hosokawa, 1998).

Mammalian CESs comprise a multigene family whose gene products are localized in the endoplasmic reticulum of many tissues, such as the liver, kidney, intestine, lung, and brain, however, not all isozymes are present in all tissues. There is a great deal of overlap of substrate acceptance among the isoforms (Yamada et al., 1994; Satoh and Hosokawa,

1998). For example, *p*-nitrophenyl acetate is a substrate for many CES isozymes (Mentlein et al., 1980; Heymann and Mentlein, 1981; Hosokawa et al., 1990).

Earlier analytical methods made use of pH-stat analysis (Heymann and Mentlein, 1981). In weakly buffered solutions, the amount of acid released by enzymatic hydrolysis can be recorded continuously by the pH-stat technique. Many other assay methods have used spectrophotometric analysis. The methods described here are based on the use of spectrophotometric analysis and are applicable to most substrates (Berge, 1979; Talcott, 1979; Heymann and Mentlein, 1981; Hosokawa et al., 1990). Furthermore, these assay systems have been developed as fast techniques for analyzing the hydrolysis in tissues or cultured cells (Mori et al., 1999).

The fluorometric method (see Basic Protocol 2) was developed for assaying the hydrolysis of aromatic amides (Heymann et al., 1981). Normally, it is not possible to assay the hydrolysis of these amides by a photometric assay because the rate of cleavage of amides by CES is usually low. The fluorometric assay described here is the most-sensitive method for cleavage of amides.

Recently, many HPLC methods have been developed for identifying metabolites. Thus, HPLC methods can also be used to identify and quantify metabolites from esters and amides (Satoh et al., 1994; Kurita and Kaneda, 1999; Mori et al., 1999). The HPLC method described here (see Basic Protocol 3) is useful for identifying and quantifying metabolites for which the hydrolytic reaction yields several esters and amides.

Critical Parameters and Troubleshooting

In CES assays, incubation time is critical. For some substrates, such as *p*-nitrophenyl acetate, palmitoyl-CoA, and CPT-11, the reaction is not linear beyond 5 to 10 min. The Michaelis constant (K_m) of CES is dependent on the structure of the substrate and is also dependent on tissues, species, or isozymes. For example, the K_m value for CPT-11 is in the range of 3 to 200 μM. Since the use of an optimal amount of protein and substrate is required for linear product formation, it is necessary to establish the optimal conditions for unknown substrates.

When dissolving the hydrophobic substrates of esters and amides, the type of organic solvent is critical for CES assay. Ethanol and methanol must not be used and the concentration of other organic solvents should be <1% in the assay mixture.

When solubilizing the CES from microsomes in purification procedures, it is necessary to use some detergent. Many detergents can affect the CES activities. High concentrations of detergents, such as 1.0% (v/v) Triton X-100, 1.0% (v/v) cholic acid, and 1.0% (v/v) Emulgen 911, decrease the CES activity by 10% to 50%. But low concentrations of detergents such as 0.001% to 0.05% Triton X-100 can increase the CES activity in microsomes. Therefore, the effect of detergent towards each substrate must be determined before detergent is employed in the CES assay.

Anticipated Results

This section provides examples of assays that were analyzed by each of the three methods described in this unit.

Basic Protocol 1

A microsome preparation from rat liver was analyzed for activity towards *p*-nitrophenyl acetate, malathion, butanilicaine, and palmitoyl-CoA. The general assay requirements are described in Basic Protocol 1.

p-Nitrophenyl acetate. The specific conditions of this assay were pH 8.0, 50 µl of 0.2 mg/ml rat liver microsomes, and a substrate concentration of 900 µM. The release of *p*-nitrophenol was monitored by UV/VIS spectrophotometer at 405 nm. The assay was incubated 1 to 2 min at 30°C.

Specific activity (µmol/min/mg protein) was calculated using the following formula with Δabsorbance/min = 0.612, Δblank/min = 0.025:

$$\frac{(\Delta\text{absorbance/min} - \Delta\text{blank/min}) \times 1.0}{16.4 \times 0.05 \times \text{protein (mg/ml)}} =$$

$$\frac{(0.612 - 0.025) \times 1.0}{16.4 \times 0.05 \times 0.2} = 3.58 \text{ (µmol/min/mg)}$$

Malathion. The specific conditions of this assay were pH 7.5, 100 µl of 2.0 mg/ml rat liver microsomes, and a substrate concentration of 300 µM. The reduction of INT was monitored by UV/VIS spectrophotometer at 500 nm. The assay was incubated 5 to 10 min at 37°C.

Specific activity (µmol/min/mg protein) was calculated using the following formula with Δabsorbance/min = 0.325, Δblank/min = 0.045:

$$\frac{(\Delta\text{absorbance/min} - \Delta\text{blank/min}) \times 2.01}{13.75 \times 0.1 \times \text{protein (mg/ml)}} =$$

$$\frac{(0.325 - 0.045) \times 2.01}{13.75 \times 0.1 \times 2.0} = 0.204 \text{ (µmol/min/mg)}$$

Butanilicaine. The specific conditions of this assay were pH 8.6, 50 µl of 2.5 mg/ml rat liver microsomes, and a substrate concentration of 5 mM. The formation of 2-chloro-6-methylaniline was monitored by UV/VIS spectrophotometer at 285 nm. The assay was incubated 3 to 10 min at 30°C.

Specific activity (µmol/min/mg protein) was calculated using the following formula with Δabsorbance/min = 0.027:

$$\frac{\Delta\text{absorbance/min} \times 1.0}{2.080 \times 0.05 \times \text{protein (mg/ml)}} =$$

$$\frac{0.027 \times 1.0}{2.080 \times 0.05 \times 2.5} = 0.103 \text{ (µmol/min/mg)}$$

Palmitoyl-CoA. The specific conditions of this assay were pH 7.4, 100 µl of 0.6 mg/ml rat liver microsomes, and a substrate concentration of 40 µM. The 5-thio-2-nitro-benzoic acid produced was monitored by UV/VIS spectrophotometer at 412 nm. The assay was incubated 1 to 2 min at 30°C.

Specific activity (µmol/min/mg protein) was calculated using the following formula with Δabsorbance/min = 0.128, Δblank/min = 0.004:

$$\frac{(\Delta\text{absorbance/min} - \Delta\text{blank/min}) \times 1.0}{13.6 \times 0.1 \times \text{protein (mg/ml)}}$$

$$\frac{(0.128 - 0.004) \times 1.0}{13.6 \times 0.1 \times 0.6} = 0.152 \text{ (µmol/min/mg)}$$

Basic Protocol 2

Microsomes prepared from rat liver were analyzed for activity towards acetanilide and phenacetine. The general assay requirements are described in Basic Protocol 2. The

specific conditions of this assay were pH 8.6, 100 µl of 10 mg/ml rat liver microsomes, and a substrate concentration of 10 mM and 20 mM, phenacetine and acetanilide, respectively. The assays were incubated 30 min at 37°C and then were stopped with 500 µl of 1.2 M TCA solution.

The specific activity (nmol phenetidine formed/min/mg protein) of phenacetine was calculated using the following formula:

$$\frac{0.1\times(\text{sample [fluorescence]}-\text{blank [fluorescence]})\times 1.0\times 1000}{(\text{standard [fluorescence]}-\text{blank [fluorescence]})\times 0.1\times \text{time (min)}\times \text{protein (mg/ml)}} =$$

$$\frac{0.1\times(98-3)\times 1.0\times 1000}{(60-3)\times 0.1\times 30\times 10} = 5.56\ (\text{nmol/min/mg})$$

Basic Protocol 3

Microsomes prepared from rat liver were analyzed for activity towards CPT-11. The general assay requirement is described in Basic Protocol 3. The specific conditions of this assay were pH 7.4, 100 µl of 10 mg/ml rat liver microsomes, and a substrate concentration of 100 µM. The assays were incubated 10 min at 37°C, and then were stopped with 200 µl of 0.05 N HCl solution.

The specific activity (pmol of SN-38 formed/min/mg protein) of CPT-11 was calculated using the following formula:

$$\frac{\text{SN38 (pmol/ml)}\times 1.0}{0.1\times \text{time (min)}\times \text{protein (mg/ml)}} =$$

$$\frac{68.5\times 1.0}{0.1\times 10\times 2.3} = 29.8\ (\text{pmol/min/mg})$$

The amount of SN-38 was derived from a calibration curve.

CES is located in the lumen of the endoplasmic reticulum. Microsomal preparations of organ tissue contain the endoplasmic reticulum. The total yield of microsomal organ protein from rat liver is ~20 mg protein/1 g liver weight (see Support Protocol 1). The total yield of microsomal protein obtained from 1×10^8 V79 cells expressing CES isozome is ~1 mg (see Support Protocol 2).

Time Considerations

For all assays, the total time required depends, in part, on the duration of the reaction and the level of activity, and can range from 1 min to 2 hr. Photometric assays require 1 to 15 min. Fluorometric assays require 1 to 2 hr. HPLC assays require 10 to 20 min and an additional 2 hr for HPLC analysis.

Literature Cited

Berge, R.K. 1979. Purification and characterization of a long-chain acyl-CoA hydrolase from rat liver microsomes. *Biochim. Biophys. Acta.* 574:321-333.

Heymann, E. and Mentlein, R. 1981. Carboxylesterases-amidases. *Methods Enzymol.* 77:333-344.

Heymann, E., Mentlein, R., and Rix, H. 1981. Hydrolysis of aromatic amides as assay for carboxylesterases-amidases. *Methods Enzymol.* 77:405-409.

Hosokawa, M. and Satoh, T. 1993. Differences in the induction of carboxylesterase isozymes in rat liver microsomes by perfluorinated fatty acids. *Xenobiotica* 23:1125-1133.

Hosokawa, M., Maki, T., and Satoh, T. 1987. Multiplicity and regulation of hepatic microsomal carboxylesterases in rats. *Mol. Pharmacol.* 31:579-584.

Hosokawa, M., Maki, T., and Satoh, T. 1988. Differences in the induction of carboxylesterase isozymes in rat liver microsomes by xenobiotics. *Biochem. Pharmacol.* 37:2708-2711.

Hosokawa, M., Maki, T., and Satoh, T. 1990. Characterization of molecular species of liver microsomal carboxylesterases of several animal species and humans. *Arch. Biochem. Biophys.* 277:219-227.

Hosokawa, M., Hirata, K., Nakata, F., Suga, T., and Satoh, T. 1994. Species differences in the induction of hepatic microsomal carboxylesterases caused by dietary exposure to di(2-ethylhexyl)phthalate, a peroxisome proliferator. *Drug Metab. Dispos.* 22:889-894.

Kurita, A. and Kaneda, N. 1999. High-performance liquid chromatographic method for the simultaneous determination of the camptothecin derivative irinotecan hydrochloride, CPT-11, and its metabolites SN-38 and SN-38 glucuronide in rat plasma with a fully automated on-line solid-phase extraction system, PROSPEKT. *J. Chromatogr. B. Biomed. Sci. Appl.* 724:335-344.

Mentlein, R., Heiland, S., and Heymann, E. 1980. Simultaneous purification and comparative characterization of six serine hydrolases from rat liver microsomes. *Arch. Biochem. Biophys.* 200:547-559.

Mentlein, R., Lembke, B., Vik, H., and Berge, R.K. 1986. Different induction of microsomal carboxylesterases, palmitoyl-CoA hydrolase and acyl-L-carnitine hydrolase in rat liver after treatment with clofibrate. *Biochem. Pharmacol.* 35:2727-2730.

Mori, M., Hosokawa, M., Ogasawara, Y., Tsukada, E., and Chiba, K. 1999. cDNA cloning, characterization and stable expression of novel human brain carboxylesterase. *F.E.B.S. Lett.* 458:17-22.

Satoh, T. and Hosokawa, M. 1998. The mammalian carboxylesterases: From molecules to functions. *Annu. Rev. Pharmacol. Toxicol.* 38:257-288.

Satoh, T., Hosokawa, M., Atsumi, R., Suzuki, W., Hakusui, H., and Nagai, E. 1994. Metabolic activation of CPT-11, 7-ethyl-10-[4-(1-piperidino)-1-piperidino]carbonyloxycamptothecin, a novel antitumor agent, by carboxylesterase. *Biol. Pharm. Bull.* 17:662-664.

Talcott, R.E. 1979. Hepatic and extrahepatic malathion carboxylesterases. Assay and localization in the rat. *Toxicol. Appl. Pharmacol.* 47:145-150.

Yamada, T., Hosokawa, M., Satoh, T., Moroo, I., Takahashi, M., Akatsu, H., Yamamoto, T. 1994. Immunohistochemistry with an antibody to human liver carboxylesterase in human brain tissues. *Brain Res.* 658:163-167.

Key References

Berge, 1979. See above.

A modification of this method is described in Alternate Protocol 3.

Heymann and Mentlein, 1981. See above.

A modification of this method is described in Basic Protocol 1.

Heymann et al., 1981. See above.

A modification of this method is described in Alternate Protocol 2 and Basic Protocol 2.

Hosokawa et al., 1987. See above.

A modification of this method is described in Support Protocol 1.

Mori et al., 1999. See above.

A modification of this method is described in Support Protocol 2.

Satoh et al., 1994. See above.

A modification of this method is described in Basic Protocol 3.

Talcott, 1979. See above.

A modification of this method is described in Alternate Protocol 1.

Contributed by Masakiyo Hosokawa
Chiba University
Chiba, Japan

Tetsuo Satoh
Biomedical Research Institute
Chiba, Japan

Analysis of the Aryl Hydrocarbon Receptor (AhR) Signal Transduction Pathway

The aryl hydrocarbon receptor (AhR) is a soluble, ligand-dependent transcription factor that mediates many of the biological and toxicological actions of a structurally diverse group of natural and synthetic hydrophobic chemicals, including the environmental contaminant 2,3,7,8-tetrachlorodibenzo-*p*-dioxin (TCDD; Safe, 1990; Schmidt and Bradfield, 1996; Denison et al., 1998a,b). Exposure to AhR agonists results in a variety of effects, the most studied of which is the induction of gene expression (Fig. 4.8.1). Following ligand binding, the cytosolic ligand-AhR complex undergoes transformation during which it translocates into the nucleus and dissociates from two molecules of hsp90 (a heat shock protein of 90 kDa), p20, and at least one additional protein termed XAP2, AIP, or ara9. Following its association with at least one nuclear factor, the AhR nuclear translocator (Arnt) protein, the AhR complex is converted into its high affinity DNA-binding form. The binding of the transformed heteromeric ligand-AhR-Arnt complex to its specific DNA recognition site, the dioxin responsive element (DRE), leads to chromatin and nucleosome disruption, increased promoter accessibility, and increased rates of transcription of an adjacent gene. The AhR signal transduction pathway is present in a diverse range of species, tissues, and cell types, and to date, the majority of genes which respond to AhR ligands have been shown to utilize the AhR-DRE-dependent mechanism of action.

This unit describes several procedures for detecting the AhR and characterizing its functional activity. Measurement of AhR ligand binding is accomplished by two different methods. The sucrose density gradient (SDG) binding assay (see Basic Protocol 1) provides the greatest amount of information and allows direct determination and visualization of the binding of [^{3}H]TCDD to cytosolic AhR, but it is time consuming and not

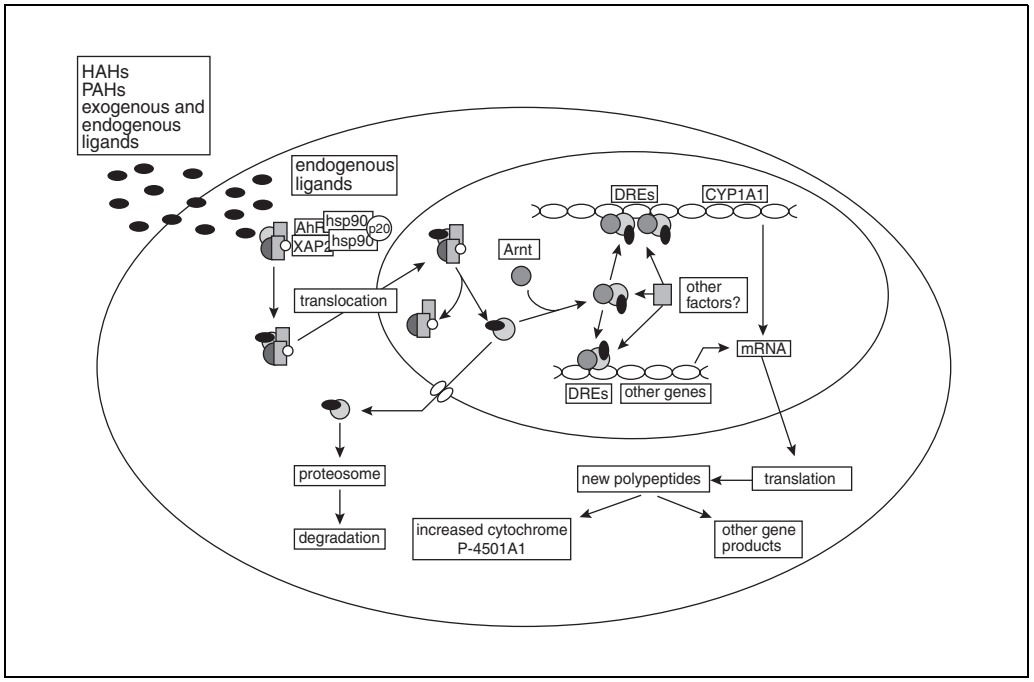

Figure 4.8.1 Molecular mechanism of Ah receptor-dependent regulation of gene expression. Abbreviations: AhR, aryl hydrocarbon receptor; Arnt, AhR nuclear translocator protein; DRE, dioxin responsive element; HAHs, halogenated aromatic hydrocarbons; PAHs, polycyclic aromatic hydrocarbons.

Contributed by Michael S. Denison, Jane M. Rogers, S. Renee Rushing, Carol L. Jones, Selwyna C. Tetangco, and Sharon Heath-Pagliuso

Current Protocols in Toxicology (2002) 4.8.1-4.8.45

amenable to analysis of large numbers of samples. In contrast, the hydroxyapatite (HAP) binding assay (see Alternate Protocol 1) is relatively rapid, requires less equipment, and is amenable to analysis of relatively large numbers of samples, but it does not provide direct visualization of [^{3}H]TCDD-specific binding.

Measurement of AhR transformation and DNA binding is carried out using a gel retardation analysis (GRA; see Basic Protocol 2 or Alternate Protocol 2 for competitive GRA). GRA and SDG analysis of nuclear extracts from treated cells provide a measure of AhR transformation, nuclear translocation, and DNA binding in intact cells. All of these procedures can be carried out using cytosolic ligand–AhR complexes transformed in vitro, nuclear ligand–AhR complexes transformed in vivo, or in intact cells. Detection of AhR in tissue samples can be accomplished by demonstration of specific ligand binding or by direct measurement of AhR protein or mRNA using immunoblot analysis (see Basic Protocol 3), RT-PCR (see Basic Protocol 4), or northern blot analysis (see Basic Protocol 5). AhR ligand–dependent induction of expression of a specific gene known to be regulated by the AhR—e.g., cytochrome P4501A1 (CYP1A1) or P4501B1 (CYP1B1)—provides indirect evidence for the presence of the AhR signaling system in tissues or cells in culture and is commonly accomplished by examining mRNA levels for the gene of interest by RT-PCR or northern blot analysis.

Support protocols are included for preparation of hepatic cytosol (see Support Protocol 1), cytosol from cultured cells (see Support Protocol 2), nuclear extract (see Support Protocol 3), ^{32}P-labeled probes for GRA (see Support Protocol 4), and total RNA (see Support Protocol 5).

CAUTION: When working with radioactivity, and TCDD or other carcinogens, take extreme care to avoid contaminating work areas and personnel. Use these materials only in appropriately designated areas with all necessary precautions, including the use of laboratory coats, protective eyewear, and disposable benchtop paper, gloves, plasticware, and glassware. In addition, follow all chemical and radiation safety guideline for handling and disposal of these materials (also see *APPENDIX 1A*). It is particularly important that when handling any hazardous chemical dissolved in DMSO or other solvent that appropriate solvent-resistant nitrile gloves are used. Latex gloves provide little or no barrier to solvent penetration and subsequent chemical exposure. Finally, given the hazards associated with TCDD and related chemicals, laboratory use of these chemicals usually requires prior permission of the local chemical and radiation safety officers.

NOTE: All DMSO should be 99% pure.

BASIC PROTOCOL 1

SUCROSE DENSITY GRADIENT ANALYSIS OF CYTOSOLIC Ah RECEPTOR LIGAND BINDING

The sucrose density gradient (SDG) method allows direct determination and visualization of the binding of [^{3}H]TCDD to cytosolic AhRs and its competitive displacement by other AhR ligands. Cytosolic samples incubated with [^{3}H]TCDD in the absence or presence of an unlabeled competitor ligand, such as 2,3,7,8-tetrachlorodibenzofuran (TCDF), are centrifuged through a linear 10% to 30% (w/v) sucrose gradient and, following fractionation, the distribution of radioactivity throughout the gradient is determined. The peak of radioactivity that is competitively eliminated by TCDF represents the amount of [^{3}H]TCDD specifically bound to the AhR. The ability of other chemicals to competitively bind to the AhR can be determined in the same manner by adding these chemicals in place of TCDF in the incubation. Although this method is somewhat time consuming and is not amenable for analysis of large numbers of samples, it provides important additional information that is not obtained using solid phase AhR ligand binding methods like

hydroxylapatite binding (HAP; see Alternate Protocol 1). The procedure described here is based on the method of Tsai and Okey (1981) and uses 5-ml gradients in a vertical tube rotor (which reduces centrifugation time to 2.5 hr as compared to 16 hr for swinging bucket rotors). Other tube sizes and rotors can be used with appropriate adjustments for volumes and centrifugation times (Okey et al., 1979).

Materials

Cytosol sample (see Support Protocols 1 and 2)
Bio-Rad protein assay
HEDG buffer (see recipe)
1 µM [^{3}H]TCDD in DMSO (specific activity 10 to 50 Ci/mmol; Eagle-Picher Technologies or Terrachem)
DMSO
100 µM TCDF in DMSO (Accustandard, Cambridge Isotope Laboratories, or Wellington Laboratories)
Test ligand in DMSO
Dextran-coated charcoal (see recipe)
60% (w/v) sucrose in HEDG or HEDGK4 (see recipes)
200 cpm/µl [^{14}C]formaldehyde-labeled protein sedimentation standards (e.g., BSA, catalase; Dottavio-Martin and Ravel, 1978)
Scintillation cocktail

12 × 75–mm glass culture tubes
Heat-sealable, vertical, 13 × 51–mm ultracentrifuge tubes (Beckman) and sealing device
Sucrose gradient maker and fractionator (optional)
Ultracentrifuge with slow acceleration/deceleration modes and vertical rotor (Beckman VTi65.2 or equivalent), 4°C
18-G solid-metal wire
7-ml scintillation vials
Needle (optional)
Liquid scintillation counter with dual isotope counting function

NOTE: All steps should be performed at 4°C.

Incubate sample

1. Determine the protein concentration of the cytosol sample using the Bio-Rad protein assay. Adjust the sample to a protein concentration of 5 mg/ml with HEDG buffer.

2. For each binding incubation, prepare two 12 × 75–mm glass culture (incubation) tubes, one for total and one for nonspecific binding. Prepare a third tube if another compound is also to be assessed for binding inhibition. To each incubation tube add 500 µl cytosol and keep on ice.

   Glass culture tubes are recommended for incubations since a loss of radioactivity may result with some plastics.

3. For each set of incubations (i.e., total binding and nonspecific binding samples), add 5 µl of 1 µM [^{3}H]TCDD in DMSO to each tube. Then add 5 µl DMSO (carrier solvent) to the total binding sample tube and 5 µl of 100 µM TCDF in DMSO to the nonspecific binding sample tube. If the ability of another chemical to competitively bind to the AhR is also being assessed, add 5 µl [^{3}H]TCDD and 5 µl test ligand in DMSO at the desired concentration to the third tube.

   The standard SDG binding reaction uses final chemical concentrations of 10 nM [^{3}H]TCDD and 1 µM TCDF. These concentrations are generally sufficient for saturation

of AhR binding in the above conditions. Although use of higher TCDD concentrations have been reported, use of TCDD at concentrations over 50 nM is not recommended because of its limited aqueous solubility. This is also the reason TCDD is not used as a competitor—i.e., TCDF has a greater solubility. The concentration of test compound necessary to observe competitive AhR binding is dependent upon its affinity for the AhR and as such, multiple analyses may be required using a range of competitor concentrations.

Incubate in dextran-coated charcoal to remove free and loosely bound [^{3}H]TCDD

No incubation period or charcoal treatment is necessary when using nuclear extracts prepared from cells or tissues that have been incubated with [^{3}H]TCDD (in the absence or presence of TCDF). Aliquots of these sample preparations can be loaded directly onto the gradients as described below (step 9).

4. Incubate samples 2 hr at 4°C.

5. While the cytosol is incubating, prepare charcoal pellets by pipetting 700 µl dextran-coated charcoal into a 1.5-ml microcentrifuge tube and microcentrifuging 10 min at ~12,000 to 15,000 rpm, 4°C. Prepare one charcoal tube per sample incubation.

   These charcoal treatment conditions have been optimized for guinea pig hepatic cytosol at 5 mg protein/ml buffer. The optimal protein-charcoal concentration for AhR binding analysis must be experimentally determined when cytosol from other species or tissues are to be used. Once the protein/charcoal ratio has been established, it should be maintained if cytosol containing more or less protein is used. Too high a charcoal concentration can result in stripping of ligand from the receptor and too low a concentration will result in lack of complete removal of free and loosely bound [^{3}H]TCDD. This is especially important when analyzing AhR from species that have reduced affinity for TCDD (i.e., human and nonmammalian species).

6. Aspirate the supernatant from the tube without disturbing the charcoal pellet. Store the pellets at 4°C until needed.

7. After the incubation period (step 4), transfer the 500-µl binding reaction into appropriately labeled microcentrifuge tubes containing charcoal pellets. Vortex immediately and incubate 10 min at 4°C.

8. Microcentrifuge the tubes 10 min at high speed (i.e., ~12,000 to 15,000 rpm), 4°C. Transfer 400 µl supernatant into a fresh 1.5-ml microcentrifuge tube without disturbing the charcoal pellet. Keep tubes on ice.

Load sample on the gradient and centrifuge

9. Prepare 4.7-ml linear 10% to 30% (w/v) gradients of sucrose in HEDG (cytosolic samples) or HEDGK4 (nuclear extracts) in heat-sealable, vertical, 13 × 51–mm ultracentrifuge tubes using one of several commercial sucrose gradient makers, or by simply successively layering five 1-ml aliquots of buffer containing decreasing amounts of 60% (w/v) sucrose (i.e., 10%, 15%, 20%, 25%, and 30% w/v sucrose). Before allowing the gradients to linearize, remove 300 µl from the top of the gradient (this provides the space needed for sample addition).

   The sucrose stock is prepared at 60%, since this concentration appears to be inhibitory to the growth of contaminating organisms (growth has been observed in 30% sucrose stock solutions).

   The sucrose will diffuse into a linear gradient if left for 1 hr at room temperature or overnight at 4°C. Gradients can be prepared in advance and stored frozen at −20°C. The linear sucrose gradients will remain intact for up to a year or more if kept frozen and then slowly thawed in an ice bath just before use.

10. Layer 300 µl of each sample onto a linear sucrose gradient. If desired, add 5 µl (1000 cpm) of each 200 cpm/µl [^{14}C]formaldehyde-labeled protein sedimentation standard as internal controls to allow accurate alignment of different gradients, more accurate estimation of specific binding, and determination of the sedimentation coefficient of the AhR complex.

    [^{14}C]Catalase (CAT; 11.3 S) and [^{14}C]BSA (4.4 S) are common internal standards and are easily radiolabeled using [^{14}C]formaldehyde as described in detail by Dottavio-Martin and Ravel (1978).

11. Seal the cooled gradient tubes with the appropriate sealing device (there are several options for sealing vertical rotor tubes) and load them into a prechilled vertical ultracentrifuge rotor (Beckman VTi65 or equivalent). Centrifuge 2.3 hr at 416,000 × *g* (65,000 rpm for a VTi65 rotor), 4°C, in an ultracentrifuge with programmed slow acceleration and deceleration.

    CAUTION: *It is extremely important to make sure that the tubes have been completely sealed before loading into the rotor. A leaking tube will not only contaminate the rotor and centrifuge, but will cause the rotor to become unbalanced, which can be dangerous. The adequacy of the seal can easily be assessed by gently squeezing the tubes after sealing and making sure that no liquid leaks out of the tube.*

    The slow acceleration and deceleration mode feature must be available on the ultracentrifuge to be able to use a vertical tube rotor. If this feature is not available, the gradients must be centrifuged in a swinging-bucket rotor. The slow acceleration/deceleration modes are needed to ensure that the gradients do not mix during their transition from vertical to horizontal orientation during centrifugation.

12. After centrifugation, puncture the top of the heat-sealed tubes with a heated 18-G solid metal wire and collect twenty-five 200-µl fractions from each gradient directly into 7-ml scintillation vials using a commercially available gradient tube fractionator or by simply puncturing the bottom of the tube with a needle and collecting two-drop fractions.

13. Add 5 ml scintillation cocktail to each vial, cap, and shake. Determine the amount of radioactivity in each vial/fraction in a liquid scintillation counter. Perform dual isotope counting for all gradients containing both [^{3}H]TCDD and [^{14}C]protein standards

    The solution will appear cloudy after shaking, but this will not affect scintillation counting efficiency. If after shaking, the gradients are not uniformly cloudy, then the amount of sample in each vial is not the same.

14. Determine the specific binding of [^{3}H]TCDD by subtracting the radioactivity present in each fraction of a gradient containing [^{3}H]TCDD and TCDF (nonspecific binding) from the radioactivity in the corresponding fractions from a gradient containing [^{3}H]TCDD alone (total binding; also see Anticipated Results).

HYDROXYAPATITE SOLID-PHASE ANALYSIS OF Ah RECEPTOR LIGAND BINDING

ALTERNATE PROTOCOL 1

The hydroxyapatite (HAP) binding assay is basically similar to the SDG assay (see Basic Protocol 1) in that it allows determination of the amount of specific binding of [^{3}H]TCDD to cytosolic proteins and its competitive displacement by AhR ligands. This assay has several advantages over the SDG assay in that it is relatively simple, rapid, not extremely labor intensive, and is amenable to analysis of relatively large numbers of samples. A disadvantage of the HAP assay is that the results only provide information as to whether the addition of a specific competitor chemical reduces [^{3}H]TCDD binding to cytosolic

proteins. It does not absolutely confirm that the reduction in bound radioactivity actually results from competitive displacement of [^{3}H]TCDD from the AhR as would be visualized with the SDG assay. Since it is always possible that the reduction in binding can result from a loss of [^{3}H]TCDD binding to some nonspecific site or sites (as is commonly observed with [^{3}H]TCDD which is not of high chemical purity), it is always prudent to confirm competitive binding of test compounds to AhRs using the SDG assay.

Additional Materials *(also see Basic Protocol)*

Hydroxyapatite (HAP; Bio-Rad Biogel HTP)
HEG buffer (see recipe)
Cytosol (see Support Protocol 1 or 2)
200 nM [^{3}H]TCDD in DMSO (specific activity 10 to 50 Ci/mmol; Eagle-Picher Technologies or Terrachem)
20 µM TCDF in DMSO (Accustandard, Cambridge Isotope Laboratories, or Wellington Laboratories)
HEGT buffer (see recipe)
95% ethanol

Buchner funnel containing #1 Whatman filter paper with vacuum source
1-ml micropipettor in which the opening of the disposable pipet tip has been enlarged
Benchtop centrifuge with swinging bucket rotor for microcentrifuge tubes

NOTE: All binding assay steps are performed at 4°C

Prepare HAP slurry

1. Gently resuspend 15 g dry hydroxyapatite (HAP) resin in 10 to 15 vol room-temperature HEG buffer. Allow the HAP to settle for 10 min and then decant the supernatant containing the fine HAP particles. Repeat 2 to 3 times, or until the supernatant is relatively clear.
2. After the last decantation, resuspend the HAP in HEG buffer and pour into a Buchner funnel containing #1 Whatman filter paper. Wash the HAP several times with HEG buffer under vacuum until the wash pH is 7.5.

   ~500 ml HEG buffer is used for the wash.
3. Scoop the vacuum-dried HAP into a bottle, add 30 ml HEG buffer (2 ml/gram original dry-weight HAP) and gently resuspend with swirling. Store the slurry up to 2 months at 0° to 4°C.

   Do not use a stir bar to resuspend the HAP as the resin may fragment and release fine particles that will be lost during the washing steps and add to assay variability.

Perform HAP binding assay

4. Determine the protein concentration of the cytosol sample using the Bio-Rad protein assay and adjust the sample to a protein concentration of 2 mg/ml with HEDG buffer.

   The 2 mg/ml protein concentration has been optimized for both [^{3}H]TCDD binding saturation and for HAP binding. If higher protein concentrations are needed, increase the [^{3}H]TCDD/TCDF in the incubation and the amount of HAP in the binding assay tubes proportionately.
5. For each binding incubation, prepare two 12 × 75–mm glass culture (incubation) tubes, one for total and one for nonspecific binding. Prepare a third tube if another test inhibitor is also to be assessed. To each incubation tube add 500 µl cytosol.

   Glass culture tubes are recommended for incubations since a loss of radioactivity may result when using some plastics.

6. For each set of incubations (i.e., total binding and nonspecific binding samples), add 5 µl of 200 µM [^{3}H]TCDD in DMSO to each tube (2 nM final concentration). Then add 5 µl DMSO (carrier solvent) to the total binding sample tube and 5 µl of 20 µM TCDF (200 nM final concentration) to the nonspecific binding sample tube. If the ability of another chemical to competitively bind to the AhR is also being assessed, add 5 µl [^{3}H]TCDD and 5 µl of the test ligand in DMSO at the desired concentration to the third tube.

7. Incubate the samples 2 hr in a room-temperature water bath.

8. While the sample is incubating, add 0.25 ml HAP slurry to a set of labeled 1.5-ml microcentrifuge tubes (2 tubes per incubation) using a 1-ml micropipettor in which the opening of the disposable pipet tip has been enlarged to allow easy pipetting of the HAP slurry. Store the tubes at 4°C.

   The HAP in the stock solution will settle out during storage and must be gently resuspended with swirling prior to use. Because it is a slurry, the HAP can be problematic to pipet, thus the need for the enlarged tip.

9. After the incubation period, transfer 0.2 ml (0.4 mg protein) of the incubation into an appropriately labeled microcentrifuge tube containing the HAP. Resuspend the mixture gently but thoroughly with vortexing and incubate 30 min at 0° to 4°C, with gentle vortexing every 10 min. If desired, count 25-µl aliquots of the remaining incubation mixture to determine the total [^{3}H]TCDD present in the binding incubation.

   Resuspend the HAP pellets by gentle vortexing since vigorous vortexing may fragment the HAP, resulting in loss of these "fines"(and their bound proteins) during the washing steps. Also make sure that the HAP pellet in each microcentrifuge tube is completely broken up by the initial vortexing, since failure to do so will result in reduced protein binding to the HAP and underestimation of the amount of bound [^{3}H]TCDD.

10. Add 0.9 ml of HEGT buffer to each tube. Cap the tubes, mix by vortexing, and centrifuge in a benchtop centrifuge with swinging bucket rotor for microcentrifuge tubes 2 min at 1500 rpm, 4°C.

11. Remove the supernatant by aspirating without disturbing the pellet. Wash the HAP pellet twice more with 1 ml HEGT buffer.

12. After the last wash, add 1.0 ml of scintillation cocktail to each tube, vortex the mixture, and transfer it into a 7-ml scintillation vial with a Pasteur pipet.

13. Wash the incubation tube and the Pasteur pipet with 0.75 ml of 95% ethanol and transfer this wash into the scintillation vial using the same Pasteur pipet.

14. Add 4 ml scintillation cocktail to each vial, cap, and shake. Determine the amount of radioactivity in each vial/fraction in a liquid scintillation counter.

15. Determine the specific binding of [^{3}H]TCDD by subtracting the radioactivity present in the tube containing [^{3}H]TCDD and TCDF (i.e., non-specific binding) from the radioactivity present in the corresponding tube containing [^{3}H]TCDD alone (i.e., total binding). Express AhR ligand binding as the number of femtomoles [^{3}H]TCDD specific binding per milligrams protein (see Anticipated Results).

SUPPORT PROTOCOL 1

PREPARATION OF HEPATIC CYTOSOL

The method as described is used to prepare cytosol from liver tissue; however, it can be used with any tissue by incorporating minor alterations in homogenization buffer volume.

Materials

Liver (or tissue) samples
HEDG buffer (see recipe)
Bio-Rad protein assay

Cheesecloth
Polytron or motorized Teflon-glass homogenizer
40-ml Oakridge polypropylene capped centrifuge tubes
Sorvall SS34 rotor or equivalent
Funnel plugged with glass wool
25-ml polycarbonate ultracentrifuge tubes
Beckman SW70Ti (or equivalent)

Additional reagents and equipment for liver perfusion (*UNIT 14.2*)

NOTE: Perform all steps at 4°C.

1. Sacrifice the animal. Open the abdominal cavity and cut the vena cava immediately above the liver with scissors. Slowly perfuse the liver with HEDG buffer using a syringe inserted into the hepatic portal vein to remove the blood.
2. Place tissue in a beaker and mince into small pieces with scissors.
3. Wash tissue with HEDG buffer until the rinse is clear.

   Livers should be perfused and the minced tissue washed as thoroughly as possible to minimize the amount of blood associated with the tissue. This is because there are several serum proteins which can bind TCDD, resulting in elevated background binding of [^{3}H]TCDD if cytosol is to be used in the binding assays (Denison et al., 1986).
4. Pass the last wash through cheesecloth to remove excess buffer and put the minced and washed liver pieces into a clean beaker and weigh.
5. For each gram of tissue, add 1 to 1.5 ml HEDG buffer to the beaker.
6. Homogenize tissue with a Polytron homogenizer or in a motorized Teflon-glass homogenizer on ice.

   Homogenates prepared using a Polytron or similar type of tissue disrupter tend to warm up during the homogenization process. Thus, make sure to homogenize using only short bursts and keep the beaker on ice to prevent samples from heating up.
7. Transfer the homogenate into a 40-ml Oakridge polypropylene-capped centrifuge tube. Centrifuge in a Sorvall SS34 rotor or equivalent 20 min at 21,000 × *g*, 4°C.
8. Pour the supernatant through a funnel plugged with glass wool into a flask.

   This step removes much of the lipid that is present in the homogenate.
9. Pour the supernatant into 25-ml polycarbonate ultracentrifuge tubes, balance, and cap. Centrifuge in a Beckman SW70Ti ultracentrifuge rotor (or equivalent) for 1 hr at 105,000 × *g*, 4°C.
10. Carefully collect the resulting supernatant (cytosol) from below the surface lipid layer using a Pasteur pipet, minimizing the amount of lipid collected, and transfer into another tube.

    Alternatively, the lipid layer can be aspirated off the top of the supernatant prior to collecting the cytosol, but typically more cytosol is lost using this method.

11. Store cytosol samples at −80°C in small aliquots (i.e., 200 to 400 µl) in 500-µl microcentrifuge tubes. Determine sample protein concentration in one aliquot using Bio-Rad protein assay.

    Cytosol has been stored in this manner for more than 7 years with no significant loss of AhR functionality.

PREPARATION OF CYTOSOL FROM CELLS IN CULTURE

SUPPORT PROTOCOL 2

This method as described has been used to prepare cytosol from a variety of cells in culture with little or no modification.

Materials

Confluent 100- or 150-mm plates of cells
Phosphate-buffered saline (PBS; see recipe)
0.5% (w/v) trypsin/0.05% (w/v) tetrasodium EDTA (Life Technologies)
HED buffer (see recipe)
HED2G buffer (see recipe)
Bio-Rad protein assay

Teflon glass homogenizer
4-ml Sorvall polycarbonate microultracentrifuge tubes
Sorvall RCM100 microultracentrifuge and RPT80 rotor, or equivalent

1. Wash confluent 100- or 150-mm plates of cells twice with 5 ml phosphate buffered saline (PBS).

   Cytosol is generally prepared from twenty 100- or ten 150-mm plates of confluent cell cultures.

2. Detach cells from the plate by adding 0.5% (w/v) trypsin/0.05% (w/v) tetrasodium EDTA and transfer into a 15-ml tube. Collect the cells by centrifuging 5 min at 1000 × *g*, room temperature.

3. Wash the cell pellet once with 10 ml cold 1× PBS.

   NOTE: *All subsequent procedures should be carried out at 4°C.*

4. Resuspend cells in HED buffer at a ratio of 1 ml HED per ten 100-mm plates of cells and transfer into a Teflon glass homogenizer.

5. Homogenize cells with 15 strokes. Mix the resulting homogenate with an equal volume of HED2G buffer, bringing the final concentration of glycerol to 10% (v/v). Transfer homogenates into 1.5-ml microcentrifuge tubes.

6. Microcentrifuge the diluted homogenate 5 min at ~12,000 × *g*, 4°C.

7. Collect the supernatant and transfer into 4-ml Sorvall polycarbonate microultracentrifuge tubes. Centrifuge in a Sorvall RCM100 microultracentrifuge and Sorvall RPT80 rotor, or equivalent, 1 hr at 105,000 × *g*, 4°C.

8. Store the resulting supernatant (cytosol) frozen at −80°C or in liquid nitrogen until use (up to 1 year). Determine protein concentrations using the Bio-Rad assay.

BASIC PROTOCOL 2

GEL RETARDATION ANALYSIS OF AhR-DNA BINDING

The gel retardation assay is a relatively simple procedure for separation of protein-free DNA from protein-bound DNA and the subsequent identification of ligand-dependent AhR-Arnt-DRE complex formation. This procedure can be used with cytosol that has been incubated with or without an AhR ligand (agonist) in vitro or nuclear extracts prepared from cells or tissues exposed to an AhR ligand or carrier solvent in vivo. The binding of AhR to the DRE is assessed by examining its ability to bind to DNA oligonucleotides or DNA fragments containing putative DREs by gel retardation analysis. The DRE-dependent nature of AhR DNA complex formation can also be determined using competitive gel retardation analysis with wild-type and mutant DRE oligonucleotides (see Alternate Protocol 2). Procedures for both cytosol and nuclear extracts are described.

Materials

95% ethanol
1× and 10× TAE buffer (see recipe)
30% acrylamide/0.8% bisacrylamide (*APPENDIX 3F*)
10% (w/v) ammonium persulfate (APS), fresh
TEMED (*N*,*N*,*N*′,*N*′-tetramethylethylenediamine)
Cytosol (see Support Protocols 1 and 2) or nuclear extracts (see Support Protocol 3)
Bio-Rad protein assay
HEDG buffer (see recipe)
Chemical to be tested
HEDGK8 buffer (see recipe)
Cytosolic and nuclear poly(dI·dC) (Roche Diagnostics) in HEDG buffer
^{32}P-labeled double-stranded wild-type DRE-oligonucleotide (see Support Protocol 4)
10× Ficoll GRA gel-loading buffer (see recipe)
HEDGK4 buffer (see recipe)

Polyacrylamide gel electrophoresis (PAGE) apparatus (e.g., V16-2; Life Technologies) with 1.5-mm spacers (*APPENDIX 3F*)
Syringe with bent needle
Peristaltic pump with two pump heads and appropriate tubing
Micropipettor with gel-loading tip or 50-µl Hamilton syringe
3 MM blotting paper

Additional reagents and equipment for PAGE (*APPENDIX 3F*) and detection and quantitation of radiolabeled proteins in gels and blots (*APPENDIX 3D*)

NOTE: When water is indicated in the procedure, use MilliQ-purified water or equivalent

Prepare the nondenaturing gel

1. Wash the glass plates of the polyacrylamide gel electrophoresis (PAGE) apparatus and rinse with plenty of water followed by 95% ethanol. Assemble washed glass plates and 1.5-mm spacers for casting of the gel as described (*APPENDIX 3F*).

   Plates are washed with water and rinsed with ethanol to ensure detergent removal. Trace amounts of detergent may affect protein-DNA complex formation.

2. For each gel to be poured, combine 4.5 ml of 10× TAE, 34 ml water, and 6 ml 30% acrylamide/0.8% bisacrylamide solution in a flask. To this mixture, add 0.45 ml fresh 10% ammonium persulfate and 22.5 µl TEMED. Swirl gently to mix and degas under vacuum.

   The volumes can be scaled up or down depending upon the number and size of the gels required.

3. Immediately pour the gel between the plates, ensure that no bubbles are formed and insert a comb. Allow the gel to polymerize (~20 min).

   Combs with 1-cm-wide teeth are recommended. For running larger numbers of samples, combs with 0.5-cm-wide teeth can be used, but the volume of sample loaded in the lane must be reduced accordingly to reduce smearing of the protein-DNA complexes.

4. Carefully remove the combs and bottom spacer, attach the plates to the gel box and fill the reservoirs with 1× TAE buffer. Flush out the wells with buffer and remove any air bubbles trapped between the glass plates beneath the gel by washing with 1× TAE buffer using a syringe with a bent needle.

5. Attach a peristaltic pump via appropriate tubing and recirculate the buffer between the top and bottom reservoirs at a moderate speed. Prerun the gel 2 hr at 130 V.

   Buffer recirculation is important when using this low ionic strength buffer, otherwise the buffering capacity will be exhausted and the resulting change in pH will disrupt protein-DNA complex formation. Alternative buffers with a greater buffering capacity have been described, but the effect on AhR DNA binding should be examined if buffer conditions are changed from that described here. An electrophoresis apparatus that is not completely enclosed is needed both to allow construction of a simple system for buffer recirculation and to provide the option of running two gels simultaneously in the same apparatus (e.g., Life Technologies V16-2 gel apparatus).

Prepare binding reactions

For binding reactions using cytosol

6a. Determine the protein concentration of the cytosol using the Bio-Rad protein assay and adjust the sample to a protein concentration of 8 mg/ml for cytosol samples from tissues and 2 to 4 mg/ml for cytosol samples from cultured cells with HEDG buffer. Keep samples at 4°C until ligand addition.

7a. Aliquot 125 µl diluted cytosol into 500-µl microcentrifuge tubes, one tube for each ligand, as well as tubes for the appropriate control solvent or solvents.

8a. To each tube add 2.5 µl of the chemical to be tested at the desired concentration(s) or control solvent or solvents. Incubate the tubes in a room-temperature water bath for 2 hr.

   For TCDD, the final concentration in the incubation is generally 10 to 20 nM in DMSO.

9a. After the incubation, combine 10 µl control or treated cytosol (from step 8a), 4 µl HEDG buffer, 3 µl HEDGK8 buffer, and 4 µl of cytosolic poly(dI·dC) in HEDG buffer in a 500-µl microcentrifuge tube. Mix gently and incubate 15 min at 20°C.

   The poly(dI·dC) concentration used with cytosolic samples is generally in the range of 100 to 400 ng per incubation; however, the exact amount of poly(dI·dC) required in a given incubation is not only species- and tissue-specific, but also dependent upon the protein concentration and the specific lot and source of poly(dI·dC) used. Identical concentrations (based on their absorbance at 260 nm) of different lots of the same poly(dI·dC) product from the same company are not necessarily equally effective as carrier DNA. Thus, with each new lot number of poly(dI·dC) used, the optimal concentration needed for maximal AhR-DRE complex formation must be established. The optimal ratio of protein/poly(dI·dC) must be maintained in order to generate maximal protein-DNA complex formation.

10a. Add 4 µl of ^{32}P-labeled double-stranded wild-type DRE oligonucleotide (~100,000 cpm) to each tube and incubate 15 min at 20°C.

11a. Add 3 µl of 10× Ficoll GRA gel-loading buffer to each tube (the solution will turn blue).

   The sample is now ready to load onto the gel.

For binding reactions using nuclear extracts

6b. Determine the protein concentration of the nuclear extract using the Bio-Rad assay.

7b. Adjust the sample to a protein concentration of 1.5 to 2 mg/ml with HEDGK4 buffer (although lower concentrations can be used).

The nuclear extracts of the matched control and treated nuclear extract must be diluted to the same protein and salt concentrations.

8b. Combine 5 µl nuclear extracts from control or treated cells with 7 µl HEDG buffer, 5 µl HEDGK4 buffer, and 4 µl of nuclear poly(dI·dC) solution (in HEDG) in a 500-µl microcentrifuge tube.

Because of the large amount of DNA binding proteins in nuclear extracts, the poly(dI·dC) concentration used with nuclear samples is generally in the range of 1 to 4 µg per incubation; however, the optimal amount of poly(dI·dC) needed for nuclear extracts from a given cell line or tissue must be determined experimentally.

9b. Mix gently and incubate 15 min at 20°C.

10b. Add 4 µl of ^{32}P-labeled DRE oligonucleotide to each tube and incubate 15 min at 20°C.

The final KCl concentration should be between 80 to 160 mM.

11b. Add 3 µl of 10× Ficoll GRA gel-loading buffer to each microcentrifuge tube (the solution will turn blue).

The sample is now ready to load onto the gel.

Run the gel

12. Turn the power supply and peristaltic pump off.

13. Flush the wells with 1× TAE and carefully load 20 µl of each sample into the appropriate 1-cm wide well of the prerun gel using either a micropipettor equipped with a gel-loading tip or a 50-µl Hamilton syringe (be sure to rinse the syringe between samples).

For 0.5-cm-wide wells, load only 10 to 15 µl sample.

14. Restart the peristaltic pump and electrophorese the samples at ~80 V until they have completely entered the gel and then increase the power to ~130 V (*APPENDIX 3F*). Stop the gel once the dye front has reached ~4 cm from the bottom of the gel (~2 to 2.5 hr for a 15- to 20-cm gel).

During the run, the glass plates should be slightly warm. If they get hot, reduce the voltage. Since the bromphenol blue dye runs slightly slower than the 25-bp oligonucleotide probe used in the standard protocol, the free [^{32}P]-labeled oligonucleotide will run off the gel if the dye front is run too close to the end of the gel.

Remove and dry the gel

15. Turn off the peristaltic pump and the power supply, remove the plates from the apparatus and carefully remove the side spacers. Gently pry the plates apart with a spatula, being careful to keep the gel adhered to only one plate. Notch a corner of the gel for orientation.

If the gel sticks to the plates and/or folds over onto itself as the plates are separated, gentle shaking of the folded gel and plate under a slow flow of water will allow the gel to resume its original shape without tearing. Be careful not to wash the gel off the plate.

16. Roll a piece of 3 MM blotting paper onto the exposed gel (making sure to keep track of the gel orientation). Lift the blotting paper up slowly to peel the gel away from the plate.

17. Cover the gel with a piece of plastic wrap. Trim off the excess paper and plastic wrap, and dry under vacuum with heat (i.e., in a gel dryer).

    A 20-cm^2 gel of 1.5 mm thickness will dry in ~1 hr at 80°C.

18. After the gel is dried, appose it to film and place at −80°C with one or two intensifying screens (*APPENDIX 3D*).

    The time needed for adequate exposure of the dried gels to X-ray film can vary greatly and is dependent on the amount and specific activity of the [^{32}P]DNA probe used and the amount of protein DNA complex formed. DNA-binding complexes can be readily quantitated by use of a phosphorimager or by excision of the desired bands from the dried gel and measurement of the radioactivity by liquid scintillation counting. Alternatively, densitometric analysis of the autoradiograms will provide a relative estimate of complex formation.

COMPETITIVE GEL RETARDATION ANALYSIS OF AhR-DNA BINDING

ALTERNATE PROTOCOL 2

This procedure allows confirmation of the sequence specificity of binding of a given DNA-binding protein and provides an avenue to confirm that a particular protein-DNA complex contains the AhR-Arnt complex. Relative to the AhR, this can be confirmed both by the demonstration of the ligand (TCDD)-dependence of formation of the specific protein-DNA complex and confirmation of the nucleotide specificity of DNA binding of the protein. Competitive displacement of the induced AhR-DRE protein DNA complex by oligonucleotides containing a wild-type DRE element (i.e., one which is known to bind the ligand AhR-Arnt complex) and the lack of competitive displacement by mutant DRE oligonucleotides (i.e., which fail to bind the AhR complex) support the identity of the protein-DNA complex as containing the AhR. Competitive gel retardation analyses using oligonucleotides containing a series of nucleotide substitutions (mutations) within the DRE have defined the nucleotides critical for formation of the ligand AhR-Arnt DRE complex. Competitive displacement curves with DNA containing known and unknown DREs can be used to estimate the relative affinity of the AhR complex for the competitor DREs (Yao and Denison, 1991; Shen and Whitlock, 1992). This procedure has been used with both cytosolic and nuclear AhR extracts. The steps in this alternate protocol are identical to those described for the method above (see Basic Protocol 2), except that the binding reactions with the cytosol and nuclear extracts are modified as described.

Additional Materials *(also see Basic Protocol 2)*

Cytosolic and nuclear poly(dI·dC) in HEDG buffer (see recipe for buffer; Roche Diagnostics)
Competitor DNA in HEDG buffer: unlabeled wild-type and mutant DRE oligonucleotides (see recipe), or other competitor DNA fragments

For cytosolic samples

9a. After the incubation, combine 10 µl control or treated cytosol, 3 µl HEDGK8 buffer, and 4 µl cytosolic poly(dI·dC) in HEDG buffer (see Basic Protocol 2, step 9a) in a 500-µl microcentrifuge tube. Mix gently and incubate for 15 min at 20°C.

10a. Add 4 µl competitor DNA in HEDG buffer or HEDG buffer alone, and 4 µl of ^{32}P-labeled double-stranded wild-type DRE oligonucleotide to each tube. Incubate 15 min at 20°C.

For nuclear extracts

8b. Combine 5 µl nuclear extracts from control or treated cells with 3 µl HEDG buffer, 5 µl HEDGK4 buffer, and 4 µl of nuclear poly(dI·dC) in HEDG buffer (see Basic Protocol 2, step 8b) in a 500 µl microcentrifuge tube.

9b. Mix gently and incubate 15 min at 20°C.

10b. Add 4 µl competitor DNA in HEDG buffer or HEDG buffer alone and 4 µl of ^{32}P-labeled DRE oligonucleotide to each tube. Incubate 15 min at 20°C.

Competitor DNA is commonly added at a 10- to 50-fold molar excess relative to the labeled DNA oligonucleotide. At a 10-fold excess, an identical unlabeled DNA fragment should theoretically reduce the amount of specific protein-DNA complexes by 10-fold. The specific competitor generally used is the same DNA fragment that was radiolabeled, while the nonspecific competitor DNA can be a DNA fragment of an unrelated sequence. To confirm the presence of the AhR in the induced protein DNA complex, the optimal nonspecific control competitor is a DNA fragment that is identical to the radiolabeled probe fragment except for the presence of a targeted mutation within the DRE core sequence which eliminates binding of the transformed AhR complex (see Support Protocol 4 for specific oligonucleotides).

SUPPORT PROTOCOL 3

PREPARATION OF NUCLEAR EXTRACTS FROM CELLS IN CULTURE

This method involves isolation of nuclear proteins from cell cultures that have been incubated with or without TCDD, [^{3}H]TCDD, or another AhR agonist. After chemical treatment, cells are collected, washed, and incubated with hypotonic buffer. The swollen cells are harvested by scraping, homogenized, and the nuclei pelleted. The crude nuclear pellet is washed and resuspended in high-salt buffer which releases soluble nuclear proteins. Following centrifugation, the nuclei are pelleted and the high-salt nuclear extract (supernatant) is collected.

Materials

Culture medium
1 µM TCDD in DMSO
DMSO
100-mm plates of confluent cells
10 mM HEPES buffer (see recipe)
MDH buffer (see recipe)
MDHK buffer (see recipe)
HEDGK4 buffer (see recipe)
Bio-Rad protein assay

6-ml Dounce homogenizer with loose-fitting pestle cooled on ice
15-ml polyethylene tubes
1-ml micropipettor with a pipet tip in which the opening has been enlarged
0.5-ml polypropylene microultracentrifuge tubes
Sorvall RCM100 microultracentrifuge and RP100AT2 rotor, or equivalent

1. Prepare an appropriate amount of culture medium containing either 1 nM TCDD or 0.1% (v/v) DMSO by adding 1 µl of 1 µM TCDD in DMSO or DMSO alone per milliliter medium in a test tube. Mix and add 2 ml treated medium to 100-mm plates of confluent cells. Incubate 1 hr in a 37°C tissue culture incubator.

A typical preparation uses six 100-mm plates of cells for each treatment.

Treatment of cells which contain a lower affinity AhR (i.e., human and nonmammalian species) requires 10 nM TCDD. The optimal TCDD concentration needed for maximal response in a given cell type should be determined empirically.

2. Place plates of cells on ice, decant medium, and wash the cells twice with 5 ml of 10 mM HEPES buffer each. Add 2 ml HEPES buffer to each plate and incubate for 15 min in a 37°C incubator.

   NOTE: *All subsequent steps should be carried out at 4°C.*

3. Aspirate HEPES buffer and add 1 ml MDH buffer per plate.
4. Collect cells by scraping and transfer them into a 6-ml Dounce homogenizer.
5. Homogenize cells using 15 to 20 strokes with a loose fitting pestle cooled on ice, and transfer the homogenate into a 15-ml polypropylene tube.
6. Centrifuge the homogenate 5 min at ~1000 × *g*, 4°C.
7. Remove the supernatant, add MDHK buffer (2 ml per 100-mm plate), resuspend the pellet with vortexing, and again centrifuge 5 min at 1000 × *g*, 4°C. Discard the supernatant and wash the crude nuclear pellet one more time.
8. Add 1 ml MDHK buffer to the tube and resuspend the crude nuclear pellet by gently vortexing. Transfer the mixture into a 1.5-ml microcentrifuge tube with a 1-ml micropipettor using a pipet tip in which the opening has been enlarged.

   Do not use a Pasteur pipet since the pellet will stick to the glass and be lost. Make sure to transfer all of the resuspended pellet.

9. Centrifuge the tube 5 min at 1000 × *g*, 4°C. Remove the supernatant.
10. Resuspend the crude nuclear pellet with HEDGK4 buffer (50 µl per plate confluent cells) by mixing gently by flicking the tube. Incubate 20 min on ice, mixing every 5 min. Microcentrifuge 15 min at ~12,000 to 15,000 × *g*, 4°C.

    The final protein concentration of the nuclear extract can be increased or decreased by decreasing or increasing the volume of HEDK5 buffer added to the pellet.

11. Transfer the supernatant (crude nuclear extract) into 0.5-ml polypropylene microultracentrifuge tubes. Centrifuge in a Sorvall RCM100 microultracentrifuge and RP100AT2 rotor, or equivalent, 1 hr at 105,000 × *g*, 4°C.
12. Store the resulting supernatant (crude nuclear extract) frozen at −80°C in 25-µl aliquots.
13. Determine protein concentrations using Bio-Rad protein assay.

    The desired working protein concentration should be ≥2 mg/ml.

PREPARATION OF ^{32}P-LABELED DOUBLE-STRANDED OLIGONUCLEOTIDES FOR GEL RETARDATION ANALYSIS

SUPPORT PROTOCOL 4

The two major methods for radiolabeling DNA for gel retardation analysis are end labeling and nick translation. End labeling generally produces a more highly labeled DNA fragment than nick translation and therefore is most commonly used for preparation of gel retardation analysis probes. In this protocol, the single-stranded oligonucleotides are reannealed and phosphorylated on their 5′-end using T4 polynucleotide kinase and [γ-^{32}P]ATP. After removal of the free [γ-^{32}P]ATP, the probe is diluted to the desired concentration and is then ready for gel retardation analysis.

Materials

DRE oligonucleotides, single-stranded and purified (wild type and mutant; see recipe)
Oligonucleotide reannealing buffer (see recipe)

10 U/µl T4 polynucleotide kinase (New England Biolabs) and 10× T4 kinase buffer (see recipe)
5000 to 8000 Ci/mmol [γ-^{32}P]ATP
TE buffer (see recipe)
Sephadex G-50 spin column (e.g., CpG Spin-pure G-50; also see recipe) equilibrated with TE buffer
HEDG buffer (see recipe)
20 µg/ml ethidium bromide in TE buffer

Heated rotary evaporator (e.g., Speedvac; Savant)
0.5-ml screw-cap microcentrifuge tubes
UV transilluminator

Reanneal single-strand oligonucleotides

1. Determine the DNA concentration of the purified single-stranded DRE oligonucleotides (wild type and mutant) by measuring the absorbance of an aliquot of each at 260 nm and using the following conversion:

   One A_{260} unit = 34 µg DNA/ml for single-stranded oligonucleotides.
2. Combine 225 µg of each of the two complementary oligonucleotides into a 1-ml microcentrifuge tube.
3. Evaporate to dryness in a heated rotary evaporator.
4. Dissolve the DNA in 75 µl oligonucleotide reannealing buffer and incubate 5 min at 90°C.
5. Turn off the heat and allow the tubes to slowly cool to room temperature.
6. Determine the DNA concentration of the reannealed DNA oligonucleotides by measuring the absorbance of an aliquot of each at 260 nm and using the following conversion:

   One A_{260} unit = 50 µg DNA/ml for double-stranded oligonucleotides.

Radiolabel double-stranded oligonucleotides

7. In a 0.5-ml screw-cap microcentrifuge tube, combine the following in order:

   25 µl water
   10 µl 20 to 25 ng/µl dsDNA oligonucleotide
   5 µl 10× T4 kinase buffer
   8 µl 5000 to 8000 Ci/mmol [γ-^{32}P]ATP
   2 µl 10 U/µl T4 DNA polynucleotide kinase

   The T4 kinase buffer supplied by the manufacturer can be used or the buffer can be made in house.
8. Incubate the reaction 30 min at 37°C.
9. To each reaction mixture add 50 µl TE buffer.
10. Pipet the radiolabeled reaction mixture directly onto a Sephadex G-50 spin column equilibrated with TE buffer. Centrifuge 2 min at 1000 × *g*, room temperature.

    This step removes the majority of unincorporated radiolabeled nucleotides.
11. Transfer the radiolabeled DNA sample in the collection tube following centrifugation into a 0.5-ml screw-cap microcentrifuge tube.
12. Dilute the sample 1:4 with HEDG buffer and count 4 µl sample by liquid scintillation.

    If the labeling was successful, the radioactivity of the original Sephadex eluant should be ~1 × 10^6 cpm/µl.

13. Dilute the radiolabeled stock solution with HEDG buffer to 100,000 cpm/4 µl for use in the gel retardation assay (see Basic Protocol 2 and Alternate Protocol 2).

The specific activity of the radiolabeled probe can be readily determined by measuring both the radioactivity and the amount of DNA in an aliquot of the final radiolabeled stock. The amount of DNA can be accurately estimated using the spot quantitation method described below.

Perform spot quantitation

For competitive gel retardation analysis, the specific activity of the radiolabeled probe must be determined in order to prepare accurate competitor concentrations.

14. Spot a 1- to 2-µl aliquot of the sample (1 to 20 ng DNA) onto a piece of plastic wrap that has been placed on a UV transilluminator. Do the same for a range of DNA standard concentrations from 1 to 20 µg/ml. Add an equal volume 20 µg/ml ethidium bromide in TE to each spot. Mix by repeated pipetting with a micropipettor.

15. Photograph the spots and estimate the DNA concentration of the sample by direct comparison of its fluorescence intensity to those of the standards.

CAUTION: *Do not look at the UV light without wearing an appropriate full-face shield that efficiently blocks the UV light.*

IMMUNOBLOT OF AhR AND Arnt

BASIC PROTOCOL 3

Immunoblot analysis is a useful technique for direct detection of the presence and size of a specific protein using an antibody specific for that protein. This procedure can be used with whole cell lysates, cytosol, or nuclear extracts (prepared from cells or tissues exposed to an AhR ligand). In this technique, proteins in a sample extract are denatured and separated in a denaturing polyacrylamide gel (also see *APPENDIX 3F*). The proteins are transferred onto a nitrocellulose or PVDF membrane and the AhR or Arnt is bound by anti-AhR or -Arnt antibodies, which are subsequently bound by a secondary antibody coupled to horseradish peroxidase (HRP). Detection of the antibody complex is readily observed using a chemiluminescent substrate for HRP and subsequent autoradiography.

Materials

4× PAGE running gel buffer (see recipe)
4× PAGE stacking gel buffer (see recipe)
95% ethanol
Immunoblot tank buffer (see recipe)
Mammalian cells or whole cell lysate, cytosol (see Support Protocols 1 and 2), or nuclear extracts (see Support Protocol 3)
PBS (see recipe)
1× trypsin (Life Technologies)
Lysis buffer, fresh (see recipe)
Bio-Rad protein assay
2× immunoblot treatment buffer, frozen (see recipe)
Prestained protein standards (e.g., Bio-Rad Kaleidoscope), frozen
Towbin transfer buffer (see recipe)
Nitrocellulose (Amersham Hybond-ECL) or PVDF (NEN Polyscreen) transfer membrane
100% methanol (for PVDF membranes only)
Phosphorescent paint (obtain from an art supply store or hobby shop)
Blotto (see recipe)

Primary antibody: rabbit anti-AhR and mouse anti-Arnt antibodies (Affinity Bioreagents, Novus Biologicals, or Santa Cruz Biotechnology)
TBST (see recipe)
Secondary antibody: Anti-rabbit or -mouse antibody conjugated to horseradish peroxidase (Pierce)
Tris buffered saline (TBS; see recipe)
Renaissance Western Blot Chemiluminescence Reagent Plus, Enhanced Luminol (NEN Life Science Products)
Stripping buffer (see recipe)

100-mm tissue culture plates
Chromatography paper (Whatman 3 MM or equivalent)
Transfer apparatus (Idea Scientific)
Plastic sheet protectors
Autoradiography film
Rocking platform (Labquake)
Shallow plastic box or tray with lid, slightly larger than blot

Additional reagents and equipment for PAGE (*APPENDIX 3F*) and autoradiography (*APPENDIX 3D*)

NOTE: When water is indicated in the procedure, use MilliQ-purified water or equivalent.

Prepare the gel

1. Prepare a 10 × 8–cm minigel with a 10% running and 4% stacking gel as described (*APPENDIX 3F*) using 4× PAGE running gel buffer and 4× PAGE stacking gel buffer. Make sure to first wash the plates with water and then 95% ethanol to remove detergent and wipe dry with Kimwipes. Use immunoblot tank buffer in the reservoirs.

Prepare samples

If using cytosol, nuclear extracts, or in vitro synthesized AhR or Arnt from rabbit reticulocyte lysates, skip to step 7.

2. Grow mammalian cells to confluence in 100-mm tissue culture plates. One plate per treatment should be sufficient.

   In general, tissue or cell extracts prepared by any of the protocols in this unit (see Support Protocols 1 to 3) will yield sufficient AhR or Arnt for detection by immunoblot analysis. Liver cytosol extracts prepared for use in gel retardation analysis experiments (see Support Protocol 1), when diluted to 2 to 3 mg protein/ml, make excellent positive controls for immunoblot experiments.

3. Rinse each plate twice with PBS. Add 1 ml of 1× trypsin and incubate 5 min at room temperature. Harvest cells by scraping and transfer them into separate 1.5-ml microcentrifuge tubes. Microcentrifuge 20 sec at 2000 rpm. Rinse twice with 1 ml PBS each and discard the supernatant.
4. Add 1.2 ml fresh lysis buffer, suspend cells and incubate 30 min at 4°C with shaking.
5. Microcentrifuge the cell lysate 15 min at 12,000 rpm, 4°C. Transfer 1 ml cleared lysate to a clean microcentrifuge tube and discard the pellet.
6. Measure sample protein concentration by Bio-Rad protein assay.

   This protocol will yield a protein concentration of 0.6 to 1 mg/ml. Lysate may be stored indefinitely at –80°C.

Perform electrophoresis

7. If using frozen samples, thaw on ice. Thaw 2× immunoblot treatment buffer and prestained protein standards at room temperature.

8. If necessary, dilute samples with water to 2 to 3 mg protein per milliliter.

   The protein concentration needed is dependent upon the AhR/Arnt concentration in the sample and preliminary experiments may need to be run to determine the optimal protein concentration to use for a given extract. For mouse hepatoma (hepa1c1c7) cells, a protein concentration of 2 to 3 mg/ml is sufficient.

9a. *For nonreticulocyte samples:* Mix 20 µl of each sample with 20 µl of 2× immunoblot treatment buffer.

9b. *For reticulocyte lysate samples:* Dilute 3 µl of a standard 20-µl reaction with 7 µl water and 10 µl of 2× treatment buffer. Boil samples 3 min and cool on ice.

   Reticuloctye lysates must be diluted significantly due to the high salt concentration of these samples, otherwise these samples will resolve poorly in the denaturing gel.

10. Briefly microcentrifuge the samples at full speed and load 7 µl prestained protein standards in the outermost wells of the gel. Load up to 30 µl (40 to 60 µg protein) of sample per lane. Electrophorese 1 hr at 20 mA/gel (*APPENDIX 3F*).

    Proteins smaller than ~20 kDa, such as the smallest two Kaleidoscope standard proteins, will not resolve in a 10% gel and will migrate with the dye front.

Prepare and blot membrane

11. Disassemble the electrophoresis unit. Lift the top plate from the gel and cut off and discard the stacking gel. Notch one corner of the gel to allow maintenance of gel orientation. Squirt water on edge of gel and carefully work the gel loose from plate. Place the gel into a plastic container containing several milliliters of Towbin transfer buffer (i.e., enough to cover the gel). Incubate the gel 20 min with shaking at room temperature.

12. With gloved hands, carefully cut the nitrocellulose or PVDF transfer membranes to gel size (8 × 6 cm). For each gel, cut two pieces of chromatography paper to a size slightly smaller than the pads in transfer unit.

    Dry membranes are very fragile and should never be handled with bare hands.

13. *For PVDF membranes only:* Wet membrane in 100% methanol for 15 sec. Rinse in water 2 min.

14. Place the membrane in the container with the gel for 5 min. Moisten chromatography paper with Towbin transfer buffer.

15. Assemble the transfer apparatus according to manufacturer's instructions, making sure to remove any bubbles, especially those between the membrane and gel.

    Two gels may be simultaneously transferred using an Idea Scientific transfer unit, but make sure that they are staggered and not placed directly above each other.

16. Transfer proteins to the membrane 45 min at 24 V for one gel, or 1 hr for two.

    Examination of the gel after transfer will reveal that much of the topmost band in the protein standard lane has not transferred; however, the AhR and Arnt are much smaller than this protein and they transfer much more efficiently.

17. *For PVDF membranes only:* Immerse in 100% methanol for 10 sec.

18. Place membrane, protein side up, on a paper towel on the lab bench and allow to dry for at least 15 min.

19. Mark the positions of the protein standards with a small dot of phosphorescent paint.

    The ability of the paint to glow in the dark will allow the positions of the weight standards to appear on the autoradiograph.

    The dry blot may be wrapped in plastic wrap and stored overnight at 4°C or indefinitely at −20°C. Sandwich the blot between two pieces of cardboard for extended storage.

Probe blot with antibodies

Perform all incubations at room temperature with rocking.

20. Block additional protein binding sites on the membrane blot by immersing it in Blotto (protein side up) in a plastic container and incubating for 30 min.

    The volume of solutions used is dependent upon the size of the container. For probing with antibody, the liquid should just cover the blot; during blocking and washing steps, use twice this volume. In the containers with a 10.5 × 8.5 cm base, 5 and 10 ml are used, respectively.

21. Remove the solution, add fresh Blotto and incubate an additional 30 min.

    Blotto is used twice in order to minimize background.

22. Remove the solution and incubate the blot with primary antibody diluted (e.g., 1:5000) in Blotto for 60 min.

    Titration may be necessary for different antibody preparations.

23. Wash membrane six times for 5 min each with TBST.

24. Incubate blot with anti-rabbit or -mouse secondary antibody conjugated to horseradish peroxidase, diluted 1 to 2 µl antibody/5 ml Blotto (e.g., 1:5000 or 2:5000) for 45 min.

25. Wash membrane five times for 5 min each with TBST. Wash once for 5 min with Tris buffered saline (TBS).

26. Mix equal volumes of each reagent supplied in the Renaissance Western Blot Chemiluminescence Reagent Plus kit (3.5 ml each per blot). Incubate membrane in the freshly prepared solution for exactly 1 min in a clean plastic container.

27. Remove membrane from solution with forceps and blot off excess. Do not overdry the membrane. Place membrane inside sheet protector.

28. Expose the blot to autoradiographic film for 1 min and develop (*APPENDIX 3D*).

    If necessary, adjust exposure time and repeat. Both the phosphorescent protein standards and the chemiluminescent proteins will appear on the autoradiographic film.

29. Compare the position of the proteins (chemiluminescent) on the blot to the position of the protein molecular weight standards (phosphorescent) to allow estimation of the size of the AhR.

    Immunoblots using anti-AhR antibodies commonly contain multiple protein bands in addition to the AhR. The authors have not identified any AhR antibody that will only produce a single band on immunoblots; however, the major band on the blot should be that of the AhR, which should be ~95 to 120 kDa in size (depending on the species examined).

30. Once an adequate autoradiogram has been obtained, rinse the blot 5 min with TBS at room temperature to remove excess chemiluminescent reagent, and wrap the wet blot in plastic wrap. Store up to 4 weeks at 4°C.

    If the membrane is to be reprobed with another antibody it will need to be stripped prior to reuse.

Strip the membrane (optional)

31. Immerse the membrane in stripping buffer and incubate 30 min at 50°C.
32. Wash membrane six times for 5 min each with TBST at room temperature.
33. Incubate membrane for exactly 1 min in freshly prepared chemiluminescence reagent.
34. Place membrane in plastic sheet protector. Expose film for 30 min and develop to make sure that the membrane is adequately washed (no chemiluminescent signal should be observed; *APPENDIX 3D*).
35. Wash membrane four more times for 5 min each with TBST at room temperature.

The blot may now be reprobed with antibody as described above.

DETECTION OF HUMAN AND MOUSE AhR, Arnt, CYP1A1, and CYP1B1 mRNA BY RT-PCR

BASIC PROTOCOL 4

The reverse transcriptase–polymerase chain reaction (RT-PCR) is perhaps the most sensitive technique developed to measure gene expression in tissues or cells. RT-PCR can be used to determine the presence and abundance of a message and also to clone a particular cDNA product. In the protocol described here, the reverse transcriptase enzyme synthesizes the first strand of cDNA from mRNA, and then the second strand of cDNA is synthesized and PCR amplification is performed using Platinum *Taq* DNA polymerase. The mixture containing the polymerase, oligonucleotide primers, and dNTPs is cycled several times (20 to 30) through a series of temperatures that allows the DNA to denature, anneal to the primers, and amplify the product. Although a number of one-enzyme/one-step kit technologies have been developed, the best results are generally obtained using a two-step approach which results in maximum integrity and efficiency of each enzyme. This protocol describes the optimal procedure for amplification and detection of the C57BL/6 mouse and human AhR, Arnt, CYP1A1, and CYP1B1 mRNAs. Minor modifications in this protocol will allow amplification of these products in other species using appropriate primer sets and amplification conditions. For more information concerning PCR, refer to *APPENDIX 3C*.

Materials

Single-stranded oligonucleotide primers (Table 4.8.1)
Total RNA (see Support Protocol 5)
Oligo$(dT)_{12\text{-}18}$ primer (Life Technologies or InVitrogen)
200 U/µl Superscript II reverse transcriptase with 5× first-strand buffer and 0.1 M dithiothreitol (DTT; Life Technologies or InVitrogen)
2 mM dNTP mix (Life Technologies or InVitrogen)
Random hexamers (Life Technologies or InVitrogen)
25 mM $MgCl_2$
5 U/µl Platinum *Taq* DNA polymerase (InVitrogen) and 10× PCR buffer (Life Technologies)
1% agarose gel in 1× TAE buffer (see recipe)
1 mg/ml ethidium bromide solution (see recipe)
100 bp or 1 Kb DNA ladder (Life Technologies)

Thin-walled PCR tubes
PCR thermocycler with heated lid
100 bp or 1 Kb DNA ladder (Life Technologies)
DNA/RNA gel electrophoresis apparatus and power supply

Additional reagents and equipment for performing agarose gel electrophoresis (*APPENDIX 3A*)

Table 4.8.1 PCR Primers for Amplification of Human and Mouse AhR, Arnt, CYP1A1, CYP1B1, and Housekeeping Gene Products (GAPDH and HPRT)

Target	5′-primer	3′-primer
Human PCR primers		
AhR	5′-GTGACTTGTACAGCATAATG-3′	5′-ATCTTCTGACACAGCTGTTG-3′
Arnt	5′-GAATTGGACATGGTACCAGG-3′	5′-AAGCTGATGGCTGGACAATG-3′
CYP1A1	5′-CCTTTGAGAAGGGCCACATC-3′	5′-GATGGGTTGACCCATAGCTT-3′
CYP1B1	5′-TATCCTGATGTGCAGACTCG-3′	5′-TCCTTGTTGATGAGGCCATC-3′
GAPDH	5′-GAGCCACATCGCTCAGAC-3′	5′-CTTCTCATGGTTCACACCC-3′
Mouse PCR Primers		
AhR	5′-GTGTCTGCCATTGTCTCTGTTC-3′	5′-CAATACAGACAAACAAATAGGCAG-3′
Arnt	5′-CCCCTCCTGTAACCATTGTC-3′	5′-ACGGAGGGAGAGGACTTTTAT-3′
CYP1A1	5′-CCAGGATGCTCACCCGCCCAG-3′	5′-ATGTAGGGTGAACAGAGGTGC-3′
CYP1B1	5′-AATGAGGAGTTCGGGCGCACA-3′	5′-GGCGTGTGGAATGGTGACAGG-3′
HPRT	5′-GTAATGATCAGTCAACGGGGGAC-3′	5′-CCAGCAAGCTTGCAACCTTAACCA-3′

CAUTION: Ethidium bromide is a mutagen and should be handled, stored, and disposed of with appropriate care.

NOTE: Use RNase-free water for solutions that come in direct contact with the RNA.

Oligonucleotide PCR Primers

1. Resuspend the single-stranded oligonucleotide primers in RNase-free water. Determine the DNA concentration by measuring the absorbance of an aliquot of each at 260 nm and using the following conversion:

   One A_{260} unit = 34 µg/ml for single-stranded oligonucleotides.

   Store primers at −20°C until use.

Perform first-strand cDNA synthesis using oligo(dT)$_{12\text{-}18}$ primer

2a. For a 20 µl reaction volume, incubate 2 µg total RNA and 200 ng oligo(dT)$_{12\text{-}18}$ primer for 10 min at 70°C to denature the RNA and then quickly chill the tubes on ice.

3a. To each reaction tube, add 4 µl of 5× first strand buffer, 2 µl of 0.1 M DTT, 1 µl of 2 mM dNTP mix, and RNase-free water to a final volume of 19 µl. Mix the reaction components gently and allow to equilibrate at 37°C for 2 min.

The 5× first-strand buffer consists of 250 mM Tris·Cl, pH 8.3, 375 mM KCl, and 15 mM $MgCl_2$. The buffer, along with 0.1 M DTT, is supplied with Superscript II reverse transcriptase.

4a. Add 1 µl (200 U) Superscript II reverse transcriptase and further incubate at 37°C for 1 hr. Terminate the reaction by heating 15 min at 70°C and adding 230 µl sterile water to each reaction. Store reactions up to 6 months at −20°C.

Perform first-strand cDNA synthesis using random hexamers

2b. Mix 5 µg total RNA with 100 ng random hexamer primers in a reaction volume of 12 µl. Incubate the mixture 10 min at 70°C to denature the RNA and then quickly chill the tubes on ice.

3b. Add 4 µl of 5× first strand buffer, 2 µl of 0.1 M DTT, and 1 µl of 2 mM dNTP mix to the reaction tube. Incubate 10 min at room temperature and then 2 min at 42°C.

4b. Add 1 µl (200 U) Superscript II reverse transcriptase and incubate 50 min at 42°C. Terminate the reaction by heating 15 min at 70°C. Store reactions up to 6 months at –20°C.

PCR amplify

5. For a 50 µl PCR amplification reaction, add the following to a thin-walled PCR tube:

   1 µl synthesized cDNA
   0.5 µl of 2 mM dNTP mix (20 µM final)
   1 µl of 25 mM $MgCl_2$ (0.5 mM final)
   5.0 µl of 10× PCR buffer
   50 pmoles of each primer (from step 1)
   1.25 U Platinum *Taq* DNA polymerase.

   The PCR primers for amplification of the human and mouse AhR, Arnt, CYP1A1, CYP1B1, glyceraldehyde 3-phosphate dehydrogenase (GAPDH), and hypoxanthene phosphoribosyl transferase (HPRT) are presented in Table 4.8.1. Primers for these specific gene products from other species can readily be found in the published literature or they can be easily and efficiently designed using software programs such as Oligo 5.0 (Molecular Biology Insights). Primers can be synthesized inexpensively by a large number of commercial labs. GAPDH, HPRT, and β-actin are housekeeping genes whose expression can be used to demonstrate successful RT-PCR reactions and to normalize for variations in sample loading. In addition to the primers described here, primer sets for β-actin and GAPDH are also commercially available from Clontech Laboratories.

   Platinum Taq DNA Polymerase is one of many "hot start" polymerases. Such enzymes are often bound to an inhibitor and thus maintained in an inactive state until they reach 94°C whereby the inhibitor is released and the enzyme becomes activated. Hot start polymerases generally increase the sensitivity and specificity of the reaction and eliminate the effort associated with manual hot start methods.

   Use of thermocyclers without heated tops requires the addition of an oil overlay to prevent loss of the reaction to the top of the tube during thermocycling. If multiple reactions are to be performed, a master mix can be prepared to minimize variations in pipetting between reactions. Be sure to confirm the amplification conditions, magnesium concentrations and cycle number since variations can occur between PCR machines.

   10× PCR buffer consists of 500 mM KCl, 15 mM $MgCl_2$, 0.01% gelatin, and 100 mM Tris·Cl, pH 8.3 (at room temperature), and is supplied with Platinum Taq DNA polymerase.

6. Amplify cDNA samples using the programs given in Table 4.8.2.

   The number of cycles should be optimized to ensure amplification within the linear range of cycle number versus amount of product formed.

7. Electrophorese a 15-µl aliquot of each PCR reaction in a 1% agarose gel in 1× TAE buffer containing 0.24 µg/ml ethidium bromide (*APPENDIX 3A*).

   The ethidium bromide is added to the heated agarose gel solution prior to pouring.

8. Visualize the PCR products under UV light and determine the size of the amplified products by direct comparison to 100 bp or 1 Kb DNA molecular weight markers included in the same gel.

   The sizes of the expected fragments are shown in Table 4.8.3.

Table 4.8.2 PCR Program for Amplification of RT-PCR Products

Primer	Initial step[a]	Denaturation[b]	Annealing[b]	Extension[b]	Extension/hold
Human PCR primers					
AhR	2 min at 94°C	45 sec at 94°C	1 min at 55°C	1 min at 72°C	10 min at 72°C
Arnt	2 min at 94°C	45 sec at 94°C	1 min at 55°C	1 min at 72°C	10 min at 72°C
CYP1A1	2 min at 94°C	45 sec at 95°C	1 min at 55°C	1 min at 72°C	10 min at 72°C
CYP1B1	2 min at 94°C	45 sec at 95°C	1 min at 55°C	1 min at 72°C	10 min at 72°C
Mouse PCR Primers					
AhR	2 min at 94°C	45 sec at 94°C	1 min at 64°C	1 min at 72°C	10 min at 72°C
Arnt	2 min at 94°C	45 sec at 94°C	1 min at 58°C	1 min at 72°C	10 min at 72°C
CYP1A1	2 min at 94°C	1 min at 95°C	30 sec at 64°C	2 min at 72°C	10 min at 72°C
CYP1B1	2 min at 94°C	1 min at 95°C	30 sec at 64°C	2 min at 72°C	10 min at 72°C

[a]The initial step is to both denature the primers and activate the enzyme.

[b]These steps are to be performed for 30 to 35 cycles.

Table 4.8.3 Expected Size of the RT-PCR Amplification Products Using the Specific Primers Described in Table 4.8.1

	Expected PCR Product Size (bp)	
Gene Product	Human	Mouse
AhR	310	797
Arnt	310	647
CYP1A1	460	448
CYP1B1	320	797
GAPDH	430	—
HPRT	—	177

BASIC PROTOCOL 5

NORTHERN BLOT DETECTION OF HUMAN CYP1A1

Northern blot analysis is a useful technique for detecting the presence and size of mRNA for a particular gene, and whether the abundance of the message is altered by a particular treatment. Either total RNA or poly(A)$^+$ mRNA is isolated from tissues or cells and separated on a denaturing formaldehyde/agarose gel. The RNA is transferred to a nylon membrane and the message of interest is subsequently detected by hybridization with a radioactively or nonradioactively labeled cDNA probe. Transcripts can be quantified using a phosphorimager (Molecular Dynamics) and normalizing the signal to that obtained for a control message such as GAPDH or β-actin. Although northern blot analysis will detect moderately to highly expressed messages in total RNA, isolation of poly(A)$^+$ mRNA may be required to detect rare messages (also see *APPENDIX 3E*). Although the procedure described here is for northern blot analysis of CYP1A1 mRNA, it can readily be adapted for detection of AhR and Arnt mRNA, the cDNAs of which are available from numerous laboratories.

Materials

Total RNA sample (see Support Protocol 5)
RNase-free H_20
1 mg/ml ethidium bromide (see recipe)
Northern sample buffer (see recipe)

1× MOPS buffer (see recipe)
NaOH/SSC (see recipe)
Tris/SSC (see recipe)
10× SSC (see recipe)
hCYP1A1 plasmid (pBR322 vector; ATCC #57258)
*Eco*RI restriction endonuclease
GAPDH or β-Actin cDNA probes (Clontech Laboratories; optional)
Oligolabeling kit (Amersham Pharmacia Biotech):
  Reagent mix
  Klenow fragment
[α-^{32}P]dCTP (3000 Ci/mmol)
Spin-Pure Sephadex G50 spin column or equivalent
Scintillation cocktail
Northern hybridization buffer, 65°C (see recipe)
0.5× and 2× SSC (see recipe)/0.1% (w/v) SDS

Fluorescent ruler
Whatman 3 MM paper
1-ml screw-cap microcentrifuge tube
95°C water bath
Roller bottle hybridization oven and appropriate bottle
Additional reagents and equipment for northern blot analysis (*APPENDIX 3E*), agarose gel purification (*APPENDIX 3A*), and autoradiography (*APPENDIX 3D*)

NOTE: Use RNase-free water (Life Technologies) for solutions that come in direct contact with the RNA.

Prepare, run, and transfer gel

1. Prepare a formaldehyde/agarose gel as described (*APPENDIX 3E*).
2. Combine 10 to 20 µg total RNA, adjusted to 5 µl with RNase-free water, with 20 µl Northern sample buffer in a 0.5-ml microcentrifuge tube. Heat to 65°C for 15 min and immediately chill on ice. Add 1 µl of 1 mg/ml ethidium bromide, mix well, and briefly microcentrifuge to collect contents in the bottom of the tube.
3. Load 25 µl into a lane of the gel and electrophorese at 47 V for 3 to 3.5 hrs in 1× MOPS buffer (i.e., until the bromphenol blue band migrates ~75% the length of the gel).
4. View the gel under UV light to check the integrity of the 28S and 18S ribosomal bands.

   The human 28S band (5.0 Kb) should be approximately twice the intensity of the 18S band (1.9 Kb). If there is significant smearing or degradation of these bands, it is an indication that the RNA is degraded. If this is the case, it is best to prepare a new sample of RNA.

5. Use a fluorescent ruler to record the migration of the ribosomal bands and photograph the gel.
6. *For mRNA >6 Kb (optional):* Soak the gel 10 min in NaOH/SSC and then 10 min in Tris/SSC.

   Soaking the gel in NaOH/SSC results in partial lysis of the RNA and allows for more efficient transfer to the membrane.

7. Soak the gel 15 min in 10× SSC, discard the solution, and resoak in fresh 10× SSC for an additional 15 min.

8. Translocate the mRNA to the membrane by upward transfer as described (*APPENDIX 3E*), except use 10× SSC.

9. View the nylon "blot" under UV light to ensure the transfer was successful.

   The ethidium-stained ribosomal bands should be visible.

10. Place the membrane, RNA side up, on a piece of Whatman 3 MM filter paper and crosslink the RNA to the membrane as described (*APPENDIX 3E*). Place the blot between two pieces of Whatman 3 MM paper and bake in a vacuum oven 1 hr at 80°C.

Radiolabel the cDNA probe

11. Create a 1000-bp CYP1A1 probe by digesting 1 µg hCYP1A1 plasmid with 20 U *Eco*RI restriction endonuclease according to the manufacturer's instructions. Electrophorese the digest on a 1% agarose gel in 1× TAE buffer and gel-purify the appropriate fragment (*APPENDIX 3A*).

    A number of kits are currently available for gel purifying DNA fragments. Qiagen's gel extraction kit is simple, rapid, and inexpensive. This method involves cutting the appropriate fragment from the gel, dissolving it in the buffer provided, binding the DNA to a column, and washing several times before eluting the desired DNA fragment.

12. Radiolabel probes for CYP1A1 and if desired, either GAPDH or β-actin, using the Oligolabeling Kit (or equivalent) and the recommended protocols (briefly described below in steps 13 to 15).

    Probes for GAPDH or β-actin should also be used to normalize for sample loading and can be obtained from collaborative colleagues or from Clontech Laboratories. If detection of AhR and/or Arnt is desired, cDNA probes for these gene products are also readily obtained from numerous investigators.

13. Combine 50 ng DNA probe with water to a total volume of 34 µl in a 1-ml screw-cap microcentrifuge tube. Heat 3 min in a 95°C water bath to denature the DNA. Immediately place on ice 5 min and briefly microcentrifuge at top speed to collect contents in the bottom of the tube.

14. To this tube, add 10 µl reagent mix (dATP, dGTP, dTTP, and random hexadeoxyribonucleotides), 5 µl of 3000 Ci/mmol [α-^{32}P]dCTP (50 µCi), and water to a total of 49 µl. Add 1 µl Klenow fragment, mix gently, and incubate 37°C for 1 hr.

    This incubation results in random priming (labeling) of the resulting nascent DNA fragment.

15. Remove unincorporated nucleotides by running the sample through a Spin–Pure Sephadex G-50 spin column or equivalent as described by the supplier. Count 1 µl radioactive probe in 5 ml scintillation cocktail.

    A good "hot" probe should be between 1 to 2 × 10^6 cpm/µl; however, probes with lower specific activity may still work well, depending on the amount of desired mRNA in the sample. Radiolabeled probes may be kept at −20°C for 7 to 10 days; however, probes labeled at high specific activity will undergo significant radiolytic degradation if kept for much longer than 10 days. Thus, optimal results are obtained with a freshly labeled probe.

Hybridize and wash the blot

16. Place the membrane in a roller bottle with the RNA-bound side facing the inside of the bottle. Add 10 ml of 65°C northern hybridization buffer. Prehybridize the blot at 65°C in a roller bottle hybridization oven for 1 hr or more.

17. Incubate 1×10^7 cpm radiolabeled probe in 100 µl water in a screw-cap microcentrifuge tube for 3 min at 95°C. Chill immediately on ice and then add to the solution in the roller bottle. Allow to hybridize with mixing overnight at 65°C.

    The desired probe concentration should be ~1×10^6 cpm/ml northern hybridization buffer.

    If a hybridization roller apparatus is not available, prehybridization and hybridization can also be carried out at the same temperatures in a plastic box weighed down in a water bath.

18. Discard the hybridization solution into a radioactive waste container and wash the blot three times for 5 min each at 65°C in the hybridization oven with 10 ml of 2× SSC/0.1% (w/v) SDS. Measure the radioactive background of the blot in an area that should not have any RNA (i.e., a corner of the blot) with a Geiger counter. If the counts are still significantly above background, then wash the blot for an additional 15 to 30 min with 15 ml 0.5× SSC/0.1% SDS.

19. Continue washing the blot until the radioactivity of the blot is near background levels. Quickly wrap the blot in plastic wrap without letting it dry out and expose to X-ray film with one or two intensifying screens overnight at −80°C (*APPENDIX 3D*).

    The time required for adequate exposure of the blot to X-ray film can vary greatly and is dependent on the amount of CYP1A1 mRNA, the specific activity of the radiolabeled probe used, and the degree of hybridization.

ISOLATION OF TOTAL RNA

SUPPORT PROTOCOL 5

There are many kits and technologies available for isolating total RNA from animal tissues and cells. The procedure described here uses the RNeasy mini kit from Qiagen and their recommended protocol and supplied buffers. This protocol, briefly described below, has proven to yield total RNA of very high purity and integrity. In general, one RNeasy mini spin column, which consists of a silica gel based membrane, was found to be suitable for isolating ~50 µg of total RNA from one 100-mm plate of confluent cells. The maximum binding capacity of each column is 100 µg RNA. If the number of plates of cells are increased, the amount of solution used must be increased proportionately. An alternative method, which has also proven very useful, is the TRIzol reagent from Life Technologies. TRIzol is a phenol and guanidine isothiocyanate solution that lyses the cells and inactivates RNases. Following homogenization and addition of chloroform, centrifugation separates the solution into an organic and an aqueous phase. RNA partitions into the aqueous phase and is recovered by precipitation with isopropyl alcohol. RNases are ubiquitous, very stable and can easily be introduced into the RNA sample. Consequently, when working with RNA, great care should be taken to wear gloves at all times and to use RNase-free disposable plasticware whenever possible.

Materials

100-mm plates of confluent control (DMSO) and treated (TCDD) cells
Medium
RNeasy mini kit (Qiagen) containing:
  Qiagen denaturing buffer
  RNeasy mini spin column and collection tube
  Wash buffers
14.2 M 2-mercaptoethanol
100% and 70% ethanol, cold
3 M sodium acetate, RNase free (see recipe)
40 U/µl RNaseOUT recombinant ribonuclease inhibitor (Life Technologies)

1-ml plastic syringe with 20-G needle
65°C water bath

Additional reagents and equipment for trypsinizing cells (see Support Protocol 2).

NOTE: Use RNase-free water (Life Technologies) for solutions that come in direct contact with the RNA. All steps are performed at room temperature. Once RNA is isolated, it should be kept on ice or at −80°C.

1. Trypsinize plates of control (DMSO) and treated (TCDD) cells as described in the kit instructions (also see Support Protocol 2, step 2). Add the trypsinized cell suspension to 10 ml medium and then pellet the cells by centrifuging 5 min at 300 × *g*.
2. Remove the supernatant and resuspend the cell pellet by vortexing in 600 µl Qiagen denaturing buffer, supplied in the RNeasy mini kit, and 1% (v/v) 2-mercaptoethanol per one 100 mm-plate of cells (5×10^6 to 1×10^7 cells).

   This step ensures lysis of the plasma membrane and release of the RNA. RNases are inactivated in the presence of the denaturing solution which allows for isolation of intact RNA.
3. Homogenize the lysate by passing it through a sterile 1-ml plastic syringe with 20-G needle 20 times.

   This step reduces the viscosity of cell lysates and shears high-molecular-weight genomic DNA.

   Use one sterile syringe and needle per treatment.
4. To optimize binding of the RNA sample to the column, add an equivalent volume of 70% ethanol to the lysate, load the sample onto an RNeasy mini spin column sitting in a collection tube, and microcentrifuge the column 15 sec at 12,000 to 15,000 rpm.

   Successive aliquots may be loaded onto the column but remember to discard the flow-through after each addition.
5. Wash the column with the two different Qiagen wash buffers provided and microcentrifuge after each buffer addition for 15 sec at 12,000 to 15,000 rpm.
6. Transfer the column to a new collection tube, add 50 µl RNase-free water onto the column and microcentrifuge 1 min at 12,000 to 15,000 rpm. Add an additional 50 µl water to the column and microcentrifuge again to obtain a final RNA sample volume of ~100 µl.

   The resulting total RNA may be used directly for techniques such as RT-PCR where the concentration of RNA is not critical. In this case, the RNA concentration is determined as described in step 10 and the sample stored frozen at −80°C until use; however, to obtain the high concentration of RNA typically needed for use in northern blot analysis, it is recommended that the RNA be precipitated and resuspended in a smaller volume as described below.
7. To concentrate the RNA sample, add 10 µl RNase-free 3M sodium acetate and ~1 ml cold 100% ethanol to the RNA and vortex to mix. Store 2 hr to overnight at −80°C.
8. Collect the RNA precipitate by microcentrifuging 15 min at 12,000 to 15,000 rpm, 4°C. Wash the pellet with 1 ml of cold 70% ethanol.
9. Air dry the RNA pellet for 5 min, resuspend in 20 µl RNase-free water, and incubate in a 65°C water bath for 10 min to completely dissolve the RNA. Add 1 µl (40 U) of RNaseOUT recombinant ribonuclease inhibitor to the sample. Store frozen at −80°C until use (up to 1 year).

10. Calculate RNA concentration by determining the absorbance of an aliquot of the sample at 260 nm and using following information:

One A_{260} unit = 40 µg/ml RNA.

REAGENTS AND SOLUTIONS

*Use Milli-Q-purified water or equivalent in all recipes and protocol steps. For common stock solutions, see **APPENDIX 2A**; for suppliers, see **SUPPLIERS APPENDIX**.*

Blotto

Mix 5 g Carnation nonfat dry milk in 100 ml TBST (see recipe). Heat gently while stirring until milk dissolves. Do not allow the solution to become too hot to touch. Filter and chill on ice. Use fresh.

Final concentrations are 10 mM Tris·Cl, pH 8.0 (APPENDIX 2A), 150 mM NaCl, 0.05% (v/v) Tween 20, and 5% (w/v) nonfat milk.

DRE oligonucleotides, single stranded

Wild-type DRE oligonucleotides:

5′- GATCTGGCTCTTCTCACGCAACTCCG -3′

3′- ACCGAGAAGAGTGCGTTGAGGCCTAG -5′

Mutant DRE oligonucleotides:

5′- GATCTGGCTCTTCTCAC**A**CAACTCCG -3′

3′- ACCGAGAAGAGTG**T**GTTGAGGCCTAG -5′

Bold type indicates the single base mutation within the DRE core recognition site which disrupts AhR DNA binding (Yao and Denison, 1991)

Dextran-coated charcoal

Dissolve 50 mg of ~100,000 g/mol dextran in 100 ml HEDG buffer (see recipe) with stirring, followed by the addition of 500 mg Norit A charcoal (Fisher). Store up to 6 months at 4°C.

Ethidium bromide solution

Mix 50 mg ethidium bromide in 50 ml water and mix well. Store up to 6 months at 4°C in the dark.

CAUTION: *Ethidium bromide is a mutagen and must be handled carefully.*

Ficoll GRA gel-loading buffer

Mix 25 mg bromphenol blue, 2.5 g Ficoll 400, and 10 ml water in a 50-ml conical tube with cap. Mix on a shaker overnight at room temperature. Transfer 1-ml aliquots into 1.5-ml microcentrifuge tubes and microcentrifuge at ~12,000 rpm for 15 min, room temperature. Avoiding the pellet of undissolved material, transfer 800 µl supernatant to new 1.5-ml tubes. Store up to 6 months at room temperature.

Avoid transferring any undissolved dye particles into the final tubes since high concentrations of dyes added to GRA incubations act as DNA intercalating agents and disrupt protein-DNA binding interactions. The presence of excess dye in a given incubation/GRA lane (i.e., uneven addition) is readily apparent by comparing the blue color intensity between lanes of the gel.

HED buffer

Dissolve 5.96 g HEPES (FW 238.3 g/mol) and 372 mg disodium EDTA in 800 ml water, and adjust pH to 7.5 with 10 N NaOH. Add water to 1000 ml. Store up to 1 month at 4°C. Just prior to use, add 154 mg DTT.

Final concentrations are 25 mM HEPES, pH 7.5, 1 mM EDTA, and 1 mM DTT.

HED2G buffer

Dissolve 5.96 g HEPES, 372 mg disodium EDTA, and 200 ml glycerol in 800 ml water, and adjust pH to 7.5 with 10 N NaOH. Add water to 1000 ml. Store up to 1 month at 4°C. Just prior to use, add 154 mg DTT.

Final concentrations are 25 mM HEPES, pH 7.5, 1 mM EDTA, 1 mM DTT, and 20% (v/v) glycerol.

HEDG buffer

Dissolve 5.96 g HEPES, 372 mg disodium EDTA, and 100 ml glycerol in 800 ml water. Adjust pH to 7.5 with 10 N NaOH. Add water to 1000 ml. Store up to 1 month at 4°C. Just prior to use, add 154 mg DTT.

Final concentrations are 25 mM HEPES, pH 7.5, 1 mM EDTA, 1 mM DTT, and 10% (v/v) glycerol.

HEDGK4 buffer

Dissolve 5.96 g HEPES, 372 mg disodium EDTA, 100 ml glycerol, and 29.82 g KCl in 800 ml of water, and adjust pH to 7.5 with 10 N NaOH. Add water to 1000 ml. Store up to 1 month at 4°C. Just prior to use, add 154 mg DTT.

Final concentrations are 25 mM HEPES, pH 7.5, 1 mM EDTA, 1 mM DTT, 10% (v/v) glycerol, and 400 mM KCl.

HEDGK8 buffer

Dissolve 5.96 g HEPES, 372 mg disodium EDTA (disodium), 100 ml glycerol, and 59.65 g KCl in 800 ml of water, and adjust pH to 7.5 with 10 N NaOH. Add water to 1000 ml. Store up to 1 month at 4°C. Just prior to use, add 154 mg DTT.

Final concentrations are 25 mM HEPES, pH 7.5, 1 mM EDTA, 1 mM DTT, 10% (v/v) glycerol, and 800 mM KCl.

HEG buffer

Dissolve 5.96 g HEPES, 372 mg disodium EDTA, and 100 ml glycerol in 800 ml water, and adjust pH to 7.5 with 10 N NaOH. Add water to 1000 ml. Store up to 1 month at 4°C.

Final concentrations are 25 mM HEPES, pH 7.5, 1 mM EDTA, and 10% (v/v) glycerol.

HEGT buffer

Add 5 ml Tween 80 (0.5% v/v final) to 1000 ml HEG buffer (see recipe) using a 5 ml micropipettor in which the opening of the disposable pipet tip has been enlarged to allow easy pipetting. Once the solution has been added, eject the tip into the buffer solution, add a magnetic stir bar, and stir until all of the Tween 80 goes into solution. Leave the tip stirring until the residual amount that remained in the tip after pipetting has also dissolved. Store up to 6 months at 4°C.

HEPES buffer

Dissolve 2.38 g HEPES (10 mM final) into 800 ml water and adjust the pH to 7.5 with 10 N NaOH. Add water to 1000 ml and store up to 2 months at 4°C.

Immunoblot tank buffer

Dissolve 3.03 g Tris·Cl (121.1 g/mol) and 14.4 g glycine into 1000 ml water, and transfer into a storage bottle. There is no pH adjustment. Add 1 g SDS and invert the bottle several times to mix. Store up to 2 months at room temperature.

Final concentrations are 25 mM Tris·Cl, 192 mM glycine, and 0.1% (w/v) SDS.

Immunoblot treatment buffer, 2×

Mix 2.5 ml of 0.5 M Tris·Cl, pH 6.8 (*APPENDIX 2A*), 4.0 ml of 10% (w/v) SDS, 2.0 ml glycerol, 2.0 mg bromphenol blue, and 0.31 g DTT. Add water to 10 ml. Store in 0.5-ml aliquots up to 6 months at −20°C.

Final concentrations are 125 mM Tris·Cl, pH 6.8, 4% (w/v) SDS, 20% (v/v) glycerol, 0.02% bromphenol blue, and 200 mM DTT.

Lysis buffer

Mix 1.5 ml PBS (see recipe), 7.5 µl Triton X-100, 15 µl of 0.5 M EDTA, pH 8.0 (*APPENDIX 2A*), 15 µl of 0.2 M phenylmethylsulfonyl fluoride (PMSF), and 15 µl protease inhibitor cocktail for use with mammalian cell and tissue extracts in DMSO (Sigma). Make fresh immediately prior to use and chill on ice.

Final concentrations are 58 mM Na_2HPO_4, 17 mM NaH_2PO_4, pH 7.5, 68 mM NaCl, 0.5% (v/v) Triton X-100, 5 mM EDTA, 2 mM PMSF, and 1% (v/v) protease inhibitors.

MDH buffer

Dissolve 61 mg $MgCl_2$ and 0.596 g HEPES in 80 ml water, and adjust the pH to 7.5 with 10 N NaOH. Add water to 100 ml. Store up to 1 month at 4°C. Just prior to use, add 154 mg DTT.

Final concentrations are 2 mM $MgCl_2$, 1 mM DTT, and 2 mM HEPES, pH 7.5.

MDHK buffer

Dissolve 610 mg $MgCl_2$, 5.96 g HEPES, and 7.456 g KCl in 800 ml water. Adjust the pH to 7.5 with 10 N NaOH, and add water to 1000 ml. Store up to 1 month at 4°C. Just prior to use, add 154 mg DTT.

Final concentrations are 3 mM $MgCl_2$, 1 mM DTT, 25 mM HEPES, pH 7.5, and 100 mM KCl.

MOPS, 10×

Combine 42 g MOPS (FW 209.26), 17 ml of 3 M sodium acetate, and 20 ml of 0.5 M EDTA (disodium; *APPENDIX 2A*) in 900 ml of water. Adjust pH to 7.0 with 10 N NaOH and add water to 1000 ml. Store up to 1 month at 4°C.

Final concentrations are 200 mM MOPS, pH 7.0, 50 mM sodium acetate, and 10 mM EDTA.

NaOH/SSC

Mix 2.5 ml of 10 N NaOH (*APPENDIX 2A*) and 25 ml of 20× SSC (see recipe), and add water to 500 ml. Store up to one month at room temperature.

Final concentrations are 500 mM NaOH, 150 mM NaCl, and 15 mM sodium citrate.

Northern hybridization buffer

Combine 12.5 ml of 1 M monobasic sodium phosphate, pH 7.5, 0.1 ml of 0.5 M EDTA, pH 7.5 (*APPENDIX 2A*), 35 ml of 10% (w/v) SDS (*APPENDIX 2A*), and water to 50 ml. Store up to 6 months at room temperature.

Final concentrations are 25 mM sodium phosphate, pH 7.5, 1 mM EDTA, and 7% (w/v) SDS.

Northern sample buffer

Combine 0.75 ml formamide, 0.24 ml formaldehyde, 0.15 ml of 10× MOPS (see recipe), and 0.2 ml of 50% (v/v) glycerol/0.25% bromphenol blue in water. Store up to 1 month at −20°C.

Oligonucleotide reannealing buffer

Dissolve 405 mg Tris·Cl, 132 mg $MgCl_2$, 16 mg spermidine, and 242 mg EDTA in 45 ml water, and adjust the pH to 7.5 with 12 N HCl. Adjust volume to 50 ml with water. Store up to 6 months at −20°C. Just prior to use, add 154 mg DTT.

Final concentrations are 67 mM Tris·Cl, pH 7.5, 1.3 mM $MgCl_2$, 7 mM DTT, 1.3 mM spermidine, and 13 mM EDTA.

PAGE running gel buffer, 4×

Dissolve 36.3 g Tris·Cl (121.1 g/mol) in 150 ml water and adjust the pH to 8.8 with 12 N HCl. Bring to 200 ml with water. Store up to 1 month at 4°C in the dark.

Final concentration is 1.5 M Tris·Cl, pH 8.8.

PAGE stacking gel buffer, 4×

Dissolve 3.0 g Tris (121.1 g/mol) in 40 ml water and adjust the pH to 6.8 with 12 N HCl. Bring to 50 ml with water. Store up to 1 month at 4°C in the dark.

Final concentration is 500 mM Tris·Cl, pH 6.8.

Phosphate buffered saline (PBS)

Dissolve 1.55 g $Na_2HPO_4 \cdot 7\ H_2O$, 0.23 g NaH_2PO_4, and 400 mM NaCl in 80 ml water, and adjust to pH 7.4 with 1 N NaOH. Add water to 100 ml. Store up to 3 months at room temperature.

Final concentrations are 58 mM Na_2HPO_4 and 17 mM NaH_2PO_4, pH 7.4, and 68 mM NaCl.

Sephadex G-50 spin column

There are numerous commercially available Sephadex-G-50 spin columns for DNA radiolabeling experiments (such as the Spin-pure G-50 columns from CpG) and detailed instructions are provided for their use by the manufacturer. Alternatively, spin columns are relatively easy to make. To prepare a spin column, plug a 1-ml plastic syringe with a small amount of glass wool and fill the syringe with a Sephadex G-50 slurry in TE buffer (see recipe) using a long 9-in. Pasteur pipet. Insert the syringe into a 15-ml Corex tube which contains a capless 1.5-ml microcentrifuge tube for sample collection (the tip of the syringe should reach into the tube itself). Centrifuge the column in a swinging bucket rotor in a benchtop centrifuge for 2 min at 1000 × g, room temperature. Discard the capless microcentrifuge tube containing the excess packing buffer and replace it with a clean capless tube and reinsert the column into the tube. This spin column is now ready for radiolabeled sample addition. Use fresh.

Sodium acetate, 3 M

Dissolve 123 g sodium acetate in 240 ml water (RNase-free if appropriate) and adjust pH to 4.6 with glacial acetic acid. Add water to 500 ml. Store up to 1 year at room temperature.

SSC, 0.5×, 2×, 10×, and 20×

Make 20× SSC by dissolving 175.3 g NaCl and 88.2 g sodium citrate into 600 ml water. Add water to 1000 ml. Store up to 2 months at room temperature. Dilute to appropriate concentration (e.g., 0.5×, 2×, 10×) as necessary.

Final concentrations of the 20× solution are 3 M NaCl and 300 mM sodium citrate.

Stripping buffer

Dissolve 0.757 g Tris·Cl, 2 g SDS, and 781 µl 2-mercaptoethanol in 80 ml water. Adjust the pH to 6.8 with 12 N HCl and add water to 100 ml. Store up to 1 month at room temperature.

Final concentration is 62.5 mM Tris·Cl, pH 6.8, 2% (w/v) SDS, and 100 mM 2-mercaptoethanol.

T4 kinase buffer

Mix 660 µl of 1 M Tris·Cl, pH 7.5 (*APPENDIX 2A*), 10 µl of 1M spermidine, 100 µl of 1 M $MgCl_2$, 150 µl of 1 M DTT, 40 µl of 500 mg/ml BSA, and 100 ml water. Store in 50-µl aliquots up to 1 year at −80°C.

Final concentrations are 623 mM Tris·Cl, pH 7.5, 9 mM spermidine, 94 mM $MgCl_2$, 141 mM DTT, and 20 mg (w/v) BSA.

TAE buffer, 1× and 10×

Mix 67 ml of 1 M Tris·Cl, pH 8.0 (*APPENDIX 2A*), 11 ml of 3 M sodium acetate (see recipe), and 20 ml of 0.5 M EDTA, pH 8.0 (*APPENDIX 2A*) in 700 ml of water. Adjust volume to 1000 ml. Store up to 4 months at room temperature. Dilute with water to make 1× working solution.

Final concentrations are 67 mM Tris·Cl, pH 8.0, 33 mM sodium acetate, and 10 mM EDTA.

TBS (Tris buffered saline)

Dissolve 8.77 g NaCl in 800 ml water. Add 10 ml of 1 M Tris·Cl, pH 8.0 (*APPENDIX 2A*). Add water to 1000 ml. Store up to 6 months at room temperature.

Final concentrations are 10 mM Tris·Cl, pH 8.0 and 150 mM NaCl.

TBST

Mix 50 µl of Tween 20 in 100 ml TBS (see recipe). Prepare fresh.

Final concentrations are: 10 mM Tris, pH 8.0, 150 mM NaCl, 0.05% (v/v) Tween 20.

TE buffer

Dissolve 1.21 g Tris (121.1 g/mol) and 0.37 g disodium EDTA into 800 ml water. Adjust the pH to 8.0 with 12 N HCl. Add water to 1000 ml. Store up to 6 months at room temperature.

Final concentrations are 10 mM Tris·Cl, pH 8.0, and 0.1 mM EDTA.

Towbin transfer buffer

Dissolve 3.03 g Tris·Cl (121.1 g/mol), 14.4 g glycine, 0.1 g SDS, and 200 ml methanol into 600 ml water. There is no pH adjustment. Add water to 1000 ml. Store up to 1 month at room temperature.

Final concentrations are 25 mM Tris·Cl, 192 mM glycine, 20% (v/v) methanol, and 0.01% (w/v) SDS.

Tris/SSC

Mix 50 ml of 1 M Tris·Cl, pH 7.5 (*APPENDIX 2A*) with 25 ml of 20× SSC (see recipe), and add water to 500 ml. Store up to 2 months at room temperature.

Final concentrations are 100 mM Tris·Cl, pH 7.5, 150 mM NaCl, and 15 mM sodium citrate.

COMMENTARY

Background Information

The existence of the AhR signal transduction pathway was originally suggested by the results of biochemical and genetic studies on the mechanism of induction of cytochrome P_1 450 (now referred to as CYP1A1). Utilizing a dextran-coated charcoal (DCC) binding assay, Poland and coworkers (1976) provided the first direct evidence for the existence of a [^{3}H]TCDD-specific binding protein (the AhR) in hepatic cytosol from mice. Subsequent studies revealed that the mechanism of AhR action resembled that established for steroid hormone receptors and their regulation of gene expression, although the AhR is now known to be a member of a distinctly different family of nuclear transcription factors termed basic helix-loop-helix-PAS proteins (Schmidt and Bradfield, 1996); however, researchers examining AhR and AhR action have continued to adapt experimental approaches and techniques used in the analysis of steroid hormone receptor

action to characterize the AhR and AhR-dependent gene expression. The methodological approaches described in this unit allow measurement and analysis of each step of the AhR signal transduction pathway, from initial ligand binding to gene expression.

The presence and/or expression of the AhR and Arnt in cell or tissue extracts has been demonstrated by measurement of AhR mRNA using northern blot (Hoffman et al., 1991; Burbach et al., 1992) or RT-PCR analysis (Hakkola et al., 1997), and AhR protein (using immunoblot analysis; Holmes and Pollenz, 1997). Although detection of mRNA for a given gene product in a sample extract clearly demonstrates expression of the desired gene, it provides no information as to whether the resulting protein is actually produced in the target cell/tissue. Confirmation of the presence of the AhR/Arnt in a given cell or tissue extract requires use of an AhR- or Arnt-specific antibody in immunoprecipitation and/or immunoblot analysis. In addition, these reagents can also be used to demonstrate AhR/Arnt expression in intact tissues and cells using immunohistochemical and in situ approaches (Tscheudschilsuren et al., 1999). These approaches and others have been used to demonstrate the presence and expression of the AhR in a wide variety of species and tissues (Hahn, 1999). In addition to direct detection of the proteins, the presence of the AhR and/or AhR-dependent signal transduction pathway can be determined by functional analysis (AhR ligand binding, nuclear localization, and DNA binding and gene expression).

Several approaches have been described for the analysis of AhR ligand binding and the majority of these assays utilize [^{3}H]TCDD as the radioligand. These assays are based on the measurement of bound [^{3}H]TCDD in the absence and presence of an excess of unlabeled competitor ligand (generally TCDF). The reduction in [^{3}H]TCDD ligand binding in the presence of TCDF provides a quantitative measure of the amount of [^{3}H]TCDD specific binding. The DCC binding assay, a procedure based on the ability of the charcoal to bind and remove unbound and loosely bound [^{3}H]TCDD from the binding incubation, was used in initial analysis of AhR ligand binding (Poland et al., 1976); however, the extremely high levels of nonspecific [^{3}H]TCDD binding commonly observed with this assay made accurate and consistent ligand binding assessment problematic. The hydroxyapatite (HAP) assay (see Alternate Protocol 1) is based on the ability of proteins in the [^{3}H]TCDD binding incubations to bind to the HAP and the free or loosely bound radiolabel is removed by repeated washing of the HAP pellet with buffer containing Tween 80 detergent (Gasiewicz and Neal, 1982). A similar rapid binding assay based on the ability of protamine sulfate to quantitatively precipitate [^{3}H]TCDD binding proteins has been described (Denison et al., 1984) and like the HAP assay, free or loosely bound radiolabel is removed by repeated washing of the pellet with buffer containing detergent. Perhaps the most sensitive AhR ligand binding assay that has been developed utilizes a high-specific-activity [^{125}I]2-iodo-3,7,8-trichlorodibenzo-*p*-dioxin ligand (Bradfield and Poland, 1988); however, the relatively short half-life of the radiolabel requires periodic preparation of new radio-iodination reactions to be carried out. In addition, the limited availability of the reagent necessary to prepare the radioiodinated ligand and the additional biohazard and containment associated with the use of this radiolabel, makes this assay somewhat impractical for general ligand binding analysis. Still, when extremely high sensitivity ligand binding assays are needed, use of the [^{125}I]ligand binding assay should be considered. Even given its slightly lower sensitivity, the relatively high specific activity of the [^{3}H]TCDD ligand (10 to 50 Ci/mmol) is generally sufficient for most analysis, and coupled with the commercial availability of this radioligand in high purity makes it the ligand of choice for most AhR ligand binding analysis.

The HAP assay has been used by numerous investigators and it allows relatively rapid binding analysis of large numbers of samples. It is the approach the authors most often use when determining ligand binding affinity (i.e., by saturation binding analysis) and for large-scale screening for competitive AhR ligands; however, although the HAP assay might reveal a decrease in [^{3}H]TCDD binding in the presence of a competitor chemical, this assay does not absolutely confirm that the reduction in bound radioactivity actually results from competitive displacement of [^{3}H]TCDD from the AhR, since only radioactivity present in the HAP pellet is being measured. Since it is always possible that the reduction in binding can result from a loss of [^{3}H]TCDD binding to some nonspecific site or sites, it is always prudent to confirm the direct competitive displacement of [^{3}H]TCDD from the AhR by unknown chemicals using the SDG assay (see Basic Protocol 1). This method allows separation of proteins

by size and shape in the gradient, and as such, it allows direct determination and visualization of the binding of [^{3}H]TCDD to the cytosolic AhR and its competitive displacement by unlabeled AhR ligands (Okey et al., 1979; Tsai and Okey, 1981; Denison et al., 1986). The presence of other [^{3}H]TCDD binding peaks and elevated binding background commonly observed with radiolabeled material of lower purity (resulting from radiolysis of the chemical and/or due to the reduced purity of the starting material used for [^{3}H]-labeling) is readily observed using the SDG assay. In addition to analysis of cytosolic AhR ligand binding, SDG analysis can also be carried out using nuclear extracts from intact cells exposed to [^{3}H]TCDD in the absence and presence of unlabeled TCDF competitor. Although the SDG method is somewhat time consuming and is not amenable for analysis of large numbers of samples (as compared to the HAP method), it does allow measurement of AhR ligand binding and direct confirmation of the ability of a chemical or chemicals to displace [^{3}H]TCDD from the AhR. Overall, the HAP and SDG assays provide complementary approaches to measure ligand binding, with each assay having unique advantages and disadvantages.

Measurement of AhR transformation and DNA binding is carried out using gel retardation analysis (see Basic Protocol 2) and can be performed using either crude cytosol or nuclear extracts. Gel retardation analysis provides a sensitive and specific assay system to examine and characterize the binding of transformed ligand AhR complex to its specific DNA recognition site, the dioxin responsive element (DRE), and is based on the ability of protein-bound DNA complexes to be separated from protein-free DNA in nondenaturing polyacrylamide gels (Denison et al., 1988a,b; Denison and Yao, 1991). This technique is a significant improvement over earlier techniques that measured the DNA binding activity of transformed AhR complexes by their ability to bind to DNA cellulose (Cuthill and Poellinger, 1988; Prokipcak et al., 1990). This latter assay only assesses the ability of the AhR complex to bind to DNA and does not differentiate between nonspecific and specific DNA binding. Although transformation of the AhR into its DNA binding form requires its dimerization with Arnt, a nuclear protein, AhR transformation and DNA binding in vitro can be carried out using cytosol preparations (Denison and Yao, 1991; Yao and Denison, 1991). This is due to the fact that Arnt is readily released from the nucleus during cell homogenization and thus is present and available to bind to the AhR in cytosol preparations. Thus, gel retardation analysis using cytosolic preparations provides an avenue for rapid analysis of large numbers of chemicals or chemical mixtures for their ability to stimulate AhR transformation and DNA binding in vitro; however, although this method allows demonstration of the direct ability of a chemical to activate the AhR in vitro, it does not provide any information as to whether the chemical can stimulate AhR transformation and DNA binding in intact cells. Final confirmation of this is carried out by gel retardation analysis of nuclear extracts prepared from control and chemical-treated cells. Detection of transformed AhR complexes in nuclear extracts from exposed cells in a ligand-dependent manner confirms the ability of the inducing chemical to stimulate AhR transformation, nuclear accumulation, and DNA binding of the ligand AhR complex in intact cells. The DNA binding activity of the nuclear AhR complexes is indirectly confirmed by the fact that these AhR complexes are only released from the nuclei by conditions that disrupt protein DNA interactions (i.e., high salt or the addition of DNA intercalating agents). The presence of nuclear AhR complexes can also be demonstrated by SDG analysis of nuclear extracts from cells treated with [^{3}H]TCDD in the absence or presence of unlabeled TCDF (Prokipcak et al., 1990).

The above methodological approaches allow detection and characterization of the functionality of the AhR; however, the mere presence of the AhR and Arnt as well as nuclear accumulation of transformed AhR complexes do not guarantee that the AhR signal transduction pathway is fully functional in a given tissue or cell line. Since AhR and Arnt have been identified in cells which lack inducible AhR-dependent gene expression (Walsh et al., 1996), the functional activity of the AhR signal transduction pathway should be confirmed by demonstration of TCDD-inducible, AhR-dependent gene expression (see Basic Protocols 4 and 5). Inducible expression of a gene known to be regulated by the AhR (such as CYP1A1 and CYP1B1) provides indirect evidence for the presence of a functional AhR signaling system in the target tissue. Measurement of induction of CYP1A1/1B1 gene expression is readily accomplished by examining mRNA levels for each enzyme by northern blot analysis and/or measurement of increased CYP-dependent enzyme activity (i.e., ethoxyresorufin *O*-deethylase activity in the case of CYP1A1;

Safe, 1990). Demonstration of TCDD-inducible expression of a DRE-linked reporter gene in transfected cells has also been used to confirm the presence of a fully functional AhR signal transduction pathway in a given cell line (Garrison et al., 1996). In some instances, CYPs are not inducible in a given tissue/cell, although a functional AhR signaling pathway is present. In this instance, analysis of the expression (mRNA, protein) of other genes known to be induced in a TCDD- and AhR-dependent manner (reviewed in Denison et al., 1998a) should be carried out. Overall, the above procedures for detection of the AhR, Arnt, and AhR-dependent gene expression are well established and all of the necessary reagents are readily available from researchers and commercial sources.

Critical Parameters and Troubleshooting

Sucrose density gradient (SDG) analysis of cytosolic AhR binding

Perhaps one of the most important parameters to consider in the AhR ligand binding assay (see Basic Protocol 1) is in regards to the [^{3}H]TCDD ligand itself, specifically in regard to its radio- and chemical purity. If the batch of [^{3}H]TCDD used for ligand binding assay is not of high purity, then increased background nonspecific binding can occur, leading to inaccurate estimates of AhR ligand binding, causing binding affinity to be inaccurate. Another important issue with regard to the amount of [^{3}H]TCDD in a binding assay is when the competitive binding by weak AhR ligands is being examined. If [^{3}H]TCDD is added to an incubation at much higher concentrations than needed to saturate the AhR (i.e., 20 to 40 nM), it is very unlikely that a weak ligand (one with a K_d in the low to mid micromolar range) would be able to compete effectively. This is due to the fact that the "free" [^{3}H]TCDD (which has a K_d in the picomolar range) would compete more effectively for the AhR because of its significantly greater binding affinity. In this instance, the authors have found that by increasing the concentration of the weak competitor and reducing the [^{3}H]TCDD concentration to just saturating (i.e., 5 nM per 5 mg cytosolic protein/ml), thus minimizing the amount of "free" [^{3}H]TCDD available to compete, that direct ligand binding of weak AhR ligands to the AhR can be observed (Denison et al., 1998c).

A second important parameter to consider with the SDG assay is that of the concentration of DCC used to strip unbound and loosely bound [^{3}H]TCDD from solution prior to centrifugation. The concentration of DCC added to the incubation is critical since too little will not remove the [^{3}H]TCDD and too much can strip [^{3}H]TCDD off the AhR. The authors have found that the DCC concentration described in this unit is optimal for rat, mouse, and guinea pig cytosolic AhRs; however, the DCC concentration should be optimized for each specific system and extract. For those AhRs with low TCDD binding affinity (i.e., human and nonmammalian species) DCC at the above concentration will likely strip off some of the ligand from the AhR, resulting in underestimation or lack of observable [^{3}H]TCDD specific binding. In fact, this is the reason that little [^{3}H]TCDD binding to human AhR was detected for many years. In order to analyze [^{3}H]TCDD binding to these lower affinity AhRs, the DCC concentration must be reduced. Preliminary SDG analysis using various DCC concentrations will allow optimization of the concentration needed to detect ligand binding in specific samples. In addition, sodium molybdate (20 mM) has been shown to help stabilize the AhR and is commonly included in buffers when analysis of low affinity AhR is planned.

Hydroxyapatite (HAP) solid-phase analysis of AhR ligand binding

Although the HAP assay (see Alternate Protocol 1) is less complicated than the SDG assay, there are still several aspects that need to be considered. Like the SDG assay, concerns regarding the purity and solubility limitations of TCDD also apply in the HAP assay and as a rule, the authors almost never exceed 10 nM [^{3}H]TCDD in an incubation containing 2 mg protein/ml. One major problem which can arise with the HAP assay is high [^{3}H]TCDD background activity in the HAP pellets. Inclusion of one or more additional washes with the Tween 80–containing wash buffer should reduce the background to acceptable levels, although it should be noted that the background [^{3}H]TCDD will never drop to zero (see Table 4.8.1 for an example of typical binding and nonspecific background results). Although one might be tempted to increase the amount of Tween 80 in the wash buffer in order to reduce background activity, it is best not to do this since the increased detergent could also strip the [^{3}H]TCDD off the AhR. In fact, for those receptors with lower TCDD binding affinities

(i.e., humans and nonmammalian species), the amount of detergent currently in the assay may strip some ligand from these AhRs. Thus, the HAP assay may need to be modified to accurately measure AhR ligand binding in species with low-affinity AhRs. Reductions in the amount of Tween 80 in the wash buffer and inclusion of additional wash steps would be possibilities to consider if problems arise in these specific situations. Another parameter that is important if alterations in the assay protocol are being considered is the limited protein binding capacity of the HAP. If the amount of specific binding detected by HAP is relatively low, do not immediately assume that it is possible to simply add more incubation mixture to the HAP pellet. If the protein binding capacity of the HAP pellet is exceeded, then the additional protein will not bind but be lost during the buffer washes, resulting in an underestimation of ligand binding activity.

Gel retardation analysis of AhR-DNA binding

There are several critical parameters relative to the electrophoresis and binding reactions that can affect the results obtained with the gel retardation assay method. Using the low ionic strength TAE buffer electrophoresis conditions described for the gel retardation assay, buffer recycling is absolutely required. Failure to recycle the buffer will exhaust its buffering capacity and the resulting change in pH of several units which develops between the top and bottom reservoirs will disrupt protein DNA complex formation. Alternative buffers using a greater buffering capacity have been described, but their utility in analysis of AhR-DNA binding remains to be determined.

The type and amount of nonspecific carrier DNA added to the binding incubation is also critically important in gel retardation assays. The authors have tested numerous types of carrier DNAs and found that poly(dI·dC) consistently produced the greatest amount of TCDD-inducible protein DNA complex formation. Other carrier DNAs do work in the assay, but they were found to competitively reduce the amount of TCDD-inducible complex at only moderate competitor concentrations. Although high concentrations of poly(dI·dC) will also competitively inhibit TCDD-inducible protein [^{32}P]DRE complex formation, transformed AhR complexes bind to poly(dI·dC) at a 1400-fold lower affinity compared to the DRE (Yao and Denison, 1991), and as long as the amount of poly(dI·dC) is maintained at a moderate ratio it is an effective carrier DNA in AhR gel retardation assays. On the other hand, if too little or no carrier DNA is added to DNA binding reactions using nuclear extracts, all of the radiolabeled probe will remain bound in the well and none will enter the gel. In contrast, if too little or no carrier DNA is added to DNA binding reactions using cytosolic extracts, the complexes still enter the gel and are resolved normally, but additional protein DNA complexes will be produced and the total amount of AhR-DRE complex formation is reduced (Yao and Denison, 1991); therefore, the optimal ratio of protein to poly(dI·dC) must be maintained. The poly(dI·dC) concentration used with cytosolic samples is generally in the range of 100 to 400 ng per incubation and the amount for nuclear extracts is 1 to 3 μg per incubation; however, the exact amount of poly(dI·dC) needed in a given incubation is not only species- and tissue-specific, but also dependent upon the protein concentration and the specific lot of poly(dI·dC) used. Identical concentrations (based on their absorbance at 260 nm) of different lots of the same poly(dI·dC) product (from the same company) are not necessarily equally effective as carrier DNA. Thus, with each new lot number of poly(dI·dC) used, the optimal concentration needed for maximal AhR DRE complex formation needs to be established.

Immunoblot of AhR and Arnt

A key issue with regard to the immunoblotting protocols (see Basic Protocol 3) is to minimize proteolysis and degradation of the protein sample. This is manifested by smearing of the proteins in the gel and/or loss of proteins. Accordingly, keep the samples on ice prior to boiling and make sure to add sufficient amounts of the protease inhibitor cocktail to the lysis buffer. It is also important to note that AhR antibodies will bind nonspecifically to proteins in addition to the AhR and as such, multiple antibody positive bands will always be present on immunoblots using AhR antibodies. In the authors' hands, two smaller bands always appear on AhR immunoblots, one at ~45 and one at ~25 kDa. Immunoblots with Arnt antibodies tend to be much cleaner.

Detection by RT-PCR and northern blot analysis

Perhaps the most important factor in ensuring success in RT-PCR (see Basic Protocol 4) or northern blot analysis (see Basic Protocol 5) is the quality of the RNA sample. Since RNases

are very stable, ubiquitous, and active enzymes, it is important to avoid contaminating the RNA sample with them either during the RNA isolation procedure or during RNA analysis. A clean work area, and the use of gloves and sterile disposable plasticware when working with RNA will help minimize RNase contamination. RNA obtained from the Qiagen RNeasy columns is generally of high purity; however, other methods of RNA isolation may not yield such clean RNA. The ratio of the absorbance readings at 260 and 280 nm (A_{260}/A_{280}) will give some indication of the purity of the sample. Pure RNA has an A_{260}/A_{280} ratio of 1.8 to 2.1 in TE buffered at pH 7.5 to 8.0. A low A_{260}/A_{280} ratio indicates contamination with protein and may require an additional acidic extraction step with phenol/chloroform/isoamyl alcohol, pH 4.3 to 4.7 (*APPENDIX 3A*). The integrity of the RNA can also be determined by examining an aliquot of the RNA by denaturing agarose gel electrophoresis and ethidium bromide staining. A nondenaturing gel can be used but be sure to use nuclease-free water for the gel and dye. The 18S and 28S ribosomal bands should appear as sharp bands and there should be ~2:1 ratio between ethidium bromide staining of the 28S and 18S bands. With significant RNA degradation, the 28S band will degrade to an 18S-like species. If there is a large amount of smearing towards the positive electrode or if the 18S band appears more intense than the 28S band it is best to isolate fresh RNA before continuing with the experiment.

When conducting RT-PCR using primers other than those indicated in this protocol, a number of variables including primer concentration, magnesium chloride concentration, annealing temperature, and cycle number may have to be optimized and determined empirically (*APPENDIX 3C*). Optimal magnesium chloride concentration can range from 1.5 to 4.0 mM. The use of a gradient cycler such as the Robocycler Gradient 40 from Stratagene allows rapid optimization of several parameters simultaneously.

Anticipated Results

Ligand binding

Techniques for measurement of AhR ligand binding can vary significantly; however, the ultimate quantitation of the amount of [^{3}H]TCDD-specific binding by these methods is essentially the same. In all cases, the amount of [^{3}H]TCDD bound to the AhR (specific binding) is the difference between the amount of [^{3}H]TCDD bound in the absence of competitor (total binding) and the total amount of [^{3}H]TCDD bound in the presence of TCDF or other chemical (nonspecific binding).

HAP assay results of the binding of [^{3}H]TCDD to guinea pig hepatic cytosol are shown in Table 4.8.4. Subtraction of the [^{3}H]TCDD (dpms) present in a nonspecific binding sample (column 2) from the [^{3}H]TCDD (dpms) present in the total binding sample (column 1) yields the amount of [^{3}H]TCDD specifically bound to proteins in the HAP pellet (column 3); however, final binding results are expressed as the number of fmoles of [^{3}H]TCDD specifically bound/mg protein. To normalize the specific binding to that in 1 mg of protein, the HAP-specific binding results in column 3 are multiplied by 2.5, since 0.4 mg protein (0.2 ml of the original 2 mg/ml incubation) was added to the HAP pellet. The resulting values (column 4) represent the total amount of [^{3}H]TCDD specific binding (dpms) per milligram cytosolic protein. To determine the actual concentration of [^{3}H[TCDD bound, the disintegrations per minute/milligram protein value must be corrected to a molar concentration. This is accomplished by simply correcting the specific binding value using the specific activity of the [^{3}H]TCDD used in the experiment. The specific activity of [^{3}H]TCDD commonly used for AhR binding assays is in the range of

Table 4.8.4 Results and Calculations of the Specific Binding of [^{3}H]TCDD[a] to Guinea Pig Hepatic Cytosol as Determined Using the HAP Binding Assay

Total binding (dpm/HAP pellet)	Nonspecific binding (dpm/HAP pellet)	Specific binding (dpm/HAP pellet)	Specific binding (dpm/mg protein)	Specific binding (fmoles/mg protein)
3697	2212	1485	3712	84.4
3710	2172	1538	3845	86.6
3617	2235	1382	3455	77.8

[a]The specific activity of the radiolabel was 20 Ci/mmol (1 Ci = 2.22×10^{12} dpm).

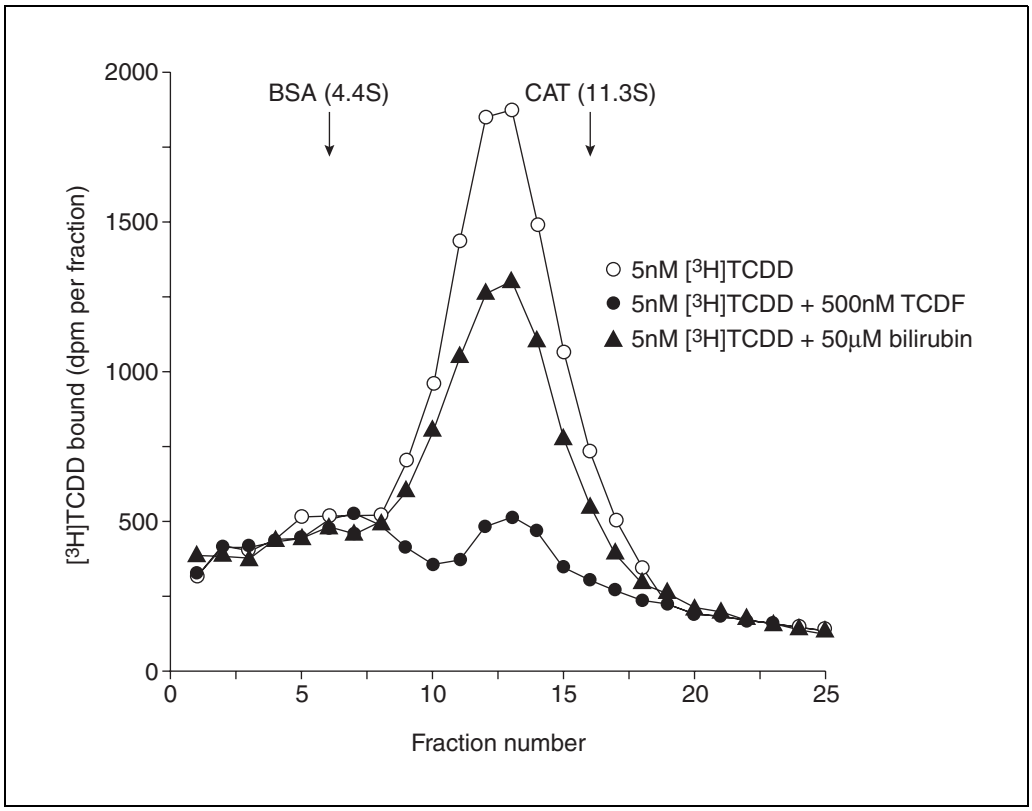

Figure 4.8.2 Sucrose density gradient analysis of the competitive binding between [^{3}H]TCDD, TCDF, and bilirubin to guinea pig hepatic cytosol. Guinea pig hepatic cytosol (5 mg protein/ml) was incubated with 5 nM [^{3}H]TCDD in the absence or presence of 1 μM TCDF or 50 μM bilirubin for 1 hr at 4°C. Aliquots (300 μl) of each incubation were analyzed by sucrose density gradient centrifugation.

10 to 30 Ci/mmol. For these experiments, the specific activity of the radiolabel was 20 Ci/mmol, and since 1 Ci is equal to 2.22×10^{12} dpm, the specific activity of the radiolabeled [^{3}H]TCDD is 4.44×10^{13} dpms/mmol or 44.4 dpms/fmole. The specific binding (dpm/milligram) is divided by the specific activity of the [^{3}H]TCDD (44.4 dpm/fmole) and the final calculated amount of [^{3}H]TCDD specific binding to guinea pig hepatic cytosol in these triplicate HAP binding incubations was between 77.8 and 86.6 fmoles/mg protein (column 5).

With the SDG assay, the calculation of specific binding requires comparison of the radioactivity gradient profiles of two different tubes after alignment of one tube of total binding ([^{3}H]TCDD alone) and one tube of nonspecific binding ([^{3}H]TCDD + TCDF). In the standard SDG experiments, [^{14}C]BSA and [^{14}C]CAT are included in each gradient as internal sedimentation control. Alignment of the [^{14}C]BSA and [^{14}C]CAT peaks between two gradients corrects for any differences in the linearity between the two gradients and allows for a more accurate calculation of [^{3}H]TCDD-specific binding. An example of a typical sucrose gradient result of [^{3}H]TCDD specific binding to guinea pig hepatic cytosol (the same cytosol used in the HAP assay) after alignment of the internal markers is shown in Figure 4.8.2. The specific binding peak is readily identified by those fractions in the total binding sample gradient ([^{3}H]TCDD) which have higher amounts of radioactivity than those in the corresponding fractions of the nonspecific binding gradient ([^{3}H]TCDD + 500 nM TCDF). Thus, the [^{3}H]TCDD-specific binding peak in the results presented in Figure 4.8.2 is contained within fractions 9 to 18. The total specific binding (7171 dpms) in the gradient in Figure 4.8.2, was calculated by subtracting the sum of the radioactivity in fractions 9 to 18 of the nonspecific binding sample (3789 total dpms) from the sum of the radioactivity in fractions 9 to 18 of the total binding sample (10,960 total dpms). To normalize the specific binding to that in 1 mg of protein, the total specific binding value (7171 dpms) was divided by 1.67, since 1.67 mg of cytosolic protein (0.3 ml of the 5 mg/ml incubation) was layered onto the gradient, resulting in a specific binding 4294 dpms/mg protein. Correction for the specific activity of

the [^{3}H]TCDD (44.4 dpms/fmole) revealed that the specific binding of [^{3}H]TCDD to guinea pig hepatic cytosol in the sample gradient in Figure 4.8.2 was 96.7 fmoles/mg protein. Although multiple gradients must be run in order to obtain a statistically accurate measure of the variability of this value, the specific binding measured by the SDG assay is comparable to that obtained using the HAP assay.

The relative competitive binding by another AhR ligand can also be compared using HAP and SDG assays. In this instance, the amount of specific binding is determined using both TCDF and the additional competitor for nonspecific binding measurements. An example of the ability of 50 μM bilirubin (a relatively weak ligand) to compete with [^{3}H]TCDD-specific binding is shown in Figure 4.8.2. Subtraction of the amount of radioactivity in fractions 9 to 18 of the bilirubin gradient (8179 dpms) from that in the same fractions of the total binding gradient (10,960 dpms) provides a measure of the competitive displacement of [^{3}H]TCDD binding by bilirubin (2781 dpms, corrected for protein to 1665 dpms/mg). Given that the amount of displacement of [^{3}H]TCDD obtained with TCDF (4294 dpms/mg) represents 100% displacement, the ratio of the amount of displacement obtained with bilirubin to that obtained with TCDF provides a relative measure of the potency of bilirubin. This comparison indicates that 50 μM bilirubin was only effective at displacing 42% of the total [^{3}H]TCDD-specific binding in this guinea pig hepatic cytosolic sample (2781 divided by 4294 dpm/mg). Not only can similar analysis of the ability of other chemicals to compete with [^{3}H]TCDD binding to the AhR be carried out using the HAP assay, many more samples can be analyzed at one time using the HAP assay.

In addition to allowing gradient alignment and more accurate measurements of ligand binding, inclusion of the internal standards [^{14}C]BSA and [^{14}C]CAT also allow accurate estimation of the sedimentation coefficient (S) of the AhR (i.e., the [^{3}H]TCDD-specific-binding peak) in a given gradient. Sedimentation coefficients provide some insight into the size and shape of a protein or protein complex since these factors affect the movement of the proteins through the gradient during centrifugation. With regard to the AhR, a sedimentation coefficient of 8S to 10S for the AhR corresponds to the >300 kDa multiprotein cytosolic form of the AhR (bound with XAP2, p20 and 2 molecules of hsp90), a sedimentation coefficient of 4S to 5S corresponds to the monomeric AhR subunit (~100 kDa), and a sedimentation coefficient of ~6S corresponds to the AhR-Arnt heterodimer (~200 kDa). Direct comparison of the position of the peak of the [^{3}H]TCDD-specific binding in Figure 4.8.2 (fraction 12.5) to that of the two internal sedimentation controls—[^{14}C]BSA (4.4S); fraction 6—and [^{14}C]CAT (11.3S); fraction 16—reveals that the [^{3}H]TCDD binding peak has a calculated sedimentation coefficient of ~8.9S, corresponding to the multiprotein AhR complex.

DNA binding

Typical autoradiograms from gel retardation analysis of nuclear and cytosolic extracts are shown in Figure 4.8.3. For orientation on the figure, samples are loaded at the top of the gel and they migrate downward. The fastest moving band at the bottom of each of the lanes represents unbound [^{32}P]DNA, while the slower moving bands represent individual protein-DNA complexes. There are distinct differences between the protein complexes formed using nuclear and cytosolic extracts. With nuclear extracts (Fig. 4.8.3A) one major and two minor protein DNA complexes are detected, while with cytosolic extracts (Fig. 4.8.3B), two major protein DNA complexes are observed. With both extracts, complex A represents the TCDD-AhR-DRE complex and is formed in a TCDD-inducible manner—compare the DMSO- (lane 1) versus TCDD-treated (lane 2) samples. Competitive gel retardation analysis demonstrates the specificity of this protein DNA complex for the DRE since it is eliminated by the addition of a 100-fold excess of unlabeled DRE oligonucleotide (lane 3), but not by an excess of DNA containing a mutated DRE sequence which fails to bind the AhR (lane 4 of Fig. 4.8.3A and lane 6 of Fig. 4.8.3B). The other major protein DNA complex formed when using cytosolic extracts (complex B) represents a constitutive protein DNA complex (i.e., it is formed in the absence and presence of TCDD). Competitive displacement of protein-[^{32}P]DNA complex B by an excess of single-stranded DNA oligonucleotide (lane 4 of Fig. 4.8.3.B), but not by purified double-stranded DRE-containing DNA which lacks any single-stranded DNA (lane 5 of Fig. 4.8.3B), indicates that complex B represents the binding of a protein or proteins to the small amount of single-stranded DRE oligonucleotide remaining after reannealing and ^{32}P-labeling. The absence of this complex when the DRE oligonucleotide is ^{32}P-labeled by Klenow fill-in reactions (which does not generate any

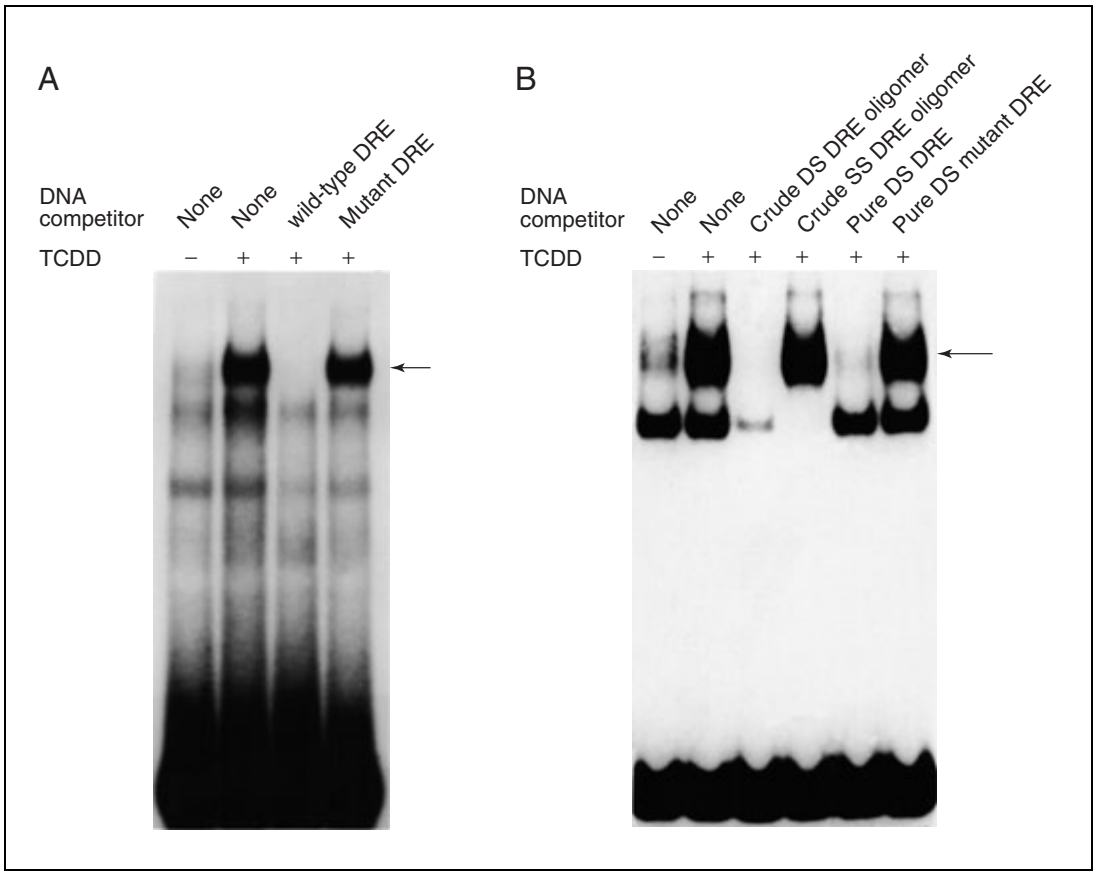

Figure 4.8.3 Typical gel retardation analysis of nuclear and cytosolic extracts. (**A**) Nuclear extracts (6 μg protein/ml) prepared from mouse hepatoma (hepa1c1c7) cells incubated for 1 hr at 37°C with DMSO (lane 1) or 1 nM TCDD (lanes 2 to 4), were incubated with wild-type (wt) [^{32}P]DRE oligonucleotide in the absence (lanes 1 and 2) or presence of a 100-fold molar excess of unlabeled wtDRE (lane 3) or mutant (m) DRE (lane 4) oligomer, and protein-DNA complexes were determined by gel retardation analysis. The arrow indicates the position of the induced protein DNA complex. (**B**) Rat hepatic cytosol (8 mg protein/ml) incubated for 2 hr at room temperature with DMSO (lane 1) or TCDD (lanes 2 to 6), was incubated with [^{32}P]wtDRE oligonucleotide in the absence (lanes 1 and 2) or presence of a 100-fold molar excess of unlabeled reannealed double-stranded wtDRE oligomer (lane 3), single-stranded wtDRE oligomer, (lane 4), pure double-stranded wtDRE (lane 5) or mDRE (lane 6), and protein-DNA complexes were determined by gel retardation analysis. Reprinted from Denison and Yao (1991).

radiolabeled single-stranded DNA) supports this conclusion; however, since formation of complex B actually provides a useful internal control (for sample loading) this residual single-stranded DNA is not removed from the oligonucleotide mixture after the reannealing step.

Gene expression

Typical results from immunoblot, RT-PCR, and northern blot analysis of various components of the AhR signal transduction pathway are shown in Figure 4.8.4. Immunoblot analysis of a whole cell lysate from mouse hepatoma (hepa1c1c7) cells using polyclonal antibodies to AhR and Arnt is shown in Figure 4.8.4A. The protein bands corresponding to the immunoreactive 95 kDa AhR and 85 kDa Arnt are indicated, as are the positions of the prestained protein standards. It is important to note that the AhR and Arnt antibodies bind nonspecifically to proteins in addition to the AhR or Arnt and as such, multiple antibody-positive bands will always be present on immunoblots using these antibodies. Although the identity of these additional immunoreactive proteins is unknown, some of them may represent AhR or Arnt, protein degradation products. Detection of AhR, Arnt, and CYP1A1 expression by RT-PCR analysis of RNA isolated from human choriocarcinoma (JEG3) cells that had been treated with DMSO (–) or TCDD (+) is shown in Figure 4.8.4B. PCR products corresponding to the 310-bp AhR, the 310-bp Arnt, the 460-bp CYP1A1, and the 430-bp GAPDH are detected in both DMSO- and TCDD-treated samples. As

expected, CYP1A1 was only detected in the presence of TCDD. Although these results are not quantitative, approaches for quantitative RT-PCR for these gene products have been described (Hakkola et al., 1997). Northern blot analysis of CYP1A1 mRNA isolated from human ovarian carcinoma (BG-1) cells that had been treated with DMSO or 10 nM TCDD is shown in Figure 4.8.4C. As with the RT-PCR analysis, CYP1A1 mRNA was only detected in cells treated with TCDD. The relative migration of the CYP1A1 mRNA (2.56 Kb) falls between that of the 28S (5.0 Kb) and the 18S (1.9 Kb) ribosomal RNA bands, while GAPDH (1.27

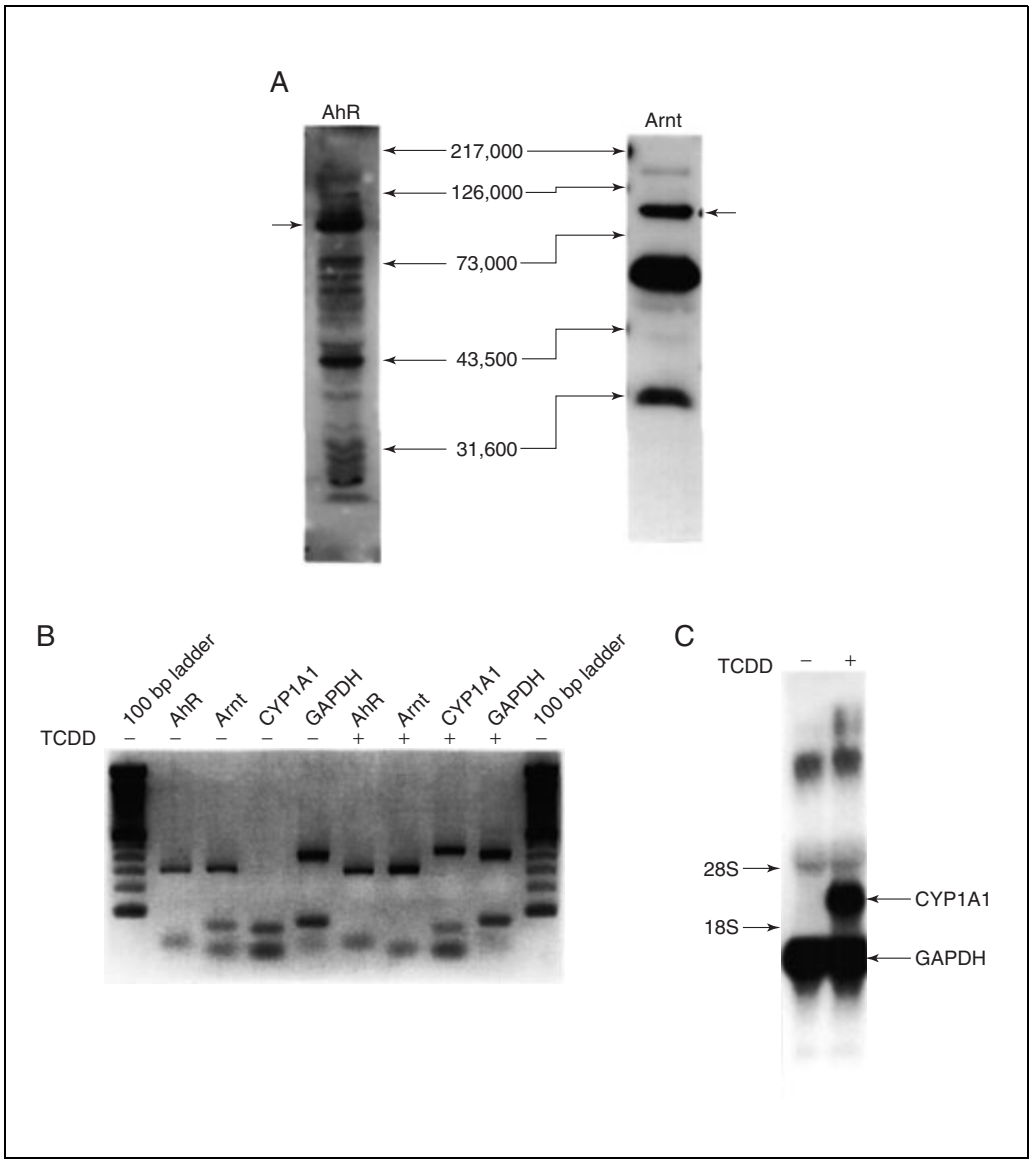

Figure 4.8.4 Analysis of the AhR signal transduction pathway by immunoblotting, RT-PCR, and northern blotting. (**A**) Immunoblot analysis of a whole cell lysate from mouse hepatoma (hepa1c1c7) cells using polyclonal antibodies to the AhR and monoclonal antibodies to Arnt. The positions and sizes of the Kaleidoscope protein standards (BioRad) are shown. The arrows indicate the positions of the AhR and Arnt proteins. Additional bands on the AhR immunoblot are common with all antibodies tested so far. (**B**) RT-PCR analysis of RNA isolated from human choriocarcinoma (JEG3) cells that had been treated with DMSO or TCDD (5 nM) for 24 hr at 37°C. PCR products corresponding to the AhR (310 bp), Arnt (310 bp) and GAPDH (430 bp) are detected in both DMSO- and TCDD-treated samples. A PCR product corresponding to that of the CYP1A1 (460 bp) was only detected in the TCDD-treated sample. The 100 bp DNA standards are shown in lanes 1 and 10. (**C**) Northern blot analysis for CYP1A1 mRNA isolated from human ovarian carcinoma (BG-1) cells that had been treated with DMSO or 10 nM TCDD for 24 hr at 37°C. The positions of CYP1A1 (2.56 Kb) and GAPDH (1.27 Kb) mRNAs and the relative positions of the human 28S (5.0 Kb) and 18S (1.9 Kb) ribosomal bands are indicated.

Kb) runs slightly faster than the 18S ribosomal band.

Time Considerations

AhR ligand binding analysis by SDG analysis (see Basic Protocol 1) is somewhat time-consuming and labor intensive during several steps, and the total time is dependent upon the number of sample gradients to be analyzed. The maximum number of gradients is dependent upon the capacity of the rotor (commonly eight or sixteen samples). For sixteen gradients, the overall procedure, from initial sample incubation until the fractionated samples are loaded into the scintillation counter takes ~8 hr. For a full rotor run of sixteen samples, the sample preparation and incubation takes 2.5 hr, charcoal treatment and gradient loading takes ~1 hr, centrifugation takes ~2.5 hr, and gradient fractionation another 1 to 2 hr. Scintillation counting of the gradient fractions adds significantly to the analysis time (~1.2 hr per 25 fraction gradient; >19 hr for counting of sixteen gradients). By staggering incubations and utilizing a vertical tube rotor for centrifugation, 32 gradients can be analyzed by a single person in one day. If a swinging bucket rotor is used, overnight centrifugation (16 hr) is required with a maximum of 6 gradients (Okey et al., 1979).

HAP binding analysis (see Alternate Protocol 1) is relatively rapid and the overall protocol time is dependent upon the number of samples to be analyzed. For example, complete analysis of 24 binding reactions (not including scintillation counting time) can be completed in ~4 hr. Set up of the incubations should take less than 30 min, even when large numbers of samples are to be run. The samples incubate for 2 hr and HAP binding of sample aliquots takes 30 min. Complete washing of HAP pellets is dependent upon the number of samples and the tube capacity of the centrifuge rotor, but 24 samples can be completed in less than 30 min. Washing times can be reduced significantly with the use of a repeating pipettor to add wash buffer and a vacuum aspirator to remove the wash supernatant. Incubations and washes can also be staggered so that large numbers of samples can be analyzed simultaneously. A convenient stopping point is immediately after the last wash of the pellets; the samples can sit at room temperature until they are transferred into the scintillation vials. Scintillation counting is commonly for 5 min per sample. One person can run over 100 samples in a single day.

Gel retardation analysis (see Basic Protocol 2) is relatively rapid once the radiolabeled probe is prepared. The overall procedure itself takes 5 to 6 hr, although only a small fraction of this time is labor intensive. Less than 1 hr is needed to complete the set up of the gels and the incubations with TCDD or other test chemicals. The samples are incubated and the gels prerun simultaneously for 2 hr. Set up and incubation of the DNA binding reactions and loading of the gels takes <1 hr (depending upon the number of samples to be analyzed) and electrophoresis takes 2 to 2.5 hr to complete. Gels are commonly dried for 1 hr at 80°C, although the time for drying can be shorter. The time necessary for autoradiography of the dried gels can vary significantly and it depends on the specific activity of the radiolabeled DNA and the amount of protein DNA complex formation. Autoradiographic results can be obtained in as little as 3 to 4 hr under optimal conditions.

Once the sample extract is in hand, immunoblot analysis (see Basic Protocol 3) can be completed in 1 long day or divided into 2 days. The authors usually complete the preparatory work (i.e., gel and sample preparation, electrophoresis, and transfer) on the first day and probe the blot on the second day; however, if the gels and samples are prepared ahead of time, electrophoresis, transfer, and probing the membrane may be completed in 1 day. Stripping and reprobing a blot may also be completed in 1 day.

For analysis of mRNA by RT-PCR (see Basic Protocol 4) or northern blotting (see Basic Protocol 5), the authors isolate RNA using the RNeasy Mini Kit from Qiagen (see Support Protocol 5). Isolation of enough material for RT-PCR analysis can be completed in <1 hr. For northern blot analysis, a more concentrated RNA sample is needed and this necessitates an additional two hour precipitation step. RT-PCR analysis can be easily accomplished in 1 day. First-strand cDNA synthesis takes ~1.5 hr and the PCR reactions take an additional 1.5 to 2 hr to complete depending on the number of cycles to be run. PCR reactions can also be set up and run overnight providing the temperature is maintained at 4°C after the cycles are completed. The resulting PCR products are viewed by ethidium bromide staining on an agarose gel, which adds an additional hour to the procedure.

In contrast, northern blot analysis takes 3 days. The cDNA fragment to be radiolabeled can be digested and isolated from its plasmid in advance and stored at −20°C for later use. The enzymatic digestion, gel separation, and fragment isolation should be completed in ~3.5

hr. A sufficient quantity of the desired fragment should be isolated so that it can be used in many northern experiments. On the first day, the agarose/formaldehyde gel is poured and the RNA samples denatured while the gel solidifies (~1 hr). The gel takes ~3 to 3.5 hr to run and the RNA is transferred to the membrane overnight. On the second day, the blot is dried for one hour and the probe is radiolabeled which takes ~1.5 hr. After successful labeling of the probe has been confirmed, the blot can be prehybridized for 1 hr and then hybridized with the radiolabeled probe overnight. On the third day, the blot is washed (~1 hr) and can either be placed on a phosphorimager screen or autoradiographic film overnight and subsequently developed.

Literature Cited

Bradfield, C.A. and Poland, A. 1988. A competitive binding assay for 2,3,7,8-tetrachlorodibenzo-*p*-dioxin and related ligands for the Ah receptor. *Molec. Pharmacol.* 34:682-688.

Burbach, K.M., Poland, A., and Bradfield, C.A. 1992. Cloning of the Ah-receptor cDNA reveals a distinctive ligand-activated transcription factor. *Proc. Natl. Acad. Sci. U.S.A.* 89:8185-8189.

Cuthill, S. and Poellinger, L. 1988. DNA binding properties of dioxin receptors in wild-type and mutant mouse hepatoma cells. *Biochemisty* 27:2978-2982.

Denison, M.S. and Yao, E. 1991. Characterization of the interaction of transformed rat hepatic Ah receptor with a dioxin responsive transcriptional enhancer. *Arch. Biochem. Biophys.* 284:158-166.

Denison, M.S., Fine, J., and Wilkinson, C.F. 1984. Protamine sulfate precipitation: A new assay for the Ah receptor. *Anal. Biochem.* 142:28-36.

Denison, M.S., Vella, L.M., and Okey, A.B. 1986. Structure and function of the Ah receptor for 2,3,7,8-tetrachlorodibenzo-*p*-dioxin: Species differences in molecular properties of the receptor from mouse and rat hepatic cytosol. *J. Biol. Chem.* 261:3987-3995.

Denison, M.S., Fisher, J.M., and Whitlock, J.P., Jr. 1988a. Inducible, receptor-dependent protein-DNA interactions at a dioxin-responsive transcriptional enhancer. *Proc. Natl. Acad. Sci. U.S.A.* 85:2528-2532.

Denison, M.S., Fisher, J.M., and Whitlock, J.P., Jr. 1988b. The DNA recognition site for the dioxin-Ah receptor complex: Nucleotide sequence and functional analysis, *J. Biol. Chem.* 263:17721-17724.

Denison, M.S., Phelen, D., and Elferink, C.J. 1998a. The Ah receptor signal transduction pathway. *In* Xenobiotics, Receptors and Gene Expression (M.S. Denison and W. Helferich, eds.) pp. 3-33, Taylor and Francis, Philadelphia.

Denison, M.S., Seidel, S.D., Rogers, W.J., Ziccardi, M., Winter, G.M., and Heath-Pagliuso, S. 1998b. Natural and synthetic ligands for the Ah receptor. *In* Molecular Biology Approaches to Toxicology (A. Puga and K.B. Wallace, eds.) pp. 393-410, Taylor and Francis, Philadelphia.

Denison, M.S., Phelan, D., Winter, G.M., and Ziccardi, M.H. 1998c. Carbaryl, a carbamate insecticide, is a ligand for the hepatic Ah (dioxin) receptor. *Toxicol. Appl. Pharmacol.* 152:406-414.

Dottavio-Martin, D. and Ravel J. M. 1978. Radiolabeling of proteins by reductive alkylation with [^{14}C]formaldehyde and sodium cyanoborohydride. *Anal. Biochem.* 87:562-565.

Garrison, P.M., Aarts, J.M.M.J.G., Brouwer, A., Giesy, J.P., and Denison, M.S. 1996. Ah receptor-mediated gene expression: Production of a recombinant mouse hepatoma cell bioassay system for detection of 2,3,7,8-tetrachlorodibenzo-p-dioxin-like chemicals. *Fund. Appl. Toxicol.* 30:194-203.

Gasiewicz, T.A. and Neal, R.A. 1982. The examination and quantitation of tissue cytosolic receptors for 2,3,7,8-tetrachlorodibenzo-*p*-dioxin using hydroxylapatite. *Anal. Biochem.* 124:1-11.

Hahn, M.E. 1999. The aryl hydrocarbon: A comparative perspective. *Comp. Biochem. Physiol.* C121:23-53.

Hakkola, J., Pasanen, M., Pelkonen, O., Hjukkanen, J., Evisalmi, S., Anttila, S., Rane, A., Mantyla, M., Purkunen, R., Saarikoski, S., Tooming, M., and Raunio, H. 1997. Expression of CYP1B1 in human adult and fetal tissues and differential inducibility of CYP1B1 and CYP1A1 by Ah receptor ligands in human placenta and cultured cells. *Carcinogenesis* 81:391-397.

Hoffman, E.C., Reyes, H., Chu, F.-F., Sander, F., Conley, L.H., Brooks, B.A., and Hankinson, O. 1991. Cloning of a factor required for activity of the Ah (dioxin) receptor. *Science* 252:954-958.

Holmes, J.L. and Pollenz, R.S. 1997. Determination of aryl hydrocarbon receptor nuclear translocator protein concentration and subcellular localization in hepatic and nonhepatic cell culture lines: Development of quantitative western blotting protocols for calculation of aryl hydrocarbon receptor and aryl hydrocarbon receptor nuclear translocator protein in total cell lysates. *Molec. Pharmacol.* 52:202-211.

Okey, A.B., Bondy, G.P., Mason, M.E., Kahl, G.F., Eisen, H.J., Guenthner, T.M., and Nebert, D.W. 1979. Regulatory gene product of the Ah locus: Characterization of the cytosolic inducer-receptor complex and evidence for its nuclear translocation. *J. Biol. Chem.* 254:11636-11648.

Poland, A., Glover, E., and Kende, A.S. 1976. Stereospecific, high affinity binding of 2,3,7,8-tetrachlorodibenzo-*p*-dioxin by hepatic cytosol: Evidence that the binding species is receptor for induction of aryl hydrocarbon hydroxylase. *Molec. Pharmacol.* 251:4936-4946.

Prokipcak, R.D., Denison, M.S., and Okey, A.B. 1990. Nuclear Ah receptor from mouse hepa-

toma cells: Effects of partial proteolysis on relative molecular mass and DNA-binding properties. *Arch. Biochem. Biophys.* 283:476-483.

Safe, S. 1990. Polychlorinated biphenyls (PCBs), dibenzo-*p*-dioxins (PCDDs), dibenzofurans (PCDFs), and related compounds: Environmental and mechanistic considerations which support the development of toxic equivalency factors (TEFs*). Crit. Rev. Toxicol.* 21:51-88.

Schmidt, J.V. and Bradfield, C.A. 1996. Ah receptor signaling pathways. *Annu. Rev. Cell Devel. Biol.* 12:55-89.

Shen, E.S. and Whitlock, J.P., Jr. 1992. Protein-DNA interactions at a dioxin-responsive enhancer: Mutational analysis of the DNA-binding site for the liganded Ah receptor. *J. Biol. Chem.* 267:6815-6819.

Tsai, H.W. and Okey, A.B. 1981. Rapid vertical tube rotor gradient assay for binding of 2,3,7,8-tetrachlorodibenzo-*p*-dioxin to the *Ah* receptor. *Canad. J. Physiol. Pharmacol.* 59:927-931.

Tscheudschilsuren, G., Hombach-Klonisch, S., Kuchenhoff, A., Fischer, B., and Klonisch, T. 1999. Expression of the aryl hydrocarbon receptor and aryl hydrocarbon receptor nuclear translocator during early gestation in the rabbit uterus. *Toxicol. Appl. Pharmacol.* 160:231-237.

Walsh, A.A., Tullis, K., Rice, R.H., and Denison, M.S. 1996. Identification of a novel cis-acting negative regulatory element affecting transcription of the CYP1A1 gene in rat epidermal cells. *J. Biol. Chem.* 271:22746-22753.

Yao, E.F. and Denison, M.S. 1991. DNA sequence determinants for binding of transformed Ah receptor to a dioxin responsive element. *Biochemistry* 31:5060-5067.

Contributed by Michael S. Denison, Jane M. Rogers, S. Renee Rushing, Carol L. Jones, Selwyna C. Tetangco, and Sharon Heath-Pagliuso
University of California, Davis
Davis, California

Measurements of Flavin-Containing Monooxygenase (FMO) Activities

The flavin-containing monooxygenases (FMOs, EC 1.14.13.8) are a family of xenobiotic-metabolizing enzymes that catalyze the flavin-adenine dinucleotide (FAD)-, NADPH-, and O_2-dependent oxidation of numerous xenobiotics containing nitrogen, sulfur, phosphorus, or selenium heteroatoms. The FMOs have been thoroughly described in a number of mammalian species, including the pig, rabbit, human, rat, and mouse, and more recently in fish. At least five different isoforms have been described by amino acid or cDNA sequencing and are classified as FMO1 to FMO5.

Many FMO substrates are also substrates for cytochrome P450s (CYPs). Since both FMOs and CYPs are membrane-bound enzymes that are sedimented during the preparation of microsomes, it can be difficult to distinguish which metabolites are produced by one or the other of these enzymes. To study the relative contributions of these two enzymes with common substrates, methods have been developed to measure the contribution of each of these enzyme systems. The most useful of these is a combination of two methods; the first involving inhibition of CYPs through the use of an antibody to cytochrome P450 reductase, thus allowing measurement of FMO activity alone. The second procedure involves the heat treatment of microsomal preparations (1 min at 50°C), which inactivates the heat labile FMO, leaving activity of CYPs intact. However, since the lung FMO (FMO2) is more heat stable than the liver forms, use of the anti-reductase with lung microsomal preparations is necessary.

Studies of drug and pesticide metabolism can also be conducted with the use of purified preparations of FMO isoforms as expressed in *E. coli*, yeast, baculovirus, and others. In these studies, NADPH oxidation can be used to determine whether a particular isoform has activity towards a given substrate. Although this procedure has proven useful for a wide variety of substrates, there is at least one case where NADPH oxidation occurred in the absence of FMO protein, indicating that appropriate controls are essential for proper interpretation of results.

Although there are a variety of substrates that can be used for the characterization of FMO activities, methimazole and *n*-octylamine are two substrates that are widely used for such characterization. Methimazole can be metabolized by FMO1 to FMO4 and to a slight extent by FMO5 while *n*-octylamine is a good substrate for FMO5.

This unit describes methods used for measuring the presence of FMOs using two basic procedures. NADPH oxidation (see Basic Protocol 1) is an important screening method used to identify potential FMO substrates; often using recombinant FMO isoforms. Because methimazole is a substrate that is easily oxidized by most FMO isoforms, methimazole oxidation (see Basic Protocol 2) is also commonly used for the characterization of FMO isoforms. Methods are also provided to determine the relative contributions of FMO versus CYP from microsomal tissues (see Basic Protocol 3).

NADPH OXIDATION

BASIC PROTOCOL 1

NADPH oxidation is a useful method to determine if a substrate is metabolized by FMOs. Previous studies have validated the stoichiometric relationships between substrate addition, NADPH oxidation, and oxygen consumption for a variety of FMO substrates (Tynes and Hodgson, 1985). This method monitors NADPH consumption by following the decrease in spectral measurement of NADPH at 340 nm. Since endogenous NADPH is high in microsomal preparations, this method is not recommended for measurement of FMOs in microsomal preparations unless NADPH cytochrome P450 reductase is inhib-

Contributed by Randy L. Rose

Current Protocols in Toxicology (2002) 4.9.1-4.9.11

ited by antibodies. The magnitude of such inhibition should be carefully checked to ensure that subsequent oxidations are significantly less than prior to the addition of the antibody. It is also important to check that the substrate and products of the reaction do not interfere with this wavelength for successful quantitation.

Materials

2× tricine/KOH buffer, pH 8.5 (see recipe)
10 mM nicotinamide adenine dinucleotide phosphate, reduced form (NADPH; see recipe)
Enzyme (usually purified or recombinant FMO)
0.1 M substrate (see recipe for suggestions on preparation and storage)

1.5-ml UV grade (methacrylate) cuvettes, 1-cm path-length
Spectrophotometer
37°C water bath

1. Add the following ingredients to a 1.5-ml sample cuvette (total 1 ml).

   500 µl 2× prewarmed tricine/KOH buffer, pH 8.5
   10 µl 10 mM NADPH
   Enzyme plus prewarmed water to a final reaction volume of 990 µl.

2. Prepare a reference cuvette with the same ingredients as the sample cuvette, but without 10 mM NADPH.

3. Place sample and reference cuvettes in the spectrophotometer and measure the decrease of OD at 340 nm.

   This provides the background rate of NADPH oxidation.

4. Add 10 µl of 0.1 M substrate to the sample cuvette, mix by inversion, and again record the decrease of OD at 340 nm.

5. Calculate NADPH oxidase activity. Applying Beer's Law: $A = \varepsilon cl$. The extinction coefficient for NADPH oxidation (ε) at 340 nm is 6200 $M^{-1}cm^{-1}$. The cell path-length (l) is 1 cm and A is the measured absorptivity at λ_{max}.

$$c = \frac{\Delta A/\text{min}}{\varepsilon l}$$

$$c = \frac{\Delta A/\text{min}}{(6200\ \text{liter/mol cm})(1\ \text{cm})(1000\ \text{ml/liter})(1\ \text{mol}/10^9\ \text{nmol})}$$

$$c = (\Delta A/\text{min})(161\ \text{nmol/min})(\text{ml}/x\ \text{mg protein}) = \text{nmol/min/mg protein}$$

BASIC PROTOCOL 2

METHIMAZOLE/DTNB ASSAY

The measurement of FMO activity in microsomal fractions is best accomplished by monitoring methimazole oxidation as originally described by Dixit and Roche (1984). Methimazole (*N*-methyl-2-mercaptoimidazole) is a highly specific substrate for the FMO and is somewhat unusual in that it is a poor substrate for CYPs. The measurement of methimazole oxidation relies upon the ability of its disulfide conjugate (formed after oxidation of methimazole) to rapidly and completely oxidize nitro-5-thiobenzoate (TNB) to DTNB (Fig. 4.9.1). This reaction is accomplished following the reduction of DTNB to TNB by DTT, allowing for subsequent oxidation of TNB to DTNB, which can be followed spectrophotometrically. The reaction has been a favorite method for characterization of FMO activity in microsomes as well as for the characterization purified or recombinant FMO isoforms. It is a preferred substrate because it can be used over a wide range of

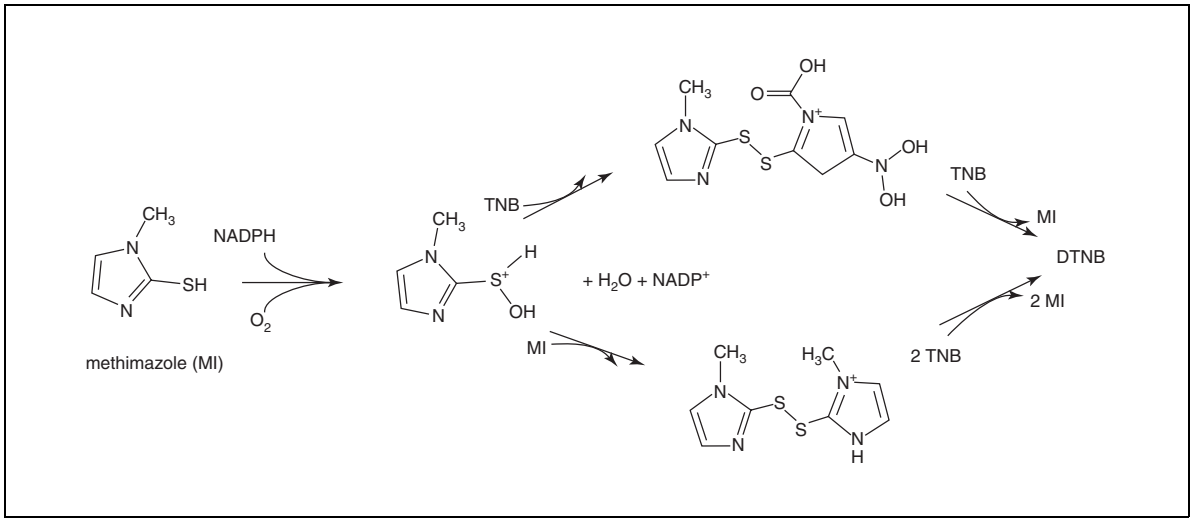

Figure 4.9.1 Oxidation of methimazole and reaction of the oxidized product with TNB to generate DTNB (modified from Dixit and Roche, 1984).

concentrations, is easily assayed, and can be used for both microsomal and purified preparations. This substrate is most suitable for studies of FMO isoforms 1 to 4, having less suitability for FMO5 due to the much higher K_m value of FMO5. For studies of FMO5 expression, NADPH oxidation using *n*-octylamine as substrate has proven to be a suitable alternative method.

Materials

2× tricine/KOH buffer, pH 8.5 (see recipe)
1 mM 5,5′-dithio-bis(2-nitrobenzoic acid) (DTNB; see recipe)
10 mM nicotinamide adenine dinucleotide phosphate, reduced form (NADPH; see recipe)
2 mM dithiothreitol (DTT; see recipe)
100 mM methimazole (see recipe)
Inhibitors (optional)
Microsomes
Enzyme

Spectrophotometer
37°C water bath
1.5-ml UV grade (methacrylate) cuvettes, 1-cm path-length

1. Turn on spectrophotometer (412 nm) and 37°C water bath. Warm 2× tricine/KOH buffer, pH 8.5, to 37°C.
2. Prepare 1 mM DTNB, 10 mM NADPH, 2 mM DTT, 100 mM methimazole, and inhibitors.

   Methimazole may be frozen and used again. It is best if a fresh solution of NADPH is used. DTT and DTNB must be fresh preparations.

3. To sample and reference cuvettes, add the following (total volume 1 ml):

   500 µl 2× tricine/KOH buffer, pH 8.5
   10 µl 2 mM DTT
   60 µl 1 mM DTNB
   10 µl 10 mM NADPH

continued

x µl microsomes
x µl water
total volume 990 µl.

The solution turns yellow when DTT and DTNB are mixed.

4. Wait 30 to 60 sec, then record the substrate-independent rate for 2 min until a good baseline is established.
5. Add 10 µl of 100 mM methimazole to the sample cuvette, mix, wait 30 to 60 sec, then record the reaction rate for at least 2 min.
6. If inhibitors are used, add 1 to 10 µl of inhibitor to sample cuvette, wait 30 sec for equilibration, then re-record the reaction rate.
7. Measure the change in absorbance that occurs between 1 and 2 min.
8. Calculate nitro-5-thiobenzoate (TNB) oxidation activity. The extinction coefficient for TNB oxidation (ε) is 28,000 $M^{-1}cm^{-1}$ at pH 8.4. Applying Beer's Law: $A = \varepsilon\, c\, l$ and incorporating protein concentration,

$$c = \frac{\Delta A/\text{min}}{(28{,}000\ \text{liter/mol cm})(1\ \text{cm})(1000\ \text{ml/liter})(1\ \text{mol}/10^9\ \text{nmol})}$$

$$= (\Delta A/\text{min})(1\ \text{nmol}/0.028\ \text{ml})(\text{ml}/x\ \text{mg protein}) = \text{nmol/min/mg protein}.$$

BASIC PROTOCOL 3

DETERMINATIONS OF FMO VERSUS CYP CONTRIBUTIONS TO METABOLISM FOR COMMON SUBSTRATES

Both the CYPs and FMOs catalyze the microsomal oxidations of a variety of drugs and pesticides. Since both enzyme families are membrane bound enzymes that are sedimented during microsomal preparations, it is often difficult to determine which has the predominant role in the oxidations being examined. In some cases, a substrate may first be oxidized by one of these enzyme systems and then subsequently oxidized by the other. By preferentially inhibiting either the FMO activity or the CYP activity in microsomal incubations the relative contributions of both enzyme systems can be determined. To do this, FMOs can be eliminated from the microsomes by a brief heat treatment (90 sec at 50°C) or the metabolic contributions of CYPs can be eliminated either by use of general CYP inhibitors (e.g., *N*-benzylimidazole) or by use of antibodies to cytochrome P450 reductase as described below.

Materials

Microsomes
100 mM potassium phosphate buffer, pH 7.4 (see recipe)
NADPH regenerating system (see recipe)
Substrate (see recipe for suggestions of preparation and storage)
Antibodies to NADPH cytochrome P450 reductase (BD Biosciences)
2× tricine/KOH buffer, pH 8.5 (see recipe)
1 mM *N*-benzylimidazole (NBI; prepare from 300 mM stock; see recipe)
50°C water bath

For FMO inactivation (heat treatment)

1a. Add microsomes to 100 mM potassium phosphate buffer, pH 7.4, so that the final concentration is 0.1 to 0.8 mg/ml.

Potassium phosphate buffer, pH 7.4, is used when examining CYP contribution to metabolism.

2a. Heat microsomes (in the absence of NADPH regenerating system and substrate) for 90 sec at 50°C.

3a. Add 25 µl NADPH regenerating system and the appropriate substrate. Incubate for 5 to 15 min, 37°C, and monitor product formation as necessary.

For CYP inactivation (antibody inhibition)

1b. Preincubate microsomes with anti-reductase antibody (1 to 2 mg/mg microsomal protein) in 500 µl of 2 × tricine/KOH buffer, pH 8.5, for 5 to 7 min at 4° C.

Tricine/KOH buffer, pH 8.5, is used when measuring the contribution of FMO.

2b. Add 25 µl NADPH regenerating system and the appropriate substrate to a final volume of 1 ml.

3b. Incubate for 5 to 15 min, and monitor product formation as necessary.

For CYP inactivation (chemical inhibition)

1c. Preincubate microsomes with 3.3 µl NBI stock solution for 5 min at 37°C in 500 µl of 2× tricine/KOH buffer, pH 8.5.

Tricine/KOH buffer, pH 8.5, is used when measuring the contribution of FMO.

2c. Add 25 µl NADPH regenerating system and the appropriate substrate to a final volume of 1 ml.

3c. Incubate for 5 to 15 min at 37°C, and monitor product formation as necessary.

REAGENTS AND SOLUTIONS

*Use Milli-Q-purified water or equivalent in all recipes and protocol steps. For common stock solutions, see **APPENDIX 2A**; for supplies, see **SUPPLIERS APPENDIX**.*

5,5′-dithiobis(2-nitrobenzoate) (DTNB), 1 mM

Dissolve 10 mg DTNB in 25 ml of 2× tricine/KOH buffer (see recipe). Prepare fresh.

Dithiothreitol (DTT), 2 mM

Dissolve 15 mg dithiothreitol per 50 ml deionized water. Prepare fresh.

Methimazole, 100 mM

Dissolve 11.4 mg methimazole in 1 ml methanol. Store up to 2 months at 4°C.

Nicotinamide adenine dinucleotide phosphate, reduced (NADPH), 10 mM

Dissolve 8.3 mg NADPH in 1 ml deionized water.

N-benzylimidazole (NBI), 300 mM

Dissolve 24 mg NBI in 0.5 ml acetonitrile:water (1:1).

NADPH regenerating system

Add 4.2 mg $NADP^+$ to 14.1 mg glucose-6-phosphate and 20 U of glucose-6-phosphate dehydrogenase in a final volume of 0.5 ml of reaction buffer. Dispense into 25-µl aliquots per 1 ml assay volume, bring final concentrations to 0.25 mM $NADP^+$, 2.5 mM glucose-6-phosphate, and 1 U glucose-6-phosphate dehydrogenase. If NADPH-RGS is left over, it may be used up to 2 weeks if stored frozen at −20°C.

Potassium phosphate buffer (pH 7.6), 100 mM, with 0.1 mM EDTA

Combine 2.176 g KH_2PO_4 and 14.64 g K_2HPO_4 in 1 liter of water. Add 33.6 g disodium EDTA. Adjust to pH 7.6 with 1 M HCl or NaOH if necessary. Store up to 6 months at 4°C.

Substrate solutions

Prepare 200- to 500-µl aliquots of stock solutions in water, ethanol, methanol, or dimethylsulfoxide to obtain final concentrations in the incubation mixture of 10 to 100 mM. Do not exceed solvent concentrations >5 to 10 µl per milliliter.

Tricine/KOH buffer (pH 8.5), 2×

Add 35.8 g tricine and 0.744 g disodium EDTA per 1 liter. Adjust to pH 8.4 with KOH. Store up to 6 months at 4°C.

COMMENTARY

Background Information

The flavin-containing monooxygenase enzymes (FMO, EC 1.14.13.8) have been characterized from several mammalian species, including humans, rabbits, mice, rats, and pigs. This enzyme, isolated from the endoplasmic reticulum, catalyzes the oxygenation of a variety of nucleophilic nitrogen-, sulfur-, and phosphorus-containing drugs, pesticides, and other xenobiotics (Ziegler, 1980; 1988; Hodgson et al., 1995). The ability of these enzymes to oxygenate a variety of xenobiotics is important in both activation and detoxication processes. Interestingly, unlike the related CYP enzymes, FMOs do not seem to be induced by their own substrates. Although several endogenous substrates have been identified (Elfarra, 1995), the physiological role of these enzymes has not been established.

The oxidative reactions carried out by both FMOs and cytochrome P450s (CYPs) generally result in the production of less toxic metabolites that can then be subsequently conjugated and/or excreted; although in some cases, increased toxicity can result. Not only can the products of these enzymes vary, but different isomers of the same product may also be produced (Hodgson et al., 1997). Because tissue and subcellular locations of these enzymes are essentially the same, it is often difficult to separate their respective oxidative activities. However, methods have been developed to determine the relative contributions of FMO and CYPs, including the manipulation of microsomes in which both enzymes are found. The best method to determine the contribution of CYP activity to the overall metabolism of specific substrates involves heat inactivation of FMOs. Since FMOs are more heat labile than CYPs (with the exception of the lung FMO2), brief heating of microsomal preparations to 50°C for 90 sec effectively eliminates the FMO contribution to metabolism with minimal inactivation of CYPs.

To more fully examine the relative contribution of FMO enzyme activity within microsomes, two methods have been used successfully. The traditional method involves use of an antibody to NADPH cytochrome P450 reductase to abolish the CYP contribution to metabolism. More recently, a general CYP inhibitor (*N*-benzylimidazole, NBI) has been used by some investigators to discriminate between CYP and FMO activity. The combination of heat treatment with antibody treatment was used to characterize the contributions of FMO versus CYP activities towards the pesticide substrate, phorate, in various tissues (Kinsler et al., 1988) and under different induction and inhibition treatments (Kinsler et al., 1990). Use of NBI was shown to nearly completely eliminate CYP metabolism of up to seven diagnostic CYP substrates without harming FMO-mediated metabolism (Grothusen et al., 1996). Use of this CYP inhibitor in place of an inhibitory antibody reduces the need to perform exploratory assays in the case of the antibody to determine optimal concentrations for CYP inactivation. By comparing uninhibited metabolism rates with those obtained following FMO inactivation (heat treatment) versus those obtained following CYP inactivation (NBI or NADPH cytochrome P450 reductase antibody treatment) assignments of FMO and CYP contributions to the production of specific metabolites can be realized.

FMO-specific substrate oxidations can also be performed using purified preparations of enzyme either from microsomes (Sabourin et al., 1984) or from heterologously expressed preparations. The first purified FMO was obtained from pig liver microsomes (Zeigler and Mitchell, 1972), and its catalytic mechanism was extensively characterized. Subsequently, purification procedures were developed for the rat, mouse, rabbit, guinea pig, and macaque. Differences observed in the modulation of FMO activities by metal ions from FMOs de-

rived from partially purified rabbit lung and liver FMO resulted in the suggestion that these tissues might possess different forms of the enzyme (Devereux et al., 1977). Subsequent studies more conclusively demonstrated that purified lung and liver FMOs were catalytically and immunochemically distinct (Williams et al., 1984; Tynes et al., 1985). Sequencing of the corresponding cDNAs yielded evidence of distinctly different but related genes (Lawton et al., 1990). To date, five distinct FMO genes (designated FMO1 to FMO5) have been identified by amino acid or cDNA sequencing (Lawton et al., 1994). Orthologous genes share at least 80% amino acid identity, while homologous FMOs are 52% to 57% identical. Highly related forms (>98% identity) within a single species are the result of allelic variation.

At least one human polymorphism of FMOs has been described. In this case, different mutations of the FMO3 gene result in the inability of human subjects to metabolize trimethylamine (Cashman et al., 1997). Subjects with this autosomally recessive disorder exude a characteristic "fish odor" resulting from their excretion of large amounts of unmetabolized trimethylamine.

One of the interesting features of FMOs involves their tissue-specific expression. Williams et al. (1984) and Tynes et al. (1985) demonstrated that the pulmonary (FMO2) and hepatic (FMO1) forms from the rabbit were immunochemically and catalytically distinct. It was also shown that both FMO1 and FMO2 were present in rabbit kidney, but that in the lung and liver, only one form was present (FMO2 and FMO1, respectively). FMO3 expression was demonstrated in rabbit liver but not in kidney or lung, while FMO4 was found in rabbit kidney, but not liver or lung (Burnett et al., 1994). Expression of FMO5 was highest in liver, followed by kidney, and was absent in lung (Atta-Asafo-Adjei et al., 1993).

Possible physiological functions of FMOs are indicated not only by tissue-specific expression but also by variations in FMO levels according to gender, nutritional status, diurnal rhythms, and pregnancy (Williams et al., 1985). Gender and developmental differences in the expression of FMO have been characterized in several species. In mice, oxidation of FMO substrates has long been known to be greater in females than in males. Based on protein and mRNA levels in CD-1 mice, it was shown that FMO3 was expressed only in females and that FMO1 was expressed to a greater extent in females than in males. In contrast, the lesser abundant hepatic isoform, FMO5, was expressed to an approximately equal extent in both males and females. Northern blotting methods did not detect either FMO2 or FMO4 in livers of mice from either gender (Falls et al., 1995). Studies examining the roles of testosterone, 17 β estradiol, and progesterone demonstrated that testosterone is involved in the modulation of the activities of FMO isoforms 1 and 3 (Falls et al., 1997).

Developmentally in CD-1 mice, FMO1 is already expressed by gestational day 13 and continues to increase in expression until 2 weeks of age when expression is equivalent in males and females (Cherrington et al., 1998). By 4 weeks of age, at which time mice are becoming sexually mature, FMO1 levels decline in males to levels less than one-half those of females. In contrast, FMO3 is not present at any level in either sex until 2 weeks post-partum. By 4 weeks of age, FMO3 is present in both males and females at a level similar to those seen in adult females. By 6 weeks of age (post-puberty), FMO3 is no longer apparent in the adult male due to the repressive effects of testosterone. Some similarities between mice and humans exist in that FMO1 is the principal FMO in human fetal tissues while FMO3 is the primary expressed form in adults. However, no gender differences in humans have been described.

Although the FMOs have been studied and well characterized in several mammalian species, considerably less is known about this family of enzymes in other vertebrates and invertebrates. In fish, FMO activity has been shown to be directly correlated with osmotic regulation, suggesting a possible physiological role. Activity towards typical FMO substrates is indicative that FMOs are present in invertebrates, but corresponding transcripts or proteins have yet to be identified (Schlenk, 1998).

Critical Parameters

NADPH oxidation in conjunction with the use of recombinant FMO or purified FMO preparations is an excellent way to determine if a given drug or pesticide is metabolized by FMO. However, certain precautions should be considered prior to the use of this method. First, neither the substrate nor product should absorb strongly at 340 nm. Strong absorbance at this wavelength would interfere with the disappearance of NADPH as it is used in the reaction. Second, some substrates may interact with re-

combinant proteins resulting in a spontaneous oxidation of NADPH as occurred with tamoxifen. In these cases, more direct measurements of substrate oxidation, such as quantitation by HPLC and/or radioisotope detection, may be necessary.

Detergents are often used during enzyme purification to solubilize the enzymes prior to placing them on columns for separation. Early observations indicated that detergent-solubilized FMO enzymes retained activity, while CYPs lost activity upon solubilization. As a result, some early studies used detergents such as Emulgen 911 as a means to inhibit oxidations due to CYP (Tynes and Hodgson, 1985). Further examination of this method as a technique to identify the FMO contributions to metabolism indicated that for certain substrates, detergents including Emulgen 911, Triton X-100, and cholate, are also inhibitory to FMO metabolism (Venkatesh et al., 1991).

Although NADPH oxidation is a valid method for determining whether a chemical is metabolized by CYPs or FMOs, its use in microsomal preparations for these purposes is not strongly encouraged because of several potential difficulties. It is difficult, for example, to be able to properly distinguish between CYP metabolism and FMO metabolism without properly inhibiting one or the other system as discussed in Basic Protocol 3. In addition, there are some cases where NADPH can be oxidized in the absence of substrate, particularly when using microsomal preparations. These oxidations may or may not be enzymatic. In some of these cases, addition of substrate can actually result in decreasing the NADPH oxidation rate. In these cases, it may not be appropriate to subtract the rate of substrate-independent NADPH oxidation from the rate of substrate-dependent oxidation. Usually, substrate-independent oxidation is <5% of substrate-dependent NADPH oxidation and can be ignored.

Troubleshooting

See Table 4.9.1 for a troubleshooting guide.

Anticipated Results

Table 4.9.2 illustrates the use of NADPH oxidation (see Basic Protocol 1) as a means to measure metabolism of several pesticides and other xenobiotics in mouse liver, lung, and kidney microsomes (Tynes and Hodgson, 1985). In this example, microsomal enzymes were used to determine possible involvement of FMOs in the metabolism of these compounds. To eliminate cytochrome P450 metabolism, microsomal enzymes were incubated on ice in 5 mg of NADPH cytochrome P450 antireductase IgG/mg of microsomal protein prior to initiation of the incubation. The inclusion of 3 mM *n*-octylamine had previously been demonstrated to increase both K_m and V_{max} for several substrates by ~25%. Note that the endogenous rate of NADPH oxidation shown at the bottom of the table was subtracted from activity levels shown.

NADPH oxidation levels shown are typical of many substrates. Consumption of molecular oxygen and the rate of appearance of oxidized products were demonstrated by Tynes and Hodgson (1985) to be equivalent to the rate of disappearance of NADPH. The activity level of thiourea in liver microsomes is near the maximal level that can be expected from this assay. Similar levels might also be expected for methimazole, cysteamine, and *N*,*N*-dimethylaniline as all of these shared common maximal velocities in kinetic studies.

Table 4.9.3 is an illustration of results obtained after inhibition of FMO activity by heat treatment and CYP activity by antireductase treatment as described in Basic Protocol 3. In this example, the antipsychotic drug, thioridazine is metabolized by both CYP and FMO to several products, including sulfoxide and *N*-oxide metabolites. Production of these metabolites was observed directly by high-performance liquid chromatography. It is interesting to note that one product, thioridazine 2-sulfoxide *N*-oxide (2SONO) is produced to approximately the same extent in all incubations, including boiled microsomes. This is indicative of a metabolite that is produced by autoxidation, rather than by metabolic processes.

The application of heat (45°C for 90 sec) resulted in significant decreases in two metabolites, northioridazine (NOR), and thioridazine *N*-oxide (NO). For NOR, the decrease was 50% of the original activity while for the NO 87% of the activity was eliminated by heat treatment. For the two other metabolites (not including 2SONO), heat treatment had minimal effects. These results suggest a minimal role of FMO in the metabolism to the 2SO and 5SO products and an important role of FMO in metabolism to the NO product. A possible role of FMO is also implicated by this data for metabolism to NOR.

Much of the data derived from heat treatment was verified by the pre-incubation of

Table 4.9.1 Troubleshooting Guide to Analysis of FMO Activity

Problem	Possible cause	Solution
High rates of NADPH oxidation independent of presence of FMO	Futile cycling of NADPH in presence of substrate	Find alternate method to NADPH oxidation
Results not consistent with loss of NADPH (i.e., baseline increases)	Substrate or product of reaction interferes with absorption at 340 nm	Scan substrate or product and monitor direct product formation and/or substrate disappearance
Prolonged initial lag phase of NADPH oxidation in the presence of substrate	Transient intermediates	Add 1 mM glutathione
Rapid, nonlinear initial rate of NADPH oxidation	Substrate insolubility in solution	Decrease substrate concentration or find alternate method to get substrate into solution

Table 4.9.2 Rates of Metabolism by the Flavin-Containing Monooxygenase in Rat Liver, Lung and Kidney Microsomes (Tynes and Hodgson, 1985)

Substrate	Concentration (mM)	Activity (nmol/min/mg of microsomal protein)[a]		
		Liver	Lung	Kidney
Organophosphate and carbamate insecticides				
Phorate	0.1	3.4 ± 0.6	1.4 ± 0.5	1.6 ± 0.7
Disulfoton	0.1	4.3 ± 0.6	1.8 ± 0.5	2.4 ± 0.2
Aldicarb	0.1	1.9 ± 0.4	0.3 ± 0.1	0.7 ± 0.1
Croneton	0.1	3.2 ± 1.5	1.2 ± 0.2	n.d.[b]
Other xenobiotics				
α -Naphthylthiourea	0.1	4.6 ± 0.7	1.4 ± 0.4	n.d.[b]
Methyl phenyl sulfide	0.1	5.4 ± 0.3	1.9 ± 0.2	n.d.[b]
Diethylphenylphosphine	0.1	4.0 ± 1.4	0.8 ± 0.2	n.d.[b]
Thiourea[c]	1.0	8.3 ± 1.3	2.8 ± 0.6	9.1 ± 1.7
Endogenous NADPH oxidation rate		2.9 ± 0.4	0.6 ± 0.3	1.5 ± 0.6

[a]All incubations included 5 mg antireductase IgG/mg of microsomal protein and 3 mM *n*-octylamine. Velocities represent substrate-stimulated minus endogenous rates. Rates are the mean ±SD.

[b]n.d., not determined.

[c]Thiourea completely saturates the enzyme at a concentration of 1 mM; these rates approximate the maximal velocities of these microsomal preparations.

microsomes with NADPH cytochrome P450 antireductase. In this example, antireductase treated microsomes completely or nearly abolished metabolism to NOR and 2SO; implicating a major role of CYPs in formation of these metabolites. The puzzling effect of heat treatment in the reduction of the NOR metabolite is less puzzling if one considers that production of the NO product by FMO is likely to lead to subsequent formation of NOR. In the case of the 5SO and NO products, which were inhibited in the antireductase treatments by ~50%, the data indicates that both P450 and FMO are nearly equally responsible for formation of these products.

Time Considerations

For NADPH oxidation, the preparation of substrate, reagents and buffers requires 1 hr. Each assay takes 5 to 10 min.

For methimazole oxidation, the preparation of substrate, reagents, and buffers requires 2 hr. Each assay takes 10 min.

For FMO versus CYP contributions, the preparation of substrate, reagents, and buffers requires 2 hr. Each assay takes 5 to 15 min.

Table 4.9.3 Metabolism of Thioridazine by Control and Treated Mouse Liver Microsomes (Blake et al., 1995)

Treatment	Metabolites[a] (nmol/mg/min)[b]				
	NOR	2SO	5SO	2SONO	NO
Control microsomes	0.26 ± 0.03	1.49 ± 0.09	0.57 ± 0.04	0.13 ± 0.01	0.23 ± 0.00
Boiled microsomes[c]	0[f]	0[f]	0[f]	0.09 ± 0.03	0[f]
Heat-treated microsomes[d]	0.13 ± 0.00[f]	1.15 ± 0.08	0.65 ± 0.05	0.15 ± 0.02	0.03 ± 0.01[f]
Antireductase-treated microsomes[e]	0[f]	0.03 ± 0.01[f]	0.23 ± 0.06	0.09 ± 0.02	0.13 ± 0.02

[a]Incubations were performed at 37°C for 30 min, before extraction. Metabolites are northioridazine (NOR), thioridazine 2-sulfoxide (2SO), thioridazine 5-sulfoxide (5SO), thioridazine 2-sulfoxide *N*-oxide (2SONO), and thioridazine *N*-oxide (NO).

[b]N ≥ 4. Numbers represent mean ± SE.

[c]Microsomes were boiled for 2 min prior to substrate addition.

[d]Heat treatment was at 50°C for 90 sec.

[e]Rabbit antibodies to NADPH cytochrome P450 reductase were incubated with microsomes for 10 min at 37°C using 2 mg antireductase per mg microsomal protein. This amount of antireductase was shown in preliminary assays to inhibit >90% cytochrome c reducatase.

[f]Significantly different from control microsomes, $p < 0.05$.

Literature Cited

Atta-Asafo-Adjei, E., Lawton, M.P., and Philpot, R.M. 1993. Cloning, sequencing, distribution, and expression in *Eschericia coli* of flavin-containing monooxygenase 1C1. *J. Biol. Chem.* 268:9681-9689.

Blake, B.L., Rose, R.L., Mailman, R.B., Levi, P.E., and Hodgson, E. 1995. Metabolism of thioridazine by microsomal monooxygenases: relative roles of P450 and flavin-containing monooxygenase. *Xenobiotica* 25:377-393.

Burnett, V.L., Lawton, M.P., and Philpot, R.M. 1994. Cloning and sequencing of flavin-containing monooxygenases FMO3 and FMO4 from rabbit and characterization of FMO3. *J. Biol. Chem.* 269:14314-14322.

Cashman, J.R., Bi, Y-A, Lin, J., Youil, R., Knight, M., Forrest, S., and Treacy, E. 1997. Human flavin-containing monooxygenase form 3: cDNA expression of the enzymes containing amino acid substitutions observed in individuals with trimethylaminuria. *Chemic. Res. Toxicol.* 10:837-841.

Cherrington, N.J., Cao, Y., Cherrington, J.W., Rose, R.L., and Hodgson, E. 1998. Physiological factors affecting protein expression of flavin-containing monooxygenases 1, 3 and 5. *Xenobiotica* 7:673-682.

Devereux, T.R., Philpot, R.M., and Fouts, J.R. 1977. The effects of Hg^{2+} on rabbit hepatic and pulmonary solubilized, partially purified *N*,*N*-dimethylaniline *N*-oxidases. *Chem. Biol. Interact.* 15:277-287.

Dixit, A. and Roche, T.S. 1984. Spectrophotometric assay of the flavin-containing monooxygenase and changes in its activity in female mouse liver with nutritional and diurnal conditions. *Arch. Biochem. Biophys.* 233:50-63.

Elfarra, A.A. 1995. Potential role of the flavin-containing monooxygenases in the metabolism of endogenous compounds. *Chem.-Biol. Interact.* 96:47-55.

Falls, J.G., Blake, B.L., Cao, Y., Levi, P.E., and Hodgson, E. 1995. Gender differences in hepatic expression of flavin-containing monooxygenase isoforms (FMO1, FMO3, and FMO5) in mice. *J. Biochem. Toxicol.* 10:171-177.

Falls, J.G., Ryu, D.-Y., Cao, Y., Levi, P.E., and Hodgson, E. 1997. Regulation of mouse liver flavin-containing monooxygenases 1 and 3 by sex steroids. *Arch. Biochem. Biophys.* 342:212-223.

Grothusen, A., Hardt, J., Brautigam, L., Lang, D., and Bocker, R. 1996. A convenient method to discriminate between cytochrome P450 enzymes and flavin-containing monooxygenases in human liver microsomes. *Arch. Toxicol.* 71:64-71.

Hodgson, E., Blake, B.L., Levi, P.E., Mailman, R.B., Lawton, M.P., Philpot, R.M., and Genter, M.B. 1995. Flavin-containing monooxygenases: Substrate specificity and complex metabolic pathways. *In* Molecular Aspects of Oxidative Drug Metabolizing Enzymes: Their Significance in Environmental Toxicology, Chemical Carcinogenesis and Health (E. Arinc, J.B. Schenkman, E. Hodgson, eds.) pp. 225-235, NATO ASI Series, Vol. H90, Springer-Verlag, Berlin Heidelberg.

Hodgson, E., Cherrington, N., Coleman, S.C., Liu, S., Falls, J.G., Cao, Y., Goldstein, J.E., and Rose, R.L. 1997. Flavin-containing monooxygenase

and cytochrome P450 mediated metabolism of pesticides: From mouse to human. *Rev. Toxicol*. 2:231-243.

Kinsler, S., Levi, P.E., and Hodgson, E. 1988. Hepatic and extra-hepatic microsomal oxidation of phorate by the cytochrome P450 and FAD-containing monooxygenase systems in the mouse. *Pestic. Biochem. Physiol.* 31:54-60.

Kinsler, S., Levi, P.E., and Hodgson, E. 1990. Relative contributions of the cytochrome P450 and flavin-containing monooxygenases to the microsomal oxidation of phorate following treatment of mice with phenobarbital, hydrocortisone, acetone and piperonyl butoxide. *Pestic. Biochem. Physiol*. 37:174-181.

Lawton, M.P., Gasser, R., Tynes, R.E., Hodgson, E., and Philpot, R.M. 1990. The flavin-containing monooxygenase enzymes expressed in rabbit liver and lung are products of related but distinctly different genes. *J. Biol. Chem*. 265:5855-5861.

Lawton, M.P., Cashman, J.R., Cresteil, T., Dolphin, C.T., Elfarra, A.A., Hines, R.N., Hodgson, E., Kimura, T., Ozols, J., Phillips, I.R., Philpot, R.M., Poulsen, L.L., Rettie, A.E., Shephard, E.A., Williams, D.E., and Ziegler, D.M. 1994. A nomenclature for the mammalian flavin-containing monooxygenase gene family based on amino acid sequence identities. *Arch. Biochem. Biophys.* 308:254-257.

Sabourin, P.J., Myser, B.P., and Hodgson, E. 1984. Purification of the flavin-containing monooxygenase from mouse and pig liver microsomes. *Int. J. Biochem.* 16:713-720.

Schlenk, D. 1998. Occurrence of flavin-containing monooxygenases in non-mammalian eukaryotic organisms. *Comp. Biochem. Physiol. C. Pharmacol. Toxicol. Endocrin.* 121:185-195.

Tynes, R.E. and Hodgson, E. 1985. Catalytic and substrate specificity of the flavin-containing monooxygenase in microsomal systems: Characterization of the hepatic, pulmonary and renal enzymes of the mouse, rabbit, and rat. *Arch. Biochem. Biophys.* 240:77-93.

Tynes, R.E., Sabourin, P.J., and Hodgson, E. 1985. Identification of distinct hepatic and pulmonary forms of microsomal flavin-containing monooxygenase in mouse and rabbit. *Biochem. Biophys. Res. Commun.* 126:1069-1075.

Venkatesh, K., Levi, P.E., and Hodgson, E. 1991. The effect of detergents on the purified flavin-containing monooxygenase of mouse liver, kidney and lungs. *Gen. Pharmacol.* 22:549-522.

Williams, D.E., Hale, S.E., Muerhoff, A.S., and Masters, B.S.S. 1985. Rabbit lung flavin-containing monooxygenase. Purification, characterization and induction during pregnancy. *Molec. Pharmacol.* 28:381-390.

Williams, D.E., Ziegler, D.M., Nordin, D.J., Hale, S.E., and Masters, B.S.S. 1984. Rabbit lung flavin-containing monooxygenase is immunologically and catalytically distinct from the liver enzyme. *Biochem Biophys. Res. Commun.* 125:116-122.

Zeigler, D.M. 1980. Flavin-containing monooxygenases: Catalytic mechanism and substrate specificities. *In* Enzymatic Basis of Detoxication (W.B. Jakoby, ed.), vol. 1, pp. 201-225, Academic Press, New York.

Zeigler, D.M. 1988. Flavin-containing monooxygenases—Catalytic mechanism and substrate specificities. *Drug Metabolism Reviews* 19:1-32.

Zeigler, D.M. and Mitchell, C.H. 1972. Microsomal oxidase 4. Properties of a mixed-function amine oxidase isolated from pig liver-microsomes. *Arch. Biochem. Biophys*. 150:116-125.

Contributed by Randy L. Rose
North Carolina State University
Raleigh, North Carolina

Assays for the Classification of Two Types of Esterases: Carboxylic Ester Hydrolases and Phosphoric Triester Hydrolases

Esterases (EC 3.1) are a large, heterogeneous group of enzymes classified under the general category of hydrolases (EC 3). Possessed by virtually all organisms, esterases hydrolyze a wide variety of substrates that contain ester linkages. It is well known that some esterases are involved in detoxication or activation of exogenous compounds, such as therapeutic drugs, anesthetics, and pesticides. Additionally, metabolism of certain chromogenic esters allow for esterase detection and quantitation. These enzymes also hydrolyze endogenous esters, although the substrates and their physiological roles have been difficult to determine.

This unit provides assay protocols to quantitate two common classes of esterases that are known to metabolize xenobiotics in a number of organisms. The first class is called the carboxylic ester hydrolases (CEHs; EC 3.1.1). Within this group are the B-esterases, which are inhibited by organophosphates. The CEH assay (see Basic Protocol 1) colorimetrically measures endpoint metabolism of the substrate 1-naphthyl acetate to the product 1-naphthol (Fig. 4.10.1A). The other class of esterases to be assayed is the phosphoric triester hydrolases (PTEHs; EC 3.1.8). Within this class is A-esterase, which also is referred to as paraoxonase due to its ability to metabolize the insecticide, paraoxon, as well as other organophosphates. The PTEH assay (see Basic Protocol 2) colorimetrically measures endpoint metabolism of the substrate, methyl paraoxon (dimethyl-*p*-nitrophenylphosphate), to the product *p*-nitrophenol (Fig. 4.10.1B).

Esterases are commonly found in serum and in both the microsomal and soluble fractions of cells. Therefore, whole homogenates from tissues or cultured cells can be used in either assay after clarification by a single centrifugation ($10{,}000 \times g$). A serum, tissue, or cell sample can be subjected to both protocols to determine the presence of one or both classes of esterases, and to quantitate respective enzyme activities. Alternatively, these assays can aid in the identification of a purified CEH or PTEH.

CAUTION: The Material Safety Data Sheet (MSDS) on methyl paraoxon labels this compound as "highly toxic." 1-Naphthol and phenyl thiourea are labeled "toxic," while Fast Blue B Salt and sodium dodecyl sulfate (SDS) are labeled "harmful." 1-Naphthyl acetate is labeled with "caution." Handle these materials under a chemical fume hood when making stock and assay solutions. Investigators should access and read the MSDS of all chemicals prior to their use to be aware of hazards, proper handling procedures, and appropriate safety wear. At the end of experiments, extreme care should be taken to appropriately package, label, and temporarily store all chemical waste that is generated from performance of these protocols. Promptly contact the hazardous waste office of the institution for proper disposal instructions.

MEASUREMENT OF CARBOXYLIC ESTER HYDROLASE (CEH) ACTIVITY

BASIC PROTOCOL 1

This method measures hydrolysis of the carboxylic ester substrate, 1-naphthyl acetate to the product, 1-naphthol, in an endpoint assay. The product then forms a complex with Fast Blue B Salt to yield a purple-blue color, which is detectable spectrophotometrically at 595 nm. Several concentrations of 1-naphthol are used to create a standard curve for estimation of CEH activity in samples. Multiple samples can be analyzed simultaneously, as the assay is formatted for a microtiter plate reader using 96-well plates. The procedure is rapid, with a total incubation time of 35 min. With a total reaction volume of 200 µl, only a small volume of sample is necessary.

Contributed by Douglas D. Anspaugh and R. Michael Roe
Current Protocols in Toxicology (2002) 4.10.1-4.10.14

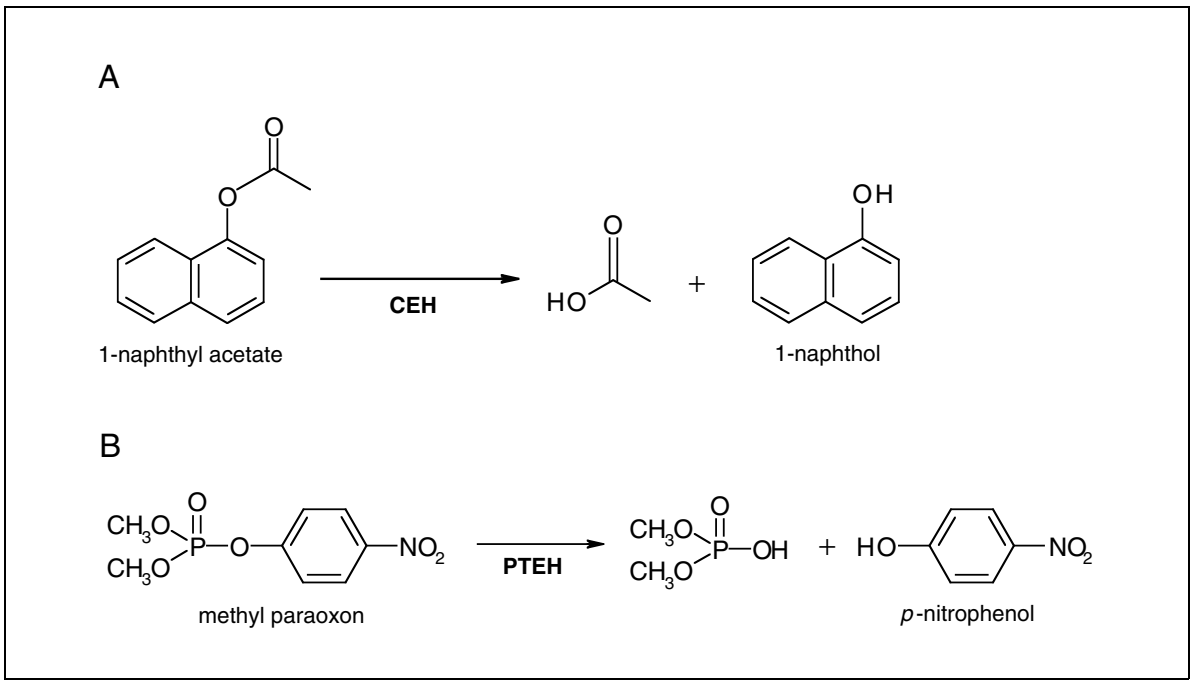

Figure 4.10.1 (**A**) Metabolism of 1-naphthyl acetate by carboxylic ester hydrolases (CEHs). (**B**) Metabolism of methyl paraoxon by phosphoric triester hydrolases (PTEHs).

Materials

100 µmol/ml 1-naphthol (see recipe)
200 mM 1-naphthyl acetate (see recipe)
0.3% (w/v) Fast Blue B Salt solution containing 3.4% (w/v) SDS (see recipe)
100 mM methyl paraoxon (see recipe)
Enzyme sample (purified protein or clarified homogenate)
100 mM sodium phosphate assay buffer, pH 7.4 (see recipe)

Spectrophotometer for microtiter plates with temperature control
Plastic 96-well, flat-bottom microtiter plates

Prepare samples and solutions

1. Turn on the microtiter plate spectrophotometer and select the endpoint mode for reading absorbance at 595 nm. Also, set the incubator to the desired assay temperature.

   Samples from mammals, birds, and E. coli normally are incubated at 37°C. An incubation temperature of 30°C may be more appropriate for fish, insect, reptile, and plant samples.

2. From stock solutions, make fresh assay solutions of 1-naphthol (100, 50, 25, 12.5, 6.25, 3.13, nmol/ml), 1-naphthyl acetate (1 mM), and methyl paraoxon (10 mM). Use sodium phosphate assay buffer for these dilutions. Also, prepare a 0.3% (w/v) Fast Blue B Salt solution containing 3.4% (w/v) SDS in distilled water (see recipes).

3. Perform preliminary CEH assays with several dilutions of enzyme sample to determine an enzyme concentration that is within the linear range for substrate hydrolysis. Make sample dilutions in ice-cold sodium phosphate assay buffer.

   A regression of sample concentration versus absorbance (OD_{595}) should produce a straight line that intersects the origin in the linear range of the assay.

4. Prepare an adequate volume of the sample concentration in the linear range of the assay for addition (steps 8 and 9) of 70 µl to each well that requires enzyme sample.

Use ice-cold sodium phosphate assay buffer for sample dilutions. Keep enzyme samples on ice before the addition of substrate.

CEH activity calculations may be inaccurate if the sample concentration assayed does not produce a linear rate of substrate hydrolysis.

Different sample preparations may vary significantly in CEH activity. If quantitating multiple samples, be aware that concentrations within the linear range of substrate hydrolysis for one sample may be different for other samples.

Avoid any delays during the execution of steps 5 to 15.

Perform CEH assay

5. For the standard blank, add 175 µl sodium phosphate assay buffer to each of three empty wells of a 96-well microtiter plate.
6. For the standards, add 175 µl to each of three empty wells for each 1-naphthol concentration (3.13, 6.25, 12.5, 25, 50, and 100 nmol/ml).
7. For the sample blank, add 75 µl of sodium phosphate assay buffer to each of three empty wells.

   This blank will detect color formation from non-enzymatic sources.

   Do not confuse sample blanks with the standard blanks (step 5). These two types of blanks differ in content.

8. For each sample, add the following in sequence to each of three empty wells:

   5 µl sodium phosphate assay buffer
   70 µl enzyme sample

9. For each sample plus methyl paraoxon treatment, add in sequence the following to each of three empty wells:

   5 µl 10 mM methyl paraoxon
   70 µl enzyme sample

   To calculate percentage inhibition, see CEH Activity Calculations below. Methyl paraoxon at the assay concentration should inhibit B-esterases (carboxylesterases, acetylcholinesterases, and cholinesterases), which generally are in abundance in many types of samples.

   Additional sample wells can be included to evaluate other inhibitors or activators of CEH activity.

10. Immediately place the plate into the microtiter plate spectrophotometer and incubate for 10 min at the assay temperature.

    If the spectrophotometer has an automix function, enable it to shake-mix the contents of the plate wells at the beginning and end of each incubation period throughout the assay.

    This incubation period allows for the methyl paraoxon to inhibit B-esterases.

11. Remove the plate from the spectrophotometer. Add 100 µl of 1.0 mM 1-naphthyl acetate substrate to all wells *except* those containing the standard blank and the standards.
12. Place the plate back into the spectrophotometer and incubate for 15 min at the assay temperature.
13. Remove the plate and add 25 µl of 0.3% Fast Blue B Salt solution containing 3.4% SDS to all wells of the assay.

14. Return the plate to the spectrophotometer and incubate for 10 min at the assay temperature.

    This incubation period allows for color development from the conjugation of naphthol-Fast Blue B.

Read samples

15. Read simultaneously the absorbance of each well at 595 nm.

16. Remove the microtiter plate from the spectrophotometer. Appropriately package and label hazardous waste from the assay, and arrange for prompt removal and disposal by the hazardous waste office of the institution.

SUPPORT PROTOCOL 1

CEH SPECIFIC ACTIVITY CALCULATIONS

The following steps for activity calculations are based on acquisition of raw absorbance readings from the endpoint mode of a microtiter plate spectrophotometer. Spectrophotometers with accompanying computer and software may be programmable for automated blank subtraction, standard curve plotting and enzyme activity calculations.

1. Subtract the mean absorbance of the three standard blank wells from the absorbance of each well that contains 1-naphthol standards. Then calculate the mean absorbance (blank subtracted) of each standard concentration from the three replicate wells per concentration.

2. Create a standard curve by plotting each 1-naphthol concentration versus its corresponding absorbance.

   After plotting the standard curve, make sure that the best-fitted line passes through the origin of the graph. Also, the correlation coefficient (r^2 value) of the line typically should be ≥0.9. If necessary, the standard curve should be repeated until these criteria are met.

3. Subtract the mean absorbance of the three sample blank wells from the absorbance of each well that contains sample and sample plus methyl paraoxon.

   The blank-subtracted absorbance value of each sample well must be between the minimum and maximum OD_{595} values of the 1-naphthol standard curve. If necessary, adjust the sample concentration and repeat the assay until the sample absorbance is in this range.

4. Use the linear regression equation of the standard curve to determine the concentration (nmol/ml) of 1-naphthol produced in each of the wells containing sample and sample plus methyl paraoxon.

   For example, with the equation $y = mx + b$, the concentration (x) can be determined by applying the blank-subtracted sample absorbance (y). The slope of the line is m, and b is the y-intercept.

5. Measure the protein concentration (mg/ml) of each sample.

6. Calculate the CEH specific activity for each well containing sample and sample plus methyl paraoxon using the following parameters: the concentration of 1-naphthol produced, the assay dilution factor of the enzyme sample, incubation time, and the protein concentration of the enzyme sample.

$$\frac{\text{nmol/ml 1-naphthol} \times \text{sample dilution factor}}{\text{incubation time (min)}} \times \frac{1\ \text{ml}}{\text{mg protein}}$$
$$= \text{nmol min}^{-1}\ \text{mg protein}^{-1}$$

7. For each sample and sample plus methyl paraoxon treatment, calculate the mean specific activity of CEH from the three replicate wells per treatment.
8. To calculate the percentage of CEH inhibition by methyl paraoxon, use the following equation:

$$\frac{(\text{specific activity of sample}) - (\text{specific activity of sample + methyl paraoxon})}{(\text{specific activity of sample})} \times 100$$

MEASUREMENT OF PHOSPHORIC TRIESTER HYDROLASE (PTEH) ACTIVITY

BASIC PROTOCOL 2

This method measures hydrolysis of the phosphoric triester substrate, methyl paraoxon. The yellow product, *p*-nitrophenol, is detectable spectrophotometrically at 405 nm. Several concentrations of *p*-nitrophenol are used to create a standard curve for estimation of PTEH activity in samples. Multiple samples can be analyzed simultaneously, as the assay is formatted for a microtiter plate reader using 96-well plates. This procedure is rapid, with a total incubation time of 45 min. With a total reaction volume of 300 µl, only a small volume of sample is necessary.

Materials

100 µmol/ml *p*-nitrophenol (see recipe)
100 mM methyl paraoxon (see recipe)
Enzyme sample (purified or clarified homogenate)
100 mM Tris·Cl assay buffer, pH 8.0 (see recipe)

Spectrophotometer for microtiter plates with temperature control
Plastic 96-well, flat-bottom microtiter plates

Prepare samples and solutions

1. Turn on the microtiter plate spectrophotometer and select the endpoint mode for reading absorbance at 405 nm. Also, set the incubator to the desired assay temperature.

   Samples from mammals, birds, and E. coli normally are incubated at 37°C. An incubation temperature of 30°C may be more appropriate for fish, insect, reptile, and plant samples.

2. For stock solutions, make fresh assay solutions of *p*-nitrophenol (100, 50, 25, 12.5, 6.25, 3.13 nmol/ml), and methyl paraoxon (2 mM). Use Tris·Cl assay buffer for these dilutions.
3. Perform preliminary PTEH assays with several dilutions of enzyme sample to determine an enzyme concentration that is within the linear range for substrate hydrolysis. Make sample dilutions in ice-cold Tris·Cl assay buffer.

   A regression of sample concentration versus absorbance (OD_{405}) should produce a straight line that intersects the origin in the linear range of the assay.

4. Prepare an adequate volume of the sample concentration in the linear range of the assay for addition (step 8) of 289 µl to each well that requires enzyme sample. Use ice-cold Tris·Cl assay buffer for sample dilutions. Keep enzyme samples on ice before the addition of substrate.

   PTEH activity calculations may be inaccurate if the sample concentration assayed does not produce a linear rate of substrate hydrolysis.

Different sample preparations may vary significantly in PTEH activity. If quantitating multiple samples, be aware that concentrations within the linear range of substrate hydrolysis for one sample may be different for other samples.

Avoid any delays during the execution of steps 5 to 10.

Perform PTEH assay

5. For the standard blank, add 300 µl of 100 mM Tris·Cl assay buffer to each of three empty wells of a 96-well microtiter plate.
6. For the standards, add 300 µl to each of three empty wells for each *p*-nitrophenol concentration (3.13, 6.25, 12.5, 25, and 100 nmol/ml).
7. For the sample blank, add the following to each of three empty wells of the microtiter plate:

   11 µl of 2 mM methyl paraoxon
   289 µl of 100 mM Tris·Cl assay buffer

   This blank will measure the non-enzymatic rate of substrate hydrolysis.

   Do not confuse sample blanks with the standard blanks (step 5). These two types of blanks differ in content.
8. For each sample, add the following to each of three empty wells of the microtiter plate:

   11 µl of 2 mM methyl paraoxon
   289 µl of enzyme sample
9. Immediately place the microtiter plate into the spectrophotometer and incubate for 45 min at the assay temperature.

   If the spectrophotometer has an automix function, enable it to shake-mix the contents of the plate wells at the beginning and end of the incubation period.

   Within the first few minutes of incubation, a fraction of methyl paraoxon will bind and inhibit B-esterases. The remainder of the organophosphate then acts solely as a substrate for PTEH.

Read samples

10. Read simultaneously the absorbance of each well at 405 nm.
11. Remove the microtiter plate from the spectrophotometer. Appropriately package and label hazardous waste from assay, and arrange for prompt removal and disposal by the hazardous waste office of the institution.

SUPPORT PROTOCOL 2

PTEH SPECIFIC ACTIVITY CALCULATIONS

The following steps for activity calculations are based on acquisition of raw absorbance readings from the endpoint mode of a microtiter plate spectrophotometer. Spectrophotometers with accompanying computer and software may be programmable for automated blank subtraction, standard curve plotting, and enzyme activity calculations.

1. Subtract the mean absorbance of the three standard blank wells from the absorbance of each well that contains *p*-nitrophenol standards. Then calculate the mean absorbance (blank subtracted) of each standard concentration from the three replicate wells per concentration.

2. Create a standard curve by plotting each *p*-nitrophenol concentration versus its corresponding absorbance.

   After plotting the standard curve, make sure that the best-fitted line passes through the origin of the graph. Also, the correlation coefficient (r^2 value) of the line typically should be ≥0.9. If necessary, the standard curve should be repeated until these criteria are met.

3. Subtract the mean absorbance of the three sample blank wells from the absorbance of each well that contains sample.

   The blank-subtracted absorbance value of each sample well must be between the minimum and maximum OD_{405} values of the p-nitrophenol standard curve. If necessary, adjust the sample concentration and repeat the assay until the sample absorbance is in this range.

4. Use the linear regression equation of the standard curve to determine the concentration (nmol/ml) of *p*-nitrophenol produced in each of the wells containing sample.

   For example, with the equation $y = mx + b$, the concentration (x) can be determined by applying the blank-subtracted sample absorbance (y). The slope of the line is m, and b is the y-intercept.

5. Measure the protein concentration (mg/ml) of each sample.

6. Calculate the PTEH specific activity for each well containing sample using the following parameters: the concentration of *p*-nitrophenol produced, the assay dilution factor of the enzyme sample, incubation time, and the protein concentration of the enzyme sample.

$$\frac{\text{nmol/ml } p\text{-nitrophenol} \times \text{sample dilution factor}}{\text{incubation time (min)}} \times \frac{1\text{ ml}}{\text{mg protein}}$$
$$= \text{nmol min}^{-1}\text{ mg protein}^{-1}$$

7. For each sample, calculate the mean specific activity of PTEH from the three replicate wells.

REAGENTS AND SOLUTIONS

Use Milli-Q-purified water or equivalent in all recipes and protocol steps. For common stock solutions, see ***APPENDIX 2A****; for supplies, see* ***SUPPLIERS APPENDIX****.*

Fast Blue B Salt solution, 0.3% (w/v) containing 3.4% (w/v) SDS

In a foil-covered container, dissolve 30.0 mg of Fast Blue B Salt (~90%; Aldrich) in distilled water for a total volume of 3.0 ml. In a separate container, add 340.0 mg of SDS (sodium dodecyl sulfate salt) in distilled water for a total volume of 7.0 ml. To dissolve the SDS, gently swirl its container by hand to minimize foaming. When both chemicals are dissolved, add the SDS solution to the Fast Blue B Salt solution container. Mix by gentle hand swirling. This solution is stable for ~2 hr.

Fast Blue B Salt is light sensitive and must be kept in darkness except when weighing, and during addition of this solution to the assay.

CAUTION: *SDS is a respiratory irritant. A dust mask should be worn during weighing and mixing of SDS.*

Methyl paraoxon, 100 mM

Stock solution: Add 24.71 mg of methyl paraoxon (99.1%; Chem Service) to 100% ethanol for a final volume of 1.0 ml. Vortex until dissolved. Store in a tightly sealed container for up to 1 month at 4°C.

Inhibitor solution for CEH assay (10 mM): Make fresh daily by diluting the stock solution with 100 mM sodium phosphate assay buffer, pH 7.4 (see recipe).

Substrate solution for PTEH assay (2 mM): Make fresh daily by diluting the stock solution with 100 mM Tris·Cl assay buffer, pH 8.0 (see recipe).

CAUTION: *Methyl paraoxon is highly toxic! Appropriate protective gloves and eyewear should be worn, and a chemical fume hood should be used when making and diluting solutions.*

1-Naphthol, 100 µmol/ml

Stock solution: Add 14.42 mg of 1-naphthol (99+%; Aldrich) to 100% ethanol for a total volume of 1.0 ml. Vortex until dissolved. Store in a tightly sealed container for up to 1 month at −20°C.

CEH standard assay solutions (100, 50, 25, 12.5, 6.25, and 3.13 nmol/ml): Make fresh daily by diluting the stock solution with 100 mM sodium phosphate assay buffer, pH 7.4 (see recipe).

1-Naphthyl acetate, 200 mM

Stock solution: Add 37.24 mg of 1-naphthyl acetate (99+%; Sigma) to 100% ethanol for a total volume of 1.0 ml. Vortex until dissolved. Store in a tightly sealed container for up to 1 month at −20°C.

CEH substrate assay solution (1 mM): Make fresh daily by diluting the stock solution with 100 mM sodium phosphate assay buffer, pH 7.4 (see recipe).

p-Nitrophenol, 100 µmol/ml

Stock solution: Add 13.91 mg of *p*-nitrophenol (99%; Fluka Chemical) to 100% ethanol for a total volume of 1.0 ml. Vortex until dissolved. Store in a tightly sealed container for up to 1 month at −20°C.

PTEH standard assay solutions (100, 50, 25, 12.5, 6.25 and 3.13 nmol/ml): Make fresh daily by diluting the stock solution with 100 mM Tris·Cl assay buffer, pH 8.0 (see recipe).

Sodium phosphate assay buffer, 100 mM (pH 7.4)

Monobasic stock solution, 1 M: Add 11.996 g of monobasic sodium phosphate (NaH_2PO_4) to distilled water for a total volume of 100 ml. Heat to dissolve if necessary. Store for up to 2 months at 4°C. Heat to re-dissolve if precipitation occurs.

Dibasic stock solution, 1 M: Add 14.196 g of dibasic sodium phosphate (Na_2HPO_4) to distilled water for a total volume of 100 ml. Heat to dissolve if necessary. Store for up to 2 months at 4°C. Heat to re-dissolve if precipitation occurs.

Sodium phosphate assay buffer, 100 mM (pH 7.4): At 25°C, add 2.26 ml of 1 M monobasic stock solution and 7.74 ml of 1 M dibasic stock solution to 90 ml of distilled water. Mix thoroughly and measure to assure a pH of 7.4. If pH is not 7.4, remake assay buffer with new monobasic and dibasic stock solutions. Store for up to 2 months at 4°C.

For homogenization of insects, add phenyl thiourea (PTU) to the assay buffer. Under a chemical fume hood, heat-dissolve the PTU in a small volume of water, and then add to the assay buffer for a concentration of 0.01% (w/v). PTU will present blackening of the sample by inhibiting tyrosinases.

Tris·Cl assay buffer, 100 mM (pH 8.0)

Dissolve 1.211 g of Tris base in distilled water for a total volume of 80 ml. Adjust the pH to 8.0 with concentrated HCl. Bring total volume to 100 ml with distilled water. Store up to 1 month at 4°C.

For homogenization of insects, add phenyl thiourea (PTU) to the assay buffer. Under a chemical fume hood, heat-dissolve the PTU in a small volume of water, and then add to the assay buffer for a concentration of 0.01% (w/v). PTU will prevent blackening of the sample by inhibiting tyrosinases.

COMMENTARY

Background Information

Esterases are monomeric (mol. wt. 40,000 to 60,000) or heteromeric (mol. wt. ≤200,000) proteins present in the soluble and microsomal cell fractions. Some may have post-translational modifications, including glycosylation and the addition of lipids (Urich, 1994). The types of esterases present and levels of activity can be highly variable from one species to another, and may differ even between individuals of the same species. Several factors can influence these differences, including life stage, hormones, sex, diet, food quality, genetic polymorphism, disease, and environmental conditions. Some esterases are associated with specific tissues, while others are ubiquitous within an organism (Devorshak and Roe, 1998).

The esterases cleave aliphatic esters of short-chain carboxyl acids, aromatic esters, aromatic amides, phosphoesters, and thioesters. The physiological function of many esterases is still obscure, but they probably are essential because their genetic codes have been preserved throughout evolution (Van Zutphen et al., 1988; Urich, 1994). Several studies have suggested that human serum esterases are involved in metabolizing various classes of lipids, such as mono- and triacylglycerols (Tsujita and Okuda, 1983; Shirai et al., 1988). Accumulation of such lipids may be caused by poor esterase metabolism, which has been implicated in the development of human atherosclerosis and myocardial infarction (McElveen et al., 1986; Mackness, 1989). A well-known endogenous esterase substrate is acetylcholine, which is specifically metabolized by acetylcholinesterase in nerve tissue for proper impulse transmission. In insects, an esterase has been discovered that is highly specific for the endogenous substrate, juvenile hormone (JH). JH esterase metabolism of JH at critical time points is essential for proper insect development and metamorphosis (Roe et al., 1993). In general, however, evidence of specific endogenous substrates for esterases is scarce.

Numerous exogenous esterase substrates, including xenobiotics, have been identified. Typically, esterase metabolism of xenobiotics is a detoxication mechanism that produces a less toxic, more water-soluble compound for excretion. In some cases however, the parent compound is activated by esterases, rendering higher toxicity to the intermediates or final products. Examples of exogenous substrates include ester and amide derivatives of drugs, nerve gases (tabun, sarin, and DFP), plasticizers that contain phthalic acid esters, herbicides with phenoxyacetic and picolinic acid esters, and several classes of insecticides (Hodgson and Levi, 1994). Development of resistance in insects to the organophosphate, pyrethroid, and carbamate insecticides has been attributed to esterases. The mechanism of resistance usually is associated with increased esterase production, which enhances detoxication or sequestration of the insectisides (see Devorshak and Roe, 1998).

In 1953, Aldridge proposed a classification system of esterases based upon their interaction with organophosphorus compounds (OPs). "A"-esterases hydrolyze OPs like paraoxon, methyl paraoxon, and diisopropylphosphorofluoridate (DFP), while "B"-esterases are inhibited by OPs. With A- and B-esterases, the OPs are substrates for the enzyme. But in the case of the B-esterases, these compounds act as suicide substrates by binding their phosphoryl moieties to the enzymes (Walker, 1989).

Since the time of Aldridge's discovery of A- and B-esterases, hundreds of types of esterases have been discovered. The Enzyme Commission of the International Union of Biochemistry and Molecular Biology (IUBMB, 1992) has classified these esterases based upon their metabolic activities toward a variety of artificial substrates. This classification system has been

criticized heavily for several reasons (Pen and Beintema, 1986; Urich, 1994). First, artificial substrates are used, since neither the endogenous substrate nor the biological function is known for most esterases. Second, substrate preferences can be highly overlapping between the defined classes. Third, many esterases exist in multiple forms (isozymes) due to genetic polymorphism, or as a result of variable glycosylation and other post-translational modifications. Fourth, other enzymes have esterase activity, such as serine proteases. Also, proteins that usually are not considered to be enzymes, like serum albumins, can have esterase activity. Finally, only a few esterases have been purified extensively for characterization. When working with unpurified homogenates, substrate metabolism may result from more than one type of esterase, or perhaps from a protein other than an esterase. Because of these pitfalls, the classification system used today lends itself to problems of ambiguity and redundancy. Ideally, the classification of esterases would be similar to that of enzymes such as the cytochrome P450s, which is based on a genealogical tree constructed from the relativity of nucleic acid and peptide sequences. Unfortunately molecular genetics data on esterases are insufficient at this time to derive such nomenclature. Until the volume of molecular data is adequate to develop this type of classification system for esterases, suggestions for improvement (e.g., Heymann 1989; Walker, 1989) of the current system should be considered and implemented when deemed appropriate.

Despite the difficulties and controversy associated with the identification and classification of esterases in the past, Aldridge's scheme still is used today to distinguish and quantitate esterases that metabolize OPs, and those that are inhibited by these compounds. However, the methodology of detecting these esterases, and the nomenclature (discussed below) has changed significantly. Originally, Aldridge used *p*-nitrophenyl esters (acetate, propionate, and butyrate) as substrates in a manometric, rather than a colorimetric method. Enzyme activity was estimated kinetically, based on the CO_2 liberated from bicarbonate buffer by the acid produced during hydrolysis (Aldridge, 1953). A- and B-esterases were distinguished by the difference in activity between reactions with, and without paraoxon. The disadvantages of this assay include a tedious protocol, low sensitivity of detection, and use of large sample volumes. Also, it was time consuming since only one sample could be measured at a time. The esterase protocols presented here have the advantages of being colorimetric and miniaturized for multi-well microtiter plates. This simpler format allows for rapid, simultaneous quantitation of multiple samples. Additionally, these assays are very sensitive and require less sample material. Other colorimetric esterase assays have been published previously (see below), but these macroassay procedures utilized large sample volumes and were limited to one sample reading at a time.

The first assay presented (see Basic Protocol 1) is for the measurement of carboxylic ester hydrolases (CEHs; EC 3.1.1). Currently, there are 66 subclasses of enzymes within this group, including the B-esterases, which are inhibited by OPs. B-esterases include carboxylesterase (EC 3.1.1.1), acetylcholinesterase (EC 3.1.1.7), and cholinesterase (EC 3.1.1.8). Besides the B-esterases, there is a wide variety of other CEHs, such as arylesterase (EC 3.1.1.2), sterol esterase (EC 3.1.1.13), α-amino acid esterase (EC 3.1.1.43), insect juvenile hormone esterase (EC 3.1.1.59), and several lipases and lactonases. Originally, the assay for CEHs was miniaturized and modified by Abdel-Aal et al. (1990) from macroassays by Gomori (1953) and van Asperen (1962). This procedure measures hydrolysis of the substrate, 1-naphthyl acetate, to the product, 1-naphthol. Although some researchers consider 1-naphthyl acetate to be specific for carboxylesterases, the protocol presented here is titled more generally due to the possibility that other CEHs can metabolize this substrate. To determine if metabolism of 1-naphthyl acetate was a result of B-esterases, esterase activity can be quantitated from samples with, and without the addition of methyl paraoxon.

The second protocol described (see Basic Protocol 2) is for detection of phorphoric triester hydrolases (PTEHs; EC 3.1.8). Currently, there are only two subclasses of esterases in this group. Besides A-esterase, now called aryldialkylphosphatase (EC 3.1.8.1) by the IUBMB, the other member is diisopropyl-fluorophosphatase (EC 3.1.8.2), or DFP-ase. Both of these enzymes metabolize OPs, including esters of phosphonic and phosphinic acids, and those with phosphorus anhydride bonds (IUBMB, 1992). The assay is a modification of a microtiter plate procedure developed by Devorshak and Roe (2001), which is based on a macroassay described by Furlong et al. (1988). The substrate is methyl paraoxon, which when

metabolized by PTEHs, yields the yellow-colored product, *p*-nitrophenol. The assay discriminates against B-esterases, as this activity is inhibited by the organophosphorus substrate.

Several inhibitors and activators of PTEH activity have been documented (Aldridge, 1953; Shishido and Fukami, 1972; Konno et al., 1990; Devorshak and Roe, 2001). Perhaps the most effective PTEH inhibitors are mercuric compounds such as *p*-chloromercuribenzoate (PCMB). Other metal ions such as Ag^{+}, Cd^{2+}, Cu^{2+}, and Sn^{4+} can also inhibit PTEHs, as well as PO_4 and ethylenediaminetetraacetic acid (EDTA). In general, these inhibitors are not as potent as mercury, and results differ widely among various biological samples. PTEH activity may be enhanced by addition of Ca^{2+}, Co^{2+}, and Mn^{2+}. These ions act as important cofactors for PTEH activity, and may be present naturally in samples from serum or whole homogenates from cells or tissues. Purified PTEH samples, however, may require addition of one or more of these cofactors to elicit activity. In mammals, Ca^{2+} appears to be the most important cofactor, while Co^{2+} and Mn^{2+} activate insect PTEH activity (Dauterman, 1976). Inhibition of PTEH by Hg^{2+} and the metal chelator EDTA, and activation by divalent cations suggests that PTEH may have a cysteine residue involved in the catalytic mechanism. This is not the case for the B-esterases, which have a serine at the active site of the enzyme (Aldridge, 1989).

Utilizing both protocols, one can determine quickly if biological samples contain CEHs, PTEHs, or both types of esterases. Furthermore, esterase activity can be detected in the pmol min^{-1} mg $protein^{-1}$ range. With the miniaturized microtiter plate design of these assays, multiple, small-volume samples can be tested simultaneously. Finally, additional treatments can be added to either assay for screening of classical or putative inhibitors or activators of these esterases.

Critical Parameters and Troubleshooting

Sample preparation

Small particles suspended in the supernatants of sample homogenates following centrifugation (10,000 × *g*) can cause erroneous absorbance readings. This suspended material can be eliminated by filtration of supernatants through glass wool. The glass wool should be cleaned with HPLC-grade hexane and then air-dried before use. Supernatants of samples can be assayed fresh or can be stored at –20° to –80°C until the time of assay. When freezing, make small aliquots of each sample to avoid repetitive freeze-thawing that could decrease enzyme activity. Always hold samples on ice immediately after thawing and until addition to the microtiter plate.

It is advisable to include in all assays a positive control sample (if available) that is known to have detectable activity of the esterase of interest. Modifications to the assay protocol may be necessary if activity is detectable in the positive control, but not in an unknown sample. For example, increasing sample concentration or incubation time may be necessary to detect low levels of activity. Additionally, some esterases are more active at slightly higher or lower pH than is listed in the protocol. Samples can be assayed at a range of pH values to determine optimal conditions for esterase activity. If the adjustment of assay conditions does not elicit detectable enzyme activity, it may be possible that the sample either has no activity, or it is too low for detection.

Assay conditions

For CEH and PTEH assays, enzyme activity measurements will be inaccurate if the enzyme concentration is not within the linear range of substrate hydrolysis. As described in Basic Protocols 1 and 2, preliminary assays may be necessary to identify an appropriate enzyme concentration.

The substrates, 1-naphthyl acetate and methyl paraoxon, are considered to be specific for carboxylic ester hydrolases and phosphoric triester hydrolases, respectively. Despite this consideration, it should be realized that there is the possibility for the substrates to be metabolized by other enzymes.

Whenever inhibitors or activators are added to the assays in a solvent, rather than an aqueous diluent, the total percentage of solvent (including substrate addition) in the final reaction volume should never exceed 1.0%. Higher solvent percentages could significantly affect enzyme activity.

When performing CEH assays, potassium phosphate should not be substituted for sodium phosphate buffer. Potassium will precipitate upon the addition of Fast Blue B-SDS solution in the assay.

Concerning the PTEH assay, there are several parameters that are critical for successful activity quantitation. Perhaps most important is proper pH of the enzymatic reactions. If the assay pH is too basic, high background may

Table 4.10.1 Results from Carboxylic Ester Hydrolase (CEH) Assay

	CEH activity (nmol min^{-1} mg $protein^{-1}$)	% Inhibition by methyl paraoxon[a]
Mouse liver	171	100
Porcine liver	13,713	99
Tobacco budworm	64	98

[a]Final assay concentration of 667 μM.

Table 4.10.2 Results of the Phosphoric Triester Hydrolase (PTEH) Assay

	PTEH activity (pmol min^{-1} mg $protein^{-1}$)
Mouse liver	42
Porcine liver	5
Tobacco budworm	100

result from non-enzymatically hydrolyzed methyl paraoxon. If the assay pH is too acidic, the *p*-nitrophenol product loses its yellow color, and PTEH activity will not be detectable. For ideal activity measurements with low background, the assay should be pH 8.0 to 8.5. PTEH activity is highest at this pH range in mammals and insects. Also, the use of Tris·Cl buffer (pH 8.0) is highly recommended for sample preparation and assay reactions in PTEH assays. Other buffers may have constituents that affect PTEH activity. For instance, buffers containing phosphate ions or ethylenediaminetetraacetic acid (EDTA) can reduce or even fully inhibit PTEH activity.

Anticipated Results

Mouse liver, porcine liver, and the tobacco budworm, *Heliothis virescens* (whole body, 5th stadium larva) were analyzed for CEH (Table 4.10.1) and PTEH (Table 4.10.2) specific activity by following the two protocols above. Whole homogenates were prepared from mouse liver and tobacco budworm in Tris·Cl buffer (pH 8.0) by use of a Polytron PT10/35 homogenizer (Brinkman Instruments). The homogenates were centrifuged for 15 min at 10,000 × *g*, and then filtered through glass wool. The porcine liver (41 U/mg) was ordered as a crude lyophilized powder from Sigma Chemical, and was resuspended in Tris·Cl assay buffer, pH 8.0. Samples were diluted in sodium phosphate assay buffer, pH 7.4, for CEH assays and Tris·Cl assay buffer, pH 8.0, for PTEH assays. Protein concentrations were determined by the Bio-Rad assay with bovine serum albumin as the standard.

Basic Protocol 1

See the CEH protocol for general assay requirements. Assays were performed at pH 7.4, and incubated with substrate for 15 min. The incubation temperature for mouse liver and porcine liver was 37°C, while the tobacco budworm sample was incubated at 30°C. Protein concentrations used for assays were 180, 382, and 37 μg for mouse, porcine, and tobacco budworm, respectively. For inhibitor treatments, methyl paraoxon (667 μM final assay concentration) was added to the sample for a 10-min incubation before addition of substrate. The specific activity (nmol min^{-1} mg $protein^{-1}$) and % inhibition by methyl paraoxon for each sample were calculated using the formulae in the CEH Calculations (see Support Protocol 1). See Table 4.10.1 for results.

Basic Protocol 2

See the PTEH protocol for general assay requirements. Assays were performed at pH 8.0, and incubated with substrate for 45 min. The incubation temperature for mouse liver and porcine liver was 37°C, while the tobacco budworm sample was incubated at 30°C. Protein concentrations used for assays were 2.30, 0.03, and 3.81 μg for mouse, porcine, and tobacco budworm, respectively. The specific activity (pmol min^{-1} mg $protein^{-1}$) for each sample was calculated using the formula in the PTEH Cal-

culations (see Support Protocol 2). See Table 4.10.2 for results.

Time Considerations

For both assays, the total time required to perform the reactions depends on the number of samples and inhibitors to be analyzed. If adequate activity is detected with the incubation times listed for each protocol, the CEH assay can be performed in 45 to 60 min, while the PTEH assay may take 60 to 75 min. This time estimation does not include the preparation of buffers, standards, substrates, or enzyme dilutions.

Literature Cited

Abdel-Aal, Y.A.I., Wolff, M.A., Roe, R.M., and Lampert, E.P. 1990. Aphid carboxylesterases: Biochemical aspects and importance in the diagnosis of insecticide resistance. *Pestic. Biochem. Physiol.* 38:255-266.

Aldridge, W.N. 1953. Serum Esterases 1. Two types of esterase (A and B) hydrolysing *p*-nitrophenyl acetate, propionate, and butyrate, and a method for their determination. *Biochem. J.* 53:110-117.

Aldridge, W.N. 1989. A-esterases and B-esterases in perspective. *In* Enymes Hydrolyzing Organophosphorus Compounds (E. Reiner, W.N. Aldridge, and F.C.G. Hoskin, eds.) pp. 1-14. John Wiley and Sons, New York.

Dauterman, W.C. 1976. Extramicrosomal metabolism of insecticides. *In* Insecticide Biochemistry and Physiology (C.F. Wilkinson, ed.) pp. 149-176. Plenum, New York.

Devorshak, C. and Roe, R.M. 1998. The role of esterases in insecticide resistance. *Rev. Toxicol.* 2:501-537.

Devorshak, C. and Roe, R.M. 2001. Purification and characterization of a phosphoric triester hydrolase from the tufted apple bud moth, *Platynota idaeusalis* (Walker). *J. Biochem. Mol. Tox.* 15:55-65.

Furlong, C.E., Richter, R.J., Seidel, S.L., and Motulsky, A.G. 1988. Role of genetic polymorphism of human plasma paraoxonase/arylesterase in hydrolysis of the insecticide metabolites chlorpyrifos oxon and paraoxon. *Am. J. Hum. Genet.* 43:230-238.

Gomori, G. 1953. Human esterases. *J. Lab. Clin. Med.* 42: 445-453.

Heymann, E. 1989. A proposal to overcome some general problems of the nomenclature of esterases. *In* Enymes Hydrolyzing Organophosphorus Compounds (E. Reiner, W.N. Aldridge, and F.C.G. Hoskin, eds.) pp. 226-235. John Wiley and Sons, New York.

Hodgson, E. and Levi, P.E. 1994. Metabolism of toxicants: Phase I reactions. *In* Introduction to Biochemical Toxicology, 2nd ed. (E. Hodgson and P.E. Levi, eds.) pp. 75-112. Appleton & Lange, Conn.

International Union of Biochemistry and Molecular Biology, Nomenclature Committee. 1992. Enzyme Nomenclature 1992. Academic Press, San Diego.

Konno, T., Kasai, Y., Rose, R.L., Hodgson, E., Dauterman, W.C. 1990. Purification and characterization of a phosphotriester hydrolase from methyl parathion-resistant *Heliothis virescens*. *Pestic. Biochem. Physiol.* 36:1-13.

Mackness, M.I. 1989. Possible medical significance of human serum 'A'-esterases. *In* Enzymes Hydrolyzing Organophosphorus Compounds (E. Reiner, W.N. Aldridge, and F.C.G. Hoskin, eds.) pp. 202-213. John Wiley and Sons, New York.

McElveen, J., Mackness, M.I., Colley, C.M., Peard, T., Warner, S., and Walker, C.H. 1986. Distribution of paraoxon hydrolytic activity in the serum of patients after myocardial infarction. *Clin. Chem.* 32:671-673.

Pen, J. and Beintema, J.J. 1986. Nomenclature of esterases. *Biochem. J.* 240:933.

Roe, R.M., Jesudason, P., Venkatesh, K., Kallapur, V.L., Anspaugh, D.D., Majumder, C., Linderman, R.J., and Graves, D.M. 1993. Developmental role of juvenile hormone metabolism in Lepidoptera. *Amer. Zool.* 33:375-383.

Shirai, K., Ohsawa, J., Saito, Y., and Yoshida, S. 1988. Effects of phospholipids on hydrolysis of trioleoylglycerol by human serum carboxylesterase. *Biochim. Biophys. Acta* 962:377-383.

Shishido, T. and Fukami, J. 1972. Enzymatic hydrolysis of diazoxon in rat tissue homogenates. *Pestic. Biochem. Physiol.* 2:39-50.

Tsujita, T. and Okuda, H. 1983. Carboxylesterases in rat and human sera and their relationship to serum aryl acylamidases and cholinesterases. *Eur. J. Biochem.* 133:215-220.

Urich, K. 1994. Ester hydrolases, ATPases and carboanhydrases. *In* Comparative Animal Biochemistry. pp. 657-684. Springer-Verlag, New York.

van Asperen, K. 1962. A study of housefly esterases by means of a sensitive colorimetric method. *J. Insect Physiol.* 8:401-416.

Van Zutphen, L.F.M. and Den Bieman, M.G.C.W. 1988. Gene mapping and linkage homology. *In* New Developments in Biosciences: Their Implications for Laboratory Animal Science (A.C. Beynen and H.A. Solleveld, eds.) pp.197-200. Martinus Nijhoff Publishers, Dordrecht.

Walker, C.H. 1989. The development of an improved system of nomenclature and classification of esterases. *In* Enymes Hydrolyzing Organophosphorus Compounds (E. Reiner, W.N. Aldridge, and F.C.G. Hoskin, eds.) pp. 236-245. John Wiley and Sons, New York.

Key References

Abdel-Aal et al., 1990. See above.

Describes, in detail, the carboxylic ester hydrolase assay (called 1-naphthyl acetate esterase assay in that publication) that was modified and miniatur-

ized for microtiter plate format. A modification of this procedure is presented in Basic Protocol 1.

Aldridge, 1953. See above.

Original description of A- and B-esterase distinction.

Devorshak and Roe, 2001. See above.

Describes, in detail, the phosphoric triester hydrolase assay that was miniaturized for microtiter plate format. This procedure was modified (see Basic Protocol 2) to provide endpoint absorbance data.

Contributed by Douglas D. Anspaugh and R. Michael Roe
North Carolina State University
Raleigh, North Carolina

Techniques for Measuring the Activity of Carboxylic Acid:CoA Ligase and Acyl-CoA:Amino Acid *N*-Acyltransferase: The Amino Acid Conjugation Pathway

A wide variety of carboxylic acid compounds are metabolized to their amino acid conjugates via a pathway that exists primarily in liver and kidney (Vessey, 1997). This conjugation occurs in two steps and is catalyzed by two distinct classes of enzymes:

$$\text{R-COOH} + \text{CoASH} + \text{ATP} \xrightarrow{\text{(Ligases)}} \text{R-CO-SCoA} + \text{AMP} + \text{PP}_i \quad \text{(step 1)}$$

$$\text{R-CO-SCoA} + \text{H}_2\text{N-CHR-COOH} \xrightarrow{\text{(Transferases)}} \text{R-CO-NH-CHR-COOH} + \text{CoASH} \quad \text{(step 2)}$$

In the first step, xenobiotic carboxylic acids and fatty acids are activated by acyl-CoA ligases, which catalyze formation of a thioester bond between the carboxylic acid moiety and coenzyme A in a reaction that results in pyrophorylytic cleavage of ATP to AMP. The activated xenobiotic is then conjugated with an amino acid (usually glycine) in a second reaction catalyzed by *N*-acyltransferases. Conjugation of carboxylic acid xenobiotics with an amino acid is important in that it can decrease toxicity or biological activity and enhance excretion. Activated short-chain and medium-chain fatty acids are subsequently metabolized by either oxidation or pathways for complex lipid synthesis.

Methods for determining the rates of reaction of carboxylic acid:CoA ligases include direct measurement of CoA-adduct formation by radiochemical (see Basic Protocol 1), spectrophotometric (see Alternate Protocol 2), or HPLC assays (see Alternate Protocol 4), as well as measurement of radiolabeled pyrophosphate (PP_i) release upon ATP cleavage (see Alternate Protocol 1) and detection of AMP by coupled spectrophotometric and fluorometric assays.

Methods for determining rates of reaction of acyl-CoA with glycine (or glutamine) catalyzed by the acyl-CoA amino acid *N*-acyltransferases include monitoring either the release of CoA by reaction with 5,5′-dithiobis(2-nitrobenzoate) (DTNB; see Basic Protocol 2), radioassay (see Alternate Protocol 6), HPLC (see Alternate Protocol 7), or the disappearance of the CoA thioester bond by UV spectroscopy (see Alternate Protocol 5).

NOTE: Accurate determination of binding constants requires accurate reagent concentrations.

DIRECT MEASUREMENT OF CARBOXYLIC ACID:CoA LIGASE ACTIVITY USING A RADIOLABELED CARBOXYLIC ACID

BASIC PROTOCOL 1

This assay measures the formation of the CoA adduct directly using a radiolabeled carboxylic acid substrate. Multiple aliquots are removed from the reaction mixture at timed intervals into tubes containing EDTA, which stops the reaction. They are then extracted with butanol to remove unreacted substrate, leaving radiolabeled acyl-CoA product in the aqueous phase. This simplified sample protocol illustrates this approach for determining rates of reaction at varied concentrations of carboxylic acid substrate, in this case optimized for [^{14}C]benzoate, with fixed concentrations of ATP and coenzyme A. If desired, other substrates (see Reagents and Solutions), other ATP or coenzyme A concentrations, or other variable parameters can be used to thoroughly investigate the

Contributed by Michael Kelley and Donald A. Vessey
Current Protocols in Toxicology (2002) 4.11.1-4.11.16

system at hand. Controls are generally not needed; although, one could leave out the CoA if desired.

Materials

Kill/acidification mix (see recipe) in dispenser set to deliver 0.4 ml
Water-saturated butanol (see recipe) in dispenser set to deliver 1 ml
1 M Tris·Cl, pH 8.0 at 30°C (*APPENDIX 2A*)
1 M KCl
100 mM $MgCl_2$
5 mM coenzyme A (see recipe)
Radiolabeled carboxylic acid substrate (e.g., 100 μM 80 cpm/mol [^{14}C]benzoate; see recipe)
1 mM ATP (see recipe)
Carboxylic acid:CoA ligase preparation (see Commentary)
Scintillation fluid

Positive-displacement pipet (e.g., Drummond)
30°C water bath
Vacuum pipettor
Scintillation vials

CAUTION: When working with radioactivity, take appropriate precautions to avoid contamination of the experimenter and the surroundings. Carry out the experiment and dispose of wastes in an appropriately designated area, following the guidelines provided by the local radiation safety officer (also see *APPENDIX 1A*). Also note that short-chain fatty acids are volatile and should be maintained in sealed tubes to avoid contamination of storage areas.

Prepare tubes containing reaction-terminating "kill" reagents

1. For each of five substrate concentrations, label a set of four 12 × 75–mm "kill" tubes with time points appropriate to determine the initial rate of reaction (i.e., twenty tubes).

   The reaction time points are chosen so that the rate is large enough for accurate determination, without significantly changing the substrate concentration over the course of the reaction; therefore, true initial rates are ensured. This is more difficult at substrate concentrations at or below K_M, as the reaction is not linear over long time courses. For the fast rate of the example (Fig. 4.11.1A), where the reactions are linear over 1 min, time points as short as 0, 20, 40, and 60 sec can be chosen by an experienced researcher.

2. Add the appropriate kill/acidification mix into each tube from a dispenser set to deliver 0.4 ml, followed by water-saturated butanol from a dispenser set to deliver 1 ml.

   The butanol may be added just before extraction if ventilation is inadequate and the vapor is objectionable.

Prepare reaction tubes

3. Prepare a mixture of the four invariant reagents in sufficient volume for the number of reactions according to Table 4.11.1.

   For the reagents that are not varied in the study, it is both easier and more accurate to prepare a mix in the appropriate proportions and then pipet this mix into each tube. A vacuum pipet (e.g., Pipetman) may be used, which while slightly less accurate is convenient and highly consistent, ensuring minimal variation of the fixed reagent concentrations when large numbers of assays are done.

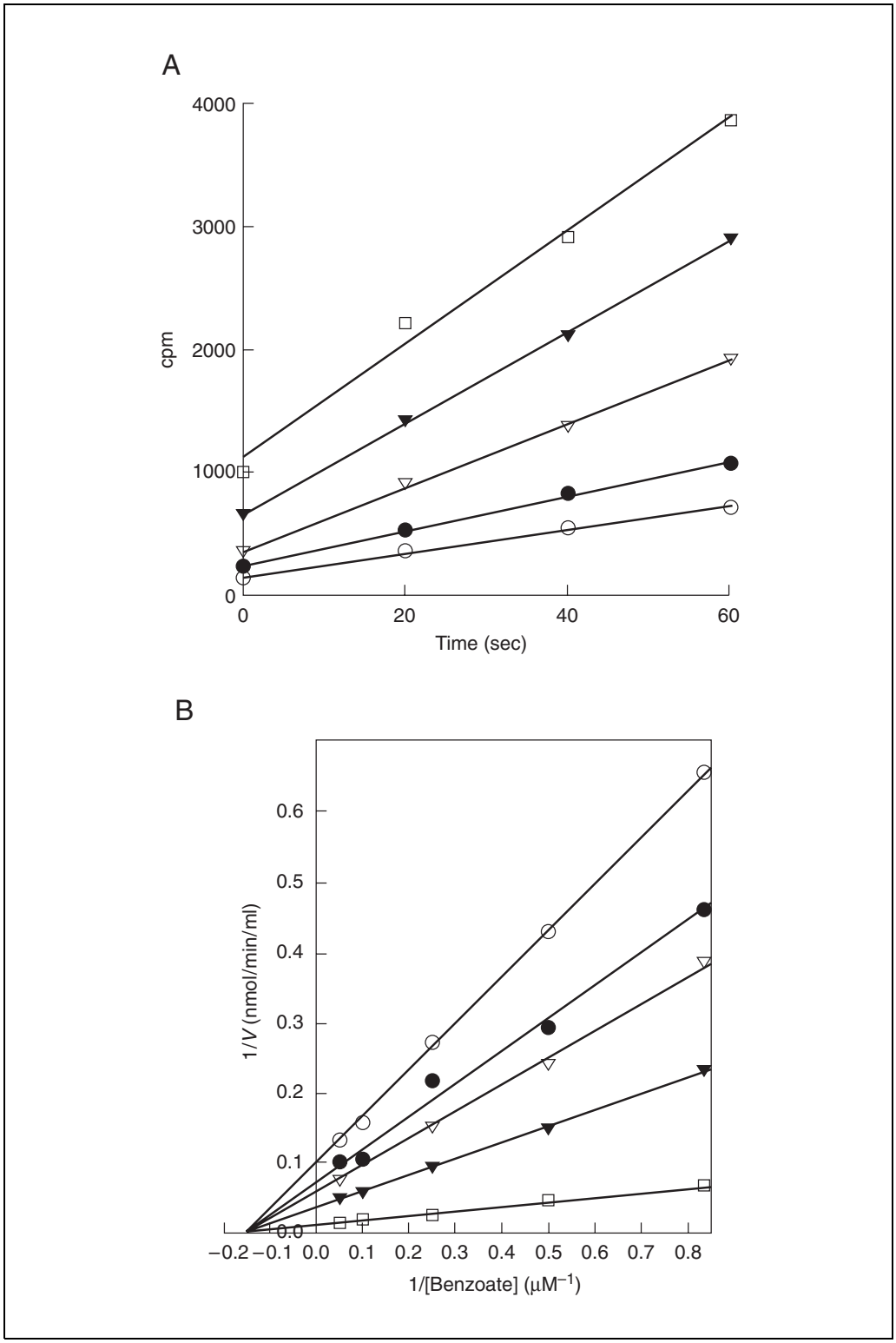

Figure 4.11.1 (**A**) Data from the scintillation counter are plotted as counts per minute (cpm) versus reaction time using 300 μM ATP and [^{14}C]benzoate concentrations of 1.2 (open circles), 2 (closed circles), 4 (open triangles), 10 (closed triangles), and 20 μM (open squares). Rates (uncorrected for extraction loss) are calculated from these data, which represent one-tenth of the total reaction, using the formula: [radioactivity (cpm)/incubation time (min) × dilution factor]/specific activity of substrate (cpm/pmol) = amount acylated product (pmol)/min/volume enzyme = *V*. (**B**) Reciprocals of these rates (1/*V*) are plotted versus the reciprocal of the benzoate concentration for these 300 μM ATP rates (open squares), as well as for rates conducted at ATP concentrations of 15 μM (open circles), 20 μM (closed circles), 29 μM (open triangles), and 50 μM (closed triangles).

Table 4.11.1 Invariant Reagent Mix

Reagent	Volume per individual assay (µl)	Volume to prepare invariant reagent mix (ml)[a]	Final concentration
1 M Tris·Cl, pH 8.0 at 30°C	50	1.3	100 mM
1 M KCl	25	0.65	50 mM
100 mM $MgCl_2$	25	0.65	5 mM
5 mM coenzyme A	50	1.3	500 µM

[a]Final volume is sufficient for 25 individual assays.

In the example shown (Fig. 4.11.1A), the rates of five reactions, each containing a different benzoate concentration but a constant concentration of ATP, were determined. The final reaction volume is 0.5 ml to allow removal of 100-µl aliquots of the reaction to the kill tubes at each of the desired time points. For example, in this series each reaction contains 100 mM Tris·Cl, pH 8.0 at 30°C, 50 mM KCl, 5 mM $MgCl_2$, 500 µM coenzyme A, 300 µM ATP, and either 1.2, 2, 4, 10, or 20 µM [^{14}C]benzoate. The reaction was initiated with 5 µl of N-acyltransferase preparation.

4. To accurately achieve the desired concentrations, prepare a stock solution of radiolabeled carboxylic acid substrate at a known specific activity (e.g., 10 to 100 cpm/pmol) and a concentration chosen for maximum accuracy of pipetting.
5. Pipet radiolabeled substrate at the desired concentration and specific activity (e.g., 100 µM 80 cpm/pmol [^{14}C]benzoate) into separate reaction tubes with a positive-displacement micropipet.

   For example, for a kinetic study of variable concentrations of carboxylic acid (Fig. 4.11.1), pipet 6, 10, 20, 50, and 100 µl of 100 µM benzoate into separate tubes.

6. Add 150 µl of 1 mM ATP and 150 µl of the invariant reagent mix (step 3) to each of the 300-µM ATP reaction tubes with a positive-displacement pipet.
7. Adjust the volume of each reaction with water such that when enzyme is added, the final volume will be 0.5 ml and place in a 30°C water bath.

Initiate reaction and remove aliquots at timed intervals

8. Initiate each reaction by adding an assayable amount of carboxylic acid:CoA ligase preparation using a positive-displacement micropipet.
9. Vortex the tube gently and, using a vacuum pipettor, transfer a 100-µl aliquot to the first (zero time) kill tube while simultaneously starting timing.
10. Remove subsequent 100-µl aliquots to the assigned kill tubes at the predetermined times.

    When the time course of the reaction is >1 min, several reactions can be run at once by initiating and killing successive reactions at intervals as allowed by the time course.

Extract unreacted radiolabeled substrate

11. Vortex the kill tubes thoroughly and place in a bench-top centrifuge. Centrifuge briefly at top speed, room temperature, until a clear separation of the aqueous and butanol layers is achieved (~5 sec).
12. Remove the top butanol layer by vacuum aspiration, then repeat the extraction by adding 1 ml water-saturated butanol.

    For very nonpolar substrates, such as myristate and palmitate, where a second extraction causes excessive loss of the CoA adduct, use only one extraction. Slightly longer centrifugation times may be required if larger amounts of protein are assayed. The vacuum aspiration system needs to be equipped with an inline filter.

Determine counts remaining in aqueous layer of each kill tube

13. Quantitatively remove 250 µl extracted aqueous phase of each kill tube to a scintillation vial containing 10 ml scintillation cocktail and count using a liquid scintillation counter.

Determine reaction rates

14. Display the reaction rate by plotting the data as counts per minute (cpm) versus reaction time (Fig. 4.11.1A).

15. After determining the initial rates of reaction, compute the rate of appearance of radioactive product over time.

    Each scintillation vial contains one-half of the aqueous phase of each kill tube, and each kill tube contains one-fifth of the total assay volume. The displayed rates therefore represent one-tenth of the product formed by the enzyme protein that was assayed.

16. Quantitate product by dividing these rates by the specific radioactivity of the substrate to convert counts per minute to moles.

    The results can be conveniently expressed as moles of product formed per minute per milliliter enzyme solution. For comparison purposes, it is useful to determine the protein concentration of the enzyme solution so that the results can be expressed on a per milligram protein basis. Any standard protein determination procedure can be used, but in general each procedure will yield a slightly different value. Thus, it is important to use the same protein determination method as was used in the study to which the results are to be compared.

MEASUREMENT OF RADIOLABELED ATP CLEAVAGE BY CARBOXYLIC ACID:CoA LIGASE

ALTERNATE PROTOCOL 1

This assay measures the rate of radiolabeled [γ-^{33}P]ATP cleavage to radiolabeled pyrophosphate (PP_i) and AMP. Unreacted ATP is removed by adsorption to activated charcoal and the remaining pyrophosphate is measured by liquid scintillation counting.

Additional Materials *(also see Basic Protocol 1)*

ATP-assay kill mix (50 mM Na_2EDTA/5 mM K_2HPO_4) in a dispenser set to deliver 1.9 ml
Unlabeled carboxylic acid substrate (e.g., 1 mM hydrocinnamic acid)
[γ-^{33} P]ATP of known concentration and specific activity (e.g., 10 mM, 6.8 cpm/pmol; also see recipe for radiolabeled carboxylic acid substrates for specific activity determination)
Phosphoric and sulfuric acid-washed activated charcoal (e.g., Sigma)

CAUTION: When working with radioactivity, take appropriate precautions to avoid contamination of the experimenter and the surroundings. Carry out the experiment and dispose of wastes in an appropriately designated area, following the guidelines provided by the local radiation safety officer (also see *APPENDIX 1A*).

Prepare kill tubes

1. Label a set of four 12 × 75–mm kill tubes for time points appropriate to the time course of the reaction being studied.
2. Add ATP-assay kill mix into each tube from a dispenser set to deliver 1.9 ml.

Prepare reaction tubes

3. Construct an appropriate mixture of the four invariant reagents to achieve the desired assay concentrations, such as that described in the example for the previous assay (see Basic Protocol 1, step 3 and Table 4.11.1).

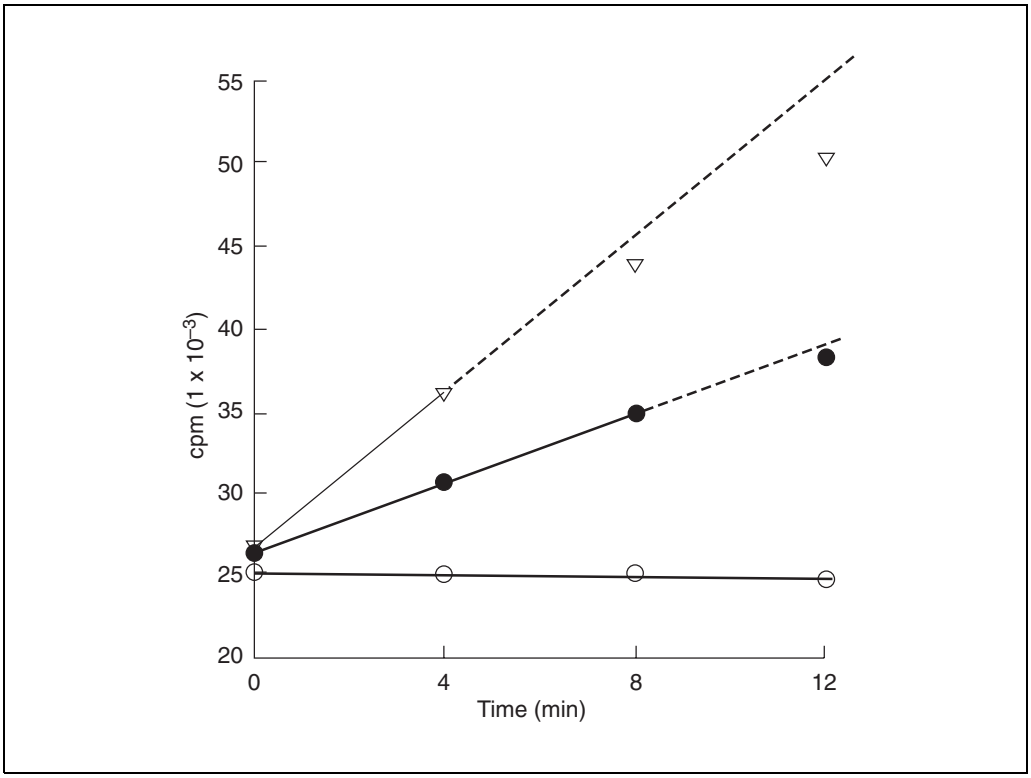

Figure 4.11.2 Data from the scintillation counter are plotted as cpm (divided by 1×10^3 for convenience) versus reaction time for the substrates hydrocinnamic acid (open triangles) and indole-3-propionic acid (closed circles), as well as a control reaction omitting CoA (open circles). Rates are calculated from these data, which represent one-tenth of the total reaction using the following formula: [radioactivity (cpm)/incubation time (min) × dilution factor]/specific activity of ATP (cpm/pmol) = amount inorganic phosphate formed (pmol)/min/volume enzyme = *V*.

4. To each reaction tube add the invariant reagent mix, unlabeled carboxylic acid substrate (e.g. 1 mM hydrocinnamic acid), 25 µl [γ-^{33}P]ATP of known concentration and specific activity (e.g., 10 mM 6.8 cpm/pmol), and sufficient water such that the final volume of the assay after enzyme addition is 0.5 ml.

   Final concentrations in this example are as follows: 100 mM Tris·Cl, pH 8 at 30°C, 50 mM KCl, 2 mM $MgCl_2$, 200 µM hydrocinnamic acid, 250 µM coenzyme A, and 500 µM [γ-^{33}P]ATP (assumed).

   [γ-^{33}P]ATP is typically supplied at >1000 Ci/mmol. Small amounts may be added to precisely made solutions of unlabeled ATP to achieve specific radioactivities of 10 to 100 cpm/pmol or more without significantly changing the concentration.

   In the example (Fig. 4.11.2), 100 µl ligase preparation was reacted with 200 µM hydrocinnamic acid at 250 µM coenzyme A and 500 µM [γ-^{33}P]ATP.

Initiate reaction and remove aliquots at timed intervals

5. Initiate each reaction at 30°C with 100 µl carboxylic acid:CoA ligase preparation and transfer 100-µl aliquots to kill tubes at the predetermined times (step 1).

   The reactions can be initiated at staggered intervals so that many reactions can be conducted simultaneously.

Adsorb unreacted ATP

6. Add 0.2 g phosphoric and sulfuric acid–washed activated charcoal to each kill tube and vortex at 10-min intervals over 30 min.

7. Sediment the charcoal from the kill tubes by centrifuging in a bench-top centrifuge 1 min at 1000 × *g* (3,000 rpm), room temperature. Transfer 1.5 ml supernatant to a second set of appropriately labeled tubes.
8. Centrifuge again (see step 7) to remove most of the fine charcoal particulate.

Determine counts remaining in each kill tube

9. Quantitatively remove 1 ml supernatant from each kill tube to a vial containing 10 ml scintillation cocktail and count using a liquid scintillation counter.

Determine reaction rates

10. Display reaction rate by plotting the data as cpm versus reaction time (min) and check that the rates are linear.

    Each scintillation vial contains one-half of the volume of each kill tube, which contained one-fifth of the total assay volume; therefore, the displayed rate represents one-tenth of the activity of the protein assayed.

11. Divide these rates by the specific radioactivity of the [γ-^{33}P]ATP to convert cpm to moles.
12. Repeat the assay without coenzyme A to determine rates of [γ-^{33}P]ATP hydrolysis independent of this substrate.

    This is especially important with crude preparations.

SPECTROPHOTOMETRIC ASSAY OF CARBOXYLIC ACID:CoA LIGASE ACTIVITY USING DTA

ALTERNATE PROTOCOL 2

Some ligase forms may be assayed accurately spectrophotometrically by exploiting the strong absorbance at 376 nm (ε_M = 34,000) of the CoA adduct of 2,4,6,8-decatetraenoic acid (DTA; Garland et al., 1970); however, not all ligases have DTA activity (Vessey, 1997).

Additional Materials *(also see Basic Protocol 1 and Alternate Protocol 1)*

5 mM DTA (see recipe)
Recording spectrophotometer, thermostatically-controlled at 30°C

1. Prepare a 1-ml cuvette containing the desired concentrations of invariant reagents (e.g., Table 4.11.1) and unlabeled substrate, minus *N*-acyltransferase and ATP:

100 µl	1 M Tris·Cl, pH 8.0 at 30°C (100 mM final)
50 µl	1 M KCl (50 mM final)
50 µl	100 mM $MgCl_2$ (5 mM final)
5 µl	5 mM DTA (25 µM or 0.5% w/v final)
50 µl	5 mM coenzyme A (250 µM final)
690 µl	H_2O.

   In this example, 25 µl ligase preparation will be assayed in a reaction initiated with 3 mM (30 µl of 100 mM) ATP.

2. On a recording spectrophotometer, thermostatically-controlled at 30°C, observe the absorbance at 376 nm over 1 min, which should not change with time.
3. Add carboxylic acid:CoA ligase preparation (25 µl in the current example) and again observe the absorbance change.

   A blank (ATP-independent) rate, seen as a small steady increase in A_{376} with time, may be unavoidable when extraneous protein is added with impure preparations. Adjust the amount of protein added as necessary so that this blank rate, if present, is as small as possible in the slowest accurately determinable reactions.

4. Initiate the reaction with ATP (e.g., 3 mM) and observe the rate of change of absorbance at 376 nm.

   This initiation order ensures that the net rate is ATP-dependent.

5. Repeat the experiment but omit the coenzyme A to confirm dependence on both cosubstrates.

ALTERNATE PROTOCOL 3

INDIRECT ASSAY OF CARBOXYLIC ACID:CoA LIGASE USING AMP FORMATION COUPLED TO NADH OXIDATION

This assay couples the formation of AMP to NADH oxidation via adenylate kinase, myokinase, phosphoenol pyruvate/pyruvate kinase, and lactate dehydrogenase. NADH oxidation is monitored spectrophotometrically at 340 nm (Kasuya et al., 1996). This assay is less sensitive than those discussed above (see Basic Protocol 1 and Alternate Protocols 1 and 2), but can be used with any carboxylic acid substrate. The sensitivity can be increased by following NADH oxidation fluorometrically with excitation at 340 nm and monitoring at 465 nm (Rodriguez-Aparicio et al., 1991). The assay is limited in its applicability because it cannot be used with crude extracts nor with any preparation containing ATPase, ADPase, or AMPase activity.

ALTERNATE PROTOCOL 4

MONITORING CARBOXYLIC ACID:CoA LIGASE ACTIVITY BY HPLC DETERMINATION OF ACYL-CoA PRODUCT FORMATION

Several investigators have described assays employing different HPLC systems for separating the acyl-CoA product from CoA and ATP (Bronfman et al., 1986; Knights and Roberts, 1994; Brugger et al., 1996; Gregus et al., 1996). The acyl-CoA is then quantitated with a UV detector. The sensitivity of this assay is dependent on the sensitivity of the UV detector.

BASIC PROTOCOL 2

MONITORING CoA RELEASE USING A DTNB-COUPLED ASSAY TO DETERMINE *N*-ACYLASETRANSFERASE ACTIVITY

The most commonly employed assay for CoA release uses 5,5′-dithiobis(2-nitrobenzoate) (DTNB), which forms an intensely yellow adduct when reacted with sulfhydryl compounds. Reactions contain buffer and DTNB (combined for solubility; see Reagents and Solutions), monovalent cation, acyl-CoA substrate, and amino acid as required for the study. A continuously recording spectrophotometric assay can be conducted by following CoA release with DTNB at 412 nm (Webster et al., 1976).

As DTNB can react with sulfhydryl groups on proteins, it is preferable to observe the blank (nonspecific) rate of change of absorbance. Any significant absorbance change due to protein reaction is first measured, then the reaction is initiated with amino acid. This usually cannot be done when glutamine is the acceptor amino acid, which due to its low solubility and high K_M will occupy a large proportion of the assay volume. The N-acyltransferase sample must be free of sulfhydryl-containing compounds such as DTE, DTT, mercaptoethanol, or cysteine.

Materials

1 mM DTNB (see recipe)
1 M KCl
1 mM benzoyl-CoA
N-acyltransferase preparation (see Commentary)
Acceptor amino acid (i.e., glycine or glutamine)
Recording spectrophotometer, thermostatically-controlled at 30°C

1. Prepare a cuvette containing for each of the concentrations of substrates to be studied:

100 µl	1 mM DTNB (100 µM final)
80 µl	1 M KCl (80 mM final)
50 µl	1 mM benzoyl-CoA (50 µM final)
710 µl	H_2O

In this example, 10 µl N-acyltransferase preparation will be assayed in a 1 ml reaction volume initiated with 50 mM (50 µl of 1 M) glycine.

2. Observe the absorbance at 412 nm in a continuously recording spectrophotometer thermostatically-controlled at 30°C. Add *N*-acyltransferase preparation (10 µl in this example) and observe the rate of change in absorbance for 1 min, which should be minimal. Decrease the amount of protein if necessary.

3. Initiate the reaction by adding acceptor amino acid.

In this example, use 50 µl of 1 M glycine for a final concentration of 50 µM.

4. Quantitate the reaction rate from the net rate of absorbance change (to correct for any nonspecific protein reaction and acyl-CoA thiolase activity) by dividing by the extinction coefficient for DTNB at 412 nm, pH 7.0 to 8.0 (ε_M = 13,600), to obtain the concentration of coenzyme A released in the 1-ml reaction volume (see Fig. 4.11.3).

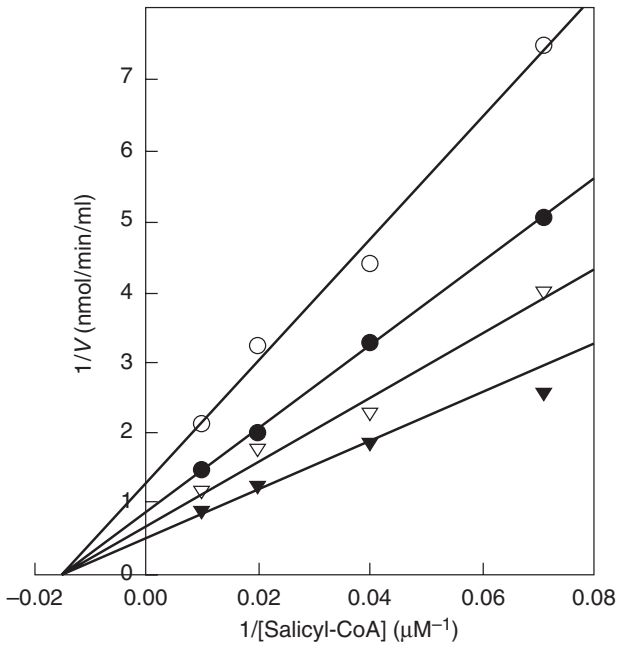

Figure 4.11.3 Lineweaver-Burk double reciprocal plots of the rates of salicyl-CoA glycine conjugation (as nanomoles per minute per milliliter enzyme) versus the concentration of salicyl-CoA for four different glycine concentrations: 5 (open circles), 10 (closed circles), 20 (open triangles), and 50 mM (closed triangles). Rates are calculated from the absorbance change with time using the extinction coefficient for DTNB: (ΔOD_{412}/incubation time (min)/volume enzyme)/[(13.6 AU liters/mmol) × 1000 ml/liter] = amount product formed (mmol)/min/100 µl enzyme = *V*.

ALTERNATE PROTOCOL 5

DIRECT ASSAY OF *N*-ACYLTRANSFERASE ACTIVITY BY MONITORING THE DISAPPEARANCE OF THIOESTER BOND ABSORBANCE

The reaction can also be followed spectrophotometrically by observing the disappearance of acyl-CoA thioester bond absorbance in the ultraviolet range.

Additional Materials *(also see Basic Protocol 2)*

0.5 M Tris·Cl, pH 8.0 at 30°C (*APPENDIX 2A*)
1-ml quartz cuvettes

1. Prepare the reaction in a 1-ml quartz cuvette as described in the previous assay (see Basic Protocol 2, step 1), but use 0.5 M Tris·Cl, pH 8.0 at 30°C instead of 1 mM DTNB.
2. Observe the absorbance at the appropriate wavelength for the chosen acyl-CoA in a continuously recording spectrophotometer thermostatically controlled at 30°C (see Table 4.11.2).
3. Initiate by adding acceptor amino acid (usually 50 µl of 1 M glycine).

Table 4.11.2 Absorption Wavelengths and Corresponding Extinction Coefficients for Acyl-CoA Substrates

Substrate	λ_{MAX}	ε_M
Benzoyl-CoA	280 nm	7,300
Phenylacetyl-CoA	236 nm	4,300
Salicyl-CoA	296 nm	3,400

ALTERNATE PROTOCOL 6

RADIOACTIVE ASSAYS FOR *N*-ACYLTRANSFERASES

An alternate radioassay (James and Bend, 1978) utilizes a radiolabeled acyl-CoA adduct with a different procedure. The reaction mixture is deproteinized with TCA and the product extracted with ethyl acetate.

If the carboxylic acid is extremely nonpolar, it is possible to utilize radiolabeled glycine and extract the glycine conjugate into butanol. The authors have used this method to assay the *N*-acyltransferases involved in bile acid conjugation (Vessey et al., 1977).

CAUTION: When working with radioactivity, take appropriate precautions to avoid contamination of the experimenter and the surroundings. Carry out the experiment and dispose of wastes in an appropriately designated area, following the guidelines provided by the local radiation safety officer (also see *APPENDIX 1A*).

ALTERNATE PROTOCOL 7

HPLC ASSAYS FOR *N*-ACYLTRANSFERASES

The reaction can also be followed by HPLC analysis of the appearance of products (i.e., acyl-CoA) in deproteinized assay extracts as described by Kasuya (1990) or by measuring the disappearance of acyl-CoA.

REAGENTS AND SOLUTIONS

Use Milli-Q-purified water or equivalent for all recipes and protocol steps. For common stock solutions, see ***APPENDIX 2A****; for suppliers, see* ***SUPPLIERS APPENDIX****.*

ATP and coenzyme A

The strong adenine absorbance at 260 nm can be used to ensure consistent concentrations of these substrates. This is important when K_M comparisons are to be made with experiments performed at different times. These compounds are subject to oxidation and hydrolysis and should be freshly made each week and stored frozen (i.e., <0°C). The millimolar extinction coefficient of ATP at 260 nm is ~15 and varies slightly with pH (Dawson et al., 1986). The millimolar extinction coefficient of CoA is 16.8 at 260 nM.

DTA, 5 mM

Prepare 2,4,6,8-decatetraenoic acid (DTA; Toronto Research Chemicals) at a concentration of 5 mM in dimethyl sulfoxide (DMSO). Store up to 1 week at <0°C. Store left over powder indefinitely at <0°C (i.e., in the freezer) to minimize oxidation.

DMSO appears to be less inhibitory to ligases than other usable solvents (e.g., ethanol) and can be used at lower final concentrations in the assay as it dissolves DTA readily.

DTNB, 1 mM

5,5′-dithiobis(2-nitrobenzoate) (DTNB) is poorly soluble and readily oxidizes in water; therefore, weigh out an appropriate amount of the yellow powder, and combine with an appropriate volume of 0.5 M Tris·Cl, pH 8 at 30°C (*APPENDIX 2A*) to make a 1 mM solution. Once the solution is made, measure the absorbance of an aliquot at 412 nm. Store at <0°C until the initial A_{412} increases significantly.

DTNB is also known as Ellman's reagent.

Kill/acidification mix

These mixtures contain EDTA (Table 4.11.3), which stops the reaction by chelating Mg^{2+}. Most also contain succinic acid, chosen to achieve the acidic conditions which favor maximum extraction of the unreacted substrate (which depends upon the butanol:water partition coefficient and the pK_a of the carboxylic acid group) with minimum loss of the CoA adduct. Tetrasodium EDTA is used when possible as it is freely soluble. These mixtures are effective for assays conducted in 100 mM Tris buffer in the pH range of 7.1 to 8.0. Adjustments may be necessary to achieve optimal pH when other buffer systems are used.

Radiolabeled carboxylic acid substrates

For water-soluble nonvolatile substrates, dry the radioisotope in a fume hood under nitrogen in a glass tube to eliminate ethanol from the assay. Redissolve in water to the desired concentration based on the stated specific radioactivity.

Table 4.11.3 Kill/Acidification Mixes for Various Substrates Used in Direct Measurement of Ligase Rate

Substrate	Kill/acidification mix
Myristate or palmitate	12 mM Na_2EDTA, pH 7.0
Benzoate, decanoate, 2,4-dichlorophenoxyacetate, hexanoate, naphthylacetate, octanoate, phenylacetate, or valproate	12 mM Na_4EDTA/30 mM succinic acid, pH 4.5
Butyrate, propionate, or salicylate	12 mM Na_4EDTA/200 mM succinic acid, pH 3.6

For substrates which contain long alkyl chains (e.g., palmitic acid), dissolve in ethanol as they are poorly water soluble. However, ensure that they are prepared at sufficiently high concentration that the assay is no more than 1% to 2% ethanol, as ethanol can affect the reaction.

For butyric and propionic acids, which are volatile liquids at standard temperature and pressure, handle as the sodium salt, which is a solid.

Determine specific activity using a scintillation counter of known efficiency. Adjust the specific activity by combining with an equal concentration of unlabeled carboxylic acid.

For example, the sodium salt of [^{14}C]benzoate is supplied as a 50 mCi/mmol solution in ethanol. When counted in a 90% efficient scintillation counter, 2.2 × 10^6 dpm/μCi is equivalent to 2.0 × 10^6 cpm/μCi, and the supplied [^{14}C]benzoate is 100 cpm/pmol. When dissolved in water such that 10 μl contains 100,000 cpm, the reagent is 1 mM 100 cpm/pmol [^{14}C]benzoate. This solution can be mixed with a precise solution of unlabeled 1 mM sodium benzoate to produce the specific radioactivity required for the study.

Water-saturated butanol

Add water to rapidly stirring *n*-butanol until the mixture is cloudy. Allow excess water to settle and pour the upper clear butanol phase into the dispenser. This reagent is stable indefinitely.

Butanol is saturated with water to avoid volume reduction in the aqueous phase.

COMMENTARY

Background Information

Carboxylic acid-CoA ligases

Three distinct classes of acyl-CoA ligase are separable from liver mitochondria. A freeze-thaw lysate can be fractionated by DEAE chromatography to yield a soluble short-chain fatty acid:CoA ligase, which does not have activity with xenobiotic carboxylic acids (SC ligases), and at least two soluble forms which activate xenobiotic carboxylic acids as well as short- and medium-chain fatty acids (XM ligases). Ligases with activity toward long- and very long-chain fatty acids are found in the membrane fraction (long-chain and very long-chain fatty acid:CoA ligases). Care should be taken to identify the separate activity peaks and to chromatograph again as necessary, especially when studying effects of a compound with greatly varying activity and binding affinity toward another narrowly-separated ligase subform.

Ligases catalyze a trisubstrate reaction in which activation of a xenobiotic or fatty acid to a coenzyme A-conjugate requires hydrolysis of ATP. Kinetic characterization is complex, as the binding of one cosubstrate, particularly carboxylic acid–containing substrates of widely varying structures, can modulate the binding of the others. Both monovalent and divalent cations affect activity in a substrate-dependent manner. It is important to remain mindful of the potential of these variable co-substrates and ionic effects to confound standard kinetic analyses by introducing uncontrolled effects, such as those which vary with different relative stoichiometries. Complex effects are usually apparent as nonlinear Dixon or Lineweaver-Burk plots. Conventional modeling of rates, binding constants, and competition patterns will demonstrate conditions under which the data are internally consistent and fit these models, and conditions where the data diverge from these models in a meaningful pattern.

N-acyltransferases

Acyl-CoA:amino acid *N*-acyltransferases determine the nature of the amino acid conjugate (Vessey, 1997). In mammals, glycine conjugates predominate, but glutamine conjugates of arylacetic acids are seen in primates. The addition of a methyl group to the β-methylene group of an arylacetic acid (e.g., 2-phenylpropionate) blocks conjugation in primates. One enzyme form, "aralkyl" *N*-acyltransferase (ArAlk), conjugates the CoA adducts of substituted benzoates, medium-chain fatty acids, and certain branched-chain alkyl acids. Another enzyme form, "arylacetyl" *N*-acyltransferase (AAc), only conjugates the CoA adducts of arylacetic acids (e.g., naphthylacetate, indoleacetate, phenoxyacetate, phenylacetate).

Acyl-CoA:amino acid *N*-acyltransferases are soluble enzymes located in the matrix space of the mitochondria of both liver and kidney. These enzymes can be extracted from mitochondria by a simple freeze-thaw lysis, and the two forms can be easily separated by chromatofocusing chromatography (Kelley and Vessey, 1990).

Kinetic studies of bovine liver AAc and ArAlk revealed that they differ not only in their specificity for acyl-CoAs, but also in their acceptor amino acid specificity. The ArAlk accepts only glycine while the AAc has a low but measurable rate with glutamine as the acceptor amino acid. Both forms follow sequential Bi Bi mechanisms (Vessey, 1997). Kinetic analysis of ArAlk and AAc suggested that they were almost completely product-inhibited by in vivo concentrations of CoA. The extent of this end-product inhibition by CoA is greatly reduced by adding K^+ to the assay; however, for in vitro assays in which CoA is not added, K^+ is inhibitory to both ArAlk and AAc (Kelley and Vessey, 1990). Thus, to measure the highest possible rates, K^+ should be omitted from assays, while to measure kinetic constants that exist under in vivo conditions, K^+ should be added.

In man and rhesus monkey, the conjugation of benzoic acid and phenylacetic acid has been shown to be due to the existence of two distinct enzymes, a glycine-specific benzoyl-CoA transferase and a glutamine-specific arylacetyl transferase. The human benzoyl-CoA transferase (ArAlk) does not differ significantly from bovine ArAlk. While human glutamine-specific arylacetyltransferase has a specificity for acyl-CoAs similar to that of bovine AAc, it differs in that it has such poor affinity for glycine that the inefficient acceptor glutamine is the preferred substrate. When assaying for this activity, concentrations of glutamine should be in excess of 50 mM (300 mM is the limit of solubility).

A significant source of interference when assaying the *N*-acyltransferases is acyl-CoA hydrolase activity. Mitochondria contain low level hydrolase activity toward most acyl-CoAs. This activity is characterized by very high K_M values for acyl-CoA (usually in excess of 0.5 mM) and so is less of a problem for substrates for which the *N*-acyltransferase has a low K_M.

Critical Parameters and Troubleshooting

Precise measurement of substrate concentrations and the amount of enzyme is essential for production of useful kinetic data. This can be accomplished by using positive-displacement pipets (e.g., Drummond) for critical measurements, ensuring that sets of reactions with small differences in substrate concentration are precise.

Carboxylic acid-CoA ligase assay

This assay (see Basic Protocol 1) is suitable for detailed kinetic studies as it can be optimized to accurately determine large numbers of reaction rates over the necessarily large ranges of activity and substrate concentration. As a given form of ligase might activate a wide variety of substrate structures with widely varying velocities and binding constants, the time course of the reaction must be adjusted in order to maximize accuracy while measuring the true initial reaction rate. Substrates that are slowly activated, bind with low affinity, or partition poorly into butanol are more difficult to assay accurately, and adjustments of the amount of enzyme protein, specific radioactivity of the substrate, and acidity of the kill/acidification mix must be made. Adjust the specific radioactivity, enzyme concentration, and time points such that the most difficult rate to determine (e.g., concentrations of any of the three cosubstrates at or below K_M) is as large as possible, while still linear over the time course. The time course can be altered for the other reactions of the study if desired. The enzyme concentration should be held constant to avoid any nonlinearity and a minimal volume of enzyme should be used, especially if glycerol or salts are used to stabilize the enzyme preparation, as they can greatly affect the rates under some conditions.

Choose specific radioactivity appropriate to the study. In the example (Fig. 4.11.1), an enzyme form that activates benzoate with good binding and rate was studied at benzoate concentrations below K_M. A relatively small amount of protein was assayed for a short time using benzoate of undiluted specific radioactivity. For studies at higher benzoate concentrations, the specific radioactivity could be decreased to 10 cpm/pmol and the time course increased to several minutes. If this form were studied with butyrate, for which the velocity and binding affinity are poor and the extraction less efficient, the study would call for more protein to be assayed over longer periods of time with butyrate used at a high concentration but at diluted specific radioactivity.

When it is necessary to relate the reaction rates of different carboxylic acid substrates, the differences in extraction losses of the CoA

adducts must be accounted for. These differences depend upon the structure of the substrate and the kill/acidification mix used, and should be determined using the appropriate CoA adduct. When the assay and extraction protocols are used as described, extraction losses of the CoA adduct of ~30% are typically observed. Differential extraction losses become significant as conjugation rates of substrates of substantially varying chemical structure are compared, necessitating determination of and correction for extraction efficiency in such comparisons. There is generally an ~25% loss of acyl-CoA product into the butanol layer in the assays described. This loss can be precisely determined for any acyl-CoA by carrying a known amount of the acyl-CoA through the extraction process and directly measuring the recovery (usually by following the $O.D._{360}$ of the CoA).

The charcoal adsorption method (see Alternate Protocol 1) is cumbersome, and because it relies on a 1:1 stoichiometry of pyrophosphate release to monitor CoA-adduct formation, nonspecific "blank" rates of ATP hydrolysis must be determined. Hydrolysis can be negligible in purified preparations but significant in cruder ones. For these reasons this assay is most useful for the study of the activation of substrates that are unavailable radiolabeled. Adsorption of radiolabeled inorganic phosphate ($^{33}PP_i$) to charcoal is minimized by including phosphate in the kill mix. Use of the phosphoric and sulfuric acid–washed activated charcoal is important. ATP is available labeled with ^{33}P, which has a half-life of 25 days. It is less hazardous and has a longer half-life than ^{32}P. Count the stock isotope daily to maintain stoichiometry.

The DTA spectrophotometric assay (see Alternate Protocol 2) is less sensitive than the radioassay, and protein can cause a "blank" (nonspecific absorbance increase) reaction. DTA is not a substrate for all of the medium-chain fatty acid:CoA ligases, nor for short-chain fatty acid ligases.

While direct observation of the decrease in absorbance of the thioester bond (see Alternate Protocol 5) avoids some of the problems due to an increase in nonspecific absorbance which occurs in the DTNB-linked reaction (see Basic Protocol 2), the smaller extinction coefficients make this assay less sensitive. In addition, the shorter wavelengths are subject to high background absorbance due to UV-absorbing compounds and proteins, and potentially also via light scattering. Also, to reduce the possibility of interference by acyl-CoA hydrolase activity, more highly purified enzyme preparations are required.

Anticipated Results

Ligase assay: Direct measurement of radiolabeled product (see Basic Protocol 1). This is the best method for determining kinetic constants, as small differences in rates can be measured with accuracy sufficient to produce meaningful kinetic data. As the time course and the specific radioactivity of the substrate can be adjusted over wide ranges, it is also good for comparing rates that vary greatly.

Ligase assay: ATP cleavage (see Alternate Protocol 1). As this method measures ATP cleavage, rates must be verified as specific to the ligase reaction (dependent on substrate or CoA). The cumbersome and time-consuming charcoal adsorption of the uncleaved ATP makes this assay unsuitable for large numbers of reactions, but most useful for studying substrates unavailable in radiolabeled form.

Ligase assay: DTA (see Alternate Protocol 2). For the ligase subforms that metabolize DTA, this spectrophotometric assay is quick and convenient. The rate is determined directly from the display of absorbance change over time, allowing rapid adjustments to produce readable, linear rates, while ATP initiation ensures specificity; however, the operational concentration range of DTA is limited.

Ligase assay: AMP/NADH coupled (see Alternate Protocol 3). This spectrophotometric assay is less sensitive than the DTA assay due to the relatively low extinction coefficient of the NADH. It is also less convenient due to the balancing of several linked enzymes.

Ligase assay: HPLC (see Alternate Protocol 4). This assay, as with all HPLC assays, requires considerable development time and appropriate standards. It is laborious if an HPLC run is required for each time point. Its sensitivity is dependent upon the sensitivity of the HPLC detector.

N-Acyltransferase assay: DTNB (see Basic Protocol 2). This spectrophotometric assay determines activity directly from the absorbance change of DTNB reaction with the free sulfhydryl group of the CoA liberated in the course of the reaction; it is therefore subject to nonspecific sulfhydryl reaction, which limits its use. It is however quick, and the high extinction coefficient makes the assay very sensitive for a spectrophotometric assay.

N-Acyltransferase assay: Thioester bond absorbance (see Alternate Protocol 5). In another spectrophotometric assay, the reaction is

followed by measuring the disappearance of the substrate thioester bond. The thioester bond absorbance is measured directly and rates are determined quickly from the rate of decrease of absorbance. This method is not susceptible to nonspecific sulfhydryl reaction. It is however less sensitive than DTNB due to lower extinction coefficients.

N-Acyltransferase assay: Radiolabeled CoA adduct (see Alternate Protocol 6). Radiolabeled CoA adducts are generally available only for short and long chain fatty acids.

N-Acyltransferase assay: HPLC (see Alternate Protocol 7). This assay requires considerable development time, and then an HPLC run for each time point. It is only as sensitive as the method of detection.

Time Considerations

Ligase assay: Direct measurement of radiolabeled product (see Basic Protocol 1). Once conditions (e.g., time course, specific radioactivity, amount of enzyme) are determined to give linear rates within the parameters of the study, many assays can be efficiently conducted simultaneously, then extracted and loaded into scintillation vials at once, allowing a kinetic study involving a large number of assays to be completed within a day, allowing overnight for scintillation counting.

Ligase assay: ATP cleavage (see Alternate Protocol 1). While the time courses of reaction are similar to other assays, the 30 min charcoal absorption step, multiple centrifugations and extensive handling make this assay much more time consuming thus allowing fewer assays to be completed daily as compared with the ligase assay using direct measurement of radiolabeled product (see Basic Protocol 1). The length of time to set up and analyze the reaction (i.e., not including actual reaction time) is ~3 hrs per 12 samples for the experienced researcher.

Ligase assay: DTA (see Alternate Protocol 2). Once the reagents are prepared, cuvettes can be prepared, reactions run, and rates determined all within a few minutes per sample.

Ligase assay: AMP/NADH coupled (see Alternate Protocol 3). The setup time for this assay is system dependent as the experimenter must balance the levels of several linked enzymes. Thus there may be considerable time spent optimizing reactions. Once set up, though, it is quick.

Ligase assay: HPLC (see Alternate Protocol 4) and N-acyltransferase assay: HPLC (see Alternate Protocol 7). HPLC assays usually require considerable development time to get them up and running. To do kinetics requires an HPLC run for each time point. Thus, this type of assay can be quite time consuming.

N-Acyltransferase assay: DTNB (see Basic Protocol 2) and N-acyltransferase assay: Thioester bond absorbance (see Alternate Protocol 5). Since these assays are more or less the inverse of one another (i.e., one measuring appearance of a product the other disappearance of a substrate), they have similar time requirements. Once reagents are prepared, cuvettes can be pipetted and rates determined at a rate of a few minutes per sample.

N-Acyltransferase assay: Radiolabeled CoA adduct (see Alternate Protocol 6). Assuming a suitable radiolabeled substrate exists, this is a rapid and sensitive assay.

Literature Cited

Bronfman M., Amigo L., and Morales, M.N. 1986. Activation hypolipidaemic drugs to acylcoenzyme A thioesters. *Biochem. J.* 239:781-784.

Brugger, R., Alia, B.G., Reichel, C., Waibel, R., Menzel, S., Brune, K., and Geisslinger, G. 1996. Isolation and characterization of rat liver microsomal R-ibuprofenoyl-CoA synthethase. *Biochem. Pharmacol.* 52:1007-1013.

Dawson, A., Elliott, D.C., Elliott, W.H., and Jones, K.M. 1986. Data for Biochemical Research, Third Edition. Clarendon Press, Oxford.

Garland, P.B., Yates, D.W., and Haddock, B.A. 1970. Spectrophotometric studies of acyl-coenzyme A synthetases of rat liver mitochondria. *Biochem J.* 119:553-564.

Gregus, Z., Fekete, T., Halaszi, E., and Klaassen, C.D. 1996. Lipoic acid impairs glycine conjugation of benzoic acid and renal excretion of benzoylglycine. *Drug Metab. Disp.* 24:682-688

James, M.R. and Bend, J.R. 1978. A radiochemical assay for glycine *N*-acyltransferase activity. *Biochem. J.* 172:285-291.

Kasuya, F., Igarashi, K., and Fukui, M. 1990. Glycine conjugation of the substituted benzoic acids in vitro: Structure-metabolism relationship study. *J. Pharmacobio. Dyn.* 13:432-440.

Kasuya, F., Igarashi, K., Fukui, M., and Nokihara, K. 1996. Purification and characterization of a medium chain acyl-coenzyme A synthetase. *Drug Metab. Dispos.* 24:879-883.

Kelley, M., and Vessey, D.A. 1990. The effects of ions on the conjugation of xenobiotics by the aralkyl-CoA and arylacetyl-CoA *N*-acyltransferases from bovine liver mitochondria. *J. Biochem. Tox.* 5:125-135.

Knights, K.M. and Roberts, B.J. 1994. Xenobiotic acyl-CoA formation: Evidence of kinetically distinct hepatic microsomal long-chain fatty acid and nafenopin-CoA ligases. *Chemico-Biol. Interact.* 90:215-223.

Rodriguez-Aparicio, L.B., Reglero, A., Martinex-Blanco, H., and Luengo, J.M. 1991. Fluorimetric determination of phenylacetylCoA ligase from Pseudomonas putida: A very sensitive assay for a newly described enzyme. *Biochim. Biophys Acta* 1073:431-433.

Vessey, D.A. 1997. Enzymes involved in the formation of amide bonds. *In* Comprehensive Toxicology Vol. 3, Biotransformation (Guengerich F.P., ed.), p. 455-475. Elsevier Science, Oxford.

Vessey, D.A., Crissey, M.H., and Zakim, D. 1977. Kinetic studies on the enzymes conjugating bile acids with taurine and glycine in bovine liver. *Biochem. J.* 163:181-183.

Webster, L.T. Jr., Siddiqui, U.A., Lucas, S.V., Strong, J.M., and Mieyal, J.J. 1976. Identification of separate acyl-CoA:glycine and acyl-CoA:glutamine N-acyltransferase activities in mitochondrial fractions from liver of rhesus monkey and man. *J. Biol. Chem.* 251:3352-3358.

Contributed by Michael Kelley and Donald A. Vessey
Veterans Administration Medical Center
San Francisco, California

Determination of Paraoxonase 1 Status and Genotypes at Specific Polymorphic Sites

Paraoxonase 1 (PON1; EC 3.1.1.2/EC 3.1.8.1) is encoded by the first of three tandem genes on human chromosome 7. It was thought that PON1 and arylesterase were different enzymes. Subsequent research, however, has shown that they are not; thus, the enzyme has two EC designations. The *PON1* gene is followed by paraoxonase 3 (*PON3*) and paraoxonase 2 (*PON2*). A main physiological role of PON1 appears to be the metabolism of toxic oxidized lipids. In addition to its physiological role, PON1 also hydrolyzes a number of xenobiotic compounds including toxic organophosphorus insecticides, nerve agents, and some drugs (a process that activates some and inactivates others). The catalytic efficiency of hydrolysis of the xenobiotic compounds determines whether the hydrolysis of a specific compound is physiologically important in modulating the effect of exposure to the specific compound. A polymorphism at position 192 (Q192R) affects the catalytic efficiency of a number of PON1 substrates. In addition to the coding-region polymorphism that affects the catalytic efficiency of PON1, there are a number of other polymorphisms in the 5′ regulatory region that have been characterized. One of these (C108T) has a significant effect on the expression and plasma levels of PON1. Recently, >140 new PON1 single-nucleotide polymorphisms (SNPs) have been described, but most have not yet been characterized for effects on PON1 expression (Brophy et al., 2002; Costa and Furlong, 2002; Costa et al., 2003).

The most important consideration for a given individual is the actual level of PON1 in his or her plasma; for determining the risk of exposure to some compounds, the amino acid present at position 192 is also important. This is most reliably assessed by a two-substrate analysis that provides both an accurate determination of the amino acid at position 192 as well as PON1 plasma levels. The authors have designated the identity of the position 192 polymorphism and the PON1 level as an individual's PON1 status. Although it might be possible to determine all of the PON1 SNPs for a given individual, doing so would not provide an accurate assessment or prediction of the individual's "PON1 status."

This unit describes the enzymatic method used to establish an individual's PON1 status (see Basic Protocol 1) as well as protocols for determining SNPs at characterized positions in the PON1 gene (see Basic Protocol 2 and see Alternate Protocols 1 to 5). It is not possible to overemphasize the importance of using the PON1 status determination as opposed to SNP analysis for examining the relationship of an individual's PON1 status to disease or risk associations. The two-substrate enzyme analysis provides an accurate assessment of an individual's PON1 level and position 192 functional status (i.e., the individual's PON1 functional genomics), whereas the SNP analyses cannot provide this information. Disagreements between the PON1 functional status and genotyping at position 192 can identify individuals with mutations elsewhere in their PON1 gene. Comparisons of PON1 status and regulatory region SNPs and haplotypes can provide information on the effects of various SNPs on plasma PON1 levels.

PHENOTYPING INDIVIDUALS FOR PARAOXONASE STATUS

BASIC PROTOCOL 1

The two-substrate assays are carried out using a Molecular Devices SPECTRAmax *PLUS* Microplate Spectrophotometer or equivalent instrument. Initial rates of substrate hydrolysis are determined, and rates of diazoxon hydrolysis (*y* axis) are plotted against the rates of paraoxon hydrolysis (*x* axis). Hydrolysis of paraoxon produces *p*-nitrophenol, which is monitored at 405 nm; hydrolysis of diazoxon produces 2-isopropyl-4-methyl-6-hydroxypyrimidine (IMHP), which is monitored at 270 nm (Fig. 4.12.1). As noted above,

Contributed by Rebecca J. Richter, Rachel L. Jampsa, Gail P. Jarvik, Lucio G. Costa, and Clement E. Furlong

Current Protocols in Toxicology (2004) 4.12.1-4.12.19

this method separates individuals into the three phenotypes of $PON1_{192}$ activity, $PON1_{192Q/Q}$, $PON1_{192Q/R}$, and $PON1_{192R/R}$ (Fig. 4.12.2). As seen in Figure 4.12.2, the functional position 192 genotype is accurately inferred (Jarvik et al., 2000). In addition, PON1 activities within a genotype provide information on the levels of PON1 in the plasma of a given individual within that genotype group, a key bit of information that is relative to an individual's sensitivity to a specific organophosphate. This point is readily visible in Figure 4.12.2. Note that both groups of homozygotes fall on the trend lines, whereas the heterozygote data points are scattered. This means that other polymorphisms in the respective promoter regions (or other regulatory polymorphisms) result in more of one $PON1_{192}$ alloform relative to the other being expressed in a given individual.

Kinetic values determined on the Microplate Spectrophotometer are in mOD/min, which are converted to U/liter (μmol substrate hydrolyzed per min per liter of plasma) using conversion factors obtained by a linear regression analysis of initial rate data from a standard spectrophotometer (e.g., Beckman DU-70). This converts the data relative to a standard 1-cm path length, which then makes use of the standard molar extinction coefficient for either *p*-nitrophenol or IMHP. Alternatively, the Molecular Devices plate reader can give a path length value, which can be used in a formula to correct to a 1-cm light path for U/liter of each end product being measured. The latter approach is much less time consuming.

The PON1 phenotype at position 192 can be verified by genotyping the individual's DNA as described (see Basic Protocol 2). The authors have found this PON1 functional genomic analysis to be highly accurate, however, and it does not require verification (Jarvik et al., 2000). Some inactive *PON1* alleles can be identified by comparing *PON1* genotype at position 192 with the PON1 status analysis. For example, finding an individual who genotypes as a $PON1_{192Q/R}$ heterozygote but whose PON1 status functional analysis indicates a $PON1_{192Q}$ or $PON1_{192R}$ homozygote, shows that one of the alleles is nonfunctional. This is another major advantage of the PON1 status analysis, it provides the functional genomics of PON1.

The use of different temperatures for the two assays is based only on historical development considerations. The conditions were maintained so as to compare recent results with past results. It should be possible to run the paraoxonase at 23°C. A correction factor could be determined if it is useful to compare results with other published studies.

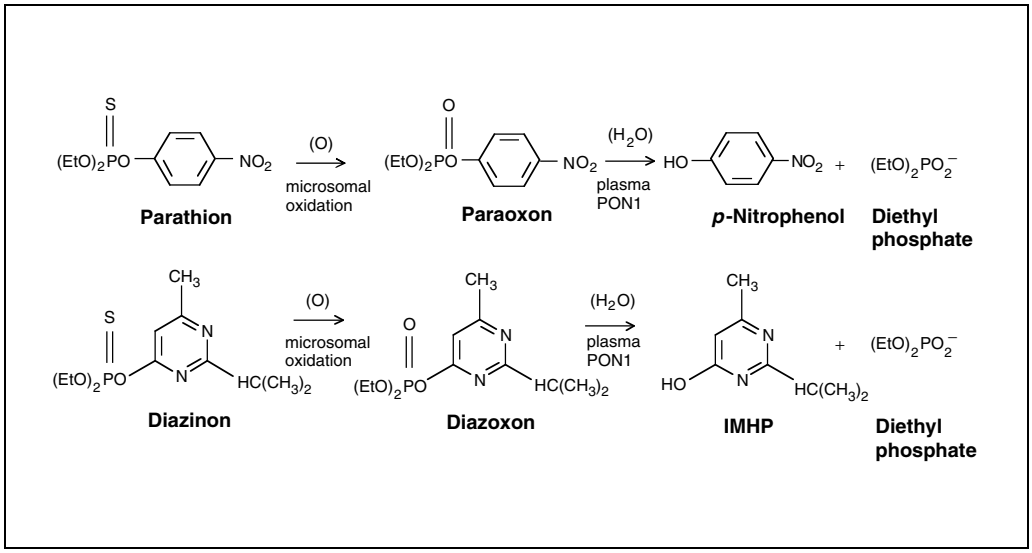

Figure 4.12.1 Metabolism of parathion and diazinon via the cytochrome P450/PON1 pathway. Abbreviations: EtO, CH_3CH_2O; IMHP, isopropyl-4-methyl-6-hydroxypyrimidine.

Materials

Plasma samples: blood samples collected in lithium heparin (green-top) tubes, centrifuged 5 min at 500 × *g*, 4°C, to remove cells
Dilution buffer (see recipe)
Paraoxon (Chem Service)
Assay buffer (see recipe), 37° and 23°C
Diazoxon (Chem Service)

Standard flat-bottom 96-well plates (Dynatech)
50-ml polypropylene tube (Falcon)
37°C water bath
Plate reader (e.g., SPECTRAmax PLUS Microplate Spectrophotometer; Molecular Devices), 37°C
UV-transparent 96-well plates (Costar)
15-ml screw-cap tubes (Falcon)
Conventional spectrophotometer (e.g., DU-70; Beckman), optional

CAUTION: Utmost care must be used with these organophosphate substrates, as they are potent cholinesterase inhibitors. All substrate-containing waste needs to be hydrolyzed in strong NaOH solution. Wear gloves and goggles for all assays and procedures using diazoxon or paraoxon. In a fume hood, add wastes to 5 N NaOH and let stand overnight. Then wash the wastes down the drain with lots of water (Mueller et al., 1983).

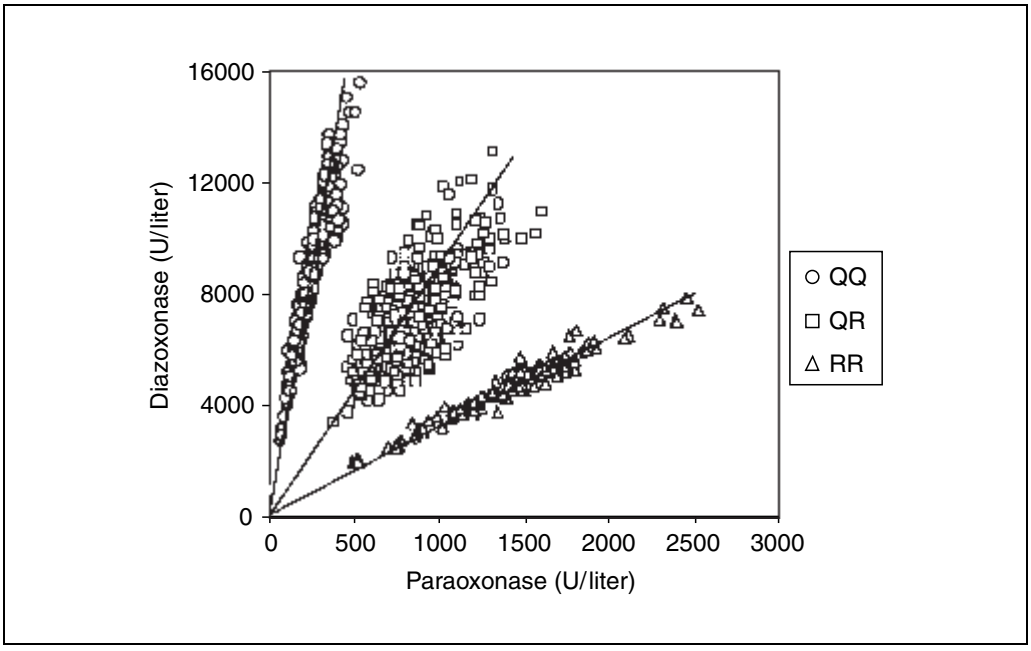

Figure 4.12.2 Determination of the functional genomics of plasma PON1 using citrate-stored plasma. Plotting the rates of hydrolysis of diazoxon versus paraoxon for plasma (or serum) samples from a population divides the population into three distinct groups: individuals functionally homozygous for $PON1_{192Q}$ (QQ), heterozygotes ($PON1_{Q/R192Q/R}$; QR) and individuals homozygous for $PON1_{192R}$ (RR). Whereas PCR analysis of the position 192 polymorphism may reveal that an individual possesses one copy of each allele, this analysis will pick up alleles in heterozygotes that are inactivated by any number of mutations (i.e., the analysis provides the functional status of an individual's PON1 genomics).

Measure paraoxonase activity

1. Dilute plasma samples 1:10 in dilution buffer just before use and mix samples thoroughly.

   It is best to microcentrifuge the plasma sample for 1 min at 14,000 rpm, 4°C, after thoroughly mixing (especially if the sample has just been thawed) to clear the sample of any particulate matter.

   If possible, samples should be diluted in 0.6-ml microcentrifuge tubes that have been set up in a rack so that an 8-channel pipet can quickly withdraw samples for high-throughput loading of the 96-well plate.

2. Pipet 20 µl diluted plasma into wells of a standard flat-bottom 96-well plate in triplicate.

3. Add 12.9 µl paraoxon to 50 ml prewarmed (37°C) assay buffer in a 50-ml tube (e.g., Falcon 352098; 1.2 mM final). Cap tube and shake vigorously and very carefully over a sink. Store in a 37°C water bath while performing the assay. Prepare fresh each hour.

   Paraoxon must be as pure as possible, because free p-nitrophenol interferes with the assay. Chem Service is an excellent source of very pure substrate.

   Gan et al. (1991) provide a method for substrate purification; however, the authors do not recommend purifying paraoxon because it is highly toxic. It is best to buy pure material.

   Paraoxon solution must be made fresh in prewarmed (37°C) assay buffer.

4. Add 200 µl of 1.2 mM paraoxon solution to each sample in the plate.

5. Quickly place plate in a prewarmed plate reader.

6. Set the plate reader to mix for the first 5 sec and then to monitor the initial rates of hydrolysis at 405 nm, taking readings each 15 sec for 4 min. Use only the initial linear rates for calculations.

7. Set plate reader software to measure the pathlength of each well in centimeters after the assay is complete. Set plate reader temperature to return to room temperature (23°C).

   Time must be allowed for the temperature of the plate reader to re-equilibrate before diazoxonase activity can be measured. Alternatively, diazoxonase can be measured first, and then the plate reader can be warmed to 37 °C.

Measure diazoxonase activity

8. Dilute plasma samples and set up a 96-well plate as described in steps 1 and 2, using a UV-transparent 96-well plate.

9. Add 2.8 µl diazoxon to 10 ml assay buffer (23°C) in a 15-ml tube (Falcon 352097; 1.0 mM final), cap securely, and shake vigorously but carefully. Prepare fresh each hour.

10. Add 200 µl of 1.0 mM diazoxon solution to each sample in the plate.

11. Quickly place plate in the plate reader (at room temperature).

12. Set the plate reader to mix for the first 5 sec and then to monitor the initial rates of hydrolysis at 270 nm, taking readings each 15 sec for 4 min. Use only the initial linear rates for calculations.

13. Set the plate reader software to measure the pathlength of each well in centimeters after the assay is complete.

Convert activity to units per liter

To convert without using pathlength correction

14a. Run replicate samples for paraoxonase and diazoxonase activity in the microtiter-plate spectrophotometer and a conventional spectrophotometer. Determine the conversion factor for mOD/min from the above plate reader assay to U/liter. Continue with step 19.

Conversion factors determined in the authors' laboratory using this approach are as follows.

Paraoxonase assay: plate reader mOD/min × 11.4 = U/liter

Diazoxonase assay: plate reader mOD/min × 53.2 = U/liter

To convert using pathlength correction feature

14b. Calculate paraoxonase activity using the absorbance of *p*-nitrophenol and the following equation:

$$A = \varepsilon \times l \times c$$

where A is absorbance (i.e., the OD), ε is the extinction coefficient of *p*-nitrophenol (18 $mM^{-1}cm^{-1}$), l is the pathlength of the well, and c is the concentration of *p*-nitrophenol. Rearranging this equation gives:

$$c = \frac{A}{(\varepsilon \times l)}$$

$$c\,(\mathrm{mM}) = \frac{\mathrm{OD}}{18\ \mathrm{mM}^{-1}\ \mathrm{cm}^{-1} \times\ l\ (\mathrm{cm})}$$

15b. Calculate moles *p*-nitrophenol in solution as follows:

Concentration (M) = mol/liter

mM = mmol/liter = µmol/ml

µmol = mM × ml

Hence, µmol *p*-nitrophenol = c (mM) × total vol (ml)

Because 20 µl sample is assayed in 200 µl assay buffer, the total volume is 220 µl (0.22 ml). Thus,

$$\mu\mathrm{mol}\ p\text{-nitrophenol} = \frac{\mathrm{OD}}{18\ \mathrm{mM}^{-1}\ \mathrm{cm}^{-1} \times\ l} \times 0.22\ \mathrm{ml}$$

and therefore:

$$\mu\mathrm{mol}\ p\text{-nitrophenol / min} = \frac{\mathrm{OD / min}}{18\ \mathrm{mM}^{-1}\ \mathrm{cm}^{-1} \times\ l} \times 0.22\ \mathrm{ml}$$

where µmol *p*-nitrophenol/min is the amount that is produced per minute by 20 µl of diluted sample.

16b. Calculate the amount of *p*-nitrophenol that will be produced by 1 liter of sample as follows:

μmol/min/liter = (μmol *p*-nitrophenol/min)/2×10^{-6} liter

where 2×10^{-6} liter (i.e., 2 μl) is the amount of the original plasma sample (before dilution).

17b. Because the readings from the plate reader are shown as mOD/min, modify the equation further by converting OD to mOD. Thus, the complete equation is:

$$\mu\text{mol/min/liter} = \left(\frac{\text{mOD/min}}{18\ \text{mM}^{-1}\text{cm}^{-1} \times l} \times \frac{10^3\ \text{mOD}}{\text{OD}} \times 0.22\ \text{ml} \right) / 2 \times 10^{-6}\ \text{liter}$$

which simplifies to:

$$\mu\text{mol/min/liter} = \frac{(\text{mOD/min}) \times 0.22}{1000 \times 18 \times l \times \left(2 \times 10^{-6}\right)}$$

$$= \frac{0.22\ \text{mOD/min}}{0.36\, l}$$

$$= \frac{6.1\ \text{mOD/min}}{l}$$

The pathlength correction feature is a standard component of the SPECTRAmax PLUS software. For other plate readers, the manufacturer's instructions must be consulted.

18b. Calculate diazoxonase activity using the formulas for paraoxonase (steps 14b to 17b) but substitute the extinction coefficient for 2-isopropyl-4-methyl-6-hydroxypyrimidine (IMHP; 3 $\text{mM}^{-1}\text{cm}^{-1}$).

This should yield a conversion factor of 36.7 for diazoxonase instead of 6.1 for paraoxonase.

Analyze activity

19. Plot initial rates of diazoxon hydrolysis on the *y* axis versus rates of paraoxon hydrolysis on the *x* axis.

This analysis will clearly separate a population into three groups: individuals homozygous for the Q alloform ($PON1_{192Q/Q}$), heterozygotes ($PON1_{192Q/R}$), and individuals homozygous for the R alloform ($PON1_{192R/R}$).

BASIC PROTOCOL 2

PARAOXONASE 1 GENOTYPING FOR POLYMORPHISM 192QR

The 192R polymorphism of the paraoxonase 1 gene ($PON1_{192R}$) has a native *Alw*I restriction site at codon 192. To genotype this polymorphism, a 99-bp polymerase chain reaction (PCR) product containing the site is amplified. When cut with *Alw*I, it produces 63-bp and 36-bp bands if the 192R codon is present; no digestion occurs if the 192Q codon is present.

Materials

~100 ng/µl purified human DNA
10× Opti-prime buffer #3 (Stratagene)
16 µM forward primer 192: 5′-TAT TGT TGC TGT GGG ACC TGA G-3′
16 µM reverse primer 192: 5′-CAC GCT AAA CCC AAA TAC ATC TC-3′
10 mM dNTPs
Dimethyl sulfoxide (DMSO), molecular biology grade
2 U/µl *Vent* DNA polymerase (NEB)
5 U/µl *Taq* DNA polymerase (Promega)
100 mM $MgSO_4$ (*APPENDIX 2A*)
5 U/µl *Alw*I and NEBuffer #4 (NEB)
6× Blue/orange loading dye (Promega)
Low-molecular-weight DNA ladder (standards for 25- to 100-bp fragments)
0.1 µg/ml ethidium bromide (see recipe) diluted in water *or* comparable staining solution

0.2-ml PCR tubes
Thermal cycler (e.g., PE 9700; PE Biosystems)
37°C water bath
Camera and UV light box or other instrument for recording the stained gel image

Additional reagents and equipment for DNA agarose gel electrophoresis (*UNIT 2.2*)

Prepare PCR Reactions

1. Make up the following on ice in a 0.2-ml PCR tube for each sample for hot-start PCR.

   2.0 µl ~100 ng/µl purified human DNA
   2.0 µl 10× Opti-prime buffer #3
   1.0 µl 16 µM forward primer 192
   1.9 µl 16 µM reverse primer 192
   0.4 µl 10 mM dNTPs
   1.0 µl DMSO
   11.6 µl H_2O
   19.0 µl total.

   This PCR requires a hot start, which involves adding the polymerase when the sample has reached denaturing temperature (the final volume after addition of polymerase is 20 µl).

   When more than one sample is being analyzed, it is convenient to make up a master mix of appropriate volume to divide between the PCR tubes, with subsequent addition of the individual DNA samples.

   It is preferable to include characterized DNA control samples for all three polymorphisms: 192QQ, 192QR, and 192RR.

2. Make up the following polymerase mix on ice for each sample.

   0.1 µl 2 U/µl *Vent* DNA polymerase
   0.2 µl 5 U/µl *Taq* DNA polymerase
   0.2 µl 100 mM $MgSO_4$
   0.5 µl H_2O
   1.0 µl total.

   A master mix can also be made for the polymerases.

Run PCR program

3. Program a thermal cycler to run the following cycling procedure.

First cycle:	5 sec	75°C (hot start)
	3 min	93°C (denaturation)
35 cycles:	1 min	93°C (denaturation)
	30 sec	61°C (annealing)
	1 min	72°C (extension)
Final step:	7 min	72°C (extension).

4. Load tubes into thermal cycler and begin the PCR program. Pause thermal cycler during the first 5 sec at 75°C and add 1 µl polymerase mix to each sample and continue the program.

Digest PCR products

5. Prepare the following on ice for each PCR sample. Save the remaining undigested, amplified DNA for comparison on the agarose gel.

   10.0 µl DNA from PCR amplification
   1.0 µl 5 U/µl *Alw*I
   2.0 µl 10× NEBuffer #4
   7.0 µl H_2O
   20.0 µl total.

   Incubate >2 hr at 37°C.

   As before, it is convenient to make up a master mix of appropriate volume to divide between the tubes.

Run agarose gel

6. Add 2 µl of 6× Blue/orange loading dye to each undigested sample and 4 µl to each digested sample. Also add loading dye to low-molecular-weight DNA ladder as per supplier's recommendations.
7. Place gel in electrophoresis tank and fill with 0.5× TBE buffer to cover the gel no more than 1 mm. Load the ladder into one well of a 3% (w/v) agarose gel made with 0.5× TBE and alternately load 10 µl of matched undigested and digested samples into the other wells.

   A small-toothed comb should be used when pouring the gel to allow ~15 µl per well.

8. When ready, close lid to tank and attach leads. Apply voltage of 1 to 5 V/cm. Run gel until the blue dye reaches a point ~75% down the gel.

   Actual gel run times may need to be determined for each manufacturer's instrument.

9. Stain gel in 0.1 µg/ml ethidium bromide or equivalent stain solution for 20 min. Destain gel in water for additional 20 min.

   CAUTION: *Appropriate safety precautions should be taken when working with ethidium bromide solutions.*

Analyze gel

10. Photograph stained gel using a camera and UV light box or other imaging system.

    CAUTION: *Appropriate safety equipment must be used with UV light.*

11. Determine the genotype as follows:

Complete digestion	192RR
Partial digestion	192QR
No digestion	192QQ.

PARAOXONASE 1 GENOTYPING FOR POLYMORPHISM –909CG

In the paraoxonase 1 gene (*PONI*), a native *Bsm*AI site is present with the –909G polymorphism; it is appropriate for distinguishing between the –909G and –909C alleles. This is complicated by a second *Bsm*AI site shifted 2 bp away from the first that is present in the –909C allele. Because a PCR product would fully digest with *Bsm*AI with either polymorphism, the second site associated with –909C is destroyed using the mismatch in the forward primer. The forward primer is large enough with its nonbinding DNA to be visible after the PCR product is restriction digested. When amplified, the PCR product is 256 bp, which digests when the –909G allele is present, producing 50-bp and 206-bp fragments. No digestion occurs with the –909C polymorphism.

Additional Materials *(also see Basic Protocol 2)*

10× *Taq* polymerase buffer (Promega)
25 mM $MgCl_2$ (Promega or *APPENDIX 2A*)
25 µM forward primer –909: 5′-TAT TAT AAT ATA TTA TAT CAT TCA CAG TAA CAG CAG ACA GCA GAG AAA AGA-3′
25 µM reverse primer –909: 5′-AAC ATG TCA CTG TGG CAT ATA TAA TGC TC-3′
5 U/µl *Bsm*AI and NEBuffer #3 (NEB)
Low-molecular-weight DNA ladder (standards for 50- to 250-bp fragments)
55°C water bath

1. Make up the following on ice in a 0.2-ml PCR tube for each sample.

   2.0 µl ~100 ng/µl purified human DNA
   1.5 µl 10× *Taq* polymerase buffer
   1.2 µl 25 mM $MgCl_2$
   0.1 µl 25 µM forward primer –909
   0.1 µl 25 µM reverse primer –909
   0.3 µl 10 mM dNTPs
   0.75 µl DMSO
   0.2 µl 5 U/µl *Taq* DNA polymerase
   8.85 µl H_2O
   15.0 µl total.

   When more than one sample is to be analyzed, it is convenient to make up a master mix of appropriate volume to divide between the PCR tubes, with subsequent addition of the individual DNA samples.

   It is preferable to include characterized DNA control samples for all three polymorphisms: –909CC, –909CG, and –909GG.

2. Program a thermal cycler to run the following cycling procedure.

First step:	2 min	94°C (denaturation)
35 cycles:	30 sec	93°C (denaturation)
	30 sec	69°C (annealing)
	30 sec	72°C (extension)
Final step:	2 min	72°C (extension).

3. Load tubes into thermal cycler and begin the PCR program.

4. Prepare the following on ice for each PCR sample. Save the remaining undigested, amplified DNA for comparison on the agarose gel.

   5.0 µl DNA from PCR amplification
   0.5 µl 5 U/µl *Bsm*AI
   1.0 µl 10× NEBuffer #3
   3.5 µl H_2O
   10.0 µl total.

   Incubate >2 hr at 55°C.

   As before, it is convenient to make up a master mix of appropriate volume to divide between the tubes.

5. Load matched undigested and digested samples as described (see Basic Protocol 2, steps 6 and 7), using 2 µl loading dye for each sample and a low-molecular-weight DNA ladder for 50- to 250-bp fragments.

6. Resolve samples by electrophoresis according to manufacturer's specifications (see Basic Protocol 2, step 8).

7. Stain gel and record gel image as described (see Basic Protocol 2, steps 9 and 10).

8. Determine the genotype as follows:

   Complete digestion –909GG
   Partial digestion –909CG
   No digestion –909CC

ALTERNATE PROTOCOL 2

PARAOXONASE 1 GENOTYPING FOR POLYMORPHISM –162GA

A native *Bst*UI restriction site in the paraoxonase 1 gene (*PON1*) at −162G allows differentiation between the −162G and −162A alleles by PCR amplification and digestion. The PCR amplifies a 1210-bp product that digests into 674- and 536-bp segments when −162G is present. No digestion occurs with the −162A polymorphism.

Additional Materials *(also see Basic Protocol 2)*

10× Opti-prime buffer #1 (Stratagene)
25 µM forward primer −162: 5′-GCT ATT CTT CAG CAG AGG GT-3′
25 µM reverse primer −162: 5′-TGA ATC TGT AGC CAG GGC AC-3′
10 U/µl *Bst*UI (NEB)
NEBuffer #2 (NEB)
1× TAE (see recipe)
1-kb DNA ladder (Promega) or equivalent
60°C water bath

1. Make up the following on ice in a 0.2-ml PCR tube for each sample.

   0.5 µl ~100 ng/µl purified human DNA
   1.5 µl 10× Opti-prime buffer #1
   0.12 µl 25 µM forward primer −162
   0.12 µl 25 µM reverse primer −162
   0.3 µl 10 µM dNTPs
   0.75 µl DMSO
   0.2 µl 5 U/µl *Taq* DNA polymerase
   11.5 µl H_2O
   15.0 µl total.

When more than one sample is to be analyzed, it is convenient to make up a master mix of appropriate volume to divide between the PCR tubes, with subsequent addition of the individual DNA samples.

It is preferable to include characterized DNA controls for all three polymorphisms: −162AA, −162AG, and −162GG.

2. Program a thermal cycler to run the following cycling procedure.

First step:	2 min	94°C (denaturation)
30 cycles:	30 sec	94°C (denaturation)
	30 sec	56°C (annealing)
	30 sec	72°C (extension)
Final step:	2 min	72°C (extension).

3. Load tubes into thermal cycler and begin the PCR program.

4. Prepare the following on ice for each PCR sample. Save the remaining undigested, amplified DNA for comparison on the agarose gel.

   5.0 µl DNA from PCR amplification
   0.5 µl 10 U/µl *Bst*UI
   1.0 µl 10× NEBuffer #2
   3.5 µl H_2O
   10 µl total.

   Incubate >2 hr at 60°C.

   As before, it is convenient to make up a master mix of appropriate volume to divide between the tubes

5. Add 2 µl of 6× Blue/orange loading dye to each undigested and digested sample. Also add loading dye to 1-kb DNA ladder as per supplier's recommendations.

6. Load the ladder into one well of a 1% (w/v) agarose gel made with 1× TAE and alternately load 10 µl of matched undigested and digested samples into the other wells.

   A small-toothed comb should be used when pouring the gel to allow ~15 µl per well.

7. Resolve samples by electrophoresis in 1× TAE according to manufacturer's specifications (see Basic Protocol 2, step 8).

8. Stain and record gel image as described (see Basic Protocol 2, steps 9 and 10).

9. Determine the genotype as follows:

Complete digestion	−162GG
Partial digestion	−162AG
No digestion	−162AA

PARAOXONASE 1 GENOTYPING FOR POLYMORPHISM −108TC

ALTERNATE PROTOCOL 3

In the paraoxonase 1 gene (*PONI*), there is no usable native restriction site that differentiates between the position −108 alleles. To resolve this problem, a reverse primer is used that introduces a *Bst*UI site when −108C is present. This primer is long enough that when the PCR product is digested, the resulting fragments are visible on a 3% (w/v) agarose gel. The digestion results in 52- and 67-bp bands from the 119-bp product when −108C is present and no digestion when −108T is present.

Additional Materials *(also see Basic Protocol 2)*

10× *Taq* polymerase buffer (Promega)
25 mM $MgCl_2$ (Promega or *APPENDIX 2A*)
25 µM forward primer −108: 5′-GAC CGC AAG CCA CGC CTT CTG TGC ACC-3′
25 µM reverse primer −108: 5′-TAT ATT TAA TTG CAG CCG CAG CCC TGC TGG GGC AGC GCC GAT TGG CCC GCC GC-3′
10 U/µl *Bst*UI and NEBuffer #2 (NEB)
Low–base pair DNA ladder (standards for 50- to 125-bp fragments)
60°C water bath

1. Make up the following on ice in a 0.2-ml PCR tube for each sample.

   2.0 µl ~100 ng/µl purified human DNA
   1.5 µl 10× *Taq* polymerase buffer
   1.2 µl 25 mM $MgCl_2$
   0.1 µl 25 µM forward primer −108
   0.1 µl 25 µM reverse primer −108
   0.3 µl 10 mM dNTPs
   0.75 µl DMSO
   0.2 µl 5 U/µl *Taq* DNA Polymerase
   8.85 µl H_2O
   15.0 µl total.

   When more than one sample is to be analyzed, it is convenient to make up a master mix of appropriate volume to divide between the PCR tubes, with subsequent addition of the individual DNA samples.

   It is preferable to have characterized DNA controls for all three polymorphisms: −108CC, −108CT, and −108TT.

2. Program a thermal cycler to run the following cycling procedure.

First step:	2 min	94°C (denaturation)
25 cycles:	30 sec	94°C (denaturation)
	30 sec	63°C (annealing)
	30 sec	72°C (extension)
Final step:	2 min	72°C (extension).

3. Load tubes into thermal cycler and begin the PCR program.

4. Prepare the following on ice for each PCR sample. Save the remaining undigested, amplified DNA for comparison on the agarose gel.

   5.0 µl DNA from PCR amplification
   0.5 µl 10 U/µl *Bst*UI
   1.0 µl 10× NEBuffer #2
   3.5 µl H_2O
   10 µl total.

   Incubate >2 hr at 60°C.

   As before, it is convenient to make up a master mix of appropriate volume to divide between the tubes.

5. Load matched undigested and digested samples as described (see Basic Protocol 2, steps 6 and 7), using 2 µl loading dye for each digested and undigested sample and a low-molecular-weight DNA ladder for 50- to 125-bp fragments.

6. Resolve samples by electrophoresis in 0.5× TBE buffer according to manufacturer's specifications (see Basic Protocol 2, step 8).
7. Stain and record gel image as described (see Basic Protocol 2, steps 9 and 10).
8. Determine the genotype as follows:

Complete digestion	−108CC
Partial digestion	−108CT
No digestion	−108TT

PARAOXONASE 1 GENOTYPING FOR POLYMORPHISM 55LM

ALTERNATE PROTOCOL 4

The paraoxonase 1 gene (*PONI*) has a native *Nla*III restriction site at the 55M codon. In this genotyping strategy, a 386-bp polymerase chain reaction (PCR) product containing the site is amplified. When cut with *Nla*III, it produces a 296-bp and 90-bp band when 55M is present. No digestion is observed with DNA containing the 55L codon.

Additional Materials *(also see Basic Protocol 2)*

10× *Taq* polymerase buffer (Promega)
25 mM $MgCl_2$ (Promega or *APPENDIX 2A*)
25 µM forward primer 55: 5′-AGA GGA TTC AGT CTT TGA GGA AA-3′
25 µM reverse primer 55: 5′-CTG CCA GTC CTA GAA AAC GTT-3′
10 U/µl *Nla*III and NEBuffer #4 (NEB)
10× BSA (NEB)
Low–base pair DNA ladder (suitable for 100- to 400-bp fragments)

1. Make up the following on ice in a 0.2-ml PCR tube for each sample.

0.5 µl ~100 ng/µl purified human DNA
2.0 µl 10× *Taq* polymerase buffer
1.6 µl 25 mM $MgCl_2$
0.2 µl 25 µM forward primer 55
0.2 µl 25 µM reverse primer 55
0.2 µl 10 mM dNTPs
0.2 µl 5 U/µl *Taq* DNA polymerase
15.1 µl H_2O
20.0 µl total.

When more than one sample is to be analyzed, it is convenient to make up a master mix of appropriate volume to divide between the PCR tubes, with subsequent addition of the individual DNA samples.

It is preferable to have characterized DNA controls for all three polymorphisms: 55LL, 55LM, and 55MM.

2. Program a thermal cycler to run the following cycling procedure.

First step:	5 min	94°C (denaturation)
35 cycles:	30 sec	94°C (denaturation)
	30 sec	61°C (annealing)
	30 sec	72°C (extension)
Final step:	7 min	72°C (extension).

3. Load tubes into thermal cycler and begin the PCR program.

4. Prepare the following on ice for each PCR sample. Save the remaining undigested, amplified DNA for comparison on the agarose gel.

   5.0 µl DNA from PCR amplification
   0.3 µl 10 U/µl *Nla*III
   1.0 µl 10× NEBuffer #4
   1.0 µl 10× BSA
   2.7 µl H_2O
   10.0 µl total.

   Incubate >2 hr at 37°C.

   As before, it is convenient to make up a master mix of appropriate volume to divide between the tubes.

5. Add 3 µl of 6× Blue/orange loading dye to each undigested sample and 2 µl to each digested sample. Also add loading dye to low-molecular-weight DNA ladder for 100- to 400-bp fragments as per supplier's recommendations.

6. Load the ladder into the well of a 2% (w/v) agarose gel made with 0.5× TBE and alternately load 10 µl of matched undigested and digested samples.

   A small-toothed comb should be used when pouring the gel to allow ~15 µl per well.

7. Resolve samples by electrophoresis in 0.5× TBE according to manufacturer's specifications (see Basic Protocol 2, step 8).

8. Stain and record gel image as described (see Basic Protocol 2, steps 9 and 10).

9. Determine the genotype as follows:

Complete digestion	55MM
Partial digestion	55LM
No digestion	55LL

ALTERNATE PROTOCOL 5

PARAOXONASE 1 GENOTYPING FOR POLYMORPHISM 194WX

The paraoxonase 1 gene (*PONI*) has a native *Bst*NI restriction site at 194W. With this strategy, a 99-bp polymerase chain reaction (PCR) product containing the site is amplified. (This is the same fragment that is amplified for the codon 192 genotyping; see Basic Protocol 2.) When cut with *Bst*NI, it produces 73- and 26-bp bands when 194W is present; no digestion occurs with 194X.

Additional Materials *(also see Basic Protocol 2)*

10 U/µl *Bst*NI and NEBuffer #2 (NEB)
10× BSA (NEB)
60°C water bath

1. Set up and run PCR reactions as described (see Basic Protocol 2, steps 1 to 4), except use 0.7 µl of 100 mM $MgSO_4$ in the polymerase mix and add no water (1.0 µl final volume).

2. Prepare the following on ice for each PCR sample. Save the remaining undigested, amplified DNA for comparison on the agarose gel.

   10.0 µl DNA from PCR amplification
   1.0 µl 10 U/µl *Bst*NI
   2.0 µl 10× BSA
   2.0 µl 10× NEBuffer #2
   5.0 µl H_2O
   20.0 µl total.

   Incubate >2 hr at 60°C.

   As before, it is convenient to make up a master mix of appropriate volume to divide between the tubes.

3. Load matched undigested and digested samples, run gel, and stain gel and record gel image as described (see Basic Protocol 2, steps 6 to 10).

4. Determine the genotype as follows:

Complete digestion	194WW
Partial digestion	194WX
No digestion	194XX

   The 194XX genotype has not yet been observed.

REAGENTS AND SOLUTIONS

Use Milli-Q-purified water or equivalent for the preparation of all buffers and in all protocol steps. For common stock solutions, see ***APPENDIX 2A;*** *for suppliers, see* ***SUPPLIERS APPENDIX****.*

Assay buffer

Dissolve 116.8 g NaCl (2 M final) in ~800 ml water containing 100 ml of 1 M Tris·Cl, pH 8.5 (0.1 M final) and 2.0 ml of 1 M $CaCl_2$ (2.0 mM final). Bring volume to 1 liter with water. Store up to 6 months at room temperature.

Dilution buffer

Combine 10 ml of 1 M Tris·Cl, pH 8.5 (10 mM final) and 2.0 ml of 1 M $CaCl_2$ (2.0 mM final) and bring volume to 1 liter with water. Store up to 6 months at room temperature.

Ethidium bromide, 1 mg/ml

Weigh 0.1 g ethidium bromide and add to 100 ml water. Store in a light-protected bottle at 4°C indefinitely. Dilute 1:10,000 in running buffer or water to stain gel.

CAUTION: *Ethidium bromide is a mutagen, is moderately toxic, and must be handled carefully. Gloves should be worn at all times to avoid contact. Solutions should be discarded in accordance with institutional guidelines.*

TAE, 50×

Add 242 g Tris base and 18.61 g $Na_2EDTA{\cdot}2H_2O$ to 800 ml water. Add 57.1 ml glacial acetic acid and bring volume to 1 liter with water. Mix until all solid is dissolved. Store up to 6 months at room temperature.

COMMENTARY

Background Information

The human high-density-lipoprotein (HDL)-associated enzyme paraoxonase 1 (PON1; EC 3.1.8.1 or 3.1.1.2) is encoded by a gene on human chromosome 7 q21-22 (Humbert et al., 1993). Two common coding region polymorphisms have been described, 55LM and 192QR (Hassett et al., 1991; Adkins et al., 1993). The latter affects catalytic efficiency of hydrolysis of a number of different substrates (Davies et al., 1996; Furlong et al., 2000). In addition to these coding-region polymorphisms, five polymorphisms in the 5′ regulatory region have been described: −108TC, −126GC, −162GA, −832GA, and −909CG (Brophy et al., 2001). The −108TC polymorphism has the largest effect on PON1 expression of these five polymorphisms, with the −108C allele generating on average approximately twice the amount of plasma PON1 as the −108T allele generates. Recently, eight new polymorphisms in the 5′ regulatory region have been described, but they are not yet characterized, which is also true of >140 polymorphisms in PON1 introns. One new functional coding region polymorphism, W194X, has been described and characterized (Jarvik et al., 2003; see Internet Resource).

Early investigations centered around the role of the PON1 polymorphisms in resistance to organophosphorus insecticides (reviewed in Costa et al., 2002; La Du, 2002). More recent studies have focused on the role of the *PON1* polymorphisms in vascular disease (reviewed in Lusis et al., 2000; Brophy et al., 2002; Mackness et al., 2002; Shih et al., 2002). These studies merit special comments. Nearly all of the studies investigating the relationship between *PON1* polymorphisms and vascular disease have considered only *PON1* genotype(s) and have ignored the equally or more important consideration of PON1 levels. The mechanism of prevention of vascular disease appears to be related to the ability of PON1 to degrade biologically active oxidized lipids (Watson et al., 1995; reviewed in Navab et al., 2002). Fundamental biochemical principles dictate that the more PON1 molecules present in the plasma, the faster an individual can detoxify toxic organophosphate compounds or oxidized lipid molecules. Thus, it is important to analyze both PON1 quantity as well as quality.

PON1 knockout mice show a dramatic increase in sensitivity to chlorpyrifos oxon (Shih et al., 1998) and diazoxon (Li et al., 2000). Resistance can be restored by injecting purified PON1. The degree of resistance provided by the injected purified PON1 depends on the catalytic efficiency of the position 192 alloform injected ($PON1_{192Q}$ or $PON1_{192R}$). Because it is both the level and catalytic efficiency of PON1 that determine sensitivity to organophosphate exposures (Li et al., 2000), and probably risk for vascular disease as well (Jarvik et al., 2000), it does not make sense to analyze for PON1 genotype alone. A simple two-substrate analysis, when used with a population analysis, provides an individual's PON1 status relative to the rest of the population. Plotting the rates of diazoxon hydrolysis versus paraoxon hydrolysis (Fig. 4.12.2) for individuals within a population clearly divides the subjects into three groups: individuals homozygous for $PON1_{192Q}$, heterozygotes ($PON1_{192Q/R}$), and individuals homozygous for $PON1_{192R}$ (Richter and Furlong, 1999).

Figure 4.12.2 illustrates a typical population distribution using the method for determination of PON1 status (see Basic Protocol 1). Whereas most of the authors' studies make use of heparin plasma, this figure shows that PON1 status can also be determined using stored citrate plasma. Plasma for a given study should all be prepared with the same preservative because there are some small differences in activity between citrate- and heparin-stored plasma samples (serum has also been used in the authors' laboratory). EDTA plasma cannot be used because EDTA irreversibly denatures PON1. If only stored EDTA plasma samples are available, it is recommended that PON1 levels be determined via immunoassay protocols (Blatter Garin et al., 1994).

Interindividual variability of PON1 levels can be at least 13-fold within a given $PON1_{192}$ genotype (Q/Q, Q/R, R/R; Davies et al., 1996). A number of factors govern the levels of plasma PON1. These include polymorphisms in the 5′ regulatory region of the *PON1* gene, possibly the as yet uncharacterized polymorphisms in the 3′ UTR of PON1, various coding region mutations such as the nonsense mutation at codon 194, and mutations in splice or acceptor sites and possibly enhancer sequences that have not yet been characterized. In addition to regulatory factors upstream from, within, and downstream from the *PON1* gene, other transacting factors, often referred to as genetic background factors, also influence the level of expression of PON1. One example is the devel-

opmental regulation of expression of PON1 controlled by as yet uncharacterized factors, which in turn will also most likely be genetically variable. Thus, while it is neither feasible nor sufficient to examine all of the different genetic factors that contribute to the variability in PON1 expression, it is straightforward to evaluate the final result of all of these effects (i.e., the level of expression and functional genomics of *PON1*). The two-substrate analysis provides an accurate analysis of an individual's PON1 status (position 192 functional genotype and level of expression) using high-throughput assay methods.

Methods are also provided for genotyping a number of the *PON1* DNA polymorphisms (see Basic Protocol 2 and see Alternate Protocols 1 to 5). It should be noted, however, that the authors do not recommend the use of PON1 genotype alone for determining susceptibility to specific exposures or for determining PON1-associated risk for specific diseases. The PON1 status determination provides essential information not provided by genotyping *PON1* polymorphisms or even more sophisticated haplotype analysis. The genotyping methods may be useful for forensic procedures or other applications such as gene frequency determination for specific populations.

Critical Parameters and Troubleshooting

The most critical parameter for determining PON1 status is to be sure that the rates used to generate the data points are derived from the linear portions of the rate versus time plots. Examination of the rate curves from the plate reader will provide the information necessary to make this determination. If some of the higher rates become nonlinear versus time, rates over shorter times can be selected. For plasma with slow rates of hydrolysis, times can be selected that provide appropriate linear rates.

It is also important that plasma not be drawn into EDTA tubes, as EDTA irreversibly inhibits PON1. Lithium-heparin has been used as the anticoagulant of choice. As noted in this unit, however, citrate plasma may also be used. For a given study, the same anticoagulant should be used, as there may be differences in activity between plasma drawn into different anticoagulants. See Table 4.12.1 for troubleshooting PON1 genotyping.

Table 4.12.1 Troubleshooting Guide to PON1 Genotyping

Problem	Possible cause	Suggested solution
No or low PCR amplification	Not enough DNA	Check DNA concentration of samples
		Increase cycle number
	EDTA or other contaminant in DNA sample	Get new samples without EDTA
		Remove EDTA with purification column
	Improper reagent mixing	Mix all components properly
Incorrect or ambiguous results	Digestion not complete	Increase incubation time
	Wrong incubation temperature	Check temperature
	Poor quality restriction enzyme	Purchase new enzyme and store properly
	Restriction enzyme not fresh	Check expiration date
	Mis-genotyped	Find new reliable controls
	Cross-contamination	Use aerosol-resistant tips
	Gel was not run long enough	Run gel until bands are well separated
	Agarose gel not prepared correctly	Make sure gel is well mixed and without bubbles or contaminants

Anticipated Results

The results obtained from the two-substrate analysis of PON1 status should generate a distribution such as that seen in Figure 4.12.2. If they do not, the most likely problem would be the use of rates derived from the nonlinear portion of the hydrolysis rate curves.

The gene frequencies obtained from the SNP analyses will vary according to the ethnic composition of the sampled population. For example, the gene frequency of the $PON1_{192Q}$ allele in populations of Northern European origin should be approximately 0.7. For populations of Asian or African origin, the gene frequency for $PON1_{192Q}$ will be significantly lower, perhaps as low as 0.3.

Time Considerations

The determination of PON1 status by the two-substrate procedure can be completed in a single day for 32 individuals when the samples are run in triplicate and rates are determined for the two substrates, paraoxon and diazoxon.

Each genotyping experiment can be completed in ~8 hr when assaying 28 samples. It can be convenient to break up the procedure by stopping after the PCR or digestion step and freezing the experiment overnight so that it can be finished in 2 days.

Literature Cited

Adkins, S., Gan, K.N., Mody, M., and La Du, B.N. 1993. Molecular basis for the polymorphic forms of human serum paraoxonase/arylesterase: Glutamine or arginine at position 191, for the respective A or B allozymes. *Am. J. Hum. Genet.* 52:598-608.

Blatter Garin, M.C., Abbott, C., Messmer, S., Mackness, M., Durrington, P., Pometta, D., and James, R.W. 1994. Quantification of human serum paraoxonase by enzyme-linked immunoassay: Population differences in protein concentrations. *Biochem. J.* 304:549-554.

Brophy, V.H., Costa, L.G., Richter, R.J., Hagen, T., Shih, D.M., Tward, A., Lusis, A.J., and Furlong, C.E. 2001. Polymorphisms in the human paraoxonase (*PON1*) promoter. *Pharmacogenetics* 11:77-84.

Brophy, V.H., Jarvik, G.P., and Furlong, C.E. 2002. *In* Paraoxonase (PON1) In Health and Disease: Basic and Clinical Aspects (L.G. Costa and C.E. Furlong, eds.) pp. 53-77. Kluwer Academic Press, Boston.

Costa, L.G. and Furlong, C.E., eds. 2002. *In* Paraoxonase (PON1) In Health and Disease: Basic and Clinical Aspects. Kluwer Academic Press, Boston.

Costa, L.G., Li, W.-F., Richter, R.J., Shih, D.M., Lusis, A.J., and Furlong, C.E. 2002. PON1 and organophosphate toxicity. *In* Paraoxonase (PON1) In Health and Disease: Basic and Clinical Aspects (L.G. Costa and C.E. Furlong, eds.) pp. 165-183. Kluwer Academic Press, Boston.

Costa, L.G., Cole, T.B., Jarvik, G.P., and Furlong, C.E. 2003. Functional genomics of the paraoxonase (PON1) polymorphisms: Effects on pesticide sensitivity, cardiovascular disease, and drug metabolism. *Annu. Rev. Med.* 54:371-392.

Davies, H.G., Richter, R.J., Keifer, M., Broomfield, C.A., Sowalla, J., and Furlong, C.E. 1996. The effect of the human serum paraoxonase polymorphism is reversed with diazoxon, soman and sarin. *Nat. Genet.* 14:334-336.

Furlong, C.E., Li, W.-F., Richter, R.J., Shih, D.M., Lusis, A.J., Alleva, E., and Costa, L.G. 2000. Genetic and temporal determinants of pesticide sensitivity: Role of paraoxonase (PON1). *Neurotoxicology* 21:91-100.

Gan, K.N., Smolen, A., Eckerson, H.W., and LaDu, B.N. 1991. Purification of human serum paraoxonase/arylesterase. Evidence for one esterase catalyzing both activities. *Drug Metab. Dispos.* 19:100-106.

Hassett, C., Richter, R.J., Humbert, R., Chapline, C., Crabb, J.W., Omiecinski, C.J., and Furlong, C.E. 1991. Characterization of cDNA clones encoding rabbit and human serum paraoxonase: The mature protein retains its signal sequence. *Biochemistry* 30:10141-10149.

Humbert, R., Adler, D.A., Disteche, C.M., Hassett, C., Omiecinski, C.J., and Furlong, C.E. 1993. The molecular basis of the human serum paraoxonase activity polymorphism. *Nat. Genet.* 3:73-76.

Jarvik, G.P., Rozek, L.S., Brophy, V.H., Hatsukami, T.S., Richter, R.J., Schellenberg, G.D., and Furlong, C.E. 2000. Paraoxonase (PON1) phenotype is a better predictor of vascular disease than is PON1(192) or PON1(55) genotype. *Arterioscler. Thromb. Vasc. Biol.* 20:2441-2447.

Jarvik, G.P., Jampsa, R., Richter, R.J., Carlson, C.S., Rieder, M.J., Nickerson, D.A., and Furlong, C.E. 2003. Novel paraoxonase (PON1) nonsense and missense mutations predicted by functional genomic assay of PON1 status. *Pharmacogenetics* 13:291-295.

La Du, B.N. 2002. Historical considerations. *In* Paraoxonase (PON1) in Health and Disease: Basic and Clinical Aspects (L.G. Costa and C.E. Furlong, eds.) pp. 1-25. Kluwer Academic Press, Boston.

Li, W.F., Costa, L.G., Richter, R.J., Hagen, T., Shih, D.M., Tward, A., Lusis, A.J. and Furlong, C.E. 2000. Catalytic efficiency determines the *in-vivo* efficacy of PON1 for detoxifying organophosphorus compounds. *Pharmacogenetics* 10:767-779.

Lusis, A.J. 2000. Atherosclerosis. *Nature* 407:233-241.

Mackness, M.I., Durrington, P.N., and Mackness, B. 2002. The role of paraoxonase in lipid metabolism. *In* Paraoxonase (PON1) in Health and Disease: Basic and Clinical Aspects (L.G. Costa and C.E. Furlong, eds.) pp. 79-88. Kluwer Academic Press, Boston.

Mueller, R.F., Hornung, S., Furlong, C.E., Anderseon, J., Giblett, E.R., and Motulsky, A.G. 1983. Plasma paraoxonase polymorphism: A new enzyme assay, population, family, biochemical, and linkage studies. *Am. J. Hum. Genet.* 35:393-408.

Navab, M., Hama, S.Y., Wagner, A.C., Hough, G., Watson, A.D., Reddy, S.T., Van Lenten, B.J., Laks, H., and Fogelman, A.M. 2002. Protective action of HDL-associated PON1 against LDL oxidation. *In* Paraoxonase (PON1) in Health and Disease: Basic and Clinical Aspects (L.G. Costa and C.E. Furlong, eds.) pp. 125-136. Kluwer Academic Press, Boston.

Richter, R.J. and Furlong, C.E. 1999. Determination of paraoxonase (PON1) status requires more than genotyping. *Pharmacogenetics* 9:745-753.

Shih, D.M., Gu, L., Xia, Y.-R., Navab, M., Li, W.-F., Hama, S., Castellani, L.W., Furlong, C.E., Costa, L.G., Fogelman, A.M., and Lusis, A.J. 1998. Mice lacking serum paraoxonase are susceptible to organophosphate toxicity and atherosclerosis. *Nature* 394:284-287.

Shih, D.M., Reddy, S., and Lusis, A.J. 2002. CHD and atherosclerosis: Human epidemiological studies and transgenic mouse models. *In* Paraoxonase (PON1) in Health and Disease: Basic and Clinical Aspects (L.G. Costa and C.E. Furlong, eds.) pp. 93-123. Kluwer Academic Press, Boston.

Watson, A.D., Berliner, J.A., Hama, S.Y., La Du, B.N., Faull, K.F., Fogelman, A.M., and Navab, M. 1995. Protective effect of high density lipoprotein associated paraoxonase. Inhibition of the biological activity of minimally oxidized low density lipoprotein. *J. Clin. Invest.* 96:2882-2891.

Internet Resource

http://pga.gs.washington.edu

The web site for the University of Washington–Fred Hutchinson Cancer Research Center Variation Discovery Resource (SeattleSNPs) includes information on the W194X coding-region polymorphism.

Contributed by Rebecca J. Richter,
Rachel L. Jampsa, Gail P. Jarvik,
Lucio G. Costa, and Clement E. Furlong
University of Washington
Seattle, Washington

Human Cytochrome P450: Metabolism of Testosterone by CYP3A4 and Inhibition by Ketoconazole

The cytochrome P450 (CYP) monooxygenase system comprises a superfamily of heme-containing enzymes expressed in many mammalian tissues, with the highest levels found in liver. These enzymes are capable of catalyzing the metabolism of a wide range of both endogenous and exogenous substrates. Human CYP3A4 is one of the most important and abundant drug-metabolizing CYP isoforms in human liver microsomes—it accounts for ~40% of the total CYP in human liver microsomes. CYP3A4 not only metabolizes xenobiotics but is also responsible for the metabolism of endogenous compounds such as testosterone. Assessing the role of CYP3A4 in drug metabolism often requires a well characterized CYP3A4 selective substrate to probe CYP3A4 activity. Among the different CYP3A4 assays available, the regioselective and stereoselective hydroxylation of testosterone is one of the most commonly used metabolism assays for the assessment of CYP3A4 activity in humans and other species. Testosterone hydroxylation assays may be used in drug metabolism studies to help assess enzyme induction, predict drug-drug interactions, characterize structure-activity relationships, and facilitate drug candidate selection. This unit begins by describing the HPLC method for measuring testosterone oxidation, which is a simple screening method (see Basic Protocol 1). Determination of testosterone metabolism by this protocol is also a very sensitive method to detect the inhibition of CYP3A4 by chemicals of interest.

Chemical inhibition studies (see Basic Protocol 2) take advantage of the specificity of the particular isoform involved in the metabolism of the chemical of interest. To understand potential interactions with other CYP3A4 substrates and effects of polymorphisms, it is important to determine whether CYP3A4 is responsible for metabolism of the chemical of interest. One method to determine the role of a CYP isoform is to use a selective chemical inhibitor. If such an inhibitor significantly inhibits the metabolic activity of CYP3A4, this indicates that CYP3A4 is responsible for the metabolism; otherwise, one may infer that CYP3A4 plays little role in the metabolism. Ketoconazole, an imidazole fungicide, is a selective inhibitor of CYP3A4. Basic Protocol 2 describes a method of using ketoconazole to determine the role of CYP3A4 in metabolism, with testosterone as a model substrate.

TESTOSTERONE OXIDATION BY CYP3A4

BASIC PROTOCOL 1

Testosterone oxidation is predominantly catalyzed by CYP3A4 and, therefore, is often used as a diagnostic pathway for CYP3A4 activity. This procedure takes advantage of the specificity of CYP3A4 toward testosterone metabolism and is a sensitive method for the measurement of testosterone metabolites.

Materials

0.1 M potassium phosphate buffer, pH 7.4, with 5 mM $MgCl_2$ (see recipe)
100 mM testosterone stock (Steraloids, Inc.; dissolve 28.841 mg testosterone in 1 ml methanol; store up to 3 months at −20°C)
NADPH regenerating system (see recipe)
1 pmol/μl CYP3A4 (BD Bioscience)
Methanol, ice-cold
Testosterone metabolites in methanol for standard curve (see recipe and Table 4.13.1)

Contributed by Khawja A. Usmani and Jun Tang
Current Protocols in Toxicology (2004) 4.13.1-4.13.9

Table 4.13.1 HPLC Retention Times for Testosterone and Hydroxylated Testosterone Metabolites[a]

Common name	Chemical name	Retention time (min)
6α-Hydroxytestosterone	4-Androsten-6α,17β-diol-3-one	14.38
15β-Hydroxytestosterone	4-Androsten-15β,17β-diol-3-one	15.11
6β-Hydroxytestosterone	4-Androsten-6β,17β-diol-3-one	16.25
11-Ketotestosterone	4-Androsten-17β-ol-3,11-dione	18.24
16β-Hydroxytestosterone	4-Androsten-16β,17β-diol-3-one	19.34
11β-Hydroxyandrostenedione	4-Androsten-11β-ol-3,17-dione	19.68
2α-Hydroxytestosterone	4-Androsten-2α,17β-diol-3-one	20.68
2β-Hydroxytestosterone	4-Androsten-2β,17β-diol-3-one	21.55
Androstenedione	4-Androsten-3,17-dione	24.92
4-Hydroxyandrostenedione	4-Androsten-4-ol-3,17-dione	27.20
Testosterone	4-Androsten-17β-ol-3-one	28.90

[a]Testosterone and its metabolites are purchased from Steraloids, Inc.

1-ml HPLC vials
HPLC system and reagents (Table 4.13.2)

Perform reaction

1. Add the following ingredients to a 1.5-ml microcentrifuge tube (total 250 μl).

   221 μl potassium phosphate buffer, pH 7.4, with 5 mM $MgCl_2$
   4 μl of 6.125 mM testosterone in methanol (prepare from 100 mM stock; final concentration in reaction, 100 μM)
   12.5 μl NADPH regenerating system.

2. Preincubate for 3 min at 37°C.
3. Initiate reaction by adding 12.5 μl of ice-cold 1 pmol/μl CYP3A4 (final concentration 50 pmol/ml).
4. Incubate for 10 min at 37°C water bath with gentle shaking.

Analyze by HPLC

5. Terminate the reaction by the addition of 250 μl of ice-cold methanol.
6. Vortex for 5 sec.
7. Microcentrifuge 10 min at maximum speed, room temperature.
8. Transfer 400 μl of supernatant to a 1-ml HPLC vial.
9. Analyze testosterone metabolite concentrations by reversed-phase HPLC using the conditions described in Table 4.13.2. Analyze a series of testosterone metabolites (see Table 4.13.1 and Reagents and Solutions) in parallel to create a standard curve.

   The recommended injection volume is 50 μl.

10. Detect the products by their absorbance at 247 nm and quantify them by comparing the absorbance to standard curves of testosterone metabolites.
11. Obtain concentrations of metabolites by extrapolation of peak heights from a standard curve.

Table 4.13.2 Reversed-Phase HPLC Conditions for Separation of Testosterone and its Potential Metabolites

Conditions	Information
Mobile phase A	5% tetrahydrofuran/95% H_2O[a]
Mobile phase B	100% methanol
Gradient	0–1 min (30% B) 1–10 min (30%–60% B) 10–22 min (60%–65% B) 22–28 min (65%–80% B) 28–30 min (80%–90% B) 30–32 min (90% B)
Flow rate	0.5 ml/min
Column	Phenomenex Prodigy ODS(3), 3 μm, 150 × 4.6 mm, 100 Å
Detector	Absorbance at 247 nm
Retention times	see Table 4.13.1
Limits of detection	For most testosterone metabolites, ~0.04 μM, except for 6β-hydroxytestosterone (0.15 μM) and 4-hydroxyandrostenedione (0.30 μM)

[a]Do not use HPLC mobile phase A for more than 1 week, because the concentration of tetrahydrofuran changes; prepare fresh every week, otherwise retention time may shift.

INHIBITION OF CYP3A4-MEDIATED TESTOSTERONE 6β-HYDROXYLASE BY KETOCONAZOLE

BASIC PROTOCOL 2

Ketoconazole is one of the most frequently used selective chemical inhibitors for CYP3A4. Although some researchers preincubate microsomes with ketoconazole to obtain a substantial inhibition before adding a substrate, most find that adding substrate and ketoconazole to microsomes simultaneously achieves the required inhibition, because of the potency of ketoconazole. The assay described here is a straightforward method to study the inhibition of CYP3A4 activity by ketoconazole.

Materials

1 pmol/μl CYP3A4 (BD Bioscience) or liver microsomes (*UNIT 4.3*; 20 mg protein/ml)
0.1 M potassium phosphate buffer, pH 7.4, with 5 mM $MgCl_2$ (see recipe)
25 mM testosterone (Steraloids, Inc.) in methanol (store up to 3 months at −20°C)
0.5 mM ketoconazole stock (Sigma) in DMSO (store up to 3 months at −20°C)
NADPH regenerating system (see recipe)
Methanol, ice-cold
6β-hydroxytestosterone in methanol for standard curve (see recipe for testosterone metabolites)

1-ml HPLC vials
HPLC system and reagents (Table 4.13.2)

Additional reagents and equipment for measurement of testosterone metabolites by HPLC (see Basic Protocol 1)

Perform reaction

1. Quickly thaw CYP3A4 or human liver microsomes and place on ice.
2. Add 451 μl of 100 mM potassium phosphate buffer (pH 7.4) with 5 mM $MgCl_2$ to each of a series of 1.5-ml plastic microcentrifuge tubes representing different concentrations of ketoconazole to be tested (see step 4, below).

3. To each tube, add 2 μl of 25 mM testosterone (to make a final concentration of 100 μM) or 2 μl of methanol as a solvent control for substrate.
4. To each tube, respectively, add 2 μl of a different concentration of ketoconazole in DMSO to make final concentrations of 0, 0.02, 0.2, and 2 μM.

   Ketoconazole is soluble in DMSO but is less soluble in acetonitrile and methanol. Make a 0.5 mM ketoconazole stock solution and dilute to 0.05 and 0.005 μM to obtain final concentrations of 2, 0.2, or 0.02 μM in the reaction mixture. Add an equal volume (2 μl) of DMSO to obtain a 0 μM ketoconazole control.

   CAUTION: *DMSO is hazardous; avoid skin contact.*
5. Add 25 μl of NADPH-regenerating system or 25 μl of 100 mM potassium phosphate buffer (pH 7.4) with 5 mM $MgCl_2$ as a control for potential non-CYP-mediated reactions.
6. Vortex tubes and preincubate 3 min at 37°C.
7. Add 20 μl of ice-cold 1 pmol/μl CYP3A4 (final concentration, 40 pmol/ml) or 20 μl of ice-cold 20 mg/ml human liver microsomes (final concentration, 800 μg/ml to start the reaction; vortex the tube and incubate for 10 min in a 37°C water bath with gentle shaking.

Analyze by HPLC

8. Stop the reaction by adding 250 μl of ice-cold methanol.
9. Microcentrifuge 10 min at maximum speed, room temperature.
10. Transfer 500 μl of the supernatant to a 1-ml HPLC vial.
11. Analyze testosterone 6β-hydroxylase by reversed-phase HPLC using the conditions described in Table 4.13.2. Analyze a series of testosterone metabolites (see Table 4.13.1 and Reagents and Solutions) in parallel to create a standard curve.

    The recommended injection volume is 50 μl.
12. Detect the products by their absorbance at 247 nm and quantify them by comparing the absorbance to standard curves of testosterone metabolites.

REAGENTS AND SOLUTIONS

Use Milli-Q-purified water or equivalent for the preparation of all solutions and in all protocol steps. For common stock solutions, see ***APPENDIX 2A****; for suppliers, see* ***SUPPLIERS APPENDIX****.*

NADPH regenerating system

Add 4.2 mg $NADP^+$ (sodium salt; Sigma) to 14.1 mg glucose-6-phosphate (monosodium salt; Sigma) and 20 U of glucose-6-phosphate dehydrogenase in a final volume of 0.5 ml of the same potassium phosphate buffer as the reaction buffer. Dispense into 25-μl aliquots per 1-ml assay volume, bring final concentrations to 0.25 mM $NADP^+$, 2.5 mM glucose-6-phosphate, and 1 U glucose-6-phosphate dehydrogenase. Excess solution may be used for up to 2 weeks if stored frozen at −20°C.

Potassium phosphate buffer, pH 7.4, 100 mM, with 5.0 mM $MgCl_2$

Combine 0.517 g KH_2PO_4 and 2.822 g K_2HPO_4 in 200 ml of water. Add 0.205 g $MgCl_2$ (hexahydrate; Fisher). Adjust to pH 7.4 with 1 M HCl or NaOH if necessary. Store up to 6 months at 4°C.

Testosterone metabolites

Make solutions of each of the testosterone metabolites (Steraloids, Inc.) in methanol, all of which are 50 μM. Take half of the 50 μM solution and add an equal volume of methanol to get a 25 μM concentration. Repeat the procedure to get the 0.1 μM concentration. Inject 50 μl testosterone metabolites on HPLC system and make a standard curve of each metabolite of testosterone based on the peak heights on Microsoft Excel.

The metabolites may be stored up to 3 months at −20°C

COMMENTARY

Background Information

Cytochrome P450s (CYPs) are the main enzymes responsible for the Phase I reactions, which are considered to be one of the rate-limiting steps of the overall drug metabolism process (Madan et al., 2001). In some cases, the products of Phase I reaction are more active or toxic than their corresponding parent compounds (Neal, 1980). Of the several human CYP enzymes, those of the CYP3A subfamily have major importance because they are the most abundant of the human CYP isoforms. Substrate specificity of the CYP3A subfamily is extremely broad, and these enzymes have been shown to be expressed in tissues of particular relevance to drug disposition, such as liver, intestine, lung, kidney, and brain (Shimada et al., 1994, Thummel and Wilkinson 1999, Madan et al., 2001). At least three members of the CYP3A subfamily have been described as having functional proteins in humans: CYP3A4, CYP3A5, and CYP3A7. It has been reported that CYP3A4 in humans represents up to 50% of the cytochrome P450 expressed in liver and 70% of that in small intestine (Kolars et al., 1994, McKinnon et al., 1995). Initial data suggested that CYP3A5 accounted for only a small percentage of total hepatic CYP3A content in only about 20% of samples. However, recent data have indicated that CYP3A5 might exceed 50% of the total CYP3A in some individuals (Kuehl et al., 2001). Expression of CYP3A7 functional protein is mainly confined to the fetal liver, although in some cases it has been detected in adults (Schuetz et al., 1994). P450-dependent hydroxylation appears to be a major pathway of oxidative metabolism of testosterone in mammals. CYP3A4 is one of the major isoforms responsible for testosterone metabolism, and 6β-hydroxytestosterone is the major testosterone metabolite. It has been shown (Usmani et al., 2003) that, among members of the CYP3A subfamily, CYP3A4 produced the highest amount of testosterone metabolites (88.5%) compared with 3A5 (6.9%) and 3A7 (4.6%). The same study indicated that among members of the CYP3A subfamily CYP3A4 produced the highest amount of 6β-hydroxytestosterone (90.6%) compared with 3A5 (7.1%), and 3A7 (2.2%). Other major TST metabolites formed by CYP3A4 were 15β-hydroxytestosterone, 2β-hydroxytestosterone, and 4-hydroxyandrostenedione. Other members of the CYP3A subfamily, CYP3A5 and 3A7, also oxidized testosterone, but their activity was 10 to 20 fold less than that of CYP3A4 (Usmani et al., 2003). Several studies have shown that CYP3A4 is the major P450 involved in the metabolism of testosterone in human liver microsomes. Either inhibition or induction can modulate the activity of an enzyme; P450s may exhibit stimulation or inhibition in the presence of certain xenobiotic compounds. It has been suggested that CYP3A4 is an allosteric enzyme, even though the identity of the allosteric site is not known (Shimada and Guengerich 1989; Lee et al., 1995). In addition, little is known about the active-site topology of CYP3A4, although it is generally recognized that the active site of this enzyme has the capacity to accommodate large molecules and even more than one substrate (Shou et al., 1994). Inhibition may, in some interactions, be more serious than enzyme induction, since inhibition happens more rapidly, not taking time to develop, as with induction (Guengerich, 1997). It is very important to know that a chemical of interest inhibits or induces CYP3A4 activity. Testosterone oxidation is one of the most important tools employed as a diagnostic test for CYP3A4 activity and its inhibition or induction. Basic Protocol 1 describes a method to study the activity of CYP3A4. This method can be used for inhibition or induction studies of CYP3A4 by chemicals of interest in human hepatocytes or in recombinant CYP3A4. Similarly testosterone oxidation can be used as a diagnostic test for CYP3A5 and CYP3A7 isoforms (Lee et al., 2003).

CYP3A4 is responsible for the P450-mediated metabolism of ~50% of marketed pharmaceuticals, although the levels vary by as much as 20-fold among individuals (Shimada et al., 1994, Rodrigues, 1999). Due to the large number of drug molecules metabolized by CYP3A4, potent inhibition can have a detrimental effect on another drug. It is very important to determine reaction phenotyping of a given drug or test compound, i.e., to understand all reaction pathways of the drug and the CYP isoforms catalyzing these reactions (see Internet Resources). One of the tools used to analyze reaction phenotyping is the use of selective chemical inhibitors to identify the CYP isoforms responsible for the reaction (Rodrigues, 1999). The information obtained from a reaction phenotyping study can predict effects of polymorphism. For example, if a phenotyping study found that a drug is predominantly metabolized by certain CYP isoforms, then it is predictable that this drug would have low clearance in a person with a mutated allele of this isoform (Dai et al., 2001). Reaction phenotyping studies can also identify potential drug-drug interactions, i.e., the metabolism of a test drug may change if it is coadministered with another drug that significantly inhibits or induces the CYP isoform that predominantly catalyzes the metabolism of the test drug, or a test drug may significantly affect the metabolism of a coadministered drug by inhibiting or inducing the CYP isoform responsible for the metabolism of the latter (Varhe et al., 1994; von Moltke et al., 1996).

CYP3A4 is the most abundant CYP isoform in human liver and is involved in the metabolism of more than half of currently used drugs as well as a number of steroids, environmental chemicals, and carcinogens (Shimada et al., 1994). It is important to identify the involvement of CYP3A4 in the metabolism of a test compound. Ketoconazole has been used as a selective chemical inhibitor for CYP3A4 in reaction phenotyping studies (Jonsson et al., 1995; Moody et al., 1997; Oda and Kharasch, 2001). Ketoconazole is an imidazole fungicide. The mechanism underlying its antifungal activity, like other azole fungicides, is the inhibition of ergosterol synthesis by binding of the unsubstituted nitrogen (N-3) of its imidazole moiety to the heme iron and binding of its N-1 substituent to the apoprotein of a fungal CYP (Vanden Bossche et al., 1989). The affinity and selectivity of azole fungicides for CYP are determined by the nitrogen heterocycle and the hydrophobic N-1 substituent. Ketoconazole not only inhibits fungal CYP, which makes it a good fungicide (Gascoigne et al., 1981), but it is also a potent CYP3A4 inhibitor, which results in adverse interactions with other drugs (Mosca et al., 1985; Brown et al., 1985; Back and Tjia, 1985; Varhe et al., 1994). Ketoconazole is a very potent and selective mixed-type CYP3A inhibitor with a $K_i \leq 0.3$ μM (Maurice et al., 1992; Bourrie et al., 1996; von Moltke et al., 1996; Satoh et al., 2000).

Basic Protocol 2 describes a method to study inhibition of testosterone metabolism by ketoconazole. This method can be used for reaction phenotyping or inhibition studies of other chemicals of interest. For example, a test compound can be used as a potential CYP3A4 substrate to replace testosterone for a reaction phenotyping study of the test compound (for more detail about phenotyping studies, see Rodrigues 1999). For inhibition studies, a test compound can be used as a potential CYP3A4 inhibitor to replace ketoconazole (for more detail about inhibition studies, see Madan et al. 2001).

Critical Parameters and Troubleshooting

For a reaction phenotyping study, it is necessary to make sure that CYP3A4 activity is significantly inhibited (% inhibition > 83%) while the other CYP isoforms are not significantly affected (Rodrigues, 1999). It has been shown that ketoconazole is selective for CYP3A at an $[I]/K_i$ ratio as high as 30 (Bourrie et al., 1996), although CYP2C9 can also be inhibited at high concentrations (20 μM) of ketoconazole (Zhang et al., 2002). To obtain an IC_{50} value, a series of concentrations of ketoconazole from 0- to 10-fold K_i is sufficient. For a single point concentration, 1 or 2 μM of ketoconazole is often used (Desta et al., 2000; Venkatakrishnan et al., 2001).

Because inhibition effect is calculated as a comparison of activities in the presence or absence of the inhibitor, ketoconazole, an addition of equal volume of solvent into the tube for 0 μM ketoconazole is important. Organic solvent, especially DMSO, has been shown to damage microsomes (Madan et al., 2001). Therefore, an appropriate control for these solvents is necessary.

The concentration of testosterone used in Basic Protocols 1 and 2 is 100 μM, which is around its K_m (Usmani et al., 2003). High concentrations of testosterone (400 to 800 μM) have been shown to inhibit testosterone metabolism. The substrate concentration affects the percent of inhibition, especially

Table 4.13.3 Testosterone Hydroxylation by CYP3A4 Expressed in Baculovirus-Infected Insect Cells

Testosterone metabolites	nmol/nmol CYP3A4/min
6α-Hydroxytestosterone	0.22 ± 0.02
15β-Hydroxytestosterone	3.18 ± 0.11
6β-Hydroxytestosterone	157.7 ± 6.00
11-Ketotestosterone	1.04 ± 0.04
16β-Hydroxytestosterone	0.44 ± 0.01
11β-Hydroxyandrostenedione	1.70 ± 0.02
2α-Hydroxytestosterone	0.19 ± 0.01
2β-Hydroxytestosterone	7.05 ± 0.23
Androstenedione	0.27 ± 0.01
4-Hydroxyandrostenedione	2.23 ± 0.24

when inhibition is competitive. It is important to choose a substrate concentration close to its K_m, because, at this concentration, the percent inhibition will be independent of substrate concentration (Rodrigues, 1999). As for inhibition by ketoconazole, which is a mixed-type inhibitor (Bourrie et al., 1996), choose a substrate concentration at a level equal to or less than K_m, so as not to affect percent of inhibition (Rodrigues, 1999).

It needs to be emphasized again that microsomal protein concentration and time of incubation should be kept in the linear range. Microsomal protein concentration needs to be as low as possible in order to minimize the nonspecific binding of substrate to proteins (Rodrigues, 1999).

persomes; BD Biosciences) may be used. The general assay requirements are described in Basic Protocol 2. The specific conditions of this assay were pH 7.4, 0.4 mg/ml human liver microsomes or 20 pmol/ml recombinant CYP3A4 (Supersomes), a substrate concentration of 100 μM testosterone, and inhibitor concentrations of 0.02 to 2 μM ketoconazole. The assay was incubated for 10 min at 37°C and was stopped with 250 μl ice-cold methanol.

The specific activity (nmol 6β-hydroxytestosterone formed/min/mg microsomal protein or nmol CYP3A4) was calculated according to the Basic Protocol 1. Percent of inhibition or percent of control was calculated using the following formula:

$$\%\ \text{inhibition} = \frac{\text{activity with solvent only} - \text{activity with ketoconazole in solvent}}{\text{activity with solvent only}} \times 100\%$$

$$\%\ \text{control} = \frac{\text{activity with ketoconazole in solvent}}{\text{activity with solvent only}} \times 100\%$$

Anticipated Results

This section gives an example of an assay that was performed by the method described in this unit. Table 4.13.3 is an illustration of results for Basic Protocol 1, obtained after the concentrations of metabolites were obtained by extrapolation of peak height from a standard curve.

Human liver microsomes from commercially available sources were analyzed for testosterone 6β-hydroxylase activity in the presence or absence of ketoconazole. Alternatively, recombinant CYP3A4 (e.g., Su-

The result using this protocol is shown in Figure 4.13.1. Testosterone 6β-hydroxylation activity was inhibited 95% when using 2 μM ketoconazole. An IC_{50} of 0.2 μM for the inhibition of testosterone 6β-hydroxylation has been reported (Baldwin et al., 1995).

Time Considerations

After all the reagents have been prepared, the enzyme assay requires a 3-min preincubation followed by 10 min of incubation. Time for HPLC run is described in the Basic Protocol 1, which is ~40 min per sample.

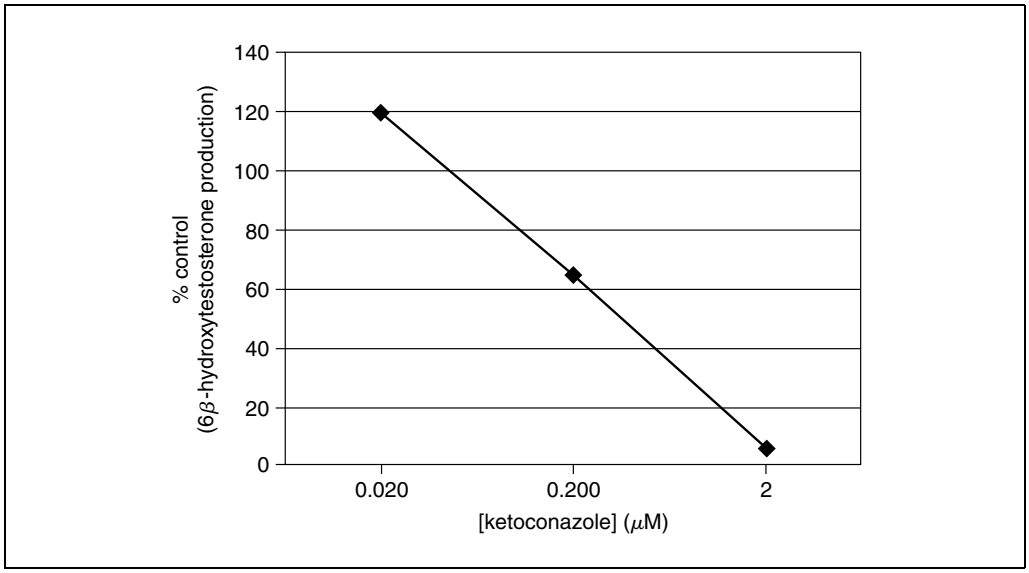

Figure 4.13.1 Inhibition of testosterone 6β-hydroxylation in the presence of ketoconazole (J. Tang, unpub. observ.).

Literature Cited

Back, D.J. and Tjia, J.F. 1985. Inhibition of tolbutamide metabolism by substituted imidazole drugs in vivo: Evidence for a structure-activity relationship. *Br. J. Pharmacol.* 85:121-126.

Baldwin, S.J., Bloomer, J.C., Smith, G.J., Ayrton, A.D., Clarke, S.E., and Chenery, R.J., 1995. Ketoconazole and sulphaphenazole as the respective selective inhibitors of P4503A and 2C9. *Xenobiotica* 25:261-270.

Bourrie, M., Meunier, V., Berger, Y., and Fabre, G. 1996. Cytochrome P450 isoform inhibitors as a tool for the investigation of metabolic reactions catalyzed by human liver microsomes. *J. Pharmacol. Exp. Ther.* 277:321-332.

Brown, M.W., Maldonado, A.L., Meredith, C.G., and Speeg, K.V. Jr. 1985. Effect of ketoconazole on hepatic oxidative drug metabolism. *Clin. Pharmacol. Ther.* 37:290-297.

Dai, D., Tang, J., Rose, R.L., Hodgson, E., Bienstock, R.J., Mohrenweiser, H.W., and Goldstein, J.A. 2001. Identification of variants of CYP3A4 and characterization of their abilities to metabolize testosterone and chlorpyrifos. *J. Pharmacol. Exp. Ther.* 299:825-831.

Desta, Z., Soukhova, N., Mahal, S.K., and Flockhart, D.A. 2000. Interaction of cisapride with the human cytochrome P450 system: Metabolism and inhibition studies. *Drug Metab. Disp.* 28:789-800.

Gascoigne, E.W., Barton, G.J., Michaels, M., Meuldermans, W., and Heyhants, J. 1981. The kinetics of ketoconazole in animals and man. *Clin. Res. Rev.* 1:177-187.

Guengerich, F.P. 1997. Role of cytochrome P450 enzymes in drug-drug interactions. *Adv. Pharmacol.* 43:7-35.

Kolars, J.C., Lown, K.S., Schmiedlin-Ren, P., Ghoh, M., and Fang, C. 1994. CYP3A4 gene expression in human gut epithelium. *Pharmacogenetics* 4:247-259.

Kuehl, P., Zhang, J., Lin, Y., Lamba, J., Assem, M., Schuetz, J., Watkins, P.B., Daly, A., Wrighton, S.A., Hall, S.D., Maurel, P., Relling, M., Brimer, C., Yasuda, K., Venkataramanan, R., Strom, S., Thummel, K., Boguski, M.S., and Schuetz, E. 2001. Sequence diversity in CYP3A promoters and characterization of the genetic basis of polymorphic CYP3A5 expression. *Nat. Genet.* 27:383-391.

Jonsson, G., Astrom, A., and Andersson, P. 1995. Budesonide is metabolized by cytochrome P450 3A (CYP3A) enzyme in human liver. *Drug Metab. Disp.* 23:137-142.

Lee, C.A., Kadwell, S.H., Kost, T.A., and Serabjit-Singh, C.J. 1995. CYP3A4 expressed by insect cells infected with a recombinant baculovirus containing both CYP3A4 and human NADPH-cytochrome P450 reductase is catalytically similar to human liver microsomal CYP3A4. *Arch. Biochem. Biophys.* 319:157-167.

Lee, S.J., Usmani, K.J., Chanas, B., Ghanayem, B., Xi, T., Hodgson, E., Mohrenweiser, H.W., and Goldstein, J.A. 2003. Genetic findings and functional studies of human CYP3A5 single nucleotide polymorphisms in different ethnic groups. *Pharmacogenetics* 13:461-472.

Madan, A., Usuki, E., Burton, L.A., Ogilvie, B.W., and Parkinson, A. 2001. In vitro approaches for studying the inhibition of drug-metabolizing enzymes and identifying the drug-metabolizing enzymes responsible for the metabolism of drugs. *In* Drug-Drug Interactions: From Basic Pharmacokinetic Concepts to Marketing Issues (A.D. Rodrigues, ed.) pp. 217-294. Marcel Dekker, New York.

Maurice, M., Pichard, L., Daujat, M., Fabre, I., Joyeux, H., Domergue, J., and Maurel, P. 1992. Effects of imidazole derivatives on cytochromes P450 from human hepatocytes in primary culture. *FASEB J.* 6:752-758.

McKinnon, R.A., Burgess, W.M., Hall, P.M., Roberts-Thomson, S.J., Gonzalez, F.Z., and McManus, M.E. 1995. Characterization of *CYP3A* gene subfamily expression in human gastrointestinal tissues. *Gut* 36:259-267.

Moody, D.E., Alburges, M.E., Parker, R.J., Collins, J.M., and Strong, J.M. 1997. The involvement of cytochrome P450 3A4 in the *N*-demethylation of L-α-acetylmethadol (LAAM), norLAAM, and methadone. *Drug Metab. Disp.* 25:1347-1353.

Mosca, P., Bonazzi, P., Novelli, G., Jezequel, A.M., and Orlandi, F. 1985. In vivo and in vitro inhibition of hepatic microsomal drug metabolism by ketoconazole. *Br. J. Exp. Path.* 66:737-742.

Neal, R.A. 1980. Microsomal metabolism of the thiono-sulfur compounds: Mechanisms and toxicological significance. *In* Reviews in Biochemical Toxicology. Vol. 2. (E. Hodgson, J.R. Bend, R.M. Philpot, eds.) pp. 131-171. Elsevier North Holland, New York.

Oda, Y. and Kharasch, E.D. 2001. Metabolism of *levo*-α-acetylmethadol (LAAM) by human liver cytochrome P450: Involvement of CYP3A4 characterized by atypical kinetics with two binding sites. *J. Pharmacol. Exp. Ther.* 297: 410-422.

Rodrigues, A.D. 1999. Integrated cytochrome P450 reaction phenotyping: Attempting to bridge the gap between cDNA-expressed cytochromes P450 and native human liver microsomes. *Biochem. Pharmacol.* 57:465-480.

Satoh, T., Fujita, K., Munakata, H., Itoh, S., Nakamura, K., Kamataki, T., Itoh, S., and Yoshizawa, I. 1999. Studies on the interactions between drugs and estrogen: Analytical method for prediction system of gynecomastia induced by drugs on the inhibitory metabolism of estradiol using *Escherichia coli* coexpressing human CYP3A4 with human NADPH-cytochrome P450 reductase. *Analyt. Biochem.* 286:179-186.

Schuetz J.D., Beach D.L., and Guzelian P.S. 1994. Selective expression of cytochrome P450 CYP3A mRNAs in embryonic and adult human liver. *Pharmacogenetics* 4:11-20.

Shimada T. and Guengerich F.P. 1989. Evidence for cytochrome $P450_{NF}$, the nifedipine oxidase, being the principle enzyme involved in the bioactivation of aflatoxins in human liver. *Proc. Natl. Acad. Sci. U.S.A.* 86:462-465.

Shimada, T., Yamazake, H., Mimura, M., Inui, Y., and Guengerich, F.P. 1994. Interindividual variations in human liver cytochrome P-450 enzymes involved in the oxidation of drugs, carcinogens and toxic chemicals: Studies with liver microsomes of 30 Japanese and 30 Caucasians. *J. Pharmacol. Exp. Ther.* 270:414-423.

Shou M., Grogan J., Mancewicz J.A., Krauaz K.W., Gonzalez F.J., Gelboin H.V., and Korzekwa K.R. 1994. Activation of CYP3A4: Evidence for the simultaneous binding of two substrates in a cytochrome P450 active site. *Biochemistry* 33:6450-6455.

Thummel, K.E. and Wilkinson, G.R. 1999. In vitro and in vivo drug interactions involving human CYP3A. *Annu. Rev. Pharmacol. Toxicol.* 38:380-430.

Usmani, K.A., Rose, R.L., and Hodgson, E. 2003. Inhibition and activation of the human liver microsomal and human cytochrome P450 3A4 metabolism of testosterone by deployment-related chemicals. *Drug Metab. Disp.* 31:384-391.

Vanden Bossche, H., Marichal, P., Gorrens, J., Coene, M.-C., Willemsens, G., Bellens, D., Roels, I., Moereels, H., and Janssen, P.A.J. 1989. Biochemical approaches to selective antifungal activity. Focus on azole antifungals. *Mycoses* 32:35-52.

Varhe, A., Klaus, M.B., Olkkola, T., and Neuvonen, P.J. 1994. Oral triazolam is potentially hazardous to patients receiving systemic antimycotics. *Clin. Pharmacol. Ther.* 56:601-607.

Venkatakrishnan, K., von Molke, L.L., and Greenblatt, D.J. 2001. Application of the relative activity factor approach in scaling from heterologously expressed cytochromes P450 to human liver microsomes: Studies on amitriptyline as a model substrate. *J. Pharmacol. Exp. Ther.* 297:326-337.

von Moltke, L.L., Greenblatt, D.J., Harmatz, J.S., Duan, S.X., Harrel, L.M., Cotreau-Bibbo, M.M., Pritchard, G.A., Wright, C.E., and Shader, R.I. 1996. Triazolam biotransformation by human liver microsomes in vitro: Effects of metabolic inhibitors and clinical confirmation of a predicted interaction with ketoconazole. *J. Pharmacol. Exp. Ther.* 276:370-379.

Zhang, W., Ramamoorthy, Y., Kilicarslan, T., Nolte, H., Tyndale, R.F., and Sellers, E.M. 2002. Inhibition of cytochromes P450 by antifungal imidazole derivatives. *Drug Metab. Disp.* 30:314-318.

Key References

Madan et al., 2001. See above.

Describes in detail the methods for inhibition and reaction phenotyping studies.

Rodrigues, 1999. See above.

Describes in details the method for reaction phenotyping study.

Internet Resources

http://www.fda.gov/cder/guidance/clin3.pdf

FDA, 1997. Guidance for Industry: Drug metabolism/drug interaction studies in the drug development process: Studies in vitro. U.S. Food and Drug Administration, Rockville, Md.

Contributed by Khawja A. Usmani and Jun Tang
North Carolina State University
Raleigh, North Carolina

Biotransformation Studies Using Rat Proximal Tubule Cells

The mammalian kidneys fulfill an important excretory function and, as a consequence, are frequently exposed to potentially toxic compounds. Within the kidneys, the cells of the proximal tubule are considered to be the main target for nephrotoxic substances, as they are the first to be exposed to the glomerular ultrafiltrate, and they actively transport a wide variety of charged organic and inorganic compounds. Moreover, proximal tubule cells (PT cells), in particular, express multiple biotransformation enzymes, enabling these to actively metabolize many endogenous substrates including hormones, as well as drugs and xenobiotics. This capacity makes the PT vulnerable to various (bioactivated) compounds, for instance, the susceptibility of the PT to glutathione-derived *S*-conjugates is well-described (Commandeur et al., 1995). Thus, the assessment of the biotransformation potential of PT cells is important in the evaluation of toxicological and kinetic properties of diverse substances. Biotransformation (iso)enzyme expression and activity can be determined in situ (immunostaining) as well as in cell-based assays. This unit describes several methods for the determination of biotransformation enzyme activities both in subcellular fractions (see Basic Protocol 2) and in intact PT cells (see Basic Protocol 1). Upregulation of these enzyme activities by specific inducers is only possible in intact cells, while inhibition experiments can be conducted in intact cells as well as in subcellular fractions.

An enriched population of PT cells can be obtained in several ways, including microdissection of the kidneys and subsequent cell isolation as described elsewhere (Stanton et al., 1986; Takenaka et al., 1998), or via in situ perfusion of the kidneys, followed by cell purification (see Support Protocol 1). A number of different methods for cell purification have been described, including centrifugation over a density gradient. Isolated cells can be cultured directly (see Support Protocol 2), or can be processed to subcellular preparations (see Support Protocol 3). The procedure to isolate cells by in situ perfusion is straightforward and relies on common laboratory equipment, making it easily adaptable to each laboratory setting. Although the protocols described here are optimized for the rat model, simple modifications will allow application for other species, including mouse, rabbit, pig, or any other experimental animal species.

In brief, rats are anaesthetized and the kidneys are isolated from the main blood stream and connected to a perfusion system. The perfusion consists, in principle, of three steps commencing with the use of a calcium-free phosphate buffer containing EGTA (EGTA scavenges calcium, which is an important element in the tight cell junctions) to remove all blood from the kidneys, followed by perfusion with a EGTA-free buffer (EGTA inhibits collagenase activity) and, finally, a collagenase-containing solution is used to reduce the tissue integrity. Note that collagenase exerts its optimal activity in cleaving the tight cell-cell junctions only in the presence of calcium ions (Seglen, 1976).

Following perfusion, the kidneys are placed in an ice-cold BSA solution and the cortex is mechanically separated from the renal medulla and its surrounding tissue. The obtained suspension of cortical cells is washed with BSA-containing buffers before layering the cells onto Nycodenz solutions for gradient centrifugation. Following centrifugation, PT cells are present at the interface of the Nycodenz layers and can be easily recovered and transferred to culture flasks where they are cultured in supplemented DMEM/F12 medium, which is commercially available.

Contributed by G. J. Schaaf, R. F. M. Maas, and J. Fink-Gremmels
Current Protocols in Toxicology (2004) 4.14.1-4.14.16

Table 4.14.1 An Overview of Useful Methods for the Assessment of Activity of Some Relevant Biotransformation Enzymes in Rat PTCs[a]

Substrate	Metabolite/reaction product	Phase I enzyme primarily involved	Samples	Analytical method	References
7-Ethoxyresorufin	Resorufin	CYP 1A1	Monolayers/ microsomes	Spectrophotometer	Burke and Mayer (1974)
Metoxyresorufin	Resorufin	CYP 1A2	Monolayers/ microsomes	Spectrophotometer	Burke et al. (1994)
Caffeine	3.7 X	CYP 1A2	Monolayers/ microsomes	HPLC	Butler et al. (1989)
	1.3X	CYP 1A2	Monolayers/ microsomes	HPLC	Butler et al. (1989)
Tolbutamide	4-hydroxytolbutamide	CYP 2C11	Monolayers/ microsomes	HPLC	Knodell et al. (1987)
Testosterone	16α-hydroxytestosterone	CYP 2C11	Monolayers/ microsomes	HPLC	Wortelboer et al. (1990)
	2α-hydroxytestosterone	CYP 2C11	Monolayers/ microsomes	HPLC	Wortelboer et al. (1990)
Dextromethorphan	Dextrorphan	CYP 2D1	Monolayers/ microsomes	HPLC	Dayer et al. (1989)
		Phase II enzyme involved			
CDNB	Glutation conjugation	GST	Cell homogenates	Spectrophotometer	Habig et al. (1974)
L-Glutamine	Hydrolysis	GGT	Cell homogenates	Spectrophotometer	Blackmon et al. (1992)
TFE-cys	β-elimination	β-lyase	Cell homogenates	Spectrophotometer	Commandeur et al. (1991)
Naphthol	Glucuronic acid conjugation	UGT 1A6	Monolayers/ microsomes	HPLC	Wortelboer et al. (1992)
	Sulphate conjugation	ST	Monolayers/ microsomes	HPLC	Wortelboer et al. (1992)

[a]Abbreviations: CDNB, 1-chloro-2,4 dinitrobenzene; GGT, gamma-glutamyltranspeptidase; GST, glutathione-*S*-transferase; ST, sulfotransferase; TFE-cys, S-(1,1,2,2 tetrafluoroethyl)-L-cysteine; UGT, UDP-glucuronyltransferase.

During culture, the biotransformation capacity of PT cells decreases rapidly, therefore, the cells can only be used for a few days. The most rapid decline occurs with CYP450 enzymes, whereas Phase II enzymes remain stable for many days (for details, see Schaaf et al., 2001). The activity of biotransformation enzymes, in particular, those of the CYP450 enzyme family, is much lower than that of other organs, e.g., the liver. Both factors, the intrinsic low activity and the time-dependent loss of biotransformation capacity, have to be taken into account in the design of biotransformation studies with PT cells.

Biotransformation Studies Using Rat Proximal Tubule Cells

Biotransformation enzyme activity can be measured by using a large variety of model substrates, selected according to the targeted (iso)enzyme, or the animal species under investigation. Two examples of such enzyme activity assays will be provided (see Basic Protocols 1 and 2). A detailed database of model substrates and inducers and

Table 4.14.2 Suggested Assay Conditions to Determine the Biotransformation Enzyme Activity in Primary Cultured PT Cells and Microsomal PT-Fractions by Means of HPLC[a]

Substrate	Concentration	Solvent for substrate	Incubation time[b]	Internal standard	Extraction fluid	Mobile phase for HPLC analysis
Caffeine	5 mM	Water	1 hr	20 µl (50 mg/ 1 water) 7-(β-hydroxypropyl)-theophylline	Chloroform:2-propanol 85:15 6 ml	100 µl acetonitril/ 55 mM NaAC in water pH 4.0
Tolbutamide	800 µM	DMSO	1 hr	25 µl (140mg/L) chloropropamide in MeOH/water 1:1	6 ml dichloromethane after acidification with 25 µl 4 N HCl/ml	200 µl acetonitrile/ water pH 2.8 (with phosphoric acid)
Testosterone	250 µM	MeOH	0.5 hr	100 µl (12.5 mg/l MeOH) 11β-hydroxy testosterone	6 ml dichloromethane	130 µl methanol/ Water (1:1)
Naphthol	1 mM	MeOH	30–60 min	[c]	[c]	[c]

[a]Phase I (CYP450) enzyme activity are best assayed using microsomal fractions. Phase II enzymes can easily be determined in primary cultured PT-cells as their expression is stable in time.

[b]Incubation times for the CYP450 enzymes (see Table 4.14.1) using microsomal fractions. When measured in primary cultured PT-cells optimal incubation times vary considerably.

[c]No extraction applied. Incubation medium directly analyzed by HPLC.

inhibitors of biotransformation enzymes is available online (*www.gentest.com*) allowing a problem-orientated selection of reagents. As an example, a selection of useful methods for the relevant enzymes expressed in the rat PT cells is provided in Table 4.14.1.

MEASURING BIOTRANSFORMATION ENZYME ACTIVITY IN PRIMARY CULTURED PT CELLS

BASIC PROTOCOL 1

In cultured cells, the activity of virtually all biotransformation enzymes expressed in the corresponding cell type can be measured. Determination is also possible after enzyme induction either in vivo (intact animal prior to cell isolation) or in vitro when intact cells are incubated with inducers.

Materials

Substrate stock solutions (Table 4.14.1)
Serum-free culture medium (see recipe)
Primary cultured rat proximal tubule cells (plated at 5×10^4 cells/cm^2 in. 60-mm dishes; see Support Protocol 2)
Phosphate buffered saline (PBS; *APPENDIX 2A*)
Rubber policeman

1. Prepare substrate solution by diluting the stock solution to the desired concentration in serum-free medium (for examples see Tables 4.14.1 and 4.14.2).
2. Rinse the primary cultured rat proximal tubule cell cultures two times with sterile PBS.
3. Incubate cells with 3 ml fresh serum-free medium containing the substrate (from step 1) at 37°C.

   Incubation times and linearity of product formation vary with substrate and need to be predetermined in an initial experiment.

4. Collect medium and store at –20°C until analysis (see Table 4.14.2).
5. Scrape cells using a rubber policeman, suspend in 1 ml PBS, and store at −20°C until determination of protein content and Westerm blotting.

   Protein concentration can be determined using commercially available assay kits (e.g., Pierce, Bio-Rad; also see Support Protocol 3) and Western blotting can be conducted using standard procedures.

BASIC PROTOCOL 2

MEASURING CYP450 ACTIVITY USING SUB-CELLULAR PT CELL FRACTIONS

The general protocol describes the principles of the methods applied to determine the activity of individual CYP450 enzymes as exemplified by the method for determining the tolbutamide 4-hydroxylation rate. The suggested volumes and incubation time are based on the experiments as described by Schaaf et al. (2001). Several methods for the determinations of other CYP450s can be found in the published literature (see Table 4.14.1).

Materials

2× concentrated cofactor mixture (see recipe)
Subcellular fractions (microsomal suspension containing ∼100 μg protein; see Support Protocols 1 and 3)
Incubation buffer (see recipe)
Substrate stock solution
Internal standard (see Table 4.14.2)
Extraction fluid (see Table 4.14.2)
Nitrogen source

10-ml glass tubes with caps
37°C water bath

NOTE: The substrate stock should preferably be prepared in incubation buffer. If the selected substrate is insoluble in buffer, DMSO, alcohol, or other solvents can be added. These solvents may have a direct effect on CYP450 activity (Hickman et al., 1998) so include solvent-only controls when solvents are used.

Prepare incubation mixture

1. Dilute 10 μl of 1000× substrate stock solution in 990 μl incubation buffer. Prepare the reaction mixture by mixing the following on ice in 10-ml glass tubes:

   500 μl 2× concentrated cofactor mixture
   100 μl microsomal suspension containing ∼100 μg protein
   Incubation buffer to achieve a total final volume of 1 ml (including substrate)
   40 μl substrate (add last to prevent initiation of the reaction).

   The volume of substrate is part of the total 1 ml.

2. Initiate the reaction by placing the incubation mixture in a 37°C water bath. Incubate for 30 min and then terminate the reaction by placing the sample on ice.

   The incubation period depends on the purity of the microsomal preparation and substrates used. Test several incubation periods and substrate concentrations to check linearity of product formation.

Analyze biotransformation products

3. Add an appropriate internal standard to the incubation mixture (see Table 4.14.2).
4. Add extraction fluid. Cap the tubes and mix (vortex) for 30 sec (see Table 4.14.2).

5. Centrifuge the samples 10 min at 3000 × *g*, 10°C, (this usually results in a satisfactory phase separation).
6. Collect the organic phase and evaporate to dryness under a gentle stream of nitrogen.
7. Resuspend the residue in the appropriate mobile phase for HPLC analysis (see Table 4.14.2). Analyze by HPLC (see CP Molecular Biology *UNITS 10.12 & 10.13*).

ISOLATION OF RAT PROXIMAL TUBULE CELLS

SUPPORT PROTOCOL 1

The procedure described below yields a more than 70% pure population of proximal tubule cells and usually 20–40 × 10^6 viable cells from one rat.

Materials

70% ethanol
10× HH buffer (see recipe)
50× EGTA stock solution (see recipe)
Collagenase B (Boehringer Mannheim)
Bovine serum albumin (BSA, fraction V; Sigma)
0.5 M $CaCl_2$ (see recipe)
Wistar Hannover rats with an average body weight of 225 g (Charles River)
100 mg/kg sodium pentobarbital solution, 60 mg/ml Nembutal, or any other anaesthetic drug
Heparin (5000 IE/ml)
36% (w/v) Nycodenz stock solution (see recipe)
PBS (sterile, GIBCO)
Complete cell culture medium (see recipe)

Perfusion apparatus (see Fig. 4.14.1) consisting of:
  37°C water bath
  Electric pump
  Bubble trap
  Organ bath
  Tubing
100-ml cylinder
250-ml bottles
100-ml bottles
50-ml bottle
250- and 100-ml beakers
0.22-μm sterile filters
Animal surgery table
Small set of surgical instruments including scissors, forceps, and clamps
18 G, 51 mm Abbocath T canula (Venisystems)
100-mm petri dish
Nylon gauze filters (80-μm)
12-ml tubes

Prepare perfusion apparatus and solutions

1. Rinse the perfusion apparatus (see Fig. 4.14.1) for 15 min with 70% ethanol to obtain sterile conditions, and then rinse with sterile water for 20 min. Prewarm the water bath to 37°C.
2. Collect the following sterile glassware (with lids):

   100-ml cylinder
   250-ml bottles

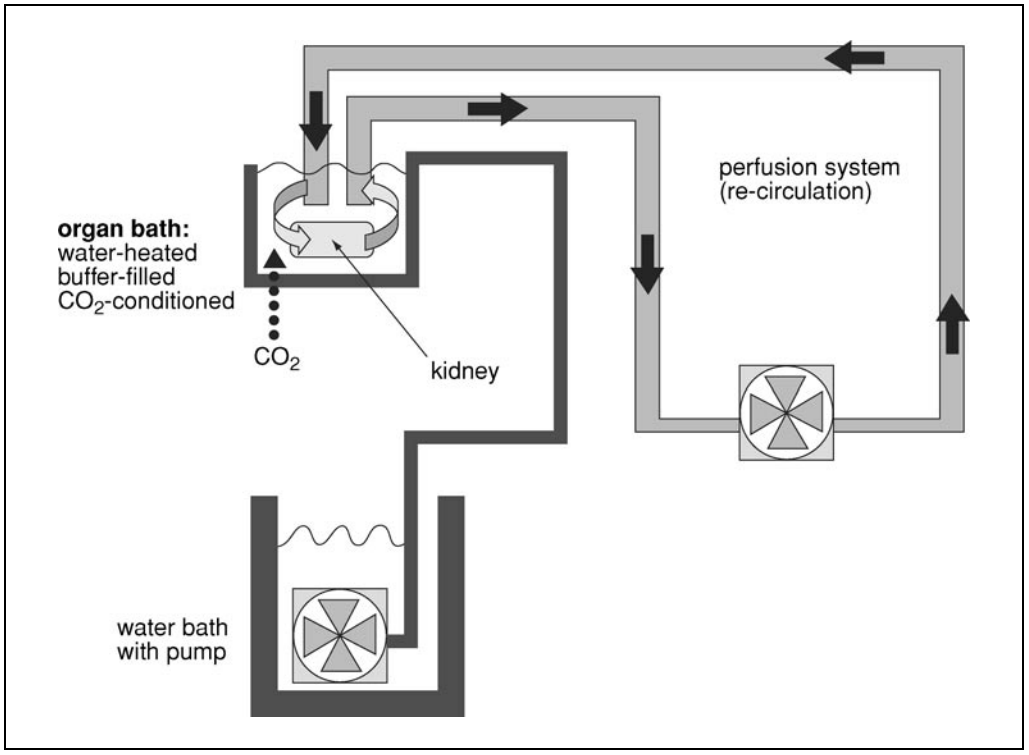

Figure 4.14.1 Kidney perfusion system.

100-ml bottles
50-ml bottle
250- and 100-ml beaker.

3. Prepare two 100-ml solutions of 1× HH buffer by diluting 10× HH stock buffer 1:10 with sterile double-distilled water. Transfer the first HH buffer solution (basis for BSA-HH buffer) into a 250-ml beaker and the second into a 200-ml bottle (basis for perfusion buffer II).
4. Prepare 30 ml of 10× HH buffer (basis for perfusion buffer III) into a 100-ml beaker.
5. Prepare a 150 ml HH-EGTA buffer (basis for perfusion buffer I) in a 250-ml bottle by mixing 15 ml of 10× HH buffer, 3 ml 50× EGTA stock solution, and 132 ml sterile double-distilled. Circulate perfusion buffer I in the perfusion system for ~20 min at a maximum flow rate of 7.5 ml/min.
6. Deposit 2.5 g BSA on the surface of 100 ml HH buffer in the 250-ml beaker (prepared in step 3) and allow it to dissolve slowly (BSA-HH buffer).
7. Dissolve 40 mg collagenase B in 30 ml 1× HH buffer in the 100-ml beaker from step 4. Filter-sterilize directly through a 0.22-μm filter and add 240 μl of 0.5 M $CaCl_2$. Keep sterile collagenase solution on ice (perfusion buffer III).
8. Add 360 μl of 0.5 M $CaCl_2$ to the BSA-HH buffer (step 6) as soon as the BSA is completely dissolved and filter the solution through a 0.22-μm filter into a sterile 100-ml bottle. Keep solution on ice.

Perform surgery

9. Anesthetize a Wistar Hannover rat, e.g., with 100 mg/kg sodium pentobarbital or any other anesthetic agent. Wait until surgical anesthesia is reached.

This rat strain has the advantage to possess only small amounts of connective tissue in the kidneys compared to other commercially available rat strains, allowing easy cell separation.

10. Place the animal on an appropriate surgery table on its back and inject heparin solution (0.1 ml/100 g) i.v. either into the vena femoralis or into one of the tail veins.
11. Open abdominal cavity up to diaphragm but leave the diaphragm intact.
12. Expose aorta and kidneys by carefully repositioning the liver, stomach, and intestines, preferably to the right side of the animal. Cut connective tissues where appropriate avoiding extensive bleeding.
13. Ligate the mesenteric and coeliac arteries. Ligate aorta and inferior vena cava distal to the renal arteries, but leave these ligatures open.
14. Insert an 18-G canula into the aorta proximal to the renal arteries and secure.
15. Close the ligatures of the distal vena cava and aorta (see step 13) and, at the same time, incise the left renal vein to ensure spontaneous outflow.

Perfuse kidneys

16. Connect the aortic canula to the perfusion apparatus (avoid air bubbles) and start perfusion with 150 ml perfusion buffer I at a minimal flow rate. Gently increase flow rate to 7.5 ml/min.

    The kidneys should turn pale instantly. Remaining blood (red patches) can be released by gentle manual massage of the kidneys. Injection of heparin solution into the perfusion buffer aids to remove small thrombi and may be used as a fail-safe routine.

17. Entirely remove the liver, stomach, and intestines while taking care not to interrupt renal circulation.
18. Using small sharp scissors, cut the vena cava distal to the ligatures and lift the kidneys, dissecting all connective tissues. Then, cut the aorta proximal to the canula.

    The kidneys should now be completely liberated and can be transferred to the organ bath of the perfusion systems. The perfusion buffer flow should never be interrupted during the extirpation procedure.

19. Replace perfusion buffer I in the perfusion system with 100 ml prewarmed perfusion buffer II, avoiding flow interruption and/or air bubbles. Continue perfusion for an additional 10 min.
20. Replace perfusion buffer II with 30 ml prewarmed perfusion buffer III containing collagenase. Perfuse for 20 min at a flow rate of 7.5 ml/min in a recirculation system.

    As the collagenase-containing buffer exits the kidney, collect it and use it for recirculation.

21. Disconnect kidney from the perfusion system and transfer to a sterile 100-mm petri dish filled with 20 ml cold, sterile BSA solution and keep on ice.

Prepare cell suspensions

22. Separate kidneys from remaining connective tissue and transfer the individual kidneys to clean medium-containing dishes on ice.
23. Remove the renal capsules using small sterile forceps.

    The kidneys should have lost tissue integrity and cohesion by now.

24. Gently scrape the cortical cells from the medulla, which is the tighter matter with a lighter color. Discard remaining medulla and pelvic sections of the kidneys.

    The cortical cells should come off easily if the perfusion was successful.

25. Resuspend the cortical cells and filter the cell suspension over nylon gauze into a sterile beaker. Keep beaker on ice.
26. Add 20 ml complete fresh BSA-HH buffer to the cells, mix gently, and filter by applying aliquots of the suspension to nylon gauze.
27. Dispense the filtered cell suspension into six sterile 12-ml tubes and centrifuge 5 min at 80 × *g*, 4°C.
28. Discard the supernatant and collect the cell pellets in 10 ml BSA-HH buffer. Centrifuge the suspension 5 min at 80 × *g*, 4°C.

Purify PT cells

29. Prepare 1 ml ice-cold 9% Nycodenz solution by diluting the 36% Nycodenz stock solution with sterile BSA buffer.
30. Prepare 3 ml of 14% Nycodenz solution by diluting the 36% Nycodenz stock solution with sterile BSA buffer.
31. Resuspend the cell pellet in the 14% Nycodenz solution in a sterile 12-ml tube. Keep on ice.
32. Carefully layer 1 ml of 9% Nycodenz solution on top of the Nycodenz-cell mixture and then add 0.5 ml BSA-HH buffer. Do not shake the tube. Centrifuge the Nycodenz gradient-cell mixture 4 min at 2300 × *g*, 4°C.

    The band between the two Nycodenz layers (interface) contains the PT cells.

33. Transfer the PT cells from the interface to a clean sterile 12-ml tube containing 5 ml sterile PBS using a small sterile pipet.
34. Briefly centrifuge 5 min at 80 × *g*, 4°C, and wash cells two times by sequentially centrifuging 5 min at 80 × *g*, 4°C, to remove remaining Nycodenz.
35. Finally, resuspend cells in sterile culture medium (DMEM/F12), analyze viability and purity (see Support Protocols 4 and 5), and follow Support Protocol 2 to obtain primary PT cultures, *or* store cell pellet up to 3 months at –70°C until further use for the preparation of sub-cellular fractions.

SUPPORT PROTOCOL 2

ESTABLISHING PRIMARY PT CELL CULTURES

This protocol describes the procedure of bringing the isolated cells into primary culture. Primary rat PT cells typically grow in isolated colonies and retain an epithelial morphology for 1 week.

Materials

Cell suspension (Support Protocol 1)
Complete culture medium (see recipe)
Serum-free DMEM/F12 medium (see recipe)

Collagen-coated 60-mm dishes (see Support Protocol 6)
37°C, 5% CO_2 incubator

1. Determine concentration of viable cells in the individual isolate (see Support Protocol 4).
2. Dilute cell suspension to 0.25 × 10^6 cells/ml in complete culture medium and plate 4 ml cell suspension on collagen-coated 60-mm dishes.
3. Swirl the dishes gently to evenly distribute the cells

4. Incubate the cells in a 37°C, 5% CO_2 incubator.

5. Change to serum-free DMEM/F12 medium after 24 hr.

   Attachment of cells may not be complete after 24 hr. Careful aspiration of the culture supernatant followed by a brief centrifugation (e.g., 5 min at 80 × g) provides a cell pellet, which can be resuspended in fresh medium (without serum) and added to the original dish to improve the cell number in the primary culture.

PREPARATION OF MICROSOMAL AND CYTOSOLIC FRACTIONS FROM PT CELLS

SUPPORT PROTOCOL 3

This protocol describes a basic procedure for the preparation of microsomal and cytosolic fractions from PT cells obtained as described in Support Protocol 1.

The procedure can be applied to freshly isolated cell pellets or cells that have been cultured. For example, using the total cell yield from one isolation (20–40 × 10^6 cells), this procedure yields a cytosolic fraction with an average protein content of 5 mg and a microsomal fraction containing ~1.0 mg protein. Both fractions can subsequently be used to measure the activity of biotransformation enzymes.

As interference of protease inhibitors in subsequent assays cannot be excluded, they are not included in this general protocol. It is therefore essential to perform all individual steps at 4°C.

The protein content from the obtained subcellular fractions can be assayed with commercially available protein assay kits (e.g., Pierce), although high glycerol concentrations (see below) in microsomal fractions might interfere with some of those assay protocols.

Materials

Cell pellet, fresh or frozen
KCl/EDTA solution (see recipe)
Liquid nitrogen
Glycerol buffer (see recipe)

Refrigerated ultracentrifuge with fixed-angle rotor
Potter-Elvehjem homogenizer with PTFE pestle (5-ml working capacity)
8.5-ml ultracentrige tubes (e.g., Nalgene UltraBottle Assemblies)
Ultra Turrax T8 homogenizer equipped with an 8-mm diameter dispersing element

1. Prior to use, cool the ultracentrifuge and rotor to 4°C.
2. Slowly thaw the frozen cell pellet on ice.
3. Add 2.5 ml KCl/EDTA solution to the cell pellet.
4. Transfer to Potter-Elvejhem homogenizer and homogenize cell suspension on ice at 1100 rpm until a clear suspension is obtained (usually 4 to 8 strokes).
5. Transfer the homogenates to a 8.5-ml ultracentrifuge tubes and equilibrate.
6. Centrifuge 25 min at 10,000 × *g*, 4°C, to obtain a cell-free homogenate.
7. Carefully transfer the supernatant to clean ultracentrifuge tubes and centrifuge 75 min at 100,000 × *g*, 4°C.

   The obtained supernatant is the cytosolic fraction.

8. Separate the supernatant, snap-freeze appropriate aliquots (e.g., 250 µl) in liquid nitrogen, and store up to 3 months at –70°C until needed.

9. Resuspend the microsomal fraction in 1 ml glycerol buffer using the ultra-Turrax T8 homogenizer (or equivalent).
10. Snap-freeze 100-µl aliquots in liquid nitrogen and store up to 3 months at –70°C until needed.

    Thawed fractions cannot be refrozen.

SUPPORT PROTOCOL 4

DETERMINING CELL VIABILITY AND NUMBER OF ISOLATED PT CELLS

Cell viability should be >70% to ensure successful subsequent culturing. Cell viability needs to be determined for each isolation.

The most common method to assess cell viability is trypan blue exclusion analysis. The method is based on the principle that viable cells exclude the dye as a result of membrane integrity, while non-viable cells lose this capacity and become stained (i.e., turn blue). A detailed protocol is presented with manufacturer's instructions for trypan blue dye (Sigma-Aldrich; also see *APPENDIX 3B*). Certain steps (e.g., dilutions, volumes) need to be adapted for use with PT cells.

Materials

PT cell suspension (Support Protocol 1)
0.4% (w/v) trypan blue solution (Sigma) in PBS
1.5-ml microcentrifuge tubes
Hemacytometer with coverslips
Microscope

1. Transfer 50 µl of PT cell suspension into a 1.5-ml microcentrifuge tube.
2. Add 200 µl of 0.4% trypan blue solution to the cell suspension (creating a dilution factor of 5). Mix thoroughly and let stand for ~5 min at room temperature; do not exceed 15 min as trypan blue is toxic for cells at longer incubation periods.
3. Transfer a small amount of the trypan blue–cell suspension to a chamber on the hemacytometer and view under a microscope at 100× magnification.

   Non-viable cells will stain deep blue, viable cells remain unstained.

4. Count cells according to the manufacturer's instructions for the hemacytometer. Count both viable and non-viable cells

   If >10% of the cells appear clustered, repeat the entire procedure after having dispersed the original cell suspension by vigorous pipetting.

   If <20 or >100 cells are observed in the counted (25) squares, repeat the procedure after adjusting the concentration of the original cell suspension.

5. Retrieve a second sample and repeat the counting procedure to ensure accuracy.
6. Calculate cell number and percent viability by using the fact that 25 squares (each 0.04 mm^2) of the hemacytometer represent a total volume of 0.1 mm^3, and 1 cm^3 equal to 1 ml. The subsequent cell concentration per milliliter (and the total number of cells) can be determined.

   Total cell number = cells per milliliter × the number of milliliters in the original cell suspension
   Cell viability (%) = [total viable cells (unstained)/total cell (stained and unstained) number] × 100

DETERMINING THE PURITY OF PT CELL PREPARATION BY SELECTIVE UPTAKE OF FLUORESCEIN

SUPPORT PROTOCOL 5

This second quality control parameter, used to quickly assess the purity of the isolate, should be performed following each of the first few isolation attempts.

Proximal tubule cells, especially those from the S1 and S2 segments of the tubule and to a lesser extent those from the S3 segment, will accumulate fluorescein. After a maximum incubation time of 15 min, all viable PT cells will be fluorescent under the fluorescence microscope. Cells from the S2 segment can be observed after only a 2- to 3-min incubation period. Other cells originating from the renal cortex, which may contaminate the isolate, have a much lower capacity to accumulate fluorescein. These cells will be (almost) invisible under the microscope. Typically, a >70% pure PT cell population is obtained.

Materials

Cell suspension (Support Protocol 1)
Serum-free culture medium (see recipe)
50 μM sodium fluorescein reagent (see recipe)
200 mM sodium azide solution (see recipe)
PBS containing 5% (w/v) BSA
37°C water bath
Fluorescence microscope: excitation wavelength between 470 and 490 nm, emission wavelength between 520 and 555 nm

1. Determine cell concentration of the isolate using the trypan blue exclusion procedure (see Support Protocol 4).
2. Resuspend 2×10^5 freshly isolated cells into 100 μl of serum-free culture medium.
3. Pre-incubate cells for 5 min in a 37°C water bath.
4. Gently shake the cell suspension and add 4 μl sodium fluorescein reagent (final concentration of 2 μM). Incubate 15 min at 37°C.
5. Add 10 μl of 200 mM sodium azide solution (final concentration 20 mM).
6. Resuspend cells in 5 ml PBS/5% BSA. Centrifuge 5 min at 1000 rpm, room temperature, and resuspend the cell pellet in 100 μl serum-free medium.
7. View the cells under a fluorescence microscope using 40× magnification
8. Count at least 100 fluorescent cells under the microscope using a hemacytometer.
9. Determine total number of cells by counting cells the same area under standard phase-contrast conditions.
10. Calculate the purity (%) of the isolated cell suspension as follows: (fluorescent cells/total number of cells in the same area) × 100%.

COATING CELL CULTURE SURFACES

SUPPORT PROTOCOL 6

Coating cell culture dishes or plates is used to promote cell attachment and cell adherence, at the same time preventing rapid de-differentiation of cells.

Materials

Collagen solution (see recipe)
PBS (GIBCO)
60-mm culture dishes, culture flasks, or culture plates

1. Prepare a 20 μg/ml collagen rat tail type I solution by diluting the 2 mg/ml stock with 0.2 N acetic acid.
2. Cover the surfaces of the plates, dishes, or flasks with the collagen working solution.
3. Incubate for at least 30 min at room temperature.
4. Remove the collagen working solution.
5. Rinse with sterile PBS and use directly or store up to 2 weeks at 4°C with a layer of PBS to protect the coating.

REAGENTS AND SOLUTIONS

Use Milli-Q purified water or double-distilled or deionized water for all recipes and in all protocol steps. Water should have a resistance of 18 MOhm/cm. Cell culture medium and all other solutions for cell culture need to be sterile and should be handled in a laminar flow cabinet. For common stock solutions, see ***APPENDIX 2A****; for suppliers, see* ***SUPPLIERS APPENDIX****.*

$CaCl_2$, 0.5 M

For 100 ml: Dissolve 21.9 g $CaCl_2 \cdot 6\ H_2O$ (Aldrich) in 80 ml water. Adjust volume to 100 ml. Sterilize by autoclaving or filtering through a 0.22-μm filter. Store up to 6 months at room temperature.

Co-factor mixture, 2×

89.4 mg $MgCl_2 \cdot 7H_2O$ (Merck; 60 mM final)
15.3 mg NADP (Sigma; 4 mM final)
14.2 mg NADH (4 mM final)
14.1 mg of glucose-6-phosphate (10 mM final)
Bring to 5 ml with 50 mM phosphate buffer, pH 7.4
Add 26 μl glucose-6-phosphate dehydrogenase (Roche; 2 U fianl)
Prepare fresh

Collagen solution

Make up a stock solution of 20 μg/ml rat tail type I collagen in 0.2 M acetic acid by pipetting 10 mg from the collagen stock solution (BD Biosciences) into a 500-ml sterile bottle. Add ~400 ml sterile water and 500 μl concentrated acetic acid, then adjust to a volume of 500 ml with sterile water. Store up to 3 months at 4°C.

Complete cell culture medium

To 500 ml DMEM/F12 (phenol red–free; GIBCO), add:

50 ml heat inactivated FBS (GIBCO; 10% v/v final)
5 ml penicillin/streptomycin (GIBCO; 100 μg/ml final)
5 ml 200 mM L-glutamine (BioWhittaker; 2 mM final)
5 ml supplement G (GIBCO; 10 μg/ml insulin, 5.5 μg/ml transferrin, and 6.7 ng/ml sodium selenite final)
Store up to 2 weeks at 4°C

EGTA solution, 50x

For a 100-ml solution, dissolve 0.951 g EGTA (Sigma; 25 mM final) in 80 ml water. To completely dissolve EGTA, add a few drops of 4 M NaOH. Adjust the volume to 100 ml with water. Sterilize by autoclaving or filtering through a 0.22-μm filter. Store up to 3 months at room temperature.

Glycerol buffer

2.8 g KH_2PO_4 (Merck; 50 mM final)
4.2 g Na_2HPO_4 (Sigma; 50 mM final)
33.6 mg Na_2-EDTA·$2H_2O$ (Sigma; 0.1 mM final)
500 ml H_2O
Add 200 ml glycerol (Sigma; 20% v/v final)
Adjust pH to 7.4 with 4 N NaOH and 4 N phosphoric acid
Bring to 1 liter with H_2O
Store up to 2 months at 4°C

HH buffer, 10x (pH 7.4)

20.02 g NaCl (Sigma; 1.37 M final)
0.932 g KCl (Merck; 50 mM final)
0.493 g $MgSO_4·7H_2O$ (Merck; 8 mM final)
0.117 g Na_2HPO_4 (Sigma; 3.3 mM final)
0.599 g KH_2PO_4 (Merck; 4.4 mM final)
5.46 g $NaHCO_3$ (Sigma; 260 mM final)
14.98 g HEPES (Sigma; 250 mM final)
240 ml H_2O
Adjust pH to 7.4 with 4 N HCl
Bring to 250 ml with H_2O
Sterilize by autoclaving for 15 min at 121°C at 1 bar or filter through a 0.22-μm filter
Store up to 6 months at 4°C

Incubation buffer

2.8 g KH_2PO_4 (Merck)
4.2 g Na_2HPO_4 (Sigma)
800 ml H_2O
Adjust pH to 7.4 with 4 N NaOH and 4 N phosphoric acid
Bring volume to 1 liter with H_2O
Store up to 1 month at 4°C

KCl/EDTA solution

11.5 g KCl (Merckl 1.15% w/v final)
33.6 mg Na_2-EDTA·$2H_2O$ (Sigma; 0.1 mM final)
900 ml H_2O
Bring volume to 1.0 liter
Store up to 3 months at 4°C

Nycodenz stock solution, 36% (w/v)

Deposit 36 g of analytical-grade Nycodenz (Nycomed Pharma) on the surface of 80 ml HH biffer (see recipe). Allow Nycodenz to dissolve in the HH buffer at 4°C. Adjust volume to 100 ml with deionized water. Sterilize by filtration through a 0.22-μm filter into a sterile 100-ml bottle. Store up to 1 month at 4″C.

Serum-free cell culture medium

Make up complete cell culture medium (see recipe) without 10% FBS.

Sodium azide solution

Dissolve 65.01 mg sodium azide in 5 ml PBS (GIBCO; 200 mM final). Prepare fresh on the day of use, protect from UV light using aluminium foil.

Sodium fluorescein reagent

Dissolve 18.8 mg sodium fluorescein in 10 ml of PBS (5 mM final concentration). Prepare fresh. Dilute 100 times to prepare a 50 μM solution.

COMMENTARY

Background Information

The cells of the proximal tubule are considered to be the main target for nephrotoxic substances. This vulnerability is explained by the presence of a variety of cellular transport mechanisms resulting in the active uptake and accumulation of numerous (toxic) substances, as well as the expression of biotransformation enzymes, which may activate (or deactivate) accumulated compounds.

Model systems consisting of enriched PT cells in primary culture have considerable advantages over "mixed" model systems (such as kidney slices), for they allow studies of cell-specific transport mechanisms as well as biotransformation-dependent effects of drugs and xenobiotics. PT cells in primary culture retain, at least for several days, their differentiated traits and, therefore, are superior to most immortal cell lines (e.g., LLC-PK_1), which have lost their biotransformation activity (Schaaf et al., 2001) and do not express renal-specific transporters including the organic anion transporters (Boom et al., 1992; Cox et al., 1993).

Various methods for the isolation of PT cells have been described previously (Stanton et al., 1986; Baer et al., 1997). The techniques described in this unit make use of standard laboratory equipment, and the surgical procedure requires minimal training. The use of a Nycodenz gradient for cell separation is supported by the observation that it is relatively inert to the PT cells compared to other widely used sucrose gradients including Percoll and Ficoll. Following isolation, for each cell preparation, the cell viability of the isolate needs to be carefully checked. Moreover, as the proximal tubule cell has very distinct features, the purity of the isolate should be quickly assessed by immunohistochemical and biochemical means (sodium-fluorescein transport).

The presented protocol for cell isolation was established for rats but may be applied to other animal species with minor modifications. It is worthwhile to mention that within a given animal species like rats, small physiological or anatomical differences might exist. The authors selected, for example, the Wistar Hanover strain (Charles River), as these animals have a smaller amount of connective tissue in the kidneys compared to other Wistar (outbreed) strains, renal perfusion is more easily performed, and digestion with collagenase results in the a sufficient number of free viable cells.

The isolated cells can be used for a variety of applications, including basic toxicity studies, biotransformation-dependent toxicity studies, and experiments to study transport and cellular distribution of drugs and xenobiotics.

Critical Parameters

The protocols are established to obtain a reproducible yield of cells, representing a highly pure population of rat proximal tubule cells. In turn, the preparation involves many steps, and the total preparation time is rather long (~4 hr). The most critical steps are the rapid and complete perfusion of the kidneys, the generation of a homogeneous single-cell suspension (prior to Nycodenz centrifugation), and the accurate preparation of the Nycodenz gradients.

Troubleshooting

Low yield

Insufficient perfusion of the kidneys due to surgical errors will considerably decrease cell yield. This includes incomplete separation of the renal perfusion system from the main body circulation (insufficient buffer flow) and obstruction by intra-renal thrombi. These thrombi can sometimes be removed by manually massaging the kidneys, or they should be avoided by injecting heparin during anesthesia or adding a heparin solution to the perfusion buffer I.

Ineffective separation

The renal cortex is comprised of 80% PT cells. Therefore, a significant fraction (>60%) of the original cell suspension should reside in the interface of the Nycodenz gradient, while the remaining cells (including distal tubule cells) are a pellet at the bottom of the tube. Any other distribution of the cell suspension indicates that the optimal Nycodenz gradient was not established and the two Nycodenz fractions have mixed during preparation. Thus, the correct density of the stock solution should be controlled (spectrophotometrically according to the manufacturer's recommendations),

and the technique to prepare the cell-Nycodenz gradient mixture (preventing mixing of the individual layers) monitored. Finally, the centrifugation step might impair the outcome if abrupt acceleration and deceleration disturb the gradient.

An ineffective separation results in impure cell populations and attempts toward reseparation usually result in a considerable decrease in cell viability. Moreover, at longer culture periods, fibroblast overgrowth serves as an indication of inefficient separation.

Low cell viability

Several reasons may contribute to a low cell viability of the plated cells (<70%). The most frequently observed difficulties are: an extended preparation and perfusion period, lack of oxygen, and mechanical injuries during the isolation steps. A possibility, which is often overlooked, is the presence of trace amounts of cleaning detergents in the glassware and tubings.

Low attachment efficiency

Directly related to low cell viability, is the fact that the plated cells may appear to have not efficiently attached as indicated by the absence of cell colonies (typical growth pattern for this type of cells) following an overnight culture. All factors described in the previous paragraphs can contribute to this. In particular, the washing steps following Nycodenz-gradient centrifugation are of importance for cell viability and performance in culture. Cells that have not attached in the first 24-hr culture period can be collected, washed by centrifugation (5 min at 80 × *g*, 4°C), resuspended in (serum-free) culture medium, and re-plated in the same dishes from which they were collected.

Biotransformation assays

The most critical step in the biotransformation experiments with intact cells is the intrinsic cytotoxicity of many model substrates, the uncontrollable cellular uptake (unless monitored with radiolabeled substrates), and the possible non-linearity of the enzymatic reactions, particularly in the presence of enzyme inducers or inhibitors. A thorough examination of all confounding factors should precede any major experiment.

Anticipated Results

Starting with a young adult rat weighing 250 to 300 g, the described procedure will routinely yield 20–40 × 10^6 PT cells. The purity of the isolated cell population is >80% and the viability of the cells exceeds 70%. When PT microsomes are prepared, ~1 mg microsomal protein should be obtained. The primary cultured cells should retain the typical epithelial-like morphology for 1 week, more specific differentiated functions will decrease significantly within the first days of culture.

Time Considerations

A typical isolation, including all preparative steps, usually takes 3 to 6 hr. Total preparation of the buffers and solutions take 30 to 45 min. Rinsing the perfusion system requires 60 min, the surgical procedure requires 60 to 90 min (including the perfusion step), and the preparation of the cell suspension takes ~90 min. Whenever possible, basic buffers and solutions should be prepared in advance.

Literature Cited

Baer, P.C., Nockher, W.A., Haase, W., and Scherberich, J.E. 1997. Isolation of proximal and distal tubule cells from human kidney by immunomagnetic separation. Technical note. *Kidney Int.* 52:1321-1331.

Blackmon, D.L., Watson, A.J., and Montrose, M.H. 1992. Assay of apical membrane enzymes based on fluorogenic substrates. *Anal. Biochem.* 200:352-358.

Blackmore, M. 1996. Rat renal cortical slices: Maintenance of viability and use in in vitro nephrotoxicity testing. *Toxicol. In Vitro.* 11:723-729.

Boom, S.P., Gribnau, F.W., and Russel, F.G. 1992. Organic cation transport and cationic drug interactions in freshly isolated proximal tubular cells of the rat. *J. Pharmacol. Exp. Ther.* 263:445-450.

Burke, M.D. and Mayer, R.T. 1974. Ethoxyresorufin: Direct fluorimetric assay of a microsomal *O*-dealkylation which is preferentially inducible by 3-methylcholanthrene. *Drug Metab. Dispos.* 2:583-588.

Burke, M.D., Thompson, S., Weaver, R.J., Wolf, C.R., and Mayer, R.T. 1994. Cytochrome P450 specificities of alkoxyresorufin *O*-dealkylation in human and rat liver. *Biochem. Pharmacol.* 48:923-936.

Butler, M.A., Iwasaki, M., Guengerich, F.P., and Kadlubar, F.F. 1989. Human cytochrome P-450PA (P-450IA2), the phenacetin O-deethylase, is primarily responsible for the hepatic 3-demethylation of caffeine and *N*-oxidation of carcinogenic arylamines. *Proc. Natl. Acad. Sci. U.S.A.* 86:7696-7700.

Commandeur, J.N., Stijntjes, G.J., Wijngaard, J., and Vermeulen, N.P. 1991. Metabolism of L-cysteine S-conjugates and *N*-(trideuteroacetyl)-L-cysteine S-conjugates of four fluoroethylenes in the rat. Role of balance of deacetylation and acetylation in relation to the nephrotoxicity of mercapturic acids. *Biochem. Pharmacol.* 42:31-38.

Commandeur, J.N., Stijntjes, G.J., and Vermeulen, N.P. 1995. Enzymes and transport systems involved in the formation and disposition of glutathione S-conjugates. Role in bioactivation and detoxication mechanisms of xenobiotics. *Pharmacol. Rev.* 47:271-330.

Cox, P.G.F., Van Os, C.H., and Russel, F.G.M. 1993. Accumulation of salicylic acid and indomethacin in isolated proximal tubular cells of the rat kidney. *Pharmacol. Res.* 27.

Dayer, P., Leemann, T., and Striberni, R. 1989. Dextromethorphan *O*-demethylation in liver microsomes as a prototype reaction to monitor cytochrome P-450 db1 activity. *Clin. Pharmacol. Ther.* 45:34-40.

Habig, W.H., Pabst, M.J., and Jakoby, W.B. 1974. Glutathione S-transferases. The first enzymatic step in mercapturic acid formation. *J. Biol. Chem.* 249:7130-7139.

Hickman, D., Wang, J.P., Wang, Y., and Unadkat, J.D. 1998. Evaluation of the selectivity of in vitro probes and suitability of organic solvents for the measurement of human cytochrome P450 monooxygenase activities. *Drug Metab. Dispos.* 26:207-215.

Knodell, R.G., Hall, S.D., Wilkinson, G.R., and Guengerich, F.P. 1987. Hepatic metabolism of tolbutamide: Characterization of the form of cytochrome P-450 involved in methyl hydroxylation and relationship to in vivo disposition. *J. Pharmacol. Exp. Ther.* 241:1112-1119.

Schaaf, G.J., de Groene, E.M., Maas, R.F., Commandeur, J.N., and Fink-Gremmels, J. 2001. Characterization of biotransformation enzyme activities in primary rat proximal tubular cells. *Chem. Biol. Interact.* 134:167-190.

Seglen, P.O. 1976. Preparation of isolated rat liver cells. *Methods Cell Biol.* 13:29-83.

Stanton, R.C., Mendrick, D.L., Rennke, H.G., and Seifter, J.L. 1986. Use of monoclonal antibodies to culture rat proximal tubule cells. *Am. J. Physiol.* 251:780-786.

Takenaka, M., Imai, E., Kaneko, T., Ito, T., Moriyama, T., Yamauchi, A., Hori, M., Kawamoto, S., and Okubo, K. 1998. Isolation of genes identified in mouse renal proximal tubule by comparing different gene expression profiles. *Kidney Int.* 53:562-572.

Wortelboer, H.M., de Kruif, C.A., van Iersel, A.A., Falke, H.E., Noordhoek, J., and Blaauboer, B.J. 1990. The isoenzyme pattern of cytochrome P450 in rat hepatocytes in primary culture, comparing different enzyme activities in microsomal incubations and in intact monolayers. *Biochem. Pharmacol.* 40:2525-2534.

Wortelboer, H.M., de Kruif, C.A., van Iersel, A.A., Noordhoek, J., Blaauboer, B.J., van Bladeren, P.J., and Falke, H.E. 1992. Effects of cooked brussels sprouts on cytochrome P-450 profile and phase II enzymes in liver and small intestinal mucosa of the rat. *Food Chem. Toxicol.* 30:17-27.

Key References

Cummings, B.S., Zangar, R.C., Novak, R.F., and Lash, L.H. 1999. Cellular distribution of cytochromes P-450 in the rat kidney. *Drug Metab. Dispos.* 27:542-548.

Provides the first overview of CYP450 (protein) expression in rat proximal and distal tubular cells determined in microsomal fractions.

Masereeuw, R., van den Bergh, E.J., Bindels, R.J., and Russel, F.G. 1994. Characterization of fluorescein transport in isolated proximal tubular cells of the rat: Evidence for mitochondrial accumulation. *J. Pharmacol. Exp. Ther.* 269:1261-1267.

Describes the technique of isolation of proximal tubualr cells for short term use in suspension (ro measure cellular uptake/transport) in detail.

Schaaf et al., 2001. See above.

An overview of phase 1 and phase 2 biotransformation activities in primary cultured proximal tubule\ar cells.

Internet Resources

www.gentest.com

This site provides relevant examples of model substrates for the measurement of CYP450 acriviry.

Contributed by G. J. Schaaf,
R. F. M. Maas, and J. Fink-Gremmels
Utrecht University
Utrecht, The Netherlands

TaqMan Real Time–Polymerase Chain Reaction Methods for Determination of Nucleotide Polymorphisms in Human *N*-Acetyltransferase-1 (*NAT1*) and -2 (*NAT2*)

N-acetyltransferase 1 (*NAT1*) and *N*-acetyltransferase 2 (*NAT2*) exhibit allelic variation and genetic polymorphism associated with increased susceptibility towards drug toxicity and environmental disease (Hein et al., 2000a; Butcher et al., 2002). The variant *NAT1* (Table 4.15.1) and *NAT2* (Table 4.15.2) alleles possess various combinations of single nucleotide polymorphisms (SNPs), deletions, and/or insertions compared to the reference alleles, that are sometimes inappropriately termed "wild-type." Combinations of nucleotide polymorphisms define alleles. The consensus listing of *NAT1* and *NAT2* alleles is maintained by an international committee and published at: *http://www.louisville.edu/medschool/pharmacology/NAT.html* (Hein et al., 2000b).

REAL-TIME TAQMAN ANALYSIS OF *NAT1* AND *NAT2*

BASIC PROTOCOL

TaqMan allelic discrimination methods have been developed to rapidly determine *NAT1* (Doll and Hein, 2002) and *NAT2* (Doll and Hein, 2001) genotypes. The SNPs selected for *NAT1* genotype determinations are: $C^{97}T$ (R^{33}Stop), $C^{190}T$ ($R^{64}W$), $G^{445}A$ ($V^{149}I$), $C^{559}T$ (R^{187}Stop), $G^{560}A$ ($R^{187}Q$), $A^{752}T$ ($D^{251}V$), $T^{1088}A$ (3′UTR), and $C^{1095}A$ (3′UTR). The SNPs selected for *NAT2* genotyping determinations are: $G^{191}A$ ($R^{64}Q$), $C^{282}T$ (silent), $T^{341}C$ ($I^{114}T$), $C^{481}T$ (silent), $G^{590}A$ ($R^{197}Q$), $A^{803}G$ ($K^{268}R$), and $G^{857}A$ ($G^{286}E$). All *NAT2* and *NAT1* alleles, except very rare ones, are detected with these SNP determinations.

The authors provide detailed methods and materials for using the 7700 Sequence Detector from Applied Biosystems. These methods can be adapted for other instruments from Applied Biosystems or other manufacturers.

The specific primers and probes for *NAT1* and *NAT2* genotype determinations are listed in Tables 4.15.3 and 4.15.4, respectively.

Materials

2× TaqMan Universal PCR Master Mix (Applied Biosystems)
3 μM primers (see Tables 4.15.3 and 4.15.4; Applied Biosystems)
4 μM fluorescent probes: normal, turbo, and MGB (see Tables 4.15.3 and 4.15.4; Applied Biosystems)
5 to 25 ng/μl high-quality genomic DNA samples
Optical 96-well plates (Applied Biosystems)
Optical caps (Applied Biosystems)
Sequence detector (e.g., 7700 Sequence Detector, Applied Biosystems) and computer

Contributed by David W. Hein and Mark A. Doll
Current Protocols in Toxicology (2004) 4.15.1-4.15.11

Table 4.15.1 Human *NAT1* Alleles[a]

NAT1 allele	Nucleotide change(s)	Amino acid change(s)
*NAT1*3*	$C^{1095}A$	None
*NAT1*4*	None	None
*NAT1*5*	$G^{350,351}C$, $G^{497\text{-}499}C$, $A^{884}G$, Δ^{976}, Δ^{1105}	R117T, R166T, E167Q
*NAT1*10*	$T^{1088}A$, $C^{1095}A$	None
*NAT1*11A*	$C^{-344}T$, $A^{-40}T$, $G^{445}A$, $G^{459}A$, $T^{640}G$, Δ9 between 1065-1090, $C^{1095}A$	V149I, S214A
*NAT1*11B*	$C^{-344}T$, $A^{-40}T$, $G^{445}A$, $G^{459}A$, $T^{640}G$, Δ9 between 1065-1090	V149I, S214A
*NAT1*11C*	$C^{-344}T$, $A^{-40}T$, $G^{459}A$, $T^{640}G$, Δ9 between 1065-1090, $C^{1095}A$	S214A
*NAT1*14A*	$G^{560}A$, $T^{1088}A$, $C^{1095}A$	R187Q
*NAT1*14B*	$G^{560}A$	R187Q
*NAT1*15*	$C^{559}T$	R187Stop
*NAT1*16*	[AAA] immediately after 1091, $C^{1095}A$	None
*NAT1*17*	$C^{190}T$	R64W
*NAT1*18A*	Δ3 between 1064-1087, $T^{1088}A$, $C^{1095}A$	None
*NAT1*18B*	Δ3 between 1065-1090	None
*NAT1*19*	$C^{97}T$	R33Stop
*NAT1*20*	$T^{402}C$	None
*NAT1*21*	$A^{613}G$	M205V
*NAT1*22*	$A^{752}T$	D251V
*NAT1*23*	$T^{777}C$	None
*NAT1*24*	$G^{781}A$	E261K
*NAT1*25*	$A^{787}G$	I263V
*NAT1*26A*	[TAA] insertion between 1065 and 1090, $C^{1095}A$	None
*NAT1*26B*	[TAA] insertion between 1065 and 1090	None
*NAT1*27*	$T^{21}G$, $T^{777}C$	None
*NAT1*28*	[TAATAA]deletion between 1065 and 1090	None
*NAT1*29*	$T^{1088}A$, $C^{1095}A$, Δ^{1025}	None

[a]From *http://www.louisville.edu/medschool/pharmacology/NAT.html*

Prepare reagents

1. Thaw an aliquot of 2× TaqMan Universal PCR Master Mix, primers, and probes at 37°C.

   TaqMan Universal PCR Master Mix (Applied Biosystems) is optimized for TaqMan reactions and contains AmpliTaq Gold DNA polymerase, AmpErase, dNTPs with UTP, and a passive reference to correct for well-to-well variation. None of the above reagents are toxic or require special care. All reagents should be aliquoted, to minimize freezing and thawing, and stored at −20°C.

   Primers and probes for each SNP are listed in Tables 4.15.3 and 4.15.4. The primers and probes are diluted, in sterile DNAse-free water, to a concentration of 3 μM and 4 μM respectively prior to being aliquoted and stored at −20°C.

   Fluorescent probes should be kept out of direct sunlight to avoid degradation.

Table 4.15.2 Human *NAT2* Alleles[a]

NAT2 allele	Nucleotide change(s)	Amino acid change(s)
*NAT2*4*	None	None
*NAT2*5A*	$T^{341}C$, $C^{481}T$	I114T
*NAT2*5B*	$T^{341}C$, $C^{481}T$, $A^{803}G$	I114T, K268R
*NAT2*5C*	$T^{341}C$, $A^{803}G$	I114T, K268R
*NAT2*5D*	$T^{341}C$	I114T
*NAT2*5E*	$T^{341}C$, $G^{590}A$	I114T, R197Q
*NAT2*5F*	$T^{341}C$, $C^{481}T$, $C^{759}T$, $A^{803}G$	I114T, K268R
*NAT2*5G*	$C^{282}T$, $T^{341}C$, $C^{481}T$, $A^{803}G$	I114T, K268R
*NAT2*5H*	$T^{341}C$, $C^{481}T$, $A^{803}G$, $T^{859}C$	I114T, K268R, I287T
*NAT2*5I*	$T^{341}C$, $A^{411}T$, $C^{481}T$, $A^{803}G$	I114T, L137F, K268R
*NAT2*5J*	$C^{282}T$, $T^{341}C$, $G^{590}A$	I114T, R197Q
*NAT2*6A*	$C^{282}T$, $G^{590}A$	R197Q
*NAT2*6B*	$G^{590}A$	R197Q
*NAT2*6C*	$C^{282}T$, $G^{590}A$, $A^{803}G$	R197Q, K268R
*NAT2*6D*	$T^{111}C$, $C^{282}T$, $G^{590}A$	R197Q
*NAT2*6E*	$C^{481}T$, $G^{590}A$	R197Q
*NAT2*7A*	$G^{857}A$	G286E
*NAT2*7B*	$C^{282}T$, $G^{857}A$	G286E
*NAT2*10*	$G^{499}A$	E167K
*NAT2*11A*	$C^{481}T$	None
*NAT2*11B*	$C^{481}T$, 859del	S287 frameshift
*NAT2*12A*	$A^{803}G$	K268R
*NAT2*12B*	$C^{282}T$, $A^{803}G$	K268R
*NAT2*12C*	$C^{481}T$, $A^{803}G$	K268R
*NAT2*12D*	$G^{364}A$; $A^{803}G$	D122N, K268R
*NAT2*13*	$C^{282}T$	None
*NAT2*14A*	$G^{191}A$	R64Q
*NAT2*14B*	$G^{191}A$, $C^{282}T$	R64Q
*NAT2*14C*	$G^{191}A$, $T^{341}C$, $C^{481}T$, $A^{803}G$	R64Q, I114T, K268R
*NAT2*14D*	$G^{191}A$, $C^{282}T$, $G^{590}A$	R64Q, R197Q
*NAT2*14E*	$G^{191}A$, $A^{803}G$	R64Q, K268R
*NAT2*14F*	$G^{191}A$, $T^{341}C$, $A^{803}G$	R64Q, I114T, K268R
*NAT2*14G*	$G^{191}A$, $C^{282}T$, $A^{803}G$	R64Q, K268R
*NAT2*17*	$A^{434}C$	Q145P
*NAT2*18*	$A^{845}C$	K282T
*NAT2*19*	$C^{190}T$	R64W

[a]From *http://www.louisville.edu/medschool/pharmacology/NAT.html*

Table 4.15.3 Primers and Fluorogenic Probes for *NAT1* SNP Determinations[a,b]

Primer or probe	Sequence
97-Forward primer (58-85)	5′-gacttggaaacattaactgacattcttc-3′
97-Reverse primer (131-107) [74 bp]	5′-caatggatgttaaggttctcaaagg-3′
97C-TaqMan MGB probe (90-104)	FAM-ccagatc**C**gagctgt
97T-TaqMan MGB probe (90-105)	VIC-ccagatc**T**gagctgtt
190-Forward primer (143-165)	5′-tggacttaggcttagaggccatt-3′
190-Reverse primer (220-198) [78 bp]	5′-gatgattgacctggagacaccat-3′
190C-TaqMan MGB probe (196-185)	FAM-caccc**G**atttc
190T-TaqMan MGB probe (195-183)	VIC-accc**A**atttctt
445-Forward primer (395-416)	5′-ggcagcctctggagttaatttc-3′
445-Reverse primer (506-481) [70 bp]	5′-tactgttcccttctgatttggtctag-3′
445G-TaqMan MGB probe (439-452)	FAM-ccttgt**G**tcttccg
445A-TaqMan MGB probe (437-454)	VIC-tgccttgt**A**tcttccgtt
559/560-Forward primer (497-521)	5′-gggaacagtacattccaaatgaaga-3′
559/560-Reverse primer (595-571) [99 bp]	5′-ttgttcgaggcttaagagtaaagga-3′
559C/560G-TaqMan MGB probe (552-566)	FAM-caaatac**CG**aaaaat
559C/560A-TaqMan MGB probe (552-569)	VIC-caaatac**CA**aaaaatcta
559T/560G-TaqMan MGB probe (552-567)	TET-caaatac**TG**aaaaatc
752-Forward primer (713-734)	5′-ccctcacccataggagattcaa-3′
752-Reverse primer (793-765) [81 bp]	5′-tttctatttcttcctcactcagagtcttg-3′
752A-TaqMan MGB probe (743-762)	FAM-acaatacag**A**tctaatagag
752T-TaqMan MGB probe (743-762)	VIC-acaatacag**T**tctaatagag
1088/1095-Forward primer (1041-1066)	5′-gaaacataaccacaaaccttttcaaa-3′
1088/1095-Reverse primer (1136-1112) [96 bp]	5′-aaatcaccaatttccaagataacca-3′
1088T/1095C-TaqMan MGB probe (1105-1079)	FAM-atctttaaaa**G**acattt**A**ttattatta
1088A/1095A-TaqMan MGB probe (1106-1079)	VIC-catctttaaaa**T**acattt**T**ttattatta
1088T/1095A-TaqMan MGB probe (1106-1078)	TET-catctttaaaa**T**acattt**A**ttattattat

[a] Adapted from Doll and Hein, 2002. Nucleotide positions are indicated in parentheses. PCR product size is indicated in square brackets. Nucleotide-specific polymerase chain reaction (PCR) primers and fluorogenic probes were designed using Primer Express (version 1.5; Applied Biosystems). The fluorogenic MGB probes were labeled with a reporter dye (either FAM or VIC or TET) specific for one of the possible nucleotides identified at eight polymorphisms in the *NAT1* coding region or 3′ UTR. The fluorogenic probes for the 559/560 and the 1088/1095 are distinguished using a three-probe system that has both nucleotide polymorphisms in the same probe. This is necessary because the 559/560 and 1088/1095 are too close together to use the conventional two-probe TaqMan assay. The nucleotide-specific primers amplify a segment of the *NAT1* gene flanking the probes.

[b] Abbreviations: bp, base-pair; FAM, 6-carboxyfluorescein; MGB, minor groove binder; *NAT1*, *N*-acetyltransferase 1; PCR, polymerase chain reaction; SNP, single-nucleotide polymorphism; TET, tetrachloro-6-carboxyfluorescein; UTR, untranslated region; VIC, a proprietary dye from Applied Biosystems.

2. Prepare a master solution of 2× TaqMan Universal PCR Master Mix, primers, and probes to have 12 µl solution/sample. Make up the solution with the following composition:

   50% 2× TaqMan Universal PCR Master Mix
   10% each appropriate primer
   2.5% each of two or three appropriate probes
   25% sterile, DNAse-free H_2O.

Table 4.15.4 Primers and Fluorogenic Probes for *NAT2* SNP Determinations[a]

191-Forward primer (131-149)	5′-gtgggcaagccatggagtt-3′
191-Reverse primer (242-220) [112 bp]	5′-gtggtcagagcccagtacagaag-3′
191A-TaqMan probe (204-179)	FAM-acaccacccacccTggtttcttctta- TAMRA
191G-TaqMan probe (202-181)	VIC-accacccacccCggtttcttct-TAMRA
282-Forward primer (196-216)	5′-gggtggtgtctccaggtcaat-3′
282-Reverse primer (321-299) [126 bp]	5′-gtgaaccatgccagtgctgtatt-3′
282C-TurboTaqMan probe (270-293)	FAM-agggtatttttaCatccctccagt-TAMRA
282T-Turbo TaqMan probe (270-294)	VIC-agggtatttttaTatccctccagtt-TAMRA
341-Forward primer (278-305)	5′-tttacatccctccagttaacaaatacag-3′
341-Reverse primer (377-359) [100 bp]	5′-ccagacccagcatcgacaa-3′
341T-TaqMan probe (349-329)	FAM-tgccgtcaAtggtcacctgca-TAMRA
341C-TaqMan probe (349-329)	VIC-tgccgtcaGtggtcacctgca-TAMRA
481-Forward primer (438-458)	5′-gccttgcattttctgcttgac-3′
481-Reverse primer (549-525) [112 bp]	5′-ctttggcaggagatgagaattaaga-3′
481C-TaqMan probe (495-468)	FAM-cctgatttggtccaGgtaccagattcct-TAMRA
481T-TaqMan probe (495-467)	VIC-cctgatttggtccaAgtaccagattcctc-TAMRA
590-Forward primer (483-506)	5′-ggaccaaatcaggagagagcagta-3′
590-Reverse primer (636-609) [154 bp]	5′-agacgtctgcaggtatgtattcatagac-3′
590G-TaqMan probe (577-604)	FAM-acgcttgaacctcGaacaattgaagatt-TAMRA
590A-TaqMan probe (577-606)	VIC- acgcttgaacctcAaacaattgaagatttt-TAMRA
803-Forward primer (763-789)	5′-tttaaaactctcactgaggaagaggtt-3′
803-Reverse primer (839-819) [77 bp]	5′-acgagatttctccccaaggaa-3′
803A-Turbo TaqMan probe (816-790)	FAM-cttaaatatatttTtcagcacttcttc-TAMRA
803G-Turbo TaqMan probe (817-791)	VIC-tcttaaatatatttCtcagcacttctt-TAMRA
857-Forward primer (768-792)	5′-aactctcactgaggaagaggttgaa-3′
857-Reverse primer (912-888) [146 bp]	5′-tgggtgatacatacacaagggtttat-3′
857G-TaqMan probe (842-870)	FAM-ccaaacctggtgatgGatcccttactatt-TAMRA
857A-TaqMan probe (841-869)	VIC-cccaaacctggtgatgAatcccttactat-TAMRA

[a] Adapted from (Doll and Hein, 2001). Nucleotide positions are indicated in parenthesis. PCR product sizes are indicated in brackets. SNP-specific polymerase chain reaction (PCR) primers and fluorogenic probes were designed using Primer Express (Applied Biosystems). The fluorogenic probes are labeled with a reporter dye (either FAM or VIC) and are specific for one of the two possible bases identified at seven SNPs in the *NAT2* coding region.

[b] Abbreviations: bp, base-pair; FAM, 6-carboxyfluorescein; *NAT2*, *N*-acetyltransferase 2; PCR, polymerase chain reaction; SNP, single-nucleotide polymorphism; TAMRA, 6-carboxytetramethylrhodamine; VIC, a proprietary dye from Applied Biosystems.

Once all the components have been added, mix briefly by vortexing.

Aerosol-free tips should be used for all pipeting to minimize risk of cross-contamination.

3. Pipet 10 µl of the mix into the appropriate number of wells of an optical 96-well plate.
4. Add 1 µl of genomic DNA (5 to 25 ng) to the appropriate wells (one DNA sample/well). Place optical caps on wells.

   Make sure not to damage the caps when putting them on the 96-well plate.
5. Vortex plate to mix the genomic DNA into the mixture. Transfer the 96-well plate to the 7700 sequence detector.

Prepare the 7700 Sequence Detector

6. Turn on the 7700 Sequence Detector and computer.

   Turn on the 7700 Sequence Detector at least 30 min in advance.

7. Open the sequence detector software and close the screen that appears by clicking the upper left-hand corner.

8. Click on File and scroll to New Plate. Select Single Reporter, 7700 Sequence Detector, and Real-time, and click OK.

9. Highlight the wells that are being used in the run, click on Sample Type, and scroll to Unknown.

10. Change the dye layer to VIC, click on Sample Type, and scroll to Sample Type Setup. Click the Add button and scroll down to bottom row where New Control in the name column is indicated. Change the acronym to Unknown, change the name to Unknown, pick a color, change the reporter to VIC, and click OK when finished.

11. Click on Sample Type and scroll to Unknown.

12. If using either the 559/560 or 1088/1095-primer/probe combination for *NAT1* genotype determination, repeat steps 10 and 11 using TET as the dye layer and reporter.

13. Click on Thermocycler conditions and in stage 3 of the program, change 95°C to 92°C for *NAT1* genotype assays, change 60°C to 62°C for *NAT2* genotype assays, and click OK.

    The NAT1 PCR reactions begin with two initial hold steps (50°C for 2 min, followed by 95°C for 10 min) and 40 cycles of a two-step PCR (92°C for 15 sec, 60°C for 1 min). The NAT2 PCR amplification reactions begin with two initial hold steps (50°C for 2 min, followed by 95°C for 10 min) and 40 cycles of a two-step PCR (95°C for 15 sec, 62°C for 1 min).

14. Click on File, assign a name, and click Save.

15. Click the Show Analysis button and then the Run button.

    The run will be completed in ~2 hr.

    The fluorescence intensity of each sample is measured at each temperature change to monitor amplification of the NAT1 or NAT2 gene. The nucleotide present at each SNP is determined by the fluorescence ratio of the two SNP-specific fluorogenic probes. The fluorescence signal increases when the probe with the exact sequence match binds to the single-stranded template DNA and is digested by the 5′-3′ exonuclease activity of AmpliTaq-Gold DNA polymerase (Applied Biosystems). Digestion of the probe releases the fluorescent reporter dye (FAM, VIC, or TET) from the quencher dye (TAMRA).

Analyze completed run

16. Once the run is complete, click on Analysis and scroll to Analyze. Click OK.

    This screen informs whether or not the samples were amplified by polymerase chain reaction (PCR). Amplification is evident by an increase in the relative number (ΔRN).

17. Click on File and scroll to Save. Close this run by clicking in the upper left-hand corner.

18. Click on File and scroll to New Plate. Change the plate type to Allelic Discrimination and click OK.

19. Highlight the wells that were used in the run. Click on Sample Type and scroll to Unknown.

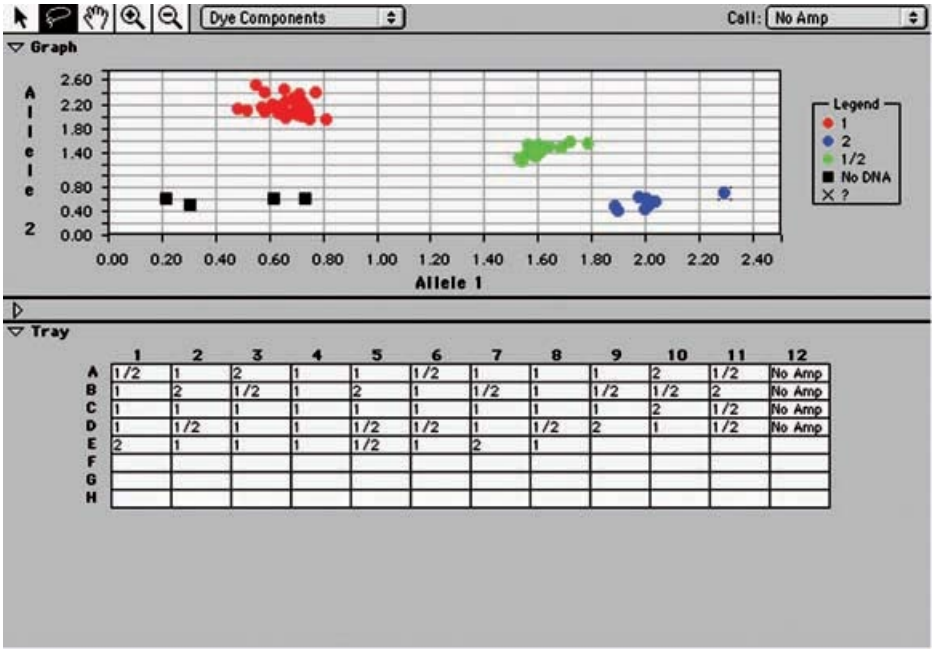

Figure 4.15.1 SNP data from the 7700 Sequence Detector. The top graph illustrates SNP fluorescence data for individual samples in the 96-well plate. The red circle cluster at upper left shows samples that are "1" or homozygous for one nucleotide (usually the more frequent one). The green circle cluster in the center shows samples that are "1/2" or heterozygous for the SNP. The blue circle cluster at lower right shows samples that are "2" or homozygous for the other nucleotide (usually the less frequent one). These values are imported into the bottom spreadsheet as described in the Basic Protocol. Thus, as shown in the database, the sample in well A-1 is in the green center cluster and is heterozygous for the two nucleotides; the sample in well A-2 is in the red upper left cluster and is homozygous for the common nucleotide; and the sample in well A-3 is in the blue cluster at lower right and is homozygous for the less common nucleotide. All cells in the 12th column (data illustrated as black squares) were negative controls (no DNA template). This black and white facsimile of the figure is intended only as a placeholder; for full-color version of figure go to *http://www.currentprotocols.com/colorfigures*.

20. Click on the Show Analysis button.
21. Click on Post-PCR Read and let the instrument proceed until it is done.
22. Click on Analysis and scroll to Analyze.
23. Click on Analysis and scroll to Allelic Discrimination. Click on Normalize button and scroll to Dye Components.
24. Click on the magnifying glass and then click on the graph to bring the graph to scale.

    There should be at least three identifiable groups as illustrated in Figure 4.15.1.

25. Click on the lasso and circle the grouping in the upper left. Change the call to allele 1. Circle the grouping of Xs that are in the bottom right and change the call to allele 2. Circle the grouping of Xs that is in the middle and change the call to allele $^1/_2$.
26. Print the graph and the corresponding 96-well tray that contains the results. Click on File and scroll to Save As. Give the post-PCR read a name and click Save.

    The results can be exported or copied to Excel or other programs for further analysis.

    The process of preparing the samples, preparing the 7700 Sequence Detector, and analyzing the run must be repeated for each SNP in human NAT1 and NAT2.

COMMENTARY

Background Information

NAT1 and *NAT2* encode *N*-acetyltransferase isozymes that catalyze the acetylation of many aromatic and hydrazine drugs as well as many aromatic and heterocyclic amine carcinogens present in the environment, industry, and the diet (Hein et al., 2000a; Butcher et al., 2002). Both *NAT1* and *NAT2* possess intronless, protein-coding, 870-bp exons. A related pseudogene, *NATP*, also has been identified (Vatsis et al., 1995). These *NAT* loci are separated by <500 kb in the orientation *NAT1:NATP:NAT2* in the 8p22 region of chromosome eight (Upton et al., 2001). *NAT1* and *NAT2* share 87% nucleotide identity in the coding region, translating to only 55 amino acid differences (Vatsis et al., 1995; Hein et al., 2000a).

*NAT1*4* is defined as the reference allele and over 25 variant alleles have been identified in human populations (Table 4.15.1). The *NAT1* alleles have genetic polymorphisms in both the coding and untranslated regions. The *NAT1*10* allele, a common allele associated with rapid acetylator phenotype in some but not all studies (Hein et al., 2000a; Upton et al., 2001), possesses SNPs in the 3′-untranslated region. Many published genotype methods are designed only to distinguish a small subset of SNPs and do not distinguish *NAT1*10* from *NAT1*14A* and other *NAT1* alleles. Since *NAT1*10* is often associated with environmental disease, it is particularly important that the *NAT1*10* allele frequency be determined accurately. Several *NAT1* alleles (*NAT1*14, *15, *17, *19*, and **22*) are associated with reduced *NAT1* catalytic activity and slow acetylator phenotype (Butcher et al., 1998; Hughes et al., 1998; Lin et al., 1998; Fretland et al., 2001b). Frequencies for some of the *NAT1* and *NAT2* alleles are rare reflecting nucleotide diversity rather than genetic polymorphism (defined as frequency of at least 1%).

*NAT2*4* is defined as the reference allele and >30 *NAT2* allelic variants have been identified in human populations (Table 4.15.2). The *NAT2* variant alleles possess one or a combination of nucleotide substitutions in the *NAT2* coding region. Seven of these: $G^{191}A$ ($R^{64}Q$), $C^{282}T$ (silent), $T^{341}C$ ($I^{114}T$), $C^{481}T$ (silent), $G^{590}A$ ($R^{197}Q$), $A^{803}G$ ($K^{268}R$), and $G^{857}A$ ($G^{286}E$) have frequencies in human populations exceeding 1% depending upon the ethnic group (Hein et al., 2000a; Butcher et al., 2002). For example, the $G^{191}A$ substitution common to the *NAT2*14* gene cluster is relatively frequent in African populations (Delomenie et al., 1996; Loktionov et al., 2002), but it is virtually absent in Caucasian populations. *NAT2* alleles possessing the $C^{190}T$ ($R64W$), $G^{191}A$ ($R64Q$), $T^{341}C$ ($I114T$), $G^{364}A$ ($D122N$), $A^{411}T$ ($L137F$), $A^{434}C$ ($E145P$), $G^{590}A$ ($R197Q$), and/or $G^{857}A$ ($G286E$) missense SNPs are associated with slow acetylator phenotypes (Leff et al., 1999; Fretland et al., 2001a; Hein, 2002; Svensson and Hein, in press). The *NAT2* slow acetylator phenotypes are most likely not homogenous, but rather reflect varying levels of slow acetylator phenotype due to different mechanisms among the various SNPs (Leff et al., 1999). The original *NAT1* and *NAT2* genotyping methods were designed to detect the most frequent SNPs (usually three or four) by polymerase chain reaction (PCR) restriction fragment length polymorphism (RFLP) analysis. These assays had the potential for genotype misclassifications (Hein et al., 2000a; Deitz et al., 2004). Several improved PCR-RFLP genotyping assays for *NAT1* and *NAT2* polymorphism assay have been developed subsequently (Doll et al., 1995; Delomenie et al., 1996; Deitz et al., 1997; Lo-Guidice et al., 2000; Cascorbi et al., 2001; Vaziri et al., 2001; Loktionov et al., 2002). Although these assays are still frequently utilized for *NAT1* and *NAT2* genotyping, they are very labor intensive and incomplete digestion of the PCR products can lead to misinterpretation of the results (Cascorbi and Roots, 1999).

Major advantages of the methods described here are that they do not require post-PCR processing (such as enzyme digestion) or the use of radioactivity. Since the methods amplify relatively small segments of *NAT1* or *NAT2*, they are effective for human DNA samples derived from buccal cells or paraffin-embedded tissues.

In addition to other real-time PCR–based assays, alternative methods for determining *NAT1* and *NAT2* nucleotide polymorphisms include automated DNA sequencing, allele-specific oligonucleotide and enzyme-linked immunosorbent assay (ELISA)-based oligonucleotide ligation assays (reviewed in Hein et al., in press).

Critical Parameters

Since *NAT1*, *NAT2*, and *NATP* are highly homologous, PCR primers must be specific for *NAT1* or *NAT2*. Since most *NAT1* and *NAT2* alleles have multiple nucleotide

substitutions, it is important to phase their location on one or the other of the homologous chromosomes in the diploid genome (Cascorbi and Roots, 1999). Genotype misclassification also occurs when variant *NAT* alleles sharing a common nucleotide polymorphism are not distinguished. This should be avoided or minimized since it causes substantial bias in epidemiology investigations, particularly if gene-environmental interactions are considered.

All assays should be set up in a place that is clean and free of any plasmid or genomic DNA contamination. This method is very sensitive and will amplify even the smallest quantities of template DNA, so care must be taken to prevent contamination of foreign DNA. The 96-well plate can be cut to size if <96 samples are run in a single run. As soon as the DNA samples have been added to the appropriate wells, the optical caps should be placed on the optical tubes. When placing the optical caps on the optical tubes, make sure not to damage the optical caps in any way or it will affect the result of that sample. No-DNA-template amplification controls should be carried out to demonstrate no contamination of foreign DNA. Other controls that should be included are positive controls for each SNP. It is important that the DNA concentration be in the range of 5 to 25 ng/assay, however, much less DNA can be used for plasmid controls.

The nucleotide substitutions at 559/560 and 1088/1095 are distinguished using a three-probe system that has both nucleotide polymorphisms in the same probe. This is necessary because the 559/560 and the 1088/1095 substitutions are too close together to use the conventional two-probe TaqMan assays. The 559/560 and 1088/1095 polymorphisms are not analyzed the way the other polymorphisms are analyzed. To determine whether and how many polymorphisms exist in a sample, look at the increase in fluorescence of the three probes. If only the FAM signal increases, then the sample is homozygous for 559C/560G or 1088T/1095C depending on which primer/probe set is used. If only the VIC signal increases, then the sample is homozygous for 559C/560A or 1088A/1095A depending on the primer/probe set used. If only the TET signal increases, then the sample is homozygous for 559T/560G or 1088T/1095A depending on which primer/probe set was used.

Assignment of haplotype or allele requires phasing the SNPs. This may be ambiguous due to the overlapping nature of the nucleotide substitutions that occur among the allelic variants. In these instances, the entire *NAT1* or *NAT2* sequence should be amplified by PCR as previously described (Doll et al., 1995; Deitz et al., 1997). The PCR product is then cloned directly into pCR-TOPO (Invitrogen) following manufacturer's instructions. This vector takes advantage of the 3′-A overhang added there by the *Taq* DNA polymerase during PCR. It also takes advantage of the topoisomerase gene that is covalently bound to the 3′-T overhang of the pCR-TOPO vector. This topoisomerase enzyme facilitates the direct ligation of the PCR product into the vector. Colonies possessing a single *NAT1* or *NAT2* allele can be used as a template for the genotyping assay or sequencing. A method to unambiguously assign the *NAT2* genotype using allele-specific PCR combined with RFLP has been described (Delmonie et al., 1996).

Anticipated Results

Figure 4.15.1 illustrates the data generated by the 7700 Sequence Detector and its transfer to a database. The frequency of *NAT1* and *NAT2* SNPs, alleles, genotypes, and phenotypes differs markedly between ethnic groups (e.g., Delomenie et al., 1996; Upton et al., 2001; Doll and Hein, 2002; Loktionov et al., 2002).

Time Considerations

It is most efficient to test all samples for one SNP before proceeding on to the next SNP. However, when processing small numbers of samples, different SNPs can be done in a single run. It requires ~2.5 hr for experienced users to assess one SNP in 96 samples. Preparation for each run can be accomplished in ~15 min with use of master mixes and multi-channel pipets. Setting up the sequence detector takes ~5 min. Once set up, each run takes ~2 hr of instrument time. Following completion of the run, data transfer to the database can be accomplished in ~10 min. For large experiments, economy of time and expense is achieved with instruments that can incorporate 384-well plates.

Literature Cited

Butcher, N.J., Boukouvala, S., Sim, E., and Minchin, R.F. 2002. Pharmacogenetics of the arylamine *N*-acetyltransferases. *Pharmacogenomics J.* 2:30-42.

Butcher, N.J., Ilett, K.F., and Minchin, R.F. 1998. Functional polymorphism of the human arylamine *N*-acetyltransferase type 1 gene caused by C190T and G560A mutations. *Pharmacogenetics* 8:67-72.

Cascorbi, I. and Roots, I. 1999. Pitfalls in *N*-acetyltransferase 2 genotyping. *Pharmacogenetics* 9:123-127.

Cascorbi, I., Roots, I., and Brockmoller, J. 2001. Association of *NAT1* and *NAT2* polymorphisms to urinary bladder cancer: Significantly reduced risk in subjects with NAT1*10. *Cancer Res.* 61:5051-5056.

Deitz, A.C., Doll, M.A., and Hein, D.W. 1997. A restriction fragment length polymorphism assay that differentiates human *N*-acetyltransferase-1 (*NAT1*) alleles. *Anal. Biochem.* 253:219-24.

Deitz, A.C., Rothman, N., Rebbeck, T.R., Hayes, R.B., Chow, W-H., Zheng, W., Hein, D.W., and Garcia-Closes, M., 2004. Impact of misclassification in genotype-exposure interaction studies. Example of *N*-acetyltransferase 2 (*NAT2*), smoking, and bladder cancer. *Cancer Epidem. Biomark. Prev.* 13:1543-1546.

Delomenie, C., Sica, L., Grant, D.M., Krishnamoorthy, R., and Dupret, J.M. 1996. Genotyping of the polymorphic *N*-acetyltransferase (*NAT2**) gene locus in two native African populations. *Pharmacogenetics* 6:177-185.

Doll, M.A., Fretland, A.J., Deitz, A.C., and Hein, D.W. 1995. Determination of human *NAT2* acetylator genotype by restriction fragment-length polymorphism and allele-specific amplification. *Anal Biochem.* 231:413-420.

Doll, M.A. and Hein, D.W. 2001. Comprehensive human *NAT2* genotype method using single nucleotide polymorphism-specific polymerase chain reaction primers and fluorogenic probes. *Anal. Biochem.* 288:106-108.

Doll, M.A. and Hein, D.W. 2002. Rapid genotype method to distinguish frequent and/or functional polymorphisms in human *N*-acetyltransferase-1 (*NAT1*). *Anal. Biochem.* 301:328-332.

Fretland, A.J., Leff, M.A., Doll, M.A., and Hein, D.W. 2001a. Functional characterization of human *N*-acetyltransferase 2 (*NAT2*) single nucleotide polymorphisms. *Pharmacogenetics* 11:207-215.

Fretland, A.J., Doll, M.A., Leff, M.A., and Hein, D.W. 2001b. Functional characterization of nucleotide polymorphisms in the coding region of human *N*-acetyltransferase 1. *Pharmacogenetics* 11:511-520.

Hein, D.W. 2002. Molecular genetics and function of *NAT1* and *NAT2*: Role in aromatic amine metabolism and carcinogenesis. *Mutat. Res.* 506-507:65-77.

Hein, D.W., Doll, M.A., Fretland, A.J., Leff, M.A., Webb, S.J., Xiao, G.H., Devanaboyina, U.-S., Nangju, N.A., and Feng, Y. 2000a. Molecular genetics and epidemiology of the *NAT1* and *NAT2* acetylation polymorphisms. *Cancer Epidem. Biomarker Prev.* 9:29-42.

Hein, D.W., Doll, M.A., and Nerland, D.E., In press. Methods for *N*-acetyltransferase (*NAT1* and *NAT2*) genotype determination. *In* Principles of Clinical Pharmacogenomics and Introduction to Pharmaco Proteomics (S.H.Y. Wong, M.W., Linder, and R. Valdes Jr., eds.), AACC Press, Washington, D.C.

Hein, D.W., Grant, D.M., and Sim, E. 2000b. Update on consensus arylamine *N*-acetyltransferase gene nomenclature. *Pharmacogenetics* 10:291-292.

Hughes, N.C., Janezic, S.A., McQueen, K.L., Jewett, M.A.S., Castranio, T., Bell, D.A., and Grant, D.M. 1998. Identification and characterization of variant alleles of human acetyltransferase *NAT1* with defective function using p-aminosalicylate as an in-vivo and in-vitro probe. *Pharmacogenetics* 8:55-66.

Leff, M.A., Fretland, A.J., Doll, M.A., and Hein, D.W. 1999. Novel human *N*-acetyltransferase 2 alleles that differ in mechanism for slow acetylator phenotype. *J. Biol. Chem.* 274:34519-34522.

Lin, H.J., Probst-Hensch, N.M., Hughes, N.C., Sakamoto, G.T., Louie, A.D., Kau, I.H., Lin, B.K., Lee, D.B., Lin, J., Frankl, H.D., Lee, E.R., Hardy, S., Grant, D.M., and Haile, R.W. 1998. Variants of *N*-acetyltransferase *NAT1* and a case-control study of colorectal adenomas. *Pharmacogenetics* 8:269-281.

Lo-Guidice, J.-M., Allorge, D., Chevalier, D., Debuysere, H., Faxio, F., Lafitte, J.-J., and Broly, F. 2000. Molecular analysis of the *N*-acetyltransferase 1 gene (*NAT1**) using polymerase chain reaction-restriction fragment-single strand conformation polymorphism assay. *Pharmacogenetics* 10:293-300.

Loktionov, A., Moore, W., Spencer, S.P., Vorster, H., Nell, T., O'Neill, I.K., Bingham, S.A., and Cummings, J.H. 2002. Differences in *N*-acetylation genotypes between Caucasians and Black South Africans: Implications for cancer prevention. *Cancer Detection Prev.* 26:15-22.

Svensson, C.K., and Hein, D.W., In press. Phenotypic and genotypic characterization of *N*-acetylation. *In* Drug Metabolism and Transport: Molecular Methods and Mechanisms (L.H. Lash, ed.) The Humana Press, Totowa, N.J.

Upton, U., Johnson, N., Sandy, J., and Sim, E. 2001. Arylamine *N*-acetyltransferases- of mice, men and microorganisms. *Trends Pharmacol. Sci.* 22:140-146.

Vatsis, K.P., Weber, W.W., Bell, D.A., Dupret, J.-M., Price-Evans, D.A., Grant, D.M., Hein, D.W., Lin, H.J., Meyer, U.A., Relling, M.V., Sim, E., Suzuki, T., and Yamazoe, Y. 1995. Nomenclature for *N*-acetyltransferases. *Pharmacogenetics* 5:1-17.

Vaziri, S.A.J., Hughes, N.C., Sampson, H., Darlington, G., Jewett, M.A.S., and Grant, D.M. 2001. Variation in enzymes of arylamine procarcinogen biotransformation among bladder cancer patients and control subjects. *Pharmacogenetics* 11:7-20.

Key References

Butcher et al., 2002. See above.

Review of the role of NAT1 and NAT2 polymorphisms on drug response.

Doll and Hein, 2001. See above.

Original report of NAT2 genotype method described in this unit.

Doll and Hein, 2002. See above.

Original report of NAT2 genotype method described in this unit.

Hein et al., 2000a. See above.

Review of the role of NAT1 and NAT2 polymorphisms on cancer risk.

Hein et al., In press. See above.

Review of different NAT1 and NAT2 genotyping methods.

McQueen, C.A. 2001. Measuring the activity of arylamine *N*-acetyltransferase (*NAT*). *In* Current Protocols in Toxicology., 4.6.1-4.6.13. John Wiley & Sons, New York.

Describes common protocols for measuring N-acetyltransferase catalytic activity.

Internet Resources

http://www.louisville.edu/medschool/pharmacology/NAT.html

Website for NAT1 and NAT2 alleles.

Contributed by David W. Hein and Mark A. Doll
University of Louisville School of Medicine
Louisville, Kentucky

Evaluation of the Cytochrome b_5/ Cytochrome b_5 Reductase Pathway

This unit provides protocols for measuring the activity of the cytochrome b_5/cytochrome b_5 reductase pathway ex vivo using the reduction of ferrihemoglobin in erythrocytes (see Basic Protocol 1) or leukocytes (see Alternate Protocol), for evaluating mRNA expression of cytochrome b_5 and cytochrome b_5 reductase in leukocytes using qRT-PCR (see Basic Protocol 2), and for obtaining heterologous expression of the soluble forms of each protein in *E. coli* (see Basic Protocol 3). A method for preparing red blood cell lysate is described in Support Protocol 1; a method for preparing peripheral blood mononuclear cells is described in Support Protocol 2.

Cytochrome b_5 and its reductase can directly detoxify arylhydroxylamine compounds and bioactivate amidoxime prodrugs. Although factors that affect the expression of this pathway have not been well studied, ascorbate deficiency, malarial infection, and antithyroid and neuroleptic drugs have been reported to affect the expression and/or activity of this pathway.

FERRIHEMOGLOBIN REDUCTION AS A MARKER OF CYTOCHROME b_5 REDUCTASE ACTIVITY IN ERYTHROCYTES

BASIC PROTOCOL 1

Methemoglobin (Hb^{3+}) is a natural substrate for cytochrome b_5 reductase. However, the reduction of methemoglobin (Hb^{3+}) to hemoglobin (Hb^{2+}) is too slow to determine the in vitro activity of the enzyme in clinical samples. Alternatively, the rate of NADH-dependent reduction of a methemoglobin-ferrocyanide complex can be used as a marker for cytochrome b_5 reductase activity. An increase in optical density due to the reduction of this complex is monitored spectrophotometrically at 575 nm. For red blood cells, activity is normalized to hemoglobin content, while for other cell types (see Alternate Protocol) activity is normalized to milligram of protein added to the reaction mixture.

Materials

0.027 M disodium EDTA, pH 7.0: dissolve 392 mg Na_2EDTA in 50 ml H_2O; adjust pH to 7.0 using 1 M NaOH
50 mM sodium citrate buffer, pH 4.7 (see recipe)
0.5 mM potassium ferricyanide: dissolve 3.292 mg $K_3Fe(CN)_6$ in 20 ml H_2O (prepare fresh; protect from light)
1.224% (w/v) human hemoglobin (see recipe)
RBC lysate from subject of interest, diluted 1:20 (see Support Protocol 1)
2 mM NADH: dissolve 2.836 mg NADH in 2 ml H_2O (degrades in solution at room temperature; prepare fresh within 1 hr of use.)
1.5-ml amber microcentrifuge tubes
Quartz spectrophotometer cuvettes
Spectrophotometer

Prepare reaction mixture

1. To a 1.5-ml amber microcentrifuge tube, add the following reagents, prewarmed to 37°C, in the order given:

   19 µl 0.027 M EDTA, pH 7.0
   98 µl 50 mM sodium citrate buffer, pH 4.7
   294 µl 0.5 mM potassium ferricyanide

Contributed by Lauren A. Trepanier, Sunil U. Bajad, and Joseph R. Kurian
Current Protocols in Toxicology (2005) 4.16.1-4.16.17

196 µl 1.224% human hemoglobin
323 µl distilled water.

Prepare two reaction mixtures per sample, one for a control reading (which will receive no NADH in step 7) and one for an experimental reading.

2. Mix well by vortexing for 1 min.

   The reaction mixture should be amber colored (confirm by drawing up a small aliquot in a glass Pasteur pipet).

3. Add 20 µl of diluted (1:20) red blood cell lysate.

Take readings

4. Transfer to a quartz spectrophotometer cuvette.
5. Incubate 10 min at 37°C. During the incubation period, turn on the visible light source and allow the lamp to warm up.
6. Transfer cuvette to spectrophotometer.
7. Add 50 µl water (for control reading) or 50 µl 2 mM NADH (for experimental reading) to cuvette.
8. Read optical density (OD) at 575 nm at 1-min intervals for 12 min.

Calculate results

9. Discard data for first 2 min.

   For the first 2 min, the reaction rate is nonlinear.

10. Calculate ΔOD (i.e., $OD_{12\ min} - OD_{2\ min}$) for control and NADH-treated samples.
11. Determine enzyme activity using the following formula:

$$\mu\text{mol ferriHb reduced/min/g Hb} = \frac{\Delta\ \text{OD sample} - \Delta\ \text{OD control}}{[\text{Hb}]} \times 238$$

[Hb] is the hemoglobin concentration (in g/dl from co-oximeter measurement; see Support Protocol 1) in the stock RBC lysate. The factor 238 is obtained from the optical density difference between ferrohemoglobin and ferrihemoglobin (1/42), the time over which readings are made (1/10 min), conversion from g/dl to g/ml (100×), and the dilution factor for the stock RBC lysate (1/20 dilution of stock, and diluted again 50-fold in reaction, so 1000×).

SUPPORT PROTOCOL 1

PREPARATION OF RBC LYSATE

Red cell lysates can be used to measure various cytosolic enzyme activities in erythrocytes. This method uses ice-cold distilled water to osmotically disrupt washed red cells.

CAUTION: Human blood should be considered a biohazard; be sure to wear gloves when carrying out this protocol.

Materials

Heparinized blood
Phosphate-buffered saline, pH 7.4 (PBS; *APPENDIX 2A* or purchase from Sigma)
Stabilizing solution (see recipe)

Tabletop centrifuge
1.5-ml amber microcentrifuge tubes
Co-oximeter (Instrumentation Laboratory; *http://www.ilus.com/*)

1. Centrifuge 2 to 10 ml heparinized blood 10 min at 650 × *g*, room temperature, and discard plasma.
2. Add 10 vol PBS to the RBCs, centrifuge 8 min at 1450 × *g*, room temperature, and discard supernatant. Repeat this wash procedure two more times. After final wash, remove as much PBS as possible.
3. Transfer 200 µl of the washed RBCs to a 1.5-ml amber microcentrifuge tube, add 200 µl ice-cold distilled water, and vortex vigorously for 1 min to lyse RBC. Use this RBC lysate immediately (diluting as in step 5) or store up to 2 months (may retain optimal activity longer) at −80°C.
4. Determine hemoglobin (Hb) concentration of 200 µl of the stock lysate (in g/dl) using a co-oximeter in microsample mode, according to manufacturer's instructions.
5. For the ferrihemoglobin reduction assay (see Basic Protocol 1), dilute stock lysate from step 3 1:10 by adding 360 µl stabilizing solution to 40 µl lysate, then centrifuge 20 min at 11,000 × *g*, room temperature, to remove cell debris. Collect the supernatant and further dilute by adding an equal volume of stabilizing solution.

   Thus, the final dilution of the lysate for use in Basic Protocol 1 will be 1:20.

FERRIHEMOGLOBIN REDUCTION ACTIVITY IN MONONUCLEAR LEUKOCYTES

ALTERNATE PROTOCOL

Mononuclear leukocytes predominantly express the membrane-bound forms of cytochrome b_5 reductase and cytochrome b_5. Like soluble forms in RBCs, membrane-bound forms can also reduce the ferrihemoglobin complex. Hence, the same method can be used to determine the level of activity of these enzymes in mononuclear leukocytes. The only difference is that the activity is normalized to the total protein concentration in the cell lysate instead of hemoglobin content.

Additional Materials *(see Basic Protocol 1)*

Leukocytes (PBMC; see Support Protocol 2)
Bath sonicator
Bradford protein assay kit (Bio-Rad)

Prepare PBMC lysate

1. Aliquot 2 × 10^6 leukocytes in a 1.5-ml microcentrifuge tube (amber tubes not necessary).

   Peripheral blood mononuclear leukocytes can be isolated from human blood using any reported protocol. Final cell suspension should be brought up in 100 µl or less, in order to get high protein concentration.

2. Sonicate cells in a bath sonicator for 30 sec, place on ice for 2 min, and repeat two times.
3. Freeze lysate at −80°C for 10 min, then thaw at room temperature.
4. Sonicate again for 30 sec to fully lyse cells.
5. Determine protein concentration of a small aliquot diluted 1:10, using a Bradford assay kit.

   When using the Bio-Rad protein assay kit, use 1 µl lysate plus 9 µl sterile water plus 200 µl Bio-Rad protein assay dye and read OD at 570 nm. Use human albumin, up to 1.0 mg/ml, for the standard curve.

Determine enzyme activity

6. Perform the enzyme assay (see Basic Protocol 1) except use PBMC lysate in place of RBC lysate.

   If more than 20 μl of cell lysate is needed to provide 50 μg protein, the volume of water included in the reaction mixture can be reduced accordingly to maintain a total final reaction volume of 1 ml.

7. Calculate enzyme activity based on the following formula (modified from that used in Basic Protocol 1):

$$\mu\text{mol ferriHb reduced/min/mg protein} = \frac{\Delta \text{ OD sample} - \Delta \text{ OD control}}{420} \times 20$$

   The factor 420 reflects the optical density difference between ferrohemoglobin and ferrihemoglobin (1/42) and the time over which the readings are made (1/10 min). The factor 20 converts 50 μg of added protein to 1 mg.

SUPPORT PROTOCOL 2

ISOLATION OF PERIPHERAL BLOOD MONONUCLEAR CELLS

The method below may be used to prepare leukocytes (peripheral blood mononuclear cells; PBMC) used in the Alternate Protocol and Basic Protocol 2.

CAUTION: Human blood should be considered a biohazard; be sure to wear gloves when carrying out this protocol.

Materials

Heparinized whole blood from subject of interest, freshly obtained
Hanks' Balanced Salt Solution (HBSS; *APPENDIX 2A*) containing 5 mM EDTA, pH 7.4
Lymphocyte Separation Medium (LSM; Mediatech Inc.)
ACK lysis buffer (Cambrex Biosciences; *http://www.cambrex.com*)
Phosphate-buffered saline (PBS; *APPENDIX 2A*)

50-ml conical centrifuge tubes
Tabletop centrifuge

Perform density gradient separation

1. Place 10 ml heparinized whole blood from subject of interest in a 50-ml conical centrifuge tube. Dilute blood to a total volume of 30 ml with HBSS containing 5 mM EDTA, pH 7.4.

   Smaller volumes of blood can be used, but do not scale down the other reagents.

2. Underlay blood slowly with 10 ml Lymphocyte Separation Medium.
3. Centrifuge 18 min at 600 × *g*, room temperature.
4. Remove plasma layer to within 1 cm of the white buffy coat containing mononuclear leukocytes.
5. Transfer the buffy coat gently into a fresh 50-ml conical tube.

   Inclusion of some red blood cells and plasma is not detrimental.

Lyse red blood cells

6. Dilute the buffy coat to 50 ml with HBSS containing 5 mM EDTA, pH 7.4.
7. Centrifuge 7 min at 250 × *g*, room temperature, to pellet the leukocytes. Discard the supernatant.

8. Add 2 ml of AKC lysing buffer to the cell pellet to lyse any residual red blood cells. Resuspend by gentle manual rocking. Incubate 3 min at room temperature.

Isolate PBMC

9. Dilute cell pellet to 50 ml with HBSS containing 5 mM EDTA, pH 7.4.

10. Centrifuge 7 min at 250 × *g*, room temperature. Discard supernatant. Resuspend cells in any buffer as required for subsequent use. For ferrihemoglobin reduction (Alternate Protocol), resuspend PBMC in 100 ml PBS, pH 7.4.

QUANTITATIVE REVERSE TRANSCRIPTASE POLYMERASE CHAIN REACTION FOR EXPRESSION OF CYTOCHROME b_5 REDUCTASE AND CYTOCHROME b_5

BASIC PROTOCOL 2

Quantitative reverse transcriptase polymerase chain reaction (qRT-PCR) is the most sensitive technique for the detection and quantification of mRNA expression. Quantification of mRNA using qRT-PCR can be performed using several different methodologies, and many kits are available. For this protocol, mRNAs for cytochrome b_5 reductase (b_5R) and cytochrome b_5 (cyt b_5) are quantified using SYBR Green dye (Molecular Probes) as a reporter, because it is simple to use, sensitive, and inexpensive. To compensate for variations in pipetting, RNA quality, or efficiency of reverse transcription, an endogenous control must also be amplified, such as 18S rRNA used in this protocol. For final calculation of the amount of mRNA in original samples, the relative standard curve method is used.

Materials

Source for RNA: e.g., peripheral blood mononuclear cells (PBMC; see Support Protocol 2)
RNA-preserving solution: e.g., RNA*later* (optional; Ambion)
Phosphate-buffered saline, pH 7.4 (PBS; *APPENDIX 2A*)
RNA isolation kit: e.g., RNAqueous-4PCR (Ambion)
DNase/RNase-free H_2O
cDNA preparation kit: e.g., SYBR Green PCR/RT-PCR kit (Applied Biosystems)
Primers (prepare in DNase/RNase-free H_2O; store in aliquots at −20°C):
  6.66 μM 18S rRNA forward primer: 5′-CGCCGCTAGAGGTGAAATTCT-3′
  6.66 μM 18S rRNA reverse primer: 5′-CGAACCTCCGACTTTCGTTCT-3′
  10.0 μM b_5R forward primer: 5′-AGGGCAAAGGGAAGTTCGCCAT-3′
  10.0 μM b_5R reverse primer: 5′-ACAGACTTCACTGTCCTGATGATA-3′
  10.0 μM cyt b_5 forward primer: 5′-CTGCACCACAAGGTGTACGA-3′
  10.0 μM cyt b_5 reverse primer: 5′-ACCTCCAGCTTGTTCCCTTA-3′
UV spectrophotometer
DNase/RNase-free pipet tips with filters
250-μl clear DNase/RNase-free tubes
Standard thermal cycler (for reverse transcription)
96-well PCR plates (e.g., Bio-Rad)
Real time PCR cycler (e.g., Bio-Rad iCycler)
Optical quality sealing tape (e.g., Bio-Rad)
Tabletop centrifuge with microtiter plate carrier

Isolate mRNA prepare cDNA

1. Isolate cells of interest (see Support Protocol 2).

   If RNA is not to be used on the same day, cells can be stored in an RNA-preserving solution such as RNAlater (Ambion) using the kit protocol (i.e., resuspend cells of interest in small volume of PBS and add 5 to 10 volumes of RNAlater). Store cells at 4°C for use within 1 month, or at −20°C or −80°C for longer periods.

2. Isolate total RNA using RNAqueous-4PCR kit according to the manufacturer's instructions.
3. Dilute an aliquot of the isolated RNA such that the concentration will be appropriate for measuring the OD_{260}/OD_{280} ratio, e.g., if the volume of isolated RNA in solution is 100 µl, dilute 30 µl to a volume of 600 µl with DNase/RNase-free water.
4. Using a UV spectrophotometer, read the OD of the diluted sample at 260 nm and then at 280 nm.

   The ratio OD_{260}/OD_{280}, indicating the purity of nucleic acid relative to protein contamination, should be between 1.8 and 2.1.
5. Calculate concentration of RNA in microgram/milliliter as:

   $OD_{260} \times$ dilution factor (see step 3) $\times$ 40.

   Nucleic acid at a concentration of 40 µg/ml gives an OD of 1 at 260 nm.
6. On the same day that the RNA is prepared, prepare cDNA using 250 ng RNA and the SYBR Green PCR/RT-PCR kit, according to the manufacturer's instructions. Store cDNA (in 20-µl aliquots) at −20°C until further use. Prepare negative-control cDNA using either no reverse transcriptase or no RNA.

Perform real-time quantitative PCR

7. Place the SYBR Green master mix (stored at 4°C) from the PCR/RT-PCR kit on ice. Calculate the total volume required for the experiment by multiplying the number of samples in duplicate/triplicate by 13 µl. Transfer this volume (plus ~10% extra) to a transparent 250-µl DNase/RNase-free tube on ice.

   The SYBR Green master mix contains buffer, nucleotides, and Taq DNA polymerase for the PCR reaction. Transferring the needed amount of master mix to a separate tube allows one to avoid contamination of the stock solution, and will also allow closer observation during pipetting to avoid bubble formation.
8. Place a 96-well PCR plate on a 96-well plate stand or a clean surface within a biosafety hood.

   If there are very few samples, it is possible split the PCR plate along the perforations and keep the remaining part for future use. Because the outer wells give variable results due to sample evaporation, select the inner wells to load the samples. Try to keep the layout simple by selecting one row for one gene.

   The PCR plate should be prepared in a biosafety hood to avoid aerosolized contamination.
9. Thaw primer stocks and dilute 1:10 with DNase/RNase-free water (e.g., 10 µl primer stock plus 90 µl water). Thaw cDNA (from step 6) and dilute 20 µl cDNA sample with 20 µl DNase/RNase-free water.
10. Add the following reagents to each well in the order indicated:

    12.5 µl SYBR Green master mix
    3.75 µl forward primer (diluted per step 9)
    3.75 µl reverse primer (diluted per step 9)
    5.00 µl diluted cDNA (from step 9).

    Adding reagents in the order indicated will help preserve the valuable cDNA sample in case of pipetting error while adding other reagents.

    The volume of cDNA solution added here (5.00 µl) should contain ~12.5 ng of cDNA if reverse transcription from 250 ng RNA was complete.

    Include controls with water, or with "cDNA" prepared using no reverse transcriptase or no RNA (see step 6).

11. Cover all wells in the plate with optical tape as follows. Carefully peel off white paper backing from the optical tape while holding the backing tabs on each end of the tape. Save the paper backing. Hold the outer tabs of the transparent tape with the sticky side facing down. Place the sticky side of the tape on the plate while stretching it slightly, so that the whole plate is covered.

    Do not touch the inner surface of the tape (fingerprints will obstruct the fluorescence signal that passes through it during data acquisition). The backing tabs should be outside the plate. Do not touch the covered plate.

12. Use the peeled-off paper backing to press the film down over the surface of the plate by smoothing the shiny side of the backing against the plate surface. Press firmly with fingers so that all wells are smoothly covered.

13. Centrifuge 5 min at 270 × *g*, room temperature, then transfer the plate to the thermal cycler.

14. Perform PCR using the following cycling parameters:

1 cycle:	3 min	95°C	(initial denaturation)
40 cycles:	30 sec	95°C	(denaturation)
	60 sec	60°C	(annealing).

    These parameters have been optimized for 18S, b_5R, and cyt b_5 in order to increase sensitivity, reduce primer dimers, and obtain reproducible results.

    Real time PCR measures RNA message levels indirectly by determining the number of cycles a sample requires to exceed an arbitrary threshold of fluorescent PCR product. The number of cycles (C_t) is related to original copy number (RNA after conversion to cDNA) by means of a standard curve of C_t at various dilutions of known quantities of cDNA.

Prepare standard curves for 18S, b_5R, and cyt b_5

15. Use 500 ng of RNA to prepare cDNA (see step 6).

    More starting RNA is used to make cDNA for a standard curve than for a single subject assay.

16. Perform serial dilutions of the cDNA sample to have at least six concentration points on each standard curve, covering the expected range of message in the samples (for example, 1:1, 1:2, 1:4, 1:8, 1:16, and 1:32).

17. Perform quantitative real-time PCR on the serial dilutions using the cycling parameters in step 14.

18. Plot log total RNA on the *y* axis and C_t values (number of cycles until copy number exceeds an arbitrary threshold, set by the cycler software) on the *x* axis.

    For individual samples, plug C_t for that sample into the standard curve to quantitate original amount of RNA in ng. To normalize for the efficiency of reverse transcription, divide ng of target RNA by ng of 18S RNA. The resulting data is a dimensionless ratio that reflects relative expression among subjects, tissues, or conditions.

Check for specificity of primers

19. Determine melting curve as programmed into cycler to control for contamination by unrelated amplicons or primer dimers.

    Determination of a melting curve usually involves a gradual increase in temperature in 0.5°C increments from 50° to 100°C. PCR product is monitored for loss of fluorescence, indicating denaturation of double-stranded DNA.

    When change in fluorescence is plotted over time, a single peak should be seen. Additional peaks indicate more than one product, or primer dimers, in the reaction mix.

BASIC PROTOCOL 3

EXPRESSION OF HUMAN RECOMBINANT SOLUBLE CYTOCHROME b_5 REDUCTASE OR CYTOCHROME b_5 IN *E. COLI*

This protocol describes a facile method for expressing and purifying the soluble forms of cytochrome b_5 reductase (b_5R) or cytochrome b_5 (cyt b_5), which have been successfully utilized in reconstitution assays for xenobiotic metabolism in vitro and in the production of polyclonal antibodies in vivo. The following protocol was established using pCR T7 TOPO TA expression vectors with ampicillin resistance. These systems are recommended for b_5R (pCR T7/NT TOPO) and cyt b_5 (pCR T7/CT TOPO) expression. The purification described uses 6×-histidine tags and nickel affinity chromatography. No activity differences were observed with the use of tagged versus untagged proteins in xenobiotic metabolism assays. The following protocol may be used for expression and purification of either b_5R or cyt b_5. Some steps are specific to one or the other protein; these are clearly noted.

Materials

b_5R and cyt b_5 cDNA, human soluble forms (contact the authors at *latrepanier@svm.vetmed.wisc.edu*)
pCR T7 TOPO TA expression vector (Invitrogen): NT or CT
Chemically competent *E. coli*: e.g., One Shot Chemically Competent Cells [BL21(DE3) cells] from Invitrogen
SOC medium (supplied with the One Shot Chemically Competent Cells from Invitrogen)
LB broth (see recipe)
100 mg/ml ampicillin stock solution (see recipe)
10 mM IPTG (see recipe)
Binding buffer, pH 8.0 (see recipe)
Complete Mini Protease Inhibitor Cocktail tablets (Roche Diagnostics; optional)
Lysozyme (Sigma; optional)
Ni-NTA agarose resin (25 ml ethanol suspension; Invitrogen)
Elution solutions 1, 2, and 3 (see recipe)
SDS-PAGE loading buffer: add 50 µl 2-mercaptoethanol (Sigma) to 950 µl Laemmli sample buffer (Bio-Rad); prepare fresh for each purification
Tris-HCl precast polyacrylamide gels (Bio-Rad) compatible with Mini PROTEAN 3 Electrophoresis Cell: 12% gel (for b_5R expression) or 15% (for cyt b_5 expression)
1× Tris-glycine electrode buffer (see *UNIT 2.2* for 10× buffer)
Phosphate-buffered saline, pH 7.4 (PBS; *APPENDIX 2A* or purchase from Sigma)
Bradford protein assay kit (Bio-Rad)
2 mM hemin (see recipe)
QIAprep Plasmid Prep kit (Qiagen)
42°C water bath
37°C warm room with rotary shakers
100- and 2000-ml Erlenmeyer flasks, sterile
250-ml culture tubes
Refrigerated centrifuge capable of holding 250-ml culture tubes, capable of 12,000 × *g*
Safety goggles and ear plugs
Sonic Dismembranator with microtip attachment (Fisher)
15- or 50-ml conical polypropylene centrifuge tubes
10-ml Poly-Prep columns (Bio-Rad)
0.5-ml microcentrifuge tubes
Mini PROTEAN 3 Electrophoresis Cell (Bio-Rad)
95°C heating block

Dialysis cassettes (Pierce): 10,000 MWCO (for b_5R expression) or 3,500 MWCO (for cyt b_5 expression)
1000-ml beaker
15-ml Centriplus centrifugal concentrators (Millipore): 10,000 NMWL (for b_5R expression) or 3,000 NMWL (for cyt b_5 expression)
Additional reagents and equipment for protein electrophoresis and gel staining (*APPENDIX 3F*) and dialysis and concentration of protein solutions (*APPENDIX 3H*)

NOTE: All solutions and equipment coming into contact with living cells must be sterile, and aseptic technique should be used accordingly.

Prepare plasmid

1. Insert b_5R or b_5 cDNA into the appropriate pCR T7 TOPO TA expression vector (NT for b_5R and CT for b_5) according to the protocols provided by the supplier of the vector. Purify the plasmid using a QIAprep Plasmid Prep kit.

   The b_5R construct should have a N-terminal histidine tag; the cyt b_5 construct should have a C-terminal histidine tag.

   NT is used for b_5 reductase and CT for cyt b_5. The authors chose these empirically because the noncatalytic hydrophobic tail for membrane bound b_5 reductase is N-terminal, and they predicted that a His tag (or any extra tag) on the N-terminus of soluble b_5R would therefore be less likely to interfere with function; conversely, the hydrophobic tail for membrane-bound cyt b_5 is on the C-terminus.

Transform E. coli

2. Add 7 µl of the b_5R– or cyt b_5–containing plasmid preparation to the tube provided with the One Shot Chemically Competent Cells containing 50 µl SOC medium and chemically competent *E. coli*. Mix gently, then incubate on ice 5 to 10 min.

   Do not vortex or pipet up and down.

   There are several chemically competent cell preparations available; for this protocol, BL21(DE3) cells are recommended.

3. Heat-shock the cells for 30 sec in a 42°C water bath, taking care not to shake the tube. Immediately transfer the tube to ice.

4. Add 250 µl of room temperature SOC medium. Cap the tube tightly and shake horizontally on a rotary shaker at ~200 rpm for 45 min at 37°C.

Inoculate bacteria

5. To a sterile 100-ml Erlenmeyer flask, add 10 ml of LB broth, 10 µl of 100 mg/ml ampicillin stock (final concentration in broth, 100 µg/ml), and the transformed *E. coli* cells from the transformation steps (see step 4). Shake at ~200 rpm on the rotary shaker for 18 hr at 37°C.

   The culture will become cloudy. This step may be extended if the culture has not become cloudy.

6. After 18 hr, increase the culture size by adding the entire culture from step 5 to a sterile 2000-ml Erlenmeyer flask containing 1000 ml LB broth and 1 ml of 100 mg/ml ampicillin stock.

   After autoclaving the medium, culture and ampicillin can be added when the outside of the flask is cool enough to be touched.

7. Shake on rotary shaker at ~175 rpm for 4 to 8 hr at 37°C or until the culture becomes cloudy and reaches an optical density of 0.8 at 600 nm. Measure the optical density periodically by sampling 1 ml from the culture and analyzing on a spectrophotometer.

Be careful not to allow the culture to proceed beyond an optical density of 0.8. Protein overexpression and sequestration through lipid vacuolization might otherwise occur during the expression step, which ultimately leads to low protein recoveries.

Express protein

8. Induce expression by adding 10 ml of 10 mM IPTG stock solution (final concentration 100 μM). Shake on rotary shaker at ~200 rpm for 16 hr at room temperature.

   Culture with b_5R will become pale yellow; culture with cyt b_5 will become orange.

9. Transfer cultures to 250-ml culture tubes. Centrifuge 10 min at 9000 × *g*, room temperature.

   Cells expressing b_5R will be yellow; cells expressing cyt b_5 will be red.

10. Discard supernatant and resuspend pelleted cells in a minimal amount (e.g., as little as 5 ml per pellet) of binding buffer, pH 8.0. Freeze cells at −80°C.

    Cells may be kept at −80°C for up to 60 days.

    A protease inhibitor cocktail tablet (e.g., Complete Mini Protease Inhibitor Cocktail from Roche Diagnostics) may be added here to protect the overexpressed enzyme from degradation during lysate preparation. Follow manufacturer's suggested protocol for protease inhibition.

Prepare lysate

11. After 10 min (or after storage), thaw the cell suspension by placing tube in a 37°C water bath for 10 min. Freeze cells ≥10 min at −80°C, then thaw again as before to lyse cells.

    Lysozyme may be added to a final concentration 1 mg/ml after thawing to enhance lysis. After lysozyme addition, incubate on ice for 30 min with frequent mixing, then proceed to the next step.

12. Put on safety goggles and ear plugs. Sonicate the cell suspension using a Fisher Sonic Dismembranator with a microtip adaptor, at 30% power. Perform ten repetitions of a cycle of 30-sec sonication bursts followed by 30 sec on ice.

    The microtip should be fully immersed in the lysate but not touching the bottom of the culture tube.

13. Clear the lysates by centrifuging for 20 min at 12,000 × *g*, 4°C, to bring down the cellular debris. Collect supernatant and proceed directly to affinity purification.

    The supernatant with b_5R should be yellow and with cyt b_5 should be red. The pellet usually retains some of its color.

Carry out Ni-NTA batch binding affinity purification

14. Pour an appropriate amount of the ethanol suspension of Ni-NTA agarose resin into a 15- or 50-ml conical polypropylene centrifuge tube.

    A suggested starting point is 1 ml of resin per 5 ml of cleared lysate. The binding capacity of Ni-NTA is 5 to 10 mg of protein per ml of resin. The resin accounts for ~35% of the Ni-NTA/ethanol mixture. If, for example, 3 ml of resin is required, use 3/0.35, or ~8.6 ml, of the Ni-NTA/ethanol mixture.

15. Remove the ethanol by centrifuging the resin 30 to 60 sec at 9000 × *g*, room temperature. Pour off the supernatant (ethanol) and resuspend the resin in an equal volume of water. Repeat this wash step three to five times.

16. Equilibrate the resin with binding buffer by centrifuging the resin as described in step 15 pouring off the supernatant (water), and resuspending in an equal volume of binding buffer, pH 8.0. Repeat this step three to five times, then centrifuge the resin, discard the supernatant (binding buffer), and proceed to step 17.

17. Add 5 ml of cleared lysate (from step 15) per 1 ml of resin and mix thoroughly. Slowly agitate the mixture on a rotary shaker 1 hr at 4°C to allow the His-tagged protein to bind to the nickel resin.

18. Centrifuge the resin as described in step 15 and collect the supernatant. Save a portion of the supernatant to determine binding efficiency at a later point.

    At this point the resin should be yellow to green for b_5R and red to purple for cyt b_5.

19. Remove residual (unbound) lysate by resuspending the resin in binding buffer, centrifuging the resin as in step 15, and discarding the supernatant. Repeat this step five times.

20. Resuspend resin in 2 vol elution solution 1 (containing 20 mM imidazole). and transfer suspension to a 10-ml Poly-Prep column for elution.

    For example, if resin is 5 ml, resuspend with 10 ml binding buffer.

21. Allow the resin to fall by gravity to form a packed column with the elution solution on top. Begin collecting 1-ml fractions in numbered glass tubes by opening the bottom of the Poly-Prep column.

22. Continue to pour elution solution 1 onto the column as fractions are being collected. For each milliliter of resin, pour a total of 5 ml of elution solution 1 over the column.

    For example, pour a total of 25 ml of elution solution over 5 ml of packed resin.

23. After a sufficient amount of elution solution 1 has been poured over the column, continue releasing contaminants by switching to elution solution 2 (containing 40 mM imidazole). For each milliliter of resin, pour 3 ml of elution solution 2 over the column.

    For example, pour a total of 15 ml of elution solution 2 over 5 ml or packed resin.

24. Begin eluting the b_5R or cyt b_5 off the resin with elution solution 3 (containing 125 mM imidazole). Continue pouring this solution over the column until the protein is entirely eluted and the resin returns to a light blue color. Store eluted 1-ml fractions at 4°C.

Perform SDS-PAGE purity analysis

25. In separate, numbered 0.5-ml microcentrifuge tubes, add 10 µl of each eluted fraction and 10 µl of SDS-PAGE loading buffer. Vortex each tube and heat at 95°C for 5 min.

26. Load 10 µl of each sample into a separate well of a Tris-HCl precast polyacrylamide gel.

    b_5R samples should be run on a 12% gel; cyt b_5 samples should be run on a 15% gel.

27. Run the gel in a Mini PROTEAN 3 Electrophoresis Cell at 150 V for 90 min, with 1× Tris-glycine electrode buffer as the running buffer.

    APPENDIX 3F provides additional details concerning protein electrophoresis.

28. Stain the gel using a method of choice (*APPENDIX 3F*).

    Coomassie stain (e.g., Bio-Safe Coomassie from Bio-Rad) is recommended for ease of use.

29. Identify the bands of desired purity on the gel. Pool the corresponding eluted fractions from step 24.

    His-tagged soluble b_5R is 36 kDa; His-tagged soluble cyt b_5 is 16.5 kDa.

    The amount of contamination can be estimated as a percentage of total band staining within a specific row of the gel. Usually when contamination bands comprise 10% or less of the total staining in a particular lane, it is determined to be acceptably pure.

30. If b_5R and or cyt b_5 samples are of adequate purity, proceed with the remainder of the protocol. If increased purity is desired, continue with the dialysis steps (through step 35, then repeat Ni-NTA affinity purification (steps 14 to 24).

Repeating affinity purification a second time should result in samples with ≥99% purity as determined by silver staining.

Dialyze and concentrate the purified material

31. Load the pooled eluted samples into a dialysis cassette and equilibrate cassette according to the manufacturer's instructions.

b_5R samples should be dialyzed in 10,000-Da molecular weight cutoff (MWCO) cassettes; cyt b_5 samples should be dialyzed in 3,500-Da MWCO cassettes. Different cassette volumes are available (e.g., 1 to 3 ml or 3 to 12 ml) depending on the sample size.

32. Place the cassette in 900 ml of PBS, pH 7.4, in a 1000-ml beaker. Add a magnetic stir bar, place the beaker on a magnetic stirring plate at 4°C and allow the cassette to rotate for 3 hr.

33. Remove the cassette and place it in a fresh 1000-ml beaker with 900 ml of PBS, pH 7.4. Continue stirring for 3 hr.

34. Remove the cassette and place it in a fresh 1000-ml beaker with 900 ml of PBS, pH 7.4. Continue stirring for 12 hr.

This step can exceed 12 hr and may be done overnight.

35. Collect the sample from the cassette.

36. Concentrate the sample using a Centriplus centrifugal concentrator and refrigerated centrifuge according to the manufacturer's recommendations for the concentrator. Do not concentrate beyond 3 mg/ml protein. Also see *APPENDIX 3H*.

Use a 10,000-Da nominal molecular weight limit (NMWL) device for b_5R, and a 3,000-Da NMWL device for cyt b_5. Manufacturers' rotation force recommendations may vary. Centrifuge the 15-ml Centriplus devices 15 min at 8000 to 9000 × g, 4°C.

37. Collect the supernatant and determine the sample concentration. (e.g., using the Bio-Rad kit for the Bradford method).

38a. *For b_5R:* Store purified b_5R at 4°C (will retain optimal activity up to 3 weeks) or up to 6 months at −80°C. Avoid multiple freeze-thaw cycles.

38b. *For cyt b_5:* Load with hemin as described in the remaining steps.

Load cyt b_5 with hemin

39. Add 2 mM hemin solution to the cyt b_5 sample at a molar ratio of 4:1 hemin/cyt b_5.

Before using cyt b_5 in xenobiotic metabolism assays, it is essential to load the E. coli–expressed protein with the metalloporphyrin that is present in human hemoproteins. Hemin, or chloroprotoporphyrin IX iron (III), is an iron-containing protoporphyrin IX complex with a chloride ion disturbing full coordination of the iron. It is a precursor to the endogenously active heme, which is the moiety responsible for hemoprotein activity. The hemin chloride ion is lost during incorporation into cyt b_5, resulting in full coordination of the iron and conversion of hemin to heme. This conversion is the ultimate step in activating E. coli–expressed human cyt b_5.

40. Lightly vortex the mixture, then place it on a rotary shaker at 4°C overnight.

41. Remove excess hemin with a 15-ml 3,000 NMWL Centriplus concentrator and refrigerated centrifuge according to the manufacturer's recommendations for the concentrator, centrifuging 10 min at 8000 to 9000 × g, 4°C.

Alternatively, dialysis may be performed as described in steps 31 to 35 to remove excess hemin. However, the time allowed for dialysis should be doubled in each step (i.e., 3 hr becomes 6 hr and 12 hr becomes 24 hr).

42. Determine concentration of cyt b_5 again as in step 37.

43. Store purified cyt b_5 at 4°C; it will retain optimal activity for 3 weeks. Alternatively, store up to 6 months at −80°C. Avoid multiple freeze-thaw cycles.

REAGENTS AND SOLUTIONS

Use Milli-Q-purified water or equivalent in all recipes and protocol steps. For common stock solutions, see ***APPENDIX 2A****; for suppliers, see* ***SUPPLIERS APPENDIX****.*

Ampicillin stock solution, 100 mg/ml

Dissolve 0.5 g ampicillin in 5 ml distilled water to prepare 100 mg/ml stock. Store in 1-ml aliquots up to 6 months at −20°C.

Binding buffer, pH 8.0

Dissolve 2.4 g NaH_2PO_4 and 23.376 g NaCl in 1 liter of distilled water. Adjust pH to 8.0. Store up to 60 days at 4°C.

Final concentrations are 20 mM NaH_2PO_4 and 400 mM NaCl.

Elution solutions

Elution solution 1 (20 mM imidazole): Add 667 µl of 3 M imidazole stock (see recipe) to 100 ml binding buffer, pH 8.0 (see recipe).
Elution solution 2 (40 mM imidazole): Add 1.33 ml of 3 M imidazole stock (see recipe) to 99 ml of binding buffer, pH 8.0 (see recipe).
Elution solution 3 (125 mM imidazole): Add 4.17 ml of 3 M imidazole stock (see recipe) to 96 ml of binding buffer, pH 8.0 (see recipe).
Elution solutions 1, 2, and 3 may be stored up to 60 days at 4°C.

Hemin, 2 mM

Dissolve 0.130 g hemin (>99% purity; Sigma) in 10 ml dimethyl sulfoxide (DMSO). The solution will be dark blue. Prepare fresh for each purification.

Human hemoglobin, 1.224% (w/v)

Dissolve 0.1224 g purified human hemoglobin (Sigma) in 10 ml warm water and vortex for 10 min. Do not keep on ice, as a precipitate may form. Prepare fresh.

Imidazole stock solution, 3 M

Dissolve 20.424 g imidazole in 100 ml distilled water. Adjust pH to 8.0 using 1 M NaOH. Store up to 60 days at 4°C.

The solution will be light yellow at this concentration.

Isopropyl β-D-thiogalactopyranoside (IPTG), 10 mM

Dissolve 0.119 g IPTG in 50 ml distilled water. Store in 11-ml aliquots up to 6 months at −20°C, protected from light.

Luria Bertani (LB) Broth

Dissolve one LB broth tablet (Sigma) per 50 ml distilled water and sterilize by autoclaving. Add ampicillin solution after flask has cooled to touch as described in Basic Protocol 3. Use broth within 24 hr of preparation.

Alternatively, make the broth by combining 10 g tryptone, 5 g yeast extract (both available from Fisher), 10 g NaCl, 200 µl of 5 N NaOH, and 1 liter of water. Sterilize the broth and add ampicillin solution as described above. Use within 24 hr of preparation.

Sodium citrate buffer, pH 4.7 (50 mM)

Dissolve 2.1 g citric acid (anhydrous) and 2.94 g sodium citrate dihydrate in 990 ml water. Adjust the pH to 4.7 using 10 M HCl, and bring the volume to 1 liter with distilled water. Store up to 1 week at 4°C.

Stabilizing solution

0.01 ml 2-mercaptoethanol
2 ml of 10% (w/v) disodium EDTA, pH 7.0
198 ml H_2O
Store up to 1 week at 4°C

Prepare the 10% EDTA stock solution by combining 10 g disodium EDTA with 100 ml distilled water and adjusting the pH to 7.0 using 1 M NaOH.

COMMENTARY

Background Information

NADH cytochrome b_5 reductase (b_5R; EC 1.6.2.2; diaphorase I; NADH:ferricytochrome b_5 oxidoreductase) is a FAD-containing protein with soluble and membrane-bound forms, each the product of the same gene through alternative promoters and alternative splicing (Tomatsu et al., 1989; Leroux et al., 2001). The hemoprotein cytochrome b_5 (cyt b_5) is also expressed in soluble and membrane-bound forms and is also the product of a single gene (Giordano and Steggles, 1991). The cyt b_5 and b_5R proteins together mediate electron transfer from NADH to fatty acid desaturases (Oshino et al., 1971) and P450 oxidases (Hildebrandt and Estabrook, 1971). In erythrocytes, these enzymes play a primary role in maintaining hemoglobin in its reduced state (Hultquist and Passon, 1971). In addition, b_5R mediates the reduction of the partially oxidized form of ascorbate, ascorbyl free radical, back to ascorbate (Ito et al., 1981; Shirabe et al., 1995). The cyt b_5 and b_5R proteins also appear to directly catalyze the reduction of hydroxylamine and amidoxime metabolites (Kurian et al., 2004). The described techniques can be used to evaluate variability in the expression and/or activity of this pathway.

Critical Parameters and Troubleshooting

Ferrihemoglobin reduction as a marker of cytochrome b_5 reductase activity

If poor activity is seen overall in Basic Protocol 1 or the Alternate Protocol, consider the following measures.

1. Prepare fresh potassium ferricyanide.
2. Prepare fresh NADH. NADH degrades in solution at room temperature and should not be used more than 1 hr after preparation.
3. Warm all the solutions to 37°C.
4. Make sure that the purified hemoglobin is not kept on ice.

qRT-PCR for expression of cytochrome b_5 reductase and cytochrome b_5

Quality of RNA is of the utmost importance in carrying out Basic Protocol 2, as contamination by genomic DNA leads to inaccurate results. The RNA elution solution (a component of the RNA isolation kit) should be heated to 95° to 100°C prior to use. For pipetting the DNase-inactivating agent (another component of RNA isolation kit used in step 2 of Basic Protocol 2), use a pipet tip with a broad opening (such as a 10- to 20-µl tip, as opposed to a 1- to 10-µl tip; the tip may be trimmed to widen the end). It is important that the white slurry be uniformly suspended during pipetting.

Because small volumes of reagents must be pipetted, pipettors should be calibrated regularly. Also, tips should be changed whenever residual volume is noted between samples; a small change in pipetting volume can result in variable data due to the high sensitivity of the assay.

If the C_T values become higher than those originally obtained with fresh reagents, the reverse transcriptase used for cDNA preparation may be degraded. Repeat cDNA preparation with fresh RT enzyme.

Expression of human recombinant soluble cytochrome b_5 reductase or cytochrome b_5 in E. coli

For problems that may arise in purification (Basic Protocol 3), along with their possible causes and solution, see Table 4.16.1.

Table 4.16.1 Troubleshooting Guide for Cytochrome b_5 Reductase or Cytochrome b_5 Expression

Problem	Possible cause	Solution(s)
Culture did not become cloudy (E. coli cell population has not grown)	Cells may have been too violently disturbed during transformation	Be gentle while introducing the plasmid to the cells.
	Ampicillin concentration may be too high	Make sure the final concentration of ampicillin in the LB broth is 100 μg/ml.
	Rotary shaker may have been turned off for extended periods (e.g., in a common equipment room)	Resume incubation with shaking.
	Incubation times may be too short or temperatures may be too high or too low	Confirm suggested time and temperature ranges for incubation from the protocol.
Pelleted cells are not expected color (expression has not occurred)	IPTG solution not optimal	Check IPTG concentration. Make sure IPTG has not expired. Make sure IPTG was not exposed to light prior to induction.
	Induction was not optimal	Make sure induction time, temperature, and IPTG concentrations were as specified.
		Make sure culture optical density was between 0.6 and 0.8. Low expression may be a result of too few cells containing the expression plasmid.
Lysate supernatant is not expected color	*E. coli* cells were not fully lysed	Increase the number of cycles of sonication with the microtip sonicator. Also, try adding lysozyme during lysate preparation.
	Overexpressed proteins were liposome-encapsulated and therefore inaccessible	Do not allow cultures to grow beyond an optical density of 0.8 and do not allow induction to proceed beyond 16 hr. Also, do not induce at temperatures >25°C.
Resin not expected color after batch binding (protein does not bind resin)	Resin is not equilibrated to the binding buffer (pH 8)	Optimal histidine tag in nickel affinity chromatography is at pH 8.0 (due to the pK_a of histidine). Be certain to follow the protocol for Ni-NTA resin equilibration.
	b_5R or cyt b_5 histidine tag is not accessible	b_5R should be N-terminally histidine tagged and cyt b_5 should be C-terminally tagged
b_5R or cyt b_5 do not elute	Imidazole concentration is too low in elution buffer	Make sure that the imidazole stock solution is 3 M, not expired (past 60 days), and not precipitated. If precipitated, warm the solution slightly and stir until the precipitate is dissolved. Follow suggested protocol for preparing elution solution.

continued

Table 4.16.1 Troubleshooting Guide for Cytochrome b_5 Reductase or Cytochrome b_5 Expression, continued

Problem	Possible cause	Solution(s)
b_5R or cyt b_5 elute with contaminants, before final elution buffer is poured over column	Less than optimal conditions; binding buffer may not be exactly at pH 8.0; elution solutions may not be the specified concentration or pH; and fewer than normal contaminants may interfere with expected imidazole-to-column interaction[a]	Make sure that buffers and elution solutions are at correct pH values. Use elution solution concentrations as relatively firm guidelines. Adjust imidazole concentrations as necessary.
		Decrease lysate:resin ratio (e.g., to 2:1).
Protein has lost activity	Protein's active life has expired	Both proteins should maintain optimal activity for 3 weeks when stored at 4°C; do not use beyond this point.
	Proteins stored at too high a concentration may precipitate	Store proteins at ≤3 mg/ml (between 0.5 and 3 mg/ml is optimal).

[a]Fewer than normal contaminants mean that the lysate may not contain the expected amount of contamination and consequently contains significantly more b_5 or b_5R. Less contaminants mean that the column can overload with the protein of interest and leave fewer sites for excess protein of interest to interact with the column. Also, the interactions tend to be less specific, as many single proteins converge on one column bead. As a result, when contamination should be eluted, the desired protein may actually begin to elute. This is actually a very rare situation.

Anticipated Results

Ferrihemoglobin reduction as a marker of cytochrome b_5 reductase activity

Reported normal values for NADH cytochrome b_5 reductase activity in adults are 3.4 ± 0.5 μmol FerriHb reduced/min/g Hb (Beutler, 1975). However, when using pure hemoglobin (see Basic Protocol 1), the mean activity that the authors have obtained is 4.6 ± 1.0 μmol FerriHb reduced/min/g Hb. For mononuclear leukocytes (see Alternate Protocol), preliminary data suggest a range of 10 to 20 nmol FerriHb reduced/min/μg protein in normal human subjects.

Although factors that affect the expression of cytochrome b_5 and its reductase have not been well studied, ascorbate deficiency, malarial infection, and antithyroid and neuroleptic drugs have been reported to affect the expression and/or activity of this pathway.

qRT-PCR for expression of cytochrome b_5 reductase and cytochrome b_5

Using the method described in Basic Protocol 2, the efficiency of the PCR reaction for all the three genes [efficiency = $10^{(-1/\text{slope})}$–1] is between 90% and 100% (where slope is that of the standard curve). The standard curves (log total RNA on *y* axis and C_T values on *x* axis) for all three genes are also linear up to a 32-fold dilution.

The range of C_T values obtained for different genes in experimental samples is: 10 to 15 for 18S RNA, 28 to 35 for b_5R, and 30 to 40 for cyt b_5.

Using the C_T value for a given sample, determine the corresponding log RNA concentration from the appropriate standard curve equation. Calculate the inverse log to obtain an RNA value. Finally, divide the values obtained for b_5R or cyt b_5 RNA by the values obtained for 18S rRNA for normalization. Report the values as RNA normalized for 18S rRNA.

Melting curve analysis is performed to check the specificity of the reaction; most instruments have protocols installed in the software for doing this. Melting curve analysis should indicate only one peak for each gene.

Expression of human recombinant soluble cytochrome b_5 reductase or cytochrome b_5 in E. coli

Average amounts of purified enzyme recovered per liter of initial culture are 8 to 10 mg for b_5R and 10 to 12 mg for cyt b_5. The lower value in this range refers to the amount expected after repeating the Ni-NTA affinity purification a second time to achieve a >99% pure enzyme. The higher value in the range is expected after one column purification, which results in a >95% pure enzyme.

Time Considerations

Ferrihemoglobin reduction as a marker of cytochrome b_5 reductase activity

Isolation of RBCs, and preparation of lysate (Support Protocol 1) and reagents takes ∼1 hr. Analysis of each patient sample (with and without NADH; Basic Protocol 1) takes 30 to

35 min. overall. To save time, start preparing another sample while the previous one is being read in the spectrophotometer.

qRT-PCR for expression of cytochrome b_5 reductase and cytochrome b_5

Basic Protocol 2 as a whole takes 1.5 days. On day 1, isolate PBMCs, isolate RNA, and prepare cDNA. On day 2, prepare PCR plate and perform the run. The protocol for PCR cycling takes ~2.5 hr. Additional time is required if a melting curve is also being performed. If the qRT-PCR instrument is a shared facility, a total of 3 to 4 hr should be booked.

Expression of human recombinant soluble cytochrome b_5 reductase or cytochrome b_5 in E. coli

Basic Protocol 3 in its entirety may be comfortably completed over 5 to 6 days. Ideally the protocol should be carried out according to the following timeline.

Day 1: Proceed through inoculation (step 5).

Day 2: Proceed through expression (step 8).

Day 3: Proceed through Ni-NTA Affinity Purification (step 24).

Day 4: Proceed through dialysis and concentration (through step 34).

Day 5: Finish the protocol for b_5R purification (through step 38a), or proceed to hemin loading (see Basic Protocol 3, steps 39 to 42) for the cyt b_5 purification.

Day 6: Finish the protocol for cyt b_5 purification.

After gaining experience with specific techniques, it may be possible to increase efficiency and combine steps from separate days. Alternatively, listed below are several intervals in the protocol where it is possible to pause without adversely affecting results.

1. The pelleted cells obtained after completing expression may be kept at −80°C for up to 60 days before proceeding to lysate preparation.

2. The fractions collected in Ni-NTA affinity purification may be stored at 4°C for up to 7 days before proceeding to dialysis and concentration. However, be aware that if fractions contain purified enzyme at a concentration above 3 mg/ml, precipitation may occur and disturb ultimate recovery.

3. Hemin loading of cyt b_5 is not immediately necessary. Cyt b_5 samples may be stored at 4° or −80°C before hemin loading. However, keep in mind the considerations regarding storage and activity of purified enzymes when deciding whether or not to delay hemin loading.

Literature Cited

Beutler, E. 1975. A Manual of Biochemical Methods. 2nd ed. Grune & Stratton, New York.

Giordano, S. and Steggles, A. 1991. The human liver and reticulocyte cytochrome b_5 mRNAs are products from a single gene. *Biochem. Biophys. Res. Commun.* 178:38-44.

Hildebrandt, A. and Estabrook, R. 1971. Evidence for the participation of cytochrome b_5 in hepatic microsomal mixed-function oxidation reactions. *Arch. Biochem. Biophys.* 143:66-79.

Hultquist, D. and Passon, P. 1971. Catalysis of methaemoglobin reduction by erythrocyte cytochrome b_5 and cytochrome b_5 reductase. *Nature New Biol.* 229:252-254.

Ito, A., Hayashi, S., and Yoshida, T. 1981. Participation of a cytochrome b_5-like hemoprotein of outer mitochondrial membrane (OM cytochrome b) in NADH-semidehydroascorbic acid reductase activity of rat liver. *Biochem. Biophys. Res. Commun.* 101:591-598.

Kurian, J., Bajad, S., Miller, J., Chin, N., and Trepanier, L. 2004. NADH cytochrome b_5 reductase and cytochrome b_5 catalyze the microsomal reduction of xenobiotic hydroxylamines and amidoximes in humans. *J. Pharmacol. Exp. Ther.* 311:1171-1178.

Leroux, A., Vieira, L., and Kahn, A. 2001. Transcriptional and translational mechanisms of cytochrome b_5 reductase isozyme generation in humans. *Biochem. J.* 355:529-535.

Oshino, N., Imai, Y., and Sato, R. 1971. A function of cytochrome b_5 in fatty acid desaturation by rat liver microsomes. *J. Biochem. (Tokyo)* 69:155-167.

Shirabe, K., Landi, M., Takeshita, M., Uziel, G., Fedrizzi, E., and Borgese, N. 1995. A novel point mutation in a 3′ splice site of the NADH-cytochrome b_5 reductase gene results in impaired NADH-dependent ascorbate regeneration in cultured fibroblasts of a patient with Type II hereditary methemoglobinemia. *Am. J. Hum. Genet.* 57:302-310.

Tomatsu, S., Kobayashi, Y., Fukumaki, Y., Yubisui, T., Orii, T., and Sakaki, Y. 1989. The organization and the complete nucleotide sequence of the human NADH-cytochrome b_5 reductase gene. *Gene* 80:353-361.

Internet Resources

http://www.ambion.com/techlib/basics/rtpcr

Web site with basic background for the qRT-PCR technique.

Contributed by Lauren A. Trepanier, Sunil U. Bajad, and Joseph R. Kurian
University of Wisconsin–Madison
Madison, Wisconsin

Measurement of Xenobiotic Carbonyl Reduction in Human Liver Fractions

This unit describes procedures for studying the metabolism of a xenobiotic by human liver carbonyl reducing enzymes. In the body, these enzymes catalyze the phase I reduction of potentially toxic aldehyde and ketone moieties to their respective alcohols, facilitating conjugation and/or excretion. In addition to detoxification, carbonyl reducing enzymes participate in steroid and prostaglandin metabolism, housekeeping, stress response, neurotransmission, mutagenesis, and carcinogenesis. The enzymes that catalyze carbonyl reduction are divided into four superfamilies: medium-chain dehydrogenases/reductases (including alcohol dehydrogenases), aldo-keto reductases, quinone reductases, and short-chain dehydrogenases/reductases (including microsomal and cytosolic carbonyl reductases).

Carbonyl reducing enzymes differ in subcellular location, cofactor dependence, and susceptibility to chemical inhibitors, enabling their characterization with simple in vitro experiments. Generally, the xenobiotic is incubated with pooled human liver microsomes or cytosol in the presence or absence of cofactors. Experimental methods for carbonyl reducing enzymes are similar to approaches for cytochrome P450 enzymes, except for the availability of isoform-specific reagents. Purified enzymes, heterologously-expressed isozymes, and isoform-selective inhibitors are well-characterized and commercially available for cytochrome P450 studies. Analogous protein preparations and reagents are not yet widely available for carbonyl reducing enzymes. Without these materials, it is impossible to identify the specific isoform within a family of carbonyl reducing enzymes responsible for metabolism. A more practical objective is to determine which carbonyl reducing enzyme(s) participates in metabolism, and this is the chief objective of the protocols described in this unit. More definitive studies require recombinant or purified carbonyl reducing enzymes along with detailed enzyme kinetic and inhibition experiments with precise analytical methods for quantitation of metabolites.

NADPH-dependent reactions in microsomes include carbonyl reduction and/or other pathways, including the oxidative pathways catalyzed by cytochrome P450 enzymes. Some of the methods outlined in this unit include conditions for examining P450-mediated reactions concurrently with carbonyl reduction. These experiments incorporate differences in the properties of P450 and carbonyl reducing enzymes in order to evaluate their roles in metabolism, and they include the use of inhibitors, recombinant P450 preparations, and pH dependence.

Basic Protocol 1 outlines preliminary experiments to characterize the cofactor dependence and subcellular location of enzymes involved in metabolism and to optimize reaction conditions. Once metabolism by carbonyl reducing enzymes has been established, chemical inhibitors selective for a family of carbonyl reducing enzymes can aid in distinguishing among their activities (see Basic Protocol 2). Determining the effect of pH on metabolism can help to characterize reactions catalyzed by carbonyl reducing enzymes (see Basic Protocol 3). Finally, recombinant P450 enzyme preparations can be employed to examine cytochrome P450–mediated reactions independently from carbonyl reduction (see Basic Protocol 4).

NOTE: To examine the metabolism of a xenobiotic with the protocols outlined in this unit, an analytical method is required for measurement of the metabolite(s) produced. Most commonly, the xenobiotic (parent) and metabolites are separated chromatographically

Contributed by M. Jane Cox Rosemond
Current Protocols in Toxicology (2005) 4.17.1-4.17.25

by HPLC with UV, radiochemical, or mass spectrometric (MS) detection. Ideally, the identity of the carbonyl reduced product is confirmed by mass spectrometry at some point during the investigations. Analysis of metabolites by HPLC with MS detection is covered in *UNIT 4.4*. Additional HPLC references are provided in the Commentary.

NOTE: The reduction of unsymmetrical ketones to their respective alcohols generates chiral centers. References on the subject of stereochemistry and metabolism are provided in the Commentary, and published investigations in which the stereochemistry of carbonyl reduction was monitored are noted in Table 4.17.7.

BASIC PROTOCOL 1

DETERMINATION OF SUBCELLULAR LOCATION AND COFACTOR DEPENDENCE OF A CARBONYL REDUCING ENZYME

Conduct these preliminary experiments to assess the involvement of particular carbonyl reducing enzymes in metabolism and to establish optimal reaction conditions. Test cytosol with the cofactors NADH or NADPH, and microsomes with NADPH. Most carbonyl reducing enzymes of human liver are active in these conditions (Table 4.17.1). Run, in parallel, control incubations in the absence of added cofactor. Some suggested initial parameters are listed in Table 4.17.2. Once the results from initial experiments are evaluated, adjust parameters (e.g., reaction time and protein concentration) to maximize turnover.

NOTE: Some residual cofactor may be present in subcellular fraction preparations; thus, a small amount of background metabolism may be observed.

NOTE: Wear personal protective equipment (e.g., laboratory coat, safety glasses, gloves) when working with materials derived from human tissue such as human liver subcellular fractions.

Table 4.17.1 Cofactor Dependence and Subcellular Location of Carbonyl Reducing Enzymes[a,b]

Subcellular location	Enzyme superfamily	Enzyme	Cofactor[c]
Cytosol	Medium-chain dehydrogenase/reductase	Alcohol dehydrogenase (ADH)	NAD(H)
	Aldo-keto reductase (AKR)	AKR1A, AKR1B, AKR1C, AKR1D, AKR6, AKR7[d]	NADPH[e]
	Quinone reductase	NAD(P)H:quinone oxidoreductase 1 (NQO1)	NADPH or NADH, interchangeably
		NRH:quinone oxidoreductase (NQO2)	NRH
	Short-chain dehydrogenase/reductase (SDR)	Carbonyl reductase (CR,CBR)	NADPH
Microsomes	SDR	11β-Hydroxysteroid dehydrogenase (11β-HSD)	NADPH

[a] Abbreviation: NRH, dihydronicotinamide riboside.

[b] A general reference for Table 4.17.1 is Oppermann and Maser (2000).

[c] The predominant cofactor for each enzyme system is given.

[d] The following human liver AKR isoforms have been the subjects of some published studies of xenobiotic metabolism: AKR1A1 (aldehyde reductase), AKR1B (aldose reductases), AKR7 (aflatoxin aldehyde reductase), and AKR1C1, 1C2, and 1C4 (dihydrodiol dehydrogenases).

[e] One member of the AKR1C family, AKR1C4, utilizes NADH or NADPH (Atalla et al., 2000).

Table 4.17.2 Suggested Assay Parameters for Preliminary Experiments[a,b]

Component	Conditions
Buffer	100 mM potassium phosphate, pH 7.4
Protein	1 mg/ml
Substrate	1, 10, 100 μM
Cofactor	2 mM NADPH, 2 mM NADH (cytosol) 2 mM NADPH (microsomes) 2 mM NADPH-regenerating system (for reaction times >30 min) 2 mM NADPH (microsomes)
Incubation time	30 min
Temperature	37°C
Controls	0 min, no cofactor

[a]Final concentrations of reaction components are given in the table.
[b]Consult the Commentary section for alternative assay conditions that have been reported in the literature (Table 4.17.7).

Materials

Pooled human liver subcellular fractions (cytosol, microsomes; BD Biosciences, In Vitro Technologies, Xenotech), −80°C
1 M potassium phosphate buffer, pH 7.4 (see recipe)
Cofactors:
2 mM NADH (see recipe)
2 mM NADPH (see recipe)
For NADPH-regenerating system:
Glucose 6-phosphate dehydrogenase (see recipe)
Regenerating system cofactor mixture (see recipe)
1000× xenobiotic substrate solutions (see recipe)
Reagents for stopping reactions (Table 4.17.7)
Chromatography buffers and solutions
Thermomixer or shaking water bath, 37°C
1.5-ml microcentrifuge tubes
Additional reagents and equipment for HPLC and analysis (*UNIT 4.4*)

1. Turn on shaking water bath or Thermomixer and warm to 37°C.
2. Thaw pooled human liver subcellular fractions by gently warming them by hand. Place on ice immediately upon thawing.

   Keep the protein preparations on ice when not in use.

3. Add the following reagents, in order, to a 1.5-ml microcentrifuge tube for a final reaction volume of 1 ml. Minimally, run samples in duplicate; include more replicates depending on reproducibility.

   a. For cytosolic incubations, add:
   789 μl H_2O (779 μl with regenerating system)
   100 μl 1 M potassium phosphate, pH 7.4
   100 μl 10 mg/ml cytosol
   (10 μl 100× glucose-6-phosphate dehydrogenase, with regenerating system)
   1 μl 1000× xenobiotic substrate solution.

   b. For microsomal incubations, add:
   839 μl H_2O (829 μl with regenerating system)
   100 μl 1 M potassium phosphate, pH 7.4

50 µl 20 mg/ml microsomes
(10 µl 100× glucose-6-phosphate dehydrogenase, with regenerating system)
1 µl 1000× xenobiotic substrate solution.

The final volumes of reagents will vary depending on the concentration of protein in the subcellular fraction preparation and the concentration of the xenobiotic substrate achievable based on solubility. Adjust the amount of water for a final volume of 1 ml.

Prepare samples on the laboratory bench at room temperature. If desired, pre-warm samples 5 min at 37°C before initiating reactions.

4. Initiate reactions by the addition of cofactor (10 µl of 0.2 M stock or 10 µl of regenerating system cofactor mixture). For control samples without cofactor, add a 10-µl aliquot of buffer only. Start a timer.

   Add the cofactor droplet to the inside lid of the microcentrifuge tube to control the timing of reactions. To start reactions, close the cap and gently mix the contents by inverting the tube two to three times.

   Alternative ways to start reactions are: (1) initiate reactions with substrate instead of cofactor, or (2) initiate reactions with enzyme if the substrate is sufficiently soluble in the absence of protein and there is no lag in enzyme activity based on temperature.

5. Prepare 0-min control samples. Remove an aliquot (e.g., 100-µl) immediately after adding cofactor. Without delay, add stopping reagent to the 0-min samples and mix.

   Details about stopping reagents are provided in step 7.

   For a rapidly metabolized substrate, remove the 0-min aliquot, then add the stopping reagent followed by the appropriate volume of cofactor (1:100 dilution of cofactor). As an example: remove 100 µl from the 1-ml incubation mixture and place into a 1.5-ml microcentrifuge tube on ice. Add 100 µl of acetonitrile and mix. Then, add 1 µl of cofactor.

6. Incubate the tubes with gentle shaking at 37°C, either in a water bath or Thermomixer (set at 500 rpm). For time-point samples, remove an aliquot (e.g., 100-µl) at the appropriate interval following the initiation of reactions.

   Until the degree of turnover is assessed, extensive sampling at multiple time-points is unnecessary. As an alternative, sample a small number of time-points in addition to the 0-min control (e.g., 5, 30 min).

   Adjust the volume removed at each time-point based on the amount of sample required for analysis. Ensure that the overall incubation volume is sufficient to allow for removal of all time-point samples.

7. Terminate the reactions with an appropriate stopping method, taking into consideration the solubility and stability of the xenobiotic/metabolites (analytes) and the analytical method.

   Common methods for stopping reactions include the addition of organic solvent or rapid acidification or alkalinization, followed by placing the samples on ice. Examples of methods for stopping reactions are provided in the Commentary, Table 4.17.7. In general, the best conditions for stopping reactions will depend on the analytes; usually some optimization is required.

   A suggested stopping procedure is as follows: remove a 100-µl aliquot at each time-point (e.g., 0, 5, 30 min). Add 0.5 to 1× volume of organic solvent (e.g, acetonitrile), vortex to mix, and then incubate for 10 to 15 min at room temperature. Proceed to step 8.

   Increase the volume of organic solvent (up to ~ 3× reaction volume) if a 0.5 to 1× dilution is insufficient to recover analytes. Ensure that the amount of stopping reagent does not excessively dilute the samples and interfere with detection of analytes. Develop an alternative stopping procedure if samples become too dilute.

   In some cases, a solvent extraction procedure may be required to concentrate the analytes. Include an internal standard in the stop solution for samples requiring extraction before

analysis (refer to Table 4.17.7 for examples). An internal standard should have properties distinct from the parent or metabolites to enable its detection independently from other analytes.

Although it is a common practice, placing terminated reactions on ice need not be routine. Some analytes may be insoluble at low temperature, reducing recovery.

Have an appropriate sample processing method in place that allows for optimal recovery of analytes before conducting large-scale experiments. Aim for reproducible recovery of >80%.

8. Centrifuge the terminated reactions 5 min at 17,000 × *g*, room temperature, to remove any precipitate. Remove an aliquot of the supernatant for analysis.

   For radiolabeled substrates, remove two aliquots of supernatant, one aliquot for liquid scintillation counting (for calculation of recovery), and one aliquot for HPLC analysis. For HPLC, inject 10,000 to 15,000 dpm per sample.

9. Repeat experiments, varying parameters such as protein concentration and incubation time, to optimize reaction conditions, achieve maximal turnover and, if preferred, establish conditions for linearity of the reaction rate with respect to protein concentration and time. For example, conduct incubations with protein concentrations ranging from 0.01 to 2 mg/ml. Vary the incubation times from minutes to several hours, depending on turnover. Substitute NADPH-regenerating system for NADPH if reaction times are >30 min due to the instability of NADPH in solution.

   If non-enzymatic substrate conversion is suspected, include the following controls: (1) incubations without protein, and (2) incubations with heat-inactivated enzymes. Heat-inactivate protein preparations by heating 30 min at 60°C (Breyer-Pfaff and Nill, 1995).

USE OF CHEMICAL INHIBITORS IN THE STUDY OF CARBONYL REDUCING ENZYMES

BASIC PROTOCOL 2

Carbonyl reducing enzymes differ in their sensitivity to chemical inhibitors, providing a convenient means of distinguishing between the activities of different enzyme families.

Ideally, conduct inhibition experiments with the substrate concentration at or near the apparent K_m of the reaction. In the absence of a K_m value, select a range of concentrations (e.g., 1, 10, 100 μM). For a xenobiotic in drug development, select a substrate concentration based upon the clinical C_{max}, if known. References about conducting kinetic experiments and K_m determinations are provided in the Commentary.

For convenience, initially test inhibitors at a single concentration (e.g., 100 μM). After assessing the data from preliminary experiments, plan to test at least two different inhibitors of each enzyme family, at two concentrations. Include inhibitors of cytochrome P450 enzymes alongside inhibitors of carbonyl reducing enzymes if P450-mediated metabolism is suspected. As a guide, a list of selected chemical inhibitors of carbonyl reducing enzymes and concentrations is provided in Table 4.17.3. An expanded list of inhibitors with kinetic data provides more choices (Rosemond and Walsh, 2004).

Conduct incubations at the optimal conditions established in preliminary experiments (see Basic Protocol 1, parameters listed in Table 4.17.2). Reagents and procedures are the same as Basic Protocol 1; the only differences are the inclusion of chemical inhibitors and corresponding vehicle controls. For the purpose of illustration, a sample method for a xenobiotic having cytosolic and microsomal NADPH-dependent metabolism is described in this protocol. Carbonyl reducing enzymes of both subcellular fractions can be probed with the inhibition experiments in this protocol. In this example, the K_m of the substrate is 20 μM, incubation time is 15 min, and protein concentration is 1 mg/ml.

Table 4.17.3 Chemical Inhibitors for Studies with Carbonyl Reducing Enzymes[a]

Subcellular location	Enzyme	Selected inhibitors	Suggested concentration range[b]	Suggested vehicle[c]	Selected references
Cytosol	ADH	4-Methylpyrazole[d]	0.6–1 mM	Water	Stone et al., 1995; Shimoda et al., 1998; Walsh et al., 2002
		Cimetidine	0.2–6.4 mM	Water	
	AKR	Flufenamic acid	10–100 μM	Alcohol	Atalla et al., 2000; Rosemond et al., 2004
		Phenolphthalein	10–100 μM	Alcohol	
	NQO1	Dicumarol	0.01–1 mM	Aqueous alkaline	Wu et al., 1997; Long and Jaiswal, 2000; Ross et al., 2000
		Phenindone	0.01–1 mM	Alcohol, alkaline	
	NQO2	Benzo(a)pyrene[e]	0.01–1 mM	DMSO	Wu et al., 1997; Long and Jaiswal, 2000
		Quercetin	0.01–1 mM	DMSO: alcohol	
	SDR (CR)	Menadione	0.01–1 mM	Alcohol	Ahmed et al., 1979; Inaba and Kovacs, 1989; Shimoda et al., 1998; Atalla et al., 2000; Maser et al., 2000; Rosemond et al., 2004
		Quercetin	0.01–1 mM	Alcohol, aqueous alkaline	
		Quercetrin	0.01–1 mM	Alcohol	
		Ethacrynic acid	0.01–1 mM	Alcohol	
Microsomes	SDR (11β-HSD)	Glycyrrhetinic acid	0.1–100 μM	Alcohol	Diederich et al., 2000; Maser et al., 2003; Rosemond et al., 2004
		Chenodeoxycholate	0.1–100 μM	Alcohol	
	P450[f] (for comparison)	Aminobenzotriazole (ABT)	1–5 mM	Water	Ortiz de Montellano et al., 1984; Trivier et al., 1993; Dalmadi et al., 2003; Turpeinen et al., 2004
		Proadifen (SKF525A)	0.1–1 mM	Water	
		Metyrapone	0.2–2 mM	Water	

[a] Abbreviations: ADH, alcohol dehydrogenase; AKR, aldo-keto reductase; CR, carbonyl reductase; 11β-HSD, 11β-hydroxysteroid dehydrogenase; NQO1, NAD(P)H:quinone oxidoreductase 1; NQO2, NRH:quinone oxidoreductase; SDR, short-chain dehydrogenase/reductase.

[b] A wide range of inhibitor concentrations is proposed where specific references for human liver enzymes were not found.

[c] The suggested vehicle is based on information from The Merck Index (Budavari, 1996) or the listed reference.

[d] 4-Methylpyrazole inhibits class I ADH isozymes only.

[e] CAUTION: Benzo(a)pyrene is a suspected carcinogen (Budavari, 1996).

[f] Monoclonal antibodies have been employed as inhibitors of cytochromes P450. For reference, see Gelboin et al. (1999) and Donato and Castell (2003).

NOTE: Some inhibitors (e.g., quercetin) and substrates of carbonyl reducing enzymes (e.g., warfarin, haloperidol, and metyrapone) are also inhibitors of P450. Consider the possibility of coincident P450 inhibition when evaluating experimental results from microsomes.

Materials

Pooled human liver subcellular fractions (cytosol, microsomes; BD Biosciences, In Vitro Technologies, Xenotech)
1 M potassium phosphate buffer, pH 7.4 (see recipe)
1000× inhibitor solution (see Table 4.17.3 and recipes):
For cytosol:
Phenolphthalein, flufenamic acid (AKR probes)
Menadione, quercetrin (CR probes)
For microsomes:
Glycyrrhetinic acid, chenodeoxycholate (11β-HSD probes)
Aminobenzotriazole (P450 probe)
Vehicle solutions (solvent for dissolving inhibitors, to be tested as controls):

1000× xenobiotic substrate solution (see recipe)
Reagents for stopping reactions (see Table 4.17.7)
Chromatography buffers and solutions
Cofactors: 2 mM NADPH (see recipe)

Thermomixer or shaking water bath, 37°C
1.5-ml microcentrifuge tubes

Additional reagents and equipment for HPLC and analysis (*UNIT 4.4*)

1. Turn on water bath or Thermomixer and warm to 37°C.
2. Thaw pooled human liver subcellular fractions by gently warming them by hand. Place on ice immediately upon thawing.

   Keep the protein preparations on ice when not in use.

3. Add the following reagents, in order, to a 1.5-ml microcentrifuge tube for a final reaction volume of 1 ml. Minimally, run samples in duplicate; include more replicates depending on reproducibility.

   a. For cytosolic incubations, add:
   788 µl H_2O
   100 µl 1 M potassium phosphate buffer, pH 7.4
   100 µl 10 mg/ml cytosol
   1 µl 1000× inhibitor or vehicle
   1 µl 1000× xenobiotic substrate solution (20 mM stock, in this example).

   b. For microsomal incubations, add:
   838 µl H_2O
   100 µl 1 M potassium phosphate buffer, pH 7.4
   50 µl 20 mg/ml microsomes
   1 µl 1000× inhibitor or vehicle
   1 µl 1000× xenobiotic substrate solution (20 mM stock, in this example).

   If preferred, preincubate samples with the inhibitor by warming samples for 5 min at 37°C after the addition of inhibitor. Then, add the substrate followed by cofactor.

4. Perform Basic Protocol 1, steps 4 to 9. Initiate the reactions with cofactor or buffer (for controls) and incubate samples. After a 15-min incubation (in this example), terminate reactions, then process and analyze the samples.

   If inhibitor stock solutions are prepared in several solvents, the total number of vehicle controls can be reduced by running the vehicle solution containing the highest concentration of organic solvent. For example, if one inhibitor is dissolved in DMSO/water (1:1), and another inhibitor is dissolved in 100% DMSO, then run only the 100% DMSO control. There should be no interference from solvent alone if the overall concentration of organic solvent from the addition of substrate and inhibitor is in the range of 0.1% to 0.2%.

DETERMINING pH DEPENDENCE OF CARBONYL REDUCING ENZYMES

BASIC PROTOCOL 3

Many cytosolic carbonyl reducing enzymes have acidic pH optima in the range of pH 5.5 to 6.5 (Table 4.17.4). Also, many carbonyl reducing enzymes function reversibly as oxidoreductases, or dehydrogenases. NADPH-dependent carbonyl reducing enzymes function in the reductive direction at physiological pH but will function oxidatively at alkaline pH (>10) and high substrate concentration (Felsted and Bachur, 1980). References for studies in which both reactive directions were investigated are noted in the Commentary (Table 4.17.7).

Table 4.17.4 Comparison of pH Optima and Reactions Catalyzed by Human Liver Carbonyl Reducing Enzymes[a]

Subcellular location	Enzyme	Cofactor[b]	pH optimum[c]	Function[d]	Selected references[e]
Cytosol	ADH	NAD^+	7.5–10.5	Oxidation of alcohols; reduction of quinones	Blair and Vallee, 1966
	AKR	NADPH	5.5–6.5	Reduction of endogenous and xenobiotic carbonyls, C-C double bonds	Felsted and Bachur, 1980; Atalla et al., 2000
	NQO1	NAD(P)H	7.0–7.4	Two-electron reduction of quinones	Ross et al., 2000
	NQO2	NRH	7.0–7.4	Two-electron reduction of quinones	Long and Jaiswal, 2000
	CR	NADPH	5.5–6.5	Reduction of endogenous and xenobiotic carbonyls	Felsted and Bachur, 1980; Forrest and Gonzales, 2000
Microsomes	11β-HSD	NADPH	7.4	Reduction of endogenous and xenobiotic carbonyls	Maser et al., 2003
	P450 (for comparison)	NADPH	7.4	Several types of oxidative reactions; endogenous and xenobiotic substrates	Guengerich, 2004

[a]Abbreviations: ADH, alcohol dehydrogenase; AKR, aldo-keto reductase, CR, carbonyl reductase; 11β-HSD, 11β-hydroxysteroid dehydrogenase; NQO1, NAD(P)H:quinone oxidoreductase 1; NQO2, NRH:quinone oxidoreductase 2; NRH, dihydronicotinamide riboside.

[b]The predominant cofactor is given.

[c]The pH ranges come from the listed references or from typical assay conditions reported in the literature.

[d]Several of these enzymes function reversibly as oxidoreductases. NADPH-dependent enzymes function mainly in the reductive direction while NADH-dependent enzymes function mainly oxidatively.

[e]A general reference for Table 4.17.4 is Oppermann and Maser (2000).

Follow this protocol for a cytosolic, NADPH-dependent enzyme system functioning in the reductive direction. Run reactions at the optimum conditions established during initial experiments (see Basic Protocol 1, parameters listed in Table 4.17.2), and evaluate the pH dependence over the range of pH 5.0 to 7.4 with phosphate buffers.

NOTE: The oxidation of carbonyl reduced products in microsomes can be catalyzed by cytochrome P450 enzymes. For example, haloperidol undergoes reduction by cytosolic carbonyl reductase and aldo-keto reductases, producing reduced haloperidol. Reduced haloperidol is oxidized by cytochrome P450, regenerating haloperidol (Kudo and Ishizaki, 1999). The interconversion of haloperidol and reduced haloperidol was observed in clinical studies (Chakraborty et al., 1989).

Materials

Pooled human liver cytosol subcellular fraction (BD Biosciences, In Vitro Technologies, Xenotech)
1M potassium phosphate buffer, pH 5.0, 5.5, 6.0, 6.5, 7.0, 7.4 (see recipes)
1000× xenobiotic substrate solution (see recipe)
Reagents for stopping reactions (Table 4.17.7)
Chromatography buffers and solutions
Cofactor: 2 mM NADPH (see recipe)

Thermomixer or shaking water bath, 37°C
1.5-ml microcentrifuge tubes

Additional reagents and equipment for HPLC and analysis (*UNIT 4.4*)

1. Turn on water bath or Thermomixer and warm to 37°C.
2. Thaw pooled human liver cytosol subcellular fraction by gently warming by hand. Place on ice immediately upon thawing.

   Keep the protein preparation on ice when not in use.

3. Add the following reagents, in order, to a 1.5-ml microcentrifuge tube for a final reaction volume of 1 ml. Minimally, run samples in duplicate; include more replicates depending on reproducibility.

   789 µl H_2O
   100 µl 1 M potassium phosphate, replicates at each pH 5.0, 5.5, 6.0, 6.5, 7.0, 7.4
   100 µl 10 mg/ml cytosol
   1 µl 1000× xenobiotic substrate solution

4. Perform Basic Protocol 1, steps 4 to 9. Initiate reactions with NADPH (10 µl of 0.2 M stock or buffer, for controls) and incubate samples. Follow with termination of reactions, sample processing, and analysis.

DISCRIMINATING BETWEEN CYTOCHROME P450 AND CARBONYL REDUCING ENZYMES WITH RECOMBINANT P450 PREPARATIONS

BASIC PROTOCOL 4

These experiments can help to distinguish between reactions mediated by carbonyl reducing enzymes (or other non-P450 enzymes) and cytochromes P450. Recombinant P450 isoforms (1A2, 2A6, 2B6, 2C9, 2C19, 2D6, 2E1, and 3A4) are combined into a single preparation containing human P450 enzymes but no human carbonyl reducing enzymes. This preparation is run in parallel with pooled human liver microsomes, which contain P450 in addition to carbonyl reducing enzymes. As a control, microsomes prepared from cells untreated with recombinant P450 vectors are included. These background control preparations contain no human P450 or carbonyl reducing enzymes, though they may contain carbonyl reducing enzymes endogenous to the expression system (Table 4.17.5).

Table 4.17.5 Suggested Assay Parameters for Recombinant P450 Experiments

Component	Conditions
Pooled human liver microsomes (human carbonyl reducing enzymes, human P450)	Run at the optimal protein concentration established in initial experiments[a]
Recombinant P450 mixture (no human carbonyl reducing enzymes, human P450)	Run at the optimal protein concentration established in initial experiments[a]
Recombinant control protein (no human carbonyl reducing enzymes, no human P450)	Run at the optimal protein concentration established in initial experiments[a]
Buffer, substrate concentration, incubation time	Run at the optimal conditions established in initial experiments
Cofactor (2 mM final)	NADPH or NADPH-regenerating system
Temperature	37°C
Controls	0 min, no cofactor

[a]In this protocol, the protein concentration was based on the sample recipe in Table 4.17.6.
[b]If possible, test all three protein preparations at the same protein concentration.

Table 4.17.6 Sample Recipe for a Recombinant P450 Mixture[a,b]

Initial product concentrations (from vendor)			Recombinant mixture preparation					Final concentrations in incubations	
P450	Initial protein concentration (mg/ml)[c]	Initial P450 content (pmol/ml)	Volume per P450 (ml)	Total volume of protein	Protein (mg/ml)	P450 (pmol/ml)	Amount recombinant mix per 1 ml incubation (ml)	Protein (mg/ml)	P450 (pmol/ml)
1A2	6	1000	0.5	3.75 ml of 5.83 mg/ml	0.80	133	0.254	0.20	30
2A6	10	1000	0.5		1.3	133		0.33	30
2B6	7	1000	0.5		0.93	133		0.24	30
2C9	3	1000	0.5		0.40	133		0.11	30
2C19	3	1000	0.5		0.40	133		0.11	30
2D6	6	1000	0.5		0.80	133		0.20	30
2E1	4	2000	0.25		0.27	133		0.07	30
3A4	7	1000	0.5		0.93	133		0.24	30
								Final total protein concentration in incubations = 1.5 mg/ml	

[a]The recombinant P450 mixture helps to discriminate between P450- and non-P450-mediated metabolism. Aliquots of each recombinant cytochrome P450 isoform are combined to create an artificial human microsomal preparation with P450 and no other human microsomal enzymes. The quantities of each isoform will vary depending on the concentration of protein and P450 in each product. These characterizations are typically performed by the supplier (e.g., BD Biosciences, Invitrogen). P450 isoforms are mixed so that the final concentration of each P450 in the incubation mixture is 30 pmol/ml.

[b]The use of recombinant P450 mixtures is discussed in Crespi and Miller (1999).

[c]A typical protein concentration for control recombinant microsomal preparations is 5 mg/ml.

Materials

Pooled human liver microsomes (BD Biosciences, In Vitro Technologies, Xenotech), gently thawed and placed on ice
1 M potassium phosphate buffer, pH 7.4 (see recipe)
1000× xenobiotic substrate solution (see recipe)
Recombinant P450 mixture (see Table 4.17.6), gently thawed and placed on ice
Recombinant control preparation, gently thawed and placed on ice
Cofactor:
2 mM NADPH (see recipe)
For NADPH-regenerating system:
Glucose 6-phosphate dehydrogenase (see recipe)
Regenerating system cofactor mixture (see recipe)
Reagents for stopping reactions (Table 4.17.7)
Chromatography buffers and solutions
Thermomixer or shaking water bath, 37°C
1.5-ml microcentrifuge tubes
Additional reagents and equipment for HPLC and analysis (*UNIT 4.4*)

1. Turn on water bath or Thermomixer and warm to 37°C.
2. Thaw microsomes by gently warming by hand. Place on ice immediately upon thawing.

   Keep the protein preparations on ice when not in use.

3. Add the following reagents, in order, to a 1.5-ml microcentrifuge tube for a final reaction volume of 1 ml. Minimally, run samples in duplicate; include more replicates depending on reproducibility.

   a. For microsomal incubations, add:

      814 µl H_2O (804 µl with regenerating system)
      100 µl 1 M potassium phosphate buffer, pH 7.4
      75 µl 20 mg/ml microsomes
      (10 µl 100× glucose-6-phosphate dehydrogenase, with regenerating system)
      1 µl 1000× xenobiotic substrate solution.

   b. For recombinant P450 incubations, add:

      635 µl H_2O (625 µl with regenerating system)
      100 µl 1 M potassium phosphate buffer, pH 7.4
      254 µl 5.83 mg/ml recombinant P450 mixture
      (10 µl 100× glucose-6-phosphate dehydrogenase, with regenerating system)
      1 µl 1000× xenobiotic substrate solution.

   c. For recombinant control incubations, add:

      593 µl H_2O (583 µl with regenerating system)
      100 µl 1 M potassium phosphate buffer, pH 7.4
      296 µl 5 mg/ml control recombinant microsomes
      (10 µl 100× glucose-6-phosphate dehydrogenase, with regenerating system)
      1 µl 1000× xenobiotic substrate solution.

      If the enzymatic activity of the recombinant P450 mixture is in doubt, confirm the viability of the mixture with a P450 probe substrate (positive control). Methods for traditional HPLC-based assays in addition to fluorescent probe substrate assays may be found in Donato et al. (2004). More fluorescent P450 methods may be found at http://www.gentest.com (website for BD Biosciences).

4. Perform Basic Protocol 1, steps 4 to 9. Initiate reactions with cofactor (or buffer, for controls) and incubate the samples. Collect multiple time-point samples if desired. Follow with termination of reactions, sample processing, and analysis.

REAGENTS AND SOLUTIONS

Use Milli-Q-purified water or equivalent in all recipes and protocol steps. For common stock solutions, see ***APPENDIX 2A****; for suppliers, see* ***SUPPLIERS APPENDIX****.*

Glucose 6-phosphate dehydrogenase (50 U/ml)

Dissolve 250 U glucose 6-phosphate dehydrogenase in 5 ml of 0.1 M potassium phosphate buffer, pH 7.4 (see recipe). Freeze in 0.2-ml aliquots. Store up to 1 year at −20°C.

The premeasured vials of lyophilized glucose 6-phosphate dehydrogenase are convenient since the enzyme powder is electrostatic and difficult to weigh accurately. Purchase vials containing a known amount (units) of dehydrogenase.

NADPH-regenerating system cofactor mixture, 100×

Combine the following:
765 mg $NADP^+$ (mol. wt. 765.4)
238 mg $MgCl_2$ (mol. wt. 95.21)

continued

705 mg glucose 6-phosphate (mol. wt. 282.1)
5 ml 0.1 M potassium phosphate, pH 7.4 (see recipe for 1 M)
Freeze in 0.2-ml aliquots
Store up to 1 year at −20°C

Nicotinamide adenine dinucleotide phosphate (reduced NADPH), 0.2 M

Dissolve 166.7 mg reduced NADPH (mol. wt. 833.4) into 1 ml of 0.1 M potassium phosphate buffer, pH 7.4 (see recipe for 1 M). Prepare fresh on each experimental day and keep on ice except during use.

Nicotinamide adenine dinucleotide (reduced NADH), 0.2 M

Dissolve 148.3 mg reduced NADH (mol. wt. 741.6) into 1 ml of 0.1 M potassium phosphate buffer, pH 7.4 (see recipe for 1 M). Prepare fresh on each experimental day and keep on ice except during use.

Potassium phosphate buffer, 1 M (pH 7.4)

Prepare a 1 M solution of monobasic potassium phosphate by adding 136.1 g anhydrous KH_2PO_4 to 1 liter water. Prepare a 1 M solution of dibasic potassium phosphate by adding 174.2 g anhydrous K_2HPO_4 to 1 liter water. Combine 1 part monobasic with 3 parts dibasic and check the pH. Continue to mix monobasic and dibasic buffers to pH 7.4. Store up to 6 months at 4°C.

To make 0.1 M potassium phosphate buffer, pH 7.4:

Dilute 10 ml of 1 M potassium phosphate buffer, pH 7.4, into 90 ml of water. Check pH and readjust to pH 7.4 with concentrated acid (H_3PO_4 or HCl) or base (KOH or NaOH) if necessary. Store up to 6 months at 4°C.

Potassium phosphate buffers, 1 M (pH 5.0, 5.5, 6.0, 6.5, 7.0)

Prepare a 1 M solution of monobasic potassium phosphate by adding 136.1 g anhydrous KH_2PO_4 to 1 liter water. Prepare a 1 M solution of dibasic potassium phosphate by adding 174.2 g anhydrous K_2HPO_4 to 1 liter H_2O. Combine 1 part monobasic with 3 parts dibasic and check the pH. Continue to mix monobasic and dibasic buffers as needed to the desired pH value (5.0, 5.5, 6.0, 6.5, or 7.0). Prepare ∼100 ml at each pH. Store up to 6 months at 4°C.

For brief periods (up to 1 week), store buffers at room temperature. To prevent microbial contamination, buffers may be sterile-filtered prior to storage. For example, 1 liter of buffer can be sterile-filtered into four 250-ml filter units to protect the integrity of the bulk buffer stock. Recommended filtering units include vacuum filter/storage systems with 0.22-μm cellulose acetate filters (Corning and Nalgene).

Xenobiotic substrate or inhibitor solution, 1000×

Prepare in aqueous solution if possible. Minimize the amount of organic solvent in reaction mixtures; for example, if the substrate or inhibitor is soluble only in DMSO, prepare the solution as concentrated as possible.

A convenient stock concentration is 1000× the final test concentration. If initial test concentrations are 1, 10, and 100 μM, then the corresponding stock solutions should be 1, 10, and 100 mM, respectively. Dilute the substrate or inhibitor 1:1000 by adding 1 μl per 1 ml incubation.

The basic protocols call for the addition of 1 μl of 1000× substrate or inhibitor stock per 1 ml incubation. If desired, adjust the concentration of stock solution to avoid pipetting this small volume, as long as the final concentration of organic solvent is kept to a minimum (e.g., 10 μl of 100× substrate). Include controls with organic solvent to ensure that the solvent alone is not inhibitory. With radiolabeled substrates, ensure that the correct amount of radioactivity is included in incubations. If necessary, combine radiolabeled and unradiolabeled (cold) substrate to reach the proper final substrate concentration and to detect metabolites with sufficient radiochemical signal.

COMMENTARY

Background Information

Carbonyl reducing enzymes catalyze the reversible phase I oxidoreduction of ketone and aldehyde moieties of xenobiotic and endogenous substrates to their respective alcohol moieties. Catalysis by carbonyl reducing enzymes is accomplished via two-electron hydride transfer from the nicotinamide cofactor to the carbonyl carbon. In detoxification, carbonyl reduction facilitates xenobiotic elimination by generating hydroxyl metabolites that become substrates of conjugative enzymes and/or undergo excretion. Carbonyl reducing enzymes are widely distributed in tissues including liver, lung, brain, heart, kidney, spleen, testis, and blood. Both soluble and membrane-bound forms exist. Some endogenous substrates are steroid hormones, glucocorticoids, monosaccharides, prostaglandins, and fatty acids. Carbonyl reducing enzymes are known more for their physiological roles than their roles in xenobiotic metabolism. Some examples of xenobiotic substrates include NSAIDS, quinones, anthracycline antiobiotics, fenofibrate, haloperidol, menadione, metyrapone, naltrexone, warfarin, and tobacco-related nitrosamines. General review references for carbonyl reducing enzymes include: Maser (1995), Forrest and Gonzales (2000), Oppermann and Maser (2000), and Rosemond and Walsh (2004).

There are more than 60 different isoforms of carbonyl reducing enzymes in humans. These enzymes can be grouped according to gene sequence, active site components, enzyme mechanism, and three-dimensional structural features of the cofactor binding site (for an overview, see Oppermann and Maser, 2000). The four superfamilies of carbonyl reducing enzymes are: medium-chain dehydrogenases/reductases (including alcohol dehydrogenases), aldo-keto reductases, quinone reductases, and short-chain dehydrogenases/reductases (including microsomal and cytosolic carbonyl reductases).

With the in vitro experiments described in this unit, the number of carbonyl reducing enzymes contributing to metabolism of a particular xenobiotic substrate can be condensed to an enzyme family or families. These experiments exploit the differences in subcellular localization, cofactor dependence, and susceptibility to chemical inhibitors among carbonyl reducing enzymes, and are conducted with subcellular fractions available commercially or prepared experimentally.

Examples of experimental methods for carbonyl reducing enzymes taken from published literature are given in Table 4.17.7, including references for purification and recombinant protein expression. Historically, liver has been the major source of carbonyl reducing enzymes, particularly the cytosolic aldo-keto reductases and carbonyl reductases. The major microsomal xenobiotic-metabolizing carbonyl reductase, 11β-HSD, has been the subject of some recent investigations (Bannenberg et al., 2003; Maser et al., 2003; Wsól et al., 2004).

Procedures for investigating carbonyl reducing enzymes typically include spectrophotometry, TLC, and HPLC. Spectrophotometric methods (monitoring the disappearance of absorbance at 340 nm due to consumption of NADPH or NADH) have been employed to follow cofactor-dependent carbonyl reducing activity during protein purification or subcellular fraction preparation. TLC has been utilized for separation and identification of carbonyl reduced products. HPLC with radiochemical, UV, or mass spectrometric detection is the most frequently cited analytical approach. The pesticide metyrapone can serve as a positive control (probe) substrate in an HPLC-based assay for carbonyl reduction. Metyrapone undergoes ketone reduction to metyrapol by carbonyl reducing enzymes of cytosol and microsomes. Incubation conditions and HPLC analytical methods for metyrapone have been published (Maser et al., 1991; Maser and Bannenberg, 1994; Bannenberg et al., 2003).

The experiments described in this unit cover all of the currently known carbonyl reducing enzymes of human liver. Subcellular fraction-cofactor combinations not included in this unit can be tested in case the xenobiotic is a superior substrate for an unidentified enzyme system. For example, no carbonyl reducing enzymes of human liver mitochondria have been described in the published literature, although a mitochondrial NADPH-dependent carbonyl reducing enzyme of mouse, guinea pig, and pig lung has been described (Forrest and Gonzales, 2000). New carbonyl reducing enzymes remain to be discovered; so, for certain substrates, it may be worthwhile to test combinations that cover all of the possibilities in vitro.

Table 4.17.7 A Sampling of Methods for Human Liver Carbonyl Reducing Enzymes from Published Literature[a]

Substrate (K_m)[b] (Ref.)	Experimental details[c]	Comments	Analysis
Acetohexamide, befunelol, 4-benzoylpyridine, daunorubicin, ethacrynic acid, haloperidol, ketoprofen, loxoprofen, metyrapone, naloxone, naltrexone, 4-nitrobenzaldehyde (Ohara et al., 1995)	100 mM potassium phosphate, pH 6.5 0.04 mg/ml enzyme (purified AKR1A1, AKR1C1, AKR1C2, AKR1C4, CR) NADPH-regenerating system 1 mM substrate 2 ml/sample, 1 hr, 30°C Stop: 1 ml 1 M sodium carbonate, pH 10.0 Organic extraction	—	TLC
Benfluron (Skálová et al., 2002)	100 mM sodium phosphate, pH 7.4 3 mg/ml microsomes or cytosol 2 mM NADPH-NADH mixture 1.5 mM benfluron 0.3 ml/sample, 30 min Stop: 0.1 ml 26% aqueous ammonia solution or 1 M NaOH, ethyl acetate extraction.	Anaerobic conditions investigated (argon)	HPLC, TLC
Benfluron (Skálová et al., 2002)	100 mM sodium phosphate, pH 7.4 71 μg/ml purified 11β-HSD; or 47 μg/ml purified CR NADPH-regenerating system 0.2 mM benfluron 0.05 ml/sample, 30 min Stop: cool to 0°C, 0.02 ml 26% aqueous ammonia solution, ethyl acetate extraction	—	HPLC, TLC
Cortisone (4 μM); ketoprofen (20 μM); metyrapone (370 μM)[d] (Hult et al., 2001)	15 mM Tris·Cl, pH 7.4 10–2000 μg microsomes, S9[e] or purified recombinant 11β-HSD 0.5 mM NADPH or regenerating system 2–2500 μM substrate, 10–60 min Stop: 3× vol acetonitrile	Reductive enzymatic activity of recombinant 11β-HSD not maintained during purification	HPLC
Cortisone (14 μM) (Maser et al., 2002)	10 mM sodium phosphate, pH 7.4 2–5 mg/ml purified 11β-HSD NADPH-regenerating system 2–75 μM substrate 0.05 ml/sample, 3 hr Stop: 0.15 ml acetonitrile	Reverse reaction investigated (pH 9.0, $NADP^+$)	HPLC
Doxorubicin (0.28 mM); daunorubicin (0.31 mM) (Loveless et al., 1978)	20 mM potassium phosphate, pH 7.4 1–2 mg/ml protein 1 mM NADPH 0.05–1 mM substrate 0.5 ml/sample, 15 min Stop: equal volume of ice-cold isopropanol, then ammonium sulfate to saturation	—	TLC

continued

Table 4.17.7 A Sampling of Methods for Human Liver Carbonyl Reducing Enzymes from Published Literature[a], *continued*

Substrate (K_m)[b] (Ref.)	Experimental details[c]	Comments	Analysis
3,7-DMX (pentoxyfylline), ethacrynic acid, naltrexone, naloxone, oxisuran, tienilic acid (Ahmed et al., 1979)	80 mM potassium phosphate, pH 6.0 10 mg/ml cytosol 0.18 mM NADPH 1 mM substrate 1 ml/sample, 2 hr Stop: immersion in boiling water bath; 1 M sodium carbonate, pH 10, ethyl acetate extraction	—	TLC, MS
Haloperidol (0.5–0.6 mM) (Inaba and Kovacs, 1989)	Potassium phosphate, pH 7.4, 0.2% KCl 20–40 mg/ml microsomes, cytosol, or S9 NADPH-regenerating system 10–1000 μM substrate 1 ml/sample, 15 min Stop: equal volume ice-cold 0.25 M NaOH, organic extraction	Anaerobic conditions investigated (nitrogen)	GC
Haloperidol (0.25 mM) (Eyles and Pond, 1992)	0.2 mM potassium phosphate, pH 7.4 2–3 μg/ml cytosol or whole blood NADPH-regenerating system 2–123 μM haloperidol 1 ml/sample, 15 min Stop: 1 ml ice-cold 0.25 M NaOH with internal standard (chlorohaloperidol), organic extraction	Stereochemistry of reaction studied	HPLC
Haloperidol (0.38 mM); timiperone (0.03 mM) (Someya et al., 1991; Shimoda et al., 1998)	100 mM potassium phosphate, pH 7.4, 0.2% KCl 0.1–0.2 mg/ml cytosol or microsomes NADPH-regenerating system 0–500 μM substrate 1 ml/sample, 15 min Stop: immersion into ice bath, addition of heptane-isoamyl alcohol (97:3), organic extraction	Reverse reaction investigated (Someya et al., 1991)	HPLC
Metyrapone (Maser et al., 1991)	50 mM sodium phosphate, pH 7.4 16 mg/ml cytosol or microsomes NADPH-regenerating system 1 mM metyrapone 75 μl/sample, 30 min Stop: 3× vol ice cold acetonitrile	—	HPLC
Naltrexone (0.03 mM) (Porter et al., 2000)	100 mM potassium phosphate, pH 7.4 0.125 mg/ml cytosol or microsomes 0.14 mM NADPH (cytosol) or NADPH-regenerating system (microsomes) 5–150 μM naltrexone 0.2 ml/sample, 60 min Stop: ice-cold methanol	Isocitrate dehydrogenase regenerating system	HPLC

continued

Table 4.17.7 A Sampling of Methods for Human Liver Carbonyl Reducing Enzymes from Published Literature[a], *continued*

Substrate (K_m)[b] (Ref.)	Experimental details[c]	Comments	Analysis
Naltrexone (1.4, 0.13, 0.04 mM for AKR1C1, 1C2, 1C4, respectively); dolasetron (0.064, 0.03, 0.22 mM for AKR1C1, 1C2, 1C4, respectively; not saturable, CR) (Breyer-Pfaff and Nill, 2004)	100 mM Tris·Cl, pH 7.4, 25 mM KCl 1–40 μg/ml purified AKR or CR NADPH-regenerating system 0–2 mM naltrexone; 0–0.12 mM dolasetron 0.36 ml/sample, 10–20 min Stop: 0.2 N perchloric acid, cool on ice	—	HPLC
NNK (2.5 mM, cytosol; 2.3 mM, microsomes) (Maser et al., 2000)	100 mM sodium phosphate, pH 7.4 6–10 mg/ml cytosol or microsomes NADPH-regenerating system 0.1–5 mM NNK 60 min Stop: 0.15 ml ice-cold acetonitrile	Lung subcellular fractions examined	HPLC
NNK (0.2, 0.3, 0.8 mM for AKR1C1, 1C2, 1C4, respectively; 7 mM for CR) (Atalla et al., 2000)	100 mM sodium phosphate, pH 7.4 0.2–12.5 μg/ml purified AKR1C1, AKR1C2, AKR1C4, CR NADPH-regenerating system 0.05–8 mM substrate 0.4 ml/sample, 30 min Stop: denature protein 3 min 100°C, cool on ice	Enzyme isolation described; universal buffer for pH dependence studies (pH range 4.5–11.5)	HPLC
NNK (12.03 mM) (Maser et al., 2003)	10 mM sodium phosphate, pH 7.4 2–5 mg/ml purified 11β-HSD 10 μM–50 mM NNK NADPH-regenerating system 0.05 ml/sample, 60 min Stop: 0.15 ml acetonitrile	Enzyme isolation described; [^{3}H]-Radiolabeled substrate utilized	HPLC
NNK (Breyer-Pfaff et al., 2004)	100 mM Tris·Cl, pH 7.4, 25 mM KCl 2–150 μg/ml purified AKR, CR, or 11β-HSD NADPH-regenerating system 10–1000 μM NNK (or 1 μM tritiated NNK) 1–2 ml/sample, 60 min Stop: cool on ice, organic extraction	Stereochemistry investigated	TLC, HPLC
E-10-oxo-nortriptyline (1.8 μM, cytosol) *Z*-10-oxo-nortriptyline (1.5 μM, cytosol) (Breyer-Pfaff and Nill, 1995)	60 mM Tris·Cl, pH 7.4, 10 mM $MgCl_2$, 24 mM KCl, 100 mM sucrose 0.25–0.8 mg/ml cytosol or microsomes; or, 11 mU/ml recombinant CR NADPH-regenerating system 5–20 μM substrate 1–2 ml/sample; 1–3 min Stop: equal volume *tert*-butyl methyl ether, 0.25 ml/ml saturated Na_3PO_4, organic extraction	Reverse reaction and stereochemistry investigated with tritiated cofactor; pH optimum (*E*) = 6.5; pH optimum (*Z*) = 6.0; pH optimum of reverse reaction (*E* and *Z*) = 10	HPLC

continued

Table 4.17.7 A Sampling of Methods for Human Liver Carbonyl Reducing Enzymes from Published Literature[a], *continued*

Substrate (K_m)[b] (Ref.)	Experimental details[c]	Comments	Analysis
E-10-oxo-nortriptyline *Z*-10-oxo-nortriptyline (R)- and (S)-ketotifen For AKR1C1 and 1C2, K_m values: 2.6–53 μM (Breyer-Pfaff and Nill, 2000)	100 mM Tris·Cl, pH 7.4, 8 mM $MgCl_2$, 25 mM KCl 0.6–12 μg purified AKR1C1, AKR1C2, or CR NADPH-regenerating system 6–10 substrate concentrations (5× below to 5× above K_m) 0.36 ml/sample, 4–20 min Stop: 0.04 ml 2 N perchloric acid, put on ice	Reverse reactions and stereochemistry examined. Enzyme isolation described	HPLC
Rofecoxib (100–200 μM, cytosol) (Slaughter et al., 2003)	100 mM sodium phosphate, pH 7.4, 3 mM $MgCl_2$ 5–6 mg/ml S9 or cytosol 1 mM nicotinamide cofactor (10 mM malate, cytosol) 100 μM substrate 0.5 ml/sample, up to 24 hr Stop: 2:1 acetonitrile:methanol (3× volume)	Complex metabolic pathways; malic acid-based regenerating system for cytosol; NAD^+-regenerating system. Reverse reactions investigated	HPLC
Warfarin (Hermans and Thijssen, 1989)	20 mM Tris·Cl, pH 7.4, 150 mM KCl 6 mg/ml cytosol or microsomes NADPH-regenerating system 0.2 mM substrate 0.36 ml/sample, 10 min Stop: 0.5 ml ice-cold acetonitrile (Stop solution contained internal standard, acenocoumarol), organic extraction	Stereochemistry examined	HPLC
Warfarin (1.55 mM) (Moreland and Hewick, 1975)	100 mM potassium phosphate, pH 7.4 3–6 mg/ml cytosol 1.3 mM substrate (0.13–2.08 mM) NADPH-regenerating system 2.5 ml/sample, 50 min Stop: 0.5 vol 3 N HCl, organic extraction	—	TLC
Wortmannin (119 μM) (Holleran et al., 2004)	100 mM potassium phosphate, pH 6.0 1:20 dilution of purified recombinant CR 0–300 μM wortmannin 1.5–3 mM nicotinamde cofactor, 25 μM FAD, 0.1% BSA 0.2 ml/sample, 5 min Stop: 5× volume ethyl acetate, organic extraction	Expression and purification of human CR	HPLC

[a] Abbreviations: AKR, aldo-keto reductase; CR, carbonyl reductase; 11β-HSD, 11β-hydroxysteroid dehydrogenase; 3,7-DMX, 3,7-dimethyl-1-(5-oxohexyl)-xanthine; NNK, 4-methylnitrosamino-1-(3-pyridyl)-1-butanone.

[b] Most substrates are available from standard commercial sources, such as Sigma-Aldrich. Some nonstandard sources for other chemicals are: NNK, Midwest Research Institute; (R)-warfarin, Ultrafine Chemicals; timiperone, Pharm Chemical Shanghai/Lansheng. Commercial sources for benfluron and nortryptyline metabolites are not known.

[c] Incubations were performed at 37°C unless indicated otherwise.

[d] The K_m values for cortisone, ketoprofen, and metyrapone were determined with yeast S9 or microsomal fractions containing recombinant human 11β-HSD (Hult et al., 2001).

[e] S9 is a subcellular fraction preparation (supernatant) from a 9000 × *g* centrifugation of homogenized liver tissue. The S9 fraction contains microsomes and cytosol.

Table 4.17.8 Troubleshooting Guide to Analysis of Carbonyl Reductase Enzymes

Problem	Possible cause	Solution
No or low turnover	Incubation time too short	Extend incubation time
	Cofactor depleted	Utilize regenerating system; prepare fresh solutions of NADH, NADPH daily
	Suboptimal pH	Test other pH
	Concentration of organic solvent too high	Reduce amount of solvent to <0.2% if possible, or try a different solvent
	Xenobiotic test compound precipitating out of solution	Start at lower concentration; add compound after adding protein to samples
	Incubation time too long (products either precipitate out of solution or are unstable)	Shorten incubation time; monitor stability of parent, products
	Conditions unsuitable	Test alternate subcellular fraction/cofactor combinations; test known substrate (i.e., positive control) to ensure viability of the test system
	Too vigorous mixing of samples	No vortexing; mix gently by hand; reduce Thermomixer mixing speed
Inconsistent results	Substrate insoluble	Check samples closely for precipitated test compound
	Inefficient sample processing	Revise sample processing methods
No detection (radiolabeled substrate)	Error in calculation	Review calculations
	Inefficient sample processing	Revise sample processing methods

Critical Parameters and Troubleshooting

It is imperative to determine the optimal conditions for performing the incubations, for processing the samples to achieve maximal recoveries, and for analyzing the products of reactions. Guidance for optimization of experimental parameters is incorporated in the Basic Protocols. A troubleshooting guide is provided in Table 4.17.8.

Anticipated Results

The results may be easily interpreted in the case of a single carbonyl reducing enzyme mediating the metabolism of a xenobiotic. As an illustration: ketone reduction occurs only in cytosol with NADPH, is inhibited by flufenamic acid and phenolphthalein, is not inhibited by menadione, and has an optimal pH 6.0. These data clearly implicate aldo-keto reductases and rule out other enzymes.

A more likely outcome is that the xenobiotic is metabolized by multiple enzymes. These studies are complicated by the fact that subcellular fractions are crude enzyme sources, unlike purified or recombinant preparations. But, even with crude fractions, it is possible to eliminate some of the potential enzymes contributing to metabolism with the experiments described in this unit.

The investigation of carbonyl reducing enzymes may be carried a step further by estimating kinetic parameters. For example, an apparent K_m value of 2 μM (cytosol) versus 1 mM (microsomes) indicates that the xenobiotic is a much better substrate for cytosolic than microsomal carbonyl reducing enzymes. Chemical inhibition experiments may be conducted at the substrate concentration approximating the apparent K_m value. The relative potency of chemical inhibitors can help to further assess the roles of different carbonyl reducing enzymes. Finally, a pH dependence study and characterization of cytochrome P450 involvement help to complete the overall metabolic picture.

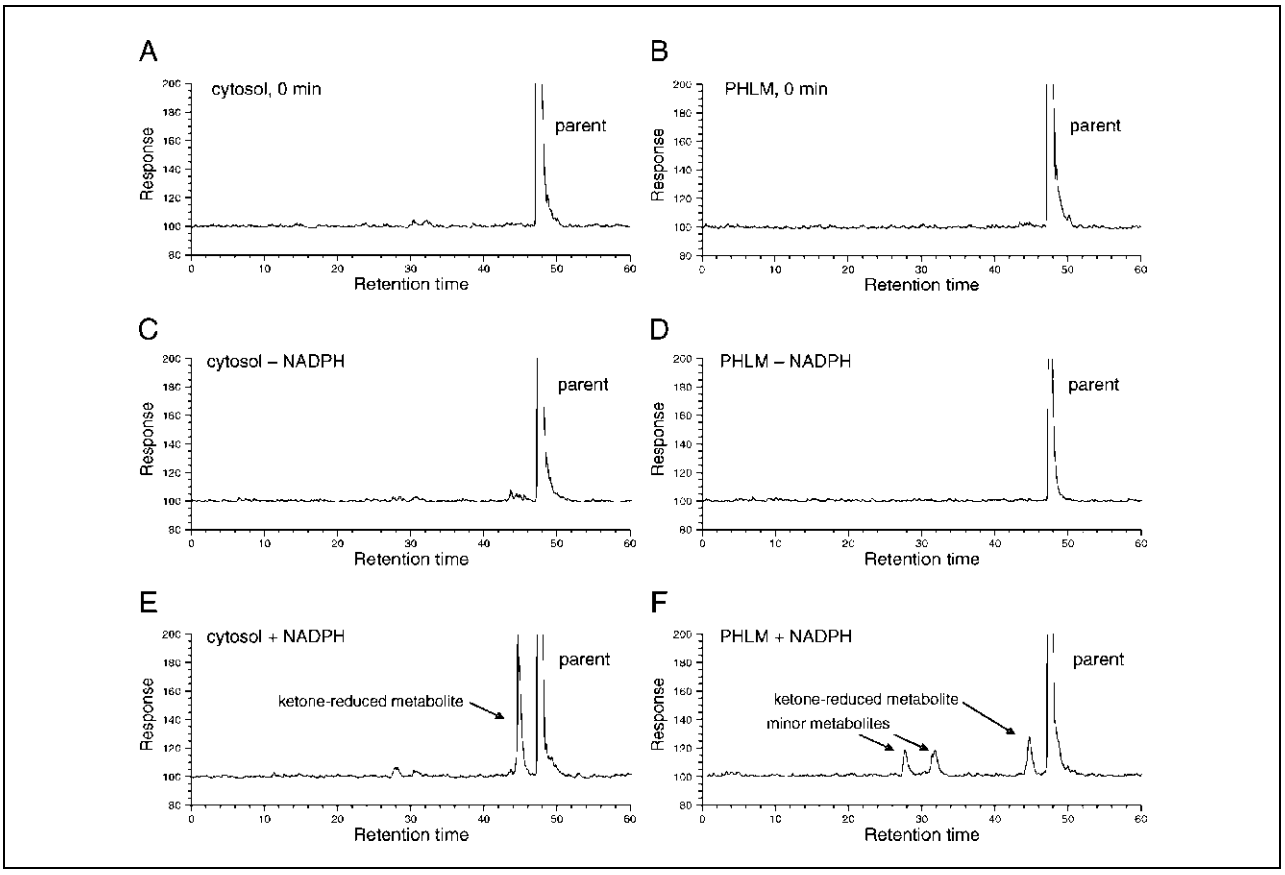

Figure 4.17.1 Representative radiochemical profiles from experiments with human liver subcellular fractions. Reaction mixtures included 100 mM potassium phosphate buffer, pH 7.4, 1 mg/ml pooled human liver subcellular fractions, and 2 μM [^{14}C]-radiolabeled substrate (parent). Reactions were initiated with 2 mM NADPH cofactor or buffer (control), followed by incubation for 30 min at 37°C and analysis by HPLC with radiochemical detection. Results from experiments with cytosol are shown in **A, C**, and **E**; results with microsomes (PHLM) are shown in **B, D**, and **F**. (**A,B,C,D**) No metabolism was detected in the control samples (0-min time point, no-cofactor control). In the presence of NADPH, the ketone-reduced metabolite (identity confirmed by mass spectrometry) was the major product in cytosol and microsomes (**E** and **F**). Thus, the xenobiotic is a substrate of NAPDH-dependent carbonyl reducing enzymes of both subcellular fractions. Some additional minor metabolites were detected in microsomal samples (**F**).

Examples of results illustrate how, in practice, the different methods generate information about carbonyl reduction pathways (Figs. 4.17.1 to 4.17.4). In these examples, the substrate is a [^{14}C]-radiolabeled benzophenone derivative in which reduction of the diphenyl ketone moiety is the major route of metabolism. The xenobiotic is a substrate of cytosolic and microsomal carbonyl reducing enzymes, and metabolites are analyzed by HPLC with radiochemical detection. Some representative radiochemical profiles comparing metabolism in cytosol and microsomes are shown in Figure 4.17.1. Some results with inhibitors of carbonyl reducing enzymes are shown in Figures 4.17.2A (cytosol) and 4.17.2B (microsomes). Figure 4.17.3 shows a pH-dependence study, and Figure 4.17.4 shows a comparison of metabolism in pooled human liver microsomes and recombinant P450 enzymes.

Time Considerations

Allow time for ordering (1 to 2 hr) and obtaining (up to 1 week) reagents. Prepare buffers and stock solutions of substrate and inhibitors ahead of time (1 to 2 days).

Gather supplies for HPLC analysis, such as the analytical column and solvents or buffer components. Set up the HPLC instrument ahead of time. Make sure the column is ready for samples and that the separation conditions are appropriate. Allow 1 to 3 days or more depending on the availability of a chromatographic method. References are provided at the end of this section for HPLC analytical method development (see Key References).

For a substrate that is radiolabeled, allow extra time for calculating stock concentrations, amounts for HPLC analysis and radiochemical detection, and amounts deposited in waste. When calculating the correct amount for HPLC analysis, remember to incorporate

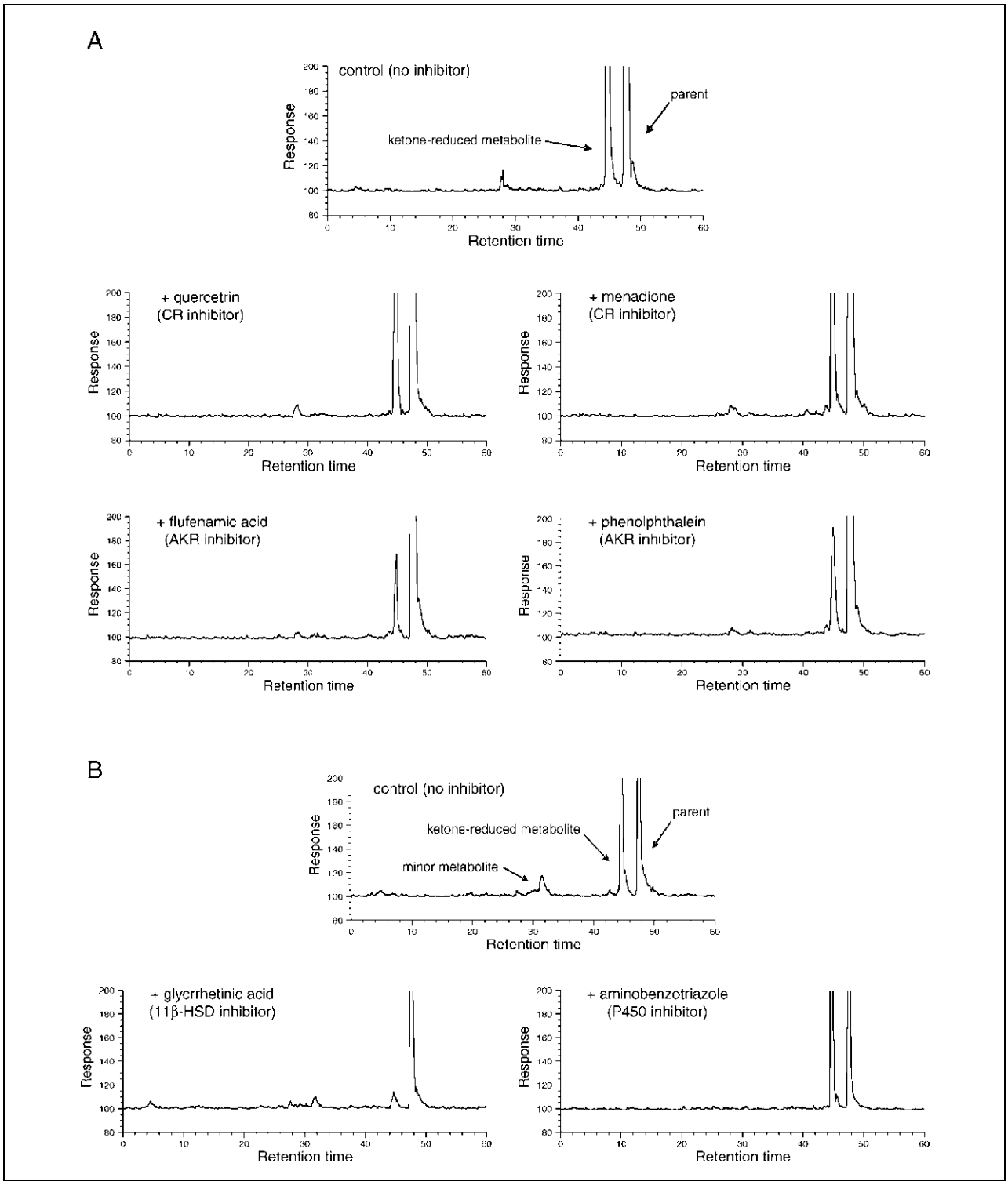

Figure 4.17.2 Legend at right.

Figure 4.17.2 *(at left)* (**A**) Representative radiochemical profiles from experiements with inhibitors of cytosolic carbonyl reducing enzymes. Reaction mixtures included 100 mM potassium phosphate buffer, pH 6.0, 1 mg/ml pooled human liver cytosol, 100 μM inhibitor, and 2 μM [^{14}C]-radiolabeled substrate (parent). Control samples without inhibitor contained vehicle only (<0.2% solvent). Reactions were initiated with NADPH-regenerating system, followed by incubation for 4 hr at 37°C and analysis by HPLC with radiochemical detection. The inhibitors selected for these experiments were: quercetrin and menadione (targeting carbonyl reductase, CR); flufenamic acid and phenolphthalein (targeting aldo-keto reductases, AKR). Ketone reduction was impacted more by the AKR probes (70% to 80% inhibition, calculated from peak areas) than the CR probes (15% to 20% inhibition), suggesting that the xenobiotic is a better substrate of AKRs than CRs. (**B**) Representative radiochemical profiles from experiments with inhibitors of microsomal carbonyl reducing enzymes. Reaction mixtures included 100 mM potassium phosphate buffer, pH 7.4, 1 mg/ml pooled human liver microsomes, and 2 μM [^{14}C]-radiolabeled substrate (parent). Control samples without inhibitor contained vehicle only (<0.2% solvent). Reactions were initiated with NADPH-regenerating system, followed by incubation for 2 hr at 37°C and analysis by HPLC with radiochemical detection. The inhibitors selected for these experiments were: 18β-glycyrrhetinic acid (targeting 11β-hydroxysteroid dehydrogenase, 11β- HSD) and aminobenzotriazole (targeting cytochrome P450). Only a trace amount of ketone-reduced metabolite formed in the presence of 10 μM 18β-glycyrrhetinic acid, implicating 11β-HSD in metabolism. In the presence of the non-specific P450 inhibitor, 1 mM ABT, minor metabolites were not detected, and there was an increase (+25%) in the amount of ketone-reduced metabolite compared to vehicle controls (calculated from peak areas). One interpretation is that ABT inhibited the formation of minor metabolites, allowing the carbonyl reduction pathway to predominate.

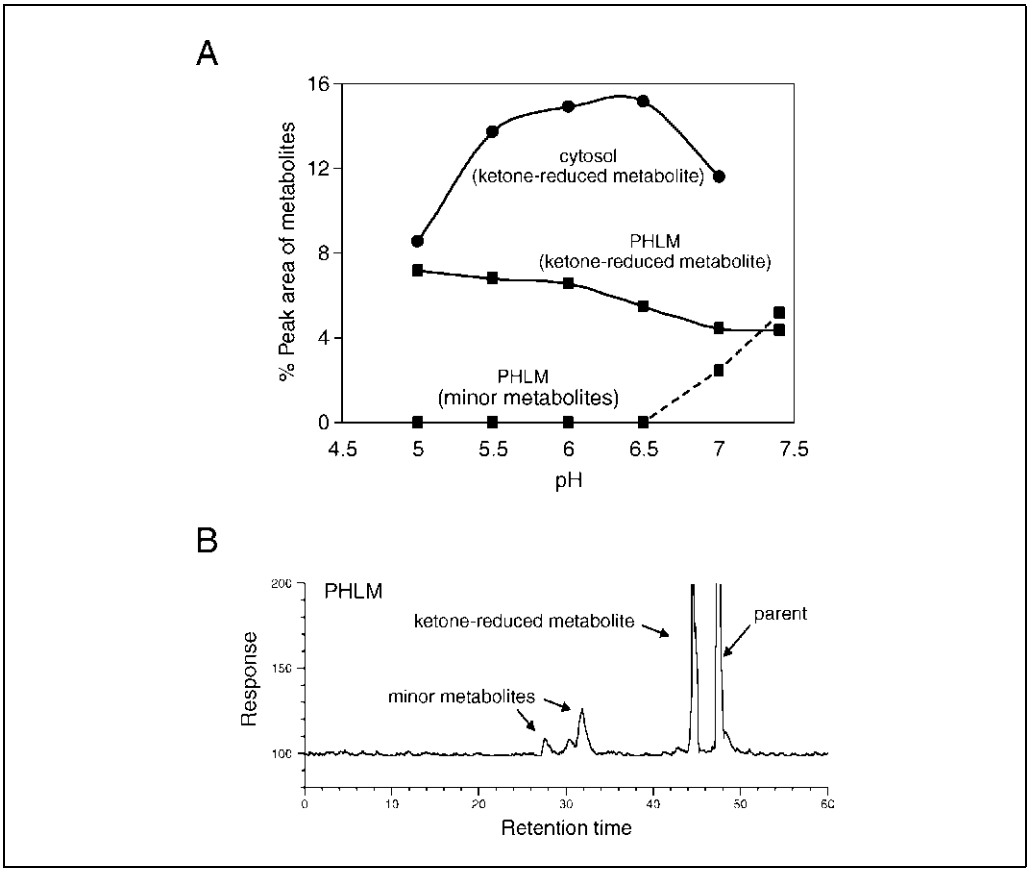

Figure 4.17.3 pH dependence of metabolism in cytosol and microsomes. Reaction mixtures contained 100 mM potassium phosphate buffer, pH 5.0 to 7.4, 1 mg/ml pooled human liver cytosol or microsomes, and 1 μM [^{14}C]-radiolabeled substrate (parent). Reactions were initiated with 2 mM NADPH, followed by incubation for 30 min at 37°C and analysis by HPLC with radiochemical detection. (**A**) Results from the pH dependence study. (**B**) A representative radiochemical profile of microsomal metabolites. To produce the plot in **A**, the % peak areas were calculated: (metabolite peak area/total peak area in chromatogram) × 100. The ketone-reduced product formed preferentially at pH 5.5 to 6.5, consistent with carbonyl reducing enzymes. Minor metabolites formed only in microsomes and at pH >6.5, consistent with P450 enzymes.

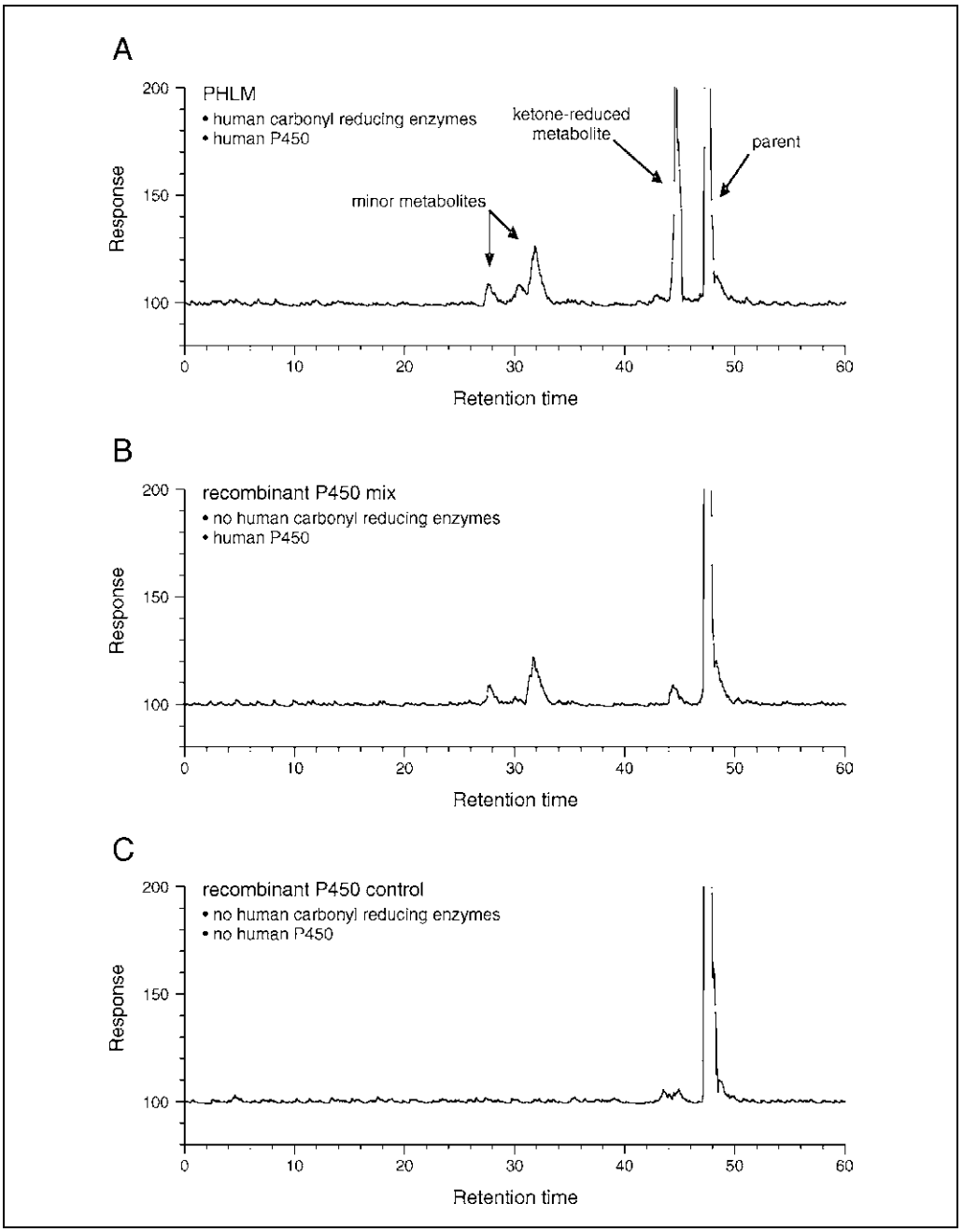

Figure 4.17.4 Representative radiochemical profiles from experiments with pooled human liver microsomes and recombinant cytochrome P450 preparations. Reaction mixtures included 100 mM potassium phosphate buffer, pH 7.4, 1.5 mg/ml protein, and 1 μM [^{14}C]-radiolabeled substrate (parent). Reactions were initiated with NADPH-regenerating system, followed by incubation for 2 hr at 37°C and analysis by HPLC with radiochemical detection. (**A**) In pooled human liver microsomes (PHLM), the ketone-reduced metabolite and minor metabolites formed (peak labels). (**B**) The minor metabolites were also detected in incubations with the recombinant P450 mixture (pool of heterologously expressed P450 enzymes: 1A2, 2A6, 2B6, 2C9, 2C19, 2D6, 2E1, 3A4). (**C**) None of the metabolites were detected in incubations with recombinant control microsomes (microsomes lacking native human P450 activity, prepared from insect cells infected with wild-type virus). These results implicate P450 enzymes in the formation of the minor metabolites and indicate that the non-P450 enzyme(s) responsible for ketone reduction reside in pooled human liver microsomes.

volume changes that occur upon stopping reactions and processing samples.

After the initial preparation of HPLC equipment, buffers, protein reagents, inhibitor, and substrate stock solutions, the time for setting up assays is minimal (allow ~1 hr for thawing enzymes, preparing cofactor solutions, and labeling tubes for samples and tubes for stopping reactions).

In preliminary experiments, minimize the number of samples until analytical techniques and sample processing methods are in place. Increase the number of samples as appropriate; for example, a convenient experiment size for 1 day of incubations (with short incubation times, <30 min), sample processing (with simple procedures), preparation for analysis, and HPLC instrument setup can range from 30 to 45 samples. In experiments with long incubation times (hours) or elaborate sample processing steps, plan for a smaller number of samples. Preferably, analyze the samples as soon as they are prepared. Store (i.e., freeze or refrigerate) samples only if analytes are stable in the storage conditions. Confirm the stability by directly comparing the contents of freshly prepared with stored samples. Ensure that the contents of stored samples are representative of the contents of freshly-prepared samples.

Acknowledgments

The author gratefully acknowledges John S. Walsh for advice and direction in conducting studies of carbonyl reducing enzymes, and Cosette Serabjit-Singh for critical review of the manuscript.

Literature Cited

Ahmed, N.K., Felsted, R.L., and Bachur, N.R. 1979. Comparison and characterization of mammalian xenobiotic ketone reductases. *J. Pharmacol. Exp. Ther.* 209:12-19.

Atalla, A., Breyer-Pfaff, U., and Maser, E. 2000. Purification and characterization of oxidoreductases catalyzing carbonyl reduction of the tobacco-specific nitrosamine 4-methylnitrosamino-1-(3-pyridyl)-1-butanone (NNK) in human liver cytosol. *Xenobiotica* 30:755-769.

Bannenberg, G., Martin, H.J., Bélai, I., and Maser, E. 2003. 11β-Hydroxysteroid dehydrogenase type 1: Tissue-specific expression and reductive metabolism of some anti-insect agent azole analogues of metyrapone. *Chem. Biol. Interact.* 143-144:449-457.

Blair, A.H. and Vallee, B.L. 1966. Some catalytic properties of human liver alcohol dehydrogenase. *Biochemistry* 5:2026-2034.

Breyer-Pfaff, U. and Nill, K. 1995. Stereoselective reversible ketone formation from 10-hydroxylated nortriptyline metabolites in human liver. *Xenobiotica* 25:1311-1325.

Breyer-Pfaff, U. and Nill, K. 2000. High-affinity stereoselective reduction of the enantiomers of ketotifen and of ketonic nortriptyline metabolites by aldo-keto reductases from human liver. *Biochem. Pharmacol.* 59:249-260.

Breyer-Pfaff, U. and Nill, K. 2004. Carbonyl reduction of naltrexone and dolasetron by oxidoreductases isolated from human liver cytosol. *J. Pharm. Pharmacol.* 56:1601-1606.

Breyer-Pfaff, U., Martin, H.J., Ernst, M., and Maser, E. 2004. Enantioselectivity of carbonyl reduction of 4-methylnitrosamino-1-(3-pyridyl)-1-butanone by tissue fractions from human and rat and by enzymes isolated from human liver. *Drug Metab. Dispos.* 32:915-922.

Budavari, S. (ed.). 1996. The Merck Index, 12th ed. Merck and Co. Inc., Whitehouse Station, N.J.

Chakraborty, B.S., Hubbard, J.W., Hawes, E.M., McKay, G., Cooper, J.K., Gurnsey, T., Korchinski, E.D., and Midha, K.K. 1989. Interconversion between haloperidol and reduced haloperidol in healthy volunteers. *Eur. J. Clin. Pharmacol.* 37:45-48.

Crespi, C.E. and Miller, V.P. 1999. The use of heterologously expressed drug metabolizing enzymes-state of the art and prospects for the future. *Pharmacol. Ther.* 84:121-131.

Dalmadi, B., Leibinger, J., Szeberényi, S., Borbás, T., Farkas, S., Szombathelyi, Z., and Tihanyi, K. 2003. Identification of metabolic pathways involved in the biotransformation of tolperisone by human microsomal enzymes. *Drug Metab. Dispos.* 31:631-636.

Diederich, S., Grossmann, C., Hanke, B., Quinkler, M., Herrmann, M., Bähr, V., and Oelkers, W. 2000. In the search for specific inhibitors of human 11β-hydroxysteroid dehydrogenase (11β-HSDs): Chenodeoxycholic acid selectively inhibits 11β-HSD-1. *Eur. J. Endocrinol.* 142:200-207.

Donato, M.T. and Castell, J.V. 2003. Strategies and molecular probes to investigate the role of cytochrome P450 in drug metabolism: Focus on in vitro studies. *Clin. Pharmacokinet.* 42:153-178.

Donato, M.T., Jiménez, N., Castell, J.V., and Gómez-Lechón, M.J. 2004. Fluorescence-based assays for screening nine cytochrome P450 (P450) activities in intact cells expressing individual human P450 enzymes. *Drug Metab. Dispos.* 32:699-706.

Eyles, D.W. and Pond, S.M. 1992. Stereospecific reduction of haloperidol in human tissues. *Biochem. Pharmacol.* 44:867-871.

Felsted, R.L. and Bachur, N.R. 1980. Mammalian carbonyl reductases. *Drug Metab. Rev.* 11:1-60.

Forrest, G.L. and Gonzales, B. 2000. Carbonyl reductase. *Chem. Biol. Interact.* 129:21-40.

Gelboin, H.V., Krausz, K.W., Gonzalez, F.J., and Yang, T.J. 1999. Inhibitory monoclonal antibodies to human cytochrome P450 enzymes: A new avenue for drug discovery. *Trends Pharmacol. Sci.* 20:432-438.

Guengerich, F.P. 2004. Cytochrome P450: What have we learned and what are the future issues? *Drug Metab. Rev.* 36:159-197.

Hermans, J.J.R. and Thijssen, H.H.W. 1989. The in vitro ketone reduction of warfarin and analogs. Substrate stereoselectivity, product stereoselectivity and species differences. *Biochem. Pharmacol.* 38:3365-3370.

Holleran, J.L., Fourcade, J., Egorin, M.J., Eiseman, J.L., Parise, R.A., Musser, S.M., White, K.D., Covey, J.M., Forrest, G.L., and Pan, S.S. 2004. In vitro metabolism of the phosphatidylinositol 3-kinase inhibitor, wortmannin, by carbonyl reductase. *Drug Metab. Dispos.* 32:490-496.

Hult, M., Nobel, C.S.I., Abrahmsen, L., Nicoll-Griffith, D.A., Jörnvall, H., and Oppermann, U.C.T. 2001. Novel enzymological properties of human 11β-hydroxysteroid dehydrogenase type 1. *Chem. Biol. Interact.* 130-132:805-814.

Inaba, T. and Kovacs, J. 1989. Haloperidol reductase in human and guinea pig livers. *Drug Metab. Dispos.* 17:330-333.

Kudo, S. and Ishizaki, T. 1999. Pharmacokinetics of haloperidol: An update. *Clin. Pharmacokinet.* 37:435-456.

Long, D.J. II and Jaiswal, A.K. 2000. NRH:quinone oxidoreductase2 (NQO2). *Chem. Biol. Interact.* 129:99-112.

Loveless, H., Arena, E., Felsted, R.L., and Bachur, N.R. 1978. Comparative mammalian metabolism of adriamycin and daunorubicin. *Cancer Res.* 38:593-598.

Maser, E. 1995. Xenobiotic carbonyl reduction and physiological steroid oxidoreduction. The pluripotency of several hydroxysteroid dehydrogenases. *Biochem. Pharmacol.* 49:421-440.

Maser, E. and Bannenberg, G. 1994. 11β-Hydroxysteroid dehydrogenase mediates reductive metabolism of xenobiotic carbonyl compounds. *Biochem. Pharmacol.* 47:1805-1812.

Maser, E., Gebel, T., and Netter, K.J. 1991. Carbonyl reduction of metyrapone in human liver. *Biochem. Pharmacol.* 42:S93-S98.

Maser, E., Stinner, B., and Atalla, A. 2000. Carbonyl reduction of 4-(methylnitrosamino)-1-(3-pyridyl)-1-butanone (NNK) by cytosolic enzymes in human liver and lung. *Cancer Lett.* 148:135-144.

Maser, E., Völker, B., and Friebertshäuser, J. 2002. 11β-Hydroxysteroid dehydrogenase type I from human liver: Dimerization and enzyme cooperativity support its postulated role as a glucocorticoid reductase. *Biochemistry* 41:2459-2465.

Maser, E., Friebertshäuser, J., and Völker, B. 2003. Purification, characterization and NNK carbonyl reductase activities of 11β-hydroxysteroid dehydrogenase type I from human liver: Enzyme cooperativity and significance in the detoxification of a tobacco-derived carcinogen. *Chem. Biol. Interact.* 143-144:435-448.

Moreland, T.A. and Hewick, D.S. 1975. Studies on a ketone reductase in human and rat liver and kidney soluble fraction using warfarin as a substrate. *Biochem. Pharmacol.* 24:1953-1957.

Ohara, H., Miyabe, Y., Deyashiki, Y., Matsuura, K., and Hara, A. 1995. Reduction of drug ketones by dihydrodiol dehydrogenases, carbonyl reductase and aldehyde reductase of human liver. *Biochem. Pharmacol.* 50:221-227.

Oppermann, U.C.T. and Maser, E. 2000. Molecular and structural aspects of xenobiotic carbonyl metabolizing enzymes. Role of reductases and dehydrogenases in xenobiotic phase I reactions. *Toxicology* 144:71-81.

Ortiz de Montellano, P.R., Mathews, J.M., and Langry, K.C. 1984. Autocatalytic inactivation of cytochrome P450 and chloroperoxidase by 1-aminobenzotriazole and other aryne precursors. *Tetrahedron* 40:511-519.

Porter, S.J., Somogyi, A.A., and White, J.M. 2000. Kinetics and inhibition of the formation of 6β-naltrexol from naltrexone in human liver cytosol. *Br. J. Clin. Pharmacol.* 50:465-471.

Rosemond, M.J.C. and Walsh, J.S. 2004. Human carbonyl reduction pathways and a strategy for their study in vitro. *Drug Metab. Rev.* 36:335-361.

Rosemond, M.J.C., St. John-Williams, L., Yamaguchi, T., Fujishita, T., and Walsh, J.S. 2004. Enzymology of a carbonyl reduction clearance pathway for the HIV integrase inhibitor, S-1360: Role of human liver cytosolic aldo-keto reductases. *Chem. Biol. Interact.* 147:129-139.

Ross, D., Kepa, J.K., Winski, S.L., Beall, H.D., Anwar, A., and Siegel, D. 2000. NAD(P)H:quinone oxidoreductase 1 (NQO1): Chemoprotection, bioactivation, gene regulation and genetic polymorphisms. *Chem. Biol. Interact.* 129:77-97.

Shimoda, K., Shibasaki, M., Inaba, T., Cheung, S.W., Someya, T., and Takahashi, S. 1998. Carbonyl reduction of timiperone in human liver cytosol. *Pharmacol. Toxicol.* 83:164-168.

Skálová, L., Nobilis, M., Szotáková, B., Kondrová, E., avlík, M., Wsól, V., Pichard-Garcia, L., and Maser, E. 2002. Carbonyl reduction of the potential cytostatic drugs benfluron and 3,9-dimethoxybenfluron in human in vitro. *Biochem. Pharmacol.* 64:297-305.

Slaughter, D., Takenaga, N., Lu, P., Assang, C., Walsh, D.J., Arison, B.H., Cui, D., Halpin, R.A., Geer, L.A., Vyas, K.P., and Baillie, T.A. 2003. Metabolism of rofecoxib in vitro using human liver subcellular fractions. *Drug Metab. Dispos.* 31:1398-1408.

Someya, T., Inaba, T., Tyndale, R.F., Tang, S.W., and Takahashi, S. 1991. Conversion of bromperidol to reduced bromperidol in human liver. *Neuropsychopharmacology* 5:177-182.

Stone, C.L., Hurley, T.D., Peggs, C.F., Kedishvili, N.Y., Davis, G.J., Thomasson, H.R., Li, T.K., and Bosron, W.F. 1995. Cimetidine inhibition of human gastric and liver alcohol

dehydrogenase isoenzymes: Identification of inhibitor complexes by kinetics and molecular modeling. *Biochemistry* 34:4008-4014.

Trivier, J.M., Libersa, C., Belloc, C., and Lhermitte, M. 1993. Amiodarone *N*-deethylation in human liver microsomes: Involvement of cytochrome P450 3A enzymes. (First report). *Life Sci.* 52:PL91-PL96.

Turpeinen, M., Nieminen, R., Juntunen, T., Taavitsainen, P., Raunio, H., and Pelkonen, O. 2004. Selective inhibition of CYP2B6-catalyzed bupropion hydroxylation in human liver microsomes in vitro. *Drug Metab. Dispos.* 32:626-631.

Walsh, J.S., Reese, M.J., and Thurmond, L.M. 2002. The metabolic activation of abacavir by human liver cytosol and expressed human alcohol dehydrogenase isozymes. *Chem. Biol. Interact.* 142:135-154.

Wsól, V., Szotáková, B., Skálová, L., and Maser, E. 2004. The novel anticancer drug oracin: Different stereospecificity and cooperativity for carbonyl reduction by purified human liver 11β-hydroxysteroid dehydrogenase type 1. *Toxicology* 197:253-261.

Wu, K., Knox, R., Sun, X.Z., Joseph, P., Jaiswal, A.K., Zhang, D., Deng, P.S.K., and Chen, S. 1997. Catalytic properties of NAD(P)H:quinone oxidoreductase-2 (NQO2), a dihydronicotinamide riboside dependent oxidoreductase. *Arch. Biochem. Biophys.* 347:221-228.

Key References

Snyder, L.R., Kirkland, J.J., and Glajch, J.L. 1997. Practical HPLC Method Development, 2nd ed. John Wiley and Sons, New York.

McClure, T.D. 2003. Detection of Metabolites Using High-Performance Liquid Chromatography and Mass Spectrometry. *In* Current Protocols in Toxicology (M.D. Maines, L.G. Costa, E. Hodgson, D.J. Reed, and I.G. Sipes, eds.) pp. 4.4.1-4.4.18. John Wiley & Sons, Hoboken, N.J.

References describing HPLC procedures.

Gross, A.S., Somogyi, A., and Eichelbaum, M. 2003. Stereoselective drug metabolism and drug interactions. *In* Handbook of Experimental Pharmacology 153 (Stereochemical Aspects of Drug Action and Disposition) pp. 313-339. (K. Starke, ed.) Springer-Verlag, New York.

Testa, B. 1986. Chiral aspects of drug metabolism. *Trends Pharmacol. Sci.* 7:60-64.

Reddy, I.K. and Mehvar, R., ed. 2004. Chirality in Drug Design and Development. Marcel Dekker, N.Y.

References describing stereochemistry procedures.

Allison, R.D. 1997. Kinetic assay methods. *In* Current Protocols in Molecular Biology (Ausubel, F.M., Brent, R., Kingston, R.E., Moore, D.D., Seidman, J.G., Smith, J.A., and Struhl, K., eds.), pp. A.3H.1-A.3H.11. John Wiley & Sons, New York.

Copeland, R.A. 2000. Enzymes: A Practical Introduction to Structure, Mechanism, and Data Analysis, 2nd ed., John Wiley & Sons, New York.

Cornish-Bowden, A. 2004. Fundamentals of Enzyme Kinetics, 3rd ed. Portland Press, Ltd. Colchester, UK.

Cornish-Bowden, A. 1995. Analysis of Enzyme Kinetic Data. Oxford Univ. Press. Oxford, UK.

References describing enzyme kinetics.

Internet Resources

http://www.med.upenn.edu/akr/

A very useful Website for the aldo-keto reductase superfamily.

http://www.gentest.com/

For fluorescence assays to confirm enzymatic activity of recombinant P450 mixture (BD Biosciences).

http://www.abnova.com.tw

http://www.biocatalytics.com

Websites for suppliers of heterologously expressed carbonyl reducing enzymes.

Contributed by M. Jane Cox Rosemond
GlaxoSmithKline
Research Triangle Park, North Carolina

CHAPTER 5
Toxicokinetics

INTRODUCTION

Toxicokinetics is a specialized area of toxicology that blends pharmacokinetic procedures with those of toxicology. It involves understanding the processes that govern the absorption, distribution, metabolism, and excretion of chemicals by the body. In general, these processes can be referred to as input (absorption), translocation (distribution), and output (metabolism, excretion). The rates of each process can be derived and used to describe in mathematical terms the time course for chemical and metabolite disposition in the body. Each process is governed by a number of physicochemical, biochemical, and physiological factors that profoundly affect how the body handles a particular chemical. For example, the state of hydration of the skin is an important physicochemical factor that influences chemical absorption by that route. Also, metabolic enzymes can have a profound effect on the input and output processes for a chemical. Thus, factors that increase the rate of biotransformation (enzymatic metabolism) of a chemical can profoundly affect input (increased formation of a toxic metabolite) or output (increased detoxification) processes that govern the temporal patterns of response to a particular chemical. These factors include induction and/or inhibition of xenobiotic-metabolizing enzymes, and interindividual variations may result from the presence of polymorphisms in these enzymes. Reduction of adipose tissue mass reduces a storage compartment for lipophilic chemicals and thus can alter their rate of elimination from the body. Since toxicants are frequently present as complex mixtures, the way in which one toxicant can affect the toxicokinetics of another is important and will be considered in subsequent units.

This chapter presents a series of methods for determining rates of absorption, distribution, and elimination of chemicals. In addition, mathematical approaches for determination of toxicokinetic parameters are discussed. As the chapter evolves, more complex modeling approaches will be presented. Since toxicokinetic models provide effective means of extrapolating animal data to the human situation, methods for obtaining human data will be presented. Chapter 4, which focuses on techniques for determining rates and routes of biotransformation of chemicals, should be considered a companion chapter to this one. Such information is critical in understanding chemical toxicity and in comparing animal and human data.

UNIT 5.1 describes an in vitro system for assessing percutaneous absorption of chemicals that can be applied to skin from a variety of animal species, including humans. The system can also provide information on the metabolism of chemicals by the skin.

UNIT 5.2 covers in vivo approaches for measuring absorption through the skin. The basic procedure uses rats, but is applicable to other species; modifications for assessing absorption of volatile compounds are also provided. A second approach presented is a procedure for assessing dermal absorption of chemicals by humans. Discussion of the legal and ethical aspects of the use of human volunteers in such studies is included.

UNIT 5.3 is an introductory unit that provides basic information on the processes that govern pharmacokinetics/toxicokinetics. It provides definitions and formulas that describe

Contributed by I. Glenn Sipes and Ernest Hodgson
Current Protocols in Toxicology (2005) 5.0.1-5.0.2

various output processes.The author stresses the importance of interrelationships among the various physiological and biochemical parameters that ultimately determine plasma half-life, clearance, tissue retention, etc. Important information is presented with respect to the experimental design for toxicokinetic studies as well as complicating factors that need to be considered in the design and analysis of such studies. The unit concludes with data analysis of an example study.

UNIT 5.4 provides a protocol for the establishment and use of the isolated perfused porcine skin flap (IPPSF). The IPPSF is used to measure the rate and extent of absorption of chemicals through skin. It involves an ex vivo preparation with intact anatomical structure and microcirculation. Metabolism of toxicants during transit through the skin can also be measured. Not only can the external environment and internal factors be controlled in this system, but porcine skin is also more closely related, anatomically and physiologically, to human skin than the skin of any other available experimental animal. The IPPSF has proven to be an invaluable model of toxicant uptake by human skin.

UNIT 5.5 describes another method for the measurement of skin penetration of toxicants or other xenobiotics, namely the flow-through diffusion cell system. The present protocol emphasizes porcine skin and thus provides a precise alternative to *UNIT 5.4*, the isolated perfused porcine skin flap (IPPSF). The diffusion cell enables the experimenter to isolate and focus on the role of the stratum corneum and the viable epidermis rather than the complex in vivo-like model represented by the IPPSF. Although porcine skin is utilized because it is the best known surrogate for human skin, this method has also been used for investigations of skin penetration in rodent, humans, and other primates.

UNIT 5.6 on toxicant transport by P-glycoprotein concerns events at the cellular level that are important to toxicokinetics. Transporter proteins are currently of considerable interest and P-glycoprotein is one of the best known. This transporter is widely distributed, generally on the apical side of cells in organs of elimination; it is found in hepatocytes, in enterocytes, in the brush border of proximal tubule cells of the kidney, as well as in other tissues. It brings about the efflux from these cells of many xenobiotics, including therapeutic drugs and many toxicants.

Although collection of urine and bile has been carried out for several decades, it is nevertheless still critically important in toxicokinetic studies. *UNIT 5.7* is particularly timely as it deals with continuous collection of urine and bile from the mouse rather than from the rat or larger mammals normally used. Because the mouse is the animal of choice for genetic manipulation, careful and accurate collection of body fluids is essential to determine toxicokinetic parameters in such genetic constructs as humanized and knockout mice.

I. Glenn Sipes and Ernest Hodgson

Measurement of Bioavailability: Measurement of Absorption Through Skin In Vitro

BASIC PROTOCOL

Measurement of skin absorption is essential for all new drugs intended for skin application (those for use in treating skin conditions and those aimed to penetrate the skin for the treatment of systemic diseases), as well as agrochemicals not intended for direct skin application, but to which there may be accidental skin exposure during occupational use. In studying skin bioavailability, both in vitro and in vivo (*UNIT 5.2*) techniques can be employed. In vitro methodologies have certain advantages over their in vivo counterparts in that they are simpler, faster, more reproducible, and more economical. By employing human skin, in vitro methods reduce the use of animals and overcome the necessity for extrapolation between species. In addition, they allow the study of skin absorption in isolation from systemic events. The use of fresh skin (maintained under conditions that ensure continuous viability of the tissue) provides a barrier that is representative of the in vivo situation. The most valuable in vitro techniques are those employing freshly excised animal or human skin in flow-through diffusion cells, since this ensures that the skin remains metabolically active throughout the course of the experiment, allowing skin absorption and skin metabolism to be studied simultaneously.

This protocol describes one particularly useful in vitro method, the flow-through diffusion-cell skin absorption model (SAM), which can be utilized to investigate the percutaneous absorption of chemicals following topical application. Skin from various species can be employed (e.g., human, rat, mouse, guinea pig, pig), and freshly obtained skin remains metabolically active in the flow-through diffusion cell for ≥24 hr, allowing skin metabolism to be assessed at the same time as skin bioavailability. For accurate assessment of skin absorption and metabolism, it is advisable to use radiolabeled compounds, although unlabeled compounds may be used if a suitably validated analytical technique is available. Either full-thickness skin or thinner sections (isolated epidermis or epidermis plus a little upper dermis) may be used. Following application of the compound to the skin surface for the desired length of time, it is possible to assess uptake into the skin, passage across the skin into the receptor fluid bathing the underside of the tissue, and residual material remaining on the skin surface, enabling a full mass balance to be achieved. A diagram of the diffusion cells (both occluded and unoccluded versions) and a photograph of the SAM system are presented in Figure 5.1.1.

The key to success with this procedure is to prepare the skin adequately prior to placing it in the diffusion cells. This involves removing all subcutaneous fat and tissue carefully. When epidermal membranes or epidermis plus a little dermis are employed, it is advisable to establish the integrity of the membrane prior to absorption studies (for example, by measuring electrical resistivity or the permeation of a marker substance such as tritiated water). It is not necessary to establish the integrity of full-thickness skin, since this tissue is generally not subjected to any potentially damaging treatment prior to experimentation.

CAUTION: Human skin is a biohazard and should be handled with caution. Gloves, goggles, and a face mask should be used throughout. Perform as much of the procedure as possible in a safety cabinet, handling samples with care so as to prevent aerosol generation. Ensure surgical samples are pathogen free. All persons handling human and animal tissue should be vaccinated against hepatitis B virus; other precautions may be required, depending on the source of the skin. Ethical approval for use of human skin should be obtained from the local hospital ethics committee, and patients' consent to donate their skin for research should be obtained.

Contributed by Sharon A.M. Hotchkiss

Current Protocols in Toxicology (1999) 5.1.1-5.1.14

CAUTION: When working with radioactivity, take appropriate precautions to avoid contamination of the experimenter and the surroundings. Carry out the experiment and dispose of wastes in an appropriately designated area, following the guidelines provided by the local radiation safety officer (also see *APPENDIX 1A*).

Materials

Receptor fluid: HHBSS (see recipe) or tissue culture medium
Skin sample (human or animal)
70% and 100% (v/v) ethanol
Enzyme solution (e.g., Dispase, Sigma; optional)

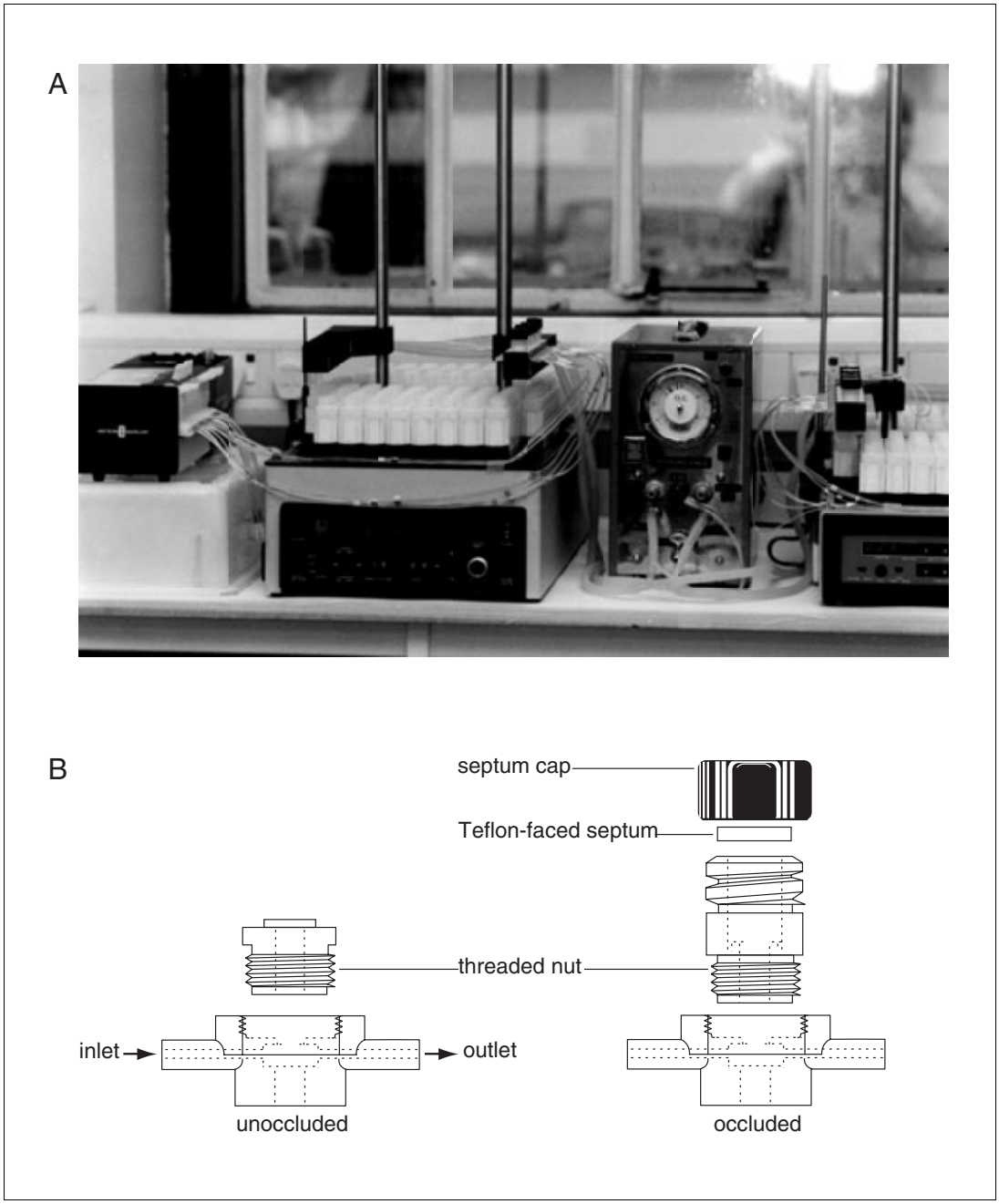

Figure 5.1.1 (**A**) Complete SAM system (1, pump; 2, fraction collector; 3, diffusion cells; 4, water circulator). The second fraction collector (at the right) is not needed. (**B**) Diagrammatic representation of in vitro flow-through diffusion cells, shown for both occluded and unoccluded systems.

Test compound (usually radiolabeled; >98% pure)
Vehicle: e.g., dimethyl sulfoxide (DMSO), ethanol, or water
Scintillation fluid (e.g., Ecoscint, National Diagnostics)
2% (v/v) aqueous soap solution (liquid hand soap, e.g., Labguard microbial hand soap, Day Impex; optional)
Decontamination liquid (e.g., Decon from Decon Laboratories)
Skin digest solution (see recipe)
4.4 M nitric acid (HNO_3)

Skin absorption model (SAM) system (Fig. 5.1.1), including:
Fraction collector (Crown Glass)
Flow-through diffusion cells (Crown Glass)
Receptor fluid reservoir
Heated water circulator set at 36°C (Churchill)
Peristaltic pump (Watson-Marlow)
Teflon septa and caps (for occluded skin experiments; Crown Glass)
20-ml plastic and glass scintillation vials
Heated mantle blocks (Crown Glass)
Vacuum filtration system with 0.45-µm filter
Dermatome (e.g., Padgett electric model; optional)
Surgical tools (scissors, scalpel, forceps)
Rubber mat or cork board
Circular steel cutter with 1.7-cm-diameter circular cutting edge (custom made at the Imperial College School of Medicine)
Hammer
0.63-µm-bore orange-white marprene or polyvinyl chloride (PVC) tubing (Watson-Marlow)
10-µl Hamilton syringe and blunt-ended needle
Gauze swabs cut into ~1.5-cm^2 pieces
70°C shaking water bath
Spreadsheet software (e.g., Microsoft Excel)

Set up equipment

1. Prepare the fraction collector of a SAM system by ensuring that all racks are filled with 20-ml plastic scintillation vials. Set digital settings for the collection interval (e.g., hourly) and the duration of the experiment (e.g., 24 hr).

2. Place seven flow-through diffusion cells of the SAM system in a heated mantle block and ensure that they are correctly oriented. Position the heated mantle block such that all drops of liquid from underneath the cells fall into the scintillation vials.

   Seven or fourteen diffusion cells can be run concurrently. Doubling the procedure requires a second heated mantle block (one for each seven cells).

   The side arms of the diffusion cells are of two types: the biggest aperture is in the inlet arm (which connects via tubing to the pump) and the smallest aperture is in the outlet arm (from which the receptor fluid flows out into the vials). The outlet hole is designed to be smaller to ensure a slight back pressure in the diffusion cell, to aid mixing, and to reduce bubble formation under the skin.

3. Prepare the receptor fluid.

   HHBSS has been determined to be the most acceptable receptor fluid for most purposes. If the compound is highly lipophilic, a solvent (e.g., 50% aqueous ethanol) or supplements (e.g., PEG or BSA) may be required (see Critical Parameters).

HHBSS or a tissue culture medium are essential when skin metabolism is to be studied, as these receptor fluids maintain the skin in a metabolically viable condition for ≥24 hr. An ethanolic receptor fluid will not support skin viability for more than a few minutes.

4. Filter the receptor fluid by vacuum filtration using a 0.45-µm filter (to remove air bubbles) and transfer the liquid to the SAM receptor fluid reservoir.

5. Switch on the heated water circulator of the SAM system (set at 36°C) and allow the heated mantle block and diffusion cells to warm up.

   Setting the water circulator to 36°C results in a skin surface temperature of ~32° to 33°C.

Prepare skin circles

6. Obtain a fresh skin sample, rinse with 70% ethanol, and place in a petri dish on ice.

   Human skin should be obtained as fresh as possible from donors. Typically, large regions of tissue are required (e.g., breast reduction, apronectomy).

   Animal skin (e.g., male Fischer 344 rat, body weight ~175 to 250 g) should be obtained following light anesthesia (with ether or halothane) and appropriate euthanasia (any humane form, e.g., cervical dislocation). The dorsal region should be clipped with animal clippers and removed using a sharp scalpel and scissors, taking care not to nick the skin.

7. Cut away as much subcutaneous tissue as possible with scissors and scalpel. If a thinner membrane is required, remove dermis as appropriate, using a dermatome (for samples consisting of epidermis and upper dermis) or an enzyme solution (for epidermis only).

   For further details, see Critical Parameters discussion of skin membrane.

8. Place the skin epidermal side up on a rubber mat or corkboard.

9. Cut out circles of skin, 1.7 cm in diameter, using a circular steel cutter and hammer. Place each skin circle in a petri dish (epidermal side down), and cover lightly with tissue paper or foil.

10. Place a circle of skin epidermal side up into each diffusion cell body, gently easing the tissue with forceps to allow the tissue to meet the edges of the cell. Secure the threaded nut in each diffusion cell.

Attach receptor fluid reservoir

11. Start the peristaltic pump of the SAM system and prime the tubes from the receptor fluid reservoir. Run the flow at maximum speed (75 ml/hr) for ~1 min and ensure that there are no air bubbles in the lines.

12. Attach a 0.63-µm marprene or PVC tube from the receptor fluid reservoir to the inlet arm of each diffusion cell, taking extreme care not to introduce any air bubbles into the system.

13. Run the peristaltic pump at maximum speed until the receptor fluid is flowing under all the skin circles and the eluent drips into the 20-ml scintillation vials.

14. Allow the receptor fluid to bathe the underside of the skin for 20 to 30 min at the required flow rate (1.5 ml/hr is suitable for most experiments).

Apply test chemical

15. While the skin and receptor fluid are equilibrating, make up a test compound solution in a suitable vehicle.

    Doses can range from a few ng/cm^2 skin to mg/cm^2 skin, depending on the compound under study and its likely level of contact with human skin.

    It is preferable to use a radioactive chemical (usually ^{14}C- or ^{3}H-labeled). For example, depending on the absorption properties of the compound, ~0.2 µCi of ^{14}C per skin circle will usually suffice.

16. Measure the specific activity of the test compound solution accurately and in triplicate by liquid scintillation spectrometry.

17. Following equilibration of the skin in the SAM system for 20 to 30 min, move the fraction collector rack (containing 20-ml vials) into position. Gently apply 5 to 10 µl test compound solution to each skin circle using a 10-µl Hamilton syringe with a blunt-ended needle.

    Apply the dose solution to the center of the exposed area of the skin, only lightly touching the skin to remove the last drop of the dose solution from the needle.

18. *Optional:* If the diffusion cells are to be occluded, cover each cell with a Teflon septum and cap (Fig. 5.1.1B), making sure the cap is finger tight.

    This is done if the experiment aims to investigate the effect of occlusion on skin penetration (see Critical Parameters).

19. Collect receptor fluid for the desired length of time (e.g., every 2 hr for up to 72 hr). Throughout the experiment, add 15 ml scintillation fluid to each collected fraction, mix, and measure the radioactivity.

Disassemble equipment and measure radioactivity

20. At the end of the experiment, switch off the water circulator, fraction collector, and pump, and disconnect the tubing from the cells. Rinse out the reservoir flask, thoroughly, and replace the liquid with 70% ethanol, leaving this to pump through the tubes for ~15 min.

21. If cells were occluded, unscrew each cap and place it with its septum in a beaker containing 10 ml of 100% ethanol (one beaker per cap and septum). Unscrew each threaded nut and place in a beaker containing 50 ml of 100% ethanol (one per nut).

    In addition to the receptor fluid measured above, four separate radioactivity measurements will be made for each sample: from the cap, the cell and matching threaded nut, a skin swab, and the skin circle.

22. Swab the skin at least twice (sometimes up to ten times) with 1.5-cm^2 gauze swabs soaked in 2% aqueous soap solution or 100% ethanol (depending on the chemical's solubility) and place the swabs in 20-ml plastic scintillation vials, each containing 10 ml of 100% ethanol.

23. Place each skin circle into a separate 20-ml scintillation vial and freeze at −20°C for later analysis of residual radioactivity in the skin. Place each diffusion cell body in the appropriate beaker with its matching threaded nut.

24. Cover the beakers with Parafilm/nescofilm and leave the caps, swabs, and cells/threaded nuts to soak overnight.

25. The next day, place triplicate 1-ml aliquots of all liquid samples (i.e., swabs, caps, cells/threaded nuts) into 20-ml scintillation vials, add 10 ml scintillation fluid, and count for residual radioactivity.

26. Clean the diffusion cells and caps by placing each cell body, threaded nut, cap, and septum into a plastic beaker containing ~800 ml of a weak solution of decontamination liquid (e.g., ~1% Decon solution). Leave to soak overnight. The next day, rinse each cell unit thoroughly with tap water followed by distilled water and leave to soak in distilled water overnight. Dry the cells thoroughly with tissue, paying special attention to the side arms.

24-hour absorption study ^{14}C-custard
cells 1 to 4 occluded, 5 to 7 unoccluded

fresh human skin
machine 1

Cell no.:	1	
Dose vol:	5	µl
Dose dpm:	318490	(0.143 µCi)
Dose ng:	7900	
Vehicle:	100%	EtOH
Flow rate:	1.5	ml/hr
Receptor phase:	HHBSS	
Skin SA:	0.32	cm^2
Skin weight:	0.2276	g

Interval	Hr	Volume	Volume Counted	DPM	Total DPM	% Dose	Cum. % Dose	Cum. Dose (ng)	% Dose /hr	ng/hr	ng/cm^2 /hr
0-2	2	3.0	3.0	2388	2388	0.75%	0.75%	59.23	0.37%	29.62	92.55
3-4	2	3.0	3.0	12458	12458	3.91%	4.66%	368.25	1.96%	154.5	482.8
5-6	2	3.0	3.0	16542	16542	5.19%	9.86%	778.57	2.60%	205.2	641.1
7-8	2	3.0	3.0	17272	17272	5.42%	15.28%	1206.99	2.71%	214.2	669.4
9-10	2	3.0	3.0	16266	16266	5.11%	20.39%	1610.46	2.55%	201.7	630.4
11-12	2	3.0	3.0	15462	15462	4.85%	25.24%	1993.99	2.43%	191.8	599.3
13-14	2	3.0	3.0	14844	14844	4.66%	29.90%	2362.19	2.33%	184.1	575.3
15-16	2	3.0	3.0	13754	13754	4.32%	34.22%	2703.35	2.16%	170.6	533.1
17-18	2	3.0	3.0	12672	12672	3.98%	38.20%	3017.67	1.99%	157.2	491.1
19-20	2	3.0	3.0	11884	11884	3.73%	41.93%	3312.45	1.87%	147.4	460.6
21-22	2	3.0	3.0	10656	10656	3.35%	45.28%	3576.77	1.67%	132.2	413
23-24	2	3.0	3.0	9554	9554	3.00%	48.28%	3813.75	1.50%	118.5	370.3
Swab		10.0	1.0	3687	36870	11.58%		914.54			
C. wash		50.0	1.0	55	2750	0.86%		68.21			
T. cap		10.0	1.0	5064	50640	15.90%		1256.10			
Skin		1.5	1.5	52000	52000	16.33%		1289.84			
Total recovery							92.94%	7342.44			

Figure 5.1.2 Sample spreadsheet for analysis of skin absorption data. Data are shown for receptor fluid (at 2-hr intervals from 0 to 24 hr), swabs, cell wash (C. Wash), Teflon cap wash (T. Cap), and skin circles. Cumulative (cum.) % dose is absorption as a percent of the applied dose. The rate of absorption per diffusion cell is given in ng/hr, and the rate of absorption per cm^2 of skin is given in ng/cm^2/hr.

27. When the skin sample analysis is to be conducted, remove the skin circles from the freezer and allow to thaw at room temperature. Transfer the tissue to a tared glass scintillation vial and weigh.

28. Add an aliquot of skin digest solution to each skin circle (1.5 ml to human skin, 1 ml to rat skin), cap the vial, and place in a shaking water bath at 70°C for 1 to 2 hr.

29. Remove the vial, allow to cool to room temperature, and add 0.5 ml of 4.4 M HNO_3. Check that the pH is neutral (pH 7 exactly).

30. Add 10 ml scintillation fluid, mix well, and count for radioactivity against a quench curve made up using untreated human or rat skin spiked with a known amount of radioactivity.

Analyze results

31. Prepare a computer spreadsheet (e.g., using Microsoft Excel; see Fig. 5.1.2) and enter dpm data to determine the recoveries on the skin surface, within the skin, in the receptor fluid, on the diffusion cells, and on the caps.

32. Calculate total recovery and absorption. Calculate absorption as a percent of the applied dose and also in absolute amounts (e.g., $\mu g/cm^2$).

Absorption is defined as recovery in the receptor fluid. Skin levels may also be considered as "absorbed" in terms of dermal exposure, although these skin residues may not necessarily be systemically available.

Total recoveries (the sum of all assayed compartments) should be >90% unless the compound is volatile.

Further analyses may involve calculation of steady-state flux, permeability constants (K_p), and lag times (see Background Information). Where appropriate, statistical analysis may be conducted (for example, to compare absorption of a given compound under both occluded and unoccluded conditions).

REAGENTS AND SOLUTIONS

Use Milli-Q-purified water or equivalent for all recipes and protocol steps. For common stock solutions, see ***APPENDIX 2A****; for suppliers, see* ***SUPPLIERS APPENDIX****.*

HHBSS (HEPES-buffered Hanks' balanced salt solution)

Weigh 19.6 g Hanks' balanced salt solution (HBSS; premade powder, Sigma), 11.9 g HEPES acid, and 0.7 g sodium bicarbonate into a conical flask and add ~800 ml Milli-Q-purified water (or equivalent). Add 10 ml of 10 mg/ml gentamicin solution and stir using a magnetic stirrer. Adjust pH to 7.3 using 1 M NaOH and adjust volume to two liters with water. Prepare fresh for each experiment.

Skin digest solution

Add 20 g sodium hydroxide to 150 ml Milli-Q-purified water and cool on a bucket of ice. Add 75 ml methanol and 25 ml Triton X-405, and mix thoroughly with a magnetic stirrer. Prepare fresh on the day of use.

COMMENTARY

Background Information

Brief review of other techniques

A wide variety of in vitro techniques are available for the study of skin bioavailability (absorption and metabolism; Table 5.1.1). The most commonly used approaches employ animal or human skin in diffusion chambers, either static or flow-through, where the skin is placed horizontally and exposed to the atmosphere to separate the donor and receptor compartments (Franz, 1975; Bronaugh et al., 1982; Bronaugh and Stewart, 1985; Hotchkiss et al., 1990, 1992a,b, 1993). Skin absorption, and metabolism if desired, is determined by the analysis of the parent compound and/or metabolites (e.g., by high-performance liquid chromatography or by gas chromatography/mass spectrometry) appearing in the receptor fluid under the skin, and the skin may also be analyzed to determine any parent compound and metabolites within the tissue. Where radiolabeled compounds have been applied, microautoradiographic techniques may be used to visualize the compound in the skin and determine the precise anatomical location of the absorbed chemical.

Other in vitro techniques have proven to be of some value for skin absorption studies, including fresh skin explants in short-term organ culture (Kao and Hall, 1987) and an elaborate isolated, perfused porcine skin-flap model (Riviere et al., 1986). Isolated human skin (Kreidstein et al., 1991) and pig ears (de Lange et al., 1994) have also been perfused. These perfused skin preparations have the advantage of using the skin's own microcirculation to carry nutrients to the cells and remove the penetrant compounds. However, they are also time consuming to perform and require competent technical skills.

So-called reconstructed human skin or human skin equivalents have been recently developed, fueled by the difficulties encountered in obtaining fresh human skin, and are currently under investigation as skin absorption models. These skin equivalents are essentially collagen matrices containing skin fibroblasts with an overlaid layer of epidermal keratinocytes. Sev-

Table 5.1.1 In Vitro Methods for the Evaluation of Percutaneous Absorption/Metabolism in Different Samples

Organs/tissue	Cells	Subcellular fractions
Diffusion chambers (static and flow-through)	Isolated cells (e.g., keratinocytes, melanocytes, fibroblasts,, Langerhans cells)	Homogenates (whole skin, epidermis, or dermis)
Short-term organ culture		Microsomes
Isolated perfused porcine skin flap	Cell lines	Cytosolic fraction
Skin slices/chopped skin	Epidermal keratinocyte cultures	Purified enzymes
Whole human hair follicles	Hair follicle keratinocyte cultures	
Human skin punch biopsies		
Reconstructed human skin		
Human skin equivalents		

eral skin equivalents have been tested to determine percutaneous absorption and, although the stratum corneum is not properly formed in these systems and absorption is often orders of magnitude higher than human skin, some are now commercially available.

In vitro/in vivo correlations

Some in vitro systems have been shown to provide predictive models for in vivo absorption. Franz (1975) reported good correlations between the in vitro absorption of hippuric acid, benzoic acid, and chloramphenicol through human skin in a static diffusion cell and previously published in vivo data. Bronaugh et al. (1982) also reported that the static cell provided a good model for the percutaneous absorption of benzoic acid, urea, and acetylsalicylic acid through rat skin. The use of skin in flow-through diffusion cells has significant advantages over its use in static cells. For one, it more closely resembles the true skin barrier as it exists in vivo, due to the continuous flow of a physiological receptor fluid across the underside of the skin, which mimics dermal blood flow, maintains skin viability by providing nutrients and oxygen and by carrying away waste products, aids in the partitioning of lipophilic compounds into the receptor fluid, and minimizes sample collection problems. Various studies have shown that the flow-through diffusion cell system provides a good model for predicting the in vivo percutaneous absorption of a wide range of compounds in human and animal skin (Bronaugh and Stewart, 1985; Hotchkiss et al., 1990, 1992a,b; Mint et al., 1994; Beckley-Kartey et al., 1997).

Skin reservoir

There is considerable debate over whether one should consider the material present within the skin, in an in vitro percutaneous absorption experiment, as absorbed compound. In theory, residual chemicals within the skin are available for subsequent systemic absorption and will not be removed by conventional washing procedures. In support of this, a linear relationship has been shown to exist between the amount of a chemical present in rat stratum corneum 30 min following application in vivo and the total amount absorbed (excreted and in epidermis and dermis) in 4 days (Rougier et al., 1985), indicating that measurement of the amount of chemical in the stratum corneum reservoir may allow the prediction of total systemic absorption. Conversely, the kinetics of absorption of some topically deposited chemicals from the skin into the systemic circulation may be so slow that skin desquamation may remove the stratum corneum reservoir layers before further systemic absorption may occur. The presence of a cutaneous reservoir for potentially hazardous or pharmacologically active compounds may result in continued systemic exposure, even after topical contact has ceased.

Quantification of absorption: permeability constant, flux, and lag time

In simple terms, the absorption of a chemical through the skin can be regarded as a diffusion process and is therefore governed by Fick's first law of diffusion at steady state. There is a period immediately after skin exposure where diffusion increases to reach steady state. This lag time is compound specific and ranges from minutes to days.

Once the system reaches steady state, the rate of absorption of a chemical across a membrane is proportional to the applied concentration and can be represented by $J = K_p \times DC$, where J is the steady-state rate of absorption (flux), K_p is the permeability constant, and DC is the concentration difference of the penetrant across the membrane. The permeability con-

stant is in turn defined by $K_p = (K_m \times D)/\delta$, where K_m is the partition coefficient of penetrant between tissue (stratum corneum) and vehicle, D is the diffusion constant, and δ is the diffusion path length (stratum corneum thickness). Thus, the permeability constant (cm/hr) increases with the solubility of the penetrant in the stratum corneum and decreases with increasing skin thickness. Combining these equations gives $J = (K_m \times D \times DC)/\delta$. These equations may be applied to most percutaneous absorption studies and, with certain exceptions, will give reasonable approximations.

In vitro studies can be carried out using two types of dosing conditions: either infinite dose or finite dose. An infinite dose of topically applied compound will ensure that steady-state kinetics are maintained over the entire time course, enabling the true permeability coefficient (K_p) to be calculated. A finite dose will more likely represent the in vivo situation, whereby only small amounts of chemical are applied to the skin and apparent steady-state kinetics are only reached for a brief period of time.

Critical Parameters

A number of factors appear to be important in determining how well a chemical penetrates into the skin, and should therefore be considered as potential influencing factors in an in vitro experiment. These include the chemical's physicochemical properties (e.g., solubility, molecular volume, volatility), the amount applied, whether any other chemical is applied at the same time, the duration of skin exposure, whether the surface of the skin is covered, skin temperature and moisture content, and whether the skin is damaged or diseased. The precise site of application is also a factor determining the rate and extent of skin absorption, as is the age of the skin, the species, and structural differences such as skin thickness and the number of hair follicles (Hotchkiss, 1995).

The critical parameters, in terms of obtaining good in vitro percutaneous absorption data that is representative of the in vivo situation, fall into two main categories: choice of skin membrane and choice of receptor fluid.

Skin membrane

The single most important factor to ensure good in vitro data is to prepare the skin very carefully by removing all subcutaneous tissue prior to placing it in the diffusion cell. The simplest skin membrane type is full-thickness skin, which is easy to handle and prepare and is routinely employed (Frantz et al., 1990; Hotchkiss et al., 1990, 1992a,b, 1993). It is quite in order to commence any new study using full-thickness skin; however, it should be remembered that for highly lipophilic compounds (e.g., those with an octanol-water partition coefficient [$P_{o/w}$] > 4) the dermis of the skin is hypothesized to act as an additional barrier to skin penetration in vitro. This may limit the chemical's partitioning from the skin into the receptor fluid in an in vitro system and, hence, the in vitro system may underestimate the true in vivo absorption. The dermal barrier is not present in vivo because the cutaneous blood supply lies in the upper dermis, close to the epidermal-dermal junction, insuring that the chemical can diffuse into the bloodstream without having to traverse the entire thickness of the dermis.

One cannot always predict, from lipophilicity alone, if the dermis will present a problem for a particular compound, because certain highly lipophilic molecules are metabolized in the skin to more polar metabolites that may readily partition out from the tissue into the receptor fluid. When a problem is anticipated, it is wise to remove the dermis, or as much of it as possible, prior to conducting the percutaneous absorption study. This should preferably be done by mechanical means with a dermatome, but can also be done thermally by immersion in hot water, enzymatically by Dispase separation, or chemically by sodium bromide treatment. Bear in mind, though, that heat and chemical treatment will deactivate xenobiotic metabolizing enzyme activity in the skin. In addition, preparation of epidermal sheets is difficult in hairy skin, since the hair follicles penetrate deep into the dermis and can compromise the barrier properties of these epidermal sheets. The dermatome method removes the majority of the dermis and can give skin samples of accurate thickness. The typical thickness of dermatomed tissue used in in vitro experiments is 200 to 300 μm for rat skin, and 300 to 1000 μm for human and pig skin (Bronaugh and Stewart, 1985; Potts et al., 1989; Storm et al., 1990).

If epidermal membranes rather than full-thickness skin are to be used, great care with handling the fine epidermal sheets is required. Typically, these sheets of skin are very thin (~100 μm) and delicate, and therefore should not be transferred to the diffusion cells using forceps (as one does for full-thickness skin). Instead, they should be floated on water and the diffusion cells should be submerged underneath to allow the membrane to settle in the cell.

Skin freshness. Where metabolism is to be studied, the skin must be obtained as fresh as possible, ideally within 1 hr of excision from either the human individual or animal. This is important because the enzymes in the skin may decline rapidly following excision. At present, the viability of skin in the SAM system has only been assessed up to 24 hr and cannot be guaranteed for longer periods. Of course, the viability of the tissue should be specifically defined in terms of the enzymes involved: cytochrome P-450 enzymes may decline very rapidly post excision (e.g., within 8 hr), whereas esterase enzymes may be active for considerably longer (e.g., >24 hr).

Nonviable tissue. Some experimenters elect to use nonviable skin—e.g., previously frozen tissue or human autopsy specimen—for skin bioavailability studies. The argument in support of this approach is that the stratum corneum, the major barrier to skin penetration, is comprised of nonliving keratinocytes and therefore it is not essential to have viable tissue for in vitro studies. There is some value to this approach in cases where fresh skin is in short supply, but by far the most appropriate skin membrane is one where the epidermal tissue is metabolically active, so that a true picture of the bioavailability, including any metabolites produced during skin penetration, may be obtained. In the author's experience, the absorption of chemicals through previously frozen skin is not always the same as through fresh skin, and therefore this membrane type should not be used unless there is no viable alternative.

Inter-individual variation. There is widespread inter-individual variation between humans in the percutaneous absorption of chemicals. For instance, the inter-individual variation in percutaneous absorption of 4,4′-methylenebis(2-chloroaniline) (MbOCA) and 4,4′-methylene dianiline (MDA) between ten different human subjects is large, with a three- to four-fold range in absorption (Hotchkiss et al., 1993). Similarly, a four-fold variation in diethyl phthalate absorption through eight subjects' skin has been observed in vitro (Mint et al., 1994). Thus, care should be taken when drawing conclusions from data in a single individual, as absorption may be considerably higher or lower in another subject. For this reason, it is recommended that skin samples from at least three different individuals (or animals) be used.

Species. Species differences in absorption are a particularly important consideration. Where human skin is not readily accessible, rodent (typically rat and mouse) skin can be employed, and both haired and hairless varieties are available (Bartek et al., 1972; Kao et al., 1988; Hotchkiss et al., 1990, 1992a,b; Beckley-Kartey et al., 1997). In general, human skin is less permeable to xenobiotics than the skin of laboratory animals (Bartek et al., 1972; Mint et al., 1994). Skin absorption would appear to be relatively high in the rat and rabbit and lower in the pig and monkey, with the latter two species providing a closer approximation than rodents to human skin. The lower percutaneous absorption (increased barrier properties) in human skin compared with rat tissue is possibly due to a combination of the increased skin thickness (3 mm compared with 2 mm) and decreased hair follicle density (10/cm^2 compared with 300/cm^2). However, on occasion, and particularly under occlusive conditions, the percutaneous absorption of some chemicals (e.g., phenol and MDA) is greater through human skin than through rat tissue, which may, in part, be due to the increased thickness of (male) rat stratum corneum (~35 μm thick) compared with that of human (~20 μm thick; Hotchkiss et al., 1993). Since rodents are typically employed for skin absorption studies, and marked species differences in percutaneous absorption between rat and human skin have been observed, care should be taken when relying upon animal data to provide a model for extrapolation to the human exposure situation. Other species' skin have been utilized in in vitro models, including monkey, rabbit, guinea pig, pig, snake, and frog. Pig skin appears to be particularly useful since it is similar in structure to human skin. However, as a general rule, there is no substitute for human skin.

Anatomical region. The anatomical region of skin exposed to a chemical in the in vitro system may have a profound effect on its absorption. Although the rank order of skin site permeability would appear to be compound specific, scrotal skin appears to be the most permeable, scalp and face are intermediate, and palms, soles, and arms are the least permeable (Maibach et al., 1971). These data are in broad agreement with site-dependent differences in stratum corneum thickness: the stratum corneum thickness is thinnest on the eyelids and scrotum (10 μm) and thickest on the palms and soles (1 mm; Scheuplein and Bronaugh, 1983; Scott et al., 1991).

Dose. The dose of a chemical applied to the skin in the in vitro system will have an effect on the extent of percutaneous absorption (Hotchkiss et al., 1990a,b). In general, increasing the dose will increase absorption, because

the rate of diffusion is proportional to the amount of diffusant (Fick's law).

Occlusion. Occlusion of the skin surface in an in vitro experiment may enhance the percutaneous absorption of some chemicals, although not of others (Bucks et al., 1989; Hotchkiss et al., 1990, 1992a,b, 1993; Mint et al., 1994). For example, the absorption of MDA through human skin in vitro is significantly increased by occlusion (from 13% to 32%; Hotchkiss et al., 1993). Occlusion blocks evaporation of water from the skin surface (transepidermal water loss), which results in an increase in skin hydration. Under normal circumstances, the stratum corneum contains 5% to 15% water, but this can be enhanced to 50% by occlusion. Occlusion may also increase skin temperature—with increases up to 5°C being observed—by preventing the cooling evaporation of water, which may further enhance percutaneous absorption (Bucks et al., 1989).

Skin temperature. Under normal conditions, skin temperature is ~32°C, although this varies with factors such as external air temperature, clothing, occlusion, rubbing, and exercise. A number of authors have reported the enhanced absorption of a wide range of chemicals (including levamisole, salicylate, and phenols) through animal skin as its temperature is increased. This may result from enhanced diffusion and/or increased cutaneous blood flow. However, absorption is not always enhanced by increasing skin temperature (Blank et al., 1967).

Vehicle. The vehicle or formulation in which a chemical is applied to the skin may affect its in vitro absorption. For example, *N*-nitrosodiethanolamine penetrates the skin 200 times faster from a lipophilic vehicle (olive oil) than from an aqueous vehicle (water; Scheuplein and Bronaugh, 1983). Ethanol, 2-phenylethanol, and DMSO vehicles have been shown to enhance the absorption of benzyl acetate through rat skin in vitro (Hotchkiss et al., 1992b).

Skin metabolism. For any in vitro percutaneous absorption study, it is important to consider the potential impact of cutaneous metabolism on the bioavailability of the chemical. The degree of cutaneous metabolism will determine whether a chemical is absorbed across the skin barrier intact or as one or more metabolites. The skin contains many of the xenobiotic metabolizing enzymes identified in the liver (Hotchkiss, 1998). Skin absorption may potentially be affected by skin metabolism, since the metabolites may be absorbed at different rates owing to their different physicochemical properties. Vice versa, skin metabolism may potentially be affected by skin absorption, since the slower a chemical is absorbed the greater the chance it will be metabolized. Cutaneous enzymes have been shown to inactivate toxic chemicals such as the organophosphorous pesticides, and indeed cutaneous esterase enzyme activity may be so efficient that topically applied esters may be completely metabolized during skin absorption (see review, Hotchkiss, 1998). In contrast, other skin enzymes may activate relatively harmless substances into toxic metabolites, including cutaneous cytochrome P4501A (CYP1A)–mediated activation of the polycyclic aromatic hydrocarbons benzo(a)pyrene and dimethylbenz(a)anthracene to toxic compounds sufficiently reactive to bind to cellular DNA and cause skin cancer (see review, Hotchkiss, 1998).

Receptor fluid

The choice of receptor fluid is the second critical consideration. Ideally, one would select a receptor fluid that maintains skin viability (e.g., HHBSS or tissue culture medium) and thus allows skin metabolism to proceed during percutaneous absorption. In addition, the receptor fluid should not be a limiting factor in terms of the solubility of the penetrant. Once again, a problem may arise with highly lipophilic compounds as these will have difficulty partitioning out from the lipid skin into the relatively aqueous receptor fluid (although skin metabolism may generate polar products that can partition more readily). In these cases, one can consider substituting the typical receptor fluid with 50% aqueous ethanol or supplementing the existing receptor fluid with up to 6% (w/v) PEG (polyethylene glycol-20 oleyl ether) or up to 4% (w/v) BSA (Bronaugh and Stewart, 1985; Suber et al., 1991). However, 50% ethanol and PEG will not maintain tissue viability, and therefore metabolism cannot be studied using these receptor fluids. The addition of albumin has its limitations in studies where skin metabolism is to be investigated, because albumin has been shown to have intrinsic hydrolytic activity with the potential for interference in the measurement of the bioavailability of esters. In general, the flow rate of the receptor fluid is set between 1.5 and 3 ml per hour, with faster flow rates having no effect on the absorption of benzoic acid or caffeine (Bronaugh and Stewart, 1985; Frantz et al., 1990).

Troubleshooting

A number of factors may lead to poor recoveries of radioactivity following an in vitro skin

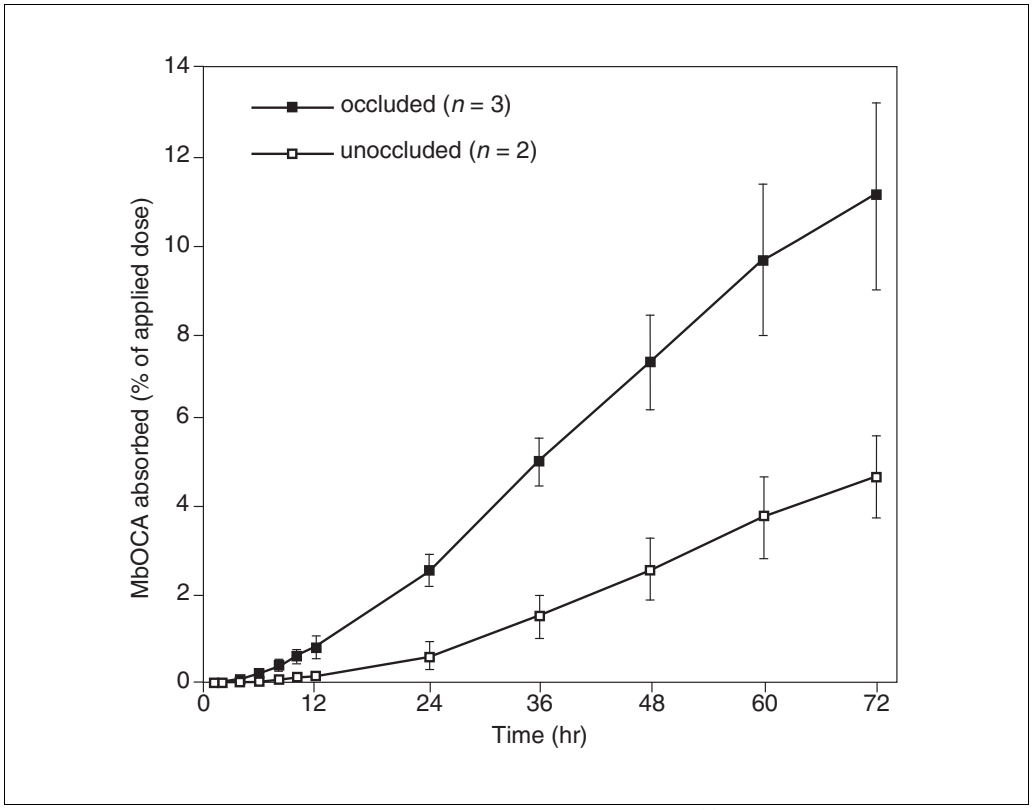

Figure 5.1.3 Typical in vitro percutaneous absorption profile of ^{14}C recoveries in receptor fluid following topical application of [^{14}C]4,4′-methylene-bis(2-chloroaniline) (MbOCA) to human skin. Mean ±SD.

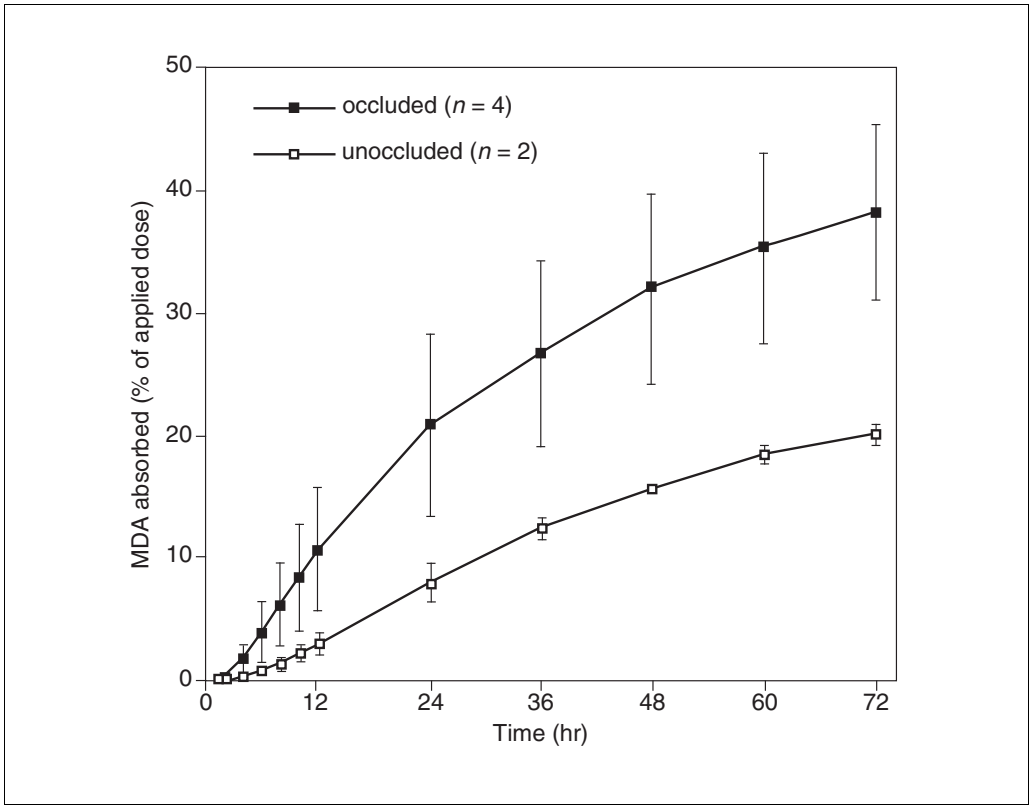

Figure 5.1.4 Typical in vitro percutaneous absorption profile of ^{14}C recoveries in receptor fluid following topical application of [^{14}C]4,4′-methylene dianiline (MDA) to human skin. Mean ±SD.

penetration study. Volatile compounds may be lost to the atmosphere at a variety of stages in the process, including evaporation from the needle or skin at the time of application, evaporation from the skin during the course of the experiment, and evaporation from the vials of receptor fluid in the fraction collector. For volatile compounds, it is advisable to apply the compound to the skin surface quickly and then immediately occlude the skin. Vials of receptor fluid should be capped immediately, rather than allowing them to sit on the faction collector for long periods of time. Conversely, if recoveries of radioactivity are unexpectedly high, consider whether the apparatus has been contaminated in some way or inadequately cleaned following a previous experiment. Always wash the diffusion cells, caps, and tubing thoroughly between experiments. Particular care should be taken when using tissue culture medium as a receptor fluid, as this may provide an ideal growth medium for bacteria and fungi in the nonsterile conditions of the open laboratory, resulting in buildup and eventual blockage of the tubing.

Anticipated Results

In vitro experiments using the SAM system are anticipated to generate percutaneous absorption profiles for the compounds under study analogous to those shown for the aromatic amines MbOCA (Fig. 5.1.3) and MDA (Fig. 5.1.4). In the case of MbOCA, the in vitro absorption through unoccluded human skin into the receptor fluid is very low, reaching only 4% (11% if occluded), and a typical absorption profile shows a lag phase of ~10 hr before an approximately linear increase in absorption that lasts for up to 72 hr. The apparent permeability constant (K_p) for the percutaneous absorption of MbOCA is 0.30×10^{-5} cm/hr (unoccluded) and 1.02×10^{-5} cm/hr (occluded). In the case of MDA, the absorption through human skin is more extensive than for MbOCA, reaching 20% (38% if occluded), and a typical absorption profile shows a lag phase of ~2 hr before a rapid increase in absorption approaching an equilibrium at 72 hr. The apparent permeability constant (K_p) for the percutaneous absorption of MDA is 3.09×10^{-5} cm/hr (unoccluded) and 8.34×10^{-5} cm/hr (occluded; Hotchkiss et al., 1993).

The graphically displayed profiles of absorption for most chemicals fall into two types. *Infinite dose* profiles have approximately steady-state absorption over the entire time course, where either the dose is high or the absorption through the skin is very slow and does not result in a significant depletion of the material remaining to be absorbed. *Finite dose* profiles show a decreasing rate of absorption, where either the dose is low or the rate of absorption is so rapid that there is depletion of the compound on the skin surface.

Time Considerations

The time taken to prepare the skin and to equilibrate the SAM system is usually on the order of 1 to 2 hr. The duration of the percutaneous absorption experiment depends on the desired exposure or collection time—ranging from relatively short-term (e.g., 8 hr) to long-term (e.g., 5 days)—but most bioavailability experiments will be of 24 or 72 hr duration. During this time, the procedure is fairly labor intensive, as the vials must be constantly removed and counted for radioactivity. Alternatively, fluor must be added and vials capped continuously; however, counting is lengthy so it is best not to count them all at the end. Once the experiment has been performed, allow extra time for data entry onto the computer spreadsheet and further analysis. Samples of skin for digestion can be collected from a number of experiments, stored in the freezer, and digested together at a later date, hence saving time and reagents.

Literature Cited

Bartek, M.J., LaBudde, J.A., and Maibach, H.I. 1972. Skin permeability in vivo: Comparison in rat, rabbit, pig and man. *J. Investig. Dermatol.* 58:114-123.

Beckley-Kartey, S.A.J., Hotchkiss, S.A.M., and Capel, M. 1997. Comparative in vitro skin absorption and metabolism of coumarin (1,2-benzopyrone) in human, rat and mouse. *Toxicol. Appl. Pharmacol.* 145:34-42.

Blank, I.H., Scheuplein, R.J., and Macfarlane, D.J. 1967. Mechanisms of percutaneous absorption. iii. The effect of temperature on the transport of non electrolytes across the skin. *J. Investig. Dermatol.* 49:582-588.

Bronaugh, R.L. and Stewart, R.F. 1985. Methods for in vitro percutaneous absorption studies. IV. The flow-through diffusion cell. *J. Pharm. Sci.* 74:64-67.

Bronaugh, R.L., Stewart, R.F., Congdon, E.R., and Giles, A.L. Jr. 1982. Methods for in vitro percutaneous absorption studies. I. Comparison with in vivo results. *Toxicol. Appl. Pharmacol.* 62:474-480.

Bucks, D.A.W., Maibach, H.I., and Guy, R. 1989. Occlusion does not uniformly enhance absorption in vivo. *In* Percutaneous Absorption. Mechanisms, Methodology, Drug Delivery. (R.L. Bronaugh and H.I. Maibach, eds.) pp. 13-27. Marcel Dekker, New York.

de Lange, J., van Eck, G.R., Bruijnzeal, P.L.B., and Elliott, G.R. 1994. The rate of percutaneous permeation of xylene, measured using the perfused pig ear model, is dependent on the effective protein concentration of the perfusing medium. *Toxicol. Appl. Pharmacol.* 127:298-305.

Frantz, S.W., Dittenber, D.A., Eisenbrandt, D.L., and Watanabe, P.G. 1990. Evaluation of a flow through diffusion in vitro skin penetration chamber method using acetone-deposited organic solids. *J. Cut. Oc. Toxicol.* 9:277-299.

Franz, T.J. 1975. Percutaneous absorption. On the relevance of in vitro data. *J. Investig. Dermatol.* 64:190-195.

Hotchkiss, S.A.M. 1995. Skin absorption of occupational chemicals. *In* Handbook of Occupational Hygiene, installment 46, pp .1-38. Croner, Surrey, U.K.

Hotchkiss, S.A.M. 1998. Dermal metabolism. *In* Dermal absorption & toxicity assessment (M.S. Roberts and K.A. Walters, eds.) pp .43-101. Marcel Dekker, New York.

Hotchkiss, S.A., Chidgey, M.A.J., Rose, S., and Caldwell, J. 1990. Percutaneous absorption of benzyl acetate through rat skin in vitro. 1. Validation of an in vitro model against in vivo data. *Food Chem. Toxicol.* 28:443-447.

Hotchkiss, S.A.M., Hewitt, P., Caldwell, J., Chen, W.L., and Rowe, R.R. 1992a. Percutaneous absorption of nicotinic acid, phenol, benzoic acid and triclopyr butoxyethyl ester through rat and human skin in vitro. Further validation of an in vitro model by comparison with in vivo data. *Food Chem. Toxicol.* 30:891-899.

Hotchkiss, S.A.M., Miller, J.M., and Caldwell, J. 1992b. Percutaneous absorption of benzyl acetate through rat skin in vitro. 2. Effect of vehicle and occlusion. *Food Chem. Toxicol.* 30:145-153.

Hotchkiss, S.A.M., Hewitt, P., and Caldwell, J. 1993. Percutaneous absorption of 4,4′-methylene-bis-(2-chloroaniline) and 4,4′-methylene dianiline through rat and human skin in vitro. *Toxic. In Vitro* 7:141-148.

Kao, J. and Hall, J. 1987. Skin absorption and cutaneous first-pass metabolism of topical steroids: In vitro studies with mouse skin in organ culture. *J. Pharmacol. Exp. Ther.* 241:482-487.

Kao, J., Hall, J., and Helman, G. 1988. In vitro percutaneous absorption in mouse skin: Influence of skin appendages. *Toxicol. Appl. Pharmacol.* 94:93-103.

Kreidstein, M.L., Pang, C.Y., Levine, R.H., and Knowlton, R.J. 1991. The isolated perfused human skin flap: Design, perfusion technique, metabolism and vascular reactivity. *Plast. Reconstr. Surg. 87:741-749.*

Maibach, H.I., Feldmann, R.J., Milby, T.H., and Serat, W.F. 1971. Regional variation in percutaneous penetration in man. *Arch. Environ. Health* 23:208-211.

Mint, A., Hotchkiss, S.A.M., and Caldwell, J. 1994. Percutaneous absorption of diethyl phthalate through rat and human skin in vitro. *Toxicol. In Vitro* 8:251-256.

Potts, R.O., McNeil, S.C., Desbonnet, C.R., and Wakshull, E. 1989. Transdermal drug transport and metabolism. II. The role of competing kinetics events. *Pharm. Res.* 6:119-124.

Riviere, J.E., Bowman, K.F., and Monterio-Riviere, N.A. 1986. The isolated perfused porcine skin flap (IPPSF). 1. A novel in vitro model for percutaneous absorption and cutaneous toxicity studies. *Fundam. Appl. Toxicol.* 7:444-453.

Rougier, A., Dupuis, D., Lotte, C., and Roguet, R. 1985. The measurement of the stratum corneum reservoir. A predictive model for in vivo percutaneous absorption studies: Influence of application time. *J. Investig. Dermatol.* 84:660-666.

Scheuplein, R.J. and Bronaugh, R.L. 1983. Percutaneous absorption. *In* Biochemistry and Physiology of the Skin (L.A. Goldsmith, ed.) pp. 1255-1295. Oxford University Press, Oxford.

Scott, R.C., Corrigan, M.A., Smith, F., and Mason, H. 1991. The influence of skin structure on permeability: An intersite and interspecies comparison with hydrophobic penetrants. *J. Investig. Dermatol.* 96:921-925.

Storm, J.E., Collier, S.W., Stewart, R.F., and Bronaugh, R.L. 1990. Metabolism of xenobiotics during percutaneous absorption: Role of absorption rate and cutaneous enzyme activity. *Fundam. Appl. Toxicol.* 15:132-141.

Suber, C., Wilhelm, K.P., and Maibach, H.I. 1991. In vitro skin pharmacokinetics of acitretin: Percutaneous absorption studies in intact and modified skin from three different species using different receptor solutions. *J. Pharm. Pharmacol.* 43:836-840.

Contributed by Sharon A.M. Hotchkiss
Imperial College School of Medicine
London, United Kingdom

Measurement of Bioavailability: Measuring Absorption Through Skin In Vivo in Rats and Humans

Humans are exposed dermally to various chemicals, either voluntarily in the case of therapeutic agents for treatment of local conditions or as a route of administration for systemic effects, or involuntarily in the case of occupational or environmental exposure. In either case a knowledge of the systemic exposure resulting from dermal exposure plays a key part in evaluating either pharmacological or toxicological effects.

A protocol design for rats is discussed here (see Basic Protocol 1), with the recognition that it will generate data that probably overestimate absorption in humans and therefore represent a worst case. A similar protocol can be used for other species such as pig, a species recognized as being a closer model to human, but with some practical limitations imposed by the greater size of the animal. An Alternate Protocol is discussed which would be applicable for volatile compounds.

Studies to assess dermal absorption in humans (see Basic Protocol 2) are invaluable to assist in extrapolating toxicological data from animals to humans as part of the risk assessment process. There are special considerations to be taken into account, namely a general reluctance to perform such studies for compounds other than human pharmaceuticals. Given a formal ethical review process, however, there is no logical reason why appropriately designed and controlled studies should not be undertaken (Hayes, 1983; Wilks and Woolen, 1994). Some practical limitations will of course restrict the type of data that can be obtained in studies with humans as opposed to animals.

Laboratory workers performing these protocols should be adequately experienced and trained and fulfill the necessary regulatory and safety requirements for working with radiochemicals and laboratory animals. It is likely that such laboratories will already be performing animal metabolism studies with radiolabeled materials, and hence have access to, and be trained in the use of, liquid scintillation counters and animal metabolism cages.

Where radiolabeled compounds are used, the radiolabel (normally carbon 14) should be situated in a metabolically stable position(s) such that there is minimal formation of $^{14}CO_2$. The radiochemical purity should be as high as possible, preferably >98%. The specific activity of the test compound required will depend upon the dose level used.

NOTE: All protocols using live animals must first be reviewed and approved by an Institutional Animal Care and Use Committee (IACUC) or must conform to governmental regulations regarding the care and use of laboratory animals.

CAUTION: When working with radioactivity, take appropriate precautions to avoid contamination of the experimenter and the surroundings. Carry out the experiment and dispose of wastes in appropriately designated areas, following the guidelines provided by local radiation safety officers (also see *APPENDIX 1A*).

MEASUREMENT OF DERMAL ABSORPTION IN THE RAT

BASIC PROTOCOL 1

The rat strain should be the same as that used in toxicology and metabolism studies. In general, particularly if rat metabolism data are already available, the use of one sex is sufficient. While there may be sex differences in metabolism, distribution, and excretion, such differences in dermal absorption are not expected. It is common either to use males

Contributed by Stephen V. Bounds and David R. Hawkins
Current Protocols in Toxicology (1999) 5.2.1-5.2.10

or to use the more sensitive sex based on toxicological data. The radiolabeled test material is applied to a protected area of the skin and absorption is measured by analyzing the material remaining in the skin and tissues and excreted by the animal.

Materials

Radiolabeled test compound (labeled with ^{14}C or ^{3}H) at >98% purity
Adult male rats, 8 to 12 weeks old, 225 to 250 g (at least four per data point)
Solvents such as acetone or methanol
Oxidizer
Sodium hydroxide
Triton X-405

Animal clippers
Spacer: saddle (silicon rubber) or O-ring (Teflon, or nonabsorbent rubber)
Adhesive (cyanoacrylate: e.g., Superglue)
Gauze (metal mesh or plastic) to fit above spacer
Application device, e.g., syringe or calibrated pipet (Gilson or equivalent)
Metabolism cages (Jencons)

1. Prepare the test compound formulation.

   The test compound should be applied in a vehicle that is appropriate to the nature of the exposure being assessed. Ideally the compound should be a solution in a liquid formulation that can be applied uniformly to the skin surface. In the case of pesticides, this may mean standard formulations developed for their use. For pharmacological products this may mean creams or emulsions representative of likely in-use preparations. A realistic application volume for liquid formulations would be 10 µl/cm^2; for a study using a radiochemical, the specific activity should be sufficient to allow application of ~0.5 MBq (~14 µCi) to a 12-cm^2 area of skin. This will allow detection of a dermal absorption of <0.5% of the dose.

2. The day prior to dosing, prepare the application site by shaving an area of each animal's dorsal skin, being careful to avoid abrading the skin surface.

3. Immediately prior to dosing, apply a spacer (part of a protective device, see below), such as a silicone rubber saddle or O-ring, to the back of the animal, enclosing the application site. Secure the spacer with cyanoacrylate adhesive.

   As an example, Figure 5.2.1 shows a protective device consisting of a spacer (e.g., rubber ring or rectangle) to which is secured a metal or plastic gauze.

   The entire protective device should be of sufficient height and robustness that when the animal arches its back or moves around, no part of the device is in direct contact with the application area. The device should allow air circulation (for semi-occluded) but should not allow the animal to lick or rub the dose site against the holding cage. It should also

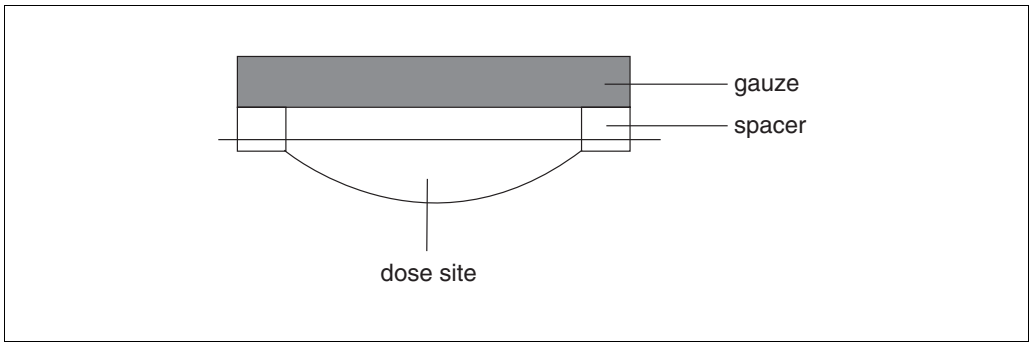

Figure 5.2.1 Schematic of saddle arrangement used to protect the dose application site (cross-section).

allow the animal sufficient movement to be able to eat and drink within the metabolism cage. An alternative is to use a collar that restricts the animals' movement. Semi-occlusion allows the skin to be equilibrated with the surrounding air and hence maintained in a normal hydration state.

4. Apply the formulation with a pipet to ~12 cm^2 of skin within the spacer. Ensure that the dose is aspirated without air bubbles and that it is spread as evenly as possible over the dose area. The pipet tip can be used as a dose spreader and retained for analysis.

   For example, for an application area of 3 × 4 cm (12 cm^2) and an application volume of 10 µl/cm^2, a total dose of 120 µl would be required.

5. After application, glue the gauze to the spacer, covering the treated area. Ensure that it does not touch the dose site, that it cannot be removed by the animal, and that it does not restrict the animal's movement.

6. For a liquid formulation, perform dose assays with the same calibrated pipet used for dosing. Pipet the dose assay aliquots directly into a volumetric flask and dilute to volume with an appropriate solvent such as acetone or methanol, prior to taking further aliquots of this solution for liquid scintillation counting. Assay the dose assays taken prior to dosing immediately to check that the radioactivity concentration was correct prior to dosing. Measure the remaining dose assays as soon as possible after dosing. Calculate the applied dose from the mean of these assays minus the residual activity remaining on the dose spreader for each animal.

   The purpose of these assays is to be able to determine the actual dose delivered using, where possible, the same dosing apparatus (syringe or pipet) and to keep a check on the homogeneity of the dose formulation. The number and frequency of the dose assays will vary from formulation to formulation depending on the formulation type. For example, for a well-mixed solution, three dose assays may be taken immediately prior to dosing, three after dosing is complete, and additional dose assays during the dosing procedure between each group of animals. For a less homogenous dose formulation, such as an emulsion, more frequent dose assays would need to be taken.

Collect samples

7. Immediately after test compound application, house the rat in an individual metabolism cage that allows separate collection of urine and feces, and volatile metabolites or $^{14}CO_2$ in expired air. When the exposure period to the applied dose is 8 hr (i.e., excess dose washed off after 8 hr), urine and feces should be collected separately from animals over the intervals 0 to 8 hr and 8 to 24 hr, and over 24-hr intervals thereafter until the experiment is terminated.

   Termination times for groups of animals can vary according to the objectives and nature of the test compound, but possible times are 8, 24, 48, and 72 hr. It is necessary to collect volatile metabolites or $^{14}CO_2$ in expired air when any absorbed material is excreted as $^{14}CO_2$ or other volatile metabolites.

8. Wash the metabolism cages with water or other suitable solvent, such as acetone or methanol, at the end of the collection. Retain the washes for measurement of radioactivity.

9. At 8 hr (or other defined time), remove the gauze from the spacer and wash the treated area five times with cotton wool swabs moistened with soap solution or other cleansing agent, such as aqueous ethanol, that would have minimal effect on the dermal uptake of the test compound. Dry the area with cotton wool and then resecure gauze to the spacer.

   During the washing period the animal should be held over the metabolism cage to collect any excreta voided during this process.

10. At each of the selected times, euthanize the animals by an overdose of anesthetic (i.e., halothane:oxygen). Remove blood by cardiac puncture. Remove the spacer and gauze (retaining them for analysis) and dissect the treated skin—including a 1-cm border surrounding the dose site—from the carcass. Remove the gastrointestinal tract and other tissues of specific interest for separate measurement.

Analyze samples

11. Measure the total radioactivity in all samples (dose assays, dose spreader, urine, feces, cage washes, tissues and organs, carcass, dose site swabs, rubber spacer, and gauze) by liquid scintillation spectrometry either by direct addition of liquid sample aliquots to a suitable scintillation fluid or after pre-treatment. Extract the saddle, gauze, and cotton wool swabs with an organic solvent (such as acetone or methanol) suitable for dissolution of the test compound and analyze extracts.

    It is expected that the recovery of the applied dose from all sources will be in the range of 90% to 110%.

    Pretreatment consists of either combustion in an oxidizer followed by trapping of the carbon dioxide or solubilization with a suitable reagent, such as a solution of 80 g sodium hydroxide in 600 ml water, 300 ml methanol, and 100 ml Triton X-405.

12. In some cases significant amounts of the applied dose may be present in the treated skin sample taken at the termination of the experiment. Assess the localization of this material within the skin using microautoradiography or by skin-stripping.

    Without experimental evidence, it is not possible to state whether this material will be absorbed or whether it will be lost externally by exfoliation of skin cells. To obtain more definitive data on the ultimate fate of this material, dose and treat additional groups of animals in the same way as the main groups, but using extended collection times. Assess the quantity of material excreted and remaining in the treated skin at times such as 5, 10, and 15 days. If absorbed, the depletion of material from the skin should correlate with material excreted.

ALTERNATE PROTOCOL

MEASUREMENT OF ABSORPTION OF VOLATILE COMPOUNDS

Dermal penetration of volatile compounds can be assessed in much the same way as described above by including carbon filters under the gauze above the dose site (Susten et al., 1986; Winter and Sipes, 1993). Perform a preliminary in vitro test to check the efficiency of the carbon filters and saddle arrangement: secure the saddle to some excised rat skin (or a glass plate), dose, then secure the gauze and filters. Place this in vitro apparatus in a metabolism cage or glass chamber within an incubator set at the rat body temperature (37.8°C). Pass air through the apparatus and through a series of traps; collect any volatile material that has passed the filter. At 8 hr after dosing, determine the distribution of dose from analysis of the dose site, saddle, gauze, filters, cage wash, and volatile traps.

If the carbon filter arrangement is efficient, then very little dose (e.g., <1%) is recovered from the cage wash and volatile traps, while quantitative recovery of radioactivity (>90%) is still maintained. It is very important to confirm the efficiency of the carbon filter arrangement, as otherwise the rat could absorb dose from inhalation rather than dermal penetration. Also, any radioactivity collected from the volatile traps connected to the metabolism cages for the in vivo experiment is assumed to have originated from expired air and hence included as absorbed dose. In order to minimize the time taken to dose the rats and secure the saddle and filters, the use of a light anesthetic at dosing can be useful.

MEASUREMENT OF DERMAL ABSORPTION IN HUMAN VOLUNTEERS

Information on dermal absorption in humans can be obtained either from routine occupational or environmental exposure monitoring (although these may include more than one route of exposure) or from controlled dose administration studies to human volunteers. Only the latter will give information on the quantitative relationship between a dose (exposure) and absorbed material circulating in blood or excreted. This information provides the basis for routine monitoring in workplace populations, the general population, or—in the case of medicinal products—in patients. Conducting human volunteer studies as part of drug development is a widely accepted practice, but the justification and ethical acceptability for performing studies with other chemicals are subject to more debate. However, the scientific value is indisputable, because volunteer studies can provide accurate and reliable information that has a practical value for the assessment of the safety of chemicals resulting from human exposure.

Legislation governing the use of human volunteers exists in most countries, although there are some inherent differences due to cultural or legal considerations. Any study must take into account the ethical aspects, particularly where there is no direct benefit to the subject—which is the case for all nonpatient volunteer studies, whether drug or chemical. The guidelines most universally adopted are in the World Medical Association Declaration of Helsinki (Recommendations Guiding Physicians in Biomedical Research Involving Human Subjects) which was first adopted in 1964 and has undergone subsequent modifications. Some of the general conditions that need to be met are as follows: a formal risk-benefit analysis has been carried out, the objectives are scientifically sound, the responsible investigators are appropriately qualified, informed consent of volunteers has been obtained, there is a detailed experimental protocol, and all studies have been approved by an independent ethics committee consisting of medical and nonmedical scientific and lay persons who act independently of the study sponsor. The key information required in the submission for ethical committee approval is toxicity data, to allow an assessment of the risk to the volunteers. The extent of toxicity data required will depend on the nature of the compound and may vary between countries. In general, for pharmaceutical development, there is a desire to obtain human data very early in the development process, and single low-dose studies can be conducted after limited toxicity data in two nonhuman species. For other chemicals, such as pesticides, studies are only likely to be conducted at later stages of development when chronic toxicity data are available. It is to be expected that more support data will be required for nonpharmaceuticals, but something less than chronic toxicity data should be acceptable.

Studies should be performed in a clinic under medical supervision by suitably qualified personnel, while analysis of samples should be laboratory based. Many of the details of test compound information and application, samples collected, and times will depend on the nature of the compound, its biological properties, and the situation in which human exposure would occur. Similar studies in animals should be carried out initially as described in Basic Protocol 1 and Alternate Protocol, and the results taken into account in designing the human study. Clinical investigations also have particular requirements for treatment of the volunteers, and for all these reasons, it is not possible to describe in detail a definitive protocol. The key stages and suggested procedures are described.

NOTE: All studies with human subjects must be approved by the Institutional Review Board (IRB), which must adhere to the Office for the Protection from Research Risk (OPRR) guidelines or other applicable governmental regulations for using human subjects.

Selection of Volunteers

Studies should be restricted to normal healthy males (three to six subjects), age range 30 to 60 years, and body weight ±15% of ideal for height/frame size. Various exclusion criteria should be applied by the clinical unit, such as subjects receiving any medication, participation in any clinical trial in the previous 3 months or in a study involving radioisotopes during the previous 12 months, known allergy or intolerance to related compounds, and any active skin condition or excessive hair in the area designated for dose application.

Subjects should undergo a pre-study screening within 14 days prior to administration; this should include a full medical history, physical examination, and laboratory tests including hematology screen, plasma biochemistry screen, plasma virology screen, urinalysis, and screening for drugs in urine. Subjects should normally be resident in a controlled clinical unit for the duration of the study and no alcohol or medication should be permitted. Standard meals should be provided in amounts commensurate with the individual. To encourage urine production, subjects should be asked to drink 200 ml of water at intervals such as pre-dose and 2, 4, 6, and 8 hr after dosing. The physiological condition of the subjects should be observed throughout the study, and blood pressure, respiration rate, and pulse rate monitored.

A post-study screening, performed at discharge after completion of the study, should include a physical examination and laboratory investigation of blood, plasma, and urine. Subjects should be requested to report any adverse events to the principal clinical investigator or his/her deputy.

Treatment Area

Select an area of skin representative of the area likely to be exposed and that allows controlled uniform application of the test compound and convenient maintenance of the integrity of the treated area post-application: e.g., the forearm or (most preferable) the back. Mark an area of ~100 cm^2 on the selected site using indelible ink and surround it with adhesive tape. Apply ~0.5 ml of the test compound, preferably in a suitable liquid formulation such as dissolved in 70% (v/v) aqueous ethanol. Use a syringe with a pipet tip to distribute the solution evenly over the area, allowing time for natural drying. Expose the treated area to air to dry for 30 min from the start of application. At this time cover the area with a gauze dressing (semi-occlusion) secured externally to the treated area to provide protection during the exposure phase. The duration of exposure will be determined by the compound, its usage, and the objective of the experiment. A typical exposure period is 6 to 8 hr; when a radiolabeled compound is used, that is usually the maximum time allowed based on assessment of radiological exposure. After the specified time, wash off unabsorbed material on the skin using cotton wool swabs and a solvent. The solvent will depend upon the objectives of the experiment but could be any solvent suitable for the compound, such as aqueous ethanol, or soapy water to simulate washing. It is possible to obtain some assessment of material remaining on the skin or in the stratum corneum by using transparent adhesive tape to take successive skin strips (~10 to 15) of a small part of the treated area (e.g., 2.5 cm^2). After washing, cover the area with a gauze dressing until the end of the experimental period (e.g., 3 to 5 days). At this stage, take further skin strips from a different treated area.

Sample Collection

The samples collected will depend upon the objectives of the study and the analytical methodology being used. When a radiolabeled compound is used, the intention is to collect all samples that can be measured to obtain information on the fate of the dermal dose, the rate and extent of absorption, rates and routes of excretion, and blood/plasma kinetics.

The samples should therefore consist of (1) urine collected in labeled pre-weighed containers at appropriate intervals, such as a pre-dose urine void and then periods of 0 to 2, 2 to 4, 4 to 6, 6 to 12, and 12 to 24 hr, and then 24-hr intervals until the end of the experiment; (2) feces, such as pre-dose, 12-hr, and then daily samples; and (3) blood samples (~9 ml) withdrawn by syringe or indwelling cannula from a suitable forearm vein into labeled lithium heparin tubes. The total blood withdrawal should be limited so as to be without impact on the subject volunteer or the integrity of the study: a total of ~150 ml over 5 days is suggested. Exact sampling times may vary according to the compound, but a possible regimen consists of pre-dose and the following times after the start of the application: 0.5, 1, 2, 4, 6, 8, 10, 12, 24, 36, 48, 72, 96, and 120 hr. The packed cell volume can be determined using a microhematocrit technique at pre-dose and at other selected sampling times, such as 2 and 24 hr post-dose. If analysis of plasma samples as well as or instead of whole blood is desired, centrifuge blood samples 10 min at $1200 \times g$, 4°C, and transfer the separated plasma to polypropylene vials.

Sample Analysis

Total radioactivity should be determined in all biological samples, skin washes, protective gauze dressings and skin strippings using standard procedures as indicated for the rat protocol. The results can be expressed as percentage of the administered dose and milligram (or microgram) equivalents either as amount in the total sample or as a concentration. If sufficient radiolabel is absorbed, other analytical techniques can be used to determine the nature of absorbed or excreted radiolabel (i.e., parent molecule/metabolites).

COMMENTARY

Background Information

Because animal models are used to assess toxicological potential, a knowledge of dermal absorption is invaluable, more particularly since dose-response relationships in systemic toxicity are often assessed using oral administration. It is well known that dermal absorption in animals exhibits large interspecies differences (Wester and Noonan, 1980). Absorption in rats, in particular, is often much higher than in humans. However, the rat is relevant as the rodent species most commonly used for toxicological assessment. Rats are also convenient to use due to availability, ease of handling for dose application, the feasibility of ensuring quantitative collection of excreta samples, and a size that provides a suitable skin area for application.

Measurement of bioavailability is being interpreted here as the extent of absorption of a dermally applied dose. It is not being interpreted as the systemic availability of the dermally applied compound, which is the strict interpretation of bioavailability in the context of pharmaceuticals, where interest is often more specifically focused on systemic exposure to the pharmacologically active compound. In this latter case, bioavailability is a function of both absorption and metabolism of the compound before it reaches the systemic circulation and may often be compared to a reference intravenous dose. However, the protocols described here could also be used to obtain this type of information.

Some aspects of a protocol design will depend upon the type of analysis being performed on collected samples. The definitive approach to assessing dermal absorption is to use radiolabeled compounds because this facilitates measurement of compound-related material (including metabolites) in the biological samples. Hence, in this case, it is not necessary to know the identity of metabolites in order to establish what proportion of a topically applied dose is absorbed. Alternatively, if the compound is excreted unchanged or the identity of a major excreted metabolite and its relationship to total excretion are known, specific analytical methods [e.g., high-performance liquid chromatography (HPLC), gas chromatography (GC), or gas chromatography/liquid chromatography–mass spectrometry (GC/LC-MS)] could be used. The protocol designs described here apply to studies using radiolabeled compound, although the technical aspects of compound application, maintenance of the test system, and sample collection would also apply to alternative analytical approaches.

Critical Parameters

For studies where radiolabeled compounds are being used in humans, separate authorization is required for the administration of a specified amount of radioactivity in terms of total dose and amount per unit area of skin. In the UK the approval process is governed by the Administration of Radioactive Substances Advisory Committee (ARSAC). The approval process requires submission of data obtained from equivalent experiments in animals that include measurement of the time-course of radioactivity concentrations in treated skin and tissues that allows an assessment of radiological exposure. The guideline is that the exposure of the human volunteer resulting from the experiment should be less than that occurring from exposure to natural sources of radioactivity during a year. These procedures are country-specific; in the USA, experiments must be conducted in accordance with the Atomic Energy Commission's guidelines.

The key specific issues pertinent in human volunteer studies can be summarized as follows:

1. Good Clinical Practice (GCP)

Compliance with the following as appropriate:

a. Declaration of Helsinki (1964), as amended Tokyo (1975), Venice (1983), and Hong Kong (1989).

b. EEC Note for Guidance: Good Clinical Practice for Trials in Medicinal Products in the European Community (approved by Committee for Proprietary Medicinal Products, July 1990, operative July 1991).

c. Current GCP documentation (21CFR parts 50, 56, and 312) issued by Food and Drug Administration (FDA), U.S.A.

d. Good Clinical Practice for Trials on Drugs issued by Pharmaceutical Affairs Bureau, Ministry of Health and Welfare, Japan (1989).

2. Good Laboratory Practice (laboratory investigation)

Performance of laboratory investigations in compliance with regulations pertaining to the country where the study is conducted and which has international acceptance.

3. Ethics Approval

Approval of study protocol by Independent Ethics Committee.

4. Approval to Administer Radioactivity (where appropriate)

In the UK, conducted through ARSAC: Administration of Radioactive Substances Advisory Committee, Department of Health, Alexander Fleming House, Elephant & Castle, London, SE1 6BY.

5. Informed Consent

Requirement that, prior to enrollment, all subjects give written informed consent to participate in the study, after the purpose, nature, and risks of the study have been fully explained both verbally and in writing. Each subject is advised that he or she is free to withdraw from the study at any time without any obligation to disclose reason for doing so.

6. Medical Cover

Availability of medical cover by a principal clinical investigator or his/her deputy.

Troubleshooting

The single most problematic aspect of human studies concerns the significance of less-than-quantitative accountability of the applied dose when a radiolabeled compound is used. Besides inaccuracies in measurement of the dose, there are essentially three possible reasons, namely, (1) errors in collection and analysis of samples, (2) incomplete recovery such as retention in the treated skin, and (3) incomplete excretion from the body and loss by volatilization from the treated site. These problems may have been encountered in the animal studies where it is possible to make the necessary checks and measurements, but data in animals do not always predict what may occur in a human study. Some indication of the problem might be obtained by comparison of data from individual subjects. Anomalous data from one subject might indicate a problem with sample collection or analysis. Incomplete excretion of absorbed material might be reflected in data on rates of excretion during the various collection periods. If substantial amounts of the dose were measured in the last samples collected, it is possible that further amounts would have been measured in subsequent samples.

However, volatilization from the skin is likely to be a main factor when recoveries are substantially less than 90% of the applied dose. Losses may occur even for compounds not considered to be highly volatile. If this phenomenon is suspected, some additional investigations, possibly simulated in vitro experiments, should be considered to provide supporting data. Such experiments could consist of application of a known amount of material to a skin sample and measurement of losses of compound from the surface.

Anticipated Results

Assessments of total dermal absorption and hence the total body burden require measurements of the compound and all its metabolites

in excreta. In the case of rodent studies using a radiolabeled compound, a complete balance of material can be obtained by taking measurements on treated skin and carcass at the end of the experiment. In this case it is expected to be able to obtain a total recovery of >90% of the administered dose. Summation of the amounts of the dose in urine, feces, and the carcass provides a value for the total absorption. An ambiguity exists if material was retained in the treated skin and was not removable by washing. The question raised is whether this material would eventually have been absorbed. It is unreasonable to assume that all this material will be absorbed, and its fate may vary from case to case, but depletion by external exfoliation may well be a major route. This phenomenon is likely to be a function of the physicochemical properties of the test compound and may be caused through some physical or covalent binding to the skin structures that effectively makes the materials unavailable for absorption. Even if the material was absorbed, this is clearly a very slow process and would provide only a very low systemic exposure concentration. An extended experimental collection period can provide an indication of the fate of this material, as described above in the rat protocol (see Basic Protocol 1).

Data obtained from human studies are of necessity more limited in providing opportunities for a complete recovery of the applied dose. The nonaccountable aspects are volatilization from the skin after application and retention in tissue or treated skin. The protocol described here is primarily one to assess human systemic exposure under simulated use conditions, and clearly enables a comparison of this exposure with laboratory animals used in toxicology studies. Some human studies using radiolabeled compounds to assess dermal absorption have been reported for diazinon (Wester et al., 1993) and pyrethrin and piperonyl butoxide (Wester et al., 1994).

For both laboratory animals and human studies, chromatographic analysis of samples (blood, urine, etc.) will provide information on the proportions and amounts of the parent compound and its metabolites. The study then becomes a metabolism investigation by the dermal route. The importance of these data is that they give the relationship between extent of absorption and the concentration-time profile or amounts of a specific component. This information can then be used in the design of further experiments to compare bioavailability using different formulations or dose rates. It also provides the means to make a transition from using radiolabeled compound to using unlabeled compound and conventional specific analytical methods.

Time Considerations

The largest amount of time required for a human study is the planning phase, which involves obtaining ethical approval, screening and selection of volunteers, and scheduling the study in a clinical unit. This process will depend upon the organizations involved but could take 2 to 3 months. The in-life phase of study will take 5 to 7 days and subsequent analysis of samples and collation of data will take a few weeks depending on the scale of the experiment. For an animal study, planning and organization may take about one month, the in-life phase about 7 days, and subsequent sample analysis etc. a few weeks.

Literature Cited

Hayes, W.J. 1983. Ethical considerations involving studies of pesticides and other xenobiotics in man. *In* IUPAC Pesticide Chemistry: Human Welfare and Environment, Vol. 3. Mode of Action, Metabolism & Toxicology (J. Miyamoto and P.C. Kearney, eds.) pp. 387-394. Pergamon Press, London.

Susten, A.S., Dames, B.L., and Nieneier, R.W. 1986. In vivo percutaneous absorption studies of volatile solvents in hairless mice. I. Description of a Skin-Depot. *J. Appl. Toxicol.* 6:43-46.

Wester, R.C. and Noonan, P.K. 1980. Relevance of animal models for percutaneous absorption. *Int. J. Pharmaceutics* 7:99-110.

Wester, R.C., Sedik, L., Melendres, J., Logan, F., Maibach, H.I., and Russell, I. 1993. Percutaneous absorption of diazinon in humans. *Fd. Chem. Toxicol.* 31:569-572.

Wester, R.C., Bucks, D.A.W., and Maibach, H.I. 1994. Human in vivo percutaneous absorption of pyrethrin and piperonyl butoxide. *Fd. Chem. Toxicol.* 32:51-53.

Wilks, M.F. and Woollen, B.H. 1994. Human volunteer studies with non-pharmaceutical chemicals: Metabolism and pharmacokinetic studies. *Hum. Exp. Toxicol.* 13:383-392.

Winter, S.M. and Sipes, I.G. 1993. The disposition of acrylic acid in the male Sprague-Dawley rat following oral or topical administration. *Fd. Chem. Toxicol.* 31:615-621.

Key References

Anonymous. 1993. Subdivision F. Hazard Evaluation—Humans and Domestic Animals: Proposed New Guideline Section 85-3. Dermal Absorption Studies of Pesticides. *Fed Regist.* 58202-54350.

Declaration of Helsinki, 1983 (revised version, October 1983). *In* Good Clinical Practice in Europe (M.E. Allen, ed.) pp. 73-76. Rostrum, Romford, U.K.

Environmental Protection Agency (EPA). 1993. Dermal Exposure Assessment: Principles and Application. EPA Report No. EPA/600/8-92/022B. U.S. Department of Commerce, Washington, D.C.

Organisation for Economic Co-operation and Development (OECD) Environmental Health and Safety Division. Proposal for Two New Guidelines on Percutaneous Absorption. OECD Environmental Health and Safety Division Discussion Document, ref. ENV/EHS/HK/ mc/94.103. OECD, Paris.

U.K. Department of Health. 1984. Notes of Guidance on the Administration of Radioactive Substances for Purposes of Diagnosis, Treatment or Research. Administration of Radioactive Substances Advisory Committee, Enclosure HN 84 5. U.K. Department of Health, London, U.K.

World Medical Association. 1982. Proposed International Guidelines for Biochemical Research Involving Human Subjects. World Health Organization, Geneva.

Contributed by Stephen V. Bounds and David R. Hawkins
Huntingdon Life Sciences
Huntingdon, England

Measurement of Disposition Half-Life, Clearance, and Residence Times

AIMS AND OBJECTIVES

The interaction of an exogenous compound, drug, or toxicant with a biological system involves at least three general processes that can be characterized as input (absorption), translocation (distribution), and output (elimination). The latter two events are often referred to as disposition. An additional and critical characteristic of such an interaction is the pharmacologic response or toxic effect. This unit is concerned with the former processes, and especially with output or elimination, which comprise the study area referred to as pharmacokinetics or toxicokinetics.

The approach taken in developing this unit will first involve providing an understanding of the process, along with definitions. This will be followed by discussion of experimental design issues, complicating factors to consider, and data analysis with a completely worked-out example. Because of the relatively limited space available here, not all concepts can be thoroughly developed; the reader will be referred to appropriate references. It will also be useful to keep in mind, when reading through this unit, the interrelationships among the parameters discussed. These interrelationships will be emphasized as the concepts are developed.

CHARACTERIZING THE ELIMINATION/DISPOSITION PROCESS (OUTPUT)

Loss of a substance from the body, generally referred to as elimination and assumed to be an irreversible process, may be quantified by three fundamental measures: rate of loss, a rate constant or associated term (e.g., half-life or residence time), and clearance. Rate of loss is not typically useful, because it is usually directly related to the plasma concentration of the substance, which is most often changing with time. Rate of loss may have some utility if the substance is at steady state (a good example is an endogenous substance such as creatinine, or an exogenous compound where steady state has been achieved with long-term intravenous infusion) or if the loss process is constant. The latter behavior is seen with some substances (e.g., ethanol, salicylate, and phenytoin) above a certain plasma concentration. In the vast majority of instances, however, the loss process for exogenous substances has been shown (or is assumed) to adhere to the principles of *first-order kinetics*. The latter principle is simply stated as: rate of loss from the body is directly proportional to the concentration (C) or amount (X) of the substance in the body (concentration is raised to the power of one and, thus, "first-order")—i.e., rate of loss $\propto C$. The proportional relationship is represented by a constant, the apparent overall first-order elimination rate constant, K, which has units of reciprocal time (t^{-1} or $1/t$)—i.e., rate of loss = $-K \times C$. The minus sign indicates loss of substance. For simplicity, the preceding and subsequent discussions will assume that dosing is achieved with an intravenous (i.v.) bolus dose (i.e., the entire dose is given at once). There is need to make an assumption concerning the model that best describes the display of concentration-time data. It is easiest to begin by assuming the simplest possible model, a one-compartment model. The meaning of this is discussed below.

Since rate per se is not particularly useful, the rate expression needs to be integrated over time (from time zero to infinity) to obtain a relationship that describes the elimination process in the form of C as a function of time, t. The integration of a first-order process results in an exponential equation:

$$C = C^0 e^{-K \times t}$$

Equation 5.3.1

where e is the base of natural logarithms and C^0 is the value of the hypothetical initial concentration at time zero. Most scientists will do almost anything to be able to present data in the form of a straight line, $y = (m \times x) + b$, where m is the slope and b is the intercept. This is easily accomplished by taking natural logarithms (ln, base e) or common logarithms (log, base 10) of both sides of Equation 5.3.1:

$$\ln C = \ln C^0 - k \times t$$

$$\log C = \log C^0 - \frac{k}{2.3} \times t$$

$$\Downarrow \quad \Downarrow \quad \Downarrow \quad \Downarrow$$

$$y = b - m \times x$$

Equation 5.3.2

Contributed by Michael Mayersohn
Current Protocols in Toxicology (2000) 5.3.1-5.3.29

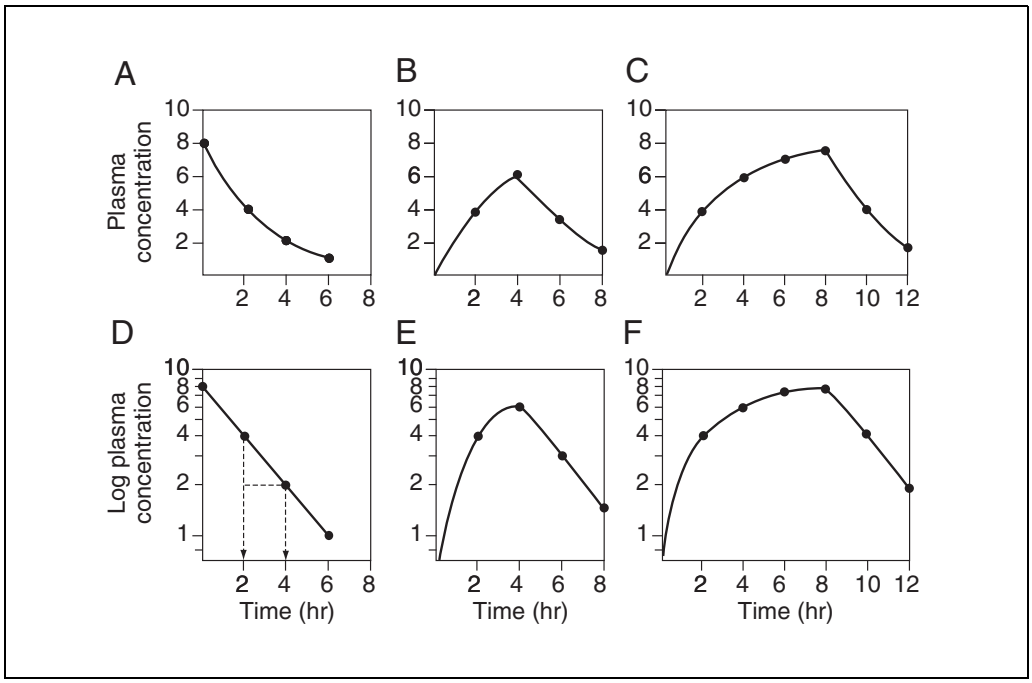

Figure 5.3.1 Plasma drug concentration–time profiles plotted on regular (Cartesian) coordinates following: (**A**) an intravenous (i.v.) bolus; (**B**) a short infusion; and (**C**) a long-term infusion. (**D-F**) The same data shown in A-C, respectively, have been re-plotted onto semilogarithmic axes in panels D-F. Used with permission of Saguaro Press.

Plots of plasma concentration versus time following an i.v. bolus dose, short-term i.v. infusion, and a long-term i.v. infusion are illustrated in Figure 5.3.1 (panels A to C). Concentrations decline in an exponential fashion, described by Equation 5.3.1. In contrast, if the same data are plotted on semilogarithmic axes, as represented by Equation 5.3.2, graphs D to F are obtained. The latter graphs contain more information than the former, and such semilogarithmic plots are the starting point for almost any pharmacokinetic analysis. In a semilog plot of plasma concentration (C; y-axis) versus time (t; x-axis), the slope of the line is given by $-K/2.3$, and the intercept is equal to C^0 following an i.v. bolus dose.

(It is of interest to note that semilogarithmic graph paper used to be called "ratio paper" and is best suited to the plotting of data that change in an exponential fashion. The term "ratio" was used to indicate that numbers in the same ratio to each other are the same distance apart on the logarithmic scale. Thus, the following pairs of numbers that are in the same ratio [of 5 to 1] are separated by the same distance: 10/2; 100/20; 600/120. Similarly, numbers that represent the same percentage increase or decrease are separated by the same distance on the logarithmic scale. Thus, the following pairs of numbers, which represent a 10% decrease, will be separated by the same distance: 100/90; 10/9; 20/18. Another characteristic of semilog graph paper is the number of "cycles" represented. Each cycle is an order of magnitude or a factor of 10. Two-cycle semilog paper will encompass a 100-fold range from, for example, 1 to 10 to 100 or 0.01 to 0.1 to 1.0.)

The first-order rate constant, K, which has units of reciprocal time, represents a fractional rate of loss of drug from the body. Thus, if K had a value of 0.05 hr^{-1}, it would be approximately correct to say that, after 1 hr, ~5% of what was in the body at the beginning of that hour was eliminated. One hour later, another 5% would be lost (but 5% of a smaller quantity). A K value of 0.1 hr^{-1} indicates that there would be a 10% loss of the starting quantity per hour. This is an approximation only, since K really represents an instantaneous rate of loss. For example, assume an initial amount in the body of 100 units and $K = 0.1$ hr^{-1}. After 1, 2, and 3 hr, the amount remaining in the body would be ~90, 81, and 73 units.

A more useful and easily understood parameter, which is inversely related to K, is referred to as *half-life* ($t_{1/2}$). Half-life is the time needed for plasma concentration or the amount of drug in the body to decline by 50%. There are several qualifications to this definition, as will be discussed. The estimation of $t_{1/2}$ is shown in Figure 5.3.1D. The concentrations of 8 and 4 units intersect the log-linear line at times

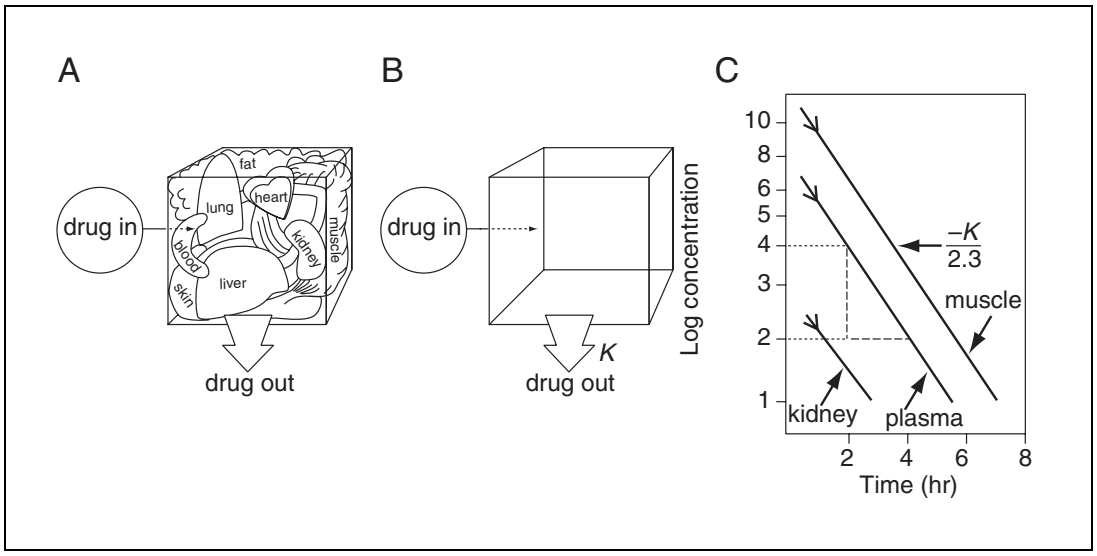

Figure 5.3.2 Schematic representation of the one-compartment model showing i.v. bolus input and drug output. (**A**) All body organs and tissues are scrunched into a single box (compartment) to indicate that these are lumped together because of similar kinetic behavior (kinetic homogeneity). Please note that there is no anatomical reality to this figure. (**B**) Typical representation of a one-compartment model. (**C**) Semilogarithmic plot of drug concentrations versus time in plasma and other selected tissues. Note that all lines are log-linear and parallel to each other (kinetic homogeneity), do not increase with time immediately after dosing, and do not superimpose (lack of concentrational homogeneity). Used with permission of Saguaro Press.

corresponding to 2 and 4 hr, respectively. The difference, 2 hr, is the half-life for that drug. The relationship between K and $t_{1/2}$ is given by $t_{1/2} = 0.693/K$. One can either calculate K from the slope of the line (by regression analysis) to estimate $t_{1/2}$, or else estimate $t_{1/2}$ from the graph and calculate K. One important point to note about this relationship is that dose does not appear; $t_{1/2}$ *is independent of dose* of drug for a first-order kinetic process.

Before applying the above analysis, it is useful to have an understanding of the model that is being depicted. A *one-compartment model* will accurately describe plasma concentration–time data if one basic assumption about the drug is met—following administration, the drug is immediately distributed throughout the body. This instantaneous distribution essentially means that drug distribution from the blood to other tissues occurs so rapidly that typical blood-sampling protocols will not permit it to be seen. Figure 5.3.2 illustrates one way to visualize such a model with drug input and output. Many, but not all, body organs and tissues have been scrunched into a large box (Fig. 5.3.2A); clearly, no attempt has been made to be anatomically correct in this depiction. This rendering is presented as a reminder that our models, no matter how simple, must reflect the existence of real body organs and tissues. The model, shown in 5.3.2B, appears as a simple box or as a single compartment not cluttered with body components and with no concern for anatomy. This model simply reflects the assumption underlying its creation; all parts of the body behave the same kinetically and, therefore, can be lumped together. Figure 5.3.2C, which is a semilog plot of plasma and other tissue concentrations with time, indicates several important aspects of the behavior of the model. First, concentrations in all sampled tissues are described by a log-linear straight line; this follows from our assumption of first-order elimination kinetics. The half-life calculation is illustrated for the plasma data; $t_{1/2}$ is equal to 2 hr. Second, all lines are parallel to each other. In other words, these tissues behave in a *kinetically homogenous* manner. In contrast, the concentrations do not superimpose, and therefore there is no concentrational homogeneity. The latter occurs because of differences in tissue binding of drug (in this instance the order of binding is: muscle>plasma>kidney). Finally, since we have assumed instantaneous distribution, all concentrations decline with time following dosing (i.e., there is no increase immediately following i.v. bolus dosing; even though we know that this must happen, it happens so quickly that we cannot see it using traditional blood sampling). *The one-compartment model*

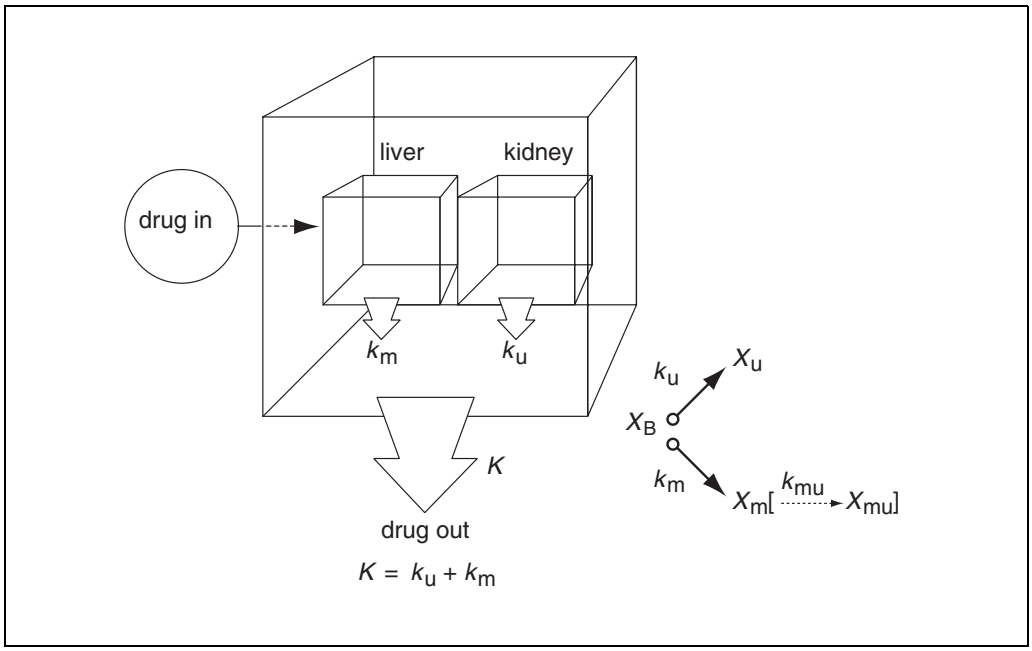

Figure 5.3.3 Schematic representation of elimination from a one-compartment model (left). The kidney and liver independently contribute to the overall elimination of drug. The apparent overall first-order elimination rate constant (K) is the sum of the rate constants for urinary excretion of drug by the kidney (k_u) and enzymatic metabolism by the liver (k_m). A simple symbolic scheme is shown on the right. Also shown by dashed line is the excretion of metabolite into the urine (k_{mu}). The latter process has no bearing on drug elimination. Used with permission of Saguaro Press.

lumps all body regions together, into a single space, since all regions behave the same way kinetically.

Reexamining Figure 5.3.2C, the only data that we will likely have generated are those from blood sampling and not from sequential tissue sampling. The fluid sampled is always blood (unless microdialysis is being applied) from which we can assay blood, plasma, or serum. For now, it is not necessary to distinguish among these different biofluids. The plasma concentration–time data are plotted on semilog graph paper (or using a software program, whereupon the data will be seen on a computer screen) and an estimate of the slope is obtained (using linear regression). From the slope, values for the apparent, overall first-order elimination rate constant (K) and $t_{1/2}$ are obtained. This overall rate constant is the sum of all individual eliminating organ rate constants.

The latter point is noted in Figure 5.3.3. The model shown is a representation of a one-compartment model with renal excretion and hepatic metabolism. The symbolic notation (right side of figure) indicates that these two kinetic processes are parallel (or competitive) and that the overall rate constant, K, is the sum of the individual rate constants for urinary excretion (k_u) and hepatic metabolism (k_m). It should be noted that half-lives are not additive. It is also important to recognize that subsequent (or "downstream") events, such as urinary excretion of a metabolite (represented by k_{mu}), have nothing to do with elimination of parent drug. The downstream process may be important because the metabolite is active or toxic, but its existence has no bearing on the disposition of parent drug or the value of K.

The meaning, but not the calculation of half-life, becomes more complicated when it is necessary to describe the disposition of a drug with a more complex model. Whenever drug distribution from the blood to body tissues following an i.v. bolus dose is not instantaneous but occurs at a measurable rate, the drug is said to have *multicompartmental* characteristics. We can no longer lump all body tissues and organs into one compartment. It is necessary to separate one group of tissues from another group—one rapidly receiving drug and the other receiving drug at a slower, measurable rate. This is illustrated in Figure 5.3.4A where there are two connected boxes (compartments) each with a different group of tissues. The group of tissues on the left, which includes blood, receives the compound rapidly (e.g., liver and kidney). The other group of tissues on the right, including muscle, skin, and fat, receives the compound more slowly. This two-

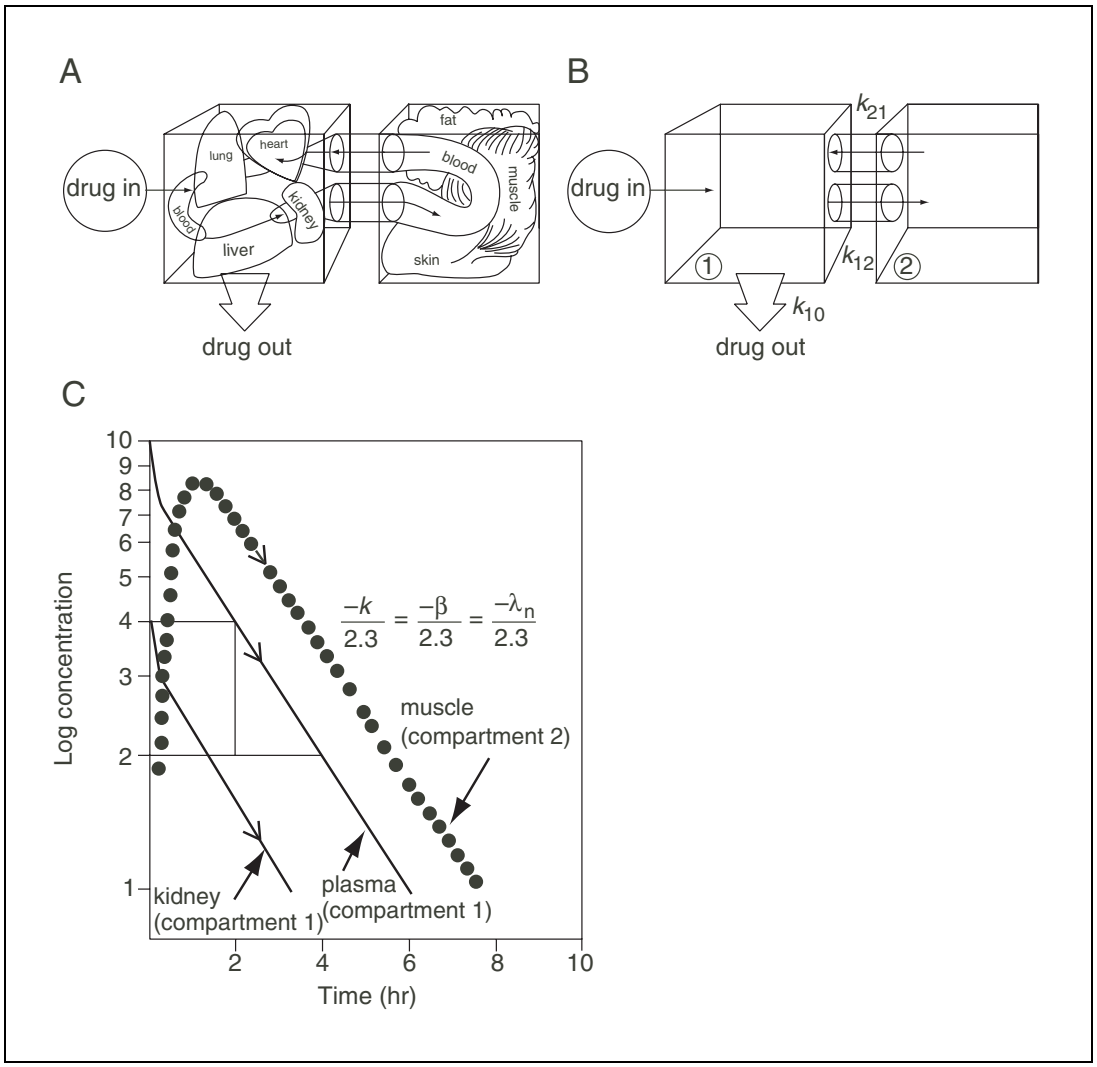

Figure 5.3.4 (**A**) An "anatomical" version of a two-compartment model illustrating the presence of specific organs and tissues in each of the two compartments connected by the blood stream. Tissues lumped together in the compartment on the left receive drug rapidly, whereas tissues lumped into the compartment on the right receive drug slowly. (**B**) Hypothetical two-compartment model devoid of any consideration of tissues. Compartment 1 ("central") receives and eliminates drug, whereas, compartment 2 ("peripheral") receives drug slowly. The intercompartmental first-order rate constants are shown (i.e., k_{12} and k_{21}) as well as the elimination rate constant (k_{10} or k_{el}). (**C**) Concentration-time profiles (semilog axes) of plasma and tissues in rapid equilibrium with plasma (e.g., kidney; compartment 1) and tissues in slow equilibrium with plasma (e.g., muscle; compartment 2). Used with permission of Saguaro Press.

compartmental representation in Figure 5.3.4B ignores the tissues contained in each box but their presence is assumed. The compartment receiving and eliminating drug is referred to as compartment 1 (or "central") and the other compartment is referred to as compartment 2 (or "peripheral"). The intercompartmental first-order rate constants, k_{12} and k_{21} and the rate constant associated with drug elimination, k_{10} (or k_{el}), are shown in the model. The corresponding concentration-time data are illustrated in Figure 5.3.4C. The concentrations of drug in those tissues represented in compartment 1, which receive drug rapidly (plasma and kidney are shown), initially decline rapidly (the distributive phase), and then in a log-linear manner (post-distributive phase). In contrast, drug concentrations in those tissues that receive drug more slowly (compartment 2; muscle is shown) initially rise and then decline in a log-linear manner in parallel with plasma.

The estimation of half-life is shown in Figure 5.3.4C and it is determined in the same way as outlined previously. The only qualification is that the data must be in the log-linear or post-distributive or terminal phase. It is for this reason that half-life is best referred to as a "terminal" $t_{1/2}$ or a "disposition" $t_{1/2}$. The for-

mer term indicates which data are being used for the estimation of half-life and the latter term makes clear that half-life depends upon distribution as well as elimination. The term "elimination" half-life is less descriptive and "biological" half-life is likely to be confused with response and, for that reason, use of the two latter terms is not encouraged.

The slopes noted in Figure 5.3.4C incorporate one of several symbols: K, β, or λ_n. The two latter terms arise from the equation describing the plasma concentration-time profiles of a multicompartmental model, in this case a two-compartment model:

$$C = Ae^{-\alpha t} + Be^{-\beta t}$$

Equation 5.3.3

$$C = A_1e^{-\lambda_1 t} + A_2e^{-\lambda_2 t}$$

Equation 5.3.4

By definition, $\alpha > \beta$ (or $\lambda_1 > \lambda_2$), and the terminal slope, which always represents the slowest process, is given by β or λ_n (in this case, λ_2). The rate constants, α and β, are hybrid constants in that they depend upon other constants in the model (i.e., k_{12}, k_{21}, and k_{10}). The coefficients (A's and B's) represent intercepts on the y-axis.

An important point to appreciate about $t_{1/2}$ is that it is not an independent parameter, but rather $t_{1/2}$ depends upon two other parameters: apparent volume of distribution (V) and clearance (CL):

$$t_{1/2} = \frac{0.693\,V}{\mathrm{CL}}$$

Equation 5.3.5

The *apparent volume of distribution* is an abstract concept made more difficult by the variety of different volume terms that may be estimated. This volume is rarely a real physiological space and, for that reason, its meaning causes confusion. Volume serves as a proportionality constant between blood concentration and the amount of substance in the body, and it gives an indication of the magnitude of distribution (or movement) out of the vascular system (i.e., the greater the apparent volume, the more extensive is the distribution). Fundamentally, the apparent volume represents the space that a substance occupies if it is uniformly present throughout the body at the same concentration as in blood or plasma. The latter is the reference fluid used for calculation of volume. That is, the apparent volume is a "volume equivalent" of plasma. For example, if plasma and liver concentrations of a substance were 1 and 10 mg/liter, respectively, every liter of liver would be equivalent to 10 liters of plasma. This disparity in concentration among tissues and the consequent value of apparent volume is a function of tissue binding. Apparent volumes in the rat may be as small as ~0.2 liter/kg (gentamicin) or as large as ~30 liter/kg for chlorpromazine and even higher for other compounds, such as insecticides.

Why should apparent volume of distribution or movement of a substance out of the bloodstream into tissues affect $t_{1/2}$? In order for a drug to be eliminated from the body it must be in the blood stream and carried to the eliminating organs (primarily the liver and kidney). If most of the compound in the body resides in tissues and not in the blood stream, that compound is not readily accessible to the organs of elimination and will, as a consequence, be slowly eliminated. The greater the apparent volume, the slower this process and the longer the $t_{1/2}$.

The other part of the half-life relationship noted in Equation 5.3.5 involves a term referred to as *clearance*. This idea of clearance is perhaps the most important concept in pharmacokinetics, and it has numerous applications. Clearance determines concentrations at steady state (resulting from multiple dosing) and it permits the evaluation and prediction of drug disposition in the body. Although clearance is used to characterize elimination, it differs from $t_{1/2}$ in that it reflects the efficiency of removal by an eliminating organ. Clearance (CL) has units of flow, i.e., volume per time, and it is defined as that volume of blood (or plasma) from which the substance is completely removed per unit of time to account for the rate at which the material is being eliminated. On the assumption of first-order kinetics, the basic relationship that defines clearance is

$$\mathrm{CL} = \frac{\text{rate of elimination}}{\text{plasma concentration}} = \frac{\dfrac{d\ (\text{amount})}{dt}}{C}$$

Equation 5.3.6

This relationship is virtually identical in form to an equation noted previously in describing first-order kinetics: $dC/dt = K \times C$ versus $d(\text{amount})/dt = \mathrm{CL} \times C$. The proportionality

constant in the former case, K, has units of reciprocal time, whereas the proportionality constant in the latter case, CL, has units of flow. The former constant depends upon apparent volume (as noted in Equation 5.3.5); clearance does not. Each eliminating organ has its own value for clearance and the sum of all such clearances is referred to as *systemic clearance*, CL_S, or total body clearance. In order to measure organ clearance experimentally in the whole animal, one has to be able to quantitate the mass of compound appearing in a terminal compartment with time. For example, clearance into urine (renal clearance), bile (biliary clearance), and expired breath (pulmonary clearance) can be measured since the compound under study can be completely collected. This is not the case for systemic or metabolic clearance. Another relationship, therefore, needs to be used in order to calculate those clearances, as well as any other organ clearance. The integral of Equation 5.3.6 for systemic clearance is:

$$CL_s = \frac{\frac{d\ (\text{amount})}{dt}}{C} = \frac{\int_0^\infty \frac{d\ (\text{amount})}{dt}}{\int_0^\infty C \times dt} = \frac{\text{dose}}{AUC_0^\infty}$$

Equation 5.3.7

where dose is the i.v. bolus dose (or the dose actually absorbed by some nonvascular route) and AUC_0^∞ is the area under the plasma concentration–time curve from time zero to infinity (i.e., area under a curve is the mathematical equivalent of integrating the equation that describes that curve). (The area may be estimated two ways: by fitting the data to an appropriate equation from which the parameters of the equation are obtained and used to calculate area, or via an area-approximation method such as the trapezoidal rule or spline function, among others. Some investigators like to look upon an area as an index of exposure to that substance; the greater the area, the greater the exposure. The latter will typically vary with dose or it may be different among subjects.) Multiplying the numerator by the fraction of the dose metabolized or excreted unchanged into the urine will provide corresponding estimates of metabolic or renal clearances, respectively.

Clearance is best understood with reference to Figure 5.3.5. In-flowing (i.e., arterial) blood enters an organ with a flow of Q_{in} and a substrate concentration of C_{in}. Out-flowing (i.e., venous) blood exits the organ with a flow Q_{out} ($Q_{in} = Q_{out}$) and a substrate concentration of C_{out}. If the organ is responsible for elimination of that substance, $C_{out} < C_{in}$. The relationship between these concentrations is embodied in the extraction ratio (ER):

$$\text{extraction rate} = ER = \frac{C_{in} - C_{out}}{C_{in}}$$

Equation 5.3.8

If $C_{in} = C_{out}$, this is a noneliminating organ and ER = 0. If $C_{out} = 0$, then ER = 1 (i.e., all of the substance has been removed from the in-flowing blood, the most efficient removal process possible). A compound with an intermediate ER value (0.5) is illustrated in Figure 5.3.5. Flow to this hypothetical organ is 10 ml/min. During a short interval of time, say, 1 min, the concentration entering the organ is 10 units/ml, and upon exit the concentration is reduced to 5 units/ml. The value for ER is (10 − 5)/10, or 0.5 The organ has removed 50% of the substance entering the in-flowing blood. The amount extracted or eliminated by the organ is one-half of the amount entering: 0.5 × 10 ml × 10 units/ml = 50 units. This is shown in Figure 5.3.5 as the material retained in the organ. Since that amount of substance (50 units) is contained in 5 ml of blood, the organ clearance is 5 ml per unit of time, in this instance, 1 min. Another way to state that calculation is that clearance is the product of ER and Q (i.e., 0.5 × 10 ml/min = 5 ml/min). According to Equation 5.3.6, clearance may be calculated as the rate of elimination divided by the corresponding blood concentration. The rate of elimination is 50 units/min, divided by the incoming concentration of 10 units/ml, giving a clearance of 5 ml/min.

The relationship between extraction ratio and clearance is illustrated with the "double rainbows" shown in Figure 5.3.6. The organ extraction ratio is often arbitrarily divided into three equal segments: low (ER < 0.33), intermediate (ER, 0.33 to 0.67), and high (ER > 0.67) extraction. The corresponding organ clearances, behind the ER rainbow, are related to the latter via blood flow, since CL = ER × Q. The clearance rainbow is divided into three comparable regions: low (or restrictive), intermediate, and high (or nonrestrictive) clearance.

Notice that organ clearance can never exceed organ blood flow following i.v. dosing: a substance cannot be cleared any faster than it is delivered (via blood flow) to the eliminating organ. Indeed, the clearance of high-ER compounds (ER ≈ 1) essentially measures organ blood flow (e.g., *p*-aminohippurate for measuring renal blood flow; indocyanine green for measuring liver blood flow). If we consider two specific eliminating organs, the liver and kid-

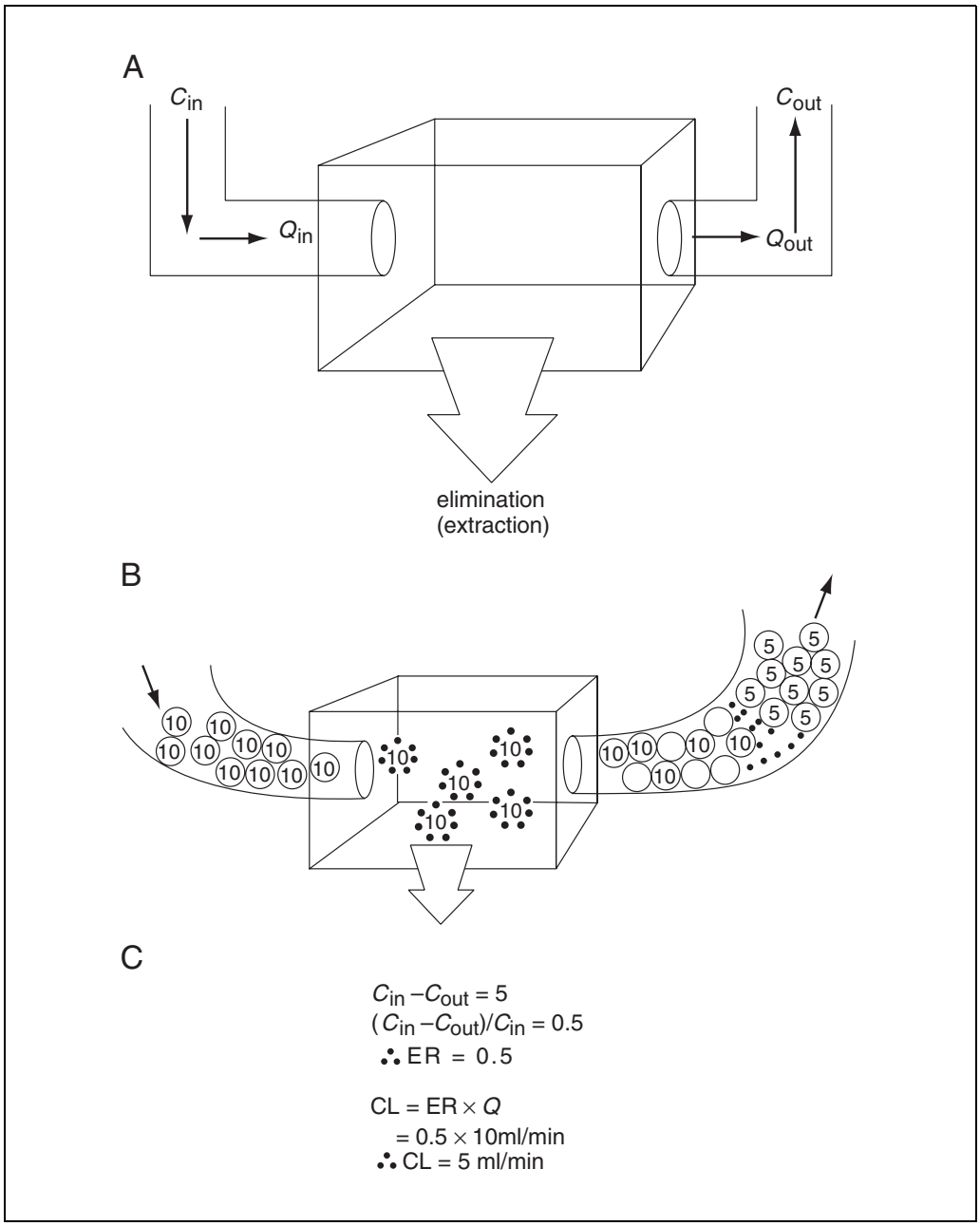

Figure 5.3.5 (**A**) Representation of blood flowing through an organ that eliminates or extracts a substrate from the in-flowing blood (Q_{in}) at an entering concentration of C_{in}. The resulting out-flowing blood ($Q_{out} = Q_{in}$) and concentration, C_{out}, allow determination of extraction ratio. (**B**) A hypothetical eliminating organ receiving 10 ml blood/min (each circle = 1 ml) at an initial concentration of 10 units/ml. The exiting concentration is 5 units/ml, the equivalent of 5 ml of blood has been extracted and the corresponding mass of substrate remains in the eliminating organ. (**C**) The extraction ratio, ER, is determined as the difference between the in and out concentrations divided by the in concentration. ER is equal to 0.5. Organ clearance, CL, is then determined from the product of ER and blood flow, Q, to be 5 ml/min. Used with permission of Saguaro Press.

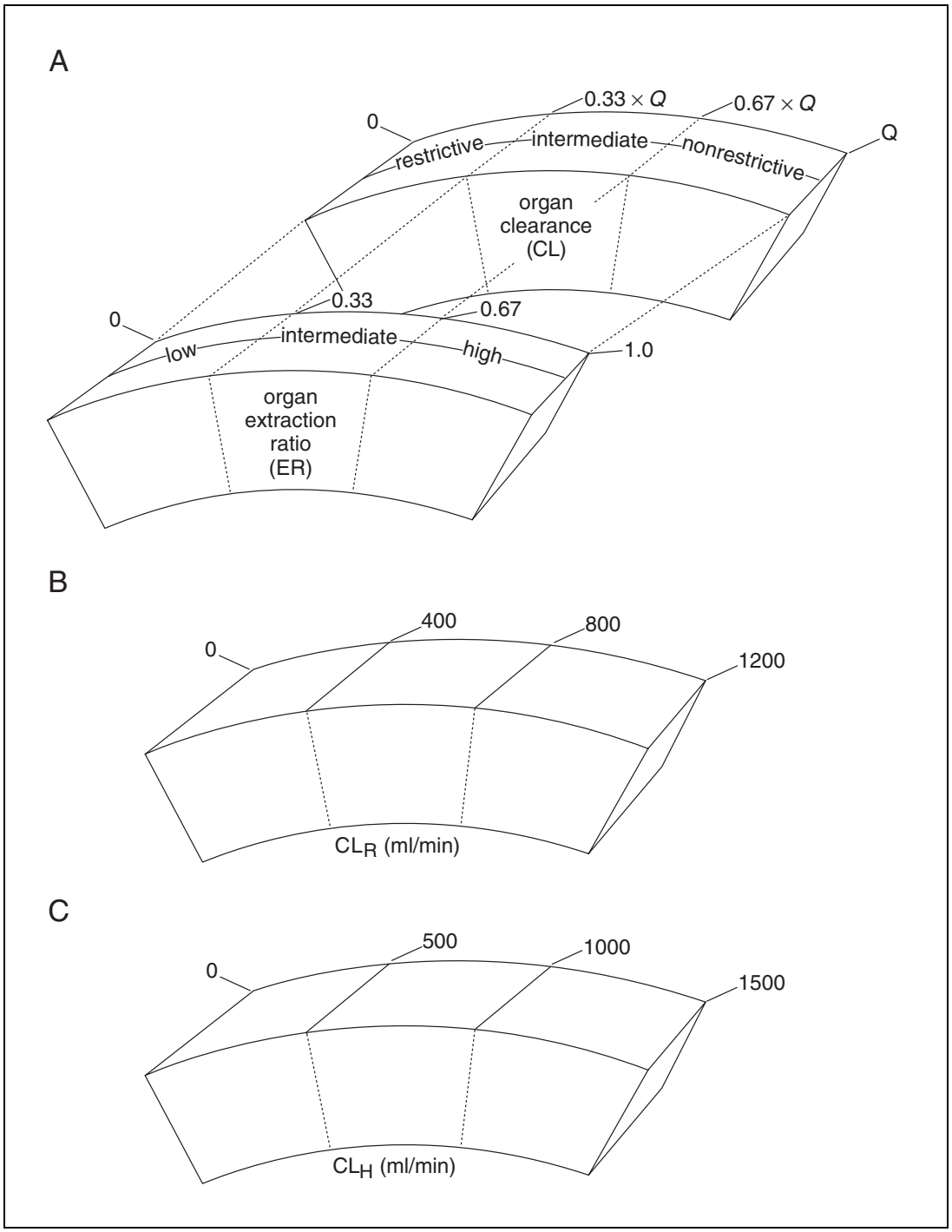

Figure 5.3.6 A "double rainbow" illustrating the range of values and the relationship between extraction ratio and organ clearance. The extraction ratio (ER) rainbow is divided into three equal parts: low, intermediate, and high extraction. Organ clearance, CL, is related to ER by organ blood flow and values range from 0 to organ blood flow. The clearance rainbow is divided into equal parts: low or restrictive ($<0.33 \times Q$), intermediate [$(0.33 \times Q)$ to $(0.67 \times Q)$] and high or nonrestrictive ($>0.67 \times Q$) clearance. The actual clearance values for two eliminating organs in humans, the kidney (**B**) and the liver (**C**), are illustrated at the bottom of the figure. The maximum hepatic and renal clearance values will not exceed blood flows to those organs, 1500 and 1200 ml/min, respectively. Used with permission of Saguaro Press.

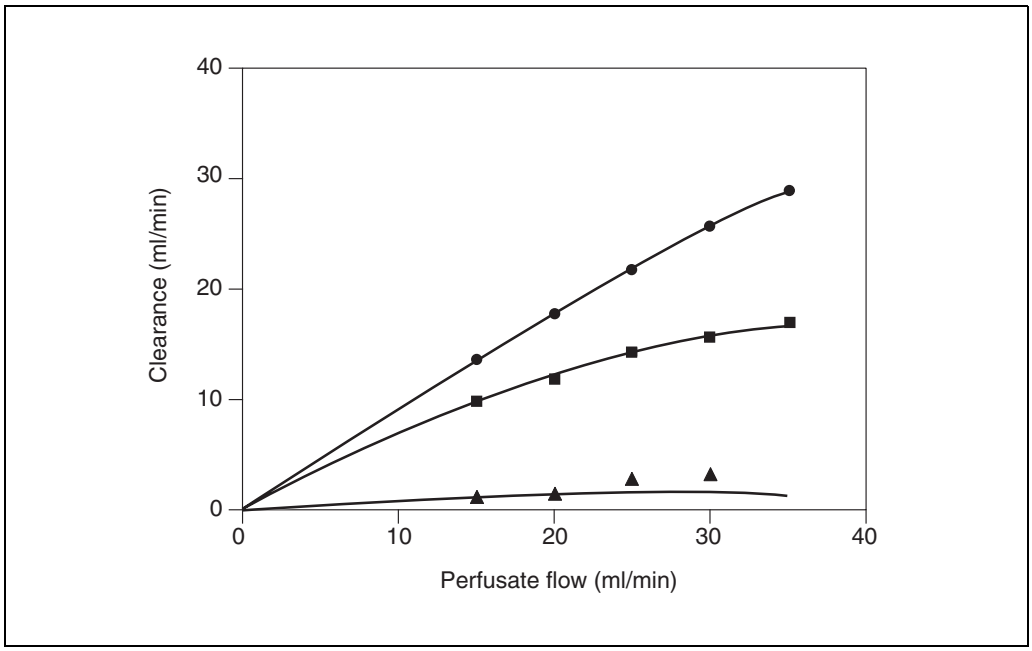

Figure 5.3.7 Clearance as a function of perfusate flow as determined in an isolated perfused rat liver. Note the dependence of clearance on flow for lidocaine (circles) and ethanol (squares) which have high and intermediate extraction ratios (0.91 and 0.65), respectively. In contrast, the clearance of antipyrine (triangles), which has a low extraction ratio (0.07), is independent of flow. Data taken from Sinha et al. (2000). Used with permission of Saguaro Press.

ney, the corresponding clearance "rainbows" are illustrated at the bottom of the figure. The average blood flows to the liver and kidney in humans are ~1500 and 1200 ml/min, respectively, as noted on the extreme right of the "rainbows." Figure 5.3.7 illustrates the relationship between clearance and perfusate flow for high (lidocaine), intermediate (ethanol), and low (antipyrine) clearance compounds as determined in an isolated perfused rat liver (Sinha et al., 2000).

A particularly useful expansion of the ER relationship, based upon a simple model of an eliminating organ (Wilkinson and Shand, 1975) is known variously as the venous equilibrium, blood flow-limited, or well-stirred model:

$$ER = \frac{CL_{int}}{CL_{int} + Q}$$

Equation 5.3.9

Since clearance is the product of ER and Q:

$$CL = \frac{CL_{int} \times Q}{CL_{int} + Q} = \frac{f_U \times CL_{U,int} \times Q}{f_U \times CL_{U,int} + Q}$$

Equation 5.3.10

The above relationship embodies all of the factors that can possibly influence organ clearance: f_U, unbound fraction of compound in plasma; CL_{int}, intrinsic clearance; $CL_{U,int}$, unbound intrinsic clearance; and Q, blood flow. Any change in clearance must be mediated through one or more of the parameters in Equation 5.3.10. Intrinsic clearance, CL_{int}, is the inherent ability of the organ to clear the compound in the absence of any blood flow restrictions. For example, a measure of intrinsic metabolic clearance could be obtained by adding the substrate to a test tube containing an enzyme or homogenized liver preparation. Since the latter value may be affected by substrate binding in the preparation, another term, unbound intrinsic clearance, $CL_{U,int}$, is defined. Unbound intrinsic clearance represents the intrinsic ability to metabolize in the absence of any substrate binding in the test tube. Having some knowledge of the clearance of the compound, i.e., whether it is low or high, permits simplification of the relationships above, which in turn provides insight into those factors that may influence clearance (and, therefore, half-life). Therefore, for a compound with low clearance (low ER),

$$CL_{int} = f_U \times CL_{U,int} << Q, \text{ and}$$
$$CL \approx f_U \times CL_{U,int}$$

Equation 5.3.11

For such a compound, only changes in plasma protein binding or unbound intrinsic clearance will affect clearance. An example is antipyrine, whose clearance is small and therefore independent of flow (see Fig. 5.3.7). In contrast, for a compound with a high clearance (high ER),

$$CL_{int} = f_U \times CL_{U,int} >> Q, \text{ and}$$
$$CL \approx Q$$

Equation 5.3.12

For such compounds, only a change in organ blood flow will affect clearance. An example is lidocaine, whose clearance depends only upon flow (see Fig. 5.3.7). (These simplifying concepts and the resulting approximate relationships provide invaluable insight and predictions with respect to the effect on drug disposition of such factors as drug-drug interactions, disease states, and physiological disorders.) Several excellent reviews have been published which present these clearance concepts (Wilkinson and Shand, 1975; Wilkinson, 1987; Rowland and Tozer, 1995a).

Another approach to the characterization of the rate of elimination (and other processes) which has received considerable attention in recent years is referred to as *statistical moment theory*, *residence time analysis*, or *noncompartmental analysis*. The acronym SHAM has been used to describe this approach; the acronym is derived from the following abbreviations: *S*, slope; *H*, height; *A*, area; and *M*, moment. Each of these measures, which describes attributes of a plasma concentration-time curve, may be used by themselves or in combination to completely characterize various aspects of the disposition process (e.g., *M*/*A* = mean residence time; Lassen and Perl, 1979). The use of slope (to get K and $t_{1/2}$), height (to get certain volumes), and area (to get clearance and volume) have already been discussed. The idea of a *moment* is applied to concentration versus time data and is normalized in order to obtain additional information about disposition, as noted below. Many biological sciences such as biochemistry and physiology (and physical sciences such as chemical engineering) have traditionally characterized elimination processes in a manner different from the way that it has developed in pharmacokinetics (as outlined previously). Those fields are more likely to employ one of the following (generally interchangeable) terms to characterize elimination: *time constant*, *turnover time*, or *mean residence time* (MRT). The time constant is the time necessary for the plasma concentration to decline to 37% of its initial value (i.e., 63% loss versus 50% for $t_{1/2}$). That time can be calculated from $1/K$ (versus $0.693/K$ for $t_{1/2}$), where K is the same first-order overall elimination rate constant discussed previously, and if a one-compartment model applies. Another way to look at this value is that it represents the amount of time necessary for an endogenous pool of substance (e.g., albumin) to completely replenish itself or "turn over." Finally, this time represents the average amount of time that molecules of an exogenous substance spend in the body after gaining access to the body, which corresponds to the mean residence time, MRT. In a simple (i.e., one-compartment) system, the time constant and MRT are easily related to half-life; $MRT = 1.44 \times t_{1/2}$. The relationship is more complex for a multicompartment system (Mayersohn and Hamilton, 1993). In physiological or biochemical terms, MRT is the relationship between some mass and a corresponding flux (rate) or between some volume and a corresponding flow. For example, the mean circulation time of blood in an adult human male is governed by total blood volume (~5 liters) and total blood flow (or cardiac output; ~5 liters/min). Mean circulation time is ~1 min (i.e., 5 liters/5 liters/min). The turnover time of the endogenous albumin pool in an adult human is determined by the mass of the pool (~300 g) and its elimination (or catabolic) rate (~10 g/day). The turnover time for the albumin pool is ~30 days (i.e., 300 g/10 g/day).

In analogy to the preceding relationships, a mean residence time for an exogenous i.v. bolus dose of drug or toxicant is given by the ratio of an apparent volume term (referred to as the steady-state volume) and the corresponding systemic clearance of the compound:

$$\text{mean residence time} = MRT = \frac{V_{ss}}{CL_s}$$

Equation 5.3.13

Note that the dependence of MRT upon volume and clearance is identical to that for $t_{1/2}$ (Equation 5.3.5); however, different volume terms are involved. The major advantage of expressing elimination in terms of MRT rather than $t_{1/2}$ is that the former is nonparametric and may be calculated directly from the data (it also

offers a method to calculate V_{SS}; Benet and Galeazzi, 1979; Perrier and Mayersohn, 1982a,b). In general, moments are easier to estimate; the parameters may not be. In addition, we generally need more data to estimate parameters compared to moments.

Moment analysis has other uses which include, for example, the characterization of movement within and through compartments (McNamara et al., 1987; Kong and Jusko, 1988), estimation of metabolite residence time after parent administration (Veng-Pedersen, 1986), and estimation of mean absorption time in conjunction with i.v. and non-i.v. data (Riegelman and Collier, 1980).

A statistical view of a mean residence time can be illustrated by analogy to i.v. drug dosing (e.g., Karol, 1989). Envision 100 people simultaneously entering a large room that you rented for a New Year's Eve party. These people all enter at time = 0, linger in the room, and leave the party by exiting at different times. Beginning at time zero, a record is kept of the time of exit and how many people exit at that time (this is how you discover who your friends really are). Table 5.3.1 summarizes the data.

We want to calculate from these data the average amount of time your friends spend at the party by being in the room (in analogy to a substance's MRT in the body). A calculation similar to a weighted mean is done: add the product of time of exit (t) and the number exiting at that time (n) and divide that product by the sum of all those exiting (N):

$$\text{mean time} = \frac{(10\times17)+(12\times23)+\ldots+(35\times14)}{(17+23+\ldots+14)} = 20.9 \text{ min}$$

Equation 5.3.14

Your friends spend an average of 20.9 min at the party (this does not appear to have been a very successful party!).

In general:

$$\text{MRT} = \frac{\sum_{i=1}^{n} t_i \times N_i}{\sum_{i=1}^{n} N_i}$$

Equation 5.3.15

When dealing with drug or toxicant elimination, we do not consider discrete events (such as people leaving a room) because there are billions of molecules and an infinite number of corresponding events (i.e., times of exit). Rather than summing as in Equation 5.3.15, the relationship is integrated over time zero to infinity. Since the molecules will exit the body according to some explicit relationship (which need not be known, e.g., $C = C^0 \times e^{-Kt}$), the term N_i may be replaced by some appropriate expression for plasma concentration as a function of time. Assuming constant clearance:

$$\text{MRT} = \frac{\int_0^\infty t \times C \times dt}{\int_0^\infty C \times dt} = \frac{\text{AUMC}_0^\infty}{\text{AUC}_0^\infty}$$

Equation 5.3.16

The denominator is the area under the concentration-time curve discussed previously. The numerator is the area under the first moment of the concentration-time curve, AUMC, which is obtained from a plot of $t \times C$ versus t. The ratio, AUMC/AUC, is called the "normalized first moment," which gives information about a

Table 5.3.1 Data Used for the Estimation of a "Mean Residence Time"

Time of exit (min): t	Number exiting: n	Cumulative number exiting
10	17	17
12	23	40
18	6	46
22	19	65
30	21	86
35	14	100

mean value. The subsequent normalized moments (2nd, 3rd, etc.) give additional information about, for example, the variance around the mean, measure of skewness or symmetry, measure of peakedness (kurtosis), etc. The latter moments tend to be unstable and are not often calculated. The terminal area for the AUMC plot is not determined in the same way as for the C versus t curve (i.e., $AUC_0^\infty = C_{last}/K$) but rather with use of the following relationship:

$$AUMC_0^\infty = \frac{C_{last}}{K^2} + \frac{t \times C_{last}}{K}$$

Equation 5.3.17

There are numerous other mean residence and transit times that may be calculated and which help to define certain properties of disposition and more completely characterize the system, but a discussion of these is beyond the scope of this chapter (see, e.g., Lassen and Perl, 1979; Kong and Jusko, 1988).

EXPERIMENTAL DESIGN ISSUES

The design of any experiment must be appropriate in order that unequivocal answers will be obtained to the questions being asked. Anything less is a waste of time, effort, and money. We will assume here that the question being asked is how can we best describe the disposition kinetics of a substance as a function of one or more variables (e.g., dose and route of administration)? A fairly consistent list of experimental design issues needs to be addressed, regardless of the nature of the substance.

Preliminary Considerations

Before beginning any animal experiment, consideration of two issues will assist in making the study successful. First, the analytical method must be in place. The analytical validation should provide answers to the questions: how sensitive, how selective, how reproducible, and how robust. The results of any pharmacokinetic study are only as meaningful as the quality of the analytical method. This point cannot be over-emphasized. Sensitivity will help establish the minimum dose (and resulting plasma concentrations) and the duration of sampling. The selectivity will ensure that the data, subsequent analysis, and parameter values are uniquely associated with the parent compound administered (and not, for example, a metabolite). Reproducibility makes the data and subsequent analysis more reliable and meaningful. Robustness ensures that the assay is sufficiently rugged so that it is not overly influenced by changes in day-to-day conditions and environment. The person who is expected to assay the authentic samples should be given unknown samples spiked with the compound of interest (in the appropriate fluid matrix), prepared by another member of the laboratory, to assure the reliability of the results.

A second essential step to a successful study, often neglected but well worth the effort, is to conduct a preliminary experiment. This one experiment or series of experiments will answer one very fundamental question: is it possible to perform the study and can the questions posed be answered? If not, this is the time to rethink the study and the experiments. The data obtained from this preliminary experiment will permit optimization of virtually all of the important experimental variables, such as: dose, sample volume, times and duration of sampling, and animal response. What constitutes a "preliminary" experiment will vary from investigator to investigator. Basically, it represents the minimal experimental effort necessary to approximately characterize the variables. Those variables, when known, will result in the design of an experiment that will provide the data necessary to answer the questions posed or hypothesis to be tested. Typically, this preliminary experiment will indicate, among other things, most of the following—(1) if the assay is working properly; (2) the type of pharmacokinetic model and kinetics of elimination involved; (3) the duration of blood sampling and the best times of sampling; (4) the minimum blood volume needed to provide reliable analytical data; (5) the need to change dose; and (6) the safety to the animal of the dose chosen Other issues that may be addressed in this preliminary experiment, but which require additional effort, would include the degree of plasma protein binding, presence of metabolites, and recovery of the compound in urine, bile, feces, or expired air.

The results of the preliminary experiment will provide useful information that will then permit optimization of the experimental design. Alternatively, the preliminary experiment may be only partially successful, in the sense that not all of the needed information is obtained. Finally, the preliminary experiment may be a "failure," in the sense that, for example, no measurable plasma concentrations are observed. If either of the two latter situations arises, additional preliminary experiments need to be conducted. However, preliminary

experimental results like these should not be considered failures, because such results clearly indicate the need to revise the initial experimental design. This information, while perhaps not what was anticipated, could save great effort, time, and expense.

Some investigators will go one step further and perform a "positive control" experiment, whose results are, from experience, completely predictable. For example, a dose of a compound with which there is considerable experience in that laboratory will be given to an animal and the data analyzed and compared to previous results. This is done to determine if critical aspects of the experiment are working properly. Such an experiment will allow, among other things: (1) assessment of the student's or technician's ability to prepare and administer the compound, obtain samples, and perform the assay properly; (2) evaluation of the analytical instruments to be certain that they are working properly; and (3) evaluation of the ability to properly analyze the resulting data. There is much to be said for this type of experimental control, but in the author's experience it is a seldom-used safeguard.

General Design

Characterizing the disposition kinetics of a substance is generally accomplished using one of three sampling strategies: (1) intense sampling of single animals; (2) less intense sampling of several animals; (3) sparse sampling of many animals. The two former designs, especially the first, are most often used, but the last approach has gained considerable attention in recent years, especially within the pharmaceutical industry. In the first design, three to six individual animals are separately dosed with compound and intensive blood sampling proceeds according to some regimen. Data from each animal are analyzed and parameters obtained. The parameters are averaged and a measure of variance expressed (e.g., standard deviation). Individual plasma concentration–time curves can be prepared to describe disposition. The within-animal data generally provide a good description of the disposition of the compound, and comparisons among animals give some estimate of inter-animal variation (albeit limited information about the population). A disadvantage to this approach is that surgery is generally required in order to place a permanent catheter, which permits multiple sampling over time. The second design follows the same sampling scheme as the first, but blood samples are taken from among a number of different animals and at different times; thus, complete concentration-time curves are not obtained in individual animals. For example, samples 1 through 3 are taken from animals A and B; samples 4 through 6 are taken from animals C and D, etc. One obtains a single concentration-time curve with some estimates of variance at each time, depending upon the number of animals sampled per time. The analysis of these data results in a single set of parameter values with no estimation of variance. An advantage to this approach is that a limited number of blood samples (and limited blood volume) is taken and, therefore, surgical placement of a catheter is generally not necessary.

Another design, used in recent years in the pharmaceutical industry, which is less suited for an academic environment, is similar to the previous approach but involves fewer samples from even larger numbers of animals. This design relies on a sparse amount of data per animal but a sufficiently large number of animals that a good estimation of population parameters is obtained. The study groups are generally those associated with long-term toxicity testing (i.e., the study group per se or a parallel "satellite" group). Since one wants to interfere with the animals as little as possible, only a limited number of blood samples will be taken from any one animal (perhaps only one). The resulting data are then treated with specialized computer-based fitting programs (e.g., NONMEM; Beal and Sheiner, 1992), which permit development of both pharmacokinetic and error models to describe disposition of the compound. This approach maximizes the use of animals and provides unique population information. The sampling design strategies for such studies can become quite complicated and will not be discussed here. The readers are referred to several publications that address these issues (Nedelman et al., 1993; Ette et al., 1994; Tanigawara et al., 1994; Van Bree et al., 1994; Nedelman and Gibiansky, 1996; Tse and Nedelman, 1996; Gething and Daley-Yates, 1997; Mahmood, 1997).

Blood Sampling Protocol

A critical issue in the design and ultimate success of any pharmacokinetic study, in terms of obtaining accurate and useful parameter values, is the frequency and duration of blood sampling. These decisions are never arbitrary but should be based upon the results of preliminary studies. The final design will primarily be governed by issues of analytical sensitivity and how much blood volume can be withdrawn; we

Table 5.3.2 Approximate Number of Blood Samples That May Be Obtained from Rats of Different Weights

Blood volume removed (%)	100-g rat				200-g rat			
	Sample volume (µl)							
	100	200	300	500	100	200	300	500
15%	9	4[a]	3[a]	2[a]	18	9	6	3[a]
20%	12	6	4[a]	2[a]	24	12	8	4[a]
25%	15	7	5[a]	3[a]	30	15	10	6
30%	18	9	6	3[a]	36	18	12	7

[a]Too few samples, indicating unacceptable protocol.

want to maximize the former and minimize the latter. Clearly the choice of animal species will have a significant impact upon such design issues; the smaller the animal the more critical the concerns. Mice offer a considerable challenge because of the limited blood volume and, most often, several animals undergo limited (e.g., 1 or 2) sampling at selected times (as described above) in order to obtain a composite description of concentration versus time. Blood volume and number of samples are less an issue in larger animals such as rabbits and dogs. However, in a practical sense, especially in the pharmaceutical industry, there is only a limited quantity of a new chemical entity that would be available early in the preclinical discovery process, and this limits the size of the dose and therefore the selection of animal species. It is essential in that situation that only a rodent be selected for initial experiments.

The author assumes here that the majority of investigators study rats rather than mice or animals larger than rats. Furthermore, it is assumed that serial blood samples are obtained from individual unanesthetized, free-moving animals, either from a previously placed indwelling venous (or arterial) catheter or via another technique that permits multiple sampling (e.g., tail cutting; Tse and Jaffe, 1991). The former approach has become so popular that many companies now provide a service whereby the animals can be purchased with an indwelling venous catheter (at considerable cost, of course). However, the general principles outlined here will apply to serial sampling of individual animals or to cases where sampling does not involve individual animals, but rather select samples from different animals. In general, the basic aim of the study is to obtain sufficient information to completely characterize the disposition kinetics of the compound of interest. When this is not the case, then other concerns need to dictate the sampling protocol (e.g., an estimate of $t_{1/2}$ only will require limited sampling and an estimate of plasma protein binding will require only several selected samples).

The total number of blood samples and the volume per sample will be limited by what the investigator believes to be an acceptable volume of total blood removal. Blood volume per sample is generally determined by assay sensitivity. The more sensitive the assay, the less blood needs to be removed per sample and the less invasive and disruptive the procedure. Another issue here is the duration of time during which blood is removed—i.e., is the total volume removed over a short time or during an experiment that lasts for several days? The effect of blood loss on the disposition kinetics of a substance needs to be considered, but with the exception of alteration in plasma protein binding (Hulse et al., 1981), little is known about this issue. One experimental technique used by some investigators, to minimize the effect of blood loss, is to replace the blood removed with saline or blood from a donor animal. Table 5.3.2 gives some indication of the approximate number of blood samples that can be taken, assuming a certain level of total blood loss and and a given volume per sample. These calculations are done for animals of 100 and 200 g and assumes that blood volume represents ~6% of total body weight. It should be stressed that if the fluid being assayed is serum or plasma, the numbers in the table need to be cut in half (assuming a hematocrit of ~0.5).

The numbers marked with the superscript letter "a" represent too few samples and an unacceptable protocol. Seldom can one obtain sufficiently reliable information from <6 blood samples. Generally, one tries to obtain ~10 blood samples per animal; more is always better. As a general rule, blood sampling should

proceed for at least 3 to 4 terminal half-lives; the longer the better. However, the latter issue is governed by the sensitivity of the assay. Using this guideline will minimize the need to rely upon extensive (and potentially incorrect) extrapolation of the data. This rule refers to parent compound. If there is interest in formed metabolite(s) with a longer terminal half-life than the parent drug, then sampling needs to be extended appropriately.

At what times should the samples be obtained? The answer to this question is determined by the results of the preliminary experiment, the purpose of the study, and some practical issues (such as normal working hours). Ideally, one has good estimates of the parameters of the model describing the concentration-time curve, but this is seldom the case. If that is indeed the case, the samples are chosen as a function of the distributive and terminal half-lives. To obtain a good estimate of terminal half-life, more samples need to be taken after distribution is complete. In order to best describe the model, especially if it is multi-compartmental, early time samples need to be obtained. Early, intensive sampling would likely also be necessary for obtaining pharmacodynamic data as part of the experimental design (assuming rapid response). If the purpose of the experiment is to describe completely the concentration-time curve in order to obtain a reasonable model and good estimates of half-life and area, the times need to be spread out over the entire duration of sampling. Assuming that a maximum of ten samples can be obtained and an i.v. bolus dose is given, the earlier sample times might include: 5 min (seldom earlier) or 10 min, 0.25 hr, 0.5 hr, 0.75 hr, and 1 hr. The remaining samples would be used to best define the terminal half-life. The latter sample times may be described relative to half-life: i.e., 1, 2, 3, 4 and 5 × $t_{1/2}$. The exact sample times are adjusted and a compromise reached based upon assay sensitivity and the actual clock time. In practice, the most difficult sample times are between 8 and 24 hr, since few experimenters want to remain in the laboratory around the clock. A cursory examination of the literature will indicate this sample void for compounds with half-lives greater than ~3 or 4 hr. If, for example, the compound had a distributive phase (but not defined well) and a terminal half-life of ~2 hr, the following sample times would be reasonable: 0.0833, 0.167, 0.25, 0.5, 1, 2, 4, 6, 8, and 10 hr. The choice becomes more complicated if fewer samples are allowed. If only six samples can be obtained, the following schedule would be reasonable: 0.167, 0.5, 1, 2, 6, and 8 hr. The fewer samples the less precise the model and the less accurate will be all parameters (e.g., $t_{1/2}$, V, and CL).

The above is a guideline only and is not inscribed in stone. One needs to exercise reasonable flexibility in choice of sample design based upon preliminary results. Some compounds have very short half-lives (e.g., cocaine, ~20 min), while others have long half-lives in rats (e.g., the dioxin derivative, TCDD, ~20 days).

How many animals should be included in a study? The answer to this question depends upon the purpose of the study and the variance associated with the parameters of interest. If the study is designed to compare the effect of one or more variables on the disposition of the compound (e.g., effect of another drug or influence of disease or age), then a sufficient number of animals needs to be used to provide a reliable statistical answer having the necessary power to detect differences. The actual number of animals will depend upon the variance in the parameters that will be compared (e.g., $t_{1/2}$ or CL). The appropriate statistical considerations need to be made, keeping in mind the assumptions behind the statistical tests that will be used (e.g., see Bolton, 1997). In contrast, there are no statistical guidelines if the purpose of the study is not to make comparisons but rather to define the disposition kinetics of the compound. Useful information will be obtained from three or six or more animals; the more animals the more reliable the population estimates become. It is fairly common to conduct a study to characterize the pharmacokinetics of a compound in four to six animals and, for the most part, with the typical variance found, this seems a reasonable number for providing reliable initial estimates.

What Fluid to Sample?

Although it is always a blood sample that is taken from an animal, the question arises, which fluid should be assayed—whole blood, plasma, or serum? While blood may be the preferred fluid, it is seldom assayed, generally for reasons of analytical cleanliness (a notable exception is determination of "blood alcohol" concentrations, but most often a head space gas chromatographic assay is used). Plasma and serum are essentially the same fluid; the only difference is that serum, which is obtained from coagulated blood, is devoid of fibrinogen. Since

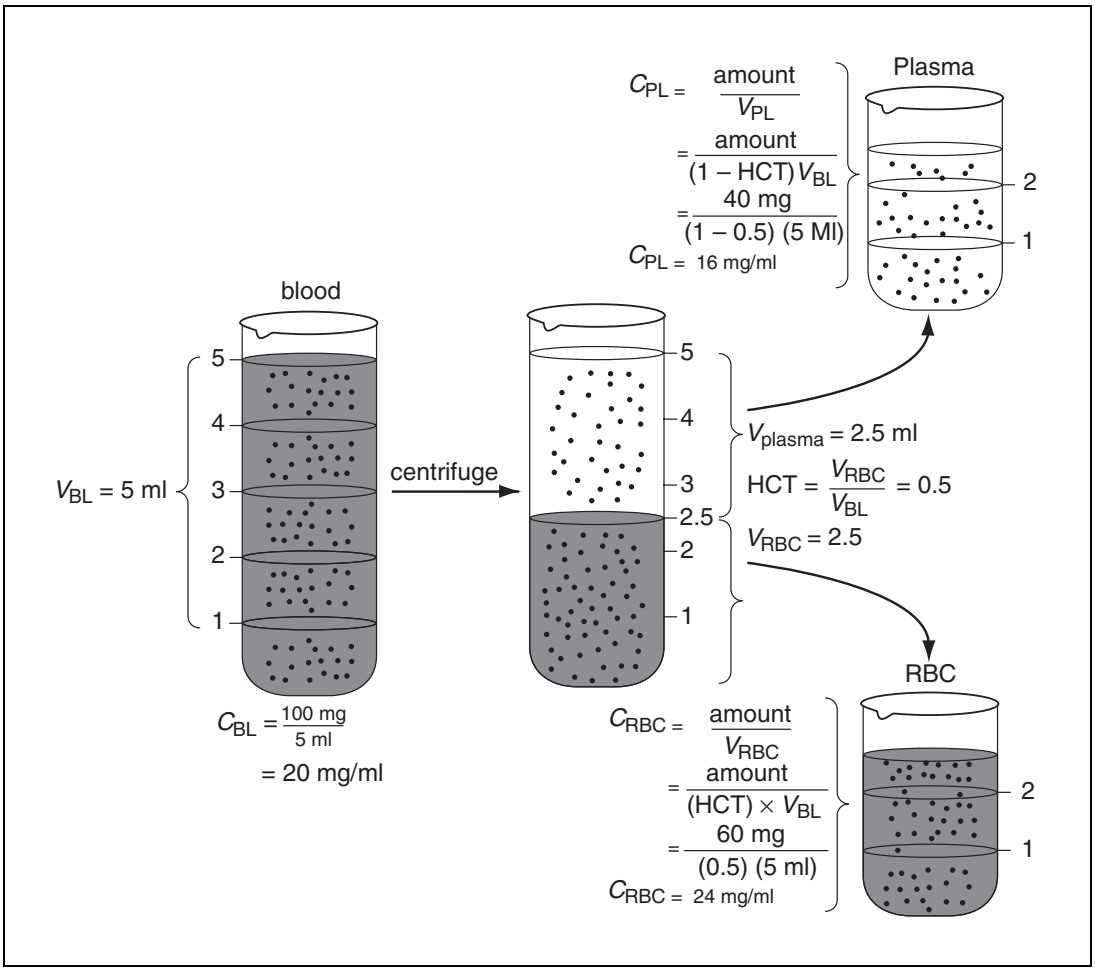

Figure 5.3.8 Illustration of the experimental determination of blood, plasma, and red blood cell concentrations of a drug. A 5-ml blood sample is determined by assay to have a drug concentration of 20 mg/ml (left). After centrifugation, the red blood cells (RBC) occupy a volume of 2.5 ml as does the plasma volume. The hematocrit, therefore, is 0.5 (2.5/5.0). The RBCs are assayed and found to have a drug concentration of 24 mg/ml (bottom right). The plasma is assayed and determined to have a drug concentration of 16 mg/ml (top right). The blood-to-plasma concentration ratio is 1.25 (viz., 20/16). HCT represents hematocrit. Used with permission of Saguaro Press.

it is blood that carries the compound to eliminating organs, all expressions of organ extraction and clearance should be made in reference to blood concentrations of the compound. This is seldom the case, however, as it is plasma concentrations that are virtually always measured and reported in the literature. While for most applications plasma clearance remains a useful and meaningful measure, it may on occasion be necessary to relate plasma clearance to blood clearance. The latter requires determination of the blood-to-plasma concentration ratio. That ratio is most easily determined experimentally with use of a radioactive form of the compound, but any selective assay should suffice. The blood (an authentic sample or one with added unlabeled compound) is spiked with sufficient radiolabeled compound. After equilibration at 37°C, the blood is counted and an aliquot of the blood is centrifuged, plasma obtained, and this plasma is also counted. Knowing the hematocrit of the blood, concentrations in each fluid are calculated and the resulting ratio determined. This is illustrated in Figure 5.3.8. Since rate of elimination is the product of either blood or plasma concentration and the corresponding clearance term, plasma clearance can be converted into blood clearance (Rowland and Tozer, 1995b).

$$\text{rate of elimination} = \mathrm{CL}_{\text{blood}} \times C_{\text{blood}} = \mathrm{CL}_{\text{plasma}} \times C_{\text{plasma}}$$

Equation 5.3.18

$$CL_{blood} = CL_{plasma}\left(\frac{C_{plasma}}{CL_{blood}}\right)$$

Equation 5.3.19

Ideally, the blood-to-plasma concentration ratio should be determined as a function of concentration over the expected or measured concentration range in the study. In this way, any concentration dependence in red blood cell partitioning can be detected. Such a study can be easily combined with evaluation of plasma protein binding. The blood samples are spiked with radioactive compound over the appropriate concentration range (achieved by adding unlabeled compound or using authentic blood samples). An aliquot of blood is counted. The blood is centrifuged and an aliquot of plasma is counted. Assuming there is sufficient plasma, the remainder may be used to assess plasma protein binding by any appropriate method (e.g., ultrafiltration). This optimal approach minimizes the need for extra blood samples and both concentration ratios and plasma protein binding are determined from the same samples, minimizing the variance associated with using different sets of blood samples.

There are a number of experimental issues here that are of concern. The first involves use of indwelling catheters for short or long-term blood sampling. While this is the most practical means of serial sampling in the free-moving animal, placement of such catheters have been associated with short-term weight loss (greatest with carotid artery and least with jugular vein placement; Yoburn et al., 1984) and changes in corticosterone plasma concentrations (Fagin et al., 1983; Tsukamoto et al., 1984). Perhaps more relevant are the direct changes noted in the pharmacokinetics of several compounds as a consequence of catheter placement. Terao and Shen (1983) noted that long-term placement of a venous catheter resulted in a substantial increase in the plasma concentrations of the acute-phase protein, α_1-acid glycoprotein (AGP), which primarily binds basic compounds, and a decrease in albumin concentrations, which primarily binds acidic compounds. These protein changes resulted in increased binding of l-propranolol to AGP and decreased binding of phenytoin to albumin and consequent changes in several pharmacokinetic parameters. The results of Chindavijak et al. (1988) and Torres-Molina et al. (1992) suggest not only changes in plasma protein binding but alterations in hepatic metabolism which may affect both low and high extraction ratio compounds. These time-dependent changes, which occur over several days, may argue against a cross-over design for those compounds whose disposition may be affected by the presence of a catheter.

Another potential problem associated with the use of indwelling catheters is related to the use of anticoagulants, especially heparin, to maintain catheter patency. Heparin, upon systemic administration, is known to mobilize free fatty acids, which in turn compete for binding sites on proteins, especially albumin (Brown et al., 1981). The consequent alteration in plasma protein binding may cause changes in the pharmacokinetic parameters (e.g, V, CL, and $t_{1/2}$) of certain drugs. Therefore, when flushing an indwelling catheter it is best to minimize the volume of anticoagulant used and try to restrict injection to the end of the catheter only. Alternatively, one can instill and use normal saline for flushing the catheter.

Often the indwelling venous catheter is used for i.v. dosing as well as for blood sampling. Following the i.v. dose, the catheter should be flushed with normal saline (~0.5 ml) to be certain that the dose is actually delivered to the systemic circulation and to wash the surface of the catheter. There is some concern about assuming that the compound given does not adsorb to the surface of the catheter. This potential for adsorption (and, therefore, overestimation of the actual dose injected) should be evaluated from simple in vitro experiments. The dosing solution should be passed through an appropriate length of catheter into a test tube. The catheter is then flushed with normal saline, as is done in vivo, and the washings combined with the dosing solution in the test tube. The total dose recovered in the test tube should be determined by assay and compared to the actual dose. If there is substantial loss of compound by adsorption, the dose needs to be accurately estimated or administered into another vein (e.g., tail vein).

A final concern is with the use of anesthetics which, depending upon the animal preparation, may be a significant issue. The anesthetic choice is of less concern when an indwelling catheter is placed and the experiment proceeds 2 or more days after the exposure to the anesthetic. The latter assumes, of course, that there are no residual effects of the anesthetic on, for example, hepatic function, which might interfere with metabolic processes. In contrast, if the animal is maintained anesthetized throughout the entire experiment during which time blood

samples are obtained, then the choice of anesthetic may be a critical one. Several investigators have compared anesthetic effects on the pharmacokinetics of antipyrine, a compound often used to assess hepatic oxidative metabolism. If the animals are maintained under anesthesia with parenterally administered anesthetics such as pentobarbital, urethane, or ketamine/xylazine, the clearance of antipyrine decreases and half-life increases. The change in antipyrine kinetics is very substantial for several of those agents, (e.g., CL, 3.20 versus 6.21 ml/min × kg for ketamine and control, respectively; Gumbleton and Benet, 1991). Similar observations were made by Tse et al. (1992), who found that the gaseous anesthetic isoflurane is the preferred agent, although long-term use of almost any anesthetic, including isoflurane, is to be avoided. A more complete review of anesthetic effects on pharmacokinetics and pharmacodynamics may be found in an especially thorough and useful text concerned with numerous experimental issues in animal pharmacology (Claassen, 1994).

Dosing Methods and Sites

There are numerous issues related to the "how" and "where" of dosing that have an impact on estimation of half-life, clearance, and residence times. Unequivocal data and meaningful disposition parameter values are only obtained following intravenous or intra-arterial dosing. The method of dosing may include bolus as well as short- and long-term infusions (as seen in Fig. 5.3.1). There are basically two issues that need to be considered when a non-vascular route of administration is used. The first is the rate of absorption, which, if very slow, will result in an incorrect estimate of disposition half-life. If the absorption process, expressed with an apparent first-order rate constant, k_a, is slower than the disposition rate constant, K ($k_a << K$), then the terminal slope will reflect absorption (or input) and not disposition. The slowest (or rate-limiting) process in a sequence of steps (e.g., absorption site → compound in body → compound eliminated) will always determine the value of the terminal slope. This situation is sometimes referred to as a "*flip-flop*" model. Plasma concentrations resulting from absorption will be described by the following relationship:

$$C = A \times (e^{-K \times t} - e^{-K_a \times t})$$

Equation 5.3.20

where A (units of concentration) is a constant given by a value on the y axis. The concentration-time data will rise and then fall with a terminal slope representing either k_a or K, depending upon which is smaller. It does not matter how sophisticated the analysis of this curve is—a nonvascular dose may or may not give rise to the correct value for disposition half-life. The only way to know for certain is to give an i.v. or intra-arterial dose whose slope, by definition, will be that of disposition. Therefore, frequently used routes of administration such as subcutaneous (s.c.), intramuscular (i.m.), or oral will either give the correct value or an overestimate of disposition half-life. An example of this phenomenon is illustrated in Figure 5.3.9, which is a plot of cocaine plasma concentrations following an i.v. bolus and s.c. dose of 7.5 mg/kg in rats (Sukbuntherng et al., submitted). Absorption following the s.c. dose is slow and the concentration-time data appear to provide a half-life much greater than that seen following i.v. dosing. This type of temporal profile is also expected to affect the response-time relationship, and this should be kept in mind when such measurements are being taken. The most likely explanations for the occurrence of a "flip-flop" situation include: compounds with poor membrane permeability (e.g., very polar or large molecule); compounds with very limited aqueous solubility; formulations that release compound slowly (e.g., oily vehicle or suspension placed s.c. or i.m.); or limited or altered blood flow to the site of absorption. The last factor might explain the slow absorption of cocaine following s.c. dosing—the compound causes constriction of blood vessels and reduces blood flow.

Moment analysis can be applied here for the estimation of a mean absorption (or input) time (MAT), which is the average amount of time that the compound spends at the absorption site. For an i.v. infusion, the mean absorption time is simply the infusion time divided by 2 (e.g., if infusion lasts for 60 min, MAT = 60/2 = 30 min). The calculation of a MAT requires knowledge of MRT (from i.v. dosing; see Equation 5.3.13 and related discussion above):

$$\text{MAT} = \left[\frac{\text{AUMC}_0^\infty}{\text{AUC}_0^\infty}\right]_{\text{non-i.v.}} - \text{MRT}$$

Equation 5.3.21

In a simple system, MAT and k_a are related (MAT = $1/k_a$). Mean absorption time offers a

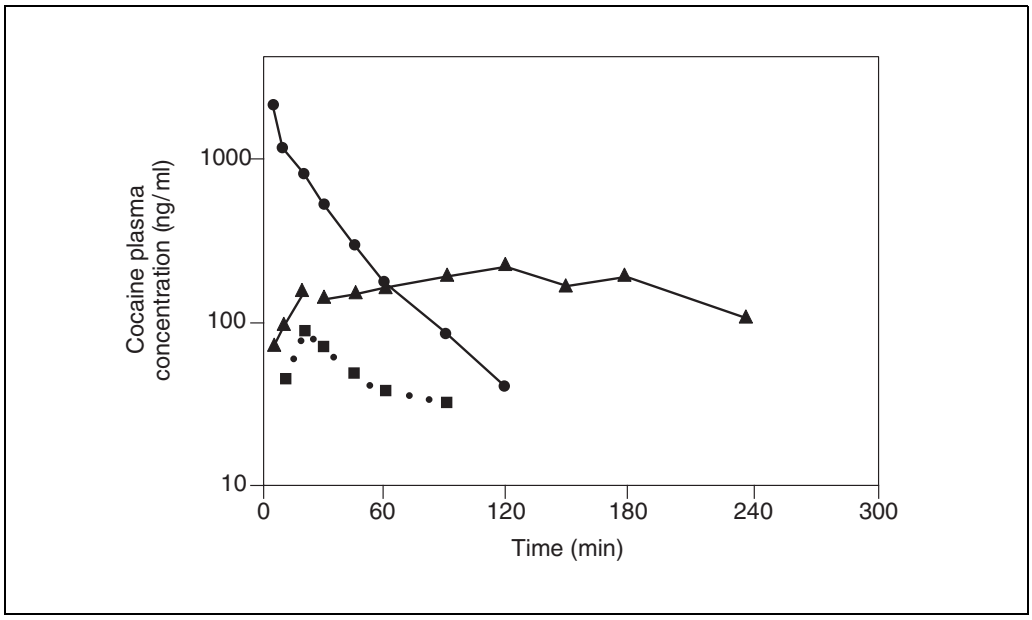

Figure 5.3.9 Average cocaine plasma concentrations as a function of time following an i.v. bolus dose of 7.5 mg/kg (circles) and a subcutaneous dose (triangles) of 7.5 mg/kg cocaine given to three rats. An oral dose of cocaine (17.9 mg/kg) was given to one rat (squares). Based upon the data in Sukbuntherng et al. (submitted). Used with permission of Saguaro Press.

measure of the rate of absorption, which complements that of an absorption rate constant.

Another approach that may also be taken, but which will not be discussed here, is to perform a *deconvolution* analysis, which provides a means of viewing the rate of absorption as a function of time. Deconvolution, which means "uncurling," is a mathematical attempt to separate (or "uncurl") the absorption process from the sum of input and disposition processes, which are represented in the concentration-time data following nonvascular dosing. The latter approach graphically illustrates the input process as the compound continues to be absorbed.

The second issue with regard to site of administration is with respect to the completeness of absorption. Estimates of completeness of absorption are often expressed as the *fraction of the dose absorbed or systemic bioavailability* (F). Expressing a previous relationship (Equation 5.3.7) in a more general manner, taking into consideration an absorption process:

$$\mathrm{AUC}_0^{\infty} = \frac{F \times \mathrm{dose}}{\mathrm{CL_s}}$$

Equation 5.3.22

For an i.v. dose, $F = 1$, so this factor does not appear in the numerator of Equation 5.3.7. Clearly, if $F < 1$, which it may be for a variety of reasons, the resulting AUC_0^{∞} will not provide a correct estimate of clearance (or apparent volume). The ratio of areas following nonvascular and i.v. dosing is often used to calculate the *absolute bioavailability* (after adjusting for any differences in doses), which is simplified by assuming constant clearance:

$$F_{\mathrm{absolute}} = \frac{(\mathrm{AUC}_0^{\infty})_{\text{non-i.v.}} \times (\mathrm{CL_s})_{\text{non-i.v.}}}{(\mathrm{AUC}_0^{\infty})_{\text{i.v.}} \times (\mathrm{CL_s})_{\text{i.v.}}} \times \frac{(\mathrm{dose})_{\text{i.v.}}}{(\mathrm{dose})_{\text{non-i.v.}}}$$

$$\cong \frac{(\mathrm{AUC}_0^{\infty})_{\text{non-i.v.}}}{(\mathrm{AUC}_0^{\infty})_{\text{i.v.}}} \times \frac{(\mathrm{dose})_{\text{i.v.}}}{(\mathrm{dose})_{\text{non-i.v.}}}$$

Equation 5.3.23

Figure 5.3.9 illustrates this issue following the oral administration of cocaine. The absolute oral bioavailability of cocaine is estimated to be only ~5% ($F = 0.05$). This is in marked contrast with s.c. dosing which, while slow, is essentially complete ($F = 1$). Low, incomplete nonvascular absorption may occur for a variety of reasons, including limited aqueous solubility, limited membrane permeability, saturable (dose-dependent) transport process, or presys-

temic (first-pass) elimination (e.g., degradation in gut fluid or metabolism by the intestinal membrane, liver, or bacterial flora). The low oral absorption of cocaine is probably attributed to the latter effect, which can be summarized in the following way:

$$F = f_{\text{released}} \times (1 - \text{ER}_{\text{gut fluid}}) \times (1 - \text{ER}_{\text{gut wall}}) \times (1 - \text{ER}_{\text{liver}})$$

Equation 5.3.24

The terms in parentheses, (1 − ER), represent the fractions that survive that particular metabolic process and f_{released} is the fraction of the dose released by the oral dosage form into the gut fluids.

There are numerous experimental factors which can affect the rate and completeness of absorption from a nonvascular site and which in turn will affect the concentration-time data and the correctness of many derived pharmacokinetic parameters including $t_{1/2}$, V, and CL_S. Such issues include the solubility of the compound in the formulation used for dosing, the pH and volume of the vehicle administered, and the tissue site chosen for dose administration. These should not be considered trivial issues, as they can have a major impact on the interpretation of the experiment. There is a fairly rich (generally, older) literature concerned with these experimental variables, which the investigator needs to consider in the proper design of an optimal experiment. Many of these are issues discussed elsewhere (Claassen, 1994).

COMPLICATING FACTORS AND OTHER ISSUES TO CONSIDER

The following discussion reviews several complicating issues, which need to be considered in the design and analysis of pharmacokinetic studies. Only a limited discussion of these issues will be presented here.

Dose-Dependencies (Nonlinearities)

All of the preceding discussions have made one important assumption, that of first-order kinetics, sometimes referred to as *linear or dose-independent kinetics*. A broad definition of a linear system is one in which output is directly related to input—double input results in double output. A complete definition of a linear system would include the *principle of superposition* and the idea of *time invariance*. The principle of superposition states that following dosing, concentration-time data divided by dose will superimpose onto one curve when plotted as a function of time. Time invariance states that the system will behave the same way regardless of time. With a linear system, the values for the input and output parameters will not change with dose. This condition does not always apply, and it is less likely to apply in toxicokinetic studies where very often unusually large, toxic doses are examined.

Any process of absorption, distribution, and elimination may become nonlinear as a function of dose, and there are numerous examples from the drug literature to indicate this (e.g., for a thorough discussion, see Rowland and Tozer, 1995c). The classic example of this type of process is given by the oxidative metabolism of ethanol by alcohol dehydrogenase, which may be described by the Michaelis-Menten enzyme kinetics equation:

$$\text{rate of metabolism} = v = \frac{V_{\max} \times C}{k_m + C}$$

Equation 5.3.25

where v is velocity or rate, $V_{\max}$ is the maximal rate, C is plasma concentration, and k_m is the Michaelis constant. The Michaelis constant has units of concentration, and it represents the concentration needed to obtain one-half of the maximal rate (i.e., one-half of $V_{\max}$). That symbol, k_m, should not be confused with a metabolic rate constant (with units of 1/time). The above equation takes the form of a hyperbola, a relationship frequently seen in biology, describing a nonlinear system or saturable process (often related to binding). We can simplify this relationship by considering the two extremes of concentration, low and high. At low concentrations, $C << k_m$, and the denominator can be approximated by k_m. Therefore, the rate of metabolism will be described as follows:

$$\text{rate of metabolism} \cong \left(\frac{V_{\max}}{K_m} \right) \times C$$

Equation 5.3.26

The ratio of constants in parentheses is also a constant and can be represented by the rate constant discussed previously, K (or a metabolic rate constant). In other words, at low plasma concentrations, rate is directly related to concentration, which is a statement of first-order kinetics. When concentrations get large, such that, $C >> k_m$, the k_m in the denominator can be ignored and the concentration terms cancel. At high concentrations, rate may be expressed as:

$$\text{rate of metabolism} = V_{max}$$

Equation 5.3.27

The above relationship indicates that no matter how concentration (or dose) increases, the rate will not change; it remains constant. This is a statement of *zero-order kinetics*. At concentrations in between the two extremes, there is mixed kinetics.

The above situation can be simply related to clearance, since clearance is the expression of rate relative to plasma concentration:

$$CL = \frac{\text{rate}}{C} = \frac{V_{max} \times C}{(k_m + C) \times C} = \frac{V_{max}}{k_m + C}$$

Equation 5.3.28

Thus, when, $C << k_m$, ignore C in the denominator and CL will be a constant given by V_{max}/k_m. In contrast, at high concentrations, $C >> k_m$, the denominator in Equation 5.3.28 becomes larger and larger as C increases. This results in a decrease in CL as concentration (or dose) increases, which in turn results in an increase in half-life (recall that $t_{1/2} = 0.693 \times V/CL$). This happens for ethanol and at least two other drugs, phenytoin and salicylate, and for numerous toxic chemicals such as dioxane. There are significant implications to this saturable process, especially in the clinical and toxicological response to the compound. The above analysis represents a very general treatment of any process of elimination, and is not limited to enzyme metabolism but includes renal excretion and biliary excretion, among other processes.

In order to detect nonlinear behavior in elimination, it is necessary to administer ≥3 different doses and to cover as wide a range of plasma concentrations as possible. An indication of nonlinear elimination can be inferred under the following circumstances: (1) when the concentration-time data divided by dose will not superimpose to form one curve; (2) when the concentration-time data are not strictly exponential (i.e., not log-linear) after distribution is complete; and (3) when the half-life appears to be changing with time (i.e., the terminal slope becomes more and more steep with time as concentrations decline). In addition, the areas under the curves will not increase in direct proportion to dose, but rather out of proportion. There are other ways to determine the existence of nonlinear elimination (in metabolism or renal excretion) that rely upon collection of urine metabolites and other experimental procedures (Levy, 1968). There are numerous other forms of nonlinearity in elimination such as, metabolite inhibition of metabolism.

Some care needs to be applied when interpreting a concentration-time curve whose data are relatively incomplete—that is, where only one or two half-lives of elimination have been examined. Virtually all data, whether adhering to first-order or zero-order elimination kinetics, will provide a log-linear relationship over a narrow concentration range, and, therefore, suggest first-order kinetics. This was noted in a report that examined the elimination kinetics of 4-methylpyrazole, which was shown to follow nonlinear elimination kinetics in the dog (Mayersohn et al., 1985). An illustration of the plasma concentration-time plot of the latter compound is shown in Figure 5.3.10, which illustrates several of the points noted above.

Measurement of Total Radioactivity or Use of a Nonselective Assay

We noted in a previous section how slow or incomplete absorption from the site of dosing could influence the estimation of parameter values and alter the interpretation of the experiment ("flip-flop" model and $F < 1$). There is an analogous situation that can occur on output rather than on input, but which reflects the identical principle; the slowest step in a sequence of steps will dictate the meaning and value of the terminal slope. The sequence of steps in this instance is: parent drug → metabolite → metabolite elimination. One of these two steps must be rate-limiting and, depending upon what chemical form is measured, will determine the meaning of the slope of concentration versus time. An incorrect value for the terminal disposition half-life may be obtained for a compound that undergoes metabolism when a radiolabled form of the compound is dosed and total radioactivity is measured, or, what is essentially the same issue, if a nonspecific chemical assay is used to quantify the parent compound. The terminal half-life obtained under either of the above circumstances will be equal to or will exceed the correct disposition half-life. The latter will occur if any of the metabolites being quantified are themselves lost from the body more slowly than the parent compound. In the case of a nonspecific assay, the metabolite may be measured along with parent compound. In the case of measurement of total radioactivity, the metabolite eliminated more slowly than the parent compound

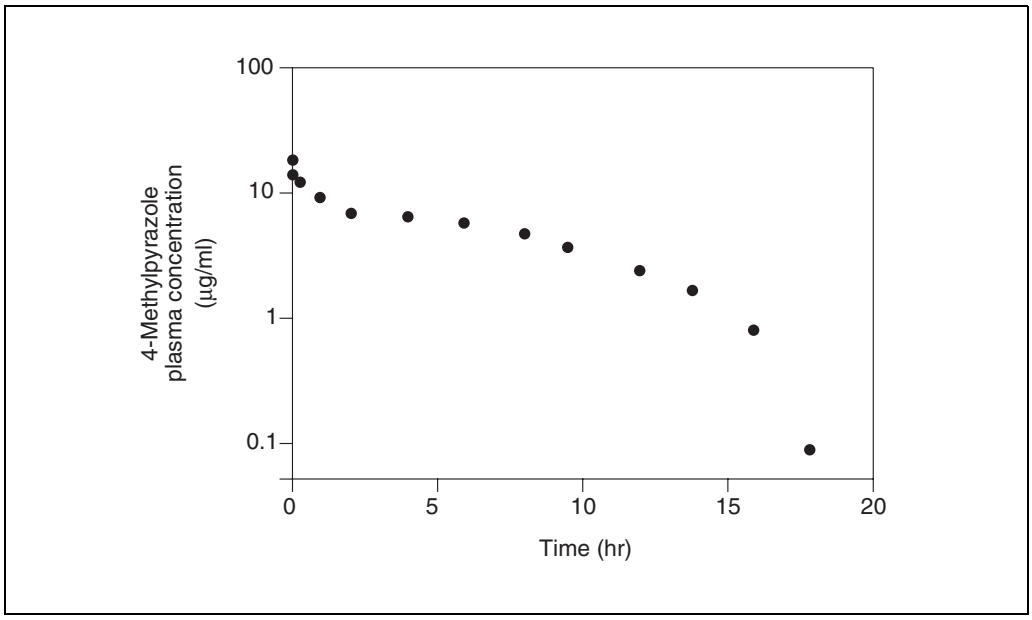

Figure 5.3.10 Plasma concentration-time profile of 4-methylpyrazole following an i.v. bolus dose of 10 mg/kg to one dog. Note that the shape of the curve suggests a nonlinearity in disposition. Based upon the experiment reported by Mayersohn et al. (1985), but data not provided in publication. Used with permission of Saguaro Press.

may contain the radiolabel in its structure, and contribute to the total radioactivity measured. An example of this disparity in terminal half-life based upon total radioactivity or that associated with the parent compound is illustrated in Figure 5.3.11. The compound, salmeterol, was given to rats as an i.v. dose (2 mg/kg) and radioactivity was measured—both total and that associated with parent compound (Manchee et al., 1993). There is obviously a very substantial discrepancy between total radioactivity and that related to parent compound, which would appear to reflect high plasma concentrations of formed radioactive metabolites. One or more metabolites are eliminated far more slowly than the parent compound.

An additional problem with radiolabeled compounds is the possibility of isotope exchange with, for example, water if the compound is tritium (^{3}H)–labeled, or where there is an exchange of ^{14}C with any of a myriad of endogenous carbon-containing molecules. The resulting apparent half-life will reflect the half-life of the slowest of all of the labeled compounds eliminated from the body. Unusually long elimination half-lives may be explained by the latter occurrence, but it is more difficult to attribute half-life to a metabolite per se if no specific information is available about the parent compound. This illustrates, once again, the critical need for a selective assay.

A similar analytical issue exists when there are enantiomeric forms of the parent compound (as well as subsequent metabolites). Unless an effort is made to develop an enantiomerically selective assay, the concentration measured will be that of the racemic mixture. Since enantiomers often behave differently in terms of pharmacokinetic and pharmacodynamic parameters (e.g., Tucker and Lennard, 1990; Eichelbaum and Gross, 1996), a selective assay is desirable. Alternatively, if the pure enantiomers are available for dosing, studies can be done on the individual forms.

"Effective" or "Accumulation" Half-Life

Advances in analytical chemistry, especially the now routine application in the pharmaceutical industry of high-performance liquid chromatography (HPLC) in conjunction with mass spectrometry (see *UNIT 4.4*), has resulted in exquisitely sensitive methods for quantitation of exogenous substances. These sensitive assays permit the evaluation of disposition for a longer time following dosing, which in turn has given rise to an apparent need for more complex multicompartmental models to describe the data. These models inevitably include a very long terminal half-life. While these long terminal half-lives may be correct, and most likely reflect slow redistribution from tissues to blood, they are often not a useful parameter.

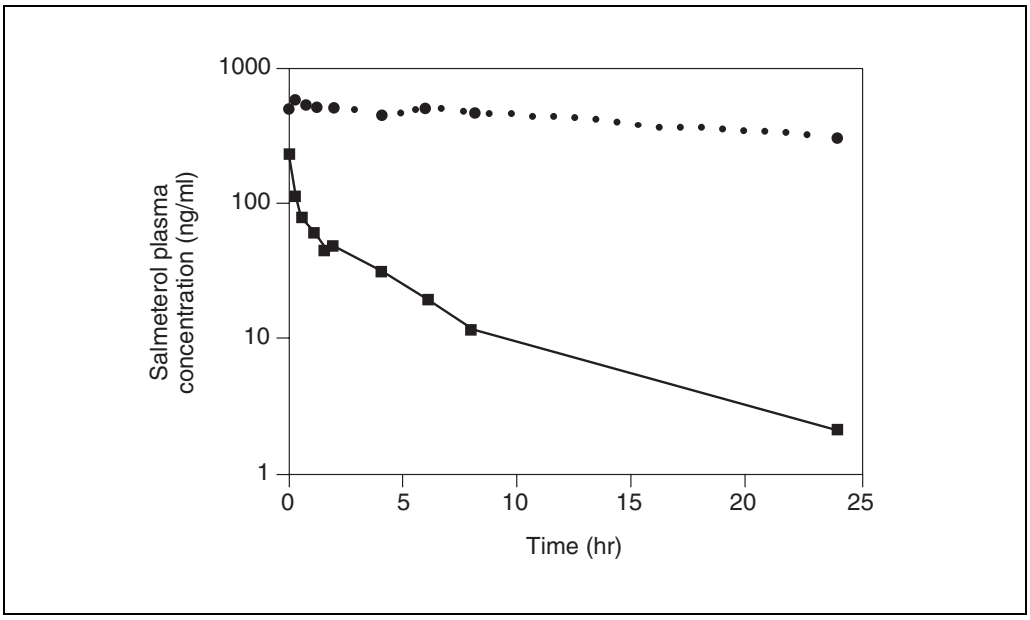

Figure 5.3.11 Salmeterol plasma concentrations as a function of time following the i.v. bolus administration of 2 mg/kg to rats. Concentrations are related to total radioactivity (circles) or that associated with parent compound (squares). Note the very large discrepancy in terminal half-life based upon the chemical form being quantified. The total radioactivity includes radiolabeled formed metabolite(s). Based upon recovery and replotting of graphical data in Manchee et al. (1993).

The reason for the latter statement is based upon the fact that the long terminal half-life occurs only after most of the dose of the compound has been eliminated from the body and because that long half-life does not determine how the drug *accumulates* in the body as a result of multiple dosing. The magnitude to which a compound accumulates in the body is a function of half-life and the dosing (or exposure) interval (τ, expressed in units of time); accumulation increases when half-life is long and when the dosing interval is short. For that reason there is need for a practical "accumulation" (or "effective") half-life that will actually determine the extent of accumulation upon multiple dosing. This effective half-life will always be less than the very long terminal half-life measured with a sensitive assay, and it is calculated on the basis of the actual accumulation of the compound (Kwan et al., 1984). Readers interested in multiple dosing and accumulation (not discussed in this unit) and effective half-life are referred to the previous reference.

DATA ANALYSIS: A WORKED EXAMPLE

The following section will provide a complete example of a fairly representative data set that would be obtained from the experimental designs discussed in preceding sections. The author has taken an actual literature example and used tabular data. Note, however, that it is possible to recover graphical data from publications using digitizing techniques that have been shown to be quite accurate (Mayersohn and Tannenbaum, 1998). The data have been treated by noncompartmental and compartmental (model-fitting) methods in order to illustrate how the final parameter values compare.

Example: Creatinine Disposition in the Dog Following an i.v. Bolus Dose

These data have been taken from an early publication (Dominguez et al., 1935). A dose of 6.6 g creatinine was given as an i.v. bolus to a dog (20.2 kg). The resulting plasma concentrations were corrected for the endogenous creatinine concentration. Table 5.3.3 provides a listing of the concentration-time data along with estimates of areas (AUC and AUMC). The areas were determined with use of the linear trapezoidal rule in a Microsoft Excel spreadsheet.

The area calculations for an i.v. bolus dose can be divided into three segments:

1. The first area is approximated by a rectangle: $C_1 \times t_1$; e.g., $812 \times 0.200 = 162.4$.
2. All of the remaining individual areas are estimated with use of the linear trapezoidal rule: $(1/2) \times (C_1 + C_2) \times (t_2 - t_1)$; e.g., $(1/2) \times (812 + 702) \times (0.292 - 0.20) = 69.4$.
3. The terminal (or remaining) area from the last measured time (t_n) to time infinity, is

Table 5.3.3 Creatinine Plasma Concentration-Time Data and Area Calculations

Time (hr)	Creatinine plasma conc. (μg/ml)	AUC (μg × hr/ml)	$C \times t$ (μg × hr/ml)	AUMC (μg × hr^2/ml)
0.200	812	162.4	162.4	16.2
0.292	702	69.4	204.8	16.8
0.567	422	154.6	239.1	61.0
0.783	411	90.2	322.0	60.8
1.025	316	87.8	323.9	78.0
1.542	242	144.2	373.1	180.1
2.042	205	111.8	418.5	197.9
3.042	169	187.0	514.0	466.3
4.033	125	145.8	504.2	504.9
5.033	86	105.5	432.9	468.5
6.058	77	83.5	466.5	460.9
7.042	66	70.3	464.8	457.9
8.075	50	59.9	403.8	448.7
Sum:		1472.4		3418.1

calculated from the last measured concentration (that is on a regression line, as noted below) divided by the terminal rate constant: C_n/β; e.g., 50/β.

The total area under the curve is the sum of the above areas:

$$\mathrm{AUC}_0^{\infty} = \mathrm{AUC}_0^{t_1} + \mathrm{AUC}_{t_1}^{t_n} + \mathrm{AUC}_{t_n}^{\infty}$$

Equation 5.3.29

The total area to time 8.075 hr is 1472.4 μg × hr/ml. An estimate needs to be obtained of the terminal rate constant, β. This is discussed below.

The same general process is used for determination of the area under the moment curve, AUMC, with some exceptions.

1. The first area is approximated by a triangle: $(1/2) \times C_1 t_1 \times t_1$; e.g., (1/2) × 162.4 × 0.200 = 16.2.

2. All of the remaining individual areas are estimated with use of the linear trapezoidal rule: $(1/2) \times (C_1 t_1 + C_2 t_2) \times (t_2 - t_1)$; e.g., (1/2) × (162.4 + 204.8) × (0.292 − 0.20) = 16.8.

3. The terminal (or remaining) area needs to be calculated differently from that for AUC. The terminal area is calculated from the two following terms: $C_{tn}/\beta^2 + C_n t_n/\beta$. Generally, the actual values for C_{tn} and $C_n t_n$ are used along with the estimate for β obtained from regression of the concentration-time data.

Figure 5.3.12 illustrates the results of the noncompartmental and compartmental analysis of the concentration-time data. A decision needs to be made, using the former approach, about which data points constitute the terminal phase (i.e., those points that form the terminal, log-linear phase). This is generally not a difficult decision if the data are reasonably uniform. In this instance, the data points from 2 hr and beyond were selected. The solid line illustrates the linear regression of those seven points. The equation of the line was:

$$C = 324\ \mu\mathrm{g/ml} \times e^{-0.235 \times t} \quad (r^2 = 0.98)$$

Equation 5.3.30

The terminal rate constant had a value of 0.235 hr^{-1}, which corresponds to a terminal half-life of 2.95 hr. That value is then used for estimation of the terminal areas of AUC and AUMC, as noted above. In the former case, the rate constant is divided into the last concentration value that lies on the regression line. The latter concentration needs to be calculated from the regression equation. In this instance, the value at 8.075 hr is 49 μg/ml. The terminal area, therefore, is equal to: 49 μg/ml ÷ 0.235 hr^{-1}, or 208.5 μg × hr/ml. The total area, therefore, is the sum of: 208.5 + 1472.4 = 1680.9 μg × hr/ml.

The terminal AUMC is given by:

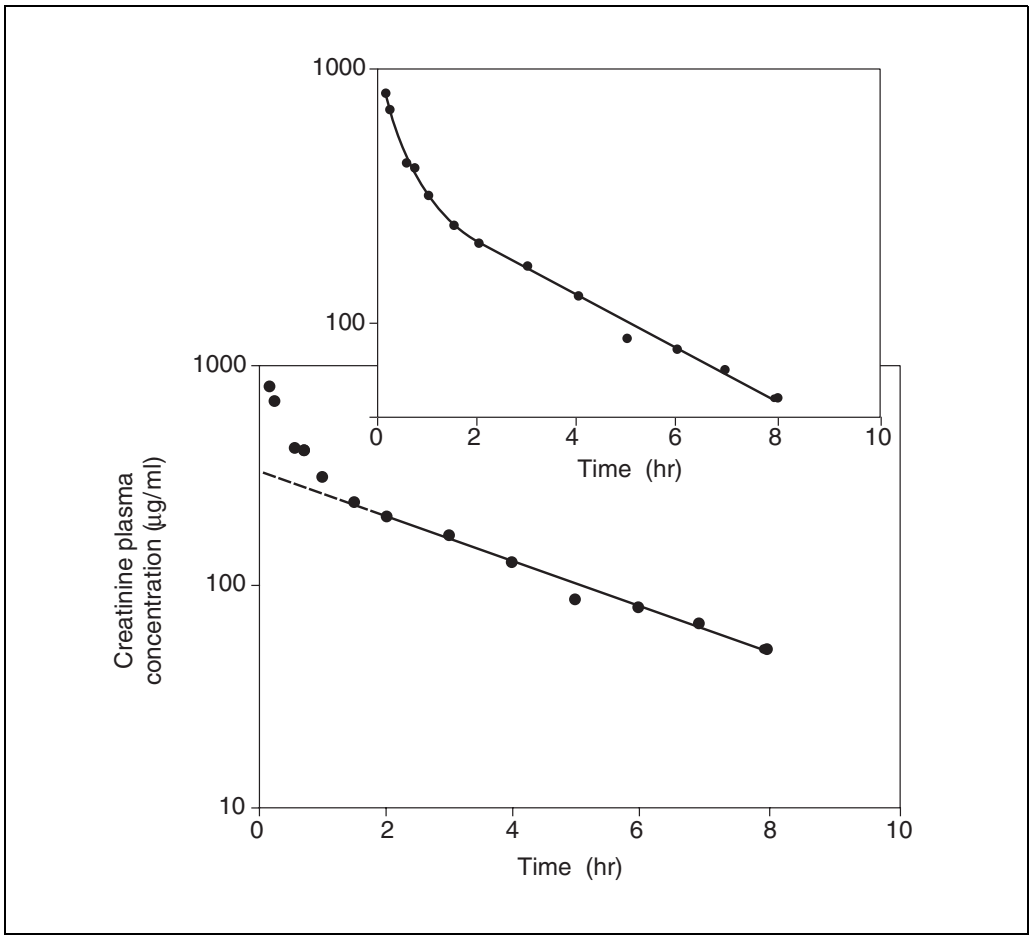

Figure 5.3.12 Semilog plot of creatinine plasma concentration as a function of time following an i.v. bolus dose of 6.6 g creatinine to one dog. The bottom graph illustrates the noncompartmental approach to data analysis. The solid line is the linear regression fit of the data points thought to represent the terminal phase. The terminal rate constant was determined to be 0.235 hr^{-1}. The inset graph illustrates a compartmental analysis of the data using the WinNonlin program. The solid line represents the nonlinear regression fit to the data. The terminal rate constant was determined to be 0.233 hr^{-1}. See text for discussion.

$$\begin{aligned}\mathrm{AUMC}_{\mathrm{terminal}} &= \frac{50\ \mu g/ml}{(0.235\ hr^{-1})^2} \\ &\quad + \frac{403.8\ \mu g \times hr/ml}{(0.235\ hr^{-1})} \\ &= 905.4 + 1718.3 \\ &= 2623.7\ \mu g \times hr^2/ml\end{aligned}$$

Equation 5.3.31

The total value for AUMC is the sum of: 3418.1 + 2623.7 = 6041.8 $\mu g \times hr^2/ml$.

We can now estimate several additional important pharmacokinetic parameters.

1. *Systemic clearance, CL_S:* This value is obtained from:

$$\frac{\text{i.v. dose}}{\mathrm{AUC}_0^{\infty}} = \frac{6600\ mg}{1680.9\ mg \times hr/liter}$$

Equation 5.3.32

A value of 65 ml/min is obtained. Since the compound is cleared only by renal pathways and, presumably, by glomerular filtration, the value calculated represents renal clearance, CL_R. If we assume that this plasma clearance is about equal to blood clearance, an estimate of renal extraction ratio can be obtained (i.e., the blood to plasma concentration ratio is about equal to 1). A literature value for renal blood flow in the dog is 21.6 ml/min × kg. CL_R in our dog is 65 ml/min × 20.2 kg or 3.22 ml/min × kg. The renal extraction ratio is given by, $CL_R/Q_R = 3.22/21.6 = 0.15$. This is a relatively

Table 5.3.4 Comparison of the Pharmacokinetic Parameters of Creatinine Obtained by Noncompartmental and Compartmental Analyses

Parameter	Compartmental	Noncompartmental
β (hr^{-1})	0.233	0.235
$t_{1/2}$ (hr)	2.97	2.96
AUC_0^∞ ($\mu g \times hr/ml$)	1701.2	1680.9
CL_S (ml/min)	64.7	65.0
V_β (liter)	16.7	16.6

small extraction ratio, indicating low or restrictive clearance of creatinine.

2. *Apparent volume of distribution: V_β or V_{area}*: this value is obtained from:

$$\frac{CL_s}{\beta} = \frac{(65\ ml/min) \times (60\ min/1\ hr)}{0.235\ hr^{-1}}$$
$$= 16.59\ liter = 0.82\ liter/kg$$

Equation 5.3.33

3. *Mean residence time, MRT:* This value is obtained from:

$$\frac{AUMC_0^\infty}{AUC_0^\infty} = \frac{6041.8\ \mu g \times hr^2/ml}{1680.9\ \mu g \times hr/ml} = 3.59\ hr$$

Equation 5.3.34

Mean residence time can also be used to estimate another apparent volume of distribution referred to as the steady-state volume (V_{SS}). [V_{SS} is determined from MRT $\times$ CL_S = 3.59 hr $\times$ (65 ml/min) (60 min/1 hr) = 14.0 liters or 0.69 liter/kg.] There are also a variety of other residence and transit times that may be of interest (see Lassen and Perl, 1979, for additional information). For this example, mean residence time in the central compartment (~1.5 hr); mean residence time in the peripheral compartment (~2.0 hr); mean transit time in the central compartment (~0.49 hr); mean transit time in the peripheral compartment (~1.0 hr); and the average number of times that creatinine returns to the peripheral compartment (~3).

How different would the results have been if the data were analyzed by compartmental methods using nonlinear regression? Not very different at all, as shown by the comparisons in Table 5.3.4.

Notice how similar the parameter values are; they are virtually identical. This is expected for data that are reasonably well behaved.

LITERATURE CITED

Beal, S.L. and Sheiner, L.B. 1992. NONMEM User's Guides. NONMEM Project Group, University of California, San Francisco.

Benet, L.Z. and Galeazzi, R.L. 1979. Noncompartmental determination of the steady-state volume of distribution. *J. Pharm. Sci.* 68:1071-1074.

Bolton, S. 1997. Pharmaceutical Statistics, 3rd ed., pp. 189-210. Marcel Dekker, New York.

Brown, J.E., Kitchell, B.B., Bjornsson, T.D., and Shand, D.D. 1981. The artifactual nature of heparin-induced drug protein binding alterations. *Clin. Pharmacol. Ther.* 30:636-643.

Chindavijak, B., Belpaire, F.M., De Smet, F., and Bogaeert, M.G. 1988. Alterations of the pharmacokinetics and metabolism of propranolol and antipyrine elicited by indwelling catheters in the rat. *J. Pharmacol. Exp. Ther.* 246:1075-1079.

Claassen, V. 1994. Neglected factors in pharmacology and neuroscience research. *In* Techniques in the Behavioral and Neural Sciences, Vol. 12 (J.P. Huston, ed.) pp. 405-414. Elsevier Science Publishing, New York.

Dominguez, R., Goldblatt, H. and Pomerene, E. 1935. Kinetus of elimination of substances injected intravenously (experiments with creatinine). *Amer. J. Physiol.* 114:240-254.

Eichelbaum, M. and Gross, A.S. 1996. Stereochemical aspects of drug action and disposition. *Adv. Drug Res.* 28:1-64.

Ette, I.I., Kelman, A.W., Howie, C.A., and Whiting, B. 1994. Influence of inter-animal variability on the estimation of population pharmacokinetic parameters in preclinical studies. *Clin. Res. Regul. Affr.* 11:121-139.

Fagin, K.D., Shinsako, J., and Dallman, M. 1983. Effects of housing and chronic cannulation on plasma ACTH and corticosterone in the rat. *Am. J. Physiol.* 245:E515-E520.

Gething, P.A. and Daley-Yates, P.T. 1997. A sparse sampling, mixed effects approach to toxicokinetic analyses. *Drug Info. J.* 31:521-527.

Gumbleton, M. and Benet, L.Z. 1991. Drug metabolism and laboratory anesthetic protocols in the rat: Examination of antipyrine pharmacokinetics. *Pharm. Res.* 8:544-546.

Hulse, M., Feldman, S., and Bruckner, J.V. 1981. Effect of blood sampling schedules on protein drug binding in the rat. *J. Pharmacol. Exp. Ther.* 218:416-420.

Karol, M.D. 1989. Mean residence time and the meaning of AUMC/AUC. *Biopharm. Drug Dispos.* 11:179-181.

Kong, A.-N. and Jusko, W.J. 1988. Definitions and applications of mean transit and residence times in reference to the two-compartment mammillary plasma clearance model. *J. Pharm. Sci.* 77:157-165.

Kwan, K.C., Bohidar, N.R., and Hwang, S.S. 1984. Estimation of an effective half-life. *In* Pharmacokinetics—A Modern View (L.Z. Benet, G. Levy, and B.L. Ferraiola, eds.) pp. 147-162. Plenum Press, New York.

Lassen, N.A. and Perl, W. 1979. Tracer Kinetic Methods in Medical Physiology, pp. 102-112. Raven Press, New York.

Levy, G. 1968. Dose dependent effects in pharmacokinetics. *In* Importance of Fundamental Principles in Drug Evaluation (D.H. Tedeschi and R.E. Tedeschi, eds.) pp. 141-172. Raven Press, New York.

Mahmood, I. 1997. A comparative computer simulation study of three different sparse-sampling methods for the estimation of steady-state area under the concentration-time curve (AUC) and maximum concentration (C_{max}) in toxicokinetics. *J. Pharm. Sci.* 86:579-583.

Manchee, G.R., Barrow, A., Kulkarni, S., Palmer, E., Oxford, J., Colthup, P.V., Maconochie, J.G., and Tarbit, M.H. 1993. Disposition of salmeterol xinafoate in laboratory animals and humans. *Drug Metab. Dispos.* 21:1022-1028.

Mayersohn, M. and Hamilton, R. 1993. The relationship between the terminal disposition half-life and mean residence time in multicompartment models. *Drug Metab. Dispos.* 21:1172-1173.

Mayersohn, M. and Tannenbaum, S. 1998. On reclaiming data from the literature: Literature data "R and R" (recovery and reanalysis) with a commentary by G. Levy, using other people's data in publications. *Am. J. Pharm. Ed.* 62:363-373.

Mayersohn, M., Owens, S.M., Lopez Anaya, A., Bliss, M., and Achari, R. 1985. 4-Methylpyrazole disposition in the dog: Evidence for saturable elimination. *J. Pharm. Sci.* 74:895-896.

McNamara, P.J., Fleishaker, J.C., and Hayden, T.L. 1987. Mean residence time in peripheral tissue. *J. Pharmacokinet. Biopharm.* 15:439-450.

Nedelman, J.R. and Gibiansky, E. 1996. The variance of a better AUC estimator for sparse, destructive sampling in toxicokinetics. *J. Pharm. Sci.* 85:884-886.

Nedelman, J.R., Gibiansky, E., Tse, F.L.S., and Babiuk, C. 1993. Assessing drug exposure in rodent toxicity studies without satellite animals. *J. Pharmokinet. Biopharm.* 21:323-334.

Perrier, D. and Mayersohn, M. 1982a. Noncompartmental determination of the steady-state volume of distribution for any mode of administration. *J. Pharm. Sci.* 71:372-373.

Perrier, D. and Mayersohn, M. 1982b. Noncompartmental determination of the steady-state volume of distribution for any mode of administration [erratum]. *J. Pharm. Sci.* 71:1427.

Riegelman, S. and Collier. P. 1980. The application of statistical moment theory to the evaluation of in vivo dissolution time and absorption time. *J Pharmacokinet. Biopharm.* 8:509-534.

Rowland, M. and Tozer, T.N. 1995a. Clinical Pharmacokinetics—Concepts and Applications, 3rd ed., pp. 158-181. Williams and Wilkins, Baltimore.

Rowland, M. and Tozer, T.N. 1995b. Clinical Pharmacokinetics—Concepts and Applications, 3rd ed., pp. 160, 502-503. Williams and Wilkins, Baltimore.

Rowland, M., and Tozer, T.N. 1995c. Clinical Pharmacokinetics—Concepts and Applications, 3rd ed., pp. 394-418. Williams and Wilkins, Baltimore.

Sinha, V., Brendel, K., and Mayersohn, M. 2000. A simplified isolated perfused rat liver apparatus: Characterization and measurement of extraction ratios of selected compounds. *Life Sci.* 66:1795-1804.

Sukbuntherng, J., Hutchaleelaha, A., Martin, D.K., Pak, Y., and Mayersohn, M. Cocaine disposition kinetics and absorption in the rat: Influence of dose and route of administration. Submitted for publication.

Tanigawara, Y., Yano, I., Kawakutsa, K., Nishimura, K., Yasuhara, M., and Hori, R. 1994. Predictive performance of the Bayesian analysis: Effects of blood sampling time, population parameters, and pharmacostatistical model. *J. Pharmacokinet. Biopharm.* 22:59-71.

Terao, N. and Shen, D.D. 1983. Alterations in serum protein binding and pharmacokinetics of *l*-propranolol in the rat elicited by the presence of an indwelling venous catheter. *J. Pharmacol. Exp. Ther.* 227:369-375.

Torres-Molina, F., Aristorena, J.-C., Garcia-Carbonell, C., Granero, L., Chesa-Jimenez, J., Pla-Delfina, J., and Peris-Ribera, J.-E. 1992. Influence of permanent cannulation of the jugular vein on pharmacokinetics of amoxycillin and antipyrine in the rat. *Pharm. Res.* 9:1587-1591.

Tse, F.L.S. and Jaffe, J.M. 1991. Preclinical Drug Disposition—A Laboratory Handbook, pp. 47-53. Marcel Dekker, New York.

Tse, F.L. and Nedelman. 1996. Serial versus sparse sampling in toxicokinetic studies. *Pharm. Res.* 13:1105-1108.

Tse, F.L.S., Nickerson, D.F., and Aun, R. 1992. Effect of isoflurane anesthesia on antipyrine pharmacokinetics in the rat. *Pharm. Res.* 9:1515-1517.

Tsukamoto, H., Reidelberger, R.D., French, S.W., and Largman, C. 1984. Long-term cannulation model for blood sampling and intragastric infusion in the rat. *Am. J. Physiol.* 247:R595-R599.

Tucker, G.T. and Lennard, M.S. 1990. Enantiomer-specific pharmacokinetics. *Pharmacol. Ther.* 45:309-329.

Van Bree, J., Nedelman, J., Steimer, J.-L., Tse, F., Robinson, W., and Niederberger, W. 1994. Application of sparse sampling approaches in rodent toxicokinetics: A prospective view. *Drug Info. J.* 28:263-279.

Veng-Pedersen, P. 1986. A simple method for obtaining the mean residence time of metabolites in the body. *J. Pharm. Sci.* 75:818-820.

Wilkinson, G.R. 1987. Clearance approaches in pharmacology. *Pharmacol. Rev.* 39:1-47.

Wilkinson, G.R. and Shand, D.G. 1975. A physiological approach to hepatic drug clearance. *Clin. Pharmacol. Ther.* 18:377-390.

Yoburn, B.C., Morales, R., and Inturrisi, C.E. 1984. Chronic vascular catheterization in the rat: Comparison of three techniques. *Physiol. Behav.* 33:89-94.

Contributed by Michael Mayersohn
University of Arizona
Tucson, Arizona

Isolated Perfused Porcine Skin Flap

The isolated perfused porcine skin flap (IPPSF) is used to determine the rate and extent of absorption of chemicals through skin. This ex vivo model system allows cutaneous toxicology and pharmacology studies to be conducted in viable skin that has a normal anatomical structure and intact microvasculature. The latter is a unique advantage of this system as other in vitro systems do not have this intact microvasculature. Porcine skin is also anatomically and physiologically similar to human skin (Fig. 5.4.1), therefore, data from studies utilizing this ex vivo model can, in some cases, be used to predict dermato-pharmacokinetics and dermatotoxicity of test chemicals in humans (Monteiro-Riviere, 1991). The porcine skin flap can be used to assess dermal metabolism and bioavailability as it eliminates the confounding influence of systemic metabolic processes.

This unit describes surgical preparation of the isolated perfused porcine skin flap and operation of the IPPSF system. Surgical preparation of the porcine skin flap (see Support Protocol) involves a two-stage surgical procedure under aseptic conditions after which the closed or tubed skin preparation is removed from the pig and the main arterial supply is cannulated. The operation of the IPPSF system (see Basic Protocol) is very labor intensive compared to most in vitro skin diffusion cell systems as it involves real time monitoring of flap viability and intensive sample collection during and at the end of these experiments.

NOTE: All protocols using live animals must first be reviewed and approved by an Institutional Animal Care and Use Committee (IACUC) and must conform to governmental regulations regarding the care and use of laboratory animals.

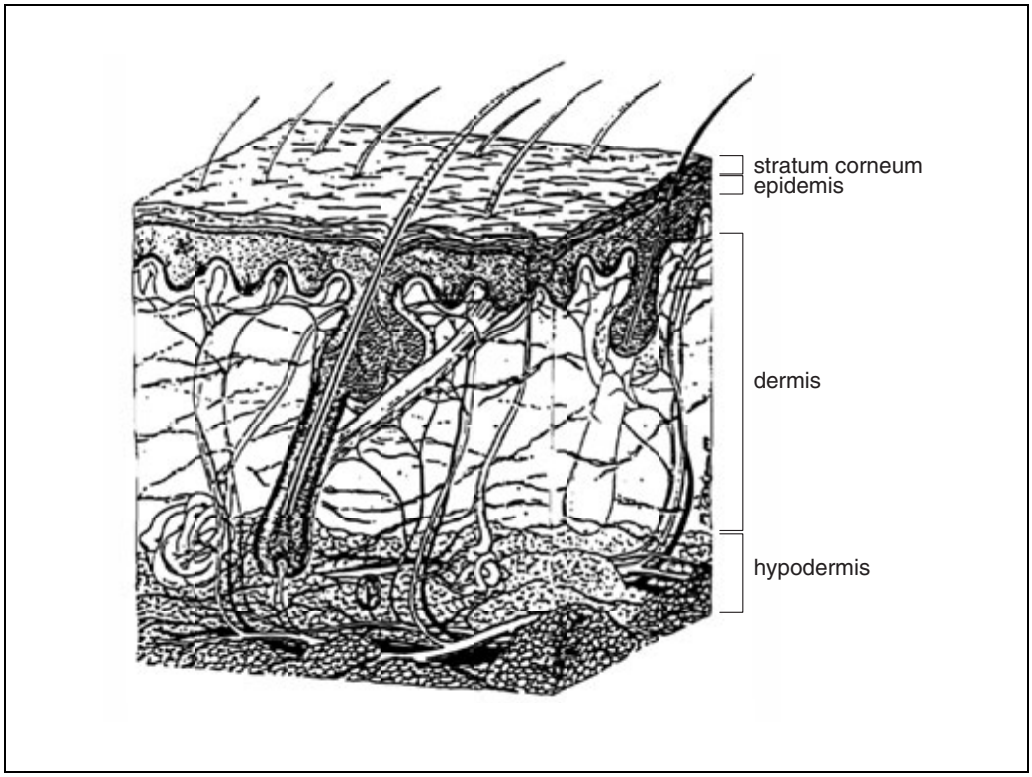

Figure 5.4.1 Illustration of mammalian skin indicating the main diffusion compartments: stratum corneum, viable epidermis, dermis, and hypodermis.

Contributed by Ronald E. Baynes
Current Protocols in Toxicology (2001) 5.4.1-5.4.9

BASIC PROTOCOL

OPERATION OF THE ISOLATED PERFUSED PORCINE SKIN FLAP

After Stage II as described in the Support Protocol, the flap is placed in a cradle where it is perfused with bovine serum albumin medium, and the effluent is collected at selected time points. The flap cradle is placed in a custom-designed temperature- and humidity-regulated chamber (Fig. 5.4.2) made specifically for this purpose. Flap viability, perfusate flow and pressure, and environmental temperature and humidity are also monitored during the course of the experiment.

Materials

Porcine skin flap (see Support Protocol)
Oxygenated Krebs-Ringer bicarbonate buffer
4.5% bovine serum albumin medium (see recipe)
Air supply: 95% oxygen/5% carbon dioxide
Skin Bond (e.g., Skin-Bond, Smith & Nephew)
Test chemical solution, with or without radiolabel
1% (v/v) soap solution (e.g., ivory soap)
Ethyl acetate
OCT Compound (Tissue-Tek, Miles)
Liquid nitrogen
10% (v/v) neutral buffered formalin

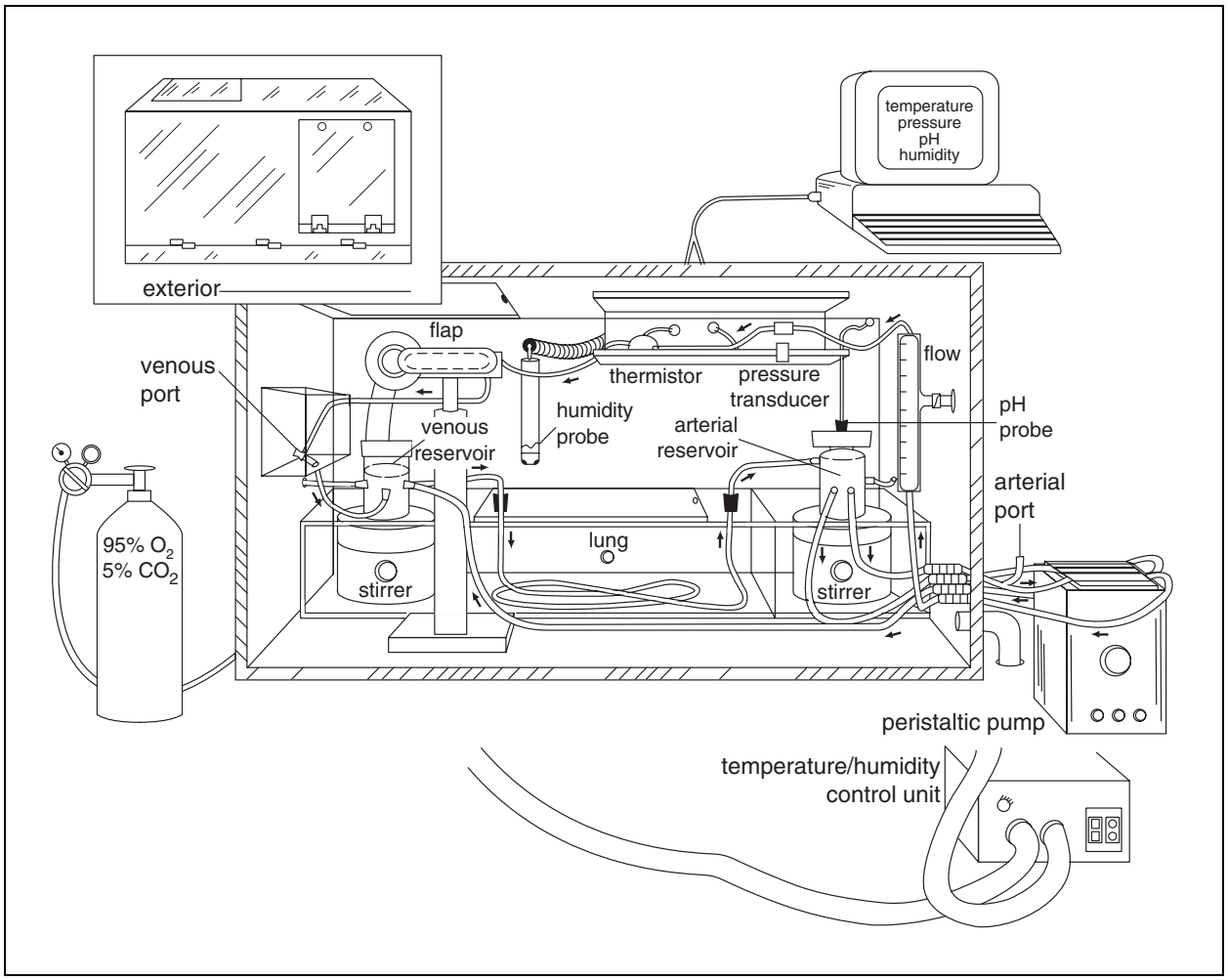

Figure 5.4.2 Schematic of the perfusion chamber used to maintain a viable IPPSF at controlled temperature, humidity, pressure, and perfusate flow.

Soluene 350 (Packard Instrument)
Sodium hypochlorite
Isopropyl alcohol

Custom-designed flap chamber made of 0.5-in thick Plexiglass and containing:
- Custom-designed humidifier
- Custom-designed media reservoirs
- Hygrometer
- Thermometer
- Peristaltic pump
- Silastic and tygon tubing
- Pressure transducer
- pH meter
- Magnetic stirers

3 × 7–cm flexible template (e.g., Stomahesive, ConvaTec-Squibb)
Glucose analyzer (e.g., Glucose Analyzer 2, Beckman)
5-ml and 20-ml capped scintillation vials (e.g., Sarstedt)
2 × 2–in. gauze
Cellophane tape
Razor blade or scalpel
Forceps
Aluminum foil boat

Perfuse porcine skin flaps

1. Perfuse porcine skin flaps via the cannula at ~1.0 ml/min (3 to 7 ml/min/100 g) with oxygenated (95% O_2/5% CO_2) Krebs-Ringer bicarbonate buffer and 4.5% bovine serum albumin medium. Add the prepared medium to the reservoir, and place the reservoir on a magnetic stirer positioned in the skin flap chamber. Maintain skin flaps at 37°C, 50% to 60% relative humidity, perfusate pH at 7.4, and mean arterial pressure ranging from 30 to 70 mmHg.

   These values are consistent with in vivo values reported in the literature.

2. Perfuse skin flap for 1 hr to equilibrate and to collect predose samples to determine glucose utilization and background levels.
3. After 1 hr of perfusion, disconnect flap from the perfusion system. Apply a 3 × 7–cm flexible template to the skin surface with Skin-Bond to provide a surface area of 5.0 cm^2 for applying dosing solutions.
4. Immediately reconnect the flap, and apply as much as 100 µl of the test chemical to the dose site within the stomahesive.

   Doses exceeding 100 µl may result in pooling and/or run off of the dose into the cradle and contamination of collected samples.

Collect venous perfusate samples

5. Collect venous perfusate samples at 30-min intervals for the first 2 hr post-dosing and then at 1 hr intervals for 6 hr for a total of 8 hr.

   Skin flap viability begins to decline after 8 hr.

6. Assess skin flap viability by monitoring vascular resistance (VR; perfusate pressure/flow) and cumulative glucose utilization (CGU). Monitor CGU by collecting arterial perfusate samples collected at hourly intervals and then compare with venous samples to determine arterial-venous glucose extraction. Use a glucose analyzer to measure glucose in both arterial and venous samples.

   VR is defined as the ratio of arterial pressure to perfusate flow rate.

Clean and process skin flap

7. At the end of the 8-hr perfusion, remove the stomahesive and save in a scintillation vial for further analysis. Rinse the suture line, which is the portion of skin in contact with the effluent, with ~10 ml distilled water to remove remnants of test chemical.
8. Swab the dose site with a single 2 × 2–in. gauze pad soaked with 1% soap solution and swab dry with a dry 2 × 2–in. gauze pad.

   The latter is important to ensure that the skin surface is dry for effective tape stripping.
9. Save swab pads in a scintillation vial for further analysis.

   This represents surface levels at 8 hr after perfusion.
10. Tape dose site 12 times with cellophane tape and store in a scintillation vial.
11. Solubilize cellophane tape with ~15 ml ethyl acetate and save for analysis.

    This sample represents the stratum corneum levels at termination.
12. Excise skin from the dose site with a razor blade or scalpel. Weigh tissue sample, and divide into three approximately equal weight portions.

Freeze tissue specimen

13. Using forceps, carefully place the central portion of the dose site, with cut surface facing up, in OCT compound in an aluminum foil boat. Ensure that entire epidermal surface is in contact with the bottom of the foil boat and freeze the contents in liquid nitrogen.

    This frozen section will be later placed in a cryostat to determine depth of penetration (~40-μm intervals) of the test chemical.
14. Of the two remaining portions of the dose skin, place one portion in 10% buffered formalin.

    The sample will be processed, and stained with hematoxylin and eosin for histological examination.
15. Place the other skin portion in OCT compound as described in step 13, except with cut surface facing down in the aluminum foil boat. Freeze remaining skin flap in liquid nitrogen and store at −80°C for further analysis.

    This skin sample can be saved for enzyme histochemical studies.
16. As these are mass balance studies, separate the frozen flap into skin and fat samples and solubilize the tissues in Soluene 350 for 48 hr at 50°C before further analysis.
17. Clean the skin flap chamber after removal of the flap, and perfuse lines with sodium hypochlorite for 12 min; isopropyl alcohol for 12 min; and water for 30 min.

SUPPORT PROTOCOL

SURGICAL PREPARATION OF PORCINE SKIN FLAP

IPPSFs are created from the ventral abdomen of the pig in two surgical stages. In Stage I (Fig. 5.4.3), two flaps per pig, each lateral to the ventral midline, are prepared but not removed from the pig. After careful dissection and suturing, the pig is allowed to recover for 48 hr to allow for granulation of the surgical area. After a recovery period of 48 hr, the flap is cannulated and then removed from the pig.

Materials

8-week-old weanling female Yorkshire pigs (Looper Farms, Hickory, NC)
Preanesthetic: 0.04 mg/kg atropine sulfate; 1.5 mg/kg xylazine hydrochloride; 11 mg/kg ketamine hydrochloride
Anesthesia: halothane
Betadine
Alcohol
Heparinized saline: 0.5 ml heparin in 50 ml physiological saline

Gowns and towels, disposable
Endotracheal tube (size 5.5 mm)
Hair clippers
Scalpels
Suture material (no. 0 and no. 2 chromic catgut; Prolene no. 3.0; Ethicon no. 3.0)
Surgical wrap and bandage (e.g., Teflon pad and elasticon)
Tygon tubing (0.023-in i.d., 0.038-in o.d.)
Hemostats

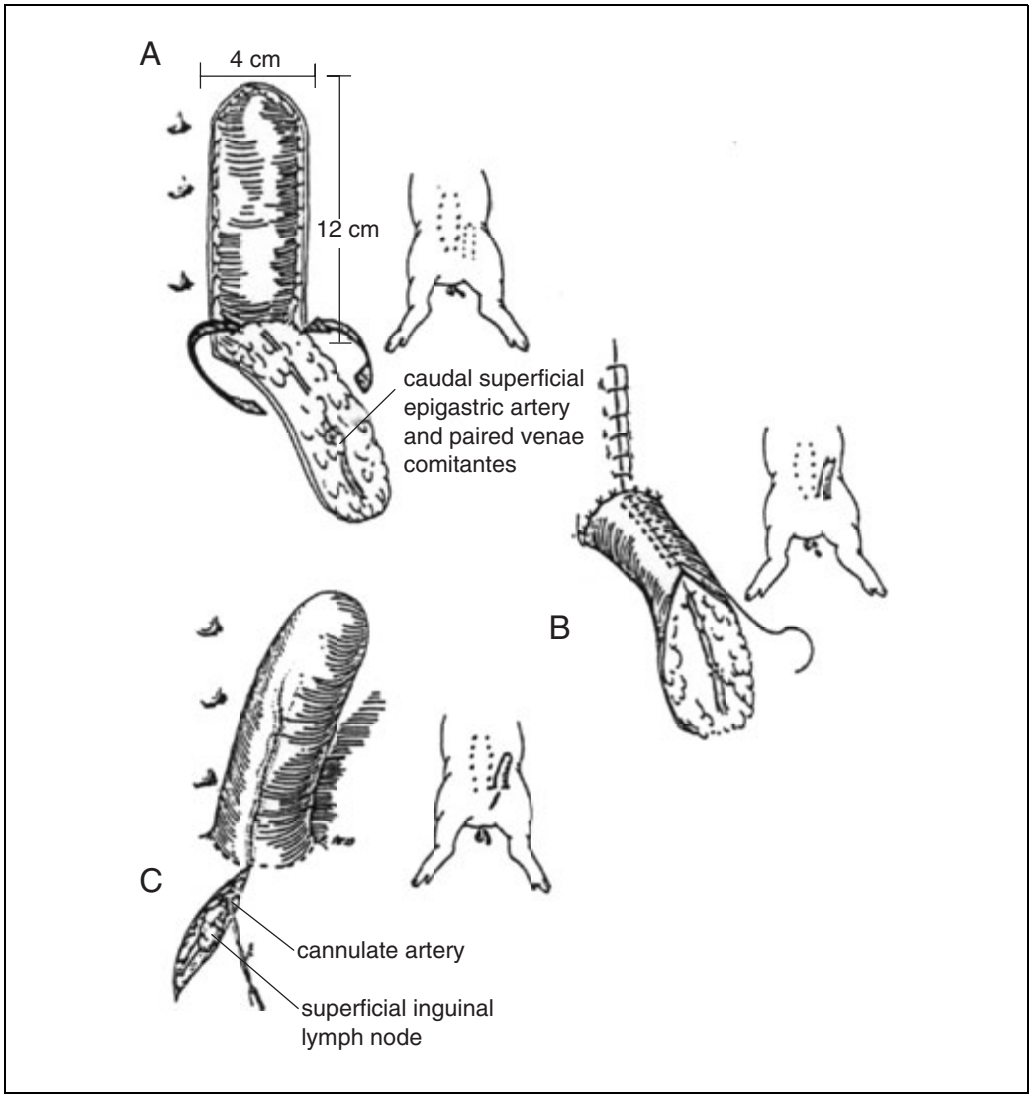

Figure 5.4.3 Surgical procedure for creating flaps. (**A**) A single pedicle axial pattern skin flap is raised and (**B**) tube completing the Stage I procedure. (**C**) Two days later, the caudal superficial epigastric artery is cannulated, and the flap is removed and transferred to the perfusion chamber in Figure 5.4.2.

Prepare pigs

1. Acclimatize and weigh pigs 1 to 2 weeks before surgical procedure.

   Acclimitization helps calm the animals and makes them easier to handle and restrain.

2. Premedicate with 1.5 mg/kg xylazine hydrochloride and 11 mg/kg ketamine hydrochloride prior to tracheal intubation; anesthetize with halothane using an anesthesia machine.

3. Place animal in dorsal recummbancy. Prepare each pig for routine aseptic surgery by clipping hair from the caudal abdominal and inguinal regions and surgically scrubbing three times each with betadine and alcohol. Don a disposable surgical gown. Use towel clamps to clamp disposable towels over the caudal region of the pig leaving the surgical area free for Stage 1 procedures.

   For surgical techniques see Knecht et al. (1987).

Stage I: Dissect flap

4. In Stage I, first mark an area 4 × 12–cm of skin on either side of the midline in the caudal abdominal and inguinal region.

   This demarcated area is perfused by the caudal superficial epigastric artery (CSEA) and its associated paired venae comitantes. For inexperienced individuals, prior trial dissection of this area may be required to ensure that the CSEA is located within the marked area.

5. Incise this marked area and use a scalpel with forceps to dissect the subcutaneous tissue while ensuring the CSEA is not compromised. Use gauze to remove excess blood.

   At the end of Stage I, only this artery and closely associated but limited subcutaneous tissues will be attached to the pig.

6. Appose the caudal incision area and suture. Trim remaining fat from skin flap edges, and suture the opposing edges with a simple interrupted suture pattern to form a tubed fold of skin. For suturing use 3.0 Proline to tube the flap; 0 catgut to close the abdomen, 2.0 catgut to close the subcuticular; and 3.0 Ethicon to close the sites of the flap.

7. Repeat steps 5 and 6 for the opposite marked area such that two sutured flaps are formed but remain attached to the pig.

8. Allow the two flaps to lie on the abdomen of the pig, and wrap with Teflon pad and elasticon before allowing the pig to recover from anesthesia.

Stage II: Cannulate and remove flap

9. Perform Stage II 48 hr after Stage I. Premedicate and anesthetize the pig as described in step 2.

10. Cannulate CSEA with 0.023-in Tygon tubing held in place with several sutures around the artery and tubing. Use a 10-ml syringe with a 21- or 23-G needle to flush the cannula with heparinized saline to ensure correct cannulation and that the CSEA is not blocked with blood clots.

11. After identifying the CSEA, remove surrounding tissue with scissors. Nick the artery with scissors to facilitate entry of the tubing. Clamp the artery with a hemostat before removing the flap from the pig, remove the flap, and then suture. Place the cannulated flap into the custom-designed skin flap cradle. Ensure that the suture line is facing down.

    The pig can be recovered for other research purposes or humanely euthanized.

REAGENTS AND SOLUTIONS

Use Milli-Q-purified water or equivalent in all recipes and protocol steps. For common stock solutions, see ***APPENDIX 2A****; for suppliers, see* ***SUPPLIERS APPENDIX****.*

Bovine serum albumin medium (2 liters)

13.78 g NaCl
0.71 g KCl
0.56 g $CaCl_2$
0.32 g KH_2PO_4
O.58 g $MgSO_4 \cdot 7H_2O$
5.50 g $NaHCO_3$
2.40 g dextrose
90.0 g BSA, Fraction V
Water to 2 liters

Add ~1700 ml water and a stir bar to a clean 4000-ml beaker. Add all reagents except BSA to beaker and mix well, adjusting pH to ~7.4 with NaOH and/or HCl. Add BSA slowly to beaker while stirring until all has gone into solution. It may take ~1 hr for all BSA to dissolve. Add 0.25 ml of 250 mg/ml amikacin (Gensia Laboratories, Ltd.). Bring volume up close to 2000 ml. Mix well and pH to 7.45 ± 0.03 with NaOH and/or HCl. Remove stir bar; pour solution into a 2000-ml volumetric flask. Bring volume to 2000 ml with water. Divide equally into six clean, autoclaved 500-ml plastic reagent bottles. Label and freeze immediately. Store up to 3 weeks. When thawing for use, add 10 ml of 1000 USP U/ml sodium heparin and 0.1 ml of 250,000 U/ml penicillin G sodium (note that this drug expires in 7 days).

COMMENTARY

Background Information

There have been numerous efforts to assess dermal absorption and cutaneous toxicity of chemicals using various in vitro and in vivo methods. The in vitro methods are limited largely because absorption is assessed in skin sections or whole skin without an intact microvasculature. In vivo models require companion intravenous studies to determine absolute dermal bioavailability, and they are usually unable to determine "first pass" cutaneous metabolism for topically applied drugs or pesticides. Isolated kidney, liver, and lung perfusion systems have been developed. However, very few isolated perfused skin systems have been developed because it has been difficult to identify a "closed" vascular system as observed with other organ systems. Isolated rabbit and pig ear systems have been developed (Behrendt and Kampffmeyer, 1989; Dick and Scott, 1992); however, the major disadvantages are that the arterial supply to tissues in the ear (e.g., cartilage, muscle) is very different from that in skin in other body regions, and the skin in the ear is structurally different (hair density and adnexial structures) compared to skin in other body regions.

Successful preparation of the isolated perfused porcine skin flap (IPPSF) depends primarily on identification, catheterization, and perfusion of the caudal superficial epigastric artery (CSEA), which directly supplies skin in the caudal abdominal region of weanling pigs. The IPPSF is strictly an ex vivo model that can be advantageous over most in vitro and in vivo systems in that there is an intact functional cutaneous microcirculation, and dermal absorption and cutaneous toxicity studies can be conducted simultaneously with the same skin flap.

Data generated from the IPPSF have been used to make predictions that have correlated well with in vivo absorption data for several drugs and insecticides (Riviere et al., 1986, 1995; Wester et al., 1998). IPPSFs can be used to study depth of penetration, skin distribution, transdermal drug delivery, and systemic targeting of anticancer drugs to tumor-bearing flaps (Chang et al., 1994; Vaden et al., 1994; Baynes et al., 1996). Iontophoretic delivery of various drugs (e.g., lidocaine, arbutamine) and hormones (e.g., LHRH) have also been demonstrated (Riviere et al., 1991, 1992; Heit et al., 1993). IPPSFs are physiologically and bio-

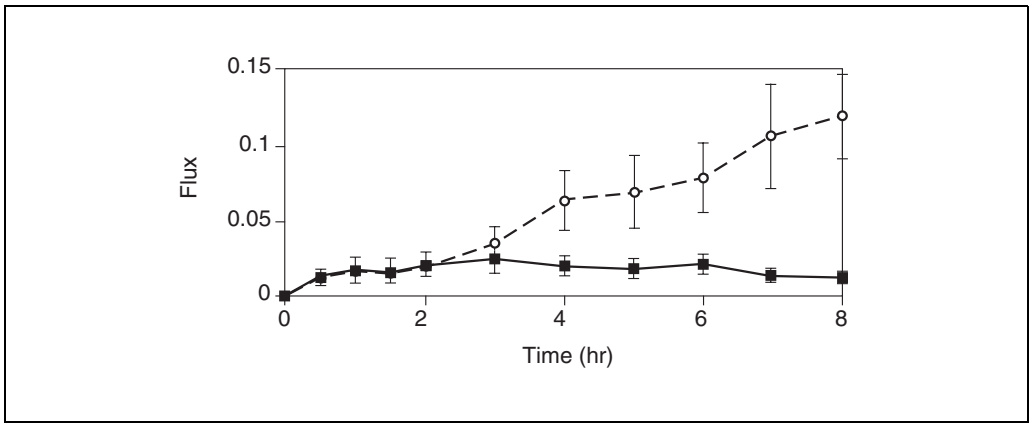

Figure 5.4.4 Flux-time profile for benzidine in acetone (solid line) and DMSO (dashed line) applied to IPPSFs.

chemically viable and have been used successfully to assess cutaneous toxicity of topically applied chemicals (King and Monteiro-Riviere, 1991; Spoo et al., 1992; Monteiro-Riviere, 1993; Zhang et al., 1995). This feature becomes relevant if the local effects of cytotoxic (e.g., solvents, fuels, surfactants) and vasoactive chemical (e.g., methyl nicotinate) components in chemical mixtures are to be assessed (Baynes et al., 1997; Allen et al., 2000).

In addition to the time and cost required to surgically prepare IPPSFs, the major drawback to IPPSFs is that systemic-mediated immunological or physiological, and neural feedback responses to topically applied toxicants cannot be observed. The other limitation is that IPPSF studies should not be conducted beyond 8 to 12 hr because IPPSF viability begins to decrease beyond this time point. In spite of these limitations, the IPPSF is more economical than animal and human in vivo studies. It has also been utilized by industry in preclinical drug development studies.

Critical Parameters and Trouble Shooting

It is important to develop a flap in a region where there are no gross morphological abnormalities in the skin. Using compromised skin can result not only in erroneous absorption profiles but also in blister formation on the dose site area during perfusion.

Cannulation of the CSEA during Stage II surgery is critical. It is possible that during Stage I surgery or during the healing process between Stage I and Stage II, that the artery may become compromised, making cannulation very difficult to almost impossible. One way to avoid this would be to adequately secure the flap after Stage I surgery.

Even after successful catheterization, high pressures may be observed in the flap. This may be due to blood clots in the CSEA. This can be corrected by first flushing the CSEA in the flap immediately after Stage II with heparinized saline and then immediately connecting the cannula to the perfusion system. High pressures can also result from a "kinked" vessel or tubing. Make certain that all tubing is free of kinks and that the cannula and vessel are straight.

Anticipated Results

This section gives an example of the kind of data that can be generated from use of the IPPSF and how absorption parameters can be calculated from a given data set. In this example, IPPSFs were exposed to benzidine for 8 hr to assess absorption in an acetone and DMSO vehicle. The plot in Figure 5.4.4 depicts the flux-time profile of benzidine diffusion through skin. At least 4 to 5 replicates are conducted per test chemical for IPPSF experiments. Systemic absorption is defined as the total amount of radioactivity detected in the perfusate for the entire 8-hr perfusion period. Skin surface penetration is defined as the sum of total absorption and total radioactivity in the tissues. The latter includes all skin and fat samples taken and analyzed after the 8-hr perfusion. Penetration into the stratum corneum layer at 8 hr is based on levels detected in the tape strips. The radioactivity remaining on the skin surface is defined as the amount of radioactivity detected in the skin swab samples. The following ratios can also be calculated to assess the relative disposition in skin: Relative Systemic Absorption (Absorption/Penetration); Relative Skin Surface Penetration (Penetration/Skin Surface); Stratum Corneum/Dosed Skin; and Stratum Corneum/Skin Surface.

Time Considerations

Surgical preparation of the IPPSF requires ~3 hr for Stage I and ~1 hr for Stage II. This time allows for restraint of the animal and for the anesthetics to take effect. Most of the IPPSF experiments do not last longer than 9 hr; 1 hr to equilibrate and to collect pre-dose samples and no longer than 8 hr to perfuse the flap. The cleaning process and collection of tissue samples at the end of the perfusion, which must occur immediately after completion of the perfusion, usually takes 1 to 2 hr.

Literature Cited

Allen, D.G., Riviere, J.E., and Monteiro-Riviere, N.A. 2000. Induction of early biomarkers of inflammation produced by keratinocytes exposed to jet fuels Jet-A, JP-8, and JP-8(100). *J. Biochem. Molecular Toxicol*. 14:231-237.

Baynes, R.E., Brownie, C., Freeman, H., and Riviere, J.E. 1996. In vitro percutaneous absorption of benzidine in complex mechanistically defined chemical mixtures. *Toxicol. Appl. Pharmacol*.141:497-506.

Baynes, R.E., Monteiro-Riviere, N.A., Qiao, G.L., and Riviere, J.E. 1997. Cutaneous toxicity of the benzidine dye direct red 28 applied as mechanistically-defined chemical mixtures (MDCM) in perfused porcine skin. *Toxicol. Lett*. 93:159-169.

Behrendt, H. and Kampffmeyer, H.G. 1989. Absorption and ester cleavage of methyl salicylate by skin of single-pass perfused rabbit ears. *Xenobiotica* 19:131-141.

Chang, S.K., Williams, P.L., Dauterman, W.C., and Riviere, J.E. 1994. Percutaneous absorption, dermatopharmacokinetics and related bio-transformation studies of carbaryl, lindane, malathion, and parathion in isolated perfused porcine skin. *Toxicology* 91:269-280.

Dick, I.P. and Scott, R.C. 1992. Pig ear skin as an in vitro model for human skin permeability. *J. Pharm. Pharmacol*. 44:640-645.

Heit, M., Williams, P.L., Jayes, F.L., Chang, S.K., and Riviere, J.E. 1993. Transdermal iontophoretic peptide delivery. In vitro and in vivo studies with luteinizing hormone releasing hormone (LHRH). *J. Pharm. Sci*. 82:240-243.

King, J.R. and Monteiro-Riviere, N.A. 1991. Effects of organic solvents on the viability and morphology of isolated perfused porcine skin. *Toxicology* 69:11-26.

Knecht, C.H., Allen, A.R., Williams, D.J., and Johnson, J.H., eds. 1987. Fundamental Techniques in Veterinary Surgery, 3rd ed. W.B. Saunders Co., Philadelphia, PA.

Monteiro-Riviere, N.A. 1991. Comparative anatomy, physiology, and biochemistry of mammalian skin. *In* Dermal and Ocular Toxicology: Fundamentals and Methods (D.W. Hobson, ed.) pp. 3-71. CRC Press, Boca Raton, Fla.

Monteiro-Riviere, N.A. 1993. The use of isolated perfused skin in dermatotoxicology. *In Vitro Toxicol*. 5:219-233.

Riviere, J.E., Bowman, K.F., Monteiro-Riviere, N.A, Dix, L.P., and Carver, M.P. 1986. The isolated perfused porcine skin flap (IPPSF). I. A novel in vitro model for percutaneous absorption and cutaneous toxicology studies. *Fundam. Appl. Toxicol*. 7:444-453.

Riviere, J.E., Sage, B.S., and Williams, P.L. 1991. The effects of vasoactive drugs on transdermal lidocaine iontophoresis. *J. Pharm. Sci*. 80:615-620.

Riviere, J.E., Williams, P.L., Hillman, R., and Mishky, L. 1992. Quantitative prediction of transdermal iontophoretic delivery of arbutamine in humans using the in vitro isolated perfused porcine skin flap IPPSF. *J. Pharm. Sci.* 81:504-507.

Riviere, J.E., Monteiro-Riviere, N.A., and Williams, P.L. 1995. Isolated perfused porcine skin flap as an in vitro model for predicting transdermal pharmacokinetics. *Eur. J. Pharm. Biopharm*. 41:152-162.

Spoo, J.W., Rogers, R.A., and Monteiro-Riviere, N.A. 1992. Effects of formaldehyde, DMSO, benzoyl peroxide, and sodium lauryl sulfate on isolated perfused porcine skin. *In Vitro Toxicol*. 5:251-260.

Vaden, S.L., Page, R.L., Williams, P.L., and Riviere, J.E. 1994. Effects of hyperthermia on cisplatin and carboplatin in the isolated, perfused tumor and skin flap. *Int. J. Hyperthermia* 10:563-572.

Wester, R.C, Melendres, J., Sedik, L., Maibach, H., and Riviere, J.E. 1998. Percutaneous absorption of salicylic acid, theophylline, 2, 4-dimethylamine, diethyl hexyl phthalic acid, and p-aminobenzoic acid in the isolated perfused porcine skin flap compared to man in vivo. *Toxicol. Appl. Pharmacol*. 151:159-165.

Zhang, A., Riviere, J.E., and Monteiro-Riviere, N.A. 1995. Topical sulfur mustard induces changes in prostaglandins and interleukin 1alpha in isolated perfused porcine skin. *In Vitro Toxicol*. 8:149-157.

Key Reference

Riviere, et al., 1986. See above.

The first paper to describe development of the skin flap and its application in dermal absorption and cutaneous toxicology studies.

Contributed by Ronald E. Baynes
North Carolina State University
Raleigh, North Carolina

Porcine Skin Flow-Through Diffusion Cell System

The flow-through diffusion cell system is used to determine the rate and extent of absorption of chemicals through skin in vitro. Skin from rats, mice, primates, and humans can be used in these experiments. However, porcine skin maybe preferred not only because of its availability but also because of its anatomical and physiological similarity to human skin (Fig. 5.4.1). It is often problematic finding disease-free fresh human skin, and if found, an unacceptably high degree of intersample variation may be introduced. The stratum corneum cell layer in humans (10 to 50 μm) and pigs (15 μm) is nonviable and is considered the rate-limiting barrier in percutaneous absorption of many compounds (Monteiro-Riviere, 1991). Much of the research has concentrated on stratum corneum, although the viable epidermis (80 μm in humans and 60 μm in pigs) and dermis are now thought to contribute significantly to the percutaneous penetration of compounds and ultimately their rate and extent of absorption. This in vitro system may be used for assessment of dermal metabolism and bioavailability without confounding contribution of the liver normally associated with in vivo methods.

This unit describes the surgical preparation of porcine skin sections and the operation of the flow-through diffusion cell system. Surgical preparation of porcine skin (see Support Protocol) involves specific humane procedures for removal of porcine skin and preparation for the diffusion cell. The operation of the diffusion cell system (see Basic Protocol) involves dosing and sample collection during and at the end of these experiments.

CAUTION: If radioactive test compounds are used, take appropriate precautions to avoid contamination of the experimenter and the surroundings. Carry out the experiment and dispose of wastes in appropriately designated areas, following the guidelines provided by your local radiation safety officer (also see *APPENDIX 1A*).

NOTE: All protocols using live animals must first be reviewed and approved by an Institutional Animal Care and Use Committee (IACUC) and must conform to governmental regulations regarding the care and use of laboratory animals.

OPERATION OF THE FLOW-THROUGH DIFFUSION CELL SYSTEM

BASIC PROTOCOL

The flow-through diffusion cell system consists of three major components; namely, (1) the diffusion cell in specifically engineered heating blocks, (2) peristaltic pump and tubing, and (3) sample collecting apparatus. The artificial medium can vary but should be physicochemically similar to serum. Bovine serum albumin is added to the medium to mimic the oncotic pressure in serum in vivo. Saline and other fluids have been used as receptor fluids, but these media may interfere with the viability of the skin and may not truly represent partitioning into blood in vivo. The aim here is to perfuse the dermal surface of the prepared skin sections with the artificial medium, dose the epidermal surface with the test chemical, collect perfusate samples at desired time points after dosing, and finally obtain surface, stratum corneum, and skin samples at the end of the perfusion experiment. These experiments are usually not longer than 8 to 12 hr as dermal viability begins to be lost at about this time. The system described below allows for perfusion of 14 diffusion cells under desired environmental conditions.

Contributed by Ronald E. Baynes
Current Protocols in Toxicology (2001) 5.5.1-5.5.8

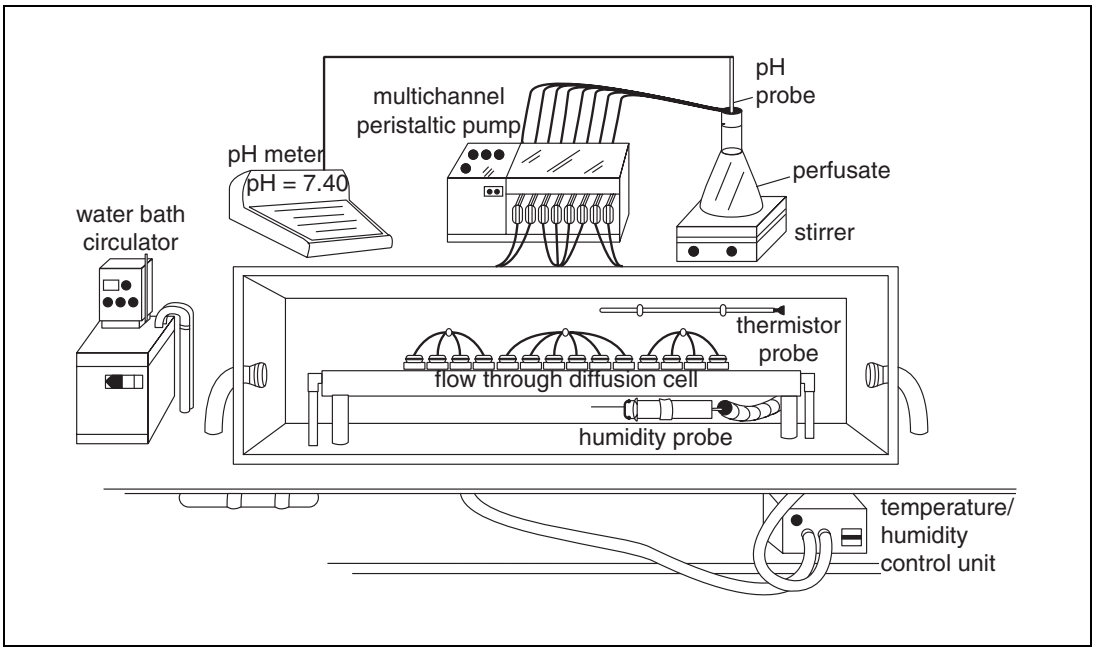

Figure 5.5.1 Illustration of the flow-through diffusion cell system in an environmentally controlled chamber.

Materials

Artificial medium
Skin punch biopsy sections (see Support Protocol)
Bovine serum albumin medium (*UNIT 5.4*)
Test compound
1% (v/v) soapy solution
Sodium hypochlorite
Isopropyl alcohol

Two-compartment Teflon flow-through diffusion cells (Crown Glass)
Heating blocks
Tygon tubing
Brinkmann constant-temperature circulator (Brinkmann)
Peristaltic pump
Fraction collector
Humidifier
Hygrometer and thermometer
pH meter
20-ml scintillation vials
Cotton swabs (e.g., Q-tips)
Cellophane tape
Magnetic stirrer

Set up flow-through diffusion cell apparatus

1. Set up a flow-through diffusion cell apparatus; an example is depicted in Figure 5.5.1.

   If the test substance is hazardous or a control of environmental conditions is desired, the flow-through diffusion cell system can be enclosed in an environmentally controlled chamber (Fig. 5.5.1). This chamber can be made of a light inert material such as plexiglass.

2. Load 7 diffusion cells into each heating block and connect inlet and outlet arms to tubing leading to the peristaltic pump and scintillation vials, respectively. Maintain temperature of the bovine serum albumin (BSA) medium and flow-through diffusion

cell at 37°C in both heating blocks using a Brinkmann constant-temperature circulator.

3. Prior to loading the skin sections in the cell, perfuse the entire system with the BSA medium to remove air bubbles from the inlet tubing connecting peristaltic pump to diffusion cells, the diffusion cells, and the outlet tubing from the diffusion cells.

   Rubber or other artificial membranes can be used at this time in place of skin sections to ensure removal of air bubbles and that BSA medium flow rates range from 4.0 to 5.0 ml/hr.

Load and perfuse skin sections

4. Load skin punch biopsy sections (see Support Protocol) into diffusion cells and ensure that there are no air bubbles at the dermis-medium interface. Perfuse skin sections with BSA medium, maintained between pH 7.4 and 7.5, at a flow rate of 4.0 to 5.0 ml/hr.
5. Maintain the heating block at 37°C.
6. Begin collecting BSA medium samples in scintillation vials for 15 to 30 min prior to dosing to obtain background levels, to ensure that there are no leaks in the system, and to ensure that flows are within range of desired flow rates.

Add test compound and collect medium samples

7. Dose skin surface with small volume of test compound.

   For example, use ~10 µl for a surface area of 0.32 cm^2. Excess volume may result in contamination and erroneous readings at early time points.

8. Collect BSA medium samples at short time points (e.g., 5, 10, 20, 30, and 45 min) for the first hour and longer time points thereafter.

   This is important if flux, permeability, and lag time are desired parameters.

Collect skin samples

9. At the end of the perfusion, obtain skin surface samples by swabbing each skin surface with one cotton swab soaked in 1% soapy solution and then with a second dry swab.
10. Obtain stratum corneum samples by tape stripping each skin section six times with cellophane tape. Save these samples along with the remaining skin section for further analysis by chromatographic or radiochemical analysis.

    Radiolabelled BSA medium and tissue samples can be combusted in a Packard Model 307 Tissue Oxidizer (Packard Chemical) and then analyzed by a Packard Liquid Scintillation Counter (Packard Chemical) for total [^{14}C or ^{3}H] determinations.

11. After tissue samples have been obtained, perfuse the entire system at maximum flow rates with the following liquids to remove remnants of the test chemical from the perfusion lines and diffusion cells: sodium hypochlorite solution for 30 min; isopropyl alcohol for 30 min; and water for 45 min. Discard the aqueous and alcohol waste appropriately, especially if the dosing compound was radiolabeled.

SURGICAL PREPARATION OF PORCINE SKIN

SUPPORT PROTOCOL

Skin can be obtained from any anatomical region of the pig's body. Skin from the dorsum (back) of the pig is preferred because the surrounding musculature and skeleton facilitates dermatoming and does not require prior excision of skin. Because of the nature of this procedure, euthanasia of the animal is required prior to dermatoming. After dermatoming skin to correct thickness, punch biopsies of the dermatome skin are then loaded into the diffusion cell system.

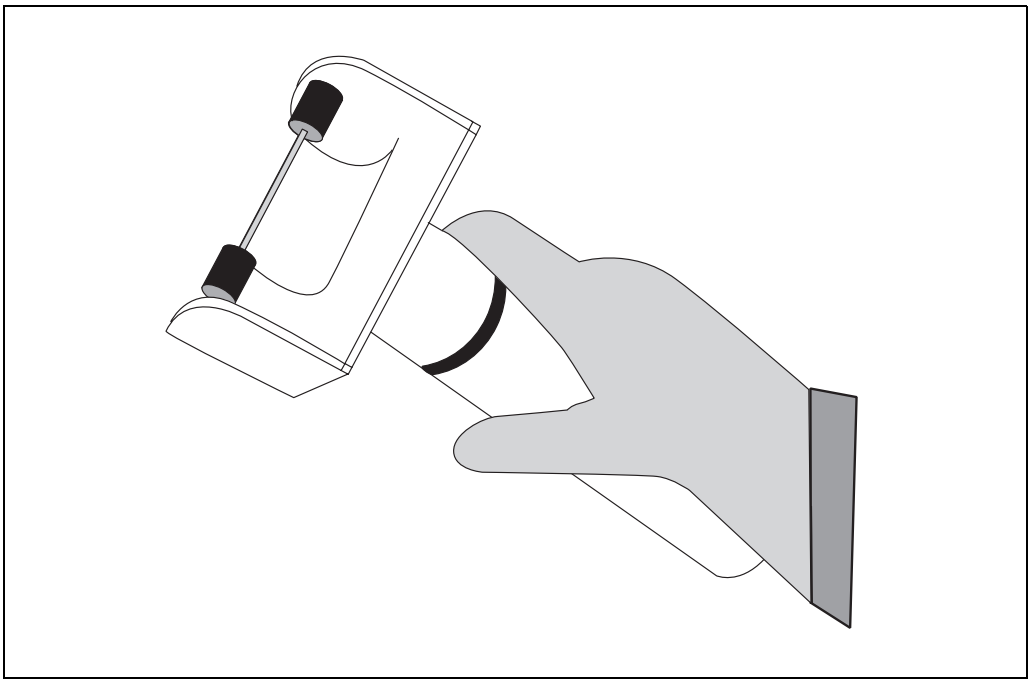

Figure 5.5.2 An illustration of the Padgett Electro Dermatome in removing sheets of skin.

Materials

8-week-old weanling female Yorkshire pigs (e.g., Looper Farms)
Preanesthetic: ketamine hydrochloride (11 mg/kg body weight); xylazine hydrochloride (1.4 mg/kg body weight)
Pentobarbitol sodium (100 mg/kg body weight)
Physiological saline

Gauze
Dermatome and blades (e.g., Padgett electric model; optional)
Scissors and forceps
16-mm steel biopsy punch
Micrometer

1. Acclimatize 8-week-old weanling female pigs 1 to 2 weeks before surgical procedure and clip the hair from the dorsum (back) of the pig 24 to 48 hr prior to dermatoming skin.
2. Tranquilize pig with ketamine (11 mg/kg body weight) and xylazine (1.5 mg/kg body weight) sequentially. Then euthanize with pentobarbitol solution (100 mg/kg body weight). Clean any debris from the back of the pig with dry gauze, and examine for gross morphological abnormalities in the skin.
3. Set dermatome to 200 to 300 μm prior to dermatoming skin.

   This setting should provide a thickness of ~200 μm, which is representative of stratum corneum, viable epidermis, and a small portion of the dermis. The aim here is to minimize the contribution of the dermis layer to diffusion of the test compound. Some individuals may use higher or lower dermatome settings to obtain a skin thickness within the 200- to 300-μm range.

4. Dermatome the skin as shown in Figure 5.5.2 applying constant pressure and utilizing a forceps to help guide the dermatomed skin through the dermatome.

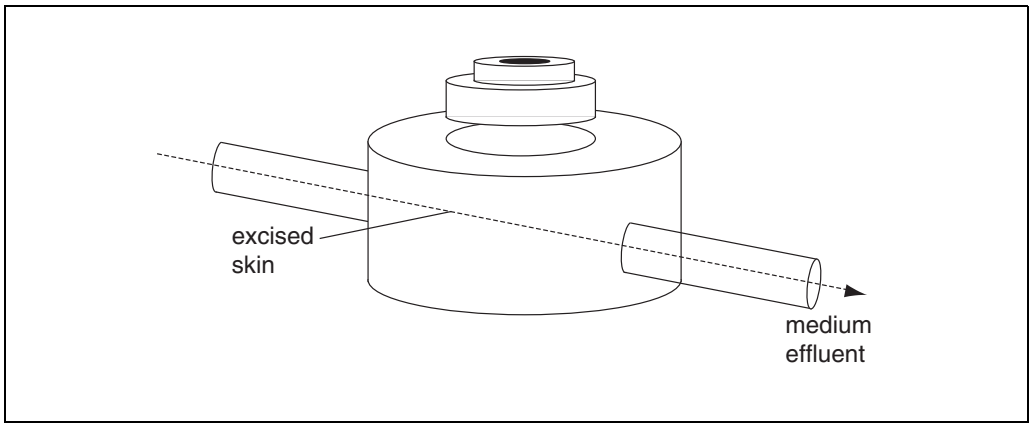

Figure 5.5.3 Illustration of the Teflon flow-through diffusion cell; also indicated are the inlet and outlet arms of the cell through which the medium perfuses.

5. Place dermatomed skin, dermis side down, on gauze presoaked with physiological saline and use within 1 to 2 hr to ensure viability. Examine both sides of dermatomed skin for lesions and use a micrometer to ensure that skin sections 200- to 300-μm thick are selected.

6. Use a 16-mm biopsy punch to provide skin disks that will be loaded into a two-compartment Teflon flow-through diffusion cell (Fig. 5.5.3).

   Depending on the diameter of the diffusion cell selected, dosing area will vary from 0.32 to 0.64 cm^2.

COMMENTARY

Background Information

Improvements in in vitro technology within the last 20 years have allowed for accurate measurements of dermal absorption and metabolism of topically applied drugs and pesticides. Static cell diffusion systems with two-chamber cells were initially used to quantitate percutaneous absorption of drugs and toxicants. The two-chambered cell can be used when steady state kinetics is required to study mechanisms of absorption and for comparing permeation through skin to Fickian diffusion (Bronaugh and Collier, 1993). However, skin is excessively hydrated with this two-chamber system and the donor chamber does not mimic environmental conditions. The flow-through diffusion cell systems (a one-chamber system) as first described by Bronaugh and Stewart (1985) have contributed significantly to quantitating the rate and extent of dermal absorption of drugs and pesticides in humans, rodents, and pigs. In many instances, permeation of lipophilic and hydrophilic drugs in these in vitro systems were comparable to permeation in vivo.

The major benefit of the flow-through diffusion system over the static diffusion system is that the skin is more likely to be viable and the penetrating drug or pesticide molecule is continually removed from the skin, which is analogous to the continual perfusion of blood in vivo (Bronaugh and Stewart, 1985; Grummer and Maibach, 1991). The receptor volume of the diffusion cell is usually small (<0.5 ml) so that it can be completely flushed out during sample collection intervals. Flow rates are usually set at 5 to 10 times the receptor volume (e.g., 2.5 to 5 ml/hr) to allow for adequate removal of the absorbed drug molecules. For these reasons, average flow rates described in this protocol are within this range, 4.0 ml/hr. Other studies have also demonstrated that changes in perfusion rate (Crutcher and Maibach, 1969; Chang and Riviere, 1991), receptor fluid constituents (Bronaugh and Stewart, 1984), environmental conditions (Chang and Riviere, 1991), and skin section thickness (Scott et al., 1991) will dramatically alter penetration of the marker chemical. Review of current literature suggests that the latter variable is often overlooked in the design of in vitro percutaneous studies.

For lipophilic chemicals such as carbaryl and permethrin, penetrating molecules are thought to enter the systemic circulation in vivo at the dermis/epidermis interface and do not

necessarily traverse the full thickness of the dermis. In in vitro experiments, the aqueous dermis can act as a significant, additional artificial barrier for penetrating lipophilic chemicals such as DDT (Reifenrath et al., 1991). Several studies have difficulty demonstrating good agreement between in vitro and in vivo absorption with lipophilic chemicals because of the presence of excess dermis in final skin preparations (Bronaugh and Stewart, 1984; Bronaugh and Collier, 1993). Whereas for more hydrophilic chemicals, good agreement between in vitro and in vivo absorption data is more often achieved. Several other studies have demonstrated that use of skin sections containing mostly epidermis and minimal dermis results in good agreement with in vivo data. For example, cypermethrin did not penetrate in vitro through rat whole skin, but penetrated epidermal membranes and predicted the in vivo absorption in rats (Scott and Ramsey, 1987). Having considered these findings, the flow-through diffusion cell experiments described in this protocol utilizes excised skin sections (200 to 300 μm) with minimal dermis. Furthermore, bovine serum albumin is used as the receptor fluid because it mimics blood and it facilitates partitioning of toxicologically important chemicals, which are often lipophilic, from the skin sections into the receptor fluid.

Critical Parameters and Troubleshooting

Skin sections should be removed at least 48 hr after clipping to ensure adequate time for recovery of the stratum corneum. Recall that the stratum corneum layer is the rate-limiting layer, and its integrity must be maintained if valid comparisons are going to be made.

Dermatoming requires some skill and practice, but the operator can quickly learn to consistently prepare skin at the desired thickness. Dermatoming of skin from anatomical regions of the pig other than the dorsum or skin from other species will require securing dissected skin on firm foam blocks prior to dermatoming. This exercise requires more practice and can result in uneven skin samples. Poor dermatoming and very thin sections can produce highly variable results as the path lengths for molecular diffusion can vary, resulting in considerable variability in absorption of the test chemical.

These are usually mass balance studies, and it is important to account for the dose delivered to the skin surface. It is also important to accurately know the dose that was delivered to the skin surface because this is the frame of reference from which the flux, permeability, and extent of absorption will be determined. The applied dose, usually expressed as $\mu g/cm^2$, can be obtained from the average predose and postdose samples in the original dose vial. This is especially important for very volatile test chemicals. Recall that very small volumes (10 to 20 μl) are usually applied to the skin surface.

Anticipated Results

This section gives examples of the kind of data that can be generated from perfusion of skin in flow-through diffusion cell systems and how diffusion parameters can be calculated from a given data set.

In this first example, porcine skin sections were exposed to 40 $\mu g/cm^2$ of ^{14}C-carbaryl for 8 hr to assess absorption in different vehicles, acetone and DMSO. The plot in Figure 5.5.4 depicts the flux of carbaryl dosed in acetone or DMSO as it diffuses through the skin. At least 4 to 5 replicates are conducted per test chemical for flow-through diffusion cell experiments. Absorption is defined as the total amount of radioactivity detected in the perfusate for the entire 8-hr perfusion period. Penetration is defined as the sum of total absorption and total radioactivity in the skin. Penetration into the stratum corneum layer at 8 hr is based on levels detected in the tape strips. The radioactivity remaining on the skin surface was defined as the amount of radioactivity detected in the skin swab samples. The following ratios can also be calculated to assess the relative disposition in skin such as: (1) relative systemic absorption (absorption/penetration); (2) relative skin surface penetration (penetration/skin surface); (3) stratum corneum/dosed skin; and (4) stratum corneum/skin surface.

Theoretically, Fick's law of diffusion describes the rate of percutaneous absorption through the intercellular pathway in skin. That is, rate of diffusion or flux = $[D \times A \times K \times \Delta C]/H$, where D is the diffusion coefficient or diffusivity, A is the surface area, K is the partition coefficient for stratum corneum/vehicle or octanol/water, ΔC is drug concentration difference across the membrane, H is membrane thickness, and permeability can be obtained from $[D/H] \times K$. The determinants (D, A, K, and ΔC) of diffusion rates for a given skin section may be altered experimentally through manipulation of drug or pesticide formulations. This system can therefore be used to quickly compare absorption of drug or chemical formulations.

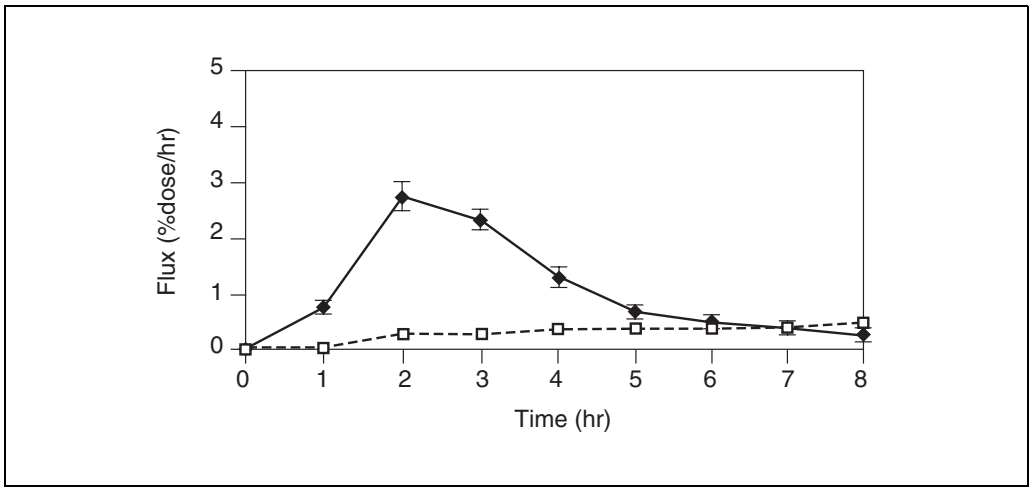

Figure 5.5.4 Flux (%dose/hr) versus time profiles for carbaryl in acetone (circles) or DMSO (squares) vehicles in a flow-through diffusion cell system.

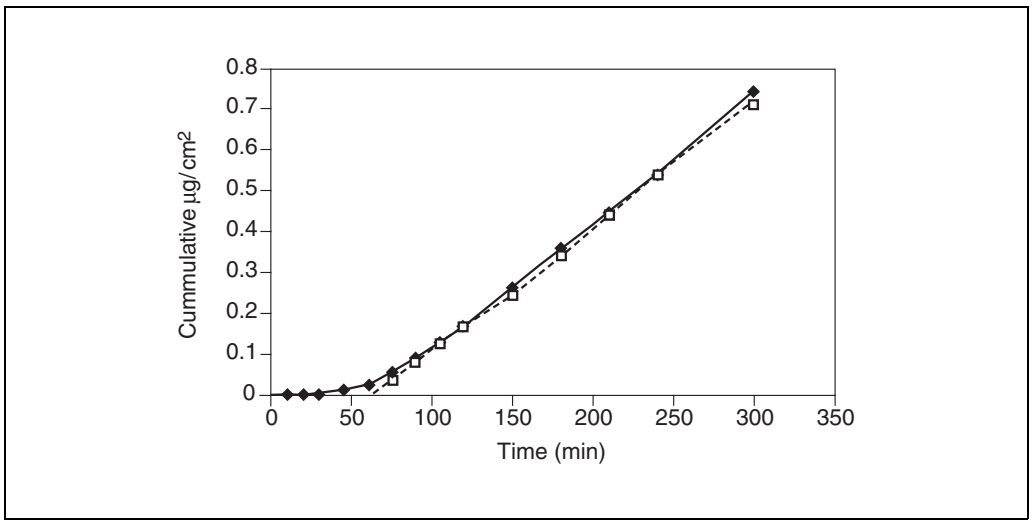

Figure 5.5.5 Cumulative absorption (µg/cm^2) versus time profile for ^{14}C-naphthalene diffusion in JP-8 jet fuel in porcine skin sections.

In the second example, porcine skin sections were exposed to ^{14}C-naphthalene (µg/cm^2) for 5 hr to assess naphthalene absorption in JP-8 fuel. The plot in Figure 5.5.5 depicts the cumulative absorption of naphthalene in porcine skin and how graphically flux, permeability, and lag time can be obtained from this experiment. Flux (µg/cm^2/hr) can be determined at steady state from the slope of the cumulative mass per unit area versus time (hr) curve. Permeability (cm/hr) can be determined from the ratio of individual fluxes to the concentration (µg/cm^3) of initial topical dose. Diffusivity (cm^2/hr) can be determined by obtaining the lag time before steady-state flux is reached. This lag time (τ) is obtained by extrapolating the steady state portion of the curve back to the time- or *x*-axis and is related to diffusivity (D) and membrane thickness (L) by the following equation: $D = L^2/6\tau$, where $L = 250$ µm or selected membrane thickness.

Time Considerations

Bovine serum albumin medium is usually prepared 24 to 48 hr in advance, and it can take up to 1 hr to dissolve the BSA. Surgical preparation requires ~20 min to first anesthetize and euthanize the pig humanely and ~10 to 15 min to dermatome the skin from the dorsum.

Loading the skin in the 14 diffusion cells can take as long as 15 min to ensure that air bubbles are removed from the medium immediately below the skin. Dosing and sample collection can vary depending on the duration of the perfusion experiment. Sometimes, 8-hr experiments are performed to mimic occupational

exposure scenarios for the average worker in the agriculture or chemical industry.

Literature Cited

Bronaugh, R. and Collier, S. 1993. In vitro methods for measuring skin permeation. *In* Skin Permeation (J.L. Zatz, ed.) pp. 93-111, Allured Publishing, Wheaton, Ill.

Bronaugh, R.L. and Stewart, R.F. 1984. Methods for in vitro percutaneous absorption studies III: Hydrophobic compounds. *J. Pharm. Sci*. 73:1255-1258.

Bronaugh, R.L. and Stewart, R.F. 1985. Methods for in vitro percutaneous absorption studies IV: The flow-through diffusion cell. *J. Pharm. Sci*. 74:64-67.

Chang, S.K. and Riviere, J.E. 1991. Percutaneous absorption of parathion in vitro in porcine skin: Effect of dose, temperature, humidity, and perfusate composition on absorptive flux. *Fundam. Appl. Toxicol*. 17:494-504.

Crutcher, W. and Maibach, H.I. 1969. The effect of percutaneous rate on in vitro percutaneous penetration. *J. Investig. Dermatol*. 53:264-269.

Grummer, C. and Maibach, H.I. 1991. Diffusion cell design. *In* In Vitro Percutaneous Absorption: Principles, Fundamentals and Applications (R.L. Bronaugh and H.I. Maibach, eds.) pp. 7-16, CRC Press, Boca Raton, Fla.

Monteiro-Riviere, N.A. 1991. Comparative anatomy, physiology, and biochemistry of mammalian skin. *In* Dermal and Ocular Toxicology: Fundamentals and Methods (D.W. Hobson, ed.) pp. 3-71, CRC Press, Boca Raton, Fla.

Reifenrath, W.G., Hawkins, G.S., and Kurtz, M.S. 1991. Percutaneous penetration and skin retention of topically applied compounds: An in vitro–in vivo study. *J. Pharm. Sci*. 80:526-532.

Scott R.C. and Ramsey, J.D. 1987. Comparison of the in vivo and in vitro percutaneous absorption of a lipophilic molecule (Cypermethrin, a pyrethrin insecticide). *J. Investig. Dermatol*. 89:142-146.

Scott, R.C., Corrigan, M.A., Smith, F., and Mason, H. 1991. The influence of skin structure on permeability: An intersite and interspecies comparison with hydrophilic penetrants. *J. Investig. Dermatol.* 96:921-925.

Key References

Bronaugh and Stewart, 1985. See above.

This paper describes the use and advantages of flow-through diffusion cells in assessing in vitro dermal absorption of chemicals.

Chang and Riviere, 1991. See above.

This paper describes the use of flow-through diffusion cells in an environmentally controlled system in order to assess environmental effects on in vitro dermal absorption of chemicals.

Contributed by Ronald E. Baynes
North Carolina State University
Raleigh, North Carolina

Toxicant Transport by P-Glycoprotein

P-glycoprotein (P-gp) is an ~170-kDa membrane-bound glycoprotein that has been shown to efflux a wide variety of drugs, including chemotherapeutic agents, as well as toxicants. In mammals, P-gp is located on the apical side of organs of elimination, such as the brush border of the proximal tubules in the kidney, the enterocytes of intestinal cells, and the canalicular membrane of hepatocytes. This localization indicates that P-gp plays an important role in eliminating toxicants from the organism or acts to prevent their uptake in the gastrointestinal tract. P-gp is also present in capillary endothelial cells and is important in maintaining the integrity of the blood-brain barrier and the testicular-blood barrier.

P-glycoprotein transport activity can be measured from tissues, from whole cultured cells, or membrane preparations from cultured cells or tissues. The activity is measured in amount of toxicant transported per unit time or amount transported per unit time per milligram of protein. Typically, transport is measured using either a radiolabeled substrate or unlabeled substrate that can readily be detected by high-performance liquid chromatography (HPLC) or gas chromatography (GC) and measuring its uptake and/or elimination into cultured cells or tissue pieces (see Basic Protocol 1). The procedure described in this unit will only cover steps for using a radiolabeled substrate, although the initial steps before detection are very similar to the procedure using unlabeled substrate. A variation of this procedure examines uptake of a radiolabeled substrate into cellular membrane vesicles (see Basic Protocol 2 and Support Protocol for vesicular preparation). Another method for examining P-gp-mediated transport uses polarized epithelial cells, such as Caco-2 cells, cultured in two-chambered vertical diffusion chambers (Transwells), examining the movement of a radiolabeled toxicant from the basolateral to apical side of the culture dishes (see Basic Protocol 3). The last protocol describes an indirect method of examining transport activity, determining whether a compound can compete or inhibit the transport of a known P-glycoprotein substrate doxorubicin (see Basic Protocol 4). This procedure is a quick screening method, avoiding the expense of radiolabeled compounds and the time involved when preparing membrane vesicles. However, this method cannot distinguish whether a toxicant is actually a substrate or an inhibitor of P-glycoprotein.

CAUTION: When working with radioactivity, take appropriate precautions to avoid contamination of the investigator and the surroundings. Carry out the experiment and dispose of wastes in an appropriately designated area following the guidelines provided by the local radiation safety officer (also see *APPENDIX 1A*).

CELLULAR EFFLUX OF RADIOLABELED TOXICANTS

BASIC PROTOCOL 1

This protocol describes methods for loading cells with a toxicant of interest and then assessing its rate of efflux by liquid scintillation counting of the cells and of the cell culture medium. This procedure can be completed in 1 day and only requires access to standard cell culture items and a radiolabeled toxicant. This procedure can also be modified to examine the efflux of non-radiolabeled compounds by either GC or HPLC.

Materials

Transfected cultured cells expressing P-gp after transfection with a vector containing P-gp cDNA along with a mock-transfected control or tissue, e.g., liver or intestine

Appropriate cell culture medium (e.g., RPMI 1640 supplemented with 10% fetal bovine serum)

Contributed by Lisa J. Bain

Current Protocols in Toxicology (2003) 5.6.1-5.6.13

[^{14}C] or [^{3}H]-labeled toxicant, diluted sufficiently with unlabeled toxicant to provide a 1 to 20 µM solution having 100,000 to 300,000 dpm per 5 µl
5 mM verapamil stock (see recipe)
PBS (*APPENDIX 2A*), ice cold
30% scintillation cocktail (e.g., Scintisafe or equivalent)

12-well culture plates
20-ml scintillation vials
Scintillation counter

Additional reagents and equipment for counting cells (*APPENDIX 3B*)

1. If using cultured cells, harvest cells and dilute to 1×10^6 cells/ml after counting with a hemacytometer (*APPENDIX 3B*). Place 1 ml of cell suspension into a 12-well culture plate along with an additional 1 ml cell culture medium. Plate out enough cells so that each time point can be performed in triplicate.

   For a typical seven-time point efflux assay using both P-glycoprotein-expressing and mock-transfected cells, and with time points at 0, 2, 5, 7, 10, 15, and 30 min, plate 21 wells for each cell line.

2. Incubate cells overnight in a 37°C, 5% CO_2 humidified incubator to allow cells to attach. If using tissues, prepare a crude primary cell suspension as described in Support Protocol, step 1b, count cells (*APPENDIX 3B*), and place 1×10^6 cells into 2 ml cell culture medium in a 12-well culture plate.

   The assays with tissues should be conducted in triplicate using medium with or without the addition of verapamil. For a typical seven-time point efflux assay, use 42 wells.

3. For cultured cell lines with both a transfectant and a mock control, after an overnight attachment period, remove cell culture medium and replace with 2 ml medium containing 5 µl of the radiolabeled toxicant of interest. For primary cells, add 5 µl of the radiolabeled toxicant directly to the culture medium, and add 5 µl of 5 mM verapamil to half of the wells (10 µM verapamil final concentration). Incubate cells or tissues for 4 hr in a 37°C, 5% CO_2 humidified incubator.

4. After 4 hr, aspirate the medium from the wells, and wash the cells two times with 1 ml ice-cold PBS, being careful to handle and dispose of the radiolabeled material properly. Add 1 ml of 37°C prewarmed cell culture medium to each well.

5. At the appropriate time points, remove the cell culture medium and place into labeled 1.5-ml microcentrifuge tubes. Wash the cells or tissue with 1 ml ice-cold PBS two times, aspirating off the washes. Then, add 0.5 ml PBS and scrape cells from the plate. Add 100 µl of the cell culture medium or 0.5 ml of the cell suspension to a 20-ml scintillation vial containing 15 ml of 30% Scintisafe scintillation cocktail and determine the amount of radioactivity transported into the medium or accumulated in the cells by counting on a scintillation counter.

   These same procedures can be used to examine the cellular efflux of unlabeled toxicants that can be measured by gas chromatography (GC) or high-pressure liquid chromatography (HPLC). The investigator would need to work out the time course of accumulation of the toxicant, as well as additional cleanup steps and the appropriate detection methods.

ACCUMULATION OF TOXICANTS INTO CELLULAR MEMBRANE VESICLES

This procedure describes methods of measuring toxicant uptake into plasma membrane vesicles. Although the procedure is relatively quick, preparing the vesicles is a 12 to 15 hr procedure. However, this procedure negates the effects of toxicant uptake and metabolism that may be problematic in the other procedures.

Materials

Membrane vesicles (see Support Protocol)
ATP and AMP solutions (see recipe)
1000 U/ml creatine kinase in Tris-sucrose buffer (store 150-µl aliquots in 0.5-ml microcentrifuge tubes for up to 1 month at −20°C)
Tris-sucrose buffer (see recipe), ice cold
0.5 µCi of 418.2 nM [^{3}H]vincristine (see recipe)
[^{14}C] or [^{3}H]-labeled toxicant, diluted sufficiently with unlabeled toxicant to provide a 10 nm to 10 µM solution having 0.5 µCi per 350 µl Tris-sucrose buffer
22 µM verapamil in Tris-sucrose buffer (see recipe)
50% scintillation cocktail (Scintisafe Plus or equivalent)

0.22-µm membrane filters, 25-mm diameter (e.g., Millipore)
Sampling vacuum manifold for 25-mm filters (e.g., Millipore)
Vacuum pump
Flat-tipped forceps
7-ml scintillation vials
Scintillation counter

IMPORTANT NOTE: Ensure that everything is set up before beginning the experiment as there is a very short period between each sampling time point.

Prepare reagents

1. Heat water bath to 37°C. For each vesicular preparation to be tested, thaw on ice 400 µg membrane vesicles, one tube each of ATP, AMP, and 1000 U/ml creatine kinase for each compound to be tested, plus vincristine as a positive control. Label twenty-four 0.5-ml microcentrifuge tubes with an "a" and twenty-four 0.5-ml microcentrifuge tubes with a "b," and place on ice.

   The tubes will be used in batches of three to perform assays in triplicate for each vesicular preparation, for each compound (vincristine or the toxicant), using either AMP or ATP.

2. Place twenty-four 1.5-ml microcentrifuge tubes on ice and add 1 ml ice-cold Tris-sucrose buffer to each one.

Prepare tubes and filter apparatus

3. To each of three "b" tubes add 6.5 µl Tris-sucrose buffer, 27.5 µl [^{3}H]vincristine solution, 10 µl ATP solution, and 11 µl creatine kinase solution. Keep on ice. To each of three "a" tubes, add 30 µg vesicle preparation and enough Tris-sucrose buffer to make a final volume of 60 µl. Keep on ice.

4. Place twelve 0.22-µm filters on each port of the sampling manifold and hook it up to the vacuum pump. To wet the filters before beginning the assay, pipet 1 ml of ice-cold Tris-sucrose buffer onto each filter and turn on vacuum. Keep the vacuum pump running for the entire set of three tubes.

Start assay

5. Place one of the "b" tubes in the 37°C water bath and preincubate for 1 min. To start the assay, add 50 µl from the warm "b" tube into an "a" tube, place in the 37°C water bath, and start the stop watch (final concentrations: 1 mM ATP, 10 mM $MgCl_2$, 10 mM phosphocreatine, 10 U creatine kinase, and 100 nM [^{3}H]vincristine). Discard the remainder of "b" as radioactive waste.

6. Remove a 20-µl aliquot from the tube at 30 sec, put into one of the 1.5-ml microcentrifuge tubes containing 1 ml Tris-sucrose buffer to immediately stop the reaction. Pipet the entire 1.02 ml onto one of the prewetted 0.22-µm membrane filters and vacuum filter. Then, add 3 ml Tris-sucrose buffer and allow liquid to filter into waste container and repeat two more times with an additional 3 ml of Tris-sucrose buffer. Remove additional aliquots from the tube at 1 min, 2 min, and 3 min and repeat the stop step, filter onto a different 0.22-µm membrane filter, and repeat the washing step.

   At the end of this assay, samples will be filtered onto four membranes and one of the triplicate samples is completed.

7. Repeat steps 5 and 6 for the second and third replicate.

8. After all twelve filters have been used, turn off the vacuum and remove the filters with flat tipped forceps. Place each filter into a prelabeled individual 7-ml scintillation vial. Add 5 ml scintillation cocktail and determine the amount of radioactivity associated with each filter by scintillation counting.

Assess specificity

9. To ensure that the radioactivity associated with the filters is not just nonspecific binding, repeat the assay and substitute AMP for ATP. To three additional 0.5-ml microcentrifuge tubes labeled "b," add to each tube 6.5 µl Tris-sucrose buffer, 27.5 µl [^{3}H]vincristine solution, 10 µl AMP solution, and 11 µl creatine kinase solution. Keep on ice. To three "a" tubes, add to each tube 30 µg vesicle preparation and enough Tris-sucrose buffer to make a final volume of 60 µl. Keep on ice.

10. Repeat steps 4 to 8 for AMP-containing samples.

11. If the vesicular preparation was from transfected cells, repeat steps 3 to 10 with the mock-transfected cells. If the vesicular preparation was from other cultured cells or tissues, repeat steps 3 to 10 while using verapamil as a specific inhibitor of P-glycoprotein-mediated transport. Modify step 3 such that to each tube "b," add 4.5 µl Tris-sucrose buffer and 2 µl verapamil solution, rather than 6.5 µl Tris-sucrose buffer.

Measure nonspecific binding

12. Perform a nonspecific-binding assay to determine how much [^{3}H]vincristine or radiolabeled-toxicant is binding to the filters. To each of two 0.5-ml microcentrifuge tubes, add 66.5 µl Tris-sucrose buffer, 27.5 µl radiolabeled compound, 10 µl ATP solution, and 11 µl creatine kinase solution. Filter through the sampling manifold as described above and determine the amount of radioactivity associated with each membrane, which will be the blank.

13. Subtract the average DPM of the blank samples from that of the other samples to determine the amount of radioactivity associated with the vesicles. Calculate an average for each time point and compound, convert the DPM into pmol transported/mg protein, and plot as a graph with time on the *x*-axis and pmol/mg transported on the *y*-axis.

   For a toxicant to be a substrate of P-gp, the rate of uptake must be greater in the ATP-utilizing samples compared to the AMP-utilizing samples, but it must also be greater

in either the transfected P-gp expressing cells than the mock-transfected cells, or greater in the toxicant vesicles without verapamil than those vesicles incubated with the toxicant plus verapamil.

APICAL TRANSPORT OF TOXICANTS IN CACO-2 CELLS CULTURED ON TRANSWELL INSERTS

BASIC PROTOCOL 3

This protocol describes methods for assessing basolateral to apical transport of toxicants in Caco-2 cells cultured on Transwell inserts. Once the cells on the inserts form the appropriate tight junctions, this is a relatively quick and robust method for examining transport. The limitations are the cost of the Transwells and the time required for the cells to become ready to use.

Materials

Caco-2 cells
Cell culture medium, such as DMEM with high glucose (4.5 g/liter) supplemented with 10% fetal bovine serum
Hank's balanced salt solution (*APPENDIX 2A*) containing 25 mM HEPES, pH 7.4 (HBSS/HEPES)
[^{3}H]- or [^{14}C]-labeled toxicant of interest diluted with unlabeled toxicant to provide a final solution of 1 to 100 µM containing 0.5 µCi/2.5 ml transport medium
5 mM verapamil (see recipe)
50% scintillation cocktail (e.g., Scintisafe Plus or equivalent)

6-well transwell plate (Costar) with 0.45-µm polyester inserts
37°C, 5% CO_2 humidified incubator
7-ml scintillation vials
Scintillation counter

1. Seed 5×10^5 Caco-2 cells/insert on a 6-well transwell plate with 0.45-µm polyester inserts and add 1.6 ml cell culture medium to the apical side and 2.5 ml to the basolateral side. Plate cells such that experiments can be run in triplicate for each compound, for each side of the transwell, and with and without verapamil. For every toxicant tested, set up at least twelve plates. Incubate for 21 days in a 37°C, 5% CO_2 humidified incubator, which is when the tight junction has formed and P-gp expression is near maximum.
2. Before the transport experiments, remove the cell culture medium and replace with an equal volume of warm (37°C) HBSS/HEPES, and incubate 30 min in the 37°C, 5% CO_2 humidified incubator.
3. To start the transport experiments, replace the medium on the apical side with fresh HBSS/HEPES and the basolateral side with HBSS/HEPES containing 0.5 µCi [^{3}H]- or [^{14}C]-radiolabeled toxicant. In transport inhibition assays when verapamil is to be added, add 5 µl verapamil/ml HBSS/HEPES to both sides of the transwell (final concentration is 10 µM verapamil). Incubate for 4 hr in a 37°C, 5% CO_2 humidified incubator and remove a 50-µl aliquot from each compartment at 0-, 0.5-, 1-, 2-, 3-, and 4-hr timepoints.
4. Place each aliquot into a 7-ml scintillation vial containing 5 ml of 50% scintillation cocktail and determine the amount of radioactivity contained in each aliquot by scintillation counting.
5. To determine the rate of transport, convert the DPM from the scintillation counter into nanomoles or picomoles transported per cm^2 of insert surface (the 6-well insert is 4.7 cm^2). Plot on a graph versus time in hours.

For a toxicant to be actively transported by P-gp, the transport from the basolateral side to the apical side should be significantly greater than the transport from the apical to basolateral side. Also, the addition of P-gp inhibitor verapamil should decrease the rate of basolateral-to-apical transport significantly.

6. Determine the apparent permeability coefficient, P_{app} (cm/sec). This is calculated as:

$$P_{app} = dQ/dt \times 1/60 \times 1/c_o \times 1/A$$

where dQ/dt is the increase in toxicant in the receiving chamber (µg/min), c_o is the initial toxicant concentration in the donor chamber (µg/ml), and A is the area of the culture insert in cm^2 (in this case, it is 4.7 cm^2). Use the P_{app} values to determine statistical differences between treatments.

BASIC PROTOCOL 4

INHIBITION OF DOXORUBICIN UPTAKE BY TOXICANTS

This procedure describes toxicant inhibition of doxorubicin accumulation in cultured cells. It is a relatively fast procedure that can be completed in 1 day. The only requirement is to have access to a fluorescence spectrophotometer. However, this assay is not a true assay for transport, as it can only determine whether a toxicant is either a substrate or an inhibitor of P-gp-mediated transport.

Materials

P-glycoprotein expressing cultured cells, such as Caco-2 cells, or transfected cells expressing P-gp after transfection with a vector containing P-gp cDNA and a mock-transfected control
10 mM doxorubicin-HCl stock (see recipe)
Toxicant of interest dissolved in PBS, saline, ethanol, or acetone at a 200-fold concentrate of the final concentration for the assay
5 mM verapamil stock (see recipe)
PBS (*APPENDIX 2A*), ice cold
Extraction solution (see recipe)

1.5-ml microcentrifuge tubes
96-well plates
96-well fluorescence spectrophotometer (e.g., SpectraMax Gemini or equivalent; or a single-cuvette fluorimeter)

Additional reagents and equipment for counting cells (*APPENDIX 3B*)

NOTE: Doxorubicin is a suspected carcinogen. Use appropriate precautions when handling.

1. Harvest P-glycoprotein expressing cultured cells and dilute to 1×10^6 cells/ml after counting on a hemacytometer (*APPENDIX 3B*). Place 1 ml cell suspension in autoclaved 1.5-ml microcentrifuge tubes, using enough cells so that all assays can be performed in triplicate.

2. Add 5 µl of 10 mM doxorubicin-HCl (final concentration 50 µM) along with 5 µl of the toxicant of interest (final concentration 1:200 of stock). Perform controls using only doxorubicin and a positive control containing doxorubicin and 2 µl of 5 mM verapamil (final concentration of 10 µM). Incubate tubes for 4 hr in a 37°C incubator.

3. Centrifuge cells 2 min at 200 × *g*, 4°C. Pour off the culture medium into an appropriate waste container, and resuspend cells in 1 ml ice-cold PBS to wash. Centrifuge 2 min at 200 × *g*, 4°C, and repeat the washing step one additional time. Remove all PBS with a pipet after final wash.

4. Add 1 ml extraction solution to each tube, vortex for 30 sec, and incubate 1 hr at room temperature. Vortex again and pellet cellular debris by centrifuging 2 min at 1000 × *g*, 4°C.

5. Remove 200 µl of solution from each tube, put into a 96-well plate, and measure the amount of doxorubicin extracted from each cell pellet on a 96-well fluorescence spectrophotometer at 470 nm excitation and 585 emission in relative fluorescent units.

   If using a fluorescence spectrophotometer with a single cuvette, use all of the extraction solution for the measurements.

6. Set the fluorescence of the tubes containing only doxorubicin as 0% and the positive control tubes containing both doxorubicin and verapamil as 100%. Using linear regression, calculate the percentage of doxorubicin in the toxicant-containing pellet. If the percentage is >75%, consider the toxicant to interact with P-glycoprotein.

   To determine whether the compound is actually a transport substrate, one must perform one of the additional protocols described here.

PREPARATION OF MEMBRANE VESICLES

SUPPORT PROTOCOL

This procedure details the preparation of cellular membrane vesicles from either cultured cells or from tissues. This is an extremely long procedure, typically requiring ~12 to 15 hr to complete. Although it is recommended that the procedure be completed in 1 day, there is a stopping point at the end of step 7. It is suggested that the remainder of the protocol be completed the following day.

Materials

P-glycoprotein expressing cultured cells in 100-cm^2 culture dishes, such as Caco-2 cells, or transfected cells expressing P-gp after transfection with a vector containing P-gp cDNA and a mock-transfected control or tissue such as liver or intestine
PBS (*APPENDIX 2A*), ice cold
0.05% collagenase (Sigma type I) in PBS
Hypotonic lysis buffer containing protease inhibitors (see recipe)
0.4% trypan blue (Sigma or equivalent)
Tris-sucrose buffer (see recipe)
38% (w/v) sucrose (see recipe)
Bio-Rad protein assay kit

40-µm mesh nylon screen
Hemacytometer
Confocal microscope
Motor-driven Potter-Elvehjem homogenizer (e.g., Dyna-Mix Stirrer, Fisher, or equivalent)
Dounce homogenizer
12-ml polycarbonate round-bottom tubes
Centrifuge with a Beckman SW-40 rotor or equivalent
1-ml pipets
27-G needle and 1-ml syringe
1.5-ml cryovials

NOTE: After step 1, perform all procedures at 4°C.

Lyse cells

1a. *Preparation from cultured cells:* Harvest cells from twenty to thirty 100-cm^2 culture dishes and wash two times with ice-cold PBS. Centrifuge cell suspension 5 min at 200 × *g*, 4°C.

1b. *Preparation from tissue:* Cut 5 g of fresh frozen tissue into small pieces, incubate with 0.05% collagenase in PBS while mixing for 10 min, and press through 40-µm mesh nylon screen. Centrifuge tissue suspension 5 min at 200 × *g*, 4°C.

2. Resuspend cells in 75 ml hypotonic lysis buffer containing protease inhibitors and incubate 2 hr on ice on a rotating shaker (150 rpm) to gently break open the cells. Examine the effectiveness of this procedure by removing 0.1 ml of suspension and mixing with 0.1 ml of 0.4% trypan blue. Incubate 1 min at room temperature, place a drop of dye suspension onto a hemacytometer, and examine under a confocal microscope.

   Intact cells will not take up the dye while cells with compromised cellular membranes will take up the dye, and thus appear blue. At least 90% of the suspension should stain blue.

Collect membranes

3. Centrifuge the cell suspension 45 min at 100,000 × *g*, 4°C, to pellet the membrane fraction. Discard the supernatant.

4. Resuspend the pellet in 30 ml hypotonic lysis buffer and gently homogenize using a motor-driven Potter-Elvehjem homogenizer set at 500 rpm. Keep the suspension on ice at all times and use 30 strokes of the homogenizer such that each stroke (up and down) takes ~20 sec. Take a 1-min break after every ten strokes.

5. Centrifuge the homogenate 10 min at 10,000 × *g*, 4°C. Remove the supernatant and set aside. Resuspend the pellet in 10 ml of Tris-sucrose buffer and homogenize with a Potter-Elvehjem homogenizer for 20 strokes, again taking a 1-min break after every ten strokes. Centrifuge this suspension 10 min at 10,000 × *g*, 4°C.

6. Combine the supernatant with the supernatant from the first centrifugation, and centrifuge 45 min at 100,000 × *g*, 4°C. Decant supernatant.

7. Homogenize the pellet in 15 ml Tris-sucrose buffer with 30 strokes with a tight-fitting Dounce homogenizer.

   If needed, one can stop the procedure at this point by snap-freezing the homogenate in liquid nitrogen and storing at −80°C overnight. On the following morning, thaw the homogenate on ice before continuing the protocol.

Isolate plasma membrane

8. Pipet 7 ml of 38% sucrose into 12-ml polycarbonate round-bottom tubes. Slowly and carefully layer the membrane homogenate on top of the denser sucrose layer, maintaining separate layers. Top off the tubes with additional Tris-sucrose buffer to balance all tubes properly, place into the centrifuge, and screw lids on tightly. Centrifuge the membrane suspension in a swinging bucket rotor 2 hr at 205,000 × *g* (SW-40 rotor 40,000 rpm), 4°C.

   This step separates the plasma membranes (found at the interface of the two layers) from endoplasmic reticulum and Golgi membranes (found at the bottom of the tubes).

9. Use a 1-ml pipet to remove 1 to 2 ml of the Tris-sucrose buffer, being careful not to disturb the interface, then use a 1-ml pipetman to "vacuum" off the membranes at the interface. Make the homogenate up to 15 ml with Tris-sucrose buffer and homogenize the preparation 30 strokes with a tight-fitting Dounce homogenizer. Centrifuge the homogenate 45 min at 100,000 × *g*, 4°C. Decant the supernatant.

Prepare vesicles

10. Resuspend the pellet in 0.6 ml Tris-sucrose buffer and pass the suspension through a 27-G needle attached to a 1-ml syringe 30 times to prepare the vesicles. Determine the protein concentration of the vesicular aliquots using the Bio-Rad protein assay kit or an equivalent procedure. Dispense 30-µl aliquots of the vesicular preparations into cryovials, snap freeze in liquid nitrogen, and store frozen in liquid nitrogen or at −80°C.

REAGENTS AND SOLUTIONS

Use Milli-Q-purified water or equivalent for all recipes and protocol steps. For common stock solutions, see ***APPENDIX 2A****; for suppliers, see* ***SUPPLIERS APPENDIX****.*

ATP and AMP solutions

Dissolve 312.8 mg phosphocreatine di(tris) salt (Sigma), 140.3 mg magnesium chloride hexahydrate, and 65 mg potassium carbonate in 6 ml of Tris-sucrose buffer (see recipe). Divide in half (3 ml each), and add 20.1 mg ATP (dipotassium salt dihydrate, Sigma) to 3 ml and 12 mg AMP to the other 3 ml. Dispense and store in 100-µl aliquots in 0.5-ml microcentrifuge tubes for up to 1 month at −20°C.

Doxorubicin-HCl, 10 mM

Dissolve 5.44 mg doxorubicin-HCl in 1 ml sterile saline (final 10 mM). Store for a maximum of 3 weeks at 4°C.

Extraction buffer

Add 5 ml of 12 N HCl to 45 ml water, then add 50 ml absolute ethanol for a final volume of 100 ml (final 0.6 N HCl in 50% ethanol/water). Store for up to 1 month at room temperature.

Hypotonic lysis buffer

Add 0.416 g EDTA to 90 ml water, pH to 8.0 with 1 N NaOH, and make up to 100 ml (final 10 mM EDTA). Store at room temperature for up to a month. In a separate bottle, add 69.98 mg sodium phosphate monobasic and make up to 990 ml with water. Add 10 ml of 10 mM EDTA (Final: 0.5 mM sodium phosphate monobasic, 0.1 mM EDTA). In an additional bottle, add 70.98 mg dibasic sodium phosphate and make up to 990 ml with water. Add 10 ml of 10 mM EDTA (final 0.5 mM dibasic sodium phosphate, 0.1 mM EDTA). Mix the monobasic and dibasic solutions until pH is at 7.0. Store for up to 1 month at 4°C. Add protease inhibitors (see recipe) immediately before use.

Protease inhibitors

100 mM phenylmethylsulfonyl fluoride (PMSF): Add 174.2 mg PMSF to 10 ml DMSO to make up a solution with a final concentration of 100 mM. Add 10 µl of 100 mM PMSF/ml of hypotonic lysis buffer (see recipe) immediately before use. Store up to 1 month at room temperature.

*154 µ*M aprotinin: Add 1 mg aprotinin to 1 ml water. Add 2.2 µl of 154 µM aprotinin/ml of hypotonic lysis buffer (see recipe) immediately before use. Store up to 2 months at −20°C.

2.1 mM leupeptin: Add 1 mg leupeptin to 1 ml water. Add 0.5 µl of 2.1 mM leupeptin/ml of hypotonic lysis buffer (see recipe) immediately before use. Store up to 2 months at −20°C.

Sucrose, 38% (w/v)

Add 0.596 g HEPES to 90 ml water and pH to 7.4. Make up to 100 ml and then add 38 g sucrose. Store up to 1 month at 4°C.

Tris-sucrose buffer

Add 4.844 g Tris and 341.5 g sucrose, make up to 3.8 liters with water, and pH to 7.4. Bring to 4 liters with water (final 10 mM Tris, 250 mM sucrose). Store up to 1 month at 4°C.

Verapamil, 5 mM

Dissolve 2.45 mg verapamil in 1 ml DMSO. Make fresh daily.

For 22 μM: Dilute 2 μl of 5 mM verapamil into 452 μl Tris-sucrose buffer (see recipe). Make fresh daily.

[^{3}H]vincristine

Add 2 μl [^{3}H]vincristine (10 Ci/mmol; Amersham) to 329.9 μl Tris-sucrose buffer (see recipe). Make up a 10 mM solution of unlabeled vincristine by dissolving 9.23 mg in 1 ml water. Make up a 10 μM solution by diluting 1 μl of 10 mM vincristine into 999 μl Tris-sucrose buffer (see recipe). Add 14.64 μl of 10 μM vincristine solution to the radiolabeled Tris-sucrose solution (final: 0.5 μCi of 418.2 nM vincristine solution).

COMMENTARY

Background Information

P-glycoprotein (P-gp) is a 170-kDa glycoprotein that transports a wide variety of drugs (for a current review, see van Tellingen, 2001), as well as toxicants (Schinkel et al., 1994; Bain and LeBlanc, 1996; Bain et al., 1997). In mammals, P-gp is located on the apical side of organs of elimination, including the proximal tubules in the kidney, the enterocytes of intestinal cells, and the canalicular membrane of hepatocytes (Thiebaut et al., 1987). This localization suggests that P-gp plays an important role in effluxing toxicants from the organism. P-gp is also present in capillary endothelial cells and is important in maintaining the integrity of the blood-brain barrier and the testicular-blood barrier (Cordon-Cardo et al., 1989; Thiebaut et al., 1989).

P-glycoprotein transport activity can be measured from tissues, from whole cultured cells, or membrane preparations from cultured cells or tissues. Historically, the easiest way to study transport of toxicants was using cells in culture and determining the amount of substrate accumulated within the cells. Using this type of procedure was how P-gp was originally discovered (Juliano and Ling, 1976), and when it was discovered that verapamil could specifically inhibit the efflux of vincristine (Tsuruo et al., 1981), using this method and inhibiting the efflux of compounds became the technique of choice (Gottesman and Pastan, 1993). It was quickly realized that other proteins besides P-gp contributed to the phenomenon of altering cellular accumulation and efflux of drugs, and different methods were needed to determine the relative contributions of P-gp to the efflux. Transfected cell lines were made to ensure overexpression of P-gp and minimize the contribution of other transport proteins in altering the apparent uptake and elimination (Ueda et al., 1987). To circumvent alterations in metabolism as well as the potential for the apparent accumulation to be due to nonspecific binding, the use of cellular membrane vesicles was employed (Horio et al., 1988; Leier et al., 1994; Wheeler et al., 2000). Caco-2 cells have more recently been used to examine transport, and also have been used to determine whether metabolites of the toxicant may be potential P-gp substrates (Artursson et al., 1996; Walle, 1996).

The doxorubicin inhibition assay (see Basic Protocol 4) was originally described by Egorin et al. (1974) and then modified by Bain and LeBlanc (1996) as a way to screen a large number of toxicants relatively quickly and easily. However, this method can only discern whether a toxicant interacts with P-gp and cannot distinguish between a P-gp substrate and a P-gp inhibitor. It is a good initial assay to perform before the other, more time-consuming assays mentioned in this unit. The toxicant efflux method (see Basic Protocol 1) was published by Fojo et al. (1985), although modifications have been made by a great number of investigators. This is the most extensively used method to measure P-gp-mediated cellular efflux of toxicants. In performing this procedure, one has the choice of using unlabeled toxicants and measuring their efflux by either GC or HPLC (Bain and LeBlanc, 1996).

The vesicular uptake method (see Basic Protocol 2) was described by Horio (1988) and modified by Ishikawa (1989), then slightly modified to the procedure described in this unit. Using this protocol negates the effects of metabolism on P-gp-mediated transport. Once all materials are in place, it is a relatively rapid procedure, although it does require a time-consuming step of preparing the vesicles (Ishikawa et al., 1990). It can also distinguish between active and passive transport by using both ATP and AMP. It typically provides the largest differences in rates of transport versus any other procedure.

The transport of toxicant by Caco-2 cells (see Basic Protocol 3) was described by Hilgers et al. (1990) and is most recently reviewed by Krishna et al. (2001). In this assay, Caco-2 cells are cultured on transwell plates typically for 20 to 30 days, as P-glycoprotein reaches maximum expression in Caco-2 cells in ~21 days (Anderle et al., 1998). This assay can also be used to determine whether metabolites of the parent toxicant are transport substrates of P-gp. All of the assays described in this unit (except Basic Protocol 4) can effectively measure P-glycoprotein-mediated transport; differences lie as to whether metabolism of a toxicant is important for the questions being asked by the investigator.

Critical Parameters and Troubleshooting

For all assays described in this unit, one of the most critical parameters to consider is the actual concentration of toxicant used in the procedures. The ranges given in the protocols are simply suggested starting points, and the actual concentration needed should be determined by the experimenter. The rate of uptake or efflux must be in the linear range to properly perform the experiment, and there must be enough of the toxicant to discern a difference between two different cell lines, between the addition or deletion of verapamil, or between apical-to-basolateral versus basolateral-to-apical flux. The other important parameter to determine in the protocols is the time points employed for measuring transport in the assays. Again, the times given in the unit are starting points in terms of what has worked in the past. However, depending on the toxicant, more or less time may be required to ensure that the rate of accumulation or efflux is linear and that it can be detected by the appropriate method, such as scintillation counting.

For the vesicular transport described in Basic Protocol 2, one must determine whether there is actual transport across the membrane vesicles rather than just nonspecific binding to the membrane. This can be determined by several methods: ensuring that a time course is performed with appropriate time points, that both AMP and ATP are used to distinguish active transport, and that there is an osmotic dependence on accumulation. The procedure described here is simply a starting point; the actual time needed to observe measurable accumulation may be longer. To determine osmotic dependence, one usually performs the assay while altering the concentration of sucrose in the assay medium, from 250 mM to 1000 mM (Wheeler et al., 2000). The amount of radioactivity associated with the vesicular preparation should be proportional to the amount of sucrose contained in the medium.

The final consideration relates to Basic Protocol 3 and the necessity to ensure that the cells have produced tight junctions. This can be accomplished foremost by culturing the cells on the Transwells for 20 to 30 days. One can also measure the transepithelial resistance using an ohm meter; the resistance should be >160 Ωcm^2 (Krishna et al., 2001). One can also include [^{3}H]- or [^{14}C]-mannitol on either side of the inserts. If the transport of mannitol is <0.5%, one can reasonably assume that the tight junctions are intact and functioning properly.

Anticipated Results

The results typical for the cellular accumulation described in Basic Protocol 1 are up to a ten-fold difference in accumulation, depending on the toxicant used, which translates into picomoles transported per minute. This procedure has the added advantage of not necessarily requiring a radiolabeled compound to perform the assay. Basic Protocol 2 details the transport by membrane vesicles in which one may see a 100-fold difference in uptake, typically measured in terms of pmol transported/min/mg protein. With Basic Protocol 2, one can exclusively measure active transport when these assays are repeated in the presence of AMP rather than ATP. This procedure tends to be more sensitive than Basic Protocol 1 because potential problems associated with metabolism and passive transport of the toxicant that may effect results may be circumvented. However, Basic Protocol 2 must be performed with radioisotopes, which may not readily be available for many toxicants

of interest, and it requires a lengthy isolation procedure to make the membrane vesicles. In Basic Protocol 3, one can measure P_{app} values of up to 40 with actual amounts transported as nmol/cm^2. Differences between basolateral-to-apical transport, for a substrate of P-glycoprotein, versus apical-to-basolateral transport may be two- to 30-fold different, depending on the substrate used. Typically, Basic Protocol 4 can detect differences of up to five fold in the inhibition of transport of doxorubicin in transfected cell lines. The differences are smaller (usually two to three fold) when using primary or non-transfected cells. The advantages to this protocol are the lack of use of a radiolabeled toxicant, and that it is a relatively quick assay. The disadvantage is that one cannot distinguish between a P-gp substrate and a P-gp inhibitor, as the assay will only discern whether or not the toxicant interacts with P-glycoprotein.

Time Considerations

Basic Protocols 1 (cellular efflux of toxicants) and 4 (inhibition of doxorubicin uptake) can be completed easily in 1 day. Basic Protocol 2 (transport into membrane vesicles) is a faster assay, typically requiring 3 hr to complete, however, vesicles must first be prepared (see Support Protocol), which can take 12 to 15 hr to complete. Basic Protocol 3 (transport in Caco-2 cells cultured in transwells) requires ~5 hr to complete, but the cells must be seeded ~3 weeks prior to performing the assay. Basic Protocol 4 (transport of doxorubicin) requires ~6 hr to complete.

Literature Cited

Anderle, P., Niederer, E., Rubas, W., Hilgendorf, C., Spahn-Langguth, H., Wunderli-Allenspach, H., Merkle, H.P., and Langguth, P. 1998. P-glycoprotein (P-gp) mediated efflux in Caco-2 cell monolayers: The influence of culturing conditions and drug exposure on P-gp expression levels. *J. Pharm. Sci.* 87:757-762.

Artursson, P., Palm, K., and Luthman, K. 1996. Caco-2 monolayers in experimental and theoretical predications of drug transport. *Adv. Drug Deliv. Rev*. 22:67-84.

Bain, L.J. and LeBlanc, G.A. 1996. Interaction of structurally diverse pesticides with the human MDR1 gene product P-glycoprotein. *Toxicol. Appl. Pharmacol.* 141:288-298.

Bain, L.J., McLachlan, J.B., and LeBlanc, G.A. 1997. Structure-activity relationships for xenobiotic transport substrates and inhibitory ligands of P-glycoprotein. *Environ. Health Perspect*. 105:812-818.

Cordon-Cardo, C., O'Brien, J.P., Casais, D., Rittman-Grauer, L., Biedler, J.L., Melamed, M.R., and Bertino, J.R. 1989. Multidrug-resistance gene (P-glycoprotein) is expressed by endothelial cells at blood-brain barrier sites. *Proc. Natl. Acad. Sci. U.S.A.* 86:695-698.

Egorin, M.J., Hildebrand, R.C., Cimino, E.F., and Bachur, N.R. 1974. Cytofluorescence localization of adriamycin and daunorubicin. *Cancer Res*. 40:2243-2254.

Fojo, A.T., Akiyama, S.-i., Gottesman, M.M., and Pastan, I. 1985. Reduced drug accumulation in multiply drug-resistant human KB carcinoma cell lines. *Cancer Res*. 45:3002-3007.

Gottesman, M.M. and Pastan, I. 1993. Biochemistry of multidrug resistance mediated by the multidrug transporter. *Annu. Rev. Biochem*. 62:385-427.

Hilgers, A.R., Conradi, R.A., and Burton, P.S. 1990. Caco-2 cell monolayers as a model for drug transport across the intestinal mucosa. *Pharm. Res.* 7:902-10.

Horio, M., Gottesman, M.M., and Pastan, I. 1988. ATP-dependent transport of vinblastine in vesicles from human multidrug-resistant cells. *Proc. Natl. Acad. Sci. U.S.A.* 85:3580-3584.

Ishikawa, T. 1989. ATP/Mg^{2+}-dependent cardiac transport system for glutathione S-conjugates. A study using rat heart sarcolemma vesicles. *J. Biol. Chem*. 264:17343-17348.

Ishikawa, T., Muller, M., Klunemann, C., Schaub, T., and Keppler, D. 1990. ATP-dependent primary active transport of cysteinyl leukotrienes across the liver canalicular membrane. *J. Biol. Chem*. 265:19279-19286.

Juliano, R.L. and Ling, V. 1976. A surface glycoprotein modulating drug permeability in Chinese hamster ovary cell mutants. *Biochim. Biophys. Acta*. 455:152-162.

Krishna, G., Chen, K., Lin, C., and Nomeir, A.A. 2001. Permeability of lipophilic compounds in drug discovery using in-vitro human absorption model, Caco-2. *Int. J. Pharm.* 222:77-89.

Leier, I., Jedlitschky, G., Buchholz, U., Cole, S.P., Deeley, R.G., and Keppler, D. 1994. The MRP gene encodes on ATP-dependent export pump for leuokotriene C4 and structurally related conjugates. *J. Biol. Chem.* 268:27807-27810.

Schinkel, A.H., Smit, J.J.M., van Tellingen, O., Beijnen, J.H., Wagenaar, E., van Deemter, L., Mol, C.A.A.M., van der Valk, M.A., Robanus-Maandag, E.C., te Riele, H.P.J., Berns, A.J.M., and Borst, P. 1994. Disruption of the mouse mdr1a P-glycoprotein gene leads to a deficiency in the blood-brain barrier and increased sensitivity to drugs. *Cell* 77:491-502.

Thiebaut, F., Tsuruo, T., Hamada, A.H., Gottesman, M.M., Pastan, I., and Willingham, M.C. 1987. Cellular localization of the multidrug resistance gene product in normal human tissues. *Proc. Natl. Acad. Sci. U.S.A.* 84:7735-7738.

Theibaut, F., Tsuruo, T., Hamada, H., Gottesman, M.M., Pastan, I., and Willingham, M.C. 1989. Immunohistochemical localization in normal tissues of different epitopes in the multidrug transport protein P170: Evidence for localization in brain capillaries and cross-reactivity of one antibody with a muscle protein. *J. Histochem. Cytochem*. 37:159-164.

Tsuruo, T., Iida, H., Tsukagoshi, S., and Sakurai, Y. 1981. Overcoming of vincristine resistance in P388 leukemia in vivo and in vitro through enhanced cytotoxicity of vincristine and vinblastine by verapamil. *Cancer Res*. 41:1967-1972.

van Tellingen, O. 2001. The importance of drug-transporting P-glycoproteins in toxicology. *Toxicol. Lett*. 120:31-41.

Ueda, K., Cardarelli, C., Gottesman, M.M., and Pastan, I. 1987. Expression of a full length cDNA for the MDR1 gene confers resistance to colchicine, doxorubicin, and vinblastine. *Proc. Natl. Acad. Sci. U.S.A*. 84:3004-3008.

Walle, T. 1996. Assays of CYP2C8- and CYP3A4-mediated metabolism of taxol in vivo and in vitro. *Methods Enzymol*. 272:145-151.

Wheeler, R., Neo, S.-Y., Chew, J., Hladky, S.B., and Barrand, M.A. 2000. Use of membrane vesicles to investigate drug interactions with transporter proteins, P-glycoprotein and multidrug resistance-associated protein. *Int. J. Clin. Pharmacol. Therap*. 38:122-129.

Key References

Bain and LeBlanc, 1996. See above.

Describes the toxicant efflux method described in Basic Protocol 1, as well as adaptations of this protocol for detecting unlabeled toxicants by HPLC.

Egorin et al., 1974. See above.

Describes the doxorubicin extraction and fluorescence spectroscopy methods. A modification of this method is described in Basic Protocol 4.

Ishikawa, 1989. See above.

Describes the transport of compounds by membrane vesicles using the rapid filtration technique. A modification of this method is described in Basic Protocol 2.

Ishikawa et al., 1990. See above.

Describes the preparation of cellular membrane vesicles. A modification of this method is described in Support Protocol.

Krishna et al., 2001. See above.

A good review article describing the transport of compounds by Caco-2 cells grown on Transwell inserts, as described in Basic Protocol 3.

Contributed by Lisa J. Bain
University of Texas at El Paso
El Paso, Texas

Collection of Bile and Urine Samples for Determining the Urinary and Hepatobiliary Disposition of Xenobiotics in Mice

Living organisms are constantly in contact with numerous xenobiotics (foreign compounds) such as environmental pollutants, food additives, pesticides, and drugs. These chemicals are excreted from the body either directly or, in many cases, in the form of metabolites that are often more hydrophilic than the parent compound. This excretion process is essential to life since in its absence, waste and poisonous substances can accumulate to exert deleterious effects.

Many xenobiotics and their metabolites are mostly cleared from the body by elimination in urine, bile, or both. The detection of metabolites present in urine or bile can greatly facilitate the elucidation of metabolic pathways of a test compound. Moreover, many researchers agree that quantitative and qualitative changes in metabolic pathways for a compound can be assessed in vivo by measuring the amount of the original dose excreted in the urine and bile and by determining whether there is a shift in the profile of metabolites.

The mouse is one of the most commonly used rodent species in toxicology and pharmacology research. Its use is becoming more appealing with the availability of transgenic and knockout models. For instance, the development of a number of transgenic mice expressing human biotransformation enzymes and knockout models of either biotransformation enzymes or membrane-associated transporters, as well as transcription factors controlling these processes, allows researchers to use humanized mouse models as more appropriate surrogates for human tissues in xenobiotic metabolism and disposition studies, and to address the in vivo role of biotransformation enzymes and transporters in the metabolism and excretion of xenobiotics. In these types of studies, as well as the classical in vivo studies mentioned earlier, it is often necessary to obtain urine and/or bile samples.

This unit describes procedures for collecting bile and urine samples from a mouse by cannulating the common bile duct (see Basic Protocol). A protocol for collecting bile from gall bladder–cannulated mice is also provided (see Alternate Protocol). Both protocols can be used in non-survival studies to determine the biliary and urinary dispostion for xenobiotics.

COLLECTION OF BILE AND URINE SAMPLES FROM A BILE DUCT–CANNULATED MOUSE

BASIC PROTOCOL

Excretion of xenobiotics in urine and bile is the cumulative result of metabolism and transport processes mainly present in the kidney and liver. Therefore, urine and bile can be used for metabolite profiling and identification. The contribution of specific transporters in the transmembrane movement of xenobiotics and their metabolites from the liver can also be assessed by determining the urinary and biliary disposition of test compounds in a mouse model lacking the transporter of interest. This protocol details procedures for collecting urine and bile from a bile duct–cannulated mouse following a bolus dose of a test compound.

Materials

0.9% saline (NaCl), sterile
Mice (3 to 4 months old or body weight >25 g)

Contributed by José E. Manautou and Chuan Chen
Current Protocols in Toxicology (2004) 5.7.1-5.7.7

Paraffin oil
Ketamine and xylazine mixture or other appropriate anesthetics
Test compound dissolved in appropriate sterile vehicle

Electric clippers
Scalpel blades
Cotton-tipped applicators
Surgical microscope or appropriate magnifier
3-0 silk sutures
Microdissecting forceps
Hemostatic forceps
1.2-French polyurethane tubing (Access Technologies)
Gauze pads
Temperature-control system composed of the following:
  Rectal thermistor probe for rodents
  Heating lamp
  Homeothermic control unit
1.5-ml microcentrifuge tubes
1-ml polypropylene disposable syringe
30- and 25-G needles
Analytical balance

Prepare animal and perform surgery

1. Administer ~20 ml/kg of 0.9% saline to a mouse by either gastric gavage or intraperitoneal injection (i.p.) to ensure the production of sufficient urine during the experiment if the disposition of a test compound via both urinary and hepatobiliary routes is to be assessed.

2. Anesthetize the animal with a combination of 100 mg ketamine/kg and 10 mg xylazine/kg i.p.

   The disappearance of the pedal reflex is a good indication that the surgical plane of anesthesia has been attained.

3. Clip the hair of the abdominal area with electric clippers. Place the animal in a ventral recumbent position. Make a midline ventral skin incision with a scalpel, extending from the xiphoid process at the cranial terminus to the genital area at the caudal terminus if collecting both bile and urine samples.

   A 1.5-in. incision with its cranial terminus just below the xiphoid process should be sufficient for collecting bile samples.

4. Carefully make an abdominal muscle wall and a peritoneum incision as long as the skin incision, along the linea alba.

5. With a saline-moisturized cotton-tipped applicator, gently retract the liver lobes cranially and toward the stomach side to reveal the bile duct.

   Placing a rolled-up gauze pad beneath the animal to arch its back usually makes it easier to retract the liver lobes and allows better access to the bile duct system.

6. Under a surgical microscope or magnification glass, observe the entire bile duct system including the gall bladder, cystic duct, hepatic ducts, and the common bile duct, via which bile received from the hepatic and cystic ducts is drained into the duodenum (see Fig. 5.7.1).

Insert cannula

7. Carefully place two 3-0 silk ligatures beneath the common bile duct: one adjacent to the duodenum and one near the bifurcation of the hepatic ducts, without fully

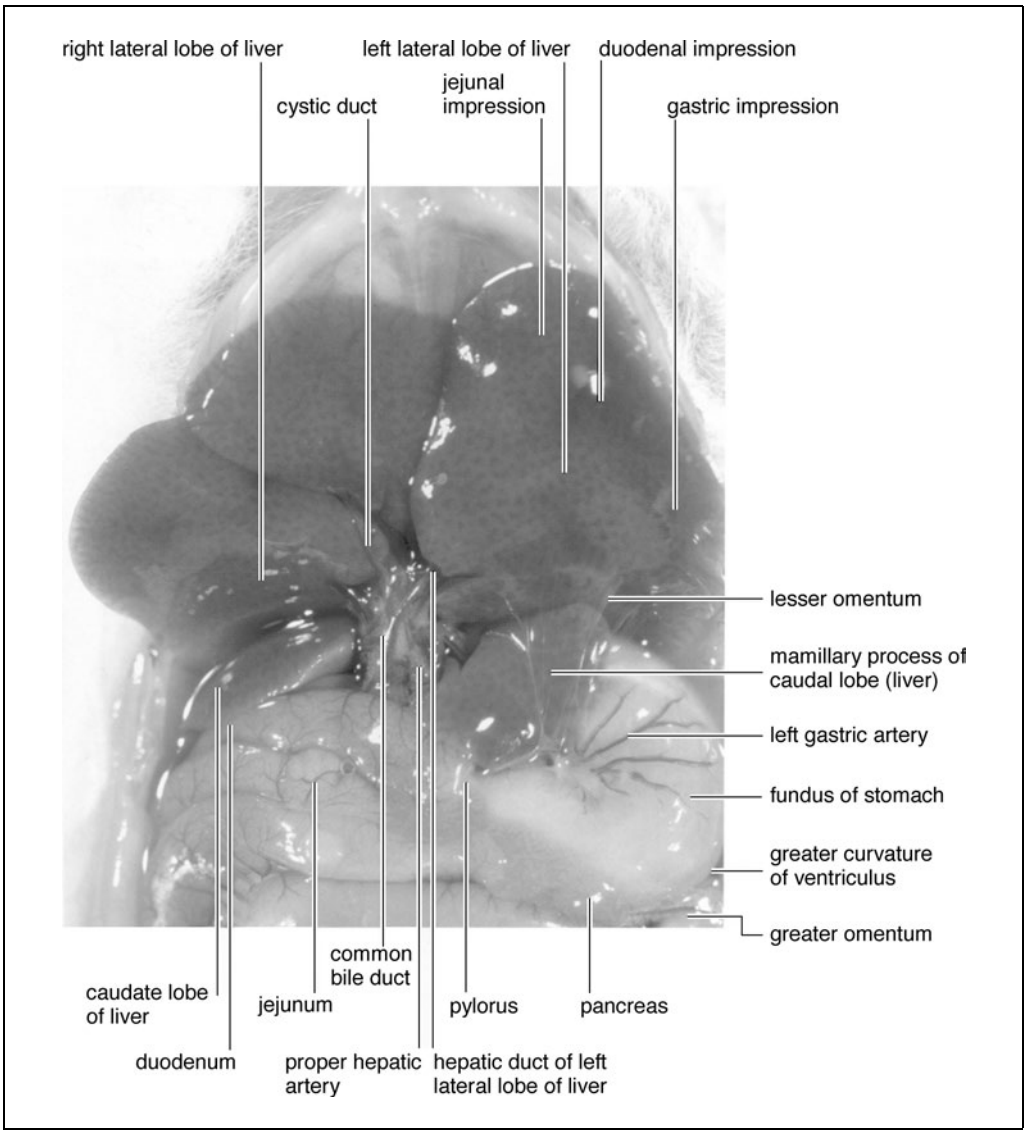

Figure 5.7.1 Diagram of the bile duct system in mice. Figure reproduced from Iwaki et al., (2001) with permission of Braintree Scientific, Inc.

isolating the bile duct between the ligatures. Tie off the first ligature and apply gentle tension to the bile duct by attaching hemostats to the threads of the ligature.

8. With the tip of a scalpel blade (size 11), make a longitudinal nick into the lumen of the bile duct between the two ligatures in a one-directional motion.

   A yellowish liquid can be observed around the nick if the blade cuts open the duct.

9. Take an ~4-in. length of 1.2-French polyurethane tubing and cut both ends at a 30° to 40° angle. Hold one end of the tubing with the bevel up, locate the opening on the bile duct, and push the tubing in until it cannot be further advanced or until its tip travels to the bifurcating point of the hepatic ducts.

10. Make sure the tip of the tubing is located within the lumen of the bile duct, then tie off the second ligature.

    Usually, bile should flow automatically into the cannula. If bile flow is not seen, adjust the position of the cannula to get rid of any kinks and attach a 1-ml syringe to the free end of the cannula and initiate the bile flow by gently withdrawing the plunger.

11. Cover the operation area with a gauze pad moistened with saline. Transfer the bile duct–cannulated mouse to an area dedicated to sample collection. Place a heat lamp ~2 feet right above the animal. Lubricate the tip of a thermistor probe with paraffin oil and gently insert into the rectum of the animal. Begin monitoring body temperature and maintain the core body temperature between 35° and 36°C.

    An alternative approach to attain appropriate body temperature is to place the animal on a thermostatted heating pad rather than under a heat lamp.

Administer test compound and collect urine

12. Collect bile into a pre-weighed microcentrifuge tube for ~10 to 15 min to establish a steady bile flow before the administration of test compound. Make sure that the free end of the cannula is in contact with the walls of the microcentrifuge tube at all times.

    This helps maintain a better and constant bile flow.

13. Externalize the urinary bladder through the midline incision. Empty its content with a 1-ml syringe attached to a 30-G needle.

14. Administer the test compound in a bolus dose via either the tail or the saphenous vein using a 25-G needle.

    If desired, the test compound can also be given i.v. at a constant rate with the use of an infusion pump.

15. Collect bile samples at time intervals between 5 and 30 min into pre-weighed microcentrifuge tubes.

    Depending on the compound being analyzed, investigators should take proper precautions to prevent alterations (e.g., oxidation, degradation) of the compound or metabolites of interest during sample collection by collecting bile into microcentrifuge tubes on ice or tubes containing an appropriate neutralizing/stabilizing reagent.

16. Monitor the anesthesia status of the animal by periodic observation of respiration, color of mucous membranes, and pedal reflex. Administer 1/5 of the initial dose of the anaesthetic i.m. to maintain anesthesia if necessary.

17. Add ~0.3 to 0.6 ml of 0.9% saline every 30 min in the abdominal cavity through the incision to prevent the animal from dehydrating.

18. At the end of the experiment, right before euthanizing the animal, withdraw urine from the urinary bladder with a syringe attached to a 30-G needle. Excise and cut open the bladder to collect any remaining urine.

19. Determine the volume of bile and urine sample by weighing on an analytical balance assuming a specific gravity of 1. Store samples at −80°C until further analysis.

ALTERNATE PROTOCOL

COLLECTION OF BILE SAMPLES FROM GALL BLADDER–CANNULATED MOUSE

Some investigators prefer to collect bile from mice by cannulating the gall bladder instead of the common bile duct. Bile samples collected this way are thought to be composed mostly of freshly excreted bile since stored bile in the gall bladder is drained before sample collection, whereas bile collected from a bile duct–cannulated mouse, especially at the beginning of sample collection, is a mixture of freshly excreted bile and stored bile. If maintaining the integrity of the gall bladder is not an important consideration in the experimental design, this method is a less complicated alternative to bile duct cannulation. Furthermore, in mice of smaller sizes (<25 g), it may be easier to collect bile samples by cannulating the gall bladder.

For materials, see Basic Protocol.

1. Follow Basic Protocol, steps 1 to 4, to anesthetize and dissect the mouse.
2. Carefully lay one 3-0 silk ligature underneath the portion of the common bile duct near the place that the cystic duct from the gall bladder merges into the common bile duct. Tie off the ligature. Place another ligature around the gall bladder and keep it open.
3. Lift the gall bladder by its tip using hemostats and make a small incision using microdissecting scissors.

   Bile will flow out as the gall bladder collapses.

4. Continue holding the tip of the collapsed gall bladder with the hemostats and insert the cannula (see Basic Protocol, step 8). Tie the ligature with a double knot.

   Bile should flow automatically into the cannula. If bile flow is not seen, follow the procedure described in Basic Protocol, step 9, annotation.

5. Follow Basic Protocol, steps 10 to 19, to monitor the animal and collect bile and urine.

COMMENTARY

Background Information

During the nineteenth century, scientists such as Oswald Schmiedeberg and Eugen Baumann discovered all of the major biotransformation pathways including oxidation, reduction, and conjugation reactions using the same type of basic methodology to obtain information on the biochemical fate of chemicals. Xenobiotics were administered to an animal or volunteer, and the urine was qualitatively analyzed for unchanged compounds or their metabolites. Using a similar approach, M.J.B. Orfila found that many metallic poisons taken up by the liver are either retained by that organ or excreted into the bile, while Abel and Rowntree reported in 1909 that a number of phthalein dyes undergo extensive biliary excretion.

Bile flow rate is usually expressed as microliter per minute per 100 g body weight. The amount of the parent compound or metabolite found in bile samples can be expressed as either concentration or mass. The mass of a compound in bile or urine is equal to the product of its concentration and the volume of excreta. When the mass of a compound is further divided by the mass of the administered dose, this represents the percentage of the administered dose excreted in the form of that compound. Additionally, one can determine the cumulative biliary excretion of a compound over time by adding the amount of the compound excreted at a given time point to the total combined amount excreted during earlier time points.

The procedure described in this unit involves bile and urine collection only. (For short-term bile collection from a rat, see *UNIT 14.5*.) Other compartments, such as blood, can also be sampled to gain a better understanding of the kinetic disposition of a xenobiotic. However, collecting multiple fluids simultaneously from a mouse can lead to excessive body fluid loss, which in turn can result in lower survival time. Because of this constraint, some investigators prefer to conduct separate studies, one addressing the hepatobiliary disposition and another investigating the plasma clearance and appearance of metabolites. In cases where the xenobiotic of interest persists in the organism beyond the study period, pharmacokinetic modeling can be used to predict the kinetic behavior of a chemical and its metabolites beyond the usual time frame for disposition studies in mice.

As stated previously, the protocol described in this unit is intended for short-term (1 to 3 hr) disposition studies. Depending on the experimental design and sampling length, investigators may want to consider collecting bile from a fully alert, unrestrained animal. This type of study is commonly done in rats, where animals are allowed to recover from anesthesia after undergoing bile duct cannulation. This procedure is described in detail in the work of Kanz and co-workers (1992). The cannulation methods used allows the bile to be returned to the gastrointestinal tract since the cannula is in the form of a biliary fistula between the bile duct and the small intestine, which can be opened for bile duct collection during the actual disposition studies. Disposition studies are initiated after several days of acclimation and recovery

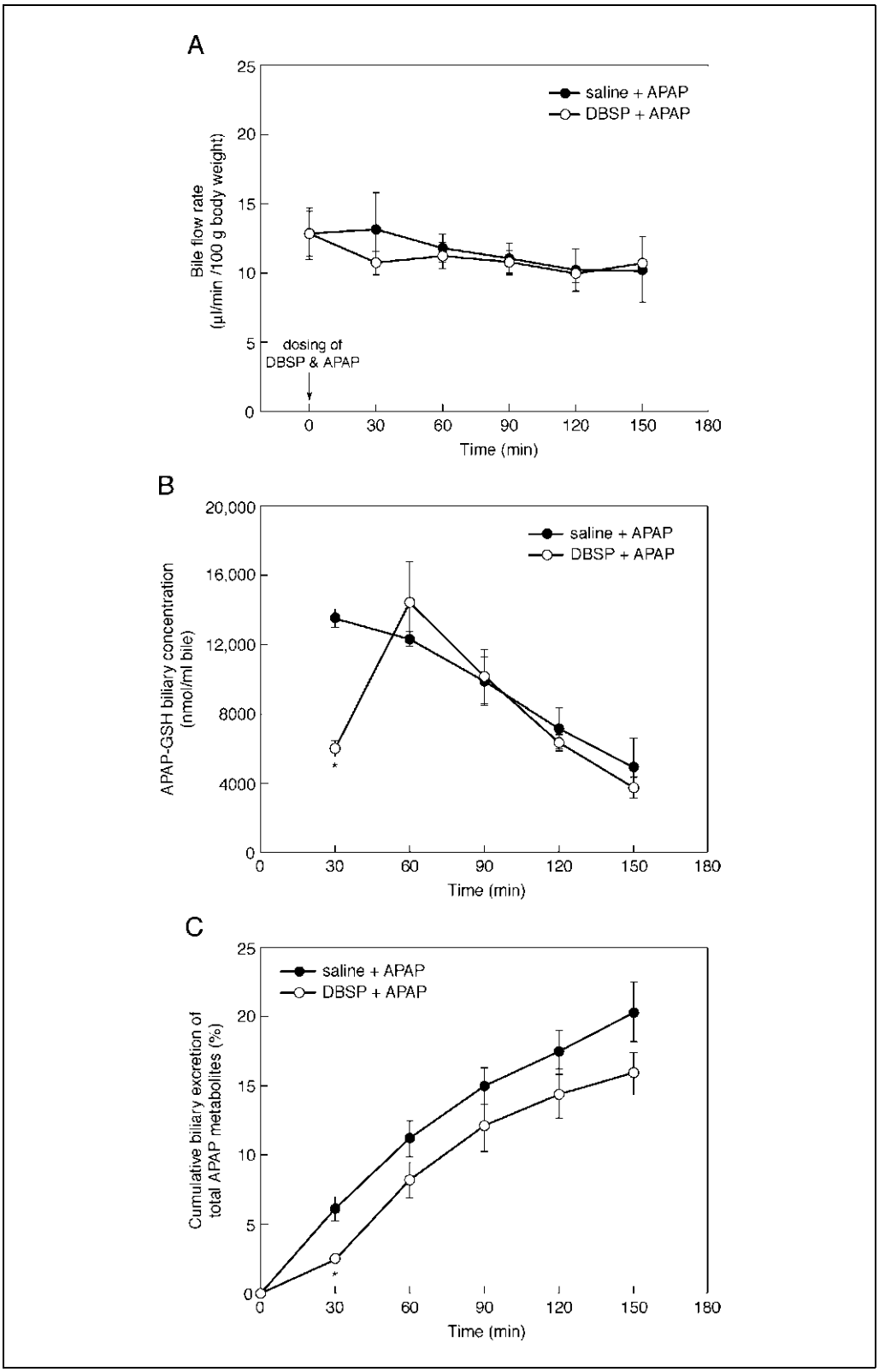

Figure 5.7.2 Effect of the non-metabolizable organic anion dibromosulphothphalein (DBSP) on bile flow rate (**A**); biliary concentration of acetaminophen-glutathione conjugate (APAP-GSH) (**B**); and the cumulative excretion of APAP and its metabolites (**C**). Following overnigt (18 hr) fasting, adult male CD-1 mice were anesthetized and the common bile duct was cannulated. Bile was collected for 15 min before mice received 120 µmol DBSP/kg immediately prior to APAP (1 mmol/kg, i.v.). Controls received saline vehicle before APAP. After APAP dosing, bile was collected for 150 min at 30-min intervals. Results are expressed as means ±SEM for 4 to 5 animals per group. *Significantly different from controls ($p < 0.05$).

from surgery. With this procedure, bile components needed for the processing and absorption of nutrients are not excluded from the small intestine during the recovery period. Proper measures are taken and certain devices are used to prevent rats from chewing on and removeing the bile duct cannula or any other implanted cannulas for collecting fluids delivering drugs. This method claims to minimize some factors that may affect the biliary disposition of xenobiotics and endogenous compounds, including anesthesia and depletion of bile acids. This method also allows for bile sampling over a longer period of time. However, there are some drawbacks associated with this approach. For example, the surgical procedure is far more complex than the non-survival methed used in mice, making it not suitable for investigators with limited surgical expertise. Moreover, it takes much longer to generate hepatobiliary disposition data using this procedure and only a few animals can be done at a time. This approach is less practical in mouse studies due to their more aggressive behavior and the lower likelihood of having a mouse retain an implanted cannula. To the authors' knowledge, biliary disposition studies using freely moving mice have not been documented. Investigators interested in using a freely moving mouse model for hepatobiliary disposition studies may want to contact companies offering surgically modified rodents. Taconic sells mice that are bile duct–cannulated.

Critical Parameters and Troubleshooting

To ensure a steady bile flow, the core body temperature of the mouse should be maintained constant since it is one of the major factors that can affect bile flow. Less bleeding and tissue damage during the operation always lead to longer survival times and fewer complications. Thus, it is recommended to avoid excessive handling of the liver, duodenum, and pancreatic tissue situated around the biliary system while cannulating the bile duct. The level of anesthesia should be closely monitored during the course of this experiment.

Unlike other larger species, rodents do not regurgitate. Therefore, it is not necessary to withhold food prior to surgery to avoid the possibility of aspiring gastric contents into the respiratory system during anesthesia. Some researchers argue that fasting may offer the benefit of limiting individual variability in biotransformation pathways resulting from differences in nutritional status among the experimental animals, while others think that it may promote better absorption of anaesthetics administered intraperitoneally.

These protocols are intended for use in non-survival studies. Thus, it is not necessary to follow aseptic procedures when performing the operation. However, it is appropriate to choose a clean, uncluttered surface in the laboratory as a surgery area.

Anticipated Results

Normally, the range of bile flow rate in bile duct–cannulated mice is between 7 and 14 μl/min/100 g body weight. Bile flow is higher at the beginning of sample collection, decreasing gradually as time progresses (Fig. 5.7.2). This drop in bile flow results from the net loss of biliary constituents via the cannula (e.g., bile salts). Bile salt secretion is a major driving force of bile flow. Some investigators prefer to maintain a more constant bile flow rate throughout the experiment by infusing a bile salt such as tauroursodeoxycholic acid (4 mM in physiological saline at a flow rate of 3 ml/hr). The survival rate for bile duct–cannulated mice generally decreases as the duration of experiment increases. Bile duct–cannulated mice are generally viable for 2 to 3 hr under anesthesia if surgery is done properly.

Time Considerations

In general, the time needed for performing the protocols described greatly depends on the skills of individual investigators and duration/intervals for sample collection. To anesthetize a mouse, it requires ~5 min. It takes ~10 to 15 min for a skilled researcher to cannulate the bile duct of a mouse. Dosing via tail vein injection requires <1 min. The procedure for emptying and withdrawing the content of the urinary bladder requires <5 min.

Literature Cited

Iwaki, T., Yamashita, H., and Hayakawa, T. 2001. A Color Atlas of Sectional Anatomy of the Mouse. Braintree Scientific, Inc. Braintree, Mass.

Kanz, M.F., Whitehead, R.F., Freguson, A.E., Kaphalia, L., and Moslen, M.T. 1992. Biliary function studies during multiple time periods in freely moving rats. A useful system and set of marker solutes. *J. Pharmacol. Toxicol. Methods* 27:7-15.

Contributed by José E. Manautou and Chuan Chen
University of Connecticut
Storrs, Connecticut

CHAPTER 6
The Glutathione Pathway

INTRODUCTION

The tripeptide glutathione (GSH) is nearly ubiquitous in cells and has been shown to participate in a multitude of cellular functions (Kosower and Kosower, 1978; Reed and Fariss, 1984; Reed, 1990; Anderson, 1998). Although many of these functions are associated with protection against reactive intermediates, including free radicals and electrophiles, maintenance of a suitable thiol redox balance with low-molecular-weight and protein thiols is also crucial for cellular homeostasis. GSH functions include the glutathione redox cycle involving glutathione peroxidase (*UNIT 7.1*) and reductase (*UNIT 7.2*); electrophile conjugation reactions via the enzymatic activities of many glutathione transferases (*UNIT 6.4*); and a role in protein synthesis, folding, activation, and inhibition. GSH synthesis (*UNIT 6.5*), transport (*UNIT 6.3*), breakdown, and turnover are vital events in cellular existence. Many methods have been developed and many studies conducted to examine the effects of GSH depletion, inhibition of GSH synthesis, and overall GSH metabolism. Recent reports have renewed interest in the role of mitochondria in many cellular processes, including apoptosis. Thus, measurement of mitochondrial GSH (*UNIT 6.2*) and events associated with mitochondrial GSH metabolism are of current interest. These features of GSH are discussed in *UNIT 6.1*, which provides an overview of GSH function and metabolism.

Measurement of GSH and glutathione disulfide (GSSG) is described in *UNIT 6.2*. The focus is on four major methods that permit precise, sensitive measurement of these to species in both cytoplasm and mitochondria. In one approach, treatment of samples with iodoacetic acid to derivatize the thiols present is followed by a second derivatization of amino groups with Sanger's reagent (1-fluoro-2,4-dinitrobenzene) and separation of the products by HPLC. The derivatives can then be detected based on their UV absorption. This procedures measures GSH, cysteine, and several disulfides and mixed disulfides, including glutathione-cysteine mixed disulfide, with subnanomole sensitivity. If picomole sensitivity is required, it can be achieved through substitution of dansyl chloride for Sanger's reagent followed by separation of the products under almost identical HPLC conditions and then fluorescence detection (the tradeoff is that successful performance of this procedure is more difficult than when Sanger's reagent is used). Alternatively, HPLC combined with electrochemical detection can be used for rapid measurement of GSH and GSSG, also with picomole level of sensitivity. Also described is an enzymatic method for measuring GSH and GSSG that involves spectrophotometric detection and provides subnanomole sensitivity.

Transport of GSH is essential to its cellular functions. Since mitochondria are unable to synthesize GSH, its high concentration within the organelles must result from transport processes that favor higher levels of mitochondrial than cytosolic GSH. Techniques for measuring GSH uptake by various cell types and by mitochondria are described in *UNIT 6.3*. Also included are methods for measuring intracellular and mitochondrial matrix volumes, a prerequisite for accurate interpretation of results.

Conjugation of glutathione with a wide variety of electrophiles is catalyzed by glutathione transferases (Hayes and Pulford, 1995). In *UNIT 6.4*, nomenclature describing the transferases is defined, along with the experimental conditions for utilizing a host of electrophile substrates that aid in characterizing the glutathione transferases being measured.

Contributed by Donald J. Reed
Current Protocols in Toxicology (2002) 6.0.1-6.0.3

Also detailed are a continuous spectrophotometric assay for glutathione transferase activity and a noncontinuous colorimetric assay in which activity is assessed at a series of separate time points.

Biosynthesis of glutathione occurs in the cytosol of virtually all cells and involves a two-step process, both steps of which are ATP dependent. In *UNIT 6.5*, HPLC-based fluorescence assays for the two enzymes of glutathione biosynthesis are described; detection in each case is by fluorescence detection of thiol products (previously derivatized with monobromobimane). The first enzyme, glutamate cysteine ligase, requires a substrate, cysteine, that is easily air-oxidized in the presence of transition metals. Thus, the assay is highly dependent upon strict adherence to the described protocol. γ-glutamyl cysteine, a substrate for the second enzyme, glutathione synthase, is even more prone to air oxidation. Successful measurement of these enzymes requires good laboratory techniques in handling substrates that are easily oxidized to products that do not serve as substrates and, if oxidized, will hamper the measurements. GSH, the final product, is also easily oxidized, to GSSG, and if this happens will not be measured, because GSSG is not detectable by the monobromobimane/HPLC procedure.

In mammals, glutathione is maintained at a high intracellular concentration (0.5 to 6 mM) and a very low extracellular concentration (0.25 to 50 μM), with a half-life in blood of 1 to 2 min. Although intracellular enzymes that catalyze the oxidation and conjugation of glutathione exist, there is a lack of any significant level of intracellular enzyme activity to degrade glutathione. A single enzyme, γ-glutamyl transpeptidase (EC 2.3.2.2) is known to initiate extracellular degradation of glutathione; the activity is located mainly in the brush border of the kidney with lesser activity in other organs and tissues. Production of glutathione by the liver, secretion mainly into the blood, and extracellular degradation are the basis for considering glutathione a physiological reservoir for cysteine. Cysteine provided in this manner is then available for uptake by various cells in the body for glutathione synthesis. Measurement of γ-glutamyl transpeptidase activity (*UNIT 6.6*) is described for a spectrophotometric assay that utilizes the transferase activity of this enzyme with γ-glutamyl-*p*-nitroanilide as the substrate and glycylglycine as the donor and acceptor substrate, respectively. The Alternate Protocol describes an assay using γ-glutamyl-3-carboxy-4-nitroanilide, which has a greater solubility than γ-glutamyl-*p*-nitroanilide.

Protocols are presented that demonstrate induction of a glutathione biosynthetic enzyme, γ-glutamylcysteine synthetase (γ-glutamate cysteine ligase, GCS, EC 6.3.2.2), a glutathione degrading enzyme, and gamma-glutamyl transpeptidase (GGT, EC 2.3.3.3) in response to oxidants (*UNIT 6.7*). Methods are described that detail the methods that can provide evidence for increased mRNA and protein content. Transcriptional (nuclear run-on analysis) and/or postranscriptional (i.e., stability of mRNA) regulation can be determined. There is also an assay for measuring GGT activity. The techniques described in *UNIT 6.7* can be used in other studies that involve induction of gene expression.

An important component in elucidating the biological significance of specific reactive products of xenobiotic bioactivation is the identification and quantitation of glutathione conjugates. *UNIT 6.8* describes, in careful detail, the measurement of glutathione conjugates. The Basic Protocol covers the use of HPLC in the measurement of glutathione conjugates, with Alternate Protocols on the radiometric assay of glutathione conjugate formation and a spectrophotometric assay for glutathione *S*-transferases. Four Support Protocols in *UNIT 6.8* provide reagents and methodology for microsomal incubations, preparation of microsomal and cytosolic fractions, purification for glutathione *S* transferases and preparative separation and isolation of glutathione conjugates for characterization by mass spectrometry and proton NMR spectroscopy.

The measurement of oxidative stress events, including changes in cellular thiol redox status, continue to demonstrate the many roles of mitochondria. Because a majority of cellular coenzyme A is found in mitochondria, the authors of *UNIT 6.9* have utilized the redox status of coenzyme A and glutathione to measure mitochondrial oxidative stress. Procedures detailed in *UNIT 6.9* provide a protocol for coenzyme A and coenzyme A-glutathione mixed disulfide determination by HPLC. To limit oxidation, reduction and thiol-disulfide exchange reactions, tissues that have been frozen in liquid nitrogen are treated with the thiol derivatizing agent, N-ethylmaleimide (NEM) as the frozen tissues are homogenized and acidified. The mixed disulfide of coenzyme A and glutathione (CoASSG) and the NEM adduct of coenzyme A (CoAS-NEM) are quantified by their 254 nm absorption during HPLC.

LITERATURE CITED

Anderson, M.E. 1998. Glutathione: An overview of biosynthesis and modulation. *Chem. Bio. Interact.* 111-112:1-24.

Hayes, J.D. and Pulford, D.J. 1995. The glutathione *S*-transferase supergene family: Regulation of GSG and the contributions of the isoenzymes to cancer chemoprotection and drug resistance. *Crit. Rev. Biochem. Mol. Biol*. 30:445-600.

Kosower, N.S. and Kosower, E. 1978. Glutathione status of cells. *Int. Rev. Cytol*. 54:109-160.

Reed, D.J. and Fariss, M.W. 1984. Glutathione depletion and susceptibility. *Pharmacol. Rev.* 36:25S-33S.

Reed, D.J. 1990. Glutathione: Toxicological implications. *Ann. Rev. Pharmacol. Toxicol*. 30:603-631.

Taniguchi, N. and Ikeda, Y. 1998. γ-Glutamyl transpeptidase: Catalytic mechanism and gene expression. *Adv. Enzymol. Relat. Areas. Mol. Biol.* 72:239-278.

Donald J. Reed

Overview of Glutathione Function and Metabolism

From the time of its discovery in 1888 by De-Rey-Pailhade (De-Rey-Pailhade, 1888a,b), glutathione (GSH) has remained of major interest for researchers in the fields of toxicology, biochemistry, molecular cell biology, and immunology. Although pathways of synthesis and breakdown have been established, transport, uptake, and some metabolic functions remain uncertain. GSH has been shown to be a major key player in reduction processes by maintaining thiol groups of intracellular proteins; by providing reducing power for cysteine, dihydrolipoate, coenzyme A, ascorbate, and vitamin E; and as a factor in the reduction of NTPs into dNTPs. GSH is involved in detoxification of endogenous and exogenous compounds, participates in synthesis of leukotrienes and prostaglandins, serves as a cofactor of various enzymes, stores and transports cysteine, and may even be involved in cell cycle regulation and thermotolerance.

Although GSH was seen for many years as a preventive molecule against results from biotransformations of xenobiotics and normal oxidative products of cellular metabolism, it is now also known to play a role in bioactivation of certain molecules, particularly several halogenated compounds.

GSH is a tripeptide with the sequence γ-Glu-Cys-Gly (Fig. 6.1.1). The disulfide derived from two GSH molecules, by oxidation of the thiol groups of each cysteine moiety, is denoted glutathione disulfide (GSSG). GSH has one peptide bond, one amide bond that is resistant to proteases, two carboxyl groups, one amino group, and one thiol group. The high number of hydrophilic groups and low molecular weight make GSH and GSSG water soluble. GSH shows two quite distinct features: it is protected from hydrolytic cleavage by regular proteases through its γ-glutamyl amide bond, and it has a high reduction potential (E^{01} = –0.33 V) due to the abundance of cysteine. Thiols are very reactive towards free radicals, donating hydrogen atoms to most carbon-, oxygen-, and nitrogen-centered radicals.

GSH is typically present at millimolar concentrations in the cell (0.5 to 10 mM) and is the most abundant low-molecular-weight peptide. Concentrations in mammalian liver are 4 to 8 mM, with nearly all glutathione present as reduced GSH, and <5% present as GSSG. Minor fractions include mixed disulfides of GSH and other cellular thiols, and minor amounts of thioethers from endogenous conjugation reactions. In most cells GSH accounts for >90% of the total nonprotein thiols. Intracellular GSH levels are tightly regulated by a complex mechanism involving control of synthesis, transport, and utilization. GSH must be regarded as an essential cellular component, as prolonged failure to maintain adequate intracellular supply is detrimental to the cell.

This overview focuses on the function, synthesis, turnover, transport, and breakdown of GSH. It also provides the reader with information on manipulation of GSH content and the importance of mitochondrial GSH. Each section emphasizes main events while providing the reader with additional references for further in-depth information.

GLUTATHIONE FUNCTION

It is widely accepted that the two major functions of GSH are (1) as a substrate for GSH peroxidase–mediated reduction of oxygen free

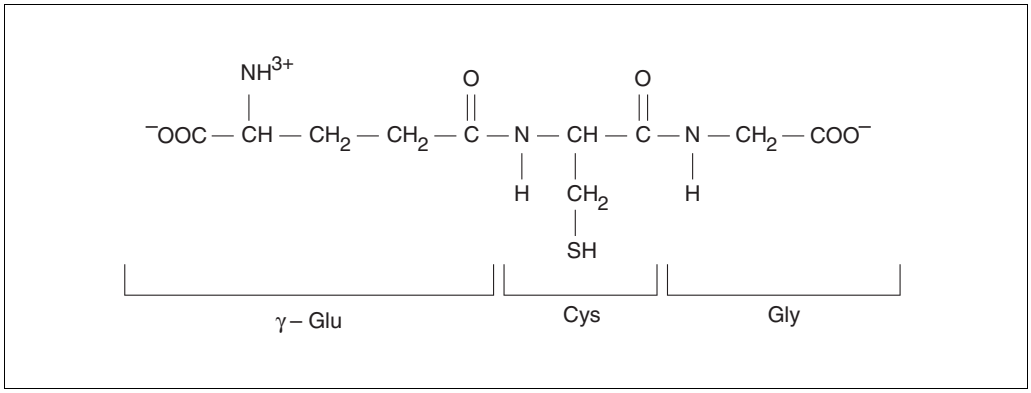

Figure 6.1.1 Structure of reduced glutathione (GSH).

Contributed by Yvonne Will
Current Protocols in Toxicology (1999) 6.1.1-6.1.18

radicals, formed naturally (as the consequence of aerobic metabolism) or through metabolism of foreign compounds that are known to cycle through oxidized/reduced states; and (2) for biotransformation of exogenous compounds catalyzed by glutathione-*S*-transferases (GSTs). Oxidative stress is defined as the imbalance between the production and detoxification of oxygen free radicals, and can be of exogenous or endogenous origin. Exogenous stress can be caused by pollutants, pesticides, drugs, and ionizing radiation. Endogenous oxidative stress results primarily from mitochondrial electron transport, but also from stimulated phagocytic cells undergoing oxidative burst, ischemia-reperfusion, inhibition of antioxidant enzymes, or induction of prooxidant enzymes. Oxidative stress can cause oxidation of cellular constituents, such as GSH protein thiols, and peroxidation of lipids. If oxygen is incompletely reduced, superoxide ($O_2^{\cdot -}$), hydrogen peroxide (H_2O_2), singlet oxygen ($^1O_2^-$), and hydroxyl radicals (HO^-) are produced. Superoxide radicals can undergo disproportionation to hydrogen peroxide and oxygen either enzymatically (with superoxide dismutase) or nonenzymatically. If hydrogen peroxide is not detoxified it will form hydroxyl radicals by the iron-catalized Haber Weiss reaction

$$Fe^{3+} + O_2^{\cdot -} + H_2O_2 \rightarrow O_2 + HO^- + HO^{\bullet} + Fe^{2+}$$

or the Fenton reaction

$$Fe^{2+} + H_2O_2 \rightarrow Fe^{3+} + HO^{\bullet} + OH^-$$

Hydroxyl radicals are highly reactive and can initiate lipid peroxidation of biological membranes. Several enzymes are involved in protecting the cell and its constituents against oxidative damage including GSH reductase, GSH peroxidase, and GSH transferases.

Glutathione Redox Cycle

The major protective system against naturally occurring reactive oxygen species is the glutathione redox cycle, which consists of GSH peroxidase, GSH reductase, and a source of NADPH. The cycle uses NADPH and indirectly NADH reducing equivalents in the mitochondrial matrix as well as in the cytoplasm to provide a recycling supply for GSH by the GSH reductase–catalyzed reduction of GSSG. In the liver, NADPH reducing equivalents are provided mainly by isocitrate dehydrogenase and to lesser degree by glucose-6-phosphate dehydrogenase, 6-phosphogluconate dehydrogenase, and malic enzyme.

GSH peroxidase, a selenium-dependent enzyme that is extemely specific for GSH, reduces hydrogen peroxide and hydroperoxides to the corresponding water or alcohol, thereby oxidizing GSH to GSSG (*UNIT 7.1*). GSH reductase plays a central role in the biochemistry of GSH, as it is responsible for keeping GSH in its reduced state, thereby maintaining an adequate GSH/GSSG ratio. The reaction occurs in two steps. The first is the reduction of GSH reductase by NADPH. Electrons are channeled through the enzyme via FAD and subsequently through a redox-active protein disulfide bond to GSSG. GSH reductase is inactivated upon reduction by its own electron donor, NADPH, and is reactivated by GSSG. GSH reductase, of all NADPH-dependent enzymes, can have the highest rate of NADPH consumption in the liver. NADPH is also consumed by fatty acid synthesis and mixed-function oxidases. At times when the glutathione redox cycle is functioning at high capacity, mixed-function oxidase activity (a major regulator of fatty acid synthesis) and other NADPH cytochrome reductase activities can be expected (Reed, 1986).

The GSH redox cycle is also involved in the detoxification of reactive drug intermediates, which are generated by bioreduction and cause oxidative stress by redox cycling. Diquat, a hepatotoxic herbicide, is an excellent example of a redox cycling compound. Using molecular oxygen in a one-electron reduction, it generates large amounts of superoxide anion radical and hydrogen peroxide within the cell. That the protective role of GSH is mediated through the GSH redox cycle was proven through the inhibition of GSH reductase by 1,3-bis-(2-chloroethyl)-1-nitrosourea (BCNU), which increases the toxicity of redox cycling compounds, including adriamycin (Babson and Reed, 1978).

Glutathione-*S*-Transferases

GSTs are a family of isoenzymes that conjugate GSH with electrophilic compounds. For many years it was believed that these reactions only served in the detoxification of xenobiotics—e.g., drugs, certain environmental pollutants, pesticides, herbicides, and carcinogens. Today we know that GSTs play a role in bioactivation of dihalomethanes and dihaloalkenes and are discussed with respect to drug resistance in cancer therapy. GSTs also have physiological catalytic functions—the isomerization of 3-ketosteroids and biosynthesis of leukotriene A4 and eicosanoids. GSTs that have peroxidase

activity are believed to play a role in preventing oxidative stress. In vitro experiments showed that GSTs can reduce fatty acid and DNA hydroperoxides: they can catalyze a Michael addition to unsaturated ketones resulting from the metabolism of dietary lipid peroxides or decomposition of fatty acid hydroperoxides. Other GST-dependent reactions have been observed in inflammation caused by the respiratory burst of immune cells. Because of their abundance (up to 10% of cytosolic protein in liver) as well as their binding properties, it has been suggested that GSTs are involved in storage and transport of hormones, metabolites, drugs, and other hydrophobic nonsubstrates (Listowsky, 1993).

GSTs are present as soluble and membrane-bound forms. GST activity is present in different subcellular fractions of most tissues and blood cells of the mammalian organism. There are four species-independent classes of cytosolic GSTs—alpha, mu, pi, and theta—and one class of microsomal GSTs. GSTs are expressed to different extents both qualitatively and quantitatively in different tissues, which suggests different susceptibility of tissues to certain xenobiotics.

Cytosolic GSTs are dimeric proteins composed of two identical or nonidentical subunits (Mannervik and Danielsson, 1988). Classes pi and theta contain homodimers, while classes alpha and mu are more complex and display multiplicity of homodimeric and heterodimeric isoenzyme forms. The subunits have a catalytic center with two binding sites: a highly specific GSH binding site (G-site) and a hydrophobic site (H-site) where acceptor substrates can be accommodated. The H-site exhibits low specificity.

Microsomal GSTs can account for as much as 3% of endoplasmic reticulum protein (Morgenstern and DePierre, 1983). It has been suggested that microsomal GSTs are involved in protection against lipid peroxidation because they have been shown to reduce fatty acid hydroperoxides (Haenen and Bast, 1983).

GSTs have not only been found in the cytosol but also in the mitochondrion, nucleus, and nucleolus. In mitochondria, a class theta GST was isolated from the matrix by Harris et al. (1991) and a class alpha by Addya et al. (1994). A transferase similar to the microsomal transferase was identified in the outer mitochondrial membrane (Nishino and Ito, 1990). Tirmenstein and Reed (1988) showed a GSH-dependent peroxidase in rat liver nuclear membranes capable of inhibiting lipid peroxidation. Because the nuclear membrane regulates transport of mRNA into the cytoplasm and aids in the process of nuclear division, protection from oxidative damage is extremely important. It is also known that DNA itself is associated with certain regions of the nuclear membrane (Tirmenstein and Reed, 1988).

In detoxification reactions, GSTs catalyze the initial reaction in the biosynthesis of mercapturic acids. The conjugates need to be transferred to the membrane-bound catabolic enzymes. More than fifteen enzyme systems are known to be involved in the formation and disposition of GSH conjugates (Commandeur et al., 1995). The first step in the catabolism of GSH conjugates is the removal of the γ-glutamyl moiety by hydrolysis or by transfer to an appropriate acceptor. This initial step is catalyzed by γ-glutamyl transpeptidase (GGT) and results in the formation of the corresponding cysteine-*S* conjugate that can subsequently be taken up by the cell for further metabolism.

Enzymes involved in the biotransformation of GSH conjugates are distributed throughout the body. As accumulation of GSH conjugates leads to inhibition of GSTs as well as GSH reductase, disposal is of absolute necessity. Transport is carried out by at least three different systems: (1) an ATP-dependent GS-X pump with broad substrate specificity that has been shown to exist in different organs and cell types; (2) a Na^+-dependent system demonstrated in basolateral membranes in the kidney and intestine; and (3) a Na^+-independent system that is probably membrane potential dependent. This latter system has been demonstrated in brush border membranes of intestinal cells and canalicular and sinosoidal membranes of liver cells. Catabolites of GSH conjugates are believed to be transported by carriers that transport amino acids and dipeptides (McGivan and Pastor-Anglada, 1994).

As the liver is the main organ for biosynthesis and disposition, hepatic transport is described in more depth. In order for GSH conjugates to be degraded by GGT (which is located in the bile canalicular membrane of the hepatocyte, the luminal membrane of the biliary epithelium, and the small intestine epithelium), conjugates have to be extruded from the hepatocyte. Extrahepatically formed conjugates can reach the liver via the blood and can be taken up by liver cells. Excretion can occur either across the canalicular or the sinusoidal membrane. GSH conjugates are preferentially excreted into the bile by the ATP-dependent GS-X pump. This transport system is inhibited competitively by GSSG and

other conjugates, but not by GSH. Transport across the sinusoidal membrane is ATP independent but membrane potential driven, suggesting that this system is the sinusoidal GSH transporter. This transport is inhibited at physiological concentrations of GSH and seems only to be of importance at high GSH conjugate concentrations, when biliary transport is saturated.

Once GSH conjugates are transported into the bile they are exposed to GGT and dipeptidases. After hydrolysis, the cysteine-*S* conjugate may be reabsorbed and acetylated within the hepatocyte to form mercapturic acids (Hinchman et al., 1991). The activity of GGT and dipeptidases, as well as the activity of reuptake transporters, determine the extent to which conjugates will be excreted. Mercapturic acids can be excreted into the bile or into the blood, depending on their molecular weight and physicochemical properties. Conjugates excreted into the blood are delivered to the kidney, while conjugates excreted into the bile must first be reabsorbed from the small intestine. For details on intestinal transport mechanisms, see Hagen and Jones (1987). In the kidney, conjugates enter the renal cells via the brush border membrane. For details on transport mechanisms, see Lash and Jones (1984).

GSTs participate in bioactivation of xenobiotics by (1) forming direct-acting GSH conjugates, (2) functioning as a transporter molecule that releases reversibly bound electrophiles at target tissues, (3) forming GSH conjugates that are bioactivated by subsequent metabolism of the GSH moiety, and (4) performing reductive bioactivation mechanisms (Commandeur et al., 1995).

An example for direct-acting GSH conjugates is the bioactivation of haloalkanes and haloalkenes. GSH conjugates form as the initial step, but are unstable and give rise to toxic metabolites. With dihalomethanes (e.g., dichloromethane), formaldehyde is formed. Dihalomethane has been shown to be tumorigenic in mice. There is evidence for DNA damage in mouse hepatocytes. Vicinal dihaloalkenes (e.g., 1,2-dichloroethane, 1,2-dibromoethane) have been shown to be mutagenic and tumorigenic. Their bioactivation leads to the formation of half-sulfur mustards that can undergo an intramolecular cyclization to give a highly reactive episulfonium ion, which may react with cellular nucleophiles.

Examples for GSH as a transporter of reversibly bound electrophiles are conjugation of isocyanates, isothiocyanates, alpha- and beta-unsaturated aldehydes, and aldehydes. These compounds form labile GSH conjugates that may again dissociate to the parent electrophile and GSH. The electrophile can then react with endogenous nucleophiles to form more thermodynamically favored adducts.

Glutathione in Protein Synthesis, Folding, Activation, and Inhibition

The activity of a variety of enzymes is known to be influenced by the GSH/GSSG ratio. Although much attention has been paid to the effect of decreased intracellular concentrations of GSH, little attention has been given to GSSG and how alterations in GSSG levels may alter cellular functions. The following discussion focuses on how GSSG is involved in synthesis, folding, and activation/inactivation of important cellular proteins.

Concentrations of GSSG reported for a variety of tissues range between 4 and 50 μM (Tietze, 1969). Kosower and Kosower (1974) reported that slight increases in GSSG concentration, even in the presence of large amounts of GSH, had effects of potential physiological relevance. These authors showed that 75 μM GSSG in the presence of 1 mM GSH shut off protein synthesis in a lysate of rabbit red blood cells. They hypothesized that GSSG had an effect on an initiation factor that is converted into a GSSG-reactive form when bound to a protein-synthesizing system.

Ruoppolo et al. (1996) studied refolding of RNase by oxidation and disulfide isomerization. The rate-limiting step for folding of disulfide-containing proteins in the endoplasmic reticulum is the formation of native disulfide bonds. The major thiol redox system in the endoplasmic reticulum is provided by GSH. The authors conclude from their studies that refolding occurs in two steps: the formation of a mixed disulfide with GSH, and the internal attack of a free SH group to form an intramolecular disulfide bond. The authors strongly believe that GSS-proteins are important folding intermediates, as shown in refolding studies of RNase A (Torella et al., 1994) and bovine pancreatic trypsin inhibitor (Weissman and Kim, 1995).

GSSG was also shown to have a direct effect on protein function by forming mixed disulfides in the active center of the enzymes, thereby either activating or inactivating the protein. Hexokinase (Eldjarn and Bremer, 1962), pyruvate kinase (Van Berkel et al., 1973), glycogen synthetase D (Ernest and Kim, 1973, 1974), adenylate cyclase (Baba et al., 1978), ribonucleotide reductase (Holmgren, 1978, 1979),

phosphorylase phosphatase (Shimazu et al., 1978; Usami et al., 1980), collagenase (Tscheche and McCartney, 1981), and 3-hydroxy-3-methylglutaryl coenzyme A reductase (HMGR; Cappel and Gilbert, 1993) have all been shown to be inactivated by GSSG, while δ-aminolevulinate synthetase (Tuboi and Hayasaka, 1972) and SoxR (Ding and Demple, 1996) have been shown to be activated by GSSG.

Van Berkel et al. (1973) studied pyruvate kinase and found two forms that have different kinetic properties and can be interconverted by oxidation/reduction of a sulfhydryl group. GSH was shown to reduce pyruvate kinase, but the kinetics were different when 2-mercaptoethanol was used. The in vitro process was very slow (6 hr for oxidation, 1 hr for reduction). The author therefore can only speculate about the in vivo existence of such a mechanism.

Ernest and Kim (1973, 1974) performed work on glycogen synthetase D. Inactivation of the enzyme was associated with the formation of a mixed disulfide between sulfhydryl groups in the enzyme by the action of GSSG. The authors found that eight sulfhydryl groups exist per subunit. Reaction of GSSG with any four lead to inactivation and dissociation of the enzyme into its subunits.

Baba et al. (1978) performed in vitro studies that showed that adenylate cyclase activity was strongly inhibited by GSSG and was reactivated upon incubation with sulfhydryl compounds including GSH. The inactivation was believed to occur through oxidation of sulfhydryl groups in the enzyme. This hypothesis was supported by the authors' finding of an increased amount of GSS-protein when adenylate cyclase was incubated with GSSG. However, questions remain about the physiological significance of this mechanism. The authors speculate by referring to Isaacs and Binkley (1977), who proposed that formation of Pro-SSG may be a mechanism for maintenance of a disulfide/sulfhydryl ratio to maintain the integrity of membranes in times of oxidative or reductive stress.

Phosphorylase phosphatase was studied by Shimazu et al. (1978) and Usami et al. (1980). GSSG was shown to inactivate the enzyme by forming a mixed disulfide with one of the two sulfhydryl groups contained in the catalytic subunit.

Tscheche and McCartney (1981) found that human polymorphonuclear collagenase could be activated by disulfide thiol exchange brought about by cysteine, GSSG, insulin, and various proteins containing accessible peripheral disulfide bonds. The activation of collagenase involves the release of an inhibitor by an oxidative process that will reform an intramolecular disulfide bond.

Cappel and Gilbert (1993) performed studies that investigated the effect of GSH/GSSG redox status on inactivation and subunit cross-linking of HMGR. The authors report that different dithiol pairs are responsible for inactivation and cross-linking. The fact that Ness et al. (1985) found cross-linked HMGR in microsome preparations when dithiothreitol was excluded in the isolation procedure gave support for the hypothesis that HMGR activity may be regulated by diurnal variations in the GSH/GSSG redox state. In vitro loss of activity showed an oxidation rate constant (K_{ox}) of 0.67 ± 0.07, while disulfide cross-linking required a K_{ox} of 0.19 ± 0.02. What does this mean? Assuming a GSH/GSSG ratio of 300 and a GSH concentration of 10 mM (which is the diurnal high for liver), 10% of HMGR would be expected to be cross-linked and 20% to be inactivated. At a diurnal low GSH/GSSG ratio of 100 and a GSH concentration of 6 mM, 25% of the enzyme would be cross-linked and 53% inactivated. The authors conclude that changes in intracellular GSH redox status needs to be added to the list of effectors that regulate the enzyme activity of HMGR.

Tuboi and Hayasaka (1972) performed in vitro studies on δ-aminolevulinate synthetase, which was shown to be activated by GSSG and also even more successfully by cystine. The authors found that a protein was also required for the activation process; this protein remains to be identified.

Ding and Demple (1996) performed work on SoxR, which is a redox-regulated transcription factor involved in defense against oxidative stress by nitric oxide or hydrogen peroxide in *E. coli*. SoxR contains 2Fe-2S clusters that can be effectively disrupted by GSH, leading to the inactivation of SoxR. The authors suggest that GSH-based free radicals are involved in this disassembly process. The same effects were observed with GSH-deficient mutants in vivo.

With the exception of Shimazu et al. (1978), all the experiments described above were carried out in vitro. This leaves the question about in vivo occurrence and relevance unanswered. Shimazu et al. injected GSSG into the portal vein of rabbits and observed a rapid increase in phosphorylase a activity in the liver, which was probably due to inactivation of phosphorylase phosphatase. Sies et al. (1974) observed that increasing GSSG levels, through injection of hydrogen peroxide into perfused liver, caused

extra release of glucose, lactate, and pyruvate. Both groups suggest that the redox state of GSH in the liver may contribute to the regulation of glycogenolysis and glycolysis.

Even though the in vitro work strongly suggests the involvement of the GSH/GSSG ratio in protein function, no further in vivo studies have been documented to date. However, the fact that changes in GSH/GSSG ratio can occur, that GSSG once produced and not immediately reduced is released from the cells at a relatively slow rate, that the amount of Pro-SSG can account for as much as 35% of total glutathione (Modig, 1968), and that the protein SS/SH ratio is not static but capable of circadian variation does not exclude the strong possibility of a regulatory function for GSSG or the GSH/GSSG ratio.

More recent studies have dealt with the effect of GSH and/or the GSH/GSSG ratio on gene expression, where both direct and indirect effects have been described. Liang et al. (1989) report that increasing GSH levels enhance binding, internalization, and degradation of interleukin 2 (IL-2), not by a direct effect on the cysteine residues of IL-2, but probably by an indirect effect on the target cells. Ginn-Pease and Whisler (1996) investigated the effect of GSH on induction of the transcription factor NFκB. NFκB transactivation response to oxidative stress proceeds in two stages. The initial step involves oxidative triggering of early membrane signaling events while the second stage requires the maintenance of a normal reducing state. In other words, optimal induction of NFκB requires a functional GSH system that can respond to oxidative stress and maintain intracellular redox homeostasis.

GLUTATHIONE SYNTHESIS AND TURNOVER

GSH Synthesis

GSH can be synthesized in the cytosol of most mammalian cells through the action of γ-glutamylcysteine synthetase and glutathione synthetase (GS; Fig. 6.1.2). Both reactions are ATP dependent. γ-Glutamylcysteine synthetase is feedback inhibited by GSH. The inhibition is not allosteric but competitive with respect to glutamate. Information on the isolation, properties, and catalytic mechanisms of the two enzymes have been extensively reviewed (Yan and Meister, 1990; Huang et al., 1993).

The rate-limiting step in GSH synthesis is the availability of cysteine (10^{-4} M), because glutamine and glycine are present at higher concentrations (10^{-3} M). Also, high levels of cysteine are known to be toxic to the cell. The liver is the main synthesizer of glutathione and is also unique in that it can synthesize cysteine from the sulfur of methionine and the carbon of serine via the cystathionine pathway (Fig. 6.1.3). This pathway becomes extremely important at times of dietary limitation or when high levels of biosynthesis of glutathione are required (Reed and Orrenius, 1977). Methionine is first converted via *S*-adenosylmethionine by demethylation to homocysteine. Homocysteine condenses with serine in a reaction catalyzed by cystathionine β-synthase to form cystathionine. This thioether does not seem to have any other metabolic function than serving as an intermediate in the cystathionine pathway. Cystathionine is then cleaved to cysteine, ammonia, and α-ketobutyrate by cystathione γ-lyase.

GSH Transport

As mentioned above, most mammalian cells can synthesize GSH. What happens to GSH after synthesis? GSH is not used just for the functions described above, but also has been shown through many studies to be exported. Export of GSH allows the cell to protect its membranes against oxidative or other forms of damage by keeping thiol groups and membrane components (e.g., vitamin E) in their reduced forms. Export of GSH may also provide a way of reducing compounds such as cystine and dehydroascorbate in the immediate environment of the cell membrane, and it may facilitate transport of certain compounds (Meister, 1991). It has been agreed that the export of GSSG

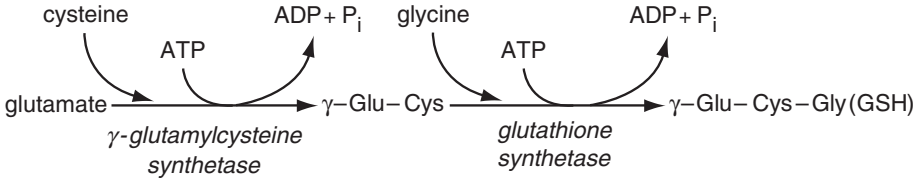

Figure 6.1.2 Synthesis of glutathione.

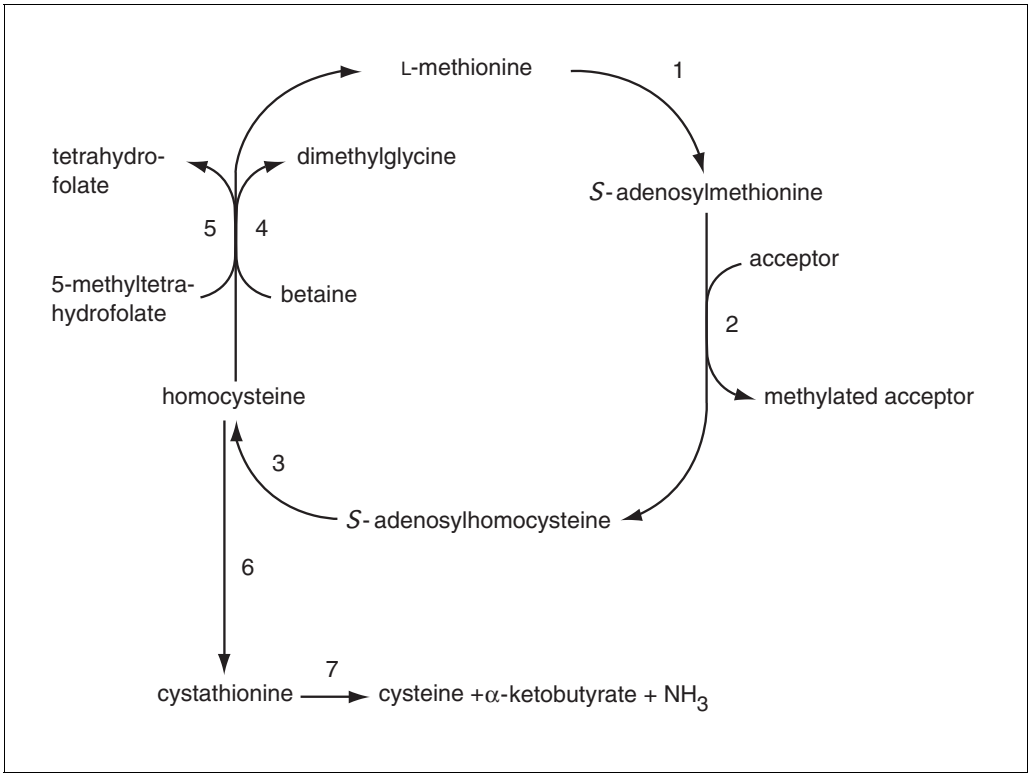

Figure 6.1.3 Cystathione pathway. Enzymes: 1, methionine adenosyltransferase; 2, *S*-adenosylmethionine methyltransferase; 3, adenosylhomocysteinase; 4, betaine-homocysteine *S*-methyltransferase; 5, 5-methyltetrahydrofolate-homocysteine *S*-methyltransferase; 6, cystathionine β-synthase; 7, cystathionine γ-lyase.

serves as a protective mechanism for the cell to eliminate formation of GSH-protein mixed disulfides and assists in the maintenance of thiol redox status or cystine/cysteine status. Export of GSH conjugates is necessary for further disposition.

Export of GSSG and of GSH conjugates seems to require ATP. Little information is available on the mechanism and the specificity of GSH export. There seems to be evidence for a membrane potential–dependent GSH transport by renal brush border membranes, but this process may be different for GSH, GSSG, and GSH conjugates, and the mechanism may also be cell specific. The liver, the main synthesizer of GSH, exports large amounts of GSH into the plasma. GSH is also transported from the liver into the bile, mainly in the form of GSSG.

GSH Breakdown

Plasma GSH derived from the liver can only be utilized by tissues that have considerable amounts of γ-glutamyl transpeptidase (GGT) activity (e.g., kidney, small intestine, and type 2 alveolar cells). Most plasma GSH, however, is transported to the kidney, where it is degraded with a half-life of 1.5 sec. Degradation of GSH begins at the cell surface and requires enzymes located both on the cell surface (GGT) as well as in the cytosol (dipeptidases; Meister and Anderson, 1983). The kidneys take up GSH from the plasma through breakdown of GSH via GGT activity.

GGT is located at the brush border of kidney epithelial cells. GSH, GSSG, and γ-glutamyl GSH react with GGT at the outer surface. The γ-glutamyl moiety is either removed by hydrolysis or transferred to a suitable amino acid acceptor, and both the γ-glutamyl amino acid and the cysteinyl glycine are transported into the cell. Cysteine is necessary in other tissues for GSH synthesis and is also returned to the liver, which closes the GSH cycle. This salvage pathway for glutathione was proven through inhibition of GGT, which raised the plasma glutathione level significantly. GSH accumulated extracellularly and was excreted with the urine. In addition to GSH, cysteine moieties and glutamyl cysteine were excreted with the urine (Reed and Ellis, 1981).

Overall Balance of GSH Turnover

It has been shown in mice that the breakdown of GSH in the kidney accounts for 80% to 90%

of the total GSH turnover (Meister, 1983). GSH efflux occurs even in the absence of GSH synthesis, which has been shown in studies where synthesis of GSH was blocked with buthionine sulfoximine (BSO). The fact that synthesis rate and export rate are very similar strongly suggests that in general there is very little intracellular degradation of GSH in the liver (Meister, 1991). The turnover of glutathione is thus largely accounted for by export of GSH, subsequent degradation by GGT, and return of cysteine moieties to tissues and liver.

GSH Uptake

The question arises if direct uptake of glutathione occurs as well. Studies have been conducted on kidney, liver, brain, and intestine. These experiments are difficult to perform because both synthesis and degradation of GSH must be completely inhibited, but the inhibitor concentrations needed for full inhibition are often toxic to the cell and won't allow kinetic measurements over long periods of time. For these reasons interpretation of results is difficult and has caused controversy about the actual existence of intact GSH uptake. Several studies on different organs and cell types were not able to show uptake of intact GSH at all (Hahn et al., 1978; Dethmers and Meister, 1981; Yoshimura et al., 1982; Tsan et al., 1989). A variety of studies have been conducted on GSH uptake in kidney. It was hypothesized that basolateral transport exists (Ormstadt et al., 1980; McIntyre and Curthoys, 1980); however, detailed studies by Abbott et al. (1984) and Inoue et al. (1986) found that there is little, if any, basolateral uptake.

Hagen and Jones (1989) performed experiments with cell suspensions isolated from kidney, intestine, and lung that showed that cells were protected from *tert*-butylhydroperoxide (TBH), menadione, and paraquat when GSH was added. GSH synthesis and breakdown were inhibited in these studies, but no enzyme activity levels were reported for the time of the experiment to ensure that the enzymes were fully inhibited.

Lash and Torkatz (1990) found that distal renal tubular cells could be protected from oxidative damage by GSH; however, the protection was abolished when BSO and α-amino-3-chloro-4,5-dihydro-5-isoxazoleacetic acid (AT-125 or acivicin) were used to inhibit GSH synthesis and degradation, respectively.

Since 1993, some more convincing studies have been conducted by Kaplowitz and colleagues. In a variety of studies, the authors identified two rat liver GSH transporters and three GSH transport activities in the brain. In the liver, the authors identified a canicular and a sinusoidal transporter, both of which have been cloned (Yi et al., 1994, 1995). Transport was independent of stimulation by ATP, and it was suggested that transport occurs bidirectionally. For more information on the mechanism on these transporters, see Fernandez-Checa et al. (1993) and Lu et al. (1994). Of the three brain GSH transport activities, one corresponded to the Na^+-independent rat canicular GSH transporter, and one was shown to be Na^+-dependent and to exhibit high- and low-affinity GSH transport (Kannan et al., 1996).

Several studies on uptake of intact GSH have been conducted in the intestine. Hunjahn and Evered (1985) and Evered and Wass (1970) used sacs of rat small intestine and reported a Na^+-independent uptake of GSH that was inhibited by triglycine and glycyl-L-leucine. This transport showed properties of carrier-mediated diffusion. Hagen and Jones (1987) showed Na^+-dependent GSH transport with in situ closed-loop vascular perfusion systems. Na^+-independent GSH transport was also shown in brush border membrane vesicles of rabbit small intestine where GGT was inhibited with acivicin (Vincencini et al., 1988).

Studies on the uptake of orally administered GSH have been contradictory. Yoshimura et al. (1982) and Martenson et al. (1990) did not find any uptake of GSH into blood plasma. In contrast, Jones and co-workers (Aw et al., 1991) administered 100 mg/kg GSH to mice and measured plasma GSH levels after 30 min and 1 hr. Plasma GSH levels increased 2.5-fold (from 30 to 75 μM) in the first 30 min and decreased back to 50 μM after 1 hr. This was in agreement with previous studies where increases in plasma GSH were observed in rats and humans after oral administration (Hagen et al., 1988). No increase in tissue GSH was found, with the exception of lung tissue. In the same study (Aw et al., 1991) the authors administered GSH to animals that were depleted in GSH by a 5-day treatment with BSO. In this study a significant increase in tissue GSH was observed in kidney, heart, lung, brain, small intestine, and skin, but not in liver. An interesting observation was the fact that brain and small intestinal GSH levels returned to control levels while the other tissues did not. The lack of an increase in liver tissue GSH level was explained by the fact that liver is the main supplier of plasma GSH and unable to take up exogenous GSH. The differences in uptake rates in the other tissues are not clear, but may be

explained by tissue-specific differences in turnover and uptake. No increase was observed when precursors of GSH (cysteine, glycine, glutamine) were administered, which suggests that uptake of intact GSH may contribute to tissue GSH levels independent of synthesis. The authors discuss four possibilities for actual GSH transport: uptake (1) through the action of transglutaminase, (2) through the action of GGT, (3) through reaction with electrophilic compounds, or (4) as a mixed disulfide with cysteine or plasma proteins like albumin. Despite the question about the uptake mechansims involved, oral administration of GSH may have a beneficial effect under pathological conditions where endogenous GSH levels are significantly decreased (Aw et al., 1991).

Intraperitoneally administered GSH did not show significant increases in the jejunal or colon mucosa. Oral administration of GSH led to an increase of mucosal GSH in colon, jejunum, and stomach (Martenson et al., 1990), but it cannot be excluded that cleavage of GSH or transpeptidation occurred with subsequent resynthesis. Plasma GSH can be increased to millimolar concentrations through intraperitoneal injection of GSH. However, this plasma increase did not significantly increase tissue GSH levels, which shows that plasma GSH is not rapidly taken up by cells.

Although the need for export of GSH is obvious and explainable, the need for uptake of GSH under normal conditions is questionable. It seems that under normal conditions degradation by GGT and subsequent resynthesis are the main route for GSH turnover. The question arises as to whether direct uptake may only exist under pathological conditions where degradation or resynthesis are diminished, or under oxidative stress when cells are not able to fully regenerate GSH from GSSG. Lash and coworkers (Visarius et al., 1996) reinvestigated the question of uptake in renal cells. Renal cellular handling of GSH involves three processes: membrane transport, oxidation, and degradation. Lash showed that renal proximal tubule cells treated with TBH were able to transport GSH across the basolateral plasma membrane, thereby increasing intracellular GSH. However, this uptake was extremely low (<6%) in the absence of acivicin and BSO, and oxidation and degradation were the main route for GSH turnover. When this route was inhibited, uptake of GSH became quite important and accounted for 30% of external GSH loss. Lash concluded that under normal conditions degradation and resynthesis are the major route for GSH turnover. Under pathological conditions (e.g., oxidative stress), cells are not able to fully regenerate GSH from GSSG and have negligible capacity to resynthesize GSH from precursor amino acids. Therefore, uptake of intact GSH may be necessary for the cell in order to maintain its GSH homeostasis (Visarius et al., 1996).

MANIPULATION OF GLUTATHIONE CONTENT

The amount of glutathione can be manipulated by depletion of GSH, through inhibition of key enzymes in the glutathione cycle or through administration of precursors of glutathione. It has been possible to manipulate glutathione levels between 10% and 150% of control levels.

Depletion of Glutathione

One of the most commonly used depleting agents is diethyl maleate (DEM), which was first introduced by Boyland and Chasseaud (1969a,b). DEM is a weak electrophile that reacts with GSH in the presence of GSH transferases. Intraperitoneal injection of DEM (0.6 to 1.0 ml/kg) reduced liver GSH to 6% to 20% of control levels for a period of up to 4 hr. However, the rate of synthesis is increased, which causes an increase in GSH to twice control levels in 24 hr. After that time GSH levels return to control values. Erythrocyte, kidney, lung, and brain GSH amounts are decreased as well, but to a significantly lesser amount than liver GSH. DEM shows a variety of side effects that suggest caution for its use and for interpretation of data. It has been shown to increase bile flow in rats and dogs, to increase hepatic microsomal heme oxygenase in rats in vivo, and to cause lipid peroxidation in isolated hepatocytes.

Another useful GSH-depleting agent is phorone (diisopropylidene acetone), which when given intraperitoneally (250 mg/kg) depletes hepatic GSH to <10% of control levels in rats. In isolated hepatocytes, phorone treatment (0.5 mM) was shown to deplete cytosolic and mitochondrial GSH by 75% and 40%, respectively (Romero et al., 1984). As with DEM administration, the rate of GSH synthesis is also increased, causing a significant increase of GSH levels above control values. Phorone has been shown to increase heme oxygenase and δ-aminolevulinic acid synthetase activity, and to decrease cytochrome P-450 and aminopyrine demethylase activity. However, unlike DEM, phorone does not seem to have an effect on protein synthesis.

Other compounds that have been used, and that deplete GSH by enzyme-catalyzed reactions, include unsaturated compounds (e.g., acrylonitrile and acrylamide) and halogenated hydrocarbons (e.g., iodomethane, chloroacetamide, 2-chloroethanol, and benzylchloride).

Kosower et al. (1969a,b) developed a variety of compounds that oxidize GSH to GSSG. These compounds are derivatives of diazenecarboxylic acid. The most widely used compound has been diazenedicarboxylic acid bis-(*N*,*N*-dimethyl)amide (diamide). GSH levels are lowered to <10% of control levels in a variety of cells; however, side effects have to be kept in mind when interpreting data. Diamide is known to cause slow oxidation of lipoic acid and pyridine nucleotides and fast oxidation of flavin nucleotides. Diamide also causes inhibition of a variety of important enzymes (e.g., protein kinase, tyrosine phosphatase, Na^+/K^+-ATPase, and glucose-6-phosphatase), and is known to cause membrane damage.

GSH can also be depleted (oxidized) using substrates for GSH peroxidase (e.g., hydrogen peroxide and THB). However, the increase in GSSG causes oxidative stress, which can make the in vivo use of hydroperoxides unattractive for certain studies.

Inhibition of GSH Synthesis

Glutathione levels can be effectively decreased by inhibiting the enzymes involved in synthesis: γ-glutamylcysteine synthetase or glutathione synthetase (GS; Fig. 6.1.2). The most useful inhibitor is BSO, which inactivates γ-glutamylcysteine synthetase. BSO is a transition-state inhibitor and mimics the transition intermediate or transition state formed in the reaction between enzyme-bound γ-glutamyl phosphate and the amino group of cysteine. BSO competes with L-glutamate for the active site of the enzyme; however, once bound and phosphorylated, the intermediate is tightly bound. BSO can be administered repeatedly either orally or intraperitoneally. Its success depends on the amount of GSH in individual tissues as well as on the turnover rate of GSH in the cells. BSO itself is not very reactive chemically and appears to be metabolized slowly. BSO therefore allows treatment over several weeks, which creates an artificial chronic GSH deficiency. BSO experiments carried out in vitro or in vivo have shown the importance of GSH in reduction and detoxification processes. It was shown that BSO-induced depletion of GSH sensitized the cells to toxic effects induced by $HgCl_2$, radiation, cyclophosphamide, morphine, and other compounds. BSO treatment also has been shown to have an effect on tumors by increasing the effects of chemotherapy and radiation once GSH is depleted.

Short-term BSO treatment (e.g., single intraperitoneal injection) leads to a rapid decline of GSH in liver, pancreas, kidney, skeletal muscle, and plasma. GSH is depleted to a maximum of 15% to 20% of control levels. The fact that glutathione cannot be further depleted led to the hypothesis that a separate GSH pool existed. This was later associated with the mitochondrial GSH pool (see Mitochondrial Glutathione). Long-term treatment with BSO over several weeks showed a decrease not only in the tissues named above but also in brain, heart, lung, spleen, and intestinal and colon mucosa. BSO therefore can be used to produce "chronic" GSH deficiency. However differences have been observed in treatment of adult versus newborn animals.

Inhibition of GS is not the method of choice to induce glutathione deficiency, because it has been shown that patients with severe inborn GS deficiency show life-threatening acidosis due to overproduction of 5-oxoproline (Meister and Larsson, 1989). When GS is inhibited, γ-glutamylcysteine accumulates; this is converted by γ-glutamylcyclotransferase to cysteine and oxoproline, which is then converted to glutamic acid by 5-oxoprolinase, resulting in severe acidosis.

Glutathione levels can also be decreased by limiting the necessary amino acids, especially cysteine and methionine. However, limitation of synthesis in this way will also have consequences with respect to protein synthesis.

Inhibition of GSH Degradation

GSH content can also be altered by inhibiting GGT. Degradation of GSH by GGT can account for as much as 80% to 90% of GSH turnover. Reed and Ellis (1981) performed in vivo treatment of rats with AT-125 (acivicin), an inhibitor of GGT. AT-125 prevented degradation of plasma GSH, which led to massive urinary excretion of GSH. This treatment lowered the hepatic GSH content, because recycling of cysteine was inhibited.

A GGT-deficient knockout mouse has recently been developed (Lieberman et al., 1996); it shows chronic depletion of GSH in certain organs. Selective depletion is thought to be due to a lack of "recovered" cysteine from the urinary GSH. The most affected organs were the liver and eye, where tissue GSH levels decreased to 20% of control levels. Pancreas, spleen, and thymus were depleted to 50% of control levels,

while brain, heart, and lung showed significant but minor depletion to 80% of control levels. Kidney GSH was not decreased at all (Lieberman et al., 1996; Will and Reed, unpub. observ.). These findings suggest that synthesis, uptake, and turnover of GSH are tissue specific.

Increasing Glutathione Levels

GSH levels can be increased by administration of GSH, GSH esters, or precursors for GS synthesis. The synthesis of GSH may be increased by increasing the amount of substrates for the two synthetases. However, since γ-glutamylcysteine synthetase is feedback inhibited by GSH, this approach may only work under certain conditions (e.g., refeeding after depletion or starvation). Introduction of cysteine is often not the best approach to increase synthesis as it is rapidly metabolized and has been shown to be toxic at high concentrations. *N*-acetyl cysteine (NAc) is a precursor for cysteine that has found therapeutic use in raising GSH levels in HIV patients and patients with respiratory diseases. The compound is transported into cells where it is deacetylated to yield cysteine. Another effective compound is L-2-oxothiazolidine-4-carboxylate (OTC), which is an analog of 5-oxo-L-proline and is a substrate for 5-oxoprolinase.

GSH levels can also be raised by supplying substrate for GS; this is a good approach because this enzyme is not feedback inhibited by GSH. γ-Glutamyl cysteine and γ-glutamyl cystine have been shown to increase the GSH concentration in the kidney. This approach is extremely useful for raising kidney GSH levels because kidney cells have an active transport system for γ-glutamyl amino acids.

The use of GSH itself to raise GSH levels has been subject to controversy. While some authors did not find any increase in plasma or tissue GSH levels after oral administration (Yoshimura et al., 1982; Martenson et al., 1990), Jones and co-workers did show increases in plasma GSH levels (Hagen et al., 1988). However, an increase in tissue GSH levels was observed only when GSH levels were previously depleted through administration of BSO (Aw et al., 1991). Therefore, administration of GSH may have a beneficial effect under pathological conditions where GSH depletion has occurred. In contrast, the administration of monoethyl or monomethyl esters has been shown to increase tissue GSH levels. Anderson et al. (1985) reported rapid uptake of intraperitoneally administered glutathione monoethyl ester into kidney, liver, spleen, pancreas, and lung. Uptake into other tissues occurred at a slower rate. The use of esters is appealing because many cells are equipped with esterases that can catalyze hydrolysis to GSH, but it must be kept in mind that the release of ethanol and methanol can have adverse effects on cellular functions.

MITOCHONDRIAL GLUTATHIONE

The fact that BSO treatment was unable to deplete liver GSH below 10% to 15% of total GSH suggested the existence of more than one pool of GSH in the liver (Edwards and Westerfeld, 1952). In 1973 it was proposed that GSH in the mitochondrial matrix provides a reservoir for reducing equivalents capable of preventing thiol groups from oxidative stress (Vignais and Vignais, 1973).

A complete redox cycle was shown to exist in liver mitochondria, containing reduced GSH, glutathione reductase, glutathione peroxidase, and NADPH (Fig. 6.1.4). This system is capable of reducing a wide range of diazenes and hydroperoxides (Jocelyn, 1978). Since mitochondria contain no catalase, they rely solely on GSH peroxidase to detoxify hydrogen peroxide. Where does the hydrogen peroxide come from? Most is of endogenous origin as a consequence of aerobic metabolism that occurs mostly in the mitochondrion. Reduction of oxygen in the respiratory chain is not absolutely complete and involves the formation of toxic intermediates. About 2% to 5% of mitochondrial oxygen consumption generates hydrogen peroxide. Hydrogen peroxide, if not reduced, leads to the formation of very reactive hydroxyl radicals that can cause lipid peroxidation. Lipid peroxidation damages membranes, nucleic acids, and proteins, thereby altering or inhibiting their function.

Meredith and Reed (1983) made the original observation that the onset of chemically induced cell injury correlated with the depletion of mitochondrial rather than cytosolic GSH. Hepatocytes were treated with ethacrynic acid, which depletes mitochondrial as well as cytosolic GSH. The authors showed that depletion of cytosolic GSH had no observable effect on cell viability, while the depletion of mitochondrial GSH caused cell injury. Cell injury occurred when the total liver GSH was depleted to 10% to 15% of normal levels.

Meredith and Reed (1982) also demonstrated different rates for GSH turnover between cytosol and mitochondria. Their finding indicated a half-life of 2 hr for cytosolic GSH versus 30 hr for mitochondrial GSH. The fact that mitochondrial GSH content (10 mM) is higher

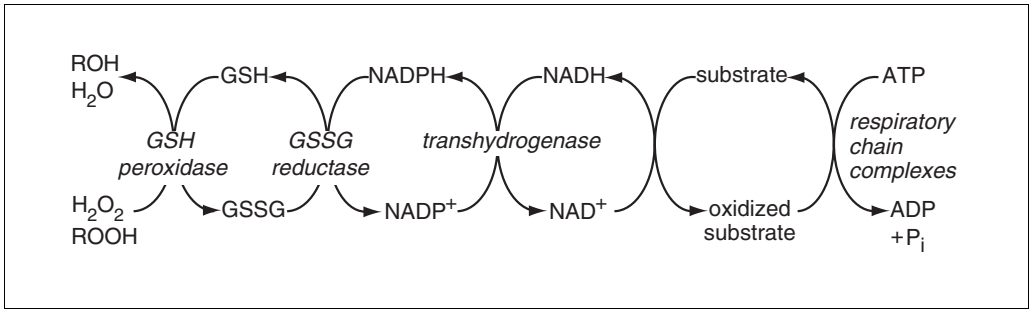

Figure 6.1.4 Mitochondrial GSH redox cycle.

than cytosolic (7 mM) suggests the importance of mitochondrial GSH. The ratio of GSH/GSSG in mitochondria under normal conditions is ~18:1. This ratio can change through oxidative stress of either endogenous or exogenous origin. A change in the GSH/GSSG ratio has adverse effects on mitochondria and subsequently on cells. For example, age-related changes in the mitochondrial GSH/GSSG ratio have been observed by Garcia de la Asuncion et al. (1996). These authors examined mitochondrial GSH/GSSG ratios and oxidative damage to mitochondrial DNA in liver, brain, and kidney in 6-, 18-, and 24-month-old mice and rats. The following results and conclusions were obtained: (1) GSH becomes more oxidized with age. (2) Oxidative damage in mitochondrial DNA increases with age. (3) A correlation (r = 0.95) exists between decreases in the GSH/GSSG ratio and increases in oxidative damage. (4) Changes in mice were much more severe than in rats. Animals with a longer maximum lifespan (rats) had less oxidation than animals with a shorter lifespan (mice). However, within a given species, older animals showed significant oxidation of GSH and mitochondrial DNA when compared to younger animals. Oxidation of GSH through TBH treatment caused release of GSSG from perfused liver (Sies et al., 1974) and isolated hepatocytes (Ekloew et al., 1984). However, TBH treatment of isolated mitochondria caused GSSG formation without subsequent release (Olafsdottir and Reed, 1988).

What would be the consequence of GSSG accumulation in the mitochondria? Accumulation of GSSG will lead to oxidation of thiol groups in mitochondria, which may explain the observation that loss of mitochondrial GSH rather than cytosolic GSH correlates with some types of cell injury (Meredith and Reed, 1983; Olafsdottir and Reed, 1988). Many mitochondrial proteins are highly sensitive to changes in the cellular thiol status, including Ca^{2+}-dependent ATPases, metabolic carriers, and proteins controlling permeability changes in the inner mitochondrial membrane. Ca^{2+}-dependent ATPases serve as membrane-bound Ca^{2+} pumps to maintain cytoplasmic Ca^{2+} at low levels. Interference with Ca^{2+} levels and increase in intracellular Ca^{2+} are known to be involved in cell injury (Bellomo and Orrenius, 1985). Homeostasis of Ca^{2+} and thiols in mitochondria are believed to be closely linked, either directly (Beatrice et al., 1984) or through pyridine nucleotides (Lehninger et al., 1978).

Many metabolic carriers of the inner mitochondrial membrane contain sulfhydryl groups. Oxidation of these groups leads to changes and inhibition of transporting capacities that can result in mitochondrial dysfunction (Le-Quoc and Le-Quoc, 1985). Changes in anion transport as well as transport of monovalent and divalent cations across the inner mitochondrial membrane have been observed when sulfhydryl groups were modified. However, the relationship between thiol modification and membrane properties is often difficult to explain. The question remains whether the effect of the thiol reagent on permeability results from reaction with a protein that specifically controls permeability, or if it is a consequence of a nonspecific perturbation.

This question gets even more complicated when dealing with the question of how the glutathione status may control the proteins that are involved in mitochondrial permeability transition. Many studies have shown that oxidative stress increases permeability in mitochondria. The permeability increase is favored by Ca^{2+} accumulation and causes equilibration of low-molecular-weight solutes (≤1500 Da), depolarization, uncoupling, and release of the previously accumulated Ca^{2+}. This phenomenon is now termed mitochondrial permeability transition (MPT). Studies conducted by Lehninger et al. (1978) linked oxidation of pyridine nucleotides to Ca^{2+} efflux, which could be reversed by reduction of pyridine nucleotides. Changes in permeability were observed, not knowing at this

time that MPT was probably involved. In 1984 the question was revisited by Pfeiffer and coworkers (Beatrice et al., 1984) who were able to independently modulate NADPH/$NADP^+$, NADH/NAD^+, and GSH/GSSG ratios. They came to the conclusion that the latter ratio was the relevant factor for changing permeability. This study was challenged, however, by previously conducted studies by Carbonera and Azzone (1988) and Hoek and Rydstrom (1988). Carbonera and Azzone showed that MPT induced by inorganic hydroperoxides was inhibited by butylhydroxytoluene while GSH remained oxidized. Hoek and Rydstrom showed that oxidation of GSH by 1,3-bis-(2-chloroethyl)-1-nitrosourea (BCNU), which prevents nucleic acid oxidation, was not followed by Ca^{2+} release.

Although results were not in concert, it was agreed that there seemed to be a strong influence of pyridine nucleotides and GSH on permeability transition, which challenged Bernardi and co-workers to revisit this question. In studies conducted from 1992 to 1996, these authors came to the following conclusions. (1) MPT induction is voltage dependent (Bernardi, 1992). The pore gating potential is shifted towards a more negative membrane potential by thiol oxidation, resulting in a higher probability for pore opening. On the other side, thiol reduction shifts the gating potential toward a less negative membrane potential, resulting in lower probability to pore opening. (2) The MPT gating potential is modified by oxidation/reduction at two different sites that are experimentally distinguishable (Constantini et al., 1996). One site, the P site, is modulated through the oxidation/reduction state of pyridine nucleotides even at times where GSH is fully reduced. The other site, the S site, can be activated even when pyridine nucleotides are fully reduced (Petronilli et al., 1994). In other words, MPT pore opening correlates to both oxidation/reduction of pyridine nucleotides through the P site and presumably GSH through the S site. TBH treatment, by oxidizing both pyridine nucleotides and GSH, could therefore have an effect on both sites. Mitochondrial dysfunction (as a result of MPT) is now considered a key event in a variety of forms of cell death (e.g., ischemia, neurodegeneration, and apoptosis).

Mitochondria cannot synthesize GSH. Griffith and Meister (1985) discovered that mitochondria contain neither γ-glutamylcysteine synthetase nor GS. Therefore an uptake mechanism must exist to shuttle GSH into the mitochondria. Several groups have reported the existence of a mitochondrial anion channel (Selwyn et al., 1979; Garlid and Beavis, 1986; Sorgato et al., 1987). The described channel, which has broad specificity for many anions and is controlled by Mg^{2+} and H^+, would allow a mechanism for loading extramitochondrial components.

Martenson et al. (1990) conducted studies on the kinetics of GSH transport in isolated liver mitochondria. The authors found that the transport system had either a high- or low-affinity component depending on the external GSH concentration. At a GSH concentration <1 mM, a high-affinity component was observed with a K_m of 60 μM and a V_{max} of 0.54 nmol/min/mg protein. At GSH levels of 1 to 8 mM, a low-affinity component was found with a K_m of 5.4 mM and a V_{max} of 5.79 nmol/min/mg protein. Both processes were stimulated by ATP and ADP and inhibited by the uncoupler carbonyl cyanide *p*-(trifluoromethoxy)phenylhydrazone (FCCP). Efflux of GSH from preloaded mitochondria was shown to be biphasic with an external GSH concentration of 0.15 mM. At external GSH concentrations of 8 mM, 60% of the GSH initially present in the matrix disappeared from the matrix in 15 sec, but was recovered in the matrix after 120 sec. This phenomenon was interpreted by the authors as follows: at high external GSH concentrations there is a rapid flow of external GSH into the intermembranous space, which facilitates reuptake of GSH into the matrix.

A transport system for GSH exists in isolated liver mitochondria (Kurosawa et al., 1990). These data indicated that high external concentrations of GSH and a proton gradient constitute the motive force to bring external GSH into the mitochondria. As cytosolic GSH is present at high concentrations in living cells, the authors assume that this motive force functions under physiological conditions. Isolated liver mitochondria in state 4 (basal respiration on substrate without ADP) incubated with GSSG had increased GSH levels, which suggests that GSSG is taken up and reduced by oxidation of NADPH. The observation of GSSG uptake seems to be unphysiological at first glance. However, GSH reductase and GSH peroxidase have been shown to be located in the intermembrane space and the matrix, which indicates that these enzymes are accessible to substrates from both the extra- and intramitochondrial space (Flohe and Schlegel, 1971; Sandri et al., 1990). Therefore, an uptake mechanism may very well exist in vivo.

Kaplowitz and colleagues (Garcia-Ruiz et al., 1995) were able to successfully express a rat

hepatic mitochondrial GSH carrier in *Xenopus laevis* oocytes and showed that the mitochondrial GSH carrier differed from the previously described sinusoidal and canalicular carriers. The carrier was stimulated by ATP and inhibited by glutamate.

Uptake of GSH by kidney mitochondria has been examined by McKernan et al. (1991) and Schnellmann (1991). In order to understand the mechanism of mitochondrial GSH transport several facts need to be considered. GSH contains two free carboxyl groups and one free amino group and thus has a net charge of −1 at neutral pH. The thiol group contains a dissociable proton with a pK_a of 9.2. This means that at cytosolic pH of 7.4, more or less none (<1%) of the GSH is in the thiolate form, which would mean a net charge of −2. In the mitochondrial matrix at pH 7.8, ~4% of the GSH is in thiolate form. In addition, a membrane potential exists, with the mitochondrial matrix negative relative to the cytosol. The membrane potential, the pH gradient, as well as the net charge of GSH provide a driving force against the uptake of GSH. Therefore, there must be a counteracting driving force in order for GSH uptake to exist. Several anion transporters are known to exist in mitochondria; they are involved in transport of citric acid cycle intermediates against the driving force. One or more of those carriers may be in part responsible for GSH uptake. That neither ΔpH nor the membrane potential are required for transport of GSH into renal mitochondria was shown by McKernan et al. (1991), who observed that the uncoupler 2,4-dinitrophenol and the protonophore carbonyl cyanide *m*-chlorophenyl hydrazone had no negative effect on GSH uptake. However, KCN, ATP, and Ca^{2+} inhibited transport, suggesting an indirect dependence on mitochondrial energetics or adenine nucleotide transport.

Substrate specificity for GSH uptake was examined by measuring the effects of mono- and dicarboxylates (Smith et al., 1996). Monocarboxylates did not have any effect, while malate and succinate did show effects, suggesting that GSH uptake may involve exchange with dicarboxylates. Additionally, glutamate inhibited GSH uptake, suggesting that the glutamyl moiety of GSH may be a recognition site for transport. In summary, GSH uptake into (at least) renal mitochondria is Na^+ independent, and apparently membrane potential independent, involves a net transfer of charge across the membrane, and is inhibited by glutamate and γ-glutamyl compounds, including GSH conjugates (Smith et al., 1996).

Studies by Jocelyn (1975) indicated that the retention and release of mitochondrial GSH is a highly regulated process. Isolated mitochondria retained most of their GSH, indicating that the inner mitochondrial membrane is impermeable to GSH. Only some was lost through outward diffusion, which suggests that the transport mechanism functions to conserve mitochondrial GSH during times of cytosolic depletion (Griffith and Meister, 1985). The addition of phosphate increased the efflux rate. During short-term incubations, no considerable amounts of GSSG were formed unless oxidizing agents were added. GSSG was retained by mitochondria unless phosphate was added to the incubations. Addition of phosphate probably induced MPT, opened the pore, and allowed efflux of mitochondrial components. Studies showing that no GSSG was released from TBH-treated, isolated mitochondria suggested that an efflux pathway for GSSG under non-MPT conditions is absent in mitochondria (Olafsdottir and Reed, 1988).

The question of GSH uptake and release under conditions of MPT was further examined by Savage et al. (1991). MPT was induced with calcium and phosphate (CaP), and nearly 100% GSH was released from the mitochondria in 5 min. Efflux was completely prevented when mitochondria were incubated with cyclosporin A, a known inhibitor of MPT. The authors also showed that GSH could be loaded into mitochondria. Mitochondria were briefly incubated with CaP to induce the transition, and 1 mM GSH was added to the suspensions. Mitochondria took up the GSH at a rate of 0.5 nmol/min/mg protein, which was higher than the uptake rate of mitochondria that were not pretreated with CaP. However, sustained opening of the pore would cause extensive release of mitochondrial components rather than exchange or even uptake; in other words only occasional opening and closing of the pore allows such a mechanism.

LITERATURE CITED

Abbott, W.A., Bridges, R.J., and Meister, A. 1984. Extracellular metabolism of glutathione accounts for its disappearance from the basolateral circulation of the kidney. *J. Biol. Chem.* 259:15393-15400.

Addya, S., Mullick, J., Fang, J.K., and Avadhani, N.G. 1994. Purification and characterization of a hepatic mitochondrial glutathione S-transferase exhibiting immunochemical relationship to the alpha-class of cytosolic isoenzymes. *Arch. Biochem. Biophys.* 310:82-88.

Anderson, M.E., Powrie, F., Puri, R.N., and Meister, A. 1985. Glutathione monoethyl ester: Preparation, uptake by tissues, and conversion to glutathione. *Arch. Biochem. Biophys.* 239:538-548.

Aw, T.Y., Wierzbicka, G., and Jones, D.P. 1991. Oral glutathione increases tissue glutathione in vivo. *Chem. Biol. Interact.* 80:89-97.

Baba, A., Lee, E., Matsuda, T., Kihara, T., and Iwata, H. 1978. Reversible inhibition of adenylate cyclase activity of rat brain caudate nucleus by oxidized glutathione. *Biochem. Biophys. Res. Commun.* 85:1204-1210.

Babson, J.R. and Reed, D.J. 1978. Inactivation of glutathione reductase by 2-chloroethyl nitrosourea-derived isocyanates. *Biochem. Biophys. Res. Commun.* 83:754-762.

Beatrice, M.C., Stiers, D.L., and Pfeiffer, D.R. 1984. The role of glutathione in the retention of Ca^{2+} by liver mitochondria. *J. Biol. Chem.* 259:1279-1287.

Bellomo, G. and Orrenius, S. 1985. Altered thiol and calcium homeostasis in oxidative hepatocellular injury. *Hepatology* 5:876-882.

Bernardi, P. 1992. Modulation of the mitochondrial cyclosporin A-sensitive permeability transition pore by the proton electrochemical gradient. Evidence that the pore can be opened by membrane depolarization. *J. Biol. Chem.* 267:8834-8839.

Boyland, E. and Chasseaud, L.F. 1969a. Glutathione *S*-aralkyltransferase. *Biochem. J.* 115:985-991.

Boyland, E. and Chasseaud, L.F. 1969b. The role of glutathione and glutathione *S*-transferases in mercapturic acid biosynthesis. *Adv. Enzymol. Relat. Areas Mol. Biol.* 32:173-219.

Cappel, R.E. and Gilbert, H.F. 1993. Oxidative inactivation of 3-hydroxy-3-methylglutaryl-coenzyme A reductase and subunit cross-linking involve different dithiol/disulfide centers. *J. Biol. Chem.* 268:342-348.

Carbonera, D. and Azzone, G.F. 1988. Permeability of inner mitochondrial membrane and oxidative stress. *Biochim. Biophys. Acta* 943:245-255.

Commandeur, J.N., Stijntjes, G.J., and Vermeulen, N.P. 1995. Enzymes and transport systems involved in the formation and disposition of glutathione *S*-conjugates. Role in bioactivation and detoxication mechanisms of xenobiotics. *Pharmacol. Rev.* 47:271-330.

Constantini, P., Chernyak, B.V., Petronilli, V., and Bernardi, P. 1996. Modulation of mitochondrial permeability transition pore by pyridine nucleotides and dithiol oxidation at two separate sites. *J. Biol. Chem.* 271:6746-6751.

De-Rey-Pailhade, J., 1888a. Sur un corps d'origine organique hydrogenant le soufre a froid. *Compte Rendus Hebdomadaire Seances de l 'Academie de Sciences* 106:1683-1684.

De-Rey-Pailhade, J. 1888b. Nouvelles recherches physiologiques sur la substance organique hydrogenant le soufre a froid. *Compte Rendus Hebdomadaire Seances de l'Academie de Sciences* 107:43-44.

Dethmers, J.K. and Meister, A. 1981. Glutathione export by human lymphoid cells: Depletion of glutathione by inhibition of its synthesis decreases export and increases sensitivity to irradiation. *Proc. Natl. Acad. Sci. U.S.A.* 78:7492-7496.

Ding, H. and Demple, B. 1996. Glutathione-mediated destabilization in vitro of [2Fe-2S] centers in the SoxR regulatory protein. *Proc. Natl. Acad. Aci. U.S.A.* 93:9449-9453.

Edwards, S. and Westerfeld, W.W. 1952. Blood and liver glutathione during protein deprivation. *Proc. Biol. Exp. Med.* 79:57-59.

Ekloew, L., Moldeus, P., and Orrenius, S. 1984. Oxidation of glutathione during hydroperoxide metabolism. A study using isolated hepatocytes and the glutathione reductase inhibitor 1,3-bis(2-chloroethyl)-1-nitrosurea. *Eur. J. Biochem.* 138:459-463.

Eldjarn, L. and Bremer, J. 1962. The inhibitory effect at the hexokinase level of disulphides on glucose metabolism in human erythrocytes.*Biochem. J.* 84:286-291.

Ernest, M.J. and Kim, K.-H. 1973. Regulation of rat liver glycogen synthetase. *J. Biol. Chem.* 248:1550-1555.

Ernest, M.J. and Kim, K.-H. 1974. Regulation of rat liver glycogen synthetase D. *J. Biol. Chem.* 249:5011-5018.

Evered, D.F. and Wass, M. 1970. Transport of glutathione across the small intestine of the rat in vitro. *Proc. Physiol. Soc.* 209:4P-5P.

Fernandez-Checa, J.C., Yi, J.-R., Garcia-Ruiz, C., Knezic, Z., Tahara, S.M., and Kaplowitz, N. 1993. Expression of rat liver reduced glutathione transport in *Xenopus laevis* oocytes. *J. Biol. Chem.* 268:2324-2328.

Flohe, L. and Schlegel, W. 1971. Glutathione peroxidase. IV. Intracellular distribution of the glutathione peroxidase system in the rat liver. *Hoppe Seylers Z. Physiol. Chem.* 352:1401-1410.

Garcia de la Asuncion, J., Millan, A., Pla, R., Bruseghini, L., Esteras, A., Pallardo, F.V., Sastre, J., and Vina, J. 1996. Mitochondrial glutathione oxidation correlates with age-associated oxidative damage to mitochondrial DNA. *FASEB J.* 10:333-338.

Garcia-Ruiz, C., Morales, A., Colell, A., Rodes, J., Yi, J.-R., Kaplowitz, N., and Fernandez-Checa, J.C. 1995. Evidence that the rat hepatic mitochondrial carrier is distinct from the sinusoidal and canicular transporters for reduced glutathione. Expression studies in *Xenopus laevis* oocytes. *J. Biol. Chem.* 270:15946-15949.

Garlid, K.D. and Beavis, A.D. 1986. Evidence for the existence of an inner membrane anion channel in mitochondria. *Biochim. Biophys. Acta* 853:187-204.

Ginn-Pease, M.E. and Whisler, R.L. 1996. Optimal NfκB mediated transcriptional responses in jurkat T cells exposed to oxidative stress are dependent on intracellular glutathione and costimulatory signals. *Biochem. Biophys. Res. Commun.* 226:685-702.

Griffith, O.W. and Meister, A. 1985. Origin and turnover of mitochondrial glutathione. *Proc. Natl. Acad. Sci. U.S.A.* 82:4668-4672.

Haenen, G.R. and Bast, A. 1983. Protection against lipid peroxidation by a microsomal

glutathione-dependent labile factor. *FEBS Lett.* 159:24-28.

Hagen, T.M. and Jones, D.P. 1987. Transepithelial transport of glutathione in vascularly perfused small intestine of rat. *Am. J. Physiol.* 252:G607-G613.

Hagen, T.M. and Jones, D.P. 1989. Role of glutathione transport in extrahepatic detoxication. *In* Glutathione Centennial, Molecular Perspectives and Clinical Applications (N. Taniguchi, T. Higashi, Y. Sakamoto, and A. Meister, eds.) pp. 423-433. Academic Press, San Diego.

Hagen, T.M., Aw, T.Y., and Jones, D.P. 1988. Glutathione uptake and protection against oxidative injury in isolated kidney cells. *Kidney Int.* 34:74-81.

Hahn, R., Wendel, A., and Flohe, L. 1978. The fate of extracellular glutathione in the rat. *Biochim. Biophys. Acta* 529:324-337.

Harris, J.M., Meyer, D.J., Coles, B., and Ketterer, B. 1991. A novel glutathione transferase (13-13) isolated from the matrix of rat liver mitochondria having structural similarity to class theta enzymes. *Biochem. J.* 278:137-141.

Hinchman, C.A., Matsumoto, H., Simmons, T.W., and Ballatori, N. 1991. Intrahepatic conversion of glutathione conjugate to its mercapturic acid: Metabolism of 1-chloro-2,4-dinitrobenzene in isolated perfused rat and guinea pig livers. *J. Biol. Chem.* 266:22179-22185.

Hoek, J.B. and Rydstrom, J. 1988. Physiological roles of nicotinamide nucleotide transhydrogenase. *Biochem. J.* 254:1-10.

Holmgren, A. 1978. Glutathione-dependent enzyme reactions of the phage T4 ribonucleotide reductase system. *J. Biol. Chem.* 253:7424-7430.

Holmgren, A. 1979. Glutathione-dependent synthesis of deoxyribonucleotides. Characterization of the enzymatic mechanism of *Escherichia coli* glutaredoxin. *J. Biol. Chem.* 254:3672-3678.

Huang, C.S., Anderson, M.E., and Meister, A. 1993. Amino acid sequence and function of the light subunit of rat kidney gamma-glutamylcysteine synthetase. *J. Biol. Chem.* 268:20578-20583.

Hunjahn, M.K. and Evered, D.F. 1985. Absorption of glutathione from the gastro-intestinal tract. *Biochim. Biophys. Acta* 815:184-188.

Inoue, M., Shinozuka, S., and Morino, Y. 1986. Mechanism of renal peritubular extraction of plasma glutathione. The catalytic activity of contralumenal g-glutamyl-transferase is prerequisite to the apparent peritubular extraction of plasma glutathione. *Eur. J. Biochem.* 157:605-609.

Isaacs, J. and Binkley, F. 1977. Glutathione dependent control of protein disulfide-sulfhydryl content by subcellular fractions of hepatic tissue. *Biochim. Biophys. Acta* 497:192-204.

Jocelyn, P.C. 1975. Some properties of mitochondrial glutathione. *Biochim. Biophys. Acta* 369:427-436.

Jocelyn, P.C. 1978. The reduction of diamide by rat liver mitochondria and the role of glutathione. *Biochem. J.* 176:649-664.

Kannan, R., Yi, J.-R., Tang, D., Li, Y., Zlokovic, B.V., and Kaplowitz, N. 1996. Evidence of the existence of a sodium-dependent glutathione (GSH) transporter. *J. Biol. Chem.* 271:9754-9758.

Kosower, N.S. and Kosower, E.M. 1974. Manifestation and changes in the GSH/GSSG status of biological systems. *In* Glutathione (L. Flohe, H.C. Benoehr, H. Sies, H.D. Waller, and A. Wendel, eds.) pp. 287-295. Georg Thieme, Stuttgart, Germany.

Kosower, N.S., Song, K.R., and Kosower, E.M. 1969a. Glutathione. I. The methyl phenyldiazenecarboxylate (azoester) procedure for intracellular oxidation. *Biochim. Biophys. Acta* 192:1-7.

Kosower, N.S., Kosower, E.M., Wertheim, B., and Correa, W.S. 1969b. Diamide, a new reagent for the intracellular oxidation of glutathione to the disulfide. *Biochem. Biophys. Res. Commun.* 37:593-596.

Kurosawa, K., Hayashi, N., Sato, N., Kamada, T., and Tagawa, K. 1990. Transport of glutathione across the mitochondrial membranes. *Biochem. Biophys. Res. Commun.* 167:367-372.

Lash, L.J. and Jones, D.P. 1984. Renal glutathione transport. Characteristics of the sodium-dependent system in the basal-lateral membrane. *J. Biol. Chem.* 259:14508-14514.

Lash, L.H. and Torkatz, J.J. 1990. Oxidative stress in isolated rat renal proximal and distal tubular cells. *Am. J. Physiol.* 259:F338-F347.

Lehninger, A.L., Vercesi, A., and Bababunmi, E.A. 1978. Regulation of Ca^{2+} release from mitochondria by the oxidation-reduction state of pyridine nucleotides. *Proc. Natl. Acad. Sci. U.S.A.* 75:1690-1694.

Le-Quoc, K. and Le-Quoc, D. 1985. Crucial role of sulfhydryl groups in the mitochondrial inner membrane structure. *J. Biol. Chem.* 260:7422-7428.

Liang, C.-M., Lee, N., Cattell, D., and Liang, S.-M. 1989. Glutathione regulates interleukin-2 activity on cytotoxic T-cells. *J. Biol. Chem.* 264:13519-13523.

Lieberman, M.W., Wiseman, A.L., Shi, Z.Z., Carter, B.Z., Barrios, R., Ou, C.N., Chevez-Barrios, P., Wang, Y., Habib, G.M., Goodman, J.C., Huang, S.L., Lebovitz, R.M., and Matzuk, M.M. 1996. Growth retardation and cysteine deficiency in gamma-glutamyl transpeptidase-deficient mice. *Proc. Natl. Acad. Sci. U.S.A.* 93:7923-7926.

Listowsky, I. 1993. Glutathione *S*-transferases: Intracellular binding, detoxication, and adaptive responses. *In* Hepatic Transport and Bile Secretion: Physiology and Pathophysiology (N. Tavolini and D. Berk, eds.) pp. 397-405. Raven Press, New York.

Lu, S.C., Kuhlenkamp, J., Ge, J.-L., Sun, W.-M., and Kaplowitz, N. 1994. Specificity and directionality of thiol effects on sinusoidal glutathione

transport in rat liver. *Mol. Pharmacol.* 46:578-585.

Mannervik, B. and Danielson, U.H. 1988. Glutathione transferases—structure and catalytic activity. *CRC Crit. Rev. Biochem.* 23:283-337.

Martenson, J., Jain, A., and Meister, A. 1990. Glutathione is required for intestinal function. *Proc. Natl. Acad. Sci. U.S.A.* 87:1715-1719.

McGivan, J.D. and Pastor-Anglada, M. 1994. Regulatory and molecular aspects of mammalian amino acid transport. *Biochem. J.* 299:321-334.

McIntyre, T.M. and Curthoys, N.P. 1980. The interorgan metabolism of glutathione. *Int. J. Biochem.* 12:545-551.

McKernan, T.B., Woods, E.B., and Lash, L.H. 1991. Uptake of glutathione by renal cortical mitochondria. *Arch. Biochem. Biophys.* 288:653-663.

Meister, A. 1983. Metabolism and transport of glutathione and other γ-glutamyl compounds. *In* Functions of Glutathione—Biochemical, Physiological and Toxicological and Clinical Aspects (A. Larsson, S. Orrenius, A. Holmgren, and B. Mannervik, eds.) pp. 1-22. Raven Press, New York.

Meister, A. 1991. Glutathione deficiency produced by inhibition of its synthesis, and its reversal; application in research and therapy. *Pharmacol. Ther.* 51:155-194.

Meister, A. and Anderson, M.E. 1983. Glutathione. *Annu. Rev. Biochem.* 52:711-760.

Meister, A. and Larsson, A. 1989. Glutathione synthetase deficiency and other disorders of the γ-glutamyl cycle. *In* The Metabolic Basis of Inherited Disorders (C.R. Scriver, A.L. Beaudet, W.S. Sly, and D. Valle, eds.) pp. 855-568. McGraw-Hill, New York.

Meredith, M.J. and Reed, D.J. 1982. Status of the mitochondrial pool of glutathione in the isolated hepatocyte. *J. Biol. Chem.* 257:3747-3753.

Meredith, M.J. and Reed, D.J. 1983. Depletion in vitro of mitochondrial glutathione in rat hepatocytes and enhancement of lipid peroxidation by adriamycin and 1,3-bis(2-chloroethyl)-1-nitrosourea (BCNU). *Biochem. Pharmacol.* 32:1383-1388.

Modig, H. 1968. Cellular mixed disulphides between thiols and proteins, and their possible implication for radiation protection. *Biochem. Pharmacol.* 17:177-186.

Morgenstern, R. and DePierre, J.W. 1983. Microsomal glutathione *S*-transferase. Purification in unactivated form and further characterization of the activation process, substrate specificity and amino acid composition. *Eur. J. Biochem.* 134:591-597.

Ness, G.C., McCreery, M.J., Sample, C.E., Smith, M., and Pendleton, L.C. 1985. Sulfhydryl/disulfide forms of rat liver 3-hydroxy-3-methylglutamyl coenzyme A reductase. *J. Biol. Chem.* 260:16395-16399.

Nishino, H. and Ito, A. 1990. Purification and properties of glutathione *S*-transferase from outer mitochondrial membrane of rat liver. *Biochem. Int.* 20:1059-1066.

Olafsdottir, K. and Reed, D.J. 1988. Retention of oxidized glutathione by isolated rat liver mitochondria during hydroperoxide treatment. *Biochim. Biophys. Acta* 964:377-382.

Ormstad, K., Lastbom, T., and Orrenius, S. 1980. Translocation of amino acids and glutathione studies with the perfused kidney and isolated renal cells. *FEBS Lett.* 112:55-59.

Petronilli, V., Constantini, P., Scorrano, L., Colonna, R., Passamonti, S., and Bernardi, P. 1994. The voltage sensor of the mitochondrial permeability transition pore is tuned by the oxidation-reduction state of vicinal thiols. Increase of the gating potential by oxidants and its reversal by reducing agents. *J. Biol. Chem.* 269:16638-16642.

Reed, D.J. 1986. Regulation of reductive processes by glutathione. *Biochem. Pharmacol.* 35:7-13.

Reed, D.J. and Ellis, W.W. 1981. Influence of gamma-glutamyl transpeptidase inactivation on the status of extracellular glutathione and glutathione conjugates. *Adv. Exp. Med. Biol.* 136:75-86.

Reed, D.J. and Orrenius, S. 1977. The role of methionine in glutathione biosynthesis by isolated hepatocytes. *Biochem. Biophys. Res. Commun.* 77:1257-1264.

Romero, F.J., Soboll, S., and Sies, H. 1984. Mitochondrial and cytosolic glutathione after depletion by phorone in isolated hepatocytes. *Experimentia* 40:365-367.

Ruoppolo, M., Freedman, R.B., Pucci, P., and Marino, G. 1996. Glutathione-dependent pathways of refolding of RNase T1 by oxidation and disulfide isomerization: Catalysis by protein disulfide isomerase. *Biochemistry* 35:13636-13646.

Sandri, G., Panfili, E., and Ernster, L. 1990. Hydrogen peroxide production by monoamine oxidase in isolated rat-brain mitochondria: Its effect on glutathione levels and Ca^{2+} efflux. *Biochim. Biophys. Acta* 1035:300-305.

Savage, M.K., Jones, D.P., and Reed, D.J. 1991. Calcium- and phosphate-dependent release and loading of glutathione by liver mitochondria. *Arch. Biochem. Biophys.* 290:51-56.

Schnellmann, R.G. 1991. Renal mitochondrial glutathione transport. *Life Sci.* 49:393-398.

Selwyn, M.J., Dawson, A.P., and Fulton, D.V. 1979. An anion-conducting pore in the mitochondrial inner membrane. *Biochem. Soc. Trans.* 7:216-219.

Shimazu, T., Tokutake, S., and Usami, M. 1978. Inactivation of phosphorylase phosphatase by a factor from rabbit liver and its chemical characterization as glutathione disulfide. *J. Chem.* 253:7376-7382.

Sies, H., Haussinger, D., and Grosskopf, M. 1974. Mitochondrial nicotinamide nucleotide systems: Ammonium chloride responses and associated metabolic transitions in hemoglobin-free perfused rat liver. *Hoppe Seylers Z. Physiol. Chem.* 355:305-320.

Smith, C.V., Jones, D.P., Guenther, T.M., Lash, L.H., and Lauterburg, B.H. 1996. Contemporary issues in toxicology. Compartmentation of glutathione: Implications for the study of toxicity and disease. *Toxicol. Appl. Pharmacol.* 140:1-12.

Sorgato, M.C., Keller, B.U., and Stuhmer, W. 1987. Patch-clamping of the inner mitochondrial membrane reveals a voltage-dependent ion channel. *Nature* 330:498-500.

Tietze, F. 1969. Enzymic method for quantitative determination of nanogram amounts of total and oxidized glutathione: Application to mammalian blood and other tissues. *Anal. Biochem.* 27:502-522.

Tirmenstein, M.A. and Reed, D.J. 1988. Characterization of glutathione-dependent inhibition of lipid peroxidation of isolated rat liver nuclei. *Arch. Biochem. Biophys.* 261:1-11.

Torella, C., Ruoppolo, M., Marino, G., and Pucci, P. 1994. Analysis of RNase A refolding intermediates by electrospray/mass spectrometry. *FEBS Lett.* 352:301-306.

Tsan, M.-F., White, J.E., and Rosano, C.L. 1989. Modulation of endothelial GSH concentrations: Effect of exogenous GSH and GSH monoethyl ester. *J. Appl. Physiol.* 66:1029-1034.

Tschesche, H. and McCartney, H.W. 1981. A new principle of regulation of enzyme activity. *Eur. J. Biochem.* 120:183-190.

Tuboi, S. and Hayasaka, S. 1972. Control of delta-aminolevulinate synthetase activity in *Rhodopseudomonas spheroides*. II. Requirement of a disulfide compound for the conversion of the inactive form of fraction I to the active form. *Arch. Biochem. Biophys.* 150:690-697.

Usami, M., Matsushita, H., and Shimazu, T. 1980. Regulation of liver phosphorylase phosphatase by glutathione. *J. Biol. Chem.* 255:1928-1931.

Van Berkel, T.J., Koster, J.F., and Huelsmann, W.C. 1973. Two interconvertible forms of L-type pyruvate kinase from rat liver. *Biochim. Biophys. Acta* 293:118-124.

Vignais, P.M. and Vignais, P.V. 1973. Fuscin, an inhibitor of mitochondrial SH-dependent transport-linked functions. *Biochim. Biophys. Acta* 325:357-374.

Vincencini, M.T., Favilli, F., and Iantomasi, T. 1988. Glutathione-mediated transport across intestinal brush-border membranes. *Biochim. Biophys. Acta* 942:107-114.

Visarius, T.M, Putt, D.A., Schare, J.M., Pegouske, D.M., and Lash, L.H. 1996. Pathways of glutathione. Metabolism and transport in isolated proximal tubular cells from rat kidney. *Biochem. Pharmacol.* 52:259-272.

Weissman, J.S. and Kim, P.S. 1995. A kinetic explanation for the rearrangement pathway of BPTI folding. *Nature Struct. Biol.* 2:1123-1130.

Yan, N. and Meister, A. 1990. Amino acid sequence of rat kidney gamma-glutamylcysteine synthetase. *J. Biol. Chem.* 265:1588-1593.

Yi, J.-R., Lu, S., Fernandez-Checa, J.C., and Kaplowitz, N. 1994. Expression cloning of a rat hepatic reduced glutathione transporter with canalicular characteristics. *J. Clin. Invest.* 93:1841-1845.

Yi, J.-R., Lu, S., Fernandez-Checa, J.C., and Kaplowitz, N. 1995. Expression cloning of the cDNA for a polypeptide associated with rat hepatic sinusoidal reduced glutathione transport: Characteristics and comparison with the canicular transporter. *Proc. Natl. Acad. Sci. U.S.A.* 92:1495-1499.

Yoshimura, K., Iwauchi, Y., Sugiyama, S., Kuwamura, T., Odaka, Y., Satoh, T., and Kitagawa, H. 1982. Transport of L-cysteine and reduced glutathione through biological membranes. *Res. Commun. Chem. Pathol. Pharmacol.* 37:171-186.

Contributed by Yvonne Will
Oregon State University
Corvallis, Oregon

Measurement of Glutathione and Glutathione Disulfide

Evaluation of cellular thiol status should include quantification of both reduced (GSH) and oxidized (GSSG) forms of glutathione. This unit describes the methods currently used to quantify both GSH and GSSG, as well as other thiols and disulfides. The main focus is on the use of high-performance liquid chromatography (HPLC) systems to separate cellular thiols with detection by the following methods: (1) ultraviolet (see Basic Protocol 1), (2) fluorescence (see Alternate Protocol 1), and (3) electrochemical (see Alternate Protocol 2). In addition, the use of enzymatic spectrophotometric analysis for glutathione measurement is described (see Basic Protocol 2). HPLC provides a rapid, sensitive, highly versatile, and reproducible means of separating and quantitating sulfur-containing amino acids and related derivatives from a variety of biologic samples. The preparation of samples from a variety of biologic sources is also presented (see Support Protocols 1, 2, and 3).

DERIVATIZATION AND ANALYSIS OF GSH AND GSSG BY HPLC WITH UV DETECTION

BASIC PROTOCOL 1

The HPLC method of Farris and Reed (1987) described here is a modification of an earlier method by Reed et al. (1980). It is based on the initial formation of *S*-carboxymethyl derivatives of free thiols by a reaction with iodoacetic acid. This is followed by addition of Sanger's reagent, 1-fluoro-2,4-dinitrobenzene (FDNB), to convert primary amine groups to their 2,4-dinitrophenyl (DNP) derivatives. Reverse-phase ion-exchange HPLC with a 3-aminopropyl column is used to separate the amino acid DNP derivatives, and the eluted DNP derivatives are measured by ultraviolet (UV) detection at 365 nm. This is a highly versatile method that can be applied to a variety of biological samples to accurately measure several sulfur-containing compounds including GSH, GSSG, and protein-glutathione mixed disulfides (Table 6.2.1). The limits of detection for this method are 50 and 25 pmol/injection onto the column for GSH and GSSG, respectively.

Materials

Perchloric acid (PCA) extract of freshly dissected tissue (see Support Protocol 1), cultured cells (see Support Protocol 2), or hepatocytes (see Support Protocol 3)
0.4 mM γ-glutamyl glutamate (γ-Glu-Glu; see recipe)
100 mM iodoacetic acid (IAA) in 0.2 mM *m*-cresol purple (see recipe)
1% (v/v) 1-fluoro-2,4-dinitrobenzene (FDNB) in 100% HPLC grade ethanol (store at 4°C in a dark container covered with foil)
$KOH/KHCO_3$ solution (see recipe)
0.4 mM GSH (see recipe)
0.4 mM GSSG (see recipe)
Mobile phase A (see recipe)
Mobile phase B (see recipe)

HPLC column: 20-cm × 4.6-mm-i.d. column with 5-μm Exsil silica derivatized with 3-aminopropyltriethoxy silane (CEL Associates; see Reed et al., 1980)
HPLC system:
Pump with gradient capability (Spectra-Physics P200, Spectra-Physics)
UV detector (365 nm; Alltech 200, Alltech)
Recording integrator (Hewlett Packard 3390, Alltech)
Autosampler (optional; Labtronix)

continued

Contributed by Debbie Mustacich
Current Protocols in Toxicology (1999) 6.2.1-6.2.14

Table 6.2.1 Amino Acids and Related Compounds Measured by HPLC[a]

Order of elution	Compound	Retention time (min)
Sulfur-containing compounds		
1	Homocystine	6.68
3	Cystathionine	7.84
4	Cystine (CySS)	8.31
5	Homocysteic acid	12.13
6	Homocysteine	13.18
7	Cysteinylglycine	13.21
8	Penicillamine	13.28
9	γ-Glutamylcysteine	13.49
11	Cysteic acid	15.57
12	Cysteine (CyS)	17.13
13	γ-Glutamyl glutamate (ISTD)	21.95
14	Cysteinyl-glutathione disulfide (CySSG)	22.95
15	Glutathione (GSH)	25.95
16	Glutathione disulfide (GSSG)	30.15
Other compounds		
2	Glutamate (Glu)	7.51
10	Aspartate (Asp)	14.74

[a]Retention times vary with mobile-phase gradient and length and age of column.

Hamilton gas-tight syringe or equivalent (100 µl and 1.0 ml; e.g., Hamilton 1700 series)
Side-arm Erlenmeyer filtration flask (PyrexPlus, 1 or 2 liter)
Millipore filtration apparatus to fit side-arm flask
Millipore polypropylene filters, type HV, pore size 0.45 µm

1. Remove 0.25 ml of the PCA extract, and add to a 2.0-ml microcentrifuge tube containing 50 µl of 0.4 mM γ-Glu-Glu.

   Samples should be derivatized in triplicate.

   The use of γ-glutamyl glutamate as an internal standard for both samples and standards increases the accuracy of the method to >95% as determined for GSH, GSSG, and cysteinyl-glutathione disulfide.

2. Add 50 µl of 100 mM IAA (dissolved in 0.2 mM *m*-cresol purple) to the above tube.

   The solution should turn pink.

   The m-cresol purple included in the IAA solution not only functions as a pH indicator but also acts as a preservative; iodoacetic acid dissolved in m-cresol purple maintains alkylating activity for at least 7 days at 4°C.

3. Add 0.24 ml $KOH/KHCO_3$ solution.

   A precipitate will form and the solution should turn a light purple (pH 8 to 9); add more $KOH/KHCO_3$ solution to bring pH into that range, if necessary.

   The instantaneous pH change, due to the addition of the $KOH/KHCO_3$ solution, in the presence of IAA aids in protecting samples from derivatization-induced thiol oxidation.

4. Incubate 60 min in the dark at room temperature.

   For GSH, the formation of S-carboxymethyl derivatives (following the addition of IAA and $KOH/KHCO_3$ solution) occurs within 5 min (Farris and Reed, 1987).

5. Add 1 ml of 1% FDNB. Cap the mixture, vortex briefly, and store 1 hr at room temperature and then overnight at 4°C.

   Samples should turn yellow. Keep the derivatized samples in the dark by covering tubes with a thick black cloth or aluminum foil.

   The addition of FDNB results in the formation of N-DNP derivatives within 1 hr at room temperature and 4 hr at 4°C. The S-carboxymethyl and N-DNP derivatives are stable for at least 2 weeks at 4°C.

6. Purge HPLC system and begin running mobile phase (80% A/20% B) through the column at a flow of 1.0 ml/min. Maintain this flow rate throughout the gradient that follows.

   The system should be allowed to equilibrate for ~1 hr prior to loading samples.

7. Set up the gradient: from 0 to 8 min, use 80% A/20% B; from 8 to 28 min, use a linear gradient to a final ratio of 1% A/99% B. Hold the mobile phase at 99% B until the final compound, usually GSSG, has eluted.

   The gradient should be adjusted to give the best possible separation of peaks and may need to be lengthened as the column ages.

8. Remove samples from the refrigerator (4°C) and microcentrifuge 1 min at 13,000 × *g*, room temperature.

   Always centrifuge samples just prior to loading into manual or autosampler loops.

9. Rinse the stainless steel loop (total volume = 150 µl) of either a manual injector or an autosampler with 80% methanol using a 1-ml gas-tight syringe. Load 100 µl of the supernatant containing the *N*-DNP derivatives into the loop. Follow this with 20 µl of 80% methanol. Return samples to 4°C.

   Derivatized samples may be stored up to 2 weeks at 4°C.

   Figure 6.2.1 shows a representative HPLC chromatogram of a select mixture of DNP derivatives.

   It is important not to introduce air bubbles into the injector loop(s) and/or column.

10. Prepare a standard curve by running the same derivatization and HPLC gradient with various dilutions of 0.4 mM GSH and GSSG. Quantitate GSH and GSSG as well as other cellular thiols and disulfides in the biological samples by comparison with this standard curve.

    The samples for the standard curve may be prepared and derivatized in triplicate the day prior to the experiment using the reagents prepared for the experiment.

    A range of known quantities of the compounds of interest (GSH and GSSG), along with a constant amount of γ-Glu-Glu (10 to 20 nmol), are derivatized and analyzed by the HPLC/UV technique, and response factors are determined for the compounds. The response factors are then used to quantitate the compounds of interest in each sample.

    The use of internal standards in both samples and standards accurately corrects for alterations in derivatization efficiency and stability, chromatographic conditions (i.e., age of the lamp and/or column), and injection volumes.

DERIVATIZATION AND ANALYSIS OF GSH AND GSSG BY HPLC WITH FLUORESCENCE DETECTION

ALTERNATE PROTOCOL 1

Martin and White (1991) have modified the UV method in Basic Protocol 1 by reacting the *S*-carboxymethyl derivatives, formed following addition of IAA, with dansyl chloride rather than FDNB. The use of dansyl chloride to produce fluorescent derivatives of GSH and GSSG results in increased sensitivity as compared to the UV method, with detection limits for GSH and GSSG reaching 1 pmol and 2 pmol per injection on column, respectively. The drawback to this more sensitive method is that if derivatization with

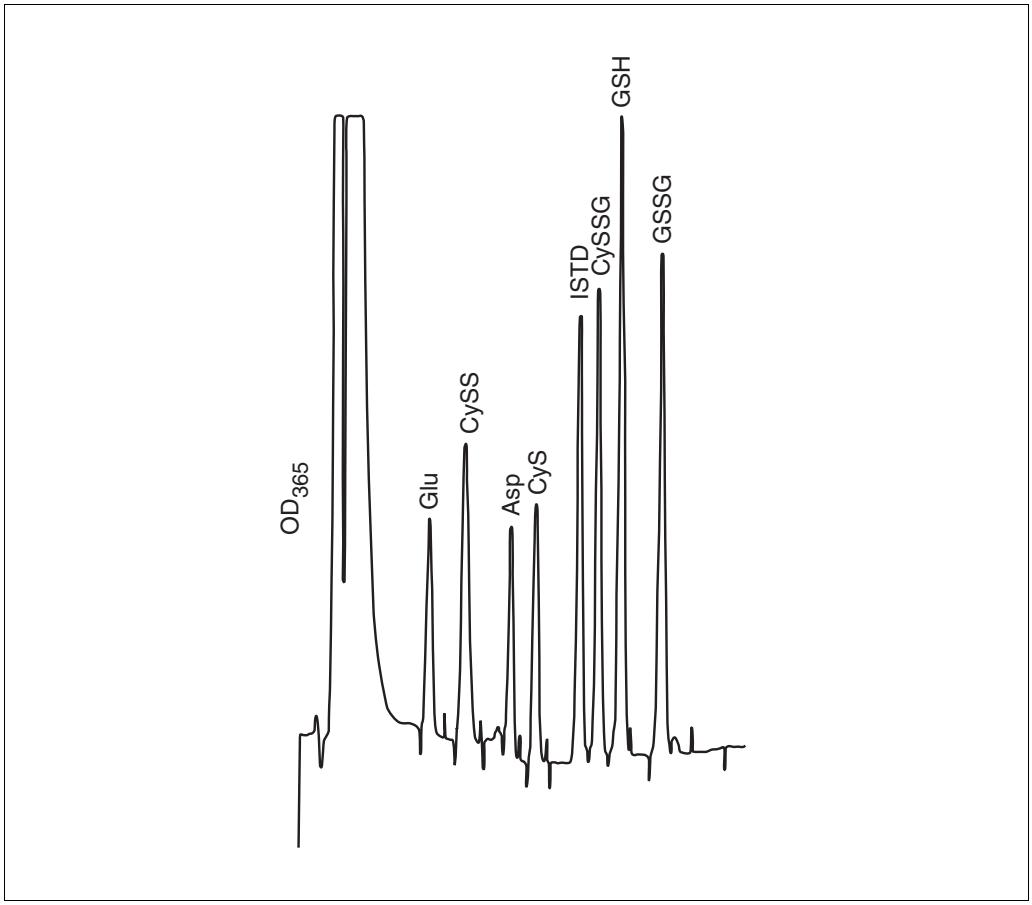

Figure 6.2.1 High-performance liquid chromatograph of a mixture of N-dinitrophenyl-S-carboxymethyl derivatives, including GSH and GSSG. Separation and UV detection were performed under conditions described in Basic Protocol 1. Abbreviations are defined in Table 6.2.1.

dansyl chloride is not complete, a portion of the GSSG is monodansylated and coelutes with the dansylated GSH. Such coelution makes the quantification of GSH and GSSG difficult. Jones et al. (1998) have evaluated the use of dansyl chloride to measure glutathione in human plasma.

Additional Materials *(also see Basic Protocol 1)*

PCA/DEPA indicator solution (see recipe)
1 mg/ml dansyl chloride in acetonitrile
2.0 M LiOH in metal-free water
50 mM IAA in metal-free water (make fresh daily)
0.1 mM γ-Glu-Glu (see recipe)
Fluorescence detector (Hewlett Packard model 1046A; 328 nm excitation and 541 nm emission)

1. Prepare samples (see Support Protocols 1, 2, and 3), replacing PCA/BPDS with PCA/DEPA indicator solution.
2. Remove 200 µl of the acid extract to a microcentrifuge tube.

   Samples should be derivatized in triplicate.
3. Add 5 µl of 0.1 mM γ-Glu-Glu and 20 µl IAA (50 mM).

   Using 0.2 M cresol purple instead of water eliminates the need for hourly preparation of the IAA solution.

4. Add sufficient 2 M LiOH to bring the pH into the range of 8 to 8.5. Vortex briefly and store in the dark for 30 min.

   The approximate amount of 2 M LiOH required may be determined empirically prior to the day of the experiment.

   A precipitate will form and the solution will become mauve in color following addition of LiOH.

   This procedure has been modified to decrease the presence of monodansylated GSSG and its interference with the accurate measurement of derivatized GSH (D. Jones, Emory University, pers. comm; Jones et al., 1998). This is accomplished by substituting 1 M KOH in saturated $K_2B_4O_7$ solution for 2 M LiOH. Sufficient KOH/$K_2B_4O_7$ solution is added to bring the pH of the sample to 9.0 ± 0.2.

5. Add an approximately equal volume of 1 mg/ml dansyl chloride to make a total sample volume of 500 µl. Place samples in the dark and store for 24 hr at room temperature.

   Samples may be stored up to 48 hr at 4°C prior to analysis.

6. Microcentrifuge 1 min at 13,000 × *g*, room temperature.

7. *Optional:* Remove excess dansyl chloride by extracting the derivatized sample with 500 µl of chloroform.

   Sensitivity may be increased by performing this step. (For details, see Martin and White, 1991.)

8. Analyze the supernatant (or the upper aqueous phase from the chloroform extraction, which will contain the dansyl glutathione adducts) on an HPLC system (see Basic Protocol 1, steps 6 to 10), using a fluorescence detector with an excitation wavelength of 328 nm and an emission wavelength of 541 nm.

   A modification of the elution has been reported (Jones et al., pers. comm.) in which the pH of solvent B is reduced to 4.6 (modified solution: 640 ml methanol, 200 ml stock sodium acetate solution, 125 ml glacial acetic acid, and 50 ml metal-free water) so that any monodansylated GSSG that is present will not coelute with the derivatized GSH.

DERIVATIZATION AND ANALYSIS OF GSH AND GSSG BY HPLC WITH ELECTROCHEMICAL DETECTION

ALTERNATE PROTOCOL 2

Electrochemical detection (EC) is the most recent advance for thiol quantification in biological samples. There are two general methods of EC detection, amperemetric and coulometric. Amperemetric methods reach limits of detection of 5 pmol per injection for both GSH and GSSG; however, limits of detection as low as 0.125 pmol GSH and 0.425 pmol GSSG per injection have been reported for coulometric methods using analytical cells with high sensitivity (Krien et al., 1992; Rose and Bode, 1995). EC methods are particularly useful in studies of extrahepatic tissues or cells where limited quantities of material are available. The method described here is based on that of Lakritz et al. (1997), in which the limits of detection have been demonstrated to be 1.63 pmol and 0.8 pmol per injection for GSH and GSSG, respectively.

Additional Materials *(also see Basic Protocol 1)*

Mobile phase: 50 mM NaH_2PO_4/0.05 mM octane sulfonic acid/2% (v/v) acetonitrile adjusted to pH 2.7 with phosphoric acid

200 mM methane sulfonic acid (MSA) containing 5 mM diethylenetriaminepentaacetic acid (DTPA)

Coulometric electrochemical detector with porous graphite electrodes (ESA model 5200, ESA)

Glass Dounce homogenizer

5-µm, 0.4 × 20–cm ODS2 HPLC column

1a. *For freshly dissected tissues:* Remove tissues from animal (see Support Protocol 1, steps 1 to 5) and quickly place fresh (unfrozen) tissue in 200 mM MSA/5 mM DTPA.

The volume of MSA/DTPA used is dependent on the amount of tissue available and the expected concentration of GSH/mg protein.

1b. *For cultured cells:* Scrape cultured cells into 200 mM MSA/5 mM DTPA (see Support Protocol 2, steps 1 to 4, substituting MSA/DTPA for PCA/BPDS).

MSA/DTPA solutions should be kept on ice.

2. Homogenize tissue or cells in 200 mM MSA/5 mM DTPA in a glass Dounce homogenizer.

Samples should be kept on ice during homogenization. The number of strokes depends upon the amount of tissues or cells, as well as whether homogenization is performed by hand or using a drill.

3. Centrifuge for 5 min at 14,000 × *g*, 4°C, and remove supernatant.

Supernatant can be stored at −80°C for subsequent replicate assays; samples are stable for up to 6 weeks.

Protein quantitation (Lowry et al., 1951) should be performed on the acid precipitate to determine the concentration of GSH, GSSG, or other thiol/disulfide of interest, per milligram protein.

4. Dilute supernatant (acid extract) 1:1 with mobile phase. Inject 10 µl onto the preequilibrated column and elute with mobile phase. Monitor elution with a coulometric electrochemical detector using the following settings: guard cell +950 mV, electrode 1 +400 mV, electrode 2 +880 mV.

The column should be equilibrated with mobile phase for 1 hr prior to loading.

Unlike in the two previous HPLC methods, an internal standard is not added to the samples. GSH and GSSG are quantified by use of a standard curve without the inclusion of an internal standard.

BASIC PROTOCOL 2

DERIVATIZATION AND ANALYSIS OF GSH AND GSSG BY ENZYMATIC DETECTION

The enzymatic recycling assay of Griffith (1980) is a modification of an assay developed by Tietze (1969). These assays are sensitive and specific for the quantification of "total glutathione" (GSH and GSSG, measured in GSH equivalents) in a sample; however, the assay must be performed twice on each sample in order to quantitate both GSH and GSSG. The method of Griffith is based on the oxidation of GSH by 5,5′-dithiobis(2-nitrobenzoic acid) (DTNB) to form GSSG and 5-thio-2-nitrobenzoic acid (TNB) coupled with reduction of GSSG to GSH by glutathione reductase in the presence of NADPH. The rate of TNB formation is proportional to the sum of GSH and GSSG present in the sample and is monitored at 412 nm. Quantification of GSSG is accomplished by derivatizing the GSH present in the sample with 2-vinylpyridine prior to enzymatic analysis, thus preventing GSH from participating in the reaction. The amount of GSH in the sample is then calculated by subtracting the value determined for GSSG from that determined for the sum of GSH and GSSG in the sample. Sian et al. (1997) demonstrated linearity to 16 pmol GSSG per cuvette using this method.

Materials

1% (w/v) picric acid
Stock buffer: 143 mM sodium phosphate and 6.3 mM sodium EDTA in metal-free water, pH 7.5
0.3 mM NADPH in stock buffer (prepare fresh daily and store at 4°C)

6 mM DTNB in stock buffer (store for 2 weeks at −20°C)
50 U/ml GSH reductase in stock buffer (store for 2 weeks at −20°C)
2-Vinylpyridine (Fluka; store at −20°C and use undiluted; replace if reagent becomes brown or viscous)
Triethanolamine
Spectrophotometer (412 nm; Alltech 200, Alltech)

1. Prepare samples (see Support Protocols 1, 2, and 3, substituting 1% picric acid for the PCA/BPDS protein precipitating reagent).

   CAUTION: *Use care when using picric acid in the laboratory. Picric acid, a component of explosives and matches, explodes when heated rapidly and by percussion. In addition, this reagent will stain skin, clothing, counters, and floors if allowed to come in contact with these surfaces.*

   Griffith (1980) suggests the use of 1% picric acid, rather than 5-sulfosalicylic acid as suggested by Anderson (1985), because it may eliminate the need for addition of triethanolamine (always check the pH of the acid extract).

   If a metal chelator, such as, EDTA or BPDS, is added to the acid of choice in this step, it must be determined that the chelator does not interfere with the enzymatic assay by running a control assay with and without chelator.

   Use aliquots of the supernatant of the picric acid extract for the determination of both total GSH and GSSG and the pellet for protein analysis.

2. For GSSG determination, add 100 µl of the acid extract supernatant to a microcentrifuge tube, followed by 2 µl of 2-vinylpyridine. Cap and vortex.

3. Check the pH of the extract/2-vinylpyridine solution. If it is not >5.5, add a sufficient volume of triethanolamine to bring the pH up to between 6 and 7.

   Do not increase the pH above 7.0.

   Triethanolamine is difficult to pipet because of its viscosity. Griffith suggests using an 8-µl Drummond Microcap to deliver up to 6 µl of this compound. Add the triethanolamine to the inside of the microcentrifuge tube above the level of the sample/standard, cap, and vortex vigorously.

4. Allow the samples to derivatize for 60 min at room temperature.

5. During the above incubation period, add 700 µl of 0.3 mM NADPH, 100 µl of 6 mM DTNB, and an aliquot of picric acid extract to a test tube. Add metal-free water to a total volume of 1 ml.

   For example, if sample volume is 100 µl, add 100 µl of water. These samples will be used for total glutathione determination.

6. Warm test tubes from step 5 in a 30°C water bath for 10 to 15 min.

7. Transfer the mixture from one test tube to a cuvette containing 10 µl of 50 U/ml GSH reductase and monitor A_{412} continuously until it exceeds 2.0 absorbance units. Continue for all samples.

   The rate of TNB formation is usually linear between 1 and 2 absorbance units.

8. Repeat steps 5 to 7 using the GSSG samples from step 4.

   The derivatized samples are used to determine oxidized glutathione (GSSG).

   2-vinylpyridine may separate from the aqueous sample during the derivatization period; however, do not mix the samples prior to removing the aliquot for analysis.

9. Generate a standard curve using known amounts of GSH dissolved in the protein precipitating agent (1% picric acid) and processed as described in steps 5 to 7. Quantify total glutathione by comparing the underivatized samples to this curve.

   All points on the standard curve should be run in triplicate.

10. Generate a second standard curve using GSSG (dissolved in the protein precipitating reagent) treated with both 2-vinylpyridine (60-min derivatization) and triethanolamine (if used in the samples) prior to enzymatic analysis. Quantify GSSG by comparing derivatized samples to this curve.

    All points on the standard curve should be run in triplicate. GSH levels are determined by subtracting the results from step 10 from the results in step 9.

    Recently, Eady et al. (1995) reported that they were unable to determine GSH levels in some of their cell lines by the Tietze enzymatic recycling method due to the presence of an inhibitory agent that was not identified. Therefore, when using enzymatic assays, it is important to determine if inhibitory agents are present in the samples to be assayed. This can be determined by supplementing cell extracts with known quantities of GSH and assaying both the GSH-supplemented and -unsupplemented cell extracts by the Tietze enzymatic method (Eady et al., 1995).

SAMPLE PREPARATION FOR ANALYSIS OF GSH AND GSSG

Support Protocols 1, 2, and 3 describe the preparation of samples from different sources—tissues, monolayer cells, and hepatocytes—for the determination of intracellular GSH and GSSG. While these protocols have been written with Basic Protocol 1 in mind, they may be modified for use with any of the basic or alternate protocols.

NOTE: Consult Basic Protocols 1 and 2 and Alternate Protocols 1 and 2 to determine the appropriate reagents for preparing the acid extract.

SUPPORT PROTOCOL 1

Preparation of Samples from Freshly Dissected Tissues

Tissue is dissected from the animal and frozen in liquid nitrogen. It is then pulverized, refrozen, and extracted with acid. A modification of this procedure has been developed for the measurement of mitochondrial thiols (Reed, 1994).

NOTE: All protocols using live animals must first be reviewed and approved by an Institutional Animal Care and Use Committee (IACUC) or must conform to governmental regulations regarding the care and use of laboratory animals.

Materials

Animal to be used for tissue studies
1 g/ml sodium pentobarbital
0.9% saline (NaCl; *APPENDIX 2A*) in metal-free water, prewarmed to 37°C
Liquid nitrogen
PCA/BPDS (see recipe)

Peristaltic pump (Barnant 72501-000, VWR)
5-ml cryogenic specimen containers (Nalgene, Fisher)
Mortar and pestle
Ultrasonic cell disrupter (Cole Parmer 4710, Cole Parmer)

1. Anesthetize animal with sodium pentobarbital at a dose of 60 mg/kg body weight (i.p.; dosage determined for rats).
2. Open the abdominal and thoracic cavities and draw blood from either the heart or the inferior vena cava to euthanize the animal.

   Draw blood from the same source for all animals. This blood may be used in assays, if desired.

3. Insert tubing attached to a peristaltic pump into the hepatic portal vein and perfuse the liver with 37°C saline.

4. Remove the liver and, while holding it above a liquid nitrogen–filled cryogenic container, quickly slice the liver into several pieces with scissors, allowing the pieces to fall into the container. Replace the lid on the cryogenic container and store samples in liquid nitrogen or at −70°C for up to 24 hr.

5. Remove additional organs of interest from the anesthetized animal. Rinse each organ with 0.9% NaCl and place it in a cryogenic container filled with liquid nitrogen. Replace lid and store as for liver samples.

   Tissues with high levels of γ-glutamyl transpeptidase, such as kidney and pancreas, should not be frozen and stored in liquid nitrogen, but must be homogenized immediately in PCA/BPDS following removal from the body in order to prevent the loss of both GSH and GSSG (Anderson, 1985; Potter and Tran, 1993). Following homogenization of fresh tissue in PCA, skip to step 9 below.

6. Pour a small amount of liquid nitrogen into a large mortar and pulverize the frozen tissue samples to a fine powder with a pestle. Return the powdered sample to the cryogenic container and store in liquid nitrogen or at −70°C until ready to begin step 7.

   Do not allow the sample to thaw until it has been added to the PCA/BPDS solution.

7. Weigh 50 to 100 mg of the frozen, powdered tissue into a microcentrifuge tube containing 1 ml PCA/BPDS.

   Prompt addition of PCA/BPDS to frozen biological specimens is essential to the rapid termination of metabolic processes and to the prevention of thiol oxidation in tissues, cells, cell organelles, and fluids.

   BPDS has excellent copper- and iron-chelating properties and is used instead of EDTA, because EDTA interferes with the HPLC measurement of GSSG.

8. Sonicate the sample on ice for 30 sec using a power setting of 4.5.

9. Freeze the sonicated, homogenized sample in liquid nitrogen and allow it to thaw on ice.

10. Microcentrifuge the thawed sample 3 min at 15,000 × *g*, room temperature. Remove the supernatant (acid extract) and proceed directly to derivatization for determination of acid-soluble sulfur-containing compounds, i.e., GSH, GSSG, and sulfur-containing amino acids (see Basic Protocols 1 and 2; see Alternate Protocols 1 and 2).

    The protein precipitate can be used for the quantification of proteins and protein-mixed disulfides or DNA.

    Work by Roberts and Francetic (1993) suggests that the acid extract can also be stored up to 12 months at −70°C before derivatization.

Preparation of Samples from Cultured Cells

SUPPORT PROTOCOL 2

Cultured adherent cells are being used in an increasing number of studies investigating the role of both GSH and GSSG in normal cell growth, metabolism, and death, as well as the role of GSH in protection from exogenously caused oxidative damage. As with tissues, it is important to stop all metabolic activity in the cell monolayer as quickly as possible. Scraping cell monolayers from dishes directly into PCA/BPDS has been found to give the highest yields and most reproducible results for GSH in cell culture as compared to trypsinization or scraping monolayer cells into PBS (Thioudellet et al., 1995; D.J. Mustacich and D.J. Reed, unpub. observ.).

Materials

Cultured adherent cells
PBS (*APPENDIX 2A*), ice cold
PCA/BPDS (see recipe)

1. Remove medium from tissue culture dish and rinse cell monolayers with 5 ml ice-cold PBS.
2. Remove the PBS and rinse cells a second time with another 5 ml ice-cold PBS.
3. Determine the total amount of PCA/BPDS to be used and immediately add half of this amount to the monolayer.

   The amount of PCA/BPDS is often in the range of 1 to 5 ml but will need to be adjusted depending on the cell number and level of GSH in control cells.
4. Scrape the cells from the dish while covered with PCA/BPDS and transfer suspended cells to a 15-ml (or other appropriately sized) conical centrifuge tube.
5. Repeat steps 3 and 4 with the second half of the PCA/BPDS, and pool both suspensions.
6. Sonicate the cell suspension on ice for 30 sec using a power setting of 4.5 and centrifuge 5 min at 10,000 × *g*, 4°C.
7. Remove the supernatant (acid extract). Proceed immediately to derivatization (see Basic Protocols 1 and 2; see Alternate Protocols 1 and 2) or store extract at −70°C until derivatized.

   Since cell counts cannot be performed on cells scraped directly into PCA/BPDS, proteins should be quantitated on the precipitated pellet for determination of GSH and other thiols per milligram protein.

SUPPORT PROTOCOL 3

Preparation of Sample from Hepatocytes

Experiments utilizing isolated hepatocytes (see Farris et al., 1985, for preparation of isolated hepatocytes) to investigate the mechanism(s) of chemical toxicity and cell death require separation of viable cells from nonviable cells to distinguish events that result in cell death from those that result from cell death. Figure 6.2.2 illustrates a technique used to separate viable from nonviable cells and terminate metabolic processes and thiol oxidation in one quick step (Farris et al., 1985).

Materials

PCA/BPDS (see recipe)
Dibutyl phthalate (Sigma)
Isolated hepatocytes

1. Add 0.55 ml PCA/BPDS to a 2.0-ml microcentrifuge tube.
2. Carefully layer 0.45 ml dibutyl phthalate (d = 1.046) over the PCA/BPDS (d = 1.06) and centrifuge 1 min at 13,000 × *g*, room temperature.
3. Carefully layer 0.75 ml of isolated hepatocyte suspension over the dibutyl phthalate layer.
4. Microcentrifuge 1 min at 13,000 × *g*, room temperature.

   This results in viable hepatocytes being forced through the dibutyl phthalate layer into the PCA/BPDS, which lyses the hepatocytes, thereby releasing the intracellular contents of the hepatocytes into the PCA/BPDS layer. The medium and nonviable cells remain above the dibutyl phthalate layer.
5. Remove a portion of the PCA/BPDS layer. Either derivatize immediately (see Basic Protocols 1 and 2; see Alternate Protocols 1 and 2) or store at −70°C until derivatized.

   As shown in Figure 6.2.2, intracellular GSH and GSSG, as well as other cellular thiols and disulfides, are located in the PCA/BPDS layer (bottom layer).

   Extracellular constituents, such as GSH and GSSG, may be measured by derivatizing the medium that remains above the dibutyl phthalate layer (Fig. 6.2.2).

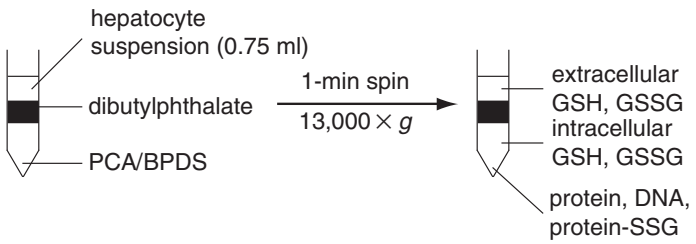

Figure 6.2.2 Analysis of intracellular contents and cell viability by the dibutyl phthalate separation method. PCA, perchloric acid; GSH, glutathione; GSSG, glutathione disulfide; protein-SSG, protein-glutathione mixed disulfide.

REAGENTS AND SOLUTIONS

Use Milli-Q-purified water or equivalent for all recipes and protocol steps. For common stock solutions, see ***APPENDIX 2A****; for suppliers, see* ***SUPPLIERS APPENDIX****.*

γ-Glutamyl-glutamate (γ-Glu-Glu), 0.1 mM

Prepare a stock solution of 4 mM γ-Glu-Glu in water containing 15 mM bathophenanthrolinedisulfonic acid (BPDS). This can be made in a quantity of 5 ml or more and then divided into aliquots of 25 µl (in microcentrifuge tubes) and stored at −20°C indefinitely. On the day of the experiment, remove one or more tubes and add 975 µl PCA/BPDS (see recipe) to each tube. Vortex and place on ice.

Make fresh working samples immediately prior to use.

γ-Glutamyl-glutamate (γ-Glu-Glu), 0.4 mM

Prepare a stock solution of 4 mM γ-Glu-Glu in water containing 15 mM bathophenanthrolinedisulfonic acid (BPDS). This can be made in a quantity of 5 ml or more and then divided into aliquots of 100 µl (in microcentrifuge tubes) and stored at −20°C indefinitely. On the day of the experiment, remove one or more tubes and add 900 µl PCA/BPDS (see recipe) to each tube. Vortex and place on ice.

Make fresh working samples immediately prior to use.

GSH (reduced glutathione), 0.4 mM

Prepare a stock solution of 4 mM GSH (free acid) in water containing 15 mM bathophenanthrolinedisulfonic acid (BPDS). Dilute 1:10 in PCA/BPDS (see recipe) to obtain working solution.

Make both solutions immediately prior to derivatization of standard curve.

GSSG (oxidized glutathione), 0.4 mM

Prepare a stock solution of 4 mM GSSG (free acid) in water containing 15 mM bathophenanthrolinedisulfonic acid (BPDS). Dilute 1:10 in PCA/BPDS (see recipe) to obtain working solution.

Make both solutions immediately prior to derivatization of standard curve.

Iodoacetic acid (IAA) in 0.2 mM m-cresol purple, 100 mM

Make a 0.2 mM solution of *m*-cresol purple by dissolving 8.1 mg *m*-cresol purple in 10 ml water. Dissolve 20.8 mg iodoacetic acid (sodium salt) in 1 ml of the 0.2 mM *m*-cresol purple to make a 100 mM solution. Store in the dark in a container designed for light-sensitive compounds for up to 1 week at 4°C.

The use of m-cresol purple in the IAA solution not only functions as a pH indicator but also acts as a preservative. Iodoacetic acid dissolved in m-cresol purple maintains alkylating activity for at least 7 days at 4°C.

$KOH/KHCO_3$ solution

Make 10 M KOH by dissolving 56.1 g KOH in 100 ml water. Make 3 M $KHCO_3$ by dissolving 60.1 g $KHCO_3$ in 200 ml water. Combine 40 ml of 10 M KOH with 160 ml of 3 M $KHCO_3$. Store up to 1 week at room temperature.

Mobile phase A

Add 800 ml water to 3.2 liters methanol (HPLC grade).

It is important to always make the mobile phases in the same manner. The solution may be made up to 24 hr in advance and stored at room temperature.

Mobile phase B

Make a 4.0 M sodium acetate stock solution by adding 544 g sodium acetate trihydrate to 224 ml water, then add 756 ml glacial acetic acid. Stir solution over low heat until sodium acetate is in solution. Allow stock solution to cool, then add 800 ml of the stock sodium acetate solution to 3.2 liters of 80% methanol (mobile phase A; see recipe). Mix and filter with a 0.45-μm polypropylene filter.

Store the stock sodium acetate solution at room temperature for up to 1 month. Mobile phase B may be made up to 24 hr in advance and stored at room temperature.

PCA/BPDS

Make a 10% (v/v) solution of perchloric acid (PCA) in water by diluting 70% PCA commercial stock. Dissolve 53.65 mg bathophenanthrolinedisulfonic acid (BPDS) in 100 ml of the 10% PCA to create a 1 mM solution. Store at 4°C. Make fresh weekly.

PCA/DEPA

35.7 ml 70% (v/v) perchloric acid (PCA; 5% final)
0.393 g diethylenetriaminepentaacetic acid (DEPA; 0.2 M final)
6.2 g boric acid (0.2 M final)
2.5 mg cresol red indicator (5 mg/ml final)
H_2O to 500 ml
Store at 4°C. Make fresh weekly.

COMMENTARY

Background Information

Glutathione, the most abundant low-molecular-weight nonprotein thiol found in cells, exists mainly in the reduced state (GSH), with <5% of the total existing as glutathione disulfide (GSSG) under normal physiologic conditions. The GSH/GSSG redox cycle, one of the major endogenous antioxidant systems, protects cells from injurious events resulting from exposure to toxic chemicals, as well as the normal oxidative products of cellular metabolism. The large GSH/GSSG ratio creates a challenge for detection, since very low levels of GSSG need to be accurately determined, and oxidation of GSH to GSSG has to be prevented during sample preparation and derivatization. This is particularly important in studies where alterations in the GSH/GSSG ratio resulting from the presence of endogenous or exogenous compounds are being determined over time. In Basic Protocol 1, thiol oxidation and thiol-disulfide interchange are inhibited during sample preparation and derivatization by (1) the prompt treatment of biologic samples with perchloric acid (PCA) containing a metal chelator (BPDS), (2) the continued presence of BPDS during derivatization, and (3) the instantaneous pH change in the presence of iodoacetic acid (IAA) resulting in the rapid formation of *S*-carboxymethyl derivatives of GSH.

Over the years, analytical methods of glutathione quantification have reflected the demands of current research. Sample preparations with acid extract concentrations of GSH in the micromolar range are easily analyzed with enzymatic or HPLC/UV detection techniques. However, there has been increasing emphasis on measuring the GSH/GSSG ratio within subcellular organelles and extrahepatic tissues. Some of these samples require more sensitive detection methods due either to the low levels of GSH and/or GSSG present or to small sample size.

Analysis of GSH, GSSG, and other sulfur-containing compounds by HPLC/UV is appropriate for freshly dissected tissues (see Support Protocol 1), cultured cells (see Support Protocol 2), hepatocytes (see Support Protocol 3), mitochondrial preparations, serum, and plasma (see Farris and Reed, 1987). However, this method should not be used for the measurement of GSSG in whole blood. A modification of the Farris and Reed method for measuring GSSG in whole blood has been developed in which *N*-ethylmaleimide (NEM) rather than IAA is used to prevent GSH oxidation (Asensi et al., 1994). However, the NEM method cannot be used for GSSH quantification because the GSH-NEM adduct decomposes, resulting in the formation of three separate HPLC peaks. In order to accurately measure both GSSG and GSH in whole-blood samples, a second method must be used for the measurement of GSH. The glutathione-*S*-transferase assay for GSH, developed by Brigelius et al. (1983), can be used in combination with the NEM method for the determination of both GSH and GSSG in whole blood.

Critical Parameters and Troubleshooting

One of the most important determinants of accurate assessment of the GSH/GSSG ratio is fast and careful sample preparation and derivatization. As discussed in Support Protocol 1, tissue samples with low levels of γ-glutamyl transpeptidase (such as liver, heart, brain, and spleen) may be frozen in liquid nitrogen and stored at −70°C for 24 hr prior to derivatization. However, tissues and cells containing high levels of γ-glutamyl transpeptidase (such as kidney) need to be homogenized immediately, without freezing, in PCA/BPDS in order to avoid enzymatic degradation. In addition, derivatized samples should be maintained in the dark at all times by covering them with a thick black cloth or aluminum foil.

When selecting a method, it is important to verify its ability to quantify the thiol or disulfide of choice in the system being studied. To this end recovery studies should be performed in which known amounts of the thiol of interest are added to samples at levels similar to endogenous levels. The thiol is then quantified in both supplemented and unsupplemented samples and percent recovery of the thiol is determined. For the methods described in this unit, recovery should be at least 90%.

The addition of GSH to a sample during acid precipitation, followed by derivatization and quantification of both GSH and GSSG in supplemented and unsupplemented samples, can be used to determine the extent to which GSH is being oxidized to GSSG during the procedure. Farris and Reed (1987) determined that <0.7% of GSH is converted to GSSG during sample preparation and derivatization with their method, and suggest that GSSG levels be corrected for this oxidative artifact. Furthermore, AT125 (acivicin), an inhibitor of γ-glutamyl transpeptidase, can be used to determine the extent to which GSH may be being enzymatically degraded in the system of choice during preparation (Reed and Ellis, 1982).

Finally, a coefficient of variance should be determined for the selected assay by quantifying the thiol of choice in replicate samples (five or more replicates per sample). The coefficient of variance should be <10% for all of the protocols described here.

Anticipated Results

GSH and GSSG levels will vary depending on the species, cell or tissue type, and/or subcellular organelle chosen for study. Most mammalian cells contain GSH at millimolar concentrations; therefore, the amount of material available may determine which assay is chosen for a particular study. The UV method described here has been used for the analysis of most of the organs in the rat and mouse, as well as mitochondrial preparations from liver, kidney, and lung. The limits of detection for each method are given in the protocol introductions.

Time Considerations

Many of the reagents for these assays can be made in advance. In addition, separate tubes should be labeled for the various steps in the procedure the day before the experiment (cryo containers for tissue samples to be frozen, and microcentrifuge tubes for the acid precipitation and derivatization procedures). Finally, the standard curve samples may be prepared and derivatized the day before the experiment using the reagents prepared for the experiment. Depending on the number of samples to be analyzed, preparation for the experiment may require 4 to 6 hr the first time the assay is performed. This time includes making the reagents and mobile phases and setting up and derivatizing the standard curve. Sample preparation time on the day of the experiment will vary with the choice of biologic material. The removal of organs from an anesthetized animal takes minutes, while preparation of hepatocytes requires 1 to 2 hr. HPLC analysis by the UV method

may take 35 to 45 min per sample depending on the age of the column; therefore, use of an autosampler is recommended, particularly if large numbers of samples will be analyzed.

Literature Cited

Anderson, M.E. 1985. Determination of glutathione and glutathione disulfide in biological samples. *Methods Enzymol.* 113:548-555.

Asensi, M., Sastre, J., Pallardó, F.V., García de la Asunción, J., Estrela, J.M., and Viña, J. 1994. A high-performance liquid chromatography method for measurement of oxidized glutathione in biological samples. *Anal. Biochem.* 217:323-328.

Brigelius, R., Muckel, C., Akerboom, T.P.M., and Sies, H. 1983. Identification and quantitation of glutathione in hepatic protein mixed disulfides and its relationship to glutathione disulfide. *Biochem. Pharmacol.* 32:2529-2534.

Eady, J.J., Orta, T., Dennis, M.F., Tratford, M.R.L., and Peacock, J.H. 1995. Glutathione determination by the Tietze enzymatic recycling assay and its relationship to cellular radiation response. *Br. J. Cancer* 72:1089-1095.

Farris, M.W. and Reed, D.J. 1987. High-performance liquid chromatography of thiols and disulfides: Dinitrophenol derivatives. *Methods Enzymol.* 143:101-109.

Farris, M.W., Brown, M.K., Schmitz, J.A., and Reed, D.J. 1985. Mechanism of chemical-induced toxicity. I. Use of a rapid centrifugation technique for the separation of viable and nonviable hepatocytes. *Toxicol. Appl. Pharm.* 79:283-295.

Griffith, O.W. 1980. Determination of glutathione and glutathione disulfide using glutathione reductase and 2-vinylpyridine. *Anal. Biochem.* 106:207-212.

Jones, D.P., Carlson, J.L., Samiec, P.S., Sternberg, P. Jr., Mody, V.C. Jr., Reed R.L., and Brown, L.A. 1998. Glutathione measurement in human plasma. Evaluation of sample collection, storage and derivatization conditions for analysis of dansyl derivatives by HPLC. *Clin. Chim. Acta.* 275:175-184.

Krien, P.M., Margou, V., and Kermici, M. 1992. Electrochemical determination of femtomole amounts of free reduced and oxidized glutathione. Application to human hair follicles. *J. Chromatogr.* 576:255-261.

Lakritz, J., Plopper, C.G., and Buckpitt, A.R. 1997. Validated high-performance liquid chromatography–electrochemical method for determination of glutathione and glutathione disulfide in small tissue samples. *Anal. Biochem.* 246:63-68.

Lowry, J.C., Rosebrough, N.J., Farr, A.L., and Radall, R.J. 1951. Protein measurement with the Folin phenol reagent. *J. Biol. Chem.* 193:265-275.

Martin, J. and White, I.N.H. 1991. Fluorimetric determination of oxidised and reduced glutathione in cells and tissues by high-performance liquid chromatography following derivatization with dansyl chloride. *J. Chromatogr.* 568:219-225.

Potter, D.W. and Tran, T. 1993. Apparent rates of glutathione turnover in rat tissues. *Toxicol. Appl. Pharm.* 120:186-192.

Reed, D.J. 1994. A centrifuge filtration separation of cells, and the measurement of constituents. *Methods Toxicol.* 1(B):421-430.

Reed, D.J. and Ellis, W.W. 1982. Influence of γ-glutamyl transpeptidase inactivation on the status of extracellular glutathione and glutathione conjugates. *In* Biological Reactive Intermediates IIA. (R. Snyder, D.V. Parke, J.J. Kocsis, D.J. Jollow, C.D. Gibson, and C.M. Witmer, eds.) pp. 75-86. Plenum, New York.

Reed, D.J., Babson J.R., Beatty, P.W., Brodie, A.E., Ellis, W.W., and Potter, D.W. 1980. High-performance liquid chromatography analysis of nanomole levels of glutathione, glutathione disulfide, and related thiols and disulfides. *Anal. Biochem.* 106:55-62.

Roberts, J.C. and Francetic, D.J. 1993. The importance of sample preparation and storage in glutathione analysis. *Anal. Biochem.* 211:183-187.

Rose, R.C. and Bode, A.M. 1995. Analysis of water-soluble antioxidants by high-pressure liquid chromatography. *Biochem. J.* 306:101-105.

Sian, J., Dexter, D.T., Cohen, G., Jenner, P.G., and Marsden, C.D. 1997. Comparison of HPLC and enzymatic recycling assays for measurement of oxidized glutathione in rat brain. *J. Pharm. Pharmacol.* 49:332-335.

Thioudellet, C., Oster, T., Leroy, P., Nicolas, A., and Wellman, M. 1995. Influence of sample preparation on cellular glutathione recovery from adherent cells in culture. *Cell Biol. Toxicol.* 11:103-111.

Tietze, F. 1969. Enzymatic method for quantitative determination of nanogram amounts of total and oxidized glutathione: Applications to mammalian blood and other tissues. *Anal. Biochem.* 27:502-522.

Contributed by Debbie Mustacich
Arizona Cancer Center
Tucson, Arizona

Measurement of Glutathione Transport

The development of methods for accurately measuring the transport of glutathione (GSH) or any metabolite across cellular membranes requires that compartments be efficiently separated. Although some contamination of the space of interest (e.g., intracellular space) is usually unavoidable, quantification of this contamination is critical so that corrections can be made. With GSH as the transport substrate, the redox status of the molecule must be maintained during transport incubations and sample processing. The thiol group of the GSH cysteinyl residue can be readily oxidized in extracellular compartments, either by oxidases or by auto-oxidative processes, particularly in alkaline compartments. In addition, the g-glutamyl residue can be cleaved by g-glutamyltransferase (GGT; EC 2.3.2.2), which is present in large excess in lumenal membranes of several epithelial tissues, such as the renal proximal tubule and small-intestinal epithelium. This oxidation and degradation must be prevented to accurately quantitate the content of GSH in different compartments.

This unit will describe methods for measuring GSH transport into renal proximal tubular cells (see Basic Protocol 1 and Alternate Protocol 1) and into renal cortical mitochondria (see Basic Protocol 2 and Alternate Protocol 2). While these procedures generally apply to measurement of GSH transport in cells or subcellular fractions from other tissues, properties of the kidneys most clearly illustrate the need for appropriate procedures to measure GSH flux accurately. Methods are described for rapidly stopping transport processes at specified times, isolating proximal tubule cells (Support Protocol 1), separating compartments by filtration or centrifugation procedures (Support Protocol 2), quantification of the volume of transport compartments and contaminating space (Support Protocol 4), and ensuring the integrity of the transported substrate by HPLC (Support Protocol 3; also see *UNIT 6.2*). Other methods for incubation and analysis of GSH transport in renal mitochondria have been previously described (Lash, 1995).

CAUTION: When working with radioactivity, take appropriate precautions to avoid contamination of the experimenter and the surroundings. Carry out the experiment and dispose of wastes in an appropriately designated area, following the guidelines provided by the local radiation safety officer (see *APPENDIX 1A*).

NOTE: All protocols using live animals must first be reviewed and approved by an Institutional Animal Care and Use Committee (IACUC) or must conform to governmental regulations regarding the care and use of laboratory animals.

MEASUREMENT OF GSH UPTAKE IN PROXIMAL TUBULAR CELLS FROM RAT KIDNEY

BASIC PROTOCOL 1

This protocol describes a procedure for quantifying GSH uptake by renal proximal tubular (PT) cells. Two critical points in the accurate determination of flux of GSH across renal plasma membranes are that: (1) GSH be neither significantly oxidized nor degraded during transport incubations or sample processing; and (2) contamination of intracellular space with material from the extracellular space be minimized or accounted for so that corrections can be made. The first point is addressed by pretreating cells with acivicin, which is an irreversible inhibitor of GGT (Reed et al., 1980), and by adding an antioxidant during sample processing to prevent auto-oxidation. The second point is addressed by rapid centrifugation of cells through Percoll and monitored by quantifying extracellular volume using a radiolabeled, impermeable solute (i.e., [^{14}C]sucrose; see Support Protocol 4). The following protocol may be used for measuring GSH uptake at incubating concentrations of 0.5 mM or higher using HPLC analysis. A more sensitive method for measuring GSH uptake using radiolabeled substrate is presented in Alternate Protocol 1, which can be used with GSH concentrations as low as 1 μM.

Contributed by Lawrence H. Lash

Current Protocols in Toxicology (1999) 6.3.1-6.3.14

Materials

10× acivicin stock solution (see recipe)
Freshly isolated renal PT cell suspension in 25-ml polypropylene Erlenmeyer flasks (see Support Protocol 1)
10× GSH stock solution (see recipe)
p-aminohippurate (PAH; Sigma)
p-[glycyl-1-,^{14}C]-aminohippuric acid (40 to 60 mCi/mmol; NEN Life Science)
20% (v/v) Percoll (Sigma) in 0.9% (w/v) NaCl
Normal saline: 0.9% (w/v) NaCl (*APPENDIX 2A*)
70% (v/v) perchloric acid
1.5 mM L-γ-glutamyl-L-glutamate (Sigma; prepare fresh in deionized water)
1.5 mM bathophenanthroline disulfonate (Sigma; prepare fresh in deionized water)

25-ml polypropylene Erlenmeyer flasks (e.g., Nalgene)
Dubnoff shaking metabolic incubator (Precision Scientific)
1.5-ml polyethylene microcentrifuge tubes

Treat cells to inhibit GGT activity

1. Add 1 vol of 10× acivicin stock solution to 9 vol renal PT cells (1–5 × 10^6 cells/ml) in a 25-ml polypropylene Erlenmeyer flask.

   Total volume in Erlenmeyer flasks should not exceed 3.0 ml. The final concentration of acivicin is 0.25 mM. Typically, one rat will yield sufficient cells for three to five incubations.

2. Incubate on a Dubnoff metabolic shaking incubator for 15 min at 60 cycles/min, 37°C.

3. Keep cells on ice until needed for transport experiments.

Perform transport incubations

4. In 25-ml Erlenmeyer flasks, gently mix 9 vol of acivicin-pretreated, renal PT cell suspension with 1 vol 10× GSH stock solution.

   Total volume should not exceed 3.0 ml.

   It is important to include a control for measurement of GSH transport in renal proximal tubular cells to demonstrate that the cells are functioning properly. This is accomplished by measuring the transport of a well-characterized substrate, such as p-aminohippurate (PAH). Substitute 1 mM PAH containing 0.1 μCi of p-[glycyl-1-,^{14}C]-aminohippuric acid for the 10× GSH stock solution and process as with the test samples. After step 8, measure radioactivity as described in Alternate Protocol 1, steps 2 to 4, using the ^{14}C channel.

5. Incubate on a Dubnoff shaking metabolic incubator at 60 cycles/min, 37°C.

6. At specified incubation time points (e.g., 1, 2, 3, 5, 10, 15, 20, and 30 min), remove 0.5-ml aliquots and layer on top of 1.0 ml of 20% Percoll in 1.5-ml microcentrifuge tubes at room temperature.

Measure transport

7. Immediately microcentrifuge each sample for 30 sec at 13,000 × *g*, room temperature.

8. Completely remove supernatant with a Pasteur pipet and drain tube dry.

9. Resuspend cell pellets in 0.5 ml normal saline. Add 0.1 ml of 70% (v/v) perchloric acid, 0.05 ml of 1.5 mM L-γ-glutamyl-L-glutamate, and 0.05 ml of 1.5 mM bathophenanthroline disulfonate. Mix vigorously on a vortex mixer.

10. Place 0.5 ml of the acid extract from step 9 into a new 1.5-ml microcentrifuge tube. Store on ice until ready for HPLC analysis of GSH content (see Support Protocol 3).

MEASUREMENT OF GSH TRANSPORT USING RADIOLABELED GSH

ALTERNATE PROTOCOL 1

A more sensitive method of measuring GSH transport uses radiolabeled GSH. This assay can be used with GSH concentrations as low as 1 μM.

Additional Materials *(also see Basic Protocol 1)*

10× GSH stock solution (see recipe) containing 0.01 μCi/ml L-[^{3}H]glycyl-GSH (20 to 50 Ci/mmol; NEN Life Science)
5-ml polyethylene scintillation vials

1. Pretreat PT cells with acivicin and perform time course of incubation with GSH (see Basic Protocol 1, steps 1 to 8), except use 1 vol 10× GSH stock solution containing 0.01 μCi/ml of L-[^{3}H]glycyl-GSH per vol cell suspension, instead of the solution containing cold GSH alone.

   [^{35}S]GSH may be used instead of the ^{3}H-labeled compound.

2. Resuspend each cell pellet in 0.5 ml normal saline. Add 0.1 ml of 70% (v/v) perchloric acid and 0.1 ml of normal saline, then mix vigorously on a vortex mixer.

3. Place 0.5 ml of the acid extract from step 2 in a 5-ml polyethylene scintillation vial.

4. Add 2 ml of scintillation fluid and determine radioactivity by liquid scintillation counting using the ^{3}H channel.

5. Calculate the amount of GSH transported by the following equation:

$$\frac{\text{cpm}}{\text{counting efficiency}} \times \text{dilution factor (ml}^{-1}) \times \text{specific activity (mol/Ci)} \times \frac{1\ \text{Ci}}{2.22\times10^{12}\ \text{cpm}} \times \frac{1\ \text{ml}}{y\times10^{6}\ \text{cells}} = \text{mol GSH transported}/10^{6}\ \text{cells}$$

   where cpm is the result from scintillation counting (see step 4) and *y* (multiplied by 10^6) is the original number of cells in the assay (see step 1).

   The dilution factor is obtained by considering the dilution of the cells during acivicin pretreatment (10/9), the dilution in the incubation (10/9), and the portion sampled for measurement (1/0.5 = 2). Hence, using the dilutions described above, the overall sample dilution = 2.469 ml $^{-1}$ cells.

ISOLATION OF PT CELLS FROM RAT KIDNEY

SUPPORT PROTOCOL 1

This protocol is used to isolate proximal tubule cells from the rat kidney for GSH transport studies. Perfused kidneys are treated with collagenase to release PT cells, which are collected after Percoll gradient centrifugation (Lash and Tokarz, 1989; Lash, 1996).

Materials

Rats (Sprague-Dawley or Fisher 344, 2- to 4-month-old males or 2.5- to 6-month-old females, 175 or 250 g body weight)
50 mg/ml sodium pentobarbital in saline
0.2% (w/v) heparin
Perfusion buffer: Hanks' balanced salt solution (HBBS; *APPENDIX 2A*) without calcium and with 0.12 mM magnesium and 0.5 mM EGTA
Collagenase solution (see recipe)
1× Krebs-Henseleit buffer (see recipe)
45% (v/v) Percoll (Sigma) in HBSS (*APPENDIX 2A*) without calcium and with 0.12 mM magnesium
HBSS (*APPENDIX 2A*) without calcium and with 0.12 mM magnesium

Surgical instruments
4-O silk ligatures
Peristaltic perfusion pump (e.g., MasterFlex), tubing, and cannulas (MasterFlex size 16 to give 0.2 to 20 ml/min; 19-G, cone-shaped)
50-ml round-bottom polycarbonate centrifuge tubes
Sorvall RC-2B or equivalent centrifuge
25-ml polypropylene Erlenmeyer flasks (e.g., Nalgene)
Rubber serum-bottle stoppers (Fisher or VWR)
95% O_2/5% CO_2 gas cylinder with regulator valve

1. Anesthetize rats with an intraperitoneal injection of sodium pentobarbital (0.1 ml of a 50 mg/ml solution in saline per 100 g body weight). Prevent blood clotting by injecting 0.2 ml of 0.2% (w/v) heparin into the tail vein just before surgery.
2. Open the peritoneal cavity by making a midventral incision and free the aorta from the surrounding connective tissue and the adjacent inferior vena cava. Place a 4-O silk ligature around the aorta approximately 0.5 inches below the renal artery and a second ligature around the aorta as high up in the abdomen as possible. Ligate the celiac and superior mesenteric arteries to prevent diversion of perfusate.
3. Make an oblique incision through approximately 50% of the diameter of the aorta above the lower ligature, then insert a cone-shaped 19-gauge cannula into the aorta. Secure the cannula with a new ligature.
4. Perfuse kidneys in situ with 37°C perfusion buffer for 10 min at 5 ml/min with recirculation. Remove the kidneys and euthanize the animal by bilateral pneumothorax and exsanguination.
5. Transfer kidneys to a beaker containing 50 ml of 37°C collagenase solution and perfuse with recirculation for 15 to 18 min at 8 ml/min.
6. Remove kidneys from collagenase and release cortical cells into 40 ml fresh 1× Krebs-Henseleit buffer by removing the renal capsule and connective tissue with scissors and gently squeezing with forceps.

   Cortical cells, although primarily of proximal tubular origin, also contain cells from other nephron segments, including the distal convoluted tubules, cortical collecting tubules, and cortical collecting duct. To obtain an enriched preparation of proximal tubular cells, further processing is required (see steps 7 to 9).

7. Layer 5 ml of renal cortical cell suspension on top of 35 ml of 45% Percoll solution in a 50-ml round-bottom, polycarbonate centrifuge tube and centrifuge 30 min at 20,500 × *g*, 0° to 4°C.
8. Harvest the top 8 ml of the gradient (containing the cells), free pool cells from all gradients, and dilute pooled suspension 5-fold with calcium-free and low-magnesium HBSS. Centrifuge in a tabletop centrifuge 5 min at 1000 × *g*, room temperature, and decant the supernatant to remove Percoll.
9. Resuspend cell pellet in Krebs-Henseleit buffer to a concentration of 2–5 × 10^6 cells/ml and place 2- to 3-ml aliquots in 25-ml polypropylene Erlenmeyer flasks. Purge the flasks for 1 min with 95% O_2/5% CO_2, and seal with rubber serum-bottle stoppers. Keep on ice until used for experiments.

   Degree of purity or enrichment of the PT cell preparation can be assessed by measurement of marker enzymes or functional responses (Lash and Tokarz, 1989). Marker enzymes for PT cells include γ-glutamyltransferase and alkaline phosphatase, both of which are present on brush-border membranes and are at high activities in PT cells but very low in other nephron cell types. Hexokinase can be measured as a distal tubular cell marker and should be present at very low activity in PT cells. Cellular respiration in PT cells, which can be measured with a Clark-type oxygen electrode, should be stimulated by addition of succinate

or other citric acid cycle intermediates. In contrast, these metabolites do not affect cellular oxygen consumption in other nephron cell types, because they are not transported across the plasma membranes in those cells.

MEASUREMENT OF GSH UPTAKE IN SUSPENSIONS OF MITOCHONDRIA FROM RAT KIDNEY CORTEX

BASIC PROTOCOL 2

The incubation protocol described below is for measurement of uptake of GSH by mitochondria at an incubation concentration of 0.5 mM or higher using HPLC analysis. For measurement of lower concentrations, see Alternate Protocol 2.

Materials

10× acivicin stock solution (see recipe)
Freshly isolated mitochondrial suspension from rat renal cortical homogenates (1 to 3 mg protein/ml; see Support Protocol 2)
50 mM dithiothreitol (DTT) in mitochondrial isolation buffer (prepare fresh)
Mitochondrial isolation buffer (see recipe)
Metabolite (optional; e.g., malate or 2-oxoglutarate)
10× GSH stock solution (see recipe)
Extraction solution (see recipe)

25-ml polypropylene Erlenmeyer flasks (e.g., Nalgene)
1.5-ml polyethylene microcentrifuge tubes
Dubnoff shaking metabolic incubator (Precision Scientific)
Centrifuge capable of delivering 10,000 × *g*

Pretreat mitochondria to inhibit GGT activity

1. Add 1 vol 10× acivicin stock solution and 1 vol 50 mM DTT to 8 vol renal cortical mitochondrial suspension (1 to 3 mg protein/ml) in 25-ml polypropylene Erlenmeyer flasks.

   Total volume in Erlenmeyer flasks should not exceed 3.0 ml. The final concentration of acivicin is 0.25 mM. Typically, one rat will yield sufficient cells for 3 to 5 incubations.

2. Incubate on a Dubnoff metabolic shaking incubator for 15 min at 60 cycles/min, 25°C.
3. Keep mitochondrial suspensions on ice until needed for transport experiments.

Perform transport incubations

4. *To measure exchange of GSH for intramatrix metabolites other than inorganic phosphate (e.g., malate); optional:* Incubate acivicin/DTT-pretreated mitochondria with 10 mM of the metabolite (e.g., malate or 2-oxoglutarate) for 5 min at 25°C, to preload cells with metabolite. Centrifuge the preloaded mitochondrial suspension for 2 min at 10,000 × *g*, room temperature. Remove supernatant and resuspend at the same protein concentration as before in fresh mitochondrial isolation buffer.

   GSH uptake into renal cortical mitochondria is largely accounted for by the activity of two carriers, the oxoglutarate carrier (OGC) and the dicarboxylate carrier (DCC; Chen and Lash, 1998). Preloading mitochondria with either inorganic phosphate or a dicarboxylate substrate (e.g., malate, succinate, malonate) can provide information about the function of one or the other carrier if initial rules are measured. As the DCC exchanges dicarboxylates for inorganic phosphate, it will only be active in the presence of inorganic phosphate. In contrast, the OGC exchanges 2-oxoglutarate for other dicarboxylates and will only be active in the presence of dicarboxylates on both sides of the mitochondrial inner membrane.

5. In 25-ml Erlenmeyer flasks, gently mix 9 vol acivicin- and DTT-treated renal cortical mitochondria (preloaded or not) with 1 vol 10× GSH stock solution. Incubate on a Dubnoff shaking metabolic incubator at 60 cycles/min, 25°C.

   Total volume should not exceed 3.0 ml.

6. At specified incubation time points (e.g., 1, 2, 3, 5, 10, 15, 20, and 30 min), remove 0.5-ml aliquots and place in 1.5-ml polyethylene microcentrifuge tubes.
7. Immediately centrifuge mitochondrial aliquots for 30 sec at 13,000 × *g*, room temperature.
8. Remove supernatant, resuspend pellets in 30 ml ice-cold mitochondrial isolation buffer, and centrifuge again for 30 sec at 13,000 × *g*, room temperature.

Measure transport

9. Resuspend pellets in 0.7 ml extraction solution and mix vigorously on a vortex mixer.
10. Place 0.5 ml of the acid extract from step 9 into a new 1.5-ml microcentrifuge tube. Store on ice until ready for HPLC analysis of GSH content (see Support Protocol 3).

ALTERNATE PROTOCOL 2

MEASUREMENT OF MITOCHONDRIAL TRANSPORT USING RADIOLABELED GSH

Basic Protocol 2 is limited by the sensitivity of the assay method. As with cellular GSH transport (see Basic Protocol 1 and Alternate Protocol 1), a more sensitive measurement of mitochondrial GSH transport can be performed using radiolabeled GSH. The protocol below is applicable to measuring uptake of GSH at any incubating concentration of GSH; it can be used with any incubating concentration of GSH, but is applicable to lower concentrations, down to 1 μM GSH.

Additional Materials *(also see Basic Protocol 2)*

10× GSH stock solution (see recipe) containing 0.01 μCi/ml L-[3H-glycyl] GSH (20 to 50 Ci/mmol; NEN Life Science)
10% (v/v) perchloric acid
5-ml polyethylene scintillation vials

1. Pretreat and (optionally) preload mitochondria, and perform time course of incubation with GSH (see Basic Protocol 2, steps 1 to 8), using 10× GSH stock solution containing 0.01 μCi/ml of L-[^{3}H-glycyl]-GSH instead of the solution containing cold GSH alone.

   [^{35}S]-GSH may be used instead of the ^{3}H-labeled compound.

2. Resuspend pellets in 0.5 ml of 10% (v/v) perchloric acid and mix vigorously on a vortex mixer.
3. Place 0.5 ml of the acid extract into a 5-ml polyethylene scintillation vial. Add 2 ml scintillation fluid and determine radioactivity by scintillation spectroscopy using the ^{3}H-channel.
4. Calculate initial rate of GSH uptake.

   The first-order rate constant of GSH uptake, k, is calculated by performing linear curve-fitting on the plot of $\ln[P_{total}/(P_{total} - P_t)]$ versus time. P_{total} represents the total uptake of GSH at equilibrium, which is estimated by performing an exponential decay curve-fitting on the time course data of GSH uptake. P_t represents the GSH uptake at time t. Thus, the initial rate of GSH uptake is determined from the first-order rate equation $v = k(P_{total})$.

SUPPORT PROTOCOL 2

ISOLATION OF MITOCHONDRIA FROM RAT RENAL CORTEX

The method for preparation of isolated mitochondria from rat renal cortex has been described elsewhere and will not be presented here in detail. Refer to Lash and Sall (1993) for a more thorough description.

Materials

Rats (Sprague-Dawley or Fisher 344, 2- to 4-month-old males or 2.5- to 6-month-old females, 175 to 250 g body weight)
50 mg/ml sodium pentobarbital in saline
0.2% (w/v) heparin
Mitochondrial isolation buffer (see recipe), without EGTA

Hand-held Dounce homogenizer (40-ml capacity)
50-ml round-bottom, polycarbonate centrifuge tubes
Sorvall RC-2B or equivalent centrifuge

1. Anesthetize rats with an intraperitoneal injection of sodium pentobarbital (0.1 ml of a 50 mg/ml solution in saline per 100 g body weight). Prevent blood clotting by injecting 0.2 ml of 0.2% (w/v) heparin into the tail vein just before surgery.
2. Open the peritoneal cavity by making a midventral incision. Euthanize the animal by bilateral pneumothorax and exsanguination, then remove the kidneys and place in 2 to 3 ml of ice-cold mitochondrial isolation buffer in a petri dish.
3. Decapsulate kidneys by making a small incision with scissors on one end and peeling the capsule around the kidney. Slice cortices into small pieces, transfer to homogenizer, add 30 ml of ice-cold mitochondrial isolation buffer, then homogenize with 10 to 15 strokes of the hand-held Dounce homogenizer.
4. Isolate mitochondria by differential centrifugation in the following three steps.
   a. Centrifuge homogenate 10 min at 650 × *g*, 0° to 4°C. Transfer supernatant into another tube.
   b. Centrifuge supernatant 5 min at 15,000 × *g*, 0° to 4°C.
   c. Remove supernatant and resuspend pellet in 30 ml isolation buffer. Centrifuge again for 5 min at 15,000 × *g*.
5. Remove supernatant and resuspend pellet in mitochondrial isolation buffer (without EGTA) at a protein concentration of 1 to 5 mg protein/ml. Keep mitochondria on ice until used in transport experiments.

   Protein concentration in suspensions of isolated mitochondria are determined with the Coommassie Blue G dye from Bio-Rad. The Lowry method cannot be used, as the sucrose in the isolation buffer interferes with the assay.

HPLC ANALYSIS OF GSH AND RELATED COMPOUNDS

SUPPORT PROTOCOL 3

This HPLC method is based on that described by Fariss and Reed (1987) and involves derivatization of thiols (e.g., GSH) with iodoacetic acid and of amino groups with 1-fluoro-2,4-dinitrobenzene. Separation of derivatives is achieved by reversed-phase, ion-exchange chromatography. Methanol is used in the mobile phase to rapidly elute the excess 2,4-dinitrophenol and the dinitrophenyl derivatives of basic and neutral amino acids. The low pH of the acetate in the mobile phase (pH = 2.5) maintains the bonded-phase amino groups in the protonated form. Selective elution of the acidic dinitrophenyl derivatives is accomplished by increasing the sodium acetate concentration of the mobile phase, and the eluted derivatives are measured by their absorbance at 365 nm. An internal standard (L-γ-glutamyl-L-glutamate) corrects for errors in dilution and alterations in derivatization efficiency, derivatization stability, and chromatographic conditions.

Materials

Acid extract of PT cells (see Basic Protocol 1, step 10) or mitochondria (see Basic Protocol 2, step 10)

100 mM iodoacetic acid (free acid; made fresh in deionized water)
Neutralization solution (see recipe)
1% (v/v) 1-fluoro-2,4-dinitrobenzene in ethanol (made fresh)
HPLC mobile phases (see recipe)

Tabletop centrifuge (e.g., Clay Adams Dynac)
HPLC column: μBondapak amine 10 μm cartridge (8 mm × 10 cm; Waters)

Derivatize sample

1. Add 50 μl of 100 mM iodoacetic acid to 0.5 ml of acid extract.

   The acid extract contains the internal standard (L-γ-glutamyl-L-glutamate) and antioxidant (bathophenanthroline disulfonate).

2. Bring the acidic solution to pH 8 to 9 by adding 0.48 ml of neutralization solution and incubate for 10 min in the dark at room temperature.

3. Add 1 ml of 1% (v/v) 1-fluoro-2,4-dinitrobenzene. Cap the reaction mixture and mix with a vortex mixer. Store overnight at 4°C.

4. Centrifuge the *S*-carboxymethyl-*N*-dinitrophenyl derivatives for 15 min at 1000 × *g* in a tabletop clinical centrifuge to remove insoluble material. Store supernatant at 4°C in the dark until analysis.

   Samples are stable for up to 2 weeks.

Separate by HPLC

5. Perform HPLC analysis by monitoring absorbance at 365 nm using the following elution conditions.

   Maintain mobile phase at 75% A/25% B for 5 min at a flow rate of 1.5 ml/min;
   Run 30-min linear gradient to 1% A/99% B;
   Hold mobile phase at 1% A/99% B until last compound (usually GSSG) has eluted (10 to 15 min);
   Run 1 min linear gradient to 80% A/20% B;
   Hold at 80% A/20% B for 5 min to reequilibrate to initial conditions.
   These separation conditions will vary depending on the efficiency of the column, which decreases with the age of the column. As resolution decreases, the acetate concentration may need to be lowered and/or the gradient made more shallow.

SUPPORT PROTOCOL 4

MEASUREMENT OF INTRACELLULAR OR MITOCHONDRIAL MATRIX VOLUME

The contamination of intracellular (intramitochondrial) space with extracellular (extramitochondrial) material must be accounted for when measuring GSH uptake so that corrections can be made. This can be accomplished by quantifying the extracellular volume using a radiolabeled, impermeable solute and comparing this with total volume determined using radiolabled water.

Materials

Isolated cells (see Support Protocol 1) or mitochondria (see Support Protocol 2)
Substrate of interest (e.g., GSH or malate)
[U-^{14}C]Sucrose (1.7 mCi/mg; Amersham)
[^{3}H]$_2$O (1 mCi/ml; Amersham)

Additional materials and equipment for GSH transport determination and sample processing (see Basic Protocol 1 or Basic Protocol 2).

1. Incubate isolated cells or mitochondria with the substrate of interest in the appropriate buffer containing 0.1 μCi/ml of [U-^{14}C]sucrose and 1 μCi/ml of [^{3}H]$_2$O.
2. At various time points, remove 0.5-ml aliquots of the isolated cell or mitochondrial suspensions and process by centrifugation as in Basic Protocol 1 or Basic Protocol 2, steps 6 and 7.
3. Determine the radioactivity of pellet and supernatant fractions separately using the ^{14}C and ^{3}H channels.
4. Calculate intracellular or mitochondrial matrix volume according to the following equation:

$$V_{cell} \text{ or } V_{matrix} = V_{H_2O} - V_{sucrose}$$
$$= ([\text{Net (H)}_{pellet}/A^{3}H] - [\text{Net (C)}_{pellet}/A^{14}C]) \times 1/\text{mg protein}$$

where V_{cell} or V_{matrix} are the volume of ^{3}[H]$_2$O in the pellet (V_{H_2O}) minus the volume of [U-^{14}C]sucrose in the pellet (Vsucrose), V_{H_2O} is the total pellet volume calculated from net ^{3}H counts divided by specific ^{3}H counts ($A^{3}H$), and $V_{sucrose}$ is the extracellular or extramitochondrial medium calculated from the net ^{14}C counts divided by specific ^{14}C counts ($A^{14}C$); $A^{3}H$ and $A^{14}C$ are determined by standard samples containing only a known amount of either [^{3}H]$_2$O or [U-^{14}C]-sucrose.

REAGENTS AND SOLUTIONS

*Use Milli-Q-purified water or equivalent for the preparation of all buffers. For common stock solutions, see **APPENDIX 2A**; for suppliers, see **SUPPLIERS APPENDIX**.*

Acivicin stock solution, 10×

Prepare a 2.5 mM (10×) stock solution of L-(αS,5S)-α-amino-3-chloro-4,5-dihydro-5-isoxazoleacetic acid (acivicin; Sigma) in Krebs-Henseleit buffer (see recipe). Store at –20°C for up to 1 month.

Collagenase solution

Prepare a 0.15% (w/v) solution of collagenase, type I (Sigma) in Hanks' buffered salt solution (HBSS; *APPENDIX 2A*) with 1.2 mM magnesium and 2 mM calcium chloride. Prepare fresh daily.

Extraction solution

Stock solutions:
70% (v/v) perchloric acid
1.5 mM L-glutamyl-L-glutamate (Sigma)
1.5 mM bathophenanthroline disulfonate (BPDS; Sigma)
0.9% (w/v) NaCl (normal saline; *APPENDIX 2A*)

Add 1 vol 1.5 mM L-γ-glutamyl-L-glutamate, 1 vol BPDS, and 2 vol 70% perchloric acid to 10 vol 0.9% NaCl. Prepare fresh.

GSH stock solution, 10×

Prepare a 1 to 100 mM (choose concentration as needed) solution of reduced glutathione (GSH) in Krebs-Henseleit buffer (see recipe) for isolated cells or mitochondrial isolation buffer (see recipe) for isolated mitrochondria. Prepare fresh daily and keep on ice.

HPLC mobile phases

Mobile phase A: Prepare a solution of 80% (v/v) HPLC-grade methanol in water.

Mobile phase B: Prepare 2.6 M sodium acetate stock solution by adding 272 g sodium acetate and 122 ml of water to 378 ml of glacial acetic acid. Stir with low heat until sodium acetate is in solution. Cool and filter with a 4.0- to 5.5-µm polypropylene filter. Add 200 ml of the sodium acetate stock solution to 800 ml of 80% (v/v) methanol to yield 0.5 M sodium acetate in 64% (v/v) methanol.

Krebs-Henseleit buffer

Stock solution: Prepare a 10× stock solution as follows:

1.18 M NaCl
48 mM KCl
12 mM $MgSO_4 \cdot 7H_2O$
9.6 mM KH_2PO_4
250 mM $NaHCO_3$
25 mM $CaCl_2 \cdot 2H_2O$
250 mM HEPES

Prepare the 10× stock solution in advance and store in a 1-liter polycarbonate bottle at 0° to 4°C for up to 1 month. Add all of the ingredients except $CaCl_2$ and allow to dissolve with stirring. Purge the 10× stock with 95% O_2/5% CO_2 for 30 min, then slowly add the $CaCl_2$ in small aliquots with slow stirring to prevent precipitation of calcium phosphate.

CAUTION: *If the $CaCl_2$ is added too quickly, a cloudy precipitate will form and the solution must be discarded and prepared again.*

Working solution: Prepare the working Krebs-Henseleit buffer (1×) just prior to use by mixing 1 vol 10× stock with 9 vol deionized water. After bubbling with 95% O_2/5% CO_2 for 30 min, adjust the pH of the buffer to 7.4 with 1 M HCl or 1 M NaOH as needed.

Mitochondrial isolation buffer

20 mM triethanolamine·HCl, pH 7.4
225 mM sucrose
3 mM potassium phosphate, pH 7.4
5 mM $MgCl_2$
20 mM KCl
0.1 mM phenylmethylsulfonyl fluoride (PMSF, 99% purity; Sigma)
2 mM EGTA (added only in preparatory steps except final resuspension and incubation of mitochondria)
Adjust pH to 7.4 with 1 M HCl or 1 M KOH as needed
Prepare buffer in advance and store in a 1-liter polycarbonate bottle at 0° to 4°C for up to 1 month

Phenylmethylsulfonyl fluoride is added to inhibit proteolysis.

Neutralization solution

Make a working solution by adding 1 vol of 10 M KOH to 4 vol of 3 M $KHCO_3$, for a final concentration of 2 M KOH/2.4 M $KHCO_3$. Store up to 2 months at 0° to 4°C.

COMMENTARY

Background Information

Until the late 1970s the dogma was that many tissues, in particular the liver, had transport systems for efflux of GSH into the extracellular space but that GSH was not transported into cells as the intact tripeptide. Observations with isolated, perfused kidneys in the late 1970s through the mid 1980s (Fonteles et al., 1976; Griffith and Meister, 1979; Häberle et al., 1979; Anderson et al., 1980; Ormstad et al., 1982; Rankin and

Curthoys, 1982; Rankin et al., 1985) provided evidence that either endogenous or administered GSH was extracted from plasma by both a basolateral and a lumenal mechanism. While the latter was ascribed to glomerular filtration, degradation by brush-border enzymes (i.e., GGT and dipeptidase), and uptake of the constituent amino acids by renal PT cells (Griffith and Meister, 1979; Lash et al., 1988), there was controversy over whether a basolateral transport mechanism for the intact tripeptide of GSH actually existed or if the apparent basolateral extraction of plasma GSH was due to degradation by extralumenal GGT followed by renal cellular uptake of the constituent amino acids and intracellular resynthesis of GSH (Anderson et al., 1980; Abbott et al., 1984; Inoue et al., 1986).

This controversy was resolved by the biochemical description of a Na^+-dependent transport process for uptake of GSH in basolateral membrane vesicles (Lash and Jones, 1983, 1984) and isolated kidney cells (Hagen et al., 1988) and the further demonstration that this system also mediated the uptake of GSH *S*-conjugates (Lash and Jones, 1985). Basolateral uptake of GSH was subsequently shown to be a general property of many epithelial cells, including those found in the small-intestinal jejunum (Lash et al., 1986; Hagen and Jones, 1987), type II pulmonary alveolar cells (Hagen et al., 1986; Bai et al., 1994), and retinal pigment epithelial cells (Davidson et al., 1994; Zlokovic et al., 1994; Kannan et al., 1995; Lu et al., 1995; Mackic et al., 1996).

Within renal PT cells, as well as isolated hepatocytes, GSH is known to be compartmentalized into distinct cytosolic and mitochondrial pools. There are two possible sources of mitochondrial GSH—de novo synthesis from precursor amino acids and transport of GSH from the cytosol. As the enzymes for synthesis of GSH are localized predominantly, if not exclusively, in the cytosol (Griffith and Meister, 1985), transport must supply the mitochondria with their pool of GSH. Because the GSH molecule has a net charge at physiological pH and there exists a pH gradient and membrane potential across the mitochondrial inner membrane, GSH transport into mitochondria cannot occur passively but must occur by a specific, carrier-mediated process. Several investigators subsequently demonstrated the presence of specific, carrier-mediated uptake of GSH in hepatic (Kurosawa et al., 1990; Martensson et al., 1990; Garcia-Ruiz et al., 1995) and renal (McKernan et al., 1991; Schnellmann, 1991) mitochondria. GSH is taken up into renal cortical mitochondria in electroneutral exchange for dicarboxylates such as malate and succinate (McKernan et al., 1991; Chen and Lash, 1997), suggesting that transport is mediated, at least in part, by the dicarboxylate and oxoglutarate carriers that are present in the mitochondrial inner membrane of mitochondria in kidney and several other tissues, including the liver (Klingenberg, 1979; Palmieri et al., 1996).

Critical Parameters

Measurement of transport

This unit examines GSH uptake by isolated renal PT cells and renal cortical mitochondria. Although the kidney has several unique properties with regard to the disposition and metabolism of GSH, the principles should apply to analysis of GSH uptake in isolated cells or mitochondria from most mammalian tissues.

Methods for accurate measurement of GSH transport must take into account not only concerns that exist with measurement of transport of any substrate, but concerns that are specific to the study of GSH transport. General concerns about the accuracy of transport measurements include efficient separation of compartments, prevention of changes in compartment volume during transport measurements and sample processing, and loss of transported substrate during sample processing. Compartment volumes can be readily quantified by use of radiolabeled water, which gives total space, and a radiolabeled impermeant molecule, such as sucrose (see Support Protocol 4). This is a critical parameter to monitor in many cases. With isolated mitochondria, matrix volume can often change due to metabolic state. Antimycin A (2 μM) can be added to incubations to inhibit substrate metabolism and thus substrate-induced changes in matrix volume. Loss of transported substrate during sample processing can be eliminated by addition of a specific, irreversible inhibitor of transport in the incubation stop solution, if one is available. Alternatively, efflux of transported substrate can be measured under the same conditions of sample processing (usually 0° to 4°C, <5 min) and can be shown to be negligible (Chen and Lash, 1998).

Concerns specific to the study of GSH transport include prevention of GSH oxidation and degradation. Oxidation of GSH during sample processing is usually prevented by stopping transport under acidic conditions and including an antioxidant, such as bathophenanthroline disulfonate (BPDS). BPDS is used in preference to EDTA, because the latter contains free amino groups and interferes with detection of GSH by the HPLC method described in Support Protocol

3. Degradation of GSH is not a major concern in tissues such as skeletal muscle or the liver, which have negligible amounts of GGT activity. In the kidney, however, extremely high activity of GGT is present on the brush-border membrane (Lash et al., 1988). Consequently, the presence of even a small amount of contaminating brush-border membranes in a preparation of basolateral membranes (Lash and Jones, 1984) or isolated mitochondria (McKernan et al., 1991) can result in a significant amount of degradation of GSH. This concern is minimized by pretreatment of the preparation with an irreversible inhibitor of GGT, such as acivicin. One must be cautious not to use too high a concentration of acivicin. Although acivicin is a specific glutamine antagonist at relatively low concentrations (usually <1 mM), it becomes a nonspecific alkylating agent at higher concentrations and can inhibit GSH transport (Lash and Jones, 1984). In suspensions of isolated renal cells, which possess both brush-border and basolateral membranes, it is essential to inhibit GGT activity. Buthionine sulfoximine (BSO) can also be added to inhibit GSH synthesis, thereby excluding the possibility that detection of intact GSH arose due to extracellular degradation of GSH, uptake of the constituent amino acids, and intracellular resynthesis of GSH.

In this unit, two methods are described for analysis of transported GSH: analysis by HPLC and use of radiolabeled GSH. The HPLC method has the advantage of demonstrating recovery of intact tripeptide. With the radiolabel method, which must be used when incubating concentrations of GSH are lower than the HPLC limit of detection (<0.5 mM), samples can be spiked with unlabeled GSH and fractions from the HPLC eluate can be collected to demonstrate that the radiolabeled molecule coincides with the derivative of intact GSH.

Sensitivity of method

Sensitivity of the HPLC method is based, in part, on the number of stationary amine groups available with which the chromophore can interact, as well as the sensitivity of the detector. With variable wavelength detectors, disulfides are measured at concentrations as low as 0.5 nmol/ml or 25 pmol/injection, and thiols are measured at concentrations as low as 1.0 nmol/ml or 50 pmol/injection. Approximately 5- to 10-fold greater sensitivities can be achieved with some fixed-wavelength, filter-type detectors. In addition to GSH and GSSG, other relevant compounds that are measurable by this method include glutamate, cystine, cysteine, aspartate, γ-glutamyl-L-cysteine, and the mixed disulfide of GSH and cysteine (also see *UNIT 6.2*).

As the time period during which both isolated renal cells and isolated mitochondria are viable is somewhat limited (2 to 3 hr for isolated cells and 30 min for isolated mitochondria after removal from storage on ice), it is critical that experiments be conducted as soon as possible after preparation of the cell or mitochondrial suspension.

Troubleshooting

Potential problems with measurement of GSH uptake can arise from three areas: (1) quality of the biological preparation, (2) alterations in GSH status during incubation or sample processing, or (3) artifacts during sample processing. There are numerous methods to assess the quality of the biological preparation being used, and these have been detailed elsewhere (e.g., Lash, 1989, 1993, 1996; Lash and Sall, 1993). Problems with the viability of isolated cells or mitochondria will often lead to changes in membrane permeability and hence, changes in apparent transport. If analysis of intracellular or intramitochondrial contents after incubation with GSH reveals significant oxidation or degradation of GSH, incubation conditions should be carefully checked to see if the pH is correct and if acivicin pretreatment is effective. If the incubating pH is too alkaline, auto-oxidation of GSH is more likely to occur. Although previous studies have shown than a 15-min preincubation of renal tissue with 0.25 mM acivicin inhibits ≥98% of GGT activity, this should be assessed if degradation is a problem. As mentioned above, concentrations of acivicin of >1 mM can lead to nonspecific alkylation of proteins. Potential artifacts during sample processing can be assessed by measurement of compartment volumes and determination of sample recovery.

Methods for the accurate measurement of GSH uptake by renal cortical mitochondria from the rat may be compromised by the following factors.

1. The presence of even small amounts of contaminating brush-border membranes, which contain GGT, can lead to significant degradation of GSH, thus either causing underestimation of uptake or making measurement of uptake impossible.

2. Efflux of transported GSH can occur during sample processing, which can lead to underestimation of uptake.

3. Contamination of the mitochondrial pellet with extramitochondrial medium can take place, thus leading to overestimation of uptake.

4. Changes in mitochondrial matrix volume during transport measurements with or without other added substrates can lead to altered transport kinetics.

5. Induction of the membrane permeability transition during transport measurements with or without other added substrates can markedly alter membrane permeability to GSH.

Anticipated Results

The choice of either the HPLC or radiolabel method for quantifying GSH uptake in either cells or mitochondria is wholly dependent on the incubating concentration of GSH and the sensitivity of the HPLC detector. Typically, a limit of detection of 25 to 50 pmol GSH is seen with the HPLC method. This is usually adequate with incubating concentrations of ≥0.5 mM. Using radiolabeled GSH and scintillation counting, incubating concentrations of GSH as low as 1 μM have been successfully used. This lower range is critical because physiological concentrations of GSH in renal plasma are 5 to 20 μM, depending on species. In contrast, renal mitochondria are typically exposed to 1 to 5 mM GSH in the cytosol.

Using two kidneys from 175- to 250-g male rats as starting material, the typical yield of isolated renal PT cells is 30×10^6 cells and that of isolated renal cortical mitochondria is 15 to 25 mg of mitochondrial protein. In both cases, this is usually enough material for 10 to 15 individual samples.

Time Considerations

The amount of time required to measure GSH uptake in isolated renal cells or mitochondria can be divided into three phases: (1) biological preparation, (2) transport incubations and sample preparation, and (3) analysis of GSH. The first and third phases require significantly more time than the second phase. The isolated cell preparation method requires ~3.5 hr to complete. If GSH transport is assessed in cells from other tissues, this time will of course vary depending on the method used to prepare the cells. The mitochondrial isolation method typically requires 45 min to 1 hr to complete. The HPLC method requires ~1 hr per sample while the radiolabel method requires ~5 to 10 min per sample, depending on the number of counts per sample. Longer counting times should be used at low incubating concentrations of GSH to decrease counting error. In contrast to the times required for the first and third phases, the actual transport incubations are done in real time and typically take at most 60 min for experiments with isolated cells and at most 30 min for experiments with isolated mitochondria. In both cases, sample preparation then requires 2 to 5 min per sample.

Literature Cited

Abbott, W.A., Bridges, R.J., and Meister, A. 1984. Extracellular metabolism of glutathione accounts for its disappearance from the basolateral circulation of the kidneys. *J. Biol. Chem.* 259:15393-15400.

Anderson, M.E., Bridges, R.J., and Meister, A. 1980. Direct evidence for inter-organ transport of glutathione and that the non-filtration mechanism for glutathione utilization involves γ-glutamyl transpeptidase. *Biochem. Biophys. Res. Commun.* 96:848-853.

Bai, C.L., Brown, L.A., and Jones, D.P. 1994. Glutathione transport by type II cells in perfused rat lung. *Am. J. Physiol.* 267:L447-L455.

Chen, Z. and Lash, L.H. 1998. Evidence for mitochondrial uptake of glutathione by dicarboxylate and 2-oxoglutarate carriers. *J. Pharmacol. Exp. Ther.* 285:608-618.

Davidson, P.C., Sternberg, P., Jr., Jones, D.P., and Reed, R.L. 1994. Synthesis and transport of glutathione by cultured human retinal pigment epithelial cells. *Invest. Ophthalmol. Vis. Sci.* 35:2843-2849.

Fariss, M.W. and Reed, D.J. 1987. High-performance liquid chromatography of thiols and disulfides: Dinitrophenyl derivatives. *Methods Enzymol.* 143:101-109.

Fonteles, M.C., Pillion, D.J., Jeske, A.H., and Leibach, F.H. 1976. Extraction of glutathione by the isolated perfused rabbit kidney. *J. Surg. Res.* 21:169-174.

Garcia-Ruiz, C., Morales, A., Cole, A., Rodes, J., Kaplowitz, N., and Fernandez-Checa, J.C. 1995. Evidence that the rat hepatic mitochondrial carrier is distinct from the sinusoidal and canalicular transporters for reduced glutathione. *J. Biol. Chem.* 270:15946-15949.

Griffith, O.W. and Meister, A. 1979. Glutathione: Interorgan translocation, turnover, and metabolism. *Proc. Natl. Acad. Sci. U.S.A.* 76:5606-5610.

Griffith, O.W. and Meister, A. 1985. Origin and turnover of mitochondrial glutathione. *Proc. Natl. Acad. Sci. U.S.A.* 82:4668-4672.

Häberle, D., Wahlländer, A., and Sies, H. 1979. Assessment of the kidney function in maintenance of plasma glutathione concentration and redox state in anesthetized rats. *FEBS Lett.* 108:335-340.

Hagen, T.M. and Jones, D.P. 1987. Transepithelial transport of glutathione in vascularly perfused small intestine of rat. *Am. J. Physiol.* 252:G607-G613.

Hagen, T.M., Brown, L.A., and Jones, D.P. 1986. Protection against paraquat-induced injury by exogenous GSH in pulmonary alveolar type II cells. *Biochem. Pharmacol.* 35:4537-4542.

Hagen, T.M., Aw, T.Y., and Jones, D.P. 1988. Glutathione uptake and protection against oxidative

injury in isolated kidney cells. *Kidney Int.* 34:74-81.

Inoue, M., Shinozuka, S., and Morino, Y. 1986. Mechanism of renal peritubular extraction of plasma glutathione: The catalytic activity of contralumenal γ-glutamyltransferase is prerequisite to the apparent peritubular extraction of plasma glutathione. *Eur. J. Biochem.* 157:605-609.

Kannan, R., Yi, J.R., Zlokovic, B.V., and Kaplowitz, N. 1995. Molecular characterization of a reduced glutathione transporter in the lens. *Invest. Ophthalmol. Vis. Sci.* 36:1785-1792.

Klingenberg, M. 1979. Overview on mitochondrial metabolite transport systems. *Methods Enzymol.* 56:245-252.

Kurosawa, K., Hayashi, N., Sato, N., Kamada, T., and Tagawa, K. 1990. Transport of glutathione across the mitochondrial membranes. *Biochem. Biophys. Res. Commun.* 167:367-372.

Lash, L.H. 1989. Isolated kidney cells in the study of chemical toxicity. *In* In Vitro Toxicology: Model Systems and Methods (C.A. McQueen, ed.) pp. 231-262. Telford Press, Caldwell, N.J.

Lash, L.H. 1993. Purification of renal cortical cell populations by Percoll density-gradient centrifugation. *In* In Vitro Biological Systems: Preparation and Maintenance, Methods in Toxicology, Vol. 1, part A (C.A. Tyson and J.M. Frazier, eds.) pp. 397-410. Academic Press, San Diego.

Lash, L.H. 1995. Intracellular distribution of thiols and disulfides: Assay of mitochondrial GSH transport. *Methods Enzymol.* 252: 14-26.

Lash, L.H. 1996. Use of freshly isolated and primary cultures of proximal tubular and distal tubular cells from rat kidneys. *In* Methods in Renal Toxicology (R.K. Zalups and L.H. Lash, eds.) pp. 189-215. CRC Press, Boca Raton, Fla.

Lash, L.H. and Jones, D.P. 1983. Transport of glutathione by renal basal-lateral membrane vesicles. *Biochem. Biophys. Res. Commun.* 112:55-60.

Lash, L.H. and Jones, D.P. 1984. Renal glutathione transport: Characteristics of the sodium-dependent system in the basal-lateral membrane. *J. Biol. Chem.* 259:14508-14514.

Lash, L.H. and Jones, D.P. 1985. Uptake of the glutathione conjugate *S*-(1,2-dichlorovinyl)glutathione by renal basal-lateral membrane vesicles and isolated kidney cells. *Mol. Pharmacol.* 28:278-282.

Lash, L.H. and Sall, J.M. 1993. Mitochondrial isolation from liver and kidney: Strategy, techniques, and criteria for purity. *In* Mitochondrial Dysfunction, Methods in Toxicology, Vol. 2 (L.H. Lash and D.P. Jones, eds.) pp. 8-28. Academic Press, San Diego.

Lash, L.H. and Tokarz, J.J. 1989. Isolation of two distinct populations of cells from rat kidney cortex and their use in the study of chemical-induced toxicity. *Anal. Biochem.* 182:271-279.

Lash, L.H., Hagen, T.M., and Jones, D.P. 1986. Exogenous glutathione protects intestinal epithelial cells from oxidative injury. *Proc. Natl. Acad. Sci. U.S.A.* 83:4641-4645.

Lash, L.H., Jones, D.P., and Anders, M.W. 1988. Glutathione homeostasis and glutathione *S*-conjugate toxicity in the kidney. *Rev. Biochem. Toxicol.* 9:29-67.

Lu, S.C., Sun, W.-M, Nagineni, C.N., Hooks, J.J., and Kannan, R. 1995. Bidirectional glutathione transport by cultured human retinal pigment epithelial cells. *Invest. Ophthalmol. Vis. Sci.* 36:2523-2530.

Mackic, J.B., Jinagouda, S., McComb, J.G., Weiss, M.H., Kannan, R., Kaplowitz, N., and Zlokovic, B.V. 1996. Transport of circulating reduced glutathione at the basolateral side of the anterior lens epithelium: Physiologic importance and manipulations. *Exp. Eye Res.* 62:29-37.

Martensson, J., Lai, J.C.K., and Meister, A. 1990. High-affinity transport of glutathione is part of a multicomponent system essential for mitochondrial function. *Proc. Natl. Acad. Sci. U.S.A.* 87:7185-7189.

McKernan, T.B., Woods, E.B., and Lash, L.H. 1991. Uptake of glutathione by renal cortical mitochondria. *Arch. Biochem. Biophys.* 288:653-663.

Ormstad, K., Låstbom, T., and Orrenius, S. 1982. Evidence for different localization of glutathione oxidase and γ-glutamyltransferase activities during extracellular glutathione metabolism in isolated perfused kidney. *Biochim. Biophys. Acta* 700:148-153.

Palmieri, F., Bisaccia, F., Capobianco, L., Dolce, V., Fiermonte, G., Iacobazzi, V., Indiveri, C., and Palmieri, L. 1996. Mitochondrial metabolite transporters. *Biochim. Biophys. Acta* 1275:127-132.

Rankin, B.B. and Curthoys, N.P. 1982. Evidence for renal paratubular transport of glutathione. *FEBS Lett.* 147:193-196.

Rankin, B.B., Wells, W., and Curthoys, N.P. 1985. Rat renal peritubular transport and metabolism of plasma [^{35}S]glutathione. *Am. J. Physiol.* 249:F198-F204.

Reed, D.J., Ellis, W.W., and Meck, R.A. 1980. The inhibition of γ-glutamyl transpeptidase and glutathione metabolism of isolated rat kidney cells by L-(αS,5S)-α-amino-3-chloro-4,5-dihydro-5-isox azoleacetic acid (AT-125; NSC-163501). *Biochem. Biophys. Res. Commun.* 94:1273-1277.

Schnellmann, R.G. 1991. Renal mitochondrial glutathione transport. *Life Sci.* 49:393-398.

Zlokovic, B.V., Mackic, J.B., McComb, J.G., Kaplowitz, N., Weiss, M.H., and Kannan, R. 1994. Blood-to-lens transport of reduced glutathione in an in situ perfused guinea-pig eye. *Exp. Eye Res.* 59:487-496.

Key References

Lash, 1995. See above.

Describes other methods for uptake of mitochondrial GSH.

Contributed by Lawrence H. Lash
Wayne State University School of Medicine
Detroit, Michigan

Measurement of Glutathione Transferases

Glutathione transferases (GSTs) occur in multiple forms with different substrate specificity profiles. In the mammalian species investigated, including man, mouse, and rat, evidence for at least 20 distinct genes is available. The corresponding GST proteins are differentially expressed such that organs differ both qualitatively and quantitatively in their GST contents. Based on similarities in amino acid sequences, the GSTs have been grouped into classes of which the most well characterized are Alpha (A), Mu (M), Pi (P), and Theta (T). Members of these classes are found in the cytosol fraction of cells. There are also membrane-bound GSTs (MGSTs) that have been identified in the microsome fraction (for additional information about GST nomenclature, see Background Information).

The common functional denominator of the GSTs is their ability to catalyze the reaction of the thiol group of glutathione with electrophilic chemical groups. However, with respect to the electrophilic substrate, there is no known chemical substance that is suitable for measuring the catalytic activity of all known GSTs. 1-Chloro-2,4-dinitrobenzene (CDNB) is the substrate most commonly used. The advantages of using CDNB are that the assay is simple to perform, sensitive, and applicable to a wide range of isoenzymes. However, some GSTs do not display any detectable activity with CDNB, and additional compounds are necessary in order to monitor their activities. Alternative substrates are useful in the discrimination among different isoenzymes with overlapping specificities. Therefore, depending on the scope of the investigation, several substrates have to be used to measure GST activity in a given biological sample. Table 6.4.1 gives a list of alternative substrates and details of the assay conditions.

The majority of the recommended assays are based on spectrophotometry because of its convenience. Table 6.4.2 serves as a guide for selecting substrates suitable for distinguishing the forms of GST under consideration. The Basic Protocol provides a convenient method for continuously monitoring changes in absorbance resulting from the consumption of substrate or the formation of product. Most reactions can be monitored directly; however, when using cumene hydroperoxide as a substrate, the formation of the product glutathione disulfide is measured indirectly by coupling the reaction to glutathione reductase–catalyzed oxidation of NADPH. In addition, continuous monitoring is not always possible. When using dichloromethane as a substrate for measuring GST T1-1, an endpoint analysis must be performed. To this end, the Alternate Protocol describes a procedure in which aliquots of the reaction mixture are quenched at various time points, and the product is colorimetrically detected.

Table 6.4.3 presents specific activities of different human GSTs with selected substrates. These substrates can also be used to detect and characterize GSTs from other biological species.

CONTINUOUS SPECTROPHOTOMETRIC ASSAYS FOR GLUTATHIONE TRANSFERASE ACTIVITY

BASIC PROTOCOL

This protocol describes a simple spectrophotometric assay for measuring GST activity in cell lysates and purified enzyme preparations. A number of substrates may be used with this assay, the choice of which depends on the isoform being studied. See Table 6.4.1 for specific assay conditions for each substrate; see Table 6.4.2 for the relative utility of the different substrates in the study of the different GST isoforms.

NOTE: To be able to compare results, reactions must be performed at constant temperature. Tabulated specific activities for GSTs are usually measured at 30°C.

Contributed by Bengt Mannervik and Per Jemth
Current Protocols in Toxicology (1999) 6.4.1-6.4.10

Materials

Assay buffer (see recipe and Table 6.4.1)
Glutathione (GSH) stock solution (see recipe and Table 6.4.1; make 20 times the desired final concentration indicated in the table)
Additional reagents for measurements with cumene hydroperoxide (prepare fresh):
Cumene hydroperoxide stock solution (see Table 6.4.1)
6 U/ml glutathione reductase in assay buffer
2 mM NADPH in 10 mM Tris·Cl, pH 7.0
Cell lysate or purified enzyme solution (amount depends on the activity of the sample)

Table 6.4.1 Conditions for Spectrophotometric Assays of Glutathione Transferase Activity[a]

Substrate	Substrate stock solution	Substrate concentration in cuvette (mM)	GSH concentration in cuvette (mM)	Assay buffer	Wavelength (nm)	Extinction coefficient ($mM^{-1}cm^{-1}$)
Δ^5-Androstene-3,17-dione	6.8 mM in methanol	0.068	0.1	25 mM Tris·Cl/sodium phosphate, pH 8.3	248	16.3
1-Chloro-2,4-dinitrobenzene	20 mM in 95% ethanol	1.0	1.0	0.1 M sodium phosphate, pH 6.5	340	9.6
Cumene hydroperoxide[b]	30 mM in 95% ethanol	1.5	1.0	0.1 M sodium phosphate, pH 7.0	340	−6.2[c]
2-Cyano-1,3-dimethyl-1-nitrosoguanidine	20 mM in DMSO	1.0	1.0	0.1 M sodium phosphate, pH 7.5	295	−2.0[c]
Dichloro-methane[d]	3.2% (v/v) (~0.5 M) in 95% ethanol	5.0	10	0.1 M Tris·Cl, pH 8.5	412	8.0
1,2-Dichloro-4-nitrobenzene	20 mM in 95% ethanol	1.0	5.0	0.1 M sodium phosphate, pH 8.0	344	10
Ethacrynic acid	1.0 mM in 95% ethanol	0.05	1.0	0.1 M sodium phosphate, pH 6.5	270	5
1,2-Epoxy-3-(4-nitrophenoxy) propane	10 mM in 95% ethanol	0.5	5.0	0.1 M sodium phosphate, pH 6.5	360	0.5
4-Hydroxynon-2-enal	2 mM in acetonitrile	0.1	0.5	0.1 M sodium phosphate, pH 6.5	224	−13.75
1-Menaphthyl sulfate	10 mM in assay buffer	0.5	5.0	0.1 M sodium phosphate, pH 7.5	298	2.5
4-Nitrobenzyl chloride	5.0 mM in 95% ethanol	0.25	5.0	0.1 M sodium phosphate, pH 6.5	310	1.9

[a]See Mannervik and Widersten (1995) and Sherratt et al. (1997; dichloromethane) for original references.
[b]See Basic Protocol for additional details on cumene hydroperoxide.
[c]A negative extinction coefficient means that the absorbance decreases in the assay.
[d]See Alternate Protocol for additional details on dichloromethane. The extinction coefficient is for the adduct diacetyldihydrobutidine formed in the assay.

Electrophilic substrate (see Table 6.4.1; also see recipe for stock solution)

Spectrophotometer, thermostatically controlled
30°C water bath

1. Prepare a thermostatically controlled spectrophotometer for kinetic measurements, and select the appropriate wavelength for the chosen substrate (Table 6.4.1). Maintain assay buffer at 30°C using, e.g., a temperature-controlled water bath.

   For wavelengths shorter than 340 nm, use a quartz cuvette.

Table 6.4.2 Ranking of Substrates for Different Human Glutathione Transferases[a]

Substrate	Human glutathione transferase										
	A1-1	A2-2	A4-4	M1-1	M2-2	M3-3	M4-4	P1-1	T1-1	T2-2	MGST1
Δ^5-Androstene-3,17-dione	++	–	–	+	–	–	–	–	NA	NA	NA
1-Chloro-2,4-dinitrobenzene	++	++	+	++	++	+	+	++	–	–	+
Cumene hydroperoxide	+	+	+	+	NA	NA	NA	+	+	+	+
2-Cyano-1,3-dimethyl-1-nitrosoguanidine	NA	NA	+	–	++	–	–	NA	NA	–	NA
Dichloromethane	NA	NA	NA	NA	NA	NA	NA	NA	++	–	NA
1,2-Dichloro-4-nitrobenzene	+	+	NA	+	+	+	–	+	NA	–	+
Ethacrynic acid	+	+	+	+	+	+	+	+	–	+	–
1,2-Epoxy-3-(4-nitrophenoxy) propane	–	–	NA	+	–	–	–	+	++	–	NA
4-Hydroxynon-2-enal	+	NA	++	+	+	+	NA	+	NA	NA	NA
1-Menaphthyl sulfate	NA	NA	NA	NA	NA	NA	NA	NA	–	++	NA
4-Nitrobenzyl chloride	+	NA	NA	+	+	+	+	NA	+	–	+

[a]Assay conditions are described in Table 6.4.1 and in the Basic Protocol. Symbols: +, may be used as a substrate; ++, preferred substrate considering nonenzymatic reactivity and specific activity compared to other GSTs; –, does not serve as substrate; NA, information not available.

Table 6.4.3 Specific Activities for Human Glutathione Transferases with Different Substrates[a,b,c]

Substrate	Specific activity of human glutathione transferase (μmol/min/mg pure protein)										
	A1-1	A2-2	A4-4	M1-1	M2-2	M3-3	M4-4	P1-1	T1-1	T2-2	MGST1
Δ^5-Androstene-3,17-dione	10	—	—	0.1	—	—	—	—	NA	NA	NA
1-Chloro-2,4-dinitrobenzene	80	80	7.5	180	220	7	1.4	105	—	—	24
Cumene hydroperoxide	10	10	1	0.6	NA	NA	NA	0.03	3	7	3
2-Cyano-1,3-dimethyl-1-nitrosoguanidin	NA	NA	0.1	—	120	—	—	NA	NA	—	NA
Dichloromethane	NA	NA	NA	NA	NA	NA	NA	NA	0.4	—	NA
1,2-Dichloro-4-nitrobenzene	0.2	0.8	NA	0.03	2	0.04	—	0.1	NA	—	NA
Ethacrynic acid	0.2	0.1	1.9	0.08	0.2	0.2	0.1	0.9	—	0.3	—
1,2-Epoxy-3-(4-nitrophenoxy) propane	—	—	NA	0.1	—	—	—	0.4	18	—	NA
4-Hydroxynon-2-enal	6	NA	190	3	4	2	NA	2	NA	NA	NA
1-Menaphthyl sulfate	NA	NA	NA	NA	NA	NA	NA	NA	—	0.3	NA
4-Nitrobenzyl chloride	NA	NA	NA	0.2	0.2	0.03	0.04	NA	2	—	0.6

[a]Data is from the review articles by Mannervik and Widersten (1995) and Hayes and Pulford (1995), except for the value for A1-1 with 4-hydroxynon-2-enal (Hubatsch et al., 1998), and the data for A4-4 (Hubatsch et al., 1998), T1-1 (Sherratt et al., 1997), and T2-2 (Tan and Board, 1996; Hayes and Pulford, 1995).

[b]Assay conditions are essentially as described in Table 6.4.1 but for details, see the above references.

[c]—, does not serve as substrate; NA, information not available.

If using a multisample spectrophotometer, an enzyme blank, in which the volume of enzyme is replaced with assay buffer, may be read concurrently with the assay sample.

2a. *If using substrate other than cumene hydroperoxide:* Referring to Table 6.4.1, add assay buffer to the cuvette, followed by GSH and enzyme solution, adjusting the volume of buffer on the basis of the volumes of enzyme and substrate to be added so that the volume in the cuvette is 1.00 ml.

The suitable amount (mg protein per ml) in the cuvette can be estimated from the reciprocal value of (specific activity) × ε × 20 (see Table 6.4.3).

2b. *If using cumene hydroperoxide as the substrate:* In addition to the reagents in step 2a, also add 50 µl of 6 U/ml glutathione reductase and 50 µl of 2 mM NADPH (0.1 mM final). Mix by inversion and incubate 1 min in the spectrophotometer chamber.

To mix the contents of the cuvette, place a piece of Parafilm over the cuvette opening and hold tightly while inverting. Do not shake.

3. Swiftly add the electrophilic substrate and mix by inverting the cuvette 3 to 4 times. Immediately insert the cuvette into the spectrophotometer and start the measurement (change in absorbance versus time). Record the absorbance for each sample continuously or at 5- to 15-sec intervals for 2 to 5 min.

CAUTION: *Some of the substrates may be allergenic (e.g., 1-chloro-2,4-dinitrobenzene) or toxic. Use gloves and follow the precautions listed with the chemicals.*

Optimize activity measurement conditions with respect to assay time and amount of enzyme added (see Critical Parameters and Troubleshooting).

4. Perform steps 2 and 3 on each sample, rinsing the cuvette with deionized water from a squirt bottle and wiping off the outside of the cuvette using a lint-free tissue (e.g., Kimwipe) between measurements.

5. Perform calculations according to example below (in which 1-chloro-2,4-dinitrobenzene is used as the substrate).

The following were added to a cuvette for a final volume of 1.0 ml: 890 µl sodium phosphate pH 6.5; 10 µl enzyme solution (protein concentration in cuvette, 0.050 mg/ml); 50 µl of 20 mM GSH solution (concentration in cuvette, 1 mM); and 50 µl of 20 mM 1-chloro-2,4-dinitrobenzene (concentration in cuvette, 1 mM). An increase of 0.202 absorbance units/min was observed. In a blank, performed without addition of enzyme (900 µl sodium phosphate, pH 6.5, 50 µl of 20 mM GSH solution, and 50 µl of 20 mM 1-chloro-2,4-dinitrobenzene), the increase in absorbance was found to be 0.010/min (nonenzymatic reaction rate).

Enzymatic activity = (0.202 − 0.010)/(9.6 × 1) = 0.020 mM/min = 0.020 mmol/min/liter = 0.020 µmol/min/ml. By relating the activity to the protein concentration, the specific activity is obtained:

Specific activity = 0.020/0.050 µmol/min/mg protein = 0.40 µmol/min/mg protein.

The spectrophotometer gives the activity in ΔA/time unit, where ΔA is the change in absorbance at the chosen wavelength. The time is usually measured in min. The change in absorbance is proportional to the change in substrate concentration as given by the Lambert-Beer law ($A = \varepsilon lc$; where ε is the molar extinction coefficient of the substrate, l is the pathlength of the cuvette and c is the concentration of the substrate). Thus, the activity = Δc per time unit = ΔA per time unit divided by εl. In the example above $\varepsilon = 9.6$ $mM^{-1}cm^{-1}$ and $l = 1$ cm.

IMPORTANT NOTE: *It is crucial that the slopes be obtained from straight lines representing the initial rates of the reactions (see Critical Parameters).*

MEASUREMENT OF GLUTATHIONE TRANSFERASE T1-1 ACTIVITY WITH DICHLOROMETHANE AS THE SUBSTRATE

ALTERNATE PROTOCOL

The only known mammalian GSTs displaying significant activity with dichloromethane as substrate are GST T1-1 orthologs from different species. Thus, the assay below can be used to discriminate GST T1-1 from other GSTs. The activity with dichloromethane and related haloalkanes has attracted some interest, since these compounds are common pollutants. The product of the enzyme-catalyzed reaction between dichloromethane and GSH, *S*-chloromethylglutathione, reacts further nonenzymatically to yield formaldehyde, a carcinogen. A large fraction of the human population lacks GST T1-1, complicating the toxicology of dichloromethane (Hayes and Pulford, 1995; Sherratt et al., 1997). In contrast to the continuous spectrophotometric assay (see Basic Protocol) this assay employs quenching of the reaction followed by colorimetric detection of the reaction product. An advantage with this assay is the low nonenzymatic reaction rate, which can be neglected in the calculations. However, if whole-cell lysates from certain bacteria are used, the possible presence of halogenases should be taken into account.

Additional Materials *(also see Basic Protocol 1)*

Assay buffer: 0.1 M Tris·Cl, pH 8.5 (*APPENDIX 2A*)
0.5 M (3.2% v/v) dichloromethane in 95% ethanol
25% (w/v) trichloroacetic acid (TCA)
Nash reagent (see recipe)

5-ml vials, sealable
Water bath, 42°C

1. Prepare a spectrophotometer for absorbance measurements, with the wavelength set to 412 nm.
2. To a sealable 5-ml vial, add buffer, enzyme, and 250 µl of 20 mM GSH solution (5 ml total volume after addition of dichloromethane) and preincubate in a water bath at the desired temperature (usually 30°or 37°C).
3. Add 50 µl of 0.5 M dichloromethane solution, mix by inversion (do not shake), and begin incubation at the desired temperature.

   The nonenzymatic reaction is slow and can be ignored. Therefore, a blank is unnecessary.
4. Withdraw 0.5-ml aliquots at various time points and dispense into a microcentrifuge tube. Add 100 µl 25% TCA to precipitate enzyme and quench the reaction. Remove any visible precipitate by centrifugation.

   CAUTION: *TCA is corrosive. Use gloves and follow the precautions on the label.*

   The choice of time points depends on amount of enzyme added. For 25 µg/ml purified human GST T1-1, under the assay conditions depicted in Table 6.4.1, suitable time points would be 0, 5, 10, 15, and 20 min.
5. Immediately add an equal volume (0.5 ml) of Nash reagent to the TCA-treated sample and incubate 30 min at 42°C.
6. Transfer samples to cuvettes and measure the absorbance at 412 nm. Plot the absorbance versus time (min) and calculate the slope of the curve using linear regression analysis.

   The data points should be on a straight line. Omit data point(s) that deviate in a systematic fashion, e.g., if the last point is lower than would be expected with regard to previous points. This is most probably due to depletion of substrate.

7. Perform calculations as described in the Basic Protocol, step 5, using an extinction coefficient of 8.0 $mM^{-1}cm^{-1}$. Use the calculated slope as the reaction rate (ΔA/min) and ignore the nonenzymatic reaction rate.

The calculated rate μmol/min/ml) should be multiplied by 2.2 to allow for the dilution of the aliquots.

REAGENTS AND SOLUTIONS

Use Milli-Q-purified water or equivalent for all recipes and in all protocol steps. For common stock solutions, see ***APPENDIX 2A****; for suppliers, see* ***SUPPLIERS APPENDIX****.*

Assay buffer

Prepare buffer solutions according to Table 6.4.1. For sodium phosphate buffers, dissolve NaH_2PO_4 to four-fifths of the desired volume, adjust the pH value with NaOH, and add water to desired volume. Make Tris buffers in the same way, except adjust the pH value with HCl. Store up to 2 weeks at 4°C.

GSH stock solution

Make GSH stock solution in water according to Table 6.4.1. It is convenient to add 50 μl GSH solution to the cuvette in the continuous assays, hence make the stock solution 20× as concentrated as the desired concentration in the cuvette (Table 6.4.1). GSH is unstable; make fresh solution every day.

Nash reagent

Prepare in H_2O:
2 M ammonium acetate
50 mM acetic acid
20 mM acetylacetone
Store up to 2 weeks at 4°C

The Nash reagent is mixed 1:1 with aliquots from the dichloromethane assay. Acetylacetone reacts with formaldehyde, formed nonenzymatically from S-chloromethylglutathione, to give a product that absorbs at 412 nm.

Substrate stock solutions

Prepare stock solutions according to Table 6.4.1. The stock solutions are usually stable for several days at 4°C, but for accurate measurements, fresh solutions should be made. Store Δ^5-androstene-3,17-dione solution (Table 6.4.1) at −20°C.

CAUTION: *Some of the substrates may be allergenic (e.g., 1-chloro-2,4-dinitrobenzene) or toxic. Use gloves and follow the precautions on the label.*

COMMENTARY

Background Information

From a toxicological point of view, the multiple forms of GST form an ensemble that collectively effects the detoxication of a wide range of toxic electrophilic chemical compounds. It would appear that natural substrates include genotoxic electrophiles, such as alkenes, epoxides, quinones, and organic hydroperoxides, which are formed by oxidative processes in organisms under normal and pathophysiological conditions. Xenobiotics, including drugs, environmental pollutants, and diverse man-made compounds, may be activated by cytochrome P-450-catalyzed reactions (so-called phase I detoxication reactions), promoting glutathione conjugations catalyzed by GSTs (phase II reactions). Some compounds are sufficiently electrophilic to react with the sulfhydryl group of glutathione directly, but in most cases a phase I reaction is required for activation.

The overlapping substrate specificities of GSTs create difficulties in determining the presence of individual GSTs in biological samples. Accurate identification and quantification may require separation of the different GSTs by high-resolution techniques such as isoelectric focusing or chromatofocusing (Ålin et al., 1985). In

addition, analytical procedures have been developed based on reverse-phase HPLC, in which individual GST subunits are quantified. The procedure is normally based on the chromatography of a pool of GSTs that has been enriched by affinity chromatography (Ostlund Farrants et al., 1987) and requires supplementation with other procedures for the several GSTs not bound to the affinity matrix. Determination of individual subunits rather than the various possible binary combinations found in the native GSTs simplifies the analysis, but has the drawback that the possible significance of heterodimeric GSTs can be overlooked. All in all, no single chromatographic or electrophoretic procedure allows the simultaneous determination of all known GSTs in a given biological sample.

In determinations of the activity of membrane-bound GSTs, the enzyme is solubilized and assayed in the presence of detergent (Morgenstern et al., 1982). The data given for MGST1 in Table 6.4.3 have been measured with enzyme activated by pretreatment with *N*-ethylmaleimide.

A radiometric assay involving labeled *trans*-stilbene oxide as substrate has been found useful for phenotyping in lymphocytes from blood samples with respect to the expression of the polymorphic human GST M1-1 (Seidegård et al., 1985).

Antibodies, polyclonal as well as monoclonal, may be used for quantitative analysis. It appears possible to distinguish closely related isoenzymes from the same GST class (Hao et al., 1994). However, such analysis requires the availability of specific antibodies for each and every GST, and presence of heterodimeric GSTs remains an analytical problem.

The current nomenclature for human GSTs is based on recognized classes of GSTs and their subunit composition. The "soluble" GSTs are dimeric proteins composed of identical or nonidentical subunits from the same class. Thus, the homodimeric enzyme composed of two subunits 1 of the Alpha class is GST A1-1, and the heterodimer composed of subunits 1 and 2 from the same class is designated GST A1-2. This nomenclature is well established for the human enzymes (Mannervik et al., 1992), and the same designations are being developed for mouse and rat GSTs (Hayes and Pulford, 1995). For earlier nomenclatures see Mannervik and Danielson (1988) and Hayes and Pulford (1995). Heterodimers composed of subunits from different GST classes are not known to occur.

Critical Parameters

In order to get reproducible results, care should be taken when pipetting buffer, enzyme solution, GSH solution, and, perhaps most importantly, the electrophilic substrate solution, into the cuvette. The electrophilic substrate is usually dissolved in ethanol (Table 6.4.1) and is therefore more difficult to pipet than the other solutions.

Some of the electrophilic substrates in Table 6.4.1 are difficult to dissolve in buffer, and this could affect the activity measurement. Each time a new substrate is used, the enzymatic activity should be compared to substrate and buffer alone as a control. If the absorbance is not constant before the initiation of the reaction, it is most probably due to incompletely dissolved substrate. In most cases preincubation of substrate with buffer (5 to 10 min in the cuvette prior to addition of enzyme and GSH) will eliminate this problem. Also, each time enzyme activity measurements are performed, the nonenzymatic reaction rate (substrate, GSH, and buffer) should be assayed as well. Even if it has been established that the uncatalyzed reaction is negligible, it is recommended that the nonenzymatic reaction rate be routinely measured and used as an extra control of the assay conditions. If the same substrate concentrations, pH value of buffer, and assay temperature are used, the rate should equal those obtained in previous experiments. To be able to compare activity measurements with or without addition of GST, it is crucial that the experiments be performed at the same temperature and pH values, since GSTs have pH optima with most substrates.

For some substrates there is a substantial nonenzymatic reaction rate. In these cases it is desirable that the amount of enzyme added be optimized such that the reaction rate measured in the presence of enzyme is at least twice that obtained in the absence of enzyme. The nonenzymatic reaction rate increases with pH due to the ionization of the sulfhydryl group of GSH ($pK_a \approx 9$), and it is recommended that all assays be performed at neutral or slightly acidic pH values according to Table 6.4.1.

In general, the activities of GSTs are not affected by altered ionic strength or addition of detergents. However, most of the electrophilic substrates in Table 6.4.1 are hydrophobic, and addition of salts or detergents may affect their solubilities. Appropriate controls for such effects should be made when assay conditions differ significantly from those given in Table 6.4.1.

Table 6.4.4 Cytosolic Specific Activities (μmol/min per mg protein) Measured with 1-Chloro-2,4-Dinitrobenzene and GSH as Substrates[a]

Source	Specific activity	Reference
Human		
Adult liver	2	Warholm et al., 1985
Erythrocytes	0.002	Marcus et al., 1978
Fetal liver	0.6	Guthenberg et al., 1986
Placenta	0.2	Mannervik and Guthenberg, 1981
Mouse		
Liver	3.0	Warholm et al., 1986
Rat		
Kidney	0.3	Guthenberg et al., 1985a
Liver	1.0	Ålin et al., 1985
Lung	0.1	Robertson et al., 1985
Small intestine	0.1	Tahir et al., 1988
Testis	1.5	Guthenberg et al., 1985b

[a]Numerous reports of cytosolic specific activities have been published. The values given are primarily from the authors' laboratory, based on the assay protocol recommended in this unit.

Pure or partly purified enzyme or whole-cell lysates can be used as samples for assaying GST activity. However, when crude cell lysates are used as samples, the absorbance of the assay solutions at wavelengths shorter than 340 nm may be high and affect the assay (spectrophotometers work best at absorbances <1). In cases where large amounts of lysate are necessary to detect activity, resulting in high absorbance at the assay wavelength, partial purification of the GST(s) should be considered. Also, the crude lysate may contain GSH, GST inhibitors, or other small compounds that influence the measured reaction rate. These can be removed by running the sample through a gel-filtration column (e.g., a PD-10 column; Amersham Pharmacia Biotech) if the sample volume is small.

GSH is unstable, primarily owing to the oxidation of its thiol group, and the stability decreases with pH. The thiol concentration can be measured using, 5,5′-dithiobis(2-nitrobenzoate) (DTNB, 20 mM in 95% ethanol). To do this, add 50 μl DTNB stock solution to neutral phosphate buffer. Measure the absorbance at 412 nm (using a 1-cm cuvette) before and after addition of 50 μl of a GSH stock solution that has been diluted by a factor of 100 (see Table 6.4.1 and Reagents and Solutions for GSH stock solutions). The final volume should be 1.00 ml. The increase in absorbance is proportional to the amount of GSH added, with an extinction coefficient of 13.6 $mM^{-1}cm^{-1}$. The GSH concentration (c) in the stock solution (mM) equals the change in absorbance times 2000 divided by 13.6 (c = dilution × $\Delta A/\varepsilon$).

Troubleshooting

The result of a GST activity measurement of the kind described in the Basic Protocol, either from a continuous assay or a quenched assay, should be a straight line showing the change in absorbance with time. This is essential in order to get reliable and reproducible results. If a smoothly bent curve is obtained, this is most probably due to addition of too much GST. In this case, repeat the measurement with addition of smaller amounts of enzyme solution until a straight line is obtained. An irregular curve is often due to poor mixing of the reactants; repeat the measurement and mix thoroughly.

Inability to reproduce experiments performed previously could also be related to the points listed in the Critical Parameters section. Check substrates, assay buffer, and temperature. Make sure that the correct wavelength is used and that the pipettors work properly.

Anticipated Results

As pointed out in the Troubleshooting section, the result of a GST activity measurement should be a straight line. The more GST added, the steeper the slope of the line should be. The activity (corrected for the nonenzymatic reaction) should be proportional to the enzyme concentration. Again, to be able to compare results

from different measurements, not only do the the assay conditions need to be identical, but the activity curves on which calculations are based need to be straight lines.

Table 6.4.2 is a quick guide to substrates for different GSTs. Certain substrate/GST combinations have been given preferred status based on two criteria: (1) low nonenzymatic activity compared to enzymatic activity and (2) high enzymatic activity compared to other GSTs; these are represented by double plus marks. Table 6.4.3 lists specific activities for purified GSTs with different substrates. However, caution should be exercised when comparing obtained specific activities with values in Table 6.4.3. The tabulated values might have been obtained under slightly different conditions than those outlined in Table 6.4.1. Note that the data in Tables 6.4.2 and 6.4.3 apply to human GST isoenzymes.

Other mammalian species have GSTs corresponding to the human isoenzymes. Although these orthologs have different specific activities, their activity profiles are often roughly similar, and substrates used to characterize human GSTs are also suitable for studies of GSTs in other mammalian species. Table 6.4.4 gives cytosolic specific activities with CDNB as electrophilic substrate for different human, rat, and mouse tissues. Several of the electrophiles in Table 6.4.1 function as substrates for nonmammalian GSTs as well (e.g., CDNB).

Time Considerations

Several measurements can be performed in one day. Preparing buffer and substrate solutions requires ~1 hr. One continuous assay normally takes 0.5 to 10 min. Adding buffer, substrates, and enzyme solution to the cuvette takes 0.5 to 1 min. The dichloromethane assay takes 10 min to 1 hr, incubation of samples takes 30 min, and absorbance measurements take ~10 min.

Literature Cited

Ålin, P., Jensson, H., Guthenberg, C., Danielson, U.H., Tahir, M.K., and Mannervik, B. 1985. Purification of major basic glutathione transferase isoenzymes from rat liver by use of affinity chromatography and fast protein liquid chromatofocusing. *Anal. Biochem.* 146:313-320.

Guthenberg, C., Jensson, H., Nyström, L., Österlund, E., Tahir, M.K. and Mannervik, B. 1985a. Isoenzymes of glutathione transferase in rat kidney cytosol. *Biochem. J.* 230:609-615.

Guthenberg, C., Ålin, P., and Mannervik, B. 1985b. Glutathione transferase from rat testis. *Methods Enzymol.* 113:507-510.

Guthenberg, C., Warholm, M., Rane, A., and Mannervik, B. 1986. Two distinct forms of glutathione transferase from human foetal liver: Purification and comparison with isoenzymes isolated from adult liver and placenta. *Biochem. J.* 235:741-745.

Hao, X.-Y., Castro, V.M., Bergh, J., Sundström, B., and Mannervik, B. 1994. Isoenzyme-specific quantitative immunoassays for cytosolic glutathione transferases and measurement of the enzymes in blood plasma from cancer patients and in tumor cell lines. *Biochim. Biophys. Acta* 1225:223-230.

Hayes, J.D. and Pulford, D.J. 1995. The glutathione S-transferase supergene family: Regulation of GST and the contribution of the isoenzymes to cancer chemoprotection and drug resistance. *Crit. Rev. Biochem. Mol. Biol.* 30:445-600.

Hubatsch, I., Ridderström, M., and Mannervik, B. 1998. Human glutathione transferase A4-4: An Alpha class enzyme with high catalytic efficiency in the conjugation of 4-hydroxynonenal and other genotoxic products of lipid peroxidation. *Biochem. J.* 330:175-179.

Mannervik, B. and Guthenberg, C. 1981. Glutathione transferase (human placenta). *Methods Enzymol.* 77:231-235.

Mannervik, B. and Danielson, U.H. 1988. Glutathione transferases: Structure and catalytic activity. *CRC Crit. Rev. Biochem.* 23:283-337.

Mannervik, B. and Widersten, M. 1995. Human glutathione transferases: Classification, tissue distribution, structure, and functional properties. *In* Advances in Drug Metabolism in Man (G.M. Pacifici and G.N. Fracchia, eds.) pp. 408-459. European Commission, Luxembourg.

Mannervik, B., Awasthi, Y.C., Board, P.G., Hayes, J.D., Di Ilio, C., Ketterer, B., Listowsky, I., Morgenstern, R., Muramatsu, M., Pearson, W.R., Pickett, C.B., Sato, K., Widersten, M., and Wolf, C. R. 1992. Nomenclature for human glutathione transferases. *Biochem. J.* 282:305-306.

Marcus, C.J., Habig, W.H., and Jakoby, W.B. 1978. Glutathione transferase from human erythrocytes: Nonidentity with the enzymes from liver. *Arch. Biochem. Biophys.* 188:287-293.

Morgenstern, R., Guthenberg, C., and DePierre, J.W. 1982. Microsomal glutathione transferase: Purification, initial characterization and demonstration that it is not identical to the cytosolic glutathione transferases A, B and C. *Eur. J. Biochem.* 128:243-248.

Ostlund Farrants, A.-K., Meyer, D.J., Coles, B., Southan, C., Aitken, A., Johnson, P.J., and Ketterer, B. 1987. The separation of glutathione transferase subunits by using reverse-phase high-pressure liquid chromatography. *Biochem. J.* 245:423-428.

Robertson, I.G.C., Jensson, H., Guthenberg, C., Tahir, M.K., Jernström, B., and Mannervik, B. 1985. Differences in the occurrence of glutathione transferase isoenzymes in rat lung and liver. *Biochem. Biophys. Res. Commun.* 127:80-86.

Seidegård, J., DePierre, J.W., and Pero, R.W. 1985. Hereditary interindividual differences in the glutathione transferase activity towards *trans*-stilbene oxide in resting human mononuclear leukocytes are due to a particular isozyme(s). *Carcinogenesis* 6:1211-1216.

Sherratt, P.J., Pulford, D.J., Harrison, D.J., Green, T., and Hayes, J.D. 1997. Evidence that human class Theta glutathione transferase T1-1 can catalyse the activation of dichloromethane, a liver and lung carcinogen in the mouse: Comparison of the tissue distribution of GST T1-1 with that of classes Alpha, Mu and Pi GST in human. *Biochem. J.* 326:837-846.

Tahir, M.K., Özer, N., and Mannervik, B. 1988. Isoenzymes of glutathione transferase in rat small intestine. *Biochem. J.* 253:759-764.

Tan, K.-L. and Board, P.G. 1996. Purification and characterization of a recombinant human Theta-class glutathione transferase (GST T2-2). *Biochem. J.* 315:727-732.

Warholm, M., Guthenberg, C., von Bahr, C., and Mannervik, B. 1985. Glutathione transferases from human liver. *Methods Enzymol.* 113:499-504.

Warholm, M., Jensson, H., Tahir, M.K., and Mannervik, B. 1986. Purification and characterization of three distinct glutathione transferases from mouse liver. *Biochemistry* 25:4119-4125.

Key References

Hayes and Pulford, 1995. See above.

Recent review article.

Mannervik and Widersten, 1995. See above.

Recent review article on human glutathione transferases.

Contributed by Bengt Mannervik and Per Jemth
Uppsala University
Uppsala, Sweden

HPLC-Based Assays for Enzymes of Glutathione Biosynthesis

The two protocols described in this unit describe assays for the enzymes involved in glutathione (GSH) biosynthesis: glutamate cysteine ligase (GLCL, EC 3.4.4.2; also known as γ-glutamylcysteine synthetase) and glutathione synthetase (GS, EC 6.3.2.3). These enzymes carry out the two-step synthesis of GSH. The first and often rate-limiting step, catalyzed by GLCL, involves the formation of the dipeptide γ-glutamylcysteine (γ-GC) from cysteine and glutamic acid via an unusual γ-carbon peptide bond. The second step involves the addition of glycine by GS to form γ-glutamylcysteinylglycine (GSH).

The protocols detailed here were adapted from the original work by Fahey et al. (1981) and represent modifications of HPLC assays published by Hamel et al. (1992). The fluorescent thiol reactive compound monobromobimane (MBB) is used to derivatize the reaction products, which are then separated by high-performance liquid chromatography (HPLC) and quantified with fluorescence detection.

NOTE: Monobromobimane (MBB) and bimane-derivatized thiols are photolabile. Reactions should be conducted under conditions that protect them from direct light exposure (e.g., in a darkened room or in brown glass reaction tubes).

NOTE: All protocols using live animals must first be reviewed and approved by an Institutional Animal Care and Use Committee (IACUC) or must conform to governmental regulations regarding the care and use of laboratory animals.

ANALYSIS OF GLUTAMATE CYSTEINE LIGASE (GLCL) ACTIVITY IN TISSUES

BASIC PROTOCOL 1

GLCL reactions are set up using cytoplasmic preparations from tissue homogenates as the source for GLCL activity. Samples and standards are derivatized with monobromobimane, and the amount of γ-GC produced is measured by HPLC. The activity of GLCL is determined by comparison with standards.

Materials

Tissue of interest
TES/SB homogenization buffer (see recipe), ice cold
GLCL reaction cocktail (see recipe), ice cold
200 mM 5-sulfosalicylic acid (SSA; Sigma), ice cold
5 mM L-cysteine (Sigma), prepared fresh
γ-Glutamylcysteine (γ-GC; Sigma)
Glutathione (GSH; Sigma)
0.2 M *N*-ethylmorpholine (NEM; Sigma)/0.02 M KOH
25 mM monobromobimane (MBB; Thiolyte reagent, Calbiochem) in acetonitrile

15-ml Corex tubes
Polytron tissue homogenizer (Kinematic AG)

Additional reagents and equipment for HPLC (see Support Protocol)

NOTE: Cysteine, γ-GC, and GSH solutions must be made immediately prior to use, or stored on ice if made in advance. Solutions should not be made more than one hour prior to use in this assay. Cysteine should be at room temperature when it is added to the incubation tubes.

Contributed by Collin C. White, Cecile M. Krejsa, David L. Eaton, and Terrance J. Kavanagh
Current Protocols in Toxicology (1999) 6.5.1-6.5.14

Prepare tissue samples

1. Place 1 to 2 g tissue in 4 vol ice-cold TES/SB homogenization buffer in a 15-ml Corex tube. Homogenize on ice with a Polytron tissue homogenizer.

   Homogenization should be carried out on ice to prevent loss of enzyme activity due to overheating of the sample. Homogenize the tissue thoroughly, but avoid excessive homogenization as this can overheat the sample and denature proteins.

   Quantitation of activity in terms of grams of tissue requires accurate weighing and recording of tissue samples prior to analysis.

2. Centrifuge at 10,000 × *g*, 4°C, for 15 min in a floor-model centrifuge. Place sample on ice.

   Only the supernatant (cytoplasmic protein) is used in the assay.

3. Prepare triplicate baseline samples (to determine background γ-GC levels) by adding the following to three microcentrifuge tubes:

   80 µl ice-cold GLCL reaction cocktail
   50 µl water
   50 µl 200 mM ice-cold SSA
   20 µl supernatant sample.

   Place on ice ≥15 min.

   Baseline samples are ready for derivatization (step 12).

Incubate samples for enzymatic activity

4. Prepare triplicate microcentrifuge tubes containing 80 µl ice-cold GLCL reaction cocktail.

   Reaction tubes should be prepared immediately prior to assay or stored on ice to prevent degradation of the ATP.

5. At 15- to 30-sec time intervals, with the sample on ice, add 20 µl sample to each reaction tube and place in a 37°C water bath. Preincubate reaction tubes for 5 min at 37°C.

   Ten samples can be processed during each 5-min incubation if a 30-sec interval is used.

6. At the appropriate time, initiate each reaction by adding 50 µl of 5 mM L-cysteine (final reaction volume 150 µl). Vortex briefly and incubate for 5 min at 37°C.

   It is essential that any modifications to this GLCL activity assay result in a final volume of 150 µl at this step. Otherwise, modifications of the neutralization and derivatization steps will also be required.

7. Stop each reaction at the appropriate time by adding 50 µl ice-cold 200 mM SSA and vortex. Place tubes on ice ≥15 min.

Prepare standards

8. Prepare a 10 mM γ-GC standard solution in TES/SB homogenization buffer. Dilute to desired concentrations (typically 0.1, 0.25, 0.5, 0.75, and 1.0 mM) in TES/SB homogenization buffer.

   Alternatively, diluted GSH solutions can be used to construct a standard curve, because detector response factors (area units/nmol) are identical for bimane-derivatized γ-GC and GSH, and because γ-GC is relatively expensive. A γ-GC standard should be run to characterize the retention time of the γ-GC-bimane derivatization product.

9. Prepare a 10 mM GSH standard solution in TES/SB homogenization buffer. Dilute to desired concentrations (typically 0.1, 0.25, 0.5, 0.75, and 1.0 mM) in TES/SB homogenization buffer.

10. Prepare triplicate standard tubes for each standard dilution by adding the following to microcentrifuge tubes:

    80 µl GLCL reaction cocktail
    50 µl 200 mM SSA
    50 µl water
    20 µl γ-GC or GSH standard solution.

11. Prepare one blank tube as in step 10, but with 20 µl TES/SB homogenization buffer instead of standard.

Derivatize samples and standards

12. Vortex samples and standards. Centrifuge at top speed in a benchtop microcentrifuge for 2 min.

13. Add 200 µl of 0.2 M NEM/0.02 M KOH.

    The pH must be between 7.5 and 8.5 following NEM/KOH addition for efficient derivatization by MBB. It is recommended that this solution be tested on a blank prior to addition to samples, and that pH paper (e.g., colorPhast pH 2 to 9, EM Science) be used to verify pH.

14. Add 20 µl of 25 mM MBB and vortex. Incubate at room temperature in the dark for 30 min.

15. Add 200 µl of 200 mM SSA and vortex. Microcentrifuge at top speed for 2 min.

Determine enzyme activity

16. Analyze samples and standards using HPLC (see Support Protocol).

17. Average triplicates. Prepare standard curves from standards and calculate the amount of GSH and γ-GC in each sample (baseline and incubated).

18. To calculate γ-GC formation, subtract the GSH level in the baseline sample from that in the incubated sample, and then add this difference to the γ-GC level in the incubated sample.

    γ-GC is usually not detected in baseline samples.

19. Express GLCL activity in µmol γ-GC formed/min/g tissue or in nmol/min/mg protein.

    To express activity per mg protein, use the Bradford method for protein determination (see APPENDIX 3). The assay of protein in sample supernatants should be performed immediately after the GLCL assay is completed.

ANALYSIS OF GLCL ACTIVITY IN CULTURED CELLS

ALTERNATE PROTOCOL 1

In order to detect GLCL activity in cultured cells, Basic Protocol 1 can be performed with the following modifications. For convenience, one may substitute phosphate-buffered saline containing serine/borate (PBS/SB) for TES/SB. There is no difference in enzyme activities or baseline GSH levels when employing PBS/SB or TES/SB with cultured cells.

Additional Materials *(also see Basic Protocol 1)*

Cell cultures of interest
PBS/SB: PBS (*APPENDIX 2A*) containing 20 mM boric acid and 1 mM serine, pH 7.4
Probe sonicator

1. Centrifuge cell suspensions in 15- or 50-ml conical polypropylene tubes at 150 to 200 × *g*, 4°C, for 10 min. Place tubes with pelleted cells on ice, remove supernatants, and resuspend cells in ice-cold PBS/SB.

   For best results, pellet cells in medium or PBS containing 5% (v/v) serum to prevent premature rupture and leakage of cytoplasmic contents.

   If activity is to be expressed per million cells (see step 6), the cells should be counted prior to pelleting.

   Cells from suspension or adherent cultures can be used. Adherent cells should be trypsinized and pelleted prior to this step. Note that GLCL activity changes with confluency, so it is essential to test cells at the same level of confluency for consistent results.

2. Using a probe sonicator, disrupt 10 to 15 million cells in 500 µl ice-cold PBS/SB, keeping tube on ice during and after sonication. Use multiple short blasts to minimize local heating of the sample and do not oversonicate as this can affect enzyme activity.

3. Centrifuge cell sample at 14,000 rpm (maximum speed) in a microcentrifuge for 10 min at 4°C. Place on ice.

4. Prepare samples (including baseline sample) as described (see Basic Protocol 1, steps 3 to 7), but reduce the stock concentration of cysteine in step 6 to between 0.5 and 5 mM. Increase incubation time to 10 min for samples with low GLCL activity.

5. Prepare γ-GC and GSH standards (see Basic Protocol 1, steps 8 through 11) at 5, 10, 25, 50, 75, and 100 µM in PBS/SB.

6. Derivatize standards and samples (see Basic Protocol 1, steps 12 to 15) but reduce MBB in step 14 to 12.5 mM. Analyze by HPLC (see Support Protocol) using the high-sensitivity setting on the HPLC fluorescence detector. Increase the injection volume for samples with low GLCL activity. Determine GLCL activity (see Basic Protocol 1, steps 17 to 19), expressing activity as nmol/mg protein/min or as nmol/10^6 cells/min.

BASIC PROTOCOL 2

ANALYSIS OF GLUTATHIONE SYNTHETASE (GS) ACTIVITY IN TISSUES

Cytoplasmic preparations from tissue homogenates are dialyzed to remove endogenous GSH and are then analyzed for GS activity.

Materials

Tissue of interest
TES/SB homogenization buffer (see recipe), ice cold
GS reaction cocktail (see recipe), ice cold
200 mM 5-sulfosalicylic acid (SSA; Sigma), ice cold
5 mM γ-glutamylcysteine (γ-GC; Sigma), prepared fresh
Glutathione (GSH; Sigma)
0.2 M *N*-ethylmorpholine (NEM: Sigma)/0.02 M KOH
25 mM monobromobimane (MBB; Thiolyte reagent, Calbiochem) in acetonitrile

15-ml Corex tubes
Polytron tissue homogenizer (Kinematic AG)
Flow Microdialysis System (Life Technologies)

Additional reagents and equipment for HPLC (see Support Protocol)

NOTE: γ-GC and GSH solutions must be made immediately prior to use, or stored on ice if made in advance. Solutions should not be made more than one hour prior to use in this assay. γ-GC should be at room temperature when it is added to the incubation tubes.

Prepare tissue samples

1. Place 1 to 2 g tissue in 4 vol ice-cold TES/SB homogenization buffer in a 15-ml Corex tube. Homogenize on ice in a Polytron tissue homogenizer.

   Homogenization should be carried out on ice to prevent loss of enzyme activity due to overheating of the sample. Homogenize the tissue thoroughly, but avoid excessive homogenization as this can overheat the sample and denature proteins.

   Quantitation of activity in terms of grams of tissue requires accurate weighing and recording of tissue samples prior to analysis.

2. Centrifuge at 10,000 × *g*, 4°C, for 15 min in a floor-model centrifuge. Place sample on ice.

   Only the supernatant (cytoplasmic protein) is used in the assay.

3. Dialyze the entire supernatant at 4°C for 3 hr by continuous-flow dialysis (e.g., with a Flow Microdialysis system, according to manufacturer's instructions) against 2 liters of TES/SB homogenization buffer. Return to ice.

   This removes ~85% of the endogenous GSH and does not affect enzyme activity.

4. Prepare triplicate baseline samples (to determine background GSH levels) by adding the following to three microcentrifuge tubes:

   80 µl ice-cold GS reaction cocktail
   50 µl water
   50 µl 200 mM ice-cold SSA
   20 µl dialyzed sample.

   Place on ice ≥15 min.

   Baseline samples are ready for derivatization (step 12).

Incubate samples for enzymatic activity

5. Prepare triplicate microcentrifuge tubes containing 80 µl ice-cold GS reaction cocktail.

   Reaction tubes should be prepared immediately prior to assay or stored on ice to prevent degradation of the ATP.

6. At 15- to 30-sec time intervals, with the sample on ice, add 20 µl sample to each reaction tube and place in a 37°C water bath. Preincubate reaction tubes for 5 min at 37°C.

   Ten samples can be processed during each 5-min incubation if a 30-sec interval is used.

7. At the appropriate time, initiate each reaction by adding 50 µl of 5 mM γ-GC. Vortex briefly and incubate for 5 min at 37°C.

   It is essential that any modifications to this GS activity assay result in a final volume of 150 µl at this step. Otherwise, modifications of the neutralization and derivatization steps will also be required.

8. Stop each reaction at the appropriate time by adding 50 µl ice-cold 200 mM SSA and vortex. Place tubes on ice ≥15 min.

Prepare standards

9. Prepare a 10 mM GSH standard solution in TES/SB homogenization buffer. Dilute to desired concentrations (typically 0.1, 0.25, 0.5, 0.75, and 1.0 mM) in TES/SB homogenization buffer.

10. Prepare triplicate standard tubes for each standard dilution by adding the following to microcentrifuge tubes:

    80 µl GS reaction cocktail
    50 µl 200 mM SSA
    50 µl water
    20 µl GSH standard solution.

11. Prepare one blank tube as in step 10, but with 20 µl TES/SB homogenization buffer instead of standard.

Derivatize samples and standards

12. Vortex samples and standards. Centrifuge at maximum speed in a benchtop microcentrifuge for 2 min.

13. Add 200 µl of 0.2 M NEM/0.02 M KOH.

    The pH must be between 7.5 and 8.5 following NEM/KOH addition for efficient derivatization by MBB. It is recommended that this solution be tested on a blank prior to addition to samples, and that pH paper (e.g., colorPhast pH 2 to 9, EM Science) be used to verify pH.

14. Add 20 µl of 25 mM MBB and vortex. Incubate at room temperature in the dark for 30 min.

15. Add 200 µl of 200 mM SSA and vortex. Microcentrifuge at maximum speed for 2 min.

Determine enzyme activity

16. Analyze samples and standards using HPLC (see Support Protocol).

17. Average triplicates. Prepare standard curves from standards and calculate the amount of GSH in each sample (baseline and incubated).

18. To calculate GSH formation, subtract the GSH level in the baseline sample from that in the incubated sample.

19. Express GS activity in µmol GSH formed/min/g tissue or in nmol/min/mg protein.

    To express activity per mg protein rather than per mg tissue, use the Bradford method for protein determination (see APPENDIX 3). The assay of protein in sample supernatants should be performed immediately after the GS assay is completed.

ALTERNATE PROTOCOL 2

ANALYSIS OF GS ACTIVITY IN CULTURED CELLS

In order to detect GS activity in cultured cells, Basic Protocol 2 can be performed with the following modifications. For convenience, one may substitute phosphate-buffered saline containing serine/borate (PBS/SB) for TES/SB. There is no difference in enzyme activities or baseline GSH levels when employing PBS/SB or TES/SB with cultured cells.

Additional Materials *(also see Basic Protocol 2)*

Cell cultures of interest
PBS/SB: PBS (*APPENDIX 2A*) containing 20 mM boric acid and 1 mM serine, pH 7.4
Probe sonicator

1. Centrifuge cell suspensions in 15- or 50-ml conical polypropylene tubes at 150 to 200 × *g*, 4°C, for 10 min. Place tubes with pelleted cells on ice, remove supernatants, and resuspend cells in ice-cold PBS/SB.

For best results, pellet cells in medium or PBS containing 5% (v/v) serum to prevent premature rupture and leakage of cytoplasmic contents.

If activity is to be expressed per million cells (see step 6), the cells should be counted prior to pelleting.

Cells from suspension or adherent cultures can be used. Adherent cells should be trypsinized and pelleted prior to this step. Note that GS activity changes with confluency, so it is essential to test cells at the same level of confluency for consistent results.

2. Using a probe sonicator, disrupt 10 to 15 million cells in 500 µl ice-cold PBS/SB, keeping tube on ice during and after sonication. Use multiple short blasts to minimize local heating of the sample and do not oversonicate as this can affect enzyme activity.
3. Centrifuge cell sample at 14,000 rpm (maximum speed) in a microcentrifuge for 10 min at 4°C. Place on ice.
4. Perform dialysis (against PBS/SB) and prepare samples (including baseline sample) as described (see Basic Protocol 2, steps 3 to 8), but reduce the stock concentration of γ-GC in step 7 to between 0.5 and 5 mM. Increase incubation time to 10 min for samples with low GS activity.
5. Prepare GSH standards (see Basic Protocol 2, steps 9 to 11) at 5, 10, 25, 50, 75, and 100 µM GSH in PBS/SB.
6. Derivatize standards and samples (see Basic Protocol 2, steps 12 to 15) but reduce MBB in step 14 to 12.5 mM. Analyze by HPLC (see Support Protocol) using the high-sensitivity setting on the HPLC fluorescence detector. Increase the injection volume for samples with low GS activity. Determine GS activity (see Basic Protocol 2, steps 17 to 19), expressing activity as nmol/mg protein/min or as nmol/10^6 cells/min.

MEASUREMENT OF γ-GC AND GSH BY HPLC

SUPPORT PROTOCOL

HPLC analysis is used to quantify the activity of GLCL or GS in the synthesis of GSH.

Materials

Derivatized samples and standards for analysis (see Basic Protocols 1 and 2 and Alternate Protocols 1 and 2)
1 mM tetrabutylammonium phosphate (TBAP; Regis), pH adjusted to 3.0 with 10% (v/v) phosphoric acid
HPLC-grade methanol

Shimadzu SIL-6B HPLC system with autosampler, CR5A integrator, and RF-535 fluorescence detector (or equivalent)
Pellicular C18 guard column (Alltech)
150-mm reversed-phase C18 HPLC column (Alltech)

1. Set up an HPLC system with a Pellicular C18 guard column, a 150-mm reversed-phase C18 HPLC column, and fluorescence detection (excitation at 375 nm and emission at 475 nm).

If a fluorescence detector is not available, it is possible to use a UV/visible detector (380 nm). In the authors' experience, however, fluorescence detection provides at least one to two orders of magnitude more sensitivity than that obtained with UV/visible detection.

The conditions described here are optimized for the Shimadzu SIL-6B HPLC with a CR5A integrator and an RF-535 fluorescence detector. Optimal conditions for other systems will have to be determined by the investigator.

Table 6.5.1 Gradient Program for HPLC Analysis

Time (min)	% aqueous phase	% organic phase
0	95	5
1	80	20
10	70	30
12	40	60
14	40	60
16	95	5
21	95	5

Table 6.5.2 Integrator Settings for HPLC Analysis

Feature[a]	Low sensitivity	High sensitivity
Width	5	5
Drift	0	0
T DBL	0	0
Attenuation	7	9
Method	0421	0421
SPL WT	100	100
Slope	15,000	15,000
Minimum area	2,000	50,000
Stop time	16	16
Speed	5	5
Format	0	0
IS WT	1	1

[a]Abbreviations: IS WT, internal standard weight; SPL WT, sample weight; T DBL, slope and width doubling.

2. Prepare mobile phases. Use 1 mM TBAP (an ion-pairing agent), pH 3.0, as the aqueous phase, and HPLC-grade methanol as the organic phase.
3. Program the gradient as indicated in Table 6.5.1 and set the integrator as indicated in Table 6.5.2.
4. Run the column using an autosampler injection volume of 25 to 50 µl and a flow rate of 1.5 ml/min.

Because the level of activity varies with different tissue or cell line sources, the conditions must be optimized for each source to keep the level within the linear range for the assay. This may be accomplished by adjusting the sensitivity, the injection volume, and/or the attenuation settings. The final derivatized samples contain enough volume to run a couple of test injections and to adjust injection and sensitivity settings prior to running the whole set of samples. This is strongly recommended.

REAGENTS AND SOLUTIONS

*Use Milli-Q-purified water or equivalent in all recipes and protocol steps. For common stock solutions, see **APPENDIX 2A**; for suppliers, see **SUPPLIERS APPENDIX**.*

GLCL reaction cocktail

Add to 100 ml of water:
1.2 g ATP (20 mM; Sigma)
1.7 g L-glutamic acid (100 mM; Sigma)

continued

37 mg EDTA (1.0 mM)
406 mg $MgCl_2$ (20 mM)
2.42 g Tris (200 mM)
Adjust pH to 7.4
Store up to 6 months at –20°C

GS reaction cocktail

Add to 100 ml of water:
1.2 g ATP (20 mM; Sigma)
751 mg L-glycine (100 mM; Sigma)
37 mg EDTA (1.0 mM)
406 mg $MgCl_2$ (20 mM)
2.42 g Tris (200 mM)
Adjust pH to 7.4
Store up to 6 months at –20°C

TES/SB homogenization buffer

Add to 1 liter of water:
85.58 g sucrose (0.25 M)
2.42 g Tris (20 mM)
370 mg EDTA (1 mM)
1.24 g boric acid (20 mM)
105 mg L-serine (1 mM)
Adjust pH to 7.4 with 1 N HCl
Store up to 6 months at 4°C

NOTE: *The inclusion of serine and borate in the homogenization buffer is necessary to inhibit any residual γ-glutamyl transpeptidase (GGT) activity. Otherwise, GGT will consume GSH and thus affect the calculation of baseline and sample GSH concentrations.*

COMMENTARY

Background Information

Glutathione (GSH) is important in free radical scavenging, xenobiotic conjugation, and maintenance of thiol redox status; for reviews see Meister (1995) and *UNIT 6.1*. Given adequate cysteine supply, the rate-limiting enzyme in GSH synthesis is GLCL. However, under some circumstances (e.g., cirrhosis of the liver), GS has been shown to be limiting for GSH synthesis (Loguercio et al., 1992).

GLCL is a heterodimeric enzyme consisting of a 70-kDa catalytic subunit (GLCLC) and a 29-kDa subunit (GLCLR) that appears to regulate the catalytic activity of the holoenzyme (Huang et al., 1993a,b). The cDNAs for both subunits have been cloned from rat, human, and mouse cells (Yan and Meister, 1990; Gipp et al., 1992, 1995; Huang et al., 1993a; Kang et al., 1997; Reid et al., 1997a,b). The expression of the mRNAs for both GLCLC and GLCLR has been reported for various tissues in humans (Gipp et al., 1995). Regional expression of GLCLC mRNA has been localized by in situ hybridization in mouse brain (Kang et al., 1997), rat kidney (Li et al., 1996a), and rat brain (Li et al., 1996b). Moreover, both subunit genes have been mapped on human and mouse chromosomes (Tsuchiya et al., 1995; Walsh et al., 1996).

GLCLC is catalytically active as a monomer; however, the K_m for glutamate is high compared to physiological levels, suggesting that in the absence of GLCLR the enzyme would not be active in situ. GLCL activity is negatively regulated by GSH, which competes for the glutamate binding site on the enzyme and inhibits γ-GC synthesis with a K_i of ~8 mM. The holoenzyme has a lower K_m for glutamate and higher K_i for GSH than GLCLC alone (Huang et al., 1993a,b). A model for redox activation of GLCL has been proposed in which a disulfide bridge between the two subunits changes the active site conformation to favor glutamate over GSH. Through this proposed mechanism the enzyme would be activated by oxidizing conditions within the cell. Indeed, in purified enzyme preparations from rat kidney, ~70% of GLCL was disulfide-linked and had an apparent molecular weight of ~100 kDa under nonreducing conditions (Huang et al.,

1993b). These results suggest that in addition to feedback inhibition by GSH there may be a "redox switch" on GLCL that determines enzyme activity. The GLCL assay as detailed in Basic Protocol 1 is not designed to assess the effects of the GLCL regulatory subunit, as glutamate levels are not limiting in the reaction cocktail.

GLCL has been shown to be under transcriptional control, and is induced by many treatments, especially agents that cause oxidative stress (Borroz et al., 1994; O'Dwyer et al., 1996; Cai et al., 1997; Galloway et al., 1997; Sekhar et al., 1997; Tian et al., 1997; Wild et al., 1998). Recently, it was reported that GLCL activity in cells is rapidly increased by H_2O_2, suggesting that post-translational regulation of the enzyme also exists (Ochi, 1995, 1996). The mechanisms of transcriptional and post-translational activation of GLCL are unknown, although recent evidence indicates the presence of antioxidant regulatory elements in the 5′ region of the genes encoding this enzyme (Mulcahy et al., 1997). The combined effect of transcriptional and post-translational upregulation of GLCL activity may explain the rapid and sustained increase in intracellular GSH that is often seen following oxidative stress and GSH depletion. While there is evidence of tissue-specific differences in GS expression (see below), it is commonly believed that control of cellular GSH content is achieved by regulation of GLCL.

Compared to GLCL, much less effort has been spent in studies of GS. Bacterial GS has been extensively studied, but this monomeric enzyme differs substantially from the GS isolated from eukaryotic organisms. The GS gene has been cloned from frogs, rats, mice, and humans (Habenicht et al., 1993; Gali and Board, 1995; Huang et al., 1995; Shi et al., 1996a). Mammalian GS is a 118-kDa enzyme composed of two identical subunits. Humans lacking functional GS demonstrate GSH deficiency, hemolytic anemia, 5-oxoprolinurea, and in severe cases, neurological disorders (Wellner et al., 1974; Larsson and Mattsson, 1976). While only one GS gene has been mapped in humans, the differences in severity of symptoms observed in patients with GS deficiency may be due to several mutations resulting in differential impairment of GS function (Shi et al., 1996b; Dahl et al., 1997). GS is expressed at the highest levels in the kidney, which has approximately three-fold higher GS activity than liver and six- to ten-fold higher activity than brain, lung, or spleen. Lower levels of expression are seen in smooth and cardiac muscle (Shi et al., 1996a).

Although GS is not considered to be the rate-limiting step in GSH formation, there is some evidence to indicate that GS activity is influenced by oxidative stress (Sun, 1997). Recently the GS gene has been shown to have six alternative transcripts, derived as mRNA splice variants from a single gene. There is some indication of organ-specific expression, but little information is available as to the tissue distribution of the various transcripts. While the functional differences of these transcripts are unknown, the prediction that they code for proteins of three different lengths suggests that regulation of GS may occur at multiple levels (Shi et al., 1996a).

Other, non-HPLC-based assays have been used to assess the kinetics of GLCL in purified enzyme preparations from mammalian and bacterially expressed sources (Seelig and Meister, 1985) and in liver cytosol (Sun et al., 1996). The most commonly used kinetic assay is a coupled reaction between GLCL, pyruvate kinase, and lactate dehydrogenase. GLCL uses ATP in the synthesis of γ-GC; the ADP formed is phosphorylated by pyruvate kinase, which converts phosphoenol-pyruvate to pyruvate; the free pyruvate is then reduced to lactate. The rate of reaction is followed by the decrease in the absorbance of NADH, which serves as electron donor for the final reaction. A modification of this method involves the use of L-α-aminobutyrate instead of L-cysteine to reduce complications due to thiol oxidation (Seelig and Meister, 1985). A different approach has been taken by Sun et al. (1996). A fluorogenic glutathione-*S*-transferase (GST) substrate, monochlorobimane, is used to follow the production of GSH in dialyzed liver cytosols. The rate of production of the fluorescent GSH-bimane adduct is compared to GSH-bimane production in samples preincubated with buthionine sulfoximine, a specific inhibitor of GLCL. The increase in bimane fluorescence is taken as a direct measure of GLCL activity since GS and the GSTs are not thought to be rate limiting in liver.

GS activity has been measured by incorporation of radiolabeled glycine into GSH over a reaction period, or by quantification of ADP or P_i production during the reaction. Both γ-GC and L-γ-glutamyl-L-α-aminobutyrate, a non-thiol analog of γ-GC, have been used as reaction substrates for the GS activity assays. [^{14}C]GSH or [^{14}C]L-γ-glutamyl-L-α-aminobutyrylglycine is quantified by scintillation counting after sepa-

ration from unincorporated [^{14}C]Gly. ADP is measured using the pyruvate kinase/lactate dehydrogenase system described above, whereas P_i may be measured by a colorimetric reaction with molybdate (Meister, 1985).

Critical Parameters and Troubleshooting

It is necessary to prepare standards and dilutions of the samples such that the enzyme activities and the response of the HPLC detector are within linear range. To do this one must anticipate relative activities from the tissues to be tested. In general, GLCL activities are highest in kidney and liver, with lower amounts in other tissues. Brain, lung, heart, ovary, and stomach show reasonable expression of GLCL, whereas thymus, uterus, adrenal gland, and eye have little GLCL per milligram total protein.

The protocols described above are appropriate for determination of GLCL and GS activity from strongly expressing tissues such as kidney or liver. The GLCL and GS activity in other tissues or cell types must be determined empirically, as modifications of the basic assay may be required for useful assessment of enzyme activity. For example, lymphocytes, which contain very little GLCL activity per milligram protein, may be assayed at low cysteine concentrations (0.125 to 1.25 mM), which permits HPLC detection at high sensitivity without peak interference from excess cysteine. In contrast, kidney GLCL activity is so high that substrate depletion is a concern at very low cysteine concentrations. Tissues with lower activity may also be assayed with a 10-min incubation time to enhance the sensitivity of the test. In some cases it is simpler to increase or decrease the injection volume of the derivatized products than to alter the assay protocol.

The addition of serine and borate to the homogenization buffers is essential for performing these assays, especially for tissues or cells that contain significant amounts of GGT activity. A protease inhibitor mix, (which may include aprotinin, leupeptin, phenylmethylsulfonyl fluoride, Pefabloc, N^{α}-tosyl-Lys-chloromethyl ketone, and/or N^{α}-tosyl-Phe-chloromethyl ketone) may also be added routinely to homogenization and sonication buffers. This is especially important if numerous samples are to be prepared on the same day, as GLCL is subject to degradation over time even when homogenates are kept on ice.

The stability of GSH, cysteine, and γ-glutamylcysteine at normal pH is very poor. Therefore, it is important to prepare baseline samples and standards immediately before use; the low pH of the SSA solution stabilizes the GSH. In addition, while freezing cell or tissue samples at −80°C prior to homogenization preserves the enzyme activity, it will not prevent loss of GSH. Therefore the GSH "baseline" levels from this assay cannot be used as true measures of reduced GSH in the tissues or cells tested.

Following treatment with SSA, the samples must be kept on ice for at least 15 min to ensure efficient precipitation of cellular proteins. Decreased incubation times can interfere with subsequent derivatization by MBB.

The pH of the sample is critical for efficient MBB derivatization of thiols. A blank should be tested with pH paper after addition of NEM/KOH to ensure that the pH of the sample is between 7.5 and 8.5 prior to addition of MBB. If for some reason the pH is off, it may be necessary to adjust the concentration of the NEM/KOH to attain the desired pH in the sample.

GSH-MBB and γ-GC-MBB adducts are labile and must be stored carefully. The acidic pH of the assay solution following derivatization helps to stabilize the products. However the samples must be protected from light prior to HPLC analysis. If there are too many samples for one day's run, derivatized samples should be stored at −80°C until they can be processed. Storage for longer than 24 hr is not recommended.

If the final GLCL and GS activity values are to be reported per milligram protein, it is important to exercise care with the protein assay. Protein levels in homogenates should be determined on the same day as the enzyme assay is performed, since freeze-thaw cycles can alter soluble protein concentrations. In addition, it is recommended that the Bradford method be used to assay protein levels as it does not rely upon sulfhydryl binding for determination of protein concentrations.

Anticipated Results

A typical HPLC chromatogram obtained using these methods is shown in Figure 6.5.1. Peaks for cysteine, γ-glutamylcysteine, and GSH are indicated. It is convenient to analyze the results of such experiments using a spreadsheet software program (e.g., Excel).

The GSH readings from baseline samples are subtracted from the GSH readings from incubated samples. In the case of the GLCL assay, this difference is then added to the γ-GC levels obtained in incubated samples (γ-GC is usually not detected in baseline samples). The

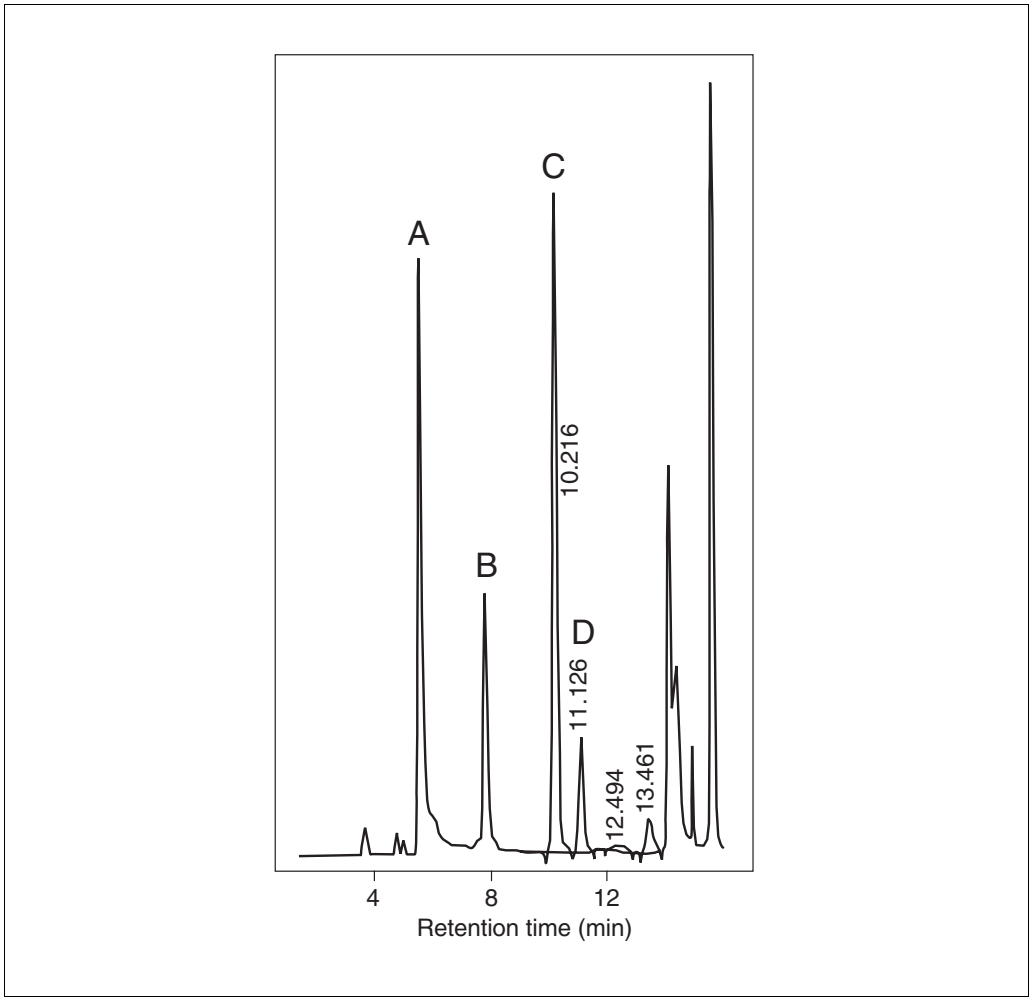

Figure 6.5.1 Typical chromatogram achieved using the GLCL protocol. Peaks corresponding to cysteine (A), free bimane (B), GSH (C), and γ-GC (D) are indicated.

total represents γ-GC formation over the course of the incubation period. In the case of the GS assay, the GSH levels in the baseline samples are simply subtracted from the GSH levels in the incubated samples to give a total of GSH formed during the incubation.

The activity can be expressed as μmol γ-GC or GSH formed/minute/gram tissue (which necessitates the accurate weighing and recording of tissues samples prior to analysis), or nmol γ-GC or GSH formed/min/mg protein. The Bradford method is recommended for protein determination. Methods that rely on bicinchoninic acid (BCA) are not advised as they may be influenced by the thiol redox status of the sample.

Time Considerations

Incubation and derivatization of samples for a typical experiment (25 to 50 reaction tubes plus standards) requires ~2 hr. Homogenization of tissues and determination of protein levels in homogenates will require additional time. HPLC analysis of samples in the autosampler described (see Support Protocol) requires ~30 min per sample. Since the derivatized samples should not be stored more than 24 hr (see Critical Parameters and Troubleshooting), the total number of standards and samples should be limited accordingly. The total number of derivatized samples to be run may be reduced in the following ways. (1) Characterize the HPLC column for retention time of γ-GC and GSH in a separate experiment. (2) Characterize the column for response factors associated with the GSH-bimane or γ-GC-bimane standards, so that a full standard curve does not need to be run with each set of samples. By thoroughly characterizing the chromatography, the investigator minimizes the number of standards that must be run alongside any given set of samples. (3) When handling error ceases to be a problem and triplicate replication is consistently good, reduce the number of GSH baseline samples in

the GLCL assay from three to two. Care should be taken to ensure that the samples are protected from light, that there is adequate paper supply in the integrator, and that there is adequate TBAP and HPLC-grade methanol for processing all of the samples and standards.

Literature Cited

Borroz, K.I., Buetler, T.M., and Eaton, D.L. 1994. Modulation of gamma-glutamylcysteine synthetase large subunit mRNA expression by butylated hydroxyanisole. *Toxicol. Appl. Pharmacol.* 126:150-155.

Cai, J., Huang, Z.Z., and Lu, S.C. 1997. Differential regulation of gamma-glutamylcysteine synthetase heavy and light subunit gene expression. *Biochem. J.* 326:167-172.

Dahl, N., Pigg, M., Ristoff, E., Gali, R., Carlsson, B., Mannervik, B., Larsson, A., and Board, P. 1997. Missense mutations in the human glutathione synthetase gene result in severe metabolic acidosis, 5-oxoprolinuria, hemolytic anemia and neurological dysfunction. *Hum. Mol. Genet.* 6:1147-1152.

Fahey, R.C., Newton, G.L., Dorian, R., and Kosower, E.M. 1981. Analysis of biological thiols: Quantitative determination of thiols at the picomole level based upon derivatization with monobromobimanes and separation by cation-exchange chromatography. *Anal. Biochem.* 111:357-365.

Gali, R.R. and Board, P.G. 1995. Sequencing and expression of a cDNA for human glutathione synthetase. *Biochem. J.* 310:353-358.

Galloway, D.C., Blake, D.G., Shepherd, A.G., and McLellan, L.I. 1997. Regulation of human gamma-glutamylcysteine synthetase: Co-ordinate induction of the catalytic and regulatory subunits in HepG2 cells. *Biochem. J.* 328:99-104.

Gipp, J.J., Chang, C., and Mulcahy, R.T. 1992. Cloning and nucleotide sequence of a full-length cDNA for human liver gamma-glutamylcysteine synthetase. *Biochem. Biophys. Res. Commun.* 185:29-35.

Gipp, J.J., Bailey, H.H., and Mulcahy, R.T. 1995. Cloning and sequencing of the cDNA for the light subunit of human liver gamma-glutamylcysteine synthetase and relative mRNA levels for heavy and light subunits in human normal tissues. *Biochem. Biophys. Res. Commun.* 206:584-589.

Habenicht, A., Hille, S., and Knochel, W. 1993. Molecular cloning of the large subunit of glutathione synthetase from Xenopus laevis embryos. *Biochim. Biophys. Acta* 1174:295-298.

Hamel, D.M., White, C., and Eaton, D.L. 1992. Determination of γ-glutamylcysteine synthetase and glutathione synthetase activity by HPLC. *Toxicol. Methods* 1:273-288.

Huang, C.S., Anderson, M.E., and Meister, A. 1993a. Amino acid sequence and function of the light subunit of rat kidney gamma-glutamylcysteine synthetase. *J. Biol. Chem.* 268:20578-20583.

Huang, C.S., Chang, L.S., Anderson, M.E., and Meister, A. 1993b. Catalytic and regulatory properties of the heavy subunit of rat kidney gamma-glutamylcysteine synthetase. *J. Biol. Chem.* 268:19675-19680.

Huang, C.S., He, W., Meister, A., and Anderson, M.E. 1995. Amino acid sequence of rat kidney glutathione synthetase. *Proc. Natl. Acad. Sci. U.S.A.* 92:1232-1236.

Kang, Y., Oiao, X., Jurma, O., Knusel, B., and Andersen, J.K. 1997. Cloning/brain localization of mouse glutamylcysteine synthetase heavy chain mRNA. *Neuroreport* 8:2053-2060.

Larsson, A. and Mattsson, B. 1976. On the mechanism of 5-oxoproline overproduction in 5-oxoprolinuria. *Clin. Chim. Acta* 67:245-253.

Li, S., Thompson, S.A., Kavanagh, T.J., and Woods, J.S. 1996a. Localization by in situ hybridization of gamma-glutamylcysteine synthetase mRNA expression in rat kidney following acute methylmercury treatment. *Toxicol. Appl. Pharmacol.* 141:59-67.

Li, S., Thompson, S.A., and Woods, J.S. 1996b. Localization of gamma-glutamylcysteine synthetase mRNA expression in mouse brain following methylmercury treatment using reverse transcription in situ PCR amplification. *Toxicol. Appl. Pharmacol.* 140:180-187.

Loguercio, C., Del Vecchio Blanco, C., Coltorti, M., and Nardi, G. 1992. Alteration of erythrocyte glutathione, cysteine and glutathione synthetase in alcoholic and non-alcoholic cirrhosis. *Scand. J. Clin. Lab. Invest.* 52:207-213.

Meister, A. 1985. Glutathione synthetase from rat kidney. *Methods Enzymol.* 113:393-399.

Meister, A. 1995. Glutathione metabolism. *Methods Enzymol.* 251:3-7.

Mulcahy, R.T., Wartman, M.A., Bailey, H.H., and Gipp, J.J. 1997. Constitutive and beta-naphthoflavone-induced expression of the human gamma-glutamylcysteine synthetase heavy subunit gene is regulated by a distal antioxidant response element/TRE sequence. *J. Biol. Chem.* 272:7445-7554.

O'Dwyer, P.J., Szarka, C.E., Yao, K.S., Halbherr, T.C., Pfeiffer, G.R., Green, F., Gallo, J.M., Brennan, J., Frucht, H., Goosenberg, E.B., Hamilton, T.C., Litwin, S., Balshem, A.M., Engstrom, P.F., and Clapper, M.L. 1996. Modulation of gene expression in subjects at risk for colorectal cancer by the chemopreventive dithiolethione oltipraz. *J. Clin. Invest.* 98:1210-1217.

Ochi, T. 1995. Hydrogen peroxide increases the activity of gamma-glutamylcysteine synthetase in cultured Chinese hamster V79 cells. *Arch. Toxicol.* 70:96-103.

Ochi, T. 1996. Menadione causes increases in the level of glutathione and in the activity of gamma-glutamylcysteine synthetase in cultured Chinese hamster V79 cells. *Toxicology* 112:45-55.

Reid, L.L., Botta, D., Lu, Y., Gallagher, E.P., and Kavanagh, T.J. 1997a. Molecular cloning and sequencing of the cDNA encoding the catalytic subunit of mouse glutamate-cysteine ligase. *Biochim. Biophys. Acta* 1352:233-237.

Reid, L.L., Botta, D., Shao, J., Hudson, F.N., and Kavanagh, T.J. 1997b. Molecular cloning and sequencing of the cDNA encoding mouse glutamate-cysteine ligase regulatory subunit. *Biochim. Biophys. Acta* 1353:107-110.

Seelig, G.F. and Meister, A. 1985. Glutathione biosynthesis: γ-glutamylcysteine synthetase from rat kidney. *Methods Enzymol.* 113:379-390.

Sekhar, K.R., Long, M., Long, J., Xu, Z-Q., Summar, M.L., and Freeman, M.L. 1997. Alteration of transcriptional and post-transcriptional expression of gamma-glutamylcysteine synthetase by diethyl maleate. *Radiation Res.* 147:592-597.

Shi, Z.Z., Carter, B.Z., Habib, G.M., He, X., Sazer, S., Lebovitz, R.M., and Lieberman, M.W. 1996a. A single mouse glutathione synthetase gene encodes six mRNAs with different 5′ ends. *Arch. Biochem. Biophys.* 331:215-224.

Shi, Z.Z., Habib, G.M., Rhead, W.J., Gahl, W.A., He, X., Sazer, S., and Lieberman, M.W. 1996b. Mutations in the glutathione synthetase gene cause 5-oxoprolinuria. *Nature Genet.* 14:361-365.

Sun, W.-M., Huyang, Z.-Z., and Lu, S.C. 1996. Regulation of γ-glutamylcysteine synthetase by protein phosphorylation. *Biochem. J.* 320:321-328.

Sun, Y. 1997. Induction of glutathione synthetase by 1,10-phenanthroline. *FEBS Lett.* 408:16-20.

Tian, L., Shi, M.M., and Forman, H.J. 1997. Increased transcription of the regulatory subunit of gamma-glutamylcysteine synthetase in rat lung epithelial L2 cells exposed to oxidative stress or glutathione depletion. *Arch. Biochem. Biophys.* 342:126-133.

Tsuchiya, K., Mulcahy, R.T., Reid, L.L., Disteche, C.M., and Kavanagh, T.J. 1995. Mapping of the glutamate-cysteine ligase catalytic subunit gene (GLCLC) to human chromosome 6p12 and mouse chromosome 9D-E and of the regulatory subunit gene (GLCLR) to human chromosome 1p21-p22 and mouse chromosome 3H1-3. *Genomics* 30:630-632.

Walsh, A.C., Li, W., Rosen, D.R., and Lawrence, D.A. 1996. Genetic mapping of GLCLC, the human gene encoding the catalytic subunit of gamma-glutamyl-cysteine synthetase, to chromosome band 6p12 and characterization of a polymorphic trinucleotide repeat within its 5′ untranslated region. *Cytogenet. Cell Genet.* 75:14-16.

Wellner, V.P., Sekura, R., Meister, A., and Larsson, A. 1974. Glutathione synthetase deficiency, an inborn error of metabolism involving the gamma-glutamyl cycle in patients with 5-oxoprolinuria (pyroglutamic aciduria). *Proc. Natl. Acad. Sci. U.S.A.* 71:2505-2509.

Wild, A.C., Gipp, J.J., and Mulcahy, R.T. 1998. Overlapping antioxidant response element and PMA response element sequences mediate basal and β-naphthoflavone induced expression of the human γ-glutamylcysteine synthetase catalytic subunit gene. *Biochem. J.* 332:373-381.

Yan, N. and Meister, A. 1990. Amino acid sequence of rat kidney gamma-glutamylcysteine synthetase. *J. Biol. Chem.* 265:1588-1593.

Contributed by Collin C. White,
Cecile M. Krejsa, David L. Eaton, and
Terrance J. Kavanagh
University of Washington
Seattle, Washington

This work has been supported by NIH grants ES04696, ES07033, ES07032, AG01751, and DOE Cooperative Agreement #DE-FCO1-95EW55084. This support does not constitute an endorsement by DOE of the views expressed herein.

γ-Glutamyl Transpeptidase Activity Assay

γ-Glutamyl transpeptidase (EC 2. 3. 2. 2) catalyzes the transfer of a γ-glutamyl group from glutathione or other γ-glutamyl compounds to amino acids or dipeptides. It also catalyzes hydrolysis of the γ-glutamyl bond (Fig. 6.6.1). When a γ-glutamyl donor acts as an acceptor, the reaction catalyzed by the enzyme leads to the formation of a γ-(γ-glutamyl)-glutamyl compound, in which case the reaction is referred to as autotranspeptidation. This enzyme is also known as γ-glutamyltransferase and is frequently abbreviated as GGT, γ-GTP, or γ-GT. It plays an important role in glutathione metabolism because the reaction catalyzed by the enzyme constitutes the first step in the degradation of glutathione. In addition, the removal of a γ-glutamyl moiety from glutathione-*S*-conjugates with xenobiotics by GGT is a step that is involved in the pathway for the formation of mercapturic acids which are excreted into urine.

For assay of GGT activity, the most common substrates are γ-glutamyl derivatives of *p*-nitroaniline or related compounds because they are convenient, give sensitive results, and are sufficiently specific for the enzyme. Since the release of *p*-nitroaniline from γ-glutamyl-*p*-nitroanilide is facilitated by the addition of an appropriate acceptor dipeptide, glycylglycine is usually used as an acceptor substrate in the assay. Although the enzyme can produce *p*-nitroaniline via hydrolysis and/or autotranspeptidation even in the absence of the acceptor, the rate of *p*-nitroaniline release is quite slow. Cleavage of the γ-glutamyl bond of the donor by the enzyme leads to the stoichiometric release of *p*-nitroaniline, which can easily be detected via spectrophotometry.

This unit describes one of the most convenient methods for the assay of GGT activity (see Basic Protocol), in which γ-glutamyl-*p*-nitroanilide and glycylglycine are used as a donor and an acceptor substrate, respectively (Fig. 6.6.2). The use of another *p*-nitroaniline derivative (L-γ-glutamyl-3-carboxy-4-nitroanilide) as the donor is also described (see Alternate Protocol).

SPECTROPHOTOMETRIC ASSAY USING γ-GLUTAMYL-*p*-NITROANILIDE FOR GGT ACTIVITY

BASIC PROTOCOL

An assay method using γ-glutamyl-*p*-nitroanilide and glycylglycine as a donor and an acceptor substrate, respectively, is most commonly used and is suitable for most samples—e.g., tissues, cultured cells, and body fluids. Although a variety of protocols involving these substrates have been reported, they are, in principle, the same as the protocol described here. γ-Glutamyl-*p*-nitroanilide is relatively insoluble in water, and its solubility is quite low at certain pH values. Activity is measured under the following conditions: 0.1 M Tris·Cl buffer, 1 mM γ-glutamyl-*p*-nitroanilide, 20 mM glycylglycine, pH 8.0.

Materials

L-γ-Glutamyl-*p*-nitroanilide (free base or HCl salt; Sigma)
0.2 N HCl
Glycylglycine free base
0.5 M Tris·Cl, pH 9.0 to 9.5 (*APPENDIX 2A*)
Sample (e.g., tissue or cell homogenate, membrane preparation, microsome suspension)
Homogenate buffer (see recipe)

Potter-Elvehjem homogenizer or Dounce homogenizer
Spectrophotometer with temperature-controlled cuvette holder
Semimicro cell (light path = 1 cm)

Contributed by Yoshitaka Ikeda and Naoyuki Taniguchi
Current Protocols in Toxicology (2000) 6.6.1-6.6.8

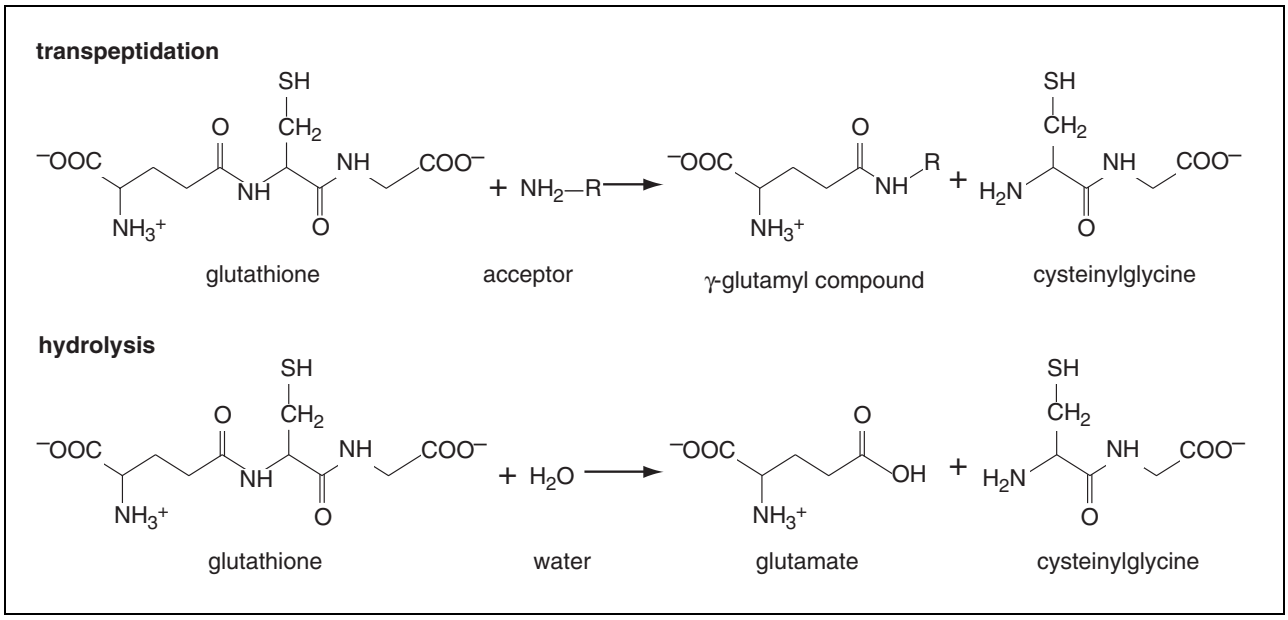

Figure 6.6.1 Reactions catalyzed by γ-glutamyl transpeptidase.

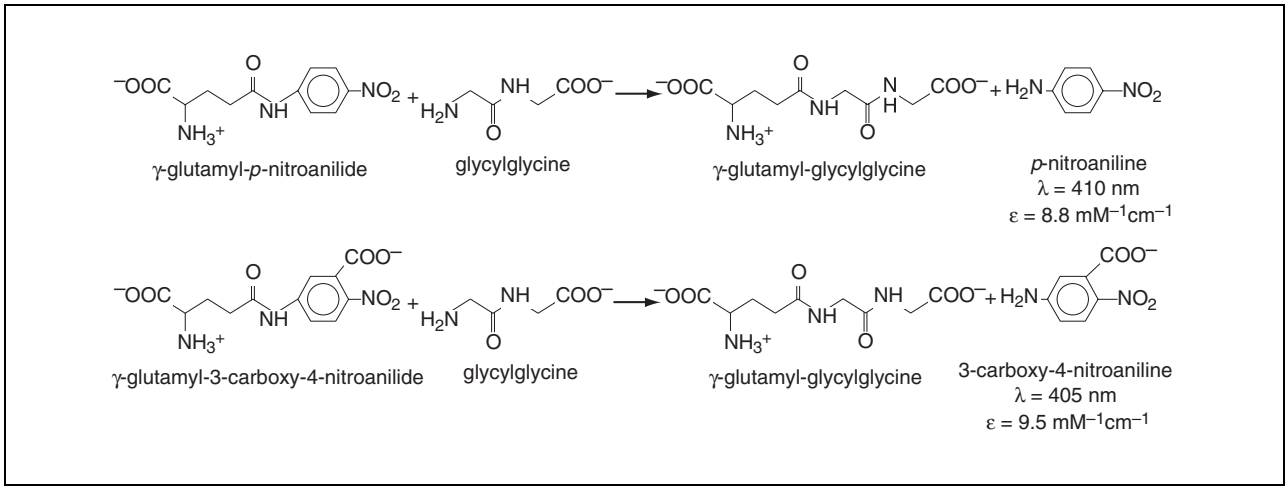

Figure 6.6.2 Reactions which occur in the γ-glutamyl transpeptidase activity assay.

Prepare assay mixture

1. Completely dissolve L-γ-glutamyl-*p*-nitroanilide (0.134 g for free base form or 0.152 g for HCl salt) in 10 ml of 0.2 N HCl.

   An acidic pH is necessary because it is difficult to dissolve the compound in water or in a buffer at pH ~6. In addition, a strong alkaline solution may cause hydrolysis of the γ-glutamyl bond of the substrate.

2. Add 350 ml water to the solution from step 1, and then completely dissolve 1.32 g of glycylglycine (free base) in the resulting mixture.
3. Add 100 ml of 0.5 M Tris·Cl, pH 9.0 to 9.5.
4. Adjust the pH to 8.0 with HCl and bring the volume up to 500 ml with water.

   This assay mixture can be stored at –20°C for up to 1 month and at 4°C for 24 hr.

Prepare sample

5. Suspend cultured cells or diced tissues in the homogenate buffer.

   The homogenate buffer may be replaced by 20 to 100 mM Tris·Cl, pH 8.0, for cells. Most of the commonly used buffers, such as phosphate buffer and HEPES buffer, can also be used as long as the pH is maintained at 7.0 to 8.0. The enzyme appears to be relatively unstable at acidic pH. In addition, borate buffer should be avoided because it can inhibit the enzyme in the presence of L-serine. Approximately 10^7 cells are resuspended in ~400 µl of the buffer.

6. Homogenize the cells or tissues using a Potter-Elvehjem or Dounce homogenizer (~10 strokes).

   In the case of cultured cells, sonication may also be applicable.

7. Centrifuge 10 min at 900 × *g*, 4°C. Retain the supernatant and discard the pellet, which contains debris.

   If the sample is sufficiently homogeneous, this step may be omitted.

Measure γ-glutamyl transpeptidase activity

8. Place 1 ml of the assay mixture (from step 4) into a cuvette (semimicro cell, light path = 1 cm), then place the cuvette into the temperature-controlled cuvette holder of the spectrophotometer and prewarm to 37°C .

9. Add 5 to 20 µl of the homogenized sample (from step 7) to the assay mixture in the cuvette, immediately seal the cuvette with Parafilm, and invert gently but quickly two or three times to mix the contents. Place cuvette in holder and start recording.

10. Record the increase in absorbance at 410 nm continuously on chart paper.

11. Read the absorbance increase per min ($\Delta A_{410}/\Delta t$) in the linear portion of the curve (initial velocity) on a chart (Fig. 6.6.3).

    If a linear response is not obtained in the recording because of excessively high activity, it will be necessary to suitably dilute the homogenate (and hence the enzyme) with a buffer, e.g., 100 mM Tris·Cl, pH 8.0.

12. Calculate the enzyme activity (U/ml of the original homogenate) as follows:

    Activity (U/ml) = $[(\Delta A_{410}/\Delta t)/\varepsilon] \times 1000/$[volume of sample (µl) added to the assay mixture]

    where the amount of the enzyme required to release 1 µmol of *p*-nitroaniline per min is defined as one unit (U).

    In the case of a diluted sample, multiplication by a dilution factor will be necessary to calculate the activity of the original homogenate.

    The molar extinction coefficient (ε) for p-nitroaniline is 8.8 $mM^{-1}cm^{-1}$. Although addition of the enzyme solution to the assay mixture changes the volume and the concentrations of substrates by a few percent, these changes are negligible in terms of the calculation of enzyme activity.

    For samples with a low activity, evaluate a change in absorbance ($\Delta A_{410}/\Delta t$) after subtracting contribution of nonenzymatic hydrolysis of the substrate, which is determined by recording in the absence of enzyme.

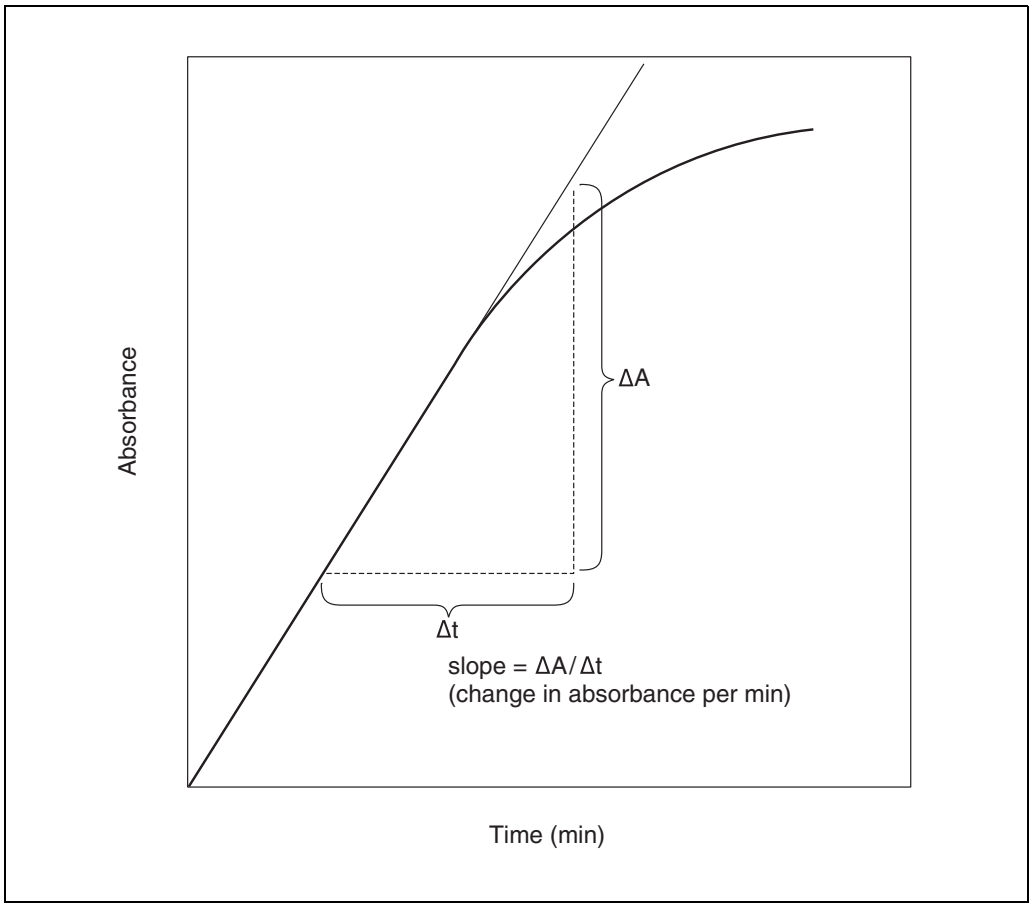

Figure 6.6.3 Estimation of the rate of the release of *p*-nitroaniline.

ALTERNATE PROTOCOL

USE OF L-γ-GLUTAMYL-3-CARBOXY-4-NITROANILIDE AS THE DONOR SUBSTRATE TO MEASURE GGT ACTIVITY

L-γ-Glutamyl-*p*-nitroanilide is the most common substrate for the GGT activity assay, but its solubility is very low at pH values of ~6. In addition, this substrate may be insoluble under certain conditions. When a specialized substrate mixture is necessary, for example, because activity must be assayed at a different pH from that used in the Basic Protocol and at which solubility becomes an issue, L-γ-glutamyl-3-carboxy-4-nitroanilide can be substituted for L-γ-glutamyl-*p*-nitroanilide. L-γ-glutamyl-3-carboxy-4-nitroanilide is more convenient for its higher solubility, but it is more expensive and relatively unstable. The ε value for carboxynitroaniline, a product of the reaction, is 9.5 $mM^{-1}cm^{-1}$.

Additional Materials *(also see Basic Protocol)*

L-γ-glutamyl-3-carboxy-4-nitroanilide (ammonium salt; Sigma)

1. Dissolve L-γ-glutamyl-3-carboxy-4-nitroanilide (ammonium salt) directly to the desired concentration in the buffer, which also contains the acceptor substrate, e.g., 20 mM glycylglycine, and other compounds that may be required for individual purposes.

   This substrate is relatively unstable and is hydrolyzed more easily than the noncarboxylated substrate. Therefore, pH value of the assay mixture should not exceed 8.0. An assay mixture which contains L-γ-glutamyl-3-carboxy-4-nitroanilide can be stored at −20°C up to ~1 week. Do not store at 4°C.

Tris buffer (pH 8.0) and several other types of buffers in which pH is 6.0 to 8.0 can be used. If necessary, the concentration of L-γ-glutamyl-3-carboxy-4-nitroanilide in the assay can be increased over 10 mM because of its high solubility.

2. Prepare cell or tissue homogenate (see Basic Protocol, steps 5 to 7).
3. Determine enzyme activity with this assay mixture (see Basic Protocol, steps 8 to 12) measuring absorbance at 405 nm (A_{405}) and using an extinction coefficient, ε, equal to 9.5 mM^{-1} cm^{-1}.

REAGENTS AND SOLUTIONS

Use Milli-Q-purified water or equivalent in all recipes and protocol steps. For common stock solutions, see ***APPENDIX 2A****; for suppliers, see* ***SUPPLIERS APPENDIX****.*

Homogenate buffer

Mix 8.6 g of sucrose with 2 ml of 1 M Tris·Cl, pH 8.0 (*APPENDIX 2A*), and 0.04 ml of 500 mM EDTA, pH 8.0 (*APPENDIX 2A*), and then dilute this with water to ~95 ml. Adjust the pH to 7.4 with HCl, and add water to a final volume of 100 ml. Store up to 1 month at 4°C.

COMMENTARY

Background Information

γ-Glutamyl transpeptidase plays a key role in glutathione metabolism because it catalyzes the first step of the degradation of glutathione (Lieberman et al., 1996) and is a member of the γ-glutamyl cycle, which involves the degradation and biosynthesis of glutathione (Meister and Anderson, 1983; Meister and Larsson, 1995).

GGT activity is most abundant in the kidney and is predominantly localized in the apical surface of the proximal microtubules. The enzyme is a membrane-bound glycoprotein and is anchored to the extracellular surface of the plasma membrane via its N-terminal transmembrane domain; as a result, glutathione is degraded by this enzyme outside the cells. The resulting cysteinylglycine is imported into the cells, and is utilized as a source of cysteine for the biosynthesis of glutathione (Meister et al., 1981; Tate and Meister, 1985). It is generally believed that the enzyme plays an important role in the maintenance of intracellular glutathione levels and appears to be involved in the protection of cells against oxidative damage. On the other hand, in the case of *S*-conjugates of chemical compounds, drugs, and xenobiotics with glutathione, their γ-glutamyl groups are removed by GGT, followed by cleavage of the glycine moiety and *N*-acetylation. These successive conversions lead to the formation of the corresponding mercapturic acids and, as a result, facilitate the excretion of those chemical compounds into urine (Meister and Anderson, 1983; Meister and Larsson, 1995). This action of GGT is directed not only towards glutathione-*S*-conjugates of foreign chemical compounds but also towards conjugates of endogenous substances, such as leukotriene C4, which is converted into leukotriene D4 by this enzyme as the result of removal of the γ-glutamyl moiety (Anderson et al., 1982). There seems to be no isozyme of GGT (Lieberman et al., 1996; Carter et al., 1997), but heterogeneities exist due to glycosylation, as shown by isoelectric focusing and electrophoresis. A related enzyme, referred to as the GGT-related enzyme or γ-glutamyl leukotrienase, is known to hydrolyze the γ-glutamyl bond of glutathione but not particular synthetic substrates (Heisterkamp et al., 1991; Carter et al., 1998).

GGT is a heterodimeric glycoprotein which consists of a large and small subunit. This enzyme is biosynthesized as a single-chain precursor and is then proteolytically cleaved into two subunits (Meister et al., 1981). It is thought that the small subunit is a catalytic one and that the substrate binding site is constituted by both the subunits, as suggested by chemical modification studies and site-directed mutagenesis (Taniguchi and Ikeda, 1998). Kinetic studies have shown that this enzyme follows a ping-pong mechanism and thus forms the γ-glutamyl enzyme intermediate in which a γ-glutamyl group from the donor substrate appears to be covalently bound to the enzyme (Tate and Meister, 1985). The functional group involved in the formation of the intermediate is believed

to be a hydroxyl group (or groups), located in the small subunit (Ikeda et al., 1995; Taniguchi and Ikeda, 1998). Substrate specificities for the donor and acceptor substrates have been the subject of extensive investigation.

GGT transfers the γ-glutamyl group of glutathione, its *S*-substituted derivatives, and γ-glutamyl compounds to a variety of amino acids and dipeptides. GGT displays a relatively broad specificity toward the leaving group, corresponding to the cysteinylglycine moiety of glutathione (Tate and Meister, 1985), as revealed by the capability of the action on *S*-substituted glutathione and synthetic γ-glutamyl donors such as γ-glutamyl-*p*-nitroanilide. This may allow GGT to react with a variety of glutathione S-conjugates and would, therefore, enable the enzyme to play a role in the metabolism of drugs and xenobiotics. On the other hand, in terms of the substrate specificity toward acceptor substrates, neutral amino acids such as cystine, methionine, glutamine, alanine, and serine are preferred as the first amino acid residue in the case of dipeptides or an amino acid acceptor. However, amino acids with a branched side chain are poor acceptors, and L-proline and α-substituted amino acids are inactive. D-isomers of those amino acids are inactive, although both L- and D-isomers of the γ-glutamyl moiety in the donor are equally active as the substrate. When L-γ-glutamyl compounds are used as the substrate in the absence of appropriate acceptor, the γ-glutamyl compound can also act as the acceptor, leading to autotranspeptidation reactions as well as hydrolysis. In the case of a D-isomer of the γ-glutamyl compound, however, the enzyme catalyzes only the hydrolysis of the γ-glutamyl bond (Thompson and Meister, 1976; Meister et al., 1981).

Kinetic analysis of GGT showed that the K_m values for L-γ-glutamyl-*p*-nitroanilide as a donor and for glycylglycine as an acceptor are 1.4 mM and 10 mM, respectively (Ikeda et al., 1996). If one wishes to determine the hydrolytic activity using L-γ-glutamyl-*p*-nitroanilide, separately from the autotranspeptidation, the concentration of the donor substrate must be sufficiently low, e.g., 10 μM or lower. Otherwise, the contribution of the autotranspeptidation to the release of *p*-nitroaniline becomes significant. Alternatively, its D-isomer should be used as the substrate because this isomer cannot act as an acceptor. However, D-γ-glutamyl-*p*-nitroanilide is not commercially available. In the hydrolysis reaction, the K_m for L-γ-glutamyl-*p*-nitroanilide is 5 to 8 μM (Thompson and Meister, 1976; Ikeda et al., 1996).

Many other methods are available for the assay of GGT activity, and the use of a fluorogenic substrate; e.g., 7-(γ-glutamyl)-4-methylcoumarylamide (γ-glutamyl-AMC) provides a more sensitive assay. The assay procedure using γ-glutamyl-AMC is described in Smith et al. (1979) and Tate and Meister (1985). Although procedures for a rate assay with a spectrophotometer are described in this unit, an end-point assay using a 96-well plate would be sufficient to roughly compare the activities of a large number of samples, for example, to determine the elution peak for the enzyme during chromatography. For this qualitative assay, 5 to 10 μl of each sample are placed into wells of the 96-well plate and 100 to 200 μl of the assay mixture is added. The plate is incubated at room temperature until a light yellow color appears, and the optical density at a wavelength ~410 nm is measured using a microtiterplate reader.

It is well known that expression of GGT is increased during chemically induced hepatocarcinogenesis in rodents, and that levels of this enzyme are also high in fetal liver, whereas its expression is quite low, nearly undetectable in normal adult liver. Therefore, this enzyme is often regarded as one of the oncofetal proteins, and it is used as a marker for hyperplastic or neoplastic nodules in chemically induced hepatocarcinogenesis in the rat (Suzuki et al., 1987).

For the measurement of GGT activity, the most common substrate is the γ-glutamyl derivative of *p*-nitroaniline or a related compound; this type of substrate is very convenient to use and sensitive. The assay involving the substrate is also sufficiently specific to the enzyme. The release of *p*-nitroaniline and 3-carboxy-4-nitroaniline from the respective γ-glutamyl derivatives is facilitated by the addition of an appropriate acceptor dipeptide, as shown in Figure 6.6.4 (Ikeda et al., 1993). Glycylglycine is known to be one of the most active acceptors and is usually contained in the assay mixture.

Critical Parameters and Troubleshooting

Although γ-glutamyl transpeptidase is capable of catalyzing both transfer and hydrolysis reactions, the transfer reaction is much faster. In the activity assay for the enzyme, therefore, the transfer reaction using glycylglycine as an acceptor for the γ-glutamyl group is usually used. The transfer reaction proceeds efficiently

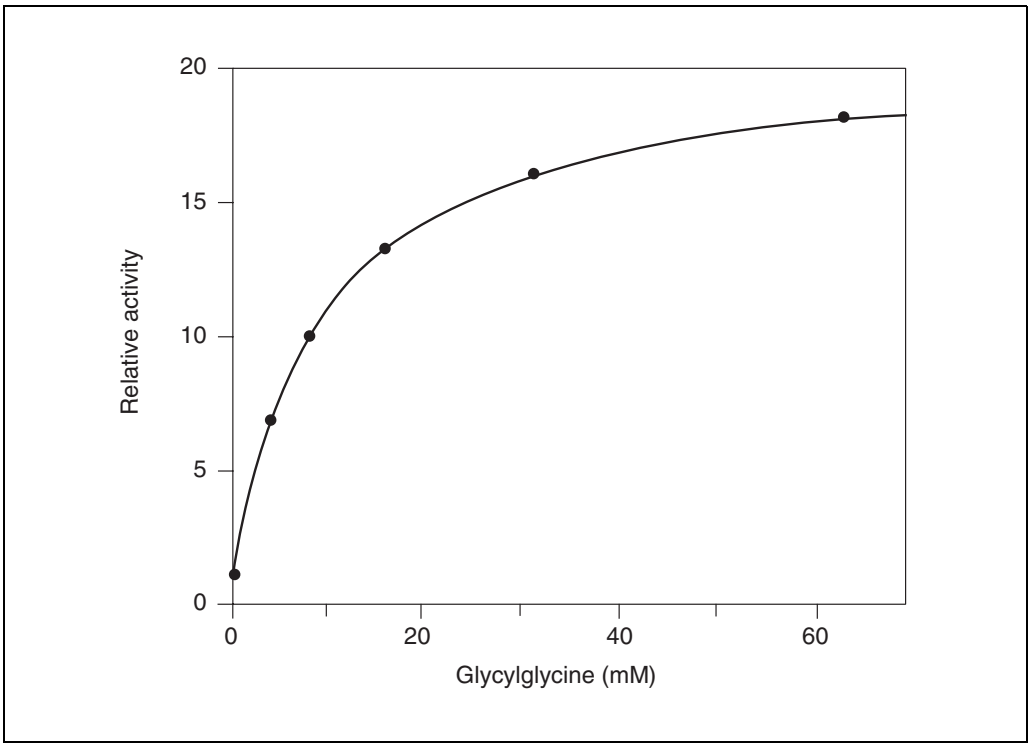

Figure 6.6.4 The effect of a dipeptide acceptor, glycylglycine.

at a relatively high pH, and thus the pH value in the assay mixture should be in excess of 8.0. However, γ-glutamyl-*p*-nitroanilide and γ-glutamyl-3-carboxy-4-nitroanilide are significantly hydrolyzed in a nonenzymatic manner at an extremely high pH.

If one wants to prepare the assay mixture at pH values around 6, for particular experimental reasons, it may be impossible to completely dissolve the γ-glutamyl-*p*-nitroanilide at the desired concentration, since the solubility of the substrate is often poor in this pH range. To avoid this solubility problem, it is desireable to use γ-glutamyl-3-carboxy-4-nitroanilide, rather than γ-glutamyl-*p*-nitroanilide. The carboxylated substrate is easily dissolved in commonly used buffers at various pH values.

When the activity for the enzyme is assayed in tissues, such as liver, in which the expression of this enzyme is quite low, it may be necessary to extract the enzyme with 0.5% to 1.0% (v/v) nonionic detergents such as Triton X-100 and Nonidet P-40. The release of the chromophore, *p*-nitroaniline is very slow because of low activity, and under such conditions, the turbidity of the sample can significantly interfere with the detection of the increase in absorbance at 410 nm. Extraction of the enzyme with detergents results in clarification of the samples, thus circumventing turbidity problems. The enzyme is easily extracted by stirring the homogenized tissues, microsomal fraction, or membrane fraction, in the buffer containing aforementioned detergents for 30 to 60 min at 4°C, followed by ultracentrifugation.

Table 6.6.1 γ-Glutamyl Transpeptidase Activities in Kidney, Liver, and Various Cultured Cells

Source	Activity (U/mg protein)
A549 cells	0.056
COS1 cells	0.0007
GGT cDNA-transfected COS1 cells	3.6
HepG2 cells	0.061
Rat kidney homogenate	1.0
Rat liver homogenate	0.0037

Anticipated Results

The specific activities of γ-glutamyl transpeptidase in various organs and cells, determined under the conditions described in the Basic Protocol, are given in Table 6.6.1.

Time Considerations

The assay, in which the release of *p*-nitroaniline is continuously monitored, requires only a few minutes for a sample with a sufficiently high activity. A much longer time (e.g., ≥30 min) may be required for samples whose activities are very low.

Literature Cited

Anderson, M.E., Allison, R.D., and Meister, A. 1982. Interconversion of leukotrienes catalyzed by purified γ-glutamyl transpeptidase: Concomitant formation of leukotriene D4 and γ-glutamyl amino acids. *Proc. Natl. Acad. Sci. U.S.A.* 79:1088-1091.

Carter, B.Z., Wiseman, A.L., Orkiszewski, R., Ballard, K.D., Ou, C.N., and Lieberman, M.W. 1997. Metabolism of leukotriene C4 in γ-glutamyl transpeptidase-deficient mice. *J. Biol. Chem. 272:12305-12310.*

Carter, B.Z., Shi, Z.Z., Barrios, R., and Lieberman, M.W. 1998. γ-Glutamyl leukotrienase, a γ-glutamyl transpeptidase gene family member, is expressed primarily in spleen. *J. Biol. Chem. 273:28277-28285.*

Heisterkamp, N., Rajpert-De-Meyts, E., Uribe, L., Forman, H.J., and Groffen, J. 1991. Identification of a human γ-glutamyl cleaving enzyme related to, but distinct from, γ-glutamyl transpeptidase. *Proc. Natl. Acad. Sci. U.S.A. 88:6303-6307.*

Ikeda, Y., Fujii, J., and Taniguchi, N. 1993. Significance of Arg-107 and Glu-108 in the catalytic mechanism of human γ-glutamyl transpeptidase: Identification by site-directed mutagenesis. *J. Biol. Chem. 268:3980-3985.*

Ikeda, Y., Fujii, J., Anderson, M.E., Taniguchi, N., and Meister, A. 1995. Involvement of Ser-451 and Ser-452 in the catalysis of human γ-glutamyl transpeptidase. *J. Biol. Chem. 270:22223-22228.*

Ikeda, Y., Fujii, J., and Taniguchi, N. 1996. Effects of substitutions of conserved histidine residues in human γ-glutamyl transpeptidase. *J. Biochem. 119:1166-1170.*

Lieberman, M.W., Wiseman, A.L., Shi, Z.Z., Carter, B.Z., Barrios, R., Ou, C.N., Chevez-Barrios, P., Wang, Y., Habib, G.M., Goodman, J.C., Huang, S.L., Lebovitz, R.M., and Matzuk, M.M. 1996. Growth retardation and cysteine deficiency in gamma-glutamyl transpeptidase-deficient mice. *Proc. Natl. Acad. Sci. U.S.A. 93:7923-7926.*

Meister, A. and Anderson, M.E. 1983. Glutathione. *Annu. Rev. Biochem.* 52:711-760.

Meister, A. and Larsson, A. 1995. Glutathione synthetase deficiency and other disorders of the γ-glutamyl cycle. *In* The Metabolic and Molecular Bases of Inherited Diseases, 7th ed., Vol. I (C.R. Scriver, A.L. Beaudet, W.S. Sly, and D. Valle, eds.) pp. 1461-1477. McGraw-Hill, New York.

Meister, A., Tate, S.S., and Griffith, O.W. 1981. γ-Glutamyl transpeptidase. *Methods Enzymol. 77:237-253.*

Smith, G.D., Ding, J.L., and Peters, J.L. 1979. A sensitive fluorimetric assay for γ-glutamyl transferase. *Anal. Biochem. 100:136-139.*

Suzuki, Y., Ishizuka, H., Kaneda, H., and Taniguchi, N. 1987. γ-Glutamyl transpeptidase in rat liver during 3′-Me-DAB hepatocarcinogenesis: Immunohistochemical and enzyme histochemical study. *J. Histochem. Cytochem. 35:3-7.*

Taniguchi, N. and Ikeda, Y. 1998. γ-Glutamyl transpeptidase: Catalytic mechanism and gene expression. *Adv. Enzymol. Relat. Areas Mol. Biol. 72:239-278.*

Tate, S.S. and Meister, A. 1985. γ-Glutamyl transpeptidase from kidney. *Methods Enzymol. 113:400-419.*

Thompson, G.A. and Meister, A. 1976. Hydrolysis and transfer reactions catalyzed by γ-glutamyl transpeptidase: Evidence for separate substrate sites and for high affinity of L-cystine. *Biochem. Biophys. Res. Commun. 71:32-36.*

Contributed by Yoshitaka Ikeda and Naoyuki Taniguchi
Osaka University Medical School
Osaka, Japan

Oxidant-Induced Regulation of Glutathione Synthesis

Protocols in this unit describe experimental methods for demonstrating induction of two glutathione biosynthetic enzymes, γ-glutamylcysteine synthetase (glutamate cysteine ligase, GCS, EC 6.3.2.2) and γ-glutamyltranspeptidase (GGT, EC 2.3.2.2), in response to oxidants. GCS is a heterodimer composed of a catalytic or heavy subunit (GCS-HS) and a regulatory or light subunit (GCS-LS). It catalyzes the first and limiting step in the de novo synthesis of reduced glutathione (GSH), forming γ-glutamylcysteine from L-cysteine and L-glutamate. GGT, on the other hand, degrades extracellular GSH to supply cells with necessary amino acids for intracellular synthesis of GSH, GCS, and GGT gene expression have been shown to be up-regulated upon treating cells with various oxidants and heavy metals. Such induction results in transient elevation of the intracellular GSH concentration that protects cells from subsequent oxidative assault. Nonetheless, to definitively show that a compound can increase the transcription rate of the GCS or GGT genes, it is necessary to perform nuclear run-on analysis (see Basic Protocol 2), which directly measures the transcription rate of the gene being studied.

The following protocols detail the methods by which one can show increased mRNA and protein content (Basic Protocols 1 to 3) of both subunits of GCS as well as GGT, and further allow the determination of the mechanism by which mRNA content is altered in response to oxidants—whether this involves transcriptional (Basic Protocol 2) and/or posttranscriptional (i.e., stability of mRNA; Basic Protocol 1) regulation. Therefore, the protocols can be applied to other studies involving induction of gene expression. Changes in the GSH content and GCS activity can be readily demonstrated using protocols reported elsewhere (*UNITS 6.5 & 6.6*). Support Protocol 3 describes an assay for measuring GGT activity. Increasing evidence suggests that glutathione synthetase (GS, EC6.3.2.3.), which produces GSH from γ-glutamylcysteine, may also be increased by oxidative stress, such as with *tert*-butylhydroperoxide (Sun, 1997; Luo et al., 1998). GS activity can be measured with a simple modification of the procedure for measuring GCS activity (*UNIT 6.5*).

CAUTION: When working with radioactivity, take appropriate precautions to avoid contamination of the experimenter and the surroundings (*APPENDIX 1A*). Carry out the experiment and dispose of wastes in an appropriately designated area, following the guidelines provided by the local radiation safety officer.

NORTHERN ANALYSIS OF γ-GLUTAMYLCYSTEINE SYNTHETASE AND γ-GLUTAMYL TRANSPEPTIDASE mRNA CONTENT

BASIC PROTOCOL 1

GCS and GGT mRNA content can be quantitated by standard northern analysis with radiolabeled probes (Brown and Mackey, 1997; *APPENDIX 3E*). After treating cells for various time periods with various oxidants added to the cell culture medium, total RNA is isolated from the cells. cDNA probes (see Support Protocol 1) are used for mRNA analysis of GCS subunits, and a cRNA probe (see Support Protocol 2) is used for GGT.

Materials

Cells to be analyzed
Oxidant, e.g. 5 to 20 μM 2,3-dimethoxyl, 4-naphthoquinone (DMUQ)
Actinomycin D
Agarose
DEPC-treated H_2O, water treated with 0.1% DEPC

Contributed by Rui-Ming Liu, Jinah Choi, and Henry J. Forman
Current Protocols in Toxicology (2001) 6.7.1-6.7.21

1× and 10× MOPS running buffer (see recipe)
37% (w/v) formaldehyde
RNA loading mixture (see recipe)
RNA molecular weight markers
2× SSC (*UNIT 3.5*)
Hybridization solution (e.g., QuikHyb, Stratagene)
Salmon sperm DNA
Radiolabeled γ-glutamylcysteine synthetase light or heavy subunit (GCS-LS or GCS-HS) cDNA probe (see Support Protocol 1) or radiolabeled γ-glutamyl transpeptidase (GGT) cRNA probe (see Support Protocol 2)
2× SSC/0.1% (w/v) SDS
0.1× SSC/0.1% (w/v) SDS, 50°C, and 70° to 75°C

65°C and boiling water baths
Nylon membrane
Capillary blot transfer system
UV cross-linker (e.g., Stratalinker 1800, Stratagene)
Hybridization oven (e.g., Hybaid), 60°C (optional)
X-ray film (e.g., Kodak X-Omat film, Eastman Kodak) or InstantImager (Packard Instrument)

Additional reagents and equipment for isolating total RNA (use commercially available reagents and protocols or see *APPENDIX 3E*), agarose gel electrophoresis (*APPENDIX 3A*), and capillary transfer and probing of RNA (see northern blotting, *APPENDIX 3E*)

CAUTION: Ethidium bromide (in RNA loading mixture) is a mutagen and must be handled carefully.

Isolate RNA

1. Set up ten plates of the cells and then treat with an oxidant. When studying the effect of an oxidant on the stability of GCS or GGT mRNA, treat cells with an oxidant in the presence and absence of actinomycin D (0.05 μg/ml for GCS) for 1, 2, 4, 6, and 8 hr in a 37°C, 5% CO_2 incubator.

   Actinomycin D is used to block the synthesis of mRNA.

2. At the appropriate time point, collect cells and isolate total RNA using commercial protocols and reagents (or refer to *APPENDIX 3A*).

   Approximately 20 μg total RNA is required per sample. RNA isolated from tissues may also be used

   This series of samples is to measure the effect of an oxidant on the stability of GCS or GGT mRNAs.

Resolve and transfer RNA

3. Melt 1.0 g agarose in 85 ml DEPC-treated water in a microwave oven. When the temperature drops to ~65°C, add 10 ml of 10× MOPS running buffer and 5 ml of 37% formaldehyde, and swirl to mix.

   CAUTION: *Work should be carried out in a chemical hood to avoid inhalation of formaldehyde.*

4. Pour ~0.5-cm thick gel into a horizontal gel electrophoresis apparatus (*APPENDIX 3A*). Allow gel to solidify for ≥30 min.

5. Attach electrophoresis unit to a power supply and pre-run the gel, submerged in 1× MOPS running buffer, at 3 to 4 V/cm for 30 min.

6. Dry 20 µg total RNA for each sample in a Speedvac evaporator. Add 15 µl RNA loading mixture to each sample as well as to RNA molecular weight markers and mix by pipetting.

   If the RNA samples are too dry, they will not go back into solution easily.

7. Incubate RNA samples 15 min in a water bath at 65°C, and then chill in an ice-water bath. Centrifuge briefly to recover sample.

8. Load samples into wells of the gel. Designate one lane for running RNA molecular weight markers. Run gel in 1× MOPS running buffer at 3 to 4 V/cm for 3 to 4 hr.

9. Wash gel briefly with DEPC-treated water and then with 2× SSC for 30 min at room temperature, shaking gently.

10. Use a capillary blot transfer system to transfer RNA from the gel to a nylon membrane in 2× SSC buffer overnight at room temperature (*APPENDIX 3E*).

11. Cross-link RNA to membrane using a UV cross-linker.

Hybridize RNA

12. Prehybridize nylon membrane with 10 ml hybridization solution in a hybridization oven at 60°C for 30 min according to manufacturer's instructions. Avoid bubbles.

    Alternatively, see APPENDIX 3A for hybridization technique without a hybridization oven.

13. Add 1 mg salmon sperm DNA to ≥5 × 10^6 cpm radiolabeled GCS-LS or GCS-HS cDNA probe or a radiolabeled GGT cRNA probe and denature probe in a boiling water bath for 5 min. Centrifuge briefly and chill probe on ice.

    Blots should be hybridized with control probes to analyze RNA loading. When measuring GCS mRNA content, the RNA should be hybridized to the GCS probe first and then the control(s), such as GAPDH cDNA or 18S rRNA probes. The GGT cRNA probe is difficult to strip off the membrane (even harder than the 18S rRNA cDNA probe). Therefore, GGT hybridization should be performed last.

    When analyzing GGT mRNA content, avoid using 18S rRNA as a loading control because its molecular weight lies close to that of GGT and because its cDNA probe is difficult to strip off the membrane.

14. Add denatured probe to the prehybridization buffer and hybridize in the hybridization oven 2 hr at 60°C.

15. Pour out the hybridization solution into an appropriate receptacle. Wash membrane twice (10 to 15 min) with 2× SSC/0.1% SDS at room temperature and then once (10 min) with 0.1× SSC/0.1% SDS at 50°C (see Critical Parameters and Troubleshooting).

    The exact time for washing will vary depending on the probe being used and the relative abundance of mRNA in the samples.

16. Wrap membrane in plastic wrap and store inside an X-ray film cassette. Expose X-ray film at −80°C or scan membrane using a InstantImager.

17. To reuse membrane, strip probe by washing membrane in 0.1 × SSC/0.1% SDS at 70° to 75°C. Store membrane tightly sealed with plastic wrap at −80°C until next hybridization.

RADIOLABELING γ-GLUTAMYLCYSTEINE SYNTHETASE LIGHT AND HEAVY SUBUNIT cDNA PROBES

To detect GCS light subunit (GCS-LS) and heavy subunit (GCS-HS) RNA, cDNA probes for each are radiolabeled with [^{32}P]dCTP. The probes are synthesized by PCR extension of cDNA fragments generated by reverse transcription of total RNA from rat epithelial L2 cells (*APPENDIX 3A*). The cDNA fragments are prepared using primers based on rat kidney GCS-LS and GCS-HS cDNA sequences. These probes hybridize with rat, mouse, and human GCS mRNA.

NOTE: This protocol is written specifically for the Rad-Prime DNA labeling system (Life Technologies) and the NucTrap push column (Stratagene). Other labeling kits, reagents, and purification methods can be used; however, the protocol will need to be modified by following the manufacturer's instructions.

Materials

5×10^6 rat epithelial L2 cells
Primers: 12.5 pmol for 50-µl reactions
  GCS-LS 5′ sense: 5′-AGACCGGGAACCTGCTCAAC-3′
  GCS-LS 3′ antisense: 5′-CATCACCCTGATGCCTAAGC-3′
  GCS-HS 5′ sense: 5′-AGACACGGCATCCTCCAGTT-3′
  GCS-HS 3′ antisense: 5′-CTGACACGTAGCTCGGTAA-3′
Rad-Prime DNA labeling system (Life Technologies), or equivalent, containing:
  1:1:1 (v/v/v) dATP/dGTP/dTTP
  2.5× reaction buffer
  Klenow fragment of *E. coli* DNA polymerase I
  Stop buffer
10 µCi/µl [α-^{32}P]dCTP (800 Ci/mmol; e.g., ICN Biomedicals)
1× STE buffer (see recipe)
Scintillation fluid (e.g., Scintisafe Econo 1 cocktail; Fisher)

37°C and boiling water baths
NucTrap push column (Stratagene)

Additional reagents and equipment for reverse transcription (*APPENDIX 3A*) and PCR (*APPENDIX 3C*)

1. Reverse transcribe total RNA from 5×10^6 rat epithelial L2 cells (*APPENDIX 3A*).
2. Use the primers for GCS-LS or GCS-HS to synthesize cDNA fragments from reverse-transcribed RNA by PCR (*APPENDIX 3C*) and purify.

   The primers for GCS-LS (sense strand of 5′ sequence at positions 122 to 141 and antisense strand of 3′ sequence at positions 1104 to 1123) span 1001 nucleotides of the GCS-LS mRNA; those for GCS-HS (sense strand of 5′ sequence at positions 105 to 124 and antisense strand of 3′ sequence at positions 890 to 909) span 804 nucleotides of GCS-HS mRNA.

3. In a microcentrifuge tube, dissolve ~25 to 50 ng of a purified cDNA fragment for GCS-LS or GCS-HS in a total volume of 21 µl using sterile water. Denature in a boiling water bath for 5 min. Immediately chill on ice.
4. Add the following components (50 µl total) and incubate 15 min at 37°C.

   3 µl 1:1:1 dATP/dGTP/dTTP
   20 µl 2.5× reaction buffer
   5 µl 10 µCi/µl [γ-^{32}P]dCTP
   1 µl Klenow fragment.

5. Add 5 µl stop buffer to the reaction mixture and place on ice.
6. Wet a NucTrap push column with 70 µl of 1× STE buffer by pushing solution through the column using a syringe.
7. Place a clean microcentrifuge tube under column. Add reaction mixture on top of the column and then push it through using the syringe. Rinse column with another 70 µl of 1× STE, collecting the solution in the same tube.
8. Take out 1 µl purified ^{32}P-labeled probe and add to 5 ml scintillation fluid in a scintillation vial. Quantify ^{32}P with a scintillation counter.

   About 0.5 to 1 million cpm/µl is expected.
9. Store purified probe up to 1 week at −80°C.

RADIOLABELING OF γ-GLUTAMYL TRANSPEPTIDASE cRNA PROBE

SUPPORT PROTOCOL 2

Because the GGT mRNA level is very low in rat lung epithelia L2 cells, a cRNA probe, not a cDNA probe, is used to detect GGT mRNA.

NOTE: This protocol is written specifically for the Riboprobe in vitro transcription system (Promega). Other labeling kits and reagents can be used; however, the protocol will need to be modified by following the manufacturer's instructions.

Materials

pBluescript γ-glutamyl transpeptidase (GGT) plasmid
*Not*I restriction enzyme and appropriate buffer
1% (w/v) agarose gel
25:24:1 (v/v/v) phenol/chloroform/isoamyl alcohol (with TE-saturated phenol, *UNIT 2.2*)
Riboprobe in vitro transcription system (Promega), or equivalent, containing:
  5× transcription-optimized buffer
  100 mM dithiothreitol (DTT; also see *APPENDIX 2A*)
  40 U/µl ribonuclease inhibitor (RNasin)
  Aqueous ATP/GTP/UTP (2.5 mM each nucleotide)
  15 to 20 U/µl T7 RNA polymerase
  RQ1 RNase-free DNase
10 µCi/µl [α-^{32}P]CTP (800 Ci/mmol; ICN Biomedicals)
DEPC-treated H_2O: water treated with 0.1% DEPC
0.1 M EDTA, pH 8.0 (*APPENDIX 2A*)
10 mg/ml tRNA (Life Technologies)
7.5 M ammonium acetate (*APPENDIX 2A*)
100% ethanol, ice cold
Scintillation fluid and counter

Additional reagents and equipment for restriction enzyme digestion, agarose gel electrophoresis, and spectrophotometric quantification of DNA (*APPENDIX 3A*)

Prepare DNA template

1. Linearize pBluescript-GGT plasmid with *Not*I restriction enzyme. Use ~1 U enzyme per 1 µg plasmid DNA and digest 2 hr at 37°C in an appropriate buffer (*APPENDIX 3A*).
2. Take 1 µl digestion solution and run on a 1% agarose gel, using 1× TBE buffer as the running buffer, at 80 V for 1 hr to confirm that digestion is complete. If digestion is not complete, add more enzyme and digest for an additional hour and check again.

3. Extract completely digested DNA using 25:24:1 phenol/chloroform/isoamyl alcohol and precipitate with ethanol (*APPENDIX 3A*). Resuspend DNA in distilled water, quantify DNA (*APPENDIX 3A*), and adjust concentration to 0.2 to 1.0 mg/ml with distilled water.

Prepare labeled cRNA

4. Use a Riboprobe in vitro transcription system and follow the protocol provided by the manufacturer to make a ^{32}P-labeled GGT cRNA probe. Briefly, add the following components to a microcentrifuge tube at room temperature in the order listed (20 µl final volume):

   4 µl 5× transcription-optimized buffer
   2 µl 100 mM DTT
   1 µl 40 U/µl RNasin
   4 µl aqueous ATP/GTP/UTP (10 nmol each)
   1 µl linearized pBluescript-GGT DNA
   5 µl 10 µCi/µl [α-^{32}P]CTP
   1 µl 15 to 20 U/µl T7 RNA polymerase
   2 µl DEPC-treated water.

   Vortex tube and centrifuge briefly. Incubate reaction mixture 60 min in a water bath at 37°C.

5. To remove DNA template, add 1 µl RQ1 RNase-free DNase and incubate 30 min at 37°C.
6. Stop the reaction by adding 5 µl of 0.1 M EDTA.

Extract and precipitate RNA

7. Add 100 µl of 25:24:1 phenol/chloroform/isoamyl alcohol to the completely digested DNA. Vortex 1 min and then centrifuge 5 min at 12,000 × *g*, 4°C. Transfer upper phase to a new tube without disturbing the interphase.
8. Add the following and chill 20 min at −80°C:

   1 µl 10 mg/ml tRNA
   50 µl 7.5 M ammonium acetate
   450 µl ice-cold 100% ethanol.

9. Centrifuge 30 min at 12,000 × *g*, 4°C.
10. Remove supernatant and air dry pellet 10 min.
11. Resuspend RNA pellet in 50 µl DEPC-treated water.
12. Add 1 µl ^{32}P-labeled RNA to 5 ml scintillation fluid in a scintillation vial. Quantify ^{32}P with a scintillation counter.

    Approximately 1 × 10^6 cpm/µl is expected.

13. Store ^{32}P-labeled RNA no more than 1 day at −80°C.

BASIC PROTOCOL 2

NUCLEAR RUN-ON ANALYSIS OF γ-GLUTAMYLCYSTEINE SYNTHETASE AND γ-GLUTAMYL TRANSPEPTIDASE GENE TRANSCRIPTION RATES

To study the effect of an oxidant on the transcription rate of the GCS or GGT genes, a transcriptional inhibitor such as actinomycin D is used to block gene transcription. A comparison of the changes in the steady-state GCS or GGT mRNA content over time between samples treated with the compound of interest plus or minus actinomycin D is made by standard northern blot analysis (see Basic Protocol 1). If actinomycin D blocks

the increase in the amount of GCS or GGT mRNA induced by an oxidant, an increased transcription rate of that gene is suggested. Nonetheless, to definitively show that a compound can increase the transcription rate of the GCS or GGT genes, it is necessary to perform nuclear run-on analysis, which directly measures the transcription rate of the gene being studied.

Generally, cells are treated with an oxidant such as 5 to 10 µg DMNQ for 1 to 3 hr, and then the nuclei are isolated. In vitro transcription is conducted with each nuclear preparation. Next, the newly synthesized mRNAs, which have been labeled with ^{32}P, are isolated and hybridized to a membrane that has been previously blotted with the cDNAs of the gene of interest and control genes.

NOTE: This protocol is written specifically for the Rapid RNA Isolation Kit (Amresco). Other kits and reagents can be used; however, the protocol will need to be modified by following the manufacturer's instructions.

Materials

Cells to be analyzed, at ~80% confluence ($\geq 20 \times 10^6$)
Oxidant (e.g., *tert*-butylhydroquinone) in cell culture medium
PBS (*APPENDIX 2A*), ice cold
NP-40 lysis buffer (see recipe)
Glycerol storage buffer (see recipe)
Target plasmid DNA, e.g., γ-glutamylcysteine synthetase light subunit (GCS-LS; Liu et al., 1998a), heavy subunit (GCS-HS; Liu et al., 1998a), or γ-glutamyl transpeptidase (GGT; Liu et al., 1998b)
Restriction enzymes (to linearize plasmid DNA) and appropriate buffers
10 N NaOH
6× and 12× SSC (*UNIT 3.5*)
2.5 M $(NH_4)_2SO_4$, autoclave and store at 4°C
1.0 M $MgCl_2$, autoclave and store at 4°C
5.0 M NaCl, autoclave and store at 4°C
0.25 M EDTA, pH 8.0 (*APPENDIX 2A*)
1.0 M $MnCl_2$, autoclave and store at 4°C
2.0 M Tris·Cl, pH 7.9 (*APPENDIX 2A*)
57 mM phenylmethylsulfonyl fluoride (PMSF) in ethanol (store at −20°C)
0.1 M dithiothreitol (DTT; *APPENDIX 2A*)
100 mM riboGTP, ATP, and CTP
40 U/µl ribonuclease inhibitor (RNasin)
DEPC-treated H_2O: water treated with 0.1% DEPC
100 mM phosphocreatine (ICN Biomedicals)
10 mCi/ml [α-^{32}P]UTP (650 Ci/mmol; e.g., ICN Biomedicals)
Glycerol
50 µg/µl yeast tRNA
10 U/µl RNase-free DNase I
DNase I buffer
2× proteinase K buffer (see recipe)
20 mg/ml proteinase K
Rapid RNA Isolation Kit (Amresco), or equivalent
70% (v/v) ethanol
Scintillation fluid
Hybridization buffer (e.g., QuikHyb, Stratagene)
2× SSC/0.1% (v/v) SDS
0.1× SSC/0.1% (v/v) SDS, 50°C

Biodyne nylon membrane (Life Technologies)
Filtration manifold system (e.g., Life Technologies) connected to vacuum pump
UV cross-linker (e.g., Stratalinker 1800, Stratagene)
Blotting paper
5-ml sterile polypropylene centrifuge tube
30°C and 42°C water baths
Spin column (e.g., Pharmacia)
20-ml glass scintillation vials and scintillation counter
Hybridization oven (e.g., Hybaid), 60°C
X-ray film (e.g., Kodak X-Omat film, Eastman Kodak) or InstantImager (Packard Instruments)

Additional reagents and equipment for restriction enzyme digestion (*APPENDIX 3A*)

Treat cells and isolate nuclei

1. Treat cells to be analyzed at ~80% confluence (total cell number should not be <20 $\times 10^6$) with an oxidant such as *tert*-butylhydroquinone (5 to 100 μM for L2 cells) in cell culture medium.

   A time course of treatments (usually from 1 to 6 hr) is generally carried out and results from these time points are compared. This protocol should be scaled up as needed.

2. Remove cell culture medium and wash cells twice with 5 ml ice-cold PBS.
3. Add 5 ml PBS and gently dislodge cells from the plastic surface by scraping with a disposable cell scraper. Transfer cells to a 15-ml centrifuge tube.
4. Centrifuge cells 5 min at 500 × *g*, 4°C. Remove as much PBS as possible. Vortex 5 sec to loosen cell pellet.
5. Add 8 ml NP-40 lysis buffer. Continue vortexing as the buffer is added and then vortex for another 10 sec.
6. Incubate lysed cells 5 min on ice, centrifuge 5 min at 500 × *g*, 4°C, and discard supernatant.
7. Repeat steps 5 and 6.
8. Resuspend pellet in 200 μl glycerol storage buffer by pipetting up and down. Quantify DNA spectrophotometrically (*APPENDIX 3A*). Store nuclei in liquid nitrogen until ready to proceed with in vitro transcription.

Bind plasmid DNA to nylon filter

9. Linearize 5 μg of each target plasmid DNA for one treatment by digesting with a restriction enzyme in its appropriate buffer (*APPENDIX 3A*). Adjust volume to a DNA concentration of 0.1 μg/μl using water.

   The plasmid DNA does not need to be purified after digestion.

   In addition to GCS DNA or GGT DNA, β-actin, glyceraldehyde phosphate dehydrogenase (GAPDH), or 18S rRNA DNA should be used as a control.

   The amount of DNA prepared should be scaled up accordingly. One slot of each target DNA is required per treatment, and 5 μg plasmid DNA is needed for each slot on the manifold. If there are six different treatment groups, 30 μg plasmid DNA is needed for each target.

10. Denature the linearized DNA by adding 0.01 vol of 10 N NaOH (0.1 N NaOH final) and incubate 30 min at room temperature.
11. Add 1 vol of 12× SSC and place DNA on ice.

12. Wet a Biodyne nylon membrane with water and then with 6× SSC. Put membrane on a filtration manifold system connected to a vacuum pump. Turn on pump and leave the release switch at the on position.

13. Pipet 100 µl linearized plasmid DNA solution (i.e., 5 µg plasmid DNA) into a slot on the manifold. Turn on the vacuum. Check that the pressure is ~12 in. Hg (305 mmHg).

14. Wash manifold slot twice with 200 µl of 6× SSC. Turn off the release switch and leave the vacuum on.

15. Carefully remove the membrane and mark the target DNA position with a pencil.

16. Cross-link DNA to the membrane using a UV cross-linker. Place membrane between sheets of blotting paper and store up to 3 months at room temperature.

Perform in vitro transcription

17. Thaw 1–5 × 10^7 nuclei (step 8) that contain ~250 µg DNA. Pipet nuclei into a 5-ml sterile polypropylene centrifuge tube and centrifuge 1 min at 10,000 × *g*, 4°C to pellet nuclei. Carefully remove storage buffer from the nuclear pellet and loosen nuclei by vortexing briefly.

    A separate reaction tube is required to analyze each treatment. These steps should be scaled up accordingly.

18. Combine the following reaction salt mixture components and add to each tube (~40 µl) of nuclei (20 µl per reaction).

    8.5 µl 2.5 M $(NH_4)_2SO_4$ (final 0.3 M)
    0.4 µl 1.0 M $MgCl_2$ (final 4.0 mM)
    4.0 µl 5.0 M NaCl (final 0.2 M)
    0.16 µl 0.25 M EDTA (final 0.4 mM)
    0.4 µl 1.0 M $MnCl_2$ (final 4.0 mM)
    5.0 µl 2.0 M Tris·Cl (final 0.1 M)
    0.2 µl 57 mM PMSF (final 0.1 mM)
    1.2 µl 0.1 M DTT (final 1.2 mM).

    To prepare enough salt mixture for all of the samples, the quantities above should be multiplied by n + 1, where n is the number of samples. This allows for minor pipetting errors.

19. Add the following to each reaction and mix gently after each addition.

    1 µl each of 100 mM riboGTP, ATP, and CTP
    8.75 µl 40 U/µl RNasin (3.5 U/µl final)
    5.25 µl DEPC-treated water
    10 µl 100 mM phosphocreatine (10 mM final)
    15 µl 10 mCi/ml [α-^{32}P]UTP.

20. Add 2 drops glycerol to tube. Incubate 30 min in a water bath at 30°C.

21. Add 4 µl of 50 µg/µl yeast tRNA and 10 µl of 10 U/µl RNase-free DNase I (75 to 100 U). Incubate 20 min at 30°C.

22. Check viscosity of the solution. Add more DNase I if the digestion is not complete (i.e., the solution is still viscous) and incubate an additional 10 min.

23. When solution is no longer viscous, add an equal volume of 2× proteinase K buffer and 5 µl of 20 mg/ml proteinase K. Incubate overnight in a 42°C water bath.

Extract RNA

24. Using a Rapid RNA Isolation Kit, add 1 ml reagent 1, vortex, and centrifuge 2 min at 10,000 × *g*, at room temperature.

25. Carefully transfer supernatant into a fresh tube. Add 1 ml reagent 2, vortex 2 min, and centrifuge 10 min at 10,000 × *g*, at room temperature.

26. Carefully transfer top layer to a fresh tube.

    The white interphase should not be disturbed.

27. Add 200 µl reagent 3 and 600 µl reagent 4. Mix by vortexing briefly after each addition. Centrifuge 5 min at 10,000 × *g*, at room temperature.

28. Transfer supernatant to a fresh tube and add 1.2 ml RNA precipitation reagent. Invert tube several times and centrifuge 10 min at 10,000 × *g*, at room temperature.

29. Remove as much of the supernatant as possible. Rinse pellet with 70% ethanol and centrifuge 5 min at 10,000 × *g*, at room temperature. Remove supernatant.

30. Resuspend pellet in 100 µl sterile nuclease-free water. Purify labeled RNA from free [α-^{32}P]UTP using a spin column.

31. Take a 1-µl aliquot of purified RNA and add to 5 ml scintillation fluid in a scintillation vial. Quantitate ^{32}P with a scintillation counter. Use immediately.

    Approximately 10^5 to 10^6 cpm/µl is expected. When comparing different RNA preparations, the same amount of radiolabeled RNA (in cpm) should be used for each hybridization.

Hybridize labeled RNA to membrane

32. Roll and place a target DNA–bound nylon membrane (step 16) inside a 20-ml glass scintillation vial.

    One membrane strip with target DNAs and control DNA is required for each treatment.

33. Add 3 ml hybridization buffer and rotate vial slowly to spread the membrane and avoid trapping any air bubbles between the membrane and the glass wall.

34. Prehybridize membrane 30 min in a hybridization oven at 60°C, and then add the radiolabeled RNA preparation into tube.

35. Hybridize 2 hr at 60°C.

36. Wash membrane twice with 2× SSC/0.1% SDS for 15 min at room temperature, and then twice with 0.1× SSC/0.1% SDS for 10 to 15 min at 50°C.

37. Wrap membrane in plastic wrap and store membrane inside X-ray film cassette. Expose an X-ray film at −80°C or scan the membrane using a InstantImager.

BASIC PROTOCOL 3

IMMUNOBLOT ANALYSIS OF γ-GLUTAMYLCYSTEINE SYNTHETASE PROTEIN CONTENT

GCS-HS and GCS-LS protein content can be determined using a standard immunoblot analysis protocol with slight modifications (also *UNIT 2.3*). After treating cells with various oxidants, cytosolic proteins are obtained and separated on a denaturing gel. Subsequently, proteins are transferred onto a PVDF membrane and probed with the appropriate antibodies.

Materials

Cells to be analyzed
PBS (*APPENDIX 2A*), ice cold
Cell extraction buffer (see recipe)
4× immunoblot sample loading buffer (see recipe)
10% Tris/glycine gel (e.g., Pre-cast Tris-glycine mini gel, Novex/Invitrogen)
SDS electrophoresis buffer (e.g., Tris-glycine SDS gel running buffer, Novex/Invitrogen or *APPENDIX 2A*)
Protein molecular weight markers
Immunoblot transfer buffer (see recipe)
Methanol
Blocking solution (see recipe)
Anti-γ-glutamylcysteine-synthetase-heavy-subunit (anti-GCS-HS) or -light-subunit (anti-GCS-LS) polyclonal antibodies
T-TBS: 0.05% (v/v) Tween 20 in TBS (see recipe)
Alkaline phosphatase (AP)–conjugated goat anti–rabbit IgG (e.g., Kirkegaard & Perry Laboratories)
Enzymatic chemiluminescence detection kit (e.g., ECL Plus, Amersham Pharmacia Biotech)

Sonicator
95°C water bath
Vertical gel electrophoresis apparatus (e.g., Novex/Invitrogen)
Polyvinylidene difluoride (PVDF) membrane (0.45-μm; e.g., Immobilon-P PVDF membrane, Millipore)
Capillary transfer apparatus (e.g., Mini Trans-Blot Cell, Bio-Rad)
X-ray film (e.g., Hyperfilm ECL, Amersham Pharmacia Biotech)

Additional reagents and equipment for determining protein concentration (*APPENDIX 3A*)

Prepare sample

1. Wash cells to be analyzed once with ice-cold PBS, collect cells, and transfer to a microcentrifuge tube.
2. Add 0.3 to 0.5 ml extraction buffer and sonicate briefly on ice. Centrifuge 20 min at 10,000 × *g*, 4°C, to pellet cell debris.
3. Transfer supernatant to a clean tube and centrifuge 1 hr at 105,000 × *g*, 4°C. Collect supernatant and determine protein concentration.

   A kit (e.g., BCA, Pierce Chemical) can be used for protein quantitation. Also see APPENDIX 3A.

4. Mix 40 μg cellular proteins 3:1 (v/v) with 4× immunoblot sample loading buffer (1× final) and heat 5 min in a water bath at 95°C to denature the GCS holoenzyme. Centrifuge briefly to recover all of the sample.

   Samples can be concentrated by centrifuging the supernatant in a concentrator (e.g., Microcon-10, Millipore).

   The quantity of cytosolic proteins used will depend on the relative abundance of GCS proteins in the sample.

Separate and transfer proteins

5. Place a 10% Tris/glycine gel in a vertical gel electrophoresis apparatus and fill apparatus with SDS electrophoresis buffer. Attach a power supply to the apparatus.

   Detailed protocols for mini-gel SDS-PAGE and immunoblotting are described in UNITS 2.2 & 2.3, respectively.

6. Load denatured sample along with appropriate molecular weight markers onto gel and run at 120 V for 1.5 to 2 hr (for mini-gel system).

   The same volume of 1× immunoblot sample loading solution should be loaded into all empty lanes.

7. Disassemble gel apparatus and open gel plates on a firm surface. Mark orientation of the gel by cutting off one corner with a knife.

8. Shake protein gel gently in transfer buffer for 15 min at room temperature to equilibrate gel.

9. Soak a PVDF membrane 30 sec in methanol, rinse 3 min in water, and then equilibrate 15 min in transfer buffer before setting up the transfer.

   The PVDF membrane must not be allowed to dry out after it is wet.

10. Transfer separated proteins to PVDF membrane using a capillary transfer apparatus per manufacturer's instructions for 2 hr at 75 V (for mini-gel system).

    The transfer system must be kept cold (4°C) during the transfer.

    CAUTION: *The transfer buffer should be disposed of in an organic-waste disposal container.*

Perform immunoblot

11. Disassemble transfer sandwich. Block membrane with blocking solution for 30 min to 1 hr at room temperature on a shaker.

12. Incubate membrane overnight at 4°C with anti-GCS-HS or anti-GCS-LS polyclonal antibodies in fresh blocking solution, shaking gently.

    Antibodies are raised against a 19–amino acid GCS-HS peptide (amino acids 295-313, NH_2-CRWGVISASVDDRTREERG-COOH) conjugated to carrier keyhole limpet hemocyanin. Light subunit antibodies can be raised against a holoenzyme purified from rat hepatocytes (Sun et al., 1996). Due to the high homology of GCS sequences among species (~95% sequence identity), human and mouse GCS equivalents are also recognized by these antibodies against the rat enzyme. GCS-LS antibodies are purified from the GCS-LS serum, according to Meyer et al. (1982, 1990). Appropriate dilutions should be determined for each antibody preparation.

13. Wash membrane with T-TBS and then incubate it with a 1:20,000 dilution of AP-conjugated goat anti–rabbit IgG in blotting solution for 1 to 2 hr at room temperature with shaking.

14. Wash with T-TBS and use enzymatic chemiluminescence detection kit (follow manufacturer's instructions) and X-ray film to detect GCS proteins.

15. Determine molecular weights of the proteins of interest by comparison with the molecular weight markers.

    The GCS-LS is ~30 kDa and the GCS-HS is 73 kDa.

SUPPORT PROTOCOL 3

γ-GLUTAMYL TRANSPEPTIDASE ACTIVITY ASSAY

The specificity of GGT toward γ-glutamyl compounds is quite broad and has allowed the development of several different activity assays (*UNIT 6.6*). The most common assay uses L-γ-glutamyl-*p*-nitroanilide, with the product detected by absorbance spectrophotometry. Another assay for the measurement of GGT activity depends upon the conversion of radiolabeled leukotriene L_4 (LTC_4) to leukotriene D_4 (LTD_4) and separation by high-per-

formance liquid chromatography. Such a method was particularly useful in assaying the activity of a γ-glutamyl-cleaving enzyme related to GGT, which does not recognize the synthetic substrates L-γ-glutamyl-7-amino-4-methyl-coumarin (γ-glutamyl-AMC) and γ-glutamyl-*p*-nitroanilide. A more sensitive assay, which is described here, was developed by using the fluorescent substrate γ-glutamyl-AMC (Smith et al., 1979). Because other enzymatic or non-enzymatic reactions may cleave γ-glutamyl compounds, the inhibitor acivicin (AT-125; L-(α*S*,5*S*)-α-amino-3-chloro-4,5-dihydro-5-isoxazoleacetic acid) is used to assess specificity of the enzymatic reaction. This is done by adding acivicin to one of the duplicate samples. The GGT activity is calculated by subtracting the fluorescence of the acivicin-containing tube from that of the acivicin-free tube.

Materials

Cells to be analyzed
Oxidant
PBS (*APPENDIX 2A*)
Acivicin (Sigma-Aldrich)
0.2 M 2-amino-2-methyl-1-3-propandiol (ammediol)/HCl buffer, pH 8.6
0.2 M glycylglycine
10 mM L-γ-glutamyl-7-amino-4-methyl-coumarin (γ-glutamyl-AMC) in methoxyethanol (e.g., Sigma-Aldrich)
Triton X-100
0.05 M glycine, cold
10 mM AMC in methoxyethanol (e.g., Sigma-Aldrich)

Sonicator
Fluorescence spectrophotometer (excitation 370 nm, emission 440 nm)

Prepare cell extract

1. Treat cells to be analyzed with an oxidant.

   A time course of treatments (usually from 6 to 24 hr) is generally carried out and results from these time points are compared. This protocol should be scaled up as needed.

2. Collect cells in 5 ml PBS in a 15-ml tube and sonicate briefly in a sonicator.
3. Centrifuge 5 min at low speed (4000 × *g*) to remove any unbroken cells, and collect supernatant (cell extract).

Set up enzymatic assay

4. Add 0.1 ml cell extract to duplicate tubes. Add 10 µM acivicin to one tube.

   The specific activity is confirmed by using 10 µM acivicin to inhibit the enzymatic reaction.

5. Dilute 10 mM AMC as needed in methoxyethanol and set up standard tubes containing 0.01 ml diluted AMC to cover a concentration range of 20 to 900 pmol/tube.
6. For each sample and standards, make up a reaction mixture containing:

   125 µl 0.2 M ammediol/HCl buffer (final 0.1 M)
   25 µl 0.2 M glycylglycine (final 20 mM)
   5 µl 10 mM γ-glutamyl-AMC in methoxyethanol (final 200 µM)
   0.25 µl Triton X-100 (final 0.1%)
   94.75 µl water.

7. Add 0.25 ml reaction mixture (cell extract) to each sample.
8. Incubate reactions 30 min in a water bath at 37°C and terminate by adding 1.5 ml cold 0.05 M glycine to each tube.

Analyze fluorescence

9. Use a fluorescence spectrophotometer to measure fluorescence of the samples and standards at 440 nm with an excitation wavelength of 370 nm.

10. Use AMC standards to generate a standard curve. Calculate product formation in the cell extract by comparison with the standard curve. To confirm the specificity of the enzyme activity, add 10 µM acivicin to one of the duplicate sample tubes to inhibit the enzyme activity in that tube.

    The advantage of this assay is that multiple samples can be assayed simultaneously. This is important when activity is low, requiring a prolonged incubation to produce a significant amount of product. Fortunately, under such conditions product formation can be linear for hours.

REAGENTS AND SOLUTIONS

Use Milli-Q-purified water or equivalent in all recipes and protocol steps. For common stock solutions, see ***APPENDIX 2A****; for suppliers, see* ***SUPPLIERS APPENDIX****.*

Blocking solution

5% (w/v) nonfat dry milk in TBS (see recipe)
Make fresh on day of experiment and keep at 4°C

Cell extraction buffer

20 mM Tris·Cl (*APPENDIX 2A*)
150 mM NaCl
1 mM $MgCl_2$
2 mM $CaCl_2$
2.5 mM EDTA, pH 8.0 (*APPENDIX 2A*)
2.5 mM EGTA
Adjust pH to 7.8 with HCl
Store up to 6 months at 4°C
Just before use add:
1 mM phenylmethylsulfonyl fluoride (PMSF) in ethanol
10 µg/ml aprotinin
10 µg/ml leupeptin

Glycerol storage buffer

50 mM Tris·Cl, pH 8.3 (*APPENDIX 2A*)
40% (v/v) glycerol
5 mM $MgC1_2$
0.1 mM EDTA, pH 8.0 (*APPENDIX 2A*)
Autoclave and store up to 6 months at 4°C

Immunoblot sample loading buffer, 4×

1 ml 1 M Tris base, pH 6.5 (0.25 M final)
1.6 ml glycerol (40% final)
0.32 g SDS (8% final)
0.4 ml 0.05% (w/v) Pyronin Y (0.005% final)
123.2 mg dithiothreitol (DTT; 0.2 M final)
H_2O to 4 ml
Store up to 6 months at −20°C

Immunoblot transfer buffer

12.2 g Tris base
57.6 g glycine
H_2O to 3.2 liters
Store up to 6 months at 4°C
On the day of experiment, add 200 ml methanol/800 ml solution and keep at 4°C until use

3-(N-Morpholino)propanesulfonic acid (MOPS) running buffer, 10×

41.8 g MOPS (200 mM final)
800 ml DEPC-treated H_2O: water treated with 1% DEPC
Adjust to pH 7 with NaOH or acetic acid
16.6 ml 3 M DEPC-treated sodium acetate, pH 5.2 (50 mM final; *APPENDIX 2A*)
20.0 ml 0.5 M DEPC-treated EDTA, pH 8.0 (10 mM final; *APPENDIX 2A*)
Add DEPC-treated H_2O to 1 liter
Filter sterilize
Store protected from light up to 3 months at room temperature
Dilute as needed with DEPC-treated H_2O

Nonidet P-40 (NP-40) lysis buffer

10 mM Tris·Cl, pH 7.4 (*APPENDIX 2A*)
10 mM NaCl
3 mM $MgCl_2$
0.5% NP-40
Autoclave and store up to 6 months at 4°C

Northern gel loading buffer

5 % (v/v) glycerol
1 mM EDTA, pH 8.0 (*APPENDIX 2A*)
0.25% (w/v) bromphenol blue
0.25% (w/v) xylene cyanol FF
Store up to 2 years at −80°C

Proteinase K buffer, 2×

0.04 M Tris·Cl, pH 7.5 (*APPENDIX 2A*)
2% (w/v) SDS (*APPENDIX 2A*)
20 mM EDTA, pH 8.0 (*APPENDIX 2A*)
Autoclave and store up to 6 months at −20°C

RNA loading mixture

28 µl northern gel loading buffer (see recipe; 10% final)
140 µl formamide (50% final)
14 µl 1 mg/ml ethidium bromide (0.05 µg final)
70 µl DEPC-treated H_2O: water treated with 0.1% DEPC
28 µl 10× MOPS running buffer (see recipe; 1× final)
Mix well and store protected from light up to 1 year at −20°C

CAUTION: *Ethidium bromide is a mutagen and must be handled carefully.*

STE buffer, 1×

10 mM Tris·Cl, pH 7.5 (*APPENDIX 2A*)
10 mM NaCl
1 mM EDTA, pH 8.0 (*APPENDIX 2A*)
Store up to 1 year at room temperature

Tris-buffered saline (TBS)

4.84 g Tris base (10 mM final)
35.06 g NaCl (0.9% final)
H_2O to 4 liters
Adjust pH to 7.6 with HCl
Store up to 6 months at 4°C (stable ≥6 months)

COMMENTARY

Background Information

Among the principal functions of reduced glutathione (GSH) is its participation in reduction of hydroperoxides and in conjugation to physiologic and xenobiotic compounds. Using depletion of GSH through conjugation reactions, inhibition of its synthesis, or inhibition of reduction of glutathione that becomes oxidized during reduction of hydroperoxides, a great number of studies have shown that low GSH content increases susceptibility to oxidative stress and xenobiotic toxicity. In contrast, it is also well established that increasing the GSH steady-state content and/or the rate of GSH synthesis provides protection against oxidative stress. Although a few types of cells can directly take up GSH from the surrounding fluid, most cells depend on de novo GSH synthesis to maintain their intracellular GSH content. Thus, it is not surprising that an increase in de novo GSH synthesis is a well-established component of adaptation to stress from oxidants and xenobiotics. This increase in GSH synthesis is due, in part, to an elevation of the protein content and enzymatic activities of both γ-glutamylcysteine synthetase (GCS) and γ-glutamyl transpeptidase (GGT), which are involved in the synthesis of GSH and the metabolism of extracellular GSH, respectively.

This unit is complementary to *UNIT 6.5*, which describes assays for enzymatic activity of GSH biosynthesis, and to *UNIT 6.6*, which describes assays for GGT. Here, the principal focus is on methods for studying the regulation of enzymes of glutathione biosynthesis at the transcriptional and translational levels with a particular focus on changes in response to oxidative or xenobiotic stress. The methods described in this unit are used to document these changes and can be used to examine the effects of other agents with the potential for regulating GSH synthesis as well.

GCS catalyzes the first step in de novo GSH synthesis. The reaction, production of γ-glutamylcysteine from glutamate and cysteine driven by ATP hydrolysis, is normally the rate-limiting step in GSH production. Under physiological conditions, GCS is substantially feedback inhibited by GSH (Richman and Meister, 1975). Therefore, when an agent causes an initial depletion of GSH, release of the GSH bound to GCS can result in a temporary enhancement of the rate of GSH synthesis (Wallig et al., 1992; Ochi, 1993). In contrast, a sustained increase in synthesis of the enzyme itself can provide a mechanism for a sustained increase in GSH. GCS is composed of two subunits: a catalytic or heavy subunit (GCS-HS; 73 kDa) and a regulatory or light subunit (GCS-LS; ~30 kDa). In the recent past, stress-induced expression of both GCS subunits has been shown to occur. Based upon experiments with recombinant proteins, GCS-LS, although not essential for catalysis, lowered the K_m for glutamate and decreased the affinity for GSH, which inhibits enzymatic activity by competing for the glutamate binding site (Richman and Meister, 1975). It was also suggested that formation of a disulfide bridge between the subunits augments the effects upon enzyme kinetics (Huang et al., 1993), although the reducing environment in the cell, in which >95% of glutathione is found in the reduced state except under major oxidative stress, would normally inhibit disulfide formation between subunits. Mulcahy et al. (1995) found that cotransfection of COS cells with both GCS-HS cDNA and GCS-LS cDNA led to a greater increase in intracellular GSH content than transfection with either subunit alone when the total amount of cDNA used was equal between cotransfection and individual transfection experiments. These data clearly suggest an important role of the light subunit for GCS activity under physiological conditions.

The regulation of GCS-HS gene expression has been extensively studied. It has been found that various agents and conditions, such as heat shock, heavy metals, substances that deplete GSH through conjugation or by inhibiting its synthesis, hormones, oxidants and antioxidants, and tumor necrosis factor, induce the expression of GCS-HS. An increased GCS-HS expression and GSH content have also been

found in drug-resistant tumor cells, implicating a potential role of this enzyme in such resistance. The regulation of the GCS-LS, on the other hand, has been less intensively studied until recently. Several compounds that induce the expression of GCS-HS have been found to induce the expression of GCS-LS as well (Galloway et al., 1997; Sekhar et al., 1997a; Tian et al., 1997). However, some hormones, such as insulin and glucocorticoid (Cai et al., 1997) or the anticancer drug cisplatin (Yao et al., 1995), have been found to induce GCS-HS but not GCS-LS, indicating dissociated regulation of the two GCS subunits. Differences in the ratio of the two GCS subunit mRNAs among various tissues further indicate that the expression of two GCS subunit genes is controlled by different mechanisms (Gipp et al., 1995). Exposure to 4-hydroxynonenal (4HNE), a reactive product of lipid peroxidation that is always present in cells, at a slightly higher-than-normal physiological concentration increased both GCS subunit proteins (Liu et al., 1998a). Nonetheless, experiments employing the protein synthesis inhibitor emetine indicated that the induction of GCS-LS by 4HNE, but not GCS-HS, required new protein synthesis. Thus, the increased transcription of GCS-LS mRNA is an indirect response to 4HNE while increased transcription of GCS-HS is a direct response to 4HNE. Previous investigations have shown that the induction of GCS-HS by other oxidants is a direct response (Shi et al., 1994; Rahman et al., 1996a,b). While the increase in transcription of both subunit mRNAs has also been shown with a variety of xenobiotic agents, 4HNE also caused an increase in the stability of both GCS-HS and GCS-LS mRNAs. Thus, an increase in the mRNAs of either of the two GCS subunits does not necessarily imply increased transcription.

Yet, increased transcription of GCS subunits does occur in response to a variety of agents. Several recent studies have suggested that transcription of the catalytic subunit of GCS (GCS-HS) can be under control of the *cis* elements κB (Urata et al., 1996; Iwanaga et al., 1998), two different AP-1 binding sites (Yao et al., 1995; Rahman et al., 1996a,b; Morales et al., 1997; Sekhar et al., 1997b; Tomonari et al., 1997a,b), and the most distal antioxidant response element (ARE; Mulcahy et al., 1997). These studies, which have relied upon reporter-gene constructs have used a variety of agents and cell types. Fewer studies have been made of the control of the regulatory subunit of GCS (GCS-LS); however, an AP-1 binding site has been suggested to control its transcription as well (Moinova and Mulcahy, 1998). Nonetheless, as described above, transcription of GCS-HS and GCS-LS are not always coordinated.

The K_m value for cysteine for GCS (0.35 mM) is close to its intracellular concentration. Therefore, the availability of cysteine may also limit the rate of GSH synthesis (Richman and Meister, 1975). For most cells, cysteine can be obtained by degradation of circulating GSH through the action of GGT, a membrane-bound enzyme (Suzuki et al., 1993; Meister, 1994). GGT transfers the γ-glutamyl moiety of GSH to an amino acid, forming a γ-glutamyl–amino acid and cysteinylglycine. Cysteinylglycine is degraded by dipeptidases on the surface of cells and the amino acids are transported into the cell (Deneke and Fanburg, 1989). The γ-glutamyl–amino acids are also transported into the cell and metabolized to release the amino acid and 5-oxoproline, which is converted to glutamate. When the acceptor amino acid for GGT activity is cystine, the resulting product, γ-glutamylcystine, can be taken up by cells and then reduced to cysteine and γ-glutamylcysteine, both of which can be used in GSH synthesis in the so-called scavenger pathway. GSH depletion or oxidative stress increases the activities of the amino acid transport systems. Another source of cysteine is its synthesis in the cystathionine pathway present in some tissues, particularly liver. The cystathionine pathway is also active in the lung and increases during hyperoxic exposure (Rusakow et al., 1993). Thus, a variety of mechanisms exist for providing cysteine for GSH synthesis.

In pulmonary epithelial cells during oxidative stress, GGT increases in coordination with GCS and provides a major source of cysteine (Liu et al., 1996). GGT has been shown to increase in response to quinones, hyperoxia, and nitrogen dioxide (Kugelman et al., 1994; Joyce-Brady et al., 1996; Takahashi et al., 1997). For the quinones, this increase has been shown to result from an increase in transcription or mRNA stability, depending upon whether the quinone redox cycles or conjugates with GSH (Liu et al., 1998b).

GGT gene regulation is complex. In humans, there are several GGT genes and a closely related protein. In rats and mice, there is only one GGT gene, but at least seven different mRNAs are made due to multiple transcription start sites and alternative splicing. Fortunately, in terms of understanding GGT, the coding region of all the GGT mRNAs is the same. It appears that only one mRNA of GGT (type III)

is normally present in lung cells after birth. In hyperoxia, the evidence suggests that this form alone increases. Following NO_2 exposure, it appears that a second fetal type reappears along with an increase in type III. GGT is a TATA-less gene, but the promoter-enhancer region of type III contains a putative ARE sequence, which has been suggested to be responsible for the increase during oxidative stress (Joyce-Brady et al., 1996).

Clearly, understanding the regulation of the expression of the two GCS genes and the GGT gene has much further to go. The methods described here can be used for determining whether alterations in mRNAs involve transcription or RNA stability and whether those are coordinated with changes in enzymatic activity (GGT) and protein content (GCS). These are important first steps in this investigation.

Critical Parameters and Troubleshooting

Northern analysis

RNA degradation must be avoided. RNase contamination, which will lead to the degradation of RNA, is the most serious and common problem during RNA isolation and analysis. Therefore, it is strongly suggested that all tubes, tips, and glassware used for RNA isolation be autoclaved and all solutions be made with fresh DEPC-treated water. If RNA is isolated from tissues, this should be performed as soon as possible once the animals are sacrificed to minimize RNA degradation.

When transferring RNA from a gel to a membrane, care should be taken to ensure that bubbles are not trapped between the gel and the membrane or the blotting paper to avoid uneven transfer.

The hybridization of the GCS cDNA probe to GCS RNA is not very strong, and therefore, extreme care should be taken while washing the membrane. Generally, membranes can be washed twice with 2× SSC/0.1% SDS at room temperature for ~10 to 15 min for GCS-HS and GCS-LS hybridizations. Then, the temperature is raised to 50°C and the membrane is washed with 0.1× SSC/0.1% SDS for another 10 min. The radioactivity on the membrane should be checked with a Geiger counter every 3 to 5 min after the first 10-min high-temperature wash. However, the exact time should be determined for each experiment. The wash solutions should be brought to the desired temperature before use.

On the other hand, the binding of the GGT cRNA probe to GGT RNA is very strong and it is very difficult to strip the probe off the membrane after hybridization. Therefore, it is suggested that the hybridization with the GGT cRNA probe be performed after the membrane has been hybridized with other probes of interest.

Nuclear run-on experiment

When isolating nuclei, it is important to make sure that the cells are lysed completely in order to get a high yield of nuclei. The optimal lysis condition varies with the cell type and therefore should be predetermined. After cells are treated with the lysis buffer for various time periods, check the cells under a microscope. The shortest time it takes to break the plasma membrane without compromising the integrity of the nucleus will be the optimum lysis time for those cells.

RNA degradation must be avoided. As in northern analysis, RNase contamination should be avoided during the isolation and handling of RNA after in vitro transcription. Autoclaved tubes, tips, and RNase-free solutions should be used.

The amount of RNA may be too small to be seen after centrifugation, and therefore RNA may be lost during isolation. It is strongly suggested that some carrier DNA, usually yeast DNA, be used when isolating RNA after in vitro transcription to increase the visibility of the RNA.

It is critical to linearize the plasmid completely as supercoiled plasmids tend to show reduced hybridization potential. A 1% agarose gel should be run after the restriction enzyme digest to make sure that the digestion is complete. It is also strongly suggested that one mark the position of the target DNA on the membrane with a pencil after removing the membrane from the filtration manifold. As in northern analysis, extreme care should be taken when washing the membrane after hybridization.

A troubleshooting guide to GCS and GGT regulation and expression is provided in Table 6.7.1.

Anticipated Results

Rat GCS-HS mRNA is ~3.7 kb in length and the protein is ~73 kDa. Typical northern analysis yields two rat GCS-LS mRNA species of 5.2 kb and 1.8 kb in length. Immunoblot analysis, on the other hand, shows one rat GCS-LS protein band, of ~30 kDa in size. It is generally considered that kidney expresses the highest levels of GCS-HS and GCS-LS as well as GGT at both the protein and mRNA levels. The

Table 6.7.1 Troubleshooting Guide to GCS and GGT Regulation and Expression

Problem	Potential reason	Solution
No RNA signal	Degraded RNA	Use autoclaved tubes and tips and DEPC-treated water for solutions.
	Membrane washed too thoroughly	Wash carefully at 50°C. Check radioactivity every 2-5 min after first 10-min wash.
No gene induction	Cells post-confluence	Treat cells at ~80% confluence.
Low signal in nuclear run-on	Incomplete cell lysis	Make sure cells are lysed completely.
	Incomplete DNA digestion	Extend digestion time.
	RNase contamination	Use RNase-free solutions and sterile tubes and tips.
Multiple bands on immunoblot	GCS holoenzyme not completely denatured	Make sure GCS holoenzyme is completely denatured. Use a 2× immunoblot sample loading solution that contains 12 M urea and 600 mM DTT. Use purified protein to identify the band.
	Antibodies not pure	Purify antibodies.

expression of GCS and GGT has been reported in numerous tissues and cells. GGT activity is very high in kidney and relatively low in adult liver.

Time Considerations

Typical northern analysis takes 1 to 2 weeks for completion. From RNA isolation through transfer of RNA to the membrane usually takes <3 days, while the actual hybridization with multiple probes takes ~1 to 1.5 weeks, including film exposure time. The actual time frame, however, will depend on the availability of the probes for hybridization and the intensity of the signal. For immunoblot analysis, sample preparation usually takes one whole day, and the rest of the procedure can be completed in 2 additional days.

Nuclear run-on analysis tends to be time-consuming. Plasmid preparation itself, which should take place before the protocol, takes ~1 to 2 weeks, but once the plasmids are isolated, they can be used several times (30 µg of each plasmid for each experiment, for an average of six different treatments per experiment). Growing and treating cells and isolating nuclei from them requires ~1 week to complete. Linearizing plasmids and binding cDNA probes to the membrane requires an additional 2 days. In vitro transcription, isolation of RNA, and hybridization requires another 2 to 3 days. Therefore, one experiment typically requires ~1 week if all plasmid cDNAs are available and the cells are ready to be treated.

Literature Cited

Brown, T. and Mackey, K. 1997. Analysis of DNA by northern and slot-blot hybridization. *In* Current Protocols in Molecular Biology (F.M. Ausubel, R. Brent, R.E. Kingston, D.D. Moore, J.G. Seidman, J.A. Smith, and K. Struhl, eds.) pp. 4.9.1-4.9.16. John Wiley & Sons, New York.

Cai, J., Huang, Z.Z., and Lu, S.C. 1997. Differential regulation of gamma-glutamylcysteine synthetase heavy and light subunit gene expression. *Biochem. J.* 326:167-172.

Deneke, S.M. and Fanburg, B.L. 1989. Regulation of cellular glutathione. *Am. J. Physiol.* 257:L163-L173.

Galloway, D.C., Blake, D.G., Shepherd, A.G., and McLellan, L.I. 1997. Regulation of human gamma-glutamylcysteine synthetase: Co-ordinate induction of the catalytic and regulatory subunits in HepG2 cells. *Biochem. J.* 328:99-104.

Gipp, J.J., Bailey, H.H., and Mulcahy, R.T. 1995. Cloning and sequencing of the cDNA for the light subunit of human liver gamma-glutamylcysteine synthetase and relative mRNA levels for heavy and light subunits in human normal tissues. *Biochem. Biophys. Res. Commun.* 206:584-589.

Huang, C.-S., Anderson, M.E., and Meister, A. 1993. Amino acid sequence and function of the light subunit of rat kidney γ-glutamyl cysteine synthetase. *J. Biol. Chem.* 268:20578-20583.

Iwanaga, M., Mori, K., Iida, T., Urata, Y., Matsuo, T., Yasunaga, A., Shibata, S., and Kondo, T. 1998. Nuclear factor kappa B dependent induction of gamma glutamylcysteine synthetase by ionizing radiation in T98G human glioblastoma cells. *Free Radic. Biol. Med*. 24:1256-1268.

Joyce-Brady, M., Oakes, S.M., Wuthrich, D., and Laperche, Y. 1996. Three alternative promoters of the rat γ-glutamyl transferase gene are active in developing lung and are differentially regulated by oxygen after birth. *J. Clin. Invest*. 97:1774-1779.

Kugelman, A., Choy, H.A., Liu, R., Shi, M.M., Gozal, E., and Forman, H.J. 1994. γ-Glutamyl transpeptidase is increased by oxidative stress in rat alveolar L2 epithelial cells. *Am. J. Respir. Cell Mol. Biol.* 11:586-592.

Liu, R.M., Hu, H., Robison, T.W., and Forman, H.J. 1996. Increased gamma-glutamylcysteine synthetase and gamma-glutamyl transpeptidase activities enhance resistance of rat lung epithelial L2 cells to quinone toxicity. *Am. J. Respir. Cell Mol. Biol.* 14:192-197.

Liu, R.M., Gao, L., Choi, J., and Forman, H.J. 1998a. Gamma-glutamylcysteine synthetase: mRNA stabilization and independent subunit transcription by 4-hydroxy-2-nonenal. *Am. J. Physiol.* 275:L861-L869.

Liu, R.M., Shi, M.M., Giulivi, C., and Forman, H.J. 1998b. Quinones increase gamma-glutamyl transpeptidase expression by multiple mechanisms in rat lung epithelial cells. *Am. J. Physiol.* 274:L330-L336.

Luo, J.L., Hammarqvist, F., Andersson, K., and Wernerman, J. 1998. Surgical trauma decreases glutathione synthetic capacity in human skeletal muscle tissue. *Am. J. Physiol.* 275:E359-E365.

Meister, A. 1994. Glutathione, ascorbate, and cellular protection. *Cancer Res.* 54:1969s-1975s.

Meyer, L.J., Milburn, S.C., and Hershey, J.W.B. 1982. Immunochemical characterization of mammalian protein synthesis initiation factors. *Biochemistry* 21:4206-4212.

Meyer, L.J., Taylor, T.B., Kadunce, D.P., and Zone, J.J. 1990. Two groups of bullous pemphigoid antigens are identified by affinity-purified antibodies. *J. Invest. Dermatol.* 94:611-616.

Moinova, H.R. and Mulcahy, R.T. 1998. An electrophile responsive element (EpRE) regulates beta-naphthoflavone induction of the human gamma-glutamylcysteine synthetase regulatory subunit gene. Constitutive expression is mediated by an adjacent AP-1 site. *J. Biol. Chem.* 273:14683-14689.

Morales, A., Garcia-Ruiz, C., Miranda, M., Mari, M., Colell, A., Ardite, E., and Fernandez-Checa, J.C. 1997. Tumor necrosis factor increases hepatocellular glutathione by transcriptional regulation of the heavy subunit chain of gamma-glutamylcysteine synthetase. *J. Biol. Chem.* 272:30371-30379.

Mulcahy, R.T., Bailey, H.H., and Gipp, J.J. 1995. Transfection of complementary DNAs for the heavy and light subunits of human gamma-glutamylcysteine synthetase results in an elevation of intracellular glutathione and resistance to melphalan [published erratum appears in *Cancer Res.* 1996;56(1):225]. *Cancer Res.* 55:4771-4775.

Mulcahy, R.T., Wartman, M.A., Bailey, H.H., and Gipp, J.J. 1997. Constitutive and beta-naphthoflavone-induced expression of the human gamma-glutamylcysteine synthetase heavy subunit gene is regulated by a distal antioxidant response element/TRE sequence. *J. Biol. Chem.* 272:7445-7454.

Ochi, T. 1993. Mechanism for the changes in levels of glutathione upon exposure of cultured mammalian cells to tertiary-butylhydroperoxide and diamide. *Arch. Toxicol.* 67:401-410.

Rahman, I., Bel, A., Mulier, B., Lawson, M.F., Harrison, D.J., Macnee, W., and Smith, C.A. 1996a. Transcriptional regulation of gamma-glutamylcysteine synthetase-heavy subunit by oxidants in human alveolar epithelial cells. *Biochem. Biophys. Res. Commun.* 229:832-837.

Rahman, I., Smith, C.A., Lawson, M.F., Harrison, D.J., and MacNee, W. 1996b. Induction of gamma-glutamylcysteine synthetase by cigarette smoke is associated with AP-1 in human alveolar epithelial cells [published erratum appears in *FEBS Lett.* 1997;411(2-3):393]. *FEBS Lett*. 396:21-25.

Richman, P.G. and Meister, A. 1975. Regulation of γ-glutamyl-cysteine synthetase by nonallosteric feedback inhibition by glutathione. *J. Biol. Chem.* 250:1422-1426.

Rusakow, L.S., White, C.W., and Stabler, S.P. 1993. O_2-induced changes in lung and storage pool thiols in mice: Effect of superoxide dismutase. *J. Appl. Physiol.* 74:989-997.

Sekhar, K.R., Long, M., Long, J., Xu, Z.Q., Summar, M.L., and Freeman, M.L. 1997a. Alteration of transcriptional and post-transcriptional expression of gamma-glutamylcysteine synthetase by diethyl maleate. *Radiat. Res.* 147:592-597.

Sekhar, K.R., Meredith, M.J., Kerr, L.D., Soltaninassab, S.R., Spitz, D.R., Xu, Z.Q., and Freeman, M.L. 1997b. Expression of glutathione and gamma-glutamylcysteine synthetase mRNA is Jun dependent. *Biochem. Biophys. Res. Commun.* 234:588-593.

Shi, M.M., Iwamoto, T., and Forman, H.J. 1994. Gamma-glutamylcysteine synthetase and GSH increase in quinone-induced oxidative stress in BPAEC. *Am. J. Physiol.* 267:L414-L421.

Smith, G.D., Ding, J.L., and Peters, T.J. 1979. A sensitive fluorometric assay for γ-glutamyl transferase. *Anal. Biochem.* 100:136-139.

Sun, Y. 1997. Induction of glutathione synthetase by 1,10-phenanthroline. *FEBS Lett*. 408:16-20.

Sun, W.M., Huang, Z.Z., and Lu, S.C. 1996. Regulation of gamma-glutamylcysteine synthetase by protein phosphorylation. *Biochem. J.* 320:321-328.

Suzuki, H., Hashimoto, W., and Kumagai, H. 1993. *Escherichia coli* k-12 can utilize an exogenous γ-glutamyl peptide as an amino acid source, for which γ-glutamyltranspeptidase is essential. *J. Bacteriol.* 175:6038-6040.

Takahashi, Y., Oakes, S.M., Williams, M.C., Takahashi, S., Miura, T., and Joyce-Brady, M. 1997. Nitrogen dioxide exposure activates γ-glutamyl transferase gene expression in rat lung. *Toxicol. Appl. Pharmacol.* 143:388-396.

Tian, L., Shi, M.M., and Forman, H.J. 1997. Increased transcription of the regulatory subunit of gamma- glutamylcysteine synthetase in rat lung epithelial L2 cells exposed to oxidative stress or glutathione depletion. *Arch. Biochem. Biophys*. 342:126-133.

Tomonari, A., Nishio, K., Kurokawa, H., Arioka, H., Ishida, T., Fukumoto, H., Fukuoka, K., Nomoto, T., Iwamoto, Y., Heike, Y., Itakura, M., and Saijo, N. 1997a. Identification of *cis*-acting DNA elements of the human γ-glutamylcysteine synthetase heavy subunit gene. *Biochem. Biophys. Res. Commun.* 232:522-527.

Tomonari, A., Nishio, K., Kurokawa, H., Fukumoto, H., Fukuoka, K., Iwamoto, Y., Usuda, J., Suzuki, T., Itakura, M., and Saijo, N. 1997b. Proximal 5′-flanking sequence of the human gamma-glutamylcysteine synthetase heavy subunit gene is involved in cisplatin-induced transcriptional upregulation in a lung cancer cell line SBC-3. *Biochem. Biophys. Res. Commun.* 236:616-621.

Urata, Y., Yamamoto, H., Goto, S., Tsushima, H., Akazawa, S., Yamashita, S., Nagataki, S., and Kondo, T. 1996. Long exposure to high glucose concentration impairs the responsive expression of γ-glutamylcysteine synthetase by interleukin-1beta and tumor necrosis factor-alpha in mouse endothelial cells. *J. Biol. Chem.* 271:15146-15152.

Wallig, M.A., Kore, A.M., Crawshaw, J., and Jeffery, E.H. 1992. Separation of the toxic and glutathione-enhancing effects of the naturally occurring nitrile,cyanohydroxybutene. *Fundam. Appl. Toxicol*. 19:598-606.

Yao, K.S., Godwin, A.K., Johnson, S.W., Ozols, R.F., O'Dwyer, P.J., and Hamilton, T.C. 1995. Evidence for altered regulation of gamma-glutamylcysteine synthetase gene expression among cisplatin-sensitive and cisplatin-resistant human ovarian cancer cell lines. *Cancer Res.* 55:4367-4374.

Contributed by Rui-Ming Liu
University of Alabama at Birmingham
Birmingham, Alabama

Jinah Choi
University of Southern California
Los Angeles, California

Henry J. Forman
University of Alabama at Birmingham
Birmingham, Alabama

Measurement of Glutathione Conjugates

Although conjugation with the nucleophile glutathione can result in products with increased toxicological activity, the vast majority of reactions that generate glutathione conjugates result in products with decreased biologic activity and increased chemical stability. Since the metabolic precursors to glutathione conjugates are generally chemically unstable, systems that efficiently trap such metabolites to form chemically stable glutathione adducts have been utilized to obtain additional structural information on reactive metabolites. There are many instances when a compound is metabolized by the cytochrome P450 monooxygenase system to multiple reactive metabolites. Differences in the cytotoxic and carcinogenic activities of these have been described extensively in the literature (Thakker et al., 1985). Thus, trapping reactive metabolites with glutathione offers a means of separately measuring each of the different precursor metabolites. In practice, these procedures work well when in vitro experimental approaches are used to address questions. When the experimental paradigm involves work conducted in vivo, measurement of mercapturic acids can often be assessed in excreta as a measure of the quantity of glutathione conjugate precursor generated.

The high polarity of glutathione conjugates and their lack of volatility have dictated the use of HPLC-based methods as a primary means of following the formation of such metabolites. Assays that are based on an initial chromatographic step (see Basic Protocol) offer obvious advantages in terms of specificity over either radiometric (see Alternate Protocol 1) or spectrophotometric (see Alternate Protocol 2) assays, but they are more time consuming. Radiometric assays, in which labeled (^{14}C, ^{3}H, or ^{35}S) parent compound is utilized in microsomal incubations (with appropriate glutathione trapping followed by extraction of unreacted parent substrate and analysis of water-soluble glutathione conjugates), offer a rapid and relatively high-throughput approach for measuring the overall rates of conjugate formation. Spectrophotometric assays in which substrates, such as 1-chloro-2,4-dinitrobenzene, that generate a product with an absorbance maximum significantly different from the parent substrate can be used to measure glutathione *S*-transferase activities with simple time-based increases in absorbance. Generally, those substrates utilized in spectrophotometric assays are not particularly reactive and, although these approaches are effective in surveys of enzyme activity, they are not as useful in assays designed for efficient trapping of reactive metabolites generated from cytochrome P450–dependent metabolic activation. Thus, a method based on continuous monitoring of conjugate formation spectrophotometrically is presented here for the purpose of providing a more complete survey of methods available for measuring glutathione conjugates, with the caveat that these approaches are used principally for the assessment of glutathione *S*-transferase activities. Since these protocols are less specific, the primary protocol presented here is based on separation of conjugates from other metabolites by HPLC followed by post-column detection and analysis. Support protocols are provided for reaction conditions (see Support Protocol 1), preparation of cytosolic and microsomal fractions (see Support Protocol 2), preparation of glutathione *S*-transferase (see Support Protocol 3), and preparation of samples for mass spectrometric or NMR analysis (see Support Protocol 4).

MEASUREMENT OF GLUTATHIONE CONJUGATES BY HPLC

BASIC PROTOCOL

Separation and quantitative measurement of glutathione conjugates can be accomplished by using an HPLC system coupled to an appropriate detection system. With the high efficiency columns currently available and with appropriate mobile phases, multiple glutathione conjugates, including those arising as diastereomers, can be measured to assess both regio- and stereoselective formation of aromatic hydrocarbon epoxides.

Contributed by Michael A. Shultz, Dexter Morin, Katherine Watt Chan, and Alan R. Buckpitt
Current Protocols in Toxicology (2002) 6.8.1-6.8.24

HPLC using a reversed-phase column with ion pairing has been used with numerous aromatic/aliphatic hydrocarbon epoxide–derived glutathione conjugates (Hernandez et al., 1980; Armstrong et al., 1981; Steele et al., 1981; Plakunov et al., 1987). Ion-exchange columns have proven effective in the isolation of conjugates derived from dichloroethylene (Dowsley et al., 1995), 4-ipomeanol (Buckpitt and Boyd, 1980), or benzo(a)pyrene (Jernstrom et al., 1982).

The method presented here has been used for the separation of 1-nitronaphthalene glutathione conjugates (Watt et al., 1999) and is similar to the method for naphthalene conjugates (Buckpitt et al., 1987). This method also has been successfully used for separation and analysis of glutathione conjugates derived from epoxides of 2-methylnaphthalene, anthracene, and benzo(a)pyrene (Shultz et al., 2001). The method utilizes reversed-phase HPLC on a Spherisorb C18 ODS 2 column with ion-pairing/ion suppression of the conjugates with triethylamine adjusted to pH 3.1 using phosphoric acid. The method is capable of separating numerous glutathione conjugates derived from attack of glutathione at the C-5, C-6, C-7, or C-8 positions (Fig. 6.8.1). Other end-capped C18 ODS-2 columns are likely to work well with slight modifications of acetonitrile concentrations in the mobile phase. Conjugates can be separated successfully using methods involving simple addition of 1% acetic acid to act as an ion suppressing/ion pairing agent. However, in practice, peak shape is not as symmetrical as with separations utilizing triethylamine/phosphoric acid. The method described here is capable of separating regio- and stereoisomers generated via formation of both the 5,6- and 7,8-epoxides of 1-nitronaphthalene. The use of [^{3}H]glutathione is included for radiochemical detection, and the generation of appropriate quantitative standards. Samples are quantitatively measured by UV detection at 256 nm. The protocol begins with the assumption that metabolites have been generated using microsomal incubations supplemented with glutathione *S*-transferase and glutathione. Refer to Support Protocol 1 for microsomal incubation conditions. Similar approaches can be adapted for incubations using isolated cells, perfused tissues, or recombinant cytochrome P450 monooxygenases.

As mentioned, the above method was developed for detecting 1-nitronaphthalene epoxides through their respective glutathione conjugates. The following is a good starting point for establishing a new protocol for detecting glutathione conjugates from other substrates of interest. The acetonitrile gradient should be optimized to yield appropriate separation of metabolites. Glutathione conjugates that are more and less polar than those generated from 1-nitronaphthalene will require lower and higher concentrations of acetonitrile, respectively, for elution. For example, glutathione conjugates from 1-nitronaphthalene are separated on a 5% to 16% acetonitrile gradient, those from anthracene required a 15% to 22% gradient, and those from benzo(a)pyrene used a 24% to 29% gradient (Watt et al., 1999; Shultz et al., 2001). While the final pH of the mobile phase has an effect on the elution of glutathione conjugates, a pH of 3.1 has been found to be optimal for many of the metabolites isolated in this laboratory. For method development, the authors recommend the use of [^{3}H]glutathione (such as presented here) or radiolabeled substrate (if available) for ease of detection and quantification of the metabolites. If standards are available, UV detection is all that is necessary for quantification of metabolite peaks. Larger quantities of glutathione adducts can be obtained by simple scale-up of the procedures outlined here (see Support Protocol 4) for analysis by mass spectrometry with electrospray ionization (to confirm suspected glutathione conjugates) and proton nuclear magnetic resonance spectroscopy (to identify sites of nucleophilic attack on an aromatic nucleus).

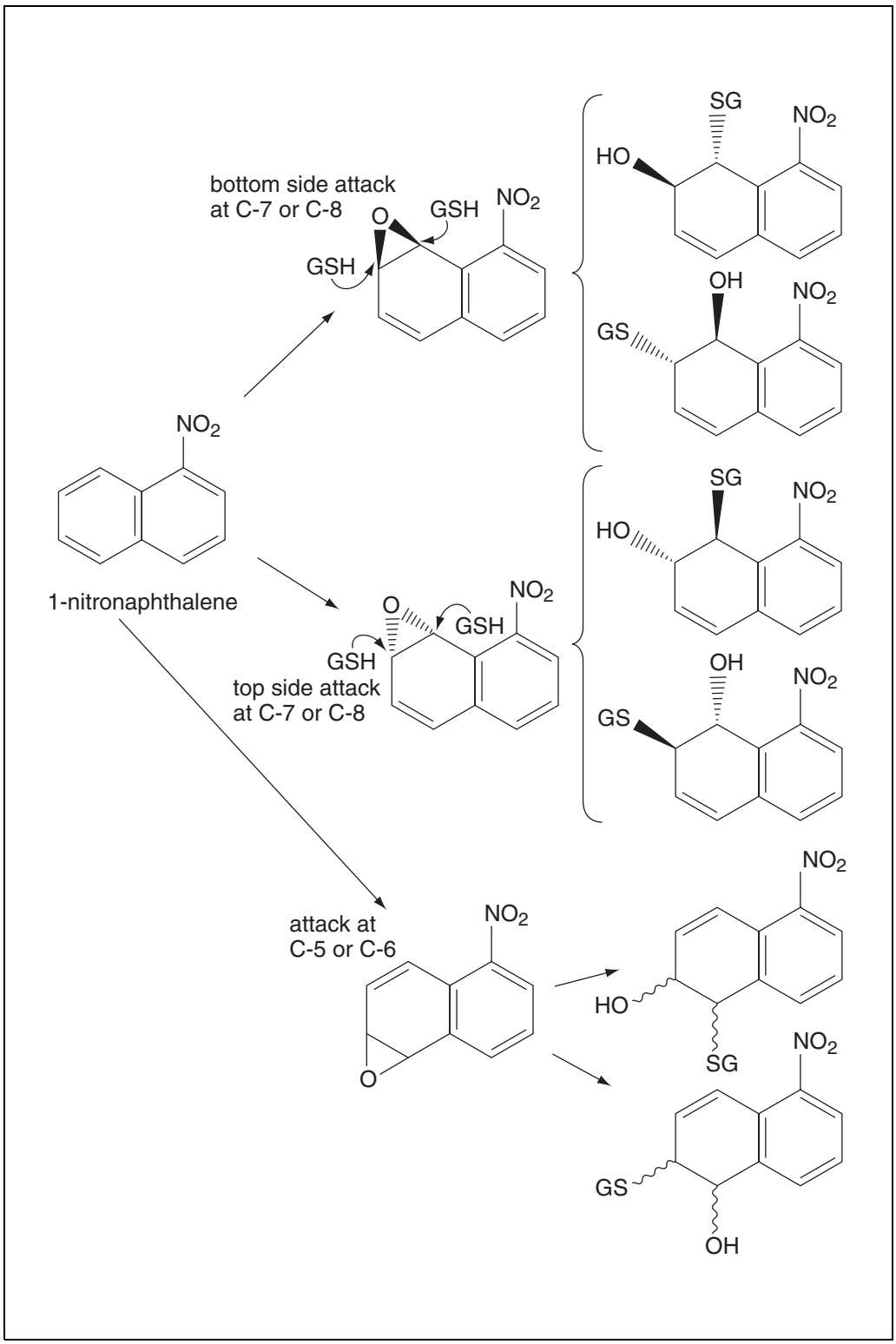

Figure 6.8.1 Diagram showing the metabolic pathways for conversion of 1-nitronaphthalene to glutathione conjugates. Note that stereochemistry is not shown for the bottom pair of products.

Materials

Sample derived from microsomal incubation (see Support Protocol 1)
100% HPLC-grade acetonitrile
Solvent A: 0.06% triethylamine, pH 3.1 (see recipe)
Solvent B: 60% acetonitrile in 0.06% triethylamine (see recipe)
Scintillation cocktail appropriate for aqueous samples

Gradient HPLC:
- 0.46 × 20–cm C18 ODS-2 Spherisorb HPLC column with 5-µm packing material and matching precolumn (Waters) or equivalent
- Injector
- Gradient pump
- UV (variable wavelength or photodiode array preferred)
- Fraction collector (e.g., Gilson model 202)
- Waste collector
- Data collection and storage device (e.g., Millennium integration and control software; Waters)

Scintillation vials

CAUTION: When working with radioactivity, take appropriate precautions to avoid contamination of the experimenter and surroundings. Carry out the experiment and dispose of wastes in an appropriately designated area following the guidelines provided by the local radiation safety officer (also see *APPENDIX 1A*).

CAUTION: The electrophilic metabolites generated for glutathione trapping are generally more toxic than the parent compounds and appropriate precautions should be taken to ensure the safety of investigators. Many of these electrophilic metabolites are potent mutagens/carcinogens and/or cytotoxicants. Appropriate protective clothing, gloves, and bench paper should be used while handling all samples.

Prepare incubated samples for HPLC

1. Vortex vials containing samples derived from microsomal incubation briefly.

   The vial contents may appear cloudy (from the precipitated protein) and may contain crystals (from precipitated buffer).

2. Transfer entire vial contents to microcentrifuge tubes using a Pasteur pipet. Microcentrifuge tubes 30 min at 14,000 rpm, 4°C, to pellet insoluble material.

3. Using a Pasteur pipet, transfer supernatant to a fresh microcentrifuge tube. Be certain to avoid transferring any of the particulate material at the bottom of the microcentrifuge tube.

4. Evaporate the supernatants to dryness in a vacuum evaporator (e.g., SpeedVac).

   CAUTION: *In cases where a volatile radiolabeled or toxic substrate is used, the use of a nitrogen evaporator (as opposed to a vacuum centrifuge) in a chemical hood is advisable. Preextraction of the incubations with a water-immiscible solvent may be advisable to remove volatile substrate and to prevent contamination.*

5. Resuspend each sample in 100 µl water and vortex well for 5 min.

6. Microcentrifuge samples briefly (~10 sec) to consolidate the entire volume.

   At this point, the samples are ready for HPLC injection. Most glutathione conjugates are quite stable. In the authors' hands, glutathione conjugates generated from aromatic hydrocarbon epoxides can be stored in 66:34 methanol/H_2O for months at −20°C without detectable loss.

Set up and equilibrate the HPLC system

7. Set up the HPLC system utilizing a 0.46 × 20–cm C18 ODS-2 Spherisorb HPLC column with 5-µm packing material and matching precolumn, an injector, gradient pump, UV detector, fraction collector, waste collector, and data collection and storage device.

   The authors' laboratory utilizes equipment from Waters/Hewlett Packard with Waters Millennium integration and control software. The fraction collector is a Gilson Model 202. For substrates that are highly fluorescent, detection with a fluorescence detector might offer optimal sensitivity. However, unless the fluorescence characteristics ($\lambda_{ex}/\lambda_{em}$) of the conjugates are known, it would be advisable to establish the HPLC methods with a UV detector. Once methods are established, the fluorescence characteristics of the conjugate(s) can be determined separately.

   In some cases isocratic separations are adequate, but for method development, a solvent delivery system capable of generating solvent gradients saves time and, with some substrates, may be necessary for complete separation of metabolites.

8. Set UV detector to monitor at 256 nm.

9. Rinse the column well with 100% HPLC-grade acetonitrile at a slow flow rate (i.e., 0.5 to 1.0 ml/min) for 15 to 30 min or until the baseline stabilizes.

10. Equilibrate the system in 95% solvent A/5% solvent B until the baseline is stable. Set up the gradient program given in Table 6.8.1.

    Note that all gradient steps assume a linear conversion between steps.

11. Set fraction collector to collect 1-min fractions of the HPLC eluent over the course of the entire gradient. Place the appropriate number of scintillation vials in the racks.

    Once the retention times of the metabolites have been established, collect only over the time at which conjugates elute. Collecting fractions for a shorter time (15 to 30 sec) can be useful for better resolution of peaks.

Inject samples, collect fractions, and count to determine regions of interest

12. Set aside a small aliquot of the sample (1% to 5% injection volume). Inject samples and begin gradient program at 1 ml/min and fraction collection. Allow the gradient program to complete.

13. Count the separate sample aliquot to determine total radioactivity injected onto the column.

    This will be used to calculate recoveries from the chromatographic step.

14. Add 5 ml scintillation cocktail to each scintillation vial. Cap, mix, and place tubes in a scintillation counter. Include a blank (i.e., 1 ml mobile phase in 5 ml cocktail) to measure background levels.

Table 6.8.1 Gradient Program for HPLC

Time (min)	Solvent A (%)	Solvent B (%)
0	95	5
60	84	16
65	0	100
85	0	100
90	95	5
110	95	5

15. Count samples using the appropriate channel for ^{3}H or $^{14}C/^{35}S$ as appropriate for the substrate being used.
16. Plot dpm/fraction versus time to generate a chromatographic profile of the metabolites.
17. Determine recovery of radioactivity.

    All (i.e., 100%) of the radioactivity injected onto the HPLC column should be recovered, although this often varies from 85% to 110% due to errors in counting and in determining an accurate background subtraction. Low recovery is an indication that the gradient is incapable of eluting all the metabolites, and the percentage of organic modifier (acetonitrile) should be increased. Be certain to dispose of all waste as radioactive waste.

Interpret data, prepare standards, and validate quantitative methods

18. Optimize the separation of any ^{3}H-labeled glutathione conjugate metabolites eluting from extracts of incubation no. 1 (see Table 6.8.2), but which are absent from control incubations (nos. 2 or 4) by adjusting acetonitrile concentrations (see Support Protocol 1 for list of incubation conditions).

    If the presumed glutathione conjugates are likely to absorb in the UV region, compare the UV trace of sample no. 1 with that of sample no. 3 (without glutathione). This comparison will be helpful in determining whether there is an "underlying" peak which elutes along with the putative glutathione conjugate.

    The first step in the further development of this methodology is to obtain additional characterization of the conjugate(s). If a photodiode array detector is used, UV_{max} for the conjugates can be determined "on-line." Otherwise, conjugate peaks can be collected for analysis in a scanning spectrophotometer.

    It is best to collect just the center two-thirds of the peak to obtain the most concentrated portion of the sample. Many spectrophotometers are capable of reading small sample volumes (i.e., 50 to 100 μl) and better spectra can be obtained by collecting the most concentrated portions of the eluting peak. These data can be utilized to optimize the wavelength of the HPLC detector. Depending upon the needs of the study, further analysis by mass spectrometry and/or NMR spectroscopy may be desirable (see Support Protocol 4).

    If the putative glutathione conjugates elute in a region where there are no obvious interfering UV peaks, then the time and expense of using radiolabeled substrate, and of collecting and counting fractions to do quantitative determinations of conjugate formation, can be eliminated. This approach requires that the investigator demonstrate that there are no interfering peaks which elute with conjugates. The blank sample (no. 3) can be used to determine this. Basing the quantitative determinations of conjugate formation on areas of peaks detected by UV absorbance will either require synthesis of sufficient quantities of conjugates so that they can be purified and weighed, or the accurate determination of extinction coefficients from UV spectra and scintillation counts of conjugates generated in incubations with known specific activities of radiolabeled substrate (either parent compound or with glutathione). In practice, measuring the UV area under the conjugate peak and the amount of radioactivity in this peak yields UV area/nmol conjugate. If radioactive standards are to be used as a basis for standardization, several standards should be analyzed with each batch of samples.

19. Sum the amount of radioactivity eluting with each conjugate peak minus background. Calculate nanomoles conjugate generated in the incubation:

$$\text{conjugate} = \frac{\text{peak} - \text{background}}{\text{substrate specific activity}}$$

    where radioactivity is expressed in dpm and specific activity is expressed as dpm per nanomole.

    These quantitative measurements assume all samples in a series of incubations include [^{3}H]glutathione.

RADIOMETRIC ASSAY OF GLUTATHIONE CONJUGATE FORMATION

ALTERNATE PROTOCOL 1

This assay depends upon substantial differences in polarity between glutathione conjugates, the parent substrate, and other metabolites. They potentially provide much higher throughput than those described above (see Basic Protocol) and are ideal for substrates generating a single glutathione conjugate or when separate analysis of multiple conjugates is unnecessary. This method is based on a thorough study published by Gill et al. (1983), which describes relatively easy methods for synthesizing radiolabeled *cis*- and *trans*-stilbene oxides. Diols and remaining epoxide can be efficiently extracted into 1-hexanol, while radiolabeled glutathione conjugates remaining in the aqueous phase can be counted. The efficiency of the extraction is very high, resulting in a reproducible assay. This method depends on the purchase or preparation of synthetic radiolabeled substrate as well as good partitioning of parent compound and metabolites other than the glutathione conjugates into 1-hexanol.

Materials

1-Hexanol
Glass culture tube with Teflon-lined screw cap (for volatile substrates)
Scintillation fluid
Scintillation vials

Additional reagents and equipment for microsomal or cytosolic incubations (see Support Protocol 1)

CAUTION: Radiolabeled probes are hazardous; see *APPENDIX 1A* for guidelines on handling, storage, and disposal.

1. Conduct microsomal or cytosolic incubations directly in extraction tubes (see Support Protocol 1). Use glass culture tubes with Teflon-lined screw caps if the substrate is volatile.

   The amount of radiolabeled substrate used depends on its turnover to glutathione conjugate. If the efficiency of extraction is high, the generation of 500 dpm glutathione conjugate should be sufficient for accurate quantitation using reasonable counting times (10 to 20 min).

   Be certain to include control incubations, which contain all reagents except glutathione. This validates that the extraction procedure removes all residual radioactivity from the incubations except glutathione conjugates. The amounts of radioactivity in these control incubations should be >100 dpm.

2. Following the appropriate time of incubation, add 500 µl of 1-hexanol.

   All volumes in the protocol assume that the volume of the incubation was 250 µl.

   The time of incubation depends upon the stability of the intermediate substrate and the rates of substrate metabolism. Optimal times will need to be established experimentally. For many studies, linearity with time and protein content will need to be determined prior to the use of the assay method for quantitative determinations.

3. Vortex tubes vigorously for 2 min. Centrifuge samples 3 min at 200 × *g*, room temperature, to separate the layers. Discard the top (hexanol) layer as radioactive waste.

4. Add another 500-µl aliquot of hexanol. Repeat step 3.

5. Discard the hexanol layer. Determine radioactivity of the aqueous layer by transferring 150 to 200 µl to a scintillation vial containing 5 ml scintillation fluid and counting in a liquid scintillation counter.

   Remove the aliquot of aqueous phase carefully since inclusion of any precipitate in the counted sample could lead to artifactually high values associated with radiolabel bound covalently to protein.

6. The nanomoles of glutathione conjugate generated during the incubation can be calculated by:

$$\text{conjugate} = \frac{\text{peak} - \text{background}}{\text{substrate specific activity}} \times \frac{\text{incubation vol.}}{\text{vol. counted}}$$

where radioactivity is expressed in dpm, substrate specific activity is expressed as dpm per nanomole, and volumes are expressed in microliters.

ALTERNATE PROTOCOL 2

SPECTROPHOTOMETRIC ASSAY FOR GLUTATHIONE *S*-TRANSERASES

One of the earliest reported and still one of the most useful assays for glutathione *S*-transferase activity depends upon monitoring the formation of glutathione conjugates of 1-chloro-2,4-dinitrobenzene (CDNB) spectrophotometrically at 340 nm. This is a popular assay for glutathione *S*-transferase activity because CDNB is a reasonably good substrate for most of the glutathione *S*-transferase isoforms. In addition to CDNB, there are other substrates that, after conjugation with glutathione, generate products with absorption spectra significantly different from that of the parent compound. Continuous monitoring of product formation in the UV or visible region provides the basis for measurement of glutathione conjugate formation. These assays can be conducted with moderate throughput on standard spectrophotometers with kinetics assemblies. The assays are readily adapted for use with microtiter plate readers with a corresponding increase in throughput. These assays are likely to be less useful in monitoring the formation of electrophilic metabolites generated during cytochrome P450–dependent metabolic activation. The protocol presented here is based on the original publication by Habig et al. (1974). In theory, these approaches could be applied to any substrate where the glutathione conjugate has a wavelength maximum which differs from that of the parent substrate. Conjugate standards are necessary for the calculation of extinction coefficients.

Materials

0.1 M sodium phosphate buffer, pH 6.5 (*APPENDIX 2A*)
3.3 mM glutathione (see recipe)
33 mM CDNB (see recipe)
Enzyme preparation (e.g., cytosol; see Support Protocol 2)
VIS spectrophotometer (e.g., Beckman DU-70) with thermostatting device

1. Turn on the spectrophotometer and allow to stabilize 15 min prior to use. Set wavelength to 340 nm in kinetics mode (if kinetics assembly is used) and thermostatting device (i.e., cuvette temperature) at 25°C.

   The specifics of this assay depend upon the type of equipment used. In the authors' laboratory, a single-beam spectrophotometer (Beckman DU-70) with a kinetics assembly is used.

Prepare blanks

2. Add 940 µl of 0.1 M phosphate buffer, pH 6.5, to a 1-ml cuvette.
3. Add 30 µl of 3.3 mM glutathione and mix contents well.
4. Add 30 µl of 33 mM CDNB, mix contents well, place cuvette in holder, rezero the instrument and record baseline for 3 min. Run a fresh blank with each set of 4 to 6 samples.

   This is the rate of nonenzymatic reaction and must be subtracted from the rate of enzymatic reaction.

Prepare and analyze samples

5. Prepare a total of four cuvettes each containing 930 to 935 µl phosphate buffer, 30 µl glutathione, and 30 µl CDNB.

   The total volume in each cuvette should be 1 ml after addition of enzyme preparation.

6. Add 5 µl buffer to the first cuvette (blank) and 5 to 10 µl enzyme preparation (e.g., cytosol) to cuvettes 2 to 4 and record increase in absorbance for 2 to 3 min.

   The change in absorbance should not exceed 0.1 AU/min. If it does, repeat the assay using less of the enzyme preparation. Significant dilution will result in lower than expected values. Work at the highest concentrations possible which still allow accurate sample pipetting.

Analyze data

7. Calculate the net increase in absorbance (i.e., enzyme − blank) per minute.

$$\frac{\left(\dfrac{\text{change in absorbance/min (sample)} - \text{change in absorbance/min (blank)}}{\text{volume of protein assayed}}\right)}{\left(\dfrac{9.6}{\text{total volume in cuvette}}\right)}$$

   where all volumes are expressed in milliliters.

   The extinction coefficient of the glutathione conjugate of 1-chloro-2,4-dinitrobenzene is 9600 $M^{-1}cm^{-1}$. One CDNB unit is defined as 1 µmol product formed per min.

MICROSOMAL INCUBATIONS

SUPPORT PROTOCOL 1

This protocol generates glutathione conjugates from substrates of interest which are metabolized to electrophilic derivatives capable of forming glutathione conjugates. The incubations are relatively straightforward and, in many cases, are capable of generating sufficiently large amounts of glutathione conjugate to be easily measured quantitatively. In addition, the extracts obtained from microsomal incubations tend to be less complex than materials obtained from perfused tissue experiments or from matrices such as urine or bile, making the separation and analysis easier.

Materials

Microsomes from tissue of interest (0.5 to 5 mg microsomal protein/ml; see Support Protocol 2) or recombinant cytochrome P450/P450 reductase
0.5 mM 5000 dpm/nmole [^{3}H]glutathione (see recipe)
50 to 100 CDNB U/ml glutathione *S*-transferases (see Support Protocol 3)
1 M $MgCl_2$
12.5 mM NADPH or NADPH regeneration system (see recipes)
0.1 M sodium phosphate buffer, pH 7.4 (*APPENDIX 2A*)
50 mM 1-nitronapthalene (see recipe)
Methanol, ice cold
1-ml glass vials with caps
37°C shaking water bath

Table 6.8.2 Basic Components of Incubations to Isolate Glutathione Conjugates[a,b]

Incubation no.	Label	5 mg/ml microsomes	0.5 mM [^{3}H]glutathione	50 U/ml glutathione *S*-transferase	NADPH regenerating system	1 M $MgCl_2$	50 mM 1-nitronaphthalene	0.1 M phosphate buffer, pH 7.4	Total volume
1	Complete	100	50	50	20	2.5	2.5	25	250
2	No nitronaphthalene	100	50	50	20	2.5	0	27.5	250
3	No glutathione	100	0	50	20	2.5	2.5	75	250
4	No NADPH regenerating system	100	50	50	0	2.5	2.5	45	250

[a] All volumes are given in microliters.

[b] All concentrations in the table refer to concentrations of the substance to be added. The final concentrations of various incubation components are specified earlier.

Perform incubations

1. Add the following components given in Table 6.8.2 to appropriate 1-ml glass vials:

   1 to 2 mg/ml microsomes (final)
   0.5 mM 5000 dpm/nmole [^{3}H]glutathione (0.1 mM final)
   50 to 100 CDNB U/ml glutathione *S*-transferase (10 U/ml final)
   1 M $MgCl_2$ (10 mM final)
   12.5 mM NADPH (1 mM final) or NADPH regeneration system (5.7 mM glucose-6-phosphate, 0.21 mM NADP, and 0.3 U/ml glucose-6-phosphate dehydrogenase final)

   Bring final volume to 250 µl with 0.1 M sodium phosphate buffer, pH 7.4.

   The final concentration of microsomes should not exceed 2 mg/ml.

   It is recommended that a "guide sheet" (e.g., Table 6.8.2) be used, outlining the addition of specific volumes of the necessary components. In studies where numerous incubations contain the same concentrations of glutathione, glutathione S-transferase, and other reagents, the use of master mixes containing all of the components is recommended to simplify and normalize the procedure. This approach is especially useful when conducting kinetic studies.

   All incubation components must be kept on ice at all times. It is advisable to precool the incubation vials on ice before adding any incubation components.

2. Gently swirl each vial to thoroughly mix the components and place on ice.

3. On ice, add 2.5 µl of 50 mM 1-nitronaphthalene (0.5 mM final). Cap each tube immediately, keeping them on ice until all tubes are capped.

   CAUTION: *Perform this step in a chemical hood to avoid any exposure to 1-nitronaphthalene, which is somewhat volatile. Keeping everything on ice minimizes the loss of substrate through volatilization. Organic solvents used to dissolve substrates should constitute no more than 1% of the total incubation volume.*

4. Place tubes in a rack, transfer to a 37°C shaking water bath, and incubate 5 to 30 min.

   For kinetic studies (determination of Michaelis constants), linearity with time and protein concentration must be established and all incubations must be conducted within the linear portions of the time and protein curves.

5. Transfer vials (in the same rack) to a slurry of ice-water at the end of the incubation.

   Keep all vials in the rack together to minimize differences in incubation time. Cool vials for 1 min to allow any volatilized 1-nitronaphthalene to condense into the aqueous phase. Uncap vials in a chemical fume hood to avoid exposure to any volatilized 1-nitronaphthalene.

6. Add twice the incubation volume (500 µl) of ice-cold methanol to each vial to completely quench the reaction.

7. Recap and place vials at –20°C overnight (minimum ≥1 hr) to precipitate the protein before continuing with sample analysis.

PREPARATION OF MICROSOMAL AND CYTOSOLIC FRACTIONS

SUPPORT PROTOCOL 2

This protocol provides the enzymes necessary to conduct the incubations to generate glutathione conjugates. There are many variations in the preparation of microsomal and cytosolic fractions and each procedure generates fractions which are capable of working well to generate glutathione conjugates from appropriate substrates.

Materials

Mouse livers
Homogenization buffer (see recipe)
0.1 M sodium phosphate buffer, pH 7.4 (*APPENDIX 2A*)

Motor-driven Potter-Elvehjem Teflon-glass homogenizers
Refrigerated ultracentrifuge (capable of 100,000 × *g*) and appropriate tubes
Cotton-tipped applicator
Hand-held glass-glass homogenizer

Additional reagents and equipment for Bradford assay of protein concentration (*APPENDIX 3G*)

CAUTION: Glass homogenizers should be placed in an ice bucket and held at the top of the vessel only. The high rotating force created during the homogenization processes can occasionally cause the homogenization vessels to shatter, resulting in a significant hazard to the operator. The use of puncture resistant gloves is strongly recommended.

CAUTION: Samples for the ultracentrifuge must be balanced within 100 mg. All rotor gaskets and the speed disk should be checked prior to use of the ultracentrifuge.

NOTE: The following procedures should be conducted at 0° to 4°C.

1. To mouse livers, add four volumes homogenization buffer per gram wet weight and homogenize using a motor-driven Potter-Elvehjem Teflon-glass homogenizer.

   The authors use 5 to 6 complete passes of the homogenizer.

2. Centrifuge homogenate 30 min at 9,000 × *g*, 2°C. Transfer the supernatant containing the cytosolic and microsomal fractions to ultracentrifuge tubes, avoiding the fat layer at the top of the tube and the fluffy layer near the interface of the cytosol with the pellet. Balance the sample tubes to within 100 mg.
3. Ultracentrifuge the supernatant 60 min at 100,000 × *g*, 2°C. Remove the supernatant, avoiding any remaining fat layer.

   The supernatant fraction can be used to partially purify glutathione S-transferases (see Support Protocol 3) or can be used directly as a source of cytosol for measurement of cytosolic glutathione transferase activities.

4. Wipe the sides of the tube with a cotton-tipped applicator to remove any remaining fat. Resuspend the pellet in homogenization buffer to approximately half the original volume. Homogenize using hand-held glass-glass homogenizer by hand, avoiding any aeration of the sample. Centrifuge the resuspended samples 60 min at 100,000 × *g*, 2°C.
5. Discard the supernatant and resuspend the pellet in 0.1 M phosphate buffer, pH 7.4, at a volume likely to provide protein concentrations ≥5 mg/ml.

   This can be calculated based on the expected yield of microsomal protein (e.g., 10 to 15 mg microsomal protein/g liver, 2 to 3 mg microsomal protein/g lung).

6. Determine protein content using the Bradford Coomassie Blue dye binding procedure (*APPENDIX 3G*).

SUPPORT PROTOCOL 3

PURIFICATION OF GLUTATHIONE *S*-TRANSFERASES

The procedures described in this support protocol are intended to provide an extract which is highly enriched in glutathione S-transferases, and are based on the method of Simmons and Vander Jagt (1977). Essentially this is a two step procedure (removal of glutathione, followed by affinity chromatography of glutathione-free cytosol), which is designed to

recover a fraction highly enriched in glutathione S-transferases. This preparation provides transferases at relatively high specific activity for use in incubations to generate glutathione conjugates.

Materials

175- to 520-µm coarse Sephadex G-25 resin
Resuspension buffer (see recipe) with and without 0.5 M NaCl
Sample (100,000 × *g* supernatant; see Support Protocol 2, step 3)
Glutathione affinity resin—i.e., glutathione-agarose (Sigma) or equivalent
Glutathione elution buffer (see recipe)
0.1 M sodium phosphate buffer, pH 7.4 (*APPENDIX 2A*)

Glass columns
Buffer resevoir
Column monitor (e.g., ISCO UA5; optional)
Amicon PM-10 membrane ultraconcentrator (10,000 MWCO) or equivalent
12,000- to 14,000-MWCO dialysis membrane

Perform Sephadex G-25 chromatography

1. Preswell 175- to 520-µm coarse Sephadex G-25 resin in resuspension buffer according to the manufacturer's instructions. Pour a bed volume at least three times the sample volume into a glass column, taking care to pour all of the resin at one time and excluding bubbles.

   The authors use a 2.5 × 70–cm column. This column has a 350-ml bed volume, which allows 100 ml cytosol to be applied.

   When not in use, store the column at 4°C in buffer with 0.05% (w/v) sodium azide to prevent bacterial contamination.

2. Equilibrate the column with 5 vol fresh resuspension buffer.

3. Apply sample to the column being careful not to disrupt the top of the resin bed. As the last of the sample enters the resin bed, add fresh resuspension buffer, again being careful not to disturb the resin bed. Then attach a buffer reservoir to the column.

   For the size stated, flow rates are 10 to 15 ml/min. Do not allow the column to go dry.

4a. *For column monitor:* Elute with resuspension buffer. Collect all of the initial peak until the absorbance at 280 nm begins to show a second peak (i.e., void volume).

   The column monitor can be run at its lowest sensitivity.

4b. *For manual isolation:* Elute with resuspension buffer. Collect all of the red-colored fractions (i.e., void volume).

   The void volume is marked by intensely red-colored proteins.

   Glutathione is retained at least two void volumes behind the initial proteins.

   This step is intended to remove glutathione from the supernatant which is isolated by ultracentrifugation of homogenized mouse liver (see Support Protocol 2).

Perform glutathione-affinity chromatography

5. Pour a chromatography column using glutathione-affinity resin and an appropriate glass column.

   The affinity resin is a glutathione agarose matrix where glutathione is attached through the sulfur. The column should contain a minimum of 1 ml resin for every 200 U glutathione S-transferase (based on CDNB activity) to be bound.

6. Equilibrate this column with 5 bed volumes resuspension buffer with freshly added DTT.
7. For a 50-ml bed volume (2.5-cm diameter column), apply eluent from the Sephadex column (step 4a or b) at a flow rate of ~1 ml/min.

   Gravity feed is recommended because the resin is soft and is easily compacted if pressurized.
8. After applying all of the supernatant, wash the column with at least five column volumes of resuspension buffer followed by five column volumes of resuspension buffer containing 0.5 M NaCl.

   If a column monitor is used, wash the column until absorbance at 280 nm returns to baseline.
9. Elute the glutathione *S*-transferases from the affinity column with glutathione elution buffer.

   Elution using two column volumes is optimal. Using less results in lower yields of transferase, while more will result in dilute enzyme which must be concentrated further on an Amicon concentrator. Thus, for a 50-ml column use 100 ml elution buffer.

10a. *For column monitor:* Collect from first baseline change to one column volume. Collect a second column volume separately.

   75% of the total glutathione S-transferase protein will come off in the first column volume and 25% will be in the second volume.

   For maximal concentration of eluted glutathione S-transferase use a column monitor.

10b. *For manual isolation:* If no column monitor is used, simply collect the first and second column volumes separately.

Concentrate and dialyze

11. Once the semipurified preparation of glutathione *S*-transferases has been collected from the column, concentrate if necessary using an Amicon PM10 membrane ultraconcentrator (10,000-MWCO) according to manufacturer's instructions. Dialyze concentrate at 4°C in 12,000- to 14,000-MWCO dialysis membrane against two changes of at least 20 vol of 0.1 M sodium phosphate buffer, pH 7.4, as soon as possible.

    Do not allow enzyme to remain at pH 9.0 overnight as significant losses of enzymatic activity will result. Do not allow the sample to concentrate to dryness as significant losses of glutathione S-transferases will result.
12. Measure glutathione *S*-transferase activity in the samples after dialysis and concentration (see Alternate Protocol 2).

    Aliquots of this preparation can be stored at −80°C for up to six months in phosphate buffer. Check enzymatic activities prior to use.

    Do not repeatedly freeze/thaw aliquots. An activity loss of ~50% will occur after a second freeze/thaw cycle.

SUPPORT PROTOCOL 4

PREPARATIVE SEPARATION AND ISOLATION OF GLUTATHIONE CONJUGATES FOR CHARACTERIZATION BY MASS SPECTROMETRY AND PROTON NMR SPECTROSCOPY

One of the advantages of establishing methodology capable of measuring individual glutathione conjugates by HPLC is that these methods can be used to isolate sufficient quantities of conjugate for further characterization by mass spectrometry and proton NMR spectroscopy. The availability of semipreparative HPLC columns coupled with enhancements in instrument sensitivity available for both mass spectrometry and proton NMR

spectroscopy has considerably decreased the amount of effort required to assign structures to the metabolites isolated. In some cases, metabolites are derived from enantiomeric epoxides and the precise structural assignments (R versus S carbon configuration) depends upon the synthesis of epoxide enantiomers. However, the regiochemistry of glutathione conjugates can be determined by appropriate NMR techniques.

There are two options for generating sufficient quantities of reactive metabolites to prepare glutathione conjugates for spectral characterization and for standards. Many reactive metabolites such as those from acetaminophen (*N*-acetyl-*p*-benzoquionone imine; Dahlin and Nelson, 1982), aflatoxin B_1 (the 8,9-epoxide; Raney et al., 1992), and naphthalene (the 1,2-epoxide; van Bladeren et al., 1984) can be synthesized. For those which are difficult to synthesize, sufficient quantities of glutathione conjugates can be obtained for spectral characterization and to serve as standards from large microsomal incubations (1 to 2 liters) by scaling up the procedures described (see Support Protocols 1 and 2).

Materials

Substrate
Methanol, ice cold
SM-16 resin (macroporous polystyrene divinyl benzene; BioRad) or equivalent
Methanol, HPLC grade
1% acetic acid or equivalent (e.g., 0.5% formic acid, 0.05% trifluoroacetic acid)
50% glacial acetic acid or equivalent (e.g., 50% concentrated formic acid, trifluoroacetic acid)
75% acetonitrile
12.4 M pyridine (99%)

Rotary evaporator and flask or large-volume centrifugal evaporator
Disposable low-pressure column
Teflon or silanized-glass containers (optional)
HPLC system:
- Semipreparative 8- to 30-mm-diameter column packed with material identical to that used in the analytical separation (see Basic Protocol)
- Gradient HPLC pump capable of delivering flow rates that vary from 5 to 40 ml/min

Lyophilizer

Additional reagents and equipment for sample preparation (see Support Protocol 1, steps 1 to 5)

Incubation and initial sample preparation

1. Incubate substrate with microsomes, glutathione *S*-transferases, and glutathione using proportionally larger quantities of starting material as described (see Support Protocol 1, steps 1 to 5).

   Once the analytical conditions have been established, the use of [^{3}H]glutathione is unnecessary; many core spectroscopy facilities will not allow radioisotopes in their facilities.

2. Stop the reaction with 2 vol ice-cold methanol and allow mixture to stand overnight at −20°C.

3. Centrifuge the reaction mixture 30 min at 5,000 × *g*, room temperature, to remove precipitated protein and salts.

4. Transfer the supernatant to a rotary evaporator flask and evaporate solvent under reduced pressure. Alternatively, use a large-volume centrifugal evaporator.

Partial purification of large samples

5. Prepare a disposable low-pressure solid-phase extraction column filled with either a C18 or a styrene-divinylbenzene-based resin (i.e., SM-16).

   The bed volume will depend upon the amount of material being bound and the binding characteristics of the resin used. If an estimate of column volume is necessary, overestimate, as the resin is reusable.

6. Rinse the solid-phase extraction column with ten column volumes of HPLC-grade methanol followed by ten column volumes of 1% acetic acid (0.5% formic or 0.05% trifluoroacetic acid).

7. Redissolve the evaporated residue from step 4 in 2% acetic acid and check the pH. Use a solution of 50% glacial acid to adjust the pH to 2.5 to 3.5.

   Note that 1% formic or 0.5% trifluoroacetic acid can be used to dissolve the evaporated sample. The pH would then be adjusted with 50% concentrated formic or trifluoroacetic acid, respectively.

8. Apply sample to the column, allowing the entire sample to wash onto the bed. Rinse with ten column volumes of 1% acetic acid (0.5% formic or trifluoroacetic acid). Discard the initial charge solution and washes.

9. Elute column with 75% acetonitrile and collect the eluate containing the glutathione conjugate(s) of interest.

   From this step on, the use of Teflon or silanized glass containers is highly recommended. If glass containers are used, they must be silanized with chlorotrimethylsilane prior to use. Significant losses will occur with standard glass surfaces. Most plasticware contains plasticizers (phthalate) which interfere with mass spectral and NMR analysis.

10. *Optional:* If the conjugate is acid labile, adjust the pH of the column eluate to neutrality with 12.4 M pyridine. Lyophilize the water/acetonitrile (pyridine) extract to dryness and reconstitute the sample in water.

    Pyridine acetate is volatile and can therefore be removed by lyophilization.

Perform final purification of samples

11. Purify conjugates by HPLC using a semipreparative 8- to 30-mm-diameter HPLC column packed with material identical to that used in the analytical separation.

    The retention times should be similar to the Basic Protocol if proportional column flows are used. The pattern of peak elution should stay the same. If possible, add a small amount of extract prepared with radioactive conjugates (prepared in Support Protocol 1) to the unlabeled sample and run these together to verify peak retention times and patterns. This only needs to be done once to determine the exact elution profile.

    Flow rate depends on the internal diameter of the column. As the internal diameter of a column doubles, the flow rate should be increased 3- to 4-fold.

    Unless the conjugates are known to be stable indefinitely at room temperature, it is best to collect samples on ice and keep them cold throughout the preparation.

    Volumes of column eluate collected will be much greater during preparative chromatography. For example, a 1-min fraction on the analytical system will have a volume of 1 ml; on the 22.5-mm diameter semipreparative system each 1-min fraction is 11.5 ml. Radioactivity can be quantitated by counting a portion of each fraction (i.e., 1 ml). This requires that more radioactivity be injected into the column or, alternatively, that shorter time intervals be used to collect fractions (such as 0.1 min). Supplies can be conserved by collecting only during those times when conjugates are eluting from the column.

12. To prepare the samples for spectroscopic analysis, lyophilize the samples to dryness and repeat steps 5 to 10.

    a. In step 8, be certain to rinse the solid-phase extraction column with 20 column volumes of equilibration solution (e.g., 1% acetic, 0.5% formic, or 0.05% trifluoracetic acid) to wash all of the triethylamine phosphate through the column.

       Each sample (peak) collected from the HPLC has triethylamine phosphate buffer in it which is incompatible with mass spectrometry and NMR spectroscopy.

    b. Elute and neutralize the sample as described in step 10.

       If very small amounts of conjugates are being purified, a C18 analytical column washed and prepared as described in step 6 can be used in place of the solid-phase extraction column. Monitoring the column eluate with a UV absorbance detector makes it easier to determine when to collect the eluate.

    c. Lyophilize samples extensively as described in step 10 to remove all volatile salts and water, being careful to exclude water vapor when venting the lyophilizer if NMR identification is required.

REAGENTS AND SOLUTIONS

*Use Milli-Q-purified water or equivalent for all recipes and protocol steps. For common stock solutions, see **APPENDIX 2A**; for suppliers, see **SUPPLIERS APPENDIX**.*

Acetonitrile, 60% in 0.06% triethylamine

Combine 600 ml 0.06% triethylamine, pH 3.1 (see recipe) with 400 ml HPLC-grade acetonitrile containing 0.06% triethylamine. Store unfiltered solution up to 5 days at 4°C. Filter through a 0.45-um filter just before use.

CDNB, 33 mM

Dissolve 6.75 mg recrystallized 1-chloro-2,4-dinitrobenzene (CDNB) in 1 ml of 100% ethanol. Store up to 1 month at −20°C in an airtight container in the dark.

This reagent is used at a final concentration of 1 mM for spectrophotometric measurement of glutathione conjugate formation.

[^{3}H]Glutathione, 0.5 mM

After receipt of a batch of 20- to 50-Ci/mmole [^{3}H]glutathione (New England Nuclear Life Science Products; Perkin Elmer), place 5- to 20-µCi aliquots in separate tubes under argon at −80°C to avoid repetitive freeze/thaw cycles.

Just prior to use, dissolve 7.6 mg glutathione in 5 ml of 0.1 M sodium phosphate buffer, pH 8.5 (*APPENDIX 2A*). Add 50 µl of this stock glutathione solution to a clean vial. Add 3 µl freshly thawed [^{3}H]glutathione to the vial and bring the solution to 500 µl with 0.1 M sodium phosphate buffer, pH 7.4. Count at least two separate 2- to 5-µl aliquots to determine the exact specific activity. The remainder should be sufficient for eight microsomal incubations at 0.1 mM, assuming an addition of 50 µl and a total reaction volume of 250 µl.

Since these steps form the basis for creating standards for the assays, they must be performed carefully.

Glutathione is readily oxidized, especially at basic pH, and the ^{3}H-labeled material is unstable.

Calculations here assume a starting specific activity of 20 Ci/mmole.

Glutathione, 3.3 mM

Dissolve 101.1 mg glutathione in 10 ml sodium phosphate buffer, pH 8.5 (*APPENDIX 2A*). Prepare just prior to use and keep cold (i.e., 4°C).

Glutathione elution buffer

Just prior to use (i.e., 1 hr or less), dissolve 0.24 g Tris base and 2.92 g NaCl in 90 ml water. Cool the solution to 4°C and add 0.76 g glutathione (50 mM final). After glutathione is dissolved, adjust the pH of the solution to 9.0 with 1 N NaOH and bring the total volume to 100 ml. Keep cold (i.e., 4°C) until use since glutathione is easily oxidized at basic pH.

Sparging the solution with He or N_2 will minimize dissolved oxygen levels and consequent disulfide formation.

Homogenization buffer

Dissolve 2.4 g Tris base and 11.5 g KCl in 800 ml water. Add 336 mg disodium EDTA. Cool to 4°C and adjust the pH to 7.4 with 6 M HCl. Adjust volume to 1 liter. Store up to 1 month at 4°C. Just prior to use add 154 mg DTT.

Final concentrations are 20 mM Tris, 1.15% KCl, 1 mM DTT, and 1 mM EDTA.

Note that the pH of Tris buffers differs substantially with temperature (dpH/dt = –0.028/1°C; also see APPENDIX 2A)

NADPH, 12.5 mM

Prepare a solution of 10.4 mg tetrasodium NADPH in 1 ml of 0.1 M sodium phosphate buffer, pH 7.4 (*APPENDIX 2A*). Prepare fresh just prior to use.

Addition of 20 μl of this solution to an incubation with a total volume of 250 μl provides a concentration of 1 mM NADPH in the incubation.

NADPH regeneration system

Dissolve 20 mg NADP and 50 mg glucose 6-phosphate in 1.0 ml of 0.1 M sodium phosphate buffer, pH 8.5 (*APPENDIX 2A*). Add 12.5 U glucose-6-phosphate dehydrogenase. Maintain protected from light at 4°C until use.

Regeneration system is only stable for ~1 hr after the addition of the dehydrogenase.

1-Nitronaphthalene, 50 mM

Dissolve 8.6 mg 1-nitronaphthalene in 1 ml methanol. Store 1 month at –20°C.

Use 2.5 μl per 250 μl incubation. The final concentration in the incubation is 0.5 mM.

Resuspension buffer

Dissolve 6.07 grams Tris base in 800 ml water. Add 372 mg disodium EDTA and cool the solution to 4°C. Adjust the pH to 7.0 using 6 N HCl and the volume to 1 liter with water. Store this solution up to 1 month at 4°C. Just prior to use add 154 mg DTT.

Triethylamine, 0.06%, pH 3.1

Add 0.6 ml HPLC-grade triethylamine to 800 ml water. Adjust the pH to 3.1 using HPLC-grade phosphoric acid. Bring volume to 1 liter with water. Store up to 1 week at 4°C. Filter through a 0.45-μm filter before use.

In some HPLC systems, which use low pressure mixing, it will be essential to sparge the mobile phase with helium prior to and during use.

COMMENTARY

Background Information

Although conjugation with glutathione occasionally results in derivatives with greater toxicologic activity (van Bladeren, 2000), the vast majority of reactions involving conjugation with glutathione result in detoxification of a wide variety of electrophilic chemicals, many of which are derived from cytochrome P450–mediated metabolism. Numerous studies have demonstrated that the balance between activation and glutathione-dependent detoxification reactions is a critical determinant in the sub-

sequent pathologic outcome of exposure to these toxicants. Accordingly, the advent of techniques for monitoring the formation of glutathione conjugates has provided important insights regarding: (1) the chemical nature of reactive metabolites generated, (2) the roles of various cytochrome P450s involved in the metabolic activation of the parent substrate, (3) the importance of various glutathione *S*-transferase isoforms in regio- and enantioselective metabolism of epoxides, and (4) the influence of other modifying factors on the overall balance between activation and detoxification reactions. In addition, the ability to monitor glutathione conjugation reactions with high sensitivity has given rise to assays capable of functionally analyzing those enzymes responsible for the activation and detoxification of drugs/environmental toxicants in well-defined subcompartments and in cells of heterogeneous tissues such as the nose, lung, kidney, and GI tract.

Three different approaches have been presented here that are capable of measuring the rates of glutathione conjugate formation. Separation and quantitative measurement of conjugates by HPLC constitutes one of the most widely used techniques for assessing the rates of reactive metabolite formation. This approach has several advantages. The sensitivity of the method depends upon the extinction coefficient of the conjugate or the specific activity of the starting substrate if radiolabeled material is utilized in the incubations. Regardless, many of these methods are sufficiently sensitive to permit the measurement of conjugates formed in microgram to low milligram tissue samples or microgram amounts of microsomal protein. This allows comparisons of glutathione conjugate formation to be conducted with target and nontarget cells in heterogeneous tissues. Moreover, these assays allow for distinction of the glutathione derived versus other metabolites. Although this is not an issue in microsomal incubations with substrates like acetaminophen that forms a single glutathione adduct (Hinson et al., 1982), this can be an important consideration if the rates of acetaminophen metabolism are being assessed in tissue slices, isolated cells, or perfused tissues because of the generation of sulfate and glucuronides in addition to the thioether metabolites. Another example is work conducted on the pulmonary metabolism of dichloroethylene where three primary metabolites are generated during microsomal incubations with dichloroethylene. Two glutathione conjugates are derived from dichloroethylene epoxide and one from an acetal which arises via metabolism of the parent compound to the dichloroacetaldehyde (Dowsley et al., 1995, 1996, 1999). Since the epoxide is the metabolite presumed to mediate the toxicity of dichloroethylene, only methods capable of distinguishing the epoxide-derived versus aldehyde-derived metabolites are useful in studies of cross-species comparisons of metabolic activity. In cases where multiple reactive metabolites are generated, glutathione conjugates derived from these metabolites, in many cases, can be separated providing the ability to examine species, cell, and tissue differences in the rates of formation of the conjugates. For example, studies on the microsomal metabolism of 1-nitronaphthalene demonstrated that pulmonary P450 monooxygenases metabolize 1-nitronaphthalene primarily to the glutathione conjugates derived from the 7,8-epoxide in both the rat and mouse, whereas the 5,6-epoxide is the predominant metabolite generated in hepatic microsomal incubations (Watt et al., 1999; Watt and Buckpitt, 2000). Similarly, the ability to separate diastereomeric glutathione conjugates has been critical to the assessments of the enantioselectivity of the glutathione *S*-transferases. An elegant example where the ability to monitor conjugation at both benzylic and allylic sites of a number of *syn*- and *anti*-diol epoxides of polycyclic aromatic hydrocarbons has been presented by Sundberg and colleagues (1997). The results show that conjugation of the R-configured benzylic carbon is strongly favored with all of the anti-diol epoxides, a result that is highly consistent with models of the A site of the glutathione *S*-transferase isoforms used in these studies.

When the study is designed to survey the activities of conjugate-generating enzymes in a particular species, cell, or tissue rather than to understand the precise chemical nature of reactive metabolites generated or the regio/stereoselectivity of conjugation, the latter two protocols (radiometric partitioning and spectrophotometric assays) can potentially provide much higher throughput at a lower cost. As long as radiolabeled parent substrate is available, the partition assays should be relatively inexpensive; highly sensitive assays will depend upon the availability of substrate with high specific activity. These assays should be readily adaptable to a wide variety of electrophilic substrates. Likewise, if the study is designed to examine the distribution of glutathione *S*-transferase activities with a specific

substrate, a spectrophotometric assay, such as that described for CDNB (see Alternate Protocol 2), can be used. Although the sensitivity of the assay could be lower than that of the HPLC or radiochemical partition assays, high sensitivity may not be necessary to answer the question being posed. The key requirement of these assays is that the product generated has a UV_{max} different from that of the parent substrate. As indicated earlier, these assays are unlikely to be of much benefit in cases where initial cytochrome P450-dependent metabolic activation of the parent substrate is required for reactive metabolite generation.

Critical Parameters and Troubleshooting

Establishing a new assay for measuring the formation of glutathione conjugate(s) with a xenobiotic in the absence of standards can be a daunting task. However, several steps can be taken to make the process easier. The first issue is to determine whether there is any indication that the compound in question conjugates with glutathione. Evidence for this can be obtained by examining depletion of glutathione in vivo. Likewise, depletion of glutathione from isolated cells or tissue subcompartments can provide presumptive evidence for the formation of glutathione conjugates. There are several well-established procedures for the measurement of this reduced tripeptide in tissues (see *UNIT 6.2*). Once this is established, the use of [^{3}H]glutathione provides a mechanism for isolating putative glutathione conjugates as long as a full series of controls is run simultaneously. It can be helpful if [^{14}C]labeled parent substrate is available, because this makes dual-label experiments possible.

If the experiment is designed to use glutathione as a trapping method for reactive metabolites generated by a cytochrome P450–dependent process, it is important to account for the overall disposition of the parent compound. For example, naphthalene is metabolized to an intermediate epoxide which can rearrange spontaneously to 1-naphthol, undergo epoxide hydrolase–mediated hydration to a dihydrodiol, and/or bind covalently to proteins. If the experiments are designed to trap all of the naphthalene epoxide formed, care must be taken to optimize glutathione and glutathione *S*-transferase concentrations. Although the use of 0.5 mM glutathione and 10 CDNB units glutathione *S*-transferases/ml was nearly optimal for trapping reactive naphthalene metabolites, these conditions could be substrate dependent and should be optimized for each substrate tested. Even under conditions where all of the substrates and cofactor have been optimized, small quantities of the epoxide are diverted to other pathways (Buckpitt et al., 1992). The ability to account for the loss of substrate and the formation of each of the products generated during the cytochrome P450–dependent metabolism almost necessitates the use of radiolabeled substrates. For those compounds that cannot be purchased or easily synthesized, the tasks of developing the methodology and validating trapping efficiencies are considerably more difficult.

There are a number of experimental steps that can be an impediment to a successful study. If there is evidence that the compound of interest is metabolized to a glutathione conjugate, but chromatographic evidence is lacking, the compound in question may deplete tissue/cellular glutathione stores by mechanisms other than conjugation (e.g., oxidation of reduced glutathione to glutathione disulfide). Another possible explanation is that the glutathione conjugate is unstable or is lost during sample preparation. If conjugates are generated in hepatocytes, they may be further metabolized to cysteinylglycine, cysteine, and/or *N*-acetylcysteine derivatives (Buonarati et al., 1989). Finally, microsomal enzyme systems used to generate reactive metabolites that are subsequently metabolized to glutathione conjugates is a multicomponent system. Lack of function at any one of these steps could lead to a negative experimental result. Individual segments of the reaction should be tested for satisfactory function. The best approach may be to utilize a positive control; either styrene or naphthalene would serve this purpose as the metabolism and conjugation of these two substrates has been described in detail previously (Steele et al., 1981; Buckpitt et al., 1987). The advantage of styrene is that the epoxide is commercially available, and the glutathione conjugates can be prepared without microsomal activation.

As mentioned earlier, if radiolabeled glutathione or parent substrate is used as the basis for assay quantitation, the specific activity of the starting material must be known precisely. In preparing substrate for use in these assays, it is worthwhile taking several samples of substrate to determine specific activity. In cases where the substrate is radiolabeled and absorbs in the UV region, it is often possible to deter-

mine specific activity precisely by UV scanning and counting samples of the actual substrate used in the reaction mixture. Knowledge of the extinction coefficient then allows precise measurements of the concentrations in the cuvette.

Anticipated Results

Analyzing HPLC chromatograms

Comparison of HPLC UV/radiochromatograms of complete incubations (microsomes, substrate, [^{3}H]glutathione, NADPH, glutathione *S*-transferase) versus those containing all components except NADPH or substrate can provide a good indication that a suspected peak is a glutathione conjugate. Figure 6.8.2 shows an example of the separation of 1-nitronaphthalene glutathione conjugates. The radiochromatogram (Fig. 6.8.2A) is from an incubation containing 1-nitronaphthalene, microsomes, NADPH-generating system, [^{3}H]glutathione, and glutathione *S*-transferases. The radiochromatogram in Figure 6.8.2C is identical except that the NADPH generating system was omitted from the incubation. Based on these profiles, peaks 1 to 7 were tentatively identified as glutathione conjugates. Later structural analysis by mass spectrometry and proton NMR spectroscopy confirmed this finding and established the regiochemistry of nucleophilic attack. In some situations, substrate-to-product turnover can be quite slow, making metabolite identification more difficult. Extending the incubation time can occasionally result in increased quantities of metabolite. The amount of metabolite per peak can be calculated using a pre-established specific activity (example: 5000 dpm/nmole) of the radiolabeled substrate. Turnover is reported as nanomoles conjugate per milligram microsomal protein (or per nanomole cytochrome P450 or milligram cytosolic protein) per minute.

As indicated earlier, the advantage of the radiometric assay over that provided in the Basic Protocol, is speed. Fifty or more samples can be processed easily in a day's time. The sensitivity of this assay will be dependent upon the specific activity of the starting substrate and on the rates of nonenzymatic reaction of the substrate with glutathione in the absence of transferase.

Spectrophotometric assays capable of monitoring glutathione conjugate formation are particularly useful for monitoring glutathione transferase activities. The use of multicell cuvette holders means that a moderate number of samples can be assessed in a single day.

Time Considerations

Measurement of glutathione conjugates by HPLC

Although the protocol for measuring glutathione conjugates by HPLC can be completed successfully in one day, it is wise to divide the steps into two to three days. The first day consists of preparing for and conducting the incubations. Depending on whether microsomes are made fresh or are from frozen specimens, this portion of the protocol can vary from 2 hr to a full day of work. Once the incubations have been quenched with methanol, they may be stored at −20°C overnight, which is a good stopping point.

On the second day, samples are prepared for HPLC, and the column is equilibrated. Long centrifugation times allow for multi-tasking. Removal of protein by centrifugation takes 30 min, and the vacuum centrifugation usually takes 3 to 4 hr. While the samples are evaporating, mobile phase should be prepared, and the column should be equilibrated.

In cases where radiolabeled substrates were used, a third day will likely be necessary. Depending upon the complexity of the samples and the corresponding length of the chromatographic runs, as few as three to four samples can be injected and counted in one day. Flow-through β detectors could simplify and speed this process, but specific activities of the starting substrate must be high as a result of generally lower sensitivity of these detectors and shorter count times. Packard Instruments offers multichannel β counters where samples are collected directly into 96-well plates containing a solid scintillant.

Radiometric assay of glutathione conjugate formation

The assay described in this protocol can be conducted in 4 to 8 hr, depending upon the number of samples. The samples can be counted overnight with results of the assay available the following morning.

Spectrophotometric assay for glutathione S-transferase

Once the enzyme preparation is available and substrates are prepared, this assay takes

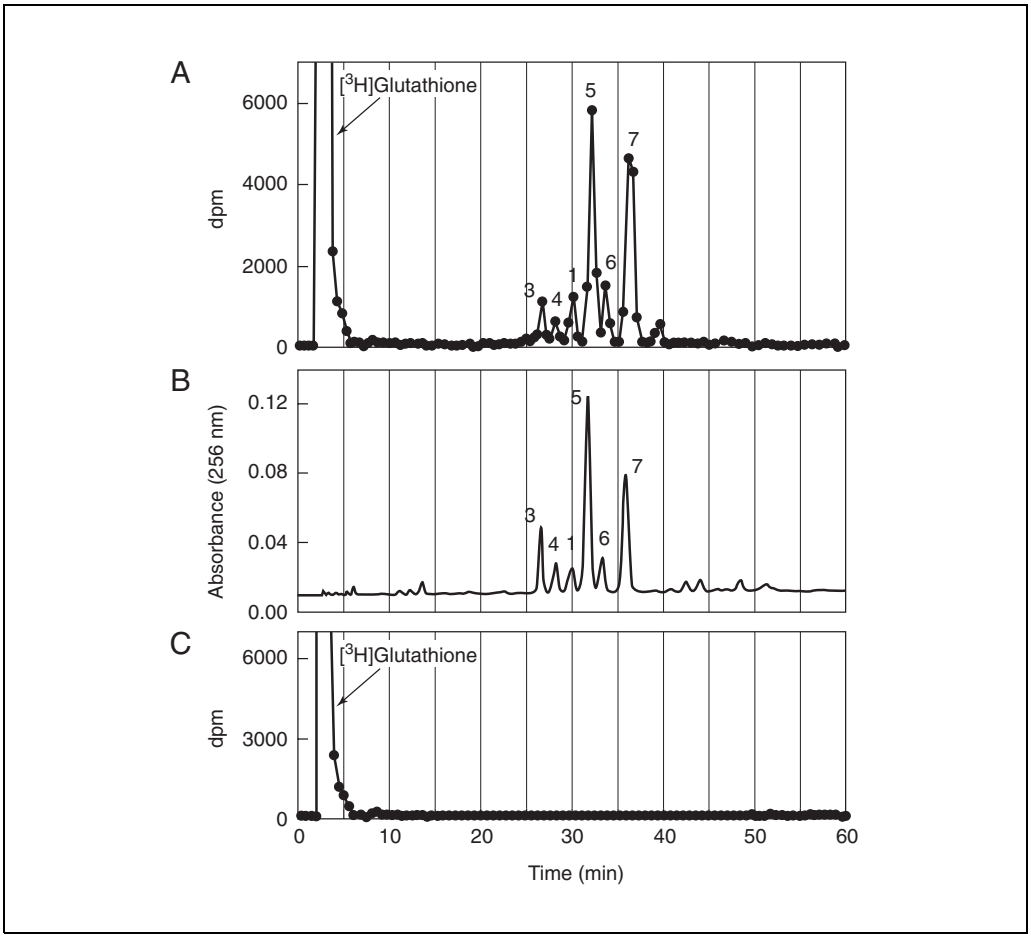

Figure 6.8.2 HPLC chromatograms showing the elution of glutathione conjugates derived from 1-nitronaphthalene. (**A**) Radiochromatogram from incubations containing [^{3}H]glutathione, 1-nitronaphthalene, microsomes, and all cofactors (Table 6.8.2). (**C**) Identical to conditions in panel A, except that the NADPH generating system was omitted from the incubations. (**B**) UV trace of conjugate elution.

<10 min for three samples and a blank. Accordingly, numerous samples can be processed in a single 4-hr period.

Microsomal incubations

Once microsomal preparations are available and all other reagents are prepared, the actual incubations to generate product can be completed in 1 to 2 hr depending upon the number of samples to be processed. Because there are multiple reagents that must be added to each vial, the authors have found that it is more time efficient to mix most of the reagents together (i.e., glutathione, transferase, NADPH regenerating solution, and buffer) and to add the variable components, such as varying concentrations of substrate or microsomes from different tissues, to the incubation separately.

Preparation of microsomal and cytosolic fractions

Preparation of microsomal and cytosolic fractions requires 4 to 6 hr from the time tissues are removed from the animal. With some degree of organization, an investigator can prepare microsomal fractions and conduct incubations during the same work day. Once the microsomal incubation is complete, samples can generally be stored at −20°C or colder for days to weeks as long as the glutathione adducts are stable in 66:34 methanol/water.

Purification of glutathione S-transferases

Cytosolic fractions prepared during the isolation of microsomal membranes can be stored at −80°C without substantial loss of enzyme activity. Gel filtration (Sephadex G-25) and glutathione affinity columns should be poured prior to the day in which the transferases are to

be affinity purified. They can be rinsed and equilibrated while the cytosolic fractions are being thawed. The two chromatographic steps (gel filtration and affinity chromatography) can be accomplished in a little more than 4 hr. Depending upon the volume of enzyme solution and the degree of concentration required, pressure dialysis requires a further 3 to 5 hrs. The preparation can be assayed and frozen in smaller aliquots for future use.

Preparative separation and isolation of glutathione conjugates for characterization by mass spectrometry and proton NMR spectroscopy

Once large incubations are completed, concentration of samples on a rotary evaporator or centrifugal concentrator can require several hours to overnight. It is advisable, unless there is information to suggest otherwise, to evaporate excess solvent (i.e., methanol/water) at room temperature. Although this adds to the time required to conduct this step, it decreases the chances that the conjugates will decompose. Column chromatography of the conjugates on SM-16 or equivalent resins requires 2 to 4 hr with further time needed for evaporation of excess solvent. Optimizing and validating the HPLC conditions for preparative chromatography can require from a few hours to several days depending upon the complexity of the separation. The time required for separation and purification of sufficient quantities of material for NMR analysis depends upon the rates at which these metabolites are generated in the incubation, whether several metabolites must be isolated, and the size of the HPLC column used. Generally, the greater the column diameter, the higher the loading capacity of the column. Further steps including neutralization of the column eluent containing the conjugates, lyophylization and repurification can take an additional several days to a few weeks.

Literature Cited

Armstrong, R., Levin, W., Ryan, D., Thomas, P., Mah, H., and Jerina, D. 1981. Stereoselectivity of rat liver cytochrome P-450c on formation of benzo(a)pyrene 4,5-oxide. *Biochem. Biophys. Res. Commun.* 100:1077-1084.

Buckpitt, A. and Boyd, M.R. 1980. The in vitro formation of glutathione conjugates with the microsomally activated pulmonary bronchiolar alkylating agent and cytotoxin, 4-ipomeanol. *J. Pharmacol. Exp. Ther.* 215:97-103.

Buckpitt, A.R., Castagnoli, N., Nelson, S.D., Jones, A.D., and Bahnson, L.S. 1987. Stereoselectivity of naphthalene epoxidation by mouse, rat and hamster pulmonary, hepatic and renal microsomal enzymes. *Drug Metab. Dispo.* 15:491-498.

Buckpitt, A., Buonarati, M., Avey, L.B., Chang, Ai-Min, Morin, D., and Plopper, C.G. 1992. Relationship of cytochrome P450 activity to Clara cell cytotoxicity: II. Comparison of stereoselectivity of naphthalene epoxidation in lung and nasal mucosa of mouse, hamster, rat, and rhesus monkey. *J. Pharmacol. Exp. Ther.* 261:364-372.

Buonarati, M., Morin, D., Plopper, C., and Buckpitt, A. 1989. Glutathione depletion and cytotoxicity by naphthalene 1,2-oxide in isolated hepatocytes. *Chemico-Biol. Interactions*, 71:147-165.

Dahlin, D.C. and Nelson, S.D. 1982. Synthesis, decomposition kinetics, and preliminary toxicological studies of pure N-acetyl-p-benzoquinone imine, a proposed toxic metabolite of acetaminophen. *J. Med. Chem.* 25:885-886.

Dowsley, T., Forkert, P.G., Benesch, L., and Bolton, J. 1995. Reaction of glutathione with the electrophilic metabolites of 1,1-dichloroethylene. *Chem. Biol. Interact.* 95:227-244.

Dowsley, T., Ulreich, J., Bolton, J., Park, S.S., and Forkert, P.G. 1996. CYP2E1-Dependent bioactivation of 1,1-dichloroethylene in murine lung: Formation of reactive intermediates and glutathione conjugates. *Tox. Appl. Pharm.* 139:42-48.

Dowsley, T., Reid, K., Petsikas, D., Ulreich, J., Fisher, R.L., and Forkert, P.G. 1999. Cytochrome P-450-dependent bioactivation of 1,1-dichloroethylene to a reactive epoxide in human lung and liver microsomes. *J. Pharmacol. Exp. Ther.* 289:641-648.

Gill, S.S., Ota, K., and Hammock, B.D. 1983. Radiometric assays for mammalian epoxide hydrolases and glutathione *S*-transferase. *Anal. Biochem.* 131:273-282.

Habig, W., Pabst, M., and Jakoby, W. 1974. Glutathione *S*-transferases: The first enzymatic step in mercapturic acid formation. *J. Biol. Chem.* 249:7130-7139.

Hernandez, O., Walker, M., Cox, R., Foureman, G., Smith, B., and Bend, J. 1980. Regiospecificity and stereospecificity in the enzymatic conjugation of glutathione with (+)-benzo(a)pyrene 4,5-oxide. *Biochem. Biophys. Res. Commun.* 96:1494-1502.

Hinson, J.A., Monks, T.J., Hong, M., Highet, R.J., and Pohl, L.R. 1982. 3-(glutathion-S-yl)acetaminophen: A biliary metabolite of acetaminophen. *Drug Metab. Dispo.* 10:47-50.

Jernstrom, B., Babson, J., Moldeus, P., Holmgren, A. and Reed, D. 1982. Glutathione conjugate and DNA-binding of (+)-trans-7,8-dihydroxy- 7,8-dihydrobenzo(a)pyrene and (+)-7,8-dihydroxy-9,10-epoxy-7,8,9, 10-tetrahydrobenzo(a)pyrene in isolated rat hepatocytes. *Carcinogenesis* 3:861-866.

Plakunov, I., Smolarek, T., Fischer, D., Wiley, J., and Baird, W. 1987. Separation by ion-pair high-performance liquid chromatography for glu-

curonide, sulfate and glutathione conjugates formed from benzo(a)pyrene in cell cultures from rodents, fish and humans. *Carcinogenesis* 8:59-66.

Raney, K.D., Coles, B., Guengerich, F.P., and Harris, T.M. 1992. The endo-8,9-epoxide of aflatoxin B1: A new metabolite. *Chem. Res. Toxicol.* 5:333-335.

Shultz, M.A., Chang, A., Morin, D., and Buckpitt, A. 2001. Metabolic capabilities of CYP2F2 with various pulmonary toxicants and its relative abundance in mouse lung sub-compartments. *J. Pharmacol. Exp. Ther.* 296:510-519.

Simons, P. and Vander Jagt, D. 1977. Purification of glutathione *S*-transferases from human liver by glutathione affinity chromatography. *Anal. Biochem.* 72:248-254.

Steele, J., Yagen, B., Hernandez, O., Cox, R., Smith, B., and Bend, J. 1981. The metabolism and excretion of styrene oxide glutathione conjugates in the rat and by isolated perfused liver, lung and kidney preparations. *J. Pharmacol. Exp. Ther.* 219:35-41.

Sundberg, K., Widersten,M., Seidel, A., Mannervik, B., and Jernstron, B. 1997. Glutathione conjugation of bay- and fjord-region diol epoxides of polycyclic aromatic hydrocarbons by glutathione transferases M1-1 and P1-1. *Chem. Res. Toxicol.* 10:1221-1227.

Thakker, D., Yagi, H., Levin, W., Wood, A.W., Conney, A., and Serina, D. 1985. Polycyclic aromatic hydrocarbons: Metabolic activation to ultimate carcinogens. *In* Bioactivation of Foreign Compounds (M.W. Anders, ed.) pp. 178-242. Academic Press, New York.

van Bladeren, P. 2000. Glutathione conjugation as a bioactivation reaction. *Chem Biol Interact.* 129:61-76.

van Bladeren, P.J., Vyas, K.P., Sayer, J.M., Ryan, D.E., Thomas, P.E., Levin, W., and Jerina, D.M. 1984. Stereoselectivity of cytochrome P-450c in the formation of naphthalene and anthracene 1,2-oxides. *J. Biol. Chem.* 259:8966-8973.

Watt, K., Morin, D., Kurth, M., Mercer, R., Plopper, C., and Buckpitt, A. 1999. Glutathione conjugation of electrophilic metabolites of 1-nitronaphthalene in rat tracheobronchial airways and liver: Identification by mass spectrometry and proton nuclear magnetic resonance spectroscopy. *Chem Res.Toxicol.* 12:831-839.

Watt, K. and Buckpitt, A. 2000. Species differences in the regio- and stereoselectivity of 1-nitronaphthalene metabolism. *Drug Metab. Dispo.* 28:376-378.

Contributed by Michael A. Shultz, Dexter Morin, Katherine Watt Chan, and Alan R. Buckpitt
University of California
Davis, California

Coenzyme A and Coenzyme A-Glutathione Mixed Disulfide Measurements by HPLC

Oxidant stresses occurring in an organism may exhibit differential expression in subcellular compartments. In many studies published to date, measurement of thiols and disulfides, most commonly glutathione (GSH) and glutathione disulfide (GSSG), have been used as biomarkers of oxidant stress status in biological models (Reed and Savage, 1995). However, assessments of oxidative status of subcellular compartments based on measurements of GSH and GSSG following isolation of subcellular fractions are problematic because of oxidation, reduction, and thiol-disulfide exchange reactions that can occur during tissue processing and isolation of subcellular fractions. Most of the current methods for sample preparation attenuate thiol redox reactions but have limitations as to either their feasibility or effectiveness in analyses of subcellular components. As one approach to circumventing these fundamental barriers, the authors of this unit have measured coenzyme A (CoASH) and coenzyme A–glutathione mixed disulfide (CoASSG) in tissue homogenates derived from tissues frozen in liquid nitrogen that have been treated with the derivatizing agent *N*-ethylmaleimide (NEM) at the time of homogenization and subsequently acidified.

The redox couple CoASH and CoASSG was chosen for analysis because CoASH is found primarily within the mitochondria (Robishaw and Neely, 1985; Tahiliani and Neely, 1987) and possesses a critical thiol group that undergoes thiol/disufilde exchange with GSH and GSSG (Gilbert, 1982). Measurements of CoASH and CoASSG levels may provide a method for assessing changes in the oxidative state within mitochondria of intact tissues. However, the important roles played by CoASH in normal cell physiology and the recent description of the potent vasoconstrictor effects of CoASSG further extend the potential implications of any changes observed in these molecular species (Schluter et al., 1995; van der Giet et al., 2001).

The following protocol describes in detail the procedures required for accurate measurement of both CoASH and CoASSG by HPLC. The method requires attention to detail, as well as the ability to adjust chromatographic conditions to optimize separation of the desired analytes from other substances encountered in specific samples.

Materials

Test animal
Liquid N_2
0.1 M sodium phosphate buffer, pH 7.4 (*APPENDIX 2A*), 4°C
1 M NEM (see recipe), 4°C
4% perchloric acid ($HClO_4$): dilute 5.1 ml concentrated (68% to 70%) $HClO_4$ to 100 ml with H_2O; prechill to 4°C at time of use
Mobile phases A, B, and C for either tertiary/quaternary or binary HPLC solvent program (see recipe)
CoAS-NEM and CoASSG standards (see recipes)

Freeze clamps: 2 × 2 × 0.5–in. aluminum blocks and stainless steel towel clamps altered to hold them (see recipe)
Mortar and pestle designed for grinding under liquid nitrogen (Fisher Scientific)
2-ml dounce homogenizer with loose and tight pestles (Wheaton; VWR)
Refrigerated centrifuge
HPLC system with UV detector (capable of measurement at 254 nm)
Precolumn filter (0.062 × 0.250-µm, 4 µm pore size; Western Analytical Inc.)
C_{18} guard column (4.6 × 125 mm, Zorbax SB; Mac-Mod Analytical, Inc.)
C_{18} analytical HPLC column (4.6 × 150 mm, Zorbax SB; Mac-Mod Analytical, Inc.)

Contributed by Lynette K. Rogers and Charles V. Smith
Current Protocols in Toxicology (2003) 6.9.1-6.9.8

Prepare samples

1. Remove tissue(s) from animal and "freeze-clamp" the tissue(s) as rapidly as possible, using the following technique:

   a. Cool 2 × 2 × 0.5–in. aluminum blocks by immersing in liquid N_2 until the rapid bubbling of the liquid has stopped, indicting that the blocks have reached a temperature close to that of the liquid N_2.

   b. Immediately upon removal from the animal, place the tissue on the horizontal surface within the open precooled aluminum blocks and flatten it with pressure while closing the clamp and submerge the tissue and the blocks once again into liquid N_2.

   c. After the bubbling subsides, remove the tissue from the liquid N_2 and the aluminum blocks.

   d. Break the flattened piece of frozen tissue into smaller pieces by striking it sharply with the handle of a pair of scissors or similar object.

   e. Wrap the broken tissue pieces in prelabeled aluminum foil and store at −80°C indefinitely until analysis.

2. Precool the mortar and pestle by pouring liquid N_2 into the mortar and placing the pestle in the liquid. Prepare the Dounce homogenizer by placing 0.78 ml of 0.1 M sodium phosphate buffer, pH 7.4, and 20 µl of 1 M NEM into the mortar of the homogenizer and placing the entire unit in ice.

3. At time of analysis, remove the tissue samples from the freezer and maintain them in liquid N_2 or on dry ice.

4. Accurately and quickly, weigh ~0.2 g of tissue and place in the liquid N_2–cooled mortar. Grind the tissue to a powder using the cooled pestle.

   IMPORTANT NOTE: *This must be done quickly, without allowing the tissue to thaw. Be sure to maintain enough liquid N_2 in the mortar to prevent the tissue from thawing.*

5. Carefully transfer the powdered tissue to the Dounce homogenizer and homogenize using 8 strokes with the loose pestle and 8 strokes with the tight pestle.

6. Transfer the homogenate to a centrifuge tube and add either 20 µl of concentrated $HClO_4$ or 1 ml of cold 4% $HClO_4$. Mix, then centrifuge 20 min at 12,000 × *g*, 4°C.

   To minimize sample dilution, one can add 20 µl of concentrated (~70%) $HClO_4$, but 1 ml of 4% $HClO_4$ is sufficient for protein precipitation; the additional dilution in some cases generates a chromatogram with less baseline noise. Samples can be maintained on ice after addition of $HClO_4$, and all prepared samples can be centrifuged at the same time.

7. Transfer the supernatant to a new tube and maintain at 4°C prior to analysis by HPLC.

Perform HPLC analysis

8. Place mobile phases A, B, and C (if tertiary or quaternary HPLC system is to be used) or mobile phases A and B (if binary HPLC system is to be used) in the appropriate containers on the HPLC.

9. Install an in-line precolumn filter, a C_{18} guard column, and a C_{18} analytical column in sequence on the HPLC.

   The precolumn filter removes particles that can plug a guard column or analytical column, and is much less expensive to replace. The use of a precolumn filter is especially important for analysis of tissue homogenates.

10. Program the HPLC mobile phase gradient as follows.

    a. For a tertiary or quaternary system:

6 min	equilibration inject	90% A, 0% B, 10% C
2 min	hold	90% A, 0% B, 10% C
20 min	linear gradient to:	5% A, 85% B, 10% C
10 min	clean-out	90% B, 10% C

    b. For a binary system:

6 min	equilibration inject	100% A
40 min	parabolic gradient to:	40% A, 60% B
5 min	linear gradient to:	100% B
10 min	clean-out	100% B

11. Inject CoAS-NEM and CoASSG standard into the HPLC in appropriate amount to generate a standard curve ranging from 0 to 500 pmol of CoAS-NEM and 0 to 50 pmol of CoASSG on column.

12. Inject the homogenized tissue samples (from step 7) and determine the concentrations of CoASH and CoASSG by comparing the respective peak areas of unknowns with peak areas obtained with injections of standards of known concentrations (Fig. 6.9.1).

    Use the equation $y = mx + b$ where y is the peak area, x is nmol of CoA species on the column, m is the slope of the standards curve, and b is the y intercept calculated from the standards curve.

    For example, for a peak area of 344357 mvolts:

$$y = (721431)x + (-7753.96)$$

$$x = \frac{344357 - (-7753.96)}{721431}$$

$$= 0.488 \text{ nmol CoASH on the column}$$

    Normalized to the grams of tissue injected (0.0028 g liver), this value becomes

$$\frac{0.488 \text{ nmol CoASH}}{0.0028} = 174.28 \text{ nmol/gram liver}$$

REAGENTS AND SOLUTIONS

Use Milli-Q-purified water or equivalent for the preparation of all reagents and in all protocol steps. For common stock solutions, see ***APPENDIX 2A****; for suppliers, see* ***SUPPLIERS APPENDIX****.*

CoAS-NEM standard

10 mM CoAS-NEM stock:
7.9 mg CoASH, sodium salt (Sigma-Aldrich)
980 µl 0.1 M sodium phosphate buffer, pH 7.4 (*APPENDIX 2A*)
20 µl 1 M NEM (see recipe)
Store in aliquots up to 1 year at −20°C

0.01 mM CoAS-NEM working standard: At time of use, dilute in 0.1 M sodium phosphate, pH 3.0 (see recipe), to yield a concentration of 0.01 mM CoAS-NEM.

Standards are more stable at pH 3.0, but the initial reaction of CoASH with NEM requires a neutral pH.

CoASSG standard

Prepare a solution of 100 nmol CoASH and 100 nmol GSH on 0.1 M sodium phosphate buffer, pH 7.4 (*APPENDIX 2A*). Add 100 nmol diamide in the same buffer, to a final volume of 1 ml. Incubate 10 min and add 1000 nmol NEM. Incubate 10 min. Add 10 µl H_3PO_4. Analyze the mixture by HPLC. Store up to 1 year at −20°C.

In the systems studied by the author, CoASSG peak precedes CoASH-NEM by 1 to 3 min. The new peak prepared by diamide oxidation coelutes with CoASSG purchased from Sigma-Aldrich. Peak areas of CoASSG are 1.1 time the eak areas observed with eqimolar amounts of CoASH-NEM, and this response factor ratio is used to CoASSG concentrations from experimentally derived standard curves for CoASH-NEM contents.

N-ethylmaleimide (NEM), 1 M

Dissolve 125.1 mg *N*-ethylmaleimide in 1 ml acetonitrile. Store in sealed container indefinitely at −20°C to prevent evaporation.

Freeze clamps

Cut two 2 × 2–in square blocks from 0.5-in sheet aluminum. Drill an 0.25-in screw hole into the center of one of the flat sides of each block. Bend towel clamps (purchased from any surgical supply company) to fit around the two blocks with the blocks resting flat against each other with the "eyes" of the towel clamps aligned with the screw hole. Place a screw through the towel clamp into the screw hole of the block to secure the clamp to the block.

HPLC mobile phases

For tertiary or quaternary HPLC solvent programming:

Mobile phase A: 25% (v/v) methanol (HPLC grade)/75% (v/v) water

Mobile phase B: 65% (v/v) methanol (HPLC grade)/35% (v/v) water

Mobile phase C: 100 mM tetrabutylammonium hydrogen sulfate (TBAS; Sigma-Aldrich)

Dissolve 34 g TBAS in 1 liter of water and adjust to pH 5.0 with NH_4OH. Filter through 4-µm filter before use.

For binary HPLC solvent programming:

Mobile phase A (10% methanol/10 mM tetrabutylammonium hydrogen sulfate): Dissolve 3.4 g of TBAS (Sigma-Aldrich) in 850 ml of water, adjust pH to 5.0 with NH_4OH, adjust volume to 900 ml with water, filter, then add 100 ml of HPLC-grade methanol.

Mobile phase B (85% methanol/10 mM tetrabutylammonium hydrogen sulfate): Dissolve 3.4 g of TBAS in 100 ml of water, adjust pH to 5.0 with NH_4OH, adjust volume to 150 ml with water, filter, then add 850 ml of HPLC-grade methanol.

Store mobile phases up to 1 month at room temperature.

If the HPLC system does not have an in-line degasser, degas the mobile phase solutions.

0.1 M sodium phosphate buffer, pH 3.0

Dissolve 1.37 g monobasic sodium phosphate in 90 ml water. Adjust the pH to 3.0 by dropwise addition of phosphoric acid.

COMMENTARY

Background Information

Assessments of oxidative stress responses within subcellular compartments of an organism have been particularly challenging. Even isolation techniques that are "really fast" require several minutes of conditions that will not prevent artifactual effects on oxidative biomarkers. Three methods commonly employed to minimize thiol redox chemistry are freezing to liquid nitrogen temperatures, alkylation of free thiol groups with electrophilic derivatizing agents, and acidification. How-

ever, important details in the use of each may be overlooked. For example, rapid freezing or "freeze-clamping" of tissues with liquid nitrogen-cooled metal blocks is superior to simply placing a piece of tissue in a plastic tube or other container and dropping the sample into liquid nitrogen. Although the same temperature is attained by both methods, the rates of cooling are substantially different. The authors have found that samples frozen initially at liquid nitrogen temperatures (−196°C) can be stored at −80°C without measurable alterations. For alkylation of thiols, *N*-ethylmaleimide (NEM) reacts significantly more rapidly than do other commonly employed reagents, such as iodoacetic acid and monobromobimane. As with freezing, the final products of derivatization are comparably effective in avoiding redox artifacts, once formed. However, greater concentrations of GSSG are observed in tissues derivatized with iodoacetic acid or monobromobimane than in tissues treated with NEM, reflecting the effects of the slower thiol alkylations by the former reagents. Although thiols and disulfides are reasonably stable under acid conditions, the authors found that processing frozen tissue samples by homogenization in acid gave significantly higher measured concentrations of CoASSG and GSSG than that observed in the same tissues derivatized with NEM prior to acidification (Table 6.9.1). In these examples of freeze-clamped tissues powdered under liquid nitrogen, the effects of acidification should be quite rapid. The results implicate reaction of oxidizing species present in tissues whose effects on GSH and CoASH, and presumably other thiols, are stimulated by acidification but can be minimized by derivatization of thiols prior to acidification.

Unfortunately, freeze-clamping of tissues is not compatible with subsequent isolation of subcellular fractions, thus presenting something of a problem for assessments of compartmental redox status in relevant biological models in vivo. To circumvent this problem, a redox-active molecule was identified in the authors' laboratory that is found primarily in the mitochondria of mammalian tissues, 75% and 95% in rat liver and heart respectively (Robishaw and Neely, 1985; Tahiliani and Neely, 1987). CoASH equilibrates with GSH and GSSG in vitro, forming and reducing, respectively, the mixed disulfide CoASSG (Gilbert, 1982). In these studies, CoASH and CoASSG levels, obtained using tissue homogenates from liquid N_2 freeze-clamped tissues derivatized with NEM and subsequently acidified as potential biomarkers of oxidative stress within the mitochondrial compartment, were investigated.

Earlier methods for measurement of CoASH described homogenizing tissues directly into 4% $HClO_4$, centrifuging the homogenates, and analyzing the supernatants. The CoASH levels in samples precipitated with $HClO_4$ alone deteriorated rapidly, and thus required homogenization of each sample just prior to analysis. The authors of this unit also measured higher concentrations of GSSG in tissue homogenate supernatants prepared with $HClO_4$ than were observed with other methods. Ansensi et al. (1994) have reported greater oxidation ex vivo with $HClO_4$ treatment than with other acids used for sample preparation.

Table 6.9.1 Effects of Sample Processing on Levels of CoASH, CoASSG, GSH, and GSSG Measured in Mouse Liver[a]

	CoASH (nmol/g liver)	CoASSG[b,c] (nmol/g liver)	GSH (μmol/g liver)	GSSG[b,c] (nmol/g)
TCA (0.6 M)	115.5 ± 10.9	7.7 ± 2.3^{I}	6.1 ± 0.8	112.4 ± 10.7^{IV}
H_3PO_4 (4%)	112.9 ± 21.0	$4.1 \pm 1.2^{I,II}$	8.8 ± 1.9	103.3 ± 9.7^{V}
NEM (pH 7.4)	125.7 ± 4.5	$1.3 \pm 0.2^{I,II,III}$	Not determined	$33.1 \pm 6.7^{IV,V,VI}$
$HClO_4$ (4%)	97.6 ± 6.6	$8.9 \pm 0.4^{II,III}$	7.3 ± 1.0	$326.4 \pm 21.1^{IV,V,VI}$

[a]Mouse livers were freeze-clamped and powdered under liquid nitrogen. The powdered liver samples were homogenized in 0.6 M trichloroacetic acid (TCA), 4% H_3PO_4 or 4% $HClO_4$; samples homogenized in 20 mM NEM were acidified by addition of 20 μl of 70% $HClO_4$. Concentrations of CoASH and CoASSG in the supernatants were measured by HPLC as described in the Basic Protocol, and GSH and GSSG were measured by the enzyme recycling method described previously by the authors of this unit (Rogers et al., 2000). Results are expressed as means ± SEM (n = 5-12 animals). Data were analyzed by one-way ANOVA with LSD post hoc.

[b]Different by one-way ANOVA, $p<0.005$.

[c]Common superscripted roman numerals indicate groups that are different by LSD.

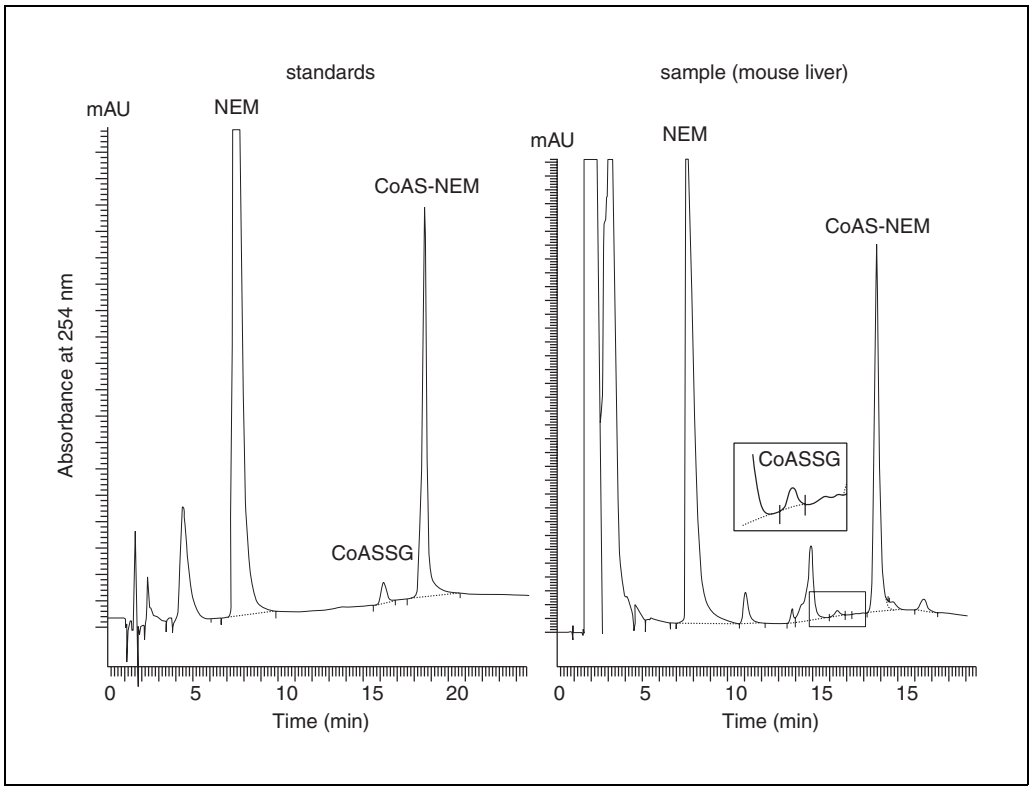

Figure 6.9.1 HPLC separation of CoASH and CoASSG. The standards injected on the column were CoAS-NEM, 1 nmol, and CoASSG, 0.1 nmol. Mouse liver tissue obtained from an animal that had been fasted 24 hr prior to sacrifice was prepared as described in the Basic Protocol, and 80 µl of the resulting supernatant were injected. The analysis was preformed on a quaternary system with UV detection at 254 nm. Analysis of the tissue sample indicated a CoASH level of 163.1 nmol/g tissue and a level of CoASSG of 0.53 nmol/g tissue.

Several acids commonly used for sample preparation and measurements of GSH, GSSG, CoASH, and CoASSG (Table 6.9.1) were therefore compared. The authors included in the analysis samples treated with the thiol derivatizing agent *N*-ethylmaleimide (NEM) and subsequently acidified with $HClO_4$. The higher levels of GSSG and CoASSG measured in acid-treated samples as compared with NEM-treated samples indicate that GSSG and CoASSG can be formed with acid treatment of samples as a product of oxidation occurring during sample preparation. NEM treatment with subsequent acidification was more effective than were any of the methods investigated that employed acidification alone for minimizing artifactual oxidation.

Methods previously developed for HPLC separation of CoASH and CoASSG have involved high-salt mobile phases that were difficult to prepare (King and Reiss, 1985), required daily preparation, and were damaging to analytical columns and the HPLC pumps. The authors chose to use a variation of the ion-pairing method described by Baker and Schooley (1981) because, using that method, it was possible to obtain good resolution of the CoAS-NEM adduct, the mobile phases were more stable, and the mobile phases were not as damaging to the to the components of the HPLC system. The HPLC analysis of the CoAS-NEM adducts also provides increased absorbance at 254 nm, due to the presence of NEM, and a sharper peak shape than that obtained for CoASH (Fig. 6.9.1). Limits of detection for CoAS-NEM of 2 pmol on column at a signal-to-noise ratio of 3:1 were observed, while the limit of detection for CoASSG was 6 pmol on column. The day-to-day coefficients of variation observed by the authors were 4.3% for CoAS-NEM and 11.2% for CoASSG.

NEM is unstable in alkaline solutions. Sacchetta et al. (1986) reported essentially complete hydrolysis of NEM in 5 min at pH 11 but <5 % hydrolysis at pH 7. The authors have not studied the effect of pH, but in the protocol described NEM is added from an anhydrous acetonitrile solution and the derivation is conducted at the physiological pH of 7.4 at which reactions of NEM with thiols is very rapid. The

samples are then acidified to precipitate proteins from the biological samples, and this helps stabilize the CoAS-NEM adduct. The CoAS-NEM adduct is sufficiently stable to allow preparation of samples and standards and injection in overnight runs, but the long-term stability has not been studied.

Critical Parameters and Troubleshooting

As noted previously, great care must be taken to minimize artifactual redox reactions during sample processing. Sample acquisition must be efficient and rapid, and sample storage must be at temperatures below −70°C. In sample preparation, the tissue must remain frozen until it is added to the NEM-containing buffer. Efficient transfer of the powdered tissue from the mortar to the buffer also requires careful attention.

The HPLC method described in the Basic Protocol is reasonably robust, requiring minimal maintenance to the equipment and relatively simple mobile phases. Problems with the HPLC separations usually lie in two areas. One is a noisy baseline. The baseline can be quieted by helium sparging the mobile phases and maintaining a back pressure on the bottles (see manufacturer for suggested pressures) and by regular changing of the precolumn filter. Changing the precolumn filter also minimizes increases in system pressure arising from multiple injections of tissue samples. The second problem with separation is interfering peaks that may obscure quantitation of the desired peak. The authors have observed differences in chromatograms arising from species, tissue, diet, or drug treatments of animals, but have found that minor adjustments in mobile-phase gradient profile usually provide the separation needed. Increasing the time course of the gradient in the portion of the solvent program that encompasses the peak of interest is usually sufficient to resolve the interfering peaks. Changing the shape of the gradient from concave to more linear or vice versa can also be employed if time sequence expansion proves not to be sufficient.

Anticipated Results

The authors have observed absolute levels of CoASH and CoASSG within a given tissue to be variable between different species or even within different strains of animals within a species. They have previously reported CoASH and CoASSG levels in the livers of ICR mice to be within the range of 101 to 130 and 0.8 to1.1 nmol/g tissue, respectively, for fed animals, and 112 to 142 and 0.9 to 1.3 nmol/g tissue, respectively, for fasted animals. Hepatic CoASH levels in these mice were decreased with acetaminophen treatment, but CoASSG levels were unchanged. In contrast, furosemide treatment caused no changes in hepatic CoASH levels, but increases were observed in CoASSG levels after 2 hr (Rogers et al., 2000). Higher levels of CoASH and CoASSG were found in control liver tissue of C57Bl/6 mice, 228 and 6.7 nmol/g tissue, respectively, and increases in concentrations of CoASSG were observed in response to 48 and 72 hours of hyperoxia exposure (Wong et al., 2001). Lung tissues were also analyzed in these animals, resulting in CoASH levels of 20.7 nmol/g tissue and CoASSG levels of 1.1 nmol/g tissue in control lungs, with levels of both analytes decreasing with time in hyperoxia. These results indicate that physiological stresses within a whole animal can cause changes in both CoASH and CoASSG levels.

Time Considerations

The HPLC analysis of CoASH and CoASSG described here is not simple, and requires a working knowledge of HPLC analyses. The amount of time required to establish or adapt this assay will depend upon the experience of the chromatographer and the particular tissues to be analyzed.

Once the system is running and optimized for the particular sample type to be analyzed, sample preparation requires only about 5 min per sample and a 30 to 45 min analysis time. Several samples can be prepared at a given time and stored at room temperature overnight, as in an unrefrigerated autoinjector, or at 4°C for up to 48 hr prior to analysis.

Literature Cited

Ansensi, M., Sastre, J., Pallardo, F.V., de la Asuncion, J.G., Estrela, J.M., and Vina, J. 1994. A high-performance liquid chromatography method for measurement of oxidized glutathione in biological samples. *Anal. Biochem.* 217:323-328.

Baker, F.C. and Schooley, D.A. 1981. Separation of S-acyl-CoA thioesters and related compounds by reversed-phase ion-pair chromatography. *Methods Enzymol.* 72:41-52.

Gilbert, H.F. 1982. Biological disulfides: The third messenger? *J. Biol. Chem.* 257:12086-12091.

King, M.T. and Reiss, P.D. 1985. Separation and measurement of short-chain coenzyme A compounds in rat liver by reversed-phase high performance liquid chromatography. *Anal. Biochem.* 146:173-179.

Reed, D.J. and Savage, M.K. 1995. Influence of metabolic inhibitors on mitochondrial permeability transition and glutathione status. *Biochim. Biophys. Acta.* 1271:43-50.

Robishaw, J.D. and Neely, J.R. 1985. Coenzyme A metabolism. *Am. J. Physiol.* 248:E1-E9.

Rogers, L.K., Valentine, C.J., Szczpyka M., and Smith, C.V. 2000. Effects of hepatotoxic doses of acetaminophen and furosemide on tissue concentrations of CoASH and CoASSG in vivo. *Chem. Res. Tox.*13:873-882.

Sacchetta, P., Di Cola, D., and Federici, G. 1986. Alkaline hydrolysis of *N*-ethylmaleimide allows a rapid assay of glutathione disulfide in biological samples. *Anal. Biochem.* 154:205-208.

Schluter, H., Meissner, M., van der Giet, M., Tepel M., Bachmann, J., Grob, I., Nordhoff, E., Karas, M., Spieker, C., Witzel, H., and Zidek, W. 1995. Coenzyme A glutathione disulfide, a potent vasoconstrictor derived from the adrenal gland. *Circ. Res.* 76:675-680.

Tahiliani, A. G. and Neely, J. R. 1987. A transport system for coenzyme A in isolated rat heart mitochondria. *J. Biol. Chem.* 262:11607-11610.

van der Geit, M., Schmidt, A., Jankowski, J., Schluter, H., Zidek, W., and Tepel, M. 2001. Coenzyme A glutathione disulfide is a potent modulator of angiotensin II-induced vasoconstriction. *Am. J. Hyper.* 14:164-168.

Wong, Y.L., Smith, C.V., McMicken, H.W., Rogers, L.K., and Welty, S.E. 2001. Mitochondrial thiol status in the liver is altered by exposure to hyperoxia. *Toxicol. Lett.* 123:179-93.

Key References

Rogers et al., 2000. See above.

Describes the method for sample preparation and HPLC analysis in this protocol and applies the protocol to a biological situation.

Baker and Schooley, 1981. See above.

Describes the original HPLC separation of both short and long chain acyl-CoA moieties and the ion-pairing chromatography adapted for this protocol.

Contributed by Lynette K. Rogers and Charles V. Smith
Children's Research Institute
The Ohio State University
Columbus, Ohio

CHAPTER 7
Assessment of the Activity of Antioxidant Enzymes

INTRODUCTION

The use of molecular oxygen to sustain life has as a metabolic byproduct the formation of superoxide and hydrogen peroxide. Glutathione (GSH)–dependent metabolism of hydrogen peroxide via GSH-dependent peroxidases is a vital process to prevent oxidative stress. These antioxidant enzymes in conjunction with glutathione reductase comprise the glutathione redox cycle (Reed, 1985, 1986). In conjunction with the superoxide dismutases, this cycle serves an essential role in limiting the production of hydroxyl radical and other reactive oxygen species that can cause indiscriminate damage to cellular constituents. As a substrate of several isoenzymes of glutathione peroxidases (*UNIT 7.1*), GSH is also used to limit the same oxidative events induced by organic hydroperoxides, including fatty acid hydroperoxides.

Methods for analyzing a variety of GSH-related enzymes are presented in *UNIT 7.1*. Glutathione peroxidase activity is measured using one of several hydroperoxide substrates, including the commercially available cumene hydroperoxide. Procedures are also given for the synthesis of phosphatidylcholine hydroperoxide to allow the measurement of GPX4 (PHGPX). Since some glutathione peroxidase activity is accompanied by glutathione transferase activity, dual assays are also included, as are chromatographic separation and immunoprecipitation techniques and assays of different isoenzymes.

Glutathione reductase is very specific for the reduction of GSSG to GSH through the use of NADPH reducing equivalents (Carlberg and Mannervik, 1975). This feature of the enzyme allows the continuous spectrophotometric assay of glutathione reductase activity (*UNIT 7.2).*

Two molecules of superoxide, the one-electron reduction product of molecular oxygen, will undergo spontaneous dismutation to yield hydrogen peroxide. This reaction is slow, however, compared to the same reaction catalyzed by superoxide dismutase (SOD) activity (Fridovich, 1995). Superoxide dismutases containing Cu and Zn (Cu,Zn-SODs) are found in both the cytoplasm and in extracellular fluids, whereas Mn-SOD is found in the mitochondrial matrix. Reduction of cytochrome *c* by superoxide produced by xanthine/xanthine oxidase forms the basis for the assay of total SOD activity presented in *UNIT 7.3*. Methods for determining the relative contributions of Cu,Zn-SOD and Mn-SOD to the total SOD activity in cell extracts are also described.

UNIT 7.5 contains protocols that permit the measurement of activity of SOD enzymes; in this case using a number of indirect competitive inhibition assays. The activities of the copper/zinc containing enzymes can be distinguished from the MnSOD activity in mammalian tissue homogenates using the differential sensitivity of these enzymes to inhibition by cyanide. In addition, a modified protocol is described in which the metal chelator, bathocuproinedisulfonic acid (BCS) is used to inhibit electron transport chain-associated interference in the assay. These assays (*UNIT 7.5*) utilize a xanthine oxidase system to generate superoxide and spectrophotomeric detection based on the reduction of nitroblue tetrazolium (NBT) which competes with SOD activity for superoxide.

Contributed by Donald J. Reed
Current Protocols in Toxicology (2002) 7.0.1-7.0.2

Cellular thiol and redox status is important for the structure and function of hundreds of thiol-containing enzymes. In addition, reducing equivalents are necessary for biosynthetic pathways, regulation of oxidative stress, and protection against oxidative damage. The ubiquitous thioredoxin system, thioredoxin (Trx) and thioredoxin reductase (TrxR), has a major role in these processes in bacterial, plant, and mammalian organisms. A hallmark of Trx, a redox-active protein, is the capacity to reduce protein disulfides. *UNIT 7.4* describes a method to measure purified Trx or TrxR by a spectrophotometric insulin-reduction assay. An alternative for biological samples is an end-point insulin-reduction assay. Mammalian-type Trx can be measured with NADPH as a direct reductant in the absence of TrxR. This assay is a coupled assay in that reduced Trx drives the reduction of Ellman's reagent, DTNB [5,5′-dithio-bis(2-nitrobenzoic acid)] to TNB (5-thio-2-nitrobenzoic acid), which is measured spectrophotometrically at 412 nm. A third protocol uses the reducing power of DTT to drive the reduction of Trx in the absence of TrxR; this reaction is ~1000-fold faster than the reduction of insulin by DTT. The reduction of insulin by Trx is another 100-fold faster than DTT reduction of insulin. Therefore, it is possible to measure the reducing capacity of Trx by a Trx-catalyzed reduction with DTT providing the reducing equivalents to Trx but not at a significant rate to insulin.

Ascorbic acid is a major water-soluble antioxidant in the cell cytoplasm and has an important role in the maintenance of redox homeostasis. Due to the power of ascorbic acid to be a reducing agent, the ease of its oxidation is always of concern during the preparation, handling, and assay of biological samples for accurate measurement of ascorbic acid and dehydroascorbic acid. *UNIT 7.6* focuses on the measurement of ascorbic acid, dehydroascorbic acid, isoascorbic acid, dehydroisoascorbic acid, and uric acid in biological samples. In addition, this unit describes the utilization of HPLC with electrochemical detection along with potential pitfalls in the analysis of these labile compounds. Protocols for the preparation of plasma, isolated-cell, and tissue samples are given in detail. A passivation procedure for the HPLC system (Support Protocol 4) is described to assist in lowering the detector background. Support Protocol 4 provides the procedures for the use of endogenous and internal standards in data analysis.

LITERATURE CITED

Arner, E.S.H, Zhong, L., and Holmgren, A. 1999. Preparation and assay of mammalian thioredoxin and thioredoxin reductase. *Meth. Enzymol.* 300:226-239.

Carlberg, I. , Mannervik, B. 1975. Purification and characterization of the flavoenzyme glutathione reductase from rat liver. *J. Biol. Chem*. 250: 5475-5480.

Fridovich, I. 1995 Superoxide radical and superoxide dismutases. *Annu. Rev. Biochem*. 64:97-112.

Mustachic, D. and Powis, G. 2000. Thioredoxin reductase. *Biochem. J.* 346:1-8.

Reed, D. J. 1985. Nitrosoureas. *In* Oxidative Stress (H. Sies, ed.) pp. 115-130. Academic Press, London.

Reed, D. J. 1986. Regulation of reductive processes by glutathione. *Biochem. Pharmacol*. 35:7-13.

Donald J. Reed

Analysis of Glutathione-Related Enzymes

This unit describes a basic spectrophotometric glutathione peroxidase (GPX) activity assay applicable to nearly any type of sample (see Basic Protocol). Variations of the Basic Protocol provide means to detect members of three gene family products with glutathione peroxidase activity, either as a collective activity or as subsets. Alternate protocols are described that can be used in conjunction with basic assay protocols to further distinguish among the six to seven major glutathione peroxidase isoenzymes (see Alternate Protocols 1 to 7). Support protocols for the preparation of substrates used in the basic variations are supplied (see Support Protocols 1 and 2) along with a support protocol for calculating specific activity (see Support Protocol 3). Short-cut methods are provided where multiple types of glutathione peroxidase activities are to be assayed. Novel reagents are discussed that can be used as an adjunct to the alternate protocols in difficult projects, and an alternate protocol is briefly described that permits the exploration of different reducing substrates (see Alternate Protocol 8). Critical issues of cell culture nutrition, sample preparation, and sample storage that need to be considered in advance of projects are discussed in the Commentary, which also provides an overview of HPLC and thin-layer chromatography systems that could be used to assay glutathione peroxidases.

STRATEGIC PLANNING

Glutathione peroxidase (GPX) is the name given to activities that catalyze the following reaction:

$$ROOH + 2GSH \rightarrow ROH + GSSG + H_2O$$

R can be hydrogen, a free fatty acyl group, cholesterol, a steroid, an ester of one of these groups, or free bases of DNA or RNA. GSH is the thiol tripeptide γ-glutamyl cysteinyl glycine, known as (reduced) glutathione and GSSG is the oxidized form of glutathione. Protein products of two unrelated gene families have glutathione peroxidase activity—the seleno-(Se)GPXs and the glutathione transferases (GSTs). A recently described non-GST, Se-independent GPX (antioxidant protein 2 or Aop2; Phelan et al., 1998), found in the ciliary body of the eye, in the olfactory epithelium, and in the skin, heart, liver, and kidney, may really be a thioredoxin peroxidase (see Background Information). However, conclusive evidence that this protein does not have glutathione peroxidase activity has not been provided. Expression of the genes for these proteins is quite variable among animal species, tissues, and derived cell lines. In the literature, glutathione peroxidase activity can refer either to the activity of a single protein (GPX1 in solid tissues or GPX3 in plasma) or to different collections of activities (GPX1, GPX2, GSTs, and GPX4) depending on the species of animal, the tissues or derived cell lines sampled, the assay conditions, and the inclination of authors. The use of different assay conditions can be fairly exclusive or inclusive as to the type of activities detected. Selective assay conditions used with unfractionated samples, or, combined with the use of sizing columns or other one-step separation methods, can be used to effectively report on individual components in many of the combinations of glutathione peroxidase proteins that are produced in tissues. The main strategic questions are as follows.

1. What should be assayed?
2. Is use of the Basic Protocol or Alternate Protocols 1 to 3 adequate to assay the glutathione peroxidase of interest, or will Alternate Protocols 4 to 7 need to be used?
3. Are there any special nutritional requirements for cultured cells to be sure that the activities will be produced?

Contributed by R.S. Esworthy, F.-F. Chu, and J.H. Doroshow

Current Protocols in Toxicology (1999) 7.1.1-7.1.32

4. Are there any special requirements for sample processing?

The successful detection of glutathione peroxidase activities in many cell lines depends on conditions established long before cell line harvesting, and, for both cell line and tissue samples, success can be dependent on the application of particular care during processing. If the study of glutathione peroxidases is new for the investigator or if the tissues or cell lines are novel and not well characterized, see Commentary for a discussion of these points.

A Basic Protocol is presented that is fairly exclusive for the assay of the major SeGPX in most solid tissues, GPX1. GPX1 is the major cytosolic and mitochondrial GPX activity. Exclusiveness of the assay is based on the use of hydrogen peroxide as substrate and on the broad distribution of GPX1 as opposed to the more limited distribution of other hydrogen peroxide–reducing isoenzymes. For cases where GPX2, GPX3, or Aop2 will be detected, see Background Information. Seven alternatives to the Basic Protocol are presented. Alternate Protocols 1 and 3 are more inclusive glutathione peroxidase assays that will detect GSTs with glutathione peroxidase activity, as well as GPX1-3. Alternate Protocol 2 is fairly exclusive for the assay of GPX4, also called phospholipid hydroperoxide GPX (PHGPX). Under some circumstances, this latter assay method can be used to detect microsomal GST with glutathione peroxidase activity, as well as a novel protein from the retina.

Protocols are presented that are useful in advance of the assays to enrich for particular glutathione peroxidase activities so that even inclusive assays (Alternate Protocols 1 and 3) can be used to determine levels of selected components. This type of strategy may be used when it is not clear which type of glutathione peroxidase activity is central to the question being asked. Animal and cell line resources that can be used to simplify the detection of subsets of the glutathione peroxidase families or used to confirm novel observations are also briefly discussed in Background Information.

Identification of the pertinent GPX activities in a toxicological study may require more thorough characterization of the sample(s) than is possible with the Basic Protocol and Alternate Protocols 1 to 3. Too often, studies of minor tissues and the GI tract are based on the false premise that the only GPX activities are from GPX1 or GSTs—or indiscriminately lump GPX1 and GST activities together. Investigations on less well characterized materials and animal species should begin with methods that could identify other isoenzymes (e.g., Alternate Protocols 4 to 7), before the decision is made that the Basic Protocol or Alternate Protocols 1 to 3 are sufficient for the purpose of the study.

Neither the Basic Protocol nor the first seven Alternate Protocols will permit the testing of alternative reducing substrates. An assay method is discussed (see Alternate Protocol 8) that can be used to examine different reducing substrates in purified samples.

BASIC PROTOCOL

MEASUREMENT OF GLUTATHIONE PEROXIDASE ACTIVITY

This protocol can be used to assay for SeGPXs 1 to 3 and Aop2. The isoenzyme subsets detected in crude samples will depend on the tissues or cell lines assayed (see appropriate Support Protocols and see Background Information). The protocol below is the method of Paglia and Valentine (1967) as modified by Lawrence and Burk (1976).

For the assay, a small volume of a clarified sample is mixed with assay buffer, as well as solutions containing GSH, NADPH, and glutathione reductase, in a cuvette rated for near-UV use. The mixture is allowed to equilibrate for 5 to 10 min. Hydrogen peroxide is then added to the mixture to begin the assay. The decline in the absorbance at 340 nm monitors the consumption of NADPH in the following reaction, which is catalyzed by glutathione reductase:

$$H^+ + GSSG + NADPH \rightarrow 2GSH + NADP^+$$

This reaction is driven by the formation of GSSG, coupling the glutathione peroxidase reaction to the change in absorbance monitored in the assay.

The coupled assay is quite adaptable. Many hydroperoxide substrates and detergents, as well as a range of pHs, different buffers, and ionic strengths can be used with this type of assay. This allows the study of the many proteins with glutathione peroxidase activity, some of which require hydroperoxide substrates other than hydrogen peroxide and conditions different from those in the Basic Protocol assay. Alternate Protocols 1 to 3 will substantially expand the repertoire of any laboratory studying glutathione peroxidases. However, there may be projects in which recourse to Alternate Protocols 4 to 8 will be needed.

Materials

Samples for analysis of glutathione peroxidase (GPX) activity
GPX-positive control (for first-time investigations; see recipe)
10 mM GSH (freshly prepared; see recipe)
2 mM β-NADPH (freshly prepared; see recipe)
5 mM H_2O_2 (see recipe)
100 U/ml glutathione reductase (see recipe)
Assay buffer: 50 mM sodium phosphate, pH 7.0 (*APPENDIX 2A*)
1.125 M sodium azide (see recipe)

Recording spectrophotometer with lamp and filters for 340-nm operation
1-ml near-uv-rated plastic cuvettes with 1-cm path (the assay can be easily scaled to smaller or larger volumes, if desired)

1. Warm up the spectrophotometer lamp.
2. Begin defrosting samples, GPX standards, if frozen, and GPX-positive controls (for first-time investigations), keeping all of these materials on ice. Assemble pipets, pipet tips, and samples at the assay site.

   Positive controls are required only for the total novice and only for the first few times that assays are performed or for troubleshooting purposes. After a few experiences with the assay, the positive control can be dispensed with unless the assay conditions are substantially altered for some purpose.

   The positive control should be prepared as a series of four or or five 1:1 serial dilutions. Do all dilutions in homogenization buffer. If the study samples are novel for the investigator, then this time can also be used to prepare dilutions. Three 1:5 serial dilutions of samples are a good starting point.

3. Prepare the 10 mM GSH, 2 mM NADPH, 5 mM H_2O_2, and 100 U/ml glutathione reductase according to their recipes (see Reagents and Solutions).

   If the GSH and NADPH have been properly handled to this point, they may be combined into a single solution for use.

4. For a 1-ml assay, add the following to a 1-ml cuvette in the order indicated:

   0.63 ml assay buffer (50 mM sodium phosphate, pH 7.0)
   0.1 ml 10 mM GSH
   0.1 ml 2 mM NADPH
   0.01 ml 1.125 M sodium azide
   0.01 ml 100 U/ml glutathione reductase.

   Add the sample in ≤0.1 ml. Add balance (to 0.1 ml) of the homogenization buffer used to process the sample (see Critical Parameters, Sample Isolation and Processing), if the sample volume is less than 0.1 ml. Mix the contents of the cuvette well and allow to equilibrate 5 to 10 min.

Blank assays should be performed first, followed by GPX positive controls, if used. To save time, up to four samples can be equilibrated at once. It is practical to perform four assays at one time on a multisampler-equipped spectrophotometer. Delays between adding substrate and recording results make it a bad practice to set up more than four assays at a time. Sample equilibration can be done in the spectrophotometer.

The assay set should begin with a blank assay containing homogenization buffer (0.1 ml) or in the case of blood plasma, phosphate buffered saline, in place of the sample in the above reaction mix. The blank is essential since hydrogen peroxide and GSH react spontaneously at a slow rate. The blank assay data will be used in the calculation of specific activity (see Support Protocol 1) at 340 nm. All assays including the blanks should be performed in duplicate. Triplicate assays are generally required only if the occasional discrepency shows up between duplicate assays.

5. Set up the spectrophotometer to give a full-scale span of 0.5 absorbance units (or other setting as determined by optimization) at 340 nm.

   The setting will depend on the actual amount of NADPH in the assay, the noise level in the recording, the types of samples, and the type of spectrophotometer. Experience will be needed to optimize the settings. Be sure to make a note of the settings so that calculations can be performed later. The assays will be run for 1 to 5 min to get data for rate determinations. Adjust the speed setting on a chart or the maximum interval for a program, accordingly. The blank(s) should run for 5 min, since it will be the slowest sample.

6. Make sure the blank is registering on the chart (if a chart recorder is used) at the higher end of the absorbance range.

   The assay follows the consumption of the absorbing species, so that the absorbance will decline as the assay proceeds. After mixing, the blank (minus H_2O_2) absorbance should be stable. If it is not, this may mean that the mixing was incomplete or that the temperature of the mixture is still equilibrating.

7. Start the chart, then add 50 µl of 5 mM H_2O_2 to the blank sample (total volume in cuvette 1 ml). Mix the sample quickly and thoroughly. Start recording the change in absorbance.

   At a setting of 0.5 absorbance full scale the blank will proceed at a rate of ~$^5/_{100}$ divisions per min (0.025 A_{340}/min). Concern is warranted only if this rate is zero or >$^{15}/_{100}$ divisions per min (0.07 A_{340}/min). However, consistency in the blank rate is expected from day to day. If this is not happening then something is wrong with the reagents or techniques.

8. Using the same procedure as for the blank (step 7), assay a dilution series of the positive control, processing the reactions one at a time.

   The purpose of the dilution series of the positive control is to test the assay mix and to establish the upper limit for the linear response of the assay. This assay will handle ~0 to 25 mU of activity (1 U = 1 µmol/min of NADPH consumed). This would correspond approximately to a rate of $^{35}/_{100}$ division/min (0.17 A_{340}/min). The dilution series of the positive control will establish that all of the reagents are good and will indicate the maximum acceptable rate that falls in the linear range (i.e., two-fold increase in sample amount produces a two-fold increase in rate after adjustment for the blank rate). After the positive control has been tested a few times, it can be dispensed with. The study samples should be well characterized by this point and they can be used for this purpose.

9. Pause at this point to determine the blank rate and maximum acceptable rate.

   During the study assays, be alert for samples whose rates approach or exceed the allowed maximum rate or are close to the blank rate. Data derived from such assays may be of limited value. Such assays may be terminated early and redone with appropriate sample amounts.

10. Using the reaction volumes described in steps 4 and 7, proceed to the assay of the study samples.

    If this is the first assay of samples, monitor the assay during equilibration to see if there is a spontaneous downward drift. If the activity of the samples is low, this small drift may have to be subtracted from the assay rate, in addition to the blank rate, to obtain accurate activity calculations. This practice may have to be continued if it is expected that activities will be low for the balance of the project(s).

    If a break is required, make sure that all of the samples and the diluted glutathione reductase are maintained at ice temperatures. After a prolonged break, the blank should be performed again. If the current blank rate is less than the initial blank rate, it may be necessary to prepare new GSH and NADPH. The blank rate is determined again with the fresh reagents.

11. Calculate the activity of the samples (see Support Protocol 3).

ASSAY OF GSTs WITH GPX ACTIVITY AND SeGPX WITH CUMENE HYDROPEROXIDE

ALTERNATE PROTOCOL 1

GPX1 and GSTs with glutathione peroxidase activity are collectively assayed using the conditions originally established by Lawrence and Burk (1976). Results collected with this assay are of little value by themselves, since too many activities are detected. It is best to combine this assay with results from the Basic Protocol (see "short-cut" method, Alternate Protocol 4) or to use this assay in conjunction with methods that can resolve SeGPX and GST activities (Alternate Protocol 6). GPX4 will not contribute significantly to the total activity measured in this protocol. It is impractical to use this variation for GPX4 and far from optimal to use it for Aop2, even with fractionation of the samples. Alternate Protocol 3 is better suited for detection of these activities.

Additional Materials *(also see Basic Protocol)*

30 mM cumene hydroperoxide (see recipe)

1. Set up spectrophotometer and reaction mixes (see Basic Protocol, step 1 to 4).

   A new blank rate must be established for this assay. Positive controls described for the Basic Protocol (see Reagents and Solutions) will work for this alternate protocol.

2. At step 7, add 50 µl of 30 mM cumene hydroperoxide, for a final 1.5-mM concentration, instead of hydrogen peroxide.

3. Peform the assays and calculate the activities (see Basic Protocol, steps 7 to 11).

ASSAY OF GPX4 (PHGPX) WITH PHOSPHATIDYL CHOLINE HYDROPEROXIDE

ALTERNATE PROTOCOL 2

GPX4 can be specifically assayed with several minor reagent modifications and a major change in the type of hydroperoxide substrate (Zhang et al., 1989; Maiorino et al., 1990). If one has a working familiarity with the Basic Protocol, the GPX4 assay will not be difficult to run. Triton X-100 (peroxide-free; Sigma, Aldrich, Boehringer Mannheim) is added from a separate stock so that the final concentration in the assay is 0.1% to 0.2% (v/v). It is essential that Triton X-100 be in the assay when GPX4 activity measurements are made. Cholate-based detergents cannot be used in the tissue preparation or in the assay, since they will denature GPX4. The pH of the assay buffer should be 7.3 to 7.6 to obtain the sensitivity needed for the assay. This will require a different buffer. A standard version of the GPX4 assay method uses a buffer of very high concentration, so that smaller volumes can be used in the assay (0.4 M Tris·Cl). Much more sample can then be used without upsetting the assay pH. This may be required for some samples (even as 20% homogenates), due to the paucity of GPX4 activity in many animal tissues and cell lines.

Tissue levels of GPX4 tend to be 0.2% to 20% of GPX1 levels (Zhang et al., 1989). Testis is an exception where the level of GPX4 exceeds that of GPX1 (Roveri et al., 1992). Dilution of samples should not be performed until an initial survey of the GPX4 levels, performed on the undiluted samples, shows that this can be done.

The most widely used differential substrate is the hydroperoxide species (PLOOH) obtained from the action of soybean lipoxygenase on phosphatidyl choline in the presence of deoxycholate (see Support Protocol 1). PLOOH can be synthesized and enriched to usable form by most laboratories. This substrate is used at 20 to 30 μM concentrations in the assay (see Support Protocol 1, step 8). This assay was developed by Zhang et al. (1989) and modified by Maorino et al. (1990).

The equipment used is the same as that used in the Basic Protocol, except that 3- to 4-ml cuvettes are used to accommodate the 2.5-ml assay volume. This is flexible, as the assay can be scaled down to 1 ml. Mixing requirements may preclude the use of <1-ml volumes.

Materials

Assay mix for GPX4 (see recipe)
100 U/μl glutathione reductase (see recipe) in ice-cold 0.4 M Tris·Cl, pH 7.4
10% (v/v) peroxide-free Triton X-100 (Sigma, Aldrich, Boehringer Mannheim) in H_2O (keep on ice)
Phosphatidyl hydroperoxide (PLOOH) substrate in methanol (see Support Protocol 1; concentration such that the substrate can be added to a final concentration of 20 to 30 μM in the assay mix by adding a 20- to 25-μl aliquot of the methanol solution)
GPX4 positive control (see recipe)
Negative control: GPX1 standard free of GPX4 (optional, but advisable for the novice; see recipe)
3- to 4-ml near-UV-rated plastic cuvettes with 1-cm path for spectrophotometer

1. Add the following to a 3- to 4-ml cuvette:

   0.5 ml assay mix for GPX4
   10 μl 100 U/μl glutathione reductase
   30 to 60 μl 10% peroxide-free Triton X-100 (final concentration 0.1% to 0.2% v/v)

   then add water to adjust the volume to 2.48 ml, less the sample volume.

   Sample volumes up to 0.5 ml are routine in this assay. The constraining factors are the possible alteration in pH and GSH concentration with the addition of sample.

   Buffer should be prepared in advance. Sodium azide can be included at a concentration of 10 mM; in that case the buffer can be used in the Basic Protocol—i.e., GPX1 can be assayed in this buffer as well.

2. Add up to 0.5 ml of the sample, positive control, or negative control, mix thoroughly, and allow an extended (e.g., 15-min) equilibration period.

   The blank for this should be homogenization buffer used for the samples (see Critical Parameters, Sample Isolation and Processing).

   Most samples probably will not require dilution. A positive control sample of rodent testis may be diluted 1:1 or 1:5 in homogenization buffer before use.

3. Carry out the assay (see Basic Protocol, steps 5 to 11), with the following variations.

   a. Set the full-scale span of the spectrophotometer at 0.2 A_{340} for chart recorders.

b. Monitor the assay equilibration phase after the sample is added since there is often a small, continuous downward drift that may be slow to cease.

This may have to be tolerated for the sake of throughput with a sample set of any size and factored into the calculations as a second rate, subtracted after the blank rate.

c. Measure the A_{340} of blanks and samples for several minutes (up to tens of minutes in some cases) to obtain good rate data because the signal-to-noise ratio is less than what is seen in the Basic Protocol.

The recommended positive control will be deceiving in this regard; it will have activity much greater than most other samples. Therefore, it is very important not to adjust the recommended parameters for the assay of samples based on the performance of a rodent testes control sample. A 1.5 to 2 A_{340} full-scale setting is used only with the positive control to determine the substrate concentration (see Support Protocol 1). However, this is the only occasion for a compressed full-scale setting.

4. Start the assay by adding 20 to 25 µl of phosphatidyl choline hydroperoxide (for a 20 to 30 µM concentration in the cuvette) and quickly but completely mixing the cuvette contents.

The PLOOH can be made while the reagents are equilibrating to room temperature or made in advance (see Support Protocol 2). An aliquot sufficient to assay the samples can be kept on ice while the balance is returned to −70°C storage.

The substrate could be hydrogen peroxide or a free fatty acid hydroperoxide (Alternate Protocol 3) rather than PLOOH. Triton X-100 would be omitted in these cases. The range of glutathione peroxidase activities detected is thereby altered, and the assay is no longer specific for GPX4. For strip-chart recorder setup, the absorbance setting and chart speeds would have to be adjusted to those used for Basic Protocol or Alternate Protocol 1.

Specific activities obtained for major organ samples with this assay will be in the range of 5 to 20 mU/mg protein. By comparison, GPX1 major organ specific activities with these conditions (with hydrogen peroxide as the substrate) are in the range of hundreds to thousands of mU/mg (Zhang et al., 1989). For the testis control, the GPX4 specific activity will be 40 to 100 mU/mg, depending on species, buffers used for extraction, and the vigor of the tissue disruption method (Esworthy et al., 1997; Roveri et al., 1992).

Interference from microsomal GST seems to be negligible (Mosialou and Morgenstern, 1989). This may be due to the requirement of microsomal GST for activation with potent thiols, the small quantities present in most sources, the microsomal localization, or the lability of this enzyme. In some eye tissues, an activity other than GPX4 or microsomal GST is detected (Lam et al., 1993). The origin of this activity is a protein with physical properties unlike any known glutathione peroxidase.

SYNTHESIS OF PHOSPHATIDYL CHOLINE HYDROPEROXIDE (PLOOH) FOR THE ASSAY OF PHGPX

SUPPORT PROTOCOL 1

The substrate derived from this method can be used to assay very specifically for GPX4, with minor exceptions (Lam et al., 1993; also see Alternate Protocol 2). GPX1-3 and most GSTs have only marginal activity with the PLOOH substrate (Maiorino et al., 1990). The substrate is used at a concentration of 20 to 30 µM. A simple and fast method (1 hr) for making the substrate was published in by Maiorino et al. (1990). The yield of substrate from the published method is sufficient for up to 50 assays.

Materials

Phosphatidyl choline (PL; Avanti Polar Lipids, Sigma, or Aldrich)
Source of nitrogen gas
0.2 M sodium borate, pH 9 (or other buffer for pH 9 to 10 range)
0.05 M sodium deoxycholate

Soybean lipoxygenase (Sigma Type IV or equivalent)
Absolute methanol
GPX4 positive control sample (see recipe)
1-ml Sep-Pak C18 cartridge column, or equivalent

Additional reagents and equipment for assaying GPX4 (see Alternate Protocol 2)

1. Dry a solution of phosphatidyl choline (PL) under nitrogen in a 50-ml beaker.

   The amount of PL stock used should yield a 0.3 mM solution in 18 to 19 ml (see step 2).

2. Resuspend the dry PL, with stirring in 18 to 19 ml 0.2 M sodium borate, pH 9, for a final concentration of 0.3 mM.

3. Add 0.05 M sodium deoxycholate stock to a final concentration of 5 mM in a volume of 20 ml. Sonicate or vigorously stir to properly dissolve the PL and to aerate the mix.

4. Add 100,000 U soybean lipoxygenase. Stir mixture 20 min to allow oxidation of the PL to PLOOH.

5. During this time, prepare a 1-ml C18 column by washing with 20 to 30 ml water, 20 to 30 ml absolute methanol, and again with 20 to 30 ml water.

6. Taking care to observe the column manufacturer's precautions about maximum flow rates, rapidly pass the oxidized PL over the column. Wash the column with 30 ml water.

   The goal of this step is to remove the sodium deoxycholate. If not removed, the detergent will interfere with the assay.

7. Slowly elute the PLOOH from the column with ~3 ml absolute methanol.

   The substrate may be ready to use at this point. However after an initial titration of the substrate (step 8), it may be found that it should be concentrated. This can be performed under a stream of nitrogen. The final eluate will probably have some water. This will limit the stability of the substrate even with careful storage (−70°C, under nitrogen). Two weeks is the longest time that the authors have been able to store a preparation.

8. Estimate the yield of the substrate by permitting a reaction with a GPX4 control sample to exhaust the hydroperoxide substrate (see Alternate Protocol 2).

   It may be necessary to run the assay reaction with GPX1 and hydrogen peroxide, or other GPX1 substrate, to determine the total OD units of NADPH that are in the assay mixture. Then, the GPX4 substrate is added to a series of positive control assays at lower and lower amounts until it is possible to see the assay running to completion well before the NADPH supply is used up. Using the millimolar extinction coefficient of 6.22 for NADPH, it is possible to calculate the amount of substrate in the reaction.

   In this case, the total OD change from the time of the addition of substrate until the substrate is consumed is divided by 6.22×10^3 OD units/mol. This value is again divided by 1000 to yield the moles of substrate in the aliquot used in the titration. Also see Support Protocol 3, step 4.

   The substrate should not drive an assay that has GPX1 and no GPX4. See Reagents and Solutions for preparation of GPX4-positive controls and GPX1 standard.

ALTERNATE PROTOCOL 3

INCLUSIVE GPX ASSAY WITH UNIVERSAL SUBSTRATES

A more inclusive version of the assay method than that described in Alternate Protocol 1 is possible with hydroperoxides of linoleic acid or arachidonic acid (Maiorino et al., 1990; Hong et al., 1989). Results collected from this alternate protocol will have little interpretative value on crude samples. It is best applied in projects where glutathione peroxidases

are resolved by some means. At a concentration of 50 μM fatty acid hydroperoxide, almost any glutathione peroxidase activity can be detected. Expense, skill at synthesis and purification, and lability of the substrates are the main barriers to the routine use of these substrates at high concentrations. The hydroperoxides are commercially available or they can be synthesized. HPLC is very useful for substrate purification following synthesis. However, it is not essential with linoleic acid hydroperoxides (see Support Protocol 2).

The assay with these substrates is best performed using the conditions described in Alternate Protocol 2, where the increased GSH concentration and higher pH of the assay buffer increase the sensitivity enough to detect GPX4 activity. However, Triton X-100 is left out of the assay when free fatty acid hydroperoxides are the substrates. Even in this variation, GPX4 may contribute little to the total activity. The assay will register activity in fractions where GPX4 has been resolved from GPX1 and GSTs. Ultimately, the quantitation of GPX4 is dependent on fractionation of the sample and/or the use of Alternate Protocol 2.

Perform Alternate Protocol 2 as described, except omit Triton X-100 from the assay and substitute linoleic acid hydroperoxide (50 μM) for phosphotidylcholine hydroperoxide in step 4 of that protocol. See Support Protocol 2 for synthesis of linoleic acid hydroperoxide. Perform a blank reaction with the linoleic acid hydroperoxide and use a sample with GPX activity as a positive control.

SYNTHESIS AND ISOLATION OF LINOLEIC ACID HYDROPEROXIDE FOR THE ASSAY OF GPX

SUPPORT PROTOCOL 2

Linoleic and arachidonic acid hydroperoxides can be purchased from Cayman Chemical. Both can be synthesized using the free fatty acids and lipoxygenases or by oxidation in air (Forman and Kim, 1989). Purification of linoleic acid hydroperoxides can be performed with or without HPLC. The authors have used the non-HPLC method of Forman and Kim (1989), described below, with good results. However, verification of the purity of the substrates is best done with HPLC or thin-layer chromatography methods. For the isolation method described here, a large fume hood is required for the many solvent extractions. A rotary evaporation device is useful, but may be replaced with a nitrogen or argon gas flow. A full H-type gas cylinder may be needed if a rotary evaporation device is not available.

Additional Materials *(also see Support Protocol 1)*

Linoleic acid (Cayman Chemical)
0.5 M sodium borate, pH 9
Petroleum ether
Ethyl acetate
70:40:1 acetonitrile/H_2O/acetic acid

Rotary evaporator or full H-type nitrogen or argon cylinder
Compressed air or oxygen tank to facilitate oxygenation of substrate
3-ml and 1-ml Sep-Pak C18 cartridge columns, or equivalent
Separatory funnels or other glassware for extractions

1. Remove solvent from the linoleic acid, if any is present, by blowing a stream of nitrogen or argon over the sample.

   Good yield is achieved by starting with 0.2 to 0.4 ml linoleic acid.

2. Resuspend linoleic acid in 50 ml of 0.5 M sodium borate, pH 9.0, using a magnetic stirrer. Aerate solution with air or pure oxygen.

3. Peroxidize the linoleic acid by adding eight aliquots of soybean lipoxygenase containing 125,000 U each, from a stock of 1,000,000 U, over a 2-hr period.
4. During this time, prepare three 3-ml C18 columns by washing with 20 ml water, 20 ml absolute ethanol, and again with 20 ml water.
5. Load one-third of the sample onto each C18 column.
6. Elute the lipid using ~8 ml methanol per column. Pool the eluate and bring to dryness under a stream of nitrogen.
7. Resuspend the lipid in 20 to 40 ml petroleum ether.
8. Extract the suspension in an equal volume of 3:1 methanol:water, then repeat with the extracted petroleum ether phase.
9. Concentrate the methanol:water extracts to 4 ml with rotary evaporation or a stream of nitrogen/argon.
10. Extract the sample twice, each time with an equal volume of ethyl acetate. Evaporate the ethyl acetate extracts to dryness under nitrogen/argon.
11. Dissolve the concentrated sample in 70:40:1 acetonitrile:water:acetic acid. Load 1-ml aliquots of the solution on 1-ml C18 columns and elute with 2 ml of 70:40:1 acetonitrile: water:acetic acid.
12. Combine fractions and concentrate as in step 9. Extract the concentrated material twice with ethyl acetate and bring to dryness as in step 10. Resuspend in 3 ml absolute ethanol.

    The yield should be at least 20 µmol, i.e., 3 ml of a 7 mM solution.

13. Store sample at –70°C in a light-proof, stoppered container that has been flushed with nitrogen.

    If properly done, the method will supply a good yield of hydroperoxides (i.e., 9 and 13 hydroperoxide isomers), with >90% purity, in one day. Other types of lipoxygenase can be used to yield other combinations of isomers (Forman and Kim, 1989).

ALTERNATE PROTOCOL 4

ASSAY OF SeGPX AND GST IN MIXTURES (DUAL ASSAYS)

There is really little value in reporting only the "total" glutathione peroxidase activities (i.e., cumene hydroperoxide, linoleic acid hydroperoxide) or attempting to draw firm conclusions about glutathione peroxidase responses to experimental conditions based on such results (see Commentary). Under the conditions described in the Basic Protocol and for Alternate Protocol 1, both substrates will come very close to saturating GPX1. The V_{max} of GPX1 for all hydroperoxides is theoretically the same. The sample activity with hydrogen peroxide will be approximately the activity of GPX1 with cumene hydroperoxide; and the difference in the activity measured with cumene hydroperoxide and hydrogen peroxide is an estimate of the fraction of activity from GSTs relative to the total cumene hydroperoxide activity. The estimate is suitable for preliminary work. More definitive means to verify the estimate are found in Alternate Protocol 6. Use of dual assays is strongly urged if these glutathione peroxidase activities will not be resolved or distinguished by other means. This will require the use of two blank reactions and two separate assays, one for each substrate. For the following steps, see Basic Protocol, Alternate Protocol 1, and Support Protocol 3 for reagents and equipment.

1. Assay one aliquot of the sample (and blank) with hydrogen peroxide (see Basic Protocol).

2. Assay a second aliquot of the sample (and blank) with cumene hydroperoxide (see Alternate Protocol 1).
3. Calculate the GPX specific activity of the sample from each assay (see Support Protocol 3).

GPX1-specific activity is obtained with H_2O_2 as the substrate (see Basic Protocol and Support Protocol 3). The GST peroxidase activity is the difference between the specific activity calculated from Alternate Protocol 1 and the specific activity calculated from Basic Protocol. Both activities can be presented as a fraction of the activity obtained with cumene hydroperoxide as substrate.

ASSAY OF GPX1 AND GPX4

ALTERNATE PROTOCOL 5

If both GPX1 and GPX4 assays are required for a project, the buffers and conditions used in Alternate Protocol 2 can be used for both isoenzymes. Triton X-100 will not interfere with the assay of GPX1 when hydrogen peroxide is the substrate, but it could be omitted when GPX1 is assayed. For accurate rates, quite different amounts of sample may have to be used to assay each activity. The spectrophotometer/recorder settings (full-scale chart settings, assay duration settings, or chart speeds) will have to be reset between assays of the isoenzymes.

Set up the sample assays and blanks in the same way as for Alternate Protocol 2, except omit Triton X-100 when GPX1 is to be assayed with hydrogen peroxide as substrate in step 4. Start the GPX1 assay with the addition of 10 µl of 5 mM hydrogen peroxide stock.

Some workers actually perform both GPX1 and GPX4 assays on a single sample aliquot by first using the GPX4 substrate, then hydrogen peroxide (sequential assay). A supply of extra concentrated NADPH stock may be required to replenish the assay between each part of the sequential assay. The spectrophotometer/recorder setting may also have to be redialed each time. For the sequential assay a 10 mM stock of β-NADPH can be prepared in the event that the GPX1 assays terminate too soon for a rate estimate due to depletion in the PHGPX assay.

For materials and equipment, see Basic Protocol and Alternate Protocol 2.

1. Proceed with the assay of PHGPX as described in Alternate Protocol 2.
2. After the PHGPX assay has run sufficiently so that a rate can be established, make a judgment about which of two procedures should be followed before proceeding to the assay of GPX1.
   a. If the PHGPX activity is very low there may be no need to let the reaction deplete the PLOOH stock before proceeding to the assay of GPX1.
   b. If the PHGPX activity is substantial, the reaction should be allowed time to deplete the PLOOH substrate before proceeding. The more PHGPX activity in the sample, the less the waiting time.
   c. An aliquot of the concentrated β-NADPH stock would be added at this point, if it appears to be needed.
3. Assay the GPX1 in the sample by adding 10 µl hydrogen peroxide.
4. Be sure to run a blank through the sequential assay.

The GPX1 activity values may be underestimated in the sequential assay because of interferences (minor) and because the maximum capacity of the assay will frequently be exceeded. The sequential assay is useful for identifying samples from columns or subcellular fractions with GPX1 or GPX4 activities where qualitative results will suffice and economy of sample is a consideration. GPX1 fractions recovered from Sephadex G-50 to

200 will not have GPX4, activity if the fractionation was competently performed. A blank rate for the PLOOH will be found in these fractions after several minutes. Human GPX1 and GPX3 samples sometimes have a rate above the blank rate for a minute or so, possibly due to PLOOH substrate deterioration. However, this spurious reaction can be distinguished from the real reaction since it is not linear. The real PLOOH blank rate is negligible in comparison to GPX1 activity rates and can be ignored when proceeding to the second part of the sequential assay. In subcellular fractions, both activities may be present. In this case, the GPX4 assay is run until the substrate is exhausted, then the GPX1 assay is performed. GPX4 contribution to activity with hydrogen peroxide is generally negligible.

ALTERNATE PROTOCOL 6

CHROMATOGRAPHIC SEPARATION AND ASSAY OF GPX ISOENZYMES

The question of whether to measure one, some, or all of the glutathione peroxidase activities in a sample requires some consideration. If it cannot be determined, a priori, which glutathione peroxidase activity is central to a question, a common substrate such as cumene hydroperoxide (Alternate Protocol 1) or better yet, linoleic acid hydroperoxide (Alternate Protocol 3), can be applied to a sample in which the isoenzymes have been resolved on a sizing column or by some other suitable methods. Then, information can be obtained for the activity of major components.

Far more methods have been described for the resolution of glutathione peroxidases than can be discussed here. Partial to complete resolution of GPX1, GSTs, and GPX4 is possible with gel-filtration columns. GPX1-3 migrate on columns of Sephadex G-100 to 200 with apparent masses of 80,000 to 100,000 Da; GSTs migrate with apparent masses of 40,000 to 55,000 Da; GPX4 has an apparent mass of 15,000 to 22,000 Da (Lawrence and Burk, 1976; Maiorino et al., 1991). Aop2 appears to have different native sizes in different tissues. In the ciliary body of the eye, the apparent mass was 110,000 Da, while in nasal epithelium the mass was estimated at 55,000 Da (Singh and Shichi, 1998; Peshenko et al., 1998). The subunit mass is 28,000 Da in the many tissues where it has been detected. However, the nature of the multimer is not known for most tissues. Thus, gel filtration methods can be used to distinguish among the more common combinations of activities found in tissues, but there will be cases where this method may not be suitable.

Materials

Column buffer with reducing agent (see recipe)
Column standards: any set of proteins with native sizes of 15,000 to 100,000 Da
Sample to be fractionated

Columns: 50 cm length × 1.5 cm diameter to 100 cm length × 2 cm diameter (see Hagel, 1998)
Tubing to connect the column and fraction collector
Sephadex G-150 to 200 (see Hagel, 1998)
Fraction collector with a capacity for up to 100 tubes (5- to 10-ml volume)

Additional reagents and equipment for assays of GPX activities (see Basic Protocol, Alternate Protocol 1, and Alternate Protocol 3)

NOTE: Perform all steps at 4°C to 10°C using a cold room or other suitable means.

Perform gel-filtration chromatography

1. Set up and standardize the column.

   This should be done a day or two in advance of fractionating the sample.The details of column setup, operation, and standardization are beyond the scope of this chapter. A good reference for gel-filtration chromatography in general is Hagel (1998).

2. Assay the unfractionated sample for GPX activity to establish that the starting activity is sufficient to be used for this purpose (see Basic Protocol).

   The sample will be diluted several-fold by the action of the gel filtration and the components will be resolved into separate fractions. If the activity is difficult to detect at this stage, it may be impossible to detect after fractionation. A larger quantity of material (5× to 10×) can be concentrated down to the 4 to 5 ml that can be loaded onto the column, or a more sensitive assay can be used.

3. A few hours prior to the fractionation of the sample, fill the column reservoir with buffer containing a fresh supply of reducing agent and flush the column with the fresh buffer.

4. Apply the sample and begin collecting fractions at a flow rate of ~0.2 to 0.5 ml/min.

   Columns with the dimensions mentioned above will handle up to 5 ml of sample.

   Collection of individual fractions can be delayed up to the point of the void volume of the column, if determined (see Hagel, 1998). However, a portion of the void sample should be kept for use in the blank assay (see step 5, below). Collect fractions so that the total amount of buffer run over the column is at least 5 column volumes.

   Fraction volumes of 2 to 6 ml should be adequate for most purposes. The run time will be several hours. It is most convenient to run the column overnight and perform the assay of the fractions first thing the next day.

5. Collect eluate just after sample is applied (i.e., from the void volume) for use as a blank.

6. Assay the fractions (Alternate Protocol 1 or 3) taking note of the volume of the unfractionated sample that was needed to detect activity and the fact that the activities will be resolved and diluted by the fractionation.

   As a time-saving measure, alternate tubes can be skipped during the initial survey of activities.

Identify the major activities

7. Plot the total activity per fraction (assuming equal volumes) as a function of fraction number.

8. Compare the locations of the activity peaks to the fractions in which the standards eluted (assuming that fraction volumes are equal) for a size estimate of the component GPX activities.

   Refer to the introduction to this protocol for the native sizes of the respective activities. In this way, the identity of the major activities can be surmised and/or some candidates eliminated. Confirmation of component identities can be made by assaying with specific substrates.

   The column can be reused many times. Flow rates and fraction volumes will have to be examined as the column is reused. By standardizing samples for total protein load, semiquantitative and quantitative comparisons can be made of individual components.

ASSAY OF GPX1 AND GPX2 AFTER SELECTIVE IMMUNOPRECIPITATION

ALTERNATE PROTOCOL 7

GPX1 and GPX2 are coproduced in the GI tract mucosal epithelium (Esworthy et al., 1998). Indirect methods suggest that GPX2 is also produced in breast tissues (epithelium) and human liver (Chu et al., 1993). Several cell lines produce GPX2; a few of these barely produce GPX1 (Esworthy et al., 1995). GPX1 and GPX2 cannot be resolved by simple one-step column methods. Several combinations of multistep column chromatography

methods that the authors have tried have produced only partial resolution (Esworthy, et al., 1998). None were adequate for quantifying the separate isoenzyme activities.

Antibodies against GPX1 generally cross-react only slightly with GPX2 and vice versa. Antibodies can be used to remove the bulk of one isoenzyme from a mixture so that the balance of the activity can be assayed (Esworthy et al., 1998). GPX1 antibodies seem to be better at this than GPX2 antibodies, and GPX2 antibodies are not available for general use. However, GPX1 antibody is commercially available and many laboratories share GPX1 antibodies. If antibody methods are used in conjunction with activity assays, immune Ig preparations depleted of plasma GPX3 will be required. This can be accomplished with many methods that are used to enrich the Ig fraction of plasma or sera (Esworthy et al., 1998). Difficult cases may also be approached using animals that underproduce GPX1, or using other reagents (see Background Information).

Materials

GPX-depleted immune (IgG) fraction of rabbit plasma (Esworthy et al., 1998): preimmune and anti-GPX1
Immunoprecipitation buffer (see recipe)
10% (w/v) suspension of washed *Staphylococcus aureus* protein A (see recipe)

Additional reagents and equipment for assay of GPX4 (see Alternate Protocol 2)

1. Incubate the plasma GPX-depleted immune fraction (IgG) with the sample (10 to 25 mU GPX activity) in immunoprecipitation buffer at 4° to 8°C in a final volume of 200 µl, for a minimum of 5 hr (up to but not exceeding 18 hr) at 4°C. Prepare blank reactions containing the same components as the sample or control reactions except substitute the sample buffer for the sample or control activity.

   Triton X-100 and GSH may have to added from separate concentrated stocks if the sample volume alone is near 200 µl.

   The optimal amount of Ig to add to the samples will have to be determined empirically. The proper amount of protein A added to the reaction (see step 2) may be affected by alterations in the amount of Ig added.

   The controls for this assay involve the use of preimmune Ig and semipurified GPX1 activity (see Alternate Protocol 6). The controls are used to demonstrate that the Ig preparation was immunoreactive with GPX and that the reactions are specific under these conditions. The depletion of plasma GPX activity from the Ig preps may not be complete. Therefore, a separate blank rate must be determined for each Ig preparation based on the volumes used in the test samples. A GPX2 control can be obtained from the GI tract of Gpx1 gene knockout mice (see Background Information).

2. Add 50 to 75 µl of a 10% suspension of washed protein A or some other Ig-binding/precipitating agent to the mixture and incubate 1 hr at 4°C.

3. Remove immune complexes by centrifuging 10 min at 10,000 × *g*, room temperature.

   This centrifugation must be done at room temperature so that the temperature of the supernatant does not interfere with the assay performed in the next step.

4. Recover the entire supernatant and assay according to Alternate Protocol 2, using hydrogen peroxide as the substrate in step 4 of that protocol.

   Alternate Protocol 2 is used because that assay system can accommodate the large sample volume and tolerate all of the sample additives.

THE FERRICYANATE METHOD OF HYDROPEROXIDE DETERMINATION TO ASSAY GLUTATHIONE PEROXIDASE

One shortcoming of the coupled method (using the Basic Protocol and Alternate Protocols 1 to 4) is that potentially interesting reducing substrates cannot be freely substituted for GSH. Glutathione reductase from most sources does not reduce a broad range of oxidized thiols. Some mixed disulfides of the type GSSX can be reduced. Thioredoxin reductase can be used as a coupling enzyme to study thioredoxin as a reducing substrate (Bjornstedt et al., 1994). Thioredoxin reductase, itself, has been found to be a reducing substrate for extracellular GPX (GPX3). There is a family of thioredoxin peroxidases with no relationship to any of the families of proteins with glutathione peroxidase activity (Chae et al., 1994). Before using thioredoxin and/or the reductase as alternative substrates, the glutathione peroxidase activities of a tissue may have to be partially or completely purified.

Alternative reducing substrates can be examined using methods that monitor hydroperoxide concentrations. Most hydroperoxide concentration assays are easy to use, very sensitive, and adaptable to glutathione peroxidase assays. The ferricyanate method of Thurman et al. (1972) can be used to assay glutathione peroxidase activity via the consumption of hydroperoxides, as a simple alternative to HPLC or thin-layer chromatography methods. The authors have used hydrogen peroxide, cumene hydroperoxide, and *t*-butyl hydroperoxide with this method. The strengths of the method are that particulates in the sample (even intact cells) can be tolerated, that it uses few costly reagents, that alternative reducing substrates can be freely explored in purified samples of glutathione peroxidases, and that the equipment requirements are less than with the coupled method. There are some weaknesses in this method, however. In crude homogenates or partially purified GPX preparations, consumption of hydroperoxides may be occurring via non-GSH-dependent means. This will be reflected in the assay results. Proper controls and/or precautions that were used in the coupled assay can determine or prevent the non-GSH dependent consumption. Neither hydroperoxide nor GSH concentrations are constant in this method, so rates will deviate from linear. A lot of sample may be required since multiple aliquots are needed to construct a hydroperoxide consumption curve. Many tubes must be labeled and set out in an orderly fashion. Manipulation of a caustic reagent (TCA) is required. Distractions cannot be tolerated once an assay has been started. It is difficult to perform more than two assays at one time. Establishing proper aliquot sampling times, size, and other parameters can be labor-intensive and time-consuming.

Additional Materials *(see Basic Protocol and Alternate Protocols)*

50% or 100% trichloroacetic acid (TCA)
10 mM ferrous ammonium sulfate
2.5 M potassium thiocyanate
Spectrophotometer

NOTE: The first step is either to carefully plan the assay so that some quantitative data can be obtained right away or to perform the assay on a trial basis using GSH as the reducing substrate so that real planning is possible. The time course of the reaction for a given sample activity can be roughly estimated from the parameters of the Basic Protocol or Alternate Protocols 1, 3, or 4. GSH is usually the best substrate for GPX, so that reactions with alternative reducing substrates should run more slowly.

1. Label a set of 1.5- to 1.7-ml plastic microcentrifuge tubes.

   These tubes will hold the TCA that will stop the enzyme reaction when an aliquot of sample is added and mixed. The labels will reflect the sample (if multiple samples are to be tested) and a time point or time point code reflecting the time lapse from the start of the reaction. Five to ten tubes may be needed per reaction.

2. Add 0.2 ml of 50% TCA or 0.1 ml of 100% TCA to each tube.

3. Prepare the reaction mixture (buffer and sample).

   The buffers can be the same as those used in the Basic Protocol or the Alternate Protocols if an enzyme preparation is to be tested. The buffers used in Alternate Protocol 3 will probably provide the best sensitivity. The volume of test enzyme will be based on a preliminary test with GSH as the reducing substrate in one of the protocols in this unit; the authors recommend using Alternate Protocol 3 conditions. The buffer could also be some type of buffered saline solution if intact cells are tested. The assay mixture will contain GSH (or test reducing source) and sample as in Alternate Protocol 3, but NADPH and glutathione reductase are not used.

4. Set up an assay reaction of sufficient volume that multiple (five to ten) sample aliquots of 0.8 to 0.9 ml can be removed.

   The reaction tube must allow mixing of contents and rapid removal of aliquots. A 15-ml screw-cap plastic centrifuge tube works well.

   A series of hydroperoxide standards is used to make a standard curve to convert the OD reading to hydroperoxide concentrations or amounts. The useful range of hydroperoxide concentrations is ~1 to 150 μM. Each type of hydroperoxide will have to have its own standard curve. A blank is prepared with sample, leaving out the substrate.

5. Set a timer and be prepared to start timing as soon as possible following addition of the substrate.

6. Start each assay with the addition of hydroperoxide, with complete mixing, and starting the timer immediately following this.

   Since the goal is to evaluate alternative reducing substrates, the hydroperoxide can be any that reacts well with ferricyanate reagent (hydrogen peroxide, cumene hydroperoxide, and t-butyl hydroperoxide will definitely work) and can be efficiently reduced by the sample enzyme when GSH is the reducing substrate. For example, if the GPX activity was a GST, t-butyl hydroperoxide should be avoided, since it is generally poor substrate for GSTs. Cumene hydroperoxide would be the best choice in that case.

7. Stop the reaction in sample aliquots, according to a predetermined schedule, by mixing aliquots with the aliquots of TCA prepared in step 2.

   Any combination of TCA and sample giving a final 10% TCA concentration can be used. This has the effect of stopping the reaction cold while the glutathione peroxidase is quickly denatured.

   A T_0 sample is made by mixing a sample aliquot with TCA, then adding a substrate volume scaled to the aliquot size.

8. When all of the sample aliquots have been taken, determine the hydroperoxide content of each aliquot by mixing the contents of each tube (1 ml vol) with 0.2 ml of 10 mM ferrous ammonium sulfate and 0.1 ml of 2.5 M potassium thiocyanate so that a color reaction (OD at 480 nm) occurs dependent on the amount of hydroperoxide remaining in the tubes.

9. Centrifuge the tubes 5 min at 14,000 × *g*, room temperature, to pellet the precipitate formed in the presence of the TCA.

10. Read the OD at 480 nm of the sample supernatant.

    The blank value (sample but no substrate) will be subtracted from the assay value before the substrate concentrations are determined from the standard curve.

CALCULATIONS OF SPECIFIC ACTIVITY

For the basic sample activity calculation, results from protein assays, DNA assays, cell counts, or other sample-quantifying methods will generally have to be available to put the data into the most useful format for analysis—i.e., specific activity. Exceptions to this may be cases where samples were fractionated on columns or where plasma, milk, or aqueous humor activity have been assayed. In such cases, enzyme activity units per fraction (volume) or unit volume may suffice for analysis or presentation. During assays, it is more convenient to record sample volumes used in each assay (with notations of any dilutions prior to assay) rather than to try and calculate sample-aliquot protein or DNA content on the spot. There is some merit to knowing the actual sample content of an assay aliquot. Specific activities can be calculated during assays, particularly with the slower GPX4 assays (Alternate Protocol 2).

Calculations will be illustrated for conversion of data to milliUnits enzyme activity per milligram protein. The use of protein content as the sample measurement is the most widely used convention; it is the only practical form for projects where purification or subcellular fractionation is performed. The enzyme activity unit is based on the international convention of 1 μmol substrate consumed or product formed per min. This convention is generally valid for coupled assays, since the GSH concentration is constant during the assay and hydroperoxide substrate concentrations up to 10 times the K_m ensure linear rates in the assay.

If a strip chart recorder was used, the settings used on the machine/chart recorder have to be recorded with each assay to translate the data. The sample calculation that follows will assume the setting of 0.5 OD/full scale, a 1-ml assay volume, and a 1-cm path length. Most spectrophotometers now come with microprocessors that compute the results to OD/min or can be programmed to perform all the calculations to the point of enzyme activity in the sample (after the blank rate has been determined and input).

1. First, read the blank assay trace as chart units per min or convert to OD/min (no other calculation need be done).

   This value will be subtracted from every assay (in like units), and the net value used as the basis to calculate specific activities.

   The spontaneous rates for each day's assays will be the same, if all the reagents have been properly measured out and were prepared from good stocks. The blank provides a quality check for the reagents. The blank should contain the same homogenization buffer(s) used for the samples added, in volumes similar to those anticipated for the sample(s). This is critical when GSH has been added to the samples for stabilization of activity. Examination of homogenates of cell lines lacking GPX activity and the tissues of selenium-deficient animals and GPX1 gene-knockout animals reveals that there is a small background above the spontaneous rate in all of these samples (0.5% to 5% wild-type levels; for exceptions, see Background Information). For many applications, accounting for the spontaneous rate with the blank is all that is required for accurate specific activity determinations.

2. Put the raw data from the assay in the form of net OD units per min to start the calculations (where net OD refers to the rate after subtraction of the blank rate).

   The spontaneous rate has to be subtracted from the sample rates for valid calculations of enzyme specific activity.

   OD/min can be determined by finding the chart interval corresponding to 1 min on the time axis and measuring the number of chart units along the OD axis that the assay trace runs through. For the blank and for samples with low activity, it will probably be necessary to base rate determinations on time intervals of 2 to 5 min. The selection of the region for the rate estimation must correspond to a part of the assay trace where a linear result occurred that is representative of the whole reaction trace (see Fig. 7.1.1).

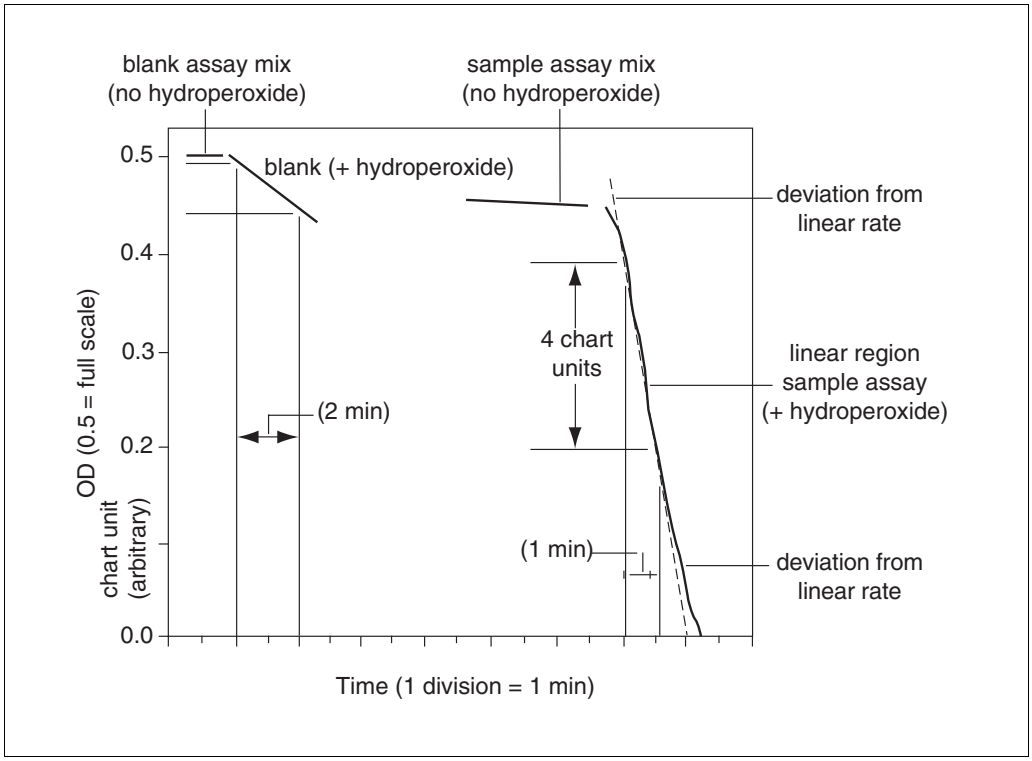

Figure 7.1.1 Schematic representation of typical spectrophotometric output during glutathione peroxidase assay under standard conditions.

3. Divide the number of OD chart subdivisions per min by the total chart subdivisions, multiplied by 0.5 OD and divided by 1 min, or the number of minutes needed to get a good estimate.

   From Figure 7.1.1, the blank trace traversed one chart subdivision (chart unit) out of 10 chart units (full scale) in 2 min. The rate is 0.5 chart units/min. The net sample rate is 4 chart units/min (total rate) – 0.5 chart units/ min (blank rate) = 3.5 chart units/min. This is converted to OD min as follows: 3.5 chart units/min ÷ 10 chart units (full scale) × 0.5 OD (full scale) = 0.175 OD/min. This is the net sample activity in OD/min.

   Accurate results cannot be expected in cases where the trace passes through more than 35% of the chart span/min or 0.17 OD/min. The reason is that the reaction rate may have exceeded the linear range. The investigator will, however, have performed a positive control series to aid in this judgment. Also, some samples will have a spontaneous rate prior to addition of hydroperoxide. It may be critical to account for this, to have accurate calculations, by subtracting this rate as for the blank rate. This is likely to be the case in GPX4 assays for most samples, and where sample activities of other GPXs are low. Cell lines grown without selenium supplementation, selenium-deficient animals, and GPX1 assays of guinea pigs are cases where this may be true.

4. Convert the OD/min results to enzyme units.

   One enzyme unit = 1 μmole substrate consumed or product formed/min. For glutathione peroxidase activity, in the coupled assay, the NADPH consumption rate is used in place of these values to calculate activity. The calculation is:

   [Net OD/min ÷ 6.22×10^3 OD/M] ÷ 1000 = mol NADPH consumed/min.

   The value 6.22×10^3 is the OD of a 1 M solution of NADPH in a path length of 1 cm. The divisor of 1000 corrects the NADPH consumption from per liter to the actual assay volume of 1 ml.

   For the example in Figure 7.1.1, this becomes [0.175 OD/min ÷ 6.22×10^5 mol/liter/OD] ÷ 1000 = 2.8×10^{-8} mol NADPH consumed/min. This converts to 0.028 U or 28 mU.

5. At this point, divide the enzyme activity units value by the amount of protein in the assayed sample aliquot, expressed in mg, to yield the sample specific activity.

The enzyme activity in this example in Figure 7.1.1 is roughly that expected for 0.08 mg of rat liver cytosol protein. The specific activity would then be calculated as 28 mU ÷ 0.08 mg = 350 mU/mg protein.

REAGENTS AND SOLUTIONS

Use Milli-Q-purified water or equivalent for all recipes and all protocol steps. For common stock solutions, see ***APPENDIX 2A****; for suppliers, see* ***SUPPLIERS APPENDIX****.*

Assay mix for GPX4 (see Alternate Protocol 2)

0.4 M Tris·Cl, pH 7.4 (*APPENDIX 2A*)
15 mM GSH (reduced glutathione)
1.25 mM NADPH (β–nicotine adenine dinucleotide phosphate, reduced form)
Prepare immediately before the assay

Allow the dry GSH and NADPH to equilibrate to room temperature 30 min prior to assay. The authors prepare the GSH and NADPH directly in the assay buffer (0.4 M Tris·Cl), but they can also be prepared separately in water.

Column buffer

0.1 M Tris·Cl, pH 7.2 (*APPENDIX 2A*)
5 mM EDTA

Prepare 2 to 4 liters of buffer without reducing agent. Store indefinitely at 4°C. Just prior to use with gel-filtration column, add 1 to 5 mM GSH, 1 to 3 mM 2-mercaptoethanol, or 0.1 to 1 mM dithiothreitol (DTT) as reducing agent.

Cumene hydroperoxide, 30 mM

Prepare a working (20×) stock of cumene hydroperoxide in water (the reagent is commercially available as a 7 to 8 M stock from Sigma and Aldrich). Use ethanol to prepare a 5× (0.15 M) stock that can be diluted 5-fold for a (30 mM) working stock.

CAUTION: *The odor of cumene hydroperoxide is quite pungent, and the chemical is hazardous. The commercial stock should be handled in a fume hood. Gloves should be worn at all times when handling this reagent.*

Drabkin's reagent

0.0016 M KCN
0.0012 M $K_3Fe(CN)_6$

This is indefinitely stable.

Glutathione reductase, 100 U/ml

Dilute the ammonium sulfate suspension of glutathione reductase to 100 U per ml in a small aliquot of ice-cold assay buffer.

The diluted glutathione reductase will be stable for two or three days at 4°C.

GPX positive control (see Basic Protocol)

This should be available for first-time investigations (see Basic Protocol). Prepare as a series of four or five 1:2 serial dilutions. Sources for the positive control could be one of the following:

1. *Murine red blood cells:* Prepare 10% (v/v) cells in 0.1× PBS (*APPENDIX 2A*), lyse by sonication, and mix 1:1 (v/v) with 2× Drabkin's reagent (see recipe). Centrifuge 10 min at 15,000 × *g*, 4° to 8°C. Store supernatant indefinitely at −70°C.

continued

2. *Rat plasma:* Dilute 1:10 in PBS (*APPENDIX 2A*). Store indefinitely at −20°C.

3. *Rat or mouse liver or kidney:* Prepare the same way as the study samples, then dilute 1/10 in homogenization buffer (see Critical Parameters). Store indefinitely at −20°C.

4. *Human or bovine GPX1:* Purchase enzyme from Sigma and prepare stocks at 200 mU/ml in homogenization buffer (see Critical Parameters) containing albumin at 0.1 mg/ml to help stabilize the stock. Divide into aliquots and store indefinitely at −20°C.

GPX1 positive control, free of GPX4 (see Support Protocol 1)

Obtain GPX1-enriched material by collecting 75,000- to 120,000-Da fractions from columns (see Alternate Protocol 6).

The starting material for this control can be erythrocytes, liver, or kidney.

GPX4 positive control (see Alternate Protocol 2 and Support Protocol 1)

Prepare a positive control GPX4 enzyme sample by making a 10% homogenate of rat or mouse testes in a buffered solution (pH 7.2) with 5 mM EDTA, 1 mM PMSF, 0.1 M NaCl, 0.2% Triton X-100, and 3 mM GSH (other reducing agents can be used).

The 10,000 × g supernatant will be very rich in GPX4 activity. GPX1 can be removed by fractionating the sample over Sephadex G-50-200 and collecting the 15,000- to 22,000-Da fractions (see Alternate Protocol 6).

GSH, 10 mM

Prepare fresh solution on each day the assay is to be performed. 30 min prior to the assay, allow the dry GSH (reduced glutathione; mol. wt. 307.3) to equilibrate to room temperature (for new batches, this will be an opportunity to subdivide the material into aliquots for storage, where each aliquot would be the amount of material consumed in a week to a month of assays). Weigh out 3.1 g per liter (scaled down to the volume required for the assay of the study samples or for 50 to 100 assays, maximum) and dissolve in room temperature assay buffer (50 mM sodium phosphate, pH 7.0; *APPENDIX 2A*).

The dry GSH should be divided into aliquots so that it is subjected to the open air at room temperature only a few times.

The GSH and NADPH will oxidize. While each working stock may last longer than the time required for 100 assays, it is best to test this gradually and then plan from experience. The working stocks of GSH and NADPH may or may not survive overnight storage in the refrigerator or freezer. The authors have had variable success using day-old assay stocks of GSH and NADPH. Because the assay is so easy and so few solutions are required, it is better to make fresh solutions each day.

Hydrogen peroxide (H_2O_2), 5 mM

Dilute ~5 to 6 µl of 30% (8 to 9 M) hydrogen peroxide into 10 ml water.

The actual concentration of hydrogen peroxide in the commercial 30% solution can be determined by using the value 0.071 as the millimolar extinction coefficient at 230 nm.

The diluted hydrogen peroxide is stable at 4°C for a few days if stored in an iron-free container. The spontaneous activity of the blank can be used to determine whether the diluted hydrogen peroxide is spent (see below).

Immunoprecipitation buffer

0.1 M NaCl
0.2% (v/v) Triton X-100
0.1 mg/ml bovine serum albumin (BSA)
3 mM GSH (reduced glutathione)
0.15 M Tris·Cl, pH 7.2 (*APPENDIX 2A*)
5 mM EGTA
Store up to 1 week at 4°C

Triton X-100 and GSH may have to added from separate concentrated stocks if the sample volume alone is near 200 μl.

NADPH, 2 mM

Prepare fresh solution on each day the assay is to be performed. 30 min prior to assay, allow the dry β-NADPH (β–nicotine adenine dinucleotide phosphate, reduced form) to equilibrate to room temperature (for new batches, this will be an opportunity to subdivide the material into aliquots for storage, where each aliquot would be the amount of material consumed in a week to a month of assays). Weigh out 1.5 g/liter (scaled down to the volume required for the assay of the study samples or for 50 to 100 assays, maximum) and dissolve in room temperature assay buffer (50 mM sodium phosphate, pH 7.0; *APPENDIX 2A*).

The dry NADPH should be divided into aliquots at the first opportunity.

The GSH and NADPH will oxidize. While each working stock may last longer than the time required for 100 assays, it is best to test this gradually and then plan from experience. The working stocks of GSH and NADPH may or may not survive overnight storage in the refrigerator or freezer. The authors have had variable success using day-old assay stocks of GSH and NADPH. Because the assay is so easy and so few solutions are required, it is better to make fresh solutions each day.

Protein A, washed, 10% suspension

Suspend protein A (from *Staphylococcus aureus* Cowan I strain, fixed cells; ICN Biochemicals) in 10 vol (w/v) Dulbecco's phosphate-buffered saline (DPBS, without calcium; Life Technologies). Centrifuge 5 min at 3000 × *g*. Pour off the supernatant and resuspend the pellet in DPBS containing 0.2% (v/v) Triton X-100. Centrifuge 5 min at 3000 × *g*, pour off the supernatant, then wash three times (to remove excess Triton X-100 and protein A fines), each time by resuspending in 10 vol DPBS, centrifuging 5 min at 3000 × *g*, and pouring off the supernatant. Resuspend the final pellet in 10 vol DPBS, and store indefinitely in 1- to 2-ml aliquots at ×20°C.

Washing the Protein A removes fine particles that will interfere with the immunoprecipitation.

Sodium azide, 1.125 M

Prepare the working stock (1.125 M) by measuring 73.12 g NaN_3 per liter into water (indefinitely stable).

Sodium azide can also be prepared in the assay buffer stock at 1.1 mM. This has the advantage that it will not be forgotten, and it prevents contamination when the buffer is stored at room temperature. Note that if azide is a component of the buffer, the buffer cannot be used for catalase assays.

COMMENTARY

Background Information

The glutathione peroxidase reaction seems to be the principal activity of SeGPX. For some SeGPX isoenzymes, glutathione may be substituted by GSNO (GPX1), 2-mercaptoethanol (GPX4), other small thiols such as cysteine and dihydrolipoic acid (GPX4), and thioredoxin (GPX3)—also see Maiorino (1994), Bjornstedt et al. (1994), and Freedman et al. (1995). Proteins with vincinal thiol groups or exposed free thiols have also been reported to serve as reducing substrates. Evidence has been presented for the utilization and possible physiological significance of GSNO and thioredoxin as substrates of SeGPX isoenzymes (Esworthy et al., 1993; Bjornstedt et al., 1994; Freedman et al., 1996). Within solid tissues, GSH is so abundant that it will be the major reducing substrate of glutathione peroxidases, regardless of the presence of other thiols. In plasma, it is not clear which reducing substrates are important.

In the major organs of most animals, the glutathione peroxidase activity detected with hydrogen peroxide as substrate will be GPX1 (Table 7.1.1). GSTs cannot use hydrogen peroxide as a substrate. Exceptions to the rule of GPX1 as the major activity are the blood plasma, where GPX3 is the sole GPX, and the mucosal epithelium of the GI tract, where GPX2 accounts for up to 50% of the activity. GPX2 may also be a major activity in human liver and in human and rodent breast tissues. GPX3 is also associated with kidney, intestine, and placenta. The GPX3 contribution to total activity in these tissues seems to be negligible based on results obtained from *Gpx1* gene knockout mice. A GPX activity is observed in the hearts of *Gpx1* gene knockout mice that is between 15% to 30% of wild-type mouse levels. The source of the activity is not known although GPX3 and Aop2 mRNAs are detectable in this organ.

In some minor organs, other putative GPX species are produced at very high levels. In the ciliary body of the eye and the nasal epithelium, Aop2 has been proposed to compete with GPX1 as the major activity detected with hydrogen peroxide (Peshenko et al., 1998;Singh and Shichi, 1998). Aop2 protein is detected in the major organs. However, it seems fairly clear that it does not contribute in a major way to the GPX activity under normal conditions. In *Gpx1* gene knockout mice, there is a small background GPX activity (0.5% to 5% of the activity of wild-type mice; 15% to 30% in heart) in the major organs (Cheng et al., 1997). This could

Table 7.1.1 Expected GPX Specific Activities[a]

	Rat			Mouse		Guinea pig
Tissue	Basic Protocol[b]	Alternate Protocol 1[b]	Alternate Protocol 2[c,d]	Basic Protocol[e,f]	Alternate Protocol 2[g,h,i]	Basic Protocol[e]
Liver	269	412	6	750	7	25
Kidney	146	212	6	350	14-28	20
Heart	225	225	2	150	4-7	20
Lung	171	171	1.5	25	21-42	5
Brain	33	45	2.5	10	—	10
Muscle	—	—	1	—	10	—
Testis	6	65	94	20	42	0

[a]Specific activity in mU/mg protein

[b]Lawrence and Burk (1978)

[c]Zhang et al. (1989)

[d]Roveri et al. (1992)

[e]Himeno et al. (1993)

[f]The values reported in Himeno et al (1993) may be higher than those found in other reports. The activity in mouse kidney and other organs relative to mouse liver seems appropriate. However, 3-fold discrepancies between various reports are common in assays of mice (using Alternate Protocol 3, rat liver has an activity of 2500 to 2900 mU/mg, while mouse liver activity is ~4200 mU/mg).

[g]Weitzel et al. (1990)

[h]Cheng et al. (1997)

[i]Esworthy et al. (1997)

arise from activities like that of Aop2 and, in some cases, GPX3. Aop2 mRNA is highly induced in skin keratinocytes as part of the early wound healing response (Munz et al., 1997). This protein may be very relevant to toxicology regardless of its final classification. However, the true nature of this protein is in dispute. Sequence homology criteria would place it among the C1-type thioredoxin peroxidases. C1-type thioredoxin peroxidases can have thiol peroxidase activity (Chae et al., 1994). Definitive evidence that GSH can serve as the donor thiol has not been provided. A strong case for GSH as a donor has recently been made specifically with Aop2, and at the same time the whole idea that the protein has any GPX activity has been strongly challenged.

Glutathione peroxidase activity can best be described as a genuine side reaction of a subset of a third protein family, i.e., GSTs. The kinetic parameters that describe the glutathione peroxidase activity of GSTs show that these enzymes may be relatively inefficient in comparison with SeGPXs (Hong et al., 1989). The K_m for GSH is low enough for the enzymes to be saturated in most cell types. However, the V_{max} with hydroperoxides tends to be very low and the K_m for many hydroperoxides is very high relative to SeGPX. Aop2 also has a very low V_{max}. However, the K_m with hydroperoxides is in the range of GPX1. Since tissue hydroperoxide levels may seldom exceed 1 μM, not all of the glutathione peroxidase activities detected with cumene hydroperoxide at 1.5 mM or linoleic acid hydroperoxide at 50 μM will have bearing on physiological roles or possibly even toxicological roles. This is the picture emerging from studies of paraquat toxicity on *Gpx1* gene knockout mice.

In some tissues, GSTs are very abundant and, in some animals and tissues, SeGPX isoenzymes are not prevalent (Lawrence and Burk, 1978). Under these conditions GSTs could contribute significantly to lipid hydroperoxide metabolism. Some GST isoenzymes have good activity with what may be regarded as physiological substrates. In the data of Hong et al. (1989), it can be seen that 15-HPETE has a K_m with GSTs that is similar to GPX1. The data of Hiratsuka et al. (1997) show that cholesterol 7-hydroperoxides are superior substrates for alpha-class GST over GPX1. However, the valid comparison would be with GPX4, which has excellent activity with cholesterol hydroperoxide substrates (Esworthy et al., 1993). If a particular physiological substrate is the object of research and is practical to use, it is best to use that substrate rather than a "model" substrate to determine whether GSTs could be effective peroxidases.

One other link between GSTs and GPX1 is the "compensatory" increase in GST activity observed when rodents were subjected to extreme selenium deprivation. This was held up as evidence for a role of GSTs as glutathione peroxidases. However, careful work with the selenium-deprived rodent model (Reiter and Wendel, 1983) and recent studies with *Gpx1* gene knockout mice (Cheng et al., 1997) show that there is no compensatory increase of GSTs with GPX1 decline. Rather, it is very low selenium levels that trigger this response, irrespective of GPX1 status.

Many studies report only results for the collective glutathione peroxidase activity with cumene hydroperoxide. In most cases, the rationale provided is doubtful at best. It is difficult to interpret what such values mean under different study conditions in the absence of supporting data on the abundance of each enzyme. The regulation of GSTs and SeGPX isoenzymes appear to be completely different. An assay that lumps GSTs with SeGPXs risks losing the signal of one in the background of the other, and therefore, losing much of the meaning.

Any assay of GPX isoenzymes (SeGPX) has inherent limitations and peculiarities due to the unusual reaction mechanism (Paglia and Valentine, 1967). Under practical assay conditions, it is not possible to saturate SeGPX isoenzymes with GSH. In fact, GPX rates are almost directly proportional to GSH concentration (0 to 5 mM) when hydroperoxide concentrations in the assay are 25 μM or greater, which is standard. This property makes the coupled assay so useful. In that assay, GSH levels are held constant, enabling linear rates to be obtained.

In the cell, where hydroperoxide levels probably do not exceed 1×10^{-6} M and GSH levels are in the millimolar range, the selenium-dependent enzymes would be nearly saturated with respect to GSH (Flohe, 1982). Under these conditions, the reaction rate (V) can be approximated as:

$$V \cong [\mathrm{ROOH}]/\Phi_{\mathrm{ROOH}} \times [\mathrm{E}_0]$$

where Φ is the Dalziel coefficients, $\Phi = 1/K$, where K is the rate constant for the respective step of the enzyme reaction, and E_0 is the enzyme concentration. K values for some commonly used hydroperoxide substrates of GPX1, GPX3, and GPX4 and the K values for GSH are found in Table 7.1.2.

Table 7.1.2 SeGPX rate constants K_1 (ROOH) and K_2 (GSH)[a]

SeGPX enzyme	Substrate[b,c]				
	K_1 (H_2O_2)	K_1 (LinOOH)	K_1 (CumeneOOH)	K_1 (PLOOH)	K_2 (GSH)
Hamster GPX1	2.9×10^6	2.3×10^6	1×10^6	ND	4.8×10^4
Human GPX1	5.2×10^6	2.7×10^6	—[d]	ND	1.5×10^4
Human GPX2	—[d]	—[d]	—[d]	—[d]	—[d]
Human GPX3	2.0×10^6	5.9×10^6	—[d]	ND	4×10^3
Porcine GPX4	1.9×10^5	1.8×10^6	1.3×10^5	7.0×10^5	5×10^3

[a]Sources: Chaudiere and Tappel (1983); Esworthy et al. (1993); Ursini et al. (1985).
[b]K_1 and K_2 have units of mM^{-1} min^{-1}. Assays conducted in Tris·Cl, pH 7.6.
[c]Abbreviations: CumeneOOH, cumene hydroperoxide; GSH, reduced glutathione; LinOOH, linoleic acid hydroperoxide; ND, no activity detected; PLOOH, phosphadidyl choline hydroperoxide.
[d]No data.

It is possible to saturate the enzyme with many hydroperoxide substrates when GSH is in the millimolar range, which is a standard assay condition. V_{max} for any hydroperoxide substrate is determined by the following equation:

$$V_{max} = [GSH]/\Phi_{GSH} \times [E_0]$$

All of the terms in this equation relate to enzyme or GSH. In other words, the theoretical V_{max} for all hydroperoxide substrates is the same. Specific activity estimations are usually derived for SeGPX isoenzymes under near-saturating conditions, so that differences among SeGPXs will largely reflect differences in the interaction of enzymes with GSH. Specific activity estimations based on maximum velocities are at variance with the parameters that describe enzyme velocities in vivo. The enzyme activity assay can be used to determine relative enzyme levels. But, for reasons mentioned above—the presence of competing reactions and limitations of substrate—in vivo, activity assays cannot be related to physiological function without elaborate modeling.

The apparent K_m for individual hydroperoxide substrates is quite different (Hong et al., 1989). This property of the reaction produces some of the variation reported for GPX activities when different substrates are used. The K_m is a variable, contingent on GSH concentration:

$$K_{m\,ROOH} = [GSH] \times \Phi_{ROOH}/\Phi_{GSH}$$

GPX isoenzyme activity rates are highly pH dependent (Paglia and Valentine, 1967). The pH dependence follows partially from the dissociation reaction, $GSH \leftrightarrow GS^- (pK_{SH}, \cong 9.) + H^+$. Other factors also affect the pH dependence of the reaction. The maximum rate occurs around pH 8.8. The spontaneous reaction is so fast at this pH that it is not practical to perform the assay under this condition. On the other hand, GPX4 activity in most tissues is barely detectable at pH 7.0. A good compromise between noise and signal is found between pH 7.3 to 7.6.

A problem with literature reports of GPX activities derives, in part, from the lack of simple optimal conditions that has led to endless variations in assay conditions, as well as the use of many substrates. This is additionally complicated in studies of cell lines, since most sera and media supply selenium in a form suboptimal for full expression of SeGPX activities (Germain and Arnson, 1977; Maiorino et al., 1991). Any report of glutathione peroxidase activity must provide the pH, GSH concentration, hydroperoxide substrates, and concentrations. Also, the report should provide information on the selenium status of the organism or cell line. It is best if this information is stated in the body of the publication even if a reference is provided for the assay method.

Alternative tissue reagents for glutathione peroxidase studies

Recently, *Gpx1* gene knockout mouse lines have been introduced (Ho et al., 1997; de Haan et al, 1998). These lines are already widely distributed, and the results of many studies using the homozygous knockout gene lines have already been published. These lines are particularly useful in studying glutathione peroxidase activities in tissues where GPX1 is (or was, in the case of the knockout line) present and obscures other activities (Esworthy et al.,

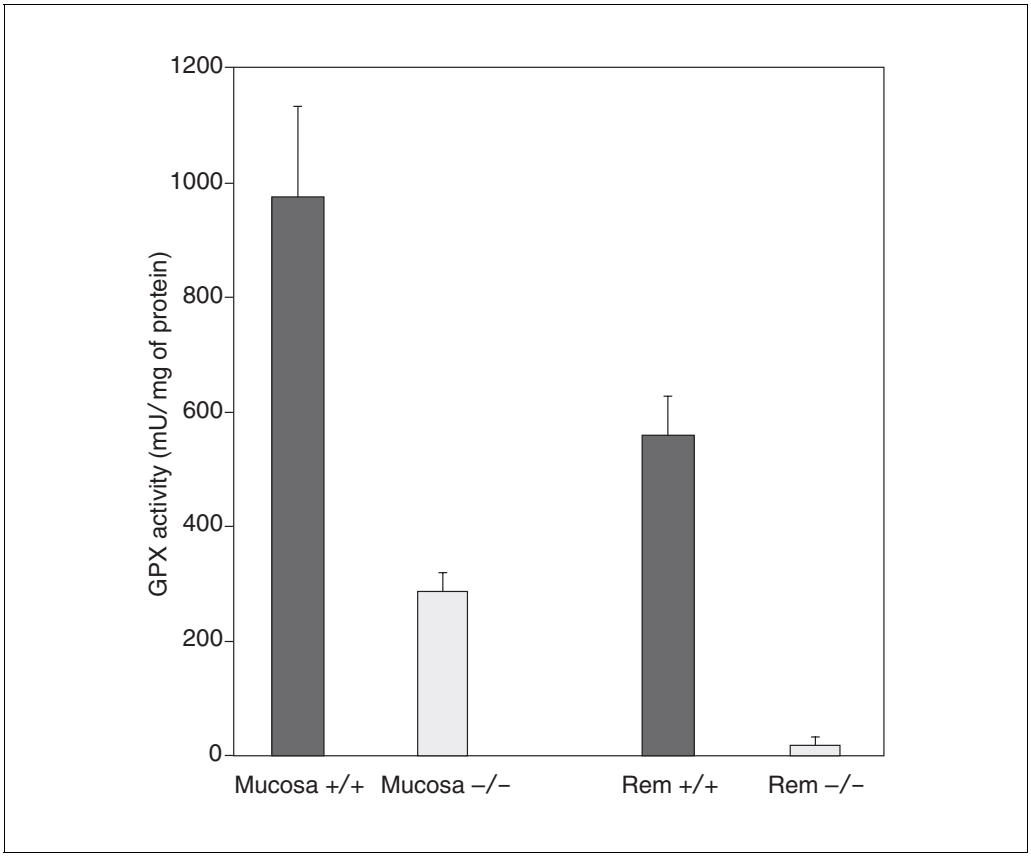

Figure 7.1.2 Glutathione peroxidase activity measured in the mucosa and muscular remnant (Rem) of mouse small intestine. The black bars show activity obtained from control mice, which have normal *Gpx1* genotype (+/+); the gray bars represent Gpx1-knockout mice with *Gpx1* (–/–) genotype. The error bars represent standard deviations obtained from four male mice. The activity was measured with H_2O_2 as the substrate.

1997, 1998). No up-regulation of other SeGPX isoenzymes, GSTs, or other antioxidant activities has been detected in these mouse lines (Cheng et al., 1997; Ho et al., 1997).

As an example of the application of the *Gpx1* gene knockout line, GPX2 is coproduced with GPX1 in the mucosal epithelium of the GI tract. It is possible to use antibodies to assay for the activity of GPX2 in the presence of GPX1. But GPX2 activity is easily detected in the *Gpx1* gene knockout line by comparison of residual GPX activity in the mucosal and the non-mucosal tissues of the GI tract toward hydrogen peroxide (see Fig. 7.1.2). Alternative mitochondrial activities could also be studied in this mouse line (Esworthy et al., 1997). The detection of Aop2 and other novel activities may be facilitated by the use of these mice.

Cell lines are reported in which SeGPXs (GPX1 and GPX4) and GST activities are altered via transgenic means (Chu et al., 1990; Mirault et al., 1991; Lavole et al., 1992; Yagi et al., 1996). Many transgenic cell lines are very useful, since the parental cell lines were picked for their lack of SeGPX isoenzyme or GST production. Nonproduction of GPX1 is very common, and nonproduction of GPX4 occurs as well (Esworthy et al., 1995). Use of paired lines can eliminate some of the interpretation problems inherent in selenium manipulation. A classic example of complications with selenium manipulation is the 100-fold amplification of the catalase gene (with up-regulation of the activity) that occurs in a few cell lines when they are selenium-depleted (Lin et al., 1995). However, selenium manipulation of SeGPX status in cell lines is an easy and often useful means for studying these enzymes (Chu et al., 1990). For both the cell lines and animals, much toxicological data is already available for altered selenium status, GSH status, and from the genetically altered lines.

Comparisons with other methods

Almost any method capable of measuring hydroperoxides or GSH can be applied to the assay of glutathione peroxidase activities. There are a wide variety of such assay methods

available, suitable to nearly any laboratory situation. Commercial kits are available for activity assays of glutathione peroxidases (Sigma), and an ELISA kit is available for determination of the levels of the SeGPX isoenzyme of the plasma (Oxis International). These methods offer huge throughput and provide most of the reagents and standards required. These kits are also expensive and may lack the range of the methods described in this unit. If a kit is adaptable to a particular study sample, it can be an attractive alternative to assembling reagents and testing assay conditions for the protocols described above. Variations of the coupled assay of Paglia and Valentine (see Basic Protocol and Alternate Protocols 1 to 7) are still the most widely used methods. With a multisampler-equipped recording spectrophotometer, tens to hundreds of samples can be assayed in a day using, e.g., variable hydroperoxides, pH, and GSH concentrations. When set up with a programmable data collection/processing system, this method is still competitive with multiwell micromethods for speed.

The glutathione reductase couple in this type of assay replaces cumbersome GSH measurements used in many older assay methods. The coupled method has the advantage that the GSH concentration in the assay does not change until the indicator NADPH runs out. This is important, since it is not practical to assay SeGPXs or Aop2 activities under conditions where GSH concentrations come anywhere near those needed to saturate the enzymes. It is possible to use many hydroperoxide substrates at up to ten times the apparent K_m of the enzymes, providing nearly linear rates for tens of seconds to minutes. This simplifies specific activity estimations and permits the reporting of activities in a conventional format. With noncoupled methods, the rates obtained are not linear. This is not a real problem. An acceptable enzyme activity unit used under these conditions, as well as calculation of the activity in these units from raw data, is described by Flohe and Gunzler (1984). The unit is a counterpart of the k unit used in catalase assays. The paper also provides conversion units that can be used to move from the k unit system to μmol NADPH consumed/min for certain assay conditions.

Many HPLC methods provide a means for following hydroperoxide consumption, alcohol product formation (sometimes both simultaneously), or GSH oxidation (Terao et al., 1988; Pascual et al., 1992; Bao et al., 1995). The published range of hydroperoxide substrates and/or alcohol products that can be completely resolved from reaction mixtures and quantified with HPLC systems is more than sufficient to study any glutathione peroxidase activity. Some workers strongly advocate this type of assay system, since both substrate and product can be monitored and there is no dependence on a coupling system that has some limitations (Pascual et al., 1992). Also, increased sensitivity in the assay of GPX4 is achieved in HPLC systems (Bao et al., 1995). If the questions of a study go beyond simple issues of glutathione peroxidase activity levels—e.g., by asking via what routes can hydroperoxides be metabolized in plasma or tissues—then systems (such as HPLC and thin layer chromatography) that can quantitate alcohol product formation and detect alternative products are essential (Terao et al., 1988). The question of whether hydroperoxides are being consumed at substantial rates in a sample in the absence of added reduced glutathione can be determined with or without HPLC systems (e.g., by the ferrithiocyanate method, Alternate Protocol 8). The throughput of HPLC methods can be substantially less than that of other methods, and multiple columns and HPLC reagents are required to study a range of hydroperoxide substrates. Thin-layer chromatography systems are also used in glutathione peroxidase assays (Esworthy et al., 1993).

Critical Parameters

Selenium status

This is an issue for cells in tissue culture. Most animal diets supply selenium at optimal levels, and Western diets ensure adequate selenium in humans. Serum for tissue culture, used at standard concentrations (5% to 20%), does not routinely supply selenium to cells in a form that is optimal for SeGPX production (Maiorino et al., 1991). Optimum production can yield cell line specific activities comparable to tissue of origin levels (Esworthy et al., 1995). However, the full details for the nutritional requirements of optimal SeGPX production in cell lines remains to be investigated.

In many studies, suboptimal SeGPX production is not a problem. SeGPX activities will be 10% to 40% of maximal values in most cases, and occasionally up to 80%. This is often adequate for detection of GPX1. In many human cell lines and some rodent cell lines, this may not be adequate for production of GPX4 or GPX2 (in those rare cases where GPX2 is the sole SeGPX produced) at detectable levels (Maiorino et al., 1991; Esworthy et al., 1995).

Tissue culture media can be supplemented with selenium in many forms (sodium selenite, selenates, selenious acid, or organoselenium compounds) to optimize SeGPX production. The serum in the medium will mask some of the supplemented selenium (Chu et al., 1990), so that the more serum in the medium, the higher the concentration of selenium needed for optimal production (30 to 300 nM). Full equilibration of cell line SeGPX to a new level with selenium modulation averages 4 to 10 days duration (Chu et al., 1990). Growth rates of the cell lines may affect this parameter. Each cell line will have to be individually examined for the minimum equilibration interval.

Sample isolation and processing

Intact tissues or cell line material can be quickly frozen for later processing. A storage temperature of at least −20°C is essential, and −70°C is recommended. With tissues or cell lines containing GPX2, −20°C storage should be confined to <1 week.

For homogenization and sample fractionation, tissues should be prepared as 10% to 20% homogenates (tissue weight/volume of buffer) in ice-cold buffer that is compatible with both good glutathione peroxidase activity recovery and the assay. If GPX2 is in the tissue, a 20% homogenate is advisable. The pH of the homogenization buffer should be between 6.5 and 7.5. The molarity of the buffering species should be low enough so that if the pH of the homogenization buffer is not the same as that of the assay buffer, the pH of the final assay mixture is not perturbed. A pH <6.5 will promote denaturation of SeGPX. With most standard tissue homogenization protocols there will be no problems. The usual precautions of keeping the samples chilled and preventing excessive foaming during disruption apply. The special requirements for recovery of particular glutathione peroxidase activities in some tissues are addressed below.

Particulates will cause problems in some assays (certainly in coupled assays) so that some means of clarifying the homogenates prior to assaying may be necessary. SeGPX1-3 and most GSTs behave as soluble proteins, although GPX1 is found in the mitochondrial inner space (up to 25% of the total activity) and may be present in the nucleus (Esworthy et al., 1997). Some SeGPX activity can be recovered from the microsomal fractions. This latter activity tends to be a very small portion of the total activity. GPX4 is generally recovered in the soluble fraction (Maiorino et al., 1990). However, a little GPX4 is found in mitochondria associated with pores in all tissues. In the testes, most of the GPX4 is bound to the outer membrane of the mitochondria (Roveri, et al., 1992). Bound GPX4 can be solubilized with the combination of high salt concentrations (at least 0.1 M) and the use of 0.2% Triton X-100. Mitochondria are also lysed under these conditions, with sonication.

Most glutathione peroxidase activity measurements are made on post-nuclear fractions. There is very little difference in the specific activities obtained for most tissues between the post-mitochondrial fraction and the 100,000 × *g* soluble fraction. However, the use of the post-nuclear fractions from tissues or clarified, detergent extracted tissues can produce significantly lower specific activities.

Reaction mixture

An equal volume of 2× Drabkin's reagent should be included when washed erythrocytes are to be assayed. Drabkin's reagent will convert the hemoglobin to cyanomethemoglobin, which will not react with hydroperoxide. Drabkin's reagent is not necessary with solid tissue preparations or the blood plasma fraction (Paglia and Valentine, 1967).

Sodium azide is included in the assay buffer to eliminate catalase activity with hydrogen peroxide. Azide can be included in the homogenization buffers, provided that catalase activity measurements are not to be performed on the samples. Azide is not needed if hydrogen peroxide will not be used as a substrate. The authors have found it most convenient to avoid using azide in homogenization buffers and to use it in the assay buffers.

The use of detergents should be carefully considered. Detergents can be used in homogenization buffers and may be required to obtain complete recovery of GPX4 and microsomal GST in the soluble fraction of homogenates. If the hydroperoxide substrate is lipid-soluble, most detergents will partially shield lipid-soluble substrates from GPX1-3 and GSTs (Maiorino et al., 1986). Hydroperoxide concentrations may have to be adjusted upward to compensate for this effect and thus maintain linear rates over the time span of an assay. Triton X-100 (<0.2%) is tolerable with assays of most glutathione peroxidase activities, except for the effect on lipid hydroperoxide partitioning. Deoxycholate definitely should not be used on human samples, unless it is to be removed before assay, as it has adverse effects on human SeGPXs (Maiorino et al., 1986; Es-

Table 7.1.3 Troubleshooting Guide to GPX Activity Measurements

Problem	Possible cause	Solution
No activity in blank	A reagent was forgotten	Use a check list until a ritual is established
	A reagent is bad	Keep the working stocks of each reagent separate before and during assays so that reagents can be easily identified.
	GSH gets oxidized in storage or in solution sufficiently to deplete the NADPH before the assay begins	Determine that this is a problem by monitoring the blank as it equilibrates immediately following the addition of all components (all components must be at room temperature and mixed for this to be valid). If the OD drops continuously, the GSH is probably bad. Adding more NADPH can sometimes remedy this problem as a short-term measure, since only a small percentage of the GSH is actually oxidized.
	The NADPH is bad	Store this as the dry powder in aliquots at −20° to −70°C. Be sure that it is the β isomer.
	pH is too low	Some buffers allow drift with aging. Measure pH of buffer, readjust to 7.0, check pH for stability.
	Inhibition of the glutathione reductase (unlikely, but possible)	Diluted glutathione reductase can go bad. The ammonium sulfate suspension of the enzyme is very stable. It is unlikely that the problem is in the commercial preparation, unless it was exposed to heat or left at room temperature for days. The remedy is generally to prepare a new dilution from the commercial stock.
Activity in blank but very little in sample	Sample was not added	Use a check list until a ritual is established
	Sample was diluted too much	Try lower dilution if possible
	Improper sample preparation or handling: e.g., homogenization was too vigorous (heating or foaming occurred); thiol in sample, if present, was oxidized and depleted the NADPH; sample needed thiol for storage but this was omitted (some GPX activities do not preserve well); or buffers in sample have lower pH and greater ionic strength than the assay buffer, resulting in wrong reaction conditions.	Repeat with fresh sample

continued

worthy et al., 1993). For GPX4, the effect is a direct inhibition of activity from all sources (including nonhuman). With human GPX1 and 3, the authors have observed an alteration of substrate range and a significant loss of activity with hydrogen peroxide if the detergent concentration is >0.5 mM. When detergents are used during tissue disruption, GPX1 is exposed to more proteases. Generally, this seems to be limited to the cleavage of the amino terminus without loss of activity. Including EDTA (1 mM) in the buffers will prevent most proteolysis of GPX1 when there are no detergents. The use of EDTA and PMSF (and/or mixtures of other protease inhibitors) will prevent proteolysis when detergents are used.

Stabilizing agents other than protease inhibitors used in protein purification, such as glycerol and some detergents, can be used to stabilize glutathione peroxidase activities and

Table 7.1.3 Troubleshooting Guide to GPX Activity Measurements, continued

Problem	Possible cause	Solution
Activity detected but rate erratic	Poor mixing of assay mix; temperature differences between components	Improper temperature equilibration or poor mixing will cause the rate to be variable. The sample and the diluted GSSG reductase should be kept at ice temperatures. The rest of the components can be kept at room temperature. This will lessen problems
	Particulate present in sample	Recentrifuge the sample or attempt to solubilize the particulate, depending on the goals of the project
	Lamp is bad or other spectrophotometer problems	Service spectrophotometer
Activity detected but reaction terminates very early	Too little NADPH; bad NADPH	Add more fresh NADPH; if this doesn't help open a fresh stock container and prepare new solution
	GSH is oxidized either in assay stock or in samples and has depleted the NADPH	Prepare a new solution from a fresh dry stock
	Too little hydroperoxide added or azide was omitted, allowing catalase to metabolize H_2O_2	Verify H_2O_2 content of commercial stock by OD_{230}. Prepare new buffer and double-check addition of azide.

prevent unwanted aggregates from forming. In dilute solutions, proteins can be added to stabilize SeGPX. However, as with detergents, serum albumin will complex with lipid hydroperoxides and slow down the rate of reduction of these hydroperoxides. Concentrations of serum albumin should be maintained so that in the assay the concentration is <1 mg/ml when lipid hydroperoxide will be used. Reducing agents are often used to stabilize SeGPX activities and thus avoid permanent activity loss that can accompany processing and storage in an open-air environment. Inactivation via this route is fairly slow at ice temperatures immediately after homogenization. Addition of reducing agents can generally be held off until after centrifugation of homogenates is accomplished. If the assays are to be performed immediately, there is often no need to consider the use of reducing agents in the homogenates. Reversible loss of GPX1 activity that is sometimes observed under these circumstances can be eliminated by preincubation of the samples in the assay buffer for 10 min. However, there are some cases where the use of reducing agents in the homogenates or other solutions is necessary. If the sample is to be dialyzed, chromatographed, or, in certain cases, simply stored before assaying (e.g., on ice for a long break or overnight at subzero temperatures), a reducing agent in the buffers or homogenates should be considered. Reducing agents interfere with many protein assays. Therefore, some provision is generally made for protein assays. This could be the use of the TCA-insoluble fraction of the homogenate. Since SeGPX will withstand some period of time in the absence of reducing reagents, samples can be split into portions for protein assays and activity assays after recovery of the soluble fraction from centrifugation.

The use of a reducing agent is recommended when GPX2 is anticipated to be a sizable portion of the activity, even when the immediate assay of the samples is planned. GPX2 is known or is indicated to be present in GI tract tissues, breast tissues, human liver, and many human cancer-derived cell lines of lung, breast, liver, and GI tract origin. Even in this instance, the addition of the reducing agent can be postponed until after a clarification step. The authors have sometimes observed reversible loss of >50% of GPX activity at ice temperatures within a few hours of recovery of post-mitochondrial supernatants of GI tract samples. As opposed to the reactivation of GPX1 by incubation in the assay buffer for 10 min, GPX2 sometimes required >½ hr of exposure to potent reducing agents such as DTT (0.1 mM) before full activity was restored. DTT (0.1 to 1 mM) is effective for

subzero storage of GPX2 activities, provided only one or two freeze-thaw cycles are anticipated, or if dialysis or other steps are confined to <24 hr before fresh DTT is supplied. At 4° to 8°C, oxidation of DTT can promote the inactivation of GPX2. This is largely reversible with addition of more DTT or dialysis against a fresh solution within a 24-hr time interval. Thereafter, the fraction of irreversible inactivation will steadily progress to completion by 48 hr. GSH, at 3 to 5 mM, is the best reducing agent for frozen storage and steps performed at 4°C.

Troubleshooting

Table 7.1.3 provices a guide to troubleshooting the measurement of GPX activity.

Anticipated Results

The variability in the production of glutathione peroxidases, the requirement for selenium in SeGPX production, and the substrate options preclude a definitive statement on anticipated results. Most murine, bovine, ovine, and primate tissue samples will have one to two types of glutathione peroxidase activity in the detectable range. Exotic animal species, uncharacterized minor tissues, and minor cell types within tissues and cell lines, in particular, may defy any preconceptions about the pivotal role of glutathione peroxidase that have been formulated from antioxidant theory. Table 7.1.1 shows values that will be obtained with some recommended control samples as well as the cautionary example of the guinea pig.

Time Considerations

In many cases, samples can be prepared and assayed within one day. If the sample size is very large, it is convenient to process the samples and do sample-content assays on one day, followed by the activity assays on the second day. The need for sample fractionation may increase the time for sample processing up to three days.

Literature Cited

Bao, Y., Chambers, S.J., and Williamson, G. 1995. Direct separation of hydroperoxy and hydroxyphosphatidylcholine derivatives: Application to the assay of phospholipid hydroperoxide glutathione peroxidase. *Anal. Biochem.* 224:395-399.

Bjornstedt, M., Xue, J., Huang, W., Akesson, B., and Holmgren, A. 1994. The thioredoxin and glutaredoxin systems are efficient electron donors to human plasma glutathione peroxidase. *J. Biol. Chem.* 269:29382-29384.

Chae, H.Z., Chung, S.J., and Rhee, S.G. 1994. Thioredoxin-dependent peroxide reductase from yeast. *J. Biol. Chem.* 269:27670-27678.

Chaudiere, J. and Tappel, A.L. 1983. Purification and characterization of selenium-glutathione peroxidase from hamster liver. *Arch. Biochem. Biophys.* 226:448-457.

Cheng, W-H., Ho, Y-S., Ross, D.A., Valentine, B.A., Combs, G.F., Jr., and Lei, X.G. 1997. Cellular glutathione peroxidase knockout mice express normal levels of selenium-dependent plasma and phospholipid hydroperoxide glutathione peroxidases in various tissues. *J. Nutr.* 127:1445-1450.

Chu, F-F., Esworthy, R.S., Akman, S., and Doroshow, J.H. 1990. Modulation of glutathione peroxidase expression by selenium: Effect on human MCF-7 breast cancer cell transfectants expressing a cellular glutathione peroxidase cDNA and doxorubicin-resistant MCF-7 cells. *Nucl. Acids. Res.* 18:1531-1539.

Chu, F-F., Doroshow, J.H., and Esworthy, R.S. 1993. Expression, characterization, and tissue distribution of a new cellular selenium-dependent glutathione peroxidase, GSHPx-GI. *J. Biol. Chem.* 268:2571-2576.

De Haan, J.B., Bladier, C., Griffiths, P., et al. 1998. Mice with a homozygous null mutation for the most abundant glutathione peroxidase, Gpx1, show increased susceptibility to the oxidative stress-inducing agents paraquat and hydrogen peroxide. *J. Biol. Chem.* 273:22528-22536.

Esworthy, R.S., Chu, F-F., Geiger, P., Girotti, A.W., and Doroshow, J.H. 1993. Reactivity of plasma glutathione peroxidase with hydroperoxide substrates and glutathione. *Arch. Biochem. Biophys.* 307:29-34.

Esworthy, R.S., Baker, M.A., and Chu, F-F. 1995. Expression of selenium-dependent glutathione peroxidase in human breast tumor cell lines. *Cancer Res.* 55:957-962.

Esworthy, R.S., Ho Y.S., and Chu, F.-F. 1997. The *Gpx1* gene encodes mitochondrial glutathione peroxidase in the mouse liver. *Arch. Biochem. Biophys.* 340:59-63.

Esworthy, R.S., Swiderek, K.M., Ho Y.-S., and Chu, F.-F. 1998. Selenium-dependent glutathione peroxidase–GI is a major glutathione peroxidase activity in the mucosal epithelium of rodent intestine. *Biochim. Biophys. Acta* 1381:213-226.

Flohe, F. 1982. Role of GSH peroxidase in lipid peroxide metabolism. *In* Biology and Medicine, Lipid Peroxides. (K. Yagi, ed.) pp. 149-159. Academic Press, New York.

Flohe, L. and Gunzler, W.A. 1984. Assays of glutathione peroxidase. *Methods Enzymol.* 105: 114-121.

Forman, H.J. and Kim, E. 1989. Inhibition by linoleic acid hydroperoxide of alveolar macrophage superoxide production: Effects upon mitochondrial and plasma membrane potentials. *Arch. Biochem. Biophys.* 274:443-452.

Freedman, J.E., Frei, B., Welch, G.N., and Loscalzo, J. 1995. Glutathione peroxidase potentiates the

inhibition of platelet function by *S*-nitrosothiols. *J. Clin. Invest.* 96:394-400.

Freedman, J.E., Loscalzo, J., Benoit, S.E., Valeri, C.R., Barnard, M.R., and Michelson, A.D. 1996. Decreased platelet inhibition by nitric oxide in two brothers with a history of arterial thrombosis. *J. Clin. Invest.* 97:979-987.

Germain, G.S. and Arneson, R.M. 1977. Selenium induced glutathione peroxidase activity in mouse neuroblastoma cells. *Biochem. Biophys. Res. Commun.* 79:119-123.

Hagel, L. 1998. Gel-filtration chromatography. *In* Current Protocols in Protein Science (J.E. Coligan, B.M. Dunn, H.L. Ploegh, D.W. Speicher, and P.T. Wingfield, eds.) pp. 8.3.1-8.3.30. John Wiley & Sons, New York.

Himeno, S., Takekawa, A., Toyoda, H., and Imura, N. 1993. Tissue-specific expression of glutathione peroxidase gene in guinea pigs. *Biochim. Biophys. Acta* 1173:283-288.

Hiratsuka, A., Yamane, B., Yamazaki, S., Ozawa, N., and Watabe, T. 1997. Subunit Ya-specific glutathione peroxidase activity toward cholesterol 7-hydroperoxides of glutathione S-transferases in cytosols from rat liver and skin. *J. Biol. Chem.* 272:4763-4769.

Ho, Y-S., Magnenat, J-L., Bronson, R.T., Cao, J., Gargano, M., Sugawara, M., and Funk, C.D. 1997. Mice deficient in cellular glutathione peroxidase develop normally and show no increased sensitivity to hyperoxia. *J. Biol. Chem.* 272:16644-16651.

Hong, Y., Li, C-H., Burgess, J.R., Chan, M., Salem, A., Srikumar, K., and Reddy, C.C. 1989. The role of selenium-dependent and selenium-independent glutathione peroxidases in the formation of prostaglandin F_{2a} *J. Biol. Chem.* 264:13793-13800.

Lam, K-W., Wang, L., Hong, B-S., and Treble, D. 1993. Purification of phospholipidhydroperoxide glutathione peroxidase from bovine retina. *Curr. Eye Res.* 12:9-15.

Lavole, L., Tremblay, A., and Mirault, M-E. 1992. Distinct oxidoresistance phenotype of human T47D cells transfected by rat glutathione *S*-transferease Yc expression vectors. *J. Biol. Chem.* 267:3632-3636.

Lawrence, R.A. and Burk, R.F. 1976. Glutathione peroxidase activity in selenium-deficient rat liver. *Biochem. Biophys. Res. Commun.* 71:952-958.

Lawrence, R.A. and Burk, R.F. 1978. Species, tissue and subcellular distribution of non Se-dependent glutathione peroxidase activity. *J. Nutr.* 108:211-215.

Lin, F., Jackson, V.E., and Girotti, A.W. 1995. Amplification and hyperexpression of the catalase gene in selenoperoxidase-deficient leukemia cells. *Arch. Biochem. Biophys.* 317:7-18.

Maiorino, M. 1994. Effect of α-lipoic acid on Se-dependent glutathione peroxidases. *In* New Strategies in Prevention and Therapy. Biological Oxidants and Antioxidants. (L. Packer and E. Cadenas, eds.) pp. 69-74, Hippokrates Verlag, Stuttgart, Germany.

Maiorino, M., Roveri, A., Gregolin, C., and Ursini, F. 1986. Different effects of triton X-100 deoxycholate, and fatty acids on the kinetics of glutathione peroxidase and phospholipid hydroperoxide glutathione peroxidase. *Arch. Biochem. Biophys.* 251:600-605.

Maiorino, M., Gregolin, C., and Ursini, F. 1990. Phospholipid hydroperoxide glutathione peroxidase. *Methods Enzymol.* 186:449-483.

Maiorino, M., Chu, F-F., Ursini, F., Davies, K.J.A., Doroshow, J.H., and Esworthy, R.S. 1991. Phospholipid hydroperoxide glutathione peroxidase is the 18-kDa selenoprotein expressed in human tumor cell lines. *J. Biol. Chem.* 24:7728-7732.

Mirault, M-E., Tremblay, A., Beaudoin, N., and Tremblay, M. 1991. Overexpression of selenoglutathione peroxidase by gene transfer enhances the resistance of T47D human breast cells to clastogenic oxidants. *J. Biol. Chem.* 266:20752-20760.

Mosialou, E. and Morgenstern, R. 1989. Activity of rat liver microsomal glutathione transferase toward products of lipid peroxidation and studies of the effect of inhibitors on glutathione-dependent protection against lipid peroxidation. *J. Biochem. Biophys.* 275:289-294.

Munz, B., Frank, S., Hubner, G., Olsen, E., and Werner, S. 1997. A novel type of glutathione peroxidase: Expression and regulation during wound repair. *Biochem. J.* 326:579-585.

Paglia, D.E. and Valentine, W.N. 1967. Studies on the quantitative and qualitative characterization of erythrocyte glutathione peroxidase. *J. Lab. Clin. Med.* 70:158-169.

Pascual, P., Martinez-Lara, E., Barcena, J.A., Lopez-Barea, J., and Toribio, F. 1992. Direct assay of glutathione peroxidase activity using high-performance capillary electrophoresis. *J. Chromatogr.* 581:49-56.

Peshenko, I.V., Novoselov, V.I., Evdokimov, V.A. et al. 1998. Identification of 28 kDa secretory protein from rat olfactory epithelium as thiol-specific antioxidant. *Free Radical Biol. Med.* 25:654-659.

Phelan, S.A., Johnson, K.A., Beier, D.A., and Paigen, B. 1998. Characterization of the murine gene encoding Aop2 (Antioxidant Protein 2) and identification of two highly related genes. *Genomics* 54:132-139.

Reiter, R. and Wendel, A. 1983. Selenium and drug metabolism. I. Multiple modulattions of mouse liver enzymes. *Biochem. Pharmacol.* 32:3063-3067.

Roveri, A., Casasco, A., Maiorino, M., Dalan, P., and Calligaro, A. 1992. Phospholipid hydroperoxide glutathione peroxidase of rat testis. *J. Biol. Chem.* 267:6142-6146.

Singh, A. and Shichi, H. 1998. A novel glutathione peroxidase in bovine eye. *J. Biol. Chem.* 273:26171-26178.

Terao, J., Shibata, S.S., and Matsushita, S. 1988. Selective quantification of arachidonic acid hydroperoxides and their hydroxy derivatives in

reverse-phase high performance liquid chromatography. *Anal. Biochem.* 169:415-423.

Thurman, R.G., Ley, H.G., and Scholz, R. 1972. Hepatic microsomal ethanol oxidation. *Eur. J. Biochem.* 25:420-430.

Weitzel, F., Ursini, F., and Wendel, A. 1990. Phospholipid hydroperoxide glutathione peroxidase in various mouse organs during selenium deficiency and repletion. *Biochim. Biophys. Acta* 1036:88-94

Yagi, K., Komura, S., Kojima, H., Sun, Q., Nagata, N., Ohishi, N., Nishikimi, M. 1996. Expression of human phospholipid hydroperoxide glutathione peroxidase gene for protection of host cells from lipid hydroperoxide-mediated injury. *Biochem. Biophys. Res. Commun.* 219:486-491.

Zhang, L., Maiorino, M., Roveri, A., and Ursini, F. 1989. Phospholipid hydroperoxide/glutathione peroxidase: Specific activity in tissues of rats of different age and comparison with other glutathione peroxidases. *Biochim. Biophys. Acta* 1006:140-143.

Key References

Esworthy et al., 1993. See above.

Presents basic information on GPX3 and the assay of this enzyme activity, as well as the assay of GPX4 by several means.

Esworthy et al., 1998. See above.

Two methods for the detection of GPX2 activity are demonstrated in this paper, one utilizing Gpx1 gene knockout mice and the other anti-GPX1 antibody.

Maiorino et al., 1990. See above.

Discusses finding and methods for studying GPX4, at length. Comparative hydroperoxide rate constants for GPX4 versus GPX1 are listed.

Paglia and Valentine, 1967. See above

Lawrence and Burk, 1976. See above.

These two references provide much basic information about glutathione peroxidases and the assay variations for GPX1 and GSTs.

Peshenko et al, 1998. See above.

Singh and Shichi, 1998. See above.

Basic information about Aop2 is presented in these two papers and the references within.

Contributed by R.S. Esworthy, F.-F. Chu, and J.H. Doroshow
City of Hope National Medical Center
Duarte, California

Measurement of Glutathione Reductase Activity

Glutathione reductase catalyzes the reduction of glutathione disulfide (GSSG) by NADPH. The product, reduced glutathione (GSH), is essential to the survival of cells of most aerobic organisms. GSH, a thiol, is a major intracellular antioxidant (normally present in cells at a concentration of 1 to 10 mM) that provides protection against hydroperoxides as well as free radicals. GSH is also involved in the inactivation of many toxic and carcinogenic electrophiles of both endogenous and xenobiotic origins through reactions catalyzed by the numerous glutathione transferases (see Chapter 6). As a substrate for glutaredoxin, GSH serves as a reductant in the ribonucleotide reductase–catalyzed biosynthesis of the DNA precursors deoxyribonucleotides. Many other cellular functions are also dependent on the presence of reduced glutathione (Mannervik et al., 1989), and the important biochemical role of glutathione reductase is obvious (Josephy et al., 1997).

Glutathione reductase occurs in all cell types. The spectrophotometric assay (see Basic Protocol) is suitable for measurement of its activity in the cytosol fraction or other particle-free samples, crude or purified.

CONTINUOUS SPECTROPHOTOMETRIC ASSAY OF GLUTATHIONE REDUCTASE

BASIC PROTOCOL

The protocol described below is based on monitoring NADPH oxidation linked to GSSG reduction. NADPH absorbs at 340 nm, and its oxidation is reflected by a decrease in absorbance at this wavelength.

NOTE: To be able to compare results, it is important to perform the reactions at constant temperature. Specific activities given are measured at 30°C.

Materials

Assay buffer: 0.2 M potassium phosphate, pH 7.0/2 mM EDTA (see *APPENDIX 2A* for preparation of potassium phosphate and EDTA stocks)
20 mM GSSG (Boehringer or Sigma) in water, prepared fresh each day
2 mM NADPH (Boehringer or Sigma) in 10 mM Tris·Cl, pH 7.0, prepared fresh each day and kept on ice
Sample to be tested for glutathione reductase activity (see Critical Parameters)

Spectrophotometer (preferably a recording instrument) with thermostat
Spectrophotometer cuvette (transparent at 340 nm, quartz or disposable) with 1-cm pathlength
Water bath (or other temperature-controlling device)

1. Prepare a spectrophotometer with thermostat for kinetic measurements. Set the measurement wavelength to 340 nm. Equilibrate assay buffer to 30°C (e.g., using a water bath).
2. Add the following to a cuvette at 30°C:

   500 µl assay buffer
   50 µl 20 mM GSSG solution
   50 µl 2 mM NADPH solution
   H_2O to give a final volume of 1.00 ml *after* sample is added in step 3.

   The amount of sample that should be added will depend on the range of concentrations and the specific activity of glutathione reductase expected in the sample. For crude cytosolic fractions, try 10 µl.

Contributed by Bengt Mannervik
Current Protocols in Toxicology (1999) 7.2.1-7.2.4

3. Add the enzyme-containing sample to the cuvette to initiate the reaction. Place a piece of Parafilm over cuvette opening, cover Parafilm with finger, and invert cuvette three or four times to mix (do not shake). Immediately place cuvette in spectrophotometer and begin recording. Moniter the reaction for 1 min, or until a 10% decrease in absorbance ($\Delta A = 0.06$) at 340 nm has occurred. Test samples in duplicate or triplicate.

   Optimize activity measurement conditions with respect to assay time and amount of enzyme added (see Critical Parameters and Troubleshooting). The time between addition of sample to start of monitoring the reaction should not exceed 10 sec. Dilute the enzyme sample if the reaction trace is not linear.

4. Between measurements, rinse cuvette with deionized water from a squirt bottle and wipe off outside of cuvette using paper tissue (Kimwipes or equivalent). Alternatively, use a new (disposable) cuvette each time.

5. As controls, also prepare one tube containing all the components listed above except GSSG, and one tube (blank) containing all the components listed except sample (i.e., adjust to correct volume with extra water). Monitor the absorbance at 340 nm of each control.

   The blank is expected to show negligible reduction; the reaction without GSSG may show low levels of reduction involving other physiologically occurring disulfides in the sample (see Background Information).

6. Adjust the values obtained for the samples by subtracting any enzymatic oxidation of NADPH observed in the absence of GSSG from the rates obtained for the samples.

7. Calculate glutathione reductase activity, with a unit of glutathione reductase activity defined as the amount of enzyme that catalyzes the reduction of 1 μmol of GSSG per minute (equivalent to oxidation of 1 μmol of NADPH per minute).

   The enzyme activity is measured in ΔA/time units, where ΔA is the change in absorbance at the chosen wavelength. The time is measured in minutes. The change in absorbance is proportional to the change in NADPH concentration as given by the Lambert-Beer law ($A = \varepsilon lc$; where ε is the molar extinction coefficient of NADPH, l is the pathlength of the cuvette, and c is the concentration of NADPH). Thus, the activity = Δc per time unit = ΔA per time unit divided by εl. In the present case, $\varepsilon = 6.2\ mM^{-1}cm^{-1}$ and $l = 1$ cm.

   IMPORTANT NOTE: *It is crucial that the slopes be obtained from straight lines representing the initial rates of the reactions.*

COMMENTARY

Background Information

Glutathione reductase plays a pivotal role in the biochemistry of the tripeptide glutathione by catalyzing the regeneration of the reduced (thiol) form from its oxidized (disulfide) state (Mannervik et al., 1989). Glutathione disulfide (GSSG) is formed by enzymatic redox reactions in which reduced glutathione (GSH) is used as a reductant—for example, in glutathione peroxidase reactions involving the reduction of organic hydroperoxides (ROOH) as well as hydrogen peroxide (R=H):

$$2\ GSH + ROOH \rightarrow GSSG + ROH + H_2O$$

Other reactions in which GSH is used as a reductant are represented by the reduction of disulfides (RSSR) catalyzed by thioltransferase:

$$2\ GSH + RSSR \rightarrow GSSG + 2\ RSH$$

The available evidence indicates that in most normal cells the major portion of the total glutathione concentration is present in the reduced form (≥95%). Maintenance of this redox state is dependent on the following glutathione reductase–catalyzed reaction and the availability of the reductant NADPH:

$$GSSG + NADPH + H^+ \rightarrow 2\ GSH + NADP^+$$

Glutathione reductase is a dimeric protein composed of identical subunits (Williams, 1991). It contains flavin adenine dinucleotide

as a redox-active prosthetic group that mediates transfer of reducing equivalents from NADPH to a disulfide group of the protein, which then reduces the substrate GSSG. Glutathione reductase from mammalian sources is highly specific for NADPH as the reductant; the activity with NADH is <1% of that with NADPH at physiological pH and ionic strength. Similarly, the specificity for the disulfide substrate is high. Of all the physiologically occurring disulfides tested as substrates, only the mixed disulfide of coenzyme A and GSH gives an activity above a few percent of that obtained with GSSG (Carlberg and Mannervik, 1975). Claims that mixed disulfides of glutathione and hemoglobin or other thiol-containing proteins serve as substrates have not been corroborated (Mannervik and Axelsson, 1975). On the other hand, as with many flavoproteins, glutathione reductase may use artificial electron acceptors as substitutes for the physiological substrate GSSG (Carlberg and Mannervik, 1986). Such "diaphorase activity" involving, for example, aromatic nitro compounds or quinones may interfere with determinations of the normal glutathione reductase activity.

Critical Parameters

Crude cytosol fractions or purified samples of biological tissues can be assayed with the spectrophotometric procedure described, as long as they are optically clear solutions without interfering turbidity. Strong color, such as is found in hemolysates, may interfere with the measurements because of high background absorbance. In general, the assay is robust and not sensitive to the presence of moderate concentrations of salt, detergents, or other additives that may be employed in the preparation of samples for analysis.

Buffer and stock solutions should be prepared in Milli-Q-purified water or equivalent. GSSG stock solution is usually stable for several days at 4°C, but for accurate measurements fresh solutions should be made daily. The NADPH solution should be made fresh daily and kept cold (preferably in an ice bucket). NADPH should be prepared in Tris·Cl buffer, as described, because it is not stable when dissolved in unbuffered water.

In order to obtain reproducible results, care should be taken when pipetting buffer, substrate, and enzyme solutions into the cuvette. Most importantly, the activity is proportional to enzyme concentration in the cuvette, and any error in the volume of enzyme sample added gives a proportional error in activity.

Even if it has been established that the uncatalyzed reaction level is negligible (see Basic Protocol), it is recommended to routinely measure the nonenzymatic reaction rate and use it as an extra check of the assay conditions. If no reaction occurs, the enzyme sample could be added. Any measurable nonenzymatic rate should be subtracted.

NADPH is somewhat unstable, and its stability decreases with pH. The initial absorbance at 340 nm in the assay system should be ~0.6 at 0.1 mM NADPH.

Troubleshooting

The progress curve of the glutathione reductase reaction should be a straight line. This is essential in order to get reliable and reproducible results. If a smoothly bent curve is obtained it is most probably due to addition of too much enzyme-containing sample. Repeat the measurement using smaller amounts of sample until a straight line is obtained. The activity (slope) should be proportional to enzyme concentration in the assay system. A curve that is not linear or smoothly bent may be due to poor mixing of the reactants. Mix thoroughly and repeat the measurement. In general, it is sufficient to follow the reaction for < 10% oxidation of NADPH ($\Delta A < 0.06$).

Inability to reproduce experiments performed previously could also be related to the points listed in the Critical Parameters section. Check substrates, assay buffer, and temperature. Make sure that the correct wavelength is used and that the pipettor works properly.

Table 7.2.1 Cytosolic Specific Activities of Glutathione Reductase

Tissue	Specific activity (μmol/min per mg protein)	Reference
Rat liver	0.10	Carlberg et al., 1981
Calf liver	0.12	Carlberg and Mannervik, 1985
Human erythrocytes	0.004	Worthington and Rosemeyer, 1974
Pig erythrocytes	0.002	Boggaram et al., 1979

Anticipated Results

As pointed out in the Troubleshooting section and Basic Protocol, the progress curve of the glutathione reductase reaction should be a straight line with a negative slope. The more enzyme is added, the steeper the slope of the line should be. Table 7.2.1 gives cytosolic specific activities of glutathione reductase for some representative tissues.

Time Considerations

Many measurements can be performed in 1 day. Preparing buffer and substrate solutions requires ~1 hr. Adding buffer, substrates, and enzyme solution to the cuvette takes 0.5 to 1 min. One measurement normally takes 0.5 to 10 min.

Literature Cited

Boggaram, V., Brobjer, T., Larson, K., and Mannervik, B. 1979. Purification of glutathione reductase from porcine erythrocytes by the use of affinity chromatography on 2′,5′-ADP-Sepharose 4B and crystallization of the enzyme. *Anal. Biochem.* 98:335-340.

Carlberg, I. and Mannervik, B. 1975. Purification and characterization of the flavoenzyme glutathione reductase from rat liver. *J. Biol. Chem.* 250:5475-5480.

Carlberg, I. and Mannervik, B. 1985. Glutathione reductase. *Methods Enzymol.* 113:484-490.

Carlberg, I. and Mannervik, B. 1986. Reduction of 2,4,6-trinitrobenzenesulfonate by glutathione reductase and the effect of $NADP^+$ on the electron transfer. *J. Biol. Chem.* 261:1629-1635.

Carlberg, I., DePierre, J.W., and Mannervik, B. 1981. Effect of inducers of drug-metabolizing enzymes on gutathione reductase and glutathione peroxidase in rat liver. *Biochem. Biophys. Acta* 677:140-145.

Josephy, P.D., Mannervik, B., and Ortiz de Montellano, P. 1997. Molecular Toxicology. Oxford University Press, New York.

Mannervik, B. and Axelsson, K. 1975. Reduction of disulphide bonds in proteins and protein mixed disulphides catalysed by a thioltransferase in rat liver cytosol. *Biochem. J.* 149:785-788.

Mannervik, B., Carlberg, I., and Larson, K. 1989. Glutathione: General review of mechanism of action. *In* Coenzymes and Cofactors, Vol. 3A (D. Dolphin, R. Poulson, and O. Avramovic, eds.) pp. 475-516. John Wiley & Sons, New York.

Williams, C.H., Jr. 1991. Lipoamide dehydrogenase, glutathione reductase, thioredoxin reductase, and mercuric ion reductase—a family of flavoenzyme transhydrogenases. *In* Chemistry and Biochemistry of Flavoenzymes, Vol. III (F. Müller, ed.) pp. 121-211. CRC Press, Boca Raton, Fla.

Worthington, D.J. and Rosemeyer, M.A. 1974. Human glutathione reductase: Purification of the crystalline enzyme from erythrocytes. *Eur. J. Biochem.* 48:167-177.

Contributed by Bengt Mannervik
Uppsala University
Uppsala, Sweden

Analysis of Superoxide Dismutase Activity

The superoxide dismutase (SOD) enzymes present unusual challenges to those who wish to quantify their activities. Their substrate, the superoxide radical ($O_2^{\cdot -}$), is quite unstable in the physiological pH range. It reacts rapidly with itself, or dismutates, with a second-order rate constant of ~10^5 $M^{-1}sec^{-1}$:

$$O_2^{\cdot -} + O_2^{\cdot -} + 2H^+ \rightarrow O_2 + H_2O_2$$

Superoxide reacts with SOD, however, with a second-order rate constant of ~2×10^9 M^{-1} sec^{-1}, about 20,000 times faster than it reacts with itself. This rate approaches diffusion limitation, the theoretical maximally efficient rate where every molecular collision leads to fruitful reaction. SOD thus has an enzymatic turnover of ~10^6 reactions per second, one of the highest known. Coupled with the fact that the cytosolic concentration of SOD is greater than the steady-state concentration of its substrate, the overall effect of the enzyme is to lower the steady-state concentration of superoxide in the cell—by a factor of ~50,000 in liver cells, for example. It should be noted that the rate of superoxide dismutation, in either the presence or the absence of the enzyme, must equal the rate of superoxide generation, as dictated by the steady-state assumption. This also means that once steady state is reached, the presence of SOD has no effect on the rate of H_2O_2 accumulation or the amount produced (which are governed by the rate of superoxide generation)—a concept that eludes many, and has led to the introduction of a certain amount of confusion in the literature by those who erroneously believe that more SOD should, somehow, lead to the production of more H_2O_2.

The standard international unit (IU) definition—1 μmol/min of product at a saturating concentration of substrate—cannot be applied to SOD. In addition to the problem of substrate instability due to nonenzymatic dismutation described above, the K_M for superoxide has been estimated to be 3.5 mM, a concentration that cannot even be approached at physiological pH. Thus, most practical assays of SOD are indirect, based on competition for superoxide between SOD and some indicator molecule that reacts avidly with the radical to produce a measurable change in absorbance. The two most widely used indicators are cytochrome *c* and nitroblue tetrazolium. Because of the arbitrary nature of SOD assays, they have cross-laboratory meaning only when compared to an accepted standard. When superoxide dismutase was first described, a set of standard assay conditions was also described, and a standard unit of activity was defined under these conditions (McCord and Fridovich, 1969; see Critical Parameters for further discussion). This standard assay is presented below (see Basic Protocol 1). Since mammals produce three distinct SODs—a cytosolic Cu,Zn-SOD, a mitochondrial Mn-SOD, and a secreted extracellular Cu,Zn-SOD—variations on the assay have been developed that are useful in distinguishing these various forms of SOD; these procedures are also included (see Alternate Protocol and see Basic Protocol 2).

ASSAY OF TOTAL SOD ACTIVITY BY THE XANTHINE OXIDASE/XANTHINE/ CYTOCHROME *c* METHOD

BASIC PROTOCOL 1

This procedure describes a spectrophotometric (visible-light) assay procedure for quantifying the activity of any solution or cell extract containing SOD, or the total activity due to any mixture of SODs. The results will be in standard, or McCord-Fridovich, units.

Materials

SOD assay cocktail (see recipe)
SOD-containing sample
Xanthine oxidase solution (see recipe)

Contributed by Joe M. McCord
Current Protocols in Toxicology (1999) 7.3.1-7.3.9

Recording, visible-wavelength spectrophotometer with thermostat set at 25°C
3-ml cuvettes

1. Place 3 ml SOD assay cocktail in a cuvette. Set the spectrophotometer reading at 550 nm to zero.
2. Add ~10 µl xanthine oxidase solution (~3 mIU) and record the rate of increase in absorbance (*A*) at 550 nm. The rate should be ~0.02 *A*/min, but it need not be exactly this value. Add more or less xanthine oxidase, if necessary, to obtain a rate in the range of 0.015 to 0.025 *A*/min. This is the control rate.

   Xanthine oxidase catalyzes the reaction of xanthine and oxygen, generating superoxide at ~1 µM/min. It will efficiently react with ferricytochrome c, reducing it to ferrocytochrome c and causing an increase in absorbance at 550 nm with a molar extinction coefficient increase of 20,000 cm^{-1} (from 9,000 to 29,000 cm^{-1}).

3. Dilute an aliquot of enzyme sample (preferably 10 to 50 µl) containing ~1 standard unit of SOD in SOD assay cocktail to 3 ml, then repeat the assay, using the amount of xanthine oxidase determined in step 2.

   This time the rate of increase in absorbance at 550 nm will be lower—under these assay conditions, the amount of SOD producing 50% inhibition of reduction of ferricytochrome c equals 1 standard unit of activity. Percent inhibition is calculated as follows:

   % inhibition = [(control rate - sample rate)/control rate] × 100.

   If the amount of inhibition produced is more than ~60% or less than ~40%, the assay should be repeated with an adjusted volume of sample until inhibition is achieved in the 40% to 60% range, where the slope of the inhibition curve (see Fig. 7.3.2A) is neither too steep nor too flat. This will produce more accurate calculations.

   This time the rate of cytochrome c reduction is lower because SOD competes with 10 µM ferricytochrome c for available superoxide. If the level of inhibition is exactly 50%, the amount of SOD is defined as a standard unit and is ~0.3 µg of mammalian Cu,Zn-SOD under these assay conditions.

4. Calculate the number of units of SOD in the sample assay using the formula:

   units = % inhibition/(100 − % inhibition).

ALTERNATE PROTOCOL

ASSESSMENT OF RELATIVE CONTRIBUTIONS OF Cu,Zn-SOD AND Mn-SOD TO TOTAL SOD ACTIVITY IN CELL EXTRACTS

Mammalian organisms have three genes that encode SODs. In most tissues, the predominant SOD is the cytosolic Cu,Zn-SOD. Mitochondria contain a Mn-SOD that is quite inducible and may also be found in the cytosol in certain species and under certain circumstances. Some tissues and extracellular fluids may contain a third SOD—extracellular SOD, or EC-SOD. EC-SOD is also a Cu,Zn-SOD and is encoded by a gene that is clearly related to the cytosolic Cu,Zn-SOD. The assay described in Basic Protocol 1 works equally well for any SOD and will simply reflect total SOD activity if a mixture of enzymes is assayed. (All SODs have roughly the same specific activity of 3000 to 5000 standard units per milligram protein.) Often, however, it may be desirable to assay the SODs separately. The Cu,Zn-SODs may be inhibited by a variety of agents including cyanide, H_2O_2, or diethyldithiocarbamate. Most methods therefore rely on assaying total activity in a sample, then reassaying under conditions where the Cu,Zn-SOD will be inhibited and only the Mn-SOD activity remains. The addition of 3 mM sodium cyanide to the assay is one simple approach that has been widely used, but this method is far from ideal. The cyanide does not cause 100% inhibition, and interferes somewhat with the xanthine oxidase/cytochrome *c* reaction. The following protocol will give more reliable analysis of Mn-SOD, and more complete inactivation of Cu,Zn-SOD.

Additional Materials (also see Basic Protocol 1)

SOD-containing sample with known total activity (see Basic Protocol 1)
25 mM sodium diethyldithiocarbamate
25 mM H_2O_2

1. To an aliquot of sample of known total SOD activity, add 1 vol of 25 mM diethyldithiocarbamate per 24 vol of sample (bringing the final concentration of diethyldithiocarbamate in the sample to 1 mM). Incubate 1 hr at 37°C.

   Diethyldithiocarbamate causes a rapid and reversible inhibition of Cu,Zn-SODs, followed by a slower, irreversible inactivation. Mn-SODs are not affected.

2. Add 1 vol of 25 mM H_2O_2 to the 25 vol of mixture, and continue to incubate for an additional 15 min at 37°C.

   Diethyldithiocarbamate can interfere with the xanthine oxidase/cytochrome c assay, so excess reagent is neutralized by reaction with equimolar H_2O_2 prior to the assay.

3. Assay the sample for SOD activity (see Basic Protocol 1, steps 2 to 4); the SOD activity observed is due to Mn-SOD.

4. Multiply the units observed by 1.08 to correct for the dilution of sample by the reagents added above, then calculate Cu,Zn-SOD activity by subtracting Mn-SOD activity from total activity.

QUANTITATIVE ASSAY OF SODs BY ACTIVITY STAINING OF ELECTROPHORETIC GELS

BASIC PROTOCOL 2

An alternative and very useful technique for the differential assay of Cu,Zn- and Mn-SODs makes use of an activity stain applicable to thin-film agarose or native polyacrylamide electrophoretic gels. Qualitative results are easily obtained, and with a little more care and effort surprisingly good quantitative results may be achieved. The method relies on the photochemical generation of superoxide radical throughout the gel, and its reaction with a soluble, pale-yellow indicator molecule, nitroblue tetrazolium chloride (NBT). As NBT reacts with superoxide, an insoluble, intensely purple precipitate called formazan is formed. This compound stains the gel uniformly purple, except at bands of SOD activity, which remain colorless due to scavenging of the radical.

Materials

SOD-containing sample with known total activity (see Basic Protocol 1)
Gel staining solutions A and B (see recipes)

Thin-film agarose gels (Universal Gel/8, Ciba-Corning Diagnostics) *or* native polyacrylamide slab gels (*APPENDIX 3*), 1-mm thick
Small rectangular dish for soaking the gel in a minimal volume of staining solution
Fluorescent desk lamp for illuminating and developing the gel
Camera, densitometer, or other device(s) for recording band intensity

Additional reagents and equipment for native PAGE (*APPENDIX 3*)

1. Prepare a thin-film agarose gel (according to manufacturer's instructions) or a native polyacrylamide slab gel (see *APPENDIX 3*). Load aliquots of sample, each containing 0.2 to 1.0 standard units SOD, into individual wells of the gel. If the gel is to be analyzed quantitatively, load at least four calibration standards containing known and varying amounts of a purified SOD, from 0.2 to 0.5 standard units, into individual wells of the gel.

The calibration standards will be used in the preparation of a standard calibration curve for each gel run. Because of the variation in staining from one gel to the next, standards must generally be included on each gel if quantification is to be expected.

2. Perform gel electrophoresis under native conditions using standard procedures (follow manufacturer's instructions for thin-film agarose gels and *APPENDIX 3* for native polyacrylamide gels).
3. When the electrophoresis is completed, mix together in subdued light 40 ml gel staining solution A and 2 ml gel staining solution B. Place this with the gel in the staining dish, and incubate in the dark for 3 to 5 min.

   Once the staining solutions are mixed together, do not expose to bright light. The solution may be reused to soak subsequent gels during the course of several days but should be discarded when it begins to turn purple.
4. Remove the gel from the staining solution, draining excess solution from its surface, and place the gel under a fluorescent desk lamp, ~6 in. (15 cm) from the tubes, so that the gel receives even illumination. Expose until the gel is uniformly purple, and the bands of SOD activity are clearly visible. This may take 10 to 15 min.

   The thin-film agarose gels have a convenient plastic backing, which makes handling easy. Polyacrylamide slab gels may be placed on a glass plate and covered with plastic film, if desired, to prevent drying during exposure.
5. When the desired color development has been achieved, remove gel from the light source and soak in water for 10 or 15 min to remove unreacted staining reagents as well as buffer salts. Photograph and/or scan the gel, wet or dried, as desired.

   Rough quantification may be achieved by visually comparing the intensity of bands of unknown samples to the known standards on the same gel. For more precise analysis, the lanes can be scanned and the areas under the curves integrated using a densitometer or a digital imaging program such as NIH Image or Matrix (QuantiVison Canada; Fig. 7.3.1). The Cu,Zn- and Mn-SODs are readily separated by electrophoresis and may be quantified

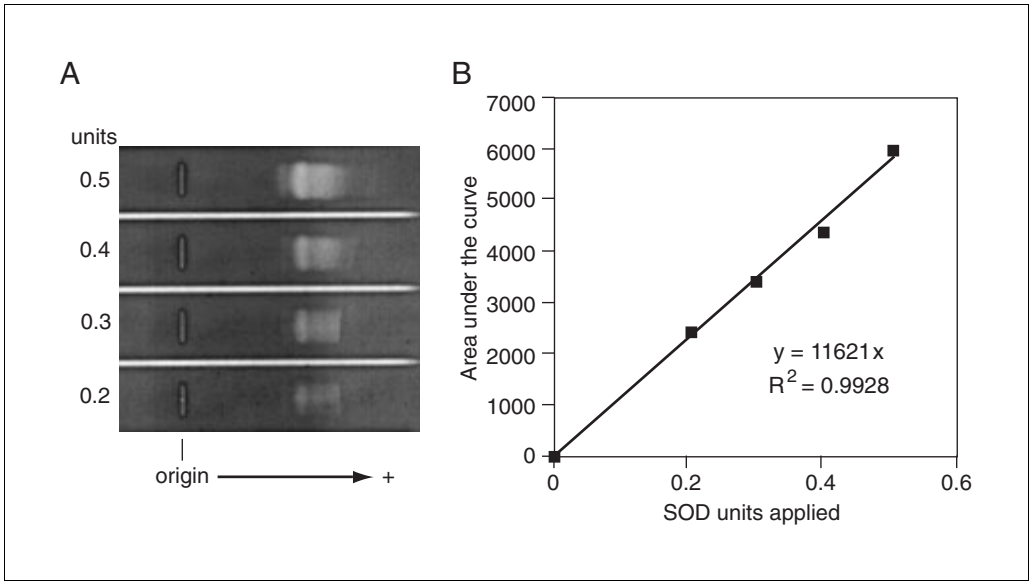

Figure 7.3.1 (**A**) A thin-film agarose gel (Universal Gel/8, Ciba-Corning Diagnostics) loaded with samples containing from 0.2 to 0.5 standard units of recombinant human Cu,Zn-SOD. The gel was electrophoresed in 0.02 M Tris/glycine buffer, pH 8.45, for 30 min at 200 V. The family of closely spaced bands reflects charge isomers, and is characteristic of the Cu,Zn-SODs. The gel was stained as described in Basic Protocol 2 and the dried gel digitally scanned (not shown) and analyzed using Matrix software (QuantiVison Canada). (**B**) The integrated area under the curve from each lane is plotted versus the amount of SOD applied.

individually by this technique. Often, the Mn-SOD is induced while the Cu,Zn-SOD level remains constant. When this is the case, the Cu,Zn-SOD may be used as an internal standard. Changes in Mn-SOD may then be reported relative to Cu,Zn-SOD, eliminating the need for external standards.

REAGENTS AND SOLUTIONS

Use Milli-Q-purified water or equivalent for all recipes and protocol steps. For common stock solutions, see ***APPENDIX 2A****; for suppliers, see* ***SUPPLIERS APPENDIX****.*

Cytochrome c stock solution, 1 mM

Prepare 1 mM ferricytochrome *c* (Sigma; from horse heart, minimum 95%) in 0.05 M potassium phosphate buffer, pH 7.8 (*APPENDIX 2A*). Store frozen at −20°C (stable indefinitely).

Gel staining solutions

Gel staining solution A:
0.05 M potassium phosphate buffer, pH 7.8 (*APPENDIX 2A*)
1 mM EDTA
0.25 mM NBT (nitroblue tetrazolium chloride)
Gel staining solution B:
0.5 mM riboflavin in water

Stock solutions of NBT and riboflavin may be used. The gel staining solutions can be stored for days in the dark at room temperature.

SOD assay cocktail

To 141 ml of 0.05 potassium phosphate buffer, pH 7.8 (*APPENDIX 2A*)/0.1 mM EDTA, add 7.5 ml of 1 mM xanthine stock solution (see recipe). Add 1.5 ml of 1 mM cytochrome *c* solution (see recipe). Check the cytochrome *c* concentration by placing an aliquot in a 1-cm cuvette and measuring the absorbance at 550 nm. Add a few crystals of solid sodium dithionite (a strong reducing agent), mix, and re-measure the absorbance. It should increase by exactly 0.20 A. If it does not, correct the cytochrome *c* concentration by adding more stock solution or diluting with sodium phosphate/xanthine mixture, as necessary. Store up to several days at 4°C or indefinitely frozen at −20°C.

Prepare an amount of cocktail appropriate for the anticipated number of assays; 150 ml is sufficient for 50 assays. Final concentrations are 0.05 M xanthine and 10 μM ferricytochrome c.

IMPORTANT NOTE: *It is critical that the cocktail contain exactly 10 μM ferricytochrome c, as this is what SOD competes against for superoxide. Any variation in this concentration will change the amount of inhibition produced by a given quantity of SOD, rendering the assay nonstandard.*

Xanthine oxidase solution

Dissolve purified bovine buttermilk xanthine oxidase (Sigma, grade III, or equivalent), at ~0.3 IU/ml in 0.05 M potassium phosphate buffer, pH 7.8 (*APPENDIX 2A*)/0.1 mM EDTA. Store frozen at −20°C.

This solution will lose some activity with repeated freezing and thawing, but the amount of xanthine oxidase added per assay is not critical, as long as it is constant between samples and their controls.

Xanthine stock solution

Prepare 1 mM xanthine (sodium salt) in 0.05 M potassium phosphate buffer, pH 7.8 (*APPENDIX 2A*). Heat to near boiling to assure complete dissolution (this concentration is near the solubility limit of xanthine). If desired, store frozen at −20°C in aliquots for future use; reheat after thawing to redissolve the xanthine prior to use.

COMMENTARY

Background Information

The metabolism of molecular oxygen is handled largely by cytochrome oxidase, the terminal oxidase in mitochondrial electron transport, which produces only H_2O as its product. From 2% to 5% of the oxygen animals inspire, however, is reduced by other pathways by one or two electrons, producing $O_2^{\cdot -}$ and H_2O_2. These cytotoxic, partially reduced forms of oxygen are produced not only by normal metabolism (resting myocardium makes superoxide at ~0.1 mM/min) but also in large amounts under pathological circumstances: by the NADPH oxidase of inflammatory cells and by injured mitochondria in post-ischemic tissues.

Because these partially reduced forms of oxygen are cytotoxic, protective antioxidant enzymes exist to convert them to water, including superoxide dismutases (SODs), catalase, and glutathione peroxidases. SOD catalyzes the reaction:

$$O_2^{\cdot -} + O_2^{\cdot -} + 2H^+ \rightarrow H_2O_2 + O_2$$

Catalase catalyzes an analogous reaction:

$$H_2O_2 + H_2O_2 \rightarrow O_2 + 2H_2O$$

Using reduced glutathione as the reducing agent, glutathione peroxidases also convert H_2O_2 to water.

Superoxide dismutases were discovered by McCord and Fridovich in 1969. The first SOD described was a cuprozinc enzyme from bovine red cells, but other members of this ubiquitous family of enzymes were quickly identified. A manganese-containing enzyme (Keele et al., 1970) and later an iron-containing enzyme (Yost and Fridovich, 1973) were isolated from *Escherichia coli*. The manganese enzyme was then found in mitochondria (Weisiger and Fridovich, 1973). Mammals possess a second cuprozinc SOD, extracellular SOD, that is secreted into extracellular fluids where it binds to cell surfaces and to components of the extracellular matrix (Marklund, 1982) and can be assayed like any other SOD. It may be separated from other SODs on the basis of its ability to bind to a column containing heparin-agarose (McCord et al., 1994).

Critical Parameters

The unique features of the reaction catalyzed by SOD dictate a very unconventional assay. Rather than being able to supply the enzyme with a saturating amount of substrate, it is necessary to continuously generate this unstable substrate in the reaction mixture where it accumulates only to levels that are perhaps as much as five orders of magnitude below its K_M value. The basis for measuring SOD activity then depends upon its ability to compete equally with a known "standard" reaction, in which this superoxide reacts with an indicator molecule, ferricytochrome *c*, under specified conditions of pH, ionic strength, temperature, and cytochrome *c* concentration. When the "control rate" is determined, essentially 100% of the superoxide is scavenged by the cytochrome *c* present. Reaction with cytochrome *c* is greatly favored over spontaneous dismutation, which would occur in the absence of an efficient scavenger molecule. The rate of disappearance of superoxide via reaction with cytochrome *c* ($R_{\text{cyt } c}$) is represented by the equation:

$$R_{\text{cyt } c} = k_{\text{cyt } c} [O_2^{\cdot -}] [\text{cytochrome } c],$$

where $k_{\text{cyt } c}$ is the rate constant for the reaction of cytochrome *c* with $O_2^{\cdot -}$. The value of this rate constant is ~6×10^5 $M^{-1}sec^{-1}$ at pH 7.8, 25°C (Simic et al., 1975). When 1 unit of SOD is present in the assay, the rate of disappearance of superoxide via catalyzed dismutation (R_{SOD}) is represented by the equation:

$$R_{SOD} = k_{SOD} [O_2^{\cdot -}] [SOD],$$

where k_{SOD} is the rate constant for the reaction of SOD with $O_2^{\cdot -}$. The value of this rate constant is ~2×10^9 $M^{-1}sec^{-1}$ at pH 7.8, 25°C for the cytosolic cuprozinc enzymes (Klug et al., 1972). When the rate of the indicator reaction is reduced by 50% (i.e., when 1 standard unit of SOD is present), the two rates by which superoxide disappears are equal:

$$k_{SOD} [O_2^{\cdot -}] [SOD] = k_{\text{cyt } c} [O_2^{\cdot -}] [\text{Cyt } c]$$

and

$$[SOD] = k_{\text{cyt } c} [\text{cytochrome } c]/k_{SOD} = 3 \times 10^{-9} \text{ M}$$

Note that the standard unit of SOD is a *concentration*, not an amount of enzyme. When the volume of the standard assay is defined as 3 ml, then the amount of a standard unit becomes 0.3 µg (using the molecular weight of 32,000 for bovine Cu,Zn-SOD). Hence, it is critical to take into account the volume of the assay reaction. If the assay were conducted with 1 ml of cocktail, 50% inhibition would be achieved at the same concentration of SOD, but the amount of enzyme added to the cuvette would be only 0.1 µg. This nonstandard unit may be converted to standard unit by simply

dividing the result by 3. Note also that the concentration of superoxide does not appear in the final equation, meaning that the unit observed depends only on the concentration of cytochrome *c*, and not on the steady-state concentration of $O_2^{\cdot -}$. Hence, for accurate analysis it is important to verify precisely the ferricytochrome *c* concentration, but the amount of xanthine oxidase added is not critical.

Similarly, the sensitivity of the standard assay changes if the pH is varied from 7.8. At pH 10, the rate constant for the reaction of $O_2^{\cdot -}$ with cytochrome *c* decreases by about an order of magnitude. The rate constant for the reaction of $O_2^{\cdot -}$ with bovine Cu,Zn-SOD, however, hardly changes at all. (The rate constant for the reaction of $O_2^{\cdot -}$ with human Mn-SOD decreases by a factor of five at pH 10.) Accordingly, if the assay is performed in a 3-ml reaction volume at pH 10, a unit of bovine Cu,Zn-SOD activity appears to be about one-tenth the "standard unit," or ~0.03 µg. Because different SODs show different effects of pH on their activities, assaying at two different pHs has been used to determine their relative contributions in a mixture (Crapo et al., 1978).

Another alteration that can be made in the assay is to substitute a different reactive indicator (against which SOD competes for superoxide) for cytochrome *c*. For example, NBT, which is used here for the gel activity stain, may also be used in solution.

IMPORTANT NOTE: An investigator may find it useful to change some of the above parameters to create modified assay conditions appropriate for specific applications. It is *crucial*, however, that any such nonstandard assay be compared to the standard assay to determine a conversion factor, and that results be published in equivalent standard units. There are numerous reports in the literature that report SOD activity only in arbitrary nonstandard units and that therefore cannot, unfortunately, be compared to studies performed in other laboratories.

A calibration curve prepared by plotting percent inhibition versus standard units of SOD will be a rectangular hyperbola, as shown in Figure 7.3.2A. Rectangular hyperbolae are linearized in double-reciprocal plots, as shown in Figure 7.3.2B. Here it may be seen that the *y* intercept equals 0.01. That is, as SOD concentration approaches infinity, the inhibition will approach 100%. The mathematical formula for a rectangular hyperbola may be conveniently rearranged as shown to allow easy calculation of units from percent inhibition when the amount of inhibition observed is not exactly 50%.

The application of a modified version of the SOD assay to agarose or acrylamide gels is a widely used technique that can give surprisingly quantitative results. Figure 7.3.1A shows a thin-film agarose gel that was stained using

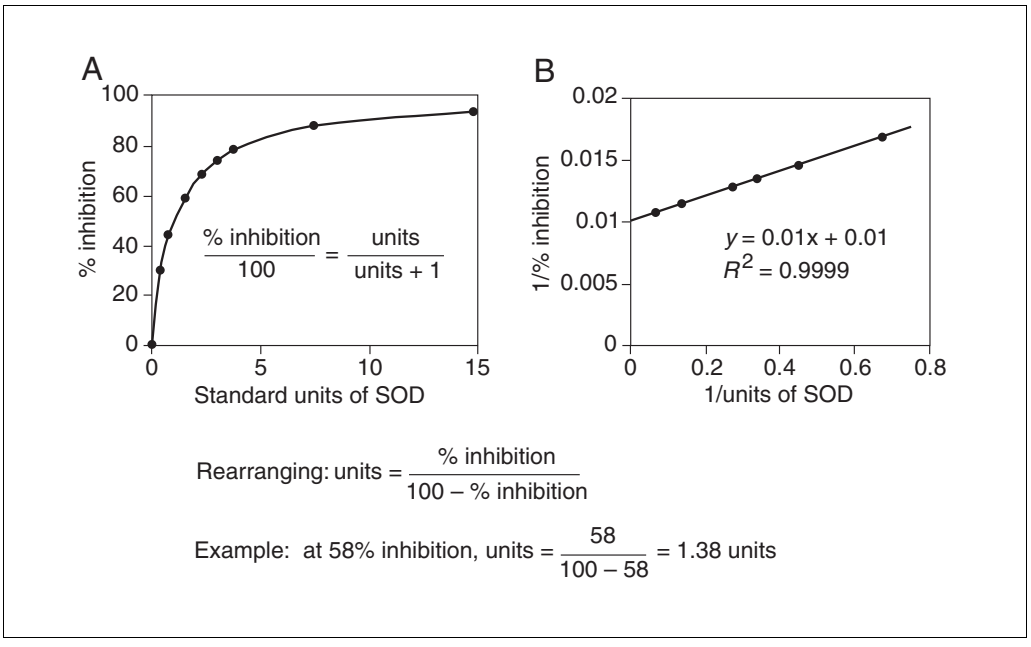

Figure 7.3.2 Calibration curves showing the relationship between units of SOD and percent inhibition of the standard assay. Purified bovine Cu,Zn-SOD was assayed under standard assay conditions to obtain the data shown. (**A**) A rectangular hyperbolic calibrating curve. (**B**) A linear double-reciprocal calibrating curve.

the technique described in Basic Protocol 2. SOD samples varied from 0.2 to 0.5 standard units per lane (60 to 150 ng of purified SOD). In this range, the values of integrated areas (Fig. 7.3.1B) under the scanned curves proved to be remarkably linear when plotted against the amount of SOD applied, even though there are theoretical reasons that the relationship should not be a linear one. In any event, the technique can provide quite quantitative results, provided that standards are run on the same gel as the unknowns and that the unknowns fall within the range of the standards' values. Because the Cu,Zn- and Mn-SODs are readily separated with this system, it is also useful and accurate for determining their relative contributions in tissue extracts that contain both types of enzymes.

Troubleshooting

All SOD assays must be interpreted cautiously, and care must be taken to include all necessary controls, because the assays are subject to the effects of a number of interfering substances. The ability to reduce ferricytochrome *c* is certainly not unique to superoxide; hence, the presence of other reducing agents in biological fluids and tissue extracts is always a concern. In Basic Protocol 1, step 3, it is often necessary, after adding the sample to the cocktail, to record a rate of absorbance change at 550 nm *before* adding xanthine oxidase. If low-molecular-weight substances are present that are capable of reducing cytochrome *c* (enzymatically or nonenzymatically), such a rate will be seen. If this rate is slow relative to the control rate (in the presence of xanthine oxidase but the absence of SOD), and if it continues linearly for several minutes, it may be noted and subtracted from all subsequent rates containing that amount of sample. Occasionally the rate will be rapid but short-lived. Here the sample may be incubated with cocktail until this background rate subsides. If ≤10% of the cytochrome *c* is reduced, one may then proceed normally. If the level of cytochrome *c* reduction is greater, the reducing agents present in the samples must be removed by dialysis or gel filtration before the samples may be accurately assayed.

Another common interference is the reoxidation of ferrocytochrome *c* by enzymes such as cytochrome oxidase, cytochrome *c* peroxidase, or lactoperoxidase. The mitochondrial cytochrome oxidase may appear to be SOD activity—instead of preventing the reduction of the cytochrome, cytochrome oxidase promptly reoxidizes cytochrome *c* using molecular oxygen as its other substrate. Fortunately, cytochrome oxidase is very sensitive to inhibition by cyanide. The addition of 10 μM sodium cyanide to the reaction mixture will eliminate interference by cytochrome oxidase without appreciably inhibiting the Cu,Zn-SODs (which requires ~3 mM; see Alternate Protocol). (Solutions of sodium cyanide should be prepared with appropriate caution, and should be freshly prepared.) Impure xanthine oxidase preparations sometimes contain an enzyme called lactoperoxidase, which can catalyze the oxidation of ferrocytochrome *c* by H_2O_2. Because there is no H_2O_2 in the assay initially, lactoperoxidase has no effect on initial rates. As the xanthine oxidase reaction progresses, however, H_2O_2 accumulates, and the reoxidation of cytochrome *c* becomes faster and faster, eventually overcoming the rate of reduction. The often surprising effect is that the change in absorbance slows, stops, and reverses, picking up speed in the negative direction until all the cytochrome is again oxidized! Purifying one's own xanthine oxidase from raw cream, using the method of Waud and Rajagopalan (Waud et al., 1975), is the best solution to this problem. Alternatively, one can try adding catalase to the assay mixture (~200 IU; Sigma, from bovine liver, crystalline suspension in water). This may effectively eliminate H_2O_2 as it is produced by xanthine oxidase, preventing its use by contaminating peroxidases.

Literally scores of SOD assay methods have been published. Many are variations on the themes described here, specially modified for particular applications, for automation, or for increased sensitivity. Others are quite novel and different. In principal, virtually any process that is superoxide dependent may be configured to serve as an assay for SOD.

Anticipated Results

Accuracy and reproducibility using Basic Protocol 1 should be well within ±5%. Because of additional steps involved in Alternate Protocol and Basic Protocol 2, variability may be somewhat higher with those assays. Likewise, variability will increase if interference with the assay, such as the presence of low-molecular-weight reductants which require correction or removal, is encountered.

Time Considerations

Once all required solutions are in hand, an unknown sample of SOD can be assayed by Basic Protocol 1, in duplicate, with duplicate

control rates, in 30 to 40 min. The Alternate Protocol, because of the incubation times, will require 1.5 to 2 hr. A thin-film agarose gel can be loaded, run, and stained according to Basic Protocol 2 in little more than 1 hr.

Literature Cited

Crapo, J.D., McCord, J.M., and Fridovich, I. 1978. Superoxide dismutases: Preparation and assay. *Methods Enzymol.* 53:382-393.

Keele, B.B., Jr., McCord, J.M., and Fridovich, I. 1970. Superoxide dismutase from *Escherichia coli B*: A new manganese-containing enzyme. *J. Biol. Chem.* 245:6176-6181.

Klug, D., Rabani, J., and Fridovich, I. 1972. A direct demonstration of the catalytic action of superoxide dismutase through the use of pulse radiolysis. *J. Biol. Chem.* 247:4839-4842.

Marklund, S.L. 1982. Human copper-containing superoxide dismutase of high molecular weight. *Proc. Natl. Acad. Sci. U.S.A.* 79:7634-7638.

McCord, J.M. and Fridovich, I. 1969. Superoxide dismutase: An enzymic function for erythrocuprein (hemocuprein). *J. Biol. Chem.* 244:6049-6055.

McCord, J.M., Gao, B., Leff, J., and Flores, S.C. 1994. Neutrophil-generated free radicals: Possible mechanisms of injury in adult respiratory distress syndrome. *Environ. Health. Perspect.* 102:57-60.

Simic, M.G., Taub, I.A., Tocci, J., and Hurwitz, P.A. 1975. Free radical reduction of ferricytochrome-C. *Biochem. Biophys. Res. Commun.* 62:161-167.

Waud, W.R., Brady, F.O., Wiley, R.D., and Rajagopalan, K.V. 1975. A new purification procedure for bovine milk xanthine oxidase: Effect of proteolysis on the subunit structure. *Arch. Biochem. Biophys.* 169:695-701.

Weisiger, R.A. and Fridovich, I. 1973. Superoxide dismutase. Organelle specificity. *J. Biol. Chem.* 248:3582-3592.

Yost, F.J., Jr. and Fridovich, I. 1973. An iron-containing superoxide dismutase from *Escherichia coli*. *J. Biol. Chem.* 248:4905-4908.

Key References

Crapo et al., 1978. See above.

A discussion of assay methodologies and variations.

McCord and Fridovich, 1969. See above.

Initial description of superoxide dismutase and the definition of the standard unit of activity.

Contributed by Joe M. McCord
University of Colorado Health Sciences Center
Denver, Colorado

Measurement of Thioredoxin and Thioredoxin Reductase

The thioredoxin system—i.e., thioredoxin (Trx), thioredoxin reductase (TrxR), and NADPH—is ubiquitous, providing reducing equivalents to essential biosynthetic enzymes like ribonucleotide reductase, and it is critical for cellular redox regulation, control of oxidative stress, and protection against oxidative damage. In recent years, particularly, the mammalian thioredoxin system has been the subject of rapidly increasing interest due to discoveries of novel functions of Trx in mammalian organisms, the disclosure that TrxR contains a catalytically-active selenocysteine residue, and identification of several isoenzymes of both Trx and TrxR (see Background Information).

Two functional properties characterize the thioredoxin family of proteins: (1) reduced thioredoxin with a an active site dithiol [Trx-$(SH)_2$] catalyzes protein disulfide reductions, and (2) oxidized thioredoxin with an active site disulfide (Trx-S_2) is reduced by thioredoxin reductase, which acquires electrons from NADPH. This is illustrated in the following reactions:

$$\mathrm{Trx-(SH)_2 + protein-S_2 \rightleftharpoons Trx-S_2 + protein-(SH)_2}$$

$$\mathrm{NADPH + H^+ + Trx-S_2 \overset{TrxR}{\rightleftharpoons} NADP^+ + Trx-(SH)_2}$$

TrxR isoenzymes from higher organisms are larger and fundamentally different from TrxR found in bacteria, yeast, or plant cells (see Commentary for further discussion). Of importance for the protocols in this unit is that the smaller TrxR enzymes of lower organisms are species-specific and usually accept only the homologous Trx as substrate, whereas the mammalian type of enzyme reduces Trx from many different organisms and also a range of other substrates. The protocols provided are used for measurement of Trx and TrxR—either measurement of total enzyme activity in biological samples or that of purified Trx or TrxR. Basic Protocols 1 and 2 and the Alternate Protocol describe specific assays based upon the reduction of Trx by TrxR, coupled with reduction of insulin disulfides by Trx. In the first assay (see Basic Protocol 1) the user continuously follows the reaction spectrophotometrically; this is preferable for use with purified enzymes, whereas the second (see Alternate Protocol) describes a more sensitive end-point assay that can be used with small amounts of enzyme or with complex samples, such as biological extracts. Another protocol describes direct measurement of DTNB reduction by TrxR (see Basic Protocol 2), a standard assay for TrxR upon which the enzyme unit is defined. The final protocol describes a method to directly analyze Trx-catalyzed protein disulfide reduction by dithiothreitol (DTT), without coupling to TrxR (see Basic Protocol 3).

SPECTROPHOTOMETRIC INSULIN ASSAY FOR MEASUREMENT OF ENZYMATIC ACTIVITY OF PURIFIED THIOREDOXINS OR THIOREDOXIN REDUCTASES

BASIC PROTOCOL 1

The thioredoxin reactions are coupled in the following protocol, using insulin as the protein substrate, since thioredoxin is rapidly oxidized by the disulfides of insulin. This assay can be used as a basic method for determining the activity of either thioredoxin or thioredoxin reductase by using a relative excess of one of the proteins.

Contributed by Elias S.J. Arnér and Arne Holmgren

Current Protocols in Toxicology (2000) 7.4.1-7.4.14

The assay is performed at room temperature (20°C ± 2°C) using the following conditions: 50 mM Tris·Cl/2 mM EDTA, pH 7.5 (TE buffer), 160 µM (1 mg/ml) insulin, and 150 µM NADPH.

NOTE: Inclusion of EDTA is necessary due to inhibition of TrxR and Trx by heavy metal ions. Insulin, however, should be hexameric zinc-containing insulin and is therefore prepared in a buffer without EDTA, as described below.

Materials

1.6 mM insulin (see recipe) in Tris·Cl, pH 7.5
50 mM NADPH (see recipe)
TE buffer, pH 7.5: 50 mM Tris·Cl, pH 7.5 (*APPENDIX 2A*) containing 2 mM EDTA
Pure control thioredoxin reductase (TrxR; IMCO)
Pure control thioredoxin (Trx; IMCO)
Protein sample to be assayed for Trx or TrxR activity
Double-beam spectrophotometer with semimicro quartz cuvettes

NOTE: Wild-type human Trx has a pronounced tendency to loose activity and aggregate due to oxidation of structural cysteine residues upon storage and freezing-thawing in air-containing buffers. This affects the assay and can be overcome by reducing the Trx sample with DTT. The *E. coli* and mutant human C62S/C73S Trx are however preferred for the assay since these thioredoxins do not have the tendency to aggregate due to oxidation and are stable upon storage.

1. Make a master mixture as follows (enough for 15 samples):

   825 µl 1.6 mM insulin (160 µM final)
   25 µl 50 mM NADPH (150 µM final)
   4650 µl TE buffer, pH 7.5
   Total volume, 5500 µl.

2a. *For measurement of Trx activity in a purified protein of interest:* Mix the following components:

   333 µl master mixture (from step 1)
   (157 – *x*) µl TE buffer, pH 7.5 (where *x* is volume of protein or Trx standard added)
   10 µl 3.75 µM pure control TrxR (~75 nM final)
   x µl purified protein or Trx standard (usually to give 0 to 5 µM Trx final)
   Total volume, 500 µl.

   Immediately after addition of the protein to be assayed for Trx activity, or the Trx standard, mix the contents of the cuvette and follow consumption of NADPH as decrease of absorbance at 340 nm, using a sample without addition of Trx as reference cuvette. Prepare a standard curve using pure control Trx (0 to 5 µM; added as ~100 µM working dilution in TE buffer, pH 7.5) for comparison of activity.

   The pure control Trx should preferably be from the homologous organism; alternatively E coli Trx or the mutant human C62S/C73S Trx may be used.

2b. *For measurement of TrxR activity in a purified protein of interest:* Mix the following components:

   333 µl master mixture (from step 1)
   (67 – *x*) µl TE buffer, pH 7.5 (where *x* is the volume of sample added)
   100 µl pure control Trx (~20 µM final)

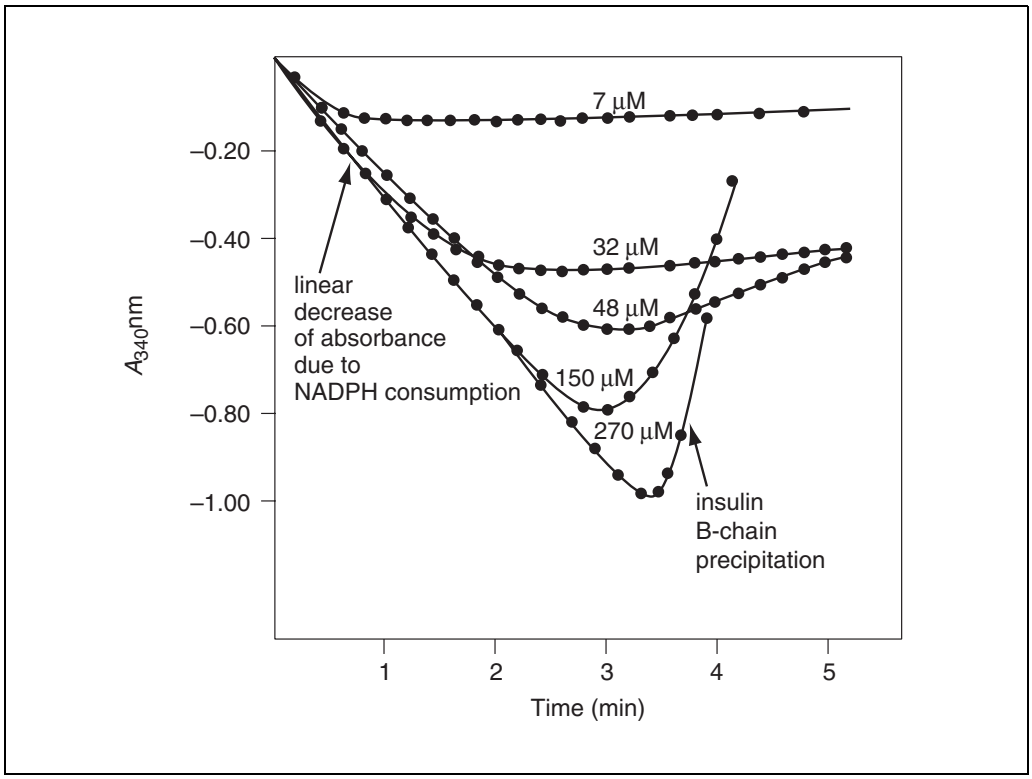

Figure 7.4.1 The spectrophotometric insulin assay. NADPH consumption is determined from the decrease of absorbance at 340 nm, during the initial linear phase. Subsequently, the absorbance increases, which is due to precipitation of reduced insulin B chains. The effects of varying insulin concentration is also shown in the figure (insulin included at 7 μM, 32 μM, 48 μM, 150 μM, and 270 μM, as shown) in an assay with 4.0 μM *E. coli* Trx, 400 μM NADPH, and 100 nM *E. coli* TrxR at pH 7.0. Adapted from Holmgren (1979a).

x μl purified protein or TrxR standard (usually to give TrxR activity equivalent to 0 to 10 nM pure TrxR)
Total volume, 500 μl.

Immediately after addition of the protein to be assayed for TrxR activity, or the TrxR standard, mix the contents of the cuvettes and then follow consumption of NADPH as decrease of absorbance at 340 nm, using a sample without addition of TrxR as reference cuvette. Prepare a standard curve using pure control TrxR [0 to 10 nM; added from 1 U/ml working dilution (250 nM for the mammalian enzyme), freshly prepared in TE buffer, pH 7.5] for comparison of activity.

The pure control TrxR should preferably be from the homologous organism; alternatively, mammalian TrxR may be used at a dilution of ~1 U/ml (~250 nM for the mammalian enzyme). For definition of units, see Basic Protocol 2.

3. Calculate the activity using the extinction coefficient of NADPH at 340 nm, i.e., 6200 $M^{-1}cm^{-1}$:

$$\text{turnover } (\text{min}^{-1}) = \frac{\text{linear initial rate of decrease at 340 nm}}{6200 \times (\text{enzyme concentration [M] in cuvette})}$$

Illustrative curves from assays similar to those described in steps 2a or 2b are shown in Figure 7.4.1, also illustrating the influence of increasing insulin concentrations. With the lower insulin concentrations, the reaction stops after the disulfides of insulin have been reduced (this may also be used to record the number of disulfides reduced in any protein,

by calculation of the amount of NADPH consumed, see below). The increase in absorbance after some time is due to turbidity caused by precipitation of reduced insulin B-chains and can be detected at all wavelengths (also see Basic Protocol 3). It is only the initial linear part of the curve, with decrease of absorbance at 340 nm, that should be used for determination of enzymatic activity; the decrease is directly proportional to the consumption of NADPH.

Note that in most cases the inclusion of a standard curve in the assay is the best way of calculating activity for a given sample protein. Also see Critical Parameters and Troubleshooting.

ALTERNATE PROTOCOL

END-POINT INSULIN ASSAY FOR MEASUREMENT OF THIOREDOXIN OR THIOREDOXIN REDUCTASE ENZYMATIC ACTIVITY IN BIOLOGICAL SAMPLES

The spectrophotometric insulin assay described in Basic Protocol 1 is not always applicable to complex biological samples, such as cell or tissue extracts, usually due to small amounts of Trx or TrxR, and more importantly due to interfering NADPH-metabolizing enzymes present in the samples, giving rise to a high background and making results difficult to interpret. This protocol is a modified procedure, whereby the number of thiols formed in the reduced insulin are determined with DTNB after the reaction has been stopped by guanidine hydrochloride, which, when using adequate control samples, will result in a correct measurement of the Trx or TrxR activities in complex protein samples.

Additional Materials *(also see Basic Protocol 1)*

200 mM HEPES buffer, pH 7.6
0.2 M EDTA (*APPENDIX 2A*)
Protein sample to be analyzed, e.g., from cell or tissue extracts
DTNB/guanidine solution (see recipe)

1. Make a master mixture as follows (enough for 30 samples):

   1295 µl 200 mM HEPES buffer (85 mM final)
   625 µl 1.6 mM insulin (0.3 mM final)
   40 µl 50 mM NADPH (660 µM final)
   40 µl 0.2 M EDTA (3 mM final)
   Total volume, 2000 µl.

2a. *For measurement of Trx activity in a complex protein sample:* Prepare two reaction mixes (A and B) per sample in the bottoms of separate semimicro cuvettes as follows:

   Reaction mix A (with TrxR)
   33 µl master mixture (from step 1)
   (7 – *x*) µl 200 mM HEPES buffer (where *x* is the volume of sample added)
   10 µl 250 nM pure control TrxR (~50 nM final)
   x µl protein sample (usually 10 to 20 µg total protein)
   Total volume, 50 µl

   Reaction mix B (without TrxR)
   33 µl master mixture (from step 1)
   (17 – *x*) µl 200 mM HEPES buffer (where *x* is the volume of sample added)
   x µl protein sample
   Total volume, 50 µl.

2b. *For measurement of TrxR activity in a complex protein sample:* Prepare two reaction mixes (A and B) per sample in the bottoms of separate semimicro cuvettes as follows:

   Reaction mix A (with Trx)
   33 µl master mixture (from step 1)

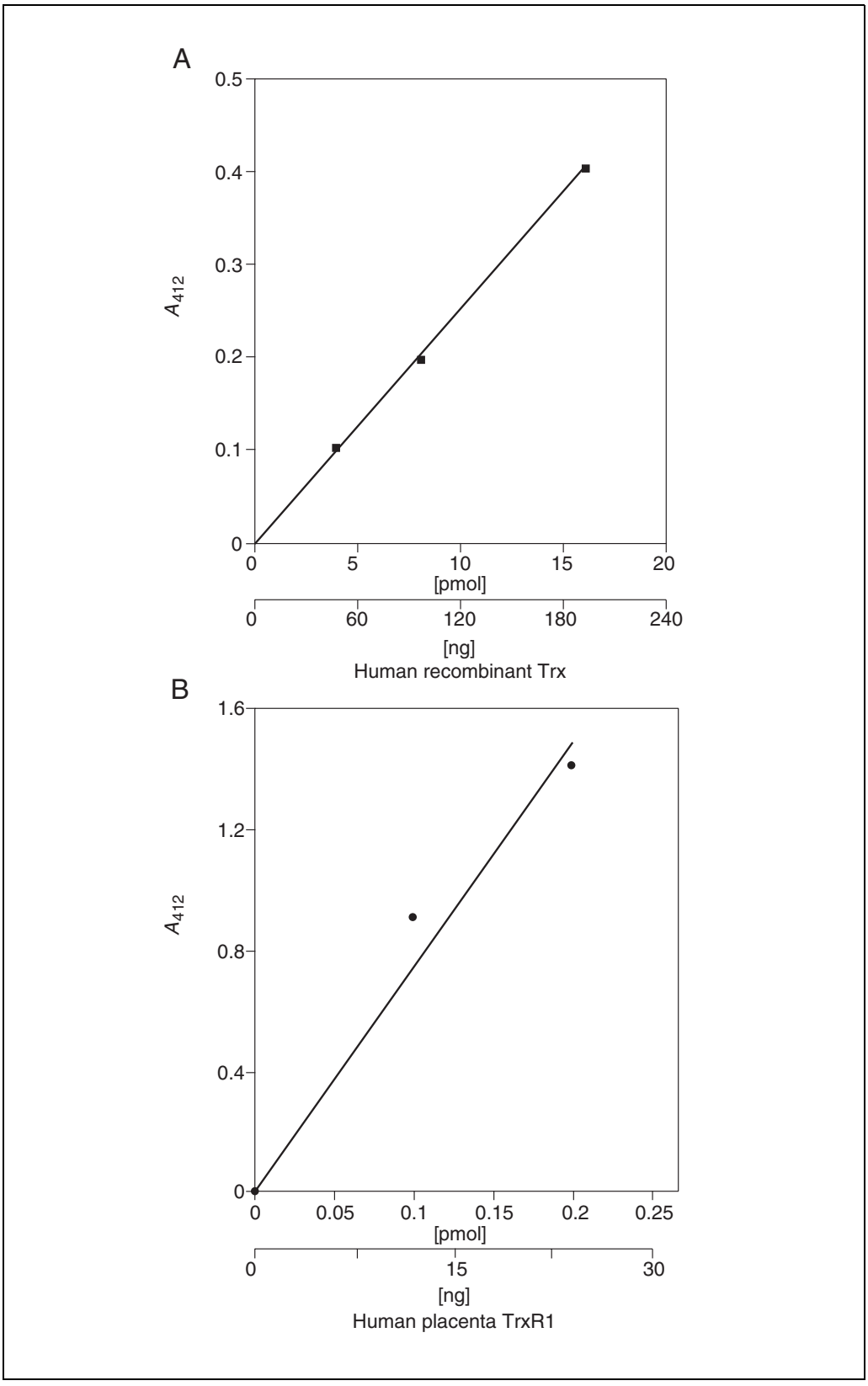

Figure 7.4.2 Standard curves of the end-point insulin assay. In (**A**) a typical standard curve for measurement of Trx is shown. The amount of human Trx (recombinant) added to the assay is shown with the resulting absorbance at 412 nm illustrated by the standard curve. In (**B**) a typical standard curve for measurement of TrxR is shown. However, this particular assay was incubated 1 hr at 37°C in order to increase the sensitivity. The amount of human TrxR (purified from placenta) added to the assay is shown with the resulting absorbance at 412 nm.

(9 – *x*) TE buffer, pH 7.5 (where *x* is the volume of sample added)
8 µl 100 µM (1.2 mg/ml) pure control Trx (15 µM final)
x µl protein sample (usually 10 to 20 µg total protein)
Total volume, 50 µl

Reaction mix B (without Trx)
33 µl master mixture (from step 1)
(17 – *x*) µl TE buffer, pH 7.5 (where *x* is the volume of sample added)
x µl protein sample (usually 10 to 20 µg total protein)
Total volume, 50 µl.

Disposable plastic cuvettes can be used if many samples are to be analyzed at one time, or, alternatively, the assay can be scaled down for use of 96-well microplates if a spectrophotometer for reading of such is available.

The protein sample will depend on the area of interest of the investigator. Be sure to include EDTA in the sample, since TrxR is easily inhibited by metal ions; also keep the pH within physiological range (7.0 to 8.0), and possibly include protease inhibitors.

A useful protein concentration in the sample is 1 to 5 µg/µl.

3. Incubate all samples 20 min at 37°C.
4. Add 500 µl DTNB/guanidine solution.

   This will denature all proteins and determine thiols with DTNB, resulting in high absorbance at 412 nm, with the extinction coefficient for the released TNB being 13,600 $M^{-1}cm^{-1}$.

5. Determine the absorbances at 412 nm of reaction mix A and reaction mix B for each sample.

   The difference (A – B) will correlate with the presence of Trx or TrxR in the protein sample, as determined in step 2a or 2b, respectively. The actual amount can be determined from a standard curve run in parallel, using pure control Trx or TrxR (see Figs. 7.4.2A and B). Preferably, this standard curve should also be performed in the presence of sample protein, to make certain that no inhibitory or stimulatory factor in the sample will affect the determination. As given here, the assay is optimized for 0 to 20 pmol Trx (0 to 200 ng; step 2a) or 0 to 2 pmol TrxR (0 to 250 ng of dimeric mammalian enzyme; step 2b). The sensitivity of the assay can however be further increased by prolonging the incubation time at 37°C.

   Some thioredoxins (e.g., human wild-type Trx) have additional structural cysteines that may oxidize and form aggregates with low or no initial activity. For frozen samples stored for longer periods of time, this becomes a problem. Such protein samples may be preincubated for 15 min at 37°C with 100 µM DTT to activate thioredoxin. However, DTT in the reaction mixture will also react with DTNB, thereby raising the background absorbance, which has to be subtracted.

BASIC PROTOCOL 2

MEASURING MAMMALIAN-TYPE THIOREDOXIN REDUCTASE

The mammalian-type thioredoxin reductase has, in contrast to the enzyme from prokaryotes, plants or yeast, a remarkably broad substrate specificity (see Commentary). One of the substrates directly reduced by mammalian TrxR and NADPH is Ellman's reagent [5,5′-dithio-bis(2-nitrobenzoic acid); DTNB]; which is used in the Alternate Protocol to measure thiols. The reaction and its products in direct reduction by mammalian TrxR are:

$$NADPH + H^+ + DTNB \rightarrow NADP^+ + 2\ TNB$$

The reaction is fast, and since the extinction coefficient of TNB is high (13,600 $M^{-1}cm^{-1}$) this assay is preferred for determination of the catalytic activity of mammalian TrxR and constitutes the basis for calculation of enzyme units.

Materials

62.5 mM (25 mg/ml) DTNB in spectroscopic grade 99% ethanol
50 mM NADPH (see recipe)
PE buffer, pH 7.0: 100 mM potassium phosphate, pH 7.0 (*APPENDIX 2A*) containing 2 mM EDTA
20 mg/ml bovine serum albumin (BSA) in water
Pure control mammalian TrxR
TrxR sample to be analyzed
Double-beam spectrophotometer with semimicro quartz cuvettes

NOTE: Inclusion of albumin in the assay protects TrxR from absorbing to the plastic surface of the vial; the disulfides of albumin are buried internally and are not reduced by the enzyme, and thereby do not interfere with the assay. The standard assay is performed at room temperature (20°C).

1. Make a master mixture as follows (enough for 10 samples):

   660 µl 62.5 mM DTNB (5 mM DTNB, 8% ethanol final)
   50 µl 50 mM NADPH (300 µM final)
   4790 µl PE buffer
   Total volume, 5500.

   IMPORTANT NOTE: *The final concentration of ethanol in the assay due to the DTNB solution should be kept <10% in the reaction mixture, due to the risk of enzyme denaturation.*

2. At time of assay, freshly dilute the pure control mammalian TrxR to 0.05 to 0.25 U/ml (~35 to 105 nM) in PE buffer containing 100 µg/ml of bovine serum albumin (added from 20 mg/ml BSA stock).

   See definition of TrxR units below.

3. Mix the following components:

   333 µl master mixture (from step 1)
   (67 – *x*) µl PE buffer (where *x* is the volume of TrxR sample added)
   x µl TrxR to be analyzed or pure TrxR standard (from step 2; usually ~5 nM final)
   Total volume, 500 µl

   Immediately after addition of TrxR, mix the contents of the cuvettes and then follow reduction of NADPH as increase of absorbance at 412 nm, using a sample without addition of TrxR as the reference cuvette. Prepare a standard curve using purified control TrxR (0 to 5 nM) for comparison of activity.

4. Calculate activity and units as follows, using an extinction coefficient of 13,600 $M^{-1}cm^{-1}$ for TNB based on the fact that two molecules of TNB are formed per DTNB molecules:

$$\text{turnover } (\text{min}^{-1}) = \frac{\text{linear initial rate of increase at 412 nm}}{13{,}600 \times 2 \times (\text{TrxR concentration [M] in cuvette})}$$

The turnover for cytosolic mammalian TrxR (TrxR1) of liver, thymus, or placenta in this standard assay is ~4000 min^{-1}.

One unit (U) of TrxR is defined as the amount catalyzing the oxidation of 1 μmol NADPH, i.e., reduction of 1 μmol DTNB (formation of 2 μmol TNB), per min, which, with a molecular mass of 115 kDa for the dimeric enzyme, amounts to ~35 U/mg.

DTNB is also used in determination of total glutathione via NADPH and glutathione reductase. Therefore, in extracts containing both GSH and glutathione reductase, the activity of TrxR could be overestimated. After removal of GSH, accurate values are obtained. Alternatively, addition of 20 μM gold thioglucose, a specific inhibitor of mammalian TrxR, allows measurement of the TrxR activity even in the presence of GSH and glutathione reductase by determination of the fraction of the activity inhibited by the gold compound (Hill et al., 1997).

BASIC PROTOCOL 3

THIOREDOXIN-CATALYZED INSULIN REDUCTION BY DTT

As stated in the introduction to this unit, the capacity of Trx to reduce protein disulfides is a hallmark of this redox-active protein, usually coupled to regeneration of active Trx by TrxR; this is the basis for Basic Protocol 1 and Alternate Protocol. This protocol describes an alternative way of analyzing the protein disulfide reduction by Trx without the use of TrxR, but instead coupled to DTT. This protocol is useful for characterization of the protein disulfide reduction by novel thioredoxins. Formation of the reduced insulin can easily be monitored by turbidimetric measurements, i.e., by following the appearance of turbidity due to precipitated reduced insulin (also see Fig. 7.4.1). The regeneration of active Trx by DTT is much faster than direct reduction of insulin by DTT (by about three orders of magnitude), and Trx-catalyzed reduction of insulin is exceptionally fast, as already mentioned above (about five orders of magnitude faster than DTT-catalyzed reduction of insulin).

NOTE: This assay, based upon turbidity measurement, is performed at pH 6.5 to increase the sensitivity of the assay due to a lower solubility of reduced insulin at this pH value.

Materials

1.6 mM insulin (see recipe) in 100 mM potassium phosphate buffer, pH 6.5
PE buffer, pH 6.5: 100 mM potassium phosphate, pH 6.5 containing 2 mM EDTA
100 mM dithiothreitol (DTT; *APPENDIX 2A*), freshly made in water
Sample: purified Trx to be analyzed
Double-beam spectrophotometer with semimicro quartz cuvettes

1. Make a master mixture as follows (enough for 10 samples):

   825 μl 1.6 mM insulin (160 μM final)
   4675 μl PE buffer
   Total volume, 5500 μl.

2. Mix the following components:

   333 μl master mixture (from step 1)
   (162 – *x*) μl PE buffer (where *x* is the volume of Trx sample added)
   5 μl 100 mM DTT (1 mM final)
   x μl Trx to be analyzed (usually 0 to 10 μM final)
   Total volume, 500 μl.

3. Measure the absorbance at 650 nm for 40 min, with an identical sample excluding Trx as reference cuvette.

   See Figure 7.4.3 for illustrative curves demonstrating this assay.

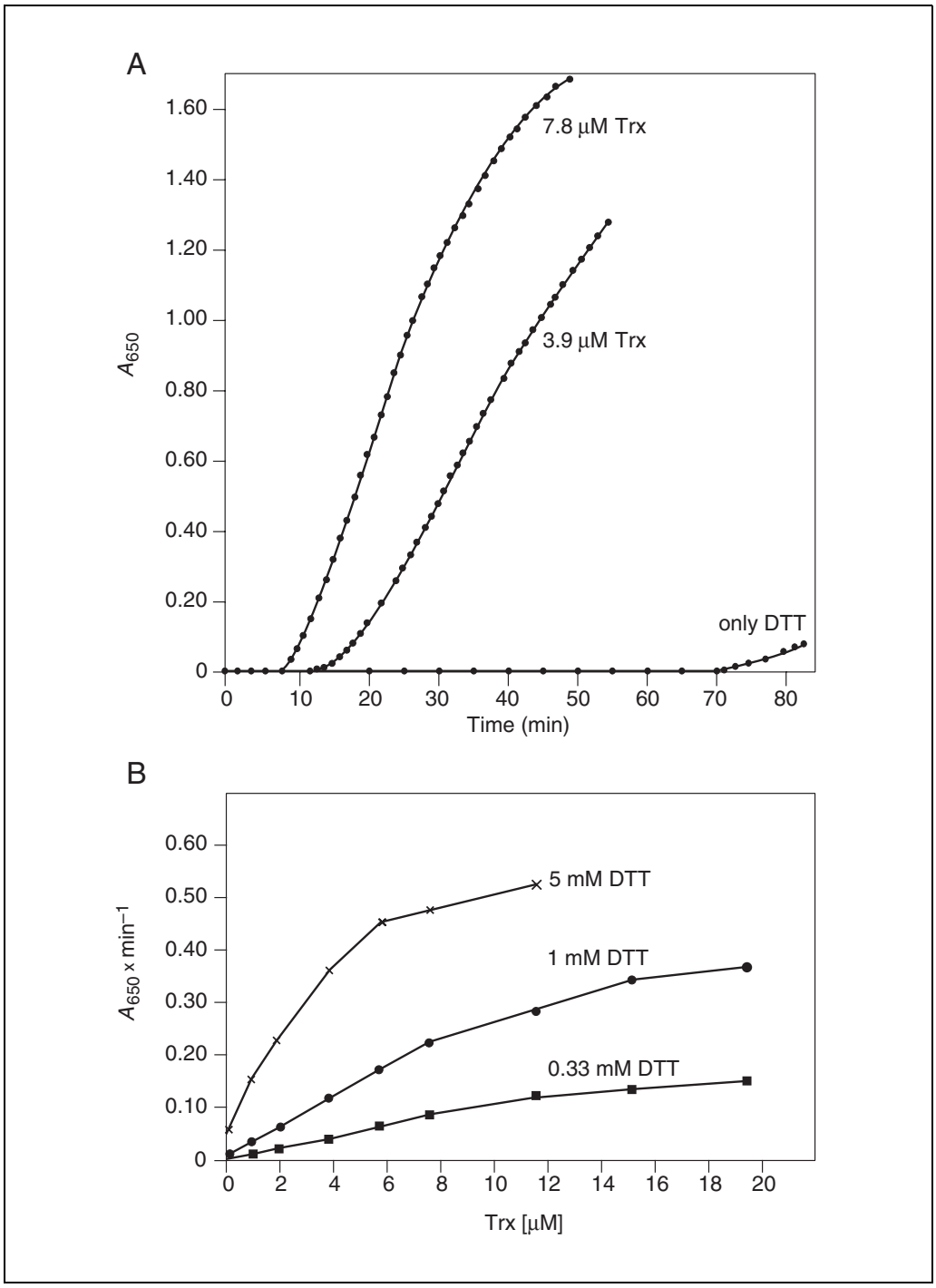

Figure 7.4.3 Reduction of insulin by DTT catalyzed by Trx. In (**A**) typical turbidimetric curves upon addition of *E. coli* Trx (3.9 or 7.8 μM, as indicated) are shown, in comparison to turbidity formed upon addition of only DTT (at pH 7.0 with 130 μM insulin and 330 μM DTT). It can be seen that both the onset of detectable precipitation as well as the slope of the curve are dependent on the Trx activity and thereby both these parameters can be used to quantitate the activity. However, the maximal rate of precipitation, given as the increase per minute of absorbance at 650 nm, is the most useful parameter. In (**B**) the effects of DTT or Trx concentrations on this reaction (at pH 6.5 with 130 μM insulin, e.g., similar to the conditions utilized in the protocol given here) are demonstrated. Note that this assay is a simple way of monitoring the Trx-catalyzed insulin reduction by DTT, but it is limited by nonlinear increase in A_{650} using high DTT levels. As seen, however, $\Delta A_{650} \times \text{min}^{-1}$ with 1 mM DTT at pH 6.5 is linear over the *E. coli* Trx concentration 0 to 10 μM (conditions utilized in Basic Protocol 3). Adapted from Holmgren (1979b).

The appearance of turbidity is not always linearily correlated to the rate of reduction of insulin. With E. coli or mammalian Trx between 0 and 10 μM Trx at pH 6.5 with 1 mM DTT, the precipitation of insulin is linearily dependent on the activity of the Trx. However, for novel thioredoxins the linearity of the assay may be different.

REAGENTS AND SOLUTIONS

Use Milli-Q-purified water or equivalent for all recipes and protocol steps. For common stock solutions, see ***APPENDIX 2A****; for suppliers, see* ***SUPPLIERS APPENDIX****.*

DTNB/guanidine solution

First make 6 M guanidine·HCl by dissolving 28.66 g guanidine·HCl in 50 ml Tris·Cl, pH 8.0 (*APPENDIX 2A*; store at room temperature). Also make 10 mM (4 mg/ml) DTNB [5,5′-dithio-bis(2-nitrobenzoic acid); Ellman's reagent] in spectroscopic grade 99% ethanol (store at −20°C in well sealed glass vials). At the time of assay, add 1 ml of the 10 mM DTNB to 9 ml of the 6 M guanidine hydrochloride, which will be enough for 20 samples; keep on ice.

CAUTION: *Guanidine·HCl is highly corrosive.*

Insulin, 1.6 mM

Make a 1.6 mM (10 mg/ml) stock solution by suspending 50 mg insulin (from bovine pancreas; Sigma) in 2.5 ml of 50 mM Tris·Cl, pH 7.5 for Basic Protocol 1 or Alternate Protocol or in 100 mM potassium phosphate, pH 6.5 for Basic Protocol 3 (see *APPENDIX 2A* for both buffers); adjust pH to 2 to 3 with 1 M HCl to dissolve the protein completely, then titrate back to the original pH of the buffer with 1 M NaOH. Finally adjust the volume with water to 5.0 ml.

This clear stock solution of insulin (10 mg/ml) can be kept at –20°C.

NADPH, 50 mM

Prepare stock vials by keeping 10-mg portions of β-NADPH (dry) in separate small microcentrifuge tubes at −20°C. Dissolve in 250 μl water at time of use (40 mg/ml, 50 mM final concentration). Store the stock solution up to 2 months at −20°C and reuse no more than two times, since the reduced β-NADPH will oxidize (and become yellow) by repeated freezing-thawing, or with time.

COMMENTARY

Background Information

At least one thioredoxin of 12 kDa exists in the cytosol of all living cells; this enzyme has a large number of activities (Holmgren, 1985, 1989, 1995; Yodoi and Tursz, 1991; Williams, 1992; Holmgren and Björnstedt, 1995). Reduced thioredoxin is a powerful protein disulfide reductase required to regenerate an active site dithiol after each catalytic cycle in, e.g., ribonucleotide reductase or methionine sulfoxide reductases. Disulfide reduction by thioredoxin is involved in redox regulation of enzymes and transcription factors. Secreted mammalian thioredoxin has co-cytokine-like activity on certain mammalian cells by an unknown mechanism but probably also involving thiol-disulfide exchange (Holmgren, 1985, 1989, 1995; Yodoi and Tursz, 1991; Holmgren and Björnstedt, 1995; Powis et al., 1995). Thioredoxin, NADPH, and thioredoxin reductase also play an important role in signal transduction and defense against oxidative stress.

Thioredoxin reductase from *Escherichia coli* has been crystallized (Williams, 1992), and a high-resolution X-ray structure shows surprisingly large differences from other members of the pyridine nucleotide-disulfide oxidoreductase family, notably glutathione reductase (Kuriyan et al., 1991; Waksman et al., 1994). *E. coli* TrxR is smaller and has a different domain organization than glutathione reductase, suggesting functionally convergent evolution of the two enzymes (Kuriyan et al., 1991). The structural features of TrxR from *E. coli* and a high specificity for its homologous Trx, are typical also for TrxR from prokaryotes, lower eukaryotes like yeast, or cytosol from plants

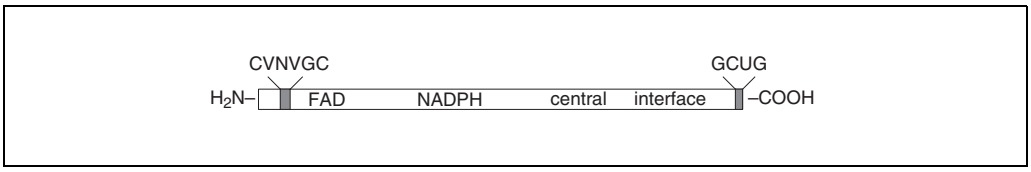

Figure 7.4.4 Schematic drawing of the mammalian cytosolic TrxR. Shown are the FAD, NADPH, central, and interface domains, based upon the high homology to glutathione reductase and other enzymes of the pyridine disulfide oxidoreductase family (Williams, 1992; Zhong et al., 1998). The sequences of the glutathione reductase–like redox active motif in the N-terminal part of the protein and the carboxyterminal motif including selenocysteine are shown by one-letter amino acid codes. Key residues with redox activity are shown in bold. U = selenocysteine.

(Kuriyan et al., 1991; Williams, 1992; Waksman et al., 1994; Dai et al., 1996).

It has long been known that mammalian TrxR has strikingly different properties when compared to the enzyme from *E. coli* and lower organisms (Holmgren, 1985, 1989; Holmgren and Björnstedt, 1995). The enzymes from calf liver and thymus and rat liver were the ones first purified to homogeneity, and they showed subunits with a molecular mass of 58 kDa (Holmgren, 1977; Luthman and Holmgren, 1982).

Recently, the mammalian TrxR was cloned and sequenced; the amino acid sequence revealed a strikingly high homology to glutathione reductase (Gasdaska et al., 1995; Zhong et al., 1998). The conserved features of all the structural components of glutathione reductase were preserved in mammalian TrxR, including a redox-active disulfide motif in the N-terminal FAD domain, the NADPH-binding domain, and the carboxyterminal interface region that governs the association of the two subunits in the homodimeric holoenzyme. Interestingly, the mammalian TrxR was also found to be a selenoprotein, carrying a catalytically active selenocysteine (Sec) residue in the penultimate carboxyterminal end (Gladyshev et al., 1996; Tamura and Stadtman, 1996; Zhong et al., 1998). Together with a neighboring cysteine residue in the conserved sequence -Gly-Cys-Sec-Gly-COOH, the selenocysteine has been suggested to be part of an open active site motif, explaining the wide substrate specificity of the enzyme. The general domain organization is shown in Figure 7.4.4.

Recently two additional mammalian TrxR isoenzymes were discovered—one mitochondrial and one mainly detected in testis—that all carry the same carboxyterminal selenocysteine-containing motif (Miranda-Vizuete et al., 1999; Sun et al., 1999; Watabe et al., 1999). In *C. elegans*, two TrxR isoenzymes were found—one a selenoprotein and one a cysteine-containing homolog (Zhong et al., 1998; Gladyshev et al., 1999). A yeast mitochondrial thioredoxin system was also newly discovered, but these enzymes were also similar to the prokaryotic type (Pedrajas et al., 1999). Several other Trx or TrxR isoenzymes exist with certainty in different organisms—some already discovered and some yet to be discovered. The protocols described in this unit are based upon the hallmarks of Trx and TrxR enzymatic activities and can be used in the initial characterizations of the novel isoenzymes as well as for the determination of their activities in different cells and tissues.

Critical Parameters and Troubleshooting

Kinetic parameters of *E. coli* and mammalian TrxR are given in Table 7.4.1. It should be emphasized that since the Trx-coupled assays given in Basic Protocol 1 and the Alternate Protocol, for practical and economic reasons, make use of limited amounts of Trx (0 to 20 μM), these assays result in nonsaturating conditions for TrxR with respect to Trx. It is therefore necessary to always include a standard curve in each experiment to enable correct extrapolation of Trx or TrxR activities in unknown samples, or, alternatively, to increase the Trx concentration to yield saturating conditions.

The presence of selenocysteine in the mammalian TrxR isoenzymes evokes several difficulties in studying these enzymes. First, the selenocysteine residue is at physiological pH in its selenolate form and is thus easily alkylated. This explains why the enzyme is easily irreversibly inhibited by electrophilic agents (see Nordberg et al., 1998; Arnér et al., 1999a, and references therein). Also, EDTA must be included in assays of the enzyme, since metal ions easily inhibit the activity. Moreover, the selenium may be lost during the purification procedure, resulting in an enzyme with lower specific activity than normal (Arnér et al., 1999a). Most important, however, is the fact

Table 7.4.1 Kinetic Parameters of *E. coli* and Mammalian TrxR[a]

		E. coli TrxR	Mammalian TrxR
E coli Trx	K_m	3.0 μM	35 μM
	k_{cat}	2000 min^{-1}	3000 min^{-1}
Mammalian Trx	K_m	No activity	2.5 μM
	k_{cat}	—	3300 min^{-1}
DTNB	K_m	No activity	0.5 mM
	k_{cat}	—	4000 min^{-1}

[a]Representative figures are taken from the literature. Note that *E. coli* TrxR is specific for its homologous Trx whereas mammalian TrxR is not. Trx and TrxR of different mammalian species are virtually fully interchangable in terms of substrate specificities and activity. The mutant C62S/C73S Trx shows essentially the same kinetic parameters as wild-type mammalian Trx.

that mammalian selenoproteins cannot normally be expressed directly in bacteria as recombinant products, due to the fact that selenocysteine—the 21st amino acid (Böck et al., 1991)—is cotranslationally inserted at the position of a UGA codon, normally conferring translational termination. The alternative decoding as selenocysteine is dependent on secondary structures in the selenoprotein mRNA, so-called selenocysteine insertion sequence (SECIS) elements, that are noncompatible between mammalian and bacterial systems (Low and Berry, 1996; Tormay and Böck, 1997). Recently, however, the authors succeeded in overcoming this species barrier by engineering SECIS elements compatible with the bacterial translation machinery, but still encoding the carboxyterminal end of mammalian TrxR, and resulting in enzymatically active recombinant enzyme (Arnér et al., 1999b). Thereby, larger amounts can now be produced, to be used as control TrxR in the protocols.

If DTT or other low-molecular-mass thiol compounds are included in the DTNB-based assays, either as described or because they were included during purification of the proteins analyzed, care must be taken because of the presence of the additional thiol groups and their reaction with DTNB. Adequate controls must be utilized, i.e., measuring control Trx or TrxR in the same DTT-containing background as that used for the samples analyzed. The NADPH-dependent reaction described in Basic Protocol 1 can be used with 0.1 to 1 mM DTT (final concentration) without affecting the rate at A_{340}. However, the range of the assay is limited by the precipitation of insulin at earlier time points due to reactions determined in Basic Protocol 3.

Some spectrophotometers with lower-intensity lamps cannot measure absorbance at 340 nm when NADPH concentrations are higher than 200 μM.

Anticipated Results

The given protocols describe determinations of Trx- and TrxR-derived enzymatic activities in purified or complex samples. The levels of these enzymes are highly dependent on cells, tissues, organelles, conditions of growth or purification protocols utilized by the investigator. As a rough guide, cytosol of *E. coli*, yeast, or mammalian cells can be considered to normally contain Trx in the range of 5 to 10 μM (~1 to 2 μg/mg protein) and TrxR in the range of ~100 nm (~200 ng/mg protein).

Time Considerations

The actual assays described in the protocols require no more than an hour in total to perform, and the reagents (except for the control enzymes) do not require much time to prepare.

Literature Cited

Arnér, E.S.J., Zhong, L., and Holmgren, A. 1999a. Preparation and assay of mammalian thioredoxin and thioredoxin reductase. *Methods Enzymol.* 300:226-239.

Arnér, E.S.J., Sarioglu, H., Lottspeich, F., Holmgren, A., and Böck, A. 1999b. High-level expression in *Escherichia coli* of selenocysteine-containing rat thioredoxin reductase utilizing gene fusions with engineered bacterial-type SECIS elements and co-expression with the *selA*, *selB* and *selC* genes. *J. Mol. Biol.* 292:1003-1016.

Böck, A., Forchhammer, K., Heider, J., Leinfelder, W., Sawers, G., Veprek, B., and Zinoni, F. 1991. Selenocysteine: The 21st amino acid. *Mol. Microbiol.* 5:515-520.

Dai, S., Saarinen, M., Ramaswamy, S., Meyer, Y., Jacquot, J.P., and Eklund, H. 1996. Crystal structure of *Arabidopsis thaliana* NADPH dependent thioredoxin reductase at 2.5 Å resolution. *J. Mol. Biol.* 264:1044-1057.

Gasdaska, P.Y., Gasdaska, J.R., Cochran, S., and Powis, G. 1995. Cloning and sequencing of a human thioredoxin reductase. *FEBS Lett.* 373:5-9.

Gladyshev, V.N., Jeang, K.-T., and Stadtman, T.C. 1996. Selenocysteine, identified as the penultimate C-terminal residue in human T-cell thioredoxin reductase, corresponds to TGA in the human placental gene. *Proc. Natl. Acad. Sci. U.S.A.* 93:6146-6151.

Gladyshev, V. N., Krause, K., Xu, X.-M., Korotkov, K.V., Kryukov, G.V., Sun, Q.-A., Lee, B.J., Wootton, J.C., and Hatfield, D.L. 1999. Selenocysteine-containing thioredoxin reductase in *C. elegans*. *Biochem. Biophys. Res. Commun.* 259:244-249.

Hill, K.E., McCollum, G.W., and Burk, R.F. 1997. Determination of thioredoxin reductase activity in rat liver supernatant. *Anal. Biochem.* 253:123-125.

Holmgren, A. 1977. Bovine thioredoxin system: Purification of thioredoxin reductase from calf liver and thymus and studies of its function in disulfide reduction. *J. Biol. Chem.* 252:4600-4006.

Holmgren, A. 1979a. Reduction of disulfides by thioredoxin: Exceptional reactivity of insulin and suggested functions of thioredoxin in mechanism of hormone action. *J. Biol. Chem.* 254:9113-9119.

Holmgren, A. 1979b. Thioredoxin catalyzes the reduction of insulin disulfides by dithiothreitol and dihydrolipoamide. *J. Biol. Chem.* 254:9627-9632.

Holmgren, A. 1985. Thioredoxin. *Annu. Rev. Biochem.* 54:237-271.

Holmgren, A. 1989. Thioredoxin and glutaredoxin systems. *J. Biol. Chem.* 264:13963-13966.

Holmgren, A. 1995. Thioredoxin structure and mechanism: Conformational changes on oxidation of the active-site sulfhydryls to a disulfide. *Structure* 3:239-243.

Holmgren, A. and Björnstedt, M. 1995. Thioredoxin and thioredoxin reductase. *Methods Enzymol.* 252:199-208.

Kuriyan, J., Krishna, T.S.R., Wong, L., Guenther, B., Pahler, A., Williams, C.H., Jr., and Model, P. 1991. Convergent evolution of similar function in two structurally divergent enzymes. *Nature* 352:172-174.

Low, S.C. and Berry, M.J. 1996. Knowing when not to stop: Selenocysteine incorporation in eukaryotes. *Trends Biochem. Sci.* 21:203-208.

Luthman, M. and Holmgren, A. 1982. Rat liver thioredoxin and thioredoxin reductase: Purification and characterization. *Biochemistry* 21:6628-6633.

Miranda-Vizuete, A., Damdimopoulos, A.E., Pedrajas, J.R., Gustafsson, J.A., and Spyrou, G. 1999. Human mitochondrial thioredoxin reductase cDNA cloning, expression and genomic organization. *Eur. J. Biochem.* 261:405-412.

Nordberg, J., Zhong, L., Holmgren, A., and Arnér, E.S.J. 1998. Mammalian thioredoxin reductase is irreversibly inhibited by dinitrohalobenzenes by alkylation of both the redox active selenocysteine and its neighboring cysteine residue. *J. Biol. Chem.* 273:10835-10842.

Pedrajas, J.R., Kosmidou, E., Miranda-Vizuete, A., Gustafsson, J.Å., Wright, A.P., and Spyrou, G. 1999. Identification and functional characterization of a novel mitochondrial thioredoxin system in *Saccharomyces cerevisiae*. *J. Biol. Chem.* 274:6366-6373.

Powis, G., Briehl, M., and Oblong, J. 1995. Redox signalling and the control of cell growth and death. *Pharmacol. Ther.* 68:149-173.

Sun, Q.A., Wu, Y., Zappacosta, F., Jeang, K.T., Lee, B.J., Hatfield, D.L., and Gladyshev, V.N. 1999. Redox regulation of cell signaling by selenocysteine in mammalian thioredoxin reductases. *J. Biol. Chem.* 274:24522-24530.

Tamura, T. and Stadtman, T.C. 1996. A new selenoprotein from human lung adenocarcinoma cells: Purification, properties, and thioredoxin reductase activity. *Proc. Natl. Acad. Sci. U.S.A.* 93:1006-1011.

Tormay, P. and Böck, A. 1997. Barriers to heterologous expression of a selenoprotein gene in bacteria. *J. Bacteriol.* 179:576-582.

Waksman, G., Krishna, T.S., Williams, C.H., Jr., and Kuriyan, J. 1994. Crystal structure of *Escherichia coli* thioredoxin reductase refined at 2 Å resolution: Implications for a large conformational change during catalysis. *J. Mol. Biol.* 236:800-816.

Watabe, S., Makino, Y., Ogawa, K., Hiroi, T., Yamamoto, Y., and Takahashi, S.Y. 1999. Mitochondrial thioredoxin reductase in bovine adrenal cortex: Its purification, properties, nucleotide/amino acid sequences, and identification of selenocysteine. *Eur. J. Biochem.* 264:74-84.

Williams, C.H., Jr. 1992. Lipoamide dehydrogenase, glutathione reductase, thioredoxin reductase, and mercuric ion reductase—a family of flavoenzyme transhydrogenases. *In* Chemistry and Biochemistry of Flavoenzymes (F. Müller, ed.) pp. 121-211. CRC Press, Boca Raton, Fla.

Yodoi, J. and Tursz, T. 1991. ADF, a growth-promoting factor derived from adult T cell leukemia and homologous to thioredoxin: Involvement in lymphocyte immortalization by HTLV-I and EBV. *Adv. Cancer Res.* 57:381-411.

Zhong, L., Arnér, E.S.J., Ljung, J., Åslund, F., and Holmgren, A. 1998. Rat and calf thioredoxin reductase are homologous to glutathione reductase with a carboxyl-terminal elongation containing a conserved catalytically active penultimate selenocysteine residue. *J. Biol. Chem.* 273:8581-8591.

Key References

Arnér et al., 1999b. See above.

Describes the purification procedure for mammalian thioredoxin and thioredoxin reductase and lists known substrates and inhibitors of mammalian thioredoxin reductase; also describes how to assay for novel substances interacting with mammalian TrxR.

Holmgren, 1977, 1979a,b. See above.

These papers describe in detail the first characterizations of the reduction of insulin by Trx, both coupled to TrxR and to DTT, and the reduction of DTNB by mammalian TrxR.

Internet Resources

http://www.imcocorp.se

The web site of IMCO, Corporation Ltd. AB, Sweden, a vendor of pure control bacterial and mammalian Trx and TrxR.

Contributed by Elias S.J. Arnér and
Arne Holmgren
Karolinska Institutet
Stockholm, Sweden

Measurement of MnSOD and CuZnSOD Activity in Mammalian Tissue Homogenates

Three basic forms of mammalian superoxide dismutase (SOD) enzymes exist and are distinguished by their size and localization. CuZnSOD is a homodimer consisting of two ~16 kDa subunits and is primarily found in the cytosolic and nuclear compartments of the cell, while MnSOD is a tetramer consisting of four ~24 kDa subunits and is primarily found in the mitochondria. Extracellular superoxide dismutase (ECSOD) is a copper- and zinc-containing tetrameric glycoprotein consisting of ~30 kDa subunits and is found predominantly in the soluble extracellular compartment but can also be bound to the surface of cells.

SOD enzymatic activity is not easily measured by direct assays, because substrate disappearance is very rapid at physiological pH. The activity of SOD enzymes can be determined by a number of indirect competitive inhibition assays based on the principle that SOD activity will inhibit the rate at which $O_2^{\cdot-}$ will reduce an indicator substrate—e.g., nitroblue tetrazolium (NBT) or cytochrome *c* in a competitive fashion. The SOD-mediated inhibition (percent inhibition) of indicator substrate reduction can then be quantitated and plotted as a function of the quantity of protein added to the reaction to construct an inhibition curve. The amount of cellular protein that causes 50% maximum inhibition can then be calculated and defined as containing one unit SOD activity. The units of SOD activity per milligram protein can then be related to the quantity of pure enzyme needed to reach 50% maximum inhibition under similar reaction conditions. The activities of the copper/zinc containing enzymes can be distinguished from the MnSOD activity in mammalian tissue homogenates using the differential sensitivity of these enzymes to inhibition by sodium cyanide. The major difficulties encountered when using such methods for the measurement of SOD activity arise from the fact that mammalian cell and tissue homogenates contain factors that directly reduce the indicator in a nonSOD inhibitable fashion, and the homogenates themselves can produce superoxide. Tissue-specific interference in the assay can cause the assay to inaccurately detect known amounts of SOD activity spiked into unknown samples. These tissue-specific assay interferences have been discussed in detail in a previous publication (Spitz and Oberley, 1989). A modified protocol for the spectrophotometric measurement of SOD activity, using xanthine oxidase and nitroblue tetrazolium (NBT) in mammalian tissue homogenates, has been developed based on the inclusion of a powerful metal chelator, bathocuproinedisulfonic acid (BCS), that inhibits electron transport chain–associated interference in the assay (Spitz and Oberley, 1989). This unit describes this modified NBT-BCS SOD assay procedure and provides a detailed protocol for use in differentiating between MnSOD and CuZnSOD activities in mammalian tissue homogenates.

NBT-BCS SUPEROXIDE DISMUTASE ACTIVITY ASSAY

BASIC PROTOCOL

The NBT-BCS SOD activity assay scheme is shown in Figure 7.5.1. The catalytic conversion of xanthine to uric acid and $O_2^{\cdot-}$ by xanthine oxidase provides an initial constant flux of superoxide in a phosphate buffered solution at room temperature. The rate of NBT reduction to blue formazan by the $O_2^{\cdot-}$ generated by the xanthine oxidase reaction is monitored spectrophotometrically at 560 nm. When increasing concentrations of pure SOD enzyme or protein homogenate containing SOD activity are added to the reaction, the rate of NBT reduction by xanthine/xanthine oxidase is progressively inhibited until maximum inhibition (typically 95%) is reached for the NBT-BCS assay. Catalase is added to the reaction to remove H_2O_2.

Contributed by Douglas R. Spitz and Larry W. Oberley
Current Protocols in Toxicology (2001) 7.5.1-7.5.11

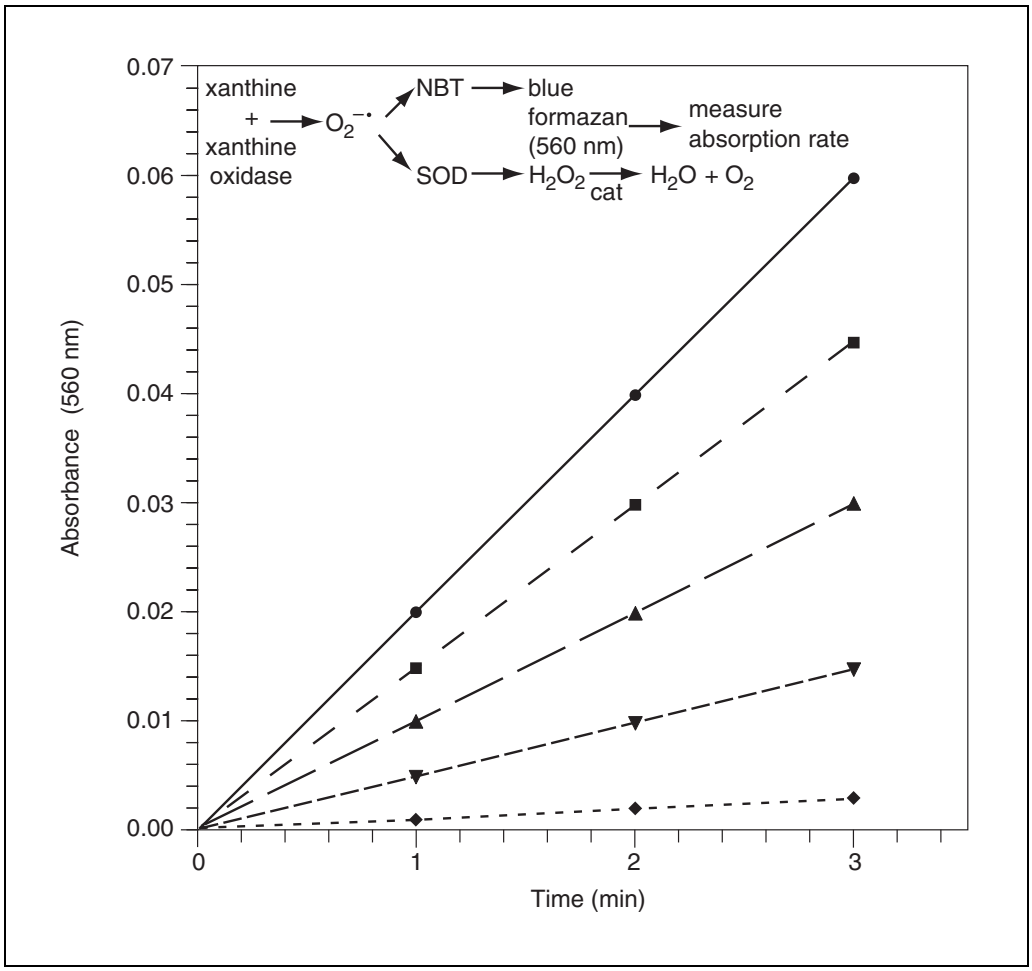

Figure 7.5.1 NBT-BCS competitive inhibition SOD activity assay. Above: an idealized reaction scheme. Below: an idealized data set showing the rates of NBT reduction monitored spectrophotometrically with increasing quantities of pure CuZnSOD standard at 0 (circles), 4 (squares), 8 (triangles), 25 (inverted triangles), and 500 (diamonds) ng. In this idealized circumstance, maximum inhibition is 95%, ½ maximum inhibition is 47.5%, and 1 unit is 8 ng.

Materials

3×10^7 cells or tissue
Phosphate buffered saline (PBS; *APPENDIX 2A*)
1.34 mM DETAPAC buffer (see recipe)
BSA in DETAPAC buffer (see recipe)
40 U/ml catalase (Sigma-Aldrich) in 0.05 M potassium phosphate buffer (see recipe); store up to 1 month at 4°C as a 4000 U/ml solution
2.24 mM nitroblue tetrazolium (NBT; see recipe)
1.18 mM xanthine (see recipe)
0.05 M potassium phosphate buffer, pH 7.8 (see recipe)
0.33 M NaCN (see recipe)
BCS (see recipe)
1 M HCl or 1 M KOH (optional)
5 µg/ml bovine CuZn superoxide dismutase (CuZnSOD; OXIS International): store up to 5 years at −20°C (avoid multiple freeze-thaw cycles)
13.2 U/ml xanthine oxidase (XO; Sigma-Aldrich), on ice

15-ml centrifuge tubes
400-W microtip sonicator (nonfragile cell culture or tissue)

Brinkman homogenizer with microtip (tissue)
10 × 75–mm borosilicate glass test tubes
Beckman 650 spectrophotometer or equivalent reading at 560 nm with 6 position automatic sample changer and enzyme kinetics software package
1-ml polystyrene cuvettes

NOTE: All solutions, unless otherwise specified, are prepared in 0.05 M potassium phosphate buffer, pH 7.8, stored at 4°C, and warmed to room temperature prior to assay. The water is double-distilled or Nanopure 18.3-megaohm purified (Barnstead/Thermolyne).

Prepare homogenate

For cell cultures

1a. Rinse cultures once with 5 ml of 4°C PBS. Scrape harvest 3×10^7 cells into 5 ml of 4°C PBS and transfer to a 15-ml centrifuge tube. Carry out all procedures at 4°C.

2a. Centrifuge 5 min at $400 \times g$, 4°C. Discard the supernatant being careful to remove as much PBS as possible. Freeze cell pellet overnight at −20°C or below to break open the cells.

3a. Thaw cell pellet. Homogenize in 0.5 ml of 1.34 mM DETAPAC buffer by repeated pipetting in a small-bore pipet tip if cells are fragile; otherwise, sonicate on ice with six 5-sec bursts from a 400-W microtip sonicator at 70% output.

This should yield a homogenate with a protein concentration of ~5 mg/ml measured using the method of Lowry et al. (1951; APPENDIX 3A).

For tissue samples

1b. Mince tissue with scissors in a petri dish containing 5 to 10 vol DETAPAC buffer on ice.

2b. Homogenize on ice using a Brinkman homogenizer with a microtip for five 2-sec bursts.

3b. Sonicate with six 5-sec bursts on ice with a 400-W microtip sonicator at 70% output.

In samples that are extremely turbid due to connective tissue in the homogenate, low-speed centrifugation (i.e., 2 min at ~50 × g, 4°C in a tabletop centrifuge) can be used to remove macroscopic clumps.

Prepare assay solutions

4. Combine stock solutions, in order, in two separate 250-ml beakers (one each for assay solution, one with and one without NaCN) as described in Table 7.5.1 to prepare assay solutions. Stir after each stock solution is added.

CAUTION: *NaCN is hazardous. Use with care and dispose of solutions containing it appropriately.*

The assay solutions are yellowish/green in color and slightly hazy after the addition of NBT. The recipe given in Table 7.5.1 is for 20 assay tubes (total volume 16 ml; 800 µl/tube), which is usually sufficient to run a complete inhibition curve (once in the presence and once in the absence of NaCN) on a homogenate containing 5 mg/ml protein as determined by the method of Lowry et al. (1951).

When running multiple samples or standards in a single day (a maximum of 12 samples and 1 standard for one person in one day; see Time Considerations), the desired multiples of these final assay solutions should be prepared and used within 6 hr. It is recommended (when possible) that all the samples from each experimental comparison be assayed within 2 days using the same stock solutions. Every day, a standard percent inhibition curve should

Table 7.5.1 Assay Solution Composition

Stock solutions	Total added volume[a] (ml)	Final concentration[b]
BSA in DETAPAC buffer	12.90	0.05 M potassium phosphate buffer; 1 mM DETAPAC; 0.13 mg/ml BSA
40 U/ml catalase	0.50	1.0 U
2.24 mM nitroblue tetrazolium (NBT)	0.50	5.6×10^{-5} M
1.18 mM xanthine	1.70	10^{-4} M
0.05 M potassium phosphate buffer or 0.33 M NaCN	0.30	0 or 5 mM CN^-
0.01 M BCS	0.10	50.0 µM

[a]The total volume of the final assay solution is 16.0 ml. Multiples of this recipe can be prepared for more than one sample.
[b]Final concentration is for each assay tube after all of the ingredients have been added.

be run using purified CuZnSOD prior to running the samples to verify that the reagents are working properly (see Fig. 7.5.2).

5. (*Optional*) Adjust final assay solutions to pH 7.8 using 1 M HCl or 1 M KOH.

   This will allow for the use of the same XO solution for both NaCN-containing and nonNaCN-containing assay tubes. If the pH is not readjusted, the XO solution may need to be diluted prior to running the NaCN-containing tubes in order to keep the rate of NBT reduction in the desired range.

Prepare blanks, samples, and standards

6. Prepare sample or standard (i.e., 5 µg/ml bovine CuZnSOD) dilutions in 0.05 M potassium phosphate buffer, pH 7.8, such that each 100 µl added to the reaction contains increasing quantities of protein (1 to 500 µg protein for each sample homogenate or 2 to 500 ng protein for the CuZnSOD standard). Adjust dilutions so that most points are taken between 10% to 60% inhibition (usually 2 to 50 µg protein for most homogenates and 2 to 50 ng for most purified CuZnSOD preparations).

   Be sure that maximum inhibition for each unknown sample is reached for both nonNaCN- and NaCN-containing tubes. Maximum inhibition is usually between 80% and 95% inhibition, requiring addition of 500 µg protein for most homogenates (500 ng for purified SOD standards). The assay is usually 10 tubes for a total SOD activity assay and 10 tubes with CN^- for a MnSOD activity assay. A dilution table and assay results for a purified CuZnSOD standard are shown in Figure 7.5.2.

7. Pipet 100 µl sample or standard into duplicate 10 × 75–mm borosilicate glass test tubes (i.e., for NaCN- and nonNaCN-containing reactions).

   Each protein dilution must be pipetted in duplicate and run with both nonNaCN- and NaCN-containing final assay solutions to obtain total SOD activity per milligram protein as well as NaCN-resistant SOD activity.

8. Prepare blanks by pipetting 100 µl of 0.05 M potassium phosphate buffer, pH 7.8, into duplicate 10 × 75–mm borosilicate glass test tubes (i.e., for NaCN- and non-NaCN-containing reactions).

   These tubes will be run with each set of samples or standards to determine the rate of NBT reduction in the absence of SOD activity for the calculation of percent inhibition in both the presence and absence of NaCN.

   One blank is run with each set of 5 samples or standards (the sample changer holds six cuvettes).

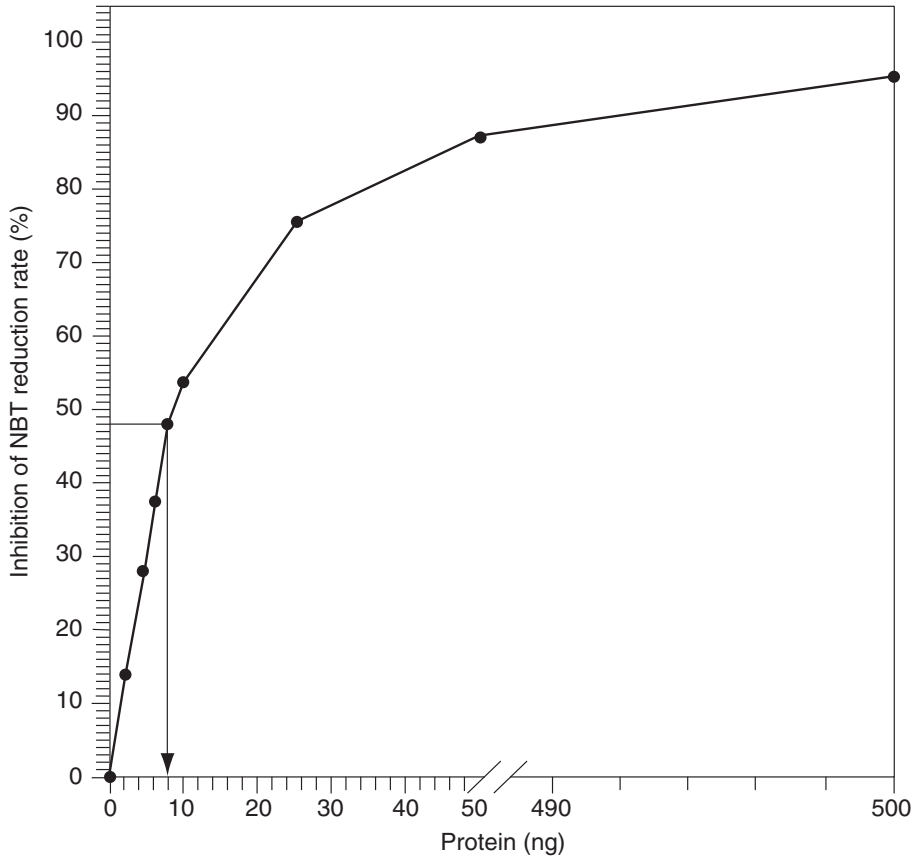

SOD (ng)	std. (µl)	buffer (µl)	total (µl)	rate	inhibition (%)
0-blank	0	100	100	0.0227	0
2	2	498	100	0.0195	13.9
4	4	496	100	0.0163	28.0
6	6	494	100	0.0142	37.3
8	8	492	100	0.0122	46.1
10	10	490	100	0.0105	53.6
25	25	475	100	0.0055	75.7
50	50	450	100	0.0029	87.2
500	100 µl undiluted SOD std.			0.0010	95.6
0-blank			100	0.0226	0

Figure 7.5.2 Top: NBT-BCS superoxide dismutase activity assay of purified 5 µg/ml CuZnSOD standard provided by OXIS International. Maximum inhibition is 95.6%, 1/2 maximum inhibition is 47.8%, and 1 unit is 8 ng. Bottom: Dilution table for this assay describing how to mix the standard and buffer to obtain the inhibition curve shown in the top figure. 100 µl of each dilution is added to 800 µl of assay reagent, then 100 µl of XO solution is added to initiate the reaction. The reaction is monitored for 2.5 min to obtain the absorption/min, which is the reported rate.

Begin competitive assay

9. Add 800 µl assay solution to blanks, standards, and samples with and without NaCN.
10. *To inactivate CuZnSOD activity:* Incubate tubes containing NaCN assay solution for each protein dilution for at least 45 min at room temperature to allow for the inhibition of CuZnSOD by CN^-.

    This can be accomplished by running all the nonNaCN-containing tubes from a series first, and then running all the NaCN-containing tubes. The NaCN-containing tubes should not be incubated >2.5 hr.

11. Dilute 10 µl of 13.2 U/ml xanthine oxidase (XO) to 3.5 ml with 1.34 mM DETAPAC buffer. Add to a nonNaCN blank first and adjust concentration as necessary to give an inhibition rate for NBT reduction in the absence of SOD between 0.016 to 0.025 AU/min (0.02 AU/min is ideal) at 560 nm using a Beckman DU-650 (or equivalent) spectrophotometer. Store XO solution on ice during the assay or the activity will diminish.

    If the desired rate is not obtained, add more XO or dilute the XO solution with DETAPAC buffer to give the desired rate.

12. Add 100 µl XO to initiate the reaction. Incubate the reaction 1 min at room temperature to allow the XO reaction to reach V_{max}.

    Xanthine oxidase (XO) is the last component added to each tube to initiate the reaction, and it should be added no more than 1 min before the sample is read.

    The XO reaction is now linear for ~5 min but should be read between 1 and 3 min following addition of XO.

Determine absorbance rate

13. Transfer reaction to a 1-ml polystyrene cuvette. Place a blank (phosphate buffer instead of sample or standard) in cuvette position 1 of the automatic sample changer and put samples or standards in cuvette positions 2 through 6. Monitor absorbance at 560 nm every 15 sec for 2.5 min. Run the standard curve (as shown in Fig. 7.5.2) first to make sure all assay conditions are optimized.
14. Record rate of change in absorbance for at least 2.5 min or until a straight line is obtained. Record rates of AU/min for blank and samples for use in calculating percent inhibition. Dispose of the cuvettes and the glassware appropriately.

    At the end of the assay the solutions should be blue.

15. Run every series (blank and 5 samples) in the same way (steps 12 to 14) until all the non-CN^- tubes are analyzed. Then repeat the same process with CN^- containing tubes.

Analyze data

16. Calculate the percent inhibition for each blank, standard, or sample:

$$\text{percent inhibition} = \frac{\text{blank rate} - \text{sample rate}}{\text{blank rate}} \times 100$$

    Blank rate is the mean of the blanks run at the beginning and the end of each sample or standard.

17. Plot percent inhibition versus protein concentration (see Fig. 7.5.2 and Fig. 7.5.3). Determine the highest maximum inhibition for each group of sample curves to be compared and calculate the amount of protein that inhibits NBT reduction by 50% maximum inhibition.

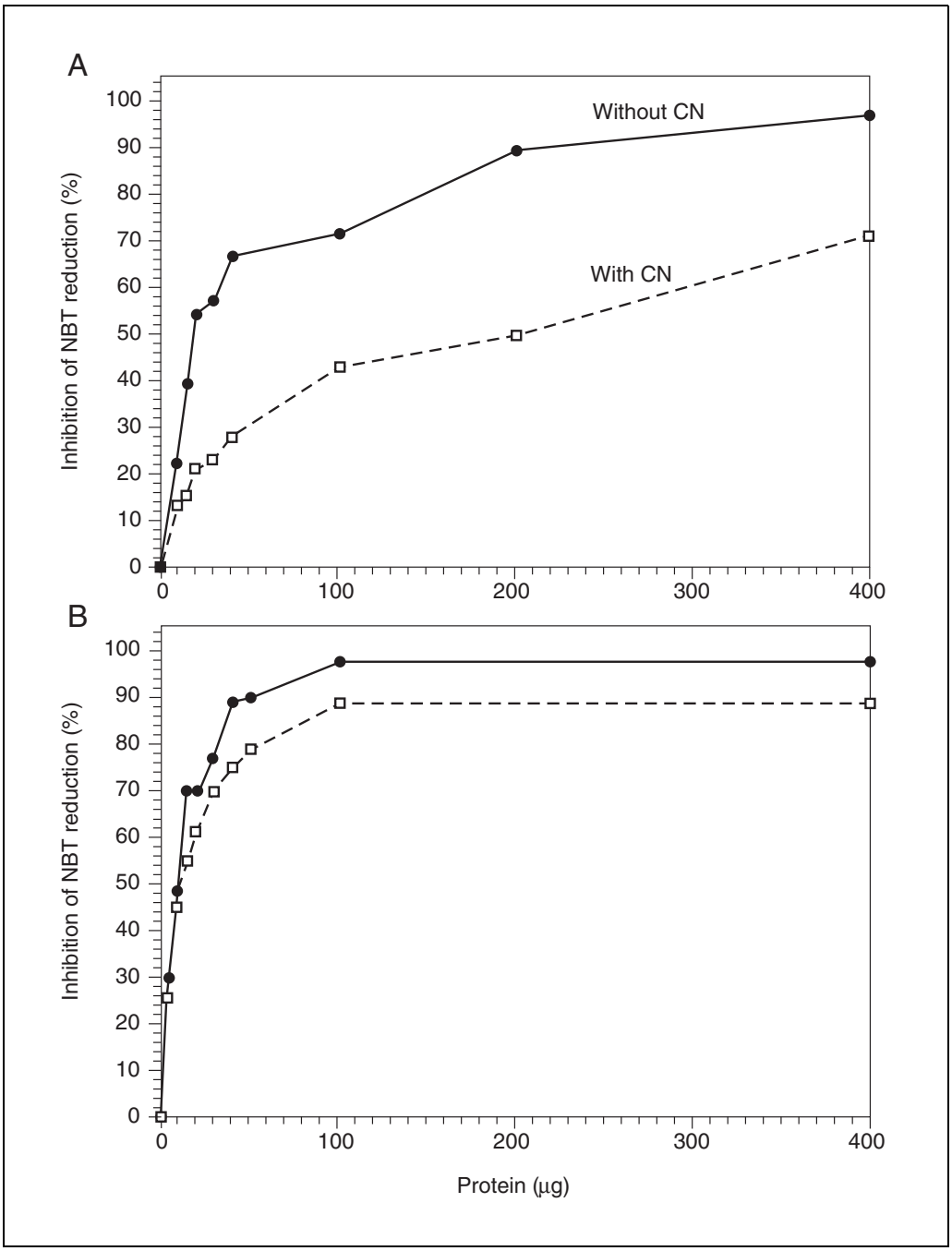

Figure 7.5.3 NBT-BCS SOD activity assay of whole homogenates from A549 human lung adenocarcinoma cells incubated in the absence (**A**) or presence (**B**) of tumor necrosis factor (TNF) and interferon (IFN) for 14 hr. The highest maximum inhibition in the two samples to be compared (A and B) for nonCN$^-$ containing reactions (solid circles) is 98%, and 1/2 maximum inhibition is 49%, while for CN$^-$ containing reactions (open squares) the highest maximum inhibition is 90% and 1/2 maximum inhibition is 45%. (Whenever a group of samples is being compared to each other, it is necessary to use the highest maximum inhibition obtained from the group to get the best relative comparison for the group. This is true for both CN$^-$ containing and nonCN$^-$ containing comparisons.) Therefore, total SOD activity is 46.5 U/mg, MnSOD activity is 8 U/mg, and CuZnSOD activity is 38.5 U/mg in the sample shown in (A). Total SOD activity is 100 U/mg, MnSOD activity is 95.2 U/mg, and CuZnSOD activity is 4.8 U/mg for the sample shown in (B).

The plot of percent inhibition verses protein concentration can be fit with a curve using a computer program (e.g., Enzfitter, version 1.03, Michaelis Menton kinetics, R.J. Leatherbarrow, Sigma Scientific) or simply by hand drawing a best fit curve through the points on engineering graph paper.

One unit of activity is defined as the amount of protein that will inhibit NBT reduction by 50% (e.g., if maximum inhibition = 95%, then 50% of maximum = 47.5%; therefore, 1 unit is defined as the amount of protein which yields 47.5% inhibition). Usually one unit of activity is 6 to 10 ng protein for purified CuZnSOD (OXIS International), 35 to 50 ng of purified MnSOD, or 10 to 20 µg protein for total SOD activity (i.e., in the absence of NaCN) in an average cell sample. Units of total SOD activity/milligram protein in the nonNaCN-containing assay can then be calculated for a given sample by taking 1000/ug protein per unit. Units of CN^- resistant (or MnSOD) activity can be calculated from a similar percent inhibition curve run in the presence of NaCN using the highest maximum inhibition obtained for samples run in the presence of NaCN.

See the examples of a standard curve (Fig. 7.5.2) or sample curves (Fig. 7.5.3) for data sets in which SOD activity was determined using this methodology. Notice in Figure 7.5.3 how the assay differentiates between CuZn- and MnSOD activity under conditions where MnSOD is being induced by exposure to tumor necrosis factor (TNF) and interferon-gamma (IF-γ).

18. Determine MnSOD activity from the CN^- containing tubes. Determine total activity from the nonCN^- tubes.
19. Calculate CuZnSOD activity, which is the total SOD activity minus the MnSOD activity.

REAGENTS AND SOLUTIONS

Use double distilled or Nanopure 18.3-megaohm purified water (Barnstead/Thermolyne) for the preparation of all buffers. For common stock solutions, see ***APPENDIX 2A****; for suppliers, see* ***SUPPLIERS APPENDIX****.*

BCS

Dissolve 0.00565 g bathocuproinedisulfonic acid (BCS) disodium salt in 1 ml of 0.05 M potassium phosphate buffer (see recipe). Store up to 2 days at 4°C.

BSA in DETAPAC buffer

Dissolve 0.0202 g BSA in 100 ml DETAPAC buffer (see recipe). Store up to 3 days at 4°C.

DETAPAC buffer, 1.34 mM

Dissolve 0.2653 g diethylenetriaminiepentaacetic acid (Sigma-Aldrich) in 500 ml 0.05 M potassium phosphate buffer, pH 7.8 (see recipe) with stirring. Store up to 1 year at 4°C.

NaCN, 0.33 M

Dissolve 0.8093 g NaCN (Fisher Scientific) in 50 ml 0.05 M potassium phosphate buffer, pH 7.8 (see recipe). Store up to 3 days at 4°C.

CAUTION: *NaCN is poisonous and care is advised in handling. It should be used and disposed of according to local health and safety regulations.*

Nitroblue tetrazolium (NBT), 2.24 mM

Dissolve 0.1832 g NBT (Sigma-Aldrich) in 100 ml 0.05 M potassium phosphate buffer, pH 7.8 (see recipe) with stirring. Store in a brown bottle (i.e., protected from light) up to 1 year at 4°C.

Potassium phosphate buffer, pH 7.8

Monobasic solution:

Dilute 10 ml 1 M potassium phosphate monobasic (Fisher Scientific; 136 gm/liter KH_2PO_4) to 200 ml with H_2O

Dibasic solution:

Dilute 50 ml 1 M potassium phosphate dibasic (Fisher Scientific; 174 gm/liter K_2PO_4) to 1 liter with H_2O

Potassium phosphate buffer:

Add monobasic solution to dibasic solution with constant stirring at room temperature until pH reaches 7.8. Store up to 1 year at 4°C.

Xanthine, 1.18 mM

Heat while stirring 0.0045 g xanthine (Sigma-Aldrich) in 25 ml 0.05 M potassium phosphate buffer, pH 7.8 (see recipe). Store up to 7 days at 4°C.

COMMENTARY

Background Information

The discovery that O_2-metabolizing cells contain enzymes that exhibit superoxide dismutase activity (SOD) has lead to an explosion of interest in the field of free radical biology (Fridovich, 1978; Halliwell and Gutteridge, 1999). These enzymes catalyze the conversion of superoxide ($O_2^{-\cdot}$) to H_2O_2 and O_2 according to the following reaction: $2O_2^- + 2H_2 \rightarrow H_2O_2 + O_2$. The SOD enzymes are thought to limit the steady state concentration of superoxide ($O_2^{-\cdot}$) formed as a byproduct of electron transport chain activity as well as mono-oxygenase enzymatic activity. Superoxide is a weak oxidant but an excellent reductant; therefore, if steady state concentrations of $O_2^{-\cdot}$ are not held in check via the action of SOD enzymes, it is believed that $O_2^{-\cdot}$ could reduce redox active metal ions such as Fe^{3+} and Cu^{2+} to potent oxidants such as Fe^{2+} and Cu^{1+}, which could promote excessive damage to critical biomolecules (e.g., lipids, proteins, nucleic acids) as well as leading to the formation of other reactive oxygen species such as hydroxyl radical (·OH), organic hydroperoxides (ROOH), alkoxyl radicals (RO·), and hydroperoxyl radicals (ROO·). In addition, $O_2^{-\cdot}$ can react with another biologically significant free radical, nitric oxide (NO·), to form peroxynitrite ($ONOO^-$), which can act as a potent oxidant capable of causing damage to critical biomolecules. For these reasons the superoxide dismutase enzymes are generally thought to play a protective role in cellular physiology and the regulation of these enzymatic activities is thought to contribute to mammalian cellular responses to a wide variety of biologically significant stresses of toxicological importance.

The NBT-BCS SOD assay was developed in order to provide an accurate and reproducible quantitative assay for CuZnSOD and MnSOD activities in whole mammalian tissue homogenates (Spitz and Oberley, 1989). This was necessary, because whole mammalian tissue homogenates contain substances that interfere with the accurate determination of SOD activity during standard addition experiments (Spitz and Oberley, 1989). The inclusion of metal chelators that also inhibit electron transport through iron-sulfur proteins was found to inhibit the interfering reactions and allow for the accurate determination of SOD activity in whole homogenates (Spitz and Oberley, 1989). Since the original development of the assay, several studies looking at the correlation between the activity measurements obtained with the NBT-BCS assay and quantities of SOD protein as determined by immunoblotting procedures have shown excellent agreement (Oberley et al., 1989; Spitz et al., 1990).

The major strength of the NBT-BCS assay is the rigorous quantitative determination of MnSOD and CuZnSOD activity in whole homogenates of mammalian tissues and cells. Whole homogenates are desirable, because when preparing the sample, one need only homogenize in 50 mM potassium phosphate buffer, pH 7.8, containing 1.34 mM DETAPAC (i.e., DETAPAC buffer). This avoids any tissue processing or extraction procedure that could remove SOD activity from the sample. In addition the NBT-BCS assay is significantly more sensitive than activity assays based on cytochrome c reduction (Spitz and Oberley, 1989). Native gel SOD activity assays (Beauchamp and Fridovich, 1971) will also provide a

Table 7.5.2 Representative Rat Tissue SOD Activity

Tissue	Activity (U/mg protein)		
	Total SOD	MnSOD	CuZnSOD
14-day lactating breast[a]	200	13	187
Breast adenocarcinoma[a]	105	12	93
Rat liver[b]	442	78	364

[a]Spitz and Oberley (1989).
[b]Brown et al. (1998).

semiquantitative determination of MnSOD and CuZnSOD activity when using whole homogenates, but these assays have difficulty discriminating between samples that display ≤2-fold differences in activity. Direct assays of SOD activity based on following the disappearance of superoxide in aqueous solutions (from potassium superoxide) have also been described (Marklund, 1985) but require doing the assay in pH ranges that alter the activity of MnSOD. Direct kinetic assays based on stopped-flow devices have also been used to accurately determine SOD activity (Wiess et al., 1993), but these assays are generally not amenable to use with whole homogenates. For these reasons the authors have found the NBT-BCS to be the most sensitive, accurate, and reproducible method for use with whole mammalian tissue homogenates.

Troubleshooting

The problems that arise during the use of the NBT-BCS assay all derive from very low activity in the sample or interfering substances that are not totally inhibited by the inclusion of DETAPAC and BCS. These include:

1. Turbidity of samples where very large amounts of protein need to be added to reach maximum inhibition. This is the problem in samples with very nonlinear rates. A low-speed ($<50 \times g$) centrifugation step to remove macroscopic pieces of connective tissue will usually solve this problem.

2. Low maximum percent inhibition (the maximum percent inhibition is <90%) due to nonSOD inhibitable NBT reduction. This problem can be solved by always constructing a complete protein versus percent inhibition curve and using the maximum percent inhibition obtained. In a series of samples being compared to one another always use the greatest maximum inhibition value obtained during that particular comparison so that all the samples are being compared using the same value.

3. Spontaneous NBT reduction occurring in the absence of exogenous xanthine oxidase (the solution in the tube will turn light purple or blue before XO solution is added). When this happens, it is always prudent to split the sample into two aliquots and do a standard addition experiment to be sure that the assay is accurately detecting known amounts of SOD activity added to the sample. Standard addition experiments are described in great detail elsewhere (Spitz and Oberley, 1989).

Anticipated Results

Overall, when utilized according to the aforementioned protocol, the NBT-BCS is the most accurate and reproducible method for discriminating between CuZn and Mn SOD activity in mammalian tissue homogenates that the authors' group of SOD researchers have found to date. Typical results from rat tissue whole homogenates are shown in Table 7.5.2.

Time Considerations

The major drawback to the NBT-BCS assay is the cost in time and supplies necessary to construct full percent inhibition versus protein concentration curves for each sample in the presence and absence of NaCN; however, by utilizing an automated spectrophotometer and pipetting the dilutions of the samples to be run beforehand, two workers can easily accomplish 12 samples and a standard curve each work day. Also the added reliability of data obtained from complete percent inhibition versus protein concentration curves justifies the additional cost and effort.

Literature Cited

Beauchamp, C. and Fridovich, I. 1971. Superoxide dismutase: Improved assays and an assay applicable to acrylamide gels. *Anal. Biochem.* 44:276-287.

Brown, K.F., Kinter, M.T., Oberley, T.D., Freeman, M.L., Frierson, H.F., Ridnour, L.A., Tao, Y., Oberley, L.W., and Spitz, D.R. 1998. Enhanced gamma glutamyl transpeptidase expression and selective loss of CuZn superoxide dismutase in hepatic iron overload. *Free Radic. Biol. Med.* 24:545-555.

Fridovich, I. 1978. The biology of oxygen radicals. *Science* 201:873-880.

Halliwell, B. and Gutteridge, J.M.C. 1999. Free Radicals in Biology and Medicine: Third Edition. Oxford University Press, Oxford.

Lowry, O.H., Rosenbrough, N.J., Farr, A.L., and Randall, R.J. 1951. Protein measurement using the folin phenol reagent. *J. Biol. Chem.* 193:265-275.

Marklund, S.L. 1985. Direct assay with potassium superoxide. *In* Handbook of Methods for Oxygen Radical Research, (R. Greenwald, ed.), p. 249. CRC Press, Boca Raton, Fla.

Oberley, L.W., McCormick, M.L., Sierra-Rivera, E., and Kasemset-St. Clair, D. 1989. Manganese superoxide dismutase in normal and transformed human embryonic lung fibroblasts. *Free Radic. Biol. Med.* 6:379-384.

Spitz, D.R. and Oberley, L.W. 1989. An assay for superoxide dismutase activity in mammalian tissue homogenates. *Anal. Biochem.* 179:8-18.

Spitz, D.R., Elwell, J.H., Sun, Y., Oberley, L.W., Oberley, T.D., Sullivan, S.J., and Roberts, R.J. 1990. Oxygen toxicity in control and H_2O_2-resistant Chinese hamster fibroblast cell lines. *Arch. Biochem. Biophys.* 279:249-260.

Wiess, R.H., Flickinger, A.G., Rivers, W.J., Hardy, M.M., Aston, K.W., Ryan, U.S., and Riley, D.P. 1993. Evaluation of activity of putative superoxide dismutase mimics: Direct analysis by stopped-flow kinetics. *J. Biol. Chem.* 268:23049-23054.

Key References

Beauchamp and Fridovich, 1971. See above.

First report on NBT-based SOD activity assays.

Spitz and Oberley, 1989. See above.

Original description of the NBT-BCS activity assay for use in mammalian tissue homogenates.

Contributed by Douglas R. Spitz and Larry W. Oberley
University of Iowa
Iowa City, Iowa

Measurement of Ascorbic Acid and Dehydroascorbic Acid in Biological Samples

Ascorbic acid (AA) and dehydroascorbic acid (DHA) play an important role in the maintenance of redox homeostasis. The concentrations of these biomolecules in such samples as plasma, isolated cells, and tissues are frequently used as markers of oxidative stress levels in a variety of experimental setups ranging from cellular biology to animal models and clinical trials. With an emphasis on HPLC with electrochemical detection (see Basic Protocol), this unit describes measurement of the antioxidant-couple AA-DHA as well as isoascorbic acid (IAA or erythorbic acid), dehydroisoascorbic acid (DHIA or dehydroerythorbic acid), and uric acid (UA) and discusses realistic expectations and potential pitfalls in the analysis of these labile compounds. The importance of sample preparation is discussed, and procedures for the proper preparation and stabilization of samples from a variety of biological origins are provided (see Support Protocols 1, 2, and 3). Furthermore, passivation of HPLC equipment for lowering detector background (see Support Protocol 4) and the use of endogenous and internal standards in data analysis (see Support Protocol 5) are described.

BASIC PROTOCOL

ANALYSIS OF ASCORBIC ACID, DEHYDROASCORBIC ACID, ISOASCORBIC ACID, DEHYDROISOASCORBIC ACID, AND URIC ACID BY HPLC WITH COULOMETRIC DETECTION

The HPLC method (Lykkesfeldt, 2000) described here with some modifications is based on the measurement of ascorbic acid (AA), isoascorbic acid (IAA), and uric acid (UA), and in a separate parallel run, total AA, total IAA, and UA in samples stabilized with *meta*-phosphoric acid (MPA; Fig. 7.6.1). The concentrations of dehydroascorbic acid (DHA) and dehydroisoascorbic acid (DHIA) are subsequently calculated by subtraction of the AA and IAA concentrations from those of total AA and total IAA, respectively. Total AA and IAA concentrations are obtained by reducing a sample aliquot with tris(2-carboxyethyl)phosphine hydrochloride (TCEP) prior to its analysis. Reversed-phase ion-pairing HPLC separates the analytes, and the compounds are quantified by coulometric electrochemical detection. This highly sensitive, specific, and fast method accurately measures AA, DHA, IAA, DHIA, and UA in a wide variety of biological samples.

Materials

Mobile phase (see recipe)
Plasma (see Support Protocol 1), isolated-cell (see Support Protocol 2), or tissue homogenate sample (see Support Protocol 3) stabilized with *meta*-phosphoric acid (MPA)
1 mM Na_2EDTA prepared from 10 mM Na_2EDTA (372 mg/100 ml)
TCEP solution (see recipe)
McIlvaine buffer (see recipe)
Standard mixture (see recipe)
5% MPA/EDTA solution (see recipe)

High-performance liquid chromatography (HPLC) system (for passivation see Support Protocol 3), including:
- Isocratic pump (Agilent 1100 series, or equivalent low-pulsation-type pump)
- Vacuum degasser (e.g., Agilent 1100 series), optional
- Column thermostat (e.g., Agilent 1100 series), 30°C
- Thermostatted autosampler, 10-µl injection volume (e.g., Agilent 1100 series), 5°C

Contributed by Jens Lykkesfeldt
Current Protocols in Toxicology (2002) 7.6.1-7.6.15

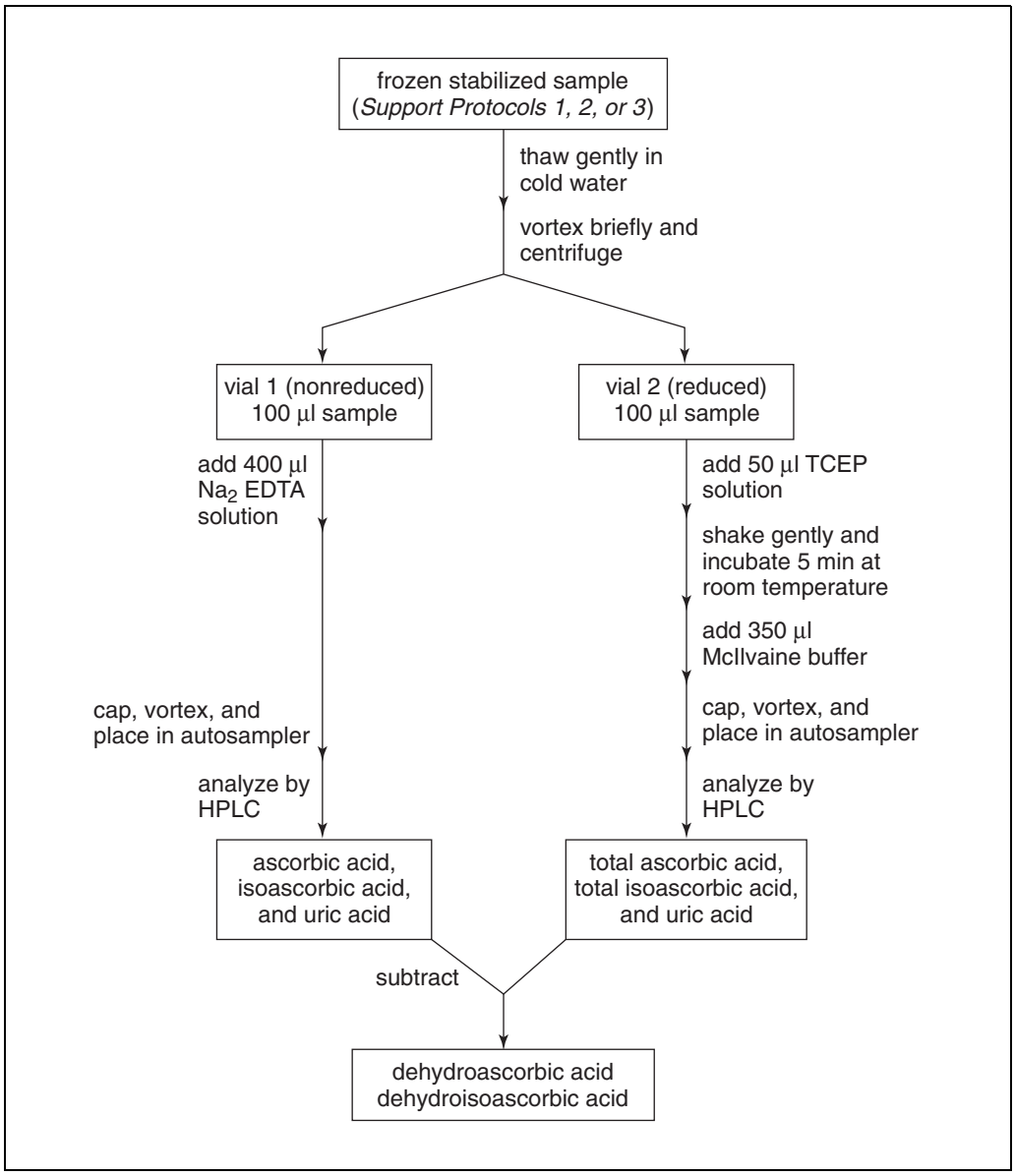

Figure 7.6.1 Sample preparation, analysis, and quantification of ascorbic acid, dehydroascorbic acid, isoascorbic acid, dehydroisoascorbic acid, and uric acid in a biological sample. The individual steps are described in detail in the Basic Protocol.

Uninterruptible power supply (UPS) for HPLC system (e.g., Smart-UPS 3000VA with extended battery pack, part nos. SU3000INET and SU48BP, respectively; American Power Conversion), optional, but highly recommended

Coulometric detector (ESA Coulochem II; ESA) and accessories, including:
- HP 35900E interface module (Agilent)
- Model 5020 guard cell (ESA)
- Model 5010 dual analytical cell (ESA)

HPLC column: 7.5-cm × 4.6-mm (i.d.) Luna C18(2) 3-µm particle size (Phenomenex)

Guard column: 4.0-mm × 3.0-mm (i.d.) SecurityGuard C18 (Phenomenex)

Microcentrifuge (e.g., Eppendorf 5417R or equivalent), 4°C

Amber HPLC vials with caps (e.g., Agilent), inserts may be required for small volumes

Set up HPLC system

1. Set up an HPLC system consisting of an isocratic pump, an optional vacuum degasser, a column thermostat, and a thermostatted autosampler. Set the autosampler to deliver a 10-µl volume. Use a UPS for the system.

   The vacuum degasser provides optimal protection against air from the mobile phase in the pump heads but can be omitted if the mobile phase is thoroughly degassed using a vacuum filtration system (e.g., Alltech Associates) or a sonicator.

   A UPS for the coulometric detector, or ideally for the entire system, provides excellent protection against surges, spikes, and shifts in current that may otherwise turn off the detector. Although optional, the use of a UPS is therefore highly recommended in facilities where a constant supply of power cannot be guaranteed.

2. Set up a coulometric detector connected via an HP 35900E interface module and fitted with a model 5020 guard cell (placed between the pump and the autosampler) operated at +450 mV and a model 5010 dual analytical cell (placed after the column) operated at −200/+400 mV.

   The current range is typically 1 to 10 µA. The precise potentials applied may change from one electrochemical cell to another, and therefore it is always important to generate voltammograms for all analytes whenever the electrochemical cell is changed and every 6 months thereafter for sensitivity control.

3a. *For new columns only:* Start up the HPLC system and flush an HPLC column with mobile phase for 1 week at a flow rate of 1 ml/min.

   Because of the ion-pairing separation principle, no retention of the analytes is observed on a new unequilibrated column. Thus, a new column needs to be thoroughly equilibrated prior to use. Recycling of mobile phase during the equilibration is not advised. The procedure may conveniently be performed on a separate HPLC pump. Gradually, retention is observed, and retention times eventually stabilize at roughly 3.5, 4.5, and 5.5 min for AA, IAA, and UA, respectively. The column can then be stored in the mobile phase ready for use on the main system. Guard columns do not need to be equilibrated and are changed as dictated by increasing back pressure.

3b. *For previously used columns:* Start up the HPLC system and flush a guard column and an HPLC column with mobile phase for ~10 min at a flow rate of 1 ml/min.

   During normal use, the system needs to equilibrate for ~10 min prior to sample loading. The flow rate can be adjusted as necessary as the column ages to maintain a 5- to 7-min run time. A column usually shows excellent performance for several thousand samples.

   Between batches of samples, the flow rate is kept at 0.05 ml/min with the detector on at all times for optimal performance. Only for major maintenance or long-term operation shutdown is the detector turned off. Mobile phase may be recycled after an appropriate rinse-out period.

Analyze sample

4. Gently thaw a plasma, isolated-cell, or tissue homogenate sample in cold water. Vortex sample and microcentrifuge 2 min at 16,000 × *g*, 4°C (Fig. 7.6.1).

   Samples are thawed and prepared in batches of eight to twenty, depending on the experience of the analyst, to limit the sample preparation time for each sample.

   Depending on how quickly samples were originally frozen during preparation (i.e., if samples were placed in a −20°C or −80°C freezer, on dry ice, or in liquid nitrogen), some fractionation of the sample may have occurred leading to very poor results if used directly. Consequently, vortexing the thawed sample, even if it appears homogeneous, can be vital. The subsequent centrifugation can be omitted if samples are consistently free of precipitate.

5. Transfer 100 µl sample to each of two separate amber HPLC vials.

   Smaller volumes down to ~5 to 10 µl of sample can be used without problems with proper adjustment of the amounts in the following steps. With smaller volumes it may be necessary to use vial inserts to ensure proper injection volume if an autosampler is used.

   Sometimes dilution can be necessary, in particular for tissue samples. In this case the 100-µl sample is diluted with 5% MPA/EDTA solution (e.g., 25 µl sample and 75 µl of 5% MPA/EDTA solution) and processed as described below.

6. To the first vial, add 400 µl of 1 mM Na_2EDTA. Cap the vial, vortex briefly, and place the 500-µl sample in the thermostatted autosampler at 5°C and analyze in the shortest time possible.

   Here and in step 8, the autosampler will inject a 10-µl aliquot from the sample onto the HPLC column. Alternatively, the sample may be manually injected onto the column.

   When analyzing multiple samples, steps 6 to 8 may be performed by using a multipipettor for increased speed and reproducibility.

   This sample represents AA, IAA, and UA. Because AA and IAA are prone to oxidation, samples should be analyzed within 12 hr, preferably less.

   Figure 7.6.2 shows representative HPLC chromatograms of various samples.

7. Add 50 µl TCEP solution to the second vial, shake gently, and leave it for 5 min at room temperature.

   Reduction of oxidized AA and IAA occurs in <5 min.

8. Add 350 µl McIlvaine buffer. Cap the vial, vortex briefly, and place the 500-µl sample in the autosampler at 5°C and analyze.

   This sample represents total AA and IAA (AA plus DHA and IAA plus DHIA, respectively) and UA. Standards and samples containing TCEP are stable in the autosampler for ≥4 days even at room temperature. Analyzing the nonreduced (step 6) and reduced (step 8) samples in pairs gives the best results in terms of quantification reproducibility and reduces the risk of error due to voltammogram shifts and changes in detector efficiency.

Prepare standards

9. Prepare a series of 100-µl standard mixture dilutions in amber HPLC vials using 5% MPA/EDTA.

   Standards containing 1 to 100 µl standard mixture diluted to 100 µl (corresponding to 1 to 100 pmol AA and IAA and 5 to 500 pmol UA per 10-µl injected sample) are used depending on the material that is analyzed.

10. Repeat steps 7 and 8 using the 100-µl standard mixture dilutions.

11. Use the HPLC data to generate a standard curve.

Quantify acid levels

12. Quantify AA, IAA, and UA by comparison to the prepared standard curve, perform relevant corrections if applicable (see Support Protocol 5), and calculate DHA and DHIA by subtraction.

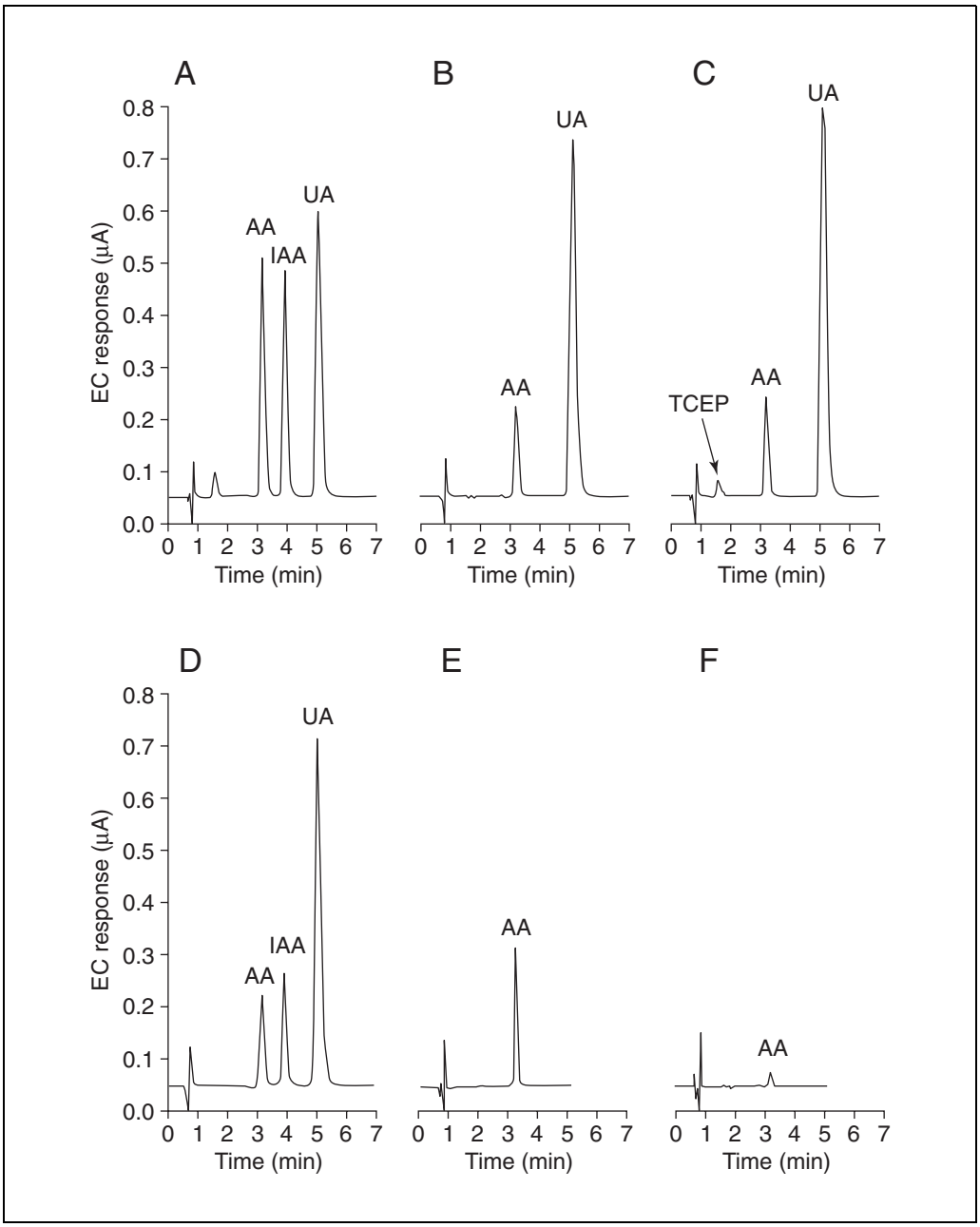

Figure 7.6.2 Separation of ascorbic acid (AA), isoascorbic acid (IAA), and uric acid (UA) by HPLC with coulometric detection. Conditions are as described in the Basic Protocol. (**A**) Standard mixture containing 100, 100, and 250 μM of AA, IAA, and UA, respectively. (**B**) Human plasma sample (male smoker, fasted overnight). AA and UA peaks correspond to 42 and 340 μM, respectively. (**C**) Same human plasma sample run in parallel after reduction with tris(2-carboxyethyl)phosphine hydrochloride (TCEP) as described. After correction for intrasample error using UA (see Support Protocol 5), the dehydroascorbic acid (DHA) concentration was calculated by subtraction to be 0.55 μM, corresponding to 1.2% of the total AA. (**D**) Plasma sample from the same individual taken 2 hr after oral administration of 1 g IAA in water. AA, IAA, and UA peaks correspond to 43, 53, and 331 μM, respectively. (**E**) Lung biopsy from pig (61 mg tissue homogenized and diluted 4-fold). AA peak corresponds to 1.3 nmol/mg tissue. (**F**) Freshly isolated hepatocytes from guinea pig. AA peak corresponds to 2.5 nmol/10^6 cells. EC, electrochemical.

COLLECTION AND STORAGE OF BIOLOGICAL SAMPLES INTENDED FOR ASCORBIC ACID AND DEHYDROASCORBIC ACID ANALYSIS

Due to the lability of the ascorbic acid (AA), dehydroascorbic acid (DHA), isoascorbic acid (IAA), and dehydroisoascorbic acid (DHIA), proper sample collection is vital in order to obtain reproducible results. The oxidation of AA and IAA starts very rapidly following blood drawing, cell lysis, or tissue homogenization, and all steps must therefore be performed as quickly and uniformly as possible. Protocols for the collection, sample stabilization, and storage conditions for plasma (see Support Protocol 1), isolated cells (see Support Protocol 2), and tissue (see Support Protocol 3) are outlined below. In general, the author stores plasma samples and other body fluids at −80°C or less and processes them within 1 to 2 months, whereas tissue and cell samples are stored at −80°C or less and processed within 1 to 2 weeks.

SUPPORT PROTOCOL 1

Preparation of Plasma Samples

This protocol can also be used to prepare samples from other body fluids.

Materials

Anticoagulated blood sample (e.g., collected in an EDTA- or heparin-containing vacutainer)
10% MPA/EDTA solution (see recipe), 4°C
Microcentrifuge (e.g., Eppendorf 5417R or equivalent), 4°C

1. Immediately following the collection of an anticoagulated blood sample, microcentrifuge a 1-ml aliquot 2 min at 16,000 × *g*, 4°C.

   When analyzing fluids other than blood, such as cerebrospinal fluid (CSF) or urine, perform only steps 2 to 4.

   A smaller amount can be used if necessary (e.g., for CSF).

   Care should be taken to avoid hemolysis, because the presence of metal ions in the plasma facilitates AA oxidation. If hemolysis is frequently observed with vacutainers, blood can be drawn more safely (albeit less conveniently) by using a butterfly needle.

2. Transfer 400 µl plasma to a microcentrifuge tube containing an equal volume of cold 10% MPA/EDTA solution and vortex.

   If necessary, the samples can be frozen at −80°C at this stage to save time during sample collection. However, sample stability has not been properly evaluated for this procedure, and it is therefore recommended that samples stored in this way be analyzed within 2 weeks.

3. Microcentrifuge the mixture 1 min at 16,000 × *g*, 4°C.

4. Store the supernatant at −80°C and process within 6 months (see Basic Protocol).

   Sample stability has only been tested up to 6 months after preparation and may be longer. In general, the author stores plasma samples and other body fluids at −80°C or less and processes within 1 to 2 months.

SUPPORT PROTOCOL 2

Preparation of Isolated-Cell Samples

Most intact, viable cells are not prone to oxidation in the same way as plasma and isolated tissues are because any dehydroascorbic acid (DHA) formed is efficiently reduced to ascorbic acid (AA) intracellularly. Once acidified, however, the cells lose this ability and should be treated as other AA-containing samples.

Materials

Isolated cells in suspension (e.g., 2×10^6 hepatocytes/ml)
10% MPA/EDTA solution (see recipe), 4°C
Microcentrifuge (e.g., Eppendorf 5417R or equivalent), 4°C

1. Mix isolated cells in suspension with an equal volume of cold 10% MPA/EDTA solution and shake vigorously for 1 min.

   The intracellular concentrations of the analytes are measured here because the extracellular concentrations are negligible following the cell isolation procedure, which includes several washes (Berry et al., 1991).

2. Microcentrifuge the mixture for 1 min at 16,000 × *g*, 4°C.

   Some researchers use disruption of the cells prior to centrifugation, but in the author's experience this is not necessary. Meta-phosphoric acid (MPA) treatment results in quantitative release of the analytes (Lykkesfeldt and Ames, 1999).

3. Store the supernatant at −80°C and process within 1 month (see Basic Protocol).

   Sample stability has only been tested up to 1 month after preparation and may be longer. In general, the author stores cell samples at −80°C or less and processes them within 1 to 2 weeks.

Preparation of Tissue Samples

SUPPORT PROTOCOL 3

Tissues can be either snap-frozen in liquid nitrogen and stored at −80°C until homogenization or homogenized prior to storage.

Materials

Isolated intact organ
PBS (*APPENDIX 2A*) or 1.15% (w/v) potassium chloride, 4°C
5% MPA/EDTA solution (see recipe), 4°C

2-ml conical Potter-Elvehjem homogenizer, on ice
Stirring motor for homogenization (e.g., IKA Eurostar digital, part no. 2482000; IKA-Werke)
Microcentrifuge (e.g., Eppendorf 5417R or equivalent), 4°C

1. Quickly rinse an isolated intact organ in PBS or 1.15% potassium chloride.

   Alternatively, the organ can be perfused in situ depending on the desired experimental protocol.

2. Dry organ surfaces gently by blotting on a piece of lint-free tissue.

3. Snap-freeze the entire organ or a suitable, freshly cut block of tissue in liquid nitrogen and store ≤1 month at −80°C until sample preparation and analysis.

   The tissue, in particular a block of tissue, should be frozen immediately. Analysis can easily be performed on 10 mg tissue, so the amount of tissue that is saved depends largely on the number of other experiments intended and convenience. This step is omitted if tissues are homogenized immediately.

4. Quickly weigh out 20 to 40 mg frozen tissue and homogenize immediately in a final 50-fold dilution of cold 5% MPA/EDTA solution (e.g., 980 µl/20 mg tissue) using a 2-ml conical Potter Elvehjem homogenizer and stirring motor. Keep the homogenizer in an ice bath.

Mechanical glass-Teflon Potter-Elvehjem homogenizers usually work well for liver and brain tissue (2 to 3 min, 750 rpm), but for lung and muscle tissue the author uses a manual glass-glass homogenizer (without a stirring motor) for better and quicker disruption of the tissue.

The use of sonication or high-speed metal shaft homogenizers for tissue disruption is not recommended because the metal rods appear to facilitate catalyzed autooxidation.

5. Microcentrifuge the mixture 1 min at 16,000 × *g*, 4°C.
6. Process samples immediately (see Basic Protocol).

Alternatively, if using fresh tissue, the sample supernatant can be stored for ≤1 month at −80°C until analyzed. Sample stability has only been tested up to 1 month after preparation and may be longer. In general, the author stores tissue samples at −80°C or less and processes them within 1 to 2 weeks.

SUPPORT PROTOCOL 4

PASSIVATION OF AN HPLC SYSTEM

When using electrochemical detectors, liquid chromatography components made from stainless steel can contribute to baseline noise and high background current due to wash-off of electrochemically active substances from the metal surfaces. In order to maximize detector performance, the chromatographic system should be cleaned (passivated) once or twice a year or when the baseline noise is too high.

Additional Materials *(also see Basic Protocol)*

6 N nitric acid
Glacial acetic acid
Unions appropriate for the high-performance liquid chromatography (HPLC) system

1. Switch off the electrochemical cell and shut down the pump of an HPLC system and coulometric detector (see Basic Protocol).

It may not be necessary to turn off the actual electrochemical detector if the electrochemical cells can be switched off separately, in which case the detector can be left on for a quicker resumption of optimal performance.

2. Remove and cap the guard column, analytical column, and electrochemical cells (guard and detector cells) and replace them with appropriate unions.

By replacing the columns and electrochemical cells with unions, the entire system is passivated while bypassing the acid-incompatible parts.

3. Pump water through the system at 1 ml/min for 1 hr while inspecting for leaks.
4. Change the water to 6 N nitric acid and pump through the system at 1 ml/min for 30 min.
5. Switch the nitric acid over to glacial acetic acid. Pump the glacial acetic acid through the HPLC system at 1 ml/min for 30 min.
6. Change the glacial acetic acid to water and pump it through the system for ≥30 hr and make sure that the pH of the effluent is approximately ≥5.0.
7. Change to the original mobile phase and pump it through the system at 1 ml/min for 30 min. Turn off the pump and replace the unions with the guard column, analytical column, and electrochemical cells. Turn on the pump and subsequently the electrochemical cells and continue equilibration.

After a short equilibration period of the electrochemical detector cell (~2 hr) the system is ready for use, but full sensitivity is usually not restored until the following day.

QUANTIFICATION OF ASCORBIC ACID AND DEHYDROASCORBIC ACID USING SUBTRACTION METHODS WITH ENDOGENOUS AND/OR INTERNAL STANDARDS

With this subtraction method, both ascorbic acid (AA) and, following the reduction of any dehydroascorbic acid (DHA), total AA levels present in the sample are analyzed. The amount of DHA originally present is then calculated by subtraction of AA from total AA. This method is also used to quantify isoascorbic acid (IAA) and dehydroisoascorbic acid (DHIA). A more detailed discussion of the problems associated with this assay principle is given below (see Background Information). Depending on the origin of the biological material and the experimental design, uric acid (UA) and IAA can be used as endogenous and internal standards, respectively.

The Use of an Endogenous Standard to Correct for Intrasample Error of Analysis

Because UA is not affected by the tris(2-carboxyethyl)phosphine hydrochloride (TCEP) reduction step, this compound can conveniently be used to correct for intrasample error of analysis—such as that due to pipetting or the apparatus—between the paired nonreduced and reduced samples. Because >99% of ascorbic acid found in biological samples isolated under nonstressing conditions is in the reduced form, this correction greatly reduces the error in the subsequent DHA (or DHIA) calculation and is therefore highly recommended. If UA is not present in the biological material under investigation, an appropriate amount (~100 μM final concentration) of exogenous UA can be added prior to sample workup. However, because additional sample handling may contribute to oxidation, this should be used primarily for optimizing procedures using test samples.

Use the following formulas for the correction:

$$AA_C = AA \times (UA_T/UA)$$
$$DHA = AA_T - AA_C$$

where AA_C is the AA concentration after correction, UA, AA, UA_T, and AA_T, are the UA and AA concentrations in the nonreduced and reduced samples, respectively. AA can be exchanged with IAA to determine the quantity of DHIA in the sample.

The Use of an Internal Standard to Correct for Artifactual Sample Oxidation

Regardless of any measures taken to avoid artifactual oxidation of AA, oxidation will occur—if not during sample collection and/or sample preparation, then during the analysis itself (i.e., on the HPLC instrument)—resulting in the production of DHA. This is particularly true for the nonreduced sample, but, even for the reduced sample, minute amounts of oxidized metabolite may be formed when AA is separated from the reducing agent on the column. For example, in samples from control material (e.g., healthy nonsmoking humans), the artifactual oxidation will constitute the majority if not all of the measured DHA (typically ~1% to 4% of the measured AA concentration). Addition of IAA to a set of samples at the time of collection or at the time of analysis can help reveal the origin and amount of artifactual oxidation during the different steps of the assay in a particular laboratory. However, due to the autooxidation of IAA itself, it may not be practical to use IAA as a general internal standard if multiple samples are collected over time as in a clinical setting. Also, the biological material should be checked to confirm that IAA is not naturally present before it is used as a standard (see Anticipated Results). When an internal standard is included, the following formula can be used to estimate the artifactual oxidation of AA:

$$DHA_C = AA_T - (AA_C \times IAA_T/IAA_C)$$

where DHA_C represents the corrected concentration of DHA; IAA_T is the total amount of IAA added; and IAA_C is the amount of IAA measured by HPLI after correction for UA as described above. Although AA and IAA have identical redox properties (Iheanacho et al., 1995), this simple equation does not take into account that the AA or IAA oxidation rate is also concentration dependent. In order to limit this error, the amount of IAA used should be in the same range as that of AA in the sample.

REAGENTS AND SOLUTIONS

*Use Milli-Q-purified water or equivalent for all recipes and protocol steps. For common stock solutions, see **APPENDIX 2A**; for suppliers, see **SUPPLIERS APPENDIX**.*

McIlvaine buffer

Dissolve 89 g $Na_2HPO_4 \cdot 2H_2O$ in 500 ml water (1 M final). Dissolve 52.5 g citric acid monohydrate in 500 ml water (0.5 M final). Adjust the pH of the citrate solution to 4.5 by adding the sodium phosphate solution (~415 ml). Filter through a 0.22-µm filter and store up to 1 year, or longer, at room temperature.

Mobile phase

Solution A:

Dissolve 17.8 g sodium dihydrogen phosphate monohydrate (129 mM final), 17.6 g anhydrous sodium acetate (215 mM final), 372 mg Na_2EDTA (1.0 mM final), and 50 mg dodecyltrimethylammonium chloride (189 µM final) in 750 ml water.

Solution B:

Dissolve 20 mg tetraoctylammonium bromide (36.6 µM final) in 250 ml methanol.

To make ~1 liter mobile phase, mix 750 ml solution A with 250 ml solution B and adjust the pH of the mixture to 5.4 with *ortho*-phosphoric acid. Store up to 1 month, or longer, at room temperature. Sonicate the mobile phase 5 min and filter on a vacuum filtration system using 0.2-µm PVDF filter membranes.

The author routinely prepares 10-liter batches.

MPA/EDTA solution, 10%

Dissolve 5.0 g *meta*-phosphoric acid (MPA) in 40 ml water (10% w/v final) and add 10 ml 10 mM Na_2EDTA (372 mg/100 ml; 2.0 mM final). Stir or shake at room temperature until the solution is homogenous (~5 to 10 min) and store at 4°C. Make fresh every 3 weeks.

For 5% MPA/EDTA, dilute 10% solution 1:1 with water.

Standard mixture

For uric acid standard:

Dissolve 8.4 mg uric acid (UA) in 100 ml 10% MPA/EDTA solution (see recipe; 0.5 mM final UA). Heat mixture 15 min at 90°C and leave to cool to facilitate dissolution. Store in 600-µl aliquots up to 6 months, or longer, at −80°C.

For ascorbic and isoascorbic acid standards:

Add 44.0 mg ascorbic acid (AA) to 250 ml water (1 mM final) at room temperature. Simultaneously dissolve 44.0 mg isoascorbic acid (IAA) in 250 ml water at room temperature. Dissolve both by inversion.

For standard mixture:

Immediately mix 50 µl 1 mM AA and 50 µl 1 mM IAA with 500 µl cold 0.5 mM UA and dilute to 1 ml with 400 µl water. Make AA and IAA solutions and the final standard mixture immediately prior to preparation of the standard curve.

When used undiluted, this standard mixture corresponds to plasma concentrations of 100 µM AA, 100 µM IAA, and 500 µM UA.

TCEP solution

Dissolve 0.72 mg tris(2-carboxyethyl)phosphine hydrochloride (TCEP, 2.5 mM final) per 1 ml 800 mM Tris buffer, pH 9.0 (see recipe). Make fresh each day.

Tris buffer, 800 mM, pH 9.0

Dissolve 9.69 g tris(hydroxymethyl)aminomethane (Tris) in 90 ml water, adjust the pH to 9.0 with ortho-phosphoric acid, and dilute to 100 ml with water. Store up to 1 month, or longer, at 4°C.

This buffer is stable for at least a year at −20°C.

COMMENTARY

Background Information

Accurate and reproducible measurements of ascorbic acid (AA) and dehydroascorbic acid (DHA) are necessary prerequisites for their application as biomarkers of oxidative stress as well as for understanding their roles in biology. AA has been referred to as "the most important water-soluble antioxidant in plasma" (Frei et al., 1989). It acts as a major radical scavenger in vivo as well as in regenerating other antioxidants such as vitamin E. AA predominately exists in its reduced state in vivo. Upon oxidation via the semidehydroascorbyl radical, the resulting DHA is transported into erythrocytes, and AA is subsequently regenerated intracellularly by one of several possible mechanisms. If not reduced, DHA is hydrolyzed irreversibly to 2,3-diketoglulonic acid, which has no antiscorbutic or antioxidant activity. The concentrations of AA and DHA in such samples as plasma, isolated cells, and tissues have been used as markers of oxidative stress levels in a variety of experiments ranging from test tube cellular biology to animal models and clinical trials (Lykkesfeldt et al., 1996, 1997, 1998, 2000; Hagen et al., 1998, 1999; Poulsen et al., 1998; Lykkesfeldt and Ames, 1999).

Assessment of AA concentrations in plasma is routinely performed in many laboratories. A wide variety of methods have been presented over the last decades employing spectrophotometry; fluorometry; gas chromatography; enzymatic assays; and capillary electrophoresis HPLC with UV, fluorescence, or electrochemical detection (reviewed by Rumsey and Levine, 2000). In some cases, AA has been measured as DHA following oxidation. Most methods of AA measurement, in particular HPLC-based methods, are capable of producing valid results if the precautions described below (see Critical Parameters and Troubleshooting) are taken. Some postsampling oxidation can even be eliminated by using tris(2-carboxyethyl)phosphine hydrochloride (TCEP) as the reductant as described in the Basic Protocol.

In contrast to AA measurements, quantification of DHA is a substantial challenge for several reasons. First of all, DHA is a highly labile compound with a half-life of only a few minutes at neutral pH (Bode et al., 1990). AA is converted to DHA nonenzymatically, and, practically speaking, it is not possible to completely avoid artifactual DHA formation at a concentration equal to a few percent of the AA in the sample unless the experiment is carried out in an oxygen-free environment. Also, DHA can be irreversibly hydrolyzed as mentioned above and thereby lost from the AA pool. Second, whereas detection of AA by coulometry is both selective and highly sensitive, no direct and sensitive method exists for the detection of DHA. Consequently, each assay principle employed for DHA involves tradeoffs. Precolumn, postcolumn, or in-line derivatization of DHA in combination with HPLC with fluorescence detection is used in the analysis of foodstuffs where the concentration of DHA is considerable (Ali and Phillippo, 1996; Kall and Andersen, 1999). However, the methods are not sensitive enough to quantify the minute amounts found in biological systems. Mass-spectrometry methods have also been employed in DHA analysis (Deutsch and Kolhouse, 1993). Although these methods have the ability to quantify small amounts, sample preparation is tedious and the operation requires very expensive equipment and often highly specialized staff. Moreover, derivatization techniques in general have the drawback of unintentionally shifting the equilibrium between AA and DHA instead of preserving it.

A different methodology of DHA quantification is the so-called subtraction method described in the Basic Protocol. Here AA is measured in one aliquot of a sample followed by

measurement of total AA (i.e., AA and DHA) in a second aliquot of the same sample. Subsequently, the DHA concentration can be indirectly assessed by subtracting the measured AA concentration from the total AA concentration. The major drawback of this assay principle is that AA and total AA concentrations are similar and usually many-fold greater than the concentration of DHA. Consequently, the resulting DHA concentration is encumbered with a relatively large error compared with a directly measured concentration. As discussed below (see Anticipated Results), one must realize that no existing method for the measurement of DHA is ideal and can completely eliminate the artifactual postsampling formation of the compound. However, the more useful and recent methods have incorporated various measures to limit this error.

Another inconvenience of subtraction methods is that the reducing agent used for the total AA measurement often has to be removed prior to HPLC analysis because of chromatographic interference. Dithiothreitol (DTT) is a convenient and powerful reducing agent commonly used in total AA analysis. However, although removal of DTT is usually not necessary before HPLC separation, the pH at which samples are usually stored in the autosampler is too low (typically <3) for DTT to have any ability to keep AA reduced. In the case of both removal and inactivity of the reducing agent, the stability of AA in the reduced samples is compromised, and rapid analysis is necessary to obtain valid results. In contrast, the reducing agent TCEP used in the Basic Protocol appears to be ideal for total AA measurement. It does not interfere with the chromatography and remains active at pH 4.5, the pH at which the samples are stored and remain stable.

The method described in the Basic Protocol is modified from Lykkesfeldt (2000) and offers several important and convenient advantages: (1) it is fast and accurate and based on a sensitive and specific analytical principle; (2) it has successfully been employed in the analysis of a wide variety of biological materials; (3) the reduced samples are stable for days, even at room temperature; (4) tedious removal of the reductant from the reduced samples prior to analysis is neither required nor desired; (5) endogenous and/or internal standards can be used to eliminate the intrasample error resulting from the subtraction methodology and to estimate the artifactual oxidation, respectively; and 6) in addition to AA and DHA, the method offers superior separation and co-analysis of IAA, UA, and, subsequently, calculation of DHIA by subtraction.

Critical Parameters and Troubleshooting

One of the most important determinants of accurate assessment of AA, IAA, and their oxidized metabolites is time. The importance of fast and meticulous sample collection, stabilization, storage, and preparation cannot be emphasized enough, as it is by far the most common reason for unanticipated results (Lykkesfeldt et al., 1995). If only the total amount of AA or IAA is of interest, the time factor is less critical albeit still important. Due to their superior stability, reduced samples prepared with TCEP are highly recommended even when the DHA or DHIA concentration is not desired. In comprehensive clinical trials, it may simply not be feasible to measure DHA if proper sample collection is not possible. Decisions regarding which of the biomarkers will be measured should therefore be made in advance so that methods to ensure proper sample handling can be taken into account in the planning phase.

When samples are collected and prepared as described in this unit, the sample stability is relatively good. However once thawed, the samples start to oxidize, and analysis of samples that have previously been thawed for other purposes or reanalysis of samples will usually not give proper results. In other words, one only has a single chance of getting it right per sample. Consequently, it is highly advisable to store biological samples in separate aliquots whenever possible.

The presence of hemolysis in plasma samples should be avoided because the resulting increase in iron concentration greatly facilitates oxidation of AA and IAA. When analyzing tissue, perfusing the tissue prior to sample collection can limit the contamination of iron from hemolysis. Tissue concentrations of AA are usually ~20- to 50-fold higher than those of plasma, so the AA contribution from the blood is very limited.

No matter how carefully the sample collection and preparation are planned and carried out, other problems such as a power failure can ruin the experiment. A power failure will stop the sample analysis, cooling of the autosampler, and data collection as a whole, whereas a deep momentary sag in voltage may often just turn off the sensitive coulometric detector resulting

in continued sample separations without detection and data collection. As mentioned above, reanalysis of the nonreduced samples is not a valid option in most cases. Besides saving several aliquots whenever possible as assurance against this type of problem, the author has installed an uninterruptible power supply (UPS). This unit supplies the power for two complete HPLC systems with attached detectors and interface units as well as the computer workstation used for controlling the equipment and data collection (the computer monitor has been left out of the UPS circuit to conserve battery power). The system will maintain full operation on both HPLC systems for ~2 hr during a full power failure. Of equal importance is the complete protection the UPS offers from momentary sags in voltage, which could otherwise accidentally turn off the coulometric detector.

Anticipated Results

AA concentrations vary considerably depending on the species, tissue type, or body fluid under investigation. In most mammalian species, tissues have AA concentrations in the low millimolar range, whereas plasma concentrations usually fall between 10 and 100 μM. IAA is not a naturally occurring compound in animals and will therefore normally not be detectable in fasted subjects. However, in plasma samples taken from humans postprandially, the IAA concentration can amount to as much as 30% of that of AA because IAA is commonly used as a food additive (Sauberlich et al., 1991). The limit of detection for this assay, which is well below these levels (<1 pmol per injection), is not an issue for most applications.

Regarding DHA or DHIA measurements, it is important to realize the limitations of not only the method presented in this unit but also any available method for DHA or DHIA measurement. Most researchers in the field agree that in a normal biological sample (e.g., a plasma sample from a healthy nonsmoking individual), the concentration of DHA is very close to zero in vivo. But artifactual oxidation will occur during sample collection, preparation, and analysis. Even if one is successful in limiting these undesirable events, DHA or DHIA concentrations of up to a few percent of the AA and IAA concentrations, respectively, will commonly be found. It is important to understand that this fact is independent of whether a subtraction method like the one present here or a direct assay is used. Consequently, practice and inclusion of proper controls is the only way of making sure that the assay is correctly performed.

Unfortunately, the true difficulties in measuring DHA and the major risk of artifactual oxidation of AA have been ignored until recently and are only starting to be more widely recognized. Consequently, a considerable proportion of the existing literature on DHA and even recently published papers continue to report values that clearly show artifactually elevated concentrations of DHA of up to 30% of the total AA in healthy subjects. A sound rule of thumb is that the AA pool in plasma, cells, and tissues of normal and healthy origin is >99% reduced in vivo. This starting point combined with meticulous practice and optimization of the procedures will help minimize artifactual formation of DHA in future experiments. Postsampling oxidation of IAA results in artifactual formation of DHIA, and thus all concerns about AA oxidation apply to IAA as well.

Time Considerations

Time is a vital parameter in the collection and stabilization of samples intended for ascorbate analysis as well as in sample preparation and analysis.

The actual sample preparation should be performed as close to the time of analysis as possible due to the lability of the analytes. However, most of the reagents for the assay can be made in advance, and the sample preparation is relatively simple. Thus once in operation, this assay is quick and allows the analysis of up to ~100 samples per day (i.e., 50 samples, nonreduced and reduced) prepared in batches of 8 to 20. The number of samples processed in one batch depends on how quickly the various steps can safely and adequately be performed. The time from when the samples are thawed to when they are placed in the autosampler should be ≤10 to 15 min. Preparation of 100 samples will take 1 to 2 hr followed by HPLC analysis for <12 hr. Although more samples could easily be prepared in a day, it is not recommended to extend the time in the autosampler beyond 10 to 12 hr for samples without reductant, and the less time spent in the autosampler the better. For long runs, a standard sample without reductant can be included for every ten samples to monitor stability. Alternatively, because the run time is normally only 5 to 7 min, the samples of the day can be prepared in two or three portions with 2 to 3 hr between each, thereby reducing the autosampler storage time for the

later samples. In contrast to samples without reductant, samples containing TCEP are stable for ≥4 days in the autosampler (Lykkesfeldt, 2000).

Equilibration of a new analytical column takes considerable time, indicating a slow modification of the stationary phase. If a separate HPLC pump is available, a spare column can conveniently be equilibrated in advance and stored in the mobile phase. Do not begin sample preparation of the biological material before making sure that the column is sufficiently equilibrated and operational. Once equilibrated, the column will usually run thousands of samples before it needs to be replaced. The guard column is changed whenever the back pressure becomes markedly increased. The author routinely starts up the HPLC system and runs a few blanks followed by a standard from the previous day (it takes ~30 min, including a 10-min start-up period) to verify that the equipment is working properly, while preparing the day's standards and reagents. This also appears to stabilize the response of the electrochemical cell. This procedure ensures that the system is working as it should before preparation of the biological samples is initiated.

After extended use, when the column starts to fail in performance, it should be replaced, and the new column thoroughly equilibrated and/or tested before continuing sample analysis. The old column may be used for other purposes, but trying to clean it with solvents or otherwise restore its performance for AA separation is not recommended due to the extensive equilibration time needed afterwards combined with the uncertainty of the outcome.

Literature Cited

Ali, M.S. and Phillippo, E.T. 1996. Simultaneous determination of ascorbic, dehydroascorbic, isoascorbic, and dehydroisoascorbic acids in meat-based food products by liquid chromatography with postcolumn fluorescence detection: A method extension. *J. AOAC Int.* 79:803-808.

Berry, M.N., Edwards, A.M., and Barritt, G.J. 1991. Laboratory Techniques in Biochemistry and Molecular Biology, Vol. 21: Isolated Hepatocytes: Preparation, Properties and Applications. Elsevier/North-Holland, Amsterdam.

Bode, A.M., Cunningham, L., and Rose, R.C. 1990. Spontaneous decay of oxidized ascorbic acid (dehydro-L-ascorbic acid) evaluated by high-pressure liquid chromatography. *Clin. Chem.* 36:1807-1809.

Deutsch, J.C. and Kolhouse, J.F. 1993. Ascorbate and dehydroascorbate measurements in aqueous solutions and plasma determined by gas chromatography-mass spectrometry. *Anal. Chem.* 65:321-326.

Frei, B., England, L., and Ames, B.N. 1989. Ascorbate is an outstanding antioxidant in human blood plasma. *Proc. Natl. Acad. Sci. U.S.A.* 86:6377-6381.

Hagen, T.M., Ingersoll, R.T., Wehr, C.M., Lykkesfeldt, J., Vinarsky, V., Bartholomew, J.C., Song, M.H., and Ames, B.N. 1998. Acetyl-L-carnitine fed to old rats partially restores mitochondrial function and ambulatory activity. *Proc. Natl. Acad. Sci. U.S.A.* 95:9562-9566.

Hagen, T.M., Ingersoll, R.T., Lykkesfeldt, J., Liu, J., Wehr, C.M., Vinarsky, V., Bartholomew, J.C., and Ames, B.N. 1999. (R)-alpha-lipoic acid-supplemented old rats have improved mitochondrial function, decreased oxidative damage, and increased metabolic rate. *FASEB J.* 13:411-418.

Iheanacho, E.N., Hunt, N.H., Stocker, R. 1995. Vitamin C redox reactions in blood of normal and malaria-infected mice studied with isoascorbate as a nonisotopic marker. *Free Radic. Biol. Med.* 18:543-552.

Kall, M.A. and Andersen, C. 1999. Improved method for simultaneous determination of ascorbic acid and dehydroascorbic acid, isoascorbic acid and dehydroisoascorbic acid in food and biological samples. *J. Chromatogr. B Biomed. Sci. Appl.* 730:101-111.

Lykkesfeldt, J. 2000. Determination of ascorbic acid and dehydroascorbic acid in biological samples by high-performance liquid chromatography using subtraction methods: Reliable reduction with Tris[2-carboxyethyl]phosphine hydrochloride. *Anal. Biochem.* 282:89-93.

Lykkesfeldt, J. and Ames, B.N. 1999. Ascorbic acid recycling in rat hepatocytes as measurement of antioxidant capacity: Decline with age. *Methods Enzymol.* 299:83-88.

Lykkesfeldt, J., Loft, S., and Poulsen, H.E. 1995. Determination of ascorbic acid and dehydroascorbic acid in plasma by high-performance liquid chromatography with coulometric detection—are they reliable biomarkers of oxidative stress? *Anal. Biochem.* 229:329-335.

Lykkesfeldt, J., Prieme, H., Loft, S., and Poulsen, H.E. 1996. Effect of smoking cessation on plasma ascorbic acid concentration. *Br. Med. J.* 313:91.

Lykkesfeldt, J., Loft, S., Nielsen, J.B., and Poulsen, H.E. 1997. Ascorbic acid and dehydroascorbic acid as biomarkers of oxidative stress caused by smoking. *Am. J. Clin. Nutr.* 65:959-963.

Lykkesfeldt, J., Hagen, T.M., Vinarsky, V., and Ames, B.N. 1998. Age-associated decline in ascorbic acid concentration, recycling, and biosynthesis in rat hepatocytes: Reversal with (R)-alpha-lipoic acid supplementation. *FASEB J.* 12:1183-1189.

Lykkesfeldt, J., Christen, S., Wallock, L.M., Chang, H.H., Jacob, R.A., and Ames, B.N. 2000. Ascorbate is depleted by smoking and repleted by moderate supplementation: A study in male

smokers and nonsmokers with matched dietary antioxidant intakes. *Am. J. Clin. Nutr.* 71:530-536.

Poulsen, H.E., Loft, S., Prieme, H., Vistisen, K., Lykkesfeldt, J., Nyyssonen, K., and Salonen, J.T. 1998. Oxidative DNA damage in vivo: Relationship to age, plasma antioxidants, drug metabolism, glutathione-*S*-transferase activity and urinary creatinine excretion. *Free Radic. Res.* 29:565-571.

Rumsey, S.C. and Levine, M. 2000. Vitamin C. *In* Chemical Analysis, Vol. 154: Modern Analytical Methodologies in Fat- and Water-Soluble Vitamins (W.O. Song, G.R. Beecher, and R.R. Eitenmiller, eds.) pp. 411-445. John Wiley & Sons, New York.

Sauberlich, H.E., Wood, S.M., Tamura, T., Freeberg, L.E. 1991. Influence of dietary intakes of erythorbic acid on plasma vitamin C analyses. *Am. J. Clin. Nutr.* 54:1319S-1322S.

Key References

Lykkesfeldt, 2000. See above.

The method on which the Basic Protocol is based. Includes stability data and reduction kinetics for TCEP.

Rumsey and Levine, 2000. See above.

Critical and comprehensive review of vitamin C analysis.

Contributed by Jens Lykkesfeldt
Royal Veterinary and Agricultural University
Copenhagen, Denmark

CHAPTER 8
Heme Synthesis Pathway

INTRODUCTION

Heme is essential for the function of all aerobic cells. As the prosthetic group of the heme proteins—a category that includes hemoglobin, myoglobin, mitochondrial and microsomal cytochromes, catalase, peroxidase, tryptophan pyrrolase, and nitric oxide synthase—heme catalyzes reactions involved in oxygen and electron transport, in the oxidative metabolism of various endogenous and exogenous chemicals, in the decomposition of hydrogen peroxide and organic peroxides, in the oxidation of tryptophan, and in the synthesis of nitric oxide. There is approximately 500 to 700 g of hemoglobin (of which 3.8% is heme) in the body of a normal 70-kg adult man. Approximately 85% of heme is synthesized in the erythropoietic bone marrow, and the remainder largely by the liver. Hepatic heme synthesis undergoes a marked induction when cytochrome P-450 synthesis is stimulated.

Inherited deficiencies or acquired defects of enzymes in the heme biosynthetic pathway lead to the disorders of heme biosynthesis, as described in *UNIT 8.1* A number of conditions, such as metal poisoning, environmental chemical exposure, drug induction, inflammation, heat shock and stress reactions, and hypoxia, can also influence the rate of heme biosynthesis and therefore the quantity of heme protein present (Fig. 8.0.1).

Figure 8.0.2 illustrates the steps involved in heme biosynthesis, with the relevant enzymes, as well as inherited enzymatic deficiencies and acquired enzymatic defects relating to this pathway. The nonspecific δ-aminolevulinate synthase (ALAS1) is under negative feedback control by heme, the end-product of the pathway, but may undergo marked induction when hepatic cytochrome P-450 synthesis is stimulated by drug treatment. Because ALAS1 induction and inhibition by chemicals (*UNIT 8.2*) directly influence cytochrome P-450 level and heme concentration (*UNIT 8.3*), this enzyme is critically important in hepatic toxicology. The erythroid-specific ALAS (ALAS2) is essential for erythroid heme syn-

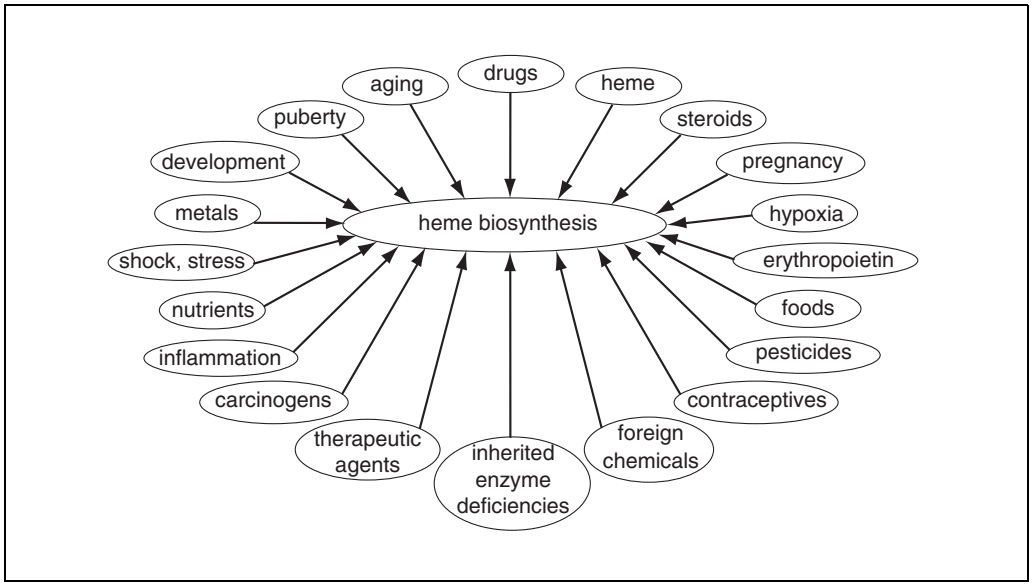

Figure 8.0.1 Conditions that influence heme biosynthesis.

Contributed by Shigeru Sassa and Mahin D. Maines
Current Protocols in Toxicology (2001) 8.0.1-8.0.3

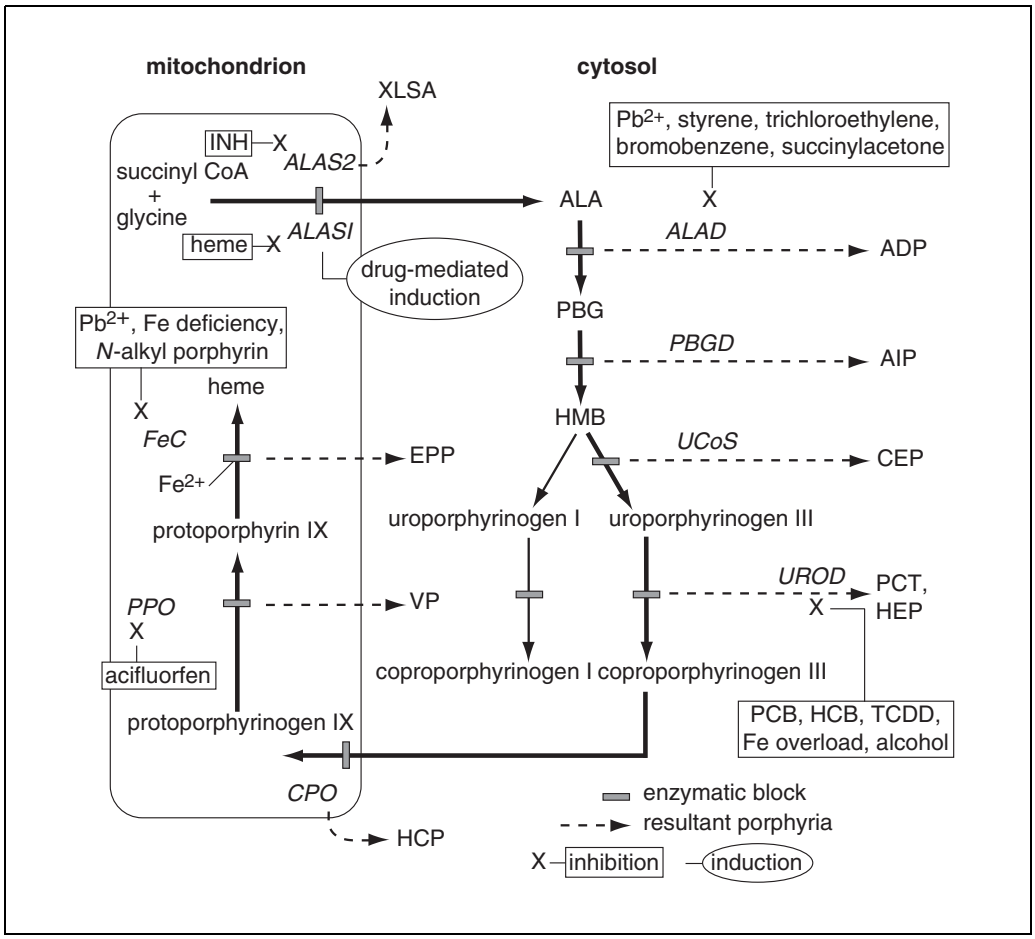

Figure 8.0.2 Heme biosynthetic pathway. Inherited enzymatic deficiencies (in boldface) and acquired enzymatic defects (with the enzyme names in italics) are indicated. Abbreviations: ADP, ALAD deficiency porphyria; AIP, acute intermittent porphyria; ALAD, δ-aminolevulate dehydratase; ALAS, δ-aminolevulinate synthase; CPO, coproporphyrinogen oxidase; EPP, erythropoietic protoporphyria; FeC, ferrochelatase; HCB, hexachlorobenzene; HCP, hereditary coproporphyria; HEP, hepatoerythropoietic porphyria; HMB, hydroxymethylbilane; INH, isonicotinic acid hydrazide; PCT, porphyria cutanea tarda; PBGD, porphobilinogen deaminase; TCDD, 2,3,7,8-tetrachlorodibenzo-*p*-dioxin; UCoS, uroporphyrinogen III cosynthase; UROD, uroporphyrinogen decarboxylase; VP, variegate porphyria; XLSA, X-linked sideroblastic anemia.

thesis, and its inherited deficiency, or inhibition by chemicals such as isoniazid, results in sideroblastic anemia (Fig. 8.0.2).

Four major heme-synthetic enzymes that are the targets of toxic effects by chemicals are ALA dehydratase (ALAD), uroporphyrinogen decarboxylase (UROD), protoporphyrinogen oxidase (PPO), and ferrochelatase (FeC). Inhibition of these enzymes results in conditions that mimic the porphyrias caused by corresponding inherited enzyme deficiencies (Fig. 8.0.2). As discussed in *UNIT 8.6*, ALAD represents one of the most sensitive sites of inhibition of heme biosynthesis by toxicological substances, including lead, styrene oxide, bromobenzene, and trichloroethylene. As described in *UNIT 8.4*, UROD activity can be inhibited by hexachlorobenzene, polychlorinated biphenyls, or dioxins, while as discussed in *UNIT 8.5*, PPO activity is specifically inhibited by acifluorfens, which because of this property are used as herbicides. Like ALAD, FeC is vulnerable to inhibition by heavy metal ions such as lead and mercury; its activity is also additionally decreased by iron deficiency and inhibited by N-alkyl porphyrins, i.e., degradation products of the heme moiety of P-450 (*UNIT 8.7*). Disruption of FeC activity leads to an accumulation of Zn-protoporphyrin in erythrocytes. Measurement of erythrocyte protoporphyrin is used

as an important clinical test for childhood lead poisoning (*UNIT 8.8*). Heme biosynthesis, therefore, is of special interest in environmental toxicology.

Differential response of heme biosynthetic pathway enzymes to drugs and environmental chemicals may result in changes in urinary, blood, tissue, and/or fecal patterns of porphyrin composition. Detecting these changes is a useful diagnostic tool. This analysis requires a relatively rapid and effective procedure for porphyrin separation and measurement. *UNIT 8.9* describes an HPLC method which meets all the stated required criteria.

Shigeru Sassa and Mahin D. Maines

The Heme Biosynthesis Pathway and Clinical Manifestations of Abnormal Function

The biosynthesis of heme is an essential process in both prokaryotes and eukaryotes. A multienzyme pathway is used in all species to convert simple precursor molecules to the complex tetrapyrrole protoporphyrin IX. Ferrous iron is then complexed with protoporphyrin IX to form heme (Fig. 8.1.1). The chemistry of porphyrins and the fully reduced porphyrinogens is unique. It is not surprising, therefore, that the enzymes comprising the heme biosynthetic pathway are highly homologous in all species. In humans, both inherited and acquired factors (such as exposure to drugs or environmental toxins) affect the activities of heme biosynthetic enzymes, giving rise to a group of diseases known collectively as the porphyrias (Kappas et al., 1995).

Porphyrins are intensely colored (the term porphyrin is derived from the Greek *porphuros*, meaning red-purple) and they display strong light absorption in the Soret band of the spectrum (~400 nm). Porphyrins fluoresce and it is this property that mediates cellular damage in the skin of patients with several types of porphyria. Although the porphyrin precursors δ-aminolevulinic acid (ALA) and porphobilinogen (PBG) do not fluoresce, neurovisceral symptoms occur when they are present in excess. These neurovisceral symptoms are extremely varied and are usually episodic. It is not known if the neurologic abnormalities are mediated by toxic effects of ALA or PBG, or by a deficiency of heme in neural cells.

Porphyric disorders in which only porphyrins are produced in excess are characterized clinically by photosensitivity restricted to light-exposed areas. Porphyric disorders in which ALA, PBG, or both are produced in excess are characterized by abdominal colic, peripheral neuropathy, paralysis, psychosis, and even coma. When both porphyrins and porphyrin precursors are produced in excess, both photosensitivity and neurovisceral manifestations are found. A practical classification of the porphyrias, based on the predominant clinical manifestations, is presented in Table 8.1.1.

Inherited heme biosynthetic defects are responsible for most forms of porphyria, but these defects are not the only abnormalities of heme biosynthesis that have clinical importance. For example, iron deficiency affects ferrochelatase activity and protoporphyrin accumulates in iron-deficient red cells. Lead, mercury, arsenic, and other metals may affect heme biosynthesis in humans (Daniell et al., 1997). Lead affects the pathway by inhibiting δ-aminolevulinate dehydratase (ALAD) and it probably also affects the function of coproporphyrinogen oxidase (CPO) and ferrochelatase (Dailey, 1997). Both ALA and porphyrins are excreted in excess in patients with lead poisoning, and the clinical syndrome, in particular the characteristic abdominal pain, resembles an acute porphyric attack.

A number of chemicals, particularly halogenated aromatic hydrocarbons, cause inhibition of hepatic uroporphyrinogen decarboxylase (UROD) activity and produce a syndrome biochemically identical to porphyria cutanea tarda (PCT; Wyckoff and Kushner, 1994). Finally, an uncommon X-linked anemia—characterized by microcytic circulating red cells, iron-laden mitochondria in red cell precursors (ringed sideroblasts), and markedly reduced synthesis of porphyrins and heme—results from mutations in the erythroid-specific form of δ-aminolevulinate synthase (ALAS; Wyckoff and Kushner, 1994).

This overview will emphasize the genetics, biochemistry, and clinical description of the porphyrias, but some of the nonporphyric disorders will also be described. Each step in the heme biosynthetic pathway will be reviewed, including the enzyme mechanism if known, molecular characterization of the relevant genes, disease phenotype, and interacting toxic mediators.

ALA SYNTHASE (ALAS)

Most of the ALA formed on earth is synthesized by plants, photosynthetic algae, and a majority of bacteria via a pathway designated the five-carbon pathway. Glutamate supplies the five-carbon backbone and three enzymes are required: glutamyl tRNA synthase, glutamyl tRNA reductase, and glutamyl 1-semialdehyde aminotransferase (Dailey, 1995). In animals and some bacteria, ALA is formed by the condensation of a glycine with succinyl-CoA (Fig. 8.1.1). In eukaryotes, the enzyme catalyzing the formation of ALA is ALA synthase (ALAS). ALAS is synthesized on ribosomes in the cytosol and then translocated to the mitochondrial matrix, the site of succinyl-

Contributed by John D. Phillips and James P. Kushner

Current Protocols in Toxicology (1999) 8.1.1-8.1.10

CoA generation by the tricarboxylic acid cycle. Pyridoxal 5′ phosphate (PLP) is a required cofactor for ALAS, and the first step in the synthesis of ALA is the formation of an enzyme-PLP-glycine Schiff base complex. The α-carbon of glycine is then deprotonated to yield a stabilized carbanion species. Succinyl-CoA then reacts with the complex and CoA is released. Finally, glycine is decarboxylated, stereospecific addition of a proton occurs, and ALA is released (Dailey, 1995).

Mammals and other higher animals express two forms of ALAS, a "housekeeping" form present in all tissues (ALAS1) and an erythroid-specific form (ALAS2; Wyckoff and Kushner, 1994; Kappas et al., 1995). The two forms of ALAS are encoded by two separate genes on different chromosomes (ALAS1 on 3p21 and

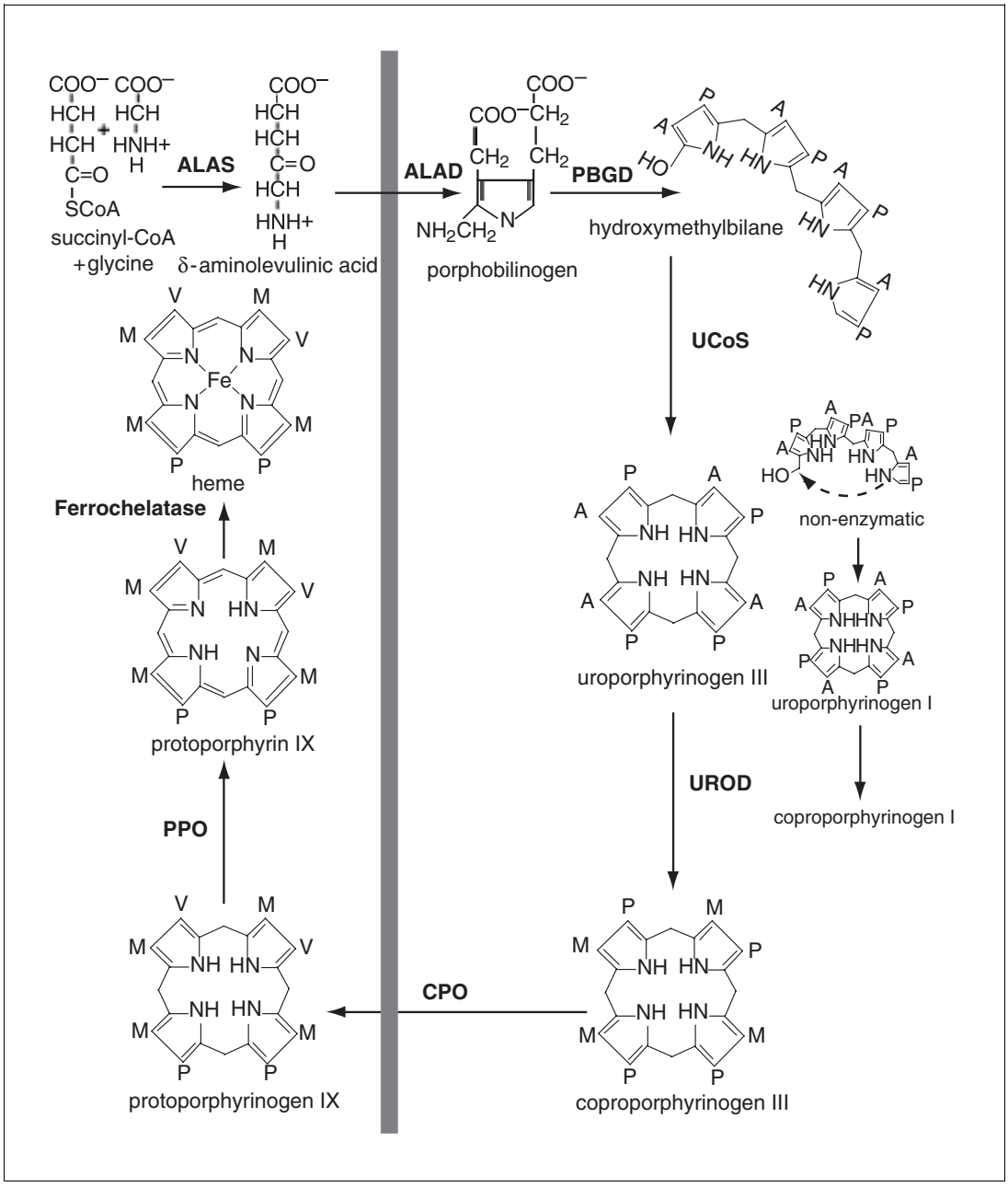

Figure 8.1.1 The heme biosynthetic pathway. Enzymatic reactions to the left of the broad shaded line occur in mitochondria. Reactions to the right of the line occur in the cytosol. Coproporphyrinogen oxidase (CPO) is located in the intermembrane space bordered by the inner and outer mitochondrial membranes. Enzymes that catalyze the reactions are indicated. Abbreviations: ALAS, δ-aminolevulinate synthase; ALAD, δ-aminolevulinate dehydratase; PBGD, porphobilinogen deaminase; UCoS, uroporphyrinogen III cosynthase; UROD, uroporphyrinogen decarboxylase; PPO, protoporphyrinogen oxidase; side chains: A, $-CH_2COO-$; P, $-CH_2CH_2COO-$; V, -CH=CH; M, $-CH_3$.

Table 8.1.1 Classification of the Porphyrias[a]

Classification	Deficient enzyme	Inheritance	Drugs or toxins involved	Laboratory findings		
				Red cells	Urine	Stool
Cutaneous photosensitivity						
Congenital erythropoietic porphyria (CEP)	Uroporphyrinogen III cosynthase	Recessive	No	Uroporphyrin I and coproporphyrin I	Uroporphyrin I	Coproporphyrin I
Porphyria cutanea tarda (PCT)	Uroporphyrinogen decarboxylase	Variable[b,c]	Yes	NA	Uroporphyrin, 7-COOH porphyrin	Isocoproporphyrin
Erythropoietic protoporphyria (EPP)	Ferrochelatase	Dominant[b]	No	Protoporphyrin	NA	Protoporphyrin
Neurovisceral symptoms						
ALAD deficiency porphyria (ADP)	ALA-dehydratase	Recessive	Yes	Zn-protoporphyrin	ALA	NA
Acute intermittent porphyria (AIP)	PBG deaminase	Dominant[b]	Yes	NA	ALA and PBG	NA
Neurovisceral and cutaneous manifestations						
Hereditary coproporphyria (HCP)	Coproporphyrinogen oxidase	Dominant[b]	Yes	NA	ALA, PBG, and coproporphyrin	Coproporphyrin
Variegate porphyria (VP)	Protoporphyrinogen oxidase	Dominant[b]	Yes	NA	ALA, PBG, and coproporphyrin	Coproporphyrin and protoporphyrin

[a]Abbreviations: ALA, δ-aminolevulinic acid; PBG, porphobilinogen; NA, not applicable.

[b]Homozygous or compound heterozygous cases have been described.

[c]PCT is transmitted as an autosomal dominant trait in some families, but in many cases no inherited defect in uroporphyrinogen decarboxylase can be demonstrated. The homozygous or compound heterozygous form of uroporphyrinogen decarboxylase deficiency is known as hepatoerythropoietic porphyria (HEP).

ALAS2 on Xq11.21). ALAS1 is the rate-limiting step in the heme biosynthetic pathway in all nonerythroid cells, and ALAS1 activity is regulated by heme. Heme regulates its own synthesis by affecting transcription of the ALAS1 gene, stability of ALAS1 mRNA, and the transport of ALAS1 protein from cytosol to mitochondria. No mutations affecting ALAS1 have been described.

The erythroid-specific ALAS2 gene is regulated quite differently, as the heme biosynthetic demands of the red cell exceed by far those of any other cell. Transcription of ALAS2 is regulated by erythroid-specific transcription factors interacting with *cis* elements in the 5′ noncoding region of the gene. Translational regulation of ALAS2 is mediated by the interaction of a *cis*-acting iron regulatory element in the 5′-untranslated region of the ALAS2 mRNA with an iron regulatory element–binding protein. When the protein is bound to the iron regulatory element, translation is inhibited. In the presence of iron, the protein dissociates, ALAS2 mRNA binds to the ribosome, and ALAS2 protein is synthesized. In the red cell, therefore, translation of ALAS2 mRNA depends on the availability of iron.

Both inherited and acquired factors affecting ALAS2 genes cause sideroblastic anemia (Wyckoff and Kushner, 1994). X-linked sideroblastic anemia, an uncommon inherited disease, generally produces a microcytic anemia in males, which is recognized in childhood. Rare cases have been noted in females when lyonization has inactivated the wild-type allele. The severity of the anemia is quite variable, but in all cases the production of porphyrins and heme by erythrocytes is subnormal. Iron stains of bone marrow reveal a halo of iron-laden mitochondria surrounding the nucleus of erythroblasts (ringed sideroblasts). X-linked sideroblastic anemia often improves with the administration of large doses of pyridoxine. Several ALAS2 mutations have been detected that affect the pyridoxal phosphate binding site but do not directly change the lysine that mediates the binding of pyridoxal phosphate.

Isonicotinic acid hydrazide (INH), which is widely used in the treatment of tuberculosis, can also cause sideroblastic anemia. INH reacts with pyridoxal to form a hydrazone that inhibits pyridoxal phosphokinase, the enzyme responsible for the synthesis of pyridoxal phosphate. A microcytic anemia occurs frequently with prolonged ingestion of INH but the anemia is usually mild. Ringed sideroblasts are invariably found in the marrow, but this abnormality and the anemia are fully reversible on withdrawal of INH or by the administration of a large, daily dose of pyridoxine.

ALA DEHYDRATASE (ALAD)

ALAD catalyzes the condensation of two molecules of ALA to form the monopyrrole porphobilinogen (Fig. 8.1.1). The enzyme has been purified from many sources, and the ALAD gene has been cloned from bacteria, yeast, plants, and mammals. The crystal structure of yeast ALAD has been solved, and the yeast enzyme, a homooctameric metalloenzyme, is highly homologous to mammalian ALADs (Erskine et al., 1997). Mammalian ALAD is an octamer of eight identical subunits, arranged as a tetramer of dimers. Each of the eight active sites has two substrate binding positions (Dailey, 1997). The ALA molecule contributing the propionate side chain of porphobilinogen and the pyrrole nitrogen binds first, at a position designated the P site. Binding of ALA at the P site is required before a second ALA molecule, which contributes the acetate side chain and the amino-methyl group, binds at the position designated the A site. Eight zinc atoms are present in mammalian ALAD, one atom per subunit. The zinc atoms exist in two different environments. One zinc atom in each dimer is required for catalytic activity. The other is bound to the protein but is not directly involved in catalysis. This noncatalytic metal has been termed a "structural zinc" and probably serves to stabilize the enzyme. The zinc atoms bind in a cysteine-rich region with sequence similarity to a motif found in zinc-finger proteins (Dailey, 1997).

Two alleles of the ALAD gene have been identified in humans. They differ by only a single nucleotide in codon 59, which changes lysine to asparagine. The lysine allele is more common and is found in 80% to 90% of the human population. Most people are homozygous for this allele. The asparagine allele is present in 10% to 20% of humans. There is no difference in ALAD activity among the three possible phenotypes (Lys-Lys, Lys-Asp, Asp-Asp), but the Asp-Asp phenotype may be associated with an altered response to lead exposure (see below; Kappas et al., 1995).

ALAD deficiency is associated with human disease, and the activity of the enzyme can be inhibited in three ways: an ALAD deficiency can be inherited, an inherited defect in tyrosine metabolism can lead to the generation of an inhibitor of ALAD, and ALAD can be inhibited by toxic metals, particularly lead.

Six cases of a clinical syndrome associated with genetically transmitted severe ALAD deficiency have been described (Wyckoff and Kushner, 1994; Kappas et al., 1995). Two were unrelated adolescent German males who developed neurovisceral symptoms, including pain in the abdomen and extremities. One of the two German cases went on to develop a mixed motor/sensory polyneuropathy. Symptoms were made worse in both cases following alcohol intake or decreased food intake. Molecular analysis in one of the German cases revealed that the patient was a compound heterozygote with two different mutant ALAD alleles. Cells from both parents had half the normal amount of ALAD activity. The third case was a two-year-old Swedish boy with retarded development, limb paralysis, respiratory insufficiency, and generalized muscle weakness. The child had repetitive episodes during which symptoms worsened, followed by periods of improvement. This case also proved to represent compound heterozygosity with a different mutation present on each ALAD allele. The Swedish boy underwent liver transplantation at the age of seven years, but basal urinary secretion of ALA did not change and there was little change in the neurovisceral symptoms. The fourth case was quite unusual, as symptoms due to a subacute polyneuropathy did not develop until the seventh decade. The last two cases occurred in Chilean siblings who developed neurovisceral symptoms in the third decade.

In all cases, patients show a marked increase in the urinary excretion of ALA. Further, they show an increase in the urinary excretion of coproporphyrin. This is surprising, because ALAD activity in these patients ranges from 1% to 12% of normal values. It is presumed that the excess of ALA which results from ALAD deficiency is toxic to nerve cells and this is causative for the neurovisceral symptoms. ALA has strong structural homology with γ-aminobutyric acid (GABA) and can activate GABA receptors on neurons. An alternate hypothesis, neither proven nor rejected, is that the neurovisceral symptoms are due to heme deficiency in neural cells.

Succinylacetone, a structural analog of ALA, is an extremely potent inhibitor of ALAD and has been widely used in vitro as an inhibitor of heme biosynthesis in cultured cells. Patients with hereditary tyrosinemia, a disorder caused by an inherited deficiency of fumarylacetoacetate hydrolase, produce large amounts of succinylacetone, and ALAD activity in their erythrocytes and liver is markedly depressed (Kappas et al., 1995). Urinary secretion of ALA is also markedly increased. Some patients with hereditary tyrosinemia develop neurovisceral symptoms similar to those seen in patients with porphyria due to ALAD deficiency and other porphyrias.

Lead is a reversible inhibitor of ALAD and probably acts by displacing zinc from the holoenzyme. Patients with lead poisoning excrete increased amounts of ALA in the urine and display clinical symptoms resembling those seen in ALAD-deficiency porphyria and other porphyric disorders, including abdominal pain, peripheral neuropathy, and other neurovisceral symptoms. Following comparable exposure to lead, individuals with the ALAD Asp-Asp phenotype have higher concentrations of lead in their blood than individuals with the Lys-Lys phenotype (Dailey, 1997). The clinical relevance of this difference is unclear. Two conflicting views have been offered. The Asp-Asp phenotype might be associated with an increased susceptibility to lead poisoning or, in contrast, the Asp-Asp phenotype might protect against lead toxicity by sequestering lead.

Lead also affects the activity of coproporphyrinogen oxidase and ferrochelatase. Urinary excretion of coproporphyrin is increased in lead poisoning but there is little evidence suggesting that excess coproporphyrin mediates any of the clinical findings. Heme synthesis in red cells is clearly affected by lead, especially in children in whom a microcytic anemia is commonly associated with lead poisoning.

PORPHOBILINOGEN DEAMINASE (PBGD)

PBGD catalyzes the polymerization of four molecules of PBG to form the unstable linear tetrapyrrole, hydroxymethyl bilane (Fig. 8.1.1; Dailey, 1995). The enzyme is cytosolic and monomeric. Human PBGD has a molecular weight of ~38 kDa, but the molecular mass varies slightly, depending on how the gene transcript is processed (see below). PBGD from bacteria was the first heme biosynthetic enzyme to be crystallized (Wyckoff and Kushner, 1994; Kappas et al., 1995). A dipyrrole cofactor is required for enzyme activity. The cofactor is assembled by the PBGD apoprotein by the deamination and polymerization of two molecules of PBG. The dipyrrole cofactor is covalently linked to the apoprotein to form the holoenzyme. During the enzymatic reaction, four molecules of PBG are deaminated and added sequentially to the cofactor to assemble a hexapyrrole. Finally, the distal tetrapyrrole is

cleaved from the cofactor and released as hydroxymethyl bilane. The cofactor remains enzyme-bound and is not turned over.

The gene encoding PBGD has been cloned from both prokaryotes and eukaryotes (Wyckoff and Kushner, 1994). The single human PBGD gene produces two different transcripts that differ at their 5′ ends. The "housekeeping" form of PBGD is derived from an mRNA in which exon 1 is spliced to exon 3. The second transcript, produced only in erythroid cells, initiates at exon 2. Translation of the housekeeping mRNA yields a protein with 17 amino acids at the amino terminus (encoded by exon 1) that are not present in erythroid-specific PBGD. Activation of transcription is controlled by two different promoters. The housekeeping promoter is located upstream of exon 1, and the erythroid promoter lies between exon 1 and exon 2.

Mutations in the PBGD gene are responsible for acute intermittent porphyria (AIP; Kappas et al., 1995). The incidence of a defective allele of PBGD in the United States has been estimated at between 5 and 10 per 100,000. AIP is transmitted as an autosomal dominant trait, but most carriers of a mutant allele never develop symptoms. Those who do, predominantly women, manifest an illness characterized by recurrent, acute attacks of abdominal pain associated with autonomic dysfunction. Constipation and even obstipation often accompanies the abdominal pain. Other abnormalities that may be present during an attack include peripheral motor neuropathy, cranial neuropathies, delirium, seizures and, rarely, death. During an attack ALAS1 is induced in hepatocytes and ALA and PBG are produced in excess and secreted in the urine, presumably because of the partial block in heme biosynthesis. As is the case with ALAD deficiency, it is not clear if the acute attacks that characterize AIP are due to neurotoxic effects of ALA (or PBG) or to a heme deficiency in neural cells. Intravenous infusions of hematin or heme-arginate have been widely accepted as appropriate treatment for acute attacks. Hematin or heme-arginate infusions induce a prompt decrease in the urinary excretion of ALA and PBG, mediated by the suppression of ALAS1 in the liver. Despite this clear biochemical effect, a controlled trial with heme-arginate generated only marginal evidence of clinical efficacy.

Acute attacks of AIP often follow the ingestion of a wide variety of drugs. Most of the drugs induce hepatic cytochrome P-450s, thereby increasing the demand for heme synthesis. Barbiturates, anticonvulsants, and sulfonamide antibiotics have been most commonly recognized as precipitating agents (Kappas et al., 1995). It is prudent, however, to recommend avoidance of all drugs whenever possible, especially drugs metabolized by P-450-dependent pathways.

Numerous PBGD mutations have been detected in patients with AIP (Wyckoff and Kushner, 1994; Kappas et al., 1995). Most mutations result in an allele that produces either no protein or an unstable protein. Mutations that affect splice junctions, introduce termination codons, cause frameshifts, or alter protein stability have all been described. Approximately 20% of mutant alleles represent point mutations that affect catalytic activity but not protein stability. Assays of PBGD activity are generally done using red cell lysates as the source of UROD. The activity of PBGD in red cells almost always parallels the activity of the enzyme in liver. In a few pedigrees, however, point mutations in exon 1 cause an enzyme deficiency that is restricted to nonerythroid cells. Rare cases have been described with severe symptoms and very large amounts of PBG in the urine. In one such case, compound heterozygosity for different point mutations affecting the same codon in exon 10 were found.

UROPORPHYRINOGEN III COSYNTHASE (UCoS)

Hydroxymethyl bilane released from PBGD will spontaneously cyclize to form uroporphyrinogen I, but in the presence of UCoS the cyclization occurs with concomitant inversion of the terminal pyrrole ring to form uroporphyrinogen III (Fig. 8.1.1). In all cells, UCoS is present in excess relative to PBGD activity. UCoS also has a high turnover number and enzymatic formation of uroporphyrinogen III is rapid. Collectively, these factors favor the synthesis of uroporphyrinogen III. In mammals, the enzyme is cytosolic. UCoS has been purified to homogeneity from prokaryotes and eukaryotes. Enzymes from these diverse sources are monomers with molecular weights of ~30 kDa, are inactivated by lead, and appear to require reactive thiols for activity. UCoS cDNAs have been cloned from several sources, and human UCoS has been mapped to chromosome 10q. Very little is known about the enzymatic mechanism of UCoS, but it is clear that hydroxymethyl bilane is the substrate and a spiro mechanism is probably involved in rearrangement of the D ring (Wyckoff and Kushner, 1994; Kappas et al., 1995).

UCoS mutations are responsible for a rare but dramatic form of porphyria called congenital erythropoietic porphyria (CEP). CEP is transmitted as a recessive trait and fewer than 300 cases have been reported. Homozygotes or compound heterozygotes generally display <10% of normal UCoS activity. There are no known interactions of UCoS with toxins or with drugs. The disease is usually detected in infancy and is often first recognized by pink or purple staining of the diapers. Staining is due to the urinary excretion of large amounts of uroporphyrin I. Extreme photosensitivity is common and severe photomutilation often occurs. The site of porphyrin overproduction is the developing erythroblast and hemolytic anemia and splenomegaly have been described in most cases. Deposition of porphyrins in the dentin of developing teeth causes both discoloration and fluorescence under UV light. The treatment of CEP is based on avoidance of exposure to sunlight through the use of protective clothing and appropriate sunscreens. Bone marrow transplantation has proven effective in several cases (Thomas et al., 1996).

Eight mutant UCoS alleles have been characterized. Six are point mutations that cause changes in amino acids, one is a deletion, and one is an insertion that produced a frameshift.

UROPORPHYRINOGEN DECARBOXYLASE (UROD)

UROD catalyzes the sequential decarboxylation of the four acetate side chains of uroporphyrinogen to form coproporphyrinogen (Fig. 8.1.1). Either the III or the I isomer of uroporphyrinogen may serve as substrate, but only coproporphyrinogen III is a substrate for the next enzyme in the pathway, coproporphyrinogen oxidase. The mechanism of decarboxylation is not known, but the enzyme does not require cofactors or prosthetic groups for activity. Human UROD is a homodimer with a monomeric molecular weight of ~41 kDa. The crystal structure of human UROD has been determined at 1.60 Å resolution (Whitby et al., 1998). There is one active-site cleft per monomer which is adjacent to that of its neighbor in the dimer. This creates a single extended cleft large enough to accommodate two substrate molecules in close proximity or to allow reaction intermediates to shuttle between monomers. The gene encoding UROD has been cloned from many species. There is no evidence to suggest tissue-specific processing of the transcript.

Subnormal activity of UROD in hepatocytes causes the most common form of porphyria in humans, porphyria cutanea tarda (PCT; Wyckoff and Kushner, 1994; Kappas et al., 1995). PCT is characterized clinically by skin fragility, bullous lesions, and hypertrichosis on sun-exposed areas. Biochemically, the disease is characterized by the accumulation of uroporphyrin in the liver (liver biopsy specimens fluoresce under long-range UV light) and the urinary excretion of these compounds in great excess.

Four variants of PCT have been described, two of which are due to UROD mutations (Wyckoff and Kushner, 1994; Kappas et al., 1995). Familial PCT (F-PCT) is transmitted as an autosomal dominant trait and accounts for about one-third of the cases of PCT. Affected individuals display half the normal amount of UROD activity in all tissues. Many UROD mutations have been identified in patients with F-PCT. The most common is a splice-site mutation leading to deletion of exon 6. Most carriers of mutant UROD alleles do not express a clinical phenotype unless additional factors that lead to further reduction of UROD activity in the liver are present. Important additional factors include alcohol abuse, exposure to the hepatitis C virus, the use of medicinal estrogens, and the development of hepatic siderosis. Depletion of hepatic iron stores through phlebotomy therapy corrects the clinical and biochemical phenotype. A second variant of PCT, designated hepatoerythropoietic porphyria (HEP), is rare and occurs in individuals with two mutant UROD alleles, either homozygotes for a single mutation or compound heterozygotes. The photosensitive dermatosis may be severe and is generally recognized in childhood. Phlebotomy is usually not effective. A third variant of PCT is called sporadic PCT (S-PCT) and accounts for ~50% to 60% of cases. In S-PCT, the UROD defect is restricted to the liver and no mutations have been identified in the UROD gene. The concentration of UROD protein in the liver is normal, even though enzyme activity is reduced, suggesting the presence of an enzyme inhibitor. Alcohol abuse, hepatitis C, and estrogen use all have been identified as risk factors and, as with F-PCT, hepatic siderosis is a nearly uniform finding. Phlebotomy therapy is effective, suggesting that iron is required for generation of the putative UROD inhibitor.

A fourth variant, designated toxic PCT, is associated with exposure to halogenated aromatic hydrocarbons. An epidemic of toxic PCT affecting more than 3000 people occurred in Turkey between 1956 and 1961. Seed wheat

treated with the fungicide hexachlorobenzene was responsible for the epidemic. Although animal models of toxic PCT, have been intensely studied (mainly in rodents), the exact mechanism by which halogenated aromatics cause inhibition of hepatic UROD activity is not known. Iron appears to be required, as does the induction of specific isoforms of cytochrome P-450.

COPROPORPHYRINOGEN OXIDASE (CPO)

CPO converts the propionate groups at positions 2 and 4 of coproporphyrinogen III to vinyls, yielding protoporphyrinogen (Fig. 8.1.1). The oxidative decarboxylation in eukaryotes requires molecular oxygen as the electron acceptor, and two molecules of CO_2 are generated. CPO has been cloned from both prokaryotic and eukaryotic species (Martasek et al., 1994). In mammals, CPO is encoded by a nuclear gene, but the enzyme is located in the mitochondrial intermembrane space, probably associated with the outer face of the inner membrane. In anaerobic prokaryotes, the CPO reaction is oxygen-independent and alternate electron receptors are used. Human CPO is a homodimer with a subunit molecular weight of 37 kDa. The enzyme mechanism has not been clarified, but inhibitor studies indicate that at least one tyrosine is required for enzymatic activity.

Mutations of the CPO gene in humans are responsible for the disease hereditary coproporphyria (HCP; Wyckoff and Kushner, 1994; Kappas et al., 1995). CPO activity is reduced to half the normal amount in all tissues, but coproporphyrin accumulates only in the liver. HCP is transmitted as an autosomal dominant trait, but rare instances of homozygous CPO deficiency have been reported and are associated with a more severe phenotype. Clinical manifestations of HCP generally occur after puberty and include both acute neurovisceral attacks similar to those seen in patients with AIP and bullous lesions on light-exposed areas as seen in patients with PCT. Approximately two-thirds of individuals heterozygous for CPO mutations never become clinically ill. The distinguishing feature in HCP is the excretion of large amounts of coproporphyrin in feces, even in the absence of clinical symptoms. During acute attacks, urinary excretion of ALA, PBG, and coproporphyrin is also increased.

The treatment of acute attacks is identical to the treatment of AIP.

PROTOPORPHYRINOGEN OXIDASE (PPO)

PPO is an integral protein of the inner mitochondrial membrane. PPO has been cloned and characterized from eukaryotic and prokaryotic sources (Dailey and Dailey, 1996). The enzyme is membrane bound in all organisms except *Bacillus subtilis*. The enzyme catalyzes the oxidation of protoporphyrinogen to protoporphyrin (Fig. 8.1.1). The mammalian enzyme requires molecular oxygen as the terminal electron acceptor. Three molecules of molecular oxygen are reduced to H_2O_2 as protoporphyrin is formed. The human enzyme is a homodimer with a subunit molecular weight of 51 kDa and contains a single, noncovalently bound molecule of FAD per dimer. PPO shares significant homologies with many oxidases containing an FAD-binding motif near the amino terminus.

Mutations of the PPO gene are responsible for variegate porphyria (VP; Wyckoff and Kushner, 1994; Kappas et al., 1995). The clinical manifestations of VP are similar to those described in patients with HCP. Both dermal photosensitivity and acute neurovisceral attacks may occur. The biochemical hallmark of VP is excessive fecal excretion of protoporphyrin and coproporphyrin. Porphyrin concentration is higher in the bile than in feces. Elevated fecal porphyrins are found in almost all patients after puberty, even in those who display no clinical phenotype. During acute neurovisceral attacks there is an increase in the urinary excretion of ALA, PBG, and coproporphyrin, but their concentrations in urine are generally normal between attacks.

The incidence of VP in South African Caucasians is ~3 per 1000, and nearly all cases are descendants of a Dutch couple settling in South Africa late in the 17th century. The ancestral PPO mutation in South Africa is R59W. The incidence of VP in other countries is not known and several other mutations of the PPO gene have been characterized.

The diphenyl-ether class of herbicides are potent inhibitors of PPO and are widely used. These herbicides also inhibit PPO from mammalian sources but no toxic effects have been clinically recognized.

FERROCHELATASE

Ferrochelatase, the final enzyme in the heme biosynthetic pathway, catalyzes the insertion of one atom of ferrous iron into the protoporphyrin macrocycle (Fig. 8.1.1). In eukaryotes, the enzyme is encoded by a nuclear gene, synthesized on cytoplasmic ribosomes, and

translocated to the mitochondria where the protein is inserted into the inner mitochondrial membrane. The active site is located on the matrix side. The active site of PPO is located in the outer side of the inner mitochondrial membrane, suggesting that a transport system is required to move protoporphyrin to the matrix side where it serves as a substrate for ferrochelatase (Wyckoff and Kushner, 1994).

Ferrochelatase is a homodimer. The mammalian enzyme contains a labile iron-sulfur cluster near the carboxyl terminus. The cluster is destroyed by nitric oxide, causing the enzyme to lose activity, but it is not known if this process reflects a physiologic regulatory role in vivo. The only crystal structure for ferrochelatase that has been solved is the enzyme from *B. subtilis*, which does not contain an iron-sulfur cluster (Al-Karadaghi et al., 1997).

Ferrochelatase will catalyze the insertion of Fe^{2+}, Co^{2+}, and Zn^{2+} into protoporphyrin and a variety of other IX isomer polymers. Ferrochelatase is inhibited by several divalent heavy metals, including Hg^{2+}, Pb^{2+}, Mn^{2+}, and Cd^{2+}. A naturally occurring inhibitor of ferrochelatase is *N*-methylprotoporphyrin, generated from the heme of cytochrome P-450. A variety of synthetic *N*-alkylporphyrins are also potent inhibitors of ferrochelatase (Dailey, 1997).

Ferrochelatase mutations are responsible for erythropoietic protoporphyria (EPP; Wyckoff and Kushner, 1994; Kappas et al., 1995). Subnormal ferrochelatase activity causes the accumulation of protoporphyrin in red blood cells. Protoporphyrin diffuses into plasma, is cleared by the liver, and secreted in bile. The protoporphyrin content of stool is increased in patients with EPP, but some of the protoporphyrin secreted into the gut is reabsorbed and processed again by the liver.

EPP is transmitted as an autosomal dominant trait. The clinical phenotype is characterized by a distinctive type of cutaneous photosensitivity. Neurovisceral attacks do not occur. Cutaneous symptoms may be limited to a sensation of burning and itching, after even brief periods of sun exposure. In some patients, edema and erythema may follow. Chronic changes include prematurely aged skin, shallow scars on the nose and cheeks, and leathery pseudovesicles over the nose and hands. In contrast to other porphyrias associated with photosensitivity, bullae, fragility, dramatic scarring, and hirsutism rarely occur. The increased content of protoporphyrin in bile leads to the formation of photoporphyrin-containing gallstones in ~10% of patients. Extreme cholestasis can lead to progressive liver disease, cirrhosis, and death, but this is a rare complication of EPP.

The diagnosis of EPP requires recognition of the clinical syndrome, coupled with findings of increased free erythrocyte protoporphyrin in red cells and an increase in fecal protoporphyrin excretion. The fecal content of protoporphyrin may vary widely because of variations in enteric reabsorption.

Treatment with orally administered β-carotene may provide systemic photoprotection but has no effect on protoporphyrin production, clearance, or excretion. Chenodeoxycholic acid may prove to be useful, as this agent diminishes the protoporphyrin content of both red cells and plasma and reduces fecal protoporphyrin excretion. Liver transplantation is the only effective therapy for the rare patients who develop severe liver disease.

A number of ferrochelatase mutants have been identified in patients with EPP, indicating that the disease is heterogeneous at the molecular level (Wyckoff and Kushner, 1994; Kappas et al., 1995; Dailey, 1997). One point mutation resulted in the formation of a catalytically inactive heterodimer composed of one normal and one mutant monomer. Ferrochelatase activity was 25% of normal, the predicted outcome if enzyme activity is restricted to dimers composed of two normal monomers.

INTERPRETATION OF URINARY PORPHYRIN EXCRETION

Nearly all hepatobiliary diseases may be associated with an increase in the urinary excretion of coproporphyrin and occasionally uroporphyrin, but not ALA or PBG. Impaired secretion of porphyrins in bile leads to an increase in urinary excretion, but there are no clinical manifestations resembling those associated with any of the porphyric disorders. Incorrect interpretation of moderate increases in urinary coproporphyrin excretion is a common cause of misdiagnosis of porphyria.

SUMMARY

With the possible exception of some forms of PCT, the porphyrias are inherited disorders. Nevertheless, most dominantly inherited porphyric traits are not associated with a manifest clinical phenotype unless a drug is ingested or exposure to a toxin occurs. The acute neurovisceral attacks of AIP, HCP, and VP are often precipitated by drugs that induce one or more of the cytochrome P-450s. Attacks in women

may occur at specific times in the menstrual cycle, implying a role for hormones in inducing attacks. The most dramatic example of environmental interactions in the pathogenesis of porphyria is PCT. Alcohol, estrogens, polychlorinated biphenyls (and other halogenated aromatic compounds), infection with the hepatitis C virus, and hepatic iron overload (due to mutations at the hemochromatosis locus or to unidentified factors) have all been implicated in precipitation of the clinical phenotype.

With the exception of heavy metals, some herbicides, and *N*-alkylporphyrins, little is known about how environmental factors interact with enzymes of the heme biosynthetic pathway. The molecular characterization of mutant genes from patients with porphyria and from microorganisms is beginning to lead to the identification of key domains required for the activity of heme biosynthetic enzymes. Structure-function relationships derived from crystal structures are beginning to unfold. The complex interactions between environmental and inherited factors affecting porphyrin metabolism are now approachable.

LITERATURE CITED

Al-Karadaghi, S., Hansson, M., Nikonov, S., Jonsson, B., and Hederstedt, L. 1997. Crystal structure of ferrochelatase: The terminal enzyme in heme biosynthesis. *Structure* 5:1501-1510.

Dailey, H.A. (ed.) 1995. Biosynthesis of Heme and Chlorophylls. McGraw-Hill, New York.

Dailey, H.A. 1997. Enzymes of heme biosynthesis. *J. Biol. Inorg. Chem.* 2:411-417.

Dailey, T.A. and Dailey, H.A. 1996. Human protoporphyrinogen oxidase: Expression, purification, and characterization of the cloned enzyme. *Protein Sci.* 5:98-105.

Daniell, W.E., Stockbridge, H.L., Labbe, R.F., Woods, J.S., Anderson, K.E., Bissell, D.M., Bloomer, J.R., Ellefson, R.D., Moore, M.R., Pierach, C.A., Schreiber, W.E., Tefferi, A., and Franklin, G.M. 1997. Environmental chemical exposures and disturbances of heme synthesis. *Environ. Health Perspect.* 105 (Suppl. 1):37-53.

Erskine, P.T., Senior, N., Awan, S., Lambert, R., Lewis, G., Tickle, I.J., Sarwar, M., Spencer, P., Thomas, P., Warren, M.J., Shoolingin-Jordan, P.M., Wood, S.P., and Cooper, J.B. 1997. X-ray structure of 5-aminolaevulinate dehydratase, a hybrid aldolase. *Nat. Struct. Biol.* 4:1025-1031.

Kappas, A., Sassa, S., Galbraith, R.A., and Nordmann, Y. 1995. The porphyrias. *In* The Metabolic and Molecular Bases of Inherited Disease (C.R. Scriver, A.L. Beaudet, W.S. Sly, and D. Valle, eds.) pp. 2103-2160. McGraw-Hill, New York.

Martasek, P., Camadro, J.M., Delfau-Larue, M.H., Dumas, J.B., Montagne, J.J., de Verneuil, H., Labbe, P., and Grandchamp, B. 1994. Molecular cloning, sequencing, and functional expression of a cDNA encoding human coproporphyrinogen oxidase. *Proc. Natl. Acad. Sci. U.S.A.* 91:3024-3028.

Thomas, C., Ged, C., Nordmann, Y., de Verneuil, H., Pellier, I., Fischer, A., and Blanche, S. 1996. Correction of congenital erythropoietic porphyria by bone marrow transplantation. *J. Pediatr.* 129:453-456.

Whitby, F.G., Phillips, J.D., Kushner, J.P., and Hill, C.P. 1998. Crystal structure of human uroporphyrinogen decarboxylase. *EMBO J.* 17:2463-2471.

Wyckoff, E.E. and Kushner, J.P. 1994. Heme biosynthesis, the porphyrias, and the liver. *In* The Liver: Biology and Pathobiology (I.M. Arias, J.L. Boyer, and N. Fausto, eds.) pp. 505-527. Raven Press, New York.

Contributed by John D. Phillips and James P. Kushner
University of Utah Medical School
Salt Lake City, Utah

Measurement of ALA Synthase Activity

In most cells, δ-aminolevulinate (ALA) synthase is the rate-limiting enzyme in heme biosynthesis. In the liver, the enzyme is inducible by drugs and toxins and it is regulated through a feedback mechanism by heme, the end-product of the pathway. Measurement of ALA synthase activity is important for determining whether accumulation of porphyrins and heme in the tissue is due to an increased activity of the enzyme. This unit describes two methods for measuring ALA synthase activity: a radiometric assay that uses ^{14}C-labeled succinate as a substrate (see Basic Protocol 1) and a colorimetric procedure that involves conversion of the product ALA to a pyrrole (see Basic Protocol 2). The concentration of the pyrrole is estimated by measuring its absorbance after reaction with Ehrlich's reagent. The radiometric procedure can be used to measure the basal activity of ALA synthase and small increases in that rate in all cells, whereas the colorimetric procedure is best suited for measuring considerable increases in activity above basal levels.

RADIOMETRIC ASSAY FOR ALA SYNTHASE

BASIC PROTOCOL 1

Compared to many enzymes of intermediary metabolism, the concentration of ALA synthase is very low in most cells or tissues. Its activity is expressed in units (U) of nmol/hr, and, in some instances, only a radiometric assay can provide sufficient sensitivity for accurate measurement of ALA synthase activity. In this protocol, tissue or cell extracts are incubated with [^{14}C]succinate and the product, [^{14}C]δ-aminolevulinate, is separated from the residual succinate and other radioactive contaminants by treatment with alkaline SDS and ion-exchange chromatography.

Materials

Control (C) and reaction (R) buffers (see recipes)
Cofactor solution (see recipe)
[2,3-^{14}C]succinate (see recipe)
Cell or tissue sample
Succinyl-CoA synthase (see recipe)
0.5 M NaOH
8.7 M acetic acid
Stop solution: 10% (w/v) SDS containing 10 mM sodium succinate and 1 mM δ-aminolevulinic acid
Dowex 50W-X8 cation exchange resin, 100-200 mesh (see recipe)
0.1 M sodium acetate, pH 3.9
Methanol/0.1 M sodium acetate, pH 3.9 (2:1, v/v)
0.01 M HCl
1.0 M Tris base (aqueous solution with unadjusted pH of ~10.5)
Aquasol II or other liquid scintillation fluid compatible with aqueous samples

2-ml screw-cap tubes (e.g., Sarstedt)
Heating blocks, 37° and 65°C
10-ml chromatography columns (e.g., Bio-Rad)
Stacking cap (e.g., Bio-Rad #731-1555), optional

Incubate extracts to form radioactive ALA

1. Prepare control and reaction cocktails by mixing: 1.0 ml C or R buffer, 0.25 ml cofactor solution, and 0.03 ml [^{14}C]succinate.

2. For each sample to be assayed or variable to be tested, transfer 0.2 ml control cocktail into a 2-ml screw-cap tube and 0.2 ml reaction cocktail into another tube.

Contributed by Peter R. Sinclair, Nadia Gorma, and Neal W. Cornell
Current Protocols in Toxicology (1999) 8.2.1-8.2.11

3. Incubate all tubes 5 min at 37°C. Add 50 µl tissue or cell extract and 10 µl diluted succinyl-CoA synthase to each control or reaction mixture. Make these additions at timed intervals (e.g., 30 to 60 sec) so that the incubations can be stopped at the same intervals.

4. Mix by gentle vortexing and incubate 20 min at 37°C.

Stop reactions with alkaline SDS

5. At the appropriate time intervals, add 1.0 ml of 10% SDS/10 mM succinate/1 mM ALA stop solution to each incubation, followed by 28 µl of 0.5 M NaOH for control samples *or* 55 µl of 0.5 M NaOH for reaction samples. Mix by vortexing immediately after adding NaOH.

   Addition of NaOH will raise the pH of the sample to 8.5 to 8.8.

6. Incubate samples 60 min at 65°C.

7. Adjust the pH to 3.6 to 3.8 by adding 50 µl of 8.7 M acetic acid to control samples and 75 µl to reaction samples.

Purify ALA by cation-exchange chromatography

8. Swirl the washed Dowex 50W-X8 (equilibrated with 0.1 M sodium acetate, pH 3.9) to obtain a uniform suspension. Pipet 3 ml of suspension into each 10-ml column. Drain under gravity flow.

   The packed resin bed volume should be ~1.5 ml.

9. Apply 1.00 ml of control sample or 1.04 ml of reaction sample from step 7 to each column. Allow sample to enter resin bed.

   These volumes are equivalent to 75% of the sample volumes.

10. Wash each column successively with: 20 ml of 0.10 M sodium acetate, pH 3.9; 20 ml of methanol/0.1 M sodium acetate, pH 3.9; and 10 ml of 0.01 M HCl.

    A screw-cap 50-ml plastic tube is convenient for collecting these eluants, which should be discarded in radioactive waste. Column washing is greatly facilitated by using a stacking cap (e.g., Bio-Rad #731-1555) that allows a second column to be "piggy-backed"onto the one containing the resin bed and by elevating the column system so that a 15-cm length of tubing can be attached to the outflow of the lower column to create a larger hydrostatic head. Remove the tubing before the elution of the radioactive product in the next step.

11. Elute [^{14}C]δ-aminolevulinate by adding 3 ml of 1.0 M Tris base directly to resin bed. Collect eluant in a clean tube.

12. Mix Tris eluant by vortexing, and place 1.0 ml into a liquid scintillation vial. Add 4 ml Aquasol II (or equivalent), mix by vortexing, and determine radioactivity as disintegrations/minute (dpm) in a scintillation counter.

13. For one reaction incubation and its respective control, measure the radioactivity in 10 µl of the 25% of the samples remaining after step 8. Mix with 0.99 ml H_2O and add the mixture to 4 ml liquid scintillation fluid as in step 12.

    This step serves to assure the accuracy of the volumes pipetted to constitute the control and reaction samples through step 7. The expected radioactivity is determined by the specific activity of the labeled succinate, and the ratio of control:reaction counts should be 1.00:1.04.

14. Calculate ALA synthase activity as follows: Divide dpm (reaction minus control) by 2200 dpm/nCi and by the specific activity (nCi/nmol) of the succinate in control and reaction cocktails. Multiply by 3 to get total nmol in the Tris eluate and again by 3

(if the incubation time was 20 min) to get nmol/hr (U). Divide by 0.75, the fraction of sample applied to the Dowex resin, to get total U in the assayed sample. Finally, divide by the volume of sample (e.g., 50 µl) put into the incubation to get U/ml of extract.

If the incubation times and assayed sample volumes are the same for all incubations, all of the factors in the calculation can be collected into one constant that can be multiplied by dpm to directly give U/ml of extract.

COLORIMETRIC ASSAY FOR ALA SYNTHASE

BASIC PROTOCOL 2

This protocol describes the assay of ALA synthase in liver or hepatocyte culture homogenates incubated with glycine (one of the enzyme's substrates) and citrate, which the mitochondria metabolize to succinyl-CoA (its other substrate). The reaction products are ALA and carbon dioxide. The assay is performed in the presence of succinyl acetone or levulinate, which inhibit the next enzyme of the heme biosynthetic pathway, ALA dehydratase. Although the dehydratase is present at a higher concentration than ALA synthase in liver, its K_M for ALA is high and it metabolizes only small amounts of ALA during the reaction. After deproteinization of the reaction mix, the ALA is reacted with acetylacetone (2,4-pentadione) to form ALA pyrrole (2-methyl-3-acetyl-4-propionic acid). Under conditions in which considerable aminoacetone is formed during the reaction of glycine with acetyl-CoA, the aminoacetone pyrrole is removed by neutralizing the solution and extracting with dichloromethane. ALA pyrrole left in the aqueous solution is then allowed to react with modified Ehrlich reagent, giving a solution with a pink color with a maximum absorption at 552 nm and a shoulder at 520 nm (see Fig. 8.2.1). The amount of ALA is calculated from the extinction coefficient.

Materials

Cultured hepatocytes or liver
Glycine medium (GM) assay buffer (no glycine; see recipe)
0.25 M glycine solution (see recipe)
15% (v/v) trichloroacetic acid (TCA) prepared from 100% (w/v) TCA
2 M sodium acetate in H_2O
8% acetylacetone (2,4-pentanedione) in 2 M sodium acetate (see recipe)
NaOH-phosphate solution (see recipe)
Dichloromethane
Modified Ehrlich reagent (see recipe)

12 × 75–mm culture tubes
Heating block or water bath, 85° to 95°C
Spectrophotometer

1. Prepare 10% (w/v) liver homogenates in GM assay buffer or scrape cultured liver cells in GM buffer using 1 ml buffer per 15-cm plate (or per two 10-cm plates) for each assay.

   Liver homogenates can also be made in 0.25 M sucrose/20 mM Tris, pH 7.4 and then a portion diluted 1:1 with 2× GM buffer.

2. Place 0.2 ml homogenate in each of three or four tubes on ice. Add 0.05 ml of 0.25 M glycine solution. Add 0.15 ml of 15% TCA to the blank (zero time) tube and mix. Incubate the other tubes 40 min in a 37°C shaking water bath. Return incubated sample tubes to ice, add 0.15 ml of 15% TCA, and mix. Allow samples to stand for 15 min, then centrifuge suspensions 10 min at 2000 × *g*.

   Glycine is added as a separate solution so that the ALA synthase reaction does not begin during preparation of homogenates.

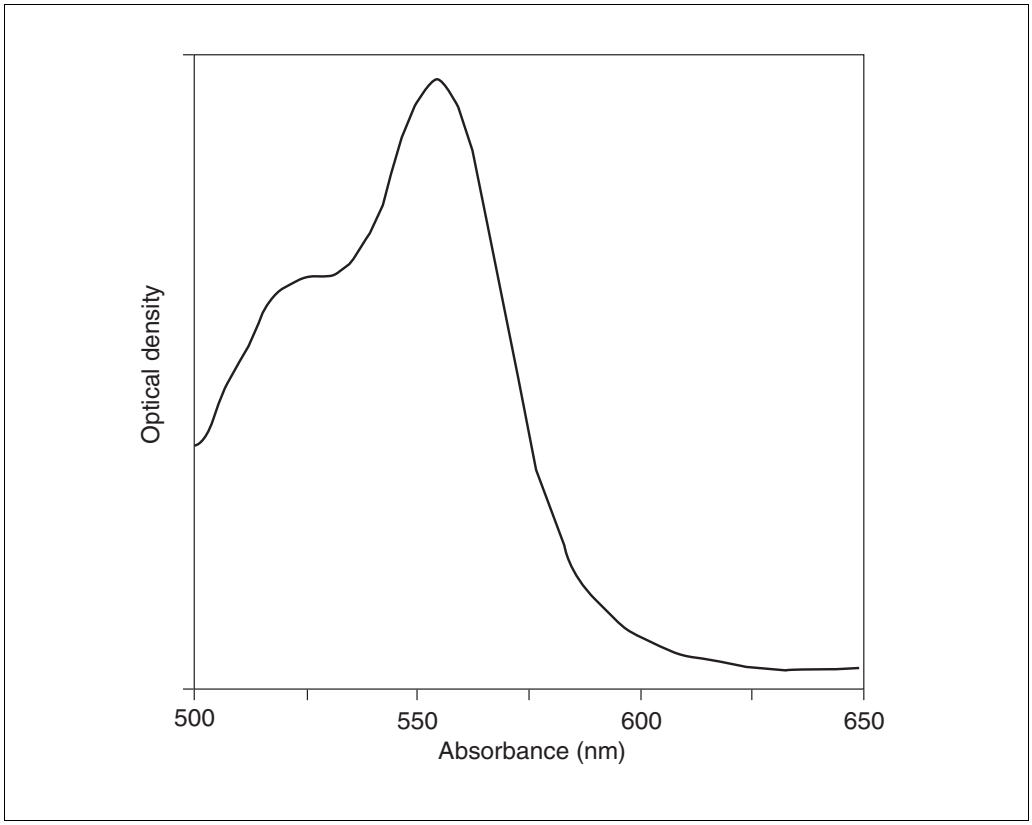

Figure 8.2.1 Absorbance spectrum of ALA-Ehrlich pyrrole.

3. From each reaction tube and blank, carefully remove 0.3 ml supernatant to another set of numbered tubes at room temperature.

   After taking TCA supernatants, samples can be stored overnight at 4°C.

4. Add 0.1 ml of 2 M sodium acetate/ 8% (v/v) acetylacetone. Mix samples and incubate 15 min at 85° to 95°C. Allow to cool.

   It is very important that the pH of the solution after addition of acetate/acetylacetone, before heating to 85°C, is between pH 4 and 5, not 2 to 3 or >5.5. The pH is most readily checked by taking a tiny drop from some tubes and applying to universal pH paper. With narrow tubes and with the lower temperature it is not necessary to cap the tubes during heating.

To measure ALA pyrrole directly

5a. Add 0.4 ml modified Ehrlich reagent and mix vigorously using a Vortex mixer.

6a. After 15 min, but not more than 45 min, scan each incubated sample from 500 to 650 nm against the zero time blank for that sample in a spectrophotometer. Measure the difference in absorbance between 552 and 650 nm. Calculate ALA concentrations using ε_{mM} of 58 for the Ehrlich pyrrole color salt. Calculate rates as nmole ALA per milligram homogenate protein (or gram tissue wet wt) per hour.

   The spectrum of the color salt should have a peak at 552 nm and a shoulder at 525 nm with a ratio of absorbances 525/552 of ~0.7, and the spectrum should be quite flat from 600 to 650 nm (Fig. 8.2.1). Other substances can react with Ehrlich reagent and cause distortion of the pure ALA pyrrole spectrum. Because prolonged incubation with Ehrlich reagent can result in absorbances due to other compounds, the Ehrlich reaction should be planned so that only as many samples are processed as can be scanned within the 45-min limit. It is recommended that an ALA standard be run through the assay to measure recovery and to obtain a typical spectrum for comparison with that obtained from cell homogenates.

To remove aminoacetone before measuring ALA pyrrole

5b. Adjust pH of sample to ~7.0 by adding 0.05 ml of 0.5 M NaOH-phosphate solution. Add an equal volume of dichloromethane and vortex vigorously. If organic and aqueous layers are not cleanly separated, centrifuge 5 min at 2000 × *g*. Remove 0.3 ml aqueous supernatant to a clean tube and add an equal volume of modified Ehrlich reagent.

This method is usually not necessary with avian liver or hepatocyte culture as aminoacetone is not a major product. Others have reported that aminoacetone is a problem in rat liver homogenate incubations. It is important for the pH to be ~7.0 for the separation of the two pyrroles by this method. The pH of the solutions should be checked by placing a small drop from some tubes on universal pH paper.

6b. Read absorbance of samples and calculate ALA concentration as in step 6a.

REAGENTS AND SOLUTIONS

Use Milli-Q-purified water or equivalent for all recipes and all protocol steps. For common stock solutions, see ***APPENDIX 2A****; for suppliers, see* ***SUPPLIERS APPENDIX****.*

Acetylacetone (2,4-pentanedione), 8%

Add acetylacetone to 2 M sodium acetate to a final concentration of 8 % (v/v). Warm the solution to 45° to 50°C and mix vigorously to make the mixture homogeneous. The solution must be made fresh prior to use.

CAUTION: *Acetylacetone is toxic. Avoid inhalation or contact with skin.*

Control (C) buffer

Per 100 ml

1.83 g of 2-{[*tris*-(hydroxymethyl)-methyl]-amino}-ethanesulfonic acid (TES; 80 mM final)

0.47 g EDTA (16 mM final)

0.65 g $MgCl_2 \cdot 6H_2O$ (32 mM final)

0.1 ml of 0.1 M sodium succinate (non-radioactive; 0.1 mM final)

Add ~90 ml H_2O

Adjust to pH 7.0 to 7.5 by adding KOH pellets, one at a time, with rapid stirring and continuous monitoring (~16 KOH pellets). Cool the solution to room temperature, and add 4 mg of pyridoxal phosphate (final concentration 0.16 mM). Use 1 M to 3 M KOH to adjust the room-temperature pH to a value that will make the pH 7.25 at 37°C; e.g., at 25°C, adjust the pH to 7.6. Bring final volume to 100 ml with H_2O.

Aliquot buffer into working portions that will be thawed only once. Store up to one month at –20°C, protected from light.

Cofactor solution

Prepare 3.3 mM coenzyme A (CoA)/26 mM GTP by dissolving 3.1 mg of the trilithium salt of CoA and either 18.9 mg of disodium GTP or 18.0 mg of trilithium GTP in 1.0 ml H_2O. If disodium GTP is used, adjust to pH ~6.5 by adding 23.5 µl of 1.5 M NaOH. If trilithium GTP is used, add 23.5 µl H_2O instead of NaOH. Prepare just prior to setting up incubations, and keep on ice until used.

The specified weights of CoA and GTP assume that the commercially available preparations contain 85% CoA or 80% GTP.

Dowex 50W-X8

100 to 200–mesh resin (e.g., from Sigma) works well in this procedure. Convert resin to the sodium form by washing with 2 vol of 2 M NaOH at 50°C three times or until the washes are colorless and odorless. Wash eight times with at least 3 vol H_2O, and equilibrate resin with 0.1 M sodium acetate, pH 3.9. Adjust the final volume of sodium acetate buffer to approximately the volume of settled resin so that pipetting 3 ml of resuspended resin will give ~1.5 ml of packed resin in a column.

Glycine medium (GM) assay buffer (no glycine)

Per 100 ml:

0.43 g Tris base (35 mM final)

0.42 g Na_2HPO_4 (30 mM final)

0.25 g Na citrate·$2H_2O$ (8.5 mM final)

0.16 g $MgCl_2·6H_2O$ (8 mM final)

5 mg pyridoxal phosphate (PLP; 0.2 mM final)

0.1 ml of 10 mM (1.6 mg/ml) succinyl acetone or 1 ml of 1 M levulinate (0.01 mM succinyl acetone or 10 mM levulinate final)

1 ml 0.5 M EDTA, adjusted to pH 8 with NaOH (5 mM final)

Adjust GM assay buffer to pH 7.4 with 1 M HCl. Filter sterilize if storing for more than one week at 4°C.

Glycine solution, 0.25 M

19 mg glycine/ml GM assay buffer. Adjust to pH 7.4 if necessary.

Modified Ehrlich reagent

Minus p-dimethylamino benzaldehyde (DMAB): For 100 ml, mix 54 ml glacial acetic acid, 23 ml of 70% (w/v) perchloric acid, and 23 ml of 1.5% (w/v) mercuric chloride dissolved in glacial acetic acid.

This solution is stable at room temperature.

On the day of use, add DMAB to a final concentration of 0.12 M; e.g., 1.8 g DMAB/100 ml Ehrlich reagent. Mix well.

CAUTION: *Ehrlich reagent is highly reactive with skin and contains Hg^{2+}. Wear appropriate gloves when handling solution.*

NaOH-phosphate solution

Mix 3 vol of 2 M NaOH with 1 vol of 0.5 M Na_2HPO_4

Reaction (R) buffer

Per 100 ml:

1.83 g of 2-{[*tris*-(hydroxymethyl)-methyl]-amino}-ethanesulfonic acid (TES; 80 mM final)

0.47 g EDTA (16 mM final)

0.65 g $MgCl_2·6H_2O$ (32 mM final)

0.1 ml of 0.1 M sodium succinate (non-radioactive; 0.1 mM final)

1.20 g glycine (160 mM final)

Add ~90 ml H_2O

Adjust to pH 7.0 to 7.5 by adding KOH pellets, one at a time, with rapid stirring and continuous monitoring (~16 KOH pellets). Cool the solution to room temperature, and add 4 mg of pyridoxal phosphate (final concentration 0.16 mM). Use 1 M to 3 M KOH to adjust the room-temperature pH to a value that will make the pH 7.25 at 37°C; e.g., at 25°C, adjust the pH to 7.6. Bring final volume to 100 ml with H_2O.

Aliquot buffer into working portions that will be thawed only once. Store up to one month at –20°C, protected from light.

[2,3-^{14}C]succinate

Commercially available [2,3-^{14}C]succinate is usually supplied as the free acid with a specific activity of ~50 mCi/mmol and a concentration of succinic acid of ~1.7 mM (e.g., DuPont NEN #NEC-201) in 10% ethanol. Convert succinate to the sodium salt by adding 1.8 mol of NaOH (from a 0.5 M solution) per mol of succinic acid. Then add 0.1 M sodium succinate, pH 7.0, and adjust the volume so the total succinate concentration is 2.22 mM.

NOTE: *In the control or reaction cocktail, 40% of the total succinate comes from the addition of the labeled material and 60% from unlabeled succinate in the C or R buffer. Thus, the specific activity of succinate in the cocktails should be 15 to 20 nCi/nmol. Determine the specific activity precisely by counting 5 to 10 µl of cocktail each time a new batch of labeled succinate is put into use. Ignore the 10% ethanol in some commercial preparations of labeled succinic acid; it causes no problem in this procedure.*

Succinyl-CoA synthase

Succinyl-CoA synthase from pig heart (e.g., Boehringer Mannheim) is available as a suspension in ammonium sulfate at 50 to 80 U/ml. Just before use, dilute a small portion of the enzyme with water to yield 10 U/ml or a total of 0.1 U in the 10 µl added to the control or reaction incubation.

COMMENTARY

Background Information

The radiometric assay described in Basic Protocol 1 can be used for all assays of ALA synthase as it has the sensitivity to measure the enzyme activity in all tissues, including basal levels or enzyme activities induced by drugs and other xenobiotics. The procedure is highly reproducible and has been used for a variety of tissues.

The radiochemical assay was developed to provide the sensitivity needed to determine ALA synthase activity in samples of such small size or low enzyme concentration as to preclude accurate measurement by the colorimetric procedure. The protocol described here is based on work by Ebert et al. (1970) and Scotto et al. (1983), and it permits the measurement of as little as 0.05 U of activity (0.05 nmol ALA formed per hour). Even smaller activities can be determined either by increasing the incubation time (in step 4) or by using a larger fraction of the Tris eluant for scintillation counting (steps 11 and 12). By comparison, the lower limit of the colorimetric assay is >0.5 U (Lien and Beattie, 1982). No systematic effort has been made to determine the upper limit of the radiochemical assay, but, with liver homogenates from rats treated with 2-allyl-2-isopropylacetamide (AIA), good proportionality was observed with 0.1 to 4 U in the assay. Results with this assay agree with those obtained with the colorimetric assay; e.g., samples that had activities of 0.61, 1.42, and 3.74 U in the radioactive assay gave 0.62, 1.35, and 3.94 U, respectively, when assayed colorimetrically. Untreated male Sprague-Dawley rats that had been starved for 24 hr had 113 ± 12 U/g of liver (n = 5), which agrees well with values determined colorimetrically (Lien and Beattie, 1982). Treatment of rats that had been starved for 24 hr with AIA (40 mg/kg body weight) caused a 12 to 15–fold increase in hepatic ALA synthase activity after 4 hr; thereafter, the activity declined gradually but was still ~10-fold greater than that in controls 18 hr after AIA injection. The latter is also in agreement with colorimetric measurements.

Using a sample of ^{14}C-aminolevulinate that had a radiochemical purity of 82%, it was found that there is negligible utilization of ALA in incubations with rat liver homogenates performed as outlined here, and that recovery of ALA added at step 1 of the protocol (but with unlabeled succinate) was 88% to 94%. No correction was made for recovery. As mentioned above, the sensitivity of the radiochemical assay makes it valuable in studies of tissues or cells with low content of ALA synthase. One example of that is a preliminary study of induction of the enzyme by succinyl acetone or polychlorinated biphenyls in isolated fish hepatocytes in which basal activity is only 15 to 20 U/g of wet weight of cells (Cornell et al., 1995).

Following the original description by Ebert et al. (1970) of the isolation of ALA by cation-exchange chromatography, several groups reported the occurrence of radioactive contaminants that co-elute with aminolevulinate, and

various approaches were proposed to eliminate those contaminants. Strand et al. (1972) used three steps of ion-exchange chromatography in which acid-stopped incubation mixtures were applied to an anion-exchange column that was used in tandem with a cation-exchange column. ALA eluted from the latter was then converted to the pyrrole and isolated by another round of anion-exchange chromatography. Bishop and Wood (1977) used a semi-automated amino acid analyzer and counted the radioactivity in the fraction corresponding to authentic ALA. Brooker et al. (1982) performed cation-exchange chromatography as described by Ebert et al. (1970), but converted ALA in the final eluate to the pyrrole, extracted it into ethyl acetate, evaporated the extract to dryness, and counted the radioactivity in the entire dried residue.

Minaga et al. (1978) reported that the major co-eluting contaminant was a breakdown product of succinyl-CoA, succinyl-cysteamine thioester, formed via the action of an amidase or peptidase. The thioester has a free amino group and is stable at a pH of ≤4.0, but at a higher pH (especially pH 8 to 10) it rapidly rearranges to succinyl-*N*-cysteamine and oxidizes to the stable disulfide, which has no free amino group. Thus, in ALA synthase incubations that are stopped with acid and adjusted to pH 3.9 for cation exchange chromatography as outlined by Ebert et al. (1970), the succinyl-cysteamine thioester will remain bound to the resin through the low pH washes, but will co-elute with ALA when an alkaline solution is applied to the column. Wolfson et al. (1980) also found that succinyl-CoA and its generating system can be the source of major contamination of the ALA fraction from cation-exchange chromatography, but they concluded that formation of the contaminant is blocked by inclusion of 10 mM EDTA in the ALA synthase incubation.

Scotto et al. (1983) confirmed and extended the work of Minaga et al. (1978), and they presented evidence that the succinyl-CoA degrading enzyme is located on the outer side of the inner mitochondrial membrane and is an amidase that requires cobalt or manganese as a metal ion cofactor. These researchers substituted alkaline SDS (pH 8.8) as the agent for stopping incubations, replacing the trichloroacetic acid that had been used by Ebert et al. (1970) and most subsequent users of the radiochemical assay of ALA synthase. The alkaline pH causes the rearrangement of the succinyl-cysteamine thioester to the stable disulfide, which does not bind to the cation-exchange resin, and SDS converts proteins in the incubation to polyvalent anions that also pass through the resin. With these changes, Scotto et al. (1983) found that the single column method of Ebert et al. (1970) gives good agreement with multi-column procedures involving conversion of ALA to its pyrrole, even when an exogenous succinyl-CoA generating system is included in the incubation mixture. Those changes are incorporated in the method outlined in Basic Protocol 1.

There are several disadvantages of this radiochemical assay. It is lengthy and labor intensive, and, while it avoids the strong acid and toxic agents needed for the colorimetric assay, it generates radioactive waste, the disposal of which is becoming increasingly difficult. The most serious disadvantage, which is also true for the colorimetric assay, is that it is a fixed-time assay that makes it laborious to determine the time course of the reaction and difficult to accurately establish kinetic parameters for ALA synthase. Recently two continuous, spectrophotometric assays have been described (Hunter and Ferreira, 1995; Shoolingin-Jordan et al., 1997) in which the activity of ALA synthase is coupled to an enzyme system that produces NADH. However, use of either of these assays is limited to somewhat purified, concentrated preparations of ALA synthase; e.g., to obtain an absorbance increase of 0.001/min would require ~10 U of the enzyme or the amount present in 0.1 gram of liver from an uninduced rat. With other tissues, that requirement would be even greater.

The colorimetric procedure has a long history of use and can be used for large numbers of samples of tissues or cultured cells. However its sensitivity is limited and so it is not recommended for studies of variation in activity in the region of 2 to 3–fold above control or at baseline or lower activities. The sensitivity can be increased by using higher concentrations of tissue or cell homogenates per incubation and scaling the procedure down, but the linearity of such assays with respect to time and protein must be checked. As described, the colorimetric assay relies on intact functioning mitochondria in the homogenate so that frozen material is less suitable. However, the authors have found that freezing liver homogenates from chick embryos at −80°C for 11 days did not result in decreased activities (G. Buzzell, N. Gorman, P. Sinclair, unpub. observ.). If activity is lost, then commercially available succinyl-CoA synthase can be added as described (Lien and Beattie, 1982).

When first establishing this assay in the laboratory, it is recommended that liver from animals given treatments known to increase ALA synthase as well as untreated animals be used. Increases in ALA synthase activity similar to those reported in the literature should be obtained before proceeding with tests of chemicals whose ALA synthase–inducing capacities are unknown.

Once increases in enzyme activities have been measured following treatment with test substances, it would be logical to test the appearance of ALA synthase protein using immunoblotting with a commercially available antibody (Agen Biomedicals) and to measure changes in ALA synthase mRNA (Hamilton et al., 1988). It should be noted that erythroid ALA synthase mRNA is transcribed from a different gene than the housekeeping gene found in liver and other tissues so that different probes are required (Riddle et al., 1989). Measurement of mRNA can be performed using Northern blotting (Riddle et al., 1989) or solution hybridization (Hamilton et al., 1988), the latter having the advantage of yielding quantitative data, but requiring DNA-free RNA prepared by CsCl density-gradient centrifugation.

An alternative procedure for measuring ALA synthase activity in cultured hepatocytes, especially in the highly inducible chick hepatocyte cultures, measures the activity in intact cells by adding the assay medium directly to the culture plates following chemical induction of ALA synthase (Sinclair and Granick, 1977). This method has been used by several laboratories and simplifies the procedure allowing more variations to be studied in a single experiment (Sassa and Kappas, 1977).

Critical Parameters and Troubleshooting

For the radiometric procedure, it is essential to control the pH as indicated at every stage of this procedure. With this assay, rat liver ALA synthase activity is maximal at pH 7.25 and decreases by only 10% to 20% at pH 7.1 or 7.4. However, the activity declines sharply at pH values outside that range. The pK of TES, 7.5 at 20°C, has a significant temperature dependence (–0.020/°C) and a small concentration dependence. It was empirically determined that, with 10% homogenates from rat liver, a pH of 7.6 at 25°C for the stock C and R buffers is necessary to obtain a pH of 7.25 at 37°C in the fully constituted incubations (steps 1 to 4 in Basic Protocol 1). For assays of different types of cell or tissue extract, replace the radioactive succinate in step 1 with unlabeled succinate, and measure the pH at step 4. If it differs from 7.25 by more than 0.05 pH units, readjust the pH of the C or R buffer.

For the SDS stop solution (used in step 5), a pH in the range of 8.5 to 8.8 is optimal for eliminating a labeled contaminant (see above) that co-elutes from Dowex 50 with ALA in assays stopped by other means (Scotto et al., 1983). Elimination of that contaminant decreases progressively at stop solutions with a pH <8.0, and the recovery of authentic ALA declines at pH values >9.0. Following the 65°C incubation with alkaline SDS, ascertain that the acetic acid addition in step 7 makes the pH 3.6 to 3.8. Likewise, take care that the Dowex 50 resin suspension and the sodium acetate wash buffer are at pH 3.9. ALA, which is quantitatively retained by the resin at pH values <4.0, begins to elute at pH 4.1. In contrast, radioactive amino acids such as glutamate and aspartate, which could be formed from [^{14}C]succinate during the incubation (step 4), elute from Dowex 50 at a pH ≥3.7. Thus, column washes at pH 3.9 separate those amino acids from ALA, which remains bound to the resin. The methanol/0.1 M sodium acetate, pH 3.9, and 0.01 M HCl washes remove the succinate that remains nonspecifically adsorbed to the resin after the first wash with 0.1 M sodium acetate, pH 3.9 (Ebert et al., 1970).

Following the low pH washes, sharp elution of ALA is effected by applying a concentrated basic solution. For that purpose, Ebert et al., 1970, used 1.0 M NH_4OH, which works well but is undesirable when the procedure is performed on an open bench. A 1.0 M solution of Tris base (e.g., Trizma base from Sigma) has an unadjusted pH of ~10.5, and is a satisfactory substitute for the NH_4OH.

The need for an exogenous succinyl-CoA generating system should be evaluated for each type of tissue and subcellular preparation. There appears to be general agreement that an added system is necessary to obtain full ALA synthase activity in homogenates of chicken (Yoda et al., 1975), mouse, or human liver (Bonkowsky and Pomeroy, 1978). However, data of Bonkowsky and Pomeroy (1978) showed only about a 10% increase in ALA synthase activity on addition of a succinyl-CoA generating system to rat liver homogenates, and they concluded that the addition is unnecessary. Brooker et al. (1982) reported that the addition was required for full expression of synthase activity in rat liver mitochondria, and they recommended also including it in assays of rat liver

homogenates. In contrast, Scotto et al. (1983) reported that an exogenous generating system actually decreased ALA production by intact rat liver mitochondria. The protocol described here has been used primarily with 10% homogenates of rat liver that were prepared with low osmolarity buffers and frozen/thawed once before assaying. Under these conditions, addition of a succinyl-CoA generating system gave a low but variable (10% to 60%) increase in ALA production, and it was decided to routinely make this addition (N.W. Cornell, unpub. observ.).

For the colorimetric procedure, as mentioned above, sufficient activity must be present to give reasonable differences in absorbance at 552 to 650 nm for the Ehrlich-pyrrole compound. Anything <0.03 OD units should be regarded as insufficient, and such low values are likely to lead to poor quality spectra as described in the method presented in Basic Protocol 2. Glycine itself gives some color in the reaction with Ehrlich reagent and minimal concentrations are used that still satisfy the high K_M of the enzyme for this substrate. The most frequent problem is the presence of nonspecific reactions of substance carried over from tissue or generated in the acetylacetone reaction, usually due to use of pH values outside the 4 to 6 region during that reaction.

It is always important to use a zero time incubation blank for each sample. This is particularly important when using tissue or cells from animals or cultures highly induced for ALA synthase as there will already be some ALA carrying over from the intact cells. There may be some porphobilinogen pyrrole (PBG) as well, which reacts directly with Ehrlich reagent, but usually there is much less PBG than the generated ALA. Another problem occurs if Ehrlich reagent is made with perchloric acid at <70% (w/v). The reagent must be mixed thoroughly with samples as the reagent is very dense.

Anticipated Results

For the radiometric assay, the actual data acquired are in counts/minute (cpm) for the 1-ml aliquots of Tris eluate mixed with scintillation fluid. Most counters now correct the counts obtained with each sample for background, quenching, and instrumental efficiency, so the output includes cpm and calculated disintegrations/minute (dpm). Each sample should be counted for sufficient time to reduce the statistical counting error to ≤5%; this requires accumulating at least 1600 total counts for each sample. In this protocol, assay of an extract with 0.05 U in 50 µl would give ~200 dpm in the 1 ml of Tris eluate, which would require ~8 to 10 min of counting.

Basal chick embryo and rat liver ALA synthase activities are in the range of 10 to 100 nmol ALA/hr/g liver. Upon induction, values increase to 2000 to 3000 nmol/g liver for chicken embryo (Hamilton et al., 1988); and for rat liver to 400 to 500 nml/hr/g liver (Scotto et al., 1983). In the cultures, activities of 0.3 to 0.6 nmol ALA/hr/mg homogenate protein are observed in livers from untreated embyros and up to 40 nmol/hr/mg protein in highly induced samples.

Time Considerations

For the radiometric assay, if the C and R buffers are prepared, a person experienced with this protocol can process 16 samples through step 11 in ~4 hr. The column chromatography requires ~2.5 hr, but it is greatly facilitated by having a linear rack with clips for holding the chromatography columns. Once the 1 ml of Tris eluant is mixed with scintillation fluid, counting can be postponed until a convenient time. If desired, the procedure can be broken up by conducting the incubation with alkaline SDS (step 6) overnight at room temperature (Scotto et al., 1983).

For the colorimetric assay, solutions should be prepared the day before the tissues samples are harvested from animals or culture. Incubations and preparation of TCA supernatants can be performed the next day, and reactions with Ehrlich reagents and reading of absorbances can be performed on the third day.

Literature Cited

Bishop, D.F. and Wood, W.A. 1977. An assay for δ-ALA synthetase based on a specific, semiautomatic determination of picomole quantities of δ-[^{14}C]aminolevulinate. *Anal. Biochem.* 80:466-482.

Bonkowsky, H.L. and Pomeroy, J.S. 1978. Assay of δ-aminolevulinic acid synthetase in homogenates of mouse, rat and human liver: Species differences in requirement for and exogenous succinyl-CoA-generating system. *Anal. Biochem.* 91:82-91.

Brooker, J.D., Srivastava, G., May, B.K., and Elliot, W.H. 1982. Radiochemical assay for δ-aminolevulinate synthase. *Enzyme* 28:109-119.

Cornell, N.W., Hahn, M.E., and Martin, H.A. 1995. Characterization and use of isolated toadfish hepatocytes for studies of heme synthesis and utilization. *Biol. Bull.* 189:227-228.

Ebert, P.S., Tschudy, D.P., Choudhry, J.N., and Chirigos, M.A. 1970. A simple micro method for the direct determination of δ-amino[^{14}C]levulinic acid production in murine spleen and liver homogenates. *Biochim. Biophys. Acta* 208:236-250.

Hamilton, J.W., Bement, W.J., Sinclair, P.R., Sinclair, J.F., and Wetterhahn, K.E. 1988. Expression of 5-aminolevulinate synthase and cytochrome P450 mRNAs in chicken embryo hepatocytes in vivo and in culture. *Biochem. J.* 255:267-275.

Hunter, G.A. and Ferreira, G.C. 1995. A continuous spectrophotometric assay for 5-aminolevulinate synthase that utilizes substrate cycling. *Anal. Biochem.* 226:221-224.

Lien, L.-F. and Beattie, D.S. 1982. Comparisons and modifications of the colorimetric assay for delta-aminolevulinic acid synthase. *Enzyme* 28:120-132.

Minaga, T., Sharma, M.L., Kun, E., and Piper, W.N. 1978. Enzymatic degradation of succinyl-coenzyme A by rat liver homogenates. *Biochim. Biophys. Acta* 538:417-425.

Riddle, R.D., Yamamto, M., and Engel, J.D. 1989. Expression of delta-aminolevulinate synthase in avaian cells: Separate genes encode erythroid-specific and nonspecific isozymes. *Proc. Natl. Acad. Sci. U.S.A.* 86:792-796.

Sassa, S. and Kappas, A. 1977. Induction of aminolevulinate synthase and porphyrins in cultured liver cells maintained in chemically defined medium. *J. Biol. Chem.* 252:2428-2436.

Scotto, A.W., Chang, L.-F.L., and Beattie, D.S. 1983. The characterization and submitochondrial localization of δ-aminolevulinic acid synthase and an associated amidase in rat liver mitochondria using an improved assay for both enzymes. *J. Biol. Chem.* 258:81-90.

Shoolingin-Jordan, P.M., LeLean, J.E., and Lloyd, A.J. 1997. Continuous coupled assay for 5-aminolevulinate synthase. *Methods Enzymol.* 281:309-316.

Sinclair, P.R. and Granick, S. 1977. Two methods for determining the activity of aminolevulinate synthetase within intact liver cells in culture. *Anal. Biochem.* 79:380-393.

Strand, L.J., Swanson, A.L., Manning, J., Branch, S., and Marver, H.S. 1972. Radiochemical microassay of δ-aminolevulinic acid synthetase in hepatic and erythroid tissues. *Anal. Biochem.* 47:457-470.

Wolfson, S.J., Allen, R.M., and Bloomer, J.R. 1980. Effect of an exogenous succinyl-CoA-generating system on the measurement of δ-aminolevulinic acid synthase activity in rat liver tissue by a radiochemical assay. *Biochim. Biophys. Acta* 611:72-78.

Yoda, B., Schacter, B.A., and Israels, L.G. 1975. δ-Aminolevulinic acid synthetase assay in chicken liver homogenates and particulate fractions. *Anal. Biochem.* 66:221-233.

Key References

Ebert et al., 1970. See above.

Provides a detailed description of the chromatographic isolation of aminolevulinate with a cation-exchange resin.

Scotto et al., 1983. See above.

Describes the development and application of the SDS procedure for stopping incubations.

Sinclair and Granick, 1977. See above.

Describes the colorimetric method and the adaptation for direct assay of activity in cultured hepatocytes.

Contributed by Peter R. Sinclair and Nadia Gorman
VA Medical Center
White River Junction, Vermont

Neal W. Cornell
Marine Biology Laboratory
Woods Hole, Massachusetts

Measurement of Heme Concentration

Heme (iron-protoporphyrin IX) is the prosthetic group of a number of hemoproteins in different tissues including hemoglobin, myoglobin, cytochrome P-450s, mitochondrial cytochromes, catalase, and peroxidases. The measurement of heme is often used as an indirect way to show the changes in liver cytochrome P-450. Heme present in the so-called "free heme" pool, which is used for the synthesis of these hemoproteins, is also the regulator of the first enzyme in the biosynthesis of heme, δ-aminolevulinate synthase. Environmental agents and mutations of the biosynthetic pathway can affect the synthesis and degradation of heme, which is most readily measured using radioactive precursors. In this unit several methods are described for measuring heme concentration in tissue homogenates or cultured cells. The basic method measures heme as the pyridine hemochrome, which has a characteristic spectrum and is readily measured spectrophotometrically (see Basic Protocol). A more sensitive fluorescence method, particularly suitable for cultured cells, is also presented (see Alternate Protocol 1). An HPLC-based method is presented for purifying and quantifying heme itself and other hemes such as heme A (see Alternate Protocol 2). Finally, the use of these basic methods to measure radioactive heme is presented for the determination of rates of heme synthesis (see Alternate Protocol 3).

SPECTROPHOTOMETRIC HEME ASSAY OF PYRIDINE HEMOCHROME

BASIC PROTOCOL

In this assay the nitrogen ligands from protein-bound heme are replaced by pyridine in alkali. The resultant hemochrome is quantitated by the difference spectrum of the reduced and oxidized compound. The sensitivity of the assay is a function of the sensitivity of the spectrophotometer and of the ability to use microcells for minimal volumes.

CAUTION: Due to the toxicity and odor of pyridine, the procedure should be performed in a hood as much as possible and cuvettes should be capped or sealed with Parafilm.

Materials

5% (w/v) tissue sample suspension: tissue homogenate, or a homogenate or sonicate of tissue culture cells (minimally, 2 mg protein)
Reagent-grade pyridine (discard if yellow)
1.0 M NaOH
Sodium dithionite crystals
3 M potassium ferricyanide

12 × 75–mm disposable glass tubes (Fisher)
Sensitive scanning spectrophotometer
Appropriate cuvettes with caps

1. Place 0.84 ml of 5% (w/v) aqueous tissue sample suspension in a 12 × 75–mm disposable glass tube.

   The volumes given throughout the assay can be reduced or increased proportionately.

2. Add 0.2 ml reagent-grade pyridine and mix by vortexing.
3. Add 0.1 ml of 1 M NaOH and mix thoroughly by vortexing.

   In tissue culture assays, NaOH can be replaced by 0.16 M sodium borate, pH 9.0.

4. Split the sample between two cuvettes and obtain a baseline absorbance spectrum from 500 to 600 nm.
5. Using the tip of a fine spatula, add a few crystals of sodium dithionite and 0.01 ml water to one cuvette and mix to reduce hemochrome.

Contributed by Peter R. Sinclair, Nadia Gorman, and Judith M. Jacobs
Current Protocols in Toxicology (1999) 8.3.1-8.3.7

Very little dithionite is needed and the amount depends in part on the volume and other reducible compounds present. The solid should be a free-running powder and should be stored in small vials in a desiccator. Discard if it becomes totally solid and buy a new stock bottle once a year.

6. Add 0.01 ml of 3 M potasium ferricyanide to the other cuvette and mix to oxidize the hemochrome.

   Ferricyanide may not be necessary, but the effect should be tested.

7. Obtain and record a spectrum of reduced versus oxidized heme between 500 and 600 nm.

   To ensure that reduction is complete, a little more dithionite can be added and the spectrum rescanned to see if any increase occurs.

8. Calculate heme concentration based on the millimolar extinction coefficient of 20.7 for the difference in absorption between the peak at 557 nm and the trough at 541 nm.

ALTERNATE PROTOCOL 1

FLUORESCENCE HEME ASSAY

In this method, the iron in heme is removed by heating in a strong oxalic acid solution and the resultant protoporphyrin is measured by fluorescence. This method needs to be optimized for each type of tissue used, but it is very sensitive. One disadvantage is that the method cannot be used when the tissue already contains a large amount of porphyrin or other substances that fluoresce at the assay wavelengths, unless the amount of this fluorescence can be accurately subtracted using a reagent blank.

Materials

Tissue culture cells or tissue (sonicate or homogenate; see Basic Protocol materials)
2 M oxalic acid solution (see recipe)
1 mg/ml heme standard solution (see recipe) or protoporphyrin standard solution (Porphyrin Products)

Heating block at 100°C
6 × 50–mm disposable glass tubes (Fisher)
Spectrofluorometer equipped with cell holder and preferably with red-sensitive phototube (Hamamatsu R928, R446, or R3896, or equivalent)

1. Collect tissue culture cells in 6 × 50–mm disposable glass tubes by centrifugation or place a small volume (up to 50 µl) in the tubes.

   Protein amount should be <10 µg/tube. The assay is linear from 1 nM to 1 µM (or 0.5 pmol to 0.5 nmol) heme per tube.

   The assay is most conveniently performed using a cell holder that holds four 6 × 50–mm tubes. Alternatively, samples can be transferred into disposable plastic cuvettes for fluorescent measurements.

2. Add 0.5 ml of 2 M oxalic acid solution and mix thoroughly.

3. Put sample tubes in a heating block set at 100°C for 30 min. Do not heat blanks.

   Blank and sample tubes contain tissue and oxalic acid, but the blanks are not heated.

4. Read fluorescence of porphyrin using 400 nm excitation and 662 or 608 nm emission, after determining that these represent the actual peaks with the instrument used.

   The 662 nm emission peak has lower fluorescence than the peak at 608 nm, but also has less scatter and other interference.

   Actual peaks vary from instrument to instrument.

5. Subtract blank values (parallel unheated samples in oxalic acid) from samples.

6. Calculate heme content based on a standard heme curve over the range of 0 to 1 nmol heme per tube, or calibrate with 1 mg/ml heme standard solution or a protoporphyrin standard.

ASSAY OF HEME AND BIOSYNTHETIC INTERMEDIATES BY REVERSED-PHASE HPLC

ALTERNATE PROTOCOL 2

This method, though considerably more elaborate than those described above, gives more precise assays for heme and also measures intermediates in the heme pathway. Other modifications permit the detection of heme A (the prosthetic group of cytochrome oxidase) and its biosynthetic intermediate, heme O (Tzagoloff et al., 1993).

CAUTION: Acetone is highly flammable and should not be used near heaters or open flames. Acetone will dissolve tissue culture plastic and should not remain in contact with plastic for >5 min.

CAUTION: When working with radioactivity, take appropriate precautions to avoid contamination of the experimenter and the surroundings. Carry out the experiment and dispose of wastes in an appropriately designated area, following the guidelines provided by the local radiation safety officer (also see *APPENDIX 1A*).

Materials

Tissue culture cells or tissue (sonicate or homogenate; see Basic Protocol materials)
Aqueous cell homogenate or tissue culture cells
Acetone/HCl/water (see recipe)
Acetone/HCl (see recipe)
Buffer A (see recipe)
HPLC-grade methanol (buffer B)
Heme/porphyrin standard injection mixture (see recipe)

HPLC system with multisolvent delivery system, absorbance detection for heme (400 nm), and fluorescence detection for porphyrins (excitation 400 nm, emission 600 nm)
C18 HPLC column (e.g., Waters μBondapak; 39 × 300 mm) and C18 precolumn

1a. *For tissue culture cells in culture dishes:* Remove culture medium from tissue culture dishes and add acetone/HCl/water (e.g., 2 ml to a 6-cm dish) directly to the cells. Remove solution and repeat extraction.

The extraction is performed with acetone/HCl/water, because in the absence of water heme is trapped in the dehydrated pellets and is then only slowly extractable using multiple extractions.

1b. *For cell homogenates:* Add an equal volume of acetone/HCl to an aqueous cell homogenate, mix vigorously, and centrifuge 10 min at 2000 × *g* using capped tubes. Transfer the extracts to glass tubes with screw-on caps. Reextract with half the original volume of acetone/HCl/water.

The second extraction is performed with acetone/HCl/water, because in the absence of water heme is trapped in the dehydrated pellets and then requires multiple extractions.

2. Mix acetone extract with an equal volume of buffer A, pH 7 to 8, and test some samples to check that the final pH is 3.5 to 4.0.

The resulting solution can be injected onto the column or stored up to 24 hr in the dark at room temperature.

3. Load 0.25 to 1.0 ml heme/porphyrin standard injection mixture on a C18 HPLC column and run gradient HPLC over 15 min with a linear gradient from 60%/40% (v/v) buffer A/buffer B to 100% buffer B.
4. Maintain at 100% buffer B for another 10 min.
5. Return to original conditions over 5 min, then maintain for 10 min before injecting the first sample.
6. Repeat steps 3 to 5 for samples.

NOTE: *The method must be optimized for each HPLC system and column due to differences in packing material and pump head volumes. The pH of buffer A may have to be optimized between pH 3.0 and 3.5 for maximal separation.*

ALTERNATE PROTOCOL 3

ASSAY OF RADIOACTIVE HEME BY SOLVENT EXTRACTION

This method is for the measurement of newly synthesized heme in tissue culture cells and is based on the specific activity of the added radioactive compound. This method can also be used for measuring total heme if labeling with radioactive δ-aminolevulinic acid (ALA) is continued for sufficient time (≥24 hr) to essentially replace all heme in the cells. The protocol described for measuring labeled heme involves a rapid solvent extraction and purification. Determination of radiolabel in heme biosynthetic intermediates can be determined by HPLC as described above (see Alternate Protocol 2). Suitable radioactive heme precursors include [^{14}C]glycine, [4-^{14}C]ALA, and [^{3}H]ALA. Because glycine will label many cellular compounds, the solvent extraction method is not suitable for preparation of heme when glycine is used as the radioactive precursor.

CAUTION: When working with radioactivity, take appropriate precautions to avoid contamination of the experimenter and the surroundings. Carry out the experiment and dispose of wastes in an appropriately designated area, following the guidelines provided by the local radiation safety officer (also see *APPENDIX 1A*).

CAUTION: Ethyl ether is highly flammable and the vapors are dense, tending to run across laboratory benches. The whole extraction and evaporation process should be performed in an explosion-proof hood. Because stored ether can develop peroxides and explode, it is best to use small bottles and to dispose of any remaining liquid by evaporation in a hood. Do not store opened bottles for >1 month.

CAUTION: Acetone is highly flammable and should not be used near heaters or open flames. Acetone will dissolve tissue culture plastic and should not remain in contact with plastic for >5 min.

Materials

Radiolabeled tissue culture cells
2 M HCl
Ethyl ether
Aqueous scintillation fluid
~45°C water bath

Additional reagents and equipment for preparing acetone extracts (see Alternate Protocol 2)

1. Prepare acid acetone extracts (see Alternate Protocol 2, steps 1a and 1b) of tissue culture cells incubated with radioactively labeled glycine or 5-aminolevulinic acid (ALA).

The amount and concentration of radioactive compound must be optimized for different cell types.

2. Place all of the acid-acetone extract in a 20-ml glass scintillation vial.
3. Add 5 ml ethyl ether and 2 ml of 2 M HCl. Screw on plastic ether- and acetone-resistant caps and vortex vigorously. Allow the layers to separate.

   Heme is extracted into the ether upper layer and labeled porphyrins into the aqueous layer.

4. Remove the bottom (aqueous) layer with a Pasteur pipet and discard. Repeat extraction of ether with another 2 ml of 2 M HCl. Repeat once more.
5. Evaporate ether by placing vial in a warm water bath (~45°C).
6. Add aqueous scintillation solution, mix well to dissolve the heme, and determine radioactivity in a suitable counter.

REAGENTS AND SOLUTIONS

Use Milli-Q-purified water or equivalent for all recipes and protocol steps. For common stock solutions, see ***APPENDIX 2A****; for suppliers, see* ***SUPPLIERS APPENDIX****.*

Acetone/HCl

97.5 ml acetone
2.5 ml concentrated HCl
Prepare fresh

Acetone/HCl/water

97.5 ml acetone
2.5 ml concentrated HCl
20 ml water
Prepare fresh

Buffer A

For HPLC gradient: Dissolve 19.3 g $NH_4H_2PO_4$ in 1680 ml double-distilled water and filter through a 0.22-µm filter. Add 1320 ml HPLC-grade methanol (final 56 mM $NH_4H_2PO_4$). Adjust pH to 3.15 with concentrated H_3PO_4. Store up to several months at room temperature.

For addition to sample: Add 10 M NaOH (*APPENDIX 2A*) to buffer A to adjust pH to 7 to 8 (requires ~0.015 ml NaOH per milliliter buffer A).

Heme standard solution, 1 mg/ml

Dissolve heme at 1 mg/ml in dimethyl sulfoxide (DMSO). Determine concentration by spectrophotometry of an ~1:300 (v/v) dilution in 40% (v/v) DMSO, using a millimolar extinction coefficient of 180 at 400 nm. Store indefinitely at room temperature.

Heme/porphyrin standard injection mixture

For 0.2 mM heme standard solution: Dissolve 2.6 mg heme in 20 ml dimethyl sulfoxide (DMSO). Check concentration by spectrophotometry of a 1:40 (v/v) dilution in 40% (v/v) DMSO, using a millimolar extinction coefficient of 180 at 400 nm. Store indefinitely at room temperature.

For 0.25 mM protoporphyrin standard solution: Dissolve 2.5 mg protoporphyrin in 20 ml dimethyl sulfoxide (DMSO). Check concentration by spectrophotometry of a 1:80 (v/v) dilution in 2.7 M HCl, using a millimolar extinction coefficient of 262 at 410 nm. Store indefinitely at room temperature.

continued

For standard solution of other porphyrins: Use a commercially available mixture (Porphyrin Products) containing 10 nmol of each porphyrin per tube. Dissolve according to supplier's instructions. Store indefinitely at room temperature.

For standard injection mixture: Use appropriate volumes of diluted standard solutions such that the injected volume contains 50 to 200 pmole heme and 5 to 20 pmole of protoporphyrin and each other porphyrin. Store indefinitely at room temperature.

Porphyrins are light sensitive. Samples containing porphyrins need to be protected from direct light and should be in dark vials when used in an autosampler.

Oxalic acid, 2 M

Prepare a 2 M solution of oxalic acid in water. Because this is close to saturation, heat solution to dissolve. Cool to room temperature and use the saturated supernatant. Store up to several months at room temperature.

COMMENTARY

Background Information

The protocols described here provide methods for determining the amount of heme in tissue samples and cultured cells. The values obtained can be compared with assays of individual hemoproteins. In liver, for example, more than half of the heme may be present in cytochrome P-450s. Following drug treatments that induce cytochrome P-450, two- to threefold increases in heme may be observed. For isolated microsomes, total heme is often compared with total cytochrome P-450, determined spectrophotometrically or immunologically, in order to determine whether the cytochrome is present as the apo or holo forms.

Four different protocols are described to measure heme. The simplest and most often used remains measurement of heme from the reduced-minus-oxidized difference spectrum of the pyridine hemochrome as originally used by Paul et al. (1953) and described in Fuhrhop and Smith (1975). The main disadvantage of this method is the use of pyridine and the requirement for a sensitive scanning spectophotometer. Use of the difference spectrum allows assay of heme in the presence of other colored compounds (such as porphyrins) and turbidity. With instruments that have the ability to determine spectra of turbid samples, this method can be used with samples that contain small amounts of heme and that scatter light. It is advisable to spike such samples with heme to ensure the method is yielding quantitative results. Dual-wavelength spectrophotometry, in which only one cuvette is required, can be used for measurement of the pyridine hemochrome. The baseline spectrum is subtracted from that of the subsequent reduced samples (Berry and Trumpower, 1987).

The fluorescence assay for heme (Sassa, 1976) is more sensitive than the pyridine hemochrome, but needs to be optimized for each tissue, adding heme to samples to determine the linear range of the response. HPLC determinations of heme are probably the most accurate, once the recovery of the extraction has been determined. It also provides a pure product and the concentrations of some other heme synthetic intermediates are also obtained (Bonkovsky et al., 1986; Jacobs et al., 1992). This HPLC method can also be used to determine radioactivity in heme in tissue culture samples, or heme can be extracted and prepared free of other radioactive heme pathway components by the solvent extraction and washing method described (Healey et al., 1981; Jacobs et al., 1998). The advantage of the latter procedure is the removal of radioactive porphyrins in the acid wash. A third wash is recommended to ensure that the heme remaining in the ether is not contaminated with porphyrins, which usually have much higher specific activities than the heme itself. Even heme labeled with ^{59}Fe can be purified in this way, in which the acid washing of the heme in ether effectively removes free ^{59}Fe (Taketani et al., 1998).

One problem with all of these methods is that total protoheme is measured, including that from hemoglobin. Therefore, perfusion should be used to remove as much blood as possible from the tissue in order to obtain useful data. It is possible to independently measure hemoglobin by converting it to methemoglobin and measuring this by the cyanide complex (Waterman, 1978).

Critical Parameters and Troubleshooting

In the pyridine hemochrome method, the condition of the solid dithionite is important, as well as ensuring that neither too little nor too

much of this powerful reductant is used for reducing the hemochrome. It is important that spectra of high quality be produced with two definite peaks at 557 and 526 nm. The spectrum of the hemochrome of pure heme should be determined for comparison. Likewise, the fluorescence spectrum of de-ironed heme (protoporphyrin) should be compared to that of pure protoporphyrin (Sassa, 1976), noting that the ratios of the two fluorescence peaks can vary with different photomultipliers.

In the heme extraction method with acetone/HCl into ether, emulsions may be produced with highly fatty tissues. These can usually be broken by cooling the samples and with centrifugation, if necessary. Although this method will give radioactive pure heme in most cases (plus a small amount of heme A), the authors have found that, using HPLC and in the presence of iron in tissue cultures, the ether fraction contains considerable radioactivity that is not heme. This probably contains heme degradation products.

Anticipated Results

These heme extraction procedures usually give ~75% to 80% recovery of heme added to samples. This number may need to be determined using spiked controls and applied as a correction factor to data obtained by this method. Heme values of 100 to 200 pmol/mg protein can be expected from chick hepatocytes (Sassa and Kappas, 1977).

Time Considerations

The pyridine hemochrome and fluorescence methods are only limited by the time taken to prepare and run the spectrum for each sample. The heme extraction for 20 to 40 samples can be performed in ~2 to 3 hr. HPLC analyses are limited by the 45-min required for each sample. However, 20 samples can be analyzed overnight with an autosampler.

Literature Cited

Berry, E.A. and Trumpower, B.L. 1987. Simultaneous determination of hemes a, b, and c from pyridine hemochrome spectra. *Anal. Biochem.* 161:1-15.

Bonkovsky, H., Wood, S., Howell, S., Sinclair, P., Lincoln, B., Healey, J., and Sinclair, J. 1986. High performance liquid chromatographic separation and quantitation of tetrapyrolles from biological materials. *Anal. Biochem.* 155:56-64.

Fuhrhop, J.-H. and Smith, K.M. 1975. Laboratory methods in porphyrin and metalloporphyrin research, pp. 48-51. Elsevier Scientific Publishing, Amsterdam.

Healey, J.F., Bonkowsky, H.L., Sinclair, P.R., and Sinclair, J.F. 1981. Conversion of 5-aminolaevulinate into haem by liver homogenates. *Biochem. J.* 198:595-604.

Jacobs, J.M., Sinclair, P.R., Gorman, N., Jacobs, N.J., Sinclair, J.F., Bement, W.J., and Walton, H.S. 1992. Effects of diphenyl ether herbicides on porphyrin accumulation by cultured hepatocytes. *J. Biochem. Toxicol.* 7:87-95.

Jacobs, J.M., Sinclair, P.R., Sinclair, J.F., Gorman, N., Walton, H.S., Wood, S.G., and Nichols, C. 1998. Formation of zinc protoporphyrin in cultured hepatocytes: Effects of ferrochelatase inhibition, iron chelation or lead. *Toxicology* 125:95-105.

Paul, K.G., Theorell, H., and Akeson, A. 1953. The molar light absorption of pyridine ferroprotoporphyrin (pyridine hemochromogen). *Acta Chem. Scand.* 7:1284-1287.

Sassa, S. 1976. Sequential induction of heme enzymes during erythroid differentiaion of mouse Friend leukemia virus–infected cells. *J. Exp. Med.* 143:305-315.

Sassa, S. and Kappas, A. 1977. Induction of aminolevulinate synthase and porphyrins in cultured liver cells maintained in chemically defined medium. *J. Biol. Chem.* 252:2428-2436.

Taketani, S., Immenschuh, S., Go, S., Sinclair, P.R., Stockert, R.J., Liem, H.H., and Muller Eberhard, U. 1998. Hemopexin from four species inhibits the association of heme with cultured hepatoma cells or primary rat hepatocytes exhibiting a small number of species specific hemopexin receptors. *Hepatology* 27:808-814.

Tzagoloff, A., Nobrega, M., Gorman, N., and Sinclair, P. 1993. On the functions of the yeast COX10 and COX11 gene products. *Biochem. Mol. Biol. Int.* 31:593-598.

Waterman, M.R. 1978. Spectral characteristics of human hemoglobin and its derivatives. *Methods Enzymol.* 52:456-463.

Key References

Bonkovsky et al., 1986. See above.

Describes basic HPLC method.

Healey et al., 1981. See above.

Describes the method of extracting radioactive heme from liver homogenates.

Contributed by Peter R. Sinclair
Veterans Administration Medical Center
White River Junction, Vermont
Dartmouth Medical School
Hanover, New Hampshire

Nadia Gorman and Judith M. Jacobs
Dartmouth Medical School
Hanover, New Hampshire

Measurement of Uroporphyrinogen Decarboxylase Activity

Uroporphyrinogen decarboxylase (UROD) catalyzes the decarboxylation of the four acetate side chains of uroporphyrinogen to form coproporphyrinogen. Both naturally occurring isomers of uroporphyrinogen (isomers I and III) are substrates for UROD, but only coproporphyrinogen III can ultimately be converted to heme. Subnormal activity of UROD in hepatocytes is the cause of porphyria cutanea tarda (PCT), the most common form of porphyria in humans. *UNIT 8.1* provides a more detailed description of the enzyme and diseases associated with deficient activity.

UROD activity can be assayed using a variety of substrates. Any of the intermediates in the conversion of uroporphyrinogen to coproporphyrinogen can serve as substrates for the enzyme (i.e., porphyrinogens with seven, six, or five carboxyl groups of either the I or III isomer series). Commercially available porphyrins can be chemically reduced to the corresponding porphyrinogens with either sodium amalgam or potassium borohydride. Uroporphyrinogen I can also be formed enzymatically.

This unit contains protocols for measuring UROD activity using substrate that is enzymatically prepared (see Basic Protocol) or chemically prepared (see Alternate Protocol). Once the substrate has been formed, the UROD assay reaction and analysis of the products in the Basic Protocol and Alternate Protocol are quite similar. There are also protocols for preparation of bacterial porphobilinogen deaminase (PBGD; see Support Protocol 1), which is used to prepare the substrate in the Basic Protocol, and erythrocyte lysates for UROD activity measurements (see Support Protocol 2).

MEASUREMENT OF UROD ACTIVITY USING ENZYMATICALLY REDUCED PORPHYRINS AS SUBSTRATES

BASIC PROTOCOL

Assaying UROD activity can be divided into three steps. The first is to form the porphyrinogen substrate for the assay. In this protocol, the enzymatic preparation of uroporphyrinogen I is described (an alternative procedure involving the chemical reduction of commercially available porphyrins is described in the Alternate Protocol). The second step is the reaction of the substrate with the source of UROD to be assayed. The third step is the separation and quantification of the reaction products. Regardless of how the substrate is generated, the second step must be started immediately, as porphyrinogens are oxidized quickly. Once the second step is completed, the products are quite stable and can be analyzed when convenient. This protocol is partially modified from Straka et al. (1982).

Materials

- 0.1 M dithiothreitol (DTT) in 0.1 M Tris·Cl, pH 7.65 (see *APPENDIX 2A* for Tris·Cl buffer)
- 2.4 mM porphobilinogen (Porphyrin Products) in 0.1 M Tris·Cl, pH 7.65 (see *APPENDIX 2A* for Tris·Cl)
- Porphobilinogen deaminase (PBGD; see Support Protocol 1), diluted in 10 mM KH_2PO_4, pH 7.6 so that 150 µl will produce 30 to 60 µM uroporphyrinogen in 30 min in the reaction mix in step 2
- N_2 source
- 0.15 M KH_2PO_4, pH 4.45 (mix 1 M KH_2PO_4 and 1 M K_2HPO_4 to a pH of 4.5 and dilute to 0.15 M with H_2O)
- UROD source to be assayed (see, e.g., Support Protocol 2)
- 0.1 M DTT in 0.1 M KH_2PO_4, pH 6.8 (see *APPENDIX 2A* for potassium phosphate buffer)

continued

Contributed by John D. Phillips and James P. Kushner

Current Protocols in Toxicology (1999) 8.4.1-8.4.13

3 M HCl
3.5 µM mesoporphyrin IX dihydrochloride (Porphyrin Products)
Methanol (HPLC grade)
Methanol/phosphate (see recipe)
Porphyrin standards, dissolved in 3.0 M HCl (Porphyrin Acids Chromatographic Marker Kit, Porphyrin Products)

12 × 75–mm tube to prepare substrate
Red lamp
Woods lamp (UV, "black light")
HPLC system fitted with a gradient maker and fluorescence detector (excitation 404 nm, emission 618 nm)
C18 column for separation of porphyrins (e.g., Waters µBondapak 3.9 × 300 mm)

Prepare reaction mix

1. Determine the number of samples to be assayed (see steps 4 and 5), including at least one blank. Prelabel assay tubes in duplicate and keep on ice to avoid delays; also calculate the amount of uroporphyrinogen I substrate solution which must be prepared in step 2.

   Each assay tube will require 0.30 ml of the uroporphyrinogen I solution that will be prepared in step 2, making allowances for pipetting errors.

Enzymatically generate uroporphyrinogen I substrate solution

2. For each duplicate sample to be assayed, including the blanks, combine the following in a 12 × 75–mm tube in the dark or under red light:

   50 µl 0.1 M DTT in 0.1 M Tris·Cl, pH 7.65
   50 µl 2.4 mM PBG
   150 µl PBGD solution (appropriately diluted; see Support Protocol 1).

   Thoroughly purge the reaction mix with N_2 gas, and top the tube with N_2 before sealing tightly. Incubate 30 to 40 min at 37°C.

   Tubes can be sealed with Parafilm or 000 stoppers depending on quantity and preference. The key is to reduce O_2 as quickly and completely as possible.

   The reaction described will produce enough uroporphyrinogen I so that there will be ~30 µM substrate in the decarboxylation reaction, a saturating concentration for UROD in most tissue lysates. See Straka et al. (1982) for additional detail.

   The amount of substrate prepared must be scaled appropriately, taking into consideration that samples are usually assayed in duplicate and that allowances must be made for pipetting errors. For instance, if 20 tubes are to be prepared in step 4 the reaction mixture above would be scaled up to 1.00 ml of 0.1 M DTT, 1.00 ml of 2.4 mM PBG, and 3.00 ml of the PBGD solution; the reaction would then be stopped using 1.00 ml of 0.15 M KH_2PO_4, pH 4.45, in step 3.

3. Place on ice and stop the reaction by adding 50 µl of 0.15 M KH_2PO_4, pH 4.45, which will inactivate PBGD by lowering the pH from 7.65 to 6.80.

   This is the optimal pH for the UROD reaction in the subsequent steps.

React assay samples with substrate

4. Working in the dark or under a red lamp to avoid photooxidation of the substrate, add the following to each assay tube, on ice:

   175 µl of UROD source to be assayed
   25 µl 0.1 M DTT in 0.1 M KH_2PO_4, pH 6.8
   300 µl of substrate from step 3.

   Top tubes with N_2, mix gently, and incubate in the dark for 30 min at 37°C.

Table 8.4.1 Solvent Gradient for HPLC Separation of Porphyrins

Time (min)	Flow rate (ml/min)	Methanol/phosphate[a]	Methanol	Slope[b]
0	1.0	100%	0%	—
13	1.0	0%	100%	5
15	1.0	0%	100%	1
15.1	1.0	100%	0%	6
25	1.0	100%	0%	1

[a]See recipe in Reagents and Solutions.
[b]Gradient curve profile as specified by Waters.

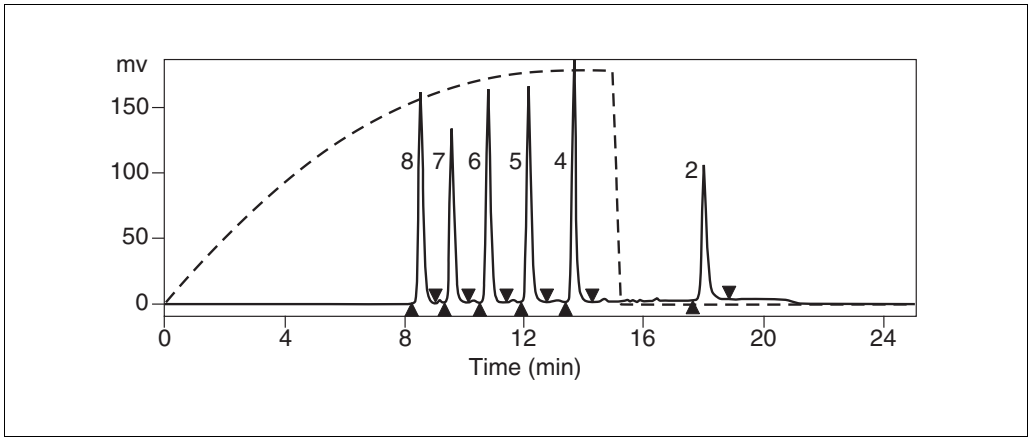

Figure 8.4.1 Chromatogram of porphyrin standards separated by reverse-phase HPLC. A 25-µl aliquot of a standard containing 62.5 pmol of each of the following porphyrins was separated with a Waters HPLC system using a C18 column: uroporphyrin (8), heptacarboxyl porphyrin (7), hexacarboxyl porphyrin (6), pentacarboxyl porphyrin (5), coproporphyrin (4), and mesoporphyrin (2). The aqueous solvent was 50% (v/v) methanol/NaH_2PO_4, pH 4.5; the organic phase was 100% methanol. A flow rate of 1 ml/min was used and the shape of the gradient is shown with the dashed line. The peaks were quantified with the Millennium software provided with the instrument.

When assaying UROD activity from a tissue homogenate or cell lysate (see Support Protocol 2), it is important to include a "no substrate" control reaction to account for any endogenous porphyrins present in the sample. A blank (substrate only, no enzyme) should also be included to verify the concentration of uroporphyrinogen I in the reaction mix.

5. Add 500 µl of 3 M HCl to each tube to stop the reaction. Place samples at room temperature under a Woods lamp for 30 min to oxidize porphyrinogens to porphyrins.

   If a Woods lamp is not available, samples can be oxidized in sunlight for 1.5 to 2 hr.

Separate and quantify reaction products

6. Microcentrifuge samples 5 min at 13,000 × *g*, room temperature, to bring down precipitated proteins.

7. Remove a 100-µl aliquot of the supernatant and mix it with 20 µl of 3.5 µM mesoporphyrin IX dihydrochloride as an internal standard.

   This serves both to be a reference for quantification and to monitor retention time of the porphyrin peaks.

   Retain the remainder of the supernatant in case samples need to be rerun on the HPLC.

8. Set up HPLC system with C18 column to separate porphyrins. Program the solvent delivery system of the HPLC as described in Table 8.4.1. Inject a 25-µl aliquot of each internal-standard-spiked sample from step 7 into the HPLC system.

9. Detect the elution of the porphyrins with a fluorescence detector set at an excitation wavelength of 404 nm and emission wavelength of 618 nm (Ford et al., 1981).

Uroporphyrin elutes first and porphyrins containing fewer carboxyl groups are retained longer.

10. Using the same HPLC technique as for the samples, analyze a standard (from the chromatographic marker kit) that contains 62.5 pmol each of 8-, 7-, 6-, 5-, 4-, and 2-carboxylporphyrins and set up a calibration profile (Fig. 8.4.1).

11. Quantify chromatogram from each sample by comparison to the standard, using software provided with the HPLC system. Express activity as nmol substrate decarboxylated per hr per mg of protein or hemoglobin, or per liter of red cells.

If UROD that has been purified to homogeneity is used, a specific activity can be calculated.

ALTERNATE PROTOCOL

MEASUREMENT OF UROD ACTIVITY USING CHEMICALLY REDUCED PORPHYRINS AS SUBSTRATES

This protocol describes the chemical reduction of porphyrins to generate porphyrinogen substrates for UROD. The porphyrin to be used is solubilized and quantified spectrophotometrically. A quantity sufficient for the assay is reduced by the addition of sodium amalgam. The pH of the porphyrinogen solution is adjusted, and the solution is incubated with the fraction containing the UROD enzyme. The total volume of the reaction is reduced by half when using chemically reduced substrates, as the porphyrins are relatively costly. The buffering capacity of the reaction has also been increased because of the alkaline nature of the chemically reduced substrate. Analysis and quantification of the reaction products is the same as described above for the enzymatically generated substrate (see Basic Protocol).

NOTE: If the pentacarboxyl porphyrinogen I isomer is used as a substrate, the UROD assay should be run at pH 5.4 (Francis and Smith, 1984). Buffers used for the assay should be adjusted to pH 5.4 in this specific case.

Additional Materials *(also see Basic Protocol)*

Porphyrin dihydrochloride (generally uroporphyrin I or III or pentacarboxyl porphyrin I or III; Porphyrin Products)
2 M NH_4OH
1.5 M HCl
1 M and 50 mM KH_2PO_4, pH 6.8 (*APPENDIX 2A*)
5% sodium amalgam (Anachemia, or as prepared in Straka et al., 1982)
1 M DTT
2 M H_3PO_4
pH paper, 5 to 10 range

Desiccator jar large enough for a tube rack and ice, with a 3-way stopcock
Spectrophotometer (able to scan from 350 nm to 550 nm)

Chemically reduce a porphyrin

1. Solubilize 5 to 10 mg of the porphyrin by adding 3 to 4 drops of 2 M NH_4OH.

2. Dilute 2-µl aliquots of the porphyrin 1:1000 and 1:10,000 with 1.5 M HCl. Scan each of these dilutions from 370 nm to 430 nm and record the absorbance at the peak.

3. Calculate the concentration of porphyrin present based on the molar extinction coefficients given in Table 8.4.2.

Table 8.4.2 Wavelength Maxima and Molar Extinction Coefficients for Porphyrins in 1.5 M HCl[a]

Substrate	Wavelength maximum (nm)	ε $(mM/l)^{-1}$ cm^{-1}
Uroporphyrin	406	541
Heptacarboxyl porphyrin	405	528
Hexacarboxyl porphyrin	404	514
Pentacarboxyl porphyrin	402	502
Coproporphyrin	400	489

[a]Values from Straka et al., 1982.

4. Dilute the porphyrin solution to 2 mM in 50 mM KH_2PO_4, pH 6.8. Top tube with nitrogen and keep on ice.

   IMPORTANT NOTE: *All subsequent steps should be performed in nitrogen-purged tubes, on ice, and in the dark or under red light to minimize oxidation.*

5. Add ~75 to 150 mg of 5% sodium amalgam (blot dry before use) per 100 µl of porphyrin solution to be reduced. Top tube with nitrogen, seal, and incubate on ice, vortexing occasionally.

   CAUTION: *Sodium amalgam is a chemical with high reductive potential, so explosions may occur. The reaction using sodium amalgam produces mercury, which must be disposed of properly. Work in a fume hood and take appropriate safety precautions.*

6. Check the reduction of porphyrin to porphyrinogen periodically by briefly examining the tube under the Woods lamp.

   When no fluorescence is visible, the reduction is complete, usually after 5 to 10 min for a 100- to 200-µl sample.

React porphyrinogen with UROD source

7. Before running the actual reactions, set up a mock reaction tube to determine the amount of H_3PO_4 required to achieve a final pH of 6.8, by adding the following to a tube in the order indicated:

   5 µl of the reduced substrate solution from step 6
   20 µl 1 M KH_2PO_4
   2.5 µl 1 M DTT
   5 µl 2 M H_3PO_4
   42.5 µl 50 mM KH_2PO_4.

   Finally, add an additional 175 µl 50 mM KH_2PO_4 (to account for the enzyme fraction to be added). Check the pH by spotting on pH paper; it should be ~6.8. If not, add 1- to 2-µl increments of 2 M H_3PO_4, checking the pH after each addition. Once a pH of 6.8 has been reached, record the amount of 2 M H_3PO_4 added and add this amount of 2 M H_3PO_4 to each of the samples to be assayed (see step 9; however, in step 8 adjust volume of 50 mM KH_2PO_4 to maintain a final total volume of 250 µl if the amount of 2 M H_3PO_4 needed is >5 µl).

8. For each sample to be assayed, add the following in the order indicated to a microcentrifuge tube on ice:

   42.5 µl 50 mM KH_2PO_4 (adjusted for volume of 2 M H_3PO_4 needed; see step 7)
   2.5 µl 1 M DTT
   20 µl 1 M KH_2PO_4
   175 µl sample of the UROD source (~1 µg of purified UROD protein) to be assayed.

   Mix each tube and place in a rack. Place the rack on ice in a desiccator and purge desiccator twice with nitrogen. Let stand for 5 to 10 min to remove oxygen.

9. Remove the tubes from the desiccator and, while blowing nitrogen over the top of the solution, add 5 µl H_3PO_4 (or volume determined in step 7) down one side of the tube, then add 5 µl of substrate (from step 6) down the other side. Cap the tubes, mix gently, and return to ice.

   Have solutions ready before removing tubes; this step should be done quickly minimizing exposure to O_2.

10. When all samples are ready, place them in a 37°C water bath and incubate in the dark for 30 min.

11. Add 250 µl 3 M HCl to stop the reaction.

12. Oxidize for 30 min under the Woods lamp, and then microcentrifuge 5 min at 13,000 × *g*, room temperature, to bring down precipitated proteins.

13. Quantify reaction products by HPLC (Basic Protocol, steps 7 to 11).

SUPPORT PROTOCOL 1

PURIFICATION OF PBGD FROM *RHODOBACTER SPHEROIDES*

The conjugation of four molecules of porphobilinogen into the tetrapyrrole hydroxymethylbilane requires the enzyme porphobilinogen deaminase (PBGD). Hydroxymethylbilane is the substrate for uroporphyrinogen III synthase and is a highly labile compound. In the absence of uroporphyrinogen III synthase there is a nonenzymatic cyclization of the hydroxymethylbilane to form uroporphyrinogen I. The purification of PBGD described (modified from Jordan and Shemin, 1973) takes advantage of the thermal stability of the enzyme. Uroporphyrinogen III synthase, on the other hand, is thermally labile and is rapidly and irreversibly inactivated in the purification procedure. The procedure outlined below provides a good yield of product and can be accomplished in ~3 days.

Materials

R. spheroides (Porphyrin Products)
10 mM KH_2PO_4, pH 7.6 (*APPENDIX 2A*)
100% ethanol, ice cold
$(NH_4)_2SO_4$
3 mM KH_2PO_4, pH 6.8
0 to 0.50 M KCl gradient in 3 mM KH_2PO_4, pH 6.8
0.01 M DTT
0.1 M Tris·Cl, pH 7.6 (*APPENDIX 2A*)
0.54 mg/ml porphobilinogen, (PBG; Porphyrin Products) in 0.1 M Tris·Cl, pH 7.6
3 M HCl
0.15 M KH_2PO_4, pH 4.45
50 mM KH_2PO_4, pH 6.8

Probe sonicator
Refrigerated centrifuge accommodating 1-liter buckets and 50-ml centrifuge tubes
Dialysis tubing, 12,000 to 14,000 MWCO
70°C water bath
DE-52 column, 50 ml bed volume, equilibrated with 3 mM KH_2PO_4, pH 6.8 (see recipe)
Concentrator (e.g., Amicon Centriprep 10)
Fraction collector
UV monitor to measure absorbance at 280 nm, or UV spectrophotometer
Woods lamp

Additional reagents and equipment for dialysis (*APPENDIX 3*)

Prepare R. spheroides lysate

1. Freeze-thaw a 100-ml sample of *R. spheroides*, twice.
2. Dilute the thick slurry with 100 ml of 10 mM KH_2PO_4, pH 7.6, and sonicate for 3 min on ice following manufacturers instructions.

   Following freeze-thaw and sonication, cells will be newly 100% lysed.
3. Place the sample in a cold room or refrigerator and gradually add 800 ml of ice-cold 100% ethanol. Stir for 2 hr, to allow protein to precipitate.
4. Centrifuge 30 min at 10,000 × *g*, 4°C. Pour off the supernatant and discard. Resuspend the pellet in 500 ml ice-cold 100% ethanol, to wash off more of the chlorophyll.
5. Centrifuge again for 30 min at 10,000 × *g*, 4°C. Drain the ethanol completely from the pellet, then resuspend the pellet in 250 ml 10 mM KH_2PO_4, pH 7.6.
6. Using a 12,000 to 14,000 MWCO dialysis membrane, dialyze the sample overnight at 4°C against 10 mM KH_2PO_4, pH 7.6.

   Several changes of buffer are required to remove all the ethanol. The authors suggest making one change before leaving at night after 2 to 3 hr of dialysis, and another change in the morning 2 to 3 hr before ending the dialysis.

Heat denature uroporphyrinogen III synthase

7. Divide the sample into 100-ml aliquots in 500-ml Erlenmeyer flasks, each containing a thermometer.
8. Place samples in a 70°C water bath and heat them until they reach 60°C. Hold this temperature for 5 min.

   Place flask briefly on ice if the temperature rises above 60°C.
9. Place the flasks on ice to cool. Transfer contents to 50-ml centrifuge tubes and centrifuge 30 min at 18,000 × *g*, 4°C. Keep the supernatant. Resuspend the pellet in 50 ml 10 mM KH_2PO_4, pH 7.6, mix well, and centrifuge as before. Combine the supernatants and measure the total volume.

Precipitate the enzyme with ammonium sulfate

10. Weigh out enough $(NH_4)_2SO_4$ to bring the $(NH_4)_2SO_4$ concentration to 32% of saturation (i.e., assuming 765 g/liter is 100%). Over 30 min, while stirring in the cold box, slowly add the $(NH_4)_2SO_4$ to the sample. Allow the solution to equilibrate for 1 hr after the last addition.

    Example: (765 g/1000 ml) (0.32) (300 ml) = 73.4 g $(NH_4)_2SO_4$ needed to make the 0% to 32% cut in 300 ml.
11. Centrifuge 30 min at 10,000 × *g*, 4°C. Keep the supernatant. Make a 32% to 55% $(NH_4)_2SO_4$ cut by weighing out more $(NH_4)_2SO_4$ based on the original volume. Add as above and allow to equilibrate for 2 hr to overnight.

    Example: (765 g/1000 ml) (0.55) (300 ml) = 126.2 g − 73.4 g = 52.8 g $(NH_4)_2SO_4$ needed to make the 32% to 55% cut.
12. Centrifuge 45 min at 18,000 × *g*, 4°C. Discard the supernatant and resuspend the pellet in 40 ml of 3 mM KH_2PO_4, pH 6.8.
13. Using a 12,000 to 14,000 MWCO dialysis membrane, dialyze against 2 liters of 3 mM KH_2PO_4, pH 6.8, at 4°C, until the pH is 6.8.

    This usually requires four buffer changes of 2 liters.

14. Centrifuge 15 min at 10,000 × *g*, 4°C, to remove any remaining precipitated protein.

Column purify the enzyme

15. Apply the supernatant to a 50-ml DE-52 column equilibrated with 3 mM KH_2PO_4, pH 6.8. Wash the column with 400 ml of the same buffer.

16. Elute the bound protein with 200 ml of 3 mM KH_2PO_4, pH 6.8, using a 0 to 0.5 M KCl gradient, and collecting 3.0 ml fractions. Monitor the eluate for protein, based on absorbance at 280 nm.

17. Assay PBGD activity in every other fraction across all protein peaks as follows:

    a. Mix 0.1 ml of fraction, 0.1 ml 0.01 M DTT, 0.225 ml 0.1 M Tris·Cl, pH 7.6, and 0.075 ml of 0.54 mg/ml PBG.
    b. Incubate 60 min at 37°C in the dark.
    c. Add of 0.5 ml 3 M HCl to stop the reaction, and oxidize under a Woods lamp for 30 min.
    d. Visually examine the assay from each fraction for fluorescence under the Woods lamp. Rank fluorescence on scale of 0 to 5.
    e. Pool all fractions with fluorescence values of ≥1.5.

    This should be ~60 ml.

18. Using a 12,000 to 14,000 MWCO dialysis membrane, dialyze pooled fractions against 10 mM KH_2PO_4, pH 7.6, then concentrate to 40 to 50 ml using an Amicon Centriprep concentrator or equivalent.

Determine necessary enzyme concentration

19. Set up assays as described in step 17, substep a, using 0.025, 0.050, 0.075, and 0.100 ml of the purified PBGD. Incubate 30 min at 37°C.

20. To each reaction add 0.10 ml 0.15 M KH_2PO_4, pH 4.45, and 0.40 ml 50 mM KH_2PO_4, pH 6.8. Incubate for an additional 30 min.

21. Add 1.0 ml of 3 M HCl to stop each reaction and analyze by HPLC (see Basic Protocol, steps 7 to 11).

22. Quantify the amount of uroporphyrinogen I made in each reaction. Determine the amount of PBGD needed to produce 30 to 40 µM uroporphyrinogen I in 30 min.

23. Adjust the concentration of the protein with 10 mM KH_2PO_4, pH 7.6, so that 150 µl will produce the required concentration of uroporphyrinogen I. Freeze 3- to 5-ml aliquots of PBGD at −70°C.

SUPPORT PROTOCOL 2

PREPARATION OF ERYTHROCYTE LYSATES FOR UROD ASSAYS

Erythrocyte UROD activity is generally reported with reference to the hemoglobin content of the blood sample. Since hemoglobin constitutes over 95% of protein in erythrocytes, simply determining the hemoglobin content of the lysate provides a reliable index of the total erythrocyte protein. Hemoglobin is converted to cyanomethemoglobin and the concentration is determined by measuring the absorption maximum at 540 nm. The concentration of cyanomethemoglobin is calculated by dividing the A_{540} by the extinction coefficient of 0.683 ml mg^{-1}. An alternative is to report UROD activity based on a defined volume of erythrocytes (McManus et al., 1988). If UROD is to be assayed in tissues other than red cells, a more direct measurement of protein may be required such as the method of Lowry et al. (1951), or a dye-binding assay (Bio-Rad).

Materials

Isoton II (Beckman Coulter)
Drabkin's reagent (see recipe)
5 mM and 0.1 M KH_2PO_4, pH 6.8
0.5 M KCl in 5 mM KH_2PO_4, pH 6.8

Heparinized Vacutainers
Tabletop centrifuge
DE-52 column, equilibrated with 5 mM KH_2PO_4, pH 6.8 (see recipe)

Lyse red blood cells

1. Draw 30-ml samples of blood in heparinized Vacutainers and centrifuge 5 min at 1000 × *g*, 4°C.
2. Remove and discard the plasma and buffy coat. Wash the red cells with an equal volume of Isoton II and centrifuge at 1000 × *g* for 5 min. Repeat the wash.
3. Osmotically lyse the red cells in a beaker with 4 vol sterile distilled water chilled to 4°C. Stir gently with a flea magnet overnight at 4°C.

   Be careful not to stir too briskly.
4. Centrifuge the lysate 25 min at 18,000 × *g*, 4°C. Carefully remove the clear red supernatant.

   Do not take any of the loose pellet on top of the firm pellet. It is best to hold the tube up to a red light to ensure that only the clear portion is harvested.

   The supernatant may be stored at –70°C pending further processing.

Measure the amount of hemoglobin

5. Dilute 20 µl of red cell lysate to a total volume of 5.0 ml (1:250 dilution) with Drabkin's reagent, and allow to stand for 10 to 60 min.
6. Measure the optical density at 540 nm and calculate the amount of hemoglobin present using the extinction coefficient of 0.683 ml mg^{-1}.

Remove hemoglobin

7. Load the equivalent of 500 mg hemoglobin onto an equilibrated DE-52 column. Wash the column with ~50 ml of 5 mM KH_2PO_4, or until the eluate is colorless.
8. Add 4 ml of 0.5 M KCl, gently resuspend the resin and let stand 1 hr.
9. Collect the 4 ml of buffer, then elute again with 3 ml of 0.5 M KCl. Collect the buffer.
10. Assay UROD activity from 80 µl of the eluate diluted with 95 µl 0.1 M KH_2PO_4 (see Basic Protocol).
11. Store 500-µl aliquots at −70°C until ready to assay. Avoid repeated freeze-thaw cycles.

    Samples of erythrocyte lysate frozen at −70°C are stable for up to one year.

REAGENTS AND SOLUTIONS

Use Milli-Q-purified water or equivalent in all recipes and protocol steps. For common stock solutions, see ***APPENDIX 2A****; for suppliers, see* ***SUPPLIERS APPENDIX****.*

DE-52 columns, equilibrated in 3 or 5 mM KH_2PO_4

Make a slurry of DE-52 resin (Whatman) in water. Let sit 1 hr, remove fines by decantation, and equilibrate by one or two washings with 0.1 M KH_2PO_4, pH 6.8 (*APPENDIX 2A*). Make a slurry of equal volumes of settled resin and 5 mM KH_2PO_4, pH 6.8, and transfer ~6 ml into a disposable 15-ml syringe fitted with a frit at the bottom (disposable columns work equally well). Equilibrate the column with 5 volumes of 5 mM KH_2PO_4, pH 6.8 (the final packed volume of resin should be ~3 ml).

Many columns can be made at one time, sealed and stored at 4°C in 5 mM KH_2PO_4, pH 6.8, containing 0.02% NaN_3. Remove NaN_3 prior to use.

For purification of PBGD prepare the DE-52 as described above. Pack a column to contain a 50-ml bed volume. Equilibrate with 10 column volumes of 3 mM KH_2PO_4, pH 6.8.

Drabkin's reagent

To 1 liter of H_2O, add:
1.0 g $NaHCO_3$ (12 mM final)
0.05 g KCN (0.768 mM final)
0.20 g $K_3Fe(CN)_6$ (0.607 mM, final).
Store up to several months at 4°C.

Methanol/phosphate

Prepare 100 mM $NaH_2PO_4 \cdot H_2O$ (13.8 g/liter). Adjust pH to 3.5 with 2 M H_3PO_4. Mix 500 ml methanol with 500 ml of the phosphate buffer and adjust pH to 4.5 with 2 M H_3PO_4. Store up to 1 week at room temperature.

Final concentration: 50% (v/v) methanol/50 mM phosphate.

COMMENTARY

Background Information

UROD activity in erythrocytes provides the basis for the commonly used classification system for porphyria cutanea tarda (PCT). Individuals with half-normal activity have familial PCT (F-PCT, or type I), a disorder transmitted as an autosomal dominant trait. When UROD activity is normal, the designation of sporadic-PCT (S-PCT, or type II) is assigned. A rare third variant of PCT, type III PCT, occurs when the defect in porphyrin production is transmitted as an autosomal dominant trait but is restricted to the liver (Kappas et al., 1995). This suggests that there are other genetic factors that can affect the expression of UROD and precipitate the PCT phenotype. In rare cases there is homozygosity (or compound heterozygosity) for mutant UROD alleles and UROD activity is extremely low (~10% of normal). These individuals are classified as having hepatoerythropoetic porphyria (HEP).

Hepatic UROD activity in individuals with all types of PCT is markedly decreased, resulting in the accumulation of uroporphyrin and its partially decarboxylated intermediates. Another characteristic feature seen in patients with all forms of PCT is the excretion of isocoproporphyrin III in the feces. This phenomenon is thought to be due to a specific reduction in levels of UROD activity in the presence of normal levels of coproporphyrinogen oxidase activity. The pentacarboxyl porphyrinogen III isomer is normally present at extremely low levels; however, when in excess due to low UROD activity it competes with coproporphyrinogen III as a substrate for coproporphyrinogen oxidase. The incompletely modified isocoproporphyrinogen III cannot be used as a substrate for subsequent steps in the pathway and is oxidized to isocoproporphyrin and excreted in the feces (Elder, 1975).

To fully characterize and correctly classify individuals with PCT it may be necessary to determine the level of UROD protein present in both liver and blood samples by immunoblotting. In cases where half-normal levels of

UROD protein are present, analysis of UROD mRNA levels by northern blotting, ribonuclease protection assays, or quantitative RT-PCR can often be informative. Mutations in the UROD locus that lead to the PCT phenotype can be simple missense mutations that result in an inactive protein or can be mutations that produce a protein with reduced stability. Large genomic deletions and nonsense mutations have been reported, which result in half-normal UROD mRNA and hence half-normal protein.

Both chick liver cell culture and rodent models of PCT have been described, where UROD activity can be inhibited by exposure to iron, polyhalogenated aromatic hydrocarbons (PAH), and combinations of both (Sassa et al., 1986; Smith et al., 1986). These models of S-PCT were developed based on the report by Schmid (1960) who identified hexachlorobenzene as the precipitating agent in ~4000 cases of S-PCT in the late 1950s. Since then this observation has been used by many investigators to identify the relationship between these types of compounds and the inhibition of UROD activity seen in hepatocytes.

Development of a UROD specific inhibitor in mice requires induction of the P-4501A2 isozyme. Mice that are homozygous null mutants for P-4501A2 (*Cyp1a2* -/-) cannot be induced to a porphyric state using the PAHs and iron (Sinclair et al., 1998). A developing hypothesis is that PAHs somehow uncouple the cytochrome P-450 cycle, leading to excessive free radical formation in the presence of excess cellular iron (De Matteis and Marks, 1996). It is unclear if the free radicals then produce the UROD specific inhibitor or if it is only an accumulation of the uroporphyrin and partially decarboxylated porphyrins (not substrates for the enzyme) that act as competitive inhibitors of UROD.

Uroporphyrinogen decarboxylase (UROD) activity has been assayed using protein from many sources. Most studies of enzyme kinetics have been done with purified or partially purified mammalian UROD (de Verneuil et al., 1980, 1983; Elder et al., 1983; Straka and Kushner, 1983). The results indicate that activity is maximal when the ionic strength of the assay buffer is ~100 mM. The optimum pH for the reaction is near 6.8 for all of the substrates with the exception of pentacarboxyl I, which has an optimal pH of ~5.4. Divalent metals have been shown to inhibit UROD activity. This is of particular interest since many patients expressing the PCT phenotype have increased hepatic iron stores and the phenotype can be corrected by depleting hepatic iron stores with phlebotomy therapy. UROD activity can be assayed from any source using the above references as guidelines for additional assay requirements.

Critical Parameters

Analysis of the reaction products can be made much simpler if an isomer of pentacarboxyl porphyrinogen is chemically reduced and used as the substrate for the assay (i.e., if there is only one reaction product). A disadvantage, however, is that some UROD mutations have been shown to alter decarboxylation of uroporphyrinogen but do not alter decarboxylation of the pentacarboxyl substrate (Wyckoff et al., 1996). In such cases UROD activity may inappropriately appear normal. The advantage to the enzymatic generation of the uroporphyrinogen I substrate is the reproducibility of the ionic strength and pH of the system. This method can also be utilized to produce radiolabeled substrate starting with labeled porphobilinogen.

If a gradient maker for the HPLC is not available for the reversed-phase separation described here, an isocratic system can be utilized. The porphyrin products of the reaction are converted to their corresponding methyl esters, separated on a silica column (Waters μPorasil or equivalent), and visualized using a detector set to read absorbance at 405 nm by spectroscopy. The process of esterification and analysis is clearly described by Straka et al. (1982). When using the isocratic method for separation it is necessary to consider losses associated with the extraction and esterification of the porphyrins.

Preparation of sodium amalgam is dangerous and uses both toxic and potentially explosive materials; if the assays are to be done rarely, purchasing the sodium amalgam is recommended (Anachemia). An alternative to sodium amalgam for the reduction of porphyrins is the use of potassium borohydride (Mukerji et al., 1984).

The most problematic aspect of the UROD assay involves the inadvertent use of oxidized substrate. This can occur if chemical reduction of a porphyrin is incomplete or if fully reduced substrate is allowed to partially oxidize. Keeping the samples purged with nitrogen is critical. Porphyrinogens are also very susceptible to photooxidation and solutions and samples should be kept covered and examined only under red light. This is especially important, as oxidized porphyrins may inhibit UROD activ-

Table 8.4.3 URO-D Activity Present in a Variety of Normal and Porphyric Tissues

Species	Tissue	Activity (U)[a]	Reference
Human	Liver (normal)	1.61 (1.27-2.42)	Straka et al., 1982.
Human	Liver (porphyric)	0.73 (0.25-1.09)	Straka et al., 1982
Human	Red cell	0.35 (0.30-0.42)	Straka et al., 1982
Rat, female	Liver (normal)	0.99 ± 0.09	Franklin et al., 1997
Rat, female	Liver (porphyric)	0.23 ± 0.07	Franklin et al., 1997
Mouse	Liver (normal)	1.25 ± 0.13	unpub. observ.

[a]Units (U) are equivalent to nmol/hr/mg hemoglobin. Range in parentheses.

ity (Lambrecht et al., 1990). If a chemically reduced substrate is being used, the pH should be checked carefully since the reaction of sodium amalgam and aqueous buffer produces hydrogen and sodium hydroxide.

Freezing and thawing of UROD, as with many proteins, can affect stability. Purified UROD is relatively stable at 4°C and can be stored for ~1 month in a solution consisting of 10% glycerol, 50 mM Tris·Cl, pH 6.8, and 2 mM 2-mercaptoethanol. When freezing aliquots of UROD, 10% glycerol is added to the buffer to stabilize the protein. When a purified source of UROD is used, bovine serum albumin (0.1 mg/ml) is added to the enzyme sample to prevent losses due to adsorption to plastic and glass. A standard time of 30 min is used in all assays to minimize oxidization of the substrate.

Troubleshooting

The most common problem encountered with enzymatic generation of substrate is the unknown concentration of PBGD being used. An initial experiment, done to determine the exact amount of PBGD to add, usually corrects this problem. Once the amount of enzyme to be added has been determined, appropriately sized aliquots are prepared and stored for later use.

The most common problem in assays using chemically generated substrate is having an alkaline pH in the final enzymatic reaction. Performing the initial test to determine the exact amount of H_3PO_4 to be added in a mock sample will help ensure that the final pH is optimal. The activity of UROD drops steeply as the pH increases above 7.0 (Elder and Wyvill, 1982, Straka and Kushner, 1983).

Anticipated Results

UROD activity is generally expressed in units (U) with 1 U equal to one nmol substrate decarboxylated per hr per mg of protein. The specific activity for both native and recombinant purified human UROD is in the range of $4–10 \times 10^3$ U, using either uroporphyrinogen I or III as substrate (de Verneuil et al., 1983; Wyckoff et al., 1996). These results have been reported for assays in which the substrate concentration is saturating (~30 μM substrate and 1 μg or less UROD protein). When assaying tissue homogenates, cell lysates, or column fractions, the amount of UROD should be in this range (Elder and Wyvill, 1982). Some typical results are given in Table 8.4.3.

Time Considerations

The time required to enzymatically produce uroporphyrinogen I and assay UROD activity in 20 samples is ~3 hr. Set up of the HPLC, preparation of buffers, and calibration of the HPLC can be done in 2 hr. Separation of the reaction products takes ~30 min per sample; therefore 20 samples requires 12 hr of HPLC time. A more rapid method for separation of porphyrins by HPLC has been described by Adjarov and Elder (1988). Data analysis for 20 samples is ~1.5 hr. The chemical reduction of a porphyrin substrate can be done in 15 to 20 min, but initial solubilization and estimation of the porphyrin concentration will take 1 to 2 hr. Time for cleanup and disposal of the sodium amalgam waste should also be considered.

Literature Cited

Adjarov, D.G. and Elder, G.H. 1988. A simplified method for determination of uroporphyrinogen decarboxylase activity in human blood. *Clin. Chim. Acta* 177:123-130.

De Matteis, F. and Marks, G.S. 1996. Cytochrome P450 and interactions with the heme biosynthetic pathway. *Can. J. Pharmacol.* 74:1-8.

de Verneuil, H., Grandchamp, B., and Nordmann, Y. 1980. Some kinetic properties of human red cell uroporphyrinogen decarboxylase. *Biochim. Biophys. Acta.* 611:174-186.

de Verneuil, H., Sassa, S., and Kappas, A. 1983. Purification and properties of uroporphyrinogen decarboxylase from human erythrocytes: A sin-

gle enzyme catalyzing the four sequential decarboxylations of uroporphyrinogens I and III. *J. Biol. Chem.* 258:2454-2460.

Elder, G.H. 1975. The differentiation of porphyria cutanea tarda symptomatica from other types of porphyria by the measurement of isocoproporphyrin in faeces. *J. Clin. Pathol.* 28:601-607.

Elder, G.H. and Wyvill, P.C. 1982. Measurement of uroporphyrinogen decarboxylase using porphyrinogens prepared by chemical reduction. *Enzyme* 28:186-195.

Elder, G.H., Tovey, J.A., and Sheppard, D.M. 1983. Purification of uroporphyrinogen decarboxylase from human erythrocytes: Immunochemical evidence for a single protein with decarboxylase activity in human erythrocytes and liver. *Biochem. J.* 215:45-55.

Ford, R.E., Ou, C.N., and Ellefson, R.D. 1981. Liquid-chromatographic analysis for urinary porphyrins. *Clin. Chem*. 27:397-401.

Francis, J.E. and Smith, A.G. 1984. Assay of mouse liver uroporphyrinogen decarboxylase by reverse-phase high-performance liquid chromatography. *Anal. Biochem*. 138:404-410.

Franklin, M.R., Phillips, J.D., and Kushner, J.P. 1997. Cytochrome P450 induction, uroporphyrinogen decarboxylase depression, porphyrin accumulation and excretion, and gender influence in a 3-week rat model of porphyria cutanea tarda. *Toxicol. Appl. Pharmacol.* 147:289-299.

Jordan, P.M. and Shemin, D. 1973. Purification and properties of uroporphyrinogen I synthetase from *Rhodopseudomonas spheroides*. *J. Biol. Chem.* 248:1019-1024.

Kappas, A., Sassa, S., Galbraith, R.A., and Nordmann, Y. 1995. The porphyrias. *In* The Metabolic and Molecular Bases of Inherited Disease, Vol. II (C.R. Scriver, A.L. Beaudet, W.S. Sly, and D. Valle, eds.) pp. 2103-2160. McGraw-Hill, New York.

Lambrecht, R.W., Jacobs, J.M., Sinclair, P.R., and Sinclair, J.F. 1990. Inhibition of uroporphyrinogen decarboxylase activity. The role of cytochrome P-450-mediated uroporphyrinogen oxidation. *Biochem. J.* 269:437-441.

Lowry, O.H., Rosebrough, N.J., Foss, A.L., and Randall, R.J. 1951. Protein measurement with the Folin phenol reagent. *J. Biol. Chem.* 193:265-275.

McManus, J., Blake and D., Ratnalke, S. 1988. An assay of uroporphyrinogen decarboxylase in erythrocytes. *Clin. Chem*. 34:2355-2357.

Mukerji, S.K., Pimstone, N.R., and Burns, M. 1984. Dual mechanism of inhibition of rat liver uroporphyrinogen decarboxylase activity by ferrous iron: Its potential role in the genesis of porphyria cutanea tarda. *Gastroenterology.* 87:1248-1254.

Sassa, S., Sugita, O., Ohnuma, N., Imajo, S., Okumura, T., Noguchi, T., and Kappas, A. 1986. Studies of the influence of chloro-substituent sites and conformational energy in polychlorinated biphenyls on uroporphyrin formation in chick-embryo liver cell cultures. *Biochem. J.* 235:291-296.

Schmid, R. 1960. Cutaneous porphyria in Turkey. *New Engl. J. Med.* 263:397-398.

Sinclair, P.R., Gorman, N., Dalton, T., Walton, H.S., Bement, W.J., Sinclair, J.F., Smith, A.G., and Nebert, D.W. 1998. Uroporphyria produced in mice by iron and 5-aminolaevulinic acid does not occur in *Cyp1a2* (–/–) null mutant mice. *Biochem. J.* 330:149-153.

Smith, A.G., Francis, J.E., Kay, S.J., and Greig, J.B. 1986. Mechanistic studies of the inhibition of hepatic uroporphyrinogen decarboxylase in C57BL/10 mice by iron-hexachlorobenzene synergism. *Biochem. J.* 238:871-878.

Straka, J.G. and Kushner, J.P. 1983. Purification and characterization of bovine hepatic uroporphyrinogen decarboxylase. *Biochemistry* 22:4664-4672.

Straka, J.G., Kushner, J.P., and Pryor, M.A. 1982. Uroporphyrinogen decarboxylase: A method for measuring enzyme activity. *Enzyme* 28:170-185.

Wyckoff, E.E., Phillips, J.D., Sowa, A.M., Franklin, M.R., and Kushner, J.P. 1996. Mutational analysis of human uroporphyrinogen decarboxylase. *Biochim. Biophys. Acta.* 1298:294-304.

Key References

Jordan and Shemin, 1973. See above.

Describes the purification of PBGD for use in the enzymatic synthesis of uroporphyrinogen I.

Straka et al., 1982. See above.

Methods described in this unit are a modification of those described in this reference. This is a very detailed manuscript that provides additional information not presented here and is a good reference for measuring activity of UROD from various sources.

Contributed by John D. Phillips and James P. Kushner
University of Utah Medical School
Salt Lake City, Utah

Measurement of Protoporphyrinogen Oxidase Activity

Protoporphyrinogen oxidase catalyzes the penultimate step in the heme biosynthetic pathway, the oxidation of protoporphyrinogen to protoporphyrin. This membrane-bound mitochondrial enzyme is of special interest, since it is the target of photobleaching herbicides and its deficiency in humans leads to one type of porphyria. The assay of protoporphyrinogen oxidase activity involves following the increase in fluorescence as the colorless, nonfluorescent protoporphyrinogen is converted to colored, fluorescent protoporphyrin by oxidation. Protoporphyrinogen, the substrate of the enzyme, is prepared from protoporphyrin by reduction with sodium amalgam.

There are two methods for following the increase in protoporphyrin fluorescence during enzymatic oxidation of protoporphyrinogen. In the indirect assay (see Basic Protocol), aliquots are removed at intervals from the reaction mixture, diluted into a measuring mixture, and the protoporphyrin fluorescence determined. In the direct assay (see Alternate Protocol 1), protoporphyrin fluorescence is monitored directly in a fluorometric cuvette containing the enzyme reaction mixture. Accumulation of protoporphyrinogen in cells actively synthesizing heme or chlorophyll is measured using Alternate Protocol 2. Protocols are included for preparing sodium amalgam (see Support Protocol 1) and *Escherichia coli* membranes (see Support Protocol 2) for detection of accumulated protoporphyrinogen.

CAUTION: All procedures involving mercury must be performed in a chemical safety hood. Proper protective equipment (chemical-resistant gloves, mercury respirator, and face shield) should be used, and the protocol should be approved by the institutional safety office.

INDIRECT ASSAY TO MEASURE PROTOPORPHYRINOGEN OXIDASE ACTIVITY

BASIC PROTOCOL

Preparation of the substrate, the most difficult step in this assay, begins with reduction of the deep red protoporphyrin solution, in a tightly closed container under nitrogen gas in the dark, by rapid addition of pulverized sodium amalgam. The colorless reduced solution is then removed from the amalgam and partially neutralized, taking care to minimize exposure to light and oxygen. Addition of an antioxidant helps prevent chemical reoxidation. The extent of reduction is monitored with a long-wave UV lamp; the best preparations will have no fluorescence. Even if the reduction is less than complete, however, as indicated by a faint red fluorescence (due to the presence of residual protoporphyrin), the substrate (protoporphyrinogen) solution may still be usable, as long as it remains colorless in visible light. A highly humid atmosphere will increase the difficulty of obtaining good reduction with sodium amalgam and should be avoided. Once the substrate is prepared it should be added to the assay without delay.

Materials

0.5 M Tris·Cl, pH 7.5 and pH 8.7 (*APPENDIX 2A*)
0.05 M Tris·Cl, pH 8.7 (*APPENDIX 2A*)
0.01 M EDTA in 0.05 M Tris·Cl, pH 8.7
0.05 M dithiothreitol (DTT) or glutathione in 0.5 M Tris·Cl, pH 7.5
Enzyme sample to be assayed, e.g., rat liver mitochondria, fibroblasts, or etiolated chloroplasts
Protein assay kit (Bio-Rad) or equivalent

Contributed by Judith M. Jacobs and Nicholas J. Jacobs
Current Protocols in Toxicology (1999) 8.5.1-8.5.13

Heat-inactivated control: enzyme sample that has been heated 15 min at 75°C
10% (v/v) Tween 20 or Tween 80 (optional)
~500 μM protoporphyrin stock solution (see recipe)
Ultra-high-purity nitrogen gas
0.01 N KOH
40% phosphoric acid, degassed with nitrogen
3.8% sodium amalgam (see Support Protocol 1)
2.7 N HCl

3-ml disposable, plastic, square spectrofluorometric cuvettes (12 × 45 mm; Fisher)
Fluorometer
Blak-Ray UV lamp (UVP 4-Watt, Fisher)
Filter funnel with fritted disc, fine porosity of 4 to 5.5 μm (Fisher)
Applicator sticks
pH paper (Hydrion pH test papers, range 6.0 to 8.0 and 8.0 to 9.5, Fisher)
Quartz spectrophotometer cuvettes

Prepare assay and measurement tubes

1. Prepare assay mixture by adding the following to small glass tubes:

   0.2 ml 0.5 M Tris·Cl, pH 7.5 to 8.7
   0.1 ml 0.01 M EDTA in 0.05 M Tris·Cl, pH 8.7 (1 mM EDTA final)
   0.1 ml 0.05 M glutathione or DTT in 0.5 M Tris·Cl, pH 7.5 (5 mM final)
   Enzyme sample containing 0.1 to 2 mg protein
   Milli-Q-H_2O to 0.74 ml.

   As well as sample tubes, prepare tubes without any enzyme and with heat-inactivated control sample (as controls for the rate of nonenzymatic protoporphyrinogen oxidation).

   Assay total protein by the Bio-Rad assay.

   The authors usually trisonicate mitochondria briefly using any low-power small sonic probe, although this is not required.

   A variety of pH values have been utilized satisfactorily over the 7.5 to 8.7 range, although protoporphyrinogen autooxidation is lower at higher pH values. Mammalian mitochondria are often assayed at pH 8.7. Plant organelles have been assayed at the lower values. The authors routinely assay rat liver mitochondria at pH 7.5 for effects of herbicide inhibitors. The final concentrations of protoporphyrinogen will be ~50 μM. Between 2 and 5 mM (final) DTT has been used in many current assays as an antioxidant in place of glutathione, since it minimizes the chemical autooxidation of protoporphyrinogen to protoporphyrin. Many enzymatic assays also employ a detergent (e.g., Tween 20 or Tween 80) at 0.03%, 0.1%, or 0.2% concentration. Detergent is not required for assay of sonicated mitochondria, and high detergent concentrations may be inhibitory to the enzyme; however, detergent is required for assay of the purified enzyme.

2. Determine the amount of measuring mixture required by multiplying the number of assay tubes by the number of time points by 1.45 ml; include an appropriate number of tubes for fluorescence standards (step 4). Prepare the appropriate quantity of measuring mixture according to the following recipe (per 100 ml):

   20 ml 0.5 M Tris·Cl, pH 8.7
   10 ml 0.01 M EDTA/0.05 M Tris·Cl, pH 8.7 (1 mM EDTA final)
   10 ml 0.05 M glutathione in 0.5 M Tris·Cl, pH 8.7 (5 mM glutathione final)
   1 ml 10% Tween 20 or Tween 80 (0.1% final)
   59 ml Milli-Q-purified H_2O.

   Dispense 1.45 ml per cuvette into 3-ml disposable spectrofluorometric cuvettes.

   The higher pH is used here to minimize chemical oxidation of protoporphyrinogen.

Prepare substrate stock and standards

3. Dilute 2 ml of ~500 μM protoporphyrin stock with 3 ml of 0.01 N KOH to obtain a working solution of ~200 μM.

4. In separate tubes, prepare protoporphyrin fluorescence standards by adding known amounts of protoporphyrin working solution to tubes of assay mixture (from step 1).

5. Set the excitation wavelength on the fluorometer to 405 nm and the emission wavelength to 633 nm. Add 50 μl of assay mixture without protoporphyrin to 1.45 ml measuring mixture and zero the fluorometer. Adjust the sensitivity of the fluorometer to read 100 fluorescent units (FU) using a 50-μl aliquot from an assay tube containing ~20 μM protoporphyrin.

   The standard should be measured in the presence of unheated as well as heated enzyme, since turbidity of the heated enzyme sample may affect fluorescence.

   The concentration of the standard will determine the sensitivity of the assay. For instance, for a very active enzyme preparation, 20 μM protoporphyrin can be used as the highest concentration. For less active material, a lower concentration is more appropriate. To assay protoporphyrinogen oxidase in fibroblasts, Brenner and Bloomer (1980) used a reference standard of 5 μM protoporphyrin that was adjusted to 25 FU. It is useful to set up a standard curve with a variety of protoporphyrin levels added to the assay mixture to test the linearity and sensitivity of the method.

Prepare protoporphyrinogen by reduction of protoporphyrin

6. Place 5 ml protoporphyrin working solution into a 25-ml rubber-stoppered Erlenmeyer flask. Deaerate the solution by flushing with nitrogen gas.

7. Grind 8 g sodium amalgam into a fine powder in the fume hood, using a mortar and pestle.

   With some amalgam preparations, larger amounts may need to be used. However, the solution becomes more difficult to neutralize if too much amalgam is used.

   IMPORTANT NOTE: *Steps 8 to 13 should be carried out under reduced light—i.e., using the minimal amount of light needed to conduct each step.*

8. Immediately add the amalgam to the protoporphyrin solution, replace the stopper, and shake vigorously using a gloved hand to secure the stopper. Gas is evolved, so point tube toward back of fume hood. Continue shaking for 2 to 5 min, venting as needed, until no fluorescence is observed when a long-wave UV lamp is shone on the solution. Add 0.25 ml of 0.05 M DTT or glutathione to the solution and remove the amalgam by filtration.

   The authors have most experience with a fritted-glass filter of fine porosity, but a syringe with a porous disc of 35-μm porosity also works. Dailey and Dailey (1997) recommend a syringe packed half full with glass wool.

9. Adjust the pH of the solution to 8.5 to 9 by dropwise addition of 40% phosphoric acid that has been degassed by bubbling with nitrogen.

   The pH should not go below 8, since autooxidation is enhanced by low pH. To determine the pH, put a drop of the solution on a strip of narrow-range pH paper using a wood applicator stick.

   Dailey and Dailey (1997) recommend neutralization with 2 M MOPS [3-(N-morpholino)propane sulfonic acid] for better pH control. The protoporphyrinogen solution should be used immediately whenever possible. Storage in the dark under nitrogen gas at room temperature for 1 hr may be possible with most preparations.

Begin assay and take spectrophotometric measurements

10. To start the reaction, add 260 µl of the protoporphyrinogen solution to each assay tube from step 1. Incubate at the appropriate temperature in a covered water bath.

    The final concentration of protoporphyrinogen added to the assay will be ~40 µM. Mammalian mitochondria are often assayed at 37°C, and plant organelles at 30°C or room temperature. If it is important to determine the actual concentration of the protoporphyrinogen solution, allow the solution to autooxidize overnight, dilute into 2.7 N HCl, determine the absorbance at 408 nm, and calculate the concentration, using the millimolar extinction coefficient (ε_{mM}) value of 297 cm^{-1} mM^{-1}. The recovery may be poor with autooxidation. For this reason, the stoichiometric recovery of protoporphyrinogen is rarely attempted. For best recovery of protoporphyrin from protoporphyrinogen, enzymatic oxidation of protoporphyrinogen with E. coli membranes should be used (see Support Protocol 2).

11. Agitate gently to mix and aerate, then remove a 50-µl aliquot of the assay mixture to 1.45 ml of measuring mixture in a disposable spectrofluorometric cuvette (prepared in step 2). Minimize exposure to light by using the least amount of light compatible with accurate pipetting. Thoroughly mix the contents of the cuvette and immediately read the fluorescence.

    Take the first aliquot as close as possible to the time of protoporphyrinogen addition.

12. Remove further 50-µl aliquots at 5- to 10-min intervals for 30 to 60 min, and measure the fluorescence as in step 11.

Calculate protoporphyrinogen oxidase activity of samples

13. Calculate the rate of protoporphyrin formation at each time interval by comparison with the reference standards, correcting for the rate of nonenzymatic protoporphyrinogen oxidation (based on the samples without enzyme and the heat-inactivated control).

    The following is a sample calculation showing how the data are used to calculate the enzyme activity in tissue preparations. If the fluorometer is adjusted to read 100 FU with measuring mixture to which 50 µl of standard (assay mixture containing 20 µM protoporphyrin) has been added (see step 4), then each FU increase in fluorescence during the assay is equivalent to 0.2 µM protoporphyrin formed from protoporphyrinogen. In a typical experiment with 1 mg/ml rat liver mitochondria, the authors observed a linear increase of 50 FU over 60 min. This is 10 µM protoporphyrin formed/hr/mg protein (50 FU × 0.2 µM = 10 µM). The heated control increased 10 FU or 2 µM in 60 min. Therefore, the rat liver mitochondria oxidized protoporphyrinogen at a rate of 8 µM/hr/mg protein. When it is necessary to verify that the product is protoporphyrin, scan the emission fluorescence from 600 nm to 650 nm (excitation 405 nm) and compare to the emission spectrum of the standard as shown in Figure 8.5.1.

14. After the assay is completed, verify that the pH of the assay mixture has not been altered by addition of an improperly acidified protoporphyrinogen solution by placing a drop of the reaction mixture on narrow-range pH paper. Dispose of all remaining pulverized sodium amalgam by adding a small amount of water. After several hours, dispose of mercury droplets formed as toxic mercury waste.

    If the pH is too high, redo the assay using a newly prepared, properly acidified protoporphyrinogen solution.

ALTERNATE PROTOCOL 1

DIRECT ASSAY TO MEASURE PROTOPORPHYRINOGEN OXIDASE ACTIVITY

In this assay, the rate of protoporphyrin formation is measured directly in a spectrofluorometric cuvette from the linear rate of increase in fluorescence as protoporphyrinogen is oxidized to protoporphyrin. A lower concentration of protoporphyrinogen is added as substrate and the pH of the protoporphyrinogen solution is decreased by use of a strongly buffered, concentrated solution of DTT. These variations eliminate the need for the technically difficult neutralization step.

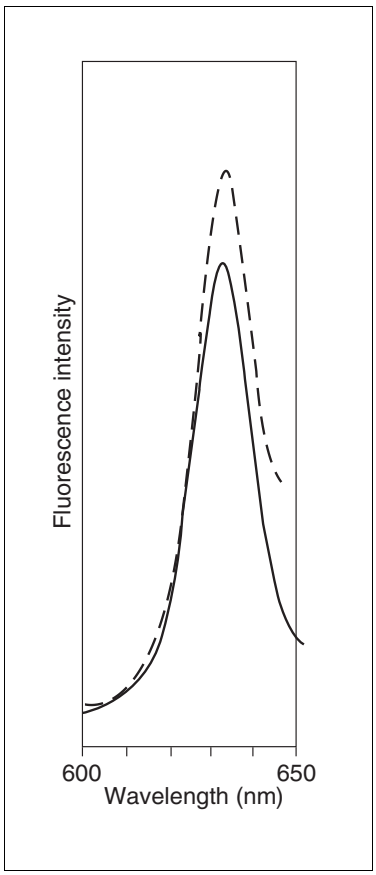

Figure 8.5.1 Fluorescence emission spectra of protoporphyrin and enzymatically oxidized protoporphyrinogen. The enzymatic reaction mixture was as described in Basic Protocol step 1 and contained (where indicated) 870 μg greening plastid protein/ml, protoporphyrin (13.5 μM), or protoporphyrinogen that had been enzymatically oxidized by the plastid enzyme. A 50-μl aliquot was added to 1.45 ml of measuring mixture as described in Basic Protocol steps 2 to 11. The fluorescence emission spectra were determined using an excitation wavelength of 410 nm with excitation and emission slits of 10 nm. The dashed line indicates the assay preparation with plasmids and oxidized protoporphyrinogen. The solid line indicates the protoporphyrin standard in the assay mix without added protoporphyrinogen or chloroplast enzyme preparation.

If enzyme sources cause turbidity, this can diminish protoporphyrin fluorescence. However, the authors have not found this to prevent measuring the relative increase in fluorescence even in the presence of relatively turbid suspensions of rat liver mitochondria or membranes from etiolated chloroplasts. The standard curve containing the enzyme should be linear. For enzyme preparations containing high background fluorescence or excessive amounts of turbidity, the indirect assay may be superior. See Critical Parameters and Troubleshooting for a discussion of interference by turbidity.

Materials

0.5 M Tris·Cl, pH 7.5 (*APPENDIX 2A*)
0.1 M EDTA in 0.05 M Tris·Cl, pH 8.7
10% (v/v) Tween 20
0.05 M and 0.1 M DTT in 0.5 M Tris·Cl, pH 7.5
Sonicated mitochondria or other enzyme sample to be assayed (see Basic Protocol)
Heat-inactivated control: enzyme sample that has been heated 15 min at 75°C
~500 μM protoporphyrin stock solution (see recipe)
Sodium amalgam (see Support Protocol 1)

3-ml, disposable spectrofluorometric cuvettes or 1.5-ml disposable semi-micro spectrophotometric cuvettes (Fisher 14-385-938; see Background Information)
Fluorometer
1-ml screw-cap microcentrifuge tubes, with securely fitted O rings
Mortar and pestle
Vortex mixer
Blak-Ray UV lamp (UVP 4-Watt, Fisher)
Applicator sticks
pH paper (Hydrion pH test papers with narrow range, Fisher)

Prepare assay and measurement tubes

1. Place spectrofluorometric cuvettes in an appropriate holder.

   Semi-micro spectrophotometric cuvettes that are clear on four sides can be used to assay volumes as small as 0.250 ml.

2. To each cuvette add the following reaction mix:

   0.1 ml 0.5 M Tris·Cl, pH 7.5
   0.1 ml 0.01 M EDTA in 0.05 M Tris·Cl, pH 8.7 (1 mM EDTA final)
   0.01 ml 10% Tween 20 (0.1% final)
   0.06 ml 0.05 M DTT in 0.5 M Tris·Cl, pH 7.5 (3 mM DTT final)
   Enzyme sample containing 0.1 to 0.4 mg protein
   Milli-Q-purified H_2O to 1 ml.

   After addition of the 0.04 ml protoporphyrinogen solution (step 7), which contains 50 mM DTT, the final DTT concentration will be 5 mM. Include controls without enzyme and with heated enzyme (see Basic Protocol, step 1).

Set up fluorometer and prepare standard curve

3. Set the fluorometer with the excitation wavelength at 405 nm, the emission wavelength at 633 nm, and the excitation slit at the narrowest setting to minimize exposure of the assay to light. Zero the instrument using a cuvette containing reaction mixture without protoporphyrin.

4. Add a dilution of ~500 μM protoporphyrin stock solution to an aliquot of reaction mixture so that the final porphyrin concentration is 0.25 μM (standard). Adjust the fluorometer so that the standard gives the maximum reading, usually 100 fluorescence units (FU).

5. Dilute the standard in reaction mixture to give final concentrations of 0.125 and 0.0625 μM, and check that these give readings 0.5 and 0.25 of the reading for the standard.

Reduce protoporphyrin to protoporphyrinogen

6. Place a small volume (0.8 ml) of ~500 μM protoporphyrin stock solution in a screw-capped 1-ml microcentrifuge tube.

7. Add 1 to 2 g very finely ground sodium amalgam rapidly with a spatula and immediately replace the cap on the tube. Vortex the tube vigorously until there is no fluorescence when viewed with a long-wave UV lamp, unscrewing the cap every 30 sec to release pressure.

   The reduction should not take longer than 3 to 5 min. Two grams of very finely ground amalgam per milliliter is usually optimal, but less can be used with the best amalgam preparations.

   Always keep the tube pointed away, since the top can be blown off by the gas generated. This procedure should be done in low light. The amalgam will settle to the bottom half of the tube after standing for several minutes. Using a dim light, check to see if settling is complete. If settling is insufficient, the authors discard and use less amalgam on the next attempt. This is rarely necessary. See step 8 for possible clarification methods.

Take spectrophotometric measurements

8. Draw off the reduced porphyrinogen with a pipet and dilute into an equal volume of 0.1 M DTT/0.5 M Tris·Cl, pH 7.5.

   The protoporphyrinogen solution can be clarified (see Basic Protocol, step 8) but the authors have not found this necessary due to the small volumes used in subsequent steps. The protoporphyrinogen should be protected from light and air. The solution should be used immediately (see Critical Parameters and Troubleshooting for storage suggestions).

9. Place cuvettes in the fluorometer and start the chart recorder or timer.
10. Add 0.04 ml protoporphyrinogen/ml reaction mixture to each cuvette to give a final concentration of 10 μM, with thorough agitation to mix and aerate.

    Since the substrate added at this concentration contains DTT to a final concentration of 2 mM, this should be taken into account when calculating the amount to add to the assay mixture to yield a final concentration of 5 mM DTT (see step 2).

11. Record the fluorescence at 633 nm of each cuvette in turn for 10 min or more at intervals of 30 sec using the chart recorder or a timer. Longer time intervals can be used with enzyme sources of low activity.

    Most fluorometers have a carrier for eight cuvettes. It is convenient to run seven samples and one heat-inactivated control to determine the nonenzymatic rate. The shutter should be opened just long enough to get a reading to minimize exposure of the sample to light.

12. Verify that the pH of the assay mixture is between 7.6 and 8.6. A pH above 8.8 is too far from the optimum pH of the enzyme.

    This can be done using a drop of the reaction mixture on narrow range pH paper .

Calculate protoporphyrinogen oxidase activity

13. Determine the increase in fluorescence units per minute for each sample and for the heat-treated control. Subtract FUs of the heated control from the FUs of the samples. The concentration of protoporphyrin in each sample can be calculated from the following (S = standard):

    sample concentration = (concentration of S/FU of S) × FU of sample

DETECTION OF ACCUMULATED PROTOPORPHYRINOGEN

ALTERNATE PROTOCOL 2

In the presence of diphenylether herbicides, protoporphyrinogen, as well as protoporphyrin, accumulates in cells that are actively synthesizing heme or chlorophyll. To detect the accumulation of protoporphyrinogen in samples treated with diphenylethers or other protoporphyrinogen oxidase inhibitors, advantage is taken of the facts that the *E. coli* enzyme for oxidation of protoporphyrinogen is not inhibited by diphenylethers and that protoporphyrinogen, but not protoporphyrin, is unstable and is degraded to undetectable non-porphyrin products in perchloric acid (PCA)/methanol.

This method should be applicable to detecting protoporphyrinogen accumulation in any tissue (crude lysates or homogenates) or enzyme assay where protoporphyrinogen is formed. The authors have used it to detect the accumulation of protoporphyrinogen in cultured hepatocytes and in suspensions of plant chloroplasts incubated with an excess of the porphyrin precursor 5-amino levulinic acid and the protoporphyrinogen oxidase inhibitor acifluorfen methyl.

Materials

Sample (reaction mixture or cell suspension) containing protoporphyrinogen (see Basic Protocol; Alternate Protocol 1)
E. coli membranes (see Support Protocol 2)
10% (v/v) PCA/methanol
~500 μM protoporphyrin stock solution (see recipe)
0.5 M Tris·Cl, pH 7.5 (*APPENDIX 2A*)

3-ml, disposable spectrofluorometric cuvettes
Fluorometer

1. Transfer a 0.5-ml aliquot of the sample to be analyzed for protoporphyrinogen to a 1.5-ml microcentrifuge tube. Add 0.5 ml of 10% (v/v) PCA/methanol and hold on ice.
2. Transfer a second 0.5-ml aliquot of sample to another microcentrifuge tube and add 0.25 mg *E. coli* membranes (final concentration 0.5 mg/ml). Incubate 30 min in the dark at 37°C in an incubator or water bath.

   About 0.01 to 0.02 ml of the ~15 mg/ml E. coli membranes will be required.
3. Meanwhile, to the first tube (on ice), add a volume of 0.5 M Tris·Cl, pH 7.5, equal to the volume of *E. coli* membranes that was added to the second tube (to keep the volumes in the two tubes equal).
4. Prepare standards containing a range of known concentrations of protoporphyrin diluted in 10% (v/v) PCA/methanol.
5. After the 30-min incubation is over, add 0.54 ml of 10% (v/v) PCA/methanol to the second sample tube.
6. Centrifuge both samples 5 min at ~9000 × *g* (e.g., 2000 to 3000 rpm in a tabletop centrifuge), room temperature, to remove the precipitated protein.

   For whole cells centrifuging 5 min at 1000 × g will be sufficient.
7. Dispense 200 µl of each the supernatant and 800 µl of 10% (v/v) PCA/methanol into spectrofluorometric cuvettes. Determine fluorescence at excitation 405 nm and emission 605 nm.
8. Calculate the concentration of protoporphyrin in each sample by comparison with the reference standards.

   If protoporphyrinogen was present in the sample, the E. coli–treated aliquot will contain a higher concentration of protoporphyrin than the untreated aliquot. The difference in the concentration of protoporphyrin between the first aliquot and the second (E. coli–treated) aliquot is the concentration of protoporphyrinogen in the sample.

SUPPORT PROTOCOL 1

PREPARING SODIUM AMALGAM

The method of preparing sodium amalgam described in Fieser and Fieser (1967) is the classical procedure using complex enclosed glassware that is usually only available in organic chemistry laboratories, but should nonetheless be used whenever possible. The method of Nicolaus et al. (1993) is more similar to the authors' method and can also be recommended. The procedure presented here is slightly modified from Brenner and Bloomer (1980) and Jacobs and Jacobs (1982), but is not recommended for inexperienced investigators. It should be done in a chemical safety hood at high setting and proper protective gear (chemical protective gloves, face shield, and mercury respirator) must be worn, as hot mercury vapors are generated. The safety committee of the investigator's institution should approve the procedure.

Materials

Mercury metal
Nitrogen gas
Sodium metal
Light mineral oil
Phosphorus pentoxide

Chemical safety hood
Face shield

Chemical protective gloves (Fisher)
Mercury respirator (Fisher)
50-ml side-arm flask
Single-hole rubber stopper with glass tube vent

1. Weigh 75 g mercury into a 50-ml side-arm flask. Secure the flask to a ring stand; place on a hot plate and pass nitrogen gas gently though the side arm, allowing it to vent through the glass tube on the stopper. Warm the mercury at low heat, using the lowest setting on the hot plate.
2. Using a heavy knife, cut a piece from a lump of sodium metal stored under light mineral oil.

   The cut surfaces of the metal should be bright silver. Trim off and discard any oxidized (white-colored) sodium.

3. Trim the piece to weigh ~2.8 g, and cut it into smaller pieces (5 mm^3).

   The authors keep the sodium immersed in light mineral oil whenever possible. This can be done using a tared beaker containing the mineral oil. The weighed sodium lump is briefly removed to a glass plate for cutting and the cut pieces are returned to the oil immediately. Quantitative addition of sodium is not as important as protection of the cut surface from a moist atmosphere.

4. One at a time, blot each piece using a paper towel, then quickly remove the stopper from the flask of mercury and drop the sodium into it. Immediately replace the stopper and continue the flow of nitrogen.

   The sodium will melt into the mercury. The reaction is vigorous and releases mercury vapor.

5. Add the rest of the sodium rapidly, piece by piece.

   As the last pieces of sodium are added, the amalgam will begin to solidify, and it may be necessary to stir it using a heavy glass rod or spatula. The flow of nitrogen gas may be briefly interrupted during these procedures.

6. After all the sodium is added, remove the amalgam from the hot plate. Stir the amalgam during cooling to break it up into smaller chunks.
7. Remove the amalgam from the flask into a 50-ml beaker. Store in an evacuated desiccator over a large dish of phosphorus pentoxide.

   In the authors' experience, the amalgam will retain its ability to reduce porphyrins for several months when stored under vacuum over phosphorus pentoxide.

PREPARATION OF *E. COLI* MEMBRANES

SUPPORT PROTOCOL 2

E. coli membranes are used to detect accumulated protoporphyrinogen in Alternate Protocol 2. The membranes are prepared by sonication and centrifugation at 144,000 × *g*.

Materials

E. coli (ATCC #25922)
Bacterial Nutrient Broth (Difco)
0.5 M Tris·Cl, pH 7.5 (*APPENDIX 2A*)
Protein assay kit (Bio-Rad) or equivalent

Centrifuge
Sonicator (e.g., Branson W185D or equivalent)
Ultracentrifuge

1. Grow *E. coli* in nutrient broth for 10 hr at 37°C with vigorous aeration.

2. Harvest cells. Centrifuge 20 min at 6000 × *g*, 4°C. Sonicate pellet using twenty 30-sec treatments and cooling cells on ice between treatments.
3. Remove unbroken cells by centrifugation for 20 min at 14,000 × *g*, 4°C.
4. Sediment the membranes 2 hr at 144,000 × *g*, 4°C. Wash once in 0.05 M Tris·Cl, pH 7.5, and resuspend in the same buffer to give a final protein concentration of ~15 mg/ml, as determined by the Bio-Rad assay.

Membranes can be stored in small aliquots at −70°C until needed.

REAGENTS AND SOLUTIONS

Use Milli-Q-purified water or equivalent in all recipes and protocol steps. For common stock solutions, see ***APPENDIX 2A****; for suppliers, see* ***SUPPLIERS APPENDIX****.*

Protoporphyrin stock solution, ~500 μM

Weigh ~2 mg of protoporphyrin into a 25-ml Erlenmeyer flask and add 7.5 ml of 0.01 N KOH in 20% ethanol. Stir 20 min away from direct light. Determine the exact concentration by adding 0.03 ml of the stock solution to 3 ml of 2.7 N HCl and measuring the absorbance at 408 nm, using the millimolar extinction coefficient (ε_{mM}) value of 297 cm^{-1} mM^{-1}.

Porphyrins are dissolved in base to facilitate reduction, but are more accurately quantitated in acidic solution. It is best to use freshly prepared protoporphyrin solutions to minimize aggregation of the protoporphyrin. The authors do not attempt to accurately weigh the protoporphyrin, but use the extinction coefficient to determine the exact concentration when this is needed. In practice, the authors' stock solutions have varied from 350 to 500 μM without any effect on enzyme activity.

COMMENTARY

Background Information

A variety of techniques have been used to measure the conversion of protoporphyrinogen to protoporphyrin. A spectrophotometric assay measuring the absorbance of protoporphyrin in both the visible and Soret (near 408 nm) regions was the first method used to show oxidation of the colorless porphyrinogen to the colored porphyrin (Poulson, 1976; Jacobs and Jacobs, 1979; Klemm and Barton, 1987). However, the distinct red fluorescence of protoporphyrin is more intense than its absorption, and is now utilized in a much more sensitive assay (Brenner and Bloomer, 1980; Jacobs and Jacobs, 1982; Labbe et al., 1985; Dailey and Karr, 1987; Camadro et al., 1993; Dailey and Dailey, 1997).

Almost any fluorometer and flurometric cuvette will be suitable for the assay; the authors have used a Perkin Elmer fluorometric spectrophotometer 650 10S equipped with a red-sensitive phototube. While the red-sensitive phototube increases sensitivity in the region of porphyrin fluorescence, it is not required. The volume of the assay will depend on the location of the light path of the spectroflurometer. It is only necessary to have 1 ml of liquid in a 3-ml cuvette to cover the light path of the Perkin Elmer 650. For assaying very small amounts of sample, the authors use disposable semi-micro spectrophotometric cuvettes that are clear on four sides. With the Perkin Elmer 650, it is possible to use as little as a 0.250-ml volume with these cuvettes by scaling down all reagents accordingly.

Critical Parameters and Troubleshooting

The most critical parameter in assays of protoporphyrinogen oxidase is the quality of the substrate, protoporphyrinogen. The authors have found that if complete reduction of protoporphyrin does not take place within 5 min, there is a problem with the sodium amalgam. Addition of more amalgam usually does not help, because the solution will become so basic that it is impossible to neutralize. On a humid day, the amalgam may take up moisture during grinding and become ineffective. Fresh amalgam is best, but stored amalgam that has remained completely dry is also suitable. Amalgam can be kept for several months in a desiccator, under vacuum, with phosphorus pentoxide used as desiccant.

Another major problem is the autooxidation of protoporphyrinogen. A variety of reducing agents have been added to the assay mixture and to the protoporphyrinogen solution in attempts to minimize chemical autooxidation. In the authors' experience, DTT is very effective at suppressing nonenzymatic protoporphyrinogen oxidation. The authors have most frequently used DTT at final concentrations of between 2 and 5 mM in the enzyme assay and also add DTT to protoporphyrinogen solutions to stabilize them before addition to the assay. Other reducing agents, such as glutathione and ascorbic acid, have been used by other researchers (Jacobs and Jacobs, 1982; Camadro et al., 1985; Camadro et al., 1993; Dailey and Dailey 1997). Protoporphyrinogen oxidase from some sources (especially plant sources) may be somewhat inhibited by DTT, and the presence of DTT also makes it more difficult to obtain quantitative recovery of protoporphyrin after chemical oxidation of protoporphyrinogen solutions by strong acids and/or light (Jacobs and Jacobs, 1982). However, the authors have found that use of an *E. coli* membrane preparation gives a good yield of protoporphyrin from protoporphyrinogen even in the presence of DTT (Jacobs and Jacobs, 1993).

Autooxidation may be more rapid with incompletely reduced protoporphyrinogen preparations, since these will contain a significant amount of unreduced protoporphyrin. Catalytic amounts of porphyrins have been reported to stimulate protoporphyrinogen autooxidation (Mauzerall and Granick, 1958). If no reductant is used, the rate of autooxidation will be substantial. A protoporphyrinogen oxidizing activity that is not inhibited by photobleaching herbicides (e.g., acifluorfen methyl), but that differs from autooxidation, has been described and may cause confusion if plant material is used (Jacobs et al., 1991; Lee et al., 1993; Yamato et al., 1994). This activity may be associated with plant peroxidases and is suppressed by DTT or ascorbate.

The preparation of protoporphyrinogen requires the reduction of protoporphyrin with 3% sodium amalgam. The authors have had little success in using other reductants, such as sodium borohydride. The method described here for making sodium amalgam must be carried out with extreme caution. The authors have not tried other methods, but preparation of small amounts of amalgam right before use by adding chips of sodium to a small amount of mercury in a beaker may be satisfactory. Other methods may be superior, if they result in less mercury vapor (Fieser and Fieser, 1967; Nicolaus et al., 1993). All procedures involving mercury, including use of the amalgam, must be done in a chemical safety hood and proper protective gear (chemical resistant gloves, mercury respirator, and face shield) should be used. The procedure should be approved by the institution's safety committee.

Determining the rate of nonenzymatic protoporphyrinogen oxidation can be another source of difficulty. Enzyme that has been heat-inactivated (15 min at 75°C) can be used, but when using crude sources of enzyme the heated preparations can become quite turbid. To partially decrease turbidity, disperse the heated enzyme with brief sonication, using a small sonic probe and a microcentrifuge tube. To correct for the quenching of protoporphyrin fluorescence by turbidity, standard curves should be set up without enzyme and in the presence of both unheated and heat-treated enzyme. The indirect assay (Basic Protocol) is less subject to interference from turbidity, since assay reactants are diluted in the measuring mixture. Turbidity can be minimized by solubilizing liver mitochondria with 1% sodium cholate (Birchfield and Casida, 1996).

Since the substrate, protoporphyrinogen, is difficult to prepare, it would be desirable to store it for several days or weeks. The authors have been able to store the substrate prepared as described in the direct assay above (see Alternate Protocol 1, step 8) by transferring it, after dilution into the DTT solution, to a 1-ml disposable tube appropriate for subsequent storage under liquid nitrogen. This gave satisfactory results in the assay after storage for several months. Other investigators have reported storage of protoporphyrinogen for many weeks frozen, under paraffin oil, discarding it only when the solution became colored (Birchfield and Casida, 1996; Camadro et al., 1993). Although the authors have no experience with this procedure, it should work for most purposes, since solutions which appear fluorescent, but remain colorless, will still contain mainly protoporphyrinogen. All frozen preparations should be thawed only once, and exposure to light and air must be minimized.

A new assay has been developed for dose-response studies of protoporphyrinogen oxidase inhibitors that eliminates the need for protoporphyrinogen as substrate (Birchfield and Casida, 1996). In this assay a radiolabeled probe, constructed from a protoporphyrinogen

oxidase–inhibiting herbicide, binds reversibly to the herbicide-binding site of the enzyme. The ability of other herbicides to interfere with binding of the labeled probe is a measure of their ability to inhibit the enzyme (Birchfield and Casida, 1996). In one recent study using a series of herbicides with variable potency, there was adequate correlation of enzyme inhibition with binding inhibition using mouse liver mitochondria as enzyme source (Birchfield and Casida, 1996). Protoporphyrinogen oxidase activity has also been assayed utilizing high-performance liquid chromatography (HPLC) with electrochemical detection to measure protoporphyrinogen disappearance (Li et al., 1987).

The decision to use the indirect (Basic Protocol) or the direct assay (Alternate Protocol 1) will depend on several factors. The indirect assay should be used if the enzyme source has high background fluorescence or high turbidity. However, the direct assay has been used for herbicide dose-response studies in both barley etioplast and rat liver mitochondrial preparations. In the direct assay, a small amount of concentrated protoporphyrinogen solution is added to the assay mixture, resulting in a final concentration of 10 μM. The 1/2 dilution of the protoporphyrinogen solution into 100 mM DTT and the 1/25 dilution of this solution (see Alternate Protocol 1, steps 8 and 10) into the assay mixture eliminates the neutralization step. If higher substrate concentrations are desired, the protoporphyrinogen solution must be neutralized before addition to the assay mixture. In the indirect assay, assay tubes can be incubated at any temperature desired. It may be preferable to use the indirect assay if the available fluorometer has no mechanism for temperature control and a specific temperature is required. Assay temperatures of between 37°C and room temperature have been used. Mammalian mitochondria are more active at 37°C, but can be assayed at room temperature for comparing effects of herbicide inhibitors.

Anticipated Results

In the indirect assay, sonicated rat liver mitochondria had a specific activity of 8 nmol protoporphyrin formed/hr/mg protein at 37°C. In the direct assay, sonicated rat liver mitochondria had a specific activity of 5 to 6 nmol protoporphyrin formed/hr/mg protein at 28°C. This specific activity is in the same range for another rat liver heme synthesis enzyme, coproporphyrinogen oxidase. Other heme synthesis enzymes show higher or lower specific activities (Bishop and Desnick, 1982).

Time Considerations

The indirect assay requires 3 hr; the direct assay 3 hr. Preparation of sodium amalgam requires 2 hr. Preparation of *E. coli* membranes requires 4 hr. These time estimates include only actual assay times after all protocols have been developed.

Literature Cited

Birchfield, N.B. and Casida, J.E. 1996. Protoporphyrinogen oxidase: High affinity tetrahydrophthalimide radioligand for the inhibitor/herbicide-binding site in mouse liver mitochondria. *Chem. Res. Toxicol.* 9:1135-1139.

Bishop, D.F. and Desnick, R.J. 1982. Assays of the heme biosynthetic enzymes. *Enzymes* 28:91-93.

Brenner, D.A. and Bloomer, J.R. 1980. A fluorometric assay for measurement of protoporphyrinogen oxidase activity in mammalian tissue. *Clin. Chim. Acta* 100:259-266.

Camadro, J.-M., Abraham, N.G., and Levere, R.D. 1985. Kinetic properties of the membrane-bound human Liver mitochondrial protoporphyrinogen oxidase. *Arch. Biochem. Biophys.* 242:206-212.

Camadro, J.-M., Matringe, M., Scalla, R., and Labbe, P. 1993. Fluorometric assay of protoporphyrinogen oxidase in chloroplasts, and in plant, yeast and mammalian mitochondria. *In* Target Assays for Modern Herbicides and Related Phytotoxic Compounds (P. Boger and G. Sandmann, eds.) pp. 29-34. Lewis Publishers, Ann Arbor, Mich.

Dailey, T.A. and Dailey, H.A. 1997. Expression, purification, and characteristics of mammalian protoporphyrinogen oxidase. *Methods Enzymol.* 281:340-349.

Dailey, H.A., and Karr, S.W. 1987. Purification and characterization of murine protoporphyrinogen oxidase. *Biochemistry* 26:2697-2701.

Fieser, L.F. and Fieser, M. 1967. Reagents for Organic Synthesis. John Wiley & Sons, New York.

Jacobs, J.M. and Jacobs, N.J. 1993 Porphyrin accumulation and export by isolated barley (*Hordeum vulgare*) plastids. *Plant Physiol.* 101:1181-1187.

Jacobs, J.M., Jacobs, N.J., Sherman, T.D., and Duke, S.O. 1991. Effect of diphenyl ether herbicides on oxidation of protoporphyrinogen to protoporphyrin in organellar and plasma membrane enriched fractions of barley. *Plant Physiol.* 97:197-203.

Jacobs, N.J. and Jacobs, J.M. 1979. Microbial oxidation of protoporphyrinogen: An intermediate in heme and chlorophyll biosynthesis. *Arch. Biochem. Biophys.* 197:396-403.

Jacobs, N.J. and Jacobs, J.M. 1982. Assay for enzymatic protoporphyrinogen oxidation, a late step in heme synthesis. *Enzyme* 28:206-219.

Klemm, D.J. and Barton, L.L. 1987. Purification and properties of protoporphyrinogen oxidase from an anaerobic bacterium *Desulfovibrio gigas*. *J. Bacteriol.* 169:5209-5215.

Labbe, P., Camadro, J.-M., and Chambon, H. 1985. Fluorometric assays for coproporphyrinogen oxidase and protoporphyrinogen oxidase. *Anal. Biochem.* 149:248-260.

Lee, H.J., Duke, M.V., and Duke, S.O. 1993. Cellular localization of protoporphyrinogen-oxidizing activities of etiolated barley (*Hordeum vulgare L.*) leaves. *Plant Physiol.* 102:881-889.

Li, F., Lim, C.K., and Peters, T.J., 1987. An hplc assay for protoporphyrinogen oxidase activity in rat liver. *Biochem. J.* 243:863-866.

Mauzerall, D. and Granick, S. 1958. Porphyrin biosynthesis in erythrocytes III. Uroporphyrinogen and its decarboxylase. *J. Biol. Chem.* 232:1141-1162.

Nicolaus, B., Sandmann, G., and Boger, P. 1993. Inhibition of protoporphyrinogen oxidase from maize. *In* Target Assays for Modern Herbicides and Related Phytotoxic Compounds. (P. Boger and G. Sandmann, eds.) pp. 29-34. Lewis Publishers, Ann Arbor, Mich.

Poulson, R. 1976. The enzymatic conversion of protoporphyrinogen IX to protoporphyrin IX in mammalian mitochondria. *J. Biol. Chem.* 251:3730-3733.

Yamato, S., Katagiri, M., and Ohkana, H. 1994. Purification and characterization of protoporphyrinogen oxidase from tobacco cultured cells. *Pestic. Biochem. Physiol.* 50:72-82.

Key References

Camadro et al., 1993. See above.

Presents slightly different methodologies than those given here, from a laboratory with extensive experience with this difficult assay (e.g., use of ascorbic acid instead of DTT as an antioxidant, and useful hints about preparing and clarifying protoporphyrinogen solutions).

Dailey and Dailey, 1997. See above.

Further descriptions of protoporphyrinogen oxidase assays.

Fieser and Fieser, 1967. See above.

Alternate procedure for sodium amalgam preparation—the classical method, using enclosed glassware, and recommended over the method described here, although biological laboratories may find it prohibitively inconvenient.

Labbe et al., 1985. See above.

First version of the direct fluorometric assay.

Nicolaus et al., 1993. See above.

Another version of the direct fluorometric assay with an alternate method for sodium amalgam preparation.

Contributed by Judith M. Jacobs and Nicholas J. Jacobs
Dartmouth Medical School
Hanover, New Hampshire

Measurement of δ-Aminolevulinate Dehydratase Activity

Vertebrate δ-aminolevulinate (ALA) dehydratase (ALAD), a cytosolic enzyme, catalyzes the second step of porphyrin formation, condensing two molecules of ALA to form one molecule of a monopyrrole, porphobilinogen (PBG). In contrast to ALA synthase (ALAS), the first and rate-limiting enzyme for porphyrin biosynthesis, ALAD activity is expressed abundantly in the liver and in erythroid tissues. The enzyme activity is also found in many other tissues. The proportion of ALAD activity to ALAS activity is ~1:100 not only in hepatic cells but also in erythroid cells. Thus, partial inhibition of ALAD activity is usually not associated with clinical symptoms.

This unit describes a colorimetric method for determining ALAD activity in mammalian blood and/or tissues (see Basic Protocol) and for measuring the extent of reactivation in lead-inhibited samples (see Alternate Protocol 1). The amount of PBG produced by the activity of ALAD can be measured by HPLC with UV detection (see Alternate Protocol 2), or the PBG can be converted to uroporphyrin and measured fluorimetrically (see Alternate Protocol 3).

Purified ALAD may be prepared from human erythrocytes (Anderson and Desnick, 1979), bovine liver (Tsukamoto et al., 1979), or rabbit or rat erythrocytes (Fujita et al., 1981). ALAD can be stored at 4°C in 55% (w/v) saturated ammonium sulfate, or in liquid nitrogen without loss of activity.

COLORIMETRIC MEASUREMENT OF ALAD ACTIVITY

BASIC PROTOCOL

ALAD activity in erythrocytes, spleen, liver, kidney, and brain can be determined using a colorimetric assay. Samples are incubated with ALA at 37°C for 60 min. The reaction is terminated with trichloroacetic acid/$HgCl_2$ and mixed well. The mixture is centrifuged and the supernatant is incubated with the modified Ehrlich's reagent. The amount of enzymatically synthesized porphobilinogen (PBG) is estimated as an Ehrlich-PBG color salt with a molar absorption coefficient of 6.2×10^4 at 555 nm (Mauzerall and Granick, 1956). One unit (U) of enzyme activity is defined as 1 μmol of PBG formed per hr at 37°C. Enzyme activity in erythrocytes or other tissues is expressed as U/ml packed cells or U/mg protein.

Materials

Blood or tissue sample
100 mM Tris-acetate buffer, pH 7.2
Protein assay dye reagent (e.g., Bio-Rad; see *APPENDIX 3*)
100 mM δ-aminolevulinic acid hydrochloride (ALA·HCl) in H_2O (Sigma; store up to 1 month at –20°C)
10% (w/v) trichloroacetic acid (TCA)/0.1 M $HgCl_2$, ice-cold (store at room temperature)
Modified Ehrlich's reagent (see recipe)

Heparinized Vacutainer
Heparinized precalibrated capillary tubes (Lancer)
Critoseal (Lancer)
Potter homogenizer
Microhematocrit centrifuge
1-ml semimicro cuvettes, 4-mm wide with 10-mm path length

Contributed by Hiroyoshi Fujita
Current Protocols in Toxicology (1999) 8.6.1-8.6.11

Prepare sample

For blood samples

1a. Collect blood samples in heparinized Vacutainer.

2a. Transfer a drop of blood to a heparinized precalibrated capillary tube, seal one end with Critoseal, and centrifuge 5 min at 10,000 × *g*, room temperature, using a microhematocrit centrifuge. Determine the hematocrit using the guide provided with the centrifuge.

3a. Lyse the remainder of the blood sample by freezing the cells 60 min or longer at –20°C and then thawing.

For tissue samples

1b. Suspend cut-up tissue in 3 vol of 100 mM Tris-acetate buffer, pH 7.2 (1:3 w/v suspension containing 25% homogenate).

2b. Homogenize by using a Potter homogenizer.

3b. Determine the protein concentration of tissue homogenates by the micro Bio-Rad assay.

Assay for ALAD

4. Set up assays in duplicate in 1.5-ml microcentrifuge tubes placed in an ice bucket. In each tube, add 50 µl lysate or homogenate to 238 µl of ice-cold 100 mM Tris-acetate buffer, pH 7.2, and mix well.

5. Add 12 µl of 100 mM ALA-HCl and incubate 60 min at 37°C.

   The reaction is usually linear for ~3 hr. An appropriate incubation time can be chosen based on the level of enzyme activity. For example, human erythroid ALAD activity is ~8 times higher than that of rats (see Anticipated Results). Therefore, for human erythroid samples the incubation could be shortened to 15 min.

6. To terminate the enzyme reaction add an equal volume (300 µl) of ice-cold 10% trichloroacetic acid (TCA)/0.1 M $HgCl_2$ and mix well. Centrifuge the mixture 5 min at ≥1000 × *g*, room temperature.

7. Transfer 500 µl of the supernatant to a fresh tube and mix with an equal volume (500 µl) of the modified Ehrlich's reagent. Prepare a blank consisting of equal volumes of 10% TCA/0.1 mM $HgCl_2$ and modified Ehrlich's reagent. Let stand 5 to 10 min at room temperature.

   The modified Ehrlich's reagent is used for these assays. The original Ehrlich's reagent gives only about half the absorbance.

8. Measure the absorbance of the Ehrlich-PBG color salt at 555 nm (A_{555}) using 1-ml semimicro cuvettes. Calculate the PBG concentration using a molar absorption coefficient of 6.2×10^4. Calculate the ALAD activity as in the following sample calculations.

   PBG concentration is calculated according to the following:

$$\frac{A_{555}}{extinction\ coefficient} \times \frac{assay\ volume}{sample\ volume} \times (dilution\ with\ TCA/HgCl_2) \times$$

$$(dilution\ with\ modified\ Ehrlich's\ reagent) \times \frac{60\ min}{15\ min} \times \frac{1}{hematocrit} \times 1000$$

When the A_{555} of normal human erythrocytes, whose hematocrit is 45%, is 0.6 after a 15-min incubation, ALAD activity is calculated as follows: $(0.6/6.2 \times 10^4) \times (300/50) \times 2 \times 2 \times 4 \times (1/0.45) \times 10^3 = (0.6 \times 6 \times 16 \times 10^3)/(6.2 \times 10^4 \times 0.45) = 2.06$ U/ml packed cells.

When A_{555} of normal rat liver is 1.1 after a 60-min. incubation, where the protein concentration of the homogenate (1:3 w/v) is 50 mg/ml, ALAD activity is calculated as follows: $(1.1/6.2 \times 10^4) \times (300/50) \times 2 \times 2 \times (1/50) \times 10^3 = (1.1 \times 6 \times 4 \times 10^3)/(6.2 \times 10^4 \times 50) = 8.5 \times 10^{-3}$ U/mg protein.

The volumes and incubation times described are suitable for measurements using 1-ml semimicro cuvettes. If micro or 100-µl ultramicro cuvettes are available, the procedure can be scaled down to 1/10.

ALAD ASSAY FOR DETECTING LEAD POISONING

ALTERNATE PROTOCOL 1

Lead poisoning has been known for centuries as an important metal poisoning in humans and is a major health problem, particularly in developing children. Because of a marked sensitivity of ALAD to lead, lead poisoning can be detected by measuring ALAD activity in a drop of blood. Another important feature is that ALAD activity can be restored to normal by treatment with dithiothreitol (DTT) or zinc (Fujita et al., 1981, 1982a). Heat treatment has also been reported to reactivate lead-inhibited ALAD activity (Chiba, 1976). Thus, the extent of inhibition by lead can also be determined as the extent of reactivation of the enzyme following incubation with DTT or Zn^{2+}, or after heat treatment.

Additional Materials *(also see Basic Protocol)*

1 M DTT (*APPENDIX 2A*; store up to 1 month at −20°C)
10 mM zinc acetate (store at room temperature)

1. Prepare hemolyzed blood samples (see Basic Protocol, steps 1a to 3a) or 25% tissue homogenates (see Basic Protocol, steps 1b to 3b).
2. To treat samples add 50 µl of sample, 3 µl of 1 M DTT, and 3 µl of 10 mM zinc acetate to 232 µl of 100 mM Tris-acetate buffer, pH 7.2, in a 1.5-ml microcentrifuge tube in an ice bath. Mix well and preincubate 15 min at 37°C.

   Prepare duplicate tubes for each assay condition. These will be the tubes with the reactivated enzyme (see step 7).

3. To prepare untreated samples (controls) add 50 µl sample to 238 µl Tris-acetate buffer, pH 7.2, in a 1.5-ml microcentrifuge tube. Place on ice.

   These will be the tubes with the nonreactivated enzyme.

4. Put the treated tubes on ice. Add 12 µl of 100 mM ALA·HCl to all (treated and untreated) tubes and incubate 60 min at 37°C.
5. Stop the enzyme incubation by adding an equal volume (300 µl) of 10% TCA/0.1 mM $HgCl_2$. Mix well and centrifuge 5 min at ≥1000 × *g*, room temperature.
6. Transfer 500 µl of supernatant to a fresh tube and add 500 µl modified Ehrlich's reagent. Let stand 5 to 10 min at room temperature. Determine the PBG concentration by reading the absorbance at 555 nm. Determine the ALAD activity in the treated (reactivated) and untreated (nonreactivated) tubes (see Basic Protocol, step 8).
7. Express enzyme activity as a ratio between the reactivated and nonreactivated enzyme. Alternatively express the activity as a ratio between the lead-bound activity to total activity, calculated as:

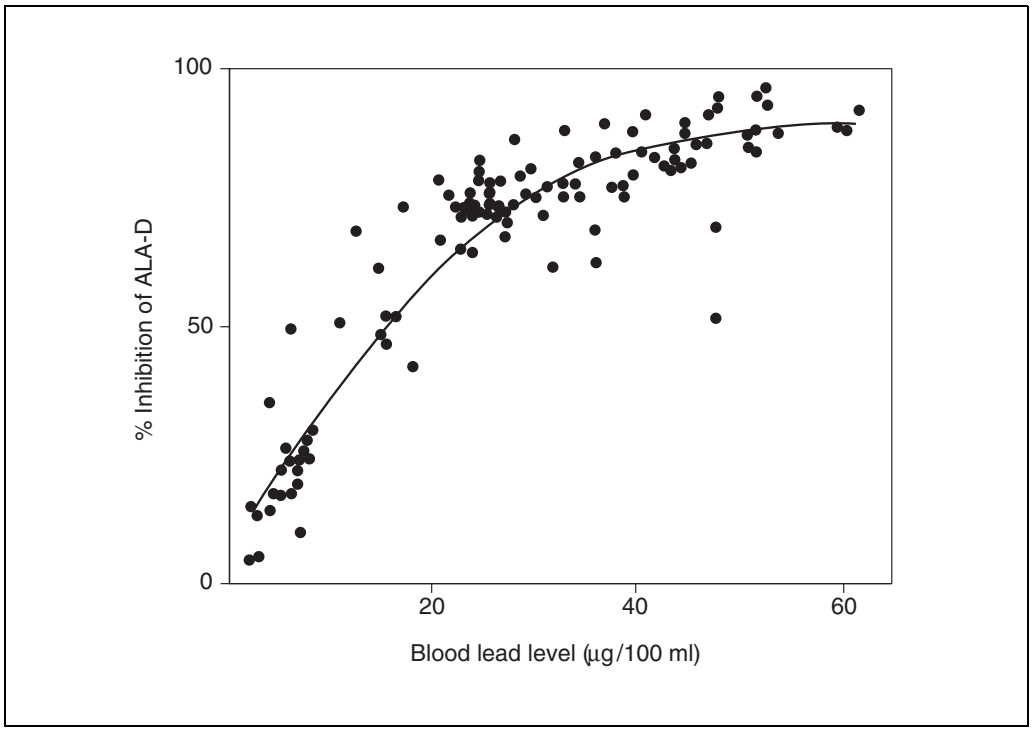

Figure 8.6.1 Correlation between inhibition ratio of ALAD and blood lead level. The inhibition ratio was calculated as described in Alternate Protocol 1. The regression curve was $y = 6.104 + 3.43x - 0.0336x^2$ (n = 108; multiple correlation coefficient 0.936; $F^2_{105} = 370.54$; $P < 0.005$). (Figure reprinted from Sato et al., 1982, with permission).

$$1 - \frac{\text{nonreactivated activity}}{\text{reactivated activity}}$$

See Figure 8.6.1. Each indicator has a good correlation with blood lead concentration.

In cases of styrene exposure (Fujita et al., 1986), trichloroethylene exposure (Fujita et al., 1984), type 1 tyrosinemia (Lindblad et al., 1977), and ADP (Doss et al., 1979), nonreactivated activity is essentially similar to reactivated activity.

ALTERNATE PROTOCOL 2

MEASUREMENT OF ALAD ACTIVITY BY HPLC

Crowne et al. (1981) reported HPLC determination of porphobilinogen after the termination of the enzyme reaction. By this HPLC method, an aliquot of the assay mixture (equivalent to ~1 µl of whole blood as enzyme source) is sufficient to determine the enzyme activity, demonstrating the extremely high sensitivity of this method.

In practice, the colorimetric determination of PBG is sensitive enough to determine ALAD activity in 5 µl of specimen when 100-µl ultramicro cuvettes are available. Thus, almost all assays are performed using spectrophotometry. However, PBG might be unstable on incubation at 37°C, so not only the amount of PBG formed but also the amount of PBG degraded should theoretically be taken into account to evaluate accurate ALAD activity. Under certain circumstances, therefore, the HPLC method should be superior to the colorimetric estimation, since ALA consumed PBG formed, and PBG degraded can be determined using the former method. According to the HPLC method, ALA consumption and PBG production in erythrocytes from 25 normal volunteers was reported to be 35.0 ± 7.7 µmol and 17.5 ± 3.84 µmol/liter RBC/min, respectively (Crowne et al., 1981). Thus, PBG degradation during incubation at 37°C for 60 min is demonstrated to be essentially nil.

Materials

5 to 50 µM PBG standards
Internal standard: 2-methyl-3-carbmethoxy-4-(3-propionic acid)-pyrrole (see recipe)
Mobile phase (see recipe)
Whole blood collected in heparinized Vacutainer
0.1 M sodium phosphate buffer, pH 6.8 (*APPENDIX 2A*) containing 10 mM δ-aminolevulinic acid hydrochloride (ALA·HCl; prepare just before use)
10% (w/v) trichloroacetic acid (TCA)/0.1 M $HgCl_2$, ice-cold (store at room temperature)
HPLC system with 5-µm particle Hypersil-SAS column (5 × 100–mm) and UV detector set at 240 nm and 0.02 AU (full scale; Shandon Southern)

1. Construct a calibration curve using standard solution of PBG ranging from 5 to 50 µM by mixing a 0.5-ml aliquot of each PBG standard with 0.1 ml of the internal standard and injecting 20 µl into the HPLC. Set the pressure at 80 bar with a flow-rate of 1.2 ml/min, and use a mobile phase consisting of 22:78 methanol/ion-pair reagent. Plot PBG concentration versus the ratio of the peaks of PBG/internal standard.

   The duration of the HPLC is <5 min.

2. Hemolyze 0.5 ml of whole blood to be tested for ALAD in 3.25 ml water.

3. Add 1.5 ml of the hemolysate (corresponding to 0.2 ml of whole blood) to 1 ml of 0.1 M sodium phosphate buffer, pH 6.8, containing 10 mM ALA. Incubate mixture 60 min at 37°C.

   ALA in 0.1 M sodium phosphate buffer should be prepared just before use because ALA is unstable under these conditions.

4. Terminate the enzyme reaction by adding 1 ml of 10% trichloroacetic acid/0.1 M $HgCl_2$, then centrifuge 5 min at ≥1000 × *g*, room temperature.

5. Mix the supernatant with the internal standard at a ratio of 5:1. Inject 20 µl of well mixed solution onto the HPLC and chromatograph as in step 1.

   Under the conditions employed, ALA, PBG, and the internal standard are well separated, with retention times of 114, 198, and 260 sec, respectively.

6. To determine ALAD activity, read PBG concentration in each assay mixture from the calibration curve.

FLUORIMETRIC DETERMINATION OF ERYTHROCYTE ALAD ACTIVITY BY HPLC

ALTERNATE PROTOCOL 3

Since PBG is considered to be sensitive to light and air oxidation, ALAD activity can be estimated after chemical conversion of PBG into stable and highly fluorescent uroporphyrin (Chakrabarti et al., 1975; Tomokuni, 1976). By fluorescence alone, however, it is difficult to separate fluorescence of the enzymatic product from fluorescence of other porphyrins in the reaction mixture. Thus, an HPLC method has been developed to enable this separation by which the amount of uroprophyrin can be used as a measure of ALAD activity .

Like the HPLC method as described in Alternate Protocol 2, the fluorometric determination is a few times more sensitive than the colorimetric determination, thus permitting ALAD assays in nonhepatic or nonerythoid tissues. The colorimetric determination is, however, sensitive enough to estimate ALAD activity in many cells.

Materials

Heparinized whole blood
0.2 M sodium phosphate buffer, pH 6.8 (*APPENDIX 2A*)
20 mM δ-aminolevulinic acid hydrochloride (ALA·HCl) in water
Authentic porphyrins: 500 μg/liter coproporphyrin I and appropriate concentration uroporphyrin I, dissolved in glacial acetic acid
10% (w/v) trichloracetic acid
Mobile phase: 500:500:10 (v/v/v) acetonitrile/aqueous 10 mM KH_2PO_4/glacial acetic acid

HPLC system with:
5-μm particle Shim-pack CLC-ODS reversed-phase column (6 × 150–mm; Shimadzu Ltd.)
Fluorescence detector with excitation wavelength of 400 nm (bandwidth 18 nm) and emission wavelength of 620 nm (bandwidth 22 nm)
100°C water bath

1. Hemolyze 0.1 ml heparinized whole blood with 1.4 ml of distilled water, then add 0.5 ml of 0.2 M sodium phosphate buffer, pH 6.8.
2. Add 0.5 ml of 20 mM ALA and incubate 60 min at 37°C.
3. Terminate the reaction by adding 1 ml of 10% trichloroacetic acid. Mix and centrifuge 5 min at ≥1000 × *g*, 4°C.
4. Transfer supernatant into fresh tube, heat 15 min at 100°C to yield uroporphyrin, then cool down in an ice bath.
5. Inject 10 μl of the assay mixture into HPLC with a flow rate of 1.5 ml/min to determine porphyrin separation and concentrations. Use mobile phase consisting of 500/500/10 acetonitrile/10 mM KH_2PO_4/glacial acetic acid. Run the authentic porphyrins to determine retention time. Also prepare a calibration curve using dilutions of coproporphyrin.

   Under these conditions, the retention times of uroporphyrin and coproporphyrin are 1.6 and 4.6 min, respectively.

6. Calculate the enzyme activity as $F_s/F_c \times 500/655 \times 3.5/0.1 \times 100$/hematocrit (mmol uroporphyrin/liter RBC/hr), where F_s = fluorescence of sample, F_c = fluorescence of coproporphyrin standard, and 655 = molecular weight of coproporphyrin.

   Since the fluorescence intensity of uroporphyrin is equal to that of coproporphyin at the same micromolar concentration under the conditions employed, the coproporphyrin standard, whose 5-μg vial is inexpensive and convenient, is used to calculate the activity instead of uroporphyrin.

   The relationship between ALAD activities determined by colorimetric assay (x) and by fluorometric assay (y) is reported as y = 0.125x – 38.761, with a correlation coefficient of 0.971 (n = 58; Tomokuni and Ichiba, 1988). Since a theoretical relationship should be y = 0.25x, more than 50% of produced PBG is lost during steps including chemical conversion into uroporphyrin.

REAGENTS AND SOLUTIONS

Use Milli-Q-purified water or equivalent in all recipes and protocol steps. For common solutions see ***APPENDIX 2A****; for suppliers, see* ***SUPPLIERS APPENDIX****.*

Ehrlich's reagent, modified

Dissolve 1 g of *p*-dimethylaminobenzaldehyde (Sigma) in a mixture of 30 ml glacial acetic acid and 16 ml 70% perchloric acid. Bring the volume to 50 ml with acetic acid. Store up to 1 week at 4°C in a dark brown bottle.

2-Methyl-3-carbmethoxy-4-(3-propionic acid)-pyrrole

Prepare an acetate buffer, pH 4.6, by diluting 57 ml of glacial acetic acid in 700 ml of water, adding 136 g of sodium acetate trihydrate, and bringing the final volume to 1 liter with water (store buffer indefinitely at room temperature). Dissolve 2 mg of δ-aminolevulinic acid hydrochloride (ALA·HCl) in 10 ml of water. Add 10 ml of the acetate buffer, pH 4.6, and heat the mixture 20 min at 100°C. Dry 1-ml aliquots and store at 4°C. Just prior to use, redissolve in 10 ml water.

Mobile phase

Dilute one 20-ml bottle of PIC-B7 (1-heptanesulfonic acid; Fluka) to 1 liter with water. Prepare this ion-pair reagent just before use or store at 4°C in the dark for a few days. Prepare mobile phase by mixing 78 parts of the ion-pair reagent with 22 parts methanol.

COMMENTARY

Background Information

ALAD activity was described for the first time by Shemin et al. (1954). Among the eight enzymes in the heme biosynthetic pathway of mammals, ALAD has one of the highest activities (Fujita et al., 1994). For example, mature human erythrocytes contain as much as 150 µg ALAD/ml packed cells (Fujita et al., 1987). While ALAD is present in erythrocytes, there is no heme synthesis in these cells since they lack mitochondrial ALA synthase, the first enzyme of heme biosynthesis.

Mammalian ALAD is a homodimer consisting of eight identical subunits, each with a molecular weight of ~35,000. Each of these subunits contains eight cysteinyl residues. Thus, one molecule of ALAD has 64 cysteinyl residues, and the enzyme activity is highly sensitive to oxidative agents (Tsukamoto et al., 1979). Furthermore, various metals, such as Ag^{+}, Hg^{2+}, Pb^{2+}, and Sn^{2+}, are known to strongly inhibit purified ALAD activity in vitro. Among these metals, Pb^{2+} and Sn^{2+} inhibit the enzyme activity also in vivo—an effect that accompanies clinical metal poisoning. Thus, the inhibition of ALAD activity is an important feature in divalent metal poisoning, and it is perhaps the most sensitive biological indicator of lead poisoning. In addition, ALAD is also inhibited by certain organic solvents, such as ethanol, trichloroethylene, bromobenzene, and styrene, and it is a useful biological index for environmental poisoning. Inhibition of ALAD by lead was originally reported by Koike (1959) and Lichtman and Feldman (1963). Since then, there have been many reports on the relationship between lead poisoning and ALAD inhibition.

Inhibition of ALAD activity is generally considered as the most sensitive indicator for low-level lead exposure. It should be noted, however, that enzyme activity in human erythrocytes has a wide range of variation which is thought to reflect different genetic backgrounds (Sassa et al., 1973). Thunell et al. (1987) reported that ~2% of 880 normal individuals have levels of ALAD activity ~50% of normal. Thus it is important to distinguish a lead-inactivated activity from a low normal activity. This distinction can be made by using DTT- and zinc-activated ALAD as described in Alternate Protocol 1.

Reactivation of lead-inhibited ALAD activity by treatment with glutathione (Haas et al., 1972), dithiothreitol (Granick et al., 1973), zinc (Finelli et al., 1975), heat treatment at 55° to 60°C (Chiba, 1976), or zinc and glutathione at 50°C (Mitchell et al., 1978) has been reported to be a useful index of lead exposure. Some methods have included DTT during enzyme incubation, and achieved an almost complete reactivation of lead-inhibited activity (Granick et al., 1973). A complete reactivation of ALAD

activity by 10 mM DTT and 100 μM zinc is more precisely documented by the comparison of ALAD protein and the completely reactivated specific activity of the protein (Fujita et al., 1981, 1982a).

The colorimetric determination of ALAD activity was first described by Gibson et al. (1955). In 1974, the European Standardized Method for ALAD assay was published (Berlin and Schaller, 1974), and it has become the main assay method. Commonly ALAD assay methods, including the European Standard method, are carried out in the presence of phosphate buffer. It should be noted, however, that lead-inhibited ALAD activity can be partially reactivated by a chelating activity of the buffer (Maes and Gerber, 1978). Thus, the use of buffers with chelating activity, such as citrate or phosphate buffers, should be carefully monitored or avoided when carrying out the assay for detecting lead poisoning (Alternate Protocol 1). This is the reason why Tris-acetate buffer, pH 7.2, is used instead of phosphate buffer, for certain assays (Fujita et al., 1981, 1982a,b). Jaffe et al. (1984) also described the use of TES-KOH buffer, pH 7.2. Thus, the ALAD assay from in vivo experiments indicates the magnitude of the inhibitory effect of a chemical hazard on ALAD. To understand the precise effect of a chemical hazard on ALAD, the in vitro relationship between the purified enzyme and the chemical hazard should be examined. Such studies will clarify, for example, the interaction between a chemical hazard and an essential SH residue of the enzyme.

Since the products of ALAD-catalyzed reactions are porphobilinogen and H^+, the purified enzyme activity can be determined as a change in pH. The formation of H^+ by ALAD can be colorimetrically monitored using bromothymol blue (5 mg/ml) at 617 nm. Under the conditions employed, a loss of 1 O.D. at 617 nm is equivalent to a formation of 0.019 M of H^+ (and PBG). The buffer for the reaction should be 10 mM Tris-acetate, pH 7.2, and ALA-HCl solution should be adjusted to pH 7.2 just before use.

In addition to toxicological inhibition, ALAD decreased activity is associated with inherited ALAD deficiency. ALAD porphyria (ADP), a rare hepatic porphyria, shows a marked deficiency in ALAD activity. This disease is due to a homozygous ALAD mutation; mutations identified in four patients to date indicate heteroallelic mutations of the ALAD gene. In one case of ADP, ALAD in erythrocyes was decreased to 45.8 μg/ml packed cells (Fujita et al., 1987b), which is markedly lower than that in normal controls (165 ± 56.8 μg/ml packed cells, $n = 18$; Fujita et al., 1987). ALAD in patients with type 1 tyrosinemia is also markedly decreased, and patients present with symptoms similar to ADP. In contrast to ADP, ALAD content in erythrocytes from a patient with type 1 tyrosinemia (~200 μg/ml packed cells) was within the normal range (Sassa et al., 1990). A comparison of ALAD concentration in the liver (ranging from 0.15 to 0.3 μg/mg protein) with that in erythrocytes (0.5 ± 0.17 μg/mg hemoglobin) suggests a preferential erythroid expression of the enzyme (Fujita et al., 1987; Sassa et al., 1990). ALAD activity in patients with tyrosinemia is inhibited by succinylacetone, an abnormal metabolite produced from tyrosine due to an inherited deficiency of fumarylacetoacetase activity. Recently, Bishop et al. (1996) reported that the tissue-specific expression of ALAD is due to a nonspecific promoter, which is located 5′ with respect to to exon 1a and an erythroid-specific promoter, 5′ with respect to exon 1b of the gene, in the liver and erythroid cells, respectively.

A genetic polymorphism of ALAD in man, with variants termed $ALAD^1$ and $ALAD^2$, was reported by Batistuzzi et al. (1981). Individuals with $ALAD^2$ phenotype were reported to have levels of blood lead higher than those with $ALAD^1$ phenotype (Astrin et al., 1987), and it has been suggested that $ALAD^2$ binds lead more effectively (Wetmur et al., 1991). A pair-matched study based on blood lead levels, however, showed that $ALAD^1$ protein and $ALAD^2$ protein were inhibited by lead to almost the same magnitude (Ziemsen, 1986). This observation suggests that lead may bind to $ALAD^1$ protein or $ALAD^2$ protein with similar affinity. Recently, a G^{177}-to-C transversion was shown in $ALAD^2$, which resulted in a Lys^{59}-to-Asn substitution (Wetmur et al., 1991). The Asn^{59} in the ALAD gene is also preserved in that position in the rat, mouse, and bovine enzyme (Wetmur et al., 1986; Bishop et al., 1986, 1989). The affinity of lead to ALAD in rat ($K_i = 6.0 \times 10^{-6}$ M) and bovine enzyme ($K_i = 2.8 \times 10^{-4}$ M) is lower than that to the human enzyme ($K_i = 1.7 \times 10^{-6}$ M); therefore, it might be possible that lead binds to the $ALAD^2$ protein, which has Asn^{59}, to a much lesser extent than to the $ALAD^1$ protein, which has Lys^{59} (Anderson and Desnick, 1979; Fujita et al., 1986). Recently, Bergdahl et al. (1997a) reported that ALAD polymorphism did not relate to lead levels but to kidney function.

In addition to genetic disease, styrene and trichloroethylene exposures are known to result

in lower ALAD activity. Styrene exposure is also associated with decreased protein, but this is presumably due to an irreversible deregulation of the enzyme by styrene and/or its oxide (Fujita et al., 1986, 1987).

Why mature erythrocytes contain a large amount of ALAD, in spite of the fact that mature erythrocytes no longer synthesize heme for hemoglobin, has not been well understood. Recently it was reported that ALAD is a 240-kDa proteasome inhibitor (CF-2; Guo et al., 1994). This may explain why ALAD is stable even after erythroid differentiation. The other possible role for ALAD protein in erythrocytes is as a 240-kDa lead-binding protein (Piomelli, 1993), since it has been reported to contain ~60% to 70% of blood lead (Bergdahl et al., 1997b). This observation is in good agreement with a regression curve between blood lead concentration (μM) as x and concentration of inhibited ALAD (subunit; μM) as y in lead-exposed workers; $y = -0.0547 + 1.448x - 0.3159x^2$, suggesting that 70% of lead is binding to ALA dehydratase when the blood lead level was lower than 3 μM (Fujita et al., 1982a).

Critical Parameters

There are a few critical points to be noted in the ALAD assay. Enzyme activity in erythrocytes can be markedly underestimated if hemolysis of the blood sample is incomplete. For example, samples frozen at −20°C for 30 min instead of 60 min show only ~50% of the complete activity. Freezing at −20°C for 60 min, or three quickly repeated freeze/thaw cycles in liquid nitrogen, is enough for complete lysis. Addition of 50% glycerol/DTT was reported to preserve ALAD activity and to facilitate detection of lead poisoning (Burns et al., 1994)

When a purified ALAD preparation is used, it loses activity rapidly because of oxidation of the sulfhydryl groups and loss of essential zinc. Therefore, activation of ALAD enzyme activity by DTT/zinc is essential. ALAD should be reactivated with 100 μM Zn^{2+} and 50 mM dithiothreitol prior to assay. Then, the reactivated enzyme should be applied to a Sephadex G-50 column (7 × 100–mm) under N_2 to remove excess dithiothreitol and zinc. Protein concentration of the reactivated enzyme is determined by measuring absorbance at 280 nm ($E^{1\%}_{1\ cm}$ = 11.8; Tsukamoto et al., 1979). Concentration of the purified enzyme, whose specific activity is 27 U/mg, in the assay mixture is usually 6 to 15 mg/ml. When the concentration of ALAD is 10 mg/ml, the absorbance of Ehrlich-PBG color salt after a 15-min reaction should be ~1. A relatively large amount of ALAD (6 to 15 mg/ml) should be used with N_2-saturated buffer and a short reaction time (15 min) to avoid oxidation during incubation.

Troubleshooting

Since the purified preparation is not stable under liquid nitrogen, it should be stored at 4°C with 55% saturated ammonium sulfate in the presence of 10 mM DTT and 100 μM zinc. In contrast to the purified enzyme, hemolysates or homogenized tissues can be stored in liquid N_2 without a significant loss of activity.

Contamination by metals may inhibit ALAD activity. Chemicals, reagents, tubes, and other items should be treated carefully to avoid contamination. Usually glass tubes and plastic labware from a freshly opened case do not present a problem When recycled glass tubes are used for assays, $HgCl_2$ should be thoroughly removed by washing with 0.1 N HNO_3 followed by exhaustive rinsing in deionized water.

Anticipated Results

When ALAD activity in human erythrocytes is determined according to the Basic Protocol, the enzyme activity for normal subjects is ~2 U/ml packed cells (Fujita et al., 1987). The ratio of nonreactivated activity to reactivated activity in normal controls is ~0.8. The relationship between nonreactivated activity and reactivated activity and blood lead concentration (μg Pb/100 ml blood) is $y = 0.0336x^2 - 3.43x + 93.90$, with a multiple correlation coefficient of 0.936, when the ratio of nonreactivated activity to reactivated activity is taken as y and the blood lead concentration is taken as x (Fujita et al., 1982a). Using hepatic biopsy tissue, ALAD activity of normal human liver is estimated to be 9×10^{-3} U/mg protein (Sassa et al., 1990). In Wistar rats after experimental lead exposure, erythrocyte nonreactivated activity in the control group (with a mean blood lead level of 9.3 μg/100 ml, $n = 6$) was 96×10^{-3} U/ml packed cells; in the low-lead-exposed group (with a mean blood lead level of 30.8 μg/100 ml, $n = 6$), 68×10^{-3} U/ml; and in high-lead exposed group (with a mean blood lead level of 90.9 μg/100 ml, $n = 6$), 20×10^{-3} U/ml packed cells. Reactivated activities for the same three groups were 136×10^{-3}, 258×10^{-3}, and 257×10^{-3} U/ml packed cells, respectively. Mean values of nonreactivated activity in the liver and in bone marrow cells in normal control rats were 8.3×10^{-3} and 8.8×10^{-3} U/mg protein, respectively; mean values of reactivated activity in the same liver and bone marrow cells were 9.5×10^{-3} and

18.9×10^{-3} U/mg protein, respectively (Fujita et al., 1985).

Time Considerations

To perform assays for ten samples in duplicate according to the Basic Protocol, it takes 3 hr, from enzyme preparation to colorimetric determination. For toxicological examinations, particularly screening for lead poisoning, it is necessary also to determine nonreactivated activity and reactivated activity. The assay for purified enzyme (from precipitation with ammonium sulfate to determination of activity) is completed within 2 hr. It takes ~2 hr to complete the preparation, preincubation, and incubation of the assay mixtures for HPLC analysis. In addition, HPLC with UV and fluorimetric detection take 5 min and 2 min, respectively, per sample. Each activity is determined in duplicate.

Literature Cited

Anderson, P.M. and Desnick, R.J. 1979. Purification and properties of δ-aminolevulinate dehydratase from human erythrocytes. *J. Biol. Chem.* 254:6924-6930.

Astrin, K.H., Bishop, D.F., Wetmur, J.G., Kaul, B., Davidow, B., and Desnick, R.J. 1987. δ-Aminolevulinic acid dehydratase isozymes and lead toxicity. *Ann. N.Y. Acad. Sci.* 514:23-29.

Batistuzzi, G., Petrucci R., Silvagni, L., Urbani, F.R., and Caiola, S. 1981. δ-Aminolevulinate dehydratase: A new genetic polymorphism in man. *Ann. Hum. Genet.* 45:223-229.

Bergdahl, I. A., Gerhardsson, L., Schutz, A., Desnick, R.J., Wetmur, J.G., and Skerfving, S. 1997a. δ-Aminolevulinic acid dehydratase polymorphism: Influence on lead levels and kidney function in humans. *Arch. Environ. Health* 52:91-96.

Bergdahl, I.A., Grubb, A., Schutz, A., Desnick, R.J., Wetmur, J.G., Sassa, S., and Skerfving, S. 1997b. Lead binding to δ-aminolevulinic acid dehydratase (ALAD) in human erythrocytes. *Pharmacol. Toxicol.* 81:153-158.

Berlin, A. and Schaller, K.H. 1974. European standardized method for the determination of δ-aminolevulinic acid dehydratase activity in blood. *Z. Klin. Chem. Klin. Biochem.* 12:389-390.

Bishop, T.R., Frelin, L.P., and Boyer, S.H. 1986. Nucleotide sequence of rat liver δ-aminolevulinic acid dehydratase DNA. *Nucl. Acids Res.* 14:10115.

Bishop, T.R., Hodes, Z.I., Frelin, L.P., and Boyer, S.H. 1989. Cloning and sequence of mouse erythroid δ-aminolevulinate dehydratase DNA. *Nucl. Acids Res.* 17:1775.

Bishop, T.R., Miller, W.M., Beall, J., Zon, L.I. and Dierks, P. 1996. Genetic regulation of δ-aminolevulinate dehydratase during erythropoiesis. *Nucl. Acids Res.* 24:2511-2518.

Burns, C.B., Sriprakash, K.S., Powers, J.R., and Currie, B.J. 1994. Method for preserving erythrocyte delta-aminolevulinic acid dehydratase activity that facilitates population studies on lead intoxication. *J. Appl. Toxicol.* 14: 365-368.

Chakrabarti, S.K., Brodeur, J., and Tardif, R. 1975. Fluorometric determination of δ-aminolevulinic acid dehydratase activity in human erythrocytes as an index of lead exposure. *Clin. Chem.* 21:1783-1787.

Chiba, M. 1976. Activity of erythrocyte δ-aminolevulinic acid dehydratase and its change by heat treatment as indices of lead exposure. *Brit. J. Ind. Med.* 33:36-42.

Crowne, H., Lim., C.K., and Samson, D. 1981. Determination of 5-aminolaevulinic acid dehydratase activity in erythrocytes by high-performance liquid chromatography. *J. Chromatogr.* 223: 421-425.

Doss, M., von Tiepermann, R., Schneider, J., and Schmid, H. 1979. New type of hepatic porphyria with porphobilinogen synthase defect and intermittent acute clinical manifestation. *Klin. Wochenschr.* 57:1123-1127.

Finelli, V.N., Klauder, D.S., Karaffa, M.A., and Petering H.G. 1975. Interaction of zinc and lead of δ-aminolevulinate dehydratase. *Biochem. Biophys. Res. Commun.* 65:303-311.

Fujita, H., Orii, Y., and Sano, S. 1981. Evidence of increased synthesis of δ-aminolevulinic acid dehydratase in experimental lead-poisoned rats. *Biochim. Biophys. Acta* 678:39-50.

Fujita, H., Sato, K., and Sano, S. 1982a. Increase in the amount of δ-aminolevulinic acid dehydratase in workers with moderate lead exposure. *Int. Arch. Occup. Environ. Health* 50:287-297.

Fujita, H., Sato, K., and Ikeda, M. 1982b. Age difference in response of erythrocyte δ-aminolevulinic acid dehydratase amount to lead administration in rats. *Ind. Health* 20:199-207.

Fujita, H., Koizumi, A., Yamamoto, M., Kumai, M., Sadamoto, T., and Ikeda, M. 1984. Inhibition of δ-aminolevulinate dehydratase in trichloroetylene-exposed rats, and the effects on heme regulation. *Biochim. Biophys. Acta* 800:1-10.

Fujita, H., Yamamoto, R., Sato, K., and Ikeda, M. 1985. In vivo regulation of δ-aminolevulinate dehydratase activity. *Toxicol. Appl. Pharmacol.* 77:66-75.

Fujita, H., Koizumi, A., Hayashi, N., and Ikeda, M. 1986. Reduced synthesis of δ-aminolevulinate dehydratase in styrene-treated rats. *Biochim. Biophys. Acta* 867:89-96.

Fujita, H., Koizumi, A., Furusawa, T., and Ikeda, M. 1987a. Decreased erythrocyte δ-aminolevulinate dehydratase activity after styrene exposure. *Biochem. Pharmacol.* 36:711-716.

Fujita, H., Sassa, S., Lundgren, J., Holmberg, L., Thunell, S., and Kappas, A. 1987b. Enzymatic defect in a child with hereditary hepatic porphyria due to homozygous δ-aminolevulinic acid dehydratase deficiency: Immunochemical studies. *Pediatrics* 80:880-885.

Fujita, H., Bishop, T.R., and Ishida, N. 1994. Toxicology and molecular biology of δ-aminolevulinate dehydratase. *In* Regulation of Heme Protein Synthesis (H. Fujita, ed.) pp. 27-39. AlphaMed, Dayton, Ohio.

Gibson, K.D., Neuberger, A., and Scott, J.J. 1955. The purification and properties of δ-aminolevulinic acid dehydratase. *Biochem. J.* 61:618-629.

Granick, J.L., Sassa, S., Granick, S., Levere, R.C., and Kappas, A. 1973. Studies in lead poisoning. II. Correlation between the ratio of activated to inactivated δ-aminolevulinic acid dehydratase of whole blood lead level. *Biochem. Med.* 8:149-159.

Guo, G.G., Gu, M., and Etlinger, J.D. 1994. 240-kDa Proteasome inhibitor (CF-2) is identical to δ-aminolevulinic acid dehydratase. *J. Biol. Chem.* 269:12399-12402.

Haas, T.H., Mache, W., Schaller K.H., Mache, K., Klavis, G., and Stumpf, R. 1972. Zur Bestimmung der Delta-Aminolävulinsäure-Dehydratase und ihrer diagnostischen Wertigkeit. *Int. Arch. Arbeitsmed.* 30:87-104.

Jaffe, E.K., Salowe, S.P., Chen, N.T., and DeHaven, P.A. 1984. Porphobilinogen synthase modification with methylmethanethiosulfonate: A protocol for the investigation of metalloproteins. *J. Biol. Chem.* 259:5032-5036.

Koike, S. 1959. Experimental studies on the activity of δ-aminolevulinic acid dehydratase in lead poisoning. *J. Nation's Health* 28:612-616 [in Japanese].

Lichtman, H.C. and Feldman, F. 1963. In vitro pyrrole and porphyrin synthesis in lead poisoning and iron deficiency. *J. Clin. Invest.* 42:830-839.

Lindblad, B., Lindstedt, S., and Steen, G. 1977. On the enzymic defects in hereditary tyrosinemia. *Proc. Natl. Acad. Sci. U.S.A.* 74:4641-4645.

Maes, J. and Gerber, G.B. 1978. Increased ALA dehydratase activity and spleen weight in lead-intoxicated rats. A consequence of increased blood cell destruction. *Experientia* 34:381-382.

Mauzerall, D. and Granick, S. 1956. The occurrence and determination of δ-aminolevulinic acid and porphobilinogen in urine. *J. Biol. Chem.* 219:435-446.

Mitchell, R.A., Drake, J.E., Wittlin, L.A., and Petering H.G. 1978. Erythrocyte porphobilinogen synthase (delta aminolevulinic acid dehydratase) activity: A reliable and quantitative indicate of lead exposure in humans. *Clin. Chem.* 23:105-111.

Piomelli, S. 1993. Effects of lead on erythrocyte function: The anemia of leading poisoning. *In* Hematology of Infancy and Childhood. (D.G. Nathan and F.A. Oski, eds.) pp. 481. W.B. Saunders, Philadelphia.

Sassa, S., Granick, S., Bickers, D.R., Levere, R.D., and Kappas, A. 1973. Studies on the inheritance of human erythrocyte δ-aminolevulinate dehydratase and uroporphryrinogen synthetase. *Enzyme* 16:326-333.

Sassa, S., Fujita, H. and Kappas, A. 1990. Succinylacetone and δ-aminolevulinic acid dehydratase in hereditary tyrosinemia: Immunochemical study of the enzyme. *Pediatrics* 86:84-86.

Sato, K., Sano, S., and Fujita, H. 1982. Increase in the amount of erythrocyte δ-aminolevulinic acid dehydratase in workers with moderate lead exposure. *Int. Arch. Occup. Enviorn. Health* 50:287-297.

Shemin, D., Abramsky, T., and Rassel, C.S. 1954. The synthesis of protoporphyrin from δ-aminolevulinic acid in a cell-free extract. *J. Am. Chem. Soc.* 76:1204-1205.

Thunell, S., Holmberg, L., and Lundgren, J. 1987. Aminolevulinate dehydratase porphyria in infancy: A clinical and biochemical study. *J. Clin. Chem. Clin. Biochem.* 25:5-14.

Tomokuni, K. 1976. Fluorometric micromeasurement of δ-aminolevulinic acid dehydratase activity in human erythrocytes as an index of lead exposure. *Ind. Health* 14:75-80.

Tomokuni, K. and Ichiba, M. 1988. Fluorometric determination of erythrocyte δ-aminolevulinate dehydratase activity by high-performance liquid chromatography. *Ind. Health* 26:75-79.

Tsukamoto, I., Yoshinaga, T., and Sano, S. 1979. The role of zinc with special reference to the essential thiol groups in δ-aminolevulinic acid dehydratase of bovine liver. *Biochim. Biophys. Acta* 570:167-178.

Wetmur, J.G., Bishop, D.F., Cantelmo, C., and Desnick, R.J. 1986. Human δ-aminolevulinate dehydratase: Nucleotide sequence of a full-length DNA clone. *Proc. Natl. Acad. Sci. U.S.A.* 83:7703-7707.

Wetmur, J.G., Kaya, A.H., Plewinska, M., and Desnick, R.J. 1991. Molecular characterization of δ-aminolevulinate dehydratase 2 (ALAD2) allele: Implications for molecular screening of individuals for genetic susceptibility to lead poisoning. *Am. J. Hum. Genet.* 49:757-763.

Ziemsen B., Angerer, J., Lehnert, G., Benkmann, H.-G., and Goedde, H.W. 1986. Polymorphism of δ-aminolevulinic acid dehydratase in lead-exposed workers. *Int. Arch. Occup. Environ. Health* 58:245-247.

Key Reference

Fujita et al., 1994. See above..

This article reviews not only toxicological but also molecular biological aspects of δ-aminolevulinate dehydratase.

Sassa, S. 1982. δ-aminolevulinic acid dehydratase assay. *Enzyme* 28:133-145.

Good description of basic assay conditions for crude enzyme preparation.

Contributed by Hiroyoshi Fujita
Hokkaido University School of Medicine
Sapporo, Japan

Measurement of Ferrochelatase Activity

Ferrochelatase, the terminal step in the heme biosynthetic pathway, catalyzes the insertion of ferrous ion into the protoporphyrin IX ring to form protoheme. The eukaryotic enzyme is located in the inner membrane of mitochondria with the active site facing the matrix. The enzyme activity is inhibited by heavy metal ions such as Pb^{2+} and Hg^{2+} and by *N*-alkylprotoporphyrins (degradation products of the heme moiety of cytochrome P-450). Although ferrochelatase cannot utilize ferric ion, it can insert zinc and cobalt ions into the porphyrin ring. Instead of protoporphyrin, artificial porphyrins including mesoporphyrin, deuteroporphyrin, and hematoporphyrin can serve as substrates (Taketani, 1994).

When zinc ion is used as a metal substrate, the enzyme reaction proceeds under aerobic conditions, and zinc-chelating activity is reflected in iron-chelating activity. Analysis of metalloporphyrins and porphyrin derivatives by high-performance liquid chromatography (HPLC) is now feasible. Also, detection of porphyrin fluorescence allows for a highly sensitive assay of ferrochelatase. Ferrochelatase can readily catalyze the insertion of ferrous, cobalt, and zinc ions into the porphyrin ring. Of these metalloporphyrins, only zinc porphyrin has fluorescence. Measuring fluorescence is a highly sensitive method compared with optical absorption. Therefore, reaction of zinc-chelation followed by analysis of zinc-porphyrins by HPLC makes for a simple and reproducible method to determine ferrochelatase activity (see Basic Protocol). It is also possible to measure cobalt-chelating activity by the same method (see Alternate Protocol 1), and to measure iron-chelating activity (see Alternate Protocol 2) spectrophotometrically. The reduced-minus-oxidized differential absorption spectra of pyridine-hemochromogen of formed heme can apply only to iron chelation (see Alternate Protocol 2). Measurement of iron- or cobalt-chelating activity was used in the past but requires large amounts of enzyme preparation for the assay. By zinc chelation it is possible to measure ferrochelatase activity on a small scale.

As described in the Commentary, measurement of zinc-porphyrin formation permits study of enzyme kinetics using small amounts of enzyme preparation. On the other hand, ferrous iron is a real substrate of ferrochelatase, and it is also informative to measure heme formation in vitro.

MEASUREMENT OF ZINC-MESOPORPHYRIN FORMATION

BASIC PROTOCOL

Mesoporphyrin and zinc ion are incubated at 37°C for 1 hr under aerobic conditions and the reaction is terminated by adding a mixture of methanol/dimethyl sulfoxide/EDTA. The resulting mixture is mixed and centrifuged, and the supernatant is withdrawn for measurement of zinc-mesoporphyrin with an HPLC equipped with a C18 column. Zinc-mesoporphyrin is measured by absorbance at 400 nm as well as by fluorescence intensity.

When zinc ion is used as a substrate, results can be altered by a nonenzymatic reaction. To prevent the nonenzymatic formation of zinc-mesoporphyrin, the molar ratio of zinc ion to mesoporphyrin should not exceed 4:1. The presence of detergents also suppresses the nonenzymatic formation of zinc-porphyrin. Tween 20 is an appropriate detergent because it does not contain fluorescence-absorbing contaminants. The addition of fatty acid to the reaction leads to a 4- to 8-fold increase in ferrochelatase activity, and some activities of ferrochelatase using homogenates from leukocytes and lymphocytes can be detected. Furthermore, saturated fatty acids such as palmitic and stearic acids will lower the nonenzymatic formation of metalloporphyrin.

Contributed by Shigeru Taketani

Current Protocols in Toxicology (1999) 8.7.1-8.7.8

Materials

1 mM mesoporphyrin solution (see recipe)
Tris/palmitate/Tween buffer (see recipe)
Enzyme source (see recipe): Mitochondrial preparation or cell homogenate (0.5 to 2.5 µg protein/µl)
2 mM zinc acetate
Stop solution: 3:7 (v/v) dimethyl sulfoxide/methanol with 0.1 mM EDTA
Ammonium acetate/methanol solution (see recipe)
Zinc-mesoporphyrin (Porphyrin Products)
Dimethylsulforide (DMSO)

Ultrasonicator
1.5-ml microcentrifuge tubes
37°C incubator
C18 column: 4-µm Novapak C18 silica column (4.6 × 150–mm; Waters) or Cosmosil 5C18-AR column (4.6 × 160–mm Nacalai Tesque)
0.2-µm precolumn filter (0.4 mm; Millipore)
HPLC system with 0.2-µm precolumn filter (2.5 × 2.5 cm), fluorescence spectrophotometric detector,and spectrophotometric visual detector

Prepare samples

1. Add 1 mM mesoporphyrin solution at a final concentration of 50 µM to Tris/palmitate/Tween buffer. Mix well and sonicate for 2 min as described in the recipe for mesoporphyrin and palmitic acid mixture in Reagents and Solutions.

   This mixture can be stored for up to 3 months in the dark at −20°C. Sonicate before use. Palmitic acid dissolved in ethanol can be used instead of sodium palmitate, but unsaturated fatty acids, including oleic acid and palmitoleic acid, are not suitable for the assay because the presence of unsaturated fatty acid leads to an increase in nonenzymatic formation of zinc-mesoporphyrin.

2. Add 20 µl cell homogenate or mitochondrial preparation (10 to 50 µg of protein) to 170 µl of the above mixture in a 1.5-ml microcentrifuge tube and mix well. Set up a second reaction mixture without enzyme as a negative control.

   As ferrochelatase is unstable below pH 7.8, the mitochondria must be prepared using solutions at pH 8.0. When using homogenates of lymphocytes or bone marrow cells as enzyme sources, solutions containing 10% to 20% glycerol should be used, as glycerol markedly stabilizes ferrochelatase.

3. Initiate reaction by adding 10 µl of 2 mM zinc acetate (final 100 µM) to each tube. Incubate 30 to 60 min in the dark at 37°C.

   The length of the incubation period depends on the enzyme preparation. When homogenates of lymphocytes or leukocytes are used, ≥60 min is needed, but prolonged incubation decreases the enzyme activity. When mitochondria from mammalian liver are used as enzyme sources, the incubation period can be <20 min because the mitochondria generally exhibit high ferrochelatase activity.

4. Terminate the enzyme reaction by adding 0.5 ml stop solution and mix by vortexing.

   After adding stop solution to the reaction mixture, the samples can be stored for up to one week at −70°C in the dark prior to HPLC analysis of zinc-mesoporphyrin.

5. Microcentrifuge samples 10 min at 14,000 × *g*, 4°C, and transfer the supernatants to new tubes.

6. Prepare standards containing various concentrations (100 to 500 nM) of zinc-mesoporphyrin dissolved in DMSO.

Perform HPLC

7. Equilibrate a C18 column with ammonium acetate/methanol solution at a flow rate of 1.5 ml/min.
8. Connect in tandem a fluorescence spectrophotometer outlet to a spectrophotometer. Adjust the detector of the spectrophotometer to 400 nm, and adjust the fluorescence spectrophotometer to excitation at 410 nm and emission at 580 nm.
9. Pass the sample through a 0.2-µm precolumn filter and then separately inject 10- to 15-µl sample onto the column.

   A precolumn filter will aid in expanding the life of the HPLC column by removing small precipitates. C18 columns such as the 4-µm Novapak C18 silica column and Cosmosil 5C18-AR column are suitable for use as a separation column.

   After all samples have been analyzed, the HPLC column should be washed with methanol for ≥30 min; maintenance of the column is of the greatest importance.
10. Read absorbance at 400 nm and fluorescence intensity of the formed zinc-mesoporphyrin. Prepare a standard curve by injection and analysis of the zinc-mesoporphyrin standards.

    Retention times of zinc-mesoporphyrin and mesoporphyrin are ~2.5 min and 3.9 min, respectively.
11. Calculate molar concentration from the different intensities of zinc-mesoporphyrin between values without or with enzyme since a small amount of zinc-mesoporphyrin is always formed nonenzymatically under the conditions described.

ASSAY OF COBALT-CHELATING ACTIVITY

ALTERNATE PROTOCOL 1

Instead of zinc acetate, this protocol uses 50 µM $CoCl_2$ as a metal substrate. Incubation conditions are the same as for zinc-chelating activity. The cobalt-mesoporphyrin formed is analyzed with an HPLC system by measuring spectrophotometric absorbance at 420 nm. As cobalt-mesoporphyrin is not fluorescent, the sensitivity of the cobalt-chelating activity is less than that seen for zinc chelation. Cobalt-mesoporphyrin is commercially available and can be used as a standard.

ASSAY OF IRON-CHELATING ACTIVITY

ALTERNATE PROTOCOL 2

In this protocol, a spectrophotometer is used to determine iron-chelating activity. The difficulty in measuring ferrochelatase activity with ferrous iron is that oxidation of ferrous ion to form ferric ion occurs in the presence of oxygen. During this reaction, hydroxy radical and peroxide are produced via a Fenton reaction, thereby destroying the porphyrin rings. Thus, oxygen must be removed from the reaction mixture by replacing oxygen gas with nitrogen or argon gas before the iron-chelating activity can be measured. A Thunberg tube is convenient and practical for obtaining anaerobic conditions.

Additional Materials *(also see Basic Protocol)*

1 M Tris·Cl, pH 8.0 (*APPENDIX 2A*)
1 mM mesoporphyrin solution (see recipe)
100 mM dithiothreitol (DTT)
10% (w/v) Triton X-100
Enzyme source (see recipe): Mitochondrial preparation or cell homogenate (0.5 to 2.5 µg protein/µl)
10 mM iron citrate (see recipe)
Nitrogen (N_2) gas
0.1 M iodoacetamide
1 N NaOH

continued

Pyridine
Sodium dithionite

Thunberg tube (Top Labo-Ware)
Spectrophotometer with scanning wavelength (i.e., Hitachi U-2010) and cuvettes

1. Prepare a 1-ml solution containing the following ingredients and add to the main tube of a Thunberg tube:

   0.1 M Tris·Cl, pH 8.0 (*APPENDIX 2A*)
   50 µM mesoporphyrin
   1 mM DTT
   0.1% (w/v) Triton X-100
   0.1 to 0.2 ml enzyme source.

2. Prepare a 1-ml solution containing 100 µM iron citrate and 0.1 M Tris·Cl and add this to the side arm.
3. Remove O_2 gas from the reaction mixture by evacuating and flushing several times with N_2 gas, and then vacuum pump to obtain reduced conditions.

   The remaining trace O_2 is removed from the reaction mixture under reduced pressure.

4. Pour the solution of the side arm into the main tube and incubate the tube 30 min at 37°C.
5. Open the side arm and add 0.5 ml of 0.1 M iodoacetamide to stop the reaction.
6. Add 0.5 ml of 1 N NaOH and 0.5 ml pyridine.
7. Divide the mixture into two cuvettes. Add a few grains of fresh, free-flowing sodium dithionite to one cuvette and mix well to reduce mesoheme. Put the cuvette containing sodium dithionite–free mixture into the reference cell box of the spectrophotometer.

   Use fresh, dry sodium dithionite, as it is ineffective when old or damp.

8. Monitor the reduced minus oxidized differential absorption spectrum by scanning from 500 to 570 nm, and measure the difference in absorbance at 531 nm and 547 nm ($\Delta A = A_{547} - A_{531}$).
9. Calculate the mesoheme formed using the equation mesoheme (nmol) = $1000 \times 3.5 \times \Delta A + 21.7$, where 1000 is µmol/nmol, 3.5 is the final volume, and 21.7 is ε_{mM} ($\Delta A_{547-531\ nm}$ for mesoheme).

REAGENTS AND SOLUTIONS

*Use Milli-Q-purified water or equivalent in all recipes and protocol steps. For common stock solutions, see **APPENDIX 2A**; for suppliers, see **SUPPLIERS APPENDIX**.*

Ammonium acetate/methanol solution

Adjust 1 M ammonium acetate to pH 5.18 with 6 M HCl. Mix 100 ml ammonium acetate with 900 ml methanol. Pass the solution through a 0.22-µm membrane filter (Millipore GVHP-type) under vacuum. Store up to several months at room temperature.

Enzyme source

For mitochondria: Suspend minced liver in 6 vol of 10 mM Tris·Cl, pH 7.8 (*APPENDIX 2A*), containing 0.25 M sucrose and homogenize in a glass homogenizer with a Teflon pestle. Centrifuge the suspension 10 min at $600 \times g$, 4°C, to remove cell debris. Centrifuge the supernatant 10 min at $10{,}000 \times g$, 4°C, to sediment the mitochondria. Wash the pellet twice with 10 mM Tris·Cl, pH 7.8, and suspend the mitochondria in the same solution. Store at −70°C until use (up to 1 month).

For homogenates of cultured cells or peripheral blood lymphocytes: Suspend 5×10^6 cells in 500 µl of 10 mM Tris·Cl buffer, pH 7.8 (*APPENDIX 2A*), containing 20% glycerol and 1 mM DTT. Sonicate the suspension 2 min at 4°C, and centrifuge 5 min at $600 \times g$, 4°C. Use the resulting supernatant for enzyme assay or store at −70°C prior to use (stable for ≥1 month).

The sample of cells can also be stored at −70°C for 1 month.

Iron citrate solution, 10 mM

Dissolve 3.4 mg ammonium ferrous sulfate and 2.7 mg sodium citrate in 1 ml H_2O. Flush the solution with nitrogen gas for 2 min and store up to 3 months below 0°C.

Mesoporphyrin and palmitic acid mixture

100 µl of 1 mM mesoporphyrin (see recipe)
200 µl of 10 mM sodium palmitate
30 µl of 10% (w/v) Tween 20
100 µl of 1 M Tris·Cl buffer, pH 8.0 (*APPENDIX 2A*)
470 µl H_2O

Sonicate the mixture at room temperature for 2 min. Determine the concentration of mesoporphyrin spectrophotometrically in 0.1 N HCl, using the extinction coefficient $\varepsilon_{\mu M} = 445$ at 399 nm.

Mesoporphyrin solution, 1 mM

Dissolve 2 mg mesoporphyrin IX into 0.5 ml of 0.1 N KOH by vigorous vortexing. Add 0.5 ml ethanol and mix the resulting solution well. Store at −30°C until use (up to 1 year).

Tris/palmitate/Tween buffer

0.1 M Tris·Cl, pH 8.0 (*APPENDIX 2A*)
1 mM sodium palmitate
0.3% (v/v) Tween 20
Store up to several months at 4°C

COMMENTARY

Background Information

All living organisms can synthesize heme (Taketani, 1994). The activity of ferrochelatase was first demonstrated by Goldberg et al. (1956) with homogenates of chicken erythrocytes; they measured incorporation of iron-59 into protoporphyrin. Although mammalian tissues including liver, kidney, and bone marrow cells exhibit a relatively high ferrochelatase activity, microorganisms and plant cells generally exhibit low activity. Ferrochelatase is located in mitochondria of mammalian livers, and measurement of iron-chelating activity (see Alternate Protocol 2) with mitochondria is routine. The formed heme can be determined by difference spectra of pyridine-hemochromogen. With this procedure, it is difficult to do kinetic studies or to measure low ferrochelatase activity. Assay of zinc-chelating activity, followed by HPLC analysis, facilitates kinetic studies using small amounts of enzymes from bacteria, plants, and mammals. The protocol described here is a simple approach to measure ferrochelatase activity of various organisms. This procedure is highly reproducible and sensitive, so it can be applied using a very small amount of enzyme or when the enzyme source exhibits very low ferrochelatase activity.

HPLC analyses of porphyrins and metalloporphyrins for ferrochelatase were apparently first reported by Li et al. (1987), with a more detailed procedure later reported by Rossi et al. (1988). These procedures included measurement of ferrochelatase activity of human blood peripheral lymphocytes, which contain extremely low ferrochelatase activity. A blood sample is the only simple, viable material that can be used to examine human enzyme activities. For blood samples, the only method with sufficient sensitivity for measurement of ferrochelatase activity is incorporation of radioactive iron into the formed heme, which is then extracted for counting. However, the radiochemical assay presents technical difficulties. Iron-59 with specific radioactivity that decays over time is available in the form of ferrous

ion and is stored under anaerobic conditions. After incubation, labeled heme must be extracted with organic solvents to separate the free iron. The development of HPLC methods paved the way for simpler assays.

Activation of ferrochelatase activity by fatty acid was first performed when enzyme from rat liver mitochondria was solubilized and highly purified (Sawada et al., 1969). It was then demonstrated that ferrochelatase homogeneously purified from rat liver and yeast requires fatty acid to measure the enzyme activity (Taketani and Tokunaga, 1981; Camadro and Labbe, 1988). A later sensitive assay using HPLC showed that fatty acid suppresses nonenzymatic and activates enzymatic formation of zinc-mesoporphyrin when detergents such as Tween 20 (polyoxyethylenesorbitan monolaurate) and Tween 40 (polyoxyethylenesorbitan monopalmitate) are present in the reaction mixture (Rossi et al., 1988). Saturated fatty acids including palmitic and stearic acids are more effective and less expensive than unsaturated fatty acids. Phospholipids or neutral lipids are without untoward effects on the reaction. Mechanisms involved in activation of ferrochelatase activity by fatty acids remain unknown.

Critical Parameters

Zinc-chelatase activity is mostly reflected in iron-chelatase activity. The level of ferrochelatase activity determined by measuring the formation of zinc-mesoporphyrin is reliable. However, the kinetics of mesoheme formation are not always the same as those of zinc-mesoporphyrin formation. For example, sensitivity for ferrochelatase inhibitors such as Pb^{2+} and sulfhydryl agents is higher with heme formation than with zinc-porphyrin formation. When examining the kinetics of ferrochelatase, first confirm the results by comparing measurements of zinc-chelating and iron-chelating activities (see Alternate Protocol 2).

When effects of metals on ferrochelatase activity are examined, Tris·Cl buffer is not suitable for use because metal-chloride complexes frequently precipitate out, causing the concentration of metals to be nonhomogenous in the reaction mixture. Instead of Tris·Cl buffer, Tris·acetate buffer is recommended for use.

Although mesoporphyrin is an artificial porphyrin derivative that is a relatively stable porphyrin and can serve as a substrate of ferrochelatase, porphyrins should be handled in the dark because porphyrin is generally destroyed by light. Protoporphyrin, a natural substrate of ferrochelatase, is less soluble or stable than mesoporphyrin. Therefore, insertion of metals into protoporphyrin is much less than that into mesoporphyrin.

Ferrochelatase becomes unstable below pH 7.8 and the solubility of porphyrin decreases remarkably below pH 7.4. If enzyme activity is measured below pH 7.4, no activity can be detected even in the presence of fatty acid and glycerol. Thus, enzyme sources should be prepared at a pH of ~8.0 and the enzyme reaction must be carried out at pH 8.0.

Zinc-mesoporphyrin is easily destroyed because dissociation of zinc ion from the mesoporphyrin ring occurs under acidic conditions. Therefore, the use of acidic solutions (pH <4.5) should be avoided throughout all procedures described in this unit.

Sonication of the mixture containing sodium palmitate, mesoporphyrin, and Tween 20 is important to obtain reproducible results. When sonication is insufficient to completely disperse mesoporphyrin into the mixture, the amount of zinc-mesoporphyrin formed varies because the undispersed mesoporphyrin and zinc-mesoporphyrin are precipitated by the addition of methanol/DMSO/EDTA solution. The mixture of mesoporphyrin and palmitic acid should be sonicated prior to use.

Troubleshooting

The main reason for failure to obtain reproducible data of ferrochelatase activity is improper preparation of enzyme sources, especially when using homogenates from cultured cells, bone marrow cells, reticulocytes, and peripheral blood T lymphocytes. Solutions containing 20% glycerol at pH 8.0 are a sine qua non for preparation of homogenates. If an enzyme preparation without glycerol is used, the enzyme activity dramatically decreases with time. When mitochondria from rabbit reticulocytes are left on ice for 1 hr, the activity decreases to 50%; however, addition of glycerol to the enzyme solution markedly maintains the enzyme stability. When mitochondria from tissues are used for the assay, the solution containing glycerol is not needed for the preparation. However, ferrochelatase becomes unstable when mitochondria are solubilized with detergents. The presence of 20% glycerol and 1 mM DTT stabilizes the solubilized enzyme. Reasons for the different stability among enzyme sources are yet to be forthcoming.

Although the present method is the most sensitive and simplest currently available, $\geq 10^6$ cells are needed for triplicate assays. Even if the enzyme preparation is expected to have low activity that requires long incubation, >1 hr incubation time will not lead to a linear enzyme reaction.

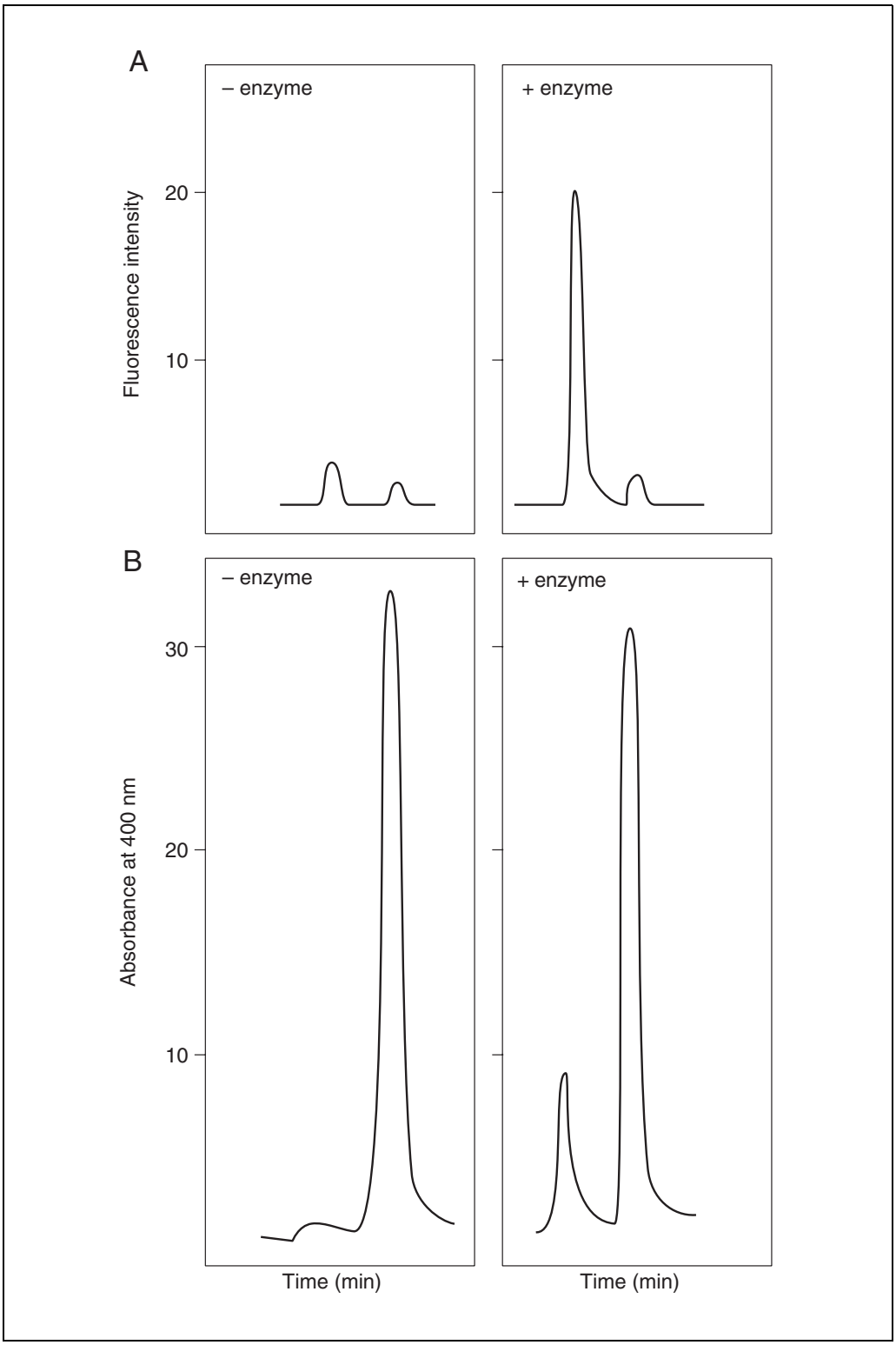

Figure 8.7.1 HPLC analysis of zinc-chelating activity with mouse macrophage RAW264.7 cells (left, no enzyme; right, with enzyme). (**A**) Fluorescence of zinc-mesoporphyrin (first peak) and mesoporphyrin (second peak) with excitation at 410 nm and emission at 580 nm. (**B**) Absorbance of zinc-mesoporphyrin and mesoporphyrin at 400 nm. Assay of ferrochelatase using homogenates (50 μg protein) of RAW264.7 cells and chromatographic conditions are described (see Basic Protocol).

Therefore, incubation time should be limited to 1 hr.

When the enzyme preparation contains a considerable amount of heme, absorbance of endogenous heme can be observed spectrophotometrically at ~400 nm. The retention time of heme by HPLC analysis is located between zinc-mesoporphyrin and mesoporphyrin, and the peak of heme sometimes overlaps that of zinc-mesoporphyrin. Since heme is nonfluorescent, fluorescence of zinc-mesoporphyrin can be measured.

Strong detergents such as Triton X-100 and Nonidet P-40 should never be used in any procedures used for measuring zinc-chelating activity because these compounds have several strong fluorescence-absorbing contaminants that interfere with measurement of zinc-porphyrin by HPLC. Tween 20 is recommended to solubilize porphyrins and to assay ferrochelatase activity because it does not interfere with fluorescence or with visual absorbance.

Anticipated Results

Zinc-chelating activity was measured with homogenates of a mouse macrophage cell line, and formation of zinc-mesoporphyrin was analyzed by HPLC under the conditions described in this unit. Figure 8.7.1 shows separation of zinc-mesoporphyrin from mesoporphyrin by HPLC. Even in the absence of ferrochelatase, a small peak of fluorescence of zinc-mesoporphyrin was observed with emission at 580 nm. Intensity of zinc-mesoporphyrin fluorescence is greatest with excitation at 410 nm and emission at 580 nm, while that of mesoporphyrin is greatest with excitation at 410 nm and emission at 630 nm. Therefore, adjusting the fluorescence spectrophotometer for emission at 630 nm causes a decrease in the intensity of zinc-mesoporphyrin fluorescence, in contrast to the increase in mesoporphyrin fluorescence. By increasing the amounts of ferrochelatase, the peak of zinc-mesoporphyrin increases linearly. At 400 nm, zinc-mesoporphyrin shows parallel increases in absorbance and the intensity of fluorescence. As a standard assay, the above adjustment is suitable for detection of zinc-mesoporphyrin, but the emission can vary between 580 and 630 nm when the enzyme preparation has high activity.

Time Considerations

With acquisition of the cells, triplicate HPLC assays of four samples will require 3 hr to complete. After terminating the assay, ≥30 min are needed to wash the HPLC column with 100% methanol. Preparation of all solutions used for the assay requires 2 to 3 hr, and all solutions can be stored at 4°C for several months. Alternate Protocol 1 requires 2 to 3 hr and Alternate Protocol 2 requires 2 hr.

Literature Cited

Camadro, J.M. and Labbe, P. 1988. Purification and properties of ferrochelatase from the yeast *Saccharomyces cerevisiae*. Evidence for a precursor form of the protein. *J. Biol. Chem.* 263:11675-11682.

Goldberg, A., Ashenbrucker, M., Cartwright, G.E., and Wintrobe, M.M. 1956. Studies on the biosynthesis of heme in vitro by avian erythrocytes. *Blood* 11:821-833.

Li, F., Lim, C.K., and Peters, T.J. 1987. An HPLC assay of rat liver ferrochelatase activity. *Biomed. Chromatogr.* 2:164-168.

Rossi, E., Costin, K.A., and Garcia-Webb, P. 1988. Ferrochelatase activity in human lymphocytes as quantified by a new high-performance liquid-chromatographic method. *Clin. Chem.* 34:2481-2485.

Sawada, H., Takeshita, M., Sugita, Y., and Yoneyama, Y. 1969. Effect of lipid on protoheme ferrolyase. *Biochim. Biophys. Acta* 178:145-155.

Taketani, S. 1994. Molecular and genetic characterization of ferrochelatase. *In* Regulation of Heme Protein Synthesis (H. Fujita, ed.) pp. 41-54. AlphaMed Press, Dayton, Ohio.

Taketani, S. and Tokunaga, R. 1981. Rat liver ferrochelatase. Purification, properties and stimulation by fatty acids. *J. Biol. Chem.* 256:12748-12753.

Key References

Furukawa, T., Kohno, H., Tokunaga, R., and Taketani, S. 1995. Nitric oxide-mediated inactivation of mammalian ferrochelatase in vivo and in vitro: Possible involvement of the iron-sulphur cluster of the enzyme. *Biochem. J.* 310:533-538.

Description of ferrochelatase activity of mouse macrophage cell line and recombinant human ferrochelatase expressed in E. coli. Some results are shown in Figure 8.7.1.

Rossi et al., 1988. See above.

Description of assay conditions of zinc-mesoporphyrin formation by HPLC.

Taketani, 1994. See above.

Description of properties and kinetics of ferrochelatase and genetic demonstration of mammalian ferrochelatase.

Contributed by Shigeru Taketani
Kansai Medical University
Moriguchi, Osaka

Measurement of Erythrocyte Protoporphyrin Concentration by Double Extraction and Spectrofluorometry

The scope of this unit is limited to the determination of erythrocyte protoporphyrin (EP) for clinical diagnostic purposes using a primary reference method (see Basic Protocol). This method, which is used by the New York State Department of Health (NYS DOH), is based upon published methods and methods developed by other public health laboratories in the U.S., including the Centers for Disease Control (CDC) and the Wisconsin State Laboratory of Hygiene (WSLH). The method is very similar to that recommended by the National Committee for Clinical Laboratory Standards (NCCLS), except where indicated in the Commentary section (see Background Information). It is recommended for laboratory participants in the EP Proficiency Testing Program operated by the NYS DOH, and is also suitable for use in programs operated by the WSLH and the Pennsylvania Department of Health. This unit also contains protocols for assessing the presence of impurities in ethyl acetate (see Support Protocol 1) and for removing these impurities by glass distillation (see Support Protocol 2).

Procedures for determining EP via direct zinc protoporphyrin (ZPP) fluorescence in whole blood using portable instrumentation based on front-surface fluorometry (i.e., hematofluorometry) are relatively simple and are provided by the instrument manufacturers. Procedures for the separation and determination of specific porphyrin species using liquid chromatographic techniques are not well established and are beyond the scope of this unit.

MEASURING ERYTHROCYTE PROTOPORPHYRIN CONCENTRATION

BASIC PROTOCOL

Porphyrins and heme components are extracted from whole blood into an ethyl acetate/acetic acid mixture. Porphyrins are then separated from heme by back extraction into a hydrochloric acid solution and are quantitatively determined by molecular fluorometry using a spectrofluorometer calibrated with protoporphyrin IX (PPIX) standard solutions. Note, however, that the exact concentration of the standards must first be established using molecular absorbance, Beer's Law, and the millimolar absorptivity of PPIX.

Materials

5-µg protoporphyrin IX standards (Porphyrin Products)
Protosolv (Porphyrin Products)
1.5 M HCl (see recipe)
Blood specimens in 10-ml evacuated collection tubes with EDTA anticoagulant (purple-cap Vacutainers, Becton Dickinson or equivalent)
Quality control (QC) samples
4:1 (v/v) ethyl acetate/acetic acid solution (see recipe)

50-, 100-, and 200-µl fixed-volume micropipets
10-ml glass volumetric pipet (class A preferable)
Light-tight cabinet or box suitable for storing a rack(s) of culture tubes protected from light
UV/visible absorption spectrophotometer equipped with standard 1-cm^2 quartz cells
2-ml glass volumetric flasks (class A preferable) wrapped in aluminum foil
Adjustable or fixed-volume micropipets in the range 400 to 1600 µl

Contributed by Patrick J. Parsons
Current Protocols in Toxicology (1999) 8.8.1-8.8.12

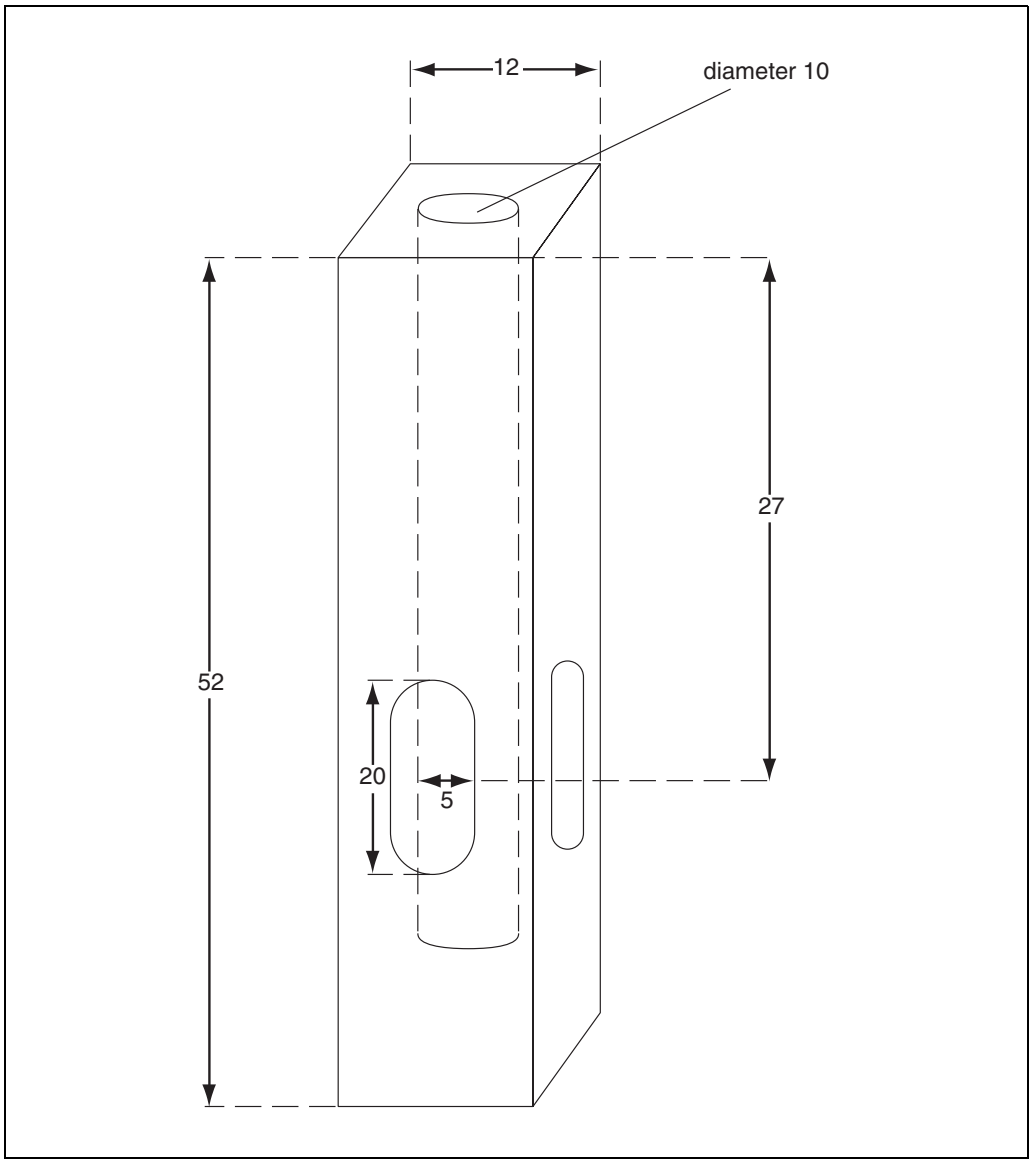

Figure 8.8.1 Schematic diagram of a cell holder modified to accommodate standard 10 × 75–mm glass culture tubes. Note that the holder, which can be easily machined from a 2 × 2 × 7–cm aluminum block, must have entrance/exit windows set at right angles to permit detection of fluorescence from the HCl phase of the extract. Dimensions (in mm) are reprinted from document C42-A (NCCLS, 1996) with permission from the NCCLS.

10 × 75–mm borosilicate glass culture tubes (Kimble, Corning or Scientific Products)

Microplate with 0.5-ml wells

1-liter actinic glass bottle-style pipets (Repipet, Barnstead/Thermolyne or equivalent) with 1-ml glass dispensers

Small benchtop centrifuge suitable for 10 × 75–mm glass culture tubes (Sero-Fuge, Clay Adams or equivalent)

Photographic dark room fluorescent tube filters (e.g., Macolite Toob Gard or EncapSulite safelite filters or equivalent)

Spectrofluorometer equipped with a red-sensitive photomultiplier tube (Hamamatsu R 928 or equivalent) and a cell holder modified to accommodate standard 10 × 75–mm glass culture tubes (Fig. 8.8.1)

NOTE: All plastic materials provided with the dispenser (i.e., uptake tubes and/or dispensing tips of the Repipet dispenser) must be replaced with glass devices to ensure the integrity of the ethyl acetate. This may require the services of a glassblower to modify commercially available devices.

NOTE: Standards and samples must be protected from exposure to bright light as much as possible throughout the procedure. Use yellow photographic filters for fluorescent tube lights. These tube-style filters are placed over standard fluorescent tube lights to reduce exposure from UV wavelengths.

Prepare PPIX calibration standard stock solution

1. Reconstitute 5 µg protoporphyrin IX by adding 100 µl Protosolv to the vial. Mix the contents gently without inverting the tube. Cap the vial and place in a darkened cabinet for 10 min to allow complete dissolution of the material.

   The vial should be capped to reduce loss of volatile components due to evaporation.

   Several alternative reagents may be used in place of the 5-µg PPIX standard, including protoporphyrin IX dimethyl ester or disodium salt (Porphyrin Products, Sigma). The exact concentration must be standardized using molecular absorbance as described below (see steps 3 to 5). Protoporphyrin IX dimethyl ester is hydrolyzed before use (Gunter et al., 1989).

   Some laboratories use coproporphyrin I or coproporphyrin III (Porphyrin Products) as secondary standards because of their greater stability compared to PPIX. Equivalent "protoporphyrin IX" values are assigned to these solutions, which are used to calibrate the spectrofluorometer on a daily basis. However, a correction factor for each new batch of coproporphyrin materials must be determined using PPIX.

2. Add 10 ml of 1.5 M HCl to the vial using a glass pipet and mix the contents by inverting the tube.

   The concentration of protoporphyrin IX is ~50 µg/100 ml.

Measure molecular absorbance of PPIX in the stock solution

3. Fill a 1-cm^2 quartz spectrophotometer cell with PPIX stock solution. Fill a 1-cm^2 spectrophotometer reference cell with 1.5 M HCl.

4. Place the sample and reference cells in an absorbance spectrophotometer and scan the spectrum between 395 and 420 nm. Record the maximum absorbance (A) at λ_{max} of the band relative to HCl.

   A sample spectrum is shown in Figure 8.8.2. Because there may be some variations in the spectrophotometer, it is safest to scan the sample and visually identify the peak to record the absorbance at its maximum.

   The exact mass of PPIX in the tube is not known and is only nominally estimated at 5 µg. Therefore, the molecular absorbance of PPIX in solution is required to calculate the true concentration of the stock solution.

5. Calculate the exact stock concentration (c) of PPIX using the equation c (µg/100 ml) = $A \times 233$.

   This equation is derived by molecular absorbance according to Beer's Law, which says that $A = m\varepsilon cl$, where A is measured absorbance at λ_{max}, $m\varepsilon$ is millimolar absorptivity (241 liters $mmol^{-1}$ cm^{-1}), and l is the cell path length in cm (1 cm). By rearrangement, c (mmol/liter) = $A/m\varepsilon l = A/241$. Using the PPIX relative molecular mass (562.3 g/mol), the equation then becomes c (µg/ml) = $A \times (562.3/241) = A \times 2.33$, or c (µg/100 ml) = $A \times 233$.

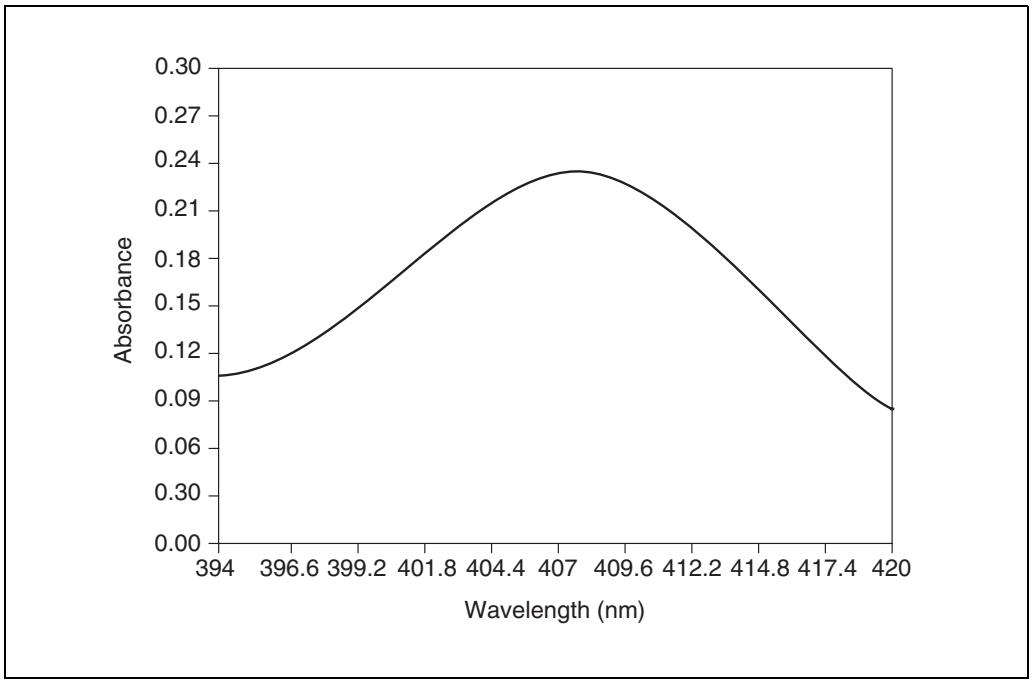

Figure 8.8.2 Typical absorbance band for a PPIX standard solution (51.8 µg/100 ml) in the 395- to 420-nm region of the spectrum. Note that λ_{max} is at 407.0 nm. Scan rate: 300 nm/min.

NOTE: *The 241 value for mε was adopted in the early days of EP testing and was based upon the best available data at the time. Although the correct mε value is now known to be 297 liter mmol^{-1} cm^{-1} (Gunter et al., 1989), the 241 value is still widely used. See Background Information for a more detailed discussion of this issue.*

Prepare working calibration standards

6. Wrap five 2-ml volumetric flasks in aluminum foil to protect the solutions from light.
7. Using an adjustable micropipet, transfer 1600, 1200, 800, and 400 µl stock solution into four flasks and label them 40, 30, 20, and 10 µg/100 ml, respectively. Label the fifth flask as the blank or zero standard.
8. Bring each flask to its 2-ml volume using 1.5 M HCl.

   This yields standards S_t, S_3, S_2, S_1, and S_b respectively, where S_t = top standard and S_b = blank.

9. Transfer 50 µl of each standard into duplicate 10 × 75–mm glass culture tubes. Prepare a third tube for the top standard, S_t.

   The extra S_t is used for adjusting and optimizing the spectrofluorometer.

10. Calculate the exact concentration of each PPIX working standard by multiplying the stock concentration (233 × A; step 5) by the dilution factor (volume of standard added/total volume).

Prepare blood specimens and QC samples

11. Bring all blood specimens and QC samples to room temperature and mix by inversion or by placing them on a rotator.

    Whole blood specimens are obtained either by venipuncture and collected in evacuated tubes (≥2 ml) with EDTA (Vacutainers; Becton Dickinson or equivalent) or by finger stick and collected in a microcollection tube with EDTA (Microtainers; Becton Dickinson or equivalent). Heparinized blood is also acceptable. QC samples are either lyophilized or frozen whole blood.

12. Transfer 200 µl deionized water into a 0.5-ml microplate well (dilution well).
13. Using a micropipet, withdraw 50 µl well-mixed whole blood. Remove any excess blood adhering to the pipet tip by wiping it with a laboratory tissue, being careful not to touch the open end of the tip.
14. Dispense the 50-µl blood sample into the dilution well and mix thoroughly by withdrawing and dispensing (i.e., pumping) the blood/water mixture several times until the solution in the tip appears clear.
15. Using a clean tip, transfer 50 µl diluted blood into a 10 × 75–mm glass culture tube. Prepare all blood specimens and QC samples in duplicate.

Extract calibration standards, blood specimens, and QC samples

16. Using a glass bottle–style pipet, add 1 ml of 4:1 ethyl acetate/acetic acid solution to all standards, QC samples, and blood samples. Thoroughly mix for 10 sec by vortexing.

    To ensure complete mixing, hold the glass tube at the top during vortexing.

17. Centrifuge 3 min at 1000 × *g* (~3000 rpm for a rotor radius of 10 cm), room temperature.
18. Decant each supernatant into a clean glass culture tube making sure the last drop is transferred by touching the two tubes. Discard the tube containing the cell debris.
19. Using another glass bottle–style pipet, transfer 1.0 ml of 1.5 M HCl to each sample and standard. Mix for 10 sec by vortexing.
20. Centrifuge 1 min at 1000 × *g*, room temperature.

    Two distinct liquid phases, ethyl acetate/acetic acid (brown) and HCl (clear), should be clearly visible.

21. Clean the surface of each tube with a laboratory tissue to remove any dust, grease, or fingerprints. Store extracted samples in a light-tight box while the spectrofluorometer is being calibrated.

    This tube will function as the sample cell when inserted into the cell holder of the spectrofluorometer.

Take fluorescence readings

22. Ensure that the excitation lamp of a spectrofluorometer is properly aligned. Set the slit width to 10 nm and adjust the gain accordingly.

    NOTE: *Spectrofluorometers vary from one manufacturer to another. Consult the operator's manual to optimize the various parameters. The instrument should be equipped with a red-sensitive detector (e.g., a photomultiplier tube) capable of enhanced sensitivity above 600 nm.*

23. For older spectrofluoromotors, where the monochromator is adjusted manually, set the excitation wavelength to 408 nm and use the extra S_t tube to scan the emission wavelength from 645 to 680 nm to locate the precise wavelength for maximum intensity. With modern computer-controlled instruments, this step may not be necessary.

    NOTE: *A scan of PPIX fluorescence spectrum shows two bands: one at 662 nm and another at 607 nm (Fig. 8.8.3). The 607-nm band is more intense than the one at 662 nm, which is broader and much easier to peak, although a little less sensitive. One consequence of the improved sensitivity of the 607-nm band is decreased precision. Since sensitivity is not a critical issue in this analysis, the improvement in precision at the 662-nm band is preferred.*

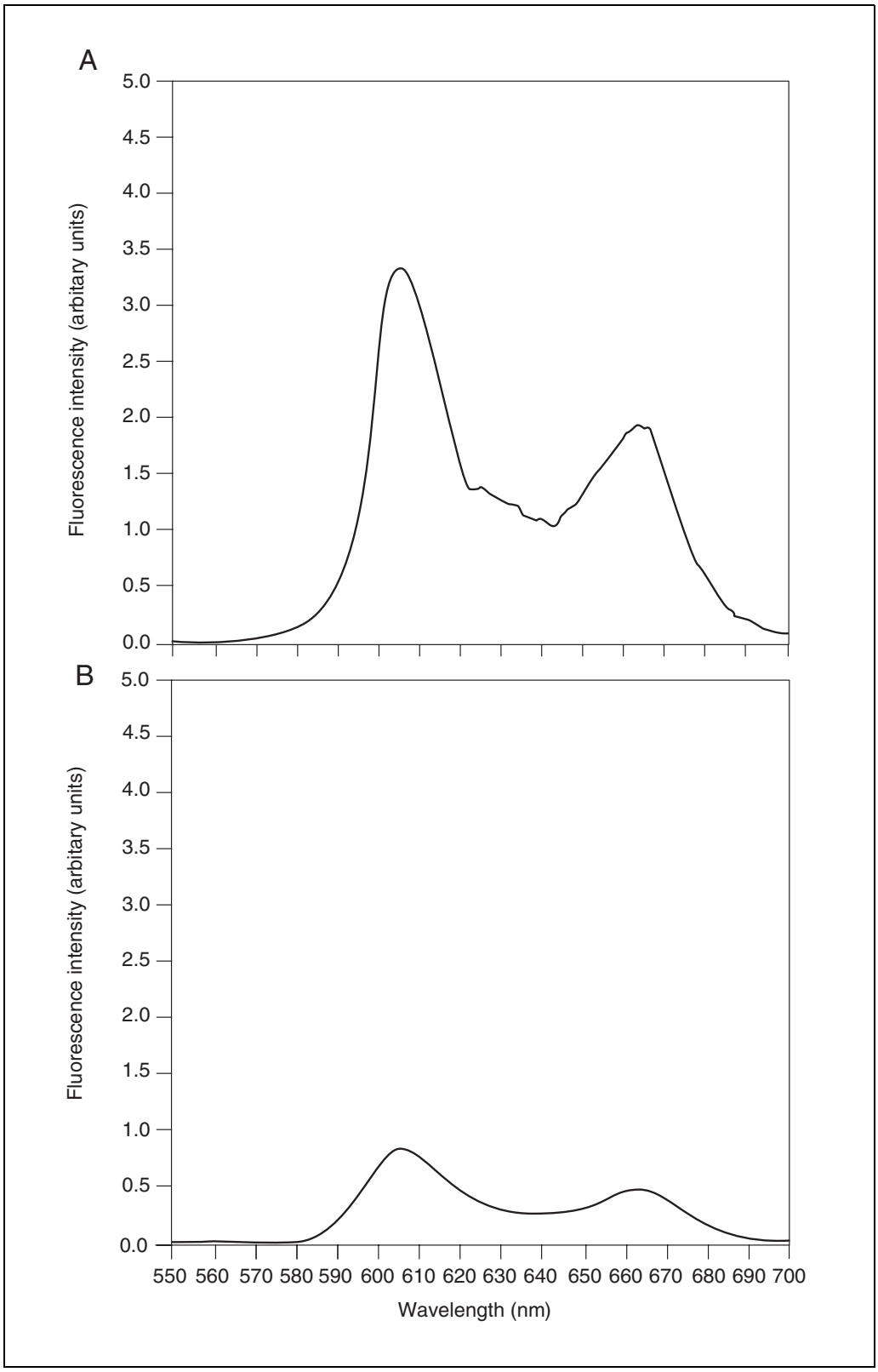

Figure 8.8.3 Typical fluorescence spectra for (**A**) a PPIX standard solution (52.9 μg/100 ml) and (**B**) an extracted human blood sample containing free erythrocyte protoporphyrin. Both measurements were made using a Perkin-Elmer LS5OB Luminescence spectrophotometer with excitation at 408 nm and a slit width of 10 nm.

24. Use one of the blank tubes (S_b) to "blank adjust" the instrument to zero. Check that the zero standard has no fluorescence relative to deionized water.

    If the blank does fluoresce, the reagents may contain interfering fluorescent materials.

25. Analyze standards in duplicate and in the sequence S_b, S_1, S_2, S_3, S_t.

26. Run any secondary standards or QC samples following the primary standards. Ensure that the results for any QC samples are within an acceptable range before continuing with blood samples for clinical testing.

    Acceptable standards are ±6 μg/100 ml or ±15%, whichever is greater.

27. Analyze all blood samples in duplicate.

Calculate PPIX concentration in samples

28. Prepare a standard curve by plotting the relative fluorescence intensity for each calibration standard (y axis) versus the exact PPIX concentration (step 10; x axis).

29. Compute the line of best fit ($y = mx + b$) by least-squares linear regression.

30. Calculate the PPIX concentration in diluted blood from the line of best fit. Multiply this value by 5.2 to account for the extraction efficiency (96% or 1.04 in whole blood) and the 5-fold dilution of blood with water.

    There are conflicting views on the efficiency of extracting porphyrins from whole blood samples. Unpublished data from the author's laboratory based on fifteen diluted blood samples repeatedly extracted with three successive aliquots of ethyl acetate/acetic acid solution showed that 96% ± 1% of the total extractable protoporphyrin was recovered in the first extraction. Thus, one can assume that the extraction efficiency is 96% provided that all extractable protoporphyrin was removed in the three successive extractions, and that the distribution of protoporphyrin IX between the aqueous and organic phases is the same for blood extracts and aqueous PPIX standards. At the present time, there are no reports of any residual protoporphyrin in the extracted cell debris.

    The top standard, S_t, is equivalent to a blood sample with an EP concentration ~200 μg/100 ml (taking into account the 5-fold dilution of blood samples). If any samples or control materials have fluorescence intensities above the top standard, additional dilution will be necessary. A 500-μl aliquot of the clear aqueous HCl phase of the final extract should be transferred, using a 500-μl fixed-volume pipet, into a clean glass culture tube. This is diluted with 2 ml of 1.5 M HCl and vortexed for 3 sec. The reduced fluorescence intensity is measured and the EP concentration is multiplied by another factor of 5 to correct for the additional dilution.

IDENTIFYING AND RESOLVING PROBLEMS WITH ETHYL ACETATE QUALITY

Some commercial supplies of ethyl acetate contain impurities such as oxidizing agents that can quench PPIX fluorescence, thus reducing relative fluorescence intensity. The problem almost always appears as low or inconsistent results for internal or external QC samples. Some problems can be traced to the use of plastic laboratory ware. All ethyl acetate solutions should be stored in glass bottles rather than plastic, as ethyl acetate can leach materials that quench fluorescence. Using clean, acid-washed, well-dried glass apparatuses for all reagents and procedures will eliminate many problems. If the problem cannot be traced to plastic ware, then the quality of the ethyl acetate used for the extraction is suspect. It is preferable to purchase bottles containing two liters or less because ethyl acetate that is left exposed to air may become oxidized, thus producing quenching agents. One test that can indicate the potential for a problem with quenching agents is the

potassium iodide (KI) test (see Support Protocol 1). If the KI test is positive, the ethyl acetate can be redistilled from glass in the laboratory (see Support Protocol 2).

SUPPORT PROTOCOL 1

Testing Ethyl Acetate Stock For Quenching Impurities

Materials

Potassium iodide
Ethyl acetate to be tested

1. Prepare a 10% (w/v) potassium iodide solution by dissolving 10 g KI in 100 ml water. Use only for the KI test and discard immediately after use.
2. Transfer 50 ml ethyl acetate into a 100-ml glass beaker and place it on a white surface (e.g., paper).
3. Add 10 ml of 10% KI solution, swirl to mix, and examine the color.

   A distinct yellow color, due to the oxidation of iodide, indicates that the ethyl acetate stock contains impurities that will quench PPIX fluorescence. Avoid using any ethyl acetate batch that yields a positive KI test. Use only supplies that do not produce a yellow color upon addition of 10% KI. If a suitable clean supply of ethyl acetate cannot be located, the material can be cleaned as described below (see Support Protocol 2).

SUPPORT PROTOCOL 2

Ethyl Acetate Cleanup by Glass Distillation

Materials

Ethyl acetate
2-liter round-bottom glass boiling flask (standard taper 24/40)
Teflon boiling stones
Column and condenser apparatus, including:
~15-inch glass fractionation column with standard taper 24/40 ground-glass joints, wrapped
in insulation and aluminum foil
~15-inch glass condenser with elbow to connect with collection vessel (standard taper 24/40)
2 ring stands and a lab jack
500-W heating mantle (Glas-Col or equivalent)
Rheostat (0-120 V output, 1500 W; Glas-Col or equivalent)
2-liter glass collection bottle with standard taper 24/40 ground glass joint opening

CAUTION: This is a hazardous procedure that must be done under a laboratory hood. Ethyl acetate and its vapors are highly flammable. When a bad batch of ethyl acetate has been identified, all pipet bottles should be washed with a clean batch to prevent cross-contamination.

1. Pour 1.5 liters commercial ethyl acetate into a 2-liter round-bottom flask. Add a few Teflon boiling stones.
2. Connect flask to a column and condenser arrangement. Turn on the water flow to the condenser.
3. Set the rheostat to an arbitrary setting of 75 until the ethyl acetate is almost boiling. Decrease heating to arbitrary setting 65.

   Don't heat the flask too rapidly at the start or ethyl acetate will be ejected directly up into the fractionating column.

   Condensed ethyl acetate should be produced steadily as rapid but distinct drops.

4. Discard the first 100 to 200 ml condensate. Use to rinse the collection/storage bottles.

   CAUTION: *Do not allow the flask to boil dry; this is not only hazardous but will require starting over. To avoid this problem, use a timer and decrease the heating rate further upon collecting ~800 ml.*

5. Collect ~1.0 to 1.2 liters condensed ethyl acetate and transfer to a clean, amber bottle. Store up to 1 month at room temperature.

   The procedure may be repeated one more time without emptying the round-bottomed flask.

   Even after redistillation, always check the ethyl acetate reagent before use by repeating the KI test.

REAGENTS AND SOLUTIONS

Use Milli-Q-purified water or equivalent in all recipes and protocol steps. For common stock solutions, see ***APPENDIX 2A****; for suppliers, see* ***SUPPLIERS APPENDIX****.*

Ethyl acetate/acetic acid solution, 4:1 (v/v)

Pour 800 ml ethyl acetate into a 1-liter graduated cylinder. Add 200 ml glacial acetic acid (trace metal grade; Baker InstraAnalytical grade or equivalent). Stir well with a clean glass rod and pour into a 1-liter glass bottle–type pipet. Store up to 1 month at room temperature.

Hydrochloric acid (HCl), 1.5 M

Pour 500 ml water into a 1-liter class A volumetric flask. Carefully add 125 ml concentrated HCl (trace metal grade; Baker InstraAnalytical grade or equivalent) using a graduated cylinder. Dilute to volume with water, mix, and transfer to a bottle-type dispenser. Store up to 1 month at room temperature.

COMMENTARY

Background Information

The measurement of erythrocyte protoporphyrin (EP) for clinical testing purposes received much attention between 1970 and 1990, largely as a result of its application as a screening test for childhood lead poisoning. Lead interferes with the incorporation of iron into the porphyrin ring to form heme, a reaction catalyzed by the enzyme ferrochelatase (*UNIT 8.7*). This disruption of the final stage in heme biosynthesis leads to an accumulation of zinc protoporphyrin (ZPP) within the red blood cell. During the analysis for EP, the ZPP component, along with heme and any uncomplexed or "free" protoporphyrin, is extracted from blood using a mixture of ethyl acetate and acetic acid. The protoporphyrin is measured using fluorescence spectrometry. This method of analysis for EP has been in the literature for almost 40 years (Schwartz et al., 1960). In subsequent publications, the name "free erythrocyte protoporphyrin" (FEP) was coined to reflect that, in acid solution, the ZPP molecule dissociates to form "free" protoporphyrin IX and "free" zinc(II) ions. Thus, in ethyl acetate/acetic acid extraction methods, total EP is measured.

Working independently, several investigators (Kammholz et al., 1972; Piomelli, 1973; Sassa et al., 1973) published micromethods for EP analysis based on extraction with a mixture of ethyl acetate/acetic acid followed by determination using spectrofluorometry. Significant improvements to these methods were published (Chisolm and Brown, 1975) along with a recommendation to determine the exact concentration of the PPIX standard solutions using absorbance, Beer's Law, and a PPIX millimolar absorptivity of 241 liters $mmol^{-1}$ cm^{-1}.

The main advantage of these micromethods was that only small blood volumes (<50 µl) were required for the EP analysis, thus making it possible to conduct mass screening of children for exposure to lead. Other advantages were that the laboratory equipment required to set up the EP test was relatively inexpensive, and that the test did not suffer from the contamination errors that plagued early blood lead methods.

Prior to 1975, a blood lead concentration of ≥50 μg/dl was considered harmful to children. The EP test had good diagnostic sensitivity for predicting underlying exposure to lead at blood lead levels >30 μg/dl. The EP test was recommended by the CDC in 1975 for screening children for lead poisoning, and again in 1978, when the blood lead threshold was lowered to 30 μg/dl (CDC, 1975, 1978). In 1985, when the safe pediatric blood lead level was lowered to 25 μg/dl, the EP threshold was lowered from 40 to 35 μg/dl in line with concerns about the diagnostic accuracy of the test for predicting lower blood lead levels (CDC, 1985). When the CDC lowered the blood lead threshold to 10 μg/dl (CDC, 1991), it was evident that the EP test was no longer adequate as a predictor of underlying lead exposure (Parsons et al., 1991) and the CDC recommended that EP be replaced by a direct blood lead test.

During the 1970s, portable instrumentation was developed for the direct determination of ZPP in a single drop of blood (Blumberg et al., 1977a,b). These portable instruments, which were based on front-surface fluorometry, became known as hematofluorometers and were widely used to conduct on-site screening of children for lead poisoning. With the demise of the EP test in recent years, hematofluorometer use has declined, although the EP test still remains clinically useful in the identification of iron-deficiency anemia and in diagnosing inherited disorders of heme metabolism (e.g., erythropoietic porphyria).

Most recently, the National Committee for Clinical Laboratory Standards (NCCLS, 1996) has issued an approved guideline for EP testing. The NCCLS guideline includes a consensus method for determination of EP by ethyl acetate acetic/acid extraction that recommends using a millimolar absorptivity value (mε) of 297 liters $mmol^{-1}$ cm^{-1}. The 241 mε value was originally used by Chisolm and Brown (1975) and was based upon the best available data at the time, although numerous discrepancies were reported in the literature. However, it was not until 1989 that the correct mε value for PPIX (297 liters $mmol^{-1}$ cm^{-1}) was published (Gunter et al., 1989). Unfortunately, it has not been possible to change the long-standing practice of clinical laboratories and proficiency testing (PT) programs in the U.S. that are using the 241 value. In addition, as a vast literature and clinical database now exist for EP using the 241 mε value, there is little enthusiasm for correcting this "historical error" in the EP test.

Other differences between the NCCLS method and that described here are minor. They include decanting the product of the primary extraction of PPIX and heme components into a second culture tube for the back-extraction step with HCl, and the absence of an arithmetic correction for individual patient hematocrit or hemoglobin levels. All EP results obtained using the method described here are reported as μg/100 ml (μg/dl) of whole blood. Currently, there are three PT programs in the U.S., and all require that EP results be reported as μg/dl whole blood using the mε value of 241; no correction for hematocrit or hemoglobin is required.

Individual porphyrin species such as ZPP, PPIX, and coproporphyrin can be successfully determined in blood and urine by liquid chromatographic (LC) techniques. A number of early papers described LC methods based on separating porphyrin species on a reversed-phase column with fluorometric detection (Smith et al., 1980; Scoble et al., 1981; Chiba and Sassa, 1982). A comparison between fluorescence and absorbance detectors showed clearly that the former has better sensitivity, specificity, and reproducibility (Sagen and Romslo, 1985). Later papers have described improvements in LC methods that have used more selective extraction procedures (Ho et al., 1987) and have incorporated a more effective specimen pretreatment procedure coupled with gradient elution (Bowers et al., 1992). More recently, Sato et al. (1994) compared a conventional reversed-phased LC method (Smith et al., 1980) with a new LC method based upon elution of porphyrins on a porous polystyrene gel with a diisopropylamine/water/methanol mobile phase. They reported significant improvements over the conventional LC method including the ability to distinguish between the protoporphyrin emission peak and quenching due to heme, thus making removal of heme unnecessary. They also reported that the conventional LC method overestimated EP concentrations below 5 ng/100 ml, possibly due to dissociation of ZPP in an acid medium which yields additional protoporphyrin.

Critical Parameters and Troubleshooting

The most frequent source of problems with this analysis can be traced to the quality of the ethyl acetate supplies used for the extraction reagent (Doran and Mitchell, 1984). Impurities in this reagent can cause fluorescence quench-

ing, which leads to erroneously low results. The KI test for impurities (see Support Protocol 1) is generally reliable in this respect, but results can be misleading because of the subjective nature of the color intensity. If the quality of the ethyl acetate is suspect and the KI test is inconclusive or, perhaps weakly positive, the ethyl acetate should be redistilled or obtained from an alternative supply.

The protection of blood samples and reagents from exposure to bright lights, particularly sunlight or fluorescent tube light, is highly desirable as porphyrins are susceptible to photooxidation, which can result in erroneously low values. Blood samples are easily protected by wrapping them in aluminum foil. Avoid using plastic microcollection devices with protective filters for bilirubin measurements. These filters do not protect blood samples for the EP assay. In the laboratory, using low-cost photographic filters (which fit over standard fluorescent tubes) and reduced UV radiation are a convenient way of reducing photooxidation of samples and reagents. Extracted blood samples and standard solutions should be stored in a light-tight box while the spectrofluorometer is calibrated.

The use of plasticware in the laboratory should be avoided, as organic reagents may leach out impurities that can interfere in the analysis. This may require some modifications to ensure that all-glass pipet bottles are used. The key to success is to ensure that all laboratory ware is thoroughly clean and well dried before use. Access to reliable quality control materials is essential to assuring that clinical results are reliable. The availability of such materials is becoming more difficult as the test becomes less widely used. Thus, the onus is on the laboratory performing the test to develop such materials. The operators of the PT programs for EP may be able to help in this respect. One alternative is to prepare QC materials in house and to validate them through interlaboratory studies.

Anticipated Results

The absorbance measurement of PPIX standard solutions should result in a single band with λ_{max} at 407 nm as shown in Figure 8.8.2. The fluorescence spectra expected for PPIX in standard solutions and in extracted blood samples are shown in Figure 8.8.3. Quantitative results for EP quality control materials should fall within ±6 µg/dl of the target value for concentrations <40 µg/dl, or within ±15% of the target for values ≥40 µg/dl. These criteria are currently the same as those expected of participants in several U.S. PT for EP.

Normal clinical test results for EP vary slightly between men, women, and children based upon data derived from the Second National Health and Nutrition Examination Survey studies (NHANES II; Yip et al., 1984). However, the NHANES II data were calculated with an mε value of 297, and a correction must be made to convert those data into equivalent EP results measured using the 241 value. After excluding those subjects with iron-deficiency anemia and elevated blood lead levels (NCCLS, 1996), the 95th percentile NHANES data for men, women, and children yields rounded upper threshold values of 35, 37, and 38 µg/dl whole blood, respectively. Note that these values are close to the most commonly accepted upper threshold value for EP, 35 µg/dl whole blood, recommended by the CDC in their 1985 document for screening children exposed to lead.

Time Considerations

The limited stability of PPIX standards in acid solution (a matter of hours rather than days) requires some attention to timing. For example, it is unwise to perform sample extractions before the instrumentation has been set up, calibrated, and optimized. If at all possible, the sample and standard extractions and the fluorometric readings should be carried out in a single operation and not separated by a long interval (e.g., a lunch break). The entire procedure, including reporting results, can be easily accomplished in a typical 8-hr day if no problems are encountered. The number of blood samples that can be processed in a typical day will depend on the technologist's skills, but usually can be up to 50 in duplicate including calibration and quality control.

Literature Cited

Blumberg, W.E., Eisinger, J., Lamola, A.A., and Zuckerman, D.M. 1977a. The hematofluorometer. *Clin. Chem.* 23:270-274.

Blumberg, W.E., Eisinger, J., Lamola, A.A., and Zuckerman, D.M. 1977b. Zinc protoporphyrin level in blood determined by a portable hematofluorometer: A screening device for lead poisoning. *J. Lab. Clin. Med.* 89:712-723.

Bowers, M.A., Aicher, L.D., Davis, H.A., and Woods, J.S. 1992. Quantitative determination of porphyrins in rat and human urine and evaluation of urinary porphyrin profiles during mercury and lead exposures. *J. Lab. Clin. Med.* 120:272-281.

CDC (Centers for Disease Control). 1975. Increased lead absorption and lead poisoning in young

children [Report]. U.S. Department of Health, Education, and Welfare, Atlanta, Ga.

CDC (Centers for Disease Control). 1978. Preventing lead poisoning in young children [Report]. U.S. Department of Health, Education, and Welfare, Atlanta, Ga.

CDC (Centers for Disease Control). 1985. Preventing lead poisoning in young children [Report]. U.S. Department of Health and Human Services, Atlanta, Ga.

CDC (Centers for Disease Control). 1991. Preventing lead poisoning in young children [Report]. U.S. Department of Health and Human Services, Atlanta, Ga.

Chiba, M. and Sassa, S. 1982. Analysis of porphyrin carboxylic acids in biological fluids by high-performance liquid chromatography. *Anal. Biochem.* 124:279-285.

Chisolm, J. Jr. and Brown, D.H. 1975. Micro-scale photofluorometric determination of "free erythrocyte pophyrin" (protoporphyrin IX). *Clin. Chem.* 21:1669-1682.

Doran, D. and Mitchell, D.G. 1984. Problems in the determination of erythrocyte protoporphyrin by ethyl acetate-acetic acid extraction. *Ann. Clin. Biochem.* 21:141-145.

Gunter, E.W., Turner, W.E., and Huff, D.L. 1989. Investigation of protoporphyrin IX standard materials used in acid-extraction methods, and a proposed correction for the millimolar absorptivity of protoporphyrin IX. *Clin. Chem.* 35:1601-1608.

Ho, J., Guthrie, R., and Tieckelmann, H. 1987. Quantitative determination of porphyrins, their precursors and zinc protoporphyrin in whole blood and dried blood by high-performance liquid chromatography with fluorimetric detection. *J. Chromatogr.* 417:269-276.

Kammholz, L.P., Thatcher, L.G., Blodgett, F.M., and Good, T.A. 1972. Rapid protoporphyrin quantitation for detection of lead poisoning. *Pediatrics* 50:625-631.

NCCLS (National Committee for Clinical Laboratory Standards). 1996. Erythrocyte protoporphyrin testing; Approved guideline. 1 pp. NCCLS Document C42-A, Wayne, Pa.

Parsons, P.J., Reilly, A.A., and Hussain, A. 1991. Observational study of erythrocyte protoporphyrin as a screening test for detecting lead exposure in children: Impact of lowering the blood lead action threshold. *Clin. Chem.* 37:216-225.

Piomelli, S. 1973. A micromethod for free erythrocyte porphyrins: The FEP test. *J. Lab. Clin. Med.* 81:932-940.

Sagen, E. and Romslo, I. 1985. Determination of porphyrins by high performance liquid chromatography: Fluorescence detection compared to absorbance detection. *Scand. J Clin. Lab. Invest.* 45:309-314.

Sassa, S., Granick, J.L., Granick, S., Kappas, A., and Levere, R.D. 1973. Studies in lead poisoning. I. Microanalysis of erythrocyte protoporphyrin levels by spectrophotometry in the detection of chronic lead intoxication in the subclinical range. *Biochem. Med.* 8:135-148.

Sato, H., Ido, K., and Kimura, K. 1994. Simultaneous separation and quantification of free and metal-chelated protoporphyrins in blood by three-dimensional HPLC. *Clin. Chem.* 40:1239-1244.

Schwartz, S., Berg, M.H., Bossenmaier, I., and Dinsmore, H. 1960. Determination of porphyrins in biological materials. *In* Methods of Biochemical Analysis, Vol. VIII (D. Glick, ed.) pp. 221-294. Interscience Publishers, New York.

Scoble, H.A., McKeag, M., Brown, P.R., and Kavarnos, G.J. 1981. The rapid determination of erythrocyte porphyrins using reversed-phase high performance liquid chromatography. *Clin. Chim. Acta* 113:253-265.

Smith, R.M., Doran, D., Mazur, M., and Bush, B. 1980. High-performance liquid chromatographic determination of protoporphyrin and zinc protoporphyrin in blood. *J. Chromatogr.* 181:319-327.

Yip, R., Johnson, C., and Dallman, P.R. 1984. Age-related changes in laboratory values used in the diagnosis of anemia and iron deficiency. *Am. J. Clin. Nutr.* 39:427-436.

Contributed by Patrick J. Parsons
Wadsworth Center, New York State
Department of Health,
and The University at Albany
Albany, New York

HPLC Methods for Analysis of Porphyrins in Biological Media

Porphyrins are formed as intermediates in the biosynthesis of heme (see Fig. 8.9.1). This process takes place in essentially all eukaryotic tissues. In mammalian, avian, and aquatic species, heme biosynthesis is characterized by formation of porphyrins with 8, 7, 6, 5, 4, and 2 carboxyl groups. Formation of 8-carboxylporphyrin(ogen), or uroporphyrinogen, is mediated by the catalytic activities of δ-aminolevulinic acid (ALA) synthetase, ALA dehydratase, porphobilinogen deaminase, and uroporphyrinogen III synthetase, while the successive decarboxylation and subsequent oxidation of 8-carboxylporphyrinogen to 2-carboxylporphyrin (protoporphyrin) are mediated by uroporphyrinogen decarboxylase, coproporphyrinogen oxidase, and protoporphyrinogen oxidase, respectively. Incorporation of ferrous iron (Fe^{2+}) into protoporphyrin to form heme is catalyzed by ferrochelatase (heme synthetase).

Differential alteration of heme biosynthetic pathway enzyme activities by drugs or environmental chemicals may result in changes in urinary, blood, fecal, and/or tissue porphyrin excretion patterns as well as in altered porphyrin concentrations in target tissues. Changes in tissue or excreta porphyrin levels are potentially useful, both in the diagnosis of chemical effects and as an indicator of toxicant exposure. The measurement of porphyrins in this manner requires a relatively rapid and efficient method of porphyrin recovery from biological media as well as a sensitive and readily applicable procedure for porphyrin separation and quantitation.

This unit describes analytical procedures for the extraction of porphyrins from urine, feces, blood, and tissues (Support Protocol 1 to 7). Each extraction procedure differs somewhat from the others, because biological media vary in the complexity of the matrix from which porphyrins must be extracted. The protocols described below maximize the recovery of porphyrins from the specific medium under consideration. An HPLC-spectrofluorometric procedure (see Basic Protocol) is also described which provides for the quantitative separation and analysis of porphyrins that have been extracted from any biological medium.

NOTE: All protocols using live animals must first be reviewed and approved by an Institutional Animal Care and Use Committee (IACUC) and must follow officially approved procedures for the care and use of laboratory animals.

SEPARATION AND QUANTITATION OF PORPHYRINS BY HPLC

BASIC PROTOCOL

Naturally occurring porphyrins may be separated according to the number of carboxyl groups. The analysis of porphyrins extracated from biological fluids and tissues (see Support Protocols 1 to 7) by HPLC provides characteristic profiles and facilitates rapid diagnosis of inherited or chemically induced disorders of porphyrin metabolism.

Materials

Porphyrin extract (see Support Protocol 5, 6, or 7)
Combined porphyrin standard: Porphyrin Acid Chromatographic Marker Kit (Porphyrin Products)
HPLC-grade methanol
0.05 M sodium phosphate buffer, pH 3.5 (see recipe)
Helium (for sparging or degassing mobile phase solutions)
HPLC system equipped with two programmable solvent-metering pumps, a gradient programmer, an automatic variable volume sample injector, and a fluorescence detector

Contributed by James S. Woods and P. Lynne Simmonds
Current Protocols in Toxicology (2001) 8.9.1-8.9.17

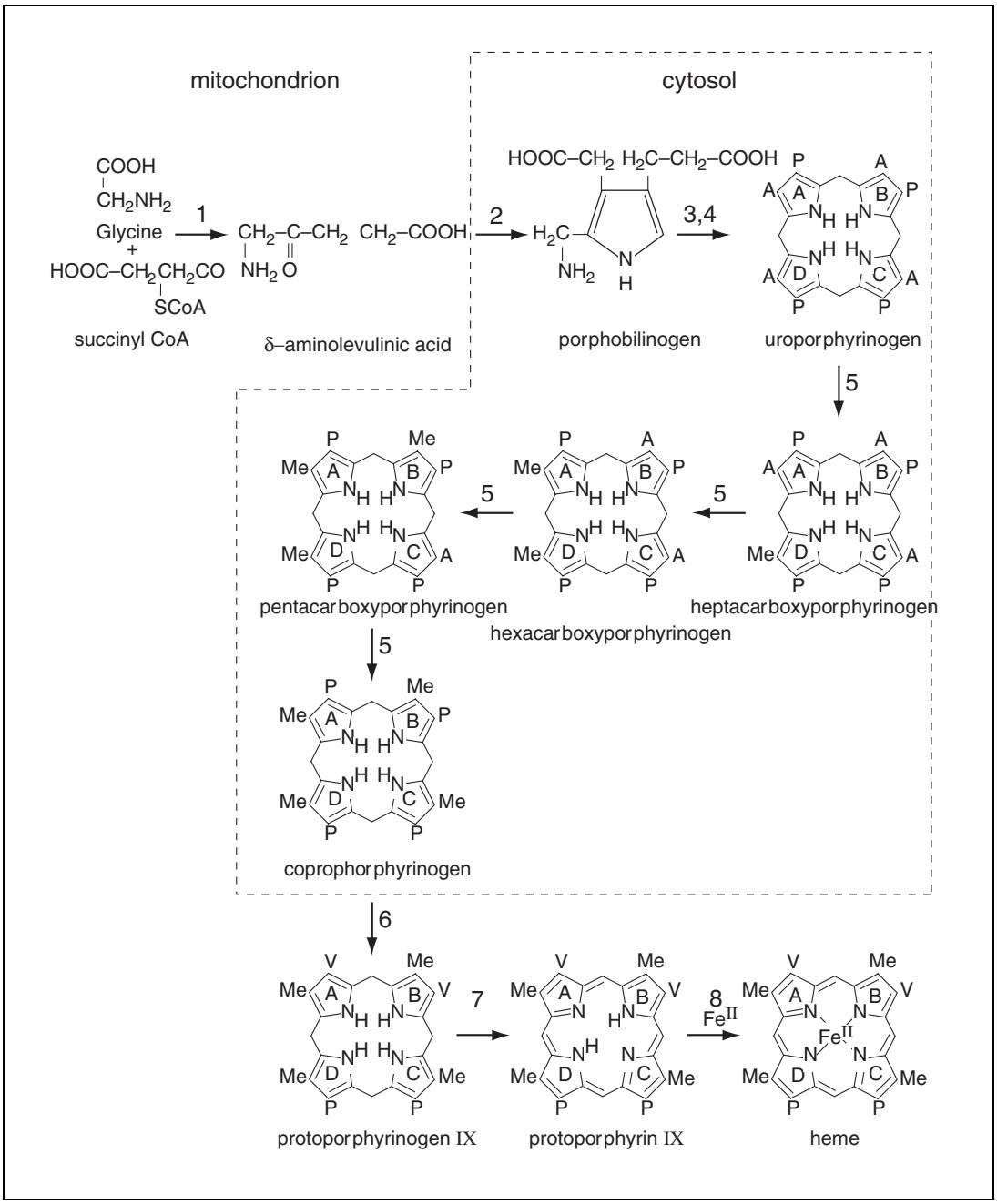

Figure 8.9.1 Role of porphyrins in biosynthesis of heme. Abbreviations: A, acetic acid; Me, methyl; P, propionic acid; V, vinyl.

C-18 250 × 4.6–mm 5-µm analytical HPLC column (e.g., Alltech Econosphere) and SS prefilter element (frit)
C-18 guard column
Column heater
Amber HPLC vials, caps and 300- to 500-µl inserts (size appropriate for specific instrument employed by the investigator)
Filters for mobile phase solvents (Millipore, type HVLP, 0.45-µm)

Perform HPLC separation

1. Initially, use a 10-µl (animal) or 50-µl (human) volume sample of the urinary porphyrin extract for HPLC-spectrofluorometric analysis. For tissue or excreta

Table 8.9.1 Mobile Phase Gradient Program[a]

Time (min)	Reservoir A (methanol)	Reservoir B (buffer)
0	50	50
4	65	35
8	85	15
22	99	1
27	10	90
28	10	90
30	50	50

[a]Filter and degas A and B just prior to use.

porphyrin determinations, use a 50- to 100-µl volume sample of porphyrin extract, whereas for blood, use a 10-µl sample.

Typically, porphyrin concentrations in rodent urine are up to 10-fold greater than those in human urine. Hence, a smaller volume of rodent urine extract may be employed for HPLC analysis. It may be necessary to determine empirically what volume of extract works best for porphyrin measurements by the analytical system employed by the individual investigator.

2. Prior to initiation of sample injections, calibrate the peak integration system by first injecting 50 µl of a combined porphyrin standard onto the column, with each of the six porphyrins in the standard mixture representing 50 pmol.
3. Inject the samples.

   Samples are most effectively injected onto the HPLC column using an autosampler that features an automatic injection system, such as the Waters 717 Plus Autosampler. For extended-run periods (overnight, week-ends) in which samples are loaded hours prior to the actual time of injection, employ an autosampler that has a temperature control feature, so that the samples can be maintained at a constant temperature (15°C or less) to prevent thermal decomposition of porphyrins prior to measurement.

4. Following injection, separate porphyrins using a gradient mobile phase in which reservoir A contains 100% HPLC-grade methanol and reservoir B contains 0.05 mM monobasic sodium phosphate, pH 3.5.
   a. Program the gradient as shown in Table 8.9.1. Use a flow rate of 1.0 ml per min.
   b. Maintain the column at 40°C during all operations using a column heater.
   c. Continuously sparge (degas) fluids in both reservoirs with helium throughout the HPLC operation in order to prevent gas build-up in the pump heads with subsequent erosion of solvent delivery and flow.

   This program provides for the separation and quantitation of 8-, 7-, 6-, 5-, 4-, and 2-carboxyl porphyrins with a sensitivity to detect 0.5 pmol. Complete resolution of all porphyrins is achieved within 25 min following sample injection (see Fig. 8.9.2).

Detect and quantitate porphyrins spectrophotometrically

5. Using a fluorescence monitor (such as the Waters model 474) that is interfaced with the outflow of the HPLC column, detect porphyrins by exciting at the wavelength of the Soret region, 390 to 410 nm, and measuring the emission at 600 to 630 nm.

   Each porphyrin responds maximally at slightly different excitation and emission wavelengths. Initially, set the excitation wavelength at 395 nm and the emission wavelength to 620 nm. Under most circumstances, these settings allow the determination of 8- through 2-carboxyl porphyrins, as well as zinc protoporphyrin, with enough sensitivity to detect 0.5 pmol. The investigator should determine empirically the optimal settings for the specific detection equipment employed.

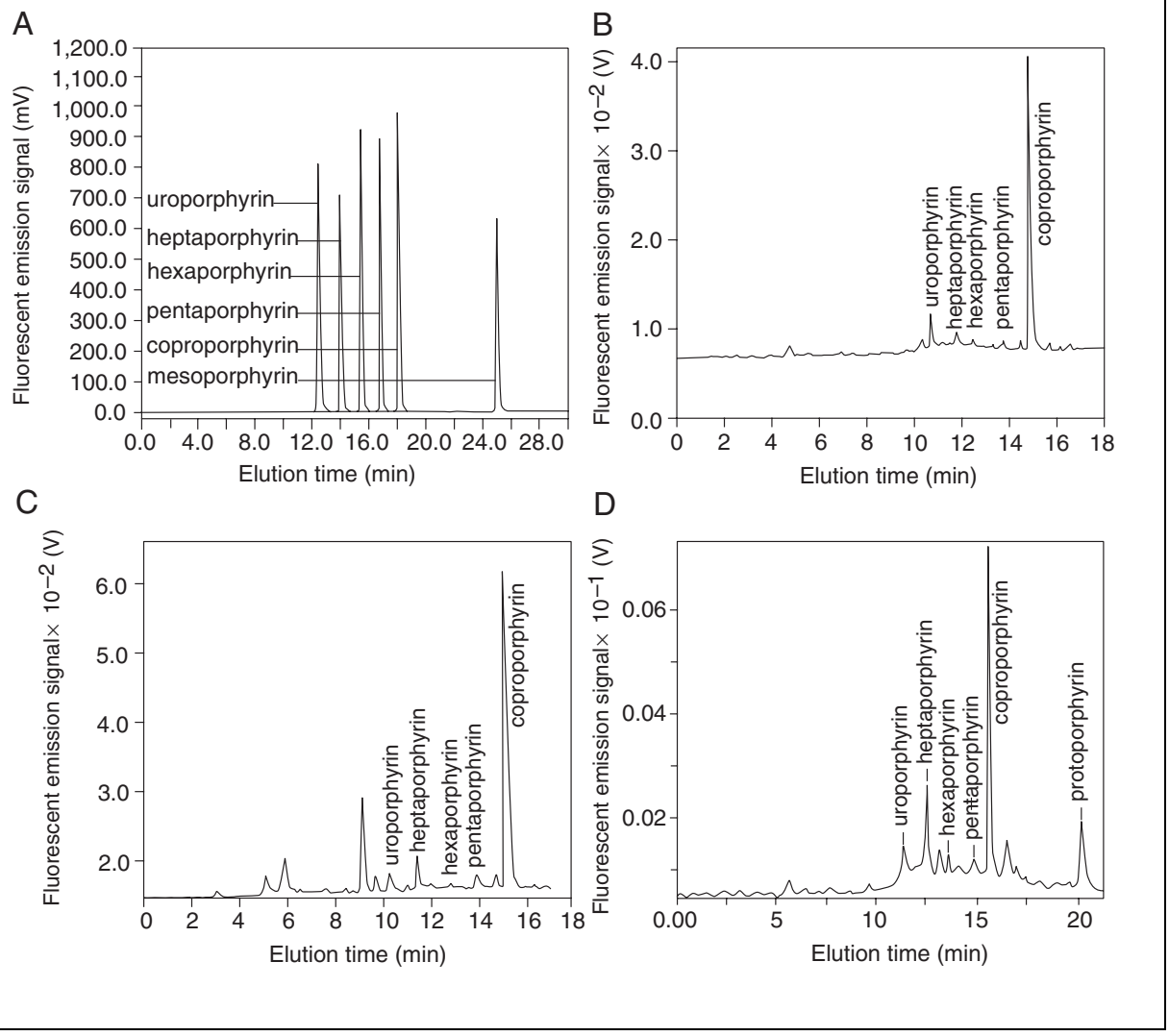

Figure 8.9.2 Anticipated chromatograms from: (**A**) porphyrin chromatographic acid standards, 100 pmol each, injection volume, 25 µl; (**B**) male human urine, injection volume, 50 µl (Bowers et al., 1992a); (**C**) Fischer 344 male rat urine, injection volume, 50 µl (Bowers et al., 1992a);(**D**) Fischer 344 male rat liver, injection volume, 50 µl (Woods and Miller, 1993).

SAMPLE COLLECTION PROCEDURES FOR PORPHYRINS

SUPPORT PROTOCOL 1

Animal Urine

Urine samples from rodents and other animal species are most effectively collected from metabolism cages that are designed to house individual animals and that permit separation of urine from feces, spilled food, hair, and other solid contaminants.

Materials

Sodium bicarbonate
Disodium EDTA
Test animals
Distilled water

Metabolism cages (Hoeltge, Inc.) that permit separation of urine from feces and other solid materials
Graduated polypropylene flasks (50-, 100-ml, or larger depending of size of animal used)

1. Before beginning urine collections, add ~50 mg sodium bicarbonate and ~4 mg disodium EDTA to each urine collection container.

   The bicarbonate prevents coprecipitation of porphyrins, which sometimes occurs at the acid pH of urine, and the EDTA precludes possible complexation of porphyrins with metals that might be present in the urine.

2. Collect a 24-hr urine sample under light-proof conditions (to avoid photochemical oxidation of urinary porphyrins over the collection period) using either dark colored or foil-wrapped glass or polypropylene flasks of sufficient size to permit collection of the entire sample. Position the flask immediately under the outlet of the collection funnel that is mounted beneath the floor of the wire-bottomed cage. Allow animals free access to drinking water during the collection period, but take care to ensure that drinking water cannot spill into the urine sample.

   For mice or rats, graduated 50- or 100-ml flasks are sufficient for the anticipated 10 to 30 ml 24-hr urine excretion volume. It is not necessary to keep the flasks on ice during the collection period if the room temperature is maintained at 21°C (70°F) or less.

3. At the end of the collection period, measure the total urine volume in each flask.

   If the total 24-hr sample is <10 ml and/or appears to be contaminated with feces, food, or other solid matter, it should not be used.

4. Either process the urine for porphyrin analysis immediately following collection (see Support Protocol 5), or freeze it at −20°C until analysis can be performed (preferably within 2 weeks).

   If it is anticipated that porphyrins will not be measured within a 2-week period following collection, freeze the samples at −80°C until analysis can be performed. Samples can be retained at −80°C for up to 6 months without significant porphyrin deterioration.

Human Urine

SUPPORT PROTOCOL 2

Human urine samples for porphyrin analysis can be collected in standard 100-ml clinical urine collection cups. While 24-hr samples are preferred for clinical studies, randomly collected "spot" urine samples are sufficient for porphyrin determination, if collected from all subjects at the same time of day.

Materials

Sodium bicarbonate
Disodium EDTA
Human subject(s)
100-ml clinical urine collection cups with orange screw-on lids (one per subject per void; Starplex Scientific, Fisher)
2.5-liter dark brown polypropylene bottles with screw-on lids (one per subject per 24-hr period; Biomedical Polymers, VWR)
Female urinals (as required; Commode Specimen Collection System, Fisher)

1. Add ~250 mg of sodium bicarbonate and ~25 mg of disodium EDTA to the containers that are used to collect human urine (either the clinical collection cup for spot samples or the larger 2.5-liter bottle for the 24-hr collection).

The bicarbonate prevents coprecipitation of porphyrins, which sometimes occurs at the acid pH of urine, and the EDTA precludes possible complexation of porphyrins with metals that might be present in the urine.

2. Collect urine samples from subjects in collection cups or female urinals. If 24-hr urine collections are required, then combine all separate urine voids that are collected over a 24-hr period in a single opaque (brown) 2.5-liter polypropylene bottle, and keep it refrigerated during the collection period.

   If a 24-hr collection is made, retain at least 25 ml for duplicate porphyrin analyses. For off-site collections made as part of field studies, freeze 25-ml aliquots and ship frozen samples on dry ice to the analytical laboratory by overnight delivery service.

SUPPORT PROTOCOL 3

Feces

Analysis of fecal polyphyrins is performed when determination of protoporphyrin, which does not appear in urine, and 4- through 6-carboxyl porphyrin excretion is required. Timing of collection is important for this purpose.

Materials

Metabolism cages (Hoeltge, Inc.) that permit separation of urine from feces and other solid materials *or* Commode Collection System (for human feces; Fisher)

For animal feces

1a. Collect animal feces as described above for urine collections, using individual metabolism cages that are designed to separate solid from liquid waste. Retain at least 0.5 g for duplicate porphyrin analysis.

For human feces

1b. Collect human feces using a Commode Specimen Collection System, such as that offered by Fisher (CMS/Fisher, Fisherbrand). Retain at least 0.5 g for duplicate porphyrin analyses.

SUPPORT PROTOCOL 4

Blood

Porphyrin determinations in blood focus primarily on ethrocyte protoporphyrin IX and zinc protoporphyrin IX concentrations. Proper collection of blood samples is essential for this purpose. Timing of collection is unimportant.

Materials

Sterile 10-ml syringe and needle or 10-ml Vacutainer tube (Becton Dickinson) with EDTA as anticoagulant

1. Draw subcutaneous venous blood samples from animals or humans using either a sterile 10-ml syringe or a 10-ml Vacutainer tube with EDTA as the anticoagulant. After the tube has been filled with blood, immediately invert several times to prevent coagulation.

   Whole blood collected in this manner can be stored at 10°C for up to 1 month.

   CAUTION: *Do not freeze, as this will lyse red cells, thereby precluding the ability to measure erythrocyte porphyrins independently from those in white blood cells or plasma. If only erythrocyte porphyrins are of interest, separate erythrocytes from other blood constituents prior to freezing.*

PORPHYRIN EXTRACTION PROCEDURES

Porphyrin extraction procedures vary somewhat depending upon the complexity of the biological matrix of the medium, e.g., urine, blood, feces, or tissue. Extraction of porphyrins from urine is relatively easily accomplished using polar solvents such as methanol and mineral acid (e.g., HCl), whereas extraction from feces, blood, or solid tissues such as liver or kidney, requires repetitive treatment with nonpolar solvents such as ethyl acetate or acetonitrile to ensure complete porphyrin recovery. The following porphyrin extraction procedures provide for efficient extraction of porphyrins from urine, tissues, fecal matter and blood.

CAUTION: These procedures must be carried out under reduced light, i.e., out of direct sunlight or fluorescent overhead lighting), to protect porphyrins from photo-oxidation. Preferred lighting is >560 nm (5600 Å). Acrylic red or yellow sheaths/tube guards (Platt Electric Supply) are available that slip over fluorescent light tubes and can be cut to fit.

Urine Porphyrin Extraction

SUPPORT PROTOCOL 5

Rodent urine differs from human urine in that it contains relatively high concentrations of riboflavin and other fluorescing materials that might potentially interfere with the spectrofluorescent detection of specific urinary porphyrins. The following analytical procedure was developed to permit separation of potentially interfering urinary contaminants as well as to provide for improved porphyrin recovery. This procedure is suitable for measurement of porphyrin levels in both animal and human urine as well as for detection of small changes in urinary porphyrin concentrations resulting from porphyrinogenic chemical exposures.

Materials
HPLC-grade methanol
10 mM sodium phosphate buffer, pH 3.5 (see recipe)
1 N and 6 N HCl
Urine sample (see Support Protocol 1 or 2)
35% (v/v) HPLC-grade methanol in 10 mM sodium phosphate buffer, pH 3.5 (see recipe for buffer)
10 mM sodium phosphate buffer, pH 7.5 (see recipe)
80% (v/v) HPLC-grade methanol/20% (v/v) 10 mM sodium phosphate buffer, pH 7.5 (see recipe for buffer)
Nitrogen source

C-18 Bond Elute columns with 10-ml reservoirs (size 10 ml/250 mg; Varian) *or* C-18 Sep-Pac columns (Waters) and 10-ml plastic syringes to be used as column barrel
Vacuum manifold system: e.g., Baker SPE 10 vacuum extraction system or Millipore 1225 Sampling Manifold
15-ml conical polystyrene centrifuge tubes with screw-on caps
Adjustable pipettor (Gilson 5000-µl) and tips to fit *or* 10-ml serological pipets and electric pipettor (Drummond)
Beckman J2-27 or equivalent centrifuge
20-ml glass or plastic scintillation vials with Mylar/Teflon-lined lid (Research Products International)
60°C water bath or heating block
Glass 5¾-in. Pasteur pipets
4-mm Millex-HV 0.45-µm membrane filters (Millipore)
1-ml plastic syringe
10-ml plastic syringe plunger

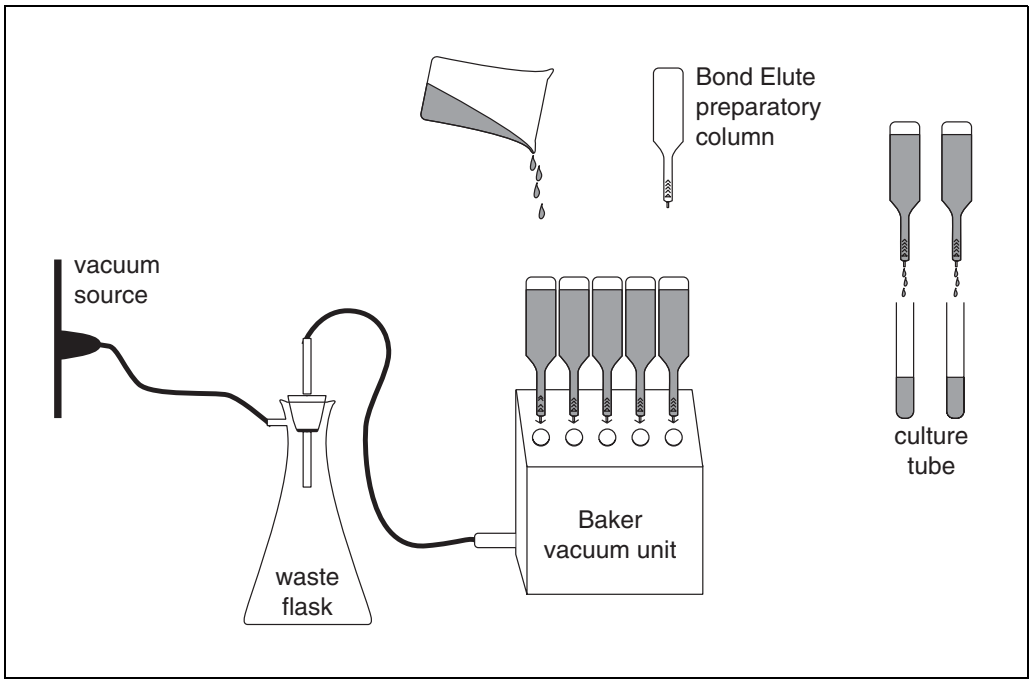

Figure 8.9.3 Setup for preparatory columns.

Amber HPLC vials to fit autosampler used (e.g., 1-ml amber shell vials for 96-position autosampler tray) and 300- to 500-µl inserts with bottom springs (Alltech Associates or Waters)

Pretreat the C-18 preparatory columns

1. For each urine sample, prepare one C-18 Bond Elute preparatory column (or C-18 Sep-Pak cartridge fitted to a 10-ml plastic syringe barrel), as shown in Figure 8.9.3.
2. Fit the outflow end of each preparatory column into one of the openings of a vacuum manifold system (Fig. 8.9.3).
3. Pass 10 ml of 100% HPLC-grade methanol through the column, followed by 10 ml of 10 mM sodium phosphate buffer, pH 3.5, under slight vacuum to facilitate flow.

   CAUTION: *Methanol is flammable and a cumulative poison. Work in a hood with safety glasses and protective gloves and clothing.*

4. Turn off the vacuum. Do not allow the cartridges to become dry.

   For rodent urinary porphyrin analysis, 6 ml is required for a single porphyrin determination. In most cases, it is desirable to analyze each individual sample in duplicate. Thus, 12 ml of urine is required for each animal determination. For human urine porphyrin determinations, use 10 ml for each individual assay (20 ml for duplicate determinations).

Extract porphyrins from urine

5. Separate a 6-ml aliquot (10 ml for human) of the urine sample into a capped 15-ml polystyrene conical centrifuge tube.
6. Centrifuge the sample 10 min at 2000 × *g*, room temperature, in Beckman J2-27 or equivalent centrifuge, to remove any insoluble and/or suspended matter.
7. Using an adjustable pipet, carefully transfer the supernatant to a 20-ml glass or plastic scintillation vial. Discard the sediment.

8. Using a pH meter or pH paper, adjust the solution to approximately pH 2.5 with a few drops of 6 N hydrochloric acid (HCl). Do not allow the pH to fall below 2.0.

   Use 10% NaOH to back-titrate, if necessary.

9. Pass the pH-adjusted urine solution through a preparatory column that has been preconditioned with methanol and phosphate buffer as described in steps 1 to 4.

   A small piece of gauze placed on top of the C-18 column is recommended to prevent clogging of the column.

10. Allow the urine solution to drip by gravity through the column until flow stops (a slight vacuum may be used if the solution fails to flow or stops flowing). Alternatively, use the 10-ml syringe plunger to assist the flow.

    CAUTION: *Do not apply continuous pressure or vacuum to facilitate this process initially, as this may cause small amounts of porphyrins to pass through the column. Porphyrins are retained on the column, while potentially interfering fluorescent contaminants, such as riboflavin, pass through and can be discarded.*

    At this stage, porphyrins are retained at the top of the column along with some contaminants. If high concentrations of porphyrins are present, they are visible with the naked eye as a dark red band. Lower concentrations can be visualized using a hand-held UV light.

11. To facilitate separation of remaining contaminants, wash the column sequentially as follows:

    a. First with 10 ml of 10 mM sodium phosphate buffer, pH 3.5.
    b. Second with 40 ml of 35% HPLC grade methanol in 10 mM sodium phosphate buffer, pH 3.5.
    c. Third with 3 ml of 10 mM sodium phosphate buffer, pH 3.5.
    d. Finally with 10 ml of 10 mM sodium phosphate buffer, pH 7.5.

    This final wash adjusts the column for elution of porphyrins.

    The preceding four wash steps may be facilitated by use of a moderate vacuum.

12. Place a 13 × 100–mm glass culture tube under each column to collect porphyrins to be eluted in the following steps.

13. To elute porphyrins, first pass 1 ml of 100% methanol, followed by 2 ml of a mixture of 80% methanol/20% 10 mM sodium phosphate buffer, pH 7.5, through the column.

    The initial drops of 100% methanol may be pushed through the column using the 10-ml syringe plunger to facilitate gravity dripping.

14. When porphyrin elution is completed, place the culture tube containing the porphyrin solution into a 60°C water bath or heating block. Discard the preparatory column.

15. Evaporate the methanol/buffer eluant to complete dryness under nitrogen gas.

    This step is best accomplished in a hood by attaching a Pasteur pipet to the nitrogen tank by flexible tubing and directing a slow stream of nitrogen through the tip of the Pasteur pipet against the inside of the test tube just above the surface of the liquid/porphyrin solution. Multiple samples may be dried simultaneously using a manifold, as shown in Figure 8.9.4.

16. Following complete evaporation of the liquid, dissolve the dried residue in the bottom of the tube that contains the concentrated porphyrins in 500 µl of 1 N HCl. Let stand at least 5 min, then vortex briefly (3 to 5 sec) to ensure complete dissolution of porphyrins.

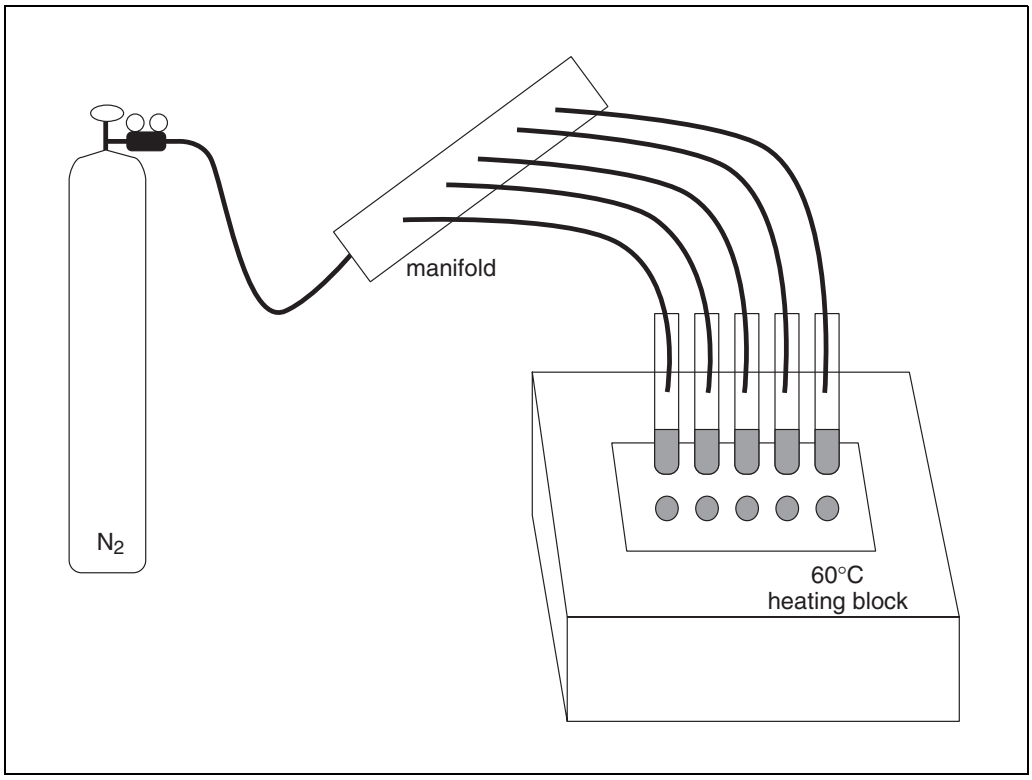

Figure 8.9.4 Setup for drying multiple samples using a manifold.

Up to 3 ml of HCl may be necessary to reconstitute the porphyrins if high concentrations are expected (such as when animals have been treated for prolonged periods with a porphyrinogenic drug or chemical).

17. Filter the reconstituted porphyrin solution through a 4-mm Millex-HV 0.45-µm membrane in order to remove small amounts of phosphate or other particulate matter that may have eluted with the porphyrins from the preparatory column and that could otherwise clog the HPLC injector system. Perform filtration in the following manner:

    a. Fit a 4-mm Millex-HV 0.45-µm membrane to a 1-ml plastic syringe with the plunger removed.

    CAUTION: *Larger filter sizes decrease percent recovery dramatically. Do not use nylon filters.*

    CAUTION: *Do not use nylon filters.*

    b. Using a 3-ml plastic pipet, transfer the reconstituted porphryin solution into the barrel of the syringe.

    c. Insert the plunger into the syringe and force the porphyrin solution through the attached 4-mm Millex-HV 0.45-µm membrane into an amber HPLC vial fitted with a 1.5-ml insert.

    Alternatively, any particulate matter can be removed by centrifugation for 10 min at 2000 × g. Centrifugation requires use of appropriate adaptors for the glass culture tubes to the centrifuge rotor employed.

18. Analyze solutions for porphyrin content (see Basic Protocol) or freeze at −20°C for up to 2 weeks prior to HPLC analysis.

Tissue and Fecal Porphyrin Extraction

Tissue or excreta porphyrin levels are of interest in the diagnosis of chemical effects on porphyrin metabolism and are also indicators of toxicant exposures. The following protocol may be employed as a relatively rapid and efficient method for porphyrin recovery from tissues as well as mammalian fecal or avian urofecal matter.

Materials

HPLC-grade acetonitrile
HPLC-grade distilled H_2O
Fecal (see Support Protocol 3) or tissue sample
1 N HCl
50:50 1 N HCl acetonitrile mixture
Nitrogen source

C-18 Bond Elute columns with 10-ml reservoirs (size 10 ml/250 mg; Varian) *or* C-18 Sep-Pac columns (Waters) and 10-ml plastic syringes to be used as column barrel
Vacuum manifold system: e.g., Baker SPE 10 vacuum extraction system *or* Millipore 1225 Sampling Manifold
Brinkman Power-Gen homogenizer (VWR) or equivalent
15-ml glass round-bottom centrifuge tubes, for homogenization
Beckman J2-27 or equivalent centrifuge
Adjustable pipettor (Gilson 5000-µl) and tips to fit *or* 10-ml serological pipets and electric pipettor (Drummond)
50-ml round bottom test tubes
32°C water bath or heating block
Glass 5¾-in. Pasteur pipets
50-ml glass round-bottom centrifuge tubes, for drying
4-mm Millex-HV 0.45-µm membrane filters (Millipore)
1-ml plastic syringe
10-ml plastic syringe plunger
Amber HPLC vials to fit autosampler used (e.g., 1-ml amber shell vials for 96-position autosampler tray) and 300- to 500-µl inserts with bottom springs (Alltech Associates or Waters)

Pretreat the C-18 preparatory columns

1. For each sample, prepare one C-18 Bond Elute preparatory column (or C-18 Sep-Pak cartridge fitted to a 10-ml plastic syringe barrel), as shown in Figure 8.9.3.
2. Fit the outflow end of each preparatory column into one of the openings of a vacuum manifold system (Fig. 8.9.3).
3. Pass 10 ml 100% HPLC-grade acetonitrile, followed by 15 ml HPLC-grade distilled water, through the column, under slight vacuum to facilitate flow.

   CAUTION: *Acetonitrile is flammable and a potential carcinogen. Work in a hood with safety glasses and protective gloves and clothing.*

4. Turn off the vacuum. Do not allow the cartridges to become dry.

Extract porphyrins from biological tissue or fecal matter

5. Working in a hood, place 0.1 to 0.2 g of tissue or fecal matter into a 15-ml round-bottom glass centrifuge tube containing 5 ml of a 50:50 mixture of 1 N hydrochloric acid (HCl) and concentrated acetonitrile.

6. Homogenize the tissue or fecal sample using a Power-Gen (or comparable) homogenizer.
7. Centrifuge the resulting homogenate 15 min at 3000 × *g*, 7°C, in a Beckman J2-27 or equivalent centrifuge.
8. Transfer 10 ml of the supernatant into a 100-ml beaker on ice, using a 10-ml serological pipet (or 5 ml twice with the 5000-µl pipettor).
9. Resuspend the pellet in an additional 6 ml of 50:50 1 N HCl acetonitrile mixture and vortex vigorously until the pellet is fully resuspended.
10. Centrifuge again for 15 min at 3000 × *g*, 7°C. Discard the pellet.
11. Combine the supernatant with the supernatant from the first spin in the 100-ml beaker.
12. Bring the total volume to 70 ml with HPLC-grade distilled water.
13. Pass the entire 70 ml of supernatant through a preparatory column that has been preconditioned with acetonitrile and water as described in steps 1 to 4.
14. Allow the supernatant to drip by gravity through the column until flow stops by continuously adding supernatant so that the liquid level remains above the top surface of the C-18 material, until the entire 70 ml of supernatant has passed through the column.

    A slight vacuum may be used to if the solution fails to flow or stops flowing. Do not apply pressure or continuous vacuum to facilitate this process initially, as this may cause small amounts of porphyrins to pass through the column.

15. When all of the extract has passed through the column, gently push (air purge) the excess solution through the cartridge using a 10-ml syringe plunger applied to the top of the column.
16. Dispose of the column eluate as hazardous waste.

    At this stage, porphyrins are retained at the top of the column along with some contaminants. If high concentrations of porphyrins are present, they are visible with the naked eye as a dark red band. Lower concentrations can be visualized using a hand-held UV light.

17. Place a 50-ml round-bottom test tube under each preparatory column and elute the porphyrins from the column into the test tube with 10 ml of acetonitrile.
18. When porphyrin elution is completed, place the test tube containing the acetonitrile-porphyrin solution into a 32°C water bath or heating plate and evaporate the acetonitrile to complete dryness under nitrogen gas.

    This step is best accomplished by attaching a Pasteur pipet to the nitrogen tank by flexible tubing and directing a slow stream of nitrogen through the tip of the Pasteur pipet against the inside of the test tube, just above the surface of the acetonitrile/porphyrin solution. Multiple samples may be dried simultaneously using a manifold, as shown in Figure 8.9.4.

19. Following complete evaporation of the acetonitrile, dissolve the dried concentrated porphyrins in the bottom of the tube in 500 µl of 1 N HCl. Let stand at least 5 min, then vortex briefly (3 to 5 sec) to ensure complete dissolution of the porphyrins.
20. Filter the reconstituted porphyrin solution through a 4-mm Millex-HV 0.45-µm membrane in order to remove small amounts of phosphate or other particulate matter that may have eluted with the porphyrins from the preparatory column and that could otherwise clog the HPLC injector system. Perform filtration in the following manner:

a. Fit a 4-mm Millex-HV 0.45-µm membrane to a 1-ml plastic syringe with the plunger removed.

CAUTION: *Larger filter sizes decrease percent recovery dramatically.*

CAUTION: *Do not use nylon filters.*

b. Using a 3-ml plastic pipet, transfer the reconstituted porphryin solution into the barrel of the syringe.

c. Insert the plunger into the syringe and force the porphyrin solution through the attached 4-mm Millex-HV 0.45-µm membrane into an amber HPLC vial fitted with a 1.5-ml insert.

Alternatively, any particulate matter can be removed by centrifugation for 10 min at 2000 × g. Centrifugation requires use of appropriate adaptors for the glass test tubes to the centrifuge rotor employed.

21. Analyze solutions for porphyrin content or freeze at −20°C for up to 2 weeks prior to HPLC analysis (see Basic Protocol).

Blood Porphyrin Extraction

SUPPORT PROTOCOL 7

Principal interest in blood porphyrins focuses on erythrocyte porphyrin measurements. Several methods for the analysis of erythrocyte porphyrins have been described. An extraction procedure that allows for analytical recoveries of protoporphyrin IX as well as zinc protoporphyrin IX is presented here. This procedure avoids extraction of porphyrins from the organic phase into aqueous HCl, thereby preventing conversion of Zn protoporphyrin to the free protoporphyrin IX.

Materials

Blood sample (see Support Protocol 4)
3:1 (v/v) ethyl acetate/glacial acetic acid containing 50 pmol mesoporphyrin IX (Porphyrin Products) as internal standard
Amber HPLC vials to fit autosampler used (e.g., 1-ml amber shell vials for 96-position autosampler tray) and 300- to 500-µl inserts with bottom springs (Alltech Associates or Waters)

1. Pipet 100 µl of whole blood into a microcentrifuge tube.
2. Working in a hood with protective clothing, gloves and safety glasses, add 300 µl of 3:1 ethyl acetate/acetic acid containing 50 pmol internal standard mesoporphyrin IX.
3. Vortex for 30 sec, then microcentrifuge 5 min at maximum speed.
4. Carefully remove the supernatant into an amber HPLC vial.
5. Analyze solutions for porphyrin content (see Basic Protocol) or freeze at −20°C for up to 2 weeks prior to HPLC analysis.

REAGENTS AND SOLUTIONS

Use Milli-Q-purified water or equivalent for all recipes and protocol steps. For common stock solutions, see ***APPENDIX 2A****; for suppliers, see* ***SUPPLIERS APPENDIX****.*

Sodium phosphate buffer, pH 3.5, 50 mM

Dissolve 6.9 g $NaH_2PO_4 \cdot H_2O$ in 1 liter of water. While stirring, adjust the pH to 3.5 with 20% (v/v) H_3PO_4 (phosphoric acid). Use 10% (w/v) NaOH to readjust the pH, if necessary. Store up to 1 month at 4°C.

Sodium phosphate buffer, pH 3.5, 10 mM

Dissolve 1.38 g $NaH_2PO_4 \cdot H_2O$ in 1 liter of water. While stirring, adjust the pH to 3.5 with 20% (v/v) H_3PO_4 (phosphoric acid). Use 10% (w/v) NaOH to readjust the pH, if necessary. Store up to 1 month at 4°C.

Sodium phosphate buffer, pH 7.5, 10 mM

Dissolve 1.38 g $NaH_2PO_4 \cdot H_2O$ in 1 liter of water. While stirring, adjust the pH to 7.5 with 10% (w/v) NaOH. Readjust to pH 7.5 using 20% (v/v) H_3PO_4 (phosphoric acid) if necessary. Store up to 1 month at 4°C.

COMMENTARY

Background Information

Chromatographic analytical techniques for measuring porphyrins in biological media were first developed to study porphyrins in urine, feces, and blood of patients with genetically inherited disorders of porphyrin metabolism (Nacht et al., 1970; *UNIT 8.1*). In more recent decades, numerous classes of drugs and environmental chemicals have been found to produce changes in tissue or excreta porphyrin levels (McColl and Moore, 1981; Maines, 1984; Marks, 1985; Woods, 1995), and HPLC techniques have evolved rapidly to accommodate the investigation of these effects (Ford et al., 1981; Scoble et al., 1981; Schreiber et al., 1983; Lim and Peters, 1984; Woods et al., 1984, 1991; Li et al., 1986; Kennedy and Maslen, 1989; Ho, 1990; Bowers et al., 1992a; Woods and Miller, 1993).

Although HPLC is a powerful technique for porphyrin separation and quantitation, the prechromatographic procedures employed in the extraction of porphyrins from biological media determine the accuracy of the total method to a large extent. Historically, extraction procedures involved the conversion of naturally occurring free porphyrin carboxylic acids to methyl esters, which were subsequently separated using normal-phase HPLC (Carlson and Dolphin, 1976; Seubert and Seubert, 1982). These procedures offered the advantage of increased stability and solubility in solution, but were tedious and time-consuming and often resulted in loss of porphyrins during the extraction and esterification procedures. Additionally, the esterification steps introduced problems such as incomplete and differential porphyrin esterification, as well as modification of vinyl side groups. In contrast, the use of procedures that permit the quantitative extraction of free porphyrins from biological media without esterification, as described in this unit, obviates many of these concerns and, additionally, allows analysis of porphyrins by the widely utilized and technically superior reversed-phase HPLC chromatographic columns employed today.

Free porphyrins, as well as the metalloporphyrin, zinc protoporphyrin, fluoresce intensely when irradiated with long-wave ultraviolet light. Hence, fluorescence detection is employed as a sensitive means for porphyrin quantitation. Detection of porphyrins is achieved by exciting at the wavelength of the Soret region, 390 to 410 nm, and measuring the emission at 600 to 630 nm. Each porphyrin responds maximally at slightly different excitation and emission wavelengths. Excellent results have been obtained in terms of the detection of all extracted porphyrins in biological substances using an excitation wavelength in the range of 395 to 400 nm and an emission wavelength of 620 nm (Woods et al., 1991; Bowers et al., 1992a,b; Woods and Miller, 1993). Spectrofluorometric analysis at these parameters permits the quantitative detection of 8- through 2-carboxyl porphyrins, as well as for zinc protoporphyrin, with a sensitivity to detect 0.5 pmol in the column effluent.

Critical Parameters

Porphyrins are subject to degradation by photo-oxidation. To protect porphyrins from photo-oxidation, use opaque or foil-wrapped collection bottles and store them in covered containers. Carry out all extraction procedures under reduced light, i.e., out of direct sunlight or fluorescent overhead lighting. Preferred lighting is >560 nm (5600 Å). Acrylic red or yellow sheaths/tubes guards are available that slip over fluorescent light tubes and can be cut to fit (Platt Electric Supply).

EDTA is added to prevent potential metal complexation of porphyrins. Care should be taken to use metal-free reagents to avoid introduction of metals into the porphyrin medium.

Do not freeze whole blood samples if erythrocyte porphyrin determinations are desired. Freezing will lyse the cells, making it impossi-

ble to separate erythrocyte porphyrins from those from other blood components.

In the urinary porphyrin extraction procedures, pH changes are used to maximize separation of porphyrins from fluorescent contaminants. A slightly alkaline pH during collection, storage, and centrifugation avoids porphyrin loss from oxidation and coprecipitation during centrifugation. Subsequently, the pH is lowered to ~2.5 just before application to the preparatory column to fully oxidize all reduced porphyrins (porphyrinogens) in the sample. A pH higher than 3.0 results in inconsistent binding to the C-18 preparatory column from one extraction procedure to another or between duplicate samples within the same trial. Undesirable contaminants are maximally removed from the preparatory column at pH 3.5. Caution must be exercized, since if the washing solution exceeds 35% methanol, porphyrins will be eluted from the C-18 packing material prematurely. Elution is highest at pH 7.5, so the last wash prepares the samples for elution into the collection tubes. Porphyrins precipitate out of solution at pH 4; therefore, samples must be kept above or below this pH value.

Urine samples should be slightly alkaline when centrifuged in step 2 to prevent coprecipitation of porphyrins out of solution. Usually, the sodium bicarbonate added as a preservative in the collection bottle (50 mg $NaHCO_3$ per 125-ml flask; 5 g $NaHCO_3$ per 2.5-liter amber bottle) is ample to achieve >pH 7.5. When samples are centrifuged, they should be at room temperature for maximum recovery. Ice-cold samples will have ~5% less recovery.

Sample solutions must pass through the preparatory columns slowly to be retained on the C-18 packing material; therefore, do not apply continuous pressure or vacuum to facilitate this process initially. If flow stops or fails to start, apply as little pressure as necessary to produce flow of 1 drop per sec.

Do not use nylon filters in the final porphyrin filtration step. Nylon completely retains porphyrins at low pH and partially at any pH. Increasing the Millex filter size also substantially reduces recovery. 4-mm filters decrease porphyrin recovery minimally, by ~3%.

Troubleshooting

During porphyrin extraction from tissues or excreta, sediment can build-up to such an extent that the solution will not pass through the preparatory column. If this occurs, precondition another column and pour the remaining sample into it. Continue with the wash steps. The flow usually improves after the first 35% methanol wash. After this is done there will be two columns that must be eluted into the same collection tube (6 ml total).

If the Millex syringe filters keep popping off the syringe when filtering the final porphyrin concentrate into the HPLC vial, too much pressure is being applied. If a filter plugs up, release pressure on the sample by pulling the plunger out half way, tip the syringe so the filter is up, remove the plugged filter and replace it with a new one, then continue to filter the remaining sample.

If no peaks or very small peaks are detected following injection of the porphyrin concentrate onto the analytical column, porphyrins could be present but undetectable due to a problem with the HPLC system. Check that the porphyrin standards can be detected. If even these are not apparent, the flow cell of the spectrofluorometric detector may be dirty. Try cleaning it per the manufacturer's instructions. On the other hand, the porphyrins can be lost during handling or in the extraction process. The most likely causes of this are incorrect collection or storage conditions (too much light, lack of refrigeration, or samples frozen in acidified state), or incorrectly made wash buffers (methanol higher than 35%, pH higher than 3.5). All aqueous buffers should be pH adjusted before organic solvents such as methanol are added.

Filter HPLC solvents and samples to remove particulates. Particulates can plug the HPLC pumping system and are very difficult to locate and remove. Degas the HPLC mobile phase solvents prior to use and sparge the reservoirs continuously with helium during analyses. If dissolved air is present in the solvents, it can come out of solution when the two solvents are combined in the HPLC mixing chamber and accumulate in the pump heads. Air is more compressible than the mobile phase liquids, so each stroke of the piston will deliver less solvent. As an air bubble grows, the gradient will deteriorate. Peaks may elute together, late, or not at all when this happens.

Change solvents and pressure gradually to protect the HPLC analytical column.

Abrupt solvent changes or high operating pressure can also damage the column. If the liquid that collects in the waste bottle becomes cloudy, high pressure may have forced C-18 packing material out of the column. In this case, the column must be replaced. Avoid getting air in the column. If air has built up in the pump heads or a solvent reservoir has inadvertently been allowed to run dry, disconnect the column

Table 8.9.2 Normal Values (Means ± SD) for Human Urinary Porphyrins (Bowers et al., 1992a)

Porphyrin	Amount detected	
	pmol/ml	μg/liter
Uroporphyrin	9.7 ± 5.7	8.4 ± 3.8
Heptaporphyrin	2.6 ± 2.4	2.0 ± 1.9
Hexaporphyrin	1.2 ± 0.3	0.9 ± 0.2
Pentaporphyrin	2.0 ± 1.0	1.4 ± 0.8
Coproporphyrin	61.1 ± 18.8	40.0 ± 13.5

Table 8.9.3 Normal Values (means ± SD) for Liver, Kidney, and Urine Porphyrins in the Male Fischer 344 Rat (Bowers et al., 1992a; Woods and Miller, 1993)[a]

Porphyrin	Liver (pmol/g)	Kidney (pmol/g)	Urine (pmol/24 hr)
Uro	1.9 ± 1.5	9.1 ± 1.5	373 ± 188
Hepta	2.8 ± 1.2	4.2 ± 1.8	211 ± 99
Hexa	0.2 ± 0.1	0.7 ± 0.3	68 ± 40
Penta	1.7 ± 1.5	6.0 ± 2.0	119 ± 76
Copro	44.5 ± 13.0	82.9 ± 3.2	1341 ± 280
Proto	4.2 ± 2.3	8.1 ± 3.2	0
Total	61.0 ± 14.3	107.5 ± 18.1	2112 ± 341

[a]Pay attention to strain, gender, and age variability (Bowers et al., 1992a).

while resolving the problem. Do not leave phosphate buffer in the column, as it will precipitate out and clog the column. Always flush the HPLC system by gradually, changing to 90% water/10% methanol for sufficient time—20 column volumes × flow (ml/min)—to thoroughly remove the phosphate buffer before changing to storage conditions (usually 100% methanol).

Apparently abnormally high uroporphyrin levels may be due to degradation of the C-18 packing material. This occurs when the silica packing material is subjected to pH <2.0, which results in degradative products from the C-18 HPLC column that coelute with uroporphyrin.

Drifting peak retention times are usually due to build-up of gas in pump heads. pH variations will also cause retention-time shifts.

Phosphate buffer precipitating in valves can cement moving parts together. Change phases gradually and flush thoroughly (20 columns volumes) with 50:50 methanol/H_2O after all runs to prevent phosphate buildup.

High back-pressure can be caused by blocked column frits. Try reversing the flow and flushing with methanol/H_2O or sonicating the frit to dislodge particles from the inlet frit. If the pressure remains high, replace the frit. High pressure can also mean it is time to change the HPLC guard column or the analytical column itself.

Poor separation of porphyrin peaks is mostly due to problems with the delivery of mobile phase solvents. Check for blocked frits, an empty helium gas tank, plugged check valves, leaks (often at a newly installed guard column) or air in the pump heads.

Anticipated Results

Tables 8.9.2 and 8.9.3 provide quantitative urinary and/or tissue porphyrin yields that have been achieved using the protocols described in this unit. Figure 8.9.2 presents anticipated chromatograms (HPLC elution profiles) of porphyrins extracted from various sources.

Time Considerations

Thirty tissue or urine samples can be effectively extracted in 1 day. Subsequently, each sample will require 33 min for HPLC analysis, once the HPLC is set up and equilibrated. Conversion of the output of the spectrofluorometric

detector to porphyrin concentrations (pmol/ml or other units) is readily accomplished using established computer software programs. The actual time will depend on the capabilities of the software available to the user.

Literature Cited

Bowers, M.A., Aicher, L.D., Davis, H.A., and Woods, J.S. 1992a. Quantitative determination of porphyrins in rat and human urine and evaluation of urinary porphyrin profiles during mercury and lead exposures. *J. Lab. Clin. Med*. 120:272-281.

Bowers, M.A., Luckhurst, C.L., Davis, H.A., and Woods, J.S. 1992b. Investigation of factors influencing urinary porphyrin excretion in rats: Strain, gender and age. *Fundam. Appl. Toxicol*. 19:538-544.

Carlson, R.E. and Dolphin, D. 1976. High pressure liquid chromatographic techniques for the separation of complex mixtures of occurring porphyrins naturally. *In* Porphyrins in Human Diseases (M. Doss, ed.) pp. 465-471. S. Karger, Basel.

Ford, R.E., Ou, C.N., and Ellefson, R.D. 1981. Liquid-chromatographic analysis for urinary porphyrins. *Clin. Chem*. 27:397-401.

Ho, J.W. 1990. Determination of porphyrins in human blood by high performance liquid chromatography. *J. Liq. Chromatogr*. 13:2179-2192.

Kennedy, S.W. and Maslen, A.L. 1989. Separation of porphyrin isomers by high-performance liquid chromatography. *J. Chromatogr*. 493:53-62.

Li, F., Lim, C.K.. and Peters, T.J. 1986. Analysis of urine and faecal porphyrins by HPLC coupled to an advanced automated sample processor. *Biomed. Chromatogr*. 1:94-95.

Lim, C.K. and Peters, T.J. 1984. Urine and faecal porphyrin profiles by reversed-phase high-performance liquid chromatography in the porphyrias. *Clin. Chim. Acta* 139:55-63.

Maines, M.D. 1984. New developments in the regulation of heme metabolism and their implications. *CRC Crit. Rev. Toxicol*. 12:241-314.

Marks, G.S. 1985. Exposure to toxic agents: The heme biosynthetic pathway and hemoproteins as indicator. *CRC Crit. Rev. Toxicol*. 15:151-179.

McColl, K.E.L. and Moore, R. 1981. The porphyrias. An example of pharmacogenetic disease. *Scott. Med. J*. 26:32-40.

Nacht, C., San Martin De Vaile, L.C., and Grinstein, M. 1970. Human porphyria cutanea tarda. Isolation and properties of the urinary porphyrins. *Clin. Chim. Acta* 27:445-452.

Schreiber, W.E., Raisys, V.A., and Labbe, R.F. 1983. Liquid-chromatographic profiles of urinary porphyrins. *Clin. Chem.* 29:527-530.

Scoble, H.A., McKeag, M., Brown, P.R., and Kavarnos, G.J. 1981. The rapid determination of erythrocyte porphyrins using reversed-phase high performance liquid chromatography. *Clin. Chim. Acta* 113:253-265.

Seubert, A. and Seubert. S. 1982. High-performance liquid chromatographic analysis of porphyrins and their isomers with radial compression columns. *Anal. Biochem.* 124:303-307.

Woods, J.S. 1995. Porphyrin metabolism as indicator of metal exposure and toxicity. *In* Handbook of Experimental Pharmacology: Toxicology of Metals-Biochemical Aspects, Vol. 115 (R.A. Goyer and M.G. Cherian, eds.) pp. 119-125. Springer-Verlag, Berlin.

Woods, J.S. and Miller, H.D. 1993. Quantitative measurement of porphyrins in biological tissues and evaluation of tissue porphyrins during toxicant exposures. *Fundam. Appl. Toxicol*. 21:291-297.

Woods, J.S., Eaton, D.L., and Lukins, C.B. 1984. Studies on porphyrin metabolism in the kidney. Effects of trace metals and glutathione on renal uroporphyrinogen decarboxlase. *Mol. Pharmacol.* 26:336-341.

Woods, J.S., Bowers, M.A., and Davis, H.A. 1991. Urinary porphyrin profiles as biomarkers of trace metal exposure and toxicity: studies on urinary porphyrin excretion patterns in rats during prolonged exposure to methyl mercury. *Toxicol. Appl. Pharmacol*. 110:464-476.

Key References

Bowers et al., 1992a. See above.

Contains detailed information on HPLC analysis of human and rat urinary porphyrins and describes the effects of prolonged lead and mercury exposure on urinary porphyrin excretion.

Bowers et al., 1992b. See above.

Describes the influence of age, sex, and strain on urinary porphyrin excretion in rats.

Martin, M.D., McCann, T., Naleway, C., Woods, J.S., Leroux, B.G., and Bollen, A-M. 1996. The validity of spot urine samples for low-level occupational mercury exposure assessment and relationship to porphyrin and creatinine excretion rates. *J. Pharmacol. Exp. Ther.* 277:239-244.

Describes diurnal variations in urinary excretion of porphyrins among men and women and establishes the validity of random ("spot") sampling for assessment of 24-hr porphyrin excretion rates.

Woods and Miller, 1993. See above.

Contains detailed information on HPLC analysis of tissue porphyrins and the effects of drug and metal treatments on liver and kidney porphyrin concentrations in rats.

Contributed by James S. Woods and
P. Lynne Simmonds
University of Washington
Seattle, Washington

CHAPTER 9
Heme Degradation Pathway

INTRODUCTION

The heme oxygenase (HO) system consists of three isozymes, members of the HSP32 family of oxidative stress–inducible proteins. Two, HO-1 and HO-2, are catalytically active and the third, HO-3, is marginally active. Unlike larger heat-shock proteins such as HSP70 and HSP90 that have chaperonin functions, HSP32 proteins catalyze degradation of the heme molecule. An overview of this degradative pathway is provided in *UNIT 9.1*.

Increased activity of HO isozymes can be used as an indication of exposure to oxidative stress. Catalytic activity of HO produces carbon monoxide (CO), biliverdin, and iron. To date there is no convenient method to detect iron release due to HO activity. For all practical purposes, however, the heme oxygenase system is the only biochemical system that produces CO and biliverdin; therefore, measurements of the formation of these compounds accurately reflect HO system activity. CO and biliverdin are produced in a 1:1 molar ratio, and experiments comparing production of the two compounds by in vitro reconstituted systems have shown good agreement in the molar quantities measured.

UNIT 9.2 describes the detection of CO production as an indication of HO activity. CO production can be measured directly by gas chromatography in cell- or tissue-expressed and purified preparations in vitro. It may also be measured in exhaled air, which can give a good indication of heme degradation activity of the organism. Instead of measuring biliverdin, it is more convenient to measure its reduction product bilirubin, which is produced in the next reaction in the heme degradation pathway, catalyzed by the enzyme biliverdin reductase.

UNIT 9.3 describes measurement of heme oxygenase activity by spectrophotometric analysis of bilirubin formation. There are other methods of measuring HO reaction products, including HPLC (*UNIT 9.6*). Because heme oxygenase isozymes are bound to the endoplasmic reticulum, isolated microsomal fractions can be used as the enzyme source, which reduces interference with the spectral analysis by other cellular constituents.

Measuring enzyme activity based on the formation of either CO or biliverdin/bilirubin does not distinguish the activities of HO-1 and HO-2. To estimate the relative contributions of the two proteins would require isozyme-specific inhibitors, which at this time are not readily available; metalloporphyrin inhibitors, which are commonly used to block HO activity, inhibit both isozymes. Fortunately, quite specific, non-cross-reacting antibodies to HO-1 (mono- and polyclonal) and HO-2 (polyclonal) are available commercially. A good estimate of the isozymes' relative contributions can therefore be obtained by immunoblotting, also described in *UNIT 9.3*. HO-1, HO-2, and HO-3 have been cloned and expressed as fusion proteins in *Escherichia coli*; a support protocol describes the purification of these fusion proteins for use in the assays or in other structure/function analyses. A second support protocol describes the isolation from tissues of microsomes that contain HO-1 and HO-2.

For studies of biliverdin reductase activity itself, *UNIT 9.4* describes an activity assay for detection of the enzyme at kinetic levels in either tissue extracts or cell extracts. (In

Contributed by Mahin D. Maines
Current Protocols in Toxicology (2003) 9.0.1-9.0.2

contrast, in HO activity assays using cell homogenates, biliverdin reductase is usually not rate limiting for heme degradation because it is present in most tissues in excess of HO isozymes, and moreover an excess is added to the assay system.) The reductase has two pH optima and preferentially uses a different cofactor at each. Using pH-specific buffers make it possible to measure the enzyme activity at both optima. A second method of measuring biliverdin reductase levels is immunoblotting using commercially available, highly specific, high-titer polyclonal antibodies to the reductase. Finally, detection of the multiple isoforms of biliverdin reductase (which exhibits extensive microheterogeneity in both molecular weight and isoelectric point) by two-dimensional gel electrophoresis is also described. This assay is significant because the isoform population may be affected by an organism's exposure to chemicals.

As described in *UNIT 9.5*, the tissue distribution pattern of heme degradation pathway enzymes can be visualized by histochemical analyses at both the transcript level (by in situ hybridization) and the protein level (by immunodetection). Histochemical methods are invaluable for discerning which cell populations express which isozyme of heme oxygenase. The methods are also useful for detecting populations of cells that respond to a stimulus by expressing an isozyme of heme oxygenase. At the tissue level, the response of heme oxygenase genes to various stimuli can be detected by northern blot hybridization and RT-PCR, which will be covered in future supplements.

As noted above, the products of heme oxygenase activity are amenable to measurement by various techniques. *UNIT 9.6* describes a recently developed method for measurement of HO activity by HPLC. The method measures both biliverdin and bilirubin simultaneously and can be used with different cell and tissue preparations.

As described in *UNIT 9.1*, HO-1 is the stress/heat shock–inducible form of heme oxygenase, and its increased expression is primarily due to transcriptional activation of the *ho-1* gene. HO-2 is the glucocorticoid-responsive isozyme; the response is at both the level of transcription and translation. *UNIT 9.7* describes methods for the assessing transcriptional activation of the *ho-1* gene by analyzing promoter activity in transient and stable transfection systems. Transient transfection is the method most commonly used and involves transfection of cells using reporter genes. Stable transfection of the *ho-1* promoter has also been used, usually when *ho-1* promoter exhibits less-than-satisfactory behavior in transient transfection assays. This unit also contains a method for purification of high-quality plasmid DNA for cell transfection. Induction of HO-1 gene expression is generally considered an indicator of cellular stress response. HO-1 gene expression can be assessed by RT-PCR when limited tissue is available yet a high degree of sensitivity is required. *UNIT 9.8* describes an RT-PCR technique for quantification of HO-1 mRNA.

A critical factor in the biophysical characterization of a protein is its availability in a purified form. Because heme oxygenase functions in diverse physiological processes, it is of importance to characterize the protein from a mechanistic and a structural aspect. *UNIT 9.9* focuses on the human HO-1 isoform and describes high-yield expression and purification, as well as spectrophotometric techniques utilized in physical characterization of the protein.

Additional units will describe methods for quantitation of HO-2 and biliverdin reductase in human tissue samples by RT-PCR.

Mahin D. Maines

Overview of Heme Degradation Pathway

Heme—also called iron (Fe)-protoporphyrin IX or hemin (Fig. 9.1.1)—can be degraded through several enzymatic and chemical mechanisms. In mammals, the most efficient pathway for enzymatic heme degradation involves the heme oxygenase (HO) system. HO enzymes oxidatively cleave heme's porphyrin ring, generating stoichiometric quantities of biliverdin (Fig. 9.1.1) and carbon monoxide (CO). Chelated Fe is also released during the cleavage reaction (reviewed in Maines, 1992).

In mammals (and certain species of fish), biliverdin—the green pyrrolic product of HO activity—is subsequently converted to bilirubin by the cytosolic enzyme biliverdin reductase (Kutty and Maines, 1981). Bilirubin is the yellow pigment found in bile (Fig. 9.1.1).

The reduction of biliverdin by the reductase is coupled to the oxidation of the pyridine nucleotide cofactors NADH and NADPH. BVR reductase is unique among all enzymes described to date in that it has two distinct pH optima, 6.7 and 8.6, and it uses a different cofactor at each pH (Kutty and Maines, 1981). NADH is used at the acidic pH and NADPH is used in the basic range. The enzyme is highly conserved in its primary structure and biochemical properties as revealed by molecular characterization of the proteins from human and rat (Fakhrai and Maines, 1992; Maines et al., 1996). Biliverdin reductase has been identified as a zinc metalloprotein (Maines et al., 1996), and the protein shows extensive microheterogeneity due to post-translational modification (Huang et al., 1989).

Two catalytically active forms of HO, HO-1 and HO-2 (Maines et al., 1986), have been fully characterized. Recently a third isoform was identified (McCoubrey et al., 1997a), but its contribution to physiological heme degradation is likely to be minimal, because its HO activity in the presence of heme is low.

Both enzymatic and chemical mechanisms for heme degradation require molecular oxygen (O_2) and a reducing agent to activate the O_2 and reduce the heme iron from Fe^{3+} to Fe^{2+} (or maintain the iron in the Fe^{2+} state). In the HO-catalyzed reaction, NADPH acts as the reducing agent. In chemically catalyzed reactions, sodium dithionite or ascorbate provide the reducing equivalent.

For both enzymatic and chemical reactions, activation of O_2 by the electron donor initiates the multistep process of oxidative cleavage of the methene carbon bridges (Sano et al., 1986; Liu et al., 1997). The chemical mechanism, also called coupled oxidation, can cleave any one of heme's four carbon bridges, the α, β, γ, and δ carbon bridges. Thus chemical degradation leads to the formation of all four isomers of biliverdin. Biliverdin isomers are distinguished by which methene bridge was cleaved: e.g., biliverdin IXα is formed as a result of cleavage at the α-carbon bridge.

When heme b is the substrate, HO cleaves the molecule specifically at the α-methene bridge and the carbon atom is subsequently released as CO. For each molecule of heme oxidized by the HO system, three molecules of O_2 and NADPH are used. HO is designated a mixed-function oxidase, because it generates one mole of H_2O for each mole of O_2 consumed in the reaction.

Cells also use other minor enzymatic pathways to degrade heme. For example, in the mitochondria of heart tissue, an NADH-dependent heme-degrading system cleaves the heme molecule at the α-methene carbon bridge (Kutty and Maines, 1987). Heme can also be degraded by proteins such as xanthine oxidase (XO) and NADPH–cytochrome P450 reductase in the presence of H_2O_2. In the XO- or P450-catalyzed reactions, however, the products of heme degradation are not biliverdin or CO, but a mixture of pyrrolic complexes. A comprehensive description of the various heme-degrading systems is provided in Maines (1992).

HO-1 and HO-2 are produced by two different genes. The isozymes share little similarity in amino acid composition or sequence, and their genes differ in their nucleotide sequence, transcript size and number, organization and structure, and chromosomal location (Shibahara et al., 1985; Müller et al., 1987; Rotenberg and Maines, 1990; Sun et al., 1990; McCoubrey et al., 1992, 1995; McCoubrey and Maines, 1994). In addition, the two isoforms differ in their cell type and tissue distribution (Maines, 1992).

Both HO-1 and HO-2 are single-copy genes; however, HO-1 protein is produced from a single transcript of ~1.8 kb, whereas HO-2 is produced from two or more different-sized mRNAs. Most tissues and cell types in mammalian species express at least two different-

Contributed by Mahin D. Maines

Current Protocols in Toxicology (1999) 9.1.1-9.1.5

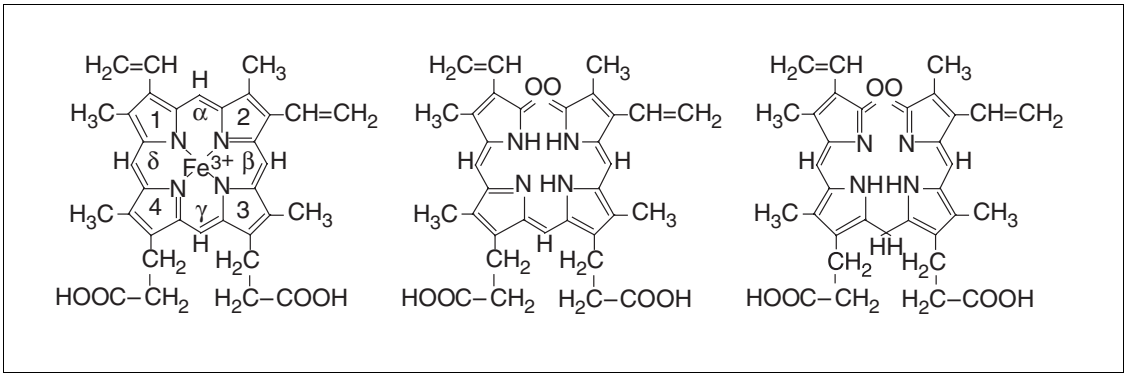

Figure 9.1.1 Chemical structures of heme (left), biliverdin (center), and bilirubin (right).

sized HO-2 transcripts, ~1.3 kb and ~1.7 to 1.9 kb. In the rat testis, however, five different transcripts for HO-2, ranging in size from ~1.3 to ~2.1 kb, have been identified. These transcripts show a developmentally regulated pattern of expression (McCoubrey et al., 1995). Different HO-2 transcripts arise from use of three different 5′ untranslated regions (UTRs) and two different polyadenylation signals (McCoubrey et al., 1992).

HO-1, also known as heat shock protein 32 (HSP32), was initially identified in 1974 as an enzyme that is induced by metals (Maines and Kappas, 1974). HO-1 expression is now known to be exquisitely sensitive not only to metals, but to all kinds of stimuli and agents that cause oxidative stress and pathological conditions, including heat shock, ischemia, glutathione depletion, radiation, hypoxia, hyperoxia, and cellular transformation and disease (Maines, 1992). In fact, no other enzyme studied to date is affected by as many diverse stimuli as is HO-1.

Induction of HO-1 by stress, such as heat shock, occurs in a coordinated fashion within different organs of an animal. The response is very rapid and fairly short-lived. For instance, in the heart, liver, kidneys, and brain of heat-shocked rats, HO-1 induction reaches its maximum in 1 hr, and the concentration of enzyme returns to normal ~6 hr after the stress (Maines, 1992).

HO-2, discovered in 1986 (Maines et al., 1986), is not induced by the factors that increase HO-1 expression (Trakshel et al., 1986a); HO-2 is responsive only to adrenal glucocorticoids (Weber et al., 1994). The consensus sequences necessary for binding regulatory factors—such as heat shock factors, AP-1 (activator protein-1), NF-κB (nuclear factor κB), and metal-dependent transcription factors—are present in the HO-1 gene promoter region (Müller et al., 1987; Alam et al., 1994), whereas the HO-2 gene contains only one functional glucocorticoid response element (GRE) consensus sequence (McCoubrey and Maines, 1994; Raju et al., 1997). Its GRE, however, is not a strong transcriptional promoter, and glucocorticoids exert a prominent regulatory effect on HO-2 expression at the protein level. At this time, it's not known whether glucocoticoids increase translation rate or protein turnover.

Total HO specific activity, which represents the sum of HO-1 and HO-2 activities, varies greatly among organs. The highest HO activity is usually found in the spleen, testes, and brain. In the brain and testes, HO-2 is the primary enzyme responsible for heme degradation. The spleen is the only organ in which HO-1 is the predominant HO isozyme under normal, unstressed conditions. The liver, however, displays an impressive level of HO-1 after exposure to oxidative stress.

As far as we know, HO-1 and HO-2 have similar catalytic mechanisms, substrate specificities, and cofactor requirements. The catalytic site of both enzymes consists of a conserved sequence of 24 amino acids that forms the "heme pocket" (Rotenberg and Maines, 1991). The heme pocket, which is hydrophobic and contains an essential histidine (McCoubrey et al., 1997b), recognizes the porphyrin ring of the metalloporphyrins but not the chelated metal. Therefore, various synthetic metalloporphyrins can bind to the heme pocket and prevent the natural substrate, Fe–protoporphyrin IX, from accessing the active site (Maines, 1981; Rublevskaya and Maines, 1994; McCoubrey et al., 1997b). Zn- and Sn-protoporphyrins have been used to inhibit heme degradation in clinical and laboratory settings (Vreman et al., 1993; Drummond et al., 1996). To a large degree such complexes are specific for HO isozymes, but they do not distinguish between HO-1 and HO-2. They can also affect nitric oxide (NO)

synthase and guanylyl cyclase activities. Metalloporphyrins can be used effectively to inhibit isolated purified protein preparations or to inhibit heme degradation altogether.

Recently an immunosuppressive peptide (D2702) has been identified as an effective inhibitor of HO-1 (Iyer et al., 1998). This peptide inhibits HO-1 in vivo and in vitro. The kinetics of its inhibition of HO-1 differ from its effects on HO-2, making the peptide a poor inhibitor of the latter isozyme. When using HO-1 inhibitors in vivo, however, it is important to note that inhibition is virtually always followed by a rebound induction at a later time point (Maines, 1984; Iyer et al., 1998).

Although major differences between HO-1 and HO-2 exist, each isozyme is evolutionarily conserved in its primary amino acid and nucleotide sequences. Therefore, antibodies and nucleotide probes can be used to study the proteins and genes from different species. HO-1 from rat, mouse, and human show >80% homology in their amino-acid sequences. For the HO-2 gene, the cDNA nucleotide sequence from rat, rabbit, and human is >90% homologous. Among the HO-1 and HO-2 proteins that have been sequenced, homology decreases to a mere 42% (Maines, 1992).

All of the products of HO activity are now suspected to be biologically active: CO, like NO, is thought to function as a signal molecule that regulates the generation of cGMP in biological systems (reviewed in Maines, 1997); Fe released by HO activity regulates the expression of genes, including the gene that encodes NO synthase; and biliverdin and bilirubin are both potent antioxidants (Stocker et al., 1987). In addition, the catalytic activity of the HO system plays a crucial role in maintaining homeostasis of cellular heme and hemoprotein levels (Maines, 1984, 1988); among the many hemoproteins and heme-activated enzymes are NO synthase, soluble guanylyl cyclase, and the cytochrome P450s.

In addition to its regular functions, HO-2 may have another, somewhat intriguing function: the protein may act as a cellular "heme or heme ligand sensor" (Maines, 1997; McCoubrey et al., 1997b). The 3′ UTR of HO-2 mRNA harbors two copies of a sequence 100% identical to the oxygen-sensing consensus sequence of erythropoietin, 5′-TTTTGCA-3′ (McCoubrey et al., 1992, 1997b). The sequence falls between the two poly(A) signals in the rat ~1.9-kb HO-2 transcript and in the equivalent ~1.7-kb transcript in humans. Moreover, in addition to its catalytic heme pocket, HO-2 possesses two additional high-affinity heme binding sites, called heme regulatory motifs (HRMs; McCoubrey et al, 1997a,b). Only seven cellular proteins identified to date contain HRMs (Rotenberg and Maines, 1991), including HO-2 and HO-3 (McCoubrey et al., 1997a). All HRMs have absolutely conserved cysteine-proline core residues. The cysteine residues of the HO-2 HRMs bind heme with high affinity but are not involved in heme catalysis. As a sensor, HO-2 may help regulate genes that are regulated by oxygen radicals, heme, or iron, including the ferritin, inducible NO synthase, and HO-1 genes. Also, by binding NO, HO-2 could function as an intracellular "sink" for NO.

Because HO-1 and HO-2 generate the same end products—biliverdin, CO, and Fe—measurement of any one of these products will reflect the combined activity of both isozymes. Detecting the activities of the individual isozymes is made even more difficult by the fact that both forms are present in all tissues examined to date, albeit in quite different proportions. Further, no inhibitors that are specific for one isozyme have yet been identified.

HO activity can be evaluated by measuring the generation of any one of the three different products of heme catalysis. For technical reasons, however, release of iron is seldom used to assess HO activity because this requires the use of radiolabeled Fe–protoporphyrin IX (heme).

Heme degradation by the HO isozymes requires the concerted activity of NADPH–cytochrome P450 reductase, which provides the reducing equivalents necessary for both the reduction of iron to the ferrous (Fe^{+2}) state (the form that binds oxygen) and the activation of molecular oxygen. The HO isozymes and the reductase colocalize to the endoplasmic reticulum. Therefore, the availability of the reductase can become limiting when measuring HO activity in tissues that have proportionally low concentrations of reductase and high concentrations of the HO isozymes, such as oxidatively stressed hepatic tissue or normal testis (Trakshel et al., 1986b).

Furthermore, other monooxygenase enzymes also rely on cytochrome P450 reductase to activate molecular oxygen using electrons provided by NADPH. Thus, the HO isozymes may have to compete with cytochrome P450 drug-metabolism systems for reducing equivalents. Awareness of the role of cofactors for HO activity becomes even more crucial when bilirubin is measured as the indicator of HO

activity. Biliverdin reductase, which must be present in such an assay system, also uses NADPH as a cofactor and has a rapid rate of reaction (Kutty and Maines, 1981). However, biliverdin reductase can also use NADH, whereas the HO system does not use NADH effectively.

Compounds that react with sulfhydryl groups, including metals such as Cd and Hg (Kutty and Maines, 1981; Maines, 1992), inhibit biliverdin reductase activity. Such inhibitors do not affect HO activity because HO-1 does not have any cysteine residues, and although HO-2 does contain cysteine residues, they are not involved in heme catalysis (McCoubrey et al., 1997b). Sulfhydryl reagents can inhibit overall heme degradation, however, by inhibiting biliverdin reductase. NADPH cytochrome P450 reductase is also inhibited by sulfhydryl reagents (Trakshel et al., 1986).

Immunoblotting can be used to assess the relative tissue concentrations of HO isozymes and their individual response to inducing agents. The two proteins have different predicted molecular weights: HO-1 is ~32 kDa and HO-2 is ~36 kDa. The commercially available antibodies to HO-1 and HO-2 do not cross-react and they have been used effectively for detecting individual HO isozymes by various analytical methods, including immunoblotting, immunohistochemistry, and radioimmunoassay (Sun et al., 1990; Ewing and Maines, 1992; Ewing et al., 1994).

LITERATURE CITED

Alam, J., Cai, J., and Smith, A. 1994. Isolation and characterization of the mouse heme oxygenase-1 gene. Distal 5′ sequences are required for induction by heme or heavy metals. *J. Biol. Chem.* 269:1001-1009.

Drummond, G.S., Valaes, T., and Kappas, A. 1996. Control of bilirubin production by synthetic heme analogs: Pharmacologic and toxicologic considerations. *J. Perinatol.* 16:S72-S79.

Ewing, J.F. and Maines, M.D. 1992. In situ hybridization and immunohistochemical localization of heme oxygenase-2 mRNA and protein in normal rat brain: Differential distribution of isozyme 1 and 2. *Mol. Cell. Neurosci.* 3:559-570.

Ewing, J.F., Raju, V.S., and Maines, M.D. 1994. Induction of heart heme oxygenase-1 (hsp32) by hyperthermia: Possible role in stress-mediated elevation of cyclic 3′:5′-guanosine monophosphate. *J. Pharmacol. Exp. Ther.* 271:408-414.

Fakhrai, H. and Maines, M.D. 1992. Expression and characterization of a cDNA for rat kidney biliverdin reductase: Evidence suggesting the liver and kidney enzymes are the same transcript product. *J. Biol. Chem.* 267:4023-4029.

Huang, T.J., Trakshel, G.M., and Maines, M.D. 1989. Detection of ten variants of biliverdin reductase in rat liver by two-dimensional gel electrophoresis. *J. Biol. Chem.* 264:7844-7849.

Iyer, S., Woo, J., Cornejo, M.-C., Gao, L., McCoubrey, W.K., Maines, M.D., and Buelow, R. 1998. Characterization and biological significance of immunosuppressive peptide D2702.75-84 (E>V) binding protein: Isolation of heme oxygenase-1. *J. Biol. Chem.* 273:2692-2697.

Liu, Y., Moenne-Locccoz, P., Loehr, T.M., and Ortiz de Montellano, P.R. 1997. Heme oxygenase-1 intermediates in verdoheme formation and the requirement for reduction equivalents. *J. Biol. Chem.* 272:6909-6917.

Kutty, R.K. and Maines, M.D. 1981. Purification and characterization of biliverdin reductase from the rat liver. *J. Biol. Chem.* 256:3956-3962.

Kutty, R.K. and Maines, M.D. 1987. Characterization of an NADPH-dependent haem-degrading system in ox heart mitochondria. *Biochem. J.* 246:467-474.

Maines, M.D. 1981. Zinc-protoporphyrin is a selective inhibitor of heme oxygenase activity in the neonatal rat. *Biochim. Biophys. Acta* 673:339-350.

Maines, M.D. 1984. New developments in the regulation of heme metabolism and their implications. *Crit. Rev. Toxicol.* 12:241-314.

Maines, M.D. 1988. Heme oxygenase: Function, multiplicity, regulatory mechanisms, and clinical applications. *FASEB J.* 2:2557-2568.

Maines, M.D. 1992. Heme Oxygenase: Clinical Applications and Functions. CRC Press, Boca Raton, Fla.

Maines, M.D. 1997. The heme oxygenase system: A regulator of second messenger gases. *Annu. Rev. Pharmacol. Toxicol.* 37:517-554.

Maines, M.D. and Kappas, A. 1974. Cobalt induction of hepatic heme oxygenase; with evidence that cytochrome P450 is not essential for this enzyme activity. *Proc. Natl. Acad. Sci. U.S.A.* 71:4293-4297.

Maines, M.D., Polevoda, B.V., Huang, T.J., and McCoubrey, W.K. 1996. Human biliverdin IXα reductase is a zinc-metalloprotein; Characterization of purified and *Escherichia coli* expressed enzymes. *Eur. J. Biochem.* 235:372-381.

Maines, M.D., Trakshel, G.M., and Kutty, R.K. 1986. Characterization of two constitutive forms of rat liver microsomal heme oxygenase: Only one molecular species of the enzyme is inducible. *J. Biol. Chem.* 261:411-419.

McCoubrey, W.K., Jr. and Maines, M.D. 1994. The structure, organization, and differential expression of the gene encoding rat heme oxygenase-2. *Gene* 139:155-161.

McCoubrey, W.K., Ewing, J.F., and Maines, M.D. 1992. Human heme oxygenase: Characterization and expression of a full length cDNA and evidence suggesting the two HO-2 transcripts differ by choice of polyadenylation signal. *Arch. Biochem. Biophys.* 295:13-20.

McCoubrey, W.K., Eke, B., and Maines, M.D. 1995. Multiple transcripts encoding HO-2 in rat testis: Developmental and cell specific regulation of transcripts and protein. *Biol. Reprod.* 53:1330-1338.

McCoubrey, W.K., Huang, T.J., and Maines, M.D. 1997a. Isolation and characterization of a cDNA from the rat brain that encodes hemoprotein heme oxygenase-3. *Eur. J. Biochem.* 247:725-732.

McCoubrey, W.K., Huang, T.J., and Maines, M.D. 1997b. Heme oxygenase-2 is a hemoprotein and binds heme through heme regulatory motifs that are not involved in heme catalysis. *J. Biol. Chem.* 272:12568-12574.

Müller, R.M., Taguchi, H., and Shibahara, S. 1987. Nucleotide sequence and organization of the rat heme oxygenase gene. *J. Biol. Chem.* 262:6795-6802.

Raju, V.S., McCoubrey, W.K., Jr., and Maines, M.D. 1997. Regulation of heme oxygenase-2 mRNA and protein by glucocorticoids: Characterization of a functional GRE. *Biochim. Biophys. Acta* 1351:89-104.

Rotenberg, M.O. and Maines, M.D. 1990. Isolation, characterization, and expression in *Escherichia coli* of a cDNA encoding rat heme oxygenase-2. *J. Biol. Chem.* 265: 7501-7506.

Rotenberg, M.O. and Maines, M.D. 1991. Characterization of a cDNA encoding rabbit brain heme oxygenase-2 and identification of a conserved domain among mammalian heme oxygenase isozymes: Possible heme binding site? *Arch. Biochem. Biophys.* 290:336-344.

Rublevskaya, I.N. and Maines, M.D. 1994. Interaction of Fe-protoporphyrin IX and heme analogues with purified recombinant heme oxygenase-2, the constitutive isozyme of the brain and testes. *J. Biol. Chem.* 269:26390-26395.

Sano, S., Sano, T., Morishima, I., Shiro, Y., and Maeda, Y. 1986. On the mechanism of the chemical and enzymatic oxygenation of α oxyprotohemin IX to Fe-biliverdin IXα. *Proc. Natl. Acad. Sci. U.S.A.* 83:531-535.

Shibahara, S., Müller, R., Taguchi, H., and Yoshida, T. 1985. Cloning and expression of cDNA for rat heme oxygenase. *Proc. Natl. Acad. Sci. U.S.A.* 82:7865-7869.

Stocker, P., Yamamoto, Y., McDonach, A.F., Glazer, A.N., and Ames, B.N. 1987. Bilirubin is an antioxidant of possible physiological importance. *Science* 235:1043-1047.

Sun, Y., Rotenberg, M.O., and Maines, M.D. 1990. Developmental expression of heme oxygenase isozymes in rat brain: Two HO-2 mRNAs are detected. *J. Biol. Chem.* 265:8212-8217.

Trakshel, G.M., Kutty, R.K., and Maines, M.D. 1986a. Purification and characterization of the major constitutive form of testicular heme oxygenase: The non-inducible isoform. *J. Biol. Chem.* 261:11131-11137.

Trakshel, G.M., Kutty, R.K., and Maines, M.D. 1986b. Cadmium-mediated inhibition of testicular heme oxygenase activity: The role of NADPH-cytochrome *c* (P450) reductase. *Arch. Biochem. Biophys.* 251:175-187.

Vreman, H.J., Ekstrand, B.C., and Stevenson, D.K. 1993. Selection of metalloporphyrin heme oxygenase inhibitors based on potency and photoreactivity. *Pediatr. Res.* 33:195-200.

Weber, C.M., Eke, B.C., and Maines, M.D 1994. Corticosterone regulates heme oxygenase-2 and NO synthase transcription and protein expression in rat brain. *J. Neurochem.* 63:953-962.

Contributed by Mahin D. Maines
University of Rochester School of Medicine
Rochester, New York

Detection of Heme Oxygenase Activity by Measurement of CO

BASIC PROTOCOL

Heme oxygenase (HO, E.C. 1.14.99.3) is the first and rate-limiting enzyme in the heme degradation pathway. In the presence of NADPH–cytochrome P-450 reductase, HO catalyzes the following reaction, producing equimolar amounts of carbon monoxide (CO) and biliverdin:

$$\text{hemin (ferriprotoporphyrin IX)} + 6\text{NADPH} + 3\text{O}_2 \rightarrow \text{biliverdin} + \text{CO} + \text{Fe}^{3+} + 3\text{H}_2\text{O} + 3\text{NADP}^+$$

The biliverdin is immediately reduced to bilirubin, the pigment associated with jaundice. HO exists as two active isozymes, the inducible HO-1 and the constitutive HO-2. A third isozyme (HO-3) is ~90% identical to HO-2 in its amino-acid sequence but shows little HO activity (McCoubrey et al., 1997).

HO activity can be assayed by several methods, most of which rely on measurements of the rate of product formation. Bilirubin formation can be monitored in purified microsomal preparations by a coupled enzyme reaction using biliverdin reductase (see *UNIT 9.3*). Such assays require labor-intensive sample preparation and involve spectrophotometric quantification of the bilirubin formed in the aqueous phase or extracted into an organic phase.

A more direct procedure, described in this unit, involves the quantification, by gas chromatography, of HO-generated CO. This method is specific, sensitive, reproducible, and simple. CO determination can be used to study HO activity in all types of tissue at various stages of tissue fractionation and in tissue slices. The assay is also useful for studying, in vitro, the effects of various HO inhibitors, including the highly colored metalloporphyrin derivatives of heme.

HO activity in preparations from animal or plant tissue can be determined by measuring the production of CO. The protocol described in this unit measures the CO produced in a sealed reaction vial following the interaction of HO in a tissue preparation with hemin and NADPH.

Tissue homogenates are centrifuged at 13,000 × *g* and the supernatants (or other fractions purified to a greater or lesser extent) are incubated for 15 min at 37°C with 50 µM methemalbumin as substrate in the absence (blank) or presence (total) of NADPH in septum-sealed, CO-free vials. The reaction is terminated by quick-freezing samples to –78°C. The CO thus produced diffuses into the headspace of the reactor, where it can be quantified by gas chromatography (GC) on a molecular-sieve column with a reduction gas detector.

HO activity is expressed as nanomoles of CO produced per hour per milligram of protein. The method allows analysis of as little as 2 µl of rat tissue homogenate (20% w/v), prepared from 0.4 mg of liver (~40 µg total protein), for example. The assay measures the CO produced by all HO isozymes present in the sample.

When analyzing a large number of samples in 1 day, having two analysts work in conjunction can increase the sample throughput rate to up to ~300 vials per day. One analyst can isolate the tissues, perform the HO assays, and determine the amount of protein in the samples, while the other processes the tissues, prepares the samples, calibrates the instrument, and analyzes the CO content of the samples.

Contributed by Hendrik J. Vreman and David K. Stevenson

Current Protocols in Toxicology (1999) 9.2.1-9.2.10

NOTE: Because CO can be produced through photooxidative reactions between organic molecules in the samples and endogenous (e.g., riboflavin) or exogenous photooxidizers (e.g., metalloporphyrins), it is important that the steps involving CO generation and quantification be performed under conditions of reduced light.

Materials

Tissue or cell samples
0.1 M potassium phosphate, pH 7.4 (*APPENDIX 2A*)
0.9% (w/v) NaCl (optional, *APPENDIX 2A*)
HO substrate (see recipe)
4.5 mM NADPH (see recipe)
NADPH–cytochrome P-450 reductase (optional)
Anhydrous magnesium perchlorate (anhydrone; Fisher)
GC calibration gas: 10.8 µl CO/liter air (Scott Specialty Gases)
CO gas, 99.9% pure (e.g., Matheson Gas Products), optional

12 × 32–mm amber vials with polypropylene screw caps fitted with septa (e.g., Alltech Associates)
Vial racks (e.g., Fisher or equivalent)
Hamilton gas-tight syringe with repeating dispenser
2.5-mm-thick blue silicone sheets (Alltech Associates), for use in making septa
Hopcalite (CuO/MnO) catalytic converter (Trace Analytical)
Vial-purging assembly (see Fig. 9.2.1A)
Headspace-sampling assembly (see Fig. 9.2.1B)
0.0625-in. (1.59-mm) o.d. sleeve connector
18-G side-port needles, 5 and 7 cm
68 × 0.53–cm (i.d.) stainless steel column
40- to 60-mesh molecular sieve, 13X (Alltech Associates)
Gas-flow meter (J & W Scientific)
Gas-chromatograph system with reduction gas detector (Trace Analytical)
Sample injection valve with Model 451 Recycling Intervalometer (Gralab Instruments Division)
Recorder: 10-mV recorder (Linear Instrument) or integrating recorder (e.g., CR-3A, Shimadzu Scientific Instruments)
20-G side-port needle.

Additional reagents and equipment for determination of protein concentration (*APPENDIX 3*)

Prepare sample

1. Collect tissues or cells and rinse with ice-cold 0.1 M potassium phosphate, pH 7.4, or 0.9% NaCl. Keep tissue on ice.

   Whenever possible, flush or blanch tissue in situ or immediately after removal to eliminate circulating hemoglobin (a potential source of substrate). The assay can be performed on any cell or tissue type.

2. Homogenize fresh tissue in 4 vol ice-cold 0.1 M potassium phosphate (or 9 vol potassium phosphate for tissue with high levels of HO activity, e.g., spleen). Transfer tissue homogenates into microcentrifuge tubes.

3. Centrifuge homogenate 1 min at 13,000 × *g*, 4°C.

   A minimum of 100 µl of supernatant is needed for the assay, so prepare at least 200 µl of homogenate. The assay may be performed on crude enzyme preparations or on HO enzymes purified from specific subcellular compartments, e.g., from nuclear, mitochrondrial, microsomal, or soluble fractions. Purified isozymes can also be used.

4. Aspirate and discard any lipid from the supernatant surface. Transfer supernatant to a clean microcentrifuge tube without disturbing pellet.

5. Remove an aliquot of supernatant for determination of protein concentration.

Perform HO reaction

6. For each sample, assemble a set of five reaction vials into a rack. Label three vials "total" and the other two "blank."

   Total CO production (from HO activity and other sources) will be measured from the vials labeled "total," and the blanks will be used to measure any CO generated by non-HO activity.

   For conveniently handling large numbers of reaction vials, use commercially available 102-peg racks with 5 × 16 pegs, modified by shortening the pegs from 45 mm to 22 mm. These racks are also useful for storing clean vials.

7. Using 1.0-ml Hamilton syringes with repeating dispensers, add to all sample vials 20 µl HO substrate and 20 µl tissue preparation (from step 4). To the total samples, add 20 µl NADPH; to the blank samples, add 20 µl 0.1 M potassium phosphate, pH 7.4.

   Reactants should be pipetted in a manner that will prevent cross contamination: i.e., pipet substrate onto the bottom of the vial, tissue preparation onto the vial wall close to the bottom, and NADPH and buffer onto the wall just above the tissue preparation.

   The production of CO also requires the presence of NADPH–cytochrome P-450 reductase. This enzyme should be added when using highly purified tissue preparations from organs that have small amounts of reductase activity (e.g., brain or heart), or when reductase inhibitors are included in the reaction medium.

8. Seal vials with septum-fitted screw caps and mix liquids by swirling rack.

   Septa (8 mm diameter) are cut from 2.5-mm-thick, high-temperature blue silicone sheets (Alltech Associates).

9. Transfer rack to water bath and incubate 5 min at 37°C.

10. Prepare CO-free air by passing compressed air through a Hopcalite catalytic converter (see Fig. 9.2.1A).

11. Purge each vial for 2 sec with CO-free air at a flow rate of 200 to 300 ml/min using the vial-purging assembly (t = 0 min).

    If caps are wetted with distilled water prior to purging, the vial-purging assembly will penetrate the septa more smoothly (see Fig. 9.2.1A).

12. Incubate samples an additional 15 min at 37°C (t = 15 min). Remove vials from the water bath in the same sequence and at the same rate that they were purged. Dry vials with a towel and place them into a rack set in crushed dry ice.

13. Cover vials with a black plastic sheet and analyze headspace gas for CO as soon as possible.

    The septum material produces small amounts of CO at ambient temperatures, but the production rate is negligible at −78°C.

Quantify CO

14. Confirm that the GC injection-valve controller, detector, and recorder are functioning properly. Check and record carrier flow rate, column temperature, detector settings, and recorder settings. Verify that the carrier gas flow rate is ~30 ml/min and column temperature is 140°C.

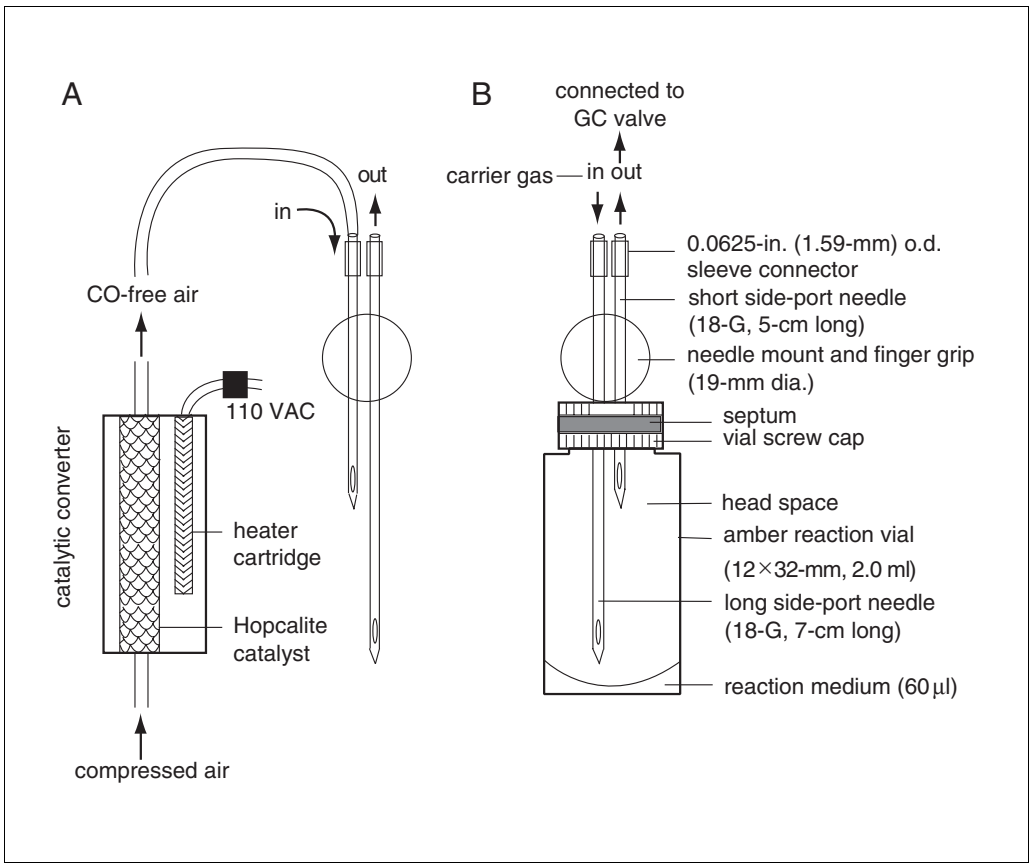

Figure 9.2.1 Double-needle assemblies for vial purging (**A**) or headspace sampling (**B**). The assemblies are identical except for the direction of the gas flow through the needles. (**A**) Compressed air is passed through a heated (~120°C) catalytic converter containing Hopcalite (CuO/MnO) catalyst. The catalyst oxidizes any CO to CO_2. The resulting CO-free gas is used to purge the headspace of the reaction vial just prior to incubation. When the assembly is removed from the vial after purging, the vial pressure will equilibrate to atmospheric pressure via the long needle after the shorter purging gas–inlet needle has been withdrawn. (**B**) The long needle introduces carrier gas into the vial and the short needle serves as an outlet. Such an arrangement will prevent vial liquid from being forced into the injection valve by the flow of carrier gas.

The ten-port pneumatic sample injection valve, fitted with a headspace-sampling assembly (Fig. 9.2.1B), injects the gas sample through a water-vapor trap filled with anhydrous magnesium perchlorate (Fisher), onto the 68 × 0.53–cm (i.d.) stainless steel column packed with 40- to 60-mesh molecular sieve 13X (Alltech Associates). The carrier gas flows through the column at a rate of ~30 ml/min to separate the vial gases on the basis of molecular size. The carrier gas then transports the reactor gas to the detector.

Under these operating conditions, the elution time for CO is ~90 sec, and as little as 1 pmol of CO is detectable. A 10-mV recorder can be used to chart the detector response (peak height) at a speed of 20 cm/hr. Integrating recorders are more efficient and convenient for determining CO peak areas accurately and rapidly.

15. Attach a clean, septum-fitted, capped vial to the headspace-sampling assembly (Fig. 9.2.1B) and turn on the valve controller to initiate the cycling of the valve between the injection phase (15 sec) and analysis phase (90 sec). Release carrier gas by puncturing the septum with a 20-G side-port needle.

Injection of the vial headspace gas onto the GC column will purge the vial of CO but will also leave the vial pressurized with carrier gas. This pressure must be released before standard gas is added to the vial.

16. Prepare a standard curve by injecting into the depressurized vial, one at a time, aliquots of 50, 100, 150, 200, and 250 µl standard gas (representing ~24, 48, 72, 96, and 120 pmol CO, respectively).

    If CO production is expected to be very high, greater volumes (up to 1000 µl) of CO standard gas may be introduced. However, with most GC systems, the standard curve ceases to be linear for quantities of CO >120 pmol. Higher quantities can be determined quite accurately through interpolation.

    Standard gas may be purchased or can be prepared by mixing 20 µl pure CO gas (99.9%; e.g., Matheson Gas Products) with 1000 µl of CO-free gas in a 1000-µl Hamilton acrylic syringe sealed with a septum fitted into an 18-G needle hub without the needle. The CO concentration in the syringe should remain stable for ~8 hr.

17. Plot the detector response (peak area, mV·sec) against pmol CO injected. Calculate the slope, in pmol CO per mV·sec.

    The plot for detector response should be linear from the origin up to 120 pmol.

18. Attach each HO reaction vial to the headspace-sampling assembly during the analysis phase of the previously injected sample. Record the detector response to CO as the area under the CO peak (retention time of ~0.7 min), expressed in mV·sec.

    If numerous samples are to be analyzed, check the slope of the standard curve hourly by injecting 250 µl CO standard gas into a CO-free depressurized vial. Compare with the peak area determined during the preparation of the initial standard curve.

19. Record data. Calculate the mean peak heights for total and blank samples during the analysis phase.

20. Measure protein content of processed tissue samples.

    HO activity can be expressed or normalized in several ways. The most widely accepted practice involves expressing activity as nanomoles of product formed (in this case CO) per hour per milligram protein. Thus determination of HO activity requires measurement of the protein concentration of the sample.

    Many protein determination methods can be used. Each methodology has its own sets of advantages and disadvantages and not all yield the same values for a given tissue preparation. The authors use the Lowry method (Lowry et al., 1951) because of its widespread use and sensitivity.

Calculate HO activity

21. Calculate HO activity as follows:

$$\text{HO activity (nmol/ hr/ mg protein)} = \text{total} - \text{blank (pmol CO)} \times \frac{\text{nmol}}{1000\ \text{pmol}} \times \frac{60\ \text{min/ hr}}{15\ \text{min}} \times \frac{\text{ml prep}}{\text{mg protein}} \times \frac{1}{0.02\ \text{ml prep}}$$

    The factor 15 min is the reaction time. In some instances, HO activity may be more appropriately expressed in terms of activity per unit (mg) fresh weight of tissue. Normalization of activity on the basis of fresh weight may be preferred, for example, when working with intact tissue slices, cells, and preparations with widely varying concentrations of HO-inactive protein. In such cases, calculate HO activity according to the following equation:

$$\text{HO activity (nmol/ hr/ mg fresh tissue)} = \text{total} - \text{blank (pmol CO)} \times \frac{\text{nmol}}{1000\ \text{pmol}} \times \frac{60\ \text{min/ hr}}{15\ \text{min}} \times \frac{\text{ml prep}}{\text{mg fresh tissue}} \times \frac{1}{0.02\ \text{ml prep}}$$

REAGENTS AND SOLUTIONS

Use Milli-Q-purified water or equivalent for all recipes and protocol steps. For common stock solutions, see ***APPENDIX 2A****; for suppliers, see* ***SUPPLIERS APPENDIX****.*

HO substrate (150 μM heme/15 μM albumin)

Dilute 1 vol of 1.5 mM heme/0.15 mM albumin methemalbumin (see recipe) with 9 vol of 0.1 M potassium phosphate, pH 7.4 (*APPENDIX 2A*). Prepare fresh daily.

Methemalbumin, 1.5 mM heme/0.15 mM albumin

Dissolve 9.9 mg hemin (Sigma) in 2.5 ml of 0.4 M Na_3PO_4. Add H_2O to 8 ml and dissolve 100 mg of bovine serum albumin (A7030, Sigma). Gradually adjust to pH 7.4 using 1.0 N HCl (~0.75 ml) in a 1-ml gas-tight Hamilton syringe with a repeating dispenser while stirring vigorously. Add H_2O to 10.0 ml. Store up to 14 days at 4°C.

NADPH, 4.5 mM

4.3 mg β-nicotinamide adenine dinucleotide phosphate, reduced form (Na_4NADPH; Sigma)
1.0 ml 0.1 M potassium phosphate, pH 7.4
Prepare fresh daily

COMMENTARY

Background Information

Heme oxygenase plays an important role in homeostasis in cells and tissues. Not only does the enzyme play a key role in the degradation of heme (Maines, 1992), but it also produces CO, a gas with potential physiologically activity. Like nitric oxide, CO has been shown to modulate cyclic guanosine 5′-monoposphate concentrations (Maines, 1997). Furthermore, bilirubin, a prominent end product of the heme degradation pathway, has been shown to possess significant antioxidant properties, particularly in neonates just after birth (Dennery et al., 1995). Finally, HO has been shown to be a heat-shock protein and to respond to oxidative stress (Maines, 1997). Although activation of HO during heat shock or oxidative stress is being examined through measurements of HO gene transcription (mRNA) and translation (HO protein), it will be of interest to determine whether gene regulation and protein production also modulate HO activity. Thus, HO activity measurements are becoming increasingly relevant and important.

Several methods for the determination of HO activity in animal tissues have been described. The most commonly used method measures spectrophotometrically the amount of bilirubin produced by the sequential reactions of HO and biliverdin reductase in reconstituted microsomal preparations (Tenhunen et al., 1968; Tenhunen, 1972; Maines, et al., 1977). The use of a linked, multienzyme assay for the determination of HO presents difficulties for both experimental design and interpretation of results (Lodola et al., 1979). First, sample preparation and activity measurements are time consuming. Second, the spectrophotometric technique for the determination of the bilirubin produced requires a low absorptivity, transparent sample matrix, and an excess of biliverdin reductase. Furthermore, the molar extinction coefficient for bilirubin needed for the calculation of HO activity depends on the reaction matrix (aqueous or organic), and must be determined for each tissue preparation if accuracy is to be achieved (Tenhunen et al., 1968).

A different and more direct HO assay was first described by Cavallin-Stahl et al. (1978) using methodology initially developed for the determination of CO in blood. This method, which was subsequently modified by Sunderman et al. (1982), does not require biliverdin reductase and measures the CO produced from the oxidation of heme to biliverdin by HO. CO is trapped with added hemoglobin and is subsequently released into the headspace of a second reaction vessel by the action of potassium ferricyanide [$K_3Fe(CN)_6$]. The CO in the headspace is then reduced to methane and quantified by GC. HO activity measurements using the GC method are reported to correlate well with those of the spectrophotometric assay (Vreman et al., 1988).

The protocol presented in this unit provides a simpler, more sensitive, and better integrated method by omitting the trapping step. Instead, CO is measured directly from the reaction vial headspace by a reduction gas detector (Vreman et al., 1984; Vreman and Stevenson, 1988). The

detector can specifically measure trace levels (parts per billion or pmol) of reducing gases—i.e., those that are capable of combining with oxygen (O_2), including CO and hydrogen (H_2).

When directed through a heated bed of mercuric oxide (HgO), gases such as CO undergo the following reaction:

$$HgO + CO \xrightarrow{270°C} CO_2 + Hg \uparrow$$

The amount of mercury vapor produced during this reactions is directly proportional to the inlet CO concentration. It is detected by means of an ultraviolet light photometer located immediately downstream from the reaction bed. The high molar ultraviolet light absorption coefficient gives this detector its unusual sensitivity.

Further, because CO is the only gas generated, in equimolar quantities, from the degradation of heme to biliverdin or bilirubin in the presence of NADPH and O2 (Vreman et al., 1988), use of the reduction gas detector makes this assay specific for the detection of HO activity.

The procedure is rapid, simple, specific, and accurate. It permits the measurement of HO activity in an unlimited variety of tissue extracts and tissue slices (Meffert et al., 1994). Because no direct spectrophotometric measurements of HO reaction products are involved, highly colored or photosensitizing inhibitors, such as metalloporphyrins, can be studied using this method (Vreman et al., 1993). The original method (Vreman and Stevenson, 1988) involved using 20 µl of undiluted methemalbumin (2 mM heme/0.15 mM albumin) to yield a final reaction concentration of 800 µM heme. This concentration is much higher than that used for spectrophotometric methods (<100 µM). Because HO inhibition is competitive in nature, the authors have subsequently decreased the heme concentration to 50 µM; this change enabled the method to be more responsive to HO inhibitor studies.

Critical Parameters

This protocol is used to accurately detect and measure trace amounts of an odorless and invisible gas (Vreman and Stevenson, 1988). The handling and quantification of gases present unique problems in the laboratory. It is important to recognize that gas molecules are compressible, small, and mobile through Brownian motion. All these factors can promote rapid loss through the inappropriate handling of samples. The protocol describes the dispensing of gas with syringes open to the atmosphere. This technique works well, but must be completed as quickly as possible.

It is also important to recognize issues related to the permeability of gases through materials with relatively open molecular structure, including plastics such as polyethylene or polypropylene (in contrast to glass). Thus the composition of vessels used in the procedure may also play a role in CO losses. Furthermore, some organic materials (including some plastics, silicone, and rubber; see Levitt et al., 1995) may spontaneously produce CO at ambient temperatures or in the presence of light. This could contribute to falsely elevated assay results. Most problems of this nature can be kept to a minimum by keeping assay vials cool and dark, running appropriate blank controls, and by completing analyses as rapidly as possible.

HO activity in tissue samples may not remain stable. Stability varies from preparation to preparation. Timely assay of tissue preparations is important for reproducible and accurate results.

The GC system has great sensitivity towards CO, which readily passes through it. However, a large number of other, mostly organic, molecules can be retained on the molecular sieve column and can thereby affect its molecular separating characteristics or reduce the HgO in the reaction bed. Thus, it is important to keep the headspace gas as simple as possible by using, besides air, only inert gases such as nitrogen (N_2) and O_2 if the gaseous phase of the HO reaction needs to be altered. The use of organic solvent solutions for reactants (e.g., DMSO or pyridine) should be avoided or carefully researched in advance. Call Trace Analytical Customer Service (650-364-6895) with any questions about system compatibility. The system is absolutely and totally incompatible with the use of volatile halogenated hydrocarbons (e.g., chloroform and some anesthetics).

Some processes, such as photooxidation (Vreman et al., 1990a) or lipid peroxidation (Vreman et al., 1998), could contribute to CO generation in reaction vials. However, analysis of a blank reaction mixture will correct for these possible sources of error.

H_2, produced by microorganisms, is another reduction gas that may sometimes be present with CO. This potential interferant (with a retention time of 0.3 min) will be separated from CO (retention time of 0.7 min) on the molecular sieve column (Ostrander et al., 1982).

The combination of these discriminating steps contributes to the great specificity of this HO assay.

Table 9.2.1 GC Troubleshooting Guide

Problem	Possible cause	Solution
No CO peaks or peaks with erratic area and retention time	Faulty CO standard or poor sampling or transfer of standard	Check for plugged or leaky syringe
	Poor or no carrier flow through the vial or column	Check the detector outlet flow rate (which should be 30 ml/min) and peak retention time
		Check for proper position needle assembly through septum
	Reaction vial septum leaks when attached to headspace-sampling assembly	Check septum with soap solution with controller in inject mode
	Loose valve or carrier line fittings	Check valves and line fittings with soap solution
	Poor injection valve functioning	Check operation and actuation of valve and valve controller.
	Inappropriate column or detector temperature	Column temperature should be 140°C; detector temperature should be 270°C
	Ultraviolet light source burned out	Replace light source (Trace Analytical)
Gradual loss of sensitivity to CO	Introduction of water vapor onto column	Check column moisture trap or replace anhydrone and perform a new calibration curve
	Depletion of reaction bed	Replace reaction bed (Trace Analytical)
Baseline drift	Column contaminated	Recondition or replace column

Troubleshooting

Because CO is a gas, its quantification with the GC system poses unique problems. Unlike working with liquids, handling and transferring gases can result in a loss of material that cannot be detected until it is too late for recovery. However, loss of sample can be prevented through the careful use of well-planned techniques. The GC system itself can also, sometimes spontaneously, cause analysis failure.

When no CO peaks, or peaks with erratic area and retention times, emerge during analysis of CO-containing samples, the causes listed in Table 9.2.1 should be considered.

Table 9.2.1 also lists the possible causes and solutions for a gradual loss of sensitivity to CO in the GC system. Because the detection of CO depends on the chemical conversion of HgO to Hg gas, the reaction bed will become depleted of HgO as the Hg evaporates. Thus, the system will gradually (over ~2 year) lose its sensitivity to CO. This diminishing sensitivity should not affect daily CO analyses. With normal use, the column should be usable for up to 2 years. When the column fails, as detected by unstable and high baseline, it should be disconnected from the detector and reconditioned for 16 hr at 200°C, repacked with new column or replaced with a new column.

Anticipated Results

Table 9.2.2 shows representative results obtained using this methodology.

The results are not given as absolute values to be used for comparisons. They should be considered as representative values or trends for HO activity that may be encountered when different tissues from different species in various developmental stages are assayed. These results also represent HO activities in tissues observed after in vivo and in vitro perturbations that either increase (heme) or inhibit (metalloporphyrins) HO activity. In addition to these perturbations, there are many other parameters that may also play a significant role in the magnitude of the measured HO activities. These include, for instance, the route of administration of HO affectors (IP, IV, etc.), the time between administration and HO activity measurements, and the HO purification and concentration steps. It is our policy to always include an appropriate reference tissue as an assay check.

Table 9.2.2 Representative HO Activity Values Obtained Using the CO Method[a,b]

Treatment	HO activity (nmol CO/hr/mg protein)					
	Liver	Spleen	Brain	Kidney	Skin	Intestine
Newborn rhesus monkey (in vivo intravenous treatment)[c]						
Control	0.19 ± 0.10	0.62 ± 0.20	0.46 ± 0.14	0.12 ± 0.07	0.04[d]	0.30 ± 0.12
Heme	0.33 ± 0.23	0.78 ± 0.14	0.68 ± 0.28	0.32 ± 0.15	0.12 ± 0.02	0.41 ± 0.42
Heme + ZnPP[b]	0.08 ± 0.06	0.28 ± 0.03	0.60 ± 0.26	0.30 ± 0.13	0.10 ± 0.12	0.23 ± 0.12
Newborn Wistar rat (in vivo intraperitoneal treatment)[e]						
Control	0.43 ± 0.21	2.19 ± 0.66	—	—	—	—
CrMP	0.08 ± 0.04	0.98 ± 0.65	—	—	—	—
Adult Wistar rat (in vitro treatment)[f]						
Control	0.47 ± 0.10	2.23 ± 0.96	0.97 ± 0.34	0.17 ± 0.12	—	—
ZnBG	0.06 ± 0.03	0.04 ± 0.06	0.34 ± 0.20	ND	—	—

[a]Abbreviations: ZnPP, zinc protoporphyrin; CrMP, chromium mesoporphyrin; ZnBG, zinc deuteroporphyrin bis glycol; ND, not determined.

[b]All HO activity values measured from 1-min 13,000 × *g* supernatants from homogenized tissue using 50 μM heme as a substrate.

[c]Data taken from Vreman et al. (1990b). For each group of animals, control or treated, $n = 4$ except where otherwise noted.

[d]$n = 1$.

[e]Data taken from Vallier et al. (1993). For control animals, $n = 10$; for treated animals $n = 11$.

[f]Data taken from Vreman et al. (1992). For control and treated animals, $n = 3$.

Linearity. In preparations from rat liver and other tissues, HO activity is linear for up to 30-min of reaction time and up to 500 μg protein from the supernatant resulting from a 1-min 13,000 × *g* centrifugation. CO quantitation by this method is linear to 120 pmol.

Reproducibility. As an example of the within-run reproducibility of the method, assay of CO from 20-μl samples ($n = 10$) of adult rat liver and spleen yielded the following results [mean CO (pmol) ± SD (C.V.)]: for liver, 137 ± 4 (4%) total CO, 30 ± 4 (13%) blank, and 106 ± 4 (4%) net CO; for spleen, 440 ± 10 (2%) total CO, 49 ± 2 (4%) blank, and 391 ± 10 (2%) net CO.

Sensitivity. The limit of detection for CO is ~1 pmol. However, 10 pmol CO per vial is generally recommended as a practical working limit. Under current reaction conditions, ~1 μl (10 to 20 μg protein) of a 1-min 13,000 × *g* rat liver supernatant will produce 10 pmol of CO.

Time Considerations

The typical HO activity assay for ~6 tissue samples or 30 reactions requires ~4 to 5 hr. Sample preparation, including organ dissection and pretreatment, homogenization, and microsome isolation, should take 1 to 2 hr. Setting up and performing the HO reaction requires 1.5 hr. Quantitation of CO, including instrument calibration and sample analysis, requires 1.5 hr. Protein concentrations can be determined while CO is being measured. Finally, calculations can be performed in an hour, with most completed during the CO quantification phase.

An experienced analyst can perform and analyze ~160 HO reactions in a typical 8-hr day. With two analysts working together, the throughput rate can be increased to ~300 reactions per day.

Literature Cited

Cavallin-Stahl, E., Jonsson, F.-I., and Lundh, B. 1978. A new method for determination of microsomal haem oxygenase (E.C. 1.14.99.3) based on quantitation of carbon monoxide formation. *Scand. J. Clin. Lab. Invest.* 38:69-76.

Dennery, P.A., McDonagh, A.F., Spitz, D.R., Rodgers, P.A., and Stevenson, D.K. 1995. Hyperbilirubinemia results in reduced oxidative injury in neonatal Gunn rats exposed to hyperoxia. *Free Radic. Biol. Med.* 19:395-404.

Levitt, M.D., Ellis, C., Springfield, J., and Engel, R.R. 1995. Carbon monoxide generation from hydrocarbons at ambient and physiological temperature: A sensitive indicator of oxidant damage? *J. Chromatogr.* 695:324-328.

Lodola, A., Hendry, A.F., and Jones, O.T.G. 1979. Haem oxygenase: A reappraisal of the stoichiometry. *FEBS Lett.* 104:45-50.

Lowry, O.H., Rosebrough, H.J., Farr, A.L., and Randall, R.J. 1951. Protein measurement with the Folin phenol reagent. *J. Biol. Chem.* 193:265-275.

Maines, M.D. 1992. Heme Oxygenase: Clinical Applications and Functions. CRC Press, Boca Raton, Fla.

Maines, M.D. 1997. The heme oxygenase system: A regulator of 2nd-messenger gases. *Annu. Rev. Pharmacol. Toxicol.* 37:517-554.

Maines, M.D., Ibrahim, N.G., and Kappas, A. 1977. Solubilization and partial purification of heme oxygenase from rat liver. *J. Biol. Chem.* 252:5900-5903.

McCoubrey, W.K., Jr., Huang, T.J., and Maines, M.D. 1997. Isolation and characterization of a cDNA from the rat brain that encodes hemoprotein heme oxygenase-3. *Eur. J. Biochem.* 247:725-732.

Meffert, M.K., Haley, J.E., Schuman, E.M., Schulman, H., and Madison, D.V. 1994. Inhibition of hippocampal heme oxygenase, nitric oxide synthase, and long term potentiation by metalloporphyrins. *Neuron* 13:1225-1233.

Ostrander, C.R., Stevenson, D.K., Neu, J., Kerner, J.A., and Moses, S.W. 1982. A sensitive analytical apparatus for measuring hydrogen production rates. I. Application to studies in small animals. Evidence of the effects of an α-glucosidehydrolase inhibitor in the rat. *Anal. Biochem.* 119:378-386.

Sunderman, F.W., Jr., Downs, J.R., Reid, M.C., and Bibeau, L.M. 1982. Gas chromatographic assay for heme oxygenase activity. *Clin. Chem.* 28:2026-2032.

Tenhunen, R. 1972. Method for microassay of microsomal heme oxygenase activity. *Anal. Biochem.* 45:600-607.

Tenhunen, R., Marver, H.S., and Schmid, R. 1968. The enzymatic conversion of heme to bilirubin by microsomal heme oxygenase. *Proc. Nat. Acad. Sci. U.S.A.* 61:748-755.

Vallier, H.A., Rodgers, P.A., and Stevenson, D.K. 1993. Inhibition of heme oxygenase after oral vs intraperitoneal adminstration of chromium porphyrins. *Life Sci.* 52:79-84.

Vreman, H.J. and Stevenson, D.K. 1988. Heme oxygenase activity as measured by CO production. *Anal. Biochem.* 168:31-38.

Vreman, H.J., Kwong, L.K., and Stevenson, D.K. 1984. Carbon monoxide in blood: An improved micro-blood sample collection system, with rapid analysis by gas chromatography. *Clin. Chem.* 30:1382-1386.

Vreman, H.J., Stevenson, D.K., Henton, D., and Rosenthal, P. 1988. Correlation of carbon monoxide and bilirubin production by tissue homogenates. *J. Chromatog. Biomed. Appl.* 427:315-319.

Vreman, H.J., Gillman, M.J., Downum, K.R., and Stevenson, D.K. 1990a. In vitro generation of carbon monoxide from organic molecules and synthetic metalloporphyrins mediated by light. *Dev. Pharmacol. Ther.* 15:112-124.

Vreman, H.J., Rodgers, P.A., and Stevenson, D.K. 1990b. Zinc protoporphyrin administration for suppression of increased bilirubin production by iatrogenic hemiolysis in rhesus neonates. *J. Pediatr.* 117:292-297.

Vreman, H.J., Lee, O.K., and Stevenson, D.K. 1992. In vitro and in vivo characteristics of the heme oxygenase inhibitor: ZnBG. *Am. J. Med. Sci.* 302:335-341.

Vreman, H.J., Ekstrand, B.C., and Stevenson, D.K. 1993. Selection of metalloporphyrin heme oxygenase inhibitors based on potency and photoreactivity. *Pediatr. Res.* 33:195-200.

Vreman, H.J., Wong, R.J., Sanesi, C.A., Dennery, P.A., and Stevenson, D.K. 1998. Simultaneous production of carbon monoxide and thiobarbituric acid reactive substances in rat tissue preparations by an iron/ascorbate system. *Can. J. Physiol. Pharmacol.* 76:1057-1065.

Key References

Maines, 1992. See above.

This book provides a comprehensive review of heme oxygenase.

Maines, 1997. See above.

This review presents the most up-to-date information on the heme oxygenase system.

Vreman and Stevenson, 1988. See above.

This paper provides technical details on measuring HO activity by assaying CO production.

Vreman et al., 1984. See above.

This article presents technical details on determining CO concentrations by GC.

Contributed by Hendrik J. Vreman and David K. Stevenson
Stanford University Medical Center
Stanford, California

Detection of Heme Oxygenase 1 and 2 Proteins and Bilirubin Formation

Changes in the amounts of the two heme oxygenase (HO) isozymes at the level of expressed protein may be detected by measurement of heme oxygenase activity (see Basic Protocol 1) or by immunoblot analysis (see Basic Protocol 2). Measurement of enzyme activity is useful for examining overall increases or decreases in total HO levels. The protocol described in this unit relies on a coupled assay, performed in the presence of excess biliverdin reductase, to measure the conversion of heme to bilirubin, which is quantified spectrophotometrically. The activity assay does not, however, distinguish between the contribution of HO-1 and HO-2, because, with minor exceptions, the substrates for both isozymes are the same and the products are identical. In contrast, immunoblotting provides a means to examine the expression of each protein individually. The differences in the primary amino acid compositions of the two isozymes is reflected in the specificity of their antisera: antibody prepared against HO-1 shows essentially no detectable cross-reactivity with antibody prepared against HO-2.

The two HO isozymes can be found in the microsomal fraction of cells and tissues and in the membrane fraction prepared from bacterial cells expressing full-length recombinant HO-1 or HO-2. This unit describes the preparation of microsomal fractions from tissue and cell extracts (see Support Protocol 1) or from bacterial cultures (see Support Protocol 2), the assessment of heme oxygenase activity by the measurement of bilirubin formation (see Basic Protocol 1), and the examination of HO protein levels by immunoblotting (see Basic Protocol 2).

SPECTROPHOTOMETRIC HEME OXYGENASE ASSAY

BASIC PROTOCOL 1

HO activity can be detected using a coupled heme degradation assay supplemented with biliverdin reductase (BVR). HO converts heme to biliverdin, which is subsequently reduced to bilirubin by BVR. The complete conversion of heme to bilirubin also requires the cofactor NADPH and cytochrome *c* (P450) reductase (CCR). The latter activity is high in fresh microsomal preparations, so addition of exogenous CCR is usually not necessary. However, if membrane fractions have been frozen and thawed, supplementing the assay with purified CCR is recommended to compensate for the loss of activity associated with storage. Bilirubin can be readily detected using a scanning spectrophotometer. The reactions should be carried out under reduced lighting to limit the destruction of bilirubin, which is photosensitive. The presence of Triton X-100 in the reaction prevents the formation of aggregates of enzyme and of heme, which can greatly reduce the efficiency of the reaction. It is essential that the final protein concentration in the assay be <1 mg/ml as higher concentrations can lead to spectral interference.

Materials

1 mM heme (see recipe), prepared fresh
30 U/ml biliverdin reductase (BVR; e.g., StressGen Biotechnologies) *or* kidney cytosolic fraction (see Support Protocol 1)
Cytochrome *c* reductase (CCR; e.g., Sigma or StressGen Biotechnologies), optional
Heme oxygenase (HO) assay buffer (see recipe)
Microsomal fraction (adjust protein concentration to <8 mg/ml with resuspension buffer)
Resuspension buffer (see recipe)
Triton X-100 (optional)

Contributed by William K. McCoubrey, Jr.
Current Protocols in Toxicology (1999) 9.3.1-9.3.9

2.75 mM NADPH (see recipe)
Chloroform, chilled on ice (optional)

Glass tubes, 13 × 100–mm or 12 × 75–mm
Scanning spectrophotometer

Perform reaction

1. Place three glass tubes in an ice bath to chill.
2. To one tube, add 18 µl of 1 mM heme and either 30 µl of 30 U/ml BVR (0.9 U total), *or* 100 µl kidney cytosolic fraction. If using bacterial cell extracts or microsomal preparations that have been frozen and thawed, add 0.12 U CCR to tube. Bring volume to 1.2 ml with HO assay buffer.

   When performing multiple assays it is best to prepare a master mix of buffer, heme, BVR, and CCR (if needed) and then to bring volume of tube to 1.2 ml. This ensures that conditions are identical for all samples.

   Addition of CCR is not necessary when freshly prepared microsomes are used, but will not interfere with the reaction.

3. Add 150 µl microsomal fraction. If necessary, dilute microsomal protein with resuspension buffer to <8 mg/ml, so that the final protein concentration in the assay is <1 mg/ml.

   If the protein sample being used is not in resuspension buffer, add Triton X-100 to the reaction mixture to a final concentration of 0.04%.

4. Mix tube briefly and return to ice bath. Label remaining two tubes as reference and test. Add 60 µl HO assay buffer to reference tube and 60 µl of 2.75 mM NADPH to test tube.
5. Add 600 µl reaction mixture (from step 3) to test and reference tubes.
6. Incubate test and reference tubes ≤30 min at 37°C in the dark with constant shaking.

   Incubation time will vary depending on the activity of the protein in the sample. A typical reaction time is 8 min, but the incubation could take as long as 30 min if HO activity is low. Longer incubations are not recommended, as they do not give quantitative results because of the thermal lability of the enzymes and product.

7. Stop the reaction by returning tubes to the ice bath. Cover the ice bath to protect bilirubin from photolysis.

Measure reaction product

8. Using the solution in reference tube, blank the scanning spectrophotometer between 410 and 610 nm.

   Using a scanning spectrophotometer rather than taking readings at two wavelengths is necessary because the maximum absorbance of bilirubin can vary between 460 and 475 nm, depending on conditions that cannot be optimized when using crude preparations. The continuous scan also allows measurement of a typical bilirubin peak rather than artifactual differences between the anticipated maximum and minimum wavelengths.

To measure bilirubin directly

9a. Scan the test reaction.

10a. Determine the difference in absorption between 470 and 530 nm. Calculate the concentration of bilirubin using an extinction coefficient of 40 mM^{-1} cm^{-1}.

   One unit of activity is defined as the amount that produces 1 nmol bilirubin/hr.

To extract bilirubin before measuring

9b. Add 1.5 vol cold chloroform to test reaction. Mix gently for a few seconds and return to ice. Repeat mixing two additional times.

Try to avoid forming an emulsion which will subsequently require separation. If an emulsion does form, hold the tube on ice or centrifuge at low speed until the phases separate.

Extracting bilirubin with chloroform prior to scanning increases the sensitivity of the assay by eliminating residual heme and raising the extinction coefficient of the product, which is higher in chloroform.

10b. Using chloroform as a reference, determine the difference in absorption of the chloroform phase between 450 and 530 nm. Calculate the concentration of bilirubin using an extinction coefficient of 58 mM^{-1} cm^{-1}.

Again, one unit of activity is defined as the amount that produces 1 nmol bilirubin/hr.

IMMUNOBLOTTING FOR HEME OXYGENASE 1 AND 2

BASIC PROTOCOL 2

Conditions for electrophoresis and immunoblotting are identical to those used for biliverdin reductase (see *UNIT 9.4 & UNIT 2.3*). The only modification is that acetone precipitation is performed on samples with low protein concentration (e.g., brain HO-1) prior to electrophoresis. To precipitate proteins, add 3 vol ice-cold acetone to samples and microcentrifuge 20 min at 10,000 × g, 4°C. Remove acetone and air dry the pellet for 5 min prior to adding 1× SDS-PAGE sample buffer.

Primary antibodies to rat HO-1 and HO-2 are commercially available (StressGen; see *SUPPLIERS APPENDIX*). The dilutions of the primary antibodies for each application need to be empirically determined, but a dilution of 1:100 to 1:250 usually works well for immunoblotting.

PREPARATION OF MICROSOMAL FRACTION FROM TISSUE

SUPPORT PROTOCOL 1

HO isozymes associate with intracellular membranes through their hydrophobic tails. Preparing HO isozymes involves homogenizing tissue samples and disrupting cell membranes. A low-speed centrifugation step removes particulates and the supernatant is then subjected to ultracentrifugation to separate the membrane fraction from the cytosol. The cytosolic portion can be used as a source of biliverdin reductase. The microsomes are resuspended in a buffer containing Triton X-100, which disrupts the hydrophobic interactions that bind the enzymes to the membranes.

Materials

Fresh or flash-frozen tissue
0.9% (w/v) NaCl in distilled H_2O, ice cold
Homogenization buffer (see recipe), ice cold
Resuspension buffer (see recipe)

Surgical scissors
Dounce homogenizer with tight-fitting Teflon pestle
Variable-speed drill
Centrifuge with fixed-angle rotor and tubes (e.g., Beckman J2 and JA20 rotor)
Ultracentrifuge with fixed-angle rotor (e.g., Beckman L8 and 50Ti rotor)

NOTE: Microsomes can be prepared from either fresh or frozen tissue. All steps must be carried out on ice or at 4°C unless otherwise noted.

1. Rinse fresh tissue or thaw frozen tissue in 50 ml ice-cold 0.9% NaCl, then weigh tissue.

   In general, 0.5 to 1 g of tissue is a convenient quantity for use in this protocol, although the amount may be scaled up or down depending on availability of tissue.

2. Add 5 vol (ml/g) ice-cold homogenization buffer to tissue.

   5 vol works well for most tissue. However, when working with liver, use 4 vol of buffer; for brain use 10 vol.

3. Using surgical scissors, mince tissue and then pour tissue and buffer into Dounce homogenizer. Homogenize sample until smooth using a Teflon pestle attached to a variable-speed drill. Set drill to ~200 rpm and homogenize tissue for 10 strokes.

4. Centrifuge 20 min at 10,000 × *g* (10,000 rpm in JA20 rotor), 4°C.

5. Transfer supernatant to an ultracentrifuge tube. Be careful to avoid transfering loose particulates.

6. Centrifuge 1 hr at 100,000 × *g* (50,000 rpm in 50Ti rotor), 4°C.

7. Transfer supernatant (cytosolic fraction) to appropriate storage tube and store at −80°C.

   When prepared from tissues that contain high concentrations of BVR (see UNIT 9.4), such as kidney, this fraction may be used as a source of BVR for HO assays (see Basic Protocol 1).

8. Resuspend microsomal pellet in a volume of resuspension buffer equivalent to 0.5 to 1 ml/g of tissue processed.

   It may be helpful at this step to use a small pestle on a drill to assist in disrupting the pellet.

9. Transfer microsomes to appropriate storage tube. Use immediately for determination of protein concentration and HO assay (see Basic Protocols 1 and 2) or store at −80°C.

SUPPORT PROTOCOL 2

PREPARATION OF BACTERIAL CELL EXTRACTS

HO fusion proteins, expressed from bacterial plasmids containing HO cDNAs coupled to vector-encoded sequences, are relatively stable in *E. coli.* Therefore, maximal yields of HO can be obtained following overnight growth of bacterial cultures to saturation. As is the case for the native HO proteins prepared from tissue, the hydrophobic tails of full-length cloned proteins cause association of the expressed recombinant HO with the membrane fraction of bacterial cell lysates. Lysates are prepared utilizing multiple cycles of freezing and thawing followed by brief sonication. In this protocol, Triton X-100 is included during lysis, so the HO protein is contained in the supernatant rather than in the pellet in the initial centrifugation step. The relatively high proportion of the fusion protein in the bacterial cells makes initial separation of membrane and cytosolic fractions unnecessary. However, as bacterial cells do not possess significant CCR activity, assays for HO activity require addition of that enzyme to the coupled reaction even when extracts have not been frozen before use. The protocol describes preparation of extracts from a 40-ml culture, but the volume can be scaled up or down as needed.

Materials

Bacteria on culture plate or in overnight culture
Liquid culture medium (e.g., 2× TY medium or superbroth; *APPENDIX 3A*) containing appropriate antibiotic (e.g., 50 to 100 µg/ml ampicillin)
Isopropyl-β-D-thiogalactopyranoside (IPTG), optional

0.1% (w/v) NaCl in distilled H_2O
Resuspension buffer (see recipe)

Centrifuge and rotor (e.g., Beckman J2 and JA20 rotor)
Water bath, room temperature
Sonicator

Additional reagents and equipment for culturing bacteria (*APPENDIX 3*)

1. Inoculate 40 ml of liquid medium containing the appropriate concentration of antibiotic with a single colony or with 0.4 ml (0.01 vol) of overnight culture. If vector requires IPTG for expression of recombinant protein, incubate culture 3 to 4 hr at 37°C before adding the appropriate concentration (1 to 3 mM) of inducer. Continue incubation overnight (16 to 18 hr).

   The flask used should be of sufficient volume (typically at least five times the volume of the medium) to allow for proper aeration.

   All subsequent steps must be carried out on ice or at 4°C unless otherwise noted.

2. Collect bacterial cells by centrifuging 12 min at 2000 × *g* (4000 rpm in JA20 rotor).

3. Wash pellet by resuspending in 4 to 5 vol of 0.1% NaCl (with respect to the volume of packed cells). Repeat centrifugation.

   The resuspended pellet may be transferred to a microcentrifuge tube if the volume allows. In this case, microcentrifuge 2 min at 6000 rpm.

4. Resuspend washed cells in 4 to 5 vol resuspension buffer and freeze in dry ice.

   The cells may be stored indefinitely at −80°C at this stage with virtually no loss of activity.

5. Thaw cells by immersing tube in cold tap water. Shake tube occasionally to mix sample and to minimize the time cells spend at elevated temperatures.

6. Repeat freeze-thaw cycle two additional times.

7. Sonicate samples three to four times using 15- to 20-sec bursts and allowing the suspension to cool for several minutes in between.

   There is usually a noticeable change in the opacity of the suspension when the cells have lysed sufficiently.

8. Centrifuge 20 min at 10,000 × *g*.

9. Transfer supernatant to an appropriate tube and use immediately for HO activity analysis or store at −80°C.

REAGENTS AND SOLUTIONS

*Use Milli-Q-purified water or equivalent for all recipes and protocol steps. For common stock solutions, see **APPENDIX 2A**; for suppliers, see **SUPPLIERS APPENDIX**.*

Heme, 1 mM

Dissolve 6.52 mg hemin (Sigma) in 250 µl of 0.1 N NaOH. Vortex until completely dissolved. Add 0.1 g Tris base, 132 mg bovine serum albumin (fraction V), and 9.5 ml H_2O. Vortex until BSA is completely in solution. Add 0.2 ml of 0.1 N HCl, vortex, and store on ice in the dark.

This solution should be used as soon as possible after preparation as aggregates of heme will form upon storage.

Heme oxygenase (HO) assay buffer

3.402 g KH_2PO_4
13.064 g K_2HPO_4
950 ml H_2O
Add 2 ml 0.5 N EDTA
Adjust to pH 7.4 with 1 N KOH
Filter and store up to 1 year at 4°C

Homogenization buffer

10 ml 1 M Tris·Cl, pH 7.5 (*APPENDIX 2A*)
790 ml H_2O
Add 85.58 g sucrose
Stir to dissolve
Add H_2O to 1 liter
Filter sterilize and store up to 6 months at 4°C

NADPH, 2.75 mM

2.3 mg β-NADPH (Sigma)
1 ml HO assay buffer (see recipe)
Store on ice, protected from light, and use immediately

Alternatively, this solution may be stored frozen at −20°C for a week or more; however, repeated thawing and refreezing should be avoided.

Resuspension buffer

369 ml H_2O
10 ml 1 M Tris·Cl, pH 7.5 (*APPENDIX 2A*)
100 ml glycerol
1 ml 0.5 M EDTA (*APPENDIX 2A*)
20 ml 10% (v/v) Triton X-100
Filter sterilize and store up to 6 months at 4°C

COMMENTARY

Background Information

In all mammalian species examined to date, heme oxygenase (HO) activity is produced largely by two isozymes: an inducible form, HO-1 (also known as heat shock protein 32; Keyes and Tyrell, 1989), and a constitutively expressed form, HO-2 (Maines et al., 1986). The proteins are encoded by distinct single-copy genes (Müller et al., 1987; McCoubrey and Maines, 1994), and they differ significantly in their amino acid composition and sequence (Shibahara et al., 1985; Rotenberg and Maines, 1990). Of particular note, HO-1 contains no cysteine residues, whereas HO-2 has three, two of which are present within its heme regulatory motifs (HRMs). HRMs are involved in heme-regulated functions in several proteins (Zhang and Guarente, 1995). They constitutively bind heme in HO-2 but are not involved in catalysis (McCoubrey et al., 1996). The differences in primary amino acid sequence between HO-1 and HO-2 are also reflected in the specificity of antibodies raised against each isozyme; polyclonal rabbit antisera are isozyme specific, exhibiting no cross-reactivity.

Both isozymes share an identical region of 24 amino acids, thought to be the heme-binding and catalytic pocket (Rotenberg and Maines, 1991). The recently described HO-3 (McCoubrey et al., 1997) differs from HO-1 and HO-2 in this domain and has almost no detectable heme oxygenase activity. Like HO-2, HO-3 is a hemoprotein that contains an HRM. Despite ≈90% amino acid identity between the two proteins, antiserum to HO-2 does not recognize HO-3. Although they diverge in amino acid composition, the carboxyl termini of all heme oxygenases so far sequenced have a conserved hydropathy profile. The terminal sequences are highly hydrophobic in nature and thus serve as a membrane binding domain (McCoubrey and Maines, 1993).

Heme oxygenase activity can be detected in most tissues, although the highest levels are found in spleen, testes, and brain. The relative contribution of the isozymes varies from tissue

to tissue. In spleen, HO-1 predominates, even under normal conditions. In contrast, although HO activity levels in the brain are comparable to that of spleen, HO-1 protein is nearly undetectable and is expressed in few neurons in the absence of induction. Exogenous stimuli have little effect on HO-2 levels. HO-1 activity, however, increases dramatically in many tissues in response to several factors, including heat shock and treatment with bromobenzene, hematin, lipopolysaccharide, or metal ions, such as cadmium.

Microsomal HO catalyzes the initial step in degradation of the heme moiety of hemoproteins: the cleavage of the α-meso carbon bridge to produce the open tetrapyrole, biliverdin (Tenhunen et al., 1968; Maines et al., 1977). In this reaction the bound iron is released and carbon monoxide (CO) is produced; HO activity is the sole source for the in vivo production of CO in mammalian systems (reviewed in Maines, 1992, 1997).

In principle, it is possible to quantify HO activity by measuring the production of any of the three products released after the oxidative cleavage of the heme molecule; all are produced in stoichiometric amounts by the enzyme. However, measurement of bilirubin formation using the coupled assay described in this unit is highly sensitive and more specific than measuring the other products. Direct measurement of biliverdin is possible, but, because it has a comparatively low extinction coefficient, detection of this product is less sensitive than for bilirubin. Although the release of chelated iron could be monitored using a radiolabeled derivative, any cleavage of heme has the potential to release the bound metal moiety. Because nonenzymatic cleavage occurs in microsomal preparations, this approach is not practical. Monitoring CO production (*UNIT 9.2*) would be more specific, but its measurement can be confounded by the release of the gas following the oxidative cleavage of any of heme's four meso-carbon bridges; HO-mediated cleavage is specific to the α-methane bridge and produces biliverdin IXα, for which BVR has a very high specificity. Thus, measuring the production of bilirubin is more specific than measuring the release of CO. In addition, measuring CO production requires expertise in gas chromatography; measurement of bilirubin concentration can be performed in any laboratory with a scanning spectrophotometer.

Critical Parameters

The simplest yet most common problem preventing the collection of usable data from the HO activity assay is inaccurate pipetting. These errors are magnified when samples have relatively low levels of HO activity. Heme has a very strong and broad absorption peak at ~390 nm (the Soret band). A slight error in the distribution of the reaction mixture between test and reference tubes can lead to differences in heme concentration and to detection of a heme peak when the tubes are compared. When activity is low, the heme peak remains large and the bilirubin peak is small. Under these conditions, the upper shoulder of the heme peak may obscure all or part of the bilirubin peak, making accurate determination of the magnitude of the latter difficult or impossible. Because of the small volume used for the assay and the amount of heme present (15 μM), even a few microliters difference can make a large difference in the quality of the assay.

Although the heme solution may be used over the course of more than 1 day if kept cold and in the dark, when quantitative results are required, daily preparation of fresh solution is necessary. Over time, visible aggregates will form in the solution and lead to a decrease in the concentration of available heme. More importantly, the presence of particulates in the assay may make obtaining an accurate spectrum impossible. Likewise, it is better to prepare fresh NADPH than to use a frozen stock, especially when the accuracy of absolute values is critical. Insufficient concentrations of detergent will also adversely affect the amount of bilirubin produced. A final concentration of 0.04% Triton X-100 in the assay is ideal and allows for a small margin of error without significant reduction in apparent activity. When assays are conducted on protein preparations that lack Triton X-100, the assay buffer should be supplemented to obtain a final detergent concentration of 0.04%.

For immunoblotting, selection of the appropriate antibodies and dilutions is essential. Follow suppliers' recommendations when possible. For untested applications, dilutions must be determined empirically.

Troubleshooting

As noted previously, the most common errors in the coupled HO assay are caused by poor pipetting technique. These inaccuracies often manifest themselves as abnormal spectra, in many cases causing an apparently linear increase or decrease in absorption between 450 and 600 nm. Careful examination and recalibration of pipettors will often rectify this problem. Mixing all of the reaction components,

except NADPH and buffer, with the microsomal preparation minimizes the number of different additions to the test and reference tubes.

It should be noted that a slight excess of the reaction mix is prepared so that a small amount remains in the mixing tube; this reduces the risk of pipetting unequal volumes into the test and reference tubes. When processing multiple samples, prepare a master mixture containing all the reaction components except protein. Use $(N + 0.5) \times$ the volume of each component (where N is the number of assays to be performed) and aliquot 1.2 ml of the mixture to each mixing tube. Such preparation allows more accurate comparisons of the HO activity values obtained because all the reactions are identical except for the protein added.

If the spectrum suggests a large contribution of residual heme, as can sometimes happen when HO activity is low, the concentration of heme in the reaction mix can be lowered as much as 3-fold (to 5 μM) without adversely affecting the kinetics or the magnitude of the bilirubin peak. Also, as noted in Basic Protocol 1, the incubation time can be increased to 30 min to boost the amount of bilirubin produced. Finally, when HO activity is extremely low, bilirubin may be extracted with chloroform and its spectrum obtained by comparison with a chloroform blank. Such extraction is also helpful when there is a contribution of a residual heme peak, as heme is not soluble in chloroform.

Measurement of less HO activity than expected is often an indication of insufficient CCR in the reaction. This is sometimes the case when performing an unsupplemented assay with fresh microsomal preparations that have been stored for an extended period following preparation, or when assay temperatures have been allowed to fluctuate above 4°C. Supplementing the assay with purified CCR usually alleviates this problem.

The presence of particulates in the microsomal preparation can also lead to irreproducible peaks or valleys in the spectral profile. This problem can be eliminated by centrifuging microsomes at $10{,}000 \times g$ prior to performing the HO assay (Support Protocol 1, step 4). HO proteins will remain in the supernatant and particulates should pellet under such conditions.

The most common problem in immunoblotting is uneven transfer of the protein to the membrane. This is generally due to the presence of bubbles in the transfer sandwich, which can be eliminated by careful layering of the components. Insufficient or excessive transfer times or voltages can also lead to decreased signal. Inclusion of prestained markers can allow monitoring of transfer efficiency.

Anticipated Results

The limits of detection of the HO assay depend on the sensitivity of the spectrophotometer being used and, in part, on the protein concentration of the microsomal preparation. Assuming that a ΔOD of 0.001 can be measured accurately, which is possible with many current spectrophotometers, the standard 8-min assay should accurately measure ≥1.7 U/ml HO activity in the microsomal preparation. If the protein concentration is the maximum 8 mg/ml, this corresponds to a specific activity of 0.2 U/mg. The assay sensitivity may be further increased by using a longer incubation time, so that <0.1 U/mg could be reliably detected. It should be noted that when protein concentration is low, it is possible to add a larger amount of the microsomal preparation by reducing the amount of assay buffer accordingly.

Microsomal HO activity varies greatly with tissue type. Microsomes prepared from the spleen, testis, and brain of an untreated rat may have activities of >10 U/mg. Small intestine, epididymis, and seminal vesicles yield specific activities from 0.4 to 0.7 U/mg, and HO activity in other tissues falls between these values (Maines, 1988). The activity of bacterial lysates depends on the activity of the promoter and the growth conditions, but can easily exceed that of tissue microsomes. Given the range of the assay, it is relatively easy to observe both increases and decreases in HO activity.

Using immunoblot analysis, HO-2 is readily detectable in most tissues. In untreated animals, the HO-1 level is at the limit of detection in many tissues, but can show dramatic increases in response to stress (Ewing and Maines, 1991).

Time Considerations

The time required for tissue preparation will vary with the number of animals being processed and the number of tissues to be collected, as well as the experience of the person doing the dissections. Microsomal preparation will require 2 to 3 hr depending on the number of samples. Preparation of the bacterial cell lysate following overnight growth will take ~1.25 to 1.5 hr for small cultures (25 to 100 ml) and ~2 to 2.5 hr for larger cultures due to the longer times necessary for the freeze-thaw cycles. Determination of protein concentration requires 30 to 60 min, and set up for 6 to 10 assays,

including preparation of fresh heme and NADPH, takes another hour. Calibration of the spectrophotometer can usually be accomplished during the incubation, and this period along with collection of spectra will take an hour. Thus, a single experimenter can obtain data in a single day if only a limited amount of dissection is required.

For immunoblotting, preparation of samples, electrophoresis, and transfer of proteins to the membrane can be accomplished by a single investigator in one day. For practical purposes, it is generally advisable to block overnight and to perform the antibody treatments and substrate development, which take 4.5 to 6 hr, the next day.

Literature Cited

Ewing, J.F. and Maines, M.D. 1991. Rapid induction of heme oxygenase-1 mRNA and protein by hyperthermia in the rat brain: Heme oxygenase-2 is not a heat shock protein. *Proc. Natl. Acad. Sci. U.S.A.* 88:5364-5368.

Keyse, A.M. and Tyrell, A.M. 1989. Heme oxygenase is the major 32 kDa stress protein induced in human skin fibroblasts by UVA radiation, hydrogen peroxide and sodium arsenite. *Proc. Natl. Acad. Sci. U.S.A.* 86:99-103.

Maines, M.D. 1988. Heme oxygenase: Function, multiplicity, regulatory mechanisms and clinical applications. *FASEB J.* 2:2557-2568.

Maines, M.D. 1992. Heme oxygenase and heme degrading enzymes. *In* Heme Oxygenase: Clinical Applications and Functions (M.D. Maines, ed.) pp. 43-108. CRC Press, Boca Raton, Fla.

Maines, M.D. 1997. The heme oxygenase system: A regulator of second messenger gases. *Annu. Rev. Pharmacol. Toxicol.* 37:517-554.

Maines, M.D., Ibrahim, N.G., and Kappas, A. 1977. Solubilization and partial purification of heme oxygenase from rat liver. *J. Biol. Chem.* 252:5900-5903.

Maines, M.D., Trakshel, G.M., and Kutty, R.K. 1986. Characterization of two constitutive forms of rat liver heme oxygenase: Only one molecular species is inducible. *J. Biol. Chem.* 261:411-419.

McCoubrey, W.K., Jr. and Maines, M.D. 1993. Domains of rat heme oxygenase-2: The amino terminus and histidine 151 are required for heme oxidation. *Arch. Biochem. Biophys.* 302:402-408.

McCoubrey, W.K., Jr. and Maines, M.D. 1994. The structure, organization and differential expression of the gene encoding rat heme oxygenase-2. *Gene* 139:155-161.

McCoubrey, W.K., Jr., Huang, T.J., and Maines, M.D. 1996. Heme oxygenase-2 is a hemoprotein and binds heme through heme regulatory motifs that are not involved in heme catalysis. *J. Biol. Chem.* 272:12568-12574.

McCoubrey, W.K., Jr., Huang, T.J., and Maines, M.D. 1997. Isolation and characterization of a cDNA from the rat brain that encodes hemoprotein heme oxygenase-3. *Eur. J. Biochem.* 247:725-732.

Müller, R.M., Taguchi, H., and Shibahara, S. 1987. Nucleotide sequence and organization of the rat heme oxygenase gene. *J. Biol. Chem.* 262:6795-6802.

Rotenberg, M.O. and Maines, M.D. 1990. Isolation, characterization and expression in *Escherichia coli* of a cDNA encoding rat heme oxygenase-2. *J. Biol. Chem.* 265:7501-7506.

Rotenberg, M.O. and Maines, M.D. 1991. Characterization of a cDNA-encoding rabbit brain heme oxygenase-2 and identification of a conserved domain among mammalian heme oxygenase isozymes: Possible heme-binding site? *Arch. Biochem. Biophys.* 290:336-344.

Shibahara, S., Müller, R., Taguchi, H., and Yoshida, T. 1985. Cloning and expression of cDNA for rat heme oxygenase. *Proc. Natl. Acad. Sci. U.S.A.* 82:7865-7869.

Tenhunen, R., Marver, H.S., and Schmid, R. 1968. The enzymatic conversion of heme to bilirubin by microsomal heme oxygenase. *Proc. Natl. Acad. Sci. U.S.A.* 61:748-755.

Zhang, L. and Guarente, L. 1995. Heme binds to a short sequence that serves a regulatory function in diverse proteins. *EMBO J.* 14:313-320.

Contributed by William K. McCoubrey, Jr.
University of Rochester
Rochester, New York

Detection of Biliverdin Reductase Activity

The initial step of the heme catabolic pathway is the oxidation of the porphyrin ring to form the open tetrapyrrole biliverdin IXα. In mammals, and in some species of fish, biliverdin is subsequently reduced to the bile pigment bilirubin. This reaction is catalyzed by the cytosolic enzyme biliverdin reductase (BVR). The enzyme is unique in that it has two pH optima, 6.7 and 8.7, and preferentially uses a different cofactor at each optimum—NADH and NADPH, respectively. BVR activity can be detected in nearly every tissue type, with the highest concentrations in liver and kidney. Purified from tissue, BVR exists as at least ten isoforms that differ in their isoelectric points and tissue distribution. BVR can be prepared from cytosolic fractions from tissue (see Basic Protocol 1) or from extracts from bacterial expression cultures (see Support Protocol). This unit presents a kinetic assay for the measurement of BVR activity at both pH optima (see Basic Protocol 1). In this assay, bilirubin is detected using a scanning spectrophotometer. BVR protein can be detected by immunoblotting (see Basic Protocol 2), and its isoelectric variants can be separated by two-dimensional isoelectric focusing (two-dimensional gel electrophoresis; see Basic Protocol 3). Subcellular localization of BVR should be determined by immunocytochemical analysis

KINETIC ASSAY OF BILIVERDIN REDUCTASE ACTIVITY

BASIC PROTOCOL 1

A cytosolic fraction is prepared from tissue and its BVR activity is determined by spectrophotometric measurement of the reaction product, bilirubin. To measure BVR activity at its different pH optima, two assay buffers are prepared: buffer of pH 8.7 is used when NADPH is the cofactor; buffer of pH 6.75 is used for NADH. Assays are performed under conditions of reduced lighting to prevent photolytic degradation of the substrate and product.

Materials

Fresh or flash-frozen tissue
0.9% (w/v) NaCl in distilled H_2O, ice cold
Homogenization buffer (see recipe)
BVR assay buffers, pH 8.7 and 6.75 (see recipes)
300 μM biliverdin (see recipe)
20 mg/ml bovine serum albumin (BSA)
Cofactor buffer (see recipe)
1 mM NADPH in BVR assay buffer, pH 8.7 (see recipe for buffer, store on ice; use within 2 hr)
10 mM NADH in cofactor buffer (see recipe for buffer; store on ice; use within 1 hr)

Surgical scissors
Dounce homogenizer with tight-fitting Teflon pestle
Variable-speed drill
Centrifuge with fixed-angle rotor and tubes (e.g., Beckman J2 with JA20 rotor)
Ultracentrifuge with fixed-angle rotor (e.g., Beckman L8 with 50Ti rotor)
13 × 100–mm or 12 × 75–mm glass tubes
Scanning spectrophotometer

NOTE: Microsomes can be prepared from either fresh or frozen tissue. Enzyme preparation is carried out on ice or at 4°C, and the assay is performed at room temperature.

Prepare cytosolic fraction

1. Rinse 0.5 to 1 mg tissue in 50 ml ice-cold 0.9% NaCl.
2. Add 9 vol (v/w) homogenization buffer to tissue.

Contributed by Tian-Jun Huang
Current Protocols in Toxicology (1999) 9.4.1-9.4.10

3. Using surgical scissors, mince tissue in buffer and pour into Dounce homogenizer. Homogenize sample until smooth using a Teflon pestle attached to a variable-speed drill. Set drill to ~200 rpm and homogenize tissue for 10 strokes.

4. Centrifuge 20 min at 10,000 × *g*, 4°C.

   In most cases, the specific activity of BVR in the 10,000 × g supernatant is sufficiently high that the activity assays can be performed at this point. If desired, an additional high-speed centrifugation step can be performed to separate heme oxygenase and other microsomal proteins from the cytosolic BVR.

5. Transfer supernatant to an ultracentrifuge tube, being careful to avoid transferring loose particulates.

6. Centrifuge 1 hr at 100,000 × *g*, 4°C.

7. Collect supernatant for BVR activity assay.

Perform BVR assay

8. At room temperature, prepare a combination solution containing 960 µl BVR assay buffer (pH 8.7 for use with NADPH or pH 6.75 for NADH), 10 µl of 300 µM biliverdin, and 10 µl of 20 mg/ml BSA. (If performing the assay in the absence of BSA, add an additional 20 µl assay buffer).

   NADH and NADPH assays are identical except that an assay buffer of pH 6.75 is used for NADH and a buffer of pH 8.7 is used for NADPH. Assays are performed under conditions of reduced lighting to prevent photolytic degradation of the substrate and product. BSA is included to stabilize BVR, but may be omitted in preparations that have a high concentration of total protein.

9. In cuvettes, prepare reference reactions as follows: Add 490 µl combination solution (step 8), 50 µl homogenization buffer, and 60 µl assay buffer, pH 8.7 (for assays using NADPH) *or* 60 µl cofactor buffer (for assays using NADH).

10. Place reference cuvette in scanning spectrophotometer and record the spontaneous change in absorbance at 468 nm (or 450 nm if BSA is not present) over 30 to 60 sec.

11. To test reaction cuvette add 490 µl combination solution, 50 µl cytosol, and 60 µl of 1 mM NADPH *or* 60 µl of 10 mM NADH. Mix sample and immediately record the change in absorbance at the same wavelength used for reference sample. Monitor rate over several time intervals (e.g., 4 × 15 sec) to ensure that reaction is linear. Correct the test spectrum for absorbance in the absence of cofactor by subtracting the reference spectrum (step 10).

    It is frequently necessary to dilute the cytosolic preparations in homogenization buffer to ensure that the reaction remains linear for the duration of the assay. If the reaction rate decreases over time, the substrate is becoming depleted. Repeat the assay with a diluted (1:10) enzyme.

12. Calculate concentration of bilirubin using an extinction coefficient of 63 $mM^{-1}cm^{-1}$ (or 53 $mM^{-1}cm^{-1}$ when assaying in the absence of BSA).

    One unit of activity is defined as the amount producing 1 nmol bilirubin/min.

BASIC PROTOCOL 2

IMMUNOBLOTTING ASSAY FOR BILIVERDIN REDUCTASE

Proteins are separated according to molecular weight by acrylamide gel electrophoresis and then transferred to a membrane. The membrane is incubated with a nonspecific blocking solution and then with a BVR-specific antiserum produced in rabbits. A secondary antibody, directed against rabbit immunoglobulin and conjugated to horseradish peroxidase, is then added. The location of protein-antibody complexes is then

visualized by adding a colorimetric substrate for the peroxidase. When selecting a primary antibody, note that BVR-specific antisera show pronounced species specificity. Antibodies raised against human BVR react very poorly with the rat reductase. Antibodies to a given species, however, will recognize all BVR isoforms from that species.

Materials

Protein samples in 1× SDS sample buffer (*APPENDIX 2A*)
Prestained or dye-labeled protein molecular-weight markers
Transfer buffer (see recipe)
1× and 5× PBS (see recipe)
Blocking solution (see recipe)
Rabbit anti-BVR antiserum (e.g., StressGen)
Antibody diluent (see recipe)
1× PBS containing 0.5% (w/v) sodium cholate (PBS/cholate)
Horseradish peroxidase–conjugated anti–rabbit IgG antiserum (e.g., Bio-Rad or Cappel)
4-Chloronaphthol
Methanol
30% (v/v) H_2O_2
0.2-μm-pore nitrocellulose sheets *or* nylon-backed equivalent

Additional reagents and equipment for SDS-polyacrylamide gel electrophoresis (SDS-PAGE; *APPENDIX 3*) and electrotransfer of proteins (*UNIT 2.3*)

Perform electrophoresis and transfer proteins to membrane

1. Prepare a gel for SDS-PAGE using a 12.5% separating gel and a 3.5% stacking gel.
2. Load samples and molecular weight markers.
3. Run electrophoresis until bromphenol blue dye front reaches the bottom of gel.
4. Separate plates, cut stacking gel away with a clean razor blade, and submerge separating gel in transfer buffer.
5. Transfer proteins to nitrocellulose membrane (see *UNIT 2.3*).

Treat membrane with antibodies

6. Examine membrane to confirm transfer of proteins. Remove membrane and rinse briefly several times with 1× PBS.

   Before removing the membrane from the transfer chamber, confirm the effectiveness of transfer by noting the transfer of the molecular-weight markers to the membrane. If the process is incomplete, and the membrane and gel have not yet been separated, the transfer can be repeated.

7. Add sufficient blocking solution to completely cover the membrane and incubate overnight at 4°C with gentle rocking.

   The blocking step may also be carried out at 37°C for 1 to 2 hr.

8. Remove blocking solution and briefly rinse membrane twice with 1× PBS.

   The blocking solution can be stored at 4°C and reused at least a dozen times.

9. Dilute BVR antiserum 1:200 in antibody diluent. Add enough BVR antiserum to cover membrane (typically 10 ml) and incubate 1 to 2 hr at room temperature with gentle rocking.
10. Remove primary antibody and store solution at 4°C.

    The diluted antibody may be used up to five times without significant loss of sensitivity.

11. Rinse membrane briefly with PBS/cholate at room temperature. Cover membrane with PBS/cholate and incubate 10 min at room temperature with gentle rocking.
12. Remove PBS/cholate and cover membrane with 1× PBS. Incubate 10 min at room temperature with gentle rocking. Rinse membrane briefly with PBS/cholate.
13. Dilute horseradish peroxidase–conjugated goat anti–rabbit Ig serum 1:500 in antibody diluent. Add enough diluted secondary antibody to cover membrane. Incubate 1 to 2 hr at room temperature with gentle rocking.
14. Rinse membrane briefly with PBS/cholate. Cover with PBS/cholate and incubate 10 min at room temperature with gentle rocking. Repeat 10-min wash with fresh PBS/cholate.

    The diluted secondary antibody may be stored at 4°C and reused up to three times.

15. Rinse membrane briefly with 1× PBS. Cover with more 1× PBS and incubate 5 min at room temperature with gentle rocking. Repeat 5-min wash with fresh 1× PBS.

Detect antibody complexes

16. Prepare developing solution: Dissolve 15 mg 4-chloronaphthol in 5 ml methanol. Add 6 ml of 5× PBS and 19 ml H_2O.

    NOTE: *Solutions should be prepared on ice and the following steps carried out in reduced lighting.*

17. Place membrane in developing tray. Add 30 µl of 30% H_2O_2 to the chloronaphthol solution and immediately transfer solution to tray.
18. Incubate membrane at room temperature with gentle rocking in the dark. Check color development periodically. When band intensity is sufficient, transfer membrane to 1× PBS to stop the development.

    Developing time may vary from 1 to 30 min depending on the amount of BVR protein present. When the membrane begins to appear noticeably blue or violet in color, the probability of obtaining a good signal-to-background ratio decreases significantly.

BASIC PROTOCOL 3

TWO-DIMENSIONAL GEL ISOELECTRIC FOCUSING

Changes in BVR expression may be reflected by changes in the distribution of its isoforms, which can be resolved by two-dimensional isoelectric focusing. Protein samples are subjected to isoelectric focusing (IEF) in tube gels essentially by the method of O'Farrell (1975). After electrophoresis, the gel is removed from the tube and placed onto a denaturing polyacrylamide gel. Proteins are separated by SDS-PAGE and the resulting gel is either stained or developed as a immunoblot as described in Basic Protocol 2.

Materials

Urea
IEF acrylamide mix (see recipe)
Ampholytes pH 5-8, pH 4-6.5, and pH 3.5-10
10% (w/v) ammonium persulfate
TEMED
Lysis buffer (see recipe)
Overlay solution (see recipe)
Upper electrode buffer: 0.02 N NaOH
Lower electrode buffer: 0.01 M H_3PO_4
Sample for analysis
Gel equilibration buffer (see recipe)

3-ml syringe
10-cm gel tube–loading needle (e.g., Bio-Rad)
IEF tubes, 1.5 mm × 12.5 cm (e.g., Bio-Rad)
IEF apparatus (e.g., Bio-Rad)
Gel tube–extrusion needle (e.g., Bio-Rad)
Glass test tube, ≥15 cm in length

Additional reagents and equipment for SDS-PAGE (*APPENDIX 3*), electrotransfer (*UNIT 2.3*), staining proteins in gels (*APPENDIX 3*), and immunodetection (see Basic Protocol 2)

Prepare tube gels

1. Dissolve 5.5 g urea in 1.33 ml IEF acrylamide mix. Add 0.225 ml ampholyte pH 5-8, 0.225 ml ampholyte pH 4-6.5, and 0.05 ml ampholyte pH 3-10. Bring volume to 10 ml with H_2O. Warm to 37°C until urea is dissolved.
2. Degas solution for 15 min, then add 15 µl of 10% ammonium persulfate and 7 µl TEMED.
3. Pour solution into syringe fitted with gel tube–loading needle.
4. Seal bottom of gel tube with Parafilm, then fill tube with acrylamide solution to a depth of 10 cm. Add solution slowly to avoid introducing bubbles.
5. Overlay acrylamide solution with 20 µl H_2O by slowly pouring down the side of the tube to avoid mixing at the interface. Allow solution to polymerize for 1 hr.
6. Remove water from the top of the gel using a syringe with a pipettor. Add 15 µl lysis buffer followed by 15 µl overlay solution. Remove Parafilm from bottom of tube.
7. Carefully fill tube with upper electrode buffer.
8. Place tubes in holder in IEF apparatus. Fill top and bottom reservoirs with upper and lower electrode buffers, respectively.
9. Prefocus the gel by electrophoresing 15 min at 200 V, 30 min at 300 V, and 1 hr at 400 V.

Prepare sample and perform electrophoresis

10. In a microcentrifuge tube, add solid urea to protein sample until solution is saturated. Then add 1 µl lysis buffer for each 5 µl of sample.

    For purified BVR protein, 3 to 5 µg of sample can be easily detected on a stained gel. If using cytosolic extract, load 100 to 200 µg of protein and perform an immunoblot to detect BVR.

11. After prefocusing, remove IEF tube from apparatus and remove overlay and lysis buffer.
12. Load sample onto top of gel and carefully overlay with 15 µl overlay buffer. Fill remainder of tube with upper electrode buffer.
13. Return tube to IEF apparatus and electrophorese 17 hr at 400 V.
14. Increase voltage to 800 V and electrophorese for an additional 1 hr.
15. Shut off power. Remove upper chamber and then tube.
16. Attach a gel tube–extrusion needle to a 3-ml syringe and fill the syringe with H_2O.

17. Insert the needle into the tube, running the tip against the tube's inside surface, until the tip rests between the gel and the tube.

    Allow the tip to penetrate only a few millimeters below the top of the gel. Do not push the gel with the needle.

18. Very slowly apply pressure to the syringe, carefully rotating the tube at the same time.

    The gentle stream of water will detach the gel from the tube.

19. As the gel is extruded from the bottom of the tube, allow the needle to advance further into the tube. When the needle has been inserted as far as it will go, remove it and use air pressure to expel the gel into a large tray of water.

20. Collect gel in a test tube submerged in the water.

    It is essentially impossible to handle the gel directly without damaging it.

21. Decant the water from the tube and replace with gel equilibration buffer.

22. Incubate tube 20 min with gentle rocking.

Electrophorese the SDS-PAGE dimension

23. Pour a separating gel and stacking gel for SDS-PAGE using 1.5-mm spacers and a preparative comb that produces a loading well that is wider than the length of the tube gel (see *APPENDIX 3*).

24. Remove most of the equilibration buffer from the tube and allow gel to slide out onto a piece of Parafilm. Use a spatula to straighten the gel out on the Parafilm.

25. Carefully slide the gel into the loading well. Try to avoid trapping air bubbles.

26. Perform electrophoresis and transfer proteins to a nitrocellulose membrane (see *UNIT 2.3*). Stain gel for proteins or develop as an immunoblot (see Basic Protocol 2, steps 6 to 18).

SUPPORT PROTOCOL

PREPARATION OF BVR FUSION PROTEIN FROM BACTERIAL CELL EXTRACTS

BVR expressed from plasmids containing cloned BVR cDNA is not stable in some strains of *Escherichia coli* if the cells are grown past log phase. However, significant yields of the BVR–β galactosidase fusion protein can be obtained from cultures grown to relatively late log phase. As is the case for native BVR, the fusion protein is found in the cytoplasmic fraction of the lysates. Lysates are prepared by several cycles of freezing and thawing followed by sonication and centrifugation at 10,000 × *g*. Preparation of bacterial cell lysates is identical to that described in *UNIT 9.3,* Support Protocol 2, except that homogenization buffer is substituted for resuspension buffer in the lysis step. BVR activity is then analyzed as described in Basic Protocol 1 (steps 8 to 12).

These crude lysates have sufficient BVR activity that they can be used to supplement heme oxygenase assays (see *UNIT 9.3*) without the further purification.

Because the stability of the fusion protein varies from one bacterial strain to another, a preliminary time-course study should be performed determine the optimal harvest time for the bacteria.

REAGENTS AND SOLUTIONS

Use Milli-Q-purified water or equivalent for all recipes and protocol steps. For common stock solutions, see ***APPENDIX 2A****; for suppliers, see* ***SUPPLIERS APPENDIX****.*

Antibody diluent

6 g bovine serum albumin
40 mg Thimerosal (Sigma)
40 ml 5× PBS (see recipe)

Add 10 ml normal goat serum and bring volume to 200 ml with H_2O. Centrifuge 15 min at 20,000 × *g*, 4°C. Filter sterilize and store up to 6 months at 4°C.

Biliverdin, 300 µM stock

1 mg biliverdin dihydrochloride (Sigma)
5.08 ml methanol
Keep on ice in reduced light
Prepare fresh daily

Blocking solution

6 g bovine serum albumin
40 mg Thimerosal (Sigma)
40 ml 5× PBS (see recipe)

Add 20 ml normal goat serum and bring volume to 200 ml with H_2O. Centrifuge 30 min at 20,000 × *g*, 4°C. Filter sterilize and store up to 6 months at 4°C.

BVR assay buffer, pH 6.75

Dissolve 3.95 g KH_2PO_4 and 3.66 g K_2HPO_4 in 400 ml H_2O. Add 5 ml 0.1 M EDTA (*APPENDIX 2A*) and adjust to pH 6.75 with KOH. Bring volume to 500 ml with H_2O. Autoclave to sterilize and store at 4°C for up to 6 months.

BVR assay buffer, pH 8.7

Dissolve 6.057 g Tris base in 400 ml H_2O. Add 5 ml 0.1 M EDTA (*APPENDIX 2A*) and adjust to pH 8.7 with HCl. Bring volume to 500 ml with H_2O. Store up to 6 months at 4°C.

Cofactor buffer

Adjust 2 ml BVR assay buffer, pH 6.75 (see recipe), to pH ~7.8 by adding 0.1 ml of 1 N NH_4OH. Bring volume to 4 ml with H_2O.

If preparing larger volumes, buffer can be stored up to 6 months at 4°C.

Gel equilibration buffer

10 ml glycerol
4 ml 2-mercaptoethanol
16 ml 10% (w/v) SDS
10 ml 0.5 M Tris·Cl, pH 6.8
2 ml 0.05% (w/v) bromphenol blue
40 ml H_2O
Store up to 1 year at 4°C

Homogenization buffer

10 ml 1 M Tris·Cl, pH 7.5 (*APPENDIX 2A*)
790 ml H_2O
85.58 g sucrose
H_2O to 1 liter
Filter sterilize and store up to 6 months at 4°C

IEF acrylamide mix

141.9 g acrylamide
8.1 g bisacrylamide
H_2O to 500 ml
Filter through Whatman no. 1 filter paper
Store up to 1 year at 4°C

Lysis buffer

5.7 g urea
2 ml 10% Nonidet P-40
0.2 ml pH 5-8 ampholytes
0.2 ml pH 4-6.5 ampholytes
0.1 ml pH 3-10 ampholytes
0.5 ml 2-mercaptoethanol
H_2O to 10 ml
Prepare fresh daily

Overlay solution

5.5 g urea
0.1 ml pH 5-8 ampholytes
0.1 ml pH 4-6.5 ampholytes
0.05 ml pH 3-10 ampholytes
H_2O to 5 ml
Prepare fresh daily

Phosphate-buffered saline (PBS), 5×

10.8 g KH_2PO_4
55.7 g K_2HPO_4
175.3 g NaCl
3 liters H_2O
Adjust pH to 7.4 with KOH
Bring volume to 4 liters with H_2O
Store indefinitely at room temperature
To obtain 1× PBS, dilute 4:1 with H_2O before use

Transfer buffer

25 mM Tris·Cl, pH 8.3 (*APPENDIX 2A*)
192 mM glycine
20% (v/v) methanol
Store up to 1 year at room temperature

COMMENTARY

Background Information

In mammals and some species of fish, the cytosolic enzyme biliverdin reductase (BVR) reduces biliverdin IXα—the open tetrapyrole product of the oxidative cleavage of heme by heme oxygenase—to bilirubin (Singleton and Laster, 1965; Colleran and O'Carra, 1970; Tenhunen et al., 1970). In mammals, bilirubin is subsequently glucuronidated by bilirubin UDP-glucuronosyltransferase and excreted. BVR reduces the γ bridge of biliverdin using either NADH or NADPH as a cofactor. The optimal pH for BVR activity differs for each of the pyridine nucleotides. Optimal activity is seen at pH 6.75 with NADH and at 8.7 when NADPH is used as the cofactor for the enzyme purified from rat (Kutty and Maines, 1981). Human biliverdin IXα reductase also shows similar cofactor specificity and pH optima, although the pH optimum for NADH is broader for human BVR than for the rat enzyme (Maines and Trakshel, 1993; Maines et al., 1996).

Whether isolated from rat or human tissue, BVR is strongly inhibited by thiol agents, suggesting that cysteine residues are important for

enzymatic activity. Both rat and human BVRs have been cloned and expressed in *E. coli* (Fahkrai and Maines, 1992; Maines et al., 1996) and the critical nature of the cysteine residues has been confirmed by site-directed mutagenesis of the rat enzyme (McCoubrey and Maines, 1994). Rat and human BVRs share 83% identity in amino acid sequence and differ in length by a single additional amino acid residue present in the human protein. On SDS-PAGE the rat enzyme has a mobility comparable to its predicted size (~34 kDa); however, human BVR migrates anomalously, yielding an apparent size of 39 to 42 kDa. Human BVR expressed from the cDNA also shows an abnormal mobility. The explanation for this phenomenon remains to be elucidated. Despite the relatively strong sequence homology between rat and human BVR, antisera raised to the enzymes show pronounced species specificity. Antibodies raised against the human form have extremely low immunoreactivity toward the rat protein.

Purified BVR exists as a large number of isoelectric variants. At least ten isoforms can be detected by two-dimensional gel electrophoresis using protein purified from various tissues (Huang et al., 1989); the relative abundance of isoforms varies among tissues. Several variants are also detected when the enzyme is expressed in bacteria (Maines et al., 1996), which suggests that at least some variants may be the result of post-translational modifications common to both prokaryotes and eukaryotes. Recently it has been demonstrated that differential phosphorylation plays a significant role in generation of the variant isoforms (Huang et al., manuscript in preparation). It is likely that phosphorylation regulates enzyme activity. Thus, changes in the distribution of the variants may reflect a regulation of BVR at the post-translational level.

Critical Parameters

The most common error in detection of BVR activity results from improper preparation or storage of reagents. Biliverdin is not soluble in aqueous solutions, and failure to completely dissolve the substrate in methanol before adding it to the reaction mixture may result in spectral interference and an inaccurate measurement of BVR activity. Similarly, exposing biliverdin to light may cause it to degrade, thus altering the kinetics of the reaction.

Cofactor instability can also lead to spurious results. Although NADPH solutions remain stable for many hours if kept on ice, they should be prepared as close to the time of use as possible. Rapid use is even more essential for NADH, which is comparatively unstable in solution and should be used immediately after preparation.

For Basic Protocol 2, all of the critical parameters normally pertinent to immunoblotting will apply. Of particular note for BVR blots is the species specificity of antisera. Polyclonal sera prepared against rat BVR recognize the human enzyme poorly, and antisera prepared against human BVR recognize the rat protein to an extremely limited degree. Thus selecting the appropriate antibody is essential for success of the procedure.

For two-dimensional gel electrophoresis (Basic Protocol 3), all considerations relevant to electrophoresis and immunoblotting apply. In particular, caution should be used to avoid introduction of air bubbles into the gels. Bubbles are frequently trapped between the tube gel and the surface of the second gel and can prevent an even transfer of the protein, which leads to artifacts. The small-diameter IEF tubes must be cleaned scrupulously and rinsed well prior to use to avoid the buildup of bubbles, which can effectively block the tube. Care must be taken when overlaying solutions in the tubes to avoid similar problems. As noted in the protocol, extrusion of the gel is accomplished using the water in the syringe, not the needle, as the latter can easily tear the gel.

Troubleshooting

As noted above, degradation of the cofactor solutions, especially NADH, can decrease the success and reproducibility of the assay. As a general rule, when activities appear lower than anticipated, it is wise to repeat the assay with fresh cofactor. Also, BVR activity is maximal when the substrate concentration is in the 3- to 5-μM range. Use of concentrations above or below this range will yield reduced estimates of activity. Thus, care should be taken in the preparation of stock and reaction solutions.

When sample preparations may contain very high levels of BVR activity, it is possible that addition of too much protein will lead to inaccurate estimates of activity. If too much BVR is present, so much substrate may be converted to product initially that the reaction will no longer be in the linear range during the spectrophotometric scan. In some cases the biliverdin may be virtually exhausted before the scan begins. Such a situation sometimes occurs when using purified protein or bacterial cell extracts that express high concentrations of

BVR fusion protein. Frequently, dilution of the protein preparation will remedy this problem. Additionally, the reaction rate should be determined by taking an average of activities measured during several short periods, rather than a single long period (e.g., four readings over 15 sec rather than one reading lasting 1 min). A decrease in the initial activity rate during the later intervals would suggest nonlinear kinetics, and the assay should be repeated with a reduced amount of protein.

In addition to the critical parameters noted above, most difficulties in immunoblotting and IEF arise from the technical problems typical of SDS-PAGE or to problems with the antibody solutions. Upon initial use, polyclonal antisera may detect proteins in addition to BVR. Such activity is particularly likely when crude bacterial extracts are used, as the hosts (generally rabbit) are frequently exposed to *E. coli* antigens and may develop antibodies to some of them. These antibodies are generally relatively low in titer compared to the antibodies raised against the immunogen and their activity is reduced with subsequent reuse of the serum. However, excessive reuse of the working antibody solutions eventually results in decreased signal sensitivity. If maximum sensitivity is required in examining bacterial lysates, it may be necessary to preabsorb the serum with lysates prepared from the same *E. coli* strain lacking BVR cDNA.

Anticipated Results

Preparations of rat liver and kidney cytosol generally yield specific activities in the range of 1 U/mg of total protein. Bacterial cell extracts typically have 10 to 20 times the specific activity of tissue preparations. The number and relative distribution of isoelectric variants will differ depending on the tissue being examined and the treatment regimen. In general both kidney and liver will show five or six isoform bands.

Time Considerations

Dissection of tissue and preparation of cytosolic fractions or collection of bacterial cells and preparation of lysate requires ~2 hr. Determination of protein concentrations and preparation of reagents for the kinetic assay takes ~1 hr, and the assay and calculations require 1 to 2 hr depending on the number of samples. Immunoanalysis is typically performed over the course of 2 days but can be accomplished in 1 day if the blocking step is carried out at 37°C. The first phase of two-dimensional gel electrophoresis requires a full day, due to the 17-hr electrophoresis step. The second dimension and immunoblotting usually takes 2 days.

Literature Cited

Colleran, E. and O'Carra, P. 1970. Specificity of biliverdin reductase. *Biochem. J.* 119:16P-17P.

Fahkrai, H. and Maines, M.D. 1992. Expression and characterization of a cDNA for rat kidney biliverdin reductase: Evidence suggesting the liver and kidney enzymes are the same transcript product. *J. Biol. Chem*. 267:4023-4029.

Huang, T.J., Trakshel, G.M., and Maines, M.D. 1989. Detection of ten variants of biliverdin reductase in rat liver by two-dimensional gel electrophoresis. *J. Biol. Chem.* 264:7844-7849.

Kutty, R.K. and Maines, M.D. 1981. Purification and characterization of biliverdin reductase from rat liver. *J. Biol. Chem*. 256:3956-3962.

Maines, M. and Trakshel, G.M. 1993. Purification and characterization of human biliverdin reductase. *Arch. Biochem. Biophys.* 300:320-326.

Maines, M.D., Polevoda, B.V, Huang, T.J., and McCoubrey, W.K., Jr. 1996. Human biliverdin IXα reductase is a zinc-metalloporphyrin: Characterization of purified and *Escherichia coli* expressed enzymes. *Eur. J. Biochem*. 235:372-381.

McCoubrey, W.K., Jr. and Maines, M.D. 1994. Site-directed mutagenesis of cysteine residues in biliverdin reductase: Roles in substrate and cofactor binding. *Eur. J. Biochem*. 222:597-603.

O'Farrell, P.H. 1975. High resolution two dimensional gel electrophoresis of proteins. *J. Biol. Chem.* 250:4007-4021.

Singleton, J.W. and Laster, L. 1965. Biliverdin reductase of pig liver. *J. Biol. Chem*. 240:4780-4789.

Tenhunen, R., Ross, M.E., Marver, H.S., and Schmid, R. 1970. Reduced nicotinamide dinucleotide phosphate dependent biliverdin reductase: Partial purification and characterization. *Biochemistry* 9:298-303.

Contributed by Tian-Jun Huang
New York Blood Center
New York, New York

Histochemical Analysis of Heme Degradation Enzymes

Histochemical analysis of the heme degradation system provides critical insights into the cellular localization, expression, and regulation of enzymes responsible for catabolism of the heme molecule. Assessment of the expression and regulation of select mRNAs and protein by in situ hybridization histochemistry (ISH; see Basic Protocol 1) and immunohistochemical approaches (IHC; see Basic Protocol 2 and Alternate Protocols 1 to 3) allows, respectively, for visualization and analysis of specific cellular sites of expression. Immunohistochemistry represents an important adjunct to gross biochemical, molecular, and activity measurements of tissue enzyme protein and transcripts (see *UNITS 9.2, 9.3 & 9.4*). Successful application of histochemical technique is as much an art as it is science. As such, the protocols described here constitute basic histochemical procedures for analysis of the heme degradation system, but some empirical modifications may be necessary to optimize the application for the special requirements of a particular experimental design, tissue source, or type of tissue. Additional protocols describe preparation of tissues for ISH and IHC (see Support Protocol 1) and adsorbing antibody with antigen to demonstrate specificity of staining (see Support Protocol 2).

DETECTION OF HEME OXYGENASE 1 AND 2 TRANSCRIPTS BY ISH

BASIC PROTOCOL 1

Cloning and characterization of the genes for rat heme oxygenase 1 (HO-1; Shibahara et al., 1985) and heme oxygenase 2 (HO-2; Rotenberg and Maines, 1990) have allowed for derivation of specific cDNA probes and characterization of transcripts coding for HO isozymes from a variety of tissue sources across mammalian species, including rodent and human (reviewed in Maines, 1992, 1997). ISH has been successfully applied to reveal the cellular localization of HO gene expression in brain (Ewing and Maines, 1992; Verma et al., 1993) and testis (Maines and Ewing, 1996). This nonisotopic approach, using digoxigenin labeling of cDNA, affords a highly sensitive technique without the hazards inherent in using radioisotopes. Furthermore, immunochemical detection of the HO-1/HO-2 cDNA-mRNA hybrids can be completed in 1 day, whereas techniques utilizing autoradiographic detection of radiolabeled probes can take weeks to obtain proper exposure. Using this method, specific mRNA can be detected in a heterogeneous cell population where only a subpopulation may be transcribing the HO-1/HO-2 gene.

This protocol describes in situ detection of HO-1 or HO-2 mRNAs. Selective cDNA probes that encode complementary sequence to either HO-1 or HO-2 mRNAs are produced and tagged with digoxigenin. Paraffin-embedded tissue is prepared under conditions that preserve the integrity of the target mRNAs and is then treated to allow penetration of the digoxigenin-labeled HO-1/HO-2 cDNA probes. Prepared tissue is incubated overnight with the appropriate cDNA probe to allow formation of cDNA/mRNA hybrids. The tissue is washed under conditions of sufficient stringency to reduce nonspecific adherence of cDNA probes with tissue components. Finally, the authentic cDNA/mRNA hybrids are immunochemically visualized.

Contributed by James F. Ewing

Current Protocols in Toxicology (1999) 9.5.1-9.5.22

Materials

10× PCR buffer (see recipe)
2 mM dNTP mix (2 mM each of dATP, dGTP, dCTP, and dTTP)
100 mM stocks of HO-1 or HO-2 sense and antisense primers (Midland Certified Reagent Co.):
HO-1 primers: 5′-TGCACATCCGTGCAGAGAAT-3′ (+71 to +90) and 5′-AGGAAACTGAGTGTGAGGAC-3′ (+814 to +833)
HO-2 primers: 5′-GAAGTGAGGGCAGCACAAAC-3′ (−32 to −13) and 5′-CTTCTTCAGCACCTGGCCT-3′ (+486 to +504)
5 U/µl *Taq* DNA polymerase (U.S. Biochemical)
10 to 20 µl/ml template plasmid DNA
Mineral oil
Chloroform
1% (w/v) agarose gel (see recipe)
1× TAE buffer (see recipe) containing 0.5 µg/ml ethidium bromide (added from 5 mg/ml ethidium bromide stock; see recipe)
3 M sodium acetate, pH 5.2 (*APPENDIX 2A*)
70% and 100% ethanol
TE buffer, pH 8 (see recipe)
GeneClean kit (Bio 101)
Digoxigen-dNTP labeling mix (see recipe)
Slides containing paraffin-embedded tissue sections of interest (see Support Protocol 3)
Xylene
Graded ethanol series: 50%, 60%, 70%, 80%, 90%, and 100% (v/v) ethanol
Phosphate-buffered saline (PBS; *APPENDIX 2A*)
0.2 N HCl
2×, 1×, 0.5×, 0.25×, and 0.05× SSC (see recipe for 20×)
10 µg/ml proteinase K working solution (see recipe; preincubate 45 min at 37°C before use)
4% (w/v) paraformaldehyde
Prehybridization buffer (see recipe)
Buffer I (see recipe)
Blocking solution (see recipe)
Anti-digoxigenin antibody-alkaline phosphatase conjugate (Fab fragments; Boehringer Mannheim)
Buffer II (see recipe)
Developer solution (see recipe)
Aqueous mounting medium

Programmable thermal cycler
Coplin jars
Humidified chambers: large plastic culture dishes lined with RNase-free H_2O-saturated Whatman filter paper
Glass coverslips

Additional reagents and equipment for agarose gel electrophoresis (*UNIT 2.2* & *APPENDIX 3*)

Prepare double-stranded templates for HO-1/HO-2 by PCR

To exclude vector sequence and yield a probe with defined ends, the target is amplified from double-stranded template prior to generation of single-stranded probes.

1. Combine the following in a 0.5-ml microcentrifuge tube:

   76.5 µl distilled water
   10 µl 10× PCR buffer
   10 µl 2 mM dNTP mix
   1 µl 100 mM HO-1 or HO-2 sense primer stock solution (100 pmol)
   1 µl 100 mM HO-1 or HO-2 antisense primer stock solution (100 pmol).

2. Add 0.5 µl of 5 U/µl *Taq* DNA polymerase and 1 µl (20 ng) of the appropriate template plasmid.

   Appropriate negative controls may include a reaction mixture without Taq DNA polymerase enzyme and another without template plasmid. The template plasmid can be generated by RT-PCR of mRNA from rat spleen (HO-1) or rat testes (HO-2).

3. Vortex mixture and gently overlay with 70 µl mineral oil.

4. Carry out PCR in a programmable thermal cycler using the following amplification cycles:

1 cycle:	2 min	94°C	(denaturation)
30 cycles:	1 min	94°C	(denaturation)
	1.5 min	57°C	(annealing).
	4 min	70°C	(extension)
Final step:	10 min	70°C	(hold)

5. Cool at 4°C, add 100 µl chloroform, then vortex for 15 sec. Transfer the top (aqueous) phase to a clean microcentrifuge tube.

   Upon chloroform addition the mineral oil will settle to the bottom of the microcentrifuge tube.

6. Remove 5 µl of the aqueous phase and analyze by electrophoresis on a 1% (w/v) agarose gel in 1× TAE buffer containing 0.5 µg/ml ethidium bromide (see *UNIT 2.2* & *APPENDIX 3A*).

7. After electrophoresis, visualize the amplified fragment using a UV light source (see *UNIT 2.2* & *APPENDIX 3*). A bright fluorescent band should be visualized on the gel following amplification relative to negative controls.

Purify the double-stranded DNA template

8. If the HO-1/HO-2 cDNA has been suitably amplified, add 10 µl of 3 M sodium acetate, pH 5.2, and 300 µl of ice-cold 100% ethanol to the remainder of the aqueous phase to precipitate the amplified DNA fragment. Vortex and place on dry ice for 10 to 20 min.

9. Microcentrifuge 15 min at 10,000 × *g*, 4°C. Decant the supernatant and rinse the pellet containing the cDNA by adding 70% ethanol and microcentrifuging 5 min at 10,000 × *g*, 4°C. Decant the supernatant, air dry the pellet, and resuspend it in 20 µl TE buffer, pH 8.

10. Electrophorese sample on two lanes of a 1% (w/v) standard agarose gel in 1× TAE buffer containing 0.5 µg/ml ethidium bromide (see *UNIT 2.2* & *APPENDIX 3A*).

11. Visualize the purified material using a UV-light source and excise the bands corresponding to the size of the desired HO-1 (763-bp)/HO-2 (563-bp) fragment.

12. Purify the fragment away from the agarose using the GeneClean kit, according to the manufacturer's instructions.

13. Quantitate the final DNA concentration of the sample by comparison with standards in a 1% agarose gel, and store sample at −20°C.

Label single-stranded probes

14. Starting with the double-stranded template, prepare single-stranded sense and antisense probes by asymmetric PCR and purify as described above for preparation of the double-stranded template (steps 1 to 13), with the following modifications at the indicated steps.

    a. In step 1, for each single-stranded probe (sense and antisense), use only one of the two HO-1/HO-2 primers in the reaction mixture.

       HO-1 primer, +71 to +90, is used to generate the sense orientation, whereas the complement of +814 to +833 is used for antisense. HO-2 primer, −32 to −13, is used to generate the sense orientation, whereas the complement of +486 to +504 is used for antisense.

    b. Also in step 1, use 10 µl digoxigenin-dNTP labeling mix instead of 10 µl of the standard 2 mM dNTP stock in the reaction mix.

    c. In step 2, use 5 µl (2 ng/µl) of the double-stranded HO-1/HO-2 fragment from (step 13) as the template, instead of the plasmid template.

    d. The total volume of the reaction is maintained at 100 µl by the addition of the appropriate amount of RNase-free water.

       The probe is stored at −20°C and is stable for at least 6 months.

Experimental day 1: Pretreat tissue

15. To increase diffusion of HO-1/HO-2 cDNA probes into cells, clear tissue of paraffin by placing slides twice sequentially, each time for 10 min, in Coplin jars containing xylene.

    See Support Protocol 1 for preparation of tissue.

16. Rehydrate the tissue by sequential incubations of 3 min each in graded ethanol solutions from 100% to 50% in increments of 10%.

17. Equilibrate the tissue in PBS with three sequential incubations for 3 min each.

18. Denature the tissue by immersing in in 0.2 N HCl and incubating 20 min.

19. Incubate tissue for 15 min in 2× SSC.

20. Equilibrate the tissue in PBS with two sequential incubations for 3 min each.

21. Apply 10 µg/ml proteinase K to the tissue section on the slide and incubate 30 min at 37°C in a humidified chamber.

    Depending on the tissue type the length of digestion may have to be optimized for maximal probe penetration.

22. Rinse the deproteinated tissue with PBS to remove excess enzyme, then incubate tissue in 4% (w/v) paraformaldehyde for 5 min at 4°C . Rinse tissue briefly in PBS, then air dry for 10 min.

    Depending on the tissue type the length of fixation may have to be optimized.

Prehybridize and hybridize tissue

23. Pipet prehybridization buffer onto the dry tissue section and incubate the slides in a humidified chamber for 1 hr at room temperature.

24. Rinse tissue in 2× SSC for 15 min. Dehydrate slides by sequential incubations of 3 min each in graded ethanol solutions from 50% to 100% in increments of 10% (i.e., in the opposite order from step 16).

25. Dilute the HO-1/HO-2 cDNA probe (from step 14) to 2 ng/ml in prehybridization solution. Pipet this hybridization solution onto the dry tissue.

In addition to the HO-1/HO-2 antisense probe, the appropriate HO-1/HO-2 sense probe should be run in parallel and at the same concentration. The latter constitutes a negative test, or control, for HO-1/HO-2 mRNA. Also, a control in which no probe is applied to the tissue should be tested under in situ hybridization conditions to confirm the absence of endogenous alkaline phosphatase activity in tissue sections.

26. Gently apply Parafilm coverslips, taking care to exclude all air bubbles. Transfer slides to humidified chambers, seal the cover of each chamber with Parafilm, and incubate 16 hr at 37°C.

    "Parafilm coverslips" are applied as follows. Gently grasp the end of a precut rectangular piece of Parafilm with a pair of forceps. Lay the edge of the Parafilm at the end of the slide and gently place the coverslip onto the tissue by slowly decreasing the angle between the Parafilm and the slide. This technique will allow even distribution of probe solution and displacement of air bubbles.

Experimental day 2: Post-hybridize and perform immunohistochemistry

27. Perform post-hybridization treatment of tissue by sequentially incubating in Coplin jars containing: 2× SSC (40 min, 25°C), 1× SSC (40 min, 25°C), 0.5× SSC (40 min, 37°C), 0.25× SSC (40 min, 25°C), and 0.05× SSC (40 min, 25°C), respectively, prior to immunochemical localization.

    Time and stringency may have to be varied depending on the tissue source.

28. Rinse tissue briefly in buffer I, then block tissue by treating for 30 min with blocking solution at 25°C.

29. Dilute anti-digoxigenin antibody–alkaline phosphatase conjugate 1/500 in blocking solution. Replace the blocking solution from the previous step with this diluted primary antibody and incubate 1 hr at 25°C in a humidified chamber.

30. Rinse the tissue twice with buffer I, each time for 10 min at 25°C to remove excess primary antibody.

31. Equilibrate the tissue for 10 min in buffer II, then begin incubating in developer solution in the dark, while monitoring color development in the tissue every 30 min using a microscope. If the staining intensity is not sufficient, return the slide to the developer for another 30-min incubation period. Otherwise proceed to step 32.

    Slides may either be immersed in developer or the developer applied to the section directly.

    The hybrids of HO-1/HO-2 cDNA and mRNA will be indirectly visualized as deposits of purple formazan dye in cells within the tissue.

32. When staining intensity is satisfactory, terminate reaction by rinsing slides in distilled water.

33. Coverslip (glass) slides using aqueous mounting medium and store in a light-tight container.

IMMUNOHISTOCHEMICAL ANALYSIS OF HEME DEGRADATION SYSTEM IN FREE-FLOATING SECTIONS

BASIC PROTOCOL 2

Immunohistochemistry (IHC) has been widely applied to reveal the cellular localization of HO gene expression in a variety of tissues (see Table 9.5.1). Using this method, specific sites of protein expression can be detected in a heterogeneous cell population where only a subset of cells may be translating the HO-1/HO-2 gene. The IHC procedures describe how to localize HO system components with specific antibody preparations that are commercially available.

Table 9.5.1 Histochemical Analysis of Heme Degradation System in Various Species and Tissues

Organ system	Species	Reference	Comments
Nervous	Rat	Ewing and Maines, 1991. *PNAS* 88:5364	HO-1/-2 expression and heat shock response in adult
		Ewing et al., 1992. *J. Neurochem.* 58:1140	Detailed pattern of HO-1 protein expression in normal and thermal-stressed adult
		Ewing and Maines, 1992. *Mol. Cell. Neurosci.* 3:4559	Detailed pattern of HO-2 protein and transcript expression in adult; comparison with HO-1
		Ewing and Maines, 1993. *J. Neurochem.* 60:1512	Effect of glutathione depletion on HO-1/-2 protein expression in adult brain
		Ewing et al., 1993. *J. Neurochem.* 61:1015	Expression HO-1/-2 and BVR proteins in normal and heat shock brain
		Maines et al., 1993. *Mol. Cell. Neurosci.* 4:389	Effect of glutathione depletion on HO-1/-2 expression in the neonate
		Verma et al., 1993. *Science* 259:381	HO-2 transcript expression in adult brain
		Weber et al., 1994. *J. Neurochem.* 63:953	Effect of glucocorticoid on HO-2 protein expression
		Vincent et al., 1994. *Neuroscience* 63:223	HO-1/-2 and NOS colocalization in adult brain
		Maines et al., 1995. *J. Neurochem.* 64:1769	Effect of corticosterone on HO-1 heat shock response
		Dwyer et al., 1995. *Neuroreport* 6:973	HO-2 protein expression in spinal cord
		Ewing and Maines, 1995. *Brain Res.* 672:29	Age-related changes in BVR protein expression
		Yamanake et al., 1996. *Neurosci. Res.* 24:403	HO-2 protein expression in cerebellum
		Maines et al., 1996. *Brain Res.* 722:83	Effect of corticosterone on expression of HO-2 protein and transcript in the neonate
		Kaistinaho et al., 1996. *Eur. J. Neurosci.* 8:2265	Effect of transient focal ischemia on HO-1 protein expression
		Takeda et al., 1996. *Neurosci. Lett.* 205:169	Effect of transient forebrain ischemia on HO-1/-2 protein expression
		Matz et al., 1996. *J. Neurosurg.* 85:892	Expression of HO-1 protein and transcript following subarachnoid injection of lysed blood
		Geddes et al., 1996. *Neurosci. Lett.* 210:205	Effect of focal and global ischemia on HO-1/-2 protein expression
		Raju et al., 1997. *Biochim. Biophys. Acta.* 1351:89	Effect of corticosterone on HO-2 protein and transcript expression in COS cells
		Matz et al., 1997. *J. Neurosurg.* 40:152	Effect of intracerebral hemorrhage on HO-1/-2 protein expression
	Mouse	Maines, 1998. *J. Neurochem.* 70:2057	HO-1 expression in transgenic mice
	Human	Smith et al., 1994. *Am. J. Path.* 145:42	HO-1 protein expression in brain with Alzheimer's disease
		Schipper et al., 1995. *Annal. Neurol.* 37:758	HO-1 protein expression in senescent brain and brain with Alzheimer's disease
		Smith et al., 1995. *Mol. Chem. Neuropath.* 24:227	HO-1 protein expression in sensory ganglia

continued

Table 9.5.1 Histochemical Analysis of Heme Degradation System in Various Species and Tissues, continued

Organ system	Species	Reference	Comments
	Guinea Pig	Vollerthun et al., 1995. *Neuroreport* 7:173	HO-2 protein expression in postganglionic neurons
		Vollerthun et al., 1996. *Histochem. Cell. Biol*. 105:453	HO-2 protein expression in sensory ganglia
Cardiovascular	Rat	Ewing et al., 1994. *J. Pharmacol. Exp. Ther.* 271:408	Effect of thermal stress on HO-1/-2 protein expression in heart and cardiovasulature
	Guinea Pig	Hassall and Hoyle, 1997. *Neuroreport* 8:1043	HO-2 and NOS protein expression in intracardiac neurons
Digestive	Mouse	Miller et al., 1998. *Gastroenterology* 114:239	HO expression in small intestine
Reproductive	Rat	Ewing and Maines, 1995. *Endocrinology* 136:2294	Testicular expression of HO-1/-2 protein and transcript in normal and thermal-stressed adult
		McCoubrey et al., 1995. *Biol. Reprod.* 53:1330	Developmental pattern of HO expression in testis
		Maines and Ewing, 1996. *Biol. Reprod*. 54:1070	HO-1 stress response in testis
	Mouse	Matejevic et al., 1996. *Acta Histochem*. 98:173	Assessment of HO-2 protein expression in murine placental structures
Respiratory	Rat	Lee et al., 1996. *Am. J. Resp. Cell. Mol. Biol*. 14:556	Effect of hyperoxia on HO-1 protein expression
Urogenital	Pig	Werkstrom et al., 1997. *Brit. J. Pharmacol*. 120:312	HO-1/-2 protein expression in bladder and urinary tract
	Human	Maines and Abrahamsson, 1996. *J. Urol*. 47:727	HO-1 protein expression in normal, hyperplastic and prostatic tumor tissue
		Hedlund et al., 1997. *J. Autonomic Nervous System* 63:115	HO and NOS expression in prostate
Visual	Rat	Nishimura et al., 1996. *Neurosci. Lett*. 205:13	Effect of light adaption on HO-1/HO-2 protein expression in retina
Various	Rat	Grozdanovic and Gossrau, 1996. *Acta Histochem*. 98:203	Survey of HO-2 protein expression

Briefly, frozen tissue is prepared under conditions that preserve both the integrity of the tissue and the select antigenic proprerties of the target protein needed for antibody binding. Tissue is treated to allow entry of antibody directed against the target protein. The tissue is washed under conditions of sufficient stringency to reduce nonspecific adherence of antibody with tissue components. Tissue is then incubated with secondary antibody and washed. Finally, the authentic antibody-antigen complexes are visualized using an immunochemical detection system typically consisting of a tertiary antibody conjugated to peroxidase followed by diaminobenzidine treatment. Consequently, sites of protein expression are stained brown.

NOTE: Tissue preparations for IHC primarily fall into two categories, depending on the method used for handling post fixation: paraffin-embedded sections and frozen sections. In turn, frozen tissue sections may be subjected to IHC procedure as mounted sections or free-floating sections. This latter format is commonly applied to analysis of components of the heme degradation system in brain tissue.

Materials

Frozen tissue sections (Support Protocol 1)
0.1 M sodium phosphate buffer, pH 7.3 (*APPENDIX 2A*)

PBTX: 0.3% (v/v) Triton X-100 in 0.1 M sodium phosphate buffer, pH 7.3 (store up to 1 month at 4°C)
Antibody buffer: PBTX (see above) containing 10% (v/v) normal goat serum (NGS)—filter through 0.45-µm filter fitted to a syringe; prepare fresh
Primary antibody: HO-1, HO-2, or BVR antibody (StressGen)
Secondary antibody: goat anti-rabbit γ-globulin (Organon Teknika Cappel)
Tertiary antibody: peroxidase-anti-peroxidase antibody (Organon Teknika Cappel)
0.05 M Tris·Cl, pH 7.5 (*APPENDIX 2A*)
0.5% (w/v) 3,3-diaminobenzidine tetrahydrochloride dihydrate (DAB) in 0.05 M Tris·Cl, pH 7.5 (prepare fresh; filter through Whatman filter paper)
3% (v/v) hydrogen peroxide (prepare fresh from 30% hydrogen peroxide)
Graded ethanol series: 50%, 60%, 70%, 80%, 95%, and 100% (v/v) ethanol
Xylene
Cytoseal 60 mounting medium

Small paint brushes
Netted compartments (Brain Research)
Tabletop shaker
60 × 15–mm tissue culture dishes (Falcon)
Superfrost Plus slides (Fisher)
Slide warmer
Glass coverslips
Large crystallization dishes

Experimental day 0

1. On the night before the experiment is to begin, soak tissue for 16 hr in 0.1 M sodium phosphate buffer, pH 7.3, at, 4°C with gentle agitation on a tabletop shaker.

   Tissue is transferred to netted compartments which are then placed in large crystallization dishes containing 0.1 M sodium phosphate buffer, pH 7.3.

   This incubation serves to remove the cryoprotectant from the sections.

Experimental day 1: Expose to primary antibody

2. With a small paintbrush, transfer tissue into netted compartments and then place the compartments into a large crystallization disk containing 0.1 M sodium phosphate buffer, pH 7.3.

   Many sections may be processed in a single netted compartment.

3. Wash sections three times with 0.1 M phosphate buffer, pH 7.3, each time by incubating 5 min at room temperature with shaking.

   All washes are performed on a tabletop shaker at room temperature unless otherwise specified. The speed of shaking should allow for gentle movement of the tissue within the netted compartment.

4. Wash sections three times in PBTX, each time by incubating 5 min.

5. Block the tissue by incubating 20 min in antibody buffer.

6. Transfer tissue into 60 × 15–mm culture dishes containing primary antibody (HO-1, HO-2, or BVR) diluted to the appropriate concentration in antibody buffer. Incubate from overnight to ≤4 days in a cold room (4°C).

   The final concentration of antibody depends on the specific antibody preparation being used and may need to be empirically determined.

Experimental day 2: Expose to secondary antibody

7. Transfer the tissue out of the dishes containing the primary antibody into netted compartments with PBTX. Wash tissue with eight changes of PBTX, at room temperature, over a period of 2 to 3 hr.
8. Preincubate the tissue sections in antibody buffer for 20 min.
9. Transfer the tissue out of the netted compartments into 60 × 15–mm culture dishes containing goat anti-rabbit γ-globulin (GAR) secondary antibody diluted 1/1000 (v/v) in antibody buffer.

   If a primary antibody is derived from a source other than rabbit, then the choice of secondary antibody should be adjusted accordingly for specificity.

10. Incubate tissue in secondary antibody overnight in a cold room.

Experimental day 3: Expose to tertiary antibody

11. Transfer the tissue into netted compartments containing PBTX. Wash the tissue with eight changes of PBTX over a period of 1.5 to 3 hr.
12. Preincubate tissue sections in antibody buffer for 20 min.
13. Transfer tissue sections into culture dishes containing peroxidase-anti-peroxidase tertiary antibody diluted 1:500 (v/v) in antibody buffer. Incubate tissue in tertiary antibody for 1 hr at room temperature.
14. Transfer tissue into netted compartments containing 0.1 M sodium phosphate buffer, pH 7.3. Wash tissue with eight changes of 0.1 M sodium phosphate buffer, pH 7.3, over a period of 1 to 2 hr.
15. Wash tissue twice, each time for 10 min, in 0.05 M Tris, pH 7.5.

Detect bound antibodies

16. Incubate tissue in 0.5% DAB/0.05 M Tris·Cl, pH 7.5.

    CAUTION: *Development reagents should be prepared and used in a fume hood. 3,3-diaminobenzidine tetrahydrochloride dihydrate (DAB) is a carcinogen. DAB solutions may be inactivated by addition of full-strength bleach. Furthermore, DAB-tainted glassware should be decontaminated by rinsing with bleach prior to further cleaning. All DAB-containing solutions should be handled as chemical waste in accordance with institutional guidelines.*

17. Add 33 ml of 3% hydrogen peroxide to 100 ml of freshly prepared 0.5% DAB/0.05 M Tris·Cl, pH 7.5. Immediately begin incubating tissue in this developer solution and continue incubation up to 15 min, visually inspecting selected sections under a microscope frequently to assess the progress of development.

    The reaction product is brown.

18. Terminate the development process by washing the tissue sections three times, each time for 10 min, in 0.05 M Tris, pH 7.5.
19. Wash tissue sections three times, each time for 15 min, in 0.1 M sodium phosphate buffer, pH 7.3. Store sections in 0.1 M sodium phosphate buffer, pH 7.3, at 4°C until further processing.

Process tissue sections

20. Mount sections onto Superfrost Plus slides with a paintbrush.
21. Dry the mounted sections covered at 37°C on a slide warmer.
22. Dehydrate the tissue by immersing the slides successively, each time for 3 min, in Coplin jars containing 50%, 60%, 70%, and 80% (v/v) ethanol solutions, respectively.

Then, immerse slides twice, each time for 3 min, in 95% ethanol, and finally three times, each time for 3 min, in 100% ethanol.

23. Immerse slides three times in xylene, each time for 15 min, to clear the sections.

    Removal of water content and treatment with xylene is required for good resolution of the cellular architecture of the tissue.

24. Coverslip slides using Cytoseal 60 mounting medium.

ALTERNATE PROTOCOL 1

IMMUNOFLUORESCENCE LOCALIZATION OF HEME DEGRADATION SYSTEM USING FREE-FLOATING FROZEN SECTIONS

Generally, there are two primary approaches to the visualization of protein/antibody complexes: colorimetric and fluorimetric. Fluorimetric detection is an extremely powerful strategy that has been elegantly applied to visualize a wide variety of target proteins.

This procedure details the detection of the heme degradation system by fluorimetric detection using goat anti-rabbit γ-globulin (GAR) secondary antibody conjugated to fluorescein isothiocyanate. These procedures are a modification of those described in Basic Protocol 2.

Additional Materials *(also see Basic Protocol 2)*

Secondary antibody: fluorescein (FITC)-conjugated goat anti-rabbit γ-globulin (Organon Teknika Cappel)
70% (v/v) glycerol
Fluorescence microscope

1. For frozen sections, carry out steps 1 to 8 of Basic Protocol 2.

   From this point onward, tissue sections should be manipulated under conditions of dimmed lighting to avoid photobleaching of the fluorescent signal. All incubations are performed in the dark. It is convenient to cover incubation vessels with aluminum foil to ensure light-tight conditions.

2. Transfer the tissue out of the netted compartments into culture dishes containing FITC-conjugated goat anti-rabbit γ-globulin diluted 1/10,000 (v/v) in antibody buffer.

   If a primary antibody is prepared from a source other than rabbit, then the choice of secondary antibody should be adjusted accordingly for specificity. Also, appropriate dilution of the fluorescently labeled secondary antibody and optimal duration of incubation may have to be empirically determined.

3. Incubate tissue in secondary antibody overnight in a cold room.

4. Transfer the tissue into netted compartments containing 0.1 M sodium phosphate buffer, pH 7.3. Wash the tissue with eight changes of 0.1 M sodium phosphate buffer, pH 7.3, over a period of 1.5 to 3 hr.

5. Mount tissue on Superfrost Plus slides and dry overnight on a slide warmer at 37°C.

6. Briefly rehydrate tissue by placing slides in a Coplin jar containing 0.1 M sodium phosphate buffer, pH 7.3, for 2 to 3 min.

7. Apply a glass coverslip using 70% (v/v) glycerol.

8. Wrap completed slides in foil and store at 4°C until ready to visualize using a fluorescence microscope.

IMMUNOHISTOCHEMICAL LOCALIZATION OF HEME DEGRADATION SYSTEM USING PARAFFIN-EMBEDDED TISSUE

Infiltration of tissue with paraffin wax (paraffin embedding) is a popular way to preserve tissue for IHC. In the hands of a skilled practitioner, paraffin-embedded tissue can be sectioned much more thinly than frozen tissue. As a result, paraffin sections typically yield superior resolution of individual cells than that obtained using frozen sections. However, it is noteworthy that paraffin embedding requires harsher chemical treatment of tissue than does processing of frozen sections. Consequently, with paraffin embedding there is greater risk for disruption of target protein such that antibody recognition is lost. Many antibodies that work perfectly well in procedures using frozen sections are useless with paraffin sections.

The following IHC procedures detail localization of HO system components in sections preserved by fixation and paraffin embedding. Briefly, paraffin is removed from the tissue using xylene and the sections are rehydrated. Tissue is incubated with primary antibody, washed, incubated with a biotinylated secondary antibody, and washed again. Finally, tissue is incubated with streptavidin conjugated with peroxidase, and washed prior to visualization of antibody-antigen complexes.

Additional Materials *(also see Basic Protocol 2)*

Paraffin-embedded sections on slides (Support Protocol 1)
Phosphate-buffered saline (PBS; *APPENDIX 2A*)
Endogenous peroxidase inhibitor (see recipe)
PBS containing 0.3% (v/v) Triton X-100
PBS containing 0.3% (v/v) Triton X-100 and 10% (v/v) normal goat serum (NGS)
HO-1, HO-2, or BVR antibody (StressGen)
Zymed histological staining kit containing biotinylated goat anti-rabbit antiserum (secondary antibody) peroxidase-streptavidin conjugate, and development solution (Zymed)
Humidified chambers: large plastic culture dishes lined with H_2O-saturated Whatman filter paper
Glass coverslips

Prepare sections

1. Incubate paraffin-embedded tissue (5- to 10-µm thick) three times in xylene, each time for 3 min.
2. Incubate tissue three times in 100% ethanol, each time for 3 min.

   Once a bottle of ethanol is opened it will take up moisture from the atmosphere, rendering it less than absolute. It is advisable to replace the bottle of ethanol on a weekly basis, depending upon use.

3. Incubate tissue for 3 min in 80% ethanol, then for 3 min in 70% (v/v) ethanol.
4. Incubate tissue for 5 min in PBS, then in endogenous peroxidase inhibitor for 7 min.
5. Wash tissue four times in PBS, each time for 5 min.
6. Incubate tissue twice in PBS containing 0.3% Triton X-100, each time for 5 min.

Block tissue

7. Apply 250 µl of PBS containing 0.3% Triton X-100 and 10% NGS to each slide, transfer to a humidified chamber, and incubate 20 min at 25°C .

   This step is intended to block nonspecific binding sites in the tissue. Depending on the tissue type and source or the antibody being employed, the duration of the blocking step may have to be optimized.

8. Drain slides of excess blocking solution.

   It is convenient to tilt slides at a 45° angle onto a paper towel to remove the bulk of the solution. The remainder of the blocker may be removed by carefully placing a Kimwipe adjacent to the tissue to absorb remaining solution. However, it is important that the slides not be allowed to dry, or high background will be observed. Thus, prompt replacement of blocker with primary antibody is necessary. It is advisable to process a limited number of slides through each step to ensure timely and consistent tissue treatment.

Expose to primary antibody

9. Apply 100 µl of primary antibody diluted to the appropriate concentration in PBS containing 0.3% Triton X-100 and 10% NGS.

   The optimal primary antibody concentration will vary among antibody preparations and tissue type; so this needs to be empirically determined. For most antibody preparations, a 1/250 (v/v) dilution gives good results.

10. Apply Parafilm coverslips to each slide.

    "Parafilm coverslips" are applied as follows. Gently grasp the end of a precut rectangular piece of Parafilm with a pair of forceps. Lay the edge of the Parafilm at the end of the slide and gently place the coverslip onto the tissue by slowly decreasing the angle between the Parafilm and the slide. This technique will allow even distribution of antibody and displacement of air bubbles.

11. Transfer slides to a humidified chamber, seal with Parafilm, and incubate overnight at 4°C .

Expose to secondary antibody

12. Remove humidified chamber from refrigerator or cold room and equilibrate to room temperature for 1 hr.

13. Wash tissue four times with PBS, each time for 3 min.

    Parafilm coverslips may be efficiently removed by immersing the slides in a Coplin jar containing PBS. Thereafter, excess primary antibody is rinsed from the slides by placing them in Coplin jars containing PBS.

14. Drain sections and place slides back in humidified chambers. Pipet 100 µl of biotinylated goat anti-rabbit secondary antibody onto the sections, close chamber, and incubate 20 min at room temperature.

15. Wash slides four times with PBS, each time for 3 min. Drain sections and place them back in the humidified chambers.

Expose to conjugate

16. Pipet 100 µl of peroxidase-streptavidin conjugate onto each section, close the humidified chambers and incubate 15 min at room temperature.

17. Transfer sections to Coplin jars containing PBS and wash four times with PBS, each time for 3 min.

Develop slides

18. Prepare development solution (Zymed kit) immediately prior to use, in accordance with the manufacturer's instructions, and keep in the dark.

19. Pipet developer onto sections and incubate at room temperature for up to 15 min.

20. Terminate development by rinsing sections twice with distilled water, each time for 10 min.

21. Apply glass coverslips with mounting solution provided with the Zymed kit.

Mounting solution should be warmed to 37°C prior to use.

22. Examine slides for cells giving a positive (brown) reaction.

IMMUNOFLUORESCENCE LOCALIZATION OF HEME DEGRADATION SYSTEM FOR PARAFFIN-EMBEDDED SECTIONS

ALTERNATE PROTOCOL 3

This procedure details the fluorimetric detection of enxymes of the heme degradation system using goat anti-rabbit γ-globulin (GAR) secondary antibody conjugated to fluorescein isothiocyanate. The procedures are modified from Alternate Protocol 2.

Additional Materials *(also see Basic Protocol 2 and Alternate Protocol 2)*

Secondary antibody: fluorescein isothiocyanate (FITC)–conjugated goat anti-rabbit γ-globulin (Organon Teknika Cappel)
Phosphate-buffered saline (PBS; *APPENDIX 2A*)
70% (v/v) glycerol

Humidified chambers: large plastic culture dishes lined with H_2O-saturated Whatman filter paper
Glass coverslips
Fluorescence microscope

1. Carry out steps 1 to 14 of Alternate Protocol 2.

   From this point onward, tissue sections should be manipulated under conditions of dimmed lighting to avoid photobleaching of the fluorescent signal. All incubations are performed in the dark. It is convenient to cover incubation vessels with aluminum foil to ensure light-tight conditions.

2. Transfer slides to a humidified chamber and apply 100 µl of FITC-conjugated goat anti-rabbit antibody diluted 1/1000 in antibody buffer. Apply a Parafilm coverslip and seal the humidified chamber.

   "Parafilm coverslips" are applied as follows. Gently grasp the end of a precut rectangular piece of Parafilm with a pair of forceps. Lay the edge of the Parafilm at the end of the slide and gently place the coverslip onto the tissue by slowly decreasing the angle between the Parafilm and the slide. This technique will allow even distribution of antibody and displacement of air bubbles.

   If a primary antibody is derived from a source other than rabbit, then the choice of secondary antibody should be adjusted accordingly for specificity. Also, appropriate dilution of the fluorescently labeled secondary antibody and optimal duration of incubation may have to be empirically determined.

3. Incubate tissue in secondary antibody for 20 min at room temperature.
4. Remove slides from the humidified chamber and wash tissue four times with PBS, each time for 3 min.

   Excess secondary antibody is rinsed from the slides by placing them in Coplin jars containing PBS.

5. Drain sections and mount glass coverslips on each slide with 70% glycerol.
6. Wrap completed slides in foil and store at 4°C until ready to visualize using a fluorescence microscope.

PREPARATION OF TISSUE FOR ISH AND IHC

SUPPORT PROTOCOL 1

Tissue fixation and subsequent chemical treatment(s) are critical to the preservation of cellular architecture and target integrity (i.e., mRNAs and protein). The ultimate quality of histochemical data is greatly influenced by conditions used at this stage.

This protocol details the procedures for perfusion and fixation of tissue from both adult and neonatal rats. Optimal conditions for fixation treatment will vary and may have to be empirically determined.

NOTE: All protocols using live animals must first be reviewed and approved by an Institutional Animal Care and Use Committee (IACUC) and must follow officially approved procedures for care and use of laboratory animals.

Materials

Adult or neonatal rat
Sodium pentobarbital
0.9% (w/v) NaCl
Perfusion fixative (see recipe)
Graded sucrose solutions: 0.1 M sodium phosphate buffer (*APPENDIX 2A*) containing 10%, 20%, and 30% (w/v) sucrose (store up to 1 week at 4°C)
Cryoprotectant (see recipe)

Dissecting instruments
Intravenous catheter (18-G for adult rat; 22-G for 14- to 28-day neonate; Becton Dickinson) or 30-ml syringe with 25-G needle (for 7-day neonate)
Superfrost Plus slides (Fisher)
Perfusion apparatus including peristaltic pump
Microtomes (Reichert-Jung)
Compartmentalized boxes

Anesthetize the animal

1. Weigh the adult or neonatal rat and anesthetize it by intraperitoneal injection of 50 mg/kg sodium pentobarbital.
2. After the animal is asleep, firmly pinch the foot with a pair of forceps.

   If there is no response, then proceed with the surgery.
3. Place the animal on its back. Open the abdominal cavity with a midline incision to the sternum.

   Positioning the animal on a refrigerator rack placed over a sink or basin is convenient for animal manipulation and drainage of perfusate.

Insert the catheter

4. Make a diagonal cut to each side of the sternum through the rib cage, extending to either side of the neck.

   Care should be taken not to sever any vessels or puncture the heart.
5. Clamp the sternum back with hemostatic forceps to give access to the heart.
6. Cut the connective tissue surrounding the diaphragm and make a lateral cut on each side of the animal to allow proper drainage of the perfusate.
7. Lift the lungs to expose the descending aorta and occlude the vessel using hemostatic forceps.

   Only occlude the descending aorta if the organ(s) of interest are in the upper body. Full-body perfusion is obtained by omitting this step.
8. Make a small incision in the right atrium.

   Be sure to have the intravenous catheter at hand and perfusion apparatus set up and functional prior to this step.

9. Insert the intravenous catheter into the left ventricle. Remove the needle and carefully position the catheter so that the tip of the device resides within the aortic arch.

The optimal size of the catheter for transcardial perfusion is either 18-G for adult rats or 22-G for 14- to 28-day-old neonatal animals, respectively. For 7-day-old neonates transcardial perfusion may be performed manually using a 30-ml syringe fitted with a 25-G needle. Manual perfusion of these young animals is technically demanding since the heart is very small and great care must be taken not to pierce through the organ. Extra time should be allotted for these manual procedures.

Begin perfusion

10. Connect the catheter to the perfusion apparatus and begin a flow of 0.9% (w/v) NaCl into the animal.

For an adult animal, infuse 250 ml of 0.9% (w/v) saline over 15 min. For a 7- to 28-day-old animal, infuse 60 to 70 ml over 10 min. Manually infuse the 7-day-old neonate with 20 to 30 ml 0.9% NaCl over ~3 min. Monitor the progress of the perfusion by assessing the animal's eyes and gums for a blanched appearance at the end of this step.

11. Switch the flow to perfusion fixative.

It is common to see turgor and twitching of the upper extremities at the initial flow of fixative. Perfuse the adult with 500 ml of fixative over 30 min. Perfuse 14- to 28-day-old rats with 200 ml of fixative over 30 min. For 7-day-old neonates, infuse ~100 ml of fixative. After this step, the extremities and tip of the nose should be stiff.

Collect and section tissue(s)

12. Disconnect the animal from the perfusion apparatus and collect tissue.

For many tissues, post-fixation is recommended following initial perfusion/fixation procedure. Post-fixation times and temperature vary considerably among tissues. For example, adult rat brain tissue is post-fixed for 1 hr at room temperature, whereas post-fixation of this tissue from 7- to 28-day-old animals is extended to 16 to 24 hr at 4°C. Similarly, adult testis is post-fixed up to 16 hr at 4°C prior to further processing. In many cases, fixation time must be empirically determined to optimize detection of HO protein or mRNAs. For ISH application, overfixation of tissue severely diminishes HO mRNA signal obtained.

For brain tissue to be used for IHC of frozen sections

13a. Post-fix 1 hr at room temperature (adult rat brains) or 16 to 24 hr (for brains from 7- to 28-day-old rats) by allowing the tissue to remain submerged in the fixative. Cryoprotect following post-fixation by placing the organ in graded 10% increments of sucrose solutions (from 10% up to 30% w/v sucrose) for 1 to 2 days each at 4°C.

The organ is completely equilibrated with each solution when it sinks to the bottom of the vessel.

14a. Section brain tissue for IHC using a freezing sliding microtome. Cut the brain into 30- to 50-µm thick sections. Store intact brain or sections in cryoprotectant in compartmentalized boxes at −20°C until immunohistochemical staining is to be performed.

Best recovery of brain tissue from 7- to 14-day-old rat is obtained using sections >40-µm-thick. Furthermore, neonatal cerebellar tissue remains intact throughout the procedure if cut in sagittal orientation.

For other tissues

13b. After fixation and optional post-fixation, paraffin-embed tissue and section at 5- to 10-µm thickness onto Superfrost Plus glass slides using a microtome.

A typical processing schedule for paraffin-embedding of tissue is 10% (v/v) neutral buffered formalin (1.5 h); 10% neutral buffered formalin (1.5 h); 60% (v/v) ethanol (30 min); 80%

(v/v) ethanol (45 min); 95% (v/v) ethanol (50 min); absolute ethanol (50 min); absolute ethanol (30 min); absolute ethanol (30 min); xylene (1 h); xylene (30 min); paraffin (30 min); paraffin (30 min); paraffin (1 h).

14b. Store slides at ambient temperature in slide cases until use.

SUPPORT PROTOCOL 2

PREPARATION OF PREADSORBED SERUM CONTROL

Appropriate reagent controls should be run in parallel with histochemical procedures. The use of preadsorbed antisera is an important control for the authenticity of antibody-antigen complexes detected by IHC procedure. Below is the procedure for preparation of preadsorbed antisera for IHC of the heme degradation system, along with notes on their use.

Materials

Primary antibody (see appropriate protocol)
Purified HO-1, HO-2, or BVR protein (StressGen)
Antibody buffer (see Basic Protocol 2)

1. Pipet equal amounts of primary antibody into two 1.5-ml polypropylene microcentrifuge tubes.
2. Add pure antigen to give a final protein concentration >1 mg/ml to the antiserum to be adsorbed. Add an equal amount of diluent without antigen to the control antiserum.
3. Incubate the mixtures for 2 hr at room temperature.
4. Dilute mixtures to their final working concentration with antibody buffer. Store aliquots at −20°C until use. Incubate serum aliquots overnight at 4°C prior to use.
5. Use the control and preadsorbed antisera in parallel throughout histochemical procedures.

Adsorption of antisera may be confirmed in a dot-blot format. Briefly, dilute antigen serially in 10-fold increments. Apply known quantities of diluted antigen to small strips of nitrocellulose blotting medium and air dry. Process strips for immunoblotting (UNIT 2.3). Preadsorbed antibody should no longer yield signal observed with unadsorbed antisera. Likewise, use of preadsorbed antisera under histochemical conditions should abolish signal observed in sections treated with control antiserum. No further processing is necessary.

REAGENTS AND SOLUTIONS

*Use Milli-Q-purified water or equivalent in all recipes and protocol steps. For common stock solutions, see **APPENDIX 2A**; for suppliers, see **SUPPLIERS APPENDIX**.*

Agarose gel, 1% (w/v)

Suspend 1 g low-melting agarose in 100 ml 1× TAE buffer (see recipe) containing 0.5 μg/ml ethidium bromide (added from 5 mg/ml stock; see recipe). Heat with stirring until solids are dissolved. Allow to cool in a 60°C water bath prior to pouring the gel (see *UNIT 2.2* & *APPENDIX 3*).

Agarose solutions can be prepared ahead of time and stored at room temperature. It is often convenient to melt the agarose in a microwave oven prior to each use.

Blocking solution

100 mM Tris·Cl, pH 7.5 (*APPENDIX 2A*)
150 mM NaCl
2% (v/v) normal sheep serum
0.5% (w/v) bovine serum albumin (BSA)
Store up to 1 week at 4°C

Buffer I

100 mM Tris·Cl, pH 7.5 (*APPENDIX 2A*)
150 mM NaCl
Store up to 1 month at 25°C

Buffer II

100 mM Tris·Cl, pH 9.5
100 mM NaCl
50 mM $MgCl_2$
Store up to 1 month at 25°C

Cryoprotectant

Dissolve 300 g sucrose in 500 ml 0.1 M sodium phosphate buffer, pH 7.3 (*APPENDIX 2A*). Add 300 ml ethylene glycol and stir until solution is thoroughly mixed. Make solution up to 1 liter with 0.1 M sodium phosphate buffer, pH 7.3. Store at 4°C.

CAUTION: *Ethylene glycol is hazardous.*

Final concentrations: 0.05 M sodium phosphate, pH 7.3, containing 30% (w/v) sucrose and 30% (v/v) ethylene glycol.

Denhardt's solution, 50×

Dissolve 1 g polyvinylpyrrolodone, 1 g BSA, and 1 g Ficoll in 77 ml RNase-free water (see recipe). Bring volume up to 100 ml with RNase-free water and filter sterilize. Divide solution into aliquots and store at −20°C for up to several months.

Final concentrations are 1% (w/v) polyvinylpyrrolidone, 1% (w/v) BSA, and 1% (w/v) Ficoll.

Developer solution

Prepare a stock solution of 0.122 M nitroblue tetrazolium chloride (NBT) in 70% (v/v) DMSO. Prepare a stock solution of BCIP (5-bromo-4-chloro-3-indolyl phosphate *p*-toluidine salt) by dissolving 10 mg of BCIP in 200 µl *N*,*N*-dimethylformamide. Prepare the solutions immediately prior to use and keep in the dark.

Mix 250 µl of the NBT stock solution (0.61 mM final), 177 µl of the BCIP stock solution (0.52 mM final), and 12 mg levamisole (0.024% w/v final) with 50 ml buffer II (see recipe). Prepare immediately prior to use and keep in the dark.

Digoxigenin-dNTP labeling mix

Mix 285 µl RNase-free water (see recipe), 350 µl 1 mM digoxigenin-11-dUTP, 65 µl 10 mM dTTP, and 100 µl each of 10 mM dATP, dGTP, and dCTP. Store frozen in aliquots at −20°C for several months.

Final concentrations: 1 mM dATP, 1 mM dCTP, 1 mM dGTP, 0.65 mM dTTP, and 0.35 mM digoxigenin-11-dUTP

Endogenous peroxidase inhibitor

Combine 40 ml phosphate-buffered saline (PBS; *APPENDIX 2A*), 5 ml 30% (v/v) H_2O_2, and 5 ml methanol. Prepare immediately prior to use.

Final concentrations: 3% (v/v) H_2O_2, and 10% (v/v) methanol.

Ethidium bromide, 5 mg/ml

Dissolve 50 mg ethidium bromide in 10 ml RNase-free water (see recipe). Store at room temperature protected from light up to several months.

CAUTION: *Ethidium bromide is a carcinogen. Gloves should be worn at all times to avoid contact. Solutions should be discarded in accordance with institutional guidelines.*

Fish sperm DNA

Dissolve fish (salmon) sperm DNA (Sigma) in RNase-free water (see recipe) to 10 mg/ml. Shear by passing through tuberculin syringes sequentially fitted with 18- to 27-G needles, then sonicate briefly. Store in aliquots frozen at −20°C until use.

Formamide, deionized

Stir formamide with 1% (w/v) Bio-Rad AG501-X8 resin for 1 hr at room temperature. Separate the formamide from the resin by filtration through general-use filter paper. Aliquot and store at −20°C prior to use.

PCR buffer, 10×

Mix 5 ml of 1 M Tris·Cl, pH 8.3, 12.5 ml of 2 M KCl, 750 µl of 1 M $MgCl_2$, and 2.5 ml of 2% (w/v) gelatin. Adjust volume to 50 ml using RNase-free water (see recipe). Filter sterilize and store frozen in aliquots indefinitely.

Final concentrations of components in the 10× buffer are: 100 mM Tris·Cl, 500 mM KCl, 15 mM $MgCl_2$, and 0.1% (w/v) gelatin. The 1× buffer is 10 mM Tris·Cl, pH 8.3, 50 mM KCl, 1.5 mM $MgCl_2$, and 0.01% (w/v) gelatin.

Perfusion fixative

Heat 500 ml of distilled water to 90°C. Turn off heat, add 40 g paraformaldehyde to the water, and stir until the solids are dissolved (the solution will now appear milky white). Clarify the solution with dropwise addition of 1 N NaOH.

Dissolve 15 g sucrose in 500 ml 0.2 M sodium phosphate buffer, pH 7.3 (*APPENDIX 2A*). Add this solution to the clarified paraformaldehyde solution. Filter the mixture using Whatman general-use filter paper. Store overnight at room temperature or up to 1 week at 4°C.

CAUTION: *Paraformaldehyde is toxic and all procedures should be performed in a fume hood.*

Final concentrations: 0.1 M phosphate buffer containing 4%(w/v) paraformaldehyde and 1.5% (w/v) sucrose

Prehybridization buffer

Mix 25 ml deionized formamide (see recipe), 10 ml 20× SSC (see recipe), 1 ml 50× Denhardt's solution (see recipe), and 12.8 ml RNase-free distilled water (see recipe). Heat denature an aliquot of 10 mg/ml fish sperm DNA (see recipe) by boiling for 10 min followed by quenching on ice. Add 1.25 ml denatured fish sperm DNA just prior to use.

Final concentrations are 50% (v/v) formamide, 4× SSC, 1× (v/v) Denhardt's solution, and 0.25 mg/ml heat-denatured fish sperm DNA

Proteinase K, 10 µg/ml

Stock solution: Prepare 10 mg/ml proteinase K in RNase-free water. Divide into convenient aliquots and store up to several months at −20°C.

Working solution: Add 10 µl of 10 mg/ml proteinase K to 10 ml phosphate-buffered saline (PBS; *APPENDIX 2A*). Warm the fresh solution to 37°C for 30 min before use.

RNase-free water

Add 1 ml diethylpyrocarbonate (DEPC) to 1 liter distilled water. Shake well and autoclave.

SSC, 20×

Dissolve 88.2 g sodium citrate and 173.3 g NaCl in 800 ml distilled water. Adjust solution pH to 7 with 10 N NaOH and adjust volume to 1 liter with distilled water. Add 1 ml diethylpyrocarbonate (DEPC), mix well, and sterilize by autoclaving.

Store at room temperature up to 1 month. From this stock prepare 4×, 2×, 1×, 0.5×, 0.5×, 0.25× and 0.05× SSC by appropriate dilution with RNase-free water (see recipe).

TAE buffer, 1×

Dissolve 4.84 g Tris base in 700 ml RNase-free distilled water (see recipe). Add 1.14 ml glacial acetic acid and 2 ml 0.5 M EDTA, pH 8. Adjust volume to 1 liter with RNase-free distilled water. Filter sterilize or autoclave and store at room temperature up to several months.

TE buffer, pH 8

Dissolve 158 mg Tris hydrochloride in 80 ml RNase-free distilled water (see recipe). Adjust pH to 8 with 1 N NaOH. Add 200 µl 0.5 M EDTA, pH 8 (*APPENDIX 2A*). Adjust volume to 100 ml with RNase-free water, sterilize by autoclaving, and store at room temperature up to several months.

COMMENTARY

Background Information

Rabbit anti-rat polyclonal antibody preparations (HO-1, HO-2, and BVR) and HO cDNA(s) are utilized in the above protocols to localize immunoreactive protein and transcripts, respectively, of enzymes of the heme degradation system. These protocols represent the first comprehensive compendium of current histochemical methodologies used to define the pattern of expression of the HO system in the newborn (Maines et al., 1996) and adult rat brain (Ewing et al., 1993). The procedures described herein have the virtue of being nonradioactive, and are applicable to systemic organs, such as the cardiovascular system (Ewing et al., 1994) and the male reproductive system (Maines and Ewing, 1996), as well as to cultured cells (Raju et al., 1997). Visualization of the cellular HO system aids in assessment of potential sites of carbon monoxide, iron, and bile pigment production.

Heme is synthesized in a complex series of enzymatic steps that begin with Δ-aminolevulinate synthase and end with ferrochelatase. The resultant metalloporphyrin, Fe-protoporphyrin IX (Fe-PP, heme, hemin, protoheme, ferro-protoporphyrin, ferri-protoporphyrin) is utilized in a variety of functions when associated with proteins (reviewed in Maines, 1992). Heme is integral to life, and it carries out oxidative reactions and electron-transfer processes and delivers molecular oxygen (O_2) to cells. In addition, this essentially square-planar tetrapyrrole is the molecular cornerstone of gaseous cell signaling, wherein it serves as source of carbon monoxide (CO) and is a general cellular target for this monoxide and nitric oxide (NO). In most cases, mammalian tissue has a very high capacity to generate CO and in some organs, such as the brain, it overwhelmingly exceeds the NO generating capacity (reviewed in Maines, 1997).

Recent findings regarding the diverse biological properties of the products of heme metabolism have challenged the previous view of these entities as mere physiological waste products (reviewed in Maines, 1992, 1997). In mammals, the heme molecule can be degraded by both enzymatic and chemical means. Enzymatic catabolism of heme by the HO system utilizes NADPH as a source of reducing equivalents, leading to the activation of O_2 and initiation of a multistep process of oxidation of the methene bridges of the porphyrin ring, ultimately generating CO, biliverdin, and Fe. A comprehensive description of the various heme-degrading systems was provided by Maines (1992).

In mammals three forms of HO have been identified to date. The first form, now known as HO-1, was identified as a distinct enzyme entity nearly two decades ago (reviewed in Maines, 1992). The second enzyme, now known as HO-2, was recognized about a decade later (Trakshel et al., 1986). The third form, now known as HO-3, was most recently described (McCoubrey et al., 1997).

HO-1, HO-2, and HO-3 are different gene products (McCoubrey et al., 1997). The isoenzymes display distinct nucleotide sequences, amino acid composition, transcript number and size. HO-1, also known as the stress protein HSP32 (Keyse and Tyrrell, 1989), is the smallest of the three and has a molecular weight of ~30,000 (Shibahara et al., 1985); HO-2 and HO-3 have molecular weights of ~36,000 (Ro-

tenberg and Maines, 1990) and ~33,000 Da (McCoubrey et al., 1997), respectively.

HO-1 and HO-2 vastly differ in cell type, tissue distribution, and regulation (reviewed in Maines, 1992); in these areas little is currently known about HO-3. At this time, it is believed that all three HO enzymes have similar mechanisms of heme-based catalysis, substrate specificity, and cofactor/coenzyme requirements (McCoubrey et al., 1997), although HO-3 is a poor heme catalyst (McCoubrey et al., 1997). HO-1 is exquisitely sensitive, not only to metals, but to all kinds of stimuli and agents that cause oxidative stress and pathological conditions—e.g., heat shock, ischemia, GSH loss, radiation, hypoxia, hyperoxia, and cellular transformations and disease states (reviewed in Maines, 1992, 1997). In fact, there is no other enzyme described to date that is affected by so many stimuli of diverse nature as is HO-1. HO-2 is not induced by the factors that increase HO-1; the only chemical inducers of HO-2 identified to date are adrenal glucocorticoids (Raju et al., 1997).

All products of heme degradation are now suspected to be biologically active. CO is suspected to be, like NO, a signal molecule for generation of cGMP in biological systems. Iron released by HO activity regulates genes, including those of HO-1 (reviewed in Maines, 1992), and NO synthase (NOS; Weiss et al., 1994). Bilirubin, which is formed when biliverdin is reduced by biliverdin reductase (reviewed in Maines, 1992), is a potent antioxidant (Stocker et al., 1987). Aside from the important biological functions of HO activity products, the catalytic activity of the system plays a crucial role in maintaining cellular heme homeostasis and hemoprotein levels (reviewed in Maines, 1992); among the many hemoproteins and heme-activated enzymes are NOS and soluble guanylate cyclase. In addition, HO protects the cell from the deleterious effects of the heme molecule, which is the most effective promotor of lipid peroxidation and oxygen free radical formation (Tappel, 1961).

Critical Parameters and Troubleshooting

The IHC portion of this protocol has been optimized for use with rabbit polyclonal antibody preparations directed against HO-1, HO-2, or BVR. Any polyclonal antibody preparation may vary in character among sources and should be optimized for working concentration. The results of histochemistry should be validated by use of preadsorbed or preimmune serum as a negative control. Incomplete perfusion of tissue will result in nonspecific spotting of sections, particularly prominent within the microvasculature of the tissue. Treatment of tissue with endogenous peroxidase inhibitor (EPI) for 5 to 8 min and thorough rinsing prior to blocking and incubation with primary antibody generally solves this problem.

As with all molecular techniques utilized for visualization of mRNAs in cells and tissue, the sensitivity of target transcripts to degradation is worthy of note. It is therefore essential to maintain all reagents free of RNase, which will abolish signal via destruction of target mRNA. Furthermore, fixation time for tissue from multiple species and obtained from animals of different ages may have to be optimized for best results. In the hands of the authors, overfixation of tissue has resulted in loss of HO cDNA:mRNA signal using the digoxigenin labeling technique described in this protocol.

The heme degradation pathway is an exquisitely regulated system responsive to developmental factors, endogenous stimuli (i.e., drugs and toxins), and seemingly subtle exogenous stimuli (i.e., handling, general environment). As such, careful attention to animal handling and tissue collection procedures should be maintained throughout the execution of experimental protocols to ensure accurate and reproducible results. In retrospective studies where tissues are obtained for comparison from sources utilizing different collection and fixation protocols, caution is advised. In turn, tissue samples for analysis should be processed in parallel throughout all histochemical procedures, along with appropriate reagent controls.

Finally, the critical but little discussed subject of data collection deserves attention. As mentioned in the beginning of this unit, application of histochemistry is as much an art as a science. Proper use of these procedures requires a critical and objective eye to minimize subjectivity in data collection. A double-blind format for analysis should be used wherever possible. Furthermore, photographic documentation of histochemical data should be performed under uniform conditions of lighting, exposure, and magnification for all specimens to be compared. This is particularly critical when using immunofluorescent endpoints where photobleaching may preclude repetition of photography. A custom photolab may be utilized to obtain photomicrographs of highest fidelity to the original image.

Reagent and tissue preparation

Successful outcome of the ISH procedure (Basic Protocol 1), requires care to ensure that all glassware and reagents are free of RNase, which will destroy target mRNAs. Human skin is a common source of RNase contamination of equipment and reagents, so gloves should always be worn whenever handling anything that will come into contact with tissue samples over the course of analysis. It is common practice to designate glassware for sole use in these histochemical procedures.

For either ISH or IHC, time invested in meticulous preparation and sectioning of tissue is paramount to the overall quality of data ultimately derived. In particular, the quality of tissue perfusion, choice of fixative, and duration of fixation are often overlooked as critical determinants to successful application of these techniques.

While many of these important details are described here, the novice practitioner is encouraged to review more general considerations found in a good quality histochemistry textbook.

Probe design for HO-1/HO-2 cDNA

The HO-1/HO-2 cDNA probes are prepared by adaptation of the polymerase chain reaction (PCR) technique using digoxigenin-dUTP as previously described (Iwamura et al., 1994), with the modifications detailed in Basic Protocol 1. The probe design and amplification procedures described here specifically pertain to analysis of rat HO mRNA. Application of these probes for analysis of tissue from other species should be undertaken with appropriate caution, because complete probe homology may not exist between the rat and the species of interest. Furthermore, gene products other than HO-1/HO-2 mRNA targets may be expressed in other species which bear select sequence homology to HO-1/HO-2 cDNA probes and could yield artifacts. To avoid these problems, it is expedient to perform a search of GenBank to identify known mRNAs that could yield interference prior to initiating analysis of sections from a unique type or source of tissue. Additionally, assessment of cDNAs intended for use in ISH may be very effectively applied in a Northern blot format to confirm hybridization of probe to mRNA(s) of appropriate size and abundance in a sample representing total extract of mRNA from the tissue of interest. Northern blot analysis of HO-1/HO-2 mRNAs has been presented before (Ewing, 1996).

The digoxigenin-labeled HO-1 cDNA most successfully used for ISH is a 763-bp fragment corresponding to HO-1 nucleotides +71 to +833, as described by Shibahara et al. (1985). The two nucleotide primers used were 5′–TGCACATCCGTGCAGAGAAT–3′, homologous to HO-1 cDNA nucleotides +71 to +90, and 5′–AGGAAACTGAGTGTGAGGAC–3′, complimentary to HO-1 cDNA nucleotides +814 to +833. This HO-1 cDNA probe was selected so that it would not hybridize to HO-2 mRNA.

The digoxigenin-labeled HO-2 cDNA most successfully used for ISH is a 536-bp fragment corresponding to HO-2 nucleotides −32 to +504, as described by Rotenberg and Maines (1990). The two nucleotide primers used were 5′–GAAGTGAGGGCAGCACAAAC–3′, homologous to HO-2 cDNA nucleotides −32 to −–13, and 5′ CTTCTTCAGCACCTGGCCT–3′, complimentary to HO-2 cDNA nucleotides +486 to +504. This HO-2 cDNA probe was selected so that it would not hybridize to HO-1 mRNA. The HO-2 probe was, however, complimentary to regions common to both 1.3- and 1.9-kb homologous transcripts. Thus, HO-2 ISH utilizing this probe reflects total HO-2 mRNA expression.

Anticipated Results

Since the first presentations of histochemical analysis of heme degradation system in rat brain (Ewing and Maines, 1991) and systemic organs (Ewing et al., 1994; Ewing and Maines, 1995), the application of these IHC and ISH techniques (or variations thereof) has been extended to include a variety of mammalian tissues and species including man. Many of these studies are summarized in Table 9.5.1 and are provided as a convenient source for anticipated results from these procedures, as well as support protocols for the application of these techniques in a plethora of experimental settings and with select tissue types.

Time Considerations

The total time for ISH procedures is approximately 4 to 5 days (Basic Protocol 1). IHC analysis of free-floating sections requires 3 days (Basic Protocol 2 and Alternate Protocol 1). However, this does not take into account the time required for mounting of the frozen sections onto slides prior to final processing. IHC of a heme degradation system using paraffin sections requires 2 days (Alternate Protocols 2 and 3). Tissue perfusion and fixation are typi-

cally conducted over 2 days (Support Protocol 1). Cryopreservation of frozen tissue is performed over 2 to 4 days. Time required to section tissue will vary with the number of samples to be processed.

Literature Cited

Ewing, J.F. 1996. Methods for detection of heme oxygenase-1 and 2 transcripts: Northern blot and in situ hybridization. *In* Nitric Oxide Synthase Characterization and Functional Analysis, (M.D. Maines, Ed.), pp.112-115. Academic Press, San Diego.

Ewing, J.F. and Maines, M.D. 1991. Rapid induction of heme oxygenase-1 mRNA and protein by hyperthermia in rat brain: Heme oxygenase-2 is not a heat shock protein. *Proc. Natl. Acad. Sci. U.S.A.* 88:5364-5368.

Ewing, J.F. and Maines, M.D. 1992. In situ hybridization and immunohistochemical localization of heme oxygenase-2 mRNA and protein in normal rat brain: Differential distribution of isozyme 1 and 2. *Mol. Cell. Neurosci.* 3:4559-4570.

Ewing, J.F. and Maines, M.D. 1995. Distribution of constitutive (HO-2) and heat-inducible (HO-1) heme oxygenase isozymes in testes: HO-2 displays stage-specific expression in germ cells. *Endocrinology* 136:2294-2302.

Ewing, J.F., Weber, C.M., and Maines, M.D. 1993. Biliverdin reductase is heat resistant and coexpressed with constitutive and heat shock form of heme oxygenase in brain. *J. Neurochem.* 61:1015-1023.

Ewing, J.F., Raju, V.S., and Maines, M.D. 1994. Induction of heart heme oxygenase-1 (HSP32) by hyperthermia: Possible role in stress-mediated elevation of cyclic 3′:5′-guanosine monophosphate. *J. Pharmacol. Exp. Ther.* 271:408-414.

Iwamura, M., Wu, G., Abrahamsson, P., Di Sant'Agnese, P.A., Cockett, A.T.K., and Deftos, L.J. 1994. Parathyroid hormone–related protein is expressed by prostatic neuroendocrine cells. *J. Urol.* 43:667-674.

Keyse, S.M. and Tyrrell, A.M. 1989. Heme oxygenase is the major 32-kDa stress protein induced in human skin fibroblasts of UVA radiation, hydrogen peroxide and sodium arsenite. *Proc. Natl. Acad. Sci. U.S.A.* 86:99-103.

Maines, M.D. 1992. Heme Oxygenase: Clinical Applications and Functions. CRC Press, Boca Raton, Fla.

Maines, M.D. 1997. The heme oxygenase system: A regulator of second messenger gases. *Annu. Rev. Pharmacol. Toxicol.* 37:317-354.

Maines, M.D. and Ewing, J.F. 1996. Stress response of the rat testis: In situ hybridization and immunohistochemical analysis of heme oxygenase-1 (HSP32) induction by hyperthermia. *Biol. Reprod.* 54:1070-1079.

Maines, M.D., Eke, B.C., and Zhao, X. 1996. Corticosterone promotes increased heme oxygenase-2 protein and transcript expression in the newborn rat brain. *Brain Res.* 722:83-94.

McCoubrey, W.K. Jr., Huang, T.J., and Maines, M.D. 1997. Isolation and characterization of a cDNA from the rat brain that encodes hemoprotein heme oxygenase-3. *Eur. J. Biochem.* 247:725-732.

Raju, V.S., McCoubrey, W.K., Jr., and Maines, M.D. 1997. Regulation of heme oxygenase-2 by glucocorticoids in neonatal rat brain: Characterization of a functional glucocorticoid response element. *Biochim. Biophys. Acta.* 1351:89-104.

Rotenberg, M.O. and Maines, M.D. 1990. Isolation, characterization, and expression in *Escherichia coli* of a cDNA encoding rat heme oxygenase-2. *J. Biol. Chem.* 265: 7501-7506.

Shibahara, S., Müller, R., Taguchi, H., and Yoshida, T. 1985. Cloning and expression of cDNA for rat heme oxygenase. *Proc. Natl. Acad. Sci. U.S.A.* 82:7865-7869.

Stocker, P., Yamamoto, Y., McDonaugh, A.F., Glazer, A.N., and Ames, B.N. 1987. Bilirubin is an antioxidant of possible physiological importance. *Science* 235:1043-1047.

Tappel, A.L. 1961. Biocatalysts: Lipoxidase and hematin compounds. *In* Autooxidation and Antioxidants, vol. 1 (W.O. Lundberg, ed.). pp 325-366. John Wiley & Sons, New York.

Trakshel, G.M., Kutty, R.K., and Maines, M.D. 1986. Purification and characterization of the major constitutive form of testicular heme oxygenase: The non-inducible isoform. *J. Biol. Chem.* 261:11131-11137.

Verma, A., Hirsch, D.J., Glatt, C.E., Ronnett, G.V., and Snyder, S.H. 1993. Carbon monoxide: A putative neural messenger. *Science* 259:381-384.

Weiss, G., Werner-Felmayer, G., Werner, E.R., Grunewald, K., Wachter, H. and Hentze, M.W. 1994. Iron regulates nitric oxide synthase activity by controlling nuclear transcription. *J. Exp. Med.* 180:969-976.

Key References

Ewing and Maines, 1991. See above.

The first reported immunohistochemical localization of heme degradation system.

Ewing et al., 1993. See above.

First full comparison of pattern of expression of HO-1,HO-2, and BVR protein.

Maines, 1997. See above.

Eloquent review on the current status of the heme oxygenase field.

Contributed by James F. Ewing
ArQule, Inc.
Waltham, Massachusetts

An HPLC Method to Detect Heme Oxygenase Activity

Heme oxygenase (EC 1.14.99.3, HO), in a coupled reaction with NADPH:cytochrome P-450 reductase (EC 1.6.2.4), oxidizes heme (ferriprotoporphyrin-IX) to form biliverdin-IXα (BV), ferrous iron, carbon monoxide (CO), and water. NAD(P)H:biliverdin reductase (BVR; EC 1:3:1:24) completes the sequence of heme degradation by reducing BV to bilirubin-IXα (BR). The HO reaction fulfills an important metabolic function in regulating intracellular heme concentrations.

The classical HO assay depends on the spectrophotometric determination of bilirubin (see *UNIT 9.3*). Because BV cannot be detected by this assay, the reactions must be supplemented with an excess of exogenous BVR activity, to convert all residual BV to BR.

This unit describes a method for measuring HO activity by the simultaneous quantification of BV and BR using high performance liquid chromatography (HPLC; see Basic Protocol). The principal advantage of this technique is that it permits calculation of total HO activity even if BVR activity is limiting or absent. Thus, the protocol does not require supplementation with a BVR extract, which is not commercially available and is time-consuming to prepare. The Basic Protocol may be easily transformed into an assay for BVR activity (see Alternate Protocol).

This protocol has been developed using microsomal extracts from cultured cells (see Support Protocol). Optionally, crude cellular extract may be substituted for microsomal protein (see Support Protocol). In principle, protein preparations from organ tissue may also be used (see *UNIT 9.3*).

DETERMINING HEME OXYGENASE ACTIVITY USING HPLC

BASIC PROTOCOL

The HO enzymatic reaction consists of a microsomal extract from tissue culture cells combined with a heme substrate and β-NADPH, at 37°C. The BV and BR produced in the reaction are then extracted, separated on a reversed-phase C18 column by HPLC, and detected in the elution volume by visible spectroscopy at 405 nm. HO activity is then expressed as the picomoles of bilirubin equivalents formed (BV + BR) per fixed reaction time at 37°C and fixed protein mass.

CAUTION: Methanol is required for the assay. Use appropriate precautions for the use and storage of flammable liquids. Avoid skin and eye contact with this reagent.

NOTE: All protein extraction procedures must be performed at 4°C with precooled solutions and equipment. The photosensitive materials, including the reaction samples, should be handled under dark ambient conditions.

NOTE: The assay is labor-intensive and best performed with a team of two investigators.

Materials

Microsomal protein extract from cultured cells (see Support Protocol)
Solution A (see recipe)
Partially purified biliverdin reductase (BVR; optional)
20 mM β-NADPH (see recipe)
40 mM glucose 6-phosphate (see recipe)
1 U/μl glucose-6-phosphate dehydrogenase (see recipe)
2.5 mM protoporphyrin IX (Sn PPIX; see recipe; optional)

Contributed by Stefan W. Ryter and Rex M. Tyrrell
Current Protocols in Toxicology (2000) 9.6.1-9.6.14

2.5 mM hemin stock solution (see recipe)
Stop solution with mesoporphyrin internal standard (see recipe)
HPLC buffer A (see recipe)
HPLC buffer B: methanol (HPLC grade; Fisher; degassed 2 min with compressed He)
20 μM biliverdin and bilirubin standards (see recipes)

1.5- and 0.5-ml microcentrifuge tubes
High performance liquid chromatography (HPLC) system with two solvent reservoirs and pumps (e.g., Kontron or equivalent)
Data acquisition system (e.g., MT 450 MS-DOS or higher; Kontron or equivalent)
Autosampler (e.g., HPLC 360; Kontron, or equivalent)
Visible detector (e.g., UVIKON 720 LC microdetector; Kontron or equivalent)
Reversed-phase C18 steel cartridge HPLC column (e.g., Novapak 3.9 mm × 15 cm) *or* phenyl reversed-phase column (both available from Waters Chromatography)
Compressed helium tank

Assemble HO reaction

1. Assemble the reagents on ice in microcentrifuge tubes. Add 500 μg fresh microsomal protein extract per sample tube in a volume of 50 to 88 μl (see Support Protocol).

   Optionally, BVR may be included in the reaction. Add both microsomal (500 μg) and partially purified BVR extract (50 to 200 μg) in a volume of <88 μl. The BVR may be prepared as described by Tenhunen et al. (1970).

2. Adjust volume to 88 μl with solution A. Also add the following:

   5 μl 40 mM glucose-6-phosphate solution
   5 μl 20 mM β-NADPH
   1 μl 1 U/μl glucose-6-phosphate dehydrogenase.

   Prepare negative controls by assembling the reaction mixtures as described above with the substitution of 5 μl solution A for the NADPH solution; alternatively, substitute boiled protein extract for fresh microsomal protein. A competitive inhibitor of HO activity, such as Sn PPIX, may be introduced into the reaction as a negative control (e.g., add 1 μl of 2.5 mM Sn PPIX solution to a complete reaction to a final concentration of 25 μM).

3. Preincubate the incubation mixtures for 5 min at 37°C.

4. To initiate the reactions, add 1 μl of 2.5 mM hemin stock solution and vortex 5 sec.

   The final reaction concentrations are 5 mg/ml fresh microsomal protein, 0.5 to 2 mg/ml BVR extract (optional), 1 mM β-NADPH, 2 mM glucose-6-phosphate, 1 U/100 μl glucose-6-phosphate dehydrogenase, 25 μM hemin, 0.25 M sucrose, 20 mM Tris·Cl, pH 7.4, in a final volume of 100 μl.

5. Place tubes in a circulating water bath at 37°C in the dark.

6. Incubate reactions at 37°C for a chosen time interval, typically 5 to 60 min.

   The linear range for measured activity must be determined. A 20-min reaction time is suggested from previous studies with various human cell types. Reaction time may have to be increased up to 1 hr to detect activity from control (uninduced) cells that express low basal activity.

Prepare samples for HPLC

7. Terminate the HO reactions under dark ambient conditions by adding 1 vol (100 μl) stop solution to each tube at 20°C. Vortex 5 sec.

8. Centrifuge the stopped reaction mixtures 10 min at 15,000 × *g*, 20°C.

   The resulting colored pellet retains ~80% to 85% of the heme. The supernatant is clear with a faint yellow color.

9. Recover supernatants and transfer to 0.5-ml microcentrifuge tubes.

   These are the ethanol/DMSO extracts. Ensure that samples are free of suspended particles.

10. Place the tubes containing ethanol/DMSO extracts into an autosampler with a dark cover, and begin the sample run as soon as possible.

    If manual injection is used, store uninjected samples at room temperature protected from light until injection. If an autosampler is used, ensure that the microcentrifuge tubes are compatible with the sampling apparatus.

    Freeze-thawing the alcohol-extracted HO reaction mixtures (final step) at −70° may decrease the quality of the sample. The resulting bile pigment and internal standard (mesoporphyrin) decomposition products will appear as additional chromatographic peaks.

Prepare the HPLC apparatus

11. Connect the HPLC apparatus to a reversed-phase C18 steel cartridge HPLC column.

    A phenyl reversed-phase column also gives a good separation of reaction products.

    IMPORTANT NOTE: *This part of the protocol is best performed in advance by a second investigator.*

12. Program the HPLC to perform a linear gradient that starts from 100% HPLC buffer A at time zero and reaches 100% buffer B at 14 min, and which then reverts to 100% buffer A and remains constant until the termination at 19 min. Set the total flow rate to 1.5 ml/min.

13. Set the detector for continuous absorbance monitoring at 405 nm.

14. Degas both HPLC solutions with compressed helium for ≥2 min. Fill one reservoir with HPLC buffer A. Fill the second reservoir with buffer B.

    Ensure that the solutions are free of particles and that the pump intake heads are clean.

15. Purge the intake hoses free of air by pumping from each buffer reservoir through an open precolumn check valve.

16. Prime the HPLC column with 100% HPLC buffer A for ≥2 min prior to the first injection. Check system for leaks.

    Include a tube of mixed standards as the first sample in the run to ensure that the system is operating correctly. Prepare mixed standards in HPLC buffer A in the following final concentrations: 1 μM hemin, 1 μM BR IXα, 1 μM BV, and 0.4 μM mesoporphyrin. For assay calibration, however, prepare standards as described in steps 18 to 26.

17. After the sample analysis is complete, wash the column 60 min with 100% methanol.

Construct BR and BV standard curves

18. Dilute the 20 μM biliverdin and bilirubin standard solutions with 100% DMSO to generate a series of 10× standard solutions in the range of 2 to 20 μM.

    Perform this step under dark ambient conditions.

    Biliverdin standards may be omitted if biliverdin reductase has been added to the samples.

19. To microcentrifuge tubes at room temperature, add 500 μg microsomal protein (in <100 μl) and adjust to 100 μl with solution A.

20. Heat the protein to 37°C for 10 min in a circulating water bath.

21. Add 100 μl stop solution with internal standard and vortex 10 sec.

22. Centrifuge at 15,000 × *g* for 5 min at room temperature.
23. Transfer 135 µl of the supernatant to a fresh microcentrifuge tube.
24. Before each injection, in the dark, add 15 µl BV or BR standard from 10× concentrated stock solutions (prepared in step 18) to final concentrations ranging from 0.2 to 2 µM.

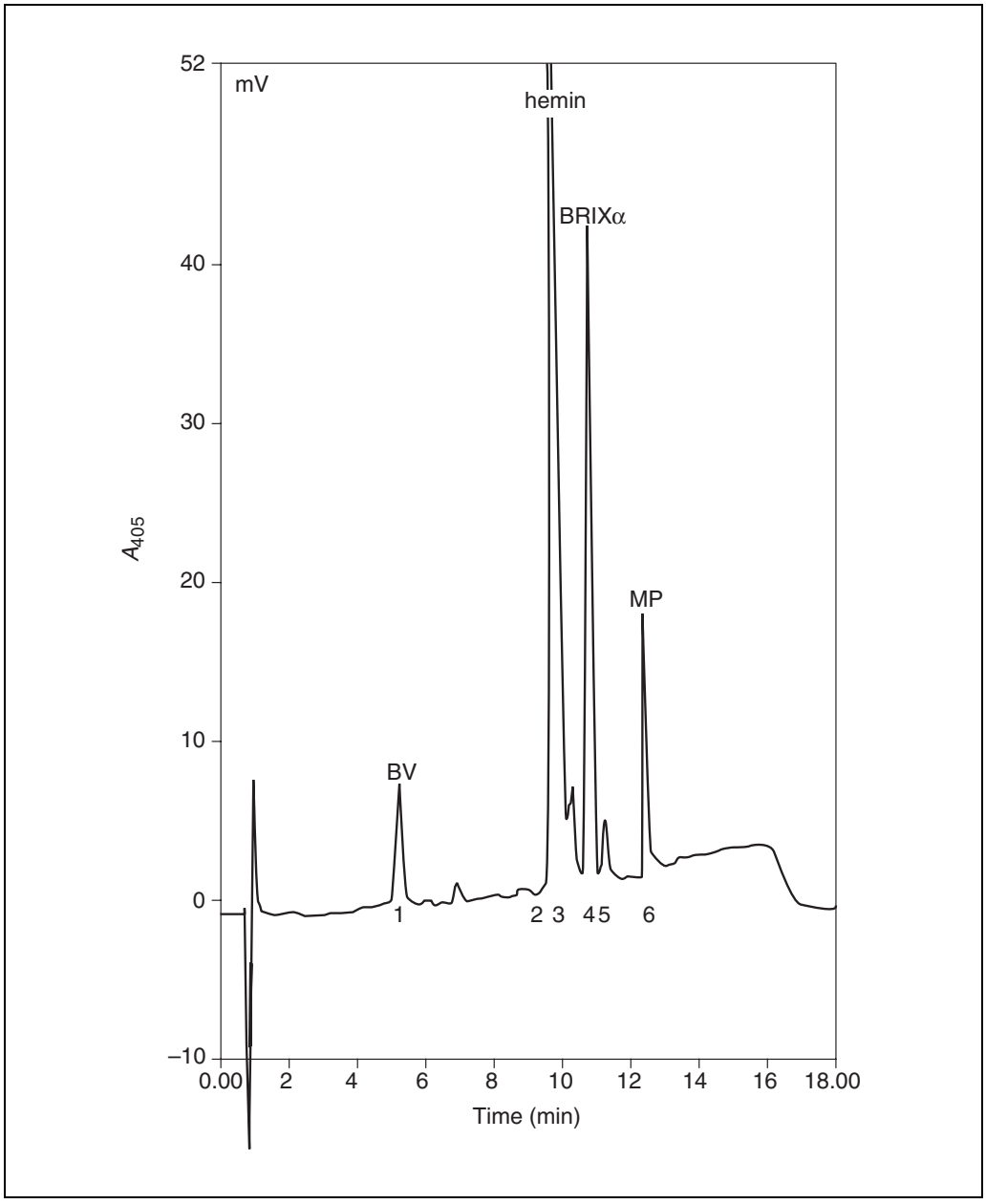

Figure 9.6.1 HPLC chromatogram showing the resolution of tetrapyrrole standards in an alcohol extract of sonicated microsomal protein solution. Final concentrations were 2 µM biliverdin (BV), 2 µM bilirubin-IXα (BRIXα), 0.35 µM BRIIIα, 0.27 µM BRXIIIα, 12.5 µM hemin, 0.4 µM mesoporphyrin (MP), corresponding to injected amounts of 240 pmol BV, 240 pmol BRIXα, and 48 pmol MP. The tetrapyrroles eluted with the following typical retention times: (1) biliverdin (BV), 5.29 min; (2) hemin, 9.8 min; (3) bilirubin structural isomer (IIIα or XIIIα), 10.39 min; (4) bilirubin-IXα (BRIXα), 10.9 min; (5) bilirubin structural isomer (IIIα or XIIIα), 11.38 min; and (6) mesoporphyrin (MP), 12.54 min. Optical density was detected at 405 nm. Reprinted from Ryter et al. (1998), with permission from Elsevier Science.

25. Inject immediately into the HPLC system.
26. Plot the detector response (integrated peak area) as a function of BV or BR concentration.

The assay protocol assumes that 100% of the BV and BR will be recovered from HO reactions by extraction in 95:5 (v/v) ethanolDMSO (in the stop solution), which is the case for HO reactions containing 500 μg protein and <2 μM BV or BR. To determine recovery efficiency, dissolve 20 μl 10× standard in 80 μl protein solution at 37°C (0.2 to 2 μM assuming a final volume of 200 μl). Add 100 μl 95:5 (v/v) ethanol/DMSO. Centrifuge 5 min at 15,000 × g. Inject the supernatant immediately into HPLC. Compare with result obtained in steps 18 to 26.

Calculate HO activity

27. Record the integrated peak areas of biliverdin-IXα, bilirubin-IXα, and mesoporphyrin from each sample chromatogram (see Fig. 9.6.1).

If an integration program is not available, then detector response in peak height (arbitrary units) may also be used.

28. From the linear standard curves, calculate the concentrations of BV and BR in an injected sample in μM (pmol/μl).
29. Calculate bilirubin equivalents (BReq) using the following formula, assuming a stopped reaction volume of 200 μl.

BReq = (pmol/μl BV + pmol/μl BR) × (200 μl).

The BReq value is equivalent to the picomoles of substrate oxidized.

In the presence of an excess of BVR activity, the equation simplifies to:

BReq = (pmol/μl BR) × (200 μl).

30. Normalize the BReq value against the relative mesoporphyrin recovery for each sample, using the following formula:

BR′eq = BReq (MP*/MP_S)

where MP* = average mesoporphyrin recovery for the entire run, and MP_S = sample mesoporphyrin recovery. Calculate the mesoporphyrin ratio directly from arbitrary detector units.

31. Calculate HO activity using the following formula:

BR′eq/(mg protein) (hr)

where hr = reaction time in linear range of assay, expressed in hours.

32. Express the final result with the units pmol BR/mg protein/hr.

PREPARATION OF MICROSOMAL PROTEIN EXTRACTS FROM CULTURED CELLS

SUPPORT PROTOCOL

This protocol is used to prepare microsomal protein extracts from cultured cells. Crude cellular extract may optionally be prepared by following steps 1 to 5 and 11 to 12 only.

Materials

Cultures of cells
Phosphate-buffered saline (PBS), pH 7.4 (*APPENDIX 2A*), ice-cold
PBS/EDTA solution (see recipe), ice-cold
Solution A (see recipe)
1000× protease inhibitor stock solutions (see recipe)

Rubber cell scrapers
15-ml centrifuge tubes (e.g., 16 × 125–mm tissue culture tubes with screw caps; Corning)
Refrigerated tabletop centrifuge (e.g., GPK centrifuge; Beckman, or equivalent)
Sonicator (e.g., Branson sonifier B-12 sonicator; Branson Ultrasonics, or equivalent)
Ultracentrifuge (e.g., Centrikon T20-60 ultracentrifuge; Kontron, or equivalent)
Fixed-angle rotor capable of 105,000 × *g* (e.g., TFT65.13 rotor; Kontron, or equivalent)
Polyallomar ultracentrifuge tubes, (e.g., 13.5-ml; Kontron)

Additional reagents and equipment for determination of protein concentration (*APPENDIX 3*)

NOTE: Perform all steps at 4°C.

Prepare crude extract

1. Place petri dishes containing cells on ice. Aspirate culture medium and rinse the monolayers twice with ice-cold PBS and drain. To each dish, add 1.0 ml ice-cold PBS/EDTA. Detach the cells with a rubber cell scraper. Recover the suspension from each dish and combine into 15-ml centrifuge tubes. Rinse each dish with an additional 1.0 ml of PBS and pool.

   Cell culture parameters must be determined experimentally for cell type and for the degree of purification desired. Microsomal preparations require ~5 × 10^7 cells pooled from two to four 150-mm monolayer cultures grown to 80% to 90% confluence. This approximation yields 1 to 2 mg microsomal protein from human HeLa cells. If crude extract is chosen for the assay, then two to three 100-mm near-confluent plates should be sufficient to yield 1 to 2 mg protein. Although this protocol has been developed using monolayer tissue cultures, in principle, any cell type may be applied.

2. Centrifuge cells 5 min at 500 × *g*, 4°C.

3. Resuspend each pellet 1:1 (v/v) in solution A containing protease inhibitors.

   Add the protease inhibitors to solution A from 1000× stock solutions immediately before use.

4. Transfer the suspension to 1.5-ml microcentrifuge tubes and sonicate on ice twice for 15 sec, at low power (20 W).

   When operating the sonicator, keep the tube completely embedded in ice. Use adequate ear protection.

5. Centrifuge the homogenates 20 min at 15,000 × *g*, 4°C. Transfer the supernatant to a clean 1.5-ml microcentrifuge tube. Repeat the centrifugation step if necessary to obtain a clear supernatant.

   The protein extraction procedure may be stopped at this point, and the crude supernatant used in the enzyme assay instead of microsomal protein (proceed to step 11). The crude extract contains HO activity and may contain BVR activity depending on the cell type. The use of crude extract is discouraged since it may accelerate column aging.

Prepare microsomal protein extract

6. Transfer the supernatant to ultracentrifuge tubes. Balance the tubes by adding solution A.

7. Centrifuge at 1 hr at 105,000 × *g*, 4°C, in fixed-angle ultracentrifuge rotor.

8. Drain the microsomal pellets at 4°C. Resuspend the pellet in 100 to 200 µl buffer A by vigorous manual pipetting (20 to 50 times) on ice. Transfer the suspension to microcentrifuge tubes. If necessary use another 100 to 200 µl buffer A to recover residual particles, and pool.

   The resulting pellet will be difficult to resuspend, due to high viscosity.

9. Sonicate the crude suspensions 10 sec on ice at low power (20 W).

10. Centrifuge the suspensions 5 min at 15,000 × *g*, 4°C.

    The final suspensions should be homogenous, with a small amount of pellet. If the supernatant is not homogenous, or if the pellet is too large, repeat steps 9 and 10.

11. Decant the supernatant to a fresh microcentrifuge tube and store on ice until use.

12. Calculate the protein concentration of the supernatant using a commercial protein assay reagent kit according to the manufacturer's instructions. Dilute microsomal protein to 6 to 10 mg/ml with solution A.

    If the microsomal protein preparations are too dilute (<6 mg/ml) increase starting material or reduce protein resuspension volume.

DETECTION OF BVR ACTIVITY

ALTERNATE PROTOCOL

The HPLC technique can be readily adapted to an assay for BVR activity with a simple transformation as described below.

Additional Materials *(also see Basic Protocol)*

Protein sample to be analyzed for BVR activity
2.5 µM biliverdin (BV) solution in DMSO (see recipe for 20 µM stock)

1. Assemble the reagents on ice in microcentrifuge tubes.

2. Add 500 µg of a protein sample to each tube in <88 µl volume.

3. Adjust volume to 88 µl with solution A, then add the following:

   5 µl 40 mM glucose-6-phosphate solution
   5 µl 20 mM β-NADPH
   1 µl 1 U/µl glucose-6-phosphate dehydrogenase.

4. Preincubate reaction mixtures 5 min at 37°C.

5. To initiate the reactions, add 1 µl of 2.5 µM BV and vortex 5 sec.

   If DMSO is used as the solvent for BV, do not exceed a final concentration of 0.25% in the reaction mixture. A buffer such as 0.1 M potassium phosphate, pH 7.4, may be substituted for solution A.

   The final reaction concentrations—dissolved in solution A—are 5 mg/ml protein extract, 1 mM β-NADPH, 2 mM glucose 6-phosphate, 1 U/100 µl glucose 6-phosphate dehydrogenase, and 25 µM biliverdin.

6. Place tubes in a circulating water bath at 37°C in the dark.

7. Incubate reactions at 37°C for a chosen time interval, typically 5 to 60 min.

8. Terminate the reactions and perform HPLC separations (see Basic Protocol, steps 7 to 17).

9. From the linear standard curves (see Basic Protocol, steps 18 to 26), calculate the concentration of BR in an injected sample in µM (pmol/µl). Calculate BVR activity

using the following formula, where MP* = average mesoporphyrin recovery for the entire run, MP_S = sample mesoporphyrin recovery, and hr = reaction time expressed in hours:

$$(\text{pmol}/\mu\text{l BR}) \times (200\ \mu\text{l})(MP^*/MP_s)$$

Express the final result in the units pmol BR/mg protein/hr.

REAGENTS AND SOLUTIONS

*Use Milli-Q-purified water or equivalent in all recipes and protocol steps. For common stock solutions, see **APPENDIX 2A**; for suppliers, see **SUPPLIERS APPENDIX**.*

Ammonium acetate, 1 M, pH 5.2

Weigh 77.0 g ammonium acetate
Add 26.0 ml glacial acetic acid
Adjust volume to 1.0 liter with Millipore-filtered water
Adjust pH to 5.2 with glacial acetic acid
Filter through 0.2-µm filter
Store up to 3 months at 4°C

Bilirubin IXα standard, 20 µM

Prepare 1.0 mM bilirubin-IXα in 100% DMSO (Sigma) by calculating the required weight of bilirubin mixed isomers (Sigma) according to percent composition (by weight) of the IXα isomer, using the following formula: [(5.84 mg × 100)/percent composition of IXα isomer], and weighing the result in milligrams. Dissolve in 10 ml DMSO. Prepare fresh immediately before use. Add 20 µl of 1.0 mM bilirubin stock to 980 µl DMSO, for a final concentration of 20 µM.

Do not store bilirubin solutions.

The BR IIIα or BR XIIIα structural isomers will appear as minor peaks on either side of the BR IXα peak in standard chromatograms, but will not interfere with the analysis.

Biliverdin IX standard, 20 µM

Weigh 6.19 mg biliverdin IX hydrochloride (Sigma). Dissolve in 10 ml 100% DMSO for a final concentration of 1.0 mM. Divide into aliquots and store up to 3 months at −20°C. Add 20 µl of the 1.0 mM stock to 980 µl 100% DMSO, for a final concentration of 20 µM.

Glucose-6-phosphate, 40 mM

Weigh 11.3 mg D-glucose-6-phosphate monosodium salt (Sigma) and dissolve in 1.0 ml solution A. Prepare fresh daily.

Glucose-6-phosphate dehydrogenase, 1 U/µl

Dissolve commercial preparation of glucose-6-phosphate dehydrogenase (G6PDH; EC 1.1.1.49, Type XV from Baker's yeast, lyophilized, sulfate free; Sigma) to a final concentration of 1 U/µl in solution A (see recipe). Divide into aliquots and store up to 3 months at −20°C.

Hemin stock solutions, 2.5 mM

Weigh 6.5 mg bovine hemin (Sigma). Dissolve in 1.0 ml 100% DMSO, for a final concentration of 10 mM. Store up to 3 months at −20°C. Immediately before use, gradually dilute the stock 1:3 (v/v) by addition of distilled water, for a final concentration of 2.5 mM.

HPLC buffer A

Pour 100 ml of 1.0 M ammonium acetate, pH 5.2 (see recipe), into a clean glass cylinder. Add 600 ml methanol (HPLC grade). Fill to 1.0 liter with Millipore-filtered water from the source. Degas 2 min with compressed helium.

Mesoporphyrin stock, 200 µM

Working in the dark, weigh 6.39 mg mesoporphyrin (Sigma). Dissolve in 10.0 ml 100% DMSO, for a final concentration of 1.0 mM. Dilute to the stock solution 1:4 (v/v) by addition of 100% DMSO, for a final concentration of 200 µM. Divide into aliquots in foil-wrapped tubes. Store up to 3 months at −20°C, protected from light. Avoid repeated freeze-thaw cycles.

β-NADPH, 20 mM

Weigh 16.7 mg nicotinamide adenine dinucleotide phosphate, reduced form (β-NADPH, tetrasodium salt; Sigma). Dissolve in 1.0 ml solution A (see recipe), for a final concentration of 20 mM. Prepare fresh daily.

PBS/EDTA solution

To 500 ml phosphate-buffered saline (PBS), pH 7.4 *(APPENDIX 2A*), add 0.5 ml of 1.0 M EDTA, pH 8.0 (*APPENDIX 2A*). Store up to 1 month at 4°C. To an aliquot add AEBSF (see recipe for protease inhibitor stock solutions) to a final concentration of 50 µg/ml immediately before use.

Protease inhibitor stock solutions, 1000×

AEBSF: Weigh 50 mg 4-(2-aminoethyl) benzolsulfonylfluoride hydrochloride (AEBSF, Pefabloc SC; Boehringer Mannheim). Dissolve by vortexing in 1.0 ml water. Store up to 2 months at −20°C.

Leupeptin: Weigh 4 mg leupeptin (Boehringer Mannheim). Dissolve by vortexing in 1.0 ml water. Store up to 6 months at −20°C.

Pepstatin: Weigh 4 mg pepstatin (Boehringer Mannheim). Dissolve by vortexing in 1.0 ml 100% DMSO. Store up to 1 month at −20°C.

Divide solutions into 20- to 50-µl aliquots for storage. See above.

Sn Protoporphyrin-IX (Sn PPIX)

Working in the dark, weigh 7.5 mg Sn PPIX dichloride (Porphyrin Products). Dissolve in 1.0 ml 100% DMSO for a final concentration of 10 mM. Divide into aliquots in foil-wrapped tubes and store up to 3 months at −20°C, protected from light. Immediately before use, gradually dilute the stock solution 1:3 (v/v) with distilled water, to a final concentration of 2.5 mM.

Solution A

Weigh 85.6 g sucrose (Sigma). Add 20 ml of 1 M Tris·Cl, then add water to 800 ml and adjust pH to 7.4 with 2 N NaOH. Adjust volume to 1.0 liter with water, autoclave, and store up to 1 month at 4°C. Add protease inhibitors (see recipe) just before use.

Stop solution with mesoporphyrin internal standard

Add 20 µl of the 200 µM mesoporphyrin stock solution (see recipe) to a 10-ml aliquot of a mixture of 95 parts ethanol 5 parts dimethylsulfoxide (v/v). Prepare immediately before use; Do not store.

COMMENTARY

Background Information

HO, a microsomal monooxygenase activity, provides the rate-limiting step in heme degradation (Tenhunen et al., 1969). HO facilitates the disposal of hemoglobin heme during the turnover of erythrocytes in the reticuloendothelial system. Furthermore, HO regulates an intracellular free heme pool that exists in equilibrium with the synthesis and degradation of hemoproteins (Maines, 1992). HO may provide an antioxidative function in the removal of free heme, a potentially harmful iron chelate (Keyse and Tyrrell, 1989). The three biologically active reaction products of HO activity—iron, BR, and CO—imply multiple physiological consequences that can arise from a single enzymatic reaction. By degrading heme, HO activity may directly affect the balance of cellular redox-active iron pools (Ryter and Tyrrell, 2000). The iron-dependent stimulation of ferritin synthesis, coupled with the equilibration of the released iron to the ferritin pool, may also represent an antioxidative process associated with HO activity (Vile and Tyrrell, 1993). Furthermore, BR, which has antioxidant properties, may affect serum antioxidant balance (Stocker et al., 1987), though its intracellular function remains obscure. The CO released by HO may act as a second messenger molecule. The coordination of CO to the heme iron of soluble guanylate cyclase activates the enzyme, resulting in the increased synthesis of 3′,5′-cyclic guanosine monophosphate (cGMP). This mechanism of action resembles that proposed for the endothelium-derived relaxing factor, nitric oxide, NO. The possible consequences of HO/CO/cGMP–dependent signaling include the regulation of vascular function (platelet aggregation, vasodilation, smooth muscle proliferation) and neurotransmission (reviewed in Maines, 1997; Durante and Schafer, 1998). Three distinct HO isozymes, representing three different genes, have been characterized (Maines et al., 1986; McCoubrey et al., 1997a): an inducible form (HO-1), and two constitutive noninducible forms (HO-2) and (HO-3). All three forms can contribute, to various extents, to the total HO activity measurable by current methods. HO-2, which occurs abundantly in testes, nervous tissue, and vascular systems, may conceivably function in CO/cGMP-dependent signaling in these tissues (Maines, 1997). Both HO-1 and HO-2 catalyze the identical biochemical reaction, but they differ in physical properties and reaction rate toward heme (Maines et al., 1986). HO-3, which is highly homologous to HO-2, has weak HO activity (McCoubrey et al., 1997a). Both HO-2 and HO-3 contain two additional heme regulatory domains (HRD) distinct from the catalytic domain (McCoubrey et al., 1997a,b).

The inducible isozyme, HO-1, may be classified as a stress protein, since its elevated synthesis occurs in cultured cells following adverse environmental conditions. Among the agents that trigger the HO-1 response are physical conditions (hyperthermia, shear stress, hypoxia, and 320- to 380-nm ultraviolet-A radiation), inflammatory mediators (cytokines, endotoxins, nitric oxide), and chemical xenobiotics (including heavy metals, thiol-reactive substances, and various oxidants). The alteration of cellular reducing potential by depletion of cellular glutathione may represent a common mechanism by which many agents, including oxidants, trigger induction of the *HO-1* gene (reviewed in Maines, 1992; Ryter and Tyrrell, 1997).

Enzymatic activity assays are important tools in studying the functional significance of the HO system. A conventional method for the detection of HO activity involves the spectrophotometric detection of BR (Schacter, 1978; Tenhunen et al., 1969) directly in micosomal protein by NADPH difference spectroscopy (λ max 464 to 468 nm). The direct measurement of BR in complex protein mixtures can be complicated by spectral interference and the fact that the molar extinction coefficient of BR varies with the consistency of the protein extract. A variation of this method, as described by Kutty and Maines (1982; also see *UNIT 9.3*), extracts the BR from the aqueous phase using chloroform. The concentration of BR is subsequently calculated from the A_{464} to A_{530} of the chloroform extract relative to a chloroform blank. The chloroform extraction of BR, however, may be inefficient. Furthermore, the use of this assay with protein from cultured cells often yields results near the lower limit of spectrophotometric detection. As a source of enzymes (HO and P-450 reductase), the assay requires an 18,000 × *g* supernatant fraction (crude extract) derived from organ, tissue, or cultured cells, which then may be further purified as the 104,000 × *g* microsomal pellet. The spectrophotometric HO assays require supplementation with exogenous tissue extracts to provide BVR activity. Since BV, the proximal product of HO activity, is difficult to measure

Table 9.6.1 Troubleshooting Guide for HPLC Measurement of HO Activity

Problem	Possible cause	Solution
No peaks in chromatogram	HPLC system malfunction	Check detector signal cable. Check detector lamp and settings.
		Check for precolumn leaks.
	Autosampler malfunction	Ensure sampling mechanism is injecting properly.
Unstable baseline	Air in system	Degas buffers and purge system.
Split peaks	Flow obstruction	Replace precolumn filter.
Peak spreading	Column wear	Invert or replace column.
Heme and mesoporphyrin peaks visible, but no BV or BR peaks appear	No detectable enzymatic activity	Review protein extraction procedures, and ensure that all steps are performed at 4°C.
		Ensure a reaction temperature of 37°C. Check quality of reaction components, especially heme and NADPH. Increase reaction time.
Additional peaks in chromatograph	Mesoporphyrin degradation	Replace mesoporphyin stock solution.
	BR degradation	Ensure dark conditions for post-reaction processing.

by spectrophotometry due to spectral interference from other reaction components, the success of the assay depends on the complete conversion of the BV to BR. BVR may be obtained from animal tissues (i.e., bovine or rat liver) in the 30,000 to 105,000 × *g* supernatant, or in partially purified form (Tenhunen et al., 1970).

Derivatives of the HO assay have included radiochemical methods, which typically use [^{14}C]heme as the HO substrate. The [^{14}C]bilirubin formed as the final product is either extracted into chloroform (Tenhunen, 1972) or isolated by thin-layer chromatography (Sierra and Nutter, 1992). The detection of CO by gas chromatography provides another alternative for estimating HO activity (see *UNIT 9.2*).

High-performance liquid chromatography (HPLC) may be conveniently used to detect bile-pigment formation. Bonkovsky et al. (1986) and Lincoln et al. (1989) developed reversed-phase HPLC methods for resolution of BV, BR, and heme extracted from biological materials, using an ammonium phosphate/methanol gradient. HPLC has been employed for the detection of BR formed in HO reactions (Lee and Ho, 1994; Lincoln et al., 1988), and has been demonstrated to be more sensitive than the spectrophotometric assay when analyzing HO activity in hepatocytes (Lincoln et al., 1988). An HPLC method was used to identify BV IXα as the product of the HO reaction (Noguchi et al., 1982). The protocol described in this unit integrates the previous methods to provide an HPLC-based HO assay that measures both BV and BR produced in the HO reaction mixture, using an ammonium acetate/methanol gradient (Ryter et al., 1998, 2000).

Critical Parameters and Troubleshooting

Bilirubin can be easily detected by HPLC and is relatively stable if reasonable precautions are taken to avoid photodegradation. While the 405 nm employed as the detection wavelength is suboptimal for detection of BV or BR, it allows simultaneous detection of both pigments, as well as hemin, at picomole sensitivity. If BVR is present in the reaction mixtures in excess, or added from an exogenous source, the BV peak will disappear to favor a single BR peak, which will simplify quantification. Protein extracts prepared from HeLa cells were found to contain substantial BVR activity in the 18,000 × *g* supernatant, which even cosedimented in 105,000 × *g* pellets. The amount of endogenous BVR present in protein samples will vary with cell type and degree of protein purification used.

Successful performance of this assay requires a high-quality protein extraction (see Table 9.6.1). To safeguard against protein degradation, a broad spectrum of protease inhibitors should be employed in all extraction solutions. Perform all steps at 4°C using pre-

Table 9.6.2 Measurement of HO Activity in Human Cell Types[a]

Cell type	Treatment condition	HO activity (pmol BR/mg microsomal protein/hr)
HtTA-1 (Hela)[b]	Control[b]	25 ± 11
HtTA-1 HO-2 overexpressing clone[b]	72 hr culture[c]	727 ± 150
HtTA-1[b]	Hemin, 10 μM[d]	278 ± 20
FEK-4 Human skin fibroblast	Control[e]	120 ± 2.5
FEK-4 Human skin fibroblast	Na-Arsenite, 50 μM[f]	350 ± 38
FEK-4 Human skin fibroblast	UVA radiation (250 kJ/m^2)[g]	450

[a]Sample values were obtained by HPLC determination of HO activity as described previously (Ryter et al., 1998, 1999). Microsomal protein derived from cultured cells was used for all determinations. Values reflect mean and standard deviation from three independent determinations.

[b]Human HeLa HtTA-1 were cultured in Earle's minimal essential medium (EMEM) supplemented with 10% FBS, 0.2% sodium bicarbonate, and antibiotics, under standard conditions (37°C, 95% air/5% CO_2) for 4 days.

[c]The heme oxygenase-II (HO-2) overexpressing HtTA-1 subclone (9D5) was cultured for 72 hr in antibiotic-free medium and then harvested for activity analysis.

[d]HtTA-1 were treated with hemin (10 mM in DMSO) applied directly to complete medium to a final concentration of 10 μM, and incubated at 37°C for 16 hr before harvest.

[e]The normal human foreskin fibroblast line FEK-4 was cultured to confluence in EMEM supplemented with 15% FCS, and 0.2% sodium bicarbonate, under standard conditions (37°C, 95% air-5% CO_2).

[f]Sodium *m*-arsenite was applied to confluent FEK-4 monolayers in PBS at 50 μM for 30 min. Subsequently, the cultures were rinsed twice with PBS, fed again with original conditioned complete medium, and restored to 37°C incubators for an additional 14 hr prior to harvest.

[g]For ultraviolet-A (UVA) radiation treatments, confluent FEK-4 monolayers were irradiated at room temperature in PBS supplemented with 0.01% Ca^{2+} and Mg^{2+}. The UVA radiation (250 kJ/m^2) was applied using a broad-spectrum (350 to 400 nm) Sellas 4 KW UVA lamp (Sellas Medizinische Gerate). The light dose was determined using an IL-1700 radiometer (International Light). Following irradiation, cells were rinsed with PBS, restored to complete conditioned medium, and incubated at 37°C for an additional 10 hr.

cooled solutions and equipment. For best results, finish the entire assay on the day of protein extraction. Freezing microsomal or crude extracts at −20°C may cause activity loss.

Assay failure may also commonly arise from mechanical problems with the HPLC apparatus (see Table 9.6.1). These problems can be avoided by proper maintenance of the equipment, including routine inspection for leaks and replacement of precolumn filters. Special care should be used to ensure that buffers and injected samples are free of particulate contamination. HPLC columns have a limited lifetime and require periodic replacement, which can drive up the cost of performing this assay. The columns must be rinsed thoroughly with methanol immediately after completion of the run. Repeated injection of the samples leads to progressive column wear, which manifests as peak spreading. The use of crude protein extract as starting material may cause accelerated column wear. Reversing the column direction when peak spreading occurs can extend column lifetime. Excess injected hemin may be retained in the column and elute during subsequent methanol rinsing. The binding of excess heme inside the column may also affect column lifetime.

A slight dark decay of BR IXα occurs when the samples are stored for long periods of time in plastic tubes. The cause of this has not been determined, but may be due to air oxidation or binding of the pigment to the plastic. Thus, long serial repetitions of equivalent samples in an autosampler result in gradual signal reduction. The authors recommend limiting autosampler runs to 20 samples. The rate of dark decay can be determined experimentally from the serial repetition of BR standards.

A weakness of HO activity assays is that they do not differentiate between HO-1 and HO-2 activity. Theoretically, based on known mRNA and protein expression patterns, basal HO activity is generally assumed to reflect constitutive HO-2 expression with a negligible contribution from HO-1. Inducible HO activity reflects the additional contribution of HO-1 activity to the background of HO-2 activity.

There are rare cases, however, where HO-2 contributes to inducible activity, such as stimulation of nervous tissue with glucocorticoid hormones (Weber et al., 1994). A thorough analysis of HO expression, therefore, might involve a combination of activity assay data supplemented with immunoblot or northern blot analyses of the protein or mRNA levels of the different isozymes.

Furthermore, in vitro enzyme assays provide only a comparative estimate of functional enzyme protein levels under the artificial condition of excess exogenous substrate. However, the availability of endogenous heme for HO activity in tissue samples cannot be addressed by the assay. Absolute activity values reported will vary depending upon the degree of protein purification used. Therefore, for comparative purposes, one should use a consistent protein extraction protocol.

Anticipated Results

Figure 9.6.1 shows a sample standard chromatogram. As little as 10 pmol of BV or BR can be detected using the HPLC parameters described. Most mammalian cell types should contain basal HO activity. Basal values from cultured cells should be in the range of 30 to 200 pmol/mg protein/hr. Table 9.6.2 shows typical results from analyses of cultured cells exposed to several inducing agents.

Time Considerations

The preparation of tissue culture samples is typically initiated 2 to 3 days prior to the assay. Treatment with inducing chemicals or other manipulations of cell culture conditions is typically performed during the 12-hr period preceding the cell harvest. These parameters will vary depending on individual experimental design. Cell scraping and preparation of crude extract typically requires 1.5 to 2 hr for 20 to 30 petri dishes. The preparation of microsomal fractions from crude extract requires an additional 1.5 hr. Allow ≥0.5 hr for determination of protein concentrations. Allow 0.5 to 1 hr for assembly of reaction mixtures, if all reagents are prepared. Allow up to 1 hr reaction incubation time. Allow 15 min for post-reaction processing. Allow an analysis time of 20 min per sample (if an autosampler is used, the investigator need not be present after the first injection). Allow several hours for manual peak integration (this may be automatic on newer HPLC systems) and calculation of HO activities.

LITERATURE CITED

Bonkovsky, H.L., Wood, S.G., Howell, S.K., Sinclair, P.R., Lincoln, B., Healy, J.F., and Sinclair, J.F. 1986. High performance liquid chromatography separation and quantitation of tetrapyrroles from biological materials. *Anal. Biochem.* 155:56-64.

Durante, W. and Schafer, A. 1998. Carbon monoxide and vascular cell function (review). *Int. J. Mol. Med.* 2:255-262.

Keyse, S.M. and Tyrrell, R.M. 1989. Heme oxygenase is the major 32-kDa stress protein induced in human skin fibroblasts by UVA radiation, hydrogen peroxide, and sodium arsenite. *Proc. Natl. Acad. Sci. U.S.A.* 86:99-103.

Kutty, R.K. and Maines, M.D. 1982. Oxidation of heme C derivatives by purified heme oxygenase. Evidence for the presence of one molecular species of heme oxygenase in the rat liver. *J. Biol. Chem.* 257:9944-9952.

Lee, T.C. and Ho, I.C. 1994. Expression of heme oxygenase in arsenic-resistant human lung adenocarcinoma cells. *Cancer Res.* 54:1660-1664.

Lincoln, B.C., Mayer, A., and Bonkovsky, H. 1988. Microassay of heme oxygenase by high performance liquid chromatography. Application to assay of needle biopsies of human liver. *Anal. Biochem.* 170:485-490.

Lincoln, B., Aw, T.Y., and Bonkovsky, H. 1989. Heme catabolism in cultured hepatocyte: Evidence that heme oxygenase is the predominant pathway and that a proportion of the synthesized heme is converted rapidly to biliverdin. *Biochim. Biophys. Acta* 992:49-58.

Maines, M.D. 1992. Heme Oxygenase: Clinical Applications and Functions. CRC Press, Boca Raton, Fla.

Maines, M.D. 1997. The heme oxygenase system: A regulator of second-messenger gases. *Annu. Rev. Pharmacol. Toxicol.* 37:517-554.

Maines, M.D., Trakshel, G.M., and Kutty, R.K. 1986. Characterization of two constitutive forms of rat liver microsomal heme oxygenase. Only one molecular species of the enzyme is inducible. *J. Biol. Chem.* 261:411-419.

McCoubrey, W.K., Huang, T.J., and Maines, M.D. 1997a. Isolation and characterization of a cDNA from the rat brain that encodes hemoprotein heme oxygenase-3. *Eur. J. Biochem.* 247:725-732.

McCoubrey, W.K., Huang, T.J., and Maines, M.D. 1997b. Heme oxygenase-2 is a hemoprotein and binds heme through heme regulatory motifs that are not involved in heme catalysis. *J. Biol. Chem.* 272:12568-12575.

Noguchi, M., Yoshida, T., and Kikuchi, G. 1982. Identification of the product of heme degradation catalyzed by the heme oxygenase system as biliverdin-IXα by reverse phase high performance liquid chromatography. *J. Biochem. (Tokyo)* 91:1479-1483.

Ryter, S. and Tyrrell, R.M. 1997. The role of heme oxygenase-1 in the mammalian stress response:

Molecular aspects of regulation and function. *In* Oxidative Stress and Signal Transduction (H.J. Forman and E. Cadenas, eds.) pp. 343-386. Chapman and Hall, New York.

Ryter, S. and Tyrrell, R.M. 2000. The heme synthesis and degradation pathways: Role in oxidant sensitivity. Heme oxygenase has both pro- and antioxidant properties. *Free Radic. Biol. Med.* 28:289-309.

Ryter, S., Kvam, E., Richman, L., Hartmann, F., and Tyrrell, R. M. 1998. A chromatographic assay for heme oxygenase activity in cultured human cells: Application to artificial heme oxygenase over-expression. *Free Radic. Biol. Med.* 24:959-971.

Ryter, S., Kvam, E., and Tyrrell, R.M. 2000. The heme oxygenases: Current methods and applications. *Methods Mol. Biol.* 99:369-391.

Schacter, B. 1978. Assay for microsomal heme oxygenase in liver and spleen. *Methods Enzymol.* 52:367-372.

Sierra, E. and Nutter, L.M. 1992. A microassay for heme oxygenase activity using thin layer chromatography. *Anal. Biochem.* 200:27-30.

Stocker, R., Yamamoto, Y., McDonagh, A., Glazer, A., and Ames, B.N. 1987. Bilirubin is an antioxidant of possible physiological importance. *Science* 235:1043-1046.

Tenhunen, R. 1972. Method for microassay of microsomal heme oxygenase activity. *Anal. Biochem*. 45:600-607.

Tenhunen R., Marver, H.S., and Schmid, R. 1969. Microsomal heme oxygenase, characterization of the enzyme. *J. Biol. Chem.* 244:6388-6394.

Tenhunen, R., Ross, M.E., Marver, H.S., and Schmid, R. 1970. Reduced nicotinamide-adenine dinucleotide phosphate dependent biliverdin reductase: Partial purification and characterization. *Biochemistry* 9:298-303.

Vile, G.F. and Tyrrell, R.M. 1993. Oxidative stress resulting from ultraviolet-A irradiation of human skin fibroblasts leads to a heme oxygenase-dependent increase in ferritin. *J. Biol. Chem.* 268:14678-14681.

Weber, C.M., Eke, B.C., and Maines, M.D. 1994. Corticosterone regulates heme oxygenase-2 and NO synthase transcription and protein expression in the rat brain. *J. Neurochem.* 63:953-962.

KEY REFERENCES

Ryter, S., Kvam, E., and Tyrrell, R.M. 1999. Determination of heme oxygenase activity by high performance liquid chromatography. *Methods Enzymol.* 300:322-336.

This paper also provides detailed methodology for the analysis of HO activity using high performance liquid chromatography.

Ryter et al., 1998. See above.

This paper shows graphic examples of the application of the HPLC technique to the detection of heme oxygenase activity.

Maines, 1992. See above.

This book provides a comprehensive account of the basic background information related to the heme oxygenase system.

Contributed by Stefan W. Ryter
Southern Illinois University School of Medicine
Springfield, Illinois

Rex M. Tyrrell
University of Bath
Bath, United Kingdom

Functional Analysis of the Heme Oxygenase-1 Gene Promoter

Heme oxygenase (HO) enzyme activity is stimulated by a diverse array of chemical compounds, bioactive agents, and environmental conditions. This stimulation is a consequence of increased expression of the HO-1 enzyme resulting primarily from an enhanced rate of *ho-1* gene transcription.

Understanding the mechanism of inducer-dependent *ho-1* gene activation requires measurement of the transcriptional activity of the *ho-1* gene promoter. Promoter activities are most commonly measured in vivo by transient transfection assays utilizing reporter genes. In such assays, plasmid DNA bearing a reporter gene under the control of the test promoter is introduced, or transfected, into target cells by chemical or other means. The cells are subsequently exposed to vehicle or inducing agents and reporter enzyme activity is measured in extracts from treated and untreated cells, generally within 24 to 72 hr after transfection. By examining reporter gene constructs containing different regions (and mutants) of the *ho-1* gene promoter in this manner, it is possible to localize the exact DNA regulatory sequences necessary for *ho-1* gene activation by a particular agent. In certain circumstances, the *ho-1* gene promoter exhibits suboptimal or aberrant regulation in transient transfection assays. Integration, or stable transfection, of an *ho-1* promoter/reporter gene construct into chromosomes, which provides a more normal chromatin environment for gene regulation, often overcomes this limitation.

The *Photinus pyralis* (firefly) luciferase gene is arguably the most commonly used reporter gene for promoter analyses. Often, in transient transfection analyses, a second reporter gene under the control of a strong, constitutively active promoter is cotransfected with the primary construct. Normalization of the primary enzyme activity in each cell extract to the activity of the secondary reporter enzyme activity corrects for any potential variations in transfection efficiency between different cell populations. The *E. coli lacZ* gene encoding β-galactosidase is commonly used as the secondary reporter gene.

This unit describes procedures necessary for transient transfection analysis of the *ho-1* gene promoter (see Basic Protocol); these include transfection of cells using calcium phosphate–DNA precipitates and measurement of luciferase and β-galactosidase activities in the same cell extract by chemiluminescence-based assays. The calcium phosphate precipitation technique is also used to generate stable transfectants (see Alternate Protocol). Finally, a method is presented for purification of high-quality plasmid DNA necessary for cell transfection (see Support Protocol).

TRANSIENT TRANSFECTION OF REPORTER GENE CONSTRUCTS INTO MAMMALIAN CELLS AND MEASUREMENT OF REPORTER ENZYME ACTIVITIES

BASIC PROTOCOL

Transient transfection analysis is the preferred method for promoter function studies, as transfections can be carried out in 1 day and the entire experiment completed within 3 to 4 days. In contrast, 3 to 4 weeks are required for generation and expansion of stably transfected cell lines (see Alternate Protocol). In the present method, a precipitate containing calcium phosphate and DNA is formed by slowly mixing a HEPES-buffered saline solution with a solution containing calcium chloride and the reporter gene plasmid DNA, and this is applied to the cells. The $CaPO_4$-DNA complexes adhere to the surface of cells and are internalized. The transfected cells are exposed to the HO-1 inducer being tested and subsequently lysed directly on the plate with a detergent-containing buffer.

Contributed by Jawed Alam

Current Protocols in Toxicology (2000) 9.7.1-9.7.21

Aliquots of lysates are used to measure luciferase and β-galactosidase activities with a single-tube luminometer.

Materials

Adherent eukaryotic cells: e.g., HeLa (human cervical epithelial adenocarcinoma), MCF-7 (human mammary epithelial adenocarcinoma), NIH 3T3 (mouse embryo fibroblast), L929 (mouse connective tissue fibroblast-like), Hepa (mouse hepatoma), or RAW 264.7 (mouse peritoneal macrophage)
Complete medium (depending on cell line used)
Plasmid containing luciferase gene under control of *ho-1* promoter (see Table 11.9.1) purified by CsCl gradient (see Support Protocol)
Plasmid containing β-galactosidase gene (see Table 11.9.1) purified by CsCl gradient (see Support Protocol)
Carrier CsCl-purified plasmid DNA (see Support Protocol)
3 M sodium acetate, pH 5.2 (see recipe)
95% ethanol
2.5 M $CaCl_2$ (see recipe)
2× HEPES-buffered saline (HeBS; see recipe)
Glycerol/PBS solution (see recipe)
Phosphate-buffered saline (PBS; *APPENDIX 2A*)
HEPES-buffered, serum-free medium (appropriate to cell line; see recipe) containing inducing agent of interest
Cell lysis buffer (see recipe)
Luciferase assay buffer (see recipe)
0.2 mM luciferin solution (see recipe)
β-galactosidase chemiluminescent substrate solution (see recipe)
Light emission accelerator (Tropix)

6-well tissue culture plates
14-ml polystyrene round-bottom tubes (Falcon)
Platform shaker or rocker
Luminometer with measuring tube
48°C bath or heating block

Additional reagents and equipment for mammalian cell culture (*APPENDIX 3B*)

NOTE: All solutions and equipment coming into contact with living cells must be sterile, and aseptic technique should be used accordingly.

NOTE: All culture incubations should be performed in a humidified 37°C, 5% CO_2 incubator unless otherwise specified.

Transfect cells with $CaPO_4$-DNA precipitates

1. The day before transfection, plate 5×10^5 cells per well of 6-well tissue culture plates and place in CO_2 incubator under standard growth conditions. Just prior to transfection, replace culture medium with 2.0 ml complete medium.

   The number of cells plated may be adjusted to account for differences in cell size and morphology and the cell density requirements at the time of induction. In general, on the day of transfection, it is important that cells be visibly separated in the wells (~50% confluent), as the ability to take up DNA is related to the surface area of the cell exposed to medium.

   APPENDIX 3B describes techniques for mammalian cell culture.

2. Ethanol precipitate DNA to be transfected as follows.

   a. In a 1.5-ml microcentrifuge tube, mix appropriate amounts of:

      CsCl-purified luciferase reporter/*ho-1* promoter plasmid DNA
      CsCl-purified β-galactosidase plasmid DNA
      CsCl-purified carrier DNA

   b. Adjust the volume to 90 µl with water.

   c. Add 10 µl of 3 M sodium acetate, pH 5.2, and 250 µl 95% ethanol.

   d. Mix and place 15 min at −70°C or overnight at −20°C.

   Ethanol precipitation sterilizes the DNA to be transfected. Plasmid DNA should be purified by two rounds of CsCl gradient centrifugation (see Support Protocol), as impurities in the DNA preparation can be deleterious to transfection efficiency.

   The total amount of DNA that is optimal for transfection will vary with cell line, from ~5 to 15 µg per well of a 6-well plate. The amount of individual reporter plasmids used for transfection will depend largely on the strengths of the ho-1 promoter (generally 5 µg) and the promoter driving expression of the lacZ gene in the cell line transfected (generally 1 to 5 µg, typically less but never more than the ho-1/luc plasmid because the β-gal plasmid contains a strong constitutive promoter). Surprisingly, the most important consideration here is the total amount of DNA used, which is determined empirically and is cell-line dependent. The range of 5 to 15 µg is based on observation and published reports. General cloning plasmids, E. coli DNA, or salmon sperm DNA are commonly used as carrier DNA.

3. Pellet DNA by microcentrifuging 5 min at 12,000 × *g* (12,000 rpm), 4°C, and remove the supernatant by aspiration or by inverting the microcentrifuge tube on a fresh Kimwipe inside a tissue culture hood. Air dry the pellet.

4. Resuspend the pellet in 450 µl sterile water and add 50 µl of 2.5 M $CaCl_2$. Mix by pipetting.

   DNA is difficult to dissolve in high salt solutions and should be resuspended completely prior to addition of $CaCl_2$.

5. Place 500 µl of 2× HeBS in a sterile, 14-ml polystyrene round-bottom tube. Add the DNA/$CaCl_2$ solution dropwise with a Pasteur pipet, mixing the solutions after every 4 to 5 drops by gentle agitation of the tube. Incubate 15 to 20 min at room temperature.

   Agitation (2 to 3 sec each) should be of sufficient strength to permit mixing but not so strong as to generate bubbles. A vortex mixer may also be used. Clear polystyrene tubes, in contrast to opaque tubes, permit easier visualization of the precipitate. The mixture should appear cloudy, similar to very dilute milk. The volume of precipitate is sufficient for two wells; if more than one inducer, or multiple concentrations of the same inducer, are being tested, adjust the amount of DNA and solution volumes proportionally. Do not prepare more than 2 ml of precipitate in a single tube of this size. Higher volumes do not permit adequate mixing, and result in suboptimal precipitation. Combine all precipitates of the same DNA mixture into a single tube prior to aliquoting into replicate wells.

6. With a 1-ml pipettor, transfer 0.45 ml of each precipitate prepared to each of 2 wells in a 6-well plate of growing cells (see step 1). Distribute the precipitates dropwise over the entire well and gently agitate to mix precipitate and medium.

7. Incubate the cells 4 to 6 hr under standard growth conditions.

   The amount of time that the precipitate should be left on the cells will vary with cell type. For hardy cells such as HeLa, L929, and NIH 3T3, the precipitate can be left on for 16 to 24 hr with concomitant enhancement in DNA uptake and reporter enzyme activities. Other cell types will not survive this amount of exposure to the precipitate. As a general rule, expose cells for the minimum amount of time sufficient to attain reasonable levels of reporter enzyme activity.

8. Remove the medium from each well, add 1 ml sterile 37°C glycerol/PBS, and leave for 1 to 2 min, room temperature. Remove the glycerol solution and wash cells twice with 2 ml 37°C PBS, then feed cells with 2 ml 37°C complete medium.

   For most cell lines, transfection efficiency is increased to varying degrees by "shocking" the cells with either glycerol or DMSO (10% to 20%). DMSO tends to be somewhat less harmful to the cells, but also may not be as effective. Shocking is unnecessary when cells are exposed to the precipitate overnight. Wash cells quickly with PBS as excessive exposure to glycerol will kill cells.

9. Incubate cells for 16 to 40 hr under standard growth conditions.

Expose cells to inducing agent

10. Remove medium by aspiration and wash each well with 1 ml 37°C PBS.

11. To duplicate wells, add 2 ml HEPES-buffered, serum-free medium containing the inducing agent or the vehicle used for the inducing agent (control). Return plates to the CO_2 incubator for 5 hr.

    For many HO-1 inducers, such as heme and heavy metals, the highest induction levels are achieved in serum-free medium, as serum proteins bind and retard cellular uptake. In serum-free medium, the optimal exposure time is generally between 3 and 8 hr, which represents a balance between the need to translate sufficient levels of reporter gene products and to maintain cell viability, as many HO-1 inducers are toxic. HO-1 inducers that are not toxic or whose actions are not inhibited by serum proteins can be added in complete medium for extended periods. In such circumstances, addition of inducing agent immediately after transfection (at the end of step 8) may provide for higher induction levels.

12. Remove induction medium by aspiration and wash each well twice with PBS.

    If luciferase assays cannot be carried out immediately, freeze plate at −70°C after removal of PBS.

Prepare cell extract

13. Add 0.5 ml cell lysis buffer to each well and agitate the plate on a platform shaker or rocker for 15 min at moderate speed, room temperature.

    Cell lysis can be monitored by examining the cells under a microscope. Lysed cells will appear shrunken and circular. Detachment of cells from the plate is not necessary for lysis and release of reporter enzymes.

Measure luciferase activity

14. Pipet 0.4 ml luciferase assay buffer into each luminometer measuring tube and an appropriate volume of luciferin solution (depending upon the luminometer) into the injection vial.

    Perform all assays in duplicate.

15. Pipet 5 to 50 µl cell lysate directly into the assay buffer within each tube and mix by gentle agitation.

16. Place tube in the luminometer and inject 100 µl luciferin solution. Measure luminescence by integrated light analysis (typically 10 to 20 sec).

    Dilute or reduce cell extract to maintain reaction within the linear range of the instrument. Reaction buffer, lysate, and substrate volumes will vary depending on instrument used. Compared to peak height analysis, integrated analysis is less affected by noise fluctuations, thus reducing variability, and this generally can detect lower levels of light emission.

    Integrated light analysis is "built into" all luminometers used for promoter analysis. Most luminometers permit adjustment of integration period (i.e., 10, 20, or 30 sec).

Measure β-galactosidase activity

17. Transfer 0.25 ml of each cell lysate (from step 13) to a 1.5-ml microcentrifuge tube and heat at 48°C for 50 min. Place tubes on ice 5 min and then microcentrifuge 5 min at 12,000 × *g*, 4°C.

    Perform all assays in duplicate.

    All mammalian cells exhibit varying degrees of endogenous β-galactosidase activity. Depending on the level, this activity may lead to background, which will decrease the overall sensitivity of the assay by lowering the signal-to-noise ratio. Mammalian and E. coli β-galactosidases exhibit differential sensitivity to heat inactivation. Because endogenous β-galactosidase activity may not be completely eliminated by heating, it is useful to measure the heat-insensitive activity in control extracts (from mock-transfected cells). For cells with low endogenous activity, such as HeLa and L929, this step may be omitted if exogenous activity is relatively high. Heated samples may be frozen at −70°C for up to 1 week without loss of activity.

18. Transfer 2 to 20 µl of each clarified cell lysate into a luminometer measuring tube. Add 100 µl β-galactosidase substrate solution (containing chemiluminescent β-Gal substrate) to each sample and gently mix. Incubate 60 min at room temperature.

    The amount of cell extract required may vary depending on the amount of expression and the instrument used. It is important to vary the concentrations of extract or time of reaction to keep the signal within the linear range of the assay. Measurements are time dependent. Substrate solution should be added to sample extracts in the same time frame as they are counted in the luminometer. For example, if it takes 20 sec to completely count a sample, then substrate solution should be added to tubes at 20-sec intervals.

19. Transfer an appropriate volume of light emission accelerator to the injection vial. Place tube with lysate/substrate solution (step 18) in luminometer and inject 100 µl accelerator. Measure integrated light emission over a 10- to 20-sec period.

STABLE TRANSFECTION OF REPORTER GENE CONSTRUCTS INTO MAMMALIAN CELLS

ALTERNATE PROTOCOL

Nonspecialized DNA transfected into mammalian cells lacks functional centromeres and is lost from the cell population with first-order kinetics. A small fraction will integrate into cellular chromosomes and be stably maintained as chromosomes replicate during subsequent cell divisions. Regulatory sequences within "transient" DNA molecules generally do not assume proper chromatin/nucleosomal structures and may exhibit suboptimal or aberrant gene regulation, particularly with respect to gene activation or repression. Differences in transcriptional activity between "transient" and "stable" sequence conformations have been observed for several promoters, including that of the *ho-1* gene and, in certain cellular contexts, some agents only activate integrated promoter sequences. Additionally, stably transfected cell lines permit rapid screening of agents (and conditions) that modulate promoter activity without repeated transfections.

To select for stable transfectants, generally representing ≤0.01% of the original population, the reporter gene plasmid is cotransfected with a second plasmid encoding a dominant selectable marker at a molar ratio of at least 5:1. Because transfected DNAs form large concatemers inside the cells, this ratio practically ensures that cells with the integrated marker gene will also incorporate the reporter gene. Cells are cultured in selection medium that permits survival only of those cells expressing the dominant marker. Resistant cells are allowed to grow until colonies are readily visible to the naked eye, and they are then collected and expanded. Several selectable marker genes are available for use in mammalian cells. The bacterial *aph* (*neo*) gene, encoding aminoglycoside phosphotransferase, is frequently used to select stable transfectants.

Additional Materials *(also see Basic Protocol)*

20 mg/ml G418 (see recipe)
Mammalian expression plasmid encoding *neo* gene and control expression vector lacking *neo* gene (e.g., pBSSK)
Bicinchoninic acid kit for protein determination (Sigma; optional)

10-cm tissue culture dishes
12- to 96-well tissue culture plates

Determine the minimum concentration of G418 necessary to prevent cell growth

1. Plate 5×10^5 cells in each of six 10-cm tissue culture dishes. After 24 hr, add serial dilutions of G418 (from 20 mg/ml stock) to individual plates at final concentrations of 0 to 1000 µg/ml in increments of 200 µg/ml and incubate under standard growth conditions.

2. Culture cells for 2 weeks, feeding with the appropriate selective medium every 3 to 4 days.

   APPENDIX 3B describes techniques in mammalian cell culture.

3. After 2 weeks, examine dishes for viable cells and determine the minimum concentration of G418 required to significantly inhibit cell growth.

   Cells differ in their susceptibility to killing by G418 and some may require even higher concentrations of the drug to evince cell death within a reasonable period of time. Cells will divide once or twice in the presence of lethal doses of G418, so the effects of the drug take several days to become apparent. The rate of cell killing diminishes dramatically if the cells reach confluency before the selection can take full effect. If necessary, plate lower numbers of cells (here and for transfection below).

Precipitate DNA and transfect cells

4. The day before transfection, plate 5×10^5 cells in a 10-cm tissue culture dish and incubate under standard growth conditions. Just prior to transfection, replace culture medium with 9.0 ml complete medium.

   Most cell lines can grow in isolation, a requirement for selecting stably transfected cells. If in doubt about the cell line being used, plate ~50 to 100 cells on a 10-cm tissue culture dish and feed every 4 days for 12 to 14 days. Examine for number of colonies by looking from underneath the plate or using a microscope. Colonies may also be quantified by removing the medium and staining the plate with 2 to 3 ml of 2% methylene blue in 50% ethanol. Colonies become visible after removal of the excess stain.

5. Ethanol precipitate the DNAs to be transfected as follows (see Basic Protocol, steps 2 to 3).

   Experimental plates—13.5 µg *ho-1* promoter/luciferase plasmid + 1.5 µg of *neo* expression vector plasmid.

   Control plate—13.5 µg *ho-1* promoter/luciferase plasmid + 1.5 µg of expression vector lacking the *neo* gene.

   Use a molar ratio between 5:1 and 15:1 of the reporter plasmid to the neo plasmid. For promoter analysis studies, it is best not to physically link the selective marker to the reporter gene transcription unit in a single plasmid. Any potential interference by the strong, constitutive promoter controlling expression of the marker gene with the regulation of the test sequences will be more pronounced at the 1:1 molar ratio in the linked plasmid. For control plates, any DNA lacking the selectable marker (e.g., pBSSK) will suffice.

6. Transfect the DNAs into the cells (see Basic Protocol, steps 4 to 9).

   For each sample, prepare 1 ml of $CaPO_4$-DNA precipitate and distribute entire volume on to a single 10-cm culture dish. For post-transfection shock, use 5 ml glycerol/PBS solution and PBS per 10-cm culture dish. Do at least two independent transfections (i.e., independent precipitates) of the experimental DNA in case one of the transfections fails.

7. Twenty-four hours after transfection, add G418 at the concentration determined in steps 1 to 3. Replace selection medium every 3 to 4 days.

   Some investigators propagate cells under nonselective conditions for 36 to 48 hr and then split the cells 1:15 into multiple plates containing selective medium. This is useful when it is necessary to isolate individual clones or to determine the number of transfectants, as one of the plates can be stained to facilitate counting. This strategy, however, is more cumbersome and less economical and usually not necessary for promoter studies.

   Different lots of G418 can have different potencies. If cell death occurs slowly or cells reach confluency, increase the G418 concentration incrementally by 100 μg/ml at each change of the medium until cell death is obvious.

Culture and expand cells

8. Culture cells in selective medium until colonies are 1 to 2 mm in diameter and readily visible to the naked eye (e.g., ~3 to 4 weeks).

9. Collect all colonies from a single plate as a pooled mixture, expand, and prepare frozen stocks at the earliest passage possible.

   Analysis of pooled clones is recommended to dilute or equalize any potential effects of specific integration sites on promoter regulation. If isolating and testing individual colonies, ≥2 to 3 such clones need to be analyzed. The number of resistant colonies obtained will depend on the efficiency of transfection, but ideally each mixture should contain ≥100 individual transfectants.

Measure luciferase activity

10. Plate stably transfected cells in multiwell plates (e.g., 12- or 96-well tissue culture plates) and culture under standard growth conditions for 2 days. Treat cells and measure luciferase activity (see Basic Protocol, steps 14 to 16).

    The use of multiwell plates allows for analysis of multiple inducers at various concentrations and periods of treatment. For example, 96-well plates are particularly advantageous for analysis of stably transfected cells if a 96-well plate format luminometer is available. The number of cells plated and volumes used for cell culture, induction, and cell lysis will vary with cell type and well format used. (See Anticipated Results for specific numbers).

11. *Optional:* Measure protein content of cell extract using a bicinchoninic acid kit to normalize luciferase data with respect to protein.

    Because the same number of cells are plated in each well, extracts are prepared with minimal manipulation, and the inducers are unlikely to significantly affect cell growth within the brief period examined, there is little variation in the amount of protein between individual cell extracts (in a given experiment), and normalization is generally unnecessary. If measuring protein, use a procedure, such as the bicinchoninic acid method, that is compatible with the concentrations of DTT and Triton X-100 in the lysis buffer.

SUPPORT PROTOCOL

PLASMID DNA PURIFICATION

High-quality plasmid DNA is essential for efficient transfection by calcium phosphate precipitation. Plasmid DNA prepared by simple or quick methods do not work well with this protocol. Best results are obtained with supercoiled plasmid DNA purified on silica or other DNA-binding matrices or by banding in cesium chloride gradients. The latter method is described here.

Materials

Plasmid-bearing *E.coli* colonies on agar plate
2× YT bacteria culture medium (see recipe)
Antibiotic (e.g., ampicillin, kanamycin)
Glucose solution (see recipe)
NaOH/SDS solution (see recipe)
Potassium acetate solution (see recipe)
Isopropanol
TE buffer, pH 8.0 (see recipe)
CsCl
10 mg/ml ethidium bromide (see recipe)
CsCl/TE buffer solution (see recipe)
CsCl/TE buffer–saturated isopropanol (see recipe)
3 M sodium acetate, pH 5.2 (see recipe)
95% or 100% and 70% ethanol

Sterile toothpicks
Culture tubes
37°C shaker incubator
2-liter flask
250-ml ultracentrifuge bottles (for a Sorvall GSA rotor)
Sorvall RC-5B superspeed centrifuge and Sorvall GSA rotor (or equivalent)
10-ml heat sealable ultracentrifuge tubes
Beckman L-70 ultracentrifuge and Beckman VTi 65 rotor (or equivalent)
Stand and clamp
18-G (or wider) needles
3- to 5-ml sterile syringes
15-ml screw-cap polypropylene tubes
Sorvall SS-34-rotor with rubber adapters (or equivalent)
1.5-ml microcentrifuge tubes

Culture E. coli cells and prepare cleared cell lysates

1. Propagate a small-scale culture of plasmid-bearing *E. coli* cells by stabbing an isolated colony from an agar plate with the end of a sterile toothpick and dropping it into a 15-ml polypropylene tube containing 2 ml of 2× YT medium and the appropriate antibiotic. Culture overnight at 37°C in a shaking incubator (200 to 250 rpm).

2. On the following day, pour all of the overnight culture into a 2-liter flask containing 500 ml of 2× YT medium and antibiotic. Culture for 12 to 18 hr at 37°C with shaking.

   Large-scale cultures may also be initiated from a single colony, bypassing step 1. In such cases, culture for 24 hr.

3. Transfer cultures into two 250-ml bottles and collect cells by centrifuging 10 min at 9000 × *g* (7500 rpm in a Sorvall GSA rotor), 4°C, using a Sorvall RC-5B superspeed centrifuge.

   Type of bottle, rotor, and centrifuge used will depend on availability.

4. Discard supernatant and resuspend each pellet in 5 ml glucose solution. Combine duplicate pellets and keep on ice.

   Use a rubber policeman or glass rod to break up pellet; incomplete resuspension will reduce plasmid DNA yield.

5. Add 20 ml NaOH/SDS solution (i.e., two times total volume of glucose solution) to lyse cells. Mix by swirling and keep on ice for 5 min.

   Lysates will be pale brownish-yellow and relatively clear. Incomplete clarification will reduce plasmid DNA yield, and generally results from excess cells. In such cases, reduce culture incubation time or proportionally increase volumes of glucose, NaOH/SDS, and potassium acetate (see below) solutions.

Partially purify plasmid DNA

6. Add 15 ml potassium acetate solution (1.5 times total volume of glucose solution). Mix by swirling and keep on ice for 5 min.

   A flocculent precipitate forms immediately and contains, along with other cellular debris, much of the E. coli chromosomal DNA.

7. Centrifuge samples as in step 3. Transfer the supernatant into a clean 250-ml centrifuge bottle.

   Some low-density particulate remains in the supernatant; it will not affect plasmid DNA purification.

8. Add 0.6 volumes of isopropanol to supernatant to precipitate DNA. Swirl or invert to mix and keep at room temperature for 5 min. Centrifuge samples as in step 3. Discard supernatant and wipe inside of bottle with Kimwipes.

   After adding isopropanol, do not store mixture at −20°C or −70°C as additional contaminating material may precipitate and affect subsequent purification.

Purify plasmid DNA by banding in a CsCl gradient

9. Resuspend pellet in exactly 8.8 ml TE buffer, pH 8.0, and add 10 to 10.2 g CsCl. Swirl or vortex to completely dissolve CsCl.

10. Transfer sample to a 10-ml heat sealable ultracentrifuge tube and add 100 µl of 10 mg/ml ethidium bromide solution to the top. Seal tube, and mix by inversion.

    Remember to balance tubes prior to sealing. Use CsCl/TE solution to increase weight. Check seal by squeezing tubes.

11. Ultracentrifuge overnight (i.e., 14 to 24 hr) at 238,000 × *g* (50,000 rpm in a Beckman VTi 65.1 rotor), 20°C.

    If the rotor or ultracentrifuge is in use or otherwise unavailable, store tubes indefinitely in the dark wrapped in aluminum foil at room temperature.

12. Remove centrifuge tubes from the rotor and immobilize with a clamp attached to a stand.

    Care should be taken not to disturb the CsCl gradient and DNA band(s) formed during centrifugation.

13. Puncture the top of the tube with an 18-G (or wider) needle (which can be left or removed). Insert an 18-G needle connected to a 3- to 5-ml sterile syringe into the side of tube, ~0.5 to 1 cm below DNA band, and move needle so that the bevel is pointed upwards and is just touching the bottom of the DNA band. Extract DNA slowly into the syringe.

CAUTION: *When inserting needle into the side, do not place fingers behind the tube. Ideally, there should be a single DNA band near the middle of the tube; RNA will be at the bottom and any precipitates will form a solid film on one side of the tube. If there are two DNA bands, remove the lower, closed-circular plasmid DNA. If the DNA band is toward the bottom of the tube, the sample withdrawn will be contaminated with RNA. The plasmid DNA is easily separated from the RNA on the second CsCl gradient. Do not use a higher-gauge needle as they tend to get clogged and may also shear large plasmid DNAs. Withdraw DNA in the smallest volume possible (e.g., ~2 to 3 ml) and do not attempt to collect the entire band. A thin band is always left behind no matter the volume removed.*

14. Transfer plasmid DNA to another ultracentrifuge tube, top with CsCl/TE solution, and seal tube. Ultracentrifuge for 6 hr at 342,000 × *g* (60,000 rpm in a Beckman VTi 65.1 rotor), 20°C.

    If it is more convenient, centrifuge overnight at 238,000 × g (50,000 rpm in Vti65.1 rotor).

15. Remove the plasmid band as described in step 13, note approximate volume, and transfer to a 15-ml screw-cap polypropylene tube. Extract three times with 1 to 2 vol CsCl/TE buffer–saturated isopropanol. Remove and discard the upper (pink), isopropanol phases containing ethidium bromide.

    The lower, DNA-containing layer should be clear after the final extraction. If necessary, carry out additional extractions. The upper phase is most easily removed using a Pasteur pipet. Any lower layer removed by pipetting is easily visible in the stem of the pipet and should be returned to the tube.

Precipitate DNA

16. Measure volume of the final lower phase and add 2 vol TE buffer, pH 8.0. Mix, then add 3 vol isopropanol (50% final concentration) and mix again. Place tubes at −20°C for 30 min to overnight to precipitate DNA.

17. Collect DNA by centrifuging for 10 min at 7600 × *g* (8000 rpm in a Sorvall SS-34 rotor with rubber adapters), 4°C.

18. Decant or aspirate supernatant and invert tube onto Kimwipes to drain any residual liquid. Be careful not to let any loosened pellet drain along with the liquid. Resuspend the pellet in 400 µl TE buffer, pH 8.0, and transfer to a 1.5-ml microcentrifuge tube. Add 0.1 vol (i.e., 40 µl) of 3 M sodium acetate, pH 5.2, and 2.5 vol (i.e., 1 ml) of 95% or 100% ethanol. Mix to precipitate DNA.

19. Pellet DNA in a microcentrifuge for 5 min at 12,000 × *g* (12,000 rpm). Decant or aspirate supernatant and wash pellet with 1 ml of 70% ethanol. Air dry pellet and resuspend in 1 ml TE buffer, pH 8.0.

    Because of the compactness of the pellet, vigorous pipetting is necessary to break up the pellet and facilitate resuspension. Alternatively, the pellet can be stored overnight in TE buffer at 4°C to allow dissolution.

20. Quantify DNA and store at 4°C.

    This procedure yields ~2 to 3 mg DNA/500 ml culture for high-copy plasmids.

REAGENTS AND SOLUTIONS

Use autoclaved Milli-Q-purified water or equivalent for all recipes and protocol steps. For common stock solutions, see ***APPENDIX 2A****; for suppliers, see* ***SUPPLIERS APPENDIX****.*

$CaCl_2$, 2.5 M

Dissolve 18.4 g $CaCl_2 \cdot 2H_2O$ in 50 ml water. Sterilize solution by filtering through a 0.22-µm filter and distribute into 5-ml aliquots. Maintain working aliquot at 4°C for up to 6 months and store remainder indefinitely at −20°C.

Cell lysis buffer

Add 1 µl of 100 mM PMSF (see recipe) and 5 µl of 0.1 M DTT (see recipe) to each milliliter of cell lysis reagent (see recipe). Prepare just before use and only the amount necessary (final concentration: 0.1 mM PMSF/0.5 mM DTT).

Cell lysis reagent

Weigh 1.23 g $MgSO_4$, 0.38 g EGTA, and 2.6 g HEPES (*N*-2-hydroxylthylpiperazine-*N*′-2-ethanesulfonic acid; sodium salt). Add water and adjust pH to pH 8.0 with NaOH. Add 5 ml Triton X-100 and adjust with water to a final volume of 500 ml (final concentration: 10 mM $MgSO_4$/2 mM EGTA/20 mM HEPES, pH 8.0/1% (v/v) Triton X-100). Store up to 6 months at 4°C.

CsCl/TE buffer–saturated isopropanol

Dissolve 240 g CsCl in 200 ml TE buffer, pH 8.0 (see recipe). Add to 300 ml isopropanol. Mix and allow the phases to separate. Use the upper phase. Store indefinitely at room temperature.

After depletion, additional isopropanol may be added and used as long as distinct phases form. Conversely, CsCl/TE solution may be added to assist phase separation.

CsCl/TE buffer solution

Dissolve 48 g CsCl in 40 ml TE buffer, pH 8.0 (see recipe). Store up to 1 month at room temperature.

Dithiothreitol (DTT), 0.1 M

Dissolve 0.15 g DTT in 10 ml water. Dispense into 0.5-ml aliquots and store indefinitely at −20°C.

Ethidium bromide, 10 mg/ml

Dissolve 1 g ethidium bromide in 100 ml water. Store indefinitely in a dark bottle or a bottle wrapped in aluminum foil at room temperature.

CAUTION: *Ethidium bromide is a powerful mutagen and is moderately toxic. Gloves should be worn when working with solutions that contain this dye, and a mask should be worn when weighing it out.*

G418, 20 mg/ml

Dissolve 1 g G418 in 50 ml complete tissue culture medium. Sterilize by filtering through a 0.22-µm filter and distribute into 10-ml aliquots. Maintain working aliquot at 4°C for up to 3 months and store remainder indefinitely at −20°C.

β-Galactosidase chemiluminescent substrate solution

1 M sodium phosphate, monobasic: Dissolve 13.8 g $NaH_2PO_4 \cdot H_2O$ in water and adjust volume to 100 ml. Store at room temperature.

1 M sodium phosphate, dibasic: Dissolve 26.8 g $Na_2HPO_4 \cdot 7H_2O$ in water and adjust volume to 100 ml. Store at room temperature.

Substrate diluent: Mix 0.7 ml of 1 M monobasic sodium phosphate and 9.3 ml of 1 M dibasic sodium phosphate stock solutions. Add 100 µl of 1 M $MgCl_2$ (*APPENDIX 2A*) and adjust volume to 100 ml (final concentration: 0.1 M sodium phosphate, pH 8.0/1 mM $MgCl_2$). Store up to 3 months at 4°C.

Substrate solution: Dilute chemiluminescent β-Gal substrate (Galacton; Tropix) 1:500 with diluent. Prepare just before use and only the amount necessary.

Glucose solution

Dissolve 9.8 g dextrose monohydrate in 955 ml water. Add 25 ml of 1 M Tris·Cl, pH 8.0 (*APPENDIX 2A*), and 20 ml of 0.5 M EDTA, pH 8.0 (*APPENDIX 2A*). Dispense into 100- to 500-ml portions and sterilize by autoclaving and store up to 6 months at 4°C (final concentration: 50 mM glucose/25 mM Tris·Cl, pH 8.0/10 mM EDTA).

Glycerol/PBS solution

Mix 130 ml glycerol with 130 ml phosphate-buffered saline (PBS; *APPENDIX 2A*). Sterilize mixture by filtering through a 0.45-µm filter. Add 125 ml of mixture to each of two 500-ml bottles of sterile PBS. Mix and store indefinitely at 4°C (final concentration: 10% v/v glycerol).

HEPES-buffered saline (HeBS) solution, 2×

Dissolve 4.1 g NaCl, 3.0 g HEPES acid, and 0.053 g Na_2HPO_4 in 200 ml water. Adjust pH to 7.05 with concentrated NaOH. Adjust volume to 250 ml with water, sterilize by filtering through a 0.22-µm filter, and test for transfection efficiency (final concentration: 50 mM HEPES, pH 7.05/280 mM NaCl/1.5 mM Na_2HPO_4). Dispense 40-ml aliquots into sterile 50-ml plastic tubes. Maintain working aliquot up to 2 months at 4°C and store remainder indefinitely at −20°C.

Efficient precipitates form only within the narrow pH range of 7.05 ± 0.05, and there can be wide variability in the efficiency of transfection obtained between batches of 2× HeBS. Precipitate formation should be checked with each new batch by mixing 0.5 ml of 2× HeBS with 0.5 ml of 250 mM $CaCl_2$ and vortexing. A fine precipitate should develop that is readily visible in the microscope.

HEPES-buffered serum-free medium

Add 10 ml of sterile 1 M HEPES, pH 7.2 (commercially prepared) to a sterile 500-ml bottle of serum-free medium appropriate to the cell line to be used (final concentration: ~20 mM HEPES). Store at 4°C until expiration date of medium.

Luciferase assay buffer

Add 1 µl of 1 M DTT (*APPENDIX 2A*) and 20 µl of 100 mM ATP (*APPENDIX 2A*) to each milliliter of luciferase reagent buffer (see recipe). Prepare just before use and only the amount necessary (final concentration: ~1 mM DTT/2 mM ATP).

Luciferase reagent buffer

Weigh 1.65 g glycylglycine, 1.85 g $MgSO_4$, 0.76 g EGTA, and 1.02 g KH_2PO_4; add water and adjust pH to 7.8 with concentrated KOH. Adjust with water to a final volume of 500 ml (final concentration: 25 mM glycylglycine/15 mM $MgSO_4$/4 mM EGTA/15 mM KH_2PO_4). Aliquot and store up to 1 year at 4°C.

Discard if excessive precipitate forms upon storage.

Luciferin solution, 0.2 mM

Dissolve 10 mg luciferin (sodium salt; Analytical Luminescence Laboratory) in 165 ml water. Transfer 10-ml aliquots into 15-ml screw-cap tubes, wrap with aluminum foil and store at −20°C for up to 1 year.

NaOH/SDS solution

Mix 0.1 volume each of 2 N NaOH (*APPENDIX 2A*) and 10% SDS (*APPENDIX 2A*) with 0.8 volume water (final concentration: 0.2 N NaOH/1% SDS). Prepare just before use and only in the amount necessary.

Phenylmethylsulfonyl fluoride (PMSF), 100 mM

Dissolve 0.17 g of PMSF in 10 ml anhydrous isopropanol and store indefinitely at 4°C.

Potassium acetate solution

Dissolve 294.4 g potassium acetate in ~600 ml water. Adjust pH to 5.0 with glacial acetic acid (~120 ml). Adjust volume to 1 liter with water (final concentration: 3 M potassium/5 M acetate). Autoclave and store indefinitely at room temperature.

Sodium acetate, pH 5.2, 3 M

Dissolve 204 g of sodium acetate trihydrate in 400 ml water. Adjust the pH to 5.2 with glacial acetic acid and adjust volume to 500 ml with water. Sterilize by autoclaving and store indefinitely at room temperature. Decant working aliquots into 50-ml screw-cap plastic tubes.

TE buffer, pH 8.0

Mix 10 ml of 1 M Tris·Cl, pH 8.0 (*APPENDIX 2A*), 2 ml of 0.5 M EDTA, pH 8.0 (*APPENDIX 2A*), and 988 ml water. Aliquot and autoclave (final concentration: 10 mM Tris·Cl/1 mM EDTA). Store indefinitely at room temperature. Decant working aliquots into 50-ml screw-cap plastic tubes.

YT bacteria culture medium, 2×

Weigh and mix 16 g tryptone, 10 g yeast extract, and 5 g sodium chloride. Dissolve in 1 liter water. Aliquot into bottles or flasks and sterilize by autoclaving. Store indefinitely at room temperature. Discard if medium turns cloudy at any time after sterilization.

COMMENTARY

Background Information

Heme oxygenase (HO) enzymes catalyze the initial and rate-limiting reaction in heme catabolism—the oxidative cleavage of b-type heme molecules to yield equimolar quantities of biliverdin IXα, carbon monoxide, and iron. This activity was identified and initially characterized in the mid- to late 1960s. Soon thereafter, several studies demonstrated that HO activity is stimulated not only by the substrate heme or during erythrophagocytosis, but also in response to agents unrelated to heme including endotoxin and heavy metals. Initial investigations using RNA synthesis inhibitors hinted at the requirement of de novo RNA synthesis, and studies with isolated polysomes confirmed that induction of enzyme activity resulted from increased levels of the mRNA encoding the isozyme now classified as HO-1. The availability of cDNA and genomic clones has established, by direct measurement of transcription rates, that induction of HO-1 expression by many if not all stimuli is regulated primarily at the level of transcription initiation. Additionally, the list of HO-1 inducers has expanded dramatically to include, among others, UV irradiation, hyperthermia, inflammatory cytokines, nitric oxide, disease states, and therapeutic drugs (Maines, 1992; Choi and Alam, 1996).

The basic mechanism of transcription is essentially identical for all genes and involves the initiation and procession of RNA synthesis by RNA polymerase and the basic transcription machinery. Temporal, spatial, tissue-specific, and inducer-dependent variations in gene expression result primarily from the binding of specific transcription factors to their target DNA sequences (*cis* elements) located within the body of the gene, downstream of the gene or, more commonly, upstream of the gene in the proximal and/or distal promoter regions. These sequence-specific DNA binding proteins, in turn, modulate the rate of transcription initiation by interacting directly, or indirectly via coactivators, with the basic transcription machinery.

Aside from the obvious requirement of procedures to isolate and sequence select eukaryotic genes, identification and functional analysis of *cis*-elements has been greatly facilitated by two technological developments: (1) the ability to transfect DNA into cells, and (2) the use of reporter genes to monitor the transcription activity of regulatory sequences.

Transfection

Naked DNA can be introduced into mammalian cells directly by microinjection, or, more commonly, by methods that promote cellular uptake. DNA uptake can be facilitated by generation of pores in the cellular membrane with electrical impulses (i.e., electroporation),

by lipid-mediated fusion to cell membranes, or with the use of chemical agents such as DEAE-dextran or calcium phosphate. The calcium phosphate coprecipitation technique has evolved from the observations of Graham and van der Eb (1973) that $CaCl_2$ enhances DEAE-dextran-mediated cellular uptake of adenovirus DNA. Further analysis indicated that enhanced uptake resulted as a consequence of the formation and cellular adsorption of DNA-$CaPO_4$ coprecipitates (the phosphate was fortuitously present in the DNA dilution buffer). Calcium phosphate precipitation is a relatively simple and inexpensive procedure, and, unlike the DEAE-dextran method, is equally effective in transient and stable transfections. Because effective precipitates form under relatively specific conditions, variability in transfection efficiencies is a potential and not infrequent problem. Another disadvantage is that this technique is not particularly effective with suspension or primary cells. Lipids, on the other hand, expedite DNA uptake into a wide variety of cells. This property, and the commercial availability of various formulations, have made lipid-mediated transfection a popular methodology in promoter function analysis, in spite of the inherently higher cost of commercial reagents.

Reporter genes

The transcriptional activity of putative regulatory sequences can be studied using homologous systems in which the test sequence directs the expression of its corresponding gene. In this approach, cloned genomic fragments encompassing the coding and flanking regions or minigenes are transfected into cells and activity is assayed by mRNA analysis. The transcripts derived from the exogenous, transfected gene can be distinguished from the endogenous mRNA by using a heterologous cell line (i.e., from a different species) or by modification of the cloned gene (i.e., deletion or insertion of foreign sequences) that generates a slightly altered product. The advantage of this strategy is that RNA measurements provide a relatively direct assessment of transcriptional activity and utilize genetic configurations similar to the endogenous gene, minimizing any potential effects of post-transcriptional processes on gene expression. Measurement of RNA levels, however, can be quite cumbersome and time-consuming, especially considering that identification of *cis* elements requires examination of numerous deletion and site-directed mutant constructs, and the homologous strategy has been superseded by a heterologous approach utilizing reporter genes. With the heterologous system, transcriptional activity is most commonly scored indirectly by measuring reporter gene product levels or enzyme activity. Such assays are generally quicker and more easily quantifiable, and the assumption that protein levels are directly proportional to transcription activity appears to be valid under most circumstances. An important criterion for a reporter gene is that it encode a protein (activity) that is not present in the target cell, or, if present, that can be distinguished from the endogenous activity. Even some mammalian genes, such as those encoding human growth hormone and interleukin 2, which are expressed in a tissue-restricted manner, or placental alkaline phosphate, which can be distinguished from most other phosphatases by its heat stability, satisfy this criterion and have been used in such a capacity. The most commonly used reporter genes, however, are derived from nonmammalian sources. For most of the 1980s, the bacterial genes encoding chloramphenicol acetyl-transferase (Gorman, 1985) and, to a lesser extent, β-galactosidase, were most frequently used for promoter analysis. Because of the construction and availability of numerous promoter/CAT plasmids, this reporter gene is still widely used. Its popularity, however, has gradually and significantly diminished since the introduction of the firefly luciferase reporter gene in 1987 (de Wet et al., 1987). The preference for luciferase is obvious when one compares the characteristics of the enzyme assays; the luciferase reaction is simpler and can be carried out in a matter of minutes as opposed to several hours, does not utilize radioisotopes (as is the case with the most common CAT assays), is more sensitive by at least 3 to 4 orders of magnitudes, and is more economical (Alam and Cook, 1990).

Genomic clones encoding HO-1 from several species have been isolated, and regulatory sequences of these genes have been characterized to varying degrees. Mouse (Alam et al., 1999), rat (Immenschuh et al., 1998; Pellacani et al., 1998), human (Takeda et al., 1994), and chicken (Elbirt et al., 1998) *ho-1* gene promoter/luciferase fusions and their derivatives have been constructed by several investigators and may be obtained from these sources. If necessary, however, *ho-1* promoter sequences may be obtained by other means such as: (1) by screening genomic libraries with traditional methods; (2) by PCR amplification of genomic DNA of species for which sequence data is available; (3) by PCR amplification of commer-

cially available genomic library arrays; and (4) from individuals (or affiliated repositories) involved in large-scale genome sequencing, after first having identified the appropriate clone(s) from sequence information in various databases. With the *ho-1* promoter sequence in hand, standard cloning into a luciferase reporter gene vector will provide the necessary chimera for transfection experiments. Initial analysis should be carried out with largest promoter construct available. Subsequent deletion and mutation of the *ho-1* sequences will localize the inducer-responsive *cis*-element(s).

Critical Parameters and Troubleshooting

The use of luciferase and the development and enhancement of chemiluminescent-based assays for other commonly used reporter enzymes, such as β-galactosidase and alkaline phosphatase, has significantly reduced the lower limit of detection for reporter proteins, in some cases to as few as 10^3 molecules (Alam and Cook, 1990). Because of this increased sensitivity, optimization of protocols to achieve maximum transfection efficiency is less of a consideration in promoter regulation analysis. Nonetheless, reasonable levels of DNA uptake are still useful, for example, when analyzing weak promoters, and particularly with the $CaPO_4$ precipitation technique, as small variations in the size and quality of the precipitate can have dramatic effects on transfection efficiencies.

The initiation, growth, and physical characteristics of precipitate complexes, and ultimately transfection efficiencies, are influenced by many factors, including the concentrations of calcium and phosphate, DNA concentration, and reaction temperature and time (Graham and van der Eb, 1973; Jordan et al., 1996). With the Basic Protocol, however, poor transfection efficiency can most often be attributed to the 2× HeBS solution or the plasmid DNA sample. Optimal transfection—and presumably the formation of highly effective $CaPO_4$-DNA complexes—occurs within the extremely narrow pH range of 7.05 ± 0.05 for the 2× HeBS solution. Values outside this pH range can result in highly dense precipitates that are toxic to cells, large complexes that are not readily internalized, or little to no precipitate (i.e., not visible under a microscope). Given these narrow limits, it is necessary to carefully calibrate the pH meter, using freshly prepared standards, just before preparation of the 2× HeBS solution. Furthermore, the pH of the 2× HeBS solution will migrate outside of the optimal range upon prolonged storage at 4°C. If deterioration in reporter enzyme activities and/or variability in the size, uniformity, or density of the precipitate complex is observed over a period of several transfections, replacement of the 2× HeBS solution should be the first step in the troubleshooting process. While some investigators have also noted deterioration of the 2.5 M $CaCl_2$ solution over time, the author has observed no decay in efficacy of such solutions stored for up to a year at 4°C.

DNA prepared by simple or quick methods should not be used for transfection by the $CaPO_4$ precipitation technique. Impurities in such preparations inhibit initiation and growth of precipitate complexes, reduce internalization of the complex by host cells, and/or promote cellular toxicity. Plasmid DNA purified by CsCl banding is generally considered the "gold standard" and DNA purified as described in the Support Protocol is rarely the source of poor transfection efficiencies. DNA purified by single banding exhibits somewhat reduced efficacy. Plasmid DNA purified by adsorption to silica or other matrices is purported to yield transfection efficiencies equal to or better than those observed with CsCl-purified DNA. In the authors' experience, such preparations are adequate but slightly less effective and give more inconsistent results when used in transfections by $CaPO_4$ precipitation.

For induction studies, another important but less obvious parameter is the molecular nature of the luciferase reporter gene and vector. Firefly luciferase is normally translocated to the peroxisomes in the firefly photocytic cells and also in transfected mammalian cells. As a consequence, this reporter enzyme has a relatively short half-life, ~3 hr in mammalian cells. A commonly used, commercially available luciferase reporter vector encodes a modified luciferase in which the peroxisome targeting sequence has been inactivated, resulting in cycloplasmic retention of the enzyme, and consequently increased stability. Other modifications within the luciferase cDNA and the vector backbone have the net effect of providing high-level, stable expression of luciferase in mammalian cells, 10- to over 100-fold greater than observed with typical vectors encoding wild-type luciferase. The modified luciferase vector is extremely useful when testing regulatory sequences with weak transcriptional activity or measuring basal expression. Promoter sequences cloned into the modified vector, however, may exhibit reduced apparent

inducibility; with the identical *ho-1* promoter sequences, wild-type luciferase constructs generate "fold induction" values 3 to 10 times higher than the modified luciferase plasmid. Presumably, this difference is a consequence of the increased basal activity observed with the modified luciferase reporter plasmid and will be more pronounced when the induction period is brief and not initiated immediately after transfection.

Test DNA

For purposes of this unit, the promoter is broadly defined as all the sequences of a gene necessary for correct transcription initiation and modulation of the rate of such initiation. Proper transcription initiation is controlled primarily by the initiation region itself and the TATA box (or analogous sequences in genes lacking identifiable TATA boxes), generally located 20 to 30 bp upstream of the transcription start site. This short region is operationally referred to as the core promoter. The rate of transcription initiation, as noted earlier, is controlled by discrete *cis* elements that may be located proximal or distal to the core promoter within the body of the gene (either in introns or exons) or in the 5′ or 3′ flanking regions. In the literature, the term "promoter" is often synonymous with the 5′ flanking region as transcription regulatory sequences are most commonly located within this segment. For instance, in the case of *ho-1* genes, all the regulatory *cis* elements thus far identified are situated in the upstream region. Therefore as a general rule, the initial reporter gene construct to be tested should contain the largest contiguous portion of the 5′ flanking region available (and clonable) including the transcription initiation site. Because not all *cis* elements may reside within such a contiguous region, another common strategy is to clone individual subfragments spanning the entire gene into a reporter plasmid containing either a homologous (i.e., derived from the gene under study) or a heterologous core promoter. This latter strategy is possible because of the modular nature of *cis* elements. With either cloning strategy, higher reporter enzyme activity resulting from the test construct relative to the parent reporter plasmid is indicative of the presence of regulatory sequences that confer basal and/or inducible transcription activity. These elements can be further localized by testing either subfragments or systematic deletion mutants of the original DNA. Confirmation of the role of a discrete element in transcription regulation generally requires site-directed mutation of that sequence in the context of the native promoter and/or the function of the element in isolation.

While the above strategies are generally applicable to all promoters, it should be noted that, as no two genes are identical, neither are two promoters alike. Even within the limited class of stress-responsive genes, mechanistic and structural differences are readily evident. For example, activation of the *ho-1*, *c-fos*, *hsp 70*, and metallothionein genes by cadmium is mediated by the cadmium- or stress-responsive, serum-responsive, heat shock, and metal regulatory elements, respectively, each of which has a unique sequence and binds to distinct transcription factors. Furthermore, while the cadmium-responsive sequences of the *c-fos*, *hsp 70*, and metallothionein genes are located relatively close to the transcription start site, those for the *ho-1* gene are situated ~4 kbp upstream. In addition, while some *ho-1* gene promoters contain sequence motifs similar to the heat shock and metal regulatory elements, none of these sequences have been shown to be activated by cadmium. Indeed, identification of elements based on similarity to consensus sequences is not necessarily indicative of function, and each promoter and each element must be tested individually and in the proper context.

Target cells

HO-1 expression is stimulated by one or more agents in practically all tissues tested, and in theory, any cell type can be used for *ho-1* promoter analysis. Consequently, the choice of cell type and its tissue of origin is dependent largely on the interests of the investigator and the physiological relevance of the inducing agent to that particular cell type. For any chosen cell type, the obvious and overriding requirement is that the test inducer activate transcription of the endogenous *ho-1* gene, a characteristic that should be confirmed prior to initiation of promoter analysis experiments. Furthermore, among different cells, those exhibiting the highest levels of induction are generally better suited for inducible promoter activity measurements, all other factors, such as transfectability, being similar. Analysis of the *ho-1* promoter, as of other promoters, is most frequently carried out using transformed or immortalized cells, since these cells are readily available, easily cultured and in general, quite conducive to DNA transfection. In most immortalized cell lines, for most inducers, the mechanisms of *ho-1* gene activation appear to be preserved. In certain circumstances, how-

ever, the transformed phenotype may result in the loss or abatement of part or all of the induction mechanism. For instance, while bromobenzene potently stimulates expression of rat hepatic HO-1, no induction is observed in several transformed hepatoma cell lines (J. Alam, unpub. observ.). One possible explanation for this discrepancy is that induction of HO-1 requires transformation of bromobenzene by one or more cytochrome P-450s, whose constitutive expression and/or activities are generally attenuated in hepatoma-derived cell lines. In theory, the absence of a particular cytochrome P-450 in immortalized cells may be overcome by ectopic expression of the enzyme or the use of the active bromobenzene metabolite, but this will require identification of the metabolizing enzyme or the actual metabolite responsible for gene induction. In such and similar circumstances, promoter analysis will require the use of primary cells or possibly even the use of transgenic mice. Finally, it should be noted that primary cells and suspension cells are generally not easily transfected with the $CaPO_4$-DNA coprecipitation technique.

Inducing agent

As noted earlier, a wide array of agents and conditions, both physiological and nonphysiological, stimulate transcription of the *ho-1* gene. A substantial list of such agents can be found in Maines (1992). These inducers are chemically and structurally diverse, ranging from such ephemeral entities as nitric oxide gas and shear stress resulting from blood flow in the vasculature to more concrete substances including heavy metals and polypeptide cytokines. This diversity is reflected in the mechanism of *ho-1* gene activation as distinct, inducer-specific *cis*-elements have been identified within *ho-1* promoters (Choi and Alam, 1996). Furthermore, additional differences are inevitable, as some agents, such as inflammatory cytokines or polypeptide growth factors, initiate the induction process by stimulation of cell-surface receptors, whereas other, membrane-permeable inducers, including heme and hydrogen peroxide, are likely to utilize a less circumscribed route to the nucleus. Most, but maybe not all inducers, however, share a common characteristic in that they promote cellular oxidative stress, either directly by generating reactive oxygen species or indirectly by depleting cellular antioxidant functions. This commonality is also reflected in the mechanism of *ho-1* gene activation by some inducers, as they utilize a common *cis*-element and its cognate DNA-binding protein (Choi and Alam, 1996).

Some practical considerations in the use of *ho-1* inducers are outlined as follows. (1) Many inducers are cytotoxic and the degree of toxicity can be cell dependent. Consequently, it is useful to establish dosage and temporal profiles for cell toxicity and HO-1 induction with each agent (in each cell line). The ultimate goal is to establish experimental conditions that permit reasonable induction of reporter gene expression without the confounding variable of cellular dysfunction. A time course is also useful because some agents can activate the *ho-1* gene in a relatively direct manner (i.e., within a few hours) whereas others evince a more delayed response, possibly because such induction is indirect, requiring the prior synthesis or generation of intermediary activators. (2) In examining the mechanism of inducer-dependent gene activation, it is often necessary to identify pharmacological compounds, such as antioxidants, steroids, or kinase inhibitors, that further modify the response. These compounds are generally added at the same time as or prior to (i.e., 0.5 to 24 hr) the addition of the inducing agent. (3) One should also consider the possibility that the test agent (either inducer or induction modifier) directly modulates the reporter enzyme activity/assay. For instance, the author has observed that PD098059, a commonly used inhibitor of mitogen-activated protein kinase kinases 1 and 2, and resveratrol, an antioxidant, inhibit the luciferase reaction, whereas hemin potently suppresses the chemiluminescent-based β-galactosidase assay described in this unit. Because it is often difficult to measure the actual intracellular concentration of test agents, the simplest and proper way to determine any modulatory effects of such compounds (at the concentrations used) on enzyme activity is to assay cell extract mixtures containing a constant amount of lysate from cells transfected with the reporter gene and varying amounts of lysates from untransfected cells exposed to the vehicle or the test agent. Purified enzyme may also be substituted for the former. (4) Many agents are soluble only in nonaqueous solutions. It goes without saying that data should be collected for transfected cells treated with the proper "vehicle" control, especially since some solvents, such as dimethyl sulfoxide and ethanol, are known to modulate HO-1 activity in certain settings. (5) Most *ho-1* inducers activate other genes and the protocol described herein (along with the caveats) is generally applicable to the functional

Table 9.7.1 Troubleshooting Guide for Transfection and Promoter Analysis

Problem	Potential cause	Possible solution
Basic Protocol		
No enzyme activity: luciferase and β-Gal	Instrument malfunction	Repeat assay using purified enzymes as positive control; repair instrument if necessary
	Incorrect plasmid used	Check integrity of plasmid by restriction endonuclease analysis
No enzyme activity: luciferase	ATP omitted from luciferase assay buffer	Prepare new assay buffer
Low activity: luciferase and β-Gal[a]	Poor transfection efficiency	Optimize transfection (Kingston et al., 1996; Rose, 1996); change cell line; change transfection method
	Incomplete cell lysis	Monitor cell lysis under microscope; prepare new lysis buffer if necessary
	Inducer is toxic to cells	Decrease concentration
Low activity: luciferase[a]	Precipitation (probably magnesium phosphate) in luciferase reagent buffer	Prepare new buffer; make sure pH and phosphate concentration are correct
	Luciferin solution old or of improper pH	Luciferin is most stable at pH between 6.1 and 6.5; discard if yellow
Low activity: β-Gal[a]	Promoter exhibits weak activity in cell line	Use β-galactosidase construct with different promoter
	Inducer inhibits activity (i.e., hemin)	Omit β-galactosidase measurements; normalize to protein content. Use different secondary reporter (i.e., CAT, AP).
Variable activity: luciferase and β-Gal	Contaminated injector lines	Thoroughly wash injectors
Variable activity: β-Gal	Incomplete inactivation of endogenous β-galactosidase activity	Reheat extract; check temperature
No or low induction of luciferase activity	*ho-1* promoter does not contain inducer-responsive element	Test other regions of *ho-1* gene
	Induction requires chromatin structure	Test stable transfectants
	Inducer must be metabolized prior to induction	Test metabolic derivatives or use cells capable of metabolizing agent
	ho-1 gene not responsive to inducer in cell line tested	Check induction of endogenous HO-1; use different cell line
	Induction occurs by a post-transcriptional mechanism	
Alternate Protocol		
Few or no stable transfectants	Cells are extremely sensitive to G418	Use different selectable marker gene and antibiotic (Mortensen et al., 1997)
	Selectable marker DNA degraded or omitted.	Check integrity of plasmids
	Poor transfection efficiency	See above

continued

Table 9.7.1 Troubleshooting Guide for Transfection and Promoter Analysis, continued

Problem	Potential cause	Possible solution
Stable transfectants on control plate	Plasmid DNAs contaminated	Check DNA stock
	Cell line contaminated with previous stable transfectants	Transfect new batch of cells from frozen stock
Support Protocol		
No plasmid band	Band at top of tube: too much CsCl	
Band at bottom of tube: too little CsCl	Carefully weigh CsCl; bake at 100°C to evaporate any moisture	
Low plasmid yield[b]	Incomplete lysis of cells	Prepare new NaOH stock
	Insufficient removal of chromosomal DNA and cellular protein	Check pH of potassium acetate solution; may not have been adjusted with acetic acid
	Low-copy plasmid	Use chloramphenicol amplification to prepare plasmid DNA (Sambrook et al., 1989)

[a]Arbitrarily defined as 3- to 4-fold above instrument background.

[b]100 to 200 µg.

analysis of other promoters. One should bear in mind, however, that certain adjustments may be necessary because of promoter-specific mechanistic differences (see above for cadmium-mediated gene regulation).

The problems commonly observed with the protocols, their most likely causes, and potential solutions are outlined in Table 9.7.1.

Anticipated Results

Results from a typical transient transfection analysis and from an experiment using stable transfectants are shown in Tables 9.7.2 and 9.7.3, respectively. For the former, 5×10^5 cells were plated in each well of 6-well plates and each well was transfected with a DNA mixture consisting of 2 µg of pHO15 luc (which contains 15 kbp of the mouse *ho-1* gene promoter), 1 µg of pCMV β-gal (*lac Z* gene under the control of cytomegalovirus regulatory sequences), and 2 µg of pBluescript II SK$^-$ (Stratagene) for 6 hr. "Mock" transfections were carried out with 5 µg of pBluescript II SK$^-$ per well. After glycerol shock, cells were incubated for 36 hr and treated with vehicle or inducing agent for 5 hr. 8% (~40, 25, and 20 µg of protein for HeLa, Hepa, and L929 cells, respectively) and 4% of the cell extracts were used for luciferase and β-galactosidase assays, respectively. The data is the average of duplicate measurements. Hepa cells stably transfected with pHO15 luc were plated in a 24-well cluster (1×10^5 cells/well) and cultured for 66 hr. Cells were treated with vehicle or inducer for 5 hr and 3.3% of each extract (~7 µg of protein) was used for luciferase assays. For each treatment, the data represent the average from triplicate wells. Several aspects of the data are noteworthy. (1) Even though the same precipitate is used, basal luciferase activity varies considerably among different cell lines. This is in part due to cell-specific differences in *ho-1* promoter activity, but mostly reflects the transfection efficiency of the calcium phosphate precipitation method in these cells. (2) For a given inducer, the level of induction will vary with cell type and the optimal concentration of a given inducer is also cell-dependent (compare effect of cadmium concentration on induction levels in HeLa or Hepa cells with that in L929 cells). (3) When using the same $CaPO_4$-DNA precipitate, transfection efficiency between populations (i.e., wells) should be similar for a given cell line, as exemplified by the consistency in the β-galactosidase activities in HeLa or Hepa cell extracts. The variations in β-galactosidase activity observed in L929 cells indicates that the inducers, at the concentration used, are toxic to these cells. (4) Some agents can affect the reporter enzymes reaction; note the reduced β-galactosidase activity in extracts from hemin-treated cells. A direct effect of hemin, but not of arsenite or $CdCl_2$, on this reaction has been confirmed with the use of purified β-galactosidase. (5) β-galactosidase activity in HeLa cell extracts is near the upper

Table 9.7.2 Transient Transfection Assay

Inducer	Conc. (μM)	Luciferase ($\times 10^3$ RLU)[a]			β-galactosidase ($\times 10^5$ RLU)[a]		
		HeLa	Hepa[b]	L929	HeLa	Hepa	L929
Arsenite	25	219	100 (8)	2.23	95.9	30.9	0.81
	50	323	108 (8)	1.57	93.6	33.6	0.32
Cadmium	20	333	163 (13)	1.63	102	30.2	0.49
	50	499	337 (26)	0.89	98.2	33.0	0.19
Hemin	10	224	53.4 (4)	1.43	5.08	0.13	0.02
Mock	—	0.22	0.23	0.23	0.02	0.02	0.02
Vehicle	—	20.4	13.0 (1)	0.81	109	31.6	1.98

[a]RLU, Relative light units.

[b]Fold induction is given in parentheses.

Table 9.7.3 Luciferase Activity in Stably Transfected Hepa Cells

Inducer	Conc. (μM)	Luciferase ($\times 10^3$ RLU)[a]	Fold induction
Arsenite	25	2975	79
Cadmium	20	3460	92
Hemin	10	1080	29
Vehicle	—	37.6	1

[a]RLU, Relative light units.

limit of detection for the instrument (1×10^7 RLU) and may not be in the linear range for the assay. These extracts should be diluted and reassayed. (6) For *ho-1* promoter-directed reporter genes, induction levels are almost invariably greater in stably transfected cells than in transiently transfected cells.

Time Considerations

Transient transfection analysis is generally carried out over a period of 3 to 5 days. This range reflects the variability in the lengths of the transfection (4 to 24 hr), of the incubation period prior to induction (typically 0 to 48 hr), and of the induction and post-induction incubations (4 to 24 hr). The hands-on time is, of course, considerably less. With practice, a given cell line can be trypsinized, counted, and plated in ~30 min. It will take a similar amount of time to ethanol precipitate 6 to 12 DNA samples. To facilitate this process, all plasmid stocks should be stored at 4°C, not frozen, and at consistent and convenient concentrations (e.g., 1 μg/μl) that permit simple, mental calculations to determine volumes used for precipitation. Most protocols recommend that cells be incubated for 2 to 4 hr in fresh medium prior to transfection. This step allows sufficient time to carry out ethanol precipitations on the same day as transfections. Because this incubation period has been eliminated in these protocols, it is more convenient to precipitate the DNA samples on the day before transfections. The actual transfection procedure, from pelleting of DNA by centrifugation to the application of $CaPO_4$-DNA precipitates on the cells, will take ~1 hr. With experience, the actual mixing of the $CaCl_2$-DNA and the 2× HeBS solutions will take ≤1 min per sample. Therefore, 6 to 12 precipitates (for 12 to 24 wells when testing one inducer) can easily be prepared before the first precipitate is ready for addition to cells.

Measurement of luciferase and β-galactosidase activities, if carried out in the same day, will take ~3 hr. The longest steps in these procedures are heat-inactivation of endogenous β-galactosidases and incubation of extracts with the β-galactosidase substrate, each of which requires ~1 hr. Therefore, after preparation of cell lysates, the first step should be to initiate the heat-inactivation procedure with a portion of the extract. The luciferase measurements can easily be carried out during this period. Once the luciferase assay buffer has been aliquoted into individual tubes, addition of extract and measurement of light output will

take ~30 sec/sample with a single tube luminometer set for a 10-sec integrated light analysis. Consequently, 24 samples can be measured in duplicate in ~30 min. There will be sufficient time to clean the luminometer before the heated extracts are ready for β-galactosidase measurements. Actual luminometer readings for β-galactosidase, as for luciferase, will take ~30 sec/sample. Often, it is more convenient to carry out the luciferase and β-galactosidase measurements on separate days. In this case, cell extracts can be frozen at −70°C prior to or after heating, although activities are slightly higher with the latter strategy.

For the Alternate Protocol, where applicable, the time required for individual manipulations is similar to that of the Basic Protocol. The main difference between these protocols is the time required to select (~3 to 4 weeks) and expand (~1 to 2 weeks) stable transfectants.

Literature Cited

Alam, J. and Cook, J.L. 1990. Reporter genes: Application to the study of mammalian gene transcription. *Anal. Biochem.* 188:245-254.

Alam, J., Stewart, D., Touchard, C., Boinapally, S., Choi, A.M.K., and Cook, J.L. 1999. Nrf2, a cap 'n' collar transcription factor regulates induction of the heme oxygenase-1 gene. *J. Biol. Chem.* 274:26071-26078.

Choi, A.M.K. and Alam, J. 1996. Heme oxygenase-1: Function, regulation, and implication of a novel stress-inducible protein in oxidant-induced lung injury. *Am. J. Respir. Cell. Mol. Biol.* 15:9-19.

de Wet, J.R., Wood, K.V., DeLuca, M. Helinski, D.R., and Subramani, S. 1987. Firefly luciferase gene: Structure and expression in mammalian cells. *Mol. Cell. Biol.* 7:725-737.

Elbirt, K.K., Whitmarsh, A.J., Davis, R.J., and Bonkovsky, H.L. 1998. Mechanism of sodium arsenite–mediated induction of heme oxygenase-1 in hepatoma cells. *J. Biol. Chem.* 273:8922-8931.

Gorman, C. 1985. High efficiency gene transfer into mammalian cells. *In* DNA Cloning II—A Practical Approach (D.M. Glover, ed.) pp. 143-190. IRL Press, Oxford.

Graham, F.L. and van der Eb, A.J. 1973. A new technique for the assay of infectivity of human adenovirus 5 DNA. *Virology* 52:456-467.

Immenschuh, S., Hinke, V., Ohlmann, A., Gifhorn-Katz, S., Katz, N., Jungermann, K., and Kietzmann, T. 1998. Transcriptional activation of the haem oxygenase-1 gene by cGMP via a cAMP response element/activator protein-1 element in primary cultures of rat hepatocytes. *Biochem. J.* 334:141-146.

Jordan, M., Schallhorn, A., and Wurm, F.M. 1996. Transfecting mammalian cells: Optimization of critical parameters affecting calcium-phosphate precipitate formation. *Nucl. Acids Res.* 24:596-601.

Kingston, R.E., Chen, C.A., Okayama, H., and Rose, J.K. 1996. Calcium phosphate transfection. *In* Current Protocols in Molecular Biology (F.M. Ausubel, R. Brent, R.E. Kingston, D.D. Moore, J.G. Seidman, J.A. Smith, and K. Struhl, eds.) pp. 9.1.4-9.1.11. John Wiley & Sons, New York.

Maines, M.D. 1992. Heme Oxygenase: Clinical Applications and Functions. CRC Press, Boca Raton, Fla.

Mortensen, R., Chesnut, J.D., Hoeffler, J.P., and Kingston, R.E. 1997. Selection of transfected mammalian cells. *In* Current Protocols in Molecular Biology (F.M. Ausubel, R. Brent, R.E. Kingston, D.D. Moore, J.G. Seidman, J.A. Smith, and K. Struhl, eds.) pp. 9.5.1-9.5.19. John Wiley & Sons, New York.

Pellacani, A., Wiesel, P., Sharma, A., Foster, L.C., Huggins, G.S., Yet, S.-F., and Perrella, M.A. 1998. Induction of heme oxygenase-1 during endotoxemia is downregulated by transforming growth factor-β1. *Circ. Res.* 83:396-403.

Rose, J.K. 1996. Optimization of transfection. *In* Current Protocols in Molecular Biology (F.M. Ausubel, R. Brent, R.E. Kingston, D.D. Moore, J.G. Seidman, J.A. Smith, and K. Struhl, eds.) pp. 9.1.1-9.1.4. John Wiley & Sons, New York.

Sambrook, J., Fritsch, E.F., and Maniatis, T. 1989. Molecular Cloning: A Laboratory Manual, 2nd ed. Cold Spring Harbor Laboratory Press, Cold Spring Harbor, N.Y.

Takeda, K., Ishizawa, S., Sato, M., Yoshida, T., and Shibahara, S. 1994. Identification of a *cis*-acting element that is responsible for cadmium-mediated induction of the human heme oxygenase gene. *J. Biol. Chem.* 269:22858-22867.

Key References

Alam and Cook, 1990. See above.

Compares advantages and disadvantages of various reporter genes commonly used in mammalian cells.

Brasier, A.R., Tate, J.E., and Habener, J.F. 1989. Optimized use of the firefly luciferase assay as a reporter gene in mammalian cell lines. *BioTechniques* 7:1116-1122.

Provides a more detailed characterization of the luciferase assay used herein.

Graham and van der Eb, 1973. See above.

Jordan et al., 1996. See above.

These two articles examine parameters essential for successful transfection by the calcium phosphate precipitation method.

Contributed by Jawed Alam
Alton Ochsner Medical Foundation
New Orleans, Louisiana

Quantitation of Human Heme Oxygenase (HO-1) Copies by Competitive RT-PCR

Heme oxygenase 1 (HO-1) is an indicator of stress conditions. The goal of this unit is to describe a microsensitive assay for human HO-1 mRNA molecules, since most clinical samples are of limited cell number and/or limited mRNA copy number. Conventional methods of mRNA analysis, such as northern blot analysis and nuclease protection mapping (*APPENDIX 3E* and *APPENDIX 3A*, respectively), are insufficient in sensitivity and/or accuracy. Competitive RT-PCR is suitable and has become the most widely used form of quantitative RT-PCR. Using competitive RT-PCR, it is not necessary to assay products exclusively during the exponential phase of the amplification procedure (Murphy et al., 1990; Cross, 1995). Serial dilutions of the sample are used with a fixed amount of competitor template (internal standard) cDNA, and this mixture is subjected to amplification. This approach is used to determine the levels of HO-1 in normal human tissues—i.e., cerebral brain, cerebellum, kidney, spleen, and fetal liver. The results of this study demonstrate that human spleen basal levels of HO-1 mRNA copies were markedly higher than the levels in fetal liver, which are higher than the kidney, which are higher than the brain (Goodman et al., 1996).

This unit describes RT-PCR analysis of tissues in a quantitative assay (see Basic Protocol). It also includes protocols to verify that the amplified product is distinguishable from the product amplified from the internal standard (see Support Protocol 1) and that the internal standard and the sample are amplified with equivalent efficiency (see Support Protocol 2).

QUANTITATIVE RT-PCR TO MEASURE HO-1 mRNA

BASIC PROTOCOL

This protocol is designed to quantitate human HO-1 mRNA in samples limited in cell number and/or mRNA copies. Varying amounts of total RNA from human tissues are used for reverse transcription. The sequences are then amplified by PCR in a tube that also contains an internal standard, equivalent in amplification efficiency (see Support Protocol 2), obtained by deleting 50 bp from the original human HO-1 gene (Yoshida et al., 1988). After amplification, templates are resolved and, when the internal standard is present in the reaction mixture, the ratio of the amplified sample versus the standard template is proportional to the amount of RNA; therefore, it is possible to calculate the number of specific mRNA molecules.

Materials

pCMV-HHO-1 plasmid (Yoshida et al., 1988)
1 U/µl *Eco*R47III and buffer (Promega)
1 U/µl *Bal*31 nuclease and buffer
2% (w/v) agarose gel (*APPENDIX 3A*)
100-bp DNA molecular weight marker VI (Boehringer Mannheim Biochemicals)
10 mg/ml ethidium bromide
0.5 M EDTA (*APPENDIX 2A*)
1 U/ml T4 DNA ligase and buffer
JM109 *E. coli* transformation-competent bacteria (*APPENDIX 3A*)
LB broth and plates or equivalent containing 10 mg/ml ampicillin (*APPENDIX 3A*)
1:3 phenol/chloroform (*APPENDIX 3A*)
Qiagen miniprep kit
1 U/ml *Hind*III restriction enzyme and buffer
1% (w/v) low-melting-temperature agarose gel (*APPENDIX 3A*)

Contributed by N.G. Abraham, S.K. Shenouda, and A. Goodman
Current Protocols in Toxicology (2002) 9.8.1-9.8.10

Tissue sample (e.g., human liver)
First-Strand cDNA Synthesis Kit (Clontech Laboratories):
DEPC-treated H_2O (*UNIT 2.9*)
10 µM oligo$(dT)_{18}$
0.1 M Tris·Cl, pH 8.3 (*APPENDIX 2A*)
0.1 M KCl
0.1 M $MgCl_2$
100 mM dNTPs in sterile deionized H_2O (Promega)
2 U/ml RNase inhibitor
100 U/ml Moloney murine leukemia virus reverse transcriptase (Bethesda Research Laboratories)
0.001% (w/v) gelatin
1 µM sense primer: 5′-CAG GCA GAG AAT GCT GAG TTC-′ (Kutty et al. 1992; CER)
1 µM antisense primer: 5′-GAT GTT GAG CAG GAA CGC AGT-3′ (Kutty et al., 1992; CER)
2.5 U/µl *Taq* DNA polymerase (Stratagene)
5 Ci/µl (185 GBq/µl) [α-^{32}P] dCTP (3000 Ci/mmol)
Mineral oil (optional)
6% (w/v) 37.5:1 acrylamide/bisacrylamide gel (*APPENDIX 3A*)
25 mM Tris·Cl, pH 8.3 (*APPENDIX 2A*)/200 mM glycine/1 mM EDTA
Thermocycler

Additional reagents and equipment for restriction endonuclease digestion, agarose gel electrophoresis, ethidium bromide staining, bacterial transformation, cell culture, phenol/chloroform extraction, determination of RNA purity by UV spectroscopy, polyacrylamide gel electrophoresis, plasmid amplification and purification (*APPENDIX 3A*), RNA isolation (Chomczynski and Sacchi, 1987; *APPENDIX 3A*), and autoradiography (*APPENDIX 3D*)

Prepare internal standard plasmid

1. In each of three 1.5-ml microcentrifuge tubes, linearize 1 µg pCMV-HHO-1 plasmid with 2 U *Eco*R47III 2 hr at 37°C, in appropriate buffer, using equal aliquots for each tube. Stop on ice.

   There is a single restriction site in human HO-1 cDNA at position 420 bp.

2. Add 2 to 5 µl plasmid to 10 µl appropriate restriction enzyme buffer to each tube and digest 5 min with 2 µl of 1 U/ml *Bal*31 nuclease, 37°C (*APPENDIX 3A*).

3. Stop the reaction by placing the tubes on ice.

4. Analyze 2 µl linearized plasmid on a 2% (w/v) agarose gel alongside 100-bp DNA molecular weight marker VI and stain with 10 mg/ml ethidium bromide (*APPENDIX 3A*). If not linearized, repeat steps 1 to 3.

5. Add 2 µl linearized plasmid to each of five 1.5-ml microcentrifuge tubes containing 10 µl *Bal*31 buffer. Add 1 to 3 µl of 1 U/µl *Bal*31 to each tube.

6. Incubate at 22°C, stopping the reaction at 5, 10, 15, 20, and 30 min by transferring the tube to ice or by adding 5 µl of 0.5 M EDTA.

   This reaction digests nucleotides and creates a truncation in the plasmid.

Ligate plasmid

7. Analyze 2 µl of each reaction on a 2% agarose gel and stain with ethidium bromide to confirm digestion has occurred.

8. Transfer 2 to 5 µl of each of the digested plasmids to a fresh tube. Ligate by adding 10 µl T4 DNA ligase buffer and 1 µl T4 DNA ligase to each tube. Incubate overnight at 16°C.
9. Stop the reaction by placing the tubes on ice.
10. Analyze 2 µl of each reaction on a 2% agarose gel and stain with ethidium bromide to confirm ligation (i.e., DNA is larger).

Transform E. coli

11. Transform 2 to 5 µl construct DNA into 1 ml JM109 *E. coli* transformation-competent bacteria (*APPENDIX 3A*).
12. Heat shock cells by incubating 5 min at 95°C.
13. Place the cells on ice.
14. Spread the bacteria on an LB plate or equivalent containing 10 mg/ml ampicillin (*APPENDIX 3A*). Incubate overnight at 37°C.

    Only the cells that are transformed with the plasmid containing the ampicillin-resistance gene will survive and form colonies.

Identify internal standard

15. Pick several colonies and extract the DNA with 1:3 phenol/chloroform (*APPENDIX 3A*).

    Alternatively, perform PCR directly on the colonies.

16. Digest the clones with *Bal*31. Analyze the digests on a 2% agarose gel to determine the size of the truncated plasmids.
17. Confirm that the plasmid contains a mutated HO-1 gene by digesting with *Eco*R47III and analyzing on a 2% agarose gel stained with ethidium bromide to confirm fragment and DNA size.
18. Select a clone with ~50 bp truncated from the original cDNA of HHO-1. Amplify the selected clone by transferring cells from the colony to 3 ml LB broth containing 10 mg/ml ampicillin. Incubate overnight in a 37°C shaker.

Purify the plasmid for internal standard

19. Extract the DNA using a Qiagen miniprep kit according to manufacturer's instructions.
20. Excise the insert from the vector by digesting as described (see steps 1 to 3), except use 2 U *Hind*III endonuclease and buffer per microgram DNA. Purify by gel electrophoresis on a 1% (w/v) low-melting-temperature agarose gel.

    This insert is used as the internal standard in the PCR reactions.

21. Cut out the appropriate band with a razor blade or scalpel, and purify DNA by phenol/chloroform extraction.

    Alternatively, the DNA can be purified using a centrifuge filtration kit (Millipore), and centrifuging 25 min at 10,000 rpm, 5°C.

Prepare RNA

22. Isolate total RNA from 1 mg of the tissue sample (e.g., human liver) using the method of Chomczynski and Sacchi (1987; *APPENDIX 3A*).

23. Quantify RNA by UV spectrophotometry (i.e., A_{260}/A_{280}; *APPENDIX 3A*). Check the quality of the RNA on a 2% (w/v) agarose gel stained with ethidium bromide.

    The ratio should be ~1.6:1.0.

Reverse transcribe RNA

24. To a microcentrifuge tube add (20 µl total volume):

    0.1 to 2 µg RNA
    12.5 µl DEPC-treated H_2O
    1 µl of 10 µM oligo $(dT)_{18}$ (0.2 µM final).

    To determine the appropriate amount of RNA to add, use an RT-PCR assay with an internal competitive RNA standard to quantify HO-1 expression. Set up a series of five RT-PCR reactions with each reaction containing a serial amount of total cellular RNA. Adjust the concentration of cellular RNA so that the PCR signal falls within the range of the internal standard RNA used.

25. Denature RNA 2 min at 70°C and place on ice.

26. Prepare reverse transcription mixture containing (30 µl total volume):

    50 mM Tris·Cl, pH 8.3
    75 mM KCl
    3 mM $MgCl_2$
    0.5 mM (each) dNTP
    1 U/µl of RNase inhibitor
    200 U Moloney murine leukemia virus reverse transcriptase.

27. Add 5 µl reverse transcription mixture to the denatured RNA and incubate 1 hr at 42°C.

28. Stop the reaction by heating 5 min at 95°C. Place the tube on ice.

Amplify RNA

29. Prepare PCR mixture (50 µl total volume):

    10 mM Tris·Cl, pH 8.3
    50 mM KCl
    0.001% (w/v) gelatin
    1.5 mM $MgCl_2$
    250 µM (each) dNTP
    1 µM (each) sense and antisense primers
    10 fg internal standard (step 21)
    2.5 U *Taq* DNA polymerase per reaction
    1 µCi [α-^{32}P]dCTP

    The primers are designed to amplify a 555-bp stretch (79 to 633 bp) of the published cDNA of the human HO-1 (Yoshida et al., 1988).

30. Add PCR mixture (80 to 100 µl) to RT reaction tube to 100 µl final volume. If the thermocycler does not have a heated lid, overlay with two drops of mineral oil.

31. Amplify by PCR using the following program:

40 cycles:	1 min	95°C	(denaturation)
	1 min	55°C	(annealing)
	2 min	72°C	(extension)
Final step:	10 min	72°C	(final extension).

Characterize amplified products

32. Analyze amplified products on a 6% (v/v) 37.5:1 acrylamide/bisacrylamide gel in 25 mM Tris·Cl, pH 8.3/200 mM glycine/1 mM EDTA (*APPENDIX 3A*).
33. After drying, analyze the gel by autoradiography (*APPENDIX 3A*).
34. Analyze autoradiogram by densitometry (*APPENDIX 3A*), or excise bands from the gel and count the radioactivity (e.g., in a scintillation counter).
35. Identify amplified templates (see Support Protocol 1) and verify that the internal standard is amplified as efficiently as the HO template (see Support Protocol 2).
36. Use the areas of HHO-1 mRNA and internal standard bands in densitometry graphs to calculate the area ratios of mRNA to the internal standard for each RT-PCR reaction.

    Where the ratio of mRNA to internal standard products equals 1 (Log_e ratio = 0), the number of mRNA molecules is the same as the known number of internal standard RNA molecules. This gives a value for the expression of HHO-1 mRNA in molecules per microgram total cellular RNA. The results are used for calculating mRNA levels when they fall within the range of internal standard RNA products. For example, at the point of RNA species equivalence, the HHO-1:mHHO-1 ratio = 1 and y = Log_e (area HHO-1/area mHHO-1) = 0, area under the curve, Asx = Log_e (molecules internal standard RNA). When y = 0, and molecules internal standard RNA = −7.969/−0.538 = 14.812, the actual number of HHO-1 mRNA molecules = $e^{14.812} = 2.71 \times 10^6$. Therefore, there are 2.71×10^6 molecules HHO-1 mRNA in 1.5 g total cellular RNA, which equates to 1.81×10^6 molecules HHO-1 mRNA/g total RNA.

DISTINGUISHING BETWEEN THE AMPLIFIED TEMPLATES

SUPPORT PROTOCOL 1

To perform quantitative analysis, it is necessary to be able to distinguish between the product from the sample tissue and that of the internal standard. Analyze several clones for the size of the mutated cDNA (mHHO-1) resulting from the digestion by *Bal*31 and for the presence of an *Eco*47III restriction site. After transformation into competent bacteria by the mutated plasmid, obtain PCR products from several clones with the indicated primers (see Basic Protocol) and analyze them on a 6% acrylamide/bisacrylamide gel (Fig. 9.8.1). For these experiments, clone 2 (lane 2) is chosen and designated pCMV-mHHO-1. This clone is also examined for size (Fig. 9.8.2). The difference in size between the original and mutated plasmids is ~50 bp (Fig. 9.8.1, lanes 2 and 3). To better evaluate the size of the PCR products, the two inserts (HHO-1 and mHHO-1) are amplified by PCR and analyzed on a 2% agarose gel. The difference in size, 50 bp, should be demonstrated as expected from the previous sizing results (Fig. 9.8.2).

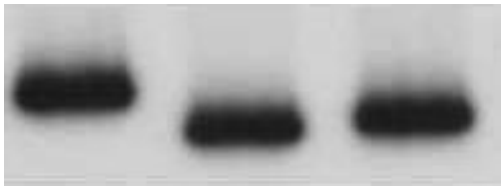

Figure 9.8.1 Analysis of different clones for the internal standard of HHO-1. A representative RT-PCR autoradiogram showing PCR products obtained from the amplification of several clones selected after modification of the Eco47III site as described. Lane 1: PCR product from pCMV-HHO-1 as a positive control for the reactions on and as a marker for original size. Lanes 2 and 3: different clones tested after mutation.

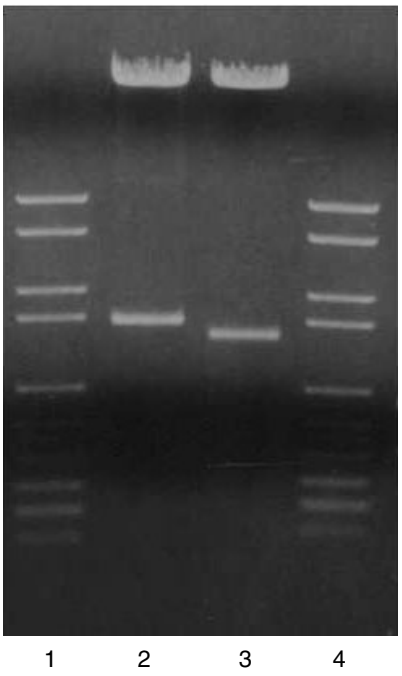

Figure 9.8.2 Analysis on 1% agarose gel of clone 2 (Fig. 9.8.1), which was selected as an internal standard. Lanes 1 and 4: 100-bp DNA molecular weight marker. Lane 2: HHO-1 insert digested with Eco47III. Lane 3: mHHO-1 insert digested with Eco47III.

SUPPORT PROTOCOL 2

COMPETITIVE VERSUS NONCOMPETITIVE AMPLIFICATION

In order to achieve a reliable quantitation, it is critical to demonstrate that the internal standard and sample template or templates are amplified equally under the reaction conditions. To determine this, examine whether the 10% (50 bp) difference in the sequence between the two templates causes a difference in amplification efficiency. Subject various amounts of total RNA (e.g., from human liver) to RT-PCR alone or as a mixture with a fixed amount (10 fg) of the mutated insert (mHHO-1). For combined PCR, add mHHO-1 to the PCR step. Reverse transcribe the RNA samples using oligo$(dT)_{18}$ primers. Identify respective templates by their difference in size examined by electrophoresis on an acrylamide/bisacrylamide gel, and quantify the amount of product by densitometry of the bands on the autoradiogram.

In Figure 9.8.3A there is a concentration dependence associated with the amount of mRNA added to the RT-PCR incubation mixture shown in the autoradiogram band. In Figure 9.8.3B, when the internal standard (mHHO-1) is included in the PCR mixture (the same amount, 10 fg and 0.1 to 2 μg of the reference RNA, were added to each reaction), the amount of amplified standard decreased as the amount of kidney RNA increased. These results indicate that the sample and internal standard templates are both amplified in the same manner and are competing for amplification: as the amount of one template increases, the chance of the other template being amplified declines.

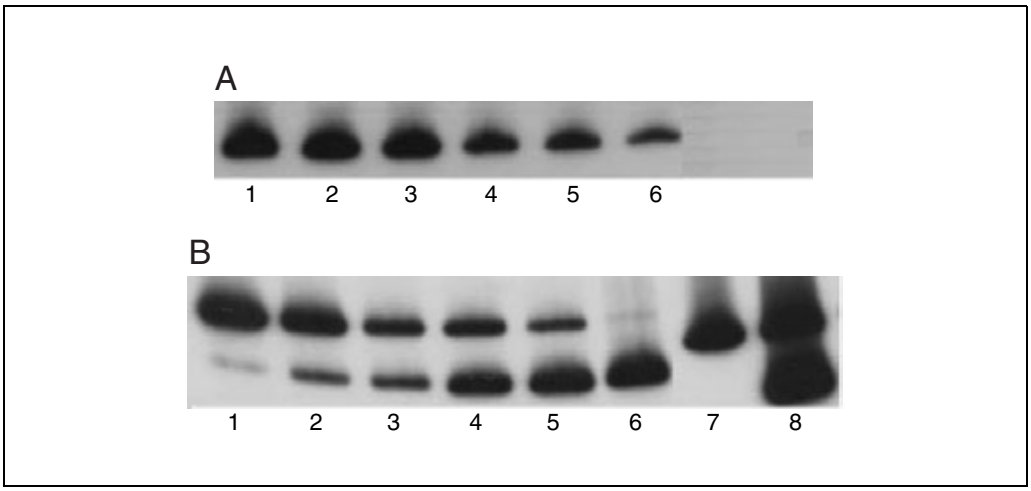

Figure 9.8.3 (**A**) Analysis of RT-PCR products obtained from total RNA of human kidney. Lane 1: 200 ng; lane 2: 100 ng; lane 3: 50 ng; lane 4: 25 ng; lane 5: 5 ng; and lane 6: 1 ng. (**B**) Competitive amplification of human kidney total RNA and mutated insert (mHHO-1). Internal standard (mHHO-1) at 10 fg is mixed with human kidney total RNA at 200, 100, 50, 25, 5, and 1 ng in lanes 1 to 6, respectively.

COMMENTARY

Background Information

The rate-limiting enzyme in heme catabolism, heme oxygenase (HO), is a stress protein, and its induction has been suggested to represent an important protective response in numerous biological processes, including defense against oxidative stress produced by heme and hemoglobin, since unmetabolized heme is a source of free radicals (Wagener et al., 1999; Yang et al, 1999; Quan et al., 2001). It is also involved in the inflammatory process (Laniado-Schwartzman et al., 1997; Otterbein et al., 2000) and it contributes to the regulation of vascular tone (Levere et al., 1990). HO-1 knockout mice (Poss and Tonegawa, 1997) and the recently reported first human case of HO-1 deficiency (Yachie et al., 1999) were both shown to have exaggerated inflammatory status. Induction of HO decreases cellular heme (pro-oxidant) content and elevates bilirubin (antioxidant) levels (Nath et al., 1992; Abraham et al., 1995). Elevation of HO activity in tumor-bearing rats (Schacter and Kurz, 1986) and in partial hepatectomized rats (Solangi et al., 1988) also results in a decrease in the content of renal and liver heme proteins such as cytochrome P450.

To date, three HO isoforms, HO-1, HO-2, and HO-3, have been identified that catalyze this reaction. HO-1 is a 32-kDa heat-shock protein, which is inducible by numerous noxious stimuli. HO-2 is a constitutively synthesized 36-kDa protein, which is abundant in brain and testes. HO-3 is related to HO-2 but is the product of a different gene, and its ability to catalyze heme degradation is much less than that of HO-1. (McCoubrey et al., 1992; Maines et al., 1997).

This unit describes a protocol designed to measure the amount of HO-1 mRNA in a given tissue sample (see Basic Protocol). Once the RT-PCR system has been shown to be specific for designated targets and the sample and the internal standard templates can be amplified with an equivalent efficiency, the quantitative nature of the system can be examined. In the course of testing for the competitiveness of the sample and internal standard templates for amplification, the authors found that 10 fg of standard was the appropriate amount required in the reaction mixture for RNA from various human tissues at the range of 1 to 100 ng to be amplified and unambiguously quantified. Because the internal standard and sample templates have been shown to be amplified equally efficiently under the conditions described (see Support Protocol 2), it is possible to determine the human HHO-1 mRNA content. The number of molecules of HHO-1 in human spleen was 3755 per nanogram total RNA, and in the fetal liver was 2440 per nanogram total RNA (Fig. 9.8.4). In contrast, cerebellum expressed the least amount of HO-1 mRNA followed by human whole cerebral brain and kidney.

In summary, it is believed that, after all proper normalizations, this competitive RT-PCR method will be a sensitive and truly quantitative way to measure the level of HO-1

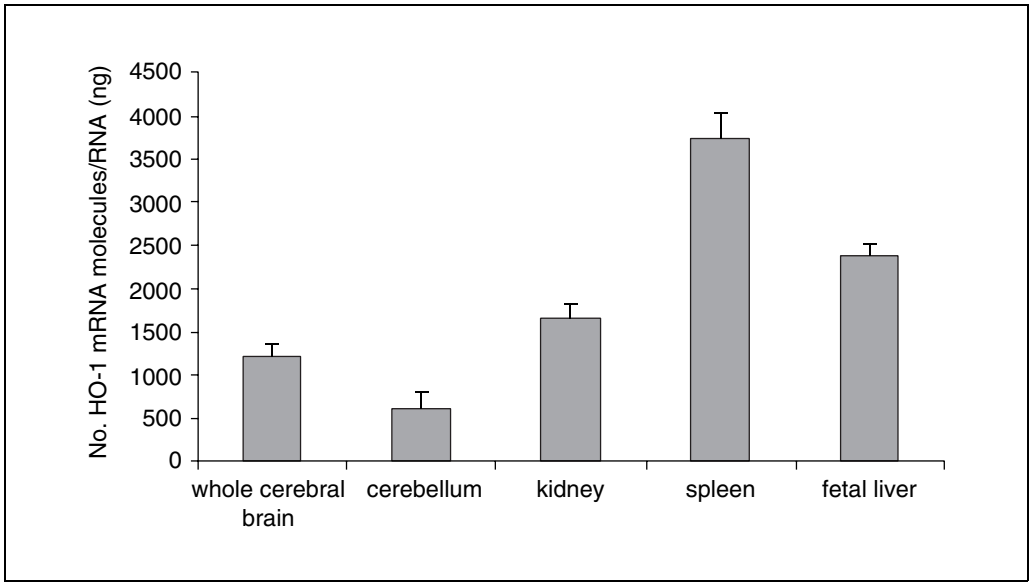

Figure 9.8.4 HHO-1 mRNA molecules in different human tissues. RT-PCR products were subjected to autoradiography and densitometric analysis to detect the number of mRNA molecules of HHO-1 compared to a known internal standard molecule as described (see Basic Protocol). See Figure 9.8.5 for the standard curve.

mRNA copies not only in normal tissues but also in other systems where HO-1 is an indicator for stress conditions.

Critical Parameters

The great power of amplification of PCR presents a challenge when the technique is used to quantify copy numbers of genes and mRNAs. Minute differences in any of the variables that affect the efficiency of amplification can dramatically alter product yield. This problem can be circumvented by co-amplifying a target sequence with a standard template so that the reaction is completed in the presence of an internal control (Becker-Andre and Hahlbrock, 1989; Wang et al., 1989; Gilliland et al., 1990). Accordingly, this system, which is used to evaluate the genetic expression of HHO-1, was developed with the following considerations in mind. First, the internal standard used was identical to the sample template in the target region; the difference being 10% in length due to mutation. Second, the primers were derived from regions where the standard and the original templates have identical sequences. Consequently, differences in the melting temperatures of cDNA templates and primer/template duplexes, which can greatly influence the amplification, are of no consequence. Furthermore, the standard and sample templates can be easily distinguished on an acrylamide gel due to their difference in size (50 bp).

As expected, the great sequence similarity between the standard and sample templates

Table 9.8.1 Troubleshooting Guide to Quantitative RT-PCR

Problem	Possible cause	Solution
The intensity of the band is not related to the concentration	Improper RNA concentration used due to error in measurements of the RNA samples	Make accurate measurements of RNA and/or perform a rapid GAPDH PCR to determine the discrepancy of the spectrophotometer and the estimated total RNA samples
Autoradiography bands appear in different positions	The water used in the PCR or RT-PCR is contaminated	Water used for preparation of various reagents must be highly purified

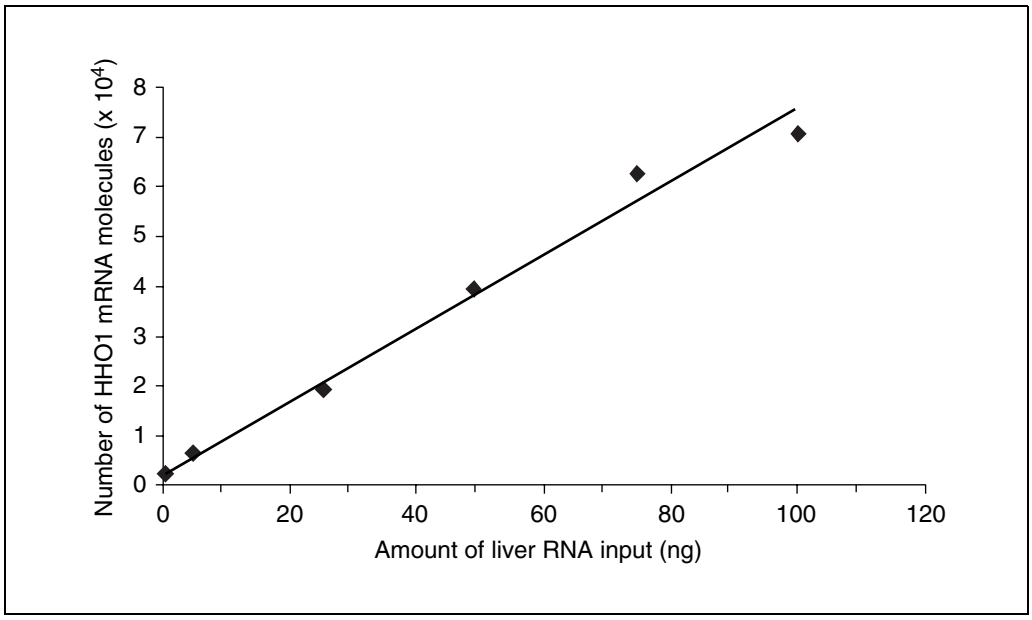

Figure 9.8.5 Competitive amplification of human kidney total RNA and mutated insert (mHHO-1). Internal standard (mHHO-1) at 10 fg is mixed with human kidney total RNA at 100, 50, 5, and 1 ng, respectively. Reaction products are analyzed on a 6% acrylamide/bisacrylamide gel. The amount of amplification human template is identified by densitometry on the autoradiogram and by counting the radioactivity of various bands after excision from the gel (the methods were compared in their results). The ratio of human RNA versus the internal standard is used to calculate the amount of HHO-1 mRNA content and this is plotted against the amount of input sample RNA. Reproduced from Abraham (1998).

rendered them good candidates for amplification. The input ratio of internal standard versus sample RNA was therefore critical for a clear-cut measurement of the amount of each template amplified. This required that RNA in each sample be individually determined. When the ratio was appropriate, a linear relationship existed between the amount of input sample RNA and the amount of amplified sample template after the latter had been normalized against the amplified internal standard. It is estimated that there are ~1670 HHO-1 mRNA molecules in each nanogram of total RNA from human kidney using this technique.

Troubleshooting

For the most common problems and solutions, see Table 9.8.1 (also see *APPENDIX 3C*).

Anticipated Results

The authors studied the HO-1 transcript expression in normal human liver tissue. Total RNA from this tissue showed a PCR cycle–dependent linear relationship with the concentrations of GAPDH mRNAs. A linear relationship also was seen between the optical density of the PCR band and the concentration of the mRNAs after RT reactions (unpub. observ.). As seen in Figure 9.8.5, the number of molecules formed under these conditions was dependent on the RNA input. Thus, optimum conditions were used to determine HO-1 expression.

The human RNAs extracted from five organs were obtained from Clontech Laboratories and were quantified by spectrophotometry. Using 15 μg of each organ RNA, the RNAs were checked by 1% agarose gel electrophoresis and ethidium bromide staining, RT-PCR, and Southern blotting, and filters were hybridized with a human HO probe (Fig. 9.8.5). The five different human organ RNAs were whole brain, cerebellum, whole kidney, whole spleen, and fetal liver. GAPDH was used to assess the quality of RNA.

Time Considerations

Three to six hours is required to generate PCR products.

Acknowledgment

The authors wish to thank Dr. Hatem Sabaawy for allowing his research results to be included in this discussion.

Literature Cited

Abraham, N.G. 1998. Quantitation of HO-1 copies in human tissues by competitive RT/PCR. *In*

Free Radicals and Antioxidant Protocols (D. Armstrong, ed.) Humana Press, Totowa, N.J.

Abraham, N.G., Lavrovsky, Y., Schwartzman, M.L., Stoltz, R.A., Levere, R.D., Gerritsen, E., Shibahara, S., and Kappas, A. 1995. Transfection of the human heme oxygenase gene into rabbit coronary microvessel endothelial cells: Protective effect against heme and hemoglobin toxicity. *Proc. Natl. Acad. Sci. U.S.A.* 92:6798-6802.

Becker-Andre, M. and Hahlbrock, K. 1989. Absolute mRNA quantitation using the polymerase chain reaction (PCR): A novel approach by a PCR aided transcript titration assay (PATTY). *Nucl. Acids Res.* 17:9437-9441.

Chomczynski, P. and Sacchi, N. 1987. Single-step method of RNA isolation by acid guanidium. *Anal. Biochem.* 162:156-159.

Cross, N.C. 1995. Quantitative PCR techniques and applications. *Br. J. Haematol.* 89:693-697.

Gilliland, G., Perrin, S., Blanchard, K., and Bunn, H.F. 1990. Analysis of cytokines mRNA and DNA: Detection and quantitation by competitive polymerase chain reaction. *Proc. Natl. Acad. Sci. U.S.A.* 87:2725-2729.

Goodman, A.I., Choudhury, M., da Silva, J-L., Jiang, S., and Abraham, N.G. 1996. Quantitative measurement of heme oxygenase-1 in the human renal adenocarcinoma. *J. Cell. Biochem.* 63:342-348.

Kutty, G., Hayden, B., Osawa, Y., Wiggert, B., Chader, G.J., and Kutty, R.K. 1992. Heme oxygenase: Expression in human retina and modulation by stress agents in a human retinoblastoma cell model system. *Curr. Eye Res.* 11:153-160.

Laniado-Schwartzman, M., Abraham, N.G., Conners, M., Dunn, M.W., Levere, R.D., and Kappas, A. 1997. Heme oxygenase induction with attenuation of experimentally-induced corneal inflammation. *Biochem. Pharmacol.* 53:1069-1075.

Levere, R.D., Martasek, P., Escalante, B., Schwartzman, M.L., and Abraham, N.G. 1990. Effect of Heme Arginate administration on BP in spontaneously hypertensive rats. *J. Clin. Invest.* 86:213-219.

Maines, M.D. 1997. The heme oxygenase system: A regulator of second messenger gases. *Annu. Rev. Pharmacol. Toxicol.* 37:517-554.

McCoubrey, W.K., Jr., Ewing, J.F., and Maines, M.D. 1992. Human heme oxygenase-2: Characterization and expression of a full-length cDNA and evidence suggesting that the two HO-2 transcripts may differ by choice of a polyadenylation signal. *Arch. Biochem. Biophys.* 295:13-20.

Murphy, L.D., Herzog, C.E., Rudick, J.B., Fojo, A.T., and Bates, S.E. 1990. Use of polymerase chain reaction in the quantitation of mdr-1 gene expression. *Biochemistry* 29:10351-10356.

Nath, K.A., Balla, G., Vercellotti, G.M., Balla, J., Jacob, H.S., Levitt, M.D., and Rosenberg, M.E. 1992. Induction of heme oxygenase is a rapid protective response in rhabdomyolysis in the rat. *J. Clin. Invest.* 90:267-270.

Otterbein, L.E., Bach, F.H., Alam, J., Soares, M., Tao, L.H., Wysk, M., Davis, R.J., Flavell, R.A., and Choi, A.M. 2000. Carbon monoxide has anti-inflammmarory effects involving the mitogen-activated protein kinase pathway. *Nat. Med.* 4:422-428.

Poss, K.D. and Tonegawa, S. 1997. Heme oxygenase-1 is required for mammalian iron utilization. *Proc. Natl. Acad. Sci. U.S.A.* 94:10919-10924.

Quan, S., Yang, L., Abraham, N.G., and Kappas, A. 2001. Regulation of human heme oxygenase in endothelial cells by using sense and antisense retroviral constructs. *Proc. Natl. Acad. Sci. U.S.A.* 98:12203-8.

Schacter, B.A. and Kurz, P. 1986. Alterations in microsomal drug metabolism and heme oxygenase activity in isolated hepatic parenchymal and sinusoidal cells in Murphy-Sturn lymphosarcoma-bearing rats. *Clin. Invest. Med.* 9:150-155.

Solangi, K., Sacerdoti, D., Goodman, A.I., Schwartzman, M.L., Abraham, N.G., and Lever, R.T. 1988. Differential effects of partial hepatectomy on hepatic and renal heme and cytochrome P450 metabolism. *Am. J. Med. Sci.* 296:387-391.

Wagener, F.A., da Silva, J.L., Farley, T., de Witte, T., Kappas, A., and Abraham, N.G. 1999. Differential effects of heme oxygenase isoforms on heme mediation of endothelial intracellular adhesion molecule 1 expression. *J. Pharmacol. Exp. Ther.* 291:416-23.

Wang, A.M., Doyle, M.V., and Mark, D.F. 1989. Quantitation of mRNA by the polymerase chain reaction. *Proc. Natl. Acad. Sci. U.S.A.* 86:9717-9721.

Yachie, A., Niida, Y., Wada, T., Igarashi, N., Kaneda, H., Toma, T., Ohta, K., Kasahara, Y., and Koizumi, S. 1999. Oxidative stress causes enhanced endothelial cell injury in human heme oxygenase-1 deficiency. *J. Clin. Invest.* 103:129-135.

Yang, L., Quan, S., and Abraham, N.G. 1999. Retrovirus-mediated HO gene transfer into endothelial cells protect against oxidant-induced injury. *Am. J. Physiol.* 277 (part 1): L127-L133.

Yoshida, T., Biro, P., Cohen, T., Muller, R.M., and Shibahara, S. 1988. Human heme oxygenase cDNA and induction of its mRNA by hemin. *Eur. J. Biochem.* 171:457-461.

Contributed by N.G. Abraham, S.K. Shenouda, and A. Goodman
New York Medical College
Valhalla, New York

Purification and Characterization of Heme Oxygenase

Heme oxygenase (EC 1.14.99.3) catalyzes the NADPH–cytochrome P450 reductase, O_2-dependent degradation of heme to biliverdin, carbon monoxide (CO), and iron (Fig. 9.9.1; reviewed in Ortiz de Montellano, 2000; Ortiz de Montellano and Wilks, 2000). Heme oxygenase (HO) is highly unusual in that it uses heme as a cofactor for its own degradation, and it is therefore unlike classic hemoproteins such as the cytochrome P450, peroxidase, or catalase enzymes. The reaction requires a total of seven electrons and three oxygen molecules for the conversion of one heme molecule to biliverdin, CO, and iron (Liu and Ortiz de Montellano, 2000). All mammalian heme oxygenases regiospecifically cleave heme at the α-*meso*-carbon to yield biliverdin IXα which, by the action of biliverdin reductase, is converted to bilirubin. The existence of two isoforms of heme oxygenase, designated HO-1 and HO-2, respectively, has been known for some time (Maines et al., 1986; Rotenberg and Maines, 1990; Shibahara et al., 1993). HO-1, a heat shock protein also known as HSP32, is induced by a number of factors including heme, heavy metals, and oxidizing agents (Maines, 1992). HO-2, which is primarily located in the brain, spleen, and testis, is largely resistant to induction, except by the adrenal glucocorticoids (Weber et al., 1994). A third isoform, HO-3, has been described recently, and a lack of catalytic activity has suggested that its function may largely be regulatory (McCoubrey et al., 1997).

In mammals, the heme oxygenase pathway is the only defined mechanism for the degradation of heme. The oxidative cleavage of heme, in addition to removing a potentially toxic agent, also provides a mechanism for the reutilization of iron. Iron recovery and reutilization is of major physiological importance, as 97% to 99% of the iron in red blood cell synthesis comes from iron recycled from heme and iron-binding proteins (Bothwell et al., 1995). The critical role of heme oxygenase in iron reutilization was further demonstrated in recent experiments with genetic HO-1 knockout mice (Poss and Tonegawa, 1997a). The HO-1 deficient adult mice developed chronic anemia associated with low serum levels, but also an increased hepatic and renal iron content resulting in oxidative damage, chronic inflammation, and tissue injury. Earlier studies had demonstrated that HO-1 is induced as a response to oxidative challenge, and that the up-regulation was an adaptive response to protect cells from such oxidative challenge (Balla et al., 1993; Otterbein et al., 1995). More recently, murine cells lacking HO-1 were found to be

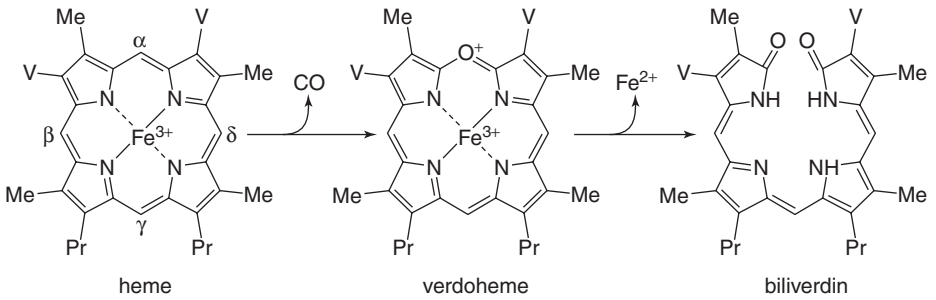

Figure 9.9.1 Enzymatic conversion of heme to biliverdin. Abbreviations are as follows; Me, methyl ($-CH_3$), V, vinyl ($-CH=CH_2$), and Pr, propionate ($-CH_2-CH_2-COOH$). The *meso*-carbons are labeled α, β, δ, γ.

Contributed by Angela Wilks

Current Protocols in Toxicology (2003) 9.9.1-9.9.17

more susceptible to the accumulation of free radicals and oxidative damage both in vivo and in vitro, confirming the role of HO-1 as an important antioxidant system (Poss and Tonegawa, 1997b). The critical role of HO-1 in both antioxidant protection and iron homeostasis highlights the unique interest in HO-1 from areas of study as diverse as cardiovascular physiology, the central nervous system, renal and hepatic function, inflammation, and transplant surgery (Immenschuh and Ramadori, 2000; Otterbein and Choi, 2000). Indeed the overexpression of HO-1 activity brought about by pharmacological agents or specific gene transfer has been postulated as having therapeutic benefits (Immenschuh and Ramadori, 2000).

Bilirubin, the final product of the oxidative cleavage of heme, has long been known as a neurotoxic agent when it rises above physiological levels, as in neonatal jaundice or Crigler-Najjar syndrome (Maines, 1992). However, bilirubin can also act as a lipid-soluble antioxidant that may have physiological relevance in the protection against intracellular oxidative damage due to free-radical formation (Stocker et al., 1987; Stocker, 1990; Dore et al., 1999; Barañano et al., 2002).

The oxidative cleavage of heme by HO releases CO as a product of the reaction, which has been proposed as a neural messenger in processes such as long-term memory potentiation, neuroendocrine regulation, and vasodilation through the action of soluble guanylyl cyclase, or sGC (Stevens and Wang, 1993; Verma et al., 1993; Snyder et al., 1998). More recently, evidence has indicated that the anti-inflammatory response and inhibition of apoptosis by CO is independent of sGC and results from direct activation of the mitogen-activated protein (MAP) kinase pathway (Otterbein et al., 2000).

Given the unique role of heme oxygenase in many diverse physiological functions, it is of fundamental importance to characterize the heme oxygenase protein from a mechanistic and structural aspect. This unit will focus on the human HO-1 isoform, on which most of the biophysical data has been obtained, and describes both high-yield expression (see Basic Protocol 1) and purification (see Basic Protocol 2) as well as spectrophotometric techniques utilized in physical characterization of the protein (see Support Protocols 2 and 3). A protocol for the preparation of NADPH–cytochrome P450 reductase, used in assays for HO, is also included (see Support Protocol 1).

A critical factor in the biophysical characterization of any protein is the ability to generate a sufficient amount of material for such studies. The advent of heterologous expression systems for HO-1 greatly advanced the biophysical and mechanistic characterization of the protein. Truncated genes for both the rat and human HO-1 were constructed lacking the C-terminal 23 amino acids corresponding to the hydrophobic membrane anchor (Wilks and Ortiz de Montellano, 1993; Wilks et al., 1995). The enzymes were expressed at high levels as catalytically active soluble forms that caused the bacterial cells to accumulate biliverdin (Wilks and Ortiz de Montellano, 1993; Wilks et al., 1995).

HIGH-YIELD EXPRESSION OF HUMAN HO-1 IN *E. COLI*

BASIC PROTOCOL 1

The expression vector for the human HO-1 gene is constructed in pBAce, a pBR322 derivative carrying the alkaline phosphatase promoter *phoA* (Craig et al., 1991). The gene is generated by the polymerase chain reaction (PCR) from the respective full length cDNA in an Okayama-Berg vector (Shibahara et al., 1985). The 5′-sense oligonucleotide encodes an *Nde*I site at the N-terminus and the 3′-antisense oligonucleotide encodes a stop codon (TAA) at the proline 23 amino acids from the C-terminus, immediately followed by a *Sal*I site (Wilks et al., 1995). The PCR product is cloned into pBAce following restriction digest with *Nde*I and *Sal*I to generate pBHO1.

The expression of HO-1 is carried out in low-phosphate induction medium containing 75 μg/ml ampicillin. A 3-ml inoculum in LB medium is set up from fresh colonies of pBHO-1-transformed *E. coli* DH5αF′ grown on LB-ampicillin plates. A 100-μl aliquot is taken from the mid-log-phase cultures grown at 30°C, and this is used to inoculate four 1-liter cultures of the same medium containing 75 μg/ml ampicillin. Cells are grown for a further 18 hr at 30°C, or until the medium becomes green.

It was noted in early experiments that *E. coli* DH5αF′ cells containing pBHO1, when grown in LB medium containing 100 μg/ml ampicillin, grew with green coloration. The expression yields in both the low-phosphate medium and LB medium under identical conditions were found to be within the same range. The advantages of using LB medium are the simpler protocol and cost effectiveness.

Materials

pBHO-1 vector (P.R. Ortiz de Montellano; *ortiz@cgl.ucsf.edu*)
E. coli DH5αF′ (Life Technologies)
LB medium and plates containing 100 μg/ml ampicillin (see recipe)
Low-phosphate induction medium (see recipe) containing 75 μg/ml ampicillin
Temperature-controlled shaking incubator (New Brunswick Model G20 or equivalent)
UV/visible spectrophotometer (Varian Cary Bio-100 or equivalent)
Low-speed centrifuge (Beckman Avanti J25-I with JA-10 rotor or equivalent model)

1. Transform (see *APPENDIX 3A*) *E. coli* DH5αF′ cells with pBHO-1 and grow the transformed cells on a fresh LB-ampicillin plate overnight at 37°C. Pick a single colony and use it to inoculate 3 ml of LB medium containing 75 μg/ml ampicillin.
2. Grow the 3-ml culture at 30°C in a shaking incubator to mid-log phase (OD_{600} ~0.5 to 0.6) by monitoring the optical density at 600 nm in a UV/visible spectrophotometer.
3. Take 100 μl of the mid-log phase cells and inoculate 1 liter of LB medium or low-phosphate induction medium containing 75 μg/ml ampicillin.
4. Grow the cells for a further 16 to 18 hr at 30°C in a shaking incubator or until the cells turn green in color. Harvest the cell pellets by centrifuging 20 min at 10,000 × *g* (5,000 rpm in a JA-10 rotor), 4°C. Store the harvested cell pellets at −80°C prior to purification of the protein (see Basic Protocol 2).

   Do not grow the cells for longer than 24 hr as partial proteolysis of the 30 kDa HO-1 to a 28-kDa inactive fragment occurs (see Critical Parameters and Troubleshooting).

PURIFICATION OF HO-1 PROTEIN

BASIC PROTOCOL 2

The purification of HO-1 by ion-exchange chromatography yields the biliverdin-bound protein. For preparations of HO-1 that are to be reconstituted with heme, the addition of heme readily displaces biliverdin from the protein to yield the heme-HO-1 complex. To obtain the apoprotein free of biliverdin, a modification to the purification protocol is required (see steps 6b to 9b).

Materials

Cell pellets (see Basic Protocol 1)
Lysis buffer I (see recipe)
Ammonium sulfate
10, 20, and 100 mM potassium phosphate buffer, pH 7.4 (*APPENDIX 2A*)

250 mM potassium chloride (KCl)
10 mM diaminopropane
Gradient from 0 to 250 mM KCl in 10 mM diaminopropane
1.5 mM hemin solution (see recipe)
NADPH–cytochrome P450 reductase (see Support Protocol 1)
2.5 to 3.0 μmol/min/mg biliverdin reductase (Mahin D. Maines; *Mahin_Maines@urmc.rochester.edu*)
Hemin/BSA solution (see recipe)
1 mM NADPH: dilute 1 M NADPH stock (see recipe) in 100 mM potassium phosphate buffer, pH 7.4 (*APPENDIX 2A*)

Fisher Scientific 60 Sonicator Dismembrator (or equivalent)
Low-speed centrifuge (Beckman Avanti J25-I with JA-10 and JA-20 rotors or equivalent) and corresponding 50-ml centrifuge tubes
Dialysis membrane, MWCO 10 kDa (also see *APPENDIX 3H*)
FPLC system (Amersham Pharmacia Biotech) with Mono-Q (HR 10/10) column *or* conventional chromatography system (peristaltic pump, fraction collector, and gradient maker) with 3 × 10–cm Q-Sepharose column (also from Amersham Pharmacia Biotech)
3 × 10–cm chromatography column packed with QAE anion-exchange resin (Amersham Pharmacia Biotech) and equilibrated with 10 mM diaminopropane, pH 9.0
1.5 × 6.0–cm chromatography column packed with Bio-Gel HTP hydroxyapatite resin (Bio-Rad) and equilibrated with 10 mM potassium phosphate buffer, pH 7.4 (*APPENDIX 2A*)
UV/visible spectrophotometer (Varian Cary Bio-100 or equivalent)
Amicon filtration unit with YM10 membrane (10 kDa molecular weight cut-off)

Additional reagents and equipment for dialysis (*APPENDIX 3H*) and SDS-PAGE (*APPENDIX 3F*)

NOTE: All procedures should be carried out at 4°C.

Disrupt cells

1. Resuspend the harvested cells in 150 ml lysis buffer I, 4°C. Stir the cell suspension for 30 min at 4°C.
2. Sonicate the cell suspension for three 1-min cycles at 2-min intervals, keeping the suspension on ice.
3. Transfer the sonicated cell suspension to four 50-ml centrifuge tubes and centrifuge 60 min at 27,000 × *g*, 4°C, to remove the cell debris.

Perform ammonium sulfate precipitation

4. Transfer the supernatant to a 250-ml graduated beaker and slowly add solid ammonium sulfate to a final concentration of 40% (w/v), stirring continuously. Stir the solution for a further 30 min, then centrifuge 20 min at 27,000 × *g*, 4°C.

   This ammonium sulfate precipitation is referred to as the "40% cut."

5. Transfer the supernatant to a 250-ml graduated beaker and add ammonium sulfate to a final concentration of 70%. Stir the suspension for 30 min and collect the precipitate by centrifugation at 27,000 × *g*, 4°C.

To obtain biliverdin-bound HO-1

6a. Resuspend the ammonium sulfate precipitates in a total of 30 to 50 ml of 10 mM potassium phosphate buffer, pH 7.4, and dialyze 4 to 6 hr (*APPENDIX 3H*) against three 3-liter changes of that buffer using an MWCO 10 kDa dialysis membrane.

7a. Purify protein by anion-exchange chromatography as follows:

i. Set up the FPLC system to produce a linear gradient of 10 mM potassium phosphate buffer, pH 7.4/250 mM KCl.

ii. Equilibrate the Mono-Q (HR 10/10) column with 10 mM potassium phosphate buffer, pH 7.4, at a flow rate of 2 ml/min.

iii. Load the dialyzed fraction (from step 6) on to the column. Wash the column with a further 50 ml of 10 mM potassium phosphate buffer, pH 7.4.

iv. Elute the protein (collecting 3-ml fractions) with a linear gradient from 0% of 250 mM KCl (100% of 10 mM potassium phosphate buffer, pH 7.4) to 25% of 250 mM KCl (75% of 10 mM potassium phosphate buffer, pH 7.4) over 20 min, hold at 25% for 10 min, and then increase linearly over 20 min to 100% of 250 mM KCl.

The fractions containing heme oxygenase elute in the first half of the gradient.

If an FPLC chromatography system is not available, a 3 × 10–cm Q-Sepharose column can be substituted using the same buffer system and a linear KCl gradient from 10 to 200 mM KCl.

8a. Remove 10-µl samples from every third fraction and run on SDS-PAGE (*APPENDIX 3F*) to determine the peak heme oxygenase–containing fractions.

9a. Pool the peak heme oxygenase fractions and dialyze (*APPENDIX 3H*) against three changes (4 to 6 hr) of 4 liters of 10 mM potassium phosphate buffer, pH 7.4, using an MWCO 10 kDa dialysis membrane. Store proteins up to 12 months at −80°C.

At this stage the protein should be 95% pure.

To obtain biliverdin-free HO-1 apoprotein

6b. Resuspend the ammonium sulfate precipitate from step 5 in 10 mM diaminopropane, pH 9.0, dialyze against three 4 liter changes of the same buffer, and apply to a 3 × 10–cm QAE anion-exchange column previously equilibrated with the same buffer.

7b. Elute the protein from the column with a gradient of 0 to 250 mM KCl in 10 mM diaminopropane, pH 9.0. Collect 3.0-ml fractions and analyze every third fraction for the HO-1 protein by SDS-PAGE (*APPENDIX 3F*).

The green biliverdin pigment remains bound to the column and the apo-enzyme is eluted.

8b. Pool the fractions containing HO-1 protein and dialyze (*APPENDIX 3H*) against three 4- to 6-hr changes of 4 liters of 20 mM potassium phosphate buffer, pH 7.4, using an MWCO 10 kDa dialysis membrane.

9b. Store the protein up to 12 months at −80°C.

Prepare the heme-HO-1 complex

10. Add 1.5 mM hemin solution to the dialyzed protein from either step 9a or 9b in a quantity sufficient to give a final molar ratio of 2:1 heme:protein.

The hemin solution should be prepared fresh and used within 30 min.

11. Apply the heme/protein solution to a 1.5 × 6.0–cm Bio-Gel HTP column previously equilibrated with 10 mM potassium phosphate buffer, pH 7.4. Wash the column with a further 50 ml of the same buffer or until no heme can be detected in the eluate. Monitor the heme by measuring the absorbance at 402 nm.

12. Elute the heme-HO-1 complex with 100 mM potassium phosphate buffer, pH 7.4, collecting 2.0 to 3.0 ml fractions. Pool the peak fractions by monitoring the absor-

bance of the heme-HO-1 complex at 405 nm. Calculate the total yield of protein from the millimolar extinction coefficient of 128 mM^{-1}.

13. If necessary, concentrate the heme-HO-1 protein to 10 mg/ml by filtration on an Amicon filtration unit with a 30-kDa MWCO YM10 membrane. Divide protein solutions into 100- to 1000-µl aliquots, and store up to 12 months at –80°C.

Assay heme oxygenase activity

14. Add the following to a 1-ml cuvette:

    10 to 50 µl heme oxygenase–containing solution (step 13; ~0.1 nmol enzyme)
    5 to 20 µl NADPH–cytochrome P450 reductase (prepared as in Support Protocol 1; 0.3 nmol)
    5 to 20 µl of biliverdin reductase (0.3 nmol)
    100 µl hemin/BSA solution (final concentration 15 µM heme/1 µM BSA)
    100 mM potassium phosphate buffer, pH 7.4, to give a final volume of 900 µl.

15. Mix the contents of the cuvette by inverting gently and zero the absorbance at 468 nm.

16. Add 100 µl of 1 mM NADPH (final concentration 100 µM), mix, and monitor the change in absorbance with time at 468 nm for 10 min. Calculate the specific activity using the millimolar extinction coefficient (ε) of 43.5 mM^{-1} cm^{-1} and the following relationships:

    $\Delta A = \varepsilon cl$

    where ΔA represents the change in absorbance per min (in the linear phase), ε represents the millimolar extinction coefficient and l represents the path length (a path length of 1 cm is routinely used). Rearranging this equation, the number of mmol of bilirubin formed per min can be calculated from:

    $c = \Delta A/\varepsilon$

    where the units are mM/min, and:

$$\text{activity (mmol/min)} = c \times \frac{\text{µl protein solution}}{1000}$$

    Finally, divide by the concentration of protein (mg) used in the assay to give the specific activity in mmol/min/mg.

SUPPORT PROTOCOL 1

PREPARATION OF NADPH–CYTOCHROME P450 REDUCTASE

NADPH–cytochrome P450 reductase is used in assays for HO-1 such as that described in steps 14 to 16 of Basic Protocol 2. The purified NADPH–cytochrome P450 reductase is obtained by a slight modification of the method of Yasukochi and Masters (1976). The pETOR vector used in the heterologous expression of the protein is described in Wilks et al. (1995).

Materials

E. coli BL21(DE3)
pETOR (pET vector containing gene for human NADPH cytochrome P450 reductase; *wilks@tx.maryland.edu*)
LB medium containing 100 µg/ml ampicillin (see recipe)
Terrific broth containing 100 µg/ml ampicillin (see recipe)

1 M IPTG stock (see recipe)
Lysis buffer II (see recipe)
Resuspension buffer (see recipe)
Bio-Rad protein assay kit
Lubrol PX detergent (polyoxyelthylene 9 lauryl ether; Sigma-Aldrich)
Column wash buffers I and II (see recipes)
Elution buffer: column wash buffer II (see recipe) containing 2.5 mM 2′-AMP
20 mM potassium phosphate buffer, pH 7.4 (*APPENDIX 2A*) containing 20% (v/v) glycerol
300 mM potassium phosphate buffer, pH 7.7 (*APPENDIX 2A*)
1 mM bovine cytochrome *c*
1 mM NADPH: dilute 1 M NADPH (see recipe) with 300 mM potassium phosphate buffer, pH 7.7 (see *APPENDIX 2A* for buffer)

UV/visible spectrophotometer (Varian Cary Bio-100 or equivalent model)
Temperature-controlled shaking incubator (New Brunswick Model G25 or equivalent model)
Low-speed centrifuge(Beckman Avanti J25-I with JA-10 rotor or equivalent model)
Fisher Scientific 60 Sonicator Dismembrator (or equivalent)
High-speed centrifuge (Beckman L8-70 with 45 Ti rotor, or equivalent)
1 × 10–cm chromatography column packed with 2′,5′-ADP-Sepharose and equilibrated with equilibration buffer (see recipe for buffer)

Grow E. coli in E. coli BL21(DE3)

1. Transform (see *APPENDIX 3A*) *E. coli* BL21(DE3) with pETOR and grow the transformed cells in 3 ml LB-ampicillin medium overnight to saturation.
2. Inoculate three 1-liter cultures of terrific broth containing 100 μg/ml ampicillin with 1 ml of the overnight culture from step 1, and grow the cells to an OD_{600} of 0.4 at 37°C in a shaking incubator.
3. Reduce the temperature of the incubator to 22°C and induce the cells by adding 1 M IPTG stock to a final concentration of 0.4 mM.
4. Grow the cells for a further 16 hr, then harvest by centrifuging 20 min at 10,000 × *g* (5,000 rpm in a JA-10 rotor), 4°C.

Purify NADPH cytochrome P450 reductase

All of the following steps should be carried out at 4°C.

5. Resuspend the cell pellets in 100 ml lysis buffer II. Stir the resuspended cells for 1 hr to ensure lysis of the cells.
6. Sonicate the lysed cells four times for 30 sec, at 1-min intervals. Centrifuge 30 min at 18,000 × *g* (10,000 rpm in JA-10 rotor), 4°C, to remove cell debris.
7. Collect the supernatant and centrifuge it again for 1 hr at 185,000 × *g* (40,000 rpm in a Beckman 45 Ti rotor), 4°C. Resuspend the pellets from this high-speed centrifugation in 30 ml resuspension buffer.
8. Determine the protein concentration by Bio-Rad protein assay kit and adjust the concentration to 3 mg/ml with resuspension buffer. Add Lubrol PX to a final concentration of 0.2 % (v/v) and stir for 1 hr.
9. Clarify the solubilized protein solution by centrifuging 1 hr as in step 7. Retain the resulting supernatant.

10. Load the supernatant onto a 1 × 10–cm 2′,5′-ADP-Sepharose column equilibrated in equilibration buffer.

11. Wash the column with an additional 50 ml of equilibration buffer followed by 50 ml of column wash buffer I. Finally wash the column with 50 ml of column wash buffer II.

12. Elute the protein from the column using elution buffer, collecting 1-ml fractions. Assay the fractions for activity using the reduction of cytochrome *c* (see steps 14 to 17). Pool the fractions containing the peak activities.

13. Dilute the pooled fractions with sufficient 20 mM potassium phosphate buffer, pH 7.4, containing 20% (v/v) glycerol, to reduce the concentration of 2′-AMP 100-fold. Remove the 2′-AMP by successively concentrating the diluted solution over an Amicon YM30 membrane.

Assay NADPH-cytochrome P450 reductase activity

14. In a spectrophotometer cuvette, add 0.1 to 1.0 μg of NADPH–cytochrome P450 reductase (usually 1 to 10 μl of the solution obtained from step 12) and 100 μl 1 mM bovine cytochrome *c* to 300 mM potassium phosphate buffer, pH 7.7, adjusting the volume of buffer to give a final volume of 900 μl.

15. Seal the cuvette with Parafilm, mix the contents gently by inversion, and zero the absorbance at 550 nm.

16. Add 100 μl of 1 mM NADPH (from 1 M stock solution) in 300 mM potassium phosphate buffer, pH 7.7, and mix the contents immediately. Monitor the increase in absorbance with time over a 5-min period or until the activity reaches a plateau.

17. Measure the initial rate and, using the millimolar extinction coefficient of 21.1 mM^{-1} cm^{-1}, calculate the specific activity (see Basic Protocol 2, steps 14 to 16).

A typical specific activity would be in the range of 1 to 15 μmol/min/mg.

SPECTROPHOTOMETRIC ANALYSIS OF THE HEME-HEME OXYGENASE COMPLEX

The unique chromophore of heme-binding proteins allows the use of a number of spectrophotometric techniques to yield detailed information on the nature of the heme ligands. Although individual spectroscopic techniques can yield valuable information, it is the combined use of techniques such as UV/visible, magnetic circular dichroism (MCD), resonance Raman, and nuclear magnetic resonance (NMR) that can provide great insight into the nature of the coordination and ligation of the heme. It is beyond the focus of this review to provide detailed methodology for all such techniques, and therefore the focus will be on the characterization of the heme-HO-1 complex by UV/visible spectroscopy. A synopsis of the information that can be gained in a more extensive spectroscopic analysis will be given below (see Background Information).

SUPPORT PROTOCOL 2

UV/Visible Spectra of the Heme-HO-1 Complex

Materials

10 to 20 μM heme-HO-1 complex (see Basic Protocol 2)
20 mM potassium phosphate buffer, pH 7.0 (*APPENDIX 2A*)
Carbon monoxide (CO) gas source
1 mM (17.4 mg/ml) sodium hydrosulfite (sodium dithionite) in 10 mM potassium phosphate buffer, pH 7.0 (see *APPENDIX 2A* for buffer), prepared immediately before use

1-cm quartz cuvettes
UV/visible spectrophotometer (Varian Cary Bio-100 or equivalent model)
1 × 10–cm Bio-Gel P-10 desalting column (Bio-Rad), equilibrated with 20 mM potassium phosphate buffer, pH 7.0 (see *APPENDIX 2A* for buffer)

1. In a 1-cm quartz cuvette, dilute heme-HO-1 complex to a final concentration of 10 μM in a final volume of 1 ml of 20 mM potassium phosphate buffer, pH 7.0. Record the spectrum of the ferric (Fe^{3+}) heme-HO-1 complex, scanning from 250 to 750 nm in a UV/visible spectrophotometer.

   The spectrum of the oxidized heme-HO-1 complex has a Soret maximum at 404 nm and a high spin marker band in the visible region at 628 nm (Fig 9.9.2).

   The Soret maxima at 404 nm for a 10 μM concentration of the heme-HO-1 complex should give an absorbance of 1.3 to 1.4.

2. To obtain the reduced, ferrous (Fe^{2+}) carbon monoxy (CO) spectrum of the heme-HO-1 complex, take the 1-ml sample and gently bubble with CO for 1 to 2 min, to saturate the solution and ensure a high content of CO in the cuvette.

   CAUTION: *CO is a poisonous gas. Carry out the CO saturation in a ventilated hood. Do not bubble vigorously or foaming and precipitation of the protein may occur.*

3. Following CO saturation, add 1 equivalent (5 to 10 μl) of a fresh 1 mM sodium hydrosulfite solution, and mix by inverting the cuvette.

   The ferrous CO heme-HO-1 complex should immediately change color from brown to red, indicating reduction and binding of the CO ligand.

4. Again record the spectrum of the ferrous CO-bound heme-HO-1 complex, scanning from 250 nm to 750 nm.

   The spectrum should increase in intensity with a Soret maximum at 420 nm and the visible α/β bands at 567 and 537 nm, respectively (Fig 9.9.2).

5. To obtain the ferrous oxy (O_2)-complex, pass 1 ml of the ferrous CO-heme-HO-1 complex over a Bio-Gel P-10 desalting column equilibrated with 20 mM potassium phosphate buffer, pH 7.0, to remove the sodium hydrosulfite.

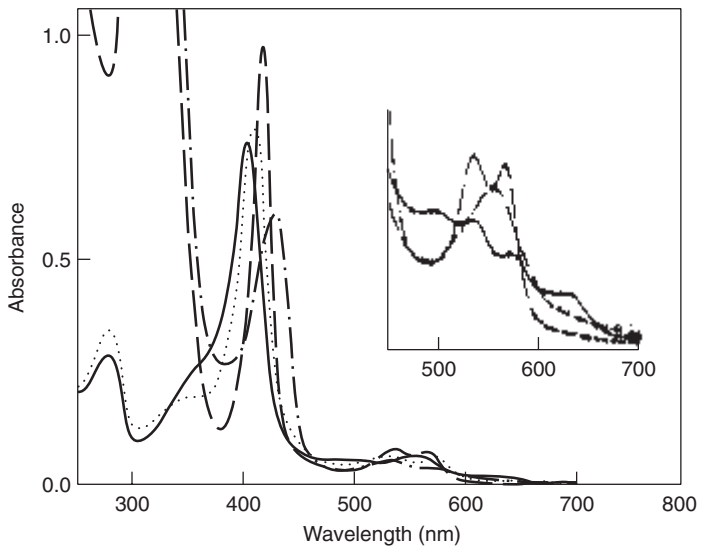

Figure 9.9.2 Absorption spectra of the purified heme-HO-1 complex: ferric heme-HO-1 (solid line); ferrous deoxy heme-HO-1 (line of alternating dots and dashes); ferrous O_2 heme-HO-1 (dotted line); ferrous CO-heme-HO-1 (dashed line).

6. Elute the ferrous O_2-heme-HO-1 complex (~2 ml) with 20 ml potassium phosphate buffer, pH 7.0.
7. Record the spectrum of the eluted ferrous O_2-heme-HO-1 complex, scanning from 250 to 750 nm.

   The spectrum of the ferrous O_2-heme-HO-1 complex has a Soret maximum at 412 nm and α/β bands at 573 and 539 nm respectively (Fig 9.9.2).

SUPPORT PROTOCOL 3

UV/Visible Spectra of Heme Oxygenase Reaction Intermediates

It has previously been shown that in the presence of CO inhibition of the heme oxygenase reaction results in the accumulation of the ferrous CO-verdoheme intermediate (Wilks and Ortiz de Montellano, 1993; Yoshida et al., 1980, 1982). The conversion of the heme-HO-1 complex to the ferrous CO-verdoheme complex can be monitored spectroscopically in the presence of the NADPH–P450 reductase system.

Materials

NADPH–cytochrome P450 reductase (see Support Protocol 1)
Heme-HO-1 (see Basic Protocol 2)
100 mM potassium phosphate buffer, pH 7.4 (*APPENDIX 2A*)
Carbon monoxide (CO) gas source
1 M NADPH (see recipe)

1-cm cuvette
UV/visible spectrophotometer (Varian Cary Bio-100 or equivalent model)

1. In a 1-cm cuvette, prepare a solution of 30 μM NADPH–cytochrome P450 reductase and 10 to 15 μM heme-HO-1 in a final volume of 1 ml of 100 mM potassium phosphate buffer, pH 7.4. Record the spectrum of the resting state ferric heme-HO-1 complex from 300 to 750 nm. Saturate the heme-HO-1 complex with CO by gently bubbling.

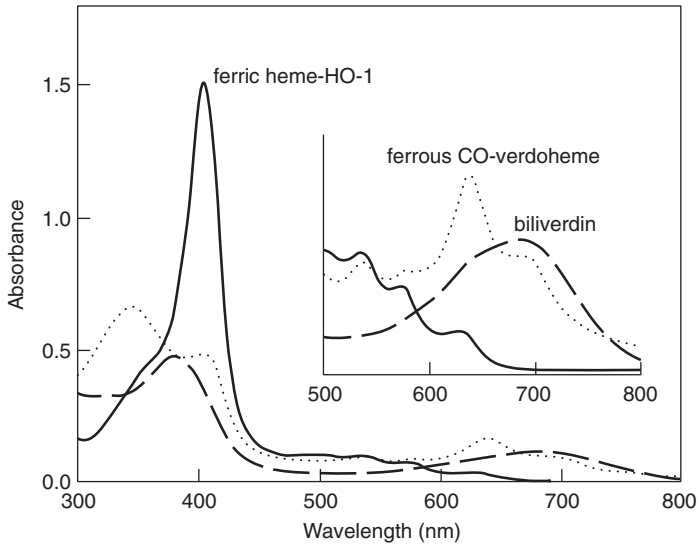

Figure 9.9.3 Conversion of the ferric heme-HO-1 complex to biliverdin-IXα in the presence of NADPH cytochrome P450 reductase: ferric heme-HO-1 (solid line); ferrous CO-verdoheme HO-1 (dotted line); biliverdin (dashed line).

2. Initiate reaction by the addition of NADPH in 10-µM increments to a final concentration of 100 µM. Monitor the spectral changes between 300 and 750 nm over a 20-min period at 1-min intervals. Add NADPH increments between scans.

   Increments are added to avoid interference with heme soret—the NADPH absorbs at 350 to 360 nm.

   The characteristic shift in Soret maximum from 404 nm to 420 nm, with the appearance of a band at 638 nm in the visible region is characteristic of the ferrous CO-verdoheme complex (Fig 9.9.3).

3. Bubble the reaction intermediate with oxygen and record the final spectrum which is typical of the final product, biliverdin (Fig. 9.9.3).

REAGENTS AND SOLUTIONS

Use autoclaved Milli-Q-purified water or equivalent for all recipes and protocol steps. For common stock solutions, see ***APPENDIX 2A****; for suppliers, see* ***SUPPLIERS APPENDIX****.*

Ampicillin, 100 mg/ml stock solution

Add 10 ml of H_2O to 1 g ampicillin. Once the ampicillin is completely in solution, filter sterilize through a 22-µm disposable syringe filter. Store in 1 ml aliquots up to 3 months at −20°C.

Column wash buffer I

300 mM potassium phosphate, pH 7.4 (*APPENDIX 2A*)
20% (v/v) glycerol
0.1 mM EDTA
Store up to 2 weeks at 4°C

Column wash buffer II

20 mM potassium phosphate, pH 7.4 (*APPENDIX 2A*)
0.15% (w/v) sodium deoxycholate
Store up to 2 weeks at 4°C

Equilibration buffer

20 mM potassium phosphate, pH 7.4 (*APPENDIX 2A*)
20% (v/v) glycerol
0.1 mM EDTA
Store up to 2 weeks at 4°C

Hemin/BSA solution

Prepare 100 µl of 1.5 mM hemin solution (see recipe) and add 0.68 mg of BSA as a carrier. Store up to 1 week at 4°C.

Although free hemin will form µ-oxo dimers, hemin bound to BSA does not form such inactive dimers.

This solution when used in the HO-1 assay gives a final concentration of 15 µM heme and 1 µM BSA.

Hemin solution, 1.5 mM

Dissolve 10 µg of hemin in 100 µl of 0.1 N NaOH. Once the hemin is completely dissolved, increase the volume to 10 ml with 10 mM potassium phosphate buffer, pH 7.4 (*APPENDIX 2A*). Filter through 0.45-µm disposable syringe filter. Prepare fresh before each use; use within 30 min of preparation.

IPTG stock solution, 1 M

Dissolve 2.38 g isopropylthio-β-D-galactoside (IPTG) in 8 ml water. Adjust the volume to 10 ml and filter sterilize through a 0.22-µm disposable filter. Store up to 8 weeks at −20°C.

LB (Luria-Bertani) medium and plates containing 100 µg/ml ampicillin

For liquid LB medium:

950 ml deionized H_2O
10 g Bacto tryptone (Difco)
5 g Bacto yeast extract (Difco)
10 g NaCl
Adjust pH to 7.0 with 5 N NaOH
Adjust volume to 1 liter
Sterilize by autoclaving 20 min on liquid cycle

For LB plates:

Add 15 mg of Bacto-agar (Difco) to 1 liter of liquid LB medium prior to autoclaving. Pour into sterile 150-mm-diameter petri dishes and allow to cool.

For LB medium or plates containing 100 µg/ml ampicillin:

After autoclaving the medium (with or without agar), allow it to cool to ~50°C and add 1 ml of 100 mg/ml ampicillin stock (see recipe) per liter for a final concentration of 100 µg/ml. Mix thoroughly. If preparing plates, pour them at this point as described above.

Low-phosphate induction medium

Prepare 1 × 10^6 stock solution of micronutrients:

37 mg $(NH_4)_6Mo_7O_{24}{\cdot}4H_2O$
247 mg H_3BO_3
84 mg $CoCl_2$
25 mg $CuSO_4$
158 mg $MnCl_2{\cdot}4H_2O$
18 mg $ZnSO_4$
H_2O to 10 ml
Filter sterilize

Prepare 1 × 10^6 stock solution of salts:

370 ml H_2O
400 ml 1 M MOPS (83.72 g/400 ml, adjusted to pH 7.4 with KOH)
40 ml 1 M Tricine (7.17 g/40 ml, adjusted to pH 7.4 with KOH)
10 ml 10 mM $FeSO_4{\cdot}7H_2O$ (27.8 mg/10 ml)
50 ml 1.9 M NH_4Cl (5.08 g/50 ml)
10 ml 276 mM K_2SO_4 (0.48 g/10 ml)
10 ml 0.5 mM $CaCl_2$ (0.74 mg/10 ml)
10 ml 528 mM $MgCl_2$ (0.5 g/10 ml)
100 ml 5 M NaCl (29.22 g/100 ml)
Add 10 ml of the 1 × 10^6 micronutrients from the above stock, filter sterilize and store at 4°C as 10× MOPS salts to be used below.

Prepare 1 liter of low-phosphate induction medium:

895 ml of sterile H_2O
100 ml 10× MOPS salts (from above)
2 g glucose
2 g casamino acids (vitamin assay grade from Difco)
75 mg ampicillin

continued

100 ml 1 M sodium phosphate (equimolar mix of Na_2HPO_4 and NaH_2PO_4)
1 ml 1.5 mM thiamine (0.506 mg/ml)
20 mg adenine
Sterilize by filtration
Store up to 1 month at 4°C

Lysis buffer I

50 mM Tris·Cl, pH 8.0 (*APPENDIX 2A*; sterilize by autoclaving 20 min on liquid cycle)
1 mM EDTA (add from 0.5 mM EDTA, pH 8.0 stock; *APPENDIX 2A*; sterilize by autoclaving 20 min on liquid cycle)
1 mM phenylmethylsulfonyl fluoride (PMSF; add from 1 M PMSF stock; see recipe)
10 µg/ml lysozyme
Use immediately

Lysis buffer II

100 mM Tris-acetate, pH 8.1
20% (v/v) glycerol
1 mM EDTA
1 mM PMSF (add from 1 M PMSF stock solution; see recipe)
1 µg/ml pepstatin
10 µg/ml leupeptin
0.1 µg/ml antipain
50 µg/ml lysozyme
Use immediately

NADPH, 1 M

Dissolve 833 mg NADPH in 1 ml of the reaction buffer for either the HO-1 assay (100 mM potassium phosphate buffer, pH 7.4; *APPENDIX 2A*) or the NADPH–cytochrome P450 reductase assay (300 mM potassium phosphate buffer, pH 7.7; *APPENDIX 2A*). Store in 100-µl aliquots for 8 weeks at −80°C

PMSF, 1 M

Dissolve 1.74 g of phenymethylsulfonyl fluoride (PMSF) in 10 ml isopropanol. Store up to 3 months in 1-ml aliquots at −20°C.

Resuspension buffer

20 mM potassium phosphate, pH 7.4 (*APPENDIX 2A*)
20% (v/v) glycerol
1 mM EDTA
1 mM PMSF (add from 1 M PMSF stock solution; see recipe)
1 µg/ml pepstatin
10 µg/ml leupeptin
0.1 µg/ml antipain
Use immediately

Terrific broth containing 100 µg/ml ampicillin

900 ml H_2O
12 g Bacto tryptone (Difco)
24 g Bacto yeast extract (Difco)
4 ml glycerol

continued

Sterilize by autoclaving for 20 min. Allow the medium to cool to 60°C and add 100 ml of 0.17 M KH_2PO_4/0.72 M K_2HPO_4 (see annotation). Finally, add 1 ml of 100 mg/ml ampicillin stock (see recipe) per liter for a final concentration of 100 μg/ml. Mix thoroughly.

The 0.17 M KH_2PO_4/0.72 M K_2HPO_4 solution is made by dissolving 2.31 g of KH_2PO_4 and 12.54 g of K_2HPO_4 in 90 ml of H_2O. After the salts have fully dissolved adjust the volume to 100 ml with H_2O and sterilize by autoclaving for 20 min.

COMMENTARY

Background Information

The methods described in this unit have set the stage for many subsequent biophysical studies of the human HO-1. The expression system and purification protocol described here routinely yield 20 to 30 mg of purified protein per liter of cells. Consequently, it has been possible to characterize heme oxygenase on a mechanistic and structural level. Such characterizations include biochemical studies and the use of biophysical techniques such as X-ray crystallography, NMR, resonance Raman, and magnetic circular dichroism (MCD).

Initial UV/visible spectra of the heme-HO-1 complex as described in this unit have provided preliminary information on the nature of the ligation. At pH 6.0, the heme-HO-1 complex has a Soret maximum at 404 nm and a charge transfer band at 632 nm, characteristic of a high-spin species. On increasing the pH from 6.0 to 10.0, the heme Soret shifts from 404 to 409 nm and the charge transfer band decreases with the appearance of α/β-bands at 539 and 574 nm respectively (Sun et al., 1993; Hawkins et al., 1994). These data suggest that a water molecule occupying the sixth ligand position is being titrated to a hydroxide with increasing pH. The UV/visible spectrum of the ferrous complex in the presence of CO with the Soret at 420 nm and α/β bands at 567 and 537 nm, respectively (Fig 9.9.2), is consistent with a histidine as the proximal ligand.

The limited information gained from the UV/visible spectrum on the nature of the proximal ligand is far from conclusive, and much more information can and has been gained from more sophisticated spectroscopic techniques including MCD. MCD, because it is a difference technique that has both positive and negative components, yields a more detailed spectrum than the corresponding UV/visible spectrum. The increased sensitivity of MCD makes it an effective "fingerprinting" technique for the determination of the ligand coordination, oxidation state, and spin state of heme-binding proteins (Cheek and Dawson, 2000). Assignment of the proximal ligand in a heme protein of unknown function is based on comparison to a protein whose proximal ligand is known. The sample to be analyzed is prepared with a known ligand such as cyanide or azide, which can then be compared to the ferric-cyano complex of heme proteins with known ligands, such as myoglobin or cytochrome *c* peroxidase. The cyanoferric heme-HO-1 complex is very similar to that of cyanoferric myoglobin, thus confirming the proximal histidine ligation (Hawkins et al., 1996).

Raman spectroscopy is a vibrational spectroscopy technique that can detect transitions between different ligation states of porphyrins as the spin-state changes (Spiro and Czernuszewicz, 1995). As in MCD experiments, the resonance Raman spectra of the heme-HO-1 complex show a marked change in the heme axial coordination and spin state with changing pH, supporting the ionization of a coordinating water molecule (Sun et al., 1993). Resonance Raman studies, as well as providing direct confirmation of histidine as the proximal ligand, has provided more detailed information on the nature of the proximal histidine. The position of a characteristic marker band for the iron-histidine stretching frequency has implications for the ionization state of the proximal histidine. The band at 216 cm^{-1} in the heme-HO-1 complex (Sun et al., 1993) is close to that of myoglobin (221 cm^{-1}; Kitagawa et al., 1979), where the proximal ligand is only weakly hydrogen bonded. The presence of a strong hydrogen bond, such as that in cytochrome *c* peroxidase, shifts the iron-imidazole stretching frequency to 233 cm^{-1}, while complete ionization gives a value closer to 246 cm^{-1} (Smulevich et al., 1988). The relatively low value for the heme-HO-1 complex can therefore be interpreted as a proximal histidine that is weakly hydrogen-bonded.

The weakly hydrogen-bonded proximal histidine in the heme-HO-1 complex has strong implications for the mechanism of oxygen activation. The ability to form an activated ferryl

by destabilizing the dioxygen bond is largely dependent on the electron density present on the proximal ligand. As the electron density increases by partial or complete deprotonation of the proximal histidine, the ability to carry out dioxygen cleavage increases. Biochemical studies have shown that a ferryl species is not an intermediate in the heme oxygenase–catalyzed degradation of heme (Wilks and Ortiz de Montellano, 1993; Wilks et al., 1994). The mechanism proposed in these studies was that of an electrophilic addition of the terminal oxygen of the protonated peroxo intermediate (Fe-O-OH) to the α-*meso*-carbon. The proposed electrophilic mechanism is consistent with the presence of a proximal ligand that is neither ionized nor hydrogen-bonded. Indeed, recent NMR studies of the heme-HO-1 complex have identified an increased electron density at the α-*meso*-carbon, which would facilitate such a mechanism (Hernandez et al., 1994).

The extensive characterization of the heme-HO-1 complex by spectroscopic techniques such as MCD, resonance Raman, and NMR has greatly aided biochemical studies in elucidating the mechanism of action of HO-1. It is also gratifying that the recently determined crystal structure of the human heme-HO-1 complex (Schuller et al., 1999) has confirmed many aspects of the previous spectroscopic studies. The successful development of high-yield expression and purification protocols has enabled the majority of such studies to be carried out. Understanding of regiospecificity and catalysis will be greatly advanced with ongoing biophysical studies on both the wild-type HO-1 and site-directed mutants.

Critical Parameters and Troubleshooting

Although expression of HO-1 in high yields is feasible in both LB-ampicillin and low-phosphate induction medium, the key factor in obtaining viable protein is to minimize proteolysis to the 28-kDa fragment. This 28-kDa protein, while readily taking up heme, is inactive and can significantly lower the specific activity of the preparation. Therefore, for preparations in which it is imperative that no proteolytic fragment be present, the expression of the protein should be monitored to determine optimal conditions for obtaining the intact protein.

The purified apo-HO-1 or the biliverdin-HO-1 can both be used to reconstitute the heme-HO-1 complex (see Basic Protocol 2). The critical factor in successful reconstitution of the protein is the preparation of the hemin solution. As emphasized in the protocol, the heme solution must be freshly prepared immediately before use, as on standing it will form μ-oxo-dimers in which two heme molecules are coordinated through their iron centers by an oxygen molecule. Hemin is not soluble in aqueous buffer at pH 7.4 and must first be dissolved in alkaline conditions. It is important to dissolve the heme in a minimal amount of 0.1 N NaOH (100 μl), so that on dilution with aqueous buffer (pH 7.4) the pH remains close to neutral. If the pH of the heme solution is too alkaline (pH 8.5 to 9.0), significant denaturation of HO-1 may occur on addition of the hemin solution to the protein.

The HO-1 activity assay relies on the successful coupling of the NADPH cytochrome P450 reductase and HO-1 enzymes, as well as the conversion of biliverdin to bilirubin by biliverdin reductase. The molar ratio of cytochrome P450 reductase to heme oxygenase should be at least 3:1; however, a large excess will result in significant uncoupling in which H_2O_2 will be produced at the expense of NADPH consumption, resulting in nonenzymatic heme degradation. In some instances it may be necessary to titrate the concentration of NADPH–cytochrome P450 reductase required to give the maximum rate of bilirubin production. An excess of biliverdin reductase is required to ensure that the conversion of biliverdin to bilirubin is not the rate-limiting factor in the assay. In the author's laboratory, both purified and partially purified biliverdin reductase have been used successfully in the reconstituted assay.

Anticipated Results

The protocol outlined for the purification of HO-1 routinely yields 100 mg of purified protein with a specific activity 3 to 6 μmol/hr/mg. Purified protein obtained from a 6-liter expression is sufficient to carry out a number of biophysical and biochemical assays, including spectroscopic analysis and X-ray crystallography. The purification of NADPH cytochrome P450 reductase routinely yields 20 mg of purified protein with a specific activity of 15 μmol/min/mg, which is sufficient to reconstitute 100 heme oxygenase activity assays.

Time Considerations

The transformation and expression of HO-1 protein (Basic Protocol 1) requires 2 days for growth and harvest of the cells. Purification of HO-1 (Basic Protocol 2) from lysis of the cells to reconstitution of the protein with heme re-

quires 3 to 4 days. Preparation of the biliverdin-free protein requires 2 days when not reconstituting with heme. The purification of the NADPH cytochrome P450 reductase (Support Protocol 1) requires 5 days for the expression and subsequent purification steps. In both Basic Protocol 2 and Support Protocol 1 a 4 to 6 hr dialysis step can be carried out overnight for convenience. Characterization of the heme-HO-1 complex by UV/visible spectroscopy (Support Protocol 2) can be carried out in 2 to 4 hr. Similarly, the turnover of the heme-HO-1 complex in the presence of NADPH cytochrome P450 reductase (Support Protocol 3) can be carried out over 2 to 3 hr.

Literature Cited

Balla, J., Jacob, H.S., Balla, G., Nath, K., Eaton, J.W., and Vercellotti, G.M. 1993. Endothelial-cell heme uptake from heme proteins: Induction of sensitization and desensitization to oxidant damage. *Proc. Natl. Acad. Sci. U.S.A.* 90:9285-9259.

Barañano, D.E., Rao, M., Ferris, C.D., and Snyder, S.H. 2002. Biliverdin reductase: A major physiologic cytoprotectant. *Proc. Natl. Acad. Sci. U.S.A.* 99:16093-16098.

Bothwell, T.H., Charlton, R.W., and Motulsky, A.G. 1995. Hemochromatosis. *In* The Metabolic and Molecular Basis of Inherited Diseases (C.R. Scriver, A.L. Beaudet, W.S. Sly, and D. Valle, eds.) pp. 2237-2269. McGraw-Hill, New York.

Cheek, J. and Dawson, J. 2000. Magnetic circular dichroism spectroscopy of heme proteins and model systems. *In* The Porphyrin Handbook, vol. 7. (K.M. Kadish, K.M. Smith, and R. Guilard, eds.) pp. 339-369. Academic Press, London.

Craig, S.P., 3rd, Yuan, L., Kuntz, D.A., McKerrow, J.H., and Wang, C.C. 1991. High level expression in *Escherichia coli* of soluble, enzymatically active schistosomal hypoxanthine/guanine phosphoribosyltransferase and trypanosomal ornithine decarboxylase. *Proc. Natl. Acad. Sci. U.S.A.* 88:2500-2504.

Dore, S., Takahashi, M., Ferris, C.D., Hester, L.D., Guastella, D. and Snyder, S.H. 1999. Bilirubin, formed by activation of heme oxygenase-2, protects neurons against oxidative stress injury. *Proc. Natl. Acad. Sci. U.S.A.* 96:2445-2450.

Hawkins, R.D., Zhuo, M., and Arancio, O. 1994. Nitric oxide and carbon monoxide as possible retrograde messengers in hippocampal long-term potentiation. *J. Neurobiol.* 25:652-665.

Hawkins, B.K., Wilks, A., Powers, L.S., Ortiz de Montellano, P.R., and Dawson, J.H. 1996. Ligation of the iron in the heme-heme oxygenase complex: X-ray absorption, electronic absorption and magnetic circular dichroism studies. *Biochim. Biophys. Acta.* 1295:165-173.

Hernandez, G., Wilks, A., Paolesse, R., Smith, K.M., Ortiz de Montellano, P.R., and La Mar, G.N. 1994. Proton NMR investigation of substrate-bound heme oxygenase: Evidence for electronic and steric contributions to stereoselective heme cleavage. *Biochemistry* 33:6631-6641.

Immenschuh, S. and Ramadori, G. 2000. Gene regulation of heme oxygenase-1 as a therapeutic target. *Biochem. Pharmacol.* 60:1121-1128.

Kitagawa, T., Nagai, K., and Tsubaki, M. 1979. Assignment of the Fe-Nepsilon (His F8) stretching band in the resonance Raman spectra of deoxy myoglobin. *FEBS Lett.* 104:376-378.

Liu, Y. and Ortiz de Montellano, P.R. 2000. Reaction intermediates and single turnover rate constants for the oxidation of heme by human heme oxygenase-1. *J. Biol. Chem.* 275:5297-5307.

Maines, M.D. 1992. Heme Oxygenase: Clinical Applications and Functions. CRC Press, Boca Raton, Fla.

Maines, M.D., Trakshel, G.M., and Kutty, R.K. 1986. Characterization of two constitutive forms of rat liver microsomal heme oxygenase: Only one molecular species of the enzyme is inducible. *J. Biol. Chem.* 261:411-419.

McCoubrey, W.K., Huang, T.J., and Maines, M.D. 1997. Isolation and characterization of a cDNA from the rat brain that encodes hemoprotein heme oxygenase-3. *Eur. J. Biochem.* 247:725-732.

Ortiz de Montellano, P.R. 2000. The mechanism of heme oxygenase. *Curr. Opin. Chem. Biol.* 4:221-227.

Ortiz de Montellano, P.R. and Wilks, A. 2000. Heme oxygenase structure and mechanism. *Adv. Inorg. Chem.* 51:359-402.

Otterbein, L.E. and Choi, A.M. 2000. Heme oxygenase: Colors of defense against cellular stress. *Am. J. Physiol. Lung Cell Mol. Physiol.* 279:L1029-L1037.

Otterbein, L., Sylvester, S.L., and Choi, A.M. 1995. Hemoglobin provides protection against lethal endotoxemia in rats: The role of heme oxygenase-1. *Am. J. Respir. Cell. Mol. Biol.* 13:595-601.

Otterbein, L.E., Bach, F.H., Alam, J., Soares, M., Tao Lu, H., Wysk, M., Davis, R.J., Flavell, R.A., and Choi, A.M. 2000. Carbon monoxide has anti-inflammatory effects involving the mitogen-activated protein kinase pathway. *Nat. Med.* 6:422-428.

Poss, K.D. and Tonegawa, S. 1997a. Heme oxygenase 1 is required for mammalian iron reutilization. *Proc. Natl. Acad. Sci. U.S.A.* 94:10919-10924.

Poss, K.D. and Tonegawa, S. 1997b. Reduced stress defense in heme oxygenase 1-deficient cells. *Proc. Natl. Acad. Sci. U.S.A.* 94:10925-10930.

Rotenberg, M.O. and Maines, M.D. 1990. Isolation, characterization, and expression in *Escherichia coli* of a cDNA encoding rat heme oxygenase-2. *J. Biol. Chem.* 265:7501-7506.

Schuller, D.J., Wilks, A., Ortiz de Montellano, P.R., and Poulos, T.L. 1999. Crystal structure of human heme oxygenase-1. *Nat. Struct. Biol.* 6:860-867.

Shibahara, S., Muller, R., Taguchi, H., and Yoshida, T. 1985. Cloning and expression of cDNA for rat heme oxygenase. *Proc. Natl. Acad. Sci. U.S.A.* 82:7865-7869.

Shibahara, S., Yoshizawa, M., Suzuki, H., Takeda, K., Meguro, K., and Endo, K. 1993. Functional analysis of cDNAs for two types of human heme oxygenase and evidence for their separate regulation. *J. Biochem. (Tokyo)* 113:214-218.

Smulevich, G., Mauro, J.M., Fishel, L.A., English, A.M., Kraut, J., and Spiro, T.G. 1988. Heme pocket interactions in cytochrome *c* peroxidase studied by site- directed mutagenesis and resonance Raman spectroscopy. *Biochemistry* 27:5477-5485.

Snyder, S.H., Jaffrey, S.R., and Zakhary, R. 1998. Nitric oxide and carbon monoxide: Parallel roles as neural messengers. *Brain Res. Brain Res. Rev.* 26:167-175.

Spiro, T.G. and Czernuszewicz, R.S. 1995. Resonance Raman spectroscopy of metalloproteins. *Methods Enzymol.* 246:416-460.

Stevens, C.F. and Wang, Y. 1993. Reversal of long-term potentiation by inhibitors of haem oxygenase [see comments]. *Nature* 364:147-149.

Stocker, R. 1990. Induction of haem oxygenase as a defence against oxidative stress. *Free Radic. Res. Commun.* 9:101-112.

Stocker, R., Yamamoto, Y., McDonagh, A.F., Glazer, A.N., and Ames, B.N. 1987. Bilirubin is an antioxidant of possible physiological importance. *Science* 235:1043-1046.

Sun, J., Wilks, A., Ortiz de Montellano, P.R., and Loehr, T.M. 1993. Resonance Raman and EPR spectroscopic studies on heme-heme oxygenase complexes. *Biochemistry* 32:14151-14157.

Verma, A., Hirsch, D.J., Glatt, C.E., Ronnett, G.V., and Snyder, S.H. 1993. Carbon monoxide: A putative neural messenger [see comments] [published erratum appears in *Science* 1994. 263:15]. *Science* 259:381-384.

Weber, C.M., Eke, B.C., and Maines, M.D. 1994. Corticosterone regulates heme oxygenase-2 and NO synthase transcription and protein expression in rat brain. *J. Neurochem.* 63:953-962.

Wilks, A. and Ortiz de Montellano, P.R. 1993. Rat liver heme oxygenase: High level expression of a truncated soluble form and nature of the meso-hydroxylating species. *J. Biol. Chem.* 268:22357-22362.

Wilks, A., Black, S.M., Miller, W.L., and Ortiz de Montellano, P.R. 1995. Expression and characterization of truncated human heme oxygenase (hHO-1) and a fusion protein of hHO-1 with human cytochrome P450 reductase. *Biochemistry* 34:4421-4427.

Wilks, A., Torpey, J., and Ortiz de Montellano, P.R. 1994. Heme oxygenase (HO-1): Evidence for electrophilic oxygen addition to the porphyrin ring in the formation of alpha-meso-hydroxyheme. *J. Biol. Chem.* 269:29553-29556.

Yasukochi, Y. and Masters, B.S. 1976. Some properties of a detergent-solubilized NADPH-cytochrome *c* (cytochrome P-450) reductase purified by biospecific affinity chromatography. *J. Biol. Chem.* 251:5337-5344.

Yoshida, T., Noguchi, M., and Kikuchi, G. 1980. A new intermediate of heme degradation catalyzed by the heme oxygenase system. *J. Biochem. (Tokyo)* 88:557-563.

Yoshida, T., Noguchi, M., and Kikuchi, G. 1982. The step of carbon monoxide liberation in the sequence of heme degradation catalyzed by the reconstituted microsomal heme oxygenase system. *J. Biol. Chem.* 257:9345-9348.

Contributed by Angela Wilks
University of Maryland
Baltimore, Maryland

CHAPTER 10
The Nitric Oxide/Guanylate Cyclase Pathway

INTRODUCTION

No other single molecule has such a multiplicity of biological effects as nitric oxide (NO). This simple molecule, which acts in a fairly specific manner, is now recognized as playing an integral part in various homeostatic mechanisms—including those of the central and peripheral nervous systems and cardiovascular system, as well as host-defense interactions—where it can directly alter vital functions; it also affects gene expression. Among NO's most crucial roles are its activities as a brain neurotransmitter and in the regulation of blood pressure. NO was cited in over 8000 papers in the 1990s. Its importance is underscored by the fact that within a few years after its production in the body was first demonstrated, it had become the most heavily studied molecule in the history of modern science. It was declared molecule of the year by *Science* in 1992; in 1998, the Nobel Prize for physiology and medicine was awarded to key investigators in the field.

UNIT 10.1 initiates this chapter by providing an overview of the NO formation pathway and elaborating on the molecule's many functions, with emphasis on those relating to the immune and vascular systems.

The next several units cover methods for detecting NO activity in a wide range of biological systems using a variety of different approaches. In *UNIT 10.2*, NO synthase activity is measured—as an indication of NO production—by a radiometric assay in which labeled arginine is used as the enzyme substrate. This approach can be applied to all types of biological systems, from cells in culture to tissue extracts.

A second strategy is based on NO's status as a free radical, possessing an unpaired electron that can react with amino acid side chains and cause nitrosylation of proteins. Detection of nitrosated proteins is an effective means to assess NO production and activity. *UNITS 10.3 & 10.4* describe several methods that can be used to detect NO metabolites and protein derivatives. Also discussed in *UNIT 10.4* is the direct detection of NO in cellular systems and chemical reactions.

An indirect means to measure NO production while directly assessing the its biological function is to measure cGMP, which is produced by activation of soluble guanylyl activity. *UNIT 10.5* describes methods for determining tissue levels of cGMP and measuring guanylyl cyclase activity. Experimenters should be cautioned that cGMP is produced by the activation of guanylyl cyclase through interaction with NO or CO. Therefore, tissue cGMP level should not be directly equated with NO synthase activity or NO production.

Histochemical analysis is a nearly indispensable tool for detecting the pattern of NO synthase expression in tissues. This method of analysis is of similar value to the visualization of the cyclic nucleotide cGMP in tissues. Protocols for such analyses are provided in *UNIT 10.6* and *UNIT 10.7*, respectively.

Contributed by Mahin D. Maines
Current Protocols in Toxicology (2000) 10.0.1-10.0.2

Nitric oxide, being a highly reactive molecule, is capable of forming various derivatives in biological systems. The biological effect of nitrogen oxide species depends on the chemistry of the intermediates formed and the chemical reactions they are involved in. Determination of which reactions are relevant to different toxicological mechanisms is challenging. *UNIT 10.8* provides methods for distinguishing between oxidative and nitrosative chemistry of different nitrogen oxide species.

Because of the centrol role of NO in host defense mechanisms and the molecule's ability to alter expression of stress-responsive genes, measurement of the transcriptional regulation of inducible NO synthase (iNOS) is often needed to assess the impact of environmental stimuli on the cell. When stimulated, high levels of iNOS are expressed, and its expression can be specifically measured by northern blot analysis and, conveniently, from nitrite formation. *UNIT 10.9* provides procedures for mRNA analysis as well as a rapid method using the Greiss reaction to measure nitrite accumulation.

Mahin D. Maines

Overview of the Pathway and Functions of Nitric Oxide

WHAT IS NO?

Nitric oxide (NO) has been recognized for many years as a toxic, reactive free radical gas. Initially, most research on NO focused on its role in air pollution, as a component of cigarette smoke, and as a byproduct of microbial metabolism. More recently, however, NO has been discovered to be present in a wide variety of biological systems. NO was first shown to be the species previously defined as endothelium-derived relaxing factor (EDRF), which mediates the ability of substances such as acetylcholine and bradykinin to dilate blood vessels (Furchgott and Zawadski, 1980; Ignarro et al., 1987; Palmer et al., 1987). NO was then discovered to be the molecule responsible for the tumoricidal and bactericidal actions of macrophages (Hibbs et al., 1987). NO was also found to be released from cerebellar granule cells after exposure to glutamate analogs, suggesting a role in nervous system function (Garthwaite et al., 1988). These and subsequent studies indicate that NO is a unique biological molecule that functions in a variety of metabolic and signaling pathways.

NO is present in biological systems as a dissolved nonelectrolyte (except in the lung and paranasal sinus where it is present as a gas) that is not stored in any subcellular compartments. It is synthesized on demand and simply diffuses from the site of formation to the site of action. NO forms covalent and noncovalent linkages with protein and nonprotein targets, including the enzyme guanylate cyclase. NO is inactivated by diffusion away from its targets and by the formation of covalent linkages to the superoxide anion or scavenger proteins. Because the biological actions of NO are not controlled by conventional means, NO depends on its small size, diffusibility, membrane permeability, and reactivity to exert its effects (Dawson and Snyder, 1994). Furthermore, because the cell cannot sequester and regulate the local concentration of NO, regulation of NO synthesis is the key to regulating its biological activity.

PATHWAY OF NO FORMATION BY NITRIC OXIDE SYNTHASE

NO is formed directly from the guanidino nitrogen of L-arginine by the enzyme nitric oxide synthase (NOS) through a process that consumes five electrons and results in the formation of L-citrulline (Fig. 10.1.1). NOS is unusual among oxidative enzymes in that most other enzymes consume one or two electrons for similar functions. Initial attempts to purify NOS were unsuccessful, owing to the rapid loss of enzymatic activity upon purification. The loss of NOS activity was eventually attributed to separation from its necessary cofactor, calmodulin; this knowledge led to its purification to homogeneity from cerebellum (Bredt and Snyder, 1990). NOS was then isolated from macrophages and endothelial tissue (Jaffrey and Snyder, 1995). Purification of NOS led to

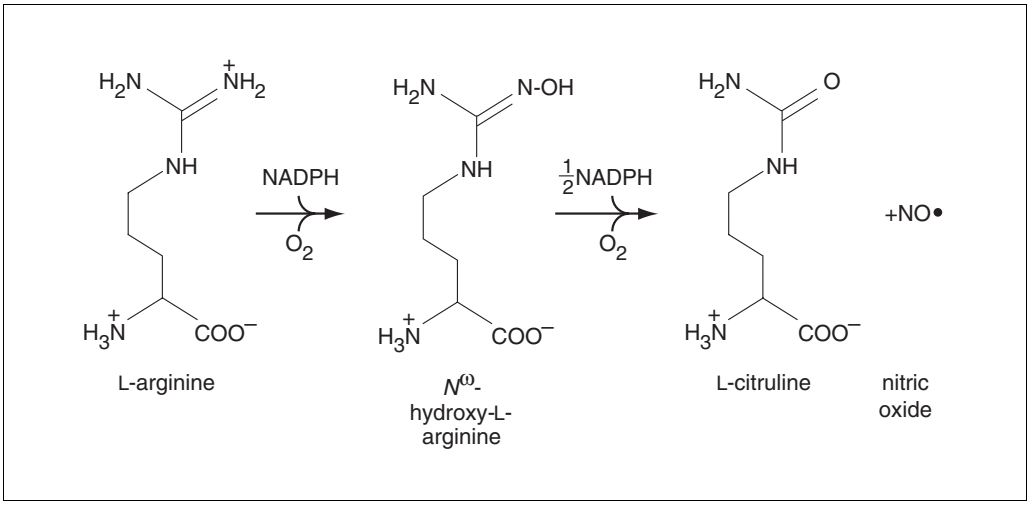

Figure 10.1.1 Biosynthesis of nitric oxide. NO is formed from L-arginine in two successive reactions. Both steps require NADPH, O_2, Ca^{2+}, and calmodulin and are enhanced by tetrahydrobiopterin.

Contributed by James F. Dillman, Valina L. Dawson, and Ted M. Dawson
Current Protocols in Toxicology (1999) 10.1.1-10.1.6

cloning of the cDNA for neuronal NOS (nNOS, type I; Bredt et al., 1991), which facilitated the subsequent cloning of macrophage NOS—also referred to as inducible NOS or immunologic NOS (iNOS, type II)—and endothelial NOS (eNOS, type III; Jaffrey and Snyder, 1995).

Cloning of NOS revealed 60% homology to cytochrome P-450 reductase (CPR) at the C-terminal portion of nNOS (Fig. 10.1.2; Bredt et al., 1991). The homology with CPR is shared by all NOS isoforms cloned and reflects the oxidative nature of NO biosynthesis. Both NOS and CPR contain specific recognition sites for NADPH, flavin mononucleotide (FMN), and flavin adenine dinucleotide (FAD), which bind NOS stoichiometrically. These are the only mammalian enzymes known to contain recognition sites for NADPH, FMN, and FAD (Dawson and Snyder, 1994). NOS also uses tetrahydrobiopterin as a cofactor. Tetrahydrobiopterin helps transform NOS into a catalytically active conformation and may also act as an oxidative-reductive cofactor. NOS contains heme, which reacts with CO. CO inhibits purified NOS, which is consistent with the participation of a cytochrome-P-450-type heme in the reaction. Moreover, NO itself appears to interact with the enzyme's heme and inhibit its own formation, thus exerting feedback inhibition (Marletta, 1994).

The catalytic form of NOS is a dimer. Dimerization requires the presence of heme, tetrahydrobiopterin, and arginine; heme and tetrahydrobiopterin become associated with the dimer during assembly. Dimerization alone is not sufficient for electron flow; calmodulin binding is also required. The mechanism of electron transfer is likely to be similar to that of the cytochrome P-450 enzymes, in that NADPH reduces FAD, which subsequently reduces FMN, which in turn transfers electrons to the ferric heme, promoting the interaction with molecular oxygen (Dawson and Snyder, 1994). Calmodulin binding appears to permit electron transfer both from NADPH to the flavins and from the flavins onto heme. The calmodulin-binding site lies between the putative P-450 oxygenase domain, which contains the heme-, tetrahydrobiopterin-, and arginine-binding sites, and the CPR domain, located in the C-ter-

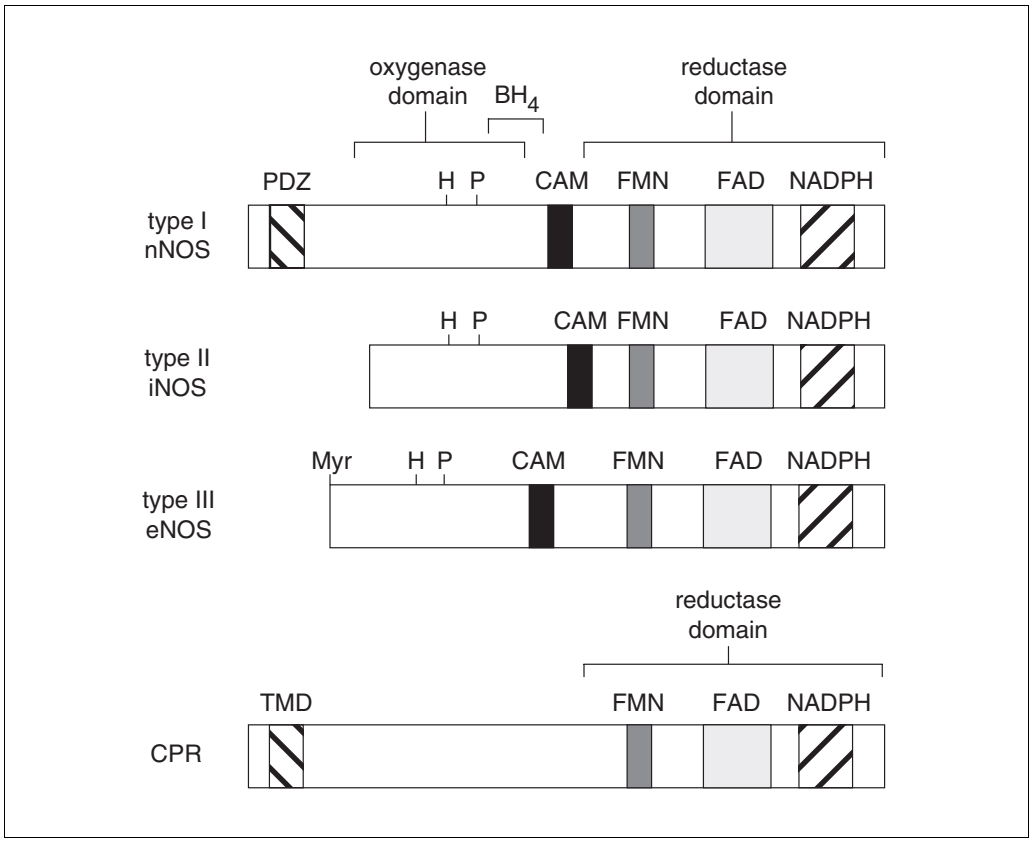

Figure 10.1.2 Isoforms of NOS compared to CPR. PDZ, PDZ domain; H, heme binding site; P, consensus sequence for phosphorylation by cAMP-dependent protein kinase; BH_4, tetrahydrobiopterin binding site; CAM, calmodulin binding site; FMN, flavin mononucleotide binding site; FAD, flavin adenine dinucleotide binding site; NADPH, NADPH binding domain; TMD, transmembrane domain; Myr, myristoylation site.

minal 60% of NOS. Elevation of intracellular calcium levels allows calmodulin to bind calcium and become competent to bind eNOS and nNOS. In contrast, the calmodulin of iNOS is very tightly bound, and thus is constitutively capable of transferring electrons to heme even in the absence of elevated intracellular calcium (Marletta, 1994).

eNOS and nNOS are constitutive, and are sometimes designated cNOS because substantial levels of basal enzyme protein exist in cells; in contrast, macrophages contain negligible levels of iNOS enzyme, and new enzyme is formed in response to stimuli. The categories defining the NOS isoforms are not absolute. Although constitutive forms of NOS were thought to be activated only by calcium-calmodulin interactions and not by new enzyme synthesis, recent findings show dramatic increases in nNOS synthesis in response to nerve damage and other stimuli. Recently, nNOS was found in non-neuronal tissues, such as skeletal muscle, respiratory and gastrointestinal epithelium, white blood cells, and pancreatic and uterine tissues. eNOS occurs in neuronal subpopulations in the brain. iNOS occurs in many tissues besides macrophages (Jaffrey and Snyder, 1995).

The constitutive and inducible forms of NOS are controlled differently. nNOS and eNOS are activated by increases in intracellular calcium. In the brain, glutamate acting at *N*-methyl-D-aspartate (NMDA) receptors triggers an influx of calcium that binds to calmodulin to activate nNOS. Glutamate can triple nNOS activity in brain slices in a matter of seconds. In endothelial cells, acetylcholine or bradykinin receptor activation stimulates the phosphoinositide cycle, generating the calcium that activates eNOS. iNOS is catalytically active in the absence of calcium, because calmodulin is tightly bound to the enzyme. Under basal conditions, macrophages have no detectable iNOS activity, whereas stimuli such as lipopolysaccharide and interferon γ stimulate new iNOS protein formation in a few hours (Nathan and Xie, 1994).

FUNCTIONS OF NO

NO in the Nervous System

NO is a regulator of neurotransmitter release. NOS inhibitors block neurotransmitter release in brain slices and synaptosomes. In synaptosomes, neurotransmitter release evoked by stimulation of NMDA receptors is blocked by NOS inhibitors, whereas release by potassium depolarization is unaffected. Presumably, glutamate acts at NMDA receptors located in NOS nerve terminals, stimulating the formation of NO, which diffuses to adjacent terminals to augment neurotransmitter release. In contrast, potassium depolarizes all terminals so that effects of the limited populations of NOS terminals are not detectable (Jaffrey and Snyder, 1995).

Stimulating NMDA receptors in cerebellar slices with glutamate or NMDA itself augments NOS activity and cGMP levels as rapidly as one can measure, and both increases are blocked by NOS inhibitors. Whether NO is the primary regulator of cGMP throughout the brain is unclear, because localization of nNOS and guanylate cyclase differ. Localizations of guanylate cyclase more closely parallel those of heme oxygenase 2, the enzyme that synthesizes carbon monoxide, which can also stimulate guanylate cyclase (Dawson and Snyder, 1994).

Initial immunohistochemical mapping of nNOS detected specific staining in many parts of the peripheral autonomic nervous system. Neurons of the myenteric plexus throughout the gastrointestinal pathway possess NOS. These nitrergic neurons, formerly termed nonadrenergic and noncholinergic (NANC) neurons, are involved in the relaxation phase of peristalsis. NOS inhibitors selectively block NANC neurotransmission (Bult et al., 1990; Desai et al., 1991). Furthermore, nNOS knockout mice display markedly enlarged stomachs with hypertrophy of the pyloric sphincter, a syndrome that resembles the human disease infantile hypertrophic pyloric stenosis (Huang et al., 1993).

Autonomic neurons of the pelvic plexus and its axonal processes that form the cavernous nerve, which innervates penile blood vessels, also contain nNOS, as do the projections of the nerve plexus into the arterial sinusoids in the periphery of the corpora cavernosa, the erectile tissue of the penis. NANC neuronal stimulation relaxes isolated cavernosal strips, and this effect is blocked by NOS inhibitors. Penile erection elicited by electrical stimulation of the cavernous nerve is blocked by low doses of NOS inhibitors (Burnett et al, 1992; Rajfer et al., 1992). nNOS knockout mice, however, display normal copulatory activity, procreate normally, and obtain erections upon stimulation of the cavernous nerve. Therefore, other mechanisms must compensate for the loss of nNOS (Huang et al., 1993).

NO may also participate in nervous system development. nNOS is expressed transiently in the cerebral cortical plate of rats, especially at

embryonic days 15 to 19, when the majority of the cells in the plate stain along with their processes, which project to the thalamus. The innervation gradually decreases after birth and is absent in adults. Similarly, embryonic sensory ganglia all stain for nNOS, as do embryonic olfactory neurons, whereas in both cases, staining is absent in adults (Jaffrey and Snyder, 1995). In long-term potentiation (LTP), enhancement of transmitter release by Schaeffer collaterals is thought to require release by pyramidal cells of a retrograde messenger. NOS inhibitors interfere with the establishment of LTP, as does hemoglobin, which binds NO. Some NOS inhibitors are active when injected directly into pyramidal cells (O'Dell et al., 1991; Schuman and Madison 1991; Haley et al., 1992). Recently, strong evidence supporting a role for NO in LTP has been obtained using transgenic mice null for both eNOS and nNOS (Son et al., 1996) and in hippocampal cultures using NOS inhibitors, NO scavengers, and photoactivatable NO donors (Arancio et al., 1996).

Studies in nNOS knockout mice provide insight into behavioral roles for NO (Nelson et al., 1995). Male knockout mice mount females indiscriminately, regardless of whether the females are in estrus or not. When wild-type male mice are housed together, they fight; but within an hour or so they establish appropriate hierarchical relationships. By contrast, male knockout mice fight almost incessantly, sometimes to the death. Thus nNOS knockouts appear to lose behavioral inhibition.

Excess production of NO in the nervous system is neurotoxic. NO has been shown to mediate glutamate excitotoxicity, which is the primary mode of neurotoxicity in cerebral ischemia (Dawson et al., 1991). nNOS knockout mice are more resistant to cerebral ischemia than are wild-type controls (Huang et al., 1994). The neurotoxic effects of NO are mediated by its interaction with the superoxide anion, which forms the highly neurotoxic species peroxynitrite, leading to the activation of pathways that deplete cellular energy substrates and result in cell death (Dawson and Snyder, 1994).

NO in the Immune System

NO is effective against various microbes, tumor cells, and alloantigens. iNOS is not detectable in healthy tissue but is expressed after immunologic challenge or injury. The induction of iNOS can be mediated by cytokines and by microbial products. In addition to macrophages and microglia, iNOS under pathologic conditions can be expressed in most tissues, including neurons, astrocytes, and endothelial cells (Nathan and Xie, 1994).

NO formation is increased during inflammation (e.g., arthritis), and several classic inflammatory symptoms are reversed by NOS inhibitors. Furthermore, unregulated NO synthesis becomes self-destructive and may play a role in disorders such as autoimmune disease, immune rejection of allografted organs, graft-versus-host disease, and sepsis. These proinflammatory effects of NO are not evident under acute physiologic conditions, in which NO can mediate anti-inflammatory functions, such as inhibition of neutrophil adhesion, cyclooxygenase activity, and cytokine formation (Schmidt and Walter, 1994). Induction of iNOS can take place under neuropathologic conditions (Iadecola, 1997). iNOS knockout mice have markedly reduced defenses against microorganisms (e.g., *Listeria* and *Leishmania*), and against the proliferation of lymphoma tumor cells. These animals are, however, resistant to carrageenan inflammation and hypotension elicited by endotoxin (MacMicking et al., 1995; Wei et al., 1995).

NO in the Vascular System

NO is a major regulator of vascular hemodynamics and is the primary messenger molecule mediating blood vessel relaxation (Ignarro et al., 1987; Palmer et al., 1987). Attempts to understand the vasodilatory effects of organic nitrates and the mechanisms of acetylcholine-induced relaxation of vascular smooth muscle led to the discovery that endothelially derived NO is critical in the regulation of vascular hemodynamics and that NO represents the long-sought endothelium-derived relaxing factor (EDRF). NO relaxes blood vessels by binding to iron in the heme at the active site of guanylate cyclase, thereby activating the enzyme to generate cGMP. Both shear stress and deformation of vascular endothelium, which accompany pulsatile flow through blood vessels, stimulate NO release through poorly defined mechanisms (Moncada and Higgs, 1993).

eNOS knockout mice exhibit deficient acetylcholine vasodilation, and their mean blood pressure is higher than that of control animals (Huang et al., 1995). eNOS may play a protective role in cerebral ischemia by maintaining regional cerebral blood flow, because transgenic mice that lack eNOS experience increased infarct volumes after middle cerebral artery occlusion (Huang et al., 1995). Endothelial functions, including NO release and action,

are clearly impaired or dysregulated in important vascular diseases such as atherosclerosis; hypertension; diabetes; reperfusion injury; and vasculopathy associated with angioplasty, bypass surgery, and transplantation, although the molecular mechanisms are as yet unclear.

SUMMARY

In a relatively short period of time, understanding of the diverse functions of NO in mammalian systems has grown immensely. Having been recognized as a bona fide cellular signaling molecule, NO has changed our understanding of what constitutes a physiologic signal. Undoubtedly, new roles for NO will be found in an even greater number of biological processes.

LITERATURE CITED

Arancio, O., Kiebler, M., Lee, C.J., Lev-Ram, V., Tsien, R.Y., Kandel, E.R., and Hawkins, R.D. 1996. Nitric oxide acts directly in the presynaptic neuron to produce long-term potentiation in cultured hippocampal neurons. *Cell* 87:1025-1035.

Bredt, D.S. and Snyder, S.H. 1990. Isolation of nitric oxide synthetase, a calmodulin-requiring enzyme. *Proc. Natl. Acad. Sci. U.S.A.* 87:682-685.

Bredt, D.S., Hwang, P.H., Glatt, C., Lowenstein, C., Reed, R.R., and Snyder, S.H. 1991. Cloned and expressed nitric oxide synthase structurally resembles cytochrome P-450 reductase. *Nature* 351:714-718.

Bult, H., Boeckxstaens, G.E., Pleckmans, P.A., Jordaens, F.H., Van Maercke, Y.M., and Herman, A.G. 1990. Nitric oxide as an inhibitory non-adrenergic non-cholinergic neurotransmitter. *Nature* 345:346-347.

Burnett, A.L., Lowenstein, C.J., Bredt, D.S., Chang, T.S.K., and Snyder, S.H. 1992. Nitric oxide: A physiologic mediator of penile erection. *Science* 257:401-403.

Dawson, T.M. and Snyder, S.H. 1994. Gases as biological messengers: Nitric oxide and carbon monoxide in the brain. *J. Neurosci.* 14:5147-5159.

Dawson V.L., Dawson T.M., London E.D., Bredt D.S., and Snyder S.H. 1991. Nitric oxide mediates glutamate neurotoxicity in primary cortical cultures. *Proc Natl. Acad. Sci. U.S.A.* 88:6368-6371.

Desai, K.M., Sessa, W.C., and Vane, J.R. 1991. Involvement of nitric oxide in the reflex relaxation of the stomach to accommodate food or fluid. *Nature* 351:477-479.

Furchgott, R.F. and Zawadski, J.V. 1980. The obligatory role of endothelial cells in the relaxation of arterial smooth muscle by acetylcholine. *Nature* 288:373-376.

Garthwaite, J., Charles, S.L., and Chess-Williams, R. 1988. Endothelium-derived relaxing factor release on activation of NMDA receptors suggests role as intercellular messenger in the brain. *Nature* 336:385-388.

Haley, J.E., Wilcox, G.L., and Chapman, P.F. 1992. The role of nitric oxide in hippocampal long-term potentiation. *Neuron* 8:211-216.

Hibbs, J.B. Jr., Taintor, R.R., and Vavrin, Z. 1987. Macrophage cytotoxicity: Role for L-arginine deaminase and imino nitrogen oxidation to nitrite. *Science* 235:473-476.

Huang, P.L., Dawson, T.M., Bredt, D.S., Snyder, S.H., and Fishman, M.C. 1993. Targeted disruption of the neuronal nitric oxide synthase gene. *Cell* 75:1273-1286.

Huang, Z., Huang, P.L., Panahian, N., Dalkara, T., Fishman, M.C., and Moskowitz, M.A. 1994. Effects of cerebral ischemia in mice deficient in neuronal nitric oxide synthase. *Science* 265:1883-1885.

Huang, P.L., Huang, Z.H., Mashimo, H., Bloch, K.D., Moskowitz, M.A., Bevan, J.A., and Fishman, M.C. 1995. Hypertension in mice lacking the gene for endothelial nitric oxide synthase. *Nature* 377:239-242.

Iadecola, C. 1997. Bright and dark sides of nitric oxide in ischemic brain injury. *Trends Neurosci.* 20:132-139.

Ignarro, L.J., Buga, G.M., Wood, K.S., Bryns, R.E., and Chaudhuri, G. 1987. Endothelium-derived relaxing factor produced and released from artery and vein is nitric oxide. *Proc. Natl. Acad. Sci. U.S.A.* 84:9265-9269.

Jaffrey, S.R. and Snyder, S.H. 1995. Nitric oxide: A neural messenger. *Annu. Rev. Cell Dev. Biol.* 11:417-440.

MacMicking, J.D., Nathan, C., Hom, G., Chartrain, N., Fletcher, D.S., Trumbauer, M., Stevens, K., Xie, Q.W., Sokol, K., Hutchinson, N., Chen, H., and Mudgett, J.S. 1995. Altered responses to bacterial infection and endotoxic shock in mice lacking inducible nitric oxide synthase. *Cell* 81:641-650.

Marletta, M.A. 1994. Nitric oxide synthase: Aspects concerning structure and catalysis. *Cell* 78:927-930.

Moncada, S. and Higgs, A. 1993. The L-arginine-nitric oxide pathway. *N. Engl. J. Med.* 329:2002-2012.

Nathan, C. and Xie, Q.-W. 1994. Nitric oxide synthases: Roles, tolls, and controls. *Cell* 78:915-918.

Nelson, R.J., Demas, G.E., Huang, P.L., Fishman, M.C., Dawson, V.L., Dawson, T.M., and Snyder, S.H. 1995. Behavioral abnormalities in male mice lacking neuronal nitric oxide synthase. *Nature* 378:383-385.

O'Dell, T.J., Hawkins, R.D., Kandel, E.R., and Arancio, O. 1991. Tests of the roles of two diffusible substances in long-term potentiation: Evidence for nitric oxide as a possible early retrograde messenger. *Proc. Natl. Acad. Sci. U.S.A.* 88:11285-11289.

Palmer, R.M.J., Ferrige, A.G., and Moncada, S. 1987. Nitric oxide release accounts for the bio-

logical activity of endothelium-derived relaxing factor. *Nature* 327:524-526.

Rajfer, J., Aronson, W.J., Bush, P.A., Dorey, F.J., and Ignarro, L.J. 1992. Nitric oxide as a mediator of the corpus cavernosum in response to nonadrenergic noncholinergic transmission. *N. Engl. J. Med.* 326:90-94.

Schmidt, H.H.H.W. and Walter, U. 1994. NO at work. *Cell* 78:919-925.

Schuman, E.M. and Madison, D.V. 1991. A requirement for the intercellular messenger nitric oxide in long-term potentiation. *Science* 254:1503-1506.

Son, H., Hawkins, R.D., Martin, K., Kiebler, M., Huang, P.L., Fishman, M.C., and Kandel, E.R. 1996. Long-term potentiation is reduced in mice that are doubly mutant in endothelial and neuronal nitric oxide synthase. *Cell* 87:1015-1023

Wei, X.-Q., Charles, I.G., Smith, A., Ure, J., Feng, G.-J., Huang, F.-P., Xu, D, Muller, W, Moncada, S., and Liew, F.Y. 1995. Altered immune responses in mice lacking inducible nitric oxide synthase. *Nature* 375:408-411.

KEY REFERENCES

Bredt et al., 1991. See above.

Reports the initial cloning of nitric oxide synthase, specifically the neuronal isoform, and led to the understanding of the functional domains of the enzyme.

Furchgott and Zawadski, 1980. See above

Reports the role for an endothelium-derived relaxing factor (EDRF) in the dilation of blood vessels, which would later be identified as nitric oxide.

Garthwaite et al., 1988. See above.

Initial report suggesting that nitric oxide plays a role in neuronal signaling. Subsequent reports would define nitric oxide as one of a new class of neurotransmitters.

Hibbs et al., 1987. See above.

Identification of a role for nitric oxide in the cytotoxic capabilities of macrophages.

Palmer et al., 1987. See above.

Identification of nitric oxide as the signaling molecule representing EDRF.

Contributed by James F. Dillman, Valina L. Dawson, and Ted M. Dawson
Johns Hopkins University School of Medicine
Baltimore, Maryland

Assay of Tissue Activity of Nitric Oxide Synthase

Nitric oxide synthase (NOS) activity can be assayed by several techniques that are based on the formation of either NO or L-citrulline. Among these methods, which include the quantitation of NO (or NO-derived metabolites) by UV/VIS spectroscopy, fluorescence spectroscopy (*UNIT 10.4*), electron paramagnetic resonance (EPR) spectroscopy, chemiluminescence or bioassay, the conversion of radiolabeled L-arginine to L-citrulline is the most widely used. The assay is very sensitive, simple to perform, and relatively robust. As described in this unit, it can be used to determine NOS activity in either intact cells (see Basic Protocol 1) or cell and tissue extracts (see Basic Protocol 2). Both protocols are based on the separation of [^{3}H]L-citrulline from [^{3}H]L-arginine by cation-exchange chromatography, a simple and time-saving technique that allows parallel processing of many samples. Detailed instructions for preparation and maintenance of the chromatography columns are also provided (see Support Protocol 1). Because the sensitivity of the assay depends critically on the purity of the radiolabeled substrate, an additional support protocol is supplied that describes the purification of [^{3}H]L-arginine by HPLC (see Support Protocol 2). Throughout all protocols, [^{14}C]L-arginine can be substituted for [^{3}H]L-arginine if desired. These procedures have been successfully applied to a broad range of cell types (see Anticipated Results for examples).

DETERMINING NOS ACTIVITY IN INTACT MONOLAYER CELLS

BASIC PROTOCOL 1

This protocol describes the determination of NOS activity in freshly isolated or cultured cells, and provides a simple and rapid means for assessing the responsiveness and sensitivity of cellular NOS to different stimuli. The method is based on the conversion of incorporated [^{3}H]L-arginine to [^{3}H]L-citrulline and can be applied to adherent or suspended cells. After appropriate isolation and/or culture procedures, cells are washed with buffer and incubated with [^{3}H]L-arginine and the compound(s) to be tested. After removal of extracellular [^{3}H]L-arginine, the reaction is terminated by lysis of the cells with HCl. To determine the amount of [^{3}H]L-arginine incorporated, a sample of the cell extract is removed and radioactivity is measured by liquid-scintillation spectrometry. The remaining extract is subjected to cation-exchange chromatography followed by the quantification of [^{3}H]L-citrulline in the eluate. Results are calculated as percent conversion of incorporated [^{3}H]L-arginine to [^{3}H]L-citrulline and corrected for blank levels obtained in the presence of a NOS inhibitor.

The procedure described here is for cell monolayers cultured in six- or twelve-well plates. It is recommended that the experiment be performed in triplicate wells for each test condition. Moreover, each set of assays requires control incubations in the presence of a NOS inhibitor, e.g., 100 µM N^G-nitro-L-arginine (L-NNA) or N^G-monomethyl-L-arginine (L-NMA).

CAUTION: When working with radioactivity, take appropriate precautions to avoid contamination of the experimenter and the surroundings. Carry out the experiment and dispose of wastes in an appropriately designated area, following the guidelines provided by the local radiation safety officer (see *APPENDIX 1A*).

NOTE: Because unlabeled L-arginine diminishes the uptake of [^{3}H]L-arginine, experiments should be performed in L-arginine-free buffer to achieve maximum sensitivity of the assay.

Contributed by Kurt Schmidt and Bernd Mayer
Current Protocols in Toxicology (1999) 10.2.1-10.2.13

Materials

Confluent monolayer culture
HEPES-buffered salt solution, pH 7.4 (see recipe), prewarmed to 37°C
10 mM N^G-nitro-L-arginine (L-NNA) or N^G-monomethyl-L-arginine (L-NMA) in water
[2,3,4,5-^{3}H]L-arginine (HPLC-purified, see Support Protocol 2) in HEPES-buffered salt solution (~10,000 cpm/µl)
Stock solution of compound to be tested, prepared as 20× stock solution in HEPES-buffered salt solution or an appropriate solvent (see step 3 annotation)
0.01 N HCl
Scintillation cocktail
Sodium acetate buffer with L-citrulline (see recipe)
[^{3}H]L-citrulline in 0.01 HCl
Dowex 50W cation-exchange columns (for preparation and maintenance of columns, see Support Protocol 1)

Incubate cells with test compound and [^{3}H]L-arginine

1. Aspirate the culture medium and wash confluent monolayer twice with 1 ml of 37°C HEPES-buffered salt solution.

   Because culture media usually contain 0.3 to 3 mM L-arginine, at least two washes are required to minimize contamination of the buffer with residual L-arginine.

2. Add 0.9 ml HEPES-buffered salt solution to the washed cells. To determine blank levels, add 9 µl of 10 mM L-NNA or L-NMA to three wells. Agitate the plate, then place it into an incubator or onto a thermostated heating block, and incubate it 10 min at 37°C.

3. Add 50 µl of 10,000 cpm/µl [^{3}H]L-arginine in HEPES-buffered salt solution (~500,000 cpm) and 50 µl of a 20-fold stock solution of the compound to be tested. Agitate the plate, then incubate it 10 min at 37°C.

   In general, stock solution(s) of test compound(s) should be prepared in HEPES-buffered salt solution. If not possible, substances may be dissolved in 0.01 N HCl, 0.01 N NaOH, or an organic solvent (e.g., dimethyl sulfoxide), but proper controls are then required to exclude solvent effects.

4. Aspirate the incubation medium, and wash monolayer twice with 1 ml ice-cold HEPES-buffered salt solution.

   CAUTION: *Incubation medium is radioactive—pay attention to correct waste disposal!*

   For complete removal of extracellular [^{3}H]L-arginine, two washing steps are required. The use of ice-cold washing buffer is strongly recommended to stop cell metabolism rapidly. In the washing buffer, 1 mM ethylene glycol bis(β-aminoethylether-N,N,N′,N′-tetraacetic acid) (EGTA) may be substituted for $CaCl_2$ to block Ca^{2+}-dependent NOS activity.

5. Add 1 ml 0.01 N HCl to the washed cells. Leave plates at least 1 hr at room temperature to ensure complete release of intracellular [^{3}H]L-arginine and [^{3}H]L-citrulline.

Determine [^{3}H]L-arginine incorporation and [^{3}H]L-citrulline formation

6. Agitate the plate; then transfer 0.1 ml HCl extract to a scintillation counting vial and sequentially add 1.9 ml water and 5 ml scintillation cocktail. Mix, then count radioactivity in a liquid scintillation spectrometer to determine the amount of incorporated [^{3}H]L-arginine.

   Typically, 5 ml scintillation cocktail will be sufficient to achieve a homogenous solution, but a larger volume may be required if a scintillation cocktail with a low sample load capacity is used.

7. Add 0.1 ml sodium acetate buffer with L-citrulline to the remaining HCl extract.

   After adding the sodium acetate buffer with L-citrulline, the pH of the samples should be between 5.0 and 5.5. Thus each time a fresh solution of either HCl or sodium acetate buffer with L-citrulline is prepared, mix 0.9 ml HCl and 0.1 ml buffer and check the pH. If necessary, change the pH of the sodium acetate buffer with L-citrulline, mix it again with HCl, and measure the pH. Repeat this procedure until the desired pH is obtained.

8. Agitate the plate; then transfer the supernatant to the cation-exchange column and collect the effluent in a scintillation counting vial. Elute residual [^{3}H]L-citrulline with 1 ml water into the same vial, and add 5 ml scintillation cocktail. Mix, then count radioactivity to determine the amount of [^{3}H]L-citrulline formed.

   Treatment of cells with HCl disrupts cell membranes, but the resulting cell debris usually remains attached to surface of the culture dishes. If, however, loosening of the cell debris is observed, samples should be centrifuged 5 min at 10,000 to 15,000 × g before being transferred to the cation-exchange column.

Determine L-citrulline recovery

9. Prepare a solution of ~10,000 cpm/ml [^{3}H]L-citrulline in 0.01 N HCl. Mix 0.9 ml of this solution with 1.1 ml water and 5 ml scintillation cocktail in a scintillation counting vial; count radioactivity (= total cpm).
10. Mix another 0.9 ml of the [^{3}H]L-citrulline solution with 0.1 ml sodium acetate buffer with L-citrulline in a test tube and transfer the sample to the cation exchange column. Elute, and determine radioactivity as described in step 8 (= recovered cpm).
11. Divide recovered cpm by total cpm to calculate recovery of L-citrulline.

    The recovery of L-citrulline is usually between 0.8 and 0.9 (i.e., 80% to 90%). Because the elution profile may vary after prolonged use or storage of the columns, it is recommended that the recovery be checked periodically (e.g., each month).

Calculate results

12. Calculate the total radioactivity of incorporated [^{3}H]L-arginine:

$$\frac{\text{cpm (step 6)} \times \text{total volume of HCl extract (1 ml)}}{\text{sample volume (0.1 ml)}}$$

$$U: \frac{1100 \text{ cpm} \times 1 \text{ ml}}{0.1 \text{ ml}} = 11{,}000 \text{ cpm } (S: 12{,}000 \text{ cpm}, I: 11{,}500 \text{ cpm})$$

NOS activity in intact cells is expressed as percent conversion of incorporated [^{3}H]L-arginine into [^{3}H]L-citrulline. As an example, results from a typical assay performed with endothelial cells in six-well plates are given (U, unstimulated; S, stimulated with a Ca^{2+} ionophore; I, stimulated with a Ca^{2+} ionophore in the presence of L-NNA).

13. Calculate the total radioactivity of [^{3}H]L-citrulline formed:

$$\frac{\text{cpm (step 8)} \times \text{total volume of HCl extract (1 ml)}}{\text{sample volume (0.9 ml)} \times \text{recovery of L-citrulline}}$$

$$U: \frac{230 \text{ cpm} \times 1 \text{ ml}}{0.9 \text{ ml} \times 0.95} = 270 \text{ cpm } (S: 2600 \text{ cpm}, I: 150 \text{ cpm})$$

14. Calculate conversion of incorporated [^{3}H]L-arginine into [^{3}H]L-citrulline:

$$\frac{[^3\text{H}]\text{L-citrulline formed}}{\text{incorporated } [^3\text{H}]\text{ L-arginine}}$$

$$U: \frac{270 \text{ cpm}}{11{,}000 \text{ cpm}} \times 100 = 2.5\% \ (S: 21.7\%, I: 1.3\%)$$

15. Subtract the value of the NOS-inhibitor control (*I*) from those of the samples (*U*, *S*) to obtain NOS-dependent conversion of L-arginine into L-citrulline:

    Unstimulated: 1.2% conversion;
    Stimulated: 20.4% conversion.

ALTERNATE PROTOCOL 1

DETERMINING NOS ACTIVITY IN INTACT SUSPENSION CELLS

NOS activity can also be measured for cells that grow in suspension. It is recommended that the experiment be performed in triplicate for each test condition. Moreover, each set of assays requires control incubations in the presence of a NOS inhibitor (e.g., 100 µM NNA or L-NMA). Materials required for this procedure are the same as those used when assaying monolayer cells (see Basic Protocol 1).

1. Collect cells from suspension cultures and centrifuge 5 min at 400 × *g*, room temperature. Wash the pellet twice with 37°C HEPES-buffered salt solution and resuspend the final pellet to a concentration of 0.2–1 × 10^6cells/ml.
2. Transfer 0.9-ml aliquots of the cell suspension to 1.5-ml microcentrifuge tubes. To determine blank levels, add 9 µl of 10 mM L-NNA or L-NMA to three tubes. Mix sample, and place tube into a 37°C water bath or heating block. Incubate cells 10 min at 37°C.
3. Add 50 µl [^{3}H]L-arginine solution and 50 µl of a 20-fold stock solution of the compound to be tested. Incubate cells 10 min at 37°C, shaking the tube occasionally.
4. Sediment cells by centrifugation, 4°C, and wash the pellet twice with 1 ml ice-cold HEPES-buffered salt solution.

   CAUTION: *Incubation medium is radioactive—pay attention to correct waste disposal!*

   According to the authors' experience with various types of cells, centrifugation can be performed at 10,000 to 15,000 × g without disruption of cell membranes. Centrifugation at high speeds reduces the time required for sedimentation (~10 sec) and thus minimizes cell metabolism during the washing procedure.
5. Resuspend the pellet in 1 ml of 0.01 N HCl, and leave tube at least 1 hr at room temperature to ensure complete release of intracellular [^{3}H]L-arginine and [^{3}H]L-citrulline.
6. Vortex sample 5 to 10 sec. Transfer 0.1 ml cell suspension to a scintillation counting vial, and sequentially add 1.9 ml water and 5 ml scintillation cocktail. Mix, then count the radioactivity in a liquid scintillation spectrometer to determine the amount of incorporated [^{3}H]L-arginine.
7. To the remaining cell suspension (0.9 ml), add 0.1 ml sodium acetate buffer with L-citrulline. Mix the sample and centrifuge 5 min at 10,000 to 15,000 × *g*, room temperature, to sediment cell debris.
8. Transfer the supernatant to the cation-exchange column, and collect the effluent in a scintillation counting vial. Elute residual [^{3}H]L-citrulline with 1 ml water in the same vial and add 5 ml scintillation cocktail. After mixing, count radioactivity to determine the amount of L-[^{3}H]citrulline formed.
9. Calculate the results (see Basic Protocol 1, steps 9 to 15).

DETERMINING NOS ACTIVITY IN CELL OR TISSUE EXTRACTS

This protocol describes a sensitive enzyme assay that allows the determination of NOS activity in cell or tissue extracts. The assay can be carried out with cell homogenates, subcellular fractions, or (partially) purified NOS. Several methods are available for disrupting the cell membranes, but the efficacy of each technique may vary, depending on the type of cells or tissues used. In general, a mechanical homogenizer is a good choice for homogenizing intact tissues, whereas isolated and cultured cells are often more efficiently disrupted by sonication. After appropriate homogenization and centrifugation, NOS activity is assayed in the presence of [^{3}H]L-arginine, NADPH, Ca^{2+}/calmodulin, flavin adenine dinucleotide (FAD), flavin mononucleotide (FMN), and (6*R*)-5,6,7,8-tetrahydro-L-biopterin (H_4biopterin). Following termination of the reaction, [^{3}H]L-citrulline is separated from [^{3}H]L-arginine by cation-exchange chromatography, and [^{3}H]L-citrulline is quantified in the eluate by liquid scintillation spectrometry. Results are corrected for blank and column recovery, and NOS activity is expressed as formation of L-citrulline per minute and milligram of protein.

NOTE: Tissues should be either used immediately on collection or rapidly frozen and stored at −70°C. Preparation of tissue extracts should be performed at 4°C to avoid loss of enzyme activity.

Materials

Cells or tissue of interest
Phosphate-buffered saline (PBS; *APPENDIX 2A*), prewarmed to 37°C
Triethanolamine buffer with EDTA (see recipe)
Assay buffer with [^{3}H]L-arginine (see recipe)
Sodium acetate buffer with EDTA (see recipe)
Scintillation cocktail
[^{3}H]L-citrulline in sodium acetate buffer with EDTA (~10,000 cpm/ml)

Ultrasonic generator *or* mechanical tissue homogenizer (e.g., Polytron, Brinkman)
Cheesecloth or 100-μm-pore-size cell strainer
Protein assay kit (e.g., Bio-Rad kit for Bradford protein assay)
Dowex 50W cation exchange columns (for preparation and maintenance of columns, see Support Protocol 1)

Prepare extracts

For cell extracts

1a. Suspend adherent cells using a rubber policeman or cell scraper, and centrifuge cells 5 min at 400 × *g*, room temperature. Wash the pellet twice with 37°C PBS, and resuspend the final pellet in a small volume (typically 2 ml per ml pellet) of ice-cold triethanolamine buffer with EDTA

2a. Disrupt the cells by sonication (typically, four 10-sec pulses).

CAUTION: *Prolonged sonication will increase the temperature of the cell extract. Thus, sonicate cells in short bursts (~10 sec); allow sample to cool 50 sec in ice water in between bursts.*

For tissue extracts

1b. Working at 4°C, weigh a portion of the tissue (typically 0.5 to 5 g) and put it into a beaker. Add a measured volume of ice-cold triethanolamine buffer with EDTA (typically 5 ml/g tissue) and mince the tissue with scissors.

Perform steps 1b, 2b, and 3 to 5 at 4°C.

2b. Disrupt the chopped tissue using a standard mechanical homogenizer.

Depending on the type of tissue, the time required for homogenization may vary from 20 (brain or liver) to 60 sec (muscle). Alternatively, soft tissues (e.g., brain and liver) may be homogenized by six to eight strokes with a Potter-Elvehjem homogenizer (800 rpm).

For tissue and cell extracts

3. Filter homogenate through multiple layers of cheesecloth or a cell strainer (pore size 100 μm) to remove cell debris.

4. Either use the homogenate immediately to determine NOS activity (step 6 onward; keep preparations on ice until just before use) or store it at −70°C.

Alternatively, use the fresh homogenate for subcellular fractionation (Castle, 1995).

Depending on the type of tissue, homogenates may be stored up to 6 months at −70°C without considerable loss of enzyme activity.

5. Determine the protein concentration by a standard protein assay (e.g., Bradford assay, kit available from Bio-Rad).

Perform NOS assay

6. Put assay tube into a test tube rack on ice. Add 50 μl assay buffer with [^{3}H]L-arginine and 10 μl of a 10-fold stock solution of the compound to tested.

It is recommended that the experiment be performed in triplicate for each test condition. Moreover, each set of assays requires incubations in the absence of enzyme extract to obtain blank values.

7. Add 40 μl homogenate (enzyme extract; 1 to 10 mg protein/ml) and vortex the sample for ~5 sec. Put the tube into a 37°C water bath or heating block, and incubate the sample for 10 min.

To determine blanks, add 40 μl water instead of enzyme extract.

8. Terminate the reaction by adding 0.9 ml ice-cold sodium acetate buffer with EDTA. Vortex sample ~5 sec, and put tube on ice.

The stopped assays can be left on ice until the batch of incubations has been completed.

9. Transfer sample to the exchange column, and collect effluent in a scintillation counting vial. Elute residual [^{3}H]L-citrulline with 1 ml water in same vial, and add 5 ml scintillation cocktail. Mix, then count radioactivity in a liquid scintillation spectrometer to determine amount of [^{3}H]L-citrulline formed.

10. To determine the radioactivity of the [^{3}H]L-arginine added to the assay, mix 50 μl assay buffer with [^{3}H]L-arginine with 2 ml water and 5 ml scintillation cocktail in a scintillation counting vial; count radioactivity.

Determine L-citrulline recovery

11. To determine the recovery of L-citrulline, prepare a solution of authentic L-[^{3}H]citrulline in sodium acetate buffer with EDTA (~10,000 cpm/ml). Mix 1 ml of this solution with 1 ml water and 5 ml scintillation cocktail in a scintillation counting vial; count radioactivity (= total cpm).

It is recommended that the experiment be performed in triplicate.

12. Load another 1 ml [^{3}H]L-citrulline solution onto the cation-exchange column. Elute, and determine radioactivity as described in step 9 (= recovered cpm). Divide recovered cpm by total cpm to obtain recovery of L-citrulline.

The recovery of L-citrulline is usually between 0.8 and 0.9 (i.e., 80% to 90%). Because the elution profile may vary after prolonged use or storage of the columns, the recovery should be checked periodically (e.g., each month).

Calculate results

13. To correct values for blank and L-citrulline recovery, subtract radioactivity of the blank from that of the sample, and divide this value by the L-citrulline recovery:

$$\frac{1200 \text{ cpm} - 80 \text{ cpm}}{0.9} = 1244 \text{ cpm}$$

NOS activity is usually expressed as picomoles of L-citrulline formed per minute per milligrams of protein. As an example, results from a typical assay performed with a cytosolic fraction of cytokine-activated murine macrophages are as follows:

Assay volume: 100 µl
Final concentration of L-arginine: 100 µM (amount per tube: 10,000 pmol)
Radioactivity of [^{3}H]L-arginine added: 67,000 cpm
Radioactivity of blank: 80 cpm
Radioactivity of sample: 1200 cpm
Recovery of L-citrulline: 90%
Amount of protein added: 0.14 mg.

14. Multiply this value by the amount of L-arginine per assay, and divide by the radioactivity of the [^{3}H]L-arginine added to obtain the amount of L-citrulline formed:

$$\frac{1244 \text{ cpm} \times 10{,}000 \text{ pmol}}{67{,}000 \text{ cpm}} = 186 \text{ pmol L-citrulline}$$

15. Divide this value by the incubation time and the amount of protein to obtain the specific NOS activity:

$$\frac{186 \text{ pmol}}{10 \text{ min} \times 0.14 \text{ mg}} = 133 \text{ pmol L-citrulline} \times \text{min}^{-1} \times \text{mg}^{-1}$$

PREPARATION AND REGENERATION OF DOWEX 50W CHROMATOGRAPHY COLUMNS

SUPPORT PROTOCOL 1

The strongly acidic cation exchanger Dowex 50W can be used to achieve a simple and efficient separation of L-citrulline from L-arginine. This protocol describes preparation of chromatography columns and regeneration of the resin.

Materials

Cation-exchange resin (Dowex 50W, H^+ form, 200 to 400 mesh, 8% cross-linked)
Chromatography columns (bed volume 1 to 2 ml, e.g., Poly-Prep columns from Bio-Rad)
Ethanol
0.5 M and 1 M NaOH
1 M HCl

1. Suspend 100 g cation-exchange resin in 500 ml water. Allow the resin to settle for 20 to 30 min and decant the supernatant. Repeat this procedure as follows:

Four times with 500 ml water
Twice with 200 ml ethanol
Twice with 200 ml water
Once with 500 ml 0.5 M NaOH
Once with 500 ml 0.5 M NaOH, preheated to ~80°C
Three times with 500 ml water
Twice with 500 ml 1 M HCl
Three times with 500 ml water.

2. Resuspend the resin in 100 ml water and pipet 1.5-ml aliquots of the suspension into chromatography columns.

   The final volume of the settled resin in the column should be 0.6 to 0.8 ml.

   With 100 g resin, 80 to 100 columns of 1- to 2-ml bed volume can be filled. The suspension of the resin can be stored with sodium azide (~0.02% w/v) at 4°C.

3. Wash columns three times with 3 ml of 1 M NaOH to transform the resin into the Na^+ form.

4. Before use, wash columns three times with 10 ml water.

   Chromatography columns are most conveniently used if they are mounted in racks with spacing identical to that of the racks of the scintillation vials to be used.

5. After each experiment, regenerate the resin by washing once with 3 ml of 1 M NaOH and store columns dry at room temperature. Repeat the treatment with NaOH once or twice a week until the next use of the columns (step 4).

   CAUTION: *NaOH wash is radioactive—pay attention to correct waste disposal!*

   According to experience, flow rates may be markedly reduced when columns are not reused within a few days. This problem can be avoided by treating unused columns with NaOH every few days (see Critical Parameters and Troubleshooting).

SUPPORT PROTOCOL 2

PURIFY [^{3}H] L-ARGININE BY HPLC

Commercially available batches of [^{3}H]L-arginine often contain radiolabeled impurities that will coelute with [^{3}H]L-citrulline on Dowex 50W cation-exchange columns. Because this results in high blank levels (up to 5%) and thus decreased sensitivity of the NOS assay, [^{3}H]L-arginine should be purified before use. This protocol describes a simple and efficient method of purifying of [^{3}H]L-arginine by HPLC that reduces blank levels in the NOS assay to 0.1% to 0.2 %.

Materials

HPLC system
50 mM sodium acetate buffer, pH 6.4 (*APPENDIX 2A*)
[2,3,4,5-^{3}H]L-arginine (100 µCi)
Scintillation cocktail
Methanol
HPLC column (Nucleosil 100 10 SA, 4 mm × 250 mm)

1. Equilibrate the HPLC column with 50 mM sodium acetate buffer (pH 6.4) for 2 to 3 hr (flow rate 0.1 ml/min). Before the run, increase the flow rate gradually to 1.5 ml/min.

2. Set up the fraction collector to obtain 20-sec (= 0.5-ml) fractions in plastic vials.

3. Inject 100 µl of the [2,3,4,5-^{3}H]L-arginine solution (100 µCi) onto the equilibrated column and start the fraction collector. Collect 50 fractions.

   Typically, the retention time of L-arginine is ~12 min, but it may increase to up to 25 min after prolonged use of the column.

4. Transfer 10 µl of each fraction into a scintillation counting vial, add 2 ml scintillation cocktail to each vial, and count radioactivity in a liquid scintillation spectrometer. Pool all fractions with a radioactivity of >100,000 cpm/10 µl, and store the solution at 4°C until use.

   IMPORTANT NOTE: *Solutions of ^{3}H-labeled compounds should not be stored frozen, as this will accelerate the exchange of ^{3}H with water.*

5. Wash the HPLC column at a flow rate of 0.1 ml/min for ~3 hr with 50 mM sodium acetate buffer (pH 6.4), then for 12 to 24 hr with Milli-Q-purified water.

   CAUTION: *Washing buffer is radioactive—pay attention to correct waste disposal!*

   If the column is not reused within the next few days, an additional wash with methanol (~1 hr) is recommended to avoid bacterial contamination of the resin. Before use, remove the methanol by washing the column for ~12 hr with Milli-Q-purified water.

REAGENTS AND SOLUTIONS

Use Milli-Q-purified water or equivalent for all recipes and protocol steps. For common stock solutions, see ***APPENDIX 2A****; for suppliers, see* ***SUPPLIERS APPENDIX****.*

Assay buffer with [^{3}H]L-arginine

200 µl 500 mM triethanolamine/HCl, pH 7.4
200 µl 5 mM $CaCl_2$
100 µl 2 mM L-arginine
20 µl 1 mg/ml calmodulin
10 µl 1 mM FAD in 50 mM triethanolamine/HCl, pH 7.4
10 µl 1 mM FMN in 50 mM triethanolamine/HCl, pH 7.4
200 µl 2 mM NADPH in 50 mM triethanolamine/HCl, pH 7.4
20 µl 1 mM H_4biopterin in 0.01 N HCl
~1,000,000 cpm (50 to 150 µl) HPLC-purified [^{3}H]L-arginine (see Support Protocol 2)
H_2O to 1 ml
Prepare just before use

Stock solutions of triethanolamine/HCl (pH adjusted with 5 M NaOH), $CaCl_2$, L-arginine, and calmodulin can be stored indefinitely at –20°C. Stock solutions of FAD, FMN, NADPH, and H_4biopterin should be prepared daily.

HEPES-buffered salt solution

50 mM HEPES (free acid)
100 mM NaCl
5 mM KCl
2.5 mM $CaCl_2$
1 mM $MgCl_2$
Adjust pH to 7.4 with 5 N NaOH
Store up to 1 month at 4°C

Sodium acetate buffer with L-citrulline

Prepare a solution of 0.2 M sodium acetate and 10 mM L-citrulline. Adjust pH to 13.0 with 5 N NaOH and store up to 1 month at 4°C.

Sodium acetate buffer with EDTA

20 mM sodium acetate
2 mM EDTA
10 mM L-citrulline
Adjust pH to 5.0 with 5 N HCl
Store up to 1 month at 4°C

Triethanolamine buffer with EDTA

Prepare a solution of 50 mM triethanolamine hydrochloride and adjust the pH to 7.4 with 5 N NaOH. Add 0.1 ml of 0.5 M EDTA (*APPENDIX 2A*) per 100 ml buffer (0.5 mM EDTA final) and store up to 1 month at 4°C. Immediately before use, add 0.1 ml 2-mercaptoethanol per 100 ml buffer (12 mM final).

COMMENTARY

Background Information

NO is a widespread messenger molecule that regulates biological processes as diverse as blood vessel relaxation, neuronal cell-to-cell communication, and immune function (*UNIT 10.1*). It is formed enzymatically by three NOS isoforms, which differ in tissue distribution and mechanisms of regulation (Mayer and Hemmens, 1997; Stuehr, 1997). The endothelial (eNOS) and neuronal (nNOS) isozymes are constitutively expressed and activated by Ca^{2+}-dependent calmodulin binding, whereas the inducible isozyme (iNOS)—which is expressed after stimulation of cells with cytokines or endotoxin—is largely Ca^{2+} independent. Although differently regulated, all isozymes catalyze the same reaction, namely an NADPH- and O_2-dependent oxidation of L-arginine to form L-citrulline and NO. Accordingly, the catalytic activities of all NOS isoforms can be measured by monitoring the formation of either L-citrulline or NO.

In this unit, a radiochemical assay is described that is based on the conversion of [^{3}H]L-arginine to [^{3}H]L-citrulline to determine tissue activity of NOS. The earliest form of this assay was reported by Iyengar et al. (1987) and was used for sequential chromatography with Dowex 50W (Na^+) and Dowex 50W (H^+) columns (method adapted from Gopalakrishna and Nagarajan, 1980) for isolation of the product. Bredt and Snyder (1989) simplified the separation procedure to a single step with Dowex 50W (Na^+), which then became the standard method for separating L-citrulline from L-arginine. As demonstrated in this unit, the radiochemical assay can be used to determine NOS activity in both intact cells and broken cell preparations. Applied to intact cells, the method provides a rapid and sensitive measure for the responsiveness of the cells to external stimuli. The values obtained, however, are not measures of absolute NOS activity, because of the difficulty of controlling the intracellular concentrations of the substrates, cofactors, and Ca^{2+}. Therefore, the whole-cell assay cannot be used to compare directly the total NOS activity in different cell types. For a reliable assay of total NOS activity, cell or tissue extracts must be prepared.

Besides the radiochemical assay, several other techniques are available for determining NOS activity. In intact cells, for instance, accumulation of intracellular cyclic guanosine 5′-monophosphate (cGMP) can be used as biochemical marker for NO formation and thus NOS activity. This method is based on the stimulation of soluble guanylyl cyclase by endogenously formed NO and the determination of cGMP by radioimmunoassay (Schmidt et al., 1989, 1992). The assay is a highly sensitive detector of NO; but like the radiochemical assay in intact cells, it does not provide an absolute measure of NOS activities.

Another commonly used method for detecting NO is the oxyhemoglobin assay. This is based on the NO-induced conversion of oxyhemoglobin to methemoglobin, which can be monitored photometrically at 401 (Feelisch and Noack, 1987) or 577 nm (Murphy et al., 1991). The assay can be used to quantify both the release of NO from cells or tissues and the NOS activity in cell or tissue extracts. The sensitivity of this method is lower than that achieved with the radiochemical assay, and proper controls with a NOS inhibitor are required to account for the possible interference of superoxide or H_2O_2 (Winterbourn et al., 1976).

Tissue activity of NOS can also be monitored by measuring the accumulation of nitrite and nitrate in culture supernatants and body fluids. First, nitrate is reduced to nitrite (by either enzymatic conversion or reduction with metallic cadmium or zinc); then the total nitrite is measured via a diazotization reaction with the Griess reagent and photometric quantitation of the azo dye at 550 nm. Owing to its low sensitivity, the assay is not suitable for detecting eNOS and nNOS activity; but it represents one of the standard procedures for determining the tissue activity of iNOS.

Not described here are alternative, more sophisticated detection methods, including bioassays, fluorescent spectroscopy, EPR spectroscopy, chemiluminescence, and electrochemical techniques. For detailed descriptions of these methods see Key References for suggested reading.

Critical Parameters and Troubleshooting

Experiments with cultured cells

When working with cell monolayers, the major concern is to avoid detaching the cells from the substratum. The most critical step is the washing procedure, because parts of the monolayer may be washed away if the buffer is poured directly onto the cells. The best way to avoid damaging the monolayer is to pipet the

buffer slowly onto the wall of the well. Because most cells require divalent cations for attachment, dissociation of the monolayer may also be observed in Ca^{2+}/Mg^{2+}-free buffers. If experiments must be performed in Ca^{2+}-free buffer, it might help to increase the Mg^{2+} concentration to 2.5 to 10 mM. EGTA, a chelator with a pronounced Ca^{2+} preference, should used instead of EDTA. If dissociation of the monolayer is still observed, the dishes should be coated with polylysine before use. For coating, dissolve 5 mg polylysine in 50 ml Milli-Q-purified water and sterilize the solution by filtration (0.22-µm filter). Add 1 ml of this solution to each well, and leave the plates for 10 min at room temperature. Remove the solution (which can be reused for further coatings) and wash the dishes twice with sterile Milli-Q-purified water. Wait until the residual water has evaporated, and use the coated plates for cell culture.

Uptake of radiolabeled L-arginine and lysis of the cells after incubation are also critical parameters when determining NOS activity in intact cells. For the protocol described, the percentage of incorporated L-arginine should be in the range of 1% to 10%. One cause of low incorporation is the presence of (residual) L-arginine or other basic amino acids, which compete with radiolabeled L-arginine at the transport site. Apparently low incorporation of L-arginine may also result from incomplete lysis of the cells. According to the authors' experience with different types of cells (e.g., endothelial cells, macrophages, and neuronal cell lines), treatment with 0.01 N HCl is sufficient for complete cell lysis. The advantage of this method is that the cell debris remains attached to the wells so the supernatant can be applied onto the columns without further centrifugation. Because treatment with 0.01 N HCl might be insufficient for disruption of other cells, lysis should be checked by solubilizing the cells with 1 N NaOH after removing the HCl extract. If substantial radioactivity is found in the NaOH extract, more concentrated HCl (e.g., 0.1 N) should be used. For column chromatography, the pH of the sample should be between 5.0 and 5.5, so the ionic strength and the pH of the sodium acetate buffer and L-citrulline must be adjusted accordingly.

Preparation of cell and tissue extracts

Although NOS activity may vary slightly depending on culture conditions (e.g., medium composition, removal of serum prior to experiments, number of cells/well during the assay), these effects are usually only marginal and any standard culture conditions are generally acceptable.

Because NOS is very labile, temperature is the most critical parameter when preparing cell and tissue extracts. Accordingly, the materials required (such as buffers, homogenization tube, rotor, and centrifuge) should be precooled and all working steps performed in a 4°C cold room. During the homogenization, tubes should be placed in ice; and if the time required for cell rupture exceeds 15 to 20 sec, the procedure should be performed in intervals and samples recooled on ice to avoid any rise in temperature.

Several methods are available for cell rupture, but the efficiency of most techniques varies, depending on the type of cells or tissues used. The mild shearing forces generated by mechanical homogenizers are usually sufficient to disrupt intact tissues but may be inappropriate for an efficient homogenization of isolated cells. For most types of cells, sonication is the best alternative, but the efficiency of the treatment must be checked by microscopy. If incomplete homogenization is observed, increase the number of bursts but not their duration, because prolonged sonication will rapidly increase the temperature of the cell extract. Alternatively, a pressure homogenizer or a bead mill can be used to disrupt the cells.

NOS assay

In general, the authors perform the assay in the presence of 100 µM L-arginine, a concentration far above the K_M value of NOS, which allows a reliable determination of maximal enzyme activity. The use of such a high substrate concentration has the additional advantage of minimizing the interference of endogenous L-arginine present in homogenates and cytosolic fractions. When low NOS activities are expected, however, the concentration of unlabeled L-arginine should be reduced to 10 µM, which will increase the amount of [^{3}H]L-arginine that is converted to [^{3}H]L-citrulline and thus the sensitivity of the assay.

All isozymes require enzyme-bound H_4biopterin, FAD, and FMN for catalytic activity. These cofactors are usually present in sufficient amounts in intact cells but should be added to the incubation buffer when assaying NOS activity in cell or tissue extracts. If not available, one or more cofactors may be omitted, but their absence will reduce NOS activity to 30% to 50%. When iNOS is assayed, $CaCl_2$ and calmodulin can be omitted.

Column chromatography

Prolonged use or storage of the Dowex columns may result in decreased flow rates, usually caused by clogged column filters or air bubbles in the column bed. This problem can usually be avoided by washing the columns with 1 N NaOH once or twice a week to prevent drying of the resin and precipitation of protein in the column filter. If poor flow rates are observed, resuspend the resin with a spatula during the washing procedure to remove any air bubbles present in the column bed. To clean clogged filters, close the outlet of the columns and leave columns filled with 1 N NaOH for 2 to 4 hr. If flow rates are still slow, suck NaOH through the column by applying vacuum to the outlet.

Anticipated Results

The NOS family consists of three isoforms, which differ in enzymatic activity, mechanism of regulation, and cellular distribution. The endothelial isoform is a membrane-bound low-output NOS that is expressed primarily in vascular endothelial cells but also in epithelial cells and cardiomyocytes. Enzyme activity requires Ca^{2+}-dependent binding of calmodulin and is, therefore, regulated by changes in Ca^{2+} concentration. In intact endothelial cells (e.g., isolated from aortas or umbilical veins) conversion of [^{3}H]L-arginine to [^{3}H]L-citrulline will be in the range of 1% to 5% under control conditions and up to 40% upon stimulation of the cells with Ca^{2+}-mobilizing agonists (e.g., bradykinin, histamine, ATP, or Ca^{2+} ionophores). In broken cell preparations (e.g., homogenates or membrane fractions of endothelial cells) maximal enzyme activity will be in the range of 5 to 20 pmol L-citrulline $\times$ min^{-1} $\times$ mg protein^{-1}.

The neuronal isoform is a cytosolic low-output NOS that is expressed primarily in neuronal cells but also in skeletal muscle. Similar to eNOS, enzymatic activity of nNOS requires Ca^{2+}-dependent binding of calmodulin. In intact neuronal cells (e.g., N1E-115 neuroblastoma cells or 108CC15 neuroblastoma $\times$ glioma hybrid cells), conversion of [^{3}H]L-arginine to [^{3}H]L-citrulline will be in the range of 1% to 5% under control conditions and up to 30% on stimulation of the cells with Ca^{2+}-mobilizing agonists. In broken cell preparations (e.g., cytosolic fractions of porcine or rat brain) maximal enzyme activity will be in the range of 20 to 150 pmol L-citrulline $\times$ min^{-1} $\times$ mg protein^{-1}.

The inducible isoform is a cytosolic high-output NOS whose expression is induced by cytokines and endotoxins in virtually all mammalian cells. In contrast to the other isoforms, iNOS binds calmodulin Ca^{2+} independently and is, therefore, not regulated by changes in Ca^{2+} concentration. Accordingly, enzymatic activity of iNOS can easily be distinguished from that of eNOS and nNOS by performing parallel experiments in the absence and presence of Ca^{2+}. The highest activity of iNOS (200 to 700 pmol L-citrulline $\times$ min^{-1} $\times$ mg protein^{-1}) can be found in the cytosolic fraction of activated macrophages (e.g., isolated alveolar or peritoneal macrophages or cell lines J774 or RAW 264.7).

Time Considerations

Determination of NOS activity in intact cells (24 samples). The entire procedure can be done in ~2 hr plus the time required for liquid scintillation spectrometry. The assay takes ~30 min; cell lysis with HCl, ~1 hr; neutralization and transfer of the samples on the Dowex column, ~10 min; and elution of L-citrulline, ~20 min.

Preparation of cell or tissue extracts. The entire procedure can be done in 30 to 90 min. Homogenization takes ~10 min; centrifugation (optional), ~1 hr; and protein determination, ~20 min.

NOS assay (24 samples). The entire procedure can be done in ~1 hr plus the time required for liquid scintillation spectrometry. The assay takes ~30 min; transfer of the samples on the Dowex column, ~10 min; and elution of L-citrulline, ~20 min.

Preparation and regeneration of Dowex columns. Initial preparation of the columns (washing the resin, filling the columns, treating with NaOH) takes ~8 hr. Washing the columns before use takes ~2 hr, and regeneration of the resin takes ~30 min.

Purification of [^{3}H]L-arginine by HPLC. Equilibration of the HPLC column requires 2 to 3 hr, separation takes ~30 min, and washing the column requires 12 to 24 hr.

Literature Cited

Bredt, D.S. and Snyder, S.H. 1989. Nitric oxide mediates glutamate-linked enhancement of cGMP levels in the cerebellum. *Proc. Natl. Acad. Sci. U.S.A.* 86:9030-9033.

Castle, J.D. 1995. Purification of Organelles from Mammalian Cells. *In* Current Protocols in Protein Science (J.E. Coligan, B.M. Dunn, H.L. Ploegh, D.W. Speicher, and P.T. Wingfield, eds.) pp. 4.2.1-4.2.56. John Wiley & Sons, New York.

Feelisch, M. and Noack, E.A. 1987. Correlation between nitric oxide formation during degrada-

tion of organic nitrates and activation of guanylate cyclase. *Eur. J. Pharmacol.* 139:19-30.

Gopalakrishna, R. and Nagarajan, B. 1980. Separation and estimation of arginine-related metabolites in tissues. *Anal. Biochem.* 107:318-323.

Iyengar, R., Stuehr, D.J., and Marletta, M.A. 1987. Macrophage synthesis of nitrite, nitrate, and *N*-nitrosamines: Precursors and role of the respiratory burst. *Proc. Natl. Acad. Sci. U.S.A.* 84:6369-6373.

Mayer, B. and Hemmens, B. 1997. Biosynthesis and action of nitric oxide in mammalian cells. *Trends Biochem. Sci.* 22:477-481.

Murphy, M.E., Piper, H.M., Watanabe, H., and Sies, H. 1991. Nitric oxide production by cultured aortic endothelial cells in response to thiol depletion and replenishment. *J. Biol. Chem.* 266:19378-19383.

Schmidt, K., Mayer, B., and Kukovetz, W.R. 1989. Effect of calcium on endothelium-derived relaxing factor formation and cGMP levels in endothelial cells. *Eur. J. Pharmacol.* 170:157-166.

Schmidt, K., Werner, E.R., Mayer, B., Wachter, H., and Kukovetz, W.R. 1992. Tetrahydrobiopterin-dependent formation of endothelium-derived relaxing factor (nitric oxide) in aortic endothelial cells. *Biochem. J.* 281:297-300.

Stuehr, D.J. 1997. Structure-function aspects in the nitric oxide synthases. *Annu. Rev. Pharmacol. Toxicol.* 37:339-359.

Winterbourn, C.C., McGrath, B.M., and Carrell, R.W. 1976. Reactions involving superoxide and normal and unstable haemoglobins. *Biochem. J.* 155:493-502.

Key References

The following references provide collections of methods used for measuring NO and NOS activity.

Everse, J. and Grisham, M.B. (eds.) 1995. Methods: A Companion to Methods in Enzymology, Vol. 7: Measurement of Nitric Oxide. Academic Press, San Diego, Calif.

Maines, M.D. (ed.) 1996. Nitric Oxide Synthase: Characterization and Functional Analysis. Academic Press, San Diego, Calif.

Titheradge, M.A. (ed.) 1998. Methods in Molecular Biology, Vol. 100: Nitric Oxide Protocols. Humana Press, Totowa, N.J.

Contributed by Kurt Schmidt and Bernd Mayer
Karl-Franzens-Universität Graz
Graz, Austria

Detection of Nitrosated Proteins

Several methods have been used to analyze nitroso compounds: the Saville assay (Saville, 1958), spectrophotometric analysis, the quinine fluorescence quenching assay (Gabor and Allon, 1994), the diaminonaphthalene assay (Cook et al., 1996), chemiluminescence analysis, and mass spectrometry analysis. Among these methods, the Saville assay is the most widely used, because it is less sensitive to interference than are the fluorescence methods and because it requires only simple chemical reagents and a spectrophotometer. The diaminonaphthalene assay (a fluorescence method) and chemiluminescence analysis are the methods of choice when high sensitivity is required; their detection limits are 10^{-7} M and 10^{-8} M, respectively, which are 10 and 100 times more sensitive than for the Saville assay. Spectrophotometric analysis is mainly used for the structural characterization of nitroso compounds, but can also serve as a rapid method for estimating the -NO content of unknown samples. Mass spectrometry analysis is employed for precise structural analysis. This unit describes the Saville assay, spectrophotometric analysis, and the quinine fluorescence quenching assay (the diaminonaphthalene assay is discussed in *UNIT 10.4*). For discussion of the principles of chemiluminescence and mass spectrometry methods, which require special instrumentation, see Commentary.

SAVILLE ASSAY TO DETECT NITROSATED PROTEINS

BASIC PROTOCOL 1

The Saville assay is the most widely used method for detecting *S*-nitroso (S-NO) compounds. It was developed by Saville (1958) and is based on the nitrite detection method of Griess (1879). In the Saville assay, the mercuric ion (Hg^{2+}) substitutes for the -NO group in S-NO, and the released -NO (in the form of HONO) is subsequently detected by the Griess reaction, which involves diazotization with sulfanilamide (SN) and subsequent derivatization with *N*-1-(naphthyl)ethylenediamine dihydrochloride (NEDD). To distinguish the released HNO_2 from free nitrite in the sample, ammonium sulfamate (ASM) and HCl are added to the sample before the Hg^{2+} substitution reaction. ASM rapidly reacts with HNO_2 to form NH_3, N_2, and H_2SO_4 but does not affect *S*-nitrosothiol (RSNO) species. It also cannot compete with SN, which is added later to react with the HNO_2 produced after Hg^{2+} is substituted for -NO. SN forms a diazonium salt with HNO_2, which then couples to NEDD to form a purple-pink azo dye.

Although the detection limit of the Saville assay is 1 μM (the final concentration of *S*-nitroso compounds in the assay mixture), the initial -NO concentration must be >5 μM, because the sample is diluted a minimum of 5-fold in the assay (as in this protocol). To analyze samples of limited quantity, use a microtiter-plate assay in which the sample is diluted 2-fold in the assay and the total assay volume is 0.2 ml (see Alternate Protocol).

Materials

Sample to be tested (nitroso compounds, nitrosated proteins, cell homogenates)
100 μM $NaNO_2$ (freshly prepared)
0.5% (w/v) ammonium sulfamate (ASM; Aldrich) in water (store at room temperature; stable 1 year or more)
2 N HCl
Hg/sulfanilamide (Hg/SN) solution (see recipe)
N-1-(Naphthyl)ethylenediamine dihydrochloride (NEDD) solution (see recipe)

1. Add 0.4 ml water to two 10-ml test tubes for blanks. For standards, add 15, 30, 60, 120, 180, 240, and 300 μl of 100 μM $NaNO_2$ to 16 × 100–mm test tubes, and dilute with water to a final volume of 0.4 ml.

Contributed by Ying-Yi Zhang and Joseph Loscalzo
Current Protocols in Toxicology (1999) 10.3.1-10.3.8

The final concentration of the standards in the total assay mixture will be 1, 2, 4, 8, 12, 16, and 20 μM, respectively.

The standard curve is linear up to 40 μM. If needed, prepare the standards in the range of 2 to 40 μM using a 200 μM $NaNO_2$ solution. Do not use HNO_2 in place of $NaNO_2$. Once solubilized, HNO_2 slowly decomposes in water into H_2O and NO.

2. Add each unknown sample (up to 0.3 ml) to its corresponding test tube, and dilute with water to a final volume of 0.3 ml.

3. Add 0.1 ml of 0.5% ASM to the unknown sample tubes; mix well.

   Do not add ASM to the standards. See annotation to step 4.

4. Add 0.1 ml of 2 N HCl to all test tubes; mix. Wait 1 to 2 min.

   This step yields two different reactions. In the tubes with standards, HCl reacts with $NaNO_2$ to form HNO_2, which will react with SN and NEDD in step 5 to form a chromophore. In the tubes with unknowns, the HNO_2 formed from the reaction of HCl and free nitrite is removed by ASM (added in step 3). This reaction takes ~1 min. To avoid significant degradation of HNO_2 in the standards, do not let this incubation step exceed 3 min.

5. Add 0.5 ml Hg/SN solution and 0.5 ml NEDD solution to all test tubes; mix. Leave at room temperature 10 min.

   A purple-red color should be visible in the standards immediately after addition of the NEDD solution. Maximum color development occurs within a few minutes and is stable for at least 1 hr.

6. Read absorbance at 540 nm against blank.

7. Use the readings for the standards to prepare a standard curve, and calculate the actual concentration of each sample as follows: actual concentration = concentration read from standard curve × 1.5/sample volume (ml).

   N-Nitrosotryptophan releases NO slowly but spontaneously. It can, therefore, be detected by the Griess reaction used in the Saville assay if the reaction time (after addition of SN and NEDD) is extended to 30 min. In this case, the presence of $HgCl_2$ does not affect the detection of the nitroso group.

ALTERNATE PROTOCOL

MICROTITER-PLATE SAVILLE ASSAY TO DETECT NITROSATED PROTEINS

The basic steps in the microtiter-plate Saville assay are the same as those of the standard assay. The annotations in the standard assay (see Basic Protocol 1) apply equally to the steps in this protocol.

Additional Materials (also see Basic Protocol 1)

40 μM $NaNO_2$ (freshly prepared)
Hg/SN/NEDD solution (see recipe)

96-well microtiter plate
Microtiter plate reader

1. Devote two columns of wells on a microtiter-plate to blanks and standards by adding 0, 5, 10, 20, 40, 60, 80, and 100 μl of 40 μM $NaNO_2$ to wells A1 to H1, and the same volume to wells A2 to H2 for duplicates. Dilute with water to a final volume of 130 μl.

   The final concentration of the standards in the total assay mixture will be 1, 2, 4, 8, 12, 16, and 20 μM, respectively.

   Standards can be made up in the range of 2 to 40 μM using an 80 μM $NaNO_2$ stock solution.

2. Add up to 100 µl of each unknown sample to an empty well; dilute with water to a final volume of 100 µl. Set up wells containing unknown samples in duplicate or triplicate.
3. Add 30 µl of 0.5% ASM to the wells with unknown samples; mix well.
4. Add 30 µl of 2 N HCl to all wells; mix. Wait 1 to 2 min.
5. Add 40 µl Hg/SN/NEDD solution to all wells; mix. Incubate 10 min at room temperature.
6. Read absorbance at 540 nm or 550 nm with standard-cutoff filter. Use wells A1 and A2 as blanks to zero the instrument.
7. Use the readings for the standards to construct a standard curve, and calculate the actual concentration of sample as follows: actual concentration = concentration read from standard curve × 0.2/sample volume (ml).

SPECTROPHOTOMETRIC ASSAY TO DETECT NITROSATED PROTEINS

BASIC PROTOCOL 2

The nitroso group in nitrosocysteine and nitrosotryptophan generates chromophores that absorb at 300 to 350 nm. By analyzing the absorption spectrum and the intensity of absorption, one can determine both the structural characteristics of the nitroso group and the concentration of -NO in the sample. Spectrophotometric analysis is not sufficiently sensitive for concentration determinations in typical biological samples, owing to the low extinction coefficient of the -NO; detection requires a minimum sample concentration of 10 µM. Nitrosoproline has a low-intensity absorption peak at 343 nm and an extinction coefficient of 91 M^{-1} cm^{-1}. Thus it is not detectable by this protocol at concentrations <100 µM.

Materials

Appropriate reference solution (see step 4 annotation)
Sample to be tested

1. Set spectrophotometer to wavelength scan mode.
2. Take baseline of the blank.

   For example, if the sample contains GSNO, then the corresponding blank will contain glutathione. In this case, the glutathione reference solution should be scanned (the blank) before the sample solution is scanned.

3. Scan the absorption of the sample from 200 to 600 nm.
4. Read absorbance at the wavelength of maximum absorption.

   The critical step in this analysis is the preparation of the reference (blank), which greatly affects the interpretation of the sample spectrum. When the reference contains only water, the observed spectrum represents the sum of the absorption of all the components in the sample. When the reference contains the same solution components as the sample except for the nitrosated molecule of interest, the spectrum reflects the absorption of the nitrosated molecule. If the reference contains all sample components including the precursor molecule that is not nitrosated, the spectrum reflects -NO group absorption exclusively.

5. Calculate the concentration of nitroso equivalents in the sample by dividing the maximum absorbance by the extinction coefficient for the specific nitroso group.

BASIC PROTOCOL 3

QUININE FLUORESCENCE QUENCHING ASSAY TO DETECT NITROSATED PROTEINS

Quenching of fluorescence emission by a chromophore that absorbs at the wavelength of a fluorophore's excitation or emission is known as the inner filter effect (primary or secondary, respectively). Gabor and Allon (1994) developed a method that exploits the inner filter effect to measure -NO content. The fluorophore used is quinine sulfate, which has an absorption spectrum that overlaps with the absorption spectra of -NO in *S*-nitroso-cysteine and *N*-nitrosotryptophan. The sensitivity of the method is 1 μM; however, because the sample must be diluted in the assay solution 10- to 100-fold (depending on the interference of other components in the biological sample), the original sample concentration must be >10 μM.

Materials

Sample to be tested
100 μM *S*-nitrosoglutathione (GSNO) solution (see recipe)
10 μM quinine sulfate
0.1 M H_2SO_4

Spectrofluorometer
Cuvettes or microcuvettes

1. For standard curve measurements, prepare mixtures containing 1 to 20 μM GSNO and 0.1 μM quinine sulfate in 0.1 M H_2SO_4, in a final volume of 3 ml (standard cuvette) or 0.3 ml (microcuvette).
2. For each standard, excite solution at 334 nm and read emission at 453 nm using spectrofluorometer.
3. For sample measurement, prepare a mixture containing unknown sample (1% to 10% of final volume) and 0.1 μM quinine sulfate in 0.1 M H_2SO_4, in the appropriate final volume (as defined in step 1). Read fluorescence as described in step 2.
4. Plot the standard curve, and read the sample nitroso concentration from the curve.

Because the quinine assay is based on the inner filter effect, any molecule that absorbs light in the 300 to 500 nm range will interfere with the assay. Myoglobin, for example, absorbs at 300 to 450 nm; at 40 μg/ml; it reduces quinine fluorescence by 30%.

REAGENTS AND SOLUTIONS

Use Milli-Q-purified water or equivalent for all recipes and protocol steps. For common stock solutions, see ***APPENDIX 2A****; for suppliers, see* ***SUPPLIERS APPENDIX****.*

GSNO solution

Mix equimolar concentrations of glutathione (Sigma) and $NaNO_2$ in 0.2 M HCl. Prepare fresh.

Hg/SN solution

0.25% (w/v) $HgCl_2$ (Sigma)
3% (w/v) sulfanilamide (Aldrich)
0.4 N HCl
Store at room temperature (stable 6 months or more)

CAUTION: *Hg^{2+} is toxic. Care should be taken not to contaminate the environment or one's hands. Sulfanilamide and $HgCl_2$ have limited solubility in H_2O; dissolve them in HCl directly.*

Hg/SN/NEDD solution

Prepare 0.4 % (w/v) $HgCl_2$ (Sigma) and 5% (w/v) sulfanilamide (Aldrich) in 0.4 N HCl, and store indefinitely at room temperature. Before use, add 20 mg NEDD (Aldrich) to 10 ml of the Hg/SN solution. Use immediately.

NEDD solution

0.1% NEDD (Aldrich)
0.4 N HCl
Keep in dark at room temperature (stable for a few days)
Discard when the solution becomes dark

COMMENTARY

Background Information

NO, NO metabolites (NO_2, N_2O_3, HNO_2, $ONOO^-$), and NO donor compounds react with proteins via three types of reactions: nitrosylation, nitration, and nitrosation. In nitrosylation reactions, NO coordinates with a metal ion in a protein to form a nitrosyl-metal complex, such as the nitrosyl-heme-Fe complex. In nitration and nitrosation reactions, a nitro (-NO_2) or nitroso (-NO) group covalently binds to an amino acid residue in a protein to form the corresponding nitroamino acid (such as nitrotyrosine) or nitrosoamino acid (such as nitrosocysteine). The likelihood of these reactions occurring in a specific protein depends on the structural characteristics of the protein and the particular NO species involved in the reaction. Thus a systematic examination of all possible reaction products is important for understanding the molecular mechanisms underlying various NO-mediated biological effects. This unit presents methods for detecting nitrosation of proteins.

Depending on the atom to which the nitroso group is attached, nitrosation is classified as *C*-, *O*-, *N*-, and *S*-nitrosation. Studies on model peptides have shown that nitrosation can occur on a cysteinyl thiol group (*S*-nitrosation); on a tyrosine phenol ring (*C*-nitrosation); or on a side-chain amine group in proline, tryptophan, arginine, lysine, glutamine, and asparagine (*N*-nitrosation). Because many of these nitrosation products are very unstable under physiologic conditions, only three nitrosoamino acids are commonly observed: *S*-nitrosocysteine, *N*-nitrosoproline, and *N*-nitrosotryptophan. The specificity of *N*-nitroso (N-NO) and *S*-nitroso (S-NO) detection is noted for each method. In addition to N- and S-specificity, the methods described in this unit are applicable to the detection of N-NO and S-NO groups in proteins and in other compounds. Thus when a biological sample is found to be nitroso positive, further structural analysis should be performed to identify the specific nitroso derivative.

Chemiluminescence

Chemiluminescence is defined as light emitted by a molecule in the course of a chemical reaction. NO generates light when it reacts with ozone by the following reaction sequence:

$$NO + O_3 \rightarrow NO_2^* + O_2$$
$$NO_2^* \rightarrow NO_2 + h\nu\ (590 - 2800\ nm)$$

Fontijin and colleagues (1970) built the first chemiluminescence detector to detect NO in air as an environmental pollutant. The sensitivity of the detector is quite high: 4 parts per billion (v/v, NO/air), corresponding to 1×10^{-13} mol/liter.

Chemiluminescence methods cannot be used to detect nitroso compounds directly, because NO must enter the reaction chamber in the gas phase. Several methods have, therefore, been developed to liberate the NO moiety from the nitroso compound in a gas form ($NO^\cdot$) and subsequently to detect it by chemiluminescence.

TEA (thermal energy analyzer)

The TEA was developed by Fine and colleagues (1975a) to detect N-NO compounds; it consists of a pyrolytic unit and a chemiluminescence detector. In the pyrolytic unit, the nitroso compound is vaporized with a flash of heat (300°C) and is homolytically cleaved in a catalytic pyrolyzer containing a mixture of WO_3 and $W_{20}\ O_{58}$. The sudden increase in thermal energy cleaves the molecule at its weakest bond. Because N-NO bonds generally have lower energy (10 to 50 kcal/mol) than the C-N, C-C, and C-H bonds (70 to 90 kcal/mol), they will be cleaved preferentially. The generated NO is carried by argon to the chemiluminescence detector for analysis. The TEA can detect nitroso compounds in the range of 10

pmol (1 μM in 10 μl), with a specificity of 100 μg/kg (nitroso compounds/total mass). Although it was originally designed to detect N-NO compounds, TEA can also detect S-NO, nitrosyl metal complexes, some nitroalkanes, nitrate esters, nitroaromatics, and inorganic nitrite and nitrate.

HPLC-TEA and GC-TEA

To improve the detection selectivity of the TEA, Fine and colleagues made two other instrumental modifications, which involve linking an HPLC unit (1976) or a gas chromatography (GC) unit (1975b) to the TEA. The GC-TEA was designed to detect volatile *N*-nitroso compounds and the HPLC-TEA nonvolatile compounds. In this instrument, the sample is first separated by HPLC and then enters the pyrolysis unit for liberation of $NO^{\cdot}$. Because both the carrier solvent and the nitroso molecule are vaporized during pyrolysis, the products leave the pyrolyzer in a vapor or gas form. The two cold traps (at 0° and −70°C)—in sequence after the pyrolyzer—condense the vapor first to liquid and then to solid, while NO is carried by argon into the chemiluminescence detector. The HPLC separation makes nitroso detection more selective; but it does not, of course, alter the sensitivity of TEA.

HPLC-photolysis-chemiluminescence

The solvent used in the HPLC-TEA-chemiluminescence instrument must be sufficiently volatile to be vaporized instantaneously to liberate NO efficiently; however, separation of biological samples is commonly performed in aqueous solution. Conboy and Hotchkiss (1989) developed a device that releases NO from nitroso compounds by photolysis at room temperature. The photolysis device, interfaced between an HPLC and a chemiluminescence detector, consists of a 3-m × 1-mm-i.d. borosilicate glass tube coiled around a 200-W mercury vapor lamp. The sample enters the glass coil after HPLC separation and helium purging (to remove O_2) and is then photolyzed by the energy provided by the UV lamp. The resulting NO is separated from the liquid matrix when passing through the two cold traps, after which it is carried by helium to the chemiluminescence detector for analysis.

Photolysis detects nitroso compounds (N-NO, S-NO), nitrosyl-metal complexes, and inorganic nitrite. The nitrite can be separated from nitroso compounds on HPLC. Without separation, the use of a 495-nm-cutoff filter can also eliminate interference from nitrite in the assay (Alpert et al., 1997). The detection limit of this method is 10 pmol (10 nM in 1 ml).

Denitrosation-chemiluminescence detection

The denitrosation-chemiluminescence method releases NO from nitroso compounds by chemical reaction and was developed by Downes and colleagues (1976) based on a denitrosation reaction. In this method, the nitroso compound is refluxed with hydrogen bromide in an acidic nonaqueous solution. The resulting nitrosyl bromide product, a gas, is carried by nitrogen to a tube containing silica heated at 350°C. The nitrosyl bromide is converted to $NO^{\cdot}$, which is then separated from the halogenated material in a cold trap and detected by chemiluminescence. The original method was later modified in several ways to distinguish thermal and acid-labile contaminants from N-NO compounds and to accelerate the analysis (for a review, see Walters, 1996). This method is still used for analysis of nitroso compounds in gastric fluid and has a detection limit of 10 pmol; it does not distinguish N-NO from S-NO compounds, because the latter can also be denitrosated by hydrogen bromide.

Mass spectrometry analysis

Mass spectrometry (MS) measures the mass of a molecule or fragments of a parent molecule in concert with the molecule's charge. The analysis is achieved by first ionizing the molecule in a gas phase and then differentiating the resulting ions according to their mass/charge ratio (*m/z*). Traditional mass spectrometers carry out the ionization step by thermal vaporization and electron bombardment, which is not suitable for proteins and thermolabile molecules, because these molecules cannot be transformed to the gas phase intact. To analyze nitrosoproteins, the mass spectrometer must be equipped with a milder ionization source, such as an electrospray ionization (ESI) or matrix-assisted laser desorption/ionization (MALDI) unit. The ionization process in the ESI unit is carried out by spraying the sample into a drying chamber through a high-voltage syringe tip; and in the MALDI unit, by desorption of the sample molecule from the sample/matrix crystal on a high-voltage metal surface with a UV laser beam. The ESI unit has the advantage of being able to interface with an HPLC-UV unit. Thus the products in a reaction mixture can be first chromatographically separated and then consecutively analyzed by ESI-MS.

NO has a relative mass of 30 Da. During nitrosation, a proton of a protein or peptide is

substituted by a -NO group; thus the mass increase of the nitrosation product will be 29 Da. MS also detects the results of other NO_x-dependent reactions, including nitration (mass increase of 45 Da) and oxidation of thiol groups (SH) into sulfonic acid groups (SO_3H) (mass increase of 49 Da). Several examples of the application of MS analysis to nitrosated peptides have been published (Mirza et al., 1995; Zhang et al., 1996; Lander et al., 1997). The S-NO bond in nitrosocysteine and the N-NO bond in nitrosotryptophan are weak bonds. Although ESI is used in the MS analysis, these bonds are still readily cleaved during ionization. Mirza and colleagues (1995) found that 50% of the S-NO bonds are cleaved at a drying gas temperature of 125°C and 100% cleaved at 200°C. The sensitivity of MS analysis is in the femtomole to picomole range.

Troubleshooting

The Saville assay and spectrophotometric analysis are straightforward and highly reproducible. In the Saville assay, if the color (pink to purple-red) is not visible after addition of all the reagents, the formation of HNO_2 in the standard tubes during Basic Protocol 1 step 4 should be confirmed. Two factors could account for lower HNO_2 concentrations in the standards than expected: (1) the pH of the $NaNO_2$ solution used in step 1 is below pH 5 or (2) there is a long delay between step 4 (addition of HCl) and step 5 (addition of Hg^{2+}/SN and NEDD). $NaNO_2$ is converted to HNO_2 in acidic solution, and HNO_2 decomposes gradually once formed. The freshness of the NEDD could also affect color development.

In the quinine fluorescence quenching assay, if HCl is used in place of H_2SO_4, the intensity of the standard emission peak is significantly reduced.

Anticipated Results

The lower limits of the Saville assay is 1 μM. With 1 to 20 μM nitroso species present in the assay solution, the corresponding absorption range is expected to be 0.05 to 1.00 OD units in the standard assay, and 0.02 to 0.40 OD units in the microtiter plate assay. Over this range of concentrations and absorptivities, the standard curve should be absolutely linear. The molar extinction coefficients of various low-molecular-weight nitroso derivatives range from 500 to 1200 cm^{-1} M^{-1}. For *N*-nitroso compounds, the molar extinction coefficients vary greatly between aromatic and nonaromatic derivatives. For example, the molar extinction coefficient for *N*-nitrosotryptophan at 335 nm is 7000 cm^{-1} M^{-1}; the molar extinction coefficient for *N*-nitrosoglutamine, by contrast, is 76 cm^{-1} M^{-1} at the same wavelength.

The concentration of nitrosoproteins in biological samples is reported to be in the micromolar range (Stamler et al., 1992; Upchurch et al., 1996), and the concentration varies with disease states (Hilliquin et al., 1997) and in different bodily fluids (Gaston et al., 1993). For example, Hilliquin and co-workers (1997) found that rheumatoid arthritis patients have an average serum *S*-nitrosoprotein concentration of 3.2 ± 2.3 μM, but their synovial fluid *S*-nitrosoprotein concentration is significantly higher at 10.1 ± 2.9 μM.

Time Considerations

When stock reagents are prepared, both the standard and microtiter-plate Saville assays take ~30 to 60 min. Dilution and pipetting of samples take 10 to 30 min to complete. Addition of the reagents requires ~10 min; color development and reading take ~15 to 20 min. The quinine assay, spectrophotometric analysis, and chemiluminescence analysis each requires 2 to 3 min for each sample reading.

Literature Cited

Alpert, C., Ramdev, N., George, D., and Loscalzo, J. 1997. Detection of *S*-nitrosothiols and other nitric oxide derivatives by photolysis-chemiluminescence spectrometry. *Anal. Biochem.* 245:1-7.

Conboy, J.J. and Hotchkiss, J.H. 1989. Photolytic interface for high-performance liquid chromatography–chemiluminescence detection of nonvolatile *N*-nitroso compounds. *Analyst* 114:155-159.

Cook, J.A., Kim, S.Y., Teague, D., Krishna, M.C., Pacelli, R., Mitchell, J.B., Vodovotz, Y., Nims, R.W., Christodoulou, D., Miles, A.M., Grisham, M.B., and Wink, D.A. 1996. Convenient colorimetric and fluorometric assays for *S*-nitrosothiols. *Anal. Biochem.* 238:150-158.

Downes, M.J., Edwards, M.W., Elsey, T.S., and Walters, C.L. 1976. Determination of a non-volatile nitrosamine by using denitrosation and a chemiluminescence analyser. *Analyst* 101:742-748.

Fine, D.H., Lieb, D., and Rufeh, F. 1975a. Principle of operation of the thermal energy analyzer for the trace analysis of volatile and non-volatile *N*-nitroso compounds. *J. Chromatogr.* 107:351-357.

Fine, D.H., Lieb, D., Rufeh, F., and Rounbehler, D.P. 1975b. Description of the thermal energy analyzer (TEA) for trace determination of volatile and nonvolatile *N*-nitroso compounds. *Anal. Chem.* 47:1188-1191.

Fine, D.H., Rounbehler, D.P., Silvergleid, A., and Ross, R. 1976. Trace analysis of polar and apolar *N*-nitroso compounds by combined high-performance liquid chromatography and thermal energy analysis. *In* Proceedings of the 2nd International Symposium of Nitrite Meat Products (B.J. Tinbergen and B. Kroll, eds.) pp. 191-198. Zeist, Wageningen, The Netherlands.

Fontijin, A., Sabadell, A.J., and Ronco, R.J. 1970. Homogeneous chemiluminescent measurement of nitric oxide with ozone: Implications for continuous selective monitoring of gaseous air pollutants. *Anal. Chem.* 42:575-579.

Gabor, G. and Allon, N. 1994. Spectrofluorometric method for NO determination. *Anal. Biochem.* 220:16-19.

Gaston, B., Riley, J., Drazen, J., Fackler, J., Ramdev, P., Mullins, M., Sugarbaker, D., Jaraki, O., Singel, D.J., Loscalzo, J., and Stamler, J.S. 1993. Endogenous nitrogen oxides and bronchodilator *S*-nitrosothiols in human airways. *Proc. Natl. Acad. Sci. U.S.A.* 90:10957-10961.

Griess, P. 1879. Bemerkungen zu der Abhandlung der HH. Weselsky und Benedikt, "Uber einige Azoverbindungen." *Ber. Deutsch. Chem. Ges.* 12:426-428.

Hilliquin, P., Borderie, D., Hernvann, A., Menkes, C.J., and Ekindjian, O.G. 1997. Nitric oxide as *S*-nitrosoproteins in rheumatoid arthritis. *Arthritis Rheum.* 40:1512-1517.

Lander, H.M., Hajjar, D.P., Hempstead, B.L., Mirza, U.A., Chait, B.T., Campbell, S., and Quilliam, L.A. 1997. A molecular redox switch on p21ras. *J. Biol. Chem.* 272:4323-4326.

Mirza, U.A., Chait, B.T., and Lander, H.M. 1995. Monitoring reactions of nitric oxide with peptides and proteins by electrospray ionization–mass spectrometry. *J. Biol. Chem.* 270:17185-17188.

Saville, B. 1958. A scheme for the colorimetric determination of microgram amounts of thiols. *Analyst* 83:670-672.

Stamler, J.S., Jaraki, O., Osborne, J., Simon, D.I., Keaney. J., Vita, J., Singel, D., Valeri, C.R., and Loscalzo, J. 1992. Nitric oxide circulates in mammalian plasma primarily as an *S*-nitroso adduct of serum albumin. *Proc. Natl. Acad. Sci. U.S.A.* 89:7674-7677.

Upchurch, G.R., Welch, G.N., and Loscalzo, J. 1996. *S*-nitrosothiols: Chemistry, biochemistry, and biologic actions. *Adv. Pharmacol.* 34:343-349.

Walters, C.L. 1996. Analytical techniques for the determination of total *N*-nitroso compounds. *Eur. J. Cancer Prev.* 5(Suppl. 1):59-61.

Zhang, Y.-Y., Xu, A.-M., Nomen, M., Walsh, M., Keaney, J.F. Jr, and Loscalzo, J. 1996. Nitrosation of tryptophan residues(s) in serum albumin and model dipeptides: Biochemical characterization and bioactivity. *J. Biol. Chem.* 271:14271-14279.

Contributed by Ying-Yi Zhang and Joseph Loscalzo
Boston University School of Medicine
Boston, Massachusetts

Fluorometric Techniques for the Detection of Nitric Oxide and Metabolites

The explosion of interest in the biology of nitric oxide (NO) over the past decade has led to the development of different methods for detecting metabolites of NO under a variety of biological conditions. Numerous techniques, ranging from chemiluminescence to electron spin resonance (ESR), have been employed to evaluate this diatomic radical and other chemical intermediates associated with NO metabolism. The assay most widely used to determine the presence of NO is the measurement of nitrite (NO_2^-) via the classical Griess reagent method (Granger et al., 1996; *UNIT 10.3*). This takes advantage of the formation of a nitrosating species in acidified nitrite solutions that will react with sulfanilamide to form a diazonium adduct. The diazonium adduct then couples with *N*-(1-naphthyl)ethylenediamine dihydrochloride (NEDD) to form a colored azo dye. The absorbance of the resulting solution is read by a UV/VIS spectrophotometer. More recently, fluorometric techniques have been developed using similar nitrosation chemistry; these techniques provide improved sensitivity for nitrite determination (Miles et al., 1996, and references therein). Both fluorometric and colorimetric techniques to determine NO (Miles et al., 1996; Nims et al., 1995) and *S*-nitrosothiols (Cook et al., 1996) at neutral pH, using the same chemical reactions, have been devised. These are useful for numerous biological experiments, especially those concerned with temporal factors. This unit describes fluorometric techniques for the detection and quantification of NO, nitrosating

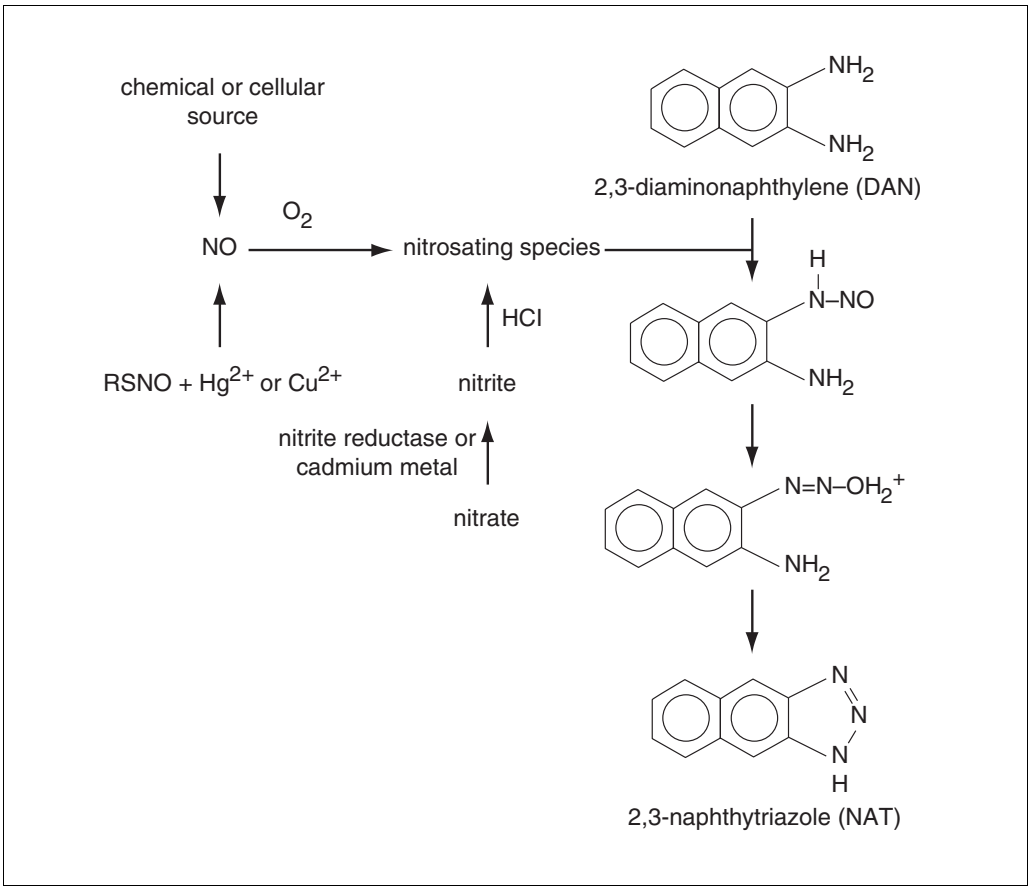

Figure 10.4.1 Reactions for analyzing nitric oxide.

Contributed by David A. Wink, Sungmee Kim, Allen Miles, David Jourd'heuil, and Matthew B. Grisham
Current Protocols in Toxicology (1999) 10.4.1-10.4.12

species, nitrite/nitrate (NO_3^-), and *S*-nitrosothiols in chemical, biochemical, and cellular experiments (Fig. 10.4.1).

This method involves the detection of nitrosating agents produced either chemically or from cellular sources. In the presence of oxygen, NO decomposes via an autoxidation reaction to form the nitrosating agent N_2O_3.

$$4\ NO + O_2 \rightarrow 2\ N_2O_3$$

The reactive intermediate can then be chemically trapped and will serve as a direct indication of the level of NO present. The reaction can be readily followed quantitatively over specified time intervals (Miles et al., 1996). The same chemical reactions can be used to detect *S*-nitrosothiol via a displacement reaction with mercury or copper (Cook et al., 1996). The fluorescence detection method described here employs the reactions whereby 2,3-diaminonaphthylene (DAN) is nitrosated to yield the fluorescent compound 2,3-naphthyltriazole (NAT; Fig. 10.4.2).

$$N_2O_3 + DAN \rightarrow NAT + NO_2^- + H^+$$

When NAT is excited with 375-nm light, it fluoresces with a maximum emission between 425 and 450 nm. For quantification, it is important to note, when calculating the amount of NO present, that one molecule of NAT is formed for every two molecules of NO (Miles et al., 1996). It is advised, however, that standard curves be prepared for all conditions.

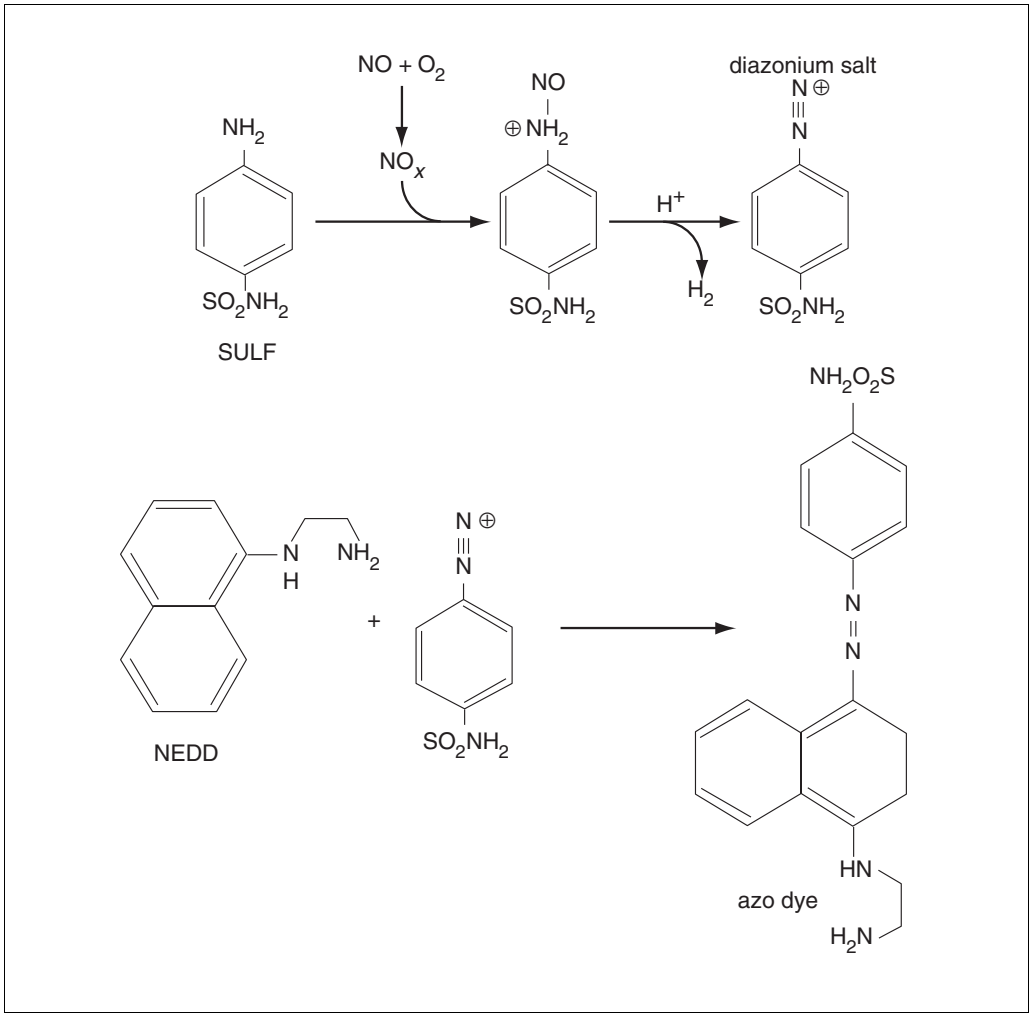

Figure 10.4.2 Reactions for chemically trapping reactive N_2O_3.

DETECTION OF NO FROM CHEMICAL REACTIONS

In the procedure that follows, DAN-containing solutions (prepared without reductants, phenol red, GSH, or vitamins, which may interfere with the assay) are exposed to either a chemical or a biological source of NO. The fluorescence is determined using a fluorometer with both excitation and emission slit widths adjusted depending on the desired sensitivity. Table 10.4.1 shows an approximate concentration range for each slit width. There is some variation among instruments, and the appropriate sensitivity level must be determined for each one.

One of the most useful aspects of this fluorescence technique is that it can be used to monitor the release of NO over the course of an experiment. For instance, one can readily determine the NO release profile over a specific time interval that results from exposing an NO-generating compound to a cell culture. This gives an indication of the temporal NO profile during the biological experiment. This protocol is a basic means of measuring NO released from different chemical or biochemical systems.

Materials

Cell culture medium with no phenol red or vitamins (see recipe)
2,3-Diaminonaphthylene (DAN)
Dimethyl formamide (DMF) or dimethylsulfoxide (DMSO)
20 to 100 mM sodium phosphate, pH 7.4 (*APPENDIX 2A*)
Nitrogen or argon gas
NO gas
Concentrated NaOH (1 or 10 M; *APPENDIX 2A*)
Sulfanilamide
N-(1-Naphthyl)ethylenediamine dihydrochloride (NEDD)
Phosphate-buffered saline (PBS; *APPENDIX 2A*)
NO-generating system to be tested

Fluorescent cuvettes (preferably quartz)
Airtight 100-µl syringe
NO gas cylinder
Fluorometer
Airtight syringe
Plastic tuberculin syringe
Syringe needles

1. Dissolve 15 mg DAN in either DMF or DMSO to give ~100 mM DAN stock solution.
2. Dissolve 200 µl DAN stock solution in 100 ml desired buffer to achieve a 0.2 mM DAN solution.

   Most common buffers can be used, such as Tris, HEPES, and PBS. Generally phosphate buffers with metal chelators such as diethylenetriaminepentaacetic acid (DETAPAC) are used.

Table 10.4.1 Relationship Between Fluorometer Slit Width and Concentration Range[a]

Slit width (nm)		Triazole concentration range (nm)
Excitation	Emission	
2.5	2.5	250-10,000
5.0	5.0	40-1500
10	10	10-40

[a]For Perkin-Elmer LS-50B.

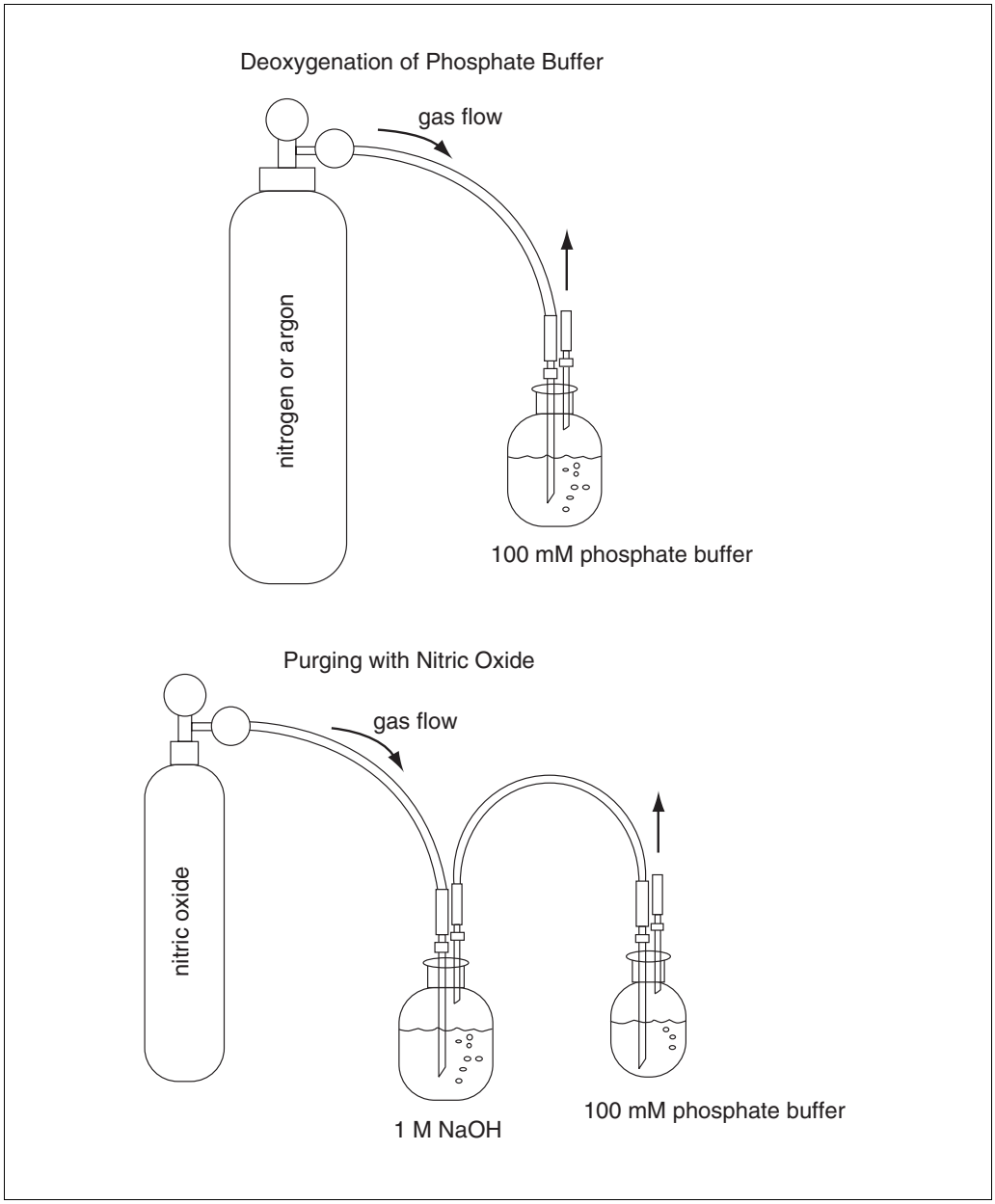

Figure 10.4.3 Apparatus used to degas buffer (top diagram) and prepare NO stock solution (bottom diagram). First degas the vial containing 100 mM sodium phosphate buffer solution by bubbling argon through the solution. Degas the solution 1 min for every milliliter of buffer. Remove the exhaust syringe needle first, then the inlet needle. The 100-mM buffer is now ready for introduction of NO. To prepare the NO-saturated phosphate buffer, connect Tygon tubing from an NO tank to a 6-in. needle (spinal tap needles are useful), and then cut a plastic 1-ml tuberculin syringe and insert into the end of the tubing. Place the needle on the tip. Fill a 500- to 1000-ml flask or bottle that can be fitted with a rubber septum halfway with 1 M NaOH. Place a rubber septum on the opening of the bottle. Stick the needle from the tank through the septum and into the solution, allowing NO to bubble through the solution. Then attach a piece of Tygon tubing to two modified plastic syringes, one with a 2-in. needle and one with a 6-in. needle. Stick the 2-in. needle through the septum into the NaOH solution container, keeping it above the level of the liquid to collect gas; stick the 6-in. needle through the septum into the container of degassed phosphate buffer. Vent the gas from the phosphate buffer into a hood using another 2-in. needle.

Compounds that absorb at wavelengths >350 nm, including phenol red, may interfere with this assay. Media should be prepared without phenol red and some vitamins.

3. To prepare NO stock solution, place 20 to 100 mM sodium phosphate, pH 7.4, in a vial with a rubber septum, and bubble nitrogen or argon through the buffer for 1 min per milliliter of buffer (a convenient setup for accomplishing this is shown in the top diagram of Fig. 10.4.3).

   The concentration should protect the solution from sudden changes in pH. Sometimes small exposure to oxygen will generate acid. A high buffer concentration prevents an acidic pH, which can nitrosate DAN, leading to potentially erroneous results.

4. Set up an apparatus to bubble NO gas first through 1 M NaOH and then through the degassed phosphate buffer (see the bottom diagram of Fig. 10.4.3). Bubble NO through this apparatus for 20 min.

   Alternatively, an NO donor, such as $[(C_2H_5)_2NN(O)NO]Na$ (DEA/NO), can be used to calibrate the fluorometric technique (Keefer et al., 1996). The solid is dissolved in 0.01 mM NaOH. Approximately 20 mg/ml will yield a 10-mM stock solution. To verify the exact concentration, take a UV/VIS spectrum of the base. The wavelength maximum at 250 nm has an extinction coefficient of 8000 M^{-1} cm^{-1}.

5. Prepare colorimetric assay solution (for standardizing the NO stock solutions or DEA/NO) by dissolving 0.5 g sulfanilamide and 30 mg NEDD in 100 ml PBS. Stir and gently heat; then filter if necessary through a 0.22- to 0.45-µm-pore-size paper or syringe filter.

   This colorimetric assay is as described by Nims et al. (1995, 1996).

6. Add a 100-µl aliquot of NO stock solution via an airtight syringe to 1 ml colorimetric solution. Allow to stand 2 min; then read the absorption at 500 nm using a UV/VIS spectrophotometer. Divide the absorbance reading by 0.012 to get the concentration of NO in the stock solution.

   Airtight syringes are required to reduce the exposure of oxygen to the NO solution. NO is unstable under aerobic conditions, and airtight syringes protect the NO from degradation before it is introduced to the colorimetric solution. To introduce the NO into the airtight syringe, first puncture the septa of the NO-saturated buffer; then draw the buffer into the syringe. Place the needle of the airtight syringe at the bottom of the air-exposed test tube that contains the colorimetric solution; then introduce the buffer.

   To standardize the amount of NO released by DEA/NO, add 10 µl to 1 ml colorimetric solution. Allow to stand at room temperature for 1 hr or at 37°C for 20 min. Read the absorption at 500 nM, and divide by 0.012 to get the amount of potential NO released by DEA/NO at neutral pH. The division accounts for the extinction coefficient and the 10× dilution. The maximum DAN concentration is 400 µM, which limits the amount of NO that can be detected. Under conditions in which large amounts of nitrosation occurs, the fluorescence intensity at 450 nm is saturated. To correct for this, simply shift to a wavelength >500 nm. This shift to a lower emission wavelength reduces the fluorescence reading per mole of NAT, providing a spectral region that will not go off scale. The lower the wavelength, the less sensitive the assay; therefore, systems that generate higher NO can be monitored. Remember to redo the standard curve at the new wavelength.

7. Add 1-, 2-, 5-, and 10-µM aliquots of NO stock solution to different test tubes via an airtight syringe to DAN solution. Allow to stand for 10 min at room temperature. To read fluorescence, excite the solutions at 375 nm and read the emission at 450 nm, to obtain a standard curve for the particular buffer or medium.

   Reducing agents such as NADPH, dithiothreitol (DTT), GSH, ascorbate, and 2-mercaptoethanol can interfere with this reaction. Be sure to obtain the standard curve with NO and the exact buffer system in which the experiment is conducted. Phenol red and vitamins also interfere with the assay and should be omitted.

8. Determine NO concentration in the NO-generating system of interest by adding 0.01 ml of the system to a tube containing 1 ml DAN buffer as described in step 6. Follow the reaction by exciting the solutions at 375 nm and reading the emissions at 450 nm.

Temporal experiments can be readily conducted to obtain real-time profiles of NO production.

BASIC PROTOCOL 2

DETECTION OF NO IN CELLULAR SYSTEMS

Basic Protocol 1 can be readily used to detect NO derived from cells (Miles et al., 1995, 1996) by testing the cell supernatant. Supernatants can be from almost any buffer system that does not contain vitamins or phenol red. Cells such as stimulated murine macrophages or rat neutrophils can generate considerable amounts of nitrite in a short period of time, which under some conditions can be detected by fluorescence methods. This protocol describes how to use the fluorescent technique to detect NO produced by cells.

Materials

Cells thought to produce NO
Cell culture medium (see recipe)
2,3-Diaminonaphthylene (DAN; see Basic Protocol 1)
Phosphate-buffered saline (PBS; *APPENDIX 2A*)
Concentrated NaOH (1 or 10 M; *APPENDIX 2A*)

1. Plate cells at 0.2–1 $\times 10^6$ cells/ml in cell culture medium. Allow the cells to attach for 1 to 2 hr.

   Cytokines or other stimuli can be introduced at this time.

2. Place 0.2 ml of DAN stock solution in 100 ml of cell culture medium. Remove the full medium, and wash the cells with PBS twice. Remove the final rinse, and place the cell culture medium with DAN on the cells and incubate for the required time.

   IMPORTANT NOTE*: For long-term storage of the medium, filter it, but omit DAN from the buffer. Add DAN just before conducting the experiment. No phenol red should be present. Vitamins commonly added to media can also interfere.*

3. After cell incubation is complete, take between 0.5 and 1 ml of cell supernatant and add sufficient 10 mM NaOH to obtain a total volume of 2 ml.

   The volume can be adjusted if a plate reader is used.

4. To read fluorescence, excite the solution at 375 nm and read the emission at 450 nm.

   This may not be an effective method for detecting NO derived from cells that use low concentrations of NO, such as bradykinin-stimulated endothelial cells. However, cells that are stimulated to generate iNOS are potentially good candidates.

5. Generate a standard curve for the buffer or medium used to grow the cells, as described in the previous protocol (see Basic Protocol 1, steps 3 to 7).

BASIC PROTOCOL 3

DETECTION OF *S*-NITROSOTHIOLS

S-nitrosothiol complexes are important metabolites in the biology of nitric oxide. This method first removes the nitrosyl from *S*-nitrosothiol adducts by mercury or copper and then oxidizes it to form a nitrosating agent that readily reacts with DAN (Cook et al., 1996).

Materials

Mercuric chloride or copper sulfate
Dimethyl formamide (DMF) or dimethylsulfoxide (DMSO)

2,3-Diaminonaphthylene (DAN)
Phosphate-buffered saline (PBS; *APPENDIX 2A*)
Glutathione
Sodium nitrite
Hydrochloric acid (HCl)
Cell extracts
Buffer samples

Rubber gloves
Fluorometer

1. Prepare a stock solution of 10 mM mercuric chloride in DMF or a 10 mM copper sulfate aqueous solution.

   CAUTION*: DMF/$HgCl_2$ solutions are highly toxic, and should be handled using rubber (not latex) gloves. Copper is less toxic; however, its sensitivity is considerably less.*

2. Prepare 0.4 mM DAN in PBS and add 1 vol of this solution to the sample.

   It is most convenient to use 1 ml of sample and 1 ml of 0.4 mM DAN.

3. Add 10 µl of either mercuric chloride or copper sulfate solution per 100 µl of sample. Allow the mixture to stand for 20 to 30 min at room temperature.

4. Dilute to 2 ml with PBS.

   Add buffer to reach the needed volume for the fluorometer. Volumes of 2 to 3 ml are generally required when using cuvettes; plate readers require less.

5. To prepare a standard curve, first generate *S*-nitrosoglutathione by mixing 33 mg glutathione with 6.9 mg sodium nitrite in 10 ml of 100 mM HCl. Allow the solution to stand 5 min at room temperature.

6. Dilute the solution 1:10 (0.1 ml to 1 ml) in PBS and read fluorescence on a UV/VIS spectrophotometer at 338 nm. Divide the absorbance by 0.09 to obtain the concentration of GSNO in the stock solution.

7. Take the stock solution and serially dilute it in PBS so that the GSNO concentrations range from 0.1 to 10 µM in the same final volume (the same volume as for the sample) and read fluorescence.

   This provides an approximation of the total amount of S-nitrosothiols in the sample.

DETERMINATION OF NITRATE BY FLUORESCENT TECHNIQUES

BASIC PROTOCOL 4

As discussed, acidified nitrite produces a powerful nitrosating agent, which can be trapped by different aromatic amines such as DAN. Nitrate can also be quantified by fluorescent methods, but only after enzymatic or cadmium pellet reduction. Kits are currently available for the enzymatic reduction of nitrate to nitrite. This section describes a protocol involving the nitrosation of DAN. Samples to be tested can be derived from biochemical, cell culture media, or in vivo fluid samples.

Materials

Hydrochloric acid (HCl)
Sample to be tested
2,3-Diaminonaphthylene (DAN)
Concentrated NaOH (1 or 10 M; *APPENDIX 2A*)
5000 U/ml lactate dehydrogenase (Sigma) diluted 1:10 in phosphate-buffered saline (PBS; *APPENDIX 2A*)
100 mM sodium pyruvate
Hydrogen peroxide

100 U/ml GSH peroxidase (Sigma)
10 U/ml *Aspergillus nitrate* reductase
Flavin adenine dinucleotide (FAD)
β-Nicotinamide adenine dinucleotide phosphate (NADPH)

1. Prepare 0.2 mM DAN in 1 N HCl.
2. Add 0.9 ml of sample to 1 ml DAN/HCl and allow the solution to stand for 2 min.
3. Add 100 µl of 10 N NaOH.
4. To read the fluorescence, excite the solution at 375 nm and read the emission at 450 nm.

   A standard curve containing nitrite can be produced by diluting various concentrations of nitrite (from 0.1 to 20 µM) in PBS and repeating steps 1 to 3. Plot nitrite concentration versus fluorescence to obtain the standard curve.

5. If the sample medium or buffer contains >10 µM NADPH or GSH, remove them by the following methods: to oxidize NADPH, add 10 µl lactate dehydrogenase in PBS and 1 µl of 100 mM pyruvate per 1 ml sample. To eliminate GSH, add 10 mM hydrogen peroxide and 5 µl of 100 U/ml GSH peroxidase and incubate 10 min. Then add DAN/HCl as in step 2.
6. Prepare a 1 mM solution of FAD and a 10 mM solution of NADPH. To 1 ml sample, add 10 µl *Aspergillus nitrate* reductase*, 5* µl of 1 mM FAD, and 3 µl of 10 mM NADPH. Incubate 30 min at 37°C.

   The sample size can be changed as long as the proportion of milliliters to liters is maintained.

   Nitrate determination uses reduction by Aspergillus nitrate reductase (1000 U/ml; Grisham et al., 1996).

7. Add 20 µl of 5000 U/ml lactate dehydrogenase and 1 µl of 100 mM sodium pyruvate and let sit 5 min. Add 1 ml DAN/HCl solution, as described in step 2, and proceed to step 4 to obtain a reading without the NADPH and GSH.

REAGENTS AND SOLUTIONS

Use deionized or distilled water in all recipes and protocol steps. For common stock solutions, see ***APPENDIX 2A****; for suppliers, see* ***SUPPLIERS APPENDIX****.*

Cell culture medium

Phosphate-buffered saline (PBS; *APPENDIX 2A*) containing:
10 mM HEPES, pH 7.4
20 mM glucose
4 mM glutamine
1 mM L-arginine
50 U/ml penicillin
50 U/ml streptomycin
Store up to 7 days at 4°C

The medium must be prepared without phenol red, as this and any other compound that absorbs at wavelengths >350 nm (such as some vitamins) will interfere with the assay. The medium should not contain serum, because it will interfere with the fluorometric assay. Solutions containing either colorimetric components or DAN can be stored at room temperature for several days. The medium should be stored in the refrigerator without DAN or the colorimetric components.

COMMENTARY

Background Information

The protocols described here provide a fluorescence method for the determination of nitrosation chemistry—which serves as an indicator of the presence of nitric oxide from either chemical, biochemical, or cellular sources—as well as the determination of *S*-nitrosothiol complexes. The protocols use the specificity of the nitrosation of 2,3-diaminonaphthylene (DAN) to yield a fluorescent triazole (Fig. 10.4.2). Although not a direct method of detecting NO, this is a sensitive indicator of its presence at neutral pH. Basic Protocol 4 was specially designed to detect NO derived from cells.

The basic principle underlying the method is that the generation of nitrosating agents at neutral pH involves the formation of nitric oxide. This can be useful for real-time quantification of NO produced from different sources. For instance, NO released from NO donors, such as NONOates, can result in nitrosative chemistry (Wink et al., 1997). As seen in Figure 10.4.4, 10-, 20-, 50-, and 100-μM samples of DEA/NO release NO over a 1-hr period, indicating the formation of NO, which then further reacts.

Critical Parameters and Troubleshooting

When starting to compare different sources of NO in the presence of a substance such as superoxide, NO may be produced, but nitrosation may be limited (Miles et al., 1995; Wink et al., 1997). Therefore, if NO is being produced, nitrosation chemistry may be diverted. If the presence of superoxide is suspected, then add superoxide dismutase (SOD) at 0.2 mg/ml. As shown in Figure 10.4.5, nitrosation is suppressed in the presence of superoxide. The addition of SOD readily restores the nitrosation. When doing cell culture experiments, be sure that SOD does not harm the cells.

Other substances that can limit the assays are sodium azide, dithiothreitol, 2-mercaptoethanol, and ascorbate. To test whether any of these substances are a problem in a medium, obtain a simple standard curve using NO-saturated aqueous solutions or NO donor drugs,

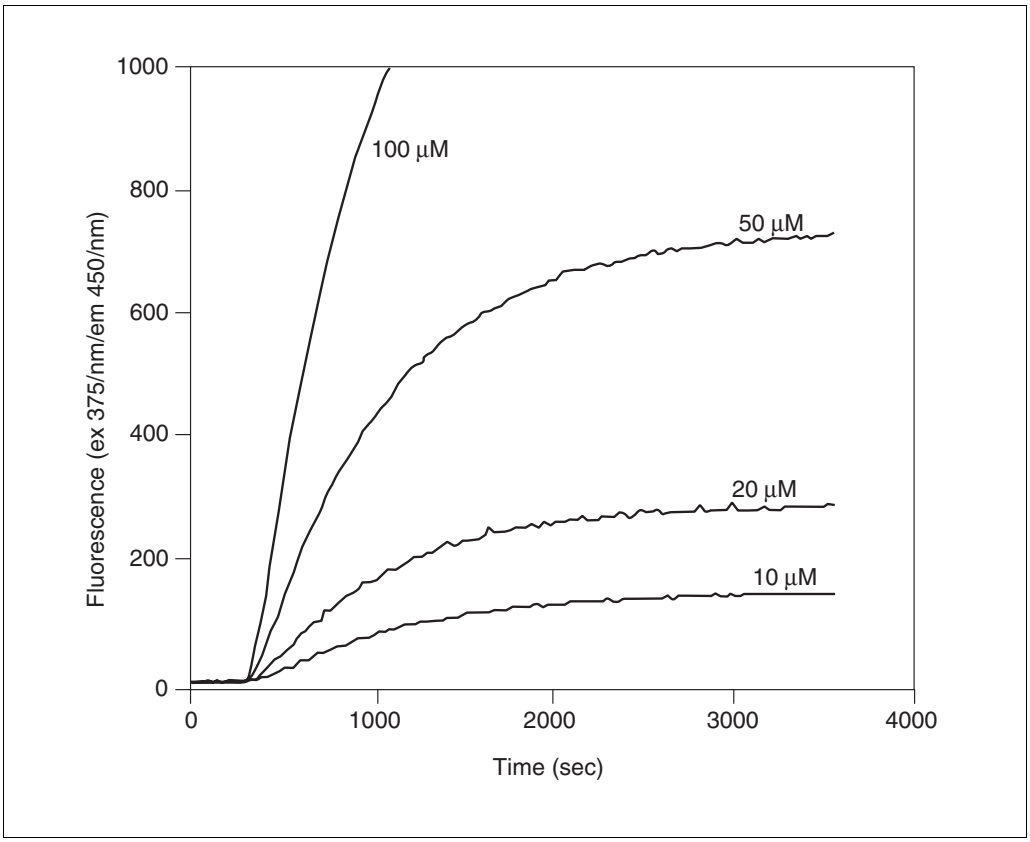

Figure 10.4.4 The formation of NAT is mediated by different concentrations of the NONOate DEA/NO in PBS buffer at room temperature.

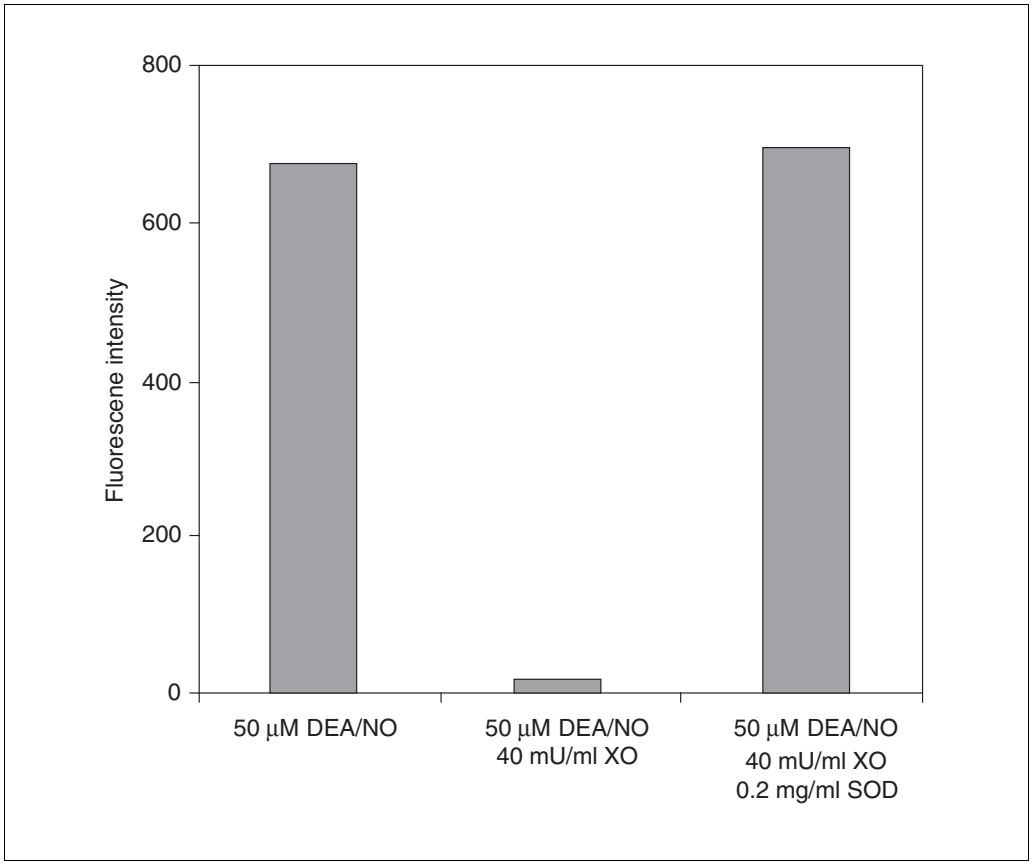

Figure 10.4.5 The effect of superoxide on nitrosation reaction by NO sources; data reported in Wink et al. (1997). The PBS buffer solution included 10 mM HEPES, 0.1 mM DETAPAC, and 0.5 mM hypoxanthine. The solutions were incubated for 1 hr at 37°C.

such as DEA/NO. Another possible source of interference is heme proteins, such as oxyhemoglobin. Heme proteins at concentrations >10 μM can interfere by creating a filter effect or by scavenging NO directly. Using NO gas or NO donors can be a reliable method.

Determining of *S*-nitrosothiol takes advantage of the fact that mercury or copper ions can readily displace NO from these adducts (Cook et al., 1996). NO is oxidized by O_2 to N_2O_3, which then nitrosates DAN. The mercuric salts are very toxic, and extreme care should be taken when handling them. Like low-molecular-weight *S*-nitrosothiol, protein *S*-nitrosothiol can be readily detected; however, BSA and other proteins are not as sensitive as low-molecular-weight *S*-nitrosothiol (Cook et al., 1996). The level of protein *S*-nitrosothiol indicates the lower limit of the actual concentration of total *S*-nitrosothiol. Colorimetric assays have also been described for these procedures (Cook et al., 1996).

Cellular determination of NO via nitrosative chemistry can be readily done using media without phenol red. Dulbecco's minimum essential medium (DMEM; Sigma) without phenol red and with L-arginine and glucose, is a good medium in which to monitor nitrosation for 24 hr (Miles et al., 1995). Under optimal conditions, 500,000 cells per 1 ml medium will give ~0.8 μM NAT in 4 hr. At slit widths of excitation/emission at 5/5 or 2.5/2.5 nm, the reading is significant. Murine macrophages that have been stimulated by interferon (INF) and lipopolysaccharide (LPS; Fig. 10.4.6) or rat neutrophils stimulated with phorbol esters generate detectable nitrosation for 4 to 8 hr after treatment.

Nitrite and nitrate can also be determined using the DAN fluorescence assay. In acidic solutions nitrite can readily nitrosate DAN. The addition of a 1 N HCl solution containing 0.2 mM DAN readily nitrosates DAN with any nitrite. There is a potential of interference from NADPH or GSH, which is a problem for experiments in which biochemical assays such as NOS are used and when nitrate is converted to nitrite via nitrite reductase. The addition of lactate dehydrogenase for 5 min readily converts these proteins. It is important to obtain standard curves each time, to ensure that the

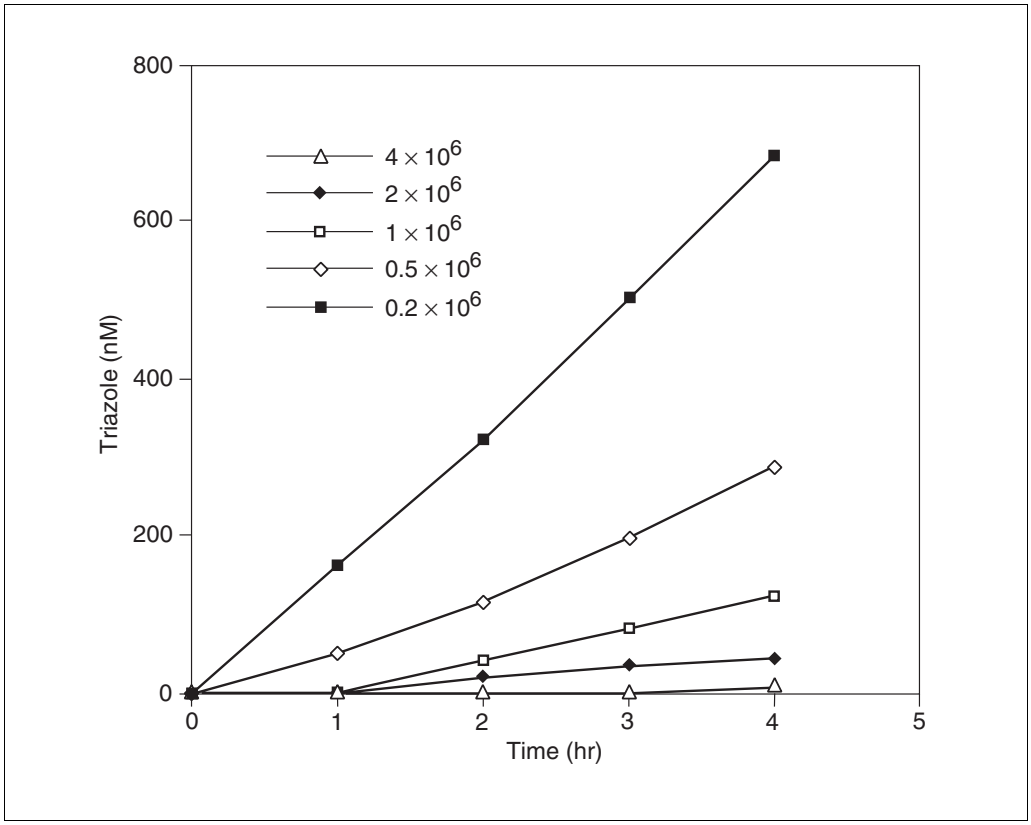

Figure 10.4.6 Nitrosation of DAN by different cell densities of RAW macrophages. Macrophages were plated in 10-cm dishes and treated overnight with interferon-γ. LPS was then added for 4 hr. The cells were rinsed, and the medium was replaced with 10 ml DMEM containing 0.2 μM DAN, 20 mM HEPES, 4 mM glutamine, 10 mM glucose, and 1 mM L-arginine.

specific experimental conditions do not interfere with the assay.

The protocols described here provide several methods for determining a variety of metabolites of NO. Although these protocols measure the analyte indirectly through nitrosating agents, they provide a good indication of the presence of NO metabolism. These protocols may need to be modified to fit the particular experiment being conducted.

Anticipated Results

The detection limit of the DAN assay is about 10 nM; however, some of the procedures described here require dilutions of 10 to 100 times, reducing sensitivity. A typical experimental detection limit ranges from 50 nM to 200 μM. Nitrosation from cell cultures has a lowest detection limit of 50 nM, and the detected nitrite concentration may be as low as 10 nM. Be sure to check for and subtract any background nitrite. The limits of detecting NO from donors and *S*-nitrosothiol range from 50 nM to 100 μM. Again, the sensitivity is determined by the type of dilution made.

Time Considerations

The assays described in this unit are not in themselves time consuming, taking 1 hr or less to perform. However, preparation and treatment of the cells prior to making these measurements may take variable amounts of time.

Literature Cited

Cook, J.A., Kim, S.-M., Teaug, D., Krishna, M.C., Pacelli, R., Mitchell, J.B., Nims, R.W., Christodoulou, D., Miles, A.M., Grisham, M.B., and Wink, D.A. 1996. Convenient colorimetric and fluorometric assays for *S*-nitrosothiols. *Anal. Biochem.* 238:150-158.

Granger, D.L., Taintor, R.R., Boockvar, K.S., and Hibbs, J.B. 1996. Measurement of nitrate and nitrite in biological system using nitrate reductase and Griess reaction. *Methods Enzymol.* 268:142-151.

Grisham, M.B., Johnson, G.G., and Lancaster, J.R. 1996. Quantitation of nitrate and nitrite in extracellular fluids. *Methods Enzymol.* 268:237-246.

Keefer, L.K., Nims, R.W., Davies, K.W., and Wink, D.A. 1996. NONOates (diazenolate-2-oxides) as nitric oxide dosage forms. *Methods Enzymol.* 268:281-294.

Miles, A.M., Gibson, M., Krishna, M., Cook, J.C., Pacelli, R., Wink, D.A., and Grisham, M.B. 1995. Effects of superoxide on nitric oxide-dependent N-nitrosation reactions. *Free Radic. Res. Commun.* 233:379-390.

Miles, A.M., Wink, D.A., Cook, J.C., and Grisham, M.B. 1996. Determination of nitric oxide using fluorescence spectroscopy. *Methods Enzymol.* 268:105-120.

Nims, R.W., Darbyshire, J.F., Saavedra, J.E., Christodoulou, D., Hanbauer, I., Cox, G.W., Grisham, M.B., Laval, J., Cook, J.A., Krishna, M.C., and Wink, D.A. 1995. Colorimetric methods for the determination of nitric oxide concentration in neutral aqueous solutions. *Methods: A Companion to Methods Enzymol.* 7:48-54.

Nims, R.W., Cook, J.C., Krishna M.C., Christodoulou, D., Poore, C.M.B., Miles, A.M., Grisham, M.B., and Wink, D.A. 1996. Colorimetric methods for the determination of nitric oxide concentration in neutral aqueous solutions. *Methods Enzymol.* 268:93-105.

Wink, D.A., Cook, J.A., Kim, S., Vodovotz, Y., Pacelli, R., Kirshna, M.C., Russo, A., Mitchell, J.B., Jourd'heuil, D., Miles, A.M., and Grisham, M.B. 1997. Superoxide modulates the oxidation and nitrosation of thiols by nitric oxide derived reactive intermediates, 1997. *J. Biol. Chem.* 272:9922-9932.

Contributed by David A. Wink and Sungmee Kim
National Cancer Institute
Bethesda, Maryland

Allen Miles, David Jourd'heuil, and Matthew B. Grisham
Louisiana State University Medical Center
Shreveport, Louisiana

Measurement of cGMP and Soluble Guanylyl Cyclase Activity

Guanosine 3′,5′-cyclic monophosphate (cGMP) was originally identified more than three decades ago, but little headway was made in elucidating its physiologic role(s) until it was established that the synthesizing enzyme, soluble guanylyl cyclase, could be activated by nitric oxide (NO; Waldman and Murad, 1987) and that NO mediated the cGMP response to excitatory amino acid receptor activation in the brain (Garthwaite et al., 1988). Since then, the ideas that NO is an important intercellular messenger molecule and that soluble guanylyl cyclase is its best characterized target have gained wide acceptance (Mayer et al., 1993). Thus measurement of tissue cGMP levels and soluble guanylyl cyclase activity have become important tools in the investigation of the NO-cGMP signal transduction pathway. Methods for both are described in this unit. cGMP levels may be determined either ex vivo or in tissues that have been maintained in vitro. Guanylyl cyclase activity may be estimated for both crude and purified enzyme preparations.

For measuring the cGMP content of tissues, radioimmunoassay (RIA) is the method of choice (Steiner et al., 1972; see Basic Protocol 1). This technique has recently been simplified by the introduction of scintillation proximity assay (SPA) technology (see Alternate Protocol 1). Two approaches are generally used to determine the activity of soluble guanylyl cyclase. In the first, unlabeled (cold) guanosine 5′-triphosphate (GTP) is the substrate, and the cGMP formed is measured by RIA (Troyer et al., 1978; see Basic Protocol 2). In the second, the conversion of radiolabeled substrate ([α-^{32}P]GTP) to product ([^{32}P]cGMP) is monitored (Schultz and Böhme, 1984; see Alternate Protocol 2).

CAUTION: When working with radioactivity, take appropriate precautions to avoid contamination of the experimenter and the surroundings. Carry out the experiment and dispose of wastes in an appropriately designated area, following the guidelines provided by the local radiation safety officer (see *APPENDIX 1A*).

NOTE: All protocols using live animals must first be reviewed and approved by an Institutional Animal Care and Use Committee (IACUC) or must conform to government regulations regarding the care and use of laboratory animals.

DETERMINATION OF TISSUE cGMP LEVELS BY RIA

BASIC PROTOCOL 1

This technique is based on the competition for binding to cGMP antiserum between a known concentration of [^{3}H]cGMP and the unlabeled cGMP contained within samples. Therefore, after the removal of unbound radiolabeled ligand and the addition of scintillant, the counts per minute (cpm) will be inversely proportional to the concentration of cGMP in the sample.

Tissue maintained in vitro is inactivated by plunging it into a small volume of boiling hypotonic homogenization buffer (aiming for a protein concentration of ~1 mg/ml) contained in a microcentrifuge tube and heating it for 3 to 5 min. Alternatively, the cGMP content of tissues may be determined ex vivo after rapidly removing and freeze clamping. Most tissues possess quanylyl cyclase activity, but liver and brain are particularly good sources of the soluble isoform.

NOTE: A cGMP RIA kit containing [^{3}H]cGMP, antiserum, cGMP standards, 10 µM cGMP, and ammonium sulfate solution is commercially available (Amersham).

Contributed by Eric Southam

Current Protocols in Toxicology (1999) 10.5.1-10.5.8

Materials

Tissue to be analyzed
Tris/EDTA buffer: 50 mM Tris/4 mM EDTA, pH 7.6 (prepare from Tris base and EDTA, and adjust pH with 1 M HCl)
~5.9 kBq/ml [^{3}H]cGMP (Amersham)
Rabbit antiserum specific for cGMP (raised according to the method of Steiner et al., 1972)
80, 40, 20, 10, and 5 nM unlabeled cGMP (standards)
10 µM cGMP (for determining nonspecific binding)
0.39 g/ml ammonium sulfate [$(NH_4)_2SO_4$], ice cold
Water-compatible scintillation fluid

Probe sonicator
Aspirator (a narrow-gauge syringe needle attached to a vacuum line works well)

Prepare soluble cGMP-containing fraction

1. Homogenize the tissue by sonication in Tris/EDTA buffer, pH 7.6.
2. Remove an aliquot of homogenate (e.g., 50 µl) for protein determination by standard methods. Centrifuge the remainder 5 min at 10,000 × *g*, room temperature, and then determine the cGMP content of the soluble fraction.

Perform the RIA

3. Place 50 µl of [^{3}H]cGMP, 100 µl of sample, and 50 µl of rabbit anti-cGMP antiserum into an appropriate number of 1.5-ml microcentrifuge tubes. For total counts, nonspecific binding, and standards, set up tubes in similar fashion in which the 100 µl of sample is replaced with 100 µl of either Tris/EDTA buffer, 10 µM cGMP, or standard dilutions of cGMP, respectively. Perform each determination in duplicate.
4. Vortex mix each tube and incubate ≥1.5 hr on ice.

   There is no disadvantage to overnight incubation, as long as all tubes are treated indentically.

5. Precipitate bound [^{3}H]cGMP by adding 1 ml ice-cold 0.39 g/ml ammonium sulfate. Vortex mix, and leave 5 min on ice.
6. Centrifuge 75 sec at 10,000 × *g*, 4°C.
7. Aspirate the supernatant, which contains unbound [^{3}H]cGMP; dissolve the precipitate by adding 1 ml distilled water and vortex mixing.

   From this stage on, tubes can be safely left at room temperature.

8. Transfer 950 µl of the resuspended precipitate to a scintillation vial, and add 10 ml scintillation fluid. Mix thoroughly.
9. Count for 5 min in a scintillation counter.

Calculate results

10. Subtract nonspecific binding from all of the other counts. Then calculate, for each standard or sample cGMP concentration, the fraction C_0/C_x, where C_0 = total counts and C_x = counts for the standard or sample.
11. To obtain the standard curve, plot C_0/C_x on the ordinate against standard concentrations of cGMP (0.5 to 8.0 pmol/100 µl) on the abscissa.

    The resulting curve is a straight line that intercepts the ordinate at 1.0 and is, therefore, described by equation:

$$C_0/C_x = (\text{slope} \times \text{cGMP concentration}) + 1$$

12. To determine unknown cGMP concentrations, rearrange the equation:

$$\text{cGMP concentration} = \frac{(C_0/C_x - 1)}{\text{slope}}$$

13. The resultant cGMP concentration has the units picomoles of cGMP per 100 µl; divide by the protein content of 100 µl of homogenate to arrive at a tissue concentration measured in picomoles per milligram of protein.

DETERMINATION OF TISSUE cGMP LEVELS BY SCINTILLATION PROXIMITY ASSAY

ALTERNATE PROTOCOL 1

Like RIA, this procedure is based on competition between a known concentration of [^{3}H]cGMP and unlabeled sample cGMP for binding to cGMP antiserum; results are calculated as for the RIA. Unlike in the RIA, the scintillant is contained within microspheres that bear anti-rabbit antibodies on their surface (SPA antibody binding beads). This means that only the [^{3}H]cGMP bound to antibody—which itself becomes bound to the fluomicrospheres—will be in close enough proximity to the scintillant within the spheres to generate a signal. There is, therefore, no need to separate bound radiolabeled ligand from unbound.

Additional Materials *(also see Basic Protocol 1)*

Anti-rabbit SPA antibody binding beads (fluomicrospheres, Amersham)
96-well microtiter plate and sealer (e.g., T-tray, Wallac)
β-plate scintillation counter

1. Dispense 50 µl of [^{3}H]cGMP, 100 µl of buffer, standards, or sample (see Basic Protocol 1, step 3), and 50 µl of rabbit anti-cGMP antiserum into each well of a 96-well plate.
2. Add 50 µl of fluomicrospheres to each well. Seal the plate and mix.

   The manufacturer recommends a 3-hr incubation at room temperature, but experience has proved this to be unnecessary.

3. Count for 5 min using a β-plate scintillation counter.
4. Calculate cGMP binding activity (see Basic Protocol 1, steps 10 to 13).

SOLUBLE GUANYLYL CYCLASE ASSAY USING RIA TO QUANTIFY cGMP PRODUCT

BASIC PROTOCOL 2

In this assay, based on the method of Troyer et al. (1978), the quantity of cGMP product formed from GTP substrate by soluble guanylyl cyclase, maintained at 37°C, is measured by RIA (or SPA). This method is suitable for either crude or purified enzyme preparations. Crude soluble guanylyl cyclase is prepared simply as described here. Typically, liver or brain tissue is used for the preparation of a crude enzyme extract. The enzyme may be purified to homogeneity as described elsewhere (Mülsch and Gerzer, 1991).

Materials

Animals whose tissues are to be analyzed
Tris/DTT buffer, ice cold: 10 mM Tris/1 mM dithiothreitol, pH 7.4 (prepare with Tris base and adjust pH with 1 M HCl; *APPENDIX 2A*)
Reaction buffer containing unlabeled GTP (see recipe)
0.1 M EDTA (*APPENDIX 2A*)
Motorized homogenizer, 4°C
Refrigerated centrifuge capable of 48,000 × *g*

Prepare a crude enzyme extract

1. Quickly remove tissue and immerse it in ~10 vol ice-cold 10 mM Tris/DTT buffer, pH 7.4, aiming for a final protein concentration of <10 mg/ml.
2. Thoroughly homogenize (~15 sec, high power) using a prechilled motorized homogenizer, 4°C.
3. Centrifuge 30 min at 48,000 × *g*, 4°C.
4. Decant the soluble fraction and keep on ice until used, or divide into aliquots and snap freeze in liquid nitrogen for long-term storage at −70°C.

Perform the enzyme assay

5. Dispense 150-µl aliquots of reaction buffer containing unlabeled GTP into 1.5-ml microcentrifuge tubes and prewarm to 37°C in a water bath.
6. Add 50 µl crude enzyme extract.
7. Incubate 10 min at 37°C.
8. To determine enzyme activity, add 40 µl of 0.1 M EDTA, and heat to 100°C in a block heater for 3 to 5 min.

   Nonspecific activity is determined by adding EDTA to the enzyme extract and heating before adding the GTP substrate.

9. Determine the cGMP content of the reaction mixture via RIA as described above (see Basic Protocol 1, steps 3 to 9).

Calculate results

10. Calculate the cGMP generated by the enzyme as described above (see Basic Protocol 1, steps 10 to 13), expressing enzyme activity as moles cGMP formed per milligram of protein per minute.

ALTERNATE PROTOCOL 2

SOLUBLE GUANYLYL CYCLASE ASSAY USING [α-^{32}P]GTP AS SUBSTRATE

Soluble guanylyl cyclase activity may also be determined by monitoring the conversion of [α-^{32}P]GTP to [^{32}P]cGMP (Schultz and Böhme, 1984). [^{32}P]cGMP must be separated from unused radiolabeled substrate by precipitating out the latter with zinc carbonate and running the sample on an alumina column. Tritium may be used in place of the very high-energy beta emitter ^{32}P as a label for this assay.

Additional Materials *(also see Basic Protocol 2)*

Reaction buffer containing [α-^{32}P]GTP (see recipe)
125 mM zinc acetate [$Zn(C_2H_3O_2)_2 \cdot 2H_2O$]
125 mM sodium carbonate ($Na_2CO_3 \cdot 10H_2O$)
Neutral alumina column (see recipe)
0.1 M Tris·Cl, pH 7.5 (*APPENDIX 2A*)
[^{3}H]cGMP containing ~5.9 kBq/ml (Amersham)
Water-miscible scintillation fluid

Perform the enzyme assay

1. Prepare the crude enzyme extract (see Basic Protocol 2, steps 1 to 4).
2. Dispense 75-µl aliquots of reaction buffer containing [α-^{32}P]GTP into 1.5-ml microcentrifuge tubes and prewarm to 37°C.
3. Prepare two additional tubes to be used for determining the efficiency of recovery (ER) in step 6. Prepare two blank tubes by adding 75 µl reaction buffer containing label, 400 µl of 125 mM zinc acetate, and 500 µl of 125 mM sodium carbonate.

4. Add 25 µl crude enzyme extract to each tube, including blank and ER tubes. Briefly vortex mix.
5. Incubate 10 min at 37°C.
6. Add 400 µl of 125 mM zinc acetate followed by 500 µl of 125 mM sodium carbonate to terminate the assay. Add 5,000 to 10,000 cpm [^{3}H] cGMP to ER tubes.

Isolate the [^{32}P]cGMP

7. Centrifuge 10 min at 2000 × *g*, room temperature.
8. Transfer 800 µl of supernatant to a neutral alumina column.
9. Elute [^{32}P]cGMP with 5 ml of 0.1 M Tris·Cl, pH 7.5; drain and repeat with a further 5 ml buffer.
10. Collect entire eluates into 20-ml scintillation vials. Add 10 ml water-miscible scintillation fluid to each vial.
11. Determine activity of samples using a scintillation counter. Also prepare two 50-µl aliquots of reaction buffer containing label (i.e., 50 pmol GTP) and count those to determine the specific activity (SA) of the labeled substrate.

Calculate results

12. Calculate soluble guanylyl cyclase activity as the ratio of recovered counts (minus blank) divided by specific activity of labeled substrate and corrected for efficiency of product recovery, per milligram of protein per minute.

$$\text{activity} = \frac{\text{cpm} - \text{blank}}{\text{SA} \times \text{ER} \times \text{mg protein} \times \text{min}}$$

where blank = counts per minute when zinc carbonate is added before the addition of the enzyme; SA = specific activity of radiolabeled substrate; and ER = efficiency of recovery of cGMP (the fraction of added cGMP recovered in the eluate) for the ER tubes.

A recovery of ~0.6 is usual. [^{3}H]cGMP is suitable for this purpose.

REAGENTS AND SOLUTIONS

Use Milli-Q-purified water or equivalent for all recipes and protocol steps. For common stock solutions, see ***APPENDIX 2A****; for suppliers, see* ***SUPPLIERS APPENDIX****.*

Neutral alumina column

Fill glass or plastic columns (7 mm i.d.) with dry neutral alumina (100 to 200 mesh) to a height of 2.5 cm. Add 8 ml of 0.1 M Tris·Cl buffer, pH 7.5 (*APPENDIX 2A*); allow buffer to drip through and the alumina to resettle. Wash with a further 2 ml of 0.1 M Tris·Cl buffer, pH 7.5.

Columns should be freshly prepared.

Reaction buffer containing [α-^{32}P]GTP

4.0 ml 2 × reaction buffer stock solution (see recipe)
0.5 ml 24 mM $MnCl_2$ (4.75 mg/ml $MnCl_2 \cdot 4H_2O$ in 50 mM Tris·Cl)
0.5 ml 8 mM [α-^{32}P]GTP (1.134 mg/ml GTP in 50 mM Tris·Cl, spiked with [α-^{32}P]GTP to arrive at ~5×10^6 cpm/ml)
1.0 ml 50 mM Tris·Cl, pH 7.5

Prepare 50 mM Tris·Cl from Tris base, adjusting the pH to 7.5 with 1 M HCl.

Final concentrations in the reaction buffer are 50 mM Tris·Cl, 4 mM IBMX, 5 mM creatine phosphate, 0.15 mg/ml creatine phosphokinase, 0.5 mg/ml BSA, 2 mM cGMP, 3 mM $MnCl_2$, and 1 mM [α-^{32}P]GTP. The working solution is diluted 3:1 in the assay.

Reaction buffer containing unlabeled GTP

2.5 ml 2× reaction buffer stock solution *without* cGMP (see recipe)
3.05 mg guanosine 5′-triphospate (GTP; sodium salt)
50 µl 0.3 M $MnCl_2$ (5.937 g $MnCl_2 \cdot 4H_2O$/100 ml 50 mM Tris·Cl)
1.20 ml 50 mM Tris·Cl, pH 7.5
Keep stirred

Prepare 50 mM Tris·Cl from Tris base, adjusting the pH to 7.5 with 1 M HCl.

Final concentrations in the reaction buffer are 50 mM Tris·Cl, 4 mM IBMX, 5 mM creatine phosphate, 0.15 mg/ml creatine phosphokinase, 0.5 mg/ml BSA, 1 mM GTP, and 3 mM $MnCl_2$. The working solution is diluted 3:1 in the assay.

Reaction buffer stock solution, 2×

Combine (per milliliter):
6.05 mg Tris base (to 50 mM)
H_2O to dissolve
1 M HCl (*APPENDIX 2A*), pH 7.5
1.776 mg 3-isobutyl-1-methylxanthine (IBMX; warm and stir to dissolve; to 8 mM)
2.551 mg creatine phosphate (disodium salt, hydrate; to 10 mM)
0.30 mg creatine phosphokinase (type I, rabbit muscle, 150 to 250 U/mg protein)
1.0 mg BSA (lay on top of buffer and let dissolve without agitation)
0.734 mg guanosine 3′,5′-cyclic monophosphate (cGMP; sodium salt; to 2 mM)
Add H_2O to full volume
Divide stock solution (e.g., 50 ml) into aliquots and store up to several weeks at −20°C

For reaction buffer with unlabeled GTP, omit cGMP from the stock solution.

COMMENTARY

Background Information

There are two isoforms of guanylyl cyclase: a membrane-bound particulate form and a soluble form. Soluble guanylyl cyclase is a heterodimer consisting of α and β subunits and is activated by the interaction of NO with its heme moiety (Mayer et al., 1993). Many tissues contain both isoforms of the enzyme, but the two are readily separated by centrifugation. Investigators should be aware, however, that the resultant soluble fraction contains other enzymes in addition to soluble guanylyl cyclase. Components of the assay reaction buffers are included to take account of some of these. 3-isobutyl-1-methylxanthine (IBMX) is a broad-spectrum inhibitor of phosphodiesterases (PDE), except the calcium/calmodulin-dependent PDE I (Mayer et al., 1993), and will, therefore, minimize the degradation of cGMP. The GTP-regenerating system, consisting of creatine kinase and creatine phosphate, is included to counteract the activity of 5′ nucleotidases and thus protect the supply of substrate. Unlabeled cGMP is included in the reaction buffer containing [α-^{32}P]GTP to minimize any loss of the labeled cyclic nucleotide product.

Essential for the activity of soluble guanylyl cyclase is the presence of a divalent metal cofactor, either Mg^{2+} or Mn^{2+}. The former cation facilitates a more pronounced response when the enzyme is stimulated by NO; the latter results in higher basal activities. It will be noted from Basic Protocol 2 that enzyme activity may terminated by chelating the metal cofactor with EDTA. Soluble guanylyl cyclase is extremely sensitive to oxidation, and the reducing agent DTT (or another equivalent thiol) is an essential additive to the homogenization buffer.

In intact tissues, the activity of soluble guanylyl cyclase depends on the various physiologic stimuli that result in the synthesis of NO. In rat brain slices, for example, cGMP levels are raised after stimulation with the excitatory amino acid glutamate in a NO-dependent manner (Southam et al., 1991). Indeed, the cGMP response is an excellent biochemical marker for glutamate receptor activation. In the absence of such stimuli—for example, when assaying crude or purified preparations of soluble guanylyl cyclase—basal levels of activity may be very low, necessitating the inclusion of a NO-donor com-

pound in the reaction mixture (see Critical Parameters and Troubleshooting).

Critical Parameters and Troubleshooting

Perhaps the greatest source of variability when estimating the cGMP content of tissues, either by RIA or by SPA, is the treatment of the tissues themselves. The effects of the animal's behavior immediately before death and of the method of killing should be considered. For example, cGMP levels in the cerebellum are influenced by stress, motor activity, and respiratory depression (Wood, 1991). Basal and stimulated cGMP levels in tissues maintained in vitro highly depend on the viability of the tissue and, therefore, on the method of preparation and maintenance. The cGMP response to 10 mM glutamate in adult rat brain slices, for example, is 10-fold greater in hand-cut slices than in chopped slices (Garthwaite et al., 1979). It should also be remembered that the cGMP content of intact tissues reflects not only the activity of guanylyl cyclases but also that of phosphodiesterases. When the NO-cGMP pathway is studied in tissues maintained in vitro, it may be desirable to promote the cGMP response by incubating in the presence of a broad-spectrum PDE inhibitor (e.g., 1 mM IBMX).

cGMP antiserum provided in cGMP RIA kits is claimed by the manufacturers to bind to cGMP with ~ 150,000 and 30,000 times greater affinity than to cAMP and guanine nucleotides, respectively, so that cross-reactivity should not be a problem. Investigators who prepare their own antiserum must carefully characterize its properties before use. Reconstituted antiserum should be stored frozen; and although it will withstand a small number of freeze-thaw cycles with minimal loss of activity, these should be minimized by dividing it into small aliquots before storage. Thawed antiserum must be thoroughly mixed before use.

Optimum antiserum-cGMP binding is achieved at low temperatures; care should be taken that the temperature does not rise above 4°C during incubation, precipitation with ammonium sulfate (which itself must be ice cold), and centrifuge steps of the RIA procedure. Because the SPA does not require separation of bound from unbound radiolabeled ligand, this protocol may be performed at ambient temperatures.

It is essential for both RIA and SPA that standards be included with each assay to control for an interassay variation. When plotted as described in the Basic Protocol 1, the standard curve should produce a straight line. This linearity should not be assumed to hold true for higher cGMP concentrations, at which the curve tends to flatten out. If the cGMP content exceeds 8 pmol/100 µl then samples should be diluted. Generally, though, provided good experimental practice is observed (accurate pipetting, for example), RIA and SPA assays of cGMP are highly reproducible. The sensitivity of the RIA technique may be enhanced from the picomole to the femtomole range by acetylating the samples and standards (Harper and Brooker, 1975).

To ensure that consistent results are obtained when assaying soluble guanylyl cyclase activity, it is essential that the conversion of substrate to product per milligram protein (or unit of purified enzyme) is constant, i.e., within the initial velocity phase. It is, therefore, necessary to demonstrate that the quantity of cGMP formed is directly proportional to time and to protein concentration, within the limits of the experimental protocol. If they are not, the most likely explanations are that the enzyme is unstable or the quantity of substrate is limiting. The following steps may be taken to optimize enzyme stability: (1) ensure that the enzyme is used as quickly as possible once prepared and stored on ice in the meantime; (2) reduce oxidation of the enzyme by incorporating a reducing agent, such as DTT, in the homogenization buffer and, if necessary, the reaction buffer; (3) add BSA to the reaction mix (particularly when using purified enzyme); and (4) inhibit dephosphorylation of the enzyme by adding a phosphatase inhibitor. In addition, the reaction period may be reduced from the 10 min indicated in the protocol. Substrate should be present in excess; but if high concentrations of enzyme (high protein content) are present, then it could conceivably become limiting. In this case, the simplest solution is to dilute the enzyme preparation.

Obtaining reproducible values for basal soluble guanylyl cyclase activity may prove problematic because the basal activity levels are low (which makes inhibition studies, in particular, difficult) and also because of spontaneous activation of the enzyme, presumably caused by variable concentrations of endogenous NO. These problems may be overcome by ensuring that sufficient NO is present in the reaction mix to cause a consistently elevated level of enzyme activity. There are several NO-donor compounds available that may be used to stimulate soluble guanylyl cyclase activity (Southam and Garthwaite, 1991). For example, 100 µM sodium nitroprusside (SNP, Sigma) is reported to increase purified bovine lung-soluble guanylyl cyclase activity 174-fold (Humbert et al., 1990).

Anticipated Results

The cGMP content of tissues is influenced by many factors (see Critical Parameters and Troubleshooting), but typical basal concentrations in rat brain slices are in the range of 1 to 5 pmol/mg protein and may rise 100-fold or more upon stimulation by glutamate receptor agonists (Southam et al., 1991). Soluble guanylyl cyclase activity measurements vary, depending largely on whether a crude extract or purified enzyme is assayed and the makeup of the reaction buffer. The basal activity of purified bovine lung enzyme, with Mg^{2+} present as a metal ion cofactor, is reported to be 12 nmol/mg/min, rising to 2100 nmol/mg/min in the presence of 100 μM SNP (Humbert et al., 1990).

Time Considerations

Tissue homogenates to be assayed for cGMP content can be safely kept frozen for several weeks without any loss of the cyclic nucleotide. About 60 samples can comfortably be assessed by RIA in 3 to 4 hr. This does not include time taken for scintillation counting but does include a 90-min incubation period. SPA is considerably quicker, because an extended incubation period is not necessary and the need for separating bound from unbound radiolabeled ligand is eliminated: the same number of samples can be assayed in ~1 hr (again, not including time taken for scintillation counting). A crude extract of soluble guanylyl cyclase takes 1 hr to prepare, and the enzyme assay a further 2 hr. If Alternate Protocol 2 has been followed, eluates from the chromatography column are counted directly. When nonradioactive cGMP is the product, either an RIA or SPA assay must be performed. Preparation of a crude enzyme extract, the assay, and determination of cGMP by RIA can all be done in a single day.

Literature Cited

Garthwaite, J., Woodhams, P.L., Collins, M.J., and Balazs, R. 1979. On the preparation of brain slices: Morphology and cyclic nucleotides. *Brain Res.* 173:373-377.

Garthwaite, J., Charles, S.L., and Chess-Williams, R. 1988. Endothelium-derived relaxing factor release on activation of NMDA receptors suggests role as intercellular messenger in the brain. *Nature* 336:385-388.

Harper, J.F. and Brooker, G. 1975. Femtomole sensitive radioimmunoassay for cyclic AMP and cyclic GMP after 2′0 acetylation by acetic anhydride in aqueous solution. *J. Cyclic Nucleotide Res.* 1:207-218.

Humbert, P., Niroomand, F., Fischer, G., Mayer, B., Koesling, D., Hinsch, K.-D., Gausepohl, H., Frank, R., Schultz, G., and Böhme, E. 1990. Purification of soluble guanylyl cyclase from bovine lung by a new immunoaffinity chromatographic method. *Eur. J. Biochem.* 190:273-278.

Mayer, B., Koesling, D., and Böhme, E. 1993. Characterization of nitric oxide synthase, soluble guanylyl cyclase, and Ca^{2+}/calmodulin-stimulated cGMP phosphodiesterase as components of neuronal signal transduction. *In* Advances in Second Messenger and Phosphoprotein Research, Vol. 28 (B.L. Brown and P.R.M. Dobson, eds.) pp 111-119. Raven Press, New York.

Mülsch, A. and Gerzer, R. 1991. Purification of heme-containing soluble guanylyl cyclase. *Methods Enzymol.* 195:377-383.

Schultz, G. and Böhme, E. 1984. Guanylate cyclase. *In* Methods of Enzymatic Analysis, Vol. 4 (H.U. Bergmeyer, J. Bergmeyer, and M. Grassl, eds.) pp. 379-389. Verlag Chemie, Weinheim, Germany.

Southam, E. and Garthwaite, J. 1991. Comparative effects of some nitric oxide donors on cyclic GMP levels in rat cerebellar slices. *Neurosci. Lett.* 130:107-111.

Southam, E., East, S.J., and Garthwaite, J. 1991. Excitatory amino acid receptors coupled to the nitric oxide/cyclic GMP pathway in rat cerebellum during development. *J. Neurochem.* 56:2072-2081.

Steiner, A.L., Parker, C.W., and Kipnis, D.M. 1972. Radioimmunoassay for cyclic nucleotides. I. Preparation of antibodies and iodinated cyclic nucleotides. *J. Biol. Chem.* 247:1106-1113.

Troyer, E.W., Hall, I.A., and Ferrendelli, J.A. 1978. Guanylate cyclase in CNS: Enzymatic characteristics of soluble and particulate enzymes from mouse cerebellum and retina. *J. Neurochem.* 31:825-833.

Waldman, S.A. and Murad, F. 1987. Cyclic GMP synthesis and function. *Pharmacol. Rev.* 39:163-196.

Wood, P.L. 1991. Pharmacology of the second messenger, cyclic guanosine 3′,5′-monophosphate, in the cerebellum. *Pharmacol. Rev.* 43:1-25.

Key References

Mayer et al., 1993. See above.

Short review describing the NO-cGMP pathway at the molecular level.

Johnson, R.A. and Corbin, J.D. (eds.) 1991. *Methods in Enzymology*, Vol. 195. Adenyl Cyclase, G Proteins, and Guanylyl Cyclases. Academic Press, San Diego.

A relatively recent volume that is an excellent source of practical information.

Contributed by Eric Southam
GlaxoWellcome Medicines Research Centre
Stevenage, United Kingdom

Histochemical Analysis of Nitric Oxide Synthase by NADPH Diaphorase Staining

Since Hope at al. (1991) and Dawson et al. (1991) first showed that neuronal nitric oxide synthase (NOS) and NADPH diaphorase are identical, NADPH diaphorase staining has been widely used to detect NOS-containing neurons in tissue sections and cell cultures. Throughout the brain and peripheral tissues, all NOS-staining cells also stain for NADPH diaphorase, and in most areas the great majority of NADPH diaphorase–containing cells also exhibit immunoreactivity for NO synthase (Dawson et al., 1991). In some tissues, such as the adrenal cortex, NADPH diaphorase can be detected where NOS cannot. However, the coincidence of neurons staining positive for NOS and NADPH diaphorase is dramatic, especially in areas such as the cerebral cortex and corpus striatum, where only ~1% to 3% of cells are positive for NOS and NADPH diaphorase and the two enzymes are co-localized in all instances (Dawson et al., 1991). The extraordinary concurrence of NOS and NADPH diaphorase implies that NOS accounts for the diaphorase staining. Transfection of NOS cDNA into the 293 human kidney cell line showed that diaphorase staining of transfected cells reflects and is proportional to the amount of NOS cDNA transfected. Moreover, the proportion of NOS and NADPH diaphorase staining in individual neurons is the same as observed for cells transfected with NOS cDNA (Dawson et al., 1991). Thus, the NOS content of each neuron can fully account for its diaphorase activity. Macrophage or immunological or inducible NOS (iNOS) and endothelial (eNOS) also have NADPH diaphorase activity.

This unit describes the procedure for NADPH diaphorase staining of neurons, but the procedure works equally well for non-neuronal cells (e.g., macrophages and endothelial cells).

This procedure describes a histochemical analysis of nitric oxide synthase through NADPH diaphorase staining (Dawson et al., 1991) in which the diaphorase enzymatic activity reduces tetrazolium dyes to a dark blue formazan precipitate in the presence of NADPH. NOS-containing cells are visualized by incubating fixed tissue or cell cultures for 30 to 90 min at 37°C in a solution containing NADPH/nitroblue tetrazolium/Tris·Cl/Triton X-100. The progress of the reaction can be observed under a microscope. NOS containing cells stain dark blue-purple. The reaction is stopped by washing off the staining solution and adding buffered salt solution.

NOTE: The key to success with this procedure is freshness of the reagents used. All solutions should be made fresh prior to use.

Materials

Cultured cells, free-floating tissue sections, or slide-mounted tissue sections
Tris-buffered saline (TBS): 50 mM Tris·Cl, pH 7.2 (*APPENDIX 2A*)/1.5% (w/v) NaCl
0.2 M sodium phosphate buffer, pH 7.4 (PB; see recipe; prepare fresh)
4% (w/v) paraformaldehyde in 0.1 M PB (see recipe; prepare fresh)
0.2% or 0.4% (v/v) Triton X-100 in TBS
NADPH diaphorase staining solution (see recipe; prepare fresh)
TBS containing 0.05% (w/v) sodium azide (optional)
Sonicating water bath

Contributed by Mirella Gonzalez-Zulueta, Valina L. Dawson, and Ted M. Dawson
Current Protocols in Toxicology (1999) 10.6.1-10.6.4

Fix tissue sections or cell cultures

1. If cell cultures are being used, aspirate off culture medium and wash cells by letting them stand in 0.5 ml of TBS per 15-mm well.

   Good positive controls are cultures or tissue sections from cerebellar granule cells.

2. Fix cells or tissue sections by covering them with 4% paraformaldehyde/0.1 M PB and letting them stand 30 min at 4°C.
3. Aspirate off paraformaldehyde and wash with TBS three times for 10 min each time by letting the cells stand in 0.5 ml of TBS per 15-mm well.

Permeabilize cells

4. Permeabilize cells by incubating them 5 min at room temperature in 0.2% Triton X-100 in TBS.

   Free-floating or slide-mounted tissue sections should be permeabilized for 30 min at room temperature in 0.4% Triton X-100 in TBS.

5. Aspirate off solution and rinse once with TBS.

Stain cells

6. Apply 0.5 ml NADPH diaphorase staining solution per 15-mm well.
7. Float dish or plate in a 37°C water bath and allow staining to proceed.

   For slide-mounted tissue sections, incubation in the staining solution should be performed for 30 to 90 min in a 37°C incubator or oven.

8. Check staining under a light microscope at 30 min and at 15-min intervals thereafter.
9. When cells stained dark blue-purple become visible, stop the reaction by washing off staining solution and adding TBS.

   The stained cells are those containing NOS. If the solution itself turns pink-purple the reaction should be stopped; the authors routinely get optimal NADPH diaphorase staining prior to this point. If the reaction is allowed to proceed beyond this point, high background staining may appear.

   Stained cultures can be kept for a few days at 4°C in TBS containing 0.05% sodium azide.

REAGENTS AND SOLUTIONS

Use Milli-Q-purified water or equivalent in all recipes and protocol steps. For common stock solutions, see ***APPENDIX 2A****; for suppliers, see* ***SUPPLIERS APPENDIX****.*

NADPH diaphorase staining solution

Prepare buffer solution, β-NADPH and NBT solutions (in separate tubes), and staining mix as follows:

Buffer solution

0.1 M Tris·Cl (pH 7.2)
0.2% (v/v) Triton X-100
0.02% (w/v) NaN_3

2 mM β-NADPH solution: 16.66 mg β-NADPH reduced form in 10 ml buffer solution.

0.4 mM NBT solution: 3.28 mg nitroblue tetrazolium in 10 ml buffer solution (the mixture may need to be sonicated for 10 to 15 min to dissolve the NBT).

Staining mix: Mix together β-NADPH and NBT solutions 1:1 (v/v). Just before application to cells, filter through a 0.22-μm filter unit (to prevent formation of dark blue precipitate).

The final concentration of the stain mix is 1 mM reduced β-NADPH and 0.2 mM NBT.

4% (w/v) paraformaldehyde/0.1 M PB

1. Prepare 8% (w/v) paraformaldehyde in distilled water (8 g in 100 ml water). Depolymerize solution by heating to 80°C and letting it stand 30 min at that temperature while stirring.

Do not exceed 80°C. If paraformaldehyde boils, start over.

CAUTION: *Wear gloves and mask while weighing and preparing paraformaldehyde. While solution is being heated, cover it with aluminum foil.*

2. Clear paraformaldehyde solution by adding 1 or 2 drops of 10 M NaOH.

Solution will change from a turbid appearance to clear.

3. Check volume and replace water that has evaporated.

4. Add 1 vol of 0.2 M PB (pH 7.4; see recipe) to make a final solution of 4% paraformaldehyde/0.1 M PB.

5. Just before use, filter solution through a 0.22-μm filter unit.

Sodium phosphate buffer (PB), 0.2 M, pH 7.4

Stock solution A: 0.2 M NaH_2PO_4 (12 g NaH_2PO_4 in 500 ml water or 13.9 g $NaH_2PO_4 \cdot H_2O$ in 500 ml water).

Stock solution B: 0.2 M Na_2HPO_4 (28.4 g Na_2HPO_4 in 1 liter water).

0.2 M PB working solution: Mix 1 part solution A with 4 parts solution B (e.g., 100 ml of A and 400 ml of B). Prepare fresh before use.

COMMENTARY

Background Information

The procedure described in this unit is a simple histochemical analysis of NOS-containing cells. It is highly reproducible if the solutions are freshly prepared before each use and the protocol is followed accurately. This approach is based on the enzymatic diaphorase activity that nitric oxide synthase possesses. NADPH diaphorase was first identified histochemically through the reduction of tetrazolium dyes in the presence of NADPH but not NADH (Thomas and Pearse, 1964). The co-localization of NOS-staining neurons and NADPH diaphorase–staining neurons is well documented (Bredt et al., 1991), and in 1991 both activities were shown to reside in the same protein (Dawson et al., 1991; Hope et al., 1991). Definite demonstration that NOS accounts for diaphorase staining came from experiments in which cells of the human kidney cell line 293 that lacked both NOS and diaphorase activities were transfected with NOS cDNA (Dawson et al., 1991). The transfected cells showed extremely similar levels of immunoreactivity for NOS and diaphorase, and the diaphorase staining correlated with the amount of transfected cDNA. Another approach taken by Hope et al. (1991) to link NOS and NADPH diaphorase was to purify diaphorase activity and show that it possesses NOS activity.

Under appropriate fixation conditions, NADPH diaphorase staining can be used to identify all NOS isoforms. For an unknown reason, NOS is resistant to paraformaldehyde fixation, whereas all other NADPH-dependent oxidative enzymes are inactivated by fixatives. The choice of fixation and permeabilization can influence the specificity of the staining and favor one isoform over another (Vaid et al., 1996). For example, the CA1 hippocampal pyramidal neurons stain prominently when tissue sections are fixed in high concentrations of glutaraldehyde (2%), but when fixed in the presence of paraformaldehyde CA1 pyramidal cells do not stain for diaphorase.

Critical Parameters and Troubleshooting

The largest source of failure in obtaining good NADPH diaphorase staining is the use of solutions that have not been freshly made before each use. This is particularly true for the paraformaldehyde solution and the staining mix. A long enough fixation time (at least 30 min) is also important.

Trouble usually arises if the staining solution is not filtered before addition to the cells, which leads to formation of abundant dark blue precipitates that greatly interfere with observation of stained cells. The pH of the buffer is not

critical, but pH 7.2 limits nonspecific NADPH diaphorase staining. A staining solution that is not light yellow immediately after preparation should be discarded. NBT may not go into solution easily, requiring sonication for 10 to 15 min. If NBT is not dissolved adequately, very poor or no staining will be obtained.

A high background staining may be seen that may impede accurate assessment of NOS-containing cells. This is usually due to an excessively long incubation time of cells in the staining solution. Moreover, if the reaction takes place for an abnormally long period of time, dark blue precipitates form that obstruct the detection of stained cells. Therefore, the progress of the reaction should be observed every 15 min. Incubation for 30 to 90 min is usually necessary, depending on the tissue and the level of NOS expression.

Anticipated Results

NADPH diaphorase staining is a simple technique that gives reproducible results if the protocol is followed carefully. Cells that contain NOS should stain dark blue-purple, and are clearly distinguishable from unstained cells. The dark blue stain is intense and homogenously distributed in the cytoplasm. The nucleus of the cell is clearly devoid of blue stain. The number of diaphorase staining cells varies with the tissue type. A good positive control are cerebellar granule cells for the high number of cells expressing NOS at high levels.

In the brain, the highest density of diaphorase staining neurons is evident in the cerebellum and the olfactory bulb. In most brain regions, diaphorase staining can be detected in 1% to 2% of the cells. In the cerebellum, positive staining is detected in up to 80% of granule cells. Other areas of high staining include the supraoptic nucleus, the superior and inferior colliculi, the caudate-putamen, and the dentate gyrus of the hippocampus. Microglia and astrocytes can also stain positive. Throughout the gastrointestinal tract, diaphorase-staining neurons are present in the myentric plexus. Staining also occurs in discrete ganglia cells and fibers in the adrenal medulla. Disphorase staining is prominent within the posterior pitutiary gland. It has also been found in the macula densa of the kidney. In the periphery, diaphorase staining is localized to the endothelium of blood vessels, in neutrophils and macrophages. In primary cultures of mature (14 days in vitro) cortical neurons, the authors routinely are able to count 100 to 120 diaphorase-positive neurons per 15 × 15–mm culture well, where cells are plated at a density of 4×10^5 cells/well.

Time Considerations

The entire procedure can be done in ~3 hr plus the time required to observe and quantify NOS positive cells under the microscope. Preparation of the 4% paraformaldehyde/0.1 M PB solution takes ~1 hr, cell fixation and permeabilization requires about 40 min, and staining takes ~1 hr.

Literature Cited

Bredt, D.S., Glatt, C.E., Hwang, P.M., Fotuhi, M., Dawson, T.M., and Snyder, S.H. 1991. Nitric oxide synthase protein and mRNA are discretely localized in neuronal populations of the mammalian CNS together with NADPH diaphorase. *Neuron* 7:615-624.

Dawson, T.M., Bredt, D.S., Fotuhi, M., Hwang, P.M., and Snyder, S.H. 1991. Nitric oxide synthase and neuronal NADPH diaphorase are identical in brain and peripheral tissues. *Proc. Natl. Acad. Sci. U.S.A.* 88:7797-7801.

Hope, B.T., Michael, G.J., Knigge, K.M., and Vincent, S.R. 1991. Neuronal NADPH diaphorase is a nitric oxide synthase. *Proc. Natl. Acad. Sci. U.S.A.* 88:2811-2814.

Thomas, E. and Pearse, A.G.E. 1964. The solitary active cells. Histochemical demonstration of damage-resistant nerve cells with a TPN-diaphorase reaction. *Acta Neuropathol.* 3:238-249.

Vaid, R.R., Yee, B.K., Rawlins, J.N., and Totterdell, S. 1996. NADPH-diaphorase reactive pyramidal neurons in Ammon's horn and the subiculum of the rat hippocampal formation. *Brain Res.* 733:31-40.

Contributed by Mirella Gonzalez-Zulueta, Valina L. Dawson, and Ted M. Dawson
Johns Hopkins University School of Medicine
Baltimore, Maryland

Immunocytochemical Analysis of Cyclic Nucleotides

Within certain limits, immunocytochemical detection of cyclic nucleotides makes it possible to study dynamic alterations in cyclic nucleotide levels under conditions that are at least partly reflective of those in living tissue. Changes in cAMP or cGMP levels can be pinpointed in cells in heterogeneous tissue. In combination with (immuno)histochemical characterization of these cells, or cells that are in contact with cyclic nucleotide–immunopositive cells, this can give insight into the regulation of cyclic nucleotides in a complex tissue. Such studies are limited by the strategy chosen to study the living tissue or cells. In principle, any approach can be used that allows for fixation of cyclic nucleotides to the protein matrix at some point in the experiment. It should be realized that immunocytochemical analysis of cyclic nucleotides is time consuming, especially when physiological or pharmacological factors are to be studied.

The first choice to be made is whether to use an in vivo or an in vitro approach. Biochemical studies of cyclic nucleotide metabolism in vivo have shown that changes in cAMP or cGMP may be very rapid, and unless special precautions are made, cyclic nucleotides levels will change during the process of isolating the tissue (Guidotti et al., 1974). Nevertheless, excellent results have been obtained using cGMP immunocytochemistry in in vivo experiments in invertebrates (e.g., Bicker et al., 1996; Ewer et al., 1994; Truman et al., 1997). In vertebrates the number of in vivo studies has been limited (Berkelmans et al., 1989; Southam and Garthwaite, 1993), and it is probably best to use tissue slices or isolated organs when different conditions, e.g., drugs or time periods, are to be studied.

This unit includes protocols for preparation and characterization of antibodies to conjugated cAMP and cGMP (see Support Protocol) and in vitro immunostaining of brain slices for cyclic nucleotides (see Basic Protocol) with modifications for in vivo fixation for immunocytochemistry (see Alternate Protocol). The basic principles are the same for cAMP and cGMP immunocytochemistry, and the relevant variations in procedural details have been indicated.

NOTE: All protocols using live animals must first be reviewed and approved by an Institutional Animal Care and Use Committee (IACUC) or must conform to governmental regulations regarding the care and use of laboratory animals.

IMMUNOCYTOCHEMISTRY FOR CYCLIC NUCLEOTIDES USING IN VITRO FIXED BRAIN SLICES

BASIC PROTOCOL

Freshly dissected brains are sectioned and treated, then fixed in vitro for staining with cGMP- or cAMP-specific antibodies. Alternatively, the tissue can be fixed in vivo before sectioning and staining (see Alternate Protocol).

Materials

Animal source of tissue
Krebs buffer, oxygenated with 5% CO_2/95% O_2 (see recipe), ice cold
Cyanoacrylate glue
Drug or toxin to be tested for effects on cGMP or cAMP levels
Formaldehyde fixative (see recipe), ice cold
Formaldehyde fixative containing 10% sucrose (see recipe)
10% (w/v) sucrose
Optimal cutting (OCT) compound (cryostat embedding medium)

Contributed by J. de Vente and H.W.M. Steinbusch
Current Protocols in Toxicology (1999) 10.7.1-10.7.17

Acrolein fixative (see recipe)
Glycine
0.1 M phosphate buffer, pH 7.0, containing 10% sucrose
TBS (see recipe)
10 mM $NaCNBH_3$ in 0.1 M sodium acetate, pH 7.45
Anti-cGMP-formaldehyde-protein *or* anti-cAMP-acrolein-protein antiserum (see Support Protocol)
TBS-T: TBS containing 0.3% Triton X-100
Secondary and tertiary antibodies conjugated with reporter molecules (e.g., FITC or Cy3; see Troubleshooting)
1:3 (v/v) TBS/glycerol
DAB staining solution (see recipe)

Grid glued to a firmly fitting teflon support ring into the multiwell tissue culture plate
12-well plates
Vibrating tissue knife: Vibratome (Technical Products) or Vibroslicer (WPI)
Cryostat
Chrome-alum-coated glass microscopic slides

Prepare brain slices

1. Sacrifice animal, then remove the brain from the skull as quickly as possible.

   This protocol describes the procedure for brain slices, but the method is, in principle, suitable for any tissue (also see Commentary). However, experience is limited with other tissues, which means that many parameters governing cyclic nucleotide metabolism, factors important for correct interpretation of the immunocytochemical results, still need to be explored.

   Probably the fastest way to remove the brain from the skull is by decapitating the animal followed by removal of the skull bones. Lift the brain upward in a rostral to caudal direction and sever the optic nerves just rostral to the optic chiasm. It is necessary to sever the optic nerves, otherwise they will dislodge the optic chiasm and the ventral part of the hypothalamus will be damaged. There are many possible modifications of this basic procedure. Some groups recommend that the animal be anesthetized and allowed to inhale pure oxygen prior to decapitation and opening of the skin layers on top of the skull. These precautions are recommended to prevent ischemic cell damage. For further details see Garthwaite et al. (1979) and Aitken et al. (1995). The complete June 1995 issue of Journal of Neuroscience Methods focuses on problems related to isolating, preparing, and maintaining brain tissue slices in vitro.

2. Cool the brain immediately by dropping it in ice-cold continuously oxygenated Krebs buffer.

3. Dissect the area(s) of interest and glue this part on a cooled support using cyanoacrylate glue.

   Do not touch the brain with your fingers. The maximum size of the brain slice is determined by dimensions of the culture wells.

4. Prepare brain slices of 300- to 400-µm thickness using a Vibratome or Vibroslicer, while the tissue is immersed in ice-cold continuously oxygenated Krebs buffer.

   Speed is the key to success in this procedure. It is also very important to handle the slices with utmost care. Two different ways of obtaining slices are commonly in use, i.e., the McIlwain tissue chopper and the Vibratome or Vibroslicer. In the authors' experience, slicing is preferred as the gentler method, resulting in better morphology (see also Garthwaite et al., 1979). Many different protocols for handling and incubation of brain slices are to be found in the literature, each advocating modifications of this basic protocol (Aitken et al., 1995). It is doubtful whether any of these recipes will save the slice when the slicing process is too slow.

The quality of a slice is most often defined operationally. Routine histochemistry to assess the quality of the slice is necessary, using histochemical stains such as hematoxylin-eosin or toluidine blue staining. Preferably, this should be done for each experiment, and it is necessary to do this when effects of drugs are studied for the first time using this approach. For a detailed discussion on the quality of the slice the reader is referred to Aitken et al. (1995).

Incubate brain slices

5. Place slices on a grid glued to a support ring in a multiwell culture plate containing 2 ml ice-cold continuously oxygenated Krebs buffer.
6. Slowly and continuously bubble 5% CO_2/95% O_2 through the buffer solution. Place culture plates in a water bath and gradually raise the temperature to 35°C.
7. Incubate slices 30 to 60 min at room temperature in the presence or absence of drug.
8. Add drug to the wells and continue the incubation for the desired period of time.

Depending on the design of the experiment, drugs may alternatively be present from the start of the incubation.

Incubation duration for the tissues in vitro is determined by the experimental setup Hoever, it is necessary to let the tissue equilibrate in buffer under the conditions used in the final experiment for ≥30 min. This equilibration time varies considerably in the literature (Garthwaite et al., 1979; Aitken et al., 1995). The necessity to include a phosphodiesterase inhibitor will be readily apparent when there is no cGMP immunostaining observed in the absence of such an inhibitor. At present, it is impossible to give definite guidelines on this point as the involvement of phosphodiesterases in cell signalling is a rapidly developing field (see Background Information).

Cyclic nucleotides are rapidly broken down by phosphodiesterases, so it may be necessary to include a phosphodiesterase inhibitor in the incubation buffer. Isobutylmethylxanthine (IBMX) at 1 mM concentration has been most commonly used (see Background Information).

Fix brain slices for immunocytochemistry and cryostat sectioning

For cGMP analysis:

9a. Place slices in ice-cold formaldehyde fixative containing 10% sucrose for 2 hr.

The cGMP-formaldehyde-protein conjugate is not indefinitely stable. However, at 4°C dissociation is negligible. Fixation of cGMP to the protein is not 100% complete. The indicated fixation time has proved to be sufficient for brain slices but may be prolonged. Slices may be kept overnight in 10% sucrose in the cold before being sectioned on a cryostat.

10a. Wash the slice 30 min in ice-cold 10% sucrose in 0.1 M phosphate buffer, pH 7.4.

It is necessary to wash out the formaldehyde because otherwise it may form an insoluble precipitate when slices are frozen with CO_2.

11a. Align slices in a plane and quick-freeze them in OCT compound using CO_2.

Aligning brain slices in a plane can be accomplished as follows. Cover a glass microscope slide with Parafilm. Place the slices on the Parafilm, positioning them carefully with a soft brush so that they will fit on the cryostat chuck. Remove adhering buffer with a piece of filter paper. Push the glass slide, face down, into Tissue-Tek OCT compound already applied to the cryostat chuck using a vertical adjustment attachment. Freeze the slices into the OCT compound with CO_2. The Parafilm ensures that the slices can be easily removed from the glass slide.

12a. Cut 5- to 20-µm sections on a cryostat and thaw-mount them onto chrome-alum-coated glass slides.

Any type of coating commonly in use to adhere sections to glass slides will do. Chrome-alum has the advantage of low cost.

13a. Store sections at −20°C.

Sections can be stored for considerable time. The authors have successfully stained sections that had been stored frozen >2 years.

For cAMP analysis:

9b. Place slices in 2 ml acrolein fixative for 2 hr.

IMPORTANT NOTE: *Special precautions must be taken for cAMP immunocytochemistry because acrolein is used as a fixative. Acrolein is a very aggressive and highly toxic compound. Addition of glycine to the fixative solution will inactivate the acrolein.*

10b. Add 20 mg glycine at room temperature and leave for 30 min more.

11b. Remove the solution and postfix the slices in formaldehyde fixative containing 10% sucrose for 1 hr.

12b. Place slices in 0.1 M phosphate buffer (pH 7.0) containing 10% sucrose for 30 min.

13b. Freeze and section as described in steps 11a to 13a.

Immunostain for cyclic nucleotides

14. Airdry the cryostat sections by letting them stand for 15 to 20 min at room temperature.

15. Wash in TBS three times, 5 min each.

16. *For cAMP only:* Treat the sections for 30 min with 10 mM $NaCNBH_3$ in 0.1 M sodium acetate, pH 7.45.

For cGMP, skip to step 17.

The cyanoborohydride treatment is necessary to reduce double bonds produced by acrolein, which may give a very high background signal when epifluorescence is used.

17. Apply the appropriate anti–cyclic nucleotide antiserum to the sections at the necessary dilution in TBS-T.

The dilution of the primary antibodies depends on the particular antiserum and the detection method used. In conjunction with the avidin/biotin detection system, use of a 1:40,000 dilution of a primary anti-cGMP antibody has been reported.

18. Leave the sections at 4°C overnight.

19. Wash 15 min each with TBS, TBS-T, and TBS.

It is advisable to limit the time of the initial washing steps as much as possible in view of the labile nature of the cGMP-formaldehyde-protein bond. These precautions are no longer necessary when the primary antibody is bound to the cGMP-epitope, as this binding is tenacious.

20. Apply the secondary antibody containing the fluorescent reporter molecule and incubate 1 hr at room temperature.

21. Repeat step 19.

22. Mount sections with 1:3 (v/v) TBS/glycerol.

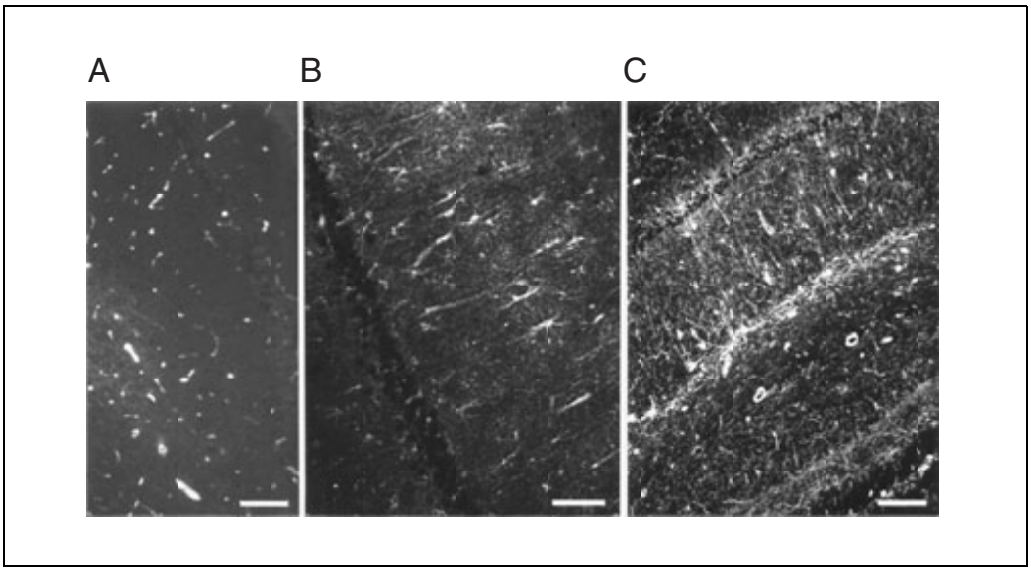

Figure 10.7.1 Cyclic nucleotide immunocytochemistry: the different localization of sGNC and pGNC using cGMP immunocytochemistry in the hippocampus. Tissue was (**A**) unstimulated; (**B**) incubated 10 min in the presence of 100 nM ANF; (**C**) incubated 10 min in the presence of 0.1 mM sodium nitroprusside. All in vitro incubations were performed in the continuous presence of 1 mM IBMX to inhibit phosphodiesterase activity. Bars represent 50 μm.

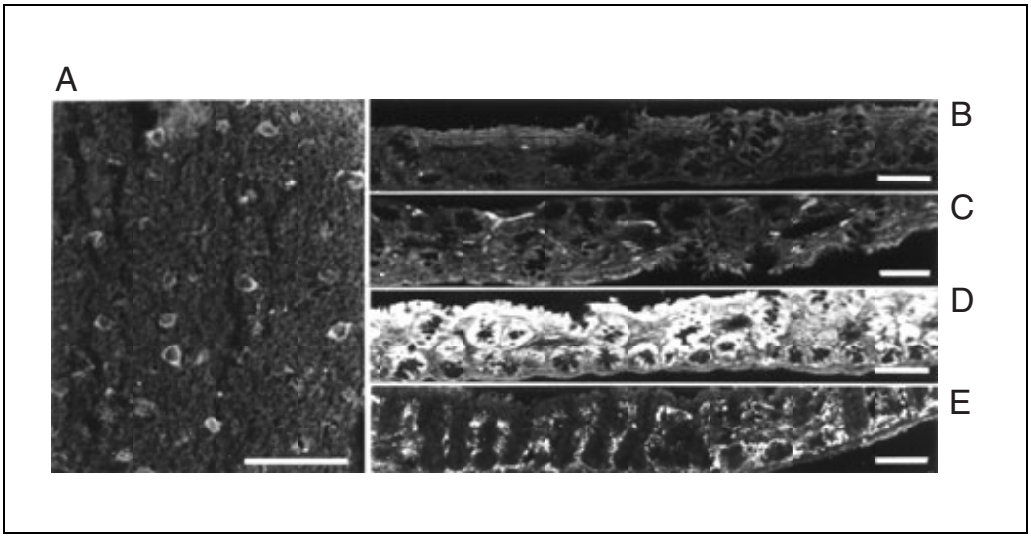

Figure 10.7.2 cAMP immunocytochemistry in (**A**) in a slice from the frontal cortex of the rat incubated 5 min in the presence of 10 μM dopamine. Demonstration of the differential localization of cGMP in the rat colon after stimulation of three different types of GNC is shown in: (**B**) unstimulated proximal colon; (**C**) proximal colon incubated 10 min in the presence of 1 μM ANF; (**D**) proximal colon incubated 10 min in the presence of 0.1 μM *Escherichia coli* enterotoxin STa; (**E**) distal colon incubated 10 min in the presence of 0.1 mM sodium nitroprusside. All in vitro incubations were performed in the continuous presence of 1 mM IBMX to inhibit phosphodiesterase activity. Bars represent 50 μm.

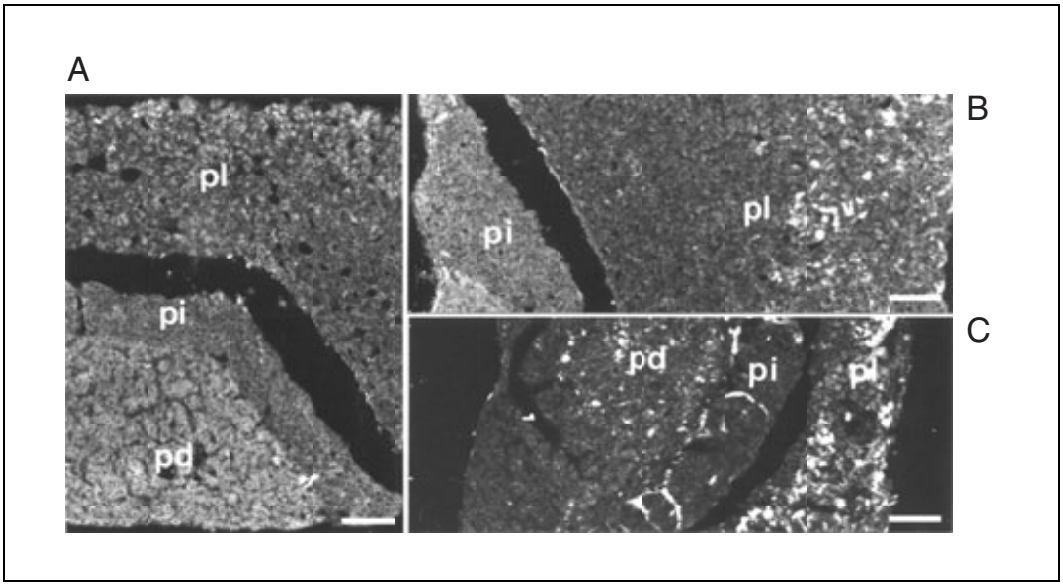

Figure 10.7.3 Differential localization of sGNC and pGNC in the hypophysis of the rat using cGMP immunocytochemistry. (**A**) unstimulated; (**B**) stimulated with 100 nM ANF; (**C**) stimulated with 0.1 mM sodium nitroprusside (pl - pars lateralis; pi - pars intermediate; pd - pars distalis). All in vitro incubations were performed in the continuous presence of 1 mM IBMX to inhibit phosphodiesterase activity. Bars represent 50 μm.

Any detection system in use with other immunocytochemical procedures can be used to visualize cGMP or cAMP. In this respect there is no difference between cyclic nucleotide immunocytochemistry and other immunocytochemical procedures. For example, the peroxidase-antiperoxidase method with diaminobenzidine visualization may also be used.

See Figures 10.7.1, 10.7.2, and 10.7.3 for examples of results.

ALTERNATE PROTOCOL

IN VIVO FIXATION FOR CYCLIC NUCLEOTIDE IMMUNOCYTOCHEMISTRY

The tissue of interest is perfused with fixative in vivo, then used for immunocytochemistry with cyclic nucleotide–specific antisera.

Additional Materials *(also see Basic Protocol)*

Animal source of tissue
Pentobarbital sodium (Nembutal)
Krebs buffer (see recipe) prepared without calcium, oxygenated with 5% CO_2/95% O_2
Drug to be tested for effects on cGMP or cAMP levels
Formaldehyde fixative (see recipe)
TBS (see recipe) containing 10% (w/v) sucrose
0.9% (w/v) NaCl (*APPENDIX 2A*)
Chrom-alum- or lysine-coated slides

1. Weigh animal, and anesthetize by i.p. injection of the appropriate volume of pentobarbital sodium (50 mg/kg).
2. Open the rib cage and transcardially perfuse the animal with 150 ml oxygenated calcium-free Krebs buffer containing the appropriate concentration of drugs.

   This should be done by someone with experience in performing perfusions (for additional perfusion details see UNIT 9.5). In the process of fixation the animal will be killed.

Fix tissue

For cGMP analysis:

3a. Perfuse the animal with 500 ml formaldehyde fixative.

4a. Remove the brain from the skull and postfix the tissue for 2 hr in the same fixative.

For cAMP analysis:

3b. Perfuse the animal with 200 ml of acrolein fixative followed by 500 ml saline solution containing 10 mg/ml glycine to inactivate the acrolein.

> IMPORTANT NOTE: *Whole-body perfusion with acrolein requires a high-quality fume hood, the use of a gas mask and special gloves, and immediate inactivation of the acrolein fixative using a saturated solution of glycine in water.*

4b. Postfix the tissue for 2 hr in formaldehyde fixative.

5. For cryostat sectioning, immerse the tissue overnight in TBS containing 10% sucrose in the cold.

> *As an alternative, the tissue can be sectioned immediately after postfixation with a Vibratome slicer. In this case, keep the tissue and the sections in a cold TBS solution.*

6. Thaw cryostat sections onto chrome-alum- or lysine-coated glass slides.

7. Proceed with immunostaining (see Basic Protocol, steps 14 to 22).

PREPARATION AND CHARACTERIZATION OF ANTISERA TO CONJUGATED CYCLIC NUCLEOTIDES

SUPPORT PROTOCOL

The key to successful visualization of cyclic nucleotides in fixed tissue is the use of antisera directed against the fixed forms of the nucleotides. This is accomplished by treating the nucleotide antigen with the appropriate fixative when generating the antiserum. The antisera against (unfixed) cyclic nucleotides that are commonly used in radioimmunoassays may be of some utility; however, their performance can be capricious, and the results are disappointing in comparison with those obtained with antibodies against fixed nucleotides.

Because of their small size, cyclic nucleotides must be fixed and conjugated to a carrier protein for use as an immunogen. After the antisera are produced, their specificity is characterized using a peroxidase-based immunodot procedure.

Materials

Carrier protein (e.g., bovine thyroglobulin, BSA, hemocyanin)
3′,5′ cGMP or 3′,5′ cAMP (sodium salt)
0.2 M sodium phosphate buffer, pH 7.0 (*APPENDIX 2A*)
Formaldehyde fixative (see recipe)
0.1 M sodium phosphate buffer, pH 7.0 (*APPENDIX 2A*), 4°C
0.1 M sodium acetate, pH 4.75 (*APPENDIX 2A*)
Acrolein fixative (see recipe)
Glycine
$NaCNBH_3$
Rabbits (or other species in which to raise antibodies)
0.9% (w/v) NaCl (*APPENDIX 2A*)
Complete and incomplete Freund's adjuvant
Fixative-treated carrier protein
Glycerol

Blocking solution: 1% (w/v) gelatin and 1% (w/v) nonfat dry milk in water
TBS (see recipe)
TBS-T: TBS containing 0.3% (v/v) Triton X-100
Anti–rabbit Ig (secondary antibody)
Rabbit peroxidase-antiperoxidase antibody
0.05 M Tris·Cl, pH 7.0 (*APPENDIX 2A*)
DAB staining solution (see recipe)

Dialysis equipment
Homogenizer, either standard Potter system or high-speed-blade (Polytron-type) system
Nitrocellulose or nylon membrane
Glass capillary micropipets

Prepare and purify cyclic nucleotide–protein conjugate

For cGMP-formaldehyde-protein conjugate:

1a. Dissolve, while stirring, 20 mg carrier protein (thyroglobulin or BSA) and 45.8 mg of cGMP (25 mM) in 5 ml of 0.2 M phosphate buffer, pH 7.0.

2a. Add 5 ml of 8% (w/v) freshly depolymerized formaldehyde in water and stir solution at least 2 hr at room temperature.

The solution will turn slightly opaque. No precipitate should develop.

3a. Purify conjugate at 4°C by dialysis against several volumes of 0.01 M phosphate buffer, pH 7.0, or by repeated ultrafiltration with the same buffer.

Purification of the conjugate should be done in the cold because of the labile nature of the cGMP-formaldehyde bond (de Vente et al., 1987).

When selecting dialysis tubing or ultrafiltration filters, take into account the molecular weight of the carrier proteins when selecting the MWCO—e.g., thyroglobulin has a molecular weight of >600,000; with BSA it is possible to use a MWCO of 65,000. Consult the manufacturer's documentation to select the proper membranes.

4a. Freeze-dry the conjugate and store at −20°C.

For cAMP-acrolein-protein conjugate:

1b. Add 10 mg carrier protein (thyroglobulin, hemocyanin, or BSA) and 25 mg cAMP to 10 ml of 0.1 M sodium acetate, pH 4.75. Add 40 µl acrolein fixative under vigorous stirring. Continue stirring 4 hr at room temperature in the dark.

CAUTION: *Acrolein is an aggressive and toxic chemical; use gloves and a fume hood.*

2b. Add 200 mg glycine and leave under the same conditions for 30 min. Add 130 mg $NaCNBH_3$ and stir for another 30 min.

Glycine neutralizes the acrolein, and $NaCNBH_3$ reduces double bonds, which may give a very high background signal when epifluorescence is used.

3b. Dialyze the conjugate solution against three changes of distilled water for 24 hr at 4°C.

When selecting dialysis tubing or ultrafiltration filters, take into account the molecular weight of the carrier proteins when selecting the MWCO—e.g., thyroglobulin has a molecular weight of >600,000; with BSA it is possible to use a MWCO of 65,000. Consult the manufacturer's documentation to select the proper membranes.

4b. Freeze-dry the conjugate solution and store desiccated at −20°C.

Collect preimmune samples

5. Collect a preimmune blood sample from the rabbit or other animal to be immunized in normal glass tubes.

   See Donovan and Brown (1999a,b) for animal care and handling and Donovan and Brown (1999c) for blood collection.

6. Leave the sample for 1 hr at room temperature. Free the clotted blood from the glass wall and place tubes at 4°C overnight.

7. Isolate the serum and store in aliquots at −80°C.

Raise antibodies against cyclic nucleotides

8. Suspend 0.5 mg of conjugate in 0.5 ml of 0.9% NaCl. Add 0.5 ml complete Freund's adjuvant and emulsify using a Potter homogenizer system or Polytron-type system.

   Other adjuvants may be used in place of Freund's adjuvant, which is considered to be a rather painful means of immunization because of the ulcers it produces. However, not all will give results as good as those obtained with Freund's, although the response of the animals is very individual. See Cooper and Paterson (1999) for general details of immunizing and collecting serum.

9. Inject the conjugate suspension (1 ml total volume) intradermally at six to eight sites on the back of the animal.

   In the specific case of raising antibodies to cGMP, it is the authors' experience that not all rabbits respond to the antigen. About one out of three rabbits responds to some extent, and only about one out of six produces a high-quality serum. In the authors' experience, the quality of the serum does not improve after five booster injections.

10. At 3-week intervals, prepare a booster injection as described above (step 8) using incomplete instead of complete Freund's adjuvant, and administer this booster injection (1 ml) intramuscularly at four sites (250 µl per site).

11. Collect immune serum 7 to 10 days after each booster injection. Isolate the serum and store it in aliquots at −80°C as described in steps 6 and 7.

    Antibodies have been raised in rabbits, mice, and sheep. Although some differences in recognition of cGMP epitopes in different cells might be expected because cGMP is fixed to different matrix proteins (de Vente et al., 1989), this problem can be overcome by combining different antisera. Antibodies against cGMP raised in rabbits and in sheep have been observed to stain exactly the same, as demonstrated by double immunostaining (de Vente, unpub. observ.).

Purify antiserum

12. Incubate the immune serum 30 min at 56°C.

13. Add 3 mg fixative-treated carrier protein to each milliliter of serum. Incubate 30 min at 37°C and then overnight at 4°C.

    As the cyclic nucleotides are fixed to the carrier protein using formaldehyde (cGMP) or acrolein (cAMP), it is necessary to study the effects of these fixatives on the carrier protein itself in the absence of the cyclic nucleotide. Therefore, the carrier protein is treated in exactly the same way as described for preparation of the conjugate except that the cyclic nucleotides are not added. This protein is used either to remove excess antibodies (those not specific for the cyclic nucleotides) from the sera or to provide a constant carrier protein concentration for conjugate dilutions in preabsorption experiments.

14. Centrifuge the serum for 15 min at 10,000 × *g*, 4°C.

15. Dilute the serum 1:1 (v/v) with glycerol and store at −20°C.

    Antisera can be stored this way for prolonged periods of time.

Test specificity of antibodies

16. Prepare conjugates as described above (steps 1 to 4), using a range of nucleotides selected for specificity testing and a carrier protein different from the one used to immunize the animals.

17. Prepare serial dilutions (1:10) of these conjugates in TBS, starting at 1 mg/ml, at constant down to 0.1 µg/ml concentration of the unconjugated protein.

    This constant concentration of unconjugated protein assures identical conditions.

18. Spot 2 µl each of these solutions onto nitrocellulose or nylon blotting membrane using glass capillary micropipets. Let dry at room temperature.

19. Soak the blot 1 hr in blocking solution.

    Blocking of the binding capacity of the blot is necessary, as otherwise the blot will be saturated with antiserum. Gelatin usually works satisfactorily and has the advantage of low cost.

20. Wash in three changes of TBS, 5 min each.

21. Incubate blot with primary antibodies (from step 15) at an appropriate dilution in TBS overnight at 4°C.

22. Wash 15 min each with TBS, TBS-T, and TBS.

23. Incubate with anti–rabbit Ig secondary antibody diluted in TBS for 30 min, then repeat step 22

    Dilution is usually as indicated by the manufacturer, otherwise it needs to be determined for each antibody separately.

24. Incubate with rabbit peroxidase-antiperoxidase antibody diluted in TBS for 30 min, and repeat step 22.

    Dilution is usually as indicated by the manufacturer, otherwise it needs to be determined for each antibody separately.

25. Wash 5 min in 0.05 M Tris·Cl buffer, pH 7.4. Add DAB staining solution and wait until the brownish color has developed sufficiently.

    The brownish color must be visible within 10 min and should be complete within 20 to 30 min. In exceptional cases it is necessary to wait longer; however, a certain nonspecific precipitation of the color might occur, and this is likely to interfere with the immunocytochemical staining when prolonged incubations are used.

26. Wash at least three times, 10 min each, with 0.05 M Tris·Cl buffer, pH 7.4. Let the blots dry at room temperature.

    Interaction of the antiserum with the spotted proteins will produce brown spots.

    Careful analysis of the results will yield information about the specificity of the antiserum. Preimmune sera must be negative. Antisera preabsorbed with antigen-protein conjugates will be negative, but at a limiting dilution of the antigen-protein conjugate, the reaction product will become visible again. Using the antiserum in different dilutions will give some indication of the antiserum dilution that might give a result with tissue samples. The dilution of antiserum used for tissue immunocytochemistry will generally be less by a factor of three to ten. A good performance of antiserum on nitrocellulose dot blots or immunoblots (western blots) is no guarantee of good performance in tissue immunocytochemistry.

REAGENTS AND SOLUTIONS

Use Milli-Q-purified water or equivalent in all recipes and protocol steps. For common stock solutions, see ***APPENDIX 2A****; for suppliers, see* ***SUPPLIERS APPENDIX****.*

Acrolein fixative, 1% (v/v)

Working in a high-capacity fume hood, dissolve 1% (v/v) double-distilled acrolein (as supplied) under vigorous stirring in 0.1 M sodium acetate, pH 4.8 (*APPENDIX 2A*).

This solution is prepared just prior to use and cannot be stored.

CAUTION: *Acrolein is highly toxic. Use gloves and a mask. Acrolein distillation needs to be carried out by a very experienced organic chemist.*

DAB staining solution

10 mM Tris·Cl, pH 7.4 (*APPENDIX 2A*)
0.01% (v/v) hydrogen peroxide
0.5 mg/ml diaminobenzidine (DAB)

This solution is prepared just prior to use and cannot be stored.

Formaldehyde fixative (4% w/v), freshly depolymerized

Add 4 g powdered paraformaldehyde to 50 ml water and add 3 drops of 1 N NaOH. Stir gently and heat the solution at 65°C until it has cleared completely. Add 50 ml of 0.2 M sodium phosphate buffer (pH 7.4).

To obtain sucrose-containing fixative, add 10% (w/v) sucrose to the prepared formaldehyde solution.

These solutions can be kept for at least 4 hr. No upper limit for storage can be given; however, it is advised to prepare them fresh for each experiment.

Other formaldehyde-based fixatives such as Zamboni (containing picric acid) or Bouin (containing picric acid, acetic acid, and commercial formalin solution) can be used equally well. There may be particular circumstances in which one of these fixatives is preferred. However, this issue has not been investigated in detail.

Krebs buffer, oxygenated

1.2 mM $CaCl_2$
121.1 mM NaCl
1.87 mM KCl
1.15 mM $MgCl_2$
24.9 mM $NaHCO_3$
11.0 mM glucose
Adjust pH to 7.4, if necessary, with 0.01 M HCl or 0.01 M NaOH.
Oxygenate with 5% CO_2/95% O_2

This buffer is best prepared by making a 10× concentrated solution of the salts without glucose, $CaCl_2$, and $NaHCO_3$. When required, the concentrated solution is diluted and oxygenated, and glucose and $NaHCO_3$ are added. Aeration is continued and the $CaCl_2$ is added from a concentrated stock solution as the final ingredient. This procedure prevents the formation of insoluble $CaCO_3$. If well oxygenated, this buffer can be kept for one working day.

In some cases it may be desirable to include phosphodiesterase inhibitors in this buffer (see Basic Protocol, step 8 annotation). Many phosphodiesterase inhibitors are rather insoluble in water and in such a case a concentrated stock solution needs to be prepared in DMSO. A final concentration of 1% DMSO in the incubation buffer has no effect on the concentration of cyclic nucleotides in rat brain tissues. IBMX dissolves slowly in aqueous medium; it will take at least 1 hr to reach a concentration of 1 mM IBMX.

Tris-buffered saline (TBS)

50 mM Tris·Cl, pH 7.4 (*APPENDIX 2A*)
0.9% (w/v) NaCl (*APPENDIX 2A*)
Store at 4°C

Phosphate-buffered saline (PBS; APPENDIX 2A) can be used equally well.

This solution is stable for prolonged times when kept cold; at room temperature it is not advised to keep it longer than 5 days.

COMMENTARY

Background Information

Cyclic nucleotides are second messengers. They relay many different signals involved in regulating growth, development, metabolism, memory formation, and memory storage. Signaling molecules either stimulate or inhibit the synthesis or breakdown of cAMP or cGMP.

cAMP is synthesized by the enzyme adenylate cyclase (ADC). Presently, eight species of ADC are known (Cooper et al., 1995), and these species are uniquely regulated by a variety of different ligands. In addition, different types of ADC show discrete expression patterns throughout the organism. For studying the role of cAMP in different cell types in heterogeneous tissue, immunocytochemical detection greatly expands the possibilities for assessing the compound's distribution. Moreover, such a technique might be able to show a discrete regulation of cAMP within different parts of a single cell.

Similar considerations apply to cGMP metabolism. cGMP is synthesized by two different classes of enzymes, the so-called particulate and soluble guanylyl cyclases (pGNC and sGNC). Both forms of cyclases are activated by different ligands and have very different structures, and both are found in vertebrates as well as in invertebrates (Wedel and Garbers, 1997).

pGNC contains an extracellular hormone-receptor domain, a membrane-spanning region, and an intracellular catalytically active portion (Wedel and Garbers, 1997). Six membrane-bound forms of GNC have been recognized in mammals. To date, some but not all endogenous ligands for these receptors have been identified. pGNC-A and -B receptors are activated by natriuretic peptides. pGNC-C is activated by guanylins and by the heat-stable fragment of *Escherichia coli* endotoxin (Wedel and Garbers, 1997). Recently, GNC activating peptides have been described in the retina, which act on both pGNC-D and -E (e.g., Gorczyca et al., 1994). The activating ligand for the neuroepithelial pGNC-F is still unknown. In invertebrates, activation of pGNC by eclosion hormone is important for the initiation of specific behavioral programs (Truman et al., 1997). From cloning studies of GNC in *Caenorhabditis elegans* came the surprising result that at least 29 gene products could be identified that appeared to encode a protein with GNC activity (Yu et al., 1997). Therefore, many more pGNCs may be discovered in mammals.

sGNC is a heterodimeric protein. In rats, two α (α_1, α_2) and two β (β_1, β_2) subunits are presently known (Harteneck et al., 1991), whereas in humans a β_3 subunit has been identified (Giuili et al., 1992). sGNC contains a prosthetic heme group and is activated by NO (Murad, 1994). Although other activators of sGNC are known—e.g., CO, OH^-, and arachidonic acid—their physiological significance is not known. NO is synthesized by nitric oxide synthase (NOS) from L-arginine and molecular oxygen, with citrulline as a coproduct (Bredt et al., 1990; Knowles and Moncada, 1994; Moncada et al., 1991). In the past 10 years several isoforms of NOS have been characterized (Moncada et al., 1991). Apart from the constitutive forms, another isoform of the enzyme can be induced by combinations of cytokines and immunostimulants. The constitutive forms of NOS are all activated through a calcium/calmodulin-dependent pathway, whereas the inducible form of NOS is intrinsically active (Knowles and Moncada, 1994). As NO has a very high affinity for sGNC (Traylor and Sharma, 1992), it is easily conceivable that sGNC might be an important target for endogenously synthesized NO (Garthwaite, 1991).

Cyclic nucleotide levels in tissue are controlled by the rates of synthesis through ADC or GNC and breakdown through phosphodiesterase (PDE) activity. The 3′,5′-cyclic nucleotide phosphodiesterases comprise a large family of enzymes that can be classified on the basis of kinetic and structural characteristics into at least eight subfamilies (Beavo and Reifsnyder, 1990). Several of these subfamilies

also contain a considerable number of isoforms (Houslay and Milligan, 1997). Recently, it has been demonstrated that members of several of these subfamilies have a specific localization in cells in restricted areas of the brain and peripheral tissues (Juilfs et al., 1997). These findings, together with known properties relating to substrate specificity (cAMP and/or cGMP) and inhibitor selectivity, point to an important role for PDE activity in regulating cyclic nucleotide–mediated signal transduction.

In addition, it has been shown that cGMP has an important role in regulating cAMP hydrolysis. cGMP stimulates PDE-2 and inhibits PDE-3 activity (both enzymes preferentially hydrolyze cAMP). The PDE-1 class of enzymes is calcium dependent, and both cAMP- and cGMP-specific forms of this type PDE are known (Beavo and Reifsnyder, 1990; Houslay and Milligan, 1997). As there is considerable PDE activity in most tissues and certainly in the brain, it is advisable to choose a suitable inhibitor of PDE activity when cyclic nucleotide immunocytochemistry is attempted.

In summary, cyclic nucleotides are important second messengers regulating ion-channel activity, protein function, cell interactions, and gene transcription, thus controlling cell structure and function. In recent years it has become clear that the cyclic nucleotide signaling cascade is more complex than was previously thought. Great variety has been observed in enzymes synthesizing cAMP or cGMP, and in addition, the number and disparity of classes of PDEs increasingly reveal their complexity. Thus evidence is accumulating that individual cells in complex tissues like the brain can have a distinct set of cyclic nucleotide synthesizing and hydrolyzing enzymes, leading to unique responses even when the receptor set of the cells are similar. Modern cyclic nucleotide immunocytochemistry can play an important role in identifying these cells in an environment that is at least partly intact. This can give clues to the function of single cells in a complex response.

Visualization of second messenger molecules is a powerful approach in studying the role of second messengers in relation to the (sub)cellular localization and/or kinetics of the second messenger response. During the last decade, technical improvements in Ca^{2+} imaging have yielded a wealth of information about the second messenger role of this ion in time and space. For cyclic nucleotides, there is presently no method available that has the same resolution as Ca^{2+} imaging. The localization of cyclic nucleotides can be studied using conventional immunohistochemical techniques. However, if the kinetics of the cyclic-nucleotide response are very fast, as in the case of odor or photon transduction (Baylor, 1996; Boekhoff and Breer, 1992), advanced biochemical techniques are necessary.

Immunocytochemical and biochemical analysis of cyclic nucleotides both require antibodies raised against cAMP or cGMP. Indeed, when antibodies against the cyclic nucleotides first became available (Steiner et al., 1972), they were immediately used in immunocytochemical studies (Wedner et al., 1972). These antibodies were raised against a 2′-succinylated cyclic nucleotide, which was coupled to a carrier protein by means of a carbodiimide reaction. All immunoassays for cAMP or cGMP presently available use this type of antibody. Although the early immunocytochemical studies showed for the first time a discrete localization of cAMP or cGMP in complex tissues, some drawbacks of the method were soon recognized. For cAMP immunocytochemistry it was necessary to use unfixed tissue material, with the accompanying severe losses of the readily water-soluble cyclic nucleotide from the tissue (Cumming et al., 1980). Although tissue fixation was shown to be compatible with cGMP immunocytochemistry (Chan-Palay and Palay, 1979), cyclic nucleotide immunocytochemistry did not find wide application. Visualization of the active pool of cyclic nucleotides proved difficult, and it was hypothesized that these antibodies recognized cAMP and cGMP bound to the respective protein kinases (Steiner et al., 1976).

Successful immunocytochemical visualization of small, water-soluble molecules requires fixation of these molecules to tissue-matrix proteins, as otherwise they will be lost during the subsequent procedural steps. The fixatives most commonly used in immunocytochemistry are formaldehyde and glutaraldehyde, which are both rather reactive chemicals. During fixation, the original structure of the hapten may be modified, as has been demonstrated for serotonin (Schipper and Tilders, 1983). Therefore, as these small molecules are nonimmunogenic, antisera should be raised against conjugates that have been prepared following a procedure similar to that used for tissue fixation (de Vente et al., 1987; Schipper and Tilders, 1983). For cAMP and cGMP, different fixation procedures

had to be worked out, which finally resulted in the raising of antisera specifically directed against acrolein-fixed cAMP and formaldehyde-fixed cGMP.

Critical Parameters

When working with isolated tissue, the isolation procedure is probably the most difficult, and most controversial, step (Aitken et al., 1995). In general, routine pharmacological methods for preparing tissues can be used and have met with success (e.g., Berkelmans et al., 1989; Chevalier et al., 1992; de Vente et al., 1989; Vaandrager et al., 1992). For the preparation of brain tissue, speed is of utmost importance. The thickness of the slice should be not more than 400 µm, and oxygenation of the slice should be optimal on all sides (Aitken et al., 1995).

As fixation of cyclic nucleotides is necessary for a reliable visualization, the choice of the fixative is critical. cAMP is not very reactive towards formaldehyde or glutaraldehyde, therefore it is necessary to use the highly reactive and highly toxic cross-linker acrolein (de Vente et al., 1993; Wiemelt et al., 1997). In the case of cGMP, the methylene bridge formed between the protein and hapten by use of formaldehyde is sufficiently stable to permit raising highly selective antibodies (de Vente et al., 1987). The reaction conditions for conjugating cGMP to a protein have been investigated in some detail. Fixation of cGMP was optimal between pH 6.0 and 7.0. A fixation time of 2 hr was taken to be sufficient as the reaction between cGMP, formaldehyde, and thyroglobulin approached equilibrium at this time point. As the retention of cGMP in a model system was improved at pH 7.4 compared to pH 6.0, a routine fixation of cGMP at pH 7.4 is indicated (de Vente et al., 1987).

Troubleshooting

The immunostaining procedure itself is reliable and there are no real pitfalls other than the normal problems related to proving specificity in immunocytochemistry. Therefore, always include negative controls. Specificity can further be studied by preabsorbing the antibodies with either cyclic nucleotides free in solution or in conjugated form (de Vente et al., 1989). As the antibodies are raised against conjugated cAMP or cGMP, it is preferred to preabsorb the primary antibodies with the respective conjugates. To avoid false positive results in the specificity test, it is necessary to use a conjugate protein different from the one used for immunizing the animal. In the authors' experience nonspecific staining of the primary antibodies is very low, and if there are problems in this direction, they are most probably related to the fixative.

In theory, the secondary and tertiary antibodies should not be a cause of erroneous results. However, in the authors' experience they are the largest source of trouble in immunocytochemistry. Large differences have been observed in the quality of immunostaining with various batches of labeled antibodies, even when they originated from the same manufacturer. Especially large differences have been noted in the nonspecific immunofluorescence associated with FITC- and Cy3-conjugated secondary antibodies. This nonspecific immunofluorescence has been observed in myelinated tissue in particular, and the authors have not been able to identify a pretreatment that removes such nonspecific staining if it is present. When double or triple immunostaining is to be performed, the experimenter must be aware that interactions between secondary antibodies may occur or that there may be nonspecific interactions between primary and unrelated secondary antibodies. False-positive reactions may also be observed when tertiary antibodies are used. Double and triple immunostaining reactions must be validated by controls for all the different combinations of antibodies that are used.

Anticipated Results

Cyclic nucleotide immunocytochemistry should result in the visualization of cGMP or cAMP in cell somata and in tissue fibers. How cGMP or cAMP immunostaining will present itself depends on the stimulus and the kind of tissue. Most experience has been obtained with the stimulation of the soluble guanylyl cyclase using a nitric oxide–donor compound, like sodium nitroprusside, and with the stimulation of the particulate form of the enzyme using atrial natriuretic factor (ANF) in mammals and eclosion hormone in insects (e.g., Bicker et al., 1996; de Vente et al., 1996; Ewer et al., 1994; Shuttleworth et al., 1993; Southam and Garthwaite, 1993; Truman et al., 1997). The effect of stimulation of cGMP synthesis in the central nervous system and in peripheral tissue slices incubated in vitro with sodium nitroprusside or ANF is demonstrated in Figure 10.7.1, 10.7.2, and 10.7.3. In the hippocampus, sodium nitroprusside stimulates soluble guanylyl cyclase

primarily in varicose fibers, a few interneurons and in some astrocytes. In contrast the effect of ANF is primarily shown in astrocytes (de Vente et al., 1989). A certain number of astrocytes contains both the soluble and the particulate guanylyl cyclase (de Vente, unpub. obs.). In the intestine it was possible to demonstrate the presence of three different types of guanylyl cyclase activity by stimulating different pieces of tissue with three different specific ligands (e.g., Vaandrager et al., 1992). In the hypophysis the authors could demonstrate that sGNC and pGNC have a different localization in the three different parts of this tissue. Activation of adenylate cyclase by dopamine is shown in the frontal rat brain, where cAMP accumulation is observed in neuronal cell somata (de Vente et al., 1993).

A sharply defined immunostaining of cGMP has been demonstrated in almost all studies using antibodies against formaldehyde-fixed cGMP and, therefore, is anticipated. Presently, it is unknown whether diffusion of cGMP out of the cellular structures has a significant role. The retention of cGMP in biological tissue is almost certainly much higher than the 30% reported for a model system (de Vente et al., 1987; de Vente et al., unpub. observ.). If some diffusion of cAMP or cGMP occurs, as described in the literature for cultured cells (Wu et al., 1993) or in in vivo microdialysis studies (e.g., Luo et al., 1994), the immunostaining of this extracellular nucleotide will be part of the background staining. It might be argued, on the basis of the sharp delineation of the cyclic GMP immunostaining that diffusion out of the tissue is negligible, which is in agreement with the published data (Tjörnhammar et al., 1986).

It may be anticipated that the use of different phosphodiesterase inhibitors may give insight into the distribution of these enzymes in tissues. It has to be realized that none of these inhibitors is a very specific drug; in the best case they are highly selective. Thus it has been shown that zaprinast, a rather selective inhibitor of the PDE-5 (cGMP hydrolyzing), in combination with a NO donor results in the accumulation of cGMP in a restricted area of the hippocampus of the rat (de Vente et al., 1996). Similarly, zaprinast was effective in raising cGMP levels in canine colon smooth muscle cells (Shuttleworth et al., 1993). As already discussed in Background Information, immunocytochemical studies on the tissue distribution of phosphodiesterases (PDEs), although limited (e.g., Juilfs et al., 1997), have provided convincing evidence that various isoforms of this class of enzymes may have a very specific distribution in subsets of cells of functionally assigned areas of every tissue. It is becoming apparent that cells can have an individual expression of a set of PDEs. Therefore, the study of cyclic nucleotide localization in heterogeneous tissue may yield different results when the same experiment is performed twice using different PDE inhibitors. Thus, although IBMX has been the PDE inhibitor of choice in many studies, it will always be necessary to study the effects of other PDE inhibitors in a particular setup when the aim is to provide definite conclusions about the involvement of cyclic nucleotides in signal transduction using the approach described in this unit.

Time Considerations

The entire procedure, incubation of the slices, fixation, sectioning, and immunostaining, can be done in 1.5 working days. The most time consuming step, incubation of the sections with the primary antibodies, can be done overnight. It takes ~4 months to raise primary antibodies in rabbits.

Literature Cited

Aitken, P.G., Breese, G.R., Dudek, F.F., Edwards, F., Espanol, M.T., Larkman, P.M., Lipton, P., Newman, G.C., Nowak, T.S., Panizzon, K.L., Raly-Susman, K.M., Reid, K.H., Rice, M.E., Sarvey, J.M., Schoepp, D.D., Segal, M., Taylor, C.P., Teyler, T.J., and Voulalas, P.J. 1995. Preparative methods for brain slices: A discussion. *J. Neurosci. Methods* 59:139-149.

Baylor, D. 1996. How photons start vision. *Proc. Natl. Acad. Sci. U.S.A.* 93:560-565.

Beavo, J.A. and Reifsnyder, D.H. 1990. Primary sequence of cyclic nucleotide phosphodiesterase isozymes and the design of selective inhibitors. *Trends Neurosci.* 11:150-155.

Berkelmans, H.S., Schipper, J., Hudson, L., Steinbusch, H.W.M., and de Vente, J. 1989. cGMP immunocytochemistry in aorta, kidney, retina, and brain tissues of the rat after perfusion with nitroprusside. *Histochemistry* 93:142-148.

Bicker, G., Schmachtenberg, O., and de Vente, J. 1996. The nitric oxide/cyclic GMP messenger system in olfactory pathways of the locust brain. *Eur. J. Neurosci.* 8:2635-2643.

Boekhoff, I. and Breer, H. 1992. Termination of second messenger signaling in olfaction. *Proc. Natl. Acad. Sci. U.S.A.* 89:471-474.

Bredt, D.S., Hwang, P.M., and Snyder, S.H. 1990. Localization of nitric oxide synthase indicating a neural role for nitric oxide. *Nature* 347:768-770.

Chan-Palay, V. and Palay, S.L. 1979. Immunohistochemical localization of cyclic GMP: Light and electron microscope evidence for involvement of neuroglia. *Proc. Natl. Acad. Sci. U.S.A.* 76:1485-1488.

Chevalier, R.L., Fern, R.J., Garmey, M., El-Dahr, S.S., Gomez, R.A., and de Vente, J. 1992. Localization of cGMP after infusion of ANP or nitroprusside in the maturing rat. *Am. J. Physiol.* 262:F417-F424.

Cooper, D.M.F., Mons, N., and Karpen, J.W. 1995. Adenylyl cyclases and the interaction between calcium and cAMP signalling. *Nature* 374:421-424.

Cooper, H.M. and Paterson, Y. 1999. Production of polyclonal antisera. *In* Current Protocols in Immunology (J.E. Coligan, A.M. Kruisbeek, D.H. Margulies, E.M. Shevach, and W. Strober, eds.) pp. 2.4.1-2.4.9. John Wiley & Sons, New York.

Cumming, R., Dickison, S., and Arbuthnott, G. 1980. Cyclic nucleotide losses during tissue processing for immunocytochemistry. *J. Histochem. Cytochem.* 28:54-55.

de Vente, J., Steinbusch, H.W.M., and Schipper, J. 1987. A new approach to immunocytochemistry of 3′,5′-cyclic guanosine monophosphate: Preparation, specificity, and initial application of a new antiserum against formaldehyde-fixed 3′,5′-cyclic guanosine monophosphate. *Neuroscience* 22:361-373.

de Vente, J., Schipper, J., and Steinbusch, H.W.M. 1989. Formaldehyde fixation of cGMP in distinct cellular pools and their recognition by different cGMP-antisera. An immunocytochemical study into the problem of serum specificity. *Histochemistry* 91:401-412.

de Vente, J., Schipper, J., and Steinbusch, H.W.M. 1993. A new approach to the immunocytochemistry of cAMP. Initial characterization of antibodies against acrolein-fixed cAMP. *Histochemistry* 99:457-462.

de Vente, J., Hopkins, D.A., Markerink-van Ittersum, M., and Steinbusch, H.W.M. 1996. Effects of the 3′,5′-phosphodiesterase inhibitors isobutylmethylxanthine and zaprinast on NO-mediated cGMP accumulation in the hippocampus slice preparation: An immunocytochemical study. *J. Chem. Neuroanat.* 10:241-248.

Donovan, J. and Brown, P. 1999a. Animal health assurance. *In* Current Protocols in Immunology (J.E. Coligan, A.M. Kruisbeek, D.H. Margulies, E.M. Shevach, and W. Strober, eds.) pp. 1.1.1-1.1.3. John Wiley & Sons, New York.

Donovan, J. and Brown, P. 1999b. Handling and restraint. *In* Current Protocols in Immunology (J.E. Coligan, A.M. Kruisbeek, D.H. Margulies, E.M. Shevach, and W. Strober, eds.) pp. 1.3.1-1.3.5. John Wiley & Sons, New York.

Donovan, J. and Brown, P. 1999c. Blood collection. *In* Current Protocols in Immunology (J.E. Coligan, A.M. Kruisbeek, D.H. Margulies, E.M. Shevach, and W. Strober, eds.) pp. 1.7.1-1.7.8. John Wiley & Sons, New York.

Ewer, J., de Vente, J., and Truman, J.W. 1994. Neuropeptide induction of cyclic GMP increases in the insect CNS: Resolution at the level of single identifiable neurons. *J. Neurosci.* 14:7704-7712.

Garthwaite, J. 1991. Glutamate, nitric oxide and cell-cell signalling in the nervous system. *Trends Neurosci.* 14:60-67.

Garthwaite, J., Woodham, P.L., Collins, M.J., and Balasz, R. 1979. On the preparation of brain slices: Morphology and cyclic nucleotides. *Brain Res.* 173:373-377.

Giuili, G., Scholl, U., Bulle, F., and Guellaën, G. 1992. Molecular cloning of the cDNAs coding for the two subunits of soluble guanylyl cyclase from human brain. *FEBS Lett.* 304:83-88.

Gorczyca, W.J., Gray-Keller, M.P., Detwiler, P.B., and Palczewski, K. 1994. Purification and physiological evaluation of a guanylate cyclase activating protein from retinal rods. *Proc. Natl. Acad. Sci. U.S.A.* 91:4014-4018.

Guidotti, A., Cheney, D.L., Trabucchi, M., Doteuchi, M., Wang, C., and Hawkins, R.A. 1974. Focused microwave radiation: A technique to minimize post mortem changes of cyclic nucleotides, DOPA and choline and to preserve brain morphology. *Neuropharmacology* 13:1115-1122.

Harteneck, C., Wedel, B., Koesling, D., Malkewitz, J., Böhme, E., and Schultz, G. 1991. Molecular cloning and expression of a new α-subunit of soluble guanylyl cyclase. Interchangeability of the α-subunits of the enzyme. *FEBS Lett.* 292:217-222.

Houslay, M.D., and Milligan, G. 1997. Tailoring cAMP-signalling responses through isoform multiplicity. *Trends Biochem. Sci.* 22:217-224.

Juilfs, D.M., Fülle, H.J., Zhao, A.Z., Houslay, M.D., Garbers, D.L., and Beavo, J.A. 1997. A subset of olfactory neurons that selectively express cGMP-stimulated phosphodiesterase (PDE2) and guanylyl cyclase-D define a unique olfactory signal transduction pathway. *Proc. Natl. Acad. Sci. U.S.A.* 94:3388-3395.

Knowles, R.G. and Moncada, S. 1994. Nitric oxide synthases in mammals. *Biochem. J.* 298:249-258.

Luo, D., Leung, E., and Vincent, S.R. 1994. Nitric-oxide dependent efflux of cGMP in rat cerebellar cortex: An in vivo microdialysis study. *J. Neurosci.* 14:263-271.

Moncada, S., Palmer, R.M.J., and Higgs, E.A. 1991. Nitric oxide: Physiology, pathophysiology and pharmacology. *Pharmacol. Rev.* 43:109-142.

Murad, F. 1994. Regulation of cytosolic guanylyl cyclase by nitric oxide: The NO–cyclic GMP signal transduction system. *Adv. Pharmacol.* 26:19-33.

Schipper, J. and Tilders, F.J.H. 1983. A new technique for studying specificity of immunocytochemical procedures: Specificity of serotonin immunostaining. *J. Histochem. Cytochem.* 31:12-18.

Shuttleworth, C.W., Xue, C., Ward, S.M., de Vente, J., and Sanders, K.M. 1993. Immunohistochemical localization of 3′,5′-cyclic guanosine monophosphate in the canine proximal colon: Responses to nitric oxide and electrical stimulation of enteric inhibitory neurons. *Neuroscience* 56:513-522.

Southam, E. and Garthwaite, J. 1993. The nitric oxide–cyclic GMP signalling pathway in rat brain. *Neuropharmacology* 32: 1267-1277.

Steiner, A.L., Parker, C.W., and Kipnis, D.M. 1972. Radioimmunoassay for cyclic nucleotides. 1. Preparation of antibodies and iodinated cyclic nucleotides. *J. Biol. Chem.* 247:1106-1113.

Steiner, A.L., Ong, S., and Wedner, H.J. 1976. Cyclic nucleotide immunocytochemistry. *Adv. Cyclic Nucleotides Res.* 7:115-155.

Tjörnhammar, M.L., Lazarides, G., and Bartfai, T. 1986. Efflux of cyclic guanosine 3′,5′-monophospohate from cerebellar slices stimulated by L-glutamate or high K^+ or *N*-methyl-*N*′-nitro-*N*-nitrosoguanidine. *Neurosci. Lett.* 38:95-99.

Traylor, T.G. and Sharma, V.S. 1992. Why NO? *Biochemistry* 31:2847-2849.

Truman, J.W., Mumby, S.M., and Welch, S.K. 1997. Involvement of cyclic GMP in the release of stereotyped behavior patterns in moths by a peptide hormone. *J. Exp. Biol.* 84:201-212.

Vaandrager, A.B., Bot, A.G.M., de Vente, J., and De Jonge, H.R. 1992. Atriopeptins and *Escherichia coli* enterotoxin STa have different sites of action in mammalian intestine. *Gastroenterology* 102:1161-1169.

Wedel, B.J. and Garbers, D.L. 1997. New insights on the functions of the guanylyl cyclase receptors. *FEBS Lett.* 410:29-33.

Wedner, H.J., Hoffer, B.J., Battenberg, E., Steiner, A.L., Parker, C.W., and Bloom, F.E. 1972. A method for detecting intracellular cyclic adenosine monophosphate by immunofluorescence. *J. Histochem. Cytochem.* 20:293-299.

Wiemelt, A.P., Engleka, M.J., Skorupa, A.F., and McMorris, F.A. 1997. Immunochemical visualization and quantitation of cyclic AMP in single cells. *J. Biol. Chem.* 272:31489-31495.

Wu, X.B., Brüne, B., Von Appen, F., and Ullrich, V. 1993. Efflux of cyclic GMP from activated human platelets. *Mol. Pharmacol.* 43:564-568.

Yu, S., Avery, L., Baude, E., and Garbers, D.L. 1997. Guanylyl cyclase expression in specific sensory neurons: A new family of chemosensory receptors. *Proc. Natl. Acad. Sci. U.S.A.* 94:3384-3387.

Key References

de Vente et al., 1987. See above.

Describes the preparation of cGMP-formaldehyde conjugates and gives details about stability, retention, and characterization.

de Vente et al., 1989. See above.

Describes at length the various methods for studying the specificity of these antibodies.

de Vente et al., 1993. See above.

Describes for the first time preparation of cAMP-acrolein conjugates and first characterization of these antibodies.

Ewer et al., 1994. See above.

Describes the first application of the antibody in insect tissue.

Shuttleworth et al., 1993. See above.

Provides an example of the importance of the choice of phosphodiesterase inhibitor.

Contributed by J. de Vente and
H.W.M. Steinbusch
Maastricht University
Maastricht, The Netherlands

Methods for Distinguishing Nitrosative and Oxidative Chemistry of Reactive Nitrogen Oxide Species Derived from Nitric Oxide

The chemistry of nitric oxide (NO) may have profound effects on biological systems depending on the reactive intermediates involved (Wink et al., 1996a). These NO-derived intermediates formed under aerobic conditions may engage in complex chemical reactions with biologically important molecules. The outcome of these reactions, as well as their ultimate effect on biological systems, depends on the selectivity of the reactive chemical species and the concentration of different substances present. For instance, the reaction between nitric oxide and oxygen can lead to a variety of chemical intermediates, depending on the phase of the reaction. In the gas phase normally associated with air pollution, the autoxidation requires two NO molecules and one oxygen molecule to form two molecules of NO_2 (nitrogen dioxide), which can further react with NO to form N_2O_3 (dinitrogen trioxide).

$$2\ NO + O_2 \rightarrow 2\ NO_2$$
$$NO_2 + NO \rightarrow N_2O_3$$

However, in aqueous solution, there appears to be a fundamental difference in the intermediates produced in the NO/O_2 reaction. Trapping experiments appear to indicate that there is no formation of free NO_2 in aqueous solution (Wink et al., 1993). Furthermore, it has been suggested that the major reactive intermediate in aqueous solution is an isomer of N_2O_3 that differs from that formed in the gas phase (Pires et al., 1994). Competitive kinetic experiments have shown that peptides containing thiols have a high affinity for N_2O_3 (Wink et al., 1994). These results indicate that the primary target of N_2O_3 in vivo is thiols, and suggest that proteins such as those containing zinc-finger motifs are susceptible to reaction with the intermediate (Kroncke et al., 1994; Wink and Laval, 1994). This reaction can affect numerous cellular functions, possibly resulting in cytotoxicity.

Other reactive intermediates formed during the metabolism of NO under in vivo conditions may have important consequences. Peroxynitrite ($ONOO^-$) is readily formed from the reaction between O_2^- and NO (Huie and Padmaja, 1993). Studies have indicated that, unlike N_2O_3, peroxynitrite does not directly nitrosate substrates (Miles et al., 1995; Wink et al., 1997). However, peroxynitrite does oxidize different substrates (lipids, DNA, proteins), which is the primary mode of reactivity in biology (Beckman et al., 1990; Pryor and Squadrito, 1996).

In this unit, conversion of two different compounds to fluorescent products will be used to distinguish between oxidative and nitrosative chemistry of different reactive nitrogen oxide species. In addition, methods will be described for determining the relative selectivity of different substances with these reactive intermediates. Conversion of 2,3-diaminonaphthylene (DAN) to 2,3-naphthyltriazole (NAT) will be used to determine the chemistry of nitrosation (see Basic Protocol 1). The oxidation of 123 dihydrorhodamine (DHR) to 123 rhodamine will be used as a probe for oxidation (see Basic Protocol 2).

DETERMINATION OF NITROSATION REACTIONS

BASIC PROTOCOL 1

The two parts of this protocol provide information necessary to determine the amount of nitrosation, as well as the relative selectivity of the nitrosating intermediates for other substances (Wink et al., 1996a). Buffers and medium often contain an array of substances, and it is not always clear when designing experiments whether these agents might interfere with an assay or experiment. The first part (consisting of steps 1 to 7) is useful

Contributed by David A. Wink, Sungmee Kim, Allen Miles, David Jourd'heuil, Matthew B. Grisham
Current Protocols in Toxicology (2000) 10.8.1-10.8.12

for determining whether substances are present in medium or buffers that limit nitrosation in a particular experiment.The second part (consisting of steps 8 to 12) is used to distinguish the relative chemical affinity for nitrosating intermediates. This is useful in determining the order of reactivity of different substances with nitrosating agents, and can be used to find efficient scavengers for nitrosating agents.

Materials

2,3-diaminonapthylene (DAN; Aldrich)
Dimethylformamide (DMF) or dimethylsufoxide (DMSO)
Buffer or medium under investigation
PBS without calcium or magnesium (*APPENDIX 2A*)
20 to 100 mM sodium phosphate, pH 7.4 (*APPENDIX 2A*)
Nitrogen or argon gas (see Fig. 10.4.3 for setup)
NO gas cylinder (see Fig. 10.4.3 for setup)
1 M NaOH
Sulfanilamide
N-(1-naphthyl)ethylenediamine dihydrochloride (NEDD; Aldrich)
Substrate to be evaluated

Bubbling apparatus for nitrogen or argon and for NO (Fig. 10.4.3), consisting of:
  Glass vials with rubber septa
  Tygon tubing
UV/visible spectrophotometer and quartz cuvettes
100-µl airtight syringe
Spectrofluorometer
13 × 75–mm glass test tubes

Determine Extent of Nitrosation in Different Buffering Systems

Prepare stock solutions

1. Prepare 100 mM DAN stock solution by dissolving 15.6 mg of DAN in 1 ml of either DMSO or DMF.
2. Dissolve 0.2 ml of the DAN stock solution in 100 ml of the buffer or medium under investigation, to make a 0.2 mM DAN/buffer solution.

   IMPORTANT NOTE: *No phenol red should be present. Also, vitamins commonly added to media can interfere as well. It is important that a standard curve be done in the medium of interest to check if any interferences are present.*
3. Prepare comparison buffer by adding 0.2 ml of DAN stock solution to 99.8 ml of PBS (without calcium or magnesium).
4. Prepare NO stock solutions as follows.
   a. Place 20 to 100 mM sodium phosphate, pH 7.4, in a vial with a rubber septum (Fig. 10.4.3).
   b. Bubble nitrogen or argon through the phosphate solution for 1 min per 2 ml of buffer.
   c. Bubble NO through the solution for 20 min per 2 ml of buffer using an apparatus such as that illustrated in Figure 10.4.3 to first bubble the NO through 1 M NaOH to purify the gas and then collect the gas in 100 mM sodium phosphate, pH 7.4.

      Alternatively an NO donor such as $(C_2H_5)_2N(NO)(NO)Na$ and DEA/NO can be used (Keefer et al., 1996). Approximately 20 mg/ml DEA/NO solid should dissolved in 0.01 mM NaOH to yield a 10 mM stock solution. To verify the exact concentration, take a UV-vis spectrum in base. The maximum absorbance at 250 nm has an extinction coefficient of 8000 cm^{-1} M^{-1}.

Standardize using colorimetric method (Nims et al., 1995)

5. Dissolve 0.5 g of sulfanilamide and 30 mg NEDD in PBS to form the colorimetric solution. Stir and gently heat. Filter if necessary.

6. Add a 100-µl aliquot of the NO stock solution via an airtight syringe to 1 ml of colorimetric solution. Allow to stand for 2 min then read the absorption at 500 nm in a UV/vis spectrophotometer. Divide the absorbance reading by 0.012 (for a 1-cm pathlength cuvette) to get the concentration of NO in the stock solution in mM.

   Alternatively, to standardize the amount of NO released by DEA/NO, add 10 µl of the stock solution of that compound (see annotation to step 4) to 1 ml of the colorimetric solution. Allow to stand 1 hr at room temperature or 20 min at 37°C. Read the absorbance at 500 nm. Take the absorbance and divide by 0.0012. This is the concentration of NO released at neutral pH by the DEA/NO stock solution.

Determine the extent of nitrosation in buffer

7. Add 100 µl of the NO stock solution (prepared in step 4) through an airtight syringe to 2 ml of the test buffer containing DAN (prepared in step 2) in the spectrofluorometer. Allow to stand for a few minutes, then read the fluorescence with excitation of 375 nm and emission of 450 nm. Repeat with the comparison buffer (PBS containing DAN; prepared in step 3). Compare fluorescence intensity.

   IMPORTANT NOTE: *The difference in fluorescence between the medium and PBS indicates the amount of potential nitrosative scavenging agents.*

Determine Relative Selectivity of Different Substances

Prepare DAN and substrate solutions

8. Make a 0.2 mM DAN solution in PBS as described in step 3.

   10 to 20 mM HEPES, phosphate, or Tris can be added for additional buffering capacity if required. If the amount of added stock NO or NO donor is <1% of the reaction volume, there should be no effect on the pH. Otherwise, check the pH.

9. Place 2 ml DAN solution (prepared in step 8) into each of a series of 13 × 75–mm glass test tubes. Add substrate to be evaluated at concentrations from 0 to 50 mM (if solubility permits).

   Samples should be analyzed in triplicate. The range of concentrations includes positive and negative controls.

Read fluorescence and analyze results

10. Read the fluorescence at 375 nm excitation and 450 nm emission.

11. Plot concentration of substrate (x-axis) versus 1/fluorescence (y-axis). Divide the slope of the line by the y intercept. Multiply the x intercepts by −1 to give the concentration of substrate required to quench 50% of the reaction with DAN.

    This is the concentration where the 50% of the intermediate is nitrosating DAN and 50% is being scavenged by the substrate. Therefore, the rates of the two pathways are identical and the rate constants can be derived from the concentration (see Background Information).

12. Compare different substrates and their relative $-x$ intercepts at a single concentration of DAN to provide the relative affinity of different substrates for a particular substrate.

BASIC PROTOCOL 2

DETERMINATION OF THE SELECTIVITY FOR DHR OXIDATION

Some reactive nitrogen oxide intermediates formed during NO metabolism can oxidize different substrates. The oxidation of different fluorescent dyes by reactive chemical species such as peroxynitrite can be used to detect these species (Crow, 1997). One such reaction is that of DHR oxidation (Kooy et al., 1994; Miles et al., 1996). This is not a specific dosimeter for a particular intermediate such as hydroxyl radical or peroxynitrite, but instead represents the presence of oxidation chemistry under a given set of conditions. Addition of different trapping agents provides a method for deciphering the species responsible for oxidation. For instance, azide is an excellent trap for nitrosating reactive nitrogen oxide species (RNOS) such as N_2O_3 (Williams, 1988). Metal chelators such as DETAPAC prevent oxidation of DHR by metal-catalyzed reactions mediated by O_2^- and H_2O_2. The following provides a method to determine selectivity, as well as the effect of scavengers on oxidation.

Materials

123 dihydrorhodamine (DHR)
Dimethylformamide (DMF)
PBS (*APPENDIX 2A*) or sample buffer
Oxidizing substances under investigation
123 rhodamine

13 × 75–glass test tubes
Spectrofluorometer

1. Dissolve 25 mg solid DHR in 5 ml of DMF. Dilute this solution three-fold in DMF to yield a 5 mM DHR stock solution.
2. Prepare dilutions of the stock solution (2 ml samples in 13 × 75–mm glass test tubes) with concentrations ranging between 5 and 200 μM DHR in medium, PBS, or sample buffer.

   DHR alone is the negative control; 123 rhodamine is the positive control.
3. Add the oxidizing substances or system to the solution and incubate for the designated time of the experiment. Prepare standard solutions using 123 rhodamine in the exact buffer used in the experiment.
4. Place the 2-ml samples in the spectrofluorometer. Excite at 500 nm and read the emission at 570 nm.
5. Plot 1/[DHR] (*x*-axis) versus 1/fluorescence intensity (*y*-axis). Divide the *y* intercept by the slope and multiply it by −1.

   This value is the concentration of DHR required to trap 50% of the chemical oxidant.

   If the reaction is competitive with DHR oxidation—i.e., formation of nitrite/nitrate—division of the first-order rate constant by this value can give the second-order rate constant for the reaction between the oxidant and DHR.
6. Once the concentration of DHR required to trap 50% of oxidant is determined, prepare a stock solution with the concentration of DHR five times that determined in step 5.

   For example, if 20 μM DHR was required to achieve 50% fluorescence, make a 100 ml stock solution of 100 μM DHR. This will ensure that most of the chemical oxidant is reacting with DHR.

7. Place 2 ml of the DHR solution prepared in step 6 into a series of glass test tubes. Add the substrate that is being evaluated at concentrations from zero to five or ten times the concentration of DHR.

   For example, if 100 μM DHR is present in the solution, then a concentration range of quenching substrates should be from 0 to 1 mM. However, this may depend on the solubility of substrate.

   Samples should be run at least in triplicate for each point for accuracy.

8. Read the resulting fluorescence by exciting the solution at 500 nm and reading the emission at 570 nm.

9. Plot the concentration of substrate (*x*-axis) versus 1/fluorescence (*y*-axis). Divide the slope of the line by the *y* intercept.

   This will give the x intercept which, when multiplied by −1, gives the concentration of substrate required to quench 50% of DHR.

10. Compare different substrates and their relative *x* intercept at a single concentration of DHR to provide the relative selectivity of different substrates for oxidants.

COMMENTARY

Background Information

The mechanism of toxicology that NO is involved in depends on the chemistry of this diatomic radical. Nitrosative and oxidative chemistry resulting from these intermediates can determine specific toxicological mechanisms (Wink et al., 1996a, 1998). Therefore, it is important to understand the reactive chemical species present and the influences they may have on various biological components both from a mechanistic standpoint and an experimental one. As discussed below, there are two ways of interrogating these intermediates. The first is a dose-dependent analysis using either DAN or DHR, which gives the relative reactivity of the RNOS with each compound with respect to other reactions such as nitrite and nitrate formation. The second allows the comparison of different compounds and their effect on scavenging nitrosative and oxidative species.

Product formation analysis

The limiting reaction for the oxidation or nitrosation mediated by different RNOS is the reaction mechanism that ultimately forms nitrite/nitrate. For example, the hydrolysis of N_2O_3 in aqueous solutions will limit the reactions this molecule can undergo with various substrates:

$$N_2O_3 + H_2O \rightarrow NO_2^-$$
$$N_2O_3 + \text{substrate} \rightarrow \text{products}.$$

From these equations, it is possible to derive an expression that will provide the ratio of rate constants for a variety of reactions. Such information should provide a better understanding of the selectivity of RNOS.

A mathematical model can be used to determine the relative affinities of various substrates for NO_x. The reaction rate constant for the substance is defined as k_s, while the reaction rate constant for the formation of nitrite is defined as k_H. The ratio of rate constants, k_s/k_H, determines the affinity of substrate (S) and the amount of product (P) that will be formed at specific substrate concentrations, or, in other words, the fraction of total NO_x that is scavenged by S. The ratio of k_s to k_H can be assessed by analyzing product formation as a function of substrate concentration. This is analogous to the Lineweaver-Burke plots commonly employed in the study of enzyme kinetics. The following mathematical derivation for scheme 1 (see Fig. 10.8.1A) will aid in the determination of the selectivity.

The ratio of product formed versus nitrite concentration is proportional to the rates of formation for each reaction pathway such that: $(dP/dt)/(d[N]/dt)$ = ratio of product formation to nitrite formation. Since $dP/dt = k_s[NO_x]S$, and nitrite formation is unimolecular because water is the solvent,

$$dN/dt = k_H[NO_x].$$

Then,

$$dP/dN = (k_s[NO_x]S)/(k_H[NO_x]).$$

Simplifying the equation gives

$$P/N = k_sS/k_H.$$

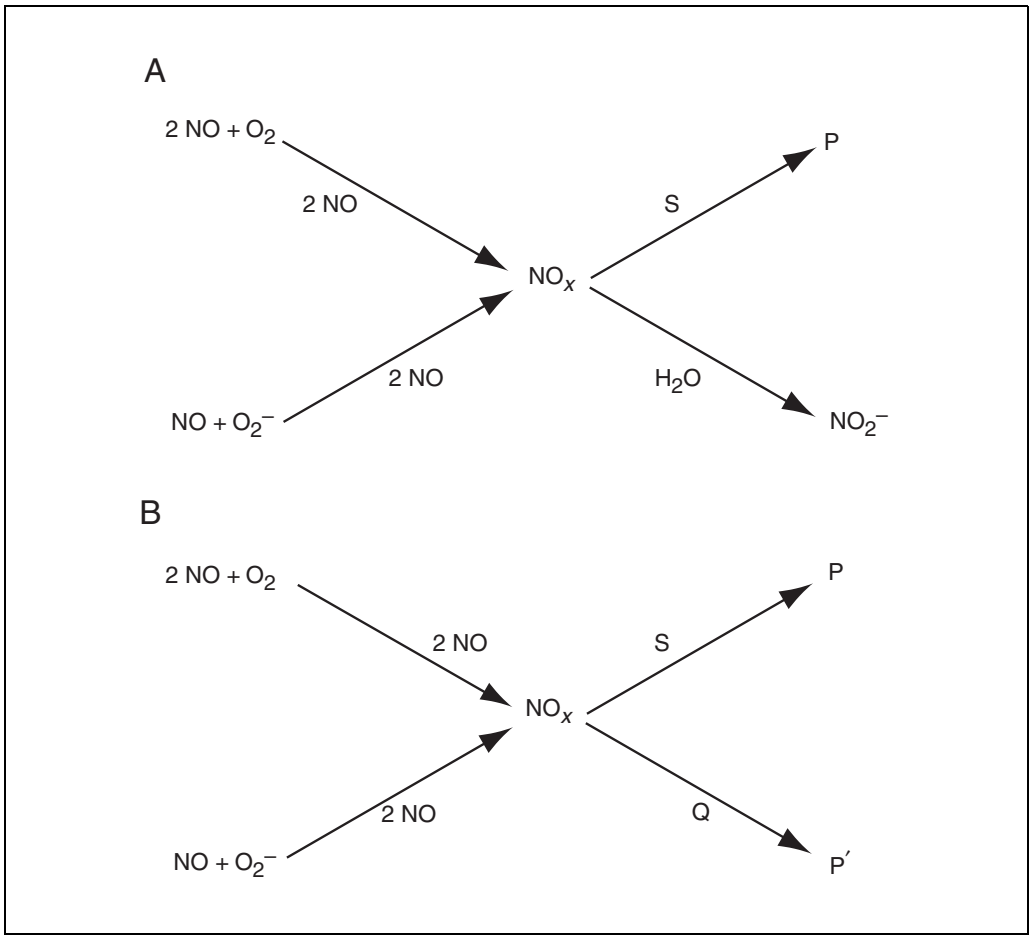

Figure 10.8.1 Reaction schemes. (**A**) Scheme 1. (**B**) Scheme 2.

Since the amount of P as it relates to amount of nitrite formed via hydrolysis is:

$$P_o = P + N$$

where P_o is equal to the maximum total amount of P formed at infinite S concentration or, in other words, the total amount of available NO_x formed. If one solves for N:

$$N = P_o - P$$

and by substitution:

$$P/(P_o - P) = k_s S/k_H$$

This can then be solved algebraically in terms of $1/P$ to yield:

$$1/P = (k_H/(k_s S) \times 1/P_o) + 1/P_o.$$

A plot of $1/S$ versus $1/P$ will give a linear plot with slope $= k_H/(k_s) \times (1/P_o)$ and y-intercept $= 1/P_o$. Therefore,

$$k_s/k_H = y\text{-intercept/slope or } -(x\text{-intercept}).$$

Using this methodology, the $-(1/x$-intercept) represents the concentration of substrate required to scavenge 50% of the available NO_x. An alternative way to express this is that the concentration of substrate required is such that the rate of product formation is equal to the rate hydrolysis of NO_x. Hence,

$$k_H = k_s[S_{0.5}],$$

which can be solved as follows:

$$k_H = k_s[S_{0.5}] = -1/x \text{ intercept.}$$

Product quenching

Another approach is to design a study of the competition between two different substrates, S and Q (for quencher) for NO_x.

The rate constant for the reaction of substrate (detection compound) is k_s, while the rate constant for the quencher is k_Q. A mathematical expression can be derived for scheme 2 (see Fig. 10.8.1B) which can yield the ratio of rate constants for k_s and k_Q. As above, the ratio of P/P' is proportional to the ratio of their rates of formation:

$$(dP/dt)/(dP'/dt) = dP/dP'.$$

Since

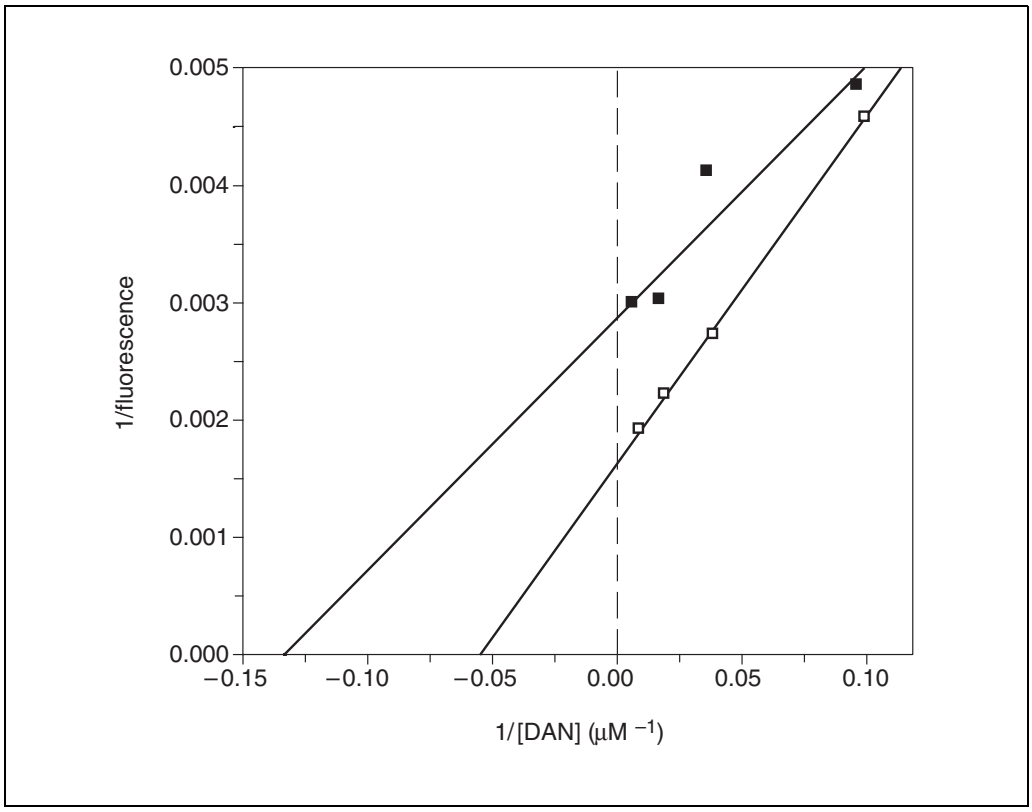

Figure 10.8.2 The effect of different concentrations of DAN on the fluorescence intensity mediated by the NO/O_2 reaction or acidic nitrite. Increasing DAN was placed in a 10 mM phosphate solution, pH 7, where NO concentration was 10 μM (open squares). Another 10 mM phosphate solution at, pH 5, with 10 mM $NaNO_2$ was exposed to different DAN concentrations (closed diamonds).

$$dP/dt = k_s[NO_x]S$$
$$dP'/dt = k_Q[NO_x]Q$$

then

$$P/P' = (k_s[NO_x]S)/(k_Q[NO_x]Q)$$

Often it is inconvenient to measure product, P'. Therefore, P' can be expressed in terms of P. In the absence of Q, P_T represents the total NO_x which is scavenged

$$P_T = P + P'$$

therefore

$$P' = P_T - P;$$

then

$$P/(P_T - P) = (k_sS)/(k_QQ).$$

Solving the above equation for $1/P$:

$$1/P = [\ (k_QQ)/(k_sS) \times 1/P_T] + 1/P_T.$$

In this type of experiment, the substrate concentration remains constant while the amount of quencher, Q, is varied. A plot of $1/P$ versus the concentration of Q yields a linear graph with slope = $(k_Q)/(k_sS) \times 1/P_T$ and y-intercept is $1/P_T$. Therefore if S is known:

$$k_Q/k_s = S \times (\text{slope}/y\text{-intercept}) \text{ or}$$
$$S \times x\text{-intercept}.$$

It is important to note that with this type of experiment, the substrate concentration should be such that >90% of the NO_x is scavenged by S.

Chemical biology of NO

There are numerous chemical reactions involving nitric oxide that are thought to be operative in biological systems. Determining which reactions are relevant to different toxicological mechanisms has been a challenge. In order to decipher the complexity of these reactions, a description known as the chemical biology of NO was formed, which equates the pertinent chemical reactions to specific biological situations (Wink et al., 1996b, 1998). The chemical biology of NO is divided into two major categories, consisting of direct and indirect effects. The direct effects are those that involve direct reactions of NO with biological targets—e.g., the reaction between NO and heme proteins such as guanylate cyclase and oxyhemoglobin. These reactions require low concentrations of NO and occur very rapidly.

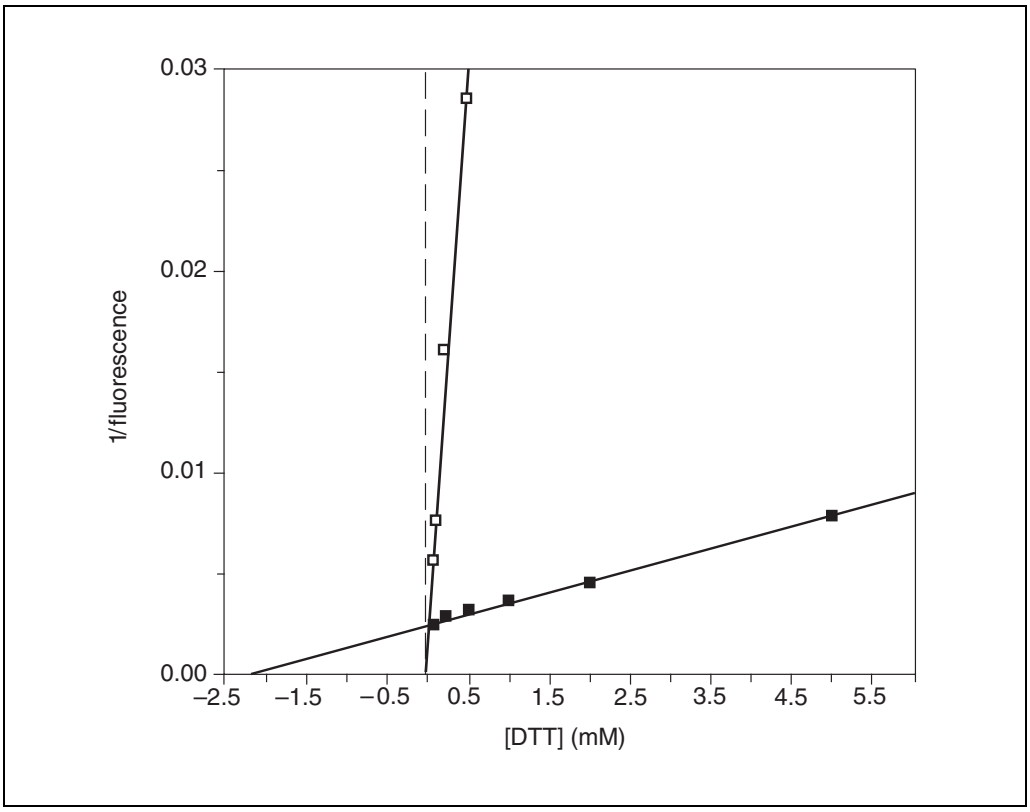

Figure 10.8.3 The effect of different amounts of DTT on the nitrosation of DAN, mediated either the NO/O_2 reaction or acidic nitrite. A 10 mM phosphate solution, pH 7, with 100 μM DAN and varying amounts of DTT was exposed to 10 μM NO (closed squares). A 10 mM phosphate solution, pH 5, with 100 μM DAN and varying amounts of DTT was exposed to 10 μM $NaNO_2$ (open squares).

Table 10.8.1 Selectivity of NO_x Toward Reaction with Various Substrates in Aqueous Solution[a]

Substrate	$k_s/k_H(M^{-1})$	Concentration required to scavenge 90% of NO_x (mM)
Amino acids	<5	2000
5-Aminosalicylic acid	2×10^3[b]	5
Ascorbate	3×10^4	0.3
Azide ion	10^5	0.1
Cysteine	5×10^3	2
Cytosine	<0.005	2×10^5
DAN	3×10^4	0.3
Dopamine	1×10^3[c]	10
Ferrocyanide	5×10^2	20
Glutathione	10^4	1
Phosphate	25	400
Tyrosine	25	400

[a]Data from Wink et al., 1996c.

[b]Obtained by monitoring of the resultant product with absorbance at 400 nm.

[c]Obtained by monitoring the formation of the resultant oxidized product by absorbance at 475 nm.

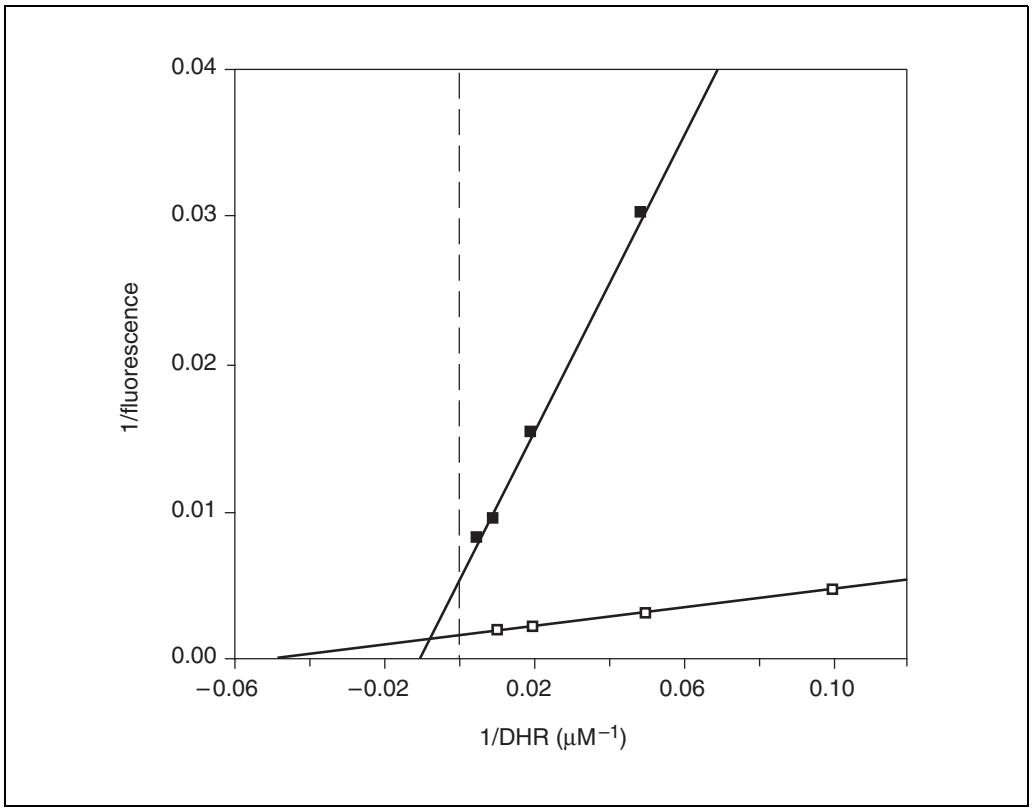

Figure 10.8.4 Concentration dependency of DHR treated with peroxynitrite or DEA/NO. PBS solutions containing 50 μM DETAPAC and 10 mM HEPES with varying concentrations of DHR was exposed to 10 μM DEA/NO (closed squares). PBS solutions containing 50 μM DETAPAC and 10 mM HEPES with varying concentrations of DHR was exposed to 10 μM peroxynitrite (open squares).

Indirect effects do not involve NO itself, but rather RNOS derived from the reaction between NO and oxygen or superoxide. These reactions require high localized concentrations of NO, generally for a prolonged period of time, and primarily generate N_2O_3 from the reaction with oxygen, while $ONOO^-$ is the preliminary product from the NO/O_2^- reaction. N_2O_3, as discussed above, mediates nitrosation reactions, while $ONOO^-$, and, to lesser extent, N_2O_3, mediate oxidative chemistry. With this in mind, the indirect effects can be cataloged into nitrosative and oxidative stress. As presented here, DAN distinguishes nitrosative pathways, while DHR indicates oxidation, allowing the determination of both categories of the indirect effects.

Nitrosation reactions in biological systems occur primarily with amines and *S*-nitrosothiols. These reactions with a variety of proteins (e.g., DNA repair proteins, ligase, alkylyltransferase, GAPDH, metallothionein, and zinc finger proteins such as Fpg and SP-1) can have profound effects such as inhibition of DNA repair proteins and formation of vasoactive substances (Wink et al., 1996a,b). The formation of N_2O_3 in vivo is primarily from three sources. Reactions such as the autoxidation of NO (Ford et al., 1993), acidic nitrite solutions (Williams, 1988), and NO reaction with peroxynitrite can all result in nitrosation reactions (Wink et al., 1997). There appear to be two isomers of N_2O_3 that differ in affinity for different substrates. The autoxidation of NO in the gas phase proceeds through the intermediate NO_2, which reacts at near diffusion control to yield N_2O_3 (Pires et al., 1994). Mildly acidic nitrite solutions can also generate N_2O_3. It has been presumed that the $ON\text{-}NO_2$ isomer of N_2O_3 is formed in both gas phase autoxidation and acidic nitrite reactions (Williams, 1988). However, the autoxidation in aqueous solution is thought to form a different isomer of N_2O_3 perhaps ONONO (Pires et al., 1994). With the methods described above, it is possible to probe the relative reactivity of these intermediates under different conditions.

When NO is exposed to a solution with varying DAN concentrations, there is an increase in fluorescence with increasing concentration of DAN. A plot of 1/[DAN] versus 1/fluorescence is linear, with $-1/x_{int} = 18$ μM

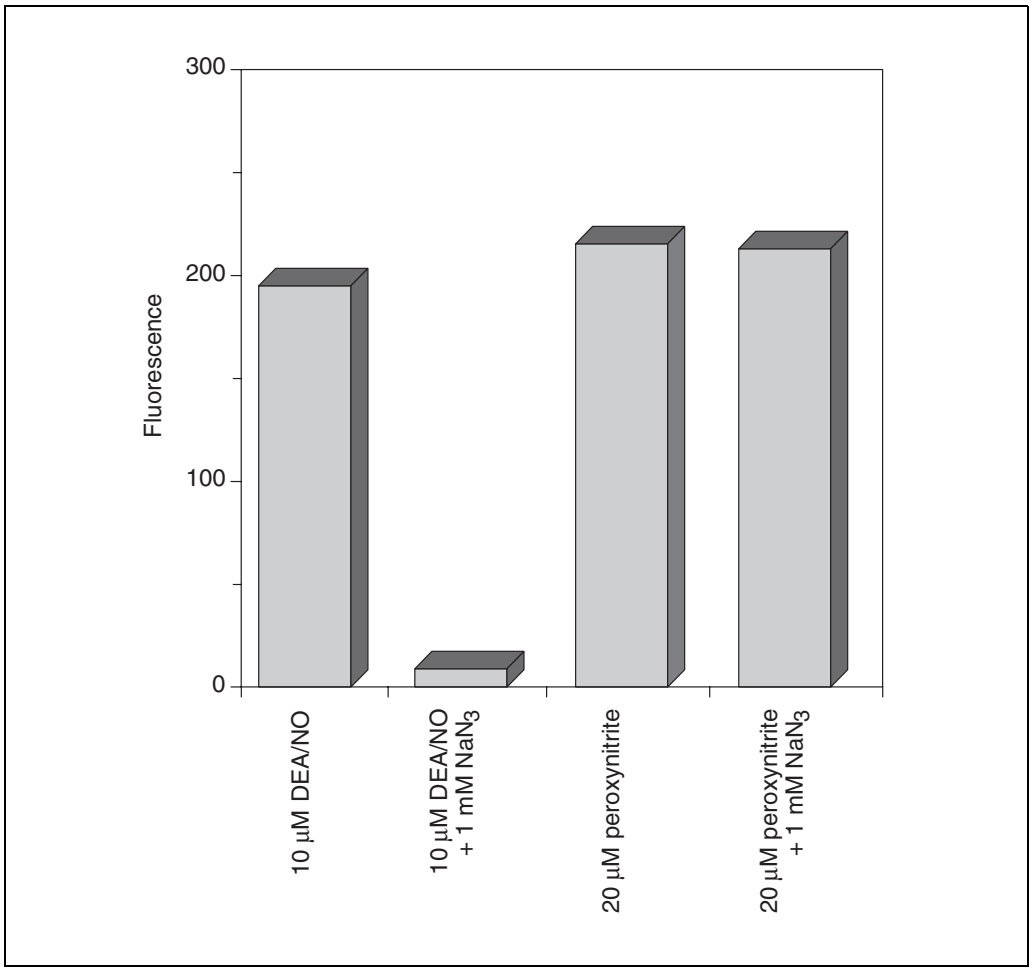

Figure 10.8.5 Comparison of azide between DEA/NO and peroxynitrite. PBS solutions with 10 mM HEPES and 50 μM DETAPAC containing 50 μM DHR were exposed to either 10 μM DEA/NO or 20 μM peroxynitrite with or without 1 mM azide.

(Fig. 10.8.2). From the equation discussed above, this gives a relative reactivity to hydrolysis of 55,000 M^{-1}:1 as defined in Figure 10.8.1. From this information, other substrates such as azide, ascorbate, dithiothreitol (DTT), and glutathione (GSH) can be compared (Table 10.8.1). As seen in Figure 10.8.3 and Table 10.8.1, the $-x_{int}$ shows that relative selectivity to hydrolysis and DAN. This suggests that the order of preference is azide, GSH, ascorbate, and DTT.

Using the method described above, the nitrosative chemistry mediated by the autoxidation reaction in aqueous solution can be compared to that in an acidic nitrite solution, pH 5. DAN nitrosation at pH 5 in the presence of 10 mM sodium nitrite is linear with time. The fluorescence value at 4 min increased with increasing concentrations of DAN. A plot of 1/fluorescence versus 1/[DAN] gives a value of $-1/x$ intercept of 7 μM (Fig. 10.8.2). This suggests a small difference in selectivity for nitrosation reaction with DAN either by the NO/O_2 reaction or by nitrite. However, if the relative selectivity for DTT is compared, there is a marked difference. In Figure 10.8.3, a plot of the concentration of DTT versus 1/fluorescence shows that the x intercept is 68 μM for acidic nitrite solution while the $-x$ intercept is 2.4 mM for the NO/O_2 reaction. This suggests that there is a selectivity difference of 35-fold for DTT between the nitrosation chemistry in acidic nitrite solution and in NO/O_2. Figure 10.8.2 and Figure 10.8.3 illustrate how these methods can be used to distinguish different chemical properties of different agents.

As described above, similar strategies can be used to probe the oxidative chemistry of peroxynitrite and N_2O_3 produced in aqueous solution. The reaction of NO with O_2^- results in the powerful oxidant peroxynitrite:

$$NO + O_2^- \rightarrow ONOO^-$$

It has been shown that when excess NO is present, peroxynitrite can be converted to form nitrosating agents, presumably N_2O_3. DHR has

often been used to quantitate oxidants in biological systems and the presence of $ONOO^-$ (Kooy et al., 1994; Crow, 1997). However, care must be taken. In Figure 10.8.4, 10 μM peroxynitrite is exposed to increasing DHR. A plot of 1/fluorescence versus 1/[DHR] is linear with $-1/x_{int}$ = 19 μM. NO released from the NONOate DEA/NO also oxidizes DHR; however, a plot of 1/DHR versus 1/fluorescence reveals an $-1/x_{int}$ of 97 μM. This suggest that peroxynitrite is a more powerful oxidant than N_2O_3. Azide can be used to distinguish oxidation mediated by peroxynitrite and nitrosating agents such as N_2O_3. 1 mM azide will quench the oxidation mediated by N_2O_3, while oxidation mediated by peroxynitrite is not quenched. As seen in Figure 10.8.5, 10 μM of the NO donor DEA/NO readily oxidizes DHR. However, in the presence of azide (an NO^+ donor scavenger), the oxidation is completely abated. Peroxynitrite-mediated oxidation, on the other hand, shows no quenching by azide. This illustrates how different oxidants can be discerned under various conditions. Under some biological conditions, specific scavengers such as azide can prove useful in deciphering the nature of the intermediates involved.

Critical Parameters and Troubleshooting

These assays are usually straightforward. However, in some media there could be azide, 2-mercaptoethanol, or dithiothreitol (DTT), which will interfere with the measurement. DAN stock solutions can be nitrosated or oxidized readily. These should be made up fresh. Also, the purity of DAN is critical. DHR stock solutions should be stored under argon in a –20°C freezer. The baseline of a measurement should not be any higher than 10% of the lowest reading.

Anticipated Results

The above techniques can provide insights into the type of chemical stress, nitrosative or oxidative, that occurs under the experimental conditions. By formulating different conditions, the RNOS involved can be deciphered. Another advantage is that new agents can be tested for their ability to quench either nitrosative or oxidative damage by different reactive intermediates. The amount of nitrosation or oxidation can be quantitated in specific media (but note vitamins will interfere with these assays).

Time Considerations

Once the equipment is set up and the reagents are ready, these assays require 1 to 2 hr.

Literature Cited

Beckman, J.S., Beckman, T.W., Chen, J., Marshall, P.H. and Freeman, B.A. 1990. Apparent hydroxyl radical production by peroxynitrites: Implications for endothelial injury from nitric oxide and superoxide. *Proc. Natl. Acad. Sci. U.S.A.* 87:1620-1624.

Crow, J. 1997. Dichlorodihydrofluorescein and dihydrorhodamine 123 are sensitive indicators of peroxynitrite in vitro: Implications for intracellular measurement of reactive nitrogen and oxygen species. *Nitric Oxide Biol. Chem.* 1:145-157.

Ford, P.C., Wink, D.A., and Stanbury, D.M. 1993. Autooxidation kinetics of aqueous nitric oxide. *FEBS Lett.* 326:1-3.

Huie, R.E. and Padmaja, S. 1993. The reaction of NO with superoxide. *Free Radic. Res. Commun.* 18:195-199.

Keefer, L.K., Nims, R.W. Davies, K.W., and Wink, D.A. 1996. NONOates (diazenolate-2-oxides) as nitric oxide dosage forms. *Methods Enzymol.* 268:281-294.

Kooy, N.W., Royall, J.A., Ischiropoulos, H., and Beckman, J.S. 1994. Peroxynitrite-mediated oxidation of dihydrorhodamine 123. *Free Radicals Biol. Med.* 16:149-156.

Kroncke, K.-D., Fechsel, K., Schmidt, T., Zenke, F.T., Dasting, I., Wesener, J.R., Bettermann, H., Breunig, K.D., and Kolb-Bachofen, V. 1994. Nitric oxide destroys zinc-finger clusters inducing zinc release from metallothionein and inhibition of the zinc finger-type yeast transcription activator LAC9. *Biochem. Biophys. Res. Commun.* 200:1105-1110.

Miles, A.M., Gibson, M. Krishna, M., Cook, J.C., Pacelli, R., Wink, D.A., and Grisham, M.B. 1995. Effects of superoxide on nitric oxide–dependent *N*-nitrosation reactions. *Free Radical Res.* 233:379-390.

Miles, A.M., Bohle, .D.S., Glassbrenner, P.A., Hansert, B., Wink, D.A., and Grisham, M.B. 1996. Modulation of superoxide-dependent oxidation and hydroxylation reactions by nitric oxide. *J. Biol. Chem.* 271:40-47.

Nims, R.W., Darbyshire, J.F., Saavedra, J.E., Christodoulou, D., Hanbauer, I., Cox, G.W., Grisham, M.B., Laval, J., Cook, J.A., Krishna, M.C., and Wink, D.A., 1995. Colorimetric methods for the determination of nitric oxide concentration in neutral aqueous solutions. *Methods* 7:48-54.

Pires, M., Ross, D.S., and Rossi, M.J. 1994. Kinetic and mechanistic aspects of the NO oxidation by O_2 in aqueous phase. *Int. J. Chem. Kinet.* 26:1207-1227.

Pryor, W.A. and Squadrito, G.L. 1996. The chemistry of peroxynitrite and peroxynitrous acid: Products from the reaction of nitric oxide with superoxide. *Am. J. Phys.* 268:L699-721.

Williams, D.L.H. 1988. Reagents involved in Nitrosation. *In* Nitrosation (D.L.H. Williams, ed.) pp. 18-37. Cambridge University Press, New York.

Wink, D.A. and Laval, J. 1994. The Fpg protein, a DNA repair enzyme, is inhibited by the biomediator nitric oxide in vitro and in vivo. *Carcinogenesis* 15:2125-2129.

Wink, D.A., Darbyshire, J.F., Nims, R.W., Saveedra, J.E., and Ford, P.C. 1993. Reactions of the bioregulatory agent nitric oxide in oxygenated aqueous media: Determination of the kinetics for oxidation and nitrosation by intermediates generated in the NO/O_2 reaction. *Chem. Res. Toxicol.* 6:23-27.

Wink, D.A., Nims, R.W., Darbyshire, J.F., Christodoulou, D., Hanbauer, I., Cox, G.W., Laval, F., Laval, J., Cook, J.A., Krishna, M.C., DeGraff, W., and Mitchell, J.B. 1994. Reaction kinetics for nitrosation of cysteine and glutathione in aerobic nitric oxide solutions at neutral pH: Insights into the fate and physiological effects of intermediates generated in the NO/O_2 reaction. *Chem. Res. Toxicol.* 7:519-525.

Wink, D.A., Hanbauer, I., Grisham, M.B., Laval, F., Nims, R.W., Laval, J., Cook, J.C., Pacelli, R., Liebmann, J., Krishna, M.C. Ford, M.C., and Mitchell, J.B. 1996a. The chemical biology of NO: Insights into regulation, protective and toxic mechanisms of nitric oxide. *Curr. Top. Cell. Regul.* 34:159-187.

Wink, D.A., Grisham, M., Mitchell, J.B., and Ford, P.C. 1996b. Direct and indirect effects of nitric oxide: Biologically relevant chemical reactions in biology of NO. *Methods Enzymol.* 268:12-31.

Wink, D.A., Grisham, M.B., Miles, A.M., Nims, R.W., Krishna, M.C., Pacelli, R., Poore, C., and Cook, J.A. 1996c. Methods for the determination of selectivity of the reactive nitrogen oxide species for various substrates. *Methods Enzymol.* 268:120-130.

Wink, D.A., Cook, J.A., Kim, S., Vodovotz, Y., Pacelli, R., Kirshna, M.C., Russo, A., Mitchell, J.B., Jourd'heuil, D., Miles, A.M., and Grisham, M.B. 1997. Superoxide modulates the oxidation and nitrosation of thiols by nitric oxide derived reactive intermediates. *J. Biol. Chem.* 272:11147-11151.

Wink, D.A., Feelisch, M., Vodovotz, Y., Fukuto, J., and Grisham, M.B. 1998. The chemical biology of NO: An update. *In* Reactive Oxygen Species in Biological Systems (D. Gilbert and C.A. Cotton, eds.) pp. 275-292. Plenum, N.Y.

Contributed by David A. Wink and Sungmee Kim
National Cancer Institute
Bethesda, Maryland

Allen Miles, David Jourd'heuil, and Matthew B. Grisham
Louisiana State University Medical Center
Shreveport, Louisiana

Inducible Nitric Oxide Synthase Expression

Nitric oxide synthases (NOSs, EC 1.14.13.39) are a family of isoenzymes that catalyze the production of nitric oxide (NO) from the oxidation of L-arginine in the presence of NADPH (Fig. 10.1.1). Multiple cofactors are required for the enzymatic reaction, including heme, tetrahydrobiopterin (BH4), calmodulin (CaM), and flavins FMN and FAD. The iNOS (Type II NOS), one of the three isoforms of NOS cloned and characterized in mammals, is inducible at the transcriptional level and, in general, is not expressed unless the cells are stimulated. In the presence of stimuli, high levels of iNOS are expressed which then produce large amounts of NO for a long period (up to days), provided L-arginine is available.

Based on the high-output characteristics of iNOS, its expression can be conveniently and specifically detected and measured. This unit describes three basic protocols to determine iNOS expression in the mouse macrophage-like cells, RAW264.7, by measurement of: (1) end-product by measuring the accumulation of nitrite (see Basic Protocol 1), (2) protein detected by immunoblotting (see Basic Protocol 2), and (3) mRNA detected by northern blot analysis (see Basic Protocol 3) using radiolabeled oligonucleotide probes (see Support Protocol). RAW264.7 cells are easily induced to express iNOS in the presence of stimuli like the bacterial product, lipopolysaccharide (LPS), and cytokines (e.g., IFN-γ). LPS alone can stimulate RAW264.7 cells and is therefore chosen to be the stimulus used in these protocols. Expression of iNOS also occurs in many other tissues besides macrophages, such as neurons, astrocytes, microglia, endothelial and smooth muscle cells, in the presence of certain stimuli.

DETECTION OF iNOS EXPRESSION BASED ON NITRITE ACCUMULATION

BASIC PROTOCOL 1

Under appropriate conditions, the NO produced from the NOS pathway undergoes a series of reactions to form stable end-products, nitrite and nitrate, which accumulate in cell culture or in body fluid. In this protocol, only the accumulation of nitrite (i.e., a portion of the NO end-products) is measured to indicate iNOS expression. The culture supernatant is collected and reacted with Griess reagents, a mixture of sulfanilamide (SULF) and *N*-(1-naphthyl)-ethylenediamine (NNED) hydrochloride in 2.5% phosphoric acid solution. Under this condition, the accumulated nitrite taken from the culture is acidified and undergoes diazotization with SULF to form a diazonium salt, which then couples to NNED and forms an azo dye. Since this azo dye has an absorption maximum at 540 nm, the absorbance measured at 530 to 570 nm (depending on the available filter in the microplate reader) is used to indicate iNOS expression.

Materials

RAW264.7 cells (ATCC #TIB 71)
Complete RPMI medium/10% FBS with antibiotics (Life Technologies; see recipe)
100 μg/ml lipopolysaccharide (LPS) working solution (see recipe)
10 mM sodium nitrite (see recipe)
Griess reagent working solution (see recipe)

100-mm-diameter tissue culture dishes
Platform shaker
Ultrasonic bath (Lab-Line Instruments)
96-well microtiter plate
Microplate reader

Contributed by Qiao-wen Xie
Current Protocols in Toxicology (2000) 10.9.1-10.9.16

NOTE: All solutions and equipment coming into contact with living cells must be sterile, and aseptic technique should be used accordingly.

NOTE: All culture incubations should be performed in a humidified 37°C, 5% CO_2 incubator unless otherwise specified.

Stimulate cells

1. Seed ~10×10^6 RAW264.7 cells in each of two 100-mm-diameter tissue culture dishes (marked as no. 1 and no. 2), with 10 ml of complete RPMI medium/10% FBS per dish.

   Only two culture dishes of cells are used here, because only two conditions are chosen in step 2—without and with LPS stimulation.

   Depending on the needs of the experiment, various numbers of cells and different kinds of culture containers (e.g., 6-well plate, 12-well plate, or others) can be used. If the culture is also to be used to detect iNOS expression by immunoblotting and northern analysis (see Basic Protocols 2 and 3), grow at least 10×10^6 cells/dish. If the culture is to be used only for the measurement of nitrite accumulation, seed 1×10^6 or 0.5×10^6 cells/well in a 12-or 24-well plate, with 1 ml complete RPMI per well.

2. In a tissue culture hood, add 10 µl of 100 µg/ml LPS working solution to dish no.2, making the final concentration of LPS 100 ng/ml. Do not add LPS to dish no.1.

   Different concentrations of LPS or other stimuli can be used, based on the experimental design. If more conditions are being studied, increase the number of culture dishes in step 1, at least one dish for each condition.

3. Incubate at 37°C for a chosen time period.

   Overnight (≥12 hr) is often chosen as a convenient time period. LPS-treated RAW264.7 cells grown overnight normally accumulate micromolar concentrations of nitrite in the culture medium. More than one time point may also be chosen, depending on the experimental design.

Prepare sodium nitrite standard

4. Freshly prepare 200 µM sodium nitrite as the standard solution by diluting the 10 mM stock solution 50-fold with water.

5. In a 96-well microtiter plate, use columns 1 and 2 for the nitrite standard. Place 100 µl of water in each well of columns 1 and 2 of rows A through H. Use wells A1 and A2 as blanks. Add 100 µl of 200 µM sodium nitrite to wells B1 and B2 and mix thoroughly by pipeting up and down. Transfer 100 µl to equivalent wells in row C. Repeat until a series of 2-fold dilution (100, 50, 25, 12.5, 6.25, 3.125, and 0 µM) is prepared in rows B through H. After mixing in row H, remove 100 µl and discard.

Measure nitrite accumulation

6. Remove 100 µl (in triplicate) of culture supernatant from each culture dish and place into corresponding wells of the same 96-well plate as the nitrite standards.

   It is recommended that the culture supernatant be placed into the wells in columns 3 to 5. For example, wells A3, A4, and A5 (row A) can be for the samples from dish 1 (without LPS), and wells B3, B4, and B5 (row B) for the samples from dish 2 (with LPS).

7. Add 100 µl of Griess reagent working solution to each of the wells containing either the water (blanks), nitrite standards, or culture samples. Incubate 5 to 10 min at room temperature after gentle mixing on an orbital platform shaker.

8. Place the 96-well plate in a microplate reader and read the absorbance at 530 to 570 nm, depending on the filter available.
9. Determine the concentration of nitrite accumulated in the culture compared to the sodium nitrite standards.

   Nitrite standards are not necessary for a quick check of nitrite accumulation, when no quantitative analysis is involved.

CONFIRMING iNOS EXPRESSION AT PROTEIN LEVEL BY IMMUNOBLOT

BASIC PROTOCOL 2

Measuring nitrite accumulation in the culture (see Basic Protocol 1) is a simple and rapid method to reveal the expression of iNOS activity. In addition, synthesis of iNOS protein and mRNA can be analyzed to confirm the expression. This protocol describes the detection of iNOS protein in the lysate of RAW264.7 cells after stimulation with LPS, by the use of an antibody specifically against iNOS in an immunoblot.

Materials

10× PBS (see recipe or purchase from Life Technologies)
Lysis buffer (see recipe)
Bradford protein assay reagent kit (Bio-Rad)
NuPAGE Tris-Acetate SDS Buffer Kit (Novex) containing:
  4× sample buffer (also see recipe)
  20× running buffer (also see recipe)
  10× sample reducing agent
Precast NuPAGE 3% to 8% Tris-acetate gel, 1.5-mm-thick, 10 wells (Novex)
Multicolored protein standards (NEN Life Science Products)
20× NuPAGE transfer buffer (Novex; see recipe)
Blocking solution (see recipe)
PVDF or nitrocellulose membrane
PBST (see recipe)
Mouse monoclonal antibody 1E8-B8 (iNOS-specific; R&D Systems)
SuperSignal West Dura Mouse IgG Detection Kit (Pierce) containing:
  Horseradish peroxidase (HRP)-conjugated anti-mouse IgG
  Luminal/enhancer solution
  Stable peroxide solution

Cell scraper (Falcon)
15-ml centrifuge tube
XCell II Mini-Cell (Novex)
XCell II Blot Module (Novex)
Polyvinylidene difluoride (PVDF) or nitrocellulose membrane: pore size, 0.2 μM
Whatman 3MM filter paper or equivalent
Kodak X-Omat AR X-ray film

Additional reagents and equipment for culturing cells and inducing iNOS expression (see Basic Protocol 1), SDS-PAGE (*APPENDIX 3*) and immunoblotting (*UNIT 2.3*)

NOTE: All solutions and equipment coming into contact with living cells must be sterile, and aseptic technique should be used accordingly.

NOTE: All culture incubations should be performed in a humidified 37°C, 5% CO_2 incubator unless otherwise specified.

Stimulate cells

1. Grow and stimulate RAW264.7 cells (see Basic Protocol 1. steps 1 to 3). After 12 to 24 hr, measure nitrite accumulation in the cultures (see Basic Protocol 1).

   Nitrite accumulation should be seen within 24 hr after adding LPS. If not, repeat step 1 before preparing cell lysate.

Prepare cell lysate

2. Detach the cells with a cell scraper and transfer the cell suspension to a 15-ml tube.

   The cell scraper can be cleaned and reused, since this step is not performed under sterile conditions.

3. Centrifuge the cells in a benchtop centrifuge 5 min at ~100 × *g*, 4°C, and remove the supernatant.

4. Wash the cell pellet twice, each time by adding 5 ml of ice-cold 1× PBS, centrifuging 5 min at 100 × *g*, 4°C, and removing the supernatant.

5. Resuspend the cells in 1 ml of ice-cold 1× PBS and transfer to a microcentrifuge tube.

6. Microcentrifuge 2 min at 1500 × *g*, 4°C, and discard the supernatant.

   If the pellet is not to be used immediately, store at −70°C.

7. Resuspend the cell pellet in 300 µl of lysis buffer.

   The volume of lysis buffer should be reduced if the concentration of protein is <2 µg/µl (see step 11).

8. Freeze and thaw three times to lyse the cells, each time by placing tubes in liquid nitrogen or in a −70°C freezer for 5 min, then placing tubes in a water bath at room temperature until thawed. Each time, briefly vortex the samples as soon as they thaw.

9. Microcentrifuge 20 min at 12,000 × *g*, 4°C, then transfer the lysate (supernatant) into a fresh microcentrifuge tube on ice.

   Store the lysate at −70°C if not to be used immediately.

10. Measure the protein concentration in the lysate by Bradford assay using the Bio-Rad protein assay reagent kit.

Separate proteins by SDS-PAGE and blot onto membrane

11. Mix 25 µl of lysate containing 50 µg of total protein with 10 µl of 4× NuPAGE sample buffer and 4 µl of 10× reducing agent, boil for 3 to 5 min, and quickly microcentrifuge to collect the sample at the bottom of the tube.

    If the protein concentration of the lysate is >2 µg/µl, dilute it with lysis buffer before mixing.

    IMPORTANT NOTE: *Conditions for steps 11 to 14 are specific for the equipment provided by Novex; conditions for equipment provided by other suppliers may have to be adjusted according to the manufacturer.*

12. Load the sample onto the lane of a pre-cast NuPAGE 3% to 8% Tris-Acetate gel. Also load prestained multicolored protein standards onto the same gel.

13. Separate the proteins on the gel by electrophoresis in a XCell II Mini-Cell using 1× NuPAGE running buffer.

14. Transfer the proteins from the gel to a PVDF (or nitrocellulose) membrane with an XCell II Blot Module, using 1× NuPAGE transfer buffer.

15. Upon completion of the transfer procedure, place the membrane in a container. Briefly rinse with 1× NuPAGE transfer buffer, immerse in blocking solution, and incubate in blocking solution at 4°C overnight with gentle rocking on a platform rocker.

Perform antibody reaction and detection of iNOS protein

16. Wash the membrane three times with PBST for 15 min, 10 min, and 5 min, respectively.
17. Dilute primary antibody 1E8-B8 ≥1:5000 in blocking solution. Immerse the membrane in the diluted primary antibody and gently shake on a platform rocker for 1 hr at room temperature.

    Alternatively, the incubation with primary antibody can be performed overnight at 4°C.

18. Wash the membrane four to six times, each time for 10 min, with PBST.
19. Dilute the secondary antibody (HRP-conjugated anti-mouse IgG) ≥1:100,000 with PBST. Immerse the membrane in the diluted secondary antibody and incubate for 40 min at room temperature with gentle shaking on a platform rocker.
20. Wash the membrane four to six times, each time for 10 min, with PBST.
21. Blot the membrane on 3MM filter paper to remove excess liquid. Measure the area of the membrane.
22. Prepare SuperSignal Western Dura substrate working solution by mixing equal parts Luminal/Enhancer solution and stable peroxide solution in quantities sufficient for the membrane area.

    The volume of substrate required is 0.125 ml/cm^2 of membrane area.

23. Incubate the membrane with substrate working solution 5 min at room temperature. Place the membrane in a plastic bag and expose to X-ray film inside a film cassette (*APPENDIX 3*).
24. Develop the X-ray film after exposure for 20 sec. If not satisfied, reexpose the membrane to additional X-ray film(s) until the optimal time to obtain a clear result is attained.

DETECTION OF iNOS EXPRESSION BY NORTHERN BLOT ANALYSIS

BASIC PROTOCOL 3

Since iNOS is induced at the transcriptional level, its expression should be detected by the synthesis of iNOS mRNA. This protocol describes a northern blot analysis to detect the mRNA synthesis of iNOS in LPS-stimulated RAW264.7 cells using an oligonucleotide probe specific for mouse iNOS.

CAUTION: When working with radioactivity, take appropriate precautions to avoid contamination of the investigator and the surroundings. Carry out experiments and dispose of wastes in an appropriately designated area, following the guidelines provided by the local radiation safety office (also see *APPENDIX 1A*).

Materials

TRI Reagent for RNA isolation (Molecular Research Center)
Chloroform
Isopropanol
75% ethanol
DEPC-treated H_2O (see recipe)

1% (w/v) agarose gel with 2% (v/v) formaldehyde (see recipe)
10× MOPS buffer (see recipe)
Loading buffer (see recipe), freshly prepared
Formamide
100% glycerol
RNA Molecular Size Standard (Life Technologies)
20× SSPE, pH 7.4 (Life Technologies; also see recipe)
50× Denhardt solution (see recipe)
10% (w/v) sodium dodecyl sulfate (SDS)
10 mg/ml herring sperm DNA (Promega)
20× SSC: 3.0 M NaCl/0.3 M sodium citrate, pH 7.0 (Life Technologies)

50-ml Oak Ridge centrifuge tubes with caps, polypropylene (Nalge)
Centrifuge (e.g., Sorvall with SS-34 rotor or equivalent)
55° to 60°C and 65° to 70°C water baths
Horizontal electrophoresis apparatus, with circulation (OWL Separation Systems)
UV lightbox
GeneScreenPlus nylon membrane (NEN Life Scientific Products)
Turboblotter Rapid Downward Transfer System (Schleicher & Schuell)
Stratalinker UV cross-linker (Stratagene)
Heat-sealable bags (Kapak)
Impulse sealer (American International Electric)

Additional reagents and equipment for culturing cells and inducing iNOS expression (see Basic Protocol 1), determining RNA concentration by spectrophotometry (*APPENDIX 3*), and preparing oligonucleotide probes specific to mouse iNOS and β-actin (see Support Protocol)

NOTE: All solutions and equipment coming into contact with living cells must be sterile, and aseptic technique should be used accordingly.

NOTE: All culture incubations should be performed in a humidified 37°C, 5% CO_2 incubator unless otherwise specified.

Stimulate cells

1. Grow and stimulate RAW264.7 cells (see Basic Protocol 1, steps 1 to 3).

Isolate total RNA from cells

2. At desired time point(s), remove the medium from the culture dish, add 5 ml of TRI Reagent to the dish, and pipet up and down several times. Transfer the homogenate to a 50-ml centrifuge tube with cap. Incubate at room temperature for 5 min for complete dissociation of the nucleoproteins.

   Due to the presence of phenol in TRI Reagent, polypropylene, but not polystyrene tubes should be used.

3. Add 1 ml of chloroform to the tube, shake vigorously for 15 sec and then incubate 2 to 15 min at room temperature. Centrifuge 15 min at ≤12,000 × *g*, 4°C.

4. Transfer the aqueous (upper) phase to a fresh 50-ml tube, add an equal volume of isopropanol, and mix well. Let stand 5 to 10 min at room temperature. Centrifuge 10 min at ≤12,000 × *g*, 4°C.

5. Discard the supernatant, then wash the RNA pellet by adding 5 ml of 75% ethanol, vortexing briefly, then centrifuging 5 min at 7500 × *g*, 4°C. Remove supernatant.

   If a break is needed, stop the experiment at this step. Keep the RNA pellet in 75% ethanol and store at −70°C to minimize RNA degradation.

6. Briefly dry the RNA pellet (but do not overdry). To dissolve the RNA, add 100 µl of DEPC-treated water to the pellet, passing the solution a few times through a pipet tip. Heat 10 to 15 min at 55° to 60°C. Transfer the RNA solution to a micocentrifuge tube.

7. Determine the RNA concentration according to the absorbance at 260 nm.

   The specific absorbtion coefficient of ssRNA is 0.025 $(\mu g/ml)^{-1}cm^{-1}$. The ratio of A_{260}/A_{280} should be 1.6 to 1.8 if the RNA is free of protein and DNA.

Separate RNA on agarose gel and blot onto membrane

8. Prepare a 1% agarose gel containing 2% formaldehyde for RNA electrophoresis. When the gel is solidified, place in a horizontal electrophoresis apparatus filled with 1× MOPS buffer.

9. Place an aliquot of RNA sample containing 10 µg of total RNA into a microcentrifuge tube and dry in a Speedvac evaporator. At the same time, dry down 5 µl of RNA standard in another tube in the Speedvac evaporator.

10. Add 20 µl of loading buffer to each tube, mix well, and heat at 95°C for 2 min, then cool immediately on ice.

11. Load the RNA standard onto the first lane in the gel. Load samples adjacent to the standard.

12. Run electrophoresis at 5 V/cm until the bromphenol blue dye has migrated at least halfway.

    Circulate the buffer, or change the buffer once, during electrophoresis.

13. Upon completion of electrophoresis, place the gel on the top of an UV light box. Take a picture with a fluorescence ruler beside the lane of RNA standard. On the picture, mark the distance of each RNA standard band from the top of the gel. Estimate the ratio of 28S rRNA (~5 kb)/16S rRNA (~2 kb), which should be ≥1 if no degradation of RNA occurs.

    Other RNA bands may also be seen on the gel: 5S rRNA (0.1 to 0.3 kb) and high-molecular-weight RNA (7 to 15 kb).

14. Soak the gel with DEPC-treated water to remove formaldehyde.

15. Blot RNA onto a GeneScreenPlus nylon membrane using the Turboblotter Rapid Downward Transfer System.

    The transfer can be finished in a few hours or overnight for convenience.

16. Cross-link the RNA to the membrane in a UV cross-linker.

    This step increases hybridization signal compared to oven baking.

Hybridize RNA on the membrane

17. Prepare oligonucleotide probes (see Support Protocol) specific to mouse iNOS and β-actin.

    β-actin is used as an internal control.

18. Place the membrane in a sealable bag with a solution containing:

    6× SSPE, pH 7.4
    5× Denhardt solution
    1% SDS
    100 µg/ml denatured herring sperm DNA.

    Use 1 ml of solution per 5 cm^2 of membrane area. Seal the bag with an impulse sealer.

    The herring sperm DNA from Promega is ready to use.

19. Place the bag into a gently shaking water bath and prehybridize at 65° to 70°C for 2 to 4 hr.

    Hybridization temperature should be ~20°C lower than the T_m of the oligonucleotides.

20. Open the bag and add iNOS-34 and β-actin oligonucleotide probes to a final concentration of 2×10^6 cpm/ml. Reseal the bag, place back in the water bath, and hybridize at 65° to 70°C for 6 to 24 hr.

21. Remove the membrane from the bag and thoroughly wash the membrane with constant agitation as follows:

    a. Three times with 6× SSC/0.1% SDS at 65° to 70°C, 30 min each time
    b. Three times with 2× SSC/0.1% SDS at 65° to 70°C, 15 min each time

    CAUTION: *Carefully handle the isotope waste.*

22. With the RNA face up, blot the membrane on a sheet of 3MM paper to remove excess liquid.

    Do not dry the membrane if rehybridization is planned.

23. Place the membrane into a plastic bag or cover with plastic wrap and expose to X-ray film (within a cassette with intensifying screens) for an optimal time at room temperature or at 70°C depending on the signal. Develop the X-ray film(s).

SUPPORT PROTOCOL

5′-END LABELING OF OLIGONUCLEOTIDE PROBES

This protocol is used to prepare oligonucleotide probes specific to mouse iNOS and β-actin by 5′-end labeling with [γ-^{32}P]ATP. The probe for β-actin is used as a control in the northern blot procedure (see Basic Protocol 3).

CAUTION: When working with radioactivity, take appropriate precautions to avoid contamination of the investigator and the surroundings. Carry out experiments and dispose of wastes in an appropriately designated area, following the guidelines provided by the local radiation safety office (also see *APPENDIX 1A*).

Materials

Oligonucleotide iNOS-34: 5′-TCT GTG CTG TCC CAG TGA GGA GCT GCG GGG AGC C-3′
Mouse β-actin oligonucleotide (Clontech)
10× kinase buffer (Promega; also see recipe)
10 mCi/ml [γ-^{32}P]ATP (6000 Ci/mmol; NEN Life Scientific Products)
10 U/µl T4 polynucleotide kinase (Promega)

65°C water bath
Quick-Spin columns (TE) for radiolabeled DNA purification, Sephadex G-25 (Boehringer Mannheim)

1. Dissolve the oligonucleotides in autoclaved distilled water to produce a 500 µM stock solution. Dilute 50-fold to 10 µM as a working solution.

   iNOS-34 is a 34-mer derived from the 5′-end of mouse iNOS cDNA; it is antisense, has 68% G/C content, the T_m is 95°C, and it is synthesized with the help of the Oligo oligonucleotide design software (Molecular Biology Insights). β-actin oligonucleotide is a 30-mer, has 63% G/C content, the T_m is 90°C, and is distributed by Clontech.

2. Add the following to a microcentrifuge tube on ice (total volume 25 µl):

   10.5 µl H_2O
   1.0 µl of 10 µM oligonucleotide (iNOS 34-mer or β-actin 30-mer)
   2.5 µl 10× kinase buffer
   10.0 µl 10 mCi/ml [γ-^{32}P]ATP
   1.0 µl (10 U) polynucleotide kinase.

   Mix well and incubate at 37°C for 30 min.

3. Heat at 65°C to inactivate the kinase.

4. Pass the reaction mixture through a Quick-Spin column (Sephadex G-25) to remove unincorporated [γ-^{32}P]ATP.

5. Count cpm per 0.1 µl of each probe in a scintillation counter.

   The probe should be >10^5 cpm/µl.

REAGENTS AND SOLUTIONS

Use Milli-Q-purified water or equivalent in all recipes and protocol steps. For common stock solutions, see ***APPENDIX 2A****; for suppliers, see* ***SUPPLIERS APPENDIX****.*

Agarose gel, 1% (w/v), with 2% (v/v) formaldehyde

For each 50 ml of gel desired, melt 0.5 g of UltraPure agarose in 42.3 ml DEPC-treated water (see recipe). Cool to 60°C, then add 5 ml of 10× MOPS buffer (see recipe), 2.7 ml of 37% formaldehyde, and 25 µl of 10 mg/ml ethidium bromide stock solution (Bio-Rad). Mix well and pour the gel on a tray in a fume hood.

Blocking solution

Dissolve 5 g of nonfat dry milk in 100 ml of PBST (see recipe; 5%, w/v final). Store at 4°C and use within a week.

Complete RPMI medium/10% FBS

To 895 ml of RPMI (with glutamine; Life Technologies), add 100 ml of heat-inactivated FBS and 5 ml of a stock solution (e.g. Life Technologies) of 10,000 U/ml penicillin/10,000 µg/ml streptomycin (10% FBS, 50 U/ml penicillin, 50 µg/ml streptomycin, final). Store up to 6 months at 4°C.

To heat inactivate FBS, thaw a 500-ml bottle of frozen FBS at 37°C and heat in a water bath at 56°C for 1 hr. Divide in aliquots at 50 ml/tube and store at −20°C until use.

Denhardt solution, 50×

Dissolve 5 g Ficoll (Type 400; Sigma), 5 g polyvinylpyrrolidone (Sigma), and 5 g fraction V bovine serum albumin (BSA; Sigma) in water to a final volume of 500 ml. Divide into 50-ml aliquots and store up to 6 months at −20°C.

DEPC-treated water

To each liter of distilled water, add 0.5 ml of diethylpyrocarbonate (DEPC) in the hood (0.5% v/v final). Incubate at 37°C overnight and then autoclave (liquid cycle) for 20 min. Store at room temperature.

Griess reagents

NNED solution: Dissolve 0.1 g *N*-(1-naphthyl)ethylenediamine (NNED) hydrochloride (Sigma) in 100 ml distilled water. Store up to 6 months at 4°C protected from light.

SULF solution: Dissolve 1 g of sulfanilamide (SULF; Sigma) in 5% (v/v) phosphoric acid (Aldrich). Store up to 6 months at 4°C protected from light.

Working reagent: Mix equal volumes of NNED and SULF solutions within 12 hr of use.

Kinase buffer, 10×, pH 7.2

Provided with T4 polynucleotide kinase (Promega)
Composition is as follows:
700 mM Tris·Cl, pH 7.2 (*APPENDIX 2A*)
100 mM $MgCl_2$
50 mM DTT
Store up to 1 year at −20°C

Lipopolysaccharide (LPS) solution

LPS stock solution (2 mg/ml): Dissolve 2 mg of lipopolysaccharide (LPS; *Escherichia coli* serotype 0111:B4; Sigma) in 1 ml of 1× PBS (see recipe, or purchase from Life Technologies) in a tube. Incubate in an ultrasonic bath (Lab-Line Instruments) for 2 hr at room temperature and then store up to 1 year at −20°C.

LPS working solution (100 μg/ml): Dilute LPS stock solution 20-fold with medium to a final concentration of 100 μg/ml and store up to 6 months at 4°C.

Vortex the LPS working solution every time before use.

Loading buffer

75 μl formamide
15 μl 10× MOPS buffer, pH 7.0 (see recipe)
25 μl 37% formaldehyde
8 μl 100% glycerol
7 μl bromophenol blue (saturated solution in water)
20 μl DEPC-treated water (see recipe)
Store up to 1 year at −70°C

Lysis buffer

Prepare 40 mM Tris·Cl buffer, pH 7.9, by a 25-fold dilution of a stock solution of 1 M Tris·Cl buffer, pH 7.9 (*APPENDIX 2A*). Add 1/1000 volume of each of the protease inhibitor stocks (see recipe).

Final concentration: 40 mM Tris·Cl, pH 7.9, 1 μg/ml each of the protease inhibitors aprotinin, leupeptin, and pepstatin, and 0.1 mM PMSF.

MOPS buffer, pH 7.0, 10×

0.4 M MOPS (pH ~7.0; Sigma)
0.1 M sodium acetate
0.01 M EDTA
DEPC-treated water (see recipe)
Store up to 3 months at room temperature

NuPAGE running buffer, 20×, pH 8.24

Purchase from Novex; composition is as follows:
1 M Tris-Cl, pH 8.24 (*APPENDIX 2A*)
1 M tricine
0.07 M SDS
Store up to at least 6 months at 4°C

NuPAGE sample buffer, 4×, pH 8.5

Purchase from Novex; composition is as follows:
4.4 M glycerol
564 mM Tris base
424 mM Tris·Cl
292 mM LDS (lithium dodecyl sulfate)
2.04 mM EDTA
0.88 mM Serva Blue G-250
0.7 mM phenol red
Store up to at least 6 months at 4°C

NuPAGE transfer buffer, pH 7.2

Purchase from Novex; composition is as follows:
500 mM Bicine
500 mM Bis-Tris
20 mM EDTA
1 mM chlorobutanol
Store up to at least 6 months at 4°C

PBS, 10×

2 g/liter KCl
2 g/liter KH_2PO_4
80 g/liter NaCl
21.6 g/liter $Na_2HPO_4 \cdot 7H_2O$
Store up to 1 year at room temperature

This formulation of 10× PBS may also be purchased from Life Technologies.

PBST

To 895 ml of distilled water, add 100 ml of 10× PBS (see recipe, or purchase from Life Technologies) and 5 ml of polyoxyethylensorbitan monolaurate (final: 1× PBS with polyoxyethylensorbitan monolaurate, 5%, v/v). Store up to 6 months at room temperature.

Protease inhibitor stocks, 1000×

1 mg/ml aprotinin (Sigma) in water, store up to 1 year at −70°C
1 mg/ml leupeptin (Sigma) in water, store up to 1 year at −70°C
1 mg/ml pepstatin (Sigma) in ethanol, store up to 1 year at −70°C
0.1 M PMSF: dissolve 8.7 g phenylmethyl sulfonyl fluoride (Sigma) in 50 ml isopropanol; store up to 1 year at room temperature protected from light

Sodium nitrite solution stock, 10 mM

Dissolve 69.0 mg of sodium nitrite (Sigma) in 100 ml of distilled water. Store at 4°C protected from light. Freshly prepare 200 μM nitrite standard solution from this stock each time it is needed.

SSPE, 20×, pH 7.4

Purchase from Life Technologies; composition is as follows:
1M Tris·Cl, pH 7.4 (*APPENDIX 2A*)
3 M NaCl
0.2 M NaH_2PO_4
0.02 M EDTA
Store up to 1 year at room temperature

COMMENTARY

Background Information

Transcriptional induction of iNOS by LPS has been well documented in mouse macrophages (Xie et al., 1992, 1993; Lorbach et al., 1993). The northern blot analysis described in Basic Protocol 3 is a direct and reliable procedure to detect iNOS expression in the LPS-stimulated RAW264.7 cells at the mRNA synthesis level, but northern analysis involves many steps and is time consuming. Since the iNOS mRNA synthesis induced by LPS leads to a consequent synthesis of iNOS protein, detection of iNOS protein by an immunoblot can also be used to indicate iNOS expression. As described in Basic Protocol 2, immunoblot analysis is a shorter procedure and directly detects iNOS protein in the cell lysate, using an antibody specific to iNOS. The iNOS-specific antibody has also been used in an immunostaining procedure to detect iNOS expression in the whole cell or in tissue samples (Xie et al., 1992; Nicholson et al., 1996; Vodovotz et al., 1996).

The fastest way to reveal iNOS expression, however, is to measure the significant nitrite accumulation in the culture based on the high-output characteristics of iNOS. The assay is conveniently performed as described in Basic Protocol 1. With tightly bound calmodulin, the enzymatic activity of iNOS is independent of elevated calcium level (Cho et al., 1992). In the presence of stimuli, high levels of iNOS are expressed and large amounts of NO are produced for ≥5 days, provided L-arginine is available (Vodovotz et al., 1994). (It is not necessary to replenish the L-arginine because the amount in cell culture medium is usually sufficient.) This characteristic of iNOS is different from that of nNOS or eNOS; the latter are constitutively expressed but at low levels and their activity is dependent on an elevated calcium level for binding of calmodulin. Both nNOS and eNOS produce small amounts of NO over a short period of time, from seconds to minutes (Malinski and Taha, 1992). Under appropriate conditions, NO undergoes a series of reactions to form stable end-products, nitrite and nitrate. Although NO itself is unstable in an aerobic environment and is difficult to measure directly, the measurement of nitrite and nitrate is commonly used as a rapid and simple method to detect NO production. Nitrite accumulation is conveniently measured by reading the absorbance at 530 to 570 nm after reacting the culture supernatant with the Griess reagent (Green et al., 1982).

To make the procedure as simple as possible, Basic Protocol 1 does not include the measurement of nitrate accumulation, which is more complicated and has an extra step to reduce nitrate into nitrite by nitrate reductase or by metallic cadmium. Since the ratio of nitrite to nitrate is frequently the same (usually 3:2 in the culture of stimulated RAW264.7 cells), measurement of nitrite alone is sufficient to serve as an indicator of iNOS expression. Due to the low sensitivity of the Griess reaction, which measures the low micromolar range of nitrite, the assay cannot detect the submicromolar nitrite produced by nNOS or eNOS, even when they are active. In fact, neither nNOS nor eNOS is active in the culture without an increase in intracellular calcium level. Therefore, measurement of nitrite accumulation in the culture is actually a procedure specific for detecting iNOS expression and activity.

All three protocols described in this unit are based on two conditions—with and without LPS treatment—i.e., iNOS is expressed or not expressed. No other conditions are yet included in the protocol. For example, the LPS-induced iNOS expression may be partially inhibited by a certain agent, as detected by a partial reduction in nitrite accumulation. In order to characterize the mechanism of inhibition, or the level of inhibition (transcriptional or posttranscriptional; translational or posttranslational) of inhibition, iNOS protein and mRNA analyses should all be performed in addition to nitrite measurement.

The three protocols described here can also be used to detect iNOS expression in other types of cells, as reported by other investigators (Table 10.9.1). However, the conditions to induce iNOS in these cells may be different from that in RAW264.7 cells, requiring stimulus other than LPS or a mixture of stimuli. Induction of iNOS in rodent cells is usually detected within a day. But it may take more than one day for iNOS to be expressed in human cells. In addition, the level of iNOS expressed in human cells is generally lower than that in rodent cells. When the expression level is very low, it requires other methods with higher sensitivity to detect iNOS induction. Very often, RT-PCR analysis is applied to substitute for northern blot.

Critical Parameters and Troubleshooting

Nitrite accumulation is always detected in RAW264.7 cells after overnight treatment with

Table 10.9.1 Expression of iNOS in Various Cell Types

Cell type	Species	Stimuli used in culture[a]	Reference
Alveolar macrophages	Rat	IFNγ + LPS, ozone	Pendino et al. (1993)
C6 glioma cells	Rat	LPS + IFNγ or TNFα	Feinstein et al. (1994)
Cardiac microvascular endothelial cells	Rat	IL-1β + IFNγ	Simmons et al. (1996)
Chondrocytes	Human	IL-1β + TNFα, or LPS	Palmer et al. (1993)
Colonic epithelial cells (HT-29)	Human	IL-1α + IFNγ + TNFα	Kolios et al. (1995)
Colorectal adenocarcinoma cells (DLD-1)	Human	(IL-1β + IFNγ) + LPS, TNFα, or IL-6	Sherman et al. (1993)
Glioblastoma cells (A-172)	Human	IFNγ + TNFα + LPS + IL-1β	Fujisawa et al. (1995)
Hepatocytes	Rat	(IL-1β + TNFα + IFNγ) ± LPS	Geller et al. (1993)
Liver epithelial cells (AKN-1)	Human	IL-1β + IFNγ + TNFα	De Vera et al. (1996)
Lung epithelial cells (A-549)	Human	IL-1β + IFNγ + TNFα	Robbins et al. (1994)
Macrophages (ANA-1)	Mouse	IFN-γ ± picolinic acid	Melillo et al. (1993)
Mesangial cells	Rat	IL-1β	Kunz et al. (1995)
	Human	IL-1β + TNFα	Saura et al. (1996)
Pancreatic β-cells	Rat	IL-1β	Kwon et al. (1995)
Primary astrocytes and microglia	Rat	LPS ± IL-1β, IFNγ, TNFα	Pahan et al. (1997)
	Human	IL-1β + IFNγ	Ding et al. (1997)
Pulmonary artery smooth muscle cells	Rat	IL-1β	Finder et al. (1997)
Synovial fibroblasts, articular chondrocytes, and osteoblasts from joint	Human	IL-1β + IFNγ + TNFα	Grabowski et al. (1996)
Vascular smooth muscle cells	Rat	cAMP-elevating agents + IFNγ, IL-1β, or TNF-α	Koide et al. (1993)

[a]Abbreviations: IFN, interferon; IL, interleukin; LPS, lipopolysaccharide; TNF, tumor necrosis factor.

100 ng/ml LPS. No significant nitrite should be accumulated in the culture without LPS treatment. If nitrite accumulation is found, the medium should be tested for LPS contamination. Medium with LPS contamination should not be used.

When nitrite accumulation is seen in the culture supernatant of LPS-treated RAW264.7 cells, the lysate from these cells should show a major band at ~130 kDa by immunoblot using an antibody specific to iNOS. If this is not the case, increase the amount of lysate protein and/or use a freshly made lysate. The sensitivity of detection method is also critical. In Basic Protocol 2, a SuperSignal West Dura Extended Duration (HRP) substrate is applied to the chemiluminescent western blot. This provides high sensitivity and long light emission for optimization of the results. Occasionally, some minor bands below 130 kDa may be seen on the blot, due to the degradation of iNOS protein. To reduce degradation, use the lysate as soon as possible and avoid multiple freeze/thaw cycles. Reagents and apparatuses from Novex greatly increase performance in Basic Protocol 2 and are therefore highly recommended.

The most important issue in northern blotting is contamination by RNase. All the containers used should be rinsed with DEPC-treated water, and the experiment should be finished as quickly as possible. A RNA pellet can be obtained from the cell culture using TRI Reagent within 1 hr. With the oligonucleotide probe, the total RNA can be used directly in northern blot analysis without mRNA purification. This shortens the experiment, and, more importantly, reduces the occurrence of contamination. Another advantage to using an oligonucleotide probe is that it can be easily stripped off the membrane, leaving the membrane free to be rehybridized with another probe(s).

Anticipated Results

Basic Protocol 1

Nitrite accumulation is always detected in the LPS-treated RAW264.7 cells, but not in the untreated cells. The 24-hr culture usually accumulates ~50 μM nitrite under the conditions described in the protocol.

Basic Protocol 2

When nitrite accumulation is seen in the culture supernatant of LPS-treated RAW264.7 cells, iNOS protein expression is detected by immunoblot. The lysate from these cells shows a major band at ~130 kDa on the blot after reaction with an antibody specific to iNOS; but the band is not seen in the lysate from the cells not treated with LPS (Fig. 10.9.1). Sometimes, minor bands below 130 kDa may be seen, due to the degradation of iNOS protein during the experimental procedure. With the use of high-sensitivity substrate, SuperSignal West Dura Extended Duration (HRP) substrate, in the chemiluminescent immunoblot, the exposure time is usually <20 sec.

Basic Protocol 3

The iNOS mRNA is synthesized in the RAW264.7 cells stimulated with LPS, but not in the cells without LPS treatment. Figure 10.9.2 is one of the results from northern analysis described in Basic Protocol 3. A band of iNOS mRNA at ~4 kb is seen from the LPS-treated sample but not the untreated sample. However, a band of β-actin mRNA at ~1.8 kb is seen from both samples, since β-actin is a housekeeping gene and should not be affected by the treatment with LPS. Therefore, β-actin is used as an internal control for RNA loading. For a more accurate analysis, the signal ratio of iNOS/β-actin mRNA should be used for an evaluation, not just the total amount of iNOS mRNA.

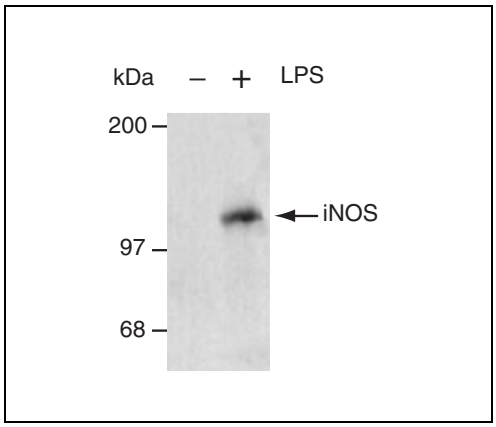

Figure 10.9.1 Immunoblot for iNOS (130 kDa) in the lysate from RAW264.7 cells treated with (+) or without (–) LPS (100 ng/ml) for 18 hr.

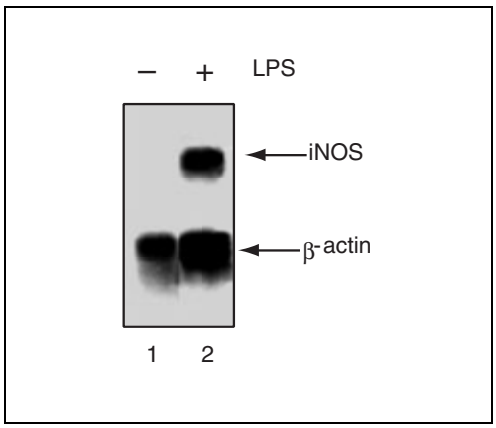

Figure 10.9.2 Northern blot of total RNA from RAW264.7 with (+) and without (–) an 18-hr treatment of LPS (100 ng/ml). The hybridization was performed with two oligonucleotide probes: one is a 34-mer specific for iNOS (4.2 kb) and the other is a 30-mer specific for β-actin (1.9 kb) as an RNA loading control.

Time Considerations

Measurement of nitrite is a rapid assay; the Griess reaction itself only takes 5 to 10 min. To prepare the fresh nitrite standard and the Griess reagent, another 10 to 20 min may be needed. In total, after all the samples are collected, the measurement of nitrite can be finished within 30 min.

With the use of materials from Novex, a lot of time can be saved in immunoblot analysis. The procedure described in Basic Protocol 2 may be finished in 2 days after the cells have been harvested. If the cells are harvested in the morning, cell lysate preparation, protein separation on gel, and blotting onto membrane can be finished on the same day. On the next day, ~5 hr are sufficient to perform the antibody reaction for detection of iNOS protein.

For Basic Protocol 3, depending on the film exposure time, it takes 4 days or more to perform the procedure after the cells are harvested. Day 1 is used to isolate total RNA; only 1 hr is needed. Day 2 is the busiest day; tasks include dissolving the RNA, measuring the RNA concentration, mixing with loading buffer and then running the electrophoresis, followed by overnight blotting to the membrane. On day 3, tasks include labeling the probe(s), prehybridization, and hybridization. Day 4 is used to wash and expose the membrane to X-ray film. If the

signal is strong, the film can be developed on day 4; if the signal is weak, one or two additional days of exposure time may be necessary.

Literature Cited

Cho, H.J., Xie, Q.-W., Calaycay, J., Mumford, R.A., Swiderek, K.M., Lee, T.D., and Nathan, C. 1992. Calmodulin is a subunit of nitric oxide synthase from macrophages. *J. Exp. Med.* 176:599-604.

De Vera, M.E., Shapiro, R.A., Kussler, A.K., Mudgett, J.S., Simmons, R.L., Morris, S.M., Jr., Billiar, T.R., and Geller, D.A. 1996. Transcriptional regulation of human inducible nitric oxide synthase (NOS2) gene by cytokines: Initial analysis of the human NOS2 promoter. *Proc. Natl. Acad. Sci. U.S.A.* 93:1054-1059.

Ding, M., St. Pierre, B.A., Parkinson, J.F., Medberry, P., Wong, J.L., Rogers, N.E., Ignarro, L.J., and Merrill, J.E. 1997. Inducible nitric-oxide synthase and nitric oxide production in human fetal astrocytes and microglia. *J. Biol. Chem.* 272:11327-11335.

Feinstein, D.L., Galea, E., Roberts, S., Berquist, H., Wang, H., and Reis, D.J. 1994. Induction of nitric oxide synthase in rate C6 glioma cells. *J. Neurochem.* 62:315-321.

Finder, J.D., Litz, J.L., Blaskovich, M.A., McGuire, T.F., Qian, Y., Hamilton, A.D., Davies, P., and Sebti, S.M. 1997. Inhibition of protein geranylgeranylation causes a superinduction of nitric oxide synthase-2 by interleukin-1 beta in vascular smooth muscle cells. *J. Biol. Chem.* 272:13484-13488.

Fujisawa, H., Ogura, T., Hokari, A., Weisz, A., Yamashita, J., and Esumi, H. 1995. Inducible nitric oxide synthase in a human glioblastoma cell line. *J. Neurochem.* 64:85-91.

Geller, D.A., Nussler, A.K., Di Silvio, M., Lowenstein, C.J., Shapiro, R.A., Wang, S.C., Simmons, R.L., and Billiar, T.R. 1993. Cytokines, endotoxin, and glucocorticoids regulate the expression of inducible nitric oxide synthase in hepatocytes. *Proc. Natl. Acad. Sci. U.S.A.* 90:522-526.

Grabowski, P.S., Macpherson, H., and Ralston, S.H. 1996. Nitric oxide production in cells derived from the human joint. *Br. J. Rheumatol.* 35:207-212.

Green, L.C., Wagner, D.A., Glogowski, J., Skipper, P.L., Wishnock, J.S., and Tannenbaum, S.R. 1982. Analysis of nitrate, nitrite and [^{15}N]nitrate in biological fluid. *Anal. Biochem.* 126:131-138.

Koide, M., Kawahara, Y., Nakayama, I., Tsuda, T., and Yokoyama, M. 1993. Cyclic AMP-elevating agents induce an inducible type of nitric oxide synthase in cultured vascular smooth muscle cells. Synergism with the induction elicited by inflammatory cytokines. *J. Biol. Chem.* 268:24959-24966.

Kolios, G., Brown, Z., Robon, R.L., Robertson, D.A., and Westwick, J. 1995. Inducible nitric oxide synthase activity and expression in a human colonic epithelial cell line, HT-29. *Br. J. Pharmacol.* 116:2866-2872.

Kunz, D., Walker, G., Eberhardt, W., Nitsch, D., and Pfeilschifer, J. 1995. Interleukin 1β–induced expression of nitric oxide synthase in rat renal mesangial cells is suppressed by cyclosporin A. *Biochem. Biophys. Res. Commun.* 216:438-446.

Kwon, G., Corbett, J.A., Rodi, C.P., Sullivan, P., and McDaniel, M.L. 1995. Interleukin 1β–induced nitric oxide synthase expression by rat pancreatic β cells: Evidence for the involvement of nuclear factor κB in the signaling mechanism. *Endocrinology* 136:4790-4795.

Lorbach, R.B., Murphy, W.J., Lowenstein, C.J., Snyder, S.H., and Russell, S.W. 1993. Expression of the nitric oxide synthase gene in mouse macrophages activated for tumor cell killing. Molecular basis for the synergy between interferon-gamma and lipopolysaccharide. *J. Biol. Chem.* 268:1908-1913.

Malinski, M. and Taha, Z. 1992. Nitric oxide release from a single cell measured in situ by a porphyrinic-based microsensor. *Nature* 358:676-678.

Melillo G., Cox, G.W., Radzioch, D., and Varesio, L. 1993. Picolinic acid, a catabolite of L-tryptophan, is a costimulus for the induction of reactive nitrogen intermediate production in murine macrophages. *J. Immunol.* 150:4031-4040.

Nicholson, S., Bonecini-Almeida, M.G., Silva, J.R.L., Nathan, C., Xie, Q.-W., Mumford, R., Weidner, J.R., Calaycay, J., Geng, J., Boechat, N., Linhares, C., Rom, W., and Ho, J.L. 1996. Inducible nitric oxide synthase in pulmonary alveolar macrophages from patients with tuberculosis. *J. Exp. Med.* 183:2293-2302.

Pahan, K., Sheikh, F.G., Namboodiri, A.M.S., and Singh, I. 1997. Lovastatin and phenylacetate inhibit the induction of nitric oxide synthase and cytokines in rat primary astrocytes, microglia, and macrophages. *J. Clin. Invest.* 100:2671-2679.

Palmer, R.M., Hickery, M.S., Charles, I.G., Moncada, S., and Bayliss, M.T. 1993. Induction of nitric oxide synthase in human chondrocytes. *Biochem. Biophys. Res. Commun.* 193:398-405.

Pendino, K.J., Laskin, J.D., Shuler, R.L., Punjabi, C.J., and Laskin, D.L. 1993. Enhanced production of nitric oxide by rat alveolar macrophages after inhalation of a pulmonary irritant is associated with increased expression of nitric oxide synthase. *J. Immunol.* 151:7196-7205.

Robbins, R.A., Barnes, P.J., Springall, D.R., Warren, J.B., Kwon, O.J., Buttery, L.D.K., Wilson, A.J., Geller, D.A., and Polak, J.M. 1994. Expression of inducible nitric oxide in human lung epithelial cells. *Biochem. Biophys. Res. Commun.* 203:209-218.

Saura, M., Perez-Sala, D., Canada, F.J., and Lama, S. 1996. Role of tetrahydrobiopterin availability in the regulation of nitric-oxide synthase expression in human mesangial cells. *J. Biol. Chem.* 271:14290-14295.

Sherman, P.A., Laubach, V.E., Reep, B.R., and Wood, E.R. 1993. Purification and cDNA sequence of an inducible nitric oxide synthase from a human tumor cell line. *Biochemistry* 32:11600-11605.

Simmons, W.W., Ungureanu-Longrois, D., Smith, G.K., Smith, T.W., and Kelly, R.A. 1996. Glucocorticoids regulate inducible nitric oxide synthase by inhibiting tetrahydrobiopterin synthesis and L-arginine transport. *J. Biol. Chem.* 271:23928-23937.

Vodovotz, Y., Kwon, N.S., Pospischil, M., Manning, J., Paik, J., and Nathan, C. 1994. Inactivation of nitric oxide synthase after prolonged incubation of mouse macrophages with IFN-γ and bacterial LPS. *J. Immunol.* 152:4110-4118.

Vodovotz, Y., Lucia, M.S., Flanders, K.C., Chesler, L., Xie, Q.-W., Smith, T.S., Weidner, J., Mumford, R., Webber, R., Nathan, C., Roberts, A.B., Lippa, C.F., and Sporn, M.B. 1996. Inducible nitric oxide synthase in tangle-bearing neurons of patients with Alzheimer's disease. *J. Exp. Med.* 184:1425-1433.

Xie, Q.-W., Cho, H.J., Calaycay, J., Mumford, R.A., Swiderek, K.M., Lee, T.D., Ding, A., Troso, T., and Nathan, C. 1992. Cloning and characterization of inducible nitric oxide synthase from mouse macrophages. *Science* 256:225-228.

Xie, Q.-W., Whisnant, R., and Nathan, C. 1993. Promoter of the mouse gene encoding calcium-independent nitric oxide synthase confers inducibility by interferon gamma and bacterial lipopolysaccharide. *J. Exp. Med.* 177:1779-1784.

Key References

Green et al., 1982. See above.

Describes in detail the reduction of nitrate to nitrite and the measurement of total nitrite in the sample by a stoichiometric diazotization reaction using the Griess reagent to form a purple azo product.

Nathan, C. and Xie, Q.-W. 1994. Regulation of biosynthesis of nitric oxide. *J. Biol. Chem.* 269:13725-13728.

Summarizes the induction and regulation of inducible nitric oxide synthase.

Contributed by Qiao-wen Xie
The Kenneth S. Warren Laboratories
Tarrytown, New York

CHAPTER 11
Neurotoxicology

INTRODUCTION

There is continuing concern about environmental neurotoxicity and the potential effects of neurotoxic chemicals on human beings, caused in part by the dearth of information about the overall magnitude of the problem. Indeed, the number of people with neurotoxic disorders, and the extent of neurologic disease and dysfunction that results from exposure to toxic chemicals in the environment, are not known. Until a few years ago, for instance, only a few of the several thousand chemicals in commercial use in the United States had been tested for neurotoxicity, though it can be hoped the recent implementation of new federal guidelines for neurotoxicity and developmental neurotoxicity will lead these gaps in data to be filled.

Exposure to neurotoxic substances either in the workplace or through consumption of contaminated food has led to several outbreaks of neurotoxicity. Examples are the pesticides leptophos and kepone, triorthotolylphosphate, methylmercury, and domoic acid. Occupational and/or environmental exposure to a number of types of chemical such as solvents (e.g., toluene, styrene), metals (e.g., lead, organotins, manganese), and pesticides (e.g., organophosphates) are also associated with neurotoxic effects involving the central and/or peripheral nervous systems. Drugs of abuse, alcohol, and some pharmaceuticals may also cause neurotoxicity, particularly in developing organisms.

This chapter focuses on a variety of approaches that can be used in neurotoxicological research. Setting the stage for the chapter, *UNIT 11.1* defines the principal issues in neurotoxicology. This is followed by three units on behavioral testing of rodents, which together provide an excellent tool to enable investigators to assess the neurotoxic potential of a chemical and its effect on cognitive functions. *UNIT 11.2* describes what is known as the functional observational battery, a first-tier screening test for neurobehavioral effects that has become very important in the regulatory arena. *UNITS 11.3 & 11.4* focus on tests of cognitive functions, which are often affected by neurotoxic chemicals. Tests of spatial memory (radial arm maze, Morris maze, and T maze), which are among the most widely used, are described in detail in *UNIT 11.3*, while advanced behavioral testing procedures for assessing cognition are described in *UNIT 11.4*.

UNIT 11.5 details testing protocols for organophosphate-induced delayed polyneuropathy, including behavioral and postmortem morphological assessment and enzyme assays. These test are a regulatory requirement for all organophosphorus pesticides. A discussion of the issues dealing with risk assessment for neurotoxicity is presented in *UNIT 11.6*, while *UNIT 11.7* provides a description of the behavioral tests (some computerized) available to detect neurotoxicity in humans.

UNITS 11.8 & 11.9 describe several models of global and focal ischemia in the mouse, which leads to neuronal degeneration.

A set of three units discuss electrophysiological approaches to neurotoxicology. *UNIT 11.10* offers a general overview on how electrophysiology can be used in toxicological studies. *UNIT 11.11* describes methods used for intracellular and extracellular recording in slices

Contributed by Lucio G. Costa
Current Protocols in Toxicology (2005) 11.0.1-11.0.2

from different brain areas. *UNIT 11.12* focuses on whole-cell path-clamp electrophysiology in cultured cells for measuring voltage-sensitive calcium channels.

UNIT 11.13 provides protocols for the assessment of sensory neuropathy in rats using thermal and mechanical stimuli. *UNIT 11.14* describes protocols to induce brain hyperthermia in rats.

Lucio G. Costa

Overview of Neurotoxicology

It is widely accepted that the nervous system can be adversely affected by chemicals in the environment (OTA, 1990; NRC, 1992). One well-known example of such a chemical (neurotoxicant) is inorganic lead, which can be found in industrial emissions, lead-based paints, food, beverages, and emissions from the burning of leaded gasolines. Organic lead compounds such as triethyl- and tetraethyllead have also been reported to be neurotoxic in humans and animals. The immature nervous system is particularly sensitive to lead, reflecting the generally accepted rule that exposure to relatively low levels of neurotoxicants during development can cause learning disorders and altered mental development.

Another environmental chemical known to produce neurotoxicity in humans is mercury, which causes sensory, motor, and speech dysfunction (NRC, 1992). One major incidence of human exposure to methylmercury occurred in the mid-1950s when a chemical plant near Minamata Bay, Japan, discharged mercury as part of its waste sludge. An epidemic of mercury poisoning developed when the local inhabitants consumed contaminated fish and shellfish. Children exposed in utero developed a progressive neurological disturbance resembling cerebral palsy. In 1971, a similar epidemic occurred in Iraq resulting from the use of methylmercury as a fungicide to treat grain. Attempts to define the threshold at which mercury produces developmental neurotoxicity remain an active research area.

Repeated exposure to organic solvents has also been reported to produce neurotoxicity in humans. For example, a peripheral nervous system neuropathy has been reported in workers exposed to methyl-*n*-butyl ketone, a dye solvent and cleaning agent. Solvents including diethyl ether, some ketones and alcohols, and various combinations thereof are commonly used in glues, cements, and paints, and can be neurotoxic when inhaled. Repeated exposure to such solvents can lead to permanent neurological effects due to severe and permanent loss of nerve cells.

Pesticides, including insecticides, fungicides, rodenticides, and herbicides, are another class of potentially neurotoxic substances. Pesticides are composed of active ingredients combined with inert substances to make thousands of different formulations. Workers overexposed to pesticides may display overt indications of neurotoxicity, including tremors, weakness, ataxia, visual disturbances, and short-term memory loss. The organophosphorus insecticides, which account for ~40% of registered pesticides, can produce a delayed neurotoxicity that involves an irreversible loss of motor function and an associated neuropathology.

Many naturally occurring chemicals have also been found to be neurotoxic (NRC, 1992). For example, neurotoxicities in humans, domestic livestock, and poultry have been associated with exposure to fungal toxins (mycotoxins) that resemble ergot alkaloids, which have neurotrophic, uterotonic, and vasoconstrictive activities. They can also have direct dopaminergic receptor activity or act as serotonergic and α-adrenoceptor antagonists. Jimson weed (*Datura stramonium*) is known to contain a number of chemicals with anticholinergic activity. An outbreak of toxic encephalopathy caused by eating mussels contaminated with domoic acid, an excitotoxin, was recently reported.

It is not known how many environmental chemicals are neurotoxic to humans. Using a generally broad definition of neurotoxicity, Anger (1990) estimated that of the ~200 chemicals to which one million or more American workers are exposed, more than one-third may have adverse effects on the nervous system at some level of exposure. O'Donoghue (1989), on the other hand, reported that of 488 compounds assessed in his chemical evaluation process, only 2.7% had effects on the nervous system.

DEFINITIONS AND CRITICAL CONCEPTS

Neurotoxicity has been defined as an adverse change in the structure or function of the central and/or peripheral nervous system following chemical exposure (Tilson, 1990). Adverse effects include alterations from baseline that diminish an organism's ability to survive, reproduce, or adapt to the environment. Neurotoxicity is a function of the properties of both the agent and the nervous system itself. Toxicity can occur at any time in the life cycle, from conception through senescence, and its manifestations can change qualitatively and quantitatively with age. The range of responses can vary from short-lived changes following acute exposures to delayed or persistent changes following acute or repeated exposures. Effects

Contributed by Hugh A. Tilson
Current Protocols in Toxicology (1999) 11.1.1-11.1.8

produced by the same neurotoxicant vary in both nature and magnitude at different dose levels. Neurotoxic effects may be progressive, with small deficits occurring soon after exposure and becoming more severe over time. At present, relatively few neurotoxic syndromes have been thoroughly characterized. However, knowledge of exact mechanisms of action is not necessary to conclude that a chemically induced change is a neurotoxic effect.

Effects of chemicals on the nervous system can be assessed using a weight-of-evidence approach that assesses the nature and severity of the response, as well as the dose, the duration, and the persistence of the effect. Neurotoxic effects may be irreversible (i.e., the organism cannot return to the state prior to exposure but is permanently changed) or reversible (i.e., the organism can return to its preexposure condition). Clear or demonstrable irreversible change in either the structure or function of the nervous system is of great concern.

It should be noted that the nervous system is known for its reserve capacity (Tilson and Mitchell, 1983). That is, repeated insult to the nervous system may lead to an adaptation to the neurotoxic insult. There are, however, limits to the capacity for adaptation; when these are exceeded, further exposure may lead to frank manifestations of neurotoxicity at the structural and functional levels. Once damaged, neurons, particularly in the central nervous system, have a limited capacity for regeneration. Reversal of neuronal damage resulting from cell death or from the destruction of cell processes may represent an activation of repair capacity, possibly decreasing future adaptability. Reversible neurotoxic changes must therefore be carefully weighed. Evidence of progressive effects (those that continue to worsen even after the causal agent has been removed), delayed-onset effects (those that occur at a time distant from the last contact with the causal agent), residual effects (those that persist beyond a recovery period), or latent effects (those that become evident only after an environmental challenge or aging) should be weighted heavily. Environmental challenges can include stress, increased physical or cognitive workload, pharmacological manipulations, and nutritional deficiency or excess. Evidence for reversibility may depend on the region of the nervous system affected, the chemical involved, and factors such as the age of the exposed population. Some regions of the nervous system such as peripheral nerve have a high capacity for regeneration, while regions in the brain such as the hippocampus are known for their ability to adapt to neurotoxic insult. For example, adaptation is likely to be seen with solvents (e.g., *n*-hexane) that produce peripheral neuropathy due to the high repair capacity of peripheral nerves. In addition, tolerance to some cholinergic effects of cholinesterase-inhibiting compounds may occur as a result of compensatory down-regulation of muscarinic receptors. It is also generally recognized that younger individuals may have a greater capacity to adapt than older individuals, suggesting that the aged may be at increased risk during neurotoxic exposure. In general, lesser weight is assigned to effects that are rapidly reversible or transient—i.e., measured in minutes, hours, or days—and appear to be associated with the pharmacokinetics (absorption, distribution, metabolism, and excretion) of the chemical and its presence in the body. Reversible changes that occur in the occupational setting or environment, however, should receive a heavy weight if, for example, exposure to a short-acting solvent interferes with operation of heavy equipment in an industrial plant.

Neurotoxic effects can be produced by chemicals that do not require metabolism prior to interacting with their target sites in the nervous system (primary neurotoxic agents) or by those that do (secondary neurotoxic agents). Chemically induced neurotoxic effects can be direct (i.e., due to an agent or its metabolites acting directly on target sites in the nervous system) or indirect (i.e., due to agents or metabolites that produce their effects primarily by interacting with target sites outside the nervous system, which subsequently affect target sites in the nervous system).

NEUROLOGICAL PRINCIPLES FOR NEUROTOXICOLOGY

Structure of the Nervous System

The nervous system is composed of two parts: the central nervous system (CNS) and the peripheral nervous system (PNS; Hammerschlag and Brady, 1989). Within the nervous system, there exist predominantly two general types of cells—neurons and glial cells. Neurons are unique in that they have axons and dendrites, extensions of the neuron along which nerve impulses travel. The structure of the neuron consists of a cell body, which contains a nucleus and organelles for the synthesis of various components necessary for the cell's functioning (e.g., proteins and lipids), dendrites, and axons. Dendrites are numerous

branched processes that emanate from the cell body and increase the neuronal surface area available to receive inputs from other sources. Neurons communicate by releasing neurotransmitters onto specific surface regions (the receptors) of other neurons. Axons are specialized processes that conduct nerve impulses away from the cell toward the terminal synapses and eventually toward other cells (neurons, muscle cells, or gland cells).

Neurons are responsible for the reception, integration, transmission, and storage of information, and certain nerve cells are specialized to respond to particular stimuli. In general, the length of the axon is tens to thousands of times greater than the diameter of the cell body. For example, the cell body whose processes innervate the muscles in the human foot is found in the spinal cord at the level of the middle back. The axons of these cells are more than a meter long. Many, but not all, axons are surrounded by layers of membrane from the cytoplasmic process of glial cells. These layers are called myelin sheaths and are composed mostly of lipid. In the PNS, the myelin sheaths are formed by Schwann cells, while in the CNS the sheaths are formed by the oligodendroglia. The myelin sheath formed by one glial cell covers only a short length of the axon, so the entire length of the axon is ensheathed in myelin composed of numerous glial cells. Between adjacent glial sheaths are very short lengths of bare axon called the nodes of Ranvier. In unmyelinated axons, a nerve impulse must travel in a continuous fashion down the entire length of the nerve. The presence of myelin accelerates the nerve impulse by allowing the impulse to jump from one node to the next.

The nerve cells of the PNS are generally found in aggregates called ganglia. In the CNS (made up of the brain and spinal cord), the neurons are segregated into functionally related aggregates called nuclei. Various nuclei together with the interconnecting bundles of axonal fibers are functionally related to one another to form higher levels of organization called systems—for example, the motor system, the visual system, and the limbic system.

Transport Processes

All types of cells must transport proteins and other molecular components from their site of production near the nucleus to the other sites in the cell. Neurons are unique in that the neuronal cell body must not only maintain the functions normally associated with its own support, but also provide support to its various processes. This support may require transport of material over relatively long distances. The delivery of necessary substances by intracellular transport down the axon (axonal transport) is vulnerable to interruption by toxic chemicals. In addition, the integrity of the function of the neuronal cell body is often dependent on a supply of trophic factors from the cells that it innervates. These factors are continually supplied to the neural cells by the process of retrograde axonal transport, often as a process of normal exchange between two or more cells. Neighboring cells play a significant role in the normal growth and maintenance of the neural cells, and a continual supply of certain trophic factors is necessary for cell functioning.

The majority of axonal transport occurs along longitudinally arranged fiber tracks called neurofilaments. This movement along neurofilaments requires energy in the form of oxidative metabolism. Toxicants that interfere with this metabolism or that disrupt the spatial arrangement or production of neurofilaments may block axonal transport and can produce neuropathy. This can been seen following exposure to many substances, such as *n*-hexane and methyl-*n*-butyl ketone.

Ionic Balance

The axonal membrane is semipermeable to positively and negatively charged ions, such as potassium, sodium, and chloride, both within and outside the axon. The ionic balance that changes following depolarization of the membrane is maintained by continual, active, energy-dependent transport of ions across the membrane. Except in sensory neurons, where it originates at the terminal receptive end of specialized axons, the nerve impulse is a traveling wave of depolarization normally originating from the cell body. This wave is propagated by openings in the membrane that allow ions to enter the cell; the resulting sudden change in the charge across the axon's membrane constitutes the nerve impulse. An amplified depolarization reaches a threshold value and spreads down the axon. The depolarization continues in this fashion until it reaches the synaptic terminal regions. There are a variety of membrane channels (e.g., calcium) that rapidly open and close during impulse generation. Sodium and potassium channels are also very common; they are very small and allow only ions of a certain size to pass. Several classes of neurotoxic agents, especially natural toxins such as tetrodotoxin, inhibit nerve impulse conduction by blocking these channels.

Neurotransmission

The terminal branches of the axon end in small enlargements called synaptic "boutons," from which chemical messengers or neurotransmitters are released to communicate with the synapse of the target cell. When a nerve impulse reaches the terminal branches of the axon, it depolarizes the synaptic boutons. This depolarization causes the release of the chemical messengers—neurotransmitters and neuromodulators—stored in vesicles in the axon terminal. Classical neurotransmitters include serotonin, dopamine, acetylcholine, and norepinephrine, and are typically secreted by one neuron into the synaptic cleft where they act on the postsynaptic membrane. Neuropeptides, another type of neurotransmitter, may travel relatively long distances through the bloodstream to receptors on distant nerve cells or in other tissues. Following depolarization, the amount of secretion is dependent on the number of nerve impulses that reach the synaptic bouton—i.e., the degree of depolarization. The chemical messengers diffuse across the synaptic cleft or into the intraneuronal space and bind to receptors on adjacent nerve cells or effector organs, thus triggering biochemical events that lead to electrical excitation or inhibition.

When information is transmitted from nerves to muscle fibers, the point of interaction is called the neuromuscular junction and the interaction leads to contraction or relaxation of the muscle. When the target is a gland cell, the interaction leads to secretion of hormones. When the target is another neuron, the process (known as synaptic transmission) is slightly more complicated: the binding of the messenger to the receptor of the receiving cell can lead to either the excitation or inhibition of certain activities in the target cell. At an excitatory synapse, the neurotransmitter-receptor interaction leads to the opening of certain ion-specific channels. The charged ions that move through these opened channels carry a current that serves to depolarize the cell membranes. At inhibitory synapses, the interaction leads to the opening of a different type of ion-specific channel that produces an increase in the level of polarization (hyperpolarization). The sum of all the depolarizing and hyperpolarizing currents determines the transmembrane potential, and when a threshold level of depolarization is reached at the axon's initial segment, a nerve impulse is generated and begins to travel down the axon.

The duration of neurotransmitter action is primarily a function of the length of time it remains in the synaptic cleft. This duration is very short due to either rapid degradation of the transmitter by specialized enzymes or by removal of the transmitter by reuptake systems that transport it back into the synaptic bouton. A toxic substance may disrupt this process in several different ways. It is important that the duration of the effect of synaptically released chemical messengers be limited. Some neurotoxicants, such as organophosphorus compounds, carbamate insecticides, and nerve gases, inhibit the enzyme acetylcholinesterase (AChE), which serves to terminate the effect of the neurotransmitter acetylcholine on its target. This results in a buildup of acetylcholine, leading to overstimulation of the target cell, and can cause loss of appetite, anxiety, muscle twitching, and paralysis. Some cholinesterase-inhibiting organophosphates can also cause a delayed neuropathy, which is discussed in greater detail in *UNIT 11.5*. Other substances, particularly biological toxins, are able to interact with the receptor molecule and mimic the action of the neurotransmitter. Some toxic substances, such as neuroactive pharmaceuticals, may interfere with the synthesis of a particular neurotransmitter, while others may block access of the neurotransmitter to its receptor molecule. Neurochemical approaches to neurotoxicology are described in greater detail elsewhere in Chapter 11.

Types of Effects on the Nervous System

The normal activity of the nervous system can be altered by many toxic substances. A variety of adverse health effects can be seen, ranging from impairment of muscular movement to disruption of vision and hearing to memory loss and hallucinations. Toxic substances can alter both the structure and the function of cells in the nervous system. Structural alterations include changes in the morphology of the cell and its subcellular structures, and can be assessed via quantitative morphometric analysis and analytical cytology. In some cases, agents produce neuropathic conditions that resemble naturally occurring neurodegenerative disorders in humans. Cellular alterations can include the accumulation, proliferation, or rearrangement of structural elements (e.g., intermediate filaments, microtubules) or organelles (mitochondria) as well as the breakdown of cells. By affecting the biochemistry and/or physiology of a cell, a toxic substance can alter the internal environment of any neural cell. Intracellular changes

can also result from oxygen deprivation (anoxia), because neurons require relatively large quantities of oxygen due to their high metabolic rate.

At the cellular level, a substance might interfere with processes such as protein synthesis, leading to a reduced production of neurotransmitters and concomitant brain dysfunction. Nicotine and some insecticides mimic the effects of the neurotransmitter acetylcholine. Other substances can alter the synthesis and release of other specific neurotransmitters or activate their receptors in specific neuronal pathways. They may perturb the system by overstimulating receptors, blocking transmitter release, inhibiting transmitter degradation, or blocking reuptake of neurotransmitter precursors. At the cellular level, the flow of ions such as calcium, sodium, and potassium across the cell membrane may also be changed and the transmission of information between nerve cells altered by certain neurotoxicants.

The role of excitatory amino acid (EAA)-mediated synaptic activation is critical for normal function of the CNS. Because endogenous EAA-mediated synaptic transmission is a widespread excitatory system in the brain and is involved in the process of learning and memory, the issue of the effects of endogenous and exogenous EAA-related toxicity has broad implications for both CNS morbidity and mortality in humans. Much of the injury and neuronal death associated with toxicity is mediated by receptors for excitatory amino acids, especially glutamic acid. When applied in sufficient excess from either endogenous or exogenous sources, EAAs have profound neurotoxic effects that can result in the destruction of neurons and, as a consequence, lead to acute phase confusion, seizures, and generalized weakness or to persistent impairments such as memory loss.

One final common path in the activation of many receptor classes appears to be an increase in free cytosolic Ca^{2+}. This increase can result in the release and activation of intracellular enzymes, which can break down the cytoskeleton and in turn cause the release of more glutamate. This has the same effects as other sources of increased EAAs, as discussed above. Some neurotoxicants appear to impair energy metabolism, which can lead to death. It is likely that reduced oxidative metabolism can also result in the partial depolarization of resting membrane potential, in the activation of ionotropic membrane receptor/channels, and in the influx of Ca^{2+} or its release from intracellular stores.

Neurophysiological methods are used to measure chemically induced changes in electrical activity in the nervous system. For example nerve conduction studies measure the speed, amplitude, and refractory period of peripheral sensory or motor nerves, while sensory evoked potentials provide a measure of responses elicited from defined sensory stimuli, such as a tone or light. Although electroencephalogram (EEG) analysis is used in a clinical setting to aid in the diagnosis of neurological diseases, its use in neurotoxicology has not been widely accepted.

Exposure to neurotoxic chemicals can also affect behavior, which is the product of various sensory, motor, and associative functions of the nervous system. Neurotoxic substances can adversely affect sensory or motor functions, disrupt learning and memory processes, or cause detrimental behavioral effects. Although changes may be subtle, the assessment of behavior may serve as a robust means of monitoring the well-being of an organism. Behavioral procedures measure the frequency, pattern, latency, or magnitude of a response, all of which may be differentially affected by neurotoxic chemicals. In the screening of chemicals for potential neurotoxicity, behavioral procedures are frequently used (see *UNITS 11.2, 11.3 & 11.4*). Advanced behavioral testing as described in these units is used to characterize the effects of chemicals on nervous system function.

CRITICAL ISSUES IN DEFINING NEUROTOXIC EFFECTS

Verifying that a chemically induced change is a neurotoxic effect is sometimes difficult. In general, alterations in the structure of the nervous system, such as neuronopathy, myelinopathy, neurodegeneration, axonopathy, and peripheral neuropathy, are neurotoxic effects. Interpretation of structural changes as being neurotoxic is dependent upon a number of methodological issues related to the sampling procedure, the method of sample fixation and preparation, and identification of artifacts.

Chemically induced changes in the function of the nervous system are measured using neurophysiological, neurochemical, and behavioral methods. Irreversible functional changes are typically regarded as neurotoxic. If the effect is reversible, the results should be assessed further using at least one of four additional criteria. For example, some chemicals that produce a reversible effect are known to have a specific neurotoxicological mechanism characterized at a higher level of nervous sys-

tem organization (e.g., cholinesterase-inhibiting insecticides produce clinical signs of cholinergic overstimulation because these compounds inhibit the breakdown of acetylcholine, leading to an overactivation of cholinergic receptors). An increase in our knowledge of neurotoxicity mechanisms will greatly reduce uncertainties in the interpretation of chemically induced changes in the nervous system.

Another criterion by which to evaluate reversible functional effects is to determine if the change covaries with another change that is known to be neurotoxic. For example, it is generally accepted that chemical-induced injury to the nervous system is a toxicological effect. Chemical-induced changes in markers that are associated with injury may therefore be regarded as neurotoxic even though they are short-lived. For example, under some conditions, an increase in the expression of glial fibrillary acidic protein (GFAP) is associated with injury to neurons. A chemical-induced increase in GFAP that is reversible would be of concern since this change is a marker for a generally accepted indicator of neurotoxicity, i.e., neuronal injury.

Reversible functional changes should always be interpreted cautiously because of the well-established ability of the nervous system to adapt to damage. Even when an initial exposure has produced only reversible changes, subsequent exposure to the same or a similar chemical could cause additional damage and result in a decreased ability to respond to further exposures. The nervous system appears to have a functional reserve that, once exhausted, can lead to overt, irreversible neurotoxicity. One method to determine if the functional reserve has been diminished by chemical exposure is to subject the system to a pharmacological or environmental challenge. For example, if an animal is exposed to a neurotoxic chemical and is apparently unaffected, subtle toxicokinetic or toxicodynamic changes may be revealed by shifts in the dose-response curve to a psychostimulant. In cases where reversible functional changes are associated with such adaptive changes, a pharmacological or environmental challenge may unmask subclinical neurological damage.

A fourth criterion that could be used to evaluate reversible changes in nervous system function relates to the occupational or environmental consequences of the effect. For example, exposure to a solvent may produce a relatively short-lived change in motor function. Such an exposure could significantly impair the performance of tasks required in the workplace, leading to a loss of productivity or unsafe performance on the job. Alcohol-induced impairment in the operation of a motor vehicle is another example. In these cases, it is important to be able to estimate the concentration required to produce the neurotoxic effect and to limit exposure to concentrations of the chemical below some defined limit or level.

NEUROTOXICOLOGY RISK ASSESSMENT

Risk assessment is an empirically based process used to estimate the probability that exposure of an individual or population to a chemical, physical, or biological agent will be associated with an adverse effect. The risk assessment process usually involves four steps: hazard identification, dose-response assessment, exposure assessment, and risk characterization (NRC, 1983). Risk management is the process whereby information obtained through the risk assessment process is analyzed to determine whether the assessed risk should be reduced and, if so, to what extent (NRC, 1983).

Hazard identification, the first step of risk assessment, is a process of examining all available experimental and animal data and the associated doses, routes of administration, and durations of exposures to determine qualitatively if an agent causes neurotoxicity in that species and under what conditions. Of particular concern in hazard identification is the use of animal data to identify hazards to humans and to determine the relative sensitivity across species and genders. Overly conservative risk assessments, based on the assumption that humans are always more sensitive than a tested animal species, may result in poor risk management decisions. Conversely, an assumption of equivalent sensitivity in a case where humans actually are more sensitive to a given agent can result in underregulation that might have a negative impact on human health.

A related issue concerns the use of data collected from healthy adult organisms, animal or human, to predict hazards in potentially more sensitive populations such as the very young, the elderly, or the chronically ill. In some cases, assessment of a neurotoxicity hazard is done without including subjects from either end of the human life span or from less-than-healthy subjects; instead, uncertainty factors are used to adjust for more sensitive populations. In addition, single- or multigeneration reproduc-

tive studies in animals may provide a source of information on neurological disorders, behavioral changes, autonomic dysfunction, neuroanatomical anomalies, and other signs of neurotoxicity in the developing animal. For the most part, the basic principles of hazard identification are the same for neurotoxicity as for any adverse effect on health.

The second step in risk assessment is dose-response assessment, which attempts to establish the relationship between the extent of damage or toxicity and the dose of a toxic substance for various conditions of exposure. Because several different kinds of responses may be elicited by a single agent, more than one dose-response relationship may need to be developed (e.g., for neurochemical and morphological parameters). The most frequently used approach for dose-response risk assessment of neurotoxicants and other noncancer endpoints is the uncertainty- or safety-factor approach (Barnes and Dourson, 1988). In general, this approach involves the determination of reference doses (RfDs) by dividing a no-observed-adverse-effect level (NOAEL) by uncertainty factors that presumably account for interspecies differences in sensitivity. Generally, an uncertainty factor of 10 is used to allow for the potentially higher sensitivity in humans than in animals and another uncertainty factor of 10 is used to allow for variability in sensitivity among humans. Hence, the RfD is equal to the NOAEL divided by 100. If the NOAEL cannot be established, it is replaced by the lowest-observed-adverse-effect level (LOAEL) in the RfD calculation and an additional uncertainty factor of 10 is introduced (i.e., the RfD equals the LOAEL divided by 1000). There are several known limitations to the NOAEL/LOAEL approach (Kimmel, 1990) and other quantitative models have been proposed (Gaylor and Slikker, 1990; Glowa and MacPhail, 1995).

The third step in risk assessment is exposure assessment, which determines the source, route, degree, duration, and interval of human exposure to an agent. The results of the dose-response assessment are combined with an estimate of human exposure to obtain a quantitative estimate of risk. As the effect of (or the exposure to) an agent approaches zero, the risk of neurotoxicity approaches zero. It should be recognized that exposure to multiple agents may produce synergistic or additive effects. Sources of exposure may include soil, food, air, water, or intended vehicle (e.g., drug formulation). Exposure can occur via many routes, including ingestion, inhalation, or direct contact with skin. The degree of exposure may be strongly influenced by a number of factors—for example, the occupation of the individual involved. The duration of exposure (i.e., acute or chronic) and interval of exposure (i.e., episodic or continuous) are variables common to all types of risk assessment, including carcinogenicity. Although not routinely used, biological markers (or biomarkers) of exposure could theoretically improve the exposure assessment process and thereby improve the overall risk assessment of neurotoxicants.

The final step in risk assessment combines hazard identification, dose-response assessment, and exposure assessment to yield the characterization of risk. This combined analysis provides an evaluation of the overall quality of the assessment and the degree of confidence in the estimates of risk and conclusions drawn, and describes risk in terms of the nature and extent of harm. The risk characterization summary communicates the results of the risk assessment to the risk manager.

LITERATURE CITED

Anger, W.K. 1990. Worksite behavioral research: Results, sensitive methods, test batteries and the transition from laboratory data to human health. *Neurotoxicology* 11:629-720.

Barnes, D.G. and Dourson, M. 1988. Reference dose (RfD): Description and use in health risk assessments. *Regul. Toxicol. Pharmacol.* 8:471-486.

Gaylor, D.W. and Slikker, W. Jr. 1990. Risk assessment for neurotoxic effects. *Neurotoxicology* 11:211-218.

Glowa, J.R. and MacPhail, R.C. 1995. Quantitative approaches to risk assessment in neurotoxicology. *In* Neurotoxicology: Approaches and Methods (L. Chang and W. Slikker, eds.) pp. 777-787. Academic Press, New York.

Hammerschlag, R. and Brady, S. 1989. Axonal transport and the neuronal cytoskeleton. *In* Basic Neurochemistry (G.J. Siegal, B.W. Agranoff, R.W. Albers, and P.B. Molinoff, eds.) pp. 457-478. Raven Press, New York.

Kimmel, C.A. 1990. Quantitative approaches to human risk assessment for noncancer health effects. *Neurotoxicology* 11:189-198.

National Research Council (NRC). 1983. Risk Assessment in the Federal Government. National Academy Press, Washington, D.C.

National Research Council (NRC). 1992. Environmental Neurotoxicology. National Academy Press, Washington, D.C.

O'Donoghue, J.P. 1989. Screening for neurotoxicity using a neurologically based examination and neuropathology. *J. Am. Coll. Toxicol.* 8:97-115.

Office of Technology Assessment (OTA). 1990. Neurotoxicity: Identifying and controlling poi-

sons of the nervous system (U.S. Congress Office of Technology Assessment, OTA-BA-436). U.S. Government Printing Office, Washington, D.C.

Tilson, H.A. 1990. Neurotoxicology in the 1990s. *Neurotoxicol. Teratol*. 12:293-300.

Tilson, H.A. and Mitchell, C.L. 1983. Neurotoxicants and adaptive responses of the nervous system. *Fed. Proc.* 42:3189-3190.

KEY REFERENCES

Chang, L. and Slikker, W. 1995. Neurotoxicology: Approaches and Methods. Academic Press, New York.

Contains a broad overview of various methods in neurotoxicology research and risk assessment.

National Research Council (NRC), 1992. See above.

A general overview of the area of neurotoxicology and risk assessment.

Tilson, H.A. and Mitchell, C.L. 1991. Neurotoxicology. Raven Press, New York.

Describes a range of methods in experimental neurotoxicology.

Tilson, H.A., MacPhail, R.C., and Crofton, K.M. 1995. Defining neurotoxicity in a decision-making context. *Neurotoxicology* 16:363-376.

Describes weight-of-evidence approach to assess chemical effects on structure and function of the nervous system.

Contributed by Hugh A. Tilson
U.S. Environmental Protection Agency
Research Triangle Park, North Carolina

Neurobehavioral Screening in Rodents

Neurobehavioral evaluations are an important component of testing for the neurotoxic potential of chemicals. Observations made during standard toxicity studies or specialized neurotoxicity studies can provide information important for identifying and/or characterizing neurotoxic effects. A protocol that includes a framework for the systematic recording of observations and manipulations, such as a functional observational battery (FOB), is an integral part of neurobehavioral screening. A neurobehavioral test battery can be composed of a variety of endpoints, usually chosen to assess an array of neurological functions, including autonomic, neuromuscular, sensory, and excitability.

The protocols in this unit are divided into (1) observational assessments and (2) manipulative tests. Each protocol is further subdivided into specific tests or endpoints (Table 11.2.1). These various endpoints may be combined into a battery of tests for neurobehavioral screening. Most or all of these protocols/endpoints should be used in the context of a broad neurobehavioral test battery, whereas judicious selection of specific endpoints may be appropriate for more focused neurological testing.

NOTE: In all protocols, the term "rat" is used to describe the test subject. These tests are equally valid in mice; instances where differences exist between mice and rats are listed.

NOTE: All protocols using live animals must first be reviewed and approved by an Institutional Animal Care and Use Committee (IACUC) or must conform to governmental regulations regarding the care and use of laboratory animals.

Table 11.2.1 Endpoints in a Neurobehavioral Screening Battery

Observational assessments (Basic Protocols 1 to 5)	Manipulative tests (Basic Protocols 6 to 8)
Activity levels:	*Neurological reflexes/reactions*:
Home-cage observations	Pupil response
Open-field observations	Palpebral reflex
Rearing	Pinna reflex
Reactivity/excitability:	Extensor thrust reflex
Reactivity	*Neuromuscular tests and postural reactions*:
Arousal	Grip strength
Gait and postural characteristics:	Landing food splay
Gait descriptions	Hopping
Postural descriptions	Righting reaction
Involuntary/abnormal motor movements:	*Sensory responses*:
Tremors	Visual test: approach response
Fasciculations	Visual test: visual placing
Clonus	Somatosensory test: touch response
Tonus	Auditory test: click response
Stereotypy	Nociceptive test: tail/toe pinch
Bizarre behaviors	Nociceptive test: flexor reflex
Clinical signs:	Proprioceptive positioning test
Lacrimation	Olfactory test
Salivation	
Hair coat	
Palpebral closure	
Ocular abnormalities	
Muscle tone/mass	

Contributed by Virginia C. Moser

Current Protocols in Toxicology (1999) 11.2.1-11.2.16

NOTE: Generally, a sample size of ten to twelve subjects per sex per treatment is sufficient. Control animals must be treated exactly the same as the other groups except that they are administered only vehicle.

OBSERVATIONAL ASSESSMENTS

This section provides observational assessments used to characterize neurological function, a description of the behaviors being observed, and possible ranking scales to be used, where applicable. The observed behaviors are innate, that is, they do not need to be taught or shaped. Thus, observations require little or no interaction between the observer and the subject, with the possible exception of holding the rat. Because the observer makes judgments regarding these behaviors, the assessments are subjective.

The rat may be observed briefly in the home cage, but such observations are quite constrained and therefore limited. The home cage may prevent clear observations due to a variety of factors including available light, position of the cage, and clarity of the cage material. For these reasons, most of these evaluations are made in an open field or arena. The observer should be positioned so as to have a clear, unobstructed view as the rat moves about. Choose an open field that is large enough for the rat to explore, has a nonslippery surface, and has a raised border to prevent the subject from escaping or falling over the edge. Typical open fields include the top of a laboratory cart with a rim, or a benchtop with metal sides enclosing the area. Cover the open field with clean absorbent paper that can be changed after each rat (or clean the area after each rat) to eliminate interfering olfactory cues. Environmental conditions (e.g., lighting and temperature) should be held constant from day to day.

The endpoints described in Basic Protocols 1 to 5 may be evaluated simultaneously by a single observer during the handling phase and open-field observation period. It is suggested that the open-field period be sufficiently long for the observer to score the animal on all the associated endpoints (e.g., 2 or 3 min).

BASIC PROTOCOL 1

Observation of Spontaneous Activity Levels

Spontaneous activity levels of the rat may be evaluated in several circumstances such as in the home cage and while exploring a novel (open-field) environment. Home-cage observations are made while the animal is undisturbed in the cage; open-field observations are made during the time that the animal is exploring the open field or arena. In addition to general activity level, rearing is used as a measure of locomotor activity and exploration and in addition indicates the ability of the animal to lift both forepaws from the surface and place its weight on its haunches. A rear occurs when the front legs of the animal are lifted completely off the surface, when the animal raises up vertically, or when the animal places its front paws or legs on the side or lip of the open-field enclosure. The exact definition of a rear is not as important as consistency across studies. Rats and mice show considerably different levels of activity.

Materials

Subject animals
Home cage
Open field
Silent laboratory counter

Perform home-cage observations

1. Approach the cage quietly so as not to disturb the rat. Do not pull out the cage or move it in any way until the measure has been made.

2. Observe the rat's spontaneous activity. Limit observation to 5 sec or less, as the presence of the observer will influence the rat's activity.
3. Rank the level of spontaneous activity displayed in the cage. Use scoring criteria with a sufficient range of scores to adequately describe the behavior. Possible scoring criteria include:

   1 = No activity (rat may be asleep or sitting motionless)
   2 = Slight (rat may move its head or body, just a very few times)
   3 = Moderate (rat moves about some)
   4 = Active (rat moves more actively around cage)
   5 = High activity (rat moves about rapidly).

Perform open-field observations

4. Place the rat in the center of an open field.
5. Observe the rat for a standard period of time (e.g., 2 or 3 min). Keep the length of open-field observation time consistent across subjects.
6. Rank the amount of activity (locomotion) in the open field, using a scale such as:

   1 = No body movement
   2 = Low (somewhat sluggish, little movement)
   3 = Somewhat low (some exploratory movements)
   4 = Low but active (mostly walking with very little or no running)
   5 = Clearly active (exploratory movements, includes walking and running)
   6 = High (very active, darting or running).

   As an alternative to ranking the level of activity, count the number of times the rat crosses unit areas (e.g., squares that have been marked on the field).

Assess rearing

7. Use a laboratory counter to tabulate rears. Be sure that the counter does not make noise, so that it does not disturb the rat.
8. Count the number of rearing responses within a fixed period of time, typically during the open-field observation time.

   The number of rearing responses observed, and the habituation of such activity, is highly dependent on the strain of rat. Evaluation of this habituation process may provide an additional neurobehavioral endpoint.

Observation of Reactivity and Arousal

BASIC PROTOCOL 2

Measures of reactivity (excitability) assess the animal's level of responsiveness to nonspecific stimuli such as handling or being placed in an open field. Arousal or alertness is inferred from watching the animal in the open field. It can be thought of as the attentiveness or vigilance of the animal. Arousal can be inferred by observing the locomotion, rearing, vibrissa movement (whisking or quick, light sweeping movements of the whiskers), and sniffing behaviors of the animal.

Materials

Subject animals
Home cage
Open field

Assess reactivity/excitability

1. Observe the level of excitability or resistance of a subject animal in response to handling and/or removal from the home cage.

   Handling may precipitate the expression of certain spontaneous neurological abnormalities, and therefore some degree of assessment should be made before handling.

   Always handle rodents gently, and hold the rat or mouse under the shoulders (not by the tail). Rough handling will greatly increase the level of excitability and may compromise subsequent tests.

2. Rank the level of reactivity/excitability using scoring criteria such as:

   1 = Low (no resistance, easy to hold or pick up)
   2 = Moderately low (slight resistance)
   3 = Moderately high (some squirming or moving around)
   4 = High (excited, squirming, twisting)
   5 = Very high (aggressive actions, e.g., biting, tail and throat rattling).

Assess arousal

3. Place the animal in an open field. Observe whisking, rearing, exploration, or responses to sudden noises for 2 or 3 min in order to make an overall ranking of arousal.

4. Rank arousal over the entire observation period, using a scale such as:

   1 = Very low (stupor, coma, or prostrate)
   2 = Low (sluggish, only some movements)
   3 = Somewhat low (slightly sluggish, some exploratory movements)
   4 = Moderate (alert, exploratory behavior)
   5 = Somewhat high (slight excitement, tenseness)
   6 = Very high (very alert, very excited or tense, sudden running or movements).

   With repeated testing, the subject may habituate to the surroundings and arousal scores may subsequently decrease.

BASIC PROTOCOL 3

Observation of Gait and Postural Characteristics

Changes in posture and movements reflect alterations in the central and peripheral nervous systems and as such are sensitive indicators of neurological dysfunction. Gait descriptions refer to movements of the limbs as the rat ambulates; postural descriptions refer to the placement of the body and spinal curvature. Clearly and explicitly describe observations of altered posture or motility, without using slang or nonspecific terms. Ranking the severity of abnormality is also useful for interpreting these changes. Assure a clear view of the rat from the top and sides to make these observations. For these measures, the period of observation is not critical.

Materials

Subject animals
Open field

Observe gait

1. Observe a rat moving about in an open field. Gently prod the animal if it does not move. Look at the movement of all four limbs in relation to one another and to the saggital plane of the body.

   The normal rat moves opposing limbs simultaneously, which allows the body to remain steady.

2. Rank the degree of gait abnormality, using a scale such as:

   1 = No abnormality
   2 = Slight abnormality
   3 = Moderate abnormality
   4 = Severe abnormality.

   Note that even "normal" rats, especially older or heavier ones, may display some gait abnormalities.

3. Describe the gait using either accepted terms (e.g., ataxia) or predefined criteria such as:

   Ataxia (uncoordinated, staggering, wobbly gait)
   Hindlimbs show exaggerated, overcompensated, and/or splayed movements
   Feet (primarily hindfeet) point outward from body
   Forelimbs drag and/or show abnormal positioning
   Walking on toes (the heels of the hind feet are perpendicular to the surface).

Observe posture

4. Observe a rat moving about in an open field. Focus observations on the positions of the back, the belly, and the saggital plane of the body.

   Observation of posture is best made while the subject is moving about. The normal rat walks upright, with the back straight and pelvis off the surface.

5. Rank the degree of postural abnormality, using a scale such as that used for gait characteristics (step 2). Describe postural alterations using criteria such as:

   Completely flattened, pelvis flat on surface
   Pelvis low, dragging somewhat
   Hunched, back raised up.

Observation of Involuntary/Abnormal Motor Movements

BASIC PROTOCOL 4

Involuntary movements include motor acts typically referred to as tremors or convulsions. Tremors indicate rhythmic, repetitive contractions/relaxations of major muscle groups, and may be localized (e.g., head or limbs) or general (whole body). Involuntary movements also include fasciculations, clonus, tonus, and stereotypy. Fasciculations also indicate rhythmic, repetitive movements, but are localized to muscle fibers. When occurring superficially, fasciculations may appear as twitching of the skin. Clonus or myoclonus refers to sudden brief episodes of contraction or relaxation of large muscle groups (muscle jerks). As opposed to tremors, clonic movements are sporadic rather than rhythmic. Tonus refers to a state of prolonged, continuous contraction of large muscle groups. Stereotypy is defined as the pronounced repetition of specific gestures or movements (i.e., excessive or repetitive behaviors that appear purposeless). In addition, the animals should be observed for "bizarre" or unusual behaviors (i.e., behaviors not normally seen in rats). Examples of stereotypic and bizarre behaviors are described below. These behaviors can be observed in the home cage or in an open field. The observation time is not critical.

Materials

Subject animals
Open field or home cage

Examine for involuntary motor movements

1. Rank the magnitude of tremors, fasciculations, and clonic and tonic movements, using a scale such as 1 (none) to 4 (severe) for each behavior.

   Specific terms for tonic movements include opisthotonus (a tetanic spasm in which the spine and extremities are bent backwards) and emprosthotonus (a tetanic contraction of the flexor muscles, curving the back and bending the body forward).

2. Describe the affected area or muscle groups.

Examine for stereotypy

3. Observe for stereotypy and indicate its presence (yes/no).

   Examples include, but are not limited to, circling in tight circles, stereotypic grooming whose duration continues well beyond the normal grooming action, persistent pacing especially in one particular direction, or head weaving back and forth. The behaviors themselves are normal; all rats groom or occasionally walk in a circle. It is rather the frequency and persistence of these behaviors that distinguish them as being stereotypic.

4. Fully describe any stereotypic behavior and indicate its frequency.

   Videotaping is an excellent means of documenting stereotypies.

Examine for bizarre behaviors

5. Observe for any bizarre behaviors and indicate their presence (yes/no).

   Bizarre behaviors should be carefully recorded. Examples include, but are not limited to, self-mutilation (or, for example, evidence of missing digits or bite marks on the tail in singly housed rodents), retropulsion (marked backwards movements), Straub tail (tail is stiff and is held in a vertical position), or writhing (a twisting motion or spasmodic pulling in of the abdominal muscles).

6. Fully describe any unusual behaviors and their magnitude and/or frequency.

   Videotaping is an excellent means of documenting abnormal or bizarre behaviors.

BASIC PROTOCOL 5

Observation of Clinical Signs

Observations of clinical signs should be made while holding the subject animal or observing it in the open field. Subject animals are observed for lacrimation and salivation, hair coat characteristics (color/staining, alopecia, and piloerection), presence and degree of eyelid closure, ocular abnormalities, and muscle tone or mass.

Materials

Subject animal
Open field

Examine for lacrimation

1. Score lacrimation on a two- or three-point scale.

   Lacrimation is evidenced by wetness around the eyes. The normal state is a low basal level of lacrimation, so it is difficult if not impossible to observe decreased lacrimation.

2. Indicate whether tears are clear or tinged red (termed chromodacryorrhea).

   Red porphyrin deposits may be chemically induced or may appear spontaneously in some strains of rats.

Examine for salivation

3. Score salivation on a two- or three-point scale.

   Salivation is evidenced by wetness around the mouth and chin. As with lacrimation, it is difficult to observe decreased salivation.

Examine hair coat

4. Indicate the presence and location of staining or abnormal coloration of the hair.
5. Indicate alopecia (thinning of the hair).
6. Indicate the presence of piloerection (hair standing on end).

   To differentiate piloerection from a scruffy or ungroomed coat, simply stroke the back of the rat in a rostral to caudal direction. Piloerection will still be apparent after stroking.

Examine for palpebral closure

7. Describe the degree of palpebral closure (degree of eyelid closure).

   This will depend on the activity level of the subject. Chemically induced ptosis, or drooping eyelids, is not reversed by handling or otherwise stimulating the rat.

8. Rank palpebral closure or indicate the presence/absence of ptosis.

Examine eyes

9. Indicate corneal opacity or cloudiness for each eye.

   Ocular abnormalities involve changes in the cornea or eyeball.

10. Indicate whether the eyeball appears to bulge (termed exophthalmia) for each eye.

Assess muscle tone/mass

11. Palpate the abdominal muscles and/or large muscle groups.

    Body tone, or resistance of the major abdominal muscles, may be assessed by the feel of the whole body. Muscle tone can also be measured by palpating the large muscle groups (e.g., thigh) and rating its resistance.

12. Indicate any changes in normal muscle tone.

    Terms such as hypotonia (completely flaccid, limp) and hypertonia (body stiff, muscles exert much resistance) can be used where appropriate.

MANIPULATIVE TESTS

A number of tests may be performed to measure specific neurological functions. The tests listed here are manipulative in that they require an interaction between the observer and the subject. As with the observational tests, many of these are subjective measures in that the observer will do the test and rate the subject's response. In addition, a few tests are quantified using simple instruments. Basic Protocols 6 to 8 describe manipulative methods commonly used to characterize neurological function, a description of the behaviors, and possible ranking scales to be used.

Assessment of Neurological Reflexes/Reactions

BASIC PROTOCOL 6

A systematic examination of neurological reflexes or reactions is important to evaluate the integrity of specific nerves or nerve pathways. A reflex is a characteristic response to a specific stimulus and typically involves simple neural circuitry (for example, an eyeblink in response to an air puff). More complex behaviors mediated by several reflex circuits are termed reactions. Because reflexes/reactions are common across many species, these findings can facilitate extrapolation of chemical effects to humans.

Materials

Subject animal
Narrow-beam light source: e.g., pocket-size flashlight (penlight) or otoscope
A fine object such as a thin wire

Test pupil reaction

1. Use a narrow-beam light source and shine the beam in a rat's eye, bringing the beam in from the side of the head.

   The pupil reaction is the response of the pupil to a light stimulus.

2. Watch for the constriction of the pupil, which occurs within seconds. Note whether the reaction is present or absent.

   In brightly lit laboratories, the rat's eyes may have to be covered briefly to dilate the pupils. Even if the pupil is difficult to see, the contraction itself is usually visible.

3. Record any obvious features of the pupil such as miosis (pin-point pupils) or mydriasis (dilated pupils).

Test palpebral reflex

4. Use a fine object such as a thin wire and touch the edge (not the point) of the object to the inside (nasal) point of the eye.

   The palpebral reflex tests the trigeminal and facial nerves in response to a light touch (somatomotor stimulus). The eyelids should quickly close.

5. Indicate the presence/absence of the reflex.

Test pinna reflex

6. Use a fine object such as a thin wire and touch the edge of the object to the skin/hair inside the ear.

   The pinna reflex is another somatomotor test of the cranial nerves. The ear should either shake or flatten against the head.

7. Indicate the presence/absence of the reflex.

Test extensor thrust reflex

8. Hold the rat in one hand. Gently press the fingertips into the plantar surface of the animal's two hindfeet.

   The extensor thrust reflex evaluates the motor/sensory components of the spinal response to pressure in the footpads. The rat will extend the hindlimbs, pushing against the fingertips, and curl the toes around the fingertips. It may be necessary to press against the hindfeet several times to elicit this response.

9. Indicate the presence/absence as well as the strength of the extensor response. Note whether the response is equal in both hindlimbs. If desired, note the number of stimuli required to elicit the response.

BASIC PROTOCOL 7

Neuromuscular Tests and Assessment of Postural Reactions

Postural reactions are necessary for the rat to maintain an upright posture and require intact sensory and motor systems. Neuromuscular tests evaluate muscular coordination and strength. Examination of both functions are necessary to test the motor/muscular systems; however, there is a large sensory component as well (see Basic Protocol 8).

This protocol describes postural and neuromuscular tests that assess grip strength, landing foot splay, hopping, and righting. Tests of grip strength provide a quantitative measure of muscle strength, which reflects the integrity of both peripheral nerves and muscles (Meyer et al., 1979). Grip strength may be measured using commercially available strain gauges with either wire-mesh screens or T bars for the rat to grab. The force at which the rat releases its hold on the screen or T bar is the measure of its grip strength. Alternatively,

an array of wires or screens can be used for the rat to grab, and a subjective assessment can be made regarding the ease with which the grasp can be broken. Landing foot splay is a test of proprioceptive function and muscle tone (Edwards and Parker, 1977). Hopping is a challenging test of postural reaction, which requires adequate balance, proprioception, coordination, and strength. The righting reaction is a test of vestibular function, but coordination and strength are necessary as well for the rat to complete this task.

IMPORTANT NOTE: Do not test landing foot splay or aerial righting if the animal is paralyzed or severely affected by treatment.

Materials

Subject animals
Strain gauge with attached wire-mesh or T bar
Paint or ink
Paper
Measuring stick or ruler

Test grip strength

For forelimb grip strength

1a. Set a rat's forepaws on the screen or T bar attached to a strain gauge. Alternatively, hold the rat until it grabs the screen/bar.

2a. Hold the rat by the base of the tail and pull the rat horizontally, smoothly and quickly, until its grip is broken.

This should be performed in one continuous motion. A slight pause may be necessary before beginning the pulling motion, to assure that the rat's digits are properly curled around the screen or bar and that the paws are not crossed. The observer should place his/her arm under the rat to catch it as soon as it releases the screen or bar.

3a. Read the dial on the gauge and reset it.

4a. Repeat two or three times and use the average of the readings.

Use only those readings that appear to be valid (e.g., rat's paws were placed properly).

For hindlimb grip strength

1b. Hold a rat with its hindfeet close to the screen or T bar attached to a strain gauge.

A platform may be helpful to support the body.

2b. Pull the rat backward, horizontally, until its hind feet grab the screen or bar. Continue to pull until the rat's grip is broken.

This should be performed in one smooth, continuous motion. A slight pause may be necessary before beginning the pulling motion, to assure that the rat's digits are properly curled around the screen or bar and that the paws are not crossed. Stop pulling before the front feet touch the screen or bar.

3b. Read the dial on the gauge and reset it.

4b. Repeat two or three times and use the average of the readings.

Use only those readings that appear to be valid (e.g., rat's paws were placed properly).

Test landing foot splay

5. Dab a small amount of paint or ink on the outer portion of the hindfeet.

Various methods can be used to mark the position of the hindfeet upon landing.

6. Hold rat in a prone position at a standard height, typically 20 to 30 cm above a piece of paper. Use a vertical measure to assure consistency in the height used.
7. Drop the rat.

   A padded surface should be used to cushion the fall and prevent injury in case the rat cannot land properly.
8. Observe where the rat lands on the paper, and immediately circle or otherwise indicate the appropriate marks.

   The rat will often either jump forward upon landing or start walking away, smearing the paint as it moves.
9. Measure the distance between the centers of the marks.
10. Repeat two or three times and use the average of the readings.

Test hopping

11. Hold the rat with three limbs tucked into the body and the body weight supported on one limb.

    Both forelimbs and hindlimbs can be tested, but hindlimb hopping is not as robust. If the rat is given too much support, it will not be compelled to use the single limb to support its weight.
12. Move the rat forward or to the side. The rat should hop the limb as the body is moved to maintain its weight-bearing position.

Test righting reactions

For surface righting

13a. Hold the rat in a supine position on a surface.

14a. Quickly release the rat.

    The rat should immediately flip to resume a normal standing posture. This reaction follows the same pattern in all rodents, with the head turning over first, followed by the forelimbs, and then hindlimbs.

15a. Evaluate the final position of the limbs to evaluate proprioceptive deficits.

    You may try to time the latency to right, but the reaction is often too fast to time with a stopwatch.

For aerial righting

13b. Hold the rat in a supine position, with your hands under the back and shoulders. Position the rat 20 to 30 cm above a surface. Use a vertical measure to assure consistency in the height used.

    Most rats can right from a distance of ≥10 cm.

14b. Quickly release the rat.

    The rat should flip over and land on its feet. A padded surface should be used to cushion the fall and prevent injury in case the rat cannot right itself. Righting follows the same progression described for surface righting (see step 14a).

15b. Score the ease of landing, using a scale ranging from normal righting to slightly uncoordinated to markedly uncoordinated. Evaluate the final position of the limbs to evaluate proprioceptive deficits.

Assessment of Sensory Responses

Sensory reactivity tests measure the responses to stimuli of different sensory modalities. Visual function is difficult to measure in rodents but is nonetheless an important sense to evaluate for potential toxicity. Two visual tests are presented here: a visual approach response and visual placing, which both measure the rat's reaction to an object coming into its field of vision. Somatosensory tests evaluate the sense of touch, pressure, or vibration. A touch response test measures the rat's reaction to a light touch stimulus. For auditory function, a click response test measures the rat's reaction to a sudden sound. For nociception, a tail-pinch or toe-pinch response test measures the rat's perception of brief pain. Additionally, the flexor reflex tests the spinal sensory/motor pathway in response to a brief, painful stimulus. This can be used to measure the sensory response as well as to evaluate muscle strength. Finally, proprioceptive positioning evaluates the awareness of the position of the limbs without visual input, and an olfactory test evaluates orientation to or sniffing of a novel odor.

Most of the stimuli are relatively crude and may not actually be specific for the sensory function being measured. Automated apparatuses, such as acoustic startle chambers, may improve the specificity of some stimuli. Tests for these responses are typically conducted while the animal is moving freely about in an open field. The animal should be positioned properly in order to do certain tests. Because a motor response is the behavior that is observed, there is a large motor component to the tests as well.

Materials

Subject animals
Odorant
Blunt object (e.g., pen or pencil, brush, wire)
Metal clicker or other sound device

Test visual approach response

1. Place a rat in an open field, ensuring that it is properly positioned away from the edge of the field.
2. Approach the rat at nose level with the end of a blunt object, such as a pen or pencil. Be sure that the stimulus is consistent from test to test.
3. Hold the stimulus ~3 cm from the face for ~4 sec to give the rat time to make a response.
4. Rank the magnitude of response to the stimulus using scoring criteria such as:

   1 = No reaction or response
   2 = Slight or sluggish reaction (flinch or startle as evidence of perception)
   3 = Obvious reaction (locomotor orientation as evidence of perception)
   4 = Clear reaction or response (more intense startle or locomotion)
   5 = Exaggerated reaction (may jump, bite, or attack).

Test visual placing

5. Hold the rat by the tail and position it above the edge of a table or cart.
6. Slowly move the rat down toward the surface or edge.

   As it approaches, the rat should extend its head and neck and reach towards the edge with the forelimbs.

7. Indicate the presence/absence of the placing response.

Test somatosensory response

8. Position the rat away from the edge of an open field.
9. Coming in from the side, touch the rump of the rat gently with a blunt object, such as a pen, pencil, brush, or wire. Be sure that the stimulus is consistent from test to test. Use a brief touch (1 to 2 sec) that is deliberate but not too forceful.
10. Score the magnitude of the response using a scale similar to that above (step 4).

Test auditory response

11. Position a sound stimulus ~5 cm above the back of the rat (i.e., outside the field of view).

    Various stimuli may be used, including a metal clicker, finger snap, or hand clap.

12. Make a sudden sound. Be sure that the stimulus is consistent from test to test.

    The rat should react immediately with pinna movement, flinch, or whole-body startle.

13. Score the magnitude of the response using a scale similar to that above (step 4).

Test tail-pinch response

14. Position the rat away from the edge of an open field. Pinch the tail ~2 to 3 cm from the tip, or pinch the toes or foot pad. Pinch hard enough to produce a reliable response in control rats, and be consistent in the intensity of the pinch from test to test.

    The very tip of the tail is relatively insensitive. The rat should react immediately with a flinch, whole-body startle, or an escape response.

    Metal tweezers may be used, or any other device that will make a quick squeeze without damaging tissues.

15. Score the magnitude of the response using a scale similar to that above (step 4).

Test flexor reflex

16. Holding the rat in one hand, use the other hand to grasp the toes on one hindlimb and gently pull the leg.
17. Briefly but sharply pinch the toes. Be consistent in the intensity of the pinch from test to test.

    The rat will immediately retract the leg.

18. Evaluate the presence/absence and the strength of the flexor response.

Test proprioceptive positioning

19. Gently hold the rat on a surface and flex a hindlimb so that the dorsal surface of the paw is down on the surface.
20. Relax the hold on the hindlimb.

    The rat should immediately return the paw to the normal position under the body.

21. Evaluate the presence/absence and the strength of the response. Note whether the response is equal in both hindlimbs.

Test olfactory response

22. Position the rat away from the edge of an open field.
23. Dip a cotton swab in an odorant and approach the rat at nose level with the swab. Be sure that the stimulus is consistent from test to test.

24. Hold the stimulus ~3 cm from the face for ~4 sec to give the rat time to make a response.

25. Indicate the presence/absence of a response, or score the magnitude of the response using a scale similar to that above (step 4).

COMMENTARY

Background Information

Neurobehavioral screening methods such as a functional observational battery (FOB) typically include a series of noninvasive observational and interactive measures that assess the neurobehavioral and functional integrity of the rat. In addition to these measures, automated tests are also often included in neurobehavioral screening. Automated tests are objective, and the observer plays no role in the assessment. The level of instrumentation is higher than the tests that have been described in these protocols. Motor activity is commonly used and is amenable to inclusion in a neurobehavioral screening battery by virtue of its ease of operation as well as its usefulness.

Motor activity is an apical endpoint in that locomotor activity requires intact sensory, motor, and integrative neural function. For that reason, motor activity has been purported to be a very sensitive measure of neuronal function (MacPhail et al., 1989). Motor activity may be measured in many types of devices (reviewed in Reiter and MacPhail, 1979). The systems used to detect activity include, for example, infrared photocells, video tracking, and running wheels. Furthermore, the chambers range from large open fields to small cages to corridors in the shape of a doughnut or a figure eight. Activity can be monitored as horizontal movements (ambulation), vertical displacements (rearing), repetitive movements (stereotypy), or any number of various parameters. Finally, the length of sessions in the chambers can vary, but should be long enough to observe habituation, or a decrease in activity from the initial exploratory phase to a lower, asymptotic level.

Neurotoxicity screening methods are becoming increasingly important in the detection of the neurotoxic potential of new and existing chemicals. In 1985, the U.S. Environmental Protection Agency (EPA) published test guidelines for neurotoxicity test methods that included motor activity and FOB; these have since been revised and their use has become more widespread (Sette, 1989). The EPA originally developed these testing guidelines to provide a more structured framework for neurotoxicity tests. These include guidance on the types of tests, testing conditions, scoring criteria, as well as a requirement for proficiency data or positive-control studies. Several protocols based on these guidelines have been developed for rats and are published (e.g., Gad, 1982; Haggerty, 1989; McDaniel and Moser, 1993; Moser et al., 1988; O'Donoghue, 1989, 1996; reviewed in Tilson and Moser, 1992). Modifications of these screening tests for use in other species have also been published, including those for mice (Tegeris and Balster, 1994), primates (O'Keeffe and Lifshitz, 1989), and dogs (Schaeppi and Fitzgerald, 1989). Note, however, that the field of neurotoxicology is advancing rapidly, and these test methods should be flexible to change as new methodology is introduced.

Numerous studies using these tests have now been conducted to evaluate a variety of chemicals under many different dosing and testing paradigms. The results of these studies document effects of pesticides (e.g., Ehrich et al., 1993; McDaniel and Moser, 1993), solvents (e.g., Daughtrey et al., 1997; Gill et al., 1995), neuropathic chemicals (e.g., Moser et al., 1992), and a variety of other chemicals (e.g., Haggerty and Brown, 1996; LeBel and Foss, 1996), as well as strain- and sex-related differences in the outcomes (e.g., Moser et al., 1991; Moser, 1996). These and other publications should be consulted to obtain information on the types of data generated, characteristic profiles of different chemical classes, and methods for data interpretation. Still, the investigator should develop a standardized protocol that is appropriate for the individual laboratory, and should conduct positive-control studies to assure reproducibility and validity of the methods for the testing situation.

Several types of data are generated using these methods, including continuous (e.g., grip strength), rank-order (e.g., gait score), count (e.g., number of rears), descriptive (e.g., type of gait), and quantal (e.g., presence/absence of piloerection). Nominal data are unordered and can include several outcomes (descriptive data) or only two outcomes (yes/no). This is the crudest form of evaluation and may be especially difficult to interpret without specific ob-

jective criteria (e.g., a definition of "abnormal"). Ordinal, or scalar, data are ranked, and the observations are recorded as a position on a scale, with each rank clearly greater than the preceding one. These data are somewhat more sensitive to small changes in behavior, seen as shifts in the distribution of group scores. The scoring criteria for individual measures should be carefully considered and defined as objectively as possible. The range of possible scores should be sufficient to describe the range of possible differences in the particular behavior, as long as the observer can distinguish these intervals consistently. Interval, or continuous, data are reported on a quantitative scale and assume a normal distribution (sometimes following suitable transformation, e.g., square root). Statistically, these types of data are handled differently and should be analyzed with the appropriate parametric or nonparametric models. When the study design calls for multiple tests on the same subject, the analysis should include a within-subject factor (repeated-measures design). Several approaches for statistical analyses have been suggested (Creason, 1989; Gad, 1989).

These tests produce a large amount of data, as do all batteries of tests. Some investigators prefer to use only expert judgment in data interpretation, whereas others feel that relying on statistically significant effects is a more defensible approach. Because innate behaviors are not under tight experimental control, there is always some variability in the data that could be misinterpreted. Furthermore, simple analyses of all the test measures of the battery could lead to randomly significant results, improper conclusions, and false positives. A possible approach for condensing the multitude of data is to examine the endpoints based on the effects within functional domains, e.g., autonomic, sensory, or neuromuscular function, or levels of general excitability and activity (Moser, 1991). Regardless of the approach used, the investigator must be thoroughly familiar with the tests and data, including the control values, to make scientifically sound conclusions.

Critical Parameters

The observations and manipulations made during these tests are recorded only by the observer. The utility of the tests is dependent on the observer's ability to detect and describe changes in the subject's behavioral or neurological function, and to consistently conduct the tests and accurately record the responses. In addition, some functional changes may be transient, especially during acute toxicity tests. Training is therefore of paramount importance, since there is no other way to calibrate the observer. There is simply no substitute for hands-on experience, particularly during the initial stages of training. Observers should have extensive experience observing and handling untreated rats and then proceed to study rats treated with chemicals known to alter function. To aid in training and recertification of personnel and to improve consistency of the protocols across laboratories, a training video and manual are available from the EPA and the American Industrial Health Council (Moser and Ross, 1996).

A preexposure, or baseline, test is often included to document possible preexisting group or individual differences. Additional testing should be performed at specified times, sufficient to establish a time course of effects. Initial range-finding studies are critical for determining (1) appropriate doses, such that the selection of doses is adequate to define the full range of effectiveness, from no effects to marked changes; and (2) appropriate time of testing to optimize detection of possible neurological effects. The importance of these study parameters cannot be overemphasized.

Observations typically proceed from the least obtrusive to the most manipulative to reduce the influence of handling on subsequent behavior. Always perform the tests in the same order for all rats. The way in which subjects are handled affects their behavior and resulting observations. Personnel involved in performing routine husbandry procedures as well as personnel involved in dosing and testing should handle the rats in a gentle and consistent manner.

These tests are labor intensive. The observer is the instrument and (unlike automated instruments) observers get tired, need lunch breaks, and get sick. To provide consistency within a study, the same observer should conduct all the tests, to the extent possible. To break the monotony of the tests, take care not to exceed reasonable limits on schedules and stagger the tests over days (see Time Considerations, below).

Pay close attention to testing conditions, and ensure that differences are never systematically related to treatment level. Variables that can be controlled include temperature, humidity, lighting, noise, odors, and environmental distractions. The latter factors are more critical than is often realized (i.e., no distractions such as telephones, radios, talking, food). Extrane-

ous noise and/or interruptions during testing must be minimized, as this may alter the behavior of the rats and therefore affect the outcome of the study.

Because most of these tests are subjective, the observer must be "blind" to the treatment conditions of the subject to reduce possible bias or anticipatory results. While this may introduce logistic problems in testing, the importance of this variable cannot be ignored.

Troubleshooting

Because these measures are relatively simple, and there is little or no instrumentation, there is little that can go wrong. All equipment should be properly calibrated. Troubleshooting for commercial equipment should follow manufacturer's instructions. Problems arise when other factors come into play, such as lack of attention by the observer or environmental distractions (see Critical Parameters).

Anticipated Results

As mentioned above, there are numerous publications on these test methods that provide typical control values and examples of chemically induced changes. Another valuable source of information is a recently published report on an international collaborative study, which addressed issues of test validity and interlaboratory reliability of the data. In that study, eight laboratories (four in Europe, four in the U.S.) conducted acute and repeated-dosing studies on seven chemicals. A specific FOB protocol and an automated measure of motor activity were used, but other experimental variables (e.g., type of activity chamber and strain of rat) were not standardized. The results, which show how the screening battery performs in a variety of laboratory settings as well as control data for all endpoints, appear in a special issue of Neurotoxicology (Moser, 1997). Some overall conclusions from this study were that (1) the control data were generally reproducible, but this depended on the individual endpoint, and (2) all participants could detect and characterize the effects of known neurotoxicants using these methods.

Time Considerations

For any FOB and/or motor activity experiment, test times must be established and schedules must be developed to accommodate these test times. An experienced observer can conduct this series of tests in 6 to 8 min, or longer if more time is needed to study the subject's condition. Thus, it may take a full day to test only 35 to 40 rats, and this may be only a half to a third of the number of rats under study. Staggering the dosing and testing is fully acceptable, but it is important to carefully counterbalance the time of testing for each dose group and sex across the days of testing.

Literature Cited

Creason, J.P. 1989. Data evaluation and statistical analysis of functional observational battery data using a linear models approach. *J. Am. Coll. Toxicol.* 8:157-169.

Daughtrey, W.C., Gill, M.W., Pritts, I.M., Douglas, J.F., Kneiss, J.J., and Andrews, L.S. 1997. Neurotoxicological evaluation of methyl tertiary-butyl ether in rats. *J. Appl. Toxicol.* 17:S57-S64.

Edwards, P.M. and Parker, V.H. 1977. A simple, sensitive and objective method for early assessment of acrylamide neuropathy in rats. *Toxicol. Appl. Pharmacol.* 40:589-591.

Ehrich, M., Shell, L., Rozum, M., and Jortner, B.S. 1993. Short-term clinical and neuropathologic effects of cholinesterase inhibitors in rats. *J. Am. Coll. Toxicol.* 12:55-68.

Gad, S.C. 1982. A neuromuscular screen for use in industrial toxicology. *J. Toxicol. Environ. Health* 9:691-704.

Gad, S.C. 1989. Statistical analysis of screening studies in toxicology with special emphasis on neurotoxicology. *J. Am. Coll. Toxicol.* 8:171-183.

Gill, M.W., Burleigh-Flayer, H.D., Strother, D.E., Masten, L.W., McKee, R.H., Tyler, T.R., and Gardiner, T.H. 1995. Isopropanol: Acute vapor inhalation neurotoxicity study in rats. *J. Appl. Toxicol.* 15:77-84.

Haggerty, G.C. 1989. Development of tier I neurobehavioral testing capabilities for incorporation into pivotal rodent safety assessment studies. *J. Am. Coll. Toxicol.* 8:53-69.

Haggerty, G.C. and Brown, G. 1996. Neurobehavioral profile of subcutaneously administered MK-801 in the rat. *Neurotoxicology* 17:913-921.

LeBel, C.P. and Foss, J.A. 1996. Use of rodent neurotoxicity screening battery in the preclinical safety assessment of recombinant-methionyl human brain-derived neurotrophic factor. *Neurotoxicology* 17:851-863.

MacPhail, R.C., Peele, D.B., and Crofton, K.M. 1989. Motor activity and screening for neurotoxicity. *J. Am. Coll. Toxicol.* 8:117-125.

McDaniel, K.L. and Moser, V.C. 1993. Utility of a neurobehavioral screening battery for differentiating the effects of two pyrethroids, permethrin and cypermethrin. *Neurotoxicol. Teratol.* 15:71-83.

Meyer, O.A., Tilson, H.A., Byrd, W.C., and Riley, M.T.A. 1979. A method for the routine assessment of fore- and hindlimb grip strength of rats and mice. *Neurobehav. Toxicol.* 1:233-236.

Moser, V.C. 1991. Applications of a neurobehavioral screening battery. *J. Am. Coll. Toxicol.* 10:661-669.

Moser, V.C. 1996. Rat strain- and gender-related differences in neurobehavioral screening: Acute trimethyl tin neurotoxicity. *J. Toxicol. Environ. Health* 47:567-586.

Moser, V.C. (ed.) 1997. Neurobehavioral screening methods. A report of the International Programme on Chemical Safety's Collaborative Study on Neurobehavioral Screening Methods. *Neurotoxicology* Vol. 18.

Moser, V.C. and Ross, J.F. 1996. Training Film and Reference Manual for a Functional Observational Battery. U.S. Environmental Protection Agency and the American Industrial Health Council, Washington, D.C.

Moser, V.C., McCormick, J.P., Creason, J.P., and MacPhail, R.C. 1988. Comparison of chlordimeform and carbaryl using a functional observational battery. *Fund. Appl. Toxicol.* 11:189-206.

Moser, V.C., McDaniel, K.L., and Phillips, P.M. 1991. Rat strain and stock comparisons using a functional observational battery: Baseline values and effects of amitraz. *Toxicol. Appl. Pharmacol.* 108:267-283.

Moser, V.C., Anthony, D.C., Sette, W.F., and MacPhail, R.C. 1992. Comparison of subchronic neurotoxicity of 2-hydroxyethyl acrylate and acrylamide in rats. *Fundam. Appl. Toxicol.* 18:343-352.

O'Donoghue, J.L. 1989. Screening for neurotoxicity using a neurologically based examination and neuropathology. *J. Am. Coll. Toxicol.* 8:97-116.

O'Donoghue, J.L. 1996. Clinical neurologic indices of toxicity in animals. *Environ. Health Perspect.* 104:323-330.

O'Keeffe, R.T. and Lifshitz, K. 1989. Nonhuman primates in neurotoxicity screening and neurobehavioral toxicity studies. *J. Am. Coll. Toxicol.* 8:127-140.

Reiter, L.W. and MacPhail, R.C. 1979. Motor activity: A survey of methods with potential use in toxicity testing. *Neurobehav. Toxicol.* 1:53-66.

Schaeppi, U. and Fitzgerald, R.E. 1989. Practical procedure of testing for neurotoxicity. *J. Am. Coll. Toxicol.* 8:29-34.

Sette, W.F. 1989. Adoption of new guidelines and data requirements for more extensive neurotoxicity testing under FIFRA. *Toxicol. Ind. Health* 5:181-194.

Tegeris, J.S. and Balster, R.L. 1994. A comparison of the acute behavioral effects of alkylbenzenes using a functional observational battery in mice. *Fundam. Appl. Toxicol.* 22:240-250.

Tilson, H.A. and Moser, V.C. 1992. Comparison of screening approaches. *Neurotoxicology* 13:1-14.

Key References

Gad, 1982; Haggerty, 1989; McDaniel and Moser, 1993; Moser et al., 1988; O'Donoghue, 1989, 1996. See above.

These references describe specific FOB protocols.

Irwin, S. 1968. Comprehensive observational assessment: Ia. A systemic, quantitative procedure for assessing the behavioral and physiologic state of the mouse. *Psychopharmacologia* (Berl.) 13:222-257.

The first description of a full observational battery

Moser and Ross, 1996. See above.

Training video and manual intended to help achieve consistency in neurobehavioral screening.

Reiter and MacPhail, 1979. See above.

A description and comparison of automated motor activity devices.

Contributed by Virginia C. Moser
Apex, North Carolina

Assessment of Spatial Memory

Behavioral tasks must be evaluated in terms of the cognitive functions they require in order to be performed. Each task is a tool that allows the researcher to achieve a specific goal—i.e., to determine the consequences of manipulations of specific brain regions. These manipulations usually fall into one of four categories: stimulation of a single brain region by drugs or small electrical current, impairment of normal function by production of a lesion or administration of appropriate pharmacologic or toxicologic agents, recording of brain activity during the performance of a specific behavioral task, or behavioral phenotyping of transgenic and knockout mice for genes expressed in specific brain regions. All of the tasks described in this unit can be used with each of these four experimental manipulations.

Performance of the radial arm maze task (see Basic Protocol 1 and Alternate Protocol 1) requires intact spatial memory abilities. Normal performance is sensitive to the effects of hippocampal damage, normal aging, and a variety of pharmacologic or toxicologic agents. Performance of the water maze task (see Basic Protocol 2 and Alternate Protocols 2 and 3) also requires intact spatial memory abilities and is particularly sensitive to the effects of aging. The major advantage of the water maze task over the radial arm maze task is that the rats do not need to be water or food deprived; they are quite motivated to escape from the water. The task is also free from errors of omission or abortive choices—i.e., the rat makes an attempt to find the platform on every trial.

This unit also describes the use of the T maze to assess spatial memory, which takes into account the alternating behavior of rats in searching for food (see Background Information). The T maze has been most extensively used to investigate specific aspects of spatial working memory, which is operationally defined as information that is only useful to a rat during the current experience with the task. This is assessed using food-deprived rats in a simple T maze (see Basic Protocol 3). A modification of the T maze allows for the assessment of reference memory, defined as information that is useful across all exposures to the task (i.e., on any day of testing; see Alternate Protocol 4). Finally, in the absence of food-deprivation, a simple T maze can be used to assess spontaneous alternation (see Alternate Protocol 5).

Rats are generally used in research employing these behavioral tasks because a considerable amount is known about their brain anatomy and chemistry. Previous experimental studies have clearly shown that rats can be used to investigate the structure/function relationships between selected brain regions and learning or memory. Eight to ten rats are included in each experimental group, a number that is sufficient for statistical analyses (e.g., an analysis of variance, ANOVA) of the behavioral data and any neurochemical assays or histopathological studies that might be performed for confirmation of the manipulations.

NOTE: All protocols using live animals must first be reviewed and approved by an Institutional Animal Care and Use Committee (IACUC) or must conform to governmental regulations regarding the care and use of laboratory animals.

USE OF RADIAL ARM MAZE TASK TO TEST BASIC WORKING MEMORY

BASIC PROTOCOL 1

The radial arm maze task has been most extensively used to investigate specific aspects of spatial working and reference memory. This task is based upon the premise that animals have evolved an optimal strategy to explore their environment and obtain food with the minimum amount of effort.

A radial arm maze can easily be built by the investigator, so cost for this equipment can be quite low compared to other behavioral testing equipment. Using the maze, however,

Contributed by Gary L. Wenk
Current Protocols in Toxicology (1999) 11.3.1-11.3.18

is quite labor-intensive and requires that a tester be present throughout the task. The maze is typically used for rats, but it can be scaled down in size (by ~75%) for use with mice.

Materials

Rats
Pharmacologic or toxicologic agents (optional)
Food reward: e.g., 1-mg piece of normal chow, flavored (chocolate) or sweetened breakfast cereal, chocolate milk, or water
Radial arm maze (Fig. 11.3.1), handmade or fully automated (Coulbourn Instruments or Columbus Instruments)

Train rats

1. Weigh each rat daily throughout training and testing to monitor health and degree of food deprivation.
2. Restrict food available to rat so that its body weight attains 85% of that prior to training. During testing and training, allow rat to gain ~5 g body weight per week.
3. Allow rat to become comfortable with the experimenter (see Critical Parameters, discussion of rat handling).
4. Give food reward in home cage for a few days prior to training in order to acclimate the rat to the reward in a familiar environment.

   Liquid rewards are preferred if the rat will be given a drug, e.g., scopolamine, that might make swallowing dry food uncomfortable.

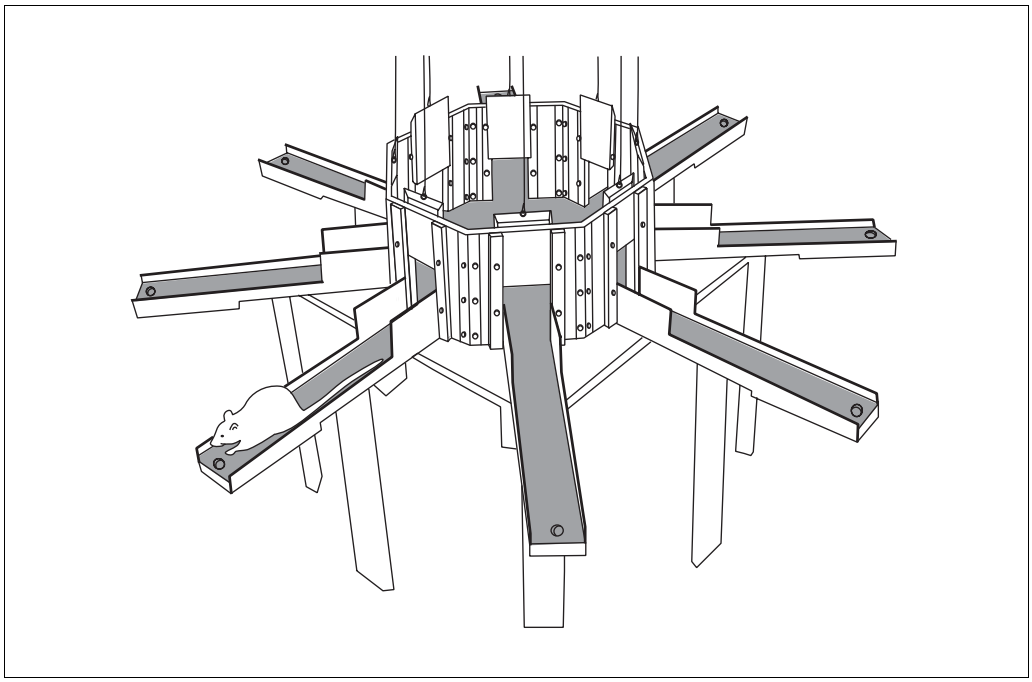

Figure 11.3.1 Eight-arm radial maze. For rats, the central platform should be ≥45 cm in diameter to accommodate the animal and allow it to turn easily between arms. A Plexiglas wall, 25 cm high, surrounds the central platform. The arms are 87 cm long and 10 cm wide, radiating from the central platform at equal angles. For mice, use shorter (35-cm), narrower (5-cm) arms and a smaller (20-cm) central platform. Each arm has a 5-mm-deep hole 1 cm from the end, which is used as a food cup, and each arm is separated from the center platform by a transparent Plexiglas guillotine door that covers a hole in the Plexiglas wall. The guillotine door can be raised or lowered to allow or prevent entry. The guillotine doors are connected by individual strings to a pulley system that allows the experimenter to open any door from one location within the testing room. Short walls (2 cm high) along the edge of the maze arms prevent the animal from falling off the maze.

5. Set up radial arm maze (see Fig. 11.3.1).

   The wooden or Plexiglas maze is set up ~1 m above the floor for easy access to the rat and food cups. It is composed of a central octagonal platform with eight arms extending from it like the spokes of a wheel. Guillotine doors that can be opened and closed individually separate the central platform from the arms. The maze should be placed in a room that contains various external cues that are visible to the rat while it is on the maze—e.g., a doorway, overhead lights, a noisy radio, and large simple designs on the walls. The maze can be handmade or a fully automated setup purchased commercially. The latter, including data analysis software, can be obtained from either Coulbourn Instruments or Columbus Instruments.

6. Place a well-handled pair of rats (preferably cagemates) on the maze at the same time.

   Using two rats reduces the time it takes for each to acclimate to the maze.

7. Spread food rewards around the entire maze to encourage exploration.

   Acclimation should require only 1 or 2 days.

8. On subsequent days, place food only on the arms, then only at the ends of the arms.

9. Finally, place rat alone on maze and food only in the food cup at end of arms. Testing can begin when rat is comfortable being picked up by the experimenter and, when placed alone on the maze, explores without hesitation and without excessive defecation or urination.

   A typical rat will be ready for testing—i.e., food-restricted and acclimated to the maze—within ~7 days. Rats should be run in the maze once a day every day (including weekends, ideally) during training and testing.

Test rats

10. Place food reward at end of each arm before each test session.

11. Place rat on central platform with all guillotine doors closed.

12. Raise all doors simultaneously. Allow rat to enter an arm. Close doors to all other arms.

13. Allow rat time to eat food and to return to central platform.

14. Close door to that arm and confine rat to the central platform area for a set time (from 0 sec to many minutes; 5 sec is ideal to begin).

    Longer waits make the task more difficult to solve—i.e., increase the length of time for which the rat must remember which arms it has entered.

15. Repeat steps 12 to 14 until all food pellets have been retrieved or until a predetermined length of time has elapsed.

16. Record the following data:

    Which arm the rat entered each time and whether it received a food reward
    Time elapsed between the beginning of the test session and the rat's obtaining all eight food rewards
    Number of correct arm choices: i.e., those that are chosen the first time
    Number of incorrect arm choices: i.e., visitations to the same arm more than once during a single test session.

    Time elapsed since the beginning of the session is considered in order to determine how fast the rat is making choices and finding the food rewards. This is also an indirect indication of motivation.

    Visitations to a previously chosen arm is considered a working memory error. Normal healthy young rats will perform this task almost perfectly every time.

    A healthy, happy, and motivated rat should learn this task, such that working memory errors are <15%, within 15 days.

17. Perform data analysis. Performance for all groups is typically expressed as either:
    a. The percentage of correct choices made in each test session in relation to the total number of arms entered,
    b. The absolute number of correct choices made in the first eight to twelve choices of each test session, *or*
    c. The percentage of correct choices made in relation to the number of incorrect choices.

    The data are best presented as a line drawing comparing a performance measure for each group versus daily test sessions. Data from 2 or 4 days of testing can also be averaged into blocks.

18. When performance is stable and choice accuracy is >85%, begin studies with pharmacologic and toxicologic agents or lesions.

    Alternatively, one can study the effects of drugs or lesions upon the acquisition of performance of this task. Drugs can be administered (or lesions produced) either prior to training to assess their effects upon acquisition, or after acquisition in order to assess their effects upon performance.

ALTERNATE PROTOCOL 1

USE OF RADIAL ARM MAZE TASK TO TEST WORKING VERSUS REFERENCE MEMORY

This protocol allows a dissociation to be achieved between working and reference types of memory, whereas the previous protocol is primarily sensitive to impairments in working memory. Working memory is operationally defined as information that is only useful to a rat during the current experience with the task, whereas reference memory is information that is useful across all exposures to the task—i.e., on any day of testing. This protocol should be performed after initial training of rats (Basic Protocol 1) has been completed.

1. Train rats in radial arm maze (see Basic Protocol 1, steps 1 to 9).
2. Place food reward at the end of only four arms of the radial arm maze before each test session.

    The arms chosen to be baited must be the same for a given rat but should vary between rats. For example, bait arms 1, 3, 6, and 8 every time that rat #1 is on the maze, bait arms 1, 4, 5, and 7 every time that rat #2 is on the maze, and so on. This task can be conducted on mazes with more or fewer arms in much the same way.

3. Place rat on maze with all doors raised and allow it to explore the maze completely and retrieve all food rewards.
4. Remove the rat from the maze for a set period of time (1 hr to 1 day).

    Longer delays make the task more difficult for the rat.

5. Bait appropriate four arms of maze for rat.

    In the example discussed above, bait arms 1, 3, 6, and 8 for rat #1.

6. Repeat step 3.
7. Record the following data:

    Number of correct entries into baited arms
    Number of entries into unbaited arms
    Number of reentries into baited arms
    Time elapsed between the beginning of the test session and the rat's obtaining all available food rewards.

    Entries into unbaited arms are reference memory errors; reentries into baited arms are working memory errors.

8. Repeat steps 2 to 7 until performance is stable and choice accuracy is high (>85%).
9. Perform data analysis. Performance for all groups is typically expressed as:
   a. The percentage of correct entries into baited arms in relation to the total number of arms originally baited (working memory performance), *and*
   b. The percentage of entries into arms that are never baited in relation to the number of unbaited arms (reference memory performance).

   The data are best presented as a line drawing comparing working and reference performance for each group versus daily test sessions. Data from 2 or 4 days of testing can be averaged into blocks.
10. Once the rat makes few, or no, reference or working memory errors, begin studies with pharmacologic or toxicologic challenges or lesions.

    Normal healthy young rats will perform this task almost perfectly every time. A healthy, happy, and motivated rat should learn this version of the task, such that working and reference memory errors are <15%, within 10 days.

USE OF MORRIS WATER MAZE TASK TO TEST SPATIAL MEMORY

BASIC PROTOCOL 2

The water maze task has been most extensively used to investigate specific aspects of spatial memory. This task is based upon the premise that animals have evolved an optimal strategy to explore their environment and escape from the water with a minimum amount of effort—i.e., swimming the shortest distance possible. The time it takes a rat to find a hidden platform in a water pool after previous exposure to the setup, using only available external cues, is determined as a measure of spatial memory. Studies with pharmacologic or toxicologic agents or lesions are initiated when performance is stable; the water maze task is particularly sensitive to the effects of aging (Brandeis et al., 1991). Alternatively, one can study the effects of drugs or lesions upon the acquisition of this task. Drugs can be administered (or lesions produced) prior to training to assess their effects upon acquisition, or after acquisition in order to assess their effects upon performance. A water maze (Fig. 11.3.2) can easily be built or purchased by the investigator, so the cost for this equipment can be quite low. Using the maze is quite labor-intensive and requires that a tester be present, or nearby, throughout the task. This maze is typically used for rats, but it can be scaled down in size (by ~50%) for use with mice.

Materials

Rats
Pharmacologic or toxicologic agents (optional)
Water maze apparatus (Fig. 11.3.2)
Tracking system and software (Columbus Instruments, HVS Image, San Diego Instruments, or CPL Systems)

Set up apparatus and begin acquisition testing

1. Set up water maze (see Fig. 11.3.2).

   A water-tight pool, painted white, should be positioned in a room with various external cues that are visible to a rat swimming in the pool, e.g., a doorway, overhead lights and camera (if desired), and large simple designs on the walls. Make water opaque by adding powdered milk or nontoxic white paint to the water. The pool should be designed so that it can be easily drained on a regular basis.
2. Insert platform into one quadrant of the pool.
3. Place rat into water with its head pointed towards the side of pool.

   The starting position should be at a different, and randomized, location each day of testing, e.g., north, south, etc.

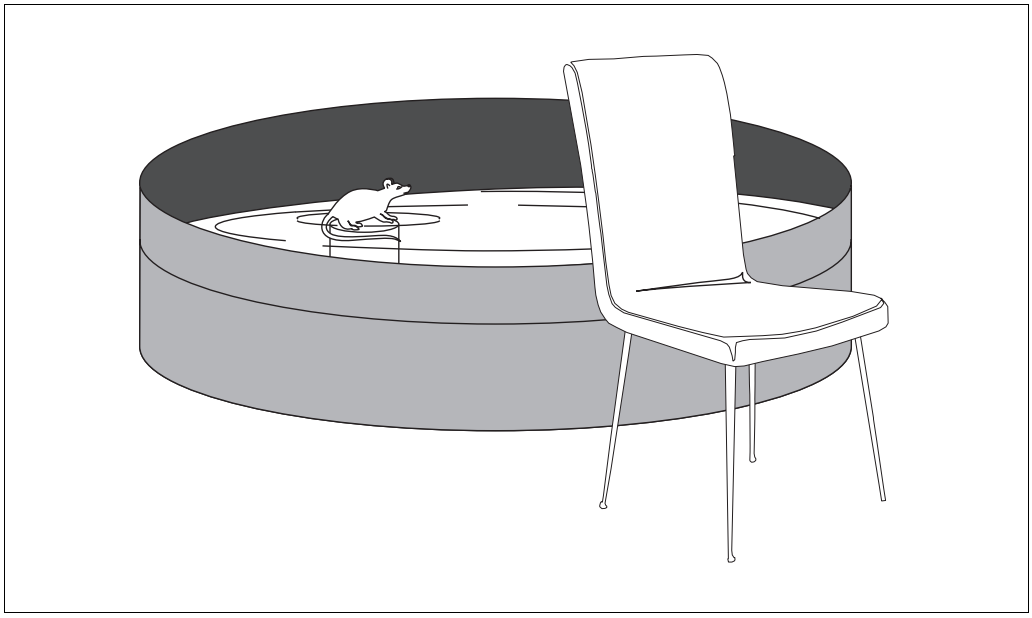

Figure 11.3.2 Morris water maze. The pool should be watertight, 200 cm in diameter and 75 cm deep, and filled with 50 cm water. The actual dimensions of the pool can be varied depending upon the space available to contain it and whether rats or mice are being tested (e.g., for mice, the pool need only be ~100 cm in diameter and 30 cm deep). The water is made opaque by adding nontoxic white paint or powdered milk. A 10-cm circular escape platform should be constructed of a water-resistant material and covered with material (e.g., cloth) that allows the animal to remain on the top when it is submerged. The platform should be made heavy enough to remain upright when submerged or may be attached to the bottom of the pool. The platform should be 48 to 49 cm in height so that it is submerged 1 to 2 cm below the surface. A chair can be positioned near the pool to allow the experimenter easy access and provide an additional cue for the animal. The water temperature should be maintained at ~20°C. It is useful to have an ample supply of towels nearby to dry animals between trials. Also, an incubator can be used to keep them warm between trials.

4. Record time (in seconds) it takes the rat to find the submerged platform. Guide rat to platform on first few trials if it requires >120 sec.

   A tracking camera, positioned ~200 cm above the center of the pool, can be used to quantify the distance swam on each trial and thereby determine swimming speed when combined with latency measurements. The tracking system can also display swim path and distance and provide additional information on search efficiency and exploration patterns during acquisition and probe trials. This equipment and associated computer software can be obtained from several commercial manufacturers.

5. Allow rat to remain on platform for 10 to 15 sec.

   This allows the experimenter time to return to an appropriate place at the side of the water pool in order to be ready for step 6.

6. Remove rat from pool. Wait 5 min.

7. Release rat into pool (from the same location) with platform in same location. Record time for rat to find platform.

8. Give each rat four trials on the first day.

Perform trials

9. On second day, insert platform in same location as on the first day.

10. Release rat with its head pointed towards the side of the water pool.

11. Record time it takes rat to find platform.

12. Give rat eight to ten trials per day with 5-min intertrial intervals for several days until performance is stable and latency to find the platform is low (<5 to 7 sec).
13. Perform data analysis. Performance is expressed as the average time it takes each rat to find the submerged platform. The data are best presented as a line drawing comparing the latency to find the platform for each group versus daily test sessions. Data from 2 or 4 days of testing can be averaged into blocks.
14. Begin studies with pharmacologic or toxicologic agents or lesions.

USE OF WATER MAZE TASK FOR SPATIAL PROBE TRIAL

ALTERNATE PROTOCOL 2

This alternate protocol should be performed after the acquisition phase of testing in Basic Protocol 2 has been completed. It is important that the rats know the location of the hidden platform before beginning this protocol. This knowledge is demonstrated by the rat swimming quickly and directly to the hidden platform. The spatial probe trial is used to test the rat's knowledge of the precise location of the platform. An accurate direction of the swimming behavior provides evidence that the rat has learned the spatial location of the platform relative to the available external cues (Sutherland et al., 1982). Although the spatial probe trial is typically performed only after performance has stabilized, some researchers perform a spatial probe trial at the end of each day of training throughout the acquisition phase, and average performance across trials.

1. Train rats in water maze (see Basic Protocol 2, steps 1 to 12).
2. Set up water pool without platform.
3. Release rat with its head pointed towards the side of the water pool.
4. Remove rat after 90 sec.
5. Record time rat spent in the quadrant that previously contained the platform and calculate as a percentage of total time in pool. If possible (i.e., if using a computer tracking system), also record the percentage of time spent in the other quadrants.
6. Perform data analysis. The data can be expressed as either:
   a. A histogram showing the average amount of time that the rats in each group spent exploring each quadrant of the pool (most typically), *or*
   b. The percentage of time the rat spent exploring the quadrant that had contained the platform in relation to the total time spent exploring the entire pool.

USE OF WATER MAZE TASK TO TEST WORKING MEMORY

ALTERNATE PROTOCOL 3

This alternate protocol can be performed after the acquisition phase of testing in Basic Protocol 2 has been completed. It is important that the rats have demonstrated that they know the location of the hidden platform before this next protocol is begun. This protocol has also been referred to as a "reversal test."

1. Train rats in water maze (see Basic Protocol 2, steps 1 to 12).
2. Release rat with its head pointed towards the side of the water pool.

   Start position should be at same location each day.
3. Record time it takes rat to find submerged platform. Allow rat to remain on platform for 10 sec. Remove rat from pool and place in holding cage for 15 sec.
4. Move submerged platform to new location.
5. Release rat from same location as in step 2.

6. Allow rat to swim for up to 120 sec. Record time it takes for rat to find platform.

   Guide rat to platform if necessary.

7. Allow rat to remain on platform for 10 sec. Remove rat from pool and place in holding cage for 15 sec.

8. Repeat steps 5 to 7 until rat swims directly and quickly to the platform. Record time on each attempt.

9. Repeat steps 4 to 8 once per day for 4 days, with the platform in a different quadrant of the pool each day.

   Latency to find the platform should decrease with each day of testing.

10. Perform data analysis. Performance is expressed as the average time it takes each rat to find the submerged platform at each new location. The data are best presented as multiple line drawings comparing the latency to find the platform for each group and for each location versus daily test sessions. Data from 2 or 4 days of testing can be averaged into blocks.

BASIC PROTOCOL 3

USE OF T MAZE TO TEST SPATIAL MEMORY

This protocol describes the use of the simple T maze (see Fig. 11.3.3) and food deprivation for the assessment of spatial working memory. The maze can easily be built by the investigator, and is much easier to construct than the radial arm maze (Fig. 11.3.1). Similar to the radial arm maze task, this task is quite labor-intensive for the investigator and requires that a tester be present throughout the time the animal is on the maze. This maze is typically used for rats, but it can be scaled down in size (by ~75%) for use with mice.

Materials

Rats
Pharmacologic or toxicologic agents (optional)
Food reward: e.g., 1-mg piece of normal chow, flavored (chocolate) or sweetened breakfast cereal, chocolate milk, or water
Split-stem T maze (Fig. 11.3.3), handmade or commercial (Coulbourn Instruments or Columbus Instruments), without hardware cloth partition, Plexiglas barrier, or curtain

Train rats

1. Weigh each rat daily throughout training and testing to monitor health and degree of food deprivation.

2. Restrict the food available to the rat so that its body weight attains 85% of that prior to training. During testing and training, allow rat to gain ~5 g per week on the restricted diet.

3. Allow rat to become comfortable with the experimenter (see Critical Parameters, discussion of rat handling).

4. Give one food reward in the home cage each day for a few days prior to training in order to acclimate the rat to the reward in a familiar environment.

   Liquid rewards are preferred if the rat will be given a drug (e.g., scopolamine) that might make swallowing dry food uncomfortable.

5. Set up the T maze without the hardware cloth partition, Plexiglas barrier, or curtain on the stem (see Fig. 11.3.3). Spread food rewards around the entire maze to encourage exploration.

   Environmental conditions and materials can be similar to those described for the radial arm maze (Basic Protocol 1).

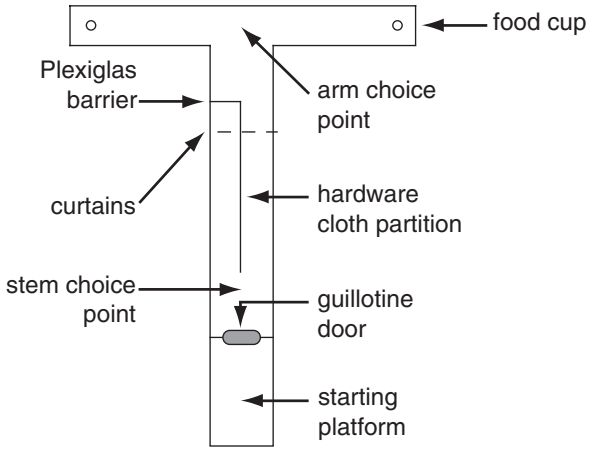

Figure 11.3.3 The split-stem T maze. For rats, the maze consists of a wooden T-shaped platform with a 87 × 20–cm stem and 40 × 10–cm arms at the end. Black Plexiglas can also be used, and is easier to clean. The entire perimeter of the platform has 5-cm walls to discourage the rat from jumping to the floor. Located 1 cm from the distal end of each arm is a food cup (1 cm wide and 1.5 cm deep). The starting platform is 25 cm long and is separated from the stem by a guillotine door (11 cm high and 6 cm wide), mounted in a frame (22 cm high and 18 cm wide). The stem is divided lengthwise into two halves by a hardware cloth partition (i.e., a taut cloth screen or some other opaque partition, 10 cm high and 20 cm long), that starts 20 cm from the guillotine door. Near the end of the partition proximal to the arms, and extending across both sides of the stem, is a white opaque cloth curtain (14 cm high) suspended in a frame that is perpendicular to the stem. A clear Plexiglas barrier (14 cm high and 8 cm wide, suspended in a frame that is perpendicular to the stem) is placed behind one of the curtains to block access to the arms from that side of the stem. A large cache of food reward is suspended under the ends of the arms, under both food cups to prevent the use of olfactory cues. A rich variety of local and distant cues should surround the maze (e.g., large objects that the animal can see from the maze). These can be removed as required by the particular demands of the experiment. The room should not be too bright, as this tends to frighten the animal. To convert this to a standard T maze (see Basic Protocol 3 and Alternate Protocol 5), the hardware cloth partition, Plexiglas barrier, and curtain can be removed from the stem.

6. Place a well-handled pair of rats (particularly cagemates) on the maze at the same time and allow them to explore.

   Having two rats present on the maze will make the rats more comfortable during this initial phase of exploration and will reduce the time it takes for each rat to acclimate to the maze.

   The acclimation period should require only 1 or 2 days. Consumed food rewards should be replaced on the maze during exploration.

7. Repeat once a day for two more days, placing food only on the arms of the maze one day, then only at the ends of the arms on the following day.

8. Place one rat on the maze with food only in the food cup at the end of the arms. Begin testing when the rat is comfortable being picked up by the experimenter and, when placed alone on the maze, explores without hesitation and without excessive defecation or urination.

   A typical rat will be ready for testing (i.e., sufficiently food-restricted and acclimated to the maze) within 7 to 10 days. Each rat should be run alone on the maze once a day every day during training and testing.

Test rats

9. Place a food reward at the end of an open arm.

10. Place a small barrier (i.e., a small block of wood or similar object) on the maze to prevent the rat from entering the other arm.
11. Place the rat on the stem behind the closed guillotine door.
12. Raise the door and allow the rat to enter the stem of the maze. Close the guillotine door quietly (and not on the rat's tail).

    This is called the forced trial. On each day, the open, baited arm for the forced trial should be randomly varied.

13. Allow rat to enter the open arm and eat the food reward. Return the rat to the starting position behind the closed guillotine door. Do not allow the rat to explore the maze.

    At this time the rat must be aware that he has consumed the food at only one location for this trial.

14. Remove the barrier to the arm and place a food reward on the arm not previously rewarded.
15. Confine rat to the starting position for a set time (from 0 sec to many min; 5 sec is ideal to begin). Use the same time for each repetition.

    Longer waiting periods make the task more difficult to solve, i.e., increasing the length of time that the rat must remember which arm it last entered.

16. Raise the guillotine door and allow the rat to enter the stem and either arm of the maze. Close the guillotine door. An arm entry can be defined as the rat either having all four feet on an arm or investigating food cup; this must be determined by the experimenter prior to testing.

    This is called a choice trial.

17. Allow rat to eat the reward and return it to the starting platform. If the rat chooses the unbaited arm, allow it to reach and momentarily explore the empty food cup and then return it to the starting platform.
18. Repeat steps 15 to 17 from one to nine times. For all subsequent choice trials, place food on the side of the maze not entered by the rat on the previous trial. Allow the rat to choose between the two arms. If the rat enters the arm that contains food, record a correct choice. If the rat enters the unbaited arm, record an error and place the rat back at the start position without a food reward.

    The food reward remains in its location until it is found and eaten—i.e., the food pellet should not be moved if it is not found. A rat can receive the maximum amount of reinforcement for choosing correctly on the first choice trial and then alternating its responses between the two arms on subsequent choice trials.

19. Record the following data:

    Number of correct entries into baited arms
    Number of reentries into unbaited arms.

    Repeated visitation to an unbaited arm is considered a working memory error. Normal healthy young rats will perform this task almost perfectly every time. A healthy, happy, and motivated rat should learn this task within 5 days—i.e., working memory errors should be <15%.

20. Begin studies of pharmacologic or toxicologic agents or lesions when performance is stable and choice accuracy is high.

    Alternatively, the effects of drugs or lesions on the acquisition of this task can be studied. Drugs can be administered (or lesions produced) prior to training to assess their effects upon acquisition, or after acquisition in order to assess their effects upon performance.

21. Express performance as the percentage of correct choices made in each test session. Present data as either:

    a. A histogram showing the percent correct choices averaged across a given test period for controls, brain-lesioned, or drug-treated groups, *or*
    b. A line drawing comparing percent correct choices for each group versus daily test sessions.

    Data from daily test sessions can also be averaged into 2-day blocks.

USE OF T MAZE TO TEST WORKING VERSUS REFERENCE MEMORY

ALTERNATE PROTOCOL 4

This protocol, like Alternate Protocol 1, allows the dissociation of working and reference types of memory, and is achieved by changing the external cues (i.e., by moving the maze to a new location), and by using an additional partition and barrier in the T maze stem during the testing phase (Fig. 11.3.3). In this case, the rat is required to associate a specific set of external cues with the memory of which side of the stem is blocked. Otherwise, the test is performed as in Basic Protocol 3.

Additional Materials *(also see Basic Protocol 3)*

Hardware cloth partition, Plexiglas barrier, and curtain for split-stem T maze (Fig. 11.3.3)

1. Train rats in the T maze (see Basic Protocol 3, steps 1 to 8). To vary the demand upon reference memory, move the maze to a different location (or construct an additional maze and place it in a different location).
2. Place the hardware cloth partition, Plexiglas barrier, and curtain on the T maze (Fig. 11.3.3).
3. Begin the forced trial (see Basic Protocol 3, steps 9 to 12). If the rat enters the side of the stem that is blocked by the Plexiglas barrier, allow the rat to make a correction and to enter the open side of the stem.
4. Complete forced trial (see Basic Protocol 3, steps 13 to 14) and perform repeated choice trials (steps 15 to 18).
5. Record the following:

    Number of correct entries into open side of stem
    Number of correct entries into baited arms
    Number of entries into blocked side of stem (reference memory errors)
    Number of reentries into unbaited arms (working memory errors).

    Normal healthy young rats will perform this task almost perfectly every time. A healthy, happy, and motivated rat should learn this version of the task within 10 days—i.e., working and reference memory errors should be <15%.

6. Begin pharmacologic, toxicologic, or lesion analyses (see Basic Protocol 3, step 20).
7. Express performance as the percentage of correct stem and arm choices made in each test session. Present stem- and arm-choice results as separate line drawings comparing percent correct choices for the controls, brain-lesioned, or drug-treated groups, versus each daily test session (for example see Hepler et al., 1985).

    Data from daily test sessions can also be averaged into 2-day blocks.

ALTERNATE PROTOCOL 5

SPONTANEOUS ALTERNATION ON A T MAZE

Sustained performance in this task is based upon the assumption that rats will explore their environment in a repeating and alternating fashion in order to optimize the amount of area investigated, even when exploration is not rewarded by food. Normal alternation performance in this task is consistent with an intact working memory ability. Pharmacologic or toxicologic challenges or discrete lesions are typically made prior to testing a rat on the alternation task.

1. Set up T maze without the hardware cloth partition, Plexiglas barrier, or curtain on the stem (Fig. 11.3.3).
2. Place a well-handled rat on the T maze starting platform.

   Because these rats are only motivated by their desire to explore the maze (i.e., they are not food-deprived), they must be completely comfortable with the experimenter and not fearful of their environment.
3. Raise the guillotine door and allow the rat to walk down the stem and choose an arm.

   A rat has made its choice when it has placed all four of its feet onto one arm. Some rats will tentatively place a foot onto each arm before making a final decision.
4. Return the rat to the starting platform for a set time (from 0 sec to many min; 5 sec is ideal to begin).
5. Repeat steps 3 and 4 nine times.
6. Record the number of entries into each arm.

   Control rats should alternate their arm choices within each test session.
7. Express results as the number of alternations divided by the total number of choices made per session. Present data as either:
   a. A histogram showing the percent correct choices averaged across a given number of tests for controls, brain-lesioned, or drug-treated groups, *or*
   b. A line drawing comparing percent alternations for each group versus each daily test session.

   Data from daily test sessions can also be averaged into 2-day blocks.

COMMENTARY

Background Information

For rats and mice, spatially organized tests are typically learned very quickly and performed very accurately. Consequently, testing these animals in a spatial task—e.g., the radial arm maze or T maze—has become very popular.

Rats can use any of three possible strategies to achieve accurate performance in spatial maze tasks. The first is a place strategy in which the rat uses remote sensory cues to navigate around the maze and obtain a reward. The second is a cue strategy in which local cues are used to help the subject find the reward. The third is a response strategy in which the rat uses a specific sequence of motor acts that are essentially independent of the available sensory cues. These strategies are not necessarily independent of one another: in order to solve the task, the rat may use them in combination. In addition, different components of these strategies may dominate during different stages of training. Therefore, in the T maze task, the rewarded arm can be distinguished from the unbaited arm by its spatial location, by local cues associated with the maze itself, or by the direction in which the rat turns to approach the goal arm.

Good performance on the radial arm maze (see Basic Protocol 1) and T maze (see Basic Protocol 3) requires intact spatial memory abilities. Normal performance is sensitive to the effects of damage to the hippocampus, to the effects of normal aging, and to a variety of pharmacologic or toxicologic agents. Performance of the Morris water maze task (see Basic Protocol 2) also requires intact spatial memory abilities and is particularly sensitive to the effects of aging. The major advantage of the

Morris water task (and of the spontaneous alternation task; see Alternate Protocol 5) over the radial arm and T maze tasks is that the rats do not need to be food- or water-deprived; in the Morris water task the rats are quite motivated to escape from the water. The Morris water task is also free from errors of omission or abortive choices—i.e., the rat makes an attempt to find the platform on every trial.

Each behavioral task must be evaluated in terms of the types of cognitive functions required to perform it. Each task is a tool that allows the researcher to achieve a specific goal, i.e., to determine the consequences of specific manipulations of the brain. These manipulations usually fall into one of four categories: (1) stimulation of a single brain region by drugs or small electrical current, (2) impairment of the normal function of a brain region by production of a lesion or administration of appropriate pharmacologic or toxicologic agents, (3) recording of activity from a brain region while the animal is performing a specific behavioral task, or (4) mutation of a gene expressed in the brain. All the tasks described in this unit can be used in each of these four experimental conditions.

Radial arm maze task

The radial arm maze task was introduced and popularized in its present form by Olton and co-workers (Olton and Samuelson, 1976). The task is a logical extension of the multiple, simultaneous choice tasks originally described by Hamilton (1911) and Tolman et al. (1946); it has been used to measure the effects of various brain manipulations upon specific aspects of memory, such as spatial working and reference memory, and can be adapted for use with rats, mice, and pigeons (Bond et al., 1981; Levy et al., 1983; Wenk et al., 1986). The large number of sequential locations that the rat can visit to obtain a reward makes the task ideal for investigating the effects of drugs or lesions upon serial order memory—i.e., whether locations visited first or last are remembered better (Kesner and Novak, 1982). The task is sensitive to the effects of brain lesions (Becker et al., 1980) and to numerous drugs (for review see Levin, 1988) that either impair or enhance performance, including inebriants such as ethanol (Devenport et al., 1983), endogenous neuropeptides such as vasopressin (Buresova and Skopkova, 1982), amnestic drugs such as scopolamine (Stevens, 1981; Watts et al., 1981; Okaichi and Jarrard, 1982), and neurotoxins such as trimethyltin (Walsh et al., 1982).

Water maze task

The water maze task was designed to address theoretical controversies that arose from using the radial arm maze task (Brandeis et al., 1989): i.e., the concept that memories about spatial information are handled by the brain quite differently than information relating to other forms of learning. The water maze task is not a better or more sensitive task than the radial arm maze task, it simply asks many of the same questions of the animal under different circumstances. Differences between the two tasks include the nature of the locomotion, walking versus swimming; the nature of the motivation, food deprivation versus avoidance of drowning; the location of available cues for finding the reward, local and distant cues versus distant cues only; and the visibility of the location of the reward, a visible food cup on the radial arm maze versus a submerged platform in the water maze task. Sometimes asking the same question in a different way has allowed researchers to discover subtle differences in the contributions of different brain regions or the effects of specific lesions or drugs. The water maze task was introduced by Morris (1981) and colleagues as a spatial localization or navigation task. The task has been extensively used to study the neurobiological mechanisms that underlie spatial learning and memory, age-associated changes in spatial navigation (Gage et al., 1984; Rapp et al., 1987; Pitsikas et al., 1990), and the ability of psychopharmacological agents (Sutherland et al., 1982; Hagan et al., 1983, 1986; McNaughton and Morris, 1987; Brandeis et al., 1991; McNamara and Skelton, 1991), lesions (Morris et al., 1982; Kolb et al., 1983), or gene mutations (Tsien et al., 1996; Crawley et al., 1997) to influence specific cognitive processes.

T maze task

The T maze task has been used to measure the effects of various brain manipulations on specific aspects of spatial memory. It can be adapted for use with rats, mice, gerbils, pigs, sheep, goats, turtles, and pigeons (Schnurr, 1971; Wenk et al., 1987; Avigan and Powers, 1995; Hosoi et al., 1995; Mendl et al., 1997). The task is sensitive to the effects of various brain lesions (Durantou et al., 1989; Aggleton et al., 1995, 1996; Beracochea and Jaffard, 1995; Sanchez-Santed et al., 1997), particularly in the hippocampus (White, 1974), and to numerous drugs or toxins that either enhance or impair spatial memory (Wenk et al., 1989;

Barone et al., 1995; Givens and Olton, 1995; Levin et al., 1996).

Spontaneous alternation behavior is a form of sensory-independent motor behaviors. Tolman (1925) first reported that rats would avoid repeated entry into the arms of a maze. Spontaneous alternation behavior was first defined in a T maze when a rat would go down one arm of a maze first and then go down the other arm on the next trial (Dennis, 1939). It has been proposed that the rat generates a sense of internal inhibition to the first arm after it has explored it and is reluctant to return to that arm on a subsequent choice. Choosing the opposite arm increases the animal's opportunity to find food. Responding in this alternating fashion can, over time and in a complicated environment, substantially increase the amount of food obtained and reduce the amount of time and energy expended (not to mention reducing the time exposed to predators). An alternation strategy would thus confer an adaptive advantage to solving the problem of finding food.

Critical Parameters

Essence of rat handling

Remain relaxed. The rat can sense your nervousness. Be consistent with your treatment and handling. Use the rat's native intelligence and your skills to provide him with the specific knowledge that he needs to perform the task. Take the rat's point of view. Handle the rat the way that you would like King Kong to handle you! Go slowly and be gentle. Do not approach the rat from behind and above; this is how a predator would attack the rat. Do not grab the rat tightly around the abdomen, as its internal organs have very little protection. Support the rat from underneath its body and hold it against yours. Run rats on the maze at the same time every day; rats are like people in that they grow accustomed to a particular schedule. Allow the rat to gain ~5 g each week during testing and training, even though it is food-restricted. Pay attention to how well groomed the animal is; a well-groomed rat is a healthy rat. If the rat is undernourished, it will feel cold to the touch. Sick rats do not provide useful data and may be in danger of dying. Find out why the rat is sick and correct the problem.

Radial arm maze task

Rats will use whatever sensory cues are available to solve the radial arm maze task and obtain a reward. Removing these cues will make performance difficult and impair choice accuracy. Reducing the salience of stimuli around the maze—e.g., completely enclosing the arms or placing the maze in a homogeneous environment—can greatly influence performance. This may force the rat to use other, more egocentric, information to solve the task, such as a sequence of left turns after every arm choice, or to depend upon intramaze cues, such as odor trails.

The guillotine doors are a critical feature of the maze in that they confine the rat to the central platform area between choices. Otherwise, the rat may develop a biased response pattern, which makes interpretation of the performance difficult: i.e., it becomes impossible to determine whether the rat remembered the correct choice or a response habit. For example, without temporary confinement between each arm choice, the rat could successfully solve this task by simply always turning right after each choice and entering the first arm away from the previously chosen one. This simple strategy does not require an accurate knowledge of the spatial environment or memory for a specific location. Unless the experimenter is primarily interested in studying response patterns, it is best to have the rat confined to the central platform prior to making each arm choice.

The number of arms the maze contains can vary depending upon the goals of the experimenter. For example, having fewer arms requires that the animal remember fewer visited places on each trial. Increasing the number of arms increases the mnemonic demands of the task by increasing the list of spatial locations in memory. In addition, an increased number of arms introduces considerably more proactive interference, i.e., interference of previous learning on current memory. Most researchers choose to use eight arms in order to minimize proactive interference (if that is desired) or to shorten the length of time it takes to test each rat. Numerous variations have been introduced in order to automate the task, reduce testing time, or provide alternative interpretations of the psychological processes that underlie normal performance (Bond et al., 1981; Okaichi and Jarrard, 1982).

Most rats are quite fearful of exploring the arms during the initial training periods. Sometimes it is better to have somewhat taller sides (6 to 8 cm) along the edges of the arms to offer more support to the rat. A taller barrier may be attached along the edges of the arms near the central platform. This prevents the rat from jumping from one arm to another and forces the rat into the central platform area between choices. The guillotine doors should be at-

tached by strings to an overhead pulley system that allows all doors, or individual doors, to be raised and lowered by one experimenter from a single location. Alternatively, individual electronic mechanisms could also be installed at a greater cost.

The food reward is typically a small piece (10 mg) of normal chow or a flavored (chocolate is a favorite) or sweetened breakfast cereal. Liquid rewards, such as chocolate milk or water, can also be used. Liquid rewards are preferred if the rat will be given a drug, such as scopolamine, that might make swallowing dry food uncomfortable.

Water maze task

Rats will use whatever sensory cues are available to solve this task and escape from the water. Removing external cues around the pool will make finding the submerged platform more difficult and increase the latency to escape. Reducing the salience of stimuli around the pool may force the rat to use other, more egocentric, information to solve the task. Rats will use a search strategy to find the platform when it is moved. They will swim close to the wall for a few laps, then move further away and continue swimming in concentric circles until they bump into the platform. Latency to find the platform and swimming distance will then decrease quickly thereafter. The greatest advantage of this task over food-motivated tasks is that most rats are more highly motivated to escape from the water. In addition, food restriction is unnecessary, which is a great advantage when testing aged animals, to which such restriction is more stressful.

Performance in the water maze task can be influenced by many factors that should be considered carefully when comparing the results of one study with another. For example, the sex and strain of the rats, the dimensions of the pool and temperature of the water, and the particular training schedule can all affect performance. One should also take into account factors that affect swimming speeds, which include body weight, muscle development, and age. See Brandeis et al. (1989) for a thorough discussion of the role of these factors in performance of the Morris water maze task.

Finally, because older rats or mice are frequently tested in the water maze, it is important to be sure that they can swim adequately and have sufficient visual acuity to use distant cues. To test this, place rat into the pool and allow it to swim to a platform that is supported above the water level. To assist rat, suspend a large visible cue above the platform. If the rat can swim directly to the visible platform without difficulty, it is ready to begin testing using the protocols outlined in this unit.

T maze task

In normal animals, choice accuracy in the T maze task varies with the duration of the delay interval introduced between choices on the maze. Choice accuracy is very good with short intervals (e.g., 5 sec), and approaches random chance performance with extremely long intervals (e.g., >1 hour). Choice accuracy is also influenced by the number of choice trials given within each testing session. When only a single choice trial follows the forced trial, choice accuracy is usually very good. When multiple choice trials are given following the forced trial, performance accuracy worsens as the number of choice trials increases. The memory of choices made earlier in the test session interferes with remembering the most recent choice. This is called proactive interference. The task can also be made more difficult by reducing the number of salient stimuli near the maze (as for the Morris water maze and radial arm maze tasks; see discussion above).

The guillotine door on the stem is a critical feature of the maze, which serves to confine the rat to the starting platform area for a predetermined delay period between choices. The guillotine door also prevents the rat from exploring the maze between choice trials. It is therefore important to quickly return the rat to the starting platform between choice trials so that the rat does not explore the opposite arm of the maze.

Troubleshooting

Radial maze and T maze tasks

The major problems associated with testing rats in open mazes are usually related to two competing factors for the rat: its fear of the maze (or experimenter) versus its motivation to explore and find the food that it knows is on the maze. Excessive fear will prevent the rat from performing. It will usually remain frozen in one place on the maze and not explore. In addition, if it is frightened it will usually defecate and urinate on the maze and squeal when being picked up. If the rat is not making choices on the maze it is impossible to know whether its mnemonic abilities are normal or impaired. Fear can be overcome by considering some of the issues presented in the discussion of rat handling above (see Critical Parameters). The most important thing the experimenter can do

is simply handle the animal more often. Also, higher barriers can be installed along the arms of the maze to provide the rat a better sense of security from falling.

A lack of motivation will produce similar results—i.e., the rat will make little or no attempt to explore the maze and find food. Motivation can be increased by a slightly greater restriction of food intake. The rat's weight and general health must be carefully monitored during food restriction. Usually the rat's weight should not drop below 80% of its free-feeding weight. For most rats, it is only necessary to reduce their weight by 15%. If the rat is aware that a safe food source exists on the maze, it will usually explore the maze to find it.

Water maze task

There are only two problems that are typically associated with this task. First, immersion of the animal into the water may cause significant stress and subsequent endocrinological changes that may interfere with the purpose of the study. These problems are usually resolved with continued exposure to the pool. However, for aged animals this stress can be sufficient to induce cardiovascular system collapse, leading to death or stroke. Second, the method by which the water is made opaque can produce problems. If powdered milk is added to the water, the pool must be drained regularly (e.g., daily) to avoid bacterial contamination and odor. If powdered white paint is used, care must be taken to ensure that it is nontoxic to the animals, which may frequently ingest small quantities of water while performing the task.

Anticipated Results and Time Considerations

Radial arm maze task

A healthy, happy, and motivated rat should learn this task within 15 days: i.e., working and reference memory errors should be <15%. This assumes that the rat is actively making choices and eating the food rewards on the maze. The rat should run quickly down the arms to retrieve the food reward and return to the central platform immediately after eating the reward. During the confinement period the rat will usually wander around the central area and quickly choose an unvisited arm as soon as the guillotine doors are raised. After a control rat has learned the task, a single test session—i.e., eight correct arm choices—should not require more than 5 to 10 min to complete. Rats given drugs or lesions may require two to three times longer to complete the test session. A healthy group of rats, including experimental and control groups, should be able to be trained and tested in Basic Protocol 1 and Alternate Protocol 1 in ~4 weeks. This estimate assumes that all rats are tested once per day.

Water maze task

Control rats may take ~30 to 60 sec to find the platform on the first day of testing. Latency should decrease significantly with subsequent trials to ~5 sec. On the probe test, the rats should spend a greater percentage of time exploring the quadrant that previously contained the platform than in the other quadrants. On both the reversal and working memory tests, the rats should first explore the quadrant that previously contained the platform and then inadvertently find the new location of the platform. On subsequent trials (usually less than five), their latency to find the platform will decrease significantly. All rats should be trained in the Basic Protocol 2 portion of this task within 1 week. The spatial probe trial (Alternate Protocol 2) can be completed in 1 day, and the reversal test (Alternate Protocol 3) within 5 days. Lesioned rats may require a few additional days of training in Basic Protocol 2 in order to reach an asymptotic level of performance. Drugs can be given each day prior to testing in this protocol; however, this will also extend the amount of time required to reach asymptotic performance. Drug administration will also prolong the number of days spent testing in the spatial probe and reversal trials; the number of days depends upon the number of doses to be tested. It is important to have drug-free and saline injection days interspersed between the drug testing days. Obviously, this will prolong the time required to complete this task.

T maze task

A healthy, happy, and motivated rat should perform this task well within 7 days: i.e., the rat should be alternating between arms at least 85% of the time. This assumes that the rat is actively making choices and eating the food rewards on the maze. The rat should run quickly down the arms to retrieve the food reward. After the confinement period, the rat should quickly choose an arm as soon as the guillotine door is raised. Food deprivation and acclimation to the maze take ~10 days. After a control rat has learned the task, a single test session should not require more than 15 min to complete. Rats given drugs or lesions may require up to twice as long to complete a session.

Literature Cited

Aggleton, J.P., Neave, N., Nagle, S., and Hunt, P.R. 1995. A comparison of the effects of anterior thalamic, mammillary body and fornix lesions on reinforced spatial alternation. *Behav. Brain Res.* 68:91-101.

Aggleton, J.P., Hunt, P.R., Nagle, S., and Neave, N. 1996. The effects of selective lesions within the anterior thalamic nuclei on spatial memory in the rat. *Behav. Brain Res.* 81:189-198.

Avigan, M.R. and Powers, A.S. 1995. The effects of MK-801 injections and dorsal cortex lesions on maze learning in turtles (*Chrysemys picta*). *Psychobiology* 23:63-68.

Barone, S., Stanton, M.E., and Mundy, W.R. 1995. Neurotoxic effects of neonatal triethyltin (TET) exposure are exacerbated with aging. *Neurobiol. Aging* 16:723-735.

Becker, J.T., Walker, J.A., and Olton, D.S. 1980. Neuroanatomical bases of spatial memory. *Brain Res.* 200:307-320.

Beracochea, D.J. and Jaffard, R. 1995. The effects of mammillary body lesions on delayed matching and delayed non-matching to place tasks in the mice. *Behav. Brain Res.* 68:45-52.

Bond, A.B., Cook, R.B., and Lamb, M.R. 1981. Spatial memory and the performance of rats and pigeons in the radial-arm maze. *Anim. Learn. & Behav.* 9:575-580.

Brandeis, R., Brandys, Y., and Yehuda, S. 1989. The use of the Morris water maze in the study of memory and learning. *Int. J. Neurosci.* 48:29-69.

Brandeis, R., Sapir, M., Kapon, Y., and Borelli, G. 1991. Improvement of cognitive function by MAO-B inhibitor L-deprenyl in aged rats. *Pharmacol. Biochem. Behav.* 39:297-304.

Buresova, O. and Skopkova, J. 1982. Vasopressin analogues and spatial working memory in the 24-arm radial maze. *Peptides* 3:725-727.

Crawley, J.N., Belknap, J.K., Collins, A., Crabbe, J.C., Frankel, W., Henderson, N., Hitzemann, R.J., Maxson, S.C., Miner, L.L., Silva, A.J., Wehner, J.M., Wynshaw-Boris, A., and Paylor, R. 1997. Behavioral phenotypes of inbred mouse strains: Implications and recommendations for molecular studies. *Psychopharmacology* 132:107-124.

Dennis, W. 1939. Spontaneous alternation in rats as an indicator of the persistence of stimulus effects. *J. Comp. Psychol.* 28:305-312.

Devenport, L.D., Merriman, V.J., and Devenport, J.A. 1983. Effects of ethanol on enforced spatial variability in the 8-arm radial maze. *Pharmacol. Biochem. Behav*. 18:55-59.

Durantou, F., Cazala, P., and Jaffard, R. 1989. Intertrial interval dependent effect of lateral hypothalamic stimulation on spontaneous alternation behavior in a T-maze. *Physiol. Behav.* 46:253-258.

Gage, F.H., Dunnett, S.B., and Bjorklund, A. 1984. Spatial learning and motor deficits in aged rats. *Neurobiol. Aging* 5:43-48.

Givens, B. and Olton, D.S. 1995. Bidirectional modulation of scopolamine-induced working memory impairments by muscarinic activation of the medial septal area. *Neurobiol. Learn. Mem.* 63:269-276.

Hagan, J.J., Alpert, J.E., Morris, R.G., and Iversen, S.D. 1983. The effects of central catecholamine depletions on spatial learning in rats. *Behav. Brain Res.* 9:83-104.

Hagan, J.J., Tweedie, F., and Morris, R.G. 1986. Lack of task specificity and absence of posttraining effects of atropine on learning. *Behav. Neurosci.* 100:483-493.

Hamilton, G.V. 1911. A study of trial and error reactions in mammals. *J. Anim. Behav.* 1:33-66.

Hepler, D., Olton, D., Wenk, G., and Coyle, J. 1985. Lesions of the nucleus basalis magnocellularis and medial septal area of rats produce qualitatively similar memory impairments. *J. Neurosci.* 5:866-873.

Hosoi, E., Swift, D.M., Rittenhouse, L.R., and Richards, R.W. 1995. Comparative foraging strategies of sheep and goats in a T-maze apparatus. *Appl. Anim. Behav. Sci.* 44:37-45.

Kesner, R.P. and Novak, J.M. 1982. Serial position curve in rats: Role of the dorsal hippocampus. *Science* 218:173-175.

Kolb, B., Sutherland, R.J., and Whishaw, I.Q. 1983. A comparison of the contributions of the frontal and parietal association cortex to spatial localization in rats. *Behav. Neurosci.* 97:13-27.

Levin, E.D. 1988. Psychopharmacological effects in the radial-arm maze. *Neurosci. Biobehav. Rev.* 12:169-175.

Levin, E.D., Wilkerson, A., Jones, J.P., and Christopher, N.C. 1996. Prenatal nicotine effects on memory in rats: Pharmacological and behavioral challenges. *Dev. Brain Res.* 97:207-215.

Levy, A., Kluge, P.B., and Elsmore, T.F. 1983. Radial arm maze performance of mice: Acquisition and atropine effects. *Behav. Neural Biol.* 39:229-240.

McNamara, R.K. and Skelton, R.W. 1991. Diazepam impairs acquisition but not performance in the Morris water maze. *Pharmacol. Biochem. Behav*. 38:651-658.

McNaughton, N. and Morris, R.G. 1987. Chlordiazepoxide, an anxiolytic benzodiazepine, impairs place navigation in rats. *Behav. Brain Res.* 24:39-46.

Mendl, M., Erhard, H.W., Haskell, M., and Wemelsfelder, F. 1997. Experience in substrate-enriched and substrate-impoverished environments affects behaviour of pigs in T-maze task. *Behavior* 134:643-659.

Morris, R.G.M. 1981. Spatial localisation does not depend on the presence of local cues. *Learn. Motiv*. 12:239-260.

Morris, R.G., Garrud, J., Rawlins, N.P., and O'Keefe, J. 1982. Place navigation impaired in rats with hippocampal lesions. *Nature* 297:681-683.

Okaichi, J. and Jarrard, L.E. 1982. Scopolamine impairs performance of a place and cue task in rats. *Behav. Neural Biol.* 35:319-325.

Olton, D.S. and Samuelson, R.J. 1976. Remembrance of places passed: Spatial memory in rats. *Exp. Psychol. [Anim. Behav.]* 2:97-116.

Pitsikas, N., Carli, M., Fidecka, S., and Algeri, S. 1990. Effect of life-long hypocaloric diet on age-related changes in motor and cognitive behavior in a rat population. *Neurobiol. Aging* 11:417-423.

Rapp, P.R., Rosenberg, R.A., and Gallagher, M. 1987. An evaluation of spatial information processing in aged rats. *Behav. Neurosci.* 10:3-12.

Sanchez-Santed, F., de Bruin, J.P.C., Heinsbroek, R.P.W., and Verwer, R.W.H. 1997. Spatial delayed alternation of rats in a T-maze: Effects of neurotoxic lesions of the medial prefrontal cortex and of T-maze rotations. *Behav. Brain Res.* 84:73-79.

Schnurr, R. 1971. Spontaneous alternation in normal and brain-damaged gerbils. *Psychol. Sci.* 25:181-182.

Stevens, R. 1981. Scopolamine impairs spatial maze performance in rats. *Physiol. & Behav.* 27:385-386.

Sutherland, R.J., Whishaw, I.Q., and Regehr, J.C. 1982. Cholinergic receptor blockade impairs spatial localization by use of distal cues in the rat. *J. Comp. Physiol. Psychol.* 96:563-573.

Tolman, E.C. 1925. Purpose and cognition: The determiners of animal learning. *Psychol. Rev.* 32:285-297.

Tolman, E.C., Ritchie, F.B., and Kalish, D. 1946. Studies in spatial learning. I. Orientation and the short cut. *J. Exp. Psychol.* 36:13-24.

Tsien, J.Z., Huerta, P.T., and Tonegawa, S. 1996. The essential role of hippocampal CA1 NMDA receptor-dependent synaptic plasticity in spatial memory. *Cell.* 87:1327-1338.

Walsh, T.J., Miller, D.B., and Dyer, R.S. 1982. Trimethyltin, a selective limbic system neurotoxicant, impairs radial arm maze performance. *Neurobehav. Toxicol. Teratol.* 4:177-183.

Watts, J., Stevens, R., and Clare, R. 1981. Effects of scopolamine on radial maze performance, male rats, implications for hippocampal role in spatial memory. *Physiol. & Behav.* 26:845-851.

Wenk, G.L., Hughey, D., Boundy, V., Kim, A., Walker, L., and Olton, D.S. 1987. Neurotransmitters and memory: The role of cholinergic, serotonergic and noradrenergic systems. *Behav. Neurosci.* 101:325-332.

Wenk, G.L., Markowska, A.L., and Olton, D.S. 1989. Basal forebrain lesions and memory: Alterations in neurotensin, not acetylcholine, may cause amnesia. *Behav. Neurosci.* 103:765-769.

Wenk, G., Sweeney, J., Hughey, D., Carson, J., and Olton, D. 1986. Choline acetyltransferase inhibition does not impair radial maze performance in rats. *Pharmacol. Biochem. Behav.* 25:521-526.

White, S.R. 1974. Atropine, scopolamine and hippocampal lesion effects on alternation performance of rats. *Pharmacol. Biochem. Behav.* 2:297-307.

Key References

Brandeis et al., 1989. See above.

Provides a general review of the many ways the water maze task has been used to study brain function and the general theoretical principles that underlie its use.

Hepler, et al., 1985. See above.

Provides an introduction to the use of the split-stem T maze to determine the effects of specific brain lesions.

Olton, D.S. 1983. The use of animal models to evaluate the effects of neurotoxins on cognitive processes. *Neurobehav. Toxicol. Teratol.* 5:635-640.

This review describes the use of many different behavioral tasks in toxicological studies.

Olton, D.S. 1985. The radial arm maze as a tool in behavioral pharmacology. *Physiol. & Behav.* 40:793-797.

Reviews the many ways in which the radial arm maze task has been and can be used to investigate the effects of lesions or drugs upon the function of specific brain regions.

Richman, C.L., Dember, W.N., and Kim, P. 1986/1987. Spontaneous alternation behavior in animals: A review. *Curr. Psychol. Res. Rev.* 5:358-391.

Provides a general review of the use of the standard T maze to study spontaneous alternation behavior.

Stanton, M.E. 1992. Animal models of cognitive development in neurotoxicology. *In* The Vulnerable Brain and Environmental Risks, Vol. 1: Malnutrition and Hazard Assessment (R.L. Isaacson and K.F. Jenson, eds.) pp. 129-146. Plenum Press, New York.

This review describes the use of many different behavioral tasks in toxicological studies.

Contributed by Gary L. Wenk
University of Arizona
Tucson, Arizona

Advanced Behavioral Testing in Rodents: Assessment of Cognitive Function in Animals

In the risk assessment of a neurotoxic chemical, it may be necessary to characterize its effects on cognitive function in rodents. *Cognitive function* refers generally to the information-processing capacity of an animal and subsumes the more discrete processes of learning, memory, attention, and performance. None of these processes is directly observable, and this fact has two important consequences. First, the existence and characteristics of these processes must be inferred from the behavior of a test subject in a specified test environment. Second, other possible sources of behavior change must be ruled out in order to attribute the behavioral effect of a chemical to a particular process. The experimental analysis of behavior provides the tools to quantify behavior; by proper arrangement of the contingencies of response and reinforcement, and by application of appropriate control procedures, the processes of interest can be specifically assessed.

Learning includes the acquisition or utilization of new behavior to solve a new problem, and is quantified by an appropriate change in behavior over time. Because the reinforcement contingencies that govern behavior change frequently in every day life, and because adaptive responses to these changes challenge the information processing capacities of animals, quantifying the behavioral transitions that occur when environmental conditions change can yield powerful techniques for assessing this cognitive function. Protocols for two procedures, acquisition of reference memory for spatial location (Morris water maze) and acquisition of strategy and use of spatial working memory (radial maze) are presented in *UNIT 11.3*. Two others are presented here: autoshaping a lever-press response (see Basic Protocol 1) and repeated acquisition in the radial maze (see Basic Protocol 2).

Memory implies the control of behavior by antecedent events (stimuli no longer present) and has been subdivided into many types in human psychology. A practical dichotomy distinguishes between *reference memory* (memory for information that remains constant across episodes, e.g., what kind of car you drive) and *working memory* (memory for information that changes across episodes, e.g., where you parked your car today). Of the two, working memory is much more labile and more likely to be impaired by intoxication, aging, and disease. Assessment of working memory can thus provide important information regarding the potential cognitive effects of a neurotoxic agent. Many procedures have been devised for assessing memory, including the radial maze (Fig. 11.3.1) and Morris water maze (Fig. 11.3.2), which are used for assessing spatial working and/or reference memory. This unit provides assessments of working memory in the operant environment with delayed matching to position (see Basic Protocol 3) and of reference memory with two-light visual discrimination (see Support Protocol).

Attention refers to a constellation of hypothetical processes by which the nervous system apprehends and organizes sensory input and generates coordinated behavior. As with memory, many varieties of attention have been described in humans, including selective and sustained attention. Although it has been a subject of psychological investigation since William James' seminal work in the late 1800s, the rigorous assessment of attention in animals has begun only recently. Because many deficits in learning and memory may arise from impaired attending to relevant events, it is important to probe for attentional dysfunction as a primary response to chemical intoxication. Visual signal detection (see Basic Protocol 4) is presented here for this purpose.

Performance refers to the pattern(s) of behavior engendered by specific environmental contingencies, usually described in terms of operant *schedules of reinforcement*. The most

Contributed by Philip J. Bushnell
Current Protocols in Toxicology (1999) 11.4.1-11.4.34

common schedules involve ratios (e.g., ten responses yields a food pellet) or intervals (e.g., the first response after 30 sec yields food). These contingencies yield characteristic temporal patterns of behavior that are consistent across a very wide variety of animal species. These schedules may also be combined in various ways: for example, a multiple schedule presents two or more simple schedules sequentially in a test session, with each schedule identified to the subject by a unique stimulus condition. Operant schedules are used primarily to assess performance baselines (i.e., does a chemical interfere with the expression of the behavior pattern engendered by that schedule) without attribution to any particular cognitive process. These schedules also provide powerful tools for the manipulation of behavior for application in other contexts (e.g., the acquisition of a fixed-interval schedule may be used to assess learning). One common performance baseline, the multiple fixed-interval/fixed-ratio (MULT FI/FR) schedule, is presented here (see Basic Protocol 5).

STRATEGIC PLANNING

Assessments of cognitive function are time consuming because they involve training animals to perform complex tasks under carefully controlled conditions. The benefits from this effort include the ability to specify the cognitive process(es) assessed by the procedure, to quantify the effect(s) of a chemical, and to document the time course of onset and recovery from intoxication. Although a good cognitive test will reduce the possibility that differences in test performance result from sensory or motor dysfunction, one should keep in mind that neurotoxic chemicals are more likely than drugs to exert multiple effects on the nervous system, and ancillary tests for noncognitive sources of altered behavior (e.g., sensory dysfunction or motor impairment) may also be necessary.

Generally, tests of cognitive function have not been applied during initial screening of novel compounds with unknown toxicity and mode of action, but are more likely be used to characterize the hazard of a compound in terms of dose-effect or dose-response relationships. In this case, some information about the neural substrate for the toxicity of a chemical should be available, and reasonably specific hypotheses about its potential effects may be generated. These hypotheses should enable one to specify, before training begins, the endpoints (i.e., specific measurements of behavior) that will constitute the critical dependent variables of the experiment. These measurements may be obtained during acquisition of a task, during parametric manipulations after the animals have reached asymptotic performance levels, or during challenges with psychoactive drugs.

This variety of endpoints is available from procedures that yield a trained animal whose behavior can be measured repeatedly. This “baseline approach” allows one to document the time course of onset, duration, and recovery from intoxication by monitoring the performance of the animal in daily tests before and after administration of the toxicant. It also permits the use of powerful within-subject statistical tests, because each animal can serve as its own control, defined by its pretreatment baseline performance.

Alternatively, the stages of training and/or criterion performance can be used to assess the effects of prior treatment from, for example, prenatal exposure to a neurotoxic agent. Tests of differences in cognitive function can then be made across groups of animals trained together identically, as long as criteria for acquisition are defined prior to training, and training is continued until each criterion is reached. Failure to reach criterion by a treated group at any stage of training, or retarded acquisition of the criterion, will indicate a learning deficit.

The number of animals required per group for an experiment will depend upon the consistency with which behavior can be controlled by the procedure, the consistency of the effect of the chemical of interest, and the magnitude of the expected effect. To

demonstrate the properties of a conditioned behavior and the capacity of an animal to perform a task, two or even one animal may be sufficient. For toxicology studies, sample sizes of eight rats per condition are generally sufficient for assessing the effects of chemicals on behaviors that have been conditioned to a baseline, including most of the protocols described here. More animals will be required for autoshaping, which involves acquisition of a new response (pressing a lever) for food. This is because of the weak response-reinforcer relationship that is characteristic of autoshaping and the consequent high variability in the number of trials necessary to elicit the response.

Animals of either sex may be conditioned using the methods described here. When it is possible to do so, including both sexes in an experiment can provide important information regarding sex differences that may emerge from close analysis of the results. For example, compared to males, female rats tend to freeze less in mazes, to acquire autoshaping responses more slowly, and to perform some signal-detection tasks less accurately. In addition, gender-specific effects of chemicals may arise (e.g., with endocrine-disrupting chemicals such as the polychlorinated biphenyls), which cannot be determined without assessment of the behavior of both sexes.

ASSESSMENT OF LEARNING: AUTOSHAPING THE LEVER-PRESS RESPONSE

BASIC PROTOCOL 1

Autoshaping refers to a procedure by which a subject is automatically shaped (i.e., "autoshaped") to a emit a criterion response to a specified manipulandum. This protocol describes a method to train a rat to press a retractable lever for food. It thereby satisfies two needs: providing a systematic, objective means to quantify acquisition of the lever-press as an operant response, and preparing the rat for learning and performing other operant tasks. With this rapid method, useful data regarding learning can be obtained in just a few days of training.

Materials

Subject rats
Precision food pellets: 45 mg for male rats, 37 mg for females (BioServ or PJ Noyes)

Operant conditioning chamber (Fig. 11.4.1; e.g., Coulbourn Instruments, MED Associates, CeNeS, or TSE Systems) including:
- Incandescent house light (~0.1 W)
- Loudspeaker for white noise
- Food cup that can be lighted from within
- Cue light: LED or incandescent bulb behind a clear lens (if using an incandescent bulb, use a glass jewel dome in front of the bulb rather than plastic, as it cannot be gnawed down by the animal)
- Retractable response lever

Pellet dispenser
Computer system and interface to control test environments and stimuli and to collect response data (see Commentary)

Set up equipment

1. Set up one or more standard operant conditioning chambers as shown in Figure 11.4.1.
2. In each chamber, place an incandescent house light (~0.1 W) and a loudspeaker at the top of the panel. Place a food cup in the center of the front wall with the lower edge of its opening positioned 1 to 2 cm above the floor of the chamber.

   Use a food cup that can be lit from within and can detect "nosepokes" (i.e., insertion of the rat's nose or paws into the cup) by means, for example, of a photobeam or a hinged door and microswitch.

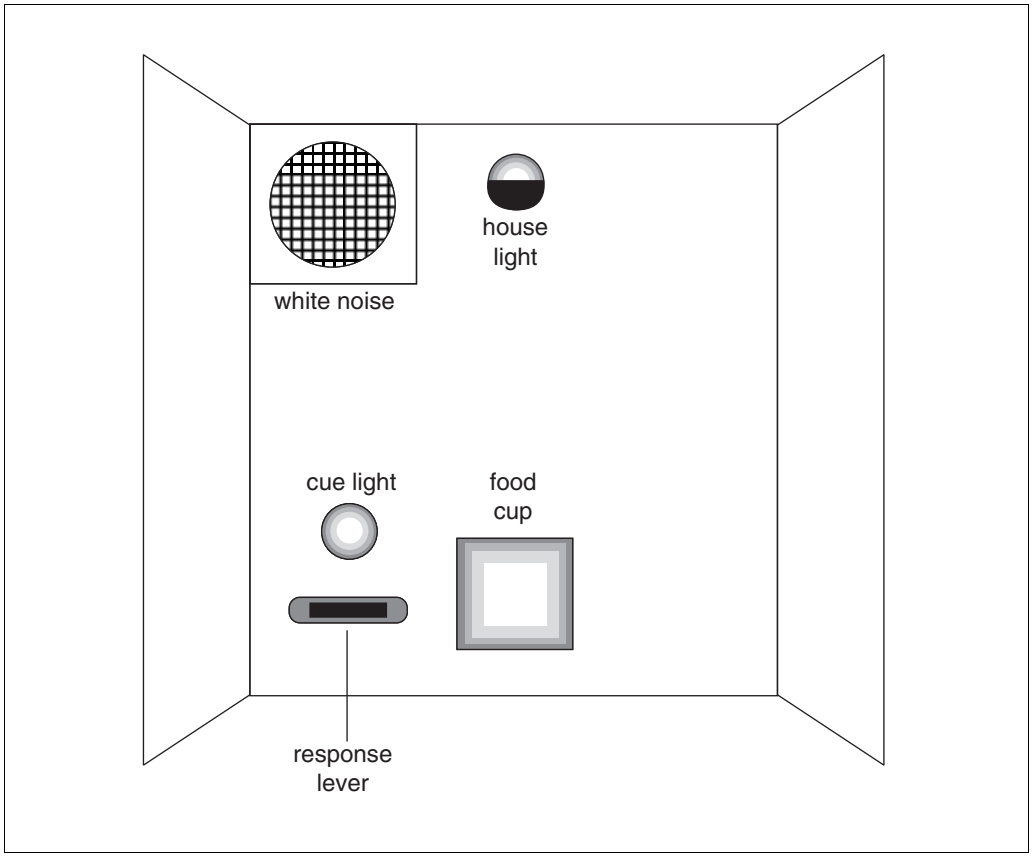

Figure 11.4.1 Configuration of an operant test chamber for autoshaping and multiple fixed-interval/fixed-ratio responding. Only the front panel of the chamber is shown. The response lever must be retractable for autoshaping but need not be for free operant studies. White noise is produced through a loudspeaker. The house light has a shade on its lower side, thus illuminating the chamber by reflecting light from the ceiling. The food cup should be illuminable from within, to indicate the presence of food.

3. Connect a pellet dispenser for delivering precision food pellets (45 mg for male rats, 37 mg for females) to the back of the food cup with clear plastic tubing. Install a retractable response lever to one side of the food cup, and a cue light immediately above the lever.

   If two or more chambers are to be used, it is good practice to set up half the chambers with the cue light and lever on the right side of the food cup and the other half with the cue light and lever on the left side of the food cup.

   In general, it helps to generate a low background level (~65 dB) of white noise through the loudspeaker or with a ventilation fan. In addition, one should provide unique stimulus conditions for the test session (e.g., illumination of the house light), the availability of food (e.g., brief illumination of the food cup or sounding of a quiet but audible tone), and for incorrect responding (e.g., a short period of darkness or an appropriate auditory cue).

Perform preliminary training

4. Establish motivation for appetitive reinforcement by keeping animals hungry on a limited diet. Begin food restriction one week prior to food cup training and continue throughout the entire study (see Critical Parameters, discussion of motivation).

5. Identify each animal uniquely (e.g., by tattoo, ear tag, tail marking, or implanted magnetic tracking device).

   If indelible markers are used to inscribe a number on the animal's tail, these must be refreshed weekly. Marking and remarking the tails can be incorporated into the handling/acclimation procedures.

6. Acclimate animals to handling for one week prior to food cup training (see *UNIT 11.3* for advice on animal handling).
7. Give the animal a few of the food pellets that will be used as reinforcers in its home cage for a few days prior to food cup training.

   This avoids the rats' natural hesitation to accept novel food (bait shyness).
8. Expose animals to test equipment, including any transfer cages that might be used to deliver the animals from their home cages to the test cages. Give the animals a day or two to acclimate to transfer cages and to the location where they will wait while others are being tested.

   The acclimation to food pellets should be done in this venue as well.

Perform food cup training

9. Day 1. Place the animal in the test chamber with a counted number of food pellets (~20) in the food cup. If the food cup has a door, prop it open on the first day. Illuminate the food cup light, and allow 20 min for the animal to consume the food and explore the chamber. Remove the animal and count the pellets remaining in the food cup. Repeat once or twice per day until all pellets are consumed.
10. Day 2. Repeat step 9 with the food cup door closed.

    If the food cup has no door, skip this step.
11. Day 3. Deliver pellets individually at random irregular intervals of ~30 sec (range, 17 to 45 sec). Illuminate the food cup at the time of pellet delivery. Measure the latency between each pellet delivery and the rat's entry into the food cup, and extinguish the light when the rat retrieves the pellet. When the latency is consistently fast (e.g., five consecutive entries with a latency ≤2 sec), food cup training is complete. Administer a maximum of 50 trials per daily session.

    Typically, 1 to 3 sessions will be needed.

Perform tests of autoshaping

12. As soon as food cup training has been completed, either in the same test session (Day 3) or in the next (Day 4), begin inserting the response lever into the chamber during each trial. Extend the response lever into the chamber and illuminate the cue light 15 sec prior to delivering each food pellet, after a variable time interval (starting with delivery of the previous pellet) ranging from 2 to 60 sec and averaging 30 sec.

    If the criterion response occurs (i.e., the rat presses the lever with sufficient force to trip the microswitch) during this 15-sec period, retract the lever, turn off the cue light, and deliver a food pellet immediately. If the criterion response does not occur, deliver a food pellet at the end of the 15-sec period, while simultaneously retracting the lever and extinguishing the cue light. In either case, illuminate the food cup light for 2 sec each time a pellet is delivered. Perform a maximum of 50 trials per daily session.
13. Repeat step 12 for up to four additional daily sessions.

Analyze data

14. Divide each 50-trial test session into five 10-trial blocks. Count the number of trials in each block during which a lever-press response occurs. Measure the response latency (the time between insertion of the lever and detection of the response) if a measure of response speed is desired.

    Acquisition of the response will be seen as an increase in the frequency of responses detected per block and a decrease in response latency across the five blocks of trials in a session.

    During autoshaping, animals will engage in responses to the source of the food (i.e., exploring the food cup, called "goal tracking") and responses to the signal that food

delivery is imminent (i.e., exploring the lever, called "sign tracking"; Schwartz and Gamzu, 1977). Thus, an ancillary measure of goal tracking can be obtained as the frequency of nosepokes (i.e., entries into the food cup) during presentation of the lever in each trial. Typically, rats will engage in goal tracking early during autoshaping and then shift to sign tracking, seen as a shift in responding from the food cup to the lever.

If autoshaping is used to prepare animals for further study, rats that do not press the lever after four sessions may be trained to do so by either of two methods. First, pellet delivery can simply be made contingent upon a response: extend and retract the lever as before, but do not deliver food upon its retraction if the criterion response does not occur. Frequently, the frustration engendered by unexpected nonreinforcement will induce the animals to explore the lever more vigorously and thus obtain food by pressing it. In rare cases, it may be necessary to leave the animal in the chamber overnight with the lever-press-food contingency in effect. (Be sure to provide water.) Failing this, the animal may be shaped by hand by the method of successive approximations (see Troubleshooting).

An alternative to the systematic pairing of the movement of a retractable lever and food delivery during a series of daily tests, as described above, involves placing the animal in an operant chamber with a nonretracting response lever for one or two long sessions (e.g., overnight). This approach relies on the normal exploratory activity of the animal to bring it into contact with the lever and with the contingent delivery of food when the lever is pressed. High success rates have been reported with this method (e.g., Van Haaren et al., 1987). Acquisition of the response can be followed by dividing the session into successive time bins. The advantages of this approach are its simplicity and high success rate. These are balanced by the need to supply water in the chamber and the fact that training a large number of animals will still require either a large number of chambers or several sequential sessions; the overall savings in time and effort may thus not be significant.

BASIC PROTOCOL 2

ASSESSMENT OF LEARNING: REPEATED ACQUISITION IN THE RADIAL MAZE

Repeated acquisition refers to a family of methods for assessing learning in which the subject first learns a rule or strategy to solve a problem and is then given a series of problems that s/he must solve. The rate of increase and asymptotic level of accuracy with which each solution is acquired provide an assessment of learning. This method resembles many situations in daily life; for example, a student in a math class learns rules of calculus and then uses them to solve differential equations. The present method capitalizes upon rats' foraging strategies, in this case quantified in terms of food-seeking behavior in the radial maze. The rat is first trained to seek food efficiently in the maze (*UNIT 11.3*) and then is given a series of daily problems to solve. These problems are defined by the location of food: a different subset of the arms of the maze is baited each day, and the rat is given a series of trials in the maze during which it learns which arms contain food that day.

Materials

Subject rats

Reinforcers for manual system: any cereal- or sugar-based foodstuff that can be delivered in small, reproducible quantities; pieces of breakfast cereal are frequently used (e.g., ¼ of a Froot Loop)

Reinforcers for automated system: precision food pellets, 45 mg for male rats, 37 mg for females (BioServ or PJ Noyes)

Radial arm maze, manual or automated (*UNIT 11.3*; Coulbourn Instruments, MED Associates, or TSE Systems)

Stopwatch (for manual system)

Food pellet dispensers (one at end of each arm for automated system)

Perform preliminary training

1. Train rats in a radial arm maze according to the basic working memory protocol (*UNIT 11.3*).

The materials differ depending upon whether a manually operated maze or an automated maze is to be used. Manual mazes are much cheaper and can be constructed from plywood, sheet metal, and paint, but require labor-intensive operation by a trained observer. Automated mazes rely upon computers to control stimulus conditions, pellet delivery, and recording of the rats' behavior (see Commentary for a fuller discussion of this trade-off). In either case, the experiment requires a radial maze with a minimum of eight identical arms and a set of doors that will confine the rat to the central arena. See UNIT 11.3 and Figure 11.3.1 for further details regarding the dimensions and layout of an appropriate maze.

For manual systems, all data must be recorded on data sheets. For automated systems, programs must be written to control timing of trials, stimulus conditions, and recording of arm-choice sequences. See Commentary for information regarding computer systems and interfaces to control the test environments and stimuli and to collect response data.

2. After the behavior of the rats has stabilized, begin providing multiple trials each day for each rat. Increase the number of trials per session by two each day until the rats perform eight trials in a session.

Perform tests of repeated acquisition

3. Repeat step 2, but instead of baiting all eight arms, select a subset of four arms randomly from the list of all possible subsets. Use this same subset for all trials in a given day, but vary the subset randomly from day to day. Terminate each trial when either all four reinforcers have been obtained or after ten choices have been made with fewer than four reinforcers obtained. Confine the rat to the central arena for an intertrial interval (ITI) of ≥ 10 sec.

   Each day the rat will obtain food only for entering the four baited arms, and not for entering the four unbaited arms. Because a different set is baited each day, the rat has to learn which arms are baited in each session, and its learning ability can be assessed repeatedly (from session to session).

   It is necesssary to run enough trials so that the error frequency for the slowest animal reaches a constant level before the end of the session. Start with about eight trials for each animal each session. The actual number will be determined by the rate at which errors decline to an asymptote of fewer than one error per trial (see Critical Parameters and see Anticipated Results).

4. Record the sequence of arm entries on each trial and whether food was obtained. Count initial entries into baited arms as correct and count entries into unbaited arms as errors.

   Learning each day's problem will be evident as a within-session reduction in error frequency. In other words, on trial 1 of each session, the rat has no information regarding which arms are baited and will be expected to make four errors (i.e., enter all eight arms to find the four with food). The number of errors should decline monotonically across trials in each session, reaching an asymptote of one error or fewer within five trials (see Anticipated Results). A baseline of consistent within-session error reduction should be achieved within 15 daily sessions (3 weeks at 5 sessions per week).

   Note that errors may also include reentries into an arm that was previously baited on that trial as well as reentries into arms that are in the unbaited set for that session. Information regarding these error types may be helpful in interpreting changes in behavior in this task; interpretation of these error types is discussed in Bushnell and Angell (1992).

ASSESSMENT OF WORKING MEMORY: DELAYED MATCHING TO POSITION

BASIC PROTOCOL 3

Working memory refers to the process engaged by remembering information that changes frequently (e.g., where you parked your car today) rather than information that remains constant for long periods of time (what kind of car you drive). Working memory is particularly relevant to toxicology because of its sensitivity to disruption by fatigue, drugs, aging, disease, and intoxication. Delayed matching to position (DMTP) is a type of

delayed-response task that is suitable for testing working memory in rats. In contrast to the radial maze, where spatial aspects of working memory are emphasized, the operant environment emphasizes temporal aspects of the process. Thus, forgetting occurs relatively quickly (e.g., within ~1 min) in operant tests and a complete retention gradient, or "forgetting function," can be generated for each subject in each daily test session. In contrast, forgetting requires hours in the radial maze.

The basic strategy for assessing working memory involves four steps: (1) present the subject with a bit of information to remember (sample); (2) remove it and wait a variable period of time (delay); (3) present that same bit of information with one or more other bits; and (4) reinforce the subject for choosing the bit that had been presented prior to the delay (choice). Choice accuracy can be reduced by increasing the number and similarity of the bits of information, the number of times the choice is repeated (trials), and most importantly the delay between sample and choice. Just two information bits are used in DMTP: the locations of two otherwise identical retractable levers mounted on one wall of an operant chamber. Finally, it is necessary to prevent the rat from simply waiting near the sample lever during the delay, to force it to choose between the two levers when they are inserted after the delay. For this purpose, the rat is trained to emit a specific delay behavior (repetitive responding into the food cup).

DMTP involves four component behaviors that must be trained in sequence: sample response, delay behavior, choice response, and food retrieval. The basic strategy involves training the terminal response (food retrieval) first and building the chain in reverse order. These steps, criteria for advancement, and the expected number of training sessions are outlined in Table 11.4.1.

Materials

Subject rats
Precision food pellets: 45 mg for male rats, 37 mg for females (BioServ or PJ Noyes)
Operant conditioning chamber (Fig. 11.4.2; e.g., Coulbourn Instruments, MED Associates, or CeNeS, or TSE Systems) including:
  Incandescent house light (~0.1 W)
  Loudspeaker for white noise
  Food cup that can be lighted from within
  Cue light: LED or incandescent bulb behind a clear lens (if using an incandescent bulb, use a glass jewel dome in front of the bulb rather than plastic, as it cannot be gnawed down by the animal)
  Two retractable response levers
Pellet dispenser
Computer system and interface to control test environments and stimuli and to collect response data (see Commentary)

Set up equipment

1. Set up equipment as for the lever-press response (see Basic Protocol 1, steps 1 to 3). In addition, mount a second retractable lever on the other side of the front wall of the test chamber (Fig. 11.4.2). Initially, center the food cup between the levers; however, design (or modify) the chamber to permit the food cup and pellet dispenser to be moved to the opposite wall part way through training.

   This latter arrangement physically separates the food cup from the choice levers, thereby reducing the effectiveness of behavioral mediating responses to bridge the delay (see Background Information). Because the animals will be earning a large proportion of their total food intake in the test environment in performing this task, be sure to use nutritionally complete food pellets as reinforcers.

Table 11.4.1 Sequence of Steps for DMTP Training

Protocol, step[a]	Procedure	Parameters	Criterion[b]	Sessions[c]
1, 1-3	Set up equipment			
1, 4-8	Preliminary training			
1, 9	Food cup 1	Food cup door open	Eat all pellets	1
1, 10	Food cup 2	Food cup door closed	Eat all pellets	1
1, 11	Food cup 3	Intermittent pellets	5 consecutive trials with latency[d] <3 sec	1
1, 12-13	Autoshape	Right lever	50 lever presses	4
	Hand shape[e]	Right lever	50 lever presses	1
3, 3	Continuous rft[f]	Right lever	50 right lever presses	1
		Left lever	50 left lever presses	1
3, 4-5	Anti-bias/delay behavior	Food cup front, 1 nosepoke[g]	100 trials	1
3, 6	Anti-bias/delay behavior	Food cup rear, 1 nosepoke	100 trials	5
3, 7	Anti-bias/delay behavior	Food cup rear, 2 nosepokes	100 trials	2
		Food cup rear, nosepoke (VI 2s)[h]	100 trials	5
3, 8	Position match	Max delay[i] 0 sec	≥80% correct	10
3, 9	Position match	Max delay 2 sec	≥80% correct at shortest delay	5
		Max delay 5 sec	≥80% correct at shortest delay	5
		Max delay 10 sec	≥80% correct at shortest delay	5
		Max delay 20 sec	≥80% correct at shortest delay	5

[a]Steps indicated for Basic Protocols 1 and 3.
[b]Criterion for advancing to the next step of training.
[c]Approximate number of sessions to expect for each training step.
[d]Latency to retrieve food pellet from food cup.
[e]If necessary, for rats that do not press the lever at the end of four sessions of autoshaping (see Troubleshooting).
[f]Rft, reinforcement. Continuous rft is equivalent to an FR1 (one response per reinforcer).
[g]Nosepoke refers to opening the food cup door.
[h]VI 2s, variable interval 2-sec. Multiple nosepokes during delay; first nosepoke after 2 sec ends delay and causes levers to insert for choice response.
[i]Maximum time between sample response and end of delay interval. As this value increases, keep shorter delays in the list; use five delay values in final schedule.

Establish food retrieval

2. Perform preliminary and food cup training as described for the lever-press response (see Basic Protocol 1, steps 4 to 12).

Establish sample response

3. Autoshape the lever-press response using one of the levers and its adjacent cue light (see Basic Protocol 1, step 13). Train the animals to press each lever for food, and ensure that they will press either lever when the two are inserted together into the chamber with illumination of their respective cue lights. Set the intertrial interval (ITI) to 10 sec. Use a choice criterion of at least one 100-trial session without a strong preference for either lever.

At this point, either choice is reinforced, as there is no basis for determining which response is "correct." Under these conditions, side preferences (or biases) must be discouraged to prevent their disruptive influence later in the study. One way to accomplish this is to present both levers together on a series of trials and count the number of times each is pressed. If the number of responses on one lever exceeds the number on the other by some criterion ratio (e.g., 60%) after five trials, insert only the other, nonpreferred lever until the ratio of

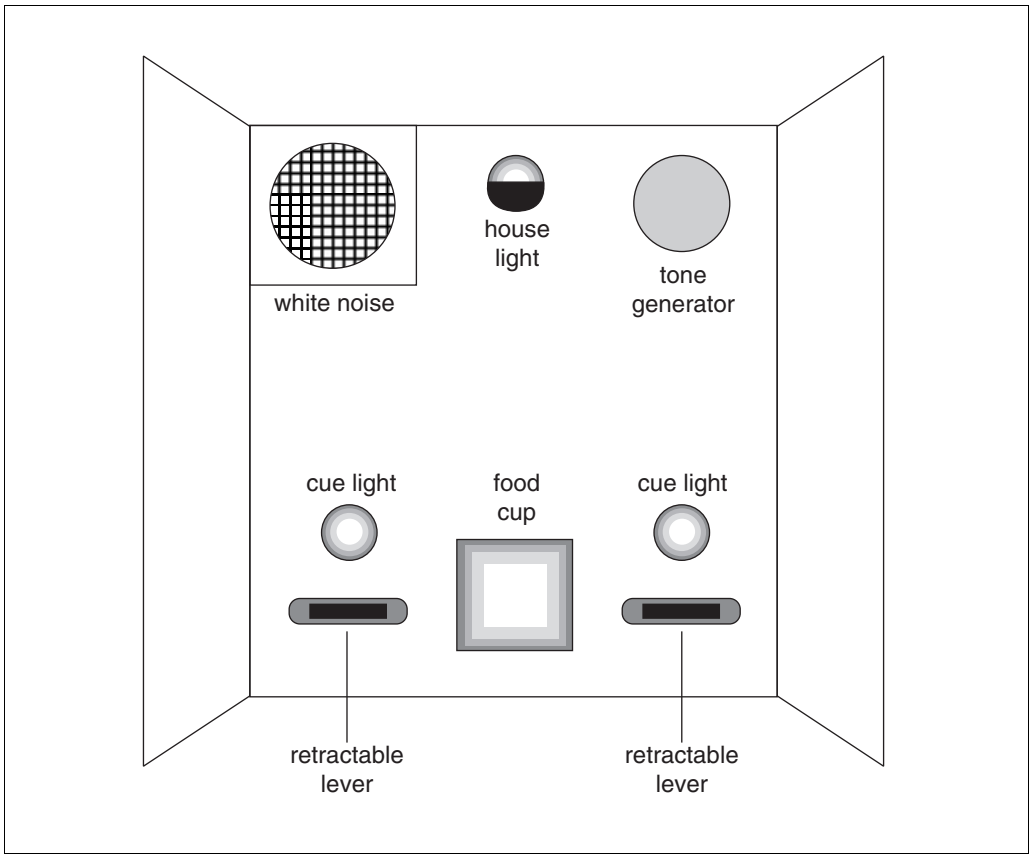

Figure 11.4.2 Configuration of an operant test chamber for delayed matching to position and visual discrimination. Only the front panel of the chamber is shown. In addition to the fixtures in Figure 11.4.1, a second retractable lever and cue light are necessary, and a tone generator is used to provide feedback for each effective nosepoke in the food cup. Early in training, the food cup should be moved to the rear wall of the chamber, to physically remove the rat from the locations of the two possible choice responses.

responses to the two levers falls below the criterion, and then insert both levers on the next trial. The delay behavior (step 4, below) can be introduced while position biases are being minimized.

Establish delay behavior

4. With the food cup between the two levers, begin each trial by turning on the food cup light, and require the rat to initiate each trial with a nosepoke into the food cup.

   Because this light has previously signaled the availability of food, the rat will open the food cup door (if there is one) or poke its nose into the cup looking for food.

5. When a nosepoke occurs, insert both levers into the chamber and reinforce a press on either one. Maintain the anti-bias contingencies of step 3. Use a criterion of at least 100 trials with a bias <60% in one 30-min session.

6. Move the food cup to the center of the rear wall of the chamber and repeat steps 4 and 5.

   Moving the food cup will disrupt performance considerably, as the rat has to relearn the physical relationships among the stimuli and manipulanda. It should be done early in training, before the rat's behavior has become strongly conditioned to the original configuration of the test environment.

7. Repeat steps 4 and 5 but require the rat to emit multiple nosepokes to initiate a trial.

   A fixed-ratio schedule (e.g., n nosepokes per trial initiation) will suffice at this point; however, a variable-interval (VI) schedule will eventually be necessary. A low ratio (e.g., 5) or short interval (e.g., 2 sec) is adequate at this time.

Delay behavior has now been established. During the delay, the rat will be kept busy making nosepokes into the food cup, and cannot simply wait near the sample lever during the delay and make its choice at the end of the delay. Note, however, that behavioral mediating strategies (analogs of rehearsal in humans) cannot be completely eliminated in memory tasks. Some rats will traverse the chamber repeatedly during the delay, returning to the location of the levers and attempting to press them in the retracted position between nosepoke responses in the food cup. If this is a concern, it will be necessary to count these "delay presses" to determine whether their frequency and location are related to the accuracy of choice at the end of the delay. Whereas mediating responses were shown long ago to affect choice accuracy in memory tasks, one study of DMTP suggested that rats do not use them effectively to increase accuracy (Bushnell, 1988).

Establish choice response

8. At the beginning of each trial, randomly select one lever as the sample and insert it into the chamber. When the rat presses it, retract it and turn on the food cup light. When the rat completes its nosepoke response requirement, insert both levers. Retract both levers when one is pressed. Reinforce with food when a matching response is made (i.e., when the rat presses on the same lever that was inserted as the sample at the beginning of that trial). If the rat presses the other lever, turn off the house light for 2 sec and do not deliver food (time out [TO]). Administer correction trials during this phase of training by presenting the same sample after each incorrect response up to a set maximum (usually 3).

   This contingency defines the matching rule as the correct response. The nonmatching rule can also be trained (i.e., reinforce each choice response to the lever not inserted as the sample on that trial). Both rules work for this task, though they differ slightly in rate of acquisition, variability of accuracy at asymptote, and sensitivity to drugs (Dunnett et al., 1989).

   Correction trials facilitate the acquisition of the matching rule by reducing the likelihood that the animal will adopt a position habit, responding only on one choice lever and accepting the 50% reinforcement rate yielded by that strategy. If three correction trials are given sequentially (i.e., the rat has made four consecutive errors), force the correct response on the next trial by withholding the incorrect choice lever. Then begin a new trial by selecting the next sample lever randomly.

   Note that correction trials should not be included in the computations of performance, as they will affect calculations of accuracy. Count correction trials and forced-choice trials separately.

Establish the retention gradient

9. Gradually increase the duration of the delay between sample and choice responses. Intermix several delay values (at least three, preferably five) during each session, ranging from essentially zero (a single nosepoke is required to terminate the delay) to a maximum of 20 or 30 sec. Select, randomly and without replacement, a value for each trial from a list, and repeat selection from the list of values 15 to 20 times during a session (e.g., if five delay values are used, each value will be used 20 times in a 100-trial session).

   For the purpose of programming the contingencies governing delay behavior (nosepoking), it is convenient to think of the list of delay values as a list of intervals in a variable-interval (VI) schedule. Thus, the nosepoke becomes the operant response for this VI schedule, the termination of which results in the opportunity to press a lever for food (rather than in food delivery). A VI schedule will engender a low, steady rate of responding. If the rate is too low, a minimum interresponse time can be imposed (e.g., a trial can be terminated if successive nosepokes are spaced >3 sec apart).

   Accuracy of choice will decline with increasing delay, revealing a retention gradient or forgetting function. The more delay values that are presented in an unpredictable sequence in each test session, the less accurately the subject can anticipate the delay length on a

given trial, increasing the reliability and consistency of the gradient obtained. That is, with just two values, the subject will learn to expect either a short or a long delay and will engage in mediating behavior appropriate to the delay. With a large number of values, the specific delay will be difficult to anticipate and thus engender less effective mediating strategies. Five delays provides a useable compromise between the theoretical optimum of an infinite number of delays and the practical optimum of two delays.

SUPPORT PROTOCOL

ASSESSMENT OF REFERENCE MEMORY: TWO-LIGHT VISUAL DISCRIMINATION

Basic Protocol 3 yields a rigorous test of working memory, yet performance of this task also requires sensory, motor, and motivational competence. A treatment that affects one of these non-mnemonic processes may impair performance of the DMTP task. One way to determine whether this impairment is due to a failure of working memory involves a test that requires all of the components of the DMTP task except working memory. This support protocol describes a test of reference memory that requires the same four component behaviors as DMTP (i.e., sample response, delay behavior, choice response, and food retrieval) trained in the same sequence. However, because the cue light *always* predicts the correct response, accuracy in this task depends upon reference memory for a cue light rather than working memory for the location of the sample lever.

Additional Materials *(also see Basic Protocol 3)*

Tone generator (e.g., Sonalert)

Perform training steps

1. Set up equipment as described for DMTP (see Basic Protocol 3, step 1).
2. Establish food retrieval, choice response, and delay behavior as described (see Basic Protocol 3, steps 2 to 6), but turn on the cue light over the sample lever at the beginning of each trial and again over the correct choice lever after the delay. Continue training until the rat initiates trials with a single nosepoke into the food cup, with the cup at the rear of the test chamber, and presses either lever with equal frequency.

Establish cue discrimination

3. At the beginning of each trial, randomly select one lever as correct and turn on the cue light above it for 2 sec prior to insertion of both levers. Reinforce a press on the lit lever with food and punish a response on the unlit lever with a TO (see Basic Protocol 3, step 8). Use a criterion for advancement of 90% correct responses to the lit lever.

   This 2-sec "cue-light advance" facilitates acquisition of cue discrimination, especially in male rats.

4. To increase the nosepoke requirement, extend the duration of the period during which the rat must make nosepokes from a single response to 5 sec.
5. Shorten the cue-light advance in stages, while maintaining accuracy at 90% or better.

   With female rats, this advance may be reduced to zero, but it may be necessary to keep it at ~1 sec to maintain criterion accuracy in males.

Establish choice response

6. Establish the sample response as for DMTP (see Basic Protocol 3, step 8) with the following exceptions.

   a. Illuminate the cue light over the sample lever while it is extended into the chamber, and extinguish it when the lever is retracted after being pressed.

b. At the end of the delay period, select one of the levers randomly as the correct lever and illuminate the cue light above it.
c. Reinforce a press on the lit lever with food, and punish a response on the unlit lever with a time out. Use a criterion for advancement of 90% correct responses to the lit lever.

The accuracy of this discrimination can be adjusted by varying the duration of the cue-light advance and/or the duration of the cue itself during the choice phase of the trial. Female rats are less sensitive to the cue-light advance, as their response latencies tend to be longer than those of the males, who tend to respond ballistically to the first lever they encounter, regardless of the cue light.

Test sessions can be run with intermixing matching and discrimination trials (e.g., Bushnell et al., 1991) or in separate test sessions or even in different rats.

7. Extend the delay interval (see Basic Protocol 3, step 9).

To make the discrimination task procedurally homologous with the matching task in Basic Protocol 3, the delay interval must be extended on a schedule identical to that used in the matching task. Thus, the only difference between the tasks will be that the discrimination task can be solved using reference memory (the cue light always indicates the correct response), whereas solution of the matching task requires working memory (the lever that is presented as the sample changes on each trial).

ASSESSMENT OF SUSTAINED ATTENTION: VISUAL SIGNAL DETECTION

BASIC PROTOCOL 4

Sustained attention refers to process(es) involved in reporting unpredictable signal events that occur repeatedly over long periods of time. The simplest methods require only that the subject make a response whenever a signal event occurs. However, these methods tend to generate high levels of false-positive responses (false alarms), which seriously complicate interpretation of correct detections (hits). The present method provides control over the rate of false alarms by using a discrete-trial, choice test format in which the rat must report, by pressing one of two levers, whether a signal did or did not occur in a variable, antecedent time interval. The subject must "pay attention" during this time interval to detect the signal reliably. In addition, the strength of the signal is varied within each session to provide a stable response baseline and a control for sensory dysfunction (see below). Finally, the attentional load is increased by making the time interval between signals long and highly variable. A summary of the training steps is outlined in Table 11.4.2.

NOTE: The term signal (as opposed to cue) is used in this protocol to be consistent conceptually with a large literature on signal detection methods and theory. A signal and a cue may be identical physical events; however, these stimuli are typically called cues in the discrimination learning literature and signals in the signal detection literature.

Materials

Subject rats

Precision food pellets: 45 mg for male rats, 37 mg for females (BioServ or PJ Noyes)

Operant conditioning chamber (Fig. 11.4.3; e.g., Coulbourn Instruments, MED Associates, or CeNeS, or TSE Systems) including:
- Incandescent house light (~0.1 W)
- Loudspeaker for white noise
- Food cup that can be lighted from within
- Signal light: LED or incandescent bulb behind a clear lens (if using an incandescent bulb, use a glass jewel dome in front of the bulb rather than plastic, as it cannot be gnawed down by the animal)
- Retractable levers

Pellet dispenser
Clear plastic tubing with inner diameter large enough to accommodate food pellets
Computer system and interface to control test environments and stimuli and to collect response data (see Commentary)

Set up equipment

1. Set up the equipment required for autoshaping (see Basic Protocol 1, steps 1 to 3), but install a second retractable lever in each operant chamber on the same wall as the

Table 11.4.2 Sequence of Steps for Sustained Attention Training

Protocol, step[a]	Procedure	Parameters	Criterion[b]	Sessions[c]
1, 1-3	Set up equipment			
1, 4-8	Preliminary training			
1, 9	Food cup 1	Food cup door open	Eat all pellets	1
1, 10	Food cup 2	Food cup door closed	Eat all pellets	1
1, 11	Food cup 3	Intermittent pellets	5 consecutive trials with latency[d] <3 sec	1
1, 12-13	Autoshape	Right lever	50 lever presses	4
	Hand shape[e]	Right lever	50 lever presses	1
1, 13	Continuous rft[f]	Signal lever	50 signal lever presses	1
4, 3	Continuous rft	Blank lever	50 blank lever presses	1
4, 4	Discrimination training	Correction trials: presignal interval[g] 10 sec, signal light above signal lever, signal duration 2 sec, signal advance[h] 2 sec, trials 100 → 240[i]	≥80% correct	15
4, 5	Discrimination training	Remove correction trials	≥80% correct	1
4, 6	Discrimination training	Signal advance 1 sec, signal duration 1 sec	≥80% correct	3
4, 7	Discrimination training	Turn off signal before lever insertion	≥80% correct	3
4, 8	Discrimination training	Signal above food cup	≥80% correct	6
4, 9	Signal detection	Postsignal interval[j]→ 2, 3, or 4 sec	≥80% correct	6
4, 10	Signal detection	Presignal interval → variable 7 sec	≥80% correct	8
4, 11	Signal detection	Signal intensities → variable	≥80% at highest signal	5
4, 12	Signal detection	Signal duration → 0.3 sec	≥80% at highest signal	10
4, 13	Signal detection	Increase background light level	≥80% at highest signal, ≤20% at lowest signal	5

[a]Steps indicated for Basic Protocols 1 and 4.

[b]Criterion for advancing to the next step of training.

[c]Approximate number of sessions to expect for each training step.

[d]Latency to retrieve food pellet from food cup.

[e]If necessary, for rats that do not press the lever at the end of four sessions of autoshaping (see Troubleshooting).

[f]Rft, reinforcement. Continuous rft is equivalent to an FR1 (one response per reinforcer).

[g]Presignal interval is equivalent to intertrial interval (ITI) at this point. Use a constant value until step 10.

[h]Signal advance is the time between onset of signal and insertion of levers. When signal advance = signal duration, the signal should be turned off when the levers are inserted.

[i]Gradually increase the number of trials from 100 to 240 during this phase.

[j]When the signal advance exceeds signal duration, the signal is turned off before the levers are inserted. Gradually lengthen the signal advance up to 3 sec, then introduce the variable signal advance values.

first and on the other side of the food cup (Fig. 11.4.3A). To facilitate training, keep the signal light immediately above the lever used in autoshaping. Designate the lever that has the signal light above it as the signal lever; designate the other one as the blank lever.

In the final test arrangement, this signal light will be moved to the top center of the panel (Fig. 11.4.3B). In addition, some means will be needed to vary the strength of the signal, which can be defined in terms of either the intensity or duration of the signal. Varying the intensity is preferred, but requires additional hardware. During training, the intensity of the signal light should be ≥10 times that of the background illumination from the house light.

Coulbourn Instruments manufactures a 256-step digital-to-analog converter (DAC) that permits manipulation of the signal intensity. When the DAC is set to 0, it completely attenuates the voltage applied to it and no signal is generated. When it is set to 255, no attenuation is applied to the voltage passed via an amplifier to the light. Intermediate settings yield signals of intermediate brightness.

Several photometric probes are available for measuring the illumination from these light sources; one adequate device is model 450 made by EG&G. It is most appropriate to measure the illuminance (incident light at the photodetector) with a cosine adapter at some location in the chamber where the rat is likely to be during the test (e.g., center of the chamber, floor level). In order to measure this illuminance in a standardized manner in all test chambers, fix the illuminance probe in a template, so the probe will be positioned at the same location each time a measurement is made. For signal durations >100 msec, illumination may be measured with the light continuously on.

Because the animals will be earning a large proportion of their total food intake in the test environment in performing this task, be sure to provide pellets that are nutritionally complete.

Perform initial lever training

2. Autoshape animals for the lever-press response (see Basic Protocol 1, steps 4 to 13) for the signal lever only. Train until each rat presses the lever reliably (50 presses in at least one 50-trial session).

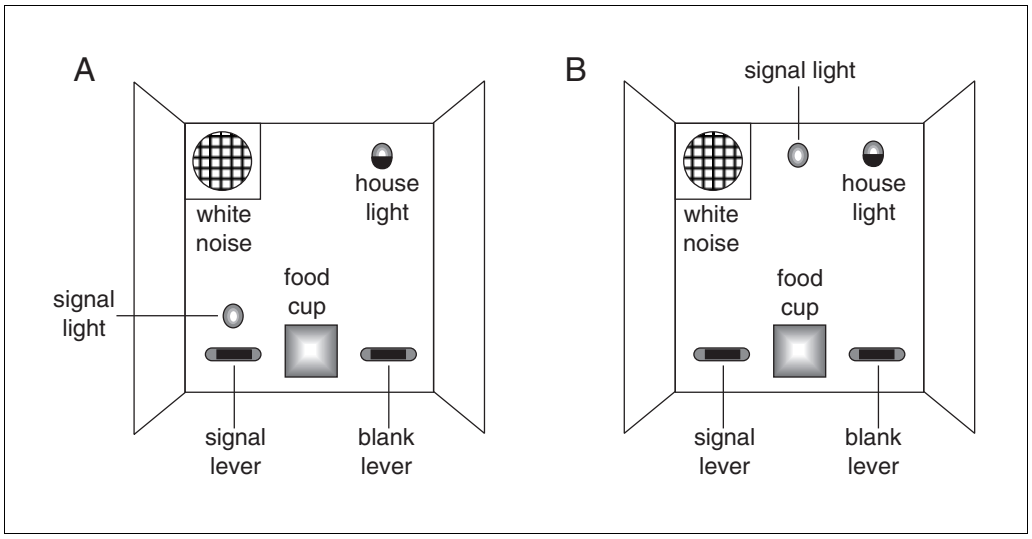

Figure 11.4.3 Configurations of an operant test chamber for testing sustained attention. (**A**) For training, the signal light is located directly above the signal lever (i.e., the lever paired with food on trials when a signal is presented). The blank lever is paired with food on trials lacking a signal. (**B**) Midway through training, after the rats have learned the response rules, the signal light is moved to the top center of the front wall of the chamber for assessment of attention.

3. Perform blank lever training by inserting the blank lever into the box as for autoshaping, but without illuminating the signal light. Train to the same criterion as above (50 presses in at least one 50-trial session).

   All rats should press this lever readily and with little delay. If any rats fail to do so, hand shaping may be required (see Commentary).

Perform tests of discrimination training

4. Present 50 signal and 50 blank trials in random sequence in daily test sessions (30 to 40 min). Separate trials with a 10-sec intertrial interval (ITI), during which the houselight is illuminated.

   a. *For signal trials:* Illuminate the signal lamp for 2 sec and then insert both levers into the chamber, leaving the signal light on. Retract both levers and turn off the signal when either lever is pressed. If the rat presses the signal lever, deliver a food pellet and illuminate the food cup. If the rat presses the blank lever, provide other cues to designate a punishment period or timeout (TO). For a typical TO, extinguish the house light for 2 or 3 sec and/or deliver a brief auditory cue that is unique to this event (a Sonalert, which generates a loud tone of ~4 kHz when supplied with 28 DC volts, is commonly used for this purpose). Follow the reinforcement or TO with the 10-sec ITI.

   b. *For blank trials:* Perform as for signal trials, but do not present a signal, and reverse the contingencies for pressing the two levers (i.e., reinforce a press on the blank lever with food, and follow a press on the signal lever with TO).

   Count the frequencies of correct and incorrect responses in each session. Continue training until each animal reaches a criterion accuracy of 80% or better in at least one 100-trial session.

   Note that there are two types of correct responses and two types of errors in this kind of signal detection task. Correct responses occur on the signal lever on a signal trial (hits) and on the blank lever on a blank trial (correct rejections). Similarly, errors occur when the signal lever is pressed during a blank trial (false alarms) and when the blank lever is pressed during a signal trial (misses).

   Trials in each session may be counted in blocks (e.g., five 20-trial blocks), but the animals will improve more across sessions than across blocks when daily sessions are given. However, session blocks may be useful for detecting equipment failures (see Troubleshooting).

   Use correction trials to facilitate acquisition of the response rules, observing appropriate cautions as described elsewhere (see Basic Protocol 3, step 8, and see Troubleshooting, discussion of poor learning).

   The 2-sec period between onset of the signal and insertion of the levers is called the signal advance, in distinction to the signal duration, which refers to the length of time that the signal is illuminated on each trial. At this point, the signal duration exceeds the signal advance, because the signal remains on after insertion of the levers.

5. Remove correction trials from the training procedure, but be prepared to reinstate them as a remedial measure as needed (i.e., if an animal fails to progress in their absence).

Modify signal parameters

6. Shorten the signal advance and signal duration in 0.5-sec decrements to 1.0 sec. Retrain to criterion (80% correct) after each change.

   Expect the rats to require 1 to 3 sessions at each stage.

7. Turn off the signal light simultaneously with insertion of the levers instead of keeping it lit until the rat makes its response. Retrain to criterion (1 to 5 sessions).

   The signal advance and signal duration are now equal; later, the signal duration will be shortened further, such that the signal terminates several seconds before insertion of the levers.

8. Move the signal light from its position above the signal lever to a position above the food cup at the top of the test chamber (Fig. 11.4.3B), thus placing it in a neutral position with respect to the levers. Retrain to criterion (2 to 10 sessions). Begin increasing the number of trials per session from 100 to the total that will be used in the final procedure, and reduce the presignal interval from 10 to 7 sec.

   Present a minimum of twelve trials (six signal and six blank) per test condition. If both signal strength and testing duration (trial blocks) are important variables, then the total number of trials per test session will equal 12 × number of strengths × number of trial blocks administered (e.g., for three trial blocks and five strengths, 12 × 3 × 5 = 180 trials). At a nominal trial rate of 5/min (ITI ≅ 7 sec), a 180-trial session will require ~40 min to complete. The number of trials should be increased gradually during steps 8 to 10, in 20- to 40-trial increments. For sessions longer than 240 trials, reduce the probability of primary reinforcement (pellet delivery) to maintain the maximum possible number of pellets earned at 240 and to prevent the rats from becoming sated (240 pellets × 45 mg/pellet = 10.8 g of food).

9. Vary the postsignal interval, while keeping the signal duration constant at 1 sec by inserting a variable time between onset of the signal and insertion of the levers. Begin with 1.5 sec and end with 2, 3, or 4 sec, randomly determined on each trial. Retrain as necessary to maintain the criterion of 80% correct accuracy (5 to 7 sessions).

   This change inserts a gap between offset of the signal and insertion of the levers.

10. Vary the duration of the presignal interval by randomly selecting a presignal interval value on each trial, keeping the average duration at 7 sec. Begin with a relatively homogeneous list of values (e.g., 5, 6, 7, 8, and 9 sec) and increase the range of values until very short (≤1 sec) and very long (≥20 sec) values are used. Retrain to criterion after each change in the list (5 to 10 sessions).

    Fleschler and Hoffman (1963) provide an algorithm for calculating constant-probability lists that are appropriate here. These lists of durations maintain a constant probability that the interval will terminate throughout the interval.

    This manipulation will cause a large drop in accuracy when first introduced; accuracy will return toward the previous baseline over about a week of testing, but will not reach the same levels. This decrement appears to be due to the increased attentional demands of the variable presignal interval. The initial decrease in accuracy and the subsequent rate of recovery should provide sensitive measures of sustained attention. Thus, this step should be monitored closely in studies assessing the effects of prior treatment with a test agent.

    Steps 11 to 14 below are designed to increase the difficulty of the task, thus lowering the proportion of hits, P(hit), to an appropriate range. Ideally, the gradient relating P(hit) to signal strength will extend from chance accuracy at the lowest signal strength to near 100% at the highest strength. See Anticipated Results for further explanation. Skip these steps if the task difficulty is appropriate after step 10.

11. *Optional:* Vary the signal strength during each session. Present trials of each signal strength in a completely randomized order or in blocks of 4 to 8.

    If a random order is used, all blank trials in the whole session are equivalent, and false alarms and correct rejections cannot be categorized in terms of signal strength. If trials are blocked, then all four response types can be categorized by intensity for purposes of data analysis.

    Varying the signal strength can be accomplished by varying its intensity, its duration, or both. Conceptually, briefer signals should increase the attentional load of the task (Muir et al., 1993), whereas dimmer signals should provide a sensory challenge rather than an attentional challenge. The degree to which these processes can be selectively challenged by these manipulations remains to be determined. However, it is clear that appropriate manipulation of the signal intensity can be used to establish increment thresholds for the sensory modality of the signal (Bushnell et al., 1997).

12. *Optional:* Vary the signal intensity. Present the brightest two values in one session and include successively dimmer signals each day to facilitate development of a generalization gradient across signal intensity (5 sessions).

13. *Optional:* Increase the background intensity of the signal light from zero (signal light off between signals) to a dim value. In other words, keep the signal light on dimly before each signal and return it to that dim value after each signal. Use a final criterion of ≥80% correct for the most salient signal and ≤20% correct (i.e., guessing) for the least salient signal (5 sessions).

    This increases the difficulty of the task by making the signal an increment in intensity. Psychophysically, increasing the background illumination raises the threshold for detecting the increment in illumination represented by the signal. Skip this step if the task is sufficiently difficult without brighter background illumination.

14. Vary the signal duration within each session, using a range of values of 1 sec to 0.1 sec, using the same strategy as for signal intensity, above.

    This method will produce a gradient of P(hit) across signal durations, as shown by McGaughy and Sarter (1995). Under the assumption that shorter signals involve a greater attentional demand than do longer signals, effects of a treatment specific to attention should reduce accuracy preferentially to short signals.

Analyze data

15. Convert the frequencies of hits, misses, false alarms, and correct rejections (see step 4) at each signal strength to proportions of hits, *P*(hit), and false alarms, *P*(fa). Calculate *P*(hit) as the frequency of hits divided by the sum of the frequencies of hits and misses (i.e., proportion of correct responses on signal trials). Calculate *P*(fa) as the frequency of false alarms divided by the sum of the frequencies of false alarms and correct rejections (i.e., the proportion of errors on blank trials).

    P(hit) and P(fa) can be used to calculate sensitivity and bias indices from signal detection theory, but this approach must be taken with caution, because interpretation of these derived measures depends upon the particular assumptions upon which their calculation is based, and explanation of their meaning invariably requires recourse to the values of P(hit) and P(fa) from which they were derived. In this author's opinion, the advantages of deriving signal detection indices, which involves trading one pair of measures [P(hit) and P(fa)] for another pair of more derived measures (sensitivity and bias), are outweighed by the effort required to calculate and explain these latter measures.

    In addition to these measures of accuracy, response time may be measured as the latency between insertion of the lever and the rat's response. Latency provides an index of motor function akin to a simple reaction time, because rats typically choose which lever to press during the postsignal interval by positioning themselves in front of one of the levers and pressing it as it is inserted into the chamber. Latency typically does not vary with signal intensity (Bushnell et al., 1994).

BASIC PROTOCOL 5

MULTIPLE FIXED-INTERVAL/FIXED-RATIO OPERANT SCHEDULE

Operant schedules are useful for assessing the degree to which one or more contingencies of reinforcement can gain control of the behavior of a subject. In addition, the rate of acquisition of the response rules and control of behavior by reinforcement contingencies can provide evidence regarding the ability of a subject to learn this information and respond accordingly. Because interval and ratio schedules generate different patterns of behavior, it is often useful to observe acquisition and performance of both types, as well as the ability of the subject to switch between schedules within a test session. Thus arises the utility of the multiple schedule, a procedure in which combinations of two or more component schedules are arranged within a test session, each with a unique stimulus associated with the schedule.

This protocol describes training steps for a multiple FR10/FI 1-min schedule for rats. In the FR10 component, every tenth lever press (response) yields a food pellet. In the FI 1-min schedule, the first response after a fixed interval of 1 min (since delivery of the previous pellet) yields a food pellet. FR schedules produce rapid responding until the ratio has been completed, followed by a period with no responding (post-reinforcement pause). In contrast, FI schedules produce a response pattern in which the response rate gradually increases across the time interval, reaching a maximum just prior to the end of the interval. If responses are plotted sequentially and cumulatively across the interval, a positively accelerated curve is revealed; this pattern is called the FI scallop.

Materials

Subject rats
Precision food pellets: 45 mg for male rats, 37 mg for females (BioServ or PJ Noyes)

Operant conditioning chamber (Fig. 11.4.1; e.g., Coulbourn Instruments, MED Associates, or CeNeS, or TSE systems) including:
- Incandescent house light (~0.1 W)
- Loudspeaker for white noise
- Food cup
- Cue light: LED or incandescent bulb behind a clear lens (if using an incandescent bulb, use a glass jewel dome in front of the bulb rather than plastic, as it cannot be gnawed down by the animal)
- Response lever, fixed or retractable
- Tone generator (e.g., Sonalert; optional)

Pellet dispenser
Computer system and interface to control test environments and stimuli and to collect response data (see Commentary)
Computer software for visualizing patterns of response in each component (MED Associates)

Set up equipment

1. Set up equipment as described for autoshaping the lever-press response (see Basic Protocol 1, steps 1 to 3).

   White noise can be provided by a loudspeaker, a ventilation fan, or both.

Perform training steps

2. If retractable levers are used, perform initial training as described for autoshaping (see Basic Protocol 1, steps 4 to 13) until each rat presses the lever reliably (50 presses in at least one 50-trial session). If fixed levers are used, illuminate the cue light prior to delivery of each pellet during the autoshaping phase.

   Hand shaping and/or overnight sessions with a continuous-reinforcement schedule (FR1; each lever press yields a food pellet) in effect are more likely to be needed with fixed levers.

3. Train ratio schedule. Insert the lever into the chamber and illuminate the house light for the duration of the session. After each rat presses the lever reliably for food on the FR1 schedule, gradually increase the number of presses required for delivery of food to a value of 10 (FR10).

   For example, a sequence of ratios with values of 1, 2, 4, 7, and 10 might be used over the course of six to ten sessions. The criterion for advancing to the next ratio is completion of a predetermined number of ratios (e.g., 20) within an allotted time (e.g., 20 min). Stability of the response rate, both within and across sessions, might also be used. See Perone (1991) for a discussion of stability criteria in the design and analysis of free operant studies.

4. Train interval schedule. Insert the lever into the chamber and illuminate the house light and the cue light for the duration of the session. Deliver a pellet immediately following the first lever press that occurs after a short (e.g., 5-sec) time interval. Gradually increase the duration of the interval across six to ten sessions, using interval values of 5, 10, 20, 40, and 60 sec.

   As above, the primary criterion for advancement is completion of a specified number of intervals (e.g., 20) in a session lasting, for example, 30 min.

5. Train multiple schedule. Insert the lever into the chamber and illuminate the house light for the duration of the session. Randomly select a sequence of FR10 and FI 1-min components (e.g., five of each) for each session. Illuminate the cue light at the start of each interval component, and turn it off at the start of each ratio component.

   The number of sessions will depend upon the criteria selected for establishing stability of the behavior in each component; 10 to 20 session are frequently needed.

Analyze data

6. Inspect individual-animal data from cumulative response records or use microanalysis of the distributions of interresponse times (IRTs) and other temporal aspects of responding.

   The traditional approach to data analysis in free operant studies is the individual-animal approach. Other techniques described for quantifying performance (summarized in Perone, 1991) can also provide a wealth of information regarding the patterns of behavior engendered by these schedules.

7. For ratio schedules, quantify performance in terms of overall response rate (ORR), running rate (RR), and post-reinforcement pause (PRP) duration.

   The ORR is the sum of all responses in all FR components divided by the sum of the durations of the FR components. The RR is calculated similarly but excluding the PRP, which is defined as the time between delivery of the pellet and emission of the first response of the next ratio.

8. For interval schedules, quantify ORR as well as the curvature of the FI scallop.

   Curvature of the FI scallop better reflects the control of behavior by time. Two such measures include the index of curvature (IOC), which quantifies the degree to which the response pattern in each interval deviates from linearity (Fry et al., 1960), and the quarter life, which is that portion of the interval required for the animal to emit the first 25% of its total responses in the interval (Herrnstein and Morse, 1957).

COMMENTARY

Background Information

Mazes versus operant chambers

Tests of cognitive function may be carried out in any of a number of devices. Typically, either mazes or operant chambers are used. The same cognitive processes may be assessed in both kinds of apparatus, so neither gains any conceptual advantage over the other. The choice of test environment is generally made instead on the practical issues involved. Mazes are simpler and much cheaper to assemble, but larger and more difficult to automate than operant chambers. A single radial-arm maze or water maze may occupy a test room that could house a dozen operant chambers. In addition, computer control over the operant test environment reduces the intensity of the labor involved in daily testing of the animals, reduces the potential for observer bias in affecting the behavior of the animals, increases the precision with which stimuli and responses can be timed, and facilitates microanalysis of response patterns. These considerations gain significance when viewed in light of the number of animals that must be tested in generating dose-effect information for toxicology studies. A variety of operant chambers are illustrated by Ator (1991). Both mazes and operant chambers are available from commercial suppliers (e.g., Coulbourn Instruments, MED Associates, CeNeS, and TSE Systems).

Motivation and reinforcement

Most often, selected behaviors are reinforced appetitively, using food. Specific techniques for maintaining hunger are detailed below. Alternatively, animals may be induced to work for water by being kept on a limited water supply (e.g., 30 min access to water each day, provided after testing and while food is available in the home cage). The primary advantage of water reinforcement is the ease with which water can be delivered to the animal with a simple water spout and solenoid valve. The primary disadvantage involves the complications associated with maintaining the health of the animal under conditions of chronic thirst. For example, rats will not eat dry lab chow without access to water, so care must be taken to provide both at the same time, and to monitor carefully the weight of the animals during the study.

Escape from aversive stimuli may also be used as motivation. Several traditional tests (e.g., active and passive avoidance) employ termination of electric shock as a negative reinforcer to control behavior. Escape from water has more recently been used, as in the Biel, Cincinnati, and Morris water mazes (the Morris water maze is described in *UNIT 11.3*).

Autoshaping

Originally described in pigeons pressing backlit keys (Brown and Jenkins, 1968), the technique has also been developed for rats (e.g., Davenport, 1974; Poplawsky and Phillips, 1986). Thorough, if dated, reviews of the phenomenon are also available (e.g., Schwartz and Gamzu, 1977). The criterion response may be either a lever press (as described above) or any other response detectable by the computer—e.g., touching the lever or a designated region in the test chamber (Messing and Sparber, 1985) or pressing a backlit pigeon key. The criterion response is elicited by pairing food with a change in the manipulandum (e.g., insertion and retraction of the response lever or illumination of the pigeon key). In essence, pairing the change in the manipulandum with food delivery causes the animal to associate the manipulandum with food and to engage in exploratory ingestive behavior directed at the manipulandum. This exploration can then serve as an operant response if its emission causes immediate delivery of food in a combined autoshaping-operant procedure (Davenport, 1974).

Not all rats will press the response lever under the contingencies described below (expect about seven of eight rats to do so), and the rate of acquisition can vary dramatically across animals within a treatment group (see Fig. 11.4.4). Thus, relatively large sample sizes are typically necessary to detect group differences in autoshaping ($n \geq 12$). A higher percentage of animals will emit touch responses than press responses, and conditioning will proceed correspondingly more quickly (Messing and Sparber, 1985). However, touch responses are more difficult to detect and quantify automatically. In addition, further work with the animals will typically be more conveniently pursued with lever-press responses. The trade-off between the rate and unanimity of acquisition with lever-touch responses and the convenience of lever-press responses should be decided by the long-term goals of the study.

Parametric manipulations, including delay and probability of reinforcement, may be used to slow the rate of acquisition (reviewed by Gleeson, 1991). These manipulations may be useful for teasing out subtle effects of a compound, particularly those that compromise processing of temporal or probabilistic information (Messing and Sparber, 1985).

Repeated acquisition

Repeated acquisition was originally demonstrated in monkeys that learned to press a series of response levers in an operant chamber in a specific sequence each day (Boren and Devine, 1968). Operant response sequence methods have been explored extensively in primates (Thompson, 1974, 1975) and adapted for rats (Cohn et al., 1993; Cohn and Cory-Slechta, 1994). These methods have been ably reviewed both conceptually (Cohn and Paule, 1995) and with respect to neuroactive chemicals (Cohn et al., 1996).

It is rather less time consuming to train rats to perform repeated-acquisition baselines in mazes, either in a three-panel runway (Ohno et al., 1992) or a radial-arm maze (Peele and Baron, 1988; Bushnell and Angell, 1992). Repeated acquisition is more tractable for rats in mazes, probably because of the spatially rich environment and the fact that the problems can be based upon the location of food rather than a specific sequence of responses. In addition, the cognitive processes that support the problem-solving strategy in the maze—i.e., combinations of working and reference memory (Bushnell and Angell, 1992)—are better understood than those involved in acquiring novel sequences of responses.

Delayed matching to position

Delayed matching to position (DMTP) was developed from delayed matching to sample as a means of testing working memory (Honig, 1978) in rodents. The method was developed by Dunnett and colleagues (Dunnett, 1985; Dunnett et al., 1989; Dunnett and Martel, 1990) to assess the neurobiological basis of working memory and the efficacy of cholinergic grafts in the remediation of CNS lesions. It has also been applied to problems in pharmacology and toxicology (Bushnell et al., 1991, 1993; Thomas et al., 1991).

Technically, DMTP is a discrete-trial delayed-response task, with all of the limitations of the delayed-response paradigm (Heise and Milar, 1984; Paule et al., 1998). In contrast to maze procedures, which assess spatial components of working memory, DMTP is one of the few practical means available for assessment of the temporal aspects of working memory in rats. The fact that delays of <30 sec are sufficient to reduce accuracy across delays means that retention gradients can be obtained in test sessions of reasonable duration. For purposes of analysis, this gradient may be approximated by a linear function whose *y* intercept and slope define the probability that the sample information was encoded and the rate at which that information is lost over time, respectively (Bushnell, 1990; Paule et al., 1998). These parameters probably reflect attending to the sample stimulus and rate of forgetting; both are important in determining the accuracy of response when the choice opportunity is provided.

DMTP may also be conducted with a control procedure for assessing reference memory to provide evidence that deficits in accuracy are specific for working memory. For example, the visual-discrimination task described in the Support Protocol requires the same motivation and motor responses demanded by DMTP, but does not require working memory. Thus, a deficit in the DMTP task without a corresponding deficit in visual discrimination strengthens the evidence for impairment of working memory. Note that this case can be made most strongly when baseline accuracy levels on the two tasks are the same (Paule et al., 1998).

Sustained attention

Sustained attention refers to the process(es) by which temporally unpredictable signal events may be detected and reported over prolonged periods of time (reviews by Parasuraman et al., 1987; Craig and Davies, 1991; Nachreiner and Hänecke, 1992). The term vigilance refers to a special type of sustained attention in which the signal events are rare and the test environment is monotonous (Mackworth, 1970; Nachreiner and Hänecke, 1992) and does not apply to the method described here (Bushnell, 1998). The signal-detection method described here for assessing sustained attention provides strong control for changes in the false alarm rate, which can complicate interpretation of studies of sustained attention (see Moore et al., 1992, for a discussion of this problem). The method described here relies upon visual stimuli, but can be implemented in other sensory modalities as well (Bushnell et al., 1994), and can produce very similar psychophysical relationships. The theory of signal detection (Green and Swets, 1974) can be applied to these data to derive indices of sensitivity (reflecting the discriminability of the stimuli) and bias (reflecting the subject's tendency to make a particular choice). However, patterns of effect in this task can be observed as readily and with much less effort by calculating the proportions of hit and false alarm, as described.

Many methods have been devised for assessing attention, both sustained and selective, and have a rich history in pharmacology and neurobiology (Robbins and Everitt, 1995; Bushnell, 1998); however, their application to toxicology is just beginning. Given the importance of attention in learning and memory, and the likelihood that changes in these latter processes may reflect more specific effects on attention, it is likely that this area will expand in the near future. For example, the five-choice serial reaction-time test (Carli et al, 1983; Muir et al., 1994) has become a standard method for studying the neurobiology and pharmacology of attention, but has not yet been used to ask neurotoxicological questions relevant to public health.

Multiple fixed-interval/fixed-ratio schedule

Since Skinner's seminal work on operant conditioning, codified by Ferster and Skinner (1957), schedule-controlled operant behavior has enjoyed a long and rich history in behavioral pharmacology and toxicology. This history has been driven largely by the precise control that can be gained over behavior in a variety of species of test animals, including humans. A great variety of simple and complex schedules have been devised and continue to fascinate students of behavior (Lattal, 1991; any issue of the *Journal of the Experimental Analysis of Behavior*). Operant conditioning focuses on the behavior of the subject per se

and, consistent with the atheoretical approach of Skinner, any association of conditioned behavior to underlying hypothetical processes is eschewed as mentalistic guesswork. Thus, whereas clear evidence of changes in schedule-controlled behavior can often be observed in response to treatment with chemical agents (e.g., Brocco and McMillan, 1983; Moser et al., 1987; Hymowitz et al., 1990), the interpretation of those changes is typically not pursued beyond the observable events themselves. The difficulties with associating schedule-controlled behavior with underlying neurophysiological and neurochemical systems, and with interpreting changes in behavioral baselines in terms of the cognitive processes of concern to public health, have impeded widespread acceptance of these methods as tools in toxicology.

Critical Parameters

Handling animals

See Critical Parameters of *UNIT 11.3* for a discussion of rat handling considerations. In addition, Ator (1991) has provided a thorough description of techniques for handling laboratory animals.

Motivation

Appetitive motivation may be maintained during training and testing by one of several means. Frequently a target body weight is established based upon a percentage (usually 80% or 85%) of the animals' free-feeding weight. Determining the free-feeding weight is not a simple matter, as rats (especially males) continue to gain weight throughout their lifetimes if permitted to do so. Thus, 85% of free-feeding weight may involve a continually increasing weight that must be monitored and adjusted throughout the study.

Alternatively, the rats may be grown to their adult weight and maintained at a constant value thereafter (Ator, 1991). Typical weights are 325 to 375 g for male Long-Evans and Sprague-Dawley rats, and 225 to 275 g for females. Frequent weighing and careful feeding are necessary to maintain weight in a target range. Algorithms for calculating daily feedings to maintain constant body weight are available (e.g., Ali et al., 1992).

Animals should be fed with standard rat chow at the end of each test day, but not immediately after removal from the test chamber (so they don't learn to wait for their food). It will also be necessary to subtract the amount of food earned during daily tests from their total allotment to maintain target body weights when the amount earned in the chambers exceeds 10% of their total daily allocation.

Finally, in preparation for each daily session, it helps to provide a short (~2-min) period in the test chamber or maze before each session to permit the animal to recover from any stress involved in transfer to the test apparatus.

Computer control of testing equipment

Unless a strictly manually operated maze is used, the computer will be an essential aspect of testing cognitive function. Even tracking systems for the Morris water maze use computerized acquisition of speed, heading, and latency data. Thus, selecting the interface and software should be considered carefully.

Many computer software packages may be used for quantifying behavior (Gollub, 1991); in addition, three commercial systems have been designed specifically for testing the behavior of small animals. State Systems wrote an early and successful state-table program called SKED-11, which runs under RSX-11 on Digital PDP-11 minicomputers. Although this computer platform is expensive and outmoded, the software is well developed and relatively flexible. In particular, the multitasking operating system permits such tasks as programming, editing, and file handling to occur while animals are being tested. Up to sixteen stations can be run simultaneously with simple programs, or fewer stations can be run with more complex programs. MED Associates adapted the state-table approach for the PC with their MED-PC system, which runs under DOS or Windows. Because of the limited multitasking availability on these platforms, the system is less flexible than SKED-11, but uses cheaper and more accessible hardware. A third system, L2-T2, was developed by Coulbourn Instruments for the PC. It appears to be suitable for simple operant schedules but handles complex test programs with difficulty. In addition, other custom software may be used, limited only by available time and ingenuity of the researcher and support staff (Gollub, 1991).

Autoshaping

The intertrial interval (ITI) can influence the course of autoshaping. In general, more lever-directed activity and pressing (sign tracking) will be elicited by longer ITIs, and more food-cup-directed activity (goal tracking) will be elicited by shorter ITIs (Van Haaren et al., 1987).

The effects of ITI depend also upon the sex and strain of the rat. Male rats tend to autoshape

faster than female rats, because of more frequent and vigorous exploration of the lever during the pairing of lever retraction with food (van Haaren et al., 1987). Consistent with this gender difference, acquisition of the lever-press response can be facilitated paradoxically by treatments that interfere with the control of fine motor movements. Thus, acute exposure to the organic solvent *p*-xylene increased the rate of acquisition of lever pressing, and this increase in rate was blocked by increasing the force necessary to press the lever (Bushnell, 1989). Because (1) responding begins with exploration of the response lever, (2) the animals were observed to be unsteady and slightly uncoordinated after exposure to xylene, and (3) acquisition of a discrimination reversal was not affected by xylene, the facilitation of autoshaping was interpreted as a reduction in motor control.

The rate of acquisition of an autoshaped response can be slowed by introducing a delay between retraction of the lever and delivery of food (Davenport, 1974; Messing and Sparber, 1985) and, under some conditions, by decreasing the probability with which food is delivered after retraction of the lever (Schwartz and Gamzu, 1977).

Repeated acquisition

Changing the number of arms in the baited set will affect the shape of the acquisition curve. If a lower proportion of arms is baited, more errors will occur on the first trial and fewer on later trials, thus steepening the daily learning curve. Increasing the proportion of baited arms should have the opposite effect (i.e., prolong the acquisition phase, but starting at a lower error level).

The number of trials per session may be adjusted as necessary, with constraints (1) that the animals all reach a low and stable error frequency by the end of the session and (2) that the test session is kept as short as practical. Note that if a treatment is expected to retard learning, then a longer session may be necessary to document the effect.

The subset of arms baited must be varied across the rats tested each day. If the same set of arms is baited each day for all rats, then those rats tested late in the day will find useable odor trails to follow (D.B. Peele, pers. comm.).

Delayed matching to position

Because of the length of the chain of responses necessary for completion of each trial in this task (i.e., sample press, delay responses, choice response, food retrieval), it is advisable to generate a unique stimulus condition or combination of stimuli for each element of the chain. These unique conditions help "pace" the rat through each trial without providing information regarding the choice response. For example, the white noise intensity might be increased after the ITI to mark the beginning of the trial, and then be reduced after collection of the food pellet.

Because a large number of trials are presented in each session in this task, proactive interference (PI) plays an important role in performance. That is, the response made on a given trial is an important factor in determining accuracy on the next trial, and is said to interfere proactively with the subject's choice on the next trial. The influence of proactive interference in working memory tasks has been demonstrated primarily by manipulations of the ITI (Roberts and Kraemer, 1982; Bushnell, 1988; Dunnett and Martel, 1990). These manipulations are based on the assumption that the influence of the previous response will dissipate with time; hence, the strength of the PI will diminish as the ITI is lengthened, and accuracy will increase. Indeed, choice accuracy appears to be closely related to the ratio of the delay interval to the ITI (Roberts and Kraemer, 1982). These considerations gain further importance when the effect of a treatment appears to be mediated through its effects on PI, as has been elegantly documented for nicotine (Dunnett and Martel, 1990).

The DMTP procedure is designed to assess working memory, but obviously requires other processes as well. Thus, in addition to the sensory and motor aspects of performing the task, the contingency governing the response in each component of a trial must be remembered. Because this information remains constant throughout the experiment, it is assumed to require reference memory. An independent assessment of reference memory can be added to this procedure by intercalating discrimination trials randomly among the matching trials (Bushnell et al., 1991). Alternatively, reference memory (e.g., visual discrimination) can be tested independently in the same animals or in others (Bushnell, 1990).

Finally, it should be noted that several variations of this method exist (e.g., White, 1985; Thomas et al., 1991), and other operant methods have been devised for assessing working memory for pharmacological and toxicological investigations—e.g., continuous nonmatch to sample (Spencer et al., 1985) and delayed alternation (Heise and Hudson, 1985).

Sustained attention

Three parameters are particularly efficacious at determining accuracy in the signal-detection task: signal strength, variability of the ITI, and trial rate. First, the intensity of the signal relative to the background illumination strongly influences the probability with which the signal will be detected and reported. This relationship is primarily perceptual, reflecting the fact that the rats are required to detect an increment in illumination. Thus, overall accuracy can be varied by adjusting the ambient illumination as well as the brightness of the signal.

Varying the signal strength (intensity or duration) is important for two reasons. First, it helps to maintain a stable performance baseline, in that the animals are reinforced consistently for detecting strong signals and inconsistently for detecting weaker signals. Second, if the signal strength is varied in terms of its intensity, and if the intensities are chosen appropriately, the shape of the gradient relating *P*(hit) to intensity can distinguish between sensory and attentional dysfunction. That is, an attention deficit is probable if a treatment shifts the gradient downward—seen as a reduced *P*(hit) at all intensities above chance—particularly if *P*(fa) is also elevated. In contrast, if the treatment shifts the *P*(hit) by intensity gradient to the right—i.e., reduced *P*(hit) only at intermediate intensities and no increase in *P*(fa)—then it is more likely that it has caused a deficit in perception of the signal (visual deficit; see Bushnell et al., 1997).

The temporal unpredictability of the signal also affects accuracy, as would be expected of a test of sustained attention. Increasing the variability of the presignal (and postsignal) intervals decreases the temporal predictability of the signal and thus can be presumed to increase the attentional load of the task (Muir et al., 1993). As predicted, increasing the variability of the ITI reduces accuracy in this task (McGaughy and Sarter, 1995); however, accuracy will improve somewhat with practice after a change from a constant to a variable ITI (Bushnell, unpub. observ.).

Accuracy also decreases with increasing trial rate (the rate at which trials are presented; Bushnell and Kelly, 1992). The decrease in accuracy with faster trial presentation rates may be due to fatigue, which develops both in peripheral sensory organs and central processing systems in human subjects in fast-paced tasks (Parasuraman, 1984).

Multiple fixed-interval/fixed-ratio schedule

The particular values of the ratio and interval applied in a multiple schedule will greatly affect the rate and temporal patterning of the behavior obtained (Lattal, 1991; Perone, 1991) and may also interact with the effects of chemicals (Branch, 1991). Thus, comparison across studies must be done carefully, with a keen eye toward differences in both the training history and schedule conditions employed.

Troubleshooting

Hand shaping when autoshaping fails

Some rats will fail to acquire the lever-press response under the conditions described for autoshaping. The behavior of these rats may have to be shaped manually. Shaping refers to a process by which an animal may be induced to emit a specific response by reinforcing behaviors that approximate that response. This method of successive approximations is used extensively in animal training and was formalized for the laboratory by Ferster and Skinner (1957). The process requires a motivated subject (hungry rat), an observer with a means to deliver a reinforcer (food pellet), and a predefined criterion response. Simply put, the observer reinforces behaviors that successively approximate the criterion response until the response is emitted by the animal on its own. A fuller description of this process is given by Gleeson (1991).

In the present context, a hungry rat in an operant chamber may be shaped to press a lever as follows. The rat is shown during the first stages of autoshaping that food will be available periodically in the food cup, accompanied by the sound of a pellet being delivered and illumination of the food cup light. As the experimenter observes the rat moving about the chamber, s/he first causes a food pellet to be delivered into the food cup whenever the rat enters the quadrant of the chamber where the lever is located. Next, food is delivered only when the rat approaches the lever, then only when it sniffs, and then touches the lever. If necessary, the rat may be induced to approach the lever by gently tapping on the panel of the test chamber behind the lever. Finally, only a press vigorous enough to cause the lever to move is reinforced. If the electronic circuitry is set up appropriately, this movement will be detected by the equipment and cause delivery of a pellet. A practiced observer should be able to shape a hungry rat to press a lever in a matter of minutes.

Equipment failures

Many things can go wrong in complex systems like operant conditioning apparatuses: light bulbs burn out, moving parts wear out, microswitches fail, pellet dispensers jam, and retractable levers malfunction. There is no way to eliminate these problems entirely, but their frequency and effects on experiments can be minimized in several ways. First, it is essential to test each piece of equipment each day prior to collecting data from the animals. Test programs need to be written so that any loose bulb or broken wire or stuck response lever results in an easily detectable and traceable fault. Second, it is essential to monitor the progress of each animal during its test session. When, for example, box 2 fails during a data-collection session, it should be obvious from the display that a problem has developed in that box (e.g., the rat has stopped responding, or for the last 5 min it responded only on the left lever, or its accuracy has fallen from 90% to 10%). Third, moving parts must be kept clean to increase their reliability and prolong their lifespan; particular attention should be paid to pellet dispensers, which accumulate dust and a sticky residue, even from "dustless" pellets. However, as discussed below, the olfactory cues in a test chamber become part of the environment, so abrupt changes in these cues from, for example, a sudden, thorough cleaning of the test cage, will seriously disrupt performance. Because of time constraints and the complexity of the equipment, thorough cleaning and sanitization is not feasible between rats, or even daily. However, judicious, regular cleaning of the most failure-prone pieces of equipment is essential; if this is incorporated into the testing routine, it will not interfere with a stable performance baseline.

Most commercially available retractable levers are extended by an electric motor, which tends to produce relatively slow movement. In addition, some older models do not reliably extend and retract repeatedly. These levers may be modified by replacing the motor with a pneumatic cylinder, which greatly increases the speed and reliability of the devices. The rate of motion of the levers under compressed air can be controlled by inserting a small orifice (e.g., a 26- or 27-guage needle) in the air line to the cylinder. Small pneumatic cylinders, solenoid valves, manifolds, and fittings for this purpose are manufactured by Clippard and are available from Carolina Fluid Components. If compressed air is not available or is unreliable in the building, a nearly silent air compressor with adequate capacity and good reliability is manufactured by Jun-Air and is available from the Newport Corporation.

Animals in wrong cages

Each test chamber is unique to a rat, despite our best efforts to make them identical; for example, many of the cues that make the chambers different to the rats are olfactory and too subtle for a human's degenerate sense of smell to discriminate. Thus, rats learn faster and perform more consistently when they are tested in the same test chamber every day. Occasionally, two or more animals may be placed inadvertently in the wrong chambers, which may or may not create obvious differences in performance. Assembling adjacent chambers with mirror-image configurations (e.g., signal lever on the left side in boxes 1, 3, and 5; signal lever on the right in boxes 2, 4, and 6) will increase the likelihood that misplaced animals will be identified quickly, because the reverse contingencies of the chambers will cause a precipitous drop in accuracy or complete response failure due to unexpected nonreinforcement. The best way to minimize these mishaps is to maintain clear identification marks on each animal and to check these marks every time an animal is moved from one cage to another.

Poor (slow) learning

Each animal will learn at its own pace. If the variability in these rates is large, the animals at the slow end of the distribution will be considered slow learners (for options regarding keeping these animals in the study versus eliminating them, see Time Considerations). The particular method used to facilitate learning in these animals will depend upon the specific contingencies in effect at the time and on the animal's training history. For example, correction trials can provide a powerful means to shape the appropriate response and are recommended for the discrimination and matching tests described here. However, some animals will learn a response strategy that depends upon the use of correction trials and avoids the necessity of learning the discrimination planned by the experimenter. This strategy involves pressing one lever on the initial presentation of a trial; if the response is correct, the food is taken. If it is incorrect, the rat simply responds on the other lever on the next presentation (the correction trial). Because the trial conditions are repeated, this strategy guarantees that this second response will be reinforced. Across a session, strict adherence to this strategy will

yield a reinforcement ratio of 66.7%, more than enough to sustain responding. Thus, an animal whose accuracy on a two-choice problem with correction trials plateaus at 60% to 70% should be suspected of having adopted this strategy. The obvious solution is to remove the correction trial contingency to obviate its benefit to the animal.

Response biases may develop in rats that are challenged by a difficult discrimination. A frequent bias involves position: a rat may choose one lever and respond preferentially on it, accepting a reduced rate of reinforcement. An effective strategy to deal with these biases is to alter the proportion of trial types away from the animal's bias. For example, if an animal learning the matching rule develops a left bias, decrease the proportion of trials in which left is the correct matching response, thus reducing the payoff associated with that bias. Similarly, if an animal learning the combined matching and discrimination protocol has high accuracy in one component and low accuracy in the other, then reduce the proportion of trials in the preferred component, thereby selectively reinforcing improvement in the nonpreferred component.

In some cases, animals may have difficulty with a discrimination and not show evidence of a bias or an alternative response strategy. It may be beneficial for these animals to make the discriminative stimulus more salient by, for example, increasing the brightness of a light or reducing the background illumination. Rarely, it may be necessary to cause the light to flash to enhance its effectiveness as a discriminative cue.

Anticipated Results

Autoshaping

Frequencies of lever presses should increase across trial blocks, reaching an asymptote of ten presses per ten-trial block within four to five sessions. As shown in Fig. 11.4.4, acquisition curves for individual rats will vary primarily with respect to the trial block when responding begins; once a rat begins to press the lever, it

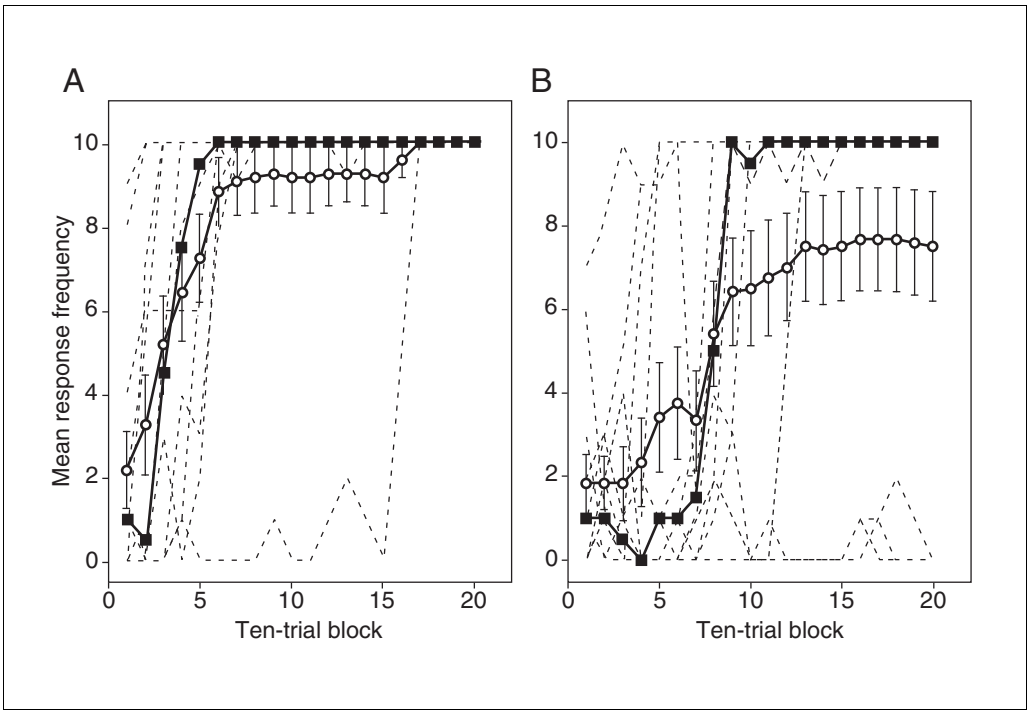

Figure 11.4.4 Representative data from an autoshaping experiment, showing the interanimal variability among male (**A**) and female (**B**) rats. The frequency of lever presses per ten-trial block is plotted as a function of trial block. Individual acquisition curves from each of twelve animals of each sex are shown as dotted lines. The means ± SEM (open circles) and medians (closed squares) are superimposed on the individual animal data (dotted lines). Note that the males tend to reach asymptotic frequencies of pressing sooner than females, that females are more variable in the time at which they begin to press, and that the slopes of the lines for animals that begin to press late are not less steep than for those that begin to press early. In other words, the rate of acquisition of responding does not depend upon the time at which the animal begins to respond.

will generally (but not always) do so quickly and reliably thereafter. Thus, the group average acquisition curve reflects averaging across time (trial block) and can be quite variable. This variability, coupled with the between-subject nature of the experiment and the reticence of 10% to 15% of rats to press the lever at all, increases the number of animals necessary for detecting treatment effects. Because of this variability, the data are often better summarized in terms of medians rather than means (Fig. 11.4.4). In some cases, each subject's acquisition curve can be aligned with respect to the block in which the first lever-press response occurs, and acquisition can be described as the slope with which each rat's response frequency approaches its asymptote.

Note also that some interanimal variability can be eliminated by requiring the rat only to touch the lever, instead of pressing it (Messing and Sparber, 1985), because more animals will touch the levers than will press them under the contingencies described. Two disadvantages of using touches instead of presses are (1) that reliable touch-detecting electric circuitry is needed and (2) that the animals are not necessarily pressing the lever when the study is finished, which reduces their usefulness for future assessments.

Repeated acquisition

Error frequencies should decline from ~4/trial on trial 1 of each session to an asymptote below 1/trial by trial 5 (Fig. 11.4.5). This within-session error reduction shows that learning is occurring and can be repeated in each daily session. Note that because each animal begins each session with about the same error frequency, interanimal variability is much reduced compared to the autoshaping data (Fig. 11.4.4). Interpretation of these data is discussed by Bushnell and Angell (1992).

Delayed matching to position

Choice accuracy should decline from near 100% at the shortest delay to ~60% at the longest (chance performance for this two-choice task is 50%). Typical data are shown in

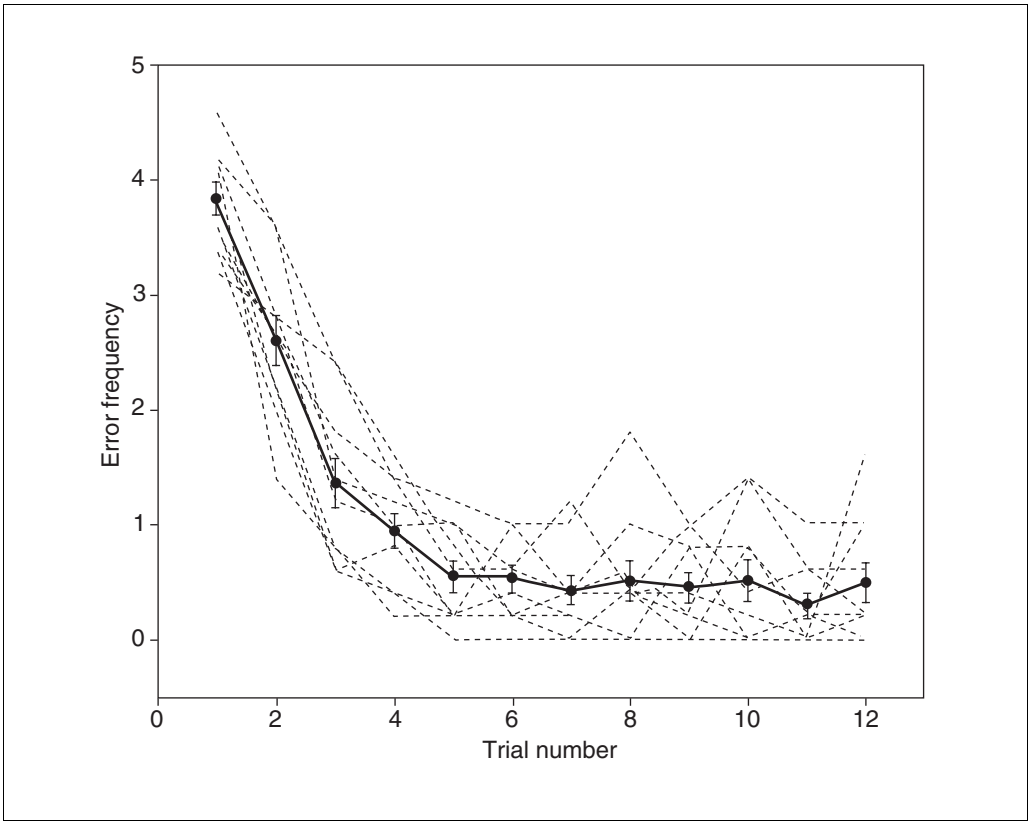

Figure 11.4.5 Representative data from a twelve-trial session of repeated acquisition in the eight-arm radial maze. The number of errors is plotted for each of ten rats (dashed lines) across twelve trials in a single test session. The mean ± SEM is also plotted (filled circles and solid line). The within-session reduction in error frequency indicates that learning is occurring. Note that each animal begins the session with ~4 errors on trial 1, that the error frequencies fall to ≤1 by about trial 5, and that the values are reasonably normally distributed around the mean at each trial.

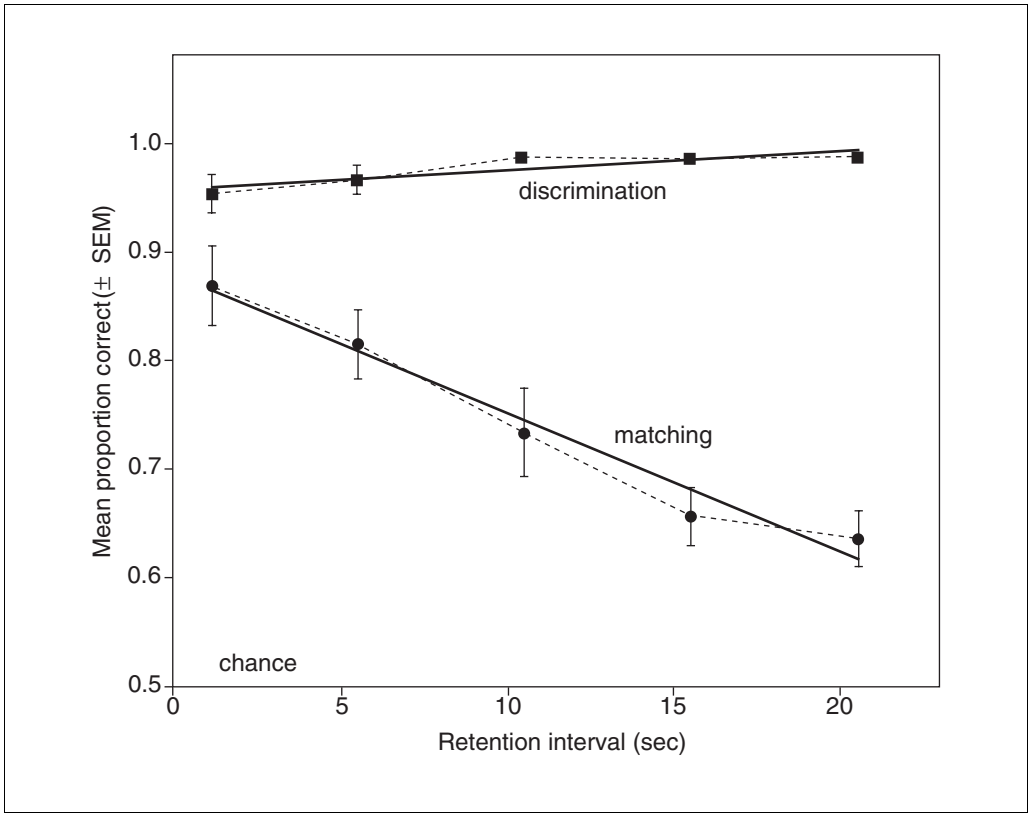

Figure 11.4.6 Representative data from a session of combined delayed matching to position (100 trials) and visual discrimination (100 trials). Points are mean choice accuracy (± SEM) for eight male rats as a function of delay on matching trials (circles), or across delays on discrimination trials (squares). The heavy lines show best-fit linear regressions through the five data points of each trial type. Note that matching accuracy falls across delays, reflecting the fact that the rats forget the trial-dependent sample information across time (working memory). Discrimination accuracy does not fall with increasing delay because the stimulus controlling discrimination accuracy (the cue light) is the same on all trials; thus, accuracy on these trials measures reference memory. Chance accuracy is 0.5 in this two-choice task.

the lower curve in Figure 11.4.6. Delays can be adjusted to establish an appropriate gradient for a given study. If the treatment of interest is expected to reduce accuracy, set the longest delay to produce no less than 70% accuracy; use a longer delay if an increase in accuracy is anticipated. If many sessions are run, expect gradual improvement in accuracy over time.

The theoretical form of the retention gradient is a negatively accelerated exponential. However, with a limited range of delay values, a linear approximation typically fits averaged data well. Linearly spaced delay values tend to produce quasi-linear retention gradients (e.g., Bushnell et al., 1993). Nonlinear gradients have also been modeled (e.g., White, 1985); the theoretical soundness of these gradients must be considered against the simplicity of linear gradients and the ease of their calculation. In any case, both approaches yield similar conclusions regarding the effects of drugs on this task.

Fitting a function to the data points provides the analytic advantage of reducing the number of statistical comparisons that are needed to test for changes in the gradient to two: slope and intercept. In addition, these parameters have interpretive value. The intercept can be considered the probability of encoding the sample stimulus at the beginning of the trial, and the slope the rate at which that information is lost over time (Heise and Milar, 1984; Bushnell, 1990; Paule et al., 1998).

If discrimination trials (see Support Protocol) are also run in this task, the accuracy should be relatively independent of delay (top curves in Fig. 11.4.6). A slight positive slope (increasing accuracy with delay) is not uncommon when matching and discrimination trials are intermixed in the same sessions. This pattern reflects interference with discrimination choice accuracy by the matching response rule, the effect of which decreases across delay, yielding

increased discrimination accuracy with increasing delay.

Sustained attention

When all values of signal strength are included, the gradient of accuracy should range from near chance performance with the weakest signals to near 100% accuracy with strongest signals (Fig. 11.4.7). Chance performance can be defined as the false alarm rate (i.e., the rate of pressing the signal lever during a blank trial), which should range from 5% to 20%, and not vary appreciably across signal intensity. If *P*(hit) at the lowest intensity is too high, increase the background illumination, which should be set during training to a level ≤0.1 times the brightest signal intensity. Interpretation of these data is discussed in Bushnell et al. (1997). *P*(hit) values for each rat at each signal intensity can also be corrected for "guessing" according to the following formula: $P^*(\text{hit}) = [P(\text{hit}) - P(\text{fa})]/[1 - P(\text{fa})]$ (Green and Swets, 1974). This correction assumes that the true proportion of hits, $P^*(\text{hit})$, is elevated by an amount proportional to *P*(fa), and removes that contribution from the observed *P*(hit).

Multiple fixed-interval/fixed-ratio schedule

Typical response patterns on the MULT FI/FR schedule were detailed by Ferster and Skinner (1957), whose data are reproduced by Lattal (1991); examples of drug effects on multiple schedules in rats can be found in Brocco and McMillan (1983). Note that the response rate is high and constant prior to reinforcement in the FR components; by contrast, responding begins slowly and increases with time prior to reinforcement in the FI components (the FI scallop). A clear and thorough analysis of the effects of two pesticides on a MULT FI 5-min/FR10 schedule is provided by Moser et al. (1987).

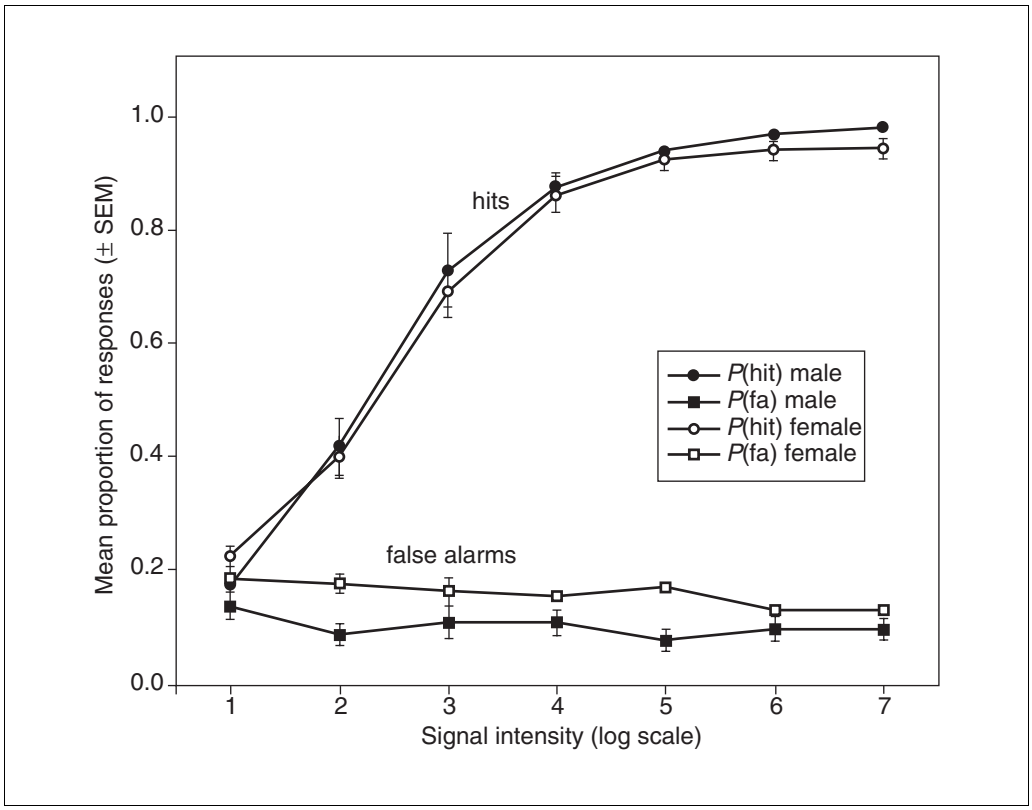

Figure 11.4.7 Representative data from a session of 300 trials of signal detection. These data show that *P*(hit) (the probability of a correct response on a signal trial; open or filled circles) increases with increasing signal intensity (in arbitrary units), whereas *P*(fa) (the probability of an incorrect response on a blank trial; open or filled square) does not vary with signal intensity. *P*(fa) provides an estimate of the probability of guessing (10% to 20%). Values are mean ± SEM for twelve animals per sex. Note that females perform slightly less well than males, primarily because of a higher false alarm rate. A decrease in attention is indicated by a decrease in *P*(hit) across all intensities, or an increase in *P*(fa), or both. A rightward shift in the *P*(hit) function—i.e., reduced *P*(hit) only at intermediate signal intensities—in the absence of an elevated *P*(fa) indicates an increase in threshold for detecting the signal, suggesting sensory impairment.

Time Considerations

Training animals is not a rapid process and achieving the baselines described in this unit requires many sessions. It is important that each animal reach the same criterion of proficiency at each stage of training, and there will necessarily be those animals that reach criterion quickly and those that reach it slowly. This fact has different consequences, depending upon whether untreated animals are being prepared for an experiment after baseline has been achieved, or whether the effects of a previous treatment with a test agent are being assessed.

In training untreated animals, there are two options for dealing with slow animals: (1) they can be retained in the study with additional time allotted for their training, or (2) they can be eliminated to speed up the process. The first option has the obvious disadvantage of taking more time, but preserves the representativeness of the sample of rats selected for the study; in other words, this sample will more accurately represent the population of all rats and will increase the generality of the results of the study. The second option restricts generalization to those rats that learn quickly, introduces a selection bias against those individuals potentially more at risk from the effects of chemical agents, and may require replacing some rats to preserve group sample sizes.

When assessing the effects of a prior treatment, slow learning must be considered as a possible result of that treatment. If some animals are to be segregated on the basis of their performance, criteria for segregation must be developed carefully and applied strictly to all treatment groups.

Autoshaping

After two weeks of acclimation to the animal facility and induction of motivation (hunger) prior to actual testing, an autoshaping study can be completed in two weeks. The first week should be spent handling the animals and acclimating them to transfer cages, test chambers, and the food pellets that will be delivered as reinforcers. The animals should be completely acclimated by the end of 1 week. Autoshaping should be accomplished during the second week, although it would be wise to allow part of a third week in case some animals acquire slowly. Each test session will last ~60 min (depending primarily upon the ITI; see Critical Parameters).

Repeated acquisition

A stable baseline of within-session error reduction should require 20 to 25 training sessions, including those described in *UNIT 11.3*. With 10 trials/session and a 10-sec ITI, each session should last no more than 10 min.

Delayed matching to position

Training to a stable baseline of DMTP performance requires ~40 test sessions (8 weeks at 5 days per week). If the visual discrimination component is also used, an additional 20 sessions (4 weeks) should be allowed to train the discrimination and integrate it into the complete schedule. DMTP test sessions of 100 trials and a maximum delay of 20 sec will require 45 to 50 min per day. To add visual discrimination, the number of trials should be doubled and each session should last 1.75 hr.

Sustained attention

Training to a stable baseline of performance in the sustained-attention task requires ~50 test sessions (10 weeks at 5 days per week). The length of each test session will depend upon the trial rate and the number of trials presented. A 300-trial session at 5 trials/min requires 60 min.

Multiple fixed-interval/fixed-ratio schedule

A simple ratio schedule can be escalated to FR10 in a matter of a week after the rat has learned to press the bar on the FR1 schedule. In contrast to mice, which will eagerly perform high ratios, rats may not perform ratios above 20 to 30 reliably (ratio strain). Performance of interval schedules may stabilize more quickly with respect to measures of patterning (e.g., index of curvature), although large differences between animals in response rate are common. Six to ten weeks (30 to 50 sessions) should be allowed for stability on a typical multiple schedule, although this estimate will depend upon the training history and stability criteria used. Daily sessions should require 30 to 45 min.

Literature Cited

Ali, J.S., Olszyk, V.B., Dunn, D.D., Lee, K.-A., Rhoderick R.R., and Bushnell. P.J. 1992. A LOTUS 1-2-3-based animal weighing system with a weight maintenance algorithm. *Behav. Res. Methods Instrum. Comput.* 24:82-87.

Ator, N.A. 1991. Subjects and instrumentation. *In* Experimental Analysis of Behavior, Part 1 (I.H. Iversen and K.A. Lattal, eds.) pp. 1-62. Elsevier Science Publishers, Amsterdam.

Boren, J.J. and Devine, D.D. 1968. The repeated acquisition of behavioral chains. *J. Exp. Anal. Behav.* 11:651-660.

Branch, M. 1991. Behavioral pharmacology. *In* Experimental Analysis of Behavior, Part 2 (I.H.

Iversen and K.A. Lattal, eds.) pp. 21-78. Elsevier Science Publishers, Amsterdam.

Brocco, M.J. and McMillan, D.E. 1983. Tolerance to *d*-amphetamine and lack of cross-tolerance to other drugs in rats under a multiple schedule of food presentation. *J. Pharmacol. Exp. Ther.* 224:34-39.

Brown, P.L. and Jenkins, H.M. 1968. Auto-shaping of the pigeon's keypeck. *J. Exp. Anal. Behav.* 11:1-8.

Bushnell, P.J. 1988. Effects of delay, inter-trial interval, delay behavior, and trimethyltin on spatial delayed response in rats. *Neurotoxicol. Teratol.* 10:237-244.

Bushnell, P.J. 1989. Behavioral effects of acute *p*-xylene inhalation in rats: Autoshaping, motor activity, and reversal learning. *Neurotoxicol. Teratol.* 10:569-577.

Bushnell, P.J. 1990. Modeling working and reference memory in rats: Effects of scopolamine on delayed matching-to-position. *Behav. Pharmacol.* 1:419-427.

Bushnell, P.J. 1998. Behavioral methods for the assessment of attention in animals. *Psychopharmacology* 138:231-259.

Bushnell, P.J. and Angell, K.E. 1992. Effects of trimethyltin on repeated acquisition (learning) in the radial-arm maze. *Neurotoxicology* 13:429-441.

Bushnell, P.J. and Kelly, K.L. 1992. Vigilance and selective attention in rats using auditory stimulus detection. *Soc. for Neurosci. Abstr.* 18:1062.

Bushnell, P.J., Padilla, S.S., Ward, T., Pope, C.N., and Olszyk, V.B. 1991. Behavioral and neurochemical changes in rats dosed repeatedly with diisopropylfluorophosphate (DFP). *J. Pharmacol. Exp. Ther.* 256:741-750.

Bushnell, P.J., Pope, C.N., and Padilla, S. 1993 Behavioral and neurochemical effects of acute chlorpyrifos in rats: Tolerance to prolonged inhibition of cholinesterase. *J. Pharmacol. Exp. Ther.* 266:1007-1017.

Bushnell, P.J., Kelly, K.L., and Crofton, K.M. 1994. Effects of toluene inhalation on detection of auditory signals in rats. *Neurotoxicol. Teratol.* 16:149-160.

Bushnell, P.J., Oshiro, W.M., and Padnos, B.K. 1997. Detection of visual signals by rats: Effects of chlordiazepoxide and cholinergic and adrenergic drugs on sustained attention. *Psychopharmacology* 134:242-257.

Carli, M., Robbins, T.W., Evenden, J.L., and Everitt, B.J. 1983. Effects of lesions to ascending noradrenergic neurones on performance of a 5-choice serial reaction task in rats: Implications for theories of dorsal noradrenergic bundle function based on selective attention and arousal. *Behav. Brain. Res.* 9:361-380.

Cohn, J. and Cory-Slechta, D.A. 1994. Assessment of the role of dopaminergic systems in lead-induced learning impairments using a repeated acquisition and performance baseline. *Neurotoxicology* 15:913-926.

Cohn, J. and Paule, M. 1995. Repeated acquisition of response sequences: The analysis of behavior in transition. *Neurosci. Biobehav. Rev.* 19:397-406.

Cohn, J., Cox, C., and Cory-Slechta, D.A. 1993. The effects of lead exposure on learning in a multiple repeated acquisition and performance schedule. *Neurotoxicology* 14:329-346.

Cohn, J. MacPhail, R.C., and Paule, M. 1996. Repeated acquisition and the assessment of centrally acting compounds. *Cognitive Brain Res.* 3:183-191.

Craig, A. and Davies, D.R. 1991. Vigilance: Sustained visual monitoring and attention. *In* Vision and Visual Dysfunction, Vol. 15: The Man-Machine Interface (J.A. Roufs, ed.) pp. 83-98. MacMillan, Basingstoke, England.

Davenport, J.W. 1974. Combined autoshaping-operant (AO) training: CS-UCS interval effects in the rat. *Bull. Psychon. Sci.* 3:383-385.

Dunnett, S.B. 1985. Comparative effects of cholinergic drugs and lesions of the nucleus basalis or fimbria-fornix on delayed matching in rats. *Psychopharmacology* 87:357-363.

Dunnett, S.B. and Martel, F.L. 1990. Proactive interference effects on short-term memory in rats: I. Basic parameters and drug effects. *Behav. Neurosci.* 104:655-665.

Dunnett, S.B., Rogers, D.C., and Jones, G.H. 1989. Effects of nucleus basalis magnocellularis lesions in rats on delayed matching and nonmatching to position tasks. *Eur. J. Neurosci.* 1:395-406.

Ferster, C. and Skinner, B.F. 1957. Schedules of Reinforcement. Prentice-Hall, Englewood Cliffs, N.J.

Fleschler, M. and Hoffman, H.S. 1963. A progression for generating variable-interval schedules. *J. Exp. Anal. Behav.* 5:529-530.

Fry, W., Kelleher, R.T., and Cook, L. 1960. A mathematical index of performance on fixed-interval schedules of reinforcement. *J. Exp. Anal. Behav.* 3:193-199.

Gleeson, S. 1991. Response acquisition. *In* Experimental Analysis of Behavior, Part 2 (I.H. Iversen and K.A. Lattal, eds.) pp. 63-86. Elsevier/North-Holland, Amsterdam.

Gollub, L.R. 1991. The use of computers in the control and recording of behavior. *In* Experimental Analysis of Behavior, Part 2 (I.H. Iversen and K.A. Lattal, eds.) pp. 155-192. Elsevier Science Publishing, Amsterdam.

Green, D.M. and Swets, J.A. 1974. Signal Detection Theory and Psychophysics. R.E. Krieger Publishing, Huntington, NY.

Heise, G.A. and Milar, K.S. 1984. Drugs and stimulus control. *In* Handbook of Psychopharmacology, Vol. 18 (L.L. Iversen, S.D. Iversen, and S.H. Snyder, eds.) pp. 129-190. Plenum, New York.

Heise, G.A. and Hudson, J.D. 1985. Effects of pesticides and drugs on working memory in rats:

Continuous delayed response. *Pharmacol. Biochem. Behav.* 23:591-598.

Herrnstein, R.J. and Morse, W.H. 1957. Effects of pentobarbital on intermittently reinforced behavior. *Science* 125:929-931.

Honig, W. 1978. Studies of working memory in the pigeon. *In* Cognitive Processes in Animal Behavior (S.H. Hulse, H. Fowler, and W.K. Honig, eds.) p. 213. Lawrence Erlbaum Associates, Hillsdale, N.J.

Hymowitz, N., Ploshnick, A., Laemle, L., and Brezenoff, H. 1990. Effects of repeated administration of soman on schedule-controlled behavior and brain in the rat. *Neurotoxicol. Teratol.* 12:47-56.

Lattal, K.A. 1991. Scheduling positive reinforcers. *In* Experimental Analysis of Behavior, Part 1 (I.H. Iversen and K.A. Lattal, eds.) pp. 87-134. Elsevier/North-Holland, Amsterdam.

Mackworth, J.F. 1970. Vigilance and Attention. Penguin, Baltimore, Md.

McGaughy, J. and Sarter, M. 1995. Behavioral vigilance in rats: Task validation and effects of age, amphetamine, and benzodiazepine receptor ligands. *Psychopharmacology* 117:340-357.

Messing, R.B. and Sparber, S.B. 1985. Greater task difficulty amplifies the facilitatory effect of *des*glycinamide arginine vasopressin on appetitively motivated learning. *Behav. Neurosci.* 99:1114-1119.

Moore, H., Dudchenko, P., Bruno, J.P., and Sarter, M. 1992. Toward modeling age-related changes of attentional abilities in rats: Simple and choice reaction time tasks and vigilance. *Neurobiol. Aging* 13:759-772.

Moser, V.C., Boyes, W.K., and MacPhail, R.C. 1987. Investigations of amitraz neurotoxicity in rats. *Fundam. Appl. Toxicol.* 9:131-139.

Muir, J.L., Page, K.J., Sirinathsinghji, D.J.S., Robbins, T.W., and Everitt, B.J. 1993 Excitotoxic lesions of basal forebrain cholinergic neurons: Effects on learning, memory and attention. *Behav. Brain Res.* 57:123-131.

Muir, J.L., Everitt, B.J., and Robbins, T.W. 1994. AMPA-induced excitotoxic lesions of the basal forebrain: A significant role for the cortical cholinergic system in attentional function. *J. Neurosci.* 14:2313-2326.

Nachreiner, F. and Hänecke, K. 1992. Vigilance. *In* Handbook of Human Performance, Vol. 3: State and Trait (A.P. Smith, and D.M. Jones, eds.) pp. 261-288. Academic Press, London.

Ohno, M., Yamamoto, T., and Watanabe, S. 1992. Effects of intrahippocampal injections of NMDA receptor antagonists and scopolamine on working and reference memory assessed in rats by a three-panel runway task. *J. Pharmacol. Exper. Ther.* 263:943-950.

Parasuraman, R. 1984. The psychobiology of sustained attention. *In* Sustained Attention in Human Performance (J.S. Warm, ed.) pp. 61-101. John Wiley & Sons, New York.

Parasuraman, R., Warm, J.S., and Dember, W.N. 1987. Vigilance: Taxonomy and utility. *In* Ergonomics and Human Factors (L.S. Mark, J.S. Warm, and R.L. Huston, eds.) pp 11-32. Springer-Verlag, New York.

Paule, M.G., Bushnell, P.J., Maurissen, J.P.J., Wenger, G.R., Buccafusco, J.J., Chelonis, J.J., and Elliott, R. 1998. Symposium overview: The use of delayed matching-to-sample procedures in studies of short-term memory in animals and humans. *Neurotoxicol. Teratol.* 20:493-502.

Peele, D.B. and Baron, S.P. 1988. Effects of scopolamine on repeated acquisition of radial-maze performance by rats. *J. Exp. Annal. Behav.* 49:275-290.

Perone, M. 1991. Experimental design in the analysis of free-operant behavior. *In* Experimental Analysis of Behavior, Part 1 (I.H. Iversen and K.A. Lattal, eds.) pp. 135-172. Elsevier/North-Holland, Amsterdam.

Poplawsky, A. and Phillips, C.L. 1986. Autoshaping a lever press in rats with lateral, medial, or complete septal lesions. *Behav. Neural Biol.* 45:319-328.

Robbins, T.W. and Everitt, B.J. 1995. Arousal systems and attention. *In* The Cognitive Neurosciences (M.S. Gazzaniga, ed.) pp. 703-720. MIT Press, Cambridge, Mass.

Roberts, W.A. and Kraemer, P.J. 1982. Some observations of the effects of intertrial interval and delay on delayed matching to sample in pigeons. *J. Exp. Psychol. Anim. Behav. Processes* 8:342-353.

Schwartz, B. and Gamzu, E. 1977. Pavlovian control of operant behavior. *In* Handbook of Operant Behavior (W.K. Honig and J.E.R. Staddon, eds.) pp. 53-97. Prentice-Hall, Englewood Cliffs, N.J.

Spencer, D.G. Jr., Pontecorvo, M.J., and Heise, G.A. 1985. Central cholinergic involvement in working memory: Effects of scopolamine on continuous nonmatching and discrimination performance in the rat. *Behav. Neurosci.* 99:1049-1065.

Thomas, J.R., Ahlers, S.T., and Schrot, J. 1991. Cold-induced impairment of delayed matching in rats. *Behav. Neural Biol.* 55:19-30.

Thompson, D.M. 1974. Repeated acquisition of behavioral chains under chronic drug conditions. *J. Pharmacol. Exp. Ther.* 188:700-713.

Thompson, D.M. 1975. Repeated acquisition of response sequences: Stimulus control and drugs. *J. Exp. Annal. Behav.* 23:429-436.

Van Haaren, F., Van Hest, A., and Van de Poll, N.E. 1987. Acquisition and reversal of a discriminated autoshaped response in male and female rats: Effects of long or short and fixed or variable intertrial interval durations. *Learn. Motiv.* 18:220-233.

White, K.G. 1985. Characteristics of forgetting functions in delayed matching to sample. *J. Exper. Anal. Behav.* 44:15-34.

Key References

Bushnell, 1998. See above.

This review article describes a large number of approaches to the assessment of attention in experimental animals, primarily rodents. It also discusses general issues regarding the assessment of hypothetical cognitive processes, and the validation of procedures for conducting those assessments.

Cohn and Paule, 1995; Cohn et al., 1996. See above.

This pair of reviews thoroughly covers the realm of repeated acquisition of response sequences, providing a history of the area and background information regarding the approach and implementation of repeated acquisition methods for assessing learning. The first paper reviews the behavioral phenomena and the second the influence of drugs and toxic chemicals on these behaviors.

Heise and Milar, 1984. See above.

This review chapter very nicely lays out the rationale and taxonomy of procedures for assessing learning and memory in animals. The section on memory is particularly useful for understanding and interpreting tests of working memory (e.g., DMTP).

Iversen, I.H. and Lattal, K.A. (eds.) 1991. Experimental Analysis of Behavior, Parts 1 and 2. Elsevier/North-Holland, Amsterdam.

These two volumes discuss clearly and in detail behavioral methods for quantifying and analyzing the behavior of experimental animals. The contributions provide a wealth of information regarding basic techniques for handling and testing animals, and for quantifying patterns of behavior engendered by a wide variety of reinforcement schedules.

Parasuraman, 1984. See above.

This review chapter detailed current knowledge of sustained attention in humans. Much of the development of sustained attention methods in animals is based upon knowledge of human performance of these tasks and the variables that affect it.

Robbins and Everitt, 1995. See above.

This chapter very clearly summarizes current knowledge about the role of the ascending arousal systems in the CNS on attention in animals, as assessed primarily with the 5-choice serial reaction-time test. It is a good general reference for understanding the neurobiological substrates of readiness and directed attention.

Schwartz and Gamzu, 1977. See above.

This chapter reviews various phenomena of autoshaping, primarily in terms of the associative processes (operant and respondent) that support this unique form of conditioning. The chapter provides a readable presentation of many of the variables found to influence acquisition and maintenance of sign-tracking behaviors, the kinds of behaviors that are supported by autoshaping contingencies, generalization to automaintenance schedules, and the theoretical analysis of the phenomenon.

Contributed by Philip J. Bushnell
National Health and Environmental Effects Research Laboratory
U.S. Environmental Protection Agency
Research Triangle Park, North Carolina

Testing for Organophosphate-Induced Delayed Polyneuropathy

Organophosphorus compounds may cause two distinct types of toxicity: acute cholinergic toxicity and organophosphate-induced delayed polyneuropathy (OPIDP). Evaluating the capability of a compound to cause OPIDP requires treatment of animals (hens) with that compound and measurement of biochemical, clinical, and, when possible, morphological parameters. Generally, hens are administered single doses of organophosphate (OP) and, if necessary, are treated to prevent cholinergic toxicity. Determination of the activity of the putative molecular target for OPIDP—neuropathy target esterase (NTE)—in brain, spinal cord, and peripheral nerve is performed after 1 or 2 days, in association with determination of acetylcholinesterase (AChE) activity. AChE is the target of the acute toxicity, and measurement of its inhibition compared to that of NTE is necessary to assess the potential of a given compound to preferentially cause either toxicity. If high AChE inhibition occurs at doses not causing NTE inhibition, the compound is unlikely to cause OPIPD because animals will not survive the higher doses required. Observation for clinical signs of OPIDP is carried out for up to 3 weeks after treatment, and morphological assessment of selected regions of the central and peripheral nervous system might be performed after 3 weeks (see Basic Protocol 1). Because OPIDP development is associated with >75% NTE inhibition, in the case of negative clinical and morphological findings, measurement of NTE activity (see Basic Protocol 2) gives an indication of the compound's potential to cause OPIDP at higher doses.

Single doses of compounds that might potentially protect from OPIDP (e.g., phosphinates, carbamates, or sulfonyl fluorides) are usually administered to hens 4 to 24 hr before administration of an effective dose of a neuropathic OP. Determination of NTE activity after treatment with these potentially protective compounds is performed at the same time point as that of the administration of the neuropathic OP. More than 30% NTE inhibition is expected to be associated with protection from a subsequent challenging dose of a neuropathic OP. Clinical and morphological observations are carried out as above. When testing a new OP, a control group of hens is pretreated with a known protective compound.

In vitro screening tests might also be useful in identifying NTE inhibitors when the parent compound does not need metabolic activation (see Alternate Protocol). Comparison with their ability to inhibit AChE will also be helpful in assessing the relative potency of the compound to preferentially cause OPIDP or acute cholinergic toxicity.

NOTE: OPs and other esterase inhibitors are generally dangerous compounds (neurotoxicants), and the pure material should be handled with care, using gloves in a chemical fume hood. In case of a spill, clean the area with a 4% to 10% solution of NaOH in 50% water/50% industrial methylated spirits, which should always be available.

NOTE: All protocols using live animals must first be reviewed and approved by an Institutional Animal Care and Use Committee (IACUC) or must conform to governmental regulations regarding the care and use of laboratory animals.

INDUCTION AND EVALUATION OF OPIDP IN HENS

BASIC PROTOCOL 1

This procedure is used to assess the potential of an OP to cause OPIDP in vivo. Neuropathic compounds are usually administered in a single dose, and are expected to cause clinical signs of OPIDP within 8 to 15 days after dosing. Protective compounds (also NTE inhibitors) are administered to a test group of the animals before the neuropa-

Contributed by Angelo Moretto
Current Protocols in Toxicology (1999) 11.5.1-11.5.14

thic OP. Assessments are made on the basis of a scoring system which classifies the animals according to the severity of the clinical findings. Hens are sacrificed and perfused ~3 weeks after treatment, and assessments are made on the basis of another scoring system,which classifies the animals according to the severity of the morphological lesions.

Materials

Adult domestic laying hens (>6 months of age, preferably 8 to 14 months), standard size, breeds, and strains
Protective compound: e.g. phenylmethylsulfonyl fluoride (PMSF)
Organophosphate to be tested
Saline or glycerol formal (or other vehicles such as dimethylsulfoxide or corn oil)
20 mg/ml atropine sulfate (e.g., Aldrich) in saline
0.1 mg/ml eserine hemisulfate (e.g., Sigma) in saline
200 mg/ml pyridine-2-aldoxime-1-methanesulfonate (e.g., Sigma; or other oxime) in saline
50 mg/ml ketamine in saline
Halothane
Oxygen
Heparin
100 mM sodium phosphate buffer, pH 7.4 (*APPENDIX 2A*)
4% paraformaldehyde, pH 7.4 (see recipe)
4% formalin: dilute 40% commercial formalin solution to 4% with 100 mM sodium phosphate buffer, pH 7.4

Animal house, equipped to rear adult hens under conditions that permit free mobility
Gavage needles
21/22-G needles for intraperitoneal, subcutaneous, and intramuscular injection
Vaporizer for anesthetic gases
Anesthetizing box (see recipe)
Wooden dissecting board appropriate for hens
Dissecting equipment including:
  Scalpels
  Forceps
  Bone cutter
  Heavy and small scissors
Perfusion apparatus: peristaltic pump (50 to 200 ml/min) with connecting tubes and a cannula (a gavage needle can be used)
Large (>5 liter) container for the perfusion solution, with faucet on bottom
5- to 50-ml plastic containers with leak-proof caps to store tissues sampled for histology

Treat animals with compounds to be tested

1. Fast hens overnight if the oral route of administration is to be used.

2. Dissolve compounds (protective compound and organophosphate) in the appropriate vehicle (saline if water-soluble; otherwise dissolve in appropriate solvent e.g., glycerol formal, corn oil, or DMSO). Prepare solution to have the desired dose administered in the following volumes of administration.

   Gavage: 1 ml/kg
   Subcutaneous injection: 0.2 ml/kg (if the test compound is poorly soluble, use up to 1 ml/kg and two sites of injection, preferably in the anterot-horacic region)

The choice of the dose of the compound under test can be based on preliminary experiments where NTE has been measured (see Basic Protocol 2). The dose should cause >70% NTE inhibition or the maximum attainable inhibition. If there is significant acute cholinergic toxicity (whose signs include mitosis, hypersalivation, diarrhea, muscle fasciculation or, if severe, paralysis), adequate treatment (step 5) will significantly increase the LD_{50}.

3. Assign animals to experimental groups including at least the following:

   a. Control (vehicle-treated) group.
   b. A group to be treated with one dose level of the compound under study.
   c. A group be pretreated with a protective compound (e.g., 30 mg/kg PMSF, subcutaneously, 24 hr before dosing, as in group "b").

   Three animals per group are generally sufficient for a yes/no evaluation. Five or more are required to estimate a dose-response relationship.

4. Pretreat group "c" with the protective compound at the appropriate time interval before administration of the test compound, with the desired doses administered in the volumes listed in step 2. Pretreat groups "a" and "b" with vehicle.

5. If treatment against cholinergic toxicity is required, inject the hens intraperitoneally, 10 min before administration of the test compound, with 1 ml/kg of a 20 mg/ml solution of atropine (20 mg/kg) and 1 ml/kg of a 0.1 mg/ml solution of eserine (0.1 mg/kg).

6. Treat groups "b" and "c" with the organophosphate, with the desired doses administered in the volumes listed in step 2. Treat group "a" with vehicle only.

7. Depending on severity of cholinergic toxicity, inject again with atropine (after dosing with the test compound) intraperitoneally, at the same dose as in step 5, as needed, and with 0.5 ml/kg of a 200 mg/ml solution of pyridine-2-aldoxime-1-methanesulfonate (100 mg/kg), every 8 to 12 hr, intramuscularly, either in the anterothoracic muscles (preferably) or in the muscles of the thigh.

   Duration of treatment with atropine and pyridine-2-aldoxime-1-methanesulfonate will depend on duration of cholinergic signs. These can be estimated in a pilot experiment which includes a prolonged (2- to 4-day) observation of the animals and/or measurement of the time course of AChE inhibition. More than 60% inhibition is associated with signs of toxicity; death occurs at >95% AChE inhibition.

Observe animals for clinical symptoms

8. Observe the hens in an open space, not in the cage, every other day for up to 21 days after treatment. After 2 to 3 min of free walking, evaluate the animals according to the following 0- to 8-point scoring system:

   0: No defects in posture, standing ability, or walking performance
   1: Minor changes in walking performance
   2: Clear changes in walking performance with some falling of the hind end
   3: Walking limited to short steps with frequent falling of the hind end
   4: Still able to walk, but often remain sitting on metatarsus
   5: Unable to walk, sitting on metatarsus, but able to stand when lifted
   6: Unable to stand when lifted
   7: Unable to stand, wings drop
   8: Unable to stand, extended legs and wings.

   Onset is usually between days 8 and 14 and peak score is reached by days 15 to 18.

   It might be necessary to sacrifice the hens for humane reasons when OPIDP is severe (grades 6 to 8) because they cannot feed or drink.

9. *Optional:* Evaluate the leg-retraction reflex by placing a hand under the breast and lifting the hen, observing whether the animal retracts its leg from the dangling position.

   A normal animal retracts its leg from the dangling position. If peripheral nerve lesions are present, the leg will remain extended and flaccid. Assess this reflex before dosing, since a few hens may have spontaneously lost it and therefore should not be used in the test.

Perform morphological assessment

10. At the end of the observation period, ~21 days, deeply anesthetize hens with an injection of 1 ml/kg ketamine (50 mg/kg intraperitoneally) followed by inhalation of 3% to 4% halothane with 1.5 liters/min oxygen in an anesthetizing box.

    CAUTION: *Perform the procedure in a chemical fume hood, and use gloves, goggles, and a mask.*

11. Remove the hen from the anesthetizing box and secure it on its back on a wooden board by tying the spread legs to the corners of the board with ropes, and pinning the head and the spread wings with needles.

12. Carefully open the abdomen with a scalpel just below the rib cage. Make and incision in the middle, below the sternum and along the rib cage, of ~10 cm, taking care not to cut the liver, which is just below the surface.

13. Cut the rib cage laterally with scissors and reflect the sternum backwards (the bone is very hard) with the attached distal part of the ribs.

14. Expose the heart and inject 1500 to 2000 U heparin into the heart. Cut the pericardium, then the wall of the right atrium, and finally the apex of the left ventricle.

15. Start the pump (100 to 150 ml/min) and insert the cannula in the left ventricle. Clamp the cannula.

    The tip of the cannula must be within the heart to obtain optimal perfusion.

16. Perfuse for ~1 min with 100 mM sodium phosphate buffer, pH 7.4, then switch to paraformaldehyde solution until the animal is stiffened, or until ~4 liters of perfusion solution (15 to 20 min in total) have been perfused.

17. Dissect the sciatic nerve (n. ischiadicum) and its main branches, the peroneal (n. peronaeus) and the tibial (n. tibialis) nerves to the ankle, the lumbo-sacral (easily recognizable by the presence of the glycogen body), the mid-thoracic and the upper cervical spinal cord, and the brain.

    Avoid tissue drying during dissection by bathing exposed tissues with 4% paraformaldehyde fixative. Manipulate tissues as little as possible with forceps. See Koch (1973) for anatomical details.

18. Keep the samples in 4% formalin, in plastic containers with leak-proof caps until processed.

19. Score axonal lesions in peripheral nerves, spinal cord tracts, cerebellum, and medulla oblongata (other areas of the brain are optional) according to the following semi-quantitative scoring system:

    0: No abnormality
    1: Occasional disruption of axons (one to four disruptions in any spinal cord slide, one or two disruptions in any peripheral nerve slide) with rare myelin abnormalities (these might be found in control animals)

2: Fragmentation/disruption of few axons (five or more in any spinal cord slide, three or more in any peripheral nerve slide) with minimal myelin changes (spheroids)
3: Extent of damage greater than in 2; changes as described in 4, but not as widespread
4: Widespread fragmentation/disruption of many axons, with variation in thickness; distortion/fragmentation of myelin sheaths; glial/Schwann cell response.

See Bickford and Sprague (1983) and Prentice and Roberts (1983) for details of scoring procedure, and Sprague et al. (1980) for description of lesions.

DETERMINATION OF NEUROPATHY TARGET ESTERASE ACTIVITY

BASIC PROTOCOL 2

This protocol describes a spectrophotometric assay to determine the activity of neuropathy target esterase (NTE) in nervous tissues. NTE activity is determined as the phenyl valerate (PV) esterase activity that is resistant to inhibition by paraoxon (a non-neuropathic organophosphate) and sensitive to inhibition by mipafox (a neuropathic organophosphate). Tissue homogenates are preincubated with these inhibitors prior to PV addition. Hydrolysis is stopped by protein denaturation (and sometimes precipitation) followed by colorimetric measurement of the phenol content of the sample.

Materials

Adult domestic laying hens (>6 months of age, preferably 8 to 14 months), standard size, breeds, and strains
Organophosphate (OP) to be tested, in appropriate solvent (see Basic Protocol 1)
Tris/EDTA buffer (see recipe), ice-cold
10 mM mipafox stock solution (see recipe)
10 mM paraoxon stock solution (see recipe)
15 and 30 mg/ml phenyl valerate (PV) stock solutions (see recipe)
0.03% (v/v) Triton X-100 in double-distilled water
SDS/AAP solution (see recipe)
0.4% (w/v) $K_3Fe(CN)_6$ in double-distilled water (stable for months at room temperature)
Modified Koenig buffer: 0.7 M glycine/0.05 M triethylamine·HCl, pH 6.0 (store up to 2 months at 4°C)
0.35 M perchloric acid/0.36 M sodium acetate
Tris/AAP buffer (see recipe)

Guillotine
Forceps
Scalpel
Polytron homogenizer (Brinkmann) with PTA 10S and 7S sondes (for brain and spinal cord, a glass-Teflon Potter-Elvehjem homogenizer can be used; for the peripheral nerve this might pose some problems and require more time)

NOTE: All procedures performed at room temperature unless otherwise specified.

Dose, sacrifice, and dissect hens

1. Administer OP to the hens (see Basic Protocol 1)

   Give the compound used to protect from OPIDP (e.g., PMSF) alone if its (protective) effect on NTE is to be tested.

2. Sacrifice hens with a guillotine, generally 24 hr after dosing.

   Three animals per group are generally sufficient to determine a dose-response relationship. Timing of sacrifice may change depending on the toxicokinetics of the compound under study.

3. Remove brain, spinal cord (lumbo-sacral), and sciatic nerves with their two major branches, down to the ankle (see Basic Protocol 1, step 17). Put tissues in ice-cold Tris/EDTA buffer.

Determine NTE

For brain and spinal cord

4a. Remove fat, meninges, and vessels. Weigh the tissues. Prepare a 10% (w/v) homogenate in Tris/EDTA buffer using a Polytron (with PTA 10S sonde, at speed 7, for 10 sec). Dilute the homogenate (for brain 1:15; for spinal cord 1:10) with Tris/EDTA buffer.

5a. Prepare paraoxon and mipafox working solutions as follows.

Paraoxon: mix 0.1 ml of 10 mM stock solution with 6.15 ml Tris/EDTA buffer.
Mipafox: mix 0.1 ml of 10 mM stock solution with 4.9 ml Tris/EDTA buffer.

6a. Assemble reaction mixtures as described in Table 11.5.1 and incubate 20 min at 37°C.

7a. Prepare working suspension of PV by adding 1 vol of 15 mg/ml PV stock solution to 30 vol of 0.03% Triton X-100. Add 1 ml of the suspension to each tube and incubate brain 15 min or spinal cord 25 min at 37°C.

The substrate that will be added to the tubes is actually a white, cloudy dispersion rather than a solution.

8a. Terminate reactions by adding 1 ml of SDS/AAP solution to each tube, then add 0.5 ml of homogenate to tube 3. Mix thoroughly and add 0.5 ml of 0.4% $K_3Fe(CN)_6$ solution to each tube. Wait at least 3 min, then measure absorbance at 510 nm.

The color is stable for at least 30 min. Under these conditions, the molar extinction coefficient (ε_{510}) for phenol (the hydrolysis product of PV) is ~13,900 M^{-1} cm^{-1}.

9a. Calculate activity in each tube according to the following equations.

Brain:

$$\frac{OD_{510}}{13{,}900}\times\left(3.5\times10^{-3}\right)\times\frac{1}{15}\times\frac{1}{0.0033}\times10^{6}$$

$$=(\mu\text{mol PV hydrolyzed})\cdot\text{min}^{-1}\cdot(\text{g tissue})^{-1}$$

Spinal cord:

$$\frac{OD_{510}}{13{,}900}\times\left(3.5\times10^{-3}\right)\times\frac{1}{15}\times\frac{1}{0.0033}\times10^{6}$$

$$=(\mu\text{mol PV hydrolyzed})\cdot\text{min}^{-1}\cdot(\text{g tissue})^{-1}$$

where 3.5×10^{-3} is the total reaction volume in liters, 15 and 25 min are the incubation times respectively, for brain and spinal cord, and 0.0033 and 0.005 g are the weights, respectively, of brain and spinal cord tissue added to the reactions on the basis of the dilutions made in step 4a and the aliquots of homogenate added to the reactions.

10a. Calculate NTE activity as the activity measured in tube 1 minus that in tube 2.

The blank (tube 3) is not used in the calculations, but it is added for control of activity in tube 2 and development of color.

Table 11.5.1 Preparation of NTE Reaction Mix for Brain and Spinal Cord

Tube	Paraoxon working solution[a]	Tris/EDTA buffer	Mipafox working solution[b]	Homogenate
1	0.25 ml	0.25 ml	—	0.5 ml
2	0.25 ml	—	0.25 ml	0.5 ml
3 (blank)	0.25 ml	—	0.25 ml	—[c]

[a]Refers to working solution prepared in step 5a; final concentration in each tube will be 40 µM.

[b]Refers to working solution prepared in step 5a; final concentration in each tube will be 50 µM.

[c]Add 0.5 ml of homogenate at step 8a, after the PV solution.

Table 11.5.2 Preparation of NTE Reaction Mix for Peripheral Nerve

Tube	Paraoxon working solution[a]	Tris/EDTA buffer	Mipafox working solution[b]	Supernatant
1	0.05 ml	0.05 ml	—	1.0 ml
2	0.05 ml	—	0.05 ml	1.0 ml
3	0.05 ml	—	0.05 ml	—[c]

[a]Refers to working solution prepared in step 5b; final concentration in each tube will be 40 µM.

[b] Refers to working solution prepared in step 5b; final concentration in each tube will be 50 µM.

[c]Add 1 ml of supernatant at step 8b, after the PV solution.

For peripheral nerve

4b. Cut the nerve into 1 to 1.5-cm segments and immerse in modified Koenig buffer at 0°C for ~2 hr. Remove the fat and collagen and desheath the nerve with fine forceps and a scalpel. Rinse the tissue in water to remove excess glycine, gently dry on filter paper, and weigh. Using a Polytron (PTA 7S sonde, at speed 7, three times for 10 sec), prepare a 40 mg/ml homogenate in Tris/EDTA buffer. Centrifuge for 10 min at 1000 × *g*, 4°C, and use the supernatant for the assay.

Tissues can be frozen after weighing (the enzymatic activity is stable for months at –80°C if tissues are frozen within hours of sampling). Loss of activity is expected if homogenates are frozen.

5b. Prepare paraoxon and mipafox working solutions as follows.

Paraoxon: mix 0.1 ml 10 mM stock solution with 1.04 ml Tris/EDTA buffer
Mipafox: mix 0.1 ml of 10 mM stock solution with 0.81 ml Tris/EDTA buffer

6b. Assemble reaction mixtures as described in Table 11.5.2 and incubate 20 min at 37°C.

7b. Prepare a working suspension of PV by adding 1 vol of 30 mg/ml PV stock solution to 30 vol of 0.03% Triton X-100. Add 1 ml of this suspension to each tube and incubate 35 min at 37°C.

8b. Terminate the reaction by adding 1 ml ice-cold perchloric acid/sodium acetate solution, then add 1 ml of the supernatant obtained in step 4b to tube 3. Mix thoroughly, keep in ice-cold bath for 5 to 10 min, then centrifuge ~5 min at 1000 × *g*, 4°C.

9b. Place 2 ml of the supernatant in a fresh tube, then add 1 ml of Tris/AAP buffer and 0.5 ml of 0.4% $K_3Fe(CN)_6$ solution. Measure absorbance at 510 nm.

Under these conditions, the ε_{510} for phenol (the hydrolysis product of PV) is ~13,900 M^{-1} cm^{-1}.

10b. Calculate activity in each tube according to the following equation:

$$\frac{OD_{510}}{13{,}900} \times \left(3.5 \times 10^{-3}\right) \times \frac{3.1}{2} \times \frac{1}{35} \times \frac{1}{0.04}$$

$$= (\mu\text{mol PV hydrolyzed}) \cdot \text{min}^{-1} \cdot (\text{g tissue})^{-1}$$

where 3.5×10^{-3} is the total reaction volume in liters, 3.1/2 is the dilution factor, 35 min is the incubation time, and 0.04 is the weight of tissue added.

11b. Calculate NTE activity as the activity measured in tube 1 minus that in tube 2.

The blank (tube 3) is not used in the calculations, but it is added for control of activity in tube 2 and development of color.

ALTERNATE PROTOCOL

DETERMINATION OF THE IN VITRO INHIBITORY POWER OF A COMPOUND ON NTE

This protocol can be applied to compounds that do not need metabolic activation. It provides information on the inhibitory power of the compound on NTE which, in combination with the inhibitory power on AChE, gives an indication of the potency to cause OPIDP relative to acute toxicity. Data might also be helpful for interspecies comparisons (including human).

Additional Materials *(also see Basic Protocol 2)*

Test compound (putative inhibitor)
Acetone

1. Prepare a 10 mM stock solution in acetone of the compound under study. Prepare working solutions in acetone at 100× the desired final assay concentration.
2. Perform steps 1 to 5a or 5b of Basic Protocol 2 (depending on the target tissue).

3a. *For fixed-time incubations:* Assemble the reaction mixtures according to Table 11.5.1 or 11.5.2 (see Basic Protocol 2, step 6a or 6b), but add 10 µl of the 100× test compound to each incubation tube (including blank) in addition to the paraoxon, buffer, and mipafox. Add homogenates and proceed as described in the remaining steps of Basic Protocol 2.

Control samples (not containing the inhibitor) should contain 10 µl acetone, although 1% acetone has no or minimal effect on NTE activity.

3b. *For a time course of inhibition:* Assemble the reaction mixtures according to Table 11.5.1 or 11.5.2 (see Basic Protocol 2, step 6a or 6b). Add 10 µl of the chosen concentration(s) of test compound at various times (0 to 20 min) after addition of homogenates to the tubes containing paraoxon, buffer, and mipafox. For each time point, proceed as described in the remaining steps of Basic Protocol 2. Calculate the percentage of activity/inhibition as compared to a control sample (10 µl of acetone alone).

REAGENTS AND SOLUTIONS

Use Milli-Q-purified water or equivalent for all recipes and protocol steps. For common stock solutions, see ***APPENDIX 2A****; for suppliers, see* ***SUPPLIERS APPENDIX****.*

4-Aminoantipyrine, 0.5%

Prepare a 0.5% (w/v) solution of 4-aminoantipyrine (4-AAP; also called 4-aminophenazone; e.g., Sigma) in 50 mM Tris·Cl, pH 8.0 (*APPENDIX 2A*).

This solution is stable for a few months if kept in the dark at room temperature.

Anesthetizing box

Custom-prepare a 20 × 15 × 10–cm Plexiglas box with a 1-cm-diameter inlet and outlet for the anesthetic gas. Have one of the walls divided into two halves—one fixed, the other capable of being opened. Make a hole ~5 cm in diameter in the center of this wall (so that it is equally divided between the two halves and will close, stock-like, around the neck of the hen). Put a ring made of soft rubber around the hole.

To put the head of the hen into the box, open the half-wall, lay the neck on the hole and close the wall.

Mipafox stock solution, 10 mM

Dissolve 1.82 mg/ml of solid mipafox (Oryza Laboratories; 10 mM final) in Tris/citrate buffer (see recipe). This solution is stable for ~3 weeks at room temperature. Prepare the working solutions on day of use (see Basic Protocol 2, step 5a or 5b).

CAUTION: *Mipafox is a dangerous neurotoxicant. Handle solid mipafox with care using gloves under a chemical fume hood. In case of spill, clean with a 4% to 10% solution of NaOH in water/industrial methylated spirits which should always on hand. There is no significant hazard in handling small volumes of the solution.*

Paraformaldehyde solution, 4%

Dissolve paraformaldehyde to 4% (w/v) in warm 100 mM sodium phosphate buffer, pH 7.4 (*APPENDIX 2A*). Store up to a few days at 4°C.

CAUTION: *Paraformaldehyde is a strong irritant. The operation should be performed under a chemical fume hood. Use gloves, goggles and a mask.*

Paraoxon stock solution, 10 mM

Dissolve 2.75 mg/ml paraoxon (Sigma) in dry acetone (obtained by placing a layer of anhydrous Na_2SO_4 at the bottom of the container). Close vial tightly to avoid evaporation of acetone. Store up to several months in a desiccator at room temperature.

When using small volumes of acetone it is advisable to cool the solution on ice to reduce evaporation.

In the past, certain paraoxon batches contained small amounts of an impurity [ethyl bis-(4-nitrophenyl) phosphate] that inhibits NTE; therefore, purification of paraoxon was necessary. The authors now use paraoxon from Sigma, which does not require purification.

CAUTION: *Paraoxon is a dangerous neurotoxicant. Handle pure paraoxon with care using gloves under a chemical fume hood. In case of a spill, clean with a 4% to 10% solution of NaOH in 50% water/50% industrial methylated spirits, which should always be kept on hand. There is no significant hazard in handling small volumes of the solution.*

Phenyl valerate (PV) stock solutions, 15 and 30 mg/ml

Dissolve phenyl valerate (PV; Oryza Laboratories) in redistilled dimethylformamide to concentrations of 15 or 30 mg/ml (depending on the tissue under study; see Basic Protocol 2). Store stock solutions up to 3 weeks (or longer) in the dark at room temperature. Prepare working suspension (see Basic Protocol 2, steps 7a and 7b) on day of use.

If PV contains an excessive amount of phenol (giving a blank absorbance of >0.150), remove it by washing PV in a separatory funnel in petroleum ether 60–80° with ice-cold 2 N NaOH followed by washing with water, drying over anhydrous sodium sulfate, and removal of solvent.

SDS/AAP solution

Prepare a 1% (w/v) solution of sodium dodecyl sulfate (SDS) in 50 mM Tris·Cl, pH 8.0 (*APPENDIX 2A*). Mix 950 ml of the SDS solution with 50 ml of 0.5% 4-aminoantipyrine (see recipe). Store up to several weeks in a dark glass bottle at room temperature.

SDS dissolves rather slowly; dissolution can be accelerated by warming in a 35° to 40°C water bath.

Tris/AAP buffer

Mix 95 ml of 0.5 M Tris·Cl, (pH 9.0 at 25°C; *APPENDIX 2A*) and 5 ml of 0.5% 4-aminoantipyrine (see recipe). Prepare fresh daily.

Tris/citrate buffer

Prepare 50 mM Tris base in water and 50 mM citric acid in water. Titrate the Tris solution with the citric acid to reach a pH of 6.0 at 25°C. Store up to 1 month at 4°C.

Tris/EDTA buffer

Add 4 ml of 0.5 M EDTA (ethylenediaminetetraacetic acid disodium salt, dihydrate; *APPENDIX 2A*) to 996 ml of 50 mM Tris·Cl, pH 8.0 at 25°C (*APPENDIX 2A*). Store up to 1 month at 4°C.

COMMENTARY

Background Information

This unit describes procedures for the assessment of the neuropathic potential of an organophosphate (OP) compound [(thio)phosphate, (thio)phosphonate, phosphoro(thio)amidate] or the ability of other esterase inhibitors (carbamates, phosphinates, and sulfonyl fluorides) to provide protection from induced delayed polyneuropathy (OPIDP) caused by OPs.

Single doses of certain OP compounds cause a peripheral neuropathy (OPIDP). This effect is independent of their ability to cause the cholinergic syndrome by inhibiting neural AChE (Lotti, 1992). OPIDP is a central-peripheral polyneuropathy characterized by degeneration (with secondary demyelination) of distal parts of long and large-diameter axons (Bouldin and Cavanagh, 1979a,b). The animal of choice for OPIDP studies is the hen (Johnson, 1982); chicks are resistant to OPIDP (Johnson and Barnes, 1970; Peraica et al., 1993). Rodents were initially believed to be resistant to OPIDP; however later experiments showed that morphological lesions resembling those of OPIDP could be demonstrated in rodents (Padilla and Veronesi, 1988), and clinical OPIDP could also be elicited in older rats (6 months of age or older; Moretto et al., 1992). Therefore, the apparent resistance was due to the young age of the commonly used animals.

The molecular target of OPIDP is believed to be a neural protein with an esterasic activity, called neuropathy target esterase (NTE, formerly known as neurotoxic esterase; Johnson, 1982; Lotti, 1992). This protein, whose physiological function or functions are unknown, was initially identified as a phosphorylation site that could be blocked by the neuropathic OP mipafox, but not by the non-neuropathic OP paraoxon. Subsequently, it was shown that esters such as phenyl valerate (PV) blocked the phosphorylation. PV is now used as substrate to detect NTE activity, which is the PV esterase activity resistant to inhibition by paraoxon and sensitive to inhibition by mipafox (Johnson, 1969, 1977, 1982). NTE inhibitors are divided into two groups: (1) neuropathic inhibitors—i.e., (thio)phosphates, (thio)phosphonates, and phosphoro(thio)amidates (group 1 compounds); and (2) non-neuropathic, protective inhibitors—i.e., phosphinates, carbamates, and sulfonyl fluorides (group 2 compounds). The latter (group 2) compounds not only do not cause OPIDP, but also protect from OPIDP when given prior to administration of group 1 compounds because they block NTE, which cannot therefore be phosphorylated. This is the best evidence that NTE is in fact the target of OPIDP. The threshold to trigger the mechanism of OPIDP is ~75% NTE inhibition—soon after dosing, the peak is reached at different times according to the toxicokinetics of the compound. Consequently, if >30% of NTE is inhibited by a group 2 compound, the animal is protected from a subsequent neuropathic com-

pound because <75% of the target remained available for phosphorylation. Therefore, a group of hens pretreated with a known protective compound should always be added as a control when testing an OP compound for OPIDP. The dose of PMSF (30 mg/kg subcutaneously) suggested in the above protocols will cause ~50% NTE inhibition, and protect hens from at least 5 times the minimum neuropathic OP dose (Lotti et al., 1995). The relevant interaction between NTE and inhibitors occurs in the axon rather than in the cell body (i.e., in peripheral nerve and in spinal cord, not in the brain; Lotti et al., 1987).

It should be noted that a few years ago, a phenomenon called promotion of OPIDP was described by two independent groups (Pope and Padilla, 1990; Lotti et al., 1991), whereby protective doses of group 2 compounds, when administered after (rather than before) a neuropathic OP, caused an exacerbation of the effects of the OP. It was later shown that some other inhibitors caused promotion at doses not inhibitory, or only marginally inhibitory, to NTE (Moretto et al., 1994; Lotti et al., 1995). It was concluded that NTE is unlikely to be the target of promotion. It was also shown that promotion is a more general phenomenon, also involving axonopathies other than OPIDP (Moretto and Lotti, 1993, Moretto et al., 1994). All protective compounds tested thus far do cause promotion when given after the neuropathic OP. A promoter (e.g., PMSF, 120 mg/kg subcutaneously) might be administered after the compound under study when a sufficiently high dose cannot be given because of acute toxicity. In this way, the neuropathic potential that might be suspected because of some NTE inhibition can be demonstrated.

The procedures for clinical observation and determination of NTE activity as described in this unit provide essential information for assessing the ability of a compound to cause OPIDP. Morphological data, though useful, are not likely to modify or add qualitatively relevant information. Moreover, it has been reported that there is a poor correlation between clinical scores and morphological scores, especially in peripheral nerves (Prentice and Roberts, 1983). Other scoring systems have been proposed (Abou-Donia and Graham, 1979; Prentice and Majeed, 1983; Roberts et al., 1983; Jortner and Ehrich, 1987) for both clinical and morphological analysis. Those presented in this unit have been used for many years and have proved to be reliable and quick to perform.

Guidelines for testing for OPIDP have been introduced for regulatory purposes (OECD, 1995a,b; also see United States Environmental Protection Agency document OPPTS 810.6100: "Delayed neurotoxicity of organophosphorus substances following acute and 28-day exposure"). These guidelines require a single oral dose and (on occasion) 28-day repeated dosing studies. In the single-dose study, one dose level at about the oral LD_{50} and a concurrent positive control (e.g., tri-*o*-cresyl phosphate) should be used. Protection or promotion experiments are not required. The repeated 28-day rat study is required if the single oral dose produces a positive response (biochemical, clinical, or morphological). However, OPIDP is not induced, it should be noted, even if some NTE inhibition is maintained for several weeks but the threshold is not reached (Lotti and Johnson, 1980). This repeated dosing experiment will not add information on the neuropathic potential of a given compound other than a comparison between the possible cumulative effect on NTE and that on AChE. For instance, spontaneous reactivation might occur for AChE, but not NTE, inhibited by dimethylphosphates, and this will result in a higher cumulative effect on the latter.

The NTE assay was first introduced by Johnson (1977) for determination in hen brain and spinal cord. It was subsequently modified to allow determination in peripheral nerves (Caroldi and Lotti, 1982; slightly modified by Moretto et al., 1989). For peripheral nerves, there are methods that differ slightly from the one presented in this unit. The authors of Barril et al. (1988) do not put nerves in modified Koenig buffer, do not desheath nerves, and add 0.32 M sucrose to the Tris/EDTA buffer. This method will result, in a greater amount of debris, in a slightly lower activity when expressed on a tissue weight basis, and in a possibly larger interindividual variability if activity is expressed per gram of tissue and not per milligram of protein, (the latter being the suggested form of expression). This quicker method of preparing the tissue might be used for in vitro inhibition studies when the precise determination of absolute activity is not required. Kayyali et al. (1991) reported that SDS induces a shift in the phenol/4-AAP chromophore spectrum with peak absorbance at 490 nm and not at 510 nm. However, since the change in ε is not very great and all data have so far been obtained at 510 nm, the method presented here uses 510 nm. Automated microassays have been proposed for NTE and other PV esterases (Correll and

Ehrich, 1991; Escudero et al., 1996). These methods do not introduce relevant qualitative modifications and require more expensive instruments, but they are useful for assessing hundreds of samples, especially when small amounts of tissues are available.

Critical Parameters and Troubleshooting

Animals. Hens used for OPIDP studies usually come from commercial egg production farms; these animals live in an environment where exposure to infectious agents, variable feed and water quality, and even exposure to chemicals (e.g., pesticides) are possible. All these factors might lead to wrong and uninterpretable results. Moreover, hens are sometimes handled by their legs, which might cause trauma and consequently cause clinical observation to be biased. Even specific-pathogen-free hens present background morphological lesions which should be taken into account when evaluating slides from treated hens. Sometimes these lesions are qualitatively similar to those associated with OPIDP (e.g., axonal swelling or degeneration), but most frequently the involved sites (e.g., brain) and types of lesion (e.g., focal gliosis, perivascular cuffing) are not typical of OPIDP (Bickford and Sprague, 1983).

Perfusion. Good hen perfusion is not easy to obtain. Better results are obtained if the tip of the cannula rests inside the heart and is not pushed too far into the aorta.

Test compounds. Stability of compounds in different solvents is generally not known. It is therefore advisable to dissolve them immediately before use (unless otherwise indicated). It should also be remembered that impurities might be present which can be much more active than the compound itself. Protection by PMSF (or other compounds) might not be complete for toxicokinetic reasons. It is possible that peak NTE inhibition by some OPs is reached a few days after dosing, when the protective effect of PMSF is reduced due to reappearance of NTE.

NTE assay. The NTE assay is relatively easy to perform and major difficulties are not expected. The pH of the reaction is not critical because NTE activity is rather stable over a wide pH range (i.e., pH 6 to 9; Johnson, 1982). However, basic pH is needed for color development. NTE is very sensitive to detergents. If using recyclable glassware, plasticware, or tubes, be sure that they are washed with little detergent and rinsed thoroughly. If the blank is too high, it is possible that the phenyl valerate spontaneously hydrolyzed, most likely in the stock solution. This decomposition might be due to light, temperature, length of storage, or to the presence of water in the dimethylformamide. In the latter case, the dimethylformamide should be redistilled. Purify phenyl valerate if the batch contains too much phenol (Johnson, 1977). The concentrations of paraoxon and mipafox are such that either small decreases or increases will not substantially change the results of the assay. However, paraoxon (at high concentrations) is a very weak, reversible NTE inhibitor, and some PV esterase activity (especially in the peripheral nerve) is sensitive to high mipafox concentrations (Vilanova et al., 1990).

Anticipated Results

Group 1 compounds are expected to cause OPIDP when inhibiting NTE by more than 75% in spinal cord and/or peripheral nerve. Clinical signs will appear between days 9 and 14 after treatment, and peak between days 15 and 18. This will depend on the severity of OPIDP, and on the toxicokinetics of the compound. It might be necessary to sacrifice the hens for humane reasons when OPIDP is severe (grades 6 to 8) because they cannot feed or drink. Clinical signs are expected to be associated with typical lesions in spinal cord and peripheral nerves. Group 2 compounds should not cause OPIDP. Group 2 compounds that cause more than 30% NTE inhibition in spinal cord and peripheral nerve should protect from OPIDP when administered prior to administration of a group 1 compound. Exceptions are represented by neuropathic compounds with slow toxicokinetics, which cause peak NTE inhibition several days after dosing, when the protective effect has either vanished or become reduced due to concomitant reappearance of NTE.

Atypical clinical signs, characterized by spasticity rather than flaccidity and accompanied by morphological lesions limited to spinal cord and medulla oblongata, may appear, which are associated with preferential inhibition of spinal cord NTE rather than peripheral nerve NTE. This may happen for toxicokinetic reasons, or because of different sensitivity to inhibition of NTE from the two tissues (Moretto et al., 1989).

Control NTE activity is expected to yield the following absorbance values at 510 nm in a typical assay.

Brain: paraoxon-resistant activity (B-activity; tube 1): 0.80 to 0.95; paraoxon-resistant,

mipafox-sensitive activity (C-activity; tube 2): 0.350 to 0.450; NTE activity (B – C): 0.40 to 0.50; blank (tube 3): ~0.10. These will correspond to an activity of 2.2 to 2.5 μmol of PV hydrolyzed·min^{-1}·g of $tissue^{-1}$.

Spinal cord: B-activity: 0.675 to 0.80; C-activity: 0.40 to 0.50; NTE activity (B – C): 0.275 to 0.35; blank: ~0.120. These will correspond to an activity of 0.6 to 0.7 μmol of PV hydrolyzed·min^{-1}·g of $tissue^{-1}$.

Peripheral nerve: B-activity: 1.10 to 1.30; C-activity: 0.75 to 1.00; NTE activity (B – C): 0.35 to 0.50; blank: ~0.15. These will correspond to an activity of. 0.09 to 0.12 μmol of PV hydrolyzed·min^{-1} g of $tissue^{-1}$.

Time Considerations

The experiments that include clinical observation last ~3 weeks. Administration of compounds and treatment against cholinergic toxicity might require the presence of a worker for several hours on the first day and every 6 to 12 hr during the following days. Clinical observation of each animal requires 3 to 5 min.

In one working day, 7 to 10 hens can be perfused and dissected by two workers. Also in one working day, brain, spinal cord, and sciatic nerves from 15 to 20 hens can be dissected, cleaned, weighed, and stored at −80°C. Approximately 50 tissue samples (30 to 40 if from peripheral nerves) can be assayed for NTE activity (assuming analysis in duplicate) in a single day. Determination of brain AChE (if deemed necessary or useful) in 50 samples requires ~2 hr with a multicell spectrophotometer, assuming that the same initial homogenate (prepared for NTE assay) is used.

Literature Cited

Abou-Donia, M.B. and Graham, D.G. 1979. Delayed neurotoxicity of *O*-ethyl-*O*-4-nitrophenyl phenylphosphonothioate: Toxic effects of a single oral dose on the nervous system of hens. *Toxicol. Appl. Pharmacol.* 48:57-66.

Barril, J.B., Vilanova, E., and Pellin, M.C. 1988. Sciatic nerve neuropathy target esterase: Methods of assay, proximo-distal distribution and regeneration. *Toxicology* 49:107-114.

Bickford, A.A. and Sprague, G.L. 1983. The significance of background neurologic lesions in acute delayed neurotoxicity studies: A comparison of neurohistopathological lesions induced in commercial hens by tri-*o*-tolyl phosphate (TOCP) with those observed in negative control hens. *Neurotoxicology* 4:283-310.

Bouldin, T.W. and Cavanagh, J.B. 1979a. Organophosphorus neuropathy. I. A teased-fiber study of the spatio-temporal spread of axonal degeneration. *Am. J. Pathol.* 94:241-252.

Bouldin, T.W. and Cavanagh, J.B. 1979b. Organophosphorous neuropathy. II. A fine-structural study of the early stages of axonal degeneration. *Am. J. Pathol.* 94:253-270.

Caroldi, S. and Lotti, M. 1982 Neurotoxic esterase in peripheral nerve: Assay, inhibition and rate of resynthesis. *Toxicol. Appl. Pharmacol.* 62:498-501.

Correll, L. and Ehrich, M. 1991. A microassay method for neurotoxic esterase determinations. *Fundam. Appl. Toxicol.* 16:110-116.

Escudero, M.A., Sogorb, M.A., and Vilanova, E. 1996. An automatable microassay for phenyl valerate esterase activities sensitive to organophosphorus compounds. *Toxicol. Lett.* 89:241-247.

Johnson, M.K. 1969. The delayed neurotoxic effects of some organophosphorus compounds: Identification of the phosphorylation site as an esterase. *Biochem. J.* 114:711-717.

Johnson, M.K. 1977. Improved assay of neurotoxic esterase for screening organophosphates for delayed neurotoxicity potential. *Arch. Toxicol.* 37:113-115.

Johnson, M.K. 1982. The target for initiation of delayed neurotoxicity by organophosphorus esters: Biochemical studies and toxicological applications. *In* Reviews in Biochemical Toxicology (E. Hodgson, J.R. Bend, and R.M. Philpot, eds.) vol. 4, pp. 141-212. Elsevier, New York.

Johnson, M.K. and Barnes, J.M. 1970. Age and the sensitivity of chicks to the delayed neurotoxic effects of some organophosphorus compounds. *Biochem. Pharmacol.* 19:3045-3047.

Jortner, B.S. and Ehrich, M. 1987. Neuropathological effecs of phenyl saligenin phosphate in chickens. *Neurotoxicology* 8:303-314.

Kayyali, U.S., Moore, T.B., Randall, J.C., and Richardson, R.J. 1991. Neurotoxic esterase (NTE) assay: Optimized conditions based on detergent-induced shifts in the phenol/4-aminoantipyrine chromophore spectrum. *J. Anal. Toxicol.* 15:86-89.

Koch, T. 1973. Anatomy of the Chicken and Domestic Birds. Iowa State University Press, Ames, Iowa.

Lotti, M. 1992. The pathogenesis of organophosphate delayed polyneuropathy. *Crit. Rev. Toxicol.* 21:465-487.

Lotti, M. and Johnson, M.K. 1980. Repeated small doses of a neurotoxic organophosphate. Monitoring of neurotoxic esterase in brain and spinal cord. *Arch. Toxicol.* 45:263-271.

Lotti, M., Caroldi, S., Moretto, A., Johnson, M.K., Fish, C.J., Gopinath, C., and Roberts, N.L. 1987. Central-peripheral delayed neuropathy caused by diisopropyl phosphorofluoridate (DFP): Segregation of peripheral nerve and spinal cord effects using biochemical, clinical and morphological criteria. *Toxicol. Appl. Pharmacol.* 88:87-96.

Lotti, M., Caroldi, S., Capodicasa, E., and Moretto, A. 1991. Promotion of organophosphate-in-

duced delayed polyneuropathy by phenylmethanesulfonyl fluoride. *Toxicol. Appl. Pharmacol.* 108:234-241.

Lotti, M., Moretto, A., Bertolazzi, M., Peraica, M., and Fioroni, F. 1995. Organophosphate polyneuropathy and neuropathy target esterase: Studies with methamidophos and its resolved optical isomers. *Arch. Toxicol.* 69:330-336.

Moretto, A., Lotti, M., and Spencer, P.S. 1989. In vivo and in vitro regional differential sensitivity of neuropathy target esterase to di-*n*-butyl-2,2-dichlorovinyl phosphate. *Arch. Toxicol.* 63:469-473.

Moretto, A., Capodicasa, E., and Lotti, M. 1992. Clinical expression of organophosphate-induced delayed polyneuropathy in rats. *Toxicol. Lett.* 63:97-102.

Moretto, A. and Lotti, M. 1993. Promotion of peripheral axonopathies by certain esterase inhibitors. *Toxicol. Ind. Health* 9:1037-46.

Moretto, A., Bertolazzi, M., and Lotti, M. 1994. The phosphorothioic acid *O*-(2-chloro-2,3,3-trifluorocyclobutyl) *O*-ethyl *S*-propyl ester exacerbates organophosphate polyneuropathy without inhibition of neuropathy target esterase. *Toxicol. Appl. Pharmacol.* 129:133-137.

Organization for Economic Cooperation and Development (OECD). 1995a. Delayed neurotoxicity of organophosphorus substances: Following acute exposure. *In* OECD Guideline for Testing of Chemicals, 418, adopted 27.07.95.

Organization for Economic Cooperation and Development (OECD). 1995b. Delayed neurotoxicity of organophosphorus substances: 28-day repeated dose study. *In* OECD Guideline for Testing of Chemicals, 419, adopted 27.07.95.

Padilla, S. and Veronesi, B. 1988. Biochemical and morphological validation of a rodent model of organophosphorus induced neuropathy. *Toxicol. Ind. Health* 4:361-371.

Peraica, M., Capodicasa, E., Moretto, A., and Lotti, M. 1993. Organophosphate polyneuropathy in chicks. *Biochem. Pharmacol.* 45:131-135.

Pope, C.N. and Padilla, S. 1990. Potentiation of organophosphorus-induced delayed neurotoxicity by phenylmethylsulfonyl fluoride. *Toxicol. Environ. Health* 31:261-273.

Prentice, D.E. and Majeed, S.K. 1983. A subchronic study (90 day) using multiple dose levels of tri-*ortho*-cresyl phosphate (TOCP): Some neuropathological observations in the domestic hen. *Neurotoxicology* 4:277-282.

Prentice, D.E. and Roberts, N.L. 1983. Acute delayed neurotoxicity in hens dosed with tri-*ortho*-cresyl phosphate (TOCP): Correlation between clinical ataxia and neuropathological findings. *Neurotoxicology* 4:271-276.

Roberts, N.L., Fairley, C., and Phillips, C. 1983. Screening acute delayed and subchronic neurotoxicity studies in the hen: Measurements and evaluations of clinical signs following administration of TOCP. *Neurotoxicology* 4:263-270.

Sprague, G.L., Sandvik, L.L., Bickford, A.A., and Castles, T.R. 1980. Evaluation of a sensitive grading system for assessing acute and subchronic delayed neurotoxicity in hens. *Life Sci.* 27:2523-2528.

Vilanova, E., Barril, J., Carrera, V., and Pellin, M.C. 1990. Soluble and particulate forms of organophosphorus neuropathy target esterase in hen sciatic nerve. *J. Neurochem.* 55:1258-1265.

Key References

Caroldi and Lotti, 1982. See above.

Description of the original method for measuring NTE activity in peripheral nerves.

Johnson. 1977. See above.

Describes the original method (but contains a typographical error on page 114, last paragraph, line 3, where the concentration of tissue should be 6.6 mg and not 0.6 mg).

Johnson, 1982. See above.

Extensive review on OPIDP, including a description of the method for measuring NTE activity in brain and spinal cord tissue.

Lotti, 1992. See above.

Most recent extensive review on OPIDP.

Lotti et al., 1987. See above.

Describes the procedures for clinical observation.

Prentice and Roberts, 1983. See above.

Describes and scores clinical signs and morphological lesions.

Contributed by Angelo Moretto
Università degli Studi di Padova
Padova, Italy

Risk Assessment and Neurotoxicology

AIMS AND OBJECTIVES

Risk assessment refers to the use of toxicological data to define the relationship between exposure to an agent and an adverse health outcome. The goal is to develop a quantitative estimate of the probability that a given health outcome results from a specific exposure to an agent for a particular length of time by a particular route. Neurotoxicity may be defined as any adverse effect on the structure or function of the central and/or peripheral nervous system by a biological, chemical, or physical agent. Neurotoxic effects may be permanent or reversible, produced by neuropharmacological or neurodegenerative properties of a neurotoxicant, or resulting from direct or indirect actions on the nervous system. Adverse effects can include both unwanted effects and any alteration from baseline that diminishes the ability of an organism to survive, reproduce, or adapt to its environment. Putting this together, neurotoxicity risk assessment seeks to define the relationship between an adverse health outcome and exposure to an agent that affects the structure or function of the nervous system.

RISK ASSESSMENT

The risk assessment process has been described by the National Research Council (NRC) as including four components: (1) hazard identification, (2) dose-response assessment, (3) exposure assessment, and (4) risk characterization (NRC, 1983). The first two components focus on characterizing the sufficiency and strength of the toxicological data. Knowledge of the dose relatedness of the data is critical to dose-response modeling and further quantitative assessment. The third component, exposure assessment, provides human exposure estimates based on therapeutic, accidental, environmental, and/or occupational exposure possibilities. The final step in the risk assessment process is to integrate all the data and determine human risk. This risk assessment process is usually conducted by a risk assessor, whereas the influence of other factors—including economic, social, and health benefits—on risk characterization is determined by a risk manager. The logic of conducting risk assessment and risk management separately is to allow the scientific toxicological data to be evaluated fully without influences from unscientific factors (NRC, 1983).

Although many government agencies provide the framework for risk assessment as a focus of their missions, the United States Environmental Protection Agency (EPA) and United States Food and Drug Administration (FDA) have the responsibility for regulation of many agents to which the U.S. public may come into contact. Because of the widespread use of risk assessment procedures by the EPA and FDA, and the potential for agents under their responsibility to produce neurotoxicity, the EPA- and FDA-recommended procedures for neurotoxicity risk assessment will be the primary focus of this review.

Neurotoxicity Risk Assessment Within the FDA

The FDA has responsibility for the safety and efficacy of drugs, biologics, and medical devices, as well as ensuring the safety of food and food-related chemicals, cosmetics, electronic products that emit radiation, and veterinary drugs. Under the food, drug, and cosmetics laws, the FDA is charged with the responsibility of regulating products that account for 25 cents out of every dollar spent by U.S. consumers (Slikker and Sobotka, 1997). Although the FDA generally follows a rather structured review and approval process in making its regulatory decisions about these products, there are few formally written guidelines. The most detailed account of the agency's approach for assessing risk of adverse health effects is described in the FDA's Redbook I (U.S. FDA, 1982). This publication described the nature and extent of toxicological testing that was considered necessary for the agency to assure the safety of foods and color additives intended for use in human foods.

Recently, a proposed set of guidelines, referred to as Redbook II, has been drafted and disseminated for public comment and revision (Sobotka et al., 1996; Slikker and Sobotka, 1997). These proposed guidelines include specific attention to neurotoxicity and describe the nature and extent of information deemed necessary for the assessment of neurotoxic potential. The Redbook II guidelines suggest a structured process of tiered testing. Each tier or stage of testing focuses on different aspects of assessment: (1) screening, (2) characterization of effects, and (3) dose-response assessment. In the first stage, chemicals are initially screened across a range of dose levels for any clinical or

Contributed by William Slikker, Jr.

Current Protocols in Toxicology (1999) 11.6.1-11.6.7

pathological signs of toxicity, including those involving the nervous system. Those chemicals showing evidence of adverse effects on the nervous system may be presumptively identified as candidates for subsequent specific neurotoxicity testing to confirm and further characterize the scope of nervous system involvement and to determine dose-response relationships, including a determination of the no-observed-adverse-effect level (NOAEL). A tiered approach to neurotoxicity testing and evaluation allows for multiple decision points at which scientifically based decisions can be made about the adequacy of available information and the need for additional testing (Sobotka et al., 1996).

The FDA has used the NOAEL from bioassay data for noncancer effects as the starting point for safety assessment of chemicals. The NOAEL was defined to be the largest dose that did not appear to result in an increase in adverse biological effects above the level measured in unexposed control animals. In determining safe intake for humans, the NOAEL was divided by a safety factor of 10 to account for possible increased sensitivity of humans compared to test animals, and another safety factor of 10 to account for sensitive individuals (Gaylor et al., 1997). Additional safety factors were often employed to account for long-term effects based on short-term experiments or other inadequacies of the experimental data. The acceptable daily intake (ADI) was simply defined as ADI = NOAEL/($F_1 \times F_2 \times$...), where F_i are safety factors (Gaylor et al., 1997). In a case where all doses showed an adverse effect greater than that seen in the controls, the lowest observed adverse effect level (LOAEL) was divided by 10 to estimate the NOAEL. Some investigations have indicated that the NOAEL can be estimated from the LOAEL by dividing by a factor of three to five (Weil and McCollister, 1963; Abdel-Rahman and Kadry, 1995; Kadry et al., 1995). The above procedure is described in detail by Barnes and Dourson (1988). They state that the ADI is an estimate (with uncertainty spanning perhaps an order of magnitude) of a daily exposure in the human population (including sensitive subgroups) that is likely to be without appreciable risk of deleterious effects during a lifetime.

Neurotoxicity Risk Assessment Within the EPA

The EPA risk assessment guidelines for Neurotoxicity Risk Assessment were finalized quite recently (EPA, 1998). They are firmly based on an earlier document, Final report: Principles of neurotoxicity risk assessment (Reiter et al., 1994). Neurotoxicity risk assessment in the EPA frequently relies on animal data and the necessity to extrapolate the outcome of the animal studies to predict human risk. Therefore, a number of default assumptions are necessary but applied with informed discretion. These assumptions are plausibly conservative in nature because they are designed to protect public health, and they are well supported by current scientific knowledge (NRC, 1994). These assumptions include: (1) neurophysiological, neurochemical, behavioral, and neuroanatomical manifestations of toxicity are of concern as a basis for risk assessment; (2) agents that elicit adverse neurotoxic effects in experimental animal studies will produce hazard in humans; (3) neurotoxic effects seen in animal studies may not always reflect those seen in humans; and (4) unless there are data to suggest otherwise, the most sensitive species will be used as a basis for human risk assessment.

BIOLOGICAL MARKERS

The appropriate selection and use of biological markers or biomarkers is fundamental for the conduct of risk assessments for neurotoxicants, and biomarkers can be used to reduce knowledge gaps and minimize assumptions. Biomarkers may be defined as indicators signaling events in a biological system and are classified into three categories: indicators of exposure, effect, and susceptibility (NRC, 1987). Exposure biomarkers involve the quantitation of exogenous agents or of the complex of endogenous substances with exogenous agents within the system. Biomarkers of effect or endpoints are measures of an endogenous component of the biological system that is recognized as an alteration of disease or pathogenesis. A biomarker of susceptibility is an indicator that demonstrates that a particular biological system is especially vulnerable to toxic insult by an exogenous agent (NRC, 1987; Slikker, 1991).

ASSESSING HUMAN NEUROTOXICITY

Because of technical and ethical considerations, neurotoxicity in humans is primarily measured by noninvasive neurophysiological and neurobehavioral methods. Clinical neurological and neuropsychological approaches have been used extensively to evaluate neurological diseases, and these same methods have been used to assess patients suspected of having

Table 11.6.1 Some Human Neurobehavioral Methods

Neurobehavioral function	Test
Sensation	Flicker fusion
	Lanthony (color vision)
Motor/dexterity	Pursuit aiming
	Finger tapping
	Postural stability
	Reaction time
	Santa Ana peg board
Cognition	Benton visual retention
	Continuous performance task
	Digit-symbol
	Digit span
	Dual tasks
	Paired associate
	Symbol-digit task
	Wechsler Adult Intelligence Scale (Revised; components)
	Wechsler Memory Scale
	Complex brain function tasks
Affect	Profile of Mood States (POMS)

neurotoxic insults (Reiter et al., 1994). In addition, many neurobehavioral methods have been proposed or used to assess neurobehavioral function in humans (Table 11.6.1). In recent years, imaging techniques—including magnetic resonance imaging (MRI) and computerized tomography (CT)—and computerized brain electrical activity mapping, as well as operant behavioral assessments, have provided noninvasive and quantitative methods for human neurotoxicity assessment (Slikker and Chang, 1998). Epidemiological approaches—including retrospective and prospective studies—provide the means for evaluating the effects of neurotoxic substances in human populations (Reiter et al., 1994; Chang and Slikker, 1995).

ANIMAL MODELS

Whereas human data are available from clinical trials for therapeutics such as drugs and biologics, initial preclinical studies to determine dose, pharmacokinetic, and safety parameters are usually performed in animal models. Use of in vivo animal studies currently serves as the principal approach for detecting and characterizing neurotoxic hazards and helping to identify factors affecting susceptibility to neurotoxicity. In vitro tests have been proposed as a means of complementing whole-animal tests and, when properly developed, may be less time consuming and more cost effective than in vivo assessments (Reiter et al., 1994). The currently used in vitro tests have certain limitations, however, including the inability to model neurobehavioral effects (e.g., memory, learning, or sensory dysfunction).

Validation of animal models, whether in vivo or in vitro, is of paramount importance and may include measures of construct, criterion, and predictive validity. Despite the biological similarity of humans and many animal models, differential susceptibility to toxicants is well documented between species. Predictive capability or concordance between human and animal models after exposure to human neurotoxicants, however, has frequently been reported (Slikker, 1994a,b; Reiter et al., 1994; Slikker and Chang, 1998). These comparable outcomes provide a firm foundation for the use of animal models in neurotoxicity risk assessment. Examples of neurotoxicity endpoints or biomarkers of effect (Reiter et al., 1994; Slikker and Gaylor, 1995b; EPA, 1998) for each of the four major disciplines of neurotoxicology (neuropathological, neurochemical, neurophysiological, and behavioral) are shown in Table 11.6.2.

Generally, the most sensitive endpoint is used to determine toxicological risk. Regardless of the endpoint category (e.g., neurochemical, histological, physiological, or behavioral), the most sensitive one is used as the basis for risk

assessment. Even relatively complex indices such as behavior can be quantified in terms of, for example, rate of responding, percent task completed, or time to complete task, and can be used to determine NOAEL or LOAEL. However, long-latency effects, regardless of the endpoint category, are more problematic. It is generally assumed that average dose or total dose is a reasonable measure of exposure when doses are not equivalent in time, rate, or route of administration and the average (or total) dose is proportional to adverse effect. This major assumption is most prudently applied if it can be supported by empirical or mechanistic data. Animals exposed pre- or postnatally to test agent may be assessed as juveniles and later in life as adults and during senescence. Multi–time point approaches in different groups of animals, or longitudinal study designs with the use of the same animals, can provide for the assessment of long-latency effects (Reiter et al., 1994; Chang and Slikker, 1995; Sobotka et al., 1996; EPA, 1998).

TRADITIONAL RISK ASSESSMENT PROCEDURES FOR NEUROTOXICANTS

The regulation of neurotoxicants has generally been based upon setting reference doses (RfDs) by dividing the NOAEL by uncertainty

Table 11.6.2 Neurotoxicological Biomarkers of Effect

Neuropathological or structural endpoints	Gross changes in morphology, including brain weight
	Histologic changes in neurons or glia (neuronopathy, axonopathy, myelinopathy)
Neurochemical endpoints	Alterations in synthesis, release, uptake, or degradation of neurotransmitters
	Alterations in second messenger–associated signal transduction
	Alterations in membrane-bound enzymes regulating neuronal activity
	Alteration of neurotoxic esterase
	Alterations in developmental patterns of neurochemical systems
	Increases in glial fibrillary acidic protein in adults
Neurophysiological endpoints	Change in velocity, amplitude, or refractory period of nerve conduction
	Change in latency or amplitude of sensory-evoked potentials
	Change in electroencephalographic pattern or power spectrum
Behavioral endpoints	Absence or altered occurrence, magnitude or latency of sensorimotor reflex
	Altered magnitude of neurological measurements, such as grip strength or hindlimb splay
	Increases or decreases in motor activity
	Changes in rate, temporal patterning, or accuracy of schedule-controlled behavior
	Changes in motor coordination, weakness, paralysis, abnormal movement or posture, tremor, ongoing performance
	Changes in touch, sight, sound, taste, or smell sensations
	Changes in learning, memory, and attention
	Occurrences of seizures
	Altered temporal development of behaviors or reflex responses
	Autonomic signs

factors that hopefully account for interspecies and intraspecies extrapolation of experimental results in animals to humans (Barnes and Dourson, 1988; Kimmel, 1990). Generally, an uncertainty factor of 10 is used to allow for potentially higher sensitivity in humans than animals and another uncertainty factor of 10 is used to allow for variability in sensitivity among humans. Hence, the RfD = NOAEL/100. If NOAEL cannot be established, it is replaced by LOAEL in the calculation of the RfD and an additional uncertainty factor of 10 is often introduced, so that RfD = LOAEL/1000. It is assumed that this approach produces a dose with no significant neurotoxic risk, but this procedure makes no attempt to estimate the potential risk as a function of dose or to even consider the potential risk at the NOAEL.

Risk assessment procedures for developmental neurotoxicity have generally followed those for adult neurotoxicity. Several aspects of development require special consideration, however, and these include agent delivery (e.g., transplacental, lactational), susceptible periods of development (e.g., organogenesis, histogenesis), and latent presentation of effects (e.g., postnatal, senescent). Although quantitative risk assessment approaches have been applied, the limited number of developmental neurotoxicity risk assessments conducted have generally followed the RfD approach (Slikker, 1994a,b; Slikker and Chang, 1998).

LIMITATIONS AND ASSUMPTIONS

There are several features of the RfD or safety factor approach that deserve consideration. First, the method assumes a theoretical threshold dose below which no biological effects of any type are observed in a heterogeneous population. Not only is the determination of a threshold dose influenced by the sensitivity of the analytical methods employed, but the theoretical bases of a threshold dose may be questioned. Unfortunately, less sensitive experiments can result in higher RfDs. If, due to normal variation in cellular function, an adverse effect can occur in untreated control subjects, then endogenous or exogenous factors may already be supplying a stimulus that is equivalent to a dose above threshold. If exposure to an agent augments this stimulus in a strictly monotone manner as dose increases, then an additional risk is expected and no threshold dose exists for that agent (Gaylor and Slikker, 1990). Secondly, the magnitudes of the safety factors used to determine RfDs—interspecies extrapolation (10) and intraspecies extrapolation (10)—are based more on best estimates than actual data (Reiter et al., 1994; Slikker and Gaylor, 1995a).

The RfD approach relies on a single experimental observation (NOAEL or LOAEL) instead of using complete dose-response data in the calculation of risk estimates. Because chemical interactions with biological systems are often specific, stereoselective, and/or saturable, a chemical's dose-response curve may not be linear. Examples include enzyme-substrate binding leading to substrate metabolism, transport, and receptor-binding, any or all of which may be a requirement for an agent's effect or toxicity. The certainty of low-dose extrapolation is markedly affected by the shape of the dose-response curve (U.S. FDA, 1971). Therefore, the use of dose-response data should enhance the certainty of risk estimations when thresholds are not assumed or determined.

QUANTITATIVE DOSE-RESPONSE-BASED RISK ASSESSMENT APPROACHES

Dose-response models have generated considerable interest and are seen by many to be more appropriate (and quantitative) than the safety-factor approach to risk assessment. Rather than routinely applying a fixed safety factor to the NOAEL (which is based on a single dose) to estimate a safe dose, these approaches use data from the entire dose-response curve (Reiter et al., 1994).

Two fundamentally different approaches in the use of dose-response data have been developed to estimate risk. Dews and coworkers (Glowa et al., 1983; Dews, 1986; Glowa and Dews, 1987) and Crump (1984) demonstrated an approach in which information on the shape of the dose-response curve was used to estimate levels of exposure associated with relatively small effects (i.e., a 1%, 5%, or 10% change in a biological endpoint). Both Dews and Crump fit a mathematical function to the data and provided an estimate of the variability in exposure levels associated with a relatively small effect. Crump (1984) proposed the benchmark dose (BMD) as a replacement for the NOAEL in setting an ADI. The BMD was defined as a dose corresponding to an excess risk of 1% to 10% above background. A lower confidence (LBMD) was placed on the BMD to account for the variability in the experimental data. It was proposed that the ADI could be estimated as the LBMD divided by appropriate safety factors. For risk levels of 1% to 5%, the LBMD could be treated as the NOAEL; at the 10% risk level,

LBMD could be LOAEL. Kodell and West (1993) provide a procedure for estimating confidence limits on the BMD for continuous data following the modeling approach of Gaylor and Slikker (1990).

In another approach developed by Gaylor and Slikker (1990, 1992) for use with continuous data, a mathematical relationship is first established between the average biological effect and the dose of a given chemical. A second step determines the distribution (variability) of individual measurements of biological effects about the dose-response curve. The third step statistically defines an adverse or "abnormal" level of a biological effect in an untreated population. The fourth step estimates the probability of an adverse or abnormal level as a function of dose utilizing the information from the first three steps. The advantages of these dose-response models are that they encourage the generation and use of data needed to define a complete dose-response curve and provide an estimate of risk and/or changes in the average response as a function of dose.

BIOLOGICALLY BASED RISK ASSESSMENT

The development of quantitative risk assessment approaches depends, in part, on the availability of information on the mechanism of action and the pharmacokinetics of the agent in question. The development and use of physiologically based pharmacokinetic models to define target tissue concentrations of neurotoxicants is an important advancement for neurotoxicity risk assessment (Kim et al., 1995; Slikker et al., 1996; Slikker and Chang, 1998). In the development of a biologically based dose-response model for the psychoactive agent methylenedioxymethamphetamine (MDMA), Slikker and Gaylor (1990) considered several factors, including the pharmacokinetics of the parent chemical, the target tissue concentrations of the parent chemical or its bioactivated proximate toxicant, the uptake kinetics of the parent chemical or metabolite into the target cell, and the interaction of the chemical or metabolite with the membrane or with presumed receptor site(s). Because these theoretical factors contain a saturable step due to limited amounts of required enzyme, reuptake, or receptor site(s), a nonlinear, saturable dose-response curve was predicted. In the case of neurochemical effects of MDMA in the rodent, saturation mechanisms were hypothesized and, indeed, saturation curves provided relatively good fits to the experimental results. Some of the advantages of the biologically based quantitative approaches over the currently used RfD risk assessment procedures include the ability to (1) utilize continuous data, (2) utilize all of the dose-response data, (3) incorporate biological information into the dose-response model, and (4) provide an actual risk of exposure to a given dose. The conclusion was that use of dose-response models based on plausible biological mechanisms provides more validity to predication than purely empirical models.

CONCLUSION

Decisions concerning the production and use of chemicals and other agents are now generally considered in terms of not just risk, but of a balance between risk, health, and economic or environmental benefit. These risk/benefit decisions, usually made by risk managers, require quantitative risk assessments. In order for the risk manager to make a decision where the benefit is estimated in quantitative terms, the risk assessment side of the equation must also be quantitative. Therefore, there is a need for risk assessment procedures for neurotoxicants that are quantitative. A single risk assessment model may not be adequate for all conditions of exposure, for all endpoints, or for all agents. Risk assessment models of the future may well include biomarkers of both effect and exposure as well as biologically based mechanistic and pharmacokinetic considerations derived from both epidemiologic and experimental test system data.

LITERATURE CITED

Abdel-Rahman, M.S. and Kadry, A.M. 1995. Studies on the use of uncertainty factors in deriving RFDs. *Hum. Ecol. Risk Assess.* 1:614-624.

Barnes, D.G. and Dourson, M. 1988. Reference dose (RfD): Description and use in health risk assessments. *Regul. Toxicol. Pharmacol.* 8:471-486.

Chang, L.W. and Slikker, W. Jr. 1995. Neurotoxicology: Approaches and Methods. Academic Press, San Diego.

Crump, K.S. 1984. A new method for determining allowable daily intakes. *Fundam. Appl. Toxicol.* 4:854-871.

Dews, P.B. 1986. On the assessment of risk. *In* Developmental Behavioral Pharmacology (N. Krasnegor, J. Gray, and T. Thompson, eds.) pp. 53-65. Lawrence Erlbaum Associates, Hillsdale, N.J.

Environmental Protection Agency (EPA). 1998. Guidelines for Neurotoxicity Risk Assessment. *Fed. Regist.* 63:26925-26954.

Gaylor, D.W. and Slikker, W. Jr. 1990. Risk assessment for neurotoxic effects. *Neurotoxicology* 11:211-218.

Gaylor, D.W. and Slikker, W. Jr. 1992. Risk assessment for neurotoxicants. *In* Neurotoxicology (H. Tilson and C. Mitchell, eds.) pp. 331-343. Raven Press, New York.

Gaylor, D.W., Axelrad, J.A., Brown, R.P., Cavagnaro, J.A., Cyr, W.H., Hulebak, K.L., Lorentzen, R.J., Miller, M.A., Mulligan, L.T., and Schwetz, B.A. 1997. Health risk assessment practices in the U.S. Food and Drug Administration. *Regul. Toxicol. Pharmacol.* 26:307-321.

Glowa, J.R., DeWesse, J., Natale, M.E., and Holland, J.J. 1983. Behavioral toxicology of volatile organic solvents. I. Methods: Acute effects. *J. Am. Coll. Toxicol*. 2:175-185.

Glowa, J.R. and Dews, P.B. 1987. Behavioral toxicology of volatile organic solvents. IV. Comparison of the behavioral effects of acetone, methyl ethyl ketone, ethyl acetate, carbon disulfide, and toluene on the responding mice. *J. Am. Coll. Toxicol*. 6:461-469.

Kadry, A.M., Skowronski, G.A., and Abdel-Rahman, M.S. 1995. Evaluation of the use of uncertainty factors in deriving RfDs for some chlorinated compounds. *J. Toxicol. Environ. Health* 45:83-95.

Kim, C.S., Slikker, W. Jr., Binienda, A., Gargas, M.L., and Andersen, M.E. 1995. Development of a physiologically based pharmacokinetic model for 2,4-dichlorophenoxyacetic acid dosimetry in discrete areas of the rabbit brain. *Neurotoxicol. Teratol*. 17:111-120.

Kimmel, C.A. 1990. Quantitative approaches to human risk assessment for noncancer health effects. *Neurotoxicology* 11:189-198.

Kodell, R.L. and West, R.W. 1993. Upper confidence limits on excess risk for quantitative responses. *Risk Anal*. 13:177-182.

National Research Council (NRC). 1983. Risk assessment in the Federal Government. Managing the Process. National Academy Press, Washington, D.C.

National Research Council (NRC). 1987. Biological markers in environmental health research. *Environ. Health Perspect*. 74:3-9.

National Research Council (NRC). 1994. Science and judgment in risk assessment. National Academy Press, Washington, D.C.

Reiter, L.W., Tilson, H.A., Dougherty, J., Harry, G.J., Jones, C.J., McMaster, S., Slikker, W. Jr., and Sobotka, T.J. 1994. Final Report: Principles of neurotoxicity risk assessment. *Fed. Regist*. 59(158):42360-42404.

Slikker, W. Jr. 1991. Biomarkers of neurotoxicity: An overview. Recent advances on biomarker research. *Biomed. Environ. Sci*. 4:192-196.

Slikker, W. Jr. 1994a. Placental transfer and pharmacokinetics of developmental neurotoxicants. *In* Principles of Neurotoxicology (L. Chang, ed.) pp. 659-680. Marcel Dekker, New York.

Slikker, W. Jr. 1994b. Principles of developmental neurotoxicology. *Neurotoxicology* 15:11-16.

Slikker, W. Jr. and Chang, L.W. 1998. Handbook of Developmental Neurotoxicology. Academic Press, San Diego.

Slikker, W. Jr. and Gaylor, D.W. 1990. Biologically based dose-response model for neurotoxicity risk assessment. *Korean J. Toxicol*. 6:204-213.

Slikker, W. Jr. and Gaylor, D.W. 1995a. Concepts on quantitative risk assessment of neurotoxicants. *In* Neurotoxicology: Approaches and Methods (L.W. Chang and W. Slikker Jr., eds.) pp. 771-776. Academic Press, San Diego.

Slikker, W. Jr. and Gaylor, D.W. 1995b. Risk assessment strategies for neuroprotective agents. *Ann. N.Y. Acad. Sci*. 765:198-208.

Slikker, W. Jr. and Sobotka, T.J. 1997. Current and future approaches to neurotoxicity risk assessment. *Ann. N.Y. Acad. Sci*. 825:406-418.

Slikker W. Jr., Crump, K.S., Andersen, M.E., and Bellinger, D. 1996. Symposium overview: Biologically based, quantitative risk assessment of neurotoxicants. *Fundam. Appl. Toxicol*. 29:18-30.

Sobotka, T.J., Ekelman, K.B., Slikker, W. Jr., Raffaele, K., and Hattan, D.G. 1996. Food and Drug Administration (FDA) proposed guidelines for neurotoxicological testing of food chemicals. *Neurotoxicology* 17:825-836.

U.S. Food and Drug Administration (FDA). 1971. Panel on carcinogenesis report on cancer testing in the safety evaluation of food additives and pesticides. *Toxicol. Appl. Pharmacol.* 20:419-438.

U.S. Food and Drug Administration (FDA). 1982. Toxicological Principles for the Safety Assessment of Direct Food Additives and Color Additives Used in Foods. Document PB83-170696, National Technical Information Service, Springfield, Virginia.

Weil, C.S., and McCollister, D.D. 1963. Relationship between short- and long-term feeding studies in designing an effective toxicity test. *Agric. Food Chem*. 11:486-491.

Contributed by William Slikker, Jr.
National Center for Toxicological Research
Food and Drug Administration
Jefferson, Arkansas

Neurobehavioral Testing in Humans

Evaluation of the effects of chemical exposure in humans is a worldwide concern. Each year more than 1000 new chemical compounds are developed for use in industry, most of which have never been evaluated for possible neurotoxic effects on humans (Anger, 1990). Human neurobehavioral research or clinical evaluations of populations exposed to chemicals must be carefully planned, and research must additionally be carefully structured.

The distinction between clinical examinations administered for the purpose of diagnosing clinical abnormalities and research designed to detect group differences is an important one. Clinical neuropsychological evaluations require highly trained professional clinical psychologists or neuropsychologists who use a semi-structured test series based on current information and guided by clinical judgment and neuropsychological constructs that structure the assessment (Lezak, 1995; White, 1995). The clinical study has much to recommend it, as it is very sensitive to adverse effects in many neurobehavioral and psychological domains. It is, however, also very time consuming, requires a highly trained and experienced professional, and is therefore very expensive relative to experimental studies, which typically employ technicians to administer preplanned tests.

Clinical diagnostic examinations are most efficient and productive when following a diagnostic path dictated by training, clinical judgment, and experience. However, experimental research takes the exact opposite tack. Testing procedures are rigorously standardized across participants (although clinical studies use standard procedures, the specific tests selected may vary across participants) with the goal of making administration procedures invariant. Variance from standardized procedures leads to variability in the data that compromises the reliability, validity, and sensitivity of the tests.

Be it clinical assessment or experimental research, it is not possible to define a single protocol that will be appropriate in all cases; the protocol will depend on the goals of the study and the chemical exposure(s) that constitute the study's independent variable. In what follows, the necessary steps to develop a protocol are described, using a clinical evaluation and health promotion project involving experimental research procedures to illustrate the process. However, this unit is focused primarily on experimental research.

Experimental or clinical studies can be conducted in the laboratory or in the field. Testing at a site remote from the clinic or laboratory requires increased planning and rigorous procedural control because the controls routinely used in laboratory research (e.g., noise control, since extraneous sounds can invalidate a test of attention) are less available and some equipment is not portable. Otherwise, laboratory and field testing should be identical in planning and execution. This discussion centers on the more logistically complex field research that has dominated neurotoxicology publications in the 1990s.

STUDY DESIGN: DEFINING THE GOAL OF THE RESEARCH

Planning begins with the question the investigator wishes to answer, cast as a hypothesis to be tested. For example, (a) xylene exposure reversibly affects attention at 50 ppm, or (b) occupational exposures to xylene are associated with deficits in attention. Hypothesis (a) is readily studied in a laboratory equipped with inhalation exposure capabilities, and hypothesis (b) is typically pursued in a location near the workplace where the exposures are occurring in order to stimulate a high recruitment rate and minimize expenses. Even if the effects of the agent under study are unknown, it is best to structure the study or assessment around a limited range of hypothesized effects based on symptom reports, results in the scientific literature, or whatever served to trigger the study. It is also best to pursue at least two exposure levels in addition to a control or zero-level exposure, although this is admittedly rarely done in human behavioral neurotoxicology (Anger, 1990; Anger et al., 1998). Doing so allows the identification of a dose-response effect, which greatly increases confidence that the chemical exposure (the independent variable) is indeed responsible for the neurobehavioral test deficits (the effect) measured.

Identifying Performance Deficits

A critical issue in the design of a study is the availability of a baseline condition. If acute exposure effects are of interest, then baseline testing adds a huge degree of sensitivity by providing the basis for within-subject compari-

Contributed by W. Kent Anger, Diane S. Rohlman, and Daniel Storzbach
Current Protocols in Toxicology (1999) 11.7.1-11.7.17

sons (i.e., before versus during or after). In the absence of baseline data, norms developed for a neurobehavioral test have occasionally been used to detect performance deficits. The use of historical or clinical norms as a means for comparison may now appear possible with the publication of large-*n* studies (e.g., Anger et al., 1997). However, this is fraught with pitfalls unless the investigator is thoroughly familiar with the tests in numerous applications including large-*n* studies. The neurobehavioral tests used in behavioral neurotoxicology research do not have norms for all ages, cultural groups, educational backgrounds, or gender, and test performance may vary between different areas of a country with the population diversity of the United States (Anger et al., 1997). The results of large-*n* studies may not be representative of specific worker populations and may include ethnic, cultural, or gender bias that is not explicit in the publication. Different equipment or test procedures or parameters could produce highly variant results that would never be recognized without a control group. These points argue powerfully for always employing a control group for any research study or clinical assessment unless there is very strong evidence that norms from a population representative of the exposed group are available.

Example

An example of a clinical evaluation and health promotion project that was evaluated both as an experimental study and an individual clinical assessment illustrates this approach in a field (i.e., nonlaboratory) milieu. Youths in Texarkana (on the border of Arkansas and Texas) obtained mercury from an abandoned neon lamp factory and then became exposed to the mercury in various ways. It was reported that some dipped quarters in the mercury to see the shiny result, thus receiving exposure through their skin. At least one person dipped a cigarette in the mercury and smoked it, providing extremely rapid high-concentration exposure to mercury fumes by inhalation.

Because only a small number of exposed individuals were available or willing to be tested, the main goal was a clinical evaluation using norms and a "control" group drawn from willing community members (unexposed classmates). Urine samples were collected from the exposed students whose primary history of mercury exposure had occurred in the prior few months; the ability to measure urine mercury, which would serve as a good biomarker of current and historical exposure, was a useful feature of this study (again, a relatively rare one). This ability to correlate neurobehavioral performance with a good exposure biomarker offered the potential for an experimental study, although the viability of the result as publishable research depended on a reasonable sample size with a range of urine mercury exposures. The inability to select the controls in a random manner from the unexposed population virtually precluded a credible cross-sectional comparison (although events would add even greater barriers). At a minimum, the results were expected to provide the basis for a clinical assessment on an individual basis. The small number of tests given by technical staff limited the depth and scope of the judgments but allowed cost-efficient evaluation (the more participants, the less expensive it would be per participant).

TEST SELECTION: BUILDING A BATTERY

Once the study design has been developed it is necessary to select a battery of tests to administer to the study participants. The initial step in building a battery is to identify the functions to be measured. This may be based on the known effects of the chemical under study, or—if the neurotoxic endpoints of the chemical are only suspected—based on the symptoms expressed by exposed individuals. It is necessary to include some established tests of neurotoxicity. A functional assessment (i.e., measurement of all neurobehavioral and cognitive functions) might be attempted, but a complete assessment would be prohibitively expensive and is not a serious option. If, as is usually the case, it is believed that the effects are only partially understood, then a consensus test battery, described below, is the safest basis for test selection. The necessary steps are first to identify primary tests and desirable secondary tests, and then to consider statistical power, the available participant pool, and the time and budget limitations that constrain the selection of a large number of tests.

Primary tests are those that essentially define the critical effects that must be measured—it is around these tests that the hypothesis is framed, and it is for these measures that there must be sufficient statistical power to detect an effect of expected size (e.g., a 10% difference from control performance). Secondary measures are potentially useful additions that are not critical but may add valuable supplementary findings for future consideration. However, a single study realistically can only answer one

or two questions unless the participant pool is unusually large (see discussion of statistical power, below).

Behavioral tests that are proven to be sensitive to neurotoxicity in human neurobehavioral research should be included in any study. The risk of using unproven tests exclusively lies in not finding an effect. In this case, it is uncertain if (1) a neurotoxic effect was present but the test was insensitive, or (2) there was no neurotoxic effect. Thus, established tests should always be used, and it is recommended that a core of standardized tests known to be sensitive to neurotoxicants be employed. This strategy has been recommended by the expert groups drawn together to develop the consensus test batteries to assess neurotoxicity (Johnson et al., 1987; Anger et al., 1994). However, inclusion of new tests that assess functions not previously studied or that might more effectively test a function known to be affected by the neurotoxic chemicals is a positive contribution to the field.

Established Tests

There is a wide assortment of established tests of functions known to be affected by neurotoxic chemicals (Anger, 1990). For a principal investigator (PI) who has not previously used neurobehavioral tests, consensus test batteries are recommended because they have established sensitivity, proven training materials, established parameters for the tests (e.g., number of trials, test difficulty), and they allow the PI to evaluate the effectiveness of the testing by examining the outcome in the control group. The two consensus test batteries developed to study neurotoxic endpoints in humans are described below.

Neurobehavioral tests typically assess performance, although questionnaire-type psychological tests (Lezak, 1995) are increasingly used because of the growing recognition that psychological factors can contribute to performance deficits and concern that some exposed people may be motivated to perform below their potential. Psychological tests that measure factors such as anxiety, depression, perceived mental or physical health status, and tendency to abuse substances are recommended to reveal situational variables that may affect performance (e.g., fear or anxiety over one's health if one is exposed to a chemical that might be harmful).

Another factor that should be measured is motivation. Companies are often concerned that a few individuals hostile to the intent of a neurobehavioral study could skew the results and produce an apparent, but false, effect. However, such individuals would more likely add substantially to the variability, which reduces the likelihood that any effect will be detected—that is, their presence is more likely to lead to a false negative than a false positive. Moreover, in the authors' experience such individuals are rarely encountered. Nonetheless, detection of these individuals allows the investigator to eliminate their data, and thus the variability they bring to the analysis. To assess motivation (e.g., Pankratz and Binder, 1997), the authors developed the Oregon Dual Task Procedure (ODTP; Anger et al., 1999), a computerized variant of the Portland Digit Recognition Task (PDRT; Binder, 1993), in which the number of errors (not the response speed or latency measure) is the measure of motivation. This measure of motivation has been validated for the PDRT (Binder, 1993) but not the ODTP.

Consensus Batteries to Detect Neurotoxicity

The first consensus test battery designed to detect deficits suggestive of neurotoxic exposures was the Neurobehavioral Core Test Battery (NCTB), developed by an expert panel convened by the World Health Organization (WHO) with leadership from the National Institute for Occupational Safety and Health (NIOSH). The NCTB was selected to provide an instrument for population screening and research, and to foster the development of a database of common tests shown to be sensitive to neurotoxic disorders (Johnson et al., 1987). The NCTB comprises seven tests (Table 11.7.1) that met three criteria: (1) they had detected statistically significant differences between exposed and control groups in workplace research; (2) technicians could, following minimal training, reliably administer them; and (3) the materials and equipment they required were inexpensive and could be administered in remote settings (Johnson et al., 1987).

In a 10-country cross-cultural study of the NCTB in unexposed control populations administered in nine different languages, mean test performance among the nine countries with similar education levels was within ~1 standard deviation (SD) between the high and low scores. Test performance from the tenth country was substantially inferior on all but the Santa Ana test. Participants from the tenth country had a mean education level of 3 years, compared to a mean education level in the remaining countries exceeding 9 years (Anger et al., 1993). This suggests that the NCTB can be

Table 11.7.1 WHO-Recommended NCTB and ATSDR-Recommended AENTB Tests

NCTB tests	AENTB tests
Cognitive	
Benton visual retention	Serial Digit Learning[a]
Digit Symbol	Symbol Digit (plus delayed recall)[a]
Digit Span	Digit Span[a]
	Raven Progressive Matrices
	Vocabulary[a]
Sensory	
	Visual acuity
	Contrast sensitivity
	Lanthony color vision
	Vibrotactile threshold
Motor	
Simple Reaction Time[a]	Simple Reaction Time[a]
Aiming II	Tapping[a]
Santa Ana	Santa Ana
	Dynamometer
Psychological	
Profile of Mood States	Mood test[a]

[a]Computerized.

administered to a broad range of populations with >10 years of education. There is an NCTB Operational Guide (obtainable from the authors) which allows use of this battery following a standardized method. The NCTB tests are widely used in neurotoxicology research (Anger, 1990), and the NCTB has been used in several studies (e.g., Liang et al., 1990).

The other consensus behavioral neurotoxicology test battery was developed by an expert committee (Anger et al., 1994) convened by the Agency for Toxic Substances and Disease Registry (ATSDR). The Adult Environmental Neurobehavioral Test Battery (AENTB) was designed to detect the effects of low-concentration exposures from hazardous waste sites. The same criteria used by the WHO expert group were applied. This expert group proposed a larger number of sensory, motor, and cognitive tests than were found in the NCTB. ATSDR has employed the AENTB to study hazardous waste exposures in three populations (Amler et al., 1994, 1995).

ATSDR has also developed the Pediatric Environmental Neurobehavioral Test Battery (PENTB), which employs observational methods to assess neurotoxicity in very young children, adding performance measures to test older children (Amler et al., 1996). This is not, strictly speaking, a consensus battery in that an open panel was not assembled with opportunity for comment from a broad array of scientists, although an expert group did develop the recommendation, and this was followed by extensive piloting and comment solicited from outside experts.

Computerized Test Batteries

Computerized tests have the potential to standardize neurotoxicity testing, and they may lead to the development of a large and consistent database, just as they have already caused an increased use of established tests. Computer-implemented tests have begun to dominate neurotoxicity testing as demonstrated in Portland, Ore., USA, during 1995 at the first symposium to examine this subject (e.g., Anger et al., 1996a). Topics of test validation (e.g., Krengel et al., 1996; White et al., 1996) and analysis (Heyer et al., 1996) were discussed, as were many new developments in this active field. The developers of the computer-based batteries, primarily university-based research scientists, can be contacted to purchase or obtain access to the batteries.

There are several computerized batteries comprised of standardized neurobehavioral tests. The first significant battery to be developed was the Neurobehavioral Evaluation System (NES and NES2; Letz, 1990); this battery is currently the most widely used. The NES2 has been used internationally, and on-screen

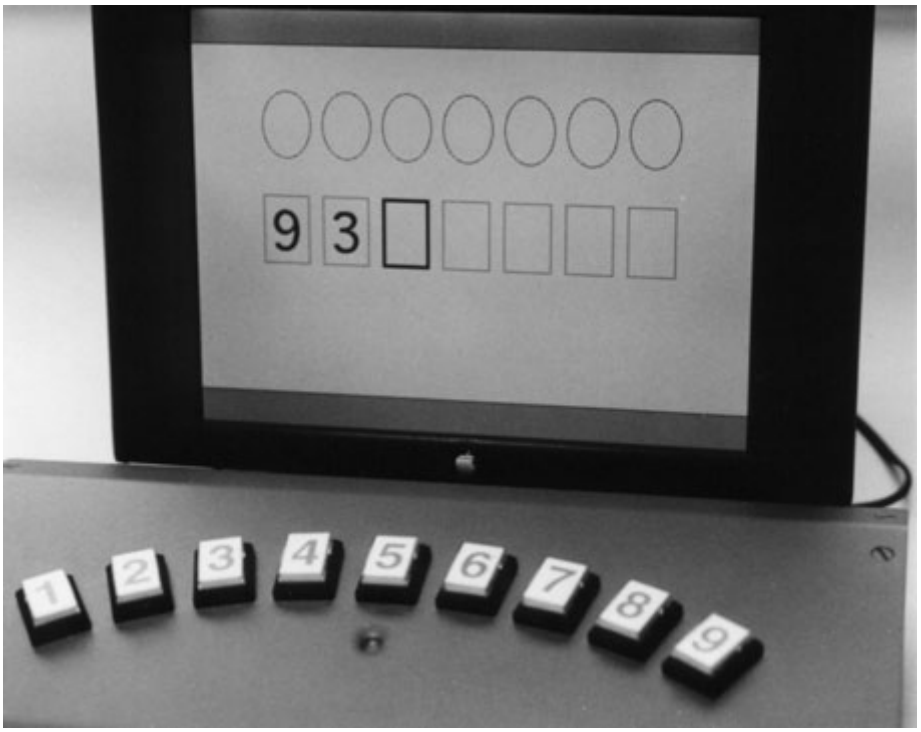

Figure 11.7.1 The 9-button DataSled response input unit is pictured set over the keyboard of a laptop computer (used for field studies due to the compact size and ease of transport). The laptop screen pictures the stimulus (dark line around the empty rectangle), indicating to participants to make their third response in the 7-digit step of the Digit Span test.

instructions are available in several languages, including English, Chinese, Japanese, Finnish, French, and Spanish (e.g., Letz, 1990). It has modifiable test parameters (e.g., number of trials), which allows researchers to adjust the test to answer specific hypotheses (e.g., does a longer test of attention reveal effects that only appear when attention is sustained over a long period of time). Because the default parameter settings vary in different versions of NES2, investigators must be careful to set the test parameters to appropriate settings to ensure that their data will be relevant to the existing database. Unfortunately, few investigators publish the parameters they have used. The NES2 (i.e., version 2 of the NES) is now evolving into the light pen–based NES3, which will debut as a screening battery with fixed parameters (Letz et al., 1996).

Sharing many properties with the NES2 is the Swedish Performance Evaluation System (SPES), available with instructions in Swedish and English. The SPES has preset, unmodifiable parameters (although of course the developer can reprogram these), saving the PI from the need to determine and set the parameters (Iregren et al., 1996). SPES consists of fourteen performance tests as well as four self-rating scales for mood, performance, and symptoms. Both the SPES and NES2 use the keyboard for input, plus a joystick for tests requiring a rapid single response (e.g., simple reaction time).

The authors have developed two computerized test batteries that are designed for the field or the laboratory. They feature the same computer system and simple and thoroughly tested instructions (Anger et al., 1996b; Kovera et al., 1996). The performance test battery, the Behavioral Assessment and Research System (BARS), was developed for presentation on a laptop computer for convenient application in the field, and a simple unintimidating response input unit, the DataSled (Fig. 11.7.1) is employed to avoid multiple problems with keyboard input (e.g., poor ergonomics for testing). The test stimuli are integrated with the instructions, which are presented in a stepped fashion (Rohlman et al., 1996), so that participants demonstrate their understanding of each test concept before moving to the next instructional stage, followed by practice on the complete test. The parameters are extensively and readily modifiable (see *http://home.att.net/~angerk*), and they have a recommended default setting.

BARS tests have now been successfully used with children as young as 5 years (Anger et al., 1996b), adults as old as 91 (Anger et al., unpub. observ.), and in people with limited education (Rohlman et al., 1996). Instructions are available in written or spoken format, in English, Spanish, and other languages. A growing database is available for review (e.g., Anger et al., 1999; Binder et al., 1999; Campbell et al., 1999).

The companion battery is the Health Screening System (HSS). This is a questionnaire-administration system, initially with twelve standard tests of physical and psychological health symptoms, personality, mood, life, and (for military veterans) combat experience. Other tests with comparable multiple-choice answers are readily added. Instructions, test items, and choices can be presented in onscreen written format, or they can be spoken via a user option selectable at any time during testing (Kovera et al., 1996). Psychological factors, not often employed in neurotoxicity assessments, are of increasing importance as subtle factors are considered (e.g., Anger et al., 1998).

Both BARS and HSS can be simultaneously administered to up to ten people by a single technician, and few questions are generated because of the intuitive nature of the instructions and tests. This is significantly more efficient than existing neurobehavioral test batteries. Other batteries such as Stollery's Automated Computerized Testing (ACT) system (Stollery, 1996) and the Automated Performance Testing System (APTS; Kennedy et al., 1987) are also available and worth consideration, as are the very popular NES2 and the SPES.

Recommendations for a minimum computerized test battery

Although the test situation, type of exposure, and time constraints dictate some of the tests to be used, it is recommended that a common core set of tests should be administered in all studies (Iregren and Letz, 1992). Data from these common tests will allow a comparison of effects across studies and can help build a general knowledge base. Iregren and Letz (1992) recommend a "Minimum Common Core Computerized Battery (MCCCB)" that consists of three tests, Simple Reaction Time, Symbol-Digit substitution, and Finger Tapping. These tests have demonstrated sensitivity to a variety of neurotoxic chemicals. To further aid comparisons, a standard set of parameters for these tests should also be used. The parameters from the NES2 version of the Symbol-Digit test and the SPES parameters for Simple Reaction Time and Finger Tapping are recommended (Iregren and Letz, 1992).

Cautions with computerized test batteries

There are many computerized test systems currently available, which vary in terms of hardware, stimulus presentation, accuracy of data collection, and ease of use. Although many of these systems include common tests (e.g., Reaction Time, Symbol-Digit, Finger Tapping) different parameter settings and screen images are used, and caution must be used when making comparisons of data across test systems. Unfortunately a description of the physical appearance of a test (available at <*http://home.att.net/~angerk*> for BARS and HSS tests) and the parameter values used is often missing from published reports. This is an even greater problem when new test systems are developed. The ease with which new test batteries can be developed is an important advance, but at the same time cause for concern: the development of new computerized tests or test batteries is not a task for the inexperienced. Caution should be used to guard against systems with unproven reliability.

Biomarkers: Exposure History

It is essential to collect information on exposure history, along with a biomarker of personal exposure, if possible. The investigator should recognize that the biomarker measure is linked to the time at which the sample is collected and may not reflect the history of exposures if they varied over time. Damage may have been accumulating over time, as well. In some cases, a history of exposures may exist if industrial hygiene and/or biological marker samples have been taken over the years in a company; this is certainly worth an inquiry if the chemical in question is a known toxicant such as mercury or lead. A specialist in biomarkers is required for an adequate treatment of this specialized subject (e.g., Travis, 1993).

Ancillary Measures

There are additional measures that are not direct tests of neurotoxicity which are recommended. It is also important to include at least one negative control test; this is a test that should not be affected by the chemical under study. Inclusion of a negative control test will calm the fears of those who believe that neurobehavioral tests are supersensitive to any

change in environment and therefore likely to give spurious results. It is also a good experimental design strategy. Furthermore, obtaining a history of occupations and jobs, as well as hobbies, is important as neurotoxic effects may be permanent and could result from previous exposure(s). These questionnaires need to be structured to fit the situation under study; standard questionnaires are printed in the initial publication describing the NCTB (Johnson et al., 1987). Although comprehensiveness of the information is important, a lengthy testing time runs the risk of tiring the participants and affecting data at the end of testing. Fifty minutes is probably the ideal session test time, although the authors regularly exceed that time without apparent adverse impact, using 7-min session breaks to refresh participants.

Example

Returning to the example of the Texarkana mercury-exposed group, the assessment was cast in terms of a research hypothesis: mercury exposure would produce increased tremor and deficits in short-term memory, possibly in a dose-response pattern. Given the short exposure period, such effects seemed unlikely, but that was the hypothesis to be tested. Thus, the hypothesis does not have to represent one's expectation, only what one wants to evaluate. The extensive history of mercury research (e.g., Anger, 1990; Echeverria et al., 1995) reduced the need to use a consensus battery, and time constraints and the desire to include a test of motivation (there was concern that the youths might be resistant to the testing) dictated the use of selected core tests rather than a complete consensus battery. Based on the demonstrated effects of metallic or inorganic mercury identified in the hypothesis, the primary tests selected were: (1) a measure of hand steadiness, and (2) the ODTP, which requires the participant to recognize a 5-digit number (from two options) after up to 25 sec of performing a distracter task. In addition to short-term recognition memory (response latency on correct trials), this test was also selected to assess motivation (the number of errors, as noted above).

The Symbol-Digit, Simple Reaction Time, and Tapping tests were also included in the battery. These tests have been widely used in neurotoxicology research, have revealed differences between groups with mercury exposure and controls, and are recommended as part of the MCCCB. For a negative control test, a subtest of the Wide Range Achievement Test III (WRAT-III), which measures reading level and has age-adjusted norms (Johnstone et al., 1996), was selected. Reading proficiency is believed (though admittedly without much direct evidence) to be insensitive to exposure to neurotoxic chemicals and is correlated with preexposure cognitive ability. Lower levels of education are associated with reduced performance on some of the neurobehavioral tests (Anger et al., 1997). Finally, the Beck Depression and Anxiety inventories (BDI and BAI) were added to the battery of tests to assess mood and psychological factors, and the SF-36 symptom checklist was included to measure perceived mental and physical health.

All of the performance tests were administered using the BARS test battery, except for the Hand Steadiness Test and the WRAT-III, which were administered individually. The psychological tests (BDI, BAI, and SF-36) were administered with the HSS. An example of a typical SF-36 "screen" is shown in Figure 11.7.2. The BARS and HSS were selected because they use a common platform and are easy to administer.

Urine mercury was selected as the biomarker. In this case, it was reasonable to expect that urine mercury would reflect the entire history of exposures of the people tested, since those exposures had begun only 3 months prior to testing.

PRELIMINARY DATA ANALYSIS PLAN AND POWER ANALYSIS

The preliminary data analysis plan should be developed at the same time as the study design and during the selection of tests and measures. It is dependent on the experimental design (e.g., comparison of an exposed to an unexposed control group, which would involve a *t*-test comparison between the groups), the levels of the independent variable (e.g., one level would be one exposed group, and two levels would be high and low exposure groups), and the number of participants available to study. It also serves to provide the basics for making a power analysis. A power analysis is unfortunately often ignored in experimental field research, especially when the need to initiate testing is urgent. However, it can be done very quickly and is necessary for understanding the outcome of any statistical analysis of neurotoxicity assessments. In most situations, a simple hypothesis is being tested and the experimental design is a comparison between an exposed and a control group. An approximate calculation can be based on the mean and standard deviation of the primary test

from published data, and the percent difference the investigator considers to be evidence of an adverse effect (e.g., 10% poorer performance by the exposed than the control group).

The power analysis allows the investigator to determine the number of participants that must provide test data to produce a credible research study (or confidence in statistical analyses of clinical field studies for which there is no control over the sample size). The number of participants needed is proportional to the ratio of the mean to the standard deviation (SD) of the primary test measure(s). Table 11.7.2 presents means and standard deviations that can provide a general guide. Obviously, the larger the standard deviation relative to the mean, the more participants are needed (put differently, the less sensitive the test is due to the high degree of variability). If the SD of the primary measure is ~20% of the mean, ~49 participants (24 in one group and 25 in the other) would be sufficient to detect a 10% deficit in the exposed versus control group. These numbers are based on three assumptions: (1) an alpha or significance level of 0.05 (often termed the 5% level); (2) a beta or undetected impairment probability

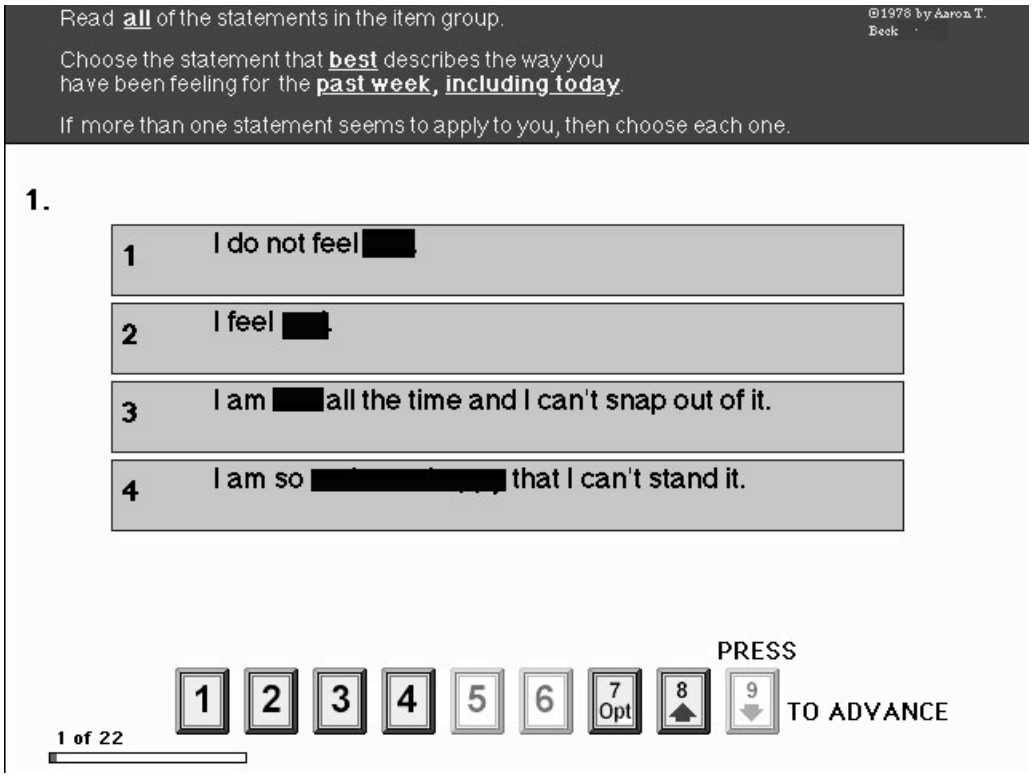

Figure 11.7.2 A typical screen from the Health Screening System (HSS) implementation of the Beck Depression Inventory. The rectangles numbered 1 to 9 at the bottom of the figure represent the physical DataSled response input unit used by participants to choose responses during the test.

Table 11.7.2 Means and Standard Deviations Required to Detect Statistically Significant Differences[a]

Mean	SD	Mean/SD ratio	*N* for difference of:[b]		
			10%	15%	20%
100	10	10%	12	5	3
100	15	15%	28	12	7
100	20	20%	49	22	12

[a]Hypothetical test mean of 100, SD, and ratio of mean to SD expressed as a percentage, and the *N* required per group to detect a 10%, 15% or 20% difference between the groups.

[b]Assumes alpha of 0.05, beta of 0.20, and a directional hypothesis (e.g., exposed individuals will have performance deficits).

of 0.20 (yielding 80% "power" to detect a true effect); and (3) one can predict the direction of an adverse effect (e.g., response speed slows down), to produce what is generally termed a directional or 1-tail test (Pagano and Evereau, 1993).

The reader should realize that these sample size numbers provide only an estimate and would differ if the PI chose alternative assumptions. For example, this power analysis is only relevant for a small number of test measures, the primary measures. If several measures are to be treated as "primary," the number must be adjusted for the number of tests used, because the more tests administered the more likely a difference between the groups will be discovered purely by chance (just as the more you flip a coin the more likely it is that you will get at least one head and at least one tail). Thus, a statistician should be consulted to discuss the many underlying factors. However, entering that discussion with the information identified in the preceding paragraph in hand (that is, with casting of the hypothesis to be tested, selection of primary measures, mean and standard deviation of those measures, and determination of how much of a deficit constitutes an adverse effect or must be detected, all completed) will allow this to be a fairly brief consultation to add some precision to the number of participants that need to be tested.

The power analysis will reveal which tests can be rationally employed in a study—since the mean/SD ratio varies considerably between tests—as well as how many tests can serve as primary measures. Further, if the number of participants is fluid or expandable, this will assist in limiting the number to an appropriate minimum. Of course, one can employ any number of secondary measures on which the outcome is reported but the results are not a basis on which the hypothesis is tested (i.e., the basis on which one concludes that the chemical did have an effect or that the exposed have a significant deficit compared to the controls). This may seem curious or even mystical, but it is simply based on the issue of chance: the more tests you administer, the more likely you are to chance upon one on which people differ.

Example

In the Texarkana example, the primary endpoints were measures of tremor and short-term memory. These were selected in part based on evidence in the literature and in part because of the authors' experience with this memory measure. Data were collected on several hundred people, and with this information a straightforward power analysis was undertaken. The ODTP served as the primary test. In data on young adults taking the ODTP (Anger et al., 1999), the mean latency is ~2000 msec (to make a choice between two options and press a button to indicate which choice) with an SD of ~400 msec; thus, the SD is ~20% of the mean. This would require an estimated 22 people in the exposed and 22 people in the control group to detect a 15% difference between the exposed and control groups, and ~12 people in each group to detect a 20% difference (see Table 11.7.2). A similar procedure can be employed when there is a body burden measure—as in Texarkana, where the relationship between the test measures can be correlated with urine mercury (which was to be the main analytic strategy). The ability to detect a 10% to 15% difference is a reasonable power level, and it reflects "deficits" that would probably be undetectable in a standard medical exam (which of course would not employ such structured neurobehavioral tests). With this preparation, the research team arrived in Texarkana prepared to test 50 people in the one day available for testing (although this number would elude the team).

IMPLICATIONS OF DEMOGRAPHIC FACTORS

A critical aspect of test selection is recognition of the key demographic factors in the test population that could affect performance on neurobehavioral tests. These factors are (1) gender (e.g., the dynamometer strength test); (2) age (e.g., people past retirement age will take much longer to complete the tests and will be slower on tests employing latency measures such as the Symbol Digit or ODTP); (3) education (e.g., performance on cognitive and motor tests will be slower in persons with <10 years of education, and tests with simple and clear instructions are highly preferred for such persons); and (4) ethnicity (e.g., tests that involve memory of Asian letters would be difficult for people whose cultural background does not include exposure to such figures). These factors may guide test selection and argue powerfully for performing pilot assessments of the tests in the population of interest and for selection of a comparable control group in cross-sectional studies (Anger et al., 1997).

Demographic data should be collected for each test participant. This should include age (obtain the date of birth and subtract that from the date of testing to get the actual age at time

of testing), years of education (discriminate between GED and 12 years; 16 is typically a BA, 17 an MA), gender, and ethnicity. If the project is funded by a federal grant, this information must be reported annually to that agency by the recipient institution.

Example

In the Texarkana example, the WRAT-III test of reading ability, which is normed on a national sample (Johnstone et al., 1996), provided an estimate of general intellectual attainment. This factor affects performance on all the planned tests. If the exposed and control participants were of comparable educational attainment, then a cross-sectional comparison might be possible, although the nonrandom nature of the sample would limit the generality of those comparisons. This was a primary concern, as the participants were expected to be of the same age and from the US majority ethnic background. Gender is a relatively minor factor on the selected tests, although it was expected to play enough of a role that it was hoped that an equal number of males and females would be tested in each group.

TEST DETAILS: THE PARAMETERS

Selection of the tests does not complete the process. The parameters (e.g., number of trials, test difficulty) for a test should be selected with care, keeping in mind the study's goals and limitations. Parameters that replicate previous administrations of a test are a good starting point because they provide a basis for comparing the data from the current study to data collected previously. However, caution should be used when comparing data from different studies, because many factors that may affect performance (e.g., size of stimuli or number of trials) can vary. The goal of testing is to select test parameters that provide a reliable and valid sample of behavior.

Test duration is a critical parameter that is often manipulated to meet time limitations. Due to the limited time available for testing and the need and desire to use a variety of tests, the duration of a test may be shortened. Test duration can be manipulated by changing the number of trials in a test or the length of a trial. Varying the duration of a test can have two effects on the performance measured. A duration that is too brief may not allow performance to stabilize. Conversely, a duration that is too long may cause fatigue to impact performance. Stable performance may develop in a single test session, but it may develop at different points in different people. Tests with a steep learning curve (such as the Symbol Digit test, in which the first trial is often discarded or only the data from the fastest trial is selected) can have a high degree of variance across participants in early trials, so the data after those trials should be chosen for analysis.

In some situations the study may be structured such that people are tested multiple times. One concern in such cases is that repeat testing may cause practice and learning effects. This may make performance from the first testing session appear lower than performance from subsequent sessions. A solution to this problem is to discard the data from the first testing session as training data. Another solution is to have multiple sets of stimuli for a test. For example, the Digit Span test presents a series of numbers and the task is to recall the numbers. If the same set of numbers are used in several sessions, over time the test participant will learn the numbers and his or her performance will improve. A solution to this problem is to have multiple sets of numbers. This idea of alternate forms is common in other testing situations. All sets of stimuli should be pilot tested ahead of time to ensure that one set is not more easy or difficult than another.

The type of stimulus that is chosen in a test can also affect performance. Changing the stimulus in a Simple Reaction Time test from a screen image ("Press 5 when the square appears") to a lighted key ("Press 5 when the 5 key lights up") increased the mean response latency significantly, from 331 msec to 371 msec in a small sample studied by the authors. The type of stimulus, as well as the size and shape of the stimulus, can affect performance. Using letters or English words can put less-educated people or non–English speakers at a disadvantage. Some tests minimize this bias by using stimuli that do not rely on words, letters, or common shapes (i.e., by using random patterns).

Variations in the presentation of the stimuli can also affect performance. The Symbol Digit test is a coding test in which numbers are paired with nine symbols and the participant must enter the numbers in a matrix that includes only the symbols but not the numbers (Figure 11.7.3 depicts the BARS implementation of this test). The test can employ fixed or random symbol-digit pairings on succeeding trials. In the fixed condition, the same symbols are paired with the same numbers on every trial. In the random condition, the same symbols are used but the

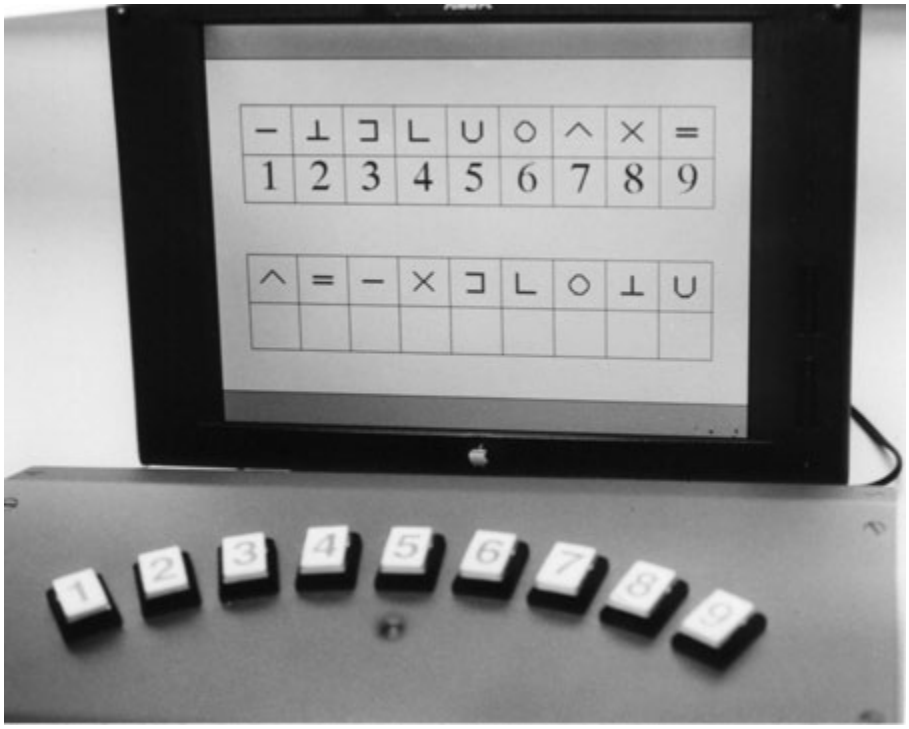

Figure 11.7.3 Test "screen" from the Behavioral Assessment and Research System (BARS) Symbol Digit coding test. At the bottom of the picture is the 9-button DataSled response input unit for participants.

numbers are rotated among the symbols on each new trial. Performance in the fixed condition tends to be significantly faster than in the random condition because people start to learn the symbol-digit pairings, which is impossible in the random condition.

Parameter settings can also be adjusted to control for the difficulty level of a test. Increasing the number of stimuli in a test requiring the participant to remember a stimulus pattern can make the test more difficult. Having a large number of stimuli or a fast presentation rate of stimuli can also add to the difficulty of a test requiring a differential response. Because of individual differences in test performance, selecting the optimal difficulty level of a test for a group may be complex. One solution is to develop a test so that the optimal parameter settings are determined by the test participant. Titrating the time between the stimulus presentations based on participant performance is one example of such an approach. When a person responds correctly to a stimulus, the intervals between the stimuli becomes shorter, so they appear more frequently. When a person responds incorrectly to a stimulus, the duration between the stimuli becomes longer. This allows each individual's performance to determine the difficulty level of the test. This strategy is employed in the BARS Selective Attention Test (SAT) for measuring attention. The SAT is a simple task in which dots appear on the screen and the participant responds on different buttons when the dots are inside but not outside two squares. Figure 11.7.4 is an example from an SAT "instruction" screen used during the training period, demonstrating the integration of the instructions with the test stimuli (Rohlman et al., 1996).

A final area of concern is the presentation order of the tests in a battery. Ideally, test order should have no effect on performance. However, if there is a concern about the order of the tests (e.g., it may be desirable that a tapping test not be followed immediately by a test of reaction time, to prevent fatigue from affecting the second test), techniques such as counterbalancing the order of the tests in the battery should be used to reduce this effect. Time constraints and equipment needs may also influence the test order.

Example

Because of the small number of participants to be tested in the Texarkana example and the desire to provide a clinical evaluation, certain test parameters were selected. The authors' laboratory maintains a large database of results from testing US veterans of the Persian Gulf (Anger et al., 1999), and it was anticipated that

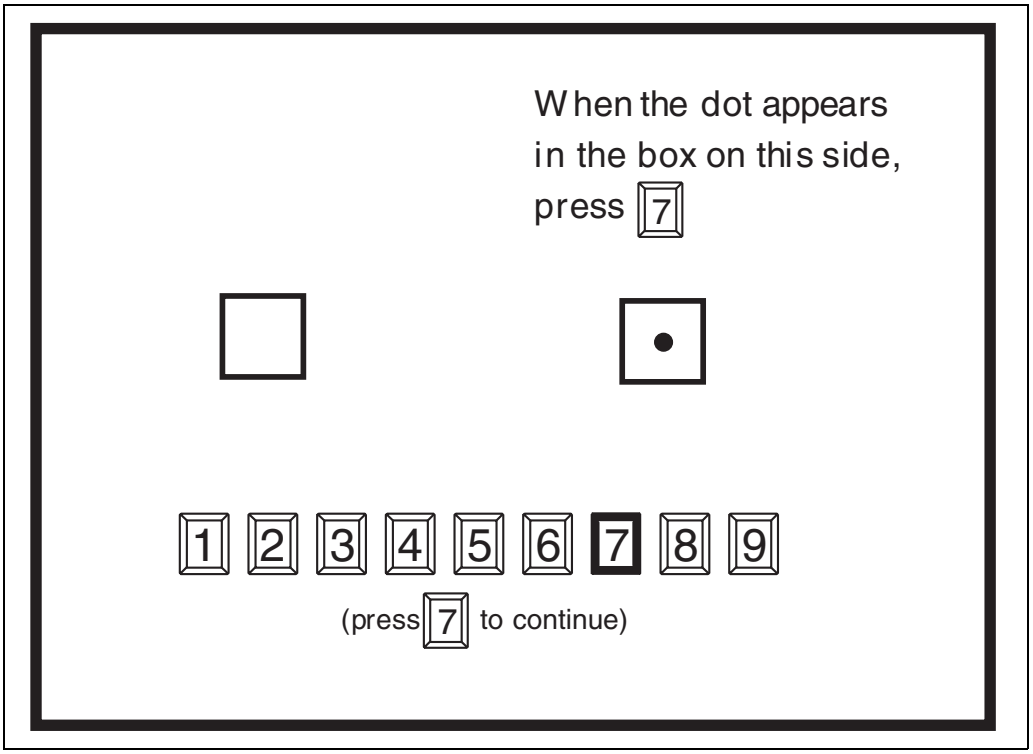

Figure 11.7.4 Instruction "screen" from the Behavioral Assessment and Research System (BARS) Selective Attention Test (SAT). The various instruction screens teach the participant which buttons to press for the various stimulus events (dots inside and outside the two boxes on the screen). The dot is enlarged during the training period which follows a series of steps that integrate the instructions with the test stimuli.

the data from the healthy control participants would serve as one basis for comparison. The same test parameters and test order that were used with the veterans were therefore selected for the Texarkana study, with a few modifications. One consideration was that the administration time recorded for the large number of tests selected was lengthy, and the amount of time participants would have for testing was unknown. Another concern was the motivation or attitude of the test participants: since the test was lengthy, early "burnout" was a possibility. For these reasons the number of trials in the Simple Reaction Time test was reduced and the test order was changed by putting the longest test at the end of the battery. This ensured that as many tests as possible could be completed in the event that the battery had to be shortened at the outset of testing (normally an unacceptable contingency, but for this unique project outside the investigators' control). These are only examples of the many considerations that affected the selection of test parameters.

TEST SETTING

The selection of an appropriate test setting depends on a variety of factors; the guidance that follows is based on the standard procedures in the authors' research. In some studies it is beneficial to divide the testing environment into several testing stations. No matter how many test stations are planned, there are certain common characteristics. The test room should be quiet. Telephones and loudspeakers must be turned off so they do not interrupt testing. The temperature in the room should be set at a comfortable level (e.g., 72°F). There should be adequate lighting, and curtains or blinds may be needed to block excessive sunshine. Sufficient table space should be provided for all of the equipment and for a writing surface, if necessary (often by purchasing folding tables at the site and then selling or donating them to local concerns after testing is finished, since shipping these in two directions often costs more than purchasing them). Electrical outlets and power strips must be provided for all equipment. The test order may influence the specific layout of the test stations.

During testing with BARS computerized tests, up to ten people are tested at one time by one research technician. The ten stations are typically located in one large room. Standard tables are placed end to end, and 1-meter-tall

panels are used to divide the tables into individual work stations that screen participants from distracters (e.g., participants who know each other tend to try to talk during testing, which will affect their data). Each station has a PowerBook laptop computer, DataSled response input unit, headphones for spoken instructions (to avoid distracting others), and a comfortable nontilting chair. There are a separate table and chair for the examiner. Food and drink are not allowed at the testing stations.

If participants are being tested as a group, as suggested above, a reception or waiting area is necessary to greet them. This area is also used to obtain informed consent and give basic instructions to the participants. It is important to have a separate waiting area during group testing because participants will arrive at different times and finish at different times.

When there are multiple testing stations, a schedule and plan of movement should be developed before testing begins. For example, the first participant to arrive may begin at Station 1, the second at Station 2, and so on. The time at each station should be set to be approximately equal in order to minimize waiting time for the participants, although arrival times often negate this plan. It should also be recognized that test completion time varies like other variables, so that almost 50% of the participants will take longer than the mean testing time.

Prior to the start of the study, it is essential to conduct a pilot study to evaluate the procedures. This includes factors such as the maximum number of participants expected at any one time, to determine if there are problems with the room layout or participant flow. Pilot participants should be as similar to the expected participants as possible, to increase the probability that any likely problems (e.g., poor test procedures or unclear instructions) will be encountered in that phase.

STUDY DETAILS: PROTOCOLS

Protocol Book

A protocol book should be assembled for each study, most conveniently in a looseleaf binder. It should contain the protocols used to administer each test in the battery as well as equipment lists, troubleshooting guidelines, copies of any data forms used in the study, a list of regular and emergency phone numbers, a picture of the testing layout, and instructions on how to record information in the log.

Instructions should be separated into "stations" if more than one test area is planned, and each page placed in a protective plastic sheet to prevent loss or damage. The protocol for each test should begin on a separate page. This allows modifications to be made easily during the development of the protocol and provides clarity for the examiner. The test protocols are developed and then pilot tested to ensure they work effectively. Any revisions should be made before the start of testing, and the protocol is not changed during the study.

The protocol for a test includes a list of the equipment and a description of the setup procedures, comprising instructions for assembling the equipment as well as the steps required to start the testing software and any calibration procedures. For noncomputerized equipment this includes the physical layout of the equipment and the procedures required. Following the setup procedures are the instructions that will be read to the test participant. They are to be read exactly as on the page. These instructions are placed in boldface or within a box to make them stand out from the procedures required to administer a test, so the examiner can locate them quickly. The procedures required to administer the test follow the instructions, and information about scoring, backing up, and/or downloading the data are presented last.

The protocol book should also contain information on how to troubleshoot problems. Problems during testing are unwelcome but likely to arise. The troubleshooting guidelines should contain information on potential participant problems, possible steps to solve them, and instructions on how to record the problem in a log book, which should be available at every test station.

Examiners

Health professionals with a BA/BS/RN in any discipline and competent health technicians can administer neurobehavioral tests reliably and effectively after 5 to 10 hr of training, at least half of which should be spent practicing with representative participants under observation by the trainer. The main requirements are that the examiner remain alert and be committed to testing in a careful and conscientious manner. Examiners must be capable of reading the instructions and following the procedural aspects of the protocol exactly.

A "professional" appearance is required—something that is difficult to define, although certain basic requirements are obvious. An examiner must be clean, wear only limited makeup, avoid jewelry, have neat hair, and use

no perfume. Examiners should begin testing each day with clean clothes that are appropriate for the test setting and population.

Examiners should be blind to whether the participants are identified as exposed or controls. Even with computerized testing, the potential for bias is to be avoided. It is important to "certify" new examiners for each study before testing begins, by requiring them to meet the standards in this section. The certification involves observing the examiner administer all the tests in the battery and grading their performance on each test. A no-errors criterion is used.

STUDY DETAILS: PROCEDURES

Recruiting

The plan for recruiting test participants generally involves both control (unexposed) as well as exposed individuals. The demographics of the two groups should be kept as equal as possible. One method of recruiting participants is to advertise in a local newspaper. The advertisement should give a brief description of the study, list any requirements, and give a phone number to call to schedule an appointment. A script should be prepared for the scheduler to read when potential recruits call. The script includes any screening questions, which must be phrased so that the potential recruit cannot glean the criterion they need to meet. For example, if the criteria require that the participants be over 25 years of age, the age of the caller is queried rather than if they are over 25. The script also includes clear directions to the testing site. Participants should be asked to bring a photo ID on the day of testing to confirm necessary demographic factors and assure the name is correct. If scheduling occurs more than a day in advance of testing, a reminder phone call is helpful to decrease the "no show" rate.

Prior to testing a packet should be prepared for each test participant that includes the consent form, a demographic data sheet, paper data forms, and the form they sign when they are paid at the end of the experiment (e.g., on the bottom of the consent form). One approach is to generate a page of labels with each participant identifier ID number to attach to all of the forms (front and back). A unique ID should be assigned to each test participant when they arrive. Participants should be assigned numbers sequentially, whether they are in the exposed or control group, to ensure blinding of the examiners and those who will score and enter data. With multiple stations, a station or test checklist may be used for tracking, and name tags with their names and IDs are useful for identifying the test participants. With multiple stations, the examiners maintain control of all data forms at their individual stations; only the station checklist (with examiner initials for each completed station) travels with the participants and their packets.

Quality Assurance

Examiner training is typically certified at the beginning of the study, but to prevent examiner drift the effectiveness of the training must be verified if the study continues for any length of time. Mid-study checks every 2 to 3 weeks, or every 20 to 30 participant test hours by an examiner, are desirable.

DATA MANAGEMENT

Data from computer files should be labeled and stored on two diskettes immediately following each test session. During the study the completed data forms should be placed in locked safes or file cabinets. The data should be kept in two physically separate and secure sites. This redundancy minimizes the possibility of irretrievable loss of data through accident or error.

The data from the paper forms are entered into a spreadsheet. To minimize entry errors, the order of entry into the spreadsheet should follow the order of the data on the paper forms. All scoring and calculations should be recorded and entered into the spreadsheet. Paper data should be entered twice by different people. When both entries are completed, the data must be compared and checked for inconsistencies—easily done in spreadsheets using an "if" statement. Any inconsistencies will be flagged, and the paper data forms can then be reviewed to determine which entry is correct. One of the spreadsheets is then modified to develop a final data file. Multiple backup copies (dated) of the data should be made frequently, and routinely at the end of every day.

DATA ANALYSIS

The analysis should begin with an inspection of the basic descriptive data—means and standard deviations. The study logs are reviewed for examiner notes that would explain data outliers or reveal data that should be excluded from the analysis. The key variables that affect neurobehavioral performance—age, education, gender, and ethnicity—are examined to identify possible differences between the exposed and control groups, taking care to

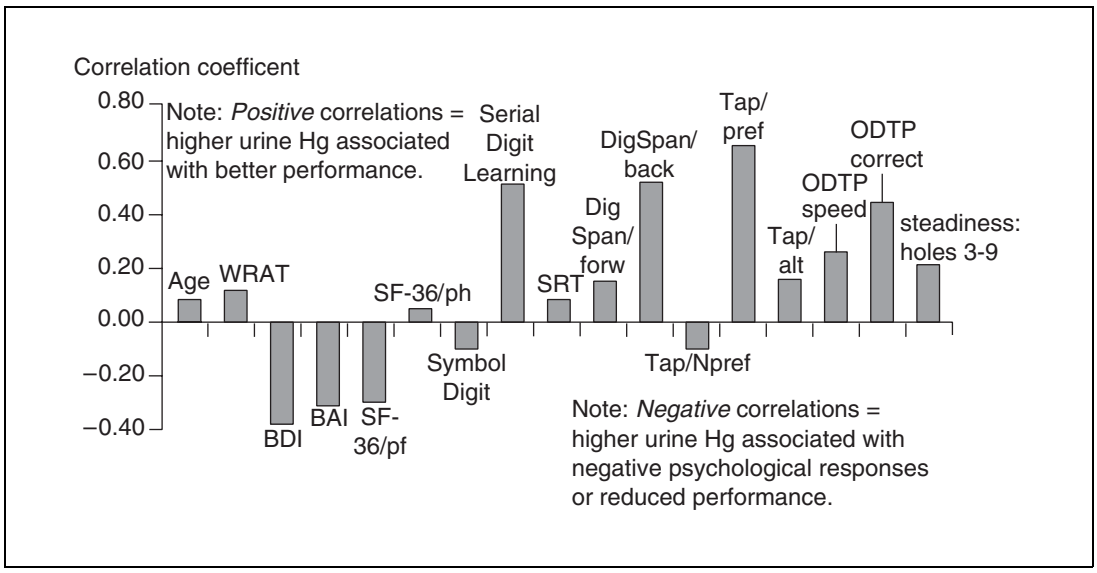

Figure 11.7.5 Urine mercury correlations with age, Wide Range Achievement Test (WRAT), psychological, and neurobehavioral test performance in eight Texarkana participants exposed to mercury. The Symbol Digit, Simple Reaction Time (SRT), and Oregon Dual Task Procedure (ODTP) scores normally presented as latencies are represented in the figure as speed for coherence of presentation (i.e., so negative or poorer performance is always represented as negative correlations); BDI (Beck Depression Inventory), BAI (Beck Anxiety Inventory), and SF-36 symptom checklist—physical functioning (SF-36/pf) and physical health (SF-36/ph)—correlations are reversed in the figure to present increased urine mercury concentrations as associated with greater distress (i.e., the adverse outcome). Three measures of fingertapping are also shown: preferred hand (Tap/pref), non-preferred hand (Tap/Npref), and alternating hands (Tap/alt). Other abbreviations: DigSpan, Digit Span.

focus on the primary measures. Simple analyses such as *t*-tests will reveal large group differences. (As a word of caution, avoid elevating a secondary measure to primary status because the groups happen to differ on that measure.) If nothing emerges, pursue more powerful analyses to identify small effects, in consultation with an experienced statistician (a powerful ally to be enlisted during the power analyses and certainly before the data are collected).

Example

The Texarkana project proved challenging from an analytic perspective. Only eight mercury-exposed participants and four controls were available for testing. Initial inspection of the results revealed that one mercury-exposed participant had clinically significant scores on the Beck Depression and Anxiety Inventories. This participant was excluded from the data analysis because depression affects test performance and was judged unlikely to be a result of the exposures (more likely a result of the situational events surrounding the mercury incidents). A second mercury-exposed participant was excluded from the analysis because of a performance on the test of motivation suggesting a lack of motivation to perform the tests, which rendered the test results suspect. This left six mercury-exposed and four control participants.

The WRAT-III reading test revealed that the mercury-exposed participants had a decidedly lower educational attainment than was expected for their current grade in school or for their age, while the controls achieved expected scores for their age and grade in school. Clearly, cross-sectional comparisons were impossible due to the small numbers and the reading-test differences, in addition to the lack of random selection noted above. While individual clinical assessments were valuable, they failed to reveal response patterns indicative of neurotoxic effect. Even more telling were the correlations between urine mercury and test results (Fig. 11.7.5). There were positive correlations between urine mercury and most performance measures, although none were significant due to the small sample size. If these differences had been associated with the mercury exposures, the expected correlation would have been negative—with higher mercury associated with lower performance scores. The trend of the psychological tests was in the expected direction, though again not significantly: higher urine mercury was minimally associated with

more symptoms of depression, anxiety, and adverse health function as perceived by the individual. Since the publicity, suggestion of adverse long-term consequences of mercury exposure, and events surrounding the mercury exposure (e.g., house evacuation during the cleanup) had a decidedly negative tenor, it is much more likely that situational events played a larger role in the psychological test results than did the mercury exposure, but there was insufficient information to draw firm conclusions on this score.

COMMENTARY

Neurobehavioral and psychological tests are frequently used to evaluate exposures to neurotoxic chemicals. A single protocol to study neurotoxic effects in humans would be desirable but dangerous. If there is little time to review the literature or consider the symptoms of the exposed population, then the NCTB (Johnson et al., 1987; Anger et al., 1993) or AENTB (Amler et al., 1994; Anger et al., 1994) consensus batteries are recommended. Manuals describing the administration of these two tests in complete detail are available. The NCTB manual is not published but may be obtained in English and Spanish versions from the authors (Anger). The AENTB manual is published (Amler et al., 1995) and is available from ATSDR (1600 Clifton Rd., Atlanta, Ga. 30333 USA).

This unit details the steps to take in developing a research study and implementing it in a laboratory or field setting. The effort is best mounted by a multidisciplinary team, including experimental psychologists for methodology, clinical psychologists to assess possible psychological implications of the exposures and to represent the interests of the exposed individual, industrial hygienists to measure the chemical in various media, neuroscientists who can propose biomarkers and suggest the possible mechanism(s) of effect(s), and statisticians who can assist with experimental design, statistical power analyses, and statistical analyses of the data.

LITERATURE CITED

Amler, R.W., Lybarger, J.A., Anger, W.K., Phifer, B.L., Chappell, W., and Hutchinson, L.J. 1994. Adoption of an Adult Environmental Neurobehavioral Test Battery (AENTB). *Neurotoxicol. Teratol.* 16:525-530.

Amler, R.W., Anger, W.K., and Sizemore, O.J. 1995. Adult Environmental Neurobehavioral Test Battery (Training Manual). US Department of Health and Human Services, Public Health Service, Agency for Toxic Substances and Disease Registry, Atlanta, Ga.

Amler, R.W., Gibertini, M., Lybarger, J.A., Hall, A., Kakolewski, K., Phifer, B.L., Olsen, K.L. 1996. Selective approaches to basic neurobehavioral testing of children in environmental health studies. *Neurotoxicol. Teratol.* 18:429-434.

Anger, W.K. 1990. Worksite behavioral research: Results, sensitive methods, test batteries and the transition from laboratory data to human health. *Neurotoxicology* 11:629-720.

Anger, W.K., Cassitto, M.G., Liang, Y-X., Amador, R., Hooisma, J., Chrislip, D.W., Mergler, D., Keifer, M., Hörtnagl, J., Fournier, L., Dudek, B., and Zsögön, E. 1993. Comparison of performance from three continents on the WHO-recommended neurobehavioral core test battery. *Environ. Res.* 62:125-147.

Anger, W.K., Letz, R., Chrislip, D.W., Frumkin, H., Hudnell, K., Russo, J.M., Chappell, W., and Hutchinson, L. 1994. Neurobehavioral test methods for environmental health studies of adults. *Neurotoxicol. Teratol.* 16:489-497.

Anger, W.K., Otto, D.A., and Letz, R. 1996a. Symposium on computerized behavioral testing of humans in neurotoxicology research. Overview of the proceedings. *Neurotoxicol. Teratol.* 18:347-350.

Anger, W.K., Rohlman, D.S., Sizemore, O.J., and Kovera, C.A. 1996b. Human behavioral assessment in neurotoxicology: Producing terminal test performance with written and shaping instructions. *Neurotoxicol. Teratol.* 18:371-379.

Anger, W.K., Sizemore, O.J., Grossmann, S.J., Glasser, J.A., Letz, R., and Bowler, R. 1997. Human neurobehavioral research methods: Impact of subject variables. *Environ. Res.* 73:18-41.

Anger, W.K., Storzbach, D., Amler, R.W., and Sizemore, O.J. 1998. Human behavioral neurotoxicology: Workplace and community assessments. *In* Environmental and Occupational Medicine (W. Rom, ed.) pp. 709-731. Lippincott, Philadelphia.

Anger, W.K., Storzbach, D., Binder, L.M., Campbell, K.A., Rohlman, D.S., McCauley, L., Kovera, C.A., and Davis, K.L. 1999. Neurobehavioral deficits in Persian Gulf veterans: Evidence from a population-based study. *J. Int. Neuropsychol. Soc.* 5:203-212.

Binder, L.M. 1993. Assessment of malingering after mild head trauma with the Portland Digit Recognition Test. *J. Clin. Exper. Neuropsychol.* 15:170-182.

Binder, L.M., Storzbach, D., Anger, W.K., Campbell, K.A., Rohlman, D.S., and members of the Portland Environmental Hazards Research Center. 1999. Subjective cognitive complaints, affective distress, and objective cognitive performance in Persian Gulf War veterans. *Arch. Clin. Neuropsychol.* 14:531-536.

Campbell, K.A., Rohlman, D.S., Storzbach, D., Binder, L.M., Anger, W.K., Kovera, C.A., Davis, K. L., and Grossmann, S.J. 1999. Test-retest

reliability of psychological and neurobehavioral tests self-administered by computer. *Assessment*. 6:21-32.

Echeverria, D., Heyer, N.J., Martin, M.D., Naleway, C.A., Woods, J.S., and Bittner, A.C. 1995. Behavioral effects of low-level exposure to HgO among dentists. *Neurotoxicol. Teratol.* 17:161-168.

Heyer, N.A., Bittner, A.C. Jr., and Echeverria, D. 1996. Analyzing multivariate neurobehavioral outcomes in occupational studies: A comparison of approaches. *Neurotoxicol. Teratol.* 18:401-406.

Iregren, A. and Letz, R. 1992. Computerized testing in neurobehavioral toxicology. *Appl. Psychol.: An Internat. Rev.*. 41:247-255.

Iregren, A., Gamberale, F., and Kjellberg, A. 1996. SPES: A psychological test system to diagnose environmental hazards. *Neurotoxicol. Teratol.* 18:485-491.

Johnson, B.L., Baker, E.L., EI Batawi, M., Gilioli, R., Hänninen, H., Seppäläinen, A.M., and Xintaras, C. (eds.). 1987. Prevention of Neurotoxic Illness in Working Populations. John Wiley & Sons, New York.

Johnstone, B., Callahan, C.D., Kapila, C.J., and Bouman, D.W. 1996. The comparability of the WRAT-R Reading Test and NAART as estimates of premorbid intelligence in neurologically impaired patients. *Arch. Clin. Neuropsychol.* 11:513-519.

Kennedy, R.S., Wilkes, R.L., Dunlap, W.P., and Kuntz, L.A. 1987. Development of an automated performance test system for environmental and behavioral toxicology studies. *Percept. Mot. Skills* 65:947-962.

Kovera, C.A., Anger, W.K., Campbell, K.A., Binder, L.M., Storzbach, D., Davis, K.L., and Rohlman, D.S. 1996. Computer-administration of questionnaires: A health screening system (HSS) developed for veterans. *Neurotoxicol. Teratol.* 18:511-518.

Krengel, M., White, R.F., Diamond, R., Letz, R., Cyrus, P., and Durso, R. 1996. A comparison of NES2 and traditional neuropsychological tests in a neurologic sample. *Neurotoxicol. Teratol.* 18:435-439.

Letz, R. 1990. The Neurobehavioral evaluation system: An international effort. *In* Advances in Neurobehavioral Toxicology: Applications in Environmental and Occupational Health. (B.L. Johnson, W.K. Anger, A. Durao, and C. Xintaras, eds.) pp. 489-495. Lewis Publishing, Chelsea, Mich.

Letz, R., Green, R.C., and Woodward, J.L. 1996. Development of a computer-based battery designed to screen adults for neuropsychological impairment. *Neurotoxicol. Teratol.* 18:365-370.

Lezak, M.D. 1995. Neuropsychological Assessment. Oxford University Press, New York.

Liang, Y.-X., Chen, Z.-Q., Sun, R.-K., Fang, Y.-F., and Yu, J.-H. 1990. Application of the WHO Neurobehavioral Core Test Battery and other neurobehavioral screening methods. *In* Advances in Neurobehavioral Toxicology: Applications in Environmental and Occupational Health (B.L. Johnson, W.K. Anger, A. Durao, and C. Xintaras, eds.) pp. 225-243. Lewis Publishers, Chelsea, Mich.

Pagano, M. and Evereau, K. 1993. Principles of Biostatistics. Duxbury Press, Belmont, Calif.

Pankratz, L. and Binder, L.M. 1997. Malingering on cognitive measures. *In* Clinical Assessment of Malingering and Deception, 2nd ed. (R. Rogers, ed.). Guilford, New York.

Rohlman, D.S., Sizemore, O.J., Anger, W.K., and Kovera, C.A. 1996. Computerized neurobehavioral testing: Techniques for improving test instructions. *Neurotoxicol. Teratol.* 18:407-412.

Stollery, B.T. 1996. The Automated Cognitive Test (ACT) system. *Neurotoxicol. Teratol.* 18:493-497.

Travis, C.C. (ed.). 1993. Use of Biomarkers in Assessing Health and Environmental Impacts of Chemical Pollutants. Plenum, New York.

White, R.F. 1995. Clinical neuropsychological investigation of solvent neurotoxicity. *In* Handbook of Neurotoxicology (L.W. Chang and R.S. Dyer, eds.) pp. 355-376. Marcel Dekker, New York.

White, R.F., Diamond, R., Krengel, M., Lindem, K., and Feldman, R.G. 1996. Validation of the NES2 in patients with neurologic patient sample. *Neurotoxicol. Teratol.* 18:441-448.

Contributed by W. Kent Anger, Diane S. Rohlman, and Daniel Storzbach
Oregon Health Sciences University
Portland, Oregon

Mouse Models of Global Cerebral Ischemia

Hippocampal neurodegeneration (HN) occurs as a result of global ischemia when blood flow to the brain is temporarily interrupted and then restarted. It can be observed in clinical cases of cardiac arrest, drowning, electrocution, and anesthesia-related accidents that are followed by successful, but somewhat delayed, resuscitation. HN can also result as a consequence of carbon monoxide inhalation (Nabeshima et al., 1991), certain hypoxemic-ischemic conditions (MacMillan et al., 1993), and as a result of measles infection (Andersson et al., 1993). HN leads to memory impairment and behavioral deficits in both humans (Beuret et al., 1993) and laboratory animals. For better understanding of the pathophysiology of this condition and molecular mechanisms involved, use of rodent replicas of HN has been recommended.

This unit describes basic surgical protocols for three models of global cerebral ischemia. These models are carried out by means of transient occlusion of both common carotid arteries (hence the name two-vessel occlusion model; see Basic Protocol 3), or in conjunction with either transient basilar artery occlusion (three-vessel occlusion model; see Basic Protocol 1) or permanent bilateral vertebral artery occlusion (four-vessel occlusion model; see Basic Protocol 2). Both controlled hypotension and ligation of the muscles on the neck can be used as adjunct procedures in all of these models to further diminish collateral blood flow to the ischemic hippocampus. These models were adapted from the laboratory rat and extensively validated in mice. The unit also describes basic histological techniques of brain tissue preparation (see Support Protocols 1 and 2) and methods for evaluation of hippocampal injury (see Support Protocols 3 to 6).

NOTE: All protocols using live animals must first be reviewed by the Institutional Animal Care and Use Committee (IACUC) and must conform to governmental regulations regarding the care and use of laboratory animals.

NOTE: Surgical instruments should be sterilized in a hot-glass-bead, dry surgical instrument sterilizer (Stoelting) and should be kept on a silicon mat for safeguarding. Instruments for perfusion should not be pooled together with instruments intended for in vivo surgeries, but should be kept separately. Microscissors (Moria) are especially valuable items for in vivo microsurgical manipulations. Several different kinds should be purchased. Instruments made of titanium are very robust and are 30% to 40% lighter than similar instruments made of Dumostar, Dumoxel, or Inox stainless steel. They are also corrosion and heat resistant and nonmagnetic, but they are hard to resharpen or recondition.

NOTE: It is recommended that the reader search *Linscott's Directory of Immunological and Biological Reagents* (2000) to find competitive pricing prior to purchase of any antibodies, histostain kits, and other reagents.

THREE-VESSEL OCCLUSION MODEL OF GLOBAL CEREBRAL ISCHEMIA

BASIC PROTOCOL 1

The purpose of this protocol is to induce a transient global ischemic episode by means of either permanent or transient occlusion of the basilar artery and simultaneous occlusion of both common carotid arteries. Throughout the procedure, the ischemic episode and the postischemic reperfusion period are thoroughly controlled by evaluation of either cortical or hippocampal regional cerebral blood flow and cortical electrical activity. Delayed neuronal death to the CA1 subregion of the hippocampus develops by the end of 72 hr and is presumed to be of apoptotic origin. The borders of the CA1 subregion can be defined by a perpendicular line connecting both dentate gyrus blades with CA1-CA2 pyramidal cell layer laterally.

Contributed by Nariman Panahian

Current Protocols in Toxicology (2000) 11.8.1-11.8.24

The three-vessel occlusion global ischemia model is recommended for investigators studying the mechanisms of delayed neuronal death and apoptotic injury. This model can be used for assessment of neuroprotective potential of novel pharmacological agents administered either systemically, intracerebroventricularly, or locally (via iontophoretic applications).

Materials

Adult mice, 20 to 28 g (e.g., Harlan Bioproducts for Science, Jackson Laboratory, Taconic Farms)
3% and 1.5% (v/v) halothane in 70% N_2O/30% O_2
Acrylic dental cement (Stoelting)
Surgical glue
Xylocaine solution: 2.5% (v/v) lidocaine solution
1000 U/ml heparin
Heparinized saline: 100 µl heparin in 100 ml saline, use immediately

Fluotec 3 halothane vaporizer equipped with air, N_2O, and O_2 flowmeter assembly (Colonial Medical Supply)
Plexiglas halothane induction chamber for rodents (Stoelting)
Homeothermic blanket for rodents with feedback-regulated maintenance of body temperature (Stoelting)
YSI thermocouple equipped with a microprobe (model 511, S.N. K076, Harvard Apparatus)
SEP/EEG gold screws: gold-wire electrophysiology contacts for EEG and/or SEP monitoring (Fine Science Tools #19003-02)
Stereotaxic frame: dual-manipulator model with swivel mouse nose adaptor (David Kopf Instruments; optional)
Periflux PF-3 laser Doppler flowmeter equipped with PF318 master probe and MTB 500-0 straight fiberoptic microtips (Perimed)
Cotton swabs
8-0, 10-0, and 11-0 black monofilament nylon atraumatic sutures (Ethicon)
Absorbtion spears, 1 box
PE-10 intramedic polyethylene tubing (Clay Adams)
Lucr-Lok stopcock (Becton Dickinson)
27.5-G needle (Becton Dickinson)
1-ml tuberculin syringes (Becton Dickinson)
20-G, 17-mm-long angiocatheter (Angiocath, Deseret Medical) and curved stilette
SAR-830/P small animal ventilator, volume and pressure cycled, with built-in pump, flowmeter, and internal valves (CWE)
Microcapnometer (Columbus Instruments)
Blood gas analyzer (800 series; Ciba-Corning)
Heparinized microhematocrit capillary tubes (Fisher Scientific)
Overhead infrared reflector lamp (120 V, 250 W, GE; Harvard Apparatus)
6-0 silk black braided monofilament suture on a cutting G-7 needle (Ethicon)
Transpore surgical adhesive tape (Baxter Medical Supply)
Rodent intensive care and temperature control unit (DW-1, ThermoCare)
Stereomicroscope consisting of:
  MZ-8 Leica stereomicroscope on a three-dimensional SMS-20 ball-bearing boom stand, WF 10×/21M HP eyepieces, and 0.8× achromatic main objective lens, FWD = 112 mm (Kramer Scientific)
  Optical carrier equipped with a double-barrel coaxial surgical illuminator integrated with EKE rheostat light source

MacLab 8/e data acquisition system equipped with ETH-400 and Bridge preamplifiers running Chart and Scope software, with blood pressure transducers, EEG, EKG electrodes, BNC cables, thermocouple (AD Instruments)

Macintosh Power PC Laptop computer

Statview v. 5 statistical package for the Macintosh (SAS Institute, Inc.)

Statistical software for power analysis: Primer of Biostatistics (McGraw-Hill)

Viking, Nicolet Pathfinder four-channel evoked potential unit (Nicolet Biomedical)

440-E animal laboratory bipolar coagulator with McPherson bipolar miniature forceps and cords (Medifor)

Software packages for image analysis: Image ProPlus v. 3.0 (Media Cybernetics)

XLC-140 caposil or calcium-filled liquid nitrogen (vapor releasing) freezing chamber (LabRepco)

Timer (VWR)

Microsurgical instruments (Fine Science Tools):

Vibration-free microdrill (11,000 rpm) with 400-μm drill bits (#18000-17)

Moria miniature scalpel (#10315-12)

Straight titanium forceps (#11602-16) or suture-tying forceps (#18025-10)

Angled fine forceps (#11063-07)

Biologie no. 5 titanium forceps, 0.05 × 0.02–mm tip (#11252-40)

Dumont no. 4 forceps (#11241-30)

Dumont microsurgery forceps with atraumatic 0.1 × 0.06–mm tips (no. 55; #11253-20)

Dumont straight-tip forceps, 0.2 × 0.12–mm tip (#11203-23)

Dumont straight ultrafine forceps, 0.05 × 0.01–mm tip (#11254-20)

Epoxy-covered forceps (#11220-21)

Moria MC40 ultrafine forceps (#11370-40)

Vessel cannulation forceps S&T (#00571-13)

Vannas-Tubingen straight titanium scissors (#150007-08)

Small-blade scissors (#15000-08) or extra-delicate mini-Vannas scissors (#15000-00)

Student Vannas spring scissors, straight (#15100-09)

Mini-Goldstein retractor (#17002-02)

Yasargil vascular clip (Aesculap FD722), closing force = 0.98 N

Battery-operated small vessel cauterizer with angled and straight 0.2-mm-diameter tips made of platinum-iridium alloy (#18000-00)

Zen temporary clips (13 × 0.4–mm, 15-g closing force; Ohwa Tsusho)

Additional reagents and equipment for assessment of hippocampal injury (Support Protocols 1 to 6)

Prepare animals for physiological monitoring

1. Provide adult mice access to food and water ad libitum and keep animals under diurnal light conditions. Weigh animals prior to surgery.

2. Induce surgical-level anesthesia with 3% halothane in 70% N_2O/30% O_2 using a Fluotec 3 halothane vaporizer in a Plexiglas halothane induction chamber. Maintain further anesthesia using 1.5% halothane in 70% N_2O/30% O_2.

   Anesthesia will be discontinued ~2 min before vascular occlusions.

3. Place the mouse supine on a homeothermic blanket for regulated maintenance of body temperature with a YSI thermocouple. Insert a rectal probe.

   Surgical procedures may be performed without temperature adjustment until step 21.

4. Turn the mouse on its belly, expose the surface of the skull, and drill two burr holes (bregma = 0; 2 mm lateral of midline) with a vibration-free microdrill using surgical stereotoxic coordinates from the Franklin-Paxinos brain atlas (1997). Perform all surgical procedures on mice using a Leica MZ-8 stereomicroscope equipped with coaxial illuminator and EKE light source.

5. Hold two SEP/EEG gold screws in place using epoxy-covered forceps and bond them permanently to the surface of the skull using acrylic dental cement. Attach wire contacts to Viking-Nicolet Pathfinder evoked-potential unit.

   If desired and for greater precision, this procedure may be done with the mouse positioned in a stereotaxic frame.

6. Attach a fiberoptic microtip (for a Doppler flowmeter) to the surface of the drilled skull (2 mm posterior of bregma; 3.5 mm lateral of midline) using surgical glue.

7. Insert an Omega thermocouple 33-G needle probe into the cerebellum for direct brain temperature measurements, and fix in place using surgical glue.

Catheterize femoral artery

8. Begin femoral arterial cutdown by cutting cutaneous tissues and fascia propria using straight student Vannas scissors and Dumont no. 4 forceps. Identify the femoral artery in a common sheath together with the femoral vein and saphenous nerve.

9. Using two cotton swabs, dissect the bundle upwards bluntly to the level of the inguinal ligament and as much upwards as possible. Carefully examine all components of the bundle and then dissect them using Dumont straight ultrafine forceps, Biologie no. 5 titanium forceps, and Dumont microsurgery forceps with atraumatic tips (no. 55). Separate the nerve, the most lateral in location, from the surface of the femoral artery.

   The surface of the femoral vein must never be touched or pulled in any way, as this will rip open its wall and result in immediate bleeding.

10. Insert Dumont straight ultrafine forceps between the femoral artery and the vein below artery profunda femoris.

    If this is not done, the animal will loose all functions of that lower extremity when the catheter is extracted, with subsequent gangrenous transformation.

11. Peel the common vascular sheath off and upwards, toward the inguinal ligament, thus skeletonizing (freeing) necessary surgical space on the vessel.

12. Use angled fine forceps to pass a 10-0 monofilament nylon atraumatic suture behind the distal portions of femoral artery and vein, and ligate them separately.

13. Position a single Yasargil vascular clip proximally on the surface of both femoral artery and vein to achieve total cessation of blood flow. Then use a pair of Dumont straight-tip forceps to tie up the knots.

14. Stretch the femoral artery out by holding its entire width with Moria MC40 ultrafine forceps at the level of the placed knot and make a small cutdown at an angle of 30° to 35° through its wall using small-blade scissors or extra-delicate, mini-Vannas scissors.

    As a rule, some blood leaks back, originating from perforant muscular branches and artery profunda itself. In this case, absorption spears should be used for hemostasis. If the mouse is <25 g in weight, a drop of xylocaine solution may be applied to the surface of the femoral artery for maximum vasodilation and visibility.

15. Mount a PE-10 intramedic polyethylene tubing to a filed-down 27.5-G needle attached to a Luer-Lok stopcock and attach it to a 1-ml tuberculin syringe filled with heparinized saline. Flush the tubing to remove any air bubbles.

    The front tip of the tubing is slightly beveled, using student Vannas scissors, for ease of intraarterial introduction.

16. Hold the tip of the catheter (27.5-G needle) with either straight titanium forceps or suture-tying forceps (depending on the surgeon's hand size), and hold the arterial wall at the cutdown site with Biologie no. 5 or Dumont no. 55 forceps. Gradually pull the artery over the PE-10 tubing (as stockings onto a foot), advancing the tubing forward until it reaches the level of the external iliac artery.

17. After cannulation, fix the PE-10 tubing in place with a 10-0 monofilament nylon suture. Close the wound with surgical glue. Attach needle-stopcock-syringe assembly to MacLab 8/e pressure transducer.

    The wound is closed permanently to make sure that the in-dwelling tubing does not get dislodged when the animal is turned over or connected to the monitoring equipment.

Intubate mouse

18. Hyperextend the neck. Using straight student Vannas scissors, make an anterior midline incision through platysma and fascia propria to expose the trachea and thus facilitate intubation under direct visual control. Cut both sternohyoid and sternothyroid muscles.

    No hemostasis is necessary and, as a rule of thumb, very little or no bleeding at all will result. If bleeding results, use a small-vessel cauterizer to stop the bleeding. If branches of the external carotid artery are accidentally severed, use the McPherson bipolar coagulator and miniature forceps to close.

19. Intubate the mouse using a 20-G, 17-mm-long angiocatheter on a curved stilette. Achieve controlled ventilation using an SAR-830/P small-animal ventilator with the following settings:

    inspiratory stroke volume ≤ 0.5 ml
    inspiratory time = 0.1 sec
    respiratory rate = 110 to 120 breaths per min.

    The microcapnometer tubing must be positioned into the lateral outlet of the intubation angiocatheter to minimize dead space and to get an accurate $EtCO_2$ reading.

Monitor respiration, body temperature, cerebral flow, blood pressure, and heart rate

20. Adjust effective ventilation flow rates by respiratory end-tidal values using microcapnometer and arterial blood gas (pCO_2, pO_2) readings (Dalkara et al., 1995). To monitor, use heparinized microhematocrit capillary tubes and sample 50 µl arterial blood directly from the 27.5-G needle firmly attached to the in-dwelling PE-10 tubing placed in the femoral artery.

    Normal readings are:

    $pC0_2$ = 35 ± 3 mm Hg
    pH^2 = 7.27 ± 0.2
    $p0_2$ = 100–150 mm Hg
    Blood pressure (BP) = 95 ± 9 mm Hg
    Heart rate = 545 ± 78 beats/min

    After blood withdrawals, the intra-arterial lines must always be flushed with heparinized saline to prevent blood clots from forming in the catheter which could disrupt blood pressure recording.

21. Maintain rectal temperature (37° to 37.5°C) by means of the homeothermic blanket coupled to the YSI thermocouple and microprobe.

22. Maintain brain temperature between 36.5° and 37.5°C by means of an overhead infrared reflector lamp.
23. Determine regional cerebral blood flow (rCBF) by laser Doppler flowmetry using a flexible fiberoptic extension of the master probe, which was previously affixed to the surface of the skull (step 6).

    Initial rCBF values are taken as 100%.

Perform three-vessel occlusion

24. Establish physiological baselines. Start continuous-recording MacLab software (Chart) and hardware connected to a Macintosh laptop computer.
25. Pass a 6-0 braided monofilament suture underneath the mouse's front incisors and tape to the operating table using Transpore surgical tape.
26. Hyperextend the mouse by applying simultaneous downward traction to the tip of the tail and upward traction to the surgical suture behind the front incisors.

    Failure to perform this maneuver will make it difficult to expose the basilar artery.

27. Further hyperextend the neck by placing two or three cotton swabs underneath it.
28. Expose the left and right carotid bundles behind the sternocleidomastoid muscles. Retract the left carotid bundle laterally and the trachea-esophagus medially with a spatula.
29. Position a mini-Goldstein retractor at the level of the hypoglossal nerve and the hyoid bone on the left side. Identify the body of the first cervical vertebra and reveal the atlanto-occipital membrane along with the basal surface of the occipital and sphenoid bones.

    Only by overextention of the neck and slight traction in the opposite direction applied to the tail and front incisors can the atlanto-occipatal membrane be stretched and the vertebro-basilar junction revealed.

    For this step experienced users may use a spatula to expand the wound.

30. Transect the dura mater with a Moria miniature scalpel and Vannas-Tubingen straight titanium scissors. Absorb the drops of cerebrospinal fluid that are released using absorption spears.

    Using the Moria miniature scalpel helps to abolish blade drag and tissue distortion. Absorption spears are synthetic sponges capable of absorbing fluids faster and retaining them three times longer than analogous cotton sponges or pieces of gauze.

31. Identify the basilar artery, both vertebral arteries, and anterior spinal artery on the surface of the brainstem. Dissect the basilar artery free of the arachnoid membrane using Dumont straight ultrafine forceps.

    Without this maneuver, it will not be possible to achieve complete clipping of the basilar artery using Zen temporary clips. The arms of the clip (not just the tip) must embrace the basilar artery in order to completely arrest blood flow. Alternatively, the basilar artery may be tied off permanently using an 11-0 Ethicon monofilament nylon suture.

32. Position Zen temporary clips on the basilar artery and the two carotid arteries using vessel cannulation forceps and immediately start the timer. Occlude the arteries for 10 to 15 min. Discontinue anesthesia 1 to 2 min before vascular occulsions.

    A clip applier for the Zen temporary clips is currently unavailable. However, the size of the grooves present on the vessel cannulation forceps matches the clip size with precise tolerances, and can be purchased at 10% of the cost of all clip appliers available on the market today.

33. Control brain temperature as needed by bringing the overhead infrared reflector lamp closer to the animal as the brain temperature drops throughout the ischemic episode.

    These conditions produce satisfactory ischemia with cortical rCBF measurements consistently reduced to ≤10% of the initial baseline values and prominent suppression of cortical electrical activity.

34. Remove clips to induce reperfusion (≥72 hr). Remove laser Doppler flowmeter and skull temperature probes.

35. Close wound with 6-0 Ethicon nylon sutures and extubate. Leave the femoral arterial catheter in place for the first 24 hr. Use Transpore surgical adhesive tape to affix catheter and Luer-Lok stopcock containing heparinized saline solution to the back of the animal.

    The catheter may be used for infusion of supplemental nutrition, crystalloid solutions (Ringer's lactate), and balanced amino acid mixture-Novamine (Kabi Pharmacia), depending on the condition of the animal.

36. Transport the mouse to a rodent intensive care and temperature control unit and keep at 28° to 31°C for 72 hr to maintain normothermia.

Assess results

37. Perform behavioral assessment during the first 2 and 6 hr after induction of global ischemia and every 24 hr thereafter. Check for the following clinical signs: impaired grasping, akinesis, locomotor hyperactivity in response to a loud finger snap, impaired ability to recognize water and laboratory chow, and loss in body weight.

38. After 3 to 7 days past reperfusion, sacrifice mice for assessment of hippocampal injury (see Support Protocols 1 to 6).

FOUR-VESSEL OCCLUSION MODEL OF GLOBAL CEREBRAL ISCHEMIA

BASIC PROTOCOL 2

The four-vessel occlusion model may not require intubation and intraischemic ventilation of animals. The model is not as laborious as the three-vessel occlusion model and can be used by investigators not adept in microsurgical techniques. In brief, the purpose of the model is to induce delayed hippocampal injury by occlusion of both vertebral and both common carotid arteries with an interval of 24 hr. Vertebral arteries are occluded permanently, while both common carotids are occluded transiently. In this model, vital brain stem structures are less likely to become ischemic, since portions of the basilar artery as well as posterior inferior cerebellar arteries (responsible for collateral circulation) are preserved, because the level of interruption of blood supply to the posterior circulation is much lower than in the three-vessel occlusion model. The possibility of ischemic preconditioning may be the only drawback related to this model—in this model, both vertebral arteries are occluded 24 hr prior to the ischemic insult to the hippocampus.

Materials

Adult mice, 20 to 28 g (e.g., Harlan Bioproducts for Science, Jackson Laboratory, Taconic Farms)

2.0% (v/v) halothane in 70% N_2O/30% O_2

Surgical glue

Standard stereotaxic frame (Stoelting or David Kopf Instruments) equipped with mouse ear bars, micromanipulators, and a specially designed Narashigi head holder, and inhalation anesthesia nose cone

Transpore surgical adhesive tape (Baxter Medical Supply)

6-0 silk black monofilament nylon atraumatic sutures (Ethicon)

Cotton swabs
1-ml syringes (Becton Dickinson)
6-0 silk black braided suture on a cutting G-7 needle (Ethicon)
Surgical gauze
Stereomicroscope consisting of:
MZ-8 Leica stereomicroscope on a three-dimensional SMS-20 ball-bearing boom stand, WF 10×/21M HP eyepieces, and 0.8× achromatic main objective lens, FWD = 112 mm (Kramer Scientific)
Optical carrier equipped with a double-barrel coaxial surgical illuminator integrated with EKE rheostat light source
Fluotec 3 halothane vaporizer equipped with air, N_2O, and O_2 flowmeter assembly (Colonial Medical Supply)
Plexiglass halothane induction chamber for rodents (Stoelting)
440-E animal laboratory bipolar coagulator with McPherson bipolar miniature forceps and cords (Medifor)
YSI thermocouple equipped with a microprobe (model 511, S.N. K076; Harvard Apparatus)
Overhead infrared reflector lamp (120 V, 250 W, GE; Harvard Apparatus)
Rodent intensive care and temperature control unit (DW-1, ThermoCare)
Hot glass bead dry surgical instrument sterilizer (Stoelting)
Timer (VWR)
Homeothermic blanket for rodents with feedback regulated maintenance of body temperature (Stoelting)
Microsurgical instruments (Fine Science Tools):
Vibration-free microdrill (11,000 rpm) with 400-μm drill bits (#18000-17)
Scalpel blade
Biologie no. 5 titanium forceps, , 0.05 × 0.02–mm tip (#11252-40)
Dumont no. 4 forceps (#11241-30)
Student Vannas spring scissors, straight (#15100-09)
Mini-Goldstein retractor (#17002-02)
Battery-operated small-vessel cauterizer with angled and straight 0.2-mm-diameter platinum/iridium alloy tips (#18000-00)
Suture-tying forceps (#18025-10)
Vessel cannulation forceps S&T (#00571-13)
Zen temporary clips (13 × 0.4–mm, 15-g closing force; Ohwa Tsusho) and clip applier
Absorbtion spears, 1 box

Additional reagents and equipment for assessment of hippocampal injury (Support Protocols 1 to 6)

Occlude vertebral arteries

1. Place the animal on a homeothermic blanket and insert rectal temperature probe.
2. Position the adult mouse with its head in a stereotaxic frame and continuously deliver 2.0% halothane in 70% N_2O/30% O_2 to the animal using a Fluotec-3 halothane vaporizer via a nose cone. Maintain halothane anesthesia throughout occlusion of the vertebral arteries.
3. Position the animal's head in the stereotaxic frame with a downward flexion of ~30°.

   This angle is optimal for alignment of alar foramina with vertebral arteries passing underneath them. It was found emperically based on analysis of many animals perfused with carbon black ink (for vascular labeling) in which the alar foramina were drilled for visual evidence of exposure of these vessels.

4. Apply downward traction to the animal's tail throughout the surgical procedure, fixing the tail in place with Transpore surgical adhesive tape.

   This maneuver helps stretch out neck muscles and facilities exposure of the alar foramina and the vertebral arteries beneath them.

5. Using a Leica MZ-8 stereomicroscope to view the field, make a surgical incision through the superficial layers of the dorsal surface of the neck using a sharp scalpel.

6. Using a scalpel blade, student Vannas scissors, and an electrocauterizer, cut the muscles longitudinally and separate them from the body of the first cervical vertebra, exposing alar foramina and the vascular arterial branches passing through them.

7. Position a mini-Goldstein retractor at the midline between the surfaces of the cut muscles, taking care not to dissect neck muscles from the occipital region of the skull. Dissect neck muscles laterally in both left and right directions to expose alar foramina of the first cervical vertebra. Use the electrocauterizer and Dumont No. 4 and Biologie No. 5 forceps as needed during the dissection.

   Dissecting neck muscles from this region of the skull hinders the animal's natural feeding and drinking activity throughout the postoperative period.

8. To ensure complete occlusion of the vertebral arteries, drill the alar foramina using a vibration-free microdrill.

   This step should always be performed, as partial or complete ossification and tortuosity are common (Panahian et al., 1996).

9. Cauterize the vertebral arteries through the alar foramina using a battery-operated small-vessel cauterizer equipped with a straight 0.2-mm-diameter platinum/iridium alloy tip.

   Hemostasis is usually easy to achieve using absorption spears and/or surgical gauze.

10. Suture the wound (skin and muscles) using 6-0 nylon atraumatic sutures and suture-tying forceps. Allow the mouse to recover for 24 hr.

    It is not necessary to maintain body temperature during occlusion of the vertebral arteries or the recovery period.

Occlude carotid arteries

11. Induce anesthesia with 2.0% halothane as above.

12. Hyperextend the neck by placing two or three cotton swabs underneath it, and gently expose both common carotid arteries, without using traction, behind the sternocleidomastoid muscles.

13. Terminate anesthesia for ~1 min, and then occlude the carotid arteries for 10 to 15 min using Zen temporary clips with the aid of a vessel cannulation forceps. Control rectal temperature with YSI thermocouple and infrared reflector lamp.

Assess results

14. During the next 10 to 15 min, assess the mouse for the presence of behavioral signs of global ischemia:

    a. Mouse becomes unconscious but responds to a tail pinch throughout the ischemic procedure and a short while after induction of reperfusion (step 15).
    b. Mouse develops mydriasis (pupil dilation) and ocular anemia (exceptionally clear to observe in albino mice; Swiss-Webster, SV-129) during ischemic episode.

c. Mouse shows behavioral signs of recovery from a global ischemic episode: impaired grasping, akinesis, locomotor hyperactivity in response to a loud finger snap, and impaired ability to recognize water and laboratory chow.

15. Remove clips and reperfuse the animal following 10 to 15 min of ischemia (as assessed by the timer). Close the wound on the front of the neck with 6-0 nylon sutures and suture-tying forceps.

16. Keep the animals in a rodent intensive care and temperature control unit for 72 hr.

17. Sacrifice the animal anytime after 72 hr for assessment of hippocampal injury (see Support Protocols 1 to 6).

BASIC PROTOCOL 3

TWO-VESSEL OCCLUSION MODEL OF GLOBAL CEREBRAL ISCHEMIA

The Smith model is performed with minor modifications to the existing protocol (Smith et al., 1984; Fujii et al., 1997). It is a model of bilateral common carotid artery occlusion supplemented with exsanguination in order to achieve intraischemic hypotension. It is also the model that requires the greatest monitoring skills. Mice must be continuously anesthetized and preferably ventilated throughout the entire procedure. This model is recommended for acute in vivo (nonsurvival) studies involving extensive monitoring (e.g., single-cell hippocampal electrophysiology). Because the animals are well anesthetized while in the stereotaxic frame, a variety of electrodes and monitoring devices can be easily incorporated into the stereotaxic setup. The author recommends inflatable vascular occluders (In Vivo Metric) for occlusion of both common carotid arteries to avoid the need to swivel animal 90° for clipping of carotid arteries. This way, the global ischemic episode will also be induced with the animal in a more natural physiological position. Vibration from such swiveling manipulations may interfere with the quality of on-line continuous physiological monitoring. The In Vivo Metric cuffs are circumferentially attached around both common carotid arteries using 8-0 Ethicon monofilament nylon sutures and their tubing is inflated with saline or air using a 10-ml syringe.

Materials

Adult mice, 20 to 28 g (e.g., Harlan Bioproducts for Science, Jackson Laboratory, Taconic Farms)

3% and 1.5% (v/v) halothane in 70% N_2O/30% O_2

Xylocaine solution

Heparinized saline: 100 µl heparin in 100 ml saline, use immediately

Surgical glue

Acrylic dental cement (Stoelting)

Fluotec 3 halothane vaporizer equipped with air, N_2O, and O_2 flowmeter assembly (Colonial Medical Supply)

Plexiglass halothane induction chamber for rodents (Stoelting)

Homeothermic blanket for rodents with feedback-regulated maintenance body temperature (Stoelting)

YSI thermocouple equipped with a microphone (model 511, S.N. Ko76; Harvard Apparatus)

Omega thermocouple with 33-G needle probe for direct brain temperature measurements (Harvard Apparatus)

Cotton swabs

8-0, 10-0, and 11-0 black monofilament nylon atraumatic sutures (Ethicon)

Absorption spears

PE-10 intramedic polyethylene tubing (Clay Adams)

27.5-G needle (Becton Dickinson)

1- and 10-ml syringes (Becton Dickinson)
Periflux PF-3 laser Doppler flowmeter equipped with PF318 master probe and MTB 500-0 straight fiberoptic microtips (Perimed)
SEP/EEG gold screws: gold-wire electrophysiology contacts for EEG and/or SEP monitoring (Fine Science Tools #19003-02)
Stereotaxic frame: dual-manipulator model with swivel mouse nose adaptor (David Kopf Instruments)
20-G and 26-G, 17-mm-long angiocatheters (Angiocath, Deseret Medical) and curved stilette
SAR-830/P small-animal ventilator, volume and pressure cycled, with built-in pump, flowmeter, and internal valves (CWE)
6-0 silk black braided suture on a cutting G-7 needle (Ethicon)
500-µl gas-tight Hamilton syringe, heparinized
Vascular occluders, 2-mm diameter (OC2A; In Vivo Metric; optional)
Transpore surgical adhesive tape (Baxter Medical Supply)
Heparinized microhematocrit capillary tubes (Fisher Scientific)
Surgical gauze
Stereomicroscope consisting of:
  MZ-8 Leica stereomicroscope on a three-dimensional SMS-20 ball-bearing boom stand, WF 10×/21M HP eyepieces, and 0.8× achromatic main objective lens, FWD = 112 mm (Kramer Scientific)
  Optical carrier equipped with a double-barrel coaxial surgical illuminator integrated with EKE rheostat light source
Microcapnometer (Columbus Instruments)
MacLab 8/e data acquisition system equipped with ETH-400 and Bridge preamplifiers running Chart and Scope software, with blood pressure transducers, EEG, EKG electrodes, BNC cables, thermocouple (AD Instruments)
Macintosh Power PC Laptop computer
Viking, Nicolet Pathfinder four-channel evoked potential unit (Nicolet Biomedical)
800 series blood gas analyzer (Ciba-Corning)
440-E animal laboratory bipolar coagulator with McPherson bipolar miniature forceps and cords (Medifor)
YSI thermocouple equipped with a microprobe (model 511, S.N. K076, Harvard Apparatus)
Omega thermocouple with 33-G needle probe for direct brain temperature measurements (Harvard Apparatus)
Overhead infrared reflector lamp (120 V, 250 W, GE; Harvard Apparatus)
Rodent intensive care and temperature control unit (DW-1, ThermoCare)
Hot glass bead dry surgical instrument sterilizer (Stoelting)
Timer (VWR)
Homeothermic blanket for rodents with feedback regulated maintenance of body temperature (Stoelting)
Laboratory scale for weighing mice
Micro-surgical instruments (Fine Science Tools):
  Vibration-free microdrill (11,000 rpm) with 400-µm drill bits (#18000-17)
  Biologie no. 5 titanium forceps, 0.05 × 0.02–mm tip (#11252-40)
  Dumont no. 4 forceps (#11241-30)
  Dumont microsurgery forceps with atraumatic 0.1 × 0.06–mm tips (no. 55; #11253-20)
  Dumont straight-tip forceps, 0.2 × 0.12–mm tip (#11203-23)
  Dumont straight ultrafine forceps, 0.05 × 0.01–mm tip (#11254-20)
  Moria MC40 ultrafine forceps (#11370-40)

Small-blade scissors (#15000-08) or extra-delicate mini-Vannas scissors (#15000-00)
Student Vannas spring scissors, straight (#15100-09)
Mini-Goldstein retractor (#17002-02)
Micro-clip applicator with 18055 series micro-serrefines (#18056-14)
Battery-operated small-vessel cauterizer with angled and straight 0.2-mm-diameter platinum/iridium alloy tips (#18000-00)
Vessel cannulation forceps S&T (#00571-13)
Yasargil vascular clip (Aesculap FD722), closing force = 0.98 N
Zen temporary clips (13 × 0.4 mm, 15-g closing force; Ohwa Tsusho)

Additional reagents and equipment for assessment of hippocampal injury (Support Protocols 1 to 6)

Catheterize femoral arteries

1. Anesthetize an adult mouse with 3% halothane in 70% N_2O/30% O_2 using a Fluotec 3 halothane vaporizer in a Plexiglas halothane induction chamber. Maintain further anesthesia using 1.5% halothane in 70% N_2O/30% O_2. Place the animal on a homeothermic blanket and insert the rectal temperature probe.

2. Position an arterial catheter (PE-10 tubing affixed to 27.5-G needle) in the femoral artery and fix in place with surgical glue (see Basic Protocol 1, steps 8 to 17). Place a second arterial catheter in the other femoral artery.

   Small-blade scissors and Moria MC40 ultrafine forceps can expedite placement of the second arterial catheter. Dumont microsurgery forceps with atraumatic tips, Dumont straight-tip forceps, and Dumont straight ultrafine forceps are helpful in dissecting, the artery from the fermoral vein.

   Placement of the second arterial line is required for adequate control of intraischemic systemic arterial blood pressure, while the first arterial line is used solely for withdrawal of blood.

Set up monitoring devices

3. Affix the probe of a laser Doppler flowmeter over an avascular region of the cerebral cortex (see Basic Protocol 1, step 6).

4. Insert a miniature Omega temperature needle probe into the cerebellum (see Basic Protocol 1, step 7).

   Both probes are either positioned and held in place using micromanipulators or simply glued to the surface of the skull using surgical glue. Positioning the animal in a stereotaxic frame will simplify these tasks.

5. *Optional:* Place EEG/SEP electrodes for complete monitoring (see Basic Protocol 1, steps 4 and 5) and connect to the Viking, Nicolet Pathfinder evoked potential unit.

6. Intubate the mouse (see Basic Protocol 1, steps 18 and 19) and ventilate under control of end tidal CO_2 ($EtCO_2$) microcapnometer and arterial blood gases, assessed using microhematocrit capillary tubes and blood gas analyzer, to prevent intraischemic respiratory arrest, hypoxia, or postischemic hyperventilation.

7. Monitor respiration, body temperature, cerebral blood flow pressure, and heart rate (see Basic Protocol 1, steps 20 and 24).

Occlude carotid arteries

8. Expose both common carotid arteries and place 6-0 braided guiding sutures underneath them for rapid guidance to their location when the mouse is swiveled.

9. Expose right and left carotid bundles (see Basic Protocol 1, steps 25 to 28).
10. Rapidly withdraw 200 to 300 µl of arterial blood into a heparinized 500-µl Hamilton gas-tight syringe, sealed from atmospheric air and kept warm on a homeothermic blanket.
11. Swivel the animal 90° (to facilitate clipping) in a dual-maniputator model stereotaxic frame and quickly place Zen temporary clips on the common carotid arteries using guiding sutures and vessel cannulation forcep.

    Guiding sutures are needed to identify common carotid arteries (CCAs) and clip them. Do not stretch CCAs excessively as this may cause irritation to the carotid glomus and the superior cervical ganglion, and this may cause lung edema after reprefusion.

    Alternatively, a pair of In Vivo Metric vascular occluders can be placed on the carotids and inflated with air or saline to induce occlusions.
12. Monitor cortical blood flow and mean arterial blood pressure using MacLab 8/e system and Macintosh laptop computer. Withdraw additional blood as necessary to achieve relative cerebral blood flow reductions of 90% (corresponding to mean arterial blood pressure of 50 to 60 mmHg).

    Mice may become physiologically unstable and even go into cardiac arrest if systemic blood pressure drops to 35 mmHg or below.

    Blood withdrawal is an efficient procedure that momentarily suppresses compensatory increases in mean arterial blood pressure caused by a surge in catecholamine release.
13. Induce reperfusion and then swivel the animal back to its original position.

    If this maneuver is performed immediately after clip occlusion, vibration may interfere with the quality of on-line physiological recordings.
14. Reinfuse the withdrawn blood slowly.

    Rapid administration of blood after unclipping results in a sustained hyperemic episode. Do not increase halothane levels in order to prevent transient intraischemic increases in mean arterial pressure, as this may result in hypothermia and higher levels of halothane may be neuroprotective in this model.

Assess results

15. Weight mice daily. Perform behaviorial assessment (see Basic Protocol 1, step 37). Sacrifice mice after 2 to 3 days for assessment of hippocampal injury (see Support Protocols 1 to 6).

PREPARATION AND STAINING OF FROZEN SECTIONS

SUPPORT PROTOCOL 1

The brains are rapidly frozen, sectioned, and stained for visualizing ischemic neuronal damage. Both thionin and hematoxylin are good nuclear stains, while eosin labels the cytoplasm of neurons.

Materials

Mice from ischemia experiments (see Basic Protocols 1 to 3)
Isopentane (2-methylbutane), −15° to −20°C
Fixative solution: 1:1:1:1 (v/v/v/v) glacial acetic acid/acetone/absolute ethanol/water
Harris hematoxylin solution, ready-made (Polyscientific)
Thionin solution (see recipe)
1% (v/v) acid alcohol (Polyscientific)
0.05% (w/v) lithium carbonate (Polyscientific)

Eosin Y alcoholic working solution (Polyscientific)
95% and 100% (v/v) ethanol
Cytoseal 60 (low-viscosity mounting medium; VWR or Stephens Scientific) or Permount (Fisher Scientific)
Xylene

Dissection tools (e.g., see Basic Protocols 1 to 3 and Support Protocol 2)
Dual-compressor cryomicrotome (Jung CM 3000; Kramer Scientific)
1600-W hair dryer
Superfrost Plus glass slides (Fisher Scientific)
25-slide containers, sealed and dessicated (VWR)
Coplin jars
24 × 50–mm coverslips (VWR)
Aluminum foil
15-ml plastic centrifuge tubes
Light microscope (e.g. Olympus AX-70)

Prepare slides

1. Rapidly dissect the brains of mice from the skull.
2. Place them in isopentane at −15° to −20°C for ~2 min.
3. Store cryoprotected brains, wrapped in foil, indefinitely at −70°C in sealed plastic 15-ml centrifuge tubes.

   IMPORTANT NOTE: *Brains submerged in isopentane cooled to low temperatures (−40°C and below) may develop freezing artifacts manifesting as "swiss cheese syndrome," which is visible after hematoxylin and eosin staining. Such artifacts are less likely to be detected if thionin staining is used instead. Thionin staining is also less likely to detect episodes of immune response/cytotoxicity after gene therapy.*

   Brains can also be frozen artifact-free with liquid nitrogen vapor in a Caposil-filled XLC-140 freezing chamber (Vonsattel et al., 1995). One advantage of this approach is that both control and treated brains can be frozen simultaneously under identical conditions. Better antigen preservation has also been reported when this method of preservation is used for such techniques as immunocytochemistry and in situ hybridization. This method is less laborious compared to isopentane or hexane cryopreservation and is a definite time saver for those routinely processing large numbers of animal tissues.
4. Cut serial 10-µm thick coronal sections of the entire hippocampus using a dual-compressor cryomicrotome according to the manufacturer's instructions.
5. Mount sections on Superfrost Plus slides.
6. Store slides in sealed and dessicated 25-slide containers indefinitely at −70° to −80°C.

   It is recommended to cut and handle all brains under RNase-free conditions and to create a "bank" of specimens for future use for experiments involving in situ hybridization, immunocytochemistry, or histochemistry (Lu and Haber, 1992).

Stain slides

7. Thaw slides briefly with a hair dryer (~30 sec).

For hematoxylin/eosin staining

8a. Fix specimens 2 min in fixative solution in a Coplin jar.

9a. Wash sections 1 min in running tap water.

10a. Incubate slides 2 to 2.5 min in Harris hematoxylin solution and wash 4 min.

11a. Dip slides into 1% acid alcohol for 1 sec and wash 4 min in running water.

12a. Transfer slides into 0.05% lithium carbonate and wash 1 min in running water.

No running water is used after this step.

13a. Incubate 1 min in Eosin Y alcoholic working solution.

14a. Dehydrate sections in two changes each of 95% and 100% ethanol (15 dips in each).

15a. Transfer slides to xylene for 5 min (or store overnight in xylene).

16a. Mount in Cytoseal 60 or Permount and cover with a 24 × 50–mm coverslip.

17a. View using a conventional light microscope.

For thionin staining alone

8b. Stain 10-µm-thick frozen sections in thionin solution for 1 to 2 min in Coplin jars.

Staining duration depends on section thickness.

9b. Wash thoroughly for 10 min in running water.

10b. Dehydrate specimens in two changes each of 95% and 100% ethanol (15 dips each).

11b. Incubate 5 min in xylene.

12b. Mount using Cytoseal 60 or Permount and add a 24 × 50–mm coverslip.

13b. View using a conventional ligh microscope.

PERFUSION FIXATION OF BRAINS FOR IMMUNOCYTOCHEMICAL EXPERIMENTS

SUPPORT PROTOCOL 2

For immunocytochemical experiments, the author recommends the use of free-floating sections cut at a thickness of 40 µm or less. For this purpose, mice are perfusion fixed with 4% paraformaldehyde in phosphate buffer (pH = 7.4).

Materials

Mice from ischemic experiment (see Basic Protocols 1 to 3)
Heparinized saline: 100 µl heparin in 100 ml saline, 4°C
4% (w/v) paraformaldehyde, chilled to 4°C (see recipe)
Cryoprotectant solution (see recipe)
Powdered dry ice
Cytoseal

Mayo Toughcut tungsten-carbide scissors (Fine Science Tools #14512-15)
Adson Graefe tissue forceps (Fine Science Tools #11030-12)
Fine straight serrated scissors (Fine Science Tools #14070-12)
Moria fine forceps with microserrations (Fine Science Tools, Moria MC31#11370-31
Straight student Vannas scissors (Fine Science Tools #15000-09)
26-G, 17-mm-long angiocatheter (Angiocath, Deseret Medical) and curved stilette
Friedman-Pearson microrongeurs (Fine Science Tools #16020-14)
20-ml scintillation vials
Sliding microtome (HM 400 R from MICROM Laborgeräte GmbH; distributed by Carl Zeiss)

Additional reagents and equipment for halothane anesthesia (see Basic Protocol 1)

1. Place mouse under 3% halothane anesthesia (see Basic Protocol 1, step 2), and expose the chest cavity. Use Mayo toughcut scissors, Adson-Graefe forceps, and fine straight serrated scissors to cut the diaphragm. Hold the beating heart with Moria fine forceps.
2. Nick the heart with straight student Vannas scissors just enough to facilitate introduction of the tip of a 26-G perfusion catheter first into the left ventricle and then into the ascending arch of the aorta. Begin perfusion with 40 to 50 ml heparinized saline.

   No longer than ~30 to 45 sec should elapse from the time the chest cavity is opened to the time a successful perfusion is initiated.
3. When the effluent is clear of blood, administer 40 to 50 ml chilled 4% paraformaldehyde solution (4° to 6°C).

   Muscle twitching starts immediately thereafter and the animal should appear very stiff. The following are signs of an unsuccessful perfusion: (1) animal fails to develop rigor mortis (does not appear stiff); (2) no muscular twitching is present during infusion of 4% paraformaldehyde; (3) blood is present in the liver, which appears to be reddish or patchily perfused (after a successful perfusion the color of the liver is yellow, with no blood present); and (4) lungs are "inflated" with saline and perfusate is coming out of the mouse's upper respiratory tract (due to accidental perforation of the intraventricular septum by the tip of the 26-G perfusion catheter and administration of the perfusion solution into the pulmonary vascular system).
4. Extract the brain from the skull using Friedman-Pearson microrongeurs. Postfix in 4% paraformaldehyde for 4 to 6 hr at 4°C. Place brain into a 20-ml scintillation vial filled with cryoprotectant solution and allow the brain to sink to the bottom (2 to 3 days at 4°C).

   Brains may be stored indefinitely in this solution.
5. Process brain for preparation of free-floating sections using powdered dry ice and a sliding microtome according to manufacturer's instructions. Cut sections that are 35 to 40 μm thick.
6. Process free-floating sections for immunocytochemistry (Panahian et al., 1999).

   Alternatively, free-floating sections may be stored in 0.1 M phosphate buffer without azide, 4°C, up to 6 months.

SUPPORT PROTOCOL 3

QUANTITATIVE AND QUALITATIVE METHODS OF EVALUATING HIPPOCAMPAL INJURY

The number of viable pyramidal neurons in the CA1 subregion is counted in a coronally cut section of the brain using 200× magnification and a microscope equipped with a reticle. Sections 6- to 10-μm thick are used for hematoxylin and eosin staining and quantitative analysis; sections 35- to 40-μm thick are used for immunocytochemistry. Damaged neurons, when stained with hematoxylin and eosin (see Support Protocol 1), appear as shrunken, eosinophilic structures with scalloped cytoplasmic membrane and pyknotic nuclei. They are concentrated in CA1 and hilar regions of the hippocampus. Pyramidal neurons are counted in a 1-mm segment of the CA1 subregion on both the right and left sides and their values are averaged to derive a quantitative score for each mouse (Clifton et al., 1989; Nabeshima et al., 1991; Ishimaru et al., 1992). The average number of pyramidal neurons in the selected 1-mm stretch of the CA1 may vary between 220 to 300 and may be dependent on the technique of histological preparation of specimens. Paraformaldehyde fixation and paraffin embedding are known to result in tissue shrinkage; however, this phenomenon is not observed in unfixed, cryoprotected specimens used for preparation of frozen sections.

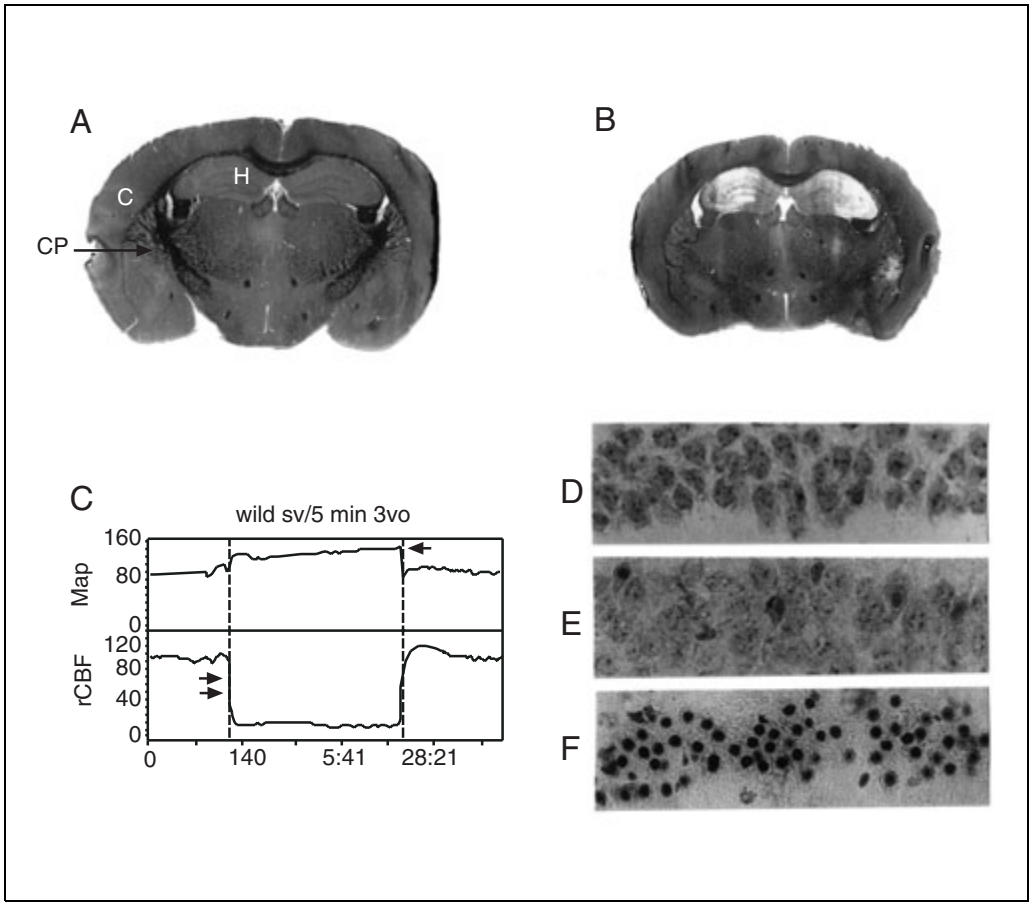

Figure 11.8.1 Three-vessel occlusion model of global cerebral ischemia in the laboratory mouse. (**A**) A hematoxylin and eosin–stained coronal section from a sham operated animal (C, cortex; H, hippocampus; CP, caudoputamen). (**B**) An ischemic episode of 15 min three-vessel occlusion followed by 72 hr reperfusion results in symmetrical injury to both hippocampi. Note that the overlying cerebral cortex is not affected. (**C**) A 5-min global ischemic episode is recorded using MacLab data acquisition system. Note a profound drop in the levels of cortical cerebral blood flow (rCBF; double arrowheads) and a compensatory increase in mean arterial blood pressure (MAP; single arrowhead). "wild sv/5 min 3vo" identifies this as an experiment in a SV129 wild-type mouse after 5 min of a 3-vessel-occulsion ischemic episode. Sham operations (**D**) and 5 min of global ischemia (**E**) result in minor injury to the CA1 hippocampal neurons. However, 15 min of global ischemia leads to complete CA1 wipeout (**F**). Magnification: A and C, 10×; D-F, 400×.

It should not be surprising to observe uneven "wipe out" of pyramidal neurons across the entire stretch of the CA1 subregion (i.e., more neurons present in the medial 1-mm stretch than in the lateral one bordering the CA2 subregion). Bilateral symmetry of hippocampal injury is the hallmark of a technically well-established model (Fig. 11.8.1). However, this may not be the case if selected ischemic intervals are shorter than 10 min. In such a case, injury to the CA1 subregion may be asymmetrical and even patchy. Thus, in order to make a meaningful interpretation of the data, pyramidal cell counts obtained from both sides of each hippocampal CA1 subregion need to be averaged. In order to detect subtle morphological differences between studied strains of mice, the author recommends that cell counts be performed throughout the entire CA1 subregion using four or five representative hippocampal coronal sections (with known distances between them) with the aid of an image analysis system (Image ProPlus; Media Cybernetics). The number of viable neurons (basophilic) is then analyzed using analysis of variance (ANOVA) followed by a recommended posthoc analysis (Statview v.5; SAS Institute). Sample size is determined by power analysis calculations (Primer of Biostatistics; also see *UNIT 1.2*).

An alternative approach is to evaluate specimens by a modified qualitative scoring method as suggested by Mòller et al. (1994):

Grade 0: No damage to any hippocampal subregions;

Grade 1: Scattered ischemic neurons in CA1 and/or hilus subregions;

Grade 2: Moderate ischemic neuronal loss in CA1 subregion (minor neuronal loss and/or edema may be present in CA2 and CA3 subregions);

Grade 3: Severe pyramidal cell loss within CA1 subregion;

Grade 4: Extensive cell loss in all hippocampal subregions.

SUPPORT PROTOCOL 4

MORPHOLOGICAL ANALYSIS OF HIPPOCAMPAL INJURY

Stratum oriens and radiale of the CA1 subregion appear more dense and eosinophylic by comparison to the dentate gyrus. Nuclear pyknosis, vacuolization, eosinophilia, cytoplasmic shrinkage, and triangulation should be considered typical features of injury during histological evaluation of the data. The number of glial cells in both of the stratum oriens and radiale of the CA1 subregion will dramatically increase after 72 hr of animal survival and can easily be detected using routine histostains (e.g., hematoxylin and eosin; see Support Protocol 1). Scattered, single, eosinophylic, triangulated (Nissl-type) neurons are frequently observed in layers 3 and 4 of the cortex bilaterally in most animals studied. Lesions typical for laminar necrosis involve cortical layers 5 and 6 and portions of the corpus callosum, as well as damage to the chorioid plexus and the wall of the lateral ventricle, and can be observed if clip occlusion intervals exceed 20 min.

SUPPORT PROTOCOL 5

PHYSIOLOGICAL PARAMETERS CONFIRMING HIPPOCAMPAL INJURY

Successful ischemic episode is evidenced by rapid decrease in both cortical and hippocampal regional cerebral blood flow values as well as flattening of the EEG and/or suppression of the SEP peaks to a flat line (Fig 11.8.1C). These changes should take place in the absence of a significant elevation in arterial blood pressure.

SUPPORT PROTOCOL 6

CLINICAL CRITERIA OF HIPPOCAMPAL INJURY

The following five clinical signs are important as predictors of the successful outcome of global ischemia models:

1. Immediate maximal dilation of both pupils and signs of ocular anemia (color changes from bright red-pink to extremely pale due to lack of filling of blood vessels) lasting throughout the global ischemic episode.
2. Absence of retrograde filling of the carotid arteries after placement of the clips during the ischemic episode.
3. A period of unconsciousness lasting up to 30 min after restoration of blood flow.
4. Traveling of longer distances in the cage by an otherwise akinetic mouse in response to loud finger snaps during the first 24 hr after induction of global cerebral ischemia.
5. Prominent weight loss by 72 hr.

REAGENTS AND SOLUTIONS

Use Milli-Q-purified water or equivalent in all recipes and protocol steps. For common stock solutions, see ***APPENDIX 2A****; for suppliers, see* ***SUPPLIERS APPENDIX****.*

Cryoprotectant solution

300 ml ethylene glycol
200 g sucrose
600 ml 0.1 M phosphate buffer, pH 7.4
Store indefinitely at 4°C

Paraformaldehyde, 4% (w/v)

Dissolve 40 g paraformaldehyde (Mallinckrodt) in 1 liter of 0.1 M phosphate buffer, pH 7.4. Heat to 60°C with constant stirring to dissolve the paraformaldehyde. Then chill for 4 hr on ice in the refrigerator (4°C) before use.

Boiling inactivates paraformaldehyde.

Thionin solution

500 mg thionin (Sigma)
37 g sodium acetate
940 ml H_2O
Mix thoroughly
Add ~30 to 35 ml glacial acidic acid to adjust the final pH to 4.2
Store up to 1 year at room temperature

COMMENTARY

Background Information

This unit describes models that cause symmetrical, reproducible, and graded injury to the hippocampus. Their purpose is to induce time-dependent delayed neuronal injury to the CA1 and hilar subregions of the hippocampus by means of transient interruption of blood supply to the hippocampus and forebrain structures. This results in intraischemic global energy failure and drops in cortical and hippocampal electrical activity. An episode of global ischemia is usually followed by postischemic hyperemia during the reperfusion period. Decrease in protein synthesis, increase/decrease in cerebral metabolic rate of glucose utilization, and induction of immediate early genes have previously been reported for this condition (Geddes et al., 1996).

Basilar artery occlusion can also be performed as a two-stage procedure. This strategy is especially useful if several groups of mice need to be processed in one day under identical experimental conditions with insufficient time for detailed physiological monitoring. In this case, the basilar artery is not dissected free of the arachnoid, but is instead ligated (through the arachnoid membrane) using atraumatic 10-0 or 11-0 Ethicon suture material. (A microneedle holder will greatly facilitate insertion of the needle underneath the basilar artery without inflicting trauma to the brainstem.) Three to four knots should be tied over the artery using two no. 55 forceps. Twenty-four hours after permanent occlusion of the basilar artery, two Zen clips are positioned on the carotid bifurcation, resulting in clip occlusion of both external and internal carotid arteries. If basilar artery and carotids are to be occluded simultaneously, there is no need to occlude both carotid arteries (external and internal).

Patent and well-established posterior collateral supply (from the circle of Willis) to the vital areas of the brainstem is an absolute prerequisite for the successful accomplishment of the hippocampal neurodegeneration model (Murakami et al., 1998). It guarantees uneventful postoperative recovery of animals and long-term survival. Surgical models of global ischemia are technically demanding procedures, requiring the use of an operating microscope, microsurgical finesse, and patience in care for operated animals.

Pilot studies examining the phenomena of selective neuronal vulnerability, delayed neuronal death, and apoptosis-related hippocampal injury were first carried out in the gerbil, because the circle of Willis in this animal is functionally incomplete (Yamada et al., 1984). These studies led to development of various techniques presently used in quantitative assessment of hippocampal injury. Different time intervals of ischemic injury ranging from 2 to 10 min have

been tested (Matsuyama et al., 1993). The outcome of the gerbil model resulted in delayed neuronal death of selectively vulnerable neurons of the CA1 hippocampal subregion. Pathophysiology of repeated ischemic occlusions as well as hippocampal preconditioning (ischemic, hypotensive, hyperthermic, pharmacological, or mechanical by means of a direct intrahippocampal injection) were extensively examined (Kato and Kogure, 1990; Yamauchi et al., 1991). Because of the high incidence of epileptic seizures, the gerbil model of hippocampal neurodegeneration remains of limited applicability. Due to advances in transgenic technology, interest in investigation of the molecular mechanisms of ischemic injury shifted largely towards the laboratory mouse.

Based on the author's experience, mice are difficult to resuscitate. Cardiac arrest may occur if the mean arterial blood pressure of the mouse drops to 35 mmHg or below. This may occur if an investigator inadvertently withdraws blood in excess of volumes required to induce hypotention in the two-vessel occlusion model. In the author's hands, the cardiac arrest model (de Garavilla et al., 1984) resulted in very high mortality and seizures. The de la Torre model, which was first developed in the rat (de la Torre and Fortin, 1991), is one of the most technically complex models. It requires direct transthoracic access to the aortic arch and ligation of both subclavian arteries to arrest flow in the vertebral arteries, followed by timed occlusion of both common carotids. The model may lead to postoperative pneumothorax and atelectasis, and may require prolonged postoperative ventilation. Detailed knowledge of vascular anatomy and rodent resuscitation techniques is an absolute requirement for any investigator attempting to successfully replicate the de la Torre model. The other major concern is the fact that the model is time consuming, making it difficult to complete experiments on a group(s) of mice in one day under similar conditions.

A model of the "new genre" is that of measles virus–mediated hippocampal neurodegeneration (Andersson et al., 1993). It has been reported in BALB/c mice after intracerebral inoculation of its hamster neurotrophic strain. The model was reported to be sensitive and successfully ameliorated by the noncompetitive *N*-methyl-D-aspartate (NMDA) antagonist MK-801, something that has long been disputed by others using a four-vessel occlusion model of hippocampal neurodegeneration in the laboratory rat (Buchan and Pusinelli, 1990).

Critical Parameters

The following parameters are crucial for establishing a successful model of hippocampal neurodegeneration. (1) There must be immediate maximal dilation of both pupils and signs of ocular anemia lasting throughout the global ischemic episode. (2) There should be absence of retrograde filling of the carotids. (3) The animal should experience a period of unconsciousness lasting for up to 15 to 30 min after restoration of blood flow. (Restoration of blood flow during reperfusion is confirmed by inspecting for filling of all three arteries. Mydriasis should resolve immediately). (4) The animal, which is otherwise akinetic, should travel longer distances in the cage in response to loud finger snap during the first 24 hr after induction of global cerebral ischemia (increased locomotor activity). (5) The animal should display a prominent weight loss by 72 hr. (6) There should be impaired forepaw grasping. (7) The animal should display transient inability to recognize water and laboratory chow. (It is recommended that mice subjected to hippocampal neurodegeneration be fed with laboratory chow soaked in water and that the animal be kept under constant observation. Solutions of Novamine and Ringers lactate may be administered to sustain these animals hemodynamically and physiologically.)

Rectal and direct brain temperatures should be monitored before, during, and after the ischemic episode. Failure to monitor and control brain temperature throughout the global ischemic episode may result in the absence of hippocampal injury. Dramatic decrease in brain temperature values will be observed after clip occlusion (rectal temperature will stay normal as the animal lies on the homeothermic blanket) and slight increase in temperature may take place after induction of postischemic reperfusion.

Every animal should be checked for the absence of retrograde filling of the carotids above positioned clips (Kuroiwa et al., 1990) and rapid dilation of both pupils (mydriasis; Panahian et al., 1996). If rapid mydriasis is not observed, partial clip occlusion and/or faulty clip mechanism should be suspected. In this case, the animal should be euthanized.

Reduction in cortical regional cerebral blood flow to ≤10% of baseline was reported to be highly correlated with significant morphological damage to the CA1 hippocampal subregion (Dirnagl et al., 1993). The same also applies for flattening of the EEG and evoked potentials. Direct hippocampal blood flow (Kuroiwa et al., 1992) can be measured as an alternative to

measuring cortical regional cerebral blood flow in this mouse model. As a means of improving the model and making it more consistent, ligation of neck muscles is recommended to arrest possible collateral circulation (Kameyama et al., 1985). Clipping both external and internal carotid arteries make CA1 lesions more consistent, symmetrical, and reproducible. Hippocampal damage after the two-vessel occlusion model is less predictable than it is in other models and is usually asymmetrical, with considerable cortical injury, pericallosal laminar necrosis, and bilateral wipe-out of the chorioid plexus, including damage to the caudate. The time course of the injury to chorioid plexa may not necessarily be delayed, but rather immediate, in parallel with the time course of laminar necrosis and ischemic damage to the caudate (first 24 hr). There is animal-to-animal variation in the volumes of blood that must be withdrawn upon clip occlusion of the common carotid arteries to achieve controlled hypotention. The most important parameters for this model are the values of mean arterial pressure, regional cerebral blood flow (which must remain well below 10%), and brain temperature. In some mice, a drop in mean arterial pressure towards the end of the experiment necessitates partial reinfusion of shed blood. Cardiac arrest may result if mean arterial pressure levels are allowed to fall to 35 mmHg or below. On an average, it requires ~1 min of close monitoring after placement of the clips to suppress possible fluctuations in mean arterial pressure and regional cerebral blood flow. Thus, it is recommended that the time of ischemic occlusion for this model be longer compared to the other models (~15 to 20 min).

The levels of end tidal CO_2 ($EtCO_2$) decline considerably from 36 ± 4 mmHg at baseline to 23 ± 6 mmHg during ischemia. Upon unclipping and reinfusion of shed blood, a dramatic rise in $EtCO_2$ is observed during the first 1 to 2 min (to 68 ± 10 mmHg); this equilibrates by the end of the second min after reperfusion. Shortly after reinfusion of shed blood, a pronounced hyperemic episode usually results (up to three to four times baseline values), lasting for up to 7 min. This rise in regional cerebral blood flow may be triggered by rapid reinfusion of shed blood. It can be avoided or significantly decreased if the shed portion of the blood is administered very slowly into the animal's circulatory system after removal of the clips. Smith et al. (1984) were one of the first groups to use flow autoradiography for confirmation of successful ischemia. The authors also made a significant contribution by demonstrating that lactate production, ATP depletion, and high levels of catecholamine release occur during the ischemic period.

The author does not withdraw blood from the superior or inferior caval veins, but rather insert two arterial femoral catheters: the first for withdrawal of arterial blood and the second for monitoring mean arterial pressure. Arterial blood is quicker to withdraw in the mouse than venous blood, especially during the clip occlusion episode when every second counts.

Disadvantages of the two-vessel occlusion model are the use of an anesthetic during the ischemic episode as well as more extensive brain damage (not limited to the hippocampus). This model is also known to alter systemic pH and cardiac function, and to cause pulmonary complications. Respiratory complications (wheezing, edema) after the Smith procedure considerably decrease upon administration of the ganglionic blocker Arfonad or intra-arterial infusion of trimethaphan camsylate (Sheng et al., 1999). Pharmacological agents (sodium bicarbonate, ganglionic blockers, α-adrenoreceptor blockers) can be successfully used to influence the outcome of this model (Smith et al., 1984). Mice that survive the procedure rarely develop "hunchback" postures, as described for this model in the rat (Smith et al., 1984).

Care should be taken to avoid severe traction on the carotids and superior sympathetic cervical ganglion, touching the brainstem, or applying pressure on the vagal nerve even with fine forceps. Such manipulations may result in instantaneous drop of arterial blood pressure. The hypoglossal nerve in the mouse intersects with both external (located medially) and internal (located laterally) carotid arteries. Experienced investigators may thus refrain from using any retractors. Special care should be taken to avoid compression of the carotid glomus and superior cervical sympathetic ganglion located underneath the carotid bifurcation. Compression of the trachea may take place if the mini-Goldstein retractor is improperly positioned. This usually leads to respiratory distress syndrome, culminating in postoperative wheezing and lung edema. Traction to the vagal nerve, superior cervical ganglion, and accidental stretching of the common carotids during application of the clips may result in increased postoperative mortality due to pulmonary edema and shock.

Troubleshooting

After lengthy ischemic episodes (15 to 20 min), some mice may not regain spontaneous respiratory activity during the reperfusion pe-

riod. This observation indicates that during the ischemic episode, significant damage has resulted to the vital respiratory and/or cardiovascular centers of the brainstem due to poor vascular collaterals. This phenomenon is largely strain dependent (Ward et al., 1990; Barone et al., 1993; Panahian et al., 1996; Fujii et al., 1997). Most of the operated mice, if taken off the ventilator (not extubated) synchronously with removal of the clips, will exhibit a brief hyperventilation episode with dramatically increased respiratory rates. They should be kept intubated and ventilated until this condition resolves and they regain full consciousness. Thus, the time of extubation may vary (15 min to 1 hr) and will depend upon reestablishment of normal respiratory activity, $EtCO_2$, and actual blood gas (ABG) values, and upon the time when the animals fully regain consciousness. It is also noteworthy to mention that ABG values are strain dependent (Dalkara et al., 1995).

Time-dependent mortality usually results from respiratory distress syndrome culminating in lung edema during the first 12 hr, or epiliptic seizures thereafter. An overall mortality of at least 30% should be expected.

Asymmetric hippocampal damage has been observed in 20% of studied mice. These observations were previously reported in the gerbil model (Clifton et al., 1989) and in two commonly used rat models: two- and four-vessel occlusion. Ligating the paravertebral neck muscles or reducing intraischemic blood pressure to 70, 60, or even 50 mmHg circumvents the problem of asymmetric hippocampal lesions. The author also recommends clipping both external (to decrease collateral flow) and internal carotid arteries on left and right sides of the neck.

In the event that no lesion results from the treatment, check the closing force of microvascular clips as their compression mechanism may deteriorate with repeated use. Purchase additional clips as back up. Carefully monitor the intracerebral temperature during the ischemic period and use the infrared lamp to bring it to normal values. Use caution when adjusting the infrared lamp, because the infrared lamp may offset the readings of the laser Doppler flowmeter probe. When blood flow to the brain of the mouse is transiently interrupted, intracerebral temperature will decline over time, whereas body temperature will stay normal. Make sure the animal spends 72 hr in the temperature-controlled unit. Occlude both external and internal carotid arteries with one clip simultaneously on both sides of the neck. Suppress the intraischemic elevation of blood pressure at any cost; use exsanguination, ganglionic blockers, or any other method to keep it below 80 mmHg. Shed blood must be reinfused very slowly intrarterially or simply discarded. Rapid administration of shed blood may cause loss of cerebral autoregulation and profound hyperemic episode. After administration of shed blood, mice may develop metabolic acidosis. Do not attempt to permanently tie off one of the carotids as recommended in the Levine-type models of hypoxia-ischemia (MacMillan et al., 1993), as this will inevitably lead to asymmetric hippocampal injury. Make sure that the basilar artery is permanently ligated or cauterized using McPherson forceps or an electrocautery device (Fine Science Tools). Twenty-four hours later, proceed with bilateral temporary occlusions of both common carotids. During the occlusion episode, confirm that mice develop mydriasis within the first 10 to 15 sec postocclusion. As another indicator, suppression of retinal blood flow can be effectively monitored using a laser Doppler flowmeter probe placed on the surface of the eye. No retrograde filling of carotids should be present. Mice must be disconnected from halothane 1 min prior to placement of clips and remain unconscious throughout the ischemic procedure and for an additional 10 to 30 min after carotid clips are removed for induction of reperfusion. If mice regain consciousness shortly after the end of the procedure, much of their CA1 subregion will remain preserved. Perform carbon black studies (Panahian et al., 1999) for confirmation of cerebrovascular anatomical anomalies.

If mice develop convulsions during the first 24 hr postocclusion, they must be immediately euthanized, since they will not last 72 hr. However, isolated convulsion episodes are common and must not be confused with rolling seizures. It is important to determine the frequency of these convulsion episodes. Convulsions may be ameliorated by briefly anesthetizing animals with 1.5% halothane and restraining them until sacrifice.

Anticipated Results

Contrary to focal ischemia, global ischemia is a replica of a state of global energy failure. Albeit transient by nature, it leads to delayed neuronal death of selectively vulnerable pyramidal neurons of the CA1 subregion as well as neurons located in the hilar region of the dentate gyrus. Damage to the hippocampus is symmetrical, without involvement of the overlying cortex and with presence of minor injury to the caudoputamen (Fig 11.8.1A-F). Damage

to the dentate gyrus is not typical for this model, but it has been noted when ischemic intervals exceed 10 min, and it is resistant to hypothermic treatment (Agardh et al., 1992).

After three-vessel occlusion, hippocampal neurodegeneration will take place between 48 to 72 hr. From 72 hr to 7 days, the stratum oriens and radiale of the CA1 subregion will be invaded by glial cells. This infiltration will be more prominent within the medial portions of the CA1 subregion. Instantaneous rise in mean arterial blood pressure (Fig. 11.8.1C) upon clip occlusion of both common carotid arteries results in increased collateral flow to the hippocampus. This hypertensive episode must be dealt with decisively, and both hemorrhagic hypotention and treatment with ganglionic blockers (Arfonad) have been suggested. Out of 250 to 300 neurons in a 1-mm region of CA1, few are injured after 5 min of global ischemia compared to sham operated mice (Fig. 11.8.1, compare panels D and E), and only 40 to 60 live neurons are left after a 10-min ischemic episode followed by 72 hr reperfusion. After 15 min of global ischemia, there is a complete wipeout of all neurons within the ischemic CA1 subregion (grade IV injury; see Support Protocol 3 and Fig. 11.8.1F).

The role of ischemic preconditioning has not been extensively studied in the mouse four-vessel occlusion model. Because it is a two-step surgical procedure, investigators should always include control animals in which both vertebral arteries have been occluded but the main ischemic episode (bilateral common carotid artery occlusion) has not been carried out. Power analysis should be performed to assess the number of mice needed for the study, based on preliminary results and values of standard deviations, using statistical software (Primer of Biostatistics). The highest mortality should be expected after two-vessel occlusion with hemorrhagic hypotension due to profound blood-brain barrier (BBB) injury in this model (Preston et al., 1993). Nevertheless, it remains a reliable model for physiological monitoring in settings of an acute experiment.

Time Considerations

The model of three-vessel occlusion is reliable and does not require the use of a stereotactic frame. In experienced hands, the surgery can be completed within 30 min (as a one-stage procedure), if the animal is not prepared for physiological monitoring. If monitoring is included, the time required is: (1) no more than 20 to 25 min for placement of SEP/EEG electrodes, fiberoptic tip of the flowprobe, and needle probe of the Omega thermocouple; (2) 7 to 10 min for femoral cutdown; (3) 3 to 5 min for intubation; and (4) 15 to 20 min for surgery.

A total of 1 hr preparation for performance of complete monitoring of the global ischemic episode is required. This is followed by 10 to 15 min of global ischemic episode itself and ≥15 to 20 min monitoring of the recovery period after induction of postischemic reperfusion. With physiological monitoring, the experiment can be performed on approximately four to six mice in 1 day. Without monitoring, that number increases to twelve to fourteen mice per day. The author recommends that all mice be intubated and ventilated, and that brain temperature be measured in every mouse throughout the entire procedure. After the model is established in the lab, monitoring may be performed on only selected animals (Panahian et al., 1996).

Literature Cited

Agardh, C.D., Smith, M.L., and Siesjö, B.K. 1992. The influence of hypothermia on hypoglycemia-induced brain damage in the rat. *Acta Neuropathol*. 83:379-385.

Andersson, T., Schwartz, R., Love, A., and Kristensson, K. 1993. Measles virus–induced hippocampal neurodegeneration in the mouse: A novel, subacute model for testing neuroprotective agents. *Neurosci. Lett.* 154:109-112.

Barone, F.C., Knudson, D.J., Nelson, A.H., Feuerstein, G.Z., and Willette, R.N. 1993. Mouse strain differences in susceptibility to cerebral ischemia are related to cerebral vascular anatomy. *J. Cereb. Blood Flow Metab.* 13:683-692.

Beuret, P., Feihl, F., Vogt, P., Perret, A., Romand, J.A., and Perret C. 1993. Cardiac arrest: Prognostic factors and outcome at one year. *Resuscitation* 25:171-179.

Buchan, A. and Pusinelli, W.A. 1990. Hypothermia but not the NMDA antagonist MK-801 attenuates neuronal damage in gerbils subjected to transient global ischemia. *J. Neurosci.* 10:311-316.

Clifton, G.L., Taft, W.C., Blair, R.E., Choi, S.C., and DeLorenzo, R.J. 1989. Conditions for pharmacological evaluation in the gerbil model of forebrain ischemia. *Stroke* 20:1545-1552.

Dalkara, T., Irikura, K., Huang, Z., Panahian, N., and Moskowitz, M.A. 1995. Cerebrovascular responses under controlled and monitored physiological conditions in the anesthetized mouse. *J. Cereb. Blood Flow Metab.* 15:631-638.

de Garavilla, L., Babbs, C.F., and Tacker, W.A. 1984. An experimental circulatory arrest model in the rat to evaluate calcium antagonists in cerebral resuscitation. *Am. J. Emerg. Med.* 2:321-326.

de la Torre, J.C. and Fortin, T. 1991. Partial or global rat brain ischemia: The SCOT model. *Brain Res. Bull*. 26:365-372.

Dirnagl, U., Thoren, P., Villringer, A., Sixt, G., Them, A., and Einhaupl, K.M. 1993. Global forebrain ischemia in the rat: Controlled reduction of cerebral blood flow by hypobaric hypotension and two-vessel occlusion. *Neurol. Res.* 15:128-130.

Franklin, K.B.J. and Paxinos, G. 1997. The Mouse Brain in Stereotaxic coordinates. Academic Press, San Diego, Calif.

Fujii, M., Hara, H., Meng, W., Vonsattel, J.P., Huang, Z., and Moskowitz, M. A. 1997. Strain-related differences in susceptibility to transient forebrain ischemia in SV-129 and C57black/6 mice. *Stroke* 28:1805-1810.

Geddes, J.W., Pettigrew, L.C., Holtz, M.L., Craddock, S.D., and Maines, M.D. 1996. Permanent focal and transient global cerebral ischemia increase glial and neuronal expression of heme oxygenase-1, but not heme oxygenase-2, protein in rat brain. *Neurosci. Lett.* 210:205-208.

Ishimaru, H., Katoh, A., Suzuki, H., Fukuta, T., Kameyama, T., and Nabeshima, T. 1992. Effects of *N*-methyl-D-aspartate receptor antagonists on carbon monoxide-induced brain damage in mice. *J. Pharmacol. Exp. Ther.* 261:349-352.

Kameyama, M., Suzuki, J., Shirane, R., and Ogawa, A. 1985. A new model of bilateral hemispheric ischemia in the rat: Three-vessel occlusion model. *Stroke* 16:489-493.

Kato, H. and Kogure, K. 1990. Neuronal damage following non-lethal but repeated cerebral ischemia in the gerbil. *Acta Neuropathol.* 79:494-500.

Kuroiwa, T., Bonnekoh, P., and Hossmann, K.A. 1990. Threshold of carotid artery back pressure for delayed neuronal injury in the hippocampus after bilateral common carotid artery occlusion in gerbils. *J. Neurol. Sci.* 97:251-259.

Kuroiwa, T., Bonnekoh, P., and Hossmann, K.A. 1992. Laser Doppler flowmetry in CA1 sector of hippocampus and cortex after transient forebrain ischemia in gerbils. *Stroke* 23:1349-1354.

Linscott's Directory of Immunological and Biological Reagents. 2000. Santa Rosa, Calif.

Lu, W. and Haber, S.N. 1992. In siu hybridization histochemistry: A new method for processing material stored for several years. *Brain Res.* 578:155-160.

MacMillan, V., Judge, D., Wiseman, A., Settles, D., Swain, J., and Davis, J. 1993. Mice expressing a bovine basic fibroblast growth factor transgene in the brain show increased resistance to hypoxemic-ischemic cerebral damage. *Stroke* 24:1735-1739.

Matsuyama, T., Tsuchiyama, M., Nakamura, H., Matsumoto, M., and Sugita, M. 1993. Hilar somatostatin neurons are more vulnerable to an ischemic insult than CA1 pyramidal neurons. *J. Cereb. Blood Flow Metab.* 13:229-234.

Mòller A, Axelsson, O., Christoffersen, P., Drejer, J. Jensen, L.H., and Nielsen, E.O. 1994. Results with calcium autagonists: The Cavalieri volume estimator. *In* New Strategies to Prevent Neuronal Damage from Ischemic Stroke (P. Kuhl, ed.) pp. 125-133. CHI Press, Cambridge, U.K.

Murakami, K., Kondo, T., Kawase, U. and Chan, P.H. 1998. The development of a new mouse model of global ischemia: Focus on the relationship between ischemia duration, anesthesia, cerebral vasculature, and neuronal injury following global ischemia in mice. *Brain Res.* 780:304-310.

Nabeshima, T., Katoh, A., Ishimaru, H., Yoneda, Y., Ogita, K., Murase, K., Ohtsuka, H., Inari, K., Fukuta, T., and Kameyama, T. 1991. Carbon monoxide-induced delayed amnesia, delayed neuronal death and change in acetylcholine concentration in mice. *J. Pharmacol. Exp. Ther.* 256:378-384.

Panahian, N., Yoshida, T., Huang, P.L., Hedley-White, E.T., Dalkara, T., Fishman, M.C., and Moskowitz, M.A. 1996. Attenuated hippocampal damage after cerebral ischemia in mice mutant in neuronal nitric oxide synthase. *Neuroscience* 72:343-354.

Panahian, N., Yoshiura, M., and Maines, M.D. 1999. Overexpression of heme oxygenase-1 is neuroprotective in a model of permanent middle cerebral artery occlusion in transgenic mice. *J. Neurochem.* 72:1187-1203.

Preston, E. Sutherland, G., and Finsten, A. 1993. Three openings of the blood-brain barrier produced by forebrain ischemia in the rat. *Neurosci. Lett.* 149:75-78.

Sheng, H., Laskowitz, D.T., Pearlstein, R.D., and Warner, D.S. 1999. Characterization of a recovery global ischemia model in the mouse. *J. Neurosci. Methods* 88:103-109.

Smith, M.L., Bendek, G., Dahlgren, N., Rosen, I., Wieloch, T., and Siesjö, B.K. 1984. Models for studying long-term recovery following forebrain ischemia in the rat. 2. A two-vessel occlusion model. *Acta Neurol. Scand.* 69:385-401.

Vonsattel, J.P., Aizawa, H., Ge, P., DiFiglia, M., McKee, A.C., MacDonald, M., Gusella, J.F., Landwehrmeyer, G.B., Bird, E.D., Richardson, E.P. Jr., and Hedley-White, E.T. 1995. An improved approach to prepare human brains for research. *J. Neuropathol. Exp. Neurol.* 54:42-56.

Ward, R., Collins, R.L., Tanguay, G., and Miceli, D. 1990. A quantitative study of cerebrovascular variation in inbred mice. *J. Anat*. 173:87-95.

Yamada, K., Hayakawa, T., Yoshimine, T., and Ushio, Y. 1984. A new model of transient hindbrain ischemia in gerbils. *J Neurosurg*. 60:1054-1058.

Yamauchi, Y., Kato, H., and Kogure, K. 1991. Hippocampal damage following repeated brief hypotensive episodes in the rat. *J. Cereb. Blood Flow Metab*. 11:974-978.

Contributed by Nariman Panahian
University of Rochester
Rochester, New York

Mouse Models of Focal Cerebral Ischemia

Stroke has been defined as a group of neurological disorders encompassing ischemic stroke, intracerebral hemorrhage (ICH) and subarachnoid hemorrhage (SAH) (Garcia et al., 1997). More than 500,000 new patients per year in the United States are affected by stroke (Fisher et al., 1999). Reproducible animal models of stroke are indispensable for investigation of pathogenesis and treatment of ischemic brain injury. Predictable location and size of infarction, as well as consistent production of neurological deficits and changes in blood flow, make it possible to evaluate the potential of novel therapeutic agents. With the advances in genetic engineering, different mouse strains with various man-made gene deletions or overexpressions (e.g., increases in the number of gene copies) are becoming available for ischemia research. Introduction of the laboratory mouse into stroke research has appropriately raised the standards of conventional physiology monitoring equipment. Throughout the past decade pioneering experiments were performed with great success using mouse species for screening of neuroprotective agents (Gotti et al., 1990; Backhauss et al., 1992). Ischemic stroke in mice can be induced using models adapted from the laboratory rat; these experiments involve craniectomy and direct exposure of the middle cerebral artery (Tamura et al., 1981; see Basic Protocol 1). Alternatively, ischemic stroke may be replicated using a coated filament obturator (Hara et al., 1996; Hata et al., 1998), which, after its endovascular introduction, is left in the intracranial portion of the internal carotid artery (ICA) to occlude the middle carotid artery (MCA) for controlled intervals of time. The general purpose of these two models is to replicate the human condition of ischemic stroke and transient ischemic attacks. Both models provide an opportunity to study novel mechanisms of neuroprotection in genetically altered mice, as well as to test pharmacologic agents for neuroprotection in both short- and long-term experiments. The filament model is used primarily to elucidate novel mechanisms of programmed cell death and brain reperfusion injury (Ma et al., 1998; Wang et al., 1998) as well as during trials for pharmacological amelioration of ischemic stroke. The Tamura-type model of permanent MCA occlusion (MCAo) is known to be statistically robust and produces minimal data scatter. It is widely used for assessing the impact of overexpression of neuroprotective genes on the course of ischemic neuronal injury in vivo (Martinou et al., 1994) as well as for the identification of genes playing major roles in neurodegeneration using knockout technology (Huang et al., 1994).

This unit describes two methods for inducing focal ischemia: one by proximal middle cerebral artery occlusion (see Basic Protocol 1) and one by permanent endovascular occlusion (see Basic Protocol 2). Alternatives of transient endovascular occlusion (see Alternate Protocol 1) and subarachnoid hemorrhage (Alternate Protocol 2) are also given. A number of protocols are described for determining the effects of ischemia induction: assessing physiological features (see Support Protocol 1), mapping of the circulation by perfusing the blood vessels with carbon black (see Support Protocol 2), determining stroke volume by staining with 2,3,5-triphenyltetrazolium chloride (see Support Protocol 3), evaluating post-treatment behavior (see Support Protocol 4), assessing stroke volume and cerebral edema (see Support Protocol 5), assessing the size of ischemic penumbra (see Support Protocol 6), and analyzing the statistics and presenting the data (see Support Protocol 7).

NOTE: All protocols using live animals must first be reviewed and approved by an Institutional Animal Care and Use Committee (IACUC) and must follow officially approved procedures for the care and use of laboratory animals.

Contributed by Nariman Panahian

Current Protocols in Toxicology (2000) 11.9.1-11.9.26

BASIC PROTOCOL 1

SUBTEMPORAL CRANIECTOMY: PROXIMAL MCA OCCLUSION

The purpose of this model is to serve as a replica of human ischemic stroke. The model is widely used for screening neuroprotective agents, assessing the therapeutic potential of overexpression of therapeutic genes, and analyzing the impact of gene knockout technology on the outcome of ischemic stroke. Occlusion of the MCA near its origin (below the level of the olfactory tract) is sufficient to induce a reproducible ischemic lesion in the cortex and caudoputamen of mice with a coefficient of variation ≤10%. The model is primarily used for permanent occlusions, but may also be used to induce transient ischemia. For this purpose, the main trunk of the MCA must be transiently occluded with a fine microclip; however, the animal will need to be re-anesthetized for clip removal and induction of reperfusion. If selected intervals of ischemia are short (30 to 90 min), it may not be necessary to disconnect the animal from anesthesia. Regional cerebral blood flow (rCBF) may be monitored to confirm intraischemic reductions in cortical cerebral blood flow as well as its re-establishment upon reperfusion, but monitoring is not mandatory. Successful MCAo is confirmed upon the awakening of the mice using a behavioral assessment (see Support Protocol 4).

Materials

Mice
2% and 3% (v/v) halothane vaporized with 30% O_2/70% N_2 (Halocarbon Laboratories)
Halothane vaporizer (e.g., Fluotec model 3; Colonial Medical Supply)
Plexiglas anesthesia induction chamber for rodents (Stoelting)
Homeothermic blanket with feedback-regulated maintenance of body temperature (Stoelting)
YSI thermocouple equipped with a rectal temperature probe (Harvard Apparatus)
Nose cone: plastic housing of 20-G angiocatheter (Angiocath, Deseret Medical)
Surgical gauze
Surgical and microsurgical instruments (*UNIT 11.8*; Fine Science Tools):
  Student Vannas scissors
  Electrocautery device
  Friedman-Pearson micro-rongeurs
  Mini-Goldstein retractor
  No. 5 forceps
  No. 55 microforceps
Stereomicroscope with 10× objective (e.g., Leica MZ-8; Leica USA)
Microdrill and 0.35- to 0.42-mm diameter ultrafine burrs (Fine Science Tools)
27.5-G blunted needle with tip bent 90° (Becton Dickinson)
30-G needle, bent (Becton Dickinson)
Gelfoam (Upjohn, Becton Dickinson)
6-0 monofilament nylon atraumatic sutures (Ethicon)
Rodent intensive care and temperature-control unit (Thermocare)

Anesthetize the mouse

1. Anesthetize mouse with 3% (v/v) halothane vaporized with 30% O_2/70% N_2 using a halothane vaporizer and a Plexiglas anesthesia induction chamber for rodents. Place the mouse on a homeothermic blanket and insert a rectal temperature probe.
2. Switch the animal to 2% halothane (v/v) vaporized with 30% O_2/70% N_2 administered by means of a nose cone.

Alternatively the animal can be intubated and artificially ventilated (see UNIT 11.8).

3. Position the mouse's head on several pieces of gauze to level it with the body.

   No restraining devices are necessary.

Dissect the MCA

4. Make a vertical skin incision half the distance between the external auditory canal and the right orbit using student Vannas scissors. Make the incision long enough to gain access to the zygomatic arch and to the coronoid and condylar processes of the mandible. Cauterize superficial facial veins in the area of the zygomatic arch with an electrocautery device to prevent bleeding. Expose the body of the zygomatic arch widely by cutting away muscle from the bone with the electrocautery device and rongeur it away using Friedman-Pearson micro-rongeurs.

   IMPORTANT NOTE: *It is desirable to avoid rongeuring in the vicinity of the orbit as severe bleeding from the retro-orbital vessels may result.*

5. Carefully position a mini-Goldstein retractor to expose the opening.

   If the mouse develops arterial or venous bleeding as a result of surgical manipulations, the experiment for that animal should be aborted.

6. After the zygomatic arch has been rongeured away, identify the mandibular nerve (a branch of the trigeminal nerve). Bluntly dissect fibers of the temporal muscle (at approximately mid-distance between auditory canal and orbit) using no. 55 microforceps in order to expose the mandibular nerve. Identify the shiny tendon of the temporal muscle. Using a stereomicroscope at 10× magnification, locate the mandibular nerve in the vicinity of its posterior side, eventually crossing it from behind, and heading underneath.

   The nerve has a thickness of ~300 to 400 μm and is easily recognizable under 10× magnification of the microscope.

7. Carefully dissect the nerve using no. 5 and no. 55 microforceps and trace it to the foramen ovale. Insert no. 5 forceps in between the mandible and the retromandibular surface of the skull (infratemporal fossa) to gain access to the foramen ovale.

8. Once the foramen ovale has been found, identify the olfactory tract (a thick white band underneath the thin skull bones), which passes above the oval foramen and upwards (heading towards 1 o'clock), making a bend and heading towards the 3 o'clock direction.

   The juncture of the mandibular nerve and olfactory tract forms an angle opening towards the nose of the animal where the bottom leg is the mandibular nerve going into the oval foramen and the top leg is the olfactory tract underneath the skull bones, forming a bend (genu olfactorii). The MCA extends upwards eventually intersecting with both legs to form a triangle. Below the intersection with the olfactory tract, the MCA gives off one or several small branches of the lenticulostriatal artery, which provides a vascular supply to the caudate nucleus. The second intersection that the MCA makes is with the inferior cerebral vein before it divides into numerous branches supplying the cerebral cortex.

Occlude the MCA

9. Perform a craniectomy using a microdrill and 0.35- to 0.42-mm diameter ultrafine burrs to drill one hole. Make craniectomy anterior and above from the oval foramen over the trunk of the MCA, which can be identified through the thin skull bones of the mouse.

   Saline cooling of the drill helps to prevent local damage to the cortex from generated heat and also helps to disperse vibration.

10. Thin the bones of the skull overlying the trunk of the MCA by drilling and peeling the bone off using a blunted, 27.5-G needle with tip bent 90°.
11. Cut open the dura mater by means of the sharp end of a bent 30-G needle.
12. Further dissect the arachnoid membrane to free the artery so that it can be slightly elevated above the surface of the cortex and then cauterized.

    IMPORTANT NOTE: *Do not apply pressure to the underlying brain tissue with instruments during surgical dissections.*

    For permanent occlusions, the MCA can be tied off using an Ethicon 11-0 monofilament nylon suture; however, such procedures require surgical finesse (Welsh et al., 1987) and may be difficult for beginners.

    The MCA can also be occluded transiently for various periods of time (this interval is usually chosen not to exceed the duration of the therapeutic window or 0 to 4 hr) using a 10-B Zen microclip (Ohwa Tsusho) and an S&T clip applier (Fine Science Tools). Five minutes prior to reperfusion, the animal is re-anesthetized with halothane, sutures are taken off and the vascular clip is removed. The wound is closed again using Ethicon 6-0 monofilament nylon sutures.

Close the wound

13. Cover the site of the craniectomy with a small piece of Gelfoam. Close the wound using Ethicon 6-0 monofilament nylon sutures.
14. Take the animal off anesthesia and allow it to recover in a rodent intensive care and temperature-controlled unit.
15. Evaluate the ischemic injury (Support Protocols 1 to 6).

BASIC PROTOCOL 2

PERMANENT ENDOVASCULAR OCCLUSION MODEL OF FOCAL ISCHEMIA

The filament model is important for those investigators interested in studying the consequences of reperfusion injury in ischemic stroke. An advantage of this model is the use of endovascular techniques for MCA occlusions without the necessity of performing a craniectomy. A disadvantage of the model is a higher incidence of brain edema (if compared to the Tamura model; see Basic Protocol 1), as well as a higher rate of technical complications and mortality. The filament model is primarily used to elucidate novel mechanisms of programmed cell death and reperfusion injury (Wang et al., 1998), as well as their possible pharmacological amelioration (Ma et al., 1998).

Two other MCA endovascular occlusion models have recently been described: an embolic model (Z. Zhang et al., 1997) and a thromboembolic model (Kilic et al., 1998). Both models involve clot preparation from donor mice and infusion into the circle of Willis to block the MCA. Both models may be transformed from permanent to transient ischemia by the administration of tissue plasminogen activator (tPA) or other "clot-busting" agents. Variability in the development of cerebral infarction as well as hemorrhagic complications should be expected if tPA is used (Wang et al., 1998).

A tight strain-dependent relationship exists between the age and weight of the animals, and the diameter of arteries of the circle of Willis (see Critical Parameters). As part of the replication of the model in the laboratory, it is important to match the diameter of the arterial vessels of the mouse against those of the filaments precoated with different thicknesses of coating material (Table 11.9.1). Based on these preliminary findings, an optimum weight range of mice that best matches specific sizes of the coated filament may be selected. It is recommended that several trial runs of filament occlusions be made

Table 11.9.1 Filament Obturator Coatings

Coating medium (supplier)	Description
Reprosil (Dental Supply International)	Hydrophilic vinyl polysiloxane dental impression material.[a] Recommended for coating of filaments made from 8-0 Ethicon monofilament nylon; this coating material is easier to shape than Cuttersil.
Xantopren (Bayer Dental) or Cuttersil (Miles Dental Products)	Silicone resins that come with elastomer activator. Recommended for coating of filaments made from 8-0 Ethicon monofilament nylon.[b]
Poly-L-lysine (Sigma)	Recommended for coating of filaments made from 7-0 Ethicon monofilament nylon (recommend using a 5-0 nylon filament).[c]
Endothelin-1 (Calbiochem-Novabiochem)	Recommended for coating filaments made from 7-0 Ethicon monofilament nylon or otherwise administered directly onto the MCA from the outside via a stereotaxic approach.[d]

[a]Fouad and Bennett (1998)

[b]Hara et al. (1996); Hata et al. (1998)

[c]Belayev et al. (1999)

[d]Sharkey et al. (1994)

ex-vivo. Such occlusions should be performed on unfixed mouse brains, as well as in mice subjected to carbon black mapping (see Support Protocol 2) of their respective arteries of the circle of Willis to confirm proper filament placement. Before endovascular insertion of the filament, the vessels of the circle of Willis should be exposed, preferably from the base of the skull, to facilitate training in mastering the surgical technique.

All transient ischemia experiments should be done in conjunction with monitoring of cortical rCBF using a laser Doppler flowmeter for confirmation of the intra-ischemic drop in rCBF values as well as confirmation of re-establishment of postischemic flow within the MCA territory.

NOTE: This model may not be advisable for stroke research on genetically altered mice with known vascular or hematological disorders.

NOTE: All surgeries should be performed on only one hemisphere of the brain (Robinson, 1979) and one gender of mouse (Fisher et al., 1999).

Materials

Coating material (Table 11.9.1)
Mice to be tested
2% and 3% (v/v) halothane in 30% O_2/70% N_2 (Halocarbon Laboratories)

6-0, 7-0, 8-0, and 10-0 monofilament nylon atraumatic sutures (Ethicon)
27.5-G needle (Becton Dickinson)
Halothane vaporizer (e.g., Fluotec Model 3; Colonial Medical Supply)
Plexiglas induction anesthesia chamber (Stoelting)
Homeothermic blanket for rodents with feedback-regulated maintenance of body temperature (Stoelting)
YSI thermocouple equipped with a rectal temperature probe (Harvard Apparatus)
SAR-830/P small animal ventilator, volume and pressure cycled, with built in pump, flowmeter, and internal valves (CWE)

Endotracheal tube: 20-G, 17-mm-long angiocatheter on a curved stilette (Angiocath, Deseret Medical)
Catheter (i.e., PE-10 polyethylene tubing; Intramedic)
Microcapnometer (Columbus Instruments)
PF-3 laser Doppler flowmeter with masterprobe (Periflux, Perimed)
Cotton swabs
Microdrill and 0.35- to 0.42-mm diameter, ultrafine burrs (Fine Science Tools)
Surgical instruments (Fine Science Tools):
Student Vannas microscissors
No. 5 and no. 55 forceps
Curved Moria forceps
Stereotaxic frame, non-ferromagnetic (Massachusetts General Hospital machine shop; optional)
Surgical glue (optional)
16-G tubing (optional)
Silicone lubricant (optional)
Gelfoam (Upjohn, Becton Dickinson; optional)
Macintosh Power PC laptop computer
MacLab/8e data acquisition system equipped with ETH-400 and bridge preamplifiers running Scope and Chart software, with blood pressure transducers, EEG and EKG electrodes, BNC cables, and thermocouple (AD Instruments)
Blood gas analyzer (800 series, Ciba-Corning)
Zen temporary clips (13 × 0.4–mm, 15 g closing force; Ohwa Tsusho)
Vessel cannulation forceps S&T (Fine Science Tools)

Additional reagents and equipment for inserting arterial catheters, positioning laser Doppler flowmeter probes for rCBF monitoring, and artificial ventilation (*UNIT 11.8*).

Prepare the coated filaments

1. Select the compound with which to coat the body and the tip of the nylon filament (Table 11.9.1).

   Selection of coating material for the filament obturator is extremely important for the successful outcome of the model.

2. Submerge the filament in coating medium for 5 to 10 sec. Afterwards, gently shape the filament (with the yet unhardened coating medium) using the left index finger and thumb in one continuous motion (see Critical Parameters). Let the coated filaments dry for 2 hr in an upward position by placing in tiny wells carved into a styrofoam container with a 27.5-G needle.

Prepare the mouse

3. Purchase adult mice weighing 22 to 24 g from any reputable vendor. Provide access to water and laboratory chow ad libitum. Weigh the mice prior to surgeries and at the time of sacrifice.

4. Induce surgical-level anesthesia with 3% (v/v) halothane vaporized in 30% O_2/70% N_2 using a halothane vaporizer and a Plexiglas anesthesia induction chamber for rodents. Maintain the mouse under 2% (v/v) halothane vaporized in 30% O_2/70% N_2 throughout surgery and insertion of the filament.

   After insertion of the filament, animals are either awakened and behaviorally tested for confirmation of successful MCA occlusion (see Support Protocol 4) or maintained under 1% (v/v) halothane vaporized in 30% O_2/70% N_2 until withdrawal of the filament and initiation of reperfusion.

5. For insertion of the filament, position the mouse on a homeothermic blanket for regulated maintenance of body temperature. Insert a rectal probe to monitor temperature.

6. Intubate with a 20-G endotracheal tube and artificially ventilate the mouse for complete monitoring of physiological parameters (*UNIT 11.8*). Monitor respiratory status ($EtCO_2$) using a microcapnometer.

   Parameters of blood pressure, heart rate, body temperature are acquired on-line and analyzed directly using MacLab sensors connected to the ETH-400 preamplifier. End-tidal CO_2 ($EtCO_2$) is determined by the microcapnometer. Regional cerebral blood flow is determined by the Perimed Periflux PF-3 laser Doppler flowmeter. Cerebrovascular resistance is calculated on-line from parameters of rCBF (%) and mean arterial blood pressure (mmHg) using the calculated values option of Chart software.

   The microcapnometer, laser Doppler flowmeter, and ventilator are connected to MacLab/8e via BNC cables for analog output.

   IMPORTANT NOTE: *In all experiments involving MRI, mice should be ventilated. The ventilator can be effectively shielded from strong magnetic fields or placed a safe distance away at the expense of an increase in the overall length of the tubing. The length of the inflow and outflow tubes does not really matter as long as the length of the Y connector (the level at which both tubes converge on the way to the intubation tube) is short enough that it does not increase the dead space, which otherwise may suffocate the mouse (Dalkara et al., 1995). The intubation tube is usually sutured to the upper lip of the mouse with 6-0 monofilament nylon sutures so as to prevent it from slipping out.*

7. Place a femoral arterial catheter for monitoring of mean arterial blood pressure and assessment of arterial blood gas status using a blood gas analyzer with a MacLab/8e pressure transducer.

8. Attach a fiberoptic PF-3 laser Doppler flowmeter masterprobe to the skull thinned by drilling in the area of distribution of the middle cerebral artery at bregma-0, and ~1 mm below the junction of the sphenoid, temporal, and parietal bones.

   For this purpose, upper portions of the temporal muscle need to be carefully detached using student Vannas scissors and fiberoptic probe fixed to the surface of the skull using surgical glue.

   For detailed procedures of arterial catheter insertion techniques, positioning of the laser Doppler flowmeter probe for rCBF monitoring, and artificial ventilation see UNIT 11.8.

9. Once the mouse is placed on the homeothermic blanket, position the mouse with the neck slightly hyperextended.

   Placement of two cotton swabs underneath the neck region is usually sufficient to hyperextend the neck.

Dissect the vessels

10. Make an anterior midline incision through the platysma and fascia propria using student Vannas microscissors.

11. Expose the carotid bundle anterior and underneath the sternocleidomastoid muscle. Bluntly dissect the common carotid artery using no. 5 and no. 55 forceps.

    Take care not to exert any traction or traumatize the vagal nerve during dissection of the common carotid artery (CCA).

12. Dissect the CCA upwards to the level of its division into the external (ECA) and internal (ICA) carotids.

The superior cervical ganglion of the cervical sympathetic tract can be easily spotted in the carotid triangle, directly underneath the carotid bifurcation (for details of rodent sympathetic tract anatomy, see Hedger and Webber, 1976). External and internal carotid arteries form a triangle with the hypoglossal nerve at the level of the hyoid bone. The external carotid artery is located medially, while the internal carotid artery is located laterally and the hypoglossal nerve horizontally, at the top of the triangle. The hypoglossal nerve appears as a prominent thick white band about the same diameter as the common carotid artery.

13. After the dissection is completed, rotate the animal's head ~60° degrees to the contralateral side in order to expose the pterygopalatine artery (PPA).

14. Apply downward traction on the ICA at its intersection with the hypoglossal nerve with no. 5 forceps to reveal the PPA, which branches off the ICA above the level of the hypoglossal nerve.

    The Pterygopalatine (PPA) artery is the only artery that branches off the ICA. It runs horizontally, while the suprahypoglossal portion of the ICA ascends vertically at a sharp angle. Traction on the ICA brings the PPA forward towards the operator.

15. After this surgical maneuver, bring the delicate curved Moria forceps underneath the PPA. Discontinue traction. Use no. 55 forceps to bring forward the end of the 10-0 monofilament nylon thread towards the Moria forceps. During this maneuver, advance the 10-0 monofilament nylon suture further around the PPA with curved Moria forceps until it is tied off.

    IMPORTANT NOTE: *Failure to perform this step will result in the filament entering the PPA during the insertion procedure.*

16. For permanent occlusion of the MCA, tie off the ECA with 10-0 monofilament nylon (as proximally as possible to prevent the filament from entering its lumen) and tie off the CCA mid-distance between the level of the clavicle and carotid bifurcation.

17. Position a second 10-0 ligature loosely underneath the carotid bifurcation.

18. Place a Zen temporary microclip on the ICA above the level of the hypoglossal nerve as far upward as possible using a clip applier (S&T vessel cannulation forceps).

    Clipping the ICA prevents arterial backflow from the vessels of the circle of Willis.

Insert the filament

19. Make a small nick in the wall of the CCA using vascular scissors at mid-distance between the first (proximal) knot and the loosely positioned ligature at the level of the CCA bifurcation.

20. Confirm that no backflow bleeding is present. Insert the coated filament until its tip reaches the level of Zen temporary microclip and tighten the 10-0 Ethicon suture around the CCA.

21. Release Zen temporary microclip with the right hand using a clip applier. In order to prevent filament "wash out" and fatal bleeding from the carotid artery (see Critical Parameters and Troubleshooting), always hold on to the rear end of the filament with no. 5 forceps positioned in the left hand.

22. Before insertion of the filament into the intercranial portion of the circle of Willis, remove all cotton swabs from underneath the neck and return the head to its normal position. Insert a coated 8-0 Ethicon nylon filament to a distance of ~12 mm (from the carotid bifurcation) until it is safely lodged in the anterior cerebral artery.

Insertion of the coated filament should be performed very gradually, avoiding any possible resistance.

23. After the filament is advanced, secure it in place to the CCA with a 10-0 Ethicon nylon ligature. Close the surgical skin incision atraumatically with 6-0 Ethicon monofilament nylon sutures. Disconnect from anesthesia and allow to recover under normothermic conditions.

Perform MRI studies to determine lesion progression (optional)

NOTE: Reperfusion can be induced anytime by withdrawal of the filament from outside of the magnet. The body temperature of the mouse positioned in the magnet is monitored by a rectal probe and maintained at 37°C by means of a water blanket or warm air current. In a pilot study, no differences in systemic arterial blood pressure, heart rate, or cortical rCBF were detected in mice monitored for 2 hr in a vertical position simulating the environment of the vertical bore 9.1 Tesla magnet (N. Panahian and S. Kennedy, unpub. observ.).

24. After insertion of the filament and confirmation of rCBF drop to ~20%, transfer the mouse to a specially made stereotaxic frame of non-ferromagnetic material.

    This frame is usually constructed to be within the bird-cage MRI coil, to effectively suppress any motion artifact (Schulz et al., 1997; van Dorstein et al., 1999).

    Later, the coil will be inserted into the bore of a vertical or a horizontal magnet.

25. Glue a 6-0 nylon thread (heavily lubricated with silicone), a meter or more in length, to the lower end of the filament and pass it through a 16-G tubing (acting as its sheath) securely attached to the animal's belly with surgical glue on its way out of the magnet.

26. Place a large piece of Gelfoam at the site of the ECA to prevent possible postreperfusion bleeding. Also tightly suture the skin with 6-0 nylon sutures to prevent external hemorrhage.

    If reperfusion is attempted during MRI, vascular clips cannot be used even if they are made of non-ferromagnetic material, as removing the clips will cause interference with magnetic gradients and negatively impact the quality of the obtained image. It is not safe to reperfuse the mouse in the magnet with the common carotid artery not clipped or not permanently tied off. This may result in profuse bleeding from the site of incision in the ECA after withdrawal of the filament during initiation of reperfusion. The filament is usually introduced into the intracranial portion of the ICA and the circle of Willis via the external carotid artery. The pterygopalatine artery (PPA) is usually left intact or electrocauterized using McPherson-type bipolars (Radionics). In cases like this, the author recommends that only 8 to 10 mm of the proximal portion of the filament are coated, and that the external carotid artery is skeletonized to the greatest possible length and tied off as far distally (away from the CCA) as possible. Thus, in order to initiate postischemic reperfusion, the surgeon pulls the coated portion of the filament into this man-made vascular "pouch" created from the remnant of the ECA and does not attempt to retrieve the filament until the animal is sacrificed to avoid the possibility of profuse arterial bleeding.

TRANSIENT ENDOVASCULAR OCCLUSION FOCAL ISCHEMIA

ALTERNATE PROTOCOL 1

If the filament is left in place (permanently) within arteries of the circle of Willis, it becomes a model of "permanent" ischemia. An alternative technique should be used for filament models involving transient occlusions. The filament in these cases should be introduced into the circle of Willis through the external carotid artery (see Basic Protocol 2) with the following variations. During MCA occlusion, do not tie off the distal portion of the CCA, but occlude it with a 10-B Zen microclip using S&T vessel cannulation forceps (Fine Science Tools) as a clip applier. Upon induction of reperfusion, withdraw

the filament, tie off the ECA, and only then, release the 10-B Zen microclip from the CCA. Suture the skin with 6-0 monofilament nylon (Ethicon), and allow the animal to recover under normothermic conditions.

ALTERNATE PROTOCOL 2

INDUCING THE FILAMENT MODEL OF SUBARACHNOID HEMORRHAGE

In order to introduce the filament model of subarachnoid hemorrhage (SAH), either a 5-0 or 6-0 nylon filament is introduced into the circle of Willis (see Basic Protocol 2) and advanced into the anterior cerebral artery (ACA). When there is resistance to further forward movement of the filament, an additional 3 to 4 mm of filament is advanced to ensure perforation of the artery. The tip of the filament is immediately withdrawn to allow reperfusion to take place. Animals are sacrificed at 30 min, 24 hr, 3 days, and 7 days and perfused transcardially with a solution of carbon black in 10% gelatin (Kamii et al., 1999). Vasospasm is evaluated ex-vivo by the diameter of the proximal portion of the MCA using the magnification of a stereomicroscope directly connected to an image analysis system or three dimensionally using the corrosion cast technique (Ono et al., 1997).

ALTERNATE PROTOCOL 3

INDUCING HEMORRHAGIC STROKE MODEL BY COLLAGENASE INJECTION

Intracerebral hemorrhage (ICH) in mice is modeled by injection of bacterial collagenase into the caudate nucleus as described by Clark et al. (1998). Hemorrhagic transformation of the ischemic stroke as well as ICH, due to their serious prognosis, are considered exclusion criteria in most preclinical and clinical studies, including treatment with "clot busting agents" like tPA. There may be different levels of susceptibility of arterial vascular elements (e.g., basal laminae) to collagenase injection in genetically altered mice, and hence a different size of hematoma formation.

Materials

Mice
2% (v/v) halothane in 30% O_2/70% N_2 (Halocarbon Laboratories)
0.150 U/µl *Clostridium histolyticum* collagenase (Sigma)
Normal saline: 0.9% (w/v) NaCl
TTC staining solution (see recipe) or H&E stain (optional)

Homeothermic blanket for rodents with feedback-regulated maintenance of body temperature (Stoelting)
YSI thermocouple equipped with a rectal temperature probe (Harvard Apparatus)
Ultraprecise stereotaxic apparatus with gas anesthesia nose cone (Kopf Instruments)
Stereotaxic drill
Microdrill with ultrafine drill bits slightly larger than 32-G needle (Fine Science Tools)
Gas-tight microsyringes (Hamilton) with 32-G stainless steel needles without bevels
Rodent intensive care and temperature-control unit (Thermocare)
Surgical wax (Ethicon)
6-0 monofilament nylon sutures (Ethicon)

Prepare mouse

1. Administer 2% halothane to anesthetize mouse. Use a homeothermic blanket and YSI thermocouple with rectal temperature probe to establish and maintain normothermia.
2. Position and align the head of the mouse in the head holder of the ultraprecise stereotaxic apparatus equipped with a gas anesthesia nose cone. Tighten the earbars

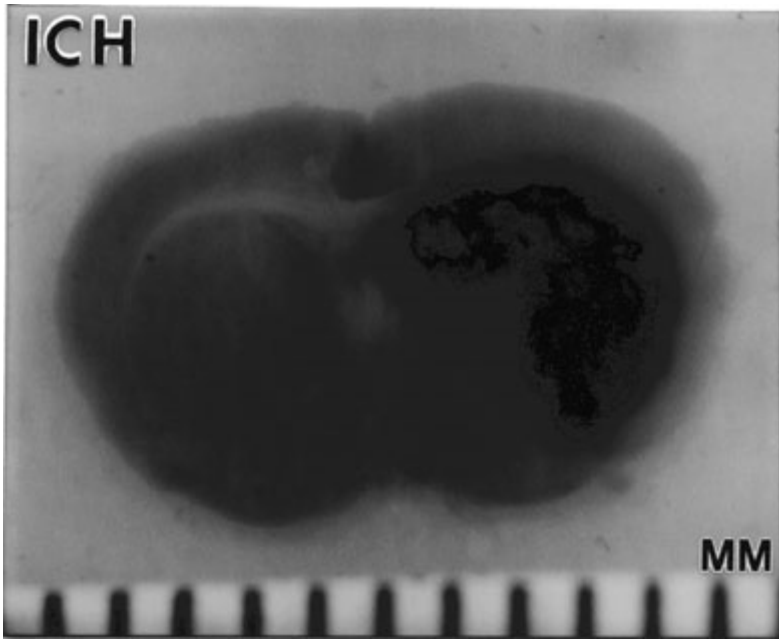

Figure 11.9.1 Hemorrhagic stroke 24 hr after stereotaxic administration of collagenase (0.075 U in 0.5 μl) into the caudate nucleus according to Clark et al. (1998). Hemorrhagic transformation and edema within this 2-mm-thick, TTC-stained coronal specimen of the mouse brain. Scale: 1 mm; magnification: 10×.

slightly, enough to prevent shifting of the stereotaxic zero point established at the intersection of Bregma and the sagittal suture.

3. Set the stereotaxic drill set-up manually to the following coordinates: anterior-posterior-(+0.7); medio-lateral-(2.0).

4. Drill the skull with the microdrill under constant saline irrigation to dissipate vibration and temperature effect on to the underlying brain.

   The diameter of the drilled burr hole only slightly exceeds that of the 32 GA needle to achieve a snug fit and prevent backflow.

Inject the mouse

5. Perform all stereotaxic injections using a gas-tight microsyringe coupled to a 32-G stainless steel needle without bevel. Gradually introduce the needle over 2 min into the brain to the depth of 3 mm.

   Bacterial collagenase can cause higher inflammatory response compared to blood infusion models of ICH. Also, the collagenase ICH model causes diffuse blood brain barrier breakdown.

6. Leave the needle in place for 20 min during the injection. Inject 0.5 μl suspension of bacterial collagenase from *Clostridium histolyticum* (0.075 U) gradually into the caudate nucleus of the mouse. Then gradually remove the needle over 2 min.

   Control animals receive 0.5 μl of normal saline instead.

7. Seal the site of the burr hole with surgical wax and suture soft tissues using 6-0 monofilament nylon sutures.

8. Transfer mouse to the rodent intensive care and temperature-control unit.

Assess results

9. Monitor animal weights and neurological status prior to surgery and every 24 hr after ICH induction until sacrifice.

10. Stain specimens with TTC staining solution (Support Protocol 3) or H&E as shown in Figure 11.9.1.

SUPPORT PROTOCOL 1

ASSESSMENT OF SYSTEMIC PHYSIOLOGICAL PARAMETERS

Systemic physiological characterization should be performed on both male and female animals of genetically engineered mice separately and matched against a hybrid strain colony. It is also important to perform these experiments on animals of uniform weight. Pelt color may differ among strains because mice are genetically inbred; however, it is important that within the same studied strain all mice have the same pelt color. Mice should always be kept in conditions of diurnal light cycle and given unrestricted access to water and laboratory chow.

Materials *(also see Basic Protocol 1 and 2)*

Mice treated to induce focal ischemia (see Basic Protocol 1 and 2) and control mice
2.5% and 1.0% to 1.5% (v/v) halothane vaporized with 30% O_2/70% N_2O (Halocarbon Laboratories)
α-Chloralose (Rochester Hospital Supply)

Homeothermic blanket (Stoelting)
Overhead infrared lamp, YSI thermocouple with rectal temperature probe (Harvard Apparatus)
Macintosh Powerbook, MacLab/8e data acquisition system with four-channel ETH-400 transducer-amplifier (AD Instruments), and appropriate software (e.g., Scope and Chart; AD Instruments)

1. For physiological monitoring, anesthetize either mice treated to induce focal ischemia (see Basic Protocol 1 and 2) or controls with 2.5% (v/v) halothane vaporized with 30% O_2/70% N_2O using a halothane vaporizer and Plexiglas anesthesia induction chamber for rodents.

2. Place the mouse supine on a homeothermic blanket and intubate with a 20-G endotracheal tube.

3. Switch the anesthesia to between 1.0% and 1.5% halothane.

4. Control the rectal temperature thoroughly by means of an overhead infrared lamp, homeothermic blanket, YSI thermocouple with rectal probe maintaining the rectal temperature at 37°C throughout the entire period of physiological monitoring.

   The overhead infrared lamp is used to quickly raise the body temperature by several degrees in a hypothermic animal. This saves time while establishing physiological baselines.

   The laser Doppler flowmeter will show erratic (artifactual) readings when the overhead infrared lamp is on.

5. Cannulate the femoral artery with PE-10 tubing for systemic arterial blood pressure measurements and sampling for confirmation of arterial blood gas status (i.e., pH, pO_2, and pCO_2) using a blood gas analyzer.

6. Change the anesthesia to 80 mg/kg α-chloralose administered intravenously upon initiation of artificial ventilation. Give the drug subsequently every hour at a dose of 40 mg/kg after the femoral vein is catheterized.

CAUTION: *Halothane anesthesia exerts negative chronotropic and inotropic effects on the hearts of mice, manifesting in decreased mean arterial blood pressure and heart rate. For baseline comparison of mean values of arterial blood pressure and heart rate, α-chloralose should be used as described (Hara et al., 1996).*

7. Connect the mouse to a CWE SAR830P ventilator and adjust effective flow rates based on the measurements of the microcapnometer.

   Inspiratory time should be set between 0.07 and 0.1 sec. The stroke volume of the ventilator must not exceed 0.5 to 0.6 ml and the respiratory rate 120 to 170 breaths/min.

8. Monitor regional cerebral blood flow (rCBF) using a Periflux PF2B laser Doppler flowmeter equipped with a flexible microprobe (Perimed), affixed directly to the surface of the skull (previously thinned by drilling; see Basic Protocol 2, step 8) overlying the MCA territory. Perform on-line data acquisition and analysis using a Macintosh Powerbook with a MacLab/8e recording unit with four-channel ETH-400 transducer-amplifier and appropriate software (e.g., Scope and Chart).

CARBON BLACK PERFUSIONS

SUPPORT PROTOCOL 2

Carbon Black perfusion of the brain arteries allows detection of vascular anomalies within the circle of Willis, detection of the borders of avascular territory after stroke, determination of the pattern of branching and topography of cortical arterial anastomoses (e.g., between branches of MCA and pericallosal artery), and determination of vascular diameter after subarachnoid hemorrhage.

Materials

Mice treated to induce focal ischemia (see Basic Protocol 1 or 2) and control mice
Heparinized saline: 100 µl heparin in 100 ml saline (0.9% w/v NaCl; use immediately)
1.6% to 1.8% (v/v) Higgins Black Magic waterproof drawing ink (Eberhard Faber)
4% (w/v) paraformaldehyde (*UNIT 11.8*)

MZ-8 Leica stereomicroscope
Styrofoam board and pins or tacks
26-G plastic catheter mounted on a 10-ml syringe
Camera (e.g., MicroCam; Polaroid)

1. Anesthetize either a mouse treated to induce focal ischemia or a control mouse with 3% (v/v) halothane vaporized with 30% (v/v) O_2/70% N_2 using a halothane vaporizer and Plexiglas anesthesia induction chamber for rodents.

2. Place the mouse belly up with extremities spread out as far as possible. Pin down the upper and lower paws to a styrofoam board (a piece of commercially available styrofoam) using pins or thumbtacks. Continue halothane anesthesia using a nose cone (see Basic Protocol 1). Introduce a 26-G plastic catheter mounted on a 10-ml syringe into the left ventricle and initiate transcardiac perfusion with 20 ml of heparinized saline.

   For details of the mouse perfusion fixation protocol see UNIT 11.8.

3. Cut open the right atrium to release the effluent. Advance the catheter into the ascending aorta and inject ~1 ml of a 1.6% to 1.8% (hypertonic) solution of Higgins Black Magic waterproof drawing ink, until the animal's tongue, lips, and paws turn black.

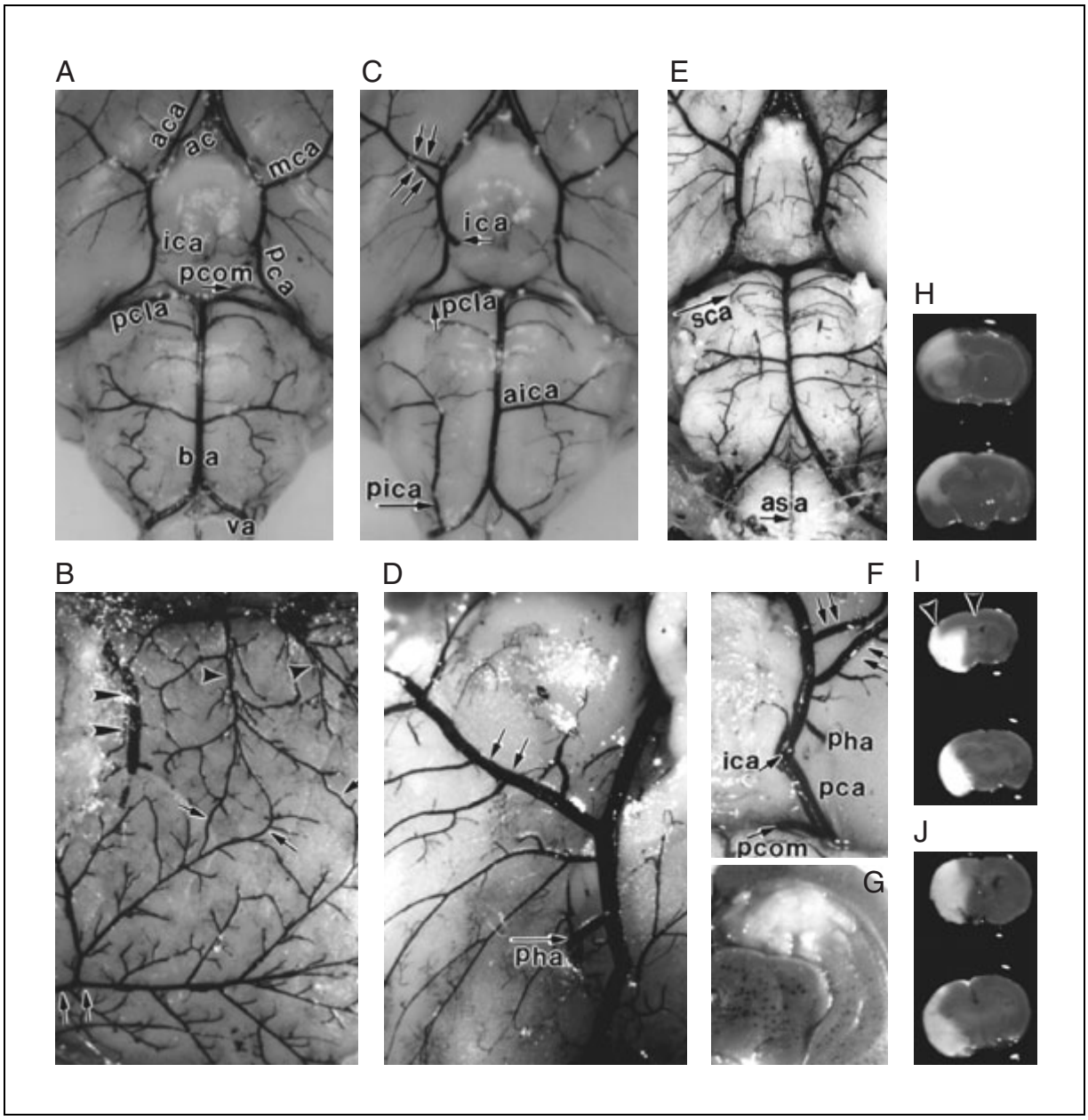

Figure 11.9.2 Carbon black vascular mapping of the brains of intact mice for demonstration of vascular anomalies (**A, C, D, E, F**) and mapping of arterial cortical collaterals (**B**, marked as small single arrows) between branches of pericallosal artery (marked with single arrow-heads) and middle cerebral artery (mca; marked with small double arrows). The level of the bregma is marked with big double arrows. Note duplications of MCA marked by small double arrows (**C** and **F**); absence of one (or both) of the posterior communicating arteries (pcom; C versus A); presence of increased posterior vascular arborizations of the MCA (D and E); absence of right anterior inferior cerebellar artery (aica , C). (**G, H, I, J**) TTC staining of mouse brains after 24 hr MCAo using either filament (G and J), Brint (H) or Tamura-type models (I). Note decreased cerebral edema in the Tamura (I) versus the filament model (J). Upper cortical regions overlying the caudate nucleus and corresponding to watershed areas (marked with arrowheads) are preserved in the Brint and Tamura models (H and I), but are compromised in the filament model (J). SV-129 mice were used in these experiments. As a result of partial filament insertion due to excessive coating material, occlusion of the posterior hippocampal artery (pha) resulted in a lesion in the upper posterior portions of the hippocampus in a C57Bl/6 mouse (G). Abbreviations: ac, anterior communicating artery; aca, anterior cerebral artery; aica, anterior inferior cerebellar artery; asa, anterior spinal artery; ba, basilar artery; ica, internal carotid artery; mca, middle cerebral artery; pca, posterior cerebral artery; pcla, posterior cerebellar artery; pcom, posterior communicating artery; pha, posterior hippocampal artery; pica, posterior inferior cerebellar artery; sca, superior cerebellar artery; va, vertebral artery.

IMPORTANT NOTE: *If the osmolarity of the final solution is lower than 1.6%, extravasation of the dye will take place resulting in the presence of dark background as well as both arterial and venous labeling.*

For labeling of fine cortical capillaries and microvessels, crystals of NaCl should be added directly to aliquots of ink, for a final hypertonic solution of 1.6% to 1.8%, without addition of particles of activated carbon. Alternatively, the carbon black perfusion solution may be prepared by adding the dye into a 10% (w/v) gelatin perfusion solution (Kamii et al., 1999).

Alternatively, ~1 ml Higgins Black Magic ink may be added to a 15% (w/v) polyacrylamide separating gel (5 ml), immediately after Temed and ammonium persulfate. This solution is used to transcardially perfuse the mouse. The gel will polymerize in arterial vessels of the brain and form a cast. Color intensity is determined by the amount of ink (B.A. Brown and N. Panahian, unpub. observ.).

Mapping of the large arterial blood vessels of the circle of Willis may be performed by directly mixing particles of activated carbon (G-60, 100 mesh; Aldrich) with Higgins Black Magic waterproof drawing ink. The final concentration of carbon particles is chosen arbitrarily and depends on the viscosity of the final solution and its ability to pass through a 22- to 26-G plastic catheter placed into the ascending aorta of mice.

4. Upon completion of perfusion, perform a small craniectomy to allow better access of fixative to the brain. Fix the brains 3 to 4 days in 4% PFA.

5. After fixation, extract the brains carefully from the skull using extra fine Friedman-Pearson microrongeurs. First separate the lower jaw and soft tissues from the skull using Friedman-Pearson rongeurs.

   IMPORTANT NOTE: *No twisting motion should be used when performing dissections with extra-fine Friedman-Pearson micro-rongeurs, as this may damage the instrument beyond repair.*

   Such dissections should be started from the base of the skull so that all major arterial branches of the brain as well as the brainstem and upper portions of the spinal cord will be preserved (Fig. 11.9.2A to F). Using the same dissection approach, the branches of the middle cerebral artery and their collaterals with pericallosal artery (in the "watershed areas") will always remain intact (Fig. 11.9.2B). Similar tactics of anatomical dissection can be used to detect the presence of vascular arterial anomalies like duplication of MCA (Fig. 11.9.2C and F), absence of one (or both) of the posterior communicating arteries (Fig. 11.9.2C), presence of increased posterior vascular arborizations of the MCA (Fig. 11.9.2D and E), absence of anterior inferior cerebellar artery (aica; Fig. 11.9.2C), as well as the presence of connections between branches of external and internal carotid arteries which may form Rete Mirabile (Fuwa, 1994).

6. Examine the vessels of the circle of Willis and their branches at 10 to 20× magnification using a Leica MZ-8 stereomicroscope equipped with a 0.8× apochromatic objective and 10× wide-angle eyepieces. Photograph anatomical specimens using a Polaroid camera (e.g., MicroCam).

TTC STAINING TO DETERMINE STROKE VOLUME

SUPPORT PROTOCOL 3

It is customary to perform analysis of stroke volume using triphenyltetrazolium chloride (TTC) staining (Bose et al., 1984; Isayama et al., 1991). Areas of the brain with active mitochondrial enzymes will stain bright red, while areas of infarcted tissue will remain white. This method cannot be used to accurately assess the area of ischemic neuronal injury during early (6 to 12 hr) and late (2 to 3 days or longer) periods of stroke, but it is widely used for detection of stroke volume at 24 hr (Fig. 11.9.2H to J and Fig. 11.9.3). Tissue stained with TTC and stored in 4% paraformaldehyde may be processed for hematoxylin and eosin (H&E) staining and immunocytochemistry.

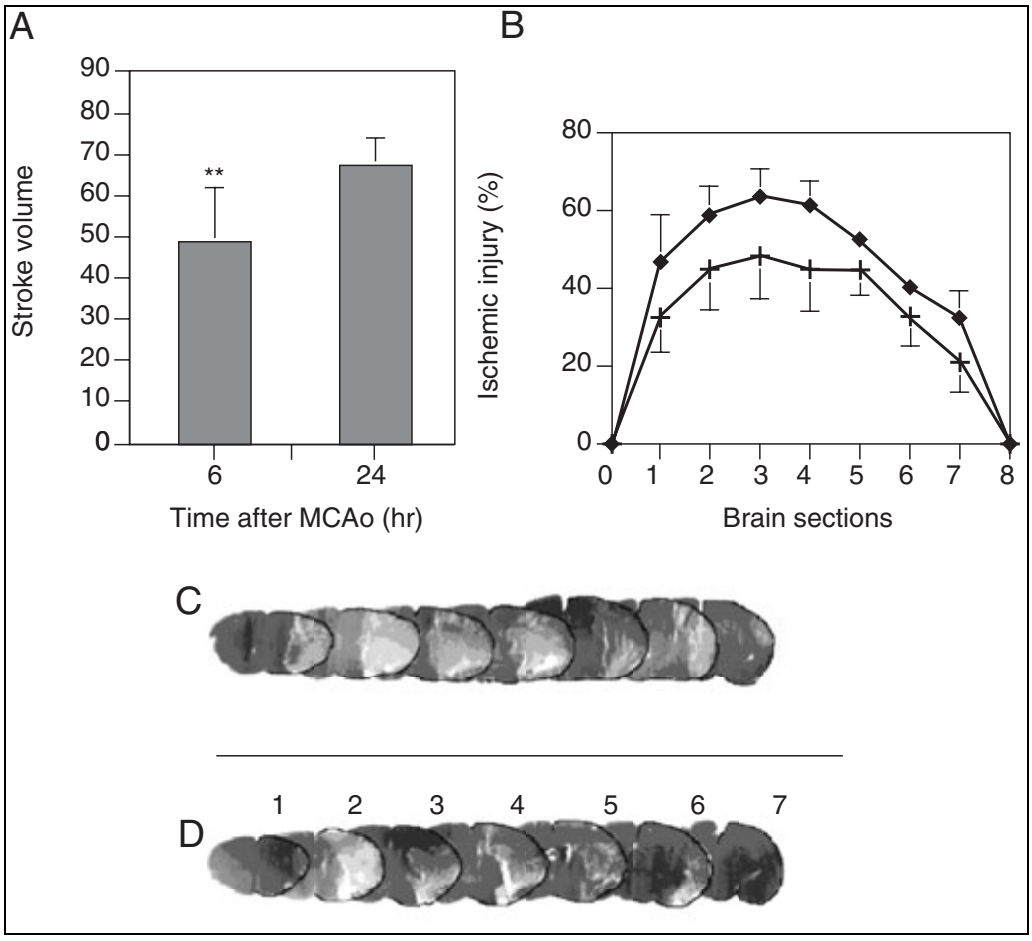

Figure 11.9.3 Analysis of stroke volume. (**A**) Cumulative stroke volume in DNX mice derived from seven representative coronal brain sections, multiplied by the distance between them. Animals were subjected to permanent MCA occlusion (pMCAo) using the subtemporal approach. (**B)** Anterior-posterior distribution of injury at 6 hr (crosses) and at 24 hr (diamonds) in DNX mice. The volume of stroke and anterior-posterior distribution was reconstructed based on hematoxylin and eosin–stained specimens. (**C**) H&E–stained coronal sections 1 to 7 were used to plot anterior-posterior distribution of the ischemic lesion at 6 hr after MCAo in DNX mice. The lesion appears to be much smaller in heme oxygenase-1 overexpressing mice (**D**).

NOTE: Due to the consequences of breakage of the blood-brain barrier and migration of inflammatory cells after 24 hr, the method subsequently becomes only marginally reliable.

Materials

Brains of control mice and mice treated to induce focal ischemia (see Basic Protocols 1 and 2)
PBS (*APPENDIX 2A*), 4°C
2% (w/v) 2,3,5-triphenyltetrazolium chloride staining solution (TTC; see recipe), prewarmed to 35° to 36°C
Brainslicer (EM Corp.) and razor blades, 4°C (stainless steel)
Spatula
Weigh boats or Petri dishes

1. Chill the brains of control mice or mice treated to induce focal ischemia in 4°C PBS for 5 min on ice.

2. Using a brainslicer and razor blades chilled to 4°C, cut the brains coronally at 1- or 2-mm regular intervals to give eight or four coronal sections, respectively.

   Both the brainslicer and razor blades must be of stainless steel and cooled to 4°C beforehand to facilitate cutting. Cooled brains also become firmer in consistency and do not stick to the surfaces of razor blades during cutting.

   It is almost impossible to consistently sample the brain tissue throughout the same anatomical areas from animal to animal using the brain matrix. Tangential distortion of brain slices due to edema and presence of midline shifting is common. Avoiding tangential distortion is difficult, as most manufacturers design brain matrixes for cutting normal rodent brains. Brain slices obtained using the matrix technique, in their anterior-posterior distribution, will not consistently correspond to exact same anatomical coordinates (locations) from animal to animal.

3. Transfer the four coronal 2-mm-thick sections per brain to a solution of 2% (w/v) 2,3,5-triphenyltetrazolium chloride (TTC) prewarmed to 35°C. Incubate for 30 min in a weigh boat or Petri dish at 35°C in a dark environment.

   TTC-stained sections may be stored up to 6 months without fading at 4° to 8°C in 10% buffered formalin (or 4% paraformaldehyde; PFA) in 20-ml scintillation vials wrapped in aluminum foil (TTC-stained material is light sensitive).

4. Estimate stroke volume and store images electronically for future reference.

BEHAVIORAL ASSESSMENT OF FOCAL ISCHEMIA

SUPPORT PROTOCOL 4

Behavioral assessment of mice after stroke is based on the criteria listed in Table 11.9.2. A cumulative behavioral score is obtained that is included in the statistical interpretation of the data (see Support Protocol 7). Behavioral functions after stroke recover faster in the mouse than in nonhuman primates because mice have a higher potential for cerebral plasticity.

IMPORTANT NOTE: Mice with grade 3 behavioral deficits are prone to severe hypothermia, thus normothermic conditions need to be continuously maintained. Hypothermia is more likely to impact transient rather than permanent focal ischemia (Ridenour et al., 1992). Contrary to rats, forearm flexion is not a reliable behavioral sign in mice and thus may not be included in statistical data analysis.

Table 11.9.2 Behavioral Score Criteria

Score	Criteria
Grade 0	No observable behavioral deficit.
Grade 1	Decreased resistance to lateral push and long radius circling.
Grade 2	Decreased resistance to lateral push, decreased grasping, weight loss (<15%), short radius circling, but normal posture at rest.
Grade 3	Leaning to the contralateral side at rest with prominent short radius circling activity, weight loss >15% by 24 hr.

ASSESSMENT OF HEMISPHERIC VOLUME OF STROKE AND CEREBRAL EDEMA

Stroke volume (V_s), measured in cubic millimeters, is derived by numerical integration of consecutive hematoxylin and eosin [or thionin (*UNIT 11.8*) or TTC (Support Protocol 3)] stained coronal sections sampled at known intervals using the following formula: V_s (mm^3) = Σ areas of hemispheric lesions (mm^2) × distance between sampled histological sections (mm).

Alternatively, percent of hemispheric injury (HS) may be calculated using the following formula: HS (%) = [Σ (areas of hemispheric lesions)/Σ (areas of ipsilateral sections)] × 100.

Seven representative coronal sections sampled at known intervals are sufficient to estimate the volume of stroke in the laboratory mouse (Fig. 11.9.3A to D). For mapping of the areas of anterior-posterior distribution of ischemic neuronal injury, the following anatomical coronal coordinates, relative to the bregma, are the most representative (taken from the mouse brain atlas; Franklin and Paxinos, 1997):

0. Bregma 2.96 mm
1. Bregma 1.98 mm
2. Bregma 1.42 mm
3. Bregma 0.98 mm
4. Bregma 0.0 mm
5. Bregma (–)1.06 mm
6. Bregma (–)2.06 mm
7. and Bregma (–)3.08 mm.

A chart of the anterior-posterior distribution of the ischemic lesion helps to identify specific anatomical areas affected by ischemia (Fig. 11.9.2B) and is also helpful in mapping out and analyzing the mechanisms of time-dependent maturation of the ischemic lesion (Du et al., 1996). It also helps to define the spread of the lesion and postischemic brain edema which may occur anterior of the bregma, posterior of the bregma, or both ways (Fig. 11.9.2C).

IMPORTANT NOTE: The distance between coronal anterior-posterior sampled areas of interest (based on frozen sections or TTC-stained sections) will appear larger if compared to the corresponding areas from the mouse brain atlas of Franklin and Paxinos (1997) in which data is reported based on formalin-fixed and paraffin-embedded specimens (brains may shrink up to 30% based on the selection of fixative and embedding medium).

It is extremely important to dissect individual components contributing to the overall size of the ischemic lesion in mice and ask the following questions: (1) What is the pattern of lesion progression (anterior, posterior, or both ways)? (2) Does the lesion progress over the course of 24 hr, 3 days, 7 days? (3) Does the lesion involve cortex, caudate-putamen, or both? (4) Does the lesion spread into areas outside of the distribution of the MCA (e.g., hippocampus, substantia nigra, and other thalamic, subthalamic, and brainstem structures)?

MCA occlusion may sometimes cause ischemic damage to the hippocampus in certain strains of mice (e.g., C57Bl/6). Ischemic damage to thalamic and subthalamic structures may result as well (partially due to the presence of vascular anomalies), and when present, usually manifests in a pronounced drop in body temperature (both after permanent and transient occlusions) and grade 3 cumulative behavioral scores (Table 11.9.2).

The Swanson correction technique of adjustment for hemispheric edema (Hara et al., 1996) should be used according to the formula:

$$V_{\text{adjusted}} = V_{\text{left hemisphere}} - (V_{\text{right hemisphere}} - \text{measured infarct volume})$$

where all volumes are measured in cubic millimeters.

The purpose of this approach is to adjust for brain swelling by correcting for infarct volume. Hemispheric edema can also be accurately measured ex vivo (applying the same principle) using MRI (Steinberg et al., 1995). Brain edema in models involving postischemic reperfusion is usually considerably higher in filament models than in Tamura craniectomies due to the fact that the site of craniectomy acts as a vent, contributes to postischemic (Cushing-type) decompression, and thus decreases brain swelling.

ASSESSMENT OF THE SIZE OF THE ISCHEMIC PENUMBRA

SUPPORT PROTOCOL 6

The dimensions of the ischemic penumbra in genetically altered mice, or those subjected to treatment with pharmacological agents, may vary. Systemic physiological parameters must be monitored in all studied animals. Critical parameters describing ischemic penumbra and its thresholds have been previously reported (Hakim, 1987; Ginsberg et al., 1996). Assessment of the size of the ischemic penumbra can be performed noninvasively in vivo using laser Doppler flowmetry and electrophysiology (Dalkara et al., 1994), or CT scanning (Lo et al., 1996) and magnetic resonance imaging (van Dorstein et al., 1999). The stretch of the ischemic penumbra can also be determined ex-vivo using a combination of techniques. It may be determined histochemically based on morphological characteristics of hematoxylin and eosin and NADPH diaphorase staining (Panahian et al., 1999), assessment of ATP synthesis, tissue pH, and cerebral protein synthesis (Hata et al., 1998), analysis of biliverdin reductase antioxidant potential (Panahian and Maines, 2000) and overexpression of heat shock proteins (Sharp et al., 2000).

STATISTICAL ANALYSIS AND DATA PRESENTATION

SUPPORT PROTOCOL 7

Statistical evaluation of neuroprotection data is performed using unpaired two-tail t-test (for two group comparisons) or analysis of variance (ANOVA) followed by posthoc analysis (in case of three or more studied groups) as recommended in Statview v. 5.0 (SAS Institute; also see *UNIT 1.2*). Physiological parameters are best compared using repeated measures ANOVA. Behavioral data are analyzed using nonparametric statistics: Mann-Whitney for two-group comparisons or Kruskal-Wallis for three or more groups of animals (Huang et al., 1994). Somatosensory evoked potentials (SEPs) and electroencephalographic (EEG) values (if monitored) may further be analyzed using software such as Igor (WaveMetrics) as well as Scope and Chart (AD Instruments). SEPs are analyzed by derived values of wave amplitude using ANOVA. Changes over time in SEP amplitude are analyzed using repeated measures ANOVA. Electroencephalographic values are analyzed using Fast Fourrier Transformation Analysis (FFT) (Dalkara et al., 1994). The minimal number of animals is determined based on the values of the coefficient of variation (ratio of the standard deviation to the mean multiplied by 100) and power analysis calculations using Primer of Biostatistics (v.3.01, McGraw Hill). Power calculations are carried out with $\alpha = 0.05$, $\beta = 0.05$, $p < 0.05$ and estimated to the power of 0.9. Meta-analysis should be carried out to minimize the number of animals essential to reject the null hypothesis and prove statistical significance. Brain specimens are always compared to control and sham-operated animals. Anterior-posterior distribution of the ischemic lesion is mapped using Cricket Graph III (Computer Associates International), and final data is presented using Canvas v. 7.0 or higher (Deneba Software).

Meta-analysis is extremely important for both preclinical and clinical trials (K.I. Maynard, unpub. observ.). Meta-analysis involves statistical analysis of summary information derived from similar but independent studies. Meta-analysis approach allows investigators to increase statistical power in order to detect an overall effect of significance, as well as to estimate the degree of benefit, assess amount of variability, and identify specific characteristics for these previously reported and analyzed studies (Normand, 1999).

REAGENTS AND SOLUTIONS

Use Milli-Q-purified water or equivalent for all recipes and protocol steps. For common solutions see ***APPENDIX 2A****; for suppliers, see* ***SUPPLIERS APPENDIX****.*

TTC staining solution

Dissolve 2 g of 2,3,5-triphenyltetrazolium chloride (TTC) in 100 ml of 0.1 M phosphate buffered saline, pH 7.4, prewarmed to 35° to 36°C. Prepare final solution in any glass or plastic container wrapped in aluminum foil because TTC solution is light sensitive. Use immediately.

COMMENTARY

Background Information

Why choose the mouse model after all?

Stroke models have been successfully reproduced in a variety of animal species: squirrel monkey (Hudgins and Garcia, 1970), gerbils (Berry et al., 1975), rabbit (Steinberg et al., 1995), cat (O'Brien and Waltz, 1973; Bose et al., 1984; Berkelbach et al., 1988), and dog (Suzuki et al., 1980). As a rule of thumb, the larger the animal species, the higher the variability in the size and location of the ischemic lesion. If compared to the cat, rabbit, or dog, the origin of the middle cerebral artery (MCA) in rodents lies further from the optic foramen; therefore, transorbital (Sundt-type) approaches to the MCA in both mice and rats are unsuitable and a subtemporal approach must be carried out instead. Extensive collateral cerebral circulation in the dog renders this species hardly fit for stroke research and requires clipping of many arterial branches for induction of a reproducible ischemic lesion (Suzuki et al., 1980). On the other hand, gerbils are not recommended for stroke research because of high mortality and higher incidence of postoperative seizures after MCAo. The arterial wall of the MCA of the cat contains a significant number of elastic elements, thus during transient MCA occlusion, the artery itself can be stretched out of the orbit using a vascular hook. Conversely, the vascular wall of the MCA in the rabbit is extremely fragile. The shape of the intracranial portion of the internal carotid artery within the cavernous sinus region of higher animal species is curved (van Loveren et al., 1991) in comparison to rodents, in which it is almost a straight line. Thus, performing endovascular filament occlusion models in dogs, cats, or rabbits may not be worthwhile to attempt due to obvious technical complexities and low chances for success. Smaller animals like mice and rats, on the other hand, are easier to handle, inexpensive, and readily available.

This unit describes basic protocols for the two most reproducible models of middle cerebral artery (MCA) occlusion in the laboratory mouse: the Tamura model (see Basic Protocol 1), which is carried out by means of a craniectomy, exposure, and direct coagulation of the MCA (adapted from the rat) and the filament endovascular occlusion model (see Basic Protocol 2), during which the calvarium is left intact, but the MCA is occluded "blindly" using a filament-obturator. Two other modifications of the subtemporal (Tamura-type) protocol are known to exist: distal MCAo at the upper level of the olfactory tract (Fig. 11.9.2A to C) and tandem MCA and ipsilateral CCA occlusion, during which the MCA is occluded more distally, at the level of the inferior cerebral vein (Brint et al., 1988).

Tamura-type models

The subtemporal approach provides clear anatomical visualization of the MCA and its branches. The trunk of the MCA is cauterized in one spot and, unlike similar models in the rat, segmental occlusion of the MCA and its branches within the stretch of MCA from the olfactory tract to the inferior cerebral vein (in order to achieve uniform size cortical lesions)

is not necessary (Menzies et al., 1992; F. Zhang et al., 1997). The whole surgical procedure is relatively quick and can be accomplished in under 10 to 15 min from the time the animal is anesthetized.

In the model of distal MCAo (at the level of inferior cerebral vein or Brint model), lenticulostriatal arteries are left intact and lesions in the caudate nucleus are considerably smaller, with minor damage to the cortical areas overlying the hippocampal region (Fig. 11.9.2H) versus those after proximal MCAo (Fig. 11.9.2I), which manifest in complete ischemic wipe-out of the caudate nucleus and extensive cortical damage in posterior hemispheric areas overlying the hippocampus. The author found that tandem occlusion of MCA (immediately above the level of the olfactory tract) and ipsilateral common carotid artery as reported by Brint et al. (1988) for the laboratory rat is not necessary to perform in the mouse as it does not affect the overall results. In a model of transient ischemia carried out using clip occlusion, ligation of the common carotid artery may unnecessarily delay postischemic recovery of cortical blood flow during the reperfusion phase of the experiment.

The Brint-type model of tandem occlusion of MCA and ipsilateral CCA may be supplemented by 1-hr clip occlusion of the contralateral CCA as previously reported for the laboratory rat (Chen et al., 1986). The site of MCA occlusion in this particular model is even more distal: at the level of or directly above the intersection of MCA with the inferior cerebral vein. Tandem models can be successfully used by investigators performing electrophysiological and iontophoretic studies or by anyone interested in performing continuous flowmetric monitoring of ischemic penumbra in nonsurvival experiments. To fit such experimental needs, the model can be easily induced with the animal positioned in a stereotaxic frame. In this case, distal clipping of the MCA may be supplemented with tandem ipsilateral/contralateral CCA occlusion using inflatable vascular occluders (In Vivo Metric). The occluder cuffs are circumferentially attached around the common carotid arteries of mice using 8-0 monofilament nylon under halothane anesthesia. Injection of saline into the tubing inflates the cuffs and compresses the vessels. Transient carotid occlusions, using the cuffs, can also be performed on unanesthetized mice to screen for the presence of vascular anomalies (e.g., absence of Pcom).

At any time, the Brint model can be transformed into the Chen-Hsu model by placing an extra clip on the contralateral carotid artery. Codman or Biemer microclips or Zen temporary clips are good choices for this purpose. The Chen-Hsu model in the mouse, unlike that in the rat, may result in ischemic damage to the caudate nucleus. Ischemic wipe-out of the putamen is uncommon. In rats, this model was proven reliable to study effects of growth factors on therapeutic neuroprotection in stroke (Speliotes et al., 1996); however, the model has also been reported to cause very delayed maturation of the ischemic lesion (Du et al., 1996).

Among some of the advantages of the Tamura-type approach to the MCA is the fact that vascular anomalies within the MCA region can be detected through the site of craniectomy, which will also decompress the brain during the postischemic period. Thus, the volume of intracerebral edema in this model is lower than it is in the filament model in which the calvarium remains intact (Fig. 11.9.2A, compare I and J). Cerebral edema (both cytotoxic and vasogenic) contributes to elevations in intracerebral pressure (ICP) and results in decreased intracerebral capillary perfusion, further increasing the size of the ischemic lesion over time. The Tamura model in the mouse can be characterized overall as a model of very low postoperative mortality (0% to 1%) and high reproducibility. The author does not have sufficient data relating to long-term behavioral, physiological, and/or biochemical differences between left-sided and right-sided lesions induced by MCAo as was reported for the laboratory rat (Robinson, 1979).

Filament occlusion models

It is a common consensus that therapeutic neuroprotection is somewhat easier to demonstrate in models of transient ischemia (provided the MCAo protocol does not exceed 2 hr). These models of transient ischemic injury were also reported to be "temperature sensitive" (Ridenour et al., 1992) and prone to postischemic cerebral edema and elevations in ICP. All of these factors contribute to statistical variability requiring greater number of animals to complete a study (Huang et al., 1994). Hemispheric lesions induced by transient filament MCAo of short duration (30 to 90 min) may lead to delayed maturation of lesions over the course of 7 to 14 days (Du et al., 1996; Endres et al., 1998). These slowly maturing lesions are apoptosis prone. The filament MCAo model in the

mouse (either permanent or transient) is by no means a "selective" procedure, as not just the MCA is occluded, but also the anterior cerebral, posterior communicating, and internal carotid arteries. This contributes to a significant decrease in collateral circulation within the region of distribution of the MCA and cortical "watershed" territories (shown in Fig. 11.9.2B and I), causing an increase in the size of the ischemic lesion accordingly. The lesion may further increase in size if a 3-hr occlusion/21-hr reperfusion paradigm is used (Fig. 11.9.2J). If only partial reduction in cortical rCBF takes place after insertion of the filament, the Chen-Hsu-type procedure (1-hr contralateral CCA clipping) to further reduce the values of cortical rCBF in the filament model must never be considered as an option because it will kill the mouse. Damage to vital brain stem structures is the likely explanation. In acute MRI experiments, it may be possible to supplement MCA filament occlusion with either bilateral or unilateral vertebral artery occlusions as described for the laboratory rat (see *UNIT 11.8*).

Critical Parameters and Troubleshooting

A very strong correlation exists between the loss of body weight and the size of the ischemic lesion. Mice developing large ischemic hemispheric lesions will exhibit short radius circling activity. Unlike rats, forearm flexion is not a reliable sign for behavioral assessment in mice (Menzies et al., 1992) and could be absent in mice that will otherwise develop severe hemispheric lesions. Mice also have low volumes of circulating blood (1 to 1.5 ml), and as a result of intraoperative bleeding, usually develop profound hypotension, which contributes to an increase in the size of the ischemic lesions. Other variables that may affect the size of the ischemic lesion include the following. (1) The strain of mice used in the study: certain strains of mice (e.g., SV-129) are less sensitive to ischemic injury than others (e.g., C57Bl/6). Ipsilateral hippocampal, thalamic, and subthalamic ischemic injuries have been noted as a result of permanent MCA occlusions at 24 hr in C57Bl/6 mice. (2) Sex differences: these have been shown to affect the outcome of MCAo, thus neuroprotection should be examined in male and female animals separately. (3) The presence of vascular anomalies. (4) Brain temperature, which primarily affects outcomes of the transient filament model. (5) Perturbations in physiological and hemodynamic parameters: these may be due to abnormal blood glucose levels, hemodilution, and volume-expansion due to constant flushing of arterial and venous catheters (e.g., due to systemic heparinization, decrease in mean arterial pressure due to frequent blood sampling for arterial blood glucose, or other tests). (6) Air emboli: this condition will manifest in decreased respiratory end tidal CO_2 ($EtCO_2$), but high arterial pCO_2 values. It may mislead investigators into lowering the respiratory rate accordingly during artificial ventilation (if arterial blood gases are not monitored). (7) Hypoxic conditions: these are encountered as a consequence of a prolonged period of halothane anesthesia (>2%) or flaws in $EtCO_2$ monitoring during artificial ventilation; if the animal remains in this condition with pCO_2 values above 55 Torr for periods exceeding 30 min, dramatic exacerbation of the ischemic lesions will result.

Filament shape and coating

The tip of the coated filament must never resemble a "club" and must have equal thickness of coating material on its body. The filament will eventually be lodged in the distal portions of the anterior cerebral artery (ACA), the diameter of which is smaller than that of the intracranial portion of the internal carotid artery (ICA). Clubbing of the tip of the filament will not facilitate its advance into these vessels and is absolutely unnecessary. Usually, a 12-mm advance from the carotid bifurcation is considered adequate for occlusion of the ICA, MCA, ACA, and posterior communicating artery (Pcom). Should there be any vascular anomalies (e.g., duplications of MCA), extra branches will get occluded by the coated side of the filament as well. The author recommends using 20-mm-long coated filaments for this purpose, marked at the 12-mm interval with red nail polish.

Poly-L-lysine does not affect the overall diameter of the suture. It only increases adhesive forces around the suture (Belayev et al., 1999), thus forcibly constricting vessels on the filament. Endothelin coating (a potent vascular constrictor) may also be used as an alternative option (Sharkey et al., 1994). In contrast, soft Reprosil and Xantopren coatings mechanically dilate the vessels as the filament is advanced forward. The author does not perform flame-heating of the filament tips due to their small size. Reprosil coating will stay well attached, allowing coated filaments to be reused a number of times, from animal to animal, contributing to the statistical consistency of the study. Both Xantopren and Cuttersil coated filaments

cannot be reused and should be made 2 to 6 hr before MCA occlusion (see Table 11.9.1).

The author prefers to use coated filaments made of 8-0 Ethicon monofilament nylon in a highly defined weight range of mice (22 to 24 g). If the intracranial vessels are too small for the inserted filament (thus preventing its advance), it is swapped for the one with slightly thinner coating; however, in heavier animals (28 to 30 g), cerebral ischemic lesions may be of inconsistent size due to lack of the "snug fit" between the wall of the vessel and that of the coated filament. For animals of this weight range, the author recommends the use of 7-0 coated nylon or prolene filaments. Neither 8-0 or 7-0 coated monofilament nylon sutures are rigid enough to cause arterial perforations. Anyone using uncoated 5-0 or 6-0 nylon sutures is at great risk of causing inadvertent arterial perforation. Interestingly, these perforations in some cases may result in hematoma formation and subarachnoid hemorrhage, leading to spasm of the MCA and its branches and formation of an ischemic lesion, leading to false-positive results and possible misinterpretation of data. Alternatively, in mice with arterial perforations, no hemispheric lesion may be noted if the filament is not removed from the ICA. Such extreme cases are strong indicators of serious technical flaws.

Filament does not advance into the intracranial portion of ICA or stops short of MCA

It is important to note the length of the filament (mm) that is introduced into the vessels. Twelve millimeters of the filament length needs to be manually advanced into the cranium from the carotid bifurcation in order to successfully block the MCA. The tip of the filament may be lodged against the stump of the PPA (~3 to 5 mm from carotid bifurcation). Thus, it is important to tie off the pterygopalatine artery (PPA) as proximally as possible to the ICA using 10-0 monofilament nylon, so as not to create an endovascular pouch. Alternatively, the filament may have excessive layers of coating material preventing it from entering the intracranial portion of the ICA or moving past the posterior hippocampal artery (~8 to 9 mm). In this case, a lesion in the upper posterior hippocampal area may result if the filament is left in place for 24 hr (Fig. 11.9.2G). If the filament cannot be advanced 12 mm, it should be partially withdrawn and inserted again. If this does not help, a filament with thinner coating should be used.

Filament is "washed out" from the ICA after removal of the upper clip

When the upper clip is released, but the filament is not secured in place with no. 5 forceps and/or a 10-0 monofilament nylon suture tied around the vessel at the level of CCA bifurcation, the filament will be washed out by the blood stream due to backflow from the circle of Willis. In this case, due to extensive blood loss, the experiment should be aborted.

Portions of filament coating material remain in the vessels

This is confirmed by examining the withdrawn filament for missing fragments of the coating material. Loss of material may lead to failure or just partial reperfusion of the ischemic hemisphere. It is recommended that after the animal is sacrificed ICA, MCA, and other arterial vessels of the circle of Willis be examined for the presence of fragmented coating material. If found, the animal should be excluded from the study.

Detecting an arterial perforation by the filament

8-0 filaments coated with Reprosil or Xantopren lack sufficient stiffness to perforate major arterial branches (Table 11.9.1). The operator will encounter mounting resistance and the filament will stop advancing if its coating is excessive or the diameter of the vessels is smaller than projected. If the filament has perforated the wall of the ICA, an alarming sign to the investigator is an absence of arterial backflow upon extraction of the filament during the reperfusion phase of the experiment. As a result of arterial perforation and subsequent subdural hematoma formation, mice may develop erroneous circling behavior to the ipsilateral side of the filament insertion (wrong direction circling). Mice usually do not die as a result of arterial perforation by the filament if it is a model of permanent MCAo; death primarily occurs in transient models, in which the physical presence of the filament is no longer there to plug the laceration. Animals may even develop a lesion due to vasospasm, triggered by blood released into the subdural and subarachnoid space. Based on these observations, a filament model of subarachnoid hemorrhage in the mouse has recently been described (Kamii et al., 1999). The condition of the animals will notably deteriorate due to the mass effect of hematoma formation, ensuing brain edema, midline shifting, and brainstem herniation. Intracerebral pressure (ICP) will noticeably rise causing further con-

striction of brain capillaries and decrease in microcirculation.

Mice develop rolling seizures during postischemic reperfusion

All animals developing seizure-related hyperactivity must be excluded from the study.

Mice demonstrate abnormal circling behavior after withdrawal of the filament

Anatomical pathways within the brain cross over to the other side. Thus, if a lesion is induced within the right cortex and caudate nucleus, the left upper and lower limbs of the mouse will become weak. Upon a light tail pinch, such animals will attempt to escape, and because the limbs on the right are stronger, mice will circle counterclockwise (away from the lesion). If an animal, upon awakening from anesthesia, attempts to circle clockwise and the surgical manipulations were performed on the right side, or in other words if the animal circles towards the lesion, hematoma formation should be suspected. This observation together with lack of signs of postischemic reperfusion based on readings of rCBF, should suggest in favor of aborting the experiment.

Possible problems during Tamura-type craniectomy

It is not recommended to drill in one spot longer than 2 to 3 sec. This may cause damage to the underlying brain tissue and edema and hemorrhagic transformation. Drilling over the surface of the MCA trunk may result in its constriction and extravasation of blood elements and plasma. The author recommends that investigators, for perfection of their microsurgical techniques, perfuse one or two mice with a saline solution of 2% Evans Blue to detect possible damage to the blood-brain barrier after drilling (Hudgins and Garcia, 1970).

Possible problems after Tamura-type craniectomies

Mice may demonstrate feeding difficulties. Excessive damage to the temporalis muscle and inadvertent damage to the bone of the lower jaw during craniectomy may cause feeding difficulties manifesting in postoperative weight loss.

Anticipated Results

Volumes of stroke after Tamura-type permanent proximal MCA occlusion (below the level of olfactory tract) should be in the range of 90 to 110 mm^3 (with incorporation of the Swanson correction for cerebral edema) and are dependent on the strain of mice used in the study and the time of sacrifice of animals. If the MCAo is performed immediately above the level of the olfactory tract, lenticulostriatal arteries are usually spared and the final lesion will be in the range of 65 to 75 mm^3. If the MCA is occluded at the level of inferior cerebral vein (Brint model) the lesions will hardly exceed 40 mm^3, but may increase to 70 mm^3 if the ipsilateral carotid artery is occluded permanently and the contralateral carotid artery is clipped transiently for 1 hr (Chen-Hsu model).

After 3 hr of transient cerebral ischemia, SV-129 mice develop smaller lesions than C57Bl/6 mice (67 ± 13 mm^3 versus 96 ± 29 mm^3; Hara et al., 1996). The size of lesions after transient filament model may vary and are entirely dependent on the duration of ischemic occlusion, duration of postischemic reperfusion, and strain of animals used in the study. This model may require a greater number of animals to reach a sufficient statistical power to yield meaningful results. The coefficient of variation must be calculated for each individual strain of mice. Placement of arterial and venous catheters, intubation of the animal, placement of laser Doppler flowmeter probes and SEP electrodes is time consuming and may not allow the investigator to screen three to four different groups of mice (4 to 5 mice per group) in one day. Collection of samples for assessment of arterial blood gas status (pO_2, pCO_2, pH, etc.) is informative; however, frequent flushing of arterial and venous lines will result in inadvertent heparinization of the animal and increased probability of intraoperative and/or postoperative bleeding. Furthermore, since the volume of circulating blood in the mouse is 1 to 1.5 ml, hemodilution and volume expansion may alter the natural course of pathophysiology of the stroke, making acquired data difficult to interpret.

Time Considerations

Tamura model

The complete surgical procedure should not take longer than 10 to 15 min per mouse to accomplish. Since there is no blood loss, and surgeries are quick, monitoring systemic parameters may be carried out in selected animals. Operation on 10 to 20 mice may be performed in one day under identical conditions.

Filament model

The exact time required for completion of the model depends on the time of establishment of reperfusion which may vary from 30 min to 3 hr.

Literature Cited

Backhauss, C., Karkoutly, C., Welsch, M., and Krieglstein, J. 1992. A mouse model of focal cerebral ischemia for screening neuroprotective drug effects. *J. Pharmacol. Methods* 27:27-32.

Belayev, L., Busto, R., Zhao, W., Fernandez, G., and Ginsberg, M.D. 1999. Middle cerebral artery occlusion in the mouse by intralumenal suture coated with poly-L-lysine: Neurological and histological validation. *Brain Res.* 833:181-190.

Berkelbach, V.D., Sprenkel, J.W., and Tulleken, C.A.F. 1988. The postorbital approach to the middle cerebral artery in cats. *Stroke* 19:503-506.

Berry, K., Wisniewski, H.M., Svarzbein, L., and Baez, S. 1975. On the relationship of brain vasculature to production of neurological deficit and morphological changes following acute unilateral common carotid artery ligation in gerbils. *J. Neurol. Sci.* 25:75-92.

Bose, B., Osterholm, J.L., and Berry, R. 1984. A reproducible experimental model of focal cerebral ischemia in the cat. *Brain Res.* 311:385-391.

Brint, S., Jacewitz, M., Kiessling, M., Tanabe, J., and Pulsinelli, W. 1988. Focal brain ischemia in the rat: Methods for reproducible neocortical infarction using tandem occlusion of the distal middle cerebral and ipsilateral common carotid arteries. *J. Cereb. Blood Flow Metab.* 8:474-485.

Chen, S. T., Hsu, C. Y., Hogan, E. L., Maricq, H., and Balentine, J.D. 1986. A model of focal ischemic stroke in the rat: Reproducible extensive cortical infarction. *Stroke* 17:738-743.

Clark, W., Gunion-Rinker, L., Lessov, N., and Hazel, K. 1998. Citicholine treatment for experimental intracerebral hemorrhage in mice. *Stroke* 29:2136-2140.

Dalkara, T., Morikawa, I., Panahian, N., and Moskowitz, M.A. 1994. Blood flow–dependent functional recovery in a rat model of focal cerebral ischemia. *Am. J. Physiol.* 267:H678-H683.

Dalkara, T., Irikura, K., Huang, Z., Panahian, N., and Moskowitz, M.A. 1995. Cerebrovascular responses under controlled and monitored physiological conditions in the anesthetized mouse. *J. Cereb. Blood Flow Metab.* 15:631-638.

Du, C., Csernansky, C.A., Hsu, C.Y., and Choi, D. 1996. Very delayed infarction after mild focal cerebral ischemia: A role for apoptosis? *J. Cereb. Blood Flow Metab.* 16:195-201.

Endres, M., Namura, S., Shimizu-Sasamata, M., Waeber, C., Zhang, M., Gomez-Isla, T., Hyman, B.T., and Moskowitz, M.A. 1998. Attenuation of delayed neuronal death after mild local ischemia in mice by inhibition of the caspase family. *J. Cereb. Blood Flow Metab.* 18:234-247.

Fisher, M., Finklestein, S.P., Furlan, A.J., Goldstein, L.B., Gorelick, P.B., Kaste, M., Lees, K.R., and Traystman, R.J. 1999. Recommendations for standards regarding preclinical neuroprotective and restorative drug development. *Stroke* 30:2752-2758.

Fouad, K. and Bennett, D.T. 1998. Decerebration by global ischemic stroke on rats. *K. Neurosci. Meth.* 84:131-137.

Franklin, K.B.J. and Paxinos, G. 1997. The Mouse Brain in Stereotaxic Coordinates. Academic Press, San Diego.

Fuwa, I. 1994. A pediatric case of carotid Rete Mirabile. *Stroke* 25:1268-1270.

Garcia, J.H., Gutierrez, J.A., and Liu, K.-F. 1997. Non-neuronal responses to short term occlusion of the middle cerebral artery. *Neurology* 49 :S27-S31.

Ginsberg, M.D., Back, T., and Zhao, W. 1996. Three-dimensional metabolic and hemodynamic imaging of the normal and ischemic rat brain. *Acta Neurochir. Suppl. (Wien)* 66:44-49.

Gotti, B., Benavides, J., MacKenzie, E.T., and Scatton, B. 1990. The pharmacotherapy of focal cortical ischaemia in the mouse. *Brain Res.* 552:290-307.

Hakim, A.M. 1987. The cerebral ischemic penumbra. *Can. J. Neurol. Sci.* 14:557-559.

Hara, H., Huang, P.L., Panahian, N., Fishman, M.C., and Moskowitz, M.A. 1996. Reduced brain edema and infarction volume in mice lacking the neuronal isoform of nitric oxide synthase after transient MCA occlusion. *J. Cereb. Blood Flow Metab.* 16:605-611.

Hata, R., Mies, G., Wiessner, C., Fritze, K., Hesselbarth, D., Brinker, G., and Hossmann, K.-A. 1998. A reproducible model of middle cerebral artery occlusion in mice: Hemodynamic, biochemical, and magnetic resonance imaging. *J. Cereb. Blood Flow Metab.* 18:367-375.

Hedger, J.H. and Webber, R.H. 1976. Anatomical study of the cervical sympathetic trunk and ganglia in the albino rat (*Mus norvegicus albinus*). *Acta Anat.* 96:206-217.

Huang, Z., Huang, P.L., Panahian, N., Dalkara, T., Fishman, M.C., and Moskowitz, M.A. 1994. Effects of cerebral ischemia in mice deficient in neuronal nitric oxide synthase. *Science* 265:1883-1885.

Hudgins, W.R. and Garcia J.H. 1970. Transorbital approach to the middle cerebral artery of the squirrel monkey: A technique for experimental cerebral infarction applicable to ultrastructural studies. *Stroke* 1:107-111.

Isayama, K., Pitts, L.H., and Nishimura, M.C. 1991. Evaluation of 2,3,5-triphenyltetrazolium chloride staining to delineate rat brain infarcts. *Stroke* 22:1394-1398.

Kamii, H., Kato, I., Kinouchi, H., Chan, P.H., Epstein, C.J., Akabane, A., Okamoto, H., and Yoshimoto, T. 1999. Amelioration of vasospasm after subarachnoid hemorrhage in transgenic mice overexpressing CuZn superoxide dismutase. *Stroke* 30:867-872.

Kilic, E., Hermann, D.M., and Hussmann, D.A. 1998. A reproducible model of thromboembolic stroke in mice. *Neuroreport* 9:2967-2970.

Lo, E.H., Hara, H., Rogowska, J., Trocha, M., Pierce, A.R., Huang, P.L., Fishman, M.C., Wolf, G.L., and Moskowitz, M.A. 1996. Temporal correlation mapping analysis of the hemodynamic penumbra in mutant mice deficient in endothelial nitric oxide synthase gene expression. *Stroke* 27:1381-1315.

Ma, J., Endres, M., and Moskowitz, M.A. 1998. Synergistic effects of caspase inhibitors and MK-801 in brain injury after transient focal cerebral ischemia in mice. *Br. J. Pharmacol.* 124:756-762.

Martinou, J.C., Dubois, D.M., Staple, J.K., Rodriguez, I., Frankowski, H., Missotten, M., Albertini, P., Talabot, D., Catsicas, S., and Pietra, C. 1994. Overexpression of BCL-2 in transgenic mice protects neurons from naturally occurring cell death and experimental ischemia. *Neuron* 13:1017-1030.

Menzies, S.A., Hoff, J.T., and Betz, A.L. 1992. Middle cerebral artery occlusion in rats: A neurological and pathological evaluation of a reproducible model. *Neurosurgery* 31:100-107.

Normand, S-L.T. 1999. Tutorial in biostatistics meta-analysis: Formulating, evaluating, combining, and reporting. *Statistics Med.* 18:321-359.

O'Brien, M.D. and Waltz, A.G. 1973. Transorbital approach for occluding the middle cerebral artery without craniectomy. *Stroke* 4:201-206.

Ono, S., Date, I., Nakajima, M., Onada, K., Ogihara, K., Shiota, T., Asari, S., Ninomiya, Y., Yabuno, N., and Ohmato, T. 1997. Three-dimensional analysis of vasospastic major cerebral arteries in rats with the corrosion cast technique. *Stroke* 28:1631-1638.

Panahian, N. and Maines, M.D. 2000. Assessment of induction of biliverdin reductase in a mouse model of middle cerebral artery occlusion. *Brain Res. Protocols* In press.

Panahian, N., Yoshiura, M., and Maines, M.D. 1999. Overexpression of heme oxygenase 1 is neuroprotective in a model of permanent middle cerebral artery occlusion in transgenic mice. *J. Neurochem.* 72:1187-1203.

Ridenour, T., Warner, D.S., Todd, M.M., and McAllister, A.C. 1992. Mild hypothermia reduces infarct size resulting from temporary but not permanent focal ischemia in rats. *Stroke* 23:733-738.

Robinson, R. 1979. Differential behavioral and biochemical effects of right and left hemispheric cerebral infarction in the rat. *Science* 205:707-710.

Schulz, J.B., Panahian, N., Chen, Y.I., Beal, M.F., Moskowitz, M.A., Rosen, B.R., and Jenkins, B.G. 1997. α-Phenyl-tert-Butyl-Nitrone facilitates postischemic reperfusion and protects against ischemic brain injury. Assessment using NMR and laser Doppler flow techniques. *Am. J. Physiol.* 272:1986-1995.

Sharkey, J., Butcher, S.P., and Kelly, J.S. 1994. Endothelin-1 induced middle cerebral artery occlusion: Pathological consequences and neuroprotective effects of MK801. *J. Autonomic Nerv. Syst.* 49: S177-S185.

Sharp, F.R., Lu, A., Tang, Y., and Millhorn, D.E. 2000. Multiple molecular penumbras after focal cerebral ischemia. *J. Cereb. Blood Flow Metab.* 20:1011-1032.

Speliotes, E.K., Caday, C.G., Do, T., Weise, J., Kowall, N.W., and Finklestein, S.P. 1996. Increased expression of basic fibroblast growth factor (bFGF) following focal cerebral infarction in the rat. *Brain Res. Mol. Brain Res.* 39:31-42.

Steinberg, G., Panahian, N., Perez-Pinzon, M., Sun, G., Modi, M., and Sepinwall, J. 1995. Narrow "therapeutic window" for NMDA antagonist protection against focal cerebral ischemia in rabbits. *Neurobiol. Dis.* 2:109-118.

Suzuki, J., Yoshimoto, T., Tranka, S., and Sakamoto, T. 1980. Production of various models of cerebral infarction in the dog by means of occlusion of intracranial trunk arteries. *Stroke* 11:337-341.

Tamura, A., Graham, D.I., McCulloch, J., and Teasdale, G.M. 1981. Focal cerebral ischemia in the rat: 1. Description of technique and early neuropathological consequences following middle cerebral artery occlusion. *J. Cereb. Blood Flow Metab.* 1:53-60.

van Dorstein, F.A., Hata, R., Maeda, K., Franke, C., Eis, M., and Hossmann, K.A. 1999. Diffusion- and perfusion-weighted MR imaging of transient cerebral ischemia in mice. *NMR Biomed.* 12:525-534.

van Loveren, H.R., Keller, J.T., El-Killiny, M., Scodary, D.J., and Tew, J.M. 1991. The Dolenc technique for cavernous sinus exploration. *J. Neurosurg.* 74:837-844.

Wang, Y.F., Tsirka, S.E., Strickland, S., Stieg, P.E., Soriano, S.G., and Lipton, S.A. 1998. Tissue plasminogen activator (tPA) increases neuronal damage after focal cerebral ischemia in wild-type and tPA-deficient mice. *Nature Med.* 4:228-231.

Welsh, F.A., Sakamoto, T., McKee, A.E., and Sims, R.E. 1987. Effect of lactacidosis on pyridine nucleotide stability during ischemia in mouse brain. *J. Neurochem.* 49:846-851.

Zhang, F., Eckman, C., Younkin, S., Hsia, K., and Iadecola, C. 1997. Increased susceptibility to ischemic brain damage in transgenic mice overexpressing the amyloid precursor protein. *J. Neurosci.* 17:7655-7661.

Zhang, Z., Chopp, M., Zhang, R.L., and Goussev, A. 1997. A mouse model of embolic focal cerebral ischemia. *J. Cereb. Blood Flow Metab.* 17:1081-1088.

Contributed by Nariman Panahian
InforMax Inc.
North Bethesda, Maryland

Principles of Electrophysiology: An Overview

NEURORECEPTORS AND ION CHANNELS

Neuroreceptors and ion channels are the fundamental sites of nerve function. In nerve fibers, opening and closing of voltage-gated ion channels such as sodium, potassium, and calcium channels generate action potentials. At nerve terminals that make synaptic contact with postsynaptic neurons or effector organs such as muscle, membrane depolarizations caused by action potentials open calcium channels. This results in Ca^{2+} influx, which in turn causes release of neurotransmitters by exocytosis. The released neurotransmitters bind to specific ligand-gated receptors on the postsynaptic membrane. The receptors are thus activated, resulting in the opening of the channel associated with them. Influx or efflux of specific ions through the open channels occurs to complete synaptic or neuromuscular transmission.

The generation and propagation of action potentials along the nerve fibers and synaptic and neuromuscular transmission form the basis for motor function, sensory function, and cognition/learning/memory in the peripheral and central nervous systems. Thus, any behaviors of animals and humans should ultimately be explained on the basis of receptor/channel functions. Neurotoxic actions of environmental toxicants, natural toxins, and therapeutic drugs at high doses are in many cases due to their interactions with various neuroreceptors and ion channels.

Neuroreceptors and ion channels may be classified into two large categories, voltage-gated ion channels and ligand-gated ion channels. Voltage-gated ion channels comprise sodium channels, potassium channels, and calcium channels, and each type of channel contains several subtypes. Neuroreceptors comprise multisubunit proteins, which form an ion channel. Many types of neuroreceptors are known, including, but not limited to, acetylcholine (ACh) receptors, glutamate receptors, γ-aminobutyric acid (GABA) receptors, glycine receptors, adrenergic receptors, and serotonin receptors. Furthermore, each of these neuroreceptors comprises several subtypes.

Simplified kinetic schemes of receptor channel activity are illustrated in Figure 11.10.1. Closed voltage-gated channels (C_c) open upon depolarizing stimulation (C_o), and eventually inactivate (C_i), as shown in scheme I of Figure 11.10.1. Neuroreceptors at resting state (R) are activated (R^*A_2) when bound by two molecules of agonist (A), a ligand, but may be desensitized ($R^*A_2{}^D$) with prolonged stimulation, as shown in scheme II of Figure 11.10.1.

Methods of Measuring Receptor/Channel Activity

The activity of receptors/channels is represented by ionic currents that result from ionic fluxes through the open channels. A large amount of ions flows through an open channel in a short period of time. For example, in an ion channel associated with the nicotinic ACh receptor, as many as 4.1×10^7 ions flow per second through a channel yielding a current of 6.6 pA (Hille, 2001). Upon stimulation either by membrane depolarizations (for voltage-gated channels) or by transmitters (for ligand-gated channels), the channel opens and closes quickly with an open time of only several milliseconds. Therefore, only electrophysiological methods can accurately follow the time course of channel activity and the resultant potential changes, e.g., action potentials.

However, other methods are also available, depending on the purpose of measurement and study. Ligand binding assays are often used, although this method is limited to the binding process, without allowing measurement of physiological functions that follow ligand

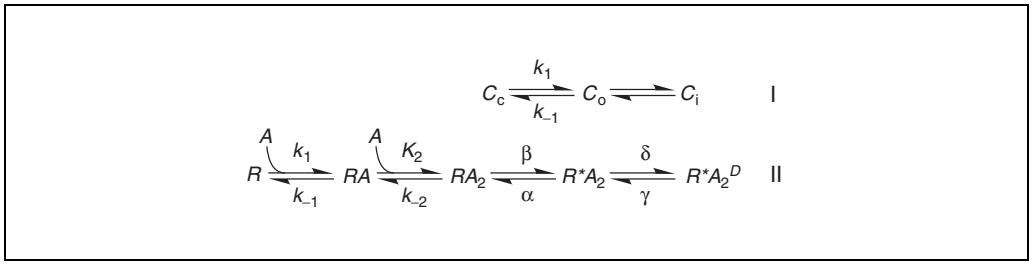

Figure 11.10.1 Simplified kinetic schemes of receptor channel activity. See text for further explanation.

Contributed by Toshio Narahashi
Current Protocols in Toxicology (2002) 11.10.1-11.10.11

binding. The advantage of this method is that it is simple, quick, and easy. The drawbacks are that the data could be misleading, as the method does not allow one to see functional changes, and that there is often more than one binding site for a ligand on a neuroreceptor/channel. For example, at least six binding sites are known to exist in the sodium channel (Catterall, 1992, 1995; Narahashi, 1998), and specific binding of [^{3}H]batrachotoxin A 20 α-benzoate to site 2 (Catterall et al., 1981) has been used often as a measure of the action of a test chemical on the sodium channel. However, this method is not sufficient, especially for screening of compounds, because there are other binding sites in the sodium channel. Similar precautions in binding experiments are applicable to other receptors and ion channels. Ion flux measurements using labeled ions have also been used often, but this method fails to follow rapid movements of permeating ions through open channels. Imaging techniques have been well developed and are being used extensively as a measure of receptor/channel activity. For example, Fura-2 can be used for the measurement of increases in the intracellular ionized Ca^{2+} concentration associated with openings of calcium channels or activation of NMDA receptors. One advantage of this method is that it is applicable to the case where routine electrophysiological techniques cannot be used. However, time resolution is not as fast as that of electrophysiological methods.

Applications of Electrophysiological Techniques

Since electrophysiological techniques allow us to measure the activity of the nervous system most accurately, they have a broad application to various types of research. These include, but are not limited to, mechanistic studies, clinical examinations, and high-throughput screenings. For clinical examinations of toxic effects of a chemical, conduction velocity of nerve action potentials is often measured and an electroencephalogram (EEG) is often performed. For high-throughput screenings of test chemicals, the two-microelectrode voltage clamp method, as applied to *Xenopus* oocytes expressing sodium channels, is being used, sometimes with the aid of a robot. Imaging techniques are also being used for high-throughput screenings. However, the most important application of electrophysiological techniques is for the study of the mechanism of action of test chemicals on neuroreceptors and ion channels.

Mechanistic Studies

While some useful information can be obtained by recording resting potential and action potential from neurons or nerve fibers, this method is far from satisfactory for elucidating the mechanism of action of test chemicals on the nervous system. Since the basis for nerve excitation and synaptic transmission resides in the activity of neuroreceptors and ion channels, it is imperative to record ionic currents associated with receptor/channel function.

The most accurate and straightforward method for recording ionic currents is the voltage clamp. This technique was originally developed by Cole (1949) for squid giant axons with 400- to 500-μm diameter and was extensively used by Hodgkin, Huxley and Katz (Hodgkin et al., 1952; Hodgkin and Huxley, 1952a,b,c,d) for the purpose of elucidating the ionic mechanism of nerve excitation. It was later adapted to muscle end-plates (Takeuchi and Takeuchi, 1959), large neurons (Hagiwara and Saito, 1959), nodes of Ranvier (Dodge and Frankenhaeuser, 1959), and smaller giant axons of lobster (80 μm in diameter; Julian et al., 1962a,b). These voltage clamp techniques were used extensively, but they could not be used for small cells such as brain neurons and smooth muscle cells. Nowadays, the two-microelectrode voltage clamp technique, originally used for large neurons (Hagiwara and Saito, 1959), is being used extensively for recording of currents from *Xenopus* oocytes expressing various receptors/channels.

A breakthrough was achieved by Neher and Sakmann (1976), who successfully recorded single-channel currents from nicotinic acetylcholine (nACh) receptors of denervated muscle fibers. This technique, called patch clamp, was later improved to record currents from an entire cell membrane (whole-cell currents) and single-channel currents from either a patch of the cell membrane (cell-attached patch clamp) or an outside-out or inside-out membrane patch (Hamill et al., 1981). The patch-clamp techniques have proven extremely versatile and useful, as they are applicable to almost any type of cells—such as brain neurons, myocytes, lymphocytes, and red blood cells—to record single-channel currents. It should be emphasized that the patch clamp is a variation of the voltage clamp, and therefore the space clamp condition, which will be described below, must be satisfied to perform patch-clamp measurements of ionic currents.

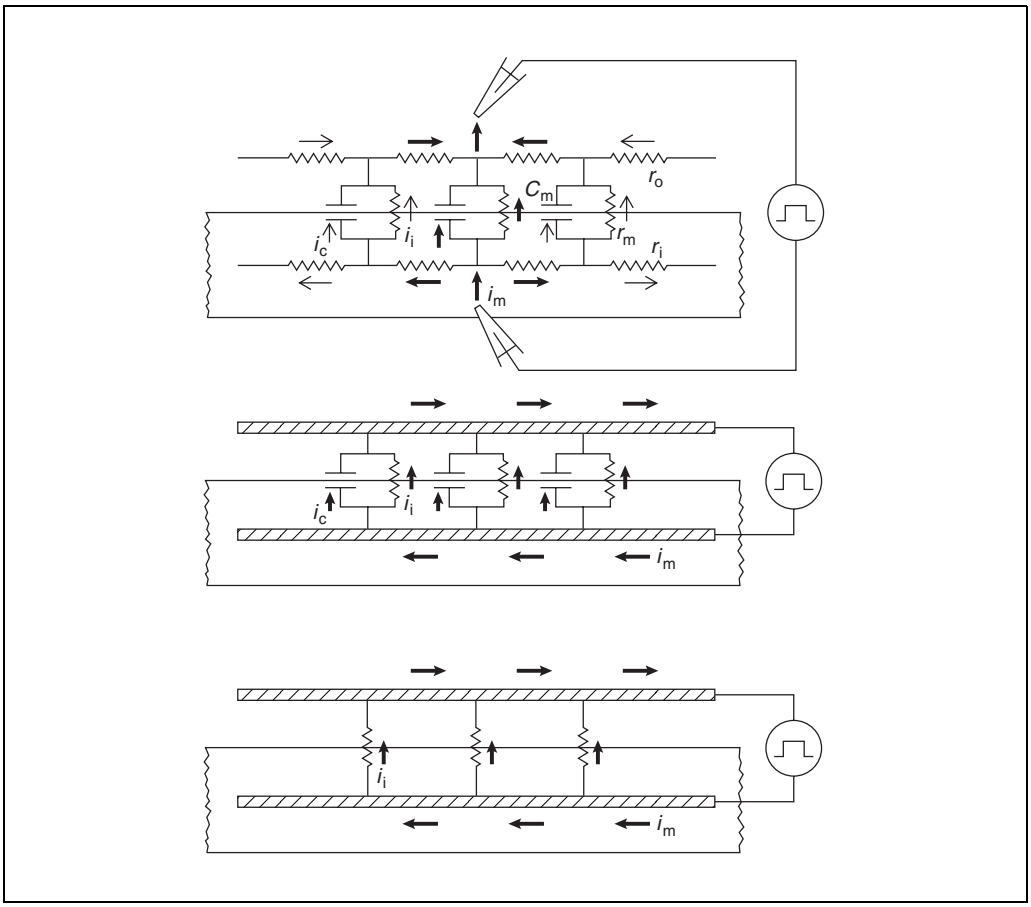

Figure 11.10.2 Current flow in an axon preparation. In the top diagram, current is applied to the axon through internal and external microelectrodes. The membrane current and longitudinal current are not uniform along the axon. In the middle diagram, current is applied through internal and external wire electrodes. The membrane current and longitudinal current are uniform along the axon (space clamp). In the bottom diagram, which illustrates the case when the axon in space clamp condition is voltage clamped, no capacitive current (i_c) flows while the membrane potential is maintained at a constant level, making it possible to measure the ionic current (i_i). Definitions: i_m, total membrane current; r_o, external resistance; r_i, internal resistance; r_m, membrane resistance; and c_m, membrane capacity. From Narahashi (1971) and used with permission of Academic Press.

BASIC PRINCIPLE OF RECEPTOR/CHANNEL FUNCTION

Electrophysiological experiments such as those by patch clamp are considerably different from other types of biomedical experiments—e.g., in biochemistry, molecular biology, immunology, and genetics—in that it is mandatory for the investigators to understand the basic principle of nerve excitation and synaptic transmission. The reasons for this lie in the fact that one must be able not only to understand the signals being recorded but also to evaluate whether the signals are of the proper shape without being contaminated by artifacts. This must be done quickly in live experiments. If patch-clamp experiments are not properly performed, the recorded signals often contain artifacts distorting the current shape and possibly leading to the wrong conclusions. Equally important is the ability of the investigators to understand and interpret any changes in electrical signals that may be caused by application of test chemicals. Contrary to many other types of in vitro experiments, electrophysiological experiments such as those by patch clamp must deal with live cells, which are often short-lived under the in vitro experimental conditions. Thus, any decisions, such as planning the next protocol, must be made quickly. This is the reason why in most cases technicians cannot properly perform patch-clamp experiments unless they have been well trained in the basic principles at the graduate school level.

Cable Properties and Voltage Clamp Principle

The principle of voltage clamp is based on the measurement of channel conductance

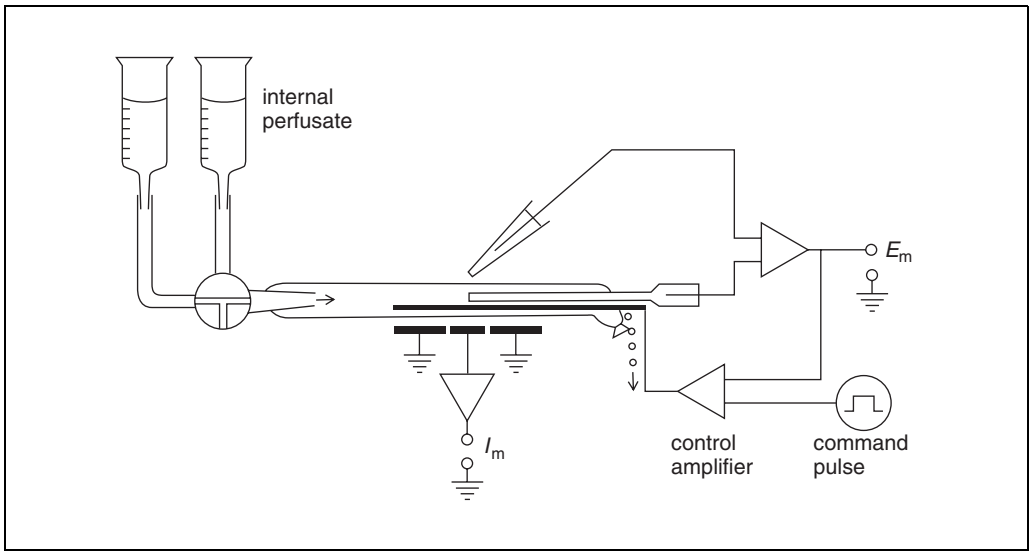

Figure 11.10.3 Voltage clamp of an internally perfused squid giant axon. See text for further explanation. Definitions: E_m, membrane potential; I_m, membrane current. From Narahashi (1984) and used with permission of John Wiley & Sons, Inc.

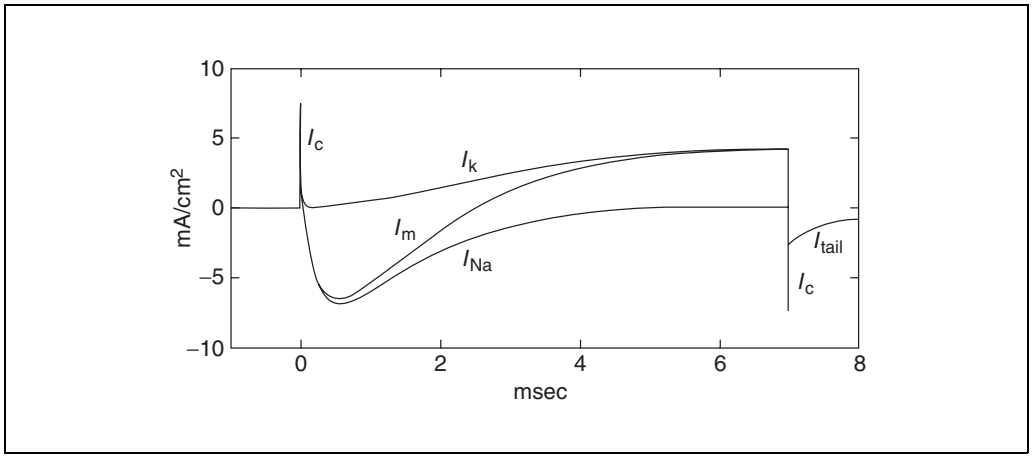

Figure 11.10.4 Membrane current (I_m) and its sodium (I_{Na}), potassium (I_K), and capacitive (I_c) current components associated with a step depolarization of the nerve membrane under voltage clamp condition. From Narahashi (1981) and used with permission of Pergamon Press.

through simultaneous recordings of both membrane potential and membrane ionic current. According to Ohm's law, the sodium conductance (g_{Na}) and the potassium conductance (g_K) are given by Equations 11.10.1 and 11.10.2:

$$g_{Na} = \frac{I_{Na}}{E - E_{Na}}$$

Equation 11.10.1

$$g_K = \frac{I_K}{E - E_K}$$

Equation 11.10.2

where I_{Na} and I_K are sodium and potassium currents, respectively, E is the membrane potential, and E_{Na} and K_K are the equilibrium potentials for sodium and potassium, respectively, as defined by the Nernst equation.

In order to clearly understand the voltage clamp principle, it is imperative to become familiar with the cable properties of a cell. Detailed analysis of cable properties is beyond the scope of this unit, and only the information that is absolutely essential for voltage clamp is described here, using the classical prototype technique as applied to the squid giant axon. This prototype is the easiest for understanding the principle of voltage clamp. The electrical equivalent circuit of a portion of an axon is shown in Figure 11.10.2. The external and internal phases of the axon are represented by

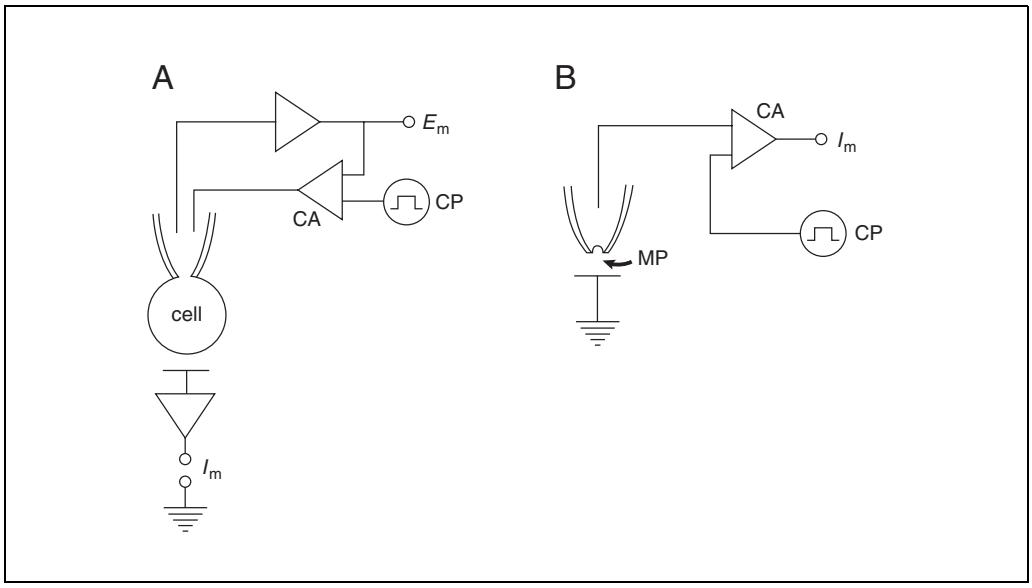

Figure 11.10.5 Schematic diagram of patch clamp. (**A**) Whole-cell patch clamp; (**B**) single-channel recording from an isolated membrane patch. Definitions: I_m, membrane current; E_m, membrane potential; CA, control amplifier; CP, command pulse; MP, membrane patch. See text for further explanation. From Narahashi (1992) and used with permission of CRC Press.

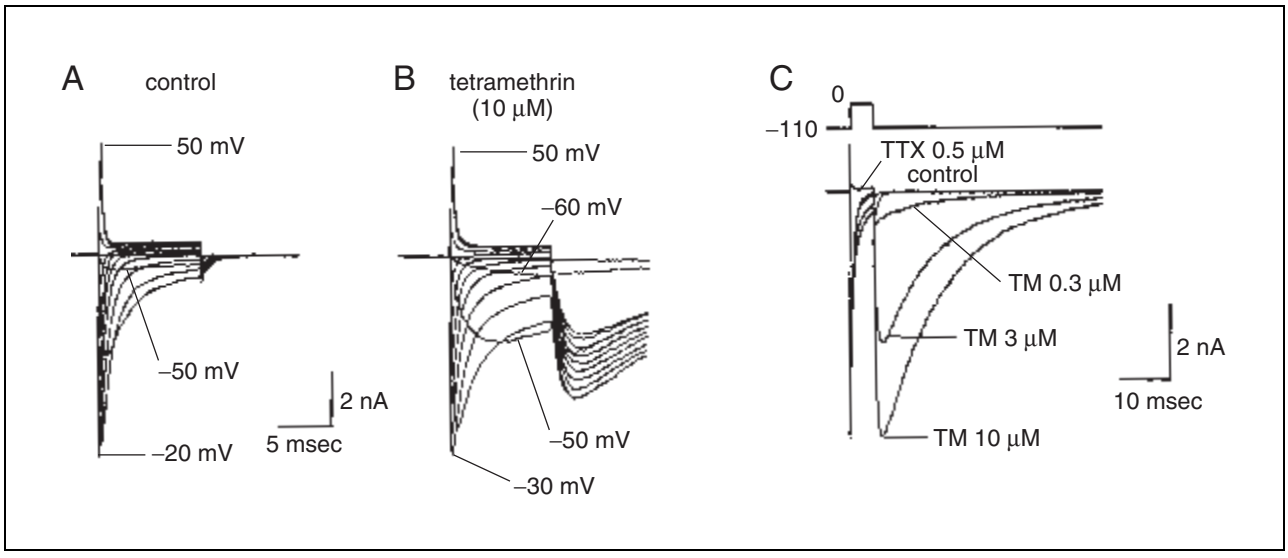

Figure 11.10.6 Effects of 10 μM tetramethrin on the current recorded from tetrodotoxin (TTX)–sensitive sodium channels in a rat cerebellar Purkinje cell. Currents were evoked by 10-msec depolarizations at a frequency of 0.1 Hz to test potentials ranging from –80 to +50 mV in 5-mV increments from a holding potential of –110 mV. (**A**) Currents under control condition. (**B**) Currents after exposure to 10 μM tetramethrin. (**C**) Concentration-dependent effect of tetramethrin. Currents were evoked by a 5-msec step depolarization to 0 mV from a holding potential of –110 mV under control conditions and in the presence of tetramethrin (0.3, 3, and 10 μM). TTX (0.5 μM) completely blocked both the peak current and tetramethrin-induced tail current. From Song and Narahashi (1996) and used with permission of The American Society for Pharmacology and Experimental Therapeutics.

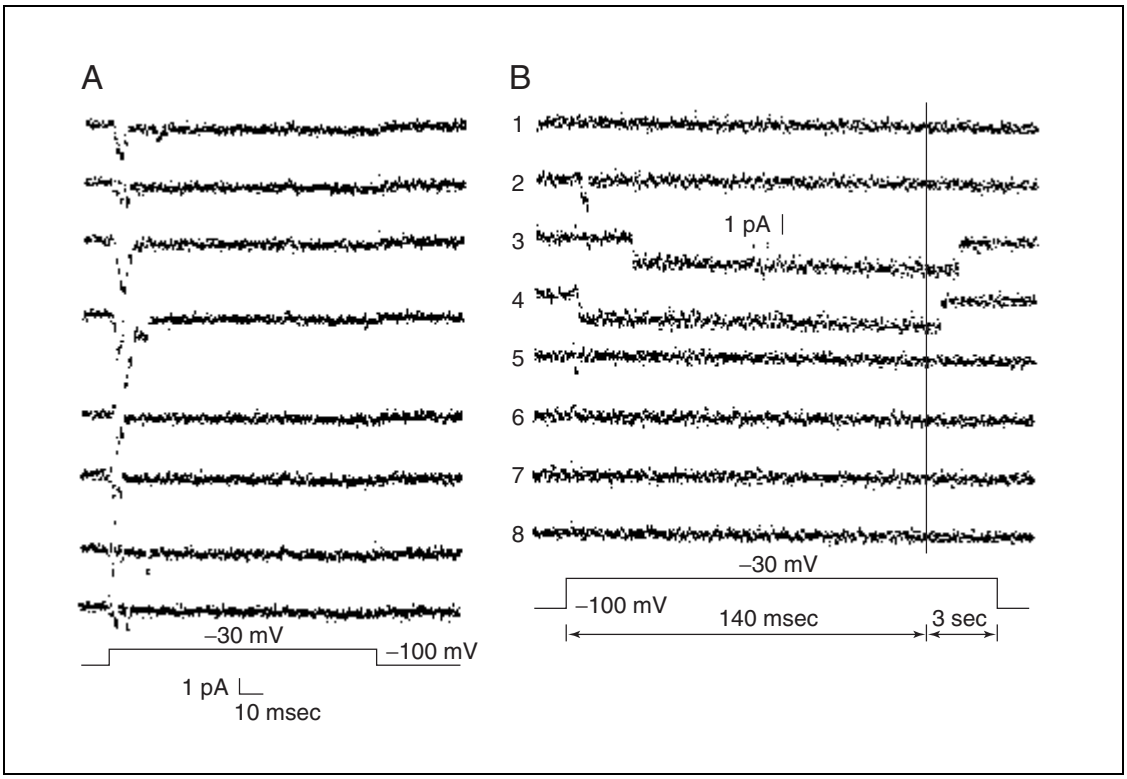

Figure 11.10.7 Effects of deltamethrin on single sodium channel currents recorded from an inside-out membrane patch isolated from a neuroblastoma cell (N1E–115). (**A**) Currents before drug treatment in response to 140-msec depolarizing steps from a holding potential of –100 mV to –30 mV with a 3-sec interpulse interval. Records were taken at a rate of 100 μsec per point. (**B**) Currents after exposure to 10 μM deltamethrin. The membrane patch was depolarized for 3140 msec from a holding potential of –100 mV to –30 mV. The interpulse interval was 3 sec. The time scale changes during the voltage step as indicated. During the first 140 msec, records were taken at a rate of 100 μsec per point and after the vertical line records were taken at a rate of 10 msec per point. From Chinn and Narahashi (1986) and used with permission of The Physiological Society.

external resistance (r_o) and internal resistance (r_i). The nerve membrane has membrane resistance (r_m) and membrane capacitance (c_m). When a current is injected to the axon through an intracellular microelectrode, the current and the resultant membrane potential change are distributed along the axon in a nonuniform manner (Fig. 11.10.2, top). The distributions of current and membrane potential change become uniform if the external and internal resistances are eliminated. This can be accomplished by placing a large, longitudinal metal electrode outside the axon and inserting a wire electrode inside (Fig. 11.10.2, middle). This condition is called space clamp, which is a prerequisite for voltage clamp. However, because of the presence of membrane capacitance, the current flowing across the membrane is complex, involving both the ionic current (i_i), through the open channels and the capacitive current (i_c). The capacitive current can be eliminated when the membrane current is measured while maintaining the membrane potential constant (Fig. 11.10.2, bottom). Thus, voltage clamp is accomplished allowing measurements of membrane ionic currents as a function of the membrane potential.

A prototype of simplified voltage clamp circuitry for the internally perfused squid giant axon is illustrated in Figure 11.10.3. The membrane potential is recorded by a glass capillary electrode inserted longitudinally to the axon while another glass capillary reference electrode is placed outside the axon. The membrane potential thus recorded is fed into a control amplifier to which a command pulse generated from a pulse generator is applied. The difference between the membrane potential and the command pulse is then amplified by the control amplifier, and a current is generated from the output of the amplifier and flows across the membrane until the membrane potential becomes equal to the command pulse. This is a feedback circuit, and the current can be measured by another amplifier (I_m).

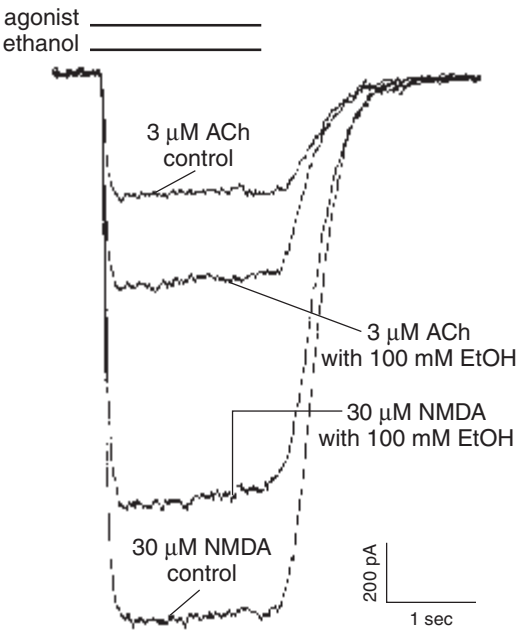

Figure 11.10.8 Effects of ethanol on ACh-induced current in α4β2-type ACh receptors and NMDA-induced current in a rat cortical neuron in long-term primary culture. Ethanol at 100 mM potentiates current induced by ACh at 3 μM while suppressing current induced by NMDA at 30 μM. Holding potential, −70 mV. From Aistrup et al. (1999) and used with permission of The American Society for Pharmacology and Experimental Therapeutics.

The membrane current (I_m) associated with a step depolarization of the membrane is schematically shown in Figure 11.10.4. Capacitive currents (I_c) flow upon step depolarization and repolarization to charge and discharge the membrane capacity, respectively. The membrane current comprises sodium current (I_{Na}) and potassium current (I_K). The equilibrium potentials for sodium (E_{Na}) and potassium (E_K) can be measured from the respective reversal potentials. Thus, sodium conductance (g_{Na}) and potassium conductance (g_K) can be calculated from Equations 11.10.1 and 11.10.2, respectively.

The classical voltage clamp as described above is difficult to apply to small cells such as brain neurons and myocytes because inserting two microelectrodes may damage the small cells quickly. Patch clamp, which is a variation of voltage clamp, has proven very powerful, as it can be applied to almost any cells to record whole-cell currents and single-channel currents (Hamill et al., 1981). Simplified schemes of patch-clamp circuitry are illustrated in Figure 11.10.5. One of the crucial points of patch clamp is a very high seal resistance (10 to 100 GW) at the orifice of the glass capillary electrode, which is placed onto the surface of the membrane. Figure 11.10.5A illustrates the circuitry for whole-cell patch clamp. After establishing the gigaohm seal, the cell membrane at the tip of the electrode is broken by applying negative pressure so that the electrode is electrically connected with the cell interior. Figure 11.10.5B shows single-channel patch-clamp circuitry using an outside-out or inside-out membrane patch (MP) isolated from the cell membrane. Single-channel current recording can also be made from a cell-attached membrane without isolating a membrane patch. Patch-clamp techniques are applicable to both voltage-gated and ligand-gated channels.

For more detailed aspects of nerve excitation, cable properties, and voltage-clamp and patch-clamp technologies, see Key References.

EXAMPLES OF CURRENT RECORDS

The effect of the pyrethroid insecticide tetramethrin on the sodium channel current recorded from rat cerebellar Purkinje neurons is illustrated in Figure 11.10.6 (Song and Narahashi, 1996). Figure 11.10.6A shows sodium currents associated with 10-msec step depolari-

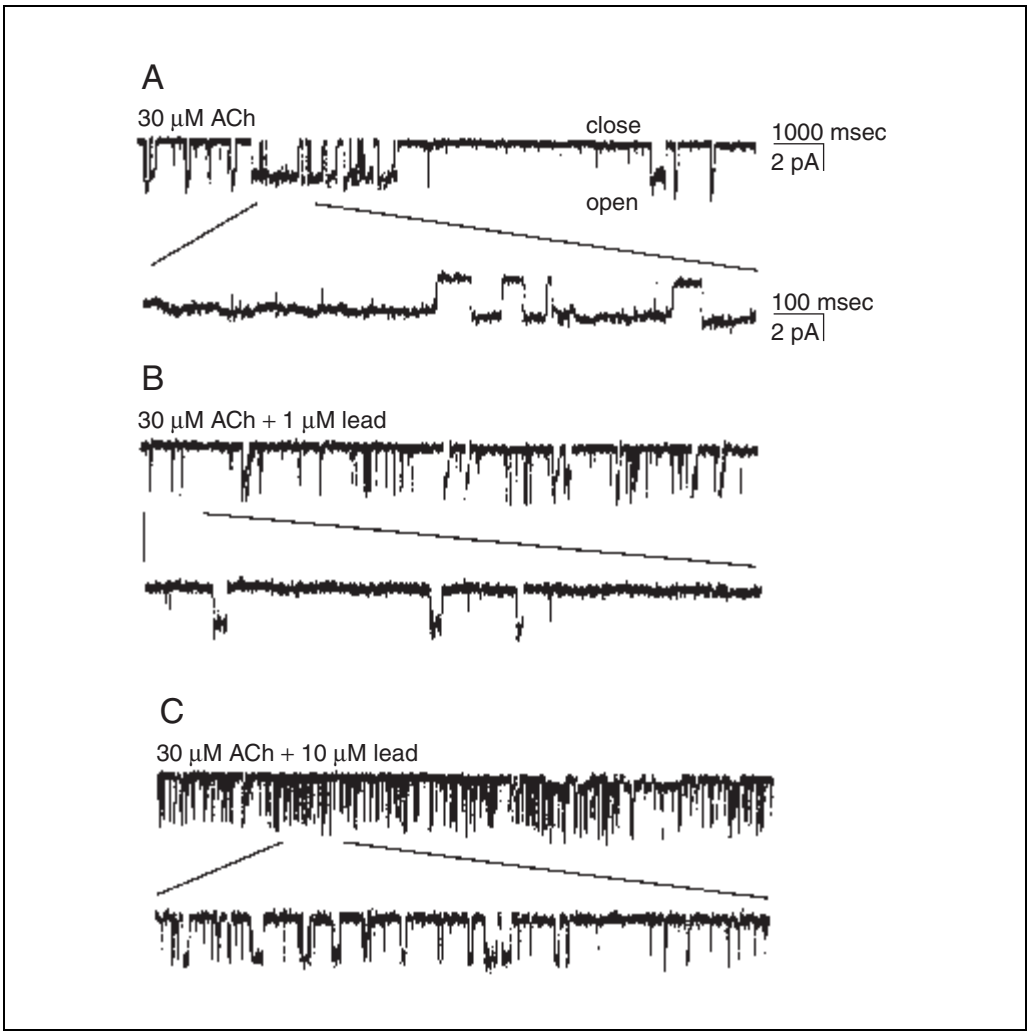

Figure 11.10.9 Single-channel currents induced by application of 30 μM ACh and coapplication of 30 μM ACh and 1 or 10 μM lead to cell-attached membrane patches of PC12 cells clamped at a membrane potential 40 mV more positive than the resting potential. (**A**) Currents induced by 30 μM ACh in the absence of lead occurred during brief isolated openings or during longer openings interrupted by a few short closures or gaps. (**B**) Coapplication of 30 μM ACh and 1 μM lead. Channel openings were shortened. (**C**) Coapplication of 30 μM ACh and 10 μM lead. Channel openings were further shortened. Small conductance state currents were observed. From Nagata et al. (1997) and used with permission of Elsevier Ltd.

zations at a frequency of 0.1 Hz to test potentials ranging from −80 mV to +50 mV in 5-mV increments from a holding potential of −110 mV. The sodium currents inactivated after reaching a peak. During application of 10 μM tetramethrin (Fig. 11.10.6B), the channel inactivation was partially inhibited, and large and slowly decaying tail currents were produced upon termination of depolarizing steps while the peak sodium currents remained unchanged. Figure 11.10.6C shows concentration dependence of tetramethrin effect on the tail current.

An example of single sodium channel currents before and during application of the pyrethroid insecticide deltamethrin at 10 μM in an N1E-115 neuroblastoma cell is shown in Figure 11.10.7 (Chinn and Narahashi, 1986). Currents were produced in an excised inside-out membrane patch by step depolarizations to −30 mV from a holding potentiation of −100 mV. Figure 11.10.7A represents several sample records of the control in which single sodium channels opened for a short period of time at the beginning of 140-msec step depolarizations. In the presence of deltamethrin (Fig. 11.10.7B), single sodium channel currents were greatly prolonged up to ~1 sec and appeared often with a long delay from the beginning of a depolarizing step. The amplitude of single-channel current was not changed by deltamethrin.

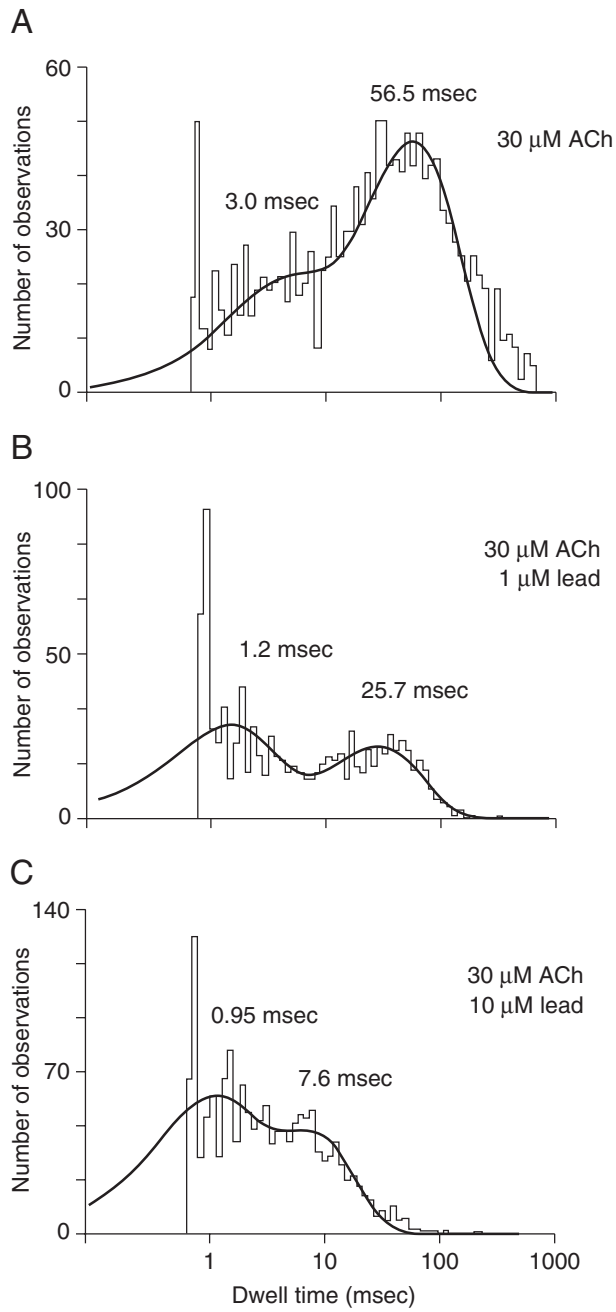

Figure 11.10.10 Open time distributions for (**A**) currents induced by 30 μM ACh; (**B**) coapplication of 30 μM ACh and 1 μM lead; and (**C**) coapplication of 30 μM ACh and 10 μM lead to cell-attached membrane patches of PC12 cells clamped at a membrane potential 40 mV more positive than the resting potential. The distributions are shown on a logarithmic time axis. The best fit of two exponential functions is shown. In (**A**; currents induced by 30 μM ACh), time constants were estimated to be 3.0 msec (75.9% of total observations) for the faster component and 56.5 msec (24.1%) for the slower component. In (**B**; coapplication of 1 μM lead and 30 μM ACh), time constants were estimated to be 1.2 msec (54.0%) for the faster component and 25.7 msec (46.0%) for the slower component. In (**C**; coapplication of 10 μM lead and 30 μM ACh), time constants were estimated to be 0.95 msec (50.5%) for the faster component and 7.6 msec (49.5%) for the slower component. From Nagata et al. (1997) and used with permission of Elsevier Ltd.

Examples of ligand-gated whole-cell currents are illustrated in Figure 11.10.8 (Aistrup et al., 1999). Acetylcholine or NMDA was applied via a U-tube system to a rat cortical neuron in long-term primary culture. ACh at 3 μM evoked an inward current, which was greatly potentiated by 100 mM ethanol. NMDA at 30 μM generated an inward current, which was suppressed by 100 mM ethanol.

Examples of ligand-gated single-channel currents recorded by the cell-attached patch clamp technique from a PC12 cell are shown in Figure 11.10.9 (Nagata et al., 1997). Currents were induced by 30 μM ACh contained in the pipet solution or by 30 μM ACh plus 1 μM or 10 μM lead contained in the pipet solution. Lead at 1 μM shortened the open time and lead at 10 μM increased the frequency of openings. The analyses of open time distribution are shown in Figure 11.10.10 indicating concentration-dependent decreases in open time by lead.

ACKNOWLEDGEMENTS

The editors of *Current Protocols in Toxicology* wish to thank Dr. Toshio Narahashi for his expert assistance in preparation and editing of this unit on electrophysiology.

LITERATURE CITED

Aistrup, G.L., Marszalec, W., and Narahashi, T. 1999. Ethanol modulation of nicotinic acetylcholine receptor currents in cultured cortical neurons. *Mol. Pharmacol.* 55:39-49.

Catterall, W.A. 1992. Cellular and molecular biology of voltage-gated sodium channels. *Physiol. Rev.* 72:S15-S48.

Catterall, W.A. 1995. Structure and function of voltage-gated ion channels. *Annu. Rev. Biochem.* 64:493-531.

Catterall, W.A., Morrow, C.S., Daly, J.W., and Brown, G.B. 1981. Binding of batrachotoxin A20-α-benzoate to a receptor site associated with sodium channels in synaptic nerve ending particles. *J. Biol. Chem.* 256:9822-9827.

Chinn, K. and Narahashi, T. 1986. Stabilization of sodium channel states by deltamethrin in mouse neuroblastoma cells. *J. Physiol.* 380:191-207.

Cole, K.S. 1949. Dynamic electrical characteristics of the squid axon membrane. *Arch. Sci. Physiol.* 3:253-258.

Dodge, F.A. and Frankenhaeuser, B. 1959. Sodium currents in the myelinated nerve fibre of *Xenopus laevis* investigated with the voltage clamp technique. *J. Physiol.* 148:188-200.

Hagiwara, S. and Saito, N. 1959. Voltage-current relations in nerve cell membrane of *Onchidium verruculatum. J. Physiol.* 148:161-179.

Hamill, O.P., Marty, A., Neher, E., Sakmann, B., and Sigworth, F.J. 1981. Improved patch-clamp techniques for high–resolution current recording from cells and cell-free membrane patches. *Pflügers Arch.* 391:85-100.

Hille, B., 2001. Ion Channels of Excitable Membranes. 3rd ed. Sinauer Associates, Sunderland, Mass.

Hodgkin, A.L. and Huxley, A.F. 1952a. Currents carried by sodium and potassium ions through the membrane of giant axon of *Loligo. J. Physiol.* 116:449-472.

Hodgkin, A.L. and Huxley, A.F. 1952b. The components of membrane conductance in the giant axon of *Loligo. J. Physiol.* 116:473-496.

Hodgkin, A.L. and Huxley, A.F. 1952c. The dual effect of membrane potential on sodium conductance in the giant axon of *Loligo. J. Physiol.* 116:497-506.

Hodgkin, A.L. and Huxley, A.F. 1952d. A quantitative description of membrane current and its application to conduction and excitation in nerve. *J. Physiol.* 117:500-544.

Hodgkin, A.L., Huxley, A.F., and Katz, B. 1952. Measurement of current–voltage relations in the membrane of the giant axon of *Loligo. J. Physiol.* 116:424-448.

Julian, F.J., Moore, J.W., and Goldman, D.E. 1962a. Membrane potentials of the lobster giant axon obtained by use of the sucrose-gap technique. *J. Gen. Physiol.* 45:1195-1216.

Julian, F.J., Moore, J.W., and Goldman, D.E. 1962b. Current-voltage relations in the lobster giant axon membrane under voltage clamp conditions. *J. Gen. Physiol.* 45:1217-1238.

Nagata, K., Huang, C.-S., Song, J.-H., and Narahashi, T. 1997. Lead modulation of the neuronal nicotinic acetylcholine receptor in PC12 cells. *Brain Res.* 754:21-27.

Narahashi, T. 1971. Effects of insecticides on excitable tissues. *In* Advances in Insect Physiology, Vol. 8 (J.W.L. Beament, J.E. Treherne, and V.B. Wigglesworth, eds.) pp. 1-93. Academic Press, London.

Narahashi, T. 1981. Mode of action of chlorinated hydrocarbon pesticides on the nervous system. *In* Halogenated Hydrocarbons: Health and Ecological Effects (M.A.Q. Khan, ed.) pp. 222-242. Pergamon Press, Elmsford, N.Y.

Narahashi, T. 1984. Drug-ionic channel interactions: Single channel measurements. *Ann. Neurol.* 16:S39-S51.

Narahashi, T. 1992. Mechanisms of neurotoxicity. Electrophysiological studies. Cellular electrophysiology. *In* Neurotoxicology. (M.B. Abou-Donia, ed.) pp. 155-189. CRC Press, Boca Raton, Fla.

Narahashi, T. 1998. Chemical modulation of sodium channels. *In* Ion Channel Pharmacology (B. Soria and V. Ceúa, eds.) pp. 23-73. Oxford University Press, Oxford.

Neher, E. and Sakmann, B. 1976. Single-channel currents recorded from membrane of denervated frog muscle fibres. *Nature* 260:779-802.

Song, J.-H. and Narahashi, T. 1996. Modulation of sodium channels of rat cerebellar Purkinje neurons by the pyrethroid tetramethrin. *J. Pharmacol. Exp. Ther.* 277:445-453.

Takeuchi, A. and Takeuchi, N. 1959. Active phase of frog's end-plate potential. *J. Neurophysiol.* 22:395-411.

Key References

Aidley, D.J. 1998. The Physiology of Excitable Cells. Cambridge University Press, Cambridge, U.K.

Gives basic electrophysiology including cable properties, mechanism of nerve excitation, and synaptic transmission.

Hille, 2001. See above.

An advanced level textbook of ion channel physiology.

Sakmann, B. and Neher, E. 1995. Single-Channel Recording. Plenum Press, New York.

Describes details of patch-clamp technology including whole-cell and single-channel patch clamp, data analyses, and other details.

Walz, W., Boulton, A.A., and Baker, G.B. (eds.). 2002. Patch-clamp analysis: advanced techniques. *In* Neuromethods, Vol. 35 (A.A. Boulton and G.B. Baker, series eds.). Humana Press, Totowa, N.J.

Describes updated versions of patch-clamp technologies, including those developed during the last decade.

Contributed by Toshio Narahashi
Northwestern University Medical School
Chicago, Illinois

Electrophysiological Studies of Neurotoxicants on Central Synaptic Transmission in Acutely Isolated Brain Slices

Normal function of the brain requires rapid and precise communication between neurons. Individual neurons in the central nervous system (CNS) communicate with each other at synapses primarily by chemical synaptic transmission. For this process, electrical properties of the membrane transduce depolarization into release of a chemical transmitter stored in the sending neuron. Any chemical that interferes with this process, at the conduction of the electrical impulse, release of the chemical messenger, or its recognition by the receiving neuron, may potentially disrupt synaptic transmission and cause neurotoxicity in the central nervous system (CNS).

Effects of neurotoxic chemicals on central synaptic transmission can be assessed using electrophysiological recording techniques in freshly isolated brain slice preparations. All conventional electrophysiological recording techniques such as extracellular microelectrode recording, intracellular microelectrode recording, whole-cell patch clamp, and single-channel recordings that are used in cultured or acutely dissociated cells can now be applied to brain slices. As a result, the excitatory or inhibitory postsynaptic potentials (EPSPs or IPSPs, respectively) or excitatory or inhibitory postsynaptic currents (EPSCs or IPSCs, respectively) may be recorded. It is also possible to study central synaptic functions and synaptic plasticity such as long-term potentiation (LTP), a long-lasting increase in synaptic transmission in the CNS in response to a brief tetanic stimulation. The advantages and disadvantages of different recording techniques and their applications to neurotoxicology are discussed in Background Information.

Theoretically, slices for electrophysiological recordings can be made from almost any region of the brain. However, the regions of brain most commonly used as slices for studying central synaptic function are those with solid laminated architectures such as the hippocampus and cerebellum. In this unit, preparations of both hippocampal (see Support Protocol 1) and cerebellar (see Support Protocol 2) slices are described. Using these two slice models, three conventional recording techniques including extracellular microelectrode recording (see Basic Protocol 1), intracellular microelectrode recording (see Basic Protocol 2), and whole-cell patch clamp recording (see Basic Protocol 3) in brain slices will be discussed.

Depending on the region of brain (e.g., hippocampus, cerebellum, or neocortex) to be sliced and the type of recordings (extra- or intracellular microelectrode recording or whole-cell patch recording) to be made, three main methods in cutting brain slices have been employed. The first method is manually cutting the slices by hand using a razor strip or bow cutter. This method is widely used for tissues such as the neocortex, olfactory cortex, and cerebellum, where a large area tangential to a surface needs to be cut. The second method is semi-manually cutting slices from a larger tissue block using a razor-containing tissue chopper. This method can be used to cut any region of the brain that can be prepared into a tissue block, as described in Support Protocol 1 for preparation of hippocampal slices. The third method is cutting slices from a smaller tissue block using an oscillation tissue slicer or vibratome. Unlike the first two methods, which produce relatively thick slices used typically for extra- and intracellular microelectrode recordings (they also can be used for whole-cell patch clamp recordings using the so-called "blind" technique), the vibratome method can cut relatively thin slices (reliably cuts 150- to 200-μm slices) suitable for whole-cell patch clamp recordings. It is especially good for cutting fresh and slightly firm tissues such as the cerebellum. The vibratome method for preparation of thin cerebellar slices is described in Support Protocol 2.

Contributed by Yukun Yuan and William D. Atchison
Current Protocols in Toxicology (2003) 11.11.1-11.11.38

STRATEGIC PLANNING

Which Type of Electrophysiological Recording Technique is Appropriate?

To study effects of neurotoxic chemicals on central synaptic transmission, the first issue to determine is what type of electrophysiological recordings (extracellular microelectrode recording, intracellular microelectrode recording, or whole-cell patch clamp recording) in the brain slice is needed for a particular experiment. In general, analysis of the field potentials (extracellular recording from a number of spatially localized cells) gives information about the average behavior of a neuronal population in response to effects of a given neurotoxic chemical, while single-cell studies (intracellular and whole-cell patch clamp recordings) give much more detailed information about the state of a particular cell during and after exposure to the neurotoxic chemical. Thus, selection of a recording method depends mainly on the primary goals of the proposed experiments. If one simply wants to screen a series of chemicals or test whether or not a given chemical affects central synaptic function, then conventional extracellular microelectrode recording in brain slices may be sufficient. If one is more interested in an in-depth analysis of the neurotoxic mechanisms underlying how a given chemical affects central synaptic transmission, then intracellular recording techniques including current clamp, discontinuous (sharp) single-electrode voltage clamp (dSEVC), and, especially, conventional whole-cell patch clamp recording would be preferable.

In addition, the availability and makeup of the electrophysiological setup, the research budget, and the investigators' experience in electrophysiological recordings are also factors in the selection of recording methods.

Which Region of Brain Tissues Should be Used for Preparation of Brain Slices?

In general, the ideal region of brain tissue for making slices should have the following characteristics: (1) slices can be prepared easily and reliably (e.g., hippocampus or cerebellum); (2) the structural landmarks are readily visible (e.g., the layers of pyramidal and granule cell in hippocampus or the layers of cerebellar Purkinje and granule cells and their fiber projections can be easily discerned); (3) the architecture is "laminated" such that the synaptic circuits are organized in a planar pattern so that they remain intact after slicing. In addition, for the purpose of neurotoxicological studies, the characteristics of the neurotoxicity of an agent, particularly the clinical symptoms, signs, and pathology resulting from exposure to the chemicals of interest, should be taken into account in selecting the region of brain tissue for slicing. For example, do particular sensory disturbances, motor dysfunctions, or behavioral changes occur? Are specific areas or regions of brain damaged? If one knows the chemical to be tested is particularly toxic to a particular brain region such as the cerebellum (e.g., methylmercury) or the hippocampus (e.g., trimethytin), then slices from these regions should be considered. Alternatively, if a chemical causes significant neural behavioral changes, loss of short-term memory, or learning disorders (e.g., lead), then regions associated with certain forms of learning and memory, such as the hippocampus, may be a better choice. If a chemical causes vision damage potentially via a central mechanism, then visual cortex slices should be considered.

What is Needed for a Basic Setup for Electrophysiological Recording in Brain Slice?

The basic components of a setup for electrophysiological recordings in brain slices are generally all similar among different laboratories; they include an antivibration table, a Faraday cage, an amplifier, a microscope, a computer, an oscilloscope, micromanipulators, a tape recorder (optional), pipet fabrication supplies (electrode puller and microforge), microelectrode holders, a recording chamber, a perfusion system, a temperature control system, and brain slicers. However, individual components may vary depending

on the requirements for a given experiment, type of recording, and the investigators' preference. Detailed electrophysiological setups in a laboratory have been described elsewhere by Penner (1995) and Finkel and Bookman (1997). Still, certain considerations for selection of some components may be worth mentioning in this unit.

Amplifier

The amplifier requirements for extracellular, intracellular, and patch-clamp recordings are different. For accurate measurement of intracellular membrane potential changes in intracellular recording, one important requirement for a microelectrode amplifier is to have a "Bridge" mode and to be able to perform "bridge balance" in order to eliminate the microelectrode voltage drop when passing currents across the microelectrode resistance. Usually, the microelectrode amplifier used for intracellular recording is also used for extracellular recording. However, because the signal for extracellular recording is typically very small and needs extensive amplification, a circuit with low-noise with a gain of at least 1000× is also required for an extracellular recording amplifier. Theoretically, all modern intracellular microelectrode amplifiers (e.g., Axoclamp-2; Axon Instrument) are capable of being used for both extra- and intracellular recordings. In addition to current clamp recordings, some intracellular microelectrode amplifiers such as the Axoclamp-2 can also be used for voltage-clamp recording in whole cells using the discontinuous single (sharp) electrode voltage clamp (dSEVC) recording method. In this type of amplifier, the single electrode performs both functions of voltage recording and current passing using time-sharing techniques, i.e., function of the electrode is switched rapidly between voltage recording (~70% of duty cycle) and current passing (~30% of duty cycle). Thus, the same system can be used for extracellular recording, conventional intracellular recording (current-clamp), and voltage-clamp recording (either patch pipets or sharp microelectrodes). Although all patch-clamp amplifiers (e.g., Axon's Axopatch 200B, Axopatch-1-D, and MultiClamp 700A; Warner's PC-505B; Bioscience Tools' WPC-100) are suitable for both single-channel and whole-cell recordings, some amplifiers may be better in one type of recording mode than others. For example, the Axopatch 200B provides very-low-noise recordings of single-channel current. Thus, if the single-channel recording is the primary method to be used in the experiments, this type of amplifier may be a better choice. On the other hand, if a whole-cell recording technique is routinely used in the experiments, then a different type of unit, such as the Axopatch 1-D amplifier, will work very well.

Recording chamber

In general, there are two types of brain slice chambers (the interface chamber and the submersion chamber) routinely used for electrophysiological recordings. The interface chamber usually consists of a small inner chamber with a fine-nylon mesh to hold the slice and an outer-bath chamber with a heating wire and oxygenation tubes. The slice is incubated in the inner chamber partially submerged in artificial cerebrospinal fluid (ACSF) with its upper surface exposed to a humidified atmosphere of 95% O_2/5% CO_2 to form an air-fluid interface. The main advantages of this type of chamber are that it provides better oxygenation of the tissue; the recording of responses, especially extracellular field potentials, is facilitated (responses are larger than those obtained in a submersion chamber); the stimulus artifacts are greatly reduced; and the temperature can easily be preheated to the desired level without a special and expensive control system. The major disadvantages are that the slice may easily dry out if the balance between input and output of medium is not adjusted perfectly; stability of the slice is not easy to maintain, and the slice on the nylon mesh can move up-and-down if the input and output of medium are not well balanced, drainage is not smooth or air bubbles appear under the nylon mesh; rapid change of the composition of the bath solution does not occur and thus exposure of slices to the test chemicals is not uniform, particularly the surface tissue; and it is not

suitable for conventional whole-cell patch-clamp recording. In the submersion type of chamber, the slice is immersed completely in oxygenated ACSF. The principal advantages are that the slice is in an environment that is more constant-free from perturbations in fluid flow, drainage, changes in "environmental" oxygen pressure, and appearance of air bubbles under the nylon mesh. Exposure of the slice to test chemicals is more uniform and the chemicals can be washed out rapidly because both sides of the slice are exposed to medium. The major disadvantages are that the field potentials are less easy to record due to shunting of currents via the bath solution; the stimulus artifacts are large; the perfusion rate has to be higher; and the series resistance may be a problem for whole-cell patch-clamp recording. Based on the authors' experience with a variety of chambers including interface and submersion chambers (home-made or commercially-produced) for neurotoxicological studies, a modified RC-26 (small volume) or RC-29 (large volume) submersion chamber assembled with a cell support (Warner Instruments) is suitable for all types of recordings in brain slices.

Perfusion system

There are many types of perfusion pumps or systems commercially available. For the purpose of general perfusion, a simple perfusion system consisting of several large syringes to feed the chamber by gravity is adequate. However, regardless of what kind of perfusion system is used, several points should be taken into consideration: the dead space or volume should be as small as possible; tubes used for perfusion should be resistant to chemicals and easy to clean and replace; and switching between solutions and control of perfusion rate should be easy. One common problem that occurs when using a multi-channel multistaltic pump to control both the perfusion and drainage of medium is that the balance between input and output of medium in the chamber is sometimes difficult to adjust. This may cause instability for recordings, especially when an interface chamber is used. This problem can usually be avoided with an RC-26-type chamber and a vacuum pump to control the drainage of the waste medium out of the recording chamber by suction (see Fig. 11.11.1).

Micromanipulators

The basic requirement for any micromanipulator is that no drift or vibration occur during recording, but requirements for fine control of movement of electrodes are different for extracellular, intracellular, and whole-cell patch-clamp recordings. For extracellular recording, a coarse-adjustment manually-operated micromanipulator such as a Narishige MP1 will work well. For intracellular recording, a manually-operated micromanipulator with fine-movement control may also work, but it will work much better if the fine movement of the micromanipulator is operated by a remote control system, as this reduces unwanted movement due to vibration applied to the manipulator by hand. For whole-cell recording in a brain slice, the manipulator should allow fine, smooth advancement of the electrode with a few microns per second or less. The best arrangement for a manipulator is when the manipulator and recording chamber are co-assembled on the same fixed platform (e.g., a Burleigh 1500 manipulator on a Gibraltar platform with an XY stage base). This greatly increases the recording stability.

Microscope

Usually, a low-power dissection microscope will work very well for extra- and intracellular microelectrode recordings in brain slices that have clear landmarks of synaptic pathways such as those from the hippocampus and cerebellum. However, for whole-cell recording in brain slices, a high-power upright microscope equipped with a Nomarski optical system is a must, unless the blind techniques are used to form the gigaohm seal. In most cases, an additional video camera system for the microscope is not necessary.

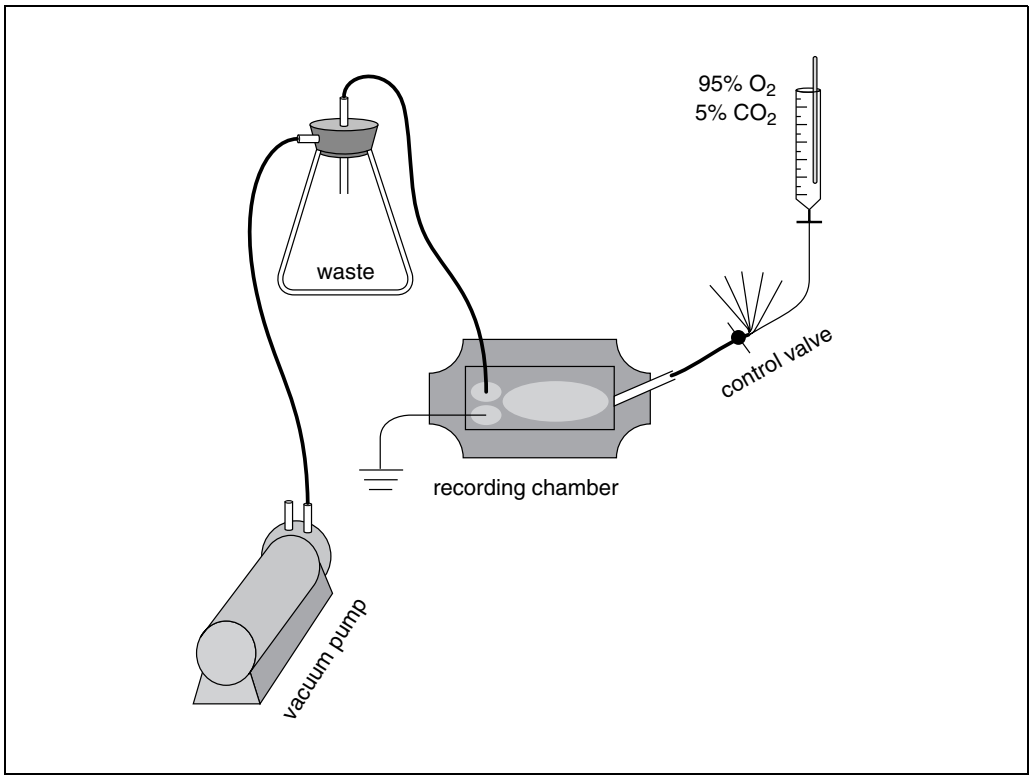

Figure 11.11.1 Schematic of the perfusion and drainage system for isolated brain slice recording. ACSF is bubbled continuously with 95% O_2/5% CO_2 in a 60-ml syringe. Six to eight input lines are controlled by a VC-6 Valve Control System (Warner Instruments) and connected to a modified RC-26 recording chamber with a glass coverslip bottom (Warner Instruments). The slice rests on a slice support so that both sides of a slice are exposed to the bath solution. The waste solution is drained away and collected into a 2000-ml flask by negative pressure with the tubing connected to a small vacuum pump (Cole-Palmer Instruments).

However, if one wishes to record from small cells, such as cerebellar granule cells or from the dendritic membranes, a video camera system may be helpful.

How to Identify Sites of Action of Neurotoxicants in Disruption of Central Synaptic Transmission?

In studying effects of neurotoxic chemicals on synaptic transmission in the CNS, one important question to ask is where and how the test chemical primarily acts to block or interfere with synaptic transmission (i.e., by pre- and/or postsynaptic mechanisms). To answer this question, several strategies can be used.

In extracellular recordings, one can compare time-courses of effects of the tested chemical on the field potentials of the postsynaptic neurons evoked by orthodromically stimulating the presynaptic fibers (Schaffer collaterals in the CA1 region of hippocampal slices) or by antidromically stimulating the axons (the alveus of hippocampal CA1 neurons) of the same population of postsynaptic neurons. The results obtained from this method may not give the precise sites where the chemical acts, but they may provide some useful clues for designing subsequent experiments.

In intracellular or whole-cell recording, quantal analysis of effects of the test chemical on spontaneously occurring and nerve-evoked postsynaptic potentials or currents can be examined. If the test chemical acts primarily by presynaptic mechanisms to reduce neurotransmitter release, then the number of quanta (i.e., quantal content) released from the presynaptic termini will be altered, the frequency of spontaneous or miniature

postsynaptic potentials or currents may be affected, but the amplitude of the postsynaptic response evoked by a quantum of transmitter (quantal size) should not be changed. In contrast, if the test chemical acts primarily at the postsynaptic sites (e.g., receptors) to antagonize the action of neurotransmitter, then the amplitudes (quantal size) of postsynaptic potentials or currents will be reduced, while the quantal content should not be changed. However, one exception is if the tested chemical (e.g., reserpine) acts presynaptically to deplete neurotransmitter and results in reduced quantal size, it may appear as a postsynaptic mechanism. Of course, if both the frequency and amplitudes of spontaneous and evoked postsynaptic responses are changed, then both pre- and postsynaptic mechanisms are likely to be involved in the effects of the test chemicals on synaptic transmission.

In intracellular or whole-cell recording, one can compare time-courses of effects of the test chemical on postsynaptic responses (EPSPs in intracellular recording or EPSCs in whole-cell voltage-clamp recording) evoked by stimulation of the presynaptic fibers or by direct application (iontophoresis, pressure ejection, or any brief pulse application) of neurotransmitters such as glutamate (Fig. 11.11.2). The rationale for comparing these responses is that fast application of neurotransmitter directly onto the dendrites of targeted neurons could mimic the process of synaptic activation yet bypass the synaptic release processes. If the test chemical acts primarily at presynaptic sites to interfere with transmitter release, then the response of the postsynaptic neuron to electrical stimulation of the presynaptic fibers would be expected to be blocked, whereas responses of the same neuron to fast application of neurotransmitter may not be affected.

One can compare time-courses of effects of neurotoxic chemicals on responses (action potentials) evoked by orthodromic stimulation of the presynaptic fibers by direct injection of depolarizing currents through the recording electrode at the postsynaptic neuronal soma, and by antidromic stimulation of the axon of the same neuron (Fig. 11.11.2). The rationale is that if the test chemical acts primarily by a synaptic mechanism to interfere with transmitter release or its postsynaptic response, then block of orthodromically-activated action potentials would be expected to occur earlier than block of action potentials evoked by current injection at the cell soma or by antidromic stimulation of the axon because the responses evoked by the latter two methods bypass the process of synaptic transmission. Actions at presynaptic versus postsynaptic sites cannot be differentiated by this method. However, if the test chemical primarily affects the processes of initiation or generation of action potentials, then time to block responses evoked by all three methods should be similar.

By analysis of the results obtained using these strategies, one can possibly identify where the test chemical has its primary action to block synaptic transmission.

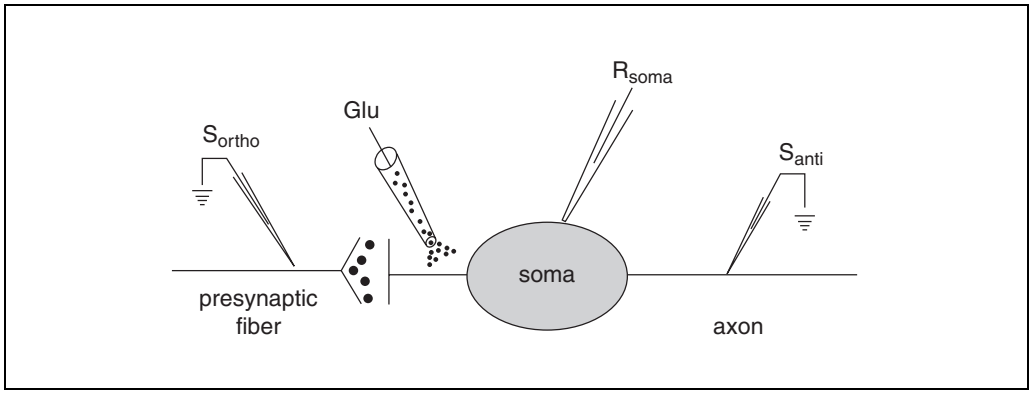

Figure 11.11.2 Schematic depiction of different methods for stimulation of a neuron. Abbreviations: Glu, direct application of glutamate onto the dendrites or soma of a neuron by iontophoresis or pressure ejection; R_{soma}, recording electrode on cell soma; S_{anti}, antidromic stimulation of the axon of the neuron; S_{ortho}, orthodromic stimulation of the presynaptic fibers.

Age of Animals for Preparation of Brain Slice

Theoretically, brain slices can be made from an animal of any age. However, it is generally believed that brain tissues of young animals have some advantages over those of older animals. For example, young animal brain tissues (1) are easier to dissect and prepare; (2) are more tolerant of anoxic damage, yielding a better chance to get good slices, and (3) use reduces the likelihood of space-clamp errors in voltage-clamp recordings. In older animals, the neurons, particularly the Purkinje cells in the cerebellum, usually have more extensive axonal and dendritic arborizations. If the process is very long or has complicated geometry, i.e., if it is highly branched, the voltage across the membrane in distant segments may differ markedly and make voltage clamp ineffective. Because membrane potentials in these distant segments of the processes will certainly deviate from the command potentials, space-clamp errors will occur. This can lead to distortions of the synaptic current recorded. In relatively young animals, while the synaptic circuits may already be established, synaptogenesis is not yet complete; as such dendritic processes may not yet have developed fully. Thus, using tissue from young animals will reduce the chances of space-clamp errors in dSEVC or whole-cell voltage-clamp recording in brain slices. If for reasons of experimental design it is necessary to use older-aged animals for slices, one can obviate some of these problems by simply pulling patches of membrane from the region of interest. This will avoid problems of space clamp.

Obviously, there are numerous other pertinent questions or considerations investigators should ask before designing experiments. For example, should the effects of a given chemical be compared on excitatory and inhibitory synaptic transmission? Should spontaneous and/or evoked synaptic responses be recorded? Should the synaptic potential (current-clamp) or currents (voltage-clamp) be measured? Should the recordings be performed at room temperature or at a temperature closer to the physiological temperature of 37°C? The authors will not discuss these issues here. Readers should refer to the detailed discussions of these and other similar issues by Langmoen and Andersen (1981), Schwartzkroin (1981), Johnston and Brown (1984), and Axon Guide (see Internet Resources).

EXTRACELLULAR MICROELECTRODE RECORDINGS IN HIPPOCAMPAL OR CEREBELLAR SLICES

BASIC PROTOCOL 1

Extracellular recording of field potentials from neurons in hippocampal slices is the most commonly used recording method for studying central synaptic function, synaptic plasticity, and pharmacological or neurotoxic effects of drugs or environmental chemicals on central synaptic transmission. Due to its well-defined tri-synaptic circuits (the perforant pathway–granule cell synapses, mossy fiber–CA3 synapses, and Schaffer collateral–CA1 synapses) and easy preparation and maintenance of stable long-lasting recording with relatively less-expensive equipment, extracellular recording in hippocampal slices is often the best starting point for those who lack, but wish to develop, experience in electrophysiological recordings in brain slices. Although this method is relatively simple, it can often be sufficient to answer general questions about effects of neurotoxic chemicals on central synaptic transmission, as well as direct further experimentation depending on the aims of the experiments.

Extracellular recording uses a relatively large tip microelectrode to record extracellular potential changes of a population of neurons in response to a given stimulus. The slices used for extracellular recording are 300 to 500 μm in thickness (see Support Protocol 1). The positioning of both recording and stimulating electrodes can be done easily with the aid of a low-power dissecting microscope. Stimulation of the presynaptic fibers (e.g., Schaffer collaterals) will evoke postsynaptic responses, which are referred to as field potentials or population spikes. Typically, an extracellular recording electrode can pick up several signal components (see Fig. 11.11.5A for an example): the presynaptic volley

corresponding to afferent spike activity, summed field excitatory postsynaptic potentials (fEPSPs), and population spikes (PSs). The amplitude, shape, and polarity of field potentials in a given slice structure may vary depending upon the relative location of the recording and/or stimulating electrodes. In this protocol, the basic steps for extracellular recording in hippocampal slices and its use in examining synaptic plasticity in brain slices will be discussed. With some minor modifications, the method can also be applied to record field potentials in other brain regions such as the cerebellum or lateral olfactory tract.

Materials

95% O_2/5% CO_2 saturated artificial cerebrospinal fluid (ACSF, see recipe)
95% O_2/5% CO_2 gas mixture source
300- to 400-μm healthy hippocampal slices (see Support Protocol 1)
3 M NaCl, optional

Perfusion system (see Fig. 11.11.1):
- 60-ml syringes
- Perfusion valve control (e.g., VC-6 valve control system, Warner Instruments)
- PE-160 tubing
- 2000-ml flask with tubing (Pyrex)
- Vacuum pump (Cole-Palmer Instruments)
- Recording chamber (interface or submersion chamber, e.g., a modified RC26 chamber assembled with a slice support, Warner Instruments)

Ag/AgCl ground electrode (e.g., REF-1L reference cell or E206 Ag/AgCl pellet electrode, Warner Instruments)

Basic electrophysiological setup:
- Microelectrode amplifier (e.g., Axoclamp-2 microelectrode clamp)
- Digidata 1200 interface (Axon Instruments)
- PC computer system installed with pClamp 8.x software
- Two manually-operated manipulators (e.g., MP1 Narishige manipulator, Narishige Scientific Instruments)
- Stimulator (Grass S88, Grass)
- Stimulus isolation unit (Grass SIU5, Grass)

Oscilloscope (Gould Instrument Systems).

Wide-bore Pasteur pipet (simply break the narrow tip end and insert it into a small rubber suction bulb)

U-shaped platinum-nylon mesh

Fiber-optic light (Dolan Jenner Industrials)

Dissection microscope (e.g., Wild M5A)

Extracellular recording pipets pulled from borosilicated glass capillaries (1.0-mm o.d., 0.5-mm i.d.; tip impedance of 5 to 15 MΩ when filled with ACSF or 3 to 4 M NaCl)

Glass microelectrode puller (e.g., Model P-97, Sutter Instruments)

Pipet filler: MicroFil MF28G needle (WPI)

Solution in-line heater SH-27B and TC-344B chamber system heater controller (Warner Instruments) or other alternative heating system (depending on the type of chamber being used), this may be required if experiments will be performed at 30° to 35°C

Concentric bipolar metal electrode or monopolar tungsten electrode (3 MΩ, FHC; alternatively, a broken-tip glass pipet filled with ACSF can also be used as the stimulation electrode)

NOTE: The oscilloscope can be replaced with the computer and monitor if appropriate software is available.

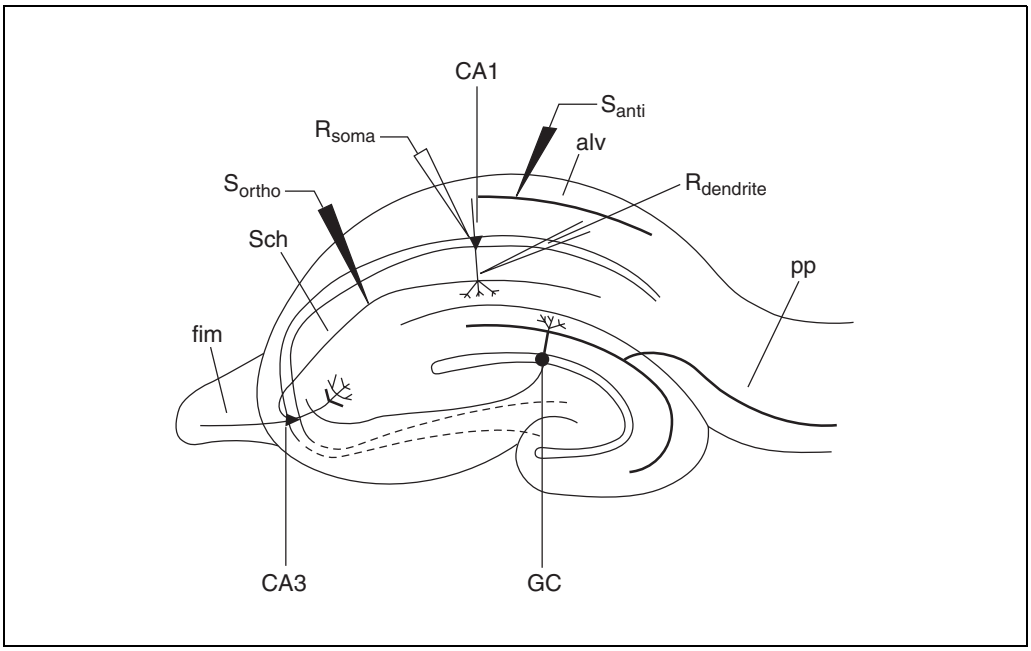

Figure 11.11.3 Schematic depiction of a structure of a transverse hippocampal slice and methods for extracellular and intracellular recordings in the CA1 pyramidal cell region by orthodromic stimulation of Schaffer collaterals and by antidromic stimulation of the alveus. Abbreviations: alv, alveus; CA1, CA1 pyramidal cell; CA3, CA3 pyramidal cell; fim, fimbria; GC, granule cells in the dentate region; PP, perforant pathway; $R_{dendrite}$, recording electrode at the apical dendrites of the CA1 pyramidal cells; R_{soma}, recording electrode at the CA1 pyramidal cell soma; S_{anti}, antidromic stimulation of the alveus; S_{ortho}, orthodromic stimulation of Schaffer collaterals.

Prepare perfusion systems and recording chamber

1. Set up the solution perfusion system and recording chamber (see Fig. 11.11.1). Turn on the vacuum. Pre-wash the recording chamber first with deionized water and then with ACSF aerated continuously with 95% O_2/5% CO_2. Make sure the reference or Ag/AgCl ground electrode is properly immersed in the bath. Turn on the basic electrophysiological setup (computer, stimulator, and amplifier) and oscilloscope.

2. Transfer a 300- to 400-µm hippocampal slice with a wide-bore Pasteur pipet into the recording chamber and gently place a U-shaped platinum frame with attached nylon mesh over the slice. Transilluminate the slice from below with a fiber-optic light. Adjust the perfusion rate to 2 to 4 ml/min and the buffer level as low as possible but be careful not to dry out the slice. Locate the CA1 pyramidal cell region under the dissection microscope (see Fig. 11.11.3).

Prepare electrodes

3. Fill an extracellular recording pipet with ACSF or 3 M NaCl, insert the pipet into the electrode holder (be sure to clean off any solution from the outside wall of the pipet) and then plug the electrode holder into the amplifier headstage (this step may vary depending on the amplifier).

4. Lower and advance the electrode into the bath. Set the oscilloscope on a proper sensitivity, i.e., mV/div level (e.g., 100 mV/div) and null the baseline. Generate 0.5 nA, 20-msec pulses from the concentric bipolar metal electrode or monopolar tungsten electrode stimulator. In "bridge mode," turn the bridge dial until the bridge is correctly balanced (see Fig. 11.11.4). Read the dial to get the electrode resistance value. Lower and advance the stimulating electrode into the bath.

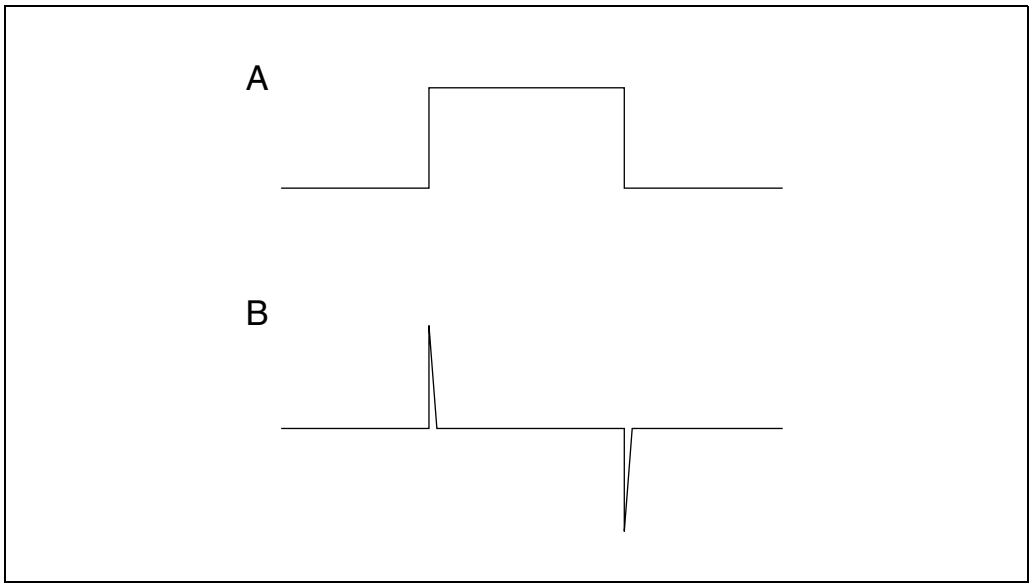

Figure 11.11.4 Schematic illustration of measurement of electrode resistance using the bridge balancing technique. (**A**) Response of electrode to a test current pulse (e.g., 0.5 nA, 20 msec), no bridge balance is used. (**B**) The bridge is correctly balanced.

Position electrodes and establish recordings

5. To record orthodromically activated fEPSPs in the CA1 region, carefully position the recording pipet ($R_{dendrite}$; Fig. 11.11.3) in the apical dendrites (stratum radiatum) of CA1 pyramidal cells and place the stimulating electrode in the Schaffer collaterals ~300 to 500 μm away from the recording electrode (S_{ortho}; Fig. 11.11.3).

6. Turn on the pulse generator to deliver stimuli at a frequency of 0.1 to 0.2 Hz, 0.1 msec, and an initial stimulus intensity (usually 3 to 5 V in the authors' experience using a Grass S88 stimulator) that produces ~50% to 60% of the maximum response.

   If no responses occur, first try to increase the stimulus intensity. If no responses still occur, reposition the stimulating electrode or the recording electrode until responses appear. If the response does not show a typical fEPSP shape, try to relocate the recording electrode at different depths and/or locations.

   Care should be taken in determining the initial stimulus intensity using the maximum responses or maximum amplitudes of fEPSPs, because when the fEPSP amplitude reaches a certain size in response to a given increased stimulus intensity, a population spike may be evoked. The appearance of a population spike in an opposite direction will certainly limit the amplitude of fEPSP for further increase (Fig. 11.11.5A) and will complicate the measurement of fEPSP amplitude, particularly if a chemical or drug were to increase the amplitude of the synaptic potential. Thus, rather than increasing the stimulus intensity to produce a peak response, it is better to set the stimulus intensity at the level at which a small population spike is just observable following the fEPSP trace. Then use this fEPSP amplitude as the peak response and reduce the stimulus intensity until it yields an fEPSP amplitude at ~50% of the peak response.

7. To record orthodromically-activated PSs in the CA1 region, simply move the recording electrode to the CA1 pyramidal cell body layer (R_{soma}; Fig. 11.11.3) while stimulating the Schaffer collaterals (S_{ortho}; Figs. 11.11.3 and 11.11.5B).

8. To obtain antidromically-evoked PSs in CA1 neurons, place the stimulating electrode in the alveus while the recording electrode remains in the CA1 pyramidal cell body layer (S_{anti} and R_{soma}; Fig. 11.11.3).

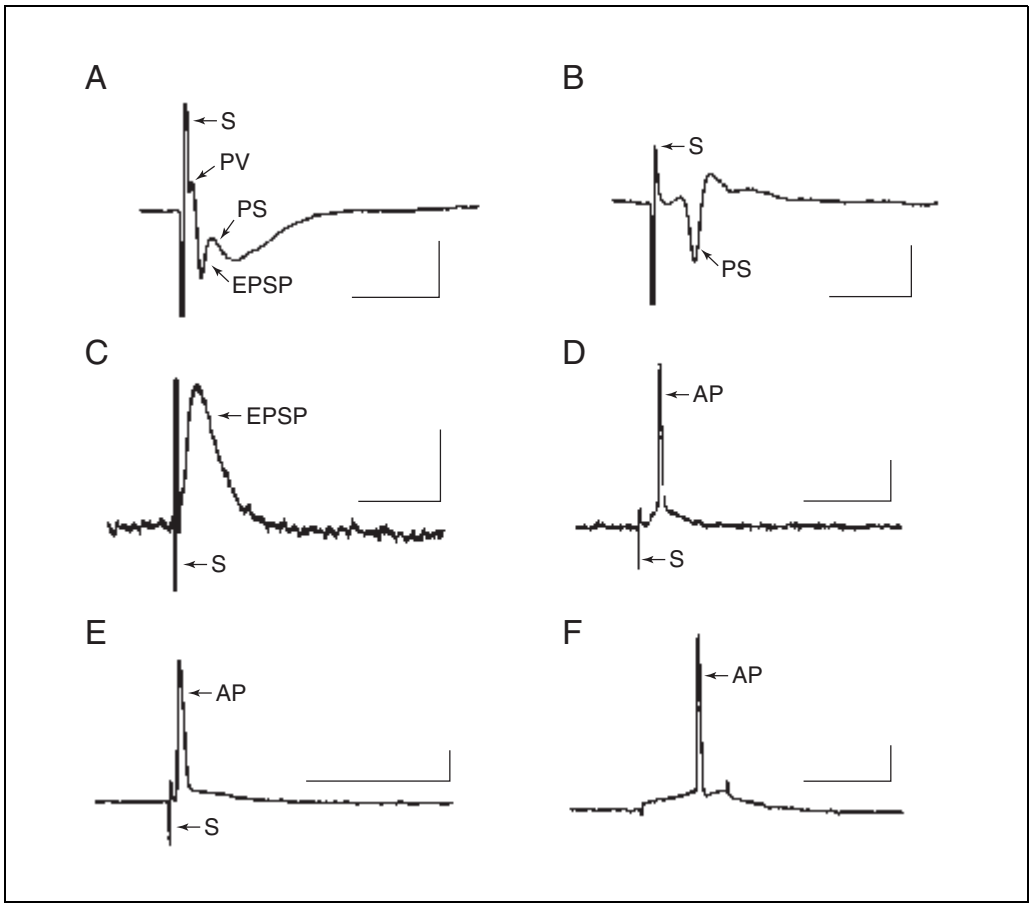

Figure 11.11.5 Representative demonstration of extracellularly recorded field potentials, intracellularly recorded excitatory postsynaptic potential (EPSP) and action potentials (APs) from the CA1 region of a hippocampal slice. (**A**) The Prevolley (PV) and the field EPSP (fEPSP) were recorded from the dendritic region of CA1 pyramidal cells by stimulating the Schaffer collaterals. Note that a positive deflection following the fEPSP was due to a strong stimulus intensity–evoked population spike (PS) at the somata. (**B**) The PS was recorded from a CA1 pyramidal cell soma area by stimulating the Schaffer collaterals. (**C**) The intracellular EPSP was recorded from an individual CA1 pyramidal cell soma by subthreshold stimulation of the Schaffer collaterals. (**D**) The AP was recorded from the same cell as in **C** but by suprathreshold stimulation of the Schaffer collaterals. (**E**) This AP was recorded from a CA1 pyramidal cell soma by antidromic stimulation of the alveus. (**F**) This AP was recorded from the same cell soma as in **E** but by injection of a depolarizing current directly through the recording electrode. "S" in each trace indicates the stimulus artifact. Calibration bars: vertical, 0.5 mV for **A** and **B**, 5 mV for **C**, 20 mV for **D**, **E**, and **F**; horizontal, 10 msec for **A**, **B**, and **E**, 20 msec for **C**, **D**, and **F**.

9. To induce long-term potentiation (LTP) of fEPSPs or PSs after the baseline response recording of fEPSPs or PSs has become stable for 30 min, apply a brief high-frequency conditioning stimulation (100 Hz, 1 sec) at the same stimulus intensity as that used to evoke the baseline responses and then return to the baseline frequency of stimulation (0.1 to 0.2 Hz, 0.1 msec) again.

   The slopes of fEPSPs or amplitudes of PSs should be increased significantly and maintained for at least 2 hr.

   Usually, field potential amplitude may increase spontaneously by 10% to 30% of the initial control value during the first 30 min of recordings. Thus exposure of slices to test chemicals and data collection should not begin until the responses have been stable for at least 30 min.

Collect data and analyze

10. To collect data in pClamp8, design a protocol in an event-detected mode in Clampex. Collect data before and after exposure to the test chemical.

11. Analysis of extracellular recording data is pretty straightforward. Analyze data using the LTP 2.22A program developed by Dr. William W. Anderson (see Internet Resources). Depending on the goals of the experiment, assess effects of the test chemical on central synaptic transmission based on the following parameters: (1) amplitudes of PSs and anti-PSs; (2) amplitude and slope of fEPSPs; (3) latency between stimulus artifact and onset of PSs or anti-PSs; (4) input/output curves (plots of presynaptic fiber volley amplitude versus stimulus intensity, fEPSP slope versus stimulus intensity, fEPSP versus presynaptic fiber volley amplitude or PS amplitude versus fEPSP slope); (5) induction and maintenance of LTP; and (6) time-courses and concentration-dependent responses to tested chemicals.

BASIC PROTOCOL 2

INTRACELLULAR RECORDING IN HIPPOCAMPAL SLICES

Unlike extracellular recording, which records responses occurring in a population of neurons, conventional intracellular recordings use a sharp electrode to penetrate the cell membrane and measure the transmembrane potential changes of that neuron at rest or in response to a given stimulus. Therefore, intracellular recording can provide more detailed information about effects of neurotoxic chemicals on the electrical behavior including resting membrane potentials, input resistance, whole-cell capacitance, synaptic responses, and action potentials (APs) of an individual neuron. Similar to extracellular recording, the initial positioning of recording and stimulating electrodes does not necessarily require a high-power microscope, this can be done simply with the aid of a dissecting microscope. However, due to the relatively small size of neurons, a much more stable recording system and more skill are required in order to obtain a stable and long-lasting intracellular recording. In this protocol, the basic steps for conventional intracellular recording in hippocampal CA1 pyramidal cells is discussed.

Materials

95% O_2/5% CO_2 saturated artificial cerebrospinal fluid (ACSF, see recipe)
95% O_2/5% CO_2 gas mixture source
300- to 400-μm healthy hippocampal slices (see Support Protocol 1)
3 to 4 M KCl or potassium acetate
Neurotransmitters of interest
500 mM glutamate in 100 mM NaCl (pH 8.0)

Perfusion system (see Fig. 11.11.1):
- 60-ml syringes
- Perfusion valve control (e.g., VC-6 valve control system, Warner Instruments)
- PE-160 tubing
- 2000-ml flask with tubing (Pyrex)
- Vacuum pump (Cole-Palmer Instruments)
- Recording chamber (interface or submersion chamber, e.g., a modified RC26 chamber assembled with a slice support, Warner Instruments)

Ag/AgCl ground electrode (e.g., REF-1L reference cell or E206 Ag/AgCl pellet electrode, Warner Instruments)
Wide-bore Pasteur pipet (simply break the narrow tip end and insert it into a small rubber suction bulb)
U-shaped platinum frame with attached nylon mesh
Microscope

Basic electrophysiological setup:
Microelectrode amplifier (e.g., Axoclamp-2 microelectrode clamp)
Digidata 1200 Interface (Axon Instruments)
PC or Macintosh computer system installed with pClamp 8.x software, MiniAnalysis 5.2.8 (Synaptosoft), or other available software
Two manipulators (one must have fine-movement control, preferably a remote, fine-movement control system—motorized, hydraulic, or piezoelectric control—e.g., MP1 Narishige manipulator, Narishige Scientific Instruments)
Grass S88 stimulator and Grass SIU5 stimulus isolation unit (Grass)
Intracellular recording pipets pulled from borosilicated glass capillaries (impedance of 80 to 120 MΩ for CA1 neurons when filled with 3 to 4 M KCl or potassium acetate

Prepare perfusion systems and recording chamber

1. Set up the solution perfusion system and chamber (see Fig. 11.11.1). Turn on the vacuum. Pre-wash the recording chamber first with deionized water and then ACSF aerated continuously with 95% O_2/5% CO_2. Make sure the reference or ground electrode is properly immersed in the bath. Turn on the computer, stimulator, amplifier, and oscilloscope.

2. Transfer a hippocampal slice into the recording chamber with a wide-bore pipet and gently place a U-shaped platinum frame with attached nylon mesh over the slice. Adjust the perfusion rate to 2 to 4 ml/min and the buffer level to an adequate level that just submerses the slice. Locate the CA1 pyramidal cell region under the microscope.

Prepare electrodes

3. Fill a glass intracellular recording pipet with 3 M KCl or potassium acetate. Insert the pipet into the electrode holder (be sure to clean off any solution from the outside wall of pipet) and insert the electrode holder into the amplifier headstage (this step may vary depending on the amplifier).

   Filling an intracellular recording pipet electrode is somewhat challenging initially. It is imperative to prevent the formation of bubbles in the tip of electrode. This is best done by taking advantage of capillary force and backfilling the electrodes. To do so, just put the backend of the electrodes in 3 M KCl or potassium acetate solution for 10 to 30 min. The solution will usually fill the tip automatically. Then back fill the rest of the tip with a Microfil, (do not fill the entire electrode yet), gently tap the electrode to remove any bubbles. Finally, back fill the rest of the electrode.

4. Lower and advance the electrode into the bath. Set the oscilloscope on a proper sensitivity, i.e., mV/div level, and null the baseline. Generate 0.5 nA, 20-msec pulses from the stimulator. In the bridge mode, turn the amplifier bridge dial until the bridge is correctly balanced (see Fig. 11.11.4) and read the electrode tip resistance from the dial. Lower and advance the stimulating electrode into the bath.

Position electrodes and establish recordings

5. To record orthodromically activated EPSPs in the CA1 pyramidal neurons, carefully position the recording electrode in the somal layer of CA1 pyramidal neurons and place the stimulating electrode in the Schaffer collaterals (S_{ortho}; Fig. 11.11.4) 300 to 500 μm away from the recording electrode (R_{soma}; Fig. 11.11.4).

6. Use the fine control on the micromanipulator to advance the electrode.

   When the tip of the electrode approaches and touches a cell, the resistance will increase and spontaneous activity of neurons can be seen as occasional small negative deflections (spikes) on the screen of the oscilloscope or computer monitor. When a large amplitude,

steady negative membrane potential drop occurs (usually −50 to −70 mV), or occasionally action potentials (60 to 80 mV in amplitude) occur, this indicates that the tip of the electrode has successfully impaled the cell membrane.

Injecting a steady negative DC current (0.1 to 0.3 nA) through the recording electrode after impalement usually helps to stabilize the cell. At this point, do not stimulate the cell, wait a few minutes to let the cell recover and allow the membrane to reseal around the electrode. After the resting membrane potential, action potential amplitude, and membrane input resistance gradually recover to the normal level, the number of spontaneous action potentials declines. The DC current injection can then be removed gradually.

Some devices can be used to aid the penetration of the cell membrane. Some investigators prefer to whistle the capacitance circuits to increase suddenly and transiently the capacitance compensation. This often leads to a successful impalement (on many amplifiers, a specific button called buzz or trick is used for this purpose). Other investigators like to penetrate the cell membrane by gently tapping the micromanipulators.

If the resting membrane potential recovers very slowly or does not recover at all, a small upward or downward movement of electrode may sometimes improve the cell membrane properties. This may indicate that the electrode tip has not penetrated the cell membrane completely, or conversely is now up against the opposite membrane or an intracellular organelle membrane. A well-penetrated CA1 pyramidal cell should typically have an action potential amplitude >60 mV, input resistance >15 MΩ and a stable resting membrane potential more negative than −55 mV.

7. After the cell has become stable, turn on the pulse generator to deliver stimuli at a frequency of 0.1 Hz, 0.1 msec, and an initial low-stimulus intensity.

   Gradually increasing the stimulus intensity should elicit a local graded positive deflection of membrane potential (i.e., EPSP). Further increasing the stimulus intensity above a certain level (threshold) will trigger a single all-or-none spike superimposed on the EPSP. Thus, the maximum EPSPs should be elicited at the stimulus intensity that is just below the threshold for spike generation (subthreshold stimulation). The evoked EPSPs normally have amplitudes of 3 to 10 mV (Fig. 11.11.5C). Usually, injecting a small, steady hyperpolarizing DC current may increase EPSP amplitude depending on the angle at which the slice is cut.

8. To initiate orthodromically activated action potentials, slightly increase the stimulus intensity just above the threshold level (suprathreshold stimulation; Fig. 11.11.5D).

   This should elicit a single action potential superimposed on the EPSP.

   Defining the threshold level for initiating action potentials is somewhat arbitrary. Usually it is defined as a stimulus intensity level for which 50% of the applied stimuli can evoke action potentials. No matter what level of stimulation will be used for initiating EPSPs or action potentials, it should be kept constant before and after exposure of slices to the test chemicals.

9. To obtain antidromically evoked action potentials in the CA1 cell soma, simply move the stimulating electrode to the alveus (S_{anti}; Fig. 11.11.3), while the recording electrode remains in the CA1 cell soma.

   Suprathreshold stimulation of the alveus usually elicits a single action potential that takes off directly from the baseline level with considerably shorter latency (Fig. 11.11.5E).

   Action potentials can be also elicited directly by injecting depolarizing currents into the CA1 pyramidal cell through the recording electrode (see Fig 11.11.5F). Low current intensity injection usually triggers only one long latency spike. With increasing current intensity, this spike may appear at progressively shorter latencies, followed by other spikes at regular intervals. Strong (1 to 3 nA), long-lasting stimulating pulses (1 to 5 sec) may trigger a high-frequency burst of spikes.

10. To evoke postsynaptic responses by direct application of neurotransmitters, use iontophoresis, pressure ejection, or other alternative fast application techniques. Apply neurotransmitters directly onto the apical dendrites of CA1 pyramidal neurons. For iontophoretic application of L-glutamate, fill a glass pipet (40 to 60 MΩ) with 500 mM glutamate in 100 mM NaCl (pH 8.0) and position it at the apical dendrites of CA1 neurons. Eject the glutamate by passing a 20 to 100 nA negative current for 30 to 40 msec with a retaining current of 0 to 5 nA.

    The retaining current keeps the glutamate from leaking out of the pipet.

    Alternatively, a picospritzer can be used for pressure ejection, e.g., Ultrafast Solution Switching System (Burleigh) or U-tube application system can be used to apply the desired neurotransmitter directly onto the apical dendrites of CA1 pyramidal cells.

    Care should be taken when using a direct application of neurotransmitters to bypass the neurotransmitter release process, because many receptors such as glutamate receptors, neuronal nicotinic acetylcholine receptors, or $GABA_A$ receptors can be easily and rapidly desensitized. This is important, because most neurotransmitter receptors desensitize if the transmitter agonist remains in continuous contact with the receptors. In order to avoid desensitization of receptors, the application pulse of transmitter should be as short as possible, while the intervals between application pulses should be as long as possible. For example, drug application could be every 10 sec with an application pulse of only 0.1 sec.

Collect data and analyze

While considerable thought should be given ahead of time to experimental design, one of the truly nice features of electrophysiological recording experiments is that one can modify the design on the fly to take advantage of the preparation as long as it remains viable. Seasoned electrophysiologists will routinely add on components to an ongoing experiment to make maximal use of a viable preparation.

11. Again, do not start exposure to test chemicals and data collection until the recording becomes stable. To acquire data in an acquisition program such as Clampex, design a protocol in event-detected mode to record evoked synaptic responses. Also, save data to a tape recorder or other system for backup and offline analysis purposes.

12. Analyze data using one of a variety of commercially available software programs such as pClamp 8.x, MiniAnalysis 5.2.8, or other available software. Depending on the aims of the experiment, assess effects of the test chemicals on synaptic transmission based on the following parameters: effects of the chemical on (1) the resting membrane potentials; (2) amplitudes and threshold of action potentials evoked by different methods; (3) latency from the stimulus artifact to the onset or peak of action potentials evoked by orthodromic or antidromic stimulation; (4) amplitude, latency from stimulus artifact to onset of intracellular EPSPs, 10% to 90% rise time, half-width (the time from the point at which the event has risen to half of the peak amplitude to the time at which it has decayed to half of the peak amplitude), and decay time; (5) time-courses and concentration-dependence of responses of the tested chemicals; (6) sites of action of chemical (presynaptic and/or postsynaptic mechanisms); and (7) ability of the tested chemical to alter the response to a known pharmacological agent.

BASIC PROTOCOL 3

WHOLE-CELL CURRENT RECORDINGS IN PURKINJE OR GRANULE CELLS IN CEREBELLAR SLICES

Compared to extra- and intracellular recordings, whole-cell patch-clamp recording in brain slices allows a more in-depth analysis of synaptic transmission between neurons in the central nervous system. Unlike patch-clamp recordings in cells that are either acutely dissociated or cultured (see *UNIT 11.12*), whole-cell patch-clamp recordings in brain slices usually require some special steps or treatments prior to making a gigaohm seal on the targeted neurons. Currently, three main methods or techniques are commonly used to obtain whole-cell recordings from neurons or glial cells in brain slices. They are so-called cleaning, blind, and blow-and-seal techniques (see Background Information). The blow-and-seal method, which combines the advantages of both the cleaning and the blind techniques, will be applied in this protocol to make whole-cell recordings in cerebellar Purkinje and granule cells. In this method, the thin cerebellar slice is placed in a submersion chamber mounted on the fixed stage of a high-power upright microscope equipped with Nomarski optics and an infrared CCD video camera system. The entire process including approaching the cell and making a seal on its membrane is visually monitored.

Materials

Thin 150- to 200-μm cerebellar slice (see Support Protocol 2)

ACSF (see recipe), ice cold and saturated with 95% O_2/5% CO_2

Intracellular pipet solution: the composition of pipet solution is highly dependent on the experimental purpose or design (see recipes for internal pipet solutions and KGlu-based pipet solution, and Critical Parameters)

Glutamate receptor blockers such as 6-cyano-7-nitroquinoxaline-2,3-dione (CNQX, 10 to 20 μM) for kainate/AMPA receptors and D,L-2-amino-5-phosphonopentanoic acid (APV, 50 to 100 μM) for NMDA receptors or CNQX, APV, and tetrodotoxin (TTX, 0.5 to 1 μM)

Electrophysiological setup:

- Axopatch 200B and Digidata 1200B interface (Axon Instrument); or a comparable circuit, microcomputer system installed with pClamp 8.x software and MiniAnalysis program 5.2.8 (Synaptosoft) or similar software for data analyses
- Two hydraulic or step-driven control micromanipulators such as the Burleigh 5000-150 series manipulators (Burleigh Instruments)
- Grass S88 stimulator and SIU5 stimulus isolation unit (Grass)

Platinum frame with attached nylon mesh

Microscope setup: Nikon E600FN (Zeiss Axioskop 2 FS or Olympus BX50WI) upright microscope equipped with Nomarski optics (at least 40× water-immersion objective, 2 mm long working distance), infrared CCD video camera system, and a black-and-white monitor (Sony). Ideally, mount the microscope on a fixed and stable platform, e.g., Gibraltar platform with an X-Y stage base, and mount all manipulators and chamber on the same platform.

Recording chamber (submersion chamber, e.g., an RC26 assembled with an SS-3 slice support, Warner Instruments)

Ag/AgCl ground electrode (e.g., REF-1L reference cell or E206 Ag/AgCl pellet electrode, Warner Instruments)

Pipet filler: MicroFil MF28G needle (WPI) or home-made pipet filler pulled from a 1-ml plastic syringe

Pipets coated with Sylgard 184 for whole-cell recording (1.5-μm o.d., 0.75-μm i.d. glass pipets) for Purkinje cells or (1.5-μm o.d., 1.0-μm i.d. glass pipets) for granule cells (see Critical Parameters)

10-ml syringes

continued

Stimulating electrode: a concentric bipolar metal electrode or monopolar tungsten electrode (3 MΩ, FHC; alternatively, a broken tip glass pipet filled with ACSF can be used as the stimulation electrode)

Prepare recording system

1. Turn on computer, amplifier, oscilloscope, and microscope. Load the data acquisition program such as Clampex of the pClamp 8.x software. Prewash the recording chamber with deionized water and then oxygenated ACSF. Check if the ground pellet is properly immersed in the bath. Check if the silver wire of the pipet holder needs to be chlorided or the pipet holder needs to be cleaned.

   The pipet holder should be cleaned regularly after use.

2. Transfer a thin (150- to 200-μm thick) sagittal cerebellar slice (see Support Protocol 2) from the holding chamber to the 150-μl RC-26 recording chamber assembled with an SS-3 slice support. Gently put a home-made platinum frame with attached nylon mesh over the slice, then perfuse the chamber continuously with oxygenated ACSF at a rate of 2 to 5 ml/min.

   The original RC-26 recording chamber does not have the SS-3 slice support; some slight modification is needed to assemble it. Even if an RC-29 recording chamber, which is assembled with the SS-3 slice support, is used, some modification may still need to be made to improve the accessibility for the electrodes.

   Regardless of the rate of perfusion used, make sure it is consistent for every experiment. This should be done before recordings begin, otherwise, it will be difficult to compare individual experiments from day to day. This is because the onset of effects of a given chemical is usually affected by the perfusion rate.

3. Lower the 40× water-immersion objective lens until it touches the bath solution to form a water column. Focus and select a healthy Purkinje cell or granule cell. For a better view of the granule cells using the video monitor, change the light path to video camera path of the microscope and switch the infrared filter into position. Adjust the light and zoom on tube to get a better image. When done, switch back to the regular light path.

   Healthy cells have smooth, soft, clearly visible, and phase-bright cell membranes under phase contrast. The healthy cell membrane can be easily dimpled by the ejected solution stream emanating from the tip of the approaching pipet with positive pressure to the back of pipet. Conversely, unhealthy cells usually have a uniform dark, rough and crinkled appearance with a shrunken cell body, or membrane with granular-like patches. Unhealthy Purkinje cells may also look like ghost cells and appear transparent.

Prepare recording pipet electrode

4. Obtain a freshly pulled and Sylgard-coated pipet for whole-cell recording in a Purkinje cell or granule cell (see Critical Parameters). Carefully polish the electrode to the desired shape and resistance (1.5 to 3 MΩ for Purkinje cell; 6 to 10 MΩ for granule cell) just before use.

5. Fill the pipet with intracellular pipet solution and insert it into the pipet holder, which is already tightly attached to the amplifier headstage.

   Filling a large-bore electrode for whole-cell recording in a large cell, such as a cerebellar Purkinje cell, is not difficult, but to fill a small-tip pipet for whole-cell recording in a much smaller cell such as a cerebellar granule cell may be challenging. One way is to drop one small drop of intracellular pipet solution on a piece of clean Parafilm and dip the tip of the pipet in the solution for a few seconds. Then back fill the pipet tip with a MicroFil MF28G needle or home-made pipet filler pulled from a 1-ml plastic syringe. Gently tap the pipet to remove any trapped air bubbles and then fill the pipet up to ~50% to 70% of its total length. Do not fill it entirely.

6. Apply gentle positive pressure to the back of the patch electrode either by mouth or through a 10-ml syringe (~0.1 ml) and then close the two-way (if using mouth) or three-way (if using syringe) valve to keep the pressure on.

   The primary purpose of applying positive pressure to the back of the pipet electrode is to prevent the particles on the surface of the bath solution from clogging the tip of the pipet electrode when the electrode tip is advanced into the bath. In addition, maintaining a positive pressure on the back of the pipet electrode is helpful in cleaning the tissue debris or surface tissue over the cell if deeper cells are chosen for recording (see below).

   Because most chemicals used in neurotoxicological experiments are very toxic, caution should be taken when using the mouth to apply positive pressure or suction to the pipet.

Position recording electrodes

7. Raise (defocus) the water-immersion objective lens slightly (do not lose the water column) to provide more working space for managing the pipet electrodes. Adjust the access angle of the recording electrode to be as large as possible.

   With the 2-mm working distance and access angle of 45° water-immersion objective (Nikon E600FN), the authors normally have a 35° to 40° electrode access angle.

   Make a mark on the manipulator once the access angle is optimally set, so subsequent attempts to adjust the electrode access angle can be made more rapidly.

8. Lower and advance the electrode tip into the bath solution, set the lowpass bessel filter at 5 kHz and a proper output gain level depending on the tip resistance of the recording pipet. Turn on the seal test switch on the amplifier or run Seal Test program in Clampex and monitor the response of the electrode to a test pulse on the computer screen or oscilloscope (experimenter's preference).

   One can directly read the electrode resistance from the built-in Seal Test program in Clampex if using pClamp 8.x software to acquire data, or alternatively calculate the electrode resistance using Ohm's law by measuring the current generated by a 10-msec and 5- to 10-mV test pulse (Fig. 11.11.6A).

   Electrode resistance should be monitored during electrode advancement. Any increase in resistance before touching the targeted cell indicates clogging of the electrode tip either by residual particles in the pipet, bath solution, or slice tissue debris; any of these will interfere with the formation of a high-resistance seal. Apply more positive pressure to clear the pipet tip or change to a new electrode.

9. Find the electrode under the 40× water-immersion objective lens. In the Seal Test mode, advance the electrode using the coarse control of the manipulator while continuously focusing on the tip of electrode until it is close to the targeted cell.

   Finding an electrode directly in the microscopic field under a 40× water-immersion objective lens is difficult for the first-time user. It can become very frustrating not to be able to find the electrode for several minutes. However, with practice, it will become easier. One way to do so is to raise the objective lens (as described in the step 7), and monitor, by eye, the advancement of the electrode tip from the side view until the electrode tip is approximately in the center of the objective lens. Then look through the eye piece and change focus to move the electrode back and forth until the shadow of the electrode is visible. Then focus directly on the electrode while advancing it towards the tissue.

10. Zero the baseline by adjusting the pipet offset of the amplifier (null the junction potential of electrode). Use the remote fine control (e.g., PCS-503 Axis Control Unit of a PCS-5200) of the manipulator to approach the selected cell soma slowly. Just before the tip of the pipet touches the cell membrane, watch for the tissue debris on the cell surface being blown away by the wave of ejected solution streaming out of the pipet tip (this helps to clean the surface of the targeted cell).

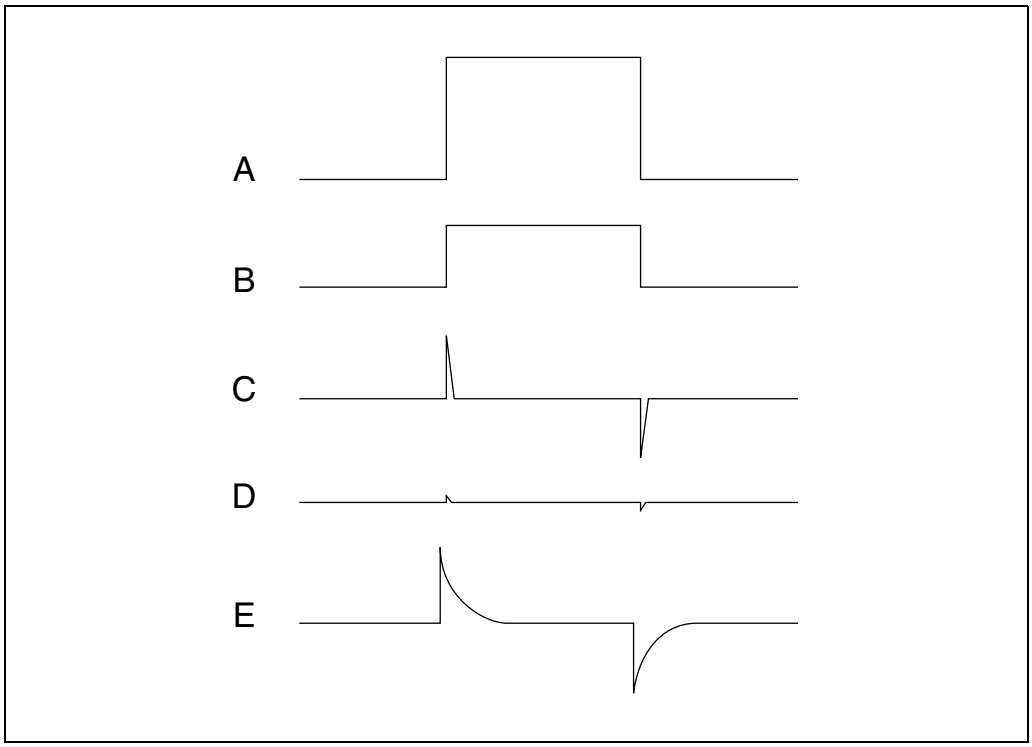

Figure 11.11.6 Schematic of steps involved in making a whole-cell recording. (**A**) Response of the patch pipet to a test pulse (e.g., 5 mV, 10 msec). (**B**) The current pulse decreases as the pipet tip touches the cell membrane (due to increased seal resistance). (**C**) Gigaohm seal formation after application of a slight negative pressure to the pipet. (**D**) After cancelling the capacitance transients. (**E**) After rupturing the cell membrane to establish whole-cell recording configuration (no whole-cell capacitance and series resistance compensation have yet been done).

If the ejected solution stream pushing away the surface tissue debris is not seen, either the pipet tip is clogged or no positive pressure is being added to the back of the pipet. In either case, a good gigaohm seal will not be obtained.

11. If recording from a Purkinje cell, continue to advance the electrode until it touches the cell and causes a slight dimple on the cell membrane. Then immediately release the positive pressure by opening the valve. At this point, the size of square current pulse on the screen of the computer or oscilloscope should decrease to ⅓ to ½ or the seal resistance should increase (Fig 11.11.6B). Apply slight negative pressure by mouth or syringe and a negative potential of −50 to −60 mV to the pipet until a gigaohm seal forms (Fig. 11.11.6C). Once the gigaohm seal is established, release the negative pressure and remove the negative holding potential.

If recording from a granule cell, these steps may be much easier if done while viewing the video monitor screen.

12. Cancel the capacitance transients by using the fast and slow pipet capacitance compensation circuits (Fig. 11.11.6D). To rupture the cell membrane, apply strong suction by mouth or use a 10-ml syringe or the zap button (see the amplifier manual for more information). Once the whole-cell recording configuration is established (Fig. 11.11.6E), examine the membrane capacitance (C_m), membrane resistance (R_m), and electrode access resistance (R_a) using the built-in Membrane Test program of Clampex or immediately perform whole-cell capacitance and series resistance compensation. Record these initial values.

Before rupturing the cell membrane, one should determine if it is important to record the initial zero-current potential (or resting membrane potential) when rupturing the mem-

brane or to monitor if the currents of interest run down or run up during dialysis of the cell with the pipet solution. To record the initial zero-current potential immediately after rupturing the membrane, run a ramp protocol over a range of voltages (e.g., from −120 mV to +80 mV, depending on the experimental aims and the cell type) immediately after rupturing the cell membrane. To monitor changes in the currents of interest during dialysis of the cell with intracellular pipet solution, run a properly designed single-voltage step immediately after rupturing the cell membrane. At the same time one should be able to make all the needed adjustments including whole-cell capacitance and series resistance compensation during the pulse intervals.

13. Start collecting data. To record spontaneous synaptic currents, run a gap-free protocol in Clampex with a membrane holding potential of −60 to 80 mV. To examine specific effects of neurotoxic chemicals on spontaneous inhibitory postsynaptic currents (sIPSPs) or miniature inhibitory postsynaptic currents (mIPSCs; Fig. 11.11.8), include glutamate receptor blockers such as 6-cyano-7-nitroquinoxaline-2,3-dione (CNQX, 10 to 20 μM) for kainate/AMPA receptors and D,L-2-amino-5-phosphonopentanoic acid (APV, 50 to 100 μM) for NMDA receptors or CNQX, APV, and tetrodotoxin (TTX, 0.5 to 1 μM) in the bath solution, in addition to using a CsCl-based pipet solution (see recipe).

    In contrast, if one is particularly interested in examining effects of chemicals on spontaneous or miniature excitatory postsynaptic currents (sEPSCs or mEPSCs), use a pipet solution with a reduced Cl^- concentration (see Reagents and Solutions). In addition, include a $GABA_A$ receptor antagonist such as bicuculline (10 to 20 μM) or picrotoxin (100 μM), or bicuculline or picrotoxin plus TTX in the bath solution.

14. To examine effects of the test chemicals on evoked synaptic responses in Purkinje cells, stimulate the climbing fibers or parallel fibers to generate climbing fiber–Purkinje cell (CF-EPSCs) or parallel fiber–Purkinje cell excitatory post-synaptic currents (PF-EPSCs). To record CF-EPSCs, establish the whole-cell recording configuration (R_{PC}; Fig. 11.11.7) on a Purkinje cell in a sagittal slice with a holding potential of −60 mV. Place a stimulating electrode (S_{CF}; Fig. 11.11.7) in the white matter or granule cell layer near the targeted Purkinje cell. Turn on the pulse generator to deliver stimuli at a frequency of 0.1 Hz, 0.1 msec and an initial low-stimulus intensity to stimulate the climbing fibers. Gradually increase the stimulus intensity until all-or-none CF-EPSC responses appear (Fig. 11.11.8).

15. To record PF-EPSCs (Fig. 11.11.8), place a stimulating electrode (S_{PF}; Fig. 11.11.7) in the molecular layer of a transverse slice and establish the whole-cell recording configuration on a Purkinje cell with a holding potential of −60 mV. Deliver stimuli at a frequency of 0.1 Hz, 0.1 msec and an initial low stimulus intensity. Gradually increase the stimulus intensity until it produces an EPSC amplitude of ~50% to 60% of the maximum response for a given cell.

16. To record the mossy fiber–activated granule cell excitatory postsynaptic currents (MF-EPSCs; Fig. 11.11.8), establish the whole-cell recording configuration (R_{GC}; Fig. 11.11.7) on a granule cell with a holding potential of −60 mV in either a sagittal or transverse slice and place a stimulating electrode in the white matter or granule cell layer near the targeted granule cell to activate the mossy fibers at 0.1 Hz, 0.1 msec, and an initial stimulus intensity that evokes EPSCs with amplitudes of ~50% to 60% of the maximum response for a given cell.

    The relative locations of stimulating and recording electrodes are important for evoking synaptic responses, particularly for CF-EPSC recordings. Adjustments of stimulating electrode location are often required to get evoked responses.

17. To generate a current-voltage (I-V) relationship of evoked synaptic responses, change the holding potentials manually from −100 to +60 mV. At each potential, record

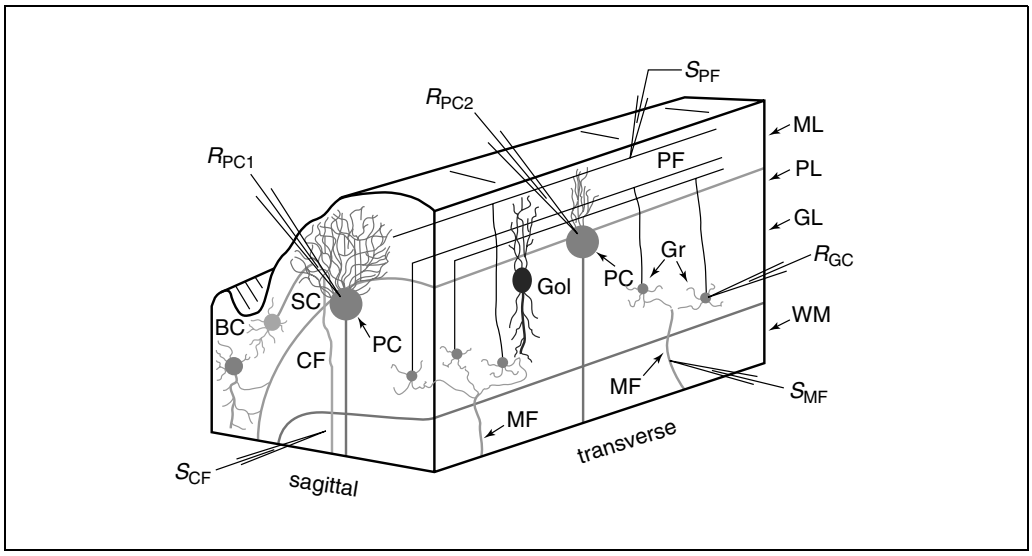

Figure 11.11.7 A schematic depiction of the architecture of the cerebellar cortex in sagittal and transverse slices, methods for whole-cell current recordings in Purkinje and granule cells, and locations of stimulating electrodes. Abbreviations: BC, basket cell; CF, climbing fiber; Gol, Golgi cell; GL, granule cell layer; Gr, granule cell; MF, mossy fiber; ML, molecular layer; PC, Purkinje cell; PF, parallel fiber; PL, Purkinje cell layer; R_{GC}, whole-cell recording electrode on a granule cell; R_{PC}, whole-cell recording electrode on a Purkinje cell in a transverse or sagittal slice; S_{CF}, stimulating electrode for climbing fiber; S_{MF}, stimulating electrode for mossy fiber; S_{PC}, stimulating electrode for parallel fiber.

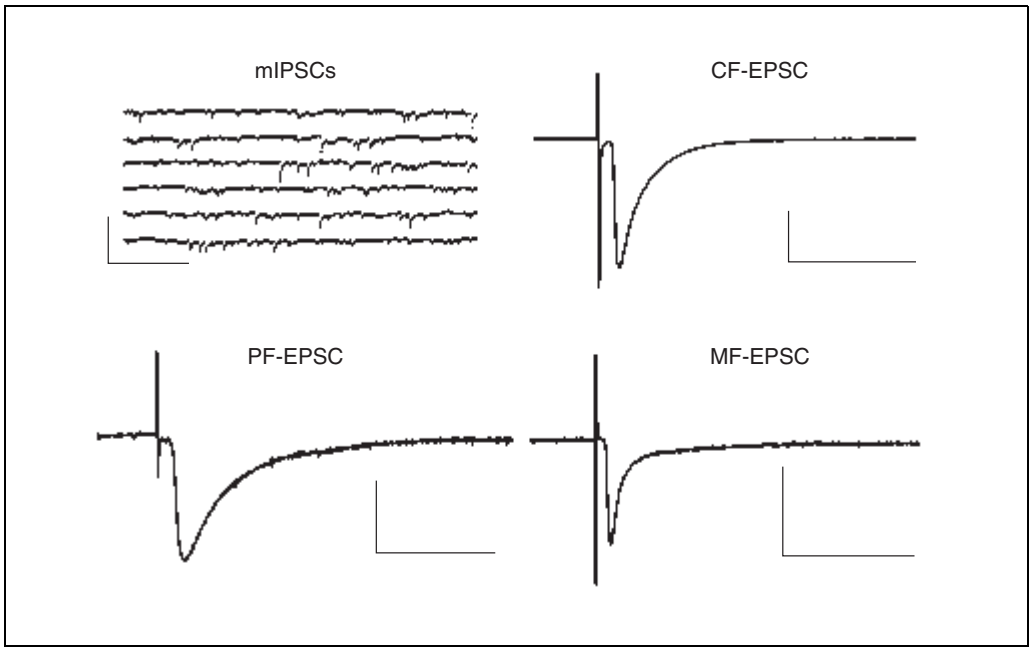

Figure 11.11.8 Representative depiction of miniature inhibitory postsynaptic currents (mIPSC), climbing fiber-Purkinje cell EPSC (CF-EPSC), parallel fiber- Purkinje cell EPSC (PF-EPSC), and mossy fiber-granule cell EPSC (MF-EPSC) recorded from a Purkinje cell or granule cell of sagittal or transverse cerebellar slices. The miniature spontaneous inhibitory postsynaptic currents (mIPSCs) were recorded from a Purkinje cell (R_{PC1}) in a sagittal slice in the presence of 0.5 μM TTX, 10 μM CNQX, and 100 μM APV. The CF-EPSC was recorded from the same Purkinje cell (R_{PC1}) by stimulation of climbing fibers with a broken-tipped glass pipet (S_{CF}) in the white matter near the Purkinje cell. The PF-EPSC was recorded from a Purkinje cell (R_{PC2}) in a transverse slice by stimulation of the parallel fiber in the molecular layer (S_{PF}). The MF-EPSC was recorded from a granule cell (R_{GC}) in a sagittal slice by stimulation of mossy fibers in the white matter (S_{MF}). Calibration bars: vertical, 200 pA for mIPSCs and MF-EPSC, 2 nA for CF-EPSC, 1 nA for PF-EPSC; horizontal, 1000 msec for mIPSCs, 20 msec for CF-EPSC, PF-EPSC, and MF-EPSC.

multiple traces (>10 traces depending on the trace-to-trace variation) for signal averaging.

Collect data and analyze

18. After the baseline recording becomes stable, expose the slice to the test chemicals and collect data. To acquire data in Clampex, design at least two different protocols. Design one protocol in the gap-free mode to record spontaneous synaptic responses. Design the other in the event-detected mode to record evoked synaptic responses. Filter currents at 1 to 5 kHz and digitize at 10 to 20 Hz. Save the data to a tape recorder, videotape, or optical disk for backup and offline analysis purposes.

19. Analyze data using Clampfit of pClamp 8.x and MiniAnalysis program 5.2.8 or other commercially available software. Assess the effects of the chemical on whole-cell synaptic currents in terms of (1) changes in frequency and amplitude of spontaneous responses; (2) changes in amplitudes of evoked responses; (3) changes in 10% to 90% rise time, half-width, or decay time of synaptic currents; (4) changes in I-V relationship, reversal potentials, or zero current potentials; (5) time-courses of effects of chemical on PF-EPSCs, CF-EPSCs, and MF-EPSCs and spontaneous synaptic currents; (6) concentration- and time-dependent responses and interaction of the test chemical with known relevant pharmacological agonists or antagonists.

SUPPORT PROTOCOL 1

PREPARATION OF ACUTELY ISOLATED HIPPOCAMPAL SLICES

This protocol is used to prepare hippocampal slices with the aid of a tissue chopper. The slices produced by this method are usually 300 to 500 μm in thickness and suitable for extracellular and intracellular microelectrode recordings, and even whole-cell patch-clamp recording using the so-called blind techniques.

NOTE: All protocols using live animals must first be reviewed and approved by an Institutional Animal Care and Use Committee (IACUC) and must follow officially approved procedures for the care and use of laboratory animals.

Materials

95% O_2/5% CO_2–saturated slicing solution (see recipe), 4°C
95% O_2/5% CO_2 gas mixture cylinder
ACSF (see recipe)
Rubber cement
10- to 30-day-old rats (either gender; Sprague-Dawley or Charles River)

500-ml glass beaker
Whatman no. 1 or no. 2 filter paper
Tissue chopper
Single-edged and high-quality double-edged razor blades
Rat guillotine
Large surgical scissors
Small sharp dissecting scissors
Rongeurs
50- or 75-mm plastic petri dishes
Blunt plastic knives (remove sharp edges and smooth with fine sandpaper)
Fine, soft artist's paintbrush
Home-made slice holding chamber (Fig. 11.11.9)

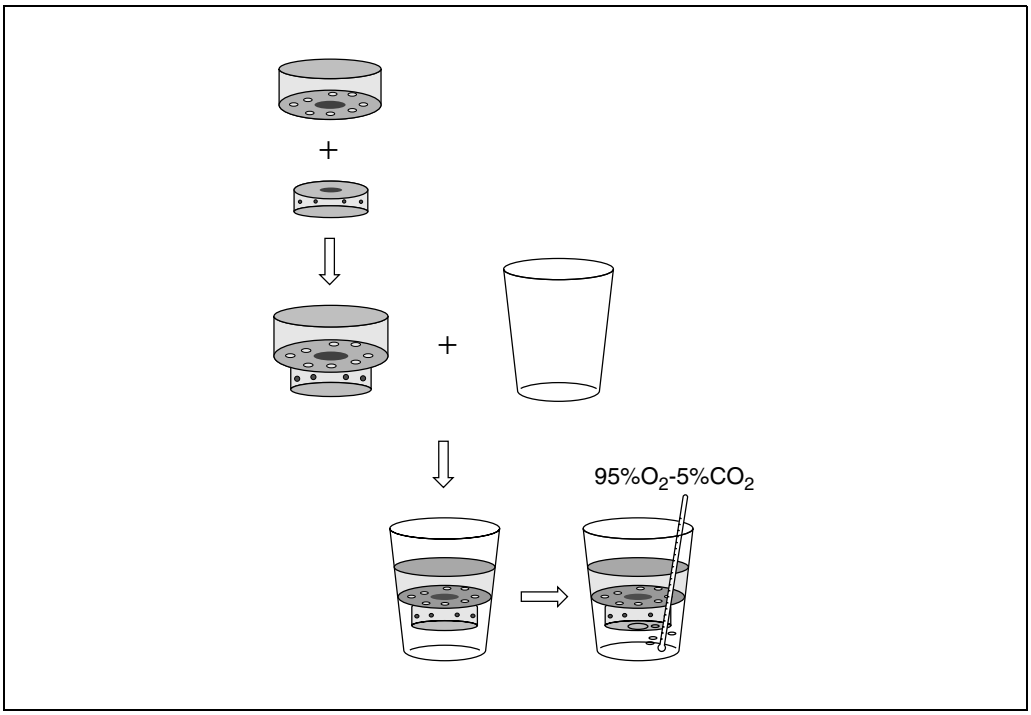

Figure 11.11.9 Diagram of a home-made slice holding chamber. To construct, drill a 20-mm diameter hole in the center and six to ten small holes around it in the bottom of a 60 × 15–cm plastic petri dish. Also, drill a 20-mm diameter hole in the bottom of a 35 × 10–plastic petri dish and several small holes in the wall. Glue a nylon mesh on top of the 35 × 10–cm plastic petri dish with super glue. Turn the 35 × 10–cm petri dish upside down and glue it to the bottom of the 60 × 15–cm petri dish (bottom to bottom). Place the two-petri-dish complex in a 100-ml plastic beaker. Add ACSF or slicing buffer and insert two small polyethylene tubes for aerating with a 95% O_2/5% CO_2 gas mixture.

Prepare slicing solution and tissue chopper

1. Make up 300 ml of cold slicing solution in a 500-ml glass beaker. Oxygenate it with a 95% O_2/5% CO_2 gas mixture for at least 15 min, and adjust pH to 7.35 to 7.4. Surround the beaker with ice and keep aerating it with the 95% O_2/5% CO_2 gas mixture. Make up 1000 ml of ACSF (see recipe).

2. Cut a piece of 3 × 5–cm Whatman no. 1 or no. 2 filter paper and glue it on the cutting platform of the tissue chopper with rubber cement. Carefully break a double-edged razor blade into two single-edged parts. Put one half into the blade clamper of the tissue chopper and loosely clamp it. Lower and gently place the blade cutting edge on the filter; make sure no gaps exist between the filter paper and the cutting edge of the blade. Then tighten the clamp. Return the chopper to the stop position and put it aside to avoid an accidental cut.

   Be sure to remove the blade from the tissue chopper after use.

Isolate hippocampus

3. Sacrifice 10- to 30-day-old rats using the proper procedures approved by an Institutional Animal Care and Use Committee and following the NIH guideline for animal care and use and then decapitate the animal with the rat guillotine.

   Anesthetics are often applied when sacrificing animals. However, care should be taken when using anesthetics for euthanasia prior to brain slice experiments, because anesthetics interact with both neurotransmitter receptors and voltage-gated channels. How readily an anesthetic can be removed from the brain will determine whether or not that agent affects the potentials or currents recorded in a slice. For example, if the purpose of a proposed

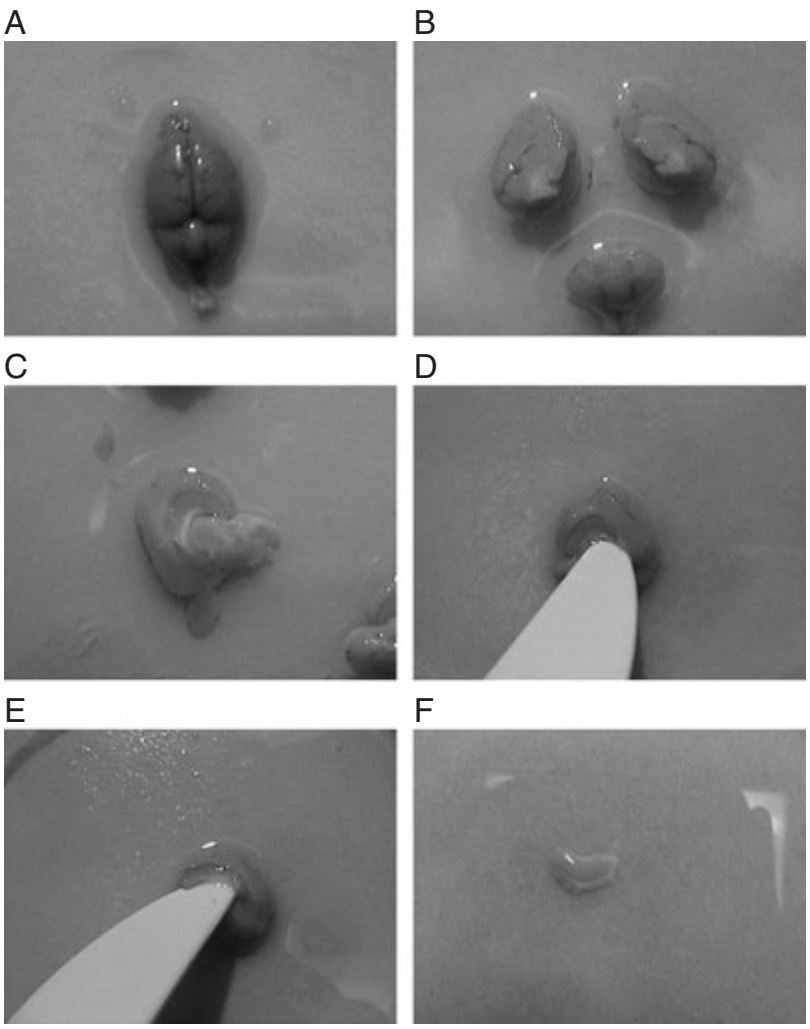

Figure 11.11.10 A photograph of a dissection of the hippocampus from rat brain. (**A**) Dorsal view of the whole brain. (**B**) Overview of the brain hemispheres and cerebellum after two cuts. (**C**) Exposure of the hippocampal formation. (**D**,**E**) Cutting the septal and temporal ends of the hippocampus. (**F**) Isolated hippocampus with the alveus side up.

experiment is to examine effects of certain insecticides on $GABA_A$ receptor–mediated inhibitory synaptic transmission, there could be pronounced interaction between the insecticide and the anesthetic, because most anesthetics can directly interact with $GABA_A$ receptors.

4. Use large surgical scissors to cut the scalp and small sharp dissecting scissors to cut the skull along the midline. Take care to avoid cutting or damaging the underlying brain tissue by keeping the tip of the scissors against the top inside wall of the skull. Pull the skull away with rongeurs.

5. Pour some cold slicing solution over the brain immediately after exposure of the brain. Remove the overlying membrane, detach all nerves and blood vessel connections, and isolate the whole brain.

6. Place the isolated brain immediately on the filter paper premoistened with the cold slicing solution in a 50- or 75-mm petri dish on ice (Fig. 11.11.10A). Wash the brain several times with the cold and oxygenated slicing solution.

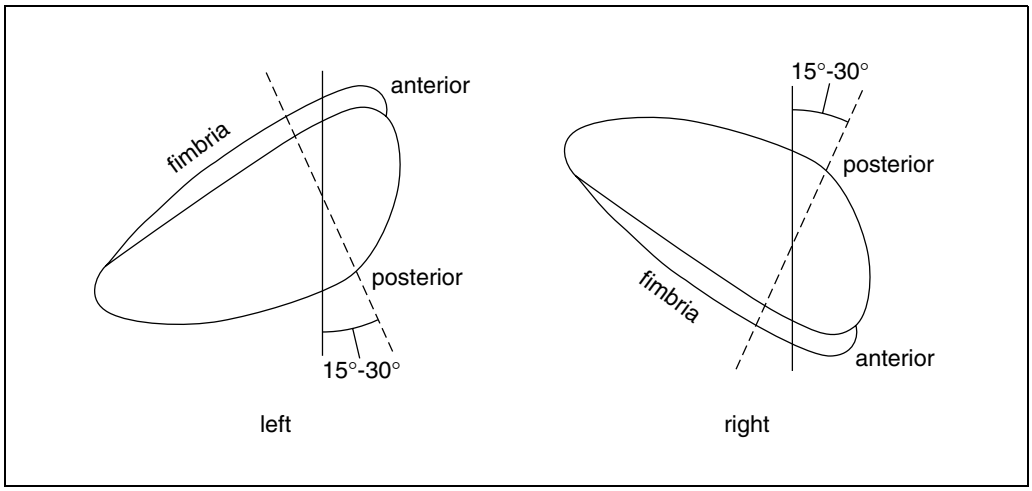

Figure 11.11.11 A diagram of the orientation and cutting angles for slicing the hippocampus. The solid lines represent the orientation of the razor blade. The broken lines indicate the transverse plane of the longitudinal axis of the hippocampus.

7. Dissect away the cerebellum and bisect the rest of the brain sagittally into two halves, rotate the hemispheres with their medial face up (Fig. 11.11.10B).

8. Gently hold down the brain-stem or hemibrain with a finger or plastic knife while using another knife to push the occipital cortex downwards until the whole medial and inferior side of the hippocampal formation are exposed (Fig. 11.11.10C). Cut both the septal and temporal ends of the hippocampus with a plastic knife (Fig. 11.11.10D,E) and rotate the knife gently to roll the hippocampus out of the brain tissue. With the hippocampal formation lying with the dentate area side down and the alveus side up, carefully trim the fimbria and free the hippocampus (Fig. 11.11.10F).

   It is essential that the brain be kept moist and cold during the isolation of the hippocampus. Although it is important to dissect quickly, take care not to damage tissue during dissection.

Slice the hippocampus

9. Thoroughly wet the filter paper on the platform of the tissue chopper with the slicing solution but without leaving excess fluid on the surface. Place one hippocampus with a fine, soft artist's paintbrush on the filter paper (the alveus side up). If the right hippocampus is used, gently rotate it clockwise to a ~15° to 30° angle; if the left hippocampus is used, rotate it counter-clockwise to a ~15° to 30° angle between the transverse plane and the longitudinal axis of the hippocampus (Fig. 11.11.11).

   Excitatory pathways are better preserved when slices are cut at an angle of 15° to 30° between the transverse axis and the longitudinal axis of the hippocampus, whereas the recurrent inhibitory pathways are better reserved if the angle is 30° to 45°.

10. Make the first transverse cut 2 to 3 mm from one end of the structure and discard it. Advance the platform 300 to 400 μm (or desired thickness of slice) and cut the tissue again. Use the wet fine, soft artist's paintbrush to transfer the slice into the home-made holding chamber containing oxygenated ACSF or slicing solution. Lift the knife and repeat the above steps five to eight times to yield five to eight slices.

    Very often, slices are damaged during transfer to the holding chamber with the wet paintbrush, especially for those who are inexperienced in slicing. To avoid this, do not immediately lift the knife after the blade cuts the tissue, but rather insert the wet paintbrush tip between the knife and the slice and then gently rotate the brush away from the blade lifting the slice to transfer it to the holding chamber.

11. Incubate slices in the holding chamber and aerate continuously with a 95% O_2/5% CO_2 gas mixture for at least 60 min before beginning any electrophysiological recordings.

Tubing used for oxygenation in the holding chamber should be small in diameter to avoid damaging slices with big bubbles. Two or more aerating tubes should be used to avoid anoxic damage to slices when using small oxygenation tubes and a low rate of oxygenation.

SUPPORT PROTOCOL 2

PREPARATION OF ACUTELY ISOLATED CEREBELLAR SLICES

This protocol describes the procedures using the vibratome method for making thin cerebellar slices for whole-cell patch-clamp recordings.

NOTE: All protocols using live animals must first be reviewed and approved by an Institutional Animal Care and Use Committee (IACUC) and must follow officially approved procedures for the care and use of laboratory animals.

Materials

95% O_2/5% CO_2–saturated slicing solution (see recipe), 4°C
95% O_2/5% CO_2 gas mixture cylinder
ACSF (see recipe)
5% agar gel block or Sylgard 184 block (see recipe)
Cyanoacrylate glue (super-glue)
10- to 20-day-old rats (either gender; Sprague-Dawley or Charles River)

500-ml beaker
Single-edged and high-quality double-edged razor blades
Automatic oscillating tissue slicer (e.g., OTS-3000-05, FHC) or equivalent
Rat guillotine
Large surgical scissors
Small, sharp dissecting scissors
Rongeurs
Whatman no. 1 or no. 2 filter papers
50- or 75-mm plastic petri dishes
No. 5 fine-tip tweezers
Wide-bore Pasteur pipet
Home-made slice-holding chamber (Fig. 11.11.9)
35° to 37°C water bath

Prepare slicing solution and tissue slicer

1. Make up 300 ml of slicing solution in a 500-ml glass beaker and oxygenate vigorously with 95% O_2/5% CO_2 gas mixture for at least 15 min (pH to 7.35 to 7.4). Surround the beaker with ice and keep aerating the solution with the 95% O_2/5% CO_2 gas mixture. Make up 1000 ml of ACSF.

2. Carefully break a double-edged razor blade into two single-edged parts. Insert the broken edge of the half blade into the blade holder of the tissue slicer and clamp it tightly (insert a small piece of filter paper to help tighten the blade).

It is recommended that the blade have a section angle of 20° to the horizontal plane.

3. Glue a small (10 × 10 × 10–mm) 5% agar block on the tissue pedestal of the slicer (Fig 11.11.11) with cyanoacrylate glue. Clean up the cutting stage of the tissue pedestal and the cutting chamber.

Prepare cerebellar tissue block

4. Sacrifice the rat using the proper procedures approved by an Institutional Animal Care and Use Committee and following the NIH guideline for animal care and use; then, decapitate the animal with a rat guillotine.

5. Use large scissors to cut the scalp and small, sharp dissecting scissors to cut the skull along the midline. Take care to avoid cutting or damaging the underlying brain tissue by keeping the tip of the dissecting scissors against the top inside wall of the skull. Pull the skull away with rongeurs.

6. Pour some cold slicing solution over the brain immediately after exposure. Remove the overlying membrane, detach all nerve and blood vessel connections and isolate the whole brain.

7. Place the isolated brain immediately on Whatman no. 1 or no. 2 filter paper premoistened with cold slicing solution in a 50- or 75-mm plastic petri dish on ice (Fig. 11.11.10A). Wash the brain several times with the cold, oxygenated slicing solution. Separate the cerebellum from the rest of the brain by a transverse cut.

   To avoid damaging the cerebellum, the authors prefer to open the skull from the front part of the head towards the rear.

8. To cut sagittal slices, remove the brain stem and spinal cord and carefully peel off the soft membrane with two no. 5 fine-tip tweezers (alternatively, slightly trim a small area of the surface of the cerebellum for cutting).

   If this soft membrane on the surface of the cerebellum is not removed, it will push the tissue during slicing and will not yield good-quality slices.

9. Make one sagittal cut to remove one lobule, leave the other lobule intact for handling at a later time.

   Some investigators like to make a block of cerebellar vermis by two sagittal cuts.

   Leaving one lobule uncut will simplify subsequent handling and gluing of the tissue onto the tissue pedestal. Moreover, it will reduce the chances of damaging the cerebellar vermis.

Mount tissue on cutting stage

10. Cover a small area of the tissue pedestal near the agar block with a thin layer of cyanoacrylate glue but do not apply excessive glue. Use no. 5 fine-tip tweezers to hold it loosely or insert into the remaining lobule of cerebellar tissue block. Mount the tissue on the cutting stage of the tissue pedestal with the ventral side (mostly white matter tissue) of the cerebellar vermis block against the agar block and the sagittal cutting end of the cerebellar vermis block against the glue layer.

    Alternatively, if the cerebellar vermis block is isolated by two sagittal cuts, one may need to use a filter paper strip to transfer and mount the tissue block on the cutting stage of the tissue pedestal (Fig. 11.11.12).

11. To prepare transverse slices, use no. 5 fine-tip tweezers to hold the remaining lobule loosely and mount the cerebellar vermis block on the cutting stage with the ventral side against the agar block and the transection face on the glue layer.

12. Immediately assemble the tissue pedestal in the cutting chamber and pour enough cold, oxygenated slicing solution to submerge the tissue block fully and continue to aerate the solution in the chamber with the 95% O_2/5% CO_2 gas mixture. Mount the slicing chamber on the tissue slicer.

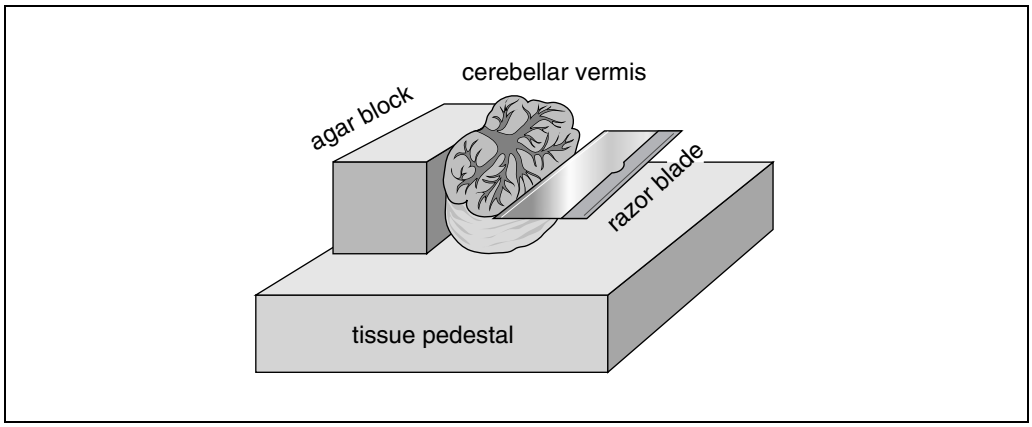

Figure 11.11.12 A diagram of the preparation of cerebellar slice using a OTS-3000-03 tissue slicer. The cerebellar vermis block is glued to the tissue pedestal with the ventral side against the agar block. The oscillation razor blade is advanced slowly into the tissue at an angle of 20° to the tissue pedestal.

Cut thin cerebellar slices

13. To cut sagittal slices, lower the blade all the way down until it is close to the level of the vermis portion. Adjust the slice thickness to 150 to 200 µm. Slice the tissue at a very slow rate of advancement and a high rate of horizontal oscillation (8 to 9 Hz). Discard the first few cuts that basically remove the remaining lobule tissue.

14. Collect five to eight slices generated from the vermis portion and transfer them with a wide-bore Pasteur pipet to the home-made slice-holding chamber containing ACSF or the slicing solution.

15. To cut transverse slices, similarly, discard the first few cuts, then collect and transfer three to five slices generated from the vermis to the home-made slice-holding chamber.

    Because the transverse slices are very easy to disperse, one may have to cut slightly thicker (e.g., 180- to 220-µm) slices than with the sagittal slices.

    It is essential that the blade cut the tissue smoothly to yield slices with even thickness. Anytime the blade pushes or compresses the tissue during slicing, this is an indication that there is residual membrane or small blood vessels remaining on the surface of the tissue block producing low-quality slices, especially in the transverse orientation. One way to recover is to back off the blade lightly and slightly trim the surface with a sharp blade, then resume cutting slices.

Incubate slices

16. Put the holding chamber in the pre-set 35°C water bath and continue to aerate the incubation solution with the 95% O_2/5% CO_2 gas mixture. Move the holding chamber out of the 35°C water bath after 60 min and leave it at room temperature until use.

    It is believed that incubation of slices at 35°C may improve the optical transparency of slices.

    The tubes used for oxygenation in the holding chamber should be small in diameter to avoid damaging slices with big bubbles. Two or more aerating tubes should be used to avoid anoxic damage to slices when using small tubes and a low rate of oxygenation.

REAGENTS AND SOLUTIONS

Use Milli-Q-purified water or equivalent in all recipes and protocol steps. For common stock solutions, see ***APPENDIX 2A****; for suppliers, see* ***SUPPLIERS APPENDIX****.*

ACSF

125 mM NaCl
2.5 mM KCl
1 mM MgCl
1.25 mM KH_2PO_4
26 mM $NaHCO_3$
2 mM $CaCl_2$
25 mM D-glucose
Adjust pH 7.35 to 7.4 by bubbling with a 95% O_2 /5% CO_2 gas mixture
Prepare fresh

ACSF can be stored up to several days at 4°C, but it must be bubbled with 95% O_2 /5% CO_2 gas before use.

Caution should be taken to avoid Ca^{2+} precipitation when preparing this solution. To prevent Ca^{2+} precipitation, add $CaCl_2$ last. In addition, it is preferable to aerate the solution first with the 95% O_2 /5% CO_2 gas mixture and then add the $CaCl_2$.

Similarly, caution should be taken with test chemicals and their solubility, particularly with heavy metals such as methylmercury and lead. These chemicals should be added to bath solution just before application. Additionally, it may be necessary to alter the anion composition to avoid precipitation of phosphate-based salts.

Internal pipet solutions

CsCl-based pipet solution:
140 mM CsCl
4 mM NaCl
0.5 mM $CaCl_2$
10 mM HEPES
5 mM EGTA
2 mM Mg-ATP
0.4 mM GTP
Adjust to pH 7.3 with CsOH
Store up to 1 month at −20°C

CsF-based pipet solution:
140 mM CsF
4 mM NaCl
0.5 mM $CaCl_2$
10 mM HEPES
5 mM EGTA
2 mM Mg-ATP
0.4 mM GTP
Adjust to pH 7.3 with CsOH
Store up to 1 month at −20°C

Potassium gluconate (KGlu)-based pipet solution

145 mM KGlu
5 mM $MgCl_2$
5 mM EGTA
10 mM HEPES
4 mM NaCl

continued

2 mM ATP
0.4 mM GTP
pH 7.3
Titrate with KOH
Store up to 1 month at –20°C

Slicing solution

125 mM NaCl
2.5 mM KCl
4 mM $MgCl_2$
1.25 mM KH_2PO_4
26 mM $NaHCO_3$
1 mM $CaCl_2$
25 mM D-glucose
Adjust pH 7.35 to 7.4 by bubbling with a 95% O_2/5% CO_2 gas mixture
Prepare fresh

Caution should be taken to avoid Ca^{2+} precipitation when preparing this solution. To prevent Ca^{2+} precipitation, add $CaCl_2$ last. In addition, it is preferable to aerate the solution first with a 95% O_2 /5% CO_2 gas mixture and then add the $CaCl_2$.

Sylgard 184

Mix one part of Sylgard 184 (Dow Corning) curing agent with 10 parts of Sylgard 184 silicone elastomer, dispense into 0.5-ml aliquots. Store up to 1 to 3 months at –20°C.

This solution is used for coating electrodes.

COMMENTARY

Background Information

Since reported by Yamamoto and McIlwain (1966) that synaptic field potentials could be evoked and recorded reliably from neurons in acutely isolated brain slices maintained in vitro, electrophysiological recordings in brain slices have become an important tool in investigating central synaptic functions. These brain-slice recordings have been widely used to study the pharmacological or neurotoxic effects of drugs or environmental chemicals on central synaptic transmission. Brain slices offer several major technical advantages over in vitro invertebrate preparations, cell culture, as well as whole brain in situ and in vivo methods for investigating mammalian CNS neurobiology, neurophysiology, and neurotoxicology. (1) Using a brain slice provides simple and precise control over the experimental conditions such as pH, temperature, and concentrations of tested chemicals, compared to the variables (e.g., blood pressure, CO_2 concentration, heart rate) that must be controlled during in vivo studies. (2) No anaesthetics, paralytics, or sedatives are necessary in slice preparations. This is particularly important if these drugs compete with the test chemicals for putative targets or interact directly with the test chemicals. (3) Using an isolated slice allows direct visual control over the positions of both recording and stimulating electrodes, avoiding the difficulties of stereotaxic techniques in vivo. The neurons being targeted can be easily located, identified, and accessed. (4) In contrast to most cell culture systems or acutely dissociated cells, the normal anatomical relationships and synaptic circuits remain relatively intact and healthy in a properly oriented brain slice. This is particularly advantageous in a highly laminated architecture such as the hippocampus and cerebellar cortex. (5) Use of an isolated slice greatly improves the stability of electrophysiological recordings and makes high-quality, long-lasting intracellular and whole-cell patch recordings possible. In short, the in vitro brain-slice recording techniques have greatly facilitated the investigation of the electrical properties and synaptic function of neurons in the CNS. Use of the brain slice has also greatly increased the knowledge of the effects of neurotoxic chemicals on the mammalian CNS in the last two decades. However, it should be kept in mind that the results obtained from in vitro brain slice experiments mimic but are not necessarily

identical to those obtained from in vivo experiments. In addition, the effective concentrations of the test chemicals used in brain slice experiments can often be much higher than those used in cell culture or acutely dissociated cells due to the larger mass of tissue providing non-specific binding sites for the drug or chemical. Moreover, the tissue acts as a diffusion barrier for drugs or chemicals, so the time course of the effect of a drug can vary significantly among surface cells and those located deeper in the brain slice. The effect of a drug on both surface cells and the deeper cells of the brain slice is still slower than on cells in culture where there is no diffusion barrier.

Electrical stimulation of neurons generates two main types of signals: either gradual changes in the membrane potentials (postsynaptic potentials, EPSPs) or all-or-none spikes (action potentials). These electrical signals can be recorded by placing a recording electrode close to a cell or a cell population (extracellular recording), by penetrating the cell membrane with a sharp pipet electrode (intracellular recording), or by forming a gigaohm seal of a glass pipet on the cell membrane of an intact cell and subsequently rupturing the membrane to gain access the cell interior (whole-cell patch-clamp recording). All of these recording techniques have been successfully applied to the brain slice preparation.

Extracellular recording refers to measurement of the potential changes across the cell membrane without penetrating the cell with a microelectrode. The extracellular signal is generated because the resistance or conductance of the extracellular fluid is not zero and the cell, whose membrane potential is not changed uniformly in response to a stimulus such that one part of the membrane is more depolarized than another part, will have current flow within it. Corresponding to the intracellular current change, there is a current flow in the extracellular fluid to complete the current circuit. The extracellular current is then picked up by an extracellular recording electrode. In general, extracellular signals are very small and, therefore, require extensive amplification. Because the signals recorded by the extracellular recording pipet electrodes are responses of a single neuron or a population of neurons, large responses can be generated only when the firing of many neighboring neurons is highly synchronized and the dipole orientation of these neurons is uniform. Therefore, the amplitude of the population spike is proportional to the numbers of neurons excited or stimulated.

Of all the recording techniques utilized for brain slices, extracellular recording is the most stable and easiest electrophysiological recording method, particularly in hippocampal slices. Extracellular recordings in hippocampal slices have been widely used to study the neurotoxic effects of chemicals—such as copper, ethanol, lead, lithium, mercury compounds, and trimethytin—on central synaptic transmission and synaptic plasticity such as long-term potentiation (LTP) or long-term depression (LTD). Recently, a new, substrate-integrated, planar microelectrode array (MEA)—a multiple-electrode extracellular recording technique—has been successfully introduced to record multiple single-unit spike activity in acutely isolated brain slices (Oka et al., 1999; Egert et al., 2002) and organotypic brain slice cultures (Stoppini et al., 1997) with up to 70 electrodes simultaneously. This provides a new, important, and potentially easy-to-use in vitro tool for the investigation of spiking neural networks and monitoring the dynamic interactions between groups of neurons on a millisecond-time scale. Extracellular recording in brain slices will remain a simple but useful in vitro tool for studying effects of neurotoxic chemicals on central synaptic function. The major advantage of extracellular recording is that it is relatively easy to make stable, long-lasting recordings with comparatively inexpensive equipment. The main disadvantages of extracellular recording are (1) because the very weak extracellular signals require higher amplification, background noise will also likely be amplified. Thus, it is important to use low-resistance pipet electrodes, a low-noise amplifier, and good shielding of the recording systems. (2) This technique cannot provide any information about changes in resting membrane potentials and input resistance, and it cannot provide detailed information about the precise sites of actions of neurotoxic chemicals on neurons. (3) It is nearly impossible to make direct comparison of amplitudes of field potentials from different individual experiments, because amplitudes of field potentials may vary greatly in different slices from the same animal, in different locations of the recording electrode in the same slice, or even in the same region of the same slice but with different depths of the electrode tips in tissue.

In contrast, intracellular recording uses a sharp electrode to penetrate the cell membrane and measure the responses of individual neurons at rest or to a stimulus. Therefore, it is possible to measure the entire gamut of changes

in the electrical behavior of a cell including resting membrane potentials, input resistance, whole-cell capacitance, action potentials, and postsynaptic potentials of an individual neuron in response to a presynaptic stimulus or direct application of neurotransmitters. It is also possible to do quantal analysis of the process of synaptic transmission and determine whether or not a given chemical affects function of the presynaptic nerve terminals. Moreover, when equipped with a bridge circuit in the intracellular recording amplifier, one can inject DC current into the cell through the same recording electrode to change the resting membrane potentials or directly excite the targeted cell. This allows one to analyze, in more detail, the site and mechanism of action of a given chemical on an individual neuron. In addition to the current-clamp recording, it is also possible to perform dSEVC by using time-sharing techniques in small cells to measure the postsynaptic currents and estimate the reversal potentials of a synaptic response. One major advantage of using dSEVC techniques is the possible avoidance of errors in the measurement due to voltage drops across the series resistance of the current-passing electrode that often occurs in whole-cell patch-clamp recordings. This is particularly useful and is an alternative choice if the series resistance of whole-cell patch-clamp recording is a major concern. In addition, because of the use of small-tip pipet electrodes, current rundown due to intracellular dialysis of the cell by the pipet solution may not be a major concern in dSEVC recordings as it is in conventional whole-cell recordings. However, the disadvantages of intracellular recordings are (1) it is difficult to make proper cell penetration and maintain a long, stable recording in small neurons. (2) Before penetrating the cell, even during recording, the bridge balance and electrode capacitance need to be properly adjusted and compensated, otherwise all measurements will be inaccurate. (3) Resting membrane potentials are influenced by the electrode tip potentials, and the tip potentials are influenced by the ionic microenvironment, which can change after penetration of a cell or by test chemicals, therefore, an exact measurement of the true membrane potentials may not be possible. (4) Penetration of the cell membrane may cause damage to the cell membrane and yield an unstable recording. (5) Because the electrodes used for the intracellular recordings usually have very sharp tips, it is difficult to inject large molecules into cells. (6) When measuring currents using the sharp intracellular electrode in dSEVC recording mode, it is generally difficult to voltage-clamp very fast responses because of constraints on the electrical circuitry or very large responses due to the amount of current needed to be injected, and the noise level is much greater than that in whole-cell patch-clamp recording.

In the last decades, the whole-cell voltage-clamp recording technique has been used widely to study synaptic transmission in brain slices (Blanton et al., 1989; Edwards et al., 1989; Konnerth, 1990; Stuart et al., 1993; Blitzer and Landau, 1994; Sakmann and Stuart, 1995; Plant et al., 1995). Compared to the extracellular and intracellular recording technique, whole-cell patch-clamp recording in brain slices offers more advantages by combining the brain-slice technique with the power of the patch-clamp techniques. First, whole-cell recording significantly improves the signal-to-noise ratio. Thus, it is better suited for detecting relatively small amplitude synaptic events, such as spontaneous or miniature EPSCs or IPSCs, than are conventional intracellular recording or the dSEVC recording (Henderson, 1993; Blitzer and Landau, 1994). Second, in whole-cell patch-clamp recording, access to the cell interior is much greater due to the relatively large tip of the recording pipet. Thus, relatively large molecules can enter the cell by diffusion from the electrode, permitting experiments involving the intracellular injection of protein and peptides, dialysis of the cell, intracellular pH-clamp, and even the intracellular application of drugs. Third, the low-resistance recording electrodes used in whole-cell patch-clamp recording are capable of passing large amounts of currents, particularly depolarizing currents, more effectively than are high-resistance sharp microelectrodes. Fourth, the whole-cell patch-clamp recording technique can be combined with other techniques such as fluorometric recording to measure simultaneous changes in currents and the intracellular ion concentration or the pH in single cells in brain slices. In addition, the whole-cell patch-clamp recording technique can also be used in combination with molecular biological tools such as single-cell RT-PCR to analyze the molecular basis for chemically induced changes in a particular ion channel or receptor. These provide a very powerful tool for studying neurotoxic mechanisms of chemicals.

Synaptic currents can be recorded using whole-cell patch-clamp recording techniques in both relatively thick (individual cells not necessarily visualized) or thin brain slices (neu-

ron cell soma or dendrites can be visualized under an upright microscope equipped with Nomarski optics and video camera systems). To date, three main techniques have been developed for making whole-cell patch-clamp recording in brain slices. These include the cleaning, blind, and blow-and-seal methods. The cleaning method was first introduced by Edwards et al. (1989). In this method, the cell membrane to be recorded from is cleaned prior to attempting to form a gigaohm seal. To do this, the debris and surface tissue over the targeted cells in the thin (150- to 200-μm) brain slice are first teased apart by gentle application of positive pressure to a broken-tipped pipet in order to eject a stream of bath solution and then removed by careful suction. The second method is the so-called blind technique introduced by Blanton et al. (1989). This procedure is similar to that used for conventional intracellular recording in thick brain slices (400 to 500 μm) and no specific optics, physical cleaning, or enzymatic treatment of tissue are required. To avoid occlusion of the pipet tip, a positive pressure is applied to the back of the pipet as it advances through the bath and slice. When the recording pipet tip contacts the cell membrane, the amplitude of the current pulses is reduced (increased resistance). Advancing the pipet a little more causes the amplitude of the current pulses to decrease further. Then a slight negative pressure is applied to the recording pipet to form a gigaohm seal and whole-cell recording is initiated. The third technique, blow-and-seal (Stuart et al., 1993), is the most commonly used method. It is a hybrid of the first two methods. In this procedure, similar to the blind technique, the tissue debris on the surface of the targeted neurons is not pre-cleaned, however, the advancement and placement of the recording electrode in thin brain slices is performed under visual control as in the clean procedure. Choosing which method to use depends on the investigator's preference, experience, and equipment.

The major problems associated with whole-cell patch-clamp recording are series resistance and current rundown. Unlike the dSEVC recording in which the single electrode handles both tasks of voltage recording and current passing using a time-sharing technique to avoid interaction between the two tasks, whole-cell patch-clamp recording uses the same pipet electrode doing both voltage recording and current passing simultaneously. The major problem associated with this is the series resistance–related voltage error in the measurement. In whole-cell voltage-clamp recording, the cell membrane potential is clamped by the command potential applied to the pipet electrode. The effectiveness of the voltage clamp depends on the size of the access resistance between the pipet electrode and the cell interior, and on the size of the currents across this resistance. In general, full access to the interior of the cell is not achieved after rupturing the cell membrane due to an obstruction caused by the broken membrane fragments or intracellular constituents. The access resistance is in series electrically with the membrane, therefore, it is also called series resistance. Any current passing through the pipet will induce a voltage drop across this series resistance and thus can introduce an error in the voltage clamp. The contribution of the access resistance to total series resistance can introduce a substantial error when making whole-cell voltage-clamp recording in brain slices. Therefore, a proper electrode coating and series resistance compensation are required to minimize this error. The rundown of currents in the whole-cell recording configuration is another common problem due to intracellular dialysis of the cell and loss of energy source, second messenger components, or a cofactor necessary to normal physiological functions. To minimize current rundown, some specific substances such as ATP and GTP should be included in the internal pipet solution.

Critical Parameters

Healthy brain slices

No matter what type of electrophysiological recording technique is to be used in brain slices, high-quality slice preparation is always the first and most important requirement for a successful experiment. Poor slices can be easily identified visually and electrophysiologically. Clearly translucent or increased whiteness of slices indicates that they are damaged and should not be used. In extracellular recording, a good slice should provide a single population spike in response to a low-intensity orthodromic stimulus. As the stimulus intensity increases, the population spike should gradually increase in size and decrease in latency. Typically, only a single spike is generated even at near maximum-intensity stimulus. On the other hand, if much higher stimulation intensity is required to evoke even small spikes, or multiple spikes are easily evoked by a low-intensity stimulus, then the slice may be damaged. In intracellular recording, in the absence of exter-

nal influences such as application of relevant drugs, a well-penetrated cell should typically have a stable membrane potential, spike amplitude, and input resistance over a long period of time. A moderate depolarizing pulse should evoke a regular, rhythmic train of spikes, which decreases in latency and increases in number as the depolarizing current intensity increases. In the whole-cell patch-clamp recording configuration, attaining a gigaohm seal or long-lasting recording on bad slices or cells is virtually impossible. Thus, the preparation and selection of healthy slices is very critical. To obtain good slices, all three crucial factors—time, care, and temperature—should be kept in mind during dissection and slicing. The shorter the time from decapitation of the animal to transfer of slices into a holding or recording chamber, the better the slices will be. Always take care not to damage the tissue mechanically during dissection and slicing, and the time should not be compromised during transfer of the slices. Always keep the tissue in cold, keeping all steps on ice if possible.

Fabrication of whole-cell recording electrodes

For a successful, low-noise whole-cell recording, optimal fabrication of the recording pipet is one of the most important steps. Detailed discussions of fabricating patch pipets have been presented elsewhere by Penner (1995) and Rae and Levis (1997). Certain concerns that are important for whole-cell recording in brain slices are discussed here. To reduce the series resistance and noise, a blunt, short-shank (bullet shape) and low-tip-resistance pipet is required for whole-cell recording. However, the geometries of recording pipets for whole-cell patch-clamp recording in brain slices are somewhat different from those used for whole-cell recording in culture or acutely dissociated cells. Due to the relatively small working space when using a water-immersion objective lens, which may impede the accessibility of the pipet to cells, the shank of the pipet is usually relatively longer than that used for conventional whole-cell recording in cultured or acutely dissociated cells. The pipet shape is nearly conical from the shoulder to the tip. When doing whole-cell recording in Purkinje and granule cells in cerebellar slices, the authors typically use two different types of glass pipets. For Purkinje cells, which are large and have extensive processes (and thus usually have large membrane capacitance), the authors prefer to use thick-walled glass to minimize the pipet capacitance. For granule cells, which are quite small, the tip of a recording pipet has to be very small, thus, having a much higher tip resistance. For granule cells, the authors usually use thin-walled glass pipets to minimize the series resistance. Because of the limited working space under a water-objective lens, the access angle for the recording pipet is relatively small. A large portion of the pipet tip is immersed in bath solution, which will cause noise and increased fast-transient capacitance. Therefore, coating the pipet tips with elastomer (e.g., Sylgard 184) is required for whole-cell recording in brain slices. Coating of the whole-cell recording pipet tip can prevent the formation of a thin film on the outside wall of a pipet, thereby reducing the associated noise, as well as the size and complexity of the fast-capacity transient. While the tips of the pipets used for whole-cell recordings in brain slices do not necessarily require fire-polishing, when they are coated with Sylgard 184, fire-polishing may be required.

The fabrication of conventional intracellular recording electrodes is not as important as that for whole-cell recording and no specific techniques are needed. However, if the tip of the intracellular recording electrode can be beveled, it will maintain the same sharpness of the electrode tip and minimize possible damage to the cell membrane when penetrating the cell. This will also reduce the high tip resistance–related background noise, particularly for dSEVC recordings.

Stability of recording systems

To maintain a stable, long-lasting recording, particularly in intracellular or whole-cell recording in brain slices, a rock-solid stable recording system is required. The slice should be well immobilized within the recording chamber. Perfusion and drainage of medium in and out of the chamber should be well balanced. All the potential sources described in The Technique Notes by Burleigh Instruments (see Internet Resources) that may cause significant pipet position drift should be eliminated.

Pipet solutions for whole-cell recording

Whole-cell recording of postsynaptic responses mediated by different neurotransmitters may require different internal pipet solutions. The choice of pipet solution primarily depends on the type of synaptic currents to be examined. For whole-cell recording of $GABA_A$ receptor–mediated inhibitory synaptic responses in Purkinje or granule cells, a CsCl-

based internal pipet solution (see recipe) is often used, whereas for glutamate-mediated excitatory synaptic responses in Purkinje or granule cells, several different pipet solutions including CsF-, potassium gluconate-, Cs-MOPs-, or $CsMeSO_3$-based solutions have been used. Care should be taken when a high concentration of F^- (CsF^--based solution) is used in the pipet solution, because F^- may interact with some types of glass pipets to cause precipitation and occlude the tip of the pipet. No matter what type of pipet solution is used, all pipet solutions should be filtered using a 0.2-µm syringe filter prior to filling the recording pipets.

The osmolarity of intracellular pipet solutions should be equal to or ~10% lower (hypoosmotic or hypotonic) than the external solution. It appears that whole-cell recordings usually last longer if the internal pipet solution is slightly hypoosmotic compared to the external solution. In some types of cells, whole-cell currents recorded with high-chloride pipet solutions may show some extent of rundown after establishing a whole-cell recording configuration. This rundown may be due to an osmotic imbalance caused by a combination of non-diffusible anions or high-molecular-weight material in the cell and highly diffusible Cl^- in the pipet solution. Very often, gluconate or even other anions are used to replace Cl^- in the pipet solution to avoid this osmotic imbalance and to obtain a more stable recording. However, one trade off of this is that using organic ions such as gluconate to replace inorganic ions such as Cl^- may increase both the pipet electrode resistance and the series resistance because organic ions have lower mobilities.

The pH of the intracellular pipet solution should be controlled at 7.2 to 7.3. Any change in intracellular pH may affect either directly or indirectly some types of currents such as inwardly rectifying potassium currents or calcium currents. Changes in intracellular pH may also cause changes in intracellular free calcium concentration, which may then secondarily affect the currents of interest. In most cases, the pipet solution is prepared as a relatively large volume of stock solution without the addition of ATP. ATP is added separately at a later time to a small volume of the stock solution to make the working pipet solution. When doing so, be sure to readjust the pH to 7.2 to 7.3, because adding an ATP salt (e.g., Mg-ATP) will lower the pH. In addition, care should be taken when acetate is used to replace Cl^- in the pipet solution, because it may cause intracellular pH changes in some types of cells.

A liquid junction potential exists between the internal pipet solution and the external solution in the whole-cell recording mode. This is another concern with which the investigator should be aware. The junction potential between solutions can be measured directly using a ceramic reference electrode filled with saturating KCl, or it can be estimated using the junction potential calculation tool provided in the pClamp8 program. This junction potential should be corrected accordingly during data analysis.

Space clamp errors

The most serious restriction on electrophysiological analysis of voltage-dependent synaptic responses in central neurons in brain slices is the lack of adequate space clamp. Space clamp effectiveness is always a concern in whole-cell voltage-clamp recording (dSEVC or whole-cell patch-clamp) of synaptic currents in neurons, especially in those neurons in slices with large soma, extensive dendritic arborizations, and/or long axons. In whole-cell recordings, voltage clamp of the cell membrane is maintained by the command potentials applied to the tip of the recording pipet. The basic assumption for whole-cell voltage-clamp is that isopotentiality exists in a spherical or round cell, i.e., all portions of the cell membrane are separated from the tip of the recording pipet by equal access resistance and the membrane is uniformly voltage clamped. A perfect space clamp is achieved when a perfect voltage clamp is applied to that portion of the membrane through which current is measured. For small round cells, this assumption probably holds true. In the CNS, however, neurons usually have extensive processes. Moreover, the membranes of the axons and dendrites are separated from the cell soma by the cytoplasmic resistance whose value is proportional to the distance from the recording site of each portion of the process membrane and the size of the cross section in that region of the cell. Just as current across the series resistance of the recording electrode will cause a voltage drop at the tip of the recording electrode, current flowing across the cytoplasmic access resistance of a dendrite or axon will also cause a voltage drop that may become substantial for the distal segment of the membrane. Thus, even though the somatic membrane potential may be voltage clamped adequately, the distal axonal or den-

Table 11.11.1 Troubleshooting Guide for Electrophysiological Recording in Brain Slices

Problems	Possible causes	Suggested solution
No test pulses showing on screen when doing Seal Test or Bridge Balance	Ground wire is not in bath solution, is not connected to the amplifier, or is broken	Check the ground pellet or wire in bath
	The silver wire in the patch pipet holder does not contact the pipet solution or the metal pin connector	Check electrode holder and make sure the silver wire is well connected with the pin connector and pipet solution
	Air bubbles exist between the electrode and extracellular or intracellular electrode holder	Make sure the electrode holder is filled with desired pipet solution before inserting the glass electrode
	Out of scale	Make sure the scaling factor on the computer and/or oscilloscope is set correctly
No postsynaptic response	Slice died due to lack of glucose in slicing or ACSF buffer (forgot to add glucose during preparation of solution)	Make new slices and be sure glucose is added to buffers
Cell is alive but no evoked postsynaptic responses occur	Synaptic inputs to this particular cell are transected or stimulating electrode is not located on the track of the presynaptic inputs	Try a different cell or try a different location with the stimulating electrode
Drift or unstable DC offset during experiments	Ground pellet in bath or silver wire in pipet is not well chlorided	Clean the wire and rechloride it
No solution stream flows out of the tip of pipet with positive pressure on the back of the pipet	Tip of the pipet is clogged by debris of glass, dust, tissue, or an air bubble	Apply strong pressure, or buzz the capacitance on amplifier, or change the pipet; clean glass pipet
	No positive pressure due to leak of tubing or two-(or three-) way valve	Check tubing and valve if they are leaking
	F^- in pipet solution interacts with glass to form precipitate at the tip of pipet	Use an alternative pipet solution
Going to whole-cell configuration before forming gigaohm seal	Membrane is too weak; applied too much negative pressure to the pipet; unhealthy cell	Find a better cell; reduce negative pressure applied to the pipet; find a better cell
Lose seal when rupturing membrane	Mechanical movement of pipet in electrode holder occurs when applying suction because the pipet in electrode holder is not sufficiently tightened or the rubber O-ring is aging	Tighten electrode holder; replace O-rings in pipet holder
	Unhealthy cell	Find a better cell
	Characteristic for certain types of cells	Try the perforated patch recording technique
Too much background noise	Recording system is not well shielded or grounded	Find the source of noise and ground it
	Pipet holder inside is wet or dirty	Clean the pipet holder regularly

dritic membrane potentials may be completely unaffected by the voltage clamp, and the time courses of synaptic currents, regenerative currents, and measurement of reversal potentials of synaptic responses will deviate substantially from the command potential. Unfortunately, unlike the series resistance of recording pipets that can be reduced by using lower-resistance electrodes and series resistance compensation with better electronics, poor space clamp cannot be reduced by simply using better electronics or electrodes. In the cerebellar slice, for example, space clamp of the small round granule cells may not be a problem. However, for the much larger cerebellar Purkinje cells with extensive dendritic arborizations, space clamp errors will be a significant concern. Thus, it is important, whenever possible, to prepare slices from young animals and to choose relatively small cells. Alternatively, one can abandon the whole-cell recording mode and make recordings of microscopic or single-channel events using the outside-out or inside-out patch recording configurations. In conjunction with so-called ensemble analyses, these techniques can allow one to extrapolate the microscopic events back to reconstruct a theoretical whole-cell or macroscopic current. These techniques are quite sophisticated though, and are beyond the scope of this unit.

Troubleshooting

Once the electrophysiological setup is well organized and shielded (grounded; see *UNIT 11.12*), most of the remaining problems are either slice-related or pipet electrode–related. The potential problems with poorly prepared slices have already been discussed. Thus, assuming that the preparation of slice was adequate, one should immediately check the electrode when one can not penetrate a cell or make a good seal, or when recordings are unstable or excessively noisy. Table 11.11.1 lists some common problems that may occur in electrophysiological recordings, particularly in whole-cell patch-clamp recordings.

Anticipated Results

Using Support Protocols 1 and 2, with practice, healthy hippocampal or cerebellar slices should routinely be obtained. The slices should be viable for at least 10 hr after preparation if properly maintained in an oxygenated environment. Using the techniques described in Basic Protocols 1 and 2, it should not be difficult to obtain stable, long-lasting extra- and intracellular recordings from hippocampal CA1 neurons. With these techniques, the authors routinely obtain reliable extra- and intracellular recordings lasting 3 to 4 hr, which should be long enough to complete experiments using even low concentrations of a given neurotoxicant. With just some minor modifications, these techniques should be also applicable to cerebellar or other brain slices to obtain long-lasting stable extra- and intracellular recordings. Using the steps described in Basic Protocol 3, the success rate for obtaining a gigaohm seal and whole-cell recordings from Purkinje cell soma could be as high as 100%. However, a much lower success rate is typical when recording from granule cells.

Time Considerations

Preparation of solutions (slicing solution and ACSF) including oxygenation may require 20 to 30 min. Sacrificing the animal and preparation of slices may require 5 to 10 min. Incubation of slices at 35°C requires ~60 min. During the period of incubation, the recording system is set up and several pipet electrodes are fabricated. Transferring the slice to the chamber and finding suitable cells may take several minutes. The actual time required for recording varies depending on the goal and type of experiments and the characteristics and concentrations of the tested chemicals. In general, at least 3 hr are required to complete one experiment from beginning to end.

Acknowledgements

The editors of *Current Protocols in Toxicology* wish to thank Dr. Toshio Narahashi for his expert assistance in enlisting and editing this unit on electrophysiology.

Literature Cited

Blanton, M.G., Lo Turco, J.J., and Kriegstein, A.R. 1989. Whole-cell recording from neurons in slices of reptilian and mammalian cerebral cortex. *J. Neurosci. Meth.* 30:203-210.

Blitzer, R.D. and Landau, E.M. 1994. Whole-cell patch recording in brain slices. *Meth. Enzymol.* 238:375-384.

Edwards, F.A., Konnerth, A., Sakmann, B., and Takahashi, T. 1989. A thin slice preparation for patch recordings from neurons of the mammalian central nervous system. *Pflügers Arch. Eur. J. Physiol.* 414:600-612.

Egert, U., Heck, D., and Aertsen, A. 2002. Two-dimensional monitoring of spiking networks in acute brain slices. *Exp. Brain Res.* 142:268-274.

Finkel, A. and Bookman, R. 1997. The electrophysiology setup. *In* Current Protocols in Neuroscience (J.N. Crawley, C.R. Gerfen, R. Mckay, M.A. Rogawski, D.R. Sibley, P. Skolnick, and S.

Wray, eds.) pp. 6.1.1-6.1.6. John Wiley & Sons. New York.

Hendersen, G. 1993. Pharmacological analysis of synaptic transmission in brain slices. *In* Electrophysiology (D.I. Wallis, ed.) pp. 89-107, Oxford, New York.

Johnston, D. and Brown, T.H. 1984. Biophysics and microphysiology of synaptic transmission in hippocampus. *In* Brain Slice (R. Dingeldine, ed.) pp. 51-86. Plenum Press, New York.

Konnerth, A., Llano, I., and Armstrong, C.M. 1990. Synaptic currents in cerebellar Purkinje cells. *Proc. Natl. Acad. Sci. U.S.A.* 87:2662-2665.

Langmoen, I.A. and Andersen, P. 1981. The hippocampal slice in vitro. A description of the technique and some examples of the opportunities it offers. *In* Electrophysiology of Isolated Mammalian CNS Preparations (J. Kerkut and H. Wheal, eds.) pp.15-50. Academic Press, London.

Oka, H., Shimono, K., Ogawa, R., Sugihara, H., and Taketani, M. 1999. A new planar multielectrode array for extracellular recording: Application to hippocampal acute slice. *J. Neurosci. Meth.* 93:61-67.

Penner, R. 1995. A practical guide to patch clamping. *In* Single-Channel Recording (B. Sakmann and E. Neher, eds.) pp. 3-30. Plenum, New York.

Plant, T.D., Eilers, J., and Konnerth, A. 1995. Patch-clamp technique in brain slices. *In* Neuromethods, Vol. 26: Patch-Clamp Application and Protocols (A.A. Boulton, G.B. Baker, and W. Walz, eds.) pp. 233-257. Human Press, Totowa, New Jersey.

Rae, J.L. and Levis, R.A. 1997. Fabrication of patch pipets. *In* Current Protocols in Neuroscience (J.N. Crawley, C.R. Gerfen, R. Mckay, M.A. Rogawski, D.R. Sibley, P. Skolnick, and S. Wray, eds.) pp. 6.3.1-6.3.31. John Wiley & Sons. New York.

Sakmann, B. and Stuart, G. 1995. Patch-pipet recordings from the soma, dendrites, and axon of neurons in brain slices. *In* Single-Channel Recording (B. Sakmann and E. Neher, eds.) pp. 199-211. Plenum, New York.

Schwartzkroin, P.A. 1981. To slice or not to slice. *In* Electrophysiology of Isolated Mammalian CNS Preparations (J. Kerkut and H. Wheal eds.) pp. 15-50. Academic Press, London.

Stoppini, L., Duport, S., and Corrèges, P. 1997. A new extracellular multirecording system for electrophysiological studies: Application to hippocampal organotypic cultures. *J. Neurosci. Meth*. 72:23-33.

Stuart, G., Dolt, H.-U., and Sakmann, B. 1993. Patch-clamp recordings from the soma and dendrites of neurons in brain slices using infrared video microscopy. *Pflügers Arch. Eur. J. Physiol.* 423:511-518.

Yamamoto, C. and McIlwain, H. 1966. Electrical activities in thin sections from mammalian brain maintained in chemically-defined media in vitro. *J. Neurochem*. 13:1333-1343.

Key References

The Axon Guide for Electrophysiology and Biophysics Laboratory Techniques. Axon Instruments. Union City, California.

A practical laboratory guide covering a broad range of topics, from the biological basis of bioelectricity and a description of the basic experimental setup, to the principles of operation of the most advanced hardware and software currently available.

Langmoen et al., 1981. See above.

An early and comprehensive description of the preparation of extracellular and intracellular recording techniques in hippocampal slices.

Stuart et al., 1993. See above.

This is the original paper describing the blow-and-seal technique for making whole-cell patch recording from a single cell in thin brain slices.

Internet Resources

http://axon.com

A Web site for downloading a free copy of The Axon Guide for Electrophysiology & Biophysics: Laboratory Techniques and the AxoBit Newsletter describing some specific methods and frequently asked questions.

http://www.ltp-program.com

A Web site for downloading a free copy of the LTP2.22A program and manual. This is useful if considering studies of long-term potentiation (LTP) in the experimental design.

http://www.synaptosoft.com

A Web site for downloading a MiniAnalysis program demo.

Contributed by Yukun Yuan and William D. Atchison
Michigan State University
East Lansing, Michigan

Whole-Cell Patch-Clamp Electrophysiology of Voltage-Sensitive Channels

Patch-clamp techniques allow one to study the function of ion channels at the level of individual channels (cell attached, inside-out, or outside-out patches) or at the level of the entire population of channels within the cell membrane (whole-cell patch). These techniques can be coupled with biochemical/pharmacological techniques to study the modulation of ion channels as well as molecular biological techniques to study the relationships between structure and function of ion channels. Thus, patch-clamp techniques offer a powerful tool for the neurobiologist and neurotoxicologist. However, patch-clamp electrophysiology is technically demanding as well as cost intensive to initiate as a laboratory technique. This unit is designed to aid a novice electrophysiologist in assembling the required equipment, making whole-cell patch recordings, and conducting initial assessments of basic parameters of ion channel function in single neurons grown in culture, as well as highlight some considerations needed for conducting toxicological experiments. Focus will be placed on recording voltage-sensitive Ca^{2+} currents, but examination of other voltage-gated ion currents is possible with simple changes in protocols and/or buffer solutions. Examination of the function of ligand-gated ion channels would require the addition of methods for rapid drug application. *UNIT 11.11* covers the application of these techniques to brain slices.

STRATEGIC PLANNING

Conducting electrophysiological assessments of ion channel function requires substantial time and effort in assembling required equipment prior to conducting an experiment. There are several important factors that must be considered to ensure success.

First, adequate isolation of any source of vibration is critical. The vibration-isolation table will eliminate most sources. However, vibrations can be transduced by cables from the microscope or headstage (these will be connected to equipment not on the vibration-isolation table). Another source of vibrations can be from the air currents within the room or those produced by someone walking past the equipment. For this and other reasons, it is preferable to place the microscope in an area that is away from heating/cooling exhausts or intakes and away from high-traffic areas. Ground floors of a building, typically, are more stable, but many electrophysiologists record successfully on higher floors.

Second, unwanted electrical noise is the bane of patch-clamp experiments and can come from a variety of sources. This includes ground loop noise, magnetically-induced pickup power sources (e.g., the microscope lamp), and radiative pickup from the overhead lights, the computer monitor, nearby equipment, and other common electrical appliances. While elimination of electrical noise at times may seem like a trial-and-error process, a methodical approach will be useful. First, placing the microscope, chamber, and headstage inside a Faraday cage can reduce radiative electrical pickup of noise from lights and other sources. Second, it is useful to identify sources of noise by starting with a minimal setup: the oscilloscope and patch amplifier. Once noise is minimized with the minimal setup, begin to add other equipment one piece at a time while monitoring and reducing noise with each addition. Most patch-clamp amplifiers have a common ground jack to which multiple ground wires can be attached using alligator clips. Thus, potential sources of noise can be grounded using this technique, and the noise present can be examined to determine if grounding of a potential source is useful. Finally, there are a number of

Contributed by Timothy J. Shafer
Current Protocols in Toxicology (2003) 11.12.1-11.12.14

precautions that can be made to minimize the potential for interference by various sources. Microscope power sources can, in most cases, be attached to the light via remote (2- to 4-feet) cables, overhead lights can be turned off, the patch-clamp amplifier and computer monitor can be placed far apart or at least shielded, and if possible, all electrical devices required for patch-clamp experiments can be powered via an electrical circuit separate from other laboratory equipment.

This covers two major aspects of setting up electrophysiology equipment. There are two additional items that are necessary. First, the patch pipet holder should contain a narrow-gauge silver wire that slides inside the patch pipet and serves as the electrode. It is necessary to have a thin coating of silver chloride (AgCl) on this wire. This can be accomplished by briefly immersing the wire in molten AgCl, or by placing the wire in a bleach solution for at least 20 min—several hours is preferable. Second, it will probably be necessary to obtain a Ag/AgCl ground pellet and solder it to a wire to connect to the headstage. Ground pellets are available from several different vendors.

In terms of actually preparing for an experiment, solutions can (in most cases) be made the afternoon before the actual experiments and kept refrigerated (or even frozen, if longer storage times are desired). Because experimental protocols and data collection are via computer software, these can be designed and written in advance of conducting experiments as well. Utilization of patch-clamp electrophysiological techniques is most successful and fruitful when large blocks of time can be spent conducting experiments. Although it is possible to collect useful data in a couple of hours or an afternoon, this is often insufficient time to be truly productive. Thus, strategic planning can include not only preparation of buffers, test solutions, and experimental protocols and design ahead of time but also scheduling time and other commitments to allow for uninterrupted, or minimal interruptions of, time in the laboratory.

One final consideration is related to the cells of interest. If one desires to record currents from cells of a particular age, or record age-related changes (e.g., changes in current expression as a function of days in vitro for a primary cell in culture), this will require advance planning in the tissue culture laboratory to assure that cells are of the proper age on the day of the experiment.

BASIC PROTOCOL

EXAMINATION OF VOLTAGE-SENSITIVE Ca^{2+} CURRENTS IN NEURONS

Voltage-sensitive Ca^{2+} channels play critical roles in the nervous system, mediating neurotransmitter release, Ca^{2+}-dependent action potentials, and signal transduction via Ca^{2+}-dependent pathways (Catterall, 1998). This latter function is thought to be important in both the developing and adult nervous systems as a mechanism of activity-dependent changes in gene expression. Ca^{2+} channels are also targets of neurotoxicants, particularly of heavy metals. Recording voltage-sensitive Ca^{2+} currents presents unique challenges for electrophysiologists. First, currents mediated via these channels are typically much smaller than those mediated by Na^+ or K^+ channels. Thus, both intracellular and extracellular solutions typically contain components to either block and/or minimize Na^+ and K^+ currents in order to isolate the Ca^{2+} current. These components often include tetraethylammonium, cesium, and barium, which block potassium currents, and tetrodotoxin or QX-314, which block sodium currents. Second, Ca^{2+} channels exhibit great diversity: both physiological as well as pharmacological methods are often required to distinguish different types of Ca^{2+} currents. Thus, it is sometimes necessary to characterize the types of current present in a cell prior to conducting experiments with chemicals of interest.

Materials

Extracellular bath solution (see recipe)
Cells plated on glass coverslips (see Support Protocol)
Intracellular (patch pipet) solution (see recipe)
Tetrodotoxin stock solution (see recipe), optional
QX-314 solution (see recipe), optional

Glass blanks for pipets
Multistage pipet puller
Microforge/heated wire polisher
Chamber to hold cells
Inverted microscope with phase-contrast, DIC, or Hoffman modulation optics
Faraday cage (can be constructed inexpensively)
Hydrolic, motorized, or piezoelectric micromanipulators
Computer with monitor
Patch-clamp amplifier
Analog to digital (A/D) conversion board
Software
Vibration isolation table
Drug delivery device (optional, but recommended)
Oscilloscope

Prepare for experiment

1. Assemble the various pieces of equipment needed to conduct experiments.

   The microscope, manipulators, and headstage for the patch-clamp amplifier will be assembled on the vibration isolation table, inside the Faraday cage. The chamber to hold the cells will be secured on the stage of the microscope, and the micromanipulator will be either attached to the microscope or mounted on a separate stand near the microscope. The headstage will be mounted on the micromanipulator so that when the pipet holder (containing a patch pipet) is attached, the tip of the microelectrode can be manipulated to touch cells viewed when coverslips are placed in the chamber attached to the microscope stage. The computer, A/D conversion board, and patch clamp amplifier need to be connected. Typically, the connection between the computer and the A/D board is one simple cable, but the connections between the amplifier and A/D board will depend on the manufacturer of the equipment and the signals which one desires to collect in computer data files. Figure 11.12.1 illustrates the typical flow of information between the various components of the patch set-up.

2. Pull six to ten patch pipets from glass blanks with a multistage pipet puller.

   Glass blanks for patch pipets come in a variety of sizes and materials, each having differing properties that offer different advantages and disadvantages. It is useful to try several different varieties to determine which glass type and size works best with the pipet puller being utilized, the cell type being recorded from, and other requirements of the experiment (e.g., lower noise). Many glass blanks also contain a filament (a thin glass fiber) attached to the inner wall. For pipets with small tip openings, this filament helps to fill the pipet with intracellular solutions without trapping air bubbles in the tip of the electrode (this will prevent adequate recordings). An additional consideration is the thickness of the glass utilized; thicker walls provide better performance for big cells with large membrane capacitance, while thinner walls can be utilized for smaller cells to reduce series resistance.

3. Polish patch pipets by bringing the tip close to a heated platinum wire, microforge/heated wire polisher, long enough to just begin melting the glass.

   It is useful to have a microforge or microscope with high magnification (600×) to polish pipets. Visually, a slight contraction of the tip of the electrode will be observed with sufficient magnification. Remove from heat at the instant this is observed. The tip of the

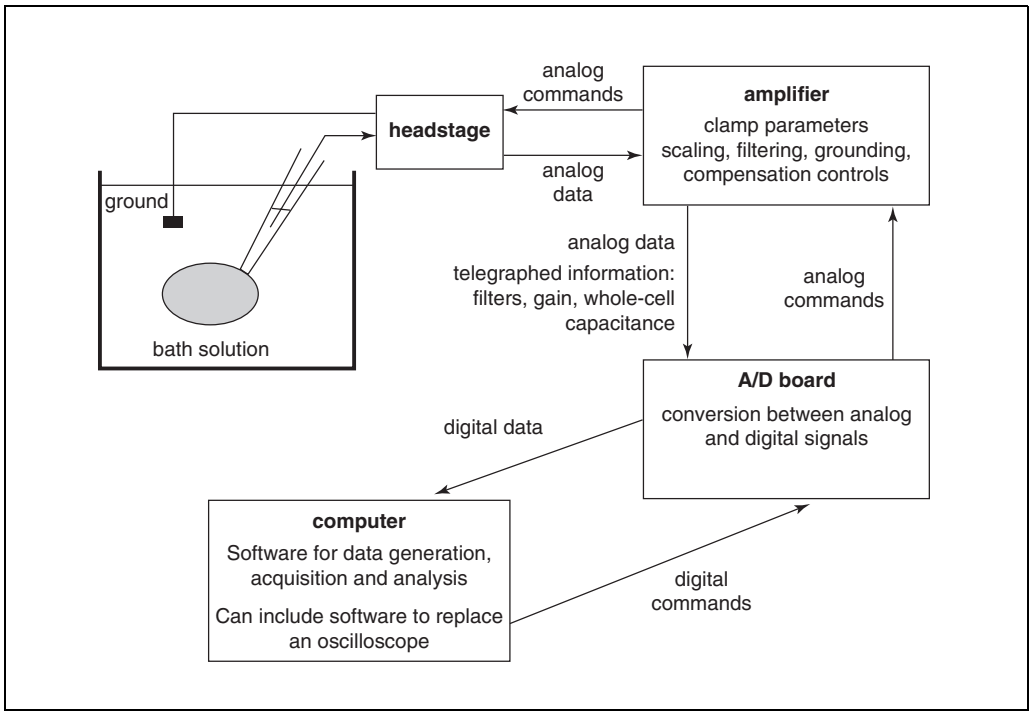

Figure 11.12.1 Diagram of patch clamp set-up and information flow. This schematic depicts the major electronic components of a patch-clamp electrophysiology setup, as well as the general functions of each component and the flow of information between them. Not depicted are other important items such as a Faraday cage, vibration-isolation table, drug delivery systems, and an oscilloscope. Many software programs have components that carry out the function of an oscilloscope. However, an oscilloscope can be useful in assessing noise and noise reduction.

electrode should be blunt, with a diameter of ~1 μm. When filled with intracellular solution, patch pipets should have a resistance of 2 to 6 MΩ, depending on the size of targeted cells. If needed, coat the tips of the pipets with Sylgard to reduce pipet capacitance.

4. Fill the chamber to hold the cells with extracellular solution and place a coverslip containing cells into the chamber. Using the microscope, select a cell to record from.

   Round- or regular-shaped cells tend to work best, and it is preferable to have a cell whose cell body is not in contact with other cell bodies, or, if possible, without extremely long neurites. These cells will be easier to maintain with an adequate space clamp.

   Although not absolutely required, having a microscope with optics providing a pseudo-three-dimensional image, such as phase-contrast, DIC, or Hoffmann modulation optics, is extremely useful. This will give the cells a three-dimensional appearance, which will facilitate manipulation of the patch pipet next to the cell without driving it into the bottom of the dish.

5. Fill a patch pipet with intracellular solution such that the end of the silver wire electrode is immersed within the intracellular solution.

   It is not necessary to completely fill the glass pipet with solution. Place the glass pipet into the pipet holder and immerse the tip into the bath solution. It is useful to apply positive pressure to the back of the pipet during this and subsequent steps. This is typically accomplished by blowing gently into a tube attached to the pipet holder (also see below), helping to prevent the pipet tip from becoming blocked with dust or debris.

6. Using the coarse and then fine adjustments on the micromanipulator, maneuver the patch pipet such that the tip of the pipet nearly touches the surface of the membrane of the cell to be recorded. Apply slight positive pressure to the pipet during this step.

7. While generating a test-pulse protocol (e.g., 5 mV depolarization for 5 msec), touch the tip of the pipet to the cell, release the positive pressure, and apply slight negative pressure (suction) to the back of the pipet.
8. Monitor the test pulse on either the oscilloscope or computer monitor to evaluate formation of a gigaohm seal between the cell membrane and patch pipet. If a gigaohm seal is detected, proceed to step 10.

   This is indicated by the elimination of current during the test pulse, such that only capacitive transients (from pipet capacitance) remain at the beginning and end of the test pulse. A cell-attached patch has now been formed.

   It will take trial and error to determine how much suction and how long to apply it in order to obtain a seal, as this will depend on the cells and environmental factors (such as the relative humidity, temperature, and other intangibles). Many people prefer to apply suction by placing a piece of tubing attached to the pipet holder into their mouth and sucking gently. This allows the experimenter to develop a feel for how much suction to apply. Depending on the substances utilized during experiments, this method may not be advisable. An alternative, safer method is to utilize a 1- or 3-ml syringe attached to the tubing via a stopcock.
9. (Conditional) In the event that the attempt is unsuccessful, obtain a new patch pipet before attempting to record from a different cell. Repeat steps 4 to 8 until a gigaohm seal is obtained.

   Formation of the gigaohm seal between the cell membrane and the surface of the glass is dependent upon having an extremely clean pipet tip surface (see Troubleshooting). Thus, a new pipet is needed for each attempt.
10. Using pipet capacitance compensation controls on the patch-clamp amplifier, reduce the pipet capacitive transients (also referred to as the fast transients) until they are eliminated.
11. In order to achieve the whole-cell configuration, apply additional negative pressure to the patch electrode or utilize the buzz button (on some amplifiers) to rupture the membrane underneath the tip of the patch pipet.

    A capacitive transient again appears at the beginning and end of the test pulse when this occurs. These transients are typically larger and longer lasting than the pipet capacitive transients and are the result of the capacitance of the cell membrane (whole-cell capacitance).
12. Using the controls on the patch-clamp amplifier, eliminate the whole-cell capacitance transients (this will be an iterative process involving the whole-cell capacitance, series resistance, series resistance compensation, and pipet capacitance compensation controls). Once whole-cell capacitance has been compensated, stop the test protocol and set membrane potential to desired holding potential or initiate control through software.
13. At this point, evaluate the cell to determine whether suitable recordings can be made, and then initiate the protocols required to evaluate various aspects of ion channel function, including activation and inactivation, current amplitude, and current-voltage response relationships.

    Depending on the conditions and cell type, stable recordings can be made for 10 to 40 min or more from each cell.

    One good indicator of the quality of the cell/recording is the steady-state holding current, which has to be injected in order to clamp the voltage at the desired membrane potential. This can often be obtained directly from the panel meters on the patch amplifier. This is a simple way of assessing the integrity of the seal resistance. Using Ohm's law ($V = I \times R$), the seal resistance (R) can be determined based on the steady-state holding current (I) and holding potential (V). The seal resistance (R) can be calculated by dividing the holding potential by the steady-state holding current. If this current is large, unstable, or increasing

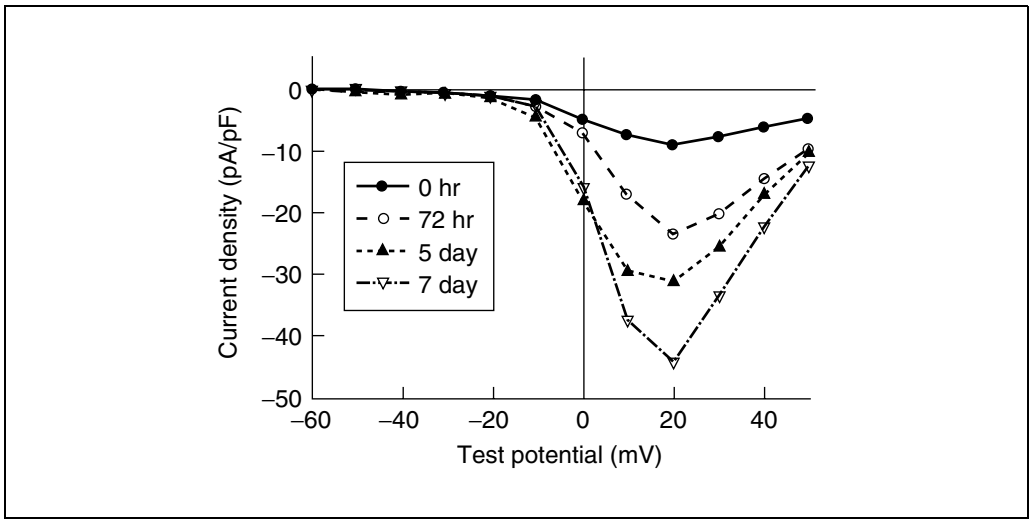

Figure 11.12.2 Current density–voltage relationship for Ca^{2+} current in PC12 cells following treatment with nerve growth factor (NGF). PC12 cells were plated onto glass coverslips and treated with NGF. At the indicated time intervals, coverslips were placed into extracellular buffer solution and whole-cell recordings were made. The current-voltage protocol described in the Basic Protocol, step 14a, was applied to cells, and then the peak amplitudes obtained at each test potential were divided by the capacitance of each cell to obtain the current density, which was plotted as a function of the test potential (in mV).

in amplitude, then the quality of data obtained will be poor. In many cases, it may not be possible to record long enough from that particular cell to complete a planned experiment.

14a. *Determining the current-voltage relationship for Ca^{2+} currents*: Generate current-voltage relationships (I/V curves) by assessing the current generated at different test potentials. A typical method to assess the I/V relationship uses a holding potential of −70 mV and delivers 140-msec depolarizing steps to the cell to evoke current responses. In the example in Figure 11.12.2, the first depolarizing step (test potential) is −60 mV, and subsequent depolarizing steps increase in 10-mV increments (e.g., to −50 mV, −40 mV, −30 mV, −20 mV, etc.) to a final level of +50 mV. From the data collected using this method, measure the peak amplitude of the Ca^{2+} current at each step level and then plot it against the test potential (mV) to generate a current-voltage plot (I/V curve).

In the example in Figure 11.12.2, the additional step of calculating current density has been taken. Typically, patch-clamp amplifiers, which have a telegraph feature (turned on), also send the whole-cell capacitance, gain settings, and other information to the computer, to be stored as part of the data file. Current density is determined by dividing the current amplitude by the whole-cell capacitance and is often calculated to normalize for differences in cell size.

14b. *Examining effects of acute neurotoxicants on Ca^{2+} currents:* In order to examine the acute effect of a neurotoxicant on Ca^{2+} currents, examine how the current amplitude or other parameters (activation, inactivation properties) change before and after application of a test compound. This method is quite simple: apply a single test potential repeatedly before, during, and, if desired, after application (washout) of a test compound, e.g., delivering a 140-msec depolarization step from a holding potential of −70 mV to +20 mV once every 10 sec. After achieving a stable baseline current, apply test compounds to the cell by a variety of methods, the simplest is a bath application, and record additional current responses. Plot the peak current amplitude versus time, although several other parameters, including end-current amplitude and activation and inactivation kinetics can also be examined.

An example of data collected utilizing this method is shown in Figure 11.12.3.

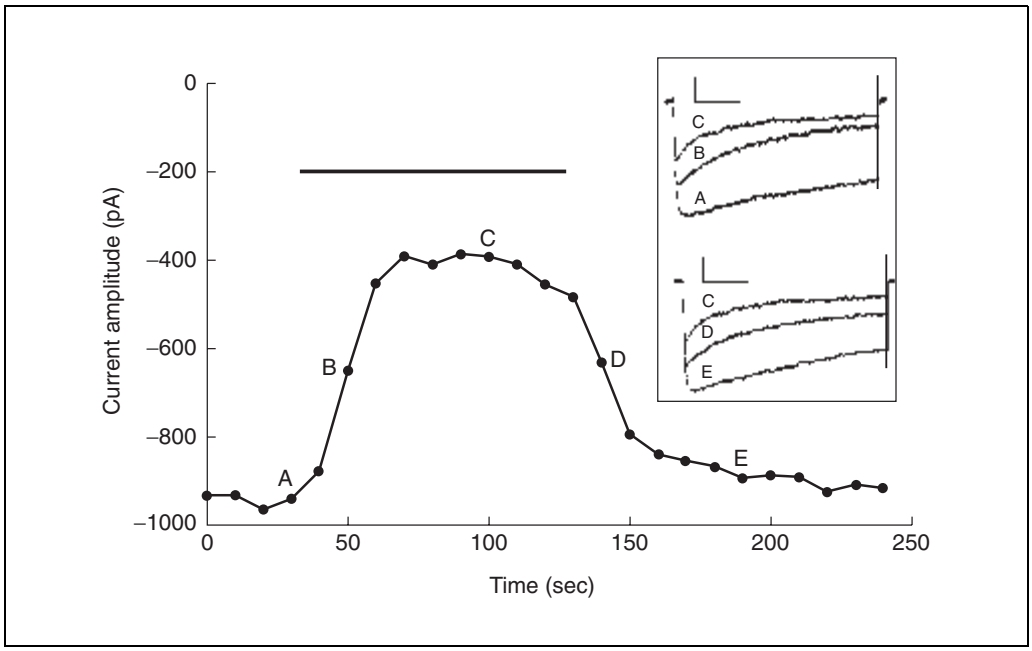

Figure 11.12.3 Reversible inhibition of Ca^{2+} currents in PC12 cells. The data presented in this figure were obtained using the protocol described in the Basic Protocol, step 14b. A test potential to +20 mV was delivered every 10 sec from a holding potential of –70 mV. When an inhibitor of Ca^{2+} channel function was applied to the bath solution (solid bar), peak current amplitude decreased rapidly. Stopping perfusion of the inhibitor (by washing) resulted in a rapid recovery of the current amplitude. The traces labeled A through E on the inset (trace C is repeated to facilitate comparisons) correspond to the points labeled A through E on the plot of the current amplitude versus time. In the inset, the scale bars correspond to 200 pA and 25 msec.

TISSUE CULTURE FOR PC12 CELLS

SUPPORT PROTOCOL

PC12 cells are a commonly used cell line for both neurobiological and neurotoxicological studies of differentiation, neurochemistry, and ion channel function. Maintenance of this cell line in culture and the preparation of plates for electrophysiology will be briefly discussed here. It should be noted that antibiotics can inhibit voltage-sensitive Ca^{2+} channels (Atchison et al., 1988) and are not used, therefore, requiring that all procedures must be conducted in a sterile environment.

Materials

PC12 cells

Dulbecco's modified Eagle medium (DMEM), supplemented with 44 mM $NaHCO_3$, 2 mM HEPES, 7.5% (v/v) fetal bovine serum (FBS), and 7.5% (v/v) horse serum

50 µg/ml poly-L-lysine

50 ng/ml human recombinant nerve growth factor (NGF) or 100 ng/ml mouse 7s NGF

25-cm^2 polystyrene culture flasks

25-mm glass coverslips, sterile

6- or 12-well polystyrene multiwell plates

15-ml conical centrifuge tubes

NOTE: All solutions and equipment coming into contact with cells must be sterile, and proper sterile technique should be used accordingly.

NOTE: All culture incubations should be performed in a humidified 37°C, 5% CO_2 incubator unless otherwise specified.

1. Seed 1×10^6 undifferentiated PC12 cells into 25-cm^2 polystyrene culture flasks containing 10 ml supplemented DMEM. Incubate cells in a 37°C humidified, 5% CO_2 incubator. Feed the cells every 3 or 4 days by removing 5 ml of medium from the flask and replacing with 5 ml of fresh supplemented DMEM.

   After 1 week, the flask will contain ~18×10^6 cells, which can be utilized for step 2.

2. To prepare cells for electrophysiological recordings, place sterile glass coverslips into 6- or 12-well polystyrene plates and cover with 2 ml of sterile, deionized water containing 50 µg/ml poly-L-lysine. Let plates stand to the side while the steps below are completed.

3. Taking a flask of undifferentiated PC12 cells, dislodge the cells by rapidly striking the flask against the palm of the hand three to five times (if cultured on uncoated polystyrene flasks, the cells dislodge easily). Transfer the cell suspension into a 15-ml conical centrifuge tube and centrifuge 10 min at ~$1000 \times g$, room temperature. Discard the supernatant and resuspend the cells in ~5 ml of fresh supplemented DMEM.

4. Remove an aliquot of cells to count and determine the cell concentration (*APPENDIX 3B*). Adjust the cell concentration to ~7.4×10^{-4} cells/ml with supplemented DMEM.

   This concentration will give an adequate number of cells for recording while also supplying numerous individual (rather than clumps of) cells.

5. Wash the plates containing the coverslips (from step 2; 25-mm coverslips in 6-well plates) two times, each wash with 2 ml of sterile deionized water, then plate 2 ml/well of cell suspension. Place in the 37°C humidified, 5% CO_2 incubator.

6a. *If undifferentiated cells are desired for recording:* Allow the cells to adhere 2 to 3 hr and examine over the next several days, until they become confluent.

6b. *If differentiated cells are desired for recording*: After 2 hr, replace the medium in the well with 2 ml/well of supplemented DMEM and 50 ng/ml of human recombinant nerve growth factor (NGF) or 100 ng/ml mouse 7s NGF. Examine the cells after they acquire a neuronal phenotype.

   After 2 to 3 days, cells will differentiate to a neuronal phenotype, although Ca^{2+} current will continue to increase for 6 to 7 days.

REAGENTS AND SOLUTIONS

*Use Milli-Q-purified water or equivalent for all recipes and protocol steps. For common stock solutions, see **APPENDIX 2A**; for suppliers, see **SUPPLIERS APPENDIX**.*

Extracellular bath solution used for recording Ca^{2+} currents

To make 500 ml:
0.735 g $CaCl_2 \cdot 2H_2O$ (mol. wt. 147; 10 mM final)
0.9 g D-glucose (mol. wt. 180.2; 10 mM final)
2.38 g HEPES (mol. wt. 238; 20 mM final)
0.102 g $MgCl_2$ (mol. wt. 203.3; 1 mM final)
3.65 g NaCl (mol. wt. 58.5; 125 mM final)
0.83 g tetraethylammonium (TEA)·Cl (mol. wt. 165.7; 10 mM final)
pH to 7.4 with 5 M NaOH
Adjust to 340 mOsm with sucrose
To record for Ba^{2+} currents: Substitute 1.22 g/500 ml or 2.44 g/liter $BaCl_2$ (mol. wt. 244; 10 mM final) for $CaCl_2$ in the above extracellular bath solution.
Store for 7 to 10 days at 4°C or for 12 months at −20°C.

Intracellular (patch pipet) solution

To make 100 ml:
0.220 g ATP (mol. wt. 551.1; 4 mM final)
2.1 g CsCl (mol. wt. 168.4; 125 mM final)
0.190 g EGTA (mol. wt. 380.4; 5 mM final)
0.180 g D-glucose (mol. wt. 180.2l 10 mM final)
0.238 g HEPES (mol. wt. 238; 10 mM final)
0.020 g $MgCl_2$ (mol. wt. 203.3; 1 mM final)
0.165 g TEA·Cl (mol. wt. 165.7; 10 mM)
pH to 7.4 with 20% (w/v) aqueous solution TEA·OH
Adjust to 310 to 315 mOsm with sucrose
Store frozen in 5-ml aliquots up to 12 months at −20°C.

This buffer is an example of an intracellular (patch pipet) solution used for recording Ca^{2+} currents from PC12 cells.

QX-314 solution

As an alternative to using tetrodotoxin in the extracellular buffer, QX-314 must be applied via the intracellular solution to block function of voltage-sensitive Na^+ channels. Make a 10 mM solution of QX-314 bromide in distilled water and heat to ~70°C to dissolve. This solution can be diluted 1:100 in intracellular solution for which the osmolarity has been reduced by 10% by the addition of distilled water. Store frozen in 0.1-ml aliquots up to 6 months at −20°C.

Tetrodotoxin stock solution

Dissolve 1 mg of tetrodotoxin into 1.56 ml of acetate buffer (pH ~4 to 5) solution to make a 2 mM stock solution. This can be diluted 1:2000 directly into the extracellular buffer to give a final concentration of 1 μM tetrodotoxin. Store for 1 to 2 months at 4°C or dispense into 0.1-ml aliquots and store up to 6 months at −20°C.

CAUTION: Tetrodotoxin is extremely toxic and potentially lethal. Extreme caution should be exercised when handling this compound. Use the QX-314 solution (see recipe) as an alternative.

COMMENTARY

Background Information

One aspect of the tissues of the nervous system that makes it unique from other tissues is the degree to which electrical excitability is a critical component of its proper function (Hille, 2001). This aspect of the nervous system also renders it particularly sensitive to toxicants which are capable of disrupting function of the numerous ion channels that control, modulate, or depend on electrical activity. There are many excellent examples of neurotoxicity produced via direct disturbance of ion-channel function (Shafer, 1999), including the effect of pyrethroid insecticides on voltage-sensitive Na^+ channels (Narahashi et al., 1998), heavy metals on voltage-sensitive Ca^{2+} channels (Audesirk, 1993; Sirois and Atchison, 1996), organochlorine insecticides on $GABA_A$ receptors, and imidacloprid on nicotinic acetylcholine receptors (nAChR). Indirectly, other classes of neurotoxicants can also disturb ion-channel function and electrical activity. For example, overstimulation of nAChR function contributes to the toxicity observed following inhibition of acetlycholinesterase by organophosphate and carbamate insecticides. Activation of muscarinic acetylcholine receptors also often results in alterations of ion-channel function, although the resulting electrical changes typically occur over a period of seconds to minutes, rather than milliseconds (as with changes mediated directly by ion channels).

Electrophysiological techniques have proven indispensable in understanding the basic function of the nervous system as well as in elucidating the cellular mechanisms of a wide variety of neurotoxicants. In the early 1980s, Hamill and co-workers (1981) made significant

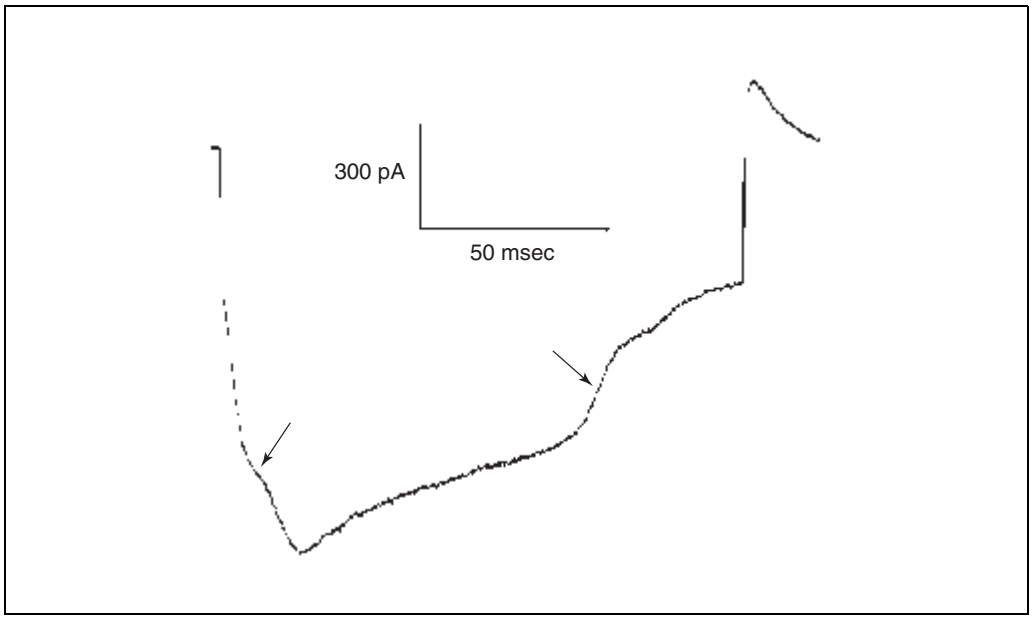

Figure 11.12.4 Example of a current trace from a cell where space clamp is poor. In this example trace, both the activation (left arrow) and inactivation (right arrow) of the Ca^{2+} current contains pronounced shoulders that indicate that the cell is inadequately space-clamped. Compare the shape of this current trace to the examples in the inset of Figure 11.12.3.

advances in recording techniques utilizing patch electrodes. Their work revolutionized the field of neurophysiology and dramatically increased the understanding of the mechanisms of action of a wide variety of insecticides, metals, and other compounds in neurotoxicology. In the future, this methodology will continue to play an important role in elucidating differences in species susceptibility and mechanisms of resistance to insecticides (Ffrench-Constant et al., 2000), as well as aid in designing novel insecticides.

Critical Parameters

There are a number of critical parameters required to obtain high-quality recordings and useful information regarding the effects of neurotoxicants on the mechanism of ion channel function. Good recordings begin with healthy cells and high-resistance seals. A number of other factors are important to ensure the integrity and reliability of the data, including correction for current rundown, minimization of electrical noise, and data collection (digitization) rates that are sufficiently fast where there is no vital information missing or lost. Of vital importance is the ability to completely control the membrane voltage at all points of the cell (space clamp). In cells with inadequate space clamp, the potential across the membrane does not change uniformly in terms of the rate and/or total change in membrane potential. Insufficient space clamp often arises because the cell is very large, has an irregular shape, contains long processes, or has established connections with other cells. An example of inadequate space clamp is shown in Figure 11.12.4. The shoulders in the current in Figure 11.12.4 are a common example of inadequate space clamp. In cells with inadequate space clamp, measurements of current amplitudes as well as kinetics are suspect, and data from cells with inadequate space clamp should be discarded.

Pulse protocol generation and data acquisition are almost always controlled via computer. Thus, it is important to understand the basics of digitization. Changes in membrane potential and current are analog events. To be controlled and stored by the computer, these analog events must be converted to digital events. When converting analog to digital, the analog signal, e.g., a membrane current, is sampled periodically and its value recorded for later reconstruction of the analog signal as a digital signal. The accuracy of reconstruction will depend on the rate at which samples are collected; the faster the rate of digitization, the more accurately the digital record will reflect the analog signal. Responses that occur more rapidly than, or close to, the sampling rate will be lost or degraded. Therefore, it is important to give some forethought to the type of signal to be recorded and the rate at which this signal occurs. Some software packages allow the sampling rate to

be changed over the course of recording a single event. For example, one may wish to examine tail current (a delayed current response that occurs upon membrane repolarization) more closely than current evoked during a depolarization and thus sample at a higher rate during that period of the recording. For specific information regarding data collection, consult the user's manual of the data acquisition software.

In order to record voltage-sensitive Ca^{2+} currents, it is necessary to block outward currents, usually carried by potassium. Thus, the solutions contain a K^+-channel blocker, tetraethylammonium (TEA), in place of K^+. Additionally, Ba^{2+}, which blocks both inwardly and outwardly rectifying K^+ channels, can be used to replace Ca^{2+}, particularly if Ca^{2+}-activated K^+ channels are present. Barium also offers an additional advantage as it does not cause Ca^{2+}-induced inactivation of Ca^{2+} currents. In order to investigate Ca^{2+} channel kinetics, it is also necessary to block function of voltage-sensitive Na^+ channels, either with tetrodotoxin or QX-314 (which must be applied intracellularly to be effective). In addition, for recording any voltage-sensitive current, it is necessary to determine the leak current present in each cell. Leak current flows in the direction of the voltage step and is linear. Typically, data-acquisition software includes online leak subtraction, which is achieved by delivery of a series of prepulses prior to delivery of the test pulse, followed by online subtraction (P/N protocols). The magnitude of the prepulses is determined by dividing the magnitude of the test pulse (P) by the number of prepulses to be delivered (N). The current flowing in response to the prepulses is averaged and scaled, then subtracted from the current subsequently recorded during the test pulse. The advantage of this protocol is that leak subtraction is simple and almost instantaneous. The disadvantage is that changes in leak associated with toxicant exposure might be overlooked because leak is not specifically examined. Manual subtraction of leak current can be conducted by writing protocols to examine this component specifically, then subtracting the leak current from the current data acquired using other protocols.

Compensation of pipet and whole-cell capacitance is an iterative process and can only be learned by experience. Most manufacturers of patch-clamp amplifiers include or make available a model cell for practice. Typically, these model cells have ports to attach the head stage, which electronically simulate a patch pipet in the bath solution, in the cell-attached patch mode and in the whole-cell patch mode. This model cell can be utilized to help minimize or eliminate unwanted electrical noise in the system and to practice adjustment of series resistance and capacitance compensations.

With respect to utilization of patch-clamp methods for toxicology, there are a couple of additional considerations. First, many neurotoxicants are highly lipophilic and difficult to wash out of biological tissues. Thus, plan to expose a coverslip to toxicant only one time. Even in the event a toxicant does have reversible effects, it may be unwise to record from multiple cells on the same coverslip because the effects of repeated exposure may be subtle. In addition, the data will have more statistical value if only one cell per coverslip is used. It should also be noted that ion-channel responses can change with the in vitro age of primary cells, passage number, or treatment (e.g., NGF) of clonal cell lines (see Fig. 11.12.2). Thus, it is either necessary to characterize such age- or passage-related changes thoroughly so that effects of toxicants can be examined during a period of stability, or to design experiments such that the same-day in vitro or passage number is utilized for each experiment. Also important in pharmacological as well as toxicological experiments is the method of application of compounds to the cells. The simplest method is to add the compound into the solution that is being perfused into the recording chamber. If the chamber volume is kept sufficiently small and/or the flow rate is sufficiently fast, rapid changes in the concentration of chemical applied to the cell are possible. A large number of perfusion devices are available that permits applications and changes in solutions in milliseconds or less and/or the ability to change through several different solutions in rapid succession, such as when generating a concentration-response curve.

Troubleshooting

For beginners, the key to successful recordings is the formation of a gigaohm seal between the patch pipet and the cell membrane. If an experienced patch-clamp experimenter is available, have them polish pipets until the beginner is adept at forming gigaohm seals. This will eliminate the variable in the learning stage. Failure to form gigaohm seals successfully is most likely to arise from improperly or inadequately fire-polished pipets, or dust, dirt, or debris on the pipet tip. Often the latter can be

seen on the tip of the pipet. Start each day with freshly made and polished pipets and store them in a covered dish until use. Alternatively, many electrophysiologists polish each patch pipet immediately prior to use. Applying positive pressure from the time the pipet enters the bath solution can help reduce the attachment of dust to the pipet tip. Filtering solutions can also reduce the amount of dust and other debris, and if needed, one can actually wash the glass blanks with deionized water followed by ethanol in order to reduce debris from the glass itself. If difficulty is encountered, begin with fire polishing and implement other steps such as filtering solutions and washing pipets only if needed. Over-polishing will typically result in sealing of the tip of the electrode. Thus, one end of the spectrum between not enough polishing and too much polishing is clearly defined.

Another key to gigaohm-seal formation is the health of the cells themselves. Unhealthy cells often have blebbed or other irregular membranes, and in many cases the membrane will rupture prior to obtaining a gigaohm seal. If this problem occurs, it may be wise to check the pH, osmolarity, and age of the buffer solution. If these parameters are within recommended ranges, then additional examination of the cells should be undertaken; bacterial contamination, serum deprivation, or depletion of nutrients in the medium (too long between additions of fresh medium) all can negatively impact the health and viability of the cells.

Anticipated Results

Utilizing the Basic Protocol and the Support Protocol, one can anticipate obtaining current-voltage relationships with a shape similar to that depicted in Figure 11.12.2. All voltage-sensitive ion channels have a characteristic I/V relationship that is determined by the electrochemical driving force across the membrane for the ion of interest. Changes in the shape of this curve in the presence of a neurotoxicant can provide information regarding the mechanism by which it inhibits ion-channel function. For example, if the toxicant inhibits current to a greater extent at high voltages and to a lesser extent at other voltages (voltage-dependent block), this suggests that the toxicant may interact with the pore of the channel. Cadmium (Chow, 1991) and other divalent heavy metals block voltage-sensitive Ca^{2+} channels (VSCC) in a voltage-dependent manner. The format chosen for expression of the data in Figure 11.12.2 allows for the illustration of some additional points. First, it is an example of a change in current characteristics over time in a clonal cell line and illustrates the need to be cognizant of such changes when conducting experiments. Age-dependent changes in ion-channel function have been reported in a variety of clonal and primary cell types. Second, when examining acute effects of toxicants, it is possible to use each cell as its own control, which will help to normalize data obtained. However, examination of subacute or chronic effects will require measuring different populations of control and toxicant-treated cells. The capacitance of the cell membrane can serve as a surrogate measure of cell size, as it is relatively constant as a function of membrane surface area and can be utilized to normalize for differences in cell size. This may be advantageous in decreasing variability and/or potentially alerting the experimenter to toxicant- or selection-induced differences in the population of cells sampled from control versus toxicant-treated cultures.

One might anticipate that exposure to neurotoxic or neuroactive substances would increase or decrease (as shown in Fig 11.12.3) the amplitude of ion channel currents. However, focusing solely on the peak amplitude of current might result in missing other important effects of toxicants on channel function. Such is the case in Figure 11.12.3. Although treatment with the toxicant decreased the peak current amplitude, two other (possibly related) effects are apparent from the current traces in the inset. First, there is a clear change in the inactivation kinetics of the treated currents; they appear to inactivate more rapidly in the presence of toxicant. Second, if the amplitude of current is measured at its peak (close to the left edge of the current traces) versus its end (to the right), it is apparent that the toxicant reduces the end current amplitude to a greater extent than it reduces the peak current amplitude. This result suggests several additional mechanistic questions to address. First, inactivation time constants should be compared in control versus treated cells. Second, because these are PC12 cells, they are likely to contain at least two (Shafer and Atchison, 1991), and possibly more types of VSCC (Colston et al., 1998). Thus, additional experiments should isolate different current subtypes and examine whether a specific subtype is more sensitive to the toxicant than others or whether the toxicant similarly affects the current amplitude and kinetics of all VSCC subtypes present. Additional informa-

tion regarding mechanisms of block can be obtained by changing the rate at which step depolarizations are applied. If a toxicant blocks current more rapidly or to a greater extent at higher frequencies of stimulation, this suggests that the toxicant has a higher affinity for the open state of the channel. Many local anesthetics produce a use-dependent block of Na^+ channels, and pentobarbital has been shown to cause use-dependent block of kainate- and quisqualate-activated currents (Marszalec and Narahashi, 1993).

Time Considerations

Successful recording of Ca^{2+} currents from a cell can take as little as 10 min, if preparation time is not considered. However, as mentioned above, large blocks of time in the laboratory will be more fruitful than shorter periods. This allows data to be collected from a sufficient number of cells to gain statistically reliable information regarding effects of toxicants on ion-channel function, as well as for failed attempts to obtain a good recording. Patience and perseverance are prerequisites for success when utilizing this technique. In addition to collecting the data, since multiple pieces of information can be obtained from a given recording (e.g., the amplitude of current at its peak and the end of the voltage step, activation times, inactivation times), data analysis can often be as or more time consuming than actual data collection.

Acknowledgements

The editors of *Current Protocols in Toxicology* wish to thank Dr. Toshio Narahashi for his expert assistance in enlisting and editing this unit on electrophysiology.

Literature Cited

Atchison, W.D., Adgate, L., and Beaman, C.M. 1988. Effects of antibiotics on uptake of calcium into isolated nerve terminals. *J. Pharmacol. Exp. Ther.* 245:394-401.

Audesirk, G. 1993. Electrophysiology of lead intoxication: Effects on voltage-sensitive ion channels. *Neurotoxicol.* 14:137-147.

Catterall, W.A. 1998. Structure and function of neuronal Ca^{2+} channels and their role in neurotransmitter release. *Cell Calcium* 24:307-323.

Chow, R.H. 1991. Cadmium block of squid calcium currents. Macroscopic data and a kinetic model. *J. Gen. Physiol.* 98:751-770.

Colston, J.T., Valdes, J.J., and Chambers, J.P. 1998. Ca^{2+} channel alpha 1-subunit transcripts are differentially expressed in rat pheochromocytoma (PC12) cells following nerve growth factor treatment. *Int. J. Dev. Neurosci.* 16:379-389.

Ffrench-Constant, R.H., Anthony, N., Aronstein, K., Rocheleau, T., and Stilwell, G. 2000. Cyclodiene insecticide resistance: From molecular to population genetics. *Annu. Rev. Entomol.* 45:449-466.

Hamill, O.P., Marty, A., Neher, E., Sakmann, B., and Sigworth, F.J. 1981. Improved patch-clamp techniques for high-resolution current recording from cells and cell-free membrane patches. *Pflügers Arch.* 391:85-100.

Hille, B. 2001. Ion channels of excitable membranes. 3rd Edition. Sinauer Associates, Sunderland, MA.

Marszalec, W. and Narahashi, T. 1993. Use-dependent pentobarbital block of kainate and quisqualate currents. *Brain Res.* 608:7-15.

Narahashi, T., Ginsburg, K.S., Nagata, K., Song, J.H., and Tatebayashi, H. 1998. Ion channels as targets for insecticides. *Neurotoxicol.* 19:581-590.

Shafer, T.J. 1999. The role of ion channels in neurotoxicity. *In* Neurotoxicology. (H.A. Tilson and G.J. Harry, eds.) pp. 99-137. Taylor & Francis, Philadelphia, PA.

Shafer, T.J. and Atchison, W.D. 1991. Transmitter, ion channel and receptor properties of pheochromocytoma (PC12) cells: A model for neurotoxicological studies. *Neurotoxicol.* 12:473-492.

Sirois, J.E. and Atchison, W.D. 1996. Effects of mercurials on ligand- and voltage-gated ion channels: A review. *Neurotoxicol.* 17:63-84.

Key References

Catterall, 1998. See above.

This review provides an excellent overview of the different types of voltage-sensitive calcium channels and their roles in neurotransmitter release.

Ffrench-Constant et al., 2000. See above.

This paper provides a review of work completed by this and other groups demonstrating that insecticide resistance to cyclodienes is the result of specific mutations in the structure of $GABA_A$ receptors. It is an excellent example of how the coupling of molecular biology techniques with electrophysiology is increasing the understanding of mechanisms of the effects of neurotoxicants.

Hamill et al., 1981. See above.

This is the seminal paper describing the use of patch-clamp techniques. Sakmann and Neher won the 1991 Nobel Prize for their related work utilizing these techniques to describe the function of ion channels at the level of an individual channel.

Hille, 2001. See above.

Also known as "The gospel according to St. Bertil"—no disrespect intended. This book by Bertil Hille provides in-depth coverage of the biophysics of ion channels from the basics such as equivalent electrical circuits in cells, Ohm's law, and the Nernst equation to more advanced topics such as the rela-

tionship between molecular structure and function, theory of gating, and mechanisms of block. It is one of the most important books for an electrophysiologist to own.

Internet Resources

http://www.axon.com/MR_Axon_Guide.html

Axon Instruments is a commercial vendor of amplifiers and other cellular electrophysiology equipment. However, the mention of this Web site is not an endorsement of their equipment. Rather, it is listed because they do make available, free of charge, a publication called The Axon Guide. This publication contains additional practical and theoretical information about path clamp electrophysiology.

Contributed by Timothy J. Shafer
U.S. Environmental Protection Agency
Research Triangle Park, North Carolina

Detection and Assessment of Xenobiotic-Induced Sensory Neuropathy

Painful peripheral neuropathy is not an uncommon result of chronic administration of medications. Perhaps the best known examples of such neuropathies are those resulting from antineoplastic agents used in the treatment of cancers and antiretroviral medications used in the treatment of HIV infection, but there are many other examples. The behavioral assessment of peripheral nerve function is therefore an important part of experiments directed at determining the toxicities of various xenobiotic compounds with intended medical purposes. The same techniques can be used to evaluate the toxic potential of industrially used or even naturally occurring compounds.

Though the specific type of painful neuropathy caused by various agents will differ, most drug-induced neuropathies are detectable using either momentary thermal or mechanical stimuli. This unit describes a pair of assays that can be performed together on the same groups of rats, and repeated over time with relatively stable baseline responses. The techniques described include the thermal paw flick assay (see Basic Protocol 1) and the mechanical von Frey fiber–based assay (see Basic Protocol 2). These protocols are quite humane and are not associated with distress or tissue damage to animals. In fact, variations of these assays are used in human clinical and experimental sensory testing. Both assays can be used repeatedly on groups of rodents undergoing prolonged exposures to the xenobiotics of interest. The use of a thermal and a second mechanical type of stimulus increases the power in being able to detect relevant sensory changes.

NOTE: All protocols using live animals must first be reviewed and approved by an Institutional Animal Care and Use Committee (IACUC) and must follow officially approved procedures for the care and use of laboratory animals.

THERMAL PAW FLICK ASSAY

BASIC PROTOCOL 1

This assay uses heat as the noxious stimulus, and the investigator times latency to removal of the hind paw from the heat as the measured parameter. This type of testing was initially described by Hargreaves et al. (Hargreaves et al., 1988). Modifications for use of mice are available (Li et al., 2001). The basic apparatus is a device capable of delivering a thermal stimulus of variable intensity coupled to a timing device. When this assay is employed to detect changes in sensory thresholds in response to the chronic administration of a xenobiotic, animals are typically assessed every 1 to 3 days. Those changes resulting in anesthesia of the hind paw will be associated with progressively prolonged latencies, whereas those resulting in the sensitization of the hind paw (thermal hyperalgesia) will be associated with declining latencies.

Materials

Rats
Thermal paw flick (Hargreaves) apparatus (IITC model 390 or similar)
Enclosures (if not included with other testing apparatus): ~15 × 15–cm area and ~30-cm high (if no lid is used) clear plastic (rats should not be restrained within enclosures)

1. Move animals from their housing facility to the testing area well ahead of the start of the experiment. Have the platform of the paw flick device at a steady-state temperature.

Contributed by J. David Clark
Current Protocols in Toxicology (2004) 11.13.1-11.13.8

The strain, gender, age, and source of rats should be concordant with those parameters used by the laboratory for biochemical or other toxicological studies.

The sample size is generally in the range of 7 to 10 rats/group for detection of 10% to 15% changes in thermal or mechanical nociceptive thresholds. Stronger experimental protocols generally employ a placebo or vehicle-treated group of animals thus allowing between-group comparisons.

The husbandry and handling of the animals should be standardized. Preferably, a single investigator should be responsible for a complete experiment.

Animals should be ordered and allowed to acclimate to the local housing facility for at least several days prior to use in behavioral experiments. Most investigators house two rats/cage with a 12:12 hr light/dark cycle and standard laboratory rat feed and water ad libitum. More reliable data are obtained when experiments are preceded by one or more mock testing sessions in which rats are transported, handled, and tested in exactly the same manner as would be in the case if actual data were being collected. Gentle handling should always be employed. The temperature of the glass testing platform is generally held a few degrees above room temperature, e.g., 27° to 30°C, to maintain a constant temperature from day to day. Temperatures above 30°C might overheat the animal.

2. Place animals on the testing platform and allow to acclimate for 20 min.

   The thermal paw flick (Hargreaves) devices generally consist of a source of thermal stimulation like a focused beam of intense light and a clear platform on which animals are placed thus allowing stimulation of the plantar surface of the hind paws. They should also allow testing of multiple animals on the same platform, have a temperature-controlled glass platform, and a timing mechanism linked to the activation and termination of the thermal source precise to at lease 0.1 sec.

   Inadequate or inconsistent acclimation times will adversely affect the quality of the data. The injection of test substances (if employed) should not occur during this acclimation period.

3. Position the source of thermal stimulation under one of the hind paws such that the beam of light will impinge upon the soft area of skin directly distal to the footpads (tori). Zero the timing device.

   The investigator should always stimulate the same hind paw of the same rat, or include in every data set measurements from both hind paws. Side-to-side variability is not uncommon. Preliminary testing can be used to determine the appropriate lamp output to obtain a 10 to 12 sec baseline latency in control animals. Do not test animals with obvious lesions of the hind paws.

4. Activate the light source/timer and leave in place until the animal lifts or flicks its hind paw. When the animal responds, stop the timer and stimulation. Make at least two and preferably three measurements for each paw tested each separated by ~2 min.

   The part of the paw tested must be in contact with the glass surface as the glass acts as a heat sink. If the paw is held above the glass the response time will be shorter. If liquid is present on the glass the response time will be longer. If urine is present it should be wiped away prior to beginning the assay. Occasionally, animals will walk away or display a non-specific behavior. Those measurements should be repeated.

5. After testing, return animals to their cages where they have access to food and water unless being used for additional testing.

   Other parameters to hold constant are: (1) personnel performing the tests; (2) time of day of testing; (3) the protocol for handling the animals including the type of gloves and protective clothing worn by investigators; (4) temperature and lighting of the room; and (5) noise level.

MECHANICAL VON FREY ASSAY

Testing for thresholds to noxious mechanical stimuli is often performed instead of or in addition to the thermal methods. In this section, a method for von Frey fiber–based assessment is presented, which is based on the methods described by Chaplan et al. (1994) to derive the 50% response threshold. Similar to the thermal technique described in Basic Protocol 1, this assay is typically applied every 1 to 3 days during the treatment of animals with the xenobiotic under study. Those changes resulting in anesthesia of the hind paw will be associated with progressively increased response thresholds, whereas those resulting in the sensitization of the hind paw (mechanical allodynia) will be associated with declining latencies.

Materials

Rats
Mesh platforms (IITC model 410 or similar)
von Frey fibers: sets of individual fibers or calibrated instruments of various designs are available (e.g., IITC model 2290 or Stoelting model 58011)
Enclosures (if not included with other testing apparatus): ~15 × 15–cm area and ~30-cm height (if no lid is used) clear plastic

1. Move animals from their housing facility to the testing area well ahead of the start of the experiment.

   The strain, gender, age, and source should be concordant with those parameters used by the laboratory for biochemical or other toxicological studies.

   The sample size is generally in the range of 7 to 10 rats/group for detection of 10% to 15% changes in thermal or mechanical nociceptive thresholds. Stronger experimental protocols generally employ a placebo or vehicle-treated group of animals thus allowing between-group comparisons.

   The husbandry and handling of the animals should be standardized. Preferably, a single investigator should be responsible for a complete experiment.

   Animals should be ordered and allowed to acclimate to the local housing facility for at least several days prior to use in behavioral experiments. Most investigators house two rats/cage with a 12:12 hr light/dark cycle and standard laboratory rat feed and water ad libitum. More reliable data are obtained when experiments are preceded by one or more mock testing sessions in which rats are transported, handled, and tested in exactly the same manner as would be the case if actual data were being collected. Gentle handling should always be employed.

2. Place animals on the mesh platform and allow to acclimate for 20 min.

   Overall size of the mesh platform should accommodate 2 to 3 animal enclosures with ~0.5 × 0.5–cm openings. The height should be >15 cm from the surface on which it is placed to allow von Frey fibers to be applied from below.

   Inadequate or inconsistent acclimation times will adversely affect the quality of the data. The injection of test substances (if employed) should not occur during this acclimation period.

3. Position equipment so that the von Frey fibers can be applied to the soft area of skin directly distal to the footpads (tori).

   The investigator should always stimulate the same hind paw of the same rat, or include in every data set measurements from both hind paws. Side-to-side variability is not uncommon. Do not test animals with obvious lesions on the hind paws.

4. Apply the first von Frey filament by applying upward pressure until a slight bend in the fiber is seen.

   Fiber sets are usually based on the Semmes Weinstein monofilament fiber progression.

   For rats, a typical set of fibers contains fibers of the following stiffnesses: 0.41, 0.70, 1.20, 2.00, 3.63, 5.50, 8.50, and 15.10 g. Fibers are applied for a maximum of 5 to 6 sec beginning with the 2.00-g fiber. They are applied in increasing stiffness until a response is obtained. A typical response is a sharp upward or lateral movement of the hind paw.

5. Once a positive response is obtained, apply the fiber of next lowest stiffness. If that fiber leads to a response, then apply the next lowest fiber, otherwise use the next higher stiffness fiber. Score a response as an "X" and the lack of response as an "O." Continue this process until four fibers have been applied after the first one causing a response.

   It is critical that each fiber be applied in the same manner and on the same hind paw location. Occasionally, a response will be equivocal and the same fiber will need to be re-applied. Fibers can be applied in rapid succession with only a few seconds passing between fiber applications. Since this up-down method is based on the successive application of fibers near the 50% response threshold, it is only necessary to perform the fiber application protocol once per test day.

6. After testing, return animals to their cages where they have access to food and water unless being used for additional testing.

   Other parameters to hold constant are: (1) personnel performing the tests; (2) time of day of testing; (3) the protocol for handling the animals including the type of gloves and protective clothing worn by investigators; (4) temperature and lighting of the room; and (5) noise level.

COMMENTARY

Background Information

Xenobiotics and sensory change

Painful peripheral neuropathy is not an uncommon result of chronic administration of medications. Perhaps the best known examples of such neuropathies are those resulting from antineoplastic agents, such as vincristine, cisplatinum, and paclitaxel, used in the treatment of cancers and antiretroviral medications, such as didanosine and stavudine, used in the treatment of HIV infection, but there are many other examples. These neuropathies can be either of transient or long-term durations and cause disability and suffering for the duration of their presence. Furthermore, the mechanisms for the neuropathies vary and can involve demylination, axonal degeneration, and death of the neuron itself. Excellent reviews discuss these issues in some detail (Peltier and Russell, 2002; Dieterich, 2003; Verstappen et al., 2003; Visovsky, 2003). Toxic peripheral neuropathies are not limited to those caused by medicinal compounds. Many naturally occurring substances and industrial byproducts have been associated with peripheral neuropathy particularly after chronic exposures. In the evaluation of new pharmaceutical candidate compounds, especially those with chemical or mechanistic similarities to compounds with known neurotoxicities, investigators should consider the possibility of painful neuropathy resulting from short- or long-term administration.

The field of pain research has been responsible for the development and validation of dozens of pain assessment techniques. Some of the chief differences between these assays involve the use of phasic (momentary) versus tonic (lasting) stimulation. The type of noxious stimulus that is used is variable as well, but generally falls within one of the following categories: thermal, mechanical, electrical, or chemical. While these assays are commonly referred to as "pain assays," keep in mind that pain has both sensory and emotional components. Because the animal's actual experiences after the application of a noxious stimulus in a laboratory cannot be positively ascertained, the results are commonly referred to as measures of "nociceptive" thresholds or behaviors referring to the fact that they result from the application of a noxious stimulus, which may or may not be experienced in a way similar to what the human experience would be.

The first test suggested for use in this unit is the paw flick assay, which uses a thermal

stimulus. This test was introduced by Hargreaves et al. (1988), and it represents an improvement on earlier methods of thermal nociceptive testing. The most commonly used alternative test utilizing thermal nociceptive input is the tail flick assay which has been in use for many decades. The tail flick assay involves positioning an animal's tail over a source of heat, usually a focused beam of light. The measurement made is the latency from the application of heat until the flick of the tail out of the path of the light. This test is robust for measuring the analgesic effects of many compounds but has several drawbacks. For example, when doing the tail flick assay, the animal needs to be restrained, which causes the animal stress. Stress-induced analgesia is a well-studied phenomenon (Fields, 2000; Bodnar and Hadjimarkou, 2003) and can confound the interpretation of results. Another problem is that the noxious stimulus is directed at an area of scaly skin on the tail of the animal. Humans do not have tails nor do they possess epidermis of the same type. Lastly, rats (and especially mice) tend to occasionally move or flick their tails for reasons unrelated to the application of noxious stimulation. This reduces the baseline latency that can be targeted in experiments. If one is hoping to detect a reduced response latency as would be expected if the animals were to develop hyperalgesia such as occurs after chronic treatment with paclitaxel (Authier et al., 2000), one would want to set a long baseline latency thus providing improved ability to detect reductions in latency. The paw flick assay circumvents many of these problems by allowing the study animals to roam freely in a non-stressful environment, directing the noxious stimulus at an area of glaborous skin similar to human palmar or plantar skin and allowing for long baselines (up to ~20 sec or so for rats) coupled with an unequivocal paw flick response essentially only seen after noxious stimulation. Disadvantages of the technique include the relative expense of the equipment, commercially available paw flick devices currently cost about two times that of a tail flick apparatus, and the greater time needed to complete the assay.

The second assay suggested in this unit is the mechanical von Frey fiber–based assay. There are alternative mechanical methods including the Randall-Sellito paw pinch assay which is also commonly used. The paw pinch assay involves placing the hind paw between the jaws of a device capable of delivering a controlled, usually ramped calibrated force that is applied until the animal attempts to remove the paw or vocalizes. This assay is widely used for the measurement of analgesic activity and in situations in which diminished sensitivity to noxious stimulation is expected. The von Frey assay outlined in this unit is widely used for the quantification of diminished mechanical sensory thresholds, which occur in some patients with painful peripheral neuropathies. Like the thermal paw flick assay, no restraint of the animal is necessary, and the test can be performed repeatedly with stable baseline responses. The equipment costs are modest if conventional nylon von Frey fibers are used. There are several disadvantages, however. The von Frey fibers are fragile and their stiffness tends to change both with repeated use over months or years in a laboratory and with differences in temperature and humidity (Levin et al., 1978). If the fibers are applied form the bottom, a force greater than the weight of the hind paw cannot be applied as that amount of force will simply lift the hind paw. Unfortunately, the baseline threshold is often not much less that the force required to lift the paw thus limiting the utility of this procedure in detecting neuropathies resulting in lowered sensory thresholds.

One might ask why more than one assay would or should be used in toxicological studies. The answer lies in the specialization of various types of nociceptors in the peripheral nervous system. In this respect, differences exist both in the types of noxious stimuli to which the nerve fibers will respond and the type of fibers which carry the nociceptive information from a single type of stimulus. For example, a noxious heat stimulus applied to the hind paw of a rat is carried by both A-δ myelinated and type C unmyelinated fibers. In fact, the rate of heating of the skin affects the mixture of fibers carrying the nociceptive information with high rates of heating causing a disproportionate number of A-δ fibers to be activated while slow rates cause a larger fraction of C fibers to participate in the response (Yeomans et al., 1996). Similar complexities exist for responses to mechanical stimuli with cutaneous nociceptive fibers of the A-δ and C types showing differential sensitivity to punctate and non-punctate stimuli as well as differential sensitization after trauma (Pogatzki et al., 2002). Each of these fiber types have correspondingly unique neurochemical characteristics and distinct areas within the spinal cord to which they project (Sandkuhler, 1996a,b). Furthermore, the distribution of neuromodulatory receptors such as opioid receptors is fiber-type specific. Thus, investigators concerned with the possibility of peripheral neuropathy might consider

casting their net widely in order to maximize the chances of detecting xenobiotic-induced alterations in nervous system function.

Critical Parameters and Troubleshooting

Several issues pertaining to the animal subjects are critical for obtaining reproducible data in animal behavioral testing. The animals in experimental groups treated in parallel or in sequential experiments need to be of the same gender, strain, and age. Animals should always be obtained from a single supplier for a set of experiments to control for genetic drift and pre-experimental husbandry conditions. The light-dark cycle, feed, temperature, bedding materials, number of animals per cage, and size of cages should all be kept constant.

Test conditions should be kept consistent for the course of the experiment. Many investigators prefer to expose animals to test conditions at least once in an independent test session before beginning to collect data. Behavioral testing is best done in dedicated space free of extraneous noise and odors and with good temperature control and with consistent lighting. Equipment should be wiped down after use with non-perfumed cleaners. The animals should be transported to the testing area well ahead of the test session and be allowed time to acclimate to any enclosures, which are used prior to beginning testing. Experiments should take place at the same time each day. Data tend to be most reliable if the animals are handled gently by the same individual during all test sessions.

The specific assays also should be performed meticulously. For example, the equipment should be the same for all experiments within a single group of studies. When using the paw flick apparatus, the glass surface should be allowed to reach target temperature well before the animals are placed upon it. The stimuli need to be applied in the same manner to a consistent area of the hind paws. The von Frey fibers need to be calibrated periodically, and damaged fibers replaced. Other parameters like the time between application of stimuli and the number of times a stimulus is applied should be standardized for a group of studies.

See Table 11.13.1 for common problems and their solutions.

Anticipated Results

The specific reproducibility of results and variance within the data collected will be influenced by many factors, some within the control of the investigators and some particular to the nature of specific protocols (Table 11.13.2). The thermal paw flick protocol has been used

Table 11.13.1 Troubleshooting Guide to Assessment of Sensory Neuropathy

Problem	Possible cause	Solution
Day-to-day baseline thermal latencies differ by >10% in control animals	Difference in acclimation period	Allow consistent period of acclimation >20 min
	Altered stimulus strength	Check lamp output
	Urine/feces on test surface	Clean surface
	Handling/husbandry changes	Maintain consistent conditions
Day-to-day baseline mechanical thresholds differ by <10% in control animals	Difference in acclimation period	Allow consistent period of acclimation >20 min
	Handling/husbandry changes	Maintain consistent conditions
	Changes in von Frey fibers	Recalibrate instrument
		Recalibrate von Frey fibers

Table 11.13.2 An Example of Data Obtained

	Thermal testing	Mechanical testing
Baseline	12.0 ± 1 sec	15.0 ± 1 g
Mild neuropathy	10.0 ± 1 sec	10.0 ± 1 g
Severe neuropathy	8.0 ± 1 sec	4.0 ± 0.5 g

Table 11.13.3 Response Pattern[a]

Fiber (g)	Response
2.00	O
3.63	O
5.50	X
3.63	O
5.50	X
3.63	O
5.50	X

[a]The value for Xf is 0.74, the value for δ is 0.224 and the value for κ is –0.458. The calculated value for the 50% threshold would be 4.34 g. This is an intuitively reasonable answer for the interpolated threshold since the 5.50 g fiber always yielded a response while the next lower 3.63 g fiber never caused a response.

by many investigators to identify changes in latencies as small as ~10% of the baseline or control values. For many treatments, the changes in mechanical thresholds tend to be more robust allowing greater sensitivity in detecting neuropathy when using mechanical assays. With preliminary data in hand, individual investigators can undertake power analyses to predict sample size requirements for particular protocols. Generally significance is sought at the 0.05 level with power of ≥90%. Group sizes of six to ten are employed by most investigators.

Analysis of the data collected will be influenced by the design of the actual experiments. In most experiments designed to detect neuropathy during or after exposure to xenobiotics, investigators will have repeated thermal and mechanical measurements for a control and an experimental group of animals. The key comparisons which will be made are: (1) between baseline nociceptive thresholds and those observed on days subsequent to the beginning of exposure to the xenobiotic, and (2) between control and experimental groups at various time points. The withdrawal latencies from noxious thermal stimulation involve time, a continuous variable. The mechanical withdrawal thresholds, if measured using a continuously variable force, can also be regarded as continuous. If a set of von Frey fibers is used according to the up-down paradigm, a more sophisticated analysis is required to determine the 50% response threshold.

The analysis of continuous variables across time and between groups is generally accomplished using a two-way ANOVA analysis with appropriate post-hoc testing. In most instances, testing for significance at the $P = 0.05$ level is considered standard. The amount of variance in the actual data obtained along with the chosen sample sizes may be used to arrive at an estimate of power if that parameter is desired.

The analysis of the non-parametric data obtained from von Frey mechanical testing is substantially more complex. A detailed discussion of the processing of such data can be found in the article by Chaplan et al. (1994) in which the approach to determining the 50% mechanical response threshold is presented. This interpolated parameter is the fiber stiffness necessary to cause a withdrawal response 50% of the time. In practice, the 50% response threshold in gram units is calculated using the following formula:

$$\text{Threshold(g)} = 10^{(\text{Xf} + \kappa\delta)}$$

Where Xf is the value in $\log_{10}$ units of the final von Frey fiber tested and δ is the mean difference in $\log_{10}$ units between the fiber forces used. For the suggested set of fibers that difference is 0.224. The parameter κ is a tabular value for the pattern of positive and negative responses. A detailed table of the possible patterns of responses and the corresponding κ values is presented by Chaplan et al. (1994). For situations in which no response is obtained for any fiber, the top fiber stiffness of 15.1 g is assigned. For situations in which responses are obtained with every fiber leads to a response, the value of the least stiff fiber is assigned. An example calculation can be seen in Table 11.13.3.

Time Considerations

The majority of the time involved in both of the tests is spent in transporting animals to the testing area, warming up the apparatus,

and allowing the animals to acclimate to the test chambers. Most of the commercial thermal paw flick devices take from 30 to 60 min to reach target temperature. With both techniques, ~20 min are required for the acclimation process. If the specific experimental design and available equipment requires that animals are tested in several groups, the total time can be quite lengthy.

Thermal paw flick testing, once the animals are acclimated, takes only a few moments for each measurement with two to three total measurements being made separated by ~5 min. For mechanical testing, ~2 min is required for each animal. In a typical experiment where two groups of eight rats are involved and four animals can be tested at a time with either technique, investigators generally test one group of rats while others are acclimating in the enclosures for the complimentary technique. The total time, including the waiting for acclimation, to do all of the behavioral testing for the two groups would be ~90 to 120 min.

Literature Cited

Authier, N., Gillet, J.P., Fialip, J., Eschalier, A., and Coudore, F. 2000. Description of a short-term Taxol-induced nociceptive neuropathy in rats. *Brain Res.* 887:239-2349.

Bodnar, R.J. and Hadjimarkou, M.M. 2003. Endogenous opiates and behavior: 2002. *Peptides* 24:1241-1302.

Chaplan, S.R., Bach, F.W., Pogrel, J.W., Chung, J.M., and Yaksh, T.L. 1994. Quantitative assessment of tactile allodynia in the rat paw. *J. Neurosci. Methods* 53:55-63.

Dieterich, D.T. 2003. Long-term complications of nucleoside reverse transcriptase inhibitor therapy. *AIDS Read* 13:176-184.

Fields, H.L. 2000. Pain modulation: Expectation, opioid analgesia and virtual pain. *Prog. Brain Res.* 122:245-253.

Hargreaves, K., Dubner, R., Brown, F., Flores, C., and Joris, J. 1988. A new and sensitive method for measuring thermal nociception in cutaneous hyperalgesia. *Pain* 32:77-88.

Levin, S., Pearsall, G., and Ruderman, R.J. 1978. Von Frey's method of measuring pressure sensibility in the hand: an engineering analysis of the Weinstein-Semmes pressure aesthesiometer. *J. Hand Surg. [Am]* 3:211-216.

Li, X., Angst, M.S., and Clark, J.D. 2001. A murine model of opioid-induced hyperalgesia. *Brain Res. Mol. Brain Res.* 86:56-62.

Peltier, A.C. and Russell, J.W. 2002. Recent advances in drug-induced neuropathies. *Curr. Opin. Neurol.* 15:633-638.

Pogatzki, E.M., Gebhart, G.F., and Brennan, T.J. 2002. Characterization of Adelta- and C-fibers innervating the plantar rat hindpaw one day after an incision. *J. Neurophysiol.* 87:721-731.

Sandkuhler, J. 1996a. Neurobiology of spinal nociception: New concepts. *Prog. Brain Res.* 110:207-224.

Sandkuhler, J., 1996b. The organization and function of endogenous antinociceptive systems. *Prog. Neurobiol.* 50:49-81.

Verstappen, C.C., Heimans, J.J., Hoekman, K., and Postma, T.J. 2003. Neurotoxic complications of chemotherapy in patients with cancer: Clinical signs and optimal management. *Drugs* 63:1549-1563.

Visovsky, C. 2003. Chemotherapy-induced peripheral neuropathy. *Cancer Invest.* 21:439-451.

Yeomans, D.C., Pirec, V., and Proudfit, H.K. 1996. Nociceptive responses to high and low rates of noxious cutaneous heating are mediated by different nociceptors in the rat: Behavioral evidence, *Pain* 68:133-140.

Contributed by J. David Clark
Stanford University and VAPAHCS
Palo Alto, California

Methods to Produce Brain Hyperthermia

Knowledge of the adverse effects of hyperthermia that are induced in human populations is limited. Sporadic reports in the past indicate that the central nervous system (CNS) is markedly affected by hyperthermia caused by seasonal increases in ambient temperature (Sharma and Hoopes, 2003; Sharma, 2004a). It is still not known, however, whether the sensitivity of the CNS to heat or the intensity of heat-related illnesses in human populations is influenced by acute or chronic vascular diseases; immunosuppression; or cardiovascular, renal, or pulmonary ailments. Thus, carefully controlled studies using hyperthermia in experimental models are needed to clarify these points.

Suitable animal models of hyperthermia that mimic clinical conditions have not been available thus far. The existing methods to induce local hyperthermia or whole-body hyperthermia (WBH) are based largely on the principles of heat treatment of tumors (Sminia et al., 1994). In these models, excessively high exposure temperatures (40° to 60°C) are used to induce local hyperthermia or WBH, which results in the death of a large number of animals. Moreover, these animal models of hyperthermia are not comparable to the local environmental situations to which human populations are normally exposed. Another model of hyperthermia has been developed to induce heat stroke in rats, rabbits, and other small mammals. The stroke models also use exposure to extreme temperatures (40° to 50°C) for 30 min to 2 hr. Because the skin temperature of laboratory animals varies between 21° and 26°C, exposure to such a high ambient temperature may result in an excessive thermal response, leading to a quick rise in body temperature above 41°C and thus causing death.

While keeping these methods in mind, the author has developed a rat model of mild hyperthermia in which the animals are exposed to 38°C for 4 hr; this method is described in the Basic Protocol. This mild hyperthermia model does not produce heat stroke and is quite comparable to average weather situations during summer months in various parts of the world including Europe and America. Alternate Protocols 1 and 2 describe two methods for inducing hyperthermia in anesthetized rats. Using this model, structural and functional changes in brain and spinal cord can be seen (Sharma, 1982, 1999). Support Protocol 2 describes the analysis of blood-brain barrier (BBB) permeability following heat stress, and Support Protocol 3 presents an easy method for measuring brain (or spinal cord) edema. Thus, the model could be useful for studying hyperthermia-induced brain dysfunction. Support Protocol 1 describes a method for quantifying the heat stress response through the analysis of gastric ulceration.

The influence of drug treatments on heat-related illnesses can also be examined using this model. Although most studies that used this model were performed on rats, it is quite likely that the model can be of use to study heat-related disorders in other small laboratory animals such as mice, guinea pigs, rabbits, and hamsters. A considerable number of human populations are suffering from cancer, diabetes, hypertension, and other heart-related illnesses. This model can be used to expand our knowledge of the sensitivity of heat-related illnesses to chronic disease conditions as well. This can be achieved by adjusting the specific modalities of heat stress (i.e., exposure temperature and duration) and by examining various stress-induced parameters in normal animals compared with animals subjected to experimental disease states.

NOTE: All protocols using live animals must first be reviewed and approved by an Institutional Animal Care and Use Committee (IACUC) and must conform to governmental regulations regarding the care and use of laboratory animals.

Contributed by Hari Shanker Sharma
Current Protocols in Toxicology (2005) 11.14.1-11.14.26

PRODUCING HYPERTHERMIA IN THE UNANESTHETIZED RAT

Further investigation using a suitable model of heat stress is needed to understand the cellular and molecular basis of the heat-induced adverse reaction in the body and to explore new therapeutic strategies in the field. This protocol results in the exposure of an unanesthetized rat to mild hyperthermia for a moderate period of time. It is also suitable for inducing hyperthermia in mice.

Materials

Rats or mice (age and sex controlled)
Paraffin oil *or* glycerine
70% (v/v) ethanol

Thermistor probe (see Internet Resources) suitable for rats or mice
Waterproof marker
Plastic cage, medium size
Thermometers, digital or ordinary mercury, with ±0.1°C accuracy
Biological oxygen demand (BOD) incubator (e.g., BS Pyromatic India, Asco, Raj Scientific Industries) or comparable heat chamber, preheated to desired temperature (e.g., 38°C)

Acclimate animal

1. One week prior to the experiment, take a rat or mouse from its cage by gently handling the animal. Do not lift the animal by the tail.

   Handling stress increases body temperature by approximately ±0.5° to 1°C. Maneuvers regarding measurement of rectal temperature also cause stress in animals, which raises body temperature (Fig. 11.14.1). Thus repeated handling is necessary to minimize stress effects during body temperature measurements.

   Lifting by the tail will induce severe stress in animals (i.e., it will increase their heart rate and respiration).

   Good-quality sterile gloves should be used while handling the animals to avoid accidental bites.

2. Place animal on a weighing pan large enough for easy movement. Record body weight, age, sex, and source of the animal. Also record date and time of the experiment.

   A preweighed restraint box, which will create unnecessary stress in the animal, should not be used.

Figure 11.14.1 *(at right)* Changes in (**A**-**C**) body temperature, (**D**) pain perception, (**E**) body weight, and (**F**) salivation in control and heat-stressed rats. (A) Handling alone alters the rectal temperature for 1 to 4 days; the rats then adapt to handling stress from day 5 onwards. A minimum of 7 days handling is necessary to avoid stress in animals. (B) Subjection of rats to heat stress at 38°C in a biological oxygen demand (BOD) incubator results in graded hyperthermia that is most severe after 4 hr. (C) The magnitude of hyperthermia is considerably less when rats are exposed to heat at 36°C. (D) Measurement of tail flick response in heat-exposed rats at 38°C did not show an analgesic or hyperalgesic response. This indicates that heat exposure did not influence normal pain pathways. (E) Changes in body weight during heat exposure of rats at 38°C. Less intake of water and evaporative heat loss through salivation appear to be the important factors in reducing the weight of rats exposed to heat stress. A significant reduction in body weight is seen after 4 hr of heat exposure. (F) Spread of saliva over snout of rats exposed to heat at 38°C. The area of spread (in millimeters) is maximum following 4 hr heat exposure in rats. This suggests that rats subjected to 4 hr heat stress did not develop heat stroke, which stops the production of saliva (see Background Information). $^{*}P < 0.05$, $^{**}P < 0.01$; ANOVA followed by Dunnet's test for multiple group comparison with one control group (A-E) or with the 30-min group (F). Values are mean ± SD of six to eight rats in each group.

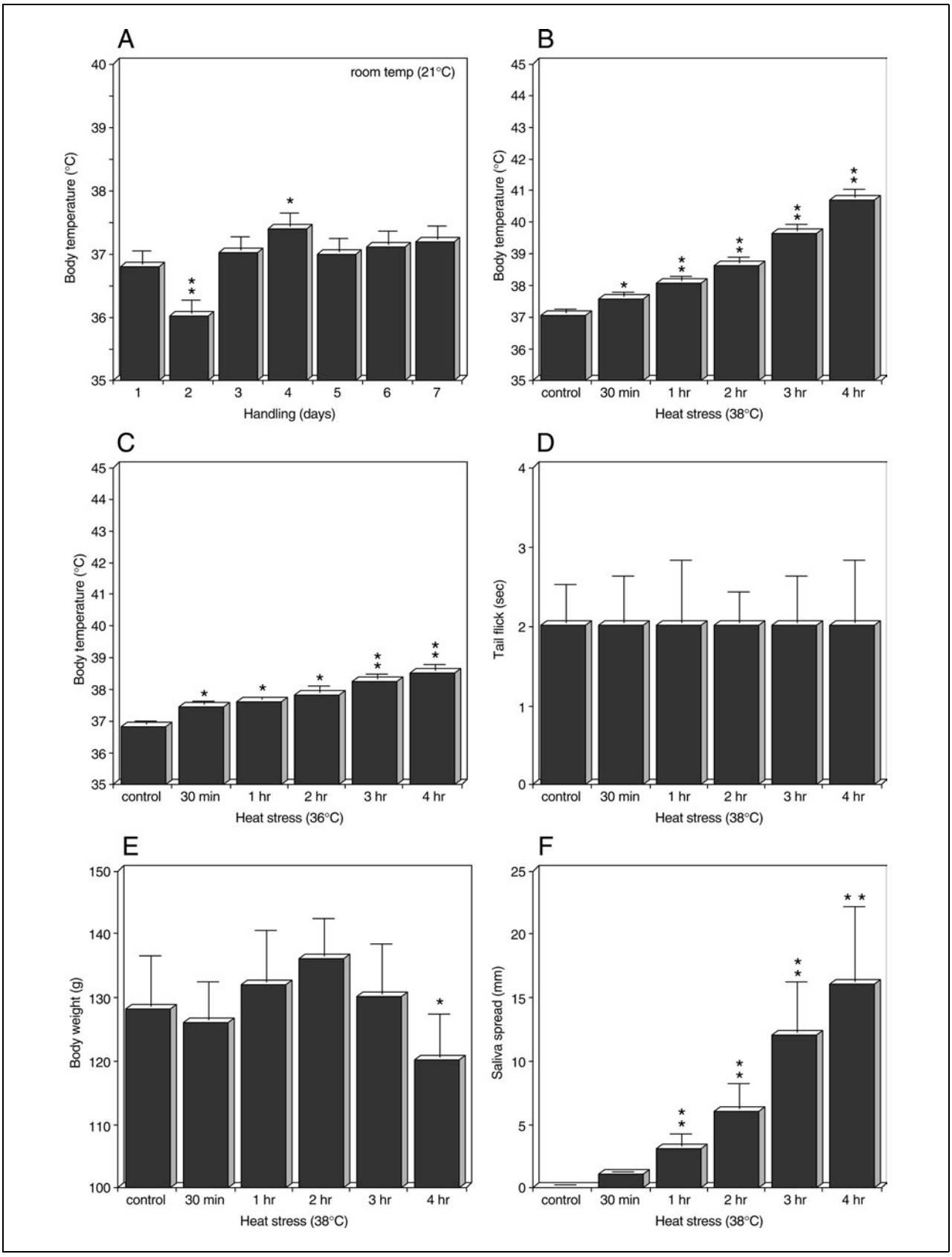

Figure 11.14.1 Legend at left.

Table 11.14.1 Heat Stress Model in the Rat[a]

Heat stress	Skin temperature (T_s)	Exposure temperature (T_e)	Heat load ($T_e - T_s$)	Relative humidity (%)	Wind velocity (cm/sec)	Exposure (hr)
BOD incubator	24°–26°C	36°–38°C	12°–14°C	47–50	24–26	1–4 (acute)
Room temperature[b]	24°–26°C	34°–36°C	10°–12°C	45–47	20–24	8–9 (1 week)

[a]Abbreviation: BOD, biological oxygen demand. Data modified from Sharma (1982) and Sharma and Dey (1987).
[b]Rats were kept at uncontrolled room temperature during the summer.

3. Hold animal gently by hand using its back skin. Avoid deep pressure on animals.
4. Dip a thermistor probe in paraffin oil or glycerin and gently insert probe deep into the rectum. Insert probe 2 cm for a mouse and 4 cm for a rat to obtain deep visceral temperature (i.e., liver temperature). Hold probe in place ≥60 sec to record a stable temperature.

   Thermistor probe size should vary according to the animals used. It is always good to have thinner thermistor probes (o.d. ~3 mm) suitable for rats or mice.

   The probe must be inserted very gently to avoid damaging internal organs and internal bleeding or microhemorrhages. For this purpose, the insertion depth should be carefully marked on the probe.

   Sometimes it is advisable to wrap the tail and the probe with adhesive tape.
5. Take the probe out gently and return animal to its cage. Clean the probe first with cotton followed by mild soap and water and sterilize it with 70% ethanol or as directed by the manufacturer. Be very careful to avoid damaging sensors on the tip of the probe.

   Care should be taken that animals don't bite the sensors

   Liquid paraffin (also known as paraffin oil or light white mineral oil) is applied topically to the thermistor. The liquid paraffin does not contain any stimulant or irritant and exerts no osmotic action. Its main use is as a lubricant, and very little of it is absorbed by the body. Its use in rectal temperature measurement is highly recommended because of its innocuous nature. Furthermore, it covers fecal masses and thus prevents absorption of toxins that may interfere with body temperature measurements.
6. Repeat steps 1 to 5 daily for all animals for 7 days.

   To avoid circadian variation, temperature measurements should be carried out at approximately the same time (±30 min) on each day.

Perform heat stress experiment

7. Place a thermometer on each shelf of a 38°C BOD incubator. Take the frontal temperature reading and compare with the inside manual thermometer. Confirm that all three temperature readings show 38°C (±0.1°C). Adjust the set temperature if needed to produce a consistent internal temperature of 38°C.

   One frequently used heat chamber is known as a BOD incubator (Table 11.14.1). The BOD incubators are made of double-wall steel construction for superior insulation and are equipped with forced air circulation for temperature uniformity inside the whole chamber (±0.5°C). These incubators can be used at a temperature range of +5° to +60° C with a precision of ±0.5°C.

   Poor air circulation within the chamber can lead to temperature variations at different shelves. If this is the case, the fan speed and air circulation should be checked.

8. At intervals of 10 to 15 min, remove an animal from its cage and record its body weight and body temperature (steps 1 to 5). Mark each animal with waterproof ink using numbers on the dorsal surface of the tail or by one to six encircling parallel lines as suitable according to the experimental set up.

   Depending on the animal handler's experience, an interval of 15 to 20 min may be used, along with a smaller number of animals for a given experiment (e.g., three to five rats), to allow adequate time for temperature measurement (step 13a or 13b).

9. Transfer animal to a medium-sized plastic cage in the BOD incubator. Place two or three animals in the cage and record the order in which they were added. Do not place more than two cages in the incubator per session and do not adjust the temperature during the first 10 min.

   For mice, two or three animals can be placed in a small-sized cage to save floor space, but crowding stress must be avoided and one must be able to record the movement and behavioral symptoms properly in individual animals. Also, placing more than six rats or mice in a BOD at once may cause minor changes in blood gases.

   Cages should contain suitable water bottles and, depending on the experimental design, food pellets.

   Placing rats into the chamber will lower the temperature slightly (±1°C) for some time (<10 min). Do not attempt to correct the internal temperature by increasing the temperature set on the front panel. The temperature is normally restored within 5 to 10 min.

Observe animal behavior

10. Observe each animal carefully from the glass window by opening the outer metal door of the BOD incubator. Follow the behavior at regular intervals (∼30 min) and look for mechanisms of heat loss (step 11) and indications of heat exhaustion (step 12; Table 11.14.2) according to the experimental protocol.

    Opening the outer metal door will not affect the internal heat chamber temperature.

    Initially, movement will increase. Exploratory behavior and an increase in locomotion, playing, and sometimes fighting is mainly due to an initial reaction to warm stress.

11. Score the incidence of spreading saliva over the snout and on parts of the belly.

    Salivation is the spreading of saliva over the snout and also on parts of the belly as an effective mechanism for heat dissipation. Because rodents lack sweat glands, this is their only effective means of lowering body temperature. Under extreme conditions, the belly

Table 11.14.2 Stress Symptoms and Physiological Variables in Control and Heat-Stressed Rats[a]

Parameters examined	Control[b] ($n = 8$)	Heat stress at 38°C in BOD chamber		
		1 hr ($n = 6$)	2 hr ($n = 8$)	4 hr ($n = 12$)
Rectal temperature (°C)	37.42 ± 0.23	38.41 ± 0.23*	39.24 ± 0.21**	41.48 ± 0.23***
Salivation	none	++	+++	++++
Prostration	none	none	none	++++
Gastric hemorrhage[c]	none	4 ± 3	8 ± 3	34 ± 8 (microhemorrhages)

[a] Abbreviations: BOD, biological oxygen demand; ++, mild; +++, moderate; ++++, severe; $^{*}P < 0.05$; $^{**}P < 0.01$; $^{***}P < 0.001$, Student's unpaired *t*-test. Data modified from Sharma (1982) and Sharma and Dey (1986b, 1987).

[b] Control rats were kept at room temperature (21° ± 1°C).

[c] The term microhemorrhages indicates that the mucosal lining of the stomach in certain regions has become proliferative and shows signs of bleeding, but individual hemorrhagic spots can not be identified (see Support Protocol 1).

can also be wet, but this may be caused by discharge of urine. Thus, spreading of saliva on the snout is a more reliable index.

The magnitude and intensity of salivation can be assessed qualitatively by observing the spread of saliva over the snout and belly. Saliva spreading over the snout is progressive in nature (Fig. 11.14.1). This can also be measured in millimeters after taking the animals out of the chamber for a short duration or at the end of the experiment.

Animals are most often observed to exhibit gnawing behavior, followed by sniffing and licking. These are normal behaviors in rodents that can become more frequent during the initial exposure (1 to 2 hr) to heat stress.

12. Carefully observe animals from 3 hr to end of experiment and score for prostration. Be certain that animals' snouts and nostrils are clear of obstructions (e.g., cage wall or small particles) during any heat prostration episodes.

The state of heat exhaustion is reflected by heat-induced prostration behavior that normally starts after 3 hr of heat stress (Table 11.14.2). In this situation, locomotion is depressed and animals become lethargic. Most animals remain confined to the corner of the cage in close association with other animals. The animals lie flat in a supine position and normally do not move. Their righting reflexes are not, however, lost. Most animals do not even move after gentle pushing. This stage is known as heat-induced prostration. At this stage the respiratory and heart rates are increased.

Heat-induced prostration can be graded qualitatively. The animals that do not move even after gentle pushing exhibit a maximum score for heat prostration. Simply lying in a prone or supine position for more than 2 min can be regarded as mild prostration.

If breathing is obstructed during heat prostration, death will occur because of asphyxia and not because of heat stress. Thus, careful monitoring of the animals from 3 hr of heat exposure and onwards is necessary.

Body temperature can be recorded once at the end of heat exposure or multiple times during the exposure.

Record body temperature

13a. *To record body temperature at the end of heat exposure:* Remove rats from the incubator one by one (separated by 5- to 10-min intervals) in the same order as they were placed in the cage (step 9). Record their body temperature at room temperature (steps 3 to 5).

Because the rats have been handled regularly and the measurements have been repeated often, only 2 to 3 min is needed for each rat.

Rats may be wrapped with a cotton towel during the recording of their body temperature. This will avoid additional temperature stress (difference between the heat chamber and room temperature). The body temperature can show a variation of $\pm 0.5^{\circ}C$ with or without the towel. (In hyperthermia experiments, changes in body temperature $>0.3^{\circ}C$ are considered significant.)

13b. *To record body temperature during heat exposure:* Remove a single animal from the cage in the chamber. Wrap it loosely with a cotton towel and record its body temperature (steps 3 to 5). Return animal to the cage in the heat chamber and wait 10 min before removing the next animal.

The heat chamber takes 5 to 6 min to readjust the temperature after an animal is removed and returned.

14. Record the body weight of individual animals after heat stress.

Most dramatic changes in body weight can be seen in animals between the third and fourth hours of heat exposure. This is the period when hyperthermia is most marked. Usually there is a decrease in body weight (<5% to 7%) after a 4-hr exposure. During this time, animals normally do not drink water. The spread of saliva and evaporative water loss could partially account for such a loss in body weight (Fig. 11.14.1).

HYPERTHERMIA INDUCED BY AN INFRARED HEAT LAMP

ALTERNATE PROTOCOL 1

Anesthetized animals can be exposed to hyperthermia using a heat lamp. Using an infrared heat lamp to induce hyperthermia is safe and also provides the opportunity to maintain the body temperature at any desired level (e.g., 42°C) for some time. This method represents passive heating, however, as physiological and psychological components of heat stress are lacking. In addition, the counter mechanisms to cope with the stress are seldom activated. This is evident by the fact that stress ulceration in the stomach is largely absent. On the other hand, the molecular mechanism of hyperthermia-induced cellular response appears to be activated by this method, as shown by the expression of heat shock proteins in the CNS and other tissues. Furthermore, histopathological examination of brains in these animals after 1 or 2 days survival following heat treatment shows mild to moderate cellular damage (H.S. Sharma, unpub. observ.). Thus, the method can be used to study the adverse effects of heat on CNS function.

Additional Materials *(also see Basic Protocol)*

Anesthetic (see Background Information and see Critical Parameters)
75-, 150-, or 200-W infrared lamp

1. Anesthetize a rat or mouse with a suitable anesthetic as permitted at your institution.
2. Insert a thermistor probe as described (see Basic Protocol, steps 3 and 4).
3. Expose animal to a 75-, 150-, or 200-W infrared lamp at a distance of 15 to 20 cm, while continuously recording body temperature.

   Care should be taken to avoid excessive heat on skin or localized heating at any point.

   The body temperature gradually rises (~1°C within 10 to 15 min depending on the wattage of the lamp used).

4. Adjust lamp height to control the body temperature rate of rise. When body temperature reaches the desired level (most commonly 42°C), maintain it for 15 to 30 min.

   Animals under anesthesia can tolerate a rectal temperature of ≤42°C. The animal may die, however, if body temperature is >42°C (i.e., 42.5°C).

5. Allow animal to revive from the anesthetic and return it to the appropriate cage.

   In these animals, no stress symptoms can be seen during heat exposure. Microhemorrhages in the stomach are also seldom seen in this model.

HYPERTHERMIA INDUCED IN HEAT CHAMBERS USING ANESTHETIZED ANIMALS

ALTERNATE PROTOCOL 2

Anesthetized animals can be exposed to elevated temperatures in heat chambers to induce hyperthermia. This method lacks the physiological and psychological effects of heat on the animals. In addition, the counter-physiological mechanisms to avoid heat are not activated; passive heating is induced, and thus the body's response to thermal stress is lacking. This method is useful, however, for studying hyperthermia-induced changes in organ function. It also results in a very low (and predictable) death rate. Using an anesthetized animal allows exposure to higher temperatures and allows exposure for a longer length of time. It is also an experimental approach that may be more readily accepted by an Institutional Animal Care and Use Committee. This protocol uses an exposure temperature of 42°C, but other temperatures can be used.

Additional Materials *(also see Basic Protocol)*

Anesthetic (see Background Information and see Critical Parameters)

1. Anesthetize a rat or mouse with a suitable anesthetic as permitted at your institution.
2. Insert a thermistor probe as described (see Basic Protocol, steps 3 and 4).
3. Place animal in a suitable cage in a 42°C BOD incubator (see Basic Protocol, step 7) for the duration of the exposure.

   These animals can be exposed to excessively high temperatures (i.e., 40° to 45°C) for a short duration of 30 min to 1 hr. The body temperature rises gradually in anesthetized rats or mice and may reach the exposure temperature within 1 hr.

   A laboratory incubator with free-flow air facilities can sometimes be used successfully instead of a BOD incubator.

4. When the body temperature reaches 42°C, maintain it for 30 min to 1 hr by adjusting the exposure temperature.

   For effective heat treatment, animals should be exposed for 1 hr. The death rate is very low and a fixed body temperature can be maintained according to the experimental design and purpose. Prolongation of heat exposure in the chamber or increasing the exposure temperature further will result in animal death, however, because of excessive heat-induced membrane and/or enzymatic damage. Thus care should be taken to avoid any further increase in body temperature >42°C.

   Under anesthesia, the control of thermoregulation is normally nonexistent. The increase in body temperature depends mainly on the level of the exposure temperature. Thus, if the anesthetized rats or mice are placed in a 38°C incubator, then their body temperature reaches 38°C within 1 to 2 hr and can be maintained for a long time (Sharma, 1982, 1999).

   For longer experiments, administration of additional anesthetic will be necessary (at ~1-hr intervals). If done properly, this will not alter the body temperature significantly. The average worker can easily administer anesthetics intraperitoneally (or by an other route) within 30 to 45 sec.

SUPPORT PROTOCOL 1

POSTMORTEM EVALUATION OF HEAT STRESS: MICROHEMORRHAGES IN THE STOMACH

Heat stress induces gastric ulceration in animals. The magnitude and intensity of gastric ulceration depend on the exposure temperature and duration (Sharma, 1982). In some cases, one can see individual hemorrhagic spots over a part of the mucosa or at various places in the inside of the stomach (Filaretova et al., 1998). In other cases, the mucosal lining of the stomach in certain regions has become proliferative and shows signs of bleeding, but no clear spots of hemorrhage can be identified (Toth, 1989). This situation is referred to as microhemorrhages. In cases where microhemorrhages are visible, some haemorrhagic spots may also be observed in other regions of the stomach in the same animal (e.g., Table 11.14.2).

To evaluate the individual responses of animals to heat stress, gastric ulceration should be evaluated at postmortem examination. The timing of euthanasia will depend on the experimental design and might be immediately after heat stress or hours or days after the initial heat exposure. Animals can be decapitated or they can be given an overdose of anesthetic to induce deep sleep before they are sacrificed.

Open the abdomen of a euthanized heat-stressed animal and remove the stomach. Make a midline incision into the stomach and wash the contents inside the stomach gently under running tap water at room temperature. Examine the mucosal wall of the entire stomach for microhemorrhages or petachae under a magnifying lens (fixation of the stomach in

formalin is not necessary). Many microhemorrhages are visible in the mucosal wall of the stomach as well as in the fundic and pyloric mucosa. Sometimes hemorrhagic spots are also seen that can be counted manually. Although hemorrhagic spots may heal to some extent after the heat stress is over, this process requires weeks and perhaps months to occur.

ASSESSING CHANGES IN BRAIN FUNCTION AFTER HEAT EXPOSURE

Apart from behavioral alterations, hyperthermia, and gastric ulceration following heat exposure, there are also subtle changes in brain function that can be evaluated within a short time. Some of the common changes in the brain following heat stress are alterations in the blood-brain barrier (BBB) permeability and development of vasogenic brain edema. Breakdown of the BBB can be visualized using several innocuous dyes, such as Evans blue, which normally binds to serum proteins after its administration into the circulation. Extravasation of Evans blue dye in the brain can be seen visually and can be documented using macrophotography (see Support Protocol 2). Alternatively, the dye that has entered the brain can also be measured using colorimetry (Sharma and Dey, 1986a). A change in BBB permeability is a measure of altered brain function, as this will induce changes in an electroencephalogram and may induce brain edema formation. The breakdown of the BBB to proteins, as shown by leakage of Evans blue, is associated with vasogenic brain edema formation and impairment of neuronal function. Edema is defined as an increase in water content that results in volume swelling of the brain. The brain water content can easily be measured (see Support Protocol 3).

Measuring Blood-Brain Barrier Permeability to Evans Blue

SUPPORT PROTOCOL 2

Evans blue (T-1824), an azo-dye, binds to serum proteins in vivo and is commonly used to determine blood volume in humans. In normal animals, the dye does not stain the brain or spinal cord because of the presence of a tight barrier between blood and brain (Rapoport, 1976). The other organs and tissues of the body are, however, stained deep blue. Thus, leakage of dye into the brain or spinal cord in experimental situations suggests a leaky blood-brain barrier (BBB). Extravasation of Evans blue in brain or spinal cord can be examined visually and eventually measured biochemically (Sharma and Dey, 1986b).

NOTE: Although this is a terminal procedure, infection can influence hyperthermia and blood-brain barrier permeability and thus all equipment and reagents used for surgical procedures should be sterile.

Materials

Rats or mice, control and heat-exposed
Equithesin solution (see recipe)
2% (w/v) Evans blue solution (see recipe)
Physiological (0.9% w/v NaCl) saline, room temperature and 4°C
4% (w/v) paraformaldehyde fixative (see recipe), optional

1-ml glass or plastic syringes, sterile
26- to 28-G needle (o.d., 0.3 to 0.4 mm)
Surgical instruments:
- Scalpel
- Forceps
- Fine scissors

Magnifying glass or stereomicroscope
Cotton wool, sterile

Intravenous perfusion setup, including infusion needle
21-G butterfly cannula (o.d., 0.8 mm)
2- or 3-way connector, optional

Additional reagents and equipment for sectioning rat brain, optional

Administer dye

1. Anesthetize a rat or mouse with equithesin anesthesia.

   In control animals, 0.3 ml/100 g body weight of equithesin is required. For heat-stressed animals, the dose should be reduced by 40% to 50%. Thus, 0.15 to 0.2 ml/100 g is sufficient to achieve the same grade of anesthesia in heat-exposed rats or mice.

2. Load a sterile 1-ml glass or plastic syringe with 2% Evans blue solution. Use 0.3 ml solution/100 g body weight.

   Usually, 0.3 ml/100 g body weight of Evans blue solution is sufficient to bind >70% of the plasma albumin in rats (Rapoport, 1976). About one molecule of Evans blue dye binds to twelve molecules of plasma albumin in circulation. Thus, enough Evans blue should be administered to bind ≥60% of plasma albumin (Sharma, 2004a).

3. Attach a 26- to 28-G hypodermic needle to the syringe and ensure that no air bubbles are present. Wipe off any dye that has leaked through the needle tip.

   Leakage of dye will stain the tissue immediately so that visualization of blood vessels is difficult.

4. Using a scalpel, excise the skin over the ventral surface of one hind leg to expose the femoral vein (∼6 to 8 mm). While working under an ordinary magnifying glass or stereomicroscope, carefully expose the femoral vein and remove membranes surrounding it. Regularly apply physiological saline to the exposed tissue and blood vessel to prevent drying.

   This will also help in clearly identifying the femoral vein.

5. Puncture the femoral vein with bevel of the needle facing upwards and insert needle ∼2 to 3 mm into the vein. Inject dye very slowly at first to see that the femoral vein is punctured correctly. When dye enters the vein freely, administer dye slowly at ∼0.8 to 1 ml/min. After completion of dye administration, carefully remove needle and plug the punctured vein with sterilized cotton wool with a little pressure.

   This will stop the bleeding within 5 to 10 sec.

6. Allow Evans blue dye to circulate for ≥5 min.

   The circulation time for dye (5 to 15 min) will not influence the permeability. This is because once the dye enters the brain it will bind to brain tissue for a long time. The circulation time for the dye (∼10 min) should, however, be kept fairly constant in a particular experimental group.

7. Attach tip of an infusion needle to a 21-G butterfly cannula and set up a commercial perfusion set to administer intravascular saline. Hang the saline perfusion bottle at 122.4 cm above the table. Check the flow of saline and remove any air bubbles from the tubing before perfusion.

   A saline perfusion bottle hung at a height of 122.4 cm corresponds to 90 mm Hg pressure multiplied by 13.6, the specific gravity of mercury, to correct the water column pressure.

8. Open the chest with a midline incision of the skin and cut the diaphragm to expose the heart. Using forceps lift the right auricle and cut with fine scissors.

9. Hold the butterfly cannula with the right hand while system is closed and gently lift the heart from the viscera and insert cannula into left ventricle. To confirm that the needle is in the left ventricle, watch for a free flow of blood into the cannula. Open the perfusion system to allow saline perfusion through the heart.

   The intracerebrovascular Evans blue dye should be washed out to assess extravasation of the dye-protein complex in the brain.

10. Perfuse with saline for 45 to 90 sec or until outgoing fluid from the right auricle is colorless.

    Usually, depending on the size of the rat and its blood volume (roughly 7 ml/100 g body weight), 30 to 45 sec is enough to wash out the remaining stained blood from the intracerebral blood vessels.

    Depending on the experimental protocol, the animal can be perfused with a formalin-based fixative or analyzed without fixation.

    Although the following steps are written for analysis of the brain, this will depend on the experimental design; the spinal cord may also be removed for analysis.

Analyze without fixation

11a. Open the skull carefully to expose the brain. Remove brain and place in cold 0.9% saline and examine for Evans blue extravasation (step 16).

    If the need arises, measurement of Evans blue in selected brain areas can be done according to previously published methods (Sharma, 1982; Sharma and Dey, 1986b). Although this method is used in unfixed tissue only, the presence of radioiodine tracers can be measured in fixed tissues as well. In the author's experience, there is no significant difference in radioactivity when counted in either unfixed or fixed material after spinal cord injury (Sharma et al., 1993).

    The brain (and/or spinal cord) should be kept in saline to prevent it from drying out. A wet surface does not, however, produce good photographs. Thus, if photographs of the brain need to be taken, it should be briefly blotted on filter paper and then photographed as quickly as possible before placing it back in saline.

Perfuse with fixative

11b. Set up another perfusion system that is filled with 4% paraformaldehyde fixative. Connect polyethylene tubing from the fixative setup to the butterfly cannula through a 2- or 3-way connector.

    A Somogyi fixative with picric acid (Somogyi and Takagi, 1982) is particularly useful if both light and electron microscopy will be used to analyze the brain sections.

12b. To perfuse the brain, open the connection to the fixative (while closing the outlet for saline) and perfuse brain with ~150 to 200 ml fixative solution (usually 6 to 8 min).

13b. Stop the perfusion by closing the system. Before perfusing another rat with saline, be sure to flush out remaining fixative in the tubing with saline.

    Presence of the fixative in the tubing during the saline perfusion in another rat will fix or coagulate the blood component immediately within the microvessels allowing poor washout of the intracerebral vessels.

14b. *Optional:* For enhanced fixation, completely wrap the whole animal in aluminum foil (excluding tail) and store overnight in a 4°C refrigerator.

    The enhanced fixation step is only necessary to prevent damage to the brain and spinal cord on their external surfaces as they are removed from the skull and the vertebral column, respectively. This is particularly important when the investigator is interested in cell changes or other morphological analyses in the cortex and/or spinal cord.

15b. Dissect out brain and place in the same fixative for 48 hr to 3 days at 4°C.

The dye in the brain will not be diluted or washed out in the fixative if kept at 4°C for ≤3 days. Complete fixation is necessary to provide an accurate assessment of neuronal structure at the microscopic level. Incomplete fixation may lead to compression during sectioning, which can give the false impression of edema, sponginess, and cell damage, even in the brains of normal animals.

Examine for extravasation

16. Visually examine the blue extravasation of dye over the dorsal and ventral surfaces of the brain. Look at the brain texture under a fluorescent lamp (white light) and

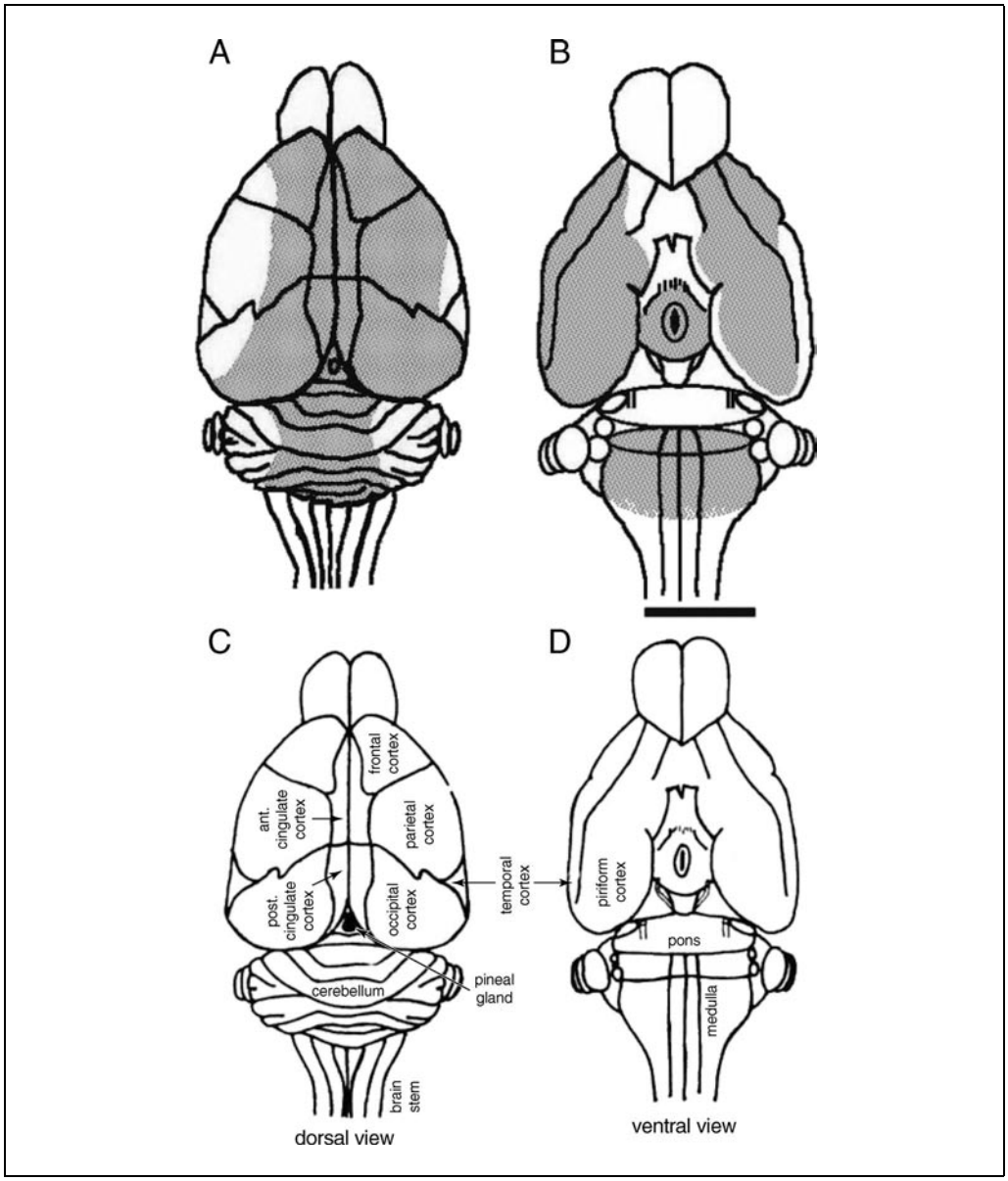

Figure 11.14.2 Representation of Evans blue albumin extravasation on the (**A,C**) dorsal and (**B,D**) ventral surfaces of the rat brain after 4 hr heat stress. Scale bar in B is 4 mm. Different regions of the cerebral cortex are divided using hypothetical solid black lines; extravasation is indicated by the shaded regions. Reprinted from The Blood-Spinal Cord and Brain Barriers in Health and Disease (H.S. Sharma and J. Westman, eds.), H.S. Sharma (2004b), Influence of serotonin on the blood-brain and blood-spinal cord barriers, pp. 117-158 and H.S. Sharma (2004a), Blood-brain and spinal cord barriers in stress, pp. 231-298, with permission from Elsevier. *This black and white facsimile of the figure is intended only as a placeholder; for fullcolor version of figure go to http://www.interscience.wiley.com/c_p/colorfigures.htm.*

compare with the brain from an normal animal. Identify the pineal gland, which always turns blue.

Extravasation of Evans blue into the cortex may be mild to moderate and may not be as blue as can be seen on the pineal gland. The pineal gland does not have a BBB. The cortical surfaces may turn light to moderate blue in certain areas (Figs. 11.14.2 and 11.14.3).

Pictures of the brain can be taken to document extravasation of Evans blue dye on the dorsal and ventral surfaces (Fig. 11.14.3).

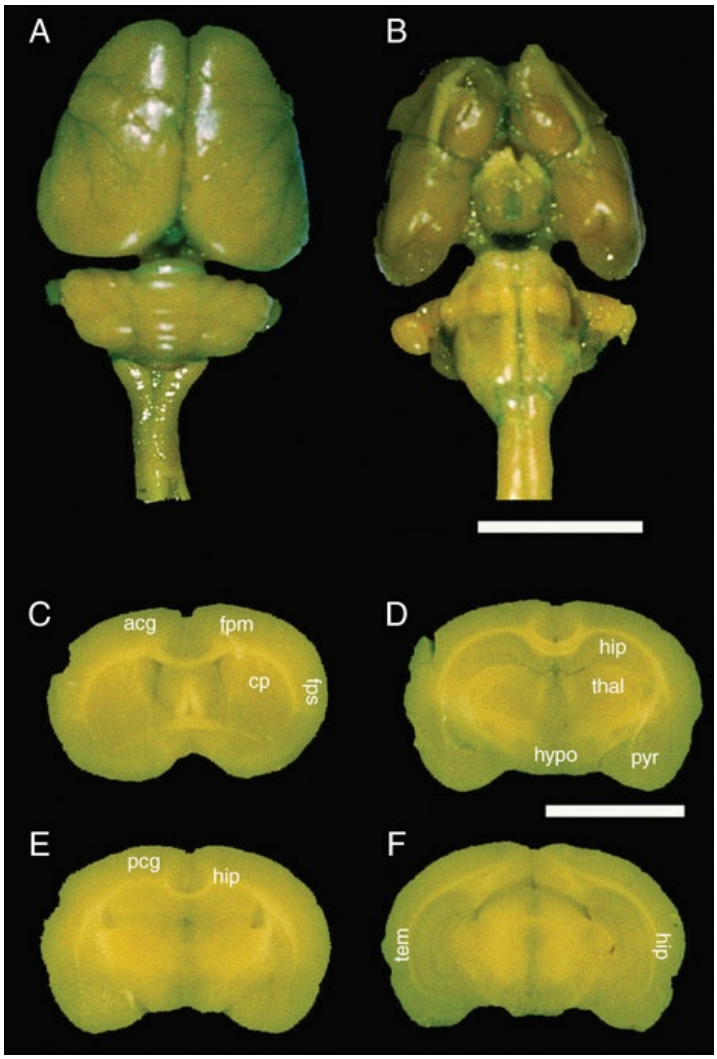

Figure 11.14.3 Evans blue extravasation on the dorsal and ventral surfaces as well as in the deeper parts of the rat brain following heat stress. (**A,B**) Mild to moderate Evans blue staining of somatosensory cortex, pyriform cortex (pyr), cerebellum, hypothalamus (hypo), pons, and brainstem are evident. (**C**-**F**) Coronal sections of rat brain from four different levels showing Evans blue extravasation in deep brain structures, such as (C) caudate-putamen (cp) and (D-F) hippocampus (hip), thalamus (thal), and hypothalamus. Abbreviations: acg, anterior cingulate cortex; fpm, frontal-parietal motor area; fps, frontal-parietal somatosensory area; pcg, posterior cingulate cortex; tem, temporal cortex. Coordinates from the bregma for coronal sections: C, +0.10 to +0.45; D, −3.25 to −3.90; E, −4.20 to −4.60; F, −5.25 to −6.65. Scale bars: B and D, 5 mm. Reprinted from The Blood-Spinal Cord and Brain Barriers in Health and Disease (H.S. Sharma and J. Westman, eds.), H.S. Sharma (2004a), Blood-brain and spinal cord barriers in stress, pp. 231-298, with permission from Elsevier. *This black and white facsimile of the figure is intended only as a placeholder; for fullcolor version of figure go to http://www.interscience.wiley.com/c_p/colorfigures.htm.*

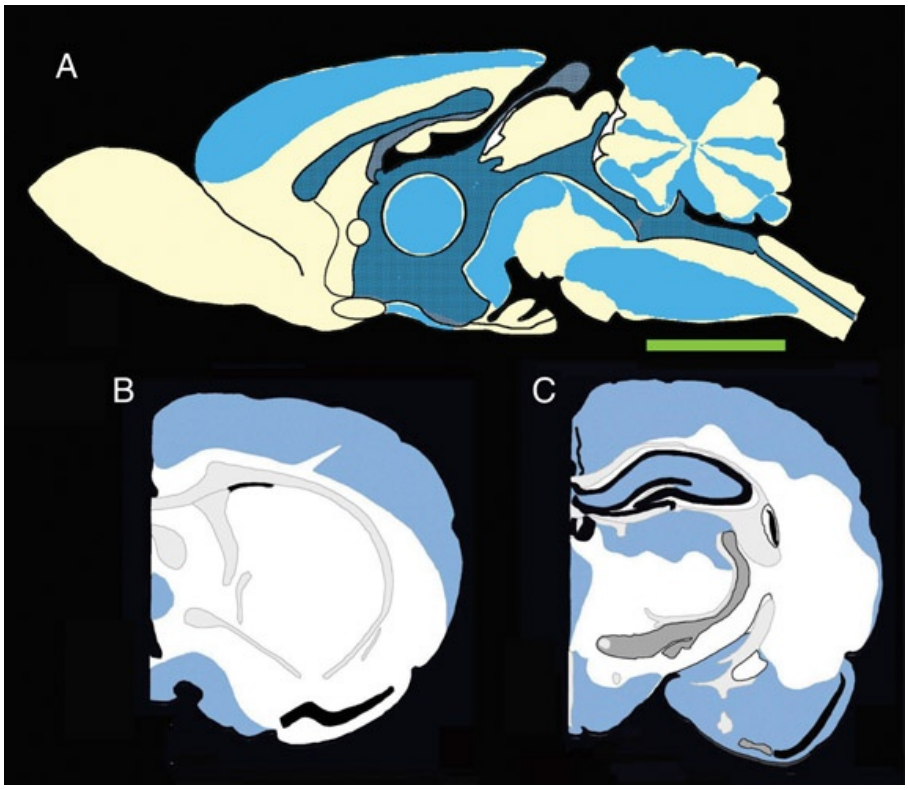

Figure 11.14.4 Extravasation of Evans blue following heat stress. (**A**) Representation of midsagittal section of the rat brain. Staining of cerebroventricular walls of the lateral ventricles, fourth ventricle, and median eminence is apparent. (**B,C**) Cross-sections of the brain passing through the caudate-putamen (+0.45 from bregma for B) and hippocampal (−3.25 from bregma for C) levels showed leakage of Evans blue in the primary somatosensory cortex, pyriform cortex, hippocampus, hypothalamus, and amygdala. Scale bar indicates 5 mm in A and 4 mm in B,C. Reprinted from The Blood-Spinal Cord and Brain Barriers in Health and Disease (H.S. Sharma and J. Westman, eds.), H.S. Sharma (2004a), Blood-brain and spinal cord barriers in stress, pp. 231-298, with permission from Elsevier. *This black and white facsimile of the figure is intended only as a placeholder; for fullcolor version of figure go to http://www.interscience.wiley.com/c_p/colorfigures.htm.*

17. Make a midline incision to see the inside penetration of the dye. Confirm that the choroid plexus has turned deep blue, as microvessels of the choroid plexus are not affected by the BBB. Examine the ventricular walls, which may show mild or faint blue staining. Using a magnifying lens, identify the extravasation of Evans blue in various regions of the brain.

    The dorsal surface of the hippocampus may also show faint staining as compared with controls.

18. *Optional:* Cut coronal sections (of one or both halves) of the brain at various levels and photograph the sections for documentation, if needed (Figs. 11.14.3 and 11.14.4).

SUPPORT PROTOCOL 3

Measurement of Brain Water Content

Another expected result in hyperthermia is an increase in brain water content representing brain edema formation. Edema is defined as an increase in water content of the nervous system that can occur in specific brain regions following several noxious insults (Cervós-Navarro and Ferszt, 1980; Sharma et al., 1998). Early clinical symptoms of brain edema include headache, nausea, vomiting, disturbances of consciousness, and occasionally coma (Reulen et al., 1990; Ito et al., 1994; Cervós-Navarro and Urich, 1995).

The edema fluid spreads over time and, depending on the magnitude and severity of the primary insult, the whole brain can be swollen within 24 hr (Cervós-Navarro and Ferszt, 1980). Progression of edema leads to herniation of the brain (Rapoport, 1976; Bradbury, 1979). A swollen brain in the closed cranial compartment results in death that is due to compression of vital centers and/or vascular infarction (Cervós-Navarro and Ferszt, 1980; Sharma et al., 1998).

Leakage of serum proteins in the brain after BBB disruption leads to vasogenic edema formation. Changes in osmotic pressure gradients across the blood-brain interface allow entry of water from the vascular compartment to the brain microfluid environment (Rapoport, 1976; Sharma et al., 1998; Sharma and Alm, 2002).

Brain edema formation can be assessed by measuring water content (Fig. 11.14.5). A simple method to determine brain water content based on dry and wet weight of the brain is described below.

Materials

Dissected rat brains after treatment with Evans blue (see Support Protocol 2), from both control and heat-stressed animals
Laboratory oven, 90°C

1. Place a whole rat brain or specific parts of it (e.g., cerebral cortex, hippocampus, cerebellum, or brainstem) on a preweighed filter paper and weigh immediately to record the wet weight of the sample. Analyze brains from heat-stressed and control animals in parallel. If dissected brain regions are used, dissect sample sizes for control and experimental brain regions as closely as possible (±50 to 80 mg).

   Because of swelling, the dry weight of the experimental group will be considerably reduced as compared with the control group. The ideal sample size for a brain is >100 mg (e.g., the wet weight of one hippocampus from a rat is ∼135 mg).

   Changes in the water content of the spinal cord can also be calculated. Spinal cord sample size should be ∼60 mg.

2. Place brain or brain parts in a laboratory oven at 90°C and dry for 48 hr.

   The oven temperature should be maintained at <100°C to avoid charring of samples.

3. Remove sample from oven and record its dry weight on the filter paper using the same electronic balance. Return sample to oven and continue drying for an additional 24 hr. Repeat weighing. If the two dry weights are constant, then total evaporation of water has occurred. If weight continues to decrease, continue repeated weighings at 12-hr intervals.

   In most cases, the dry weight is constant after 90 hr of drying.

4. Calculate the percent water content as follows: [(wet weight − dry weight)/wet weight] × 100.

   For example, the wet weight of a portion of the cerebral cortex is ∼300 mg and the dry weight of the sample is ∼70 mg. Therefore, the percent water content = (300 − 70)/300 × 100 = 76.66%.

   The whole-brain water content is considerably less (75% to 76%) than that of some regional brain samples (e.g., cerebral cortex, thalamus, hippocampus). Whole brain contains areas rich in white matter (i.e., brainstem reticular formation, pons, medulla, and parts of the cervical spinal cord). Gray matter contains more water (78% to 80%) than white matter (66% to 72%). Thus, a comparable tissue size and identical regions in control and experimental groups are important for determining regional brain water content.

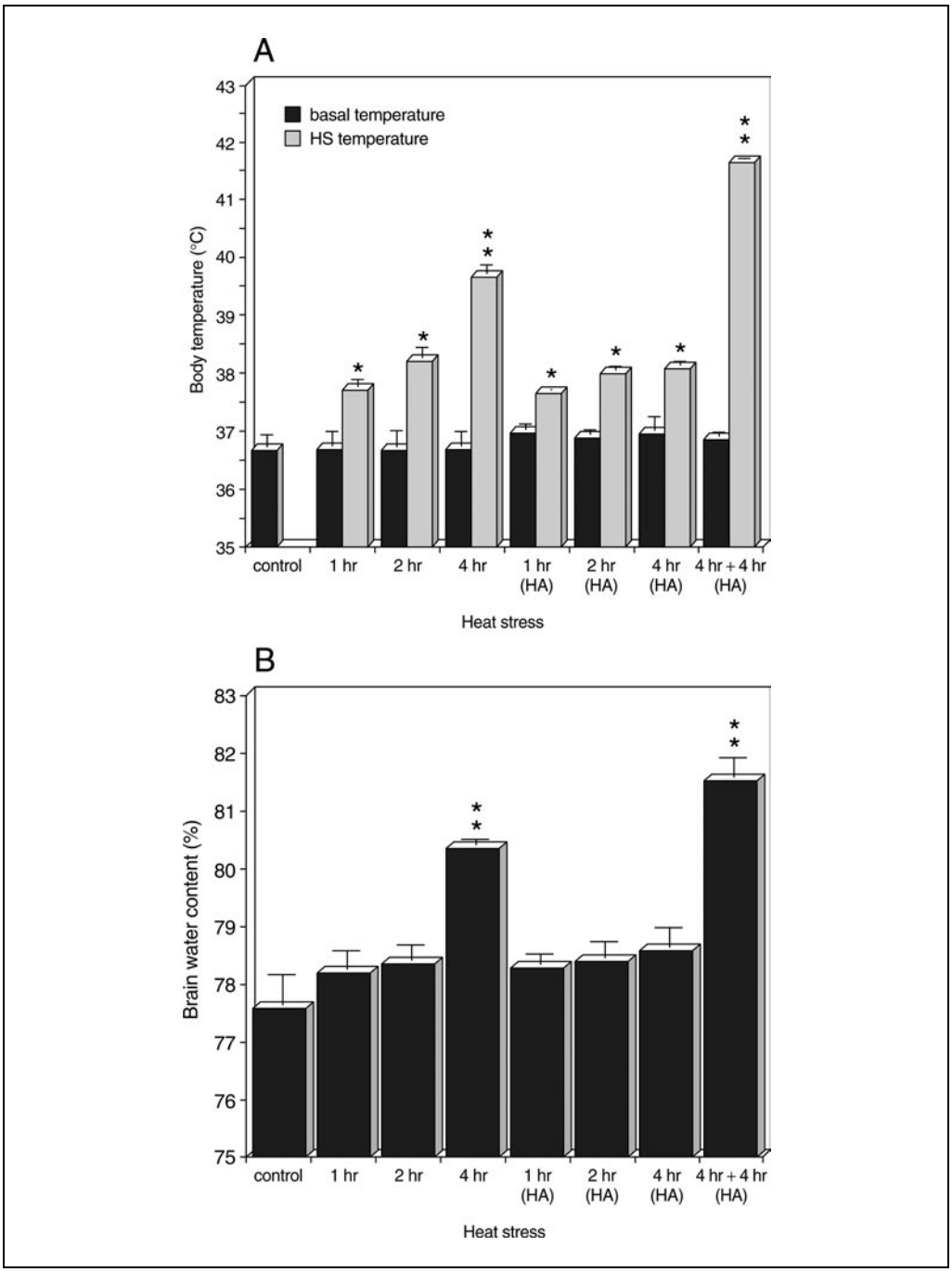

Figure 11.14.5 Changes in (**A**) rectal temperature and (**B**) brain edema formation in acute and chronic heat-exposed rats. Heat-adapted (HA) rats were exposed for 1 hr at 38°C for 7 days before the start of this experiment. A significant increase in rectal temperature was seen following 1-, 2-, and 4-hr heat exposure in the naive and HA rats, although the hyperthermia was milder in the HA rats. Brain water content increased significantly after 4 hr of heat stress (HS) at 38°C in the naive but not the HA rats. When the adapted rats were subjected to an additional 4 hr of heat exposure on the second day (4 hr + 4 hr), however, profound hyperthermia and edema formation can be seen. Values are mean ± SD from six to eight rats. $^{*}P < 0.05$, $^{**}P < 0.01$; ANOVA followed by Dunnet's test for multiple group comparison with one control group. Adapted from Sharma et al. (1986, 1992).

REAGENTS AND SOLUTIONS

Use Milli-Q-purified water or equivalent for all recipes and in all protocol steps. For common stock solutions, see ***APPENDIX 2A****; for suppliers, see* ***SUPPLIERS APPENDIX****.*

Equithesin solution

4.25 g chloral hydrate
0.97 g sodium pentobarbital
2.1 g magnesium sulfate
2.1 g propylene glycol
42.8 g ethanol, anhydrous
9 g sterile water (100 ml final vol)
Store up to 1 month at 4°C

Equithesin solution is also commercially available from Apoteket Produktion and Laboratorier.

Evans blue solution, 2%

Dissolve 2 g Evans blue (Sigma) in 90 ml sterile water. Use magnetic stirring if needed to completely dissolve the dye. Adjust volume to 100 ml. Filter solution using Whatman Filter 42 (pore size, 2.5 μm), which will take >2 hr. Store up to 1 year in a tightly sealed glass bottle at 4°C.

Paraformaldehyde fixative, 4%

Heat 500 ml double-distilled water in a 1-liter beaker to 60°C. Do not exceed 65°C. Add 40 g paraformaldehyde (4% final) and stir continuously using magnetic stirrer for several minutes. Add ~1 ml of 0.1 M NaOH and keep stirring until solution is clear. Filter solution through a Whatman no. 2 filter paper. Filter 500 ml of 0.2 M sodium phosphate buffer, pH 7.2 to 7.4 (see recipe; 0.1 M final) into container with fixative. Immediately pour solution into a 1-liter bottle that has been precooled on ice. Store up to 2 weeks at 4°C.

Sodium phosphate buffer, 0.2 M (pH 7.3)

For 1 liter, dissolve 21.8 g anhydrous sodium phosphate dibasic and 6.4 g anhydrous sodium phosphate monobasic in water. Check that pH is 7.3 (but 7.2 to 7.4 is fine). Lower the pH using phosphoric acid, if necessary, but do not use HCl. Keep bottle tightly sealed and store up to 4 weeks at 4°C in the dark.

COMMENTARY

Background Information

Heat stress

Heat-related deaths and mental illnesses have been well known since Biblical times (Contenau, 1954) as well as in the ancient Indian literature that dates back to 3000 BC. External heat injuries are associated with fire, burning, and rescue operations (Gauss and Meyer, 1917). On the other hand, heat illnesses are caused by exertion in a hot environment (Weisenburg, 1912; Malamud et al., 1946; Sterner, 1990). Heat treatment of tumors in the brain or in other parts of the body, commonly known as therapeutic hyperthermia, also induces several adverse reactions in the central nervous system (CNS; Hahn, 1982; Hoopes, 1991; Ryan et al., 1994). In addition, prolonged high fever (>40°C for several hours) because of bacterial and/or viral infections is often associated with short- or long-term mental anomalies (Hartman and Major, 1935; Alpers, 1936). Hyperthermia caused by diverse conditions influences cerebral circulation and metabolism (Siesjö, 1978; Sharma and Westman, 1998, 2000; Sharma, 1999, 2004a). The molecular mechanisms that underlie hyperthermia-induced brain dysfunction are not, however, well understood. Thus, a suitable animal model is needed to address this important problem faced by a large number of the human population to minimize their sufferings.

Heat stress represents the discomfort and physiological strain that follows physical exercise or daily work for long periods in a hot environment (air temperature >32°C; Knochel and Reed, 1994; Bouchama and Knochel, 2002). Hyperthermia denotes a rise in core body temperature above the hypothalamic set point (~37°C; Milton, 1993) that is caused by impairment of heat-dissipating mechanisms because of external (high environmental temperature) or internal (metabolic heat production) factors (Milton, 1993; Blatteis, 1997). Internal factors are often influenced by the use of drugs and acute and/or chronic diseases (Milton, 1993; Sharma and Westman, 1998).

Mild to moderate hyperthermia is characterized by a small rise in body temperature above 37°C, not exceeding 40°C (Knochel and Reed, 1994), and it is associated with heat exhaustion that causes intense thirst, weakness, discomfort, anxiety, dizziness, fainting, and headache (Milton, 1993; Bouchama and Knochel, 2002). Heat stroke represents severe heat illness that is characterized by hyperthermia >40°C associated with CNS abnormalities (e.g., delirium, convulsions, or coma; Malamud et al., 1946; Sterner, 1990; Knochel and Reed, 1994; Bouchama and Knochel, 2002). Heat stroke can occur either following exposure to environmental heat (classical heat stroke) or following strenuous exercise in a hot environment (exertional heat stroke; Knochel and Reed, 1994; Bouchama and Knochel, 2002).

Recently, heat illness caused by exposure to high ambient temperatures has been recognized as one of the most severe problems in society (Austin and Berry, 1956; Ellis, 1972; Sharma and Westman, 1998, 2000, 2004; Bouchama and Knochel, 2002). Sporadic postmortem reports of heat stroke victims suggest that the central nervous system (CNS) is one of the most vulnerable organs (Gauss and Meyer, 1917; Alpers, 1936; Malamud et al., 1946; Austin and Berry, 1956). Hyperthermia is associated with a systemic inflammatory response leading to multiorgan dysfunction in which encephalopathy predominates (Knochel and Reed, 1994; Bouchama and Knochel, 2002). In several parts of the world, heat-induced brain injury of young and adult athletes appears to be the third-largest killer, followed by cardiovascular and traumatic insults (Austin and Berry, 1956; Bouchama and Knochel, 2002).

Therapeutic hyperthermia, which induces a relatively fast increase in body temperature as compared with a hot environment or heat stroke (Bouchama and Knochel, 2002), is used to destroy deep-seated tumors in cancer patients (Hahn, 1982; Hoopes, 1991; Ryan et al., 1994). This method is still effective as a potential therapy for cancer treatment, in spite of several serious side effects (Hahn, 1982; Hoopes, 1991).

Thermal stress and nociceptive aspects

Rats exposed to heat stress do not appear to feel pain except for the discomfort caused by heat exposure. This is supported by evidence that either the mechanical or thermal nociceptive response of rats subjected to heat stress is not altered from that of an untreated group (Fig. 11.14.1). These observations are in line with the idea that this model of heat exposure does not damage the thermoreceptors and/or alter nociception. Furthermore, thermal discomfort that is seen in this model does not influence the animal's sensitivity to pain.

Heat stress and thermal load on the system

Hyperthermia induced in this model of heat stress is based on the amount of thermal overload imposed on the rats. The skin temperature in rats ranges between 24° and 25°C at room temperature (21°C). When rats are exposed to a heat chamber at 38°C, a heat overload of ~13° to 14°C (exposure temperature − skin temperature) is imposed on them (Table 11.14.1). This heat overload activates heat dissipation mechanisms to maintain normal body temperature (37 ± 0.5°C). During a 2- to 3-hr exposure, however, the rats are no longer able to maintain their body temperature effectively, leading to hyperthermia.

This heat stress–induced hyperthermia (body temperature >40°C) during 4-hr periods of heat exposure is directly related to the amount of initial heat load (i.e., the exposure temperature). Thus, exposure of rats to 36°C (a mild heat load of 11° to 12°C) results in considerably less hyperthermia (<39°C; Fig. 11.14.1).

It appears that the magnitude of heat load is crucial for the development of hyperthermia in animals following heat exposure. If the exposure temperature is increased from 38° to 39°C, most animals develop hyperthermia >41°C within 1 to 2 hr, resulting in the death of most animals (>70%) before 3 hr.

Heat stress and heat stroke

Rats subjected to heat stress in this model do not exhibit heat stroke. Heat stroke is characterized by excessively high body temperature (>41°C) with cessation of salivation and

urination and a very high mortality rate (>80%). Rats exposed to heat in this model exhibit copious salivation (Fig. 11.14.1) and urination. The body temperature normally does not exceed 41°C, and the mortality rate is quite low (<20%).

Brain temperature versus rectal temperature

Rectal temperature closely reflects brain temperature in many cases (Dickson et al., 1979; Macy et al., 1985). Thus when a probe is deeply inserted into the rectum, no difference in brain or rectal temperature was noted following whole-body hyperthermia in dogs and pigs (Dickson et al., 1979; Macy et al., 1985). In another study, when dogs with a brain tumor were exposed to 42°C for 60 min, liver and brain temperatures were only 0.1° and 0.2°C higher, respectively, than the rectal temperature. Data on the rise in brain temperature after whole-body heating in rats and mice are, however, still lacking.

Heat stress influences anesthesia

To study the morphological changes in cells and tissue after heat exposure, animals need to be anesthetized. The sensitivity of drugs to the CNS is markedly increased after heat stress (Sharma, 1982, 1999). Thus, the heat-exposed animals require an ~30% to 50% lower dose of anesthetic as compared with untreated animals, irrespective of the type of anesthetic that is chosen.

Use of anesthetics

Several anesthetics can be used in heat stress experiments depending on the local laboratory guidelines and permission from the respective authorities. A brief description of advantages and disadvantages regarding the use of particular anesthetics in heat stress is given below.

Urethane. Urethane (ethyl carbamate) is a colorless crystalline substance readily soluble in water (~1 g in 0.5 ml water at room temperature) with a neutral pH. Urethane is very safe from the anesthetic point of view because it induces only mild changes in the cardiovascular and respiratory system. Urethane normally does not influence sympathetic nervous system activity. For studies using neurophysiological parameters, urethane is a good choice for anesthesia because it mainly acts on the cortical level and does not depress the respiratory or cardiovascular centers in the brainstem.

The long-lasting effects of urethane (>12 hr) at the level of surgical anesthesia are another advantage in animal experiments (Flecknell, 1996). Thus, no maintenance doses of the anesthetic are needed. The dose of urethane that is needed for normal rats to achieve surgical anesthesia varies between 1 and 1.8 g/kg, intraperitoneally (Sharma, 1999). In the author's experience, 1.5 g/kg works very well in control rats weighing between 100 and 400 g (Sharma and Dey, 1986b). For heat-stressed animals, a reduction of ~30% to 50% of this dose is needed.

Urethane has some carcinogenic effects in animals, however, and thus the utmost care should be taken for its use in the laboratory and with respect to exposure in humans. Local safety regulations for the use and disposal of urethane should be followed strictly (Field and Lang, 1988).

Pentobarbital. Surgical-grade anesthesia in control rats can be achieved by sodium pentobarbital at a dose of 40 to 60 mg/kg, intraperitoneally. (Again, a 30% to 50% reduction of this dose is needed for heat-stressed animals.) This anesthesia, however, profoundly induces bronchial secretions that may sometimes be fatal. To avoid bronchial secretions and poor respiration during the experiment, pretreatment with atropine (0.1 mg/kg, subcutaneously, 20 to 30 min before induction of anesthesia) may be used, if this drug does not interfere with the experimental design and protocol.

The safety margin with pentobarbital anesthesia is very narrow. The effects of anesthesia are also short lasting (i.e., 60 to 80 min). Thus, for long-term experiments, maintenance doses are necessary, often at regular intervals of 45 to 60 min.

Use of pentobarbital anesthesia in heat stress is not recommended, particularly when the experiments involve neurophysiological studies (i.e., electroencephalogram or evoked potential studies). Heat stress often depresses brainstem reticular function. Thus, the use of pentobarbital anesthesia may interfere with the experiments.

Other anesthetics. A combination of ketamine and the muscle relaxant xylazine is commonly used as an anesthetic of choice in various laboratories. Under this anesthesia, however, several reflexes (e.g., blinking of eyes, swallowing, and movements of whiskers or vibrasse) are present, although the animal does not respond to pain stimuli. The duration of anesthesia is short lasting (~45 min to 1 hr) and depends on the dose used. To maintain the level of anesthesia, boosting doses are necessary. In general, 50% to 60% of the original dose is required every hour for this purpose,

although this amount should be determined empirically based on the individual objective and purpose of the experiments in question. The safety margin is considerably higher than that for sodium pentobarbital alone.

Thus, a good and safe anesthetic is still elusive. In some cases, a mixture of various anesthetics is used to produce a safe anesthesia of varying duration in animals. One such anesthetic that is widely used in small animals is equithesin. Equithesin is a mixture of sodium pentobarbital, ketamine, and a muscle relaxant (see Reagents and Solutions). The anesthetic is very safe at a dose of 3 ml/kg, intraperitoneally, for rats. Respiratory depression is seldom seen. The main drawback for this anesthetic, however, is its short duration (i.e., 30 to 40 min). Thus, repeated maintenance doses are necessary to maintain a certain level of anesthesia, and this is often difficult. The anesthetic works on the brainstem reticular formation, thus, excessive repeated doses may induce cardiovascular and respiratory depression, which may lead to animal death. The anesthetic is prepared in a mixture of lipid solvents (i.e., propylene glycol and ethanol). Thus, the anesthesia itself may influence brain function (Gaese and Ostwald, 2001). This aspect should be considered when studying the effects of drugs on brain function in animals after revival from the anesthesia.

Therapeutic hyperthermia

Whole-body hyperthermia and heat toxicity. Therapeutic hyperthermia has been used as a spontaneous cure of several kinds of tumor since the mid-19th century (Sharma and Hoopes, 2003). The technique is largely based on the ability of whole-body hyperthermia (WBH) to destroy deep-seated tumors and is effective against metastasis. Fluid loss, hemodynamic alterations, serum enzyme abnormalities, and other symptoms of variable severity are, however, commonly seen during clinical trials (Kapp and Lord, 1983). Several fatalities that occurred following heat treatment are thought to have been due to causes other than hyperthermia, per se. Recent studies, however, suggest that WBH can influence the structure and function of the CNS in a way that may contribute to some deaths during heat treatment of tumor patients (Sharma and Westman, 1998; Sharma, 1999; Sharma and Hoopes, 2003). Thus, the effective exposure temperature and CNS dysfunction over time require further investigations using this model (Kapp and Lord, 1983; Ryan et al., 1991a,b).

Clinical observations. The effects of WBH on human brain function are largely unknown (van der Zee, 1987). In brain tumor patients, the neurological outcome worsens when the brain temperature exceeds 39°C (Mellergard and Nordström, 1990). The rectal temperature adequately reflects the epidural space temperature, which is very similar to the tympanic membrane temperature (Cabanac, 1998). In human cases, endothelial cells, leukocytes, and epithelial cells are activated after WBH, and a variety of cytokines are produced (Chang, 1993; Gabay and Kushner, 1999). Increases in peripheral interleukin (IL)-1b, IL-6, IL-8, tumor necrosis factor-α (TNF-α), and the regulatory cytokine IL-10 are quite common (Katschinski et al., 1999; Bouchama and Knochel, 2002). These cytokines are involved in local and systemic inflammatory responses (Pedersen and Hoffman-Goetz, 2000). Because some of the cytokines have protective effects, several studies have recommended treatment of human tumors in the range of normally occurring fever (Chang, 1993; Cabanac, 1998; Gabay and Kushner, 1999; Katschinski et al., 1999; Pedersen and Hoffman-Goetz, 2000; Bouchama and Knochel, 2002). Patients with an advanced solid tumor tolerate 39° to 39.5°C for 3 to 6 hr and 39.5° to 40°C for 6 hr without any adverse cardiac, hepatic, or renal effects (Kraybill et al., 2002). Biopsy findings of brain pathologies were not, however, available from this study.

Brain pathology after WBH and heat stroke

Hyperthermia (40.5° to 43°C for 3 to 11 hr) following WBH results in fatality and visible organ injury (Gottschalk and Thomas, 1966). On the other hand, heat stroke–induced fatalities can be seen when the rectal temperature on admission ranges between 38° and 44°C (Bouchama and Knochel, 2002). Death occurs in 70% of cases in <24 hr (rectal temperature, 41.5° to 44°C), irrespective of hyperthermia following WBH or heat stroke (Sharma and Hoopes, 2003). In benign cases, the survival period varies between 1 and 12 days after the initial exposure (Malamud et al., 1946).

Severe brain pathologies in the cerebral cortex and cerebellum in human cases of hyperthermia are described by Malamud et al. (1946) and Gauss and Meyer (1917). This suggests that the CNS is highly vulnerable in heat-related illnesses in humans. A detailed study of other CNS regions (e.g., hippocampus, hypothalamus, and spinal cord) following heat injury at the light and electron microscopy levels has not, however, been carried out.

Local heat treatment of CNS tumors

Clinical cases. Local hyperthermia in the human nervous system is used to treat brain tumors. Tumor temperature of 42.5°C for 1 hr does not induce any adverse effects, although the temperature of normal tissue may rise as well (Zimmerman, 1940). For tumor tissue heated up to 44° to 49°C, the normal tissue temperature remained around 40°C (Tanaka et al., 1987). This heat treatment resulted in aggravation of peritumoral edema and a focal brain swelling (Tanaka et al., 1987). Deep heating has been applied in many patients, however, without apparent heat neurotoxicity (Petrovich et al., 1989). Because most studies are conducted under anesthesia, the state of brain function and cerebral metabolism as well as the effects of anesthesia on CNS function may influence the outcome (Salzman, 1990). To understand the effects of anesthetics on brain dysfunction following hyperthermia, additional work is needed.

Animal experiments. In some cases, local hyperthermia at a temperature of 42° to 43°C for 30 to 60 min is used to treat brain tumor tissue in animals (Sminia et al., 1994). Such heat doses lead to hemorrhages and necrosis in the surrounding brain tissue with limited changes in whole-body physiology (Kerner et al., 2002). Local or regional heating of the brain is often associated with edema formation and cell injury (van der Zee, 1987; Sminia et al., 1994). In experimental local brain heating, lethality after heat insult is common (Sminia et al., 1994). It appears that hyperthermia per se induces such lethality; however, this issue requires further investigation.

Previous studies on hyperthermia in animal models

Previously, several animal models have been used to study the therapeutic effects of hyperthermia on heat tolerance in various animal species. The exposure temperature, duration, survival periods, and parameters measured were, however, extremely varied. Thus, no comparisons can be made to understand the effects of therapeutic hyperthermia on CNS function (Table 11.14.3).

Exposure of dogs to 60°C hot air for 2 hr resulted in a rise in rectal and brain temperature up to 42.5°C without any signs of edema, as seen by changes in epidural pressure recordings. Histopathological studies show a generalized dilation of the subarachnoid space in three of four dogs. The details of cellular changes in the brain were not examined (Eshel et al., 1990).

On the other hand, spontaneous electrical activity or the auditory brainstem-evoked potentials in rats and cats are markedly affected following WBH (Marsh et al., 1984). Flattening of amplitude following WBH in rats occurs after a rise of rectal temperature from 36.75° to 42.65°C, corresponding to a rise in brainstem temperature from 35.25° to 41.5°C (Bulochnik and Zyablov, 1978; Marsh et al., 1984). Similar effects are seen in cats after elevation of cortical temperature to 44° to 45°C following WBH (Britt et al., 1984).

Microwave heating with 106.5 MHz for 60 min in dogs resulted in a rise of the left cardiac ventricle temperature to 42°C, and the lumbar spinal canal temperature rose to 42.5° to 43°C (Thrall et al., 1992). These dogs exhibited pelvic limb dysfunction 12 to 24 hr after hyperthermia. Histopathological examination revealed severe hemorrhage and edema in the lumber spinal cord (Eshel et al., 1990).

These observations indicate that the thermal sensitivity of nerve cells to hyperthermia varies in different regions of the CNS. A detailed mapping of thermal sensitivities of neurons in several regions of the CNS is required to further address this issue.

Brain edema

Types of brain edema. Brain edema is divided into two categories based on whether it is (1) vasogenic or (2) cytotoxic in origin (Klatzo and Seitelberger, 1967). The vasogenic brain edema formation is due to leakage of plasma proteins and water into the cerebral extracellular space because of breakdown of the BBB. Cytotoxic edema develops because of intracellular accumulation of water caused by alterations in cell metabolism (Rapoport, 1976). Heat stress produces both vasogenic and cytotoxic edema (Sharma et al., 1998).

Factors influencing brain edema formation. The protein osmotic pressure in brain is negligible. This is because the cerebrospinal fluid (CSF) protein concentration is extremely low. Furthermore, the CSF osmolality of nonprotein solutes is identical to plasma osmolality (Davson, 1967; Klatzo and Seitelberger, 1967; Rapoport, 1976). Thus, brain edema formation following CNS insults depends mainly on the leakage of the BBB. The driving force for water permeability in the brain is largely dependent on capillary hydrostatic pressure and the protein osmotic pressure (Staub, 1974; Rapoport, 1976). The rate of fluid accumulation depends on brain compliance, which varies in different regions as well as due to changes in local tissue pressure (Guyton, 1963).

Table 11.14.3 Effect of Heat on the Central Nervous System in Laboratory Animals[a]

Species	Exposure temperature (°C)	Tissue examined	Duration (min)	Pathological findings[b]
Dog	42–46[c]	Cerebral hemisphere	30	Edema, hemorrhages
	42–43.5[c]	Occipital cortex	50–70	Gray and white matter damage
	43–44[c]	Cerebral hemisphere	30	Necrosis, inflammation
	40–44[c]	Frontal cortex	30	Necrosis, gliosis
		Cerebral hemisphere		Fibrosis
Cat	45[c]	Forebrain	30	No change
	42–48[d]	Occipital cortex	50	Gray and white matter damage
	41–48[d]	Occipital cortex	50	Necrosis, inflammation
Mouse	42[e]	Spinal cord	60	Not known
	41.2–45.2[f]	Spinal cord	60	Not known
	42–3.5[e]	Spinal cord	20–100	Neuronal and vascular damage, demyelination
Rat	41.2–43.2[c]	Spinal cord	30–120	Neuronal damage, white matter necrosis, gliosis
	43.4–46[f]	Spinal cord	15–30	Not known
	42.6–43.8[c]	Spinal cord	60	Not known
Rabbit	42–43[f]	Whole brain	60	No change
	45[f]		few	Not known

[a]Compiled from Sminia et al. (1994).
[b]These observations are based on very crude pathological examinations done from 4 to 24 hr and 3, 7, 14, and 28 days after thermal insults. In some cases, details of the pathological examination were not available.
[c]Exposure to microwaves.
[d]Exposure to ultrasound.
[e]Exposure to water bath.
[f]Exposure to radiofrequencies.

Brain edema in heat-related illnesses. Edema of the leptomeninges and an increase in brain weight by several hundred grams are prominent in victims of heat-related illnesses (Malamud et al., 1946). Flattening of convolutions and softening of the brain tissue are the other features (Malamud et al., 1946; Austin and Berry, 1956).

Thus, edema appears to be the most prominent feature of hyperthermic brain injury in clinical cases. Very little emphasis is given, however, to the functional significance of brain edema formation in heat-related illnesses. Thus, further studies are needed in this direction.

Experimental hyperthermia in unanesthetized animals

Advantages. The model described in this unit simulates clinical conditions of mild to moderate hyperthermia (i.e., heat stress and heat exhaustion). The symptoms of heat stroke are largely absent in these rats. This is a physiological method to study heat-induced stress reactions in animals. This is evident by activation of the body's natural defense system against heat stress. The physiological response to actively dissipate heat from the body during heat exposure (i.e., salivation) is also operating in these rats. The stress reaction and thermoregulatory changes can easily be visualized during

heat exposure, which can help in predicting the outcome of the experiments. The exposure temperature is within the physiological range, and the chances of heat-induced degeneration of thermoreceptors and burring of skin receptors are unlikely.

Disadvantages. The level of hyperthermia may vary according to the individual response of animals to heat exposure. Thus, maintenance of a certain magnitude of hyperthermia in rats using this model is not possible. In some animals (<20%), body temperature may increase beyond 41.5°C after 4 hr heat exposure, causing death. Some animals may die 12 to 48 hr after heat exposure if the hyperthermia achieved at 4 hr is >41°C.

Critical Parameters

Thermistor probes

The use of thermistor probes (see Internet Resources) is necessary for high-accuracy temperature measurements. The size of the thermistor probe should be suitable for small laboratory animals (i.e., rats and mice). Frequent handling and measurement of body temperature are much more reliable using these probes as compared with normal thermometry. A thermistor probe can record temperature with high precision (±0.01°C) over the range of 0° to 100°C. These probes are stable over years and can measure temperature changes effectively with ±0.1°C accuracy.

Measuring brain edema

A good electronic balance able to detect ±0.01 mg should be placed in the area where the brain is dissected. The time lag between dissecting brain regions and recording the wet weight of the sample should always be kept to a minimum (~1 min). Long-time exposure of the brain samples to the environment may influence the wet weight depending on the humidity and air flow in the area where the experiment is conducted. It is not known whether control and treated brains are influenced by humidity and evaporative water loss in an identical manner.

The brain water content can be measured in animals immediately after heat exposure without the need for saline or formalin perfusion. In this case, obvious blood clots, if any, and major blood vessels over the surface of the brain should carefully be removed. The amount of blood in microvessels may vary and may affect the wet and dry weights of the samples, thus influencing the results. The influence of residual blood volume in brain capillaries can be avoided by perfusing with saline.

Pre-weighed filter papers are necessary to record the wet and dry weights of the sample. The weight of each filter varies markedly (~0.5 to 8 mg). Thus, individual recording of the weight of each filter paper is essential.

Administration of dye before versus after heat stress

Conscious rats. Administration of Evans blue dye in conscious rats either before heat stress (through a cannula implanted into the right jugular or femoral vein) or after termination of exposure (through these routes) does not influence the magnitude or intensity of extravasation in the brain tissue (Sharma, 2004a).

Influence of anesthesia. Likewise, extravasation of dye into the brain did not differ markedly when administered under anesthesia after heat stress. After heat exposure, no difference was seen in leakage of Evans blue dye in rats subjected to various kinds of anesthetics.

Duration of rest after heat stress. Opening of the BBB to Evans blue as a result of heat stress is seen up to 2 hr after the end of heat exposure in both conscious and anesthetized animals (Sharma, 2004a). Thus, to study BBB dysfunction, the dye or any other tracer can be administered in rats within a certain time interval after the termination of heat exposure. To study the reversibility of BBB function, administration of dye or tracers can be made at various time intervals after the termination of heat exposure.

Perfusion duration. The duration of saline infusion and/or formalin perfusion will not influence the magnitude and intensity of dye extravasation into the brain tissues. Because Evans blue dye will instantly bind to tissue proteins after it enters the brain, washout of the dye due to saline or formalin perfusion is quite unlikely. Care should be taken, however, to perfuse animals at ~90 mm Hg and not above to avoid rupturing microvessels, which may interfere with dye extravasation. A pressure of ~90 mm Hg is enough to keep vessels patent during the perfusion.

Anesthesia

To avoid lethality, do not administer a normal dose of anesthetics in heat-stressed rats. This effect of heat stress on anesthesia lasts even 1 to 2 hr after the end of heat exposure. For example, if normal animals require 1.5 g/kg urethane intraperitoneally for surgical-grade anesthesia, administer only 0.8 to 1 g/kg in

heat-stressed rats to achieve the same level of anesthesia. This is also true for other anesthetics, such as pentobarbital.

Anticipated Results

In general, >90% of unanesthetized rats respond to 4 hr heat stress and develop symptoms. More than 80% of rats recover after heat exposure. Approximately 20% may die during heat exposure if the body temperature exceeds 41.6°C. As mentioned above, after heat exposure, look for alterations in BBB permeability and development of brain edema. The whole brain in heat-stressed rats will show mild to moderate leakage of Evans blue (Fig. 11.14.4) and will appear swollen as compared with the control brain. The texture of brain tissue in heat-stressed rats is likely to be softer and spongy as compared with the control group. The brain weight is markedly increased. After a midsagittal section, blue staining (faint to mild) can be seen within the cerebral ventricles of heat-stressed rats (Figs. 11.14.3 and 11.14.4). Dye that has entered into the brain (Sharma, 1982; Sharma and Dey, 1987) and brain water (Sharma and Cervós-Navarro, 1990) can also be measured.

Time Considerations

Preparatory time is <30 min (to record body weight and body temperature in individual animals), after animals have undergone a week-long handling regime. Working time depends on the exposure duration and experimental design. Usually, for a 4-hr heat exposure protocol, allow 5 to 6 hr total time to complete one group of experiments on five or six rats.

Literature Cited

Alpers, B.J. 1936. Hyperthermia due to lesions in the hypothalamus. *Arch. Neurol. Psychiatry* 35:30-42.

Austin, M.G. and Berry, J.W. 1956. Observation on one hundred cases of heatstroke. *J. Am. Med. Assoc.* 161:1525-1529.

Blatteis, C. 1997. Thermoregulation: Recent progress and new frontiers. *Ann. N.Y. Acad. Sci.* 813:1-865.

Bouchama, A. and Knochel, J.P. 2002. Heat stroke. *New Engl. J. Med.* 25:1978-1988.

Bradbury, M.W.B. 1979. The Concept of a Blood-Brain Barrier. Chicester, London.

Britt, R.H., Lyons, B.E., Ryan, T., Saxer, E., Obana, W., and Rossi, G. 1984. Effect of whole body hyperthermia on auditory brainstem and somatosensory and visual evoked potentials. *In* Thermal Physiology (R.R.S. Hales, ed.) pp. 519-523. Raven, New York.

Bulochnik, E.D. and Zyablov, M.P. 1978. Effect of hyperthermia induced by a high ambient temperature on the direct cortical response. *Biull. Eksp. Biol. Med.* 84:657-660.

Cabanac, M. 1998. Selective brain cooling and thermoregulatory set-point. *J. Basic Clin. Physiol. Pharmacol.* 9:3-13.

Cervós-Navarro, J. and Ferszt, R. 1980. Brain edema: Pathology, diagnosis and therapy. *Adv. Neurol.* 20:1-450.

Cervós-Navarro, J. and Urich, H. 1995. Metabolic and Degenerative Diseases of the Central Nervous System: Pathology, Biochemistry and Genetics. Academic Press, New York.

Chang, D.M. 1993. The role of cytokines in heatstroke. *Immunol. Invest.* 22:553-561.

Contenau, G. 1954. Everyday Life in Babylon and Assyria. St. Martin's Press, N.Y.

Davson, H. 1967. Physiology of the Cerebrospinal Fluid. Churchill, London.

Dickson, J.A., Mackenzie, A., and McLeod, K. 1979. Temperature gradients in pigs during whole body hyperthermia at 42°C. *J. Appl. Physiol.* 47:712-717.

Ellis, F.P. 1972. Mortality from heat illness and heat-aggravated illness in the United States. *Environ. Res.* 5:1-58.

Eshel, G., Safar, P., Sassano, J., and Stezoski, W. 1990. Hyperthermia-induced cardiac arrest in dogs and monkeys. *Resuscitation* 20:129-143.

Field, K.J. and Lang, C.M. 1988. Hazards of urethane (ethyl carbamide): A review of the literature. *Lab. Anim.* 22:255-262.

Filaretova, L.P., Filaretov, A.A., and Makara, G.B. 1998. Corticosterone increase inhibits stress-induced gastric erosion in rats. *Am. J. Physiol.* 274:G1024-G1030.

Flecknell, P.A. 1996. Laboratory Animal Anaesthesia, 2nd ed. Section 7, Anaesthesia for Common Laboratory Species. Chapter 1, Rodents. pp. 160-181. Academic Press, London.

Gabay, C. and Kushner, I. 1999. Acute phase proteins and other systemic response to inflammation. *New Engl. J. Med.* 340:448-454.

Gaese, B.H. and Ostwald, J. 2001. Anesthesia changes frequency tuning of neurons in the rat primary auditory cortex. *J. Neurophysiol.* 86:1062-1066.

Gauss, H. and Meyer, K.A.H. 1917. Heat stroke: Report of one hundred and fifty-eight cases from Cook County Hospital, Chicago. *Am. J. Med. Sci.* 154:554-564.

Gottschalk, P.G. and Thomas, J.E. 1966. Heat Stroke. *Mayo Clin. Proc.* 41:470-482.

Guyton, A.C. 1963. A concept of negative interstitial pressure based on pressures in implanted perforated capsules. *Circ. Res.* 12:399-412.

Hahn, G.M. 1982. Hyperthermia and Cancer. Plenum Press, New York.

Hartman, F.W. and Major, R.C. 1935. Pathological changes resulting from accurately controlled artificial fever. *Am. J. Clin. Pathol.* 5:392-410.

Hoopes, P.J. 1991. The effects of heat on the nervous system. *In* Radiation Injury to the Nervous System (P.H. Gutin, S.A. Leibel, and G.E. Sheline, eds.) pp. 407-430. Raven Press, New York.

Ito, U., Baethmann, A., Hossmann, K.-A., Kuroiwa, T., Marmarou, A., and Takakura, K. 1994. Brain edema IX. *Acta Neurochir. Suppl. (Wien)* 60:1-485.

Kapp, D.S. and Lord, P.F. 1983. Thermal tolerance to whole body hyperthermia. *Int. J. Radiat. Oncol. Biol. Phys.* 9:917-921.

Katschinski, D.M., Wiedemann, G.J., Longo, W., d'Oleire, F.R., Spriggs, D., and Robbins, H.I. 1999. Whole body hyperthermia cytokine induction: A review, and unifying hypothesis for myeloprotection in the setting of cytotoxic therapy. *Cytokine Growth Factor Rev.* 10:93-97.

Kerner, T., Deja, M., Ahlers, O., Hildebrandt, B., Dieing, A., Riess, H., Wust, P. and Gerlach, H. 2002. Monitoring arterial blood pressure during whole body hyperthermia. *Acta Anaesthesiol. Scand.* 46:561-566.

Klatzo, I. and Seitelberger, F. 1967. Brain Edema. Springer-Verlag, Berlin.

Knochel, J.P. and Reed, G. 1994. Disorders of heat regulation. *In* Maxwell & Kleeman's Clinical Disorders of Fluid and Electrolyte Metabolism, 5th ed. (R.G. Narins, ed.) pp. 1549-1590. McGraw-Hill, New York.

Kraybill, W.G., Olenki, T., Evans, S.S., Ostberg, J.R., O'Leary, K.A., Gibbs, J.F., and Repasky, E.A. 2002. A phase I study of fever-range whole body hyperthermia (FR-WBH) in patients with advanced solid tumours: Correlation with mouse models. *Int. J. Hyperthermia* 18:253-266.

Macy, D.W., Macy, C.A., Scott, R.J., Gilette, E.L., and Speer, J.F. 1985. Physiological studies of whole-body hyperthermia in dogs. *Cancer Res.* 45:2769-2773.

Malamud, N., Haymaker, W., and Custer, R.P. 1946. Heat stroke. A clinicopathological study of 125 fatal cases. *Mil. Surg.* 99:397-449.

Marsh, R.R., Yamane, H., and Potsic, W.P. 1984. Auditory brain-stem response and temperature. Relationship in the guinea pig. *Electroencephalogr. Clin. Neurophysiol.* 57:289-293.

Mellergard, P. and Nordström, C.H. 1990. Epidural temperature and possible intracerebral temperature gradients in man. *Br. J. Neurosurg.* 4:31-38.

Milton, A.S. 1993. Physiology of Thermoregulation. Birkhauser, Basel.

Pedersen, B.K. and Hoffman-Goetz, L. 2000. Exercise and the immune system: Regulation, integration, and adaptation. *Physiol. Rev.* 80:1055-1081.

Petrovich, Z., Langholz, B., Gibbs, F.A., Sapozink, M.D., Kapp, D.S., Stewart, R.J., Emami, B., Oleson, J., Senzer, N., and Slater, J. 1989. Regional hyperthermia for advanced tumors: A clinical study of 535 patients. *Int. J. Radiat. Oncol. Biol. Phys.* 16:601-607.

Rapoport, S.I. 1976. Blood-Brain Barrier in Physiology and Medicine. Raven Press, New York.

Reulen, H.-J., Baethmann, A., Fenstermacher, J., Marmarou, A., and Spatz, M. 1990. Brain edema VIII. *Acta Neurochir. Suppl. (Wien)* 51:1-414.

Ryan, T.P., Hoopes, P.J., Taylor, J.H., Strohbehn, J.W., Roberts, D.W., Double, E.B., and Coughlin, C.T. 1991a. Experimental brain hyperthermia: Techniques for heat delivery and thermometry. *Int. J. Radiat. Oncol. Biol. Phys.* 20:739-750.

Ryan, T.P., Wykoff, R., and Hoopes, P.J. 1991b. An automated temperature mapping system for use in ultrasound or microwave hyperthermia. *J. Biomed. Eng.* 13:348-354.

Ryan, T.P., Trembly, B.S., Roberts, D.W., Strohbehn, J.W., Coughlin, C.T., and Hoopes, P.J. 1994. Brain hyperthermia I: Interstitial microwave antenna array techniques, the Dartmouth experience. *Int. J. Radiat. Oncol. Biol. Phys.* 29:1065-1078.

Salzman, S.K. 1990. Neural Monitoring. The Prevention of Intraoperative Injury. Humana Press, Totowa, N.J.

Sharma, H.S. 1982. Blood-Brain Barrier in Stress (Ph.D. Thesis). pp. 1-85. Banaras Hindu University, Varanasi, India.

Sharma, H.S. 1999. Pathophysiology of blood-brain barrier, brain edema and cell injury following hyperthermia: New role of heat shock protein, nitric oxide and carbon monoxide. An experimental study in the rat using light and electron microscopy. *Acta Univ. Ups.* 830:1-94.

Sharma, H.S. 2004a. Blood-brain and spinal cord barriers in stress. *In* The Blood-Spinal Cord and Brain Barriers in Health and Disease (H.S. Sharma and J. Westman, eds.) pp. 231-298. Elsevier Academic Press, San Diego.

Sharma, H.S. 2004b. Influence of serotonin on the blood-brain and blood-spinal cord barriers. *In* The Blood-Spinal Cord and Brain Barriers in Health and Disease (H.S. Sharma and J. Westman, eds.) pp. 117-158. Elsevier Academic Press, San Diego.

Sharma, H.S. and Alm, P. 2002. Nitric oxide synthase inhibitors influence dynorphin A (1-17) immunoreactivity in the rat brain following hyperthermia. *Amino Acids* 23:247-259.

Sharma, H.S. and Cervós-Navarro, J. 1990. Brain oedema and cellular changes induced by acute heat stress in young rats. *Acta Neurochir. Suppl. (Wien)* 51:383-386.

Sharma, H.S. and Dey, P.K. 1986a. Influence of long-term immobilization stress on regional blood-brain barrier permeability, cerebral blood flow and 5-HT level in conscious normotensive young rats. *J. Neurol. Sci.* 72:61-76.

Sharma, H.S. and Dey, P.K. 1986b. Probable involvement of 5-hydroxytryptamine in increased permeability of blood-brain barrier under heat stress. *Neuropharmacology* 25:161-167.

Sharma, H.S. and Dey, P.K. 1987. Influence of long-term acute heat exposure on regional blood-brain barrier permeability, cerebral blood flow and 5-HT level in conscious normotensive young rats. *Brain Res.* 424:153-162.

Sharma, H.S. and Hoopes, P.J. 2003. Hyperthermia induced pathophysiology of the central nervous system. *Int. J. Hyperthermia* 19:325-354.

Sharma, H.S. and Westman, J. 1998. Brain functions in hot environment. *Prog. Brain Res.* 115:1-527.

Sharma, H.S. and Westman, J. 2000. Pathophysiology of hyperthermic brain injury. Current concepts, molecular mechanisms and pharmacological strategies. *In* Research in Legal Medicine, Vol. 21: Hyperthermia, Burning and Carbon Monoxide (M. Oehnmichen, ed.) pp. 79-120. Lübeck Medical University Publications, Lübeck: Schmidt-Römhild Verlag, Germany.

Sharma, H.S. and Westman, J. 2004. The heat shock proteins and hemeoxygenase response in central nervous system injuries. *In* The Blood-Spinal Cord and Brain Barriers in Health and Disease. (H.S. Sharma and J. Westman, eds.) pp. 329-360. Elsevier Academic Press, San Diego.

Sharma, H.S., Dey, P.K., and Kumar, A. 1986. Role of circulating 5-HT and lung MAO activity in physiological processes of heat adaptation in conscious young rats. *Biomedicine* 6:31-40.

Sharma, H.S., Kretzschmar, R., Cervós-Navarro, J., Ermisch, A., Rühle, H.-J., and Dey, P.K. 1992. Age-related pathophysiology of the blood-brain barrier in heat stress. *Prog. Brain Res.* 91:189-196.

Sharma, H.S., Olsson, Y., Nyberg, F., and Dey, P.K. 1993. Prostaglandins modulate alterations of microvascular permeability, blood flow, edema and serotonin levels following spinal cord injury. An experimental study in the rat. *Neuroscience* 57:443-449.

Sharma, H.S., Westman, J., and Nyberg, F. 1998. Pathophysiology of brain edema and cell changes following hyperthermic brain injury. *Prog. Brain Res.* 115:351-412.

Siesjö, B.K. 1978. Brain Energy Metabolism. John Wiley & Sons, Chichester, England.

Sminia, P., van der Zee, J., Wondergem, J., and Haveman, J. 1994. Effect of hyperthermia on the central nervous system: A review. *Int. J. Hyperthermia* 10:1-30.

Somogyi, P. and Takagi, H. 1982. A note on the use of picric acid-paraformaldehyde-glutaraldehyde fixative for correlated light and electron microscopic immunocytochemistry. *Neuroscience* 7:1779-1783.

Staub, N.C. 1974. Pulmonary edema. *Physiol. Rev.* 54:678-811.

Sterner, S. 1990. Summer heat illness. *Postgrad. Med.* 87:67-73.

Tanaka, R., Kim, C.H., Yamada, N., and Saito, Y. 1987. Radiofrequency hyperthermia for malignant brain tumours: Preliminary results of clinical trials. *Neurosurgery* 21:478-483.

Thrall, D.E, Prescott, D.M., Samulski, T.V., Dewhirst, M.W., Cline, J.M., Lee, J., Page, R.L., and Oleson, J.R. 1992. Serious toxicity associated with annular microwave array induction of whole-body hyperthermia in normal dogs. *Int. J. Hyperthermia* 8:23-32.

Toth, T. 1989. An unusual stress-induced gastric lesion. *Acta Physiol. Hung.* 73:202-206.

van der Zee, J. 1987. Whole body hyperthermia. The development of and experience with a clinical method (Dissertation). Erasmus University, Rotterdam, Netherlands.

Weisenburg, T.H. 1912. Nervous symptoms following sunstroke. *J. Am. Med. Assoc.* 58:2015-2017.

Zimmerman, H.M. 1940. Temperature disturbances and the hypothalamus. *Res. Nerv. Ment. Dis. Proc.* 20:824-840.

Internet Resources

http://www.temperatures.com/thermivendors.html

A resource for thermistor probes, with links to various suppliers.

http://www.myneurolab.com/

Provides purchasing information for a 3-mm thermistor probe suitable for rats.

Contributed by Hari Shanker Sharma
Institute of Surgical Sciences
University Hospital
Uppsala University
Uppsala, Sweden

CHAPTER 12
Biochemical and Molecular Neurotoxicology

INTRODUCTION

This chapter complements the behavioral and whole-animal approaches that are provided in the preceding chapter (Chapter 11, Neurotoxicology) by addressing biochemical and molecular methodologies, as well as in vitro approaches to study neurotoxicity. By providing information on the cellular substrates involved in behavioral changes and/or correlates of neuropathological lesions, biochemical and molecular approaches are relevant to the process of assessing the impact of human exposure to neurotoxicants. Knowledge of mechanisms of action of neurotoxicants can be useful in a number of areas: it allows the design and development of proper antidotes; it is useful in predicting possible interactions with other exogenous chemicals and/or preexisting alterations; it permits the development of biomarkers of effect for use in animal toxicity studies, as well as epidemiological investigations in humans; it offers the possibility of implementing in vitro alternatives for toxicity testing; and it adds an important component to the hazard characterization aspects of risk assessment process.

UNIT 12.1 presents an overview of the different approaches that can be used to study the effect of neurotoxicants with biochemical methods. As the targets of neurotoxicants can be numerous an investigator is faced with the issue of which parameters to investigate: various steps of neurotransmission, signal-transduction pathways, intermediate metabolism, markers of oxidative stress, are among the many end-points that can be studied.

The blood-brain barrier is constituted by specialized endotheliel cells that together with astrocytes act as a selective barrier that isolates the brain from potentially noxious substances. *UNIT 12.2* presents methodologies to investigate the functions of the blood-brain barrier in a dynamic in vitro system where the passage of chemicals, as well as the functional effects of neurotoxicants, can be measured.

Cells in culture are often used for neurotoxicological studies, particularly for the study of mechanisms of toxicity. *UNIT 12.3* and *UNIT 12.4* present methods for preparing primary hippocampal neuronal cultures and primary astrocyte cultures from rat brain and their applications to neurotoxicology. *UNIT 12.5* provides a description of two applications of analytical cytology to neurotoxicology, for measurements of intracellular calcium levels and of cell-cycle parameters. *UNIT 12.6*, on the other hand, describes stereological methods that allow counting of neuronal cells. *UNIT 12.7* describes the method for preparing rat cerebellar granule cells for culture. These cells are a widely used in vitro model system for neurotoxicology studies. Reactive gliosis is a characteristic feature of toxicant-induced injury in the central nervous system, and *UNIT 12.8* describes the measurement of glial fibrillary acidic protein (GFAP), which serves as a biochemical indicator of neurotoxicity.

UNIT 12.9 describes an unique in vitro cell system, the aggregating neural cell cultures, prepared from embryonic rat or mouse brains. This tridimensional system allows direct cell-to-cell interaction and is a promising tool for in vitro neurotoxicity testing. The issue of cell-cell interaction is also addressed in *UNIT 12.10*, which describes different methods to co-culture glial cells and neurons.

Contributed by Lucio G. Costa
Current Protocols in Toxicology (2004) 12.0.1-12.0.2

UNIT 12.11 describes a method to measure the binding of metals to zinc-finger motifs of proteins, which could be useful in assessing the mechanism of toxicity of several metals, while *UNIT 12.12* provides protocols for the preparation of rat peripheral nervous system tissues for light and electron microscopy studies.

Lucio G. Costa

Biochemical Approaches to Studying Neurotoxicity

The essence of the nervous system is communication: multifarious, intricate communication between cells. In addition to the well-known neuron-to-neuron communication, there is also communication to and among the so-called supporting cells (i.e., glial or Schwann cells) of the nervous system. Communication between cells involves a variety of biochemical changes, including (but not limited to) ion fluxes, receptor stimulation, generation of second messengers, phosphorylation of proteins, receptor- or voltage-initiated opening of channels, or release of calcium. There is also a less sporadic, slower, communication between nerve cells and their targets in which they continually notify one another through chemical signals or messengers (e.g., trophic factors) that they are still there, that they are still connected. In the developing nervous system, chemical signaling molecules tell neurons when and where to grow, where not to grow, and when to stop growing. In addition to cell-to-cell communication or signaling, there is also communication within a cell, i.e., axonal transport. Moreover, in order for cell-to-cell signaling to occur properly, not only are the chemical signals and messengers integral to proper communication within the nervous system, but the structure of the cells and their connections must be optimal, making biochemical communication and maintenance of structure pivotal to the ideal functioning of the nervous system. Thus, given that the essence of the nervous system is communication, it follows that neurotoxicology may be defined as the disruption of that communication, either through perturbation of biochemical signals or messengers or through perturbation of the structure of the nervous system.

One of the basic tenets of toxicology is that the dosage makes the poison. An extension of that rule is that, in general, if enough of a chemical is administered, there will eventually be an adverse effect. Thus, the discovery that a certain toxicant produces an effect does not warrant concern until the dosage is taken into consideration. One must always be aware of how the dosage level of a chemical compares with the level expected to be encountered in the environment. It is always important to know the absorbed dose or, if possible, the dose at the presumed target site. Furthermore, if a toxic compound causes a loss in body weight or severe liver necrosis, it is possible that there will also be nonspecific alterations in nervous system biochemistry; one must always keep any neurochemical changes in perspective. The goal is to find the mechanism of action of a toxic chemical at a realistic dosage or exposure level, not an effect that is precipitated by an overall toxic response of the organism. This is even more pertinent for an in vitro testing procedure: the careful investigator should always consider the reported in vivo tissue concentration of the toxic compound and how that concentration compares to the effective concentration in any particular in vitro procedure. In all procedures, whether in vivo or in vitro, the strongest, most persuasive experimental design involves using a dose-response paradigm that includes both positive and negative controls. The dose-related response is essential to link the exposure of a toxic compound to a given neurotoxic effect. Moreover, it should be assumed that toxic compounds have multiple effects, not just a single effect. Therefore, the dose-effect assessments allow the investigator to rank order the toxic effects and possibly identify which is the proximal event, i.e., the response that is produced first or at the lowest dosage of the compound.

This unit is not intended to be a comprehensive review of the literature involving biochemical neurotoxicology. Instead, an effort has been made to supply the reader with recent examples of the various approaches to identify neurotoxicants and their modes of action. Moreover, the discussion and the majority of the references will focus on toxic compounds with environmental relevance, not toxins (plant- or animal-derived venoms or poisons) or pharmacologically relevant compounds. There are many reviews published in the last twenty years that address more specific aspects of neurochemical toxicology (e.g., Bondy, 1986; Abou-Donia et al., 1988; Costa et al., 1988; Costa, 1992).

Generally, the nervous system responds to an exposure to a neurotoxicant in a progressive way, much the same way a human responds to an illness. (1) Initially, the cells become abnormal or dysfunctional. One can measure this biochemical malaise through, for example, the induction of stress proteins, changes in second

Contributed by Stephanie Padilla

Current Protocols in Toxicology (2000) 12.1.1-12.1.7

messenger response, increased lipid peroxidation, generation of free radicals, or changes in axonal transport. In some instances, one can tell if the mature nervous system is stressed because adult cells will attempt to repair themselves by adopting a biochemical profile reminiscent of regeneration or development. One approach to studying neurotoxicology is to identify and measure these indicators of a "sick" nervous system either in vivo or in vitro, whether in the neurons themselves or in glia. (2) If the stressed nervous system is unable to repair itself, cell damage occurs. Cytotoxicity may be indicated by increased intracellular calcium concentrations, changes in energy metabolism or glucose utilization, free radical generation, loss of receptors, changes in protein phosphorylation, changes in signal transduction, changes in membrane stability or integrity, and increases in calcium-activated proteases (reviewed in Tymianski, 1996; Verity, 1992). (3) The damaged cells become dead cells, either through necrosis or increased apoptosis. It may seem self-evident, but from a biochemical approach, it is often much easier to measure stressed or damaged cells than dead cells. If a cell is dead, it generates no response at all. This means that the investigator is looking for an absence of response, which is often difficult. With stressed or damaged cells, the investigator is measuring a change in response, which, experimentally, is a more robust endpoint and is easier to detect and quantify. Therefore, in order to determine if a population of cells is dead, measuring the amount of a cell-specific marker would be the choice of tests. For example, decreased amounts of choline acetyltransferase would be a strong indication that cholinergic cells had died. Other cell-specific or region-specific markers could be chosen (see Markers). Another, indirect method for determining cell death would be to look for the "scar tissue" of the nervous system: increases in the amount of glial fibrillary acidic protein.

Although these three stages of neurotoxicity have been delineated above, the distinction between the first two (i.e., stress and damage) is extremely blurred as are the biochemical approaches for detecting these stages. Neuronal cell death, by comparison, is clear cut. Very little regenerative capacity is present in the adult central nervous system (CNS), so neuronal cell death is rarely accompanied by compensatory regeneration. There is a greater capacity for regeneration in the peripheral nervous system (PNS), but that capacity is inversely related to age.

This unit will consider the prominent biochemical approaches that are now being employed to study and identify neurotoxic compounds. All types of studies will be considered: in vivo, in vitro, single-dose, and multiple-dose studies, as well as studies using various routes of administration of the toxic compound, different species, different genders, and different ages. When designing a given study, the choice of route, species, age, gender, and dosing duration is usually made according to the human exposure scenario that the investigator wants to mimic. Below is a compendium of the main approaches in use today by the majority of neurotoxicological biochemists.

NEUROTRANSMITTER DYNAMICS

Historically, one of the most established approaches to studying neurotoxicity is to measure toxicant-induced changes in neurotransmitter dynamics. One may simply measure the level of a given neurotransmitter, but there are other diverse and integral processes surrounding neurotransmitter function in the nervous system which also may be assessed. These include synthesis, packaging, release, breakdown, and reuptake of neurotransmitters. Any of these stages in chemical neurotransmission may be affected by a neurotoxic compound, and many of these processes may be assessed using in vitro or ex vivo methods. Moreover, in an effort to understand the neurotransmitter dynamics in animals treated with a neurotoxic compound, one may isolate the synaptic endings (i.e., synaptosomes) to use as a model for in situ conditions (Lam et al., 1996).

Although the effect of a neurotoxicant on neurotransmission may be multifaceted, there are entire classes of toxic compounds that are "designed" to have an adverse effect on neurotransmission. The accepted mechanism of action of the carbamate and organophosphorus pesticides is inhibition of the enzyme acetylcholinesterase, which breaks down the neurotransmitter acetylcholine. However, even within this class of anticholinesterase pesticides, the picture is becoming much more complicated as evidence mounts that these compounds may interact with other aspects of neurotransmitter dynamics such as receptor binding and reuptake (e.g., Huff et al., 1994; Liu and Pope, 1996; Rocha et al., 1996; Ward and Mundy, 1996). In general, no matter what aspect of neurotransmitter dynamics is under investigation, this biochemical approach is strengthened by the inclusion of other nonbiochemical endpoints, such as behavioral, histo-

logical, or neurophysiological assessment (for example, Boyd et al., 1990; Fredricksson et al., 1993; Kanthasamy et al., 1994). Many good, detailed reviews have been written on the subject of neurotoxicity and neurotransmitter dynamics (Costa, 1988, 1992).

In vivo microdialysis, a method for measuring the presence of any water-soluble biochemical present in the extracellular fluid in the CNS, is often used to study neurotransmitter dynamics. The great advantage of in vivo microdialysis is that the investigator is able to measure the real-time efflux of these endogenous chemicals in freely moving, nonanesthetized experimental animals (Brodie et al., 1990). Basically, the experimenter is only limited by the sensitivity of the analytical method used (usually HPLC). In addition, it is possible to infuse compounds of interest directly into a region of the brain and then measure the response of the cells. Although this is an extremely powerful method because it identifies biochemical changes in the intact experimental animal, one must be cognizant of possible complications due to the insertion of the microdialysis probe (Layton et al., 1997) and of the fact that the basic technique does not allow the investigator to distinguish between pre- and post-synaptic release.

The receptor and the attending transduction of the chemical signaling of the neurotransmitter are key components of the communication network of the nervous system. According to the classical definition of a neurotransmitter, one has to determine or identify the receptor for the putative neurotransmitter or it ceases to have validity as a transmitter, the insinuation being that the neurotransmitter cannot elicit an effect unless there is a receptor for that transmitter. The binding of a neurotransmitter to a receptor elicits a signal, usually either changes in ion fluxes due to an opening of an ion channel or other biochemical changes due to the activation of a second messenger cascade. Showing that a toxic compound perturbs receptor and/or signal transduction is a typical, but very convincing, approach to assessing the neurotoxicity of any toxicant. Moreover, many of the receptors and signal transduction systems are amenable to study either in vivo or in vitro (Nagata et al., 1997). For example, toxic compounds are capable of causing changes in receptor number or sensitivity and perturbing the second messenger cascade (Goldstein, 1993; Costa, 1994; Tandon et al., 1994; Komulainen et al., 1995; Tonner et al., 1997). One must be careful, however, not to equate receptor number with the degree of second messenger response; experimental evidence does not support the generalization that reduced receptor number leads to reduced second messenger response (or that increased receptor number leads to increased response). Beyond the second messenger response is the phosphorylation and dephosphorylation of proteins, often referred to as the "third messenger" of the nervous system. Within the last ten years, there has been a great interest in the effects of various neurotoxicants on the activity of the second messenger–activated kinases, as the kinases are one of the biochemical mechanisms for converting an ephemeral, short-lasting neurotransmitter or ion burst into a longer-lasting, more persistent biochemical change (Kikuchi and Kim, 1993, Chen et al., 1997).

AXONAL TRANSPORT

The circulation of cellular constituents proceeds in every cell, but this circulation is especially exaggerated in neurons given the geometry of these cells. Often, the cell body is located centimeters away from the axon and nerve ending. Because most of the cellular constituents are synthesized and packaged in the cell body, these constituents have to be delivered to the other regions of the axon and dendrite via a complicated system, collectively referred to as axonal transport. This system also removes spent cellular constituents from the distant regions of the neuron and returns trophic factors back to the cell body (Oppenheim, 1996). The disruption of axonal transport is thought to be the basis for many neurotoxic responses, including the majority of peripheral neuropathies (Ochs and Brimijoin, 1993).

Traditionally, the study of axonal transport usually involved performing major surgery on animals in order to inject radiolabeled precursors into the motor roots or sensory ganglia of the sciatic nerve—the nerve that was usually affected first by the toxicant. Within the last ten years, that paradigm has changed, with an increasing usage of in vitro systems for the study of axonal transport (Brat and Brimijoin, 1992; Clarke and Sickles, 1996). More recently, axonal transport studies have also begun to concentrate on studying how neurotoxic compounds interact with the motors of anterograde and retrograde transport (kinesin and dynein, respectively), the reasoning being that if a toxicant interacts with the function of either of these proteins, perturbations in axonal transport would be predicted (Sickles et al., 1996).

IDENTIFICATION OF STRESSED OR DAMAGED CELLS

A stressed cell embarks upon a convoluted biochemical demise that may lead to cell death. There are many hallmarks of a stressed, sick, or dying cell, and not all of these hallmarks need be present (also see *UNITS 2.2 & 2.6*). Interestingly, some cells are much more susceptible to damage and death than are other cells, and, not surprisingly, there is very active research aimed at discovering the bases for this sensitivity. Usually this stress begins with changes in membrane permeability and/or an influx of calcium. This influx could be triggered by activation of glutamate receptors or perturbations in the calcium pumps, and it may activate a cascade of adverse events such as excess nitric oxide release, formation of free radicals, osmotic stress, and lipid peroxidation. All of these biochemical changes happen in normal, healthy cells and, in fact, may be integral to survival of those cells (Huxlin and Bennett, 1995). However, when these changes are generated in excess, or if the cell is unable to repair and restore itself, the cell begins to deteriorate. Therefore, any of these changes may be measured to determine if the cell has become stressed or damaged. Additionally, free radical– or oxidative stress–related injury may be a component of many neurological disorders (Dawson and Dawson, 1996). As an example of how entangled the nervous system is, many of the signal transduction systems also influence the degree of toxicity produced by a given stress response (Maiese et al., 1993).

Another method for determining whether the nervous system has been adversely affected by toxicant treatment is to measure the production of stress proteins, which are synthesized when a cell undergoes chemical or physical stress in order to protect the genome of that cell. Some commonly measured proteins are the heat shock proteins (Opanashuk and Finkelstein, 1995), but recent research indicates that other stress-activated proteins are being identified and used to measure toxic responses in both neurons and glia (Zhang et al., 1996).

MARKERS

"Marker" and "biomarker" are often-used, general terms that signify that a certain biochemical test is a sentinel for exposure to a given toxicant or is a warning that the nervous system has experienced an adverse effect. Accordingly, most biochemical markers may be classified as either markers of exposure or markers of effect, and both human and laboratory animal toxicology strive to identify and validate convenient, easily accessed markers for complicated processes.

Human Studies

Either type of marker is extremely useful in assessing human neurotoxic response to a suspected neurotoxic compound. A human biomarker must be a noninvasive surrogate for either exposure to or effect of a toxic compound. For example, inhibition of blood cholinesterase is an uncontested biomarker of exposure to anticholinesterase pesticides, and hemoglobin adducts are considered markers of exposure to acrylamide (Bergmark et al., 1993). Very few biomarkers have been validated in humans, however, mainly because only blood or urine is available for measurement of markers. One of the emerging, noninvasive methods for studying neurotoxic effects in human is imaging of either the structure or the metabolism of the brain (Brooks et al., 1997). Because detecting human exposure or chemically mediated adverse effects is the ultimate aim of many neurotoxicological studies, emphasis is placed on identifying markers for biomonitoring of humans and validating those markers in animal studies (e.g., Bergamaschi et al., 1996; for a review see Manzo et al., 1996).

Animal Studies

Many of the markers of exposure that are used for humans are also used in animal studies, but the palette of markers of effect available for use in animal studies is more diverse. Cell-specific markers are informative and useful biomarkers of effect that are often employed in animal studies. These markers are biochemical correlates of certain cell types in the brain (for a review of the use of cell- and region-specific markers, see O'Callaghan, 1992). For instance, if the investigator suspects that a certain toxic compound is causing neuronal death, that brain area may be analyzed for levels of a specific synaptic vesicle protein (a marker of synapses and, therefore, a neuronal marker) as well as glial fibrillary acidic protein (GFAP; specific to glial cells). Glial cells tend to form scar tissue in the CNS, so analyzing these two markers allows the investigator to ask two questions: are the synapses gone and has glial tissue filled in the spaces that the synapses vacated? For an example of this approach, see Morse et al. (1996).

Lately, the concept of a marker for susceptibility has arisen. Often times, certain subpopulations of cells or individuals are more sensitive to the toxic effects of a compound.

This approach to neurotoxicity is receiving considerable interest in an effort to facilitate identification of susceptible human populations. For instance, the level of detoxifying enzymes may be correlated with the susceptibility to toxic compounds either in vitro (Rising et al., 1995; Wu and Welsh, 1996) or in vivo (Mortensen et al., 1996; Li et al., 1997). Moreover, in a general sense, age, sex, nutritional status, and species may also be markers of susceptibility.

SENSITIVE SUBPOPULATIONS

One intriguing new area of study concentrates on the identification of sensitive subpopulations, i.e., are there certain individuals that are more (or less) sensitive to a toxicant? All types of sensitive subpopulations are being investigated using both in vivo and in vitro experimental designs that include differences in age, species, genetic makeup (Richter et al., 1995), and prior exposure to other toxicants (Chandler et al., 1993; Sorg et al., 1996). These investigations should provide new information on why some humans are especially debilitated by toxicant exposure, on the mechanism of a toxicant, on how to predict this sensitivity in the future, and on how, ultimately, to design new chemicals that are less toxic to certain individuals. Research on both Alzheimer's disease and multiple chemical sensitivity is expressly involved with the issue of sensitive subpopulations.

EMERGING APPROACHES

The experimental world of molecular biology has just begun to be embraced by biochemical neurotoxicologists. About five to ten years ago, there was a surge in the use of early immediate genes (e.g., *fos* and *jun*) as markers of a toxicological response in a system supposedly stressed by toxicant administration. That approach has become less popular, probably because, although it was a remarkably sensitive approach, it was also an extremely nonspecific response. Right now, only ~10% of neurotoxicological studies incorporate any technique that could be loosely defined as molecular biology. There have been successful and informative uses of various techniques such as subtractive hybridization, mRNA quantitation, in situ hybridization, and the use of transgenic or knockout mice (Toggas et al., 1992; Roberson et al., 1995). Overall, however, the use of these approaches is minimal. One would expect and hope that molecular biological techniques will represent the new wave of neurotoxicological approaches in the future.

Biochemical toxicologists strive to identify the primal or integral biochemical lesion precipitated by exposure to a toxic compound. They should also endeavor to form collaborative relationships with neurotoxicologists of other disciplines, so that the significance of the biochemical lesions may be weighed in the context of behavioral, physiological, or histological changes in the same animal (Costa et al., 1995; Evans et al., 1995; Crofton et al., 1996). This type of multifaceted effort provides a synergy between investigators and adds import and distinction to the research. In addition, when considering the neurotoxicological profile of a specific compound, it is often wise to pause once in a while and summarize the toxicity profile of that compound, taking into consideration all controlled studies from all disciplines in an effort to scrutinize what has been learned and what approaches the future research should take (see, for example, Pahwa and Kalra, 1993; Strong et al., 1996).

LITERATURE CITED

Abou-Donia, M.B., Lapadula, D.M., and Carrington, C.D. 1988. Biochemical methods for assessment of neurotoxicity. *In* Perspectives in Basic and Applied Toxicology (B. Ballantyne, ed.) pp. 1-30. Wright Publishing, London.

Bergamaschi, E., Mutti, A., Cavazzini, S., Vettori, M.V., Renzulli, F.S., and Franchini, I. 1996. Peripheral markers of neurochemical effects among styrene-exposed workers. *Neurotoxicology* 17: 753-759.

Bergmark, E., Calleman, C.J., He, F., and Costa, L.G. 1993. Determination of hemoglobin adducts in humans occupationally exposed to acrylamide. *Toxicol. Appl. Pharmacol.* 120:45-54.

Bondy, S.C. 1986. The biochemical evaluation of neurotoxic damage. *Fundam. Appl. Toxicol.* 6:208-216.

Boyd, C.A., Weiler, M.H., and Porter, W.P. 1990. Behavioral and neurochemical changes associated with chronic exposure to low-level concentration of pesticide mixtures. *J. Toxicol. Environ. Health.* 30:209-221.

Brat, D.J. and Brimijoin, S. 1992. A paradigm for examining toxicant effects on viability, structure and axonal transport of neurons in culture. *Mol. Neurobiol.* 6:125-135.

Brodie, M.E., Opacka-Juffry, J., Peterson, D.W., and Brown, A.W. 1990. Neurochemical changes in hippocampal and caudate dialysates associated with early trimethyltin neurotoxicity in rats. *Neurotoxicology* 11:35-46.

Brooks, W.M., Sabet, A., Sibbitt, W.L. Jr., Barker, P.B., van Zijl, P.C., Duyn, J.H., and Moonen, C.T. 1997. Neurochemistry of brain lesions determined by spectroscopic imaging in systemic lupus erythematosus. *J. Rheumatol.* 24:2323-2329.

Chandler, L.J., Newsom, H., Sumners, C., and Crews, F. 1993. Chronic ethanol exposure potentiates NMDA excitotoxicity in cerebral cortical neurons. *J. Neurochem*. 60:1578-1581.

Chen, H.H., Ma, T., Paul, I.A., Spencer, J.L., and Ho, I.K. 1997. Developmental lead exposure and two-way active avoidance training alter the distribution of protein kinase C activity in the rat hippocampus. *Neurochem. Res*. 22:1119-1125.

Clarke, C.H. and Sickles, D.W. 1996. Decreased GAP-43 accumulation in neurite tips of cultured hippocampal neurons by acrylamide. *Neurotoxicology* 17:397-406.

Costa, L.G. 1988. Interactions of neurotoxicants with neurotransmitter systems. *Toxicology* 49:359-366.

Costa, L.G. 1992. Effects of neurotoxicants on brain neurochemistry. *In* Neurotoxicology (H. Tilson and C. Mitchell, eds.). Raven Press, New York.

Costa, L.G., 1994. Signal transduction mechanisms in developmental neurotoxicity: The phosphoinositide pathway. *Neurotoxicology* 15:19-27.

Costa, L.G., Marinovich, M., Galli, C.L. 1988. Receptor binding techniques in neurotoxicology. *In* Recent Advances in Nervous System Toxicology (C.L. Galli, L. Manzo, and P.S. Spencer, eds.) pp. 307-349. Plenum Press, New York.

Costa, L.G., Deng, H., Calleman, C.J., and Bergmark, E. 1995. Evaluation of the neurotoxicity of glycidamide, an epoxide metabolite of acrylamide: Behavioral, neurochemical, and morphological studies. *Toxicology* 98:151-161.

Crofton, K.M., Padilla, S., Tilson, H.A., Anthony, D.C., Raymer, J.H., and MacPhail, R.C. 1996. The impact of dose rate on the neurotoxicity of acrylamide: The interaction of administered dose, target tissue concentrations, tissue damage, and functional effects. *Toxicol. Appl. Pharmacol*. 139:163-176.

Dawson, V.L. and Dawson, T.M. 1996. Nitric oxide neurotoxicity. *J. Chem. Neuroanat*. 10:179-190.

Evans, J.E., Miller, M.L., Andringa, A., and Hastings, L. 1995. Behavioral, histological and neurochemical effects of nickel (II) on the rat olfactory system. *Toxicol. Appl. Pharmacol*. 130:209-220.

Fredricksson, A., Fredriksson, M., and Eriksson, P. 1993. Neonatal exposure to paraquat of MPTP induces permanent changes in striatum dopamine and behavior in mice. *Toxicol. Appl. Pharmacol*. 122:258-264.

Goldstein, G.W. 1993. Evidence that lead acts as a calcium substitute in second messenger metabolism. *Neurotoxicology* 14:97-101.

Huff, R.A., Corcoran, J.J., Anderson, J.K., and Abou-Donia, M.B. 1994. Chlorpyrifos oxon binds directly to muscarinic receptors and inhibits cAMP accumulation in rat striatum. *J. Pharmacol. Exp. Ther*. 269:329-335.

Huxlin, K.R. and Bennett, M.R. 1995. NADPH diaphorase expression in the rat retina after axontomy—a supportive role for nitric oxide. *Euro. J. Neurosci*. 7:2226-2239.

Kanthasamy, A.G., Borowitz, J.L., Pavlakovic, G., and Isom, G.E. 1994. Dopamine neurotoxicity of cyanide: Neurochemical, histological, and behavioral characterization. *Toxicol. Appl. Pharmacol*. 126:156-163.

Kikuchi, S. and Kim, S.U. 1993. Glutamate neurotoxicity in mesencephalic dopaminergic neurons in culture. *J. Neurosci. Res*. 36:558-569.

Komulainen, H., Keranen, A., and Saano, V. 1995. Methylmercury modulates GABA-A receptor complex differently in rat cortical and cerebellar membranes in vitro. *Neurochem. Res*. 20:659-662.

Lam, H.R., Ladefoged, O., Ostergaard, G., Lund, S.P., and Simonsen, L. 1996. Four weeks' inhalation exposure of rats to p-cymene affects regional and synaptosomal neurochemistry. *Pharmacol. Toxicol*. 79:225-230.

Layton, M.E., Wagner, J.K., Samson, F.E., and Pazdernik, T.L. 1997. Redox changes in perfusates following intracerebral penetration of microdialysis probes. *Neurochem. Res*. 22:735-741.

Li, W.F., Matthews, C., Disteche, C.M., Costa, L.G., and Furlong, C.E. 1997. Paraoxonase (PON1) gene in mice: Sequencing, chromosomal localization and developmental expression. *Pharmacogenetics* 7:137-144.

Liu, J. and Pope, C.N. 1996. Effects of chlorpyrifos on high-affinity choline uptake and [^{3}H]hemicholinium-3 binding in rat brain. *Fundam. Appl. Toxicol*. 34:84-90.

Maiese, K., Boniece, I.R., Skurat, K., and Wagner, J.A. 1993. Protein kinases modulate the sensitivity of hippocampal neurons to nitric oxide toxicity and anoxia. *J. Neurosci. Res*. 36:77-87.

Manzo, L., Artigas, F., Martinez, E., Mutti, A., Bergamaschi, E., Nicotera, P., Tonini, M., Candura, S.M., Ray, D.E., and Costa, L.G. 1996. Biochemical markers of neurotoxicity. A review of mechanistic studies and applications. *Hum. Exp. Toxicol*. 15:S20-35.

Morse, D.C., Plug, A., Wesseling, W., van den Berg, K.J., and Brouwer, A. 1996. Persistent alterations in regional brain glial fibrillary acidic protein and synaptophysin levels following pre- and postnatal polychlorinated biphenyl exposure. *Toxicol. Appl. Pharmacol*. 139:252-261.

Mortensen, S.R., Chanda, S.M., Hooper, M.J., and Padilla, S. 1996. Maturational differences in chlorpyrifos-oxonase activity may contribute to age-related sensitivity to chlorpyrifos. *Biochem. Toxicol*. 11:279-287.

Nagata, K., Huang, C.S., Song, J.H., and Narahashi, T. 1997. Lead modulation of the neuronal nicotinic acetylcholine receptor in PC12 cells. *Brain Res*. 754:21-27.

O'Callaghan, J.P. 1992. Assessment of neurotoxicity using assays of neuron- and glia-localized proteins: Chronology and critique. *In* Neurotoxicology (H. Tilson and C. Mitchell, eds.) pp. 83-100. Raven Press, New York.

Ochs, S. and Brimijoin, W.S. 1993. Axonal Transport. *In* Peripheral Neuropathy, 3rd ed. (P.J. Dyck and P.K. Thomas, eds.) pp. 331-360. W.B. Saunders, Philadelphia.

Opanashuk, L.A. and Finkelstein, J.N. 1995. Relationship of lead-induced proteins to stress response proteins in astroglial cells. *J. Neurosci. Res*. 42:623-632.

Oppenheim, R.W. 1996. The concept of uptake and retrograde transport of neurotrophic molecules during development: History and present status. *Neurochem. Res*. 21:769-777.

Pahwa, R. and Kalra, J. 1993. A critical review of the neurotoxicity of styrene in humans. *Vet. Hum. Toxicol*. 35:516-520.

Richter, J.A., Brennerman, M.G., Dlouhy, S.R., and Ghetti, B. 1995. Dopaminergic parameters in the striatum and substantia nigra of seven strains of mice: Higher density in striatum of CAST compared to BALB mice. *Neurochem. Res*. 20:395-400.

Rising, L., Vitarella, D., Kimelberg, H.K., and Aschner, M. 1995. Metallothionein induction in neonatal rat primary astrocyte cultures protects against methylmercury cytotoxicity. *J. Neurochem*. 65:1562-1568.

Roberson, M.D., Toews, A.D., Bouldin, T.W., Weaver, J., Goines, N.D., and Morell, P. 1995. NGFR-mRNA expression in sciatic nerve: A sensitive indicator of early stages of axonopathy. *Mol. Brain Res*. 28:231-238.

Rocha, E.S., Swanson, K.L., Aracava, Y., Goolsby, J.E., Maelicke, A., and Albuquerque, E.X. 1996. Paraoxon: Cholinesterase-independent stimulation of transmitter release and selective block of ligand-gated ion channels in cultured hippocampal neurons. *J. Pharmacol. Exp. Ther*. 278:1175-1187.

Sickles, D.W., Brady, S.T., Testino, A., Friedman, M.A., and Wrenn, R.W. 1996. Direct effects of the neurotoxicant acrylamide on kinesin-based microtubule motility. *J. Neurosci. Res*. 46:7-17.

Sorg, B.A., Willis, J.R., Nowatka, T.C., Ulibarri, C., See, R.E., and Westbert, H.H. 1996. Proposed animal neurosensitization model for multiple chemical sensitivity in studies with formalin. *Toxicology* 111:135-145.

Strong, M.J., Garruto, R.M., Joshi, J.G., Mundy, W.R., and Shafer, T.J. 1996. Can the mechanisms of aluminum neurotoxicity be integrated into a unified scheme? *J. Toxicol. Environ. Health* 48:599-613.

Tandon, P., Padilla, S., Barone, S. Jr., Pope, C.N., and Tilson, H.A. 1994. Fenthion produces a persistent decrease in muscarinic receptor function in the adult rat retina. *Toxicol. Appl. Pharmacol*. 125:271-280.

Toggas, S.M., Krady, J.K., and Billingsley, M.L. 1992. Molecular neurotoxicology of trimethyltin: Identification of stannin, a novel protein expressed in trimethyltin-sensitive cells. *Mol. Pharmacol*. 42:44-56.

Tonner, L.E., Katz, D.I., and Heiman, A.S. 1997. The acute effect of lead acetate on glucocorticoid receptor binding in C6 glioma cells. *Toxicology* 116:109-122.

Tymianski, M. 1996. Cytosolic calcium concentrations and cell death in vitro. *Adv. Neurol*. 71:85-105.

Verity, M.A. 1992. Ca(2+)-dependent processes as mediators of neurotoxicity. *Neurotoxicology* 13:139-147.

Ward, T.R. and Mundy, W.R. 1996. Organophosphorus compounds preferentially affect second messenger systems coupled to M2/M4 receptors in rat frontal cortex. *Brain Res. Bull*. 39:49-55.

Wu, W. and Welsh, M.J. 1996. Expression of the 25-kDa heat-shock protein (HSP27) correlates with resistance to the toxicity of cadmium chloride, mercuric chloride, cis-platinum(II)-diammine dichloride, or sodium arsenite in mouse embryonic stem cells transfected with sense or antisense HSP27 cDNA. *Toxicol. Appl. Pharmacol*. 141:330-339.

Zhang, P., Milles, B.S., Rosenzweig, S.A., and Bhat, N.R. 1996. Activation of C-jun N-terminal kinase/stress-activated protein kinase in primary glial cultures. *J. Neurosci. Res*. 46:114-121.

Contributed by Stephanie Padilla
U.S. Environmental Protection Agency
Research Triangle Park, North Carolina

Development of an In Vitro Blood-Brain Barrier

The blood-brain interface is constituted by specialized endothelial cells acting as a selective barrier that allows passage of nutrients and metabolic precursors, while isolating the brain from potentially noxious substances. Cell toxicity at the level of the blood-brain barrier causes reduction of this protective shield and may result in chronic neurological disease. Conversely, an intact blood-brain barrier prevents passage of systemically administered chemotherapeutics to the brain.

Cell culture techniques have provided a useful tool to study the physiological correlates of the complex set of functions that any given cell provides to the host organ. Isolation and culturing techniques have developed dramatically in the past decades, and an increasing number of cellular "factors" have been discovered, allowing growth of differentiated cells on plastic substrates or filters. Purified cells exposed to differentiating or otherwise "permissive" factors have been shown to grow and develop a more complex phenotype in the absence of normally occurring cell-to-cell signals. This reductionistic approach to cell biology, however, does not usually provide the natural environment, and aspects of cellular responses to the physiologic environment are frequently bypassed. This is particularly true for a specialized cell type, the blood-brain barrier endothelium, continuously exposed to both cellular (perivascular glia, neurons, and blood cells) and physical (shear stress) stimuli. As a result, cultured brain endothelial cells lose their physiological properties and fail to reproduce the numerous known properties of the blood-brain barrier in vivo. To overcome the limitations of the "purified cell culturing" approach, the authors have developed a quasiphysiological cell culture apparatus that allows for endothelial cell growth and differentiation in the presence of both glia and intralumenal flow.

This unit contains protocols for setting up the model system (see Basic Protocol) and assessing the functions of the model—monitoring glucose consumption and lactate production (see Support Protocol 1), measuring transepithelial permeability (see Support Protocol 2), and assessing blood-brain barrier integrity (see Support Protocol 3).

ESTABLISHING A DYNAMIC BLOOD-BRAIN BARRIER

BASIC PROTOCOL

Cells are co-cultured using hollow fiber tubes (the capillary vessels) inside a sealed chamber (the extralumenal space or ECS) accessible by ports. The cartridge/hollow fiber culturing system (see Fig. 12.2.1) consists of artificial capillaries made from polypropylene and coated with ProNectin F (Protein Polymer Technologies) connected by gas-permeable tubing to a source of growth medium allowing exchange of O_2 and CO_2. A pulsatile pump forces medium through the lumen of the artificial capillaries allowing diffusion of nutrients out to the ECS. Percolation of medium through the 0.5-μm transcapillary pores enables permeation of proteins and solutes into the ECS; this allows nourishment of the cells loaded into the ECS and aids removal of metabolic products at a controllable rate. The pore size used in this example does not allow passage of microbial agents or eukaryotic cells; however, for experiments designed to study passage of viruses or bacteria across the blood-brain barrier, pore size can be increased up to >1 μm. Similar rules apply to the passage of cells or viruses from the ECS into the lumen. The entire apparatus resides in a water-jacketed incubator with 5% CO_2 and can be aseptically sampled by placing it inside a laminar flow hood.

There are at least two types of commercially available hollow fiber apparatuses used for growth of cells into the hollow fiber. The hardware used for these experiments was

Contributed by Damir Janigro, Kathe A. Stanness, Carl Soderland, and Gerald A. Grant
Current Protocols in Toxicology (2000) 12.2.1-12.2.11

provided by Spectrum after the original CellMax design by Cellco. Alternative hardware configurations (Genespan) do not require use of an incubator, as the cartridge itself is contained in a benchtop enclosure where oxygenation and pumping of medium is provided. The latter hardware bears promise towards a more rational approach to "benchtop" dynamic cell culturing and is currently being tested in the laboratory of Damir Janigro. Multiple sizes of cartridges are available; selection depends on the desired cell load. The lumenal surface area ranges from 70 to 320 cm^2, while the extracapillary space area ranges from 100 to 420 cm^2 (see Table 12.2.1). The coating of the lumenal artificial capillaries (i.e., fibronectin or nothing) can be customized to the cell type of interest. Cell

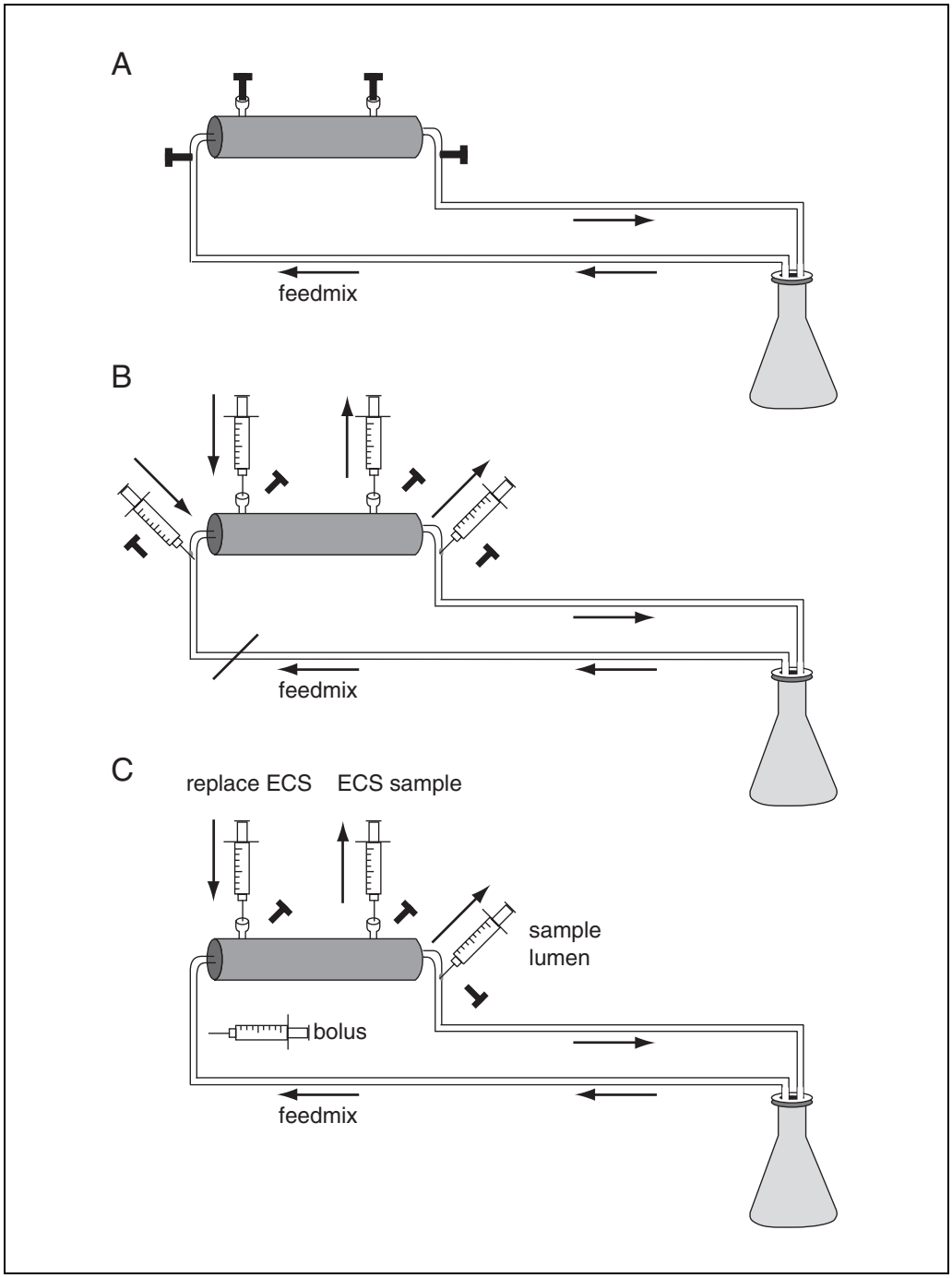

Figure 12.2.1 The cartridge/hollow fiber culturing system. (**A**) Priming and normal function; (**B**) loading of endothelial cells and glia; (**C**) testing permeability.

Table 12.2.1 Specifications for Cellmax Cartridges[a,b]

	Large cartridge	Small cartridge
Number of fibers	230	50
Lumen volume (ml)	2.7	0.5
Lumen surface (cm^2)	327	70
Endothelial inoculum (lumen)	~3–4 × 10^7 cells	~2–4 × 10^6 cells
ECS volume (ml)	7	1.4
Capillary surface area (cm^2)	423	100
Glial inoclum	~5 × 10^7 cells	~1.2 × 10^7 cells

[a]Available from Spectrum, based on the original design by Cellco.
[b]Cartridges for this purpose are polypropylene, coated cartridges.

numbers required will be specified depending on the size of the hollow fiber system purchased.

This procedure describes the main steps involved in the establishment of endothelial-glial co-culture under dynamic conditions (i.e., intralumenal flow). The initial steps are variable and depend on the cellular source that one desires to study. The first decision to be made by the investigator is whether to rely on cell lines (available commercially) or primary cultures of animal or human origin. The example outlined below refers to the use of commercially available, low-passage human endothelial cells (Cell Systems) and glial cells (Clonetics). However, the references provided at the end of this unit are used to isolate and culture endothelial and glial cells from rat or mouse brain. The following procedures imply good knowledge of aseptic cell culture techniques and access to standard equipment such as incubators and a laminar flow hood (also see *APPENDIX 3B*).

NOTE: All solutions and equipment coming into contact with living cells must be sterile, and aseptic technique should be used accordingly.

NOTE: All culture incubations should be performed in a humidified 37°C, 5% CO_2 incubator unless otherwise specified. Some media (e.g., DMEM) may require altered levels of CO_2 to maintain pH 7.4.

Materials

Human endothelial cells (Cell Systems)
Human glial cells: normal human astrocytes (NHA; Clonetics)
CS-C Complete Medium (Cell Systems) containing 10% (v/v) FBS
Gentamycin (Sigma)
Fungizone (Bio-Whittaker)
AGM BulletKit medium (Clonetics) containing 5% (v/v) FBS
Attachment factor (Cell Systems)
Versene (EDTA) and trypsin/versene (Bio-Whittaker)
DPBS, Ca^{2+}- and Mg^{2+}-free (see recipe)

75-cm^2 tissue culture flasks (Corning Costar), uncoated for glial cells and coated with 50 µg/ml attachment factor for endothelial cells
Cartridge/hollow fiber culturing system (see Fig. 12.2.1; Spectrum)
1-, 3-, 5-, and 10-ml syringes, sterile
18-G needles, blunt ended and sterile
22-G needles, sterile

Additional reagents and equipment for determining glucose levels (see Support Protocol 1)

Prepare cells

1. Grow human endothelial and glial cells to confluence in 75-cm^2 flasks coated with appropriate adhesion molecules (50 μg/ml attachment factor for endothelial cells) or on plastic (glia). Grow endothelial cells in CS-C Complete Medium supplemented with 50 μg/ml gentamicin and 0.25 μg/ml fungizone. Grow glial cells in AGM BulletKit medium, which already contains 5% (v/v) FBS.

   To coat flasks, briefly flood the surface with a solution containing the attachment factor at 50 μg/ml, then aspirate the access.

   Endothelial cells are supplied by the vendor in 25-cm^2 flasks, and each one is initially expanded to one 75-cm^2 flask. This can be further split into two or three more flasks depending on cell needs. Flasks can be expanded several times (see Cell Systems literature; provided by vendor on request).

   Normal human astrocytes (NHA) are purchased frozen with 500,000 cells per ampule, which is used to start one 25-cm^2 flask. This should be expanded first to one 75-cm^2 flask and then further expanded according to needs and speed of growth.

   The choice of substrate, while essential for traditional tissue culturing, is not relevant for the expansion of cells to be used in the dynamic in vitro blood-brain barrier, since final differentiation occurs in the hollow fibers. Another important variable, at least from the practical standpoint, relates to the time spent in traditional culture prior to seeding in the hollow fiber apparatus. If, as in this example, expansion of cell lines or highly purified cell culture is essential, it is useful to grow cells to confluence and then split the cultures until the final cell load is achieved.

2. Wean glial cells from AGM to CS-C Complete Medium by culturing first in 1:2 (v/v) CS-C/AGM for 24 to 48 hr, then in 2:1 CS-C/AGM for 24 to 48 hr, and finally in 100% CS-C.

   Co-cultures must be in the same medium (see Critical Parameters and Troubleshooting). Both cell types should be growing successfully in CS-C Complete Medium before attempting to set up co-culture.

Dissociate endothelial cells

3. Rinse endothelial cells once in 5 to 7 ml Versene (EDTA) or Ca^{2+}- and Mg^{2+}-free DPBS. Dissociate the cells by covering with 4 to 5 ml trypsin/Versene at 37°C or at room temperature until cells begin to round up.

   Dissociation time varies with cell line and stage of development; 1 to 3 min for endothelial cells and 5 to 10 min for glia are usually sufficient when the procedure is performed at room temperature.

4. Pipet detached cells into 1 ml CS-C Complete Medium and centrifuge gently (6 min at $112 \times g$, room temperature).

5. Resuspend the pellet in 5 ml CS-C Complete Medium (ten times the lumen volume) by triturating gently with a pipet bulb until no more clumps are visible.

   The lumen volume is 0.5 ml in the cartridge design used for these experiments.

Load endothelial cells into lumen

6. Detach the capillary bundle/ECS (cartridge) from the flow path and remove medium from the interior of the lumen via 5-ml syringes attached to the endports. Test this medium for glucose level, and also test a sample from the medium source and the ECS (for cell growth monitoring see Support Protocol 1).

7. Aspirate the cells into a 10-ml syringe using an 18-G blunt needle, remove needle and attach syringe to inlet port and flush back and forth with an empty 10-ml syringe attached to the outlet end until all bubbles are forced out and the capillaries are completely filled. Collect excess medium, which is forced out through the pores into the ECS, in a 5-ml syringe via the side ports, and then recap the side ports.

8. Place the cartridge in a 37°C incubator laying on one side and then rotate around its long axis for 4 to 6 hr at 45- to 60-min intervals.

   This allows the cells to settle and begin attaching to the intralumenal surface of the hollow fibers.

9. Detach the syringes and reconnect the cartridge to the flow path. Set the pump responsible for intralumenal perfusion on the lowest speed (i.e., 1 ml/min) and incubate for ≥24 hr at 37°C.

   A low speed is used to avoid pulling cells off the capillary walls. Successful growth of intralumenal endothelial cells may require periods ranging from 24 hr up to 10 days.

10. Take 200-µl samples of the lumen and ECS and analyze for glucose content (see Support Protocol 1).

Load glial cells into ECS

11. Detach glial cells from the flask with trypsin/Versene (see steps 3 and 4).
12. Resuspend the cell pellet in CS-C Complete Medium in a volume equal to the ECS not including the sideport tubing. Collect the cell suspension in a 3-ml syringe with a blunt 18-G needle.
13. Place an empty 3-ml syringe on the downstream side port and attach the cell-filled syringe upstream after removing the needle. Using equal "push-pull" pressure, inject the cells into the space and mix back and forth to chase bubbles back up the side port tubing. Allow a short period of "rest" before the flow is turned back on.
14. Close side ports with serum caps to facilitate future sampling via 22-G needles attached to 1-ml syringes. Incubate 24 to 48 hr.

    It is not necessary to rotate the cartridge after loading the ECS, as these cells are not exposed to pulsatile flow.

15. Decant medium and replace it to remove unattached cells.
16. Monitor the cultures for growth (see Support Protocol 1).

MONITORING CELL GROWTH

SUPPORT PROTOCOL 1

As the cells are not microscopically visible inside the cartridge, indicators of cell metabolism are used to monitor cell expansion. Depletion of the main carbohydrate component of the feeding mix (glucose) and accumulation of metabolically produced lactic acid are used as indicators of cell growth. The calculations for glucose consumption and lactate production rates (mg/day) are detailed elsewhere (Stanness et al., 1996, 1997). The glucose consumption and lactate production formulas are determined based on medium replacement, volume of nonreplaced medium, and previous values.

Glucose levels are measured using a Beckman Glucose Analyzer 2 with Beckman Glucose Standard (150 mg/dl) as a reference; however, any commercially available glucose detector can be used, as long as consistent mg/ml readings can be obtained. Less reliable results are obtained with glucose sticks (such as those commonly found in drug stores), and their use should be avoided. Carbohydrate metabolism produces lactic acid, which can be measured as lactate in an enzymatic assay kit (Sigma) using Sigma lactate standard solution (40 mg/dl) as a reference. Standards and samples are read on a spectrophotometer at 540 nm and converted to mg/ml. Lactate levels are then calculated using the formula lactate (mg/dl) = (A_{540} test/A_{540} standard) × 40.

Glucose consumption rate (mg/day) is calculated based on the concentration of glucose in fresh and unreplaced medium in the system, according to the following equation:

$$\frac{V_n G_n + V_o G_p - V_t G_c}{T_c - T_p}$$

where V represents added volumes of medium (ml), G is the glucose concentration (mg/dl), T is time of sampling (in fractions of days), c and p indicate the immediate and previous samples, respectively, n represents fresh medium added after previous sampling, o represents old, unreplaced medium, and t represents total medium (n + o).

Lactate production rate (mg/day) is calculated similarly:

$$\frac{V_t L_c - V_n L_n + V_o L_p}{T_c - T_p}$$

where L refers to the concentration of lactic acid in mg/ml.

To rapidly determine the mg/day values of glucose consumption and lactate production, it is recommended that a spreadsheet program (e.g., Microsoft Excel) be used to automatically determine the desired values.

SUPPORT PROTOCOL 2

MEASUREMENT OF TRANSENDOTHELIAL PERMEABILITY

The bicameral design of the hollow fiber apparatus, together with the presence of intralumenal flow, allows the measurement of "first-pass" permeability by extrapolation of pharmacokinetic equations derived from in vivo studies.

Additional Materials *(also see Basic Protocol)*

[^{14}C]sucrose (Amersham)
^{3}H-labeled drug under investigation
Additional reagents and equipment for determining glucose consumption and lactate production (see Support Protocol 1)

CAUTION: When working with radioactivity, take appropriate precautions to avoid contamination of the experimenter and the surroundings. Carry out the experiment and dispose of wastes in appropriately designated areas, following the guidelines provided by the local radiation safety officer (also see *APPENDIX 1A*).

1. Before experiments of any kind are undertaken, remove 200-µl samples from the ECS, lumen, and medium source for background levels of the tracer used (radiolabeled compound or molecule under study) and of glucose content.
2. Dilute a known concentration of the ^{3}H-labeled drug under investigation to give 5 to 10 µCi per experiment and 1 µCi [^{14}C]sucrose to a 1-ml volume and inject as a bolus directly into the proximal lumen port (upstream from the pump).

   A number of different compounds can be used as tracers. The choice of the ideal candidate depends on the experimental design and ultimately on availability of radiolabeled compound and an appropriate means of detection. For normal pharmacological studies where the permeability properties of a single molecule are to be studied, the extreme values of permeability in that particular experiment (e.g., $P_{sucrose}$ and $P_{diazepam}$) should be known. The permeability of the experimental drug can then be expressed as a percentage of $P_{sucrose}$ (or $P_{diazepam}$). In the case of high-molecular-weight compounds (e.g., polypeptides, DNA fragments, proteins), it is recommended that the permeability of a comparably sized molecule be determined (e.g., horseradish peroxidase if the experimental compound is a protein). Remember that peptides may be transported across the blood-brain barrier; hence, the reference compound must be of such a nature to exclude active transport (e.g., D-amino acid peptides).

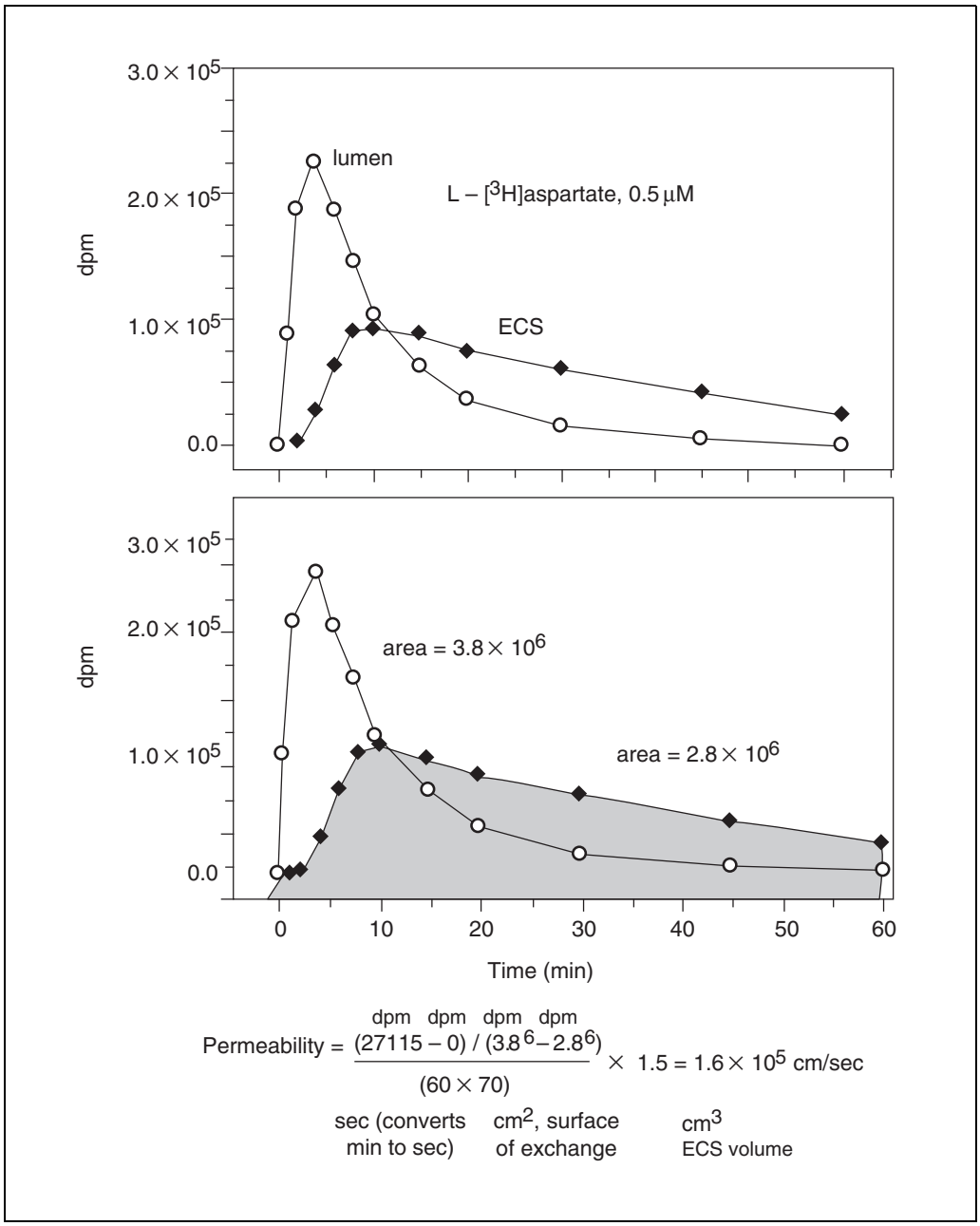

Figure 12.2.2 Testing permeability to L-aspartate.

3. Monitor the diffusion into the ECS over a period of time. Set the capillary flow at 1 dyne/cm^2 (pump setting at 1 ml/min) during the experiment and incubate in a humidified, 5% CO_2 atmosphere maintained at 37°C except during sampling.

   Although it is advisable under most experimental conditions to perform this procedure in a laminar flow hood, it is the authors' experience that, with appropriate care and respect of sterile sampling, cartridges can be sampled directly in the incubator.

4. For short-term permeability measurements, take samples from the ECS and the distal lumen at the following time points: 0, 5, 10, 20, 40, and 60 min. After each extraction (200 µl), refill the ECS content to the original volume with drug-free medium using a "push-pull" system to maintain a constant volume.

   For long-term permeability studies, samples are taken initially as described above; after the initial short-term sampling, samples are collected every 1 to 5 hr for ≥48 hr to allow

distribution to equilibrium of impermeant substances such as [^{14}C]sucrose (permeability ~10^{-7} cm/sec).

5. Analyze radiolabeled samples by liquid scintillographic detection of radioactive tracers (e.g., on a Packard Tri-Carb, 460°C) using a dual-label program to detect both ^{14}C and ^{3}H.
6. Wash excess radioactivity out of both the ECS and flow path by flushing and diluting with medium.

   Without labeled compounds, long-term experiments can be done over a period of days keeping in mind that the medium is being recycled through the system. At the end of any experiment, the medium source should be replaced with fresh medium and a glucose level taken within 24 hr.

7. Calculate the permeability/surface product by graphical integration of the concentration of the drug in the lumen and in the ECS over variable time periods (0 to 60 min; see Fig. 12.2.2). Permeability for a compound "x" is calculated by integrating the area under the ECS and lumen data points according to the following equation describing permeability (P):

$$P = \frac{K([\mathrm{x}]_{\mathrm{ecs,\ final}} - [\mathrm{x}]_{\mathrm{ecs},\ t=0})}{\int_{0 \rightarrow t\,\mathrm{lumen}} [\mathrm{x}] - \int_{0 \rightarrow t\,\mathrm{ecs}} [\mathrm{x}]}$$

   where K is a constant used to normalize rate of efflux for lumenal surface (in cm^2) and ECS volume (in cm^3), and $[\mathrm{x}]_{\mathrm{ecs,\ final}}$ and $[\mathrm{x}]_{\mathrm{ecs,\ t=0}}$ are the ECS concentrations (or dpm, cpm) of x at the extremes of the integration, and $[\mathrm{x}]_{\mathrm{lumen}}$ and $[\mathrm{x}]_{\mathrm{ecs}}$ are the areas under the respective curves.

   Mathematical formulas for the quantification of simple limited integrals are sometimes difficult to use, and graphical integration is preferred. The authors use the commercially available software Origin 6.0 (MicroCal Software) to estimate the areas underlying the profiles of intralumenal and extralumenal drug concentrations.

   Since permeability is normally expressed in cm/sec, the values obtained for P with the above equation have to be divided by 60 to transform from cm/min to cm/sec. The ratio of the concentrations in the equation used to measure P gives a nondimensional quantity. Therefore, as far as the concentrations of drugs are expressed in dimensionally consistent terms, various types of measurement values (e.g., dpm, cpm, mmol/liter) are acceptable. When using radioactive tracers, only minuscule amounts of radiolabeled drugs are used. It is important to remember that transport of drugs depends on the concentrations available for transport (or the K_D of the transporter); thus, when dealing with pharmacological studies, a therapeutic amount of unlabeled drug should be used together with the radioactive tracer. It is also important to note that drugs commonly bind avidly to plasma proteins, reducing their effective free concentrations available for transport or passive permeation.

SUPPORT PROTOCOL 3

FUNCTIONAL ASSESSMENT OF BLOOD-BRAIN BARRIER INTEGRITY

Measurement of drug permeability is time consuming and costly, since radioactive tracers and their disposal are expensive. An alternative approach can be used to indirectly obtain a rough estimate of the degree of endothelial cell differentiation. This technique takes advantages of one of the many quasi-physiological features of the dynamic in vitro blood-brain barrier. Under steady-state conditions, and in the presence of a good barrier, the levels of lumen versus ECS glucose are not equal, owing to the ablumenal-preferring distribution of glucose transporters. Thus, by simply measuring the ECS and lumenal concentrations of glucose, one can detect changes in blood-brain barrier integrity over time. If $\mathrm{glucose}_{\mathrm{lumen}}/\mathrm{glucose}_{\mathrm{ecs}}$ equals 1, there is probably no barrier formed because all the fluxes are paracellular (leak pathway); conversely, when the ratio becomes >1,

blood-brain barrier formation is occurring. An acceptable value is usually ~1.4 (lumenal glucose higher), roughly corresponding to a P_{glu} of 10^{-6} cm/sec.

Using similar considerations, one may decide to use other compounds that are, at steady state, asymmetrically distributed when the blood-brain barrier is endowed with tight junction–dependent exclusion properties. For example, the physiological ion potassium is, like glucose, more concentrated in the plasma. Potassium can be measured by a number of different analytical techniques or, if a department of laboratory medicine is located nearby, by simply treating samples as plasma samples for kalemic determination.

REAGENTS AND SOLUTIONS

Use Milli-Q-purified water or equivalent in all recipes and protocol steps. For common stock solutions, see ***APPENDIX 2A****; for suppliers, see* ***SUPPLIERS APPENDIX****.*

Dulbecco's phosphate-buffered saline (DPBS), Ca^{2+}- and Mg^{2+}-free

0.2 g/liter KCl
0.2 g/liter KH_2PO_4
6.83 g/liter NaCl
2.16 g/liter $Na_2HPO_4 \cdot 7H_2O$
4.76 g/liter HEPES
Adjust pH to 7.2 with NaOH
Sterile filter with a 0.2-µm filter
Store up to 6 months at 4°C

This formulation can be purchased from Bio-Whittaker.

COMMENTARY

Background Information

The cellular basis of the blood-brain barrier is well established and is localized at the level of the brain microvascular endothelial cells. Blood-brain barrier properties are not intrinsic to these cells, however, but are induced by the surrounding brain tissue. In the past, most studies of the blood-brain barrier have been performed in vivo. However, there are limitations to the use of whole animals for the detailed investigation of the modulation of the blood-brain barrier at the cellular level. In vitro models (i.e., isolated microvessel preparations, tissue culture systems) offer a promising alternative for studies of cellular physiology of the blood-brain barrier (Grant et al., 1998; Janigro et al., 1999); however, many of the endothelial cell culture models have been characterized by low transendothelial resistance and relatively high permeability to sucrose. Thus, these models, while versatile and simple, poorly mimic the in vivo blood-brain barrier phenotype. In vitro models of the blood-brain barrier are employed to investigate mechanisms of drug permeation and thus attempt to mimic the salient features of the blood-brain barrier in situ. Static culturing of brain endothelium typically yields low transendothelial electrical resistance and exaggerated permeability, possibly owing to nonphysiological cell growth conditions. The authors developed a dynamic in vitro blood-brain barrier model where near-physiological permeation properties are achieved by growth of endothelial cells in the presence of intralumenal flow and ablumenal glia cells.

There are at least two separate uses for in vitro models of the blood-brain barrier. Depending on the field of study, one may decide to study how drugs cross the blood-brain barrier or whether a particular substance may negatively impact on blood-brain barrier integrity. A brief discussion of these two approaches follows.

Drug permeation across cellular layers constituted by "tight" epithelial or endothelial cells is a common hindrance to effective drug delivery. Since the advent of modern psychopharmacology, it has been understood that the degree of lipophilicity of any given substance is good predictor (under most circumstances) of penetration in the central nervous system. The biological basis for this phenomenon is quite simple since cells are ensheathed by lipid membranes that are amenable for passage of similarly fatty molecules. Another predictor of drug passage is based on the molecular size (molecu-

lar weight) of the drug, with larger drugs being less permeant. It is striking, however, that lipophilicity per se fails to accurately predict passage of numerous therapeutically relevant drugs, including chemotherapeutics and antiretrovirals. It is becoming clear that pathways independent from the cellular integrity of the blood-brain barrier can exclude lipophilic drugs. Specific "reverse transport" molecules have been cloned and studied, including the ubiquitous P-glycoprotein, expressed abundantly in both epithelial and endothelial cells.

Since molecular weight and lipophilicity are not reliable predictors of central nervous system delivery, the use of realistic models has become imperative. To this end, numerous efforts have been made to establish reliable models replicating the cellular properties of the blood-brain barrier in situ. Perhaps surprisingly, and in spite of the availability of modern techniques aimed at permanent cell transformation and genetic manipulations of tissue, in vitro growth of brain endothelial cells has not produced cellular monolayers with the desirable properties (i.e., similar to in vivo). This is partially due to the fact that blood-brain barrier endothelial cells undergo physiological transformations only when exposed to cellular (perivascular glia) and intralumenal (shear stress) influences. To date, only modeling under dynamic conditions has produced results comparable to that obtained in vivo (Grant et al., 1998; Janigro et al., 1999).

Neurotoxicology has heavily relied on isolated organ models to test noxious effects of putative toxins and toxicants. Owing to growing societal concerns over whole-animal testing, and given the obvious obstacles and limitations related to human studies, studies have been routinely performed on cultured neurons or acutely on brain slices. One of the obvious limitations of this approach is the fact that some substances are not neurotoxic in their plasmatic molecular form and become neurotoxic only after passage across the endothelium. Furthermore, it is possible that—in addition to a direct effect on neurons, as estimated in vitro—substances may also affect blood-brain barrier integrity.

Similar consideration applies to studies exclusively performed in vivo. These are commonly done using control subjects, presumably with an intact blood-brain barrier. Under these conditions, a number of potentially neurotoxic compounds are excluded and will not exert central nervous system effects. The issue remains whether the same compound may become neurotoxic in the presence of an "attenuated" or outright leaky barrier. To this end, it is worth remembering that numerous common diseases and conditions negatively impact on blood-brain barrier integrity (Grant et al., 1998).

Critical Parameters and Troubleshooting

Care must be taken to prevent bubbles from forming in the tubing, as they travel to the lumen of the capillaries and strip off cells, leaving bare areas. Bubble formation leads to cell loss and capillary drying. It also decreases the flow rate, depriving cells of adequate nourishment and thus interfering with normal cell growth and differentiation. All connections must be tightened to prevent air leaks. A several-day priming of the system with complete medium allows all spaces to fill; bubbles can then be chased into the bottle before any cells are added. Prewarming medium to 37°C is helpful both for the comfort of the cells and to reduce bubble formation.

Absolute compulsiveness must be used to maintain sterility of the system. Wipe all connections with alcohol swabs before and after disconnection; use sterile syringes for each sample. Perform all sampling in a laminar flow hood, if at all possible. Once contaminated, the cartridge is useless as antibiotics alone are not usually sufficient to kill a bacterial or fungal infection.

Cells need to be monitored frequently for glucose consumption when first set up in order to establish a satisfactory feeding schedule because the cell demands in a cartridge may be very different from those in a flask. Generally the medium source is replaced two to three times per week. Extra glucose may be added to maintain the culture during a time when medium replacement is not possible. Starved cells may begin to die, fall off the capillary walls, and disrupt barrier formation. An acid pH shift (solution turns yellow) provides a visible sign of underfeeding, but hypoglycemia may occur in the absence of any significant pH change.

In co-culture, both cell populations are by design fed the same medium. If one line has been grown in a different medium it must be weaned over to the new formula before it is added to the cartridge. Generally the feed medium of choice is the one in which the more fastidious cell population grows. In this example it is the human endothelial cells lining the lumen that require their own medium formula, so the astrocytes, which are a less demanding population, are weaned over prior to loading in

the extracapillary space. As a rule, feeding the glial flasks first 1:2 (v/v) endothelial/astrocyte medium, then 2:1 endothelial/astrocyte medium, and finally 100% endothelial medium will prepare them to grow in the endothelial medium–fed cartridge.

Barrier formation cannot be hurried. Overly frequent testing with radioactive tracers stresses the cells and may delay barrier formation due to cell loss or disruption. Once the blood-brain barrier is formed, a cartridge may remain healthy up to 6 weeks. Two challenges with radiolabeled tracers per week are usually nondestructive.

Anticipated Results

The endothelial medium CS-C Complete Medium contains 300 mg/dl glucose. A rapidly growing cartridge can deplete this over a few days. It is best to replace medium when glucose levels reach 50 to 75 mg/dl. A level ≤10 mg/dl indicates a starved population of cells and results in massive accumulation of lactic acid in the bathing solution. Examples of glucose consumption and lactate production for a variety of cell types are provided elsewhere (Stanness et al., 1996, 1997; Pekny et al., 1997).

Permeability values are expressed as a velocity, but are measured vectorially since the equation used assumes that passage occurs from blood to brain (i.e., drug added to the lumen). It is possible that a significant permeation from the lumen occurs, due either to a leaky barrier or to use of highly permeant compounds. Under these conditions, the mathematical manipulation may give a negative value for P. Since this is not possible, one must adjust the limit of the integration interval to minimize the quantity of extravasated drug. This is simply achieved by changing the limits of integration to 30 (or even 20) min postinoculation. Remember to also change the values on the numerator. Typical values for poorly permeant substances such as [^{14}C]sucrose are between 2×10^{-6} and 10^{-7} cm/sec. Permeant substances such as diazepam have permeability $>10^{-5}$ cm/sec.

A hollow fiber device can be used for multiple experiments as long as drugs or radioactivity are washed out of the system between each run and background levels are monitored at each testing. The device itself can be stripped of cells by using trypsin and can then be reused in other experiments. It is best to reload with the same combination of cells in subsequent experiments. Needless to say, once sterility has been lost the device is useless. Gas sterilization of the flow path is possible, but the necessary drying of the capillary fibers precludes gas sterilization. The cartridges can be autoclaved under water for 30 min, but care must be taken that they remain wet until reused.

Time Considerations

It may take from 2 to 6 weeks for a human cell–populated cartridge to form a good barrier and be suitable for experiments. A weekly permeability measurement takes about an hour to set up, 40 to 60 min to run, and 2 to 3 hr for washing and refeeding the cartridge. Daily or biweekly samples for glucose need to be taken from the extracapillary space and medium source. At this time notes should be made about the condition of the system—color of medium, debris present, presence of bubbles or leaks. This requires only a few minutes. Glucose samples can be run as taken, can be saved at 4°C for a few days, or frozen for further analysis.

Literature Cited

Grant, G.A., Abbott, N.J., and Janigro, D. 1998. Understanding the physiology of the blood-brain barrier: The role of in vitro models. *News Physiol. Sci.* 13:287-293.

Janigro, D., Leaman, S., and Stanness, K.A. 1999. Dynamic in vitro modeling of the BBB: A novel tool for the studies of drug delivery to the brain. *Pharm. Sci. Technol.* 2:7-12.

Pekny, M., Stanness, K.A., Eliasson, C., Betsholtz, C., and Janigro, D. 1997. Impaired induction of blood-brain barrier properties in aortic endothelial cells by astrocytes from GFAP-deficient mice. *Glia* 22:1-11.

Stanness, K.A., Guatteo, E., and Janigro, D.A. 1996. A dynamic model of the blood-brain barrier "in vitro." *Neurotoxicology* 17:481-496.

Stanness, K.A., Westrum, L.E., Mascagni, P., Fornaciari, E., Nelson, J.A., Stenglein, S.G., and Janigro, D. 1997. Morphological and functional characterization of an in vitro blood-brain barrier model. *Brain Res.* 771:329-342.

Contributed by Damir Janigro and Kathe A. Stanness
Cleveland Clinic Foundation
Cleveland, Ohio

Carl Soderland
Cell Systems
Kirkland, Washington

Gerald A. Grant
University of Washington
Seattle, Washington

Culturing Rat Hippocampal Neurons

Many toxicants alter the functioning and/or development of the mammalian nervous system. The relative simplicity of neuronal culture techniques and the high degree of control over the conditions under which neurons are grown and exposed to toxicants greatly facilitate investigations into the mechanisms of neurotoxicant action. A wide variety of neuronal cultures has been used in neurotoxicology, including primary cultures from several species (most commonly rats and mice) and from various regions of the brain (including hippocampus, cerebral cortex, cerebellum, and striatum), and immortal cell lines such as PC12 and several neuroblastoma lines. Each of these options may offer advantages for specific studies; for example, site-specific neurotoxicants are probably most suitably studied in cultures from the appropriate brain region. Cultures of embryonic rat hippocampal neurons, however, have found particular favor in basic neurobiology (e.g., in studies of voltage-sensitive and ligand-gated ion channels, synaptic transmission, and neurite development). Therefore, there is a rich background literature on hippocampal neurons that the neurotoxicologist can use to formulate hypotheses, develop experimental protocols, and help understand mechanisms of toxicant action.

This unit describes procedures for isolating hippocampal neurons from embryonic rats and cryopreserving them (see Basic Protocol 1), for culturing the neurons (see Basic Protocol 2), for developing hippocampal astrocyte cultures (see Basic Protocol 3), and for coculturing neurons and astrocytes (see Basic Protocol 4).

NOTE: All protocols using live animals must first be reviewed and approved by an Institutional Animal Care and Use Committee (IACUC) or must conform to governmental regulations regarding the care and use of laboratory animals.

NOTE: All solutions and equipment coming into contact with living cells must be sterile, and aseptic technique should be used accordingly.

NOTE: All culture incubations should be performed in a humidified 37°C, 5% CO_2 incubator unless otherwise specified.

ISOLATING HIPPOCAMPAL NEURONS FROM RAT EMBRYOS

BASIC PROTOCOL 1

This procedure describes the initial isolation of hippocampi from embryonic rats and their dissociation into single neurons. All phases of the dissection must be conducted in a laminar flow hood, using sterilized instruments and surgical gloves. Dissecting tools should be stored with their working surfaces submerged in a vial of 95% ethanol when not in use. Immediately before use, they should be dipped in sterile HBSS to remove the ethanol.

When dissecting, it is best to always have a pair of forceps in one hand and a pair of forceps or scissors in the other. One pair of forceps will always be used to stabilize the head or brain tissue as the other implement is being used. Forearms and hands must be stabilized by resting them on the table and the edges of the dissecting dish, respectively, taking care that fingers aren't dipped in the HBSS.

Even though fetal brains are relatively small and the hippocampi are smaller still, anoxia and cellular damage probably begin as soon as the dam is anesthetized and continue until the neurons are dissociated from the hippocampi. Keeping the brains and hippocampi cold reduces, but does not eliminate, metabolic activity and associated cellular damage.

Contributed by Gerald Audesirk, Teresa Audesirk, and Charles Ferguson
Current Protocols in Toxicology (2000) 12.3.1-12.3.17

The highest number of healthy neurons will be obtained by a well-coordinated dissection team, in which each member of the team is highly proficient at specific tasks, thereby minimizing the total time between anesthesia and dissociation of neurons. It is useful to have one person removing brains from the skulls while a second removes the hippocampi and a third dissociates the hippocampi into a single-cell suspension. Typically, dissection of the hippocampi begins after brains have been removed from about half of a litter. Removal of the brains from the other half of the litter will usually be finished well before hippocampal dissection of the first half is complete; until dissection, these brains may be stored in a refrigerator, in a covered sterile culture dish filled with cold HBSS. Dissociation of the hippocampi from the first half-litter then begins while hippocampi are dissected from the second half. If more than one litter is to be used in a single day, three people can keep up a more-or-less continuous process of brain removal, hippocampal dissection, and hippocampal dissociation until all of the litters are finished.

Each E18 hippocampus typically provides ~0.5 to 1 million cells, almost all of which are neurons. Therefore, depending on the size of the litter, a single litter will provide ~6 to 30 million neurons. Depending on the experimental protocol, this may be far more neurons than can be conveniently used at once. For example, for morphological measurements of neuronal differentiation, neurons are typically plated sparsely (~1,000 to 20,000 cells/cm^2 or ~10,000 to 200,000 per 35-mm culture dish), so a single litter would provide enough neurons for dozens to hundreds of dishes. Further, because of the preparation and setup time, it is often convenient to dissect several litters at once. Cell suspensions may therefore be cryopreserved as described below and used at leisure. Appropriate cryopreservation results in cultures that are virtually indistinguishable from those produced by plating immediately after dissociation (Mattson and Kater, 1988).

Materials

Timed pregnant female rats (e.g., Sprague-Dawley) at gestational day 18 or 19 (E18 or E19)
95% (v/v) ethanol
HBSS (see recipe), sterile, ice cold
CMF-HBSS (see recipe), sterile, ice cold
2 mg/ml trypsin (Life Technologies) in CMF-HBSS, prewarmed (37°C)
2 mg/ml trypsin inhibitor (Sigma) in CMF-HBSS, prewarmed (37°C)
Complete EMEM (see recipe; optional) or equivalent
Cryopreservation medium (see recipe; optional), cold
Propanol (optional)

Laminar flow hood
Dissecting microscope, total magnification of ~14×
Fiber optic illuminator (e.g., Fiber-Lite, Dolan Jenner Industries)
Large magnifying glass on stand (Edmund Scientific)
CO_2 tank and tubing
Anesthetizing chamber
Dissecting pans of various sizes, all with autoclavable rubber of silicone filling for pinning tissue
~24 × 32–nm
18 × 20–nm
10-cm dia., 4-cm deep
10-cm tissue culture dish

Dissection tools (Roboz Surgical Instruments or Fine Science Tools), sterile:
Bone cutters or strong, short-bladed scissors
Rat-tooth forceps
Large and small dissecting scissors (~4- and 2-cm blades)
Microdissecting forceps (Dumont no. 5 or equivalent; old or deliberately blunted forceps work best for pinning tissues, sharpened forceps for actual dissection)
Blunt forceps
Fine dissecting pins (e.g., Minuten insect pins, Carolina Biological Supply)
Large and small spring-handled microdissecting scissors (10- and 3-mm blades, respectively)
5-ml disposable plastic tubes (e.g., Falcon), sterile
Fire-polished Pasteur pipet, sterile
Hemacytometer and coverslip
Upright compound microscope (400× total magnification)
Freezing vials (e.g., 2-ml vials from Nalgene; optional)
Vial-freezing containers (e.g., Nalgene cryo 1° freezing containers; optional)

Remove uterine horns

1. Prepare the dissection area. Ensure that all dissecting equipment is sterile and place it in a sterile laminar flow hood with a dissecting microscope and fiber optic illuminator. Ensure that all solutions are filter sterilized and place them in the hood.

   All procedures after the initial removal of the uterus from the anesthetized dam should be carried out in a sterile, laminar flow hood. A laminar flow hood with a dissecting microscope built into the front glass would be ideal, but is not necessary. A clean dissecting microscope and illuminator placed in the hood and carefully wiped down with ethanol should suffice. A large adjustable magnifying glass will facilitate removal of the fetal brains from the skulls.

2. Insert tubing connected to a CO_2 tank through the hole in the lid of an anesthetizing chamber. Allow the chamber to fill with CO_2 for 10 to 20 sec.

   The chamber can be easily constructed from a plastic cage bottom and a piece of plastic large enough to completely cover the cage top. Drill a hole in the plastic just large enough to accommodate tubing connected to a CO_2 tank.

3. Remove the lid, rapidly place a timed pregnant female rat in the chamber, and replace the lid. Wait until the rat has stopped breathing for a few seconds.

   Hippocampal neurons are usually taken from rats at day 18 or 19 of pregnancy (E18 to E19). At this stage, most of the pyramidal neurons have formed, but there are very few glial cells. If it is not desirable to keep a rat colony or to maintain pregnant rats, pregnant rats may be obtained from several companies, timed to arrive in the laboratory at E18 (or earlier).

   Longer anesthesia is unnecessary and may result in damage to fetal neurons caused by anoxia and/or pH changes.

4. Remove the dam from the anesthetizing chamber and rapidly transfer it to a large (~24 × 32-cm) dissecting pan, dorsal side up. While immobilizing the head, rapidly pull the tail so that the neck is broken. Using bone cutters or strong, short-bladed scissors, crush or sever the cervical spinal cord.

   Dissecting pans can be made from dishes filled 2 to 4 cm deep with Sylgard (Dow Corning) or similar material into which pins may be inserted during dissection. The addition of carbon black to the Sylgard before polymerization provides a black background, which greatly assists visualization of the brain during dissection.

5. Turn the dam ventral side up and sterilize the abdomen by pouring 95% ethanol over it.

6. Rinse rat-tooth forceps and short-bladed scissors in ethanol, grasp the abdominal skin with the forceps, and cut the abdomen completely open, from near the vagina to the thoracic cavity. Rinse the forceps and scissors in ethanol again.

7. Identify the uterine horns by their dark red color, with ~2-cm-long fetuses separated by constrictions. Gently grasp a horn at one of the constrictions and lift up. Remove the horns by cutting their attachments to the abdominal cavity and place in a sterile 14×20-cm dissecting dish.

   The uterine horns should be removed as rapidly as possible, because the fetuses are no longer receiving oxygen from the dam. At this stage, blood samples may be taken from the dam by cardiac puncture and/or other body parts may be removed from the dam.

   The uterine horns may come out in one or two pieces. Typical litters have six to fifteen fetuses (Sprague-Dawley rat litters average eleven fetuses).

Isolate fetal heads

8. Transfer the dissecting pan with the uterine horns to the laminar flow hood.

   Although not necessary during the removal of the uterine horns from the dams, surgical gloves should be worn during all other procedures.

9. Remove the fetuses from the uterine horns and place in cold, sterile HBSS. Using microdissecting forceps and small dissecting scissors, decapitate the fetuses and place the heads in fresh, cold HBSS in a 10-cm dissecting dish.

   For larger litters, or if the dissecting process is slow, some of the heads can be stored in HBSS in a covered sterile culture dish in the refrigerator (up to 15 min).

Dissect out fetal brains

10. Place a 10-cm circular dissecting dish in a larger dish of crushed ice and fill to ~2 cm deep with fresh, ice-cold HBSS. Orient a fetal head in the dish, with the neck down and the snout facing away. Using blunt forceps, place a dissecting pin through the snout to anchor the head.

11. Insert the tip of a pair of large spring-handled microdissecting scissors under the nearest cut edge of the skin and skull. Orient the scissor blades along the longitudinal fissure separating the hemispheres. Anchoring the head with the forceps, lift upward with the scissor blades while cutting through the skull, in order to avoid slicing the underlying brain tissue. Slice forward almost to the pin anchoring the snout.

    Initially, it may be easier to cut through the skin first, then through the transparent skull, but these steps can be combined after skill is achieved.

    It is important that the scissors be positioned exactly along the longitudinal fissure in order to avoid cutting the cerebral cortex.

12. Using two pairs of microdissecting forceps, grasp the cut edges of both skull and skin on either side of the incision and separate them, exposing the brain. Anchor each flap to the side with a dissecting pin.

13. Using the scissors held horizontally, place the blades beneath the brain, and use a few snips moving toward the snout to sever the cerebral hemispheres and cerebellum from the spinal cord.

    The scissors can now serve as a platform to lift the brain upward out of the skull.

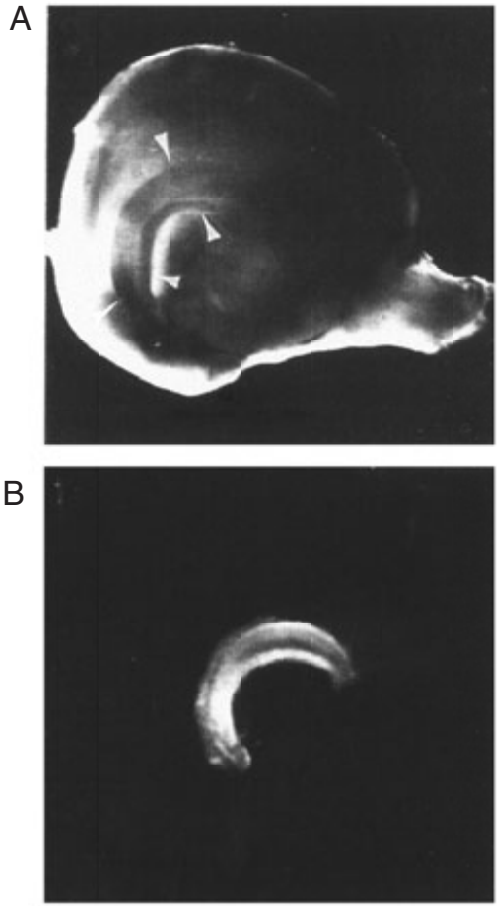

Figure 12.3.1 Hippocampal dissection. (**A**) A view of the medial surface of the left cerebral hemisphere. The arrows indicate the boundaries of the hippocampus, as described in the text. (**B**) The hippocampus after removal from the cerebral hemisphere. From Goslin and Banker (1991). Reprinted by permission of MIT Press.

14. Remove brains from all heads before continuing. Remove HBSS contaminated with blood by slowly and gently pouring it off the dissected brains, leaving them behind in the dissecting pan. Replace with fresh, ice-cold HBSS.

Dissect out hippocampi

15. Orient the brain dorsal side up with the cerebellum toward you. Insert the blades of the large spring-handled scissors between the junction of one hemisphere and cerebellum, with the blade extending along the longitudinal fissure and angled toward the midline, and use a single cut to isolate the cerebral hemisphere from the cerebellum and the brainstem. Repeat on the other side of the brain and for all the brains before removing any hippocampi.

16. Place cerebral hemispheres in a small dissecting dish that is sitting in ice. Orient one hemisphere with the medial surface upwards (Fig. 12.3.1). Anchor it with a single microdissecting pin through the severed corpus callosum just below the center of the hemisphere, allowing rotation of the tissue around the pin as needed.

A remnant of thalamus may remain attached to the medial cortex, obscuring the hippocampus (Goslin and Banker, 1991). This is easily cut away with forceps or scissors, leaving the smooth, flat medial surface of the cortex exposed. When orienting the cerebral hemisphere, the olfactory bulb, a nubbin of tissue that projects anteriorly, is a good landmark. Note in Figure 12.3.1 that the dorsal cerebral hemisphere is much more rounded than the ventral surface. The cortex is surrounded by semitransparent tissue, the meninges, in which blood vessels are embedded.

The hippocampus, located in the medial and posterior half the cerebral cortex, is a C-shaped structure whose concave portion faces the olfactory bulb. The hippocampal fissure, which forms the dorsal border of the hippocampus, is a shallow depression sometimes highlighted by a blood vessel, as seen in Figure 12.3.1. The fissure separates the dorsal margin of the hippocampus from the adjoining subicular and entorhinal cortex (Banker and Cowan, 1977). The ventral margin of the hippocampus is free, bordered by a translucent band of tissue, a developing fiber tract called the fimbria (Goslin and Banker, 1991). Immediately behind the hippocampus is the lateral ventricle.

Because the cerebral tissue is delicate and easily torn when grasped with forceps, the authors leave the meninges attached so that the tissue can be lifted by grasping the meninges. However, some researchers prefer to remove the meninges before dissecting the hippocampus. This must be done slowly and gently, stabilizing the underlying cerebral tissue with forceps to avoid tearing it.

17. Make a single cut with small microdissecting scissors from the dorsal-most part of the cerebral hemisphere (the top of the head) down through the fimbria (toward the central pin).

    This cut will define the approximate anterior boundary of the hippocampus.

18. Make a curving incision just dorsal to the hippocampal fissure, parallel to the ventral free border of the hippocampus, and extending posteriorly and ventrally. Use a final snip at the end of the curved incision to release a fingernail paring–shaped piece of tissue containing the hippocampus (see Fig. 12.3.1).

    If the meninges are still attached, remove them at this time by pulling them off gently with a pair of forceps, while stabilizing the hippocampal tissue with another pair.

19. Transfer the hippocampus to a 5-ml sterile disposable plastic tube containing 4 ml ice-cold CMF-HBSS.

    The tube may be embedded upright in crushed ice or stored in a tube rack (such as Kryorack VI) in which the tube slots are surrounded by a frozen solution.

20. Remove remaining hippocampi and add to the tube.

    Typically, the hippocampi from one litter can be processed in a single tube.

Dissociate hippocampi

21. Remove hippocampi and combine them in a 5-ml tube containing 2 ml of 2 mg/ml trypsin solution, prewarmed to 37°C. Place in 37°C water bath for 15 min.

22. Gently aspirate off the trypsin solution with a sterile pipet and add 2 ml of 2 mg/ml trypsin inhibitor solution, prewarmed. Incubate 5 min at 37°C.

23. Gently aspirate off the trypsin inhibitor solution and add prewarmed (37°C) complete EMEM (to plate the neurons immediately) or ice-cold cryopreservation medium (to preserve the neurons for later use) at 100 µl per hippocampus. Dissociate the hippocampi into a (mostly) single-cell suspension by gently pipetting through a fire-polished, sterile Pasteur pipet.

    Vigorous or excessive pipetting will result in significant cell death. It is probably better to pipet less and leave a few cell clumps than to overpipet and risk damaging many of the cells. The authors usually pipet the hippocampi only eight to ten times. Care should be taken to avoid aspirating air and causing foaming of the medium, as cell viability will be severely compromised. Finally, when fire polishing the pipets, the pipet tips should be heated just enough to smooth the opening without greatly reducing its diameter. Very small tip openings caused by excessive fire-polishing result in too much shear stress upon the cells during pipetting.

24. Place a small drop of cell suspension in a hemacytometer, apply a coverslip, and determine the cell density using an upright microscope with 400× total magnification (*APPENDIX 3B*). Add the appropriate amount of complete EMEM or cryopreservation medium to adjust the suspension to the desired cell density.

    For immediate culture (see Basic Protocol 2), there is no optimal cell density. For most applications, it is probably simplest to adjust the suspension to a fairly high density (e.g., 5–10 × 10^6 cells/ml) and dilute the resulting suspension in culture medium when the cells are plated, to obtain the density required by the experimental protocol. For cryopreservation, adjust cell density to 8 × 10^6 cells/ml.

    Some investigators use trypan blue staining (APPENDIX 3B) to distinguish live from dead cells when determining density. In the authors' experience, there is no need for trypan blue staining. Most living cells are round (possibly with a small stump of a process remaining attached to the cell body) and bright, and most dead or dying cells are clearly ragged. Counting only the round bright cells agrees very closely with results from trypan blue staining.

25. *Optional:* To cryopreserve cells, place 250-µl aliquots of cell suspension (2 × 10^6 cells) in freezing vials. Place the freezing vials in a Nalgene vial-freezing container filled with room-temperature propanol. Place the freezing container in a −70° or −80°C freezer and store for up to 1 month.

    Cryopreservation works best when a cryopreservative is added to the medium to reduce ice crystal formation and when freezing is done slowly (~1°C per min). Commercial cryopreservative media are available (e.g., Life Technologies), but simply adding dimethyl sulfoxide (DMSO) and 10% (v/v) fetal bovine serum to EMEM produces excellent results. Slow freezing may be accomplished manually, for example, by sequential cooling of the vials in a refrigerator (4 hr), a −20°C freezer (4 hr), and then a −70°C freezer. However, freezing containers greatly simplify the process.

CULTURING HIPPOCAMPAL NEURONS

BASIC PROTOCOL 2

There is no generally acknowledged optimal set of culture conditions for hippocampal neurons, in part because the appropriate plating substrate, culture medium, additives, and neuronal density may vary depending on the experimental design and aims. This protocol describes sparse plating of neurons on polylysine-coated plastic culture dishes in fairly typical Eagle's minimal essential medium containing fetal bovine serum and other supplements. See Background Information for a brief description of a few alternative media and additives that may be appropriate for certain types of experiments.

Materials

0.1 mg/ml poly-D-lysine (mol. wt. 350,000; Sigma), filter sterilized (cellulose acetate, 0.2-µm pore size)
Dissociated hippocampal cell suspension (see Basic Protocol 1)
Complete EMEM (see recipe)
10× cytosine arabinoside (typically, 10 to 100 µM) in complete EMEM, filter sterilized (optional)
Laminar flow hood
35-mm plastic cell culture dishes (Corning or Nunc)

1. Open a package of 35-mm plastic cell culture dishes in a laminar flow hood.
2. Pipet ~0.5 ml of 0.1 mg/ml poly-D-lysine solution into each dish, replace lids, and leave in the hood for 30 min.

    Many other substrates are in common use, including poly-L-lysine, polyornithine, laminin, fibronectin, collagen, and combinations of these. Several companies also sell precoated

dishes with any of several treatments (e.g., Biocoat markets dishes coated with collagen, fibronectin, laminin, poly-D-lysine, and other substrates). Poly-D-lysine and poly-L-lysine are probably the most commonly used, but the investigator should be aware that coatings, particularly protein coatings, may interact with attachment receptors on the neurons and significantly affect neuronal differentiation in culture.

3. Rinse each dish three times for 30 min each with 2 ml sterile deionized or distilled water. Aspirate off the last rinse and leave the lids ajar in the hood until the dishes are dry.

   Dishes may be used for ≥2 weeks after coating, if they are kept dry at room temperature.

4. Determine the desired number of cells per dish and calculate the volume of dissociated hippocampal cell suspension needed to contain this number. In the laminar flow hood, using sterile pipet tips, pipet the appropriate volume into 2 ml complete EMEM in each coated 35-mm culture dish. Place the culture dishes in a 37°C, 5% CO_2 incubator.

   In relatively high-density cultures (e.g., >200,000 cells plated in 2 ml medium), it may be useful to replace the medium after 2 to 4 hr to remove debris produced during trypsin digestion and cell dissociation.

   The dissociated cells will settle to the bottom of the tube if they are not used shortly after dissociation. If necessary, gently resuspend the cells with one pass through a fire-polished, sterile Pasteur pipet.

   If cryopreserved cells are used, thaw cells rapidly by filtering ~750 µl warm complete medium directly into the freezing vial (about three times the volume of the frozen cell suspension) and gently agitating in a 37°C water bath. Resuspend the cells with two or three passes through a fire-polished Pasteur pipet before dispensing into culture dishes. Replace the medium after 2 to 4 hr to remove debris and reduce the concentration of DMSO or other cryoprotectants in the culture medium. However, do not attempt to remove all of the medium during the change. A thin layer of medium should be left on the dish at all times.

5. If neurons are to be maintained more than a few days, feed once every 4 to 7 days by replacing about one-fourth to one-half of the medium with fresh complete medium.

   Probably the single greatest cause of neuronal death, other than contamination, is feeding. By the time the culture is a few days old, it becomes susceptible to glutamate-induced excitotoxicity. Most sera contain considerable amounts of glutamate, so complete replacement of medium with 10% or even 2% serum will probably cause excitotoxic cell death in relatively mature cultures. In reduced-serum or serum-free medium, this is less of a problem.

6. Reduce or eliminate proliferating glial cells to avoid astrocyte dominance of the culture. On about the second to fourth day of culture (sooner with high-serum medium, later or possibly not at all in serum-free medium), add 250 µl of 10× cytosine arabinoside to each culture.

   Neurons do not multiply in culture, but glial cells, particularly astrocytes, do. Although there are very few astrocytes in cell suspensions from E18 fetuses, they will eventually dominate the culture. This step can substitute for the first feeding.

   Although cytosine arabinoside is primarily toxic to dividing cells, in the authors' experience, it is also toxic to neurons if the concentration is too high. Further, the availability and/or toxicity of cytosine arabinoside appears to be inversely proportional to the serum concentration. Typical effective concentrations are ~10 µM in medium with 10% serum, decreasing to 1 µM in low-serum or serum-free media. It may be useful to change the medium after 1 or 2 days to remove the cytosine arabinoside.

OBTAINING HIPPOCAMPAL ASTROCYTE CULTURES

There are very few glial cells in E18 rat fetal hippocampi, but there are a few astrocytes or astrocyte progenitors (see Fig. 12.3.2B). Although it is much more efficient to obtain astrocyte cultures (or cultures of other types of glial cells) from early postnatal brain tissue, hippocampal astrocyte cultures can be produced from the neuronal cultures described above.

Because astrocytes foster neuronal survival, there will be varying numbers of neurons remaining in the initial astrocyte culture, even after the astrocytes reach confluency. Elimination of neurons can be accomplished in one of two ways: initial plating on uncoated dishes or subculturing. Astrocyte purity can be estimated by immunostaining representative dishes for the astrocyte-specific protein glial fibrillary acidic protein (GFAP). Either of the neuron-eliminating protocols usually results in astrocyte purity of 98% or better.

Materials

Dissociated hippocampal cell suspension (see Basic Protocol 1)
Complete EMEM (see recipe)

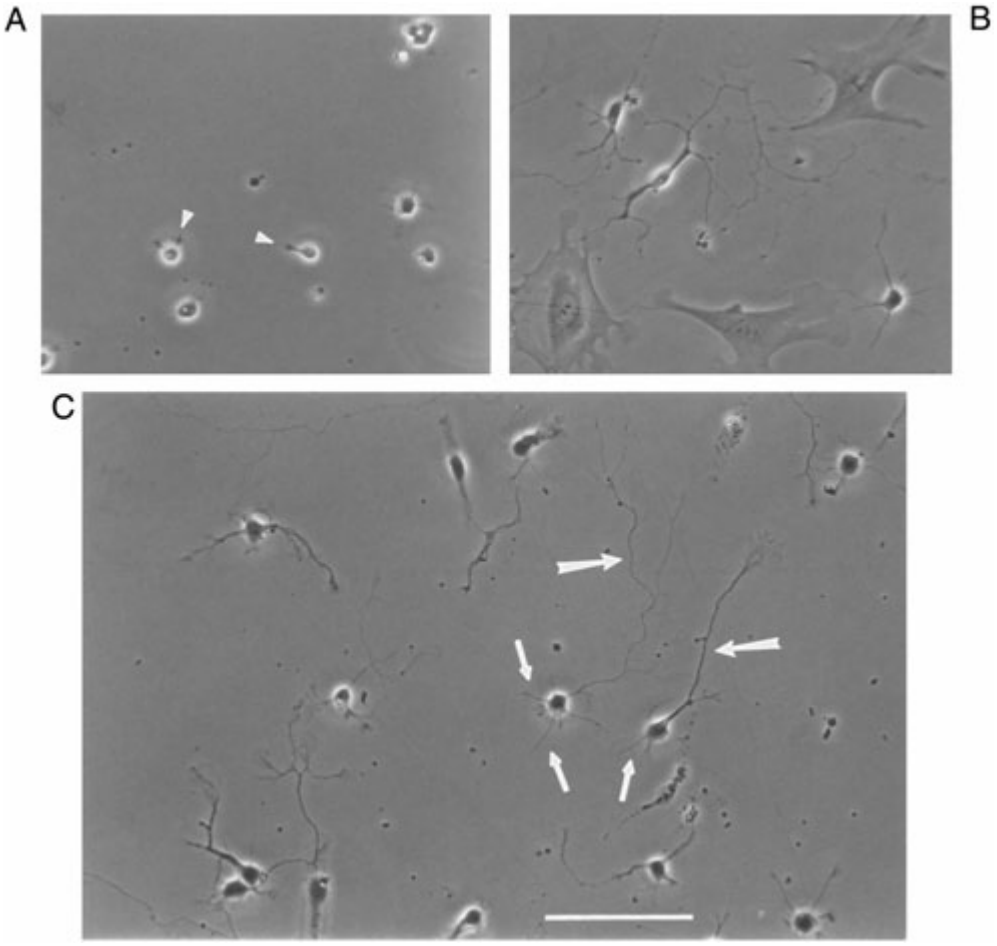

Figure 12.3.2 Typical sparse hippocampal cultures in which 100,000 E18 cryopreserved cells were plated in 35-mm plastic culture dishes coated with poly-D-lysine, using EMEM with 2% fetal bovine serum. (**A**) At 4 hr, most neurons are phase bright, and many already possess one or more short processes (arrowheads). (**B**) Occasional astrocytes (large, polygonal cells) are also found in E18 hippocampal cultures. In serum-containing medium, these will multiply over time. (**C**) At 3 days, most neurons have developed a single, long axon (large arrow) and several much shorter dendrites (small arrows), although in some neurons (e.g., upper left) there is no clear morphological distinction between axons and dendrites. Scale bar = 100 μm.

CMF-HBSS (see recipe)
2 mg/ml trypsin (Life Technologies) in CMF-HBSS

Laminar flow hood
35-mm plastic cell culture dishes, uncoated or poly-D-lysine coated (see Basic Protocol 2)
Rotary shaker (optional)
Fire-polished Pasteur pipet, sterile

To purify astrocytes at time of plating:

1a. In a laminar flow hood, plate dissociated hippocampal cell suspension at a high density in 2 ml complete EMEM/10% to 20% FBS on uncoated tissue culture dishes (≥500,000 cells per 35-mm culture dish). Incubate 24 to 48 hr in a 37°C, 5% CO_2 incubator.

See Basic Protocol 2 (step 4 annotations) for additional information on plating cells.

Neurons do not adhere well to uncoated dishes, but astrocytes do. Thus, astrocytes can be purified by washing away the unadhered neurons (below). In the authors' hands, it appears that astrocyte cultures grow more rapidly on coated dishes. Therefore, confluency may be delayed with this method.

2a. Gently shake dishes for 1 min (manually or on a rotary shaker) and remove the medium to remove most of the neurons.

3a. Immediately replace with 2 ml fresh medium containing ≥10% fetal bovine serum and return to incubator.

4a. Completely change medium once a week until astrocytes are nearly confluent.

When the neuronal suspension is initially plated at 500,000 cells/plate, it takes approximately 7 to 10 days to obtain nearly confluent astrocyte cultures. Higher plating densities will, of course, result in more rapid development of confluent astrocyte cultures.

To purify astrocytes by subcloning:

1b. In a laminar flow hood, plate the dissociated hippocampal cell suspension on poly-D-lysine-coated 35-mm culture dishes in 2 ml complete EMEM containing ≥10% fetal bovine serum. Place in a 37°C, 5% CO_2 incubator and change the medium once a week until astrocytes are nearly confluent.

See Basic Protocol 2 (step 4 annotations) for additional information on plating cells.

An initial plating density of 500,000 hippocampal cells per 35-mm plate will yield nearly confluent astrocytes in approximately 7 to 10 days.

2b. Remove medium from confluent cultures, rinse once briefly with 2 ml 37°C CMF-HBSS, and add 0.5 ml of 2 mg/ml 37°C trypsin solution to each dish. Incubate until cells have mostly detached from the dish (5 to 15 min), checking every 5 min.

The astrocytes will round up, detach from the bottom of the dish, and usually adhere to one another. Neurons do not tolerate trypsinization very well, so the subculturing both propagates astrocytes and quite effectively eliminates neurons from the secondary cultures, which should have «1% neurons.

3b. Add 1 ml complete EMEM with 10% fetal bovine serum (or other suitable serum-containing medium) and triturate the cells a few times with a fire-polished Pasteur pipet.

4b. Replate aliquots of cell suspension in new coated dishes with serum-containing medium.

Cells may be diluted if increased numbers of astrocytes are desired (e.g., plate 2 to 5 new dishes with the cells from one confluent dish).

To plate reasonably precise numbers of astrocytes in the subcultures, the cells will need to be dissociated into a (mostly) single-cell suspension and counted in a hemocytometer (APPENDIX 3B). This may require prolonged trypsinization and vigorous pipetting. Astrocytes are usually quite robust and can withstand such treatment. On the other hand, for many uses, the subcultures will be grown to confluency after replating. The authors have found that, within reason, widely varying numbers of astrocytes per dish will nevertheless reach confluency at about the same time and result in about the same number of cells per dish at confluency (as estimated by protein determinations). Therefore, depending on the experimental protocols for which the astrocytes will be used, precise cell counting may be unnecessary.

In principle, subculturing can be continued indefinitely. However, it is probably best to limit the number of times that a given astrocyte culture is divided in this way. Selection for rapidly reproducing cells, mutation, and possible spontaneous transformation may significantly alter the characteristics of astrocyte cultures after repeated subculturing. The authors usually do not subculture more than once.

COCULTURING HIPPOCAMPAL NEURONS AND ASTROCYTES

BASIC PROTOCOL 4

In the intact brain, neurons are in close association with astrocytes. In culture, neurons usually survive longer and grow better in the presence of astrocytes. Therefore, it may seem obvious that neurons should always be cocultured with astrocytes. For toxicologists, however, the decision to coculture neurons with astrocytes must be made with an awareness of the possible effects of astrocytes on the toxicant, the neurons, and the surrounding medium. For example, release of (usually unidentified) growth substances by the astrocytes will make the culture medium less defined. Further, astrocytes will remove glutamate from the medium and may sequester some toxicants. Substances released by astrocytes into the medium may bind to toxicants and alter their availability to neurons. The oxidant status of both the medium and the neuronal cytoplasm may be altered. These factors may make mechanistic experiments more difficult to interpret and dose-response curves more uncertain. Nevertheless, coculturing can be a valuable tool for in vitro neurotoxicology.

There are three fundamentally different ways to "assist" neurons with astrocytes: using astrocyte-conditioned medium, plating neurons directly on the surface of a confluent astrocyte layer, and plating astrocytes and neurons on separate surfaces so that they are in the same culture dish but not physically in contact. Although astrocyte-conditioned medium provides some assistance to neuronal survival and growth, it is not as beneficial as the other techniques (Goslin and Banker, 1991). However, using astrocyte-conditioned medium is simple and does not require any special techniques. Simply incubate the desired medium for 24 to 48 hr in dishes or flasks containing confluent astrocyte layers, and then use this medium for neuronal culturing.

Plating hippocampal neurons directly on an astrocyte layer probably provides the greatest similarity to the in vivo condition. It also has disadvantages for many experiments, because the astrocytes may visually obscure parts of the neurons, particularly fine neurites, and because the mass of the astrocytes is usually much larger than that of the neurons. To plate neurons (10,000 to 200,000 depending on the experiment) on an astrocyte layer, grow astrocytes to confluency in serum-containing medium and then add the neurons. If desired, change the medium to one that is more compatible with neuronal growth or that is optimal for a particular experimental protocol. Astrocytes typically will not overgrow neurons.

Plating neurons and astrocytes on separate surfaces may be done with two very different procedures, which might be loosely called the "closed" and "open-face" sandwich methods. In the closed sandwich method, the surfaces upon which the neurons and astrocytes are growing face each other but are kept separate by small "feet" attached to one of the surfaces. This method is somewhat complicated and will not be described here; the interested reader is referred to a complete description by Goslin and Banker (1991). The open-face sandwich method is simple yet effective. Prepare glass coverslips by soaking in concentrated nitric acid overnight to remove any contamination and to etch the surface slightly. It is convenient to use 12-mm round coverslips, which may be used for electrophysiology or imaging experiments in temperature-controlled perfusion chambers available from Warner Instrument. Rinse the coverslips with deionized water six times for 30 min each, and sterilize by autoclaving. Coat the coverslips with poly-D-lysine by placing up to five coverslips in a 35-mm culture dish and following the procedure for coating culture dishes (see Basic Protocol 2). Using sterile forceps, move the coverslips around at the beginning of each rinse to prevent them from adhering to the culture dish (if they do adhere, a short incubation in culture medium will loosen them). To coculture the neurons and astrocytes, gently place up to three coated coverslips atop a confluent layer of astrocytes in a 35-mm culture dish containing 2 ml of the medium normally used to plate neurons. Plate neurons onto the coverslips by gently pipetting them into the medium directly above each coverslip. Leave the culture dishes undisturbed in the laminar flow hood for 30 to 60 min after plating the neurons, allowing the neurons to drift down onto the coverslips and adhere. Cultures will be fine at room temperature for this length of time in HEPES-buffered medium. Then move the dishes to the incubator for a few more hours. Replace the medium as with ordinary neuronal cell cultures.

REAGENTS AND SOLUTIONS

*Use Milli-Q-purified distilled or deionized water in all recipes and protocol steps. For common solutions, see **APPENDIX 2A**; for suppliers, see **SUPPLIERS APPENDIX**.*

Ca^{2+}- and Mg^{2+}-free Hank's balance salt solution (CMF-HBSS)

Ca^{2+}- and Mg^{2+}-free HBSS (Sigma) containing:
350 mg/liter $NaHCO_3$
10 ml/liter antibiotic/antimycotic solution (Life Technologies)
10 mM HEPES buffer
Adjust to pH 7.3
Store up to 2 weeks at 4°C

Cryopreservation medium

EMEM (see recipe) containing:
19 g/liter glucose
On the day of use, add:
8% (v/v) dimethyl sulfoxide
10% (v/v) fetal bovine serum (final)

Complete Eagle's minimum essential medium (EMEM)

Phenol red–free EMEM (Sigma) containing:
1 g/liter glucose
10 ml/liter antibiotic/antimycotic solution (Life Technologies)
1 mM pyruvic acid (Sigma)
2 mM glutamine (Sigma)
25 mM $NaHCO_3$
25 mM HEPES buffer (optional)
Adjust to pH 7.3

continued

Filter sterilize into 500-ml borosilicate glass bottles (preferably with Teflon-lined bottle caps) using bottle-cap filters (cellulose acetate, 0.2-μm pore diameter; e.g., Corning)
Store up to 2 weeks at 4°C
Just before use, add 2% to 10% (v/v) fetal bovine serum (Hyclone) and warm to 37°C

Other supplements appropriate for the experimental design (e.g., B27, N2; see Commentary) can also be added.

The water must be of extremely high quality. Barnstead and Millipore, among others, manufacture deionizing systems that will produce 17 to 18 megohm tissue culture–quality water. Water may also be purchased from cell culture supply companies.

Most media are buffered principally with bicarbonate, with pH ~7.3 measured at 37°C in an incubator containing 5% CO_2/95% air. The pH may be very different at room temperature and atmospheric CO_2 concentrations (e.g., during culture setup and manipulations, such as addition of toxicants or photographing neuronal growth). The pH may also change during prolonged culturing in the incubator. For these reasons, many investigators buffer their media with 25 mM HEPES. Several companies manufacture media containing HEPES, usually adjusting the bicarbonate concentration and/or sodium chloride concentration to keep the osmotic strength similar to normal medium. If medium is made up from powders, then supplements can be added without changing the concentration of its other components.

During neuronal culturing, the importance of sterility cannot be overemphasized. Carry out all manipulations in a laminar flow hood. It is probably best to sterilize the complete medium just before use by filtering it directly into the culture dishes through a syringe filter. It is typical to use 2 ml for a 35-mm dish. If cells are not to be placed in the dishes immediately, keep the dishes in the incubator until used.

Hank's balanced salt solution (HBSS)

HBSS (Sigma) containing:
350 mg/liter $NaHCO_3$
10 ml/liter antibiotic/antimycotic solution (Life Technologies)
10 mM HEPES buffer
Adjust to pH 7.3
Store up to 2 months at 4°C

COMMENTARY

Background Information

Uses of hippocampal cultures in neurotoxicology

Hippocampal neuron cultures are favored in vitro preparations in neurobiology for studies of such diverse phenomena as neuronal differentiation, formation and functioning of synapses, electrophysiology of voltage-sensitive and ligand-gated ion channels, and calcium homeostasis. In culture, hippocampal neurons develop axonal and dendritic trees with considerable biochemical and morphological similarity to the in vivo condition. These cultures readily lend themselves to highly quantitative analyses of neurite development, including growth cone movement, differentiation of neurites into axons or dendrites, cytoskeletal involvement in neurite development, and axonal and dendritic elongation and branching. Hippocampal cultures contain a large complement of voltage-sensitive ion channels (including several types of sodium, calcium, and potassium channels) and a variety of ionotropic and metabotropic receptors (including receptors responsive to glutamate, γ-aminobutyric acid [GABA], and acetylcholine). Finally, the roles of transmembrane Ca^{2+} fluxes, Ca^{2+} release from intracellular stores, and free Ca^{2+} ion concentrations in neurite development, gene expression, synaptic plasticity, and excitotoxicity have been extensively studied in hippocampal cultures.

Hippocampal cultures have found considerable use in neurotoxicology, although probably not as much as some other systems, particularly PC12 cells. The following examples illustrate the variety of effects of toxicants that have been studied in cultured hippocampal neurons. Several toxicants, including lindane, inorganic

lead, aluminum, and ethanol, perturb specific aspects of neurite development. Inorganic lead reduces current flow through voltage-sensitive calcium and potassium channels, the *N*-methyl-D-aspartate (NMDA) subtype of ionotropic glutamate receptors, and some types of nicotinic acetylcholine receptors. Lead also increases spontaneous transmitter release. Ethanol alters current flow through NMDA and $GABA_A$ receptors. Aluminum, inorganic lead, and ethanol all cause oxidative stress. Lead and ethanol alter Ca^{2+} homeostasis. For a more extensive discussion of the uses of neuronal cultures in neurotoxicology, with some references to hippocampal cultures, see Audesirk (1997).

Alternative culture conditions

There is a bewildering array of basic media used to culture hippocampal neurons and other cell types. Many of these media, with suitable additives, enable hippocampal neurons to attach, grow extensive networks of morphologically and biochemically identifiable axons and dendrites, make effective synaptic contacts, express many intracellular molecules (e.g., cytoskeletal proteins, protein kinases, gene transcription factors), and live for many days. Probably the three most common media for hippocampal culture are the traditional Eagle's minimum essential medium (EMEM), Dulbecco's modification of MEM (DMEM), and Neurobasal. EMEM and DMEM are available from many vendors and are manufactured with many modifications, including formulations with HEPES buffer and additions or deletions of various nutrients. For radioactive labeling experiments, the ready availability of leucine- and methionine-deficient EMEM may make this the medium of choice. The investigator should consult reference texts on cell culturing for details on each of these media. In essence, however, EMEM, as its name implies, is a minimal medium, with fairly low concentrations of many nutrients and lacking several potential nutrients, including several amino acids. DMEM is much richer, with higher concentrations of many nutrients (often double) and with several additional nutrients. Neurobasal is available only from Life Technologies. It is similar to DMEM with reduced sodium chloride, rendering it quite hypoosmotic to most mammalian extracellular fluids. All of these are suitable for hippocampal cultures. Most investigators add pyruvate and glutamine (or the proprietary Glutamax from Life Technologies), which can be important energy sources for cultured cells.

Neurons need growth factors (e.g., hormones, attachment factors) for survival and development. Traditionally, these have been provided in unknown types and amounts by adding serum, usually fetal bovine serum, to the basic culture medium. More recently, several defined medium supplements have been developed. The most prevalent of these for hippocampal culture is the B27 mixture of Brewer et al. (1993), commercially available from Life Technologies. Most investigators who use B27 still plate the neurons in serum-containing medium, but then change medium after several hours or a day to B27. Brewer and Life Technologies recommend B27 in Neurobasal, but B27 in EMEM or DMEM works equally well in the authors' hands.

There are several advantages of serum-free media for neurotoxicology. First, the ingredients are defined. Although "defined" should not be confused with "physiological," at least the investigator knows what is in the medium. Second, the reduced protein levels more closely resemble the low protein content of cerebrospinal fluid and presumably brain extracellular fluid. For toxicants that may bind to proteins, this may be important. Third, potential excitotoxic effects of changing serum-containing medium are reduced or eliminated, because neither the basic medium nor the supplements usually contain glutamate. Fourth, some serum-free supplements, such as B27, do not support astrocyte proliferation very well and thus help to keep neuronal cultures relatively pure even in the absence of cytosine arabinoside.

Finally, researchers should carefully investigate the ingredients in any culture medium or supplement to ensure that they do not mimic or antagonize the actions of the toxicant under study. For example, most media contain the pH indicator phenol red. Some lots of phenol red contain a by-product introduced during manufacturing that mimics some of the actions of estrogen. Therefore, these would be unsuitable for studies of any substance thought to have estrogenic or antiestrogenic effects. Even in studies that are not directly concerned with estrogenic effects, lot-to-lot variability in estrogenicity may introduce variability in neuronal survival and development. B27 contains triiodothyronine, and would be unsuitable for studies with toxicants that may mimic or antagonize thyroid hormone effects. B27 also contains antioxidants such as superoxide dismutase, vitamin E, and glutathione. Therefore, a recent change of medium containing B27 would protect neurons against oxidative stress and prob-

ably also against glutamate excitotoxicity, as reactive oxygen species apparently contribute to excitotoxic cell death.

Critical Parameters and Troubleshooting

Even the most experienced cell culture laboratory has occasional times when cultures fail, because there are so many steps that are critical to producing healthy, contamination-free cultures (see Goslin and Banker, 1991).

Contamination

Laminar flow hoods are essential to cell culturing. Horizontal laminar flow hoods (in which the filtered air blows toward the person using the hood) typically produce the most sterile conditions toward the back of the hood and lose sterility near the front. A useful monitoring procedure is to place a series of culture dishes with complete medium at various locations in the hood, remove the lids for a few minutes, replace the lids and then incubate the dishes for a few days. The hood can then be marked at the location where the dishes begin to show contamination, and all work can be performed behind this line. Vertical laminar flow hoods (in which filtered air blows down from the top and flows out slots at the lower back and front of the hood) are less susceptible to contamination and protect the user from airborne particles. This is especially important when working with pathogens or highly toxic compounds. However, the slot at the front of the hood draws air both from the inside of the hood and from the room. It is therefore probably the most contaminated location in the laboratory. Users must consciously train themselves to work deep in the hood, away from the front slot. Conversations with hood users should be prohibited. Because hoods are typically noisy, users will automatically lean back when spoken to in order to hear better, often pulling their hands and whatever items they are holding out into the contaminated front part of the hood.

A laminar flow hood cannot maintain sterility if the solutions, pipet tips, and other items used in the hood are already contaminated. All reusable containers, glass pipet tips, and so on must be sterilized before each use, usually by autoclaving. Disposable items such as syringes, syringe filters, and culture dishes, should be opened only in the hood. Disposable plastic pipet tips can be purchased sterile or can be autoclaved. The tip box must be opened only in the hood. Even though all solutions and apparatuses are presumably sterile before they are brought into the hood, it is routine practice in the authors' laboratory to sterilize medium through a syringe filter as it is added to the culture dishes. Finally, human skin constantly sheds large numbers of microbes and dead epidermal cells (usually contaminated with microbes). Well-fitting latex gloves minimize the possibility of contamination from the user's hands without significantly affecting dexterity.

Culture viability and development

Neurons, even in uncontaminated cultures, sometimes fail to survive (acutely or after several days in culture) or develop robust neurites. This may, of course, be caused by lack of suitable attachment factors on the culture surface, by inappropriate medium (e.g., simple medium without serum or growth factors), or by errors in preparation (e.g., forgetting to add serum). Assuming that these types of problems have not occurred, there are a few likely suspects to investigate if your cultures do not grow well.

Water. Most labs use deioinized water for cell culture. If the deionizing and organic-removal cartridges are too old (or the feedstock water is too impure), the water may no longer be of suitable quality. The water from the deionizing setup usually flows through a hose; if the hose is old, algae and bacteria may be growing in it, contaminating the water with both microbes and/or toxic organics.

Cell isolation and plating. As mentioned earlier, cell damage and death probably begin as soon as the dam is anesthesized. Therefore, speed of dissection and dissociation of cells is helpful in obtaining healthy cells. To minimize cell damage and death, keep fetuses, heads, and brains cold during dissection. In dissociating cells, do not pipet too long or too vigorously, or through a very narrow-bore pipet. As the members of the dissection team become more experienced, speed, sterility, and gentleness usually improve, as does the health of the cultures. When plating cells from a relatively high-density suspension (e.g., from cryopreserved neurons), remember that the cells metabolize and may alter the medium (for example, by acidification or depletion of oxygen) if left too long at high density at warm temperatures. Finally, there is some evidence that free polylysine may be toxic to neurons, so the dishes must be adequately rinsed after coating and before use.

Culture maintenance. Be sure that the medium and supplements are maintained properly

before use. Check with the manufacturer about shelf-lives, especially in solution, and optimal storage conditions (e.g., 4° versus −20° versus −70°C). Find out if any of the medium components in use are light sensitive, and treat them accordingly. Feed the cells as seldom, and with as small a volume, as is consistent with maintaining the health of the culture. This reduces the chance of contamination and excitotoxic cell death. It is also likely that the cells "condition" the medium as they grow, and soluble conditioning factors will be removed during feeding. This is probably particularly important if astrocytes are part of the culture, as conditioned medium from astrocytes is well known to facilitate the growth of neurons. There is no golden rule about feeding, but one fourth of the culture volume exchanged twice a week is probably a good starting point.

Anticipated Results

Number of cultures

The density of neurons and therefore the number of cultures that will be obtained from a single litter depend on the purpose of the experiment. For detailed morphological examination of neurite development, neurons are generally plated quite sparsely, between 10,000 and 200,000 cells per 35-mm culture dish or equivalent surface area of coverslips or wells. For studies of intracellular signaling or gene expression, in which mRNA or proteins may be extracted from the cultures or relatively low-efficiency gene transfection may be used, 500,000 or even 1 million neurons per culture may be necessary, depending, for example, on the abundance of the mRNA or protein of interest and the sensitivity of the assay employed. Assuming 500,000 to 1 million neurons per hippocampus and 6 to 15 fetuses per litter, the number of cultures that can be plated from one litter will therefore vary from fewer than twenty to several hundred.

Culture development

Examine the cells with an inverted phase-contrast or differential interference contrast microscope, using a green filter between the light source and the cells. Although the time required for cells to settle depends on the concentration of serum and other proteins in the culture medium, healthy hippocampal neurons, either freshly dissociated or cryopreserved, should attach firmly to the bottom of the culture dish within a couple of hours of plating. Within 4 hr or so, at least some of the neurons should already extend short processes (Fig. 12.3.2A). By 24 hr, probably all of the neurons that will ever grow neurites will have done so. There may already be some differentiation of axons and dendrites, at least in length. The rate of differentiation into axons and dendrites, and the markers of differentiation that are present (e.g., long versus short length, tau versus MAP2 microtubule-associated proteins; see Goslin and Banker, 1991) varies with the culture conditions. Usually, by 2 or 3 days, most neurons display a characteristic morphology consisting of a single process (the presumed axon) that is several times longer than any of the other processes (the presumed dendrites; see Fig. 12.3.2C). By this stage, biochemical markers of axons and dendrites (e.g., tau versus MAP2) should be more abundant in the appropriate neurites. There may also be a few astrocytes in the culture (Fig. 12.3.2B).

In simple culture conditions, such as EMEM with fetal bovine serum and no astrocytes, many neurons will continue to survive and elaborate neurites for at least a few days, although by 4 or 5 days some death is usually evident. In more complete culture conditions, such as medium with B27, many neurons will thrive for ≥2 weeks, although some cell death will gradually occur. The most robust neurite growth and longest survival occur when densely plated neurons are cocultured with astrocytes (Goslin and Banker, 1991) in complex medium, particularly B27-containing medium (Brewer et al., 1993). Under these conditions, a large percentage of neurons remain vigorous for several weeks, and can be used for a variety of purposes, including studies of excitotoxicity, synaptic transmission, ion channel function, and gene expression. How closely the responses of neurons in such "mature" cultures resemble those of neurons of similar age in vivo remains largely unknown.

Time Considerations

With experience, dissociation of neurons from a single litter of fetuses takes ~2 hr from sacrifice of the dam to placement of the dissociated neurons into culture dishes or cryopreservation vials. With an efficient team of three people, tasks can overlap in time, so that neurons from as many as six litters can be obtained in 4 to 6 hr. Of course, once begun, the entire dissociation and plating or cryopreservation protocol must be completed without interruption.

Plating neurons from dissociated neuronal suspensions takes only a few minutes, once the

culture dishes have been prepared and filled with medium. Plating from cryopreserved stocks requires only 1 or 2 min longer, for rapid thawing of the cell suspension.

Literature Cited

Audesirk, G.J. 1997. In vitro systems in neurotoxicological studies. *In* Comprehensive Toxicology: Nervous System and Behavioral Toxicology (H.E. Lowndes and K.R. Reuhl, eds.) pp. 431-446. Pergamon Press, New York.

Banker, G.A. and Cowan, W.M. 1977. Rat hippocampal neurons in dispersed cell culture. *Brain Res.* 126:397-425.

Brewer, G.J., Torricelli, J.R., Evege, E.K., and Price, P.J. 1993. Optimized survival of hippocampal neurons in B27-supplemented Neurobasal, a new serum-free medium combination. *J. Neurosci. Res.* 35:567-576.

Goslin, K. and Banker, G. 1991. Rat hippocampal neurons in low-density culture. *In* Culturing Nerve Cells (G. Banker and K. Goslin, eds.) pp. 251-281. MIT Press, Cambridge, Mass.

Mattson, M.P. and Kater, S.B. 1988. Isolated hippocampal neurons in cryopreserved long-term culture. Development of neuroarchitecture and sensitivity to NMDA. *Int. J. Dev. Neurosci.* 6:439-452.

Key References

Goslin and Banker, 1991. See above.

A superb, illustrated discussion of every step of preparation of hippocampal neurons for culture.

de Hoop, M.J., Meyn, L., and Dotti, C.G. 1998. Culturing hippocampal neurons and astrocytes from fetal rodent brain. *In* Cell Biology: A Laboratory Handbook (J.E. Celis, ed.) pp. 154-163. Academic Press, San Diego.

Extremely detailed description of hippocampal culture, with emphasis on a specific methodology used in the authors' laboratory.

Contributed by Gerald Audesirk, Teresa Audesirk, and Charles Ferguson
University of Colorado at Denver
Denver, Colorado

Isolation of Neonatal Rat Cortical Astrocytes for Primary Cultures

The central nervous system (CNS) is comprised of two major cell types, the electrically excitable neurons, and the nonelectrically excitable glia. The glial cells, also known as neuroglia, can be further divided into the macroglia, consisting of astrocytes and oligodendrocytes, and the microglia. Although the term glia is sometimes used to describe a specific cell type, most often astrocytes, its proper use is to describe the entire class of nonneuronal cells. The functions of these cells are distinct. Oligodendrocytes are the myelin-producing cells in the CNS, analogous to Schwann cells in the peripheral nervous system (PNS). Microglia are similar to macrophages; they remain silent until activated, when they remove cellular debris. Astrocytes serve multiple functions within the CNS including production of growth factors, maintenance of the extracellular environment, and modulation of synaptic transmission.

Over the past two decades there has been increased focus on the role of astrocytes, not only in the normal physiology of the central nervous system, but also on their potential role as mediators of neurotoxicity (Fedoroff and Verndakis, 1986; Kimelberg and Norenberg, 1989; Murphy, 1992; Kettenmann and Ransom, 1995; Aschner and Kimelberg, 1997). It is now apparent that astrocytes are much more than just connective or structural tissue filling the space between neurons as originally envisioned—they are intimately and actively involved in maintaining the proper functioning of the CNS. Indeed, astrocytes are integral in the removal of neurotransmitters such as glutamate, and they also contain a large complement of receptors, enabling them to respond to and modulate neuronal function. These revelations have come about, in large part, due to the ability to produce high-purity primary cultures of rodent astrocytes. These cultures have led to great advances in the understanding of these often underappreciated cells (Kimelberg, 1983; Aschner and Vitarella, 1995).

The culture technique described here (see Basic Protocol) is based largely on the method first published by Frangakis and Kimelberg (1984), and has undergone minor refinement in this laboratory. The authors have recently found this technique to also work well with cells from transgenic knockout mice (Yao et al., 2000). Given the ever-increasing importance of transgenic mice to the field of toxicology, the ability to produce high-yield astrocytic cultures from these animals will allow further elucidation of the role of astrocytes in the mechanisms of neurotoxic substances. In addition, the authors have successfully obtained viable cortical astrocytes from neonatal rat brains stored at 4°C for up to 24 hr (Aschner et al., 1997).

NOTE: All steps including cell isolation and, when possible, preparation of solutions should be performed in a laminar flow hood.

NOTE: The authors recommend the use of cell culture-tested water in all steps and for preparation of all solutions. This can be obtained from Life Technologies.

NOTE: All solutions and equipment coming into contact with living cells must be sterile, and aseptic technique should be used accordingly. All nondisposable materials should be reserved for cell culture use only and cleaned thoroughly immediately after use.

NOTE: All culture incubations should be performed in a humidified 37°C, 95% air/5% CO_2, 95% relative humidity incubator unless otherwise specified.

NOTE: All protocols using live animals must first be reviewed and approved by an Institutional Animal Care and Use Committee (IACUC) or must conform to governmental regulations regarding the care and use of laboratory animals.

Contributed by Jeffrey W. Allen, Lysette A. Mutkus, and Michael Aschner
Current Protocols in Toxicology (2000) 12.4.1-12.4.15

BASIC PROTOCOL

ISOLATION AND CULTURE OF NEONATAL RAT ASTROGLIA

The astrocyte isolation method described involves enzymatic dissociation of tissue with a bacterial neutral protease (dispase). Astrocytes are recovered by repeated removal of dissociated cells from nondissociated sedimenting tissue. This method is less traumatic than techniques based on mechanical isolation, and therefore produces a greater cellular yield. Dissociation by trypsin is more rapid and produces a cellular yield similar to dispase, but dispase digestion results in higher astrocyte viability. From one litter of 1-day-old rat pups (eight to twelve pups), the authors routinely obtain a sufficient number of cells (10^8) for approximately one hundred 100-mm culture dishes. These cells reach confluency in ~3 weeks and are >95% positive for glial fibrillary acid protein (GFAP), a cytoskeletal intermediate protein localized within the CNS only in astrocytes (Eng et al., 1971). The remaining cell types within the cultures are largely oligodendrocytes, neurons, microglia, and O-2A progenitor cells. Just as astrocytes can be identified by immunoreactivity for GFAP, the other cells types can be characterized with specific antibodies (see Critical Parameters and Troubleshooting).

See Table 12.4.1 for a suggested preparation schedule for astrocyte isolation.

Materials

1-day-old Sprague-Dawley rat pups from pathogen-free time-dated pregnant dams, timed to arrive at animal facility ~1 week prior to delivery date (rat gestation is 21 days)
Halothane or other approved anesthetic
70% (v/v) ethanol
Complete S-MEM (see recipe)
Dissociation medium (see recipe), prewarmed to 37°C
Astrocyte growth medium (see recipe)
8000 U/ml DNase I solution (see recipe)
0.08% (w/v) trypan blue staining solution: 1:4 (v/v) 0.4% trypan blue (Life Technologies) in PBS (*APPENDIX 2A*)

Table 12.4.1 Timetable for Preparation of Solutions and Instruments

Time	Preparation procedure
1 or 2 days prior to isolation	Fire polish and Sigmacote Pasteur pipets
	Prepare gelatin solution for coverslips
	Prepare borate buffer, stock DNase I, and poly-L-lysine solutions
	Autoclave glass pipets, surgical instruments, 50-ml beakers with stir-bars, coverslips, and gelatin solution
1 day prior to isolation	Check for birth of pups and determine number of pups
	Treat coverslips with gelatin and poly-L-lysine; store in refrigerator overnight
Day of isolation	Check number of 1-day-old pups (i.e., to determine number of extractions)
	Prepare complete S-MEM and place 25 ml plus 10 ml/extraction on ice in 50-ml conical centrifuge tubes
	Prepare dissociation medium and place in the incubator to warm for 1 hr
	Retrieve rat pups from mother and bring to laboratory
	Proceed with dissection and dissociation

Dissecting tools, sterile:
Mayo scissors, 7-in. (17.8-mm) length, 50-mm curved blade
Fine-angled microdissecting scissors, 4-inch length, 25-mm blade
Curved forceps, 4-inch length, full curve, 0.8-mm tip width
Curved forceps, 4-inch length, full curve, 0.4-mm tip width
Dumont forceps, pattern no. 5, 110-mm length, 0.1 × 0.06–mm tip
Sterile gauze pads
Dissecting microscope or 4× to 8× lighted magnifying lamp
50-ml conical polypropylene tubes, sterile
9-in. Pasteur pipets:
Cotton plugged and sterile
Cotton plugged, fire polished, Sigmacote treated, sterile (see Support Protocol 1)
50-ml beaker and 25-mm stir bar, sterile (cover with foil prior to autoclaving)
10-ml glass serological pipets, cotton plugged and Sigmacote treated (see Support Protocol 1)
Laminar flow hood
15-ml conical polystyrene centrifuge tubes, sterile
Low-speed centrifuge with swinging bucket rotor and adapters for 50-ml conical tubes
Inverted phase-contrast microscope
Tissue culture plates of desired size for culturing astrocytes
Coated 18 × 18–mm coverslips (optional; see Support Protocol 2, up to step 6)
Vacuum source

Additional reagents and equipment for counting cells with a hemacytometer (*APPENDIX 3B*)

Dissect out fetal brain

1. Anesthetize 1-day-old Sprague-Dawley pups with halothane or other approved anesthetic.

   To anesthetize pups, place a small ball of cotton in a 50-ml tube and add a few drops of halothane. Place the pup's head into the tube until it is anesthetized. Be sure to cap the tube between uses and replenish the halothane as necessary.

   The number of pups from Sprague-Dawley rats usually varies between 8 and 15. The optimum number of pups to process at one time is 10 to 12. Use of more pups does not appreciably increase cell yield. The arrival of pregnant rats prior to delivery allows acclimatization of the animals and helps prevent delayed parturition due to transport stress. The use of time-dated rats allows scheduling of cultures on a consistent day. The authors typically prepare cultures every other Thursday from ~1-day-old pups, and therefore purchase rats that will deliver pups on Wednesday.

   Neonatal rats can very quickly become hypothermic. Placing the pups in a nest of cotton in a small open box helps the pups to stay warm when they are being transported from their cage to the laboratory. They should be kept covered as much as possible to help them maintain their body temperature.

2. Gently hold pup with thumb and forefinger around thorax and rinse head and neck of pup with 70% ethanol.

3. Using 7-in. curved Mayo scissors, decapitate a pup and place the head on a sterile gauze pad. Place body in a plastic bag for disposal.

   Scissors and forceps should be placed either on a sterile gauze pad or in a beaker of 70% ethanol between decapitations.

4. Secure the head by holding down the snout. With fine-angled microdissecting scissors, cut the skin along the midline from base of the skull to the eyes. Use 0.8-mm forceps to separate the skin and expose the skull as necessary.

5. Use a similar technique to expose the brain by cutting along the midline of the skull with the microdissecting scissors. If desired, cut away the skull flaps to ease removal of the brain.

   Placing the scissors at a slight upward angle helps prevent inadvertent damage to the underlying brain tissue.

6. With 0.8-mm-tip curved forceps, sever the olfactory bulbs at the anterior end of the brain and the spinal cord at the posterior end. Sever the cerebellum.

Isolate cortices

7. Gently slip the two sides of 0.4-mm-tip curved forceps under the cortices on either side of the brain so that the forceps are straddling the brain.

8. Gently move forceps from side to side and, with a slight back angle, pull up the cortices.

   This will separate the cortices from the rest of the brain, which remains in the head, but care should be taken not to separate the cortices from each other.

Dissect cortices

9. Place the cortices on a sterile gauze pad under a dissecting microscope with the dorsal side up and the anterior (rostral) side facing away.

10. Unfold the cortices and remove any extraneous tissue.

11. With Dumont forceps, gently tease away the meningial coverings on the cortical surface.

    Take care not to destroy the tissue by pressing the cortices into the gauze pad.

12. Turn the gauze 180° from its original orientation and gently place curved forceps under the cortices. Flip the cortices up and slightly back to expose the underside of the tissue.

    This can sometimes be difficult due to adherence of the tissue to the gauze pad. The tissue can be dislodged by gently running the forceps under the cortices.

13. Gently remove the darker hippocampal crescents with the curved 0.4-mm forceps.

14. Remove any remaining meninges with Dumont forceps.

    The total time spent removing meninges should be ~10 min per brain.

15. Place cortices in a sterile 50-ml conical polypropylene tube containing 10 ml complete S-MEM on ice.

16. Repeat steps 1 to 15 with remaining pups, placing all cortices in a single 50-ml tube on ice.

    Generally, processing more than 12 pups does not substantially increase the final number of cells obtained.

Dissociate cells

17. Carefully remove as much S-MEM as possible with a sterile, cotton-plugged, 9-in. Pasteur pipet, taking care to retain all of the cortices.

18. Add 12 ml prewarmed (37°C) dissociation medium to a 50-ml beaker with stirbar and carefully pour cortices into the beaker. Gently triturate the cortices seven to eight times using a Sigmacote-treated 10-ml glass serological pipet.

19. Stir 10 min at low speed (60 rpm) on a stir plate in a laminar flow hood.

20. While this is stirring, prepare two 15-ml conical polystyrene centrifuge tubes for each extraction to be performed. Add 5 ml room temperature astrocyte growth medium to each tube. Also thaw DNase I solution and place it on ice.

    The number of extractions is usually equal to the number of dissected brains.

21. After 10 min of gentle stirring, remove the beaker from the stir plate and place at a 45° angle for 2 to 3 min to allow the nondissociated tissue to collect at the bottom of the beaker.

    Resting the edge of the beaker on a lid from a culture dish works well.

22. Carefully aspirate 10 ml dissociated cells with a Sigmacote-treated 10-ml glass serological pipet.

    Take care not to remove the undissociated tissue pieces.

23. Place 5 ml suspension into each of the first two 15-ml centrifuge tubes containing astrocyte growth medium. Invert the mixture two to three times to mix and then allow tubes to sit undisturbed during the continuing extractions.

    The serum in the growth medium acts to inhibit dispase and prevents overdigestion of the dissociated cells.

    During this time, undissociated tissue will settle to the bottom of the 15-ml tube. This undissociated tissue will be placed back into the 50-ml beaker for further dissociation during the final two extractions.

24. Add another 10 ml prewarmed dissociation medium to the 50-ml beaker and add 100 µl of 8000 U/ml DNase I solution. Continue to stir for another 10 min.

    The removal of dissociated cells and replacement with 10 ml dissociation medium is called an extraction.

    DNase I is added after the first extraction to prevent the genomic DNA released by damaged cells from making the dissociation medium too viscous during the on-going digestion. Note that it is added only after the first extraction and is not added again.

    DNase I from pancreas is vulnerable to inactivation by physical damage. Mix all DNase I solutions carefully and do not vortex.

25. Place the 50-ml beaker at an angle for 2 to 3 min, remove 10 ml dissociated cells, and place 5-ml aliquots into a second pair of 15-ml tubes containing astrocyte growth medium.

26. Repeat extractions until there is only fibrous tissue remaining in the 50-ml beaker.

27. To remove undissociated tissue from the 15-ml tubes, insert a sterile, fire-polished, cotton-plugged, Sigmacote-treated 9-in. Pasteur pipet to the bottom of the tube and carefully aspirate the undissociated tissue. Place this tissue back into the 50-ml beaker and perform two final extractions.

    This is done only during the final two extractions because serum carried over from the completed extractions can inactivate the dispase.

Table 12.4.2 Approximate Surface Area, Plating Density, and Growth Medium Volume for Plates Used in the Production of Primary Astrocyte Cultures

Plate type	Surface area (cm^2)	Seeding density[a]	Growth medium (ml)
35-mm	9.40	1×10^5	2
60-mm	28.27	3×10^5	3
100-mm	78.54	7.5×10^5	7
150-mm	176.71	1.8×10^6	15
96-well	0.32	3.2×10^3	0.1
24-well	1.88	2×10^4	0.5
12-well	3.83	4×10^4	1
6-well	9.40	1×10^5	2

[a]Given as cells per plate or well.

Pellet cells

28. Pool dissociated cells and medium from the 15-ml centrifuge tubes into 50-ml conical tubes (one 50-ml tube for each five 15-ml tubes). Centrifuge 10 min at 400 to 1000 × *g*, 4°C, in a swinging bucket rotor to pellet the suspended cells.

    Centrifugation at room temperature is acceptable if necessary.

    If astrocytes are to be seeded on coverslips, the coverslips should have been incubating overnight in poly-L-lysine up until this point (see Support Protocol 2). This is a good time to finish their preparation.

29. Carefully aspirate medium from the cell pellets.

30. Resuspend in ~20 ml astrocyte growth medium per 50-ml tube by gentle pipetting with a Sigmacote-treated 10-ml glass serological pipet.

31. Allow cells to sit for an additional 5 min and remove any sedimented tissue as above (step 27). Discard this undissociated tissue.

32. Pool the suspended cells into 50-ml tubes on ice.

Assess cell number and viability

33. Gently mix 100 µl cell suspension with 100 µl of 0.08% trypan blue staining solution. Allow the cells to take up the trypan blue for 2 to 5 min.

    Trypan blue is used determine cell viability. Intact cells are able to exclude trypan blue while dead or damaged cells retain the dye.

34. Determine total cell number and cell viability with a hemacytometer and an inverted phase-contrast microscope (see *APPENDIX 3B*).

Plate and grow cells

35. Dilute cell suspension to 10,000 viable cells/ml with astrocyte growth medium.

36. Pipet 10,000 to 20,000 viable cells/cm^2 into tissue culture dishes and then add astrocyte growth medium to the final volume given in Table 12.4.2. To plate cells on coverslips, place a coated 18 × 18–mm coverslip in a 35-mm tissue culture dish (or 6-well plates) before adding cells and medium.

37. Incubate cells in a 37°C, 95% air/5% CO_2, 95% relative humidity incubator.

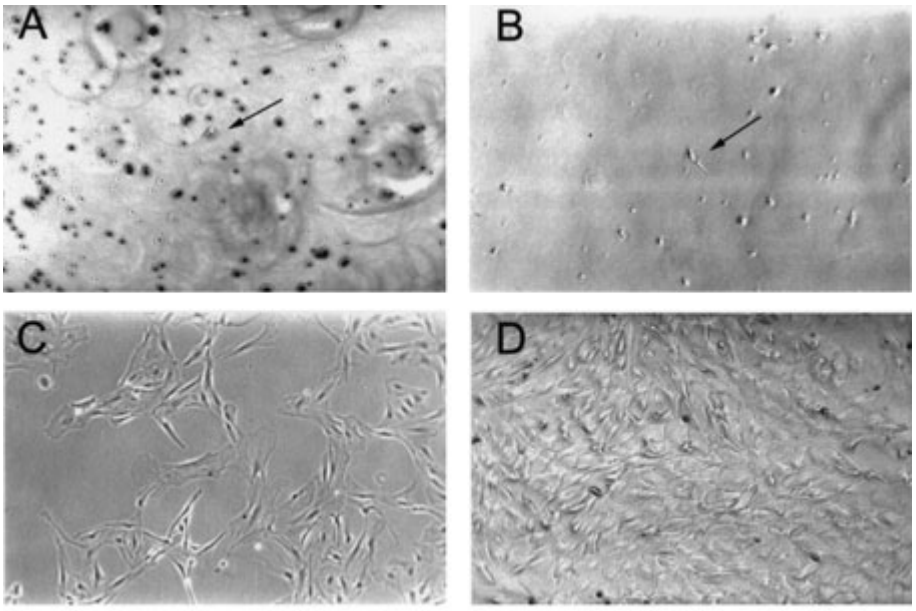

Figure 12.4.1 Primary cultures of neonatal rat astrocytes at various stages of growth (bright-field photomicrographs, 100× magnification). (**A**) 24 hr postisolation but prior to initial medium change. Note the large amount of floating debris. The arrow shows a single attached astrocyte. (**B**) 24 hr postisolation following medium change. Note only a single astrocyte (shown by the arrow) has attached to the cell culture plate in this microscopic field. (**C**) 1 week postisolation. (**D**) At 3 weeks postisolation, the astrocytes are fully confluent.

38. At 18 to 24 hr after plating, remove old growth medium with a sterile 5-in. Pasteur pipet attached to a vacuum source, and add fresh medium to the volumes as listed in Table 12.4.2 using a large disposable pipet.

    This is vital in minimizing neuronal, microglial, and oligodendrocyte contamination of cultures.

    Duplicate 2-liter heavy-walled vacuum flasks arranged in series with a hydrophobic filter (Gelman Vacushield or equivalent) between the last flask and the vacuum source should be used to prevent accidental contamination of vacuum lines. If no vacuum source is available, a peristaltic pump may be used.

    When changing medium, do not completely remove the lid of the culture plates. Instead, use one hand to hold the plate at a slight angle toward you and raise the lid ~45°. Change the Pasteur pipet frequently and any time it may have touched anything other than the inside of the culture dishes. A pipet contaminated during medium changes can easily infect the entire culture if it is not changed.

    It is not necessary to replace the medium immediately; cells may sit for a few minutes, allowing one to remove and replace medium in batches of ~20 plates. This is much more convenient than removing and then immediately replacing medium on each plate individually.

    When adding fresh medium, pipets should only be placed in the bottle of growth medium once, to prevent possible contamination from the culture plates.

39. Change medium twice per week (e.g., on Tuesday and Friday).

    Approximately 2% to 3% of the astrocytes should attach and reach confluence between 2.5 and 3.5 weeks after plating. Astrocytes at different stages of growth are represented in Figure 12.4.1. If cells do not reach confluence or begin detaching from the culture plates, the cells should be discarded and the possibility of contamination should be considered.

SUPPORT PROTOCOL 1

FIRE POLISHING AND SIGMACOTE TREATMENT OF PIPETS FOR CELL ISOLATION

Sigmacote is a prediluted silane-based coating for glass surfaces. It bonds with the uneven surface of glass pipets and provides a smooth hydrophobic barrier. The adherence of cells to the glass surface is greatly reduced, and this minimizes physical damage to the cells. Only pipets used for cell isolation, not routine changing of medium, need to be fire polished and Sigmacote treated. This is most conveniently done in batches of 30 to 50 pipets.

Materials

Sigmacote (Sigma)
9-in. Pasteur pipets
Cotton-tipped swabs
10-ml glass serological pipets, cotton-plugged

1. Fire polish the tip of a 9-in. Pasteur pipet by placing the small end in an open flame from a Bunsen burner for a few seconds. Take care not to make the diameter of the opening too small.

   This will slightly melt the borosilicate glass and will produce a smooth tip to the pipet, which helps prevent damage to the cells. However, if the opening becomes too small, increased shear forces during trituration may lead to increased cell damage.

2. Plug the large end of the Pasteur pipet with cotton removed from a cotton-tipped swab. Use the stick from the swab to push the cotton down to the notch in the neck of the pipet.

   The amount of cotton obtained from a single swab is sufficient for one pipet. With a slight pulling and twisting motion, the cotton is easily removed from the swab.

3. Treat fire-polished Pasteur pipets and 10-ml glass, cotton-plugged serological pipets with Sigmacote by drawing the viscous solution up into the pipet with a portable power pipetter. Do not allow the solution to touch the cotton plug.

   It is not necessary to fire polish or plug the glass serological pipets.

4. Allow the Sigmacote to drain back into the bottle, and allow the pipets to drain and dry completely in a beaker lined with paper towels.

5. Place coated pipets in a metal container and autoclave.

SUPPORT PROTOCOL 2

COATING COVERSLIPS FOR ASTROCYTE CULTURE

As a general rule, cultured cells do not adhere well to glass, and thus cell growth on glass coverslips can be difficult. However, many microscopic, histological, or other procedures are necessarily performed on glass, and therefore a procedure for promoting attachment of astrocytes by coating coverslips with gelatin followed by poly-L-lysine is given below.

Materials

2.5% (w/v) gelatin solution (see recipe)
1× poly-L-lysine solution (see recipe)
70% ethanol
H_2O, sterile

18 × 18–mm (no. 2) glass coverslips
Laminar flow hood with ultraviolet light
Sterile forceps
6-well tissue culture plates

1. Rinse 18 × 18–mm (no. 2) coverslips with 70% ethanol and place in an autoclavable container in multiple layers between Kimwipe tissues. Do not crowd coverslips.

   Coverslips must not overlap during autoclaving.

2. Autoclave coverslips.
3. In a laminar flow hood, use sterile forceps to remove coverslips and place them into individual wells of a 6-well tissue culture plate.
4. Add 1.5 ml sterile, room-temperature 2.5% gelatin solution to the surface of each coverslip. Allow gelatin to coat the coverslips for 30 min at room temperature.
5. Aspirate gelatin solution and add 1.5 ml of 1× poly-L-lysine solution to the surface of each coverslip.
6. Incubate plates containing coverslips at 4°C overnight to allow adherence between poly-L-lysine and the gelatin coating.
7. After isolation of cells the following day and ~1 hr before seeding cells, aspirate poly-L-lysine and wash three times with 1.5 ml sterile water.
8. After removing all water, place dishes with coverslips under the ultraviolet light of the laminar flow hood for 30 min to dry the coverslip and to crosslink the poly-L-lysine and gelatin.

   Coverslips are ready for immediate use for culturing astrocytes.

REAGENTS AND SOLUTIONS

Use Milli-Q-purified water or equivalent in all recipes and protocol steps. For common stock solutions, see ***APPENDIX 2A****; for suppliers, see* ***SUPPLIERS APPENDIX****.*

Astrocyte growth medium

900 ml minimal essential medium with Earle's salts (MEM; Life Technologies)
10 ml penicillin/streptomycin (Life Technologies; 100 U/ml penicillin, 100 µg/-liter streptomycin final)
100 ml heat-inactivated horse serum (see recipe; 10% v/v final)
1 ml Fungizone (optional)
Sterilize with a 1-liter sterile filter flask (0.2-µm pore size, cellulose acetate)
Store up to 1 month at 4°C

Penicillin/streptomycin from Life Technologies contains 10,000 U/ml penicillin G and 10,000 µg/ml streptomycin sulfate. Storing penicillin/streptomycin in 10-ml aliquots at −20°C is suggested to avoid repeated freeze-thaw cycles and because it provides the correct amount for 1 liter of medium. (See manufacturer's expiration date.)

Borate buffer

1.24 g boric acid
1.9 g borax
400 ml H_2O
Adjust pH to 8.4 with NaOH
Store at 4°C (stable for many months)

Complete S-MEM

500 ml minimal essential medium with Earle's salts, modified for suspension cultures (S-MEM; Life Technologies)
5 ml penicillin/streptomycin (Life Technologies; 100 U/ml penicillin, 100 µg/l streptomycin final)

continued

Store up to 2 months at 4°C

S-MEM has been modified to contain no Ca^{+2} which can produce cell clumping due to interactions of extracellular matrix proteins.

Penicillin/streptomycin from Life Technologies contains 10,000 U/ml penicillin G and 10,000 µg/ml streptomycin sulfate. Storing penicillin/streptomycin in 10-ml aliquots at −20°C is suggested to avoid repeated freeze-thaw cycles. (See the manufacturer's expiration date.) The use of Fungizone is not recommended.

Filter sterilization of S-MEM is optional.

Deoxyribonuclease I (DNase I) solution, 8000 U/ml

Dilute 15,000 U DNase I from bovine pancreas (type IV; Sigma) in 1.875 ml water. Mix gently; do not vortex. Sterilize with a 0.2-µm syringe filter (cellulose acetate). Store in 100-µl aliquots at −20°C for many months (see manufacturer's expiration date).

DNase I from pancreas is vulnerable to inactivation by physical damage and should not be vortexed.

Dissociation medium

Complete S-MEM (see recipe)
3 U/ml dispase (Life Technologies)

On the day of isolation, prepare 10 ml per brain plus an additional 25 ml (e.g., for 10 brains, add 375 U dispase to 125 ml complete S-MEM). Sterilize with a 150-ml sterile filter flask (0.2-µm pore size, cellulose acetate). Prewarm in a 37°C incubator for 1 hr before use. Discard any unused dissociation medium.

Gelatin solution, 2.5% (w/v)

25 mg gelatin (type A from porcine skin, bloom 300)
100 ml water
Autoclave
Store up to 6 months at room temperature

Heat-inactivated horse serum

Avoid repeated freeze-thaw cycles of horse serum (Life Technologies). To thaw frozen serum, place the bottle in a refrigerator for ~24 to 48 hr. If rapid thawing is needed, place in a water bath that is no warmer than 40°C. Dispense into aliquots in 50-ml tubes and store up to 1 year at −20°C. Thaw at room temperature over a few as hours as necessary.

Thawed serum can be stored for up to 1 week at 4°C, but freezing of aliquots is recommended.

Purchase of horse serum that has been heat inactivated by the vendor is highly recommended.

Poly-L-lysine solution, 1× and 10×

10× stock solution: Dissolve 25 mg poly-L-lysine (Sigma) in 25 ml borate buffer (see recipe). Store up to 2 months at 4°C.

1× working solution: Dilute 5 ml of 10× stock solution into 45 ml borate buffer. Filter sterilize with a 0.2-µm cellulose acetate filter. Prepare fresh each day and keep at 4°C.

Poly-D-lysine is an acceptable substitution for poly-L-lysine and may be preferred due to decreased of digestion of the D isomer by cells (Higgins and Banker, 1998). Regardless of the isomer, the large molecular weight (>300 kDa) preparations should always be used.

COMMENTARY

Background Information

Prior to the development of simple and reliable culture techniques in the late 1970s and early 1980s, the majority of studies on astrocytes dealt mainly with their morphological and developmental properties. With the advancement of cell culture techniques, investigations into the biochemical, physiological, pharmacological, and molecular aspects of astrocyte function are now possible. These cultures provide a model to study astrocytic function under controlled and reproducible conditions.

Given the wide array of functions performed by astrocytes, the range of possible uses for primary cultures is vast. A brief list includes intracellular signaling with Ca^{2+}-sensitive fluorescent dyes (*UNIT 12.5*), electrophysiological examination of ion channels and receptor function, production and secretion of growth factors, toxicant-induced astrocyte swelling, and production of free-radicals, just to name a few. The use of cell culture systems consisting of neurons grown in wells with astrocytes grown above them on inserts allows studies on the influence on neuronal function of factors released by astrocytes.

The use of primary astrocyte cell cultures rather than tumor cell lines such as the human U373 or rat C6 gliomas has both advantages and disadvantages. Tumor cell lines are less expensive and less time consuming to prepare and maintain. In addition, there should be little culture-to-culture variation in these cells. However, since the cell lines are derived from abnormal tissue, their physiology must be carefully examined. Given that the ultimate goal of most studies is to understand the function of normal astrocytes in vivo, the role of cell lines is perhaps questionable.

Of course, one must similarly be cautious when relating processes seen in culture to the in vivo situation whether the cells are primary cultures or cell lines. Indeed, there are multiple cell types within the CNS (neurons, astrocytes, oligodendrocytes, and microglia), and the complex interactions between them are not easily modeled using cell culture without losing one of the most attractive features of cell culture, the ability to study a distinct cell population. In an attempt to address some of these issues of reciprocity between neurons and astrocytes, a technique of producing astrocyte-neuron cocultures has recently been described (Aschner and Bennett, 1998; see *UNIT 12.3*).

There are multiple techniques for the isolation of astrocytes from neonatal rodents. The most common of these methods is either mechanical dissociation (McCarthy and de Vellis, 1980) through increasingly smaller-diameter nylon sieves (Cole and de Vellis, 1992), or enzymatic dissociation using either trypsin (Eng et al., 1971) or dispase (Frangakis and Kimelberg, 1984). The selection of an isolation method depends upon a number of factors, including the number and the purity of astrocyte cultures required.

To shake or not to shake? This is a common methodological question encountered in preparing primary cultures of astrocytes. The mechanical dissociation method (McCarthy and de Vellis, 1980; Cole and de Vellis, 1992) includes vigorous shaking (200 to 250 rpm for up to 24 hr at 37°C) of 7- to 8-day-old cultures grown in 75-cm^2 flasks plated at a density of at least one brain per flask. During this shaking, the astrocytes remain attached to the culture dishes, while the other cell types (neurons, microglia, oligodendrocytes, and O-2A progenitor cells) detach from the astrocytic layer and are removed by replacing the medium. The remaining astrocytes are then collected by trypsinization, replated in new culture dishes, and again allowed to grow until confluent. This procedure produces astrocytes of slightly higher purity than the procedure described here (98% versus 95%); however, it is well accepted that passage of cells changes their biochemical and immunological phenotypes (Cole and de Vellis, 1992), and thus the authors prefer a method that does not involve any passage of astrocytes.

Regardless of the method used for production of astrocytes, an important variable to consider when performing neurotoxicological studies in cultured cells is verifying that effects are not simply due to cell death following treatment. The use of standard toxicological assay such as lactate dehydrogenase (LDH) release or neutral red uptake (*UNIT 2.6*) should be performed to differentiate alterations in function from cell death.

Critical Parameters and Troubleshooting

Several critical parameters in astrocyte culture are discussed below. Table 12.4.3 presents a number of potential problems associated with production of primary astrocyte cultures, along with possible causes and solutions.

Table 12.4.3 Problems Commonly Encountered During Cell Isolation

Problem	Possible cause	Possible remedy
Clumping of cells during extractions (not to be confused with sedimentation of tissue)	Ca^{2+} present in medium	Use only S-MEM, which is Ca^{2+}-free, to prepare dissociation medium
Medium becomes viscous during extractions	No DNase I	Add DNase I (mix DNase I solutions gently; do not vortex)
Low cell yield/viability	Cell death due to excessive trituration	Use Sigmacote-treated glass pipets; do not allow air bubbles to enter cell suspension during trituration
	Prolonged dissection time	Limit dissection to 10 min per brain
	Ca^{2+} present in medium, causing cellular aggregation	Use S-MEM during cell isolation
Floating cells in cultures after initial isolation	Contaminated cultures	See Critical Parameters and Troubleshooting
	Cultures are too old	Use cultures within 3 to 4 weeks
	Loss of poly-L-lysine on coverslips	Treat coverslips with poly-L-lysine only 1 day prior to plating cells

Tissue dissection

The rapid dissection of the brain area of interest and meticulous removal of meninges is vital for the successful isolation of primary astrocytes. If the meningial removal is incomplete, fibroblast contamination can overwhelm cultures due to the faster propagation of fibroblasts compared to astrocytes. Although removal of meninges must be complete, it is recommended that no more than 10 min per brain be spent on this task. The speed and accuracy of removing the meninges will likely improve with experience.

Dissociated cell extraction

There can be lot-to-lot variability with even the highest-quality enzymes. Thus, if a rapid and continuing decrease in cell number or viability is seen, careful attention should be paid to both the age and lot number of the dispase. In general, it is good to record lot numbers of all reagents used in preparing and maintaining the cultures. Successive disappointing cell isolations may be traced to an unsatisfactory lot of enzyme or serum.

In addition, the importance of handling the dissociated cells gently cannot be over emphasized. The use of Sigmacote-treated glass pipets greatly reduces the trauma to cells during the isolation process. It is also vital to not dissociate the tissue by forceful triturations or excessively rapid mixing on the stir plate. If air bubbles are introduced into the suspension, the trituration is too harsh and will lead to a large reduction in cell viability.

Purity of cultures

The purity of the cultures can be determined by immunohistochemistry using markers for astrocytes (GFAP) and neurons (microtuble associated protein 2, MAP-2) as described previously (Aschner and Bennett, 1998). Additionally, markers for oligodendrocytes (2′,3′-cyclic-3′-phosphohydrolase, CNP; Promega; Cammer, 1990) and microglia (OX-42; Harlan Bioproducts for Science; Castellano et al., 1991) are also available.

Astrocyte cultures obtained by dispase dissociation are routinely >95% positive for GFAP by immunohistochemistry (see Fig. 12.4.2). However, this can vary between cultures, with some producing a greater degree of neuronal, oligodendrocyte, and microglial contamination. It has been suggested that using 24- to 48-hr-old rat pups may decrease the number of contaminating neurons (McCarthy and de Vellis, 1980).

Time in culture

Important variables to consider when performing studies with primary astrocyte cultures are the effects of confluency and time in culture. Unlike tumor cells, these astrocyte cultures stop growing and dividing once confluent, due to cell-cell interactions. It is strongly recommended that the effects of confluency be deter-

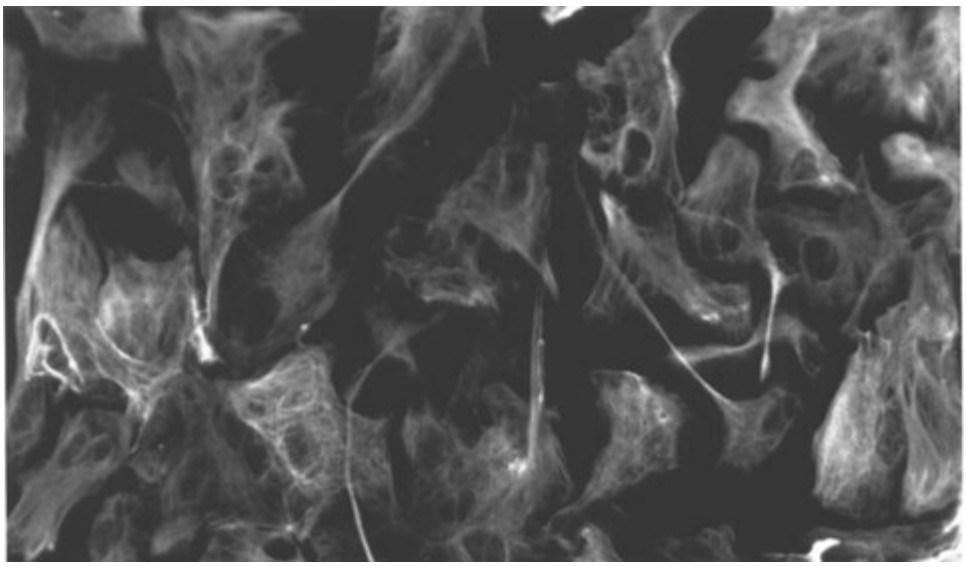

Figure 12.4.2 GFAP immunofluorescence of cultures (fluorescent photomicrograph, 400× magnification) of confluent astrocytes processed for the astrocytic marker as described previously (Aschner and Bennett, 1998). The cells are routinely >95% positive for GFAP, attesting to the purity of the cultures.

mined by treating cells at various states of confluency. In a related issue, the time in culture can have profound effects on the genotype and phenotype of the astrocytes. Thus, preliminary studies should examine temporal changes in expression of the product of interest, and subsequent studies must contain appropriate controls to account for temporal changes in expression during treatments.

Contamination

Microbial contamination of primary cell culture is probably the most common problem encountered once the initial cell isolation is successful. Contamination may be due to invasion by bacteria, yeast, fungi, molds, mycoplasma, viruses, or any combination of the above. Although isolated contamination of an individual culture plate or two is not uncommon, widespread or continual contaminations (in more than two separate isolations) requires investigation of the source of the microbes. Once contamination is suspected, the rapid and accurate identification of the offending class of microbe can aid in determining the source of contamination. If contamination of cells is suspected, the authors highly recommend that a sample be sent to a certified microbiological laboratory for identification of the class of microbe.

Any infected culture plates must be disposed of immediately. All surfaces, including microscopes, pipettors, incubators, and refrigerator door handles, should be cleaned with 70% ethanol.

Since the growth medium contains antibiotics (penicillin and streptomycin), bacterial contamination is uncommon. The addition of gentamicin sulfate may be beneficial in controlling bacterial and also mycoplasma contamination. When adding new antibiotics, begin with the lowest recommended concentrations (available in Life Technologies catalog) and perform a dose-toxicity curve in a few noninfected plates to assess effects on growth rate and cytotoxicity. In general, the highest concentration of antibiotic that doesn't adversely inhibit cell growth should be used.

In the authors' experience, the most common sources of contamination are yeast and fungi. The addition of 0.25 μg/ml Fungizone (Amphotericin B; Life Technologies) effectively halts both yeast and fungal infections. The authors do not routinely add Fungizone to the growth medium, but use it only as necessary to control sporadic infections that seem to occur mainly during spring and summer.

Cultures with yeast contamination can usually be readily identified by examination of the medium. The growth medium appears cloudy and, if phenol red is present, usually turns yellow due to acidification. The rapidly growing yeast consume the available glucose and then convert to anaerobic metabolism, which produces large quantities of lactic acid. It is this lactic acids that alters the pH (and thus the

color) of the growth medium. Microscopic examination of yeast-contaminated cultures reveals small round spores floating throughout the medium. The source of yeast is often hard to identify and thus the list of possible suspects is long. Any item to be placed in the laminar flow hood should be cleaned with 70% ethanol, but special care must be taken when laboratory water baths are used to thaw or warm reagents for cell culture.

The use of disposable plastic pipets can greatly reduce the possibility of contamination. The pipets should only be placed in the growth medium once and used to feed one stack of culture plates. This prevents transfer of contaminants from a single plate to the growth medium, which can then infect the entire culture. The Pasteur pipets used for removal of medium should similarly be changed frequently.

Fungus is often found growing directly on the astrocyte cell layers or even on the walls of culture plates. It grows rapidly to form green to yellow sponge-like circles and rapidly absorbs much of the growth medium. When a fungal infection is discovered, careful examination of the incubator is necessary, as this is often a reservoir of fungal spores. A thorough disinfection of the incubator with 70% ethanol is suggested.

Mycoplasma contamination cannot be easily detected by visual inspection of the cultures. If cultures die prior to reaching confluency or are growing slowly, mycoplasma contamination may be suspected. Once again, the authors recommend sending samples to a certified microbiological laboratory for testing of mycoplasma. Alternatively, kits designed for mycoplasma detection are commercially available (MycoTest, Life Technologies; Mycoplasma Detection Kit, Roche).

Anticipated Results

Cultured astrocytes produced by dispase digestion have a flat polygonal appearance (Fig. 12.4.1) and are >95% positive for GFAP (Fig. 12.4.2). Cell yields should be ~10^7 cells per brain, with viability ~95%. Only 2% to 3 % of seeded astrocytes actually adhere to culture plates after changing the medium at 24 hr. The development of cultures at various stages is presented in Figure 12.4.1.

A 100-mm culture plate of confluent astrocytes routinely provides a minimum of 15 µg total RNA or 150 µg cellular protein. Therefore, a single plate provides ample RNA or protein for most northern or immunoblotting procedures.

Time Considerations

The total time for the preparation of astrocyte cultures is ~6 to 8 hr depending on the number of extractions performed and the number of rat pups used for the dissections. The twice weekly change of medium (feeding) usually requires ~1 to 2 hr, but will, of course, vary with the number of plates.

Literature Cited

Aschner, M. and Bennett, B.A. 1998. Astrocyte and neuron coculturing method. *In* Methods in Molecular Medicine, Vol. 22: Neurodegeneration Methods and Protocols (J. Harry and H.A. Tilson, eds.) pp. 133-144. Humana Press, Totowa, N.J.

Aschner, M. and Kimelberg, H.K. (eds.) 1997. The Role of Glia in Neurotoxicity. CRC Press, Boca Raton, Fla.

Aschner, M. and Vitarella, D. 1995. Central nervous system glial cell cultures for neurotoxicological investigations. *In* Neurotoxicology: Approaches and Methods (L.W. Chang and W. Slikker, Jr., eds.) pp. 549-562. Academic Press, New York.

Aschner, M., Lorscheider, F.L., Cowan, K.S., Conklin, D.R., Vimy, M.J., and Lash, L.H. 1997. Metallothionein induction in fetal rat brain and neonatal primary astrocyte cultures by in utero exposure to elemental mercury vapor (Hg^0). *Brain Res.* 778:222-232.

Cammer, W. 1990. Glutamine synthetase in the central nervous system is not confined to astrocytes. *J. Neuroimmunol*. 26:173-178.

Castellano, B., Gonzalez, B., Jensen, M.B., Pedersen, E.B., Finsen, B.R., and Zimme, J. 1991. A double staining technique for simultaneous demonstration of astrocytes and microglia in brain sections and astroglial cultures. *J. Histochem. Cytochem.* 39:561-568.

Cole, R. and de Vellis, J. 1992. Astrocyte and oligodendrocyte cultures. *In* Protocols for Neural Cell Culture (S. Fedoroff and A. Richardson, eds.) pp. 65-80. Humana Press, Totowa, N.J.

Eng, L.F., Vanderhæghen, J.J., Bignami, A., and Gerstl, B. 1971. An acidic protein isolated from fibrous astrocytes. *Brain Res.* 28:351-354.

Fedoroff, S. and Verndakis, A. (eds.) 1986. Astrocytes, Vols. I, II, III. Academic Press, New York.

Frangakis, M.V. and Kimelberg, H.K. 1984. Dissociation of neonatal rat brain by dispase for preparation of primary astrocyte cultures. *Neurochem. Res.* 9:1689-1698.

Higgins, D. and Banker, G. 1998. Primary dissociated cell cultures. *In* Culturing Nerve Cells, 2nd ed. (G. Banker and K. Goslin, eds.) pp. 37-78. MIT Press, Cambridge, Mass.

Kettenmann, H. and Ransom, B.R. (eds.) 1995. Neuroglia. Oxford University Press, New York.

Kimelberg, H.K. 1983. Primary astrocyte cultures—a key to astrocyte function. *Cell Mol. Neurobiol*. 3:1-16.

Kimelberg, H.K. and Norenberg, M.D. 1989. Astrocytes. *Sci Am*. 260:66-72, 74, 76.

McCarthy, K.D and de Vellis, J. 1980. Preparation of separate astroglial and oligodendroglial cell cultures from rat cerebral tissues. *J Cell Biol.* 85:890-902

Murphy, S. (ed.) 1992. Astrocytes: Pharmacology and Function. Academic Press, New York.

Yao, C.P., Allen, J.W., Mutkus, L.A., Xu, S.B., Tan, K.H., and Aschner, M. 2000. Foreign metallothionein-I expression by transient transfection in MT-I and -II null astrocytes confers increased protection against acute methylmercury cytotoxicity. *Brain Res.* 855:32-38.

Key References

Banker, G. and Goslin, K. (eds.) 1998. Culturing Nerve Cells. MIT Press, Cambridge, Mass.

As the title implies, the book is geared toward neuronal cultures but does discuss glial cultures. It provides basic protocols, but its great strength lies in the thorough explanations and discussions of the underlying principles for each technique.

Fedoroff, G. and Richardson, A. 1992. Protocols for Neural Cell Cultures. Humana Press, Totowa, N.J.

A detailed, protocol-rich laboratory manual with numerous sections on culturing astrocytes and other glial cells. It also contains descriptions of commonly used techniques such as immunostaining and preparation of cells for electron microscopy.

Frangakis and Kimelberg, 1984. See above.

Initial description of the use of dispase for preparation of primary astrocyte cultures.

Freshney, R.I. 1993. Culture of Animal Cells: A Manual of Basic Techniques, 3rd ed. John Wiley and Sons, New York.

An excellent text and manual discussing the broad spectrum of techniques used in mammalian cell culture. Topics include designing and equipping a laboratory for cell culture, aseptic technique, preparation and maintenance of cultures, growth and quantitiation of cells, and contamination.

Contributed by Jeffrey W. Allen, Lysette A. Mutkus, and Michael Aschner
Wake Forest University School of Medicine
Winston-Salem, North Carolina

Analytical Cytology: Applications to Neurotoxicology

The protocols described in this unit provide examples of analytical cytology applied to two fundamental areas in neurotoxicology: cell-cycle regulation and cell signaling. The first protocol explains the use of dual-parameter flow cytometry to determine the effects of a toxicant on cell cycling (see Basic Protocol 1). While dual-parameter flow cytometry is only one of several available methods for detecting cell proliferation (e.g., tritiated thymidine incorporation, anti-BrdU antibody detection), it provides additional quantitative information regarding the number of completed mitotic divisions and cell-cycle phase length (i.e., G1, S, G2/M), thus giving important information on potential mechanisms of agent toxicity not easily obtained by alternative methods. Support Protocol 1 describes preparation of primary astrocytes for the flow experiment. The second protocol details the steps involved in the quantification of intracellular calcium concentrations within individual cells using scanning confocal laser microscopy (SCLM; see Basic Protocol 2). Along with the protocols describing the method that uses the fluorescent calcium probe Indo-1, a protocol for the generation of a calcium calibration curve (see Support Protocol 2) and a protocol for measuring intracellular calcium using the fluorescent calcium probe Fluo-3 (see Alternate Protocol) are provided.

The rationale behind presenting the two basic protocols, one using flow cytometry, the other SCLM, is to demonstrate how these fluorescence-based methods, both of which are widely used in analytical cytology, can be applied to neurotoxicology (also see *UNIT 2.5*).

NOTE: All solutions and equipment coming into contact with living cells must be sterile, and aseptic technique should be used accordingly.

NOTE: All incubations should be performed in a humidified 37°C, 5% CO_2 incubator unless otherwise specified.

NOTE: Fluorescent dyes are photolabile, and all manipulations with these compounds or cells loaded with these compounds should be carried out in a darkened room.

CELL-CYCLE ANALYSIS OF GLIAL CELLS BY BrdU/HOECHST FLOW CYTOMETRY

BASIC PROTOCOL 1

Flow cytometry is a well-established procedure for quantitative cell cycle analysis, and application of this technique to glial cells for use in neurotoxicological studies is described in the following protocol. Basic tissue culture techniques are described in *APPENDIX 3B* and basic flow cytometry techniques are described in the manufacturer's literature. Primary rat astrocytes are prepared as in Support Protocol 1 (also see *UNIT 12.4*). Following reseeding, astrocytes are grown for 2 days, then rinsed with phosphate-buffered saline and serum deprived for 2 days to obtain quiescence. Once the monolayer of cells is quiescent, the cells are then continuously incubated with 5-bromodeoxyuridine (BrdU), in the presence or absence of mitogen(s) and/or toxicant(s). After the desired treatment period, cells are harvested and resuspended in buffer containing Hoechst 33258. Because Hoechst cannot bind to regions of DNA that have incorporated BrdU, its fluorescence will be reduced in cells that have incorporated BrdU into DNA during DNA synthesis; used in this way, Hoechst fluorescence can provide information on the number of completed cell cycles. Prior to flow cytometric analysis, the cells are further stained with ethidium bromide, providing the second fluorescence parameter with which one can distinguish cell-cycle phases (i.e., G0, G1, S, G2/M) and cell-cycle phase transition times.

Contributed by Michelle C. Catlin, Marina Guizzetti, Rafael A. Ponce, Lucio G. Costa, and Terrance J. Kavanagh

Current Protocols in Toxicology (2000) 12.5.1-12.5.16

Materials

Monolayer cultures of primary rat astrocytes (see Support Protocol 1)
Complete DMEM medium/5% and 10% (v/v) FBS (see recipe)
Ca^{2+}, Mg^{2+}-free Dulbecco's phosphate-buffered saline (CMF-DPBS; *APPENDIX 2A*)
Serum-free medium (see recipe)
Agent to be tested for mitogenic potential
15 mM BrdU (see recipe)
Hoechst buffer (see recipe)
100× ethidium bromide (see recipe)
0.1% (v/v) trypsin in CMF-DPBS

24-well tissue culture plates
12 × 75–mm polystyrene tubes
Flow cytometer equipped with UV-excitation (351 to 362 nm lines of argon-ion laser, or 365 nm line of a mercury arc lamp)
MPLUS AV program (Phoenix Flow Systems) or equivalent flow cytometry software program for data analysis

Additional reagents and equipment for tissue culture and trypsinization of cells (*APPENDIX 3B*) and flow cytometry (*UNIT 2.5*)

1. Plate cells in 24-well plates at 5×10^5 cells/well and maintain them in complete DMEM medium/10% FBS for 2 days (*APPENDIX 3B*). Rinse cells with 37°C CMF-DPBS. Serum-deprive cells for 48 hr to bring them to quiescence by incubating in 1 ml serum-free medium.

   Depending upon the toxicant exposure conditions and the experimental outcome measurements desired, quiescent cells can be treated to determine the mitogenic, and therefore possible oncogenic, effects of a chemical or physical agent. Alternatively, the effect of treatment on the proliferative effects of known mitogens can be investigated to determine toxicant-induced effects on normal proliferative responses. The protocol described here is to assess the proliferative effect of a treatment.

2. Replace the medium with 1 ml of fresh serum-free medium in the absence or presence of chemicals or physical agents to be tested for their mitogenic potential.

   Each well is one treatment and each treatment should be carried out in triplicate.

3. At the end of the treatment, add 10 µl of 15 mM BrdU (150 µM final concentration) to each well. Incubate 48 hr.

   BrdU is photosensitive; do not expose to light. Wrap the plates in aluminum foil during the period of BrdU incubation, as exposure of cells that have incorporated BrdU to light will result in DNA strand breaks. Avoid exposing the samples to direct light from this point until flow cytometric analysis.

4. After incubation, remove the supernatant from each well, and harvest the cells from each well by adding 200 µl/well of 0.1% trypsin solution for 5 min. Neutralize trypsin by adding 200 µl of complete DMEM/10% FBS and pipet repeatedly up and down to obtain a single-cell suspension (*APPENDIX 3B*).

5. Transfer the cells from each well into an individual 1.5-ml tube and microcentrifuge 10 min at 1000 × *g*, 4°C. Remove the supernatant by aspiration and resuspend the cells in 500 µl Hoechst buffer.

   Single-cell suspensions should be checked under a microscope to ensure that there is no clumping, as this would clog the flow cytometer and result in spurious analyses.

   Cells resuspended in Hoechst must be analyzed within 8 hr. If cells will not be analyzed within that time frame, add DMSO to the Hoechst buffer to give 10% (v/v) DMSO (final

concentration) and store the cells in this solution at −20°C. Samples can be stored in this way up to 1 week. Thaw samples 15 min before flow cytometric analysis.

6. Transfer the samples to 12 × 75–mm polystyrene tubes. Add 5 µl of 100× ethidium bromide stock solution for a final concentration of 5 µg/ml, and thoroughly mix each sample.

   CAUTION: *Ethidium bromide is an animal carcinogen. Use extreme care while handling.*

   The samples are now ready for immediate flow cytometric analysis.

7. Carry out flow cytometric analysis by exciting both the stains at 351 to 362 nm (argon-ion laser) or 365 nm (mercury arc lamp). Collect Hoechst emission at 420 to 490 nm and ethidium bromide emission at wavelengths >610 nm. Collect data from 10,000 or more cells per sample for sufficient for data analysis.

PREPARATION OF PRIMARY RAT ASTROCYTES

SUPPORT PROTOCOL 1

Primary rat astrocytes are prepared as described in Guizzetti et al. (1996; also see *UNIT 12.4*).

Materials

Day-21 rat fetuses
Complete DMEM medium/10% FBS (see recipe)
75-cm^2 tissue culture flasks, poly-D-lysine coated

Additional reagents and equipment for tissue culture (*APPENDIX 3B*)

1. Mince and trypsinize cortices from day-21 fetuses (0.2% w/v trypsin in PBS for 10 min at 37°C) and wash 3 times by centrifugation at 225 × *g*, 4°C, with complete DMEM medium/10% FBS.

2. With a narrow-bore pipet, triturate tissue, filter, and plate in 75-cm^2 flasks previously coated with poly-D-lysine (10 µg/ml), at 1.5×10^5 cells/cm^2.

   To coat flasks with poly-D-lysine, cover the surface of the flask with sterile 10 µg/ml poly-D-lysine and incubate 10 min at 37°C. Aspirate the solution and rinse the flask with sterile, room temperature, double-distilled water. Let dry overnight.

3. Within 24 hours of plating, shake flasks, and add fresh medium.

4. Incubate flasks for 9 days and feed every 2 to 3 days. On day 9 of culture, shake flasks overnight, trypsinize, and reseed for experiments (see Basic Protocol 1).

ANALYSIS OF INTRACELLULAR CALCIUM IN INDIVIDUAL GLIAL CELLS USING INDO-1/AM

BASIC PROTOCOL 2

Outlined here is a protocol for the quantification of intracellular calcium concentration ($[Ca^{2+}]_i$) within individual, attached glial cells to determine the effect of a toxicant on both basal $[Ca^{2+}]_i$ and stimulus-induced $[Ca^{2+}]_i$ changes. This basic protocol describes the technique used to examine human 132 1N1 astrocytoma cells (provided by Dr. J. Heller-Brown, University of California at San Diego) using the ratiometric calcium probe Indo-1/AM. Kinetic analysis allows determination of the effect of acute or chronic incubation with a toxicant on stimulus-evoked responses, as well as any effects of the toxicant on basal calcium by scanning prior to the addition of the stimulus. For generation of a calcium calibration curve, see Support Protocol 2. An Alternate Protocol describing the measurement of $[Ca^{2+}]_i$ using Fluo-3/AM, a non-ratiometric calcium-sensitive dye, is also provided. In both this and the Alternate Protocol, 132 1N1 astrocytoma cells are loaded with a calcium-sensitive probe in Krebs'-bicarbonate buffer and rinsed; fluorescence is then measured using an SCLM (also see *UNIT 2.5*).

Materials

132 1N1 astrocytoma cells (available from Dr. J. Heller-Brown, University of California at San Diego)
Complete DMEM medium/5% FBS (see recipe)
Serum-free medium (see recipe)
Toxicant of interest
Krebs' bicarbonate buffer (see recipe)
Loading buffer (see recipe)
2 µM Indo-1/AM in loading buffer
Stimuli (e.g., serum, mitogens, glutamate)

2-well coverglass chamber slides (Nunc)
Inverted, scanning confocal microscope equipped with a mercury arc lamp or argon ion laser capable of an emission wavelength of 351 to 363 nm
445-nm long-pass dichroic filters (Omega Optical)
Neutral density filters (Omega Optical)
Two photomultiplier tubes or other fluorescent detectors (capable of quantifying fluorescence in the range of 400 to 410 nm and 500 to 530 nm simultaneously)
Data acquisition system for collecting and storing digital images
Spreadsheet software

Additional reagents and equipment for generation of a calcium calibration curve (see Support Protocol 2)

Prepare cells and reagents

1. Plate 2×10^4 cells/cm^2 (2 ml at 5×10^4 cells/ml) in a coverglass chamber slide in complete DMEM medium/5% FBS. Allow cells to grow in the incubator for 2 days in complete DMEM medium/5% FBS (or until desired confluency is reached), then serum-deprive the cells for 2 days by substituting serum-free medium. Treat with toxicant in the appropriate manner.

   Depending upon the toxicant exposure conditions and the experimental outcome measurements desired, cells can be treated chronically prior to assay, treated acutely before assay, treated and removed during an assay, or added following basal $[Ca^{2+}]_i$ determinations. The protocol described here assumes that cells have been pretreated with a toxicant for the time period of interest.

   Coverglass chamber slides are fragile; hold the chamber by the flanges to avoid leakage and breakage. It is advisable to keep them on a tray in the incubator in case of leakage. Different cell types may require special tissue culture conditions, such as precoating the coverglass chambers with poly-D-lysine or collagen to allow attachment.

2. Warm up and align laser/mercury lamp.

   Once one is comfortable with the technique, the microscope can be set up during the loading period to preserve laser or arc lamp life.

3. Tune the laser to excite in the range of 351 to 363 nm with at least 60 mW of illumination. Insert filters so that the fluorescence emission is split (e.g., 445-nm long-pass dichroic filter) and can be read simultaneously by one detector at 405 nm and the other detector at 530 nm.

   Use of an oil-immersion, 100× objective will allow for optimal resolution and is compatible with the coverslip thickness of a 2-well chamber slide.

4. Create a directory on the computer to save images and data.

   Multiple image files are generated which require a large amount of storage space. High-capacity magnetic storage devices (e.g., a ZIP drive or WORM drive) work well as a data-storage medium.

Load cells with Indo-1/AM

5. Rinse cells once with 2 ml Krebs' bicarbonate buffer and once with 2 ml loading buffer.

   If more than 2 wells are being assayed, the loading of each plate should be appropriately timed (i.e., for a 5-min scan, stagger loading by ≥20 min).

6. Incubate the cells for 1 hr at 37°C in 2 ml per well of the Indo-1/AM solution (2 μM final concentration).

   Indo-1 is light sensitive and steps involving the dye or loaded cells should be carried out in a darkened room.

7. Remove the Indo-1 AM solution and replace with loading buffer. Leave cells in loading buffer for 15 to 30 min at 37°C to allow further cleavage of the AM ester.

8. Remove loading buffer. Rinse once with 37°C Krebs' bicarbonate buffer, and add 1 ml Krebs' bicarbonate for fluorescence measurements.

Measure intracellular fluorescence

9. Secure the coverglass chamber slide on the microscope stage and prefocus under normal light. Conduct a preview scan with the laser to determine if the data acquisition settings are optimal, and adjust the focus to ensure that fluorescence from cells is maximally captured.

   If one is expecting to see an increase in calcium levels following treatment, adjust baseline fluorescence such that signals from the detector measuring 405 nm (emission of Indo-1 when bound to calcium) can increase without overshooting the range of fluorescence detection of the system. Similarly, the detector measuring 530 nm (emission of Indo-1 when not bound to calcium) should be adjusted to accommodate a stimulus-induced decrease in fluorescence.

   Different parameters may be desired for different experiments. The photomultiplier tube (PMT) percentages can be changed initially, but must be kept constant to compare ratio values between experiments and must be the same as those used for generating the standard curve. Use a UV-corrected objective of the desired magnification. Set the number of scans and scan delay depending upon the data desired (the delay will depend upon the scan speed and field size). The step (pixel) size determines the resolution and the number of pixels in the X and Y dimensions determines the field size. The scan strength can be adjusted between experiments and neutral-density filters can be used to keep fluorescence within quantifiable ranges.

10. Begin scanning/collecting data, scanning at least three times to determine the baseline level of $[Ca^{2+}]_i$. Add stimulus (e.g., serum, mitogens, glutamate), made up in Krebs' bicarbonate buffer, manually using a pipet. Collect as many time points as desired (determined by parameters).

    Be careful not to disrupt the focus when adding stimulus (i.e., don't touch the chamber slide with the pipet), and, to ensure adequate mixing of stimuli, add solutions of stimuli in a large volume (e.g., 1 ml into 1 ml in well) or mix well with a pipet.

    Care must be exercised so as not to photobleach the Indo-1 by scanning too frequently with excessive excitation power.

Analyze fluorescence data

11. With an initial (baseline) image displayed on the computer monitor, encompass individual cells with an "area" tool (e.g., polygon or circle), and save the area as a template to apply to subsequent images. Use the computer software to integrate fluorescence within each area over time. Generate a standard curve (see Support Protocol 2) to calculate the absolute $[Ca^{2+}]_i$ from the ratios. Save these values and export to a spreadsheet program for subsequent analyses as desired.

    Data analysis can be conducted any time after the experiment is finished.

SUPPORT PROTOCOL 2

GENERATION OF CALCIUM CALIBRATION CURVE

A calcium calibration curve can be generated in order to determine the absolute (nM) concentration of $[Ca^{2+}]_i$ that corresponds to a given ratio of Indo-1 dye fluorescence in the bound and unbound states.

Additional Materials *(also see Basic Protocol 2)*

Calcium Calibration Buffer Kit 1 (Molecular Probes)
Ethanol
Indo-1 free acid

1. Set up the SCL microscope and data acquisition system (Basic Protocol 2, steps 2 to 4).

   It is important that the PMT settings for the two detectors be the same as those used in the experiment. Changes in these will alter the ratio for a given concentration of calcium. The excitation intensity may differ (by use of neutral density filters and adjusting the scan strength) from that used in experiments.

2. Carefully scratch the internal surface of a 2-well coverglass chamber (use a sharp metal object) to focus on the Indo-1 solution/glass interface.

3. Adjust the pH of both the zero and high-calcium calibration buffers to 7.4 with either HCl and NaOH.

   It is important to use deionized water and plastic containers for any solutions to avoid the addition or leaching of calcium.

4. To both the zero and high calcium calibration buffers, add ethanol to a final concentration of 20% (v/v) and Indo-1 free acid to a final concentration of 10 μM.

   Ethanol helps control for differences in the viscosity between cells and the buffers (Poenie, 1990). A higher concentration of Indo-1 is used for curve generation as compared to experiments with cells, since the dye does not become concentrated in solution as it does in the cells.

5. Place the chamber securely on the microscope stage and focus on the internal surface using the scratch to focus on the plane of the solution. Move the stage such that the scratch is no longer in the field of view, add the zero calcium solution, and conduct a preview scan to focus for maximal fluorescence. Adjust the parameters to stay within the range of fluorescence detection of the system.

6. Following the directions provided with the calcium calibration buffer kit, remove the volumes of zero calcium concentration buffer and add the calculated volumes of zero and high calcium concentration buffers to determine fluorescence ratios that correspond to known concentrations of free calcium.

   Additional points on the curve can be added by using the equations shown in the kit instructions and by calculating the volumes to be removed and added.

7. Using the K_d^{EGTA} for a pH of 7.4 at 37°C (K_d^{EGTA} = 43.7 μM) and the calculation instructions provided in the kit, calculate the concentration of free calcium corresponding to each addition of high concentration calcium solution, remembering to account for the change due to the presence of ethanol.

   The calibration curve generated can be used to determine the absolute calcium concentration corresponding to the Indo-1 fluorescence ratio in a cell.

ANALYSIS OF INTRACELLULAR CALCIUM IN INDIVIDUAL GLIAL CELLS USING FLUO-3/AM

ALTERNATE PROTOCOL

When a laser with UV excitation capability is not available, or the imaging equipment does not have the ability to detect fluorescence simultaneously at two different wavelengths, Fluo-3 can be used as a calcium probe. This probe displays an increase in fluorescence quantum yield, and therefore an increase in fluorescence, when bound to calcium. With this method, the calcium measurements are highly dependent upon the dye loading, in contrast to methods that use ratiometric dyes, such as Indo-1 and Fura-2.

Additional Materials *(also see Basic Protocol 2)*

2 μM Fluo-3/AM solution, in loading buffer
35-mm plastic tissue culture dishes
Inverted, scanning confocal microscope equipped with mercury arc lamp or argon ion laser capable of emission wavelength of 488 nm
530/20-nm band pass filters

Prepare and load cells

1. Prepare and treat cells (Basic Protocol 2, step 1), substituting 35-mm dishes for coverslip chambers and Fluo-3/AM for Indo-1/AM.
2. Tune the laser to excite at 488 nm and insert filters (530/20-nm band pass filters) such that the emission intensity at 530 nm can be quantitated.
3. Load cells with Fluo-3/AM solution (see Basic Protocol 2, steps 5 to 8, but substituting Fluo-3/AM solution for the Indo-1/AM solution).

Measure intracellular fluorescence

4. Secure the tissue culture dish on the microscope stage and focus under normal light. Conduct a preview scan to determine if the data acquisition settings are appropriate and adjust the focus such that fluorescence from cells is optimal.

   If expecting to see an increase in calcium levels following treatment, set parameters (see Basic Protocol 2) such that an increase in emission intensity can be detected.

Analyze fluorescence data

5. With an initial (baseline) image displayed on the computer monitor, encompass individual cells with an "area" tool (e.g., polygon or circle), and save the area as a template to apply to subsequent images. Use the computer software to integrate fluorescence within each area over time. Express the data as relative fluorescence intensity versus time. Save these values and export them to a spreadsheet program for subsequent analyses as desired.

   Data analysis can be done any time after experiment is finished.

REAGENTS AND SOLUTIONS

Use nanopure water or equivalent in all recipes and protocol steps. For common stock solutions, see ***APPENDIX 2A****; for suppliers, see* ***SUPPLIERS APPENDIX****.*

5-Bromodeoxyuridine (BrdU), 15 mM

Dissolve 46 mg BrdU in 10 ml water; freeze in 1-ml aliquots and store up to 2 weeks at −20°C in the dark.

Complete DMEM/5% and 10% FBS medium

Dulbecco's modified Eagle medium (DMEM; low-glucose, with HEPES) containing:

continued

5% or 10% (v/v) fetal bovine serum (FBS)
1% (v/v) penicillin/streptomycin solution (10,000 U penicillin/10 mg streptomycin/ml/0.9% NaCl)
Store up to 1 month at 4°C

Ethidium bromide staining solution, 100×

On the day of the experiment, dilute the 10 mg/ml ethidium bromide (Molecular Probes) 1:20 in water for a stock solution of 500 µg/ml. Protect from light until use.

Hoechst buffer

Dissolve in <1 liter :
8.53 g NaCl (0.146 M final)
12.11 Tris base (0.1 M final)
Adjust pH to 7.4 with HCl
Add:
1 ml of 500 mM (10.165 g/100 ml) $MgCl_2$ stock solution
2.0 g bovine serum albumin (BSA; 0.2% w/v final)
1 ml Igepal CA-630 (0.1% w/v final)
5.9 mg Hoechst 33258 (5.9 µg/ml final)
Bring up to 1 liter with H_2O and store up to 1 month in a light-shielding container at 4°C

Krebs' bicarbonate buffer

To prepare 10× stock solution combine the following:
70.14 g NaCl
3.5 g KCl
1.91 g $CaCl_2$
1.63 g KH_2PO_4
2.96 g $MgSO_4 \cdot 7H_2O$
21.08 g glucose
Bring up to 1 liter with H_2O

This 10× stock solution can be made in advance and refrigerated (4°C) for a few months.

Working solution: On day of experiment, dilute 1 part 10× stock solution with 9 parts water, add 2.1 g/liter of $NaHCO_3$ and adjust the pH to 7.4 with HCl.

This will give a buffer solution that is 120 mM NaCl, 4.7 mM KCl, 1.3 mM $CaCl_2$, 1.2 mM KH_2PO_4, 1.2 mM $MgSO_4 \cdot 7H_2O$, 11.7 mM glucose, and 25 mM $NaHCO_3$.

Loading buffer

100 ml 1× Krebs' bicarbonate buffer (working solution; see recipe) containing $NaHCO_3$
1.0 g fraction V bovine serum albumin (BSA; 1% w/v final)
Adjust pH to 7.4 with HCl
Store in aliquots up to 1 year at −20°C protected from light

The volume required depends upon the number of wells assayed. 100 ml each of the Krebs' bicarbonate buffer and the loading buffer is more than sufficient for 4 wells.

Serum-free medium

Dulbecco's modified Eagle medium (DMEM; low glucose, with HEPES)
1% (w/v) fatty acid–free, fraction V bovine serum albumin (BSA)
1% (v/v) penicillin/streptomycin solution (10,000 U penicillin/10 mg streptomycin/ml/0.9% NaCl)
Store up to 1 month at 4°C.

COMMENTARY

Background Information

This unit presents several methods in analytical cytology useful for evaluating the effects of toxicants on nervous system cells. Like spectrofluorimetry, flow cytometry and attached cell scanning confocal laser microscopy (SCLM) can make use of changes in dye fluorescence properties to indicate cellular responses to toxicant exposures. However, unlike spectrofluorimetry, which generates a single value for an entire population of cells, flow cytometry and SCLM allow for examination of the responses in individual cells. Although they require complex and expensive equipment, flow cytometry and SCLM are valuable tools to investigate the effects of toxicants on CNS cellular subtypes either temporally or spatially. The nature of the question being asked will dictate whether SCLM or flow cytometry is the appropriate methodological tool.

Cell-cycle analysis

Flow cytometric analysis of cell cycling by the BrdU/Hoechst method provides quantitative information on cell proliferation, including data on the fraction of cycling cells, the number of cycles any given cell has completed, and cell-cycle phase distribution. Glial cells are incubated with BrdU, a thymidine analog that is incorporated into DNA during DNA synthesis, and are exposed to both Hoechst 33258, a fluorescent DNA stain that binds preferentially to AT base pairs, and ethidium bromide, a DNA-intercalating flurochrome. Because Hoechst fluorescence is quenched by BrdU, cells that have undergone one or more rounds of DNA replication during BrdU incubation can be distinguished from nonproliferating cells by their diminished Hoechst fluorescence. However, ethidium bromide fluorescence is not quenched by BrdU and is proportional to the amount of DNA present in the cell. Its fluorescence is minimal when cells are in the G0/G1 phase, increases during the S phase, and is maximal in the G2 phase, while it is independent of the number of mitotic cell divisions. Therefore, the use of BrdU/Hoechst and ethidium bromide in combination allows for the separation of G0, G1, S, and G2/M phases of the cell cycle for three complete cell cycles, and also allows the determination of the length of time in each phase (Rabinovitch, 1983).

The method described here is a useful tool in toxicology as it is able to reveal chemically or physically induced alterations or blocks in the cell cycle of synchronized cells. Neurooncology (M. Wei, M. Guizzetti, and L.G. Costa, unpub. observ.) and developmental neurotoxicology (Guizzetti and Costa, 1996) are two fields where this method has been applied to toxicology with positive results. With flow cytometry it is possible to test environmental exposures (either chemical or physical) for their ability to induce cell proliferation, and consequently, to be "tumor promoters" through an epigenetic mechanism. In addition, exposure to chemicals that have the ability to interfere with the cell cycle during brain development could lead to severe, long-lasting consequences for the neurobehavioral abilities of individuals, and the techniques described in this unit can be used to identify such chemicals.

This technique is also useful with unsynchronized cells. However, these flow cytograms are more difficult to interpret (Ormerod and Kubbies, 1992). Asynchronous Hoechst–ethidium bromide flow cytometric analysis has been applied in developmental neurotoxicology to examine the cell cycle kinetics of proliferating rat midbrain neuroepithelial cells exposed to either methylmercury or colchicine (Ponce et al., 1994). Use of flow cytometric Hoechst–ethidium bromide analysis is rapidly performed and provides greater information than radioactive [^{3}H]thymidine incorporation or single-parameter flow cytometry (Rabinovitch et al., 1988; Poot et al., 1990). Nevertheless, [^{3}H]thymidine incorporation, with its sensitivity in detecting DNA synthesis and its simplicity and relatively low cost, may be a better method for "routine" experiments (i.e., when information about cell cycle phase distribution or the length of cell cycle phases are not required).

To aid in the analysis and interpretation of the flow cytometric results, a positive control should be employed to monitor for variation between primary cell preparations and to ensure that the cells are responding as expected. Potential agents for use as positive controls for inhibiting cell cycling are the antimitotics, i.e., colchicine or benzimidazole analogs, or 5-azacytidine, an inhibitor of DNA synthesis. Fetal bovine serum (10%) added to the medium acts as a strong mitogen and can be used as a positive control for inducing a high percentage of cells to exit quiescence (see Fig. 12.5.1).

In addition to the protocol described here, other protocols can be designed to evaluate the time course of stimulation and provide temporal information about cell cycle characteristics fol-

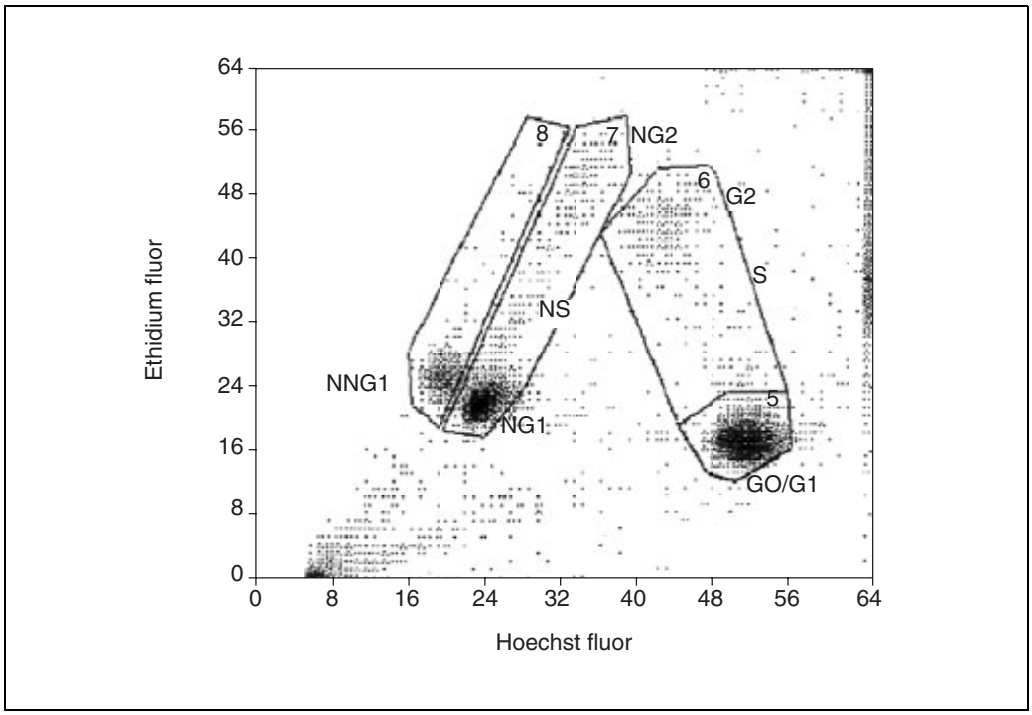

Figure 12.5.1 Flow cytometry plot for bivariate cell cycle analysis. Rat astrocytes in primary culture were stimulated with 10% FBS in the presence of BrdU for 48 hr. On the abscissa: Hoechst fluorescence emission. On the ordinate: ethidium bromide emission. G1: cells in Gap 1 phase; S: cells in synthesis phase; G2: cells in Gap 2/mitosis phases; NG1, NS, NG2: cells that have completed the first mitosis and are now in the second cell cycle (N = new); NNG1, NNS, NNG2: cells that have duplicated twice and are now in the third cell cycle.

lowing toxicant exposure. For example, it is possible to obtain information about the length of each phase of the cell cycle and to reveal abnormalities in these following toxicant exposure by incubating cells in the presence of BrdU for different lengths of time (Vogel et al., 1986).

Intracellular calcium measurement

The use of analytical cytology to measure intracellular calcium concentration allows the quantification of both basal and stimulant-mediated calcium content within individual subtypes of neural cells following toxicant exposure. The use of scanning confocal laser microscopy (SCLM) enables the researcher to distinguish between effects on the basis of the number of cells responding and the size of the maximal response, and to observe subtle effects on spatial and temporal changes in normal calcium responses following stimulation. Although the Alternate Protocol is useful, especially when the necessary excitation wavelengths for Indo-1 are not available, Basic Protocol 2 provides much more accurate quantitative data on absolute calcium levels, with few problems associated with photobleaching and interference from other ions and chemicals present. In the case of both Indo-1 and Fluo-3, the basic chemistry underlying their ability to act as calcium probes is their ability to chelate calcium. The principal difference between the two, however, is that the binding of calcium to Indo-1 results in a shift in the emission wavelength of the dye, whereas the binding of calcium to Fluo-3 increases the fluorescence intensity.

The protocols for measuring calcium provided here are only examples of many applications of SCLM as a tool in neurotoxicological research. Similar techniques, using different fluorescent probes, have investigated the levels of other ions, intracellular pH, levels of messenger RNA, cellular glutathione levels, and intercellular communication. Any of these techniques could be applied to the study of neurotoxicology using modifications to the basic protocols outlined here. Similarly, flow cytometric analysis is a useful tool in neurotoxicology beyond cell-cycle analysis; by use of various fluorescent probes and antibodies the effects of toxicants on various cellular aspects can be assessed at the single-cell or cell-population level. The techniques described in these protocols have been used in glial cells; however, they can also be used for other cell types, and in the case of SCLM, organotypic brain slices.

Some of the considerations in applying these techniques to other experimental systems are discussed below.

Critical Parameters and Troubleshooting

Many of the stains and probes used in these fluorescence assays are photolabile or cytotoxic when exposed to light. Therefore, precautions must be taken when carrying out these types of experiments to protect these compounds from light, and to protect the cells from excessive light exposure when they have been loaded or stained with the fluorescent dyes.

Flow cytometry

The method described for cell-cycle analysis is designed for primary cultures of rat astrocytes (Guizzetti et al., 1996). A similar protocol has been followed for flow cytometric analysis of the human astrocytoma 132 1N1 cell line. In this case, cells are reseeded at 5×10^4 cells/well, cultured in a complete 5% medium for 4 days, and then serum deprived. Astrocytoma cells are harvested using 0.05% trypsin. This method can be modified for use in other cell types. However, certain considerations must be made when doing so. For example, the optimal concentration of BrdU for continuous labeling is dependent on the cell type, and therefore experimental range-finding, with analysis of cytotoxicity, will be necessary to determine the optimal BrdU concentration. The extent of cell quiescence is also dependent upon the cell type studied. Although only 92% to 93% of primary rat astrocytes reach quiescence after 48 hr in serum-free medium, under the same conditions, almost all (>98%) 132 1N1 astrocytoma cells are in the G0/G1 phase, a difference that can be explained by the fact that astrocytes are usually able to produce autocrine growth factors.

A further concern for other cell types is the long duration of serum deprivation (48 hr prior to and 48 hr during BrdU incubation). If this extensive serum deprivation induces an unacceptable level of cell death (often seen as an increase in the number of nuclei with fluorescence intensity less than that of G0/G1 nuclei), it is possible to use a low serum concentration (i.e. 0.1% FBS) to induce quiescence in the cells. However, this problem can be avoided by studying asynchronous cultures. If it is not possible or desirable to artificially synchronize the cell cultures under investigation, single-parameter analysis (to determine cell cycle phase distribution) combined with dual-parameter analysis, to examine successful completion of cell division, can be used to obtain information on cell-cycle kinetics (Ponce et al., 1994).

The density of cells in suspension should be adjusted so as to provide an optimal sampling rate for the flow cytometer. In this case, the authors use $1–2 \times 10^6$ cells/ml with a sampling rate of ~300 cells/sec, which requires a minimum of 0.5 ml of cellular suspension. If the cell density is lower than this, analyzing each sample will take more time (because of slower sampling rate) or require a higher pressure to achieve the same sampling rate (which can decrease the quality of the results). In contrast, a very high cell density can result in clogging of the machine and poor reproducibility; dilution of cells in dye-containing buffer can correct for this situation. If the experimental conditions under investigation either inhibit cell proliferation or cause cytotoxicity, additional cells should be plated and harvested in order to obtain the volume and density of cells required for analysis.

Although sample preparation for cell cycle analysis is relatively straightforward, some precautions must be taken in this preparation. It is advisable to prepare each treatment in triplicate in case problems arise and samples are lost. It is also important to ensure that trypsinization is complete in order to obtain a good cell yield and avoid cell clumping, as this can give spurious flow cytometric results and clog the machine. Incomplete trypsinization is especially a problem when using primary cultures as these cells tend to have stronger cell-cell adhesion than is typical with transformed cells. Should clumping be a problem, repeated passage of the cells through a 26- to 28-G needle prior to flow cytometric analysis or slightly longer trypsinization time during harvest (e.g., 10 min) should be attempted.

Care must also be taken to avoid aspirating the pellet following centrifugation. Both harvest and centrifugation are made more difficult by the need to carry them out in the absence of direct light, although sodium lamp illumination will not cause BrdU-induced cytotoxicity and may facilitate these procedures.

Another problem that can occur during sample preparation is insufficient entry of the Hoechst stain into the cells due to an inadequate concentration of detergent (Igepal CA-630). If this occurs there will be no detection of Hoechst-associated fluorescence during flow cytometric analysis. Slightly increasing the amount of detergent, or staining the cell suspension for a longer period of time before analysis (e.g., by freezing the sample in the presence of 10%

Table 12.5.1 Affinity Constants (K_d) for Indo-1 at Varying pH

	pH = 5.5	pH = 6.0	pH = 6.5	pH = 7.0	pH = 7.4
K_d	5.75	6.28	6.48	6.61	6.75

Adapted from Lattanzio (1990).

Table 12.5.2 Affinity Constants (pK_ds) for Various Chelators and Cations, pH = 7.0, 37°C

Chelator	Mg	Ca	Mn	Fe	Co	Ni	Cu	Zn
EGTA[a]	5.2	11.0	12.1	11.8	12.3	11.8	17.7	12.9
EDTA[a]	5.4	7.3	10.7	10.9	12.7	15.3	15.5	13.1
Indo-1[b]	—	6.6	—	—	—	—	—	9.8
TPEN[c]	1.7	4.4	10.27	14.61	—	—	—	15.58
Fura-2[d]	—	6.6	—	—	—	—	—	8.0-8.1

[a]Dawson et al., 1986.

[b]Jefferson et al., 1990.

[c]Arslan et al., 1985.

[d]Grynkiewicz et al., 1985.

DMSO in Hoechst buffer) can solve this problem.

A caution regarding the use of agents that are incorporated into DNA during DNA synthesis, including both BrdU or [^{3}H]thymidine, is warranted if the toxicant or exposure conditions under investigation cause or promote DNA repair or unscheduled DNA synthesis. Because DNA is synthesized for other reasons besides cell division, exposure conditions that lead to such incorporation of either BrdU or [^{3}H]thymidine into DNA can cause spurious results upon cell-cycle analysis (with either scintillation counting, autoradiography, or flow cytometry).

Scanning confocal laser microscopy

Indo-1 has a peak emission in the calcium-free form of 475 nm. As Indo-1 binds calcium, this peak shifts towards lower wavelengths. The calcium-independent emission wavelength (i.e., the isosbestic point) is ~450 nm. However, rather than monitor changes in peak fluorescence intensity at 475 nm, the dynamic range may be increased for this dye by examining changes in emission at 530 nm, because the fluorescence diminishes at a proportionately greater rate with small increases in calcium at this wavelength as compared to 475 nm (Rabinovitch and June, 1990).

Several issues regarding Indo-1 loading should be raised. First, excessive loading of Indo-1 may lead to calcium buffering and underestimation of response following signaling. Moreover, excessive Indo-1 loading may lead to incomplete intracellular hydrolysis of Indo-1/AM (Lückoff, 1986). Because the Indo-1/AM also exhibits fluorescence properties (that are not responsive to changes in intracellular calcium), excessive incomplete hydrolysis can lead to spurious results. Second, loading of Indo-1 for long-periods of time can lead to Indo-1 intracellular compartmentalization. However, Indo-1/AM loading times may vary among different cells depending upon the activities of nonspecific esterases in the cells that cleave the acetoxymethylester (AM) group and release the active calcium probe.

Under optimal circumstances, Indo-1, Fura-2, Fluo-3, and other fluorochromes undergo fluorescence property changes upon binding calcium. However, the fluorescence properties and the calcium affinity of these dyes may be affected by such factors as temperature, pH (Table 12.5.1), viscosity, and the presence of other factors in the incubation medium (Table 12.5.2), including other divalent cations (Tsien, 1989; Owen et al., 1991; Bancel et al., 1992). Because of the sensitivity of Indo-1 cation affinities and emission spectral properties to their environment, cell-free analyses to evaluate the interaction of Indo-1 with experimental medium components are advised. Such evaluations can be conducted using spectrophotometric analysis

of Indo-1 or Fluo-3 free acids over the full spectral range of fluorescence emission in the presence and absence of medium components.

There has been criticism of the use of a cell-free method for construction of a calcium calibration curve, with some concern over the differences in viscosity between buffer and cells, which could affect the responsiveness of Indo-1 to changes in calcium concentration. To address this issue it has been suggested that 20% ethanol be used during calibration, as some of the viscosity problems have been shown to be corrected for by the addition of ethanol to buffers during calibration curve generation (Popov et al., 1988).

While Indo-1 and other calcium-sensitive fluorochromes have a relatively high specificity for calcium, they can also bind a number of other divalent cations (Table 12.5.1). Because the spectral properties of Indo-1 are affected by both the cation species present and dye concentration, evaluation of changes in the Indo-1 405 nm/530 nm emission ratio alone may not allow evaluation of the relative impact other divalent cations may have on the measured fluorescence. To determine whether other divalent cations may be affecting Indo-1 fluorescence (independent of calcium), one may monitor fluorescence changes at the Indo-1 isosbestic point (~450 nm), as changes in Indo-1 fluorescence intensity at this point cannot be attributed to calcium and may indicate interference due to other cations. Specific chelators can also be used to avoid confounding of the calcium signal by other cations. For example, tetrakis-(2-pyridylmethyl)ethylenediamine (TPEN), a relatively selective zinc chelator (Table 12.5.2), can be used in moderate zinc levels to prevent its interference with the Indo-1 fluorescence. Cell-free analyses demonstrate no direct effect of TPEN on Indo-1 fluorescence (Owen et al., 1991; Ponce, R.A. and Kavanagh, T.J., unpub. observ.).

A cell-type dependent problem that may be encountered when working with calcium probes is dye extrusion. For example, 132 1N1 astrocytoma cells do not extrude Indo-1, whereas primary rat astrocytes cultured in this laboratory required coincubation with probenecid to avoid extrusion of this dye from the cells (Gafni et al., 1997). In some cases, this efflux is mediated by organic anion transporters and can be prevented by the addition of inhibitors of this pump, such as probenecid or sulphinopyrazone (DiVirgilio et al., 1988, 1990; Arkhammar et al., 1990). In other cell types, P-glycoprotein is responsible for the extrusion of calcium probes; in these cases, this extrusion can be inhibited by addition of verapamil or cyclosporin (Brezden et al., 1994).

In addition to cell-type specific Indo-1 efflux, membrane damage may lead to dye release from cells or allow influx of non-calcium extracellular cations. To examine the role of membrane damage on intracellular Indo-1 fluorescence, Mn^{2+} addition to extracellular medium has been used as this ion will only enter the cell if the membrane is damaged. Because Mn^{2+} quenches Indo-1 fluorescence across all wavelengths, examination of cellular Indo-1 fluorescence in the absence and presence of Mn^{2+} can be used as an indicator of nonspecific membrane damage.

When performing kinetic analyses of intracellular calcium, the focus of the microscope may change or the field of observation may be shifted; such effects are especially likely to occur at the time when a stimulus is added and can confound the interpretation of Indo-1 fluorescence data. Successive fluorescence images should be watched throughout the collection period to ensure that the fluorescence intensity displayed by both detectors does not abruptly decrease, indicating a loss of focus, in which case the experiment must be repeated. It is also useful to look at the fluorescence data from individual detectors over the entire time course of the experiment to establish that any change in fluorescence seen is due to the treatment and not due to photobleaching or dye loss. One must be careful not to scan too long or with excessive excitation intensity, either during preview scans or during the experiment, as this may cause photobleaching of the dye. Under the conditions described here, this is usually not a problem with Indo-1, as it is fairly resistant to photobleaching.

One must ensure that the tissue culture dishes being used do not interfere with passage of exciting or emitted light. If the cells have a substantially higher-than-expected basal calcium level, this may be due to cellular autofluorescence. This can be corrected for by subtracting the average autofluorescence readings obtained from cells which have not been loaded with Indo-1 or Fluo-3.

Anticipated Results

The protocols described in this unit will provide the researcher with data at the individual cell level. All the protocols will qualitatively assess the effects of compounds on various aspects of cellular activity and generate figures that can indicate visually the effects of the treatments. In addition, the two basic protocols can

Table 12.5.3 Distribution of Cells in the Cell Cycles[a]

	Cell number	% of total (raw data)	% of total (adjusted data)
First cell cycle	4913	50.1	68.5
Second cell cycle	4155	42.3	28.9
Third cell cycle	744	7.6	2.6

[a]The data are expressed both as proportions of the cells present at the time of analysis ("raw data") and as "adjusted data" obtained by accounting for the number of cell divisions undergone by cells (reflecting the proportion of cells originally placed in culture).

be analyzed quantitatively to determine absolute numbers of cells in particular cell-cycle stages and absolute calcium levels and changes, in the flow cytometric experiments and SCLM experiments respectively. Details of the expected results from these two protocols are given below.

Flow cytometry

In a typical experiment, cell-cycle compartments are analyzed by plotting the Hoechst-associated fluorescence (abscissa) against ethidium bromide–associated fluorescence (ordinate). Figure 12.5.1 shows an example of cell cycle flow cytogram using bivariate (Hoechst/ethidium bromide) analysis. During DNA synthesis (S-phase), the nuclear DNA content increases; this can be observed as an increase in ethidium bromide fluorescence and a decrease in Hoechst-associated fluorescence due to the incorporation of BrdU into DNA. The G2/M phase, when all the DNA is duplicated and the cells undergo cell division, can be observed as the maximal ethidium bromide/Hoechst fluorescence (because both G2 and M have 2× DNA, they cannot be distinguished with the flow cytometric technique). Division of the cells corresponds to a drop in ethidium bromide fluorescence, a further decrease in Hoechst fluorescence (new G1 phase), and a consequent shift of the cell population to the left and down on the graph.

G0, G1, S, and G2/M phases of each of three successive cell cycles can be quantified by analysis of the respective regions of the two-parameter flow cytograms. The correct number of proliferating cells is obtained by dividing the number of cells in the second or third cycle by two and four, respectively, because in these cases the cell number is the result of one mitosis (second cycle) or two mitoses (third cycle) occurring from the beginning of BrdU incubation (Table 12.5.3). The number of noncycling G0-phase cells can be obtained by quantifying the number of G0/G1 cells that have failed to incorporate BrdU.

Scanning confocal laser microscopy

Kinetic analysis of intracellular calcium with confocal microscopy generates data from which a number of endpoints can be quantified. The scans prior to addition of the stimulant can be used to compare basal calcium levels between treated and untreated cells. The initial calcium spike can be assessed for the percentage of cells responding to the stimulus, the rate of the calcium increase, and the maximal response; these endpoints can be used to compare the control and toxicant-treated cells. It is important to assess the effect of the toxicant on the basal calcium level to properly interpret any effects on the maximal response. In addition, the effect of the toxicant on the total calcium present across time (area under the time-versus-fluorescence-intensity/calcium concentration curve), and on intracellular calcium oscillations, if present, can be determined (Barhoumi et al., 1995). An example of expected results is provided in Table 12.5.4. These calcium measurements were obtained in 132 1N1 human astrocytoma cells, using 0.01 mM carbachol as a stimulant, under control conditions or following a 24-hr incubation with the specified concentration of ethanol. Note that results, including the basal calcium concentration, will vary depending upon cell type.

The absolute $[Ca^{2+}]_i$ can be calculated using Basic Protocol 2 for calcium measurement and Support Protocol 2 for generation of a calibration curve. While the Alternate Protocol with Fluo-3 as a probe is not as quantitative, relative changes in $[Ca^{2+}]_i$ over time can be determined. Whether one uses Indo-1 or Fluo-3, pseudocolor images can be generated by most software packages, and this provides a visually interpretable assessment of the spatial/temporal effects of substances on normal calcium homeostasis.

Table 12.5.4 Expected Calcium Measurements[a]

[Ethanol] (mM)	Basal [calcium] (nM)	% cells responding	Average amplitude of response (% of basal)	Area under curve
0	67	92	498	22
25	71	43	257	17
250	83	53	236	7

[a]Measurements are made following stimulation with 0.01 mM carbachol in human 132 1N1 astrocytoma cells, under control conditions, or following a 24-hr incubation with ethanol. Experiments were carried out in calcium-free Krebs' buffer. Ethanol was present at the time of addition of carbachol. Results were analyzed to determine the basal calcium concentration, the percentage of cells responding to carbachol, the average amplitude of the response, and the area under the curve.

To study the role of extracellular calcium in the intracellular calcium response to stimuli, incubations with EGTA, EDTA, or other membrane-impermeable cation chelators are often useful. However, as these chelators may also deplete intracellular calcium over time, baseline studies should be conducted to determine whether use of the chelator is depleting intracellular stores of calcium over the experimental observation period. In cases where extracellular calcium is required to maintain steady-state intracellular calcium concentrations, special calcium-buffering systems may be applied (Denny and Atchison, 1996).

Using the protocols outlined here, kinetic analysis can be carried out to allow investigation of acute toxicant effects on intracellular calcium levels. In this case, no pretreatment is done, and the toxicant is added after establishing a baseline calcium level. With this protocol, analyses may be made of the percentage of cells affected, the rate of $[Ca^{2+}]_i$ increase/decrease, the maximal response, total calcium changes integrated over time, and any oscillatory effects that the compound causes. In addition, calcium changes within specific intracellular compartments and in specific areas within the cytosol can be assessed using confocal microscopy and calcium-sensitive dyes. If the researcher is not interested in temporal changes in calcium or the effect of a toxicant on calcium responses, but is simply interested in effects on resting calcium levels, a kinetic analysis is not necessary, and scans of multiple fields can be carried out to determine the effects of the toxicant on basal $[Ca^{2+}]_i$ in many cells.

Time Considerations

Flow cytometry

The total time for the flow cytometric procedure will vary depending on experimental and culture conditions. Treating the cells with mitogens and BrdU will take ~10 min for 24 samples (each treatment in triplicate). Harvesting, centrifuging, and resuspending cells in buffer will take 30 min. Staining the cells with ethidium bromide will take 15 min. Flow cytometric analysis of each sample will take 2 to 10 min of actual machine time per sample to collect data from 10,000 cells (depending on sampling rate and cell density). Data analysis will take ~1 hr.

Scanning confocal laser microscopy

The total time for SCLM is also dependent upon the culture conditions and experimental design being studied. Once cells have been serum deprived and pretreated (if desired) with toxicant, the experiment should take from 3 to 6 hr, depending upon loading conditions required for the cell type and the number of treatments studied. Preparation of the stock solutions can be done in advance to save time. Once cells have been loaded with dye, quantification of the fluorescence on the microscope can take 5 min, or longer if many time points are desired. It is important to remember to stagger experiments in different plates; thus the more plates that are to be examined, the longer the experiment. Due to the many solution changes and the need to stagger incubations, scanning many wells may become logistically difficult; it is not recommended that >10 wells be scanned in a given experiment.

Literature Cited

Arkhammar, P., Nilsson, T., and Berggren, P.O. 1990. Glucose-stimulated efflux of Indo-1 from pancreatic β-cells is reduced by probenecid. *FEBS Lett.* 273:182-184.

Arslan, P., Di Virgilio, F., Beltrame, M., Tsien, R.Y., and Pozzan, T. 1985. Cytosolic Ca^{2+} homeostasis in Ehrlich and Yoshida carcinomas. *J. Biol. Chem.* 260:2719-2727.

Bancel, F., Salmon, J.-M., Vigo, J., and Viallet, P. 1992. Microspectrofluorometry as a tool for in-

vestigation of non-calcium interactions of Indo-1. *Cell Calcium* 13:59-68.

Barhoumi, R., Bailey, R.H., and Burghardt, R.C. 1995. Kinetic analysis of glutathione in anchored cells with monochlorobimane. *Cytometry* 19:226-234.

Brezden, C.B., Hedley, D.W., and Rauth, A.M. 1994. Constitutive expression of P-glycoprotein as a determinant of loading with fluorescent calcium probes. *Cytometry* 17:343-348.

Dawson, R.M.C., Elliot, D.C., Elliot, W.H., and Jones, K.M. 1986. Data for Biochemical Research, 3rd ed. Oxford University Press, Oxford.

Denny, M.F. and Atchison, W.D. 1996. Mercurial-induced alterations in neuronal divalent cation homeostasis. *Neurotoxicology* 17:47-61.

DiVirgilio, F., Fasolato, C., and Steinberg, T.H. 1988. Inhibitors of membrane transport system for organic anion blocks Fura-2 excretion from PC12 and N2A cells. *Biochem. J.* 256:959-963.

DiVirgilio, F., Steinberg, T.H., and Silverstein, S.C. 1990. Inhibition of Fura-2 sequestration and secretion with organic anion transport blockers. *Cell Calcium* 11:57-62.

Gafni, J., Munsch, J.A., Lam, T.H., Catlin, M.C., Costa, L.G., Molinski, T.F., and Pessah, I.N. 1997. Xestospongins: Potent membrane permeable blockers of the inositol 1,4,5-trisphosphate receptor. *Neuron* 19:723-733.

Grynkiewicz, G., Poenie, M., and Tsien, R.Y. 1985. A new generation of Ca^{2+} indicators with greatly improved fluorescent properties. *J. Biol. Chem.* 260:3440-3450.

Guizzetti, M. and Costa, L.G. 1996. Inhibition of muscarinic receptor-stimulated glial cell proliferation by ethanol. *J. Neurochem.* 67:2236-2245.

Guizzetti, M., Costa, P., Peters, J., and Costa, L.G. 1996. Acetylcholine as a mitogen: Muscarinic receptor-mediated proliferation of rat astrocytes and human astrocytoma cells. *Eur. J. Pharmacol.* 297:265-273.

Jefferson, J.R., Hunt, J.B., and Ginsberg, A. 1990. Characterization of Indo-1 and Quin-2 as spectroscopic probes for Zn^{2+}-protein interactions. *Anal. Biochem.* 187:328-336.

Lattanzio, F.A. 1990. The effects of pH and temperature on fluorescent calcium indicators as determined with Chelex-100 and EDTA buffer systems. *Biochem. Biophys. Res. Commun.* 171:102-108.

Lückoff, A. 1986. Measuring cytosolic free calcium concentration in endothelial cells with Indo-1: The pitfall of using the ratio of two fluorescence intensities recorded at different wavelengths. *Cell Calcium* 7:233-248.

Ormerod, M.G. and Kubbies, M. 1992. Cell cycle analysis of asynchronous cell populations by flow cytometry using bromodeoxyuridine label and Hoechst-propidium iodide staining. *Cytometry* 13:678-685.

Owen, C.S., Sykes, N.L., Shuler, R.L., and Ost, D. 1991. Non-calcium environmental sensitivity of intracellular Indo-1. *Anal. Biochem.* 192:142-148.

Poenie, M. 1990. Alteration of intracellular Fura-2 fluorescence by viscosity: A simple correction. *Cell Calcium* 11:85-91.

Ponce, R.A., Kavanagh, T.J., Mottet, N.K., Whittaker, S.G., and Faustman, E.M. 1994. Effects of methyl mercury on the cell cycle of primary rat CNS cells in vitro. *Toxicol. Appl. Pharmacol.* 127:83-90.

Poot, M., Hoehn, H., Kubbies, M., Grossmann, A., Chen, Y.C., and Rabinovitch, P.S. 1990. Cell cycle analysis using continuous bromodeoxyuridine labeling and Hoechst 33258-ethidium bromide bivariate flow cytometry. *Methods Cell Biol.* 33:185-198.

Popov, E.G., Gavrilov, I.Y., Pozin, E.Y., and Gabbasov, Z.A. 1988. Multiwavelength model for measuring concentration of free cytosolic calcium using the fluorescent probe Indo-1. *Arch. Biochem. Biophys.* 261:91-96.

Rabinovitch, P.S. 1983. Regulation of human fibroblast growth rate by both noncycling cell fraction and transition probability is shown by growth in 5-bromodeoxyuridine followed by Hoechst 33258 flow cytometry. *Proc. Natl. Acad. Sci. U.S.A.* 80:2951-2955.

Rabinovitch, P.S. and June, C.H. 1990. Measurement of intracellular free calcium and membrane potential. *In* Flow Cytometry and Cell Sorting (M.R. Melamed, T. Lindmo, and M.L. Mendelsohn, eds.) pp. 651-668. John Wiley & Sons, New York.

Rabinovitch, P.S., Kubbies, M., Chen, Y.C., Schindler, D., and Hoehn, H. 1988. BrdU-Hoechst flow cytometry: A unique tool for quantitative cell cycle analysis. *Exp. Cell Res.* 174:309-318.

Tsien, R.Y. 1989. Fluorescent probes of cell signalling. *Annu. Rev. Neurosci.* 12:227-253.

Vogel, D.G., Rabinovitch, P.S., and Mottet, N.K. 1986. Methylmercury effects on cell cycle kinetics. *Cell Tissue Kinet.* 19:227-242.

Key References

Rabinovitch and June, 1990. See above.

Describes parameters for loading calcium-sensitive dyes and their detection.

Rabinovitch et al. 1988. See above.

Describes rationale and technique for BrdU/Hoechst cell cycle analysis.

Contributed by Michelle C. Catlin, Marina Guizzetti, Rafael A. Ponce, Lucio G. Costa, and Terrance J. Kavanagh
University of Washington
Seattle, Washington

Estimating Cell Number in the Central Nervous System by Stereological Methods: The Optical Disector and Fractionator

Recent advances in stereology methods allow truly unbiased estimates of the total cell and synapse number within discrete structures of the central nervous system (CNS). These new advances, based upon the disector and fractionator tools, combine unbiased counting frames, unbiased systematic random sampling, and unbiased estimates of the structure (reference) volume to produce the final estimate of total number. The estimates are unbiased because the experimental methods employed are design-based as opposed to the previously available model–based methodologies. No assumptions inherent in model-based procedures are employed. Hence the final estimates are not biased by any known or unknown assumptions about the model.

The methods are also very efficient. Proper sampling design, featuring systematic random sampling, requires that only between 100 and 300 particles (e.g., cells or synapses) per structure actually be counted. Additional effort (counting) will usually not significantly improve the results because inherent biological interanimal variation begins to predominate over the observed variation within a treatment group, once these initial 100 to 300 particles have been counted. This type of biological interanimal variation cannot be reduced by additional sampling.

Previously, the only unbiased method available for determining total cell or synapse number required complete serial reconstruction of the region of interest. This method involves no sampling or estimation. Cells or synapses are directly counted during reconstruction. Although capable of being performed in an unbiased and accurate manner, serial reconstruction is decidedly inefficient because of the enormous amount of labor required. All other previously available methods, including profile counting, profile densities, profile ratios, and the model-based methods of Abercrombie or Konigsmark, are recognized as producing either estimates with unknown amounts of bias or inaccurate results (Williams and Rakic, 1988; Coggeshall and Lekan, 1996). This unit contains protocols for estimating total cell number by optical fractionation (see Basic Protocol), N_v,V_{ref} (see Alternate Protocol 1), and physical disector (see Alternate Protocol 2), as well as glycolmethacrylate embedding (see Support Protocol 1) and Giemsa staining (see Support Protocol 2).

The stereology methods that are featured in this unit entail several concepts that are defined as follows.

Reference volume: The reference volume (V_{ref}) is the volume of the entire structure of interest. The entire structure of interest must be available at the initial stages of the sampling hierarchy. If an unknown portion of the entire structure is unavailable for sampling, then it is not possible to determine the absolute number of particles in that structure, simply because that missing region remains unknowable (see Commentary).

Optical disector: The optical disector consists of an unbiased counting frame (Fig. 12.6.1). The boundaries of the frame are determined by the exclusion lines (heavy lines in Fig. 12.6.1) and their extensions (indicated by the arrowheads in Fig. 12.6.1). Any particle (e.g., a neuron cell body) that touches the forbidden lines (i.e., out of bounds) is not counted, whereas any particle inside the frame or touching the in-bounds boundary lines is counted. Particles that touch the forbidden lines belong to the adjacent disector(s), which in practice are never used; however, one should imagine that the entire surface of

Contributed by Jay S. Charleston
Current Protocols in Toxicology (2000) 12.6.1-12.6.19

the tissue section had been tiled in disector frames. These rules ensure that each particle has the potential of being counted only once.

The disector frame is optically focused through the central portion of a relatively thick tissue section (e.g., 20 to 70 μm), and particles are counted as they come into focus. Moving the focal plane in effect turns the lines of the disector frame (i.e., in bounds and forbidden lines) into in-bounds and forbidden planes and creates a counting volume (see Fig. 12.6.2). The bottom plane of the disector volume also forms a forbidden plane. Particles touching this plane, by rule, belong to the disector volume associated with a

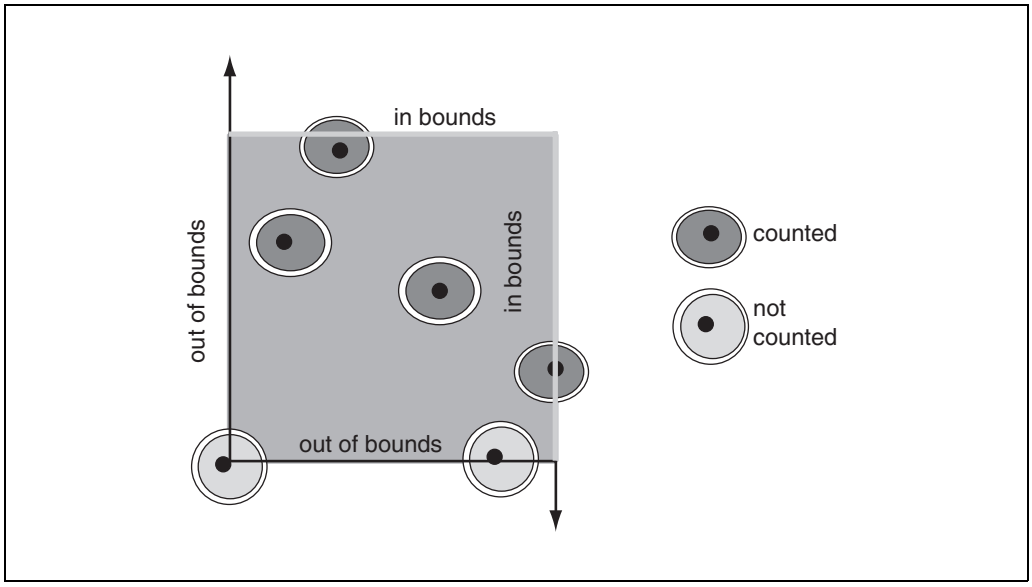

Figure 12.6.1 Disector frame and counting rules. The left and lower sides of the disector frame represent out of bounds lines. Note that the extensions of these two lines, represented by the arrows, are also out of bounds. Particles touching these lines are not counted. Particles touching the shaded area, including the in-bounds lines, are counted.

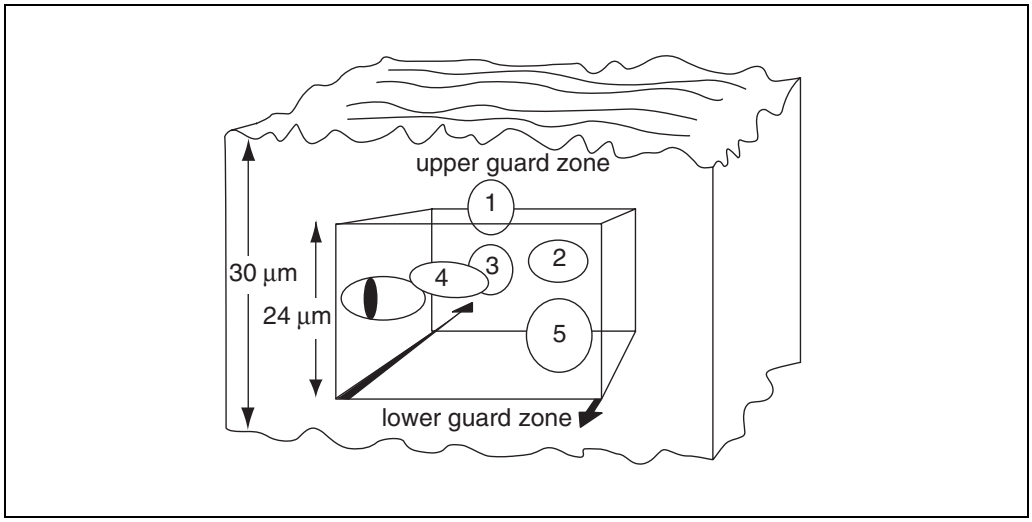

Figure 12.6.2 Optical disector. The disector frame is "moved" through the center of a relatively thick tissue section by focusing the microscope. The movement of the frame creates a counting volume. The out of bounds lines of the frame create out of bounds planes. By rule, the bottom plane is also out of bounds. The example here shows five objects belong to this volume. The sixth object intersects the out of bounds left plane (shaded area) and is not counted. The top and bottom surfaces of the section are not part of the counting volume (they are separated by guard zones), hence defects (e.g., chatter, pits) do not interfere with the counting.

disector that could have been placed immediately below the current disector (in practice this disector is also never used). The disector is a number-weighted counting probe that samples particles independently of their size or orientation.

Fractionator: The fractionator is an integral part of the sampling procedure. It is based on the simple premise that any quantity determined for a known (usually small) fraction of the entire structure can be used to determine the quantity in the entire structure by multiplying this determined quantity by the inverse of the sample fraction from which it was derived. The fractionator is ideally suited for combining with unbiased systematic random sampling (see below), which in turn can be readily combined with commonly practiced histology techniques. The optical disector can be combined with the fractionator principle to directly estimate particle number (i.e., the optical fractionator) or can be used to generate a numerical density (number counted per volume, N_v) estimate of the particles. This N_v estimate can in turn be combined with a volume estimate derived with the fractionator principle (V_{ref}) to produce an estimate of total number (the so-called N_v,V_{ref} method; see Alternate Protocol 1).

Systematic random sampling: Systematic random sampling is employed throughout the sampling hierarchy. It is random because the position of the first sample at each stage of the sampling hierarchy is determined by random chance. It is systematic in that all subsequent samples are systematically determined after the first random position has been established. For example, if an adult rat brain were slabbed in the coronal plane at 1-mm intervals, ~≥20 slabs could be expected. If every third slab were desired, a random number between 1 and 3 would be generated. If 2 were selected, then the 2nd, 5th, 8th, 11th,... slab would be selected at this sampling stage. The systematic random sampling extends across the entire sampling procedure (brain slabbing, sectioning, and disector placement;

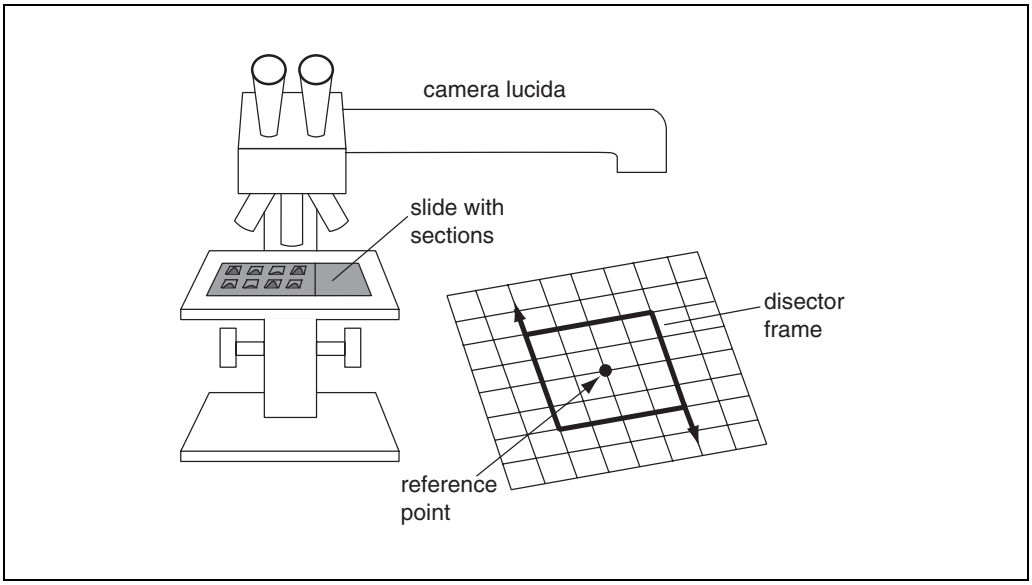

Figure 12.6.3 Optical disector microscope. A relatively inexpensive optical disector microscope can be established by projecting an image of a point grid and disector over the image of the tissue section by use of a camera lucida (drawing tube). At relatively low power, intersections of the grid lines can be counted as points for estimating the surface area of the tissue sections examined. A high-power oil-immersion lens is used when counting with the disector frame. The reference point, placed at the center of the optical path of the microscope, can be used in conjunction with the point grid to facilitate a systematic stepping across the section for placement of each disector (see Fig. 12.6.5). The linear tracking device for measurement of movement of the microscope in the *z*-axis is not shown. Mechanized stages and computer-aided video systems can also be utilized to automate these steps (e.g., see West, 1993b; Pakkenberg and Gundersen, 1997).

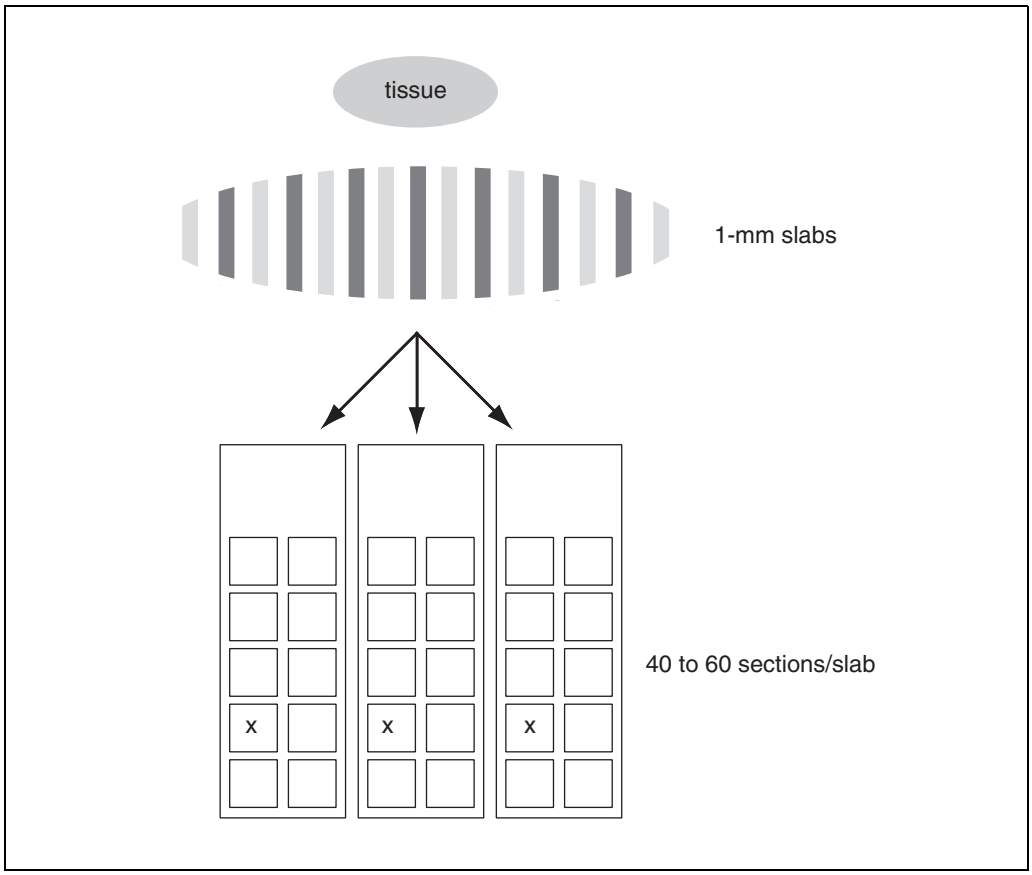

Figure 12.6.4 Systematic random sampling. A structure is systematically cut into equal slabs. In the example of a sampling design presented here, it was determined that every other slab should be sampled, and every 10th section examined. For the slabs, a random number between one and two is drawn (in this case it was 2). Therefore the 2nd, 4th, 6th, ...14th slabs are selected, embedded and sectioned. For the sections, a second random number between 1 and 10 is drawn (in this case it was 4). Therefore, the fourth section on each slide (*x*) is sampled for counting.

Fig. 12.6.3 and Fig. 12.6.4). Systematic random sampling is fair in that all portions of the original structure have equal probability of being sampled.

BASIC PROTOCOL

ESTIMATING TOTAL PARTICLE NUMBER USING OPTICAL FRACTIONATOR

The instructions for counting, provided below, represent the least demanding methods in terms of equipment for implementing the techniques. The disector counting frame and grids for disector placement can be generated by projecting them into the optical path of a microscope with the use of a camera lucida attachment (current prices for retrofitting a microscope range from ~$2,000 to $4,000; contact individual microscope manufacturer). The projected grid image can be used for stepping across the section for placing sequential disector frames. Commercially available software/hardware solutions are also available and can greatly automate the application of the methods (e.g., StereoInvestigator, MicroBrightField and Bioquant, R&M Biometrics). These solutions, featuring real-time digital-image capture, stepper-motor-driven computer-controlled microscope stages, and accessories, can cost between $30,000 and $50,000 without considering the cost of a microscope.

The optical fractionator (West et al., 1991; West, 1993a,b) combines the optical disector directly with the fractionator. The optical fractionator method is the method of choice, provided the structure of interest is represented by a naturally occurring boundary so that

a true nonarbitrary V_{ref} can be recognized (see Alternate Protocol 1 for N_v,V_{ref}, below). A point lattice is projected across the surface of a set of sections. A set of disectors is placed at every point. The ratio (fraction) of the area of the disector frame to the area per point in the point lattice is known. Therefore the sum of the total of the disector areas employed represents a known fraction of the total area of the structure (derived from the point lattice). A guard area (see Fig. 12.6.2) is established at the top and bottom of the optical disector. This fraction (disector height/section height) is also used as one component of the fractionator calculation. The number of particles counted in all the disectors is multiplied by the inverse of the known sampling fractions (including the slabs, sections, disector aerial fraction, and guard area fractions). The volume of the structure is never calculated and does not need to be calculated. This protocol represents a pure fractionator application and volume artifacts are not a confounding factor.

Materials

Test animal
4% (w/v) paraformaldehyde (see recipe), prepare fresh

Razor blades
Humidified chamber: Petri dish containing moistened filter paper *or* compartmented boxes (e.g., Brain Research Laboratories) filled with buffer
Sharp dissecting pins
Hand-operated microtome (e.g., Sorvall JB-4 or Reichert-Jung 820-II) with glass knives or disposable microtome razor blades (e.g., MB35, Shandon)
Frosted glass microscope slides (acid-cleaned in 5 N HCl for 2 min, then rinsed in H_2O)
70°C heated slide tray
Optical disector microscope
Tabletop linear tracking device (e.g., Microcator, Heidenhain)

Additional reagents and equipment for perfusion fixation (*UNIT 9.5*), glycolmethacrylate embedding (see Support Protocol 1) or cryosectioning (see *APPENDIX 3* for reference) and Giemsa staining (see Support Protocol 2)

Fix and isolate tissue

1. Perform whole-body perfusion of animal (*UNIT 9.5*) with freshly prepared 4% paraformaldehyde. Fix brain for 2 hr prior to dissection from skull to allow for dimensional stability prior to handling brain.

   Preservation of all particle types and structure (e.g., cell, synapse) is the goal. The only assumption inherent in these methods is that all target particles are preserved and that the actual boundaries of the structure of interest are preserved. It is not possible to count cells that are not preserved in the tissue and it is not possible to associate these particles with a structure whose boundaries cannot be recognized.

   The choice of fixative may be limited by requirements for other methodologies. For example, glutaraldehyde fixative may be required for optimal preservation of structure for ultrastructural examination of tissue (e.g., later characterization of synapse surface area). However, glutaraldehyde fixation may reduce immunocytochemical reactivity of the tissue.

   Immersion fixation may also be required (e.g., with human brain tissues). Several months of immersion fixation, featuring several changes of fixative, may be required to ensure adequate fixation of tissues prior to further sampling.

2. Cut the entire region of interest into systematic random slabs in the preferred plane with thin razor blades. Collect slabs in order and orientation generated (be careful not to flip left and right sides while collecting slabs) and place in a humidified chamber/box. Make a permanent physical mark (remote from target structure) with

a sharp dissecting pin after each slab is cut, which can be recognized later in the tissue sections.

Slabs should be maintained in a humidified chamber or held in compartmented boxes (e.g., Brain Research Laboratories) filled with buffer during collection to prevent surfaces from drying out as subsequent slabs are collected. Small humidified chambers can be constructed from Petri dishes fitted with filter paper that has been saturated with buffer. It is important to maintain the order of collected slabs.

Commercially available or custom-made cutting guides will greatly facilitate generation of uniform slabs (see Commentary). Embedding the entire brain in an agar matrix (see recipe) will stabilize the tissue during the slabbing step.

The use of long, thin razor blades knives (e.g., disposable microtome blades, MB35, Shandon) will facilitate a smooth cutting stroke and provide optimal surfaces of the slabs. Avoid compression and tissue distortion during this slabbing phase of the sampling. The surface of the cut slabs may yield sections that are selected later in the systematic random sampling hierarchy; therefore these faces must be preserved.

Small structures, such as a gestation-day 14 fetal mouse brains, can be conveniently processed in toto without any need for slabbing prior to processing.

3. Select a systematic random subsample of slabs (see Fig. 12.6.4).

The required frequency of slab sampling (e.g., every slab, every other slab) depends on the structure of interest and how much sequential slabs differ in regard to the particles to be counted. Several published examples featuring detailed analysis of the sampling strategy employed are available for consultation (see Commentary).

Slabs may be inspected with a stereomicroscope to ascertain which slabs contain the structure of interest. The slab before the first and after the last slab believed to contain the structure should also be embedded, as a precaution to ensure that the entire V_{ref} is collected.

Cut and prepare tissue sections

4. Section selected tissue slabs exhaustively (completely) using appropriate histology techniques.

Slabs may be embedded in paraffin or plastic (glycolmethacrylate is preferred; see Support Protocol 1), or cryosectioned. Paraffin-processed tissue is dimensionally unstable and should be avoided if possible. In addition, paraffin-processed tissue is difficult to section at thickness required for the optical disector. The less efficient physical disector (see Alternate Protocol 2) may be required for paraffin sections.

Entire slabs are serially and exhaustively sectioned.

5. Collect an appropriate systematic random subset of the sections on glass microscope slides.

For example every tenth section may be required at this stage of the sampling scheme. The fractionator concept requires that the fraction of the entire structure which is represented by the collected sections be known (hence the requirement that the collected slabs be exhaustively sectioned). Single "nice" histology slides will not suffice. Both the initial and trailing fragments of the individual slabs, as well as the full sections faces must be collected as part of this stage of the sampling hierarchy.

Sections are routinely cut at 30 µm using dry glass knives (i.e., without water-filled boat). 12-mm glass knives can completely span the height of the entire coronal plane of an adult rat brain. Larger glass knives (e.g., Ralph knives) or disposable microtome razor blades (e.g., MB35, Shandon), commonly used for cutting paraffin blocks, can be used for larger specimen blocks.

Hand-operated microtomes are ideal for this type of sectioning (e.g., Sorvall JB-4, Reichert-Jung 820-II). Knife advancement is achieved by manually advancing the knife holder with a fine-advance screw or with automatic advance as appropriate. Do not use the cutting motor on motorized microtomes due to possibility of damage to the block.

a. Grab individual glycolmethacrylate sections with forceps as they are cut. Cut one section at a time (ribbons are not possible). Float and relax sections on a 60°C water bath and pick up onto glass slides. Use normal histology procedures for paraffin and cryosections.

b. Dry completed set of glycolmethacrylate sections immediately on a 70°C heated slide tray for a minimum of 2 hr prior to staining.

Scrupulously clean microscope slides are essential for retaining the majority of sections on the microscope glass slide during the staining process. Acid cleaning (i.e., 5 N HCl, 2 min, followed by rinsing in water) is recommended even for "precleaned" slides; otherwise, an occasional "bad" batch of slides will result in costly loss of entire sets of sections.

Frosted slides are used and labeled with pencil or permanent markers (i.e., xylene- and alcohol-resistant, e.g., Securline MarkerII/Superfrost, Precision Dynamics).

Stain sections

6. Stain a systematic random subset of slides.

For example, in the rat hippocampus, every twelfth section might be examined as part of the fractionator design of the sampling protocol. Since three coronal sections of an adult rat brain can be positioned onto a standard 1 × 3–in. frosted glass slide, every fourth slide (with 3 sections), is stained. Other slides are held in reserve. Use systematic random sampling to determine which slides will be stained.

The selected staining protocol depends upon the target particles and the requirements of a particular study. Water-based stains, immunohistochemical methods, and in situ hybridization have all been used successfully with the optical disector (see Commentary).

Giemsa staining (see Support Protocol 2) works well on glycolmethacrylate-embedded tissue.

Perform systematic random sampling

7. Position the first disector frame over the tissue section without regard to any reference of the tissue section to be counted (see Fig. 12.6.5).

Placement of the disectors is easily achieved by randomly positioning a grid lattice over the image of the region of interest. This stage is also part of the systematic random sampling hierarchy; therefore do not attempt to align the grid with the region of interest. Disectors are placed only at grid points which overlay the region of interest.

8. Determine and record the thickness of the section.

Section thickness is determined by focusing from the top to the bottom of the section and recording the movement of the microscope stage with a linear tracking device. The tracking device should have a linear resolution of 0.5 μm that matches the focal plane of high oil objectives with numerical aperture >1.2. This linear tracking device will also be used to monitor disector heights and guard areas (see below).

Heidenhain produces a tabletop linear tracking device (Microcator, see Gundersen et al., 1988a,b) suitable for this purpose.

With practice, the operator will be able to learn to recognize the top and bottom of section surfaces. Practice can be gained by following capillaries that have been cut in cross-section to the respective surfaces.

9. Establish a guard area by focusing down from the top of the tissue section (Fig. 12.6.2).

This distance is read off from the linear tracking device. The guard area should be at least half the height of the particle of interest. In practice, 4 μm is a reasonable starting point.

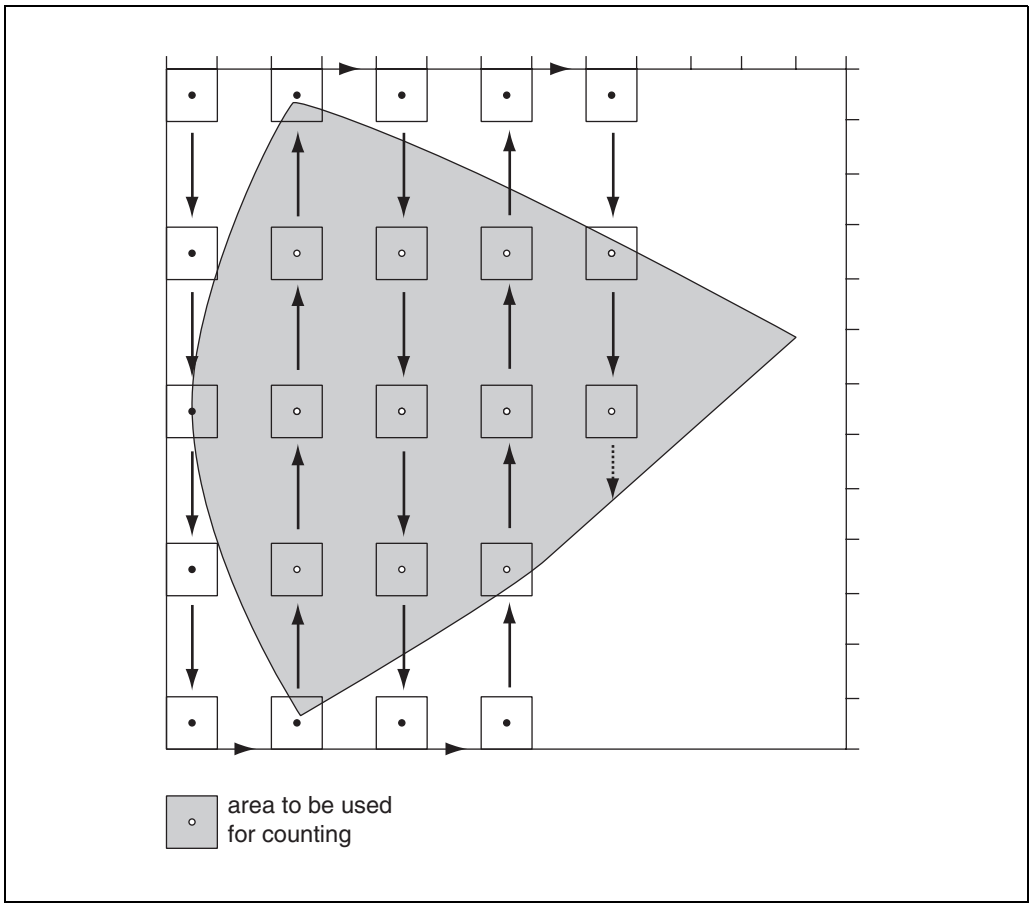

Figure 12.6.5 Systematic stepping across a section. A point is selected outside of the area of the tissue section without any reference to the tissue section (upper left corner). The microscope stage is moved systematically until the region of interest is encountered. At this point the first disector is placed. Additional disectors are placed at each subsequent position that a step encounters in the region of interest.

10. Count particles with the optical disector as they come into focus as the disector frame is "moved" down through the center of the thick section. Stop counting when the guard area at the bottom of the section is encountered (determined by monitoring the linear tracking device).

    Nucleoli make convenient counting particles assuming that there is only one per nucleus. Nuclei can also be used as counting particles.

    In practice, multiple disector frames may be combined so that common and rare objects may be counted simultaneously (e.g., see Bolender and Charleston, 1993).

11. Position all subsequent disectors by continuing the stepping process (Fig. 12.6.5) and repeating step 10.

    Set the spacing and size of disector frames so that between 100 and 200 particles of interest are encountered across the entire set of sections. The size of the disector frame is adjusted so that between one and two particles are encountered in each disector. Pilot projects should be conducted to optimize counting designs.

12. Calculate total particle number by combining total counted with sampling fractions according to the following equation (after West, 1993a,b):

    $N = \Sigma Q^{-} \times t/h \times 1/\text{asf} \times 1/\text{ssf} \times 1/\text{slsf}$

where ΣQ^- is the particle number counted, h = height of optical disector, t = section thickness, asf (area sample fraction) = area disector frame/area of each sampling grid step, ssf (section sampling fraction) = fraction of sections sampled, and slsf (slab sampling fraction) = fraction of slabs sampled.

ESTIMATING TOTAL PARTICLE NUMBER USING N_v,V_{ref}

ALTERNATE PROTOCOL 1

As stated, the optical fractionator represents the preferred method for estimating total particle number, provided that a natural V_{ref} exists. However, in some cases, investigators may be encountering situations wherein artificial structures (i.e., lesions) may vary considerably between animals. Examples would include models for artificial induction of embolic stroke, percussion injury, or lesion produced by direct infusion into the brain (e.g., 6-hydroxydopamine as a model of Parkinson's disease). In these types of models, determining the absolute number of surviving neurons or reactive glia may not be relevant if there is inherent variability in the volume of tissue involved in the lesion. In these cases, estimation of the N_v and V_{ref} may provide more relevant information. The optical fractionator does not provide this information.

It is important to note that reliance on observed N_v, a ratio of the number per volume, may directly lead the investigator to the "reference trap." The reference trap occurs when experimental treatment or outcomes involves changes to the V_{ref}. For example, edema may result in an apparent thinning of neuron (reduction in observed N_v) when no neurons may have actually been lost. This problem can be further confounded by artificial volume changes introduced by fixation, dehydration, embedment, and sectioning artifacts.

Finally, the N_v,V_{ref} method is capable of estimating the total number of particles in an equivalent manner as the optical fractionator. Simply combining N_v and V_{ref} will result in the arithmetical elimination of the volume component of the equation leaving only a number estimate.

For materials, see Basic Protocol.

1. Perform all tissue sampling and preparation (see Basic Protocol).
2. Place optical disectors and count particles with the optical disector as described in the Basic Protocol for the optical fractionator technique. Record number of optical disectors used.

   The total optical disector volume used equals the area of the disector frame multiplied by the height of the disector multiplied by the total number of disectors. N_v equals number of particles (Q^-) divided by the total disector volume.
3. Determine the volume of the sections examined by point counting. Project an image of a point lattice over each tissue section examined and count the number of points over the structure of interest.

   The section volume sampled, V(section), will be determined as:

   $V(sections) = \Sigma P(sections) \times A(point) \times meanT(sections)$

   where $\Sigma P(sections)$ is the total number of points hitting the region of interest, A(point) is the area per point (corrected for magnification), and meanT(sections) is the average section thickness (measured during disector placement).

   In practice, steps 1 to 3 are performed prior to moving to the next tissue section in the systematic random selected sequence. The optical disector is performed under high oil immersion optics. Point counting can be achieved at a much lower relative magnification (e.g., a 4× or 1× low-power objective). The lower-power objectives have a relatively short

working distance and will not contact the immersion oil. However, point counting of the section can be carried out prior to particle counting with the optical disector if desired.

In practice, a separate step of point counting may not be required to estimate the volume of a structure. The distance of the steps utilized for disector placement, and thus area per disector step (note that this is different from the area of the disector frame), is known. Therefore the total number of disectors do, in effect, form a point grid that can also be used for the estimate of the volume sampled.

4. Determine the structure volume by use of the fractionator concept.

   The reference volume, V_{ref}, will be estimated by multiplying the $V_{section}$ estimate by the inverse of the previous sampling fractions:

   $V_{ref} = V_{sections} \times f_{slabs} \times f_{sections}$

   For example, if every other slab was exhaustively sectioned, and if the volume of every 12th section was estimated, the fraction sampled would be 1/2 × 1/12 = 1/24th of the original volume. Therefore the total volume of the structure (V_{ref}) would be 24× the volume of the sampled sections.

   As a general rule of thumb, only ~100 to 200 points, spread across eight or more systematically separated sections of a structure, are all that are required to generate a sufficient estimate of the total volume of a structure.

5. Determine the total number of particles of interest in the structure by combining the N_v estimate (derived from the optical disector) with the volume estimate (derived from point counting and the fractionator).

   Combining N_v with V_{ref} results in the volume component canceling out, producing a pure number estimate.

   $N\ (cells, structure) = N_v \times V_{ref}$

ALTERNATE PROTOCOL 2

ESTIMATING TOTAL PRACTICAL NUMBER USING THE PHYSICAL DISSECTOR

The physical disector represents the first implementation of the disector counting principle. The basic premise is to compare the number of particles of interest that are unique to each of two sequential sections. The sequential section compared may be an adjacent section or represent skipped sections of known interval. Particles that are present in one section (reference section) but not the adjacent section (look-up section) belong to the volume of their respective sections (Fig. 12.6.6). No guard area is required. The optical disector is now the preferred method, due to efficiency and ease of use, for counting cells in the CNS. However, the physical disector still represents a simple method and may be of practical use in counting larger particles that do not require the use of high-powered objectives for unambiguous particle identification (e.g., Popkin and Farel, 1996; Miller et al., 1997), where high-resolution images (achieved by cutting thinner sections) are required for proper identification of particle type, or where special staining methods may not be compatible with the thicker sections that the optical fractionator requires. Finally, the physical disector can be applied to paraffin sections cut at traditional thickness (i.e., 4 to 5 μm).

Additional Materials *(also see Basic Protocol)*

One of the following setups for performing physical disector:

Camera lucida for attachment to microscope, acetate sheets, and water-soluble colored markers

Two projecting microscopes in darkened room

Commercial software/video system for capture and alignment of sequential section tracings (e.g., StereoInvestigator, MicroBrightField; Bioquant, R&M Biometrics)

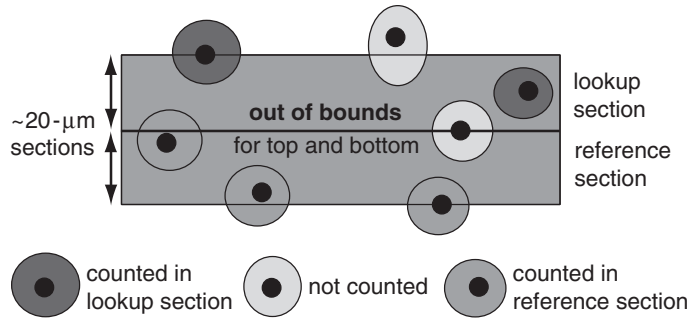

Figure 12.6.6 Physical disector counting rules. Particles unique to the reference section volume are counted (using a disector frame). In the example given here, the two adjacent sections (reference and look-up section) are shown viewed edge wise and stacked upon each other (no disector frame is visible). In practice, these two sections are not stacked on top of each other, but are shown that way here to clarify the counting rules. Nucleoli are the counting particle. The nucleolus that lies on the boundary between the two sections is not counted because its profile would be visible in both the reference and look-up section. Likewise, the nucleolus above the look-up section (which is not counted) would not even be present in the section. Only a cell fragment would be visible and not counted. Reversing the reference and look-up sections results in two disectors, thereby doubling the efficiency.

1. Prepare and section tissue (see Basic Protocol).

   Tissue thickness in the physical disector should be set as a function of at least half the height of the particle of interest.

2. Position disectors in a systematic random manner over the section (see Fig. 12.6.4).

3. Using one of the methods below, perform the physical disector. Count particles of interest in first section. Locate and align corresponding region in adjacent look-up section. Count particles of interest in look-up section. Delete from counts those particles of interest that appear in both sections.

   a. The easiest and least expensive method is to draw outlines of particles on acetate sheets using water-soluble colored markers (e.g., type used for overhead projectors) with the aid of a camera lucida attached to the microscope. First, trace reference marks (e.g., section borders, large vessel) at low power with one color of pen from the reference section. These marks will facilitate lining up the adjacent look-up section. At higher power, outline particles of interest with second color. Shift to look-up tissue section and align reference marks (first color) with new section. Trace particles of interest with third color. Determine particles of interest number by counting outlines of each appropriate color. Do not count outlines of particles that are coincident to both sections (i.e., if outlines overlap).

      Note that two separate disectors have been accomplished by reversing the order of the reference and look-up sections (i.e., the counts of the second and third colors that do not overlap).

   b. Use two projecting microscopes in darkened room (Fig. 4 in Møller et al., 1990) to alternately project images of the two adjacent sections. Mark and count particles of interest in similar manner as described above.

      Sequential sections must be mounted on separate microscope slides. Microscope stages should rotate so as to facilitate alignment of fields.

c. Use commercial software/video systems that allows for capture and alignment of sequential section tracings.

SUPPORT PROTOCOL 1

GLYCOLMETHACRYLATE EMBEDDING

The following support protocol describes steps for embedding brain tissue in glycolmethacrylate. Glycolmethacrylate is the preferred embedment medium in that it is dimensionally stable during tissue processing stages, optically transparent, and facilitates cutting relatively thick sections (20-70 μm) required for using optical disectors.

Materials

Fixed specimen
50%, 70%, 90%, and 95% ethanol
50% (v/v) ethanol/glycolmethacrylate solution
100% glycolmethacrylate (e.g., Jung Historesin; Leica Instruments)
Polymerizer
Embedding molds (e.g., EBH block holder and molds; Polyscience)

1. Dehydrate fixed specimen in graded ethanol series (50%, 70%, 90%, 95%, 95% again) 2 hr in each ethanol concentration, at 4°C.
2. Infiltrate in 50% ethanol/glycolmethacrylate solution for ≥2 hr, 4°C.

   Follow manufacturer's direction for preparing glycolmethacrylate. Glycolmethacrylate and activator are stable for several months if refrigerated.
3. Incubate in 100% glycolmethacrylate twice, each time for ≥8 hr (convenient overnight step), 4°C.
4. Polymerize in molds with labels using fresh 100% glycolmethacrylate following manufacturer's instructions. Allow to polymerize ≥3 hr prior to breaking out of mold.

   Working solution time for glycolmethacrylate is 5 to 10 min after accelerator is added; therefore mix in small batches that can be used in this time interval.

   Commercially available block holders and molds are available for small samples such as rat brain slices (e.g., EBH block holder and molds, Polyscience). Larger molds for larger samples are available (e.g., Super Metal base molds, Surgipath Medical Ind.). Coat these larger metal molds with a thin layer of petroleum jelly (e.g., Vaseline) or equivalent prior to use, to facilitate block release.

   Additional curing time of 8 hr (overnight) is recommended for consistency in sectioning characteristics. Cool large metal molds at −20°C for 1 hr, then invert under hot water to ease removal from mold.

SUPPORT PROTOCOL 2

GIEMSA STAIN PROCEDURE FOR GLYCOLMETHACRYLATE SECTIONS

Giemsa stain will primarily stain the nuclei of all cell types (Iñiguez et al., 1985; Brændgaard et al., 1990; Bjugn and Gundersen, 1993). Neuron nuclei stain moderately dark and characteristically have a single prominent nucleolus. Neurons are further differentiated by substantial staining of their Nissl substance, thereby providing for a distinct cell body shape. Nuclei of astrocytes characteristically stain very pale, have a weakly stained nucleolus, and have little if any cytoplasm stained about the perimeter of their nuclei in their cell bodies. Oligodendrocyte nuclei stain darkly and lack a single distinct nucleolus, but have considerable condensed chromatin. Microglia stain darkly, usually have an irregularly shaped nucleus, and have numerous regions of condensed chromatin. Pericytes and endothelia are also stained, but are distinguishable by their curved shape about capillaries and vessels. The neuropil itself is not stained, but may have a faint pink cast to it. Overall the thick plastic section is optically transparent.

Materials

Giemsa blood staining stock solution (Baker Analyzed, e.g., Fisher)
2% (v/v) acetic acid
50%, 70%, 90%, 95%, and 100% ethanol
100% xylene
High-viscosity mounting medium (e.g., Cytoseal 280, Stephens Scientific)

60°C water bath
Coverslips

1. Mix 10 ml Giemsa stock and 40 ml water and warm to 60°C for a working solution.
2. Add 3 to 4 drops 2% acetic acid.
3. Place slides in working solution, cover, and incubate for 70 min.

   The working solution will gradually cool.
4. Dip slides ten times in 2% acetic acid, then soak 5 min in 2% acetic acid.
5. Dehydrate in graded ethanol (50%, 70%, 90%, 95%, 100%, 100% again), 5 min in each solution.
6. Clear in 100% xylene for 10 min. Repeat.
7. Mount with coverslips.

   Mount coverslips with high-viscosity mounting medium. Edges of some sections may curl during dehydration stage. Use of 2-in. binding paper clips (Boise Express, available from stationary stores) ensures that coverslips will dry flat and tight to sections.

REAGENTS AND SOLUTIONS

Use Milli-Q-purified water or equivalent for all recipes and protocol steps. For common stock solutions, see ***APPENDIX 2A****; for suppliers, see* ***SUPPLIERS APPENDIX.***

Agar matrix

Combine 3 g agar with 100 ml water in a 250-ml Erlenmeyer flask using a stirring rod. Place flask inside a 1000-ml beaker, on stirring hot plate, with sufficient water to form a "double boiler" (dissolved agar will form a clear pale brown solution). Pour agar into mold (medium-sized weighing boats are inexpensive and disposable molds), and let cool on benchtop until cooled but still liquid. Place fixed and buffer-rinsed brain into agar, orient brain, and allow to cool until agar is completely solidified. Trim excess agar so embedded brain fits snugly into cutting guide.

The double boiler prevents scorching of the molten agar to the bottom of Erlenmeyer flask.

Paraformaldehyde in phosphate buffer, 4%

Mix 22.6 g dibasic sodium phosphate in 1 liter of water. Separately mix 12.6 g NaOH in 500 ml water. Heat 170 ml of this sodium hydroxide solution in a fume hood to 60°C (but not over 70°C). Add 40 g paraformaldehyde and stir until dissolved. Add 830 ml dibasic sodium phosphate and mix well. Filter and cool. Adjust pH to between 7.0 and 7.4. Store up to 2 weeks at 2° to 8°C.

COMMENTARY

Background Information

Recent developments in stereology, based on the optical disector and fractionator methods, have revolutionized the ability to perform unbiased cell counts in the central nervous system (Gundersen et al., 1988a,b; Mayhew, 1992; West, 1993a,b). Although only recently gaining in acceptance, these methods are now

increasingly being employed. For example, a search of the term "disector" and "fractionator" on Medline will produce over 300 published manuscripts since 1990. Furthermore, several science journals now have editorial policies that require contributors of stereology manuscripts to employ these new stereological methods or justify why they have not been employed (e.g., *J. Comparative Neurology,* Saper, 1996; *Neurobiology of Aging,* West and Coleman, 1996).

Examples in the literature can readily be found demonstrating counting in plastic sections (Brændgaard et al., 1990; Pakkenberg and Gundersen, 1997), as well as examples of in situ hybridization (West et al., 1996), and immunohistochemical methods (Mouton et al., 1997) for labeling specific cell subsets and synapses using cryosectioned material. Any embedment and compatible staining protocol can be considered for use with these new counting methods. The primary consideration remains that of ensuring that the entire V_{ref}, or a correctly generated known fraction of the V_{ref}, be used to fulfill the requirement of a true fractionator sampling design.

The new methods are design-based

The new stereology methods are design-based as opposed to the more traditional model-based methodologies. No assumptions, based on an unproved model (i.e., it is meaningless to verify a model by use of the same model), are required to generate the cell number estimates. The resulting estimates are free of any biases inherent in the model-based approach. Excellent reviews of the limitation of the model-based methods have been presented (Williams and Rakic, 1988; West, 1993a, 1999; Coggeshall and Lekan, 1996).

The new methods are efficient

The sampling design can readily be evaluated to determine the precision of the number estimate for individuals within the experimental population. The systematic random sampling that is performed at all levels of the tissue sampling hierarchy in effect generates a linear transect through the subject matter (this is why it is important to maintain all samples in the order generated). Matheron's theory of regionalized variables (Matheron, 1971) forms the theoretical basis for a quadratic approximation formula developed by Jensen and Gundersen (Gundersen and Jensen, 1987) for estimating the precision (coefficient of error, CE) of number estimates for individuals. The sampling design therefore readily allows for the assessment of the contribution of the observed coefficient of error (OCE) of the sampling in each individual relative to the observed coefficient of variation (OCV) in the study population. This in turn allows for sampling optimization and a reduced workload at all levels of the design (Gundersen and Jensen, 1987). This analysis of the sampling design should be carried out in the early stages of a new investigation (say after the first five animals have been counted) and the sampling scheme adjusted if indicated. Examples for estimating the OCE and OCV, and suggestions for optimization of sampling designs, are available in the literature (e.g., Brændgaard et al., 1990; West and Gundersen, 1990; West et al., 1991; West, 1999). The goal is to count only enough particles correctly in an individual until the interanimal variation comes to predominate the observed variation (see West, 1993a,b). At this point, additional counting produces little additional information because inherent interanimal variation is not reduced by more sampling.

The systematic random sampling scheme also provides one additional important benefit. The CE associated with systematic random sampling is inversely proportional to the number of samples ($1/N$). The CE associated with independent random sampling, however, is inversely proportional to the square root of the number of samples (i.e., $1/\sqrt{N}$). Far fewer additional samples are required with systematic sampling to improve the precision of the estimate if this is indicated for the study after initial assessment of the sampling design.

The efficiency of the methods is illustrated by the fact that ~400 neurons were required to be counted in the total human neocortex in an 80-year-old man (out of an average of 13.7×10 neurons) to produce an estimate of the total number, which could not be readily improved by additional sampling and counting (Brændgaard et al., 1990; see also Pakkenberg and Gundersen, 1997). Rarely will >100 to 200 cells need to be counted. The example cited above exceeds this number only because the neocortex was divided into four separate regions prior to sampling (parietal, frontal, temporal, and occipital poles).

The reference trap is eliminated

Experimental treatments, disease states, developmental deficits, and trauma in the CNS are all known to produce changes in the apparent volume of tissue and/or the number of cells. Differentiating between a decrease in apparent cell density due to an increase in the reference

volume (e.g., swelling that moves the cells farther apart) from a decrease in apparent cell density due to cell loss (which also results in an increase in space between cells) is problematic and leads directly to the "reference trap" (Brændgaard and Gundersen, 1986). Consideration of numerical density alone is a poor predictor of cell number (Gundersen, 1992; West, 1993a). An excellent example of a reference trap that was avoided using these methods has been presented by Pakkenberg and Gundersen (1988). This problem is further compounded by unknown effects on tissue volume due to tissue processing (fixation, dehydration, embedding, sectioning, staining). For example, fixation of tissue alone was found to produce an average 8% linear loss in monkey brain (van Essen et al., 1984) which translates into a >22% reduction in volume.

The fractionator sampling designs outlined here eliminate problems of volume changes in the V_{ref} during experimental treatment and tissue processing. The N_v,V_{ref} method, which combines the optical disector (which produces N_v estimates) with the fractionator-derived volume estimate (V_{ref}), eliminates the volume component when the final total number is calculated. The optical fractionator never requires a volume estimate. The only requirement for either of these methods is that the entire nonarbitrary structure originally be available for sampling. Small samples of the whole (such as tissue cores, needle biopsy, or randomly collected wedges of tissue), representing an unknown portion of the total structure, can never provide an unbiased estimate of the total number. They can only provide an estimate of the apparent density at that one sample site. Therefore they likely may lead to a reference trap.

The optical fractionator represents the method of choice if it is practical to implement. The volume of the structure is not (and need not be) estimated. The optical fractionator has the potential to be used with embedment media that are prone to tissue volume distortion during tissue processing (e.g., paraffin or frozen sections) thereby opening the door for using this stereological method with procedures not generally compatible with glycolmethacrylate-embedded tissues (West et al., 1996). The optical fractionator, however, is limited in its practical application by the requirement that the entire structure (or a systematic subsample of slabs from the entire structure) be sectioned exhaustively. This may preclude work with larger structures such as the human neocortex or hippocampus. For these larger types of structures, additional subsampling of the slabs can be carried out (Brændgaard et al., 1990; Pakkenberg and Gundersen, 1997), and estimations of the reference volume from sections of the subsampled tissue slabs is possible (Bolender and Charleston, 1993; Charleston et al., 1994).

Alternatively, it has been proposed that single complete sections can be collected from each slab (West and Gundersen, 1990; West, 1993b). In these cases, the volume of the structure is estimated separately by use of the Cavalieri principle (Gundersen et al., 1988a,b). However, this type of volume estimate requires that a careful assessment of tissue shrinkage be carried out because the volume estimate is made on wet tissue slabs prior to dehydration, embedment, and sectioning, whereas the N_v or number estimate is generated from the dehydrated, embedded, and sectioned material. The two estimates are no longer directly linked as they are when the volume estimate is generated from the same set of sections from which the N_v or number estimates are generated (the procedure described in this unit). The assumption that there have been no differential changes in the V_{ref} between the wet and processed tissue represents a divergence from a true design-based method.

Critical Parameters

Slabbing

The plane of slabbing should be selected to match the plane featured in a reference brain atlas. This assists in defining structure boundaries (i.e., V_{ref}) during the counting stage.

Rodent brains can be successfully slabbed in the coronal plane at ~1-mm intervals using commercially available cutting guides, or custom cutting guides can be designed and manufactured (Michel and Cruz-Orive, 1988). In the latter device, embedment of entire brain in 3% agar matrix facilitates uniform slabbing of brain and systematic random determination of the position of the slabs. Position the agar-embedded brain independent of any cutting guide. Systematic random sampling requires that the position of the first slab be random relative to the position of the region of interest. Therefore, the first slab will often be less than the full width of the selected slab width. All subsequent full-width slabs will be systematic.

Complete coronal slabs allow for left and right sides of brain to be available for stereological study. Alternatively, slabs can be accurately separated into left and right hemi-

spheres after slabbing, and one side can be devoted to stereological analysis while the other is available for alternative investigations. It is recommended that right and left hemispheres be separated after this initial slabbing stage so that the entire V_{ref} is accurately separated and preserved in each half of the brain. Freehand gross dissection of a whole brain into left and right hemispheres prior to slabbing often results in slightly unequal separation of hemispheres along the midbrain structures, thereby violating the V_{ref} concept.

Embedding

Tissue slabs shrink considerably during paraffin embedment, and tissue sections expand as a function of water temperature during "relaxing" when collected onto a water bath. These extreme dimensional changes may lead to a violation of the V_{ref} concept, especially when assuming that they are equivalent across different treatment groups. Relatively small linear dimensional changes translate into relatively large apparent density changes for particles when converted into three-dimensional space. These dimensional changes can easily mask small treatment effects. However, it should be noted that a true fractionator design can overcome the dimensional instability problem of paraffin-embedded material.

Glycolmethacrylate is dimensionally stable, optically transparent, permeable to many water-based stains, and can readily be sectioned at 1 to 70 μm. A minimum of 20 μm is recommended for the optical disector. Embedment kits (e.g., Jung Historesin and Jung Historesin Plus, Leica Instruments) and embedment molds and block holders (see Support Protocol 1 for glycomethycrylate directions) are available.

It is crucial to hydrate the glycolmethacrylate block face with water prior to cutting each section; otherwise the tissue will fracture during the cutting stroke. Touch the surface of the block with a wet paint brush and allow water in imbibe into the block face for ~4 to 5 sec before each cutting stroke.

Glycolmethacrylate imbibes water during the sectioning process and swells slightly; therefore sections will usually dry to a slightly thinner height than originally cut. In addition, the outside edges of the block trapezoid will also imbibe water and soften as cutting progresses. For this reason, the edges of the sections may develop a ruffled appearance that may impede setting coverslips after staining. The ruffles can be trimmed away from the edges of the sections with a sharp acetone-cleaned single-edge razor blade prior to drying down the sections onto the slide. Use of a stereomicroscope facilitates this step. The relatively thick sections are very robust and can tolerate considerable handling.

Troubleshooting

Histology

It is not anticipated that there will be any problems encountered in the preparation of tissues for the sample. Virtually all of the procedures described in this unit represent variations on standard histological methods (e.g., paraffin embedding, cryosections, plastic embedding) and therefore are not unique to the stereological counting procedures that are the focus of this unit. If problems are encountered with histology procedures, consult any proficient histology laboratory for fundamental advice.

The one procedure that may be somewhat unique to the stereology protocol is the cutting of relatively thick plastic sections on a standard microtome. If problems are encountered in cutting 20- to 70-μm sections, it is usually the result of not wetting the block face sufficiently with water or not allowing sufficient time for the water to be imbibed into the tissue block. Sections should cut easily. Sections that are too dry when cut will contain shattered tissue, and a noticeable "crunching" sound will be heard during the cutting stroke. Glycolmethacrylate without tissue present will cut easily. It is the infiltrated, embedded tissue that must be softened by the water. In practice, this is accomplished by wetting the entire block face.

Sampling efficiency

The method for deterimining the correct sampling intervals to produce results with sufficiently small sampling error (OCE) is described in the Basic Protocol. The goal is to sample just enough (and thereby reduce the workload) so that the observed variance which predominates is due to true individual variance and not to sampling error related to insufficient sampling. An example of the method for determining sampling efficiency for the optical fractionator method is presented in Table 12.6.1 and is based on the method of West et al. (1991). A spreadsheet template can easily be constructed to perform the calculation for each individual. The goal is to sample enough to produce an OCE for the individual that is less than half of the observed group variation for the group in which that individual belongs. Once this level

Table 12.6.1 Estimating Sampling Efficiency

Section	Q^-_1	$Q^-_1 \times Q^-_1$	$Q^-_1 \times Q^-_{1+1}$	$Q^-_1 \times Q^-_{1+2}$
1	5	25	55	80
2	11	121	176	99
3	16	256	144	320
4	9	81	180	207
5	20	400	460	60
6	23	529	60	276
7	3	9	36	48
8	12	144	192	348
9	16	256	464	464
10	29	841	841	1276
11	29	841	1276	957
12	44	1936	1452	968
13	33	1089	726	297
14	22	484	198	—
15	9	81	—	—
SUM	$\Sigma Q^-_1 = 281$	A = 7093	B = 6269	C = 5400

has been achieved for the individual, improvement of the estimate for the group mean (if desired) is achieved by increasing group number and not by additional work (counting) for the individual group members. Initially, in a new study, it is recommended that a higher rate of sampling be employed (i.e., systematically collect more sections), but particle number be estimated using a smaller fraction of collected sections. For example, collect every third section but perform particle counting on every ninth section. Perform sampling analysis and increase section frequency for counting if indicated.

The coefficient of error (CE) of the sum of the particles counted can be calculated using Equation 12.6.1. The data of estimated sampling efficiency given in Table 12.6.1 produces an estimated CE of 0.041.

$$\begin{aligned} \mathrm{CE}\Sigma Q^- &= \frac{\sqrt{(3\mathrm{A} + \mathrm{C} - 4\mathrm{B})/12}}{\Sigma Q^-} \\ &= \frac{\sqrt{(3\times 7093 + 5400 - 4\times 6269)/12}}{281} \\ &= 0.041 \end{aligned}$$

where CE is the coefficient error. ΣQ^- is the sum of the particle number counted.

Anticipated Results

This method should result in an unbiased estimate of the total particle number in a structure. The particles can be cells (e.g., neurons, astrocytes, oligodendrocytes) or particles (e.g., synapses). The N_v/V_{ref} method can also produce a separate volume estimate, but as described, volume estimates on fixed and processed tissue can lead to a reference trap. Unbiased estimates of the total number of particles in an unbiased structure can be used to compare the effects of treatment across groups.

Time Considerations

The amount of time required to process tissues for stereology counting is variable depending on the tissue. Slabbing an entire rodent or rabbit brain requires about 30 min to embed in agar and about 30 min to slab. A primate brain may require 2 hr. If the tissue will be embedded in paraffin, processing through dehydration and infiltration can be achieved in 24 hr. Automatic tissue processors can substantially increase the efficiency of this stage. Tissue embedding in glycolmethacrylate takes a minimum of 4 days, but the actual hands-on time is a few minutes at each step. Simultaneous processing of the tissue from 5 to 10 brains can increase the efficiency of this stage of the operation.

Tissue blocks must be exhaustively sectioned to satisfy the requirements of the fractionator design. Exhaustively sectioning a 1-mm block at 20 µm would produce 50 sections. The sampling design may require that every tenth section be collected. This can be achieved in <2 hr. Exhaustively sectioning a 1-mm glycolmethacrylate-embedded block at 30 µm will produce ~35 sections. Again, assuming every tenth section is collected for sampling, the process requires ~2 hr. Multiply this estimate by the total number of embedded slabs to estimate the total time required for sectioning and collecting samples. Tissue staining may require 1 to 2 hr per set. Multiple small slabs or structures (e.g., entire fetal rat brains) can be embedded in single large blocks to increase efficiency.

The actual counting procedure requires 4 to 6 hr to count neurons in a single region. Additional time allowance should be budgeted if more than one cell type is to be counted. Time should also be budgeted to allow for reasonable breaks for the person doing the counting.

Literature Cited

Bjugn, R. and Gundersen, H.J.G. 1993. Estimate of the total number of neurons and glial and endothelial cells in the rat spinal cord by means of the optical disector. *J. Comp. Neurol.* 328:406-414.

Bolender, R.P. and Charleston, J.S. 1993. Software for counting cells and estimating structural volumes with the optical disector and fractionator. *Microsc. Res. Tech.* 25:314-324.

Brændgaard, H. and Gundersen, H.J. 1986. The impact of recent stereological advances on quantitative studies of the nervous system. *J. Neurosci. Methods* 18:39-78.

Braendgaard, H., Evans, S.M., Howard, C.V., and Gundersen, H.J. 1990. The total number of neurons in the human neocortex unbiasedly estimated using optical disectors. *J. Microsc.* 157:285-304.

Charleston, J.S., Bolender, R.P., Mottet, N.K., Body, R.L., Vahter, M.E., and Burbacher, T.M. 1994. Increases in the number of reactive glia in the visual cortex of *Macaca fascicularis* following subclinical long-term methylmercury exposure. *Toxicol. Appl. Pharmacol.* 129:196-206.

Coggeshall, R.E. and Lekan, H.A. 1996. Methods for determining number of cells and synapses: A case for more uniform standards of review. *J. Comp. Neurol.* 364:6-15.

Gundersen, H.J.G. 1992. Stereology: the fast lane between neuroanatomy and brain function—or still only a tightrope? *Acta Neurol. Scand. Suppl.* 137:8-13.

Gundersen, H.J.G. and Jensen, E.B. 1987. The efficiency of systematic sampling in stereology and its prediction. *J. Microsc.* 147:229-263.

Gundersen, H.J.G., Bagger, P., Bendtsen, T.F, Evans, S.M., Korbo, L., Marcussen, N., Møller, A., Nielsen, K., Nyengaard, J.R., Pakkenberg, B., et al. 1988a. The new stereological tools: Disector, fractionator, nucleator and point sampled intercepts and their use in pathological research and diagnosis. *APMIS* 96:857-881.

Gundersen, H.J.G., Bendtsen, T.F., Korbo, L., Marcussen, N., Møller, A., Nielsen, K., Nyengaard, J.R., Pakkenberg, B., Sorensen, F.B., Vesterby, A., et al. 1988b. Some new, simple and efficient stereological methods and their use in pathological research and diagnosis. *APMIS* 96:379-394.

Iñiguez, C., Gayoso, M.J., and Carreres, J. 1985. A versatile and simple method for staining nervous tissue using Giemsa dye. *J. Neurosci. Methods* 13:77-86.

Matheron, G. 1971. The Theory of Regionalized Variables and its Application. Cahiers du Centre de Morphologie Mathématique de Fontainebleau, no. 5. Ecole National Superieure des Mines de Paris.

Mayhew, T.M. 1992. A review of recent advances in stereology for quantifying neural structure. *J. Neurocytol.* 21:313-328.

Michel, R.P. and Cruz-Orive, L.M. 1988. Application of the Cavalier principle and vertical sections method to lung: Estimation of volume and pleural surface area. *J. Microsc.* 150:117-136.

Miller, P.B., Charleston, J.S., Battaglia, D.E., Klein, N.A., and Soules, M.R. 1997. An accurate, simple method for unbiased determination of primordial follicle number in the primate ovary. *Biol. Reprod.* 56:909-915.

Møller, A., Strange, P., and Gundersen, H.J. 1990. Efficient estimation of cell volume and number using the nucleator and the disector. *J. Microsc.* 159:61-71.

Mouton, P.R., Price, D.L., and Walker, L.C. 1997. Empirical assessment of synapse number in primate neocortex. *J. Neurosci. Methods* 75:119-126.

Pakkenberg, B. and Gundersen, H.J. 1988. Total number of neurons and glial cells in human brain nuclei estimated by the disector and the fractionator. *J. Microsc.* 150:1-20.

Pakkenberg, B. and Gundersen, H.J.G. 1997. Neocortical neuron number in humans: Effect of sex and age. *J. Comp. Neurol.* 384:312-320.

Popkin, G.J. and Farel, P.B. 1996. Reliability and validity of the physical disector method for estimating neuron number. *J. Neurobiol.* 31:166-174.

Saper, C.B. 1996. Any way you cut it: A new journal policy for the use of unbiased counting methods (Editorial). *J. Comp. Neurol.* 364:5.

van Essen, D.C., Newsome, W.T., and Maunsell, J.H. 1984. The visual field representation in striate cortex of the macaque monkey: Asymmetry, anisotropies, and individual variability. *Vision Res.* 24:429-448.

West, M.J. 1993a. New stereological methods for counting neurons. *Neurobiol. Aging* 14:275-285.

West, M.J. 1993b. Regional specific loss of neurons in the aging human hippocampus. *Neurobiol. Aging* 14:287-293.

West, M.J. 1999. Stereological methods for estimating the total number of neurons and synapses: Issues of precision and bias. *Trends Neurosci.* 22:51-61.

West, M.J. and Coleman, P.D. 1996. How to count (Editorial). *Neurobiol. Aging* 17:503.

West, M.J. and Gundersen, H.J.G. 1990. Unbiased stereological estimation of the number of neurons in the human hippocampus. *J. Comp. Neurol.* 296:1-22.

West, M.J., Slomianka, L., and Gundersen, H.J. 1991. Unbiased stereological estimation of the total number of neurons in the subdivisions of the rat hippocampus using the optical fractionator. *Anat. Rec.* 231:482-97.

West, M.J., Ostergaard, K., Andreassen, O.A., and Finsen, B. 1996. Estimation of the number of somatostatin neurons in the striatum: An in situ hybridization study using the optical fractionator method. *J. Comp. Neurol.* 370:11-22.

Williams, R.W. and Rakic, P. 1988. Three-dimensional counting: An accurate and direct method to estimate numbers of cells in sectioned material. *J. Comp. Neurol.* 278:344-352.

Contributed by Jay S. Charleston
Institute of Neurotoxicology and Neurological Disorders
and Shin Nippon Biological Laboratories U.S.A.
Redmond, Washington

Isolation of Cerebellar Granule Cells from Neonatal Rats

The present unit describes the isolation of cerebellar granule cells from neonatal rats. Primary cultures of rat cerebellar granule cells consist of post-mitotic, glutamatergic neurons that undergo "maturation" in vitro (see Background Information). As a result of this maturation, the granule cells require depolarizing concentrations of extracellular KCl to survive >5 days after isolation. This unit describes isolation of the cells (see Basic Protocol), preparation of culture surfaces (see Support Protocol 1), determining cell numbers with crystal violet (see Support Protocol 2), and preparation of heat inactivated fetal bovine serum (see Support Protocol 3).

NOTE: All protocols using live animals must first be reviewed and accepted by an Institutional Animal Care and Use Committee (IACUC) and must conform to governmental regulations regarding the care and use of laboratory animals.

CAUTION: The cytosine arabinoside and crystal violet solutions are hazardous. See Material Safety Data Sheet for handling guidelines.

PREPARATION OF CEREBRAL GRANULE CELLS

BASIC PROTOCOL

To isolate the neurons, rat pups are sacrificed on postnatal day 8 and the brains removed. The cerebellum is separated from the brain and the meninges are detached. The cerebellum is then minced and the tissue digested with trypsin and deoxyribonuclease I (DNase). The tissue homogenate is suspended in complete Dulbecco's modified Eagle's medium (DMEM) and filtered through a 100-µm nylon mesh. The cells are then pre-plated in a poly-D-lysine coated T-flask to remove astrocytes. After shaking the flask to detach the neurons, the medium containing the neurons is filtered sequentially through 70- and 40-µm nylon mesh and then cells are plated onto culture dishes coated with poly-D-lysine. On day 1 and day 5 after isolation, the cells are treated with the anti-mitotic agent cytosine arabinoside (AraC) for 24 hr to remove any proliferating cells. The culture medium is changed every 3 days and the cerebellar granule cells can be used for experiments 8 days after isolation.

Materials

8-day-old postnatal Sprague-Dawley rats
70% ethanol
Antibiotic DMEM (see recipe)
2.5% (w/v) trypsin solution (e.g., Life Technologies), 4°C
100× DNase solution (see recipe)
Complete DMEM supplemented with 10% (v/v) heat-inactivated fetal bovine serum (see recipe for DMEM; see Support Protocol 3 for heat-inactivated fetal bovine serum)
Crystal violet solution (see recipe)
500× AraC solution (see recipe)

Surgical gloves
165-mm large curved operating scissors
Laboratory pad (VWR)
Animal disposal plastic bags
Curved forceps (114-mm length and 0.8-mm tip width)
115-mm delicate dissecting scissors

Contributed by Jan Oberdoerster
Current Protocols in Toxicology (2001) 12.7.1-12.7.10

Rounded weighing spatula (e.g., VWR)
100-mm an 60-mm sterile tissue culture plastic dishes with and without treatment with poly-D-lysine (e.g., Falcon; see Support Protocol 1)
Dumont forceps
115-mm angled delicate dissecting scissors
50-ml and 15-ml sterile conical tubes (e.g., Falcon)
10-ml and 25-ml sterile serological pipets
37°C water bath
10-ml syringe and 20-G needle
40-, 70-, and 100-µm sterile nylon mesh cell strainers (e.g., Falcon), sterile
75-cm^2 tissue culture flasks treated with poly-D-lysine (e.g., Falcon; see Support Protocol 1)
Inverted compound microscope
Hemacytometer (see Support Protocol 2)
Glass coverslips

NOTE: All solutions and equipment coming into contact with living cells must be sterile and aseptic techniques should be used accordingly.

NOTE: All cultured incubations should be performed in a humidified 37°C, 5% CO_2 incubator unless otherwise specified.

Dissect neonatal rat

1. Wear surgical gloves and gently hold the 8-day-old pup with thumb and forefinger between shoulder blades.

   Postnatal 8-day-old pups should be used. It is convenient to order pregnant time-mated dams from a common commercial supplier. The gestation period of a rat is 20 to 22 days.

   Steps 1 through 9 can be performed at the lab bench. All instruments should be autoclaved using autoclave bags and opened only when needed.

2. Rapidly decapitate pup onto a laboratory pad using large sterile curved scissors. Place body into plastic bag for disposal.
3. Decapitate remaining pups in the litter.

   This should be done rapidly to reduce the time that the brain remains in the cranium.

4. Place all heads onto a fresh laboratory pad and douse with 70% ethanol to reduce potential bacterial/fungal contamination.

   A standard laboratory squirt bottle is useful for gently dousing the heads with ethanol.

5. Discard surgical gloves and replace with a fresh pair.

   Surgical gloves with textured fingertips will enhance dexterity and facilitate steps 6 through 9.

Isolate neonatal rat brain

6. Grasp head with thumb and forefinger at the base of the head and place sterile forceps into the eye-sockets to firmly secure the head.
7. While holding the head in place with the forceps, cut the skin from the base of the skull to the eyes along the midline and then at right angles toward the ears with sterile dissecting scissors.
8. Insert the 115-mm sterile dissecting scissors into the base of the skull and cut along the midline. Cut away the skull flaps to expose the brain.

   Maintain a shallow cutting angle to prevent damage to the brain.

9. Use a sterile weighing spatula to remove the brain and place into a 100-mm tissue culture dish containing 10 ml ice-cold antibiotic DMEM.

   The culture dish should be maintained on ice for the duration of the isolation.

10. Repeat from step 6 until all remaining brains are isolated.

    Pool up to five brains into one 100-mm tissue culture dish.

Dissect neonatal rat cerebella

11. Move the dishes containing the brains into a laminar flow hood.

    Only sterile dissecting instruments should be used in the laminar flow hood.

12. Using a new set of sterile forceps, transfer the brains to new 100-mm tissue culture dishes containing 10 ml ice-cold antibiotic DMEM.

13. Remove one brain and place ventrally into a 100-mm tissue culture dish containing 5 ml ice-cold antibiotic DMEM.

14. Grasp brain with the forcep placed into the forebrain and gently remove the cerebellum by inserting a sterile curved forcep behind the cerebellum and pulling it away from the brain.

15. Transfer the cerebellum into a 60-mm tissue culture dish containing 3 ml ice-cold antibiotic DMEM.

    Pool up to five cerebella in one 60-mm tissue culture dish and maintain on ice.

Prepare cerebellar cells

16. Gently remove the meningial cover from the cerebellum using Dumont forceps and place cerebellum into a 60-mm tissue culture dish containing 3 ml ice-cold antibiotic DMEM.

17. Repeat procedure until all cerebella have been processed.

18. Finely mince the cerebella in the 60-mm tissue culture dish with 115-mm angled dissection scissors.

    Cerebellar pieces should be ~1 mm^2 in size.

Dissociate cells

19. Transfer all the tissues into a 50-ml conical tube with a 10-ml serological pipet and centrifuge 5 min at $1000 \times g$, 4°C.

    Handling of tissue in open tissue culture dishes/tubes should occur only in a laminar flow hood.

20. Carefully aspirate the DMEM and resuspend the pellet in 10 ml antibiotic DMEM containing 0.125% trypsin, 0.2% DNase solution. Incubate the conical tube for 15 min in a 37°C water bath.

    The remaining manipulations of the cells with culture medium (e.g., plating and subsequent "feeding" of the cells) should occur using prewarmed (i.e., ~37°C) culture medium.

21. Triturate the tissue five times using a 20-G needle attached to a sterile 10-ml syringe.

22. Centrifuge 5 min at $1000 \times g$, room temperature, and aspirate the medium. Replace with 10 ml complete DMEM with 10% heat-inactivated fetal bovine serum (DMEM/10%FBS).

23. Using a 10-ml serological pipet, strain tissue thought a 100-µm nylon mesh cell strainer into a new 50-ml conical tube.

Allow astrocytes to attach

24. Transfer the tissue homogenate into a 75-cm^2 tissue culture flask treated with poly-D-lysine (see Support Protocol 1) and incubate 15 min at 37°C.

No more than four cerebella should be plated onto one 75-cm^2 tissue culture flask.

25. Shake the flask back and forth by sliding the flask along a level surface for 1 min to detach the neurons. Remove the medium using a 10-ml serological pipet.

The back and forth motion should be rapid but slow enough so that the serum in the medium does not turn foamy.

Separate neurons

26. Strain the tissue contained in the medium through a 70-µm nylon mesh cell strainer into a new 50-ml conical tube.

27. Using a 10-ml serological pipet, strain tissue through a 40-µm nylon mesh tissue strainer into a new 50-ml conical tube.

Plate cells

28. Count the cells under an inverted compound microscope using a hemacytometer (see Support Protocol 2) by combining 20 µl cells with 20 µl crystal violet solution.

29. Plate cells at a density of 1.7×10^6 cells/cm^2 (i.e., 3×10^6 cells/well of 24-well plate; 48×10^6 cells/60-mm culture dish) onto culture dishes coated with 500 µg/ml poly-D-lysine.

30. On day 1 and day 5 after isolation, treat the cells with complete DMEM/10% FBS containing 10 µM AraC for 24 hr to remove any proliferating cells.

The characteristic "grape clusters" of cerebellar granule cells should be evident under 100× magnification after 6 days in vitro.

31. Maintain cells in complete DMEM/10% FBS in a 37°C, 5% CO_2 humidified atmosphere, and change culture medium every 3 to 4 days.

SUPPORT PROTOCOL 1

PREPARATION OF THE CULTURE SUBSTRATE OF CELL CULTURE PLATES

Cerebellar granule cells require a poly-D-lysine substrate in order to attach to the tissue culture plate. A lower concentration of poly-D-lysine is used to coat 75-cm^2 tissue culture flasks to allow the granule cells to detach after shaking (see step 25).

Materials

100× poly-D-lysine stock solution (see recipe)
Phosphate-buffered saline, pH 7.4, store at room temperature (PBS; *APPENDIX 2A*)

75-cm^2 tissue culture flasks, sterile
10-ml pipets, sterile
36-, 60-, and 100-mm tissue culture dishes, sterile

1. Work in a laminar flow hood and use sterile plates, pipets, and solutions.

2a. *Tissue culture flasks*: Coat 75-cm^2 tissue culture flasks by adding 10 ml of 50 µg/ml poly-D-lysine solution to each flask before start of tissue preparation. Coat one 75-cm^2 tissue culture flask for every 4 pups in the litter.

2b. *Tissue culture plates*: Coat tissue culture plates by adding 500 µg/ml poly-D-lysine solution to each plate before start of tissue preparation. Add 1.5 ml/35-mm culture dish, 3 ml/60-mm culture dish, and 8 ml/100-mm culture dish.

Alternatively, Poly-D-lysine can be added and left on the plates, dishes, or flasks overnight.

3. Wait ≥40 min and then rinse the flasks, plates, and dishes three times with phosphate-buffered saline. Leave the third phosphate-buffered saline rinse in flasks or plates until ready to seed cells.

Do not let the flasks or plates dry between PBS rinses.

DETERMINING CELL NUMBER WITH A HEMACYTOMETER

SUPPORT PROTOCOL 2

Cells must be counted prior to plating in order to ensure proper cell density in culture. Seeding cells at a density that is too high or too low will adversely affect cell viability. Cerebellar granule cells are tightly clustered cells that contain a small amount of cytoplasm. These qualities make cell number evaluation with the traditional trypan blue exclusion technique difficult and thus the use of crystal violet is recommended. The crystal violet solution will disrupt the cell membrane (releasing the clustered cells) and brightly stain the cell nuclei, allowing for facilitated counting of the cells with a hemocytometer.

For materials see Basic Protocol.

1. Place a clean coverslip on the counting area of the hemacytometer (see Fig. A.3B.1).
2. Combine 20 µl cells with 20 µl crystal violet solution in a 0.5-ml microcentrifuge tube.

   Work in the laminar flow hood and use sterile micropipet tips when removing the aliquot of cells.

3. Transfer ~10 µl of the crystal violet/cell solution into the groove on the edge of the hemacytometer chamber and let the solution be drawn under the coverslip by capillary action.

   Do not overfill or underfill chamber.

4. Observe under an inverted compound microscope and focus on the grid lines in the chamber at 100×.

   At this magnification, one of the nine 1-mm^2 squares should be fully visible.

5. Count the cells lying within this 1-mm^2 area. Count cells that are touching the top and left-hand lines of each square but not those on the bottom or right-hand lines.
6. Count at least four squares of the hemacytometer.
7. Each of the 1-mm^2 squares of the hemacytometer contains 0.1 µl solution. Determine cell concentration.

   To determine cell number/ml, count the number of cells present in four 1-mm^2 squares of the hemacytometer and multiply by 5000 [i.e., cell number/ml = cell number in 4 squares × 10,000 × dilution factor (2)/number squares counted (4)].

   CAUTION: *The crystal violet solution is hazardous. Refer to the Material Safety Data Sheet for handling guidelines.*

SUPPORT PROTOCOL 3

HEAT-INACTIVATION OF FETAL BOVINE SERUM

Heat-inactivation of fetal bovine serum is important to destroy heat-labile complement. Degradation of these proteins by raising the temperature of the serum to 56°C for 30 min will ensure that antibody binding will not lyse the cells. Heat inactivation may change the appearance of the fetal bovine serum and result in precipitation. This is normal and does not indicate that the serum has been compromised.

Materials

Fetal bovine serum, qualified (Life Technologies)
56°C water bath

1. Thaw the bottle of fetal bovine serum overnight at room temperature.

   Open serum bottles only in a sterile laminar flow hood.

2. Immerse the fetal calf serum bottle in the 56°C waterbath for 30 min. Swirl the bottle every 5 min to ensure proper mixing.

   The water level should be even with serum level inside the bottle.

3. Allow serum to cool for 1 hr at room temperature and store at 4°C until needed.

   If storing heat-inactivated fetal bovine serum for >3 weeks, dispense into 50-ml aliquots and store at −20°C.

REAGENTS AND SOLUTIONS

Use ultrapure water for all solutions. Filter sterilize solutions that will be used in cell culture. For common stock solutions, see ***APPENDIX 2A****; for suppliers, see* ***SUPPLIERS APPENDIX****.*

Antibiotic DMEM

DMEM (Life Technologies) containing 100 U/ml penicillin and 100 µg/ml streptomycin. Store up to 1 month at 4°C in the dark.

AraC solution, 500×

Make a 5 mM cytosine arabinoside (e.g., Sigma) solution in DMEM (Life Technologies). Dispense in 5-ml aliquots to avoid repeated freeze/thaw. Store up to 6 months at −20°C.

Complete DMEM

DMEM (Life Technologies) supplemented with:
10% (v/v) heat-inactivated fetal bovine serum (see Support Protocol 3)
24.5 mM KCl
50 mM glucose
100 U/ml penicillin
100 µg/ml streptomycin
Store up to 3 weeks at 4°C in the dark

Crystal violet solution

Make a 0.1 mg/ml crystal violet (e.g., Sigma) solution in 0.1 M acetic acid. Store up to 6 months at room temperature and protect from light.

DNase solution, 100×

Make a 2% (w/v) deoxyribonuclease I (e.g., Sigma) solution in antibiotic DMEM (see recipe). Dispense in 5-ml aliquots to avoid repeated freeze/thaw. Store up to 6 months at −20°C.

Poly-D-lysine stock solution, 100×

Make a 50 mg/ml poly-D-lysine (M.W. 150,000-300,000; e.g., Sigma) solution in ultrapure water. Store up to 6 months at 4°C in the dark.

Dilute 100× stock solution 10-fold for coating tissue culture plates or dishes or 100-fold for coating 75-cm^2 tissue culture flasks for preplating.

COMMENTARY

Background Information

Cerebellar granule cells are interneurons in the granular layer of the cerebellar cortex that represent the most numerous neuronal population in the cerebellum. The short dendrites of the cerebellar granule cells are located within the granular layer and form synapses with one of the afferent systems of the cerebellum, the glutamatergic mossy fibers. This mossy fiber input exerts a neurotrophic effect on the granule cells during development. Granule cells are the only excitatory neurons whose cell bodies are located within the cerebellar cortex and their axons project into the molecular layer of the cerebellar cortex where they bifurcate into two branches, forming parallel fibers. These parallel fibers travel to the long axis of the folium to form excitatory synapses with Purkinje cells, which act as modulators and are the only outlet for processed information from the cerebellar cortex.

As mentioned above, rat cerebellar granule cells are glutamatergic neurons. Five days after isolation, the granule cells require either K^+-induced membrane depolarization or a glutamate-receptor agonist [e.g., *N*-methyl-D-aspartate (NMDA)] to remain viable in culture (Balazs et al., 1988; Copani et al., 1995; Marini et al., 1999). This time-dependent requirement for membrane depolarization has been suggested to represent a maturation of the granule cells (Burgoyne et al., 1993; D'Mello et al., 1994; Copani et al., 1995). In the absence of depolarizing conditions that apparently mimic the in vivo stimulation by glutamatergic mossy fibers (Balazs et al., 1988), mature cerebellar granule cells undergo apoptotic cell death (D'Mello et al., 1994; Copani et al., 1995; Oberdoerster and Rabin, 1999). When maintained in complete medium (i.e., supplemented with KCl and fetal bovine serum), however, granule cells differentiate and acquire the morphology, biochemistry, and electrophysiology of mature neurons in vivo (Levi et al., 1984; Gallo et al., 1987; Cull-Candy et al., 1988; Wyllie and Cull-Candy, 1994). Mature granule cells are sensitive to excitotoxicity and changing of the culture medium has been reported to cause granule cells to undergo NMDA receptor-mediated excitotoxic cell death (Schramm et al., 1990), possibly due to glutamate present in the serum-supplemented culture medium. The authors, however, have not experienced this excitotoxicity with cultures (Oberdoerster and Rabin, 1999; Oberdoerster et al., 2000). In fact, although the first week in culture is typically characterized by a continual dying of cells, the granule cell population subsequently stabilizes and provides a uniform population of cells for up to 3 weeks in culture (Oberdoerster and Rabin, 1999).

The use of primary neuronal cultures instead of clonal cell lines has both advantages and disadvantages. The advantage of primary neuronal cultures is that the cells are derived from normal tissue as opposed to neuronal tumors (e.g., SY5Y neuroblastoma; LA-N-5 neuroblastoma). Thus, cerebellar granule cells have a normal neuronal physiology in vitro and, as pointed out previously, take on the morphological, biochemical, and electrophysiological characteristics of mature neurons. A disadvantage of primary neuronal cultures is that they are more expensive and more time consuming to produce compared to clonal cell lines. Another potential advantage of clonal cell lines is that these cultures consist of a more uniform population of cells than primary cultures. The purity of cerebellar granule cell cultures, however, is excellent. When isolated from rat pups on postnatal day 8, these cultures consist of an almost pure population of granule cells. The reason for this high purity is, at least in part, that granule cells are by far the most abundant neuronal population in the cerebellum. Furthermore, in the rat, proliferation and differentiation of cerebellar granule cells occurs postnatally and, as undifferentiated neurons survive better than differentiated neurons when seeded in culture, the viability of the neurons is enhanced. As primary cultures of rat cerebellar granule cells are post-mitotic, it is important to treat the cultures with the antimitotic agent AraC to eliminate proliferating cells such as astrocytes or fibroblasts. If the cultures are not treated with an antimitotic, the neurons can

Table 12.7.1 Potential Problems Associated with Production of Cerebellar Granule Cell Cultures

Problem	Possible cause	Solution
Medium contains viscous clumps after centrifugation	No DNase I added	Add fresh DNase I and incubate for ≥15 min at 37°C
Low cell yield prior to plating	Cerebellum not minced thoroughly prior to sieving through cell strainers	Thoroughly mince cerebellum. Increase trituration though 20-G syringe needle.
Low cell yield/viability after plating	No poly-L-lysine coating	No solution
	Prolonged dissection time	Decrease dissection time and keep tissue on ice whenever possible
Cell viability decreases after 5 days in vitro	Lack of depolarizing conditions	Add 24.5 mM KCl to cell culture medium
Floating/nonadherent cells	Contamination	Discard cells
	Old cultures	Use cultures within 2-3 weeks
Presence of proliferating cells	Cultures not treated with AraC	Treat cells with AraC on days 3 and 5 after isolation
	No preplating during isolation	Preplate cells on tissue culture flask to remove proliferating cells
	Meninges not removed during isolation	Thoroughly remove meninges during dissection

rapidly be overgrown by proliferating cells. It should be noted, however, that AraC has been shown to be cytotoxic to granule cells (Dessi et al., 1995; Saunders et al., 1997) and thus, exposure to AraC should be limited to a total of 48 hr.

Critical Parameters and Troubleshooting

A number of potential problems associated with the production of primary cultures of rat cerebellar granule cells are presented in Table 12.7.1.

Dissection of tissue

Neonatal rats (i.e., 8 days old) should be used. Rapid removal of the brains into ice-cold sterile medium is critical for good neuronal viability in vitro. The pups should be sacrificed and brains removed one at a time until the researcher is confident that the brains will not remain in the cranium for >5 to 10 min after decapitation. The tissue should be maintained on ice until enzymatic digestion with trypsin and DNase. Even though the two AraC treatments will reduce the presence of proliferating cells, thorough removal of the meningial layer is important to minimize fibroblast contamination.

Cell dissociation and maintenance in vitro

The tissue must be thoroughly minced prior to enzymatic digestion with trypsin and DNase to ensure a maximum surface area. The culture medium should not be supplemented with serum until after the enzymatic dissociation as serum contains trypsin inhibitors. Preplating of the cultures onto 75-cm^2 tissue culture flasks coated with low concentrations of poly-D-lysine (i.e., 50 µg/ml) is critical in removing contaminating astrocytes and ensuring that the neurons can easily be dislodged by shaking. A poly-D-lysine substrate (i.e., 500 µg/ml) is important for efficient granule cell plating. In addition to 10% heat-inactivated fetal bovine serum, cerebellar granule cells maintained in vitro require depolarizing concentrations of extracellular KCl (25 mM) and high glucose (50 mM; i.e. complete DMEM) to survive >5 days in vitro.

Contamination

Contamination usually involves fungi or bacteria. Long fibrous processes that may appear as mats in the culture dish typically characterize fungal contamination. Bacterial contamination, on the other hand, usually alters the color of the culture medium overnight resulting in a yellow appearance (i.e., a change in pH).

The culture medium may also appear yellow if the medium is not changed every 3 days or if the cells are plated at a very high density. To identify bacterial contamination, examine the culture with a microscope (with a 200× objective). Contaminating bacteria will appear as floating round or rod-shaped objects that are smaller than the granule cells. The presence of penicillin/streptomycin in the culture medium should reduce bacterial contamination; however, careful handling of the cells and the use of a laminar flow hood will minimize the likelihood of fungal/bacterial contamination. Further, any bottles containing solutions, pipet tips, or other disposables that are used for tissue culture should be labeled as such and should only be opened in the laminar flow tissue culture hood. If contamination of the cultures is detected, the contaminated dishes should immediately be discarded and the laminar flow hood and tissue culture incubator thoroughly cleaned and wiped down with 70% ethanol. In addition, all solutions (e.g., culture medium) that were used in maintaining the contaminated cultures should be discarded or filter sterilized.

Contamination of the granule cell cultures can also be due to the presence of impurities such as non-neuronal cells (i.e., glial cells or fibroblasts). These cells can be identified as rapidly proliferating cells that, unlike granule cells, appear flat in culture. In addition, the contaminating cells are usually significantly larger that the granule cells and often form foci of dividing cells. As mentioned previously, even though the two AraC treatments will reduce the presence of proliferating cells, thorough removal of the meningial layer and preplating the cells in poly-D-lysine coated flasks is important to minimize fibroblast and astrocyte contamination. Further, even though the majority of neurons in these cultures are granule cells, GABAergic interneurons (i.e., stellate, basket cells) account for a small number of contaminating cells. These GABAergic neurons, however, are selectively lost during the first 8 days in vitro (Aloisi et al., 1985). Identification of cerebellar granule cells in vitro is described in Anticipated Results.

Anticipated Results

Primary cultures of rat cerebellar granule cells isolated as described above should have a rounded, "cluster of grapes" appearance with long processes extending in all directions after ~5 to 6 days in vitro. Cell yields should be ~2.1 $\times 10^7$ cells per cerebellum. The number of cells will decrease for the first week in vitro, after that, the population of cells will stabilize. After ~7 days the number of cells remaining will be ~30% to 35% of the initial plated amount (Oberdoerster and Rabin, 1999). This initial loss of cells has been reported by others (Fields et al., 1982; Pantazis et al., 1993) and probably reflects the trauma of isolation as well as the exposure of the cultures to AraC.

Time Considerations

The time required for the preparation of primary cultures of rat cerebellar granule cells is ~5 to 6 hr. The time required for changing of the medium every 3 days will vary depending on the number of tissue culture plates but may range from 30 min to 2 hr.

Literature Cited

Aloisi, F., Clotti, M.T., Levi, G. 1985. Characterization of GABAergic neurons in cerebellar primary cultures and selective neurotoxic effect of serum fractions. *J. Neurosci.* 5:2001-2008.

Balazs, R., Jørgensen, O., and Hack, N. 1988. *N*-methyl-D-aspartate promotes the survival of cerebellar granule cells in culture. *Neuroscience* 27:437-451.

Burgoyne, R., Graham, M., and Cambray-Deakin, M. 1993. Neurotrophic effects of NMDA receptor activation on developing cerebellar granule cells. *J. Neurocytol.* 22:689-695.

Copani, A., Bruno, V., Barresi, V., Battaglia, G., Condorelli, D., and Nicoletti, F. 1995. Activation of metabotropic glutamate receptors prevents neuronal apoptosis in culture. *J. Neurochem.* 64:101-108.

Cull-Candy, S.G., Howe, J.R., and Ogden, D.C. 1988. Noise and single channels activated by excitatory amino acids in rat cerebellar granule neurones. *J. Physiol.* 400:189-222.

D'Mello, S., Anelli, R., and Calissano, P. 1994. Lithium induces apoptosis in immature cerebellar granule cells but promotes survival of mature neurons. *Exp. Cell Res.* 211:332-338.

Dessi, F., Pollard, H., Moreau, J., Ben-Ari, Y., and Charriaut-Marlangue, C. 1995. Cytosine arabinoside induces apoptosis in cerebellar neurons in culture. *J. Neurochem.* 64:1980-1987.

Fields, K.L., Currie, D.N., and Dutton, G.R. 1982. Development of THY-1 antigen on cerebellar neurons in culture. *J. Neurosci.* 2:663-673.

Gallo, V., Kingsbury, A., Balazs, R., and Jorgensen, O.S. 1987. The role of depolarization in the survival and differentiation of cerebellar granule cells in culture. *J. Neurosci.* 7:2203-2213.

Levi, G., Aloisi, F., Ciotti, M.T., and Gallo, V. 1984. Autoradiographic localization and depolarization-induced release of acidic amino acids in differentiating cerebellar granule cell cultures. *Brain Res.* 290:77-86.

Marini, A.M., Ueda, Y., and June, C.H. 1999. Intracellular survival pathways against glutamate re-

ceptor agonist excitotoxicity in cultured neurons. Intracellular calcium responses. *Ann. N.Y. Acad. Sci.* 890:421-437.

Oberdoerster, J. and Rabin, R.A. 1999. Enhanced caspase activity during ethanol-induced apoptosis in rat cerebellar granule cells. *Eur. J. Pharmacol.* 385:273-282.

Oberdoerster, J., Guizzetti M., and Costa L.G. 2000. The effect of phenylalanine and its metabolites on the proliferation and viability of neuronal and astroglial cells: Possible relevance in maternal phenylketonuria. *J. Pharmacol. Exp. Ther.* 295:295-301.

Pantazis, N., Dohrman, D., Goodlett, C., Cook, R., and West, J. 1993. Vulnerability of cerebellar granule cells to alcohol-induced cell death diminishes with time in culture. *Alcohol Clin. Exp. Res.* 17:1014-1021.

Saunders, P.A., Chalecka-Franaszek, E., and Chuang, D.M. 1997. Subcellular distribution of glyceraldehyde-3-phosphate dehydrogenase in cerebellar granule cells undergoing cytosine arabinoside-induced apoptosis. *J. Neurochem.* 69:1820-1828.

Schramm, M, Eimerl, S., Costa, E. 1990. Serum and depolarizing agents cause acute neurotoxicity in cultured cerebellar granule cells: Role of the glutamate receptor responsive to N-methyl-D-aspartate. *Proc. Natl. Acad. Sci. U.S.A.* 87:1193-1197.

Wyllie, D.J. and Cull-Candy, S.G. 1994. A comparison of non-NMDA receptor channels in type-2 astrocytes and granule cells from rat cerebellum. *J. Physiol.* 475:95-114.

Key References

Reberl G., Haynes L., and Lelong I.H. 1999. Nerve cell culture methodology: The medium environment. *In* The Neuron in Tissue Culture. (L.W. Haynes, ed.) pp. 323-352, John Wiley & Sons, New York.

An excellent review of potential pitfalls and methodologies in both primary and clonal neuronal cell cultures.

Contributed by Jan Oberdoerster
Aventis CropScience
Research Triangle Park, North Carolina

Measurement of Glial Fibrillary Acidic Protein

A characteristic feature of toxicant-induced injury of the developing or adult central nervous system is astrocytic hypertrophy at the site of damage (Norton et al., 1992; O'Callaghan, 1993; Norenberg, 1994; O'Callaghan et al., 1995). Astrocytic hypertrophy, also known as reactive gliosis or simply gliosis, is characterized by an accumulation of glial filaments, of which glial fibrillary acidic protein (GFAP) is the principal protein constituent (Eng, 1988). Thus, an increase in the brain concentration of GFAP serves as a biochemical indicator of neurotoxicity. In aggregate, the results of a number of studies show that a large variety of toxic insults of the CNS result in an increase in GFAP; moreover, these effects are dose-related, they correspond to regions of neural damage and they can be observed in the absence of overt cytopathology (O'Callaghan, 1993; O'Callaghan et al., 1995).

This unit describes a single method for assaying the concentration of GFAP contained in detergent homogenates of brain tissue. The method presented includes a protocol for tissue homogenate preparation (see Support Protocol 1), a protocol for assaying total brain protein in detergent homogenates (see Support Protocol 2), and a protocol for a GFAP sandwich ELISA (see Basic Protocol). Although other protocols exist for assaying GFAP (see Commentary), the sandwich ELISA is the method of choice due to its simplicity, cost, speed, and high-throughput.

GFAP SANDWICH ELISA

BASIC PROTOCOL

The GFAP sandwich ELISA is suitable for assaying the concentration of GFAP present in homogenates of brain tissue. This method has successfully been applied to analysis of at least the following species: mouse, rat, guinea pig, dog, monkey, man, chicken, pigeon, trout, and cod. Because GFAP is evolutionarily conserved, it is likely that this assay can be very broadly applied across many species. The assay does not require preparation of any special materials or reagents; all components are available from commercial sources at modest cost. However, it is dependent on the use of specific, commercially available antibody reagents. The 96-well microtiter plate format lends itself to processing large numbers of samples, and it makes the assay suitable for automation with a variety of liquid handling systems. It takes a minimum of 5 hr to process a single 96-well plate after preparation of the tissue homogenates (Support Protocol 1).

Materials

Bovine GFAP (American Research Products)
PBS/Triton: PBS containing 0.5% (v/v) Triton X-100 (Bio-Rad)
Sample: brain homogenate from treated animal (Support Protocol 1)
Rabbit anti-glial fibrillary acidic protein antibody (see recipe; Dako, cat. #Z0334)
Phosphate-buffered saline (PBS; e.g., Pierce; *APPENDIX 2A*; see recipe)
Blocking solution (see recipe)
Detection antibody solution (see recipe) consisting of mouse anti-glial fibrillary acidic protein monoclonal antibody (clone GA5; Oncogene Research Products) and alkaline phosphatase–conjugated anti-mouse IgG (Jackson Immuno Research, cat. #315-055-003)
Blocking solution containing Triton
Alkaline phosphatase substrate kit (e.g., Bio-Rad) containing:
  Alkaline phosphatase substrate: *p*-nitrophenylphosphate tablets (see recipe)
  5× diethanolamine buffer
0.4 N NaOH (e.g., Labchem)

Contributed by James P. O'Callaghan
Current Protocols in Toxicology (2002) 12.8.1-12.8.12

Vortex mixer or ultrasonic cell disruptor (e.g., PGC with 2-mm probe)
96-well flat-bottom, microtiter plates (e.g., Immulon 2, Dynatech)
Microtiter plate reader, 405 nm

NOTE: Detergents act as wetting agents, therefore, more than a single use of a pipet tip with SDS- or Triton X-100-containing samples can lead to carry-over errors. Thus, it is recommended to use a single pipet tip per sample and to withdraw the sample only a single time per tip.

Prepare standards

1. Prepare a standard, a brain homogenate (Support Protocol 1) from control, untreated animals.

   This standard should be prepared from the same species that was used to prepare the samples to be assayed for GFAP because GFAP immunoreactivity with a given set of immunodetection reagents will differ among different species. A large number of standards can be prepared in advance from a single "pool" of a 1% SDS homogenate prepared as described in Support Protocol 1. This homogenate can be aliquoted (50 µl) and stored frozen at −70°C prior to use. Thus, the GFAP standard essentially consists of a control sample. This is preferable over using a pure GFAP standard because using control tissue as a standard obviates any influence of the tissue "matrix" on the assay performance. Moreover, where absolute values of GFAP per total tissue protein are not required, data simply can be presented as arbitrary units of GFAP immunoreactivity.

   If it is deemed necessary to express the data in units of GFAP per unit of total protein, aliquots of a 1% SDS homogenate should still be used as a GFAP standard. This can be accomplished by "standardizing the standard" with addition of a known amount of pure GFAP to the 1% SDS homogenate (i.e., an internal standard; O'Callaghan, 1991). Immunoreactivity values generated from standard curves of the GFAP "spiked" homogenate and the homogenate alone then can be used to determine the concentration of GFAP in the homogenate.

   For analysis of GFAP in regions of rat brain, the authors routinely use aliquots of a hippocampal homogenate as a standard. It contains ~2.5 µg GFAP/mg total protein. Other species (e.g., mouse) contain different levels of GFAP in hippocampus.

2. To prepare dilutions of the GFAP standard, remove a tube of the GFAP standard from the freezer, thaw it at room temperature, and vortex or sonify it prior to dilution. With a rat hippocampal homogenate as a typical standard (~2.5 µg GFAP/mg total protein), use the total protein value for this homogenate (~10 mg/ml) to prepare a standard curve in PBS/Triton.

   For rat hippocampal homogenate, the protein values for the standard curve should be between ~0.25 to 10 µg/100 µl/microtiter plate well (i.e., 0.25, 0.5, 1.0, 2.5, 5.0, 7.5, 10 µg total protein/100 µl). Table 12.8.1 shows an example of dilutions needed to prepare a standard curve from a homogenate of rat hippocampus (hippocampus std.). Typically, standards are run in duplicate.

Prepare sample

3. Remove sample from the freezer, thaw at room temperature, and vortex or sonify prior to dilution.

4. Prepare dilutions of the sample in PBS/Triton to a concentration of ~10 µg total protein/100 µl.

   Samples high in GFAP (e. g., cerebellum) may need to be diluted to a concentration of 5 µg total protein/100 µl of PBS/Triton. Samples low in GFAP (e.g., striatum) may need to be diluted to 20 µg total protein/100 µl of PBS/Triton. These dilution factors are determined empirically. The best practice is to prepare multiple dilutions of each sample to ensure that

Table 12.8.1 GFAP Standard Curve Preparation

Tube no.	Total protein (µg)/100 µl/well (ng GFAP)	Hippocampus std. (10.34 mg/ml) added (µl)	Amount transferred for dilution (µl)	PBS/Triton
1	10 (25.00)	29		2971
2	7.5 (18.75)		2063 from tube no. 1	687
3	5.0 (12.50)		1833 from tube no. 2	917
4	2.5 (6.25)		1000 from tube no. 3	1000
5	1.0 (2.50)		800 from tube no. 4	1200
6	0.5 (1.25)		1000 from tube no. 5	1000
7	0.25 (0.625)		700 from tube no. 6	700

optical density readings for a given sample fall on the linear portion of the standard curve. Typically, samples (like standards) are run in duplicate.

Coat microtiter plates

5. Coat an Immulon-2 96-well flat-bottom microtiter plate with rabbit anti-GFAP antibody. Add 1.0 µg total immunoglobulin protein/100 µl PBS/well.

   Rabbit anti-GFAP antibody is used as the "capture" antibody for the sandwich ELISA.

   For each 96-well plate, ~25 µl of anti-GFAP (Dako) in 10 ml of PBS is needed.

6. Incubate the plate at 37°C for 1 hr.

   This coating step may be done at the beginning of the assay or it may be done the night before with storage in coating antibody overnight at 4°C. Perform all other incubation and reagent addition steps at room temperature.

7. Empty the plate into a sink and tap (upside down) on absorbent paper to remove excess liquid.

   This latter procedure is important to eliminate the possibility of any reagent carry-over between steps.

8. Wash plates four times with 200 µl/well PBS, tapping and blotting between each wash.

Block plates

9. Block 1 hr with 100 µl/well blocking solution.

10. Empty plate, tap on absorbent paper to remove excess liquid.

Perform sandwich ELISA

11. Load diluted standard curve and samples in a volume of 100 µl/well. Incubate for 1 hr.

    The template below (Table 12.8.2) is an example of a typical 96-well microtiter plate layout for GFAP standards and unknowns.

12. Empty plate and tap on absorbent paper.

13. Wash four times with 200 µl/well PBS/Triton, tapping and blotting between each wash.

14. Incubate for 1 hr in 100µl/well of a detection antibody solution consisting of monoclonal anti-GFAP antibody diluted 1:500 and alkaline phosphatase conjugated anti-mouse IgG diluted 1:3000 in blocking solution containing Triton.

Table 12.8.2 Microtiter Plate Template

	Standards		Samples									
Row	1	2	3	4	5	6	7	8	9	10	11	12
A	Blk	Blk	? 1	? 1	? 9	? 9	? 17	? 17	? 25	? 25	? 33	? 33
B	Std 1	Std 1	? 2	? 2	? 10	? 10	? 18	? 18	? 26	? 26	? 34	? 34
C	Std 2	Std 2	? 3	? 3	? 11	? 11	? 19	? 19	? 27	? 27	? 35	? 35
D	Std 3	Std 3	? 4	? 4	? 12	? 12	? 20	? 20	? 28	? 28	? 36	? 36
E	Std 4	Std 4	? 5	? 5	? 13	? 13	? 21	? 21	? 29	? 29	? 37	? 37
F	Std 5	Std 5	? 6	? 6	? 14	? 14	? 22	? 22	? 30	? 30	? 38	? 38
G	Std 6	Std 6	? 7	? 7	? 15	? 15	? 23	? 23	? 31	? 31	? 39	? 39
H	Std 7	Std 7	? 8	? 8	? 16	? 16	? 24	? 24	? 32	? 32	? 40	? 40

The assay is based on the use of the monoclonal antibody as a "detection" reagent and the alkaline phosphatase conjugate to bind to the detection antibody and generate a colored reaction product proportional to the amount of antigen (GFAP) present in the samples. Substitution of antibodies from other vendors may not yield suitable results.

15. Wash four times with 200 µl/well PBS/Triton. Tap and blot between each wash.

Visualize results

16. Add 100 µl/well alkaline phosphatase and substrate and incubate for 20 min.
17. Stop reaction with 100 µl/well of 0.4 N NaOH.
18. "Pop" any bubbles in the plate wells with a needle or pipet tip to ensure uniform and accurate readings of standard and sample optical density (OD). Read plate at 405 nm in a microtiter plate reader.

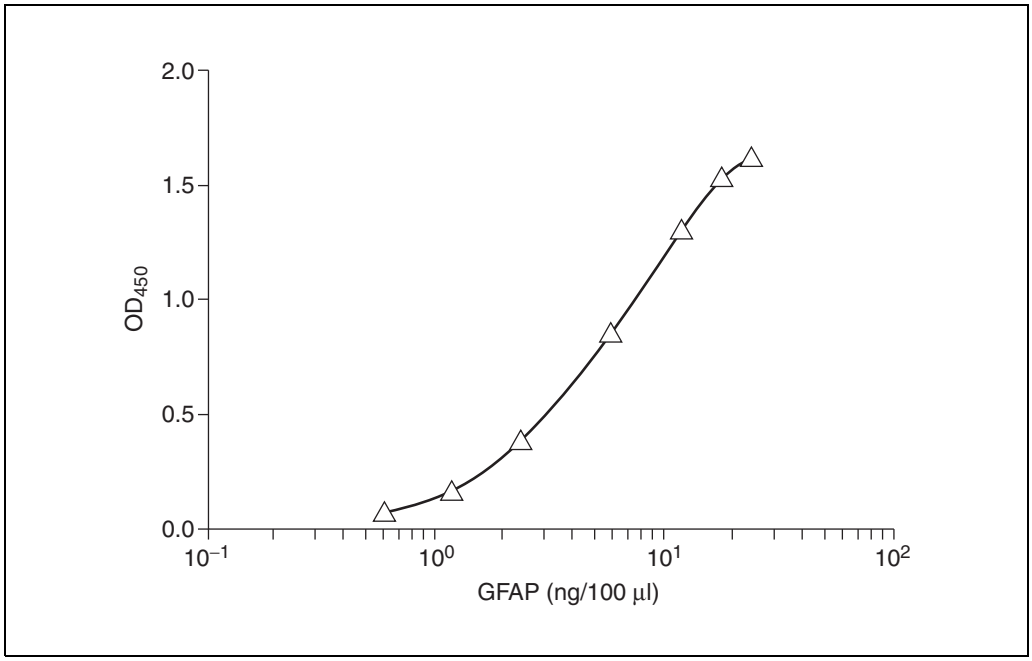

Figure 12.8.1 Sample GFAP standard curve. GFAP values in nanograms correspond to levels found in 0.25 to 10 µg total hippocampal homogenate protein. Dilutions of this homogenate were used to construct the GFAP standard curve shown.

Table 12.8.3 Sample Values for GFAP Standard Curve

Standard	Total protein (μg) (ng GFAP)	Well	OD	Mean	Std. dev.[a]	CV[a]
Blank		A1	0.001	0.0	0.001	0.0
		A2	–0.001			
STD01	10 (25.00)	B1	1.694	1.632	0.087	5.4
		B2	1.570			
STD02	7.5 (18.75)	C1	1.537	1.543	0.008	0.5
		C2	1.549			
STD03	5.0 (12.50)	D1	1.295	1.314	0.027	2.1
		D2	1.334			
STD04	2.5 (6.25)	E1	0.857	0.859	0.002	0.3
		E2	0.861			
STD05	1.0 (2.50)	F1	0.386	0.386	0.000	0.1
		F2	0.386			
STD06	0.5 (1.25)	G1	0.175	0.164	0.016	10.0
		G2	0.152			
STD07	0.25 (0.625)	H1	0.072	0.076	0.006	7.6
		H2	0.080			

[a]Abbreviations: CV, coefficient of variation; std. dev., standard deviation.

19. Calculate the GFAP concentration in each of the samples by comparing the sample OD value to those obtained for the linear portion of the GFAP standard curve.

    Software programs linked to specific plate readers should be programmed to plot OD versus GFAP values in linear versus log-linear fashion. Typically, the authors utilize the 4-parameter curve fit equation and generate curves as shown in Fig. 12.8.1 and Table 12.8.3. Most programs allow for automatic subtraction of blanks and incorporation of dilution factors.

    Data are expressed as microgram GFAP per milligram total protein or, if the absolute amount of GFAP in the standard is not available, data are expressed as GFAP-like immunoreactivity per milligram total protein. Total protein concentration in the samples is estimated from the total protein assay described in Support Protocol 2. Data can also be expressed on the basis of tissue wet weight (microgram GFAP per gram wet weight or GFAP immunoreactivity per gram wet weight). Although this approach permits elimination of the total protein assay, the authors find that the GFAP values obtained are slightly more variable.

BRAIN TISSUE PREPARATION

SUPPORT PROTOCOL 1

This protocol describes the procedure for preparing brain tissue as standards or samples for subsequent analysis of GFAP by sandwich ELISA (Basic Protocol). This procedure does not describe or recommend a specific approach for dissecting brain tissue. It is noted, however, that reliable dissections are essential for obtaining reproducible results with the GFAP ELISA (see Commentary).

NOTE: All protocols using live animals must first be reviewed and approved by an Institutional Animal Care and Use Committee (IACUC) and must follow officially approved procedures for the care and use of laboratory animals.

Materials

Control or treated animal
1% (w/v) SDS, 85° to 95°C
Dissecting instruments
Ultrasonic cell disruptor (e.g., PGC with 2-mm probe)

1. Sacrifice animal by an approved method and remove the brain as rapidly as possible.

   Animals should be sacrificed one at a time to prevent tissue degradation.

2. Dissect brain regions.

   If a number of regions are to be dissected, this process can be aided by keeping the brain firm on a cold plate (e.g., Thermoelectrics cold plate, Aldrich Chemical Co., or simply an inverted petri dish placed on ice) maintained at ~4°C. Rat or mouse brains can be dissected free hand into ten to fifteen region within ~10 min. This number of regions can be prepared on a cold plate or at room temperature without degradation of GFAP as assessed by immunoblot analysis. All brain regions can be stored frozen indefinitely in capped microcentrifuge tubes at this step in the protocol, or they can be homogenized immediately.

3. Weigh and homogenize the dissected brain parts. Tare an appropriately labeled microcentrifuge or other suitable storage tube. Place individual brain regions in a tube, obtain the weight, and immerse the tissue in 10 vol hot (85° to 95°C) 1% (w/v) SDS.

   For example, 0.1 g of tissue would be immersed in 1.0 ml of SDS.

4. While the SDS is still hot, homogenize the tissue by sonification with a 2-mm ultrasonificiation microprobe.

   A motor-driven Teflon pestle/glass homogenizer can be substituted for an ultrasonification device to homogenize most brain areas. This method is not as desirable as sonification, however, because it is much slower and often does not result in complete homogenization.

5. Store samples frozen at −70°C prior to assay.

   Samples prepared and stored in this manner retain their GFAP content for ≥5 years.

SUPPORT PROTOCOL 2

ASSAY FOR TOTAL PROTEIN

This protocol describes the procedure for assaying the concentration of total protein in the SDS-homogenates. The procedure described is essentially the bicinchoninic acid (BCA) method described by Smith et al. (1985), which is available in kit form. To assay total protein concentration of the SDS homogenates the assay must be compatible with 1% SDS. Use of the BCA assay is not an absolute requirement as other detergent-compatible methods are available (e.g., Bio-Rad DC protein assay). Bovine serum albumin (BSA) is used as the protein standard in the described procedure. Other protein standards can be substituted.

Materials

Bovine Serum Albumin (BSA), RIA grade, fraction V (Sigma)
1% (w/v) SDS (Bio-Rad)
Brain homogenates (Support Protocol 1)
BCA Protein Kit (Pierce) containing:
  Solution A
  Solution B

96-well microtiter plates
Microtiter plate reader, 562 nm

NOTE: Detergents act as wetting agents, therefore, more than a single use of a pipet tip with SDS-containing samples can lead to carry-over errors. Thus, it is recommended to use a single pipet tip per sample and to withdraw the sample only a single time per tip.

1. Prepare total protein standard stock as a 1 mg/ml solution of BSA in 1% (w/v) SDS.

   Aliquots (600 µl to 1.0 ml) of this standard can be stored frozen at −70°C for future use. Thaw as needed, but do not refreeze.

2. Prepare a total protein standard curve by making dilutions of the BSA standard in 1% SDS as follows: 1.0, 2.5, 5.0, 7.5, and 10 µg/10 µl of 1% SDS (no dilution is required for last standard).

3. Vortex each tube and add 10 µl of each standard to a well of the microtiter plate; add 10 µl of 1% SDS to a well to serve as a blank.

   Typically, standards are run in duplicate.

4. Prepare dilutions of the sample. Thaw the sample, vortex, and dilute a 10-µl aliquot with 190 µl of 1% SDS. Vortex the dilution tube and add a 10-µl aliquot into a well of a microtiter plate.

5. Add 200 µl of the BCA protein assay reagent (composed of 50:1 ratio of solution A/solution B of the Pierce BCA reagent) to each standard and sample.

6. Incubate the plate 30 min at 37°C.

   Other incubation temperatures are permissible; follow directions provided with the kit.

7. "Pop" any bubbles in the microtiter plate wells with a needle or pipet tip to ensure uniform and accurate readings. Read the plate at 562 nm.

8. Calculate the concentration of total protein in the sample from the standard curve.

   Software programs linked to specific plate readers should be programmed to plot OD versus total protein in a linear fashion. Most programs allow for automatic subtraction of blanks and incorporation of dilution factors. Because the samples are prepared in 10 vol of diluent, typically, total protein values are ~10 mg/ml.

REAGENTS AND SOLUTIONS

Use Milli-Q-purified water or equivalent for the preparation of all reagents and in all protocol steps. For common stock solutions, see ***APPENDIX 2A****; for suppliers, see* ***SUPPLIERS APPENDIX****.*

Alkaline phosphatase substrate

Mix 2 ml diethanolamine buffer on a stirrer with two *p*-nitrophenylphosphate tablets and 8 ml of deionized water. Make this solution fresh on the day of use and do not save.

Blocking solutions

Add 5 grams of non-fat powdered milk (Carnation) to 100 ml PBS (see recipe) or 100 ml PBS/Triton (see recipe). Make these solutions fresh the day of assay and do not save.

Prepare at least 100 ml of each to facilitate dissolving the powdered milk; PBS may be warmed slightly to facilitate this process.

Also, do not retain the powdered milk for longer than a month or two at room temperature. The dry milk tends to discolor and will not go into solution at shelf times longer than 2 months.

Detection antibody solution

Make up stock solutions of monoclonal anti-GFAP antibody (clone GA5; Oncogene Research Products) and alkaline phosphatase–conjugated anti-mouse IgG (Jackson Immuno Research) according to the vendors' instructions. Store both stocks at 4°C per the vendors' instructions. Add 20 µl of the monoclonal antibody solution stock and 3.3 µl of the alkaline phosphatase conjugate stock to 10 ml blocking solution containing Triton (see recipe). Make this solution fresh on the day of use and do not save.

Phosphate-buffered saline (PBS)

Mix one packet of PBS (Pierce) thoroughly with 500 ml of water to give a final concentration of: 137 mM NaCl, 1.0 mM KCl, 2 mM KH_2PO_4, 8.0 mM $Na_2HPO_4 \cdot 7H_2O$, pH 7.4. Store up to 1 month at 4°C.

PBS washes require ~20 ml/plate.

PBS/Triton

Add 2.5 ml of Triton X-100 (0.5% v/v) to 500 ml of PBS (see recipe). Store up to 1 month at 4°C.

PBS/Triton washes require ~20 ml/plate.

Rabbit anti-GFAP antibody

Add 25µl of polyclonal rabbit anti-GFAP antibody (Dako, cat. #Z0334) to10 ml PBS. Make this solution fresh on the day of use and do not save.

COMMENTARY

Background Information

It has long been known that damage to the central nervous system results in astrogliosis (gliosis, reactive gliosis, glial activation), a response to brain injury characterized by hypertrophy and, less often, hyperplasia of astrocytes, a sub-type of CNS glia (Eng, 1988; Norenberg, 1994). At the electron microscope level, astrogliosis is characterized by the accumulation of glial filaments. GFAP was found to be the major protein component of these filaments (Eng, 1988). As such, GFAP serves as a biomarker for filament accumulation and, therefore, of gliosis (Eng, 1988; Norton et al., 1992; O'Callaghan, 1993). With the development of antibodies to GFAP, immunohistochemical analysis of this protein soon documented that gliosis occurs in response to diverse insults of the CNS, including trauma, disease, and toxic exposures (Eng, 1988; Norton et al., 1992; O'Callaghan, 1993; Norenberg, 1994; O'Callaghan et al., 1995). Thus, a large body of evidence now has been accumulated demonstrating the ubiquity of the glial response to all types of CNS damage based on immunhistochemistry of GFAP. Only recently, however, have methods been introduced to assay levels of GFAP as a means of quantifying gliosis.

While GFAP immunohistochemistry has proven useful for revealing patterns of gliosis after brain injury, this approach does not lend itself to quantification or the analysis of large numbers of samples. Small (25% to 50%), but toxicologically significant increases, also may be difficult to detect by immunohistochemistry. These drawbacks, combined with the need to develop quantitative biomarkers of neurotoxicity (O'Callaghan et al., 1995) and to define quantitative aspects of toxicant- and disease-induced gliosis, have prompted the development and implementation of a number of GFAP assays. These assays have been applied to examine gliosis in specific brain areas already known to be affected by disease or other insult. In addition, they also can be broadly applied in a risk assessment context (U.S. EPA; see O'Callaghan, 1991) to screen for potential sites of neural damage resulting from toxic exposures of the CNS. Recently, analysis of GFAP has been used to demonstrate that the degree of cortical gliosis in postmortem brain tissue from victims of Alzheimer's disease correlates with the severity of dementia scores in these individuals prior to death (G. Webster Ross, unpub. observ.). Analysis of GFAP in cerebrospinal fluid (CSF) has also been applied to the human condition as an indicator of the severity of

traumatic injury to the brain (Rosengren et al., 1994). Finally, analysis of GFAP can be used as an indicator of the presence of brain or spinal cord contamination of meat (Schmidt et al., 1999).

Of the number of GFAP assays that have appeared in the literature over the last 15 years; all essentially fall into two categories: (1) solid-phase immunoassays where GFAP is immobilized on a solid support matrix and detected by mono- or polyclonal antibodies, or (2) liquid-phase assays where GFAP from brain extracts, solubilized brain tissue, or cerebrospinal fluid is "captured" by one antibody and then detected by another antibody raised in a different host species (Butler et al., 1986). The assay described in this unit is of the second type, and it has a number of advantages over the solid-phase assays. Specifically, solid-phase detection and "quantification" of GFAP most commonly involves the time-consuming resolution of a protein mixture by SDS-PAGE, followed by electrophoretic transfer to a solid support membrane. Anti-GFAP antibodies coupled to a variety of detection reagents can then be used for quantification of GFAP bound to the membranes. Unfortunately, this approach has been found to severely underestimate the concentration of GFAP in the resolved mixture of proteins and the effects of treatments known to increase GFAP (O'Callaghan et al., 1999). Other solid-phase assays for GFAP have been developed that do not rely on prior resolution of protein mixtures by SDS-PAGE (Wang et al., 1990; O'Callaghan, 1991). These assays incorporate manual spotting of brain homogenates on solid supports, with or without the aid of a template. The membranes are then incubated with anti-GFAP polyclonal or monoclonal antibodies, which, in turn, are bound by ^{125}I-labeled protein A. Quantification is achieved by gamma spectrometry or by densitometry of the autoradiogram. These assays give a linear signal over a fairly large range of spotted protein. However, they require large amounts of reagents, including radiolabeled reagents, and they do not have impressive throughput.

The sandwich ELISA for GFAP described in this unit or similar ELISAs described previously (Eng et al., 1986; Kretzschmar et al., 1985; O'Callaghan, 1991; Rosengren et al., 1994), have several advantages in comparison to the other methods for assaying GFAP described above. They are easier to perform because they have fewer steps. They are more sensitive (liquid-phase assays are generally five to ten times more sensitive than solid-phase assays). Although they may require a greater number of reagents, ELISAs adapted to the microtiter plate format permit the use of very small volumes, which results in a significant overall cost reduction. The 96-well microtiter plate format also has the advantage of speed and high throughput. From sample application to data collection, all steps can be performed in the plate. Moreover, the microtiter plate–based format permits the entire assay to be automated through the use of robotic liquid handling processors. Finally, radioactivity is not involved, making the assay safer to perform, and allowing the user to avoid costly and time-consuming radioactivity disposal procedures.

Although most of the GFAP sandwich ELISAs described to date are similar and share the advantages afforded by this technique, the assay described in this unit may have a few additional advantages. Because it is based on detergent-solubilized homogenates of a given brain area, any treatment effects can be directly related to effects in that brain area, rather than an arbitrarily defined extract or subfraction that may contain only a portion of the total GFAP in that area. Using a solubilized homogenate rather than a subfraction of a given brain area also facilitates comparisons of quantitative data on GFAP to immunohistochemical staining of GFAP in that area. Moreover, it also helps rule out inter-laboratory differences associated with assaying GFAP content in one type of extract in one lab and another type of extract/fraction in another lab. Finally, the same SDS-denatured homogenate used to assay GFAP can be subjected to multiple assays for additional glial or neuronal proteins, thereby permitting comparisons to be made among multiple markers of neurotoxicity in a single sample. For example, the dopaminergic neurotoxicant, 1-methyl-4-phenyl-1,2,3,6-tetrahydropyridine, causes a large increase in GFAP that results from damage to dopaminergic nerve terminals. This damage can be quantified by immunoassay of tyrosine hydroxylase (TH), a marker of dopamine-containing nerve terminals in the target region (O'Callaghan et al., 1990). Both markers can be assayed from aliquots of the same tissue sample and, on this basis, the authors find that larger decreases in TH predict greater increases in GFAP.

Critical Parameters and Troubleshooting

The most critical aspect of the GFAP assay is the absolute requirement for preparation of consistently dissected regions of the brain (see

Support Protocol 1). Consistent dissections yield consistent GFAP values with the use of only a few animals per dose or time point (see Anticipated Results). The particular regions to be dissected depend on the questions being addressed. If a target region is known or suspected, dissections can be limited to the region of interest. If the GFAP assay is being applied in a screening context, multiple (ten to fifteen) brain regions must be dissected in order to avoid the possibility of diluting localized increases in GFAP. The possibility exists that extremely localized increases in GFAP may fail to be detected with the assay. While GFAP immunohistochemistry is relatively insensitive in comparison to the GFAP assay, and it may not detect small increases in GFAP, it can reveal small "hot spots" of gliosis (e.g., see effects of MK-801 in Fix et al., 1995). Such discrete astrocytic responses could escape quantification with the GFAP assay due to dilution of signal by surrounding tissue. No one approach can be broadly applied to detect all toxicant-induced damage of the CNS. Therefore it is prudent to use the GFAP sandwich ELISA in conjunction with GFAP immunohistochemistry and other sensitive morphological approaches for detection of neural damage, such as silver degeneration stains (Switzer, 2000), Fluoro-Jade (Schmued and Hopkins, 2000), and stains that detect activated microglia (Streit et al., 1999).

In terms of the GFAP sandwich ELISA itself, the key requirements for optimal performance of the assay include: (1) use of the speci-

Table 12.8.4 Troubleshooting Guide for GFAP Sandwich ELISA

Problem	Possible Cause	Solution
No color reaction	Incorrect preparation of color reagent	If color reaction has not been terminated, remove reagent, add new color reagent and continue assay
	Antibody was not as specified in the protocol	Obtain correct antibody and repeat assay
	One or more antibodies were omitted or used at the wrong dilution	Repeat assay with proper reagents used at the correct dilutions
Color reaction abnormally low	Incubator was set at less that 37°C	Repeat assay with incubator temperature set at 37°C
	Antibody solution too dilute; incorrect preparation of color reagent	Repeat assay with correct reagent dilutions
Color reaction abnormally high	Alkaline phospatase substrate kit is out of date	Repeat assay with fresh kit
	Color reaction was not terminated	Repeat assay and terminate reaction with 0.4 N NaOH
Standard curve not sigmoid	Incorrect plate template set in the plate reader	Use correct plate template and reread plate
	Incorrect standard dilution	Repeat assay with correct standard dilution
Samples not on linear portion of curve	Incorrect standard dilution	Repeat assay with correct dilution of standard
	Incorrect sample dilution	Run multiple dilutions of samples to obtain OD values from the linear portion of the curve
Duplicates are not similar	Carry over from using same tip	Change tips after each use
	Poor pipetting technique	Check pipettor precision by weighing
	Plate washer malfunction	Check plate washer for even dispensing and aspiration
	Bubbles throughout the plate	Pop bubbles and reread plate
Color reaction obtained for standards and samples, but OD values not as expected	Plate read at incorrect wavelength	Read plate at 405 nm

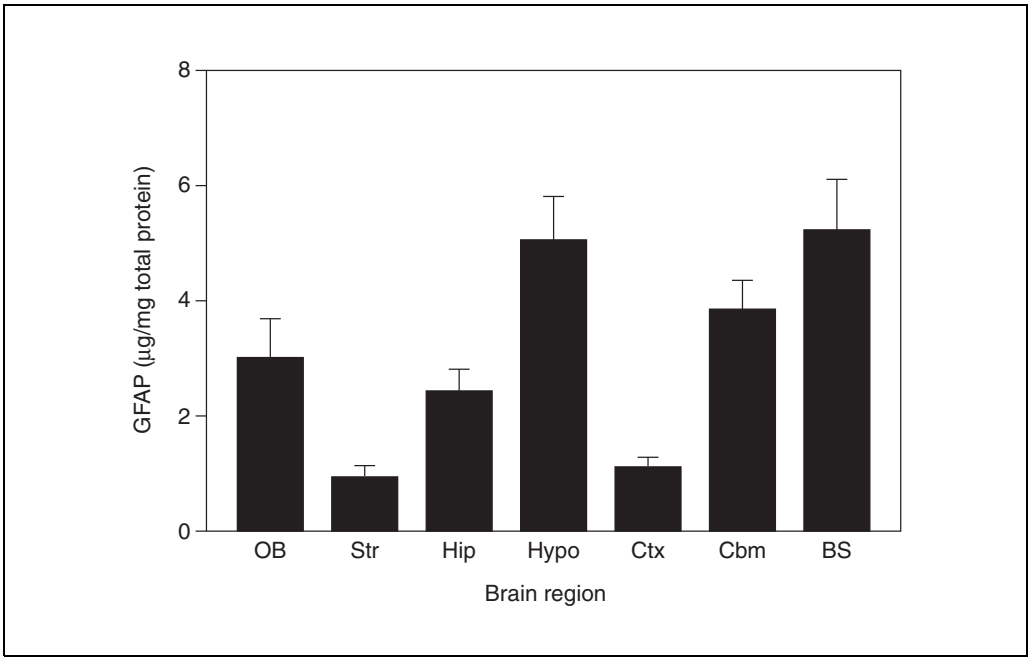

Figure 12.8.2 Levels of GFAP found in different regions of rat brain. Abbreviations: OB, olfactory bulbs; Str, striatum; Hip, hippocampus; Hypo, hypothalamus; Ctx, cortex; Cbm, cerebellum; BS, brain stem.

fied antibodies, (2) addition of the reagents at room temperature, (3) fresh (daily) preparation of all reagents containing antibodies and/or non-fat dry milk, and (4) mixing of the standards and samples prior to their dilution or addition to the microtiter plate wells. A troubleshooting guide is provided in Table 12.8.4 that covers most problems encountered with the assay.

Anticipated Results

GFAP assay values obtained for different regions of the rat brain are presented in Fig. 12.8.2. Absolute values for GFAP (microgram per milligram total protein) may vary depending on the GFAP standard used and the species subjected to evaluation. Region-to-region differences in GFAP values from untreated animals of a given species, however, should remain stable, if consistent dissections are performed.

Time Considerations

The GFAP assay requires ~5 hr for one person to process a 96-well microtiter plate. The time required to prepare brain samples depends on the number of brain areas to be dissected and on whether the areas are stored frozen prior to homogenization. With practice, ten brain areas can be prepared (and homogenized) from 50 rats in 1 day. Two people are required: one to dissect the brains and one (or more) to weigh and homogenize the tissue. The total protein assay requires ~1 hr for one person to process a 96-well microtiter plate.

Literature Cited

Butler, J.E., Spradling, J.E., Suter, M., Dierks, S.E., Heyermann, H., and Peterman, J.H. 1986. The immunochemistry of sandwich ELISAs-I. The binding characteristic of immunoglobulins to monoclonal and polyclonal capture antibodies adsorbed on plastic and their detection by symmetrical and asymmetrical antibody-enzyme conjugates. *Mol. Immunol*. 23:971-982.

Eng, L.F. 1988. Regulation of glial intermediate filaments in astrogliosis. *In* Biochemical Pathology of Astrocytes (M.D. Norenberg, L. Hertz, and A. Schousboe, eds.) pp. 79-90. A.R. Liss, New York.

Eng, L.F., Stöcklin, E., Lee, Y.-L. Shiurba, R.A., Coria, F., Halks-Miller, M. Mozsgai, C., Fukayama, G., and Gibbs, M. 1986. Astrocyte culture on nitrocellulose membranes and plastic: Detection of cytoskeletal proteins and mRNAs by immunocytochemistry and in situ hybridization. *J. Neurosci. Res*. 16:239-250.

Fix, A.S., Wightman, K.A., and O'Callaghan, J.P. 1995. Reactive gliosis induced by MK-801 in the rat posterior cingulate/retrosplenial cortex: GFAP evaluation by sandwich ELISA and immunocytochemistry. *Neurotoxicology* 16:229-237.

Kretzschmar, H.A., DeArmond, S.J., and Forno, L.S. 1985. Measurement of GFAP in hepatic encephalopathy by ELISA and transblots. *J. Neuropathol. Exp. Neurol.* 44:459-471.

Norenberg, M.D. 1994. Astrocyte responses to CNS injury. *J. Neuropathol. Exp. Neurol.* 53:213-220.

Norton, W.T., Aquino, D.A., Hozumi, I., Chiu, F.-C., and Brosnan, C.F. 1992. Quantitative aspects of reactive gliosis: A review. *Neurochem. Res.* 17:877-885.

O'Callaghan, J.P. 1991. Quantification of glial fibrillary acidic protein: Comparison of slot-immunobinding assays with a novel sandwich ELISA. *Neurotoxicol. Teratol*. 13:275-281.

O'Callaghan, J.P. 1993. Quantitative features of reactive gliosis following toxicant-induced damage of the CNS. *Ann. N.Y. Acad. Sci.* 679:195-210.

O'Callaghan, J.P., Miller, D.B., and Reinhard, J.F., Jr. 1990. Characterization of the origins of astrocyte response to injury using the dopaminergic neurotoxicant, 1-methyl-4-phenyl-1,2,3,6-tetrahydro-pyridine. *Brain Res.* 521:73-80.

O'Callaghan, J.P., Jensen, K.F. and Miller, D.B. 1995. Quantitative aspects of drug- and toxicant-induced astrogliosis. *Neurochem. Int.* 26:115-124.

O'Callaghan, J.P., Imai, H., Miller, D.B., and Minter, A. 1999. Quantitative immunoblots of proteins resolved from brain homogenates: Underestimation of specific protein concentration and of treatment effects. *Anal. Biochem*. 274:18-26.

Rosengren, L.E., Wikkelsø, C., and Hagberg, L. 1994. A sensitive ELISA for glial fibrillary acidic protein: application in CSF of adults. *J. Neurosci. Methods* 51:197-204.

Schmidt, G.R., Hossner, K.L., Yemm, R.S., Gould, D.H., and O'Callaghan, J.P. 1999. An enzyme-linked immunosorbent assay for glial fibrillary acidic protein as an indicator of the presence of brain or spinal cord in meat. *J. Food Protect*. 62:394-397.

Schmued, L.C. and Hopkins, K.J. 2000. Fluoro-Jade: Novel fluorochromes for detecting toxicant-induced neuronal degeneration. *Toxicol. Pathol*. 28:91-99.

Smith, P.K., Krohn, R.I., Hermanson, G.T., Mallia, A.K., Gartner, F.H., Provenzano, M.D., Fujimoto, E.K., Goeke, N.M., Olson, B.J., and Klenk, D.C. 1985. Measurement of protein using bicinchoninic acid. *Anal. Biochem.* 150:76-85.

Streit, W.J., Walter, S.A., and Pennell, N.A. 1999. Reactive microgliosis. *Prog. Neurobiol.* 57:563-581.

Switzer, R.C. 2000. Application of silver degeneration stains for neurotoxicity testing. *Toxicol. Pathol*. 28:70-83.

U.S. Environmental Protection Agency. Pesticide Assessment Guidelines, Subdivision F. Hazard Evaluation: Human and Domestic Animals. Addendum 10, Series 81, 82, 83, Neurotoxicity. EPA-540/09-91-123. National Technical Information Service. Springfield, VA.

Wang, S., Rosengren, L.E., Karlsson, J.-E., Stigbrand, T., and Haglid, K.G. 1990. A simple quantitative dot-immunobinding assay for glial and neuronal marker proteins in SDS-solubilized brain tissue extracts. *J. Neurosci. Methods* 33:219-227.

Contributed by James P. O'Callaghan
Center for Disease Control and Prevention
NIOSH
Morgantown, West Virginia

Aggregating Neural Cell Cultures

Aggregating cell cultures are primary cell cultures derived from embryonic tissues and consist of numerous free-floating spheroids exhibiting histotypic cellular maturation and organization. These three-dimensional cell structures form spontaneously when freshly dissociated embryonic cells are kept under gyratory agitation. After the initial reaggregation, the cells are able to migrate and reorganize themselves within the aggregates. The three-dimensional architecture, allowing direct cell-to-cell interactions and the formation of a natural cell matrix, is fundamental in the acquisition of the histotypic properties of these cultures. Aggregating cell cultures are able to reproduce a series of processes involved in organogenesis. In general, the cultures require several weeks to attain maximal cellular differentiation, and they can be maintained at this level for months. To obtain highly reproducible cultures, it is important to take into account a number of variables such as the developmental stage of the embryonal tissue, the mode of cell dissociation, the cell density at incubation, the intensity of agitation, and the composition of the cell culture medium (see Critical Parameters). This unit describes the preparation of aggregating brain cell cultures from embryonal rodent (rat and mouse) forebrains using simple mechanical dissociation of the original tissue, and a chemically defined medium for their culture. The Basic Protocol describes the technique for obtaining cultures derived from the forebrains of rat embryos, giving rise to relatively large amounts of cultures for routine tests and investigations requiring large quantities of material and/or numerous culture replicates. Of the two alternate protocols, Alternate Protocol 1 describes specific points for the preparation of mouse-derived aggregating brain-cell cultures; Alternate Protocol 2 provides the details for the preparation of neuron-enriched aggregates of both rat- and mouse-derived brain cells. All these approaches require the rigorous application of aseptic and refrigerated working conditions from the moment the uterus containing the embryos is removed from the sacrificed dam.

NOTE: All protocols using live animals must first be reviewed and approved by an Institutional Animal Care and Use Committee (IACUC) and must follow officially approved procedures for the care and use of laboratory animals.

PREPARATION OF AGGREGATING CELL CULTURES FROM RAT FOREBRAIN

BASIC PROTOCOL

This protocol is used routinely for 16-day embryonic rat forebrain. For cultures to be derived from other brain parts or other species, slight modifications are necessary (see below). The protocol is broken down into the following major stages: preliminary work, sacrifice of the dams and excision of the embryos, isolation and dissection of the embryos, mechanical dissociation of embryonic brain tissue, and initiation and maintenance of the cultures.

To estimate the number of culture flasks required, one can rely on data from previous preparations. For example, one flask is typically sufficient for 1.6 embryos using 16-day rat forebrains. Thus, with an average of 13.3 fetuses/dam, approximately twelve pregnant rats will be required to prepare 100 initial cultures. When preparing large numbers of cultures, one has to keep in mind that the duration of the culture preparation is a critical factor. Ideally, for the preparation of 100 cultures, two to three persons should participate in the first part of culture preparation: one that sacrifices the timed-pregnant animals and excises the embryos, the other(s) dissecting them under refrigerated and aseptic conditions.

Contributed by Paul Honegger

Current Protocols in Toxicology (2003) 12.9.1-12.9.17

Materials

Rats, 16-day pregnant (e.g., Sprague-Dawley)
Puck's D-GS (see recipe), 4°
96% ethanol denatured with 2% (v/v) 2-butanone, in a squirt bottle
0.4% trypan blue solution
Chemically defined medium (complete DMEM; see Support Protocol 1), 4°C

Sterile laminar flow hood with horizontal air flow
Dissecting block (optional) perfused with cooling liquid and equipped with wells to hold 60-mm petri dishes
Dissecting microscope(s), if required
Cold light source to illuminate embryos and tissues during dissection
250-ml beaker
60-mm plastic petri dishes, sterile
Guillotine for rats
Scissors (large; small and pointed; curved, Vannas)
Forceps (large; small and curved; fine, curved; extrafine, Dumont no. 5)
Disposable absorbent pads
Plastic waste bags
50-ml conical plastic tubes, sterile (e.g., Falcon)
Surgical gloves and mask
Scalpel holder and no. 11 blade
Nylon mesh bag, 200-µm and 100-µm pore size, nylon mesh purchased in large sheets from Sefar (see recipe for construction of nylon mesh bags)
Glass rods (0.6-cm diameter, 20 cm-long) with blunt, fire-polished ends
1-ml and 5-ml sterile serological plastic pipets (e.g., Falcon)
Hemacytometer and hand-held counter
100-ml or 500-ml plastic culture flask, graduated and sterile (e.g., Falcon)
25-ml and 50-ml modified Erlenmeyer flasks (see step 34)
Gas-permeable, autoclavable plastic caps for Erlenmeyer flasks (e.g., Bellco)
37°C, 10% to 11% CO_2 humidified incubator (with inside dimensions sufficient to place a gyratory shaker with large platform)
Gyratory shaker with shaking speeds up to 80 rpm, 25-mm shaking diameter with a large platform to hold up to 100 culture flasks that fits inside a CO_2 incubator, functions at 100% humidity, driven by magnetic induction rather than by a driving belt, and does not destabilize the internal temperature of the incubator
37°C water bath
Supports with a removable slanted base for media replenishment and transport of flasks—manufactured in alumina to hold 5 flasks, requiring inside dimensions of 27-cm width, 6-cm depth, 3-cm height, with removable insert (27 × 6–cm)

NOTE: All solutions and equipment coming into contact with living cells must be sterile, and aseptic technique should be used accordingly. For additional washing and sterilizing procedures, see Support Protocol 2.

Mate rats and prepare for surgery

1. Mate Sprague-Dawley rats during the daytime for 5 hr, then return them to their home cages.

   They should be mated for no longer than 24 hr. The day of separation is designated gestation day 0.

2. On the day of sacrifice (gestation day 16), place the following dissection instruments in a horizontal flow hood: the dissecting block (optional), the dissecting microscope(s) (if needed), a cold light source, a bottle of ice-cold Puck's D-GS, a bucket of ice, a 250-ml beaker for liquid waste, and a stock of 60-mm plastic petri dishes.

3. Add 5 ml of Puck's D-GS to each of two 60-mm plastic petri dishes and place them on the refrigerated dissecting block (or on ice, if no dissecting block is available).
4. Set up the operating room for the decapitation of the animals (guillotine for rats), and for the excision of the embryos (large scissors, small pointed scissors, large foreceps, small curved foreceps, adsorbent pads, squirt bottle containing denatured ethanol, and plastic bags for disposal of the carcass).
5. Under a sterile hood, add 40 ml ice-cold Puck's D-GS to 50-ml sterile plastic tube(s) destined for storage of the dissected tissue and keep on ice in the laminar horizontal flow hood; and add 25 ml ice-cold Puck's D-GS to 50-ml sterile plastic tubes (one per pregnant rat) to be used for the reception and transfer of the fetuses and place into another bucket of ice for operating.

Sacrifice dams and excise the embryos on gestation day 16

6. Wear gloves and a surgical mask. Decapitate the 16-day pregnant rat using an appropriate guillotine.

   Make sure to avoid all unnecessary stress to the animal and to follow the ethical guidelines.

7. Lay the decapitated animal on its back on an adsorbent pad. Douse the abdomen with denatured alcohol.
8. Using the large forceps, grasp a fold of skin at the base of the abdomen and gently lift. With the large scissors, cut below through skin and fascia at the midline, and extend the cut on both sides of the abdomen until the entire peritoneal cavity lays open. Displace intestines to the side to reveal the uterus.
9. With the small, curved forceps gently grasp and lift the uterine horns containing the fetuses. With the small, pointed scissors excise the uterine horns. Try to remove as much associated fat as possible during this operation. Transfer the excised uterine horns to the 50-ml plastic tube containing ice-cold Puck's D-GS.
10. Transfer the tube containing the uterine horns to the hood for dissection, place the dam's body and head into a plastic bag for disposal.
11. Repeat steps 6 to 10 until all dams have been sacrificed and the embryos recovered.

Isolate and dissect the embryos

Perform all subsequent procedures in a sterile laminar flow hood under aseptic conditions.

12. Put a petri dish containing ice-cold Puck's D-GS in the hood at the side of the dissecting block and place the uterine horns of one animal into the dish.
13. Rapidly open the uterine horns with the Vannas scissors. With the small forceps and the Vannas scissors, extract the embryos from the uterine horns and then from the amniotic sacs. Transfer them to a petri dish containing Puck's D-GS on the dissecting block.
14. Isolate the brains of all embryos in the dish one after the other as follows:
    a. Hold the head of the embryo fixed in a lateral position with the aid of the Dumont forceps.
    b. Make an extended lateral incision at the base of the brain using the Vannas scissors by cutting skin and cartilage from the region of the brain stem to the most frontal point.
    c. Extract the entire brain by lifting it through this opening using the blunt side of the closed Vannas scissors. Remove the meningeal cover as much as possible. Keep the brain and discard the rest of the embryo.

15. Using the scalpel, dissect the forebrains.
16. Transfer the dissected forebrains to the 50-ml plastic tube filled with 40 ml of Puck's D-GS.

    Up to 70 forebrains can be pooled in the same tube (batch), but replace the supernatant at regular intervals during dissection, e.g., every 20 to 30 min, adding fresh cold Puck's D-GS. Discard supernatant into waste beaker.

17. Repeat steps 12 to 16 for each pair of uterine horns.

    The duration of the dissection should not exceed 2 hr. An experienced person can dissect ~40 to 60 embryos per hour.

Rinse the collected brain tissue

18. Remove from the horizontal laminar flow hood all equipment used previously (or use another hood). Put the sterile material for the mechanical dissociation, i.e., glass rods, Nitex mesh bags with 200-µm and 100-µm pores, into the hood.
19. Place a bottle with cold Puck's D-GS in one ice bucket together with the tube(s) containing the excised brain tissue. Place two sterile 50-ml plastic tubes per batch into another ice bucket.
20. Rinse each pool of dissected tissue three times with ~40 ml of cold Puck's D-GS.
21. Add 25 ml of cold Puck's D-GS to one of the 50-ml plastic tubes.

Mechanically dissociate the tissue

22. Place a 200-µm mesh bag (with a glass funnel fitted inside) on the 50-ml conical plastic tube containing 25 ml of Puck's D-GS. Keep on ice.
23. Pour the pooled brain tissue of one batch into the bag. Rinse the funnel, if necessary, with 2 to 3 ml of Puck's D-GS. Disinfect hands (gloves) with 98% ethanol and let dry within the hood.
24. Remove the funnel, close the bag, and hold its upper end against the outer side of the tube wall. Make sure that the brain tissue remains immersed.
25. Using the sterile glass rod, gently stroke downward at the outside of the bag, to squeeze the tissue through the mesh into the surrounding solution. Repeat this movement until the bag looks empty.
26. After this first dissociation step, take the second nylon bag (100-µm mesh) attached with tape to a short glass funnel, and place it on top of an empty 50-ml conical plastic tube.
27. Using a 5-ml serological plastic pipet, transfer the cell suspension to the nylon bag, and let the suspension pass through the filter by gravity flow into the 50-ml conical tube. Toward the end of the filtration, add Puck's D-GS up to a final volume of 50 ml.

    This filtration process can be accelerated by gently moving the filtering device up and down in the tube. If there is a second batch, repeat steps 21 to 27.

28. Centrifuge the resulting filtrate(s) 15 min at $290 \times g$, 4°C, with slow acceleration and slow deceleration.
29. After centrifugation, bring the tube(s) back to the hood, wipe (disinfect) around the closure with an ethanol-soaked cloth, and put on ice. Discard the supernatant and resuspend the cells as follows.

a. Remove the supernatant using a pipet.
b. Add 2.5 ml of fresh cold Puck's D-GS and resuspend the pellet by triturating five to six strokes up and down using a 5-ml plastic pipet. Avoid foaming.
c. Bring the volume of this suspension to 50 ml with cold Puck's D-GS and take a 0.1-ml aliquot for cell counting. Transfer the 0.1-ml aliquot to 0.9 ml of Puck's D-GS.

30. Centrifuge the cell suspension(s) 15 min at $300 \times g$, 4°C, as in step 28.

Determine cell number

31. Count the cells (from step 29c, see *APPENDIX 3B*).

    a. Determine the total cell number per batch using the ten-fold diluted aliquot of step 29c. Determine cell density using a hemacytometer. For testing cell viability, add the test dye (e.g., trypan blue or nigrosin) to the Puck's D-GS used for dilution (see step b below).
    b. It may be useful (particularly in the first preparations) to also examine cell viability (determination of the percentage of cells that exclude a test dye such as trypan blue, *APPENDIX 3B*).

       Typically, 30% to 40% of the cells are stained by trypan blue. Protocols for the determination of cell viability with trypan blue are published widely (e.g., Sigma catalogue). The total cell number provided here include both stained and unstained cells.

32. At the end of the second centrifugation, remove the supernatant with a sterile plastic pipet and discard. Resuspend the pellet in Puck's D-GS by trituration to yield a total volume of 5 to 6 ml (triturate as described for step 29b).

Initiate cultures

33. Fill a 100-ml or 500-ml graduated plastic culture flask with the calculated amount of cold culture medium required to obtain a minimal final cell density of 2.7×10^6 total cells/ml. Add the cell suspension of step 32 to the medium and mix well by turning the closed flask several times upside-down. Avoid foaming.

    The size of the graduated plastic culture flask depends on the final volume of the cell suspension.

    The initial phase of reaggregation is most critical. Culture initiation must proceed rapidly to avoid prolonged periods of non-physiological conditions for the cells, and it requires optimal control of the gyratory agitation to balance between attracting and shearing forces acting on the cells. Cell aggregation starts immediately after the cell suspension has been placed in the incubator. However, during the warming period, the pH of the culture medium will rise above physiological values. In order to keep this critical period as short as possible, two persons should work together during culture initiation, one to pipet the aliquots of the cell suspension, and one to transfer the flasks to the incubator. During the initial phase, the gyratory agitation must be kept relatively low (68 rpm) to favor cell-to-cell adhesion. Thereafter, the speed of agitation is progressively increased to the final speed of agitation (80 rpm) to avoid the agglomeration (clumping) of the formed aggregates.

34. Place the required number of 25-ml Erlenmeyer flasks into the laminar (vertical, if possible) flow hood. Loosen the gas-permeable plastic caps so that they can be removed and held with the left hand while pipetting with the right hand.

    Ideally, use Schott Duran–modified flasks. Uniform Erlenmeyer-type culture flasks are required for aggregating cell cultures. It is difficult to find a large batch of uniform so-called DeLong flasks commercially (there are considerable geometric variations between batches of flasks). Therefore, it is best to purchase a large batch of standard Erlenmeyer flasks

directly from the factory (e.g., Schott Duran 25- and 50-ml Erlenmeyer flasks), if possible, with unfinished necks, and to have the necks modified by a glass blower to short straight necks (outside diameter 18 mm), fit for commercially available, autoclavable plastic caps (e.g., Bellco).

35. Transfer 4-ml aliquots of the final cell suspension to the culture flasks.

    The volume to be placed into the flasks depends on the geometry of the flask. Thus, using other types of culture vessels may require adjustment of the initial volume to obtain a similar vortex. It is recommended to adjust the volume rather than changing the protocol for the speed of agitation (see Critical Parameters).

36. Place the flasks onto the platform of a rotating gyratory shaker (68 rpm) in a 37°C, 10% CO_2 humidified incubator.

37. In the evening of the day of culture preparation (day 0), increase the agitation speed to 70 rpm.

38. On the next day (day 1), increase agitation to 74 rpm.

Transfer cultures

39. On day 2, transfer the cultures to 50-ml modified Erlenmeyer flasks equipped with gas-permeable plastic caps. Pour the content of each flask along the glass wall quickly into the new flask and repeat exactly the same movement by adding an additional 4 ml of fresh prewarmed medium, with which the original flask was rinsed.

    Ideally, no aggregates should remain attached on the wall of the new culture flask. Again, this procedure will cause an increase in the pH of the medium (as at culture initiation, see above). Therefore, care should be taken to keep this procedure as short as possible (not exceeding 30 min/series). Allow to equilibrate for 1 to 2 hr before a further series is transferred. For volume adjustments with other types of culture vessels, see step 35 and Critical Parameters.

40. After completion of the transfer, increase the frequency of agitation to 80 rpm (the maximal rotation speed).

Maintain cultures

41. On day 5, replenish the culture medium for the first time as follows:

    a. Warm the required amount of fresh culture medium in a 37°C water bath (maximum 15 min).

    b. Take the culture flasks in groups of five, put them on a support with a slanted base, and allow the aggregates to settle.

    c. With a 5-ml pipet, remove 5 ml of medium, and add an equal volume of fresh prewarmed medium.

       To avoid contamination, always use a fresh pipet when pipetting fresh medium.

42. Replenish the medium every third day (step 41) until day 14, and every other day thereafter.

43. On day 20, because of the greatly increased metabolic rate of the cultures, divide the content of each flask into two separate cultures ("split") by using the following steps.

    a. Preincubate 50-ml culture flasks with 4 ml of fresh complete medium (1 to 2 hr).

    b. Prewarm in 37°C waterbath the required amount of complete medium for replacement (see step *e* below).

    c. Use a 2-ml plastic pipet to split the cultures. Tilt the flask containing the aggregates, quickly resuspend the aggregates by short aspiration and brisk expulsion of the supernatant medium, and then quickly transfer a 2-ml aliquot to a fresh flask containing 4 ml of medium.

d. Transfer a second 2-ml aliquot in exactly the same way.

e. Replace the missing volume in the original flask with 4 ml of fresh medium.

A second split may be necessary at day 30 if the metabolic rate is too high (medium turning yellow).

MOUSE-DERIVED BRAIN CELL CULTURES

ALTERNATE PROTOCOL 1

Aggregating brain cell cultures are prepared from mouse embryos essentially as described in the Basic Protocol with only a few modifications. The brains of mice, compared to rats, mature at an accelerated rate. Therefore, mouse embryos are taken for culture preparation at an earlier stage, e.g., at gestation day 14, when preparing cultures from the telencephalon. To obtain uniform mouse-derived aggregate cultures, a two- to three-fold higher initial cell density is required as compared with rats, e.g., with 14-day mouse telencephalon, the final cell density is 7.3×10^6 total cells/ml. Furthermore, cell aggregation occurs less vigorously and the cultures show a more pronounced requirement for growth factors as compared to the rat-derived cultures. In particular, platelet-derived growth factor (PDGF) is required for oligodendrocyte proliferation and maturation, while epidermal growth factor (EGF) is mitogenic predominantly for astrocytes. Nevertheless, a considerable number of the initially proliferating glia cells is lost into the supernatant due to their migrating properties.

Taking into consideration the specificities encountered with mouse-derived cultures, Basic Protocol, steps 1, 2, 33, 37, and 38 have been modified for this protocol.

Additional Materials *(also see Basic Protocol)*

Mice, 14-day pregnant (e.g., C57/BL)

1. Mate mice overnight then return them to their home cages.

   The day of separation is designated gestation day 0.

2. Perform Basic Protocol, step 2 on gestation day 14 for mice.
3. Perform Basic Protocol, steps 3 to 32.
4. Fill a graduated plastic culture flask with the appropriate amount of cold culture medium to obtain a minimal final cell density of 7.3×10^6 total cells/ml.
5. Perform Basic Protocol, steps 34 to 37.
6. On the next day, increase agitation to 73 rpm and start treatment with growth factors and neurotrophins (minimal treatment: 20 ng/ml PDGF-BB for the development of oligodendrocytes, if desired).
7. Perform Basic Protocol, steps 39 to 43.

PREPARATION AND MAINTENANCE OF NEURON-ENRICHED AGGREGATE CULTURES

ALTERNATE PROTOCOL 2

Neuron-enriched cultures are prepared from the regular (mixed neuron-glia) cultures using cytosine arabinoside (Ara-C) to eliminate the proliferating glial cells (Honegger and Werffeli, 1988; Corthésy-Theulaz et al., 1990; Braissant et al., 2002; Honegger et al., 2002). Ara-C is added to the culture at an early stage (on days 1 and 2) and at a relatively low concentration (0.4 μM). The resulting aggregates contain >90% neurons (Honegger et al., 2002). However, the virtual absence of glial cells greatly affects neuronal survival and maturation. Therefore, supportive measures are required. This is best achieved by regularly replenishing the culture medium with conditioned medium obtained from parallel cultures of mixed-cell aggregates. This conditioned medium is diluted 1:1 with fresh medium (Honegger and Pardo, 1999). This protocol is identical to that of the Basic Protocol with modifications to steps 38, 40, 41, and 42.

Additional Materials *(also see Basic Protocol)*

2000× Ara-C (see recipe)

1. Follow Basic Protocol, steps 1 to 37.
2. On the next day, increase agitation to 74 rpm and add 2 µl of 2000× Ara-C per flask.
3. Perform Basic Protocol, step 39.
4. After completion of the transfer, increase the frequency of agitation to 80 rpm (the maximal rotation speed). Allow to equilibrate (minimum 2 hr), then add 2 µl of 2000× Ara-C solution per flask.
5. On day 5, replenish the culture medium for the first time as follows:
   a. Warm the required amount of fresh culture medium in a 37°C water bath.
   b. Replenish first cultures of the ordinary (mixed-cell) aggregates and collect their supernatant (i.e., the conditioned medium) in sterile 50-ml conical tube(s). Take the flasks in groups of five, put them on a support with slanted base, and allow the aggregates to settle.
   c. With a 5-ml pipet, remove 5 ml of medium, and add an equal volume of fresh prewarmed medium.

      To avoid contamination, always use a fresh pipet when pipetting fresh medium.

   d. Centrifuge the collected medium for 15 min at 3000 × *g*, 4°C. Mix the resulting supernatant 1:1 with fresh medium. Prewarm this medium, then go through steps *a* to *c* for media replenishment of the Ara-C-treated cultures.
6. Replenish the medium every third day until day 14, and every other day thereafter according to step 5.

SUPPORT PROTOCOL 1

PREPARATION AND USE OF CHEMICALLY DEFINED MEDIA

The basal medium used for aggregating brain cell cultures is derived from Dulbecco's modified Eagle's medium (DMEM, high glucose). The standard medium also contains high concentrations of glutamine, but low-glutamine DMEM is needed for acute experiments involving the redistribution of highly differentiated aggregates (see Critical Parameters). Because the commercially available DMEM in liquid form differs considerably in composition and osmolarity from the DMEM used for aggregate cultures, it is easier to prepare the media from the commercially available powdered medium. Thus, the following protocol describes the preparation of the two basal (incomplete) DMEM from powder mixtures, (a) the standard medium containing high glucose and high glutamine, and (b) the low-glutamine medium. Furthermore, medium completion is described (c) for both types of basal medium. Thus, the final (complete) chemically defined media are completed with the addition of metabolites, vitamins, trace elements, and hormones.

Materials

Dulbecco's modified Eagle's medium (DMEM containing high glucose (4.5 g/liter) and high L-glutamine (580 mg/liter), but no bicarbonate and no pyruvate; powder from GIBCO-Invitrogen)
Ultrapure water
Choline chloride (Sigma)
L-Carnitine (Fluka)
Lipoic acid (Sigma)
Vitamin B12 (Fluka)

50 µM $CdSO_4 \cdot 8H_2O$ (Merck)
100 µM $CuSO_4 \cdot 5H_2O$ (Merck)
50 µM $MnCl_2 \cdot 4H_2O$ (Merck)
150 µM Na_2SeO_3 (Serva)
2.5 mM $NaSiO_3 \cdot 5H_2O$ (Fluka)
5 µM $(NH_4)_6Mo_7O_{24} \cdot 4H_2O$ (Sigma)
2.5 µM $NiSO_4 \cdot 6H_2O$ (Merck)
2.5 µM $SnCl_2 \cdot 2H_2O$ (Merck)
50 µM $ZnSO_4 \cdot 7H_2O$ (Merck)
Sodium bicarbonate
CO_2 gas
Dulbecco's modified Eagle's medium (DMEM devoid of glucose, glutamine, phenol red, bicarbonate, and pyruvate powder mix, e.g., Sigma)
D-Glucose
Phenol red
100× BME vitamins (GIBCO-Invitrogen)
1 mg/ml transferrin (Sigma)
30 µM triiodothyronine (Na^+ salt; Sigma)
5 mg/ml insulin (Sigma)
20 µM hydrocortisone-21-hemisuccinate (Na^+ salt; Sigma)
3 mg/ml linoleic acid (Na^+ salt; Sigma)
Vitamin A and E solution (see recipe)
500× gentamicin sulfate stock solution (see recipe)
170 mM L-glutamine (see recipe)

10-liter glass jar (Pyrex)
Magnetic plate and stir bar
5-ml serological pipet
Hollow fiber filters (0.2-µm MediaKap-10, Spectrum Laboratories)
Peristaltic pump
500-ml bottles with gas-tight closures (Pyrex)
0.2-µm syringe filters (e.g., Acrodisc, Gelman), sterile

Prepare 10 liters of basal culture medium from powder

1a. Obtain Dulbecco's modified Eagle's medium (DMEM) powder mixture for 10 liters, containing high glucose (4.5 g/liter) and high L-glutamine (580 mg/liter), but no bicarbonate and no pyruvate.

2a. Fill a 10-liter glass jar with 9 liters of ultrapure water.

The entire preparation is at room temperature.

It is important to use water of the highest purity and devoid of pyrogens.

3a. Add the powdered medium to the water and let it dissolve under gentle continued stirring (use large magnetic stir bar).

4a. Add the following supplements:

1.35 g choline chloride
20 mg L-carnitine
2 mg lipoic acid
13.6 mg vitamin B12.

5a. Add 1 ml of each of the following 10^4-fold concentrated stock solutions of trace elements (stored frozen at −20°C):

50 µM $CdSO_4 \cdot 8H_2O$
100 µM $CuSO_4 \cdot 5H_2O$
50 µM $MnCl_2 \cdot 4H_2O$
150 µM Na_2SeO_3
2.5 mM $NaSiO_3 \cdot 5H_2O$
5 µM $(NH_4)_6Mo_7O_{24} \cdot 4\ H_2O$
2.5 µM $NiSO_4 \cdot 6H_2O$
2.5 µM $SnCl_2 \cdot 2H_2O$
50 µM $ZnSO_4 \cdot 7H_2O$

6a. Add 37 g sodium bicarbonate and immediately apply CO_2 gas (bubble through a 5-ml serological pipet into the liquid until the pH is adjusted to 7.0, color of smoked salmon).

The pH of the basal medium is kept somewhat lower than the final pH in the incubator, taking into account that the pH of the medium tends to increase during aliquot dispensing and prewarming.

7a. Measure the osmolarity of the medium and adjust to 340±2 mOsm by adding the required volume of water.

8a. Sterilize the medium by filtering through 0.2-µm hollow fiber filters and a peristaltic pump. Test the first and the last 100-ml portions of the filtrate for sterility (by incubation at 37°C or at room temperature). Dispense the remaining medium in 500-ml bottles with gas-tight closures and store at 4°C in the dark.

Maximum storage time is 1 month.

Prepare 10 liters of basal DMEM devoid of glutamine

The powder mixture of DMEM closest to the required composition can be obtained from Sigma. Besides its glutamine deficiency, it also lacks glucose, bicarbonate, and phenol red, which can be added during medium preparation.

1b. Obtain Dulbecco's modified Eagle's medium (DMEM) powder mix for 10 liters devoid of glucose, glutamine, phenol red, bicarbonate, and pyruvate.

2b. Perform steps 2a and 3a.

3b. Add the following supplements:

1.35 g choline chloride
45.0 g D-glucose
75 mg phenol red
20 mg L-carnitine
2 mg lipoic acid
13.6 mg vitamin B12.

Note that glutamine (final concentration 0.25 mM) is added only after completion of the medium (see below).

4b. Follow steps 5a to 8a.

Complete the basal DMEM

Just before use, the basal media are completed by the addition of the following sterile components (volumes are given per 500 ml of medium).

1c. Add 5 ml of 100× BME vitamins to 500 ml of basal culture medium (with or without glutamine).

With this supplementation, the concentration of the DMEM vitamins is increased. Also, biotin is added, which is not present in the regular DMEM.

2c. Add 500 µl of each of the following four 1000× concentrated stock solutions (stored frozen at −20°C):

1 mg/ml transferrin
30 µM triiodothyronine (Na^+ salt)
5 mg/ml insulin
20 µM hydrocortisone-21-hemisuccinate (Na^+ salt).

3c. Add 250 µl of 3 mg/ml linoleic acid.

Cultures >20 days may be given albumin-bound lipids (Albumax II, Gibco-BRL; final concentration 0.1% w/v) instead of linoleic acid. The Albumax II stock solution (stored at 4°C) is prepared 100-fold concentrated (10% w/v), its pH adjusted to 7.4 with 0.2 N NaOH, using phenol red (15 mg/liter final concentration, from a 50-fold concentrated sterile stock solution) as indicator.

4c. Add vitamin A alcohol and vitamin E (both are present in the medium only at trace concentrations). Of a concentrated mixture of vitamins A and E (see recipe), transfer 50-µl aliquots to 10-ml aliquots of medium, partially solubilize by sonication, and add directly to 500 ml medium after sterile filtering through 0.2-µm Gelman Acrodisc.

5c. Add 1 ml of 500× gentamicin sulfate.

6c. If medium devoid of glutamine is used (see steps 1b to 4b), add components 1c to 5c, and L-glutamine to a final concentration of 0.25 mM in the medium by adding 170 mM L-glutamine (150 µl per 100 ml of medium).

WASHING AND STERILIZING PROCEDURES

SUPPORT PROTOCOL 2

As long as there are no suitable commercially available disposable Erlenmeyer culture flasks, glass flasks have to be used and recycled. Also, it may be more economical to use recyclable glass pipets for media replenishment when working on a larger scale. However, the glassware must be free of any impurities, including traces of detergent. The detergents used should be devoid of organic additives. It is recommended to use a product line such as Neodisher (*http://www.sic.uk.com/neo_disher.htm* or *http://www.labwashers.com/models/lab_300.html*). The used culture glassware should never be allowed to dry before it is cleaned. Therefore, it must be stored immersed in a basic detergent solution (e.g., Neodisher LM-10; 5% v/v) capable of dissolving protein deposits. After washing with a special detergent (e.g., Neodisher FT), the glassware is rinsed with cold tap water and neutralized with a citric acid solution (e.g., Neodisher Z) to remove traces of detergent. Thereafter, the glassware is rinsed several times with deionized water, and finally with ultrapure water. After drying in an oven, the glassware is sterilized. The culture flasks with gas-permeable plastic caps in place are sterilized in an autoclave (120°C) with pulsed vapor. After a first sterilization, a layer of aluminum foil is wrapped around neck and cap, and the flask sterilized once more. The nylon filter bags, each with an appropriate glass funnel inside, are loosely wrapped in aluminum foil and autoclaved in a vapor-permeable box at 120°C. Cotton-plugged glass pipets are sterilized in an oven

(4 hr at 180°C). Dissecting instruments are sterilized either in the autoclave (135°C) or in a hot bead sterilizer (250°C). Instruments may also be sterilized by immersing in 70% ethanol for 5 to 10 min and letting dry inside the laminar flow hood.

REAGENTS AND SOLUTIONS

Use Milli-Q-purified water or equivalent in all recipes and protocol steps. For common stock solutions, see ***APPENDIX 2A****; for suppliers, see* ***SUPPLIERS APPENDIX****.*

Ara-C stock solution, 2000×

Add 1.92 mg cytosine arabinofuranoside (Sigma) per 10 ml water. Sterilize by filtration (0.2-µm filter). Always prepare fresh.

Gentamicin sulfate stock solution, 500×

Add 1.0 g gentamicin sulfate (Sigma) per 80 ml water. Sterilize by filtration (0.2-µm filter) and store up to 24 months at −20°C.

L-Glutamine stock solution, 170 mM

Add 24.8 mg L-glutamine (Fluka) per milliliter of water. Sterilize by filtration (0.2-µm filter). Prepare fresh or store 5 ml aliquots at −20°C.

Nylon mesh filter bags and appropriate funnels

The nylon meshes (Sefar; *http://www.sefar.com*) are sold in large sheets. Manufacture the filter bags by taking two layers of sheets, one on the other, and then dividing the bags with a hot soldering iron (40 W for 200-µm mesh and 30 W for 100-µm mesh), adjust the force applied and the rapidity of the passage such that the bags are sealed and cut at the same time.

Prepare the filter bags and appropriate funnels in the following sizes:

a. Construct 200-µm mesh bags with a 3.5-cm diameter and 14-cm length; use funnels that have a 12-cm long stem and outside diameters of 2.5 cm (top) and 1.6 cm (bottom).

b. Construct 100-µm mesh bags with a 5.0-cm diameter and 5.5-cm length; the appropriate funnels have a 4-cm long stem, and outside diameters of 4.5 cm (top) and 2.5 cm (bottom).

PBS for washing aggregate cultures prior to their harvest

6.43 g/liter NaCl
395 mg/liter KCl
540 mg/liter $Na_2HPO_4 \cdot 7H_2O$
4.5 g/liter D-glucose
24 g/liter sucrose
160 mg/liter $MgCl_2 \cdot 6H_2O$
200 mg/liter $CaCl_2$

Neutralize the solution before adding the Mg^{2+}- and Ca^{2+}-salts. Adjust to pH 7.3 and 340 mOsm then sterilize by filtration (0.2 µm filters). Store at 4°C.

This PBS is used to wash aggregate cultures before they are harvested.

Puck's D (Puck's solution D without Ca^{2+} and Mg^{2+}; Wilson et al., 1972)

8 g/liter NaCl
400 mg/liter KCl
45 mg/liter $Na_2HPO_4 \cdot 7H_2O$
30 mg/liter KH_2PO_4
1 g/liter D-glucose

continued

20 g/liter sucrose
5 mg/liter phenol red

Adjust osmolarity to 340 mOsm then sterilize by filtration (0.2 μm filter). Store up to 24 months at 4°C. Just before use, adjust the pH to 7.4 with sterile 0.2 N NaOH (~0.5 ml/500 ml).

Puck's D-GS (Puck's solution D without Ca^{2+} and Mg^{2+}, containing gentamicin sulfate)

Just before use, add to sterile Puck's D (see recipe) 1 ml of 500× of the antibiotic gentamicin sulfate per 500-ml bottle. Adjust the pH to 7.4 with sterile 0.2 N NaOH (~0.5 ml/500 ml). Store up to 24 months at 4°C.

Vitamin A and E solution

Preparation of the concentrated stock solution of vitamins A and E: dissolve 114 mg vitamin A alcohol (Fluka) in 200 μl of absolute alcohol and mix with 2.0 ml of α-tocopherol (Sigma). Store under nitrogen up to 9 months at −20°C.

COMMENTARY

Background Information

Cell culture systems, in general, provide means for the study and manipulation of living structures in vitro, which is of wide interest for practical, economical, and ethical reasons. Since the beginning of the 20th century, the number and sophistication of techniques devised for culturing isolated tissues and cells has increased at a steady pace. Today, there are a large number of culture systems of diverse complexity, ranging from single transformed cells to explanted tissue fragments. Since every culture system offers specific advantages as well as inconveniences, it is important to select the system that is most appropriate for a given task. Characteristic features of aggregating brain cell cultures include their three-dimensional architecture permitting the formation of a natural extracellular matrix and extensive cellular maturation. During the early culture period, the reaggregated cells are able to migrate and create a tissue-specific environment favoring cellular maturation and the development of specialized structures such as neurites, synapses, and myelinated axons. Therefore, aggregating cell cultures have been classified as organotypic cultures (Doyle et al., 1994). With respect to their applications in neurotoxicology, aggregating brain cell cultures were found useful to study aspects of developmental neurotoxicology (Monnet-Tschudi et al., 1995b, 2000; Zurich et al., 2000, 2002; Braissant et al., 2002). This culture system also offers the possibility to investigate cascades of neurotoxic effects occurring in response to a primary insult, as well as secondary aggravating or attenuating effects through gliosis and/or microglial activation (Monnet-Tschudi et al., 1995a, 1996, 1997; Zurich et al., 2000; Eskes et al., 2002). Besides the study of toxic processes following a chemical insult, aggregating brain cell cultures were also used as a model to investigate the consequences of hypoglycemia (Pardo and Honegger, 1999; Honegger et al., 2002). The ease of handling the free-floating aggregates, together with the high yield and high reproducibility of these cultures also makes them a suitable system for neurotoxicological routine testing (Honegger and Werffeli, 1988; Honegger and Schilter, 1992; Kucera et al., 1993).

The technique of rotation-mediated aggregating cell culture was introduced by Moscona (1961), who observed that embryonic cells taken from diverse organs and from various species were able to reaggregate spontaneously after dissociation, and to form histotypic structures when cultured under agitation for several weeks. Subsequently, the method was applied specifically to cells of the central nervous system (CNS), and predominantly morphological techniques were used for their characterization (Moscona, 1961; DeLong and Sidman, 1970). Biochemical criteria for the analysis of these cultures were used first by Seeds (1971). This approach was extended in the following decades and combined with the techniques of molecular biology. The original culture procedure was considerably modified, in particular, with respect to the method of tissue dissociation. Although enzymes (e.g., trypsin) are still used (e.g., Choi et al., 1993), Honegger and Richelson (1976) found that dissociating cells by mechanical means rendered more reproducible

cultures. The sieving technique described in this unit is a modification of the method described first by Rose (1965) and subsequently used also by Varon and Raiborn (1969). It facilitated culture preparation and greatly increased the number of replicate cultures that could be obtained. Interestingly, despite this nonselective dissociation method, only neural cells are found in the aggregates (no fibroblasts and no endothelial cells are detectable). This may be explained by the selectivity of the reaggregation process. The development of a chemically defined culture medium suitable for these cultures (Honegger et al., 1979) further simplified the culture technique and, in addition, opened new opportunities to study the role of endocrine and paracrine signaling in brain physiolgy and pathology. Over the years, an increasing number of morphological, immunocytochemical, biochemical, and molecular biological criteria were applied for the characterization of aggregating brain cell cultures. For more technical details concerning culture analyses, see Honegger and Monnet-Tschudi (2001) and Braissant et al. (2002).

Critical Parameters

Developmental stage of the embryos

The preparation of reproducible cultures requires the use of well-staged fetuses. The animals should be mated for no more than 24 hr, and the day of separation and vaginal plug control is designated as day 0. Spontaneous reaggregation occurs only with immature dissociated cells. Also, more highly differentiated cells are likely to be damaged during the mechanical dissociation process. Therefore, one must select a developmental stage that yields a maximum of relatively immature cells. This depends on the species and on the particular brain region to be used. By taking CNS tissue from different regions, it has to be kept in mind that there is a developmental caudal-to-rostral gradient in the CNS, such that the maturation of spinal cord and brainstem precedes that of the cortex.

Sterility

From the moment the uterine horns are isolated, all procedures require aseptic working conditions, and the sterility of all instruments and solutions that come in contact with the tissue and dissociated cells. In addition, the Basic Protocol prescribes the use of an antibiotic (gentamicin) in all media. While antibiotics are essential during the initial phase of culture preparation, it may be possible to omit them in more advanced cultures. During aseptic procedures, hands (gloves) must be disinfected regularly with ethanol. Also, the caps of all bottles transferred to the hood must be disinfected with ethanol. However, care must be taken to ensure that no ethanol is introduced into the liquids.

Duration of culture preparation

The dissociation, washing, and final incubation of the cells is an extremely stressful procedure for the cells, and only the immature cells can tolerate the process. To facilitate the mechanical dissociation, the tissue and cells are kept in ice-cold Ca^{2+}- and Mg^{2+}-free media during the entire preparation until the final resuspension of the cells in complete culture medium. Therefore, the duration of the procedure is critical and should not exceed a total of 4 hr.

Speed of gyratory agitation

Determining the optimal conditions for aggregation is crucial. It is important to obtain homogenous cultures, i.e., aggregates that have similar size. Also, the size of the aggregates needs to be limited to a diameter of 200 to 300 μm, to avoid the development of necrosis in the center of the aggregates due to limited diffusion of energy substrates and oxygen. Therefore, an optimum balance between adhesive and centrifugal forces must be determined, and depends on the geometry of the incubation vessel, the volume of cell suspension therein, and the speed of agitation. If using culture vessels with different shapes than those proposed in the protocol, it is recommended to vary the culture volume rather than the speed of agitation until an optimal vortex is obtained. In most cases, inhomogenous cultures indicate that the initial agitation was not sufficiently vigorous. In this respect, rat-derived brain cells reaggregate more readily, whereas mouse-derived brain cells require more careful control to avoid excessive agitation during the initial phase of aggregation. In any case, during this initial phase it is crucial to use a batch of culture vessels with identical geometry in order to obtain satisfactory replicate cultures.

Chemically defined medium

The chemically defined medium proposed here is sufficient for the growth and maturation of aggregating brain cell cultures. It should, however, be considered as a minimal culture

Table 12.9.1 Troubleshooting Guide for Neural Cell Aggregate Cultures

Problems	Possible causes	Suggested solutions
Low viable cell yield after dissociation	Mechanical dissociation too harsh	Check pore sizes of nylon sieves
		Dissociate tissue more delicately and be sure to maintain tissue in cold solution
		Resuspend and triturate cells more carefully
	Improper saline solution	Check composition and osmolarity of saline solutions
Irregular aggregates, mostly too big	Agitation too slow, particularly in the beginning	Decrease volume of cell suspension in culture vessel
	Concentration of EGF or other mitogen(s) too high	Decrease (or omit) mitogens (particularly those stimulating astrocyte proliferation)
	Initial cell density too low	Increase cell density
Most aggregates too small (e.g., at day 5)	Agitation too vigorous in the beginning	Increase volume of cell suspension in culture vessel
	Initial cell density too high	Reduce cell density
	Lack of mitotic activity	Use a mitogen or try serum (decomplemented 5% FCS)
	Toxic factor	Check media components and purity of water; make fresh medium
	Infection	Check sterility of equipment and media
Low values for total protein and cell type-specific biochemical properties	Too low level of media component(s) or toxic component in the medium	Check media components and purity of water; make fresh medium
	Damage due to prolonged periods at high pH	Reduce the duration of aggregate manipulation (including media changes), increase the pCO_2 in the incubator during the first 2 weeks of culture
	Infection that is not visible by the naked eye (e.g., mycoplasma)	Check sterility of equipment and media

medium, since the addition of certain growth factors can enhance maturational processes. The presence of serum (1% to 5%) also has beneficial effects, e.g., on the formation of myelin (Honegger and Matthieu, 1980) and on the spontaneous electrical activity of neuronal networks within highly differentiated aggregates (P. Honegger, unpub. observ.). Media preparation from powdered mixtures requires the use of pyrogen-free high-quality water, and the osmolarity of all media must be controlled.

Variability of the pH in the medium

Because of the bicarbonate/CO_2 buffering system used in DMEM, pH shifts in the medium occur frequently. Each time the cultures are manipulated outside the incubator, the pH increases because of the rapid loss of CO_2. On the other hand, pH values decrease in cultures at more advanced maturational stages because of lactate accumulation in cultures of high density. Elevated pH levels are particularly detrimental to neurons. Therefore, the time allowed

for aggregate manipulation should be kept to the strict minimum, and during recovery, the incubator has to be kept shut until a physiological pH is attained. For acute experiments with highly differentiated aggregates, it is recommended to use media with low concentrations of glutamine (0.25 mM) to prevent the spontaneous formation of ammonia. While at physiological pH the ammonium ion prevails, the diffusible neurotoxic form (NH_3) forms with increasing pH. The use of an additional or replacement buffer system (20 mM HEPES) is another option for stabilizing the pH during acute experiments lasting only a few hours.

Troubleshooting

Deficits in certain cell types or in the extent of maturation may not be apparent by the criteria discussed in Table 12.9.1. To this end, more extensive analyses are necessary using cell type-specific biochemical and immunocytochemical criteria.

Anticipated Results

Each flask of aggregating cell cultures contains ~1000 individual aggregates. They should have similar sizes with diameters not exceeding 300 to 400 μm. Although at the outset the dissociated cells appear to reaggregate in a random fashion, they are able to reorganize themselves within the resulting spherical structure. Except for the most peripheral layer where astrocytes are predominant, all four cell types (i.e., neurons, astrocytes, oligodendrocytes, and microglial cells) are found distributed throughout the sphere. Nevertheless, as observed in rat cell–derived cultures, neuronal cell bodies tend to be more concentrated in the inner half of the aggregate, while prominent neurite bundles are observed in the outer half of the aggregate where the population of oligodendrocytes is most dense. A small population of microglial cells is found scattered throughout the aggregates. Neither fibroblasts nor endothelial cells can be found in these cultures. During the first 2 weeks in vitro, most of the macroglial cells (astrocytes and oligodendroglial cells) proliferate. Thereafter, little mitotic activity is observed. The differentiation of neurons and glial cells progresses for several weeks. Synaptogenesis accelerates between the third and fourth week. During the same period, the myelination of axons progresses, and spontaneous electrical activity can be detected by extracellular and intracellular recordings. With the advancement of maturation, the metabolic rate increases drastically. More details of the criteria and techniques used for culture characterization by a multidisciplinary approach are provided elsewhere (Honegger and Monnet-Tschudi, 2001; Braissant et al., 2002).

Time Considerations

The time allowed for culture preparation is limited to 4 hr. Therefore, the number of cultures that can be prepared per batch depends primarily on the investigator's skill and on the number of participating persons. Two persons are able to prepare up to 120 individual cultures per batch. For most experimental approaches, these initial cultures can be subdivided up to six fold for experimentation. Thus, from 100 starting cultures, one can obtain up to 600 replicates. Therefore, it is important to remember that culture maintenance is relatively time-consuming. Media can be replenished for only a limited number of flasks at a time (e.g., 20 to 30) because care has to be taken to avoid extremes in pH. It is therefore convenient to use several incubators. After replenishment, the cultures require time for equilibration (1 hr for immature cultures; 30 min for mature cultures counting from the moment the CO_2 atmosphere in the incubator has recovered).

Literature Cited

Braissant, O., Henry, H., Villard, A.M., Zurich, M.-G., Loup, M., Eilers, B., Parlascino, G., Matter, E., Boulat, O., Honegger, P., and Bachmann, C. 2002. Ammonium-induced impairment of axonal growth is prevented through glial creatine. *J. Neurosci.* 22:9810-9820.

Choi, H.K., Won, L., and Heller, A. 1993. Dopaminergic neurons grown in three-dimensional reaggregate culture for periods of up to one year. *J. Neurosci. Meth.* 46:233-244.

Corthésy-Theulaz, I., Mérillat, A.-M., Honegger, P., and Rossier, B.C. 1990. Na^+-K^+-ATPase gene expression during in vitro development of rat fetal forebrain. *Am. J. Physiol.* 258:C1062-C1069.

DeLong, G.R. and Sidman, R.L. 1970. Alignment defect of reaggregating cells in cultures of developing brains of reeler mutant mice. *Dev. Biol.* 22:584-599.

Doyle, A., Griffiths, J.B., and Newell, D.G. (eds.) 1994. Cell and Tissue Culture: Laboratory Procedures. John Wiley & Sons, Chichester.

Eskes, C., Honegger, P., Juillerat-Jeanneret, L., and Monnet-Tschudi, F. 2002. Microglial reaction induced by noncytotoxic methylmercury treatment leads to neuroprotection via interactions with astrocytes and IL-6 release. *Glia* 37:43-52.

Honegger, P. and Richelson, E. 1976. Biochemical differentiation of mechanically dissociated

mammalian brain in aggregating cell culture. *Brain Res.* 109:335-354.

Honegger, P. and Matthieu, J.-M. 1980. Myelination of aggregating fetal rat brain cell cultures grown in a chemically defined medium. *In* Neurological Mutations Affecting Myelination (N. Baumann, ed.) pp. 481-488. Elsevier, Amsterdam.

Honegger, P. and Werffeli, P. 1988. Use of aggregating cell cultures for toxicological studies. *Experientia* 44:817-823.

Honegger, P. and Schilter, B. 1992. Serum-free aggregate cultures of fetal rat brain and liver cells: Methodology and some practical applications in neurotoxicology. *In* The Brain in Bits and Pieces. In vitro Techniques in Neurobiology, Neuropharmacology and Neurotoxicology (G. Zbinden, ed.) pp. 51-79. MTC Verlag, Zollikon, Switzerland.

Honegger, P. and Pardo, B. 1999. Separate neuronal and glial Na^+,K^+-ATPase isoforms regulate glucose utilization in response to membrane depolarization and elevated extracellular potassium. *J. Cereb. Blood Flow Metab.* 19:1051-1059.

Honegger, P. and Monnet-Tschudi, F. 2001. Aggregating neural cell cultures. *In* Protocols for Neural Cell Culture, 3rd edition. (S. Fedoroff and A. Richardson, eds.) pp. 199-228. Humana Press, Totowa, N.J.

Honegger, P., Lenoir, D., and Favrod, P. 1979. Growth and differentiation of aggregating fetal brain cells in a serum-free defined medium. *Nature* 282:305-308.

Honegger, P., Braissant, O., Henry, H., Boulat, O., Bachmann, C., Zurich, M.-G., and Pardo, B. 2002. Alteration of amino acid metabolism in neuronal aggregate cultures exposed to hypoglycemic conditions. *J. Neurochem.* 81:1141-1151.

Kucera, P., Cano, E., Honegger, P., Schilter, B., Zijlstra, J.A., and Schmid, B. 1993. Validation of whole chick embryo cultures, whole rat embryo cultures and aggregating embryonic brain cell cultures using six pairs of coded compounds. *Toxic. In Vitro* 7:785-798.

Monnet-Tschudi, F., Zurich, M.-G., Pithon, E., van Melle, G., and Honegger, P. 1995a. Microglial responsiveness as a sensitive marker for trimethyltin (TMT) neurotoxicity. *Brain Res.* 690:8-14.

Monnet-Tschudi, F., Zurich, M.-G., Riederer, B.M., and Honegger, P. 1995b. Effects of trimethyltin (TMT) on glial and neuronal cells in aggregate cultures: Dependence on the developmental stage. *Neurotoxicol.* 16:97-104.

Monnet-Tschudi, F., Zurich, M.-G., and Honegger, P. 1996. Comparison of the developmental effects of two mercury compounds on glial cells and neurons in aggregate cultures of rat telencephalon. *Brain Res.* 741:52-59.

Monnet-Tschudi, F., Zurich, M.-G., and Honegger, P. 1997. Aggregate cell cultures for neurotoxicity testing: The importance of cell-cell interactions. *In* Animal Alternatives, Welfare and Ethics (L.F.M. van Zutphen and M. Balls, eds.) pp. 641-649. Elsevier, Amsterdam.

Monnet-Tschudi, F., Zurich, M.-G., Schilter, B., Costa, L.G., and Honegger, P. 2000. Maturation-dependent effects of chlorpyrifos and parathion and their oxygen analogs on acetylcholinesterase and neuronal and glial markers in aggregating brain cell cultures. *Toxicol. Apl. Pharmacol.* 165:175-183.

Moscona, A.A. 1961. Rotation-mediated histogenetic aggregation of dissociated cells: A quantifiable approach to cell interactions in vitro. *Exp. Cell Res.* 22:455-475.

Pardo, B. and Honegger, P. 1999. Selective neurodegeneration induced in rotation-mediated aggregate cell cultures by a transient switch to stationary culture conditions: A potential model to study ischemia-related pathogenic mechanisms. *Brain Res.* 818:84-95.

Rose, S.P.R. 1965. Preparation of enriched fractions from cerebral cortex containing isolated, metabolically active neuronal cells. *Nature* (London) 206:621-622.

Seeds, N.W. 1971. Biochemical differentiation in reaggregating brain cell culture. *Proc. Natl. Acad. Sci. U.S.A.* 68:1858-1861.

Varon, S. and Raiborn, C.W., Jr. 1969. Dissociation, fractionation, and culture of embryonic brain cells. *Brain Res.* 12:180-199.

Wilson, S.H., Schrier, B.K., Farber, J.I., Thompson, E.J., Rosenberg, R.N., Blume, A.J., and Nirenberg, M.W. 1972. Markers for gene expression in cultured cells from the nervous system. *J. Biol. Chem.* 247:3159-3169.

Zurich, M.-G., Honegger, P., Schilter, B., Costa, L.G., and Monnet-Tschudi, F. 2000. Use of aggregating brain cell cultures to study developmental effects of organophosphorus insecticides. *Neurotoxicol.* 21:599-606.

Zurich, M.-G., Eskes, C., Honegger, P., Bérode, M., and Monnet-Tschudi, F. 2002. Maturation-dependent neurotoxicity of lead acetate in vitro: Implication of glial reactions. *J. Neurosci. Res.* 70:108-116.

Contributed by Paul Honegger
University of Lausanne
Lausanne, Switzerland

Coculturing Neurons and Glial Cells

In the development and maintenance of the nervous system there is a complex interdependency between neurons and glial cells. This relationship is vital for their individual differentiation, development, and functionality but also seems to play an important role in progressive neurodegeneration and in the modulation of neurotoxic effects.

Glial cells maintain normal functioning of the nervous system both by controlling the extracellular environment and by supplying metabolites and growth factors. Neurons may interfere with the proliferation and maturation of glial elements (Steward et al., 1991; Gegelashvili et al., 1997) and dynamically regulate the glial signaling pathway through the release of substances such as glutamate (Bezzi et al., 1998). Nevertheless, there is evidence that glia can be neurotoxic both in vivo and in vitro and can exacerbate neuronal damage caused by a variety of agents (Brown et al., 1996; Meucci and Miller, 1996; Rogrove and Tsirka, 1998; Viviani et al., 1998). This effect may be attributable to an altered supply of trophic factors to neurons, establishment of contacts, and an altered buffering of the extracellular microenvironment by glia, but also to direct release of substances toxic to neurons such as reactive oxygen species (ROS), glutamate, and some cytokines—e.g., interleukin-1β (IL-1β), tumor necrosis factor-α (TNF-α).

The general impression is that glial activation is in some way triggered by damaged neurons (Viviani et al., 2000). The hypothesis is that when a neuron is damaged it sends out signals. Usually, these are signals for help and the glia adopt a neuroprotective strategy, but sometimes, depending on the signal released or the severity of the damage, the signals elicit a lethal response. If this is the case, neural cell death could activate a self-propagating cycle sustained by neurotoxic factors released by glia, which promotes further neurodegeneration and hence more glial activation. This scheme, important in studying neurotoxicity, is part of a bicellular death pathway that has been recognized and experimentally investigated only recently.

Cocultures of different cells of the nervous system (i.e., neurons, astrocytes, and microglia) represent the easiest approach to: (1) study intercommunication between the different cell populations of the nervous system following a toxic insult, (2) evaluate its relevance in the propagation of the damage, and (3) study the molecular mechanisms involved. Other possible approaches are to use aggregate cultures of neural and glial cells and the more complex organotypic slices of hippocampus (Harry et al., 1998).

This unit, which is complementary to *UNITS 12.3 & 12.4*, describes procedures to set up a sandwich coculture system with a combination of neurons and glial cells (see Basic Protocol 1), or astrocytes and microglia cells (see Basic Protocol 2), as well as methods for the preparation of hippocampal neurons (see Support Protocol 1), glial cells (see Support Protocol 2), coated glass coverslips (see Support Protocol 4), and the separation of astrocytes and microglia from glial cells (see Support Protocol 3). A sandwich coculture is an in vitro cell system formed by two different cell populations growing on different surfaces, usually a coverslip and a petri dish. These surfaces are separated by small paraffin dots at the edges of the coverslip, on which one of the cell populations is seeded. In this way the two cell populations face each other without touching (Fig. 12.10.1) and soluble substances can diffuse between them. This cell system is therefore suitable for the study of biological responses that are due to the release of soluble mediators but not of those dependent on the contact of the two cell types.

Contributed by Barbara Viviani

Current Protocols in Toxicology (2003) 12.10.1-12.10.17

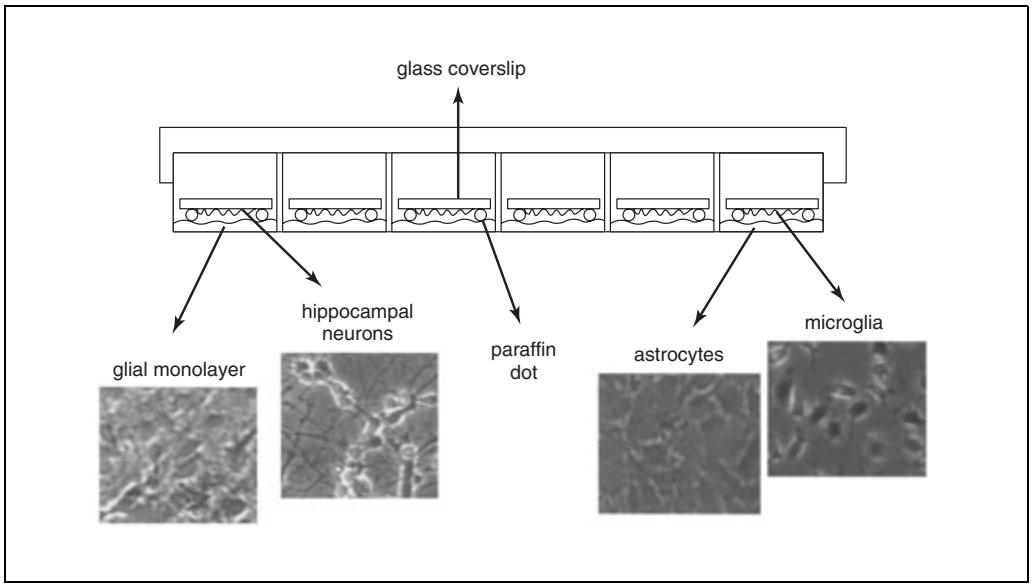

Figure 12.10.1 Scheme of a typical coculture (i.e., hippocampal neurons–glia and microglia-astrocytes) in a 24-well plate. Bright-field photographs are at 10× magnification. Note that cells populations are separated by parrafin dots on the edges of 12-mm round glass coverslips.

NOTE: All protocols using live animals must first be reviewed and approved by an Institutional Animal Care and Use Committee (IACUC) and must follow officially approved procedures for the care and use of laboratory animals.

NOTE: Working conditions must ensure the highest degree of sterility. Thus, brain tissues should be dissected and cells plated and grown under a laminar flow hood. Equipment must be sterilized before use and stored in 95% ethanol when not in use. All solutions and reagents that come into contact with tissues or cells must be sterile.

NOTE: All culture incubations should be performed in a 37°C, 5% CO_2 incubator with 95% relative humidity unless otherwise specified. As soon as prepared, cultures must be maintained in this type of incubator.

BASIC PROTOCOL 1

PREPARATION OF HIPPOCAMPAL NEURON-GLIA-SANDWICH COCULTURES

In the author's laboratory, the neuron-glia sandwich coculture is used not only to study the interaction between glia and neural cells during a toxic insult, but also to obtain a highly differentiated neural culture. Since glial cells are a valuable source of neurotrophic substances, cultures of cortical glial cells (see Support Protocol 2), consisting mainly of astrocytes and a small number of microglial cells, are prepared and allowed to reach confluence (~10 days). These monolayers can be used for up to 1 month from their preparation. Next, cultures of hippocampal neurons are prepared by plating onto glass coverslips. These coverslips are then placed above the glial monolayer as shown in Figure 12.10.1. In the author's laboratory, the coculture is set up in 24-well plates, with one coverslip for each well. This avoids overlapping of different coverslips, which can occur if petri dishes are used. The main steps in preparing a neuron-sandwich coculture are summarized in Table 12.10.1. The dissection and culture techniques described here are largely based on the method of Goslin and Banker (1991) but have undergone minor changes in the author's laboratory.

Table 12.10.1 Preparation of Neurons-Glia Coculture

Day	Action
1[a] (Thursday)	Prepare primary glial cultures
8 (Friday)	Add paraffin dots and coat glass coverslips (see Support Protocol 4)
10 (Monday morning)	Wash and condition glass coverslips
	Substitute DMEM with SFM in glial cells
10 (Monday afternoon)	Prepare and seed hippocampal neurons (see Support Protocol 1)
11 (Tuesday)	Transfer coverslips with neurons over glial cells and add cytosine arabinoside to the coculture
18 (Tuesday)	Perform experiments

[a]Note this is 10 days before hippocampal dissection.

Materials

Confluent cortical glial monolayer in 24-well plates (see Support Protocol 2)
SFM (see recipe)
Coated glass coverslips seeded with hippocampal neurons (see Support Protocol 1)
2 mM cytosine arabinoside (see recipe)
Sharpened forceps

1. On the day hippocampal neurons are to be prepared (Table 12.10.1), replace the medium in confluent cortical glial monolayers with 1 ml serum-free medium (SFM) and return them to the incubator overnight.

   The addition of SFM to glia prior to adding glass coverslips with hippocampal neurons allows conditioning to favor early phases of neural maturation. SFM is chosen since the ingredients are totally defined and the absence of serum limits the growth of glial cells together with neurons on the glass coverslip.

   Since the author's laboratory usually prepares a number of 24-well glial plates, an amount sufficient for cocultivation with neurons produced over 1 month (i.e., more than will probably be used in one experiment), the medium is replaced only in wells that will receive a coverslip plated with neural cells the following day.

2. The next morning, use one tip of a pair of sharpened forceps to lift the edge of a coated glass coverslip plated with hippocampal neurons. Seize the coverslip with the forceps, and transfer and turn it over the glial monolayer. Repeat for each well to be used.

3. To each well containing neurons and glia, add 2 mM cytosine arabinoside to a final concentration of 5 μM to reduce the proliferation of glial cells.

   Addition of cytosine arabinoside, toxic to dividing cells, is important to block astrocyte proliferation in the neuronal culture.

   In other workers' hands, cytosine arabinoside is usually added on the second to fourth day of culture. Under the experimental conditions used in the author's laboratory, such delayed addition of arabinoside did not satisfactorily reduce astrocyte contamination. This is probably because of the large number of neural cells seeded by the author (160,000/coverslip), which enriches the cell suspension with rapidly dividing astrocytes. Addition of cytosine arabinoside immediately after neuronal cells are attached allows this laboratory to obtain a 98% pure neuronal culture on the glass coverslip, as assessed by immunocytochemistry of microtubule-associated protein 2 (a marker for neurons) and glial fibrillary acidic protein (a marker for astrocytes).

   Under these experimental conditions cytosine arabinoside is not toxic to neurons.

4. Maintain the cocultures, routinely feeding once every 7 to 10 days with SFM.

Neurons are very sensitive to temperature and environmental conditions. Thus if the incubator is opened often during the day it is better to keep the plates towards the bottom where the temperature, percentage CO_2, and humidity are better preserved.

During feeding, it is important not to change the culture medium completely, since neurons depend upon glial cells to condition the medium for long-term survival. Thus, replace ~1/3 the medium each time. Under such conditions, neurons survive for several weeks and become richly innervated.

These cells reach a high degree of maturation (i.e., developed neuronal network, functional glutamatergic system, and almost complete development of the post-synaptic density) after ~7 to 9 days of culture.

SUPPORT PROTOCOL 1

ISOLATION AND SEEDING OF HIPPOCAMPAL NEURONS

The author prepares hippocampal cultures from 18-day-old fetal rats. At this stage, the generation of pyramidal neurons is complete while the generation of dentate granule cells has only just begun. Thus, the culture obtained will consist mainly of pyramidal neurons, which constitute the principal cell type in the hippocampus (85% to 90% of total neurons). From one litter of 18-day-old embryos (i.e., nine to twelve embryos), ~7×10^6 cells for 30 to 40 coverslips 12 mm in diameter (160,000 cells/coverslip) are obtained. The number of coverslips is of course related to the plating density, which has to be chosen according to the experiment to be performed and the techniques available in the laboratory.

Low-density cultures suitable for the study of the development of individual cells and their synaptic interactions or the distribution of antigens within single cells require the application of microscopic techniques because of their sparse distribution. The author's group found that a plating density of 160,000 cells/coverslip yielded a highly differentiated hippocampal culture with a sufficient number of cells for the independent measurement of several parameters of neurotoxicity by nonmicroscopic and quantifiable techniques (Table 12.10.2).

Table 12.10.2 Parameters of Neurotoxicity in Hippocampal Cultures at Low and High Density

Parameter	Low-density cultures	High-density cultures
Neural cell death	Vital dye exclusion and count of living cells	MTT test[a]
Apoptosis	Conformation of nuclei using Hoechst 33258 or propidium iodide dyes (*UNIT 2.2*)	Quantification of oligonucleosomal fragments
Intracellular Ca^{2+} homeostasis	Confocal microscopy (*UNIT 2.8*), video imaging (*APPENDIX 3A*)	Spectrofluorimetric measurement in cell population stained with Fura 2AM (*UNIT 2.5*)
Reactive oxygen species production		Spectrofluorimetric measurement in cell population stained with 6-carboxy-2',7'-dichlorohydrofluorescein diacetate
Production of cytokines	Immunohistochemistry (*APPENDIX 3A*)	Quantification by ELISA and/or RT-PCR (*APPENDIX 3A*)

[a]Source: Denizot and Lang (1986).

Since the procedures performed for isolating hippocampal neurons from rat embryos in the author's laboratory are identical to those described by Audersirk et al., the reader is referred to *UNIT 12.3* for that technique. This section provides an alternative for the dissociation of the hippocampi obtained and for growth in order to set up a sandwich coculture.

Materials

Hippocampi isolated from rat embryos (*UNIT 12.3*)
1× trypsin/EDTA solution (Sigma)
10 mg/ml DNase I stock solution (see recipe)
High-glucose MEM/10% FBS (see recipe)
0.04% (w/v) trypan blue
24-well plate containing coated coverslips (see Support Protocol 4)

Additional regents and equipment for determination of cell number and viability with a hemacytometer (*APPENDIX 3B*)

Prepare hippocampi

1. Collect hippocampi isolated from rat embryos in a sterile 1.5-ml microcentrifuge tube.
2. Centrifuge 4 min at 100 to 150 × *g*, room temperature. Carefully remove the supernatant.

   Aspiration with a pipet is recommended over a vacuum system to avoid aspirating the hippocampi along with the medium.

Trypsinize hippocampi

3. Add 400 µl of 1× trypsin/EDTA solution and 80 µl of 10 mg/ml DNase I solution. Shake gently (do not vortex) and incubate 5 min at 37°C.

   DNase is added to prevent the DNA released by damaged cells from making the dissociation medium too viscous during digestion.

4. While hippocampi are incubating, prepare four 1.5-ml microcentrifuge tubes with 400 µl high-glucose MEM/10% FBS each.
5. Gently aspirate trypsin/DNase solution with a sterile 1-ml pipet (do not use vacuum). Add 400 µl MEM/10% FBS and shake for until hippocampi are floating in the medium.

   The serum in the MEM inhibits residual trypsin and prevents overdigestion of the cells.

Wash out trypsin and DNase

6. Allow the hippocampi to pellet at the bottom of the tube.
7. Gently collect the pelleted hippocampi with a 1-ml pipet in the smallest possible volume of medium and transfer to the first of the four tubes containing MEM/10% FBS (step 4).

   Take care not to destroy the hippocampi during this and the immediately following steps.

8. Gently shake and allow the hippocampi to pellet at the bottom of the tube.
9. Repeat steps 7 and 8 another three times using the remaining tubes in succession.

   Repetitive passage through microcentrifuge tubes with fresh medium washes the hippocampi free from trypsin and DNase I. Avoiding extensive centrifugation results in a better neural culture.

Disaggregate and assess cell number and viability

10. In the last microcentrifuge tube, disaggregate the hippocampi by gently drawing up and down in a 1-ml pipet first and then a 200-µl pipet tip. Adjust the volume of the cell suspension to 1 ml using MEM/10% FBS.

    It is important to be very gentle in pipetting: too vigorous or extensive pipetting causes significant cell death. Pipetting in sequence through a 1-ml pipet and then a 200-µl pipet tip gradually yields a single-cell suspension. Note that pipet tips must be sterile.

11. Gently mix 10 µl cell suspension with 10 µl of 0.04% (w/v) trypan blue. Determine the total cell number and viability with a hemacytometer and an inverted phase-contrast microscope (see *APPENDIX 3B*).

    Trypan blue is used to distinguish viable from dead cells. Viable cells exclude trypan blue while dead or damaged cells are stained (dark blue).

Plate and prepare hippocampal neurons for the sandwich coculture

12. Pipet 160,000 cells into each well of a 24-well plate containing a coated coverslips.

13. Incubate plates overnight and place the coverslip over the confluent glial monolayer the next morning.

    Remember to keep the plates towards the bottom of the incubator where temperature, percentage CO_2, and humidity are better preserved. Neural cells will attach to the coverslip surface during this incubation.

    Since seeding medium is not suitable for hippocampal neuron survival and differentiation, remember to transfer the coverslips the day after plating.

BASIC PROTOCOL 2

PREPARATION OF ASTROCYTE-MICROGLIA-SANDWICH COCULTURES

Glia include three cell types: astrocytes, microglia, and oligodendrocytes. All glial subtypes, but particularly microglia, can express potentially neurotoxic factors when activated.

Under physiological conditions microglia have a "resting" phenotype adapted to the microenvironment of the central nervous system. However, microglia are able to respond quickly to a variety of signaling molecules. Activation at a very early stage in response to damage or alterations to the microenvironment that precede pathological changes is characteristic of microglia, and its activation often precedes reaction of any other cell type in the brain.

The author has recently observed that microglial cells can influence the response of astrocytes in producing neurotoxic substances. For instance, the production of tumor necrosis factor-α (TNF-α) after a neurotoxic insult is much higher in a culture of astrocytes and microglia than with astrocytes or microglia alone (Viviani et al., 1998; Bezzi et al., 2001). Thus, the progression of neurodegenerative events is also modulated by glia-glia interactions.

On the basis of the experience gained by the author's group in coculturing neurons and glial cells, a similar coculture system of astrocytes and microglial cells has been set up in order to study the molecular mechanisms involved in communication between these two cell populations following neurotoxic insult. First, the MEM/FBS medium present in a 24-well plate seeded with astrocytes (see Support Protocol 3) is replaced with SFM (see recipe) 1 to 2 days after the preparation of the culture. Next, the tip of a pair of sharpened forceps is used to lift the corner of a coated glass coverslip seeded with microglia (see Support Protocol 3), seize it, and transfer it over the astrocyte monolayer. In this fashion, microglial cells are juxtaposed, without direct contact, with a monolayer of astrocytes. Note that in the author's laboratory, the astrocyte-microglia coculture is usually used within 48 hr of its preparation.

ISOLATING AND CULTURING CORTICAL GLIAL CELLS

Glial cells (astrocytes, microglia, and oligodendrocytes) are obtained by mechanical and enzymatic dissociation (e.g., trypsin) of cerebral tissue from 1- to 2-day-old old rat pups (Sprague Dawley). The use of such young rats ensures the absence of viable neurons in the cell suspension. For the dissection of fetal brain and the isolation and dissection of cortices, the reader is referred to *UNIT 12.4*. From one 2-day-old pup, the author usually obtains ~5×10^6 cells.

The author uses glial cells both to obtain astrocytes and microglia, and to cocultivate hippocampal neurons. Shaking a confluent glial culture makes it possible to separate astrocytes from microglial cells and obtain two purified cultures (see Support Protocols 3). For this purpose the author's laboratory seeds 4×10^6 glial cells in 75-cm^2 culture flasks. To obtain a glial monolayer for neuron-glia coculture, cells are seeded in 24-well plates at a density of 50,000 cells/ml per well. Both the cells seeded in the wells and those seeded in the flasks reach confluence in ~10 days.

Materials

Cortices from 1- to 2-day-old Sprague Dawley rat pups (*UNIT 12.4*)
HBSS (see recipe)
10× trypsin/EDTA (Sigma)
10 mg/ml DNase I (see recipe)
High-glucose MEM/10% and 20% FBS (see recipe)
0.04% (w/v) trypan blue

35-mm petri dish
Bistoury (Aesculap)
100-µm nylon cell strainer (Falcon)
24-well plates
75-cm^2 canted-neck flasks with screw caps

Additional reagents and equipment for determining total cell number and viability with a hemacytometer (*APPENDIX 3B*)

Disassociate cells

1. Place cortices from 1- to 2-day-old rat pups in a 35-mm petri dish on ice (no medium). To obtain a homogenate of finely minced cortices, accumulate them together in the center of the dish and cut several times in different directions with a bistoury.
2. Add 2 ml HBSS and resuspend the minced cortices by drawing the mixture in and out of a disposable, sterile, 2-ml plastic pipet.
3. Remove the suspension and transfer to a 50-ml centrifuge tube.
4. Repeat steps 2 and 3 twice more to collect all of the minced cortices from the dish.

At the end of these steps minced cortices are resuspended in 6 ml HBSS.

Trypsinize cells

5. Add 750 µl of 10× trypsin/EDTA and 750 µl of 10 mg/ml DNase I to the suspension.

DNase is added to prevent the DNA released by damaged cells from making the dissociation medium too viscous during digestion.

6. Seal the capped tube with Parafilm. Vigorously agitate 15 min in a 37°C water bath to favor enzymatic digestion of the tissue. While the tube is being agitated, prepare a 50-ml centrifuge tube containing 12 ml high-glucose MEM/10% FBS.

7. After agitation, remove the tube from the shaking water bath and allow the undissociated tissue to collect at the bottom.

   Avoid centrifugation; dissociated cells must remain suspended so they can be collected.

8. Collect 5 ml dissociated cells with a disposable, sterile, plastic 12-ml pipet and transfer to the 50-ml centrifuge tube containing MEM/10% FBS (step 6).

   Take care not to include undissociated tissue pieces.

Repeat trypsinization and consolidate products

9. Add 6 ml HBSS, 750 µl of 10× trypsin, and 750 µl DNase I to the 50-ml tube containing the remaining undissociated tissue.

   The FBS in MEM (step 6) inhibits trypsin and thus prevents overdigestion of the dissociated cells.

10. Repeat steps 6 and 7, and add these dissociated cells to the 50-ml tube containing the cells from the first digestion as described in step 8.

Remove trypsin and DNase

11. Filter dissociated cells through a 100-µm nylon cell strainer and collect in a fresh 50-ml centrifuge tube.

    Filtration eliminates any pieces of tissue accidentally collected with dissociated cells.

12. Pellet pooled cells by centrifuging in a swinging-bucket rotor 5 min at 200 to 300 × *g*, room temperature.

13. Carefully remove the medium from the pelleted cells.

Dissaggregate and asses cell number and viability

14. Disaggregate the pellet by first adding 2 ml MEM/10% FBS and then gently drawing in and out of a 2-ml disposable plastic pipet until the solution becomes homogeneous. Add an additional 3 ml MEM/10% FBS for a total resuspension volume of ~5 ml.

15. Gently add 100 µl cell suspension to 200 µl of 0.04% (w/v) trypan blue. Determine total cell number and viability with a hemacytometer and an inverted phase-contrast microscope (*APPENDIX 3B*).

    Trypan blue is used to distinguish viable from dead cells. Viable cells exclude trypan blue while dead or damaged cells are stained (dark blue).

Plate and prepare glia for the sandwich coculture

16. From the 5-ml cell suspension (step 14) aspirate a volume containing a sufficient number of viable cells to prepare the desired number of 24-well plates at a ratio of 50,000 cells/well. Dilute the cell suspension to 50,000 cells/ml with high-glucose MEM/20% FBS.

    The author usually plates a sufficient number of wells for the cocultivation of neurons prepared over 1 month.

    Glial cells are plated and kept in MEM/20% FBS for 5 days, then the medium is changed to MEM/10% FBS. The cells are maintained in this medium up to 1 month.

17. Pipet 1 ml cell suspension into each well of a 24-well plate.

Plate and prepare glia to obtain astrocytes and microglia

18. From the 5-ml cell suspension (step 14), aspirate a volume containing a number of cells sufficient to prepare the desired number of 75-cm^2 canted-neck flasks with screw-caps at a ratio of ~4×10^6 cells/flask. Dilute 4×10^5 cells/ml in MEM/20% FBS.

Astrocyte and microglial cells are obtained by shaking the glial culture to divide the two cell populations (see Basic Protocol 2). Thus, it is important to use culture flasks having screw caps that can be completely tightened to prevent medium spillage during the shaking period.

19. Pipet 10 ml cell suspension into each flask.

Grow cultures to confluence

20. Incubate plates and flasks 24 hr.

21. To eliminate undetached cells, remove the medium and add 1 or 10 ml fresh MEM/20% FBS for each well or flask, respectively. Repeat 5 days later.

22. Five days later, remove MEM/20% FBS, replace with MEM/10% FBS, and continue to grow to confluence, changing the medium twice a week (e.g., Monday and Thursday or Tuesday and Friday).

    Confluence will be reached in ~10 days.

ISOLATION AND SEEDING OF CORTICAL ASTROCYTES AND MICROGLIA CELLS

SUPPORT PROTOCOL 3

The techniques described here to prepare and separate astrocytes and microglial cells are based on the methods of McCarthy and DeVellis (1980), and Giulian and Baker (1986), which have undergone some changes in this laboratory. The method is based on the selective detachment of microglial cells from astrocytes by shaking mixed glial cultures on an orbital shaker; a result of the difference in degree of attachment to tissue-culture plastic versus each other. Astrocytes are then further depleted of microglial cells by treatment with L-leucine methyl ester (L-LME), which selectively kills microglia.

Both astrocytes and microglial cultures appear >97% pure, as assessed by immunocytochemistry of glial fibrillary acidic protein (GFAP), a cytoskeletal protein found only in astrocytes, and with *Griffonia simplicifolia* isolectin B4, a selective marker of both resting and activated microglia (Cheepsunthorn et al., 2001). From each flask of confluent glial cells the author's group usually obtains ~5×10^6 astrocytes. The number of microglial cells separated by each flask is extremely variable and changes with different preparations (i.e., from ~5×10^5 to ~3×10^6 cells).

Materials

High-glucose MEM/10% and 15% FBS (see recipe)
0.04% (w/v) trypan blue solution
1× PBS (Sigma; *APPENDIX 2A*)
High-glucose MEM/10% FBS containing 5 mM L-LME (Sigma)
1× trypsin/EDTA solution (Sigma)
24-well plate containing coated glass coverslips (see Support Protocol 4)

Additional reagents and solutions for preparing confluent glial cultures in 75-cm^2 cantered-neck flasks (see Support Protocol 2) and determining cell number and viability with a hemacytometer (*APPENDIX 3B*)

Detach microglia

1. Prepare confluent glial cultures in 75-cm2 cantered-neck flasks (see Support Protocol 2).

   Use culture flasks since the caps can be completely tightened to prevent medium spill during the shaking period.

   In the author's laboratory, usually ~4×10^6 cells are seeded per flask. In these conditions glial cells reach confluence after 10 days (i.e., to obtain a confluent monolayer on Monday prepare glial cells on the Thursday two weeks before).

2. Use Parafilm to seal the flask caps and vigorously agitate on an orbital shaker 1.5 hr at 260 rpm, 37°C.

   Within 2 hr of shaking, most of the microglia can be detached from the glial monolayer and subcultured. Astrocytes remain adherent to the flask.

3. Collect the medium from the flasks in one or more 50-ml centrifuge tubes.

   Collect up to 50 ml for each tube; one 50-ml tube is enough for 6 flasks.

Equilibrate astrocytes and pellet microglia

4. Add 10 ml fresh high-glucose MEM/10% FBS to each flask with a sterile pipet.
5. To pellet the suspended cells, centrifuge the 50-ml tubes 5 min in a swinging-bucket rotor at 200 to 300 × *g*, room temperature. Meanwhile, transfer the flasks to an incubator for at least 1 hr.

   To obtain purified astrocytes, the flasks have to be shaken further overnight. Since it is usually impossible to shake the flasks in an incubator, it is better to allow the fresh medium to equilibrate before shaking again. This period usually suffices for the preparation of microglial cultures.

Dissaggregate and assess cell number and viability

6. At the end of the centrifugation discard the supernatant, add 2 ml MEM/10% FBS to microglial-cell pellet using a sterile pipet and disaggregate by drawing up and down. Add an additional 3 ml MEM/10% FBS for a total of 5 ml and resuspend to obtain a homogeneous suspension.
7. Add 100 µl cell suspension to 200 µl of 0.04% trypan blue solution and mix gently. Determine total cell number and viability with a hemacytometer and inverted phase-contrast microscope (*APPENDIX 3B*).

   Trypan blue is used to distinguish viable from dead cells. Viable cells exclude trypan blue while dead or damaged cells are stained.

Prepare and plate microglia for the sandwich coculture

8. Gently resuspend sedimented cells, then dilute to 200,000 cells/ml with MEM/10% FBS.
9. Add 1 ml suspension to each well of a 24-well plate containing coated glass coverslips.
10. Incubate 30 min.

    This short incubation period allows the adhesion of chiefly microglial cells to the substrate.

11. Gently shake the plate, remove the medium, and wash once with 1× PBS.

    By shaking and washing, loosely adhering cells like oligodendroglia are removed.

12. Add 1 ml high-glucose MEM/15% FBS to each well and transfer plates to an incubator.

Purify astrocytes

13. Transfer the flasks containing partially purified astrocytes (step 5) to an orbital shaker and agitate overnight at 260 rpm, 37°C.
14. The next morning, remove the medium and wash the monolayer three times with 1× PBS.
15. Add 10 ml high-glucose MEM/10%FBS/5 mM L-LME to each flask.

    L-LME selectively kills microglial cells and is used to reduce any microglial contamination of astrocytes.

16. Incubate 2 hr.

17. Wash twice with PBS.

Trypsinize astrocytes

18. Add 2 ml of 1× trypsin/EDTA to each flask to detach astrocytes and gently rotate so that the trypsin can spread over the surface where astrocytes are attached. Incubate 5 min.

    Do not exceed this time, otherwise there is danger of overdigestion. If it is necessary to detach astrocytes from several flasks, do not add trypsin to all of them at the same time.

    To detach cells without using trypsin, incubate the monolayer 5 min in 5 ml PBS without calcium and magnesium, supplemented with 5 mM EDTA; however, this procedure gives lower cell recovery than by trypsinization.

19. Detach astrocytes by gently shaking and washing the surface of the flask.

20. Transfer the trypsin solution containing astrocytes to a tube containing 2 ml MEM/10% FBS in each flask.

    The serum contained in the medium inactivates trypsin. Thus, to avoid overdigestion the cells resuspended in trypsin are immediately added to an equal volume of cell culture medium. If more than one flask is to be trypsinized, the cells can be pooled in a single tube containing cell culture medium. Add 1 ml of cell culture medium for each milliliter trypsin.

Prepare and plate astrocytes for the sandwich coculture

21. To pellet cells, centrifuge 10 min in a swinging bucket rotor at 100 to 200 × *g*, room temperature. Aspirate the medium and resuspend in 2 ml of MEM/10% FBS.

22. Repeat steps 7 and 8 with the astrocyte suspension.

23. Add 1 ml cell suspension to each well of a 24-well plate.

24. Transfer to an incubator.

    Astrocytes can be maintained up to 1 month.

PREPARATION OF GLASS COVERSLIPS FOR SANDWICH COCULTURES

SUPPORT PROTOCOL 4

Hippocampal neurons and microglial cells do not readily adhere to glass. Thus, to promote their attachment, maturation, and survival, coverslips are coated using poly-L-ornithine, or poly-L-lysine. In addition, three dots of paraffin are placed on each coverslip to create a narrow gap between the two cultivated cell populations.

The use of 24-well plates and 12-mm coverslips to obtain a coculture does not allow an open-face-sandwich coculture, as described for hippocampal neurons and astrocytes in *UNIT 12.3*. This is basically because the cell monolayer below the coverslip degenerates. In 24-well plates, where the well is slightly bigger than the coverslip, this means the destruction of the glial or astrocyte monolayer.

The coverslips are prepared at least one day before the hippocampal neurons (see Support Protocol 1) or microglial cells (see Support Protocol 2) are dissociated. In the author's laboratory, if hippocampi are dissected on Monday, coverslips are prepared the Friday before and kept in polyornithine at room temperature until Monday morning. Next they are washed and incubated in growth medium before being seeded with cells.

Materials

Paraffin wax
1× poly-L-ornithine solution (see recipe)
1× PBS (Sigma)
High-glucose MEM/10% FBS (see recipe)

12-mm glass coverslips
24-well tissue-culture plates
Microwave oven
5- to 10-ml sterile syringe with 0.95 × 40–mm needle
Germicide lamp (e.g., as equipped on a flow hood)

1. Place one 12-mm glass coverslip in each well of a 24-well tissue-culture plate.

   Each time, prepare the exact number of coverslips to be used. This will reduce the possibility of contamination.

2. Sterilize the coverslips by microwaving 10 min at the highest power setting.

3. Place the plates next to a beaker half full of water in order to avoid melting the plastic plates.

4. Heat paraffin wax to ~100°C. Take an ~2-ml aliquot in a 5- or 10-ml syringe and apply three small drops near the outer edge of each coverslip at roughly equal distances from each other.

   To melt paraffin, place 4 pieces in a beaker and place the beaker on a hot plate.

   By working rapidly, it is possible to place several dots over 2 to 3 coverslips. The temperature of the paraffin is very important. If it is too hot, it spreads too thin and wide, while if it is too cool, the dots do not adhere to the coverslip and will subsequently detach.

5. Resterilize the coverslips by UV irradiation for 30 min with a germicide lamp.

   The germicide lamp of a flow hood is sufficient. Avoid exposing coverslips to UV after they have been coated with polyornithine.

6. In a laminar flow hood, add 1 ml of 1× poly-L-ornithine solution in each well containing the coverslips.

   Check that the coverslips do not float in the well but are completely covered by polyornithine. To prevent floating, be sure to eliminate any air bubble under the coverslip by gently pressing over it.

7. Incubate the plates up to 2 days at room temperature or for 2 hr at 37°C.

   When plates are out of the laminar flow hood, store them sealed with Parafilm in the dark.

8. Immediately before isolating cells (see Support Protocol 2), remove polyornithine and rinse twice with 1× PBS.

   To obtain the best result in the attachment of cells and their development do not let the coverslips dry at any stage.

9. After the final rinsing add 1 ml high-glucose MEM/10% FBS and incubate until the end of cell preparation.

   When isolated and dissociated, cells will be seeded in this same medium.

   The coverslips are now ready to be seeded. Add the desired number of cells over the coverslips without changing the incubation medium.

   In the author's laboratory unused coverslips are discarded.

REAGENTS AND SOLUTIONS

Use sterile Milli-Q-purified water or equivalent for all recipes and protocol steps. For common stock solutions, see ***APPENDIX 2A****; for suppliers, see* ***SUPPLIERS APPENDIX****.*

Cytosine arabinoside, 2 mM

Dissolve 2 mg cytosine-1-β-*D*-arabino-furanoside (cytosine arabinoside) in 5 ml water. Store up to 6 months at −20°C.

DNase I, 10 mg/ml

Dissolve 100 mg of 536 Kunitz units/mg DNase I (Sigma) in 10 ml HBSS (see recipe). Store up to 6 months in 1.5-ml aliquots at −20°C.

HBSS

To 850 ml H_2O add:
Hanks Balanced Salts powder (Sigma), enough for 1 liter
10 ml 10 mM HEPES (Sigma)
10 ml penicillin/streptomycin stock solution (Sigma)
Adjust volume to 1 liter with H_2O
Sterilize using a 0.22-µm cellulose-acetate disposable vacuum-filtration system (Millipore)
Store up to 1 month at 4°C

The stock solution of penicillin/streptomycin contains 10,000 U/ml penicillin and 10 mg/ml streptomycin. Store this stock solution up to reported expiration date in 5-ml aliquots at −20°C.

High-glucose MEM/10%, 15%, or 20% FBS

500 ml minimal essential medium with Earle's salts (MEM; Sigma)
0.6% (w/v) D(+)-glucose (Sigma)
5 ml penicillin/streptomycin stock solution (Sigma)
5 ml of 200 mM L-glutamine
Shake vigorously to dissolve glucose
10%, 15%, or 20% (v/v) FBS (Sigma)
Sterilize using a 0.22-µm cellulose-acetate disposable vacuum-filtration system (Millipore)
Store up to 1 month at 4°C

Do not add FBS before shaking, otherwise there is excessive foam formation.

The stock solution of penicillin/streptomycin contains 10,000 U/ml penicillin and 10 mg/ml streptomycin (100 U and 100 µg/ml final, respectively). Store this stock solution up to indicated expiration date in 5-ml aliquots at −20°C.

See APPENDIX 3B for more information regarding preparation of medium.

Insulin, 5 mg/ml

100 mg insulin from bovine pancreas (Sigma)
20 ml sterile H_2O
100 µl glacial acetic acid
Store up to 6 months at 4°C

Poly-L-ornithine solution, 1×

Prepare a 100× stock solution by dissolving 10 mg poly-L-ornithine (Sigma) in 6.67 ml water. Store up to 6 months in 1-ml aliquots at −20°C. Dilute to 1× with water.

Progesterone, 0.1 mM

Dissolve 0.314 mg progesterone in 10 ml of ethanol. Store up to 6 months at −20°C.

Putrescine, 1 M

Dissolve 1.6 g putrescine (Sigma) in 10 ml water. Store up to 6 months at −20°C.

SFM

To 850 ml H_2O add:

Dulbecco's modified Eagle's medium nutrient mixture F-12 Ham powder (Sigma), enough for 1 liter

3.7 g $NaHCO_3$

0.11 g sodium pyruvate (1 mM final; Sigma)

1 ml 5 mg/ml insulin (see recipe)

100 mg >97% human apotransferrin (Sigma)

100 µl 1 M putrescine (1 µM final; see recipe)

120 µl 0.25 M sodium selenite (30 nM final; see recipe)

200 µl 0.1 mM progesterone (20 nM final; see recipe)

10 ml penicillin/streptomycin (100 U/ml and 100 µg/ml final, respectively; Sigma)

Adjust pH to 7.2

Adjust volume to 1 liter with H_2O

Sterilize using a 0.22-µm cellulose-acetate disposable vacuum-filtration system (Millipore)

Store for up to 1 month at 4°C.

See APPENDIX 3B for more information regarding preparation of culture medium.

Sodium selenite, 0.25 mM

Dissolve 1 mg sodium selenite (Sigma) in 10 ml water. Store up to 1 month at room temperature.

COMMENTARY

Background Information

Coculture systems provide an easy controlled way to study how a cell population can influence the function, viability, and response of another cell population. Other in vitro systems suitable for the study of the interactions between different cell populations are brain reaggregate cultures or organotypic explants. Brain reaggregate cultures are rotation-mediated aggregating cultures constructed from single-cell suspensions of fetal brain characterized by an organotypic cell association.

A more complex situation is represented by the organotypic cultures. These are derived from explants of undifferentiated embryonic brain and retain some of the structural and functional characteristics of the area of origin.

Both organotypic and reaggregate cultures differ from cocultures since they retain a three-dimensional organization. While a flat coculture system is particularly well suited to detect changes in cell function or differentiation and the interference of a neurotoxicant on these parameters, organotypic and reaggregate cultures are designed to detect changes in cellular organization by morphological and electrophysiological features. Thus, the choice of the cell system largely depends on the question to be answered.

The great advantage of a sandwich coculture system in toxicological studies over the other in vitro systems is the possibility of separating the two cell populations at any time (e.g., prior to or after a treatment) while retaining their integrity. This allows the investigator to (1) treat the cell types differently before they are exposed together to a toxicant, thus providing information on the involvement of specific mediators or biochemical pathways, (2) perform different biochemical measurements on the two cell populations separately at the end of the treatment, and (3) evaluate the effect of a toxicant on highly differentiated neurons in the presence or absence of the glial feeder layer. For example, the author used this system to study the molecular mechanisms involved in the glia-mediated neurotoxicity of the human immunodeficiency virus glycoprotein 120 (gp-120). The question of whether the production of reactive oxygen species (ROS) induced by gp-120 in glial cells could be responsible for an increased production of IL-1β from glia and

subsequent neural death was assessed (Viviani et al., 2001). For this purpose, glial cells were loaded with an antioxidant, washed, and exposed together with hippocampal neurons to gp-120. In this way, the ability of glial cells to produce ROS as a consequence of gp-120 exposure without altering the neural cells was blocked. As a control, hippocampal neurons and unloaded glia were exposed to gp-120. At the end of the treatment, glia and neurons were separated, neural cell death was assessed by the MTT test, and the results compared with the death rate of neurons exposed to gp-120 in the presence of an unloaded glial monolayer. The synthesis of IL-1β in glial cells was also measured by RT-PCR. It was observed that antioxidant pretreatment of glial cells reduced gp-120 production of IL-1β and neural cell death.

This model has also been used to monitor the influence of neural degeneration on glial response in modulating neural cell death (Viviani et al., 2000).

Because there is no contact between the cell populations, sandwich coculture allows one to study how different cell populations can reciprocally influence their functions/viability through the release of soluble mediators. The lack of contact between neurons and glia, or astrocytes and microglia may, however, represent a disadvantage since it does not mirror physiological conditions. Hippocampal neurons can be plated directly onto glial cells, as can microglia onto astrocytes, but the advantage of manipulating one of the two cell populations forming the coculture would be lost.

Critical Parameters and Troubleshooting

Three very important parameters to obtain successful primary cultures are sterility, rapidity in dissecting brain tissues and plating the obtained cells, and satisfactory reagents. Problems encountered during cell isolation and growth, their possible causes and possible remedies are reported in Table 12.10.3. Also see the equivalent section in *UNITS 12.3 & 12.4*.

Sterility

Working conditions must ensure the highest degree of sterility. This means that, wherever possible, cell isolation, culturing, and preparation of all solutions should be performed in a laminar flow hood. If nonsterile ingredients are added to a solution, the product has to be filtered through a 0.22-μm filter. To maintain sterility, solutions must never be opened outside the laminar flow hood and must be stored in small aliquots. The addition of antibiotics such as penicillin and streptomycin to the culture medium helps to avoid bacterial contamination.

The use of disposable materials for culturing cells reduces the possibility of contamination and is strongly recommended. All disposable materials (even plastic pipets) should be used only once.

Autoclave surgical instruments (i.e., 21 min at 121°C) to sterilize and store in 95% ethanol when not in use. If, during dissection, tools touch nonsterile surfaces or materials, spray them with 70% ethanol and let the ethanol evaporate before using again.

If any contamination occurs, it is wise to eliminate the contaminated cultures, prepare fresh reagents, and clean the laminar flow hood prior to new culture preparation. To clean the laminar flow hood, wash with a detergent first and then with 70% ethanol. Contaminated solutions can be filtered, but sterility has to be checked prior to use by incubating in culture dishes for a few days at 37°C.

Tissue dissection

Rapid dissection of both hippocampi and cortices is essential to obtain a successful neural or glial culture. In the author's experience the shorter the time of dissection the better the culture obtained. The author's group never exceeds 2 hr to obtain brains and dissect hippocampi and cortices. Preparation time for cultures can be considerably shortened by using a team of two people, one removing brains from the skull and the other cleaning, removing, and dissociating hippocampi or cortices.

Reagent lots

Lot-to-lot variability of reagents such as trypsin, poly-L-ornithine, and all the ingredients of SFM as well as FBS, influences the viability, development, and functionality of glia and particularly of hippocampal neurons. Wherever possible, it is better to test different lots of the same reagent before the routine cultivation of glia and neurons. Measurements to identify the best lot are: the number of cells obtained after tissue dissociation (which can depend on the lot of trypsin used), the growth rate of glial cells (dependent on serum), the cell viability, the differentiation of neural cells (dependent on the poly-L-ornithine or the ingredients of SFM). If poor neural differentiation is observed, check also that all the requisite ingredients have been added to the culture medium.

Table 12.10.3 Troubleshooting Guide to Coculturing Neurons and Glial Cells

Problem	Possible cause	Solution
Low cell viability	Prolonged dissection time	Never exceed 2 hr to obtain brain and dissect hippocampi or cortices
Poor neuronal differentiation	SFM is incomplete (e.g., without apotransferrin)	Prepare fresh SFM and check that all ingredients are added
	L-Polyornithine lot is unsatisfactory	Test different lots and choose the best
	Glial feeder layer is too old	To cocultivate hippocampal neurons use a glial feeder layer within 3 to 4 weeks
	Damaged glial feeder layer	Check the morphology of glial cultures every time before adding neurons
Floating cells in cultures	Contamination	See Critical Parameters and Troubleshooting, Sterility

Anticipated Results

Healthy hippocampal neurons readily attach to coated glass coverslips and are initially characterized as small round shapes. Within a day of coculture they extend short processes (Fig. 12.10.1). A well-developed network is clearly evident at the third or fourth day of coculture. In the following weeks, even if great morphological changes are not evident any more, hippocampal neurons develop a functional glutamatergic system and a complete post-synaptic density. Hippocampal neurons become sensitive to glutamate, showing an increase in cell death and intracellular calcium, starting from the eighth day of culture.

Glial cultures at confluence are characterized by the presence of an overwhelming percentage of astrocytes and ~5% of microglia. Astrocytes have a flat polygonal appearance and form a uniform layer over which small, dark microglial cells can be observed. Microglial cell numbers can increase considerably with aging of the culture. Once detached from astrocytes and plated on a glass coverslip, microglial cells acquire a round shape that tends to ramify as the number of days in culture increases. A "ramified" morphology is typical of resting microglia. The author's group observed no morphological difference in microglia or astrocytes cultivated alone or in coculture <48 hr from their preparation.

Time Considerations

Preparation of hippocampal neuron-glia sandwich cocultures (Basic Protocol 1) or of astrocyte-microglia-sandwich cocultures (Basic Protocol 2) requires 35 to 45 min. Hippocampal neuron-glia cocultures can be maintained up to 3 to 4 weeks. In the author's laboratory, the astrocyte-microglia coculture is used within 48 hr from its preparation.

Isolation and seeding of hippocampal neurons (Support Protocol 1) require 1.5 hr to 2 hr. Hippocampal neurons seeded by following the described protocol can be maintained without glial cells up to a couple of days.

Isolating and culturing cortical glial cells (Support Protocol 2) requires 2 hr. Cortical glial cells can be maintained up to 1 month.

Isolation and seeding of cortical astrocytes (Support Protocol 3) require 19 hr. Astrocytes can be maintained up to 1 month. Isolation and seeding of microglial cells (Support Protocol 3) require 2 hr. In the author's laboratory, microglia are maintained up to 48 hr from preparation.

Preparation of glass coverslips for sandwich cocultures (Support Protocol 4) requires 2 days when glass coverslips are incubated with poly-L-ornithine at room temperature or 3 hr when glass coverslips are incubated with poly-L-ornithine at 37 °C.

Literature Cited

Bezzi, P., Carmignoto, G., Pasti, L., Vesce, S., Rossi, D., Rizzini, B.L., Pozzan, T., and Volterra, A. 1998. Prostaglandins stimulate calcium-dependent glutamate release in astrocytes. *Nature* 391:281-285.

Bezzi, P., Domercq, M., Brambilla, L., Galli, R., Schols, D., De Clercq, E., Vescovi, A., Bagetta, G., Kollias, G., Meldolesi, J., and Volterra, A. 2001. CXCR4-activated astrocyte glutamate re-

lease via TNF-α: Amplification by microglia triggers neurotoxicity. *Nature Neurosci*. 4:702-710.

Brown, D.R., Schmidt, B., and Kretzschmar, H.A. 1996. Role of microglia and host prion protein in neurotoxicity of prion protein fragment. *Nature* 380:345-347.

Cheepsunthorn, P., Rador, L., Menzies, S., Reid, J., and Connor, S.R. 2001. Characterization of a novel brain-derived microglial cell line isolated from neonatal rat brain. *Glia* 35:53-62.

Denizot, F. and Lang, R. 1986. Rapid colorimetric assay for cell growth and survival. Modifications to tetrazolium dye procedure giving improved sensitivity and reliability. *J. Immunol Methods* 89:271-277.

Gegelashvili, G., Danbolt, N.C., and Schousboe, A. 1997. Neuronal soluble factors differentially regulate the expression of the GLT1 and GLAST glutamate transporters in cultured astroglia. *J. Neurochem*. 69:2612-2615.

Giulian, D. and Baker, T.J. 1986. Characterization of ameboid microglia isolated from developing mammalian brain. *J. Neurosci.* 6:2163-2178.

Goslin, K. and Banker, G. 1991. Rat hippocampal neurons in low-density culture. *In* Culturing Nerve Cells (G. Banker and K. Goslin, eds.) pp 251-281. MIT Press, Cambridge, Mass.

Harry, G.J., Billingsley, M., Bruink, A., Campbell, I.L., Classen, W., Dorman, D., Galli, C.L., Ray, D., Smith, R.A., and Tilson, H.A. 1998. In vitro techniques for the assessment of neurotoxicity. *Environ. Health Persp.* 106:131-158.

McCarthy, K.D. and De Vellis, J. 1980. Preparation of separate astroglial and oligodendroglial cell cultures from rat cerebral tissue. *J. Cell Biol*. 85:890-902.

Meucci, O. and Miller, R.J. 1996. gp-120-induced neurotoxicity in hippocampal pyramidal neuron cultures: Protective action of TGF-α1. *J. Neurosci.* 16: 4080-4088.

Steward, O., Torre, E.R., Tomasulo, R., and Lothman, E. 1991. Neuronal activity up-regulates astroglial gene expression. *Proc. Natl. Acad. Sci. U.S.A*. 88:6819-6823.

Rogrove, A.D. and Tsirka, S.E. 1998. Neurotoxic responses by microglia elicited by excitotoxic injury in the mouse hippocampus. *Curr. Biol.* 8:19-25.

Viviani, B. and Corsini, E., Galli, C.L., and Marinovich, M. 1998. Glia increase degeneration of hippocampal neurons through release of tumor necrosis factor-α. *Toxicol. Appl. Pharmacol.* 150:271-276.

Viviani, B., Corsini, E., Galli, C.L., Padovani, A., Ciusani, E., and Marinovich, M. 2000. Dying neural cells activate glia through the release of a protease product. *Glia* 32:84-90.

Viviani, B., Corsini, E., Binaglia, M., Galli, C.L., and Marinovich, M. 2001. Reactive oxygen species generated by glia are responsible for neuron death induced human immunodeficiency virus–glycoprotein 120 in vitro. *Neurosci.* 107:51-58.

Key References

Goslin and Banker, 1991. See above.

An excellent text and manual describing point-to-point hippocampal cell preparation and astrocyte-neuron coculture.

Harry et al., 1998. See above.

An extensive overview on several in vitro methods to study neurotoxicity, their advantages and disadvantages. A description of organ, slice and aggregate cultures is also provided.

Contributed by Barbara Viviani
University of Milan Via Balzaretti
Milan, Italy

Determining the Ability of Xenobiotic Metals to Bind a Specific Protein Domain by Electrophoresis

BASIC PROTOCOL

Environmental metals are potentially toxic and can interfere with the metal-binding motifs of various critical proteins. This unit describes an electrophoretic method that can be used to measure the ability of a xenobiotic metal to bind a zinc-finger motif. Information gained using this protocol can lead to the identification of protein targets of metals and shed better light on their mechanisms of action.

The zinc-finger motif belonging to the Cys_2-His_2 family provides a structural framework for a number of critical proteins which are essential for cellular function. Proteins that contain this motif perform a variety of functions and are present in transcription factors, enzymes, cell-surface receptors, and a number of other cellular intermediates. This protein domain is naturally tailored to serve as a specific binding region for endogenous zinc; however, this domain may be a potential target for the binding of other xenobiotic metals. The interactions of heavy metals with this protein region may lead to functional and structural perturbations of the protein.

To perform this assay, first a synthetic zinc-finger apopeptide (26 amino acids) resembling a single-finger domain of specificity protein 1 (Sp1; Fig. 12.11.1) is reconstituted with a metal of interest. Then, the ability of this metal-peptide complex to specifically bind a cognate DNA consensus sequence is examined electrophoretically. A metal that is able to bind such a peptide and maintain a specific structural configuration will interfere with the mobility of the DNA consensus sequence on an SDS-PAGE gel. As confirmed by one- and two-dimensional NMR studies (Razmiafshari and Zawia, 2001) this specific configuration requires that the metal be able to bind both the cysteine and histidine residues that are involved in the zinc-coordination sphere of this domain. The concentration, affinity, and specificity at which such a metal can bind can also be determined. This unit describes the electrophoretic method that may be used to measure the ability of a xenobiotic metal to bind the zinc-finger motif that may be present in any protein of interest.

CAUTION: Institutionally approved safety protocols must be followed when working with radioactivity. Experiments must be conducted in designated areas and the use and disposal of radioactive materials must be done according to established guidelines.

CAUTION: Radiolabeled probes are hazardous; see *APPENDIX 1A* for guidelines on handling, storage, and disposal.

NOTE: All glassware should be acid washed with 4 N nitric acid. Peptide handling must be performed with metal-free tips using metal-free tubes. To prevent peptide oxidation, all manipulations must be performed in an anaerobic environment. All buffers containing peptides and/or metal solutions should be degassed with nitrogen prior to use.

Materials

1.75 pmol/µl Sp1 consensus oligonucleotide (annealed before use):
5′-ATTCGATC*GGGGCGGGGC*GAGC-3′
3′-TAAGCTAG*CCCCGCCCCG*CTCG-5′
3000 Ci/mmol [γ-^{32}P]ATP
10× kinase buffer (see recipe)
10 U/µl T4 polynucleotide kinase
TE buffer (*APPENDIX 3C*)

Contributed by N.H. Zawia, Md. Riyaz Basha, and M. Razmiafshari
Current Protocols in Toxicology (2003) 12.11.1-12.11.8

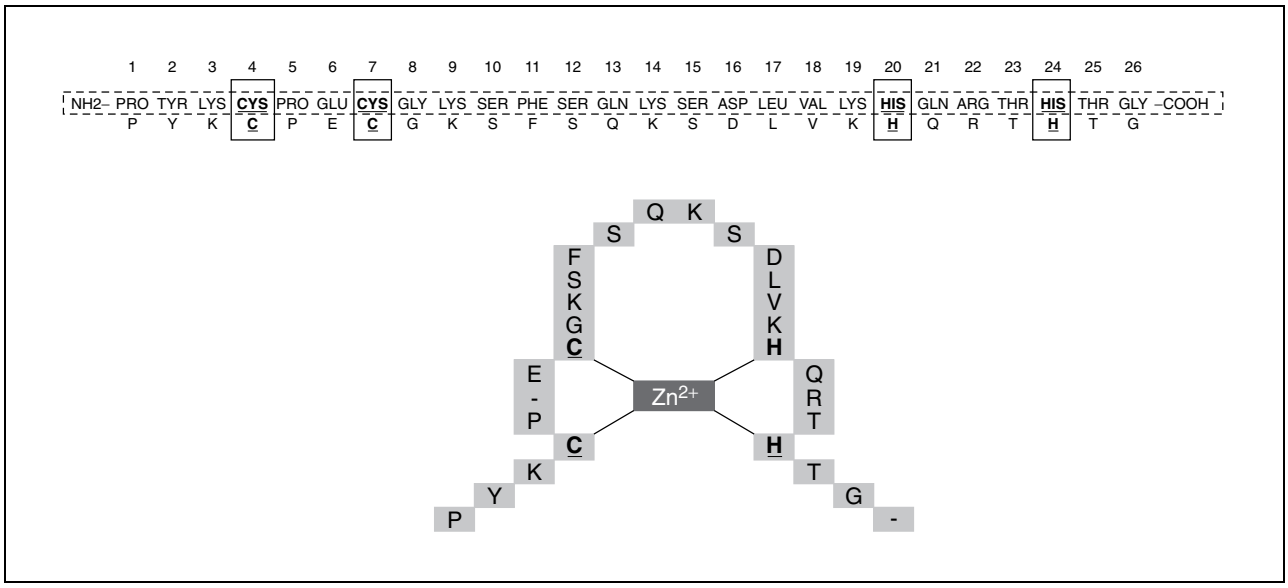

Figure 12.11.1 Schematic diagram of the amino acids sequence of a zinc-finger motif and its deduced form. This sequence was used in the studies summarized in this unit.

Synthetic zinc-finger apopeptide stock solution (see recipe)
Divalent metal solutions (see recipe)
Gel-shift binding buffer (see recipe)
Gel loading buffer (Sigma)
Sephadex G-25 spin column (Sigma)

Additional reagents and equipment for preparing and running polyacrylamide gels (*APPENDIX 3F*) and autoradiography (*APPENDIX 3D*)

Label DNA

1. Prepare the following labelling reaction mixture:

   2 µl of 1.75 pmol/µl Sp1 oligonucleotide
   1 µl of 3000 Ci/mmol [γ-^{32}P]ATP
   1 µl 10× kinase buffer
   1 µl of 10 U/µl T4 polynucleotide kinase.

   Adjust the final volume to 10 µl with water.

   The nucleotides in italics in the oligonucleotide sequence comprise the CG-rich sequence to which a transcription factor binds.

2. Incubate the reaction mixture 10 min at 37°C.

3. Dilute the resultant labeled probe to a final volume of 100 µl (optional) with TE buffer.

   Each reaction requires 55,000 to 65,000 cpm for better binding and to obtain a good signal in the autoradiogram. TE buffer helps maintain optimal reaction conditions.

4. Pass the labeled DNA probe through a Sephadex G-25 spin column for purification of labelled probe from reaction components.

Make metal-peptide complexes

5. Prepare sufficient 10 µM working solution from a synthetic zinc-finger apopeptide stock—82.5 nmole peptide (~0.25 mg) in 500 µl in buffer—for metal-binding and displacement studies.

6. Form metal-peptide complexes by preparing a series of tubes containing 0.5 µl of 10 µM synthetic peptide, and 0.5 µl of a range of low (1 to 200 µM) to high (0.4 to 3.5 mM) concentration divalent metal solutions (Zn, Ca, and metals of interest in Milli-Q-purified water).

   Zinc will serve as a positive control, while calcium, which is unable to coordinate with the Cys residues in the Cys_2-His_2 motif to form a tetrahedral structure, can be used as a negative control in these experiments.

Perform metal-peptide-DNA-binding reactions

7. Prepare the final binding reaction containing 1 µl (500 ng) purified peptide–metal complex and add 17 µl gel-shift binding buffer.
8. Incubate the reaction mixture 30 min at room temperature.
9. Add 1 µl of 0.025 ng/µl labeled DNA probe (step 4) to the above reaction mixture.

   The final reaction volume is 20 µl.

10. Incubate the resultant reaction mixture 20 min at room temperature.

Analyze the DNA-binding reaction by gel electrophoresis

11. Prepare a 15% 1.0 to 1.2-mm thick (29:1) polyacrylamide gel (*APPENDIX 3F*), and prerun 1 hr at 155 V using 90 mM Tris-borate, pH 8.3, as the running buffer.
12. Add 1 µl gel loading buffer to the sample. Load the samples (reaction mixtures) and allow for electrophoresis to proceed 3 to 3.5 hr at 155 V (15 mA; *APPENDIX 3F*).

    The color of the gel loading buffer will help when loading the gel.

13. Dry the gel and expose it to X-ray film overnight (*APPENDIX 3D*).
14. Analyze the resulting autoradiograms for shifted bands.

REAGENTS AND SOLUTIONS

*Use metal-free water (e.g., Milli-Q-purified) for all recipes and protocol steps. For common stock solutions see **APPENDIX 2A**; for suppliers, see **SUPPLIERS APPENDIX**.*

Divalent-metal solutions

Prepare 1 mM stock solutions from each metal (i.e., Zn, Ca, metal of interest) salt or nitrate in metal-free water and store up to 1 week at 4°C.

Gel-shift binding buffer

35 mM Tris·Cl, pH 8.0 (*APPENDIX 2A*)
60 mM NaCl
3 mM DTT
375 µg/ml BSA
0.2% (v/v) protease inhibitor cocktail (Sigma)
300 ng poly(dI·dC) in 10% (v/v) glycerol
Store up to 3 months at less than −20°C

Kinase buffer, 10×

700 mM Tris·Cl, pH 7.6 (*APPENDIX 2A*)
100 mM MgCl
50 mM DTT
Store up to 3 months at less than −20°C

Follow the instructions given by the company for the buffer obtained from the commercial sources (e.g., Promega).

Synthetic zinc-finger apopeptide stock solution

Synthesize a zinc-finger peptide resembling a single-finger motif of Sp1 (P-Y-K-C-P-E-C-G-K-S-F-S-Q-K-S-D-L-V-K-H-Q-R-T-H-T-G) using standard procedures. Store it as a powder at −80°C until use. Make a stock solution by dissolving 82.5 nmol (~0.25 mg) peptide in 500 µl of 100 mM HEPES (pH 7.0)/50 mM NaCl. Store up to 4 to 6 months at −20°C.

COMMENTARY

Background Information

Environmental metals are potentially toxic and can interfere with the metal-binding motifs of various critical proteins of the cell. The zinc finger is a major structural motif involved in protein–nucleic acid interactions and is present in the largest known superfamily of eukaryotic transcription factors, such as Sp1 (Dynan and Tijian, 1983). In order to maintain structural integrity, zinc ions coordinate this finger-like structure through bonds created with cysteine and histidine residues. Metal-induced perturbations of the structural integrity of this motif may alter protein function and can result in a variety of adverse effects including neurological diseases and aggressive malignancies.

A zinc-finger peptide may be utilized as a model to study the interactions of various environmental metals with this motif. This approach provides the advantage of designing apopeptides that resemble the binding sites of endogenous metals and complexing them in vitro with heavy metals suspected to bind to them. The properties of the peptide-metal complexes may then be compared to the action of these metals on an entire protein that normally contains the motif. Furthermore, details on the exact binding site of these metals to these small synthetic peptides may be examined by nuclear magnetic resonance spectroscopy. These models can help to reveal the mechanisms of action of certain metals, especially metal-induced alterations in gene expression.

Critical Parameters and Troubleshooting

The rationale for choosing the peptide used in this unit is that the residues involved in stabilizing the three-dimensional structure of the metal-bound forms of the zinc-finger domains are present in such an amino acid sequence, leading to increased affinity for metal ions (Krizek et al., 1991). Since the peptide synthesized is part of the DNA-binding domain of Sp1, one can investigate whether these metal complexes show specific DNA-binding properties. The binding and activity of zinc-finger peptides have been shown to be modulated by heavy metals (Zawia et al., 1998). Various proteins, which contain zinc-finger domains of the Cys_2-His_2 type, have been shown to bind specifically to DNA, RNA, and DNA-RNA hybrids (Shi and Berg, 1996). Also, previous DNA binding studies employing gel shift assays have suggested that single zinc-finger peptides bind to DNA only in the presence of zinc (Lee et al., 1991). Hence, for a proper metal-peptide DNA complexation and specific binding, metal ions and the peptide must cooperatively adopt the proper structure necessary for DNA sequence recognition.

The DNA-metal-peptide complex may exhibit an increased mobility on the gel. This may be due to the ability of zinc-finger proteins to cause winding and unwinding of DNA. Structural and biochemical analyses have shown that DNA was slightly unwound when bound to zinc-finger peptides (Pavletich and Pabo, 1991; Nekludova and Pabo, 1994; Shi and Berg, 1996). Although the zinc-finger motif may play a role in changing DNA shape and form, the addition of specific metals to the peptide may also change the packing structure of the peptide altering its mobility on the gel. This appears to be linked to the concentration of DNA present, because an excess of cold DNA competes and restores the accelerated band to its original position.

In the procedure describe in this unit, the following guidelines should be observed.

1. Use a concentration range for each metal because the threshold for perturbation of the motif may be different for each.

2. Follow a specific order in the reaction sequence. Prepare the peptide and metal complex first and then add the labeled DNA oligonucleotide.

3. Check the purity of the DNA consensus element, as commercially available oligonucleotides may contain mixtures of ssDNA and dsDNA, and the peptide may have different affinities for binding each of these strands.

4. Avoid or minimize the use of chelating agents such as EDTA. Although such agents

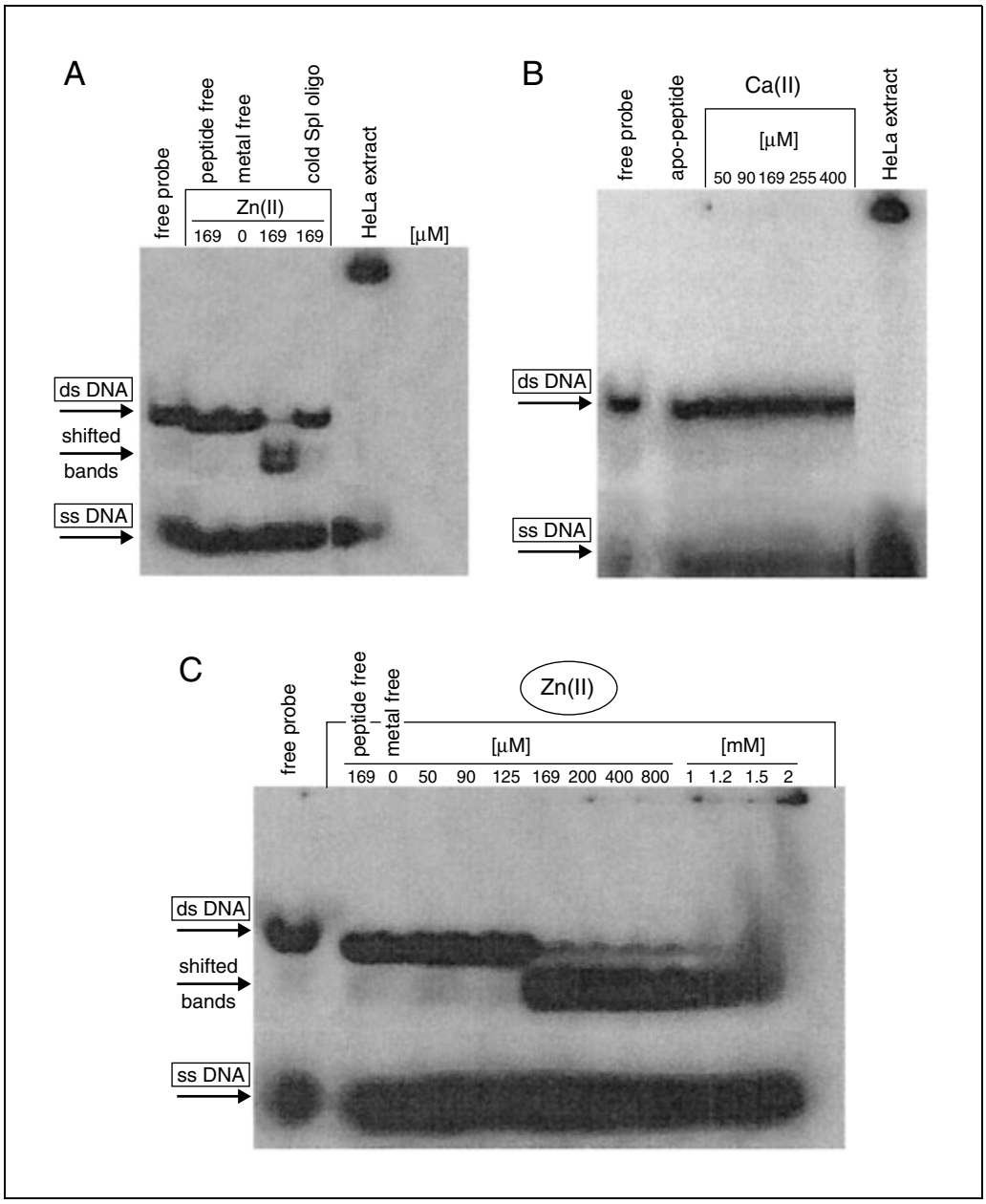

Figure 12.11.2 Concentration-dependent DNA-binding of Zn(II)- and Ca(II)-peptide complexes when reacted with a GC-box consensus DNA element. Shown are autoradiograms of (**A**) competition studies of a Zn(II)-peptide complex with hot and cold Sp1 oligonucleotide, (**B**) Ca(II)-peptide complex, and (**C**) Zn(II)-peptide complex. These reactions contained a ^{32}P-labeled oligonucleotide sequence recognized by Sp1 in each lane. The concentrations of zinc and calcium used and the shifted bands are clearly marked. Reprinted from *Toxicology and Applied Pharmacology*, 166, M. Razmiafshari and N.H. Zawia, Utilization of a synthetic peptide as a tool to study the interaction of heavy metals with the zinc finger domain of proteins critical for gene expression in the developing brain, pp. 1-12, 2000, with permission from Elsevier.

may stabilize DNA-protein complexes, they can also chelate the free metals in the reaction.

Anticipated Results

The zinc-finger motif belonging to the Cys_2-His_2 family provides a structural framework for a number of critical proteins that are essential for cellular function. To determine whether these domains are potential targets for heavy-metal perturbation, the authors examined the interaction between various metals and a synthetic Cys_2-His_2 finger peptide of the type present in the transcription factor Sp1 (Razmiafshari and Zawia, 2000). Sp1 has a DNA-binding domain composed of three contiguous zinc-finger motifs (26 residues), which binds

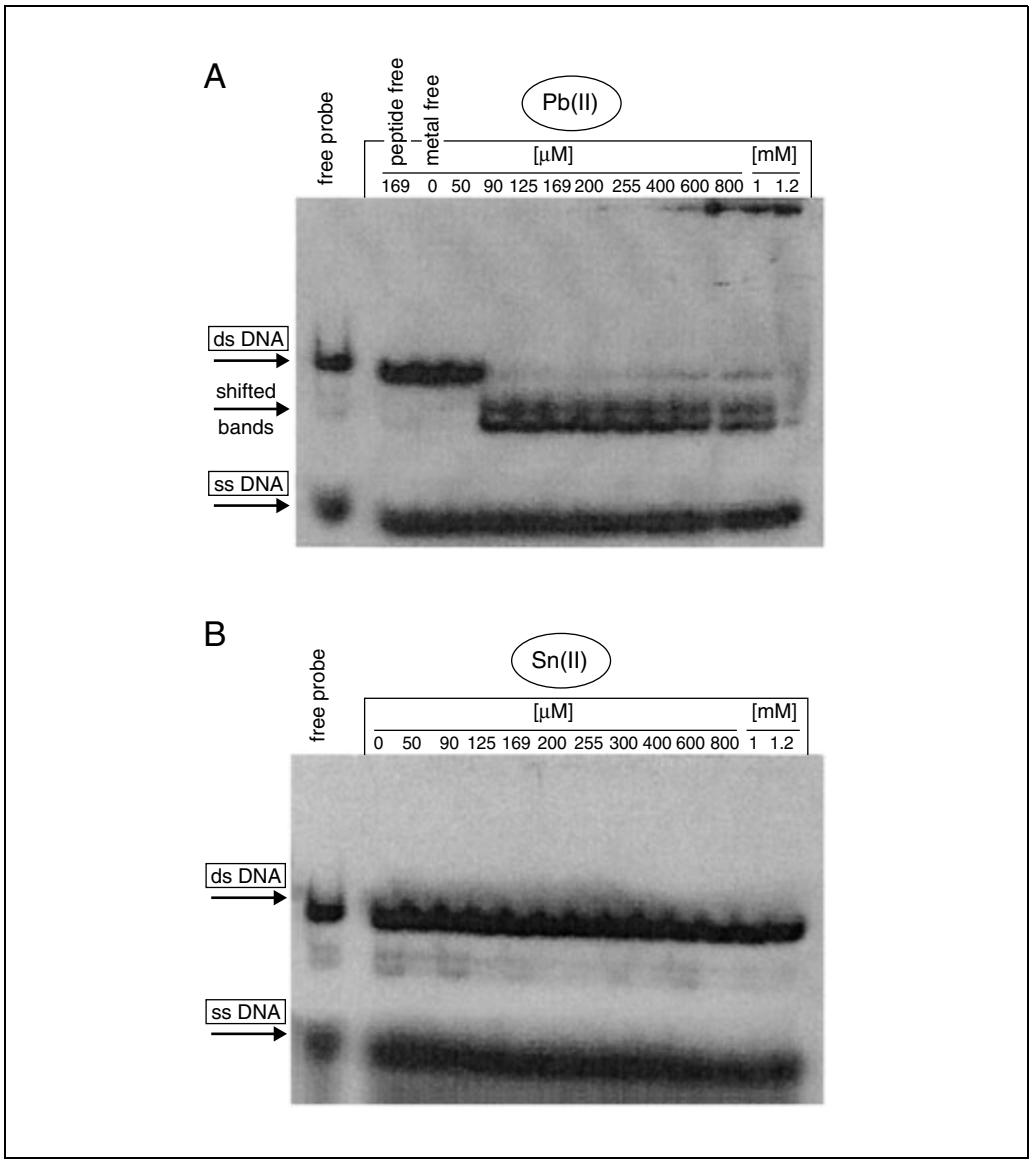

Figure 12.11.3 DNA-binding activity of metal(II)-peptide complexes when reacted with a GC-box consensus DNA sequence. Shown are autoradiograms of (**A**) Pb(II)- and (**B**) Sn(II)-peptide complexes. These reactions contained a ^{32}P-labeled oligonucleotide sequence recognized by Sp1 in each lane. The concentrations of metals used and the shifted bands are clearly marked. Reprinted from *Toxicology and Applied Pharmacology*, 166, M. Razmiafshari and N.H. Zawia, Utilization of a synthetic peptide as a tool to study the interaction of heavy metals with the zinc finger domain of proteins critical for gene expression in the developing brain, pp. 1-12, 2000, with permission from Elsevier.

to the GC box. The DNA-binding activity of these various metal-peptide complexes to their cognate DNA consensus sequence was examined electrophoretically.

Several divalent metals were complexed with the apopeptide and the resultant structural forms were analyzed using the methods outlined above. Titration experiments with the metal-peptide complexes and the DNA consensus sequence were utilized to determine optimum binding conditions. Using the optimum binding concentration of the Zn(II)-peptide complex, the binding specificity to the cognate DNA sequence was explored (Fig. 12.11.2). Under these conditions, a downward gel shift of the DNA-metal-peptide complex was observed. Gel-shift competition experiments revealed that the apopeptide in the absence of zinc ions failed to bind the double-stranded DNA. Additionally, in the absence of the peptide, zinc ions at the optimum concentration did not alter the gel mobility of the oligonucleotide (Fig. 12.11.2). Introducing a 4-fold excess of cold Sp1 oligonucleotide to the same reaction mix-

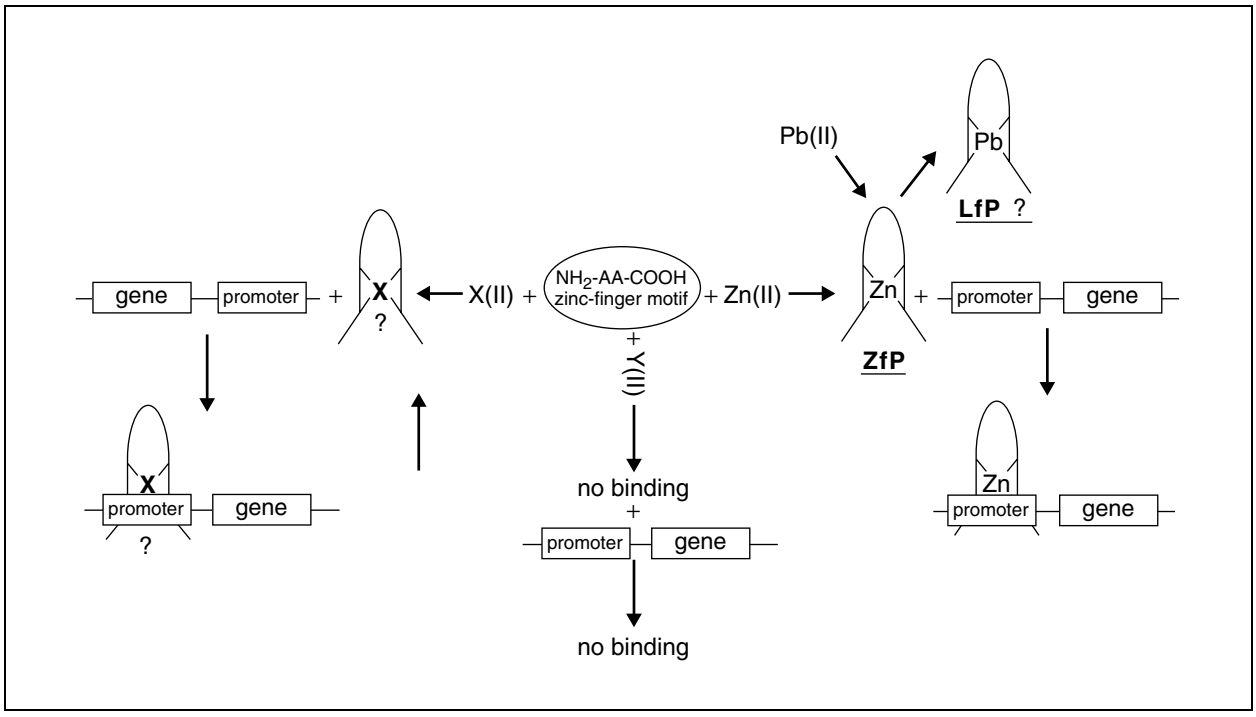

Figure 12.11.4 Predicted mechanism for the interaction of various divalent metals with the zinc-finger motif and their metal-peptide complex reactions with their DNA consensus element. Reprinted from *Toxicology and Applied Pharmacology*, 166, M. Razmiafshari and N.H. Zawia, Utilization of a synthetic peptide as a tool to study the interaction of heavy metals with the zinc finger domain of proteins critical for gene expression in the developing brain, pp. 1-12, 2000, with permission from Elsevier. Abbreviations: X(II) is Pb, Cd, or Hg; Y(II) is Ca, Ba, Mg, or Sn; ZfP, zinc-finger peptide; LfP, lead-finger peptide, AA is a sequence of 26 variable amino acids.

ture competed out the Zn(II) peptide DNA-binding ability and eliminated the shifted bands. Furthermore, Ca(II)-peptide mixtures (Fig. 12.11.2) failed to exhibit any DNA-binding activity, as demonstrated by the unchanged mobility of the DNA sequence in the presence or absence of the complexes (Fig. 12.11.2). The optimum binding concentration of the Zn(II)-peptide complex was determined to be 169 μM, using titration experiments with the metal-peptide complexes and the DNA consensus sequence. Zinc binds to this peptide in 1:1 ratio. Therefore this can happen at very low concentrations in the physiological range. However, in order to be able to detect this interaction in a gel, it is necessary to increase the amount of peptide used and proportionately the amount of metal used.

Pb(II)-peptide complexes (Fig. 12.11.3A) exhibited enhanced DNA-binding ability compared to Zn(II) (Fig. 12.11.2C). Optimal DNA-binding of the Pb(II)-peptide complex occurred at 90 μM. Pb(II) and Sn(II) are in the same group in the periodic table (IVB); however, Sn(II) failed to show any significant DNA-binding (Fig. 12.11.3). This showed that the ability to interact with the zinc-finger motif is limited to specific metals. See illustration for the properties of metals expected to interact with this motif (Fig. 12.11.4).

Time Consideration

Peptide and oligonucleotide synthesis or acquisition is the only process that may be time consuming. Once the peptide and DNA are on hand, the entire process can be accomplished in a few hours. Allow 1 hr for DNA-labeling and 1 hr for peptide complexation and DNA-binding. Running, and drying the gel may take 5 hr. Autoradiographic exposure can range from minutes to hours depending on the specific activity of the labeled DNA (*APPENDIX 3D*).

Literature Cited

Dynan, W. and Tijian, R. 1983. The promoter-specific transcription factor Sp1 binds to upstream sequences in the SV40 promoter. *Cell* 35:70-87.

Lee, M.S., Gottesfeld, J.M., and Wright, P.E. 1991. Zinc is required for folding and binding of a single zinc finger to DNA. *FEBS Lett.* 279:289-294.

Krizek, B.A., Amann, B.T., Kilfoil, V.J., Merkle, D.L., and Berg, J.M. 1991. A consensus zinc finger peptide: Design, high-affinity metal binding, a pH-dependent structure, and a His to Cys sequence variant. *J. Am. Chem. Soc.* 113:4518-4523.

Nekludova, L. and Pabo, C.O. 1994. Distinctive DNA conformation with enlarged major groove is found in Zn-finger-DNA and other protein-DNA complexes. *Proc. Natl. Acad. Sci. U.S.A.* 91:6948-6952.

Pavletich, N.P. and Pabo, C.O. 1991. Zinc finger-DNA recognition: Crystal structure of a Zif268-DNA complex at 2.1 Å. *Science* 252:809-816.

Razmiafshari, M. and Zawia, N.H. 2000. Utilization of a synthetic peptide as a tool to study the interaction of heavy metals with the zinc finger domain of proteins critical for gene expression in the developing brain. *Toxicol. Appl. Pharmacol.* 166:1-12.

Razmiafshari, M. and Zawia, N.H. 2001. Nuclear magnetic resonance (NMR) analysis of the interaction of exogenous divalent metals with zinc finger motifs in the synthetic zinc finger model. *Toxicol. Appl. Pharmacol.* 172:1-10.

Shi, Y., and Berg, J.M. 1996. DNA unwinding induced by zinc finger protein binding. *Biochemistry* 35:3845-3848.

Zawia, N.H., Sharan, R., Brydie, M., Oyama, T., and Crumpton, T. 1998. Sp1 as a target site for Pb-induced perturbations of transcriptional regulation of developmental brain gene expression. *Devel. Brain Res.* 107:291-298.

Contributed by N.H. Zawia, Md. Riyaz Basha, and M. Razmiafshari
University of Rhode Island
Kingston, Rhode Island

Morphological Measurement of Neurotoxic Injury in the Peripheral Nervous System: Preparation of Material for Light and Transmission Electron Microscopic Evaluation

An important method of assessing experimental neurotoxic injury is the pathologic examination of the nervous system. The basis of such evaluation is an organized light microscopic study of relevant tissues. While most attention has been given to histopathologic examination of the central nervous system (brain and spinal cord) and to methods relevant to such study, neurotoxicologists have placed less emphasis on the study of its projections outside the neuroaxis. Yet the latter provides an accessible portal for determination of important pathogenetic information in those neurotoxic conditions affecting the peripheral nervous system alone or in concert with central effects. Thus, pathologic study of the peripheral nervous system is an important part of neurotoxicology.

This unit reviews contemporary methods of preparing peripheral nervous system tissue for critical pathological (light and electron microscopy) study. It begins with approaches to proper fixation of tissue, using either perfusion fixation of laboratory animals or immersion fixation of dissected nerve segments (see Basic Protocol 1 and Alternate Protocol 1, respectively). These are followed by dissection of the peripheral nervous system (from perfusion-fixed animals) to allow for multilevel sampling (see Basic Protocol 2). As noted in the Commentary, the use of sections cut from epoxy resin–embedded tissue gives specimens providing excellent light microscopic resolution. Thus, methods for processing tissue for such embedding (see Basic Protocol 3), sectioning (see Basic Protocol 4), and staining (see Basic Protocol 5) are provided. Materials fixed as noted above and embedded in epoxy resin medium are suitable for transmission electron microscopy, and methods for sectioning and staining tissues for this purpose are also included (see Alternate Protocol 2). Lastly, fixed peripheral nerve is suitable for teasing and microscopic study of individual myelinated fibers, a valuable technique (see Basic Protocol 6).

CAUTION: Perform all procedures using solutions containing glutaraldehyde, paraformaldehyde, formalin, or osmium tetroxide in a chemical fume hood or on a downdraft necropsy table capable of removing noxious fumes (this latter method is not suitable for osmium tetroxide). This includes perfusion, immersion fixation, tissue dissection, and tissue trimming. Wear coveralls or laboratory coats, eye protection, and nitrile (or double latex) gloves to protect against exposure to fixatives. Collect chemical waste generated during all procedures in waste containers for proper hazardous waste disposal according to institutional policies.

NOTE: All protocols using live animals must first be reviewed and approved by an Institutional Animal Care and Use Committee (IACUC) and must follow officially approved procedures for the care and use of laboratory animals.

Contributed by S.K. Hancock, J. Hinckley, M. Ehrich, and B.S. Jortner
Current Protocols in Toxicology (2004) 12.12.1-12.12.19

PERFUSION FIXATION IN RATS

Excellent fixation is the basis for sophisticated pathological assessments of peripheral nerves (and for other regions of the nervous system). For experimental animals, such as the rat, perfusion fixation is optimal. The basic idea is to allow fixation to occur with minimal autolytic or handling artifacts: the fixative perfuses through the blood circulatory system with the animal under deep anesthesia. There are several approaches to this (Fix and Garman, 2000), but the basic steps include anesthesia, cannulation of the cardiac left ventricle/aorta, washout of blood, and administration of fixative. Fixatives for perfusion may vary depending upon desired use of tissue. As examples, glutaraldehyde enhances the quality of samples for transmission electron microscopy, but high concentrations can interfere with immunohistochemistry. For transmission electron microscopy, perfusion fixatives such as 5% glutaraldehyde or glutaraldehyde/paraformaldehyde (PF) combinations are preferred. If immunohistochemistry and electron microscopy are the objects of the study, then paraformaldehyde with a small amount of glutaraldehyde (such as 4% PF/0.2% glutaraldehyde) is suitable. All of the above are suitable for light microscopy. Specific detail is provided in this protocol for vascular perfusion of rodents. Modifications may be necessary if another species is used.

Materials

Fixative for perfusion (see recipe)
Heparinized saline washout solution (see recipe)
65 mg/ml pentobarbital sodium anesthesia solution
Rat, control or treated

Peristaltic pump with variable speed control (e.g., Masterflex pump; Cole-Parmer)
Pump tubing (e.g., Masterflex C-flex tubing, 3.1-mm i.d.) and connectors
Graduated carboys with spigots
3-way plastic Luer stopcock (Cole-Parmer)
3-in. 16-G straight stainless-steel feeding needles (Popper)
Dissecting board
Heavy push pins or plastic-coated wire
Shears
Forceps
Hemostats
Microdissecting scissors
Carcass storage bags

Set up perfusion station

1. Prepare fixative and heparinized saline. Store fixative at 4°C and saline at room temperature until use.

   Paraformaldehyde-containing fixatives must be fresh. Prepare within 1 day of the perfusion and use within 24 hr.

2. Set up the peristaltic pump. Run separate pieces of pump tubing to the spigot of each of two graduated carboys (one carboy will deliver saline, one will deliver fixative). Using a 3-way stopcock with Luer-lok fittings, join the tubing running from each carboy to a single line that is loaded into the pump. Connect the 3-in. 16-G feeding needle to the end of the tubing. Adjust the flow rate of the pump to 85 to 90 ml/min.

   It is important that saline and fixative are pumped through the animal in the correct order, so clearly label carboys and tubing running from carboy spigots with contents.

   To prevent needle from slipping off during perfusion, use a plastic, male Luer-lok fitting to connect the needle to the tubing.

3. Warm fixative to room temperature before use. Fill fixative and saline carboys.

Table 12.12.1 Guidelines to Determine Dosage of 65 mg/ml Sodium Pentobarbital for Rats

Weight (g)	Pentobarbital (ml)
150–200	0.5
201–300	0.6
301–350	0.7
351–400	0.8
>400	0.9

4. Turn on pump and open 3-way stopcock to tubing delivering fixative until the fixative fills the tubing system. Complete setup by flushing saline through the system for 1 to 2 min.

   It is important to remove all air bubbles in the tubing lines. Bend tubing at connector to carboy spigot until all air is flushed from the line.

Anesthetize animal

5. Administer pentobarbital i.p. to the rat to induce a deep plane of anesthesia.

   Rat dosage is weight-dependent. Use Table 12.12.1 to determine dosage of 65 mg/ml sodium pentobarbital for rats.

6. Place animal in a safe location and wait until adequately anesthetized. For rodents, use the tail- or foot-pinch response to determine level of anesthesia.

   If the animal is still responsive to pinch after 4 min, administer additional anesthetic in 0.2- to 0.3-ml increments.

   Do not overdose with anesthesia. If heart stops beating during anesthesia, continue with perfusion as quickly as possible. These animals can be used for light microscopy if the perfusion is successful.

7. Once deeply anesthetized, move the animal to perfusion station in chemical fume hood. Immobilize animal with dorsum down. Pin dorsum to dissecting board by stretching limbs and pushing heavy pins through the loose skin covering the four legs.

   Perfusions can also be performed on a down draft necropsy table. This has the advantage of collecting fixative/blood waste in a contained reservoir for later disposal. To immobilize, stretch limbs and fasten feet to mesh of table surface with plastic-coated wire. Twist ties are useful for this.

Prepare animal for perfusion

8. Open chest cavity. Use shears to cut through the skin immediately caudal to the end of the sternum. Cut the skin along the caudal aspect of the rib cage and along the ventral midline along the sternum. Use blunt dissection to separate the subcutaneous fascial plane on the ventral and lateral chest wall on each side. Reflect the skin.

9. Cut the ribcage and the diaphragmatic attachment to the ribs on each side. Be careful not to cut into the liver or heart while reflecting the sternum. Clamp the sternum at the xiphoid process with hemostats and fold back toward the head to expose the heart.

10. Reflect the thin, transparent pericardium surrounding the heart. Make a small cut in the apex of the heart into the left ventricle with microdissecting scissors. Insert a 16-G feeding needle through the opening upward to the base of the aorta and clamp across the ventricles with hemostats or a tissue clamp.

    It is helpful to hold the heart with the clamping instrument during placement of the needle.

Perfuse animal

11. Turn on pump to flush with saline. Incise the right atrium of the heart when it distends to allow for exit of blood and fluids.

    If the animal immediately begins to show severe muscle spasms, the tubing has not been adequately flushed with saline and/or the system is open to the fixative. Check stopcock valve and adjust as needed.

12. Flush with saline for 45 to 60 sec.

    Fluid exiting right atrium will become clear and liver will blanch.

    If lungs inflate, the gavage needle is likely not properly sited and should be repositioned. The aorta starts branching almost immediately after it leaves the heart, therefore, position the tip of the feeding needle so that it is barely visible at the base of the aorta.

13. Close stopcock valve from saline and open valve to fixative.

    Muscle spasms indicate fixative is reaching tissues. If using glutaraldehyde, light-colored tissues turn yellow as fixation takes place. If muscles do not twitch, back the needle out 2 to 4 mm. A discharge from nose, mouth, or eyes indicates too much pressure or a misplaced needle, such as in the pulmonary artery. Reduce the perfusion pump setting and/or reposition the needle.

14. Perfuse rat with 800 to 1000 ml of fixative (~10 min).

    As the perfusion continues, the muscles of the neck and legs will stiffen.

15. When the perfusion is complete, turn off the pump and remove the needle. Assess the quality and extent of the perfusion by manipulating the muscles and organs of the animal.

    In a successful perfusion, all tissues will be equally firm. If a poor perfusion has occurred, some tissue will remain flexible (such as the legs). If the perfusion is poor or has failed completely, dissect the tissue of interest immediately (see Basic Protocol 2) and use immersion fixation.

    If the perfusion is poor or has failed, carefully check the location of the needle at the completion of perfusion to determine the cause of inadequate perfusion. Adjust the placement of the needle for the next perfusion as necessary.

16. Place the animal in a sealed plastic bag and store at 4°C until tissue dissection.

    The fixative that has collected in the body cavity should be poured into a hazardous waste container prior to placing animal in storage bag. One-gallon sealable food storage bags work well for storing individual perfused carcasses.

17. Flush tubing sufficiently with saline (1 to 2 min) before perfusing the next animal.

ALTERNATE PROTOCOL 1

IMMERSION FIXATION OF PERIPHERAL NERVE

While optimal fixation of the nervous system is obtained with properly performed perfusion (see Basic Protocol 1), immersion fixation of peripheral nerve may be adequate. The latter is used to fix human nerve biopsies (Dyck et al., 1993; King, 1999). This procedure should be part of routine necropsies where perfusion is not being conducted.

Additional Materials *(also see Basic Protocol 1)*

Fixative: 10% neutral buffered formalin, 3% glutaraldehyde, or mixture of paraformaldehyde and glutaraldehyde (see recipes)
Fine, non-toothed forceps
Scalpel handles and blades
Index card
Specimen vials and labels
Dental wax pads

Dissect nerve

1. Following euthanasia of the rat, expose the nerve of interest.

   Preferred methods of euthanasia are carbon dioxide asphyxiation and pentobarbital sodium overdose (150 to 200 mg/kg i.p.).

2. With fine, non-toothed forceps, grasp the proximal level of the nerve segment to be sectioned.
3. Gently dissect the nerve free from surrounding connective tissue. Cut and lift the proximal end of the nerve with the forceps.
4. Cut the nerve with a scalpel at the distal site.
5. Gently adhere the nerve segment to an index card in an elongated state and release the forceps.

   If proximal/distal orientation is important, mark orientation on the ends of the card using a pencil or, alternatively, cut one end of the card or nerve diagonally.

Fix nerve

6. Cut out the segment of the card with the adherent nerve and immerse both in a vial of fixative.

   Use enough fixative to completely cover the card.

7. For all fixatives, except 10% formalin, fix 12 to 24 hr at 4°C. Fix tissues in 10% formalin at room temperature.

   Fix larger diameter nerves, e.g., sciatic nerve, at least 24 hr.

Trim nerve

8. Remove the index card from the vial of fixative. Using forceps, grasp an attached end of the nerve, gently peel the segment from the card, and place it on a dental wax pad.
9. Using a scalpel, trim away the ends of the nerve segment that have been cut in the unfixed state or grasped by the forceps.

   Do not let the tissue dry out during this step. Keep it moist with fixative.

   If the proximal/distal orientation has been marked on the card, cut the ends of the nerve straight and diagonally to differentiate orientation.

10. Trim nerve to suitable size for subsequent tissue processing (see Basic Protocol 2).

DISSECTION OF PERIPHERAL NERVOUS TISSUE SAMPLES FROM PERFUSION–FIXED RATS

BASIC PROTOCOL 2

Following appropriate fixation, samples of nervous tissue of interest must be obtained. Dissection of tissues may be done on the day following perfusion, or sooner if time allows. If tissues are dissected on the perfusion day, wait several hours after the perfusion before starting the dissection. Multi-level sampling of the peripheral nervous system is useful to determine a proximo-distal pattern of lesions. As an example, for the somatic nervous system of the rear leg, study of the following would represent a reasonable proximo-distal sampling of the peripheral nerves: lumbosacral dorsal root (spinal) ganglia with dorsal and ventral spinal nerve roots (see below), sciatic, tibial, and sural nerves, and selected intramuscular branches (obtained in muscle samples).

Materials

Fixative (see recipe)
Perfused animal (see Basic Protocol 1)

Specimen vials
Indelible marker
Chemical fume hood or downdraft table
Forceps
Scalpel handles and blades (no. 11 or 15)
Bone-cutting forceps
Rongeurs
Dental wax pad

Dissect peripheral nerve and dorsal root (spinal) ganglia

1. Place fresh fixative in each specimen vial. Label vials with an indelible marker and cover label with clear plastic tape.

   For perfusion-fixed animals, the fixative used will usually be that which was used for perfusion.

2. Place perfused carcass in a chemical fume hood or on a downdraft table and expose the tissues of interest using methods that subject them to the minimal amount of trauma possible.

   For example, use bone cutters or rongeurs to unroof the cranial cavity or spinal canal, without pressure on underlying nervous tissue.

3. Once the nerve is exposed, gently grasp a section of the nerve with forceps in a region distal from the area to be examined. Cut the nerve segment using a scalpel blade (no. 11 or 15) and place in a specimen vial.

   The tissue should be completely immersed in fixative.

4. To dissect dorsal root ganglia, unroof the spinal canal and remove the spinal cord.

   A useful method for the latter is the use of a periosteal elevator to lift the cord and separate it from the nerve roots. Portions of the latter will remain in the spinal canal and are most obvious in the cauda equina, noted in the lumbosacral region.

5. With a fine forceps, trace the spinal roots to the intervertebral foramena, in which the ganglion usually lies.

   This is easiest for the lumbosacral ganglia.

6. Carefully chip away the overlying bone with bone-cutting forceps or rongeurs. Grasp the nerve roots and gently pull them to provide tension. Dissect free and remove the ganglion (with attached nerve roots) using a scalpel and no. 11 blade. Place the ganglion in the specimen vial.

   If necessary, use a magnifying loupe to assist in visualizing the ganglion.

7. Store dissected tissues in fresh fixative for up to 7 days at 4°C prior to trimming for tissue processing.

Trim tissue

8. Place the tissue on a dental wax pad and, using a sharp blade, trim dissected tissues from designated sample regions to a size not exceeding 1 mm in thickness. Trim the tissue block so that it contains a full face of the region of interest.

   Use a razor blade held in a blade or needle holder or a scalpel blade for trimming. Change blades often.

9. Collect appropriate segments of peripheral nerve. Trim away tissue regions grasped by forceps during handling, as they will be artifactually damaged. Cut nerve segments for cross or longitudinal sections.

   If the proximal-distal orientation of the peripheral nerve is important, cut the ends differently, e.g., a straight cut for distal and a diagonal cut for proximal, so that the samples may be appropriately embedded.

10. Trim spinal ganglion and attached nerve roots for longitudinal embedding, which allows examination of the ganglion and both nerve roots in one section (see Basic Protocol 3).

    If cross-sections of the spinal nerve roots are needed, trim 1- to 2-mm segments for this purpose.

11. Place trimmed tissues in a labeled vial containing fresh fixative.

    Place trimmed tissues from animals perfused in formalin, which are to be processed for epoxy embedding in 3% glutaraldehyde in 0.1 M sodium phosphate buffer, pH 7.4 (see recipe).

12. Store trimmed tissues at 4°C prior to tissue processing (see Basic Protocol 3).

    It is recommended to retain reserve dissected tissue until examination of all tissues is complete. Store reserve tissue up to 6 months at 4°C, and periodically replace the fixative.

EMBEDDING TISSUES IN EPOXY RESIN

BASIC PROTOCOL 3

This protocol delineates steps in epoxy resin embedding of nerve (and other) tissue samples. Embedding in such relatively rigid medium allows sections to be cut so that they provide optimal light microscopic resolution. In addition, these tissues are suitable for transmission electron microscopic study.

Materials

Vials containing trimmed tissues in fixative (see Basic Protocol 2)
0.1 M sodium phosphate buffer, pH 7.4 (see recipe for 0.2 M sodium phosphate stock)
2% (w/v) osmium tetroxide solution in 0.1 M sodium phosphate buffer, pH 7.4 (see recipe)
15%, 30%, 50%, 70%, 95%, and 100% (v/v) ethanol
Propylene oxide
Epoxy resin embedding medium (e.g., Poly/Bed 812; Polysciences)
Chemical fume hood
Glass or plastic disposable transfer pipets
Disposable plastic beakers
Wooden applicator sticks with beveled ends
Plastic dishes (e.g., mincing dishes or weigh boats)
Flat embedding molds
60°C oven
Cardboard boxes (e.g., pill boxes)

NOTE: For all processing steps, use a transfer pipet to remove the liquid in the vial from the previous processing step and replace it with liquid from the next processing step. Recap vials at each step. Perform all steps at room temperature unless otherwise noted.

Post-fix and dehydrate tissue

1. Place specimen vials with fixed tissue in the chemical fume hood.
2. Rinse tissue at least two times, 30 min each rinse, in 0.1 M sodium phosphate buffer, pH 7.4.

   When processing a large number of samples, dispense buffer from a squirt bottle. Use 20 to 30 times the volume of tissue for buffer rinses.
3. Post-fix the tissue in 2% osmium tetroxide in 0.1 M sodium phosphate buffer for 2 hr at room temperature. Add enough osmium tetroxide to completely immerse the tissue.
4. Rinse tissue at least two times, 30 min each rinse, in 0.1 M sodium phosphate buffer, pH 7.4.

   If there is a time constraint, the second buffer rinse step may continue at 4°C overnight.
5. Dehydrate tissue 30 min in 15% ethanol, 30 min in 30% ethanol, 30 min in 50% ethanol, 15 min in 70% ethanol, 15 min in 95% ethanol, two times, 15 min each, in 100% ethanol, and two times, 15 min each, in propylene oxide.

   When processing a large number of samples, dispense ethanol solutions from a squirt bottle. The 100% ethanol must be free of water. Use a plastic disposable pipet to transfer propylene oxide into and out of vials.

   If there is a time constraint, the 70% ethanol–step may continue overnight at room temperature.

Infiltrate and embed tissue

6. Prepare a 1:1 (v/v) transition mixture of epoxy resin and propylene oxide in a disposable plastic beaker. Cover tissue with the mixture using at least 20 to 30 times the volume of the tissue. Leave for at least 12 hr at room temperature.

   CAUTION: *Use nitrile gloves when handling propylene oxide. Latex gloves are not adequate.*

   Place tissue vials on a rotator or rotating plate to improve infiltration of larger tissue pieces.
7. Prepare fresh epoxy resin. Remove the epoxy-propylene oxide mixture from the vial and dispose appropriately. Cover tissue with the fresh resin and allow to infiltrate for at least 24 hr at room temperature.

   When preparing the epoxy resin from its components, avoid rapid stirring that may beat air bubbles into the mixture. The bubbles may interfere with proper infiltration of tissue.

   It is good practice to prepare a test resin block at this point in the procedure. Place fresh resin in a flat embedding mold and polymerize for 24 hr at 60°C prior to embedding and polymerization of the tissue pieces.
8. Gently remove the tissue sample from the vial using a wooden applicator stick with a beveled end and place the sample in a plastic dish with a small amount of fresh epoxy resin. Use the wooden applicator stick to transfer the sample from the dish to a labeled embedding mold. Fill the mold with fresh epoxy resin.

   Use a pencil to write labels or use printed labels. Check that label ink does not bleed when it comes into contact with epoxy resin. Place label in a visible position in the mold that does not obscure the tissue sample.

   Embed tissues with large block faces, such as longitudinal peripheral nerve, dorsal root ganglion, and associated nerve roots, in an inverted BEEM capsule with the tip cut off. Place tissue in the cap of the capsule and gently press flat with the flat end of a wooden applicator stick. Close capsule and fill it with embedding medium. Embed peripheral nerve for cross-section in a flat embedding mold.

9. Polymerize embedded tissues for 24 to 48 hr at 60°C.
10. Remove epoxy resin blocks from molds and store in cardboard boxes (e.g., pill boxes) until sectioning (see Basic Protocol 4).

The epoxy resin blocks may be stored indefinitely in cardboard boxes at room temperature.

SECTIONING EPOXY-EMBEDDED TISSUE

BASIC PROTOCOL 4

This section defines the procedures for sectioning resin-embedded samples for light microscopy. Producing high quality sections requires training in the use of an ultramicrotome, an instrument primarily used in sectioning of transmission electron microscopy (TEM) specimens.

Materials

Epoxy resin tissue blocks (see Basic Protocol 3)
3:1 (v/v) Permount/xylene mounting medium

Ultramicrotome or Butler Block Trimmer (Electron Microscopy Sciences)
Dissecting microscope
Single-edge razor blades
Glass knives
Frosted precleaned glass microscope slides
Fine forceps
70° to 90°C hot plate
Coverslips
Chemical fume hood
Dissection needle
Bibulous paper
Microscope slide boxes
Diamond knife
Copper grids
Petri dishes, glass
Filter paper
Grid storage boxes

Additional reagents and equipment for staining sections with toluidine blue and safranin (see Basic Protocol 5) and staining thin sections (see Alternate Protocol 2)

Section tissue block for light microscopy

1. Immobilize the epoxy resin tissue block using the specimen holder of an ultramicrotome or a device such as the Butler Block Trimmer.
2. Under a dissecting microscope, roughly trim the epoxy resin block using a fresh single-edge razor blade. Using cuts oblique to the surface of the block, remove the excess epoxy resin on the sides of the tissue. Using cuts parallel to the surface, trim the resin until 0.2 to 0.4 mm of tissue has been trimmed away.

   This is the same procedure used in preparing semi-thin sections prior to transmission electron microscopy (Hayat, 1970).

   Trimming the tissue at the surface of the tissue block removes any tissue that may have been artifactually damaged during tissue trimming.

3. Using an ultramicrotome, section the tissue block with a glass knife using a 5- to 7-μm advance. Continue sectioning until sections contain a complete profile of the tissue sample. Discard the sections and replace the glass knife with a new knife.

The initial sections are discarded because they are incomplete, too thick (7 μm), and contain knife-mark artifacts due to glass knife dulling during rough trimming. Sections are collected from a new glass knife and those sections are 1-μm thick.

4. Label a frosted glass microscope slide to properly identify the tissue.
5. Cut sections at a thickness of ~1.0 μm (referred to as thick or semi-thin sections), collect each section with fine forceps, and place in a drop of water on a clean glass microscope slide.

   Sections are easiest to pick up from a knife edge if they are floating in a droplet of water. Place a drop of fingernail polish ~10 mm from the cutting edge of the glass knife. Add a drop of water to the knife edge to create a trough for the section to float in as it is cut. Scoop up each section with forceps.

   For large block faces, e.g., dorsal root ganglia and nerve roots, collect enough sections to ensure that at least one section adheres completely flat to the slide (usually six sections are sufficient).

6. Place the slide on the 70° to 90°C hot plate and heat-fix the sections to the slide for a minimum of 1 hr.

   It may be necessary to heat large tissue sections on the hot plate overnight.

   To avoid trapping air bubbles in large sections, it is helpful to let sections float in a water droplet for 1 to 2 min prior to placing the slide on the hot plate.

7. Stain sections with toluidine blue and safranin (see Basic Protocol 5).
8. Coverslip the slide in a chemical fume hood by placing a drop of the 3:1 Permount/xylene mounting medium on the slide over the tissue sections. Hold the coverslip on the edge of the solution and slowly lower the coverslip over the sections, dispersing the solution without forming air bubbles. Using a dissection needle, push extra mounting medium and any air bubbles out the side of the coverslip onto bibulous paper.
9. Dry slide overnight in the chemical fume hood.
10. Permanently label each slide and store in slide box.

Section tissue for transmission electron microscopy (TEM)

11. Identify the areas of interest from the thick sections (steps 1 to 10).

    It is helpful to use a marked hand drawing or photomicrograph of the section to identify the area to be examined by TEM.

12. Retrim the epoxy resin specimen block so that the area designated for ultrathin sectioning is in the center of the block face. Trim the block face into a trapezoid shape with the longest side no longer than 0.75 mm.

    For longitudinal peripheral nerve and spinal nerve root, trim the block face so that the nerve fibers are perpendicular to the parallel sides of the trapezoid. This will help control chatter in the section during thin sectioning.

13. Using an ultramicrotome, cut silver/silver-gold sections with a diamond knife.

    User must be experienced in the use of the ultramicrotome and diamond knife.

14. Collect sections on copper grid. Note whether sections are collected on the dull or shiny side of the grid. Collect at least two grids per specimen block. Place grids with tissue sections on filter paper in a glass petri dish.
15. Stain thin sections as outlined in Alternate Protocol 2
16. Store stained grids in a grid storage box.

    Stained grids may be stored indefinitely at room temperature.

STAINING EPOXY SECTIONS FOR LIGHT MICROSCOPY

BASIC PROTOCOL 5

This section describes the routine procedure for staining epoxy sections for light microscopy (Jortner, 2000). The stain described, a combination of toluidine blue and safranin, stains myelin intensely blue, nuclei lighter blue, collagen pink, and adipose tissue gray. Axoplasm is relatively pale, although intra-axonal inclusions are faintly stained. Other stains such as thionin and acridine orange and methylene blue and acridine orange have been recommended by other investigators (King, 1999). The toluidine blue and safranin stain procedure is as follows.

Materials

Slides with heat-fixed epoxy tissue sections (see Basic Protocol 4)
1% (w/v) toluidine blue in 1% (w/v) sodium borate (see recipe)
0.5% (w.v) safranin in 0.5% (w/v) sodium borate (see recipe)

12-ml syringes and syringe filters (0.2-μm)
70° to 90°C hot plate
Slide holder for drying slides vertically
Coverslips
Cardboard slide trays
Microscope slide boxes

1. After epoxy sections are heat-fixed to the slide (see Basic Protocol 4), cover the sections with 1% toluidine blue stain in 1% sodium borate. Use 12-ml syringes with attached 0.22-μm filters to deliver stains.
2. Reheat the slide on a 70° to 90°C hot plate until the edges of the stain begin to dry (∼1 to 2 min).
3. Gently rinse the slide in deionized, distilled water from a wash bottle and wipe the excess water from the bottom edge of the slide.
4. Cover the sections with 0.5% safranin stain in 0.5% sodium borate and heat the slide 15 to 20 sec on the hot plate.
5. Rinse the slide with water and air dry in a vertical slide holder.

   If either stain is too dark or too light, adjust the stain intensity by decreasing or increasing, respectively, the length of time the sections are heated in the stain on the hot plate.
6. Coverslip the slide (see Basic Protocol 4, step 8).
7. Store the slide in a cardboard slide tray until labeled and then store in a slide box.

STAINING SECTIONS FOR ELECTRON MICROSCOPY

ALTERNATE PROTOCOL 2

This section describes the routine procedure for staining epoxy thin sections for transmission electron microscopy.

Materials

Uranyl acetate (see recipe)
Reynold's lead citrate (see recipe)
NaOH
Thin sections collected on grids (see Basic Protocol 4, steps 11 to 16)

Parafilm
Petri dishes, glass
Glass, disposable transfer pipets
Anti-capillary forceps

Small beakers
Filter paper
Grid storage box

CAUTION: Uranyl acetate is radioactive. Wear latex gloves when handling uranyl acetate and lead citrate. Dispose of labware contaminated with uranyl acetate according to institutional radioactive waste policies.

1. Set up both uranyl acetate and Reynold's lead citrate stain chambers before starting stain procedure.
2. Place a square of Parafilm in a glass petri dish chamber and, using a glass transfer pipet, add one drop of uranyl acetate stain on Parafilm for each grid to be stained.

   Uranyl acetate is light sensitive. Protect the stain from light by covering the petri dish with a box or aluminum foil.
3. Place a square of Parafilm in a second petri dish chamber and arrange several pellets of NaOH around the Parafilm. Place one drop of Reynold's lead citrate on the Parafilm for each grid to be stained.

   Lead citrate will react with CO_2 and form a precipitate on the sections; the NaOH will scavenge any CO_2 in the chamber.

   To avoid CO_2 contamination, blow the air out of the transfer pipet before withdrawing the lead citrate from the volumetric flask. Discard the first few drops of the lead citrate. Limit the time the lid of the lead citrate chamber is opened.
4. Place each grid on a uranyl acetate stain drop with the section side down. Use fresh stain for each grid. Float the grid for 10 to 30 min.

   Stagger the times that the grids are placed on the stain by 60 sec to allow time for rinsing prior to lead citrate staining.

   The optimum staining time for uranyl acetate depends on the tissue type and may require stain trials.
5. Remove the grid from the uranyl-acetate stain droplet using anti-capillary forceps.
6. Rinse the grid in a stream of distilled, deionized water for 30 to 45 sec or rinse the grid by dipping it in two beakers of water, 20 to 30 dips in each beaker.

   Bacterial contamination can appear on the surface of a grid when the water used for rinsing is contaminated. To prevent this artifact, use wash bottles and beakers that have been cleaned with sodium hypochlorite solution (bleach) and rinsed well with distilled deionized water. For beaker-dipping rinses, filter water before use.
7. Place the grid on a fresh droplet of Reynold's lead citrate and stain from 30 sec up to 10 min.

   The optimum staining time depends on the tissue type and stain trials may be required.
8. Remove the grid from the stain and rinse thoroughly with water as in step 6. Place grid on filter paper to dry. Store stained grid in grid box.

BASIC PROTOCOL 6

PERIPHERAL NERVE FIBER TEASING

This section describes procedures for preparing teased preparations of peripheral nerve myelinated fibers for light microscopic study. Such preparations allow the nerve fibers to be examined over proximo-distal distances, assessing myelin internodes, nodal regions and axons, and are an integral part of peripheral nerve pathology studies (Krinke et al., 2000).

Materials

Fixed peripheral nerve (see Alternate Protocol 1 or Basic Protocol 2)
Fixative (see recipe)
0.05 M sodium phosphate buffer (see recipe for 0.2 M sodium phosphate buffer stock)
2% (w/v) osmium tetroxide in 0.1 M sodium phosphate buffer (see recipe)
30%, 50%, 70%, 95%, and 100% ethanol
Cedarwood oil
3:1 (v/v) permount/xylene mounting medium

Razor blades and blade holders
Scalpel handles and blades
Dental wax pads
Labeled specimen vials
Glass or plastic disposable transfer pipets
Fine forceps
Glass microscope slides
Watchmaker's forceps
Butterfly needles inserted into wooden applicator sticks
50°C oven
Glass coverslips
Cardboard slide tray
Slide boxes

NOTE: For all processing steps, use a transfer pipet to remove the liquid in the vial from the previous processing step and replace it with liquid from the next processing step. Recap vials at each step. Perform all steps at room temperature unless otherwise noted.

Trim nerve

1. Obtain a nerve that has been immersion fixed (see Alternate Protocol 1) or dissected from a perfused carcass (see Basic Protocol 2).

   Samples from most proximal levels of peripheral nerve, such as the spinal nerve roots, are difficult to tease.

2. Remove nerve from the fixative. If sample is trimmed for proximal and distal orientation (i.e., transverse cut for distal and diagonal cut for proximal levels), maintain orientation while trimming.

3. Trim nerve to a sample length of at least 1.5 cm by cutting with a sharp razor or scalpel blade on a dental wax pad. Gently trim away adipose and other extraneural tissues.

4. Place trimmed tissue samples in labeled vials containing fresh fixative.

   The tissue should be completely immersed in fixative.

Post-fix and dehydrate the nerve

5. Rinse tissue at least two times, 15 min each, in 0.05 M sodium phosphate buffer.

6. Post-fix the tissue in 2% osmium tetroxide in 0.1 M sodium phosphate buffer for 2 hr at room temperature. Add enough 2% osmium tetroxide to completely immerse the tissue.

7. Rinse tissue at least two times, 15 min each, in 0.05 M sodium phosphate buffer.

   The second buffer rinse step may continue at 4°C overnight if there is a time constraint.

8. Dehydrate the tissue 15 min in 30% ethanol, 15 min in 50% ethanol, 15 min in 70% ethanol, 15 min in 95% ethanol, and three times, 15 min each, in 100% ethanol.

   Continue the 70% ethanol step at 4°C overnight if there is a time constraint.

9. Rinse the tissue sample in cedarwood oil and drain it off.

   Use cedarwood oil in a chemical fume hood during tissue processing and in a well-ventilated area during nerve fiber teasing. Prolonged exposure to cedarwood oil may cause irritation to skin or nasal passages.

10. Replace with fresh cedarwood oil. Leave at room temperature overnight.

    If the cedarwood oil gels during the last step, place vial 15 min in 50°C oven to melt the gel, pour off the oil, and replenish with fresh cedarwood oil.

Expose nerve bundle

11. Remove the nerve from the vial and place on a clean glass microscope slide. Mark the slide to identify the sample.

    Do not compress, pinch, or crush the tissue when removing it from the vial.

    If the proximal/distal orientation of the nerve is important, mark the orientation on the label area of the slide.

12. Place a drop of cedarwood oil on top of the tissue to prevent drying.

13. Using a fine teasing instrument (e.g., watchmaker's forceps) and butterfly needles inserted into wooden applicator sticks, begin to remove excess epineural connective and adipose tissue from the nerve bundle.

    This step and steps 14 through 18 are done using a dissecting microscope.

14. Under a dissecting microscope, continue to remove excess tissue until all is stripped from the nerve bundle. Remove the stripped tissue from the slide.

15. Cut the perineurium (a cylindrical sheath of specialized fibroblastic cells surrounding fascicles of nerve fibers) with a scalpel blade. Using two forceps, pull the perineurium away from the nerve fibers by pulling half of the perineurium in one direction and the other half in the opposite direction.

    Grasp the perineurium at the ends of the sample so there is no damage to the fibers.

16. Remove stripped perineurial tissue from the slide. Continue to divide the exposed nerve bundle by gently pulling it apart from one end, using two forceps in the same manner as the perineurium.

Dissect individual nerve fibers

17. To remove an individual myelinated nerve fiber from the parent portion of the nerve bundle, use the butterfly needles to orient the bundle and fiber in a V-shape. Place the tips of the needles on the slide within the V-shape. Slowly slide the needles away from each other and gradually toward the narrowing of the V so as to separate the fiber from the bundle of individual fibers. Repeat this process until a number of individual fibers are obtained.

    Best results are achieved with the tissue wet with cedarwood oil and with fibers separated from subdivided nerve bundles having fewer than 100 fibers. Larger fibers are easier to tease out. However, take all fibers as they are separated from the bundle to provide a sampling of all fiber sizes.

18. As each fiber is separated, carefully orient it with the dissecting needles, lining it parallel to other fibers and to the shorter edge of the slide.

19. When enough fibers are obtained for the slide (usually 20 to 25), remove all remaining tissue to the vial for storage.

20. Prepare other slides using the same procedure. Collect at least 50 fibers per nerve for examination.

21. Place the slide for at least 3 days in a 50°C oven to dry. Once dried, place a drop of 3:1 Permount/xylene mounting medium on top of the fibers. Place the edge of the cover slip in the mounting medium parallel to the fibers. Slowly and carefully, lower the coverslip onto the slide.

    Once the coverslip is on the slide, do not move it. Do not press on the coverslip to remove excess mounting medium or air bubbles. Movement of the cover slip can cause disorientation of the vertically placed fibers.

22. Dry the slide overnight in a chemical fume hood. Store the slide in a cardboard slide tray until labeled and then store in slide box.

    Light microscope interpretation has been described by Krinke et al. (2000).

    The use of cedarwood oil as a medium for peripheral nerve fiber teasing was suggested to the authors by Dr. Thomas Bouldin, Department of Pathology, School of Medicine, University of North Carolina at Chapel Hill. Other media, such as glycerin, are also used (Krinke et al., 2000)

REAGENTS AND SOLUTIONS

Use Milli-Q-purified water or equivalent for the preparation of all buffers. For common stock solutions, see ***APPENDIX 2A****; for suppliers, see* ***SUPPLIERS APPENDIX****.*

Fixative solutions

3% Glutaraldehyde in 0.1 M sodium phosphate buffer, pH 7.4, solution for immersion fixation:

Add 6.0 ml of 50% glutaraldehyde to 50 ml of 0.2 M phosphate buffer, pH 7.4 (see recipe) and mix well. Add 44 ml water to the solution and continue stirring until mixing is complete. Cover container with Parafilm and store up to 1 week at 4°C.

Stock solutions of 50% and 70% glutaraldehyde are available from various suppliers. Adjust the recipe proportionately for larger volumes.

5% Glutaraldehyde in 0.1 M sodium phosphate buffer, pH 7.4, for perfusion for electron microscopy:

Add 100 ml of 50% glutaraldehyde to 500 ml of 0.2 M phosphate buffer, pH 7.4 (see recipe) and mix well. Add 400 ml water to the solution and continue stirring until mixing is complete. Cover container with Parafilm and store up to 1 week at 4°C.

Adjust the recipe proportionately for larger volumes.

4% paraformaldehyde stock solution:

For ~1000 ml, add 40 g paraformaldehyde to 1000 ml water. Heat, while stirring, for 5 min at 60°C. Slowly add drops of fresh 1 N NaOH to solution until the solution clears. Immerse paraformaldehyde solution into ice until cooled. Filter through Whatman no. 1 filter paper if necessary. Use within 24 hr and store at 4°C.

Adjust the recipe proportionally.

2% paraformaldehyde/2% glutaraldehyde in 0.1 M sodium phosphate buffer:

Cool the 4% paraformaldehyde solution (see recipe). Add 500 ml of 0.2 M sodium phosphate buffer stock solution (see recipe), 500 ml of 4% paraformaldehyde, and 40 ml of 50% glutaraldehyde to flask. Mix well. Recheck pH of solution and adjust

continued

if necessary. Cover container with Parafilm, label, and store at 4°C until needed. Use paraformaldehyde-containing solutions as soon as possible after preparation, within 48 hr.

If smaller amounts of paraformaldehyde-containing fixatives are needed, the following formula is used to calculate volumes:

$$V_1C_1 = V_2C_2$$

where V_1 = desired volume, C_1 = desired concentration, V_2 = volume of stock solution, and C_2 = concentration of stock solution.

10% neutral-buffered formalin (final 3.7% to 4%):
100 ml 37% to 40% commercial formaldehyde
900 ml H_2O
4 g NaH_2PO_4
6.5 g Na_2HPO_4 (anhydrous)
Add reagents to flask and stir until dissolved. Store up to 1 year at room temperature.

Alternatively, this solution can be purchased from a chemical supplier

CAUTION: *Prepare all solutions containing glutaraldehyde, paraformaldehyde, formalin, or osmium tetroxide in a chemical fume hood. Wear coveralls or laboratory coats, eye protection, and nitrile (or double latex) gloves to protect against exposure to fixatives.*

Heparinized saline

Add 9.0 g NaCl to a flask and bring up to 1000 ml with water. Stir until dissolved. Add 10 ml of 1000 U/ml heparin to the flask and stir. Store up to 1 month at room temperature.

Osmium tetroxide stock solution, 4%

Add 25 ml water to a brown bottle. In a fume hood, open the 1-g ampule containing the crystalline osmium tetroxide over the brown bottle. Break the ampule at the scored neck and place the entire ampule containing osmium tetroxide crystals into the brown storage bottle. Cap tightly, Parafilm, and periodically agitate or sonicate, as needed (~30 min for sonication). For storage, cap tightly, seal the bottle with Parafilm, place in a plastic storage bag, and place in a tightly covered metal can sealed with Parafilm. Store up to 4 months at 4°C.
To make up a 2% osmium tetroxide solution in 0.1 M sodium phosphate buffer, pH 7.4:
Add equal amounts of the 4% osmium tetroxide stock solution and 0.2 M sodium phosphate buffer, pH 7.4, stock solution to a clean brown bottle. Gently mix. The solution is stable stored in a brown bottle, capped tightly, and wrapped in Parafilm for up to 2 months at 4°C.

Clean the outside of the osmium ampule with scouring powder followed by soap. Rinse well with tap water followed by distilled water. Clean the brown bottle in which the osmium tetroxide stock solution will be stored in the same manner.

Osmium tetroxide crystals go into solution slowly. If possible, make up the solution at least 1 day before it is needed, and agitate periodically. It is best to make only small quantities of osmium solutions, i.e., only as much as needed for the batch of tissue being processed. If stored osmium solutions are used, check the color of the solution before use. The aqueous solution is light yellow in color. If the solution has turned black or brown during storage, do not use. Dispose of it according to procedures described below.

continued

CAUTION: *Osmium tetroxide is a heavy metal. It readily sublimes (forms a vapor) in air. These vapors are hazardous and can cause choking, eye irritation, corneal clouding, and skin discoloration. The compound is poisonous. Wear disposable nitrile gloves, laboratory coat, and eye protection at all times during preparation and handling of osmium tetroxide. Prepare and use in a chemical fume hood. Dispose of osmium-containing solutions in a hazardous waste container, as indicated by MSDS (Material Safety Data Sheet) and local environmental regulations.*

Reynold's lead citrate

In a 50-ml volumetric flask, add 1.33 g lead nitrate, 1.76 g sodium citrate, and 30 ml distilled water. Shake vigorously for 1 min. Gently shake intermittently for 30 min Add 8.0 ml of fresh 1.0 N NaOH and mix gently. Bring the volume to 50 ml with boiled, cooled distilled water. Mix by inverting the container gently until well-mixed. Store *tightly covered* (stain reacts with CO_2 in air) for up to 1 year at 4°C. Do not use stain if it contains visible precipitate.

This recipe is based on Reynolds (1963).

Safranin, 0.5% (w/v)

Add 0.5 g safranin O and 0.5 g sodium borate to a flask and bring up to 100 ml with water. Mix at least 30 min using stir plate. Filter through Whatman no. 1 filter paper using a Buchner funnel. Store up to 1 year at room temperature.

Sodium phosphate buffer stock solution, 0.2 M (pH 7.4)

Make up the following 0.2 M stock solutions:
A: 27.6 g/liter NaH_2PO_4 stock
B: 28.4 g/liter Na_2HPO_4 stock
Add ~1 part solution A to 4 parts solution B. Adjust to pH 7.4 with solution A or B, as needed. Store up to 4 months at room temperature.

Storage at 4°C will result in crystallization of the buffer solution.

Toluidine blue, 1% (w/v)

Add 1 g toluidine blue and 1 g sodium borate to a flask and bring up to 100 ml with water. Mix at least 30 min using stir plate. Filter through Whatman no. 1 filter paper using a Buchner funnel. Store the stain up to 1 year at room temperature.

Uranyl acetate stain, 2% to 5% (w/v)

Add 2 to 5 g uranyl acetate to 100 ml of 50% ethanol. Stir well. Store in brown bottle up to 1 month at 4°C.

Optimum stain concentration may be tissue dependent. Adjust uranyl acetate concentration as needed to reach desired staining quality. Stain may precipitate. If this happens, use stain from the top of the bottle for staining grids.

CAUTION: *Uranium is radioactive. Use gloves and wear a laboratory coat when preparing this solution.*

COMMENTARY

Background Information

Pathological examination of the peripheral nervous system (nerve roots, peripheral ganglia, peripheral nerves, nerve endings) is an important component in assessing neurotoxic states.

Some pathogenetic questions can be more easily addressed by study of the peripheral nervous system (Jortner, 2000). In axonopathic and neuronotoxic conditions, an important issue is the proximo-distal extent of axonal involvement. In those conditions involving the peripheral nervous system, various levels of the axon can be readily evaluated. Thus, examination of the spinal nerve roots provides proximal levels, with study of regions such as

the sciatic and tibial and/or sural nerves giving progressively more distal sites. Preterminal and terminal levels can be seen by examining intramuscular nerve branches and muscle spindles or presynaptic motor terminals.

Contemporary methods for histopathological examination of peripheral nerve have been developed for clinical application, but have relevance for experimental neurotoxicology. Three main preparative approaches are utilized (Schaumburg et al., 1992; King, 1999). (1) Conventional paraffin-embedded tissue is useful for evaluation of cellular inflammatory infiltrates and vascular changes. In addition, such specimens when appropriately fixed are the standard for immunohistochemical studies. However, subtle changes in axons, myelin, Schwann cells, and endoneurial constituents are not appreciated in sections from this type of preparation. This is due to the poorer resolution (compared to resin sections) and greater thickness of the paraffin sections (King, 1999). (2) Single-teased myelinated nerve fibers provide preparations that are useful for identification of axonal degeneration and segmental demyelination. It allows evaluation of changes along a length of the fiber. As an example, the degree of demyelination along an individual nerve fiber can only be determined in teased peripheral nerve preparations. Quantitative evaluation of the lengths of myelin internodes and fiber diameter can be done. (3) Light microscopic examination of epoxy resin-embedded tissue sections is the standard approach to assessment of peripheral nerve and ganglia. This approach allows sections of 0.5- to 1.0-μm thickness, which provide optimum light microscopic resolution (Spencer et al., 1980; King, 1999). Axons, neuronal cell bodies, Schwann cells, myelin, and the endoneurium are clearly demonstrated in appropriately stained sections obtained with this embedding procedure. As examples, degeneration, loss, and demyelination of myelinated fibers can be readily determined. The unmyelinated fibers are too small to be effectively evaluated by light microscopy. Changes in size of axons and nerve fibers can readily be assessed in cross-sections of a nerve, and thus epoxy resin embedding is a standard for such morphometric studies. Properly fixed nerve embedded in these media can also be utilized for transmission electron microscopic evaluation, allowing ultrastructural examination (King, 1999).

These diagnostic/interpretive advantages can only be obtained with properly fixed, processed, and sectioned (or teased) peripheral nerve. Such methods have long been employed by those interested in the pathology of peripheral nerve as it relates to human or animal disease. Applying these to neurotoxicology will enhance the information obtained from these pathologic studies. This unit describes methods for fixation applicable to experimental studies, tissue embedding (with an emphasis on epoxy resin procedures), sectioning and staining of such tissues for light microscopy (with some comments on relative electron microscopic procedures), and preparation of nerve tissue for fiber teasing.

Critical Parameters and Troubleshooting

Major sources of difficulty in using these protocols are in the areas of handling and fixation of tissue, embedding, and sectioning. Compression of the nerve tissue, especially in the unfixed state, leads to a series of artifacts, which can distort the appearance of myelinated fibers when viewed at the light- and electron-microscopic levels (King, 1999). Thus, it is critical to trim away the ends of nerves which have been held in forceps. When sections are too thick (>1 mm in one dimension) they may not fully infiltrate with epoxy resin embedding media. This results in sections in which the deeper regions are unevenly sectioned and poorly stained. This defect is, unfortunately, usually determined only after the sections are prepared. Lastly, since staining is done on an individual slide basis, it is important to be as consistent as possible, to avoid over- or understained sections.

Anticipated Results

The procedures outlined above should provide the pathologist with sections which would allow high resolution histological study of the peripheral nervous system. These provide clear definition of cytological elements of the nerves and ganglia in the tissue sections, which permits detailed interpretation of morphological change–related toxicant effects. These sections are of such quality that morphometric procedures can be conducted in tissues sectioned in an appropriate plane (such as cross-sections of peripheral nerve). The protocols call for sections at multiple levels of the peripheral nervous system. Examination of this nature is an important issue in neurotoxicology.

Time Considerations

Time requirements will vary, but in general the following are reasonable estimations.

Perfusion fixative and other solutions need to be made up 1 day before perfusion. For large studies, this may take 1 entire day for one person. Perfusion of a single rat takes ~20 to 30 min, with two people involved.

Dissection time devoted to dissection of the nervous system will depend on the number of samples desired. As an example, it takes the authors ~1 hr to collect samples of vagus, sural, tibial, and sciatic nerves, dorsal root ganglia as well as the entire spinal cord and brain from a rat.

Tissue processing is a long procedure, taking ~3 to 5 days. One reason for this prolonged time is that a number of steps need to run overnight. These include infiltration by the 50% propylene oxide/50% resin mixture, and infiltration by the 100% resin. These are not hands-on procedures, in that the tissues do not need to be manipulated during these procedures. Smaller specimens can be processed more rapidly, which could shorten the time committed to this exercise.

Embedding takes 48 to 72 hr and mainly consists of time the tissue remains in the embedding oven to allow the resin to polymerize. This again is not a hands-on procedure after the tissue is placed into the embedding molds in the non-polymerized resin mixture. The latter does require manipulation and takes 2 to 5 min per block.

For sectioning thick sections (for light microscopy), an experienced technician will take up to 30 min for each sample. Thin sections (for transmission electron microscopy) can take up to 45 min to 1 hr each.

Staining and coverslipping takes 6 to 10 min per slide. Staining of thin sections on grids for electron microscopy takes up to 1 hr. This is based upon times determined for optimization of the stain (see Basic Protocol 5). Multiple grids can be stained together by staggering the times.

For nerve fiber teasing, experience will reduce the time, but 2 to 4 hr per nerve is reasonably required.

Literature Cited

Dyck, P.J., Giannini, C., and Lais, A. 1993. Pathologic alterations of nerves. *In* Peripheral Neuropathy, 3rd ed. (P.J. Dyck, P.K. Thomas, J.W. Griffin, P.A. Low, and J.F. Podulso, eds.) pp. 514-595. W.B. Saunders, Philadelphia.

Fix, A.S. and Garman, R.H. 2000. Practical aspects of neuropathology: A technical guide for working with the nervous system. *Toxicol. Pathol.* 28:122-131.

Hayat, M.A. 1970. Principles and Techniques of Electron Microscopy. Van Nostrand Reinhold Co., New York.

Jortner, B.S. 2000. Mechanisms of toxic injury in the peripheral nervous system: Neuropathologic considerations. *Toxicol. Pathol.* 28:54-69.

King, R. 1999. Atlas of Peripheral Nerve Pathology. Arnold, London.

Krinke, G.J., Vidotto, N., and Weber, E. 2000. Teased-fiber technique for peripheral myelinated nerves: Methodology and interpretation. *Toxicol. Pathol.* 28:113-121.

Reynolds, E.S. 1963. The use of lead citrate at high pH as an electron opaque stain in electron microscopy. *J. Cell Biol.* 17:208-212.

Schaumburg, H.H., Berger, A.R., and Thomas, P.K. 1992. Disorders of Peripheral Nerves. 2nd ed. F.A. Davis Co., Philadelphia.

Spencer, P.S., Bischoff, F.M., and Schaumburg, H.H. 1980. Neuropathological methods for detection of neurotoxic disease. *In* Experimental and Clinical Neurotoxicology (P.S. Spencer and H.H. Schaumburg, eds.) pp. 743-757. Williams and Wilkins, Baltimore.

Contributed by S.K. Hancock, J. Hinckley, M. Ehrich, and B.S. Jortner
Virginia Polytechnic Institute and State University
Blacksburg, Virginia

CHAPTER 13
Teratology

INTRODUCTION

Teratology is the study of structural birth defects, and its name derives from the Greek word for monster, *teras*. As such, it is part of the field of developmental toxicology, a more recent term that includes all manifestations of abnormal development, including functional and behavioral impairments. During the twentieth century, a variety of environmental conditions were found to perturb the development of different species, including mammals. Full appreciation of the potential deleterious impact of exogenous substances on human embryonic and fetal development came from the discovery in 1960 in Europe of a large number of newborns with limb malformations, later linked to the use of the sedative/hypnotic drug thalidomide by pregnant women. As a result of this catastrophe, regulatory agencies began to require toxicity testing specifically addressing the possible adverse impact of any new chemical on the developing embryo and fetus.

This chapter focuses on the traditional and more recent approaches to investigate the teratogenic potential of chemicals. *UNIT 13.1* provides an introduction on the field of teratology and on its unique role within toxicology. *UNIT 13.2* examines the rat embryo culture as an in vitro method to screen for potential teratogens; this system can have useful applications also for mechanistic studies. Another model for in vitro teratology testing, micromass cultures, is described in *UNIT 13.3*. *UNIT 13.4* describes another *in vitro* model for teratology studies: the chicken embryo. Methods of assessment of in vivo prenatal developmental toxicity in rodents are described in *UNIT 13.5*. These include evaluations of skeletal and soft tissue morphology (Segment II study) as well as postnatal growth and viability (Chernoff/Kavlock assay). *UNIT 13.6* discusses an interesting in vitro system to assess the effects of chemicals on development of the palate.

Forthcoming units will address additional methodologies for screening industrial and environmental teratogens, as well as methodologies currently used to investigate specific mechanisms of teratogenesis.

Lucio G. Costa

Contributed by Lucio G. Costa
Current Protocols in Toxicology (2003) 13.0.1

Overview of Teratology

HISTORICAL PERSPECTIVE

Since the middle to late nineteenth century, teratology, the study of how congenital malformations arise, has been the subject of scientific explorations (see Warkany, 1971, for an extensive history of ancient and modern teratology). Gregor Mendel's work in the late 1800s first spawned genetic explanations for altered embryonic development, and, for a while, genetic theories were used to explain most congenital defects that occurred. Experimental mammalian teratology began in the 1920s and 30s. Hale's discovery that vitamin A–deficient diets fed to sows resulted in pigs with defects of the eyes, face, and head began a series of studies that have continued to this day on the effects of nutritional alterations during development. In particular, Warkany and colleagues in the 1940s conducted a number of studies on the effects of nutritional deficiencies on development. The importance of nutritional factors in pregnancy is still being realized, as exemplified by the discovery in the early 1990s of the role of folic acid supplementation in preventing many cases of neural tube defects. Infectious diseases were implicated as teratogens when Gregg, in 1941, discovered that infection with the Rubella virus during early pregnancy could lead to a syndrome of congenital defects. The effects of the drug thalidomide in producing limb reduction defects in children born in the late 1950s and early 1960s made it clear that chemical exposures during pregnancy can affect the developing embryo, and that the so-called "placental barrier" is not really a barrier to many agents. Following that disaster, efforts began worldwide to develop more extensive premarket testing approaches for drugs, and eventually for food additives and environmental chemicals, to prevent such occurrences. In the last 20 years, more concern has been placed on developmental effects, in addition to malformations or the study of teratology, spawning the field of developmental toxicology, as well as developmental neurotoxicology, immunotoxicology, and others.

PRINCIPLES OF TERATOLOGY AND ABNORMAL DEVELOPMENT

In the late 1960s and early 1970s, Wilson (1973) began to formulate several principles of teratology and abnormal development. These principles, further discussed in Wilson (1977), have stood the test of time and continue to serve as an excellent basis for evaluating and interpreting data on teratology and developmental toxicology. A brief summary discussion is presented here, as there are several references that discuss them in detail (e.g., Scialli, 1992; Schardein, 1993; Sadler and Hunter, 1994; Schmidt and Johnson, 1997).

Susceptibility to Abnormal Development Depends on the Genotype of the Conceptus and the Manner in Which this Genetic Composition Interacts with the Environment

A number of studies in the experimental literature show the effect of the genetic background of animals, particularly inbred strains of mice, on the incidence and types of congenital defects produced by various chemical agents. For example, certain strains of mice have a relatively high incidence of exencephaly and cleft palate. In some cases, treatment with teratogenic agents will increase the incidence of these defects in those strains that have a high background incidence to a greater extent than in those strains that show the defect less often. Species differences in susceptibility are also evident for a number of agents. For example, glucocorticoids are especially effective in producing cleft palate in mice and rabbits, but most strains of rats are highly resistant.

In humans, there are certain racial and ethnic differences in background rates of developmental alterations, but it is not always clear whether these differences are due to genetic differences or to other nutritional, social, or lifestyle differences. For example, the rate of infant mortality differs in the African-American and Caucasian populations. Some of this difference may be due to socioeconomic status and related prenatal care and nutrition. However, in comparisons between middle-class white and African-American women, African-Americans continue to show a higher infant mortality rate. Whether such differences in background rates of various developmental outcomes influence the susceptibility of certain groups of individuals to the effects of chemical exposure during development is not known. In addition, only a portion of individuals (both humans and experimental animals) exposed to a given agent will show an adverse developmental outcome. That is, the

Contributed by Carole A. Kimmel
Current Protocols in Toxicology (2000) 13.1.1-13.1.8

risk of an effect following exposure is never 100% and is often in the range of ≤10%. Because of this fact, Sokol et al. (1986) attempted to determine factors involved in susceptibility to alcohol teratogenicity. Their analysis indicated that race was a significant determinant of fetal alcohol syndrome regardless of adjustments for other possible contributing or confounding factors, such as extent of exposure and parity. Scialli and Lione (1998) have reviewed extensively the factors involved in variability of response to chemical agents related to reproductive and developmental toxicity.

More recently, efforts have been made to evaluate specific gene-environment interactions in susceptibility to various agents. Data have been published indicating an interaction between maternal cigarette smoking during pregnancy and an uncommon allele of transforming growth factor α (TGFα) which results in a 6- to 10-fold increased risk of cleft lip with or without cleft palate, or cleft palate alone (Hwang et al., 1995; Shaw et al., 1996; Shaw and Lammer, 1997). Because of the advances currently being made in identifying genes associated with certain malformations and syndromes, such interactions using genetic biomarkers of both effect and exposure are actively being pursued.

Agents that Cause Abnormal Development Vary with the Developmental Stage at the Time of Exposure

The developing embryo is constantly changing in size, number and position of cells, and degree of differentiation, and there are a number of critical events that are required for normal development. The delicate balance of these cascades of events, which lead to the formation of a normal organism, can be exquisitely sensitive to perturbations by chemical or physical agents during development. Most of the information available on critical periods comes from data during major organogenesis (i.e., gestation days 6 to 15 in mice and rats, 7 to 58 in humans). Some information is also available on periods of sensitivity for systems that develop into the fetal and postnatal periods, e.g., the nervous system, kidney, skeleton, and reproductive system. A recent workshop report (Selevan et al., 2000) summarizes the information available on pre- and postnatal critical periods of susceptibility for several organ systems and cancer.

In general, the developing embryo is most sensitive to the induction of malformations, growth retardation, and death during the period of major organogenesis, inferred from the fact that it usually requires a smaller dose (i.e., on a milligram/kilogram basis) during this time to produce effects than either earlier or later. Exposure of either parent before conception may also be an important time for induction of developmental defects. There have been several studies showing the induction of developmental effects following exposure of the father prior to conception (Olshan and Mattison, 1994; Hales and Robaire, 1997). For example, exposure to chemotherapeutic or mutagenic agents prior to conception may cause chromosomal or DNA changes in germ cells that result in heritable effects, including death, malformations, growth retardation, functional deficits, or cancer in the offspring. Experimental studies have suggested that epigenetic changes may also be responsible for some male-mediated developmental effects.

During very early embryogenesis, before implantation occurs (i.e., zygote to blastocyst stages), cells are multiplying at a rapid rate and are relatively undifferentiated; exposure to a variety of agents during this time tends to result in death or compensation and continued normal development. For several genotoxic agents, exposure during this period has been shown to result also in malformations and growth retardation. As organogenesis begins, cells become more and more differentiated and the major structure of organs is formed, although not all organs develop at the same time or rate. Exposure to many different agents during this period has been shown to cause major structural defects, as well as death, growth retardation, or postnatal functional changes.

As major organ structure is completed, organization at the histological level as well as physiological and biochemical differentiation proceeds; in most mammals, these processes occur to a varying extent during pre- and postnatal development. Exposure to a number of agents during this period may result in alterations that are detected as histopathology, growth retardation, and/or functional changes. Rodier (1976) has shown that morphological defects in brain development are induced by exposure at several specific times in late gestation to a chemotherapeutic agent, and that there are differences in the pattern of neurobehavioral effects associated with exposure at each time point. Cancer also has been induced during late fetal and neonatal stages by several genotoxic agents. Exposure during pregnancy may also affect the placenta, which can in turn affect the developing embryo/fetus. Effects on the placenta may include alterations in blood flow and

perfusion, alterations in metabolism, or in extreme cases, necrosis and separation from the uterine wall.

Later stages of development include further growth and functional maturation of organs/systems, some of this occurring at several years of age. Exposure during this period may affect the same target organs as in adults, but with different consequences because of the lack of maturity.

Data on ionizing radiation, which produces many different types of developmental effects, have been summarized by Brent (1977) and can be used to demonstrate the times in development during which various types of outcomes may be induced. For example, exposure to 100 rads during the preimplantation period results in significant embryolethality, but not many other types of effects. Exposure during early organogenesis—gestation day (gd) 8 to 10 in the rat—results in lethality, growth retardation that persists into adulthood, gross malformations, cataracts, neuropathology, and behavioral disorders. Exposure during the fetal period (gd 13 to 22 in the rat) causes less lethality, persistent growth retardation, sterility, cataracts, neuropathology, and cytogenetic abnormalities.

For functional disorders, timing of the evaluation is just as important as the timing of exposure. For example, effects on motor activity will not become apparent until a young animal or child is locomoting sufficiently to test activity patterns. Effects on cognitive function are more easily tested when children reach school age and can read and write as well as understand complex reasoning. Degenerative neurological diseases that are induced or influenced by environmental exposures may not become apparent until well into adulthood or old age. Effects on reproductive function, especially reproductive senescence, will not be detectable until adulthood. Such effects with long latency from the time of developmental exposure to the outcome observed years later are not detected easily, unless carefully controlled studies are done.

Teratogenic Agents Act in Specific Ways (Mechanisms) on Developing Cells and Tissues to Initiate Abnormal Embryogenesis (Pathogenesis)

Development is an extremely complex and carefully integrated process involving a variety of genetic controlling functions, cell interactions, and tissue interactions. All of this requires accurate timing of events, e.g., turning on and off of genes at the right time and in the correct sequence to control normal replication, cell death, differentiation, and migration of cells to their correct final positions at the appropriate time for normal tissue and organ development.

There are two types of mechanisms that must be considered in the developmental toxicity of drugs and other agents. First, there are pharmacological and biochemical mechanisms by which agents can interact with a target site and alter development, and second, there are mechanisms by which target molecules, cells, and tissues react to that initial interaction, i.e., the initial steps in pathogenesis. Although not totally distinct, both types of events must be appreciated to understand the complexities of development and how this process can be altered.

Because of the many types of processes involved in development, there are many mechanisms by which agents may potentially act to alter development. However, partial mechanisms for only a few agents have been shown. Wilson (1977) proposed a list of potential mechanisms by which agents might act on developing cells and tissues (shown in Table 13.1.1).

This list of general mechanisms by and large relates to the initial interaction of the agent at the target site or receptor. Much more specific information is now available for some agents on the ways in which they may interact with the target site to alter development. In particular, specific receptor-binding agents that act as agonists or antagonists and alter development have been studied extensively. For example, diethylstilbestrol (DES), a potent synthetic estrogen-receptor agonist, was shown to affect development of the reproductive system in both male and female offspring of women treated for premature labor in the 1950s, and in some cases it caused a rare form of vaginal adenocarcinoma that did not show up until the late teens or early

Table 13.1.1 Potential Mechanisms by Which Agents May Interfere with Development

Altered energy sources
Altered nucleic acid integrity or function
Changed membrane characteristics
Chromosomal breaks, nondisjunctions, etc.
Enzyme inhibition
Lack of precursors, substrates, etc.
Mitotic interference
Mutation (gene)
Osmolar imbalance

20s in DES daughters. Androgen receptor binding by agonists or antagonists (e.g., dihydrotestosterone, vinclozolin, hydroxyflutamide, *p,p′*-DDE) has been shown experimentally to alter reproductive development as well. Agents that bind to the retinoid receptor may also interfere with development. For example, Accutane (13-cis-retinoic acid, isotretinoin), an endogenous retinoid that is extremely important in development, was marketed for treatment of recalcitrant cystic acne in the early 1980s and caused craniofacial, cardiovascular, central nervous system, and neurobehavioral deficits in a number of children whose mothers took the drug in early pregnancy.

In addition to the initial interaction of an agent with the target site, the progression of events that follow, i.e., pathogenesis, must also be considered in the ultimate manifestation of abnormal development. Some mechanisms that may be altered are listed in Table 13.1.2. Although these general molecular and cellular mechanisms have been known for some time, much new information about them has come from recent studies in molecular and developmental biology. Some are being studied as potential pathways through which alterations in development may occur. Several of these potential mechanisms were reviewed in a recent series of articles in *Reproductive Toxicology* (vol. 11, nos. 2/3, 1997). Discussion of these and other potential mechanisms can be found in Brown (1994), and Faustman et al. (1997).

Signal transduction pathways involved in some of these processes have been identified, and this may help to elucidate more directly the initial target site of action and subsequent steps in the process that can be interfered with during development (Gerhart, 1998). For example, the signaling pathway for apoptosis may involve the *p53* tumor suppressor gene, a negative regulator of the cell cycle and a positive regulator of apoptosis, *bcl-2*, a suppressor of cell death, the ICE genes, *c-myc*, *bax*, and others. Many of these are involved in controlling the cell cycle as well as in regulating apoptosis. Apoptosis is a normal phenomenon in embryonic development, involved in remodeling of many structures in the facial area, nervous system, and limbs. A few teratogenic agents have been studied for their effects on this pathway. For example, Wubah et al. (1996) have shown that cladribine (2-chloro-2U-deoxyadenosine) induces p53-mediated apoptosis and results in eye malformations in mice treated on gd 8. Moallem and Hales (1998) showed that an analog of cyclophosphamide induced different types of cell cycle alterations, cell death, and limb malformations, depending on the p53 genetic background of the mice. The role of p53 in embryogenesis, DNA repair, and apoptosis is still unclear, as it appears to suppress teratogenesis in some cases and enhance it in others.

Table 13.1.2 Molecular and Cellular Mechanisms Important In Developmental Toxicity

Cell cycle patterns
Cell lineage
Cellular adhesive interactions
Cellular migration
Chromosomal rearrangements
DNA repair
Gamete-derived determinants of meiotic competence
Genomic imprinting
Growth and differentiation factors
Induction
Pattern formation
Programmed cell death (e.g., apoptosis)

Agents that act by any of the mechanisms listed in Table 13.1.1, or that interfere with any of the processes listed in Table 13.1.2, should be considered to have the potential for inducing developmental toxicity, and should be tested thoroughly for all types of developmental effects. The embryo appears to be able to repair a certain amount of damage and continue to develop normally, but at this point, the amount of damage that can be repaired has not been elucidated. A number of in vitro systems are being employed in the study of these mechanisms for both normal and abnormal development (see below).

The Final Manifestations of Abnormal Development Are Death, Malformation, Growth Retardation, and Functional Disorders

The four major manifestations of developmental toxicity (death, structural malformations, altered growth, and functional deficiency) are all considered adverse effects. As indicated above, the manifestations of developmental toxicity vary depending on the timing of exposure, dose, and the underlying processes that are occurring, as well as on the time of observation. These manifestations are likely to be interrelated (e.g., embryo/fetal death is frequently associ-

ated with and may be a consequence of severe malformation). Although death, malformation, and permanent functional impairment all clearly represent equally unacceptable outcomes, the significance of effects on growth or on the incidence of structural variations is sometimes questioned, particularly if these only occur at maternally toxic doses or can be shown to be reversible. However, many agents capable of producing death and malformation can also affect growth, depending on the dose and time of exposure. Growth retardation is often associated with functional impairment. While structural variations do not appear to adversely impinge on the health or longevity of affected fetuses, an increase in their incidence may indicate that the embryotoxic threshold is being approached (Kimmel and Wilson, 1973). The significance of these more subtle developmental effects also depends on the context in which they occur. For example, deficient or irregular patterns of ossification that are generalized throughout the fetal skeleton may simply reflect transient growth retardation, but such effects take on added significance when they occur without corresponding reductions in fetal weight or are more prominent in structures in which malformations also occur.

The Access of Adverse Environmental Influences to Developing Tissues Depends on the Nature of the Influences (Agents)

Access of an agent to developing tissues depends on the physico-chemical nature of the agent itself, as well as the physical, biochemical, and physiological aspects and homeostatic mechanisms of the maternal organism. Physical agents, such as ionizing radiation or hyperthermia, can impact the embryo directly and interfere with development. When the mother is exposed externally, the amount of the agent that reaches the embryo/fetus may be modified to some extent by the density of maternal tissues, but the characteristics of the agent that make it harmful developmentally will not be altered.

Chemical agents, on the other hand, are subject to a number of maternal factors that may alter, reduce, or increase the amount reaching the developing organism. For example, maternal pharmacokinetics, which include absorption, distribution, metabolism, plasma protein binding, and excretion, can all have an impact on the amount of active ingredient that is available to the developing embryo/fetus. Physiological changes in the maternal animal during pregnancy may also influence chemical delivery. Placental metabolism can play an important role in the amount of drug that crosses the placenta, as well as whether placental transport is active or passive (see review by Slikker and Miller, 1994). Although species differences in morphology of the placenta have been pointed out by a number of authors as potentially influencing placental transfer, there are very few instances where placental morphology has been demonstrated to play a role. One exception is the differential passage of nutrients as well as drugs and other agents across the yolk sac placenta, which plays a greater role in the early rodent conceptus than in the human. The primary factors that affect placental transport are uterine and placental blood flow, placental permeability, and placental metabolism. These factors change dramatically as pregnancy advances and can affect transfer significantly.

Placental permeability is affected by both physical and chemical characteristics. For example, the degree of ionization, lipid solubility, protein binding, and molecular weight of an agent may affect the ability of an agent to cross the placenta. Almost any maternally administered compound has the potential to cross the placenta, and the question is not whether a compound crosses the placenta, but at what rate, negating the concept of a "placental barrier" that protects the embryo/fetus from harmful agents to which the mother may be exposed.

Chemical biotransformation by the developing conceptus may also occur, and the same factors that influence placental transfer to the embryo/fetus also influence transfer back from the conceptus into the maternal bloodstream. In many cases, the laboratory rodent develops enzyme metabolizing systems in the early neonatal stages, whereas in humans, these events occur or begin before birth. Thus, mimicking of late human fetal exposure may require postnatal dosing of rodents. If a chemical has been conjugated by the fetus (e.g., via glucuronidation or sulfation), or metabolized to a more polar form, the rate of return to the maternal circulation will be slower than for the parent compound, resulting in an accumulation of the material in the fetal compartment.

In some cases, access of an agent to the developing conceptus may not be the deciding factor as to its potential for developmental toxicity. Instead, the effect of the agent may be primarily on the maternal system which, in turn, affects the developing organism and causes adverse effects. In the typical screening studies used for regulatory purposes, it is usually not possible to determine whether an effect is direct

on the embryo/fetus or indirect through effects on the mother. Although it is clear that embryo/fetal development can be affected by maternal toxicity, it is not well understood under what conditions and to what extent this occurs.

Daston (1994) reviews the information available on the relationship between maternal and developmental toxicity, and provides examples of situations in the mother (agents or disease states) that have been shown to affect development. These include toxicity to the placenta, altered nutritional status of the mother, decreased uterine blood flow, anemia or hypoxia, toxemia of pregnancy, autoimmune states, diabetes, acid-base disturbances, decreased milk quantity or quality, and abnormal maternal behavior. Chemical examples that have been shown to affect development by maternally mediated mechanisms include cadmium, cigarette smoking, cocaine, ethanol, and urethane. In most if not all cases, these examples have been delineated through a series of studies specifically designed to address the question of causality. Hood and Miller (1997) further discuss the role of maternally mediated effects on development and experimental approaches to assessing such effects.

Manifestations of Deviant Development Increase in Degree as Dosage Increases, from No Effect to the Totally Lethal Effect

One of the cardinal principles in determining whether or not exposure to a particular agent is related to an effect is that there is a dose-response relationship between the two. Wilson (1973) originally described the overlapping dose-response relationship between malformations, embryolethality, and maternal toxicity. In the case of an agent that causes malformations, as dose increases, the severity of malformations also tends to increase until death intervenes. If death of the conceptus occurs at higher doses as a result of malformations, a nonlinear dose-response relationship for malformations may result. Whether or not there is a low dose at which no effect will occur (i.e., a threshold) has been a controversial issue, but it is well known that compensatory growth and repair mechanisms are present in the developing organism. Several studies reported in the literature have shown that damage to a small or moderate number of cells can result in no obvious effects on development, while damage to a larger number results in malformations and death of the conceptus. Many studies have been published that focus on induction of apoptosis and alterations in the cell cycle by various agents, but the degree of insult that the embryo can tolerate has not been determined.

In recent years, a good deal of effort has been applied to mathematical modeling of the dose-response data from developmental toxicity studies (see Williams and Ryan, 1997, for a review). Such approaches are beginning to be used for risk assessment purposes by establishing a benchmark dose that can be used for comparison among agents, among types of toxicity for a given agent, or to set exposure limits. Catalano et al. (1993) also described an approach to modeling all of the prenatal outcomes of development (i.e., fetal weight, malformations, and fetal death). In recent years, several publications have resulted from efforts to develop biologically-based dose-response models for developmental toxicity (e.g., Shuey et al., 1994a,b; Kavlock and Setzer, 1996). All of these efforts have increased the understanding of dose-response relationships for developmental toxicity, but more importantly, they have highlighted the need for more understanding of the mechanisms of both normal and abnormal development for use in biologically based dose-response models.

EXTRAPOLATION OF ANIMAL FINDINGS TO HUMANS

Adverse effects seen in animal studies have been assumed to indicate a potential risk to humans. Several authors have reviewed the literature on agents known to cause developmental effects in humans and the data, though limited, strongly support this assumption (summarized by Kimmel and Kimmel, 1997). It is also clear that the occurrence of a specific adverse effect in animals does not predict that the same adverse effect will occur in another animal species, including humans; i.e., concordance of a specific effect at a specific target site in multiple species is not necessarily the case. For example, thalidomide does not cause phocomelia in rats as it does in humans, but it will increase intrauterine deaths. Valproic acid produces exencephaly (a cranial neural tube defect) in mice but not in rats, rabbits, or monkeys. Any manifestation of exposure-related developmental toxicity in animal studies can be indicative of a developmental hazard to humans. If, for example, a drug causes tail defects in mice, or an effect on Zymbal's gland in rodents, although there are no direct corollaries in man, such effects are assumed to be relevant to humans, unless it is possible to demonstrate mechanistic differences. The proximity of exposure levels that are developmentally toxic in animals to human exposure levels

is a primary consideration in evaluating human risk. For example, very large oral doses of caffeine produce ectrodactyly in rats whereas the same high levels of caffeine, administered as divided oral doses, or administered in drinking water at levels more comparable to human intake, do not.

The fact that an agent has been shown to cause developmental effects in laboratory animals and not in man does not invalidate the animal models. A few reasons for failed predictions may include: (1) appropriate studies to evaluate the association of an exposure with relevant developmental effects may not have been conducted in humans; (2) the exposure level that occurs in humans is too low to produce an effect; and (3) the incidence of effects in humans is too low to be detectable. Epidemiology studies that evaluate populations with greater phenotypic heterogeneity than in laboratory animals often do not have sufficient information for dose-response evaluations and do not typically ascertain the full spectrum of effects of an agent. Human studies are usually designed to evaluate a single outcome of pregnancy, e.g., spontaneous abortions or malformations. Thus, other possible endpoints, especially functional disorders, may go undetected. Longitudinal studies that follow exposures prior to, during pregnancy, and to infants and children, and evaluate a variety of developmental outcomes will allow linking of exposures and effects that are not possible in cross-sectional epidemiology studies.

USE OF IN VITRO SYSTEMS IN TERATOLOGY

A number of in vitro systems have been developed for use in teratology. The term "in vitro" is generally applied to any test system other than a pregnant mammal. Examples include isolated whole embryos (mammalian or nonmammalian) in culture, as well as tissue, organ, and cell culture assays. These systems afford several qualities that are useful in studying mechanisms of normal and abnormal development, e.g., isolation of the embryo from the maternal environment, removal or transplantation of specific tissues and cells, and the ability to track specific cells and molecules, to genetically alter cells, and to monitor embryo physiology.

In vitro systems have been used for two major applications in teratology and developmental toxicology: (1) screening for the effects of toxic agents; and (2) studying mechanisms of agent-induced alterations in development. Although the use of in vitro systems for mechanistic studies has many advantages (reviewed by Harris, 1997, and described in subsequent units of *Current Protocols in Toxicology*), their use in screening for teratogenic agents is extremely limited. In large part, this is because of deficiencies in the test system that have been identified above as advantages for mechanistic studies—i.e., isolation from the maternal environment that may modulate effects through pharmacokinetics, or maternal toxicity, and the fact that most systems can be maintained in vitro for only a few days in duration. This latter feature, especially for mammalian whole-embryo culture systems, limits exposure and evaluation of responses to only a small portion of the developmental stages that may be important for understanding developmental toxicity in vivo. Kimmel and Kimmel (1997) have discussed the use of in vitro developmental systems, their role in screening chemicals, and the potential for use in risk assessment. Integration of these two uses of in vitro systems, i.e., mechanistic studies and application of that information to designs for screening studies, may ultimately allow further development of in vitro assays or short-term tests to replace the large number of animals currently required for chemical testing.

LITERATURE CITED

Brent, R.L. 1977. Radiations and other physical agents. *In* Handbook of Teratology, Vol. 1 (J.G. Wilson and F.C. Fraser, eds.) pp. 153-223. Plenum Press, New York.

Brown, N.A. 1994. Mechanisms of early embryogenesis. *In* Developmental Toxicology (C.A. Kimmel and J. Buelke-Sam, eds.) pp. 15-49. Raven Press, New York.

Catalano, P.J., Scharfstein, D.O., Ryan, L.M., Kimmel, C.A., and Kimmel, G.L. 1993. A statistical model for fetal death, fetal weight, and malformation in developmental toxicity studies. *Teratology* 47:281-290.

Daston, G.P. 1994. Relationships between maternal and developmental toxicity. *In* Developmental Toxicology (C.A. Kimmel and J. Buelke-Sam, eds.) pp. 189-212. Raven Press, New York.

Faustman, E.M., Ponce, R.A., Seeley, M.R., and Whittaker, S.G. 1997. Experimental approaches to evaluate mechanisms of developmental toxicity. *In* Handbook of Developmental Toxicology (R.D. Hood, ed.) pp. 13-41. CRC Press, Boca Raton, Fla.

Gerhart, J. 1998. 1998 Warkany Lecture: Signalling pathways in development. *Teratology* 60:226-239.

Hales, B.F. and Robaire, B. 1997. Paternally mediated effects on development. *In* Handbook of Developmental Toxicology (R.D. Hood, ed.) pp. 91-107. CRC Press, Boca Raton, Fla.

Harris, C. 1997. In vitro methods for the study of mechanisms of developmental toxicity. *In* Handbook of Developmental Toxicology (R.D. Hood, ed.) pp. 465-509. CRC Press, Boca Raton, Fla.

Hood, R.D. and Miller, D.B. 1997. Maternally mediated effects on development. *In* Handbook of Developmental Toxicology (R.D. Hood, ed.) pp. 61-90. CRC Press, Boca Raton, Fla.

Hwang, S.J., Beaty, T.H., Panny, S., et al. 1995. Association study of transforming growth factor alpha (TGFα) TaqI polymorphism and oral clefts: Indication of gene-environment interaction in a population-based sample of infants with birth defects. *Am. J. Epidemiol*. 141:629-636.

Kavlock, R.J. and Setzer, R.W. 1996. The road to embryologically-based dose-response models. *Environ. Health Perspect*. 104:107-121.

Kimmel, C.A. and Kimmel, G.L. 1997. Principles of developmental toxicity risk assessment. *In* Handbook of Developmental Toxicology (R.D. Hood, ed.) pp. 667-693. CRC Press, Boca Raton, Fla.

Kimmel, C.A. and Wilson, J.G. 1973. Skeletal deviations in rats: Malformations or variations? *Teratology* 8:309-316.

Moallem, S.A. and Hales, B.F. 1998. The role of p53 and cell death by apoptosis and necrosis in 4-hydroperoxycyclophosphamide-induced limb malformations. *Development* 125:3225-3234.

Olshan, A.F. and Mattison, D.R. (eds.) 1994. Male-Mediated Developmental Toxicity. Plenum Press, New York.

Rodier, P. 1976. Critical periods for behavioral anomalies in mice. *Environ. Health Perspect*. 18:79-83.

Sadler, T.W. and Hunter, E.S. 1994. Principles of abnormal development. Past, present and future. *In* Developmental Toxicology (C.A. Kimmel and J. Buelke-Sam, eds). pp. 53-63. Raven Press, New York.

Schardein, J.L. 1993. Principles of teratogenesis applicable to drug and chemical exposure. *In* Chemically Induced Birth Defects, pp. 1-59. Marcel Dekker, New York.

Schmidt, R.R. and Johnson, E.M. 1997. Principles of teratology. *In* Handbook of Developmental Toxicology (R.D. Hood, ed.) pp. 3-12. CRC Press, Boca Raton, Fla.

Scialli, A.R. 1992. Embryology and principles of teratology. *In* A Clinical Guide to Reproductive and Developmental Toxicology. pp. 1-27. CRC Press, Boca Raton, Fla.

Scialli, A.R. and Lione, A. 1998. Variability in human response to reproductive and developmental toxicity. *In* Human Variability in Response to Chemical Exposures: Measures, Modeling, and Risk Assessment (D.A. Neumann and C.A. Kimmel, eds.) pp. 87-137. CRC Press, Boca Raton, Fla.

Selevan, S.G., Kimmel, C.A., and Mendola, P. (eds.) 2000. Identifying critical windows of exposure for children's health. *Environ. Health Perspect.* 108:451-597.

Shaw, G.M. and Lammer, E.M. 1997. Incorporating molecular genetic variation and environmental exposures into epidemiologic studies of congenital anomalies. *Reprod. Toxicol*. 11:275-280.

Shaw, G.M., Wasserman, C.R., Lammer, E.J., O'Malley, C.P., Murray, S.C., Basart, A.M., and Tolarova, M.M. 1996. Orofacial clefts, parental cigarette smoking and transforming growth factor-alpha gene variants. *Am J. Hum. Genet*. 58:551-561.

Shuey, D.L., Lau, C., Logsdon, T.R., Zucker, R.M., Elstein, K.H., Narotsky, M.G., Setzer, R.W. Kavlock, R.J., and Rogers, J.M. 1994a. Biologically based dose-response modeling in developmental toxicology: Biochemical and cellular sequelae of 5-fluorouracil exposure in the developing rat. *Toxicol. Appl. Pharmacol.* 126:129-144.

Shuey, D.L., Zucker, R.M., Elstein, K.H., and Rogers, J.M. 1994b. Fetal anemia following maternal exposure to 5-fluorouracil in the rat. *Teratology* 49:311-319.

Slikker, W., Jr. and Miller, R.K. 1994. Placental metabolism and transfer; role in developmental toxicology. *In* Developmental Toxicology (C.A. Kimmel and J. Buelke-Sam, eds.) pp. 245-283. Raven Press, New York.

Sokol, R.J., Ager, J., Martier, S., et al. 1986. Significant determinants of susceptibility to alcohol teratogenicity. *Ann. N.Y. Acad. Sci*. 477:87-102.

Warkany, J. 1971. Congenital Malformations, pp. 6-37. Year Book Medical Publishers, Chicago.

Williams, P.L. and Ryan, L.M. 1997. Dose-response models for developmental toxicology. *In* Handbook of Developmental Toxicology (R.D. Hood, ed.) pp. 635-666. CRC Press, Boca Raton, Fla.

Wilson, J.G. 1973. Environment and Birth Defects, pp. 12-34.Academic Press, New York.

Wilson, J.G. 1977. Current status of teratology—general principles and mechanisms derived from animal studies. *In* Handbook of Teratology, Vol. 1 (J.G. Wilson and F.C. Fraser, eds.) pp. 47-74. Plenum Press, New York.

Wubah, J.A., Ibrahim, M.M, Gao, X., Nguyen, D., Pisano, M.M., and Knudsen, T.B. 1996. Teratogen-induced eye defects mediated by p53-dependent apoptosis. *Curr. Biol*. 6:60-69.

Contributed by Carole A. Kimmel
U.S. Environmental Protection Agency
Washington, D.C.

Rat Embryo Cultures for In Vitro Teratology

Rat embryo culture methods have been used in industrial teratogen screening and for basic mechanistic studies in developmental toxicology. This unit describes whole-embryo protocols for (1) postimplantation embryos (see Basic Protocol 1) and (2) early fetuses (see Basic Protocol 2). Although there are many common features of culture at these stages, there are several key differences that are presented. The morning after mating is considered the beginning of gestational day 0 (gd 0), based on the observation of a vaginal plug.

NOTE: All protocols using live animals must first be reviewed and approved by an Institutional Animal Care and Use Committee (IACUC) and must follow officially approved procedures for the care and use of laboratory animals.

CULTURE OF EARLY POSTIMPLANTATION EMBRYOS (gd 9 through gd 11)

BASIC PROTOCOL 1

This protocol describes culture of postimplantation embryos. Embryos are isolated from the uterine environment and cultured in vitro for up to two days. This protocol is most frequently used in industrial screening applications and mechanistic studies because it covers the gestational stages of greatest teratogenic sensitivity.

Materials

Time-mated gravidas (≤250-g rats, gestational day 8 to 10)
Anesthetic: ether/O_2, halothane/N_2O/O_2 or isoflurane/O_2
Normal saline or Hanks' balanced salt solution (HBSS), ice-cold (see *APPENDIX 2A* for both recipes)
Embryo culture medium (see recipe), prewarmed to 37°C
20 mM potassium phosphate buffer, pH 7.4 (optional; *APPENDIX 2A*)
Compounds to be tested for effects on embryos, dissolved in DMSO if necessary
S-9 supernatant from rat liver (optional; see Support Protocol 2)
NADPH (for use with S-9 supernatant; optional)
Glucose 6-phosphate (G6P; for use with S-9 supernatant; optional)
Gas mixtures (depending on stage and length of culture):
  5% O_2/5% CO_2/90% N_2 (gd 9)
  20% O_2/5% CO_2/75% N_2 (gd 10)
  40% O_2/5% CO_2/55% N_2 (optional late gd 10)
  95% O_2/5% CO_2 (gd 11 and later)
Petri dishes, sterile
Dissecting microscope
Dissecting equipment, sterile, including:
  Forceps
  Watchmakers forceps
  Fine iris scissors
Tissue culture vessels (e.g., 125-ml medium bottles, 10-ml test tubes) with gas-tight seals, sterile
Rotator apparatus for use within incubator:
  Powered bars for round bottles
  Motorized plate for test tubes

NOTE: All solutions and equipment coming into contact with embryos must be sterile, and aseptic technique should be used accordingly.

Contributed by Alan G. Fantel, Rudolf Bechter, and David Beckman
Current Protocols in Toxicology (2000) 13.2.1-13.2.12

Obtain and prepare embryos

1. Anesthetize the gravidas on gd 9 to 11 with ether/O_2, halothane/N_2O/O_2 or isoflurane/O_2, laparotomize the animal, and excise the uterus.

   The pregnancy is timed based on the presence of sperm in vaginal smears prepared in methanol or vaginal plugs the morning after mating.

   Methods for rat embryo explantation have been thoroughly described in several publications (New, 1966, 1971).

2. Place the uterus in a petri dish containing sufficient cold normal saline or HBSS to cover it, and incise it along its antimesometrial border.

3. Under direct observation or low-power stereomicroscopy, peel off individual implantation sites with associated decidua and place them in petri dishes of cold normal saline or HBSS.

   Subsequent steps are most easily performed under the stereoscopic dissecting microscope.

4. Keeping all tissues under the surface of the salt solution and using a pair of watchmaker's forceps, dissect out and discard the Reichert's membrane and parietal yolk sac remnants, taking care not to puncture the underlying vascular membrane (visceral yolk sac).

   Although Reichert's membrane may be difficult to visualize, it covers the visceral yolk sac and can usually be gently grasped with the watchmaker's forceps and torn. In gd 9 sites, it may be visualized most easily at one pole of the implantation sac.

Culture embryos with test compound

5. Transfer embryos to culture vessel containing at least 1 ml prewarmed embryo culture medium.

   See Critical Parameters for guidelines on amount of medium to use as well as for discussion of culture technique.

6. Add compound(s) to be tested, dissolved in DMSO if necessary.

7. *Optional:* Add 5.3 µl S-9 supernatant from rat liver per ml of medium. Add NADPH to a final concentration of 5×10^{-4} M and glucose-6-phosphate (G6P) to a final concentration of 10^{-3} M.

8. Culture embryos 24 to 48 hr in a 37°C humidified incubator with the appropriate gas mixture (based on gestational day) and rotation at 30 to 60 rpm.

   For gd 9 embryos, use 5% O_2/5% CO_2/90% N_2; for gd 10 embryos use 20% O_2/5% CO_2/75% N_2; and for gd 11 and beyond use 95% O_2/5% CO_2. When embryos are cultured for 48 hr, each day the flasks are opened and reflushed with the gas mixture appropriate for the gestational day.

Evaluate treated embryos

9. At the end of the culture period, remove embryos from culture flasks and place in fresh normal saline, 20 mM potassium phosphate buffer, or HBSS.

10. Remove the embryos from the membranes using fine forceps and examine under the stereoscopic dissecting microscope.

    Common endpoints for whole-embryo culture experiments include embryonic protein content, greatest length, somite count, and morphologic development. Embryos may then be histologically processed for internal examination. They can also be stained with dyes such as Nile blue sulfate to examine cell death.

Studies of developmental toxicity in vitro frequently employ a morphologic scaling system such as that devised by Brown and Fabro (1981). This system scales 19 growth and developmental parameters, including yolk sac development, somite number, limb growth, and neural tube formation and closure, as well as other features that can be scored under the dissecting microscope. By totaling the numbers, a score is derived that can be compared with standards for gestational age between gd 9 and 12.

CULTURE OF EARLY FETAL STAGES (gd 12 to 14)

BASIC PROTOCOL 2

Culture of fetal rats is similar to embryo culture (see Basic Protocol 1) with certain exceptions, e.g., that the higher oxygen demand of later stages requires that implantation sites be placed in flasks of warmed, continuously oxygenated EBSS immediately following removal from the uterus and before the completion of dissection. Additional differences are described below. The protocol presented is based on Barber et al. (1993). This protocol has been used primarily for mechanistic studies, but it is also suitable for examining the effects of chemical exposures at later stages of development. There are significant differences in the timing of developmental events in rats and humans, so this is also an important stage for study.

Materials

Time-mated gravidas (≤250-g rats, gestational day 12 to 14)
Fetal culture medium (see recipe), prewarmed to 37°C and fully flushed with 95% O_2/CO_2
Gas mixture: 95% O_2/5% CO_2
Compounds to be tested for effects on embryos, dissolved in DMSO if necessary
S-9 supernatant from rat liver (optional; see Support Protocol 2)
NADPH (for use with S-9 supernatant; optional)
Glucose 6-phosphate (G6P; for use with S-9 supernatant; optional)

Flat-sided 625-ml tissue culture flasks
Rubber stoppers to fit tissue culture flasks
18-G hypodermic needles
Gas regulators and tubing
Side-arm Ehrlenmeyer flask
1-ml syringes
Sintered-glass diffuser
Dissecting microscope
Dubnoff metabolic incubator (Precision Scientific)

NOTE: All solutions and equipment coming into contact with fetuses must be sterile, and aseptic technique should be used accordingly.

Obtain and prepare fetuses

1. Anesthetize the gravida on gd 12 to 14 and excise the uterus. Place the uterus in a large petri dish containing HBSS and dissect individual implantation sites free. As soon as each site is removed from the uterus, place it in a flask of warmed, continuously-oxygenated EBSS. After all sites have been stripped from the uterus, transfer one fetus from the flask to a petri dish containing sterile HBSS and remove decidua, parietal yolk sac, and remnants of Reichert's membrane.

   Explantation is similar to Basic Protocol 1 except that the higher oxygen demand of later stages requires that implantation sites be placed in flasks of warmed, continuously-oxygenated EBSS immediately following removal from the uterus and before the completion of dissection.

   A major difference from earlier-stage cultures (Basic Protocol 1) is the requirement for exteriorizing the fetus. This is described in the following steps.

2. After the external membranes are removed, make an incision in the area of the visceral yolk sac nearest the fetal head, taking care not to sever the larger blood vessels.

   Although some hemorrhage normally occurs from the smaller vessels, this is usually inconsequential.

3. Reaching into the visceral yolk sac with forceps, tear open the amnion and pull the fetus outside, placing it in direct contact with the medium.

4. Place the exteriorized fetus and membranes in a common 625-ml continuously-oxygenated flask containing 125 ml of fetal culture medium. Place this flask flat side down and gently rock in the Dubnoff metabolic incubator. Use a small piece of lead to weight the bottles down and prevent them from floating in the water bath.

Preculture the exteriorized fetuses

5. Culture the fetuses in the common flask for 2 hr under the conditions described below prior to their distribution to experimental flasks.

   This preliminary incubation enables identification and elimination of fetuses that may have hemorrhaged excessively and are no longer viable. They will be evident from their pallor and reduced or absent heartbeat and yolk sac circulation.

   a. After they have been examined for viability, place fetuses in the individual *experimental* culture flasks containing 125 ml warm, oxygenated fetal culture medium and the study agent(s).

      These vessels are identical to the common flask. Medium volume is 125 ml and up to 10 fetuses may be cultured in a single flask.

   b. Culture flasks are flushed continuously throughout the culture period with O_2/CO_2 at a flow rate of 400 ml/min. This rate is most easily controlled with the use of a manometer for each flask.

   c. The screw caps supplied with the flasks are discarded and replaced with tight-fitting rubber stoppers that have been pierced by two 18-G hypodermic needles. One needle is adapted to fit gas-tight tubing, which can be accomplished by cutting off the flat (flanged) ends of 1-ml hypodermic syringes. One end is attached to the needle and the other to the tubing. The second needle serves as a vent. The rubber stoppers are fitted tightly into the necks of the flasks.

   d. In order to prevent evaporative loss of culture medium, it is necessary to humidify the gas mixture before it enters the experimental culture flasks. This is accomplished with an Ehrlenmeyer flask fitted with a side arm. The flask is filled with clean water and covered with a rubber stopper containing a sintered glass diffuser. The gas mixture (95% O_2/5% CO_2) flows through the diffuser, bubbles through the water, and exits through the side arm which is connected by tubing to the manometers, if used, or directly to the inlets of the culture flasks.

   e. The shaker is set to gently rock the flasks from long end to long end at a rate of ~30 cycles/min. Faster rates may force the fetuses onto the neck of the flask where they will dry out, or may cause hemorrhages of the yolk sac vasculature.

Perform experimental cultures

6. Prepare experimental flasks as in steps 5a to 5e, and distribute the fetuses among them using a sterile stainless steel spatula.

7. Add compound(s) to be tested, dissolved in DMSO if necessary.

8. *Optional:* Add 5.3 µl S-9 supernatant from rat liver per ml of medium. Add NADPH to a final concentration of 5×10^{-4} M and glucose-6-phosphate (G6P) to a final concentration of 10^{-3} M.

9. Place the culture flasks in the Dubnoff metabolic incubator, set to 37°C.

   Flasks are arranged flat-side-down, enabling the medium to remain below the incubating water level with the flask neck above the water line. In order to prevent the flasks from floating free, they should be weighted down.

10. Culture fetuses for up to 24 hr.

    Culture has never been successfully extended beyond the morning of gd 15.

Evaluate cultured fetuses

11. After 24 hr, remove fetuses from culture flasks and examine under the stereoscopic dissecting microscope.

    Standard measures include greatest length and protein content. The fetuses are carefully scanned for morphological staging and malformations. They may be fixed and sectioned for finer study. Limb development is especially sensitive at these later stages.

COLLECTING SERUM FOR EMBRYO CULTURE

SUPPORT PROTOCOL 1

Various medium combinations have been successfully employed for rat whole-embryo culture (New, 1979). Most have consisted entirely or in part of immediately centrifuged, heat-inactivated rat serum. The following procedure is commonly used to collect serum for whole-embryo culture.

NOTE: All solutions and equipment coming into contact with live cells must be sterile, and aseptic technique should be used accordingly.

Materials

Nonpregnant rats (often retired breeders or older males)
Anesthetic: ether/O_2, halothane/N_2O/O_2 or isoflurane/O_2

18-G needle
Sterile, nonheparinized syringe
Refrigerated centrifuge
50-ml conical centrifuge tubes
56°C water bath

1. Anesthetize nonpregnant rats with ether/O_2, halothane/N_2O/O_2 or isoflurane/O_2.
2. While under deep anesthesia, laparotomize rats and insert a large needle (18-G), attached either directly or via butterfly tubing to a sterile nonheparinized syringe, obliquely into the descending vena cava below the level of the diaphragm.
3. By gently pulling on the plunger to avoid excessive hemolysis, collect 9 to 15 ml of whole blood from each animal.
4. Sacrifice the rat by cutting the aorta above the diaphragm, after the needle is removed from the vein.
5. After removing the needle from the syringe, gently expel the blood into 50-ml conical centrifuge tubes. Immediately centrifuge 20 min at ~1500 × *g*, 4°C.
6. Remove the supernatant (serum) from the pellet (red cell layer). Incubate the serum 30 min at 56°C to inactivate complement.

   If not used immediately, the serum may then be frozen at −20° or −80°C.

   Many investigators use rat serum alone for the culture of rat and mouse embryos. See Critical Parameters for additional discussion of media.

SUPPORT PROTOCOL 2

PREPARATION OF LIVER HOMOGENATES FOR STUDIES OF BIOTRANSFORMATION

A number of systems have been employed that incorporate features of extraembryonic drug metabolism. Conspecific or allospecific liver homogenates may be prepared and added to culture medium along with appropriate cofactors. Some of the earliest successful systems employed liver from adult rats that had been preinduced with polychlorinated biphenyls, i.e., Araclor 1254 (Fantel et al., 1979; Kitchin et al., 1981), but human liver preparations have also been used (Zhao et al., 1993). Other approaches to metabolism include pretreatment of gravidas with test agents followed by culture of exposed embryos after a suitable time period (Kochar, 1975; Beaudoin and Fisher, 1981) or preparation of culture medium from the serum of nonpregnant animals previously exposed to test compounds (Schmid et al., 1982).

Materials

Adult rats
Polychlorinated biphenyls (PCB, Araclor 1254)
Corn oil
0.05 mM potassium phosphate buffer, pH 7.4

3-ml syringe and 18-G needle
Dounce homogenizer with Teflon pestle
Refrigerated centrifuge

NOTE: All solutions and equipment coming into contact with live cells must be sterile, and aseptic technique should be used accordingly.

1. Dilute Araclor 1254 in corn oil to a concentration of 500 mg/ml. Using a 18-G needle attached to a syringe, give each animal an i.p. injection of 500 mg/kg (1 ml/kg) 5 days before sacrifice.

   The Araclor acts as an oxidase inducer in the liver and will increase the metabolic activity of the S-9 preparation.

2. On day 5 after induction, sacrifice rat by cutting the thorucic aorta under deep anesthesia and remove liver.
3. Using a Dounce homogenizer with a tight-fitting Teflon pestle, homogenize rat livers in 2 vol of ice-cold potassium phosphate buffer, pH 7.4, on ice.
4. Centrifuge 20 min at 9000 × g, 4°C. Decant the supernatant into a sterile vessel on ice.

   The supernatant (S-9) used as the enzyme source is added to culture flasks at a concentration of 5.3 µl/ml. Cofactors are added including NADPH (5×10^{-4} M) as the electron donor and G6P (10^{-3} M) to assure maintenance of saturating NADPH concentrations. This system has been shown to significantly enhance the embryotoxicity of cyclophosphamide (Fantel et al., 1979) while reducing that of cytochalasin D (Fantel et al., 1981).

REAGENTS AND SOLUTIONS

Use Milli-Q-purified water or equivalent for all recipes and in all protocol steps. For common stock solutions, see ***APPENDIX 2A****; for suppliers, see* ***SUPPLIERS APPENDIX****.*

Embryo culture medium

A variety of medium compositions have been used to culture rat embryos. Rat serum (see Support Protocol 1) diluted up to 50% with Hanks' balanced salt solution (HBSS), or culture media such as Weymouth's work well (Bechter et al., 1991; Terlouw et al., 1993), but other sera, including cow (Klug et al., 1985), monkey

continued

(Klein et al., 1982), and human (Fantel et al., 1979; Chatot et al., 1980; Abir et al., 1993) have been used effectively. Fantel et al. (1979) and Chatot et al. (1980) reported considerable variability in the ability of sera from different individuals to support the growth of rat embryos. Most workers add penicillin (100 U/ml) and streptomycin (50 μg/ml) to media.

Fetal culture medium

Medium employed for fetuses may be determined by the gestational stage of the culture, with the percentage of autologous serum decreasing with age. For gd 12 and 13 cultures, medium composition may be identical to that described for embryos (see recipe for embryo culture medium), although serum concentrations as low as 25% are effective on gd 13. For gd 14, no serum is required and embryos are grown successfully in Earle's balanced salt solution (EBSS) supplemented with 0.7% bovine serum albumin (BSA). Medium volume is in the range of 12.5 ml/fetus and penicillin (100 U/ml) and streptomycin (50 μg/ml) are usually added.

COMMENTARY

Background Information

Explantation and culture of whole rodent embryos, developed largely in the laboratory of Dennis New at Cambridge in the 1960s, and 1970s, has proven to be a valuable tool for mechanistic studies in developmental toxicology as well as for teratogen screening by industry. These methods support normal growth and development during postimplantation stages, including most of organogenesis, eliminating the gravida from consideration. This permits exposure of embryos to precisely defined amounts of precisely defined agents at precisely defined developmental stages. Animal maintenance costs tend to be less, as study periods are typically reduced from the complete 21- to 22-day gestation period in rats to 1 to 2 days from exposure to autopsy.

Additional savings derive from the ability to carefully examine and precisely age-match subjects and controls prior to treatment, eliminating a potential confounding variable. Another confounder may be reduced by eliminating nonviable or moribund embryos at the outset of study. Careful age-matching and culling can reduce the total number of animals required for assay. The volume of medium used in cultures ranges from 1 ml/embryo for early postimplantation stages to ~12 ml/fetus on gd 14. Because these volumes, especially those used at earlier stages, are significantly lower than that of the typical gravida, amounts of expensive test compounds may be greatly reduced.

The inherent precision and cost savings of whole-embryo culture methods must be balanced against their limitations. These include relative increases in the time and technical skill required to explant embryos, restricted gestational stage compatible with growth in vitro, the relatively brief culture periods that are practically attainable, required exposure to nonphysiologic oxygen concentrations and, in many cases, inability to expose conceptuses to the full spectrum and proper concentrations of maternally formed metabolites. Despite the inclusion of metabolic systems (S-9 supernatant; see Support Protocol 2), exposure profiles may poorly approximate those that occur in vivo. Additionally, the nonpolar nature of many pharmaceuticals may limit concentrations to which embryos can be exposed and may require the use of additional vehicles such as ethanol or dimethylsulfoxide for solublization. Perhaps the greatest drawback is the inability of culture systems to support growth beyond early fetal stages. As a consequence of these limitations, outcomes of in vitro exposures may fail to accurately represent the results of in vivo exposures, and term effects must be extrapolated from pathological and biochemical findings at earlier gestational stages. As discussed below, the palate of abnormal outcomes of whole-embryo culture exposures is relatively limited, with disparate agents often inducing similar defects, in contrast to their in vivo activity.

Whole-embryo culture in industrial teratogen screening

The cost and time savings associated with short-term tests are useful to industry. These screens enable investigators to determine the embryotoxic and/or teratogenic potential of new drug candidates during early phases of

drug development. They can help limit costly in vivo testing to compounds that demonstrate the lowest probability of adverse effects. Candidate agents can then undergo standard animal testing prior to clinical trials and drug registration. In order to employ a screening system for compound selection, it should be validated for all compound classes in a given pipeline. It is especially important that methodologies and animal strains be held constant in screening studies. In these ways, it is possible to employ accumulated historical control and experimental data (Bechter and Terlouw, 1990) and compare test results from different experiments for compound development.

Critical Parameters

Temporal considerations

Embryo culture is temporally circumscribed, as growth beyond gd 15 has not, to the authors' knowledge, been performed successfully. Furthermore, culture for more than 48 hr is impractical and rarely performed since both medium and gas changes are required. In order to cover teratogenically sensitive stages of organogenesis, exposure studies are generally performed on gd 8, 9, or 10. The consequences of these limitations are that (1) defects induced by an agent at stages before or after the culture period may be missed; (2) defects that might have been induced by exposure during the culture period may not be evident at the end of the culture period; and (3) defects that might have been repaired prior to parturition may be observed at the end of the culture period. On the other hand, absent or incomplete repair may serve as an index of potential developmental toxicity and provide mechanistic insight.

If cultures are started in the morning to midday, culture medium must be replaced in the middle of the night. This is most easily accomplished by preparing two sets of flasks at the outset of the experiment. Fetuses can then be transferred later to the second set of flasks using a small stainless steel chemical spoon. Medium must be fully flushed with 95% O_2, a process taking 20 to 30 min.

Biotransformation, pharmacokinetics, pharmacodynamics

It may not be possible to expose embryos in culture to the full range of drug metabolites in proper concentrations during appropriate stages of gestation. As noted, several schemes have been developed that enable the incorporation of some aspects of drug metabolism, and these protocols have been useful, to an extent, in determining the role of extraembryonic biotransformation. Potential, practical problems are considered below.

A more recent experimental approach to the inclusion of biotransformation in culture was the addition of "conditioned" medium used previously for culture of hepatocytes prepared from the livers of adult animals. By harvesting medium from hepatocyte cultures at different culture times (sequential cultures) these methods enable study of the kinetics of toxification and detoxification of test compounds (Bechter et al., 1989). Other investigators have directly incorporated hepatocytes into embryo culture (coculture). Because of the experimental nature of these systems, details have been omitted. Interested readers are referred to papers by Oglesby et al. (1992) and Ozolins et al. (1995).

Medium prepared from the serum of treated animals may be unable to support embryonic growth even in the absence of the parent compound. Additionally, short-lived and reactive metabolites may be lost during the time required for medium preparation, and heat inactivation of serum may alter parent compounds and/or metabolites. Hepatic preparations tend to be relatively unstable when combined with cofactors (S-9) in culture and short-lived metabolites may be produced at the beginning of culture but not later when homogenates are no longer active.

Because teratogenic metabolites may be absent at sensitive times, other approaches have been developed. For example, by adding conditioned medium from hepatocyte cultures containing drug and metabolites to culture medium (sequential hepatocyte/whole-embryo culture, Bechter et al., 1989), metabolites may be present during the extended culture period. Metabolic capacities of the embryo, per se, and especially those of the yolk sac, are active in vitro during the culture period (Bechter and Terlouw, 1990; Terlouw and Bechter, 1992, 1993; Jones et al., 1993) and such metabolism *may* result in the formation of teratogenically relevant metabolites. Finally, because there is little information on the transfer of drugs and their metabolites from mother to fetus, those metabolites generated by these various systems may poorly represent actual exposures in vivo.

An important consideration when comparing in vitro to in vivo pharmacokinetics is the stability of metabolites under culture conditions. Furthermore, there is evidence that em-

bryos undergo some degree of adaptation to culture conditions (Brown et al., 1991), but little is known about changes in the visceral yolk sac, the primary transfer tissue. Changes in this tissue, for example, could influence the pharmacokinetics of xenobiotics. Direct experimentation is necessary to evaluate whether in vitro pharmacokinetics adequately model in vivo processes.

Culture conditions

A number of protocols have been developed to enable the warming, oxygenation, and circulation of embryo culture medium. A scheme initially adapted by New (1967) attached the embryos by remnants of Reichert's membrane to gauze mats set in glass tubes. The circulation of medium past the stationary embryos was powered by rising gas bubbles. The "Plasmom" of Robkin and Shepard (1972) employed a peristaltic pump that circulated medium through a bundle of silicon rubber tubes. These tubes were suspended in a warm bath of sterile distilled water through which the desired gas mixture bubbled. Although no longer in widespread use, these methods enabled investigators to observe and photograph embryos and to monitor physiological changes resulting from study exposures.

Today, most investigators use one of several types of motorized equipment to roll or rotate culture flasks. These include powered roller bars for round bottles and disks to which smaller test tubes or scintillation vials may be clipped and rotated. Flasks must be placed inside an incubator set to maintain temperatures between 37° and 38.5°C. Various types of glass or plastic flasks may be used, but glass is used most commonly because its wetting properties support exchange of gas with the medium. Culture vessels must have gas-tight seals. They can range from the size of small test tubes or scintillation counter vials containing 1 or 2 embryos and several milliliters of medium to 125-ml (serum) bottles containing up to a dozen embryos in 10 to 12 ml of medium. Most investigators use a ratio of ~1 ml of medium per embryo during organogenesis stages.

The gas phases required for successful embryo and fetal culture are stage-specific, and there is compelling evidence that abnormal growth and/or development result under either hypoxic or hyperoxic conditions (Morriss and New, 1979; Miki et al., 1988; Chen et al., 1999). There are several different protocols for gassing culture vessels but all include 5% CO_2 and ≤95% O_2; the balance of the mixture consists of N_2. Culture on gd 9 requires 5% O_2 while gd 10 cultures utilize 20% O_2 and gd 11 and later generally utilize 95% O_2. Some investigators employ an intermediate O_2 concentration of 40% on late gd 10. Gas is usually allowed to flow on top of the medium in large flasks via a Pasteur pipet for 10 to 20 min and in smaller flasks for 20 to 30 sec. In all instances, care must be taken to avoid bubbling the medium, which can oxidize and denature proteins. After they are flushed, bottles are tightly sealed and set to rotate in the incubator. If cultures are continued for more than 24 hr, they must be reflushed with the gas mixture appropriate for the new stage of development. Cultures generally run from 24 to 48 hr.

Scoring systems

Studies of developmental toxicity in rat embryos in vitro frequently employ a morphologic scaling system such as that devised by Brown and Fabro (1981). Although this system is useful because of common associations between developmental delay and congenital defects, and because it enables inter-laboratory comparison, it has a number of potential drawbacks. First, subtle or internal defects not associated with delays may be missed. Second, as discussed below, agents that disturb structure or function of the yolk sac in vitro may yield results that are not representative of effects in vivo. Third, reduction in growth may be transient, with recovery occurring in vivo after the culture period. Finally, growth retardation may not be observed in the in vivo syndrome of effects.

Yolk sac dysfunction

During organogenesis stages, rat embryos are highly dependent on the visceral yolk sac for maternal-embryonic transfers. Beginning on or after gd 11, the role of the chorioallantoic (labyrinthine) placenta assumes increasing importance in these functions, but since the growth, development, and function of this latter structure cannot be supported by culture methods, the vitelline placenta must perform most or all of the transfer requirements of growth and development. Under control conditions, transfer is adequate to maintain normal rates of growth and differentiation. Under the various stresses imposed by xenobiotic exposures, and without the benefit of the (potential) redundancy associated with the simultaneous function of the yolk sac and chorioallantoic placen-

tas, transfer may become insufficient. Furthermore, as the first cell layer to be exposed to test agents, the yolk sac in vitro may be especially vulnerable to their activities. Transfer differences between placental structures may be responsible for an abnormal exposure profile of cultured embryos.

Studies published during the past 20 years have employed whole-embryo culture techniques to investigate the teratogenic activities of a wide variety of chemical and physical exposures. Despite the diverse nature of these exposures, a strikingly short list of dysmorphic outcomes is commonly reported. These include reduced outgrowth of the prosencephalon/telencephalic vesicle(s), edema in the area of the rhombencephalon, abnormal flexion often manifest as failure of conversion from dorsal to ventral curvature and failure of neural tube closure. These common features may primarily represent deficits in those structures developing during the relatively restricted period amenable to whole-embryo culture. Alternatively, but not exclusively, they may represent deficits and defects resulting from inadequate transfer to and from the embryo. Although these changes are used as indices of teratogenic potential, the outcomes of in vivo exposures may well be different (see Beaudoin and Fisher, 1981).

Various inhibitors of yolk-sac function have been shown to result in abnormal development, reduced growth, or embryonic death in whole-embryo culture, including anti–visceral yolk sac serum (Freeman et al., 1982; Beckman et al., 1990, 1991; Freeman and Brown, 1994), suramin (Freeman and Lloyd, 1986), and leupeptin (Freeman and Lloyd, 1983). When examined in vivo, the effects of these agents on development mirrored those seen in vitro (Freeman and Lloyd, 1983, 1986; Brent et al., 1990; Beckman et al., 1991). Each of these agents inhibits the critical role of the visceral yolk sac in providing nutrition to the developing embryo. Anti–visceral yolk sac serum (Freeman et al., 1982; Beckman et al., 1991; Freeman and Brown, 1994) and suramin (Freeman and Lloyd, 1986) inhibit pinocytosis in the visceral yolk sac. Leupeptin (Freeman and Lloyd, 1983) and aurothiomalate (Freeman and Lloyd, 1986) inhibit lysosomal proteolysis. The resulting abnormal morphology very often includes reduced development of the CNS, edema, failure of conversion from dorsal to ventral curvature, failure of neural tube closure, prosencephalic hypoplasia, rhombencephalic edema, and misplaced and/or small somites. These findings are common in whole-embryo culture studies and may not be representative of in vivo exposures.

Hyperoxia

As noted, the oxygen requirements for whole-embryo cultures are pragmatically based. Consequently, with the possible exception of culture on gd 8 and 9, oxygen concentrations used are well above physiologic ranges for most tissues. Boveris et al. (1972) have demonstrated significantly increased formation of reactive oxygen species (ROS) in tissues under hyperoxic conditions, a process that might be favored by the high reducing potentials and low antioxidant activities of developing tissues (Allen and Venkatraj, 1992). It is therefore reasonable to expect that culture conditions may impose considerable oxidative stress on developing embryos and their membranes—stress that might increase their sensitivity to xenobiotic agents or that might exert outright toxicity. Hyperoxia may therefore represent another explanation of the common "defects" reported in whole-embryo culture experiments. Fantel (1996) has reviewed this subject, and unpublished studies by Fantel and coworkers have shown dramatic formation of superoxide anion radical by the yolk sacs of control fetuses cultured on gd 14. This subject requires further study.

Anticipated Results

A minimum of 90% of control embryos and fetuses should be viable at the end of the culture period, and no gross defects should be evident. Information on expected embryonic growth parameters can be found in Brown and Fabro (1981). Experimental conceptuses should be expected to demonstrate concentration-dependent decreases in viability, as defined by active heart beat and yolk sac circulation, and increases in growth retardation and treatment-related malformations. Percentages of embryos failing to convert from dorsal to ventral flexion, and reductions in somite count and greatest length should also be responsive to concentrations of test agents.

Time Considerations

The time taken to explant rat embryos is strongly dependent on the technical skill and experience of the investigator or technician. Rat serum is generally collected and stored frozen prior to the day of the experiment, but many laboratories collect and process blood from gravidas to use in future experiments. If this step is added, an experienced technician should

be able to explant and treat 4 litters in 4 hr. As noted, culture intervals generally range from 24 to 48 hr. The time required for analysis of the results of exposure are entirely dependent on the parameters studied and the methods used. Thus, procedures such as photography, histology, autoradiography, and enzyme assay will lengthen this phase of study.

Literature Cited

Abir, R., Ornoy, A., Hur, H.B., Jaffe, P., and Pinus, H. 1993. IgG exchange as a means of partial correction of anomalies in rat embryos in vitro, induced by sera from women with recurrent abortion. *Toxicol. In Vitro* 7:817-826.

Allen, R.G. and Venkatraj, V.S. 1992. Oxidants and antioxidants in development and differentiation. *J. Nutr*. 122:631-635.

Barber, C.V., Carda, M.B., and Fantel, A.G. 1993. A new technique for culturing rat embryos in vitro between gestation day 14 and 15. *Toxicol. In Vitro* 7:695-700.

Beaudoin, A.R. and Fisher, D.L. 1981. An in vivo/in vitro evaluation of teratogenic action. *Teratology* 23:57-61.

Bechter, R. and Terlouw, G.D.C. 1990. Xenobiotic metabolism in the isolated conceptus. *Toxicol. In Vitro* 4:480-492.

Bechter, R., Bouis, P., and Fischer, V. 1989. Primary hepatocyte culture as an activating system for xenobiotica tested in the rat whole embryo in vitro. *In* Alternative Methods in Toxicology. Vol. 7. In Vitro Toxicology New Directions (A.M. Goldberg and M.L. Principe, eds.) pp. 313-326. Mary Ann Liebert, New York.

Bechter, R., Terlouw, G.D.C., Lee, Q.P., and Juchau, M.R. 1991. Effects of QA 208-199 and its metabolite 209-668 on embryonic development in vitro after microinjection into the exocoelomic space or into the amniotic cavity of cultured rat conceptuses. *Teratog. Carcinog. Mutagen*. 11:185-194.

Beckman, D.A., Pugarelli, J.E., Jensen, M., Koszalka, T.R., Brent, R.L., and Lloyd, J.B. 1990. Sources of amino acids for protein synthesis during early organogenesis in the rat. 1. Relative contributions of free amino acids and of proteins. *Placenta* 11:109-121.

Beckman, D.A., Pugarelli, J.E., Koszalka, T.R., Brent, R.L., and Lloyd, J.B. 1991. Sources of amino acids for protein synthesis during early organogenesis in the rat. 2. Exchange with amino acid and protein pools in embryo and yolk sac. *Placenta* 12:37-46.

Boveris, A., Oshino, N., and Chance, B. 1972. The cellular production of hydrogen peroxide. *Biochem. J*. 128:617-630.

Brent, R.L., Beckman, D.A., Jensen, M., and Koszalka, T.R. 1990. Experimental yolk sac dysfunction as a model for studying nutritional disturbances in the embryo during early organogenesis. *Teratology* 41:405-413.

Brown, N.A. and Fabro, S. 1981. Quantitation of rat embryonic development in vitro: A morphological scoring system. *Teratology* 24:65-78.

Brown, N.A., Clarke, D.O., and McCarthy, A. 1991. Adaptation of postimplantation embryos to culture: Membrane lipid synthesis and response to valproate. *Reprod. Toxicol*. 5:245-53.

Chatot, C.L., Klein, N.W., Piatek, J., and Pierro, L.J. 1980. Successful culture of rat embryos in human serum: Use in the detection of teratogens. *Science* 207:1471-1473.

Chen, E.Y., Fujinaga, M., and Giaccia, A.J. 1999. Hypoxic microenvironment within an embryo induces apoptosis and is essential for proper morphological development. *Teratology* 60:215-225.

Fantel, A.G. 1996. Reactive oxygen species in developmental toxicity: Review and hypothesis. *Teratology* 53:196-217.

Fantel, A.G., Greenaway, J.C., Juchau, M.R., and Shepard, T.H. 1979. Teratogenic bioactivation of cyclophosphamide in vitro. *Life Sci.* 25:67-72.

Fantel, A.G., Greenaway, J.C., Shepard, T.H., Juchau, M.R., and Selleck, S.B. 1981. The teratogenicity of cytochalasin D and its inhibition by drug metabolism. *Teratology* 23:223-231.

Freeman, S.J. and Brown, N.A. 1994. Inhibition of yolk sac function in late gastrulation rat conceptuses as a cause of teratogenesis: An in vivo/in vitro study. *Reprod. Toxicol*. 8:137-143.

Freeman, S.J. and Lloyd, J.B. 1983. Inhibition of proteolysis in rat yolk sac as a cause of teratogenesis. Effects of leupeptin in vitro and in vivo. *J. Embryol. Exp. Morphol*. 78:183-193.

Freeman, S.J. and Lloyd, J.B. 1986. Evidence that suramin and aurothiomalate are teratogenic in rat by disturbing yolk sac–mediated embryonic protein nutrition. *Chem. Biol. Interact*. 58:149-160.

Freeman, S.J., Brent, R.L., and Lloyd, J.B. 1982. The effect of teratogenic antiserum on yolk-sac function in rat embryos cultured in vitro. *J. Embryol. Exp. Morphol*. 71:63-74.

Jones, C., Greiner, B., Wächter, F., Terlouw, G.D.C., and Bechter, R. 1993. An immunohistochemical investigation into the presence and localization of cytochrome P-450 isozymes in organogenesis-stage rat conceptal tissue. *Toxicol. In Vitro* 7:685:693.

Kitchin, K.T., Schmid, B.P., and Sanyal, M.K. 1981. Teratogenicity of cyclophosphamide in a coupled microsomal activating/embryo culture system. *Biochem. Pharmacol.* 30:59-64.

Klein, N.W., Plenefisch, J.D., Carey, S.W., Fredrickson, W.T., Sackett, G.P., Burbacher, T.M., and Parker, R.M. 1982. Serum from monkeys with histories of fetal wastage causes abnormalities in cultured rat embryos. *Science* 215:66-69.

Klug, S., Lewandowski, C., and Neubert, D. 1985. Modification and standardization of the culture of early postimplantation embryos for toxicological studies. *Arch. Toxicol.* 58:84-88.

Kochar, D.M. 1975. The use of in vitro procedures in teratology. *Teratology* 11:273-287.

Miki, A., Fujimoto, E., Ohsaki, T., and Mizoguti, H. 1988. Effects of oxygen concentration on functions of the rat visceral yolk sac endoderm in vitro. A histochemical study using whole-embryo culture technique. *Kobe J. Med. Sci.* 34: 55-70.

Morriss, G.M and New, D.A.T. 1979. Effect of oxygen concentration on morphogenesis of cranial neural folds and neural crest in cultured rat embryos. *J. Embryol. Exp. Morphol.* 54:17-35.

New, D.A.T. 1966. Development of rat embryos cultured in blood sera. *J. Reprod. Fertil*. 12:509-524.

New, D.A.T. 1967. Development of explanted rat embryos in circulating medium. *J. Embryol. Exp. Morphol*. 17:513-525.

New, D.A.T. 1971. Methods for the culture of post-implantation rodents. *In* Methods in Mammalian Embryology (J.C. Daniel, ed.) pp. 305-319. W.H. Freeman, San Francisco.

New, D.A.T. 1979. Whole-embryo culture and the study of mammalian embryos during organogenesis. *Biol. Rev*. 53:81-122.

Oglesby, L.A., Ebron-McCoy, M.T., Logsdon, T.R., Copeland, F., Beyer, P.E., and Kavlock, R.J. 1992. In vitro embryotoxicity of a series of para-substituted phenols: Structure, activity, and correlation with in vivo data. *Teratology* 45:11-33.

Ozolins, T.R., Oglesby, L.A., Wiley, M.J., and Wells, P.G. 1995. In vitro murine embryotoxicity of cyclophosphamide in embryos co-cultured with maternal hepatocytes: Development and application of a murine embryo-hepatocyte co-culture model. *Toxicology* 102:259-274.

Robkin, M.A. and Shepard, T.H. 1972. In vitro culture of somite stage rat embryos: A new technique for maintaining growth and continuously monitoring heart rate. Applications in metabolic and teratologic studies. *In Vitro* 8:151-160.

Schmid, B.P., Trippmacher, A., and Bianchi, A. 1982. Teratogenicity induced in cultured rat embryos by the serum of procarbazine treated rats. *Toxicology* 25:53-60.

Terlouw, G.D.C. and Bechter, R. 1992. Comparison of the metabolic activity of yolk sac tissue in the whole embryo and isolated yolk sac culture. *Reprod. Toxicol.* 6:85-92.

Terlouw, G.D.C. and Bechter, R. 1993. Cytochrome P-450-dependent biotransformation of QA 208-199 in cultured rat conceptuses. *Toxicol. In Vitro* 7:247-258.

Terlouw, G.D.C., Namkung, M.J., Juchau, M.R., and Bechter, R. 1993. In vitro embryotoxicity of *N*-methyl-N-7-propoxynaphthalene-2-ethylhy droxylamine QAB: Evidence for *N*-dehydroxylated metabolite as a proximate dysmorphogen. *Teratology* 48:431-439.

Zhao, J., Krafft, N., Terlouw, G.D.C., and Bechter, R. 1993. A model combining the whole embryo culture with human liver S-9 fraction for human teratogenic prediction. *Toxicol. In Vitro* 7:827-831.

Contributed by Alan G. Fantel
University of Washington
Seattle, Washington

Rudolf Bechter
Novartis Pharma Ltd.
Basel, Switzerland

David Beckman
Novartis Pharmaceuticals Corporation
East Hanover, New Jersey

Micromass Cultures in Teratology

Interest in the development and application of in vitro models of fetal development has arisen for several reasons. First, well validated in vitro models can serve as an alternative to in vivo testing, thus reducing the number of animals required for a given experiment. Second, in vitro models allow mechanistic research that is otherwise technologically difficult or impossible. Third, compared with in vivo alternatives, in vitro models offer the promise of faster and cheaper screening capabilities for potential teratogenic compounds. Recognition of these strengths led to the development and initial characterization of primary cell cultures derived from embryonic neuroepithelial cells and limb bud cells in the early 1980s (Wilk et al., 1980; Sawyer and Goetinck, 1981; Flint and Ede, 1982; Solursh et al., 1982; Flint, 1983; Flint and Orton, 1984).

Because they are derived from primary cell suspensions of undifferentiated midbrain (mesencephalic) neuroepithelium and forelimb chondrocytes, micromass cultures have been used in the study of developmental cell cycle kinetics and regulation, which are poorly modeled by transformed cell lines. Micromass cultures have also been used to examine the cellular and molecular response to known teratogenic compounds, including analysis of protein and gene expression, intracellular cation signaling, redox status, necrosis and apoptosis, and differentiation (Flint et al., 1984; Brown et al., 1986a,b; Ribeiro and Faustman, 1990; Walum and Flint, 1990; Whittaker and Faustman, 1991, 1992; Sweeney et al., 1992; Whittaker et al., 1993; Ponce et al., 1994; Seeley and Faustman, 1995; Ou et al., 1999a,b). As these studies demonstrate, micromass cultures can be successfully examined using a range of experimental tools, including flow cytometry and attached cell laser cytometry, gel electrophoresis, and light, electron, and immunofluorescence microscopy.

In this unit, methods for isolating embryos, performing microdissection, and plating cultures of midbrain neuroepithelial cells (also termed central nervous system, or CNS, cells) and limb bud (LB) chondrocytes are described (see Basic Protocol). In the Basic Protocol, it is assumed that the researcher would like to conduct experiments on the cells as they grow in culture. In the Alternate Protocol, the researcher may choose to treat the pregnant rat, isolate the embryos, and derive cultures. The objective of the Alternate Protocol is to observe the effects of maternal treatment on the growth characteristics of the cultured cells. Both protocols can provide valuable mechanistic or screening information to the investigator interested in examining the effects of environmental factors on growth and development of the nervous system and the limb. Although variations on the techniques described here are encouraged, the investigator should first obtain an understanding of the fundamental growth characteristics of these cells in culture under the conditions described below.

NOTE: All protocols using live animals must first be reviewed and approved by an Institutional Animal Care and Use Committee (IACUC) and must follow officially approved procedures for the care and use of laboratory animals.

PREPARING NEUROEPITHELIAL AND LIMB BUD CELL MICROMASS CULTURE

BASIC PROTOCOL

This protocol is used to derive micromass cultures of primary neuroepithelial cells and limb bud chondrocytes from normal (untreated) female rats. The purpose of experiments conducted using this protocol is somewhat different than that of experiments conducted using the Alternate Protocol, which is designed to examine the maternally mediated effects on embryonic cell growth characteristics.

Contributed by Rafael A. Ponce

Current Protocols in Toxicology (2001) 13.3.1-13.3.14

The basic method for culturing both primary midbrain (CNS) and limb bud (LB) cells is the same. The only major point of difference is the final plating concentration. The protocol is broken down into the following major stages: setup of dissecting room and microdissection hood, dam sacrifice and dissection, embryo isolation, embryo microdissection, tissue dissociation, cell counting and cell plating, and medium addition and in vitro treatment.

NOTE: All solutions and equipment coming into contact with living cells must be sterile, and aseptic technique should be used accordingly.

NOTE: All culture incubations should be performed in a humidified 37°C, 5% CO_2 incubator unless otherwise specified.

Materials

70% ethanol
Earle's balanced salt solution (EBSS; Life Technologies) with and without calcium and magnesium (CMF-EBSS), sterile, 37°C
4 to 8 time-mated, gestation day 12 to 12.5 rats (where gestation day 12 represents the 12th day after confirming a positive pregnancy)
50% (v/v) heat-inactivated horse serum (see recipe), 37°C
Trypsin solution (see recipe), 37°C
Sterile culture medium (see recipe), 37°C
Collagen solution (see recipe, optional)

Sterile dissecting instruments: 2 dissecting forceps and 1 pair tissue dissecting scissors (straight operating scissors)
Sterile 100-mm petri dishes
Plastic waste bags
Disposable absorbent pads
Laminar flow hood
Dissecting microscope(s) with light source
Sterile microdissecting instruments (1 to 2 sets):
  2 Dumont (watchmaker's) forceps, pattern no. 5 (Fine Science Tools)
  Pair microdissecting Wecker scissors (Fine Science Tools)
  Slotted Moria spoon (Fine Science Tools)
Data recording sheet
15-ml sterile tubes, labeled (labeled as follows: CNS1, CNS2, CNS3, LB1, LB2, LB3, CM, trypsin)
Sterile incubator trays
Pulled-glass pipets (i.d. ~0.7 mm), sterile
10-ml disposable syringes, sterile
13-mm Swinney filters (Millipore) with a 10-μm nylon mesh membrane filter (Spectrum), sterile
Hemacytometer and hand-held counter
Repeater pipettor (Eppendorf)
Sterile 0.5-ml tips for repeater pipettor
35 × 10–mm sterile primaria-coated tissue culture dishes (Falcon)

Set up dissecting room and microdissecting hood

1. Prepare sacrifice area with sterile dissecting instruments, 70% ethanol, two 100-mm petri dishes, and plastic waste bags. Prepare area by thoroughly cleaning surfaces and wipe area with 70% ethanol.

   The room where the dams will be sacrificed and dissected must be separate from the room where the dams are housed.

Preparation of the dissecting room and microdissecting hood prior to initiating animal sacrifice will greatly increase the efficiency of the protocol and will help ensure a high-quality cell culture. Separate rooms for sacrifice and the microdissection will help reduce the possibility of contamination in the cell culture.

2. Lay out a disposable absorbent pad or other surface on which the dam will be dissected. Make sure dissecting area is well lit.
3. Set up microdissecting area by wiping down interior surfaces of the laminar flow hood. Wipe down dissecting microscopes and pipettors with 70% ethanol. Lift sash of hood so that work can be done inside hood with dissecting microscopes.

   Procedures requiring use of dissecting microscopes will be conducted with the hood open. Although this disrupts the air flow in the hood, the hood should be relatively free of contamination during microdissection procedures.

4. Place 1 to 2 dissecting microscope(s) in hood along with the light source and 1 to 2 sets of sterile microdissecting instruments. Place a sterile 250-ml beaker in the hood for liquid waste.
5. Fill five 100-mm petri dishes half way with sterile EBSS. Place one dish on the stage of each dissecting microscope.

   The lid of the petri dish will be used to collect waste tissue, while the dish will be used to isolate the embryo from the uteri.

Sacrifice dam and dissect

6. Humanely sacrifice dams one at a time. Record pregnancy status, litter size, resorptions, and other observations.

   The author typically uses CO_2 asphyxiation to euthanize the dams. See Critical Parameters and Troubleshooting for discussion of alternative methods.

7. Lay dam on its back on a disposable pad with the hind feet closest to the researcher. Cleanse abdomen with 70% ethanol, which helps reduce the amount of loose fur that can fly around and get into the peritoneal cavity. Using dissecting forceps, grip a fold of skin at the midline along the lower abdomen (the base) and gently lift to create a larger skin fold that can be cut using dissecting scissors. Make a V-shaped cut through the skin and underlying muscles. Using this cut as a starting place, expose the peritoneal cavity by cutting along midline from the pubic symphysis to the lungs. Displace intestines to the side to reveal the uterus.

   Some lateral cuts at the base of the abdomen may be useful to help expose the organs. For a right-handed person, it is easier to cut with the right hand while gripping the forceps in the left hand.

8. Using dissecting forceps, locate each horn of the uterus.

   The uterus joins the vagina at the base of the pelvis.

   Locating the uterine horns can be accomplished by gently probing around the intestines with the sides of the forceps on both the left and right side of the peritoneal cavity.

9. Gently pull uterus away from surrounding organs to allow easier inspection. Be careful not to rupture intestines or other organs during this process.
10. By gently lifting the base of the uterus with dissecting forceps, identify the attachment point, and cut it with dissecting scissors. Without releasing the uterus, continue to lift the uterus by the cervical stump upward to clear the uterus from the peritoneal cavity and identify the last embryo on either side of the uterus.

    Take care to create enough tension such that the uterus can be pulled by the cervical stump so as to identify the attachment points along either side, but not so much that the uterus is torn or damaged.

11. Remove associated fat using a second set of dissecting forceps. After identifying the last embryo on either side of the uterus, remove the uterus from the dam.
12. Place uterus in a sterile petri dish and, if working in a team of two, take into the microdissection area in the laminar flow hood.

    After isolating the uterus from the dam, it should be taken to the microdissection hood for immediate microdissection. If working in a team of two, one individual can perform the sacrifice and uterine isolation while the other can prepare the microdissection hood and begin the microdissection. If one individual is performing the experiment, he/she should sacrifice all dams and isolate the uteri prior to beginning microdissection. Typically, one individual can manage 8 dams at a time, though this requires substantial experience and efficiency in order to ensure a high-quality cell culture.

13. Place dam in plastic bag for disposal.
14. Repeat steps 6 to 12 until all dams have been sacrificed and all uteri collected.

Isolate embryo

15. Rinse uterus three times in sterile EBSS and place in a petri dish containing EBSS on the dissecting microscope stage.
16. Using 2 Dumont (watchmaker's) forceps, pattern no. 5, gently tear open the uterus at each site to release the deciduum containing the embryo (see Fig. 13.3.1). First, hold the uterus between two implantation sites with Dumont forceps (the holding forceps) in one hand. Align the uterus so that the muscle edge of the uterus is at the top (antimesometrial side). Next, poke a hole through the muscle layer with the other Dumont forceps (tearing forceps) in the other hand.

    The hole should be next to the holding forceps.

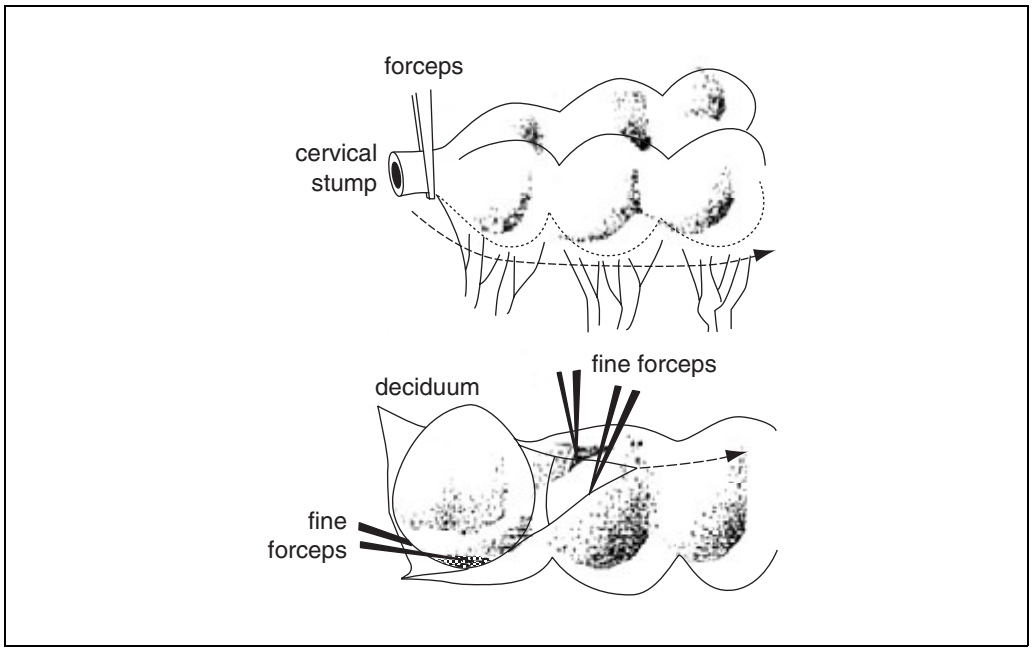

Figure 13.3.1 Removal of uterine horn from dam (top) can be accomplished by cutting the cervix and lifting the uterine horn by the cervical stump. Using a second set of forceps, gently tear away the uterine network to release the uterus (dashed line with arrow). Remove each deciduum from the uterine horn (bottom) using fine forceps. Use the set of fine forceps in the left hand to hold the uterus along the antimesometrial side at one side of the deciduum (in the case as shown, on the left side), and open the uterus along the top of the site by tearing from left to right with the forceps in the right hand. (Figure adapted from Strum and Tam, 1993).

17. Using the tearing forceps, tear away the muscle by pulling the muscle from the hole near the holding forceps across the top of the deciduum to the other side of the implantation site. Dislodge the deciduum from the uterine wall by gently teasing the deciduum away from the uterine tissue using the middle part of the forceps rather than the tips.

    Removal of the decidua may be made easier by starting at the cervical stump and working outward along either horn.

18. Place waste tissue in the petri dish lid throughout this procedure to minimize clutter in the dissecting dish.

19. Repeat steps 15 to 18 until all decidua are removed.

    Embryos from multiple uteri can be combined to generate a homogeneous cell culture unless there is an experimental reason to keep embryos from individual dams separated.

20. Fill 1 to 2 petri dishes (one/person) half way with 50% heat-activated horse serum/EBSS, 37°C, and place on the dissecting microscope stage next to the petri dish containing embryos.

21. Transfer decidua containing the embryos to 50% heat-activated horse serum/EBSS using the slotted Moria spoon. Include both embryos that were still in the embryonic sac and any that were inadvertently released by embryonic sac rupture.

22. Using two forceps, release embryos from the surrounding tissue. Gently hold the decidua along the edge of the broadest end with both sets of Dumont forceps in opposition. Open the deciduum by gently tearing laterally to reveal the embryo contained in the yolk sac.

    In most cases, use of this technique will allow the embryo to fall into the 50% heat-inactivated horse serum/EBSS. Be careful not to grasp too deeply with the forceps, as this will rupture the underlying yolk sac and possibly damage the embryo.

23. After removing the decidua from all embryos, release each embryo by teasing them out the yolk sac with the forceps. Discard decidua and yolk sac membranes in waste lid for disposal.

24. Repeat steps 22 to 23 until all embryos are freed.

Microdissect embryo

While the described steps detail the methods for collecting and plating both CNS neuroepithelial cells and limb bud cells, this procedure can be modified to plate only one or the other cell type.

25. Use a glass pipet and bulb to remove some of the 50% heat-inactivated horse serum solution and gently vacuum away tissue debris.

    If necessary transfer the embryos to fresh serum/EBSS. This will make the cell preparation and tissue isolation cleaner.

    The researcher will have to use trial and error to determine how much solution to remove. If there is too much liquid, the embryos will float and make microdissection difficult. If there is too little liquid, manipulation of the embryos will be difficult.

26. Use microdissecting scissors and forceps for tissue isolation. For a right-handed person, hold scissors in the right hand and forceps in the left.

    Scissors should be held like a pencil, between the thumb and index finger, with the tips pointing upward.

27. Move embryos to one side of the petri dish.

    As the dissection proceeds, it will be easier to move each embryo from one side to the center, where it will be dissected.

28. Slide one embryo to the center of the dish. If necessary, flip the embryo so that it is laying on its right side, with the spine on the right. Rotate the embryo so that its head is at approximately the 2 o'clock position.

    This will place the midbrain in an orientation that can easily be dissected without strain to the right hand.

29. Anchor the body of the embryo to the bottom of the dish with the side of the scissors. Use gentle pressure on the neck area or forebrain lobe of the embryo with the side of the forceps to cause the head to rotate upward during microdissection of the midbrain.

    This will allow easier access to the midbrain for dissection.

30. Dissect the midbrain (mesencephalon) away from the embryo. Start the cut by placing the open scissors at the cephalic flexure (the base of the prominent curve separating the midbrain from the hindbrain) and, making a single straight cut, dissect away the crown of tissue without including tissue from the prominent forebrain lobes surrounding the lateral ventricles at the front of the head (see Fig. 13.3.2). Collect midbrain tissue sections in a pile.

    Check the quality of the cut by examining the midbrain tissue and the remaining embryo to see whether excessive hindbrain or forebrain has been removed.

31. Rotate the embryo to obtain access to the left limb bud. Dissect the forelimb bud by placing the base of the scissors against the body and making a straight cut along the body (see Fig. 13.3.2). Flip the embryo and dissect the right forelimb bud. Collect limb bud tissues in a pile.

32. Repeat steps 27 to 31 until all embryos are dissected.

Rinse tissue

33. Count and record the number of limb buds and midbrains on the recording form.

34. Gently collect midbrain tissue sections into the tube marked "CNS1" using a glass pipet. Take care not to shear the tissue during tissue collection. Collect eight dam's worth of embryos or less in each tube to ensure proper tissue dissociation.

35. Gently collect limb bud tissue sections into tube marked "LB1" using a glass pipet.

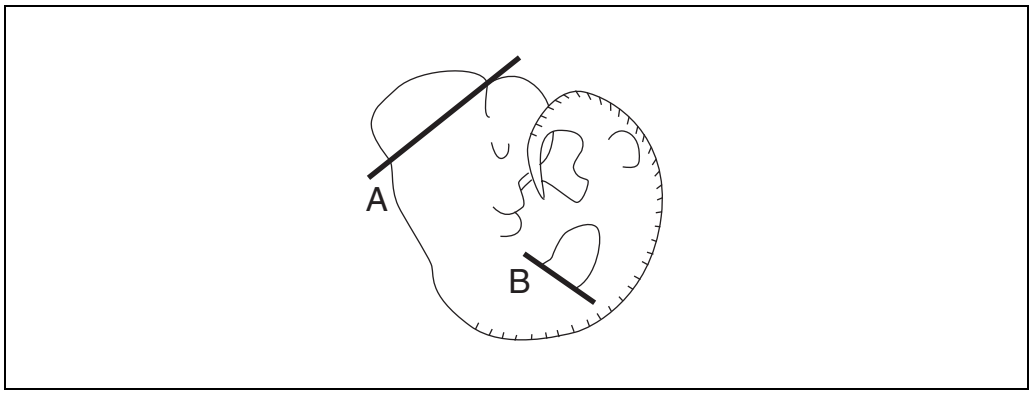

Figure 13.3.2 Dissection landmarks for midbrain (**A**) and limb bud (**B**). The midbrain is dissected away from the cephalic flexure (the indentation near the letter **A**) across the top, excluding the lateral ventricles (the prominent bulbs at the front of the head). Forelimb buds are removed by dissecting at the base of each limb bud as shown (**B**).

36. Allow tissue parts to settle and collect overlying solution. Discard solution into waste beaker. Rinse tissue parts three times or more with sterile CMF-EBSS and discard rinsate into waste beaker. Continue to rinse tissue parts until blood cells and debris are removed.

    The number of rinsing steps can be greatly reduced by maintaining a clean working environment during the tissue microdissection steps.

Dissociate tissue

37. Add 1 to 2 ml CMF-EBSS to each tube (i.e., LB1 and CNS1), and place in 37°C water bath for 20 min.
38. Use the incubation period to wipe down the work surfaces in the dissection room, laminar flow hood, and dissecting microscopes with 70% ethanol. Rinse dissecting instruments to remove debris and blood, store the light source, and discard waste tissue. After laminar flow hood has been wiped down, close sash of hood. Filter trypsin solution and prepare culture medium as necessary.
39. Pipet 10 to 15 ml culture medium in the tube marked "CM" and place tube in 37°C water bath. Pipet 10 to 15 ml trypsin solution in the tube marked "trypsin" and place tube in 37°C water bath.
40. After the first 20-min incubation, remove CMF-EBSS and add 1 to 2 ml trypsin solution to each tube.

    Make sure that addition of trypsin gently resuspends all the tissue sections to ensure good enzymatic dissociation.

41. Place each tube back into the 37°C water bath for 20 min.
42. Use the second incubation period to lay out cell culture dishes on sterile incubator trays and to complete remaining tasks from step 38, above. Pipet 180 µl culture medium into tubes labeled "CNS3" and "LB3."

    These will be used for cell counting.

43. After the trypsin incubation, remove both tubes (CNS1 and LB1) from the water bath. Wipe down exteriors of both tubes with 70% ethanol and place in a tube rack in the laminar flow hood without stirring up tissue sections.
44. Quickly remove overlying trypsin from each tube (CNS1 and LB1) and discard.
45. Add 1.3 ml of culture medium to each tube for each 6 dam's worth of embryos that were used in the experiment. Adjust the volume of medium added to each tube according to the 1.3 ml per 6-dam ratio, as needed, depending on the number of dams used in the experiment.

    The addition of culture medium will stop trypsinization.

    Steps 44 and 45 should be done quickly to avoid over-trypsinization.

46. Dissociate the cells by carefully pulling solution and tissue fragments into a pulled-glass pipet (i.d. ~0.7 mm). Use separate pulled pipets for each tissue type. Continue to pull solution up and down ~15 times, until no aggregates are visible. Avoid bubbles in the solution by keeping solution in both the pipet and tube.

    Rinsing the sterile pulled-glass pipet with culture medium immediately prior to use with the cells can reduce the tendency of cells to stick to the pipet walls.

47. Assemble the 13-mm Swinney filter and 10-ml syringe.

    Make sure to remove plunger from the syringe prior to attaching the Swinney otherwise the filter could be damaged.

48. Using one hand to hold the 10-ml syringe (with the 13-mm Swinney filter attached) over the top of the tube marked "CNS2," transfer contents of CNS1 into the syringe with a pipet. Add plunger to syringe, and gently filter the contents into CNS2. Using a new pipet, Swinney and syringe, filter the contents of LB1 into the tube marked "LB2." Discard tubes marked CNS1 and LB1.

Do not use the same filters or syringes for both culture types as this will lead to contamination of the cultures.

Count and plate cells

49. Immediately add 20 µl of the cell suspension in CNS2 to CNS3 (which contains 180 µl culture medium). Add 20 µl of the cell suspension in LB2 to LB3 (which contains 180 µl culture medium).

With a delay in this step, the cells may settle and require gentle resuspension prior to sampling. This step creates a ten-fold dilution of the cell suspension suitable for cell counting.

50. Ensure that the contents of CNS3 and LB3 are thoroughly mixed prior to sampling for cell counting by flicking each tube with a finger. Take 10 to 20 µl of cells from a tube for counting on a hemacytometer, and allow a small amount of the suspension to flow under the coverslip of the hemacytometer. Add a sufficient quantity of solution so that the entire chamber is just filled.

If too much solution is added, the volume will be off, and cell counts will be inaccurate because cells will be "floating" in the chamber.

Each hemacytometer is different, so estimation of cell number will depend on each manufacturer's specifications. Described here are the steps describing the use of the Improved Neubauer hemacytometer (also see APPENDIX 3B).

51. Count cells in 5 squares along one diagonal with a hand-held counter and record cell count on the data recording form. Repeat the cell count along the other diagonal and record. Count cells that cross the left and bottom edge of any square, and exclude those that cross the right or top edge.

If counts are widely divergent, repeat cell counting with a new aliquot.

52. Calculate the average of the cell counts and record on the data recording form. Estimate the concentration of cells in each tube according to manufacturers' instructions as in the following example for the Improved Neubauer hemacytometer:

70 cells per 5 squares
= 350 cells in entire hemacytometer chamber (which contains 25 counting squares)
$\times 10^4$ (counting chamber conversion)
$= 350 \times 10^4$ cells/ml (estimated cell concentration)
$\times$ 10 (dilution factor)
$= 3.5 \times 10^7$ cells/ml (concentration in undiluted stock).

53. Use a calibrated pipet to determine the volume of suspension in LB2 and CNS2. Record each on data recording form. Rinse the pipet with culture medium before measuring to minimize cell adherence to the walls of the pipet.

Estimate the number of dishes that can be fully plated for each cell type by dividing the volume of limb bud cells by 40 µl/dish and by dividing the volume of CNS cells by 50 µl/dish.

54. Adjust the volume in CNS2 and LB2 to achieve the desired plating concentrations. The desired plating concentrations are:

Plating concentration for limb bud cells = 2×10^7 cells/ml.

Plating concentration for CNS cells = 5×10^6 cells/ml.

55. To adjust cell concentration, multiply the concentration of cells in the undiluted stock (step 52) by the estimated volume (step 53) to determine total number of cells in each tube (LB2 and CNS2). Divide this total cell number estimate by the appropriate plating concentration for each cell type (above) to determine the total volume desired of each cell type. Record this volume on the data recording form.

    The difference between this volume estimate and the volume estimated in step 52 represents the amount of culture medium that needs to be added to that tube (CNS2 or LB2) to achieve the appropriate concentration of cells in each tube.

    Note that addition of too much volume at step 45 may result in a negative volume at this step. If this occurs, centrifuge the sample 10 to 15 min at 1500 × g, room temperature, resuspend the cells in a smaller volume of medium, and repeat cell counting procedure.

56. Add the appropriate volume of culture medium to LB2 and CNS2 as determined in step 55 to achieve the desired plating concentration of CNS cells and LB cells (see step 54). Gently mix to generate a homogenous suspension whenever filling the repeater pipettor to ensure a consistent cell concentration in the plated cell droplets.

57. Working in a laminar flow hood, use a repeater pipettor to plate five 10-µl foci per 35 × 10–mm cell culture for CNS cells and four 10-µl foci per plate for LB cells. Plate until the desired number of dishes is achieved or until cell suspension is exhausted. When plating is completed, place tray gently in incubator. Note initial incubation time on the data recording sheet.

    Use of alternatives to 35 × 10–mm dishes, such as 96-well plates or 2-well chambers, can be accomplished by coating the alternative dish with collagen. For 96-well plates, add 50 µl of 3 mg/ml collagen to each well, whereas for 2-well chambers add 200 to 300 µl per chamber. Let the chambers air dry under UV-light prior to use. These can be stored, wrapped in plastic wrap, in the refrigerator for several weeks before use.

58. Estimate the cell yield for each cell type by calculating the number of 10-µl aliquots of each solution and dividing by the number of tissue parts.

    For example, if there is 1.3 ml of limb bud cells in suspension at the correct plating concentration (as estimated at step 55), this would supply 130 10-µl aliquots (foci). If 100 limb bud sections were used to generate this volume of cells, the yield would be 1.3 foci per limb bud section. CNS yield is estimated in the same manner.

    Optimal yield for limb buds is 1.2 to 1.4 per limb bud section.

    Optimal yield for CNS cells is 10 to 14 per CNS section.

Add medium and treat

59. Add culture medium (with or without test agents) 2 hr after initial plating or later. Because the final medium volume (including the 50 µl of cell suspension) is 2 ml including the test agents, use 1.95 ml of medium with the test agents. Incubate and analyze cells accordingly to experimental protocol.

    Chemical treatments with hazardous volatile compounds, radiolabeled compounds, or photosensitizers should be conducted by constructing an air-tight chamber that can be placed in the incubator. The author's chamber is made of Plexiglas, has a removable faceplate, and two sliding shelves with 1-cm holes to allow uniform gas exchange throughout the chamber. The faceplate has two stop valves that allow initial gas charging, periodic chamber recharging, and chamber purging prior to opening with 5% CO_2/95% air from a gas cylinder. These operations can be conducted inside a fume hood if a sufficient length of tubing is used from the gas cylinder to the chamber. The temperature of the chamber can be maintained by placing the chamber inside an incubator, and humidity can be regulated

by placing petri dishes containing sterile water inside the chamber. The chamber can be made light-tight by wrapping the chamber in foil. In experiments to compare cell growth between the chamber and an incubator, no differences in cell growth have been noted by the author.

Analyses of cell cycle kinetics can be conducted with 5-bromo-2-deoxyuridine (BrdU). However, BrdU causes photo- and radio-sensitization. When using BrdU, conduct cell manipulations under low light, or sodium lamp illumination to avoid DNA damage. Use of a light-proof, air-tight cell isolation chamber as described above is ideal for such experiments.

ALTERNATE PROTOCOL

PREPARING CELLS FROM EMBRYOS OF PRETREATED DAMS

As described previously, the purpose of the experiments conducted using the Alternate Protocol differs from that of the Basic Protocol. Whereas the Basic Protocol yields cultures containing normal, healthy primary cells for study, the Alternate Protocol yields cultures with unknown viability characteristics. The uncertainty of the quality of cultured cells using this method arises due to the potential environmentally or maternally mediated influences on embryonic viability at the time of maternal sacrifice. Nevertheless, the method differs in only a few steps from the Basic Protocol, which are detailed below.

To conduct the Alternate Protocol, treat the dam in a manner consistent with the experimental inquiry (e.g., via the exposure route of interest, using the experimental doses of interest, and on the gestational days of interest). Conduct the Basic Protocol as described above, sacrificing the dam on gestation day 12. However unlike the Basic Protocol, do not aggregate embryonic tissue across treatment groups. Depending on the experimental design, it may be appropriate to aggregate embryonic tissue from multiple dams within a treatment group. Aggregation will increase the availability of cells for subsequent examination, but will reduce the statistical power because of a reduced sample size. Maintaining separation across treatment groups will require careful planning and focus on the part of the microdissector, since tissue parts must be maintained separately, and multiple cell suspension tubes (e.g., CNS1 A, CNS1 B, etc.) will be required. Depending on the experimental goals, treatment with test articles following the 2-hr attachment period may be ignored, though treatment with normal culture medium at 2 hr post-plating should still be conducted.

REAGENTS AND SOLUTIONS

Use deionized, distilled water in all recipes and protocol steps. For common stock solutions, see ***APPENDIX 2A****; for suppliers, see* ***SUPPLIERS APPENDIX****.*

Collagen solution, 3 mg/ml

Prepare collagen type I from rat tail (Sigma) as a stock solution of 3 mg/ml in 0.1% (v/v) acetic acid. For example, add 25 mg collagen to 8.3 ml reagent grade 0.1% acetic acid. Using a stir bar, slowly dissolve the collagen over 2 to 3 hr. Store the stock solution at 4°C. When ready for use, dilute 1:20 of stock solution (1 part collagen stock to 19 parts distilled water). Store up to 1 week at 2° to 8°C.

Culture medium

10% (w/v) heat-inactivated fetal bovine serum (FBS; Qualified, store frozen in a non-frost-free freezer)
2% (w/v) L-glutamine (200 mM stock, store frozen in a non-frost-free freezer)
2% (v/v) penicillin-streptomycin (store frozen in a non-frost-free freezer)
86% (v/v) Ham's F-12 nutrient mixture (store at 4°C and keep away from light)
Prepare fresh on the day of cell culture preparation.

All of the above ingredients are available from Life Technologies.

Freeze aliquots of fetal bovine serum, L-glutamine, and penicillin-streptomycin until ready for use. Because repeated freezing and thawing degrades serum stock quality, store stock in small aliquots that can be used for individual experiments. Warm in water bath or incubator (with a loose lid to allow gas exchange) until ready for use. Equilibrate in incubator during cell attachment period.

The pH should be 7.2 to 7.4. Use sterile techniques throughout to avoid contamination of the cell culture.

Horse serum

Mix 1 part horse serum (Life Technologies; store in 15-ml aliquots in non-frost-free freezer) with 1 part EBSS (Life Technologies; store at room temperature) immediately before use. Thaw in water bath immediately before use.

The pH should be 7.2 to 7.4. Prewarm to 37°C prior to use with the primary cells in culture. Use sterile technique throughout to avoid contamination of the cell culture.

Trypsin solution, pH 7.2 to 7.4

Prepare trypsin (Life Technologies; lyophilized powder) as a 0.1% (w/v) solution (or 100 mg in 10 ml) in CMF-EBSS (Life Technologies; store at room temperature). Adjust pH of trypsin to pH 7.2 to 7.4. Filter trypsin through sterile 0.22-µm mesh nylon filter. Prepare trypsin on the day of the cell culture experiment. Warm in water bath prior to use.

The pH should be 7.2 to 7.4. Prewarm to 37°C prior to use with the primary cells in culture. Use sterile technique throughout to avoid contamination of the cell culture.

COMMENTARY

Background Information

The potential application of primary CNS and limb bud cell cultures as a screening system for teratogenic compounds was demonstrated in experiments conducted by Flint and colleagues in the early 1980s (Sawyer and Goetinck, 1981; Flint and Ede, 1982; Flint, 1983; Flint and Orton, 1984; Flint et al., 1984). These validation studies, which also described the typical growth and differentiation characteristics of cells in these cultures, provided scientific evidence to support the use of these culture systems as a model of the in vivo response to teratogenic compounds. Indeed, when plated in the manner described, these primary cultures develop many characteristics in parallel to those observed in vivo, without the required addition of exogenous growth factors (Flint and Ede, 1982; Flint, 1983; Flint and Orton, 1984; Flint et al., 1984). Although originally proposed as a screening tool for teratogens, the culture of midbrain neuroepithelial cells and limb bud chondrocytes has become important in vitro test models for examining the cellular and molecular processes governing normal development and the cellular response to environmental stresses that may influence development. For example, these culture systems have been used extensively by Faustman and colleagues to examine the mechanisms underlying the developmental toxicity of *n*-nitroso compounds, metals, and pharmaceutical and agricultural compounds (Ribeiro and Faustman, 1990; Whittaker and Faustman, 1991, 1992; Sweeney et al., 1992; Whittaker et al., 1993; Faustman and Sweeney, 1994; Kidney and Faustman, 1995; Seeley and Faustman, 1995).

The protocols described here propose use of gestation day 12 to 12.5 rat embryos for the derivation of the cultures. This developmental period represents a window of vigorous cell growth in both the CNS and limb bud. In particular, the midbrain is experiencing a period of peak neuronal progenitor cell (i.e., neuroepithelial cell) replication. Because these neuroepithelial cells will stop dividing and differentiate into neurons during several days in culture, use of the gestation day 12 neuroepithelium as a source for the neuronal progenitor cells yields a culture enriched in neurons. Thus, although it is possible to derive cultures from earlier or slightly later times, the growth and differentiation conditions will vary. If the investigator chooses to use tissue from earlier gestational periods, they will be faced with limited availability of tissue. If later gestational periods are chosen, the investigator may have

fewer germinal cells and more differentiated cells, and the cultures may grow poorly.

Because both the CNS and limb bud cell cultures are derived directly from the embryo, the cell cultures are of a mixed cell type. Thus, these cultures are most suitable as a model of the developing system rather than as a model of a single specific cell type. The author has found this model to be especially suitable for examining the regulatory interactions that control development, particularly when cell lines cannot be used, such as for examining the regulatory controls governing cell proliferation (Ponce et al., 1994; Ou et al., 1997, 1999a,b).

Critical Parameters and Troubleshooting

Animal acclimation

Acclimate animals, including timed-pregnant animals, in the facility for ≥1 week prior to experimental use, dosing, or sacrifice. Such acclimation will minimize the potential for stress-induced artifacts in cell growth or viability.

Cell growth

Elapsed time between sacrifice of the dam and cell plating should be minimized as much as possible. Thus, the areas used to sacrifice the dam and to conduct embryonic microdissection should be organized, and materials and reagents should be prepared before sacrificing begins. If the cell preparation can be conducted with two people, one individual should be in charge of humanely euthanizing the dams and removing the uteri, while the other begins removing the individual embryos from the uteri. Once all the dams have been sacrificed, both individuals can work together to isolate the embryos and perform embryonic microdissection.

Cell yields are sensitive to both the somite stage and individual microdissection technique. Thus, all researchers involved in micromass culture preparation should be trained to correctly establish embryonic growth stage and to use the appropriate flexures and topological characteristics for proper tissue isolation. Identification of the extent to which members of a research group vary in technique can be gauged by monitoring cell yield.

Be careful that the light source used with the dissecting microscope is not too close to the dish in which dissection is taking place, because it can heat-stress the cells. A heat shield may also be used to protect the embryos from excessive lamp heat.

Cell growth is very sensitive to disturbances that occur during the 2-hr attachment period. The researcher should minimize disturbances that occur during this period, such as repeated incubator opening or physical shock to the dishes.

Cell growth is also sensitive to initial plating concentration. Errors in plating concentration most likely arise from errors in cell counting. Check to ensure that the proper counting procedure is being conducted with the hemacytometer. More accurate cell counts can be accomplished by counting all 25 squares, rather than just 5 squares. Make sure that the tubes marked “CNS2" and ”LB2" are well mixed by flicking the tube with the finger or by pipetting the solution up and down immediately prior to collecting the aliquots to be used in the tubes marked “CNS3" and ”LB3." Because the cells tend to settle in the tubes, failure to ensure sample homogeneity can result in inaccurate cell counts. Likewise, ensure that CNS2 and LB2 are well mixed when refilling the repeator pipettor during cell plating to maintain a consistent cell concentration in each micromass aliquot.

Harsh treatment or use of a pulled pipet that is too small during physical dissociation can create debris that can make proper cell counting difficult.

If cell growth is inconsistent or if cell yields are poor, check the CO_2 and temperature regulation. Excursions in pH and temperature can impair cell growth and viability. Also, ensure that there is sufficient water in the incubator to maintain 100% humidity.

Contamination

Problems with fungal contamination of the cell culture can arise from many sources, but are most commonly attributed to poor sterile technique. Be sure to replace pipet tips and replace gloves often. Ensure that surgical tools and reagents are sterile, and that incubators and water baths are clean.

Animal sacrifice

To avoid potential indirect effects of euthanasia solutions on cell growth characteristics, the author typically uses CO_2 asphyxiation to euthanize the dam. The author has also used ether in the past, though storage and handling concerns make ether a less preferred alternative. If other methods of sacrificing the dam are used, the investigator should consider potential effects on cell growth. Once a method is chosen,

that technique should be maintained throughout an experimental series.

Dissection

Developing an efficient dissection technique that minimizes rupture of the embryonic sac during removal of the embryo from the uterus, and that results in a consistent isolation of limb buds and midbrain sections, takes time. Like any skill, the researcher should pay attention to those techniques that work best for him or herself. Tips to consider include the following.

(1) Use two fine forceps during removal of embryo from uterus. For a right-handed person, it may be easier to hold the uterus between embryo sites with the left hand and tear with the right hand, starting from the left edge of the site. The uterus should be oriented with the muscle edge at the top. Use the tip of the forceps, held in the right hand, to poke a hole in the muscle between the two sites as a starting place to begin opening the site. (2) Note that pressure on the embryo during removal from the uterus will increase the likelihood that the embryonic sac will rupture. Thus, one should be looking for where points of pressure occur as the embryo is released from the uterus, and should gently reduce pressure, when the site is only partially opened, by opening the site along these points of pressure. (3) Use both the forceps and microdissecting scissors to flip and rotate the body as needed for access to the forelimbs and midbrain.

Recording experimental conditions

The data recording form can be an invaluable record of each experiment. Elements that should be recorded include the number of dams, pregnancy status, number of fetuses per dam, gestational stage, researchers involved in the experiment, time of initial sacrifice and time of plating, incubators and reagent lot numbers used in the experiment, calculations used to estimate yield, and cell concentration.

Anticipated Results

Limb bud cells derived from the gestation day 12 rat embryo are predominantly undifferentiated and contain little collagen or glycosaminoglycans. During 5 days in culture, these cells should undergo differentiation. Limb bud cell growth and differentiation can be monitored by numerous methods, including the use of cartilage-specific differentiation stains such as alcian blue or uptake of $^{35}SO_4^{2-}$ or ^{3}H-thymidine into proteoglycans (Faustman, 1988). Alternatively, differentiation-specific processes including aggregation, cell condensation, and cellular differentiation can be used (Flint et al., 1984; Ribeiro and Faustman, 1990).

Proper differentiation of midbrain neuroepithelial cells can be monitored by examination of cell surface markers associated with differentiation, by use of radiolabeling methods (specifically ^{3}H-GABA uptake), or by morphogenetic examination (Whittaker et al., 1993; Flint et al., 1984). When grown in culture, the undifferentiated neuroepithelial cells develop into neuronal cells that project striking neuritic extensions as early as 1 to 2 days, with more extensive development over 5 days in culture. Staining with propidium iodide or other DNA fluorochrome shows that proliferation occurs in the undifferentiated fibroblastic-like cells underlying the differentiated cells. The differentiating CNS cells tend to aggregate into clusters on top of the underlying neuroepithelial cells.

Although the author typically conducts analyses within 5 days of the initial cell culture, he has successfully grown these cells for 14 days; there was no apparent reason why these cultures could not survive longer with periodic changes to the culture medium.

Time Considerations

The author typically begins sacrifice of the dams by 8 a.m.. By having a consistent sacrifice time, the researcher will minimize this potential source of variability in embryonic growth stage. This is a point of critical concern in studies used to characterize growth stage–specific developmental mechanisms or processes.

Elapsed time between initial sacrifice and cell plating is ~4 hr for two researchers who are familiar with the protocol and for an experiment involving eight pregnant dams. The greatest degree of variation in this time estimate stems from researcher microdissection efficiency and, to a lesser extent, plating efficiency. The availability of two researchers during microdissection and plating is helpful, though one highly efficient researcher can conduct this protocol in the same, or slightly less, time. Chemical treatment after the 2-hr attachment period can take between 0.5 and 1.5 hr depending on treatment complexity, the number of plates, and the efficiency of the technician. Allowing 0.5 hr each for set-up and clean-up, total elapsed time is 7 to 8 hr.

Literature Cited

Brown, L.P., Flint, O.P., Orton, T.C., and Gibson, G.G. 1986a. Chemical teratogenesis: Testing methods and the role of metabolism. *Drug Metab. Rev.* 17:221-260.

Brown, L.P., Flint, O.P., Orton, T.C., and Gibson, G.G. 1986b. In vitro metabolism of teratogens by differentiating rat embryo cells. *Food Chem. Toxicol.* 24:737-742.

Faustman, E.M. 1988. Short-term tests for teratogens. *Mutat. Res.* 205:355-384.

Faustman, E.M. and Sweeney, C. 1994. Effects of ethylnitrosourea on expression of proto-oncogene pp60c-src and high-molecular-weight neurofilament protein in rodent embryo central nervous system cells in vitro. *Toxicol. Appl. Pharmacol.* 128:182-188.

Flint, O.P. 1983. A micromass culture method for embryonic neural cells. *J. Cell. Sci.* 61:247-262.

Flint, O.P. and Ede, D.A. 1982. Cell interactions in the developing somite: In vitro comparisons between amputated (am/am) and normal mouse embryos. *J. Embryol. Exp. Morph.* 67:113-125

Flint, O.P. and Orton, T.C. 1984. An in vitro assay for teratogens with cultures of rat embryo midbrain and limb bud cells. *Toxicol. Appl. Pharmacol.* 76:383-395.

Flint, O.P., Orton, T.C., and Ferguson, R.A. 1984. Differentiation of rat embryo cells in culture: Response following acute maternal exposure to teratogens and non-teratogens. *J. Appl. Toxicol.* 4:109-116.

Kidney, J.K. and Faustman, E.M. 1995. Modulation of nitrosourea toxicity in rodent embryonic cells by O6-benzylguanine, a depletor of O6-methylguanine-DNA methyltransferase. *Toxicol. Appl. Pharmacol.* 133:1-11.

Ou, Y.C., Thompson, S.A., Kirchner, S.C., Kavanagh, T.J., and Faustman, E.M. 1997. Induction of growth arrest and DNA damage-inducible genes Gadd45 and Gadd153 in primary rodent embryonic cells following exposure to methylmercury. *Toxicol. Appl. Pharmacol.* 147:31-38.

Ou, T.C., White, C.C., Kresja, C.M., Ponce, R.A., Kavanagh, T.J., and Faustman, E.M. 1999a. The role of intracellular glutathione in methylmercury-induced toxicity in embryonic neural cells. *Neurotoxicology* 20:793-804.

Ou, Y.C., Thompson, S.A., Ponce, R.A., Schroeder, J., Kavanagh, T.J., and Faustman, E.M. 1999b. Induction of the cell cycle regulatory gene p21 (*Waf1*, *Cip1*) following methylmercury exposure in vitro and in vivo. *Toxicol. Appl. Pharmacol.* 157:203-212.

Ponce, R.A., Kavanagh, T.J., Mottet, N.K., Whittaker, S.G., and Faustman, E.M. 1994. Effects of methyl mercury on the cell cycle of primary rat CNS cells in vitro. *Toxicol. Appl. Pharmacol.* 127:83-90.

Ribeiro, P.L. and Faustman, E.M. 1990. Chemically induced growth inhibition and cell cycle perturbations in cultures of differentiating rodent embryonic cells. *Toxicol. Appl. Pharmacol.* 104:200-211.

Sawyer, L.M. and Goetinck, J.P. 1981. Chondrogenesis in the mutant nanomelia. Changes in the fine structure and proteoglycan synthesis in high density limb bud cell cultures. *J. Exp. Zool.* 216:121-131.

Seeley, M.R. and Faustman, E.M. 1995. Toxicity of four alkylating agents on in vitro rat embryo differentiation and development. *Fundam. Appl. Toxicol.* 26:136-42.

Solursh, M., Jansen, K.L., Singly, C.T., Linsenmayer, T.F., and Reiter, R.S. 1982. Two distinct regulatory steps in cartilage differentiation. *Dev. Biol.* 94:311-325.

Strum, K. and Tam, P.P.L. 1993. Isolation and culture of whole postimplantation embryos and germ layer derivatives. *Meth. Enzymol.* 225:164-190.

Sweeney, C., Kirby, Z., and Faustman, E.M. 1992. Expression of developmentally relevant proteins by rodent embryo CNS cells in vivo and in vitro: Proto-oncogene pp60c-src and high-molecular-weight neurofilament protein. *Cell Biol. Toxicol.* 8:113-128.

Walum, E. and Flint, O.P. 1990. Midbrain micromass cultures: a model for studies of teratogenic and sub-teratogenic effects on CNS development. *Acta Physiol. Scand. Suppl.* 592:61-72.

Whittaker, S.G. and Faustman, E.M. 1991. Effects of albendazole and albendazole sulfoxide on cultures of differentiating rodent embryonic cells. *Toxicol. Appl. Pharmacol.* 109:73-84.

Whittaker, S.G. and Faustman, E.M. 1992. Effects of benzimidazole analogs on cultures of differentiating rodent embryonic cells. *Toxicol. Appl. Pharmacol.* 113:144-151.

Whittaker, S.G., Wroble, J.T., Silbernagel, S.M., and Faustman, E.M. 1993. Characterization of cytoskeletal and neuronal markers in micromass cultures of rat embryonic midbrain cells. *Cell Biol. Toxicol.* 9:359-375.

Wilk, A.L., Greenburg, J.H., Horigan, E.A., Pratt, R.M., and Martin, G.R. 1980. Detection of teratogenic compounds using differentiating embryonic cells in culture. *In Vitro* 16:269-276.

Contributed by Rafael A. Ponce
University of Washington
Seattle, Washington

Using Chicken Embryos for Teratology Studies

The chicken embryo has been used as a standard animal model for embryonic development, especially embryonic neural development, for close to a century. In the 1930s, Viktor Hamburger began studying chicken embryonic development, focusing on neural development, when he went to work in F.R. Lillie's laboratory at the University of Chicago (Purves and Lichtman, 1985). By 1951, Hamburger and Hamilton published a photographic series documenting the development of the chicken embryo throughout the 21-day incubation period (Hamburger and Hamilton, 1951, 1992; Hamburger, 1992; Sanes, 1992). Romanoff then described the development of the chicken embryonic organ systems throughout the incubation period (Romanoff, 1960) as well as a description of the factors (environmental and some chemical) that can grossly affect embryonic development (Romanoff and Romanoff, 1972). For the past half century, the chicken embryo has been consistently used as a major model for understanding mechanisms underlying control of nervous system development.

About the same time that Romanoff was publishing his seminal work on chicken embryo development, McLaughlin et al. (1963) published a toxicological survey of chemical compounds that can affect chicken embryonic development. It was McLaughlin that developed the yolk-injection method that is most effective at preventing artifactual damage to the embryonic tissues. Verrett (1976), working for the U.S. Food and Drug Administration (FDA), then used the chicken embryo as the animal model for studying the relationship between 2,3,7,8-tetrachlorodibenzo-*p*-dioxin (TCDD) and chick edema disease, a syndrome first noted in the late 1950s, and linked to dioxin in the 1960s (Firestone, 1973). In the past few decades, several groups of investigators began using the chicken embryo as a model for toxicant-induced teratological studies. Hoffman and colleagues (Hoffman and Ramm, 1972a,b; Hoffman, 1975; Hoffman and Campbell, 1978) used the chicken embryo to study chemical-induced teratogenity in a large number of studies that evaluated the teratogenic potency of a broad range of pollutants. Jelinek and colleagues (Jelinek and Marhan, 1994) developed the CHick Embryotoxicity Screening Test (CHEST) to evaluate pharmacological agents with respect to regulatory rat-rabbit procedures. Henshel et al. (1993) developed the Early Embryo Assay, a method of evaluating chick embryo potential for chemically-induced teratogenicity measured within the first week of embryonic development. This broad range of studies has shown that the chicken embryo is an excellent model for assessing potential teratogenicity, so long as the investigator understands the limitations of the design of the protocol, and so long as the investigator uses proper controls and learns how to consistently and gently work with the embryos and hatchlings.

In summary, chicken embryos are good models for teratogenicity studies because they are (a) easily obtainable; (b) relatively inexpensive when compared to other vertebrate and mammalian models; (c) easy to expose, incubate, and handle; (d) counted individually as a test unit rather than in a group such as a litter; (e) dosed individually, making it easier to control the delivered dose; (f) isolated from the mother, eliminating maternal factors such as biotransformation, which may alter the injected parent compound before it reaches the embryo; and (g) fairly non-threatening to the animal rights community because of the widespread use of chickens in agriculture.

This unit describes the steps involved in injecting and incubating fertile, domestic chicken eggs with a suspected teratogenic substance, including handling, storage, and analysis considerations. Age factors for both injection, co-dosing or repeated dosing, and sacrifice/analysis are considered, and the results of one of the authors' preliminary experiments are presented.

Contributed by Diane S. Henshel, Jamie DeWitt, and Andrea Troutman
Current Protocols in Toxicology (2002) 13.4.1-13.4.19

EGG INJECTIONS AND INCUBATION

One important step in an avian teratogenicity study is administering the toxicant to the embryo in a way that is consistent, causes little stress to the embryo, and delivers the toxicant to the embryo throughout critical periods of embryonic development. The airspace egg injection method detailed in this protocol can be used for most avian systems and can be performed with few specialized pieces of equipment. Injection into the airspace, when carried out carefully, avoids artifactual damage to the embryo due to contact between the needle and the blastoderm or developing embryo. Injection into the airspace can also be carried out at any time during the incubation period. Yolk-injection methods, described in McLaughlin et al. (1963) and Henshel (1993), are best done at the start of incubation. Both airspace and yolk injections enable embryo exposure from virtually the time of injection. Albumin injections can also be carried out at any time during the incubation process, but the toxicant primarily appears to be delivered during the last third of the incubation period when the embryo is consuming the albumin during the later rapid growth phase of development. Shell application of the toxicant is really only efficient for lipid soluble compounds. However, shell application seems to be the method that least consistently delivers the applied dose to the embryo.

Perhaps the most difficult step in this protocol is obtaining a supplier of readily available, fresh, fertilized eggs. Most agricultural universities have poultry science units that can provide low-cost eggs with relative ease. Several commercial farms will provide fertilized eggs of chickens or other birds as well.

NOTE: All protocols using live animals must first be reviewed and approved by an Institutional Animal Care and Use Committee (IACUC) or must conform to governmental regulations regarding the care and use of laboratory animals.

Materials

Eggs (any commercial or university farm; fertile and free from chemical contamination)
Egg cleaning agents (e.g., 20% povidone iodine, see recipe)
70%, 95% and 100% ethanol
Injection vehicle (see annotation to step 10; also see Critical Paramaters)
Agent to be injected mixed with the vehicle
Uncontaminated vehicle kept separate from injection agent or injection agent vehicle dilution quantity
4% paraformaldehyde or 10% formalin

Kimwipes (or other lintless wipes)
Melted paraffin and a small paintbrush for sealing injection holes
Probe: a small sharp metal object such as an awl or a compass point, sterilized by soaking in 70% alcohol for 15 min, then air dried, for piercing a small hole in the injection site
Syringes for injecting (e.g., Hamilton brand 700 series microliter syringes with cemented needles)
Circulated air incubator with a 99.5°F dry bulb and 87° to 88°F wet bulb

Prepare eggs for injection

1. After unpacking the eggs from their shipping containers and discarding the broken ones, note the overall condition of the eggs in a lab notebook or on a data sheet.

   Eggs that are shaken up too much during shipping, indicated by the number of broken eggs, will have decreased viability and increased risk of gross teratogenic defects.

2. Dip eggs gently into a container of 20% povidone iodine, and dab the shell dry with a clean, lintless wipe such as Kimwipes. Do not wipe the shells; wiping easily removes their protective layer.

   Egg shells are contaminated with bacteria from the hen and the laying site. Estimates published in the popular press suggest that ≥30% of commercial eggs are contaminated with salmonella bacteria. Fertile eggs are not put through the same heavy washing procedure as commercial eggs and are more likely to be contaminated externally with a variety of bacteria. Therefore, all eggs should be cleaned when they are first received into the laboratory. The cleaning agent, 20% povidone iodine, is gentle and effective. Povidone iodine is available in most drug stores.

3. At the time of injection, remove the eggs from storage or from the incubator and let them come to room temperature before starting injections.

   Hot eggs will absorb outside air rapidly through the hole and are more likely to get contaminated; cold eggs accumulate condensation.

4. Randomly assign eggs to dose groups.

   The authors inject their eggs in staggered batches totaling ~10 to 12 eggs (for eggs that will incubate until hatched) or 20 to 30 eggs (for early embryos) so that there is not an overwhelmingly high number of embryos or chicks coming out of the incubator at the same time. See Batches in Critical Parameters.

5. Weigh each egg in a small plastic cup cushioned with clean, lintless paper wipes to prevent the egg from rolling off the scale. Mark the weight in pencil on the side of the egg, but not on the egg equator. Also mark the egg ID number in two places, generally on the top and on the bottom.

   The authors also recommend writing the dose to be injected on the shell to prevent mistakes at the time of injection, as well as the time and day in and time and day out of the incubator for early embryos.

6. Candle each egg and mark the limits of the airspace in pencil. To candle an egg, use a home-made or commercial source of light to illuminate the inside of the egg.

   It is best to use a "cool light" candler, which uses non-tungsten light bulbs. Heat can impair egg viability.

   When candling each egg, check for cracks in the shell. For the early embryo assay, seal cracks with a thin layer of paraffin, painted on just over the crack. If the eggs will go until hatch, using cracked eggs is not recommended as the potential for excess dehydration increases the risk of later embryonic death.

Inject eggs

NOTE: All previous and further steps may be carried out in a relatively clean laboratory. However, to decrease the possibility of contamination, carry out steps 7 to 12 in a 70% alcohol-wiped laminar flow hood.

7. Prepare the injection space (hood, benchtop, etc.) with the appropriate protective material, such as an absorbent, plastic-backed bench protector.

8. Dab the shell above the airspace with 70% ethanol, let dry.

   Prior to injection, the injection site must again be cleaned with a cleaning agent. A lintless wipe squirted with 70% ethanol is effective.

9. Use the sterilized probe to gently make a hole in the shell in the middle of the air space. To protect the egg, cradle the egg in one hand while gently applying pressure to the surface of the egg.

A small dental drill has also been successfully used by some investigators. Do not fully insert the probe into the egg; just poke a hole through the shell. The probe should only go in 1 to 2 mm.

10. Draw up the appropriate amount of vehicle or agent into the corresponding syringe and inject into the injection hole using the following parameters:

    a. Eliminate air bubbles from the agent in the syringe. Air bubbles will result in less consistent dosing volumes.

    b. Wipe off excess agent from the syringe before placing the syringe into the egg. If the agent is in an oil vehicle, wipe off the syringe with a lintless wipe wet with 100% ethanol.

    c. Insert the syringe into the injection hole at a broad angle, with the hole of the needle pointing up toward the egg shell.

    d. Slowly inject the agent into the egg at the edge of the air sac so that the solution drips down the inside shell membrane of the air sac. Give the syringe a gentle twirl to dislodge any agent clinging to the tip of the needle. Be careful not to bring the needle near the blastoderm or embryonic tissue. If the injection volume is high, i.e., 1.0 µl/g of egg, or if the hole of the needle is too close to the edge of the injection hole, some agent may leak back out of the injection hole, potentially disrupting the dose administered to the egg. If there is any leakage, wipe the excess off with a clean, lintless wipe wet in 95% ethanol to prevent contamination of the paraffin.

    Use a separate syringe for each concentration and clearly mark each syringe on the body and the plunger tip so that cross-contamination among doses does not occur.

    See the Study Design section in Critical Parameters for a discussion of injection volume and vehicle/diluent choice.

    The injection vehicle chosen will depend on the relative water or lipid solubility of the chemical. For water soluble chemicals, dissolve the chemical in saline (0.7% to 0.8% NaCl), pH 7.2 to 7.4.

    For lipid soluble compounds, dissolve the material in the chosen lipid vehicle. Most chemical companies will dissolve products into the selected lipid vehicle for an additional fee. Request documentation showing an analysis of the final concentration of the material. Appropriate vehicles may include a vegetable oil (corn, soybean, sunflower, canola, safflower, peanut) or triolein. Some vegetable oils contain biologically significant concentrations of estrogenic compounds, such as genistein. If this will affect the measurement endpoint, choose another lipid vehicle. Some oils are thinner than others (e.g., safflower and sunflower) and will be less likely to occlude thin syringe needles used for injections.

    The agent to be injected is mixed with the vehicle so that the volume injected into the eggs results in the desired concentration per gram of egg. For example, if one wishes to inject in the parts per trillion concentration at 0.1 µl/g of egg, mix the agent into the vehicle based on a ~55- to 60-g egg. See the Injection Volume discussion in Critical Parameters.

11. Using a small paintbrush, seal the injection hole with a small drop of paraffin. Gently rotate the egg side to side to coat the airspace membrane with the agent.

12. If continuing injections with the same dose group, wipe the outside of the syringe with a wipe soaked with 70% or 95% ethanol. If moving on to another dose group, rinse out the syringe 10 to 15 times with clean 70% or 95% ethanol and wipe the outside of the syringe with a wipe soaked in 70% or 95% ethanol. Prior to letting the syringe dry, do a final rinse with clean 100% ethanol.

Incubate eggs

13. Once all eggs are injected, place them, with the airspace pointing up, into a circulated air incubator with a 99.5°F dry bulb and 87° to 88°F wet bulb. Make sure that the incubator has an automatic egg turner or manually turn the eggs every 3 to 4 hr.

14. Depending on the incubator, preferably space eggs so that they are not touching one another and randomize the placement of the dose groups within the incubator (see Randomization in Critical Parameters).

15. If taking the eggs to hatch, candle the eggs every day or every other day between injection and hatch. Remove eggs that have stopped developing. Such eggs will lack visible vasculature, be translucent rather than opaque, and/or excessively "sloshy." After the first week or so, it should be possible to see some movement in viable eggs. Once removed, open the dead eggs, remove the embryo, and assess the embryo for approximate age of death and abnormalities. Archive the embryo in 4% paraformaldehyde or 10% formalin for future reference and comparison to viable embryos.

EMBRYO REMOVAL AND HANDLING

BASIC PROTOCOL 2

Removing the early embryo from the egg requires patience and a gentle hand so that neither the embryo nor the vasculature is damaged. While the steps for removing 48-, 72-, and 96-hr embryos vary somewhat, the basic procedure is the same. The steps below outline the procedures for removing 48-hr embryos, with comments specific to 72- or 96-hr embryos inserted where necessary.

Materials

Hexamethyldisilazane or silane
PBS-azide (see recipe)
10% neutral buffered formalin or 4% paraformaldehyde prepared in pH-neutral buffer

Sharp-edged file or a diamond-tipped glass cutter
Pasteur pipets
Plastic beaker filled with lintless wipes, to hold eggs in fashioned "nest"
Curved and pointed forceps (no. 5 with a 45° angle)
Small dissecting scissors (e.g., Moria curved, blunt-tipped scissors, available from most fine instrument suppliers)
Pipets, disposable
Oval "donuts" made out of filter paper, ~2-cm × 1-2–cm external diameter and 1.5-cm × 0.5-cm internal diameter (for 48- and 72-hr embryos only)
Metal scooper (normally used for measuring out dry chemicals)
Petri dishes or other small containers to hold PBS-azide
Pre-labeled vials for storing embryos, filled with 10% neutral buffered formalin

Prepare silanized, fire-polished, wide-bore pipets

1. Using a sharp-edged file or a diamond-tipped glass cutter, etch a small notch around the end of a glass Pasteur pipet, just around where or before the pipet starts to narrow toward the tip.

2. Cover with a paper towel (or other cloth or fabric to hold the glass fragments). Break at the etched line using finger pressure.

3. Fire-polish the broken end in an open flame such as a Bunsen burner.

   If the opening is over-polished, it will melt together. If the opening is under-polished, sharp edges will still exist.

4. Never touch the glass until it has cooled to room temperature, ~30 min. Put the cooling pipets on a heat-safe surface or in a beaker (labeled "hot") with the heated end sticking up.
5. Coat the inside of the cooled, fire-polished pipet with hexamethyldisilazane, silane, or an equivalent anionic coating, dip the pipet in the coating solution and air dry the pipet in a laminar flow or fume hood.

Prepare egg for embryo removal

6. Remove eggs from incubator exactly 48, 72, or 96 hr from when eggs were placed into the incubator.
7. Place an egg into a plastic beaker filled with lintless wipes that forms a "nest" for the egg.
8. Remove the paraffin covering the injection hole with a pair of forceps.
9. Using the curved forceps, gently remove pieces of shell within the pencil-drawn borders of the airspace, beginning from the injection hole. Be sure to remove only small pieces at a time.
10. Once the shell is removed down to the level of the membrane covering the liquid portion of the egg, use a pair of pointed forceps to carefully peel off this membrane.

    Use extreme caution; occasionally the embryo will stick to this membrane and become damaged if the membrane is pulled off too rapidly or harshly.

Remove the embryo

11. Locate the embryo.
    a. Embryos that are 48 hr will often only have a tiny blood ring (the beginning of vasculature) or no blood ring at all. Look for a slight disturbance or clear area in the yolk membrane. The embryo will appear as a very fine, 2- to 3-mm line in the middle of the disturbance or clear area.
    b. Embryos that are 72 and 96 hr will be visible and have noticeable vasculatures.
12. Using a disposable pipet, remove a small amount of albumen, being careful not to disturb the embryo. Remove more shell so that the edge of the shell is level to the height of the liquid portion of the egg (this is to increase the working space).
13. For 48-hr embryos, place the filter paper donut over the embryo so that the embryo is in the middle of the donut. For all ages of embryos, place a few small drops of formalin on the embryo and wait a few minutes.

    The formalin helps to firm up the tissues and makes the embryo easier to handle.

14. Using small dissecting scissors, clip around the donut. For 72- and 96-hr embryos, clip around the outermost edges of the vasculature so that that the vasculature comes out with the embryo. Try to keep the vasculature intact so that it can be evaluated later for the pattern of blood vessel formation.
15. Gently insert the metal scooper underneath the donut and/or embryo and carefully lift up, clipping any pieces of membrane missed in the initial clipping. Place the donut and/or embryo into a Petri dish filled with PBS-azide.

16. Gently wash off any excess yolk clinging to the embryo, using a blunt probe or blunt forceps. Verify that the embryo is in the center of the donut or vasculature, and then use forceps, the metal scooper, or a silanized, fire-polished, wide-bore pipet to transfer the embryo to the appropriately labeled vial containing 10% formalin.

Label vials and lids with egg ID number, age, date, and any other relevant information. Since formalin can wash off permanent marker ink, label the vial itself, cover the label with labeling tape, and then label the tape. The tape protects the markings on the vial, which acts as a back-up label.

HANDLING HATCHLINGS

BASIC PROTOCOL 3

Requirements for housing and sacrificing live animals will vary from facility to facility, as well as endpoints collected by each researcher. In general, the authors recommend following the guidelines below for most teratogenicity studies involving hatchling birds.

Collect data

1. Always record the date and time of pipping (when the chick first pecks through the shell) and the date and time of hatching.

   The time between pipping and hatching can indicate the overall vigor of the chick.

2. Once the chicks have hatched, record any obvious physical and behavioral abnormalities.

3. Record the weight and crown-rump length of each chick. If doing necropsies, record the weight of the yolk sac to obtain a yolk-free body weight.

House and mark chicks

4. If no independent measurements will be made on each chick, separate chicks by dose.

5. If independent measurements will be made on each chick, mark each individual chick with either a leg or wing band or with non-toxic, permanent marking pens or paint applied to the feathers on the back and/or the head.

   Using different marker colors can indicate the dose and the number of marks can indicate the bird number. Chicks from different doses can be housed together as long as each chick is marked.

SACRIFICING CHICKS

SUPPORT PROTOCOL 1

There are three common methods for sacrificing, and the choice of which method to use will be determined, in part, by how the organs and blood must be treated for the experiment. For histology, the best method is intracardial superfusion with fixative (Method A). For larger animals, the arteries can be the route of entry of the superfusion fluids. Somewhat less optimal but still acceptable for small animals is decapitation with rapid immersion fixation (Method B). When the requirement is for blood collection, decapitation is preferred. When the requirement is for collection of fresh organ tissue, the authors' preferred method is decapitation. Some researchers choose to use CO_2 asphyxiation. This method is not recommended as it is, by far, the least humane, producing clearly panicked chicks. The net result will be a highly stressed and frightened chick with elevated corticosteroid blood levels, with all the concomitant biochemical stress changes. The 30 sec to several minutes it takes for the chicks to expire is more than sufficient to allow biochemical stress changes to occur.

Materials

Chicks
Sodium pentobarbitol (Somnotol or equivalent; see recipe)
Phosphate-buffered saline (PBS; see recipe)
0.75% avian saline (see recipe)
Fixative (heparin; see recipe)
Blood collection vial, i.e., heparinized or EDTA-treated vacutainer tube

Scalpel
Large shears (e.g., sewing shears)

Method A: Intracardial perfusion

1a. Pre-dose the chick with sodium pentobarbitol (Somnotol) injected i.m. or i.p. Wait until the chick is unresponsive to a wing or toe pinch. Stroking the chick before injection and during the wait will keep it warm and less stressed.

2a. Pin the chick down, wings spread-out, on a dissection board with fluid collection capability (a baking dish filled with paraffin works very well).

3a. Open the thoracic cavity by cutting below the rib cage, then up along the center of the rib cage, and bending the rib cage back out of the way.

4a. Use two fluids: first use a phosphate-buffered saline such as 0.75% avian saline, and then use a fixative. Use a three-way valve to switch between the solutions. Make sure there is no air in the perfusion lines or the perfusion needle. For gravity-fed perfusion (slow and more protective of tissue microarchitecture), hang the apparatus from ~2 to 3 feet above the chick.

5a. At the start of the perfusion, insert the tip of the needle into the chick's left ventricle (your right when looking down at the chick), keeping the needle parallel to the medial ventricular wall. Immediately after starting the drip, cut the chick's right atrium to allow the blood to drain and prevent back pressure in the tissues, which can damage the microarchitecture. Run the phosphate-buffered saline first until the fluids run clear (usually ~1 to 1.5 ml/g body weight), then switch to the fixative, running at least 1 to 1.5 ml/g body weight through.

A well-fixed chick will be stiff and the neck will remain rigid.

6a. Post fix the chick at 4°C in at least 2 ml fixative per gram of body weight, changing the post-fix after 48 hr.

Method B: Decapitation

1b. Keep the chick warm and unstressed until sacrifice.

2b. Using two people, with one person holding the chick and the other holding scissors (large sewing shears work best), cut off the head.

This works best if the person holding the chick tucks the legs and wings into the cupped hand holding the chick so that they do not get inadvertently snipped and if the person doing the cutting gently pulls on the head to stretch out the neck to obtain a precise cut.

3b. Quickly catch the trunk blood (if doing blood collection) as it flows out of the neck into an appropriate blood collection vial, i.e., heparinized or EDTA-treated vacutainer tube.

4b. Dissect out the most time-critical organs first, such as the brain and the liver. The dissection can be done on ice to slow tissue degradation.

5b. Immersion fix all tissues to be archived for histology. Rapid freeze tissues for biochemistry.

TREATMENT OF ORGANS

The treatment of organs from the chicks will depend on the endpoints collected by each researcher. For example, certain types of histological protocols require fixation of organs in different solutions and neurological, immunological, and enzymatic protocols often require immediate fixing or freezing of organs or sera. It is the duty of the researcher to follow the procedures dictated by the ultimate endpoint.

REAGENTS AND SOLUTIONS

Use Milli-Q-purified water or equivalent in all recipes and protocol steps. For common stock solutions, see ***APPENDIX 2A****; for suppliers, see* ***SUPPLIERS APPENDIX****.*

Avian saline, 0.75%

Dissolve 7.5 g NaCl in 900 ml distilled water. Once dissolved, bring final solution up to 1 liter using a graduated cylinder or volumetric flask. Store up to several months at room temperature in a pre-cleaned or sterilized glass bottle. Check for mold growth before use for solutions older than a few weeks. Saline used with live tissues should be freshly made or stored at 4°C for no longer than a few days.

Heparin (for perfusions)

Dissolve 0.5 ml heparin in 100 ml PBS (see recipe). Make fresh before each set of perfusions.

Phosphate buffer, 0.1 M (pH 7.4)

Mix 3240 ml of 0.2 M dibasic phosphate stock solution (see recipe), 760 ml of 0.2 M monobasic phosphate stock solution (see recipe), and 4 liters distilled water. Check the pH before adding the final 4 liters of distilled water. Adjust as necessary using the appropriate monobasic or dibasic phosphate stocks. Store up to 1 year at room temperature, following the same guidelines for dead/live tissue as for the dibasic and monobasic stock solutions.

Phosphate buffer–dibasic stock solution, 0.2 M

Dissolve 113.56 g Na_2HPO_4 (mol. wt. 141.96 anhydrous) in 2 liters of distilled water on a stir plate. Once dissolved, bring final solution up to 4 liters using a graduated cylinder or volumetric flask. Store up to 1 year at room temperature if only used with dead tissue. Replace after a few weeks if used with live tissue. Discard solution if there is any evidence of mold growth.

Phosphate buffer–monobasic stock solution, 0.2 M

Dissolve 27.5 g $NaH_2PO_4 \cdot H_2O$ (mol. wt. 137.99) in 900 ml of distilled water on a stir plate. Once dissolved, bring final solution up to 1 liter using a graduated cylinder or volumetric flask. Store up to 1 year at room temperature, following the same guidelines for dead/live tissue as for the dibasic stock solution.

Phosphate-buffered saline (PBS)

Dissolve 60 g NaCl in 8 liters of 0.1 M phosphate buffer (see recipe). Store up to 1 year at room temperature, following the same guidelines for dead/live tissue as for the stock solutions.

Phosphate buffered saline with azide (PBS-azide)

Dissolve 0.5 g sodium azide (Caution: water reactive) in 8 liters of PBS (see recipe). Store up to 1 year at room temperature.

Povidone iodine, 20%

Mix 200 ml povidone iodine (available in most drugstores) with 800 ml distilled water. Store indefinitely at room temperature. This solution can be re-used. Replace when it looks dirty, usually after ~300 eggs or when it is used up. Store the used solution separate from the fresh solution.

Sodium pentobarbitol (Somnotol)

Use 0.05 to 0.07 ml/40 to 50 g hatchling chick. Use directly from the stock bottle (65 mg/ml Somnotol stock). Store up to 1 year at room temperature.

COMMENTARY

Background Information

Description of the early embryo assay

The Early Embryo Assay (EEA) is a short-term (<5 day) bioassay used for analysis of teratogenic effects in chicken (and other avian) embryos. The EEA consists of exposing eggs to a contaminant from the start of incubation, either via maternal deposition, or injection into the yolk or the airsac. Following an appropriate incubation time, embryos are evaluated considering the effects of the toxicant on normal growth and development, and on the induction of gross abnormalities (teratogenic changes). The embryos are evaluated at various developmentally relevant time points during the period of early organogenesis. The time points chosen for evaluation are based on preliminary data that pinpoints the early developmental processes that are most likely to be affected by that toxicant or mixtures of toxicants and that identifies the time pattern for the development of the chosen species being evaluated. For 2,3,7,8-tetrachlorodibenzo-*p*-dioxin (TCDD) and the related polychlorinated biphenyls, for example, the optimal time points for embryonic evaluation are after 48, 72 and 96 hr of incubation for the chicken embryo. For other avian species, the researcher must determine the chronological age appropriate for the developmental endpoint under study. This may take some practice given that chronological age does not always equal developmental age.

After the incubation is stopped, the embryo is sacrificed by fixation with, e.g., 10% neutral-buffered formalin, removed from the egg, and evaluated in two ways. First, the embryo is developmentally staged using a stereo microscope. For each age of embryo, each tissue or organ undergoing change at that time is assessed according to its degree of development. These tissues and organs are termed "developmental indicators" and are relevant to each specific embryonic age (see Table 13.4.1). For avian embryos, the growth and development are characterized according to Hamburger and Hamilton staging (Hamburger and Hamilton, 1951). For other classes of vertebrates, a similarly detailed developmental characterization reference would be used. Next, each embryo is assessed for gross visible abnormalities of the individual tissues and organs, and of the embryo as a whole. Overall developmental delays are noted in this step. Finally, the results are evaluated statistically by dose or site to ascertain relative effects of the contaminant exposure on the growth and morphometry of each indicator tissue and organ. Abnormalities are assessed strictly by percent of observed embryos and degree affected, while the stages of each organ and the overall stage ranges observed in each embryo are compared quantitatively. All embryos exposed to a contaminant (either in the wild, at a contaminated site, or in the laboratory) are compared to "control" embryos either taken from a relatively uncontaminated reference site, or injected in the laboratory with the vehicle alone.

Benefits of the early embryo assay

By examining the embryo early, during the process of organogenesis, it may be determined whether critical stages and which stages in the process of early development are being affected, providing more clues to potential mechanisms of developmental toxic action. Furthermore, identifying the specific developmental processes that are affected enables one to utilize the developing database of information about molecular processes that control development. Thus, if it were known, e.g., that a specific gene was expressed just as somites begin to form, and a particular contaminant was documented to affect early somite formation, then an examination of whether that gene was affected by that contaminant could be undertaken. Identifying an array of such contaminant-affected genes could lead to development

Table 13.4.1 Major Developmental Indicator Organs for Embryonic Day 2 (E2), Embryonic Day 3 (E3), and Embryonic Day 4 (E4) Chicken Embryos

E2	E3	E4
Somites	Somites in tail	Somites in tail
Heart	Heart	Curvature
Curvature	Curvature	Visceral arches
Eyes	Visceral arches	Eyes
	Eyes	Brain
	Brain	Nose (nasal pits)
	Nose (nasal pits)	Ear (auditory pits)
	Ear (auditory pits)	Allantois
	Ephiphysis (pineal)	Limb buds
	Allantois	Tailbud
	Limb buds (folds)	
	Tailbud	
	Amnion	

of a suite of relatively contaminant-specific biomarker assays for developmental toxicity.

The early embryo assay has several cost and procedural benefits. The costs of collection of eggs from a sampling site can be substantial, but because the incubation is undertaken in the laboratory, the costs of subsequent trips to the sampling site are saved. Trained observers are able to analyze embryos in a period of time comparable to a necropsy analysis, especially if a well-characterized suite of abnormalities is known to occur for a given toxic agent (15 to 25 min per embryo). The eggs are relatively easy to obtain for many species of birds. Time of collection to the end of the assay (incubation of the eggs) is relatively short (up to 5 days), and sacrifice is relatively quick (on an order of minutes per embryo). Preliminary experiments using a number of different toxicants, as well as preliminary field studies examining embryos exposed to different contaminants in the field, indicate that the pattern of abnormalities observed for each toxicant is to some degree characteristic, although certain abnormalities (such as delays in heart folding or somite abnormalities) appear in embryos exposed to any one of several contaminants (Henshel et al., 1996). For example, characteristic abnormalities associated with TCDD and similarly-acting planar polychlorinated biphenyls (PCBs) in early embryonic chickens include delays in heart folding, delayed or ill-defined brain development, twisting of the embryo just below the level of the heart, asymmetric somites, and abnormal mandibular arches (Henshel, 1993; Henshel et al., 1993). Once the specific abnormalities or suite of abnormalities have been documented and shown to be consistent among species, it would be relatively straightforward for a trained technician to screen the embryos. In addition, if previously unidentified abnormalities occur, it might be possible to infer that a previously unidentified compound is present at that site.

Differences between the early embryo assay and the chick embryo screening test (CHEST)

The Chick Embryo Screening Test (CHEST) assay has been used for some time (Jelinek and Marhan, 1994; Davies and Freeman, 1995) to screen for the teratogenic potential of toxicants. The CHEST assay, however, is distinctly different from the EEA. The CHEST assay is not as portable to the field because exposure conditions are not the same as for chemicals deposited by the mother into the yolk, and ultimately does not have the same potential for development of teratogenicity and development-related biomarkers. Where the EEA begins exposure at the start of incubation, mimicking maternal deposition, the CHEST assay embryos are exposed sometime during the early phases of organogenesis, usually on embryonic (incubation) day 4 [E4], but sometimes on days 2 [E2] or 3 [E3] of incubation. Where the embryos used in the EEA are examined early, during organogenesis, the CHEST

embryos are examined late in development, usually around day 18 of incubation. One benefit of using the CHEST assay compared to the EEA is that it does examine the chick embryos relatively late in development. This enables the evaluation of which observed abnormalities have the potential to be life threatening. However, even more information would be obtained by allowing the chicks to hatch. This would provide information about hatching success as well as about teratogenic changes and growth anomalies evident at the end of the incubation period.

The first problem with using the CHEST assay for any monitoring program carried out by a large number of people in many different places is that the CHEST assay does not have a consistent protocol for exposure. This is a problem because inconsistent results might be observed with embryos exposed on different incubation days, depending on the toxicant being used. Second, exposure to the toxicant during organogenesis rather than from the start of incubation misses all effects manifested during the early embryo formation and early organogenesis phases of development, both of which are very sensitive to disturbance. Third, it is very difficult to inject the yolk of embryos past the first day of incubation since the yolk liquifies and disturbance to the liquified yolk increases the risks of experiment-induced egg mortality. Thus, one loses a critical exposure route (via the yolk) and this is the route that could be the best mimic of natural (in the wild) exposure conditions.

Differences between the early embryo assay and classical field evaluation of teratogenesis

Classical teratogenic evaluation of field-exposed egg-laying animals has consisted of evaluating both the live hatchlings and the dead embryos for gross abnormalities. This can provide clear indications of teratogenic effects, similar to the CHEST assay. However, information is often lost from the early dead embryos as they are often very decomposed by the time of evaluation. Thus, if a contaminant does affect early development, and causes a lethal deformation, it may not be easy to determine the specific developmental processes affected if the embryos are just detectable as "early dead but decomposed." Stopping incubation earlier in development allows the assessor to detect early, potentially more sensitive deformations in examinable embryos. In addition, early embryos may be more sensitive since the early embryo is the most sensitive period in embryonic development for non-specific effects. Some toxicants, such as heavy metals that affect migration in the developing nervous system (Henshel et al., 1996) or TCDD-related compounds that may specifically affect developmental control mechanisms (Henshel et al., 1993) induce effects that are best detected in the early embryo. If only hatching or reproductive success is examined, this precludes detection of physiological stresses that may have occurred during development. These physiological stresses can decrease organismal viability or vitality. The EEA allows for the detection of these early changes.

Benefits of using the early embryo assay in teratogenic monitoring

The early embryo assay provides the potential for applying reliable and sensitive teratogenic evaluation techniques to field monitoring. In conjunction with assessment of other critical parameters, such as reproductive success, teratogenic monitoring of viable and late dead hatchlings, assessment of behavioral neurotoxicity and immunotoxicity, enzyme activity and plasma hormone levels, this combined series of biomarkers will provide a relatively complete picture about the sub-lethal homeostatic mechanisms essential to survival of any individual. The EEA allows a glimpse into potentially serious, but otherwise hard to detect, early teratogenic changes, and may provide a database upon which new developmentally relevant biochemical or molecular biomarkers may be developed. Taking freshly laid eggs is not likely to impact nesting behavior, especially if one or two eggs are left in the nest. Some species, if sufficiently disturbed, will often build or locate a new nest and begin laying again. If taken to excess, this process could deplete the energy and nutrition stores of the laying female. Therefore, care should be taken not to remove too many eggs from any given nest. However, if the appropriate ages for study have been predetermined, as few as one to two embryos per nest can provide sufficient information within a colony-wide (>10 nests) study. For maximal knowledge, the authors suggest also having some method by which to evaluate exposure in at least one of the eggs from each nest sampled. Once, however, a significant knowledge base has been established regarding the relative species sensitivity and chemical sensitivities for early embryos compared to older embryos and hatchlings, the EEA may some day be considered sufficient for

identifying potential contamination problems at the screening level. Furthermore, development of this knowledge base will help future field researchers as they interpret the "decomposed" early embryos found within unhatched eggs. By studying the early embryos, there is the potential to identify the underlying mechanism of specific abnormalities that would not be identifiable in either unhatched embryos or viable hatchlings.

Additionally, since the EEA evaluates teratogenicity in embryos early in development, animal welfare certification for research projects are not difficult to obtain. Young embryos in ovo are not treated as "animals" under the National Institutes of Health animal care regulations.

Transferability to other species, including non-avian species

The EEA may be used with any species provided the basic patterns of early embryonic growth and development have been characterized in that species and verified in field collected and relatively uncontaminated specimens. The authors have found, however, that the relative rate of growth of a given species may be slower than the "standard" species. In this assay, chicken is the standard species; swallows follow a different pattern of development during some periods of development. Thus, whatever species is used, the researcher must first characterize the basic developmental rate for that species under the incubation conditions to be used in the experiment.

Critical Parameters

Study design

The most critical issue when running toxicological experiments with chicken embryos is the study design. Two factors are critical: ensuring sufficient power to evaluate the effect and ensuring that the study design enables within experiment quality controls. In order to decide the sample size for an experiment, most toxicologists follow established parameters for a "good experiment." These parameters might be 200 rats per dose per gender per age for a cancer study, or maybe 50 rats per dose per gender for an acute toxicological assessment. Using this type of thinking, standard practice tends to say that 20 eggs per dose per timing endpoint is ideal for most experiments, 15 eggs per dose per time is sufficient for most experiments, and 10 eggs per dose per timing endpoint is acceptable for a scoping or preliminary study. The problem with teratological studies is that some teratological endpoints have a very low frequency of occurring, even under what might otherwise be "ideal" inducing conditions. For example, long experience with cormorants and terns of the Great Lakes led Jim Ludwig to determine that the rate of cross-billed hatchlings occurring in even the most contaminated areas was ~0.4%, or four cross-bills observed per 1000 hatchlings assessed (Ludwig et al., 1996). At that rate of occurrence, should embryos ever develop cross-bills within a laboratory dosing study, the incidence would be so low that one could almost never be sure that the abnormalities were due to the injected toxicant.

A good study design can enable one to interpret an experiment with an across-dose mortality rate. A poor study design would leave such an experiment without recourse. There are three major parameters that must be included in the study design that goes beyond the obvious issues related to the power of the design (such as the number of eggs injected per dose and the number of doses tested).

1. *Controls*. Beyond all other types of experiments, it is critical to include both vehicle controls and non-injected controls in every group of eggs placed in the incubator. The vehicle controls are the usual controls for the toxicants injected. The non-injected eggs control for the eggs themselves (inherent viability, storage factors, handling effects, and incubator conditions). It is important to remember to treat these non-injected eggs the same as the injected eggs so that the only difference between the non-injected eggs and the other eggs is that the non-injected eggs do not receive the vehicle of the agent under study. Similarly, if the eggs are being sacrificed at more than one time point, the non-injected control eggs must also be sacrificed at each of the timed endpoints. Thus, one needs to include a set of non-injected eggs for each sacrifice time point.

2. *Batches.* Eggs come from multiple hens, which can introduce some variability, both due to factors related to the hen (age, stress levels, health) and the environment (climate and immediate temperature, time after laying and before collection, handling and storage). Thus, it is best to inject and incubate eggs in batches that include some of the sample from each dose group and each control group. To ensure intra-batch standardization and the ability to carry out a statistical quality assurance check, it is best to include at least three eggs in each dose group (and control groups) in each injection/in-

cubation batch. Five per dose group is an even better number. Then, in order to increase the net sample size for the final dose group analysis, one must set at least 3 to 4 batches of eggs for each experiment. This allows the researcher to check for consistency in eggs and incubation conditions over time. This also means that if there is a problem during the incubation period, one only has to reinject and reincubate a portion of the whole experiment, not the entire experimental set. If one were to incubate by dose group, one glitch could destroy a complete dose group, and there might not be any way to be sure that the problem was the incubation conditions and not the toxicant at that dose.

3. *Randomization*. Several factors need to be randomized. Placement of the eggs within an incubator should be randomized to minimize the possibility that a temperature gradient within the incubator differentially affects whole dosed sets of the experiment. Other factors requiring randomization include placement of eggs into dose groups, the order in which embryos are sacrificed to randomize the amount of time an embryo is at room temperature before sacrifice, and the order in which embryos are analyzed (to avoid analyzing all of one dose group at a time).

4. *Volume of injection.* Embryo mortality may result by injecting too much material (even saline) into the airsac or even the yolk. A general rule of thumb, based on preliminary experiments, is that no more than 50 µl of an oily substance, and 100 µl of an aqueous substance should be injected into the air sac. These are absolute maximum volumes for the average 50- to 60-g egg. The apparent problem is that the oil coats the embryo and causes anoxic effects. To prevent this problem, standard practice in the authors' laboratory for oil-based toxicants is to keep the volume of injection to 0.1 µl/g egg. This keeps the injection volumes well-below the 25 µl cut-off that seems to maximize egg viability. DeWitt (unpub. observ.) compared the effects of corn oil injected into the eggs at 0.1 µl/g egg and 1 µl/g egg. There was a significant difference (P = 0.005) in egg viability at these volumes (4 to 5 µl total oil versus 40 to 50 µl oil total).

5. *Vehicle/diluent.* The vehicle chosen must clearly be determined by the toxicant's solubility. However, it is important to remember that the vehicle may itself have effects on developing embryos, and the vehicle may have an impact on the relative toxicity of the toxicant in question. Several common vehicles are questionably non-toxic. Vehicles that have been used in embryos include acetone, DMSO, dioxane, as well as a number of vegetable oils, water, and saline. According to Walker (1967), some of the vehicles (such as formaldehyde and acetone) may interact with the yolk, binding the toxicant into the yolk and making it unavailable to the embryo. In this case, injecting a yolk-binding solvent vehicle into the yolk will artificially decrease the apparent toxicity of the toxicant being tested. Oils injected into the yolk will stay in a droplet and rise up under the embryo, affecting toxicant availability. Some investigators add an emulsifier, such as lecithin, to the oil. In this case, the oil emulsion spreads out under the outer member of the yolk. In this case, the embryo may take in less toxicant emulsion at a time, spread out over a longer period of time (Brunstrom and Darnerud, 1983). Some of the vegetable oils contain high enough concentrations of natural estrogenic compounds to cause masculinization of the brain or feminization of the brain or body, depending on the timing of the injection (Casanova et al., 1999). Use of such vehicles could affect a measurement endpoint. As discussed above, the choice of vehicle also affects the possible volume that may be injected. The other factor to balance against the vehicle to be used is where the researcher wants to inject the toxicant: into the yolk, the air sac, or the albumin. The yolk contains the most fat. The albumen is water-based, but the embryo does not start to "eat" the albumin until more than halfway through incubation, whereas the yolk starts to be liquified and taken up by the embryo within 1 or 2 days of the start of incubation. In summary, it is important to test the vehicle itself and evaluate both inherent toxicity, and how it interacts with the part of the egg it is injected into.

Timing issues

Timing considerations play a role both for the injection and for the sacrifice.

1. *Timing of injection/co-injection*. The embryo will start to develop as soon as the egg is incubated, even somewhat at room temperature. A number of researchers (Hoffman and Ramm, 1972a,b; Hoffman, 1975; Hoffman and Campbell, 1978; Brunstrom, 1983, 1988; Brunstrom and Darnerud, 1983; Brunstrom and Lund, 1988; Powell et al., 1996a,b; Grasman and Whitacre, 2001; Fox and Grasman, 1999) prefer to start incubating the egg first, then injecting the toxicant at embryonic day 3 or 4. This way, researchers can candle the eggs prior to injection and cull out any eggs that do not

seem to be developing normally. The problem with this approach is that the nervous system is the first system to start developing, followed closely by the heart and vasculature. If the toxicant affects the nervous system during that very early organizing phase of development, it is important that the toxicant be present during that phase in order to observe these effects. TCDD, for example, induces effects on embryos that can be detected by 48 hr of incubation. Timed experiments that evaluated heart abnormalities that occurred in chicken hatchlings injected as embryos on day 0 versus day 4 of incubation showed that the heart abnormalities were much less severe, and some abnormalities were absent (e.g., split aortic arch) in the hatchlings that were only exposed from embryonic day 4 onward (Noel and Henshel, 1996). If the researcher chooses to inject preincubated embryos, they must be aware that they may well have missed very early effects.

2. *Timing of sacrifice.* The nervous system, for example, develops in an ordered way, rostral to caudal, with a series of interdependent changes that occur at characteristic developmental stages (Purves and Lichtman, 1985). One must therefore choose the embryological endpoints with an awareness of what is supposed to happen prior to that point in development. One must also determine whether the resultant toxicological effect would be permanent or transient and adjust sacrifice ages appropriately.

Troubleshooting

Problems with chicken embryo studies often derive from several prime sources: (a) the uninjected eggs; (b) incubation conditions; (c) injection technique, volume and diluent; and (d) improper study design.

The non-injected eggs

Eggs that have been mishandled (often during shipping), allowed to overheat sometime prior to incubation, or allowed to chill at too low a temperature, will have poor viability. So long as the study design ensures that all batches of eggs include some non-injected controls, this will be evident from the cross-dose decrease in viability. In general, a 70% to 80% cross-dose or control viability is acceptable, but an 85% to 95% control viability is preferred. Consistent batch viabilities of ≤75% indicates that the eggs are being stressed or mishandled, or that the hens are reaching the end of their useful laying life. Eggs that are stored for too long also begin to lose viability. To ensure that storage is not a factor in the authors' results, eggs are held at 55°F for no more than 3 to 5 days, with 1 to 2 days being the preferred storage time. By 1 week, viability may decrease. By 2 weeks, viability is clearly affected. Any longer than 2 weeks and viability continues to decrease steadily. This change in viability will partially vary with the freshness of the eggs when put into storage, and partially depend on the storage conditions (temperature and humidity). Each laboratory should test the storage versus viability function for themselves with each new supplier or new brood of hens that provide the eggs.

Incubation conditions

Incubation conditions are critical. A slight change in incubation temperature, for example, can significantly affect the rate of embryonic development. Two degrees change of incubation temperature can result in significantly reduced viability and embryonic deformation (see detailed tables in Romanoff and Romanoff, 1972). Humidity that is too low will stress the embryo, reduce growth rate, and decrease the embryo's ability to rotate within the shell. This direct unchanging physical contact can produce gross malformations. Extended dryness may result in the death of the embryo or an embryo so weakened that it can not pip or fully hatch. Humidity that is much too high can result in excess fluid inside the shell. In this case, the excess fluid can actually drown the embryo if the humidity excess is severe. (This is less often seen with chicken embryos than with some other avian embryos. This has been seen, for example, with cormorants.) Incubation conditions need to be monitored. It is highly recommended to make sure the incubator is holding a steady temperature for at least 24 hr after being started before putting any eggs in to incubate. Thus, prior to initiating a new experiment, it is always a good idea to incubate a set of non-injected eggs and to sacrifice them at specific pre-chosen points throughout development in order to establish the growth-rate curve for the specific incubation conditions (temperature and humidity) that will be used.

Anticipated Results

The types of results will clearly depend on the study design and the endpoints chosen for analysis. In a classic toxicological experiment, with multiple doses used, two possible results may be seen for any given endpoint. First, there may be a classic dose-response curve at which there is an increase in the rate or intensity of the endpoint with increased dose applied. Many

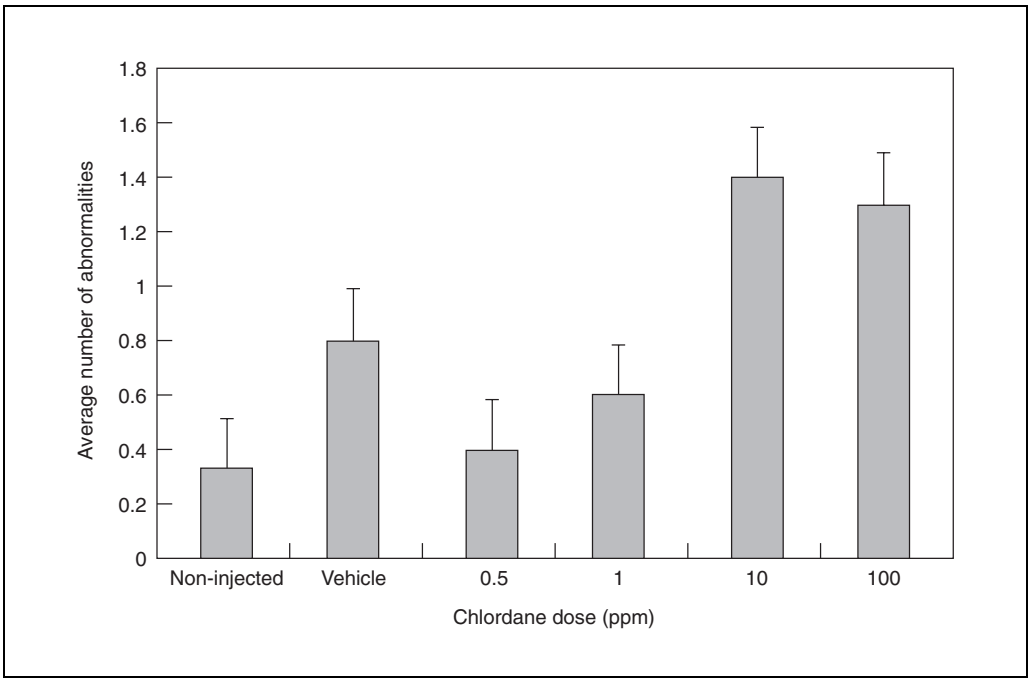

Figure 13.4.1 Average number of abnormalities in 48-hr-old domestic chicken embryos (*Gallus gallus*) exposed to technical-grade chlordane (parts per million) in ovo. Abnormalites included underdeveloped overall for age, underdeveloped organs for stage of embryo, constricted heart, asymmetric somites, abnormal spine, abnormal turning of head, and constriction of optic vesicles.

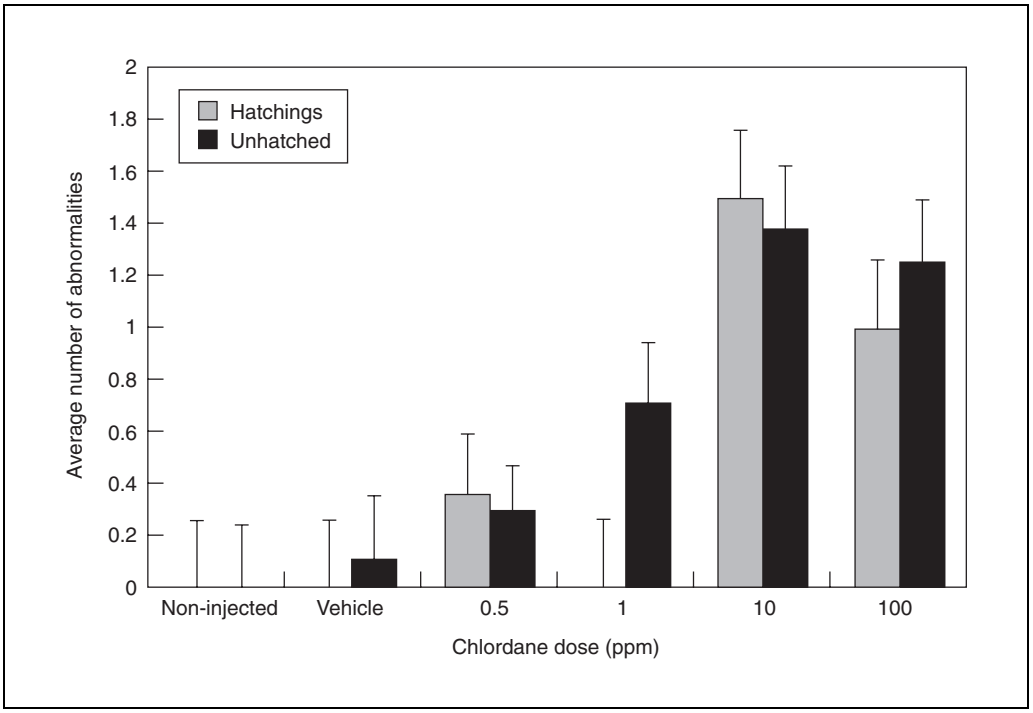

Figure 13.4.2 Average number of abnormalities in domestic hatchling or dead-at-pipping chickens (*Gallus gallus*) exposed to technical-grade chlordane (parts per million) throughout development in ovo. Abnormalites included edema, curled toes, and small size for age.

abnormalities, however, seem to occur at a higher frequency in the dosed populations, but may not occur in a pattern that matches ever-increasing frequency with ever-increasing dose.

One would say that most malformations should never occur. However, given the detectable rate of unexplained birth defects in human infants, it is clear that unexplained gross malformations do occur. This happens in chicken embryo experiments as well. The fact that some gross abnormalities occur across all doses and controls and incubators in only sporadic batches of eggs indicates to us that the most common cause relates to the handling of the eggs prior to arrival in the authors' laboratory.

Given the potential for non-specific gross malformations being induced by handling, incubation conditions, errors made during the injection process, or by other not clearly defined factors, the researcher must realize that periodically one of many gross malformations (e.g., slow developmental rate, hematomas, or generalized bleeding, twisting of the tail) may occur. These are not normally developing embryos, but the cause of the abnormality may be unclear, and may not be due to the toxicant being tested. Study designs that incorporate appropriate controls will enable the researcher to interpret the results. Study designs that lack the appropriate controls will result in difficult-to-interpret results if any of these abnormalities occur.

The following information in this section illustrates an example of the early embryo assay and a lethality study (LD50) designed to explore the teratogenic effects of chlordane, an organochlorine insecticide.

Basic Protocols 1 to 3

Eggs obtained from the Purdue University Poultry Unit (Purdue University Animal Sciences Research Farms) were prepared as directed in Basic Protocol 1, steps 1 to 5, in four different batches for the early embryo assay and in one batch for the lethality study. Technical grade chlordane (CAS number 57-74-9, Ultra-Scientific) was mixed with a safflower oil vehicle so that 0.1 µl per gram of egg resulted in either 0.5, 1, 10, or 100 parts per million concentration. Controls received the safflower oil alone or no injection at all. Doses were the same for both the early embryo assay and the LD50 study. Injection and incubation procedures followed Basic Protocol 1, steps 8 to 16.

Incubation for the early embryo assay eggs was stopped at either 48 or 96 hr of incubation. The LD50 eggs were taken to hatch unless candling revealed death, in which case the eggs were opened and the embryos were removed, aged, and assessed for external abnormalities (see Basic Protocol 1, step 16). Early embryos were removed from eggs as per Basic Protocol 2, steps 6 to 16. Hatchling chicks were examined for external abnormalities, weighed, measured, and sacrificed via decapitation (see Basic Protocol 3, Method B). Sera were collected from trunk blood that was spun in a microcentrifuge for 15 min and immediately snap frozen at −80°C. Brains were immediately removed and immersion-fixed in 10% neutral-buffered formalin. Livers were removed, weighed, and cut in half, with one half immersed in formalin and the other half immersed in glycerol and snap frozen at −80°C. See Figures 13.4.1 and 13.4.2 for results.

Time Considerations

One benefit of working with the avian embryo is that, if time is a factor for the researcher, the researcher can often choose a different endpoint or earlier stage to evaluate. Thus, the early embryo assay uses early stages of tissue development to evaluate (after 48 to 96 hr of incubation in general), reducing the total time for generation of embryos to evaluate to one 5-day week. Certain endpoints, however, are determined by the developmental timing of the embryo and cannot be changed by evaluating a slightly younger stage. Myelination, for example, starts by embryonic day 13 in the chicken spinal cord. This is much earlier than in the mammalian embryos, in which myelination generally begins postnatally. In the chicken embryo, however, myelination continues steadily over the course of embryonic days 13 through 16. Then just before day 17 myelination progresses in a burst so that by embryonic day 17, the chicken embryo spinal cord is almost as well-myelinated as the spinal cord of the hatchling chicken (21 days).

Literature Cited

Brunstrom, B. 1983. Toxicity in chick embryos of three commercial mixtures of chlorinated paraffins and of toxaphene injected into eggs. *Arch. Toxicol.* 54:353-357.

Brunstrom, B. 1988. Sensitivity of embryos from duck, goose, herring gull, and various chicken breeds to 3,3′,4,4′-tetrachlorobiphenyl. *Poult. Sci.* 67:52-57.

Brunstrom, B. and Darnerud, B. 1983. Toxicity and distribution in chick embryos of 3,3′4,4′-tetrachlorobiphenyl injected into the eggs. *Toxicology* 27:103-110.

Brunstrom, B. and Lund, J. 1988. Differences between chick and turkey embryos in sensitivity to 3,3′4,4′-tetrachloro-biphenyl and in concentration/affinity for the hepatic receptor for 2,3,7,8-tetrachlorodibenzo-*p*-dioxin. *Comp. Biochem. Physiol. C Comp. Pharmacol. Toxicol.* 91:507-512.

Casanova, M., You, L., Gaido, K.W., Archigeque-Engle, S., Janszen, D.B., and Heck, H.A. 1999. Developmental effects of dietary phytoestrogens in Sprague-Dawley rats and interactions of genistein and daidzein with rat estrogen receptors alpha and beta in vitro. *Toxicol. Sci.* 51:236-244.

Davies, W.J. and Freeman, S.J. 1995. CHick Embryotoxicity Screening Test (CHEST I and II). *Methods Mol. Biol.* 43:307-310.

Firestone, D. 1973. Etiology of chick edema disease. *Environ. Health Perspect.* 5:59-66.

Fox, L.L. and Grasman, K.A. 1999. Effects of PCB 126 on primary immune organ development in chicken embryos. *J. Toxicol. Environ. Health* 58:233-244.

Grasman, K.A. and Whitacre, L.L. 2001. Effects of PCB 126 on thymocyte surface marker expression and immune organ development in chicken embryos. *J. Toxicol. Environ. Health* 62:191-206.

Hamburger, V. 1992. The stage series of the chick embryo. *Dev. Dyn.* 195:273-275.

Hamburger, V. and Hamilton, V.L. 1951. A series of normal stages in the development of the chick embryo. *J. Morphol.* 88:49-92.

Hamburger, V. and Hamilton, V.L. 1992. A series of normal stages in the development of the chick embryo. 1951. *Dev. Dyn.* 195:231-272.

Henshel, D.S. 1993. LD50 and teratogenicity studies of the effects of TCDD on chicken embryos. *Soc. Environ. Toxicol. Chem. Abstr.* 14:652.

Henshel, D.S., Hehn, B., Vo, M.T., and Steeves, J.D. 1993. A short-term test for dioxin teratogenicity using chicken embryos. *In* ASTM STP #1216: Environmental Toxicology and Risk Assessment, 2nd Volume (W. Landis, J. Hughes, and M. Lewis, eds.) pp. 159-174. American Society for Testing and Materials, Philadelphia.

Henshel, D.S., Allen, C.A., Lam, Y., and Benson, K. 1996. A comparison of the early embryo effects of ethanol, 1,1,1-trichloroethane, atrazine, 2,4-D, methyl mercury, lead, and 2,3,7,8-TCDD. *Fundam. Appl. Toxicol.* 30:197.

Hoffman, D.J. 1975. Physiological effects of hypoxia and trypan blue in 17-day chick Embryos. *Teratology* 12:57-60.

Hoffman, D.J. and Campbell, K.I. 1978. Embryotoxicity of irradiated and nonirradiated automotive exhaust and carbon monoxide. *Environ. Res.* 15:100-107.

Hoffman, D.J. and Ramm, G.M. 1972a. Physiological effects of trypan blue on chick embryos. *J. Exp. Zool.* 182:227-232.

Hoffman, D.J. and Ramm, G.M. 1972b. Effects of hyperoxia on chick embryos injected with trypan blue. *Teratology* 5:315-318.

Jelinek, R. and Marhan, O. 1994. Validation of the Chick Embryotoxicity Screening Test (CHEST). A comparative study. *Funct. Dev. Morph.* 4:317-323.

Ludwig, J.P., Kurita-Matsuba, H., Auman, H.J., Ludwig, M.E., Cummer, C.L., Goesy, J.P., Tillitt, D.E., and Jones, P.D. 1996. Deformities, PCBs, and TCDD-equivalents in double-crested cormorants (*Phalacrocorax auritis*) and caspian terns (*Hydroprogne caspia*) of the upper Great Lakes 1986-1991: Testing a cause-effect hypothesis. *J. Gt. Lakes Res.* 22:172-197.

McLaughlin, J., Jr., Marliac, J.P., Verrett, M.J., Mutchler, M.K., and Fitzhugh, O.G. 1963. The injection of chemicals into the yolk sac of fertile eggs prior to incubation as a toxicity test. *Toxicol. Appl. Pharmacol.* 5:760-771.

Noel, S. and Henshel, D.S. 1996. Effects of in ovo exposure to TCDD on heart development in chickens. Independent research study (L490), Department of Biology, Indiana University, Bloomington, IN.

Powell, D.C., Aulerich, R.J., Meadows, J.C., Tillitt, D.E., Giesy, J.P., Stomberg, K.L., and Bursian, S.J. 1996a. Effects of 3,3′,4,4′,5-pentachlorobiphenyl (PCB 126) and 2,3,7,8-tetrachlorodibenzo-*p*-dioxin (TCDD) injected into the yolks of chicken (*Gallus domesticus*) eggs prior to incubation. *Arch. Environ. Contam. Toxicol.* 31:404-409.

Powell, D.C., Aulerich, R.J., Stromborg, K.L., and Bursian, S.J. 1996b. Effects of 3,3′,4,4′-tetrachlorobiphenyl, 2,3,3′,4,4′-pentachlorobiphenyl, and 3,3′,4,4′,5-pentachlorobiphenyl on the developing chicken embryo when injected prior to incubation. *J. Toxicol. Environ. Health* 49:319-338.

Purves, D. and Lichtman, J.W. 1985. Principles of Neural Development. Sinauer Associates, Inc. Sunderland, MA.

Romanoff, A.L. 1960. The Avian Embryo: Structural and Functional Development. The Macmillan Company, New York.

Romanoff, A.L. and Romanoff, A.J. 1972. Pathogenesis of the Avian Embryo; An Analysis of Causes of Malformations and Prenatal Death. Wiley-Interscience, New York.

Sanes, J.R. 1992. On the republication of the Hamburger-Hamilton stage series. *Dev. Dyn.* 195:229-230.

Verrett, M.J. 1976. Investigation of the toxic and teratogenic effects of halogenated dibenzo-*p*-dioxins and dibenzofurans in the developing chicken embryo. *In* Memorandum Report, U.S. Food and Drug Administration, Washington, D.C.

Walker, N.E. 1967. Distribution of chemicals injected into fertile eggs and its effect upon apparent toxicity. *Toxicol. Appl. Pharmacol.* 10:290-299.

Key References

Hamburger and Hamilton, 1951. See above.

Contains the first comprehensive overview of chicken embryonic development, with both text and photos, detailing anatomical changes from day 0 to day 21 of development.

Henshel, D.S., Sparks, D.W., Allen, C.A., Benson, K., Fox, C., Lam, Y., Sobiech, S.A., and Wagey, R. 1997. Preliminary results using the early embryo teratogenesis assay: A comparison of early embryo abnormalities with late embryo and hatchling teratogenic changes. *In* ASTM STP #1317: Environmental Toxicology and Risk Assessment: Modeling and Risk Assessment, 6th Volume (F.J. Dwyer, T.R. Doane, and M.L. Hinman, eds.) pp. 391-401. American Society for Testing and Materials, Philadelphia.

Contains an overview of the Early Embryo Assay and its comparison to older embryos and hatchling chicks.

Henshel et al., 1993. See above.

Contains an overview of the Early Embryo Assay using dioxin as a model toxicant.

Romanoff, 1960. See above.

Similar to the Hamburger and Hamilton (1951) book, chronicles the development of the chicken embryo. Chapters divided by system.

Romanoff and Romanoff, 1972. See above.

This book chronicles the types of effects that may result in chicken embryos exposed to a variety of events and agents.

Internet Resources

http://www.urbanext.uiuc.edu/eggs/

The Web site of the University of Illinois (Champagne-Urbana) Extension, Incubation and Embryology. This Web site provides a basic primer on chicken eggs, how to incubate them, and how to preserve the embryos. The site is aimed at pre-college teachers, and so some of the information is not necessarily relevant to a researcher. However, it has some good practical advice on incubation, including a nice troubleshooting page.

http://www.ucmp.berkeley.edu/vertebrates/tetrapods/amniota.html

B.R. Speer's, University of California Berkeley, 1995, Web site on the Introduction to the Amniota. This Web site provides a description of the structure of the egg as well as a nice diagram of a basic egg. A simple, but useful "atlas" of the amniote egg.

http://anatomy.med.unsw.edu.au/cbl/embryo/OtherEmb/Chicken.htm

M. Hill's, University of New South Wales, Chicken Development, Web site contains a series of lecture notes and figures utilized for a college course on embryological development. Includes an abbreviated table of the Hamburger and Hamilton (1951) stages of chicken embryonic development, as well as references to other atlases.

Contributed by Diane S. Henshel, Jamie DeWitt, and Andrea Troutman
Indiana University
Bloomington, Indiana

In Vivo Assessment of Prenatal Developmental Toxicity in Rodents

Developmental toxicity is defined as any adverse effect on the developing organism that may result from toxicant exposure prior to conception, during prenatal development, or postnatally to the time of sexual maturation. There are four major manifestations of developmental toxicity: (1) death, (2) structural abnormality, (3) altered growth, and (4) functional deficits (EPA, 1991). This unit describes two basic approaches for testing chemicals (or conditions) for their potential to cause prenatal developmental toxicity in rats and mice. Both protocols are similar in that they involve treatment of pregnant animals, followed by an evaluation of the prenatally exposed litters. The protocols differ, however, in the methodology used to evaluate the litters. In the first approach (see Basic Protocol 1), referred to as a Segment II study, the evaluation of the progeny focuses on the external, skeletal, and soft-tissue morphology of the full-term fetus. In the second basic approach (see Basic Protocol 2), often referred to as the Chernoff/Kavlock assay, the evaluation of the progeny focuses on the postnatal growth and viability of the neonates. This protocol is useful as a developmental toxicity screen and is effective in prioritizing chemicals for Segment II testing.

SEGMENT II STUDY

BASIC PROTOCOL 1

This is the standard test for developmental toxicity in rodents, and it is consistent with governmental guidelines for prenatal developmental toxicity testing (ICH, 1994; EPA, 1998b; OECD, 2000). The following Basic Protocol is presented as an overview of the study design; methodological details are provided in the ensuing Support Protocols: (1) performing cesarean sections (Support Protocol 1), (2) examination of apparently nongravid uteri (Support Protocol 2), (3) examination of fetal visceral specimens (Support Protocol 3), (4) preparation of fetal skeletal specimens (Support Protocol 4), (5) examination of fetal skeletal specimens (Support Protocol 5), and (6) statistical analysis and interpretation of the data (Support Protocol 6).

Materials

Young adult (e.g., 60- to 90-day-old) timed-pregnant rats or mice of any strain with high fecundity

Test substance

Bodian's solution (see recipe) or Bouin's solution (see recipe)

4% (w/v) NaCl

Additional reagents and equipment for care and handling of rodents (e.g., Coligan et al., 2003), cesarean section (Support Protocol 1), examination of apparently nongravid uteri (Support Protocol 2), examination of fetal visceral specimens (Support Protocol 3), preparation of fetal skeletal specimens (Support Protocol 4), and examination of fetal skeletal specimens (Support Protocol 5), and data analysis and interpretation (Support Protocol 6)

Treat and observe dams during gestation

1. Obtain timed-pregnant animals prior to gestation day (GD) 6.

   The day upon which a copulatory plug or vaginal sperm is found is designated gestation day (GD) 0.

Contributed by Michael G. Narotsky and Robert J. Kavlock

Current Protocols in Toxicology (2003) 13.5.1-13.5.25

2. Weigh the animals prior to treatment (if possible, at least 1 day prior to treatment initiation) for group assignment. Assign the animals to treatment groups using procedures that provide comparable weight distributions in all groups (see, e.g., Narotsky et al., 1997).

   Information on housing, handling, and identification of experimental rodents is available in Coligan et al. (2003).

3. Treat the animals with the test substance by a relevant route (typically by gavage) at least once per day from the point of implantation to the day prior to scheduled caesarean section.

   Rats should generally be treated on GD 6 to 20, and mice on GD 6 to 17. Animals may be dosed more frequently than once per day if this is deemed appropriate based on pharmacokinetic data.

4. Record maternal body weights and food consumption at ≤3-day intervals throughout the treatment period.

   The authors recommend recording body weights daily throughout the treatment period and 1 day after the last treatment.

5. Observe the animals for clinical signs of maternal toxicity throughout the study period. Note changes, e.g., in skin, pelage, eyes, mucous membranes, breathing, behavior, or excreta. Generally, examine the animals immediately after dosing, ~1 hr later (or when maximum effects might be anticipated), and again prior to the end of the working day.

Perform cesarean sections

6. Using a method approved by the Institutional Animal Care and Use Committee (also see AVMA, 2001), euthanize the rats on GD 21 and mice on GD 18 (to avoid losses due to early deliveries, it may be necessary to euthanize the animals 1 day earlier, i.e., on GD 20 for rats and GD 17 for mice). Weigh the gravid uterus. Deliver the litters by cesarean section. Count and classify each implantation site. Weigh and examine each live fetus for external alterations. Maintain the identity of each fetus throughout all examinations. For maternal rats, count the number of corpora lutea.

   The abovementioned procedures are described in Support Protocol 1.

7. Examine apparently nongravid uteri for resorption sites (see Support Protocol 2).

8. Preserve approximately one-half of the live fetuses of each litter in Bodian's (or Bouin's) solution for subsequent visceral examination (see Support Protocol 3).

9. Place the remaining live fetuses in 4% NaCl for subsequent preparation of skeletal specimens (see Support Protocol 4).

Examine fetal specimens

10. Examine visceral specimens for alterations (see Support Protocol 3).

11. Examine skeletal specimens for alterations (see Support Protocol 5).

Analyze and interpret data

12. Prepare data for statistical analysis. If not captured automatically during data collection, enter the data into a computerized format for subsequent data processing.

13. Statistically analyze the data using appropriate methods (see Support Protocol 6).

14. Summarize the data by preparing group summary tables and graphical presentations of the data (see Support Protocol 6).

15. Evaluate the data and draw conclusions regarding maternal and developmental toxicity of the test article (see Support Protocol 6).

CHERNOFF/KAVLOCK ASSAY

BASIC PROTOCOL 2

This is generally considered a screening assay for developmental toxicity. For most intents and purposes, the preparturition steps are identical to the methods used in a Segment II study.

Materials

Young adult (e.g., 60- to 90-day-old) timed-pregnant rats or mice of any strain with high fecundity

Test substance

Additional reagents and equipment for care and handling of rodents (e.g., Coligan et al., 2003) and examination of apparently nongravid uteri (Support Protocol 2)

Treat and observe dams during gestation

1. Obtain timed-pregnant animals prior to gestation day (GD) 6.

   The day upon which a copulatory plug or vaginal sperm is found is designated gestation day (GD) 0.

2. Weigh the animals prior to treatment (if possible, at least 1 day prior to treatment initiation) for group assignment. Assign the animals to treatment groups using procedures that provide comparable weight distributions in all groups (see, e.g., Narotsky et al., 1997).

   Information on housing, handling, and identification of experimental rodents is available in Coligan et al. (2003).

3. Treat the dams with the test substance by a relevant route (typically by gavage) on GD 6 to GD 20 (for rats) or GD 6 to GD 17 (for mice).

4. Record maternal body weights and food consumption daily throughout the treatment period and 1 day after the final treatment.

5. Observe the animals for clinical signs of maternal toxicity throughout the study period. Note changes, e.g., in skin, pelage, eyes, mucous membranes, breathing, behavior, or excreta. Generally, examine the animals immediately after dosing, ~1 hr later (or when maximum effects might be anticipated), and again prior to the end of the working day.

Examine the dams for parturition

6. After GD 20 (for rats) or GD 18 (for mice) determine observe the dams periodically for signs of parturition, while disturbing the dams as little as possible. Check the dams at the end of the working day on GD 20 (rats) or 18 (mice) and more frequently on the next 2 days. Continue periodic checking of any apparently gravid dams that have not delivered after this period.

7. For each dam, when vaginal bleeding or pup(s) are first observed, record the date (or gestation day), time, and one of the following descriptions of the status of parturition:

"Blood only" (vaginal bleeding, but no pups)
"One pup, in progress" (two or more pups delivered, but parturition not yet completed)
"Completed."

Also record any findings of prolonged labor or dystocia.

Examine the litters

8. Examine the litters on postnatal day 1 (PD 1).

   PD 1 corresponds to GD 22 regardless of the day of parturition. Alternatively, some laboratories define PD 1 as the day on which parturition was completed.

9. For each litter, record the approximate time of the PD 1 examination.
10. Place the dam in a holding cage and collect the pups. Carefully examine the cage bedding to find any buried pups.
11. Examine each pup. Record the weight (to the nearest 0.1 g), sex, and any external alterations observed. On PD 1, note the presence or absence of an abdominal milk band: i.e., milk in the stomach visible through the neonate's abdominal wall.

    In studies where sex differentiation may be affected, quantitation of the anogenital distance may be warranted.

12. Euthanize any moribund or malformed live pups that are not expected to survive using methods approved by the Institutional Animal Care and Use Committee (also see AVMA, 2001). Based on gross external findings, preserve and examine each specimen using appropriate methods to best evaluate possible visceral or skeletal defects (see, e.g., Support Protocols 3 to 5).
13. Preserve and examine any intact dead pups as deemed appropriate.
14. Return the live pups and then the dam to their home cage.
15. Examine the litters on PD 6, repeating steps 10 to 14.
16. After the PD 6 examinations, euthanize the pups in a manner approved by the Institutional Animal Care and Use Committee (also see AVMA, 2001). As deemed appropriate, re-examine/dissect select pups to confirm in-life examination findings (e.g., microphthalmia). Carcasses may be discarded.

Examine the uterus

17. Euthanize the adult females in a manner approved by the Institutional Animal Care and Use Committee (also see AVMA, 2001). Excise the dam's uterus and press the uterus between the outer surfaces of two petri dishes. Count the implantation sites while viewing the uterus against a light source.
18. For apparently nongravid females, stain and examine the uterus as described in Support Protocol 2.

SUPPORT PROTOCOL 1

CESAREAN SECTIONS

This protocol, performed as part of the Segment II study (see Basic Protocol 1), describes the procedures used to examine the uterus, deliver and examine the full-term fetuses, and designate the fetuses for subsequent examinations.

Materials

Mouse or rat from Segment II study (see Basic Protocol 1)
Physiological saline: 0.9% (w/v) NaCl
4% (w/v) NaCl
Bodian's solution (see recipe)

Surgical instruments
Dissecting microscope
Weigh boats (or petri dishes)
24- or 48-well plates
Absorbent paper and/or cardboard trays
18-well polystyrene trays (Flambeau Products Corp.)
Dry-erase marking pen (or equivalent)
Solvent-resistant specimen jars
Dissecting microscope

Additional reagents and equipment for care and handling of rodents (e.g., Coligan et al., 2003) and examination of apparently nongravid uteri (Support Protocol 2)

Examine uterine contents in situ

1. Euthanize the dam according to methods approved by the Institutional Animal Care and Use Committee (also see AVMA, 2001), and open the abdominal body wall.

2. Without incising the uterine wall, examine the uterine contents and classify each implantation site as one of the following.

    a. Metrial gland only
    b. Metrial gland plus placenta
    c. Macerated fetus
    d. Dead fetus (without areas of resorption)
    e. Live fetus (responds to tactile stimuli).

    Record the sequence of implantation sites in a systematic manner (e.g., right to left, or cervix to ovary) for each uterine horn.

Remove and weigh the gravid uterus and examine nongravid uteri

3. Excise the uterus, leaving the left ovary attached to the uterus (to distinguish the right and left horns in step 6); excise the right ovary separately, being careful to leave part of the right oviduct attached to the uterus to minimize the chance of uterine rupture. Place the tissues in petri dishes or weigh boats. Examine the carcass, especially known target organs of toxicity, for gross lesions, and record any findings.

4. Weigh the gravid uterus (with left ovary attached) to the nearest 0.1 g.

5. If the uterus appears nongravid, examine as in Support Protocol 2.

Remove ovaries for subsequent counting of corpora lutea

6. If the uterus is gravid, lay it flat on absorbent paper, noting the right and left horns as indicated by the attached (left) ovary. For rats, remove the left ovary (with some of the oviduct attached) and store with the right ovary in physiological saline for subsequent counting of the corpora lutea. Place ovaries from the same dam in the same well of a 24- or 48-well plate and label with the dam number.

Remove fetuses from uterus and examine externally

7. Open the uterus (the authors recommend using curved, blunt-tipped scissors) and confirm/correct implantation designations (see step 2). Remove each live fetus from

the uterus and, maintaining their intrauterine sequence (i.e., position within the uterus), place on absorbent paper.

8. For each live fetus, record the individual fetal weight (to the nearest 0.1 g).

9. Examine each live fetus externally for alterations. Proceed in an orderly manner to scrutinize the entire fetus, including the head (shape, pinnae, eyes, eyelids, snout, jaw, nares, lip), skin, tail, back, ventral wall, genitalia, limbs, feet, and digits (it is unnecessary to open the mouth to examine the palate at this time, since the palate will be more easily examined during the skeletal and visceral examinations). Photographically document findings as deemed appropriate.

10. Examine the external genitalia and record the sex of each fetus. Determine the sex by noting the anogenital distance (longer for males).

Designate fetuses for skeletal/visceral examination

11. Euthanize the fetuses using a method approved by the Institutional Animal Care and Use Committee. For example, inject sodium pentobarbital (~200 mg/kg) intraperitoneally.

    Protocols for euthanasia of rodents, including the pentobarbital method, are provided in AVMA (2001) and Coligan et al. (2003).

12. Systematically, and in a nonbiased manner, select approximately one-half of the fetuses from each litter for skeletal examination. For example, select alternate fetuses for skeletal examination starting with the first fetus (closest to the right ovary) in even-numbered dams and the second fetus in odd-numbered dams.

13. Place fetuses that were selected for skeletal examination in 4% NaCl. Maintaining the intrauterine sequence, place each skeletally designated fetus in a well of an 18-well plastic tray. Use a different tray for each litter.

    See Support Protocol 4 for further preparation of the skeletal specimens.

14. Individually identify each of the remaining fetuses by marking the back with a dry-erase marker (or similar ink that is resistant to Bodian's solution). Snip some skin off of the back (avoiding the identification marking) to enhance penetration of the fixative and place in a solvent-resistant specimen jar with Bodian's solution for subsequent visceral examination.

    All viscerally designated fetuses may be fixed in the same jar; the amount of fixative should be ~10 times the tissue mass being preserved (i.e., 10 ml fixative per 1 g tissue). Alternatively, place fetuses in individual compartments of a solvent-resistant tray. See Support Protocol 3 for subsequent examination of the visceral specimens.

Count the corpora lutea

15. For rats, examine the ovaries with the aid of a dissecting microscope and record the total number of corpora lutea for each dam (the ovaries and oviducts may be discarded after examination). Place any ovaries that are not examined by the end of the working day in physiological saline and refrigerate.

    For mice, the authors do not recommend counting the corpora lutea; in this species, the corpora lutea rupture easily, yielding unreliable counts (Taylor, 1986).

EXAMINATION OF APPARENTLY NONGRAVID UTERI

This method describes the procedure for staining resorption sites in rodent uteri. The procedure is used on apparently nongravid uteri to detect or confirm cases of full-litter resorption in both the Segment II and Chernoff/Kavlock protocols.

CAUTION: Due to the stench of ammonium sulfide, all work with this chemical should be conducted in a fume hood.

Materials

Uteri (see Basic Protocols 1 and 2 and Support Protocol 1)
2% (w/v) ammonium sulfide (see recipe)

Surgical instruments
Petri dishes
6-well tissue culture plate (or similar container)
Sealable specimen bags

1. Excise the uterus.
2. Press the uterus between the outer surfaces of two petri dishes and count the implantation sites while viewing the uterus against a light source.
3. Place the uterus in a compartment of a 6-well tissue culture plate for staining. Label the plate with the dam number and record the number of implantation sites.
4. Put ~5 ml of 2% ammonium sulfide solution into each uterus-containing well.
5. After at ≥15 min, but preferably after 1 to 4 hr, examine each uterus for darkly stained implantation sites. Press the uterus between two petri dishes to facilitate the examination (Fig. 13.5.1).
6. Record the number of positively stained implantation sites.
7. After all uteri are examined, seal them in a specimen bag and dispose of them.

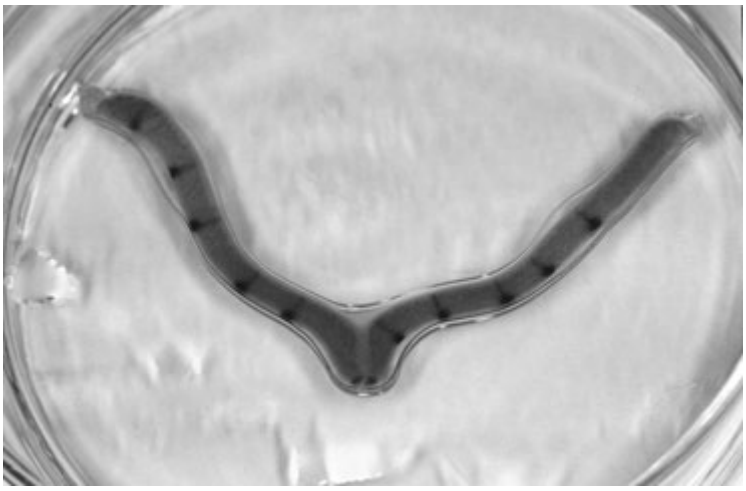

Figure 13.5.1 A rat uterus stained with 2% ammonium sulfide and viewed between two glass pretri dishes. Five stained resorption sites are visible for each uterine horn.

EXAMINATION OF FETAL VISCERAL SPECIMENS

A variety of methods may be used to examine Segment II specimens (see Basic Protocol 1) for soft-tissue defects. The following describes an examination procedure with fixed specimens. Except for examination of the brain, this procedure can be easily applied to fresh specimens.

NOTE: Since the examination involves dissection of tissues, it often precludes subsequent re-examination of many findings; thus, it is important to photographically document findings as deemed appropriate.

NOTE: When recording findings, use terminology consistent with that recommended by the International Federation of Teratology Societies Committee on Harmonization of Terminology in Developmental Toxicology (Wise et al., 1997).

Materials

Fetal specimens (see Basic Protocol 1 and Support Protocol 1) in Bodian's solution
Bodian's solution (see recipe) or Bouin's solution (see recipe)
Thymol crystals

Dissecting microscope
Dissection instruments including:
- Forceps
- Iris scissors
- Ultramicrodissection scissors
- Razor blades (or scalpels)

Air-tight vials (e.g., scintillation vials)

Vent specimen and examine externally

1. Maintaining litter identification, transfer specimens from Bodian's solution to an open container of tap water under a fume hood. After the specimen has sunk, i.e., when most of the fixative fumes have dissipated, remove the specimen for examination.
2. Examine each specimen externally for alterations of the head (i.e., general shape, pinnae, eyes, eyelids, jaw, nares, and lip), as well as the skin, tail, back, ventral wall, limbs, feet, and digits.
3. Section the specimen through the mouth (just below the pinnae) and the abdomen (leaving the diaphragm intact) yielding three portions: the head, forequarters, and hindquarters.

Examine the head

4. Remove the tongue and examine the palate for a cleft. Also examine the rugae for irregularities.
5. Make transverse sections perpendicular to the mouth and through the nasal passages, eyes, and the greatest diameter of the skull. In addition, make a mid-sagittal section through the hindbrain portion of the specimen.

   The mid-sagittal section need not go entirely through the specimen; the two halves may remain "hinged" with connective tissue.

6. Examine the head sections with particular attention to the nasal passages and septum, palate and rugae, eyes, lenses, retinae, and ventricles of the brain.

7. Score the dilation of the lateral ventricles:

   0 = essentially none
   1 = slight
   2 = moderate
   3 = severe.

Examine the forequarters

8. Examine the liver for color and texture. Carefully remove it, leaving the diaphragm intact.
9. Examine the diaphragm for herniation.
10. Cut through the length of the sternum and expose the thoracic cavity.
11. Remove the thymus with forceps and examine the major blood vessels; in particular, note the presence of the innominate artery.
12. Examine the trachea and esophagus by moving a forceps tip between the two from the larynx to the heart. In particular, note any fistulas and the right-left orientation.
13. Examine the lungs for size, lobation, and right-left orientation.
14. Examine the heart for size and orientation.
15. Section the heart perpendicular to the ventricular septum (Wilson, 1965) or use ultramicrodissection scissors to cut along the pulmonary artery and right ventricle, and then along the aorta and left ventricle (Stuckhardt and Poppe, 1984).
16. Examine the ventricular septum and valves.
17. Examine the front feet.

Examine the hindquarters

18. Carefully remove the digestive viscera and spleen and note any signs of intra-abdominal hemorrhage.
19. Examine the viscera for an accessory spleen or lobule at the caudate end of the spleen.
20. Examine the urinary bladder and the genitalia. Record the sex of the fetus; note if the external genitalia do not correspond with the internal genitalia.
21. Examine the kidneys for size and position. If the anterior tip of the left kidney is below the level of the hilus of the right kidney, or if the posterior tip of the right kidney is above the level of the hilus of the left kidney, note the kidneys as offset. If the anterior tip of the left kidney is anterior to the anterior tip of the right kidney note the kidneys as offset.
22. Gently remove the mesentery covering the ureters, then score the widest dilation of each ureter:

    0 = normal
    1 = slight
    2 = moderate
    3 = severe.

23. Section each kidney transversely through the hilus and score the dilation of the renal pelvis and the size of the papilla:

    0 = papilla intact, no dilation
    1 = papilla reduced
    2 = papilla nearly absent
    3 = papilla absent.

24. Examine the hind feet.

Store the specimen

25. Place the sections of each specimen in an *air-tight* vial for storage and tap water (with thymol crystals) sufficient to cover the tissues. Unless alterations were noted, the lower jaw and abdominal viscera (except for the urinary tract and genitalia) may be discarded. Label the vial/cap with the litter and fetus numbers of the specimen. Store indefinitely at room temperature.

SUPPORT PROTOCOL 4

PREPARATION OF FETAL SKELETAL SPECIMENS

In this protocol, the cesarean-delivered fetuses are skinned, eviscerated, and double-stained for skeletal examination. The bones are stained with alizarin red S, and the cartilage is stained with Alcian blue.

CAUTION: 95% ethanol is flammable. Store specimen trays containing 95% ethanol in a fire-safety cabinet.

Materials

Fetuses (see Basic Protocol 1 and Support Protocol 1)
4% NaCl
95% (or 100%) and 70% ethanol
150 mg/liter Alcian blue (see recipe)
1% (w/v) potassium hydroxide (KOH; see recipe)
25 mg/liter Alizarin red S (see recipe)
1:1 (v/v) glycerol/70% ethanol solution (see recipe)
2:2:1 (v/v/v) glycerol/70% ethanol/benzyl alcohol solution (see recipe)

Dissecting instruments including forceps and iris scissors
18-well polystyrene trays (Flambeau Products Corp.)
Flexible screen
Colored tape and marking pen

1. After the fetuses have been removed from the uterus, weighed, sexed, examined for external alterations, and euthanized (see Support Protocol 1), place the specimens in 4% NaCl for ~1 to 4 hr.

2. Eviscerate the fetus and completely remove the skin. Use particular care when removing skin from the extremities. Remove the thoracic and abdominal viscera as well as the subcutaneous fat between the scapulae and along the back of the neck. Be careful not to damage the skeleton. Upon completion of this step, place the fetus in a tray with 95% ethanol. Store trays with 95% ethanol in a fire-safety cabinet.

    Generally, the authors recommend that the eyes remain in situ.

3. Leave the fetuses in 95% ethanol for at least 1 day and stain according to the following schedule. To retain the specimens in their assigned cells, place a sheet of flexible screen under the lid of the tray while pouring off the solutions.

Day 1: Afternoon: Transfer the specimens to alcian blue solution. Leave overnight.
Day 2: Morning: Transfer the specimens to fresh 95% ethanol for destaining/rinsing.
Day 2: Afternoon: Transfer to 1% KOH. Leave overnight.
Day 3: Morning: Transfer to solution of alizarin red S (25 mg/l) in 1% KOH.
Day 4: Morning: Transfer to solution of 1:1 glycerol/70% ethanol.

4. If the specimens are overstained on the morning of Day 4, destain in a solution of 2:2:1 70% ethanol/glycerol/benzyl alcohol for 1 day, then transfer to 1:1 glycerol/70% ethanol.

EXAMINATION OF FETAL SKELETAL SPECIMENS

SUPPORT PROTOCOL 5

After the skeletal specimens have been prepared (Support Protocol 4), they are examined using the following protocol.

Materials

Stained fetal specimen in 1:1 glycerol/70% ethanol (Support Protocol 4)
1:1 (v/v) glycerol/70% ethanol solution (see recipe)
Glycerol

Shallow transparent dish (e.g., ashtray or petri dish)
Forceps
Dissecting microscope with base illumination
Specimen containers (e.g., jars, trays, and vials)

Prepare the specimen

1. Place the specimen in a shallow transparent dish. To minimize glare, submerge the specimen in 1:1 glycerol/70% ethanol (i.e., the solution in which the specimen is stored at the end of Support Protocol 4). Use forceps to facilitate manipulation of the specimens.

2. Examine the specimen using a dissecting microscope with a below-stage light source. Note, in particular, the anatomical features mentioned in the steps below; however, do not limit the recording of findings to these items.

   As needed, consult atlases of normal (Yasuda and Yuki, 1996; Menegola et al., 2001) and abnormal (IFTS, see Internet Resources) skeletal morphology.

   When recording findings, use terminology consistent with that recommended by the International Federation of Teratology Societies Committee on Harmonization of Terminology in Developmental Toxicology (Wise et al., 1997).

Examine the head

3. Examine the mandible and orbits for size and position.

4. Note the ossification of the calvaria.

   Reduced ossification is indicated by a discrete boundary between degrees of ossification.

5. Examine the anterior region of the suture between the frontal bones for the (normal) absence of an "interfrontal bone" and score:

   0 = absent
   1 = barely visible (with normal magnification)
   2 = readily visible
   3 = severely enlarged.

6. Score the size of the anterior fontanel (and the separation between the parietals):

   0 = minimal
   1 = slight (most typical for GD 20 rat fetuses)
   2 = moderate
   3 = severe.

7. Score the ossification of the supraoccipital:

   0 = >90% ossified
   1 = 50% to 90% ossified
   2 = >0 and <50% ossified
   3 = completely unossified.

8. Score the ossification of the hyoid:

   0 = ossified (normal)
   1 = reduced ossification
   2 = completely unossified.

9. Score palate closure. If necessary, break the mandibles for easier viewing:

   0 = palatal shelves (virtually) touching
   1 = gap between palatal shelves
   2 = cleft palate.

Examine the sternum

10. Identify by number (1 for manubrium, 6 for xyphoid) any sternebrae that are affected in the following categories: unossified; small, reduced ossification, or unilaterally ossified; bilobed or bipartite; offset. In addition, indicate the presence of an extra sternebra and identify any sternebrae that are fused and whether or not the fusion is associated with offsetting.
11. Designate a sternebra that is misaligned by at least one-half the sternebra's length as "offset." Also indicate if offsetting is due to deficient ossification.
12. If fusion between two (or more) sternebrae is present, indicate the sternebrae involved. If the fusion is associated with misalignment (i.e., offsetting), indicate this (e.g., "FO:3&4" indicates that sternebrae 3 and 4 are fused due to some offsetting of one or both sternebrae). Otherwise, "fused" indicates that the fusion was not associated with offsetting sternebrae (e.g., "FU:3&4").
13. Count the number of intact sternocostal connections. Note if there are fewer (or more) than seven intact costal cartilages on each side connecting the ribs to the sternum.

Examine the ribs

14. Examine the ribs, noting any fusions, bifurcations, or irregularities in shape (e.g., wavy) or ossification.
15. Note the presence (and side) of any cervical ribs. In addition, indicate if a cervical rib articulates with a vertebra other than C7.
16. If wavy ribs are predominant on the affected side(s), it is not necessary to identify each affected rib. For other findings, e.g., fused, specify the ribs involved.
17. Count the ribs on each side. Indicate the number of ribs if other than 13.
18. Classify the length of the last rib relative to the adjacent rib:

    Focal = rudimentary rib with no length
    Short = with length, but less than half the length of the adjacent rib
    Long = less than half the length of the adjacent rib.

Examine the vertebrae

19. Examine the vertebrae, noting the shape and ossification of the centra and arches.
20. Record the numbers of centra that are bilobed and bipartite.
21. Except for unossified, bilobed, and bipartite centra, describe any findings with respect to the specific vertebra (e.g., S1 or sacral-1) and the side (right, left, or both) affected. For the purposes of identification, designate a vertebra associated with a 14th thoracic/lumbar rib as L1.
22. Count the cervical vertebrae (and check for cervical ribs, see above). Count the number of presacral vertebrae (normally 26); indicate if other than 26. Examine the lumbosacral junction and indicate if this is asymmetrical; i.e., a vertebra shows lumbar characteristics on one side and sacral characteristics on the other side.
23. Count and record the number of ossified cervical vertebral centra.
24. Count and record the number of unossified thoracolumbosacral vertebral centra.
25. Count and record the number of ossified caudal vertebrae. Begin the count after the fourth sacral vertebra. For fetuses with a hybrid vertebra (see above), count the hybrid as the first sacral vertebra.

Examine the girdles, long bones, and feet

26. Examine the girdles and long bones. Note instances of unossified pubis, or reduced ossification of the pubis.
27. Examine the feet for any fused or misshapen structures. For each foot, record the numbers of ossified metacarpals/metatarsals and proximal phalanges.

Store the specimen

28. When ready for final storage, transfer the specimens to glycerol (with a few crystals of thymol to prevent mold growth). Store indefinitely at room temperature.

ANALYSIS AND INTERPRETATION OF DATA

SUPPORT PROTOCOL 6

This protocol addresses statistical considerations and data-interpretation issues that are especially pertinent to the Segment II and Chernoff/Kavlock studies. This is not intended to be comprehensive, but to present general concepts and references.

Materials

Statistical software (e.g., SAS, GraphPad InStat, BenchMark Dose Software)

Compile the data

1. If not already captured automatically into an electronic format at the time of data collection, enter the data into a computerized format such as an ASCII file or a spreadsheet.

   For developmental data, use the litter (not the fetus or pup) as the basic experimental unit for statistical analysis. The number of offspring is inappropriate as the sample size, since litter mates are not biologically independent from each other (Gad and Weil, 1989).

2. In the study's database, identify each female (and litter) according to its treatment group, survival, and pregnancy outcome (live litter, resorbed litter, or not pregnant). Also, identify dams with only one implantation site.
3. For each treatment group, tally the number of females that died, were not pregnant, or had only one implantation site. Exclude these females from subsequent analyses.

Calculate descriptive statistics

4. For continuous data (e.g., body weights) and counts (number of implantation sites), calculate descriptive statistics (mean ± standard error) for each treatment group. See Tables 13.5.1 and 13.5.2 for listings of endpoints.

5. For dichotomous or categorical data (e.g., male-female, live-dead-resorbed, affected-normal) calculate the percentage for each litter, then calculate the mean ± SE of the litter values.

   Determine the number and percentage of dams with full-litter resorption.

   For gestation lengths, determine the number and percentage of females delivering on each gestation day.

   For fetal-examination data, determine the incidences (number of litters per group, and each group's mean ± SE of the litter percentages) for each distinct finding, as well as for categories of related findings. Categorize findings based on syndrome, organ system, and etiology, as well as severity. For example, determine the incidence of "dilated urinary tract" as well as of each of the included findings of hydronephrosis, dilated renal pelvis, and dilated ureter.

6. Tabulate the group data.

7. Graphically represent the data as appropriate using, e.g., line graphs or bar graphs.

Calculate inferential statistics

8. Conduct appropriate inferential statistical tests (e.g., analysis of variance) to identify endpoints with significant differences between groups (Burg and Hardin, 1987; Gad and Weil, 1989; Kimmel and Price, 1990) Use appropriate multicomparison techniques (e.g., Tukey's method, least squares means, or Dunnett's test) to identify treatment groups that are significantly different from the control group.

   For gestation lengths, the authors recommend using the nonparametric Kruskall-Wallis test—i.e., rank the gestation lengths by the time and stage (just started, in progress, complete) that parturition was observed, and conduct an analysis of variance on the ranks.

   Use one-tailed tests for endpoints pertaining to survival (e.g., prenatal loss, postnatal loss).

   Analyze fetal-examination data for each distinct finding, as well as for categories of related findings (see Step 5).

   For fetal-examination findings with severity indicators (e.g., the score for the dilation of the renal pelvis), analyze incidences at each increasing level of severity (i.e., slight + moderate + severe; moderate + severe; severe).

   Use litter size as a covariate in the analysis of fetal or pup weight.

   Use the number of implantation sites as a covariate in the analysis of litter size.

   Use the number of corpora lutea as a covariate in the analysis of implantation sites.

9. Identify data points that are significantly different from controls on tables and graphs.

Interpret the data

10. Assess maternal toxicity according to the key endpoints, which include weight gain, food consumption, and clinical observations. Determine the dose levels associated with maternal toxicity and its relative severity.

    For clinical observations (e.g., behavioral changes), consider their time of onset, duration, frequency, and severity.

    For body weight data, especially consider weight gains early in the treatment period (e.g., GD 6 to 7), i.e., before the growth of the uterine contents will contribute notably to the

Table 13.5.1 Endpoints in Segment II Studies

Source of data	Endpoint
Maternal	Body weight (each time point)
	Weight gain (each interval, but especially early in treatment period)
	Extrauterine weight gain[a]
	Food consumption (each interval)
Cesarean section	*Number per dam of:*
	Corpora lutea (not for mice)
	Implantation sites
	Live fetuses
	Dead fetuses
	Resorption sites (each type, and total)
	Non-live implantation sites (dead fetuses + resorption sites)
	Percent per litter of:
	Preimplantation loss [100 × (corpora lutea – implants) ÷ corpora lutea]
	Postimplantation loss [100 × (implants – live fetuses) ÷ implants]
	Live males (or females) [100 × male fetuses ÷ live fetuses]
Fetal examinations	*For each type of examination (external, visceral, and skeletal):*
	No. of affected fetuses per litter (for each abnormality)
	Percent affected fetuses per litter [affected ÷ examined]
	No. of litters affected (litter with at least one affected fetus)
	Percent litters affected [affected litters ÷ examined litters]

[a]Extrauterine weight gain = (last gestational weight) – (pre-treatment body weight) – (gravid uterine weight).

Table 13.5.2 Endpoints in Chernoff/Kavlock Assays

Source of data	Endpoint
Maternal	Body weight (each time point)
	Weight gain (each interval, but especially early in treatment period)
	Extrauterine weight gain[a]
	Food consumption
	Gestation length
Developmental	*Number per litter of:*
	Implantation sites
	Live pups on PD 1
	Live pups on PD 6
	Live male (or female) pups
	Affected pups (e.g., with a specific abnormality, such as tail defect)
	Percent per litter of:
	Prenatal loss [100 × (implants – live pups) ÷ implants]
	Postnatal loss [100 × (live PD 1 pups – live PD 6 pups) ÷ live PD 1 pups]
	Male (or female) pups [100 × live males ÷ live pups]
	Affected pups [100 × affected live pups ÷ live pups]

[a]Extrauterine weight gain = (last gestational weight) – (pre-treatment body weight) – (PD1 live-litter weight).

weight of the dam. Differences in weight gain later in gestation may reflect developmental, rather than maternal, toxicity.

Assess developmental toxicity as a function of maternal toxicity for each litter. For example, was there correlation between endpoints of maternal toxicity (e.g., maternal body weight loss) and developmental toxicity (e.g., reduced fetal weight)?

11. Assess developmental toxicity. Endpoints are listed in Tables 13.5.1 and 13.5.2.

    For Segment II studies, especially consider postimplantation loss, fetal weight, and fetal-examination findings.

    For Chernoff/Kavlock assays, especially consider gestation length, prenatal loss, postnatal loss, pup weight (PD 1 and 6), and pup-examination findings.

    Consider competing outcomes. For example, a high resorption rate may preclude detection of malformations, as susceptible conceptuses may resorb before reaching full term.

    Subjectively compare the data with historical control data (Haseman et al., 1984; EPA, 1991; Kimmel and Price, 1990). Consider the current controls to be representative of the species if the data are within the 95% confidence interval, rather than the extremes, of the historical data (Kimmel and Price, 1990).

12. Calculate the benchmark dose (EPA, 1995, 2000) for each endpoint affected by treatment. Use, for example, BenchMark Dose Software (see Internet Resources) to facilitate the calculations.

13. Enter the control data into a database of historical control data. Note any changes in laboratory procedure that may affect the data in this study as compared to previous studies.

REAGENTS AND SOLUTIONS

Use deionized, distilled water in all recipes and protocol steps. For common stock solutions, see ***APPENDIX 2A****; for suppliers, see* ***SUPPLIERS APPENDIX****.*

Alcian blue, 150 mg/liter

3.0 g Alcian blue 8GX (e.g., Acros Organics)
16 liters 95% ethanol
4 liters glacial acetic acid
Store at room temperature; discard if Alcian blue precipitates

CAUTION: *A fume hood should be used when working with the alcohols, aldehydes, or acetic acid. Ethanol solutions at concentrations greater than 70% are flammable; use appropriate precautions (e.g., metal containers or fire-safety cabinets).*

Alizarin red S, 25 mg/liter

500 mg Alizarin red S (e.g., Acros Organics)
20 liters 1% (w/v) potassium hydroxide (see recipe)
Store up to 6 months at room temperature, protected from light.

Ammonium sulfide, 2% (w/v)

Take 1 part 20% (w/v) ammonium sulfide (purchased, e.g., from Sigma) and add sufficient water for a total of 10 parts. Prepare fresh for each use.

Bodian's solution

950 ml glacial acetic acid
380 ml formaldehyde *or* 950 ml 10% formalin
14.4 liter 95% ethanol

continued

3270 ml tap or distilled water if formaldehyde is used *or* 2700 ml if 10% formalin is used
Store indefinitely at room temperature

CAUTION: *A fume hood should be used when working with the alcohols, aldehydes, or acetic acid. Ethanol solutions at concentrations greater than 70% are flammable; use appropriate precautions (e.g., metal containers or fire-safety cabinets).*

Bouin's solution

3000 ml saturated aqueous picric acid
1000 ml formaldehyde
200 ml glacial acetic acid
Store indefinitely at room temperature

CAUTION: *Dry picric acid is explosive and is sensitive to percussion and friction. Store picric acid powder in water; ensure that the water level is always above the powder. If picric acid crystals form at screw cap, apply water prior to removing cap. A fume hood should be used when working with aldehydes or acetic acid.*

Glycerol/70% ethanol, 1:1 (v/v)

1 part 70% ethanol
1 part glycerol

Store at room temperature; solution may be reused if not too dark.

CAUTION: *A fume hood should be used when working with the alcohols, aldehydes, or acetic acid. Ethanol solutions at concentrations greater than 70% are flammable; use appropriate precautions (e.g., metal containers or fire-safety cabinets).*

Glycerol/70% ethanol/benzyl alcohol, 2:2:1 (v/v/v)

2 parts 70% ethanol
2 parts glycerol
1 part benzyl alcohol
Store at room temperature; solution may be reused if not too dark; may become too alkaline after several uses

CAUTION: *A fume hood should be used when working with the alcohols, aldehydes, or acetic acid. Ethanol solutions at concentrations greater than 70% are flammable; use appropriate precautions (e.g., metal containers or fire-safety cabinets).*

Potassium hydroxide, 1% (w/v)

200 g potassium hydroxide (KOH)
20 liters distilled water
Store up to 6 months at room temperature

COMMENTARY

Background Information

The Segment II study was first promulgated in 1966 by the Food and Drug Administration (FDA, 1966) as part of a three-segment series of studies intended to test for toxic effects on fertility (Segment I), developmental toxicity (Segment II), and effects on parturition and lactation (Segment III). Since then, the Segment II study has been harmonized across international governmental regulatory agencies (ICH, 1994) and has undergone several enhancements (e.g., a longer treatment period, staining of cartilage in skeletal specimens), but remains much the same in basic study design.

The Chernoff/Kavlock assay was first developed in 1982 (Chernoff and Kavlock, 1982) as a preliminary screening assay in mice. Modifications to the protocol have been incorporated here, in EPA testing guidelines (EPA, 1996), and elsewhere (Hardin, 1987; Kavlock et al., 1987; Wickramaratne, 1987). As a screen, it is very useful in prioritizing potentially toxic agents for testing by the more rigorous (and costlier) Segment II protocol (Hardin, 1987; Hardin et al., 1987a,b; Kavlock et al., 1987; Seidenberg and Becker, 1987; Wickramaratne, 1987; Moore et al., 1995). Compared to the Segment II protocol, the Chernoff/Kavlock as-

say is less costly and requires considerably less technical expertise. Although the Chernoff/Kavlock protocol does not detect skeletal or visceral alterations, it is important to note that it can detect other adverse effects that a Segment II protocol cannot. Because of the postnatal component of the screening protocol, it can detect changes to other endpoints that are indicative of developmental toxicity, such as functional deficits (Lau et al., 2001), morphological changes that develop postnatally (Wier et al., 1987), and changes in gestation length (Rands et al., 1982; Narotsky et al., 1994; Narotsky and Kavlock, 1995; Narotsky et al., 2001).

Generally, these protocols detect three of the four major manifestations of developmental toxicity—i.e., they can identify agents that cause death, structural abnormalities, or growth deficits, but they are limited in their ability to identify agents that cause functional deficits. Protocols with longer postnatal assessments, including those focused on developmental neurotoxicity (EPA, 1998a) or multigeneration studies (EPA, 1998c) are generally more effective at detecting functional deficits.

It should be noted that many important aspects of both the Segment II and Chernoff/Kavlock protocols are beyond the scope of this unit and are not addressed in detail here. See published guidelines for further information regarding Good Laboratory Practices (FDA, 1997), the choice of species and strain, number of animals per group, dose selection, number and spacing of dose levels (EPA, 1991; ICH, 1994; EPA, 1998b), route and frequency of administration (ICH, 1994; EPA, 1998b), animal husbandry (ILAR, 1996), euthanasia methods (AVMA, 2001), and risk assessment (EPA, 1991). The guidelines on risk assessment (EPA, 1991) address several important issues regarding data interpretation, including the usage of historical control data and the relationship between maternal and developmental toxicity. In addition, other authors have provided excellent references regarding important issues in developmental toxicity testing, such as dermal absorption studies (Kimmel and Francis, 1990), and statistical analyses (Burg and Hardin, 1987; Gad and Weil, 1989; Kimmel and Price, 1990).

Critical Parameters and Troubleshooting

A variety of methods may be used to examine visceral specimens for soft-tissue defects. The methods generally fall into two categories: the Wilson free-hand razor section technique (Wilson, 1965; Barrow and Taylor, 1969; Wilson, 1973; Weber and Weber, 1991) and the microdissection technique (Nishimura, 1974; Staples, 1977; Stuckhardt and Poppe, 1984). Both techniques are effective in detecting visceral defects; however, with adequate training, the Wilson sectioning method has been suggested to be more sensitive at detecting certain cardiac defects (Christ et al., 1991). The Wilson method must be performed on specimens fixed in Bouin's or Bodian's solution. The head is best examined with the Wilson method. Although labor-intensive, microdissection is preferably conducted with fresh specimens; this is also compatible with subsequent skeletal examination of the carcass. Alternatively, to accommodate a smaller workforce, the specimens may be fixed at the time of cesarean section,

Table 13.5.3 Example of Data Summary for a Segment II Study with Rats[a]

Dose (mg/kg/day)	0	100	200	400
No. of dams	19	13	19	15
Dams with full-litter loss	0	0	0	1
Mean ± SE per dam				
No. of corpora lutea	15.6 ± 0.4	15.3 ± 0.4	14.8 ± 0.5	15.5 ± 0.4
No. of implantations	14.2 ± 0.3	13.8 ± 0.4	3.8 ± 0.6	13.3 ± 0.8
No. of live fetuses	12.9 ± 0.6	13.2 ± 0.4	12.9 ± 0.7	11.9 ± 0.9
Preimplantation loss (%)	8.3 ± 2.4	7.3 ± 2.1	6.7 ± 3.1	13.5 ± 5.4
Postimplantation loss (%)	9.3 ± 3.2	3.7 ± 1.5	6.6 ± 2.0	15.2 ± 6.6
Fetal weight (g)	4.1 ± 0.3	4.5 ± 0.3	3.5 ± 0.2**	2.9 ± 0.2***

[a]Data from study with valproic acid (Narotsky et al., 1994). Reproduced with permission of the Society of Toxicology. Symbols: two asterisks (**), significantly different from control ($p < 0.01$); three asterisks (***), significantly different from control ($p < 0.001$).

Table 13.5.4 Example of Data Summary for Segment II Skeletal Findings in Rats[a]

Dose (mg/kg/day)	0	100	200	400
No. examined				
Litters	19	13	19	14
Fetuses	120	87	126	91
Percent incidence				
Calvaria reduced ossification	7.1 ± 2.4	16.3 ± 5.5	21.1 ± 6.9*	31.9 ± 6.4**
Hyoid unossified	9.4 ± 3.5	16.4 ± 7.7	27.0 ± 6.5*	39.6 ± 9.7***
Supraoccipital reduction/irregularity	8.8 ± 3.9	8.6 ± 3.7	27.1 ± 7.5*	44.9 ± 9.8***
Pubis unossified	7.6 ± 4.8	3.8 ± 3.8	20.0 ± 8.0	17.5 ± 9.6***
Mean score				
Supraoccipital	1.0 ± 0.0	1.0 ± 0.0	1.1 ± 0.1	1.3 ± 0.2***
Fontanel	1.4 ± 0.1	1.4 ± 0.1	1.9 ± 0.1*	2.3 ± 0.2***
Percent incidence				
Sternebrae SUR[b]	61.2 ± 8.06	3.6 ± 11.5	89.7 ± 4.6***	95.0 ± 3.7***
Sternebrae offset	25.0 ± 4.4	26.8 ± 5.6	30.0 ± 5.1	39.0 ± 6.0
Vertebrae fused	0	0	0	9.2 ± 5.1
Vertebrae duplicated	0	0	0	1.0 ± 1.0
>26 presacral vertebrae	4.0 ± 2.7	1.0 ± 1.0	9.1 ± 2.4	74.1 ± 9.3***
No. caudal ossified vertebrae	4.3 ± 0.5	4.4 ± 0.5	3.0 ± 0.4**	2.0 ± 0.4***
Fused ribs	0	0	0	13.3 ± 7.7
Lumbar ribs	12.9 ± 5.6	26.7 ± 6.9	36.0 ± 6.2*	81.3 ± 8.3***
Cervical ribs	0.7 ± 0.70	2.1 ± 1.5	0.7 ± 3.6***	
Wavy/callused ribs	1.8 ± 1.2	2.6 ± 1.7	7.0 ± 3.9	6.7 ± 2.6
Fused/duplicated/misarticulated ribs	0.9 ± 0.9	1.3 ± 1.3	2.7 ± 1.6	4.1 ± 2.3
Mean no. ossified				
Sternebrae	5.3 ± 0.3	5.5 ± 0.4	4.7 ± 0.4	3.9 ± 0.5***
Metacarpals (front limbs)	7.5 ± 0.2	7.5 ± 0.2	6.8 ± 0.3*	6.4 ± 0.2***
Front proximal phalanges	3.0 ± 0.7	3.1 ± 0.9	1.1 ± 0.5**	0.5 ± 0.3***
Front distal phalanges	9.8 ± 0.1	9.8 ± 0.2	9.5 ± 0.2	8.6 ± 0.8***
Metatarsals (hind limbs)	8.3 ± 0.2	8.6 ± 0.3	7.9 ± 0.1	7.5 ± 0.4***
Hind proximal phalanges	2.3 ± 0.7	3.2 ± 1.0	0.5 ± 0.3***	0.1 ± 0.1***
Hind distal phalanges	8.4 ± 0.9	9.2 ± 0.8	7.3 ± 1.0	7.9 ± 1.0

[a]Data from study with valproic acid (Narotsky et al., 1994). Reproduced with permission of the Society of Toxicology. Symbols: one asterisk (*), significantly different from control ($p < 0.05$); two asterisks (**), significantly different from control ($p < 0.01$); three asterisks (***), significantly different from control ($p < 0.01$).

[b]SUR, small, unossified, or reduced ossification.

Table 13.5.5 Example of Data Summary for Segment II Visceral Findings in Rats[a]

Dose (mg/kg/day)	0	100	200	400
No. examined				
Litters	19	13	19	14
Fetuses	124	87	119	87
No. fetuses affected				
Ventricular septal defect	1	0	0	0
Microphthalmia	1	0	0	0
Micrognathia, cleft palate	0	1	0	0
Mean score				
Kidney	2.8 ± 0.1	2.8 ± 0.1	3.2 ± 0.1*	3.6 ± 0.2***
Ureter	2.3 ± 0.1	2.7 ± 0.2	2.7 ± 0.2	2.9 ± 0.2
Lateral ventricles	1.0 ± 0.0	1.1 ± 0.0	1.1 ± 0.0	1.1 ± 0.0
Percent incidence				
Dilated renal pelvis	5.9 ± 2.9	8.1 ± 4.3	19.6 ± 4.9*	35.9 ± 6.2**
Dilated ureter	21.6 ± 4.1	31.5 ± 8.0	34.9 ± 5.9	35.4 ± 7.4

[a]Data from study with valproic acid (Narotsky et al, 1995). Reproduced with permission of the Society of Toxicology. Symbols: one asterisk (*) significantly different from control ($p < 0.05$); two asterisks (**), significantly different from control ($p < 0.01$); three asterisks (***), significantly different from control ($p < 0.001$).

allowing either microdissection or sectioning of the preserved specimens.

Although some regulatory guidelines suggest categorizing fetal examination findings as malformations or variations, or categorizing based on severity (major malformations, minor malformations) it should be noted that there is no generally accepted classification of malformations and variations. Furthermore, there is no scientific justification for using such classification. Instead (or in addition), the authors recommend categorizing findings based on syndrome, organ system, and etiology.

When conducting developmental toxicity studies, it is essential to have high pregnancy rates in the test animals. Pregnant animals can be obtained by breeding them in the test facility, or by purchasing timed-pregnant animals from an animal supplier. The latter approach allows some scheduling flexibility in that a larger number of test animals can be bred on the same day. However, disadvantages of buying timed-pregnant animals include the fact that the animals are subject to the stress of shipping during the preimplantation period of pregnancy (possibly contributing to low pregnancy rates) and that a quarantine period may be impossible, in addition to the increased cost.

Anticipated Results

Uterine findings

Table 13.5.3 presents an example of uterine-findings data from a Segment II study (Narotsky et al., 1994). In this example, no significant differences between groups were noted for the numbers of corpora lutea, implantation sites, or live fetuses. More importantly, the values for pre- and post-implantation loss were also comparable between groups. The values for fetal weight, however, indicated significant dose-related reductions at dosages of 200 and 400 mg/kg. Therefore, based on the fetal weight data, the test agent in this example was developmentally toxic at 200 and 400 mg/kg. On the basis of this study alone, it is unclear whether the isolated case of full-litter resorption at 400 mg/kg was treatment-related.

Skeletal findings

An example of findings from fetal skeletal examinations in a Segment II study (Narotsky et al., 1994) is presented in Table 13.5.4. Findings consistent with delayed development at dosages of 200 and 400 mg/kg include reductions in ossification (e.g., of the calvaria, hyoid, supraoccipital, sternebrae, metacarpals, phalanges, and caudal vertebrae) and an increased fontanel score. Findings indicating a toxic, and

Table 13.5.6 Example of Data Summary for a Chernoff/Kavlock Assay[a]

Daily dose (mg/kg)	No. of dams	Mean ± SE weight gain (g)		Dams with full-litter resorption (%)	Mean ± SE per litter				Pups with eye defects (%)
					Percent loss		Pup weight (g)		
		GD 6-8	GD 6-20 (adjusted)[b]		Prenatal	Postnatal	PD 1	PD 6	
0	9	0.3 ± 0.8	16.5 ± 1.2	11	14.7 ± 10.8	1.4 ± 1.4	5.4 ± 0.1	10.0 ± 0.3	0
5.1	12	0.8 ± 0.7	16.4 ± 1.7	0	4.1 ± 1.8	8.3 ± 8.3	5.2 ± 0.1	9.5 ± 0.1	0
6.8	10	0.2 ± 0.3	15.6 ± 1.8	0	10.5 ± 3.7	23.8 ± 10.0	5.1 ± 0.1*	8.3 ±0.4***	0.9 ± 0.9
9.0	10	–1.4± 0.5	7.3 ± 2.2*	0	5.0 ± 2.9	63.3 ± 13.8***	5.4 ± 0.1	9.0 ± 0.3	0
12.0	7[c]	–2.3±0.9*	–2.3± 6.5*	0	3.7 ± 2.3	59.7 ± 18.6***	5.1 ± 0.3*	8.7 ±0.6***	2.1 ± 2.1

[a]Data from study with heptachlor (Narotsky et al., 1995). Symbols: one asterisk (*), significantly different from control ($p < 0.05$); three asterisks (***), significantly different from control ($p < 0.001$).

[b]Adjusted for weight of live litter on PD 1.

[c]Includes one dam that died at term and two that died during lactation.

dose-related, effect on the development of the axial skeleton include lumbar ribs at dosages of 200 and 400 mg/kg, extra cervical ribs, extra (>26) presacral vertebrae, and rib and vertebral malformations at dosages of 400 mg/kg. Although the incidences of rib and vertebral malformations (fusion, duplication, misarticulation) did not reach statistical significance, they were attributed to treatment.

Visceral findings

Table 13.5.5 gives an example of fetal visceral examination findings in a Segment II study (Narotsky et al., 1994). Significant, dose-related increased incidences of dilated renal pelvis (also reflected by kidney scores) indicated a toxic effect at 200 and 400 mg/kg. Sporadic, non-dose-related malformations (ventricular septal defect, microphthalmia, micrognathia, cleft palate) were not attributed to treatment.

Chernoff/Kavlock assay

An example of a data summary from a Chernoff/Kavlock assay (Narotsky et al., 1995) is presented in Table 13.5.6. In this example, dose-related maternal toxicity at 9 and 12 mg/kg was evidenced by adjusted gestational weight gains (weight gain from GD 6 to 20, minus the live PD 1 litter weight). Maternal toxicity is also evident at 12 mg/kg, as indicated by significant weight losses early in the treatment period (GD 6 to 8) and by maternal deaths at term and during lactation (see footnote to Table 13.5.6). Developmental toxicity was evidenced by significantly increased postnatal loss at both 9 and 12 mg/kg dosages. Although pup weights were unaffected at dosages of 9 mg/kg, reduced pup weights at 6.8 and 12 mg/kg were attributed to treatment. Therefore, in this example, maternal toxicity was evident at 9 and 12 mg/kg; whereas developmental toxicity was evident at 6.8, 9, and 12 mg/kg. Pups with eye defects (anophthalmia or microphthalmia) occurred in one litter in each of the 6.8- and 12-mg/kg groups; based on this study alone, it was unclear whether this finding was treatment related.

Time Consideration

Typically, the in-life phase of a Segment II study (see Basic Protocol 1) or a Chernoff/Kavlock assay (see Basic Protocol 2) is ~3 to 5 weeks for mice and ~4 to 6 weeks for rats, depending on the time required to obtain sufficient mated animals for the study. The number of mated animals obtained on a given day should not exceed the number of animals that the available workforce can accommodate in one day, particularly for labor-intensive tasks such as cesarean sections. The time required to complete the cesarean sections (see Support Protocol 1) in a Segment II study may range from 1 day to 2 weeks, depending on the time required to obtain sufficient mated animals for the study. Examinations of apparently nongravid uteri (see Support Protocol 2) are done in conjunction with cesarean sections as well as Chernoff/Kavlock assays and generally require <1 hr on a given day. Preparation of fetal skeletal specimens (see Support Protocol 4) requires a minimum of 7 days; however, the ethanol fixation period is typically extended until a Monday or Tuesday so that the succeeding steps can be completed during a standard work week. The time required to complete the examinations of fetal visceral (see Support Protocol 3) and fetal skeletal specimens (see Support Protocol 5) may range from weeks to months, and is dependent on the number of specimens, the extent of the fetal abnormalities, the data-recording system, and the size and skill of the workforce.

Disclaimer

This document has been reviewed in accordance with the U.S. Environmental Protection Agency policy and approved for publication. Mention of trade names or commercial products does not constitute endorsement or recommendation for use.

Literature Cited

American Veterinary Medical Association (AVMA). 2001. 2000 Report of the AVMA Panel on Euthanasia. *J. Am. Vet. Med. Assoc.* 218:669-696.

Barrow, M.V. and Taylor, W.J. 1969. A rapid method for detecting malformations in rat fetuses. *J. Morphol.* 127:291-305.

Burg, J.R. and Hardin, B.D. 1987. Recommendations for the statistical analysis of Chernoff/Kavlock test data. *Teratog. Carcinog. Mutagen.* 7:49-54.

Chernoff, N. and Kavlock, R.J. 1982. An in vivo teratology screen utilizing pregnant mice. *J. Toxicol. Environ. Health* 10:541-550.

Christ, S.A., Randall, J.L., Read, E.J., and Smith, M.K. 1991. Comparison of fetal rat examination techniques (fixed vs. fresh) in the detection of cardiac malformations, specifically levocardia. *Teratology* 43:435.

Coligan, J.E., Kruisbeek, A.M., Margulies, D.H., Shevach, E.M., and Strober, W. 2003. Current Protocols in Immunology. John Wiley & Sons, New York.

Environmental Protection Agency (EPA). 1991. Guidelines for developmental toxicity risk assessment. *Fed. Regist.* 56:63798-63826.

Environmental Protection Agency (EPA), Office of Research and Development. 1995. The use of the benchmark dose approach in health risk assessment. EPA/630/R-94/007. EPA, Washington, D.C.

Environmental Protection Agency (EPA). 1996. Health Effects Test Guidelines OPPTS 870.3500 Preliminary Developmental Toxicity Screen "Public Draft". EPA-712-C-96-205. EPA, Washington, D.C.

Environmental Protection Agency (EPA). 1998a. Health Effects Test Guidelines OPPTS 870.6300 Developmental Neurotoxicity Study. EPA 712-C-98-239. EPA, Washington, D.C.

Environmental Protection Agency (EPA). 1998b. Health Effects Test Guidelines, OPPTS 870.3700, Prenatal Developmental Toxicity Study. EPA, Washington, D.C.

Environmental Protection Agency (EPA). 1998c. Health Effects Test Guidelines, OPPTS 870.3800, Reproduction and Fertility Effects. EPA, Washington, D.C.

Environmental Protection Agency (EPA), National Center for Exposure Assessment. 2000. Draft Benchmark Dose Technical Guidance Document. EPA/630/R-00/001. EPA, Washington, D.C.

Food and Drug Administration (FDA). 1966. Guidelines for Reproduction Studies for Safety Evaluation of Drugs for Human Use. FDA, Washington, D.C.

Food and Drug Administration (FDA). 1997. Good Laboratory Practice Regulations for Nonclinical Laboratory Studies. U.S. Code of Federal Regulations. Title 21 Part 8. FDA, Washington, D.C.

Gad, S.C. and Weil, C.S. 1989. Statistics for toxicologists. *In* Principles and Methods of Toxicology (A.W. Hayes, ed.) pp. 435-483. Raven Press, New York.

Hardin, B.D. 1987. A recommended protocol for the Chernoff/Kavlock preliminary developmental toxicity test and a proposed method for assigning priority scores based on results of that test. *Teratog. Carcinog. Mutagen.* 7:85-94.

Hardin, B.D., Becker, R.A., Kavlock, R.J., Seidenberg, J.M., and Chernoff, N. 1987a. Workshop on the Chernoff/Kavlock preliminary developmental toxicity test. *Teratog. Carcinog. Mutagen.* 7:119-127.

Hardin, B.D., Schuler, R.L., Burg, J.R., Booth, G.M., Hazelden, K.P., MacKenzie, K.M., Piccirillo, V.J., and Smith, K.N. 1987b. Evaluation of 60 chemicals in a preliminary developmental toxicity test. *Teratog. Carcinog. Mutagen.* 7:29-48.

Haseman, J.K., Huff, J., and Boorman, G.A. 1984. Use of historical control data in carcinogenicity studies in rodents. *Toxicol. Pathol.* 12:126-135.

International Conference on Harmonisation (ICH). 1994. Harmonised tripartite guideline: Detection of toxicity to reproduction for medicinal products. *In* Proceedings of the Second International Conference on International Harmonisation (P. D'Arcy and D. Harron, eds.) pp. 557-577. Queens University Press, Belfast, U.K.

Institute for Laboratory Animal Research (ILAR). 1996. Guidelines for the Care and Use of Laboratory Animals. National Academy Press, Washington, D.C.

Kavlock, R.J., Short, R.D., Jr., and Chernoff, N. 1987. Further evaluation of an in vivo teratology screen. *Teratog. Carcinog. Mutagen.* 7:7-16.

Kimmel, C.A. and Francis, E.Z. 1990. Proceedings of the workshop on the acceptability and interpretation of dermal developmental toxicity studies. *Fundam. Appl. Toxicol.* 14:386-398.

Kimmel, C.A. and Price, C.J. 1990. Developmental toxicity studies. *In* Handbook of In Vivo Toxicity Testing (D.L. Arnold, H.C. Grice, and D.R. Grewski, eds.) pp. 271-301. Academic Press, San Diego.

Lau, C., Rogers, J., Hanson, R., Barbee, B., Narotsky, M., Schmid, J., and Richards, J. 2001. Developmental toxicity of perfluorooctane sulfonate (PFOS) in the rat and mouse. *Teratology* 63:290.

Menegola, E., Broccia, M.L., and Giavini, E. 2001. Atlas of rat fetal skeleton double stained for bone and cartilage. *Teratology* 64:125-133.

Moore, J.A., Daston, G.P., Faustman, E., Golub, M.S., Hart, W.L., Hughes, C., Jr., Kimmel, C.A., Lamb, J.C.T., Schwetz, B.A., and Sciallim, A.R. 1995. An evaluative process for assessing human reproductive and developmental toxicity of agents. *Reprod. Toxicol.* 9:61-95.

Narotsky, M.G. and Kavlock, R.J. 1995. A multidisciplinary approach to toxicological screening: II. Developmental toxicity. *J. Toxicol. Environ. Health* 45:145-171.

Narotsky, M.G., Francis, E.Z., and Kavlock, R.J. 1994. Developmental toxicity and structure-activity relationships of aliphatic acids, including dose-response assessment of valproic acid in mice and rats. *Fundam. Appl. Toxicol.* 22:251-265.

Narotsky, M.G., Weller, E.A., Chinchilli, V.M., and Kavlock, R.J. 1995. Nonadditive developmental toxicity in mixtures of trichloroethylene, Di(2-ethylhexyl) phthalate, and heptachlor in a $5 \times 5 \times 5$ design. *Fundam. Appl. Toxicol.* 27:203-216.

Narotsky, M.G., Brownie, C.F., and Kavlock, R.J. 1997. Critical period of carbon tetrachloride-induced pregnancy loss in Fischer-344 rats, with insights into the detection of resorption sites by ammonium sulfide staining. *Teratology* 56:252-261.

Narotsky, M.G., Best, D.S., Guidici, D.L., and Cooper, R.L. 2001. Strain comparisons of atrazine-induced pregnancy loss in the rat. *Reprod. Toxicol.* 15:61-69.

Nishimura, K. 1974. A microdissection method for detecting thoracic visceral malformations in mouse and rat fetuses. *Cong. Anom.* 14:23-40.

Organisation for Economic Co-operation and Development (OECD). 2000. OECD Guideline for the Testing of Chemicals, Proposal for Updating Guideline 414, Prental Developmental Toxicity Study. OECD, Paris.

Rands, P.L., White, R.D., Carter, M.W., Allen, S.D., and Bradshaw, W.S. 1982. Indicators of developmental toxicity following prenatal administration of hormonally active compounds in the rat. I. Gestational length. *Teratology* 25:37-43.

Seidenberg, J.M. and Becker, R.A. 1987. A summary of the results of 55 chemicals screened for developmental toxicity in mice. *Teratog. Carcinog. Mutagen.* 7:17-28.

Staples, R.E. 1977. Detection of visceral alterations in mammalian fetuses. *Teratology* 9:A37-A38.

Stuckhardt, J.L. and Poppe, S.M. 1984. Fresh visceral examination of rat and rabbit fetuses used in teratogenicity testing. *Teratog Carcinog. Mutagen.* 4:181-188.

Taylor, P. 1986. Practical Teratology. Academic Press, New York.

Weber, M. and Weber, E. 1991. Die Rasierklingen-Schnittechnik in der teratologischen Forschung [The razor blade sectioning technique in teratological research]. *Anat. Anz.* 173:291-297.

Wickramaratne, G.A. 1987. The Chernoff-Kavlock assay: Its validation and application in rats. *Teratog. Carcinog. Mutagen.* 7:73-83.

Wier, P.J., Lewis S.C., and Traul, K.A. 1987. A comparison of developmental toxicity evident at term to postnatal growth and survival using ethylene glycol monoethyl ether, ethylene glycol monobutyl ether and ethanol. *Teratog. Carcinog. Mutagen.* 7:55-64.

Wilson, J.G. 1965. Methods for administering agents and detecting malformations in experimental animals. *In* Teratology: Principles and Techniques (J.G. Wilson and J. Warkany, ed.) pp. 262-277. University of Chicago Press, Chicago.

Wilson, J.G. 1973. Environment and birth defects. Academic Press, New York.

Wise, L.D., Beck, S.L., Beltrame, D., Beyer, B.K., Chahoud, I., Clark, R.L., Clark, R., Druga, A.M., Feuston, M.H., Guittin, P., Henwood, S.M., Kimmel, C.A., Lindstrom, P., Palmer, A.K., Petrere, J.A., Solomon, H.M., Yasuda, M., and York, R.G. 1997. Terminology of developmental abnormalities in common laboratory mammals (version 1). *Teratology* 55:249-292.

Yasuda, M. and Yuki, T. 1996. Color Atlas of Fetal Skeleton of the Mouse, Rat, and Rabbit. Ace Art Co., Osaka, Japan.

Key References

Gad and Weil, 1989. See above.

A book chapter providing statistical guidance for toxicologists.

Hood, 1997. Handbook of Developmental Toxicology. CRC Press, Boca Raton, Fla.

A practical guide for developmental toxicity testing. Encompasses areas such as study design, data presentation, data interpretation, regulatory concerns, and risk assessment.

Taylor, 1986. See above.

A handbook providing technical advice for conducting developmental toxicity studies in rats, mice, and rabbits.

Wise et al., 1997. See above.

An internationally developed glossary of terms for describing structural developmental abnormalities in common laboratory animals.

Internet Resources

http://teratology.org

Web site of the Teratology Society.

http://www.etsoc.com

Web site of the European Teratology Society.

http://www.midwest-teratology.org

Web site of the Midwest Teratology Association.

http://nbts.org

Web site of the Neurobehavioral Teratology Society.

http://www.interscience.wiley.com/jpages/1542-0752

Web site of Birth Defects Research, parts A, B, and C, the official publications of the Teratology Society.

http://hcd.org

Historical control database of preclinical developmental teratology and reproductive toxicity parameters, a joint project of the Midwest Teratology Association and the Middle Atlantic Reproduction and Teratology Association. Includes a searchable database allowing the retrieval of historical control data from contributing laboratories.

http://www.ifts-atlas.org

Atlas of developmental abnormalities in common laboratory mammals, provided by the International Federation of Teratology Societies. Includes a searchable database of images of both rare and common observations in fetuses and neonates from common laboratory mammals. Glossaries of common terms and syndromes are also included.

http://www.ich.org/pdfICH/s5a.pdf

ICH Harmonized Tripartite Guideline, Detection of Toxicity to Reproduction for Medicinal Products.

http://www.oecd.org/ehs/test/health.htm

Listing of OECD guidelines for the testing of chemicals. Text of draft guidelines are available online.

http://www.epa.gov/docs/OPPTS_Harmonized/870_Health_Effects_Test_Guidelines/Series/870-3700.pdf

U.S. EPA Health Effects Test Guidelines, OPPTS 870.3700, Prenatal Developmental Toxicity Study.

http://www.epa.gov/docs/OPPTS_Harmonized/870_Health_Effects_Test_Guidelines/Drafts/870-3500.pdf

Health Effects Test Guidelines OPPTS 870.3500 Preliminary developmental toxicity screen "Public Draft." U.S. EPA guidelines for the Chernoff/Kavlock assay.

http://www.nal.usda.gov/awic/legislat/21cfr97.htm

Good Laboratory Practice for Nonclinical Laboratory Studies.

http://www.access.gpo.gov/nara/cfr/cfrhtml_00/Title_40/40cfr799_nav_00.html

Electronic Code of Federal Regulations, Title 40, Chapter I, Part 799. Click on "799.9370" for the TSCA prenatal developmental toxicity guidelines.

http://www.epa.gov/ncea/raf/pdfs/devtox.pdf

Guidelines for Developmental Toxicity Risk Assessment (EPA, 1991). Provides guidance and discussion on interpreting data from developmental toxicity studies, and applying these data towards the assessment of risk to human health.

http://cfpub.epa.gov/ncea/cfm/bmds.cfm?ActType=default

BenchMark Dose Software, developed by the U.S. Environmental Protection Agency, can be downloaded from this Web site.

Contributed by Michael G. Narotsky and Robert J. Kavlock
U.S. Environmental Protection Agency
Research Triangle Park, North Carolina

Organ Culture of Midfacial Tissue and Secondary Palate

Palatogenesis presents an interesting model for many of the processes involved in morphogenesis in the embryo. The formation of the secondary palate requires neural crest cell migration, interaction of the palatal cells with the surrounding extracellular matrix, interaction and signaling between epithelial and mesenchymal cells, adhesion and fusion of morphological structures—which also involves cell death and transformation of cells from epithelial to mesenchymal phenotypes—and finally, differentiation into bone and stratified oral and ciliated nasal epithelia. A number of culture models are used to study these processes, including whole embryo culture, mesenchymal and micromass cell cultures, epithelial cell culture, and palatal organ culture (Tyler and Pratt 1980; Thesleff, 1981; Ferguson et al., 1984; Whitby, 1987; Pisano and Greene, 2000). A suspension palatal organ culture technique is described in this unit.

The suspension palatal organ culture method requires dissection of embryonic midfacial tissues, including the maxillary arch and secondary palatal shelves, and suspension of these "explants" in culture medium. Normal processes of palatogenesis occur during the culture period, including palatal shelf growth, elevation, and fusion. The suspension palatal organ culture model provides a tool for studies of mechanisms of normal and abnormal palatogenesis, and has applications for developmental biology and toxicology.

SUBMERGED PALATAL ORGAN CULTURE OF MOUSE MIDFACIAL TISSUES

BASIC PROTOCOL

This palatal organ culture protocol supports the outgrowth, elevation, and fusion of secondary palatal shelves. This protocol describes the dissection of the embryonic craniofacial tissue and preparation of culture medium. It specifies the gas mixtures and equipment required, the schedules for refreshing medium and gases, and the basic criteria for evaluation of the results. Modifications to the Basic Protocol are required to culture embryonic rat midfacial tissues (see Alternate Protocol). Modifications are also recommended to improve the growth and fusion of the palatal shelves (some species and strains may require adjustments to the basic model) and to support responsiveness to specific test agents (e.g., in some situations, supplementation of medium with serum may be necessary).

NOTE: All protocols using live animals must first be reviewed and approved by an Institutional Animal Care and Use Committee (IACUC) and must follow officially approved procedures for the care and use of laboratory animals.

NOTE: All solutions and equipment coming into contact with tissues to be cultured must be sterile and aseptic technique should be used accordingly. Filtration to sterilize the final solutions is performed in the laminar flow hood. Sterile media, supplements, and treatments are combined prior to culture in the laminar flow hood using sterile equipment and aseptic technique. Collection of fetuses from the dam may be performed at the laboratory bench; however, dissection of fetal tissues to be cultured, the transfer to culture flasks, and gas addition to the flasks should all occur in the laminar flow hood. All subsequent medium or gas exchanges, and any interim examination of cultures must occur in the laminar flow hood.

Contributed by Barbara D. Abbott
Current Protocols in Toxicology (2003) 13.6.1-13.6.11

Materials

Supplemented custom-modified Biggers BGJ medium (see recipe)
Dimethylsulfoxide (DMSO)
Chemical to be tested
Penicillin/streptomycin solution: 10,000 U penicillin G with 10 mg streptomycin/ml
Medical gas mixture tank of 50% O_2, 5% CO_2, 45% N_2
70% ethanol
Phosphate-buffered saline (PBS; see recipe)
Time-mated, gestation day (GD) 12 pregnant female mice (mated overnight, next morning plug-positive, confirmed mating = GD 0)

Rocker platform with adjustable tilt rate (side-to-side motion) to fit in incubator
37°C culture incubator
25-cm^2 (75-cm^2 for rat) tissue-culture flasks with tight-fitting caps (e.g., 70-ml capacity, Corning)
0.2-µm syringe filters
1-, 5-, and 10-ml syringes
Two-stage gas regulator, suitable for use with pressurized oxygen
Laminar flow hood (must be operable with door open or have ports for microscopes)
Disposable 1-ml plastic transfer pipets with bulbs, sterile
Dissecting stereo microscope(s)
Fiber-optic illuminator(s)
Gauze pads
Dissection pad (cut a black rubber stopper, size no.12 or other suitable dark rubber pad, horizontally to provide ½-in. height, sterilized by storing in a beaker of 70% ethanol)
60-mm petri dishes
Dumont forceps no. 5, stainless steel (at least 2 pairs, have extra on hand and be aware that these points are easily damaged even in routine use)
3-in. Vannas ultra-microscissors straight (Roboz Surgical or equivalent spring-loaded iridectomy scissors with very fine small blades)
Disposable no. 11 scalpels
5-in. micro-dissecting spatula (Roboz or equivalent)
4-in. dissecting forceps serrated, curved
4¼-in. curved, blunt-tip microdissecting scissors
4-in. curved, sharp-tip microdissecting scissors
5-in. straight hemostatic forceps, delicate, flat mosquito jaw (Roboz or equivalent)
Vacuum flask and vacuum hose
5-, 10-, and 25-ml disposable pipets, sterile
Vacuum pipettor

Prepare for culture

1. At least 24 hr prior to culture setup, place the rocker apparatus in the incubator and turn on, then adjust rate to provide ~15 tilts per min (left side up, moves down, and returns to original up position = 1 tilt).

   The motor will increase the temperature of the incubator chamber. Check after operation for several hours and adjust incubator temperature controls to maintain 37°C with the rocker on. Leave rocker on until completion of culture period.

2. Measure 9 ml of supplemented custom-modified Biggers BGJ medium for each 25-cm^2 flask to be prepared in step 7 into a sterile tube of appropriate volume.

   One tube will be prepared for each control and treated group.

3. Prepare 1000× stock solutions in DMSO of chemical to be tested and sterilize by filtration (for small volumes, use a syringe and 0.2-µm low-volume syringe filter).
4. Add 1 µl DMSO solvent per milliliter of supplemented custom-modified Biggers BGJ medium into the tube corresponding to the control-group flask (0.1% DMSO final).
5. Add 1 µl of the 1000× treatment stock solution of the chemical of interest per milliliter of supplemented custom-modified Biggers BGJ medium into each tube corresponding to each treated-group flask.
6. Add 5 µl penicillin/streptomycin solution per milliliter of supplemented custom-modified Biggers BGJ medium into each tube (final concentration = 50 µg streptomycin/ml and 50 U penicillin/ml).
7. Label 25-cm^2 culture flasks and transfer 9 ml of control or treated medium from each tube to its corresponding flask.

Set up for gas delivery

8. Connect the two-stage regulator to the medical gas mixture tank of 50% O_2, 5% CO_2, and 45% N_2.
9. Attach plastic tubing to the outflow valve of the regulator and position the open end of the gas tubing in the laminar flow hood.
10. Attach a sterile 0.2-µm syringe filter to the end of the gas tubing.
11. Cut the bulb off a sterile, disposable 1-ml plastic transfer pipet and attach the tapered 4-in. long pipet stem to the outflow side of the 0.2-µm syringe filter connected to the gas tubing.
12. Adjust gas flow on the regulator and direct a stream of gas through the tubing, filter, and pipet stem into the flask.

    The gas flow rate should be sufficient to agitate the medium.

13. Flush the air from the flask by streaming gas for 10 to 15 sec, replacing all the air with the gas mixture. Withdraw the pipet and immediately cap the flask tightly.
14. Place flasks horizontally on a raised platform inside the laminar flow hood workspace. Loosen cap but leave it resting over flask opening. Place several flasks at a time on the rack. If possible, have one flask of each treatment on the rack, as this permits loading of tissues from each litter across a block of treatment groups.

    Elevating the neck of the flask makes it easier to place tissues inside the flask. A test tube rack works well as a platform.

Prepare dissection area and tools

15. Place dissecting microscope(s) and fiber-optic illuminator(s) in laminar flow hood.
16. Place sterile gauze pads adjacent to microscope, on stage/platform and have additional gauze pads available in a convenient position in the hood.
17. Place dissection rubber pad on gauze, cover with another gauze pad, and soak gauze with 70% ethanol to sterilize.
18. Place the following dissecting instruments on gauze on each side of microscope in the laminar flow hood, cover with additional gauze, and soak with 70% ethanol to sterilize: Dumont forceps no. 5, spring-loaded iridectomy scissors with very fine small scissor blades (3-in. Vannas ultra-micro scissors, straight, for mouse), disposable no. 11 scalpels, and 5-in. micro-dissecting spatula.

19. Prepare a clean, absorbent paper–covered station to sacrifice the dam.
20. Add 2 to 3 ml sterile PBS to petri dishes (1 dish per litter) and place on ice.
21. Add 70% ethanol to small beaker and place dissection instruments in beaker: 4-in. serrated, curved dissecting forceps; 4¼-in. curved, blunt-tip microdissecting scissors; 4-in. curved, sharp-tip microdissecting scissors; and 5-in. straight hemostatic forceps.

Sacrifice dam and remove uterus and conceptuses

22. Euthanize time-mated (GD 12) pregnant female mice by CO_2 asphyxiation and/or cervical dislocation, according to methods approved by the Institutional Animal Care and Use Committee.

    Donovan and Brown (1995) describes the abovementioned euthanasia procedures in detail.

23. Place dam on its back and soak abdomen with 70% ethanol. Grip and lift abdominal skin with dissecting forceps, then with sharp-tip dissecting scissors, cut through skin and muscle.
24. Continue to open the abdomen through the diaphragm and rib cage. Cut lateral to midline to expose abdominal organs fully.
25. Moving the other organs aside, grip the cervical region at the base of the uterine horns and cut through the cervical tissue. As the uterine horns are raised, use the scissors to strip excess fat away from the uterus.
26. With the forceps, lift the uterus free from the abdomen and, if needed, cut at the site of each ovary to release. Place the intact uterus with contents on gauze pads.

Remove embryos from uterus

27. Clamp the tip of one uterine horn with the hemostatic forceps and lock forceps closed by engaging the clips on the handles.
28. With forceps, extend and slightly stretch the uterine horns to a linear position on the gauze, holding one end with the hemostat and the other with the forceps.
29. Use the blunt-tip dissecting scissors to open the uterus at the end furthest away from the hemostat clamp. Insert the blunt tip into the incision in the uterus near a conceptus and cut the uterine wall, cutting towards the hemostat-clamped end.
30. Cut on the other side of the cervix to open the second uterine horn.

    With practice, this method allows a rapid opening of the uterus, which exposes all of the conceptuses with yolk sac, extra embryonic membranes, and fluids intact.

31. Gently remove the conceptuses, individually, by sliding the curved forceps beneath the conceptus between the placenta and uterine wall, lifting the intact conceptus, and placing it into the PBS in the petri dish. Keep the dish covered as much of the time as possible.

    A second pair of forceps will be helpful to hold the uterus down while pinching off each conceptus.

32. After all conceptuses are transferred to the dish, place on ice, and move to the laminar flow hood for the dissection of fetal tissues.

    The petri dishes on ice can be kept just outside the hood.

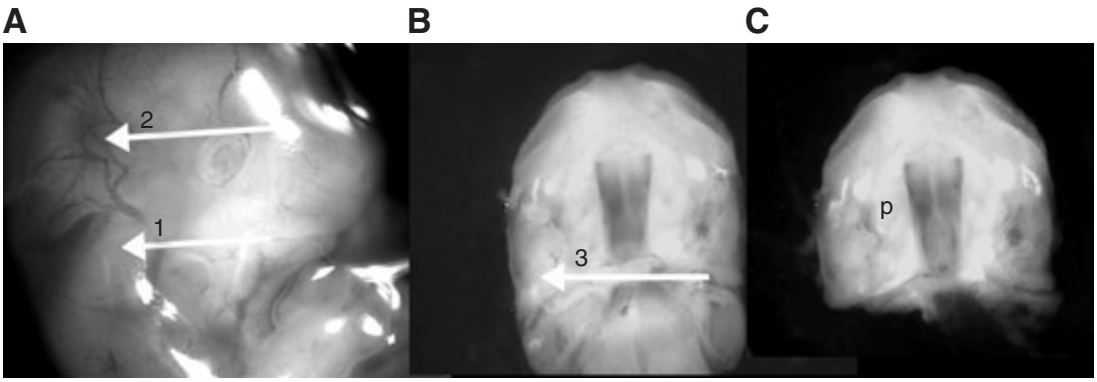

Figure 13.6.1 The gestation day 12 mouse head (plug day = 0) is shown before dissection for palatal organ culture. (**A**) The first incision is made as shown for arrow 1 through the oral cavity to separate mandible from head. The second incision is shown along arrow 2 to remove the upper cranial tissue. (**B**) After turning the midface over, exposing the palatal shelves, a final cut is made as indicated by arrow 3 to remove remaining hindbrain tissues. (**C**) The resulting midfacial region is placed in culture. The letter p indicates a palatal shelf.

Dissect mid-craniofacial region

33. Place the petri dish in the hood to open and remove one embryo at a time. Place the embryo on the black rubber platform.
34. Use two Dumont forceps to remove yolk sac, amnion, and placenta.
35. Use the Vannas ultra-microscissors to cut off the mandible and top of the head (see Fig. 13.6.1A). Insert one blade of the microscissors into the oral cavity and the other blade across the outside of the face, cut to separate the mandible and neck from the upper head.

    Forceps placed at the back of the head can be used to brace or hold head in position during the cut.

36. Make a second cut at the level of the eye to remove the upper brain tissues. Push the other tissues aside and turn the midface over, exposing the palatal shelves.
37. Trim off excess tissues and remove hindbrain tissue with a scalpel by cutting at the level of the posterior palatal shelves (see Fig. 13.6.1B).

    If any mandible, tongue, or hindbrain remains, trim off. Eyes will remain on the final midfacial explant that is now ready to transfer to the culture flask (see Fig. 13.6.1C).

38. Transfer midfacial explant by sliding a dissection spatula under the explant, pressing down on the rubber mat to assist in pickup. Open cap of flask (from step 14) and insert the spatula until it touches the medium and the tissue floats off the spatula.
39. Continue to dissect embryos from the litter until completed, or up to 30 to 35 min. Discard any embryos that are not processed within this period of time.
40. Distribute embryos from each litter across the treatment groups/flasks by placing several flasks on the platform to receive tissues in sequence as the dissections occur. Put up to four tissue samples per flask.
41. Continue to sacrifice dams as needed. After 1 hr of dissections, or when all flasks are loaded with tissues (if completed in <1 hr), flush each flask with the gas mixture as in step 13 (10 to 15 sec gas flow in each flask) and cap tightly.
42. Place flasks on the rocker platform in the 37°C incubator.

    If necessary, continue collecting tissues and repeat steps above for up to 3 to 4 hr.

Change culture medium and exchange gas

43. Replace medium and flush flasks with the gas mixture 24 hr after set up and each 24 hr thereafter.

    In most cases, the treatments are also included with the fresh medium.

44. Prewarm the supplemented custom-modified Biggers BGJ medium with DMSO solvent or treatment and penicillin/streptomycin added (as in steps 2 to 6) complete in a 37°C water bath.

45. Remove medium from flask by pouring into a beaker or by suction (keep tissues inside flask).

    For removal by suction, prepare a vacuum flask to trap the medium as it is removed. Cut a sterile, disposable transfer pipet and attach it to the end of the vacuum hose to provide a clean suction tip to place into each culture flask. Replace the pipet between treatments, if not between each flask. Although several flasks can be processed before replacing medium, try not leave tissues for more than a few minutes without medium in the flasks.

46. Pipet 9 ml fresh prewarmed medium into each flask.

47. Flush each flask with the gas mixture as in step 13 and replace on the rocker in the 37°C incubator.

    Cultures can be maintained 4 to 5 days or until palatal fusion occurs. Palatogenesis schedule and thus duration of culture depends on strain of mice chosen for cultures.

Evaluate tissue

48. At intervals during culture and at the end of culture, examine the explants under a dissecting microscope to track progress of palatal elevation and fusion.

    Palates that are attached cannot be separated even by gentle pulling with Dumont forceps on the primary palatal edges. A palatal seam will remain intact and the adjacent tissue will tear if sufficient force is used.

ALTERNATE PROTOCOL

SUBMERGED PALATAL ORGAN CULTURE OF RAT MIDFACIAL TISSUES

Rat strains differ in their requirements for successful fusion of the palates in culture. Fisher 344 rats perform well under the same conditions as the mice (four explants in 9 ml of medium for 4 to 5 days). Sprague-Dawley and CR/Lewis rats require larger, 75-cm^2 flasks with 50 ml of medium, where each flask can hold up to ten explants. The equipment, supplies, and reagents required are the same as for mouse, with the exceptions noted below. The protocol for preparation of the cultures is also the same as for mouse except as noted.

Additional Materials *(also see Basic Protocol)*

Time-mated, gestation day (GD) 14 rats (mated overnight, next morning plug-positive, confirmed mating = GD 0)

75-cm^2 tissue-culture flasks, canted-neck plug seal (caps must form gas-tight seal, no ventilated filter caps)

Vannas ultra-microscissors (spring-loaded iridectomy scissors), with slightly larger blades than used for mouse

For rat palatal organ cultures, supplemented Biggers BGJ medium (prepared as described for mouse cultures; see recipe) is supplemented with 1×10^{-11} M all-trans retinoic acid. The CR/Lewis rat palates also have a higher percentage of explants fuse if the gas is changed on day 4 to 95% O_2, 5% CO_2 and the flasks are flushed with the gas in the morning and late afternoon on day 4. Tissues are scored the next morning (day 5).

REAGENTS AND SOLUTIONS

Use Milli-Q purified water or equivalent in all recipes and protocol steps. For common stock solutions, see ***APPENDIX 2A****; for suppliers, see* ***SUPPLIERS APPENDIX****.*

All-trans retinoic acid, 1×10^{-2} M

Dissolve 3 mg retinoic acid (RA) per milliliter of filtered DMSO (final 1×10^{-2} M). Dispense into 0.1-ml aliquots into amber vials. Protect from light, store up to 1 year at −80°C.

Dilute stock with DMSO in serial dilutions as required for treatments or as a supplement to medium. Add 1 µl RA/ml medium (DMSO = 0.1%).

Apo-transferrin, 10 mg/ml

Dissolve 20 mg apo-transferrin in 2 ml sterile, distilled water. Dispense into 200-µl aliquots per 1.5-ml sterile tube. Store 10 mg/ml stock up to 1 year at −20°C.

Custom-modified Biggers BGJ medium, 1×

Reconstitute a 5-liter powder package of modified Biggers BGJ medium (see Table 13.6.1 for composition; the custom medium is supplied by Irvine Scientific) per supplier's instructions for a final concentration of 1× by adding powdered medium slowly to 4 liters distilled, deionized water with stirring. Add 14 g sodium bicarbonate and bring up to 5 liters with distilled, deionized water. Check pH (pH 7.0 to 7.5) and osmolarity (265 to 300 mOs/kg). Filter sterilize using 0.2-µm nylon or cellulose acetate filters. Store liquid medium up to 6 months at 4°C.

Bottle filter systems and autoclaved sterile glass bottles or filter units with 500-ml or 1-liter plastic storage flasks can be used for sterilization and storage.

Supplemented custom-modified Biggers BGJ Medium: Prior to use, measure 100 ml of 1× custom-modified Biggers BGJ medium with sterile graduated cylinder and

continued

Table 13.6.1 Custom-Modified Biggers BGJ Formulation[a] (with L-Glutamine 150 mg/ml, without $NaHCO_3$)

Ingredient	mg/liter	Ingredient	mg/liter
Sodium chloride	6400	*p*-Aminobenzoic acid	1.5
Potassium chloride	425	Ascorbic acid	150
Glucose (dextrose) anhydrous	4400	Nicotinic acid amide	15
Calcium lactate·$5H_2O$	600	Phenol red, Na salt	17.04
L-Arginine HCl	70	Thiamine HCl	3
L-Cysteine HCl·H_2O	135	α-Tocopherol phosphate, 2Na	0.75
L-Glutamine	150	Potassium phosphate, monobasic KH_2PO_4	113
L-Histidine HCl·H_2O	150	Magnesium sulfate, anhydrous $MgSO_4$	161.17
L-Isoleucine	23	Choline chloride	38
L-Leucine	40	Folic acid	0.15
L-Lysine HCl	225	Inositol	0.15
L-Methionine	40	Riboflavin	0.15
L-Phenylalanine	40	Vitamin B-12	0.03
L-Threonine	60	D-Biotin	0.15
L-Tryptophan	30	Pantothenic acid, Ca salt	0.15
L-Tyrosine 2Na·$2H_2O$	43.25	Pyridoxal HCl	0.15
L-Valine	50		

[a]Adapted from Shiota et al., 1990. The custom-modified Bigger BGJ formulation is supplied by Irvine Scientific.

pour into sterile plastic flask. Add 15 mg L-glutamine, cap flask tightly, and mix by inversion. Add 600 mg bovine serum albumin per milliliter of medium, cap flask tightly, and mix by gentle inversion. Filter sterilize supplemented medium using 0.2-µm nylon or cellulose acetate filters. Store up to 2 weeks at 4°C.

Additional supplements for the culture medium can include the following (also see Critical Parameters and Troubleshooting):

5 µl/ml sodium L-ascorbate solution (final 50 µg/ml; see recipe)
1% (v/v) fetal bovine serum (50% stock, 20 µl/ml medium; see recipe)
1 µl/ml sodium selenite solution (final 10 ng/ml; see recipe)
1 µl/ml apo-transferrin (final 10 µg/ml; see recipe)
L-Glutamine can be increased four times the normal level
All-trans retinoic acid (final 1×10^{-11} M; see recipe)

Fetal bovine serum, 50%

Dilute 1:1 (v/v) FBS with custom-modified Biggers BGJ medium (not supplemented, see recipe). Dispense into 3- to 5-ml aliquots per tube. Filter sterilize using 0.2-µm nylon or cellulose acetate filters. Store ≥1 year at −20°C.

Phosphate-buffered saline (PBS)

Calibrate a 4- to 6-liter Erlenmeyer flask by measuring 4 liters water with a graduated cylinder and add to flask, mark the 4-liter level on the side of the flask, and decant the water.

Add 3 liters distilled water to the Erlenmeyer flask. Weigh and add to water the following while stirring with a magnetic stir bar:
35.04 g NaCl
1.38 g $NaH_2PO{\cdot}H_2O$ (monobasic)
8.04 g $Na_2HPO_4{\cdot}7H_2O$ (dibasic)
Add distilled H_2O up to the 4-liter mark
Adjust pH to 7.4 with 1 N NaOH
Filter sterilize with a 0.2-µm filter and store in sterile 500-ml flasks ≥1 year at 4°C

Sodium L-ascorbate

Dissolve 200 mg sodium L-ascorbate in 20 ml sterile, distilled water
Dispense into 1-ml aliquots per 1.5-ml sterile tube
Store 10 mg/ml stock ≥1 year at −20°C

Sodium selenite

Dissolve 5 mg sodium selenite in 5 ml sterile, distilled water
Dilute 1:100 to give 10 µg/ml stock
Dispense 10 µg/ml solution into 1-ml aliquots per 1.5-ml sterile tube
Store aliquots ≥1 year at −20°C

COMMENTARY

Background Information

Clefts of the secondary palate are among the most frequent birth defects in live-born human infants. Across the United States in 1997, a compilation of data from states with birth defects monitoring programs (National Birth Defects Prevention Network, 1997) showed the incidence of cleft palate without cleft lip to range from 2.01 to 14.2 per 10,000 live births. Thus, the formation of the secondary palate and the mechanism for induction of cleft palate has been the focus of extensive research. Palatogenesis also presents an interesting model for many of the processes involved in morphogenesis in the embryo.

Several palatal organ and cell culture methods have been developed and some are discussed in review and overview articles (Thesleff, 1981; Whitby, 1987; Pisano and Greene, 2000). The major palatal organ culture

models include a model in which the palatal shelves are isolated and cultured on a membrane support (Tyler and Koch, 1975; Ferguson et al., 1984) and a model in which the midfacial region, including the maxillary arch, is submerged in medium in a culture flask (Lewis et al., 1980; Shiota et al., 1990; Abbott and Buckalew, 1992; Al-Obaidi et al., 1995). The system in which the palatal shelves are supported on a membrane above the medium, a Trowell-like palatal organ culture, requires skill to dissect and orient the palatal shelves. This method also requires organ culture dishes with a chamber to support the grids and membranes. Although successfully applied by many investigators in studies of chick, alligator, mouse, rat, and human secondary palatal shelves, this approach is not described in this unit (Ferguson et al., 1984; Abbott and Pratt 1987a,b; Abbott and Birnbaum, 1990, 1991).

The culture technique described here (see Basic Protocol) is the submerged culture of the entire midfacial region. This method can be performed with relatively standard culture equipment and supplies and is simpler to perform than the supported organ cultures. This model also offers several advantages over the membrane-supported palatal culture system as it permits the palatal shelves to grow, elevate, and fuse in the culture medium. The protocol presented here is a modification of a method initially described by Shiota et al. (1990). The modifications include simplifying the dissection and performing the culture in disposable flasks on a rocker platform, as well as suggesting adjustments to the culture medium supplementation, volume, and schedule for replacing medium as needed for each species, strain, or test agent. These modifications facilitated the performance of large studies and were successfully applied to mouse, rat, or human specimens (Abbott and Buckalew, 1992; Abbott et al., 1993, 1994, 1996, 1998, 1999; Shuey et al., 1994).

Critical Parameters and Troubleshooting

Developmental staging and schedule for tissue collection

Mice can be mated overnight and checked for sperm plug the next morning, which is designated GD 0. The palatal shelves appear as outgrowths of the maxillary arch between GD 11 and 11.5. The palatal shelves should be clearly visible on GD 12 (Theiler stage 20 or Carnegie stage 17) and should be vertical in orientation. A similar developmental stage for rats is found on GD 14. Be aware that different strains of mice (and even the same strain in different breeding colonies) may differ by as much as 6 to 12 hr in developmental staging. Confirm the best time for collecting tissues from the animals being used.

Maintaining tissue integrity

The embryos need to be removed from the uterus as quickly as possible. They remain in the best condition for up to 30 min on ice in PBS if the membranes and placenta stay attached. This leaves the circulatory system as intact as possible, with little or no blood loss from the conceptus before dissection. Any embryos that have ruptured yolk sac vasculature or are separated from the placenta should be dissected first. The petri dish is kept on ice to retain integrity of tissues as long as possible. The amount of time that passes between sacrifice of the dam and completed dissection of the tissues will also affect the quality of the cultures. Optimal outcomes are obtained when each litter requires <20 min to process and the cultures are completed and placed in the incubators within 1 to 2 hr after sacrifice of the first dam. Longer processing times may also produce good outcomes, but larger experiments require attention to the schedule and may need two experienced researchers. With practice, two skilled researchers can prepare 80 to 90 explants for culture in ~1 hr. It is not recommended to use any embryos that are on ice >30 min.

Factors affecting rate of palatal fusion in control cultures

A number of factors can affect the numbers of explants that fuse by the end of the culture period. Obviously, the control cultures need to be maintained long enough to permit fusion of most or all of the explants. Initially, it may be desirable to allow some flasks to remain in culture, observing daily, until all explants are fused or until no additional fusion events occur. This will define the duration required for the optimal control fusion rates. There are other factors that affect the numbers or rate of palatal fusion and some of these can be manipulated to improve the outcome. These variables include the size and number of explants per container, the volume of medium, and the vessel selected for the cultures (roller bottle versus flask). The limiting factors that are common for all of these variables are likely to be the availability of nutrients and, probably even more of

a determinant, the oxygenation of the medium. The authors' observations during variations of these factors were that too many explants, too low a medium volume, too small a vessel, and infrequent medium or gas exchanges all resulted in poor growth and fusion. In experiments, the flasks produced better results than roller bottles, and changing medium and gas daily was an improvement relative to less frequent exchanges (although every other day may be sufficient for some cultures). However, each of these variables can be manipulated as required to optimize cultures for specific strains and species.

Issues related to prevention of contamination

Bacterial and fungal contamination are generally a result of poor sterile technique and can be avoided by careful decontamination of all surfaces and instruments, and use of sterilized reagents. Filter sterilization should always be done with 0.2-μm pore size filters. All glassware should be covered with aluminum foil and autoclaved with indicator tape to show that effective levels of sterilization temperatures and times were attained. All equipment, instruments, and hood and incubator surfaces should be routinely decontaminated and sterilized with 70% ethanol. Perform as many of the procedures as possible in a laminar flow hood. Wear gloves and change them whenever there is a chance that the surfaces are contaminated. Even the water bath that is used to warm the medium needs to be as clean as possible. Once contamination occurs, all the areas used for preparing and incubating the cultures need to be thoroughly decontaminated. Awareness and vigilance to prevent contamination are far better than solving the problem after contamination occurs.

Customizing medium formulation with optional supplements

Palatal shelves have normal development and fuse in the standard control medium without addition of the optional supplements. However, depending on the test compound, additional supplements may be required to provide responses to a toxicant that are similar to those observed after an in utero exposure. This seems to depend on the mechanism of action of the compound, as the secondary palatal shelves elevate and fuse in absence of these additives. Caution should be exercised with supplements to assure that normal palatal processes occur in the presence of the additives. Excess fetal bovine serum (>1%) can interfere with palatal fusion. Be aware that each new lot of serum, even if it is from the same supplier, needs to be tested in the model to confirm that it supports normal development.

Anticipated Results

The palatal shelves of the mouse craniofacial explants elevate and contact and fuse during the 4 to 5 days of culture. In experiments with CD1 mice, the incidence of fusion after 4 days in culture was 93% (i.e., 93% of all explants were completely fused). The remaining 7% of explants showed at least partial fusion after 4 days in culture. C57BL/6N mice exhibited similar results and responded to various teratogenic exposures (e.g., all-trans retinoic acid, 5-fluorouracil, methanol, ethanol, 2,3,7,8-tetrachlorodibenzo-*p*-dioxin, dexamethasone, hydrocortisone) with failure to fuse.

The outcomes for rat palatal shelves depended on the strain of rat. F344 rat explants cultured for 5 days adhered and 82% had fused palatal shelves. Sprague-Dawley and CR/Lewis rat palates needed larger flasks, more medium, and supplementation with low levels of retinoic acid. However, 80% of these palates fused if additional gas exchanges and higher oxygen were administered on the fourth day of culture.

Time Considerations

The preparations on the day of culture prior to sacrifice and tissue collection can require 1 to 1.5 hr depending on the experience of the operator and the scale of the experiment. The amount of time required for the sacrifice and dissections will be dependent on the number of flasks required for that experiment. Plan 3 to 4 hr (all morning or all afternoon) to conduct a typical experiment as outlined below. Generally, allow 15 min per litter. A typical experimental design includes 3 flasks (12 tissues) per treatment group. Allow four tissues per flask—for C57 strains, estimate an average of eight fetuses per litter; CD1 mice and most strains of rats will average ten or more embryos per litter. Thus, a control and three concentration levels of a treatment will require 12 flasks and 48 embryonic dissections from six litters. After initial setup, the subsequent medium and gas exchange for the flasks requires ~1 hr or less each day. Evaluating the tissues under the dissecting microscope generally does not require more than a few minutes per flask and subsequent fixation and/or processing of the

specimens will depend on the objectives of the study.

Literature Cited

Abbott, B.D. and Pratt, R.M. 1987a. Human embryonic palatal epithelial differentiation is altered by retinoic acid and epidermal growth factor in organ culture. *J. Craniofac. Genet. Dev. Biol.* 7:241-265.

Abbott, B.D. and Pratt, R.M. 1987b. Retinoids and epidermal growth factor alter embryonic mouse palatal epithelial and mesenchymal cell differentiation in organ culture. *J. Craniofac. Genet. Dev. Biol.* 7:219-240.

Abbott, B.D. and Birnbaum, L.S. 1990. Rat embryonic palatal shelves respond to TCDD in organ culture. *Toxicol. Appl. Pharmacol.* 103:441-451.

Abbott, B.D. and Birnbaum, L.S. 1991. TCDD exposure of human embryonic palatal shelves in organ culture alters the differentiation of medial epithelial cells. *Teratology* 43:119-132.

Abbott, B.D. and Buckalew, A.R. 1992. Embryonic palatal responses to teratogens in serum-free organ culture. *Teratology* 45:369-382.

Abbott, B.D., Lau, C., Buckalew, A.R., Logsdon, T.R., Setzer, W., Zucker, R.M., Elstein, K.H., and Kavlock, R.J. 1993. Effects of 5-fluorouracil on embryonic rat palate in vitro: Fusion in the absence of proliferation. *Teratology* 47:541-554.

Abbott, B.D., Logsdon, T.R., and Wilke, T.S. 1994. Effects of methanol on embryonic mouse palate in serum-free organ culture. *Teratology* 49:122-134.

Abbott, B.D., Birnbaum, L.S., and Diliberto, J.J. 1996. Rapid distribution of 2,3,7,8-tetrachlorodibenzo-*p*-dioxin (TCDD) to embryonic tissues in C57BL/6N mice and correlation with palatal uptake in vitro. *Toxicol. Appl. Pharmacol.* 141:256-263.

Abbott, B.D., Probst, M.R., Perdew, G.H., and Buckalew, A.R. 1998. AH receptor, ARNT, glucocorticoid receptor, EGF receptor, EGF, TGF alpha, TGF beta 1, TGF beta 2, and TGF beta 3 expression in human embryonic palate, and effects of 2,3,7,8-tetrachlorodibenzo-*p*-dioxin (TCDD). *Teratology* 58:30-43.

Abbott, B.D., Buckalew, A.R., Diliberto, J.J., Wood, C.R., Held, G., Pitt, J.A., and Schmid, J.E. 1999. AhR, ARNT, and CYP1A1 mRNA quantitation in cultured human embryonic palates exposed to TCDD and comparison with mouse palate in vivo and in culture. *Toxicol. Sci.* 47:62-75.

Al-Obaidi, N., Kastner, U., Merker, H.J., and Klug, S. 1995. Development of a suspension organ culture of the fetal rat palate. *Arch. Toxicol.* 69:472-479.

Donovan, J. and Brown, P. 1995. Euthanasia. *In* Current Protocols in Immunology (J.E. Coligan, A.M. Kruisbeek, E.M. Shevach, and W. Strober, eds.), pp.1.8.1-1.8.4. John Wiley & Sons, New York.

Ferguson, M.W., Honig, L.S., and Slavkin, H.C. 1984. Differentiation of cultured palatal shelves from alligator, chick, and mouse embryos. *Anat. Rec.* 209:231-249.

Lewis, C.A., Thibault, L., Pratt, R.M., and Brinkley, L.L. 1980. An improved culture system for secondary palatal elevation. *In Vitro* 16:453-460.

National Birth Defects Prevention Network. 1997. Birth defects surveillance data from selected states. *Teratology* 56:115-175.

Pisano, M.M. and Greene, R.M. 2000. Palate development. In vitro procedures. *Methods Mol. Biol.* 137:267-274.

Shiota, K., Kosazuma, T., Klug, S., and Neubert, D. 1990. Development of the fetal mouse palate in suspension organ culture. *Acta. Anat.* 137:59-64.

Shuey, D.L., Buckalew, A.R., Wilke, T.S., Rogers, J.M., and Abbott, B.D. 1994. Early events following maternal exposure to 5-fluorouracil lead to dysmorphology in cultured embryonic tissues. *Teratology* 50:379-386.

Thesleff, I. 1981. Use of organ culture techniques in craniofacial developmental biology. *Proc. Finn. Dent. Soc.* 77:159-169.

Tyler, M.S. and Koch, W.E. 1975. In vitro development of palatal tissues from embryonic mice. I. Differentiation of the secondary palate from 12-day mouse embryos. *Anat. Rec.* 182:297-301.

Tyler, M.S. and Pratt, R.M. 1980. Effect of epidermal growth factor on secondary palatal epithelium in vitro: Tissue isolation and recombination studies. *J. Embryol. Exp. Morphol.* 58:93-106.

Whitby, K.E. 1987. Teratological research using in vitro systems. III. Embryonic organs in culture. *Environ. Health Perspect.* 72:221-223.

Contributed by Barbara D. Abbott
U.S. Environmental Protection Agency
Research Triangle Park, North Carolina

Overview of Behavioral Teratology

Four decades ago, a growing awareness of the potential central nervous system toxicity of many chemicals present in the environment led to extensive regulatory activity by governmental agencies in various countries, aimed at protecting populations from exposure to noxious agents. As a result, screening chemicals for possible neurotoxicity became mandatory. Among the analyses to be carried out in the neurotoxic hazard identification, behavioral teratology studies were recommended (WHO, 1986).

The discipline of behavioral teratology is based on the study of behavior as a powerful tool to identify and disentangle noxious effects of compounds known or suspected to be potentially neurotoxic early during development (Bignami, 1996; Cuomo et al., 1996; Kulig et al., 1996). Indeed, because behavior is the ultimate output of the brain, behavioral assessments can provide critical information on the noxious action exerted by selected chemicals—information that is different from, and complementary to, the information provided by neurochemical, cellular, and histological evaluations. In particular, behavioral assessments allow one to investigate the integrity of a number of brain processes, helping to identify selected structural and/or functional alterations. A large number of behavioral protocols are available that are rapid, simple, quantitative, easily replicable, and reliable as indices of brain dysfunction.

In the 1970s, the approach of classical neurotoxicology and neuroteratology, based exclusively on neuropathological and neurochemical analyses, shifted to a more comprehensive strategy that also included the study of behavioral parameters. The work by Joan M. Spyker on the deleterious effects on behavior of developmental exposure to methylmercury is considered the starting point of behavioral teratology (Spyker, 1975). This work takes into account important considerations on the use of behavioral analysis for risk assessment, providing useful working hypotheses concerning the significance and the nature of the behavioral effects observed.

The development of the discipline of behavioral toxicology and teratology has been marked by problems and difficulties concerning specific theoretical and methodological issues. For example, the concept of compensatory processes, which may or may not counterbalance and thus mask the adverse effects produced by exposure to a given noxious compound, should be carefully taken into account in order to minimize the risk of false negatives. Due to inadequate knowledge of several developmental events, most of the compensatory phenomena are not easily predicted and involve complex reorganizational processes that may occur at the neuroanatomical, neurochemical, or behavioral level. Since the development of diverse neural and behavioral systems is differentially timed, the ontogenetic analysis can represent a powerful strategy to investigate the effects of administering selected compounds on different brain functions prior to the occurrence of possible compensatory events. In fact, the literature provides examples that illustrate how selected developmental brain manipulations can induce transient phenotypic consequences that are not detectable later on, after compensatory events at a functional level have taken place (Ricceri et al., 1997, 1999).

From a methodological viewpoint, a controversial issue that characterized the initial phases of development of behavioral toxicology and teratology arose because most investigators were not aware of the importance of taking into account the litter effect, which is due to the nonindependence among observations taken on littermates. This nonindependence stems from the fact that pups tend to be more similar to each other within each litter than between litters, due to genetic and/or environmental/experiential factors (Alleva et al., 1985; Buelke-Sam et al., 1985; Chiarotti et al., 1987). Specifically, the litter, rather than the individual, represents the appropriate statistical unit in the data analysis. While parametric statistical methods generally allow one to easily manage the litter effect, particularly by mixed-model ANOVA designs, the nonparametric ones, which have to be applied when the distribution of the response variable does not respect the parametric assumptions, do not allow one to manage such an effect when working with complex experimental designs (for further considerations and for solutions aimed at minimizing the loss of statistical power, see Marascuilo and McSweeney, 1971; Winer, 1971; Chiarotti and Sparks, 2002).

Contributed by Igor Branchi, Giorgio Bignami, and Enrico Alleva
Current Protocols in Toxicology (2005) 13.7.1-13.7.6

BASIC CONSIDERATIONS IN BEHAVIORAL TERATOLOGY

Animal Species

Laboratory rodents are the animal species most commonly used in behavioral teratology studies. This is because using mice and rats provides numerous advantages: (1) ease of breeding and short gestation period, (2) large litter size (outbred mouse strains, such as Swiss CD-1, produce as many as 16 to 18 pups), (3) low maintenance costs due mainly to their relatively small size, (4) the availability of extensive background information on mouse and rat physiology and behavior, and (5) the fact that the mouse is the only species with a wide variety of inbred and noninbred strains that have specific characteristics and are easily amenable to genetic manipulations.

Primate species are also used in toxicology and teratology studies. Primates provide a major advantage compared to rodents: their high cognitive functions and their behavioral competencies, which are close to those of humans, make primates a highly appropriate model for selected in-depth analyses of potential human behavioral dysfunction due to exposure to neurotoxicants. However, both ethical considerations and cost suggest that the use of primates in scientific research should be strictly limited to cases in which a given problem cannot be solved otherwise. In fact, on the basis of primate physiology and behavior, it is supposed that these animal species are much more susceptible than others to psychophysical pain and stress.

The Ethological Perspective in Behavioral Studies

As Charles Darwin pointed out in his book *The Expression of Emotions in Man and Animals*, published in 1872, each species has evolved a species-specific behavioral repertoire shaped by its unique evolutionary history (Darwin, 1872). As a consequence, distinct species may react differently to the same stimulus or may manifest different behavioral displays as a response to the same internal drive (Crews, 1997; Katz and Harris-Warrick, 1999). Thus, the study of behavioral patterns of a given species should be carried out with consideration toward the ecoethological constraints that shaped them, since these can provide the appropriate contextual information for an accurate interpretation (Kamil and Mauldin, 1988; Martin and Bateson, 1993). This point is central to the ethological perspective in the study of behavior and should be carefully kept in mind in designing experiments as well as in interpreting data.

In order to score endpoints representative of specific behavioral competencies, experimental designs should be based on the manipulation of stimuli having a marked ecoethological relevance in the natural habitat for the species under investigation (Kamil and Mauldin, 1988; Alleva et al., 1995; Capone et al., 2002). Indeed, such relevance will determine the efficacy of the test. For instance, it has been shown that in a classical conditioning-avoidance paradigm, selected stimuli can be promptly paired, but others need repeated trials or prevent learning altogether. Rats can learn with a single trial to associate food with a nausea-inducing substance, thus developing a powerful conditioned aversion, but they require many trials to learn to avoid food associated with an electric foot shock. The relevance of this difference appears evident when considering the adaptive value of learning that allows rats to avoid eating a food that previously made them sick (Garcia and Koelling, 1966).

The wide use of animal models in neurotoxicology and teratology studies raises several issues concerning the comparison of selected behavioral responses between different species and the appropriate evaluation of the clinical relevance of behavioral alterations found in experimental models (Alleva and Sorace, 2000; Cenci et al., 2002; Watase and Zoghbi, 2003). Also in this case, the ethological perspective is an essential factor in reaching significant and reliable conclusions. For instance, in the study of behavior in animal models, the analysis of human-like symptoms in animals should be based primarily on a reasonable expectation of functional similarity of the displayed behavioral strategy, rather than on one of behavior equivalency. The crucial point is not whether a mouse would show a given behavioral impairment, but, rather, how a behavioral impairment would manifest itself in a mouse (Gerlai and Clayton, 1999; Cenci et al., 2002). Ethological studies have provided detailed descriptions of the mouse behavioral repertoire that allow an accurate analysis aimed at identifying deficits in specific behavioral abilities (Martin and Bateson, 1993; Alleva et al., 1995; Crusio and Gerlai, 1999; Crawley, 2000; Branchi and Ricceri, 2002).

Assessment of Multiple Behavioral Endpoints that Encompass Diverse Behavioral Competencies

It should be kept in mind that each behavior is a part of a complex repertoire. As a consequence, a selected behavioral competency cannot be correctly assessed without investigating different endpoints, since distinct behavioral competencies may influence each other in generating a selected behavioral response. For example, the performance of a mouse in a learning test is clearly related to its learning abilities, but a variety of other nonassociative factors, including emotional as well as stimulus and response factors, may exert an influence as great as or even greater than that of associative factors (Wolfer et al., 1998; van der Staay, 2000). Their performance in a plus-maze test is related to both their activity and their anxiety levels (Rodgers and Johnson, 1995; File, 2001). Furthermore, in order to exhaustively describe the rodent behavioral phenotype, a multitier strategy, comprising different levels of behavioral testing characterized by an increasing complexity of the responses scored, should be applied (Crawley, 2003). The lower tiers comprise the assessment of such simple behavioral and functional responses as reflexes, postures, motor coordination, and sensory abilities, among others. The higher tiers require a more complex behavioral approach, including testing of attention, anxiety, and learning and memory, which leads to a higher burden of appropriate controls aimed at avoiding erroneous inferences (e.g., confounding changes in associative and nonassociative functions in the case of learning and memory studies). This strategy allows one to exclude, or, on the contrary, to confirm, that impairments found in complex experimental situations may be due to deficits in simple physiological or behavioral functions, such as changes in response modulation or altered sensitivity to either signaling or reinforcing stimuli (Bignami, 1996; Rogers et al., 1997; Crawley, 2003).

Appropriate Test Strategies Should Be Applied at Each Age Phase

Mice and rats are altricial rodents: pups are born in a highly immature condition, with eyes and ears closed, after a short pregnancy (gestation lasts around 20 days, depending on the species and strain). At birth, they are able to crawl, to attach themselves to a nipple, and to suckle, yet they need close body contact with the mother because they are not able to thermoregulate. Several reflexes and behavioral responses appear at successive postnatal steps in parallel with somatic changes, progressively expanding pup sensory and motor capabilities (Bignami, 1996; Crawley, 2000). The subsequent, more complete behavioral repertoire increases the ability of the pup to procure food and fluid, especially after eye opening, which occurs around the end of the second postnatal week (Scott, 1953; Fox, 1965). The time of onset of selected somatic changes and the time of first appearance and subsequent complete maturation of various reflexes and responses show a remarkable regularity, providing effective tools to assess possible neurobehavioral developmental alterations (Bignami, 1996).

Thus, when exploiting behavioral studies during the first phases of development, Patrick Bateson's cardinal view of neurobehavioral development in mammals as a process akin to the metamorphosis of a caterpillar into a butterfly (Bateson, 1981), should be taken into account.

Mice Versus Rats: Species Differences Matter

The rat, in particular the *Rattus norvegicus* species, has been used in research since the mid-1800s (Sharp and La Regina, 1998). Since then, considerable knowledge on rat physiology and behavior has been produced, making this species historically the one most commonly used in the study of behavior. More recently, the mouse has been more and more extensively used in neurotoxicity and teratology studies, because of its smaller size and lower maintenance costs and because, among mammals, the mouse is the most amenable to genetic manipulations. As a consequence, many of the behavioral tests originally developed for rats began to be modified for use in mouse studies. However, in this process, the different species-specific competencies of rats and mice have not always received adequate consideration (Whishaw, 1995; Whishaw and Tomie, 1996; Frick et al., 2000). The natural habitats of the two species show important differences; for instance, while rats live in subterranean burrows near water, e.g., on river banks, mice do not. An ecological niche rich in water has allowed the rat to develop a high competency in coping with situations that require swimming. This issue has been elegantly pointed out by experiments showing that mice can learn water-based tasks but that their learning performance is quite inferior to

that of the rat (Whishaw, 1995); however, this difference is reduced when selected parameters of the experimental setting, such as pool size (Frick et al., 2000; van der Staay, 2000) and height of the pool walls (Carman and Mactutus, 2001), are appropriately modified. By contrast, the spatial learning abilities of the two species are similar when compared in dry-land mazes, such as the radial-arm maze (Whishaw and Tomie, 1996; *UNIT 11.3*). Still other factors having an ecoethological relevance may differently influence rat and mouse performances in a water maze (*UNIT 11.3*). For example, the differences in their respective predator-avoidance responses have been hypothesized to affect strategies for crossing open spaces and thus for reaching the platform (Schenk, 1987). This strengthens the notion that the learning abilities of the two species are essentially similar, except for the influence of experimental variables related to differences in their respective ecoethological characteristics (Kamil and Mauldin, 1988; Martin and Bateson, 1993).

Nonethological factors may deeply modulate animal performance in a learning test. For example, the water-based tests expose animals to cold water for a few minutes, and mice, unlike rats, can become severely hypothermic during such exposure. Thus, when testing mice in these experimental paradigms, temperature monitoring is crucial to control for this confounding factor (Iivonen et al., 2003).

These considerations should not preclude the use of tests developed for rats in mouse studies, or vice versa, but tests should be modified according to the species-specific competencies of the species under study, and the possible interference in behavioral performances arising from this process should be rigorously taken into account.

The exploitation of several rodent and nonrodent species such as gerbils, marmots, or voles in teratology and neurotoxicology studies represents a potentially important asset. Precocial–type species, such as guinea pigs or spiny mice (*Acomys cahirinus*), may provide important insights into the effects of neurotoxicant exposure at early postnatal phases, when newborns are already quite similar to adults (Pintor et al., 1986; D'Udine and Alleva, 1988). In fact, to obtain a better characterization of the complex ontogenic profile of developing humans, a comparative approach using more than two species, including precocials and altricials, is crucial to avoid biased species- or family-specific observations. The case of thalidomide is a telling example of the inadequacy of studies carried out using only a single mammalian species to identify and prevent possible adverse effects on developing humans.

Pharmacological Challenges

The use of psychoactive drugs that act on specific neurotransmitter systems represents a further useful addition to the assessment of the functional state of such systems during development. Drug challenges, such as by compounds modulating synaptic efficacy (i.e., receptor agonists and antagonists), may unmask neurobehavioral alterations not detectable under baseline testing conditions. They also can provide critical cues to the identification of changes in selected neural systems during development. For example, the use of challenges with both a monoaminergic agent (amphetamine) and a muscarinic blocker (scopolamine) at selected postnatal ages after prenatal exposure of mice to a benzodiazepine (oxazepam), showed a delay in the development of monoaminergic, but not cholinergic systems regulating locomotor activity (Alleva et al., 1985). By contrast, the use of a scopolamine challenge made it possible to show an accelerated maturation of cholinergic regulatory systems in mice neonatally treated with nerve growth factor (Calamandrei et al., 1991).

Ethical Aspects

A last, but not less important, aspect of studying behavior from the ethological perspective is that ethologically refined experimental designs meet the requirements of animal welfare, reducing the suffering of laboratory animals by taking care of their ethological needs, at least partially. This point is in line with the requirement of refinement of experimental procedures expressed by Russell and Burch (1959) in their classic book *The Principle of Humane Experimental Techniques*, a milestone in the field of improving laboratory animal well-being. It is worthy of notice that a direct consequence of the enhanced psychophysical welfare of experimental subjects is a more reliable behavioral response pattern, improving data quality (Vitale and Alleva, 1999; Alleva and Vitale, 2000). Moreover, the combination of an ecoethological approach with a progressive refinement of statistical methods can also contribute to reducing the number of animals used without reducing the power of behavioral analysis.

LITERATURE CITED

Alleva, E. and Sorace, A. 2000. Important hints in behavioural teratology of rodents. *Curr. Pharm. Des.* 6:99-126.

Alleva, E. and Vitale, A. 2000. We urgently need more data to improve the lives of laboratory animals. *Nature* 405:116.

Alleva, E., Laviola, G., Tirelli, E., and Bignami, G. 1985. Short-, medium-, and long-term effects of prenatal oxazepam on neurobehavioural development of mice. *Psychopharmacology (Berl.)* 87:434-441.

Alleva, E., Fasolo, A., Lipp, H.P., Nadel, L., and Ricceri, L. (eds.) 1995. Behavioural Brain Research in Naturalistic and Semi-Naturalistic Settings. Kluwer Dodrecht, Amsterdam.

Bateson, P. 1981. Ontogeny of behaviour. *Br. Med. Bull.* 37:159-164.

Bignami, G. 1996. Economical test methods for developmental neurobehavioral toxicity. *Environ. Health Perspect.* 104:285-298.

Branchi, I. and Ricceri, L. 2002. Transgenic and knock-out mouse pups: Growing need for behavioral analysis. *Genes Brain Behav.* 1:135-141.

Buelke-Sam, J., Kimmel, G.L., and Adams, J., (eds.) 1985. Design considerations in screening for behavioral teratogens: Results of the Collaborative Behavior Teratology Study. *Neurobehav. Toxicol. Teratol.* 7:537-789

Calamandrei, G., Valanzano, A., and Alleva, E. 1991. NGF and cholinergic control of behavior: Anticipation and enhancement of scopolamine effects in neonatal mice. *Brain Res. Dev. Brain Res.* 61:237-241.

Capone, F., Puopolo, M., Branchi, I., and Alleva, E. 2002. A new easy accessible and low-cost method for screening olfactory sensitivity in mice: Behavioural and nociceptive response in male and female CD-1 mice upon exposure to millipede aversive odour. *Brain Res. Bull.* 58:193-202.

Carman, H.M. and Mactutus, C.F. 2001. Ontogeny of spatial navigation in rats: A role for response requirements? *Behav. Neurosci.* 115:870-879.

Cenci, M.A., Whishaw, I.Q., and Schallert, T. 2002. Animal models of neurological deficits: How relevant is the rat? *Nat. Rev. Neurosci.* 3:574-579.

Chiarotti, F. and Sparks, T. 2002. Problems of behavioural teratology of rodents. *In* Behavioral Ecotoxicology (G. Dell'Omo, ed.) pp. 273-289. John Wiley & Sons, Chichester, U.K.

Chiarotti, F., Alleva, E., and Bignami, G. 1987. Problems of test choice and data analysis in behavioral teratology: The case of prenatal benzodiazepines. *Neurotoxicol. Teratol.* 9:179-186.

Crawley, J.N. 2000. What's Wrong with My Mouse?: Behavioral Phenotyping of Transgenic and Knockout Mice. Wiley-Liss, New York.

Crawley, J.N. 2003. Behavioral phenotyping of rodents. *Comp. Med.* 53:140-146.

Crews, D. 1997. Species diversity and the evolution of behavioral controlling mechanisms. *Ann. N.Y. Acad. Sci.* 807:1-21.

Crusio, W.E. and Gerlai, R.T. (eds.) 1999. Handbook of Molecular-Genetic Techniques for Brain and Behavior Research. Elsevier, Amsterdam.

Cuomo, V., De Salvia, M.A., Petruzzi, S., and Alleva, E. 1996. Appropriate end points for the characterization of behavioral changes in developmental toxicology. *Environ. Health Perspect.* 104:307-315.

Darwin, C. 1872. The Expression of Emotions in Man and Animals, 1998 ed. Oxford University Press, Oxford, U.K..

D'Udine, B. and Alleva, E. 1988. The *Acomys cahirinus* (spiny mouse) as a new model for biological and neurobehavioural studies. *Pol. J. Pharmacol. Pharm.* 40:525-534.

File, S.E. 2001. Factors controlling measures of anxiety and responses to novelty in the mouse. *Behav. Brain Res.* 125:151-157.

Fox, W.M. 1965. Reflex-ontogeny and behavioral development of the mouse. *Anim. Behav.* 13:234-240.

Frick, K.M., Stillner, E.T., and Berger-Sweeney, J. 2000. Mice are not little rats: Species differences in a one-day water maze task. *Neuroreport* 11:3461-3465.

Garcia, J., and Koelling, R.A. 1966. Relation of cue to consequence in avoidance learning. *Psychonomic Sci.* 4:123-124.

Gerlai, R. and Clayton, N.S. 1999. Analysing hippocampal function in transgenic mice: An ethological perspective. *Trends Neurosci.* 22:47-51.

Iivonen, H., Nurminen, L., Harri, M., Tanila, H., and Puolivali, J. 2003. Hypothermia in mice tested in Morris water maze. *Behav. Brain Res.* 141:207-213.

Kamil, A.C. and Mauldin, J.E. 1988. A comparative-ecological approach to the study of learning. *In* Evolution and Learning (R.C. Bolles and M.D. Beecher, eds.) Lawrence Erlbaum Associates, Hillsdale, N.J.

Katz, P.S. and Harris-Warrick, R.M. 1999. The evolution of neuronal circuits underlying species-specific behavior. *Curr. Opin. Neurobiol.* 9:628-633.

Kulig, B., Alleva, E., Bignami, G., Cohn, J., Cory-Slechta, D., Landa, V., O'Donoghue, J., and Peakall, D. 1996. Animal behavioral methods in neurotoxicity assessment: SGOMSEC joint report. *Environ. Health Perspect.* 104:193-204.

Marascuilo, L.A. and McSweeney, M. 1971. Nonparametric and Distribution-Free Methods for the Social Sciences. Brooks/Cole Publishing Company, Monterey, Calif.

Martin, P. and Bateson, P. 1993. Measuring Behaviour: An Introductory Guide, 2nd ed. Cambridge University Press, Cambridge, U.K.

Pintor, A., Alleva, E., and Michalek, H. 1986. Postnatal maturation of brain cholinergic systems in

the precocial murid *Acomys cahirinus*: Comparison with the altricial rat. *Int. J. Dev. Neurosci.* 4:375-382.

Ricceri, L., Calamandrei, G., and Berger-Sweeney, J. 1997. Different effects of postnatal day 1 versus 7 192 immunoglobulin G-saporin lesions on learning, exploratory behaviors, and neurochemistry in juvenile rats. *Behav. Neurosci.* 111:1292-1302.

Ricceri, L., Usiello, A., Valanzano, A., Calamandrei, G., Frick, K., and Berger-Sweeney, J. 1999. Neonatal 192 IgG-saporin lesions of basal forebrain cholinergic neurons selectively impair response to spatial novelty in adult rats. *Behav. Neurosci.* 113:1204-1215.

Rodgers, R.J. and Johnson, N.J. 1995. Factor analysis of spatiotemporal and ethological measures in the murine elevated plus-maze test of anxiety. *Pharmacol. Biochem. Behav.* 52:297-303.

Rogers, D.C., Fisher, E.M., Brown, S.D., Peters, J., Hunter, A.J., and Martin, J.E. 1997. Behavioral and functional analysis of mouse phenotype: SHIRPA, a proposed protocol for comprehensive phenotype assessment. *Mamm. Genome.* 8:711-713.

Russell, W.M.S. and Burch, R.L. 1959. The Principle of Humane Experimental Techniques. Methuen, London.

Schenk, F. 1987. Comparison of spatial learning in woodmice (*Apodemus sylvaticus*) and hooded rats (*Rattus norvegicus*). *J. Comp. Psychol.* 101:150-158.

Scott, J.P. 1953. The development of social behavior patterns in the mouse, in relation to natural periods. *Behaviour* 6:35-65.

Sharp, P.E., and La Regina, M.C. 1998. The Laboratory Rat. CRC Press, Boca Raton, Fla.

Spyker, J.M. 1975. Behavioral teratology and toxicology. *In* Behavioral Toxicology (B. Weiss, and V.G. Laties, eds.) pp. 311-349. Plenum Press, New York.

van der Staay, F.J. 2000. Effects of the size of the morris water tank on spatial discrimination learning in the CFW1 mouse. *Physiol. Behav.* 68:599-602.

Vitale, A. and Alleva, E. 1999. Ethological and welfare considerations in the study of aggression in rodents and nonhuman primates. *In* Animal Models of Human Emotion and Cognition (M. Haug and R.E. Whalen, eds.) pp 283-295. American Psychological Association, Washington, D.C.

Watase, K. and Zoghbi, H.Y. 2003. Modelling brain diseases in mice: The challenges of design and analysis. *Nat. Rev. Genet.* 4:296-307.

Whishaw, I.Q. 1995. A comparison of rats and mice in a swimming pool place task and matching to place task: Some surprising differences. *Physiol. Behav.* 58:687-693.

Whishaw, I.Q. and Tomie, J.A. 1996. Of mice and mazes: Similarities between mice and rats on dry land but not water mazes. *Physiol. Behav.* 60:1191-1197.

Winer, B.J. 1971. Statistical principles in experimental design. McGraw-Hill Kogakusha, Tokyo.

Wolfer, D.P., Stagljar-Bozicevic, M., Errington, M.L., and Lipp, H.P. 1998. Spatial memory and learning in transgenic mice: Fact or artifact? *News Physiol. Sci.* 13:118-123.

World Health Organization (WHO). 1986. Principles for Evaluating Health Risks from Chemicals During Infancy and Early Childhood: The Need for a Special Approach. World Health Organization Press. Geneva.

Contributed by Igor Branchi,
Giorgio Bignami, and Enrico Alleva
Instituto Superiore di Sanità
Rome, Italy

Statistical Analysis of Behavioral Data

The statistical analysis of behavioral data follows the collection and checking of data, and is aimed at assessing the effect of treatments on the observed behaviors. In the following, the author will briefly describe different behavioral tests and the response variables collected in each test, to introduce the statistical methods for the analysis of such variables. A more detailed description of the tests and of the response variables can be found in specific units of *Current Protocols in Toxicology*. The most specialized statistical terms appearing in this unit are defined under Specialized Statistical Terms, below.

When available for the analysis of a particular behavioral test, different statistical approaches to behavioral data will be described. These are often not redundant, yielding different kinds of information, and resulting in the refinement of behavioral research (Chiarotti and Puopolo, 2000). The different approaches can be characterized by different degrees of complexity which, if present, will be highlighted in each specific paragraph. For a synthetical description of the aim and characteristics of the different statistical methods that can be used for the analysis of each behavioral test data, see Table 13.8.2 at the end of this unit.

SPECIALIZED STATISTICAL TERMS

Between-Subject, Within-Subject, and Repeated Measures Factors

The between-subject factor is a factor that includes two or more levels, each of them randomly assigned to one group of independent statistical units (e.g., mice, rats, monkeys). Units in each final group are independent of each other and independent with respect to all units belonging to the other final groups.

The within-subject factor is a factor that includes two or more levels, each of them assigned to one of two or more correlated groups of independent statistical units (e.g., mice, rats, monkeys). This means that units in each final group are independent of each other, while each unit in a final group is correlated to one unit in any other final group.

The repeated measures factor is a factor that includes two or more levels, each of them assigned to each statistical unit. This means that each statistical unit is repeatedly tested under all levels of the repeated measures factor.

Normality

The assumption of normality implies that the distribution of the variable to be analyzed by parametric tests (see Statistical Tests for the Analysis of Behavioral Data, below) is normal in the population from which units (or blocks of units) are sampled. The normal distribution is a continuous frequency distribution of infinite range having a single mode (unimodal). It is characterized by two parameters: skewness and kurtosis.

Skewness describes the asymmetry of a distribution. It is equal to 0 for unimodal symmetrical distributions, such as the normal distribution, whereas it is negative for unimodal distributions with a longer left tail (towards lower values of the variable) and positive for distributions with a longer right tail (towards higher values).

Kurtosis describes the steepness of the unimodal frequency curve toward the mode. Usually, the kurtosis index is centered so that it is equal to 0 in normal distributions. Distributions with a positive, zero, and negative kurtosis index are referred to, respectively, as "leptokurtic" (heavy-tailed), "mesokurtic," and "platykurtic" (light-tailed).

Contributed by Flavia Chiarotti
Current Protocols in Toxicology (2005) 13.8.1-13.8.29

The normality assumption also states that the treatments administered to the statistical units in the different subgroups do not affect the shape of the distribution of the variable and that only the mean value of the variable changes among subgroups.

Homoscedasticity (Homogeneity of Variance)

Homoscedasticity refers to the homogeneity of variance among the independent groups being compared. In experimental designs including between-subject factors, homoscedasticity must be evaluated by comparing variances among the groups based on factor levels. When more data are collected on each statistical unit (within-subject or repeated measures factors), the data in each block (corresponding to within-subject factor levels) or in each unit (corresponding to repeated measures) should first be averaged before testing for homoscedasticity.

Sphericity

The sphericity assumption states that the variances of the differences between paired observations are equal across all groups in the sampled population. A simpler yet stricter condition is that referred to as "compound symmetry," which is met when, in the variance-covariance matrix of the sampled population, all of the variances are equal and all of the covariances are equal, although the covariances are not necessarily equal to the variances. This means that the data collected on statistical units under different conditions (corresponding to different levels of the within-subject factor or to different repeated measures) must be equally related to each other with the same correlation coefficient, ρ. Compound symmetry is sufficient, yet not necessary, for ensuring the validity of the F ratio under the general null hypothesis of no treatment effect. The F ratio is the test statistic in the parametric ANOVA. In particular, it is computed as the ratio between the variance of the effect under assessment and the variance of the error term. This ratio follows an F distribution if all the assumptions upon which the test relies are met. In other words, if compound symmetry is satisfied, then sphericity is also satisfied, but if compound symmetry is not satisfied, then sphericity must still be evaluated.

BASIC PROTOCOL 1

FOX BATTERY TEST

The Fox battery test is a battery of tests that characterize maturation of a set of sensorimotor functions, behavioral traits, and learning abilities from birth to weaning, initially developed for the assessment of behavioral ontogeny of house mice (Fox, 1965). Three main problems arise in analyzing data from a Fox battery test. First, the original response variables are ordinal scores, representing successive developmental stages achieved by the experimental subjects. Specifically, for each item, four well defined stages of mouse development can be recognized and scored: (i) absence of response (score 0); (ii) initial appearance of response (score 1); (iii) evident response (score 2); and (iv) full response (score 3). Thus, the range of data is so narrow (scale from 0 to 3) that data distribution cannot be considered as continuous. Therefore, neither parametric nor nonparametric tests can be applied, because the former require that data be normally distributed, and the latter cannot manage the large number of equal values (ties) coming from the narrow range of scores.

Second, for a better evaluation of the effect of treatments (in a broad sense) on the ontogeny of behavior, littermates receive, when possible, different treatments (obviously, under some conditions, this is very difficult or even impossible, as in the case of treatments that must be administered prenatally). Splitting litters into different treatment groups allows one to reduce at most the confounding effect of the genetic variability between litters, which would affect the assessment of treatment effect if whole litters were assigned to the same treatment group. Furthermore, littermates are tested repeatedly over days to

monitor the behavioral development. From a statistical point of view, this results in experimental designs including litters as the random blocking factor, treatments as the fixed factor within litters, and postnatal days (PNDs) as the fixed repeated measures on individual subjects. Therefore, it is not appropriate to use methods that assume the independence of observations, such as the χ^2 test, frequently performed to assess the different distribution of the scores among treatment groups day-by-day.

Finally, score profiles are expected to be monotonically nondecreasing, but sometimes they may present regressions—i.e., the score a subject achieves one day may be lower than the score achieved on the day before. This can be due to the particular situation in which the subject is at the time of testing (e.g., digestion, sleep, or even boredom), which can affect its capability and promptness in responding to stimuli.

Two solutions can be adopted to analyze Fox battery test data, as described, respectively, in steps 1a to 6a and 1b to 4b, below.

Analysis of a synthetical measure of the score profile

1a. Convert the original scores for each subject in each component of the test battery from multiple (repeated observations over time for each subject) to single (one observation per subject), by computing a synthetical measure.

To do this, different strategies can be adopted, as outlined below. Each of them presents both pros and cons.

i. For each component of the test battery, choose a particular score (usually scores 2 or 3) as adult-like response or full appearance of a somatic feature, and register the first day when the subject attains a score equal to or greater than that (for the sake of brevity, in the following this will be called first day of adult-like responding).

To choose the abovementioned threshold score, the score profile in the period of testing, collected on subjects in the control group, must be considered. Specifically, a good choice for the threshold is a score that control subjects are likely to present some days after the beginning and before the end of the testing period.

Pro: If the threshold is appropriately chosen, it is possible to detect anticipations or delays of the full response, which can be attributed to the treatment(s) under study.

Con: If the threshold score is not set at the maximum score (e.g., at score 2), it is impossible to distinguish between subjects attaining the full response with different scores (e.g., with score 2 or score 3) on the same day of testing. Moreover, subjects attaining the full response on the same day of testing with the same score, but presenting different score profiles before and/or after the attainment of the full response, will be considered equivalent.

ii. For each component of the test battery, compute the area under the curve generated by the repeated scores.

Pro: The whole score profile is considered in computing this synthetical measure. Subjects attaining the full response at the same day of test with the same score, but presenting different score profiles before and/or after the attainment of the full response, will be given different synthetical measures.

Con: Different score profiles, even in the presence of different first days of adult-like responding, can result in the same synthetical measure.

2a. Check the normality of the distribution of transformed synthetical data in each subgroup of subjects, using the Shapiro-Wilk test or the Kolmogorov-Smirnov test, Lilliefors modification (Armitage et al., 2002; Chiarotti, 2004). If the normality assumption is respected, proceed to step 3a; otherwise go to step 5a.

3a. Compare variances among subgroups using the Levene test or the Bartlett test (Armitage et al., 2002; Chiarotti, 2004). If variances are homogeneous, proceed to step 4a; otherwise go to step 5a.

4a. Perform, on the transformed synthetical data, the parametric tests for the comparison among groups appropriate for the modified experimental design (Edwards, 1985; Wilcox, 1987; Winer et al., 1991). Go to step 6a.

Remember that if the design includes repeated measures taken on the subjects, appropriate correction in case of violation of the sphericity assumption must be adopted, such as Greenhouse-Geisser or Huynh-Feldt corrections (Winer et al., 1991; Armitage et al., 2002; Chiarotti, 2004).

5a. Perform, on the transformed synthetical data, the nonparametric tests for the comparison among groups appropriate for the modified experimental design (Marascuilo and McSweeney, 1977; Brunner et al., 2002). Go to step 6a.

Note that the most commonly used statistical packages do not include nonparametric methods for the analysis of experimental designs with between-subject and within-subject or repeated measures factors. Therefore, to perform the suggested analysis, one must have access to an ad hoc software application and to the knowhow necessary for its use.

6a. Present the results (see Presentation of Results, below).

Analysis of the whole score profile by survival curves

1b. Choose the score to be considered as response, i.e., the score after which the subject that attained it will be ignored in the analysis; that score will be considered as *death*. Register, for each subject, the time from the first day of observation until the first day when the subject attains a score equal to or greater than the response; that time will be considered as *time to death*.

Subjects that do not reach the abovementioned score will be considered as censored, and will be given a time equal to the span of observation (follow-up time).

2b. Analyze *survival* data using methods such as the Kaplan-Meier survival analysis or the Cox proportional hazards model (Armitage et al., 2002).

The Kaplan-Meier survival analysis method allows one to compare survival times among two or more independent groups and to take into account at most one stratification variable. The Cox proportional hazards model method allows one to assess the independent effect on survival of more fixed or time-dependent covariates.

3b. Repeat the survival analysis using different scores as response.

It is important to note that repeated analyses on the same data can result in an increase in the probability of type I error, and that appropriate corrections (such as the Bonferroni correction; Armitage et al., 2002) should be adopted.

Pro: The described methods allow one to take into account the whole score profile.

Con: The described methods have been developed for independent data, and correlated data (such as those resulting from littermates assigned to different treatment groups) cannot be managed easily.

More complex methods can deal with survival data organized in different stages, taking into account the successive survival times in each consecutive stage. Unfortunately, these are more difficult to manage, and many of the most common statistical software applications do not perform such methods. Therefore, unless one has access to the more specialized software applications and to the knowhow necessary for their use, it may be advisable to refer to the kind of analysis suggested above in steps 1b to 3b.

4b. Present the results (see Presentation of Results, below).

ULTRASOUND VOCALIZATIONS TEST

Ultrasound vocalizations are emitted by pups in response to various conditions, such as maternal separation, low-temperature isolation, tactile stimulation, or olfactory stimulation. These vocalizations stimulate prompt expression of maternal behavior.

The response variable in the ultrasound vocalizations test (Hofer et al., 2001) is the number of calls emitted by the pups under various experimental conditions (between- or within-subject factor, according to the experimental design adopted).

For a more sophisticated analysis, vocalizations can be characterized according to the frequency modulation and the duration of the acoustic signal (sound category), as evidenced by the spectrographic analysis of calls. Moreover, ultrasound can be classified according to different frequency bands. Each vocalization is then defined by a specific sound category and frequency band. Therefore, the number of calls emitted by the pup in each sound category/frequency band combination can be considered as repeated measures on the pup.

The statistical analysis of the response variable *number of calls* passes through the following steps.

1. Check the normality of the distribution of data in each subgroup of subjects using the Shapiro-Wilk test or the Kolmogorov-Smirnov test, Lilliefors modification (Armitage et al., 2002; Chiarotti, 2004). If the normality assumption is respected, proceed to step 2; otherwise go to step 4.
2. Compare variances among subgroups using the Levene test or the Bartlett test (Armitage et al., 2002; Chiarotti, 2004). If variances are homogeneous, proceed to step 3; otherwise go to step 4.
3. Perform the parametric tests for the comparison among groups appropriate for the experimental design adopted (Edwards, 1985; Wilcox, 1987; Winer et al., 1991). Go to step 7.

   Remember that if the design includes repeated measures taken on the subjects, appropriate correction in case of violation of the sphericity assumption must be adopted, such as Greenhouse-Geisser or Huynh-Feldt corrections (Winer et al., 1991; Armitage et al., 2002; Chiarotti, 2004).

4. Consider the experimental design. If it is rather simple—i.e., no limits for the between-subject factors (treatments) and at most two levels for each repeated measures factor (days, trials)—go to step 5; otherwise go to step 6.
5. Analyze the profile on the consecutive days of testing and trials using a nonparametric test for the comparison among groups, choosing the test appropriate for the experimental design adopted—including between-subject factor(s) and repeated measures factor (days, trials) (Marascuilo and McSweeney, 1977; Brunner et al., 2002). Go to step 7.

   Remember that the most commonly used statistical packages do not include nonparametric methods for the analysis of experimental designs with between-subject and within-subject or repeated measures factors. Therefore, to perform the suggested analysis, one must have access to an ad hoc software application and to the knowhow necessary for its use.

6. Transform the original data for *number of calls* using the appropriate normalizing transformation, which must be applied separately on each observation (Edwards, 1985; Armitage et al., 2002).

Remember that the appropriate transformation must be chosen on the basis of some knowledge with regard to the theoretical and empirical distributions of data (i.e., the distributions of data in the population and in the observed samples, respectively). Note that non-normality of the UV response variable usually results from too small a number of calls under final conditions, which suggests a Poisson distribution of data. Thus, the square-root transformation is the most appropriate for normalizing data distribution. After the transformation, go back to step 1. Note that persistent violations of the assumptions of normality and homogeneity of variance after the transformation of data indicate that the performed transformation was not appropriate.

7. Present the results (see Presentation of Results, below).

BASIC PROTOCOL 3

PASSIVE AVOIDANCE TEST

Usually, in the passive avoidance test, the experimental subjects undergo repeated trials until they reach the criterion (which is, commonly, suppressing the spontaneous response for two consecutive trials), or, in case they do not reach the criterion, until they undergo the predetermined maximum number of trials. The first phase of learning (acquisition) is usually followed by an interval, and then subjects undergo one single retest trial to assess the long-term memory (memory retention).

Different kinds of data can be collected in a passive avoidance test, namely (1) number of trials to reach the criterion, (2) latency profile in the repeated trials of the learning phase, and (3) latency to step-through in the retest trial.

All the response variables are characterized by the presence of a cutoff that limits the range of values the response variable can take. In particular, latencies longer than the cutoff value are commonly arbitrarily given the cutoff value. This value is also used in the learning phase to complete the latency profile for the trials following the attainment of the criterion (usually, these trials are not performed). For all this, data usually do not follow a normal distribution. Thus, parametric methods, which use statistics based on the quantitative value of the different observations, are inappropriate.

Different solutions can be adopted for the analysis of the various response variables.

Number of trials to reach the criterion

This variable can be subjected to two different analyses as described in steps 1a to 6a and 1b to 4b, respectively.

Tests for the comparison among groups (most frequently used)

1a. Check for the presence of cutoff values. If they are present, go to step 5a; otherwise go to step 2a.

2a. Check the normality of the distribution of data using the Shapiro-Wilk test or the Kolmogorov-Smirnov test, Lilliefors modification (Armitage et al., 2002; Chiarotti, 2004). If data are normally distributed, go to step 3a; otherwise go to step 5a.

3a. Compare variances among subgroups of subjects using the Levene or the Bartlett test (Armitage et al., 2002; Chiarotti, 2004). If variances are homogeneous, go to step 4a; otherwise go to step 5a.

4a. Perform a parametric test for the comparison among groups, choosing the test appropriate for the experimental design adopted (Edwards, 1985; Wilcox, 1987; Winer et al., 1991). Go to step 6a.

5a. Perform nonparametric tests for the comparison among groups, choosing the test appropriate for the experimental design adopted (Marascuilo and McSweeney, 1977; Brunner et al., 2002). Go to step 6a.

6a. Present the results (see Presentation of Results, below).

Survival analysis (less commonly used)

1b. Set the status of the subject equal to *dead* if the subject has reached the criterion within the maximum number of trials, or *censored*, if not.

2b. Set the survival time equal to the number of trials to reach the criterion (if the subject is dead) or to the maximum number of trials (if the subject is censored).

3b. Perform the Kaplan-Meier survival analysis (Armitage et al., 2002) on these data, using *treatment(s)* as grouping variable(s).

4b. Present the results (see Presentation of Results, below).

Latency profile in the repeated trials

If the experimental subject reaches the criterion during the acquisition phase before undergoing the maximum number of trials, it is usually given the maximum latency for the remaining trials. The latency profile is then strongly affected by the limits arbitrarily set by the researcher. For this reason, parametric methods are frequently not appropriate for the analysis of this kind of data. On the other hand, nonparametric methods taking into account between-subject and repeated measures factors at the same time are not available in the most commonly used statistical packages.

1c. Convert the whole latency profile into a single response variable, using one of the two following methods.

i. Calculating the median latency value.
ii. Calculating the area under the latency curve.

2c. Analyze the single response variable using tests for the comparison among groups. To do this, follow the instructions given for the variable *number of trials to reach the criterion* (see steps 1a to 5a).

3c. Present the results (see Presentation of Results, below).

Latency to step-through in the retest trial

Subjects that have learned the task in the acquisition phase usually show memory of the task in the retest trial, unless the administered treatments interfere with memory processes. For this reason, latency in the retest trial is often affected by the presence of cutoff values which, together with the non-normality of the distribution common to most latency variables, make parametric tests not suitable for the statistical analysis. Therefore, nonparametric tests for the comparison among groups are usually the best choice, as described in steps 1d to 6d.

1d. Check for the presence of cutoff values. If they are present, go to step 5d; otherwise go to step 2d.

2d. Check the normality of the distribution of data, using the Shapiro-Wilk test or the Kolmogorov-Smirnov test, Lilliefors modification (Armitage et al., 2002; Chiarotti, 2004). If data are normally distributed, go to step 3d; otherwise go to step 5d.

3d. Compare variances among subgroups of subjects, using the Levene or the Bartlett test (Armitage et al., 2002; Chiarotti, 2004). If variances are homogeneous, go to step 4d, otherwise go to step 5d.

4d. Perform a parametric test for the comparison among groups, choosing the test appropriate for the experimental design adopted (Edwards, 1985; Wilcox, 1987; Winer et al., 1991). Go to step 6d.

5d. Perform nonparametric tests for the comparison among groups, choosing the test appropriate for the experimental design adopted (Marascuilo and McSweeney, 1977; Brunner et al., 2002). Go to step 6d.

6d. Present the results (see Presentation of Results, below).

BASIC PROTOCOL 4

MORRIS WATER MAZE TEST

Usually, the Morris water maze test consists of an acquisition phase (learning) followed by a probe trial (retention). The acquisition phase lasts for a larger number of days, and on each day of testing, the experimental subjects undergo repeated trials, spaced by an intertrial interval. The probe trial is commonly conducted after a period (minutes) from the completion of the last training trial, on the last day of the acquisition phase. For more details, see *UNIT 11.3*.

The duration of the acquisition phase (number of days, number of trials on each day, maximum duration of each trial, and intertrial interval), the duration of the period before the probe trial, and the duration of the probe trial itself are predetermined by the experimenter. These constitute the cutoffs for the different response variables that can be collected in the test.

The response variables that are collected in the acquisition phase are: (1) latency profile to reach the platform; (2) mean velocity, in the repeated days and trials within days; (3) path length, in the repeated days and trials within days; (4) time spent in the peripheral annular area close to the wall (thigmotaxis), in the repeated days and trials within days.

The response variables that are collected in the probe trial are: (1) crossings of acquisition quadrant; and (2) total time spent in the acquisition quadrant.

Latency profile to reach the platform

Usually, if the experimental subject does not find the platform within the allotted time, the experimenter manually places it onto the platform and lets it stay there for a predetermined period (seconds). The latency profile is then strongly affected by the limits arbitrarily set by the researcher. For this reason, as with passive avoidance data, the latency profile to reach the platform cannot be appropriately analyzed using parametric methods. On the other hand, nonparametric methods that take into account, at the same time, between-subject and repeated measures factors (days, trials) with more than two levels each are not available in the most common statistical packages. Therefore, proceed as follows.

1a. Convert the latency profile in each day of testing into a single response variable, using one of the two following methods.

i. Calculating the median latency value.
ii. Calculating the area under the latency curve.

2a. Check the normality of the distribution of data using the Shapiro-Wilk test or the Kolmogorov-Smirnov test, Lilliefors modification (Armitage et al., 2002; Chiarotti, 2004). If data are normally distributed, go to step 3a; otherwise go to step 5a.

3a. Compare variances among subgroups of subjects using the Levene or the Bartlett test (Armitage et al., 2002; Chiarotti, 2004). If variances are homogeneous, go to step 4a; otherwise go to step 5a.

4a. Analyze the profile on the consecutive days of testing using a parametric test for the comparison among groups, choosing the test appropriate for the experimental design adopted, including between-subject factor(s) and the repeated measures factor (days) (Edwards, 1985; Wilcox, 1987; Winer et al., 1991). Go to step 6a.

5a. Analyze the profile in the consecutive days of testing using a nonparametric test for the comparison among groups, choosing the test appropriate for the experimental design adopted (Marascuilo and McSweeney, 1977; Brunner et al., 2002). Go to step 6a.

Remember that the most commonly used statistical packages do not include nonparametric methods for the analysis of experimental designs with between-subject and within-subject or repeated measures factors. Therefore, to perform the suggested analysis, one must have access to an ad hoc software application and to the knowhow necessary for its use.

6a. Present the results (see Presentation of Results, below).

Mean velocity and path length in the repeated days and trials within days

These quantitative variables are unbounded, in that no arbitrary cutoffs are set by the experimenter. To analyze these variables, proceed as follows.

1b. Check the normality of the distribution of data using the Shapiro-Wilk test or the Kolmogorov-Smirnov test, Lilliefors modification (Armitage et al., 2002; Chiarotti, 2004). If data are normally distributed, go to step 2b, otherwise go to step 4b.

2b. Compare variances among subgroups of subjects using the Levene or the Bartlett test (Armitage et al., 2002; Chiarotti, 2004). If variances are homogeneous, go to step 3b, otherwise go to step 4b.

3b. Analyze the profile on the consecutive days of testing and trials using a parametric test for the comparison among groups, choosing the test appropriate for the experimental design adopted, including between-subject factor(s) and repeated measures factor (days and trials) (Edwards, 1985; Wilcox, 1987; Winer et al., 1991). Go to step 7b.

4b. Consider the experimental design. If it is rather simple—i.e., no limits for the between-subject factors (treatments), two levels at most for each repeated measures factor (days and trials)—go to step 5b; otherwise go to step 6b.

5b. Analyze the profile on the consecutive days of testing and trials using a nonparametric test for the comparison among groups, choosing the test appropriate for the experimental design adopted, including between-subject factor(s) and repeated measures factor (days and trials) (Marascuilo and McSweeney, 1977; Brunner et al., 2002). Go to step 7b.

Remember that the most commonly used statistical packages do not include nonparametric methods for the analysis of experimental designs with between-subject and within-subject or repeated measures factors. Therefore, to perform the suggested analysis, one must have access to an ad hoc software application and to the knowhow necessary for its use.

6b. Transform data using the appropriate normalizing transformation, which must be applied separately on each observation (Edwards, 1985; Armitage et al., 2002). After the transformation, go back to step 1b.

Remember that the appropriate transformation must be chosen on the basis of some knowledge with regard to the theoretical and empirical distributions of data (i.e., the distributions of data in the population and in the observed samples, respectively). Usually, square-root transformation is appropriate if data means and standard deviations in each treatment group are proportional, while logarithmic transformation is appropriate

in the case of strongly asymmetrical distribution, with a long upper tail. Note that persistent violation of the assumptions of normality and homogeneity of variance after the transformation of data indicate that the transformation performed was not appropriate.

7b. Present the results (see Presentation of Results, below).

Time spent in the peripheral annular area close to the wall (thigmotaxis) in the repeated days and trials within days

This quantitative variable rarely reaches the cutoff value, except when the experimental subject remains in the peripheral annular area close to the wall for the whole duration of the trial, predetermined by the experimenter. Therefore, follow the instructions given for the variables mean velocity and path length (see steps 1b to 7b).

Crossings of acquisition quadrant

This quantitative variable is superiorly unbounded. Indeed, the higher limit of this variable derives from both the predetermined duration of the probe trial (equal for all subjects) and the maximum swimming velocity that the experimental subjects can reach (different among subjects), and thus it varies from subject to subject. Therefore, follow the instructions given for the variables mean velocity and path length (steps 1b to 7b).

Total time spent in the acquisition quadrant

This quantitative variable rarely reaches the cutoff value, except when the experimental subject remains in the acquisition quadrant for the whole duration of the probe trial, predetermined by the experimenter. Therefore, follow the instructions given for variables mean velocity and path length (steps 1b to 7b).

BASIC PROTOCOL 5

SPATIAL OPEN FIELD TEST

The spatial open field test usually consists in seven repeated sessions, during which animals are put in an open-field arena. In session 1 the arena is empty; in sessions 2 to 4, four different plastic objects are placed in the arena; in sessions 5 and 6 two of these objects are displaced; in session 7, one of the objects is replaced by an unfamiliar one.

Response variables in the spatial open field test can be assigned to two main categories: *general* behaviors, such as rearing, wall rearing, grooming, top rearing, and locomotor activity (crossings), which are recorded during all sessions; and behaviors *specifically directed* towards the objects, such as object contacts, which are recorded only in the sessions when objects are presented to subjects.

For both categories, data recorded are frequencies and, in some cases, durations of behaviors—i.e., data are quantitative. Therefore, to analyze these variables, proceed as follows.

Univariate methods

1a. Check the normality of the distribution of data using the Shapiro-Wilk test or the Kolmogorov-Smirnov test, Lilliefors modification (Armitage et al., 2002; Chiarotti, 2004). If data are normally distributed, go to step 2a; otherwise go to step 4a.

2a. Compare variances among subgroups of subjects using the Levene or the Bartlett test (Armitage et al., 2002; Chiarotti, 2004). If variances are homogeneous, go to step 3a; otherwise go to step 4a.

3a. Analyze the profile on the consecutive days of testing and trials using a parametric test for comparison among groups, choosing the test appropriate for the experimental design adopted, including between-subject factor(s) and repeated measures factor (days and trials) (Edwards, 1985; Wilcox, 1987; Winer et al., 1991). Go to step 7a.

4a. Consider the experimental design: if it is rather simple—no limits for the between-subject factors (treatments), two levels at most for each repeated measures factor (days and trials)—go to step 5a; otherwise go to step 6a.

5a. Analyze the profile on the consecutive days of testing and trials using a nonparametric test for comparison among groups, choosing the test appropriate for the experimental design adopted, including between-subject factor(s) and repeated measures factor (sessions and, in case, blocks of minutes) (Marascuilo and McSweeney, 1977; Brunner et al., 2002). Go to step 7a.

Remember that the most commonly used statistical packages do not include nonparametric methods for the analysis of experimental designs with between-subject and within-subject or repeated measures factors. Therefore, to perform the suggested analysis, one must have access to an ad hoc software application and the knowhow necessary for its use.

6a. Transform data using the appropriate normalizing transformation, which must be applied separately on each observation (Edwards, 1985; Armitage et al., 2002). After the transformation, go back to step 1a.

Remember that the appropriate transformation must be chosen on the basis of some knowledge with regard to the theoretical and empirical distributions of data (i.e., the distributions of data in the population and in the observed samples, respectively). Usually, square-root transformation is appropriate if data means and standard deviations in each treatment group are proportional, while logarithmic transformation is appropriate in the case of strongly asymmetrical distribution, with a long upper tail. Note that the persistent violation of the assumptions of normality and homogeneity of variance after the transformation of data, indicate that the performed transformation was not appropriate.

7a. Present the results (see Presentation of Results, below).

Multivariate methods

1b. When many behavioral categories are collected at the same time in order to take into account the correlation among them, perform a principal component analysis (PCA) on all quantitative observations (Jackson, 1991; Armitage et al., 2002).

The statistical unit for PCA is the subject at a session. For example, if there are two levels of treatment (vehicle and drug), with 10 subjects per treatment level (for a total of 20 subjects), and 7 sessions, the resulting number of statistical units for PCA will be $2 \times 10 \times 7 = 140$. On each statistical unit, all different behaviors are recorded, making up the data set to be analyzed by PCA.

2b. Extract PCA factors and consider only the subset of factors having an eigenvalue (corresponding to the variance of the original data explained by that factor) ≥ 1.

3b. Check the cumulative proportion of variance in data space explained by that subset of factors.

Note that PCA is effective in parsimoniously describing a set of continuous, interrelated variables when the number of subset factors is much lower (i.e., <50%) than the number of the original variables and the cumulative proportion of explained variance is sufficiently large (i.e., $>0.67 = 67\%$).

4b. To interpret the subset factors, look at the correlations between them and the original variables, given by the unrotated factor loadings.

As a rule of thumb, a correlation between the original variable x and the factor $z > 0.5$ (or < -0.5) indicates that the factor z is affected by the original variable x. Lower correlations denote that the variable is less important in influencing the factor.

5b. Collect the estimated factor scores for each statistical unit on each subset factor.

6b. Analyze the factor scores, separately for each subset factor, with a parametric test for the comparison among groups, choosing the test appropriate for the experimental design adopted.

In this example, the design includes treatment as between-subject factor, subjects as random blocking factor nested under treatment, and sessions as repeated measures factors (Edwards, 1985; Wilcox, 1987; Winer et al., 1991).

7b. Present the results (see Presentation of Results, below).

BASIC PROTOCOL 6

MATERNAL BEHAVIOR ASSESSMENT

The maternal behavior assessment usually consists in the recording of dams' behavior in the presence of their offspring. For more details, see *UNIT 13.9*.

The response variables can be assigned to two main categories: (1) maternal behavior observed in the *home cage*, such as retrieval, nursing (arched-back, blanket, passive), pup care (licking, anogenital licking, stepping), dam self-care (self-grooming, eating, drinking), and other (digging, rearing, moving, resting, standing out of nest); and (2) maternal behavior in a *novel cage*, including retrieving and standing on nest, nursing, licking, digging, and self-grooming.

Methods for the analysis of maternal behavior data depend on type of data. Steps are presented for dichotomous variables which are scored as either 0 or 1, as well as for quantitative variables (also see *UNIT 13.9*).

For dichotomous variables

Original data are recorded using the instantaneous sampling; thus, they are dichotomous scores (0/1). In particular, score 0 is assigned when the behavior is not shown in the interval (seconds) of observation, while score 1 is assigned when the behavior is performed. Instantaneous sampling is repeated more times (at least eight times, preferably) at each time point; time points (hours) are repeated (usually five times) for all days of testing (days). Such data can be (1) maintained as dichotomous scores, or (2) transformed into a quantitative variable. This choice influences the methods that can be adopted for the statistical analysis.

Maintain dichotomous scores

1a. Convert the original dichotomous scores (0/1), relative to each instantaneous sample, into an overall dichotomous score (0/1, absence/presence of the behavior) relative to each time point (hour) of observation.

2a. Analyze the variable using a stepwise forward logistic regression (LR) analysis (Hosmer and Lemeshow, 2000).

In particular, the dichotomous variable (0/1) is the dependent variable in the LR model, while treatments (categorical), hours, and days of observation (continuous) are the putative explanatory variables.

Observations repeated on the same animals over days and hours are related to (dependent on) each other; this dependency must be taken into account by specifying groups (clusters) of dependent observations on animals.

3a. Present the results (see Presentation of Results, below).

Transform dichotomous scores into quantitative variables

1b. Transform the original dichotomous scores (0/1), relative to each instantaneous sample, into a quantitative variable, adding the original scores over the instantaneous sampes within each time point.

These observations (one per time point) will range from 0 (behavior never shown) to the maximum number of instantaneous samples within the time point (e.g., 8).

2b. Analyze quantitative data using univariate (steps 3c to 9c) and/or multivariate methods (steps 3d to 9d).

Univariate methods

3c. Check the normality of the distribution of data using the Shapiro-Wilk test or the Kolmogorov-Smirnov test, Lilliefors modification (Armitage et al., 2002; Chiarotti, 2004). If data are normally distributed, go to step 4c; otherwise go to step 6c.

4c. Compare variances among subgroups of subjects using the Levene or the Bartlett test (Armitage et al., 2002; Chiarotti, 2004). If variances are homogeneous, go to step 5c; otherwise go to step 6c.

5c. Analyze the profile on the consecutive days and hours of testing using a parametric test for the comparison among groups, choosing the test appropriate for the experimental design adopted, including between-subject factor(s) and repeated measures factor (days, hours) (Edwards, 1985; Wilcox, 1987; Winer et al., 1991). Go to step 9c.

6c. Consider the experimental design. If it is rather simple—i.e., no limits for the between-subject factors (treatments), two levels at most for each repeated measures factor (days, hours)—go to step 7c; otherwise go to step 8c.

7c. Analyze the profile on the consecutive days of testing and trials using a nonparametric test for the comparison among groups, choosing the test appropriate for the experimental design adopted, including between-subject factor(s) and repeated measures factor (days, hours) (Marascuilo and McSweeney, 1977; Brunner et al., 2002). Go to step 9c.

Remember that the most commonly used statistical packages do not include nonparametric methods for the analysis of experimental designs with between-subject and within-subject or repeated measures factors. Therefore, to perform the suggested analysis, one must have access to an ad hoc software application and to the knowhow necessary for its use.

8c. Transform data using the appropriate normalizing transformation, which must be applied separately on each observation (Edwards, 1985; Armitage et al., 2002). After the transformation, go back to step 3c.

Remember that the appropriate transformation must be chosen on the basis of some knowledge with regard to the theoretical and empirical distributions of data (i.e., the distributions of data in the population and in the observed samples, respectively). Usually, square-root transformation is appropriate if data means and standard deviations in each treatment group are proportional, while logarithmic transformation is appropriate in the case of strongly asymmetrical distribution, with a long upper tail. Note that the persistent violations of the assumptions of normality and homogeneity of variance after the transformation of data indicate that the performed transformation was not appropriate.

9c. Present the results (see Presentation of Results, below).

Multivariate methods

3d. Perform a principal component analysis (PCA) on all quantitative observations (Jackson, 1991; Armitage et al., 2002).

The statistical unit for PCA is the subject at a given day and time point (hour) of observation. For example, if there are two levels of treatment (vehicle and drug), 10 subjects per treatment level (for a total of 20 subjects), 13 days of observation, and 5 time points per day (65 repeated observations on each subject), the resulting number of statistical units for PCA will be $2 \times 10 \times 13 \times 5 = 1300$. On each statistical unit, all different behaviors are recorded, making up the data set to be analyzed by PCA.

4d. Extract PCA factors and consider only the subset of factors having an eigenvalue (corresponding to the variance of the original data explained by that factor) ≥ 1.

5d. Check the cumulative proportion of variance in data space explained by that subset of factors.

Note that PCA is effective in parsimoniously describing a set of continuous, interrelated variables when the number of subset factors is much lower (i.e., <50%) than the number of the original variables, and the cumulative proportion of explained variance is sufficiently large (i.e., $>0.67 = 67\%$).

6d. To interpret the subset factors, look at the correlations between them and the original variables, given by the unrotated factor loadings.

As a rule of thumb, a correlation between the original variable x and the factor $z > 0.5$ (or < -0.5) indicates that the factor z is affected by the original variable x. Lower correlations denote that the variable is less important in influencing the factor.

7d. Collect the estimated factor scores for each statistical unit on each subset factor.

8d. Analyze the factor scores, separately for each subset factor, with a parametric test for the comparison among groups, choosing the test appropriate for the experimental design adopted.

In this example, the design includes treatment as between-subject factor, subjects as random blocking factor nested under treatment, and days and hours as repeated measures factors (Edwards, 1985; Wilcox, 1987; Winer et al., 1991).

9d. Present the results (see Presentation of Results, below).

For quantitative variables

As regards retrieving and standing on nest (*UNIT 13.9*), the observed response variable is the latency to perform the behavior. As concerns nursing, licking, digging, and self-grooming, the observed response variables are the number of 30-sec intervals when the behaviors are performed during the course of the whole test (which commonly lasts 30 min). For this reason, variables are quantitative, ranging from 0 to the maximum number of intervals (e.g., 60). For all variables, the experimental design does not include repeated measures factors, i.e., it is usually simple. Therefore, to analyze these variables proceed as follows.

Tests for the comparison among groups (most frequently used)

1e. Check for the presence of observations equal to the cutoff value. If they are absent, go to step 2e, otherwise go to step 5e.

2e. Check the normality of the distribution of data using the Shapiro-Wilk test or the Kolmogorov-Smirnov test, Lilliefors modification (Armitage et al., 2002; Chiarotti, 2004). If data are normally distributed, go to step 3e; otherwise go to step 5e.

3e. Compare variances among subgroups of subjects using the Levene or the Bartlett test (Armitage et al., 2002; Chiarotti, 2004). If variances are homogeneous, go to step 4e; otherwise go to step 5e.

4e. Perform a parametric test for the comparison among groups (Edwards, 1985; Wilcox, 1987; Winer et al., 1991). Go to step 6e.

5e. Perform a nonparametric test for the comparison among groups (Marascuilo and McSweeney, 1977; Brunner et al., 2002). Go to step 6e.

6e. Present the results (see Presentation of Results, below).

Survival analysis

In addition to the analysis described in steps 1e to 6e, retreiving latency can be subjected to a survival analysis (Kaplan-Meier), which allows one to take into account the competition between mutually exclusive responses. Indeed, when the mother is slow in retreiving the pups, they can spontaneously huddle, thus creating a nest area before the mother can do it herself. In this case, the mother's response must be considered as censored (censored 1) at the time of pups' huddling, since she is no longer able to perform the selected behavior. Finally, the mother must also be considered as censored (censored 2) if neither retrieving nor huddling is observed before the cutoff time.

1f. Set the status of the subject equal to *dead* if the subject has performed the behavior, or *censored* if not (whatever the cause).

2f. Set the survival time equal to the latency to perform the behavior, if the subject is *dead*. If the subject is *censored 1*, set the survival time equal to the time of pups' huddling. If the subject is *censored 2*, set the survival time equal to the cutoff time.

3f. Perform the Kaplan-Meier survival analysis (Armitage et al., 2002) on these data using *treatment(s)* as grouping variable(s).

4f. Present the results (see Presentation of Results, below).

STATISTICAL TESTS FOR THE ANALYSIS OF BEHAVIORAL DATA

Different tests can be used to analyze behavioral data, depending on the experimental design adopted and the response variable. Tests have already been mentioned that must be used to check the assumption upon which the parametric tests rely (Shapiro-Wilk test or Kolmogorov-Smirnov test, Lilliefors modification for the normality assumption; Levene test or Bartlett test for the homogeneity of variance; Greenhouse-Geisser or Huynh-Feldt corrections for the sphericity assumption; Bonferroni correction for multiple comparisons). In addition, mention has been made of the Kaplan-Meier survival analysis, the Cox proportional hazards model, the principal component analysis (Armitage et al., 2002), and logistic regression (Hosmer and Lemeshow, 2000), which, under some conditions, can be used to test behavioral data. On the contrary, no specific mention has been made of the tests for comparison among groups regarding the measures of location. For this reason, a very brief description of such tests, either parametric or nonparametric, will be given below.

Details on all mentioned tests will not given here, because that would go beyond the aim of this unit. However, a deeper insight into statistics for the health and social sciences can be obtained from statistical textbooks (Marascuilo and McSweeney, 1977; Edwards, 1985; Winer et al., 1991; Armitage et al., 2002; Brunner et al., 2002). Finally, remember that statistical software applications are now available for all personal computers; therefore, what is important is to be able to choose the appropriate method and to appropriately describe the experimental design, rather than to know all the calculations involved in performing the tests.

Tests for the Comparison Among Groups

Parametric tests

This category of tests requires that some assumptions be respected in order to make test results reliable. Two of them are common to all parametric tests, specifically: (1) independence of observations within each final subgroup; (2) normality of the distribution of data in each subgroup. Other assumptions depend on the specific test being performed.

Student t test for two independent groups

This is the test most frequently used to compare two groups of independent subjects in cases where a single observation is available for each subject (i.e., no repeated measures). Subjects are either randomly assigned to one of two groups according to the treatment administered by the experimenter (e.g., vehicle and drug), or randomly selected by the experimenter from the population of subjects presenting one of the two modalities of the characteristic under investigation (e.g., males and females).

This test is based on the following additional assumptions: (3) independence of the observations between the two groups, and (4) homogeneity of variance between the two groups. It is important to note that the *t* test is robust against slight violations of the assumptions of normality and homogeneity of variance. Variances in the two groups can be compared, using, for example, the Bartlett, Fisher F, Cochran, or Levene test. If the variances are significantly different, tests for separate variances must be applied (e.g., Welch *t* test, Brown-Forsythe test), which are usually more conservative than the Student *t* test.

Student t test for two dependent groups (Paired t test)

This is the test most frequently used to compare two groups of correlated statistical units. In particular, *n* pairs of correlated observations are collected, coming either from *n* pairs of related subjects (e.g., littermates, one tested after the administration of vehicle and the other after the administration of drug), or from *n* subjects, each tested under both conditions (vehicle and drug), with the order of treatment administration being randomly assigned to each subject. No additional assumptions are required for this test. The paired *t* test is robust against slight violations of the normality assumption.

Analysis of variance (ANOVA)

ANOVA is a very useful method that allows one to assess the significance of the difference among two or more groups of subjects (i.e., the significance of the effect of one *treatment* factor with two or more levels). Moreover, factorial ANOVA allows one to assess the significance of the effect of more treatment factors, each with two or more levels, together with their interaction(s). For example, if male and female mice are treated with vehicle or drug, the experimental design includes four subgroups coming from the combination of sex and treatment, i.e., control males, drug males, control females, drug females. In this situation, it is possible to test the main effect of drug, the main effect of sex, and the interaction of drug and sex.

When performing the ANOVA, particular care must be put into model selection. The ANOVA model depends on the experimental design. There are three main types of experimental designs: (1) completely randomized designs, (2) randomized block designs, and (3) split-plot designs.

Completely randomized designs (CRD). In this situation, subjects belonging to the different subgroups under comparison, corresponding to the different levels or combinations of levels of the factor(s) under study, are independent within each subgroup and among subgroups. The factor or factors under study are called between-subject factor(s) or grouping factor(s).

Randomized block designs (RBD). In this case, subjects belonging to the different subgroups under comparison are independent within each subgroup and dependent among subgroups. Subgroups correspond to the different levels or combinations of levels of the factor(s) under study, which are referred to as *conditions* in the following discussion. As in the case of the paired *t* test, this situation can derive from (1) one group of subjects, or (2) more groups of related subjects (e.g., littermates). In the former case, each subject is tested under all different conditions, while in the latter case, within each group, subjects are assigned to different conditions, one subject per condition. The factor(s) under study is(are) called within-subject factor(s) or repeated measures factor(s).

Split-plot designs. Split-plot designs are a combination of CRD and RBD. A random sample of blocks (e.g., litters), each consisting of more than one subject (e.g., littermates), is extracted from a population. The blocks are randomly assigned to one out of two or more conditions, treatments or combinations of treatments—i.e., between-subject factor(s). The units within each block are randomly assigned to different treatments or to combinations of treatments—i.e., within-subject factor(s)—or are evaluated at different times—i.e., repeated measures. Between-subject, within-subject, and repeated measure factors are usually fixed-effect factors, whereas blocks and units are random-effect factors.

Nonparametric tests

This category of tests generally relies on the following assumptions: (1) independence of observations within each final subgroup, and (2) continuity of the response variable in the sampled population. The latter implies that equal observations (ties) should be unlikely. Anyway, even though a variable is continuous in theory, all measurements must be made on a discrete scale; thus equal observations can occur more frequently than expected. Usually, the first step in nonparametric tests is the transformation of the original observations into ranks. Equal observations are commonly transformed into equal ranks, corresponding to the mean of the ranks that would have been assigned to the equal observations had they been different. In the presence of ties, appropriate corrections for the test statistic must be adopted. This holds true for all tests that will be described in the following paragraphs.

Mann-Whitney U test for two independent groups

This test is the nonparametric counterpart of the Student *t* test for two independent groups. It is designed to test the hypothesis of equality of the underlying distributions. Compared to the *t* test, the *U* test has an asymptotic efficiency equal to 95.5% when the assumptions for the *t* test are respected. This means that the *U* test is almost as powerful as the *t* test in detecting differences between two independent groups, and is therefore a good alternative to the *t* test when the latter cannot be performed because of violation of the assumptions. Note that the minimum total size required by the *U* test to detect differences between the two groups under comparison is $n = 7$ (i.e., at least 2 versus 5 observations) for the one-sided test, or $n = 10$ (i.e., at least 2 versus 8 observations) for the two-sided test.

Wilcoxon test for two dependent groups

This test is the most famous nonparametric counterpart of the Student *t* test for two dependent groups. It is based on the differences between paired observations, which are transformed into ranks for successive computations. The test assumes the continuity of the distribution of such differences. This implies that differences equal to 0 are unlikely. Unfortunately, as measured observations are necessarily discrete, differences equal to 0 are more frequent than expected. Usually, such differences are dropped (this is the option adopted in most statistical software applications), reducing the effective sample size.

Note that the minimum effective sample size required by the Wilcoxon matched-pair test to detect differences between the paired groups under comparison is $n = 5$ for the one-sided test, or $n = 6$ for the two-sided test.

Kruskal-Wallis analysis of variance for independent groups

This is the nonparametric countepart of the parametric ANOVA for CRD (see above). It is designed to test the hypothesis of equality of the underlying distributions among the groups based on the different levels of one between-subject factor. Compared to parametric ANOVA, the Kruskal-Wallis ANOVA has an asymptotic efficiency equal to 95.5%, when the assumptions for the parametric ANOVA are respected. If the response variable follows a non-normal distribution, the efficiency of Kruskal-Wallis ANOVA is always greater than or equal to 86% (and it can exceed 100%, e.g., in case of uniform or exponential distributions). Kruskal-Wallis ANOVA is not too sensitive to differences in spread and shape of data distribution (thus it is not too affected by violation of normality and homogeneity of variance assumptions), while it is most sensitive to differences in centers (such as means and medians, or other indexes of location).

When the experimental design includes more than one factor (e.g., two factors, sex and treatment, with two levels each, four final subgroups), the main effects of the different factors and their interaction can be assessed by using χ^2 partitioning. This method can give the exact partitioning of the overall Kruskal-Wallis χ^2 only in the case of balanced designs, i.e., when sample sizes are equal in all final subgroups. Unfortunately, this method is not available in the most common statistical software applications.

Friedman analysis of variance for dependent groups

This is the nonparametric countepart of the parametric ANOVA for RBD. It allows one to test the hypothesis of equality of the underlying distributions among the groups, based on the different levels of one within-subject factor, against the alternative hypothesis of difference in centers (such as means and medians, or other indexes of location). Compared to parametric ANOVA, when the assumptions required by this method are respected, the Friedman ANOVA has an asymptotic relative efficiency $E = 3K/[\pi(K + 1)]$, where K is the number of groups under comparison. As it can be noted, the asymptotic relative efficiency increases as K increases, ranging from the minimum of 63.7% (when $K = 2$) to 95.5% (when K is exceptionally large).

When the experimental design includes more than one factor (e.g., two factors, day and trial, with 5 and 10 levels respectively, 50 final subgroups), the main effects of the different factors and their interaction can be assessed by using the χ^2 partitioning. This method gives the exact partitioning of the overall Friedman χ^2, when the design is balanced, i.e., when sample sizes are equal in all final subgroups (this is the usual situation, since unbalancing can derive only from missing values). Unfortunately, the χ^2 partitioning is not available in the most common statistical software applications.

Nonparametric ANOVA for split-plot designs

Data from split-plot designs cannot be analyzed using nonparametric ANOVA, unless each within-subject or repeated measures factor has only two levels. In this situation, it is possible to assess the significance of the interaction of between-subject factor(s) with within-subject factor(s) by performing the Kruskal-Wallis ANOVA, with the between-subject factor as the grouping variable, on the difference between the two levels of the within-subject factor. Unfortunately, this analysis can not be directly performed using the most common statistical software applications.

PRESENTATION OF RESULTS

Tables and figures can be used to present the results of statistical analyses. In particular, to synthesize qualitative data, use *absolute* and *percent frequencies* in the different categories of each variable. On the contrary, for quantitative data, use the appropriate indexes of location (*mean*) and variability (*variance*, *standard deviation*, *standard error*). When the distribution of data is markedly asymmetrical (presence of outliers or of cutoff values), it is preferable to use *median* and *range*, *interquartile range*, or *median absolute deviation* (Armitage et al., 2002).

In addition, when a logistic regression has been performed, present odds ratios (ORs) with the corresponding confidence interval (CI). Commonly, the 95% CI is used (Hosmer and Lemeshow, 2000).

Similarly, for Kaplan-Meier survival analysis, present the cumulative incidence (that is, the incidence of subjects achieving the response) at a given time since the beginning of observation, with the corresponding 95% CI.

Finally, remember to report the test statistics with pertinent degrees of freedom and the exact significance levels. Reporting significances as $p < 0.05$, or $p =$ ns is absolutely discouraged, except for multiple comparison tests.

In preparing tables, follow a few main rules.

1. Subdivide complex tables into two or more simpler tables.
2. Put all necessary information in the title and in legend of the table (e.g., measurement units for the variables, explanation of symbols, marginal and overall totals, denominators for computation of percentages).
3. Clearly state the source of data (if not original).

Follow the same rules in preparing figures. In addition, pay attention to the maximum number of different curves and symbols that can be managed in one figure. It has to be noted that, when reporting results of statistical analyses in figures, the significance of the comparison of two groups can be presented using asterisks, the number or type of which depends on the significance level, e.g, * = 0.05, ** = 0.01 and *** = 0.001. Different types of graphics can be used to present data, depending on the statistical method used for data analysis (Table 13.8.1). The following discussion briefly describes bar charts, box and whisker plots, histograms, Kaplan-Meier cumulative incidence curves, line diagrams, and PCA graphs (Jackson, 1991; Armitage, 2002).

Bar chart

Similar to the histogram (and frequently mistaken for it), this graphical method is very useful in the case of quantitative variables with normal or symmetrical distribution. It allows one to show the distribution of one quantitative variable for different levels of other variable(s)—i.e., grouping factor(s). The height of each rectangle is equal to the mean of the variable in the corresponding group, while the upper whisker is equal to the standard deviation (or the standard error) in the same group. For an example, see Figure 13.8.1.

Box and whisker plot

This presentation is very useful in case of quantitative variables with non-normal or asymmetrical distribution. It makes it possible to synthesize one quantitative variable (outcome) for different levels of other variable(s), i.e., grouping factor(s), by presenting some measures of location and variability. Boxes cover the interquartile range and are

Table 13.8.1 Graphical Presentations Appropriate for the Different Statistical Approaches

Statistical approach	Repeated measures?	Graphical presentation
Parametric test for comparison among groups	Without repeated measures	Bar chart Box and whisker plot
	With repeated measures	Line graph
Nonparametric test for comparison among groups	Without repeated measures	Box and whisker plot
	With repeated measures	Line graph
Kaplan-Meier survival analysis	—	Cumulative incidence curve Survival curve
Cox proportional hazards model	—	Hazard with 95% CI[a]
Principal component analysis	—	PCA graph
Logistic regression	—	Odds ratios with 95% CI[a]

[a]CI, confidence interval.

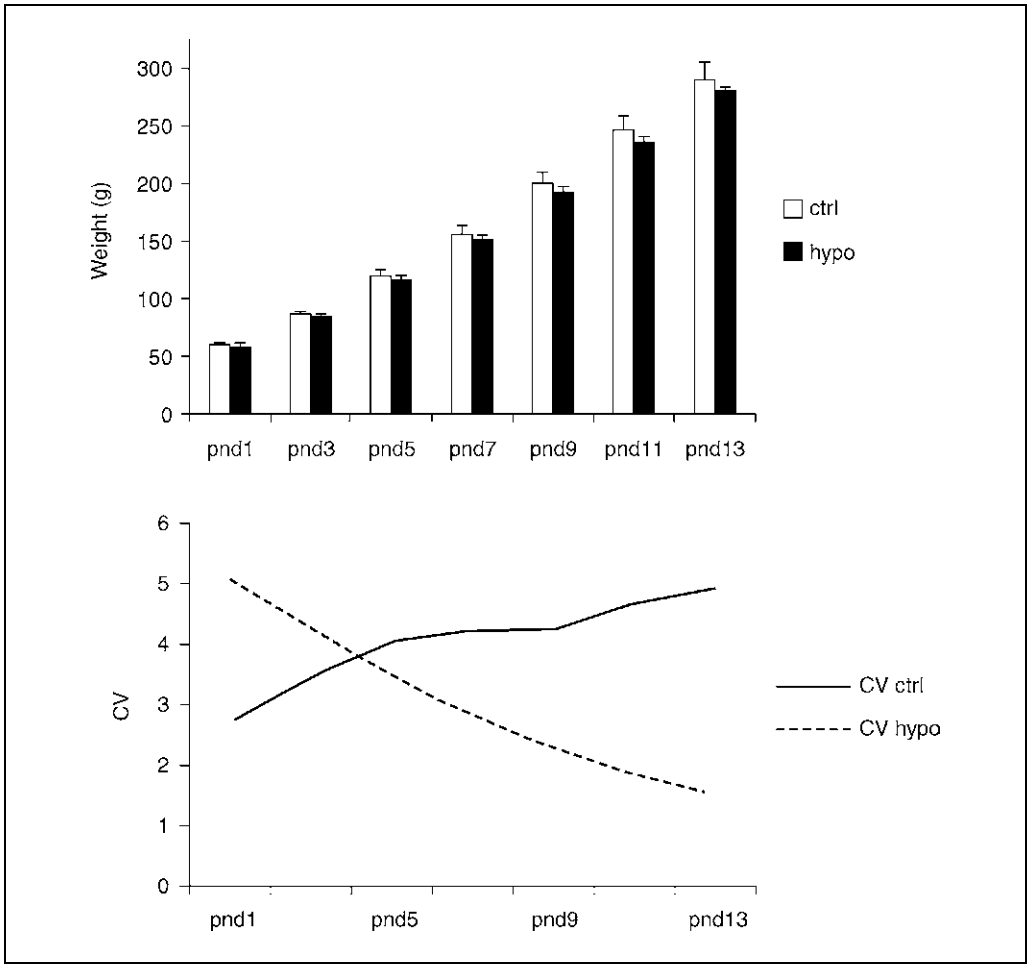

Figure 13.8.1 (**A**) Example of a bar chart. Results of parametric analysis of variance performed on litters' weight for the comparison between hypoxic (hypo) and control (ctrl) dams, every 2 days from postnatal day (pnd) 1 to pnd 13 (7 recordings). The mean litter weight is reported, with vertical bars representing standard error of mean. (**B**) The coefficient of variation (CV; i.e., the standard deviation divided by the group mean) has been plotted against PND to show the increase in this measure occurring in control litters, compared to those whose mothers had undergone hypoxia immediately after birth. Reprinted from *Neurotoxicology and Teratology*, Vol. 25, Cirulli et al. (2003). Long-term effects of acute perinatal asphyxia on rat maternal behavior, p. 575, Copyright 2003, with permission from Elsevier.

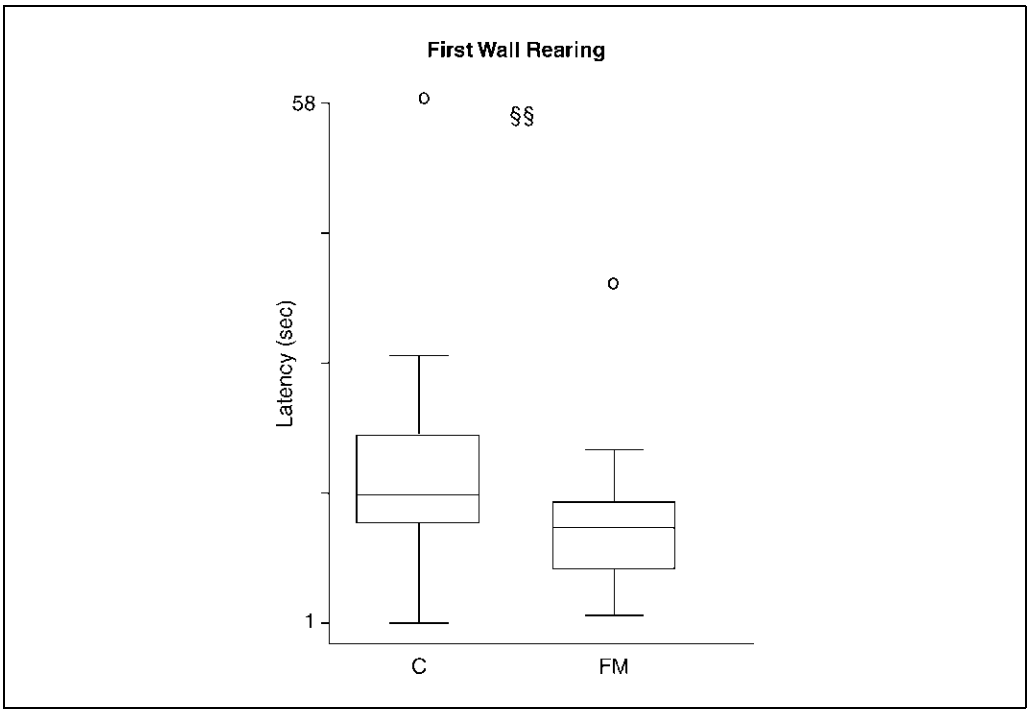

Figure 13.8.2 Example of box and whisker plot. Results of nonparametric Kruskal-Wallis analysis of variance for the comparison between two groups of CD-1 mice, one exposed to millipede aversive odor (FM) and the other to vehicle odor (C). In the figure, a box and whisker plot of latency of first wall rearing recorded in mice during the hot-plate test, performed after 15 min of exposure to the stimulus object, are reported. The line in the middle of the box represents the median. Box covers interquartile range (IQ); whiskers extend to upper and lower adjacent values. Upper value is defined as largest data point less than or equal to $x_{[75]} + (1.5 \times \text{IQ})$. Lower value is defined as smallest data point greater than or equal to $x_{[25]} - (1.5 \times \text{IQ})$. Outliers (points more extreme than the adjacent values) are represented by the letter "o." The symbol §§ represents $p < 0.001$. Reprinted from *Brain Research Bulletin*, Vol. 58(2), Capone et al. (2002). A new easy accessible and low-cost method for screening olfactory sensitivity in mice: Behavioural and nociceptive response in male and female CD-1 mice upon exposure to millipede aversive odour, p. 201, Copyright 2002, with permission from Elsevier.

divided by the median; whiskers extend to the range or some other measure of dispersion (e.g., percentile range). Observations that fall out of the whiskers represent outliers. The presence of more outliers in one direction than in the other implies asymmetry in the distribution of data. For an example, see Figure 13.8.2.

Histogram

A histogram allows one to show the frequency distribution in the different classes of a categorized quantitative variable or of a qualitative variable. Rectangles whose areas are proportional to the class frequencies are drawn on portions of the *x* axis, the width of each portion representing the class interval of the variable. In case of qualitative variables, the height of each rectangle is proportional to the frequency in the corresponding class.

Kaplan-Meier cumulative incidence curve

This graphical method allows one to represent the increase over time of the cumulative incidence of subjects showing the response. When the survival analysis is performed on behavioral developmental data, the curve represents the cumulative proportion of subjects achieving the developmental stage chosen as response. More cumulative incidence curves (one per treatment group) can be represented in one figure, using different symbols

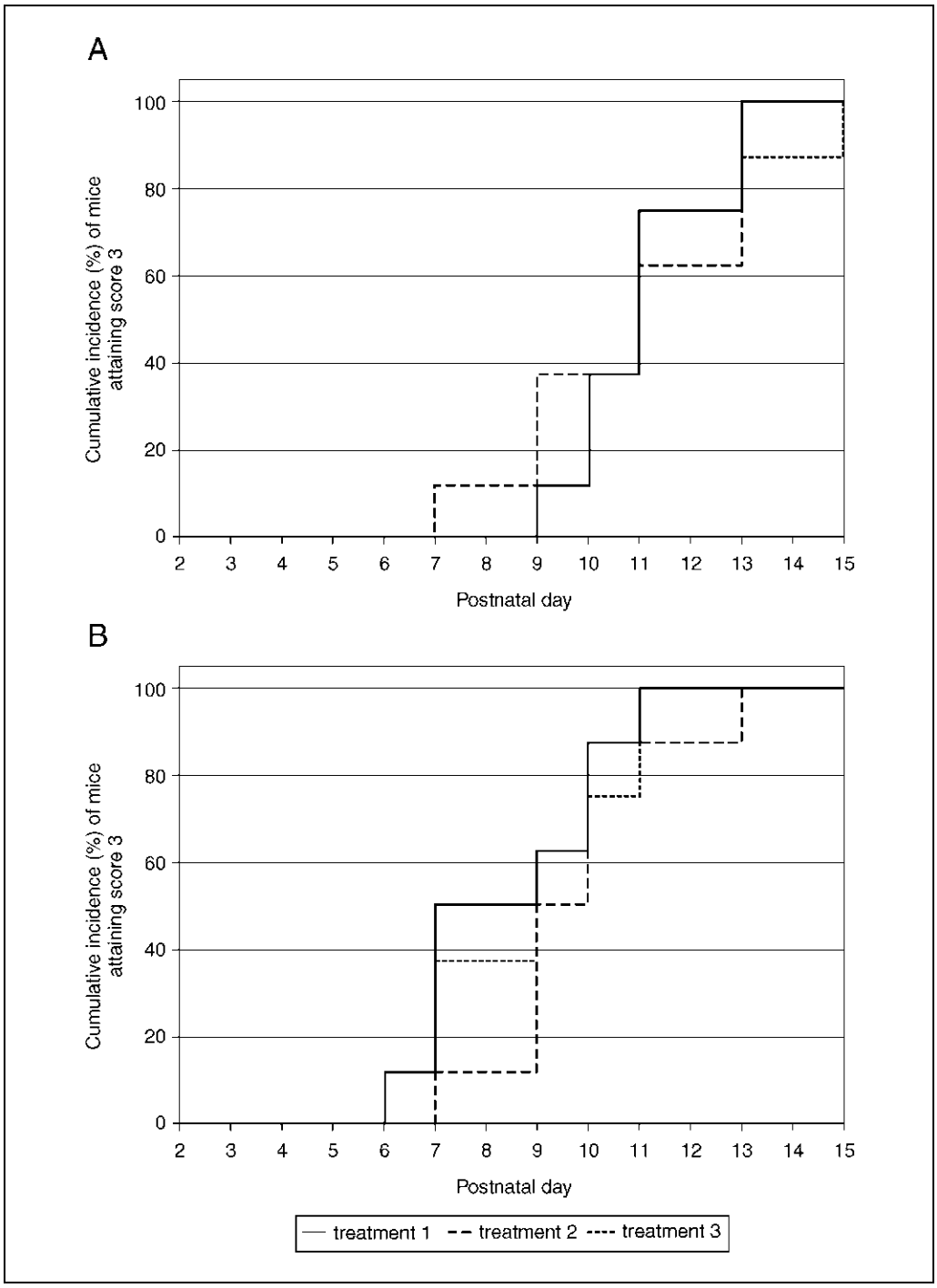

Figure 13.8.3 *(continues on next page)* Example of Kaplan-Meier cumulative incidence curve. Results of the Kaplan-Meier survival analysis performed on the swift righting score collected at postnatal days 2 to 11 and 13 to 15 on male and female mice, born from primiparous or multiparous dams, undergoing three different treatments (1, 2, and 3). (**A**) Female mice born from primiparous dams; (**B**) female mice born from multiparous dams; (**C**) male mice born from primiparous dams; (**D**) male mice born from multiparous dams. The swift righting behavior was considered as adult-like at score 3; thus that score was considered as *death*. The first day when the subject attained a score equal to 3 was considered as *time to death*. Subjects that did not reach that score were considered as *censored*, and were assigned a time equal to the span of observation (*follow-up time* = 15 days). Sex was considered as stratifying variable, while combinations of parity and treatment were considered as grouping variable (6 levels). A significant difference was observed among the six groups within each stratum ($p<0.0005$ for all tests for the comparison of survival curves). F. Chiarotti and D. Santucci (unpub. observ.).

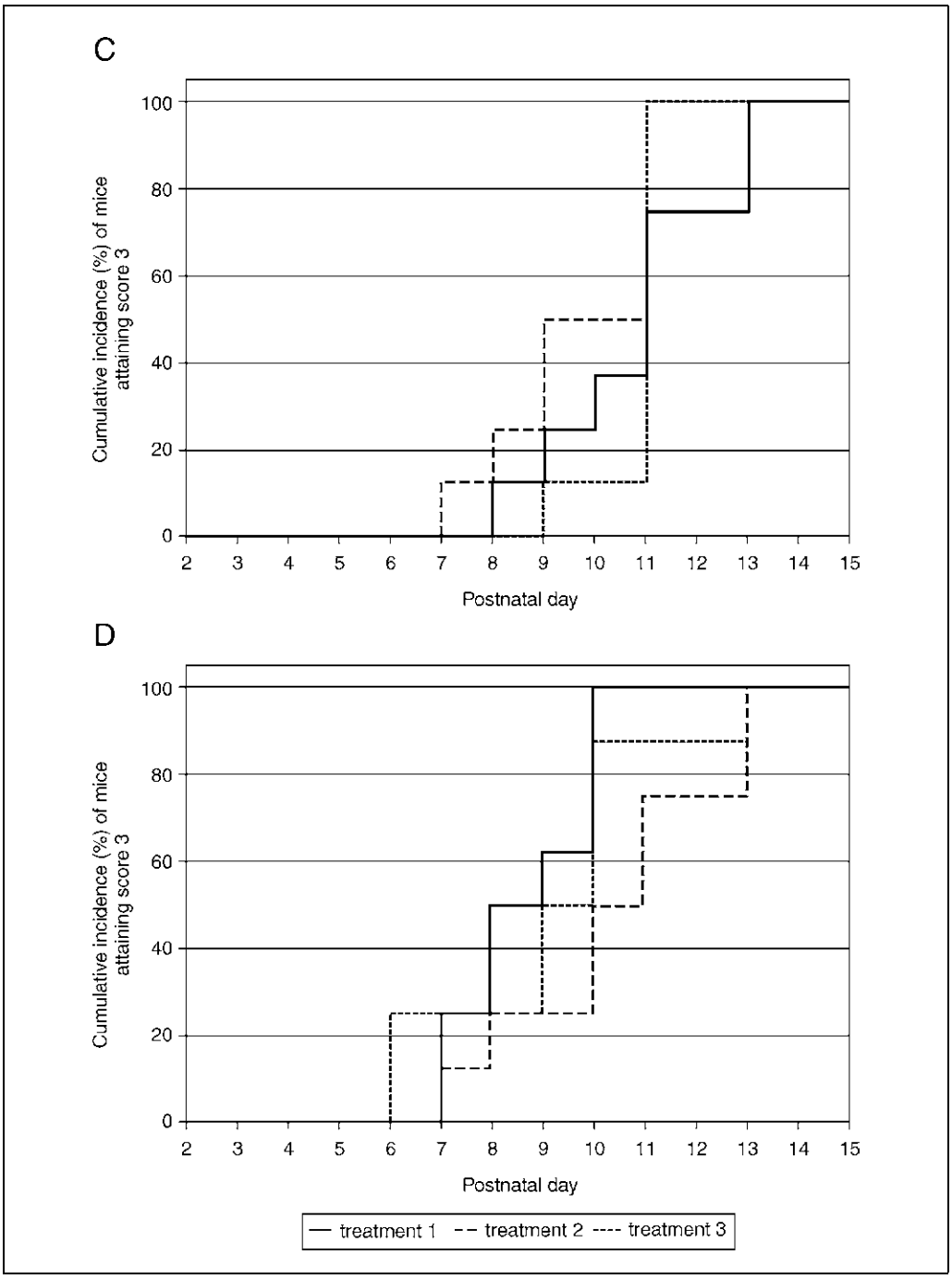

Figure 13.8.3 *(continued)*

to distinguish among different treatment groups. Sometimes the survival curves are presented, showing the decrease over time of the survival of subjects free from event. For an example, see Figure 13.8.3.

Line diagram

This technique allows one to represent data that have been collected over a period of time or over increasing doses of a drug. Mean values of the response variable are plotted as dots, and these are connected by lines showing the trend (increase, decrease or no change) over time or over doses. More curves can be presented in the same figure, one per subgroup, based on one or more between-subject factor(s). This helps to visualize

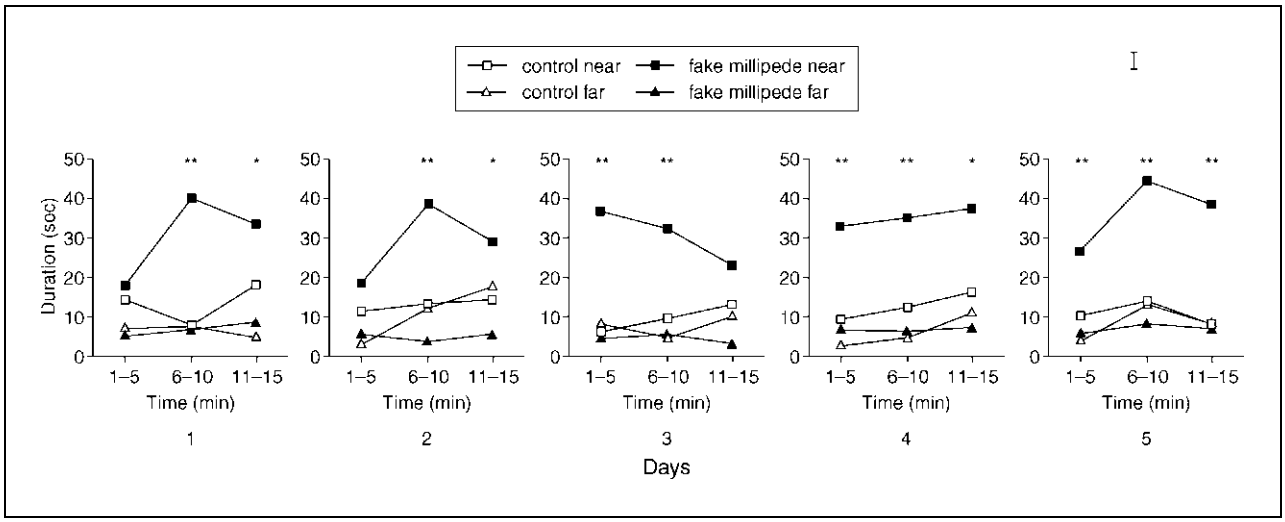

Figure 13.8.4 Example of line diagram. Results of parametric analysis of variance performed on the duration of bar holding behavior for the comparison between two groups of CD-1 mice, exposed either to millipede aversive odor (FM) or to vehicle odor (C). For each mouse, the behavior was recorded for 5 consecutive days, 15 min (3 blocks of 5 min each) per day. The behavior displayed near to the stimulus object was distinguished from the behavior displayed far from the stimulus object. In the figure, mean durations of the nonavoidance response of bar holding throghout the 5 days of testing are reported. Vertical bar on the right-hand side of the figure indicates pooled standard error of mean. This represents the best estimator of the standard error, based on more degrees of freedom, under the hypothesis of homogeneity of variance. It is computed as the square root of the ratio between the error term in the ANOVA (i.e., mean square of the residual appropriate for the assessment of the effect represented in the figure) and the number of observations contributing to each mean reported in the figure. Reprinted from *Brain Research Bulletin*, Vol. 58(2), Capone et al. (2002). A new easy accessible and low-cost method for screening olfactory sensitivity in mice: Behavioural and nociceptive response in male and female CD-1 mice upon exposure to millipede aversive odour, p. 197, Copyright 2002, with permission from Elsevier.

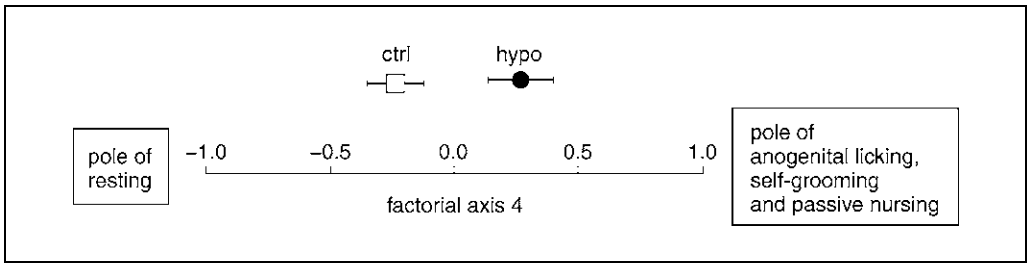

Figure 13.8.5 Example of PCA graph. Results of principal component analysis performed on maternal behavior of hypoxic and control dams, observed in the home cage. Factorial axis 4. Mean (SEM) coordinates of individuals as a function of postnatal treatment. ctrl = controls, $n = 6$; hypo = hypoxic, $n = 7$. Perinatal hypoxia affected animal's spread across the axis, increasing the probability of finding hypoxic subjects on the positive side ($p = 0.0169$). Reprinted from *Neurotoxicology and Teratology*, Vol. 25, Cirulli et al. (2003). Long-term effects of acute perinatal asphyxia on rat maternal behavior, p. 574, Copyright 2003, with permission from Elsevier.

the effect of the between-subject factor(s) on the trend over time or over doses. For an example, see Figure 13.8.4.

PCA graph

For the presentation of PCA results, monodimensional (*x* diagram) or bidimensional (*xy* diagram) graphs can be used. The graphical representation must be limited to those PCA factors that can be easily interpreted in terms of the original variables and allow a significant discrimination among the experimental groups. Each PCA factor is represented on one axis, ranging from −1 to +1. The original variables inversely correlated with

a PCA factor are reported near the negative pole of the axis representing that factor, while variables directly correlated to the factor appear near the positive pole. Along the axis, the mean values (dots) and the standard deviations (bars) relative to the subgroups differing for that PCA factor must be reported. For an example, see Figure 13.8.5.

Literature Cited

Armitage, P., Berry, G., and Matthews, J.N.S. 2002. Statistical Methods in Medical Research. 4th edition. Blackwell Science, London.

Brunner, E., Domhof, S., and Langer, F. 2002. Nonparametric Analysis of Longitudinal Data in Factorial Experiments. John Wiley & Sons, Hoboken, N.J.

Capone, F., Puopolo, M., Branchi, I., and Alleva, E. 2002. A new easy accessible and low-cost method for screening olfactory sensitivity in mice: Behavioural and nociceptive response in male and female CD-1 mice upon exposure to millipede aversive odour. *Brain Res. Bull.* 58:193-202.

Chiarotti, F. 2004. Detecting assumption violations in mixed-model analysis of variance. *Ann. Ist. Super. Sanità* 40:165-171.

Chiarotti, F. and Puopolo, M. 2000. Refinement in behavioral research: A statistical approach. *In* Progress in the Reduction, Refinement and Replacement of Animal Experimentation. Developments in Animal and Veterinary Sciences, vol. 31 (M. Balls, A.-M. van Zeller, and M.E. Halder, eds.) pp. 1229-1237, Elsevier, Amsterdam.

Cirulli, F., Bonsignore, L.T., Venerosi, A., Valanzano, A., Chiarotti, F., and Alleva, E. 2003. Long-term effects of acute perinatal asphyxia on rat maternal behavior. *Neurotoxicol. Teratol.* 25:571-578.

Edwards, A.E. 1985. Experimental Design in Psychological Research. 5th edition. Harper & Row, New York.

Fox, W.M. 1965. Reflex-ontogeny and behavioural development of the mouse. *Anim. Behav.* 13:234-241.

Hofer, M.A., Shair, H.N., and Brunelli, S.A. 2001. Ultrasonic vocalizations in rat and mouse pups. *In* Current Protocols in Neuroscience (J.N. Crawley, C.R. Gerfen, M.A. Rogawski, D.R. Sibley, P. Skolnick, and S. Wray, eds.) pp. 8.14.1-8.14.16. John Wiley & Sons, Hoboken, N.J.

Hosmer, D.W. Jr. and Lemeshow, S. 2000. Applied Logistic Regression. 2nd edition. Wiley-Interscience, New York.

Jackson, J.E. 1991. A User's Guide to Principal Components. John Wiley & Sons, New York.

Marascuilo, L.A. and McSweeney, M. 1977. Nonparametric and Distribution-Free Methods for the Social Sciences. Brooks/Cole, Monterey, Calif.

Wilcox, R.R. 1987. New Statistical Procedures for the Social Sciences: Modern Solutions to Basic Problems. Lawrence Erlbaum Associates, Hillsdale, N.J.

Winer, B.J., Brown, D.R., and Michels, K.M. 1991. Statistical Principles in Experimental Design, 3rd edition. McGraw-Hill, New York.

Contributed by Flavia Chiarotti
Istituto Superiore di Sanità
Rome, Italy

Table 13.8.2 appears on the next four pages.

Table 13.8.2 Aim and Characteristics of Statistical Methods for the Analysis of Behavioral Test Data

	Description of statistical methods						
Behavioral test	Aim	Univariate/ multivariate	Response variable	Pros	Cons	Statistical method for comparison	Degree of complexity
Fox battery	Analysis of a synthetical measure of the score profile	Univariate	First day of adult-like response	Allows detection of anticipations or delays of the full response	Does not take into account the whole curve	Test for comparison among groups	Low
			Area under the curve	Takes into account the whole curve	Does not allow one to detect anticipations or delays of the full response	Test for comparison among groups	Low
	Analysis of the whole score profile	Univariate	Adult-like response (yes vs. no) and time to adult-like response	Takes into account the whole curve	Inappropriate for correlated data (e.g., littermates assigned to different treatment groups)	Survival analysis: Kaplan-Meier-Cox proportional hazards model	Medium/ high
Ultrasound vocalizations	Evaluation of calls as for number, category, and frequency band	Univariate	Number of calls			Test for the comparison among groups	Low
Passive avoidance	Acquisition phase: analysis of the number of trials to criterion	Univariate	Number of trials to reach the criterion	Allows detection of anticipations or delays in the attainment of the criterion	Does not take into account the velocity in stepping through in the repeated trials	Test for comparison among groups	Low
			Attainment of the criterion (yes vs. no) and number of trials to reach the criterion	Allows detection of anticipations or delays in the attainment of the criterion and directly deals with subjects not attaining the criterion	Does not take into account the velocity in stepping through in the repeated trials	Survival analysis: Kaplan-Meier Cox proportional hazards model	Medium/ high

continued

Table 13.8.2 Aim and Characteristics of Statistical Methods for the Analysis of Behavioral Test Data, *continued*

	Description of statistical methods						
Behavioral test	Aim	Univariate/ multivariate	Response variable	Pros	Cons	Statistical method for comparison	Degree of complexity
Passive avoidance (*continued*)	Acquisition phase: analysis of the latency profile to step-through	Univariate	Median latency value	Takes into account the velocity in stepping through and is not affected by outliers	Not very sensitive to anticipations or delays in the attainment of the criterion	Test for comparison among groups	Low
			Area under latency curve	Takes into account the velocity in stepping through and takes into account the whole curve	Not very sensitive to anticipations or delays in the attainment of the criterion	Test for comparison among groups	Low
	Retest trial: analysis of the latency to step-through	Univariate	Latency to step-through			Test for comparison among groups	Low
Morris water maze	Acquisition phase: analysis of the latency profile to reach the platform	Univariate	Median latency value	Takes into account the velocity in reaching the platform and is not affected by outliers	Not very sensitive to anticipations or delays in the attainment of the criterion	Test for comparison among groups	Low
			Area under latency curve	Takes into account the velocity in reaching the platform and takes into account the whole curve	Not very sensitive to anticipations or delays in the attainment of the criterion	Test for comparison among groups	Low
	Acquisition phase: analysis of the mean velocity	Univariate	Mean velocity profile in repeated days and trials	Takes into account the whole profile		Test for comparison among groups	Low

continued

Table 13.8.2 Aim and Characteristics of Statistical Methods for the Analysis of Behavioral Test Data, *continued*

	Description of statistical methods						
Behavioral test	Aim	Univariate/ multivariate	Response variable	Pros	Cons	Statistical method for comparison	Degree of complexity
Morris water maze (*continued*)	Acquisition phase: analysis of the path length	Univariate	Path length profile in repeated days and trials	Takes into account the whole profile		Test for comparison among groups	Low
	Acquisition phase: analysis of the time spent in the peripheral annular area close to the wall	Univariate	Profile of the time spent in the peripheral annular area close to the wall on repeated days and trials	Takes into account the whole profile		Test for comparison among groups	Low
	Retest trial: analysis of locomotor activity	Univariate	Crossings of acquisition quadrant		Affected by animal's (hyper)activity	Test for comparison among groups	Low
	Retest trial: analysis of total time	Univariate	Total time spent in the acquisition quadrant		Is affected by animal's boredom	Test for comparison among groups	Low
Spatial open field	Analysis of behavioral pattern	Univariate	Frequency (or duration) of each: general behavior (e.g., rearing, wall rearing, grooming, locomotor activity) and behavior specifically directed towards the object (e.g., object contacts)	Allows one to assess the specific effect of treatment on each observed behavior	Does not take into account the correlation among the behavioral categories	Test for comparison among groups	Low
	Analysis of general behaviors	Mutivariate	Frequency (or duration) of all general behaviors, for each subject in each repeated session	Takes into account the correlation among the behavioral categories	May result in factors that are difficult to interpret	Principal component analysis	Medium/ high

continued

Table 13.8.2 Aim and Characteristics of Statistical Methods for the Analysis of Behavioral Test Data, *continued*

	Description of statistical methods						
Behavioral test	Aim	Univariate/ multivariate	Response variable	Pros	Cons	Statistical method for comparison	Degree of complexity
Maternal behavior	Analysis of maternal behavior in the home cage	Univariate	0/1 scores, for each behavior, time point, and day of observation	Takes into account if the behavior has been displayed or not (good for very rare behaviors)	Does not quantify display of the behavior	Logistic regression	Low/ medium
		Univariate	Number of instantaneous samples in which the behavior has been displayed, for each time point and day of observation	Allows a gross quantification of the displayment of the behaviors	Not appropriate for very rare behaviors	Test for comparison among groups	Low
		Multivariate	Number of instantaneous samples in which the behavior has been displayed, for each subject at each time point and day of observation	Takes into account the correlation among the behavioral categories	May result in factors that are difficult to interpret	Principal component analysis	Medium/ high
	Analysis of maternal behavior in a novel cage	Univariate	Latency to perform the behavior			Test for comparison among groups	Low
		Univariate	Performance of the behavior (yes vs. no) and latency to perform the behavior	Takes into account the competition between mutually exclusive responses	Inappropriate for correlated data (e.g., littermates assigned to different treatment groups)	Survival analysis: Kaplan-Meier	Medium/ high

CHAPTER 14
Hepatotoxicology

INTRODUCTION

The liver is a frequent target for chemically induced injury. This injury is manifested by a number of toxic endpoints and is detectable at levels of organization from the molecular to the gross anatomical. The significance of the liver in toxic action has several roots. First, with the possible exception of the skin, it is the largest organ in the mammalian body. Second, most xenobiotics enter the body via the gastrointestinal tract and, after absorption, are transported directly to the liver via the hepatic portal vein, making the liver the first organ perfused by chemicals absorbed by the gut. Third is the high concentration of xenobiotic-metabolizing enzymes (XMEs), particularly isoforms of cytochrome P450 (CYP). These enzymes, while primarily involved in detoxication also carry out many activation reactions, the products of which may cause hepatotoxicity or toxicity in other organ systems after being distributed throughout the body.

Because XMEs, and particularly CYP isoforms, have broad overlapping substrate specificities and because xenobiotics may serve as substrates, inhibitors and/or inducers of these enzymes, they are a common locus for toxic interactions between different xenobiotics. Thus the liver, with its high content of XMEs, is an important site for drug and other chemical interactions.

The number of toxic endpoints observed in liver is large and includes fatty liver, cell necrosis, apoptosis, cholestasis, cirrhosis, hepatitis and carcinogenesis. Similarly the range of hepatoxicants is large, including clinical drugs, drugs of abuse, industrial solvents and biologicals, the latter including both plant and fungal metabolites.

Hepatoxicity has been investigated at all levels of organization from the molecular, through the subcellular and cellular to liver slices and the isolated, perfused liver. This wide variety of causes, mechanisms and effects will form the overall basis of this chapter, starting with additional details of the importance and role of this organ in toxic action in the overview of hepatotoxicity (*UNIT 14.1*) and continuing with a most important technique, that for the isolation of hepatocytes (*UNIT 14.2*). *UNIT 14.3* describes the preparation and use of a small animal model for liver dysfunction caused by hemorrhagic shock. Blood loss continues to be a leading cause of death in many countries. About half of the victims survive the initial early death phase only to succumb later to organ failure, of which liver failure is the most important. This unit describes a rat model for such liver failure, a model needed to carry out the studies essential for clinical amelioration of this serious problem.

UNIT 14.5, on the measurement of hepatobiliary transport, describes methods for collecting bile from anesthetized mice and rats, carrying out isolated perfused rat liver studies and studies using isolating plasma membrane vesicles from the basolateral and canalicular domains of rat liver.

Ernest Hodgson

Contributed by Ernest Hodgson
Current Protocols in Toxicology (2004) 14.0.1

Overview of Hepatotoxicity

Hepatotoxicity is a collection of diverse toxic responses defined by target tissue—in this case, the liver—as opposed to other subdivisions of toxicology that are based upon a specific type of toxic effect or functional endpoint. As such, no battery of liver-specific testing protocols exists; rather, hepatotoxicity of a chemical is usually detected during acute or repeat-dose testing protocols or in clinical medicine as alterations in liver-specific serum parameters. Liver, because of its relative abundance and ease of cell dispersal, has long been a favorite tissue of biochemists and cell biologists. Thus, a rich background exists for the study of how toxicant interactions at the molecular level adversely affect liver cell function. Many of the methods for assessing generalized cellular and genetic toxic responses, xenobiotic metabolism, and regulation of glutathione homeostasis are especially pertinent here and are readily applied to cells of the liver.

FREQUENCY OF CHEMICALLY INDUCED HEPATOTOXICITY

Liver is a frequent target tissue of chemical toxicity. To illustrate the magnitude of liver susceptibility to adverse chemical effects for this overview, entries from the Environmental Protection Agency's Integrated Risk Information System (IRIS) database (see Internet Resources) were reviewed for hepatotoxic effects. For brevity, this exercise was limited to IRIS chemicals for which there are sufficient data to establish chronic oral reference doses (RfDs; i.e., estimates of human oral exposure levels that pose negligible risk of deleterious effects) and noncancer endpoints. From a total of 355 such chemicals, 141 (39%) show some evidence of hepatotoxicity. For 71% of these, hepatotoxicity is a critical effect (i.e., an adverse effect that occurs dose dependently at the lowest dosage in the most sensitive species and, thus, is used to establish the RfD).

To estimate exposure potential, those IRIS hepatotoxicants manufactured or imported at quantities of >1 million pounds per year, the so-called high production volume (HPV) chemicals, were identified (see Internet Resources). The IRIS hepatotoxicants that would be expected to pose a higher risk would then be those HPV chemicals with greater potencies as indicated by low liver "lowest observed adverse effect levels" (LOAELs). Of the 46 IRIS hepatotoxicants that are HPV chemicals, 12 have liver LOAELs ≤10 mg/kg/day, approximately one-fifth the human daily intake by weight of table salt. Most familiar among these are the industrial solvent carbon tetrachloride, herbicide 2,4-dichlorophenoxyacetic acid (2,4-D), munitions ingredient 2,4-dinitrotoluene, previous fuel additive tetraethyl lead, and plastic monomer vinyl chloride.

Also evident from this exercise is the predominance of pesticides (57%) among the IRIS hepatotoxicants. This results, in part, from the availability of large amounts of information from the comprehensive toxicity testing required for their registration. Of the IRIS pesticide hepatotoxicants with liver LOAELs ≤10 mg/kg/day, 44% are currently registered for use, while 14% are no longer registered or have severely restricted use (e.g., γ-hexachlorocyclohexane). Although banned, the latter are persistent organochlorine compounds, such as dichlorodiphenyltrichloroethane (DDT), mirex, and dieldrin, that have bioaccumulated during their earlier use such that toxicity of their residues is still of concern. Mandated reporting requirements have also enabled inclusion of a considerable number of industrial hepatotoxicants in the IRIS database. An important consideration apparent from the analysis of industrial chemicals is that the LOAELs for hepatotoxic effects of the phthalates, HPV chemicals used for manufacture of plastics, are relatively high; all are >400 mg/kg/day, except for di(2-ethylhexyl)phthalate (DEHP; LOAEL = 19 mg/kg/day).

Pharmaceuticals such as estrogenic and androgenic steroids, anesthetic halothane, retinoid acitretin, antiviral fialuridine, analgesic bromfenac, antidiabetic troglitazone, and others (Zimmerman, 1998) have exhibited hepatotoxic effects in humans, but since these substances are not found in the environment, they are not listed in the IRIS database. Although these serve as highly visible examples, the overall prevalence of chemical hepatotoxicity among pharmaceuticals relative to other chemical classes is difficult to estimate without a readily accessible, comprehensive database of animal toxicity tests. Further, when judging risks of pharmaceuticals, higher LOAELs have relevance because humans are purposely exposed, but the risk for

Contributed by Sharon A. Meyer
Current Protocols in Toxicology (2001) 14.1.1-14.1.6

hepatotoxicity must be weighed against the benefit of therapeutic effect.

Hepatotoxicity can be modified by several factors. Aggravation of hepatotoxicity from chemical-chemical interactions is of concern during concurrent therapies and environmental exposures to mixtures. Simultaneous exposures can result in competition for metabolic and excretory pathway components and thus alter toxicokinetics, whereas sequential exposures can cause induction or inhibition of molecular mediators of toxic effects. Lifestyle factors also have the potential to increase risk of hepatotoxicity. In particular, the most serious health hazard from chronic ethanol consumption is liver fibrosis, while adverse interactive effects have been noted with acetaminophen (Slattery et al., 1996). Importantly, the severity and incidence of adverse effects of chemicals on the liver can be expected to increase with the projected rise in prevalence of confounding viral hepatitis in the general U.S. population.

LIVER FUNCTION IN SUSCEPTIBILITY TO HEPATOTOXICANT TARGETING

The liver is the first internal organ to receive nutrients absorbed from the diet because its blood supply is directly connected to the intestines via the portal vein. Efferent venous blood from the intestine mixes with arterial blood upon entry into the hepatic sinusoids, the specialized capillary beds of the liver, which are fed by terminal branches of both the portal vein and hepatic artery. Although advantageous for hepatic coordination of endogenous metabolite homeostasis with newly absorbed material, this routing makes liver especially susceptible to disposition of orally administered xenobiotics. Liver parenchymal cells, the hepatocytes, are also instrumental in processing the excretory products of catabolism and their secretion by energy-dependent transporters localized to the canalicular region of the plasma membrane. Canalicular membranes from adjacent hepatocytes align to form conduits that empty into periportal bile ductules. Movement of biliary components from hepatocytes into bile ductules, and eventually their secretion into the duodenum, establishes a pathway for enterohepatic circulation of materials upon reabsorption into the portal circulation. Enterohepatic circulation not only provides a means for recovery of important nutrients and symbiotic metabolism by enteric microbes, but also increases the susceptibility of liver to toxicants by decreasing their rate of clearance.

Hepatocytes comprise ~70% of the cellular population of the liver and are the site of key anabolic reactions contributing to regulation of systemic carbohydrates, lipids, and proteins. For example, provision of systemic glucose for consumption by obligate consumers like the brain is largely dependent upon gluconeogenic activity of hepatocytes. Enzymes necessary for conversion of nonglucose energy sources to gluconeogenic precursors, such as the amino acid transaminases, are in such abundance that their leakage can be detected in the circulation and used as a surrogate indicator of hepatocyte damage. As a result of their high synthetic activity, hepatocytes are especially susceptible to effects of antimetabolites and metabolite depletion. Metabolism of lipid triglycerides and fatty acids requires substantial hepatocyte energy expenditure and thus accounts for the frequent occurrence of lipid accumulation in toxicant-exposed liver.

Other liver cell types include epithelial cells that line bile ductules and Kupffer cells, the largest reservoir of macrophages in the body. Kupffer cells are dispersed within the sinusoids and perform a major role in the liver inflammatory response through secretion of cytokines (Jaeschke et al., 1996). These function through sinusoidal endothelial cells to recruit circulating lymphocytes to damaged liver and initiate chemically induced hepatitis. Ito cells, or fat-storing cells, are a minor population that resides in the space between sinusoidal endothelial cells and hepatocytes. These cells are the site of storage of liver retinoids and can also be activated by Kupffer cell cytokines to synthesize collagen. As such, they are major cellular mediators of liver fibrosis and cirrhosis.

Hepatocytes exhibit heterogeneity depending upon their position along the sinusoid. Several sinusoids radiate from a single terminal hepatic venule or central vein, the efferent terminus of the capillary bed, and thus define a structural unit called the liver lobule. Microscopically, the lobule appears as a hexagon centered upon the central vein with alternate vertices defined by portal triads, distinct regions that contain the preterminal branches of the portal vein, hepatic artery, and bile duct. Hepatocytes are aligned in cords that run parallel with the sinusoids. Those hepatocytes nearest the central vein, the centrilobular hepatocytes, are functionally different from the periportal hepatocytes at the lobule perimeter due, in part, to the microenvironments established by oxygen and nutrient gradients that exist across the sinusoidal length (Gupta, et al.,

1999). A second classification scheme groups hepatocytes according to their relative distance from the terminal branches of the afferent vasculature. The resulting functional unit, called the acinus, defines those hepatocytes closest to the portal tract and central vein as zones 1 and 3, respectively, while those intervening in zone 2 are nearly equivalent to midlobular hepatocytes.

Hepatocyte heterogeneity can impart positional specificity to chemically induced liver injury. Sublobular regions of injury are typically defined pathologically as centrilobular or periportal (i.e., surrounding the central veins or portal tracts), while a small number of hepatotoxicants selectively damage the midlobular hepatocytes. The amount of sublobular area involved in response to a given hepatotoxicant is somewhat plastic, and depends upon dose and functional state of the liver. This sublobular pattern of injury can provide important information about the severity and mechanisms of hepatotoxicity.

Hepatocytes are physiologically specialized to metabolize xenobiotics, and metabolic activity is regulated to match functional load. Liver is rich in activities of oxidative Phase I and conjugative Phase II enzymes, for which methodology has been described elsewhere in this book (see Chapter 4). Sequential activities of these enzymes yield water-soluble metabolite conjugates of hydrophobic xenobiotics that are substrates of hepatocyte canalicular transporters. However, Phase II activities can apparently become rate limiting because unconjugated, oxidized metabolites can accumulate upon exposure to high doses of xenobiotics. Induction of cytochrome P450 enzymes, which are localized to centrilobular hepatocytes, can also lead to imbalance between Phase I and II activities and consequential production of reactive metabolites. Binding of cytochrome-P450-derived reactive metabolites to various cellular macromolecules can deleteriously affect protein function and form antigenic sites that result in localized centrilobular hepatocellular degeneration. Examples of methods for detection of protein adduction and lobular localization are presented in *UNIT 2.3*. Nucleophilic sites of nucleic acids are also susceptible to reactive metabolite adduction, which can lead to cytotoxicity and mutagenicity from the formation of cleavage sites in the polyphosphoribose strand or from promutagenic sites at modified bases. These lesions can be detected with protocols described elsewhere (see Chapter 3). Elevated cytochrome P450 activity can also lead to production of oxidative stress through leakage of reactive oxygen species from uncoupled partial reactions. Methods useful for assessment of cellular oxidative damage have been presented in *UNITS 2.4, 3.2, 7.3, 9.2, 9.3 & 9.6*.

TYPES OF TOXIC RESPONSES OF LIVER AND THEIR ASSESSMENT

A multitude of hepatic responses follows exposure to a chemical and precedes overt toxicity. The challenge for the toxicologist is to distinguish those that are intermediates leading to adverse endpoints from those that are beneficial adaptive responses. A classic example is whether the frequently observed increase in weight of chemically treated liver has toxicological significance. This response is often accompanied by increased hepatocyte size (hepatocellular hypertrophy), induction of xenobiotic metabolizing enzymes, and proliferation of associated intracellular organelles. Although these are undoubtedly adaptive responses to facilitate xenobiotic clearance, they are often a prelude to hepatotoxicity at higher dosages or following longer exposures. Of the hepatotoxicants in the IRIS database, 50% elicit an increased liver weight and/or hepatocellular hypertrophy in addition to definitive pathological indicators of hepatotoxicity or elevated serum liver enzymes. Thus, although a response may not be obviously causal to an adverse effect, its association with adverse effects of more severe exposures may be of some predictive value. The ability to make this distinction becomes more daunting as greater numbers of molecular changes are being associated with known hepatotoxicants with the application of highly efficient differential techniques.

For acute exposures, the benchmark adverse effect for toxicity is necrosis as recognized pathologically. Because cellular necrosis is accompanied by leakage of cellular contents, their detection in serum is commonly used as a noninvasive surrogate. The serum enzyme included in clinical chemistry panels most indicative of hepatocellular necrosis is alanine aminotransferase (ALT; also called serum glutamate pyruvate transaminase, SGPT). Aspartate aminotransferase (AST; also called serum glutamate oxaloacetate transaminase, SGOT) is also used, but is less specific. Sorbitol dehydrogenase (SDH) is another specific indicator of hepatocellular damage and is frequently used experimentally. Adverse hepatocellular changes that can precede overt necrosis include

fatty degeneration (steatosis), vacuolation, and deposition of various pigmented material, such as ferric heme in the hemosiderosis often seen with aryl amines (e.g., *N*,*N*-dimethylaniline) and nitroaromatics (e.g., 2,4,6-trinitrotoluene, TNT). Modest lymphocyte infiltration also usually accompanies hepatocyte degeneration and becomes pronounced with overt necrosis. Methods for histopathological and serum liver enzyme assessments will be presented in a future unit.

Impairment of bile formation (cholestasis), as a result of either hepatocyte or bile duct epithelial dysfunction, can be recognized histologically from bile deposits within canaliculi or bile ductules. Elevated alkaline phosphatase activity and bilirubin in serum also indicate cholestasis. A specific functional test for bile formation involves measurement of the clearance rate of intravenously administered bromosulfophthalene, an organic acid that is rapidly and specifically taken up by hepatocytes, conjugated, and pumped by a canalicular transporter into bile (Tennant, 1999). Direct measurement of bile flow can be monitored experimentally upon surgical cannulation of the common bile duct with subsequent administration of chemical to the intact animal or into the infusate of the isolated, perfused liver preparation. The functional integrity of the canalicular space between hepatocytes of isolated couplets and in a collagen sandwich configuration in culture (Liu et al., 1999) allows study of molecular targets of chemicals that induce hepatocellular cholestasis, such as the antipsychotic drug chlorpromazine.

Although forms of hepatocellular necrosis, steatosis, and cholestasis may also be associated with chronic exposure to hepatotoxic chemicals, fibrosis—or its more progressed form, cirrhosis—and neoplasia are more characteristic of long-term treatment. Fibrosis results from excess synthesis of extracellular matrix materials, especially collagen, by activated Ito cells. This material is deposited in the space between sinusoidal endothelial cells and hepatocytes and can be detected histologically with specific stains. Excess extracellular matrix in this perisinusoidal space can retard uptake of material from the sinusoidal fluid, a necessity for efficient hepatocyte regulation of systemic metabolites and first-pass metabolism of orally absorbed xenobiotics. Cirrhosis results when fibrosis becomes so severe that dense connective tissue bands encompass macroscopic nodular regions of liver.

The primary hepatotoxic chemical that causes cirrhosis in humans is ethanol. Early experimental models for ethanol-induced hepatotoxicity were limited by the rat's natural aversion to alcohol. Although these pair-fed, liquid-diet protocols have been instrumental for delineating effects of ethanol on induction of metabolic enzymes and interactions with other hepatotoxicants, they only achieved the less severe effect of fatty liver associated with subtoxic dosages. A more recent model in which ethanol is administered via an indwelling, intragastric feeding tube replicates the more severe alcoholic liver disease seen in humans and will be an essential tool for determining mechanistic aspects of ethanol-induced fibrosis. Recent studies with this model have emphasized the importance of Kupffer cells and free radicals as mediators of hepatotoxicity from chronic ethanol exposure (Thurman et al., 1999).

Rodent liver is often a site of chemically induced carcinogenesis observed in the two-year bioassay (Chhabra et al., 1990). Rat liver is a well-established model for the study of multistage chemical carcinogenesis. Specificity for the individual stages of initiation and promotion has been demonstrated for a variety of chemicals and has contributed to the mechanistic understanding of critical events necessary for each stage. As with other multistage models, initiation in rat liver has been shown to result from chemical modification of DNA and subsequent mutation. Compared to other models, however, rat liver has been especially informative about events associated with promotion because one of the earliest tumor precursor lesions is discernible in this system. These lesions, the altered hepatocyte foci (AHF), are small aggregates of hepatocytes distinguished by tinctoral staining and enzyme expression patterns that are also shared with subsequent neoplasias. Each AHF is presumed to be the clonal expansion of a single initiated cell; thus, information about rate of initiation and growth potential of initiated cells can be derived from AHF counts and morphometric analyses. Studies on differential properties of focal hepatocytes relative to those of surrounding liver have clearly demonstrated a role for chemical tumor promoters in creating an imbalance in cell proliferation and loss through programmed cell death (apoptosis; *UNIT 2.2*). In addition to their value for mechanistic studies, the development of these focal lesions within a relatively short treatment period (~4 months) has enabled the

development of an efficient screening assay for nongenotoxic hepatocarcinogens (Dragan et al., 1991).

An important etiological factor of human hepatocarcinogenesis is infection with hepadna viruses. Animal models that closely mimic this disease include transgenic mouse models and naturally occurring infected species, such as the woodchuck *(Marmota mona*x). These models have been valuable for understanding mechanistic aspects of virally induced carcinogenesis (Rogler et al., 1995) and evaluating efficacy of antiviral therapeutics. They also promise to be excellent experimental tools for study of viral interactions with chemicals that produce noncancerous forms of hepatotoxicity (Cullen and Marion, 1996).

CONCLUSION

This overview has presented some of the salient features of liver biology and physiology that provide the basis for a variety of experimental tools used for the study of chemical hepatotoxicity. An important protocol unit, to follow, details procedures to conduct the histopathological and clinical chemistry assessments that yield definitive evidence for adverse chemical effects on the liver. Additional units will focus on more mechanistic and functional aspects of hepatotoxicology and will present liver-specific protocols that address these types of issues. Once questions about a chemical's hepatotoxicity focus on the molecular level, these also can be approached with methods presented in units of Chapters 2, 3, 4, and 6. Collectively, these and future contributions to *Current Protocols in Toxicology* provide a wide assortment of experimental tools for the study of many of the diverse responses of the liver to toxicants (for additional background, see Arias et al., 1994).

LITERATURE CITED

Arias, I.M., Boyer, J.L., Fausto, N., Jakoby, W.B., Schachter, D., and Shafritz, D.A. 1994. The Liver. Biology and Pathobiology. Raven Press, New York.

Chhabra, R.S., Huff, J.E., Schwetz, B.W., and Selkirk, J. 1990. An overview of prechronic and chronic toxicity/carcinogenicity experimental study designs and criteria used by the National Toxicology Program. *Environ. Hlth. Persp.* 86:313-321.

Cullen, J.M. and Marion, P.L. 1996. Non-neoplastic liver disease associated with chronic ground squirrel hepatitis viral infection. *Hepatology* 23:1324-1329.

Dragan, Y.P., Rizvi, T., Xu, Y.H., Hully, J.R., Bawa, N., Campbell, H.A., Maronpot, R.R., and Pitot, H.C. 1991. An initiation-promotion assay in rat liver as a potential complement to the 2-year carcinogenesis bioassay. *Fundam. Appl. Toxicol.* 16:525-547.

Gupta, S., Rajvanshi, P., Sokhi, R.P., Vaidya, S., Irani, A.N., and Gorla, G.R. 1999. Position-specific gene expression in the liver lobule is directed by the microenvironment and not by the previous cell differentiation state. *J. Biol. Chem.* 274:2157-2165.

Jaeschke, H., Smith, C.W., Clemens, M.G., Ganey, P.E., and Roth, R.A. 1996. Mechanisms of inflammatory liver injury: Adhesion molecules and cytotoxicity of neutrophils *Toxicol. Appl. Pharmacol.* 139:213-226.

Liu, X., Chism, J.P., LeCluyse, E.L., Brouwer, K.R., and Brouwer, K.L. 1999. Correlation of biliary excretion in sandwich-cultured rat hepatocytes and in vivo in rats. *Drug Metab. Dispos.* 27:637-644.

Rogler, C.E., Rogler, L.E., Yang, D., Breiteneder-Gerleer, S., Gong, S., and Haiping, W. 1995. Contributions of hepadnavirus research to our understanding of hepatocarcinogenesis. *In* Liver Regeneration and Carcinogenesis. Molecular and Cellular Mechanisms (R.L. Jirtle, ed.) pp. 113-140. Academic Press, San Diego.

Slattery, J.T., Nelson, S.D., and Thummel, K.E. 1996. The complex interaction between ethanol and acetaminophen. *Clin. Pharmacol. Ther.* 60:241-246.

Tennant, B.C. 1999. Assessment of hepatic function. *In* The Clinical Chemistry of Laboratory Animals (W.F. Loeb and R.W. Quimby, eds.) pp. 501-517. Taylor & Francis, Philadelphia.

Thurman, R.G., Bradford, B.U., Iimuro, Y., Frakenberg, M.V., Knecht, K.T., Connor, H.D., Adachi, Y., Wall, C., Areetl, G.E., Raleigh, J.A., Forman, D.T., and Mason, R.P. 1999. Mechanisms of alcohol-induced hepatotoxicity: Studies in rats. *Front. Biosci.* 4:e42-46.

Zimmerman, H.J. 1998. Drug-induced hepatic disease. *In* Toxicology of the Liver, 2nd ed. (G.L. Plaa and W.R. Hewitt, eds.) pp. 3-60. Taylor & Francis, Washington, D.C.

KEY REFERENCES

Arias et al., 1994. See above.

A comprehensive reference book that details much of the biological and physiological background for understanding function of the normal liver and its impairment in disease.

McCuskey, R.S. and Earnest, D.L. (eds.) 1997. Comprehensive Toxicology, Vol. 9. Hepatic and Gastrointestinal Toxicology (I.G. Sipes, C.A. McQueen, and A.J. Gandolfi, eds.) Pergamon/Elsevier, New York.

Plaa, G.L. and Hewitt, W.R., eds. 1998. Toxicology of the Liver, 2nd ed. Taylor & Francis, Washington, D.C.

Two collections of review chapters devoted to toxic effects in the liver. The first includes chapters focused upon chemical-specific effects and the latter focuses on systems and mechanisms of toxic effects.

INTERNET RESOURCES

http://www.epa.gov/iris

The Integrated Risk Information System home page from the EPA.

http://www.gov/chemrtk/hpvchmlt.htm

ChemRTK and HPV Challenge Program Chemical List from the EPA's Office of Pollution Prevention and Toxics (OPPTS).

Contributed by Sharon A. Meyer
University of Louisiana—Monroe
Monroe, Louisiana

Preparation of Hepatocytes

Recent advances in laboratory procedures have made it a common practice to investigate the metabolism of new chemical entities (NCEs) and candidate drugs by various in vitro biological systems. In many instances, the in vivo metabolism of xenobiotics may increase or decrease a drug's toxicity or mutagenicity, and such metabolism may represent the underlying basis of clinically significant drug-drug interactions. Intact primary hepatocytes are one of the in vitro systems used for investigating drug metabolism and toxicity and for evaluating the in vivo disposition of drugs and other xenobiotics. In contrast to subcellular fractions, intact hepatocytes contain both Phase I (oxidative) and Phase II (conjugative) enzymes that are present in various organelles (e.g., microsomes, cytosol, mitochondria) together with the required cofactors (e.g., NADPH, uridine diphosphate-glucuronic acid, 3′-phosphoadenosine-5′-phosphosulfate). Accordingly, isolated hepatocytes provide an in vitro system for studying the integrated metabolism of drugs and other xenobiotics.

Intact viable hepatocytes can be isolated from the liver tissue of a wide variety of laboratory animals as well as from nontransplantable human livers (i.e., those donated for research). Briefly, liver tissue is perfused by a two-step collagenase digestion. The first perfusion buffer (PB-1), containing ethylene glycol-bis(β-aminoethylether)-*N*,*N*,*N*′,*N*′-tetraacetic acid (EGTA), depletes the liver of interstitial calcium and weakens epithelial cell-cell adhesion, which facilitates enzymatic digestion. The second perfusion buffer (PB-2) contains collagenase, which digests intercellular collagen required for cell-cell adhesion; this eventually leads to the complete digestion of cell-cell contacts.

In the case of laboratory animals, the best results are obtained when the liver perfusion is performed in situ during a nonrecoverable surgery (see Basic Protocol). Direct cannulation of the hepatic portal vein in an anesthetized animal allows for delivery of perfusion buffers directly into the encapsulated liver, resulting in increased perfusion efficiency and therefore greater hepatocyte yield. For previously excised livers or liver tissue (see Alternate Protocol), blood is removed by purging with a balanced salt solution, and the tissue is perfused and digested by cannulation of one or more blood vessels. Following perfusion, hepatocytes are released from the digested liver into a complete medium containing serum and hormonal supplements. Viable cells are then isolated by low-speed centrifugation and separated from dead cells through the use of a colloidal suspension of polyvinylpyrrolidone (PVP)–coated silica (Percoll). Finally, isolated viable hepatocytes are washed with fresh medium, resuspended in incubation medium, and dispensed into incubation vessels. Alternatively, hepatocytes can also be cryopreserved (see Support Protocol), although this may be associated with the loss of some hepatocellular functions, especially in the case of human hepatocytes.

CAUTION: Organs obtained from some laboratory animals and human donors may harbor infectious agents, which represent biological hazards. Take precautions to protect laboratory personnel with proper immunizations against these infectious agents as well as personal protective equipment including eye protection, gloves, and, if necessary, face masks. If possible, conduct all hepatocyte isolation steps in a Biosafety class II containment hood. Additionally, dispose of all potential biohazardous waste in a manner consistent with local laws and regulations.

NOTE: All protocols using live animals must first be reviewed and approved by an Institutional Animal Care and Use Committee (IACUC) and must follow officially approved procedures for the care and use of laboratory animals. Procedures involving the use of human-derived organs and tissues may require Institutional Review Board (IRB) approval by the Human Subjects Committee.

Contributed by Daniel R. Mudra and Andrew Parkinson

Current Protocols in Toxicology (2001) 14.2.1-14.2.13

NOTE: All solutions and equipment coming into contact with living cells must be sterile and aseptic technique should be used accordingly

NOTE: All culture incubations should be performed in a humidified 37°C, 5% CO_2 incubator unless otherwise specified.

BASIC PROTOCOL

IN SITU PERFUSION OF LABORATORY ANIMAL LIVER TO ISOLATE INTACT HEPATOCYTES

Perfusion during nonsurvival surgery is typically performed on small laboratory animals, such as mice or rats, and consistently yields a high number of viable hepatocytes. Direct cannulation of the portal vein in an anesthetized animal takes advantage of the dilated hepatic vascular system, thereby increasing the overall efficiency of the perfusion. This requires that the technician use a number of surgical techniques and that the animal be anesthetized (under a surgical plane) but alive during the initial part of the perfusion. Maintenance of aseptic technique, including the use of sterilized surgical instruments, is essential to minimize the risk of bacterial contamination of the resulting hepatocyte preparation.

Primary hepatocytes should be suspended in a hormone-supplemented complete medium and isolated by low-speed centrifugation. The percentage of viable cells in the preparation is improved through the prudent use of Percoll (Sigma-Aldrich). If possible, it is best to perform hepatocyte isolation steps in a biosafety containment hood. This will protect the analyst from undue exposure to potential biohazards as well as protect the hepatocyte suspension from possible microbial contamination.

Materials

Laboratory animal
50 mg/ml sodium pentobarbital dissolved in 5:4:1 (v/v/v) water/propylene glycol/alcohol (e.g., Nembutal, Abbott Laboratories)
Iodine surgical scrub (e.g., Betadine)
70% (v/v) ethanol
PBS (*APPENDIX 2A*), sterile
PB-1 (see recipe), sterile and oxygenated
Collagenase
PB-2 (see recipe), sterile and oxygenated
$DMEM^+$ (see recipe)
0.04% (w/v) trypan blue
90% (v/v) isotonic Percoll (Sigma-Aldrich) in PBS (*APPENDIX 2A*), store at 2° to 8°C
Culture medium (application specific)

Surgical tray
Gauze pads
Scalpel
Surgical sutures
Perfusion apparatus, including perfusion line, peristaltic pump, and oxygen source (see Fig. 14.2.1)
16-G surgical catheter
Surgical forceps
Surgical scissors, sterile
100-mesh nylon net or cheesecloth, sterile
Vacuum aspirator

Additional reagents and equipment for counting cells with a hemacytometer (*APPENDIX 3B*)

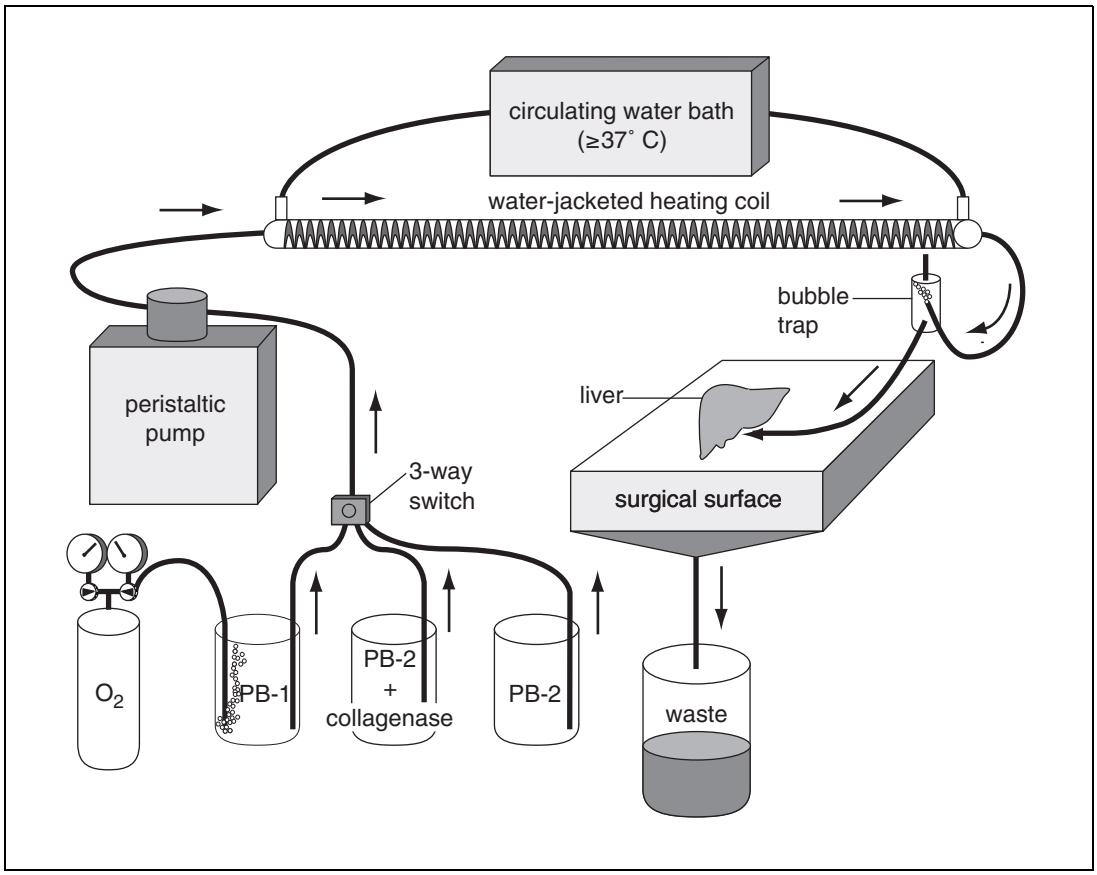

Figure 14.2.1 An example of a laboratory perfusion apparatus. This setup consists of a peristaltic pump, a heat source and a heat transfer device to maintain perfusate at 37° to 39°C, an in-line bubble trap to prevent large amounts of air from entering the liver, a carbogen (95% O_2/5% CO_2) source, and an adequate surgical procedure area. PB-1 and PB-2 are perfusion buffer 1 and 2, respectively.

Prepare animal for surgery

1. Anesthetize a laboratory animal with an appropriate dose of 50 mg/ml sodium pentobarbital.

   For most small laboratory animals (e.g., rats weighing 200 to 300 g), an intraperitoneal injection at ~60 mg/kg is sufficient to induce an anesthetic surgical plane. For larger animals (e.g., dog), the infusion of an anticoagulant before organ harvest should be considered, and a licensed veterinarian should be consulted for the appropriate surgical procedure.

2. Place animal on a surgical tray and cleanse the abdominal area with a gauze pad soaked in an iodine surgical scrub, followed by a scrub with a gauze pad soaked with 70% ethanol.

Cannulate portal vein

3. Use surgical scissors to make an initial incision through the skin and muscle wall proximal to the pubis (marked "a" in Fig. 14.2.2).

4. Cut through the abdominal skin and muscle wall with a curving incision from point "a" up to the rib cage (point "b" in Fig. 14.2.2).

   Do not cut into the diaphragm or any portion of the intestine.

5. Pull the abdominal skin and muscle above the thoracic cavity to expose the abdominal organs.

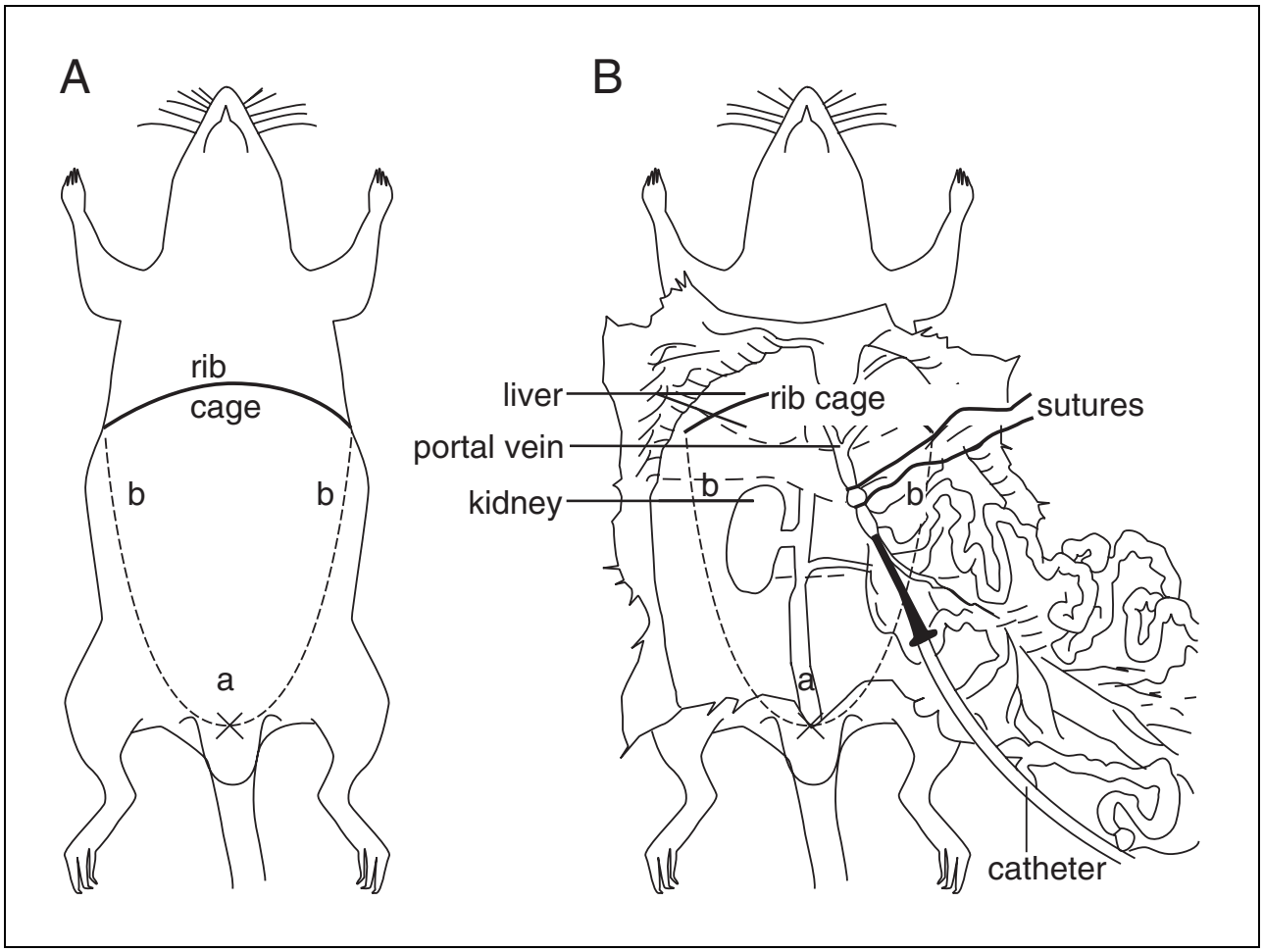

Figure 14.2.2 An example of surgical incisions on a laboratory rodent to expose the abdominal cavity. (**A**) Ventral view of an animal, with head (anterior) at the top. Each bilateral incision begins (×) at the pubis (a). The incision path follows the dotted line, up through the abdomen (b), ending at the anterior border of the rib cage as indicated. (**B**) Dissected view with intestines removed and showing positions of sutures and catheter.

6. Move the intestines from the abdominal cavity to the animal's left side using a gauze pad soaked with sterile PBS.

   If necessary, position the lobes of the liver so that the portal vein is easily accessible.

7. Place two surgical sutures loosely around the portal vein, but do not tighten.

   Blood must continue to flow through the portal vein at this time.

8. Set the peristaltic pump of a perfusion apparatus to deliver a slow drip (between 1 and 10 ml/min) of sterile oxygenated PB-1.

   Perfusion of livers for the purpose of hepatocyte isolation requires sustained perfusion of the organ at a relatively constant flow rate of 35 to 50 ml/min. Figure 14.2.1 shows one example of a perfusion system. Regardless of the source of the apparatus and its components, the assembled perfuser must provide variable flow rates, prevent air from entering the hepatic vascular system, provide a means of oxygenating the perfusion buffers, and maintain a constant perfusate temperature. For best results, all surfaces and the perfusion tubing should be cleaned with 70% (v/v) ethanol before and after each use. Before the perfusion is begun, all ethanol must be removed from the perfusion lines and replaced with PB-1.

9. Insert a 16-G surgical catheter, with the bevel of the needle facing up, into the portal vein distal to the sutures.

The size of the catheter may vary based on the size of the animal. For example, perfusion of a mouse liver may require a 22-G catheter, while perfusion of a guinea pig liver may require a 12-G catheter.

10. Provide gentle pressure to push the cannula forward, but not through, the vessel wall, so that the top portion is now proximal to both surgical sutures.

    Retrograde bleeding should now be observed at the base of the cannula.

11. Remove needle, leaving the cannula in the portal vein, and tighten sutures to secure the cannula.

Perfuse liver

12. Attach the perfusion line to the base of the cannula and immediately cut the inferior vena cava distal to the right kidney.

    The cut should be performed immediately after attachment of the perfusion line as pressure will quickly build within the liver and inferior vena cava.

13. Slowly increase the flow rate on the perfusion apparatus to between 35 and 50 ml/min.
14. Make a cut in the animal's diaphragm to expose the thoracic cavity, ceasing the animal's respiration.
15. Continue perfusion with PB-1 for 10 to 15 min.
16. Add collagenase to PB-2 at a final concentration of ~90 U/ml.

    Various categories of collagenase (e.g., Type I, Type IV.) are available from commercial vendors. Preparations may vary in activity based on the ratio of active enzyme content to contaminating proteases. The authors have found that Types I and IV collagenase (exceeding 500 U/mg) are most effective for the digestion of rat and human liver tissue. Each laboratory should determine which preparation of collagenase yields the best results for specific experimental conditions and animal species.

17. Switch perfusion apparatus to deliver oxygenated PB-2 containing collagenase. Continue perfusion for 10 to 20 min.
18. Switch perfusion apparatus to deliver oxygenated PB-2 without collagenase. Continue perfusion for 3 to 5 min.
19. Slowly decrease the flow rate (30 sec to 1 min) on the perfusion apparatus to stop the perfusion.

    During the course of the perfusion, no air should enter the liver via the perfusion lines. Air forced into the hepatic vascular system will dramatically decrease the viable cell yield.

Excise digested liver

20. Remove cannula from the portal vein and lift animal by the rib cage with surgical forceps, allowing the liver to fall forward.

    The digested liver is very soft and should be handled with care. The liver tissue should not be grasped directly with the forceps, rather grasp the surrounding vasculature or transport the liver using a surgical spatula.

21. Cut the connective tissue surrounding the liver, remove the liver from the abdominal cavity, and place it in a sterile container for processing.

    Do not cut any portion of the intestine, as this may expose the liver to intestinal flora that may contaminate the resulting hepatocyte preparation.

Process digested liver

22. Dispense DMEM$^+$ onto the digested liver such that 75% to 100% of the tissue is covered with medium.

23. Release hepatocytes into the surrounding medium by tearing Glisson's capsule (the outer membrane) using sterile surgical scissors.

    Depending on the efficiency of tissue digestion, it may be necessary to manually cut the tissue into fine pieces, thus releasing the hepatocytes into the medium. Scissors may be employed for this purpose.

24. Filter suspension using a sterile 100-mesh nylon net or, for suspensions ≥300 ml, a dual layer of sterile cheesecloth.
25. Divide filtered suspension among several sterile 50-ml centrifuge tubes.
26. Centrifuge 3 (±1) min in a low-speed centrifuge at 40 to 60 × *g*, room temperature.
27. Use a vacuum aspirator to remove supernatant fraction, add 5 to 10 ml DMEM$^+$ to each cell pellet, and gently resuspend cells. Pool cell suspensions.
28. Prepare an 8:1:1 (v/v/v) dilution of PBS/0.04% trypan blue/cell suspension (typically 50 to 100 µl of the homogeneous suspension) and count hepatocytes (*APPENDIX 3B*).

    Trypan blue is taken up by dead cells and excluded by live ones, thus allowing determination of percent viability and total cell counts.

29. Add 90% isotonic Percoll according to Table 14.2.1 and gently mix by inversion. Divide among sterile 50-ml centrifuge tubes, as needed, so that no tube contains >5 ml suspension.

Isolate cells

30. Centrifuge 5 (±1) min at room temperature according to Table 14.2.1.
31. Discard supernatant fraction by aspiration, add 5 to 10 ml DMEM$^+$ to each cell pellet, and gently resuspend.
32. Combine all remaining cells into one tube, if possible.

    The cell pellet in one 50-ml centrifuge tube must not be >10 ml.

33. Centrifuge 3 (±1) min at 40 to 60 × *g*, room temperature.
34. Discard supernatant fraction by aspiration, add a small volume of culture medium (e.g., 1 ml medium per milliliter of cell pellet), and gently resuspend.

    The culture medium may vary based on the application.

35. Combine cell suspension into one vessel.
36. Prepare an 8:1:1 (v/v/v) dilution of PBS/0.04% trypan blue/cell suspension and count hepatocytes (*APPENDIX 3B*).
37. Dilute cells with culture medium to the desired concentration and set up drug metabolism studies (see Table 14.2.2) or cryopreserve cells (see Support Protocol).

Table 14.2.1 Experimental Conditions for Percoll Centrifugation of Hepatocytes from Various Species

Species	% Percoll in DMEM$^+$	Centrifugation (× *g*)
Rat, mouse, dog	45%	60-80
Monkey	25%	40-60
Human	20-25%[a]	40-60

[a]Percoll concentration may be decreased if human hepatocytes contain high levels of intracellular fat (see Table 14.2.3).

Table 14.2.2 Recommended Experimental Conditions for Xenobiotic Metabolism Experiments

Experimental condition	Recommendation
Incubation time and medium	≤2 hr in balanced salt (e.g., Hank's, Kreb's) ≤6 hr in complete medium (e.g., DMEM+, Waymouth's, William's E)[a]
Hepatocyte concentration	1×10^6 viable cells/ml
Incubation volume	50-100 µl in 96-well plate 250 µl in 24-well plate 1.0 ml in 20-ml scintillation vial
Incubation conditions	37°C, 95% relative humidity, 95% air/5% CO_2, nonshaking incubator
To start incubations	Place multiwell plates on ice (4°C) until incubations are to be started. Enzymatic reactions will begin when cell suspensions are placed at 37°C.
To stop incubations	Place cell suspensions at or below −70°C or add an equal volume of stop reagent (e.g., concentrated acid, organic solvent).

[a]Typically it is not recommended to incubate hepatocytes in a suspension culture for >6 hr.

PERFUSION OF A PREVIOUSLY EXCISED LIVER

ALTERNATE PROTOCOL

Perfusion of a previously excised liver is typically useful for the perfusion of livers from large laboratory animals (e.g., dog, monkey) or nontransplantable human livers donated for research. This procedure can be performed on a whole liver or on a portion of a liver with a single cut face and encapsulated by Glisson's capsule. Typically, the best results are obtained when the liver is preperfused with an organ preservation solution—for example, University of Wisconsin (UW) solution (Jamieson et al., 1988)—and stored on wet ice during its transport to the laboratory. These steps will help to minimize organ damage and loss of cell viability during cold-ischemic transport. As a general rule, perfusion of an excised liver should be performed within 24 to 36 hr after harvest.

Additional Materials *(also see Basic Protocol)*

Previously excised liver
Plastic cannulas from surgical catheters (or equivalent)
Medical adhesive (e.g., Loctite 4013; Loctite)

1. If possible, insert a single perfusion line (e.g., perfuser tubing) into the portal vein and/or the hepatic artery of a previously excised liver. Secure the inserted tubing using silk sutures, umbilical tape, or medical adhesive. In the case of a cut portion of a liver, use a surgical catheter to access the portal vein. Use up to four catheters and attach each to a branch of the perfusion tubing.
2. Seal any remaining vessels on the face of the liver with medical adhesive and allow adhesive to set for the time indicated by the manufacturer.

   For best results, apply a sufficient amount of medical adhesive to seal all cut portions of the liver. This will increase the internal vascular pressure, leading to increased perfusion efficiency.

3. Start the peristaltic pump of the perfuser to deliver a slow flow rate of sterile, oxygenated PB-1 and gradually increase to between 100 and 600 ml/min. Maintain perfusion for 10 to 15 min.
4. Add collagenase (~90 U/ml) to PB-2 (see Basic Protocol, step 16).
5. Switch perfusion apparatus to deliver oxygenated PB-2 containing collagenase and perfuse 10 to 20 min.

   The waste collected here may be recirculated through the perfusion apparatus.
6. Switch perfusion apparatus to deliver oxygenated PB-2 without collagenase. Continue perfusion for 3 to 5 min.
7. Slowly decrease the flow rate on the perfusion apparatus to stop the perfusion.
8. Place the digested liver in a sterile container and isolate cells (see Basic Protocol, steps 22 to 37).

SUPPORT PROTOCOL

CRYOPRESERVATION OF HEPATOCYTES

As an alternative to the immediate use of isolated hepatocytes, the cells may be cryopreserved and stored in the vapor phase of liquid nitrogen for later use. Cryopreserved hepatocytes can be thawed and reisolated for use in integrated drug metabolism studies. Yields after thawing may vary among species, although cryopreserved hepatocytes have been shown to retain most hepatocellular functions such as active drug-metabolizing enzymes (Guillouzo et al., 1999; Li et al., 1999; Madan et al., 1999).

Additional Materials *(also see Basic Protocol)*

Isolated hepatocytes (see Basic Protocol; see Alternate Protocol)
Fetal bovine serum (FBS), heat-inactivated (*APPENDIX 3B*)
Dimethyl sulfoxide (DMSO)

Hepatocyte storage vials (must withstand −196°C)
Microprocessor-controlled programmable freezing chamber (e.g., model 1010; Forma Scientific) with thermometer
Liquid nitrogen storage unit

Prepare hepatocytes

1. Centrifuge isolated hepatocytes 3 (±1) min at 40 to 60 × *g*, room temperature.
2. Discard supernatant fraction by aspiration with a vacuum aspirator.
3. Add a sufficient volume of FBS to bring concentration to 11×10^6 viable cells/ml (as determined in Basic Protocol, step 36) and gently resuspend cell pellet.

   Although a cell concentration of 10×10^6 viable cells/ml is recommended for most applications, optimal cell concentrations may differ for specific species or applications.
4. Slowly add DMSO dropwise to a final concentration of 10% (v/v) and mix cell suspension by gentle inversion.

Prepare storage vials

5. Divide the homogenous mixture into aliquots in hepatocyte storage vials.
6. Cryopreserve hepatocytes in a microprocessor-controlled programmable freezing chamber according to the following stepwise freezing program. Use a temperature probe to measure the temperature of a sample containing only FBS and 10% (v/v) DMSO.

Cool −1°C/min until sample reaches −4°C
Cool −25°C/min until chamber reaches −25°C (sample temperature should be approximately −8° to −10°C)
Warm 15°C/min until chamber reaches −12°C
Cool −1°C/min until chamber reaches −40°C
Cool −10°C/min until chamber reaches −90°C
Hold −90°C until sample reaches −90°C.

7. Transfer vials to a liquid nitrogen storage unit.

The vial used to measure sample temperature should be discarded. For best results store the vials in the vapor phase at or below −145°C.

Thaw hepatocytes

8. Remove one or more vials of cryopreserved hepatocytes from the liquid nitrogen storage unit.
9. Place in a 37°C shaking water bath until sample is partially thawed and can be poured from the vial.
10. Gently pour thawed hepatocytes into a sterile 50-ml centrifuge tube containing 28.2 ml $DMEM^+$ and 11.8 ml of 90% isotonic Percoll.
11. Add $DMEM^+$ to obtain a final concentration of 21.5% (v/v) Percoll.
12. Centrifuge hepatocytes 5 (±1) min at room temperature according to Table 14.2.1.

Prepare cell suspension

13. Count cells as described (see Basic Protocol, steps 27 to 28).
14. Combine all remaining cells into one tube, if possible.

The cell pellet in one 50-ml centrifuge tube must not be >10 ml.

15. Prepare final suspension as described (see Basic Protocol, steps 33 to 37) and immediately deliver cells to a suspension culture containing the investigative substrate.

It is thought that cryopreserved hepatocytes may have an infinite storage life when maintained at ultra-cold temperatures (liquid nitrogen). However, rigorous studies into the long-term storage of cryopreserved hepatocytes are incomplete, and it is recommended that each laboratory monitor cell yield and viability in preparations over time.

REAGENTS AND SOLUTIONS

Use Milli-Q-purified water or equivalent (0.22-μm filtered with a resistivity ≥14 MΩ cm) in all recipes and protocol steps. Filter sterilize (0.22-μm filter) all solutions prepared with nonsterile components at the time of preparation. For common stock solutions, see ***APPENDIX 2A****; for suppliers, see* ***SUPPLIERS APPENDIX****.*

Perfusion buffer 1 (PB-1)

To ~1.8 liters water add:
13.8 g NaCl (final 118 mM)
0.7 g KCl (final 4.7 mM)
0.33 g KH_2PO_4 (final 1.2 mM)
4.2 g $NaHCO_3$ (final 25 mM)
2.0 g glucose (final 5.5 mM)
0.4 g EGTA (final 0.5 mM)

continued

Adjust to pH 7.4 with NaOH or HCl as needed
H_2O to 2 liters
Sterilize with a 0.22-μm filter
Store up to 6 months at 4°C

Perfusion buffer 2 (PB-2)

Prepare as for PB-1 (see recipe), but replace EGTA with:
4 ml 1.0 M $CaCl_2$ (final 2.0 mM)
2.4 ml 1.0 M $MgSO_4$ (final 1.2 mM)
Store up to 6 months at 4°C

Supplemented Dulbecco's modified Eagle medium (DMEM$^+$)

Two packages (13.4 g/package) DMEM without phenol red (Life Technologies)
7.4 g $NaHCO_3$ (final 44 mM)
20 ml 200 mM GlutaMAX-1 (Life Technologies; final 2 mM)
20 ml 10 mM MEM non-essential amino acids solution (MEM-NEAA, Life Technologies; final 0.1 mM)
25 ml heat-inactivated fetal bovine serum (FBS; *APPENDIX 3B*; final 5%, v/v)
781 μl 4 mg/ml insulin (final 6.25 μg/ml)
5 ml penicillin/streptomycin (100× stock: 5000 U/ml penicillin, 5000 μg/ml streptomycin)
50 μl 10 mM dexamethasone in dimethyl sulfoxide (final 1 μM dexamethasone)

Dissolve DMEM in ~1.8 liters water. Add $NaHCO_3$, GlutaMAX-1, and MEM-NEAA. Adjust pH to 7.4 with NaOH or HCl, as needed, and adjust final volume to 2 liters with water. Filter sterilize and store up to 6 months at 4°C. Before use, add FBS, insulin, penicillin/streptomycin, and dexamethasone to 500 ml medium. Store up to 1 month at 4°C.

NOTE: *DMEM and DMEM$^+$ are light sensitive and should be stored in a dark environment.*

COMMENTARY

Background Information

Recent advances have made it increasingly common to conduct experiments designed to predict the in vivo metabolism and disposition of drugs and other xenobiotics. A variety of in vitro systems has been developed to conduct these experiments. In order of increasing complexity, these are: recombinant enzymes, liver microsomes (and other subcellular fractions), postmitochondrial fraction (S9), immortalized cell lines, primary hepatocytes, and liver slices (Parkinson, 1996b; Parkinson et al., 1997). Intact primary hepatocytes offer several advantages over other in vitro systems. However, they also present unique challenges that must be considered in an experimental design.

Isolated primary hepatocytes can be obtained from various laboratory animals, as well as from nontransplantable human livers (i.e., those donated for research). The perfusion process described in this unit is based on the methods described by Berry and Friend (1969), Seglen (1976), Quistroff et al. (1989), and LeCluyse et al. (1996a,b). This process yields viable hepatocytes suitable for drug metabolism studies. The process of hepatocyte isolation includes several measures and precautions to maintain viability and hepatocellular function.

Hepatocytes have inherent characteristics that should be considered when determining their suitability for drug metabolism studies. Compared with precision-cut liver slices, isolated hepatocytes have been shown to exhibit greater rates of testosterone oxidation, 7-ethoxycoumarin O-deethylation, and 1-chloro-2,4-dinitrobenzene (CDNB) conjugation with glutathione (Ekins et al., 1995). The lower metabolic rates observed in liver slices are most likely due to a low rate of substrate and nutrient diffusion through the multiple layers of hepatocytes, which is not a problem with isolated hepatocytes.

Intact hepatocytes provide a complex biological system in which substrates are subject to metabolism by a variety of enzymes either simultaneously or sequentially. These enzymes include, but are not limited to, cytochrome

P450 enzymes (CYPs; Seddon et al., 1989; Bayliss et al., 1994) as well as sulfotransferases (STs), UDP-glucuronosyltransferases (UGTs), and glutathione *S*-transferases (GSTs; Ekins et al., 1995). This abundance of active enzymes must be considered when analyzing data obtained from hepatocyte incubations. For example, consider that a primary oxidative metabolite of interest may be rapidly glucuronidated, thereby making the oxidative metabolite nondetectable by the standard analytical method. In cases such as this, it may be desirable to reduce the incubation time or to enzymatically deconjugate metabolites (e.g., with β-glucuronidase and/or sulfatase). Furthermore, some preparations of human hepatocytes may fail to convert a substrate to a metabolite known to be formed by pooled human liver microsomes. One possible cause of this negative result is that the hepatocyte preparation is from a donor who lacked the enzyme responsible for forming the metabolite. Several drug-metabolizing enzymes are known to be polymorphically expressed (Parkinson, 1996a), and the use of individual (i.e., nonpooled) hepatocyte samples may at times result in negative metabolic results.

Finally, hepatocytes offer a unique in vitro system to study a compound's toxicological effects. Analysis of intracellular toxicological markers such as ATP levels, heat shock–protein content, rate of mitochondrial respiration, or enzyme levels in the surrounding medium—for example, lactate dehydrogenase (LDH), alanine aminotransferase (ALT), and aspartate aminotransferase (AST)—will allow for a rapid estimate of an NCE's hepatotoxic effects. Measurement of trypan blue uptake over the course of the incubation may provide insight into the possible toxic effects of the substrate. There is also growing interest in the use of microarrays to screen for changes in gene expression in order to evaluate the potential hepatotoxicity of a chemical.

Critical Parameters and Troubleshooting

It is important that hepatocytes be isolated in a medium containing the synthetic glucocorticoid dexamethasone, which maintains liver-specific functions (e.g., albumin synthesis), supports organized arrangement of the cytoskeleton, and alleviates the loss in protein synthesis typically observed in the first 24 hr after isolation (LeCluyse et al., 1996b). It is also important to note that efforts should be made to maintain high cell viability during drug metabolism studies. Typically, the initial isolation of hepatocytes may yield a preparation that is made up of only 50% to 70% viable hepatocytes. This percent viability can be greatly enhanced by centrifugation with an isotonic mixture of the PVP-coated silica, Percoll. It is important to note that apoptotic and ruptured hepatocytes are likely to be metabolically incompetent, as the cofactors necessary for drug metabolism have been diluted into the surrounding medium. Additionally, an overabundance of nonviable hepatocytes present in an incubation mixture may increase the levels of lysosomes and autolytic enzymes in the surrounding medium, thereby leading to a more rapid decline in cell viability and substrate metabolism. For these reasons, it is prudent to make efforts to increase the overall cell viability in the hepatocyte preparation.

Table 14.2.3 lists possible problems and recommended solutions that may be encountered during the hepatocyte isolation procedure. Remember that in the case of human hepatocyte isolation—and in the case of some laboratory animals (e.g., monkey)—disease and environmental factors may cause dramatic differences in the efficiency of tissue digestion and overall hepatocyte yield.

Additional problems may be encountered during hepatocyte incubations. Experimental designs may vary for numerous reasons including species specificity, the compound under investigation, and the forthcoming analytical method. Table 14.2.2 provides a brief outline of several considerations and recommendations for designing drug metabolism experiments with hepatocytes.

Anticipated Results

The percent viability of the final hepatocyte preparation will typically be ≥70% (with higher viability typically observed in preparations of rat hepatocytes). The number of hepatocytes obtained per gram of liver tissue will vary depending on the species.

Time Considerations

The perfusion procedures described in the Basic Protocol and Alternate Protocol require ~1 to 1.5 hr to complete (this does not include solution preparation, laboratory setup, or apparatus cleaning). The hepatocyte isolation procedure described in the Basic Protocol requires ~2 hr. Additional time is required once hepatocyte incubations are initiated; incubation times may range from 10 min (Zomorodi et al., 1995) to 6 hr; see Table 14.2.2. The cryopreservation

Table 14.2.3 Troubleshooting Guide for Preparation of Hepatocytes for Xenobiotic Metabolism Studies

Problem	Critical parameters and recommended measures
Difficulty in placing surgical sutures around portal vein	In laboratory rats there is typically a space in the fat tissue surrounding the portal vein. Use a pair of curved forceps to help locate this space and provide a means to thread the surgical suture around the vein.
Initial perfusion does not remove all blood (clotting is evident)	Gently pull cannula away from liver, being careful to leave it in the portal vein.
	Increase perfusion flow rate.
Poor liver digestion and low cell yield	Catheter may not be inserted properly. It is important to obtain good flow into the portal vein. Be sure catheter needle has not poked a hole in the vein, allowing perfusion buffer to leak out before reaching liver.
	Increase purity of collagenase. Utilize a collagenase high in enzymatic purity (in U/mg). Low enzyme purity is caused by proteases that will impede digestion and decrease hepatocyte viability.
	Be sure no air has entered the perfusion line.
Initial centrifugation does not yield many cells, but many cells are in supernatant	Dilute cell suspension to a point where cells efficiently pellet at a low-speed centrifugation (see Table 14.2.1). As a general rule, do not exceed 5-ml cell pellets in each 50-ml centrifuge tube.
Cell buildup at the top of the supernatant after Percoll separation	This is normal. The buildup contains mostly dead cells that are meant to be removed from the hepatocyte preparation.
No cell pellet after Percoll centrifugation	Increase centrifugation speed or time slightly.
	Decrease Percoll content. In the case of hepatocytes from human and some laboratory animals, the cells may contain high levels of intracellular fat (visible with a microscope at 100×), which will decrease the efficiency of the Percoll separation.
Percent viability is no better after Percoll centrifugation than before	Increase Percoll concentration and recentrifuge.
	When aspirating supernatant, be sure to aspirate off dead cells on top of the supernatant. If this layer is not carefully removed, the cells will be integrated with the viable cell pellet, minimizing the effectiveness of the Percoll separation.
Trypan blue count does not accurately reflect hepatocyte density	Obtain an aliquot from a homogeneous cell suspension. Any settling of the hepatocytes may lead to an errant trypan-blue count, which will lead to inaccurate cell numbers added to each hepatocyte incubation.
Cell yield is high although viability is quite low	Decrease time of perfusion with collagenase. Collagenase can be toxic to hepatocytes.
	Select a collagenase with higher purity (U/mg).
	Be sure the temperature of the perfusate is maintained between 37° and 39°C during perfusion. This is the temperature range where collagenase is most active.
	Improve hepatocyte handling techniques. Hepatocytes must be handled gently during cell isolation to avoid physical trauma to the cell membranes.
	In the case of human liver, organ damage occurring prior to perfusion may result in isolation of nonviable hepatocytes. Trypan-blue exclusion performed before Percoll centrifugation will provide initial viability information that may aid in determining the health of the original liver.

procedure requires ~1.5 hr including the stepwise freezing procedure.

Literature Cited

Bayliss, M.K., Bell, J.A., Wilson, K., and Park, G.R. 1994. 7-Ethoxycoumarin O-deethylase kinetics in isolated rat, dog and human hepatocytes. *Xenobiotica* 24:231-241.

Berry, M.N. and Friend, D.S. 1969. High yield preparation of isolated rat liver parenchymal cells. *J. Cell Biol.* 43:506-520.

Ekins, S., Murray, G.I., Burke, M.D., Williams, J.A., Marchant, N.C., and Hawksworth, G.M. 1995. Quantitative differences in phase I and II metabolism between rat precision-cut liver slices and isolated hepatocytes. *Drug Metab. Dispos.* 23:1274-1279.

Guillouzo, A., Rialland, L., Fautrel, A., and Guyomard, C. 1999. Survival and function of isolated hepatocytes after cryopreservation. *Chem. Biol. Interact.* 121:7-16.

Jamieson, N.V., Lindell, S., Sundberg, R., Southard, J.H., and Belzer, F.D. 1988. Preservation of the canine liver for 24-48 hours using simple cold storage with UW solution. *Transplantation* 46:517.

LeCluyse, E.L., Bullock, P.L., Parkinson, A., and Hochman, J.H. 1996a. Cultured rat hepatocytes. *In* Models for Assessing Drug Absorption and Metabolism (R.T. Borchardt, P.L. Smith, and G. Wilson, eds.) pp. 121-159. Plenum, New York.

LeCluyse, E.L., Bullock, P.L., and Parkinson, A. 1996b. Strategies for restoration and maintenance of normal hepatic structure and function in long term cultures of rat hepatocytes. *Adv. Drug Deliv. Rev.* 22:133-186.

Li, A., Gorycki, P., Hengstler, J., Kedderis, G., Koebe, H., Rahmani, R., de Sousas, G., Silva, J., and Skett, P. 1999. Present status of the application of cryopreserved hepatocytes in the evaluation of xenobiotics: Consensus of an international expert panel. *Chem. Biol. Interact.* 121:117-123.

Madan, A., DeHaan, R., Mudra, D., Carroll, K., LeCluyse, E., and Parkinson, A. 1999. Effect of cryopreservation on cytochrome P450 enzyme induction in cultured rat hepatocytes. *Drug Metab. Dispos.* 27:327-335.

Parkinson, A. 1996a. Biotransformation of xenobiotics. *In* Casarett and Doull's Toxicology: The Basic Science of Poisons, V (C.D. Klaassen, ed.) pp. 113-186. McGraw Hill, New York *(edition VI in press).*

Parkinson, A. 1996b. Overview of current cytochrome P450 technology for assessing the safety and efficacy of new materials. *Tox. Pathol.* 24:45-57.

Parkinson, A., Pearce, R., Madan, A., and Forster, J. 1997. Availability and preservation of human tissues, and the use of human liver microsomes in drug metabolism research. *In* The Use of Human In Vitro Systems to Support Preclinical Safety Assessment (A. Sundwall, G. Alvan, E. Lindgren, P. Moldeus, T. Salmonsson, and P. Sjoberg, eds.) pp. 17-28. Tryckgrappen. Stockholm, Sweden.

Quistorff, B., Dich, J., and Grunnet, N. 1989. Preparation of isolated rat liver hepatocytes. *In* Methods in Molecular Biology, Vol. 5: Animal Cell Culture (J.W. Pollard and J.M. Walker, eds.) pp. 151-160. Humana Press, Totowa, N.J.

Seddon, T., Michelle, I., and Chnery, R.J. 1989. Comparitive drug metabolism of diazepam in hepatocytes isolated from man, rat, monkey and dog. *Biochem. Pharmacol.* 38:1657-1665.

Seglen, P.O. 1976. Preparation of isolated rat liver cells. *In* Methods in Cell Biology, Vol. 19 (D.M. Prescott, ed.) pp. 29-83. Academic Press, New York.

Zomorodi, K., Carlile, D., and Houston, B. 1995. Kinetics of diazepam metabolism in rat hepatic microsomes and hepatocytes and their use in predicting in vivo hepatic clearance. *Xenobiotica* 25:907-916.

Key References

LeCluyse et al., 1996a,b. See above.

Describe the steps involved in in situ perfusion and enzymatic digestion of rat liver. The Basic Protocol and Alternate Protocol are based on these methods.

Madan et al., 1999. See above.

Describes the steps involved in cell isolation, cryopreservation, and thawing. The Basic Protocol and Support Protocol are based on these methods.

Contributed by Daniel R. Mudra and Andrew Parkinson
XenoTech, LLC
Kansas City, Kansas

Small Animal Models of Hemorrhagic Shock–Induced Liver Dysfunction

Blood loss and ensuing circulatory failure continues to be the leading cause of death between the ages of 1 and 45 in most western countries. About one half of the deaths result from rapid exsanguination or severe central nervous trauma within 1 hr of injury. Although progress has been made with respect to early resuscitation of trauma victims, depression/disturbances of cellular functions propagate the development of multiple organ failure and sepsis, the leading course of late death in the intensive care unit. Hepatocellular dysfunction is a key feature of the pathophysiological sequelae of trauma/hemorrhage in patients surviving the first hours and hemorrhagic hypotension has been widely used as a model for indirect liver injury in the critically ill. At least two phases of hepatic dysfunction can be distinguished: an early injury characterized by ischemia/reperfusion of the pericentral region of the liver acinus with enzyme leakage and development of acute "pericentral necrosis" and a late injury resulting from an inflammatory reaction ("ischemic hepatitis"), which is heralded by a rise in serum bilirubin (Hawker, 1991).

This unit describes a low-flow ischemia model of the liver due to hemorrhagic hypotension (see Basic Protocol) that can be used to produce a reproducible and graded injury to the pericentral region of the acinus, which is critical for metabolism of xenobiotics. This protocol allows for measurement of cardiac output and regional flow (see Support Protocol 1) and requires specially prepared tubing (see Support Protocol 2).

INDUCING HEMORRHAGIC SHOCK

BASIC PROTOCOL

Small animal models of hemorrhagic shock with or without resuscitation can be subdivided based on the physiological end point to define the severity of the ischemic insult as well as the use of anesthetics and/or heparin or infliction of a concomitant trauma (Chaudry et al., 1993). The following protocol describes an anesthetized, nonheparinized rat model of reversible hemorrhagic shock without concomitant trauma where the ischemic insult is defined by maintenance of a fixed mean arterial blood pressure over a given period of time. In addition, a resuscitation protocol is described, which restores central and liver regional hemodynamics while moderate hemodilution is tolerated similar to the current clinical standards (Bauer et al., 1996).

Materials

Male Sprague-Dawley rats (≥250 g body weight)
Sodium pentobarbital
Disinfectant
Ringers solution (see recipe)
Citrate-phosphate-dextrose solution; aseptically filtered (see recipe): suggested anticoagulant/whole blood ratio is 1.4:10; store at 4° to 8°C

Animal clippers
Heating pad
Rectal temperature probe (e.g., Thermistor 8402-20, Cole-Parmer Instrument)
Sterile surgical instruments
Polyethylene tubing (0.58-mm i.d., 0.96-mm o.d.; Intramedic PE 50, Becton Dickinson Primary Care Diagnostics), TDMAC coated (see Support Protocol 2)
Pressure transducer and data acquisition system
5-ml sterile disposable syringes

Contributed by Inge Bauer and Michael Bauer
Current Protocols in Toxicology (2002) 14.3.1-14.3.8

Induce anesthesia and prepare for surgery

1. Withhold food from animals for 12 hr prior to surgery, but allow ad lib access to water.
2. Induce general anesthesia by intraperitoneal injection of 50 mg pentobarbital/kg body weight.

   This protocol has been standardized for male Sprague-Dawley rats since there is sexual dimorphism with respect to susceptibility to ischemic injury of the liver. Since hepatic glutathione levels and intravascular volume are important determinants of bleed-out volume and hepatocellular susceptibility to redox injury, pellet food is withheld for 12 hr prior to onset of the experiment, while animals are allowed free access to water. Surgery must be performed at defined times (7:00 to 8:00 a.m.) due to the circadian profile of hepatocellular glutathione content.

3. Shave neck and apply disinfectant prior to surgical incision.
4. Place animals on a 38°C heating pad to maintain body temperature at 36° to 37°C. Monitor the body temperature using a rectal probe.

   Body temperature is an important determinant of ischemic injury.

5. Perform a tracheotomy to ensure a patent airway and allow the animal to breathe ambient air.

   The tubing should be as wide as possible to avoid airway obstruction and should not be longer than 2 cm to avoid increase in dead space. Spontaneous breathing is recommended since positive pressure ventilation will impair hepatic venous drainage and splanchnic blood flow. If artificial ventilation is required, neuromuscular blockade should be achieved with a long acting nondepolarizing neuromuscular blocking agent (e.g., 0.1 mg/kg pancuronium bromide, Sigma).

6. Cannulate the right jugular vein, the left carotid artery, or a femoral artery using polyethylene tubing (PE 50).

   To avoid clotting use PE tubing that is coated with tridodecylmethylammonium heparinate (TDMAC, see Support Protocol 2). If two arteries need to be cannulated, e.g., for insertion of a thermistor-tipped probe allowing measurement of cardiac output and invasive blood pressure reading/blood withdrawal, a carotid and a femoral artery can be used. In this case, the thermistor-tipped probe is inserted through the carotid artery and must be advanced to the aortic root, while the arterial line is placed into the femoral artery. Never cannulate two carotid arteries since bilateral ligation of the carotid arteries in combination with hemorrhagic hypotension induces brain ischemia and respiratory arrest.

7. Start a constant infusion of an isotonic Ringers solution (10 ml/kg/hr) immediately after establishing venous access to compensate for evaporative losses during surgery. Continue this infusion in time-matched sham-operated animals for the whole experiment. Measure the arterial blood pressure continuously by connecting the arterial line to a pressure transducer.

Induce hemorrhagic shock and resuscite

8. After a stabilization period of 15 min and recording of baseline hemodynamics, induce hemorrhagic hypotension by blood removal via the arterial line, collecting shed blood in 5-ml syringes containing citrate-phosphate-dextrose solution to avoid clotting.

   The required shed blood volume to achieve a mean arterial pressure (MAP) of 35 to 40 mmHg is ~2 to 2.5 ml/100 g body weight. The target pressure should be achieved within 5 min.

   The use of heparin as the anticoagulant for shed blood storage should be avoided since heparin has a substantial protective effect in this model.

9. Maintain target MAP by withdrawal of small amounts of blood (0.2 to 0.4 ml) during the early ("compensatory") phase of hemorrhage or by reinfusion of saline during the late ("decompensatory") phase.

10. Resuscitate by retransfusion of 60% of shed blood over 20 min and three times the shed blood volume of Ringers solution over 2 hr.

If the hemorrhagic hypotension is limited to 60 to 90 min, a complete recovery of central and liver regional hemodynamics can be achieved with this protocol ("reversible shock"). Longer periods may result in irreversible shock. However, even with restoration of (supra-) normal central hemodynamics, some degree of microvascular failure of the sinusoids will ensue.

MEASUREMENT OF CARDIAC OUTPUT AND REGIONAL FLOW

SUPPORT PROTOCOL 1

If measurement of cardiac output is required (for most experimental conditions this is optional), it can be achieved by the transpulmonary dilution technique (Bauer et al., 1996).

A bolus of 0.1 ml cold physiological saline is injected into the central venous line and cardiac output can be calculated from the area under the curve of the temperature reading of the thermistor tip (thermistor tip catheter, Columbus Instruments) placed in the aortic arch according to the Fick principle (e.g., on a cardiac output computer, Cardiomax II, Columbus Instruments). Although techniques using microspheres allow accurate measurements of systemic and liver regional hemodynamics (Hauptman et al., 1989; Chaudry et al., 1993; Van Oosterhout et al., 1998), the use of the thermodilution technique has the advantage that it allows repeated measurements of cardiac output. The thermodilution technique yields somewhat higher cardiac output values than other techniques due to the heat loss of the injectate from the vascular system and should therefore be reported as percent of baseline.

If measurements of regional blood flow are required, this can be achieved in the rat for most organs, including both inflows of the liver, by ultrasonic flow probes placed around the feeding vessels, e.g., hepatic artery and portal vein (T206, small animal flow meter, Transonic; Bauer et al., 1996; D'Almeida et al., 1996). In addition, high resolution intravital microscopy can be used to directly assess sinusoidal perfusion and hepatocellular mitochondrial redox state, since the sinusoid is an important site of blood flow regulation (Clemens and Zhang, 1999). While the latter technique is fairly sophisticated and requires expensive equipment, a simple method to assess microvascular perfusion and hepatocellular clearance capacity has been described using in vivo indocyanine green (ICG) clearance. After a bolus injection, plasma concentrations of ICG are measured and the maximum rate of ICG clearance (V_{max}) and Michaelis-Menten constant (K_m) are calculated (Hauptman et al., 1989; Chaudry et al., 1993).

COATING OF POLYETHYLENE TUBING WITH TDMAC

SUPPORT PROTOCOL 2

To prevent clotting, tridodecylmethylammonium (TDMAC) heparinate is used to coat the inner surface of polyethylene tubing.

CAUTION: TDMAC heparinate is highly toxic; see Material Safety Data Sheets for guidelines regarding handling, storage, and disposal. TDMAC heparinate is highly flammable, keep container tightly closed.

Materials

2% (w/w) solution (~1000 USP U/ml) TDMAC-heparin
(tridodecylmethylammonium heparinate; Polysciences)
Source of constant nitrogen flow

1. Coat the inner surface of the polyethylene tubing by refluxing in a 2% TDMAC-heparin solution.
2. Incubate 2 to 3 hr at 40° to 50°C.
3. Remove TDMAC-heparin by blowing a dry stream of nitrogen for 20 min through the tubing.
4. Air dry 1 to 3 hr at room temperature.
5. After drying, autoclave coated tubing.

REAGENTS AND SOLUTIONS

*Use Milli-Q-purified water or equivalent in all recipes and protocol steps. For common stock solutions, see **APPENDIX 2A**; for suppliers, see **SUPPLIERS APPENDIX**.*

Citrate-phosphate-dextrose solution, pH 5.6

0.327 g citric acid monohydrate
2.63 g sodium citrate dihydrate
2.32 g anhydrous glucose in injection-grade water
Bring to 100.0 ml; filter sterilize
Store up to 1 week at 4°C
Osmolality: 438 mOsmol/kg

Ringers solution

147 mM NaCl
4 mM KCl
2.3 mM $CaCl_2$
For 1 liter:
8.6 g NaCl
0.3 g KCl
0.33 g $CaCl_2$ in injection-grade water
Bring to 1000.0 ml
Filter sterilize or autoclave before use
Store up to 4 weeks at room temperature

COMMENTARY

Background Information

Various models of hypovolemic shock have been described since the original report by Penfield (1919) of a fixed-pressure model of hemorrhagic hypotension.

These models differ primarily with respect to the physiological endpoint to define the degree of injury. While fixed-pressure (as described above) or fixed-volume (i.e., defined by the amount of blood removed) models are easily used in small animal preparations, more sophisticated models, e.g., directly assessing oxygen debt, are restricted to large animals such as dogs or sheep.

The described model of hemorrhagic shock-induced injury to the pericentral region of the liver acinus allows for the infliction of a graded and defined dysfunction of those parenchymal cells of the liver primarily responsible for metabolism of xenobiotics. This dysfunction can be easily assessed by measuring clearance of drugs, such as indocyanine green (Hauptman et al., 1989; Chaudry et al., 1993). Moreover, the impact of therapeutic agents can be studied in a model closely mimicking the pathophysiology of many surgical conditions associated with development of secondary liver dysfunction.

Table 14.3.1 Typical Measurements Obtained from Hemorrhagic and Sham-Operated Animals[a,b]

Measurement	Baseline	End of shock	5 hr resuscitation
Mean arterial pressure [mmHg]	117.3 ± 5.44 (119 ± 4.33)	38.9 ± 0.50 (105.3 ± 3.23)	100.9 ± 4.35 (98.0 ± 4.98)
Heart rate [min^{-1}]	367.2 ± 8.98 (376.0 ± 11.45)	358.8 ± 19.05 (386.0 ± 16.22)	398.4 ± 15.05 (354.0 ± 8.63)
Cardiac output [% of baseline]	100.0 (100.0)	36.0 ± 3.59 (104.0 ± 4.02)	109.1 ± 6.08 (114.2 ± 5.93)
Hepatic arterial blood flow [ml/min]	3.4 ± 0.66 (3.4 ± 0.66)	0.7 ± 0.12 (3.1 ± 0.48)	2.5 ± 0.42 (2.4 ± 0.37)
Portal venous blood flow [ml/min]	19.5 ± 2.88 (19.5 ± 2.88)	7.0 ± 1.16 (17.8 ± 2.23)	18.8 ± 1.98 (15.9 ± 1.24)
pH	7.38 ± 0.01 (7.38 ± 0.02)	7.26 ± 0.02 (7.39 ± 0.02)	7.45 ± 0.01 (7.42 ± 0.01)
pO_2 [mmHg]	80.7 ± 5.47 (73.2 ± 4.68)	100.7 ± 18.07 (74.3 ± 5.10)	84.1 ± 3.49 (83.0 ± 3.69)
pCO_2 [mmHg]	51.6 ± 2.43 (49.4 ± 1.96)	34.0 ± 2.46 (41.9 ± 8.12)	40.5 ± 1.68 (40.9 ± 1.07)
Base excess [mmol/liter]	3.5 ± 0.85 (2.6 ± 0.99)	−11.8 ± 1.14 (3.5 ± 0.64)	2.8 ± 0.39 (1.5 ± 0.75)
Hemoglobin [g/100 ml]	12.71 ± 0.34 (12.35 ± 0.38)	8.72 ± 0.41 (11.38 ± 0.36)	9.87 ± 0.36 (11.58 ± 0.32)
White blood count [$\times 10_3/\mu l$]	7.05 ± 0.72 (8.16 ± 1.08)	3.57 ± 0.53 (5.43 ± 0.61)	7.17 ± 0.57 (7.52 ± 0.32)
Platelets [$\times 10_3/\mu l$]	1016.1 ± 18.05 (980.3 ± 52.17)	764.4 ± 42.71 (965.4 ± 56.67)	952.1 ± 32.67 (1020.8 ± 40.72)
α-Glutathione-*S*-transferase [μg/liter]	43.2 ± 10.33 (33.2 ± 3.79)	n.d. n.d.	557.4 ± 175.00 (61.7 ± 33.51)

[a]Data are mean ± SEM for 6 independent, individual experiments for each time point and treatment: baseline, end of shock, and after 5 hr of resuscitation; data in parentheses are obtained from time-matched sham-operated animals.

[b]Abbreviations: n.d. = not determined.

The molecular sequelae of hemorrhage and resuscitation include the activation of redox-sensitive transcription factors (most notably heat shock factor and activator protein-1) and dependent gene products such as heat shock protein 70 or heme oxygenase-1.

Critical Parameters and Troubleshooting

The amount of ischemic injury in the described model will vary with duration of hemorrhagic hypotension, the blood pressure maintained during the period of hemorrhagic hypotension, and as a function of variables affecting oxygen consumption, such as body temperature and plane of anesthesia. The liver glutathione content is a critical determinant for hepatocellular injury. The best single predictor to assess ischemic tissue injury and systemic oxygen debt is the base deficit. Repeated measurements of base deficit during hemorrhagic hypotension can help to define the degree of global ischemic injury.

Anticipated Results

Table 14.3.1 summarizes systemic and liver hemodynamics, gas exchange, acid-base status, and hepatocellular injury with the described model of reversible shock (1 hr of hemorrhagic hypotension at 35 to 40 mmHg). Values in parentheses indicate data obtained in sham-operated time-matched controls.

Figure 14.3.1 illustrates the differential expression pattern and time course of the redox-sensitive transcription factors activator protein (AP)-1 and nuclear factor (NF) κB as assessed by electrophoretic mobility shift assay. While the described model of hemorrhage and resus-

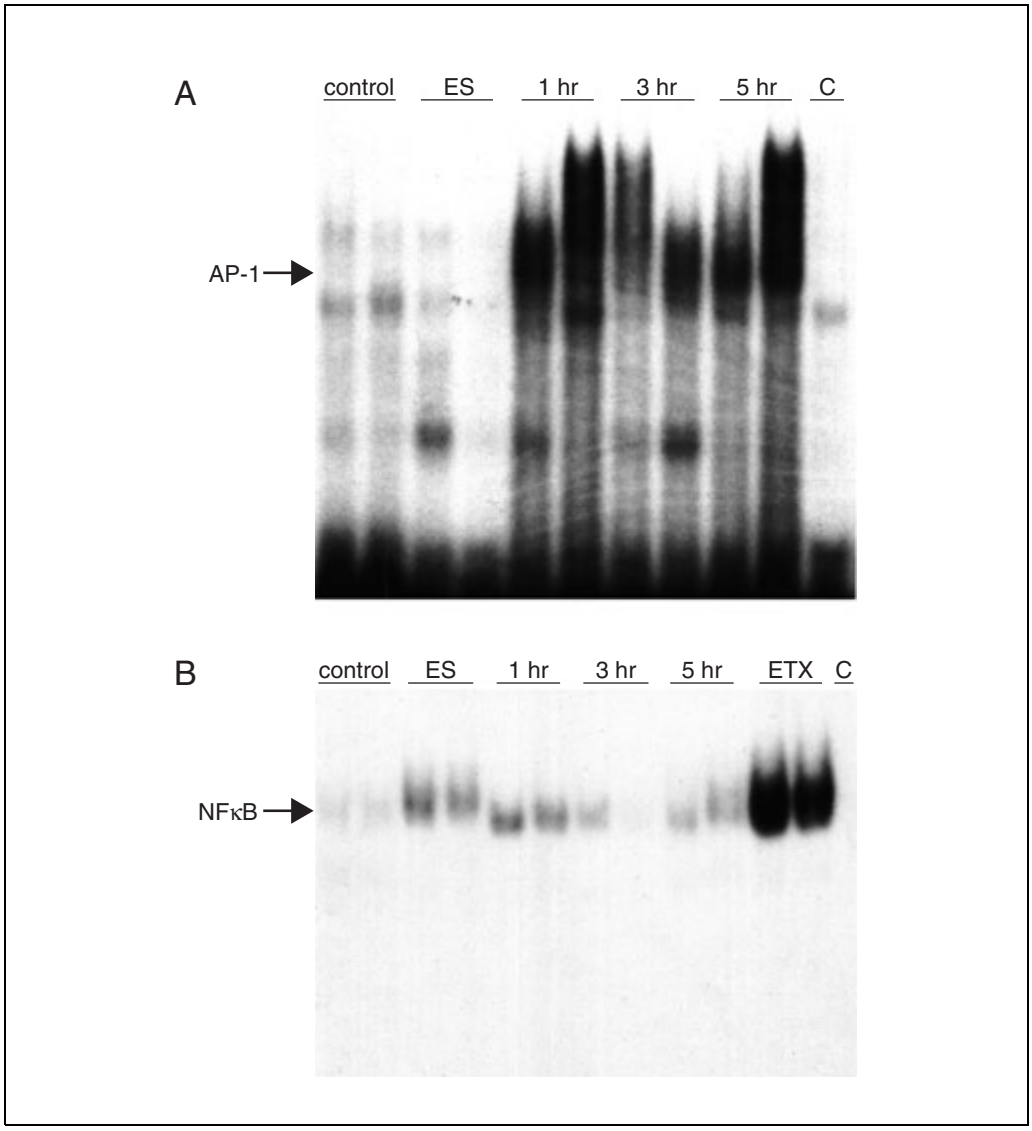

Figure 14.3.1 Differential expression of AP-1 (**A**) and NFκB (**B**) in animals subjected to hemorrhage. ES: end of hemorrhagic hypotension; 1 hr: 1 hr after onset of resuscitation; 3 hr: 3 hr after onset of resuscitation; 5 hr: 5 hr after onset of resuscitation. (**B**) ETX: NFκB binding activity in nuclear protein extracts obtained from 2 animals injected with *E. coli* endotoxin (1 mg/kg body weight) 6 hr prior to preparation of nuclear protein (positive control).

citation is a strong activator of AP-1 binding activity, only a faint activation of NFκB is observed.

Figure 14.3.2 shows the differential expression pattern and time course of transcripts encoding typical stress proteins, i.e., heme oxygenase-1, the heat shock protein hsp 70, and the acute phase reactant β-fibrinogen, as assessed by northern blot hybridization.

While hemorrhagic shock is a faint inducer of the acute phase reactant β-fibrinogen, a strong induction of the heat shock proteins hsp 32 (heme oxygenase-1) and hsp 70 over sham operated controls is associated with resuscitation from hemorrhage. The induction of hsp 70 in this model is typically biphasic with an early moderate and a late substantial increase in steady state transcripts (Fig. 14.3.2). Inter-animal variability associated with the model correlates with time course and degree of pericentral injury.

Time Considerations

The time required to perform the surgical instrumentation for hemodynamic measurements will vary depending on the parameters studied: standard tracheotomy and cannulation of a central venous and an arterial line can be achieved in <15 min while placement of transit-time ultrasound flow probes may be time-consuming and requires experience. Significant changes in hepatocellular function (e.g.,

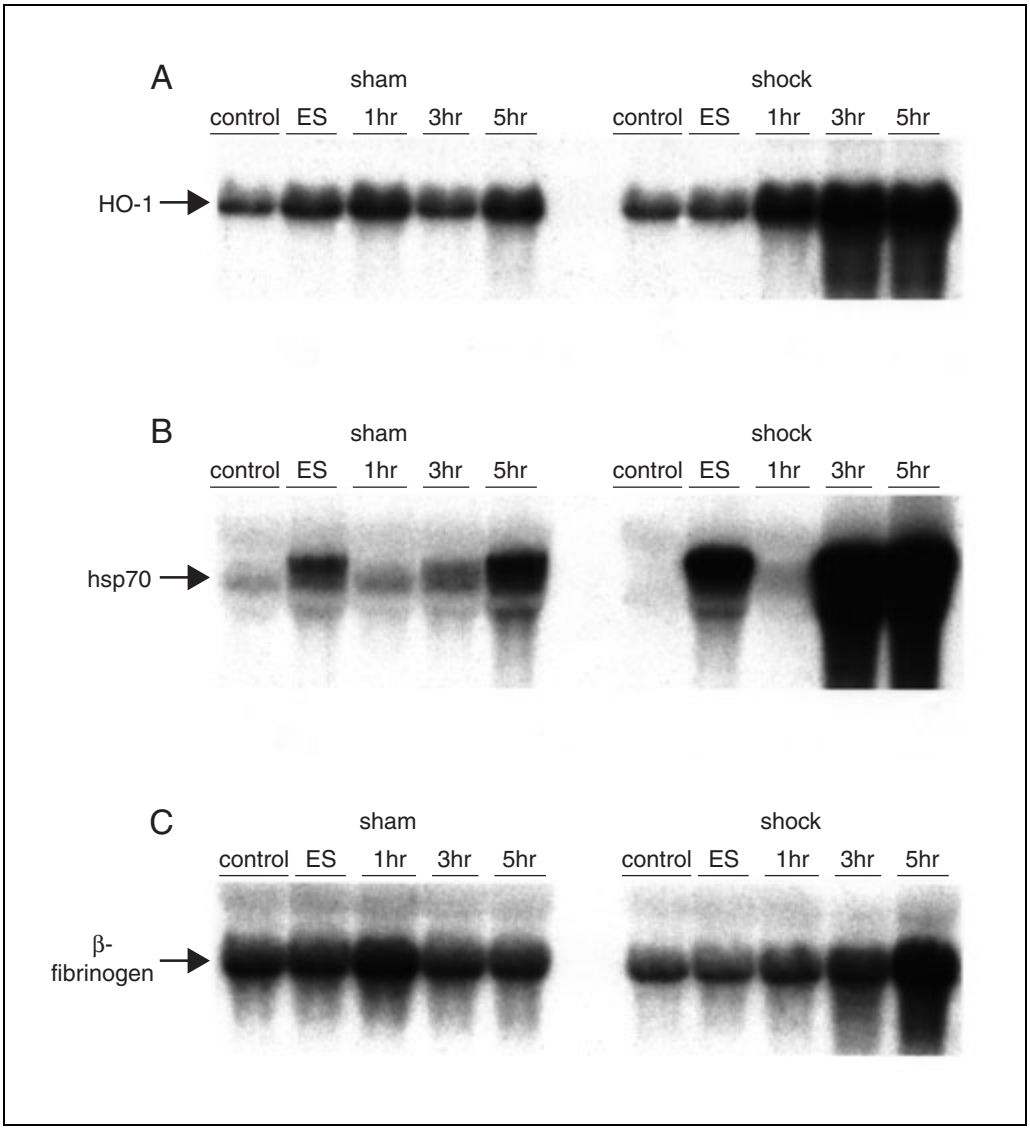

Figure 14.3.2 Differential expression of Heme oxygenase 1 (**A**), heat shock protein 70 (**B**), and β-fibrinogen (**C**) in animals subjected to hemorrhage. Left panels: samples obtained from sham-operated time-matched controls without hemorrhage; right panels: samples obtained from animals subjected to hemorrhagic hypotension (1 hr, 40 mmHg) and subsequent fluid resuscitation. ES: end of hemorrhagic hypotension; 1 hr: 1 hr after onset of resuscitation; 3 hr: 3 hr after onset of resuscitation; 5 hr: 5 hr after onset of resuscitation.

alterations in clearance capacity for ICG) and activation of transcription factors occur already during hemorrhagic hypotension or early upon resuscitation while expression of stress proteins as well as influx of inflammatory cells may require several hours (see Figs. 14.3.1 and 14.3.2).

Literature Cited

Bauer, M., Pannen, B.H.J., Bauer, I., Herzog, C., Wanner, G.A., Hanselmann, R., Zhang, J.X., Clemens, M.G., and Larsen, R. 1996. Evidence for a functional link between stress response and vascular control in hepatic portal circulation. *Am. J. Physiol.* 271:G929-G935.

Chaudry, I.H., Wang, P., Singh, G., Hauptman, J.G., and Ayala, A. 1993. Rat and mouse models of hypovolemic-traumatic shock. *In* Pathophysiology of Shock, Sepsis, and Organ Failure (G. Schlag and H. Redl, eds.) pp. 371-383. Springer, New York.

Clemens, M.G. and Zhang, J.X. 1999. Regulation of sinusoidal perfusion: In vivo methodology and control by endothelins. *Semin. Liver Dis.* 19:383-396.

D'Almeida, M.S., Cailmail, S., and Lebrec, D. 1996. Validation of transit-time ultrasound flow probes to directly measure portal blood flow in conscious rats. *Am. J. Physiol.* 271:H2701-H2709.

Hauptman, J.G., DeJong, G.K., Blasko, K.A., and Chaudry, I.H. 1989. Measurement of hepatocellular function, cardiac output, effective blood

volume and oxygen saturation in the rat. *Am. J. Physiol.* 257:R439-R444.

Hawker, F. 1991. Liver dysfunction in critical illness. *Anaesth. Intensive Care* 19:165-181.

Penfield, W.G. 1919. The treatment of severe and progressive hemorrhage by intravenous injections. *Am. J. Physiol.* 48:121-132.

Van Oosterhout, M.F., Prinzen, F.W., Sakurada, S., Glenny, R.W., and Hales, J.R. 1998. Fluorescent microspheres are superior to radioactive microspheres in chronic blood flow measurements. *Am. J. Physiol.* 275:H110-H115.

Contributed by Inge Bauer and
Michael Bauer
University of the Saarland
Homburg, Germany

Isolation of Liver Kupffer Cells

Kupffer cells (KCs), which are derived from the monocyte and macrophage cell lineage, are the resident macrophages of the liver. Though KCs make up <5% of the liver's volume, they represent ~80% of the total fixed macrophage population in the body. They play a major role in physiological processes as well as in the pathogenesis of several liver diseases.

To prepare pure cultures of parenchymal cells (PCs) and nonparenchymal cells (NPCs) including KCs for biochemical and cell physiological studies, several isolation methods have been recommended. The technique described in this unit is a simple and rapid procedure focusing on the isolation of KCs. The goal is to isolate large amounts of pure, viable, and functional cells without changing physiological properties or destroying components of the cytoplasmic membrane.

The isolation method can be used for rat (average size of 200 to 250 g) and mouse (average size of 20 to 25 g). The procedure is very similar for both rodents, and any methodological differences in the isolation of KCs from rats or mice will be explained as annotations to the individual steps. In general, the main text describes the procedure and amounts used for one rat liver.

The method described in the Basic Protocol will provide viable KCs in large amounts, which can be used for further investigations. It is based on collagenase perfusion of the liver, isopycnic sedimentation in Percoll, and selective adherence of the cells in culture. The protocol is subdivided into six main parts (animal preparation, operation procedures, liver perfusion, centrifugation, cell counting and viability check, and inoculation and culture).

The method is normally used to isolate NPCs (Kupffer and stellate cells) and PCs. Because of the authors' focus on KC isolation, only passing mention is made about the PCs and the stellate cells in the individual steps. Please see appropriate protocols for further handling of these cell fractions (Smedsrød and Pertoft, 1985).

NOTE: All solutions and equipment coming into contact with living cells must be sterile, and aseptic technique should be used accordingly.

NOTE: All culture incubations should be performed in a humidified 37°C, 5% CO_2 incubator unless otherwise specified.

Materials

Rat
50 mg/ml Nembutal sodium solution (Abbott Laboratories)
100% (v/v) ethanol
CMF-HBSS (see recipe), 37°C
0.02% (w/v) collagenase type IV in HBSS (see recipe), made fresh
PBS (see recipe)
HBSS (see recipe)
50%/25% two-step Percoll gradient (see recipe) in 50-ml conical centrifuge tubes
0.4% (w/v) trypan blue solution (Sigma)
RPMI medium 1640 (Life Technologies) containing 1× antibiotic and antimycotic solution (Sigma) and 10% (v/v) fetal bovine serum (FBS; Life Technologies)

Contributed by Matthias Froh, Akira Konno, and Ronald G. Thurman
Current Protocols in Toxicology (2002) 14.4.1-14.4.12

1/2-cc insulin syringe
Shaver
Surgical tools (sterile), including:
  Scissors
  Forceps
Pins or dots, sterile
Sterile threads (~15 to 20 cm long)
20-G catheter
Perfusion system that allows regulation of the flow rate
Petri dishes, sterile
Nylon gauze (50-μm mesh width), sterile
50-ml conical centrifuge tubes
Large-capacity centrifuge with adjustable brake, swing-out rotor, and speed up to $2000 \times g$, 4°C
Glass or plastic coverslips or tissue culture dishes, sterile

Additional reagents and equipment for counting cells with a hemacytometer and determining viability using trypan blue exclusion (*APPENDIX 3B*)

Prepare animal

1. Weigh a rat.

   Alternatively, a mouse can be used.

   The animal should always be held by the neck. If the experimenter is not experienced in handling animals, a special covered glove (rat glove) should be worn to protect from bites.

2. Anesthetize the animal using a 50-mg/ml Nembutal sodium solution injected intraperitoneally using a 1/2-cc insulin syringe (50 mg Nembutal/kg body weight).

   Either the lower right or left abdominal quadrant makes a good intraperitoneal injection point (Fig. 14.4.1A).

   The syringe should be aspirated to make certain that the needle did not enter a blood vessel.

3. Use a shaver to shave the whole abdomen and lower thorax of the animal.

4. Secure the animal to the workstation by taping its legs and sterilize its abdomen and thorax with 100% ethanol (Fig. 14.4.1A). Confirm that the animal is well anesthetized and is breathing regularly.

   The operation should be performed at a clean workstation under sufficient light. All tools (e.g., scissors, forceps, perfusion system, glass bottles, culture tubes) need to be sterilized before use.

Operate

5. Use a pair of scissors to open the abdomen by making a median incision 1 to 2 cm above the hind legs, and continuing up to the sternum. Make sure that the diaphragm is intact. Proceed with one horizontal incision on each side ending at the rib cage. Use forceps to reflect the flaps consisting of skin and muscle layers toward the head and secure them using pins or dots (Fig. 14.4.1B).

   If the isolation of KCs from more then one animal is planned, the authors recommend performing the operations successively. An alternative would be to perform the first isolation through step 20, place the supernatant on ice, carry out the second isolation up to step 20, and then finish both preparations simultaneously from step 21.

6. Pass a sterile thread under the inferior vena cava (IVC) at a level just below the liver and ligate loosely (Fig. 14.4.1C).

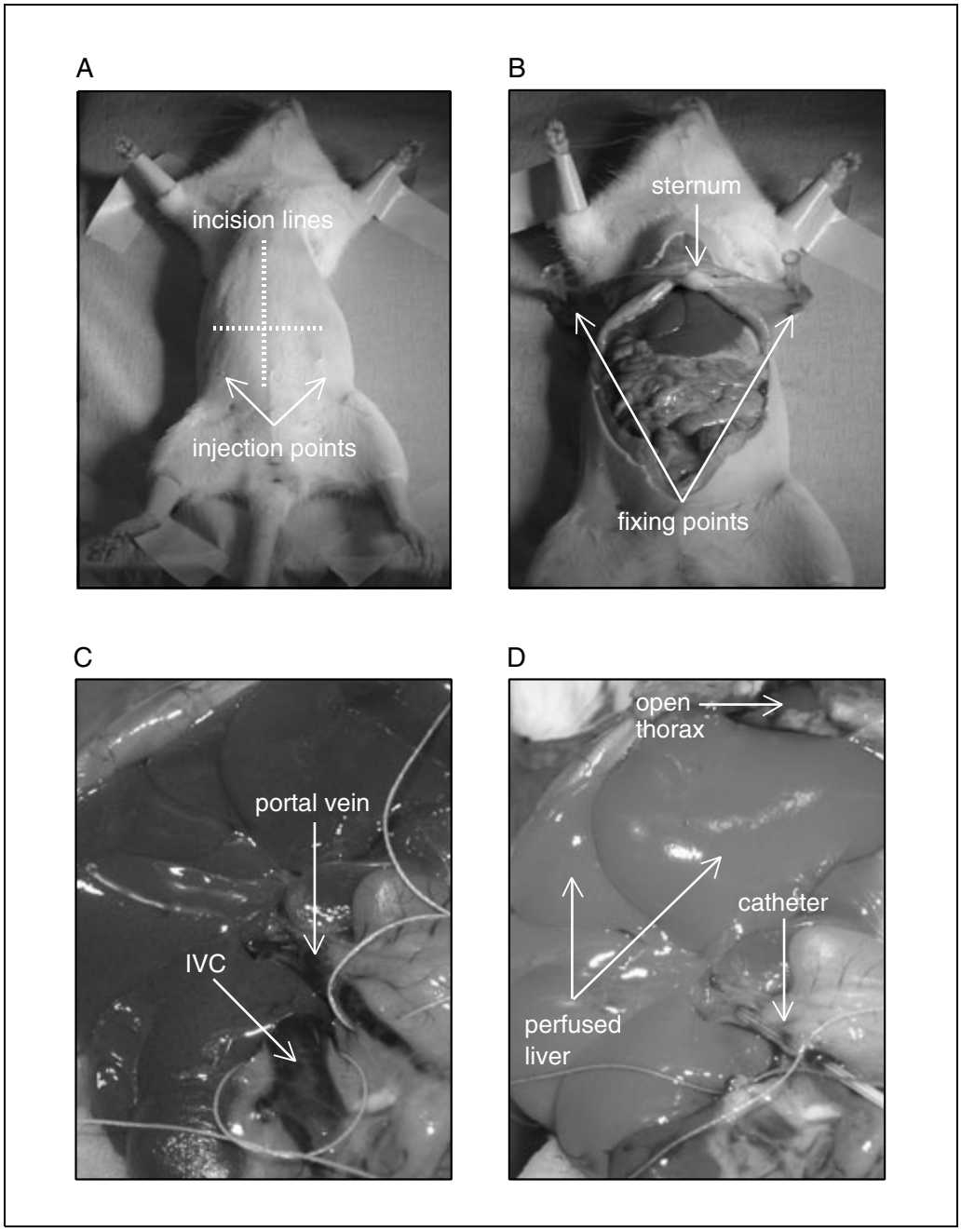

Figure 14.4.1 Animal preparation and operation procedure. (**A**) Orientation and securing of the animal to the workstation. Recommended incision lines and intraperitoneal injection points are indicated. (**B**) Opened abdomen after median and horizontal incisions. (**C**) Loosely tied threads around the inferior vena cava (IVC) and portal vein. (**D**) Perfused liver after cutting the IVC and the abdominal artery and opening the thorax. The catheter is placed in the portal vein, fixed with a thread, and the IVC is ligated. *This black and white facsimile of the figure is intended only as a placeholder; for full-color version of figure go to http://www.currentprotocols.com/colorfigures.*

7. Pass a sterile thread under the portal vein and ligate loosely (Fig. 14.4.1C).
8. Insert a 20-G catheter into the portal vein, ligate the thread tightly around the portal vein to secure the catheter, and connect a perfusion system that includes prewarmed CMF-HBSS to the catheter (Fig. 14.4.1D).

   For a mouse, a 24-G catheter is used.

   The perfusion system and catheter must be free of air. The CMF-HBSS used for the perfusion should be kept at 37°C in a water bath during the procedure.

Perfuse liver

9. Begin perfusing at a rate of 20 ml/min and cut the distal part of the IVC below the ligature and the abdominal artery to make an overflow and get the blood out of the vascular system.

   For a mouse, the IVC is cut just before the perfusion system is connected to the catheter. This is done to prevent pressure damage in the liver as a result of the small blood volume in mice. The perfusion rate is 8 ml/min.

10. Open the thorax and cut the heart.
11. Ligate the thread tightly around the IVC under the liver (Fig. 14.4.1D) and continue perfusion for 10 min.

    For a mouse, the perfusion is continued for 3 min.

    At this point the entire liver should be perfused (as indicated by a change in color from dark to light brown).

12. Change the perfusion solution to 0.02% collagenase type IV in HBSS and perfuse 10 min at a rate of 20 ml/min (200 ml total volume).

    For a mouse, 0.03% to 0.04% collagenase type IV in HBSS is perfused for 4 min at a rate of 5 ml/min (20 ml total volume).

    When the solutions are changed, a constant flow should be maintained and air must not get into the system.

    Including enzymatic digestion during the liver perfusion will yield cells that are free of desmosomes and tight junctions, which loosens cellular attachments to the extracellular matrix.

13. Remove the liver from the animal, rinse it briefly with PBS to get rid of any blood on the outside, place it in a sterile petri dish, and cover it with ~50 ml of 0.02% collagenase type IV in HBSS.

    When removing the liver, the gut must not be cut or punctured, which would release endotoxins or bacteria into the liver homogenate.

14. Gently tease the liver with forceps until it is in solution.
15. Filter the cell suspension through sterile nylon gauze to remove undigested tissue and connective tissue.
16. Transfer the filtered cell suspension to two 50-ml conical centrifuge tubes and fill them with HBSS.

Centrifuge suspensions

17. Centrifuge suspensions 3 min at 70 × *g*, 4°C (maximal brake).

    For a mouse, the suspension is centrifuged 3 min at 35 × g.

    All steps between the centrifugations are performed in 50-ml tubes that are placed on ice.

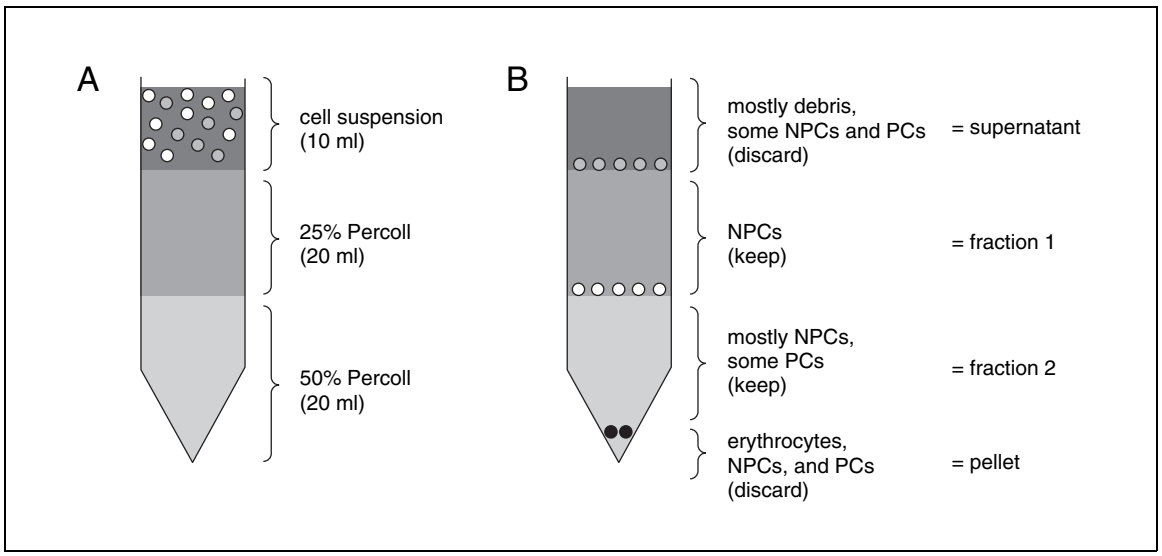

Figure 14.4.2 Isopycnic (gradient) centrifugation with Percoll. (**A**) The cell suspension, including mostly nonparenchymal cells (NPCs), is placed on a 50%/25% two-step Percoll gradient before centrifugation. (**B**) After centrifugation, the cells are separated into four fractions; fraction 1 has the highest concentration of Kupffer cells. PC, parenchymal cell.

18. Transfer supernatants to clean 50-ml tubes and place on ice. Resuspend pellets by filling tubes with HBSS to 50 ml.

    The supernatant contains mainly NPCs (Kupffer and stellate cells), whereas the pellet contains mainly PCs (mostly hepatocytes). If hepatocytes need to be collected, these pellets (and also those from step 19) can be used with an appropriate protocol (Smedsrød and Pertoft, 1985).

19. Centrifuge resuspended pellets 3 min at 70 × *g*, 4°C (maximal brake). Transfer supernatants to clean 50-ml tubes, place on ice, and discard pellets.

    For a mouse, centrifuge 3 min at 25 × g, 4°C (maximal brake). Keep the supernatant and resuspend the pellet again in HBSS. Centrifuge the resuspended pellet 3 min at 20 × g, 4°C (maximal brake).

    The additional centrifuge steps with the resuspended pellet are performed to separate the PC and NPC fractions as completely as possible.

20. Fill both supernatant tubes (steps 18 and 19) to 50 ml with HBSS if needed.

    For a mouse, all three supernatant tubes (from the three centrifugation steps) should be filled.

21. Centrifuge tubes 7 min at 650 × *g*, 4°C (maximal brake).

    The pellet contains mostly Kupffer and stellate cells and some PCs, erythrocytes, and cell debris.

22. Discard supernatants and resuspend pellets in 10 ml HBSS per tube by gently pipetting.

23. Carefully layer cell suspension from each tube onto a 50%/25% two-step Percoll gradient in a 50-ml conical centrifuge tube. Try to avoid mixing the cell suspension with the upper Percoll layer (Fig. 14.4.2A).

24. Centrifuge tubes 15 min at 1800 × *g*, 4°C (brake off).

25. Carefully remove upper layer (supernatant) from each tube and discard. Collect middle layers (fractions 1 and 2) of both tubes together into one new 50-ml tube and fill tube with HBSS (Fig. 14.4.2B). Discard pellets.

    The cells are distributed into four distinct zones in the gradient (Fig. 14.4.2B). The upper zone (supernatant) includes material that did not penetrate the upper Percoll cushion (mainly debris, damaged cells, and a few viable NPCs). The intermediate zones (fractions 1 and 2) contain mainly purified NPCs. The pellet consists of erythrocytes, NPCs, and PCs.

    If stellate cells need to be purified, fraction 1 alone should be collected using an appropriate protocol (Smedsrød and Pertoft, 1985).

26. Centrifuge pooled middle layers 7 min at 650 × *g*, 4°C (maximal brake).

27. Discard supernatant and resuspend pellet in 5 ml HBSS with gentle pipetting.

    For a mouse, the pellet should be resuspended in 1 ml HBSS.

    The actual HBSS volume in which the pellet is suspended, which will depend on the subsequent experiments that the investigator will carry out, should be determined by further experimentation.

Count cells and check viability

28. Mix 10 µl KC solution (step 27) and 10 µl of 0.4% trypan blue solution in a tube by gently pipetting.

29. Use 10 µl of the mixture to determine cell number and viability (*APPENDIX 3B*). Also check the purity (e.g., KCs, hepatocytes, bacteria, cell debris) of the cells (Fig. 14.4.3A).

    This is only a crude measure of purity and viability. Normally, assessment of cell purity requires morphological, biochemical, histochemical, or immunohistochemical methods to identify specific cells of interest. Because of difficulties identifying KCs after isolation (depending on the investigator's level of experience), cell-specific cytochemical assays (peroxidase, acid phosphatase) and morphological techniques (India ink or colloidal carbon phagocytosis) are often used. A simple method to identify KCs and exclude other cells morphologically (by light and fluorescence microscope) is to observe the uptake of latex beads in the cells (Shaw et al., 1984; Fig. 14.4.3B).

    The easiest technique for assessing cell viability is the trypan blue exclusion method (Fig. 14.4.3A). Other choices for determining cell yield and viability depend on the available time and equipment (e.g., electronic Coulter counters, channelyzers) but are usually impractical because of the cost of these instruments.

Inoculate cultures

30. Plate cells at an appropriate density on glass or plastic coverslips or tissue culture dishes and culture them in RPMI medium 1640 containing 1× antibiotic and antimycotic solution and 10% FBS for 15 min at 37°C.

    The number of cells plated will depend on the size of the coverslip or dish and on the subsequent experiments. In general, 0.5 to 50 × 10^6 cells per dish is appropriate.

    The final concentrations of the antibiotics and antimycotic are 100 U/ml penicillin G, 100 µg/ml streptomycin sulfate, and 0.25 µg/ml amphotericin B.

31. Remove nonadherent cells by replacing the culture medium.

    To obtain a pure monolayer culture of KCs, an incubation time of 15 min was chosen based on the selective adherence (i.e., attachment and spreading) of KCs to glass or plastic surfaces.

32. Culture cells for an appropriate period (usually ≥24 hr) prior to experiments.

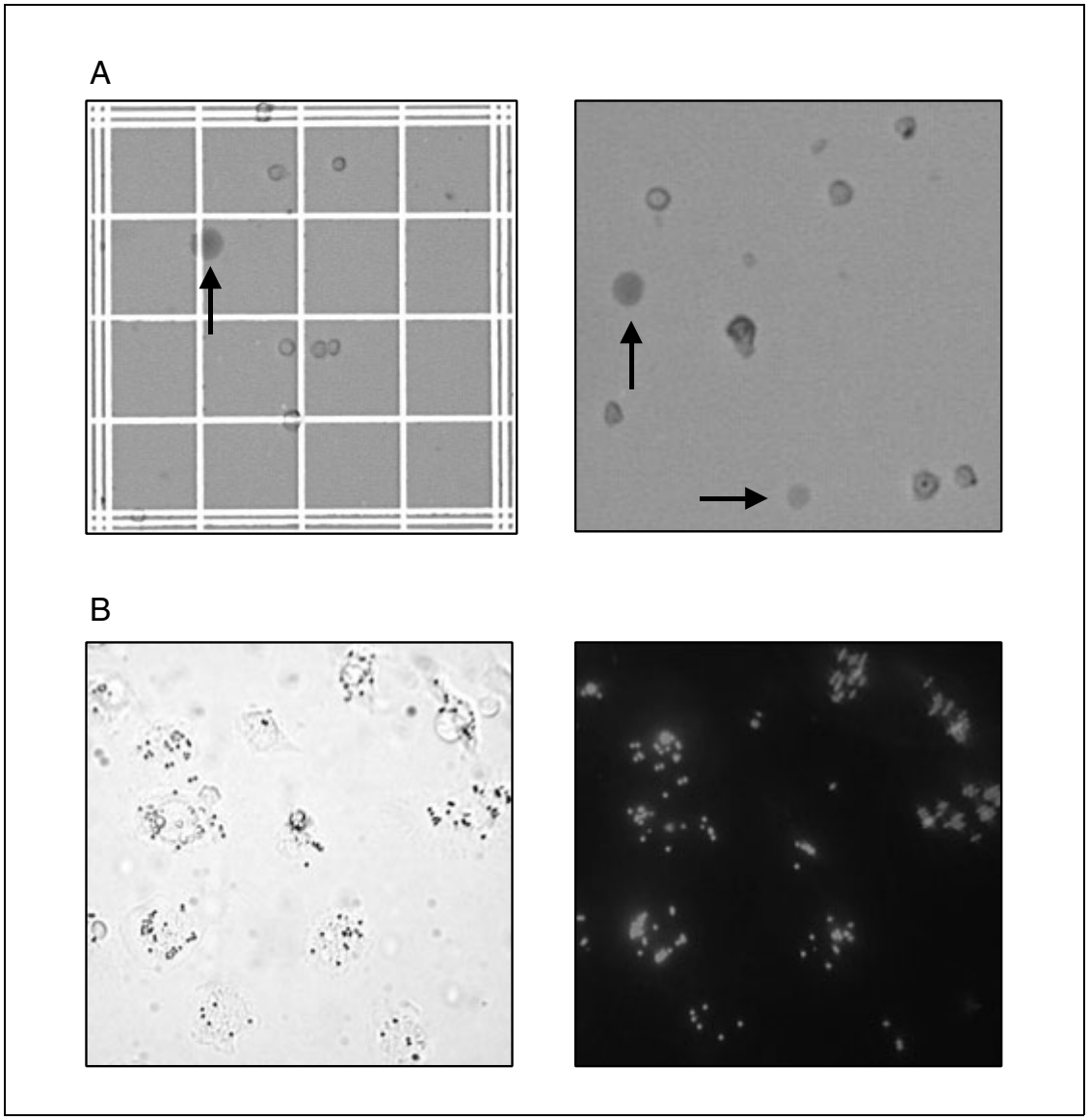

Figure 14.4.3 Assessment of Kupffer cell (KC) purity and viability. (**A**) Cell count on a hemacytometer by trypan blue exclusion (viability check). Arrows in left and right panels indicate excluded cells (blue cells). (**B**) Purity check by the uptake of latex beads in KCs. Left panel is with and right panel is without a green filter, which shows the uptake of latex beads by their fluorescence. *This black and white facsimile of the figure is intended only as a placeholder; for full-color version of figure go to http://www.currentprotocols.com/colorfigures.*

REAGENTS AND SOLUTIONS

*Use Milli-Q-purified water or equivalent in all recipes and protocol steps. For common stock solutions, see **APPENDIX 2A**; for suppliers, see **SUPPLIERS APPENDIX**.*

Ca^{2+}- and Mg^{2+}-free Hanks' balanced salt solution (CMF-HBSS)

Make up HBSS (see recipe) without $MgSO_4 \cdot 7H_2O$ and $CaCl_2 \cdot 7H_2O$. Add 0.19 g EGTA (0.5 mM final). Adjust the pH to 7.2 at room temperature with 1 M NaOH or 1 M HCl. Filter sterilize using 0.22-µm filters and store up to 3 months at 4°C.

For convenience, a 10× CMF-HBSS stock (without sodium bicarbonate, EGTA, pH adjustment, and filtration) can be made.

Hanks' balanced salt solution (HBSS)

8 g NaCl (138 mM final)
0.4 g KCl (5.4 mM final)
0.091 g $Na_2HPO_4 \cdot 7H_2O$ (0.3 mM final)
0.06 g KH_2PO_4 (0.4 mM final)
1 g dextrose (5.6 mM final)
0.2 g $MgSO_4 \cdot 7H_2O$ (0.8 mM final)
0.185 g $CaCl_2 \cdot 7H_2O$ (1.26 mM final)
0.35 g $NaHCO_3$ (4 mM final)
Add H_2O to 1 liter
Adjust pH to 7.4 at room temperature with 1 M NaOH or 1 M HCl
Filter sterilize using 0.22-μm filters
Store up to 3 months at 4°C

A 10× HBSS stock (without sodium bicarbonate, pH adjustment, and filtration) can be made.

Percoll solution, 50%

Dissolve 0.35 g $NaHCO_3$ (4 mM final) in 400 ml water and add 500 ml of 100% Percoll (Amersham Pharmacia Biotech) and 100 ml of 10× HBSS (see recipe; final density ~1.065 g/ml). Adjust pH to 7.4 at room temperature with 1 M NaOH or 1 M HCl. Filter sterilize using 0.22-μm filters and store up to 1 month at 4°C.

Percoll solution, 25%

For 20 ml, add 10 ml of 50% Percoll solution (see recipe) and 10 ml HBSS (final density ~1.037 g/ml). Always make fresh.

Phosphate-buffered saline (PBS)

8 g NaCl (138 mM final)
0.2 g KCl (2.7 mM final)
2.17 g $Na_2HPO_4 \cdot 7H_2O$ (8.1 mM final)
0.2 g KH_2PO_4 (1.5 mM final)
Add H_2O to 1 liter
Adjust pH to 7.4 at room temperature with 1 M NaOH or 1 M HCl
Filter sterilize using 0.22-μm filters
Store up to 3 months at 4°C

Two-step Percoll gradient, 50%/25%

In a 50-ml conical centrifuge tube, carefully layer 20 ml of 50% (v/v) Percoll solution (see recipe) under 20 ml of 25% (v/v) Percoll solution (see recipe). Always make fresh.

COMMENTARY

Background Information

Kupffer cells (KCs) are macrophages that reside in the hepatic sinusoids, predominantly in periportal regions of the liver, and are usually attached to endothelial cells. They show receptor-mediated, nonspecific endocytotic activity, which is important for the uptake of foreign particles, mainly microorganisms and bacterial endotoxins. The first morphological observations pointing to this specific cell type date back to the work of Wedl (1854), and a few years later to that of Eberth (1867). In 1876, Karl von Kupffer published the first general description of this phagocytic, reticuloendothelial cell, which was later named after him (Kupffer, 1876). Since then, much work has been done to explain and characterize the specific properties and functions of these cells (Jones and Summerfield, 1988; Wake et al., 1989).

KCs can be activated by numerous agents including γ-interferon, platelet-activating factor (PAF), and endotoxins. Their response to these factors includes the release of physiologically active substances such as eicosanoids, inflammatory cytokines—interleukin 1 (IL-1), interleukin 6 (IL-6), tumor necrosis factor α

(TNF-α)—transforming growth factor β (TGF-β), interferon α and β, lysosomal enzymes, and free-radical species that participate in inflammation, immune responses, and modulation of hepatocyte metabolism. The factors released by activated KCs interact with other cell types leading to specific responses such as synthesis of acute-phase proteins, glucose production, vasoconstriction, apoptosis, cell proliferation, and even tissue injury. These factors participate in hepatic injury seen in sepsis, obstructive jaundice, transplantation, endotoxin shock, alcoholic liver disease, and other types of toxicant-induced liver injury.

Over the years, several methods have been introduced and modified to purify both parenchymal and nonparenchymal cells (Alpini et al., 1994). It would be beyond the scope of this unit to give a complete overview of the advantages and disadvantages of all isolation methods for liver cells including KCs. Summaries of the most significant methods are, however, provided (for further information, see references).

To produce a cell suspension from the liver, mechanical (Branster and Morton, 1957) and enzymatic (Alpini et al., 1989) dissociation techniques have been used. Collagenase has become widely used for the enzymatic digestion of the liver, more so than other proteolytic enzymes such as pronase and trypsin. Moreover, other approaches such as immunoaffinity (Munthe-Kaas et al., 1975), selective attachment (Smedsrød and Pertoft, 1985), sorting of fluorescence-labeled cells (Morin et al., 1984), selective cytotoxicity (Alpini et al., 1989), free-flow electrophoresis (Miller et al., 1983), and centrifugal techniques have been used to purify liver cells. In fact, cell separation of a specific subpopulation is best accomplished with a combination of these methods.

The most commonly used approaches to purify cells are centrifugal techniques including counterflow elutriation (Zahlten et al., 1978) and isopycnic (Smedsrød and Pertoft, 1985), velocity, and isokinetic gradient centrifugation (Brouwer et al., 1984). These methods are based on the properties of cell size or cell density. They vary in complexity and require expensive equipment. Finding the most appropriate protocol consequently depends on the general scientific approach (e.g., investigation of one specific cell type or comparison of liver cell subpopulations) and the availability of time and equipment.

To isolate KCs, enzymatic digestion with collagenase and/or pronase (Munthe-Kaas et al., 1975) by perfusion or by direct incubation with minced liver tissue (Branster and Morton, 1957) is often used. Because certain receptors at the cell surface are destroyed by pronase and reappear only after a period of cultivation, these isolated cells can be less useful in studies of physiological processes even though the method isolates KCs in high yields. Therefore, low-temperature isolation techniques (Praaning-Van Dalen et al., 1982) are combined to reduce damage to certain cell membrane proteins.

The purification of KCs is commonly performed with methods based on cell size or density, such as isopycnic centrifugation through gradient materials including Ficoll, metrizamide (Zahlten et al., 1978), Nycodenz (Blomhoff et al., 1984), Stractan (Friedman and Roll, 1987), or Percoll (Smedsrød et al., 1985). They vary in their ease of preparation (e.g., the Stractan method is complicated), length of storage (e.g., Ficoll is unstable once made up), viscosity, osmolarity, range of usable density, cell toxicity, and cost (e.g., Ficoll is expensive). The gradient centrifugations are normally followed by counterflow elutriation (which requires special rotors and centrifuges) and/or selective attachment methods. For completion, other isolation techniques use selective preloading of KC lysosomes (e.g., with Jectofer, Zymosan, Triton WR 1339, or colloidal carbon) to alter cell density. Two other methods are injection with colloidal iron in vivo followed by magnetic separation (Rous and Beard, 1934) and enterotoxin treatment (Blomhoff et al., 1984) to selectively disrupt hepatocytes.

The isolation method described in this unit is based on the protocol by Smedsrød and Pertoft (1985) with slight modification to focus on KCs. It was originally designed as a rapid method for mass isolation of functionally intact hepatocytes and reticuloendothelial cells (stellate and Kupffer cells) from a single rat liver. Nonrecirculating collagenase perfusion is used to digest the liver, providing a cell suspension with reduced alterations in cell membrane composition and greater functional activity than have been observed with mechanical dispersion techniques or with other proteolytic enzymes like pronase. The perfusion is followed by isopycnic sedimentation in Percoll and selective attachment to purify the KCs. The advantages of performing the centrifugation with Percoll (which is composed of colloidal silica coated with polyvinylpyrrolidone and has a density of 1.130 g/ml), as opposed to other commercially available gradient materials, are

Table 14.4.1 Kupffer Cell Isolation Troubleshooting Guide[a]

Problem	Possible cause	Solution
Low animal survival before liver perfusion	Nembutal concentration too high	Weigh the animal and, if necessary, lower the Nembutal concentration (normally, 50 mg/kg body weight is used).
	Nembutal injected into a blood vessel	Aspirate to make sure that needle is intraperitoneal (Fig. 14.4.1A shows injection points).
Incomplete liver perfusion	Air in perfusion system or liver	Avoid air bubbles during portal vein cannulation.
		When changing perfusion solutions, do not let air get into the system (use an air bubble trap).
	Blood clots in the liver	Perfuse liver with recommended flow rate and make sure that the flow is constant (if necessary use heparin).
Incomplete digestion of liver	Insufficient collagenase concentration	Adjust amount of collagenase (see Critical Parameters and Troubleshooting).
	Too short perfusion time	Perfuse liver for recommended time (10 min each for CMF-HBSS and collagenase in HBSS).
	Incomplete liver perfusion	See above.
Insufficient cell separation during isopycnic (gradient) centrifugation	Percoll layers not intact before centrifugation	Avoid mixing either the two Percoll layers or the cell suspension and the upper Percoll layer (Fig. 14.4.2A).
	Incomplete cell sedimentation in Percoll after centrifugation	Check settings of the centrifuge (speed and temperature). The brake must be off.
Reduced yields of KCs	Contamination by microbes	Make sure that all buffers and solutions are sterile and store as indicated.
		All tools (including perfusion system) need to be cleaned or sterilized before use.
	Reduced number of viable KCs	Keep liver moist during the perfusion.
		After removing liver from the animal, tease liver very gently into solution.
		Try different lots of collagenase (if necessary, reduce the amount used).
	Reduced plating and culturing efficiency	Plate isolated KCs on glass or plastic surfaces (e.g., tissue culture dishes) and, if necessary, increase time until first medium change (time required for attachment and spreading).
		Change medium only at the appropriate times.
	Incomplete liver perfusion, digestion of the liver, or cell separation during isopycnic (gradient) centrifugation	See above.
Contamination of KCs with other liver cells	Too long attachment and spreading time	Decrease time between plating KCs and first medium change (normally 15-30 min).
	Insufficient cell separation during isopycnic (gradient) centrifugation	After gradient centrifugation, keep only fractions 1 and 2 and discard supernatant and pellet.

[a]Abbreviations: CMF-HBSS, Ca^{2+}- and Mg^{2+}-free Hanks' balanced salt solution; KC, Kupffer cell.

its relatively low cost and stable storage properties, not to mention the easy preparation of the Percoll solutions. Finally, a purified KC population is cultured based on the selective substrate attachment properties of these cells to plastic or glass surfaces.

The main disadvantage of the method is that other techniques can sometimes yield higher numbers of isolated cells (see Anticipated Results). However, the simplicity (e.g., no special equipment necessary), rapidity, and relatively low cost of the procedure, as well as the possibility of isolating different cell types from one animal for comparisons, clearly indicate the benefits of this method.

Critical Parameters and Troubleshooting

To prevent any kind of contamination, the protocol should be performed under sterile conditions. This includes not only sterilizing surgical tools and other equipment (e.g., glass bottles, culture dishes, perfusion system) but also confirming that solutions have not been stored longer than suggested (see Reagents and Solutions) and are free of any obvious contamination.

Another critical parameter in the isolation process is the protease used for the enzymatic digestion of the liver. Collagenase shows a great variation in enzymatic activity and specificity. Several different lots of collagenase (from different vendors and even among lots from the same vendor) may need to be tested to determine which lot best provides the anticipated result. If different lots of collagenase with different enzyme activities are used, the final collagenase concentration in HBSS for the liver perfusion may need to be adjusted.

Potential problems related to this isolation method and their causes and solutions are included in Table 14.4.1.

Anticipated Results

The final number of isolated KCs is dependent on the rodent, the specific strain, and the pretreatment of the animal (e.g., in some fibrosis or necrosis models, there will be fewer cells than in control animals). In general, the number of KCs isolated in the described method is 8 (± 1.5) $\times 10^6$ cells/g liver (purity ≥95%) for rats and 7.5 (± 1.5) $\times 10^6$ cells/g liver (purity ≥95%) for mice. The recovery rate of KCs is ~29% for rats and ~27% for mice based on the estimated number of 27 (± 3) $\times 10^6$ KCs/g liver. The yields are similar to those achieved with other procedures (Knook and Sleyster, 1976). The actual number of KCs maintained in culture can vary depending on the plating efficiency and the number of times the medium is changed. A reduction of ≤50% is possible.

Time Considerations

The estimated time for each part of the protocol is as follows:

Animal preparation: ~15 min
Operation: ~10 min
Liver perfusion: ~30 min
Centrifugation: ~45 min
Cell counting: ~10 min
Cell culture (until first medium change): ~30 min

Taken together, a total time of ~2.5 to 3 hr for the isolation of KCs should be estimated per animal.

Literature Cited

Alpini, G., Lenzi, R., Zhai, W.R., Liu, M.H., Slott, P.A., Paronetto, F., and Tavoloni, N. 1989. Isolation of a nonparenchymal liver cell fraction enriched in cells with biliary epithelial phenotypes. *Gastroenterology* 97:1248-1260.

Alpini, G., Phillips, J.O., Vroman, B., and LaRusso, N.F. 1994. Recent advances in the isolation of liver cells. *Hepatology* 20:494-514.

Blomhoff, R., Smedsrød, B., Eskild, W., Granum, P.E., and Berg, T. 1984. Preparation of isolated liver endothelial cells and Kupffer cells in high yield by means of an enterotoxin. *Exp. Cell Res.* 150:194-204.

Branster, M.V. and Morton, R.K. 1957. Isolation of intact liver cells. *Nature* 180:1283-1284.

Brouwer, A., Barelds, R.J., and Knook, D.L. 1984. Centrifugal separations of mammalian cells. *In* Centrifugation: A Practical Approach. (D. Rickwood, ed.) pp. 183-218. IRL Press, Oxford.

Eberth, C.J. 1867. Untersuchungen über die Leber der Wirbeltiere. *Arch. Mikr. Anat.* 3:423-440.

Friedman, S.L. and Roll, F.J. 1987. Isolation and culture of hepatic lipocytes, Kupffer cells, and sinusoidal endothelial cells by density gradient centrifugation with Stractan. *Anal. Biochem.* 161:1233-1247.

Jones, E.A. and Summerfield, J.A. 1988. The Liver: Biology and Pathobiology, 2nd ed. (I.M. Arias, W.B. Jakoby, H. Popper, D. Schachter, D.A. Shafritz, eds.) pp. 683-704. Raven Press, New York.

Knook, D.L. and Sleyster, E.C. 1976. Separation of Kupffer and endothelial cells of the rat liver by centrifugal elutriation. *Exp. Cell Res.* 99:444-449.

Kupffer, C. 1876. Über die Sternzellen der Leber. *Arch. Mikr. Anat*. 12:353-358.

Miller, S.B., Saccomani, G., Pretlow, T.P., Kimball, P.M., Scott, J.A., Sachs, G., and Pretlow, T.G. 1983. Purification of cells from livers of carcino-

gen-treated rats by free-flow electrophoresis. *Cancer Res.* 43:4176-4179.

Morin, O., Patry, P., and Lafleur, L. 1984. Heterogeneity of endothelial cells of adult rat liver as resolved by sedimentation velocity and flow cytometry. *J. Cell Physiol.* 119:327-334.

Munthe-Kaas, A.C., Berg, T., Seglen, P.O., and Seljelid, R. 1975. Mass isolation and culture of rat kupffer cells. *J. Exp. Med.* 141:1-10.

Praaning-Van Dalen, D.P., De Leeuw, A.M., Brouwer, A., De Ruiter, C.F., and Knook, D.L. 1982. Ultrastructural and biochemical characterization of endocytic mechanisms in rat liver Kupffer and endothelial cells. *In* Sinusoidal Liver Cells. (D.L. Knook and E. Wisse, eds.) pp. 271-278. Elsevier Biomedical Press, Amsterdam.

Rous, P. and Beard, J.W. 1934. Selection with the magnet and cultivation of reticulo-endothelial cells (Kupffer cells). *J. Exp. Med*. 59:577-591.

Shaw, R.G., Johnson, A.R., Schulz, W.W., Zahlten, R.N., and Combes, B. 1984. Sinusoidal endothelial cells from normal guinea pig liver: Isolation, culture and characterization. *Hepatology* 4:591-602.

Smedsrød, B. and Pertoft, H. 1985. Preparation of pure hepatocytes and reticuloendothelial cells in high yield from a single rat liver by means of Percoll centrifugation and selective adherence. *J. Leukoc. Biol.* 38:213-230.

Smedsrød, B., Pertoft, H., Eggertsen, G., and Sundström, C. 1985. Functional and morphological characterization of cultures of Kupffer cells and liver endothelial cells prepared by means of density separation in Percoll, and selective substrate adherence. *Cell Tiss. Res.* 241:639-649.

Wake, K., Decker, K., Kirn, A., Knook, D.L., McCuskey, R.S., Bouwens, L., and Wisse, E. 1989. Cell biology and kinetics of Kupffer cells in the liver. *Int. Rev. Cytol.* 118:173-229.

Wedl, K. 1854. Grundzüge der pathologischen Histologie. Gustav Fischer, Jena, Germany.

Zahlten, R.N., Hagler, H.K., Nejtek, M.E., and Day, C.J. 1978. Morphological characterization of Kupffer and endothelial cells of rat liver isolated by counterflow elutriation. *Gastroenterology* 75:80-87.

Key References

Alpini et al., 1994. See above.

Describes different methods for and recent advances in the isolation of NPCs and PCs and provides background information on the characterization of individual liver cells.

Smedsrød and Pertoft, 1984. See above.

Describes in detail the preparation of hepatocytes and reticuloendothelial cells using collagenase perfusion of the liver, isopycnic sedimentation in Percoll, and selective adherence of the cells—the method on which the Basic Protocol is based.

Internet Resources

www.apbiotech.com/na/

Web page of Amersham Pharmacia Biotech. A search using "Percoll" will lead to background information about the density-gradient medium.

minf.vub.ac.be/~kupffer/

Home page of The Kupffer Cell Foundation. Good resource for background information about cells of the hepatic sinusoid.

Contributed by Matthias Froh
University of Regensburg
Regensburg, Germany

Akira Konno and Ronald G. Thurman
University of North Carolina
Chapel Hill, North Carolina

For more than 30 years, Ron Thurman was an outstanding investigator in the fields of hepatic metabolism, alcoholic liver injury, and toxicology. With his passing, his large family of colleagues and friends lost a most productive and creative researcher and teacher.

Measurement of Hepatobiliary Transport

The liver is remarkably efficient at removing a multitude of compounds from circulating blood plasma and metabolizing, storing, and/or excreting these compounds and their metabolites into bile or back into the bloodstream (Boyer, 1986). Hepatobiliary transport of endogenous and exogenous compounds is mediated by the coordinated action of multiple transport systems present at the basolateral (sinusoidal) and apical (canalicular) membrane domains of hepatocytes. Over the past few years, many of these transporters have been characterized at the cellular and molecular levels, and these data have provided important insight into the normal physiology of bile formation, the pathophysiology of hepatic disorders, and the processes that mediate xenobiotic elimination and disposition (Borst and Elferink, 2002; Kato et al., 2002; Hagenbuch and Meier, 2003; Trauner and Boyer, 2003).

Several experimental model systems have been used to study hepatobiliary functions, including isolated membrane vesicles, cell lines, primary hepatocytes, and liver slices (Brandon et al., 2003). The most direct method for examining biliary excretory function, however, is to collect bile via the common bile duct in anesthetized animals or in the perfused liver. Analysis of bile volume (flow rate), pH, osmolarity, and chemical and protein composition provides invaluable information about hepatocellular function and the ability of the liver to clear toxic chemicals. Moreover, identification of drug or xenobiotic metabolites in bile provides direct evidence for the involvement of specific enzymes and transporters in their metabolism and hepatobiliary elimination.

Although bile sampling in intact animals provides the most direct information about hepatobiliary transport processes, this approach does have some drawbacks: it is often difficult to analyze and regulate blood plasma concentration of a compound or its metabolites in the whole animal, and metabolism by other organs often complicates interpretation of results. For these reasons, the isolated perfused liver model has been used extensively for studying hepatobiliary function.

The versatility of the perfused rat liver model, as well as the fact that the isolated organ remains functional for extended periods, has made it a favorite system for addressing many questions in different research areas. For toxicology, this model provides a direct means for assessing the role of the liver in the metabolism, bioactivation, toxicity, and elimination of drugs and xenobiotics. Chemicals may be added in precise amounts to the perfusate, and metabolites may be sampled directly in bile or perfusate. Hepatocellular function and viability may be addressed directly in the intact organ, thus revealing interactions among the different cell types (e.g., Kupffer cells, stellate cells, sinusoidal endothelial cells, cholangiocytes, and hepatocytes), as well as the involvement and sensitivity of cells located in different acinar zones of the liver lobule.

Because bile cannot be sampled at its primary site of formation (the bile canaliculus), the specific processes that mediate membrane transport of organic and inorganic molecules into bile have been difficult to identify and characterize using perfused liver or in vivo models. Even though chemical analysis of bile collected from the common bile duct provides some insight into these processes, it cannot directly define the events that take place on the hepatocyte canalicular plasma membrane. A solution to this dilemma was provided by the development of techniques to isolate plasma membrane vesicles that are enriched in either canalicular or basolateral membrane domains (Evans, 1969; Long et al., 1969; Meier et al., 1984). These isolated membrane subfractions are useful for establishing the localization of enzymes, receptors, channels, pumps, and transporters on

Contributed by Nazzareno Ballatori
Current Protocols in Toxicology (2004) 14.5.1-14.5.17

the different plasma membrane domains, for functionally characterizing these membrane proteins, and for examining the interaction of toxic chemicals with these processes.

This unit describes basic methods for collecting bile from anesthetized mice and rats (see Basic Protocol 1), carrying out isolated perfused rat liver studies (see Basic Protocol 2), and simultaneously isolating plasma membrane vesicles derived from the basolateral and canalicular domains of rat liver (see Basic Protocol 3).

NOTE: All protocols using live animals must first be reviewed and approved by an Institutional Animal Care and Use Committee (IACUC) and must follow officially approved procedures for the care and use of laboratory animals.

BASIC PROTOCOL 1

BILE COLLECTION IN ANESTHETIZED RATS AND MICE

This protocol is suitable for short-term bile collection in anesthetized rats or mice (<3 hr), but this time interval can be extended by several hours if supplemental fluids are given to replenish the volume lost by exhalation, evaporation, and bile collection.

Materials

Rat or mouse
50 mg/ml pentobarbital sodium

Flexible temperature probe (rectal probe; e.g., Yellow Springs Instrument)
Thermostat-controlled heat lamp or heat pad
Surgical instruments, sterile, including:
  Scalpel or blunt-end scissors
  Hemostats
  Forceps, fine
  Iridectomy scissors (i.e., fine, sharp-pointed scissors)
Suture, size 3-0
PE-10 tubing (polyethylene tubing), ≥10 cm long with beveled end (e.g., Clay Adams)
Surgical clamps, optional
1-ml microcentrifuge tubes

1. Weigh a rat or mouse and anesthetize with 50 mg/ml pentobarbital sodium (55 mg/kg, intraperitoneally). Place the animal on its back with the head oriented away from the surgeon. Monitor body temperature continuously with a flexible temperature probe and maintain it at 37°C by use of a thermostat-controlled heat lamp or heat pad. Administer additional anesthetic intraperitoneally as required throughout the experiment (~15 to 20 mg/kg every hr).

   Additional fluid is not normally required for bile collections of ≤3 hr. For longer experiments, dilute saline or glucose solutions can be administered intravenously or intraperitoneally.

2. Use a scalpel or blunt-end scissors to make a midline incision in the abdomen that extends downward from the symphysis pubis (~2 cm in length in mice and 4 cm in rats). Cut skin first and then muscle layer. Hold the two flaps open to the side with hemostats.

   By staying in the midline, bleeding is minimized.

To cannulate bile duct in rats

3a. Pull out the duodenum, find the bile duct, and, using fine forceps, isolate the bile duct from the surrounding connective tissue. Isolate a bile duct segment that is within 3 cm of the liver. Do not sever any pancreatic ducts when isolating the bile duct.

4a. Put a double suture around the bile duct (a 30-cm segment of 3-0 suture folded in half), cut the suture at the mid-point, and, using one of the two pieces, loosely tie the distal suture near the end of the bile duct.

5a. Using fine iridectomy scissors, make a nick in the bile duct at a 45° angle and insert the beveled end of a length of PE-10 tubing to within 1 cm of the liver. Tie down both sutures.

The PE-10 tubing should be ≥10 cm long to help divert the bile into a collection vessel. It is helpful to put a mark near the beveled end of the PE-10 tubing with an indelible marker, as this makes it easier to visualize the end of the tube within the bile duct.

6a. Close the muscle layer first and then the skin layer with surgical clamps or suture, being careful not to twist or bend the bile duct or cannula.

Twisting or bending the duct or cannula will obstruct bile flow.

7a. Collect bile in tared 1-ml microcentrifuge tubes at 15-min intervals, or more frequently if desired.

Bile flow rates are expected to be from 4 to 8 ml/hr/kg body weight, or about 0.25 to 0.5 ml/15 min/250 g rat.

To cannulate bile duct in mice

3b. Follow the procedure described for rats (steps 3a to 6a), except ligate the cystic duct to exclude the gallbladder and stretch the PE-10 tubing to make a smaller tube that can be inserted into the relatively small bile duct of the mouse.

The PE-10 tubing should be pulled gently with both hands until it begins elongating. It is then cut at a 45° angle at the stretched end. The goal is to reduce the outer (and inner) diameter to about one-half of its original size while being careful not to completely collapse the inner pore of the tubing.

Stretching the PE-10 tubing is also appropriate for cannulating the bile duct of a weanling rat.

4b. Collect bile in tared 1-ml microcentrifuge tubes at 15-min intervals, or more frequently if desired.

Bile flow rates are expected to be from 4 to 8 ml/hr/kg body weight, or about 0.25 to 0.5 ml/15 min/250 g rat.

PREPARING AN ISOLATED PERFUSED RAT LIVER

BASIC PROTOCOL 2

Liver perfusion is a versatile technique, both technically and in terms of the questions that may be addressed (Miller, 1973). (1) Livers may be perfused in situ or may be isolated and perfused away from the rest of the animal. For short perfusions (<1 hr), in situ perfusion may be acceptable, but for longer perfusions it is usually necessary to isolate the liver into a relatively clean environment in which temperature and humidity can be more readily controlled. (2) The perfusate may be passed only once through the liver (i.e., single-pass perfusion) or may be recirculated. Single-pass perfusions are technically easier to perform and allow a constant delivery of drugs or nutrients to the liver, but they can be expensive depending on the composition of the perfusion medium. Single-pass perfusions also tend to deplete the liver of certain factors that are continuously released

into the sinusoidal circulation, and this may be detrimental to hepatic function. Conversely, toxic metabolites may accumulate in perfusate solutions that are recirculated, and this may also be detrimental. (3) Perfusate can be passed in the normal direction (inflow through the portal vein) or in a retrograde direction, via the hepatic vein. (4) Both the portal vein and hepatic artery may be cannulated for perfusion, although perfusion through the portal vein is adequate for most studies (Miller, 1973). (5) There are also many choices of perfusate media, ranging from simple salt solution (e.g., Krebs-Henseleit buffer) to perfluorocarbon emulsions or whole blood.

This protocol describes the isolated perfusion of rat livers using recirculating Krebs-Henseleit (KH) buffer, although other buffers or approaches may be substituted with only minor modifications. This protocol is modeled after that described by Miller (1973). In brief, the bile duct, portal vein, and thoracic vena cava are cannulated, the liver is placed on a 10-cm petri dish with a 1-cm hole cut in the middle to allow the venous outflow to drain downward, this petri dish is put in a heated Plexiglas chamber, and the liver is perfused in a recirculating mode with 100 ml oxygenated KH buffer.

NOTE: Krebs-Ringer bicarbonate buffer, which has twice the concentration of calcium and magnesium that KH buffer (see recipe) has, should be used if albumin or another protein is used as an oncotic agent in the perfusate. (The albumin binds some of the calcium and magnesium, such that their starting concentrations need to be higher.)

Materials

KH buffer (see recipe)
1000 U/ml heparin
D-Glucose, aliquots of 90.1 mg stored at room temperature
pH 7 buffer (for pH meter calibration)
Rat
50 mg/ml pentobarbital sodium

12 × 75–mm test tubes or 1-ml microcentrifuge tubes
Perfusion setup (Fig. 14.5.1), including:
- Two pumps capable of delivering 10 to 50 ml/min, preferably with minimal pulsatile flow
- 250-ml Erlenmeyer flask
- Water bath, 37°C
- Tank of 95% O_2/5% CO_2
- Glass humidifier and dispersion tube
- Tygon tubing: 0.12-in. (0.32-cm) inner diameter (i.d.) and 0.25-in. (0.64-cm) outer diameter (o.d.)
- In-line filter (Millipore XX43-047-00) containing a 1.2-µm filter (Millipore RAWP-047-00) and a prefilter (Millipore AP25-042-00)
- Gas exchange mechanism: 0.5-liter jar containing 7.7 m gas-permeable silastic tubing (Dow Corning 602-235) attached to y-shaped connector
- Perfusion dish: 10-cm plastic Petri dish with a 1-cm round hole cut in the center
- 100-ml, 3-neck perfusate reservoir (e.g., Kontes Glass 606020-0224), with a plastic funnel over the central neck of this reservoir
- pH meter and electrode
- Thermometer
- Small heater and blower

Operating tray
Surgical instruments, sterile, including:
- Hemostats, two
- Iridectomy scissors (i.e., fine, sharp-pointed scissors)

Forceps, two
Heavy scissors
Blunt-end scissors or scalpel
Suture, 3-0: one 30-cm length, folded in half, and four 15-cm lengths
Bile cannula: 16-cm length of PE-10 tubing, beveled at one end
Portal vein cannula: 14- or 16-G stainless steel, blunt-end needle with slight bevel forged at the end, connected to a three-way stopcock
Thoracic vena cava cannula: 2.5-cm length of PE-205 tubing, beveled at one end
Temperature monitor with small flexible temperature probe
Dewar flask, tall
Two 1-ml syringes attached to PE-90 tubing

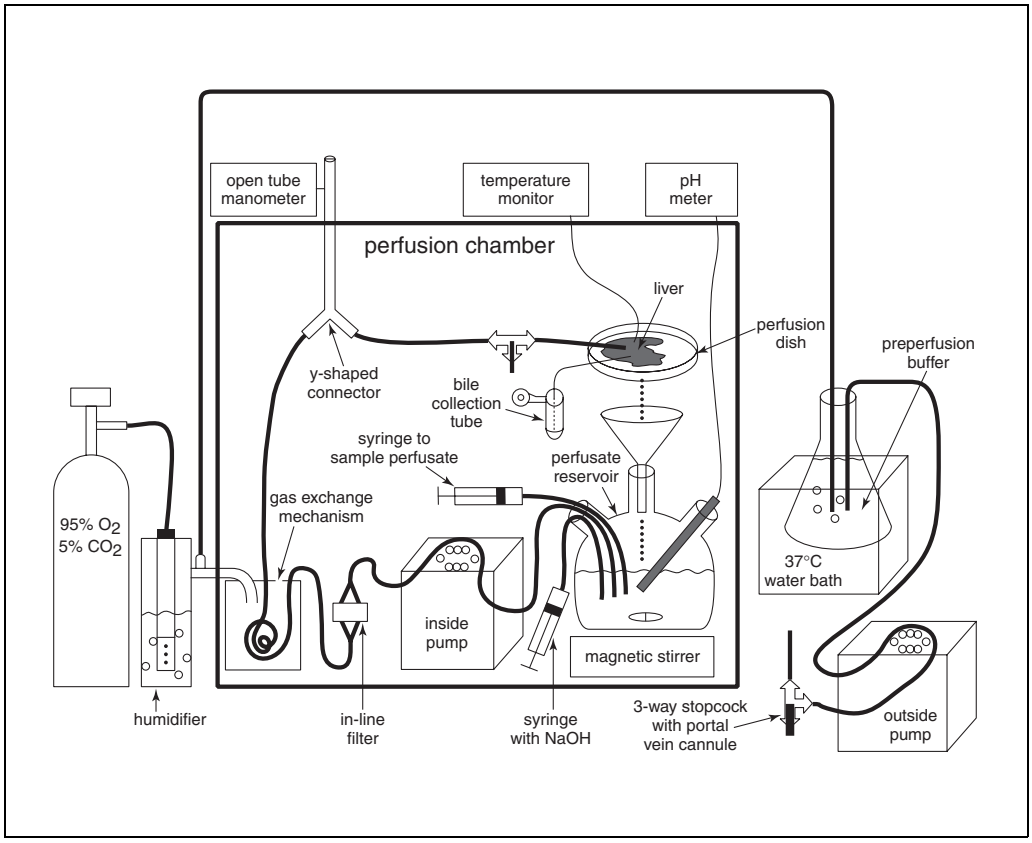

Figure 14.5.1 A perfusion chamber and preperfusion pump. The chamber contains a pump (inside pump) capable of delivering 10 to 50 ml/min, preferably with minimal pulsatile flow; an in-line filter containing a 1.2-μm filter and a prefilter; a gas exchange mechanism; a y-shaped connector; and a 100-ml, 3-neck perfusate reservoir on a magnetic stirrer. A bile collection tube is shown with the bile duct cannula, for collecting bile samples. The pump on the outside of the chamber (outside pump) and the preperfusion buffer are used in the initial perfusion during surgery. The tubing from this preperfusion pump is attached to a 3-way stopcock and a needle that will be inserted into the portal vein (i.e., the portal vein cannula). The stopcock and cannula are also shown within the perfusion chamber after they have been transferred to the inside pump for the perfusion. Humidified 95% O_2/5% CO_2 is passed into the jar of the gas exchange mechanism. As the perfusate circulates inside the gas-permeable tubing, oxygen enters the solution and carbon dioxide exits. The jar has a small hole on the top to allow excess gas to escape. The perfusion chamber also includes a small heater and blower (not shown) to maintain a constant temperature.

Prepare perfusion setup

1. Prelabel and weigh 12 × 75–mm test tubes or 1-ml microcentrifuge tubes to collect bile and perfusate samples and for liver tissue at the end of the experiment.
2. Assemble perfusion chamber and a preperfusion pump (outside pump) as illustrated in Figure 14.5.1.
3. For preperfusion buffer, place 250 ml KH buffer into a 250-ml Ehrlenmeyer flask and add 0.5 ml of 1000 U/ml heparin (~2 U/ml final). Suspend the flask in a 37°C water bath.
4. Connect a tank of 95% O_2/5% CO_2 to a dispersion tube placed within a glass humidifier that has been partially filled with water.
5. Run a length of Tygon tubing from the humidifier to the preperfusion buffer and bubble the buffer for ≥15 min. Turn on the preperfusion pump to begin to recirculate this solution at a rate of ~10 ml/min.
6. For perfusate, take 100 ml KH buffer and add a preweighed aliquot of D-glucose (90.1 mg).

Prepare chamber

7. Rinse all tubing (except for an in-line filter), gas exchange mechanism, perfusion dish, and a 100-ml, 3-neck perfusate reservoir by circulating ~80 ml preperfusion buffer through the system. Flush system completely and discard this solution.
8. Insert the in-line filter containing a 1.2-µm filter and a prefilter.

   The filter also serves as a trap for any air bubbles that may be aspirated from the perfusate reservoir.

9. Add perfusate to the perfusate reservoir. Turn on perfusion pump (inside pump) and invert the in-line filter so as to fill it with perfusate (by holding outlet upward). Set the initial flow to ~20 ml/min.

   This flow rate is increased gradually after the liver is added, to reach a setting of ~35 ml/min for a liver of 8 to 10 g (200- to 300-g rat). For optimal hepatic oxygenation, the perfusion flow rate should be ≥3.5 ml/min per gram liver when using hemoglobin-free perfusates.

10. Recirculate perfusate within the system, making sure that there are no leaks and no air bubbles. Pass humidified 95% O_2/5% CO_2 over the gas-exchange tubing.
11. Calibrate a pH electrode (using pH 7 buffer at 37°C) and insert into perfusate reservoir.

    pH adjustments are made during the experiment by delivering small aliquots of 0.15 M NaOH into the perfusate reservoir. A convenient way of delivering the NaOH is via a 3-ml plastic syringe fitted with a 23-G needle and about 50 cm of PE-50 tubing. The end of this tubing is inserted into the perfusate reservoir.

12. Close chamber door and stabilize heat to 37°C using a thermometer, a small heater, and a blower.

    The chamber should be equipped with a small heater and a blower to circulate air and maintain uniform temperature within the chamber and with a thermometer to monitor the temperature. A petri dish full of water is placed near the heater to provide moisture in the chamber.

13. Place prelabeled bile collection tubes (step 1) on ice.

Perform surgery

14. Weigh a rat and anesthetize with 60 mg/kg of 50 mg/ml pentobarbital sodium, intraperitoneally. Cover an operating tray with absorbent bench paper. Record the weight of the animal and position it on its back on top of the bench paper with its head facing away from the surgeon.

15. Using a scalpel or blunt-end scissors, make a midline incision in the abdomen that extends from the symphysis pubis to the suprasternal notch. Cut skin first and then the muscle layer. Hold the two flaps open to the side with hemostats.

    By staying in the midline, a lot of bleeding is avoided.

Cannulate bile duct

16. Pull out the duodenum and find and isolate the bile duct. Insert a folded 30-cm piece of suture underneath the bile duct, cut the suture in half, and use one piece of suture to ligate the distal end of the bile duct.

17. Use fine iridectomy scissors to make a nick in the bile duct and insert the beveled end of a bile cannula ~1 cm into the duct (Fig. 14.5.2). Align the other suture beneath the cannula. Tie down both sutures.

    It is helpful to put a mark near the beveled end of the cannula with an indelible marker, as this makes it easier to visualize the end of the tube within the bile duct.

    The second suture holds the cannula in place.

Prepare for perfusion

18. Place two 15-cm pieces of suture loosely around the portal vein, one above and one below the pancreatico-duodenal vein (Fig. 14.5.2). Put suture around portal vein only and avoid the hepatic artery.

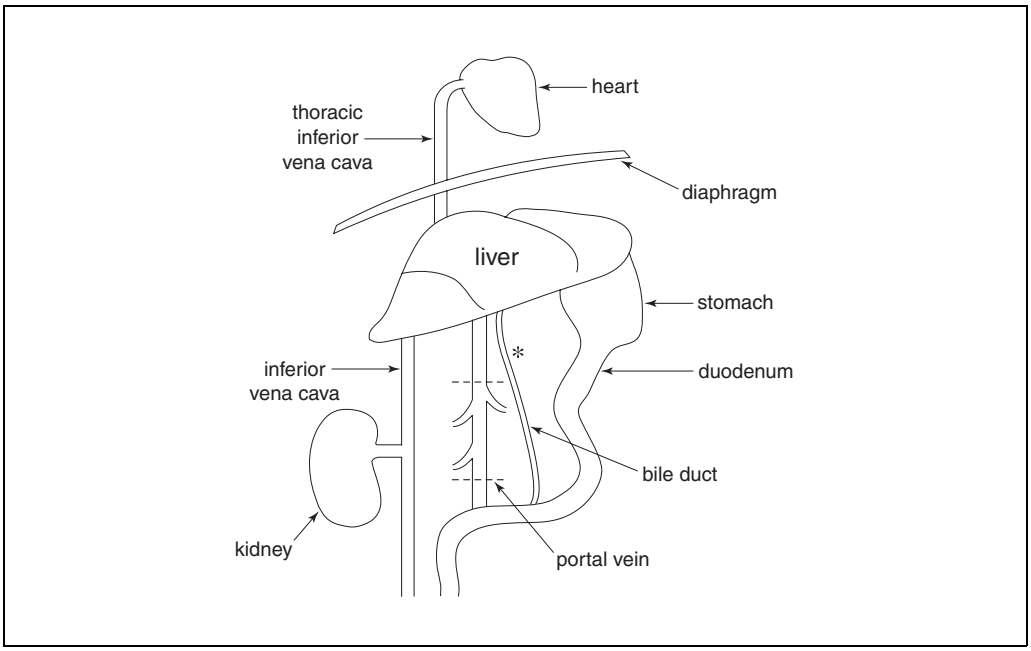

Figure 14.5.2 Anatomy of the rat abdominal cavity. The gastrointestinal tract has been retracted and moved to the right-hand side of the operating field, to expose the inferior vena cava and the right kidney of the rat. The approximate positions of the two portal vein sutures are indicated by dashed lines; the portal vein cannula is placed halfway between the sutures. The approximate position of the bile duct cannula is indicated by an asterisk; a suture is placed both above and below this site of insertion.

19. Retract the gastrointestinal tract and move it to the right-hand side of the operating field, to expose the inferior vena cava and the right kidney of the rat (Fig. 14.5.2). Place a loose 15-cm suture around the vena cava, above the animal's right kidney. Don't tie this suture down until just before portal vein cannulation.

20. Stop the inside pump and suspend the tubing from a piece of tape attached to the ceiling of the chamber. Set initial flow rate to ~20 to 25 ml/min. Make sure all of the tubing is filled with perfusate and that there are no air bubbles.

Cannulate portal vein

21. Attach a portal vein cannula to the outside pump (Fig. 14.5.2) and fill with preperfusion buffer. Place the cannula next to the rat and eliminate any air bubbles (particularly those that may be hiding in the 3-way stopcock).

    Because the pump is running, subsequent steps have to be performed in rapid succession, or the pump can be turned off temporarily.

    The portal vein can be cannulated with various types of needles. The tip of the needle must be completely smooth so as not to damage the portal vein once inserted. It is helpful to have some grooves engraved near the tip of the needle, as this will help hold the suture in place.

22. Tie the suture around the vena cava right above the animal's right kidney (Fig. 14.5.2). Ligate the distal suture (with respect to the liver) around the portal vein.

23. With fine forceps, hold the portal vein and cut a flap in the portal vein (at a 45° angle) using iridectomy scissors. Hold the flap with one hand and insert portal vein cannula with the other hand. Tie down the suture and immediately cut the vena cava below the animal's right kidney to allow blood to escape. Tie down the other suture around the portal vein cannula.

    Note that once blood flow to the liver is interrupted by ligation of the portal vein, there is a window of ~30 sec during which the cannula can be inserted before there is irreversible damage to the liver. Also, after the cannula is inserted, the inferior vena cava must be cut to avoid blood pressure buildup while liquid is pumped into the liver via the cannula.

Cannulate thoracic vena cava

24. Grab the xiphoid with hemostats and using heavy scissors cut through the ribs on both sides. Fold the resulting flap over the animal's head to expose the lungs and heart (Fig. 14.5.2). Use a hemostat to hold this flap in place.

25. Put a single loose 15-cm suture around the thoracic inferior vena cava near the diaphragm. Using iridectomy scissors, put a small hole in the vena cava next to the heart and insert a thoracic vena cava cannula. Secure the suture around the cannula.

Transfer liver to perfusion dish

26. Cut between the animal's right kidney and the suture in the vena cava, but don't cut the suture.

    Removing and transferring the liver is the most challenging part of the surgery.

27. Cut the diaphragm on the left side of the operating field (i.e., the animal's right side), all the way down to the esophagus and then on the right side, but don't cut the esophagus. Flip the largest lobe of the liver to the left to expose some connective tissue and the small lobes of the liver that need to be dissected out.

28. Cut under the bile duct and portal vein cannulas to free them from the underlying tissue. Then, while holding these two cannulas in one hand, gently lift the liver by the cannulas and cut any remaining connections between the liver and the rest of the carcass.

    The portal vein cannula is still attached to the outside pump.

29. Transfer the liver to the perfusion dish and connect the three-way stopcock to the perfusate in the chamber. As soon as the tubing is connected, turn the inside pump on and outside pump off, and immediately turn the stopcock to redirect perfusate. Disconnect the tubing coming from the preperfusion buffer.

30. Adjust the position of the liver lobes, making certain that the caval outflow cannula is centered in the perfusion dish opening and the bile duct cannula is resting over the edge of the dish, and downward to facilitate bile collection (Fig. 14.5.1).

31. Insert a small flexible probe of a temperature monitor between and underneath the large lobe of the liver, and cover the entire petri dish with a piece of clear plastic wrap.

    The plastic wrap maintains moisture over the surface of the liver.

Adjust perfusion setup

32. Make certain that bile is flowing by watching it drip into the bottom of the perfusion chamber. Gradually increase perfusion flow rate as the resistance decreases (look at the manometer; Fig. 14.5.1), to reach a perfusion flow rate of about 35 ml/min for a 10-g liver (~3.5 ml/min/g liver).

    The bile duct may be twisted in the transfer to the perfusion dish, which will prevent the flow of bile.

    The net perfusion pressure through the liver should be <6 cm water.

33. Shut off oxygen to preperfusion reservoir and check on the flow of oxygen into the jar containing the gas-exchange tubing by looking for bubbles in the gas humidifier (Fig. 14.5.1). Allow the liver to equilibrate for 10 min.

Collect bile

34. Fill a tall Dewar flask with ice, put a prechilled collection tube (step 13) into the ice, and position this close to the liver to facilitate bile collection. Using the bile duct cannula, collect bile in tube, changing the collection tube at 15-min intervals or more frequently if desired.

    Bile flow is normally 1 to 2 µl/min/g lower.

35. Take aliquots of perfusate (normally 0.5 ml) using a 1-ml syringe attached to PE90 tubing to access the perfusate reservoir through the sample port. Rinse the tubing and syringe by drawing fluid in and out of the syringe a few times before collecting the perfusate sample.

36. After all samples have been collected, confirm the perfusion flow rate by collecting the perfusate dripping from the bottom of the liver for 30 sec into a 50-ml graduated cylinder. Remove cannulas from the liver and weigh the liver. Measure perfusion pressure in the absence of the liver.

    Perfusion pressure should normally be 4 to 6 cm water.

SIMULTANEOUS ISOLATION OF RAT CANALICULAR AND BASOLATERAL LIVER PLASMA MEMBRANE VESICLES

This protocol is similar to the one devised by Meier et al. (1984; Meier and Boyer, 1990), with only minor modifications. The approach for isolating the canalicular and basolateral liver plasma membrane (cLPM and blLPM, respectively) vesicles is based on previous studies by Long et al. (1969) and Evans (1969) and utilizes two major centrifugation steps. In brief, a mixed liver plasma membrane subfraction is first separated out of a crude nuclear pellet by rate zonal flotation using a TZ-28 (Sorvall) zonal rotor. After tight homogenization, the vesiculated cLPMs are separated by high-speed centrifugation of the mixed liver plasma membranes through a three-step sucrose gradient. The membranes are collected, suspended in a buffered sucrose solution, and stored at −80°C.

Each membrane isolation requires six to eight fed male Sprague-Dawley rats (200 to 250 g) that have been kept for ≥4 days under constant environmental conditions before use. The animals are allowed food and water ad libitum and are killed between 7:00 and 8:00 a.m. The protocol can easily be scaled down to one rat liver (10 g).

NOTE: All steps are performed at 4°C with precooled solutions and equipment. The solutions (homogenization buffer and sucrose solutions) should be prepared 1 to 2 days in advance and stored at 4°C.

Materials

1 mM $NaHCO_3$, pH 7.4, ice cold
Male Sprague-Dawley rats, 200 to 250 g
50 mg/ml pentobarbital sodium, to anesthetize rats
Sucrose solutions: 8.1%, 31%, 34%, 36.5%, 38%, 44%, and 56% sucrose (see recipe), ice cold
Resuspension buffer: e.g., 250 mM sucrose/20 mM KCl/0.2 mM $CaCl_2$, buffered with 10 mM HEPES/TRIZMA, pH 7.5 (see recipe)

100-ml and 2-liter plastic beakers
250-ml and 1-liter glass beakers
7-, 40-, and 100-ml glass-glass Dounce homogenizers with loose-fitting type A and tight-fitting type B pestles
2-liter Erlenmeyer flasks
Guillotine
Scissors
Cheesecloth
250-ml plastic centrifuge tubes with caps
Superspeed centrifuge (e.g., Sorvall RC-5B), 4°C
Centrifuge rotors: Sorvall TZ-28-Zonal, GSA, TH-641, and T-865 (Sorvall Instruments), or equivalent, 4°C
Peristaltic pump
16 × 125–mm test tubes
10-ml plastic Pasteur pipets or transfer pipets
Ultracentrifuge (e.g., Sorvall OTD55B), 4°C
Spectrophotometer (700-nm wavelength)

Set up equipment

1. Place 100-ml plastic beakers (one for each animal) and a 250-ml glass beaker on ice. Fill beakers with ~50 ml of 1 mM $NaHCO_3$.
2. Place two 7-ml and a 40- and a 100-ml glass-glass Dounce homogenizers (with pestles), a 2-liter Erlenmeyer flask, a 2-liter plastic beaker, and a 1-liter glass beaker on ice.

Collect livers

3. Anesthetize six to eight male Sprague-Dawley rats using 60 mg/kg of 50 mg/ml sodium pentobarbital.

4. Using a guillotine, decapitate one rat and using scissors and forceps rapidly remove its liver. Quickly dissect away connective tissue with scissors, rinse liver in ice-cold 1 mM $NaHCO_3$ in the 250-ml glass beaker, and place in one of the 100-ml plastic beakers on ice (step 1). Immediately mince liver tissue with scissors.

5. Decapitate and remove and process livers from remaining animals, one at a time

6. Decant 1 mM $NaHCO_3$ from each of the 100-ml beakers and replace with 80 ml fresh, ice-cold 1 mM $NaHCO_3$ from the original stock bottle.

Homogenize livers

7. Homogenize each liver in 80 ml of 1 mM $NaHCO_3$ with loose-fitting pestle A, first by four strokes in precooled 100-ml Dounce homogenizer and then, in batches, by three strokes in precooled 40-ml Dounce homogenizer.

   One stroke is the equivalent of a complete up-and-down movement of the pestle.

8. Filter each homogenate through a funnel lined with four layers of cheesecloth into the 2-liter Erlenmeyer flask. Pool filtered homogenates in flask and bring total volume to 1500 ml with ice-cold 1 mM $NaHCO_3$. Remove a 1-ml aliquot for protein and enzyme determination and note final volume of homogenate (i.e., ~1500 ml).

   Alternatively, two layers of 60-grade cheesecloth can be used to filter the homogenates.

9. Pour homogenate into six 250-ml centrifuge bottles and spin in a superspeed centrifuge with a GSA rotor for 15 min at $1250 \times g_{ave}$ (3500 rpm for 15 min, including acceleration time).

10. Aspirate supernatant with water vacuum line, while holding bottle at an angle. Pour gelatinous pink pellets into a clean 100-ml Dounce homogenizer on ice. Adjust total volume to 70 ml with 1 mM $NaHCO_3$.

    The total volume of the crude nuclear pellet is ~60 to 70 ml. The final volume must not exceed 70 ml because of the capacity of the zonal rotor.

11. Homogenize with two strokes in the Dounce homogenizer with a loose-fitting pestle. Dilute crude nuclear pellet with 385 ml of 56% sucrose (i.e., 5.5 vol) and stir using the Dounce pestle in the prechilled 1-liter glass beaker.

Perform zonal density gradient centrifugation

12. Install a TZ-28 rotor in the superspeed centrifuge for dynamic loading at 3000 rpm. After reaching 3000 rpm, remove the brake and place centrifuge in the slow acceleration mode.

13. Load the following solutions using a peristaltic pump at a flow rate of ~80–90 ml/min in the order given:

    100 ml of 56% sucrose
    445 to 455 ml membrane suspension (step 11)
    400 ml of 44% sucrose
    200 ml of 36.5% sucrose
    175 to 185 ml of 8.1% sucrose (1330 ml total).

    Remove rotor-filling accessories and accelerate to 19,000 rpm for 120 min.

Collect and wash mixed membranes

14. After slow deceleration to a complete stop, unload the sample from the top of the rotor using the peristaltic pump at a flow rate of ~50 ml/min. Discard the first 750 ml and collect the rest into twenty-four 16 × 125–mm test tubes (17-ml fractions). Take a 1-ml aliquot of each fraction and measure absorbance at 700 nm (turbidity).

15. Combine ten fractions of the major turbidity peak (44%/36.5% interface) in a 1-liter graduated cylinder. Rinse tubes with 1 mM $NaHCO_3$ and add to cylinder to maximize yield.

16. Dilute pooled fractions to 1000 ml with ice-cold 1 mM $NaHCO_3$. Pour membrane suspension into four 250-ml centrifuge bottles and sediment at $6500 \times g_{ave}$ (8000 rpm) for 15 min in the GSA rotor.

17. Aspirate supernatant and rinse pellets with ice-cold 1 mM $NaHCO_3$ into a single bottle. Centrifuge 15 min at $3100 \times g_{ave}$ (5500 rpm).

18. Aspirate supernatant with water vacuum line. Using a 10-ml plastic Pasteur pipet or transfer pipet, add 10 ml of 8.1% sucrose to bottle and resuspend membranes. Transfer to 40-ml Dounce homogenizer on ice. Rinse bottle with additional 8.1% sucrose and transfer to homogenizer to give a total volume of 25 ml.

Isolate cLPMs and blLPMs

19. Homogenize mixed liver plasma membranes by 75 (three sets of 25) strokes in the 40-ml Dounce homogenizer with a tight-fitting type B pestle.

    The Dounce homogenizer is immersed in ice.

20. Sequentially pipet the following solutions into six clear TH-641 tubes:

    3.0 ml of 38% sucrose
    2.5 ml of 34% sucrose
    2.5 ml of 31% sucrose.

    Layer ~3.5 ml homogenized liver plasma membranes on top of the sucrose gradients.

21. Centrifuge tubes 3 hr in an ultracentrifuge with a TH-641 rotor at $195{,}000 \times g_{ave}$ (40,000 rpm), using relatively slow acceleration and deceleration rates to avoid disrupting the gradients.

    This centrifugation produces three distinct bands at the sucrose interfaces and a pellet at the bottom of the tube. The band on top of the 31% sucrose layer represents cLPMs, whereas the band at the 34%/38% interface corresponds to blLPMs.

Collect plasma membranes subfractions

22. Collect membrane bands on top of the 31% (cLPM) and 38% (blLPM) sucrose gradients with 10-ml plastic Pasteur pipets after carefully aspirating any overlying fluid. Divide each subfraction between two 26-ml centrifuge tubes and dilute with ice-cold 8.1% sucrose to fill the tubes.

23. Centrifuge 60 min at $105{,}000 \times g_{ave}$ (40,000 rpm) in a T-865 rotor. Decant supernatant, gently aspirate any remaining supernatant, and add resuspension buffer.

    Normally, each of the four tubes (i.e., 2 of the 31% and 2 of the 38%) will receive 0.5 to 1 ml resuspension buffer.

    The composition of the resuspension buffer is contingent on the ultimate use of the vesicles, but may consist simply of 250 mM sucrose with a pH 7.4 buffer—such as 250 mM sucrose buffered with 10 mM HEPES/TRIZMA pH 7.4 (see recipe).

24. Using 10-ml plastic Pasteur pipets, place these suspensions into precooled 7-ml Dounce homogenizers (one for 31% and one for 38% fractions). Using tight-fitting type B pestles, homogenize with fifteen strokes. Save small aliquots (three 20-µl) for protein and enzyme determination, and store the rest in 0.2 - 0.5-ml aliquots at –80°C for up to 6 months.

The normal yields from this procedure are 10 to 15 mg blLPM protein and 5 to 7 mg cLPM protein.

The membranes should be assessed for their degree of purification. Several marker enzymes have been used to test the relative purity and enrichment of blLPM and cLPM fractions (Meier et al., 1984; Meier and Boyer, 1990). For routine assessment of purification, the enzymes γ-glutamyltranspeptidase (canalicular; Rosalki and Tarlow, 1974) and Na^+,K^+-ATPase (basolateral; Scharschmidt et al., 1979) are probably the most useful.

REAGENTS AND SOLUTIONS

Use glass-distilled, Milli-Q-purified water or equivalent for the preparation of all buffers and in all protocol steps. For common stock solutions, see ***APPENDIX 2A;*** *for suppliers, see* ***SUPPLIERS APPENDIX.***

HEPES/TRIZMA stock, 500 mM

37.75 g HEPES
11.36 g TRIZMA
H_20 to 500 ml

Add this solution to a final concentration of 10 mM in resuspension solution or other solutions in which a buffer is needed, e.g., resuspension buffer or sucrose solution.

Krebs-Henseleit (KH) buffer

~1950 ml H_2O
13.80 g NaCl (118 mM final)
9.4 ml 1 M KCl (*APPENDIX 2A*; 4.7 mM final)
2.4 ml 1 M KH_2PO_4 (1.2 mM final)
4.20 g $NaHCO_3$ (25 mM final)
1.2 ml 1 M $MgSO_4 \cdot 7H_2O$ (*APPENDIX 2A*; 0.6 mM final)
2.5 ml 1 M $CaCl_2 \cdot 2H_2O$ (*APPENDIX 2A*; 1.25 mM final)
Add H_2O to 2 liters
Store up to 2 weeks at 4°C

The $MgSO_4 \cdot 7H_2O$ and $CaCl_2 \cdot 2H_2O$ should be added separately (last) to avoid precipitation.

The pH after gassing with 95% O_2/5% CO_2 for 15 to 20 min at 37°C should be ~7.5.

Krebs-Ringer bicarbonate buffer (with double the amount of $MgSO_4$ and $CaCl_2$) should be used if albumin or another protein is used as an oncotic agent in the perfusate. (The albumin binds some of the calcium and magnesium, such that their starting concentrations need to be higher.)

Sucrose solutions

Make up sucrose solutions according to recipes given in Table 14.5.1. Store solutions for up to 2 weeks at 4°C.

Even the highest sucrose solution should be clear. If yellowish discoloration is seen, filter through a 0.45-µm filter or change to a new sucrose batch.

The refractive index (n) should be checked before use with a refractometer (e.g., Bausch & Lomb). Do not use the sucrose solution if its refractive index deviates by more than ±0.0003 from the expected value.

Table 14.5.1 Sucrose solution recipes for isolation of liver plasma membrane vesicles

Percent weight (w/w)	Molarity (M)	g/liter solution (w/v)	Refractive index (*n*; 20°C)	Density (g/ml)
8.1	0.25	85.6	1.3458	1.0300
31	1.025	350.9	1.3829	1.1318
34	1.138	389.5	1.3883	1.1463
36.5	1.236	422.9	1.3930	1.1587
38	1.295	443.2	1.3958	1.1663
44	1.539	526.8	1.4076	1.1972
56	2.067	707.4	1.4329	1.2632

COMMENTARY

Background Information

The liver's complex microanatomy and reticuloendothelial system create a specialized epithelial barrier separating blood from bile (Boyer, 1986). Mammalian hepatocytes are arranged in plates or sheets that are only one cell thick and are surrounded by capillaries (sinusoids), thus maximizing surface area for exchange with plasma. The sinusoidal endothelium is highly fenestrated and has little if any basement membrane (Disse space). The sieve-like plates in the endothelial cells permit solutes up to the size of chylomicrons to pass from blood into the Disse space. As a result, xenobiotics that are soluble or that may be bound to particles of this size or smaller in blood plasma have direct access to the basolateral surface of hepatocytes.

Three distinct plasma membrane domains are present on hepatocytes: the sinusoidal, lateral, and canalicular membranes. The sinusoidal or basal surface is covered with numerous irregular microvilli that increase the surface membrane area thereby facilitating hepatic uptake. The lateral domain is a relatively smooth and straight extension of the sinusoidal membrane that projects between neighboring hepatocytes and lines the intercellular cleft. It contains gap junctions, desmosomes, and tight junctions, but no microvilli. In analogy with other epithelial cells, the sinusoidal and lateral domains together form the basolateral membrane. The apical or canalicular membrane differs histochemically and biochemically from the basolateral surface. Although the lumen of the canalicular space is only ~1 μm in diameter, the surface area is enlarged by an extensive network of microvilli, which often fill the lumen. The canalicular membrane constitutes ~13% of the plasma membrane surface.

Separation of blood spaces from the lumen of biliary spaces is accomplished largely by two belt-like junctional complexes that encircle each hepatocyte, enclosing the canaliculi and linking adjacent hepatocytes within the hepatic plate. The canalicular wall is therefore a specialized part of the hepatocellular plasma membrane. The tight junctions that separate bile from plasma were initially considered to be impermeable. It is now accepted, however, that the paracellular pathway is the major route for the movement of certain solutes and water between plasma and bile. Studies in perfused rat liver demonstrate that >75% of biliary Na^+, K^+, Cl^-, and water come directly from plasma via the paracellular pathway (Graf et al., 1984, 1987). Hepatocyte junctional complexes are of low electrical resistance and are somewhat cation selective, suggesting the presence of negative charges. Studies by Graf et al. (1987) in isolated rat hepatocyte couplets indicate that the cation selectivity of the paracellular pathway is relatively weak. Paracellular permeability appears to be regulated by hormones, Ca^{2+}, and other endogenous factors and is altered by some drugs and chemicals or during hepatic injury.

Differences in lipid and protein composition among the three plasma membrane domains generate the hepatocyte's functional polarity (Meier, 1988). The sinusoidal membrane is rich in receptors, enzymes, and transport proteins. Receptors for hormones and transmitters such as insulin, glucagon, vasopressin, and α-adrenergic agonists and for metabolites such as lipoproteins, asialoglycoproteins, transferrin, and IgA, are concentrated on this membrane domain. Hormone-sensitive adenylate cyclase and Na^+,K^+-ATPase enzyme activity are also localized to the sinusoidal membrane. Its high phagocytic and endocytic properties are re-

vealed by the presence of clathrin-coated and noncoated vesicles. Transport proteins are also abundant on the sinusoidal membrane. These proteins facilitate uptake of ions, nutrients, bile acids, and organic anions and cations, including certain drugs and xenobiotics from blood plasma. The sinusoidal membrane also has transport systems that facilitate efflux of H^+, Ca^{2+}, amino acids, and possibly other solutes from liver cells back into blood plasma.

The lateral membrane participates in cell-cell interactions but has not yet been shown to contain specific transport processes. Desmosomes and tight junctions within lateral membranes link adjacent hepatocytes and create the canalicular space, whereas its gap junctions are specialized for cell-cell communication. The canalicular membrane is also replete with membrane transport proteins. Transport systems for organic anions (MRP2), organic cations (MDR1), phospholipids (MDR2), and bile acids (BSEP), along with high specific activities of the enzymes γ-glutamyl transpeptidase, leucylnaphthylamidase, Mg^{2+}-ATPase, and alkaline phosphodiesterase are localized to the canalicular membrane.

These transporters are responsible for generating hepatic bile, which is an isoosmotic electrolyte solution containing mixed lipid micelles of bile acids, cholesterol, and phospholipids, along with porphyrins, proteins, peptides, amino acids, metals, and a variety of other endogenous and exogenous compounds (Boyer, 1986). Bile is secreted largely in response to the osmotic gradient between bile, liver tissue, and plasma, which is generated by active secretion of impermeant solutes into the canalicular spaces. Water, electrolytes, and other solutes move across the canalicular membrane as well as through the tight junctions to dissipate the osmotic gradient created by active secretion of bile acids (Sperber, 1959), glutathione (Ballatori and Truong, 1992), and possibly other solutes.

After its secretion, canalicular bile winds its way through the labyrinth of canaliculi towards the periphery of the hepatic lobule and drains into the hepatic ductules and ducts and, finally, into the common duct and gallbladder. At each of these sites, canalicular bile may be modified by both absorptive and secretory processes, and some of its components may be metabolized by membrane-bound ectoproteins (Ballatori et al., 1986, 1988; Ballatori and Truong, 1989), demonstrating that biliary epithelia are not inert conduits for bile but are actively involved in its postsecretory processing.

Overall, the complex microanatomy of bile secretion poses a special challenge in the design of experiments to investigate mechanisms of hepatobiliary transport. The intact animal and the isolated perfused liver model are the only systems that permit the simultaneous measurement of sinusoidal transport and biliary excretion; however, it is often difficult to obtain detailed kinetic data using these model systems. Other in vitro models are used more often, but all in vitro models share a major limitation, namely the inability to reproduce the ionic and ligand composition of blood and blood plasma, a critical factor in regulating xenobiotic clearance.

In the early 1980s, another useful model system was introduced: a technique for the separation of plasma membrane vesicles derived from the liver cell sinusoidal and canalicular membrane domains (Meier et al., 1984). This made it possible to examine transport at both poles of the cell separately, without interference from cell metabolic functions. With this system, the electrogenic features, energy dependence, and ion requirements could be determined with relative ease. The limitations of this system include cross-contamination with other intracellular or plasma membranes, orientation of the vesicles, functional integrity of the transport proteins or the vesicles themselves, and the relatively high degree of nonspecific binding that is often observed with hydrophobic compounds or with metals. Despite these limitations, the vesicle systems have provided invaluable information on the functional characteristics of these two hepatocellular membrane domains.

Critical Parameters and Troubleshooting

The most common complication of the in vivo bile collection method in anesthetized animals is obstruction of the bile duct or cannula. Occasionally, blood clots, biliary sludge, or air bubbles may partially or completely block bile flow. This is usually remedied by gently aspirating the end of the bile cannula with a transfer pipet or a syringe to dislodge the obstruction. If this procedure fails to dislodge the block, remove the cannula, verify that bile is dripping from the end of the bile duct, and insert a new cannula. Occasionally, the bile duct is twisted or bent during the surgery, and this may also obstruct bile flow. Visual inspection of duct anatomy and cannula orientation should reveal this complication, and the defect is usually

remedied by rotating or bending the duct or cannula in the appropriate direction.

Surgical isolation and in vitro perfusion of a rat liver require considerable manual dexterity and surgical skills and may require a significant number of practice trials to perfect the approach. For most investigators, the most difficult parts of the surgery are the cannulation of the portal vein (which should be completed within 30 sec of cutting the portal vein) and the resection of the liver from the body cavity. Considerable time should be invested in studying the gross anatomy of the rat, with a particular focus on the hepatic vascular system, and in practicing cannulating small vessels. The most common complications arise from trauma caused to the liver during surgery or transfer to the perfusion dish and from the incorrect positioning of the liver on the perfusion dish. If incorrectly positioned on the dish, some of the lobes of the liver may be twisted or bent, which would prevent adequate perfusion of those lobes. Likewise, the positioning of the portal vein, vena cava, and bile duct cannulas needs to be adjusted to mimic that in the in situ liver, thus maximizing flow through each cannula. Thorough knowledge of the gross anatomy of the liver will minimize these problems. Surgery is greatly facilitated by the use of sharp, high-quality instruments, and by a surgical lamp to brightly illuminate the operating field. Although the experiment may be performed by a single investigator, it is useful to have a surgical assistant, particularly during the training period.

The critical element of the membrane vesicle isolation protocol is temperature control, which is important for minimizing protein degradation and cross-contamination between basolateral and canalicular membranes. All solutions and equipment must be precooled on ice, and samples must not be allowed to sit for extended periods before processing. Another important element is the use of high-quality distilled or deionized water for the preparation of all solutions, and the use of high-grade sucrose for preparation of gradients and vesicle storage solutions. Sucrose solutions are prone to bacterial contamination and thus should be stored at 4°C and used within two weeks.

Anticipated Results

Bile flow rates in adult anesthetized rats are expected to be from 4 to 8 ml/hr/kg body weight or from 1.7 to 3.3 µl/min/g liver wet weight. These flow rates normally drop slowly with time of bile collection, owing largely to the interruption of the enterohepatic circulation and the consequent depletion of bile acids.

In the isolated perfused rat liver, bile flow rates are lower than in vivo (from 1 to 2 µl/min/g liver wet weight at the onset of perfusion) and also tend to decrease with time of perfusion. The lower flow rates in the isolated perfused liver as compared with the in vivo situation are explained largely by the absence of bile acids in the perfusate, as well as the gradual loss of bile acids and their precursors from liver tissue. Perfusion pressure in the isolated liver is normally from 4 to 6 cm water, and this is generally maintained throughout a perfusion period of <3 hr.

The recovery of membrane vesicle proteins ranges from 0.1 to 0.2 mg/g liver and 0.05 to 0.10 mg/g liver for basolateral and canalicular membranes, respectively, starting with a single liver homogenate. Given the capacity of the zonal rotor (i.e., starting with about 100 g liver wet weight), the yields of basolateral and canalicular membrane proteins range from 10 to 20 mg and 5 to 10 mg, respectively. In terms of marker enzyme activities, Na^+,K^+-ATPase is normally enriched 20- to 40-fold in basolateral membranes when compared with the starting liver homogenate and is only minimally enriched in canalicular membranes (2-fold). Conversely, γ-glutamyltranspeptidase is normally enriched 40- to 70-fold in canalicular membranes when compared with the starting liver homogenate and is enriched 10- to 20-fold in basolateral membranes. Thus, the basolateral membrane vesicles are normally contaminated with 10% to 20% canalicular membranes, and the canalicular membrane vesicles are normally contaminated with ~5% basolateral membranes.

Time Considerations

For the in vivo bile collections, the surgical procedure requires only ~5 to 10 min to complete, whereas for the perfused rat liver protocol, the surgical approach requires 20 to 30 min. Once the liver is on the perfusion dish, an additional 5 to 15 min is normally allowed for making adjustments to the liver's anatomical arrangement, perfusate flow rate, and temperature control, prior to initiating the experiment.

Isolation of canalicular and basolateral membranes requires ~11 hr (7:00 a.m. to 6:00 p.m.). This includes about 6.5 hr of centrifugation time.

Literature Cited

Ballatori, N. and Truong, A.T. 1989. Relation between biliary glutathione excretion and bile acid-independent bile flow. *Am. J. Physiol*. 256:G22-G30.

Ballatori, N. and Truong, A.T. 1992. Glutathione as a primary osmotic driving force in hepatic bile formation. *Am. J. Physiol*. 263:G617-G624.

Ballatori, N., Jacob, R., and Boyer, J.L. 1986. Intrabiliary glutathione hydrolysis—a source of glutamate in bile. *J. Biol. Chem*. 261:7860-7865.

Ballatori, N., Jacob, R., Barrett, C., and Boyer, J.L. 1988. Biliary catabolism of glutathione and differential reabsorption of its amino acid constituents. *Am. J. Physiol*. 254:G1-G7.

Borst, P. and Elferink, R.O. 2002. Mammalian ABC transporters in health and disease. *Annu. Rev. Biochem*. 71:537-592.

Boyer, J.L. 1986. Mechanisms of bile secretion and cholestasis. *In* Physiology of Membrane Disorders (T.E. Andreoli, J.F. Hoffman, D.D. Fanestil, and S.G. Schultz, eds.) pp. 609-636. Plenum Publishing, New York.

Brandon, E.F., Raap, C.D., Meijerman, I., Beijnen, J.H., and Schellens, J.H. 2003. An update on in vitro test methods in human hepatic drug biotransformation research: Pros and cons. *Toxicol. Appl. Pharmacol.* 189:233-246.

Evans, W.H. 1969. Subfractionation of rat liver plasma membranes. *FEBS Lett*. 3:237-241.

Graf, J., Gautam, A., and Boyer, J.L. 1984. Isolated rat hepatocyte couplets: A primary secretory unit for electrophysiologic studies of bile secretory function. *Proc. Natl. Acad. Sci. U.S.A.* 81:6516-6520.

Graf, J., Henderson, R.M., Krumpholz, B., and Boyer, J.L. 1987. Cell membrane and transepithelial voltages and resistances in isolated rat hepatocyte couplets. *J. Membr. Biol.* 95:241-254.

Hagenbuch, B. and Meier, P.J. 2003. The superfamily of organic anion transporting polypeptides. *Biochim. Biophys. Acta* 1609:1-18.

Kato, Y., Suzuki, H., and Sugiyama, Y. 2002. Toxicological implications of hepatobiliary transporters. *Toxicology* 181-182:287-290.

Long, C.S., Rubin, W., Rifkind, A.B., and Kappas, A. 1969. Plasma membranes of the rat liver: Isolation and enzymatic characterization of a fraction rich in bile canaliculi. *J. Cell Biol*. 41:124-132.

Meier, P.J. 1988. Transport polarity of hepatocytes. *Semin. Liver Dis*. 8:293-307.

Meier, P.J. and Boyer, J.L. 1990. Preparation of basolateral (sinusoidal) and canalicular plasma membrane vesicles for the study of hepatic transport processes. *Methods Enzymol*. 192:534-545.

Meier, P.J., Sztul, E.S., Reuben, A., and Boyer, J.L. 1984. Structural and functional polarity of canalicular and basolateral plasma membrane vesicles isolated in high yield from rat liver. *J. Cell Biol.* 98:991-1000.

Miller, L.L. 1973. Technique of isolated rat liver perfusion. *In* Isolated Liver Perfusion and its Applications (I. Bartosek, A. Guaitani, and L.L. Miller, eds.) pp. 11-52. Raven Press, New York.

Rosalki, S.B. and Tarlow, D. 1974. Optimized determination of γ-glutamyltransferase by reaction-rate analysis. *Clin. Chem.* 20:1121-1124.

Scharschmidt, B.F., Keeffe, E.B., Blankenship, N.M., and Ockner, R.K. 1979. Validation of a recording spectrophotometric method for measurement of membrane-associated Mg- and NaK-ATPase activity. *J. Lab. Clin. Med*. 93:790-799.

Sperber, I. 1959. Secretion of organic anions in the formation of urine and bile. *Pharmacol. Rev*. 11:109-134.

Trauner, M. and Boyer, J.L. 2003. Bile salt transporters: Molecular characterization, function, and regulation. *Physiol. Rev*. 83:633-671.

Contributed by Nazzareno Ballatori
University of Rochester School of Medicine
Rochester, New York

CHAPTER 15
Gene Targeting

INTRODUCTION

The development of murine embryonic stem (ES) cells has brought about another revolution in the biological sciences. When considering the most important experiments of the last century, one must include those resulting in the discovery that clones derived from the inner cell mass of early embryos could be propagated in culture and that resultant cells could contribute to the germ line after reinjection into blastocysts (Evans and Kaufman, 1981; Bradley et al., 1984; Robertson et al., 1986). The marriage of pluripotent ES cells with an understanding of gene targeting through homologous recombination was the additional breakthrough that allowed application of this powerful approach to the murine system (Doetschman et al., 1988; Mansour et al., 1988).

As a result of these advances, a number of truly remarkable experimental avenues are now available to the general scientific population. In essence, ES cells and related gene targeting technologies allow us to alter any locus within the mouse genome, in essentially any way that is desired. The results of this new-found ability include the generation of better mouse models of human disease and the capacity to examine mutations within a whole-animal context. Moreover, the cell lines and organ culture models that can be derived from these experiments provide powerful systems for the analysis of gene-function relationships in simpler in vitro systems.

Like any new methodology, ES cells and gene targeting can be technically demanding. Because of this challenge, one can make the mistake of being intimidated and never attempting such experiments for oneself. In the early years of these techniques, avoidance of ES cell biology and gene targeting was understandable. ES cell lines were not readily available, generation of mouse embryonic fibroblasts required a large up-front commitment, serum lots had to be checked carefully for their capacity to maintain ES cell pluripotency, and the procurement of targeting vectors and related reagents was difficult. Add to this the fact that only a few experts knew what an ES cell colony looked like further sowed the seeds of intimidation. Today, avoidance of this technology is not as defensible. Pluripotent ES cell lines, the required feeder cells, ES-validated serum lots, and parent targeting vectors are available from a number of commercial vendors. In addition, most universities have core facilities that can easily handle the injection needs of the average investigator. With these technical obstacles out of the way, the only impediment left is the normal energy barrier that prevents us from beginning any new technique in the lab.

It is certain that ES cell technology will soon become a standard approach in the field of toxicology. At the very least, toxicologists will be able to benefit greatly from the use of mutant mice that have been generated by others. The utility of this technology to toxicology is less of a prediction than an observation. Already, null alleles at *Cyp* loci have proven that certain monooxygenases play a role in the toxicity of various chemicals (e.g., Lee et al., 1996; Zaher et al., 1998; Buters et al., 1999). Similarly, null alleles at loci encoding various cytokines are demonstrating a role for these factors in the mechanisms of certain toxicants (e.g., Ladenheim et al., 2000).

The protocols that follow should provide a solid start to those individuals ready to establish ES cell technology in their own laboratories. Although these protocols are fairly

Contributed by Christopher A. Bradfield
Current Protocols in Toxicology (2001) 15.0.1-15.0.2

detailed in nature, where appropriate, we have also tried to cite additional references and manuals in ES cell and mouse biology. In addition, a considerable discussion of ES cell biology can be found in *UNIT 1.3*. Here, we start with a section describing the general maintenance of ES cells, as well as the preparation of necessary feeder cells and related reagents (*UNIT 15.1)*. This is followed with a section describing protocols for the rapid genotyping of ES cells after a gene-targeting event (*UNIT 15.2*). The current version of this chapter also includes a description of how an investigator can make aggregation chimeras (*UNIT 15.3*). this protocol allows the study of chimeric mice and serves as a starting point for germ-line transmission. Additionally, we have begun to address how an investigator can examine Cre-expression methods in recombinant mice through the use of novel and widely available "reporter mice" (*UNIT 15.4*). In future supplements, we will address the construction of targeting vectors and the fundamentals of ES cell microinjection into blastocysts.

LITERATURE CITED

Bradley, A., Evans, M., MH, K., and Robertson, E. 1984. Formation of germ-line chimaeras from embryo-derived teratocarcinoma cell lines. *Nature* 309:255-256.

Buters, J. T., Sakai, S., Richter, T., Pineau, T., Alexander, D. L., Savas, U., Doehmer, J., Ward, J. M., Jefcoate, C.R., and Gonzalez, F.J. 1999. Cytochrome P450 CYP1B1 determines susceptibility to 7, 12-dimethyl-benz[a]anthracene-induced lymphomas. *Proc. Natl. Acad. Sci. U.S.A.* 96:1977-1982.

Doetschman, T., Maeda, N., and Smithies, O. 1988. Targeted mutation of the Hprt gene in mouse embryonic stem cells. *Proc. Natl. Acad. Sci. U.S.A.* 85: 8583-8587.

Evans, M. and Kaufman, M. 1981. Establishment in culture of pluripotential cells from mouse embryos. *Nature* 292:154-156.

Ladenheim, B., Krasnova, I.N., Deng, X., Oyler, J.M., Polettini, A., Moran, T.H., Huestis, M.A., and Cadet, J. L. 2000. Methamphetamine-induced neurotoxicity is attenuated in transgenic mice with a null mutation for interleukin-6. *Molec. Pharmacol.* 58:1247-1256.

Lee, S.S., Buters, J.T., Pineau, T., Fernandez-Salguero, P., and Gonzalez, F.J. 1996. Role of CYP2E1 in the hepatotoxicity of acetaminophen. *J. Biol. Chem.* 271:12063-12067.

Mansour, S.L., Thomas, K.R., and Capecchi, M.R. 1988. Disruption of the proto-oncogene int-2 in mouse embryo-derived stem cells: A general strategy for targeting mutations to non-selectable genes. *Nature* 336:348-352.

Robertson, E., Bradley, A., Kuehn, M., and Evans, M. 1986. Germ-line transmission of genes introduced into cultured pluripotential cells by retroviral vector. *Nature* 323:445-448.

Zaher, H., Buters, J.T., Ward, J.M., Bruno, M.K., Lucas, A.M., Stern, S.T., Cohen, S.D., and Gonzalez, F.J. 1998. Protection against acetaminophen toxicity in CYP1A2 and CYP2E1 double-null mice. *Toxicol. Appl. Pharmacol.* 152:193-1999.

Christopher A. Bradfield

Embryonic Stem (ES) Cell Culture Basics

Embryonic stem (ES) cells are derived from the inner cell mass (ICM) of a 3.5-day mouse blastocyst. The ICM is that portion of the blastocyst that will form the embryo proper and at 3.5 days these cells are pluripotent with respect to developmental fate. These cells can be manipulated in culture and returned to a mouse embryo to generate an animal with a desired mutation. Perhaps the most important factor in a successful targeting project is the quality of the ES cells used. Improper culture conditions can result in ES cells that have begun to differentiate and therefore lost their pluripotency. ES cells are ordinarily maintained on a layer of mitomycin C–inactivated mouse fibroblasts, either primary mouse embryonic fibroblasts or a fibroblast cell line. The cytokine known as leukemia inhibitory factor (LIF) is added to ES cell culture medium as it has an important role in maintaining the ES cells in the undifferentiated state. Lastly, very stringent culture conditions must be employed when working with ES cells. These include feeding the cells every day and passaging every 2 to 3 days, all the while maintaining minimal time in culture.

This unit describes the techniques necessary to maintain ES cells in culture (Basic Protocol), prepare primary mouse fibroblasts (Support Protocol 1), introduce targeted modifications by homologous recombination (Support Protocol 2), select for this event (Support Protocol 3), and prepare ES cells for injection (Support Protocol 4).

NOTE: All solutions and equipment coming into contact with live cells must be sterile, and proper aseptic technique should be used accordingly. All reagents should be warmed to 37°C just before use and not left at 37°C any longer than necessary.

NOTE: Most laboratories prefer commercially supplied reagents, including PBS, for culture work because the quality of in-house-purified water is so variable.

NOTE: All culture incubations should be performed in a humidified 37°C, 5% CO_2 incubator unless otherwise specified.

ES CELL CULTURE

BASIC PROTOCOL

The key to successful culture of ES cells is to maintain the cells at the correct density. Cells split back too far will not regrow while cells allowed to become overly confluent may begin to differentiate. For more information on primary mouse embryonic fibroblasts (pMEFs), see Support Protocol 1.

Materials

0.1% (w/v) gelatin
Mitomycin C–inactivated primary mouse embryonic fibroblast (pMEF) cells in a 1.5-ml cryovial (see Support Protocol 1)
pMEF medium, 37°C (see recipe)
ES cells in a 1.5-ml cryovial (see Support Protocol 2)
ES cell medium, 37°C (see recipe)
Trypsin/EDTA: 0.05% (w/v) trypsin/53 mM Na_4 EDTA (Invitrogen)

10-cm tissue culture dish or 6- or 96-well tissue-culture plate
15-ml culture tube
Sterile medium boats (96-well plates)
Multichannel pipettor (96-well plates)

Contributed by Jennifer V. Schmidt
Current Protocols in Toxicology (2001) 15.1.1-15.1.15

Thaw pMEF feeder cells

1. Gelatinize a 10-cm tissue culture dish or 6- or 96-well plate by adding 0.1% (w/v) gelatin to cover the bottom of the dish or wells. Incubate undisturbed (5 to 30 min) while preparing pMEF feeder cells.
2. To prepare previously inactivated and frozen feeder cells—i.e., mitomycin C–inactivated primary mouse embryonic fibroblast (pMEF) cells—thaw quickly by gently shaking the 1.5-ml cryovial in a 37°C water bath until the medium is liquid. Rinse the outside of the vial with ethanol. Transfer cells to a 15-ml culture tube and add warm pMEF medium to 10 ml.

   Each frozen cryovial of mitomycin C–inactivated pMEF cells will make one 10-cm dish, 6-well, or 96-well plate of ES cell feeders.
3. Centrifuge cells 2 min at ~400 × *g*, room temperature. Aspirate medium.
4. Resuspend cell pellet in 10 ml pMEF medium to make either a 10-cm dish or 96-well plate, or 18 ml to make a 6-well plate.
5. Aspirate gelatin from the dish or plate prepared in step 1.

Plate pMEF feeder cells

6. Add the full volume resuspended pMEF cells to the gelatinized 10-cm dish, 3 ml to each well of the gelatinized 6-well plate, or transfer the cell suspension to a sterile medium boat and use a 12-channel multichannel pipettor to dispense 100 µl to each well of the gelatinized 96-well plate.
7. Incubate ≥6 hr.

   This incubation is done to allow mitomycin C–inactivated pMEF cells to attach before adding ES cells. A 12-hr incubation is preferred.

Thaw frozen ES cells

NOTE: ES cells should be started in the same size plate as they were frozen from. The authors typically freeze and thaw ES cells from individual wells of a 6-well plate, which is the method described here (steps 8 to 11). This procedure can be modified for different numbers of cells.

8. Thaw one 1.5-ml cryovial ES cells quickly by shaking gently in a 37°C water bath until the medium is liquid. Rinse the outside of the vial with ethanol. Transfer to a 15-ml culture tube and add 37°C ES cell medium to 10 ml.
9. Centrifuge 2 min at ~400 × *g*, room temperature. Aspirate the supernatant and resuspend cell pellet in 3 ml of 37°C ES cell medium.
10. Aspirate pMEF medium from one well of a new 6-well feeder-cell plate and add all of the resuspended ES cells gently to the well without detaching the feeder cells. Rock the plate back and forth by hand three or four times to distribute the cells.
11. Transfer to an incubator.
12. Change ES cell medium daily.

Split and expand ES cells

13. The day before splitting the ES cells, prepare the appropriate feeder-cell plates for the next passage (steps 1 to 7).

    ES cells should be split when ~80% confluent. Cells should never be split more than 1:5. The author's laboratory typically thaws a vial of ES cells to one well of a 6-well plate (see above), splits to the other 5 wells of the plate, and then splits to two 10-cm dishes, yielding enough cells for two electroporation reactions (see Support Protocol 2).

14. Feed ES cells with an appropriate volume ES cell medium 1 hr before trypsinization. Just prior to trypsinization, aspirate the pMEF medium from the new feeder-cell plates and replace with 37°C ES cell medium.
15. Rinse ES cells once by removing the medium, adding sufficient trypsin/EDTA to cover the bottom of the dish or individual wells, swirling briefly, and aspirating. Add 3 ml, 0.5 ml, or 35 µl trypsin/EDTA to the dish or each well of a 10-cm dish, 6-well, or 96-well plate, respectively.
16. Incubate 10 min. Check that cells have detached completely from the dish or plate. If cells have not detached incubate a minute or two longer.
17. Add an equivalent volume 37°C ES cell medium to neutralize the trypsin, and pipet cells several times through a serological pipet with a 200-µl pipet tip (i.e., yellow tip) on the end. Transfer cells to a 15-ml culture tube and add ES cell medium to 10 ml.

    pMEFs will also be passaged but because they are inactivated, they will not divide, and they will die off.
18. Centrifuge cells 2 min at ~400 × *g*.
19. Aspirate the supernatant and resuspend the cell pellet in an appropriate volume ES cell medium.
20. Pipet dropwise onto new feeder-cell dishes or plates.

PREPARATION OF PRIMARY MOUSE EMBRYONIC FIBROBLAST (pMEF) CELLS

SUPPORT PROTOCOL 1

Primary mouse embryonic fibroblasts (pMEFs) provide the ideal substrate for the culture of ES cells. These cells provide a support matrix for the ES cells and secrete factors that help keep the cells in an undifferentiated state. The feeder cells must be neomycin resistant so they are able to survive drug selection and are therefore obtained from mouse embryos transgenic for the *neo* gene. One embryo will yield ~20 plates of ES cell feeders.

Additional Materials *(also see Basic Protocol)*

Male transgenic mice homozygous for the *neo* gene (e.g., C57BL/6JTgN[pPGKneobpA]Ems, Jackson Laboratories)
Outbred nontransgenic female mice (preferably the same strain as the males)
PBS, fresh (*APPENDIX 2A*)
Freezing medium, 4°C (see recipe)
Mitomycin C medium (see recipe)

Dissecting equipment
Petri dish
Dissecting microscope
6-cm tissue culture dish
Razor or scalpel blades
10-ml serological pipets
10-ml syringe with 18-G needle
50-ml centrifuge tube
10-cm tissue culture dish
1.5-ml cryovials
Additional reagents and equipment for isolating postimplantation embryos (*UNIT 13.3*)

NOTE: All protocols using live animals must first be reviewed and approved by an Institutional Animal Care and Use Committee (IACUC) and must follow officially approved procedures for the care and use of laboratory animals.

Mate Neo transgenic mice

1. Set up mating pairs of male transgenic mice homozygous for the *neo* gene with strain-matched nontransgenic females. Check the females each morning for the presence of a copulation plug in the vagina.

   The copulation plug looks like a grain of rice and indicates that mating has occurred. The day of the plug is counted as embryonic day 0.5 (e0.5).

Isolate embryos

2. Working on a regular lab bench, sacrifice 1 to 2 pregnant females on day e13.5 to e14.5. Using dissecting equipment, remove the uterine horns from the mice (*UNIT 13.3*) and transfer into a petri dish containing PBS.

3. Move this dish to a clean area (e.g., a tissue culture room) and dissect the intact embryos into a petri dish containing fresh PBS. Release each embryo from its yolk sac and placenta, and transfer to a petri dish containing fresh PBS.

4. Cut the head off each embryo and using a dissecting microscope remove as much viscera as possible. Move each carcass into a petri dish containing fresh PBS.

5. Move the dish containing carcasses into a tissue culture hood.

   Work with 5 to 6 embryos at a time for the following volumes.

6. Put carcasses in a 6-cm tissue culture dish containing 5 ml fresh trypsin/EDTA. Mince very well with a razor or scalpel blade and incubate 5 min.

7. Add 5 ml of 37°C pMEF medium and pipet the embryo mixture up and down several times with a 10-ml serological pipet. Place an 18-G needle on a 10-ml syringe and pass the embryo mixture through the needle several times.

8. Transfer the embryo mixture to a 15-ml tissue culture tube and incubate undisturbed for 1 to 2 min to allow the largest debris to settle out.

9. Transfer the supernatant to a 50-ml centrifuge tube, add 40 ml pMEF medium, and centrifuge 2 min at ~400 × *g*, room temperature. Aspirate the supernatant and resuspend the cell pellet in 5 to 6 ml pMEF medium (i.e., 1 ml medium/initial embryo).

Plate pMEF cells

10. Treat all embryos as above and pool when finished to ensure uniformity in plating.

11. Prepare as many 10-cm tissue culture dishes as there were initial embryos, by adding 9 ml pMEF medium per dish.

12. Add 1 ml resuspended cells to each dish.

13. Transfer to an incubator, changing pMEF medium the following day and every 2 days after until cells have almost reached confluency (i.e., usually 3 to 5 days).

14. Aspirate all medium from each dish and replace with 3 ml trypsin/EDTA. Incubate 10 min. While plates are incubating, prepare four new 10-cm tissue culture dishes for each dish of pMEFs as described in step 11.

    There should be four new dishes for each starting embryo.

15. After incubation, check to see that cells have detached from the dish and add 3 ml pMEF medium to each. Pipet several times with a 10-ml serological pipet and transfer cells to a 50-ml centrifuge tube.

16. Add additional pMEF medium to 50 ml total and centrifuge 2 min at ~400 × *g*, room temperature

17. Aspirate the supernatant and resuspend the cell pellet in 4 ml pMEF medium (i.e., 1 ml per each new dish or 4 ml per each embryo).

18. Add 1 ml resuspended cells to each new dish.

19. Incubate to confluency, feeding cells with pMEF medium every 2 days.

When the pMEFs have again reached confluence, they can be frozen for later use or passaged again for mitomycin C inactivation.

Freeze cells for later use

20a. Trypsinize and centrifuge (see Basic Protocol, steps 15 to 17) but do not prepare new dishes. Aspirate the supernatant and resuspend the cell pellet in 4°C freezing medium at 1 ml per starting dish (i.e., 20 or 24 ml). Pool all cells for uniformity. Aliquot 1 ml cells into 1.5-ml cryovials and place in a −20°C freezer until frozen solid (i.e., 1 to 2 hr).

21a. Move cells to a −80°C freezer overnight. The following morning transfer cryovials to the vapor phase of a liquid nitrogen tank up to 1 year.

To continue with mitomycin C inactivation, perform steps 22 and 23.

Continue with mitomycin C inactivation

20b. Prepare four or five new plates as described in step 11.

21b. Split cells 1:4 or 1:5 and incubate to confluency (~4 to 5 days), feeding every 2 days.

Proceed to step 24.

Prepare mitomycin C–inactivated feeder cells

22. (*Optional*) If cells were frozen, thaw one or more cryovials pMEF cells quickly by gently shaking the cryovial(s) in a 37°C water bath until the medium is liquid. Transfer cells to a 15-ml tube and add 37°C pMEF medium to 10 ml. Centrifuge cells 2 min at ~400 × *g*, room temperature. While the centrifugation is proceeding, prepare five 10-cm tissue culture dishes by adding 9 ml warm pMEF medium.

23. (*Optional*) Aspirate supernatant and resuspend cell pellet in 5 ml pMEF medium per vial thawed. Add 1 ml cells to each 10-cm dish. Transfer to an incubator. Feed cells every 2 days with pMEF medium until confluent (~4 to 5 days).

24. Remove pMEF medium and replace with 6 ml mitomycin C medium per dish. Incubate 2 hr.

25. Wash cells three times gently with PBS. Trypsinize and centrifuge (see Basic Protocol, steps 15 to 17). Aspirate supernatant and resuspend cell pellets in 1 ml pMEF medium for each starting dish. Pool all cells when finished to ensure uniformity in plating.

26a. *For immediate use:* Prepare a new gelatinized dish (see Basic Protocol, step 1) for each starting dish. Transfer 1 ml to each new dish (i.e., split 1:1).

26b. *For later use:* Resuspend and freeze as described in steps 20a and 21a, omitting further trypsinization and centrifugation.

Feeder cells should be prepared at least 6, and preferably 12 hr before use, and may be used for up to 1 week after plating.

SUPPORT PROTOCOL 2

ELECTROPORATION OF ES CELLS

ES cell targeting is a laborious and time consuming endeavor. Use of a 96-well plate such as the one described in this protocol dramatically decreases the hands-on time required. One important concern during all ES cell work is to minimize the amount of time the cells spend in culture and thus the possibility they may begin to differentiate. For this reason, ES cells are never maintained as a continuously growing cell line. The author's laboratory freezes the cells in small batches, thawing and expanding them only to the extent necessary for electroporation, and freezing the targeted clones as soon as possible. One additional advantage of scaled-down protocols is that they allow the time in culture to be kept to a minimum.

Additional Materials *(also see Basic Protocol)*

Targeting plasmid
H_2O, sterile
ES cell cultures (see Basic Protocol)
G418 medium or G418/ganciclovir medium (see recipes)
Freezing medium (see recipe)

Electroporator (Bio-Rad) and appropriate cuvettes with a 4-mm gap
15-ml conical tube
96-well U- and flat-bottom plates
Microscope with 4× objective
200-µl micropipettor and tips, sterile
Styrofoam box

Additional reagents and equipment for plasmid preparation by cesium chloride equilibrium centrifugation, enzyme digestion, agarose gel electrophoresis, phenol/chloroform/isoamyl extraction, and ethanol precipitation (see Table A.3A.1 of *APPENDIX 3A*), preparing 10-cm feeder-cell dishes (see Support Protocol 1), and counting cells in a hemacytometer (*APPENDIX 3B*).

Prepare DNA for targeting

1. Prepare the targeting construct plasmid DNA by cesium chloride equilibrium centrifugation (*APPENDIX 3A*). Linearize 50 to 100 µg targeting construct with an appropriate enzyme and check a small amount of the DNA on an agarose gel (*APPENDIX 3A*) to make sure the linearization is complete.

   Instead of cesium chloride equilibrium centrifugation, the Qiagen method can be used for plasmid purification.

2. Extract DNA with phenol/chloroform, then chloroform/isoamyl alcohol and ethanol precipitate (*APPENDIX 3A*). Resuspend to a concentration of 1 µg/µl using sterile H_2O.

Electroporate ES cells

NOTE: ES cells should be electroporated when they reach 70% to 80% confluency. One 10-cm dish of ES cells at this density will yield ~2×10^7 cells (i.e., the number required for one electroporation); therefore, one targeting construct and a blank will require two 10-cm dishes of ES cells.

3. The day before electroporation, prepare three 10-cm feeder-cell dishes for each DNA electroporation (see Support Protocol 1).

   Only one feeder cell plate is necessary for the blank reaction.

4. Feed the ES cell cultures with ES cell medium 1 hr before electroporation. Just prior to electroporation, aspirate the pMEF medium from the feeder-cell dishes and replace with 9 ml of 37°C ES cell medium.

5. Trypsinize cells as described (see Basic Protocol, steps 15 to 19) and resuspend the cell pellet in 10 ml ES cell medium.

6. Add 20 µl ES cells to one chamber of a hemacytometer and count the center 25 squares (*APPENDIX 3B*). To obtain the total number of cells, multiply the number of cells in the center 25 squares by 10,000 then by the total volume of culture in milliliters.

7. Centrifuge 2 min at ~400 × *g*, room temperature. Adjust the cell concentration to 2 × 10^7 cells/800 µl with ES cell medium.

8. Mix 800 µl ES cells with 25 µg linearized DNA in a sterile microcentrifuge tube. Incubate 5 min at room temperature. Add mixture to an electroporation cuvette with a 0.4-mm gap and electroporate at settings of 250 V and 500 µF. Monitor the time constants, which should be between 7 and 10 msec.

   These settings are for a Bio-Rad electroporator and may need to be optimized for different machines.

9. Incubate the electroporated ES cells 5 min at room temperature. Use a Pasteur pipet to transfer all cells from the electroporation cuvette to a 15-ml conical tube. Adjust the cell volume to 3 ml with ES cell medium.

10. Add 1 ml reaction mixture to each of the three 10-cm feeder-cell plates. Transfer to an incubator.

    The blank reaction requires only one plate with ⅓ of the electroporated cells. This acts as a negative control and should show no colony growth in G418.

Select for drug resistance

NOTE: Drug selection should be begun 24 to 48 hr after electroporation. If selection is begun at 48 hr, cells should be fed with regular ES cell medium at 24 hr.

11. Replace ES cell medium with warm G418 or G418/ganciclovir medium. Change medium daily.

    The majority of the ES cells should begin to die after 1 to 2 days of drug selection and a large number of dead cells is normal for several days.

    DNA introduced into a cell can integrate homologously or heterologously; the frequency of homologous integration is quite low and selection is required to enrich for this event. Selection strategies incorporate a positive selectable marker such as neomycin into the targeting vector—incorporation of the neo gene renders a cell resistant to the drug geneticin, found in G418 medium. A second strategy known as negative selection is often employed to enrich for homologous recombinants. Incorporation of a negative selectable marker such as HSV-TK renders cells sensitive to the drug ganciclovir. By placing the HSV-TK gene in the targeting construct, outside of the region of homology, it will be incorporated in only those cells in which the DNA has integrated heterologously. The choice of positive alone or positive-negative selection is one of personal preference and cloning feasibility.

Pick colonies

NOTE: Colonies of ES cells should begin to be visible microscopically after 4 to 5 days of drug selection and are typically picked after 5 to 7 days of selection, when most of the background has cleared.

12. The day before picking colonies, prepare 96-well feeder-cell plates (see Basic Protocol, steps 1 to 7), for the number of clones to be picked.

    An initial analysis of 400 clones is a good number and can easily be managed by a single person.

13. When ready to pick, prepare the 96-well feeder-cell plate by replacing the pMEF medium with 100 µl of 37°C ES cell medium in each well. Prepare a 96-well U-bottom plate by adding 75 µl trypsin/EDTA to each well.

14. Move one plate ES cell colonies to a microscope with a 4× objective and use a 200-µl micropipettor set at 25 µl to pick and transfer individual colony to one of the wells of the 96-well U-bottom plate containing trypsin, using a fresh pipet tip for each clone. Repeat for all clones.

    The wells can be checked with the microscope to verify that the clone was transferred.

    ES cells are remarkably resistant to trypsin and can be left to disaggregate for up to 1 hr. Working quickly an entire 96-well plate can be picked at one time.

15. When finished picking colonies, add 75 µl ES cell medium to each well and pipet the clone up and down several times with a 200-µl micropipettor with an appropriate (i.e., yellow) tip.

16. Add disaggregated ES cells to the new feeder-cell plate, one clone per well. Transfer to an incubator.

Expand colonies

17. Feed picked clones daily with ES cell medium without drugs.

    Cells should begin to be visible in the wells after 3 to 4 days.

    Invariably all ES cell clones will not grow at the same rate. There will be some clones that are not yet confluent when the majority are ready to split. Regardless, the plate should be split when the majority of clones are ready, even if those with fewer cells may be lost.

18. The day before splitting, prepare one new 96-well feeder-cell plate (see Basic Protocol 1, steps 1 to 7), for each plate of colonies.

19. On the split day, add 0.1 % (w/v) gelatin to cover the bottom of two 96-well flat-bottom plates for each plate of clones. Let this sit while preparing to trypsinize. Replace the pMEF medium of each well of the new 96-well feeder-cell plates with 100 µl ES cell medium.

20. Rinse the ES clones with trypsin/EDTA, swirl, and aspirate. Replace with 75 µl trypsin/EDTA and incubate 10 min. While cells are trypsinizing, aspirate the gelatin in the flat-bottom 96-well plates replace with 100 µl ES cell medium in each well.

21. After incubation add 75 µl ES cell medium to each well and pipet the cells several times using a multichannel pipettor with 200-µl (i.e., yellow) tips. Transfer $\frac{1}{3}$ each clone suspension to each of the two gelatinized 96-well flat-bottom plates and the new feeder-cell plate. Transfer to an incubator.

22. Feed the ES cells on feeder cells daily with ES cell medium until confluent, then freeze plate for later retrieval.

    The cells on gelatin will be used to extract DNA (see UNIT 15.2, Basic Protocol 1). While in the author's laboratory cells are not normally fed after plating, they can be fed every 2 to 3 days if desired.

Freeze ES cell clones in 96-well plates

NOTE: Plates should be stored at −80°C for no more than a few weeks and should be placed in a position to avoid any freeze-thaw. This length of time is usually sufficient for analysis of the clone DNAs. If longer storage is necessary, the plates should be stored in the vapor phase of a liquid nitrogen tank.

23. Chill a small styrofoam box in a −80°C freezer.
24. Use a multichannel pipettor to aspirate the medium from each 96-well plate and replace with 50 µl freezing medium, 4°C.
25. Quickly wrap each plate in a double layer of Parafilm and place in the chilled box in a −80°C freezer.

Thaw and expand ES cells after genotyping

26. The day before thawing, prepare a 96-well plate of feeder cells (see Basic Protocol, steps 1 and 2). Just prior to thawing the ES clones replace the pMEF medium of each well with 100 µl of 37°C ES cell medium.

    ES cells should always be thawed to the same size plate as the one they were frozen from. For targeted cells being recovered after screening, this means thawing to a 96-well plate and sequentially expanding.

27. Remove the 96-well plate from the freezer and unwrap. Working quickly, locate the clone to be thawed and use a 200-µl micropipettor to add 200 µl of 37°C ES medium to the well; pipet up and down several times as the cells thaw. Transfer the cells to a 3-ml tube and repeat several times until all cells have been thawed and transferred. Add medium to 2 ml.

    The well can be examined under the microscope to ensure that all cells have been recovered.

28. Centrifuge the cells 2 min at ~400 × *g*, room temperature. Aspirate the supernatant, leaving ~100 µl medium in the tube. Use a 200-µl pipet tip to resuspend the cell pellet and transfer to one well of the feeder-cell plate. Repeat with all other clones to be thawed. Transfer to an incubator.
29. When cells are visible in the 96-well plate (4 to 6 days), prepare a new 24-well feeder-cell plate (see Basic Protocol, steps 1 to 7). Once cells reach 80% confluence, trypsinize as described previously (see Basic Protocol, steps 15 to 19) and plate cells from one well into one well of the 24-well plate.
30. When the cells again reach 80% confluence, expand further by plating into one well of a 6-well plate; then further again by splitting to the other 5 wells of the 6-well plate. When confluent again, freeze as 1 well/vial. Upon thawing, the clones should be genotyped (*UNIT 15.2*) to ensure the correct clone identity.

    This will give 5 vials of cells per clone for microinjection or subsequent protocols such as Cre excision. Upon thawing, the clones should be genotyped (UNIT 15.2) to ensure the correct clone identity.

TRANSFECTION OF CRE

SUPPORT PROTOCOL 3

The presence of the Neo transcription unit in a targeted locus can have unwanted effects on gene expression at the targeted locus, as well as at other nearby loci. Cre-lox technology allows the specific removal of the Neo selectable marker after gene targeting. During design of the gene targeting vector, the selectable marker is flanked by a direct repeat of 34-bp loxP sites. The Cre recombinase protein catalyzes recombination between the two loxP sites, resulting in excision of the intervening DNA segment and leaving behind a single loxP site. Cre excision is accomplished by the transient transfection of a circular Cre-expressing plasmid into the targeted ES cell clones. The circular Cre plasmid doesn't

integrate and is soon eliminated from the cells. The authors have found that the frequency of Cre-mediated excision can vary among similarly targeted ES cell clones; therefore, it is advisable to use 2 to 3 separate ES cell clones for Cre excision.

Additional Materials *(also see Basic Protocol)*

Circular Cre plasmid DNA
Targeted ES cells
H_2O, sterile
G418 medium (see recipe)

Electroporator and appropriate electroporation cuvettes with a 4-mm gap
Microscope with 4× objective lens
96-well flat-bottom plate

Additional reagents and equipment for plasmid preparation by cesium chloride equilibrium centrifugation (see Table A.3A.1 of *APPENDIX 3A*), counting cells in a hemocytometer (*APPENDIX 3B*), and Southern blotting (*UNIT 3.6* and *APPENDIX 3*).

Prepare Cre plasmid DNA

1. Prepare circular Cre plasmid DNA by cesium-chloride equilibrium centrifugation and resuspend the DNA in sterile water to a concentration of 1 µg/µl.

   Alternatively, instead of cesium chloride equilibrium centrifugation, the Qiagen method can be used for plasmid purification.

Thaw and expand ES cells

2. Thaw one vial of each targeted ES cell clone to be transfected to the appropriate sized plate and expand to at least 2×10^7 cells per clone (approximately one 10-cm plate at 80% confluence).

3. Prepare two 10-cm feeder-cell dishes (see Basic Protocol, steps 1 to 7) for each construct to be electroporated.

Transfect ES cells

4. Trypsinize cells as described (see Basic Protocol, steps 15 to 19), and resuspend the cell pellet in a total of 10 ml of 37°C ES cell medium. Add 20 µl cells to one chamber of a hemacytometer and count the center 25 squares (*APPENDIX 3B*). To obtain the total number of cells, multiply the number of cells by 10,000, then by the total number of milliliters. Centrifuge and adjust the cell concentration to 2×10^7 cells/800 µl with ES cell medium.

5. Mix 800 µl ES cells in a microcentrifuge tube with 25 µg Cre plasmid DNA. Transfer to an electroporation cuvette with a 4-mm gap and incubate 5 min at room temperature. Electroporate cells at settings of 250 V and 500 µF.

   These settings are for a Bio-Rad electroporator and may need to be optimized for different machines.

6. Resuspend each transfection reaction in 5 ml ES cell medium total. Plate the ES cells at concentrations of 1% and 0.1% (i.e., 50 and 5 µl, respectively) on the individual 10-cm feeder-cell plates prepared in step 3. Transfer to an incubator.

7. Feed plates daily for ~5 to 6 days with ES cell medium.

   Colonies should be visible at 3 to 4 days and picked after 5 to 6 days.

Pick colonies

8. The day before picking colonies, prepare sufficient 96-well feeder-cell plates (see Basic Protocol, steps 1 to 7) for the number of clones to be picked.

   An initial analysis of 200 clones per initial clone transfected is a good number.

   The number of Cre-transfected colonies that will need to be picked is largely dependent upon the transfection efficiency of the ES cells. The authors find that their efficiency of Cre-mediated recombination is between 3% and 5%; therefore, picking 100 to 200 colonies will usually give several recombinant clones.

9. Replace the pMEF medium of each well of a 96-well feeder-cell plate with 100 µl ES cell medium. Prepare a 96-well U-bottom plate by adding 75 µl trypsin/EDTA to each well.

10. Transfer one 10-cm dish of ES colonies to a microscope with a 4× objective lens and use a 200-µl micropipettor set at 25 µl to pick individual colonies.

11. Transfer each clone to one of the wells of the 96-well U-bottom plate containing trypsin/EDTA.

    The wells can be checked with the microscope to verify that the clone was transferred.

    ES cells are remarkably resistant to trypsin and can be left to disaggregate for up to 1 hr without harming the cells.

12. When finished picking colonies, add 75 µl ES cell medium to each well and pipet each clone up and down several times with a 200-µl micropipettor and appropriate tip.

13. Add disaggregated ES cells to the new feeder-cell plate at a density of one clone per well. Transfer to an incubator.

Expand and select for drug resistant colonies

14. Feed picked clones daily with ES cell medium.

    Cells should begin to be visible in the wells after 3 to 4 days.

15. Prepare two new 96-well feeder-cell plates for each plate of colonies.

    Once confluent, the transfected clones are split 1:3. One plate is used to determine sensitivity to G418, one for DNA extraction, and one plate is frozen for later retrieval.

16. On the day to split, add 0.1% (w/v) gelatin to cover the bottom of one 96-well flat-bottom plate for each plate of clones. Allow to incubate at room temperature while preparing to trypsinize.

17. Replace the pMEF medium in the wells of one of the new 96-well feeder-cell plates with 100 µl regular ES cell medium. Repeat the procedure with a second plate, except using G418 instead of ES cell medium.

18. Rinse the clone wells with 75 µl trypsin/EDTA and aspirate. Replace with 75 µl trypsin/EDTA and incubate 10 min.

19. During this incubation, aspirate the gelatin in the 96-well flat-bottom plate and add 100 µl ES cell medium to each well.

20. Add 75 µl ES cell medium to each well of the 96-well flat-bottom plates and pipet the cells several times using a multichannel pipettor with 200-µl tips. Transfer $\frac{1}{3}$ each clone suspension to the corresponding well of each of the new feeder cell and gelatin plates.

21. Transfer to an incubator. Feed cells daily with ES cell or G418 medium as appropriate.
22. Freeze the ES medium plates when most of the clones are ~80% confluent (see Support Protocol 2, steps 23 to 25)

    It will probably be a few days before G418 selection of the other plate is complete.
23. When there is a clear distinction between surviving and non-surviving clones on the plate under drug selection, score each clone for survival or death in G418. Those clones that died in G418 may have undergone Cre excision. Prepare DNA from only these clones and analyze by Southern blotting (*APPENDIX 3*) for evidence of Cre-mediated recombination.
24. Thaw those clones from the frozen plate (see Support Protocol 2) that have undergone appropriate Cre excision.

SUPPORT PROTOCOL 4

PREPARATION OF CELLS FOR MICROINJECTION

Cells for microinjection should be thawed ~5 days before the date of injection. In the author's laboratory, the protocol is to inject on a Thursday and Friday, thaw cells on Saturday, and split Tuesday for Thursday injection and Wednesday for Friday injection. This allows cells to be harvested for injection on day 2 after a split, at ~50% confluence. This protocol can be adapted to different injection schedules.

Materials

ES cell cultures (see Support Protocol 2)

1. Feed ~70% to 80% confluent ES cells 1 hr before trypsinization with ES cell medium.
2. Trypsinize and centrifuge cells as described (see Basic Protocol, steps 15 to 19). Resuspend in 10 ml ES cell medium.
3. To obtain the total number of cells, count the center 25 squares in a hemacytometer, multiply by 10,000, then by the total number of milliliters.
4. Centrifuge 2 min at ~400 × *g*, room temperature and adjust the cell concentration to 2×10^6 cells/ml with ES cell medium.
5. Plate the ES cells in a nongelatinized tissue culture plate. Incubate 15 min.

   The feeder cells will attach quickly to the plate and an enriched population of ES cells can be obtained.
6. Swirl the plate gently and pipet the enriched ES cells from the plate.

   The cells are now ready for injection into blastocysts.

REAGENTS AND SOLUTIONS

Use Milli-Q-purified water in all recipes and protocol steps. For common stock solutions, see ***APPENDIX 2A****; for suppliers, see* ***SUPPLIERS APPENDIX****.*

ES cell medium

To 500 ml high glucose DMEM, -glutamine, -pyruvate, add 75 ml heat-inactivated ES cell–qualified FBS, 5 ml of 100× L-glutamine (Invitrogen), 5 ml of 100× penicillin/streptomycin (Invitrogen), 5 ml of 2-mercaptoethanol solution (see recipe), and 50 µl LIF (Chemicon ESGrow). Store up to 2 months at 4°C. Replenish L-glutamine every 2 weeks.

NOTE: *Many companies now sell ES cell–qualified FBS; however, it is still desirable to test the serum on the ES cells used in the laboratory for its ability to inhibit differentiation of the cells.*

Freezing medium

Add additional heat-inactivated ES cell–qualified FBS to either pMEF or ES cell medium (see recipes) to a total of 20% (v/v) and DMSO to a total of 10% (v/v). Store up to 2 months at 4°C.

See note above concerning FBS.

Ganciclovir, 1000×

Make a 1 mM solution of ganciclovir in sterile water. Use a 10-ml syringe with a 0.2-µm filter to sterilize the drug and aliquot into 1-ml tubes. Store up to 1 year at 4°C.

G418/ganciclovir medium

Add 200 mg/ml geneticin (G418; see recipe) and 1 mM ganciclovir (see recipe) to ES cell medium (see recipe) at a 1:1000 dilution each. Store up to 2 months at 4°C.

G418 (geneticin), 1000×

Make a 200 mg/ml solution of active G418 (Invitrogen) in sterile water. Use a 10-ml syringe with a 0.2-µm filter to sterilize the drug and aliquot into 1-ml tubes. Store up to 1 year at 4°C.

The percentage of active drug varies with each lot and is indicated on the individual bottle.

G418 medium

Add 200 mg/ml G418 (see recipe) to ES cell medium (see recipe), at a 1:1000 dilution. Store up to 2 months at 4°C.

2-Mercaptoethanol solution

Add 7 µl of 2-mercaptoethanol to 10 ml complete DMEM (*APPENDIX 3B*). Store at 4°C and use within 2 weeks.

Mitomycin C medium

Dissolve a 2 mg vial mitomycin C (Sigma) in 2 ml PBS (*APPENDIX 2A*). Filter through a 0.2-µm syringe filter. Add the mitomycin C to pMEF medium at a 1:100 dilution. Store up to 2 weeks at 4°C or 2 months at −20°C.

pMEF medium

To 500 ml high-glucose DMEM, add 50 ml heat-inactivated FBS, 5 ml of 200 mM L-glutamine, and 5 ml of 100× penicillin/streptomycin (i.e., 10,000 U/ml penicillin and 10,000 µg/ml streptomycin). Store up to 2 months at 4°C, replenish L-glutamine every 2 weeks.

COMMENTARY

Background Information

Embryonic stem (ES) cells are derived from the inner cell mass of a mouse blastocyst at embryonic day 3.5 (e3.5). These cells are pluripotent with respect to developmental fate, an essential property for their use in gene targeting. ES cells were first isolated in 1981 and soon after shown to be capable of colonizing the germline when returned to a mouse embryo (Evans and Kaufman, 1981; Bradley et al., 1984). The ability to manipulate ES cells in culture has revolutionized the field of mouse molecular genetics and provided information on the function of many genes. Numerous groups have generated ES cell lines, with the most popular being the AB1, CCE, CJ7, D3, E14, J1, and R1 cell lines. Virtually all commonly used ES cell lines are obtained from strain 129 mice, since this strain has been shown to allow superior germline competence.

An important factor to consider when initiating a gene targeting project is the use of isogenic DNA—i.e., the DNA used to construct the gene targeting vector should be derived from a 129 mouse substrain identical or very closely related to the ES cells to be used, as recent work has shown the various 129 substrains to be genetically variable and highly

contaminated with other strain backgrounds (Simpson et al., 1997; Threadgill et al., 1997). Careful DNA-ES cell matching using a genealogy chart such as that shown in Simpson et al. (1997) will help ensure the use of properly isogenic DNA.

Proper culture of embryonic stem cells is perhaps the most critical step in any gene targeting procedure. The cells must be maintained under defined culture and cell density conditions to prevent their differentiation. Even slight differentiation can result in cells that will not contribute to the germline upon introduction into host embryos. Strict adherence to the protocols outlined here will help ensure the pluripotency of the ES cells and the success of the gene targeting project.

Critical Parameters and Troubleshooting

The most critical aspect of these protocols is to maintain the integrity of the ES cells. This includes the use of sterile technique to avoid contamination of the cells as well as following the procedures described to minimize ES cell differentiation. While strict cell culture protocols will help to maintain ES cells in the desired state, some cells may still begin to differentiate. An important skill is to learn to recognize early signs of differentiation and know how to handle them. Healthy and undifferentiated ES cells may display two characteristic morphologies depending on the particular ES cell line used. They may grow as broad and slightly raised colonies atop their feeder layers, or as more rounded up balls of cells. Either cell morphology should show highly refractile colony edges. Photos of undifferentiated ES cells can be found in the two protocol manuals listed at the end of this unit (Hogan et al., 1994; Robertson, 1997). In contrast to these pluripotent cells, cells that are beginning to differentiate will display one of two altered appearances. They may appear as tight balls of cells with darkening centers and edges that appear to be membrane-limited. Alternatively the cells may assume a flattened ring-like "donut" shape with nearly empty centers. These "donuts" will often show highly differentiated cell types at the periphery.

Differentiation will occasionally be seen during passage and expansion of ES cells. This often results from inadequate trypsinization during passage and/or the failure to obtain a single cell suspension following trypsinization. If the cells should begin to differentiate, they should be trypsinized immediately to prevent further differentiation. If the areas of differentiation are small, these cells can be removed prior to trypsinization by vacuum aspiration using a pipet with a 200-µl (i.e., yellow) tip. Passage of the remaining cells may then be able to halt any further differentiation. Most commonly, however, differentiation will be seen during drug selection when the cells are maintained without passage for many days. In the event this does occur, it is unlikely that all ES cell colonies will differentiate at the same time. The remaining undifferentiated colonies should be picked immediately and have a good chance of retaining germline competence.

Anticipated Results

This 96-well plate protocol for the handling and analysis of ES cell clones is a rapid way to manipulate large numbers of individual clones. This type of high-throughput system, however, invariably results in the loss of some clones at various steps of the protocol. Whole plates must be processed (e.g., trypsinized, frozen) when the majority of clones on the plate are ready; therefore, slower growing clones will be lost. The authors frequently lose ~10% of the original ES cell clones by the time the final plates are frozen. This reduces the numbers of clones screened only slightly and can be considered an acceptable loss. The authors have not seen any evidence to indicate that targeted clones may be slower growing and therefore selectively lost.

Time Considerations

Gene targeting is a time-consuming activity. Most often cloning of the targeting construct is the rate-limiting step in these experiments. Once the construct is prepared and ES cell work begins, the time for a single round of transfection, selection, and analysis is ~5 to 6 weeks. This time includes periods of drug selection requiring only daily medium changes, as well as periods of picking and passaging clones that will require several hands-on hours a day. Subsequent Cre-mediated excision and the time required for thawing and expansion of correctly targeted clones will result in a total time commitment of ~3 to 4 months.

Literature Cited

Bradley, A., Evans, M., Kaufman, M.H., and Robertson, E.J. 1984. Formation of germ-line chimeras from embryo-derived teratocarcinoma cell lines. *Nature* 309:255-256.

Evans, M.J. and Kaufman, M.H. 1981. Establishment in culture of pluripotential cells from mouse embryos. *Nature* 292:154-156.

Hogan, B., Beddington, R., Constantini, F., and Lacy, E. 1994. Manipulating the Mouse Genome. Cold Spring Harbor Laboratory Press, Cold Spring Harbor, N.Y.

Robertson, E.J. 1997. Derivation and maintenance of embryonic stem cell cultures. *In* Methods in Molecular Biology, Vol. 75: Basic Cell Culture Protocols (J.W. Pollard and J.M. Walker, eds.) pp. 173-184. Humana Press, Totowa, N.J.

Simpson, E.M., Linder, C.C., Sargent, E.E., Davisson, M.T., Mobraaten, L.E., and Sharp, J.J. 1997. Genetic variation among 129 substrains and its importance for targeted mutagenesis in mice. *Nature Genet.* 16:19-27.

Threadgill, D.W., Yee, D., Matin, A., Nadeau, J.H., and Magnuson, T. 1997. Genealogy of the 129 inbred strains: 129SvJ is a contaminated inbred strain. *Mammal. Genome* 8:390-393.

Key References

Hogan et al., 1994. See above.

The above reference is an excellent manual that describes both theory and practice of gene targeting in embryonic stem cells.

Kuhn, R. and Schwenk, F. 1997. Advances in gene targeting methods. *Curr. Opin. Immunol.* 9:183-188.

Another well-written review of gene targeting methods.

Muller, U. 1999. Ten years of gene targeting: Targeted mouse mutants, from vector design to phenotype analysis. *Mech. Dev.* 82:3-21.

An extremely comprehensive and up-to-date review covering all aspects of gene targeting.

Robertson, 1997. See above.

The above reference is an excellent manual that describes both the theory and practice of gene targeting in embryonic stem cells.

Contributed by Jennifer V. Schmidt
University of Illinois at Chicago
Chicago, Illinois

Genotyping Embryonic Stem (ES) Cells

The techniques described in *UNIT 15.1* describe the process of using homologous recombination in embryonic stem (ES) cells to introduce a desired mutation into a gene. The frequency of homologous recombination is quite low, and selection protocols are used to enrich for this event. Even utilizing selection, however, only a fraction of the surviving cells will contain the correct recombination event. Therefore, a screening strategy is needed to identify those cells which are properly targeted. ES cell clones may be analyzed for gene targeting events using Southern blotting (see Basic Protocol) or PCR (see Alternate Protocol) to detect products unique to the recombined locus. A protocol for isolating DNA from ES cell clones is also described (see Support Protocol).

ANALYSIS OF ES CELL CLONES BY SOUTHERN BLOT HYBRIDIZATION

BASIC PROTOCOL

Genotyping by Southern blotting requires the addition or removal of a restriction enzyme site during generation of the targeting vector. A detection strategy for homologous recombinants must use a probe located outside the targeting vector so that it will analyze the locus for a polymorphism consistent with the correct targeting event rather than random integration of the vector.

Materials

Restriction enzyme cocktail (see recipe)
96-well plate containing ES cell clone genomic DNA (see Support Protocol)
10× loading dye (see recipe)
0.8% (w/v) agarose gel in TAE (see recipe)
0.25 M HCl (optional)
Denaturing solution (see recipe)
Renaturing solution (see recipe)
10× and 5× SSC (see recipe for 20×)
0.4 M NaOH
Hybridization solution (see recipe)
Radiolabeled and denatured probe
2×, 1×, and 0.1× and SSPE (see recipe for 20×)/0.1% SDS

Humidified chamber (e.g., plastic container lined with wet paper towels)
Camera
Ruler, fluorescent
UV transilluminator
Whatman paper
Hybond N+ nylon membrane (Amersham)
Blotting bridge
Blotting paper
Gel plate or other solid top
Weight (~500 g)
65°C hybridization oven and appropriate hybridization bottle
X-ray film

Run the Southern gel

1. Add 40 µl restriction enzyme cocktail (20 to 40 units per sample) directly to each well of the 96-well plate containing ES cell clone genomic DNA (Support Protocol) and resuspend by pipetting. Incubate in humidified chamber overnight in a 37°C incubator or warm room.

Contributed by Jennifer V. Schmidt
Current Protocols in Toxicology (2001) 15.2.1-15.2.10

The design of the vector and the restriction pattern of the locus dictate the choice of restriction enzyme. It is best to use a single enzyme because double digests of genomic DNA can be problematic under the best of circumstances.

2. Mix reaction mixture with 6 µl of 10× loading dye. Load onto a 0.8% agarose gel in TAE.

   The author usually uses 20 × 25–cm gels with two 36-well combs (Amersham-Pharmacia Biotech) that allow a total of 70 samples to be run per gel.

   For more information concerning pouring and running of agarose gels, see Table A.3A.1 of APPENDIX 3A.

3. Electrophorese as necessary for separation of the expected wild-type and targeted bands and photograph with a fluorescent ruler on a UV transilluminator.

4. (*Optional*) If any of the expected bands are >10 kb, "nick" the DNA by soaking the gel in 0.25 M HCl for 15 min to ensure efficient transfer to the membrane.

   If the band sizes are all <10 kb this step can be omitted.

   HCl depurinates the DNA and the apurinic sites are cleaved by incubation in denaturation solution (see Ramirez-Solis et al., 1992).

5. Incubate the gel in denaturing solution for 15 min. Incubate in renaturing solution 15 min. Rinse with water, then repeat the incubation in renaturing solution.

Transfer DNA to membrane

6. Cut two pieces of Whatman paper and one piece of Hybond N+ nylon membrane to the size of the gel. Place these in a dish of distilled water to wet. Cut a piece of Whatman paper to the same size as the blotting bridge, but slightly longer on the ends, to use for a wick.

   The protocol described here is for upward transfer at neutral pH; however, the DNA can be transferred using either upward or downward and either neutral or alkaline pH transfer (Fig. A.3E.1).

7. Fill a large dish with 400 to 500 ml 10× SSC. Wet the wick in 10× SSC, position the bridge in the SSC, and place the wick on top of the bridge so the ends of the wick are in the solution.

8. Position the gel face down (i.e., well openings down) in the center of the wick and use a gloved finger or a pipet to remove all air bubbles from under the gel.

9. Lay the membrane on top of the gel and the two Whatman papers on top of the membrane. Be careful not to trap any air bubbles between these layers; roll a pipet over the surface to remove any air.

10. Cover the gel sandwich (i.e., wick/gel/membrane) with a thick layer of blotting papers and a solid top such as a gel plate. Place a small (~500 g) weight on top of the gel plate. Transfer ≥8 hr (preferably overnight) at room temperature.

Hybridize membrane

11. When the transfer is complete, disassemble the apparatus, take the sandwich apart, and mark the positions of the wells on the back of the membrane with a pencil or marker.

12. Lay the membrane face up on a piece of Whatman paper saturated with 0.4 N NaOH for 30 min to fix the DNA to the membrane.

13. Neutralize the membrane by rinsing in 5× SSC.

14. Drain the membrane briefly and transfer to a hybridization bottle containing 20 ml hybridization solution. Prehybridize the membrane 6 hr to overnight in a 65°C hybridization oven.

15. Add radiolabeled and denatured probe to 20 ml fresh hybridization solution at a final concentration of 10^6 cpm/ml. Add this solution to the hybridization bottle and hybridize overnight in a 65°C hybridization oven.

    The choice of probe depends on the DNA sequence available surrounding the targeted region. The probe fragment must be located outside the region of homology and usually should be between 500 bp and 1 kb in size. The probe should be tested with wild-type mouse genomic DNA to ensure it contains no repetitive sequences and detects a band of the expected size. The method of probe labeling is a matter of personal choice; however, most investigators use random-primed labeling (APPENDIX 3).

16. Wash the membrane twice in 20 ml of 2× SSPE/0.1% SDS, then once each in 20 ml 1× SSPE/0.1% SDS and enough 0.1× SSPE/0.1% SDS to cover the membrane. Blot briefly on Whatman paper and wrap in plastic wrap.

    In the author's laboratory, the first three washes are usually performed in the hybridization bottle and the fourth (~200 ml) in a plastic container.

Analyze on X-ray film

17. In the dark, place the wrapped membrane in an X-ray cassette with an appropriate sized piece of X-ray film and an intensifying screen. Expose until bands are visible.

    Exposure times of 48 hr with one intensifying screen are usually sufficient.

18. Analyze film for the presence of the expected targeted band in a subset of clones.

    All clones will show at least one band on the Southern blot; this band is derived from the wild-type allele. The locus will be the same in the feeder cells as in the ES cells, and the contribution from the feeder cells will not be distinguishable from that of the wild-type ES cells. A targeted clone will show two bands, the wild-type band and the targeted band, because it has been targeted at only one of the two alleles (see Fig. 15.2.1).

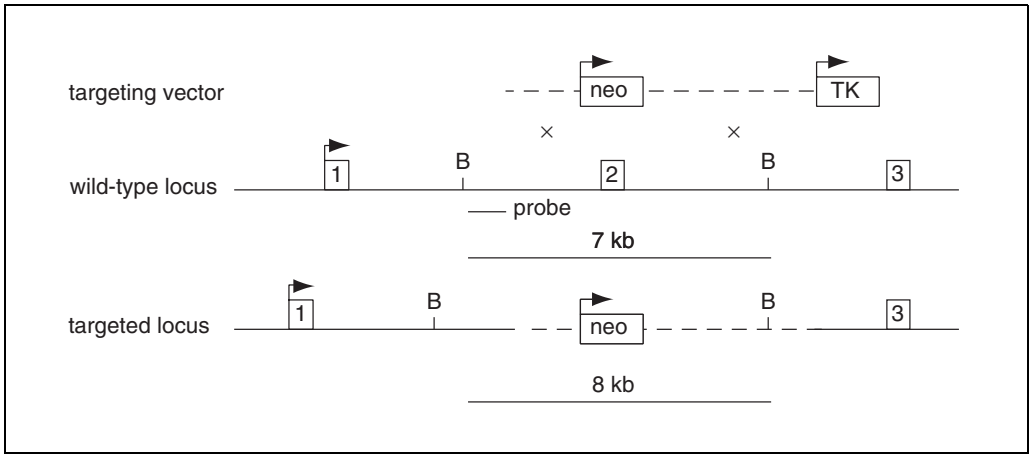

Figure 15.2.1 Southern blot detection of a homologous recombination event. The first three exons of a putative gene are shown; the targeting event replaces exon 2 with the neomycin-resistance gene. The two regions of homology (arms) of the targeting vector are depicted as dashed lines; the upstream is the shorter arm and the downstream the longer arm. The TK gene for negative selection is lost during homologous recombination. The particular gene contains a 7-kb *Bam*HI fragment in the wild-type allele that is detected by Southern blot with the indicated probe. Replacement of exon 2 with the neomycin gene results in an increase in the fragment to 8 kb in the targeted allele. Note that the probe fragment has no overlap with the targeting vector and will not detect heterologous integration events.

ALTERNATE PROTOCOL

ANALYSIS OF ES CELL CLONES BY PCR

While most people prefer to screen ES cell clones by Southern blot hybridization, a PCR assay can be designed to amplify a band specific to the correctly targeted locus. While a PCR strategy uses less DNA than Southern blotting it has a higher potential for missing positive clones. Choice of the correct primer pair is crucial for efficient PCR detection of targeted ES cell clones. The primer set must be chosen to amplify a unique product only in correctly targeted clones. This can be accomplished by using one primer located in sequences unique to the targeted locus, such as the *neo* gene, and another primer located in the locus outside of the targeted region. Detection of recombinants by PCR must be taken into account when designing the targeting construct. A construct designed for PCR analysis must be generated with one long arm and one short arm flanking the region of homology. The long arm should have enough homology for recombination, and the short arm should allow reliable PCR between the selectable marker and the DNA region outside the construct. The reproducible amplification of a PCR product limits the size of the short arm of the targeting construct to ~2 kb.

The inclusion of proper controls are essential to ensure the reliability of the PCR analysis. Use of a positive control ensures that the DNA is of sufficient quality to detect the targeted band if present and that all proper reagents were added to the PCR reaction. The ideal positive control will amplify a fragment of genomic DNA flanking the region to be targeted and will be approximately the same size. The control reaction should be run on all samples. A negative control should also be included, which is ordinarily a blank reaction to which H_2O is added in the place of DNA.

PCR conditions described here are those commonly used in the author's laboratory. Other conditions will work and may be substituted after appropriate verification. Annealing temperature will have to be optimized for each primer set (see *APPENDIX 3C*).

Materials

96-well plate containing ES cell clone genomic DNA (see Support Protocol)
TE buffer, pH 8.0 (*APPENDIX 3C*)
10× PCR buffer (supplied with the *Taq* DNA polymerase)
10 mM dNTPs (2.5 mM each dNTP)
Red juice (see recipe)
25 pmol/µl forward and reverse primers
5 U/µl *Taq* DNA polymerase (Perkin-Elmer)
0.8% (w/v) agarose or 7.5% (w/v) acrylamide gel (see recipes)

0.5-ml PCR tubes
Thermal cycler

1. Add 50 µl water or TE buffer, pH 8.0, to each well of a 96-well plate containing ES cell clone genomic DNA and resuspend the DNA by pipetting.
2. Make a sufficient volume of master mix for the number of samples plus one (i.e., to allow for pipetting loss) using the following recipe for one reaction as a guide. Keep master mix on ice while setting up the reaction to inhibit nonspecific priming (45 µl per reaction).

   5 µl 10× PCR buffer
   4 µl 10 mM dNTPs
   10 µl red juice
   1 µl each 25 pmol/µl forward and reverse primers
   0.25 µl 5 U/µl *Taq* DNA polymerase
   23.75 µl H_2O

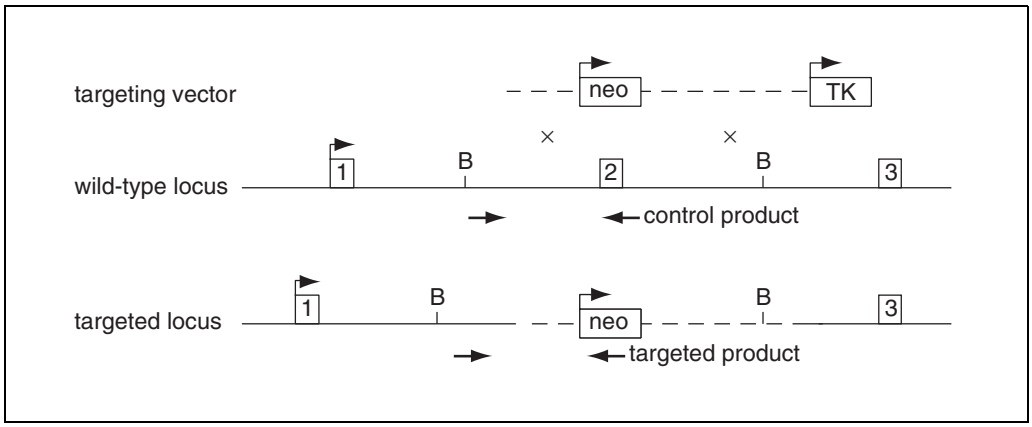

Figure 15.2.2 PCR detection of a homologous recombination event. The PCR strategy uses a primer within the selectable marker and amplification across one arm of the targeting vector to generate a unique product specific to the targeted allele. The control reaction detects a fragment found only in the wild-type allele, which should be present in all ES cell clones. Note that the length of the shorter arm of the targeting construct dictates the size of the PCR fragment that must be generated.

3. For each reaction, aliquot 45 µl master mix into 0.5-ml PCR tubes and add 5 µl ES cell genomic DNA. Keep on ice.
4. Program the thermal cycler with the appropriate conditions. Begin the cycle and when the block has reached 94°C transfer the PCR tubes directly from ice to the thermal cycler.

Initial step:	5 min	94°C	(denaturation)
35 cycles:	1 min	94°C	(denaturation)
	1 min	55°C	(annealing)
	1 min	72°C	(extension)
Final step:		4°C	(hold)

This program is a guide and may have to be optimized for individual PCR targets (APPENDIX 3C).

5. When cycling is complete, remove tubes and analyze 10 to 15 µl on a 0.8% agarose or 7.5% acrylamide gel for the presence of the targeting-specific band (see Fig. 15.2.2).

An agarose gel can be used for fragments ≥500 bp; however, for smaller fragments an acrylamide gel provides better resolution and sizing.

For more information concerning pouring and running of acrylamide and agarose gels, see Table A.3A.1 of APPENDIX 3A.

PREPARATION OF ES CLONE DNA

SUPPORT PROTOCOL

A variety of protocols have been published for the preparation of DNA in 96-well plates. The salting-out protocol described here generates DNA of sufficient quality for PCR or Southern blot analysis. As this protocol gives sufficient DNA for only one Southern blot analysis, the assay and probe should be tested ahead of time on ES cell genomic DNA.

Materials

Confluent cultures of ES cells in gelatinized 96-well feeder-cell plate (*UNIT 15.1*)
PBS (*APPENDIX 2A*)
Lysis buffer (see recipe)
75 mM NaCl in ethanol (see recipe)

70% ethanol

Multichannel pipettor
Humidified chamber (e.g., a plastic container lined with wet paper towels)
55° to 60°C incubator or hybridization oven
Tabletop centrifuge with microplate adapter

1. Using a multichannel pipettor aspirate medium from confluent ES cells on one gelatinized 96-well plate.

   If following the protocols in UNIT 15.1, there will be duplicate plates of ES cell clones for DNA extraction. Analyzing only one set of plates is recommended initially, as the duplicate plates may be held in the tissue culture incubator for another 2 to 3 days in case they are needed.

2. Working quickly, wash cells gently with PBS twice.
3. Add 50 µl lysis buffer to each well and incubate overnight in a humidified chamber (e.g., a plastic container lined with wet paper towels) in a 55° to 60°C oven.
4. Centrifuge 1 min at 2000 × *g*, room temperature, to collect condensation.
5. Add 100 µl of 75 mM NaCl in ethanol to each well and incubate 30 min at room temperature.

   DNA should be visible as strands of fibers at the edges of wells when viewed with a low-power microscope.

6. Centrifuge in a tabletop centrifuge with microplate adapter 5 min at 2000 × *g*, room temperature.
7. Invert the plate and blot gently on a paper towel to remove the ethanol solution.
8. Gently add 100 µl of 70% ethanol to each well. Centrifuge and invert the plate as described above. Repeat this rinse twice more. After the last wash air dry the plate for 15 min or until all remaining ethanol has evaporated.

   The DNA can remain dry for no longer than 30 min. Residual ethanol with impair loading onto the agarose gel. If necessary, open incubate plate at 37°C until all ethanol is gone.

   If genotyping by Southern blot hybridization, the DNA will be directly resuspended in the restriction enzyme cocktail by pipetting (see Basic Protocol). If genotyping by PCR, the DNA will be resuspended in water or TE buffer (see Alternate Protocol).

REAGENTS AND SOLUTIONS

*Use Milli-Q-purified water or equivalent in all recipes and protocol steps. For common stock solutions, see **APPENDIX 2A**; for suppliers, see **SUPPLIERS APPENDIX**.*

Acrylamide gel, 7.5% (w/v)

Add 6.25 ml of 30% acrylamide:bisacrylamide (i.e., 37.5:1) to 1.25 ml of 20× TBE (see recipe) and add 250 µl of 10% (w/v) ammonium persulfate. Bring to 25 ml with water and mix well. Prepare glass plates, spacers, and comb. Add 20 µl TEMED, mix well and pour gel between the glass plates quickly. Let gel polymerize for 30 min. Run in 1× TBE.

The gel can be wrapped in plastic wrap and stored overnight at 4°C if necessary.

CAUTION: *Acrylamide is toxic.*

Agarose gel, 0.8% (w/v)

Add 0.8 g agarose to 100 ml of 1× TAE or TBE (see recipes) in a beaker with a stir bar. Stir to suspend agarose. Microwave until all agarose particles are dissolved. Add 2 µl of 10 mg/ml ethidium bromide (*UNIT 2.2*). Transfer to a stir plate until cooled to ~55°C, then pour into casting tray. Allow gel to harden 30 min. Run in 1× TAE or TBE buffer.

CAUTION: *Ethidium bromide is a mutagen and must be handled carefully.*

For agarose gel analysis of PCR products the author's laboratory typically uses TBE buffer; however, for Southern blot analysis better band resolution is obtained with the use of TAE buffer.

The gel can be wrapped in plastic wrap and stored overnight if necessary.

Denaturing solution

Dissolve 88 g NaCl in 800 ml water. Add 50 ml of 10 M NaOH and bring volume to 1 liter. Store up to 1 year at room temperature.

Hybridization solution

62.6 ml 20× SSPE (see recipe)
12.5 ml 100× Denhardt's solution (*UNIT 2.7*)
12.5 ml 10% SDS (*APPENDIX 2A*)
162.5 ml H_2O
Heat to 65°C to dissolve ingredients
Filter through 0.2-µm filter
Add 500 µl 10 mg/ml salmon testis sperm DNA
Store up to 3 months at room temperature
Warm to 65°C before each use.

The salmon sperm DNA should be heated at 65°C before addition to the solution.

Loading dye, 10×

6.25 g Ficoll 400
60 mg bromphenol blue
60 mg xylene cyanol
H_2O to 25 ml
Incubate at 65°C with occasional shaking to dissolve ingredients
Store indefinitely at room temperature.

Lysis buffer

60 µl 1 M Tris·Cl, pH 7.5 (*APPENDIX 2A*)
120 µl 0.5 M EDTA (*APPENDIX 2A*)
12 µl 5 M NaCl (*APPENDIX 2A*)
300 µl 10% (w/v) Sarkosyl
600 µl 10 mg/ml proteinase K
4.9 ml H_2O
Prepare fresh.

This recipe makes 6 ml lysis buffer, sufficient for one 96-well plate.

NaCl in ethanol, 75 mM

For each 96-well plate add 150 µl of 5 M NaCl (*APPENDIX 2A*) to 10 ml ethanol, 4°C. The salt will precipitate out; therefore, mix before using. Prepare fresh.

Red juice

Dissolve 30 g sucrose in 50 ml water, 65°C. Add 20 mg cresol red and bring volume to 50 ml with water. Aliquot into 1.5-ml tubes and store up to 1 year at −20°C.

Renaturing solution

800 ml H_2O
88 g NaCl
79 g Tris base
2 ml 0.5 M EDTA, pH 8.0 (*APPENDIX 2A*)
Adjust pH to 7.2 with concentrated HCl
H_2O to 1 liter
Store up to 1 year at room temperature.

Restriction enzyme cocktail

400 µl 10× restriction enzyme buffer
40 µl 10 mg/ml BSA
4 µl 1 M spermidine
265 µl 20 U/µl restriction enzyme
3.3 ml H_2O
Prepare fresh.

This recipe makes 4 ml restriction enzyme cocktail, sufficient for one 96-well plate.

For less concentrated enzymes, use a larger volume of enzyme and adjust the water accordingly.

SSC, 20×

800 ml H_2O
175.3 g NaCl
88 g sodium citrate
Adjust pH to 7.0 with 1 M HCl
H_2O to 1 liter
Store up to 1 year at room temperature.

SSPE, 20×

800 ml H_2O
175.3 g NaCl
27.6 g NaH_2PO_4
40 ml 0.5 M EDTA (*APPENDIX 2A*)
Adjust pH to 7.4 with 10 M NaOH (*APPENDIX 2A*)
H_2O to 1 liter
Store up to 1 year at room temperature.

TAE, 50×

800 ml H_2O
242 g Tris base
57 ml glacial acetic acid
100 ml 0.5 M EDTA, pH 8.0 (*APPENDIX 2A*)
H_2O to 1 liter
Store up to 1 year at room temperature.

TBE, 20×

800 ml H_2O
216 g Tris base
110 g boric acid
80 ml 0.5 M EDTA, pH 8.0 (*APPENDIX 2A*)
H_2O to 1 liter
Autoclave or filter through Whatman no. 1 filter paper
Store up to 1 year at room temperature.

Autoclaving or filtering prevents precipitation of the buffer.

COMMENTARY

Background Information

The 96-well microplate DNA extraction protocol described in this unit is a continuation of the methodology presented in *UNIT 15.1*. This method has been used successfully by our laboratory and others to analyze ES cell clones (Ramirez-Solis et al., 1992). Numerous variations on this protocol have been described and may be substituted (e.g., Udy and Evans, 1994); however, it is recommended that any new protocol be tested on a small number of clones before beginning a large experiment.

Critical Parameters and Troubleshooting

Several common errors have been observed when performing this DNA extraction and analysis protocol for the first time. It is essential to centrifuge the 96-well plates after the precipitation and 70% ethanol washes or the DNA will be lost (see Support Protocol). It is also important to ensure that the DNA has completely dried before resuspending in restriction enzyme cocktail (see Basic Protocol). Residual ethanol will result in the DNA samples floating out of the wells of the agarose gel during loading. Should this happen, the remaining DNAs may often be salvaged by drying the open plates in a warm room for 30 min to evaporate the ethanol or by adding 2 to 3 times excess loading dye. If the DNAs are lost in preparation, the duplicate ES cell plate may be prepared and analyzed.

Errors during analysis of the ES cell clones are those inherent in any Southern blotting or PCR assay. Most commonly seen during Southern blot hybridization is incomplete digestion of the ES cell genomic DNA. This will manifest as high background and partial digestion bands on the Southern films and can be avoided by a pilot experiment before beginning targeting. Extraction and Southern blotting of wild-type ES cell DNA using the desired protocol and restriction enzyme will help determine the digestion conditions required for full cutting. Additionally, Ramirez-Solis et al. (1992) have tested numerous restriction enzymes for their digestion efficiency on ES cell genomic DNA extracted by the method presented here.

The most important concern in a PCR strategy is the possibility of false negative results. Because the absence of a targeted allele–specific band is interpreted as a nonrecombinant clone, the failure of this reaction for any technical reason has the potential for missing positive clones. Unfortunately there is no good way to avoid the possibility of this happening, and many laboratories, the author's included, feel the danger is high enough that all screening is done by Southern blotting. Should a PCR detection strategy be necessary or desirable, however, the possibility of false negatives can best be avoided by running the control reaction on all clones at the same time that the targeting-specific reaction is run. While this cannot completely ensure that false negatives will not occur, it will control for many variables such as DNA quality, proper reagent aliquotting, enzyme activity, and thermal cycler performance.

Anticipated Results

Gene targeting frequencies can vary greatly; in the author's laboratory frequencies ranging from 1 in every 2 to 1 in every 800 drug-selected colonies have been observed. These frequencies are dependent upon many factors, including the use of isogenic DNA (Te Reile et al., 1992), the length of homology contained within the targeting construct (Deng and Capecchi, 1992), and the accessibility of a particular locus to recombination. Initial analysis of 400 selected ES cell colonies is recommended for the protocols outlined in *UNIT 15.1*. At average targeting frequencies this is usually sufficient to obtain targeted clones. If analysis of 400 clones reveals no targeting, several diagnostic steps should be taken. First, the targeting construct should be carefully reanalyzed to assure that it is correctly constructed. One common cloning mistake is the inversion of one arm of the construct. Additionally, the diagnostic digest should be verified as accurate, perhaps by additional mapping of the locus. If the targeting construct and diagnostic digest appear correct, it is usually worthwhile to screen another 400 to 600 clones. If no positive clones are obtained after 1000 clones are screened, it may be helpful to design a slightly different targeting construct. The addition of more sequence to the flanking arms can often increase targeting frequency. If the size of the targeting vector cannot be further increased, it may be useful to flip the long and short arms of the construct, thereby including different DNA sequences even if the total amount of homology is unchanged.

Time Considerations

Extraction and analysis of the ES cell clone DNAs will take ~1 week, depending on the

autoradiographic exposure time needed. It is advantageous to prepare and analyze the ES clone DNAs as quickly as possible. The frozen ES cell clones are stable at −80°C for only a short time and should be retrieved within 2 to 3 weeks for most efficient thawing.

Literature Cited

Deng, C. and Capecchi, M.R. 1992. Reexamination of gene targeting frequency as a function of the extent of homology between the targeting vector and the target locus. *Mol. Cell. Biol.* 12:3365-3371.

Ramirez-Solis, R., Rivera-Perez, J., Wallace, J.D., Wims, M., Zheng, H., and Bradley, A. 1992. Genomic DNA microextraction: A method to screen numerous samples. *Anal. Biochem.* 201:331-335.

Te Reile, H., Maandag, E.R., and Berns, A. 1992. Highly efficient gene targeting in embryonic stem cells through homologous recombination with isogenic DNA constructs. *Proc. Natl. Acad. Sci. U.S.A.* 89:5128-5132.

Udy, G.B. and Evans, M.J. 1994. Microplate DNA preparation, PCR screening and cell freezing for gene targeting in embryonic stem cells. *BioTechniques* 17:887-894.

Key References

Ramirez-Solis et al., 1992. See above.

This reference describes a DNA extraction and Southern blotting protocol very similar to that presented in this unit.

Udy and Evans, 1994. See above.

Presents a somewhat different 96-well plate DNA extraction and analysis method.

Contributed by Jennifer V. Schmidt
University of Illinois at Chicago
Chicago, Illinois

Aggregation Chimeras (ES Cell–Embryo)

Embryo stem (ES) cells are used for introducing genetic changes into mice when the genetic change occurs at a low frequency, such as in gene targeting experiments. The genetic change is introduced into a population of ES cells, which are then screened for the correct genetic modification. Once ES cell clones with the desired change are identified, they are used to generate chimeric mice that contain a mixture of ES and wild-type cells. The chimeric mice are then bred to wild-type mice. If the germ cells (i.e., sperm or oocytes) of the chimera are derived from the ES cells, then the offspring of the chimeric mouse will be heterzygous for the transgene, and the line is said to have "gone germline."

Chimeric mice can be made either by injecting the ES cells into blastocyst-stage embryos (Stewart, 1993) or by aggregating the ES cells to 8-cell stage embryos (Wood et al., 1993). In each case, the embryo hosts are collected from superovulated female "donor" mice, and the chimeric embryos are transferred back into pseudopregnant recipient females to develop to term; however, the aggregation method requires less technical training and expensive equipment than blastocyst injection.

The following protocols are based on techniques developed in Dr. A. Nagy's laboratory (Wood et al., 1993). They describe how to flush 8-cell stage embryos from female donor mice, remove the zona pellucida to prepare the embryos for aggregation, and then aggregate them (see Basic Protocol) in a specially prepared plate (see Support Protocol 2). After overnight incubation, the ES cell/embryo aggregates are transferred into a recipient female. A protocol describing some of the mouse husbandry required during the course of the experiment is also provided (see Support Protocol 1).

NOTE: All protocols using live animals must first be reviewed and approved by an Institutional Animal Care and Use Committee (IACUC) and must follow governmental procedures for the care and use of laboratory animals.

PREPARING ES CELL–EMBRYO AGGREGATION CHIMERAS

BASIC PROTOCOL

Outbred albino (e.g., CD-1) females are superovulated (see Support Protocol 1) and mated. Two days later—i.e., 2.5 days post coitus (dpc)—these donor females are sacrificed and embryos (4 to 16 cell stage) are flushed from the oviduct and the upper part of the uterus. Individual embryos are placed into an incubator in KSOM medium until all the embryos are collected. The embryos are then treated for a brief time with acid Tyrode's solution to dissolve the zona pellucida (via the low pH), which must be removed from the embryos to allow the ES cells to adhere. ES cells and embryos are transferred to the individual depressions of an aggregation plate (see Support Protocol 2). The following morning, the majority of aggregates should have formed blastocysts. A maximum of 8 to 10 embryos are then transferred into each uterine horn of a 2.5-dpc 6-week-old CD-1 pseudopregnant recipient. In the event of a recipient shortage, it is possible to culture the aggregates (preferably morulae) for one more day and transfer them into 2.5-dpc pseudopregnant females, or to use 3.5-dpc pseudopregnant females.

ES cells are thawed onto a feeder plate three days before the aggregation and split 1 day before the aggregation as sparse single cells onto gelatinized plates. The split onto gelatinized plates should include 1:10, 1:20, and 1:30 dilutions. When the embryos have been placed in the aggregation plate, or alternatively before the embryos are treated with acid Tyrode's solution, ES cells are briefly trypsinized, which is stopped by adding

Contributed by Corrinne G. Lobe and Caiying Guo
Current Protocols in Toxicology (2001) 15.3.1-15.3.12

medium to the plate. The clumps of cells are then picked from the plate and transferred to depressions in the aggregation plate.

Before removing zona pellucida, the embryos can be stored in KSOM under oil in the incubator while the ES cells are prepared and added to the aggregation plate. It is easier to place the ES cell clumps in the aggregation wells first, followed by the embryos.

Materials

M2 medium (see recipe)
KSOM medium (see recipe)
2.5-dpc superovulated donor mice (e.g., CD-1; see Support Protocol 1)
Acid Tyrode's solution (Sigma)
ES cells (*UNIT 15.1*), trypsinized
Light mineral oil, embryo tested
2.5- or 3.5-dpc pseudopregnant recipient mice (see Support Protocol 1)
1.25% (w/v) avertin (see recipe)
70% (v/v) ethanol in a squeeze bottle

1- and 5-ml syringes with 26-G needles
100 × 15–mm petri dish, sterile
Surgical instruments: 2 straight or curved forceps with serrated tips, small straight or curved scissors, no. 5 forceps (Dumont), forceps with 1 × 2 teeth (i.e., "rat's tooth"), sharp forceps, serrefine clamps (e.g., Fine Scientific Tools), and suture clips and applier (Fine Scientific Tools)
1-ml syringe with flushing needle (see recipe)
Dissecting microscope
Finger pipet (see recipe)
Prepared aggregation plate with depressions (see Support Protocol 2)
Embryo-transfer pipet (see recipe) and appropriate mouth piece
28-G needle
Lamp

NOTE: All solutions and equipment coming into contact with living cells must be sterile and aseptic techniques should be used accordingly.

NOTE: All culture incubations should be performed in a humidified 37° C, 5% CO_2 incubator unless otherwise specified.

Prepare for oviduct removal

1. Draw a small amount of M2 medium into a 5-ml syringe attached to a 26-G needle.
2. Draw a small amount of KSOM medium into a 1-ml syringe attached to a 26-G needle.
3. Place a large drop of M2 medium from the syringe onto one side of a sterile 100 × 15–mm petri dish. Retain the remaining medium in the syringe.

Remove oviducts

4. Sacrifice all or half of the 2.5-dpc superovulated donor mice, depending on how many there are, by cervical dislocation. Using straight or curved forceps with serrated tips, and small straight or curved scissors, make a horizontal incision along the abdomen through the skin, then through the body wall. Push aside the intestines and locate the uterine horn on one side.

   Typically, 5 to 10 mice should be done at one time.

5. Pull up the uterus with the forceps and tease away the connective tissue with closed scissors. Grasp the uterus just under the oviduct with forceps and cut it first between the oviduct and the ovary, and then ~1 cm under the oviduct so as to include a bit of the uterus.

6. Place the oviduct into the large drop of M2 medium (step 3). Repeat steps 5 and 6 for each oviduct (two per animal) of each mouse, placing all oviducts in the large drop of M2 medium.

7. Use the syringe loaded with M2 medium to place several small drops (i.e., one per oviduct) in the other half of the petri dish. Place each of the oviducts into an individual drop of M2 medium.

Flush embryos from oviducts

8. Load M2 medium into the 1-ml syringe with the flushing needle by pulling the liquid up into the barrel of the syringe without the needle on, putting on the needle, flicking up the air bubbles, and pushing them out.

   Do not pull liquid up the flushing needle, only push it out.

9. Put the plate containing the oviducts (step 6) under a dissecting microscope.

10. Select an oviduct. Find the oviduct opening (infundibulum) using the flushing needle and no. 5 forceps to handle the tissue. Locate the end, grab it loosely with the no. 5 forceps in the left hand (assuming a right-handed experimenter), and carefully place the needle into the opening.

    Make sure the flushing needle and the oviduct opening are oriented in the same direction before trying to slip in the needle.

11. Once the needle is in the opening, secure it firmly by gripping more tightly with the forceps. Push some of the M2 medium from the needle into the oviduct.

    If the needle is inserted properly, the oviduct will expand as the M2 is pushed out and the embryos and debris are flushed out. Typically, 0.1 ml M2 is used to flush each oviduct.

12. After flushing, place the oviduct onto the edge of the plate with forceps. Repeat steps 9 to 12 for each oviduct.

Remove zona pellucida

13. Collect the embryos using a finger pipet and wash them through several drops of M2 medium to remove any debris.

    Transfer embryos using the finger pipet for steps 13 to 24. Some experimenters find it easier to handle the embryos using a mouthpiece and tubing connected to an embryo transfer pipet with a wide bore rather than a finger pipet.

14. In a fresh 100 × 15–mm petri dish, place a drop of M2 medium to the left and right side of the dish. Place 2 drops of acid Tyrode's solution in a vertical row in the center of the dish.

15. Transfer the embryos to the drop of M2 on the left. Empty all the M2 medium from the finger pipet, then take up some acid Tyrode's solution from the container. Return to the drop of M2 containing the embryos and displace the acid Tyrode's over the embryos. Pipet up as many embryos as can be easily pipetted up and down (usually ~50 to 60 embryos).

    In this way the embryos are taken up with a minimum amount of M2.

16. Transfer the embryos into the upper drop of acid Tyrode's solution, and then transfer them immediately to the lower drop. While observing under the dissecting microscope, continue to pipet the embryos up and down until the zona pellucida dissolves (~2 min).

    Transferring quickly between the upper and lower drops avoids dilution of the acid Tyrode's solution by M2 medium.

    The zona pellucida appears as an outline surrounding the embryo. When it dissolves, the outline will be invisible and the borders of the embryo cells will be sharper.

    Watch carefully. If the embryos incubate too long in acid Tyrode's solution, they will begin to fall apart.

17. Transfer the embryos into the drop of M2 medium on the right as soon as the dissolution is complete. Repeat steps 16 and 17 with the remaining embryos.

Aggregate embryos and ES cells

18. Place microdrops of KSOM medium onto an aggregation plate, both in and outside of the depressions. Cover the drops with light embryo-tested mineral oil.

19. Wash the embryos at least twice in KSOM drops.

20. Transfer embryos into the aggregation plate by placing them one by one inside each depression.

    It is easiest to pick up ~30 to 60 embryos at a time and put six into each microdrop with depressions, then put an embryo into each depression.

    Alternatively, add all ES cells to the wells, then use acid Tyrode's solution to treat the embryos and add them to the wells with ES cells.

21. Choose clumps of loosely connected, trypsinized ES cells and transfer them into drops of KSOM medium in a petri dish using a finger pipet. From these drops select appropriately sized clumps (8 to 20 cells) and transfer them into the microdrops on the aggregation plate without depressions.

22. Transfer clumps of ES cells into the microdrops containing depressions, using at least six clumps of ES cells per microdrop. Finally, place an ES cell clump into each depression.

23. Assemble all aggregates in this manner, check the plate, and culture overnight.

Prepare for transfer of embryos to recipient females

24. Under the dissecting microscope, use an embryo-transfer pipet to transfer the embryos from the aggregation plate to a drop of M2. Group the embryos according to number per uterus to be implanted.

25. Anesthetize a recipient 2.5- or 3.5-dpc pseudopregnant recipient mouse with 0.2 ml/10 g of 1.25% avertin.

26. Draw a small quantity of M2 medium from the side of the drop with embryos into the embryo-transfer pipet, followed by an air bubble, then more M2 medium. Repeat until there are approximately four air bubbles to allow good control of the pipet.

27. Take up approximately ten embryos. Lay the loaded pipet on the bench, with the pipet on right and the mouthpiece on the left of the microscope (for right-handers).

    For steps 27 to 37 use a fine embryo transfer pipet and mouthpiece to manipulate embryos.

Isolate uterus for transfer

28. Put the anesthetized mouse on the lid of a petri dish. Blow on the hair of its back to part it and apply 70% ethanol from a squeeze bottle to wet the hair down.

29. Make a 1-cm incision through the skin along the dorsal midline, placing the top of the incision at the hump where the ribs end.

30. Use a pair of forceps with 1×2 teeth (i.e., "rat's tooth") to hold the skin and pull the opening to the right side, while using sharp forceps to clear the connective fascia until the fat pad and ovary can be seen.

31. Make an incision through the body wall over the fat pad.

32. Use dull forceps with serrated tips to reach into the incision and grab the fat pad. Pull it out to place the ovary and uterus over the back. Clamp the fat pad close to the ovary with serrefine clamps. Lay the clamp over the back, so the uterus is stretched out over the top of the back. Move the mouse (still on the petri dish lid) to the microscope, positioning it so the clamp holding the uterus is away from the experimenter.

Transfer embryos to uterus

33. Place the mouthpiece connected to the embryo transfer pipet in the mouth. Hold the serrated forceps in one hand and a 28-G needle in the other hand.

34. While holding the fat pad at the clamp with forceps, put the needle into the uterus to make a hole in the top, narrow part of the uterus (i.e., one of the uterine horns), avoiding blood vessels.

35. Leaving the needle in, carefully put down the forceps, and pick up the embryo-transfer pipet. Pull out the needle and put the transfer pipet in the same hole, being careful to insert the transfer pipet into the lumen of the uterus.

    The 28-G needle, still in hand, can be used to pull the uterus taut by pressing against the clamp or to turn the uterus, as required.

36. Once the embryo-transfer pipet is placed well into the uterus, pull it out a little so the tip isn't against the uterine wall, and start blowing out the embryos. Continue to pull the pipet out a little as all the embryos are blown into the uterus, up to the first air bubble. Pull out the transfer pipet and clean any blood off by wiping it on the fat pad.

37. Release the clamp and use the serrated forceps to carefully put the ovary and uterus back into the body cavity, making sure to place it below the body wall. Avoid touching the ovary and uterus.

Repeat transfer with the other uterine horn

38. Pull the outside edge of the body wall over the inside edge. Rotate the plate so the mouse's head is now toward the experimenter.

39. Pull up ten more embryos into the transfer pipet.

40. Repeat the transfer into the other uterine horn.

Close incision and allow animals to recover

41. Pull the edges of the skin together over the midline with the edges up, away from the animal. While holding the edges up together, place one to two woundclips over the incision using an appropriate clip applier.

42. Place the mouse on its stomach in a fresh cage. Wrap a tissue around it and shine a lamp a safe distance away to keep the mouse warm until it recovers. After each operation, lay each successive mouse along the previous one, also for warmth.

SUPPORT PROTOCOL 1

MOUSE HUSBANDRY

Four populations of mice are required for the aggregation experiments: a stock of 4-week-old donor females (e.g., outbred CD1), which should be ordered weekly; stud males, which can be maintained as a stock and should be used only once to twice per week (i.e., cage cards should be marked with the date of each successful and unsuccessful mating, with males presenting <50% plug rate being replaced); vasectomized males, which can be ordered or prepared in house; and a stock of 6-week-old recipient females, which can be maintained and checked for estrus before being mated to vasectomized males. Vasectomized males should be removed from females for 2 weeks after surgery before using to plug recipient females. For weekly experiments, a reasonable mouse transgenic colony would consist of 20 donor females, 80 recipient females, 20 stud males, and 15 vasectomized males. Each stud and each vasectomized male can be mated with 1 to 2 donor and recipient females, respectively, at a time.

To superovulate the females that will serve as embryo donors, inject mice 2 days before mating with 0.1 cc of 20× pregnant mare serum i.p. (PMS; ~5 IU final; see recipe) and 46 hr later with 0.1 cc of 20× human chorionic gonadotropin (hCG; 5 U final; see recipe). After hCG injection place donor females with stud males and check for copulation plugs the next morning. Each plugged female will yield ~ 15 to 30 embryos; therefore, ~ 10 to 15 females are required per ES cell line to be aggregated.

SUPPORT PROTOCOL 2

MAKING AGGREGATION PLATES

A plate with depressions to hold the embryos and ES cells in contact (Wood et al., 1993) is used for aggregation, with one such plate required for every 60 embryos. Usually 3 to 4 are made for each experiment.

Additional Materials *(also see Basic Protocol)*

35 × 10–mm tissue culture dishes, sterile
Aggregation (i.e., darning) needle (BLS)

1. Place four rows of KSOM microdrops (~3 mm in diameter) into a 35 ×10–mm tissue culture dish using a 1-ml syringe and 26-G needle (3 drops in the first and fourth row, 4 to 5 drops in the second and third rows). Cover with light embryo-tested mineral oil.
2. Sterilize the aggregation (i.e., darning) needle by washing in 70% ethanol.
3. Make six depressions in the plastic of the dish, arranged in a circle, in each microdrop of the second and third rows, by pressing the aggregation needle into the plastic and making a slight circular movement. Do not twist the needle.

   This movement creates a tiny depression with a clear smooth wall. It should be deep enough to hold the embryo.

4. Place the plate in a tissue culture incubator until use.

REAGENTS AND SOLUTIONS

Use Milli-Q-purified water or equivalent for the preparation of all reagents and in all protocol steps. For common stock solutions, see ***APPENDIX 2A****; for suppliers, see* ***SUPPLIERS APPENDIX****.*

Avertin, 1.25% (w/v)

Dissolve 2.5 g of 2,2,2-tribromoethyl alcohol in 5.0 ml 2-methyl-2-butanol (*tert*-amyl alcohol). Add to 200 ml distilled water or physiological saline. Place on a magnetic stirrer until solution is in phase. Store protected from light (e.g., in a covered or brown bottle) up to 1 year at 4°C. Before use, perform a decomposition test by adding 1 drop of Congo Red to 5 ml of 1.25% avertin.

If purple color develops at pH < 5, it indicates decomposition to dibromoacetic aldehyde and hydrobromic acid and the solution should be discarded.

Dosage is 0.2 ml/10 g body weight (250 mg/kg).

Embryo-transfer pipet

Starting with one Pasteur pipet, heat the narrow end in a flame until soft. Remove from the flame and pull it out until it is the right thickness (i.e., a long and not-too-thin needle, ~1 mm in diameter). Break it at either end to get a thin glass tube ~2 in. long. Fire polish one end. Check under a dissecting microscope for a smooth bevel.

Pull out another pipet at the lower part of the neck of the pipet. Break the glass off close to the barrel. Put the thin needle into the broken off barrel. Warm a block of paraffin wax over a flame to form a drop, and let the drop fall on the joint where the needle meets the barrel. Hold the joint with the drop of wax on it close enough to the flame to heat up the glass and allow the molten wax to travel up the joint by capillary action (Fig. 15.3.1).

This pipet gives a shorter transfer pipet that is easier to hold than the long conventional drawn-out pipet. See Wood et al. (1993) for more information.

Finger pipet

Prepare a finger pipet for manipulating the embryos by flaming a 9-in. glass Pasteur pipet at a point 1 to 2 inches from the narrow end until it becomes soft. Remove the pipet from the flame and pull to obtain a long, narrow shaft of 1 to 2 in. that changes diameter gradually. Break the glass in the middle of the narrow shaft by pulling straight out while pinching slightly to generate a tip with an even end. Fire polish the end by briefly passing it through the flame. Check the tip of the resultant transfer pipet for correct size and smoothness under the dissecting microscope (See Fig. 15.3.2).

Flushing needle

Cut off the tip of a ½-in. 30-G needle and round the end using a sharpening stone. Attach to a 1-ml syringe. After each day's use, rinse the needle several times with ethanol by loading the syringe with the needle off, attaching the needle, and then pushing fluid through.

HEPES/phenol red, 10×

5.958% (w/v) HEPES
0.001% (w/v) phenol red

Add half of the final volume of water and adjust the pH to 7.4 with 1 M NaOH. Add water to volume. Store in 10-ml aliquots up to 3 months at –20°C.

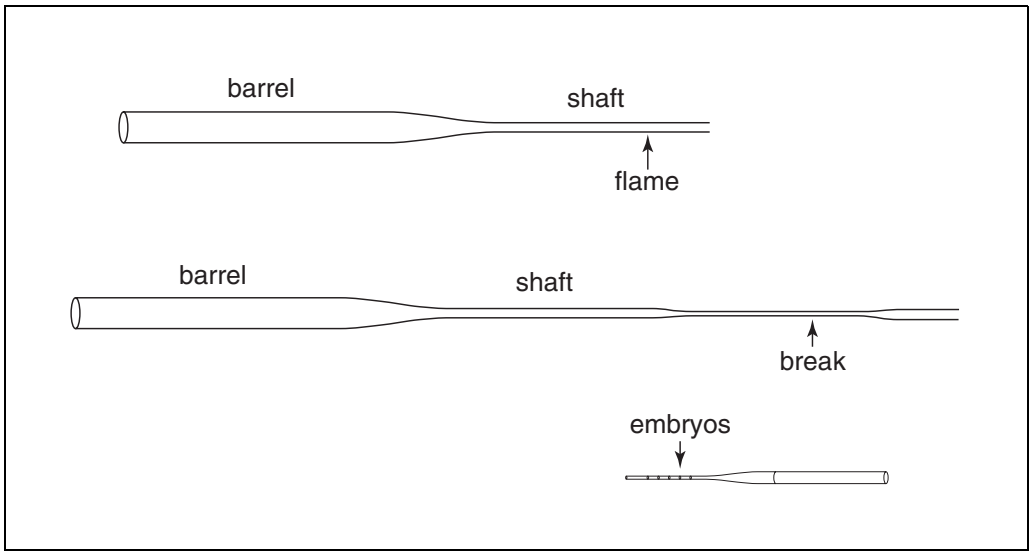

Figure 15.3.1 Schematic of a finger pipet.

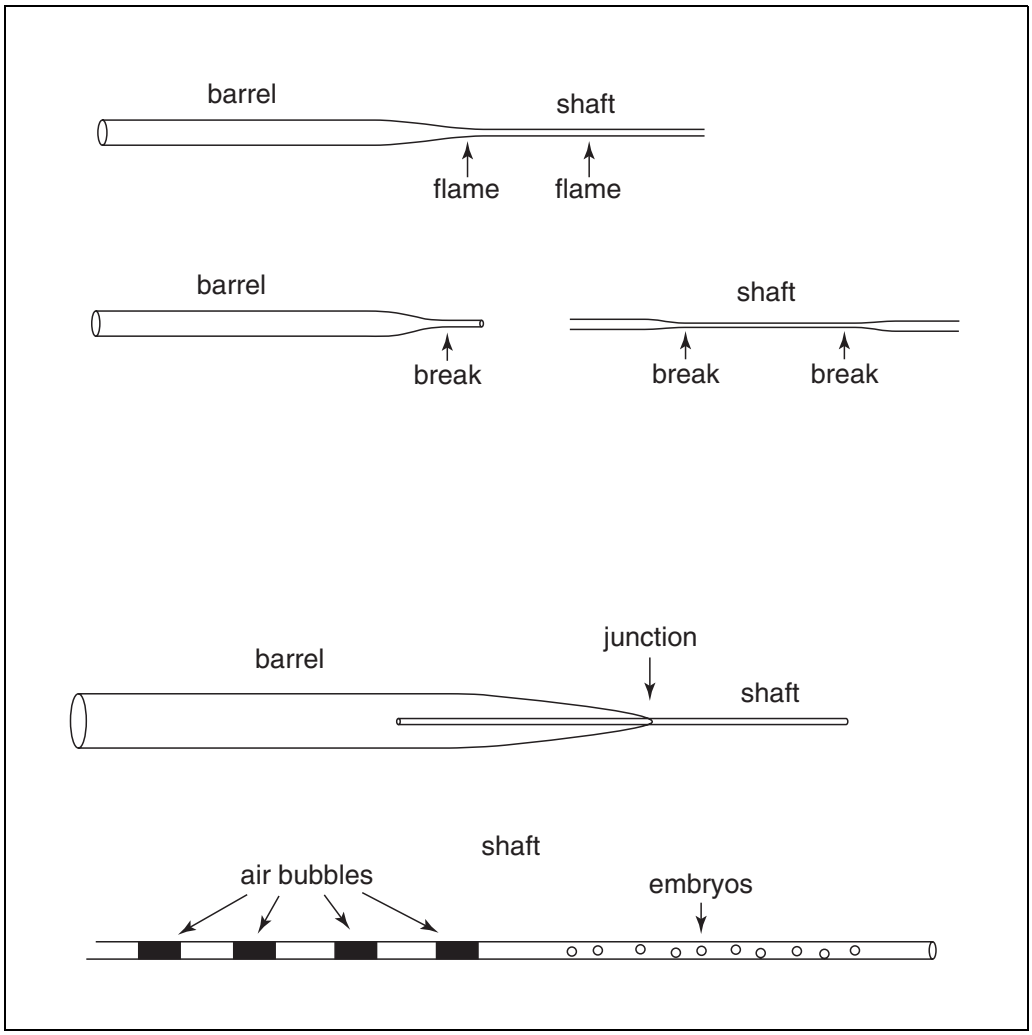

Figure 15.3.2 Schematic of an embryo-transfer pipet.

Human chorionic gonadotropin (hCG), 20×

Reconstitute 10,000 IU hCG (Wyeth-Ayerst) with the 10 ml of solution provided with hormone (1000 IU/ml). Store in 75-µl aliquots up to 3 months at −20°C. Reconstitute with 1.5 ml phosphate buffered saline (PBS; *APPENDIX 2A*) before using.

KSOM medium

10 ml 10× KSOM salts/antibiotics (see recipe)
10 ml 2.101% (w/v) $NaHCO_3$/0.001% (w/v) phenol red
1.0 ml 0.022% (w/v) sodium pyruvate
1.0 ml 0.252% (w/v) $CaCl_2 \cdot 2\ H_2O$
0.01 ml 0.372 M disodium EDTA
0.5 ml 200 mM glutamine (Life Technologies)
90 ml H_2O
400 mg BSA

Rinse all pipets and tubes thoroughly into the final flask. Add 400 mg BSA, allow to dissolve, and gently stir the medium with a magnetic stirrer, avoiding excessive frothing. Bubble 5% CO_2 through the solution in air to adjust to pH 7.4, or place in a humidified 37°C, 5% CO_2 incubator for several hours (e.g., overnight) with a loose cap. Filter sterilize through a 0.2-µm filter and aliquot into polypropylene tubes. Store in polypropylene tubes up to 2 weeks at 4°C.

The concentrated stock solutions can be stored at −80°C for 6 months, or −20°C for a shorter time (e.g., 3 months).

KSOM salts/antibiotics, 10×

5.534% (w/v) NaCl
0.186% (w/v) KCl
0.0476% (w/v) KH_2PO_4
0.0493% (w/v) $MgSO_4 \cdot 7\ H_2O$
1.87 g 60% sodium lactate syrup (rinse the boat well and add wash to the flask)
0.036% (w/v) D-glucose
0.060% (w/v) penicillin G
0.050% (w/v) streptomycin
Store in 10-ml aliquots up to 3 months at −20°C.

M2 medium

10 ml 10× M2 salts/antibiotics (see recipe)
1.6 ml 2.101% (w/v) $NaHCO_3$/0.001% (w/v) phenol red
1.0 ml 0.036% (w/v) sodium pyruvate
1.0 ml 0.252% (w/v) $CaCl_2 \cdot 2\ H_2O$
8.4 ml 10× HEPES/phenol red (see recipe)
78.0 ml H_20

Rinse all pipets and tubes thoroughly into final flask. Add 400 mg BSA, allow to dissolve, and gently stir the medium with a magnetic stirrer, avoiding excessive frothing. If necessary, readjust to between pH 7.2 to 7.4 with 1 M NaOH before making up to volume. Filter sterilize through a 0.2-µm filter and aliquot into polypropylene tubes. Test the medium and culture conditions by collecting 1-cell-stage embryos (0.5 dpc) and culturing them through the blastocyst stage. Store in polypropylene tubes up to 2 weeks at 4°C.

The concentrated stock solutions can be stored at −80°C for 6 months, or −20°C for shorter time (e.g., 3 months).

M2 salts/antibiotics, 10×

5.534% (w/v) NaCl
0.356% (w/v) KCl
0.162% (w/v) KH_2PO_4
0.293% (w/v) $MgSO_4 \cdot 7\ H_2O$
4.349 g 60% sodium lactate syrup (rinse the boat well and add wash to the flask)
1.000% (w/v) D-glucose
0.060% (w/v) penicillin G
0.050% (w/v) streptomycin
Store in 10-ml aliquots up to 3 months at −20°C.

Pregnant mare serum (PMS), 20×

Store 1000 IU/ml PMS (Wyeth-Ayerst) in 75-µl aliquots up to 3 months at −20°C. Reconstitute with 1.5 ml PBS (*APPENDIX 2A*) before using.

COMMENTARY

Background Information

Transgenic mice can be produced by injecting the transgene into the pronucleus of a one-cell stage embryo or by introducing the transgene into ES cells and then producing chimeric mice between the ES cells and a host embryo. The latter, ES cell–mediated transgenesis, is the preferred approach when a rare event such as homologous recombination is required because it is more practical to screen a large number of ES cell clones in culture than it is to screen a large number of transgenic mice. Examples of applications for ES cell-mediated transgenesis are gene targeting (Thomas and Capecchi, 1987; Doetschman et al., 1988), gene trap strategies (Friedrich and Soriano, 1991; Skarnes et al., 1992), and to prescreen transgenes for expression or copy number (Lobe et al., 1999). The disadvantage of ES cell–mediated transgenesis is the additional 3 months required to breed the chimeras and obtain transgenic offspring. As well, not all ES lines will provide germline chimeras.

If ES cell-mediated transgenesis is used, a second choice is whether to introduce the ES cells into host embryos by injection (Stewart, 1993) or by aggregation (Wood et al., 1993). The technique of ES cell–embryo aggregation has the advantage that the technique is less technical, is easier and faster to learn, and does not require expensive microinjection equipment. One potential disadvantage is that not all ES cell lines work equally well in aggregation experiments. Thus, some preliminary confirmation that a particular cell line contributes to the germ line by this approach may be useful.

Commonly used ES cell lines are derived from a male blastocyst and are therefore XY (Bradley, 1990; Doetschman et al., 1985; Nagy et al., 1993; Robertson, 1991). Germline chimeras are typically, but not exclusively, males. This has the advantage that male chimeras will provide more offspring over their lifetime than females.

For ES lines derived from a pigmented mouse strain, albino embryo donors are used, so that the degree of chimerism can be seen by coat color. For example, R1 ES cells are derived from 129 agouti mice and are commonly used with albino CD-1 female donors.

Critical Parameters

The success rate of obtaining germline chimeras is critically dependent on the potential of the ES cell line being aggregated. As discussed in other sections of this chapter, care must be taken to maintain high quality undifferentiated ES cells (see *UNIT 15.1*). The passage number should be kept to a minimum, ideally 10 to 15 passages in total. It is safest to maintain the ES cells on feeder layers of embryo fibroblasts and include LIF in the medium. It is always best for an investigator to have at least three different ES cell clones for each transgene or to gene knockout because different clones will have different abilities to contribute to the germline.

The water used to prepare M2 and KSOM medium should be of the highest possible purity. Water that has been purified by a combination of reverse osmosis and Milli-Q filtration contains minimal contaminants. The conductivity should be at least 18 MΩ. Prolonged storage of water is not advised. Clean glass bottles reserved for media use and that have been thoroughly rinsed or plastic tissue culture flasks are used to collect water and prepare stocks and media.

Table 15.3.1 Troubleshooting Guide for Preparation of Aggregation Chimeras

Problem	Possible cause	Solution
Low plug rate	Males too young or too old	Use 8-week to 9-month old males. Males with <50% plug rate should be replaced.
	Males mated too often	Males should only be mated 1 to 2 times per week
	High traffic in mouse room	Limit access to mouse room
Poor embryo yield	Superovulation ineffective	Titrate PMS or try a new batch of hormone
	Oviduct flushing is faulty	Be sure oviduct swells when flushed
ES cells not incorporated into embryo	Sides of well are rough and sticky	The aggregation well should have smooth walls. Use a small circular motion with the aggregation needle
Embryos not developing into blastocyst	Medium conditions not optimized	Test the medium by incubating flushed embryos without ES cells overnight. Virtually all should develop to blastocysts overnight.
Recipient females not pregnant	Embryo transfer is poor	Insert the transfer pipet well into the uterus. Avoid touching the uterus or ovary with the forceps.
No chimeras	ES cell clumps too big or ES line compromised, so chimeras are dying in utero	Pick smaller ES cell clumps for aggregation. Try a different ES cell clone.
Only weak chimeras	ES cell line is compromised	Use a different ES cell clone.
	ES cell clumps too small (seldom a problem; it is more common to use clumps that are too large)	Pick larger ES clumps for aggregation.
Chimeras die after birth, or survive but are sterile	ES cell line compromised	Use a different ES cell clone.

Table 15.3.2 Time Course of a Typical Experiment

Timepoint	Procedure
Day 1	Inject donors with PMS (e.g., at 2 p.m. for a 7 a.m. to 7 p.m. light cycle)
Day 3	Inject donors with hCG (e.g. at 12 noon for a 7 a.m. to 7 p.m. light cycle) and pair with stud males. Thaw ES cells to be aggregated onto feeder plate.
Day 4	Check plugs of donors. Check recipient females for estrus and pair with vasectomized males.
Day 5	Check plugs of recipients. Split ES cells to be aggregated onto gelatin plate.
Day 6	Flush embryos from donor females. Aggregate embryos with ES cells.
Day 7	Transfer ES cell–embryo aggregates into psuedopregnant recipient females
Day 22	Split pregnant recipient females into individual cages
Day 24	Pups are born

All chemicals should be of the highest grade possible. Some embryo-tested chemicals are available. Chemicals used to prepare media should be reserved only for this purpose.

Troubleshooting

Table 15.3.1 presents some common problems and their solutions.

Anticipated Results

To obtain a sufficient number of male germline chimeras, at least 120 aggregations should be done per ES cell line. This should provide ~10 male chimeras with >50% coat color chimerism, from which three germline transmitters should be obtained.

Time Considerations

Table 15.3.2 presents a time course for an average experiment.

Literature Cited

Bradley, A. 1990. Embryonic stem cells: Proliferation and differentiation. *Current Opinion in Cell Biology* 2:1013-1017.

Doetschman, T.C., Eistetter, H., Katz, M., Schmidt, W., and Kemler, R. 1985. The *in vitro* development of blastocyst-derived embryonic stem cell lines: Formation of visceral yolk sac, blood islands and myocardium. *J. Embryol. Exp. Morph.* 87:27-45.

Doetschman, T., Maeda, N., and Smithies, O. 1988. Targeted mutation of the *Hprt* gene in mouse embryonic stem cells. *Proc. Natl. Acad. Sci. U.S.A.* 85:8583-8587.

Friedrich, G. and Soriano, P. 1991. Promoter traps in embryonic stem cells: A genetic screen to identify and mutate developmental genes in mice. *Genes Dev.* 5:1513-1523.

Lobe, C.G., Koop, K.E., Kreppner, W., Lomeli, H., Gertsenstein, M., and Nagy, A. 1999. Z/AP, a double reporter for cre-mediated recombination. *Dev. Biol.* 208:281-292.

Nagy, A., Rossant, J., Nagy, R., Abramow-Newerly, W., and Roder, J. 1993. Derivation of completely cell culture-derived mice from early-passage embryonic stem cells. *Proc. Natl. Acad. Sci. U.S.A.* 90:8424-8428.

Robertson, E.J. 1991. Using embryonic stem cells to introduce mutations into the mouse germ line. *Biol. Reprod.* 44:238-245.

Skarnes, W.C., Auerbach, B.A., and Joyner, A.L. 1992. A gene trap approach in mouse embryonic stem cells: The lacZ reporter is activated by splicing, reflects endogenous gene expression, and is mutagenic in mice. *Genes Dev.* 6:903-918.

Stewart, C.L. 1993. Production of chimeras between embryonic stem cells and embryos. *Methods Enzymol.* 225:823-855.

Thomas, K. and Capecchi, M. 1987. Site-directed mutagenesis by gene targeting in mouse embryo-derived stem cells. *Cell* 51:503-512.

Wood, S.A., Allen, N.D., Rossant, J., Auerbach, A., and Nagy, A. 1993. Non-injection methods for the production of embryonic stem cell-embryo chimeras. *Nature* 365:87-89.

Contributed by Corrinne G. Lobe and Caiying Guo
Sunnybrook and Women's College Health Sciences Center and University of Toronto
Toronto, Canada

Reporter Genes to Detect Cre Excision in Mice

The development of mouse embryonic stem (ES) cells has provided the opportunity to introduce many types of genetic alterations into the mouse (*UNIT 1.3*). Recently the Cre/*loxP* system has been combined with ES cell technology to accomplish virtually any type of genetic alteration that occurs in human disease. In addition, the Cre/*loxP* system allows conditional genome alterations that are spatially and temporally restricted (Sauer, 1998).

The Cre recombinase of the P1 bacteriophage catalyzes recombination between two 34-bp consensus sequences (*loxP* sites; Sternberg and Hamilton, 1981). The *loxP* sites are palindromic except for an 8-bp asymmetric core sequence that provides each *loxP* site with an orientation (Hoess et al., 1986). If two *loxP* sites lie in the same orientation in the same DNA strand, introduction of Cre enzyme will result in recombination between the *loxP* sites and excision of the intervening DNA sequence.

The Cre/*loxP* system has become a powerful tool to make conditional alterations to the mouse genome. Typically two lines of mice are required: the first is a transgenic mouse line with *loxP* sites strategically placed in the genome using standard transgenic technologies; the second is a Cre transgenic mouse line. The transgenic mice carrying *loxP* sites are crossed to the Cre transgenic line to effect recombination in the double-transgenic offspring. Recombination can be directed to a specific tissue or stage of the animal's life, depending on the gene promoter driving Cre expression.

To fulfill the potential of this new approach, a collection of Cre transgenic mice must be developed that express Cre recombinase with a variety of tissue and temporal specificities. The establishment of these lines is an ongoing effort in many laboratories. To achieve spatial restriction, the Cre recombinase coding sequence in these transgenic mice is under the regulation of a variety of tissue-specific promoters or has been "knocked in" to a gene (see Internet Resources). Several approaches to provide inducible Cre activity in transgenic mice by administration of exogenous compounds are also now emerging, opening the possibility of restricting site-specific recombination to later stages in the animal (Furth et al., 1994; Feil et al., 1996; Kellendonk et al., 1996; Rivera et al., 1996). A major impediment to the development of these mice has been the lack of an assay for Cre excision in the transgenic mice.

To address this problem, several Cre reporter mouse lines have been developed that provide a read-out of Cre activity (Tsien et al., 1996; Akagi et al., 1997; Lobe et al., 1999; Mao et al., 1999; Soriano, 1999; Kawamoto et al., 2000; Novak et al., 2000). In some of these reporter lines, Cre excision leads to activation of a *lacZ* reporter gene. In other double-reporter lines, Cre excision causes a switch from one reporter gene to another, including chloramphenicol acetyltransferase (CAT) to *lacZ*, CAT to enhanced green fluorescent protein (EGFP), *lacZ* to human alkaline phosphatase (hPLAP), also known as the Z/AP line, or *lacZ* to EGFP, also known as the Z/EG line. Thus, when a Cre reporter mouse is crossed to a Cre transgenic mouse, the double-transgenic offspring display a change in reporter gene expression that reflects the tissue and temporal specificity of the Cre transgene.

The protocols that follow describe detection of the *lacZ*, hPLAP, and EGFP reporter genes in whole-mount embryos or tissues (Basic Protocol 1) and in tissue sections (Basic Protocol 2). Samples can be analyzed sequentially for *lacZ* and hPLAP or EGFP and *lacZ*. Support Protocols 1 and 2 provide methods for genotyping mice.

Contributed by Corrinne G. Lobe and Caiying Guo

Current Protocols in Toxicology (2001) 15.4.1-15.4.11

ANALYZING WHOLE-MOUNT EMBRYOS OR TISSUES FOR REPORTER GENE EXPRESSION

Embryos or tissues can be stained as whole mounts (i.e., without sectioning onto slides). EGFP visualization is done directly. For *lacZ* staining, samples are first fixed and then stained. Staining for hPLAP also requires tissue fixation first, as well as a heat inactivation step to eliminate endogenous alkaline phosphatase activity.

This protocol describes the detection of multiple markers. EGFP should be assayed first because the fluorescence intensity decreases over time. Likewise, hPLAP should be assayed last because the heat inactivation will eliminate *lacZ* and EGFP activity.

Materials

Dissected Cre reporter double-transgenic mouse embryos or tissues (see Support Protocols 1 and 2 for genotyping)
PBS (*APPENDIX 2A*), ice cold
100 mM sodium phosphate buffer, pH 7.3 (see recipe), optional
lacZ fixative (see recipe), ice cold
2% (w/v) paraformaldehyde/0.2% (v/v) glutaraldehyde in PBS, for large (≥E9.5) embryos only, ice cold
lacZ wash buffer (see recipe), ice cold
lacZ staining solution (see recipe)
AP wash buffer (see recipe)
AP staining solution (see recipe)
0.1% (v/v) Tween 20/2 mM $MgCl_2$ in PBS

Petri dishes
24-well and 6-well tissue culture plates
Dissecting microscope with light source and filter set for GFP visualization (Leica or BLS-Ltd.)
15- or 50-ml snap-cap tubes (e.g., Falcon), for en masse hPLAP staining
70° to 75°C water bath

CAUTION: Paraformaldehyde and glutaraldehyde are hazardous chemicals; follow appropriate precautions for handling, storage, and disposal.

NOTE: Signals will be best if initial tissue fixation and washing is done in ice-cold solutions on ice and with gentle shaking.

Visualize EGFP

1. Place a dissected Cre reporter double-transgenic mouse embryo or tissue in a petri dish containing ice-cold PBS.
2. View whole embryo or tissue under the blue-wavelength light and yellow filter of a dissecting microscope with light source and filter set for GFP visualization.

   The EGFP signal persists for 24 hr in PBS at 4°C.

Fix sample

3. Place individual embryos in 24-well plate (for small embryos) or 6-well plate (for large embryos). Rinse embryo or tissue in 100 mM sodium phosphate buffer or PBS.

4a. *For small embryos (<E9.5):* Fix 30 min in an excess of *lacZ* fixative on ice, with gentle shaking.

4b. *For large embryos:* Fix 30 min in an excess of 2% paraformaldehyde/0.2% glutaraldehyde in PBS on ice with shaking, then bisect and fix for an additional 30 to 60 min on ice in *lacZ* fixative.

4c. *For large tissues:* Fix 4 hr in an excess of *lacZ* fixative on ice with shaking, bisecting the tissue after the first hour to allow penetrance of the fixative solution.

Stain for lacZ

5. Wash embryo or tissue three times, 15 to 30 min each, in *lacZ* wash buffer.
6. Stain in *lacZ* staining solution at 37°C or room temperature for 30 min to overnight, with shaking and protection from light.

   Stain will appear blue.

7. Wash three times, 10 min each, in PBS. If not doing the hPLAP stain, store samples in *lacZ* wash buffer at 4°C for up to one month.

Stain for hPLAP

8. Fill a 6-well tissue culture plate (for individual staining) or a 15- or 50-ml snap-cap tube (for en masse staining) with PBS and place in a 70°C water bath to preheat.

   If samples are not first stained for lacZ, they should be dissected and fixed as described in steps 1 to 4, then washed as described in step 7 before staining for hPLAP. For better penetration of the hPLAP substrates, 0.02% Nonidet P-40 and 0.01% sodium deoxycholate can be included in the fixative solution.

   The plate or tube should be placed in the hot water bath in advance to ensure that it is up to temperature and should be left in the water bath for the entire 30-min incubation.

9. Rinse sample in PBS.
10. Incubate sample 30 min in PBS at 70° to 75°C to inactivate endogenous AP.
11. Rinse sample in PBS at room temperature.
12. Wash sample 10 min in AP wash buffer.
13. Stain with AP staining solution at room temperature for 5 to 10 min or at 4°C for 0.5 to 36 hr.

    Stain will appear dark purple. If staining reaction is continued too long, a brown background stain appears.

14. Wash three times for 10 min each, in 0.1% Tween 20/2 mM $MgCl_2$ in PBS.

ANALYZING TISSUE SECTIONS FOR REPORTER GENE EXPRESSION

BASIC PROTOCOL 2

To visualize Cre activity through reporter expression at the cell level, tissues or embryos are cryosectioned, and the slides are stained for expression of the relevant reporters. For EGFP reporters, slides should simply be coverslipped after fixation. For the Z/AP double-reporter mice, slides can be stained for *lacZ* first and then for AP.

Materials

Dissected Cre reporter double-transgenic mouse embryos or tissues (see Support Protocols 1 and 2 for genotyping)
PBS (*APPENDIX 2A*), ice cold
Tissue-Tek OCT
15% and 30% (w/v) sucrose in PBS, 4°C
0.2% glutaraldehyde (v/v) in PBS, 4°C

lacZ wash buffer (see recipe), 4°C
lacZ staining solution (see recipe)
AP wash buffer (see recipe)
AP staining solution (see recipe)
0.1% (v/v) Tween 20/2 mM $MgCl_2$ in PBS
Nuclear fast red stain: 5% (w/v) aluminum sulfate/0.1% (w/v) fast red (optional)
70% and 90% (v/v) ethanol in PBS
100% ethanol
1:1 (v/v) ethanol/xylene
Xylene
Mounting solution (e.g., Cytoseal; Fisher)

Petri dishes
Coverslips
Compound microscope with light source and filter set for GFP visualization (Leica or BLS-Ltd.)
Plastic molds for cryofreezing
Box for storing embedded samples, optional
Cryostat, −20°C
Poly-lysine coated slides (e.g., Fisher)
Slide box
Staining jars
70° to 75°C water bath
Light-protected container, such as a plastic food container wrapped in foil

Additional reagents and equipment for fixing samples (see Basic Protocol 1)

CAUTION: Glutaraldehyde and xylene are hazardous chemicals; follow appropriate precautions for handling, storage, and disposal.

NOTE: Signals will be best if initial tissue fixation and washing is done in ice-cold solutions on ice and with gentle shaking.

Prepare sample

1. Place a Cre reporter double-transgenic mouse embryo or tissue in a petri dish containing ice-cold PBS.

For lacZ and hPLAP staining:

2. Fix sample as described for whole mounts (see Basic Protocol 1, step 4). For EGFP visualization, fix in 4% w/v PFA in PBS. Do not use glutaraldehyde.

   Petri dishes or 6-well plates work well for containers.

3. Wash sample three times, 20 min each, in PBS.

For EGFP visualization:

4a. Rinse sample once for 2 to 5 min through Tissue-Tek OCT.

   a. Freeze sample in Tissue-Tek OCT as described in steps 6 to 8.
   b. Section sample and apply sections to slides as described in steps 9 to 10.
   c. Mount slides with coverslips and view under a compound microscope equipped with a light source and filter set for GFP visualization.

4b. Cryoprotect sample in 15% sucrose in PBS for 1 hr at 4°C followed by 30% sucrose in PBS overnight at 4°C.

5b. Place sample in Tissue-Tek OCT at 4°C for several hours (≥1 hr).

Embed and section sample

6. Fill a plastic mold (which has been labeled) with Tissue-Tek OCT. Place the sample in the center of the mold and orient it.

7. Place the mold on dry ice and hold it level, being careful to maintain the orientation of the sample. Keep the mold on dry ice until the OCT is completely frozen.

   It is best to have some dry ice in a plastic tray.

8. *Optional:* Wrap sample in plastic wrap, place in a labeled box, and store up to 1 month at −80°C.

9. Equilibrate embedded sample in the chamber of a −20°C cryostat. Cryosection block at 7 µm and place the sections onto poly-lysine coated slides.

10. Dry slides for 1 to 4 hr at room temperature.

11. Store slides at −20°C in a slide box with a little desiccant. Tape the box shut.

Fix sections

12. Allow box of slides to equilibrate to room temperature before opening the box.

13. Preheat a large staining jar with PBS in a 70°C water bath.

    This step is unnecessary if only lacZ staining is to be carried out.

14. Place slides to be stained in another staining jar.

    Unused slides can be placed back into −20°C with desiccant and stored up to 1 week.

15. Fill staining jar with cold 0.2% glutaraldehyde in PBS and fix slides 10 min.

    If only hPLAP staining is to be carried out, the slides should be washed three times, 5 min each, in PBS following fixation and then stained as described in steps 19 to 25.

Stain for lacZ

16. Remove fixative and wash slides three times, 5 min each, in *lacZ* wash buffer.

17. Stain 4 to 6 hr in *lacZ* staining solution at 37°C, protected from light.

18. When the staining is complete, rinse slides three times, 5 min each, in PBS.

    Staining is complete when blue color appears. Slides can be briefly viewed under a dissecting microscope without covering. Do not allow slides to dry.

    If only lacZ staining is to be carried out, the slides should be dehydrated and mounted at this point as described in steps 28 to 29.

Stain for hPLAP

19. Transfer slides to staining jar containing preheated PBS and incubate 30 min at 70° to 75°C to inactivate endogenous alkaline phosphatase.

    The temperature of the PBS should be checked with a thermometer. A common mistake is to not have the PBS at 70°C so that the endogenous alkaline phosphatases are not inactivated.

20. Cool slides at room temperature for 1 to 2 min.

21. Rinse slides with PBS and then wash 10 min in AP wash buffer.
22. Shake excess liquid from slides and place slides flat in a light-protected container.
23. Overlay slides with 0.5 to 1 ml AP staining solution/slide. Cover the container and, if necessary, cover with foil to protect from light.
24. Stain slides 10 to 30 min at room temperature.
25. When the stain is complete, wash the slides three times, 10 min each, in 0.1% Tween 20/2 mM $MgCl_2$ in PBS.

    Staining is complete when dark purple color appears. Color reaction can be monitored as described in step 18.

Counterstain (optional)

26. Incubate slides 5 min in PBS.
27. Incubate slides 30 sec to 5 min in nuclear fast red stain until sections are faintly pink.

    The length of incubation depends on the freshness of the nuclear fast red stain.

Dehydrate and mount slides

28. Dehydrate slides through an ethanol series as follows:

    5 min in PBS
    5 min in 70% ethanol in PBS
    5 min in 90% ethanol in PBS
    5 min in 100% ethanol
    5 min in 1:1 ethanol/xylene
    5 min in xylene
    5 min in xylene.

29. Mount with coverslips using a mounting solution. View with a compound microscope.

    lacZ expression will appear as blue-stained cells, and hPLAP expression will appear as dark purple. The AP stain localizers move to the cell periphery.

SUPPORT PROTOCOL 1

GENOTYPING Cre REPORTER MICE AND Cre TRANSGENIC MICE BY PCR

To establish the genotype of mice, genomic DNA is prepared from ear punch or tail biopsy samples, digested with a restriction enzyme, and used in Southern blot analysis (Southern, 1975). Alternatively, for Cre genotyping the DNA can be used in a PCR reaction as described below (also see *APPENDIX 3C*). In the case of mice that express a reporter such as *lacZ*, the ear punch can be used in a *lacZ* staining reaction to identify pups carrying the transgene (see Support Protocol 2). General information about transgenic mice is described in *UNIT 1.3*.

Materials

Yolk sac, tail biopsy, or ear punch from potential transgenic mouse
PBS (*APPENDIX 2A*)
1× proteinase K buffer (see recipe)
Mineral oil
dNTP cocktail: 2 mM each dATP, dCTP, dGTP, dTTP
Taq DNA polymerase
10× PCR buffer (*APPENDIX 3C*)
10 μM PCR primer for Cre recombinase:
5′-ATG TCC AAT TTA CTG ACC CC-3′
5′-CGC CGC ATA ACC AGT GAA AC-3′

50°C incubator
PCR tubes
Thermal cycler

Additional reagents and equipment for agarose gel electrophoresis (*APPENDIX 3A*)

1. Dissect yolk sac, tail biopsy, or ear punch and rinse thoroughly in PBS.

   As a positive control, a sample from the transgene-positive parent can be used. A transgene negative control should be included, which can simply be siblings in the litter.

2. Place yolk sac, tail biopsy, or ear punch in a microcentrifuge tube with 100 µl of proteinase K buffer containing 1 mg/ml proteinase K.
3. Incubate overnight in a 50°C incubator.
4. Place 10 µl proteinase K–treated material into a PCR tube with 35 µl water and overlay with two drops of mineral oil.

   Too much tissue can inhibit the PCR.

5. Incubate tube 10 min at 94°C in a thermal cycler to denature the proteinase K.
6. Bring the thermal cycler to the annealing temperature (step 7) and add:

   10 µl dNTP cocktail
   10 µl 10× PCR buffer
   2.5 µl each 10 µM PCR primer
   0.5 µl, 2.5 U/µl *Taq* DNA polymerase.

   The final concentration of dNTPs should be 200 µM. Bring the final volume to 100 µl with water.

7. Carry out PCR using the following amplification cycles:

Initial step:	4 min	94°C	(denaturation)
30 to 40 cycles:	45 sec	94°C	(denaturation)
	45 sec	58°C	(annealing)
	1 min	72°C	(extension; 1 minute per kb)
Final step:	10 min	72°C	(extension).

8. Analyze products by gel electrophoresis (*APPENDIX 3A*) on a 1.0% agarose gel.

   The amplified Cre fragment is 356 bp.

GENOTYPING Cre REPORTER MICE AND Cre TRANSGENIC MICE BY *lacZ* EXPRESSION

SUPPORT PROTOCOL 2

If mice express *lacZ*, they can be rapidly and easily genotyped by using an ear biopsy, collected when enumerating the pups, for *lacZ* stain.

Materials

Ear punch from potential transgenic mouse
PBS (*APPENDIX 2A*)
0.2% (v/v) glutaraldehyde in PBS
lacZ staining solution (see recipe)

96-well plate
37°C incubator, optional
Dissecting microscope

CAUTION: Glutaraldehyde is a hazardous chemical; follow appropriate precautions for handling, storage, and disposal.

1. Place an ear punch, 2 to 3 mm in diameter, from a potential transgenic mouse in PBS in a 96-well plate.
2. Aspirate off PBS and fix sample 5 to 15 min in 0.2% glutaraldehyde in PBS.
3. Wash three times, 5 min each, in PBS.
4. Add 50 to 100 µl *lacZ* staining solution and stain 5 min in a 37°C incubator (or at room temperature for a longer time) protected from light.

   Staining is usually visible after 5 min if fresh stain is used.

5. Examine ear punch for *lacZ* staining using a dissecting microscope.

REAGENTS AND SOLUTIONS

Use Milli-Q-purified water or equivalent for the preparation of all reagents and in all protocol steps. For common stock solutions, see ***APPENDIX 2A****; for suppliers, see* ***SUPPLIERS APPENDIX****.*

Alkaline phosphatase (AP) staining solution

2 ml 1 M Tris·Cl, pH 9.5 (*APPENDIX 2A*)
0.4 ml 5 M NaCl
1 ml 1 M $MgCl_2$
200 µl 1% (w/v) sodium deoxycholate (0.01% final)
200 µl 2% (w/v) Nonidet P-40 (NP-40; stored at 4°C; 0.02% final)
70 µl 100 mg/ml nitroblue tetrazolium (NBT; 337 µg/ml final)
70 µl 50 mg/ml 5-bromo-4-chloro-3-indolyl phosphate (BCIP; 175 µg/ml final)
16 ml water
Do not store; prepare shortly before use.

Alkaline phosphatase (AP) wash buffer

10 ml 1 M Tris·Cl, pH 9.5 (*APPENDIX 2A*)
2 ml 5 M NaCl
1 ml 1 M $MgCl_2$
87 ml water
Store indefinitely at room temperature.

lacZ fixative

43.8 ml 100 mM sodium phosphate buffer, pH 7.3 (see recipe) or PBS (*APPENDIX 2A*)
5.0 ml 1 M $MgCl_2$
0.2 ml 50% (v/v) glutaraldehyde
1.0 ml 250 mM EGTA, pH 7.3
Store up to 1 week at 4°C

For whole-mount hPLAP staining, a mixture of 0.2% (v/v) glutaraldehyde in PBS, 0.02% (w/v) NP-40, and 0.01% (w/v) sodium deoxycholate may be used in place of this fix solution to improve penetration of stain.

lacZ staining solution

70.5 ml *lacZ* wash buffer (see recipe)
3.0 ml 25 mg/ml 5-bromo-4-chloro-3-indolyl-β-D-galactoside (Xgal; dissolved in dimethyl sulfoxide)
750 µl 500 mM potassium ferrocyanide
750 µl 500 mM potassium ferricyanide

This stain can be stored for 1 to 2 weeks at room temperature, but optimal staining occurs with freshly prepared stain solution.

lacZ wash buffer

489 ml 100 mM sodium phosphate buffer, pH 7.3 (see recipe)
1.0 ml 1 M $MgCl_2$
5.0 ml 1% (w/v) sodium deoxycholate (stored at 4°C)
5.0 ml 2% (w/v) NP-40 (stored at 4°C)
Store up to 3 months at 4°C

Proteinase K buffer, 1×

10 mM Tris·Cl, pH 7.5 (*APPENDIX 2A*)
10 mM EDTA
10 mM NaCl
0.5% (w/v) Sarkosyl
For enzyme solution: 1 mg/ml proteinase K (add just before use)

Sodium phosphate buffer (pH 7.3), 100 mM

11.5 ml 1 M NaH_2PO_4
38.5 ml 1 M Na_2HPO_4
450 ml water
Store indefinitely at room temperature.

This mixture should be pH 7.3. Do not adjust with acid/base.

COMMENTARY

Background Information

The use of Cre recombinase has become a powerful tool in manipulating the mouse genome. Some applications are to activate expression of transgenes, perform conditional or tissue-specific gene knockouts, or remove the phosphoglycerate kinase promoter (PGK)-neo sequence used in gene targeting (reviewed in Lobe and Nagy, 1998). A large number of Cre transgenic mouse lines have been and continue to be developed. In order to test the tissue and temporal specificity of these transgenic lines, the Cre mice can be crossed to a reporter mouse line, and the double-transgenic offspring analyzed for reporter gene expression.

The *lacZ* reporter gene, which encodes the β-galactosidase enzyme, has been used in transgenic mice for many years. Its expression is assumed to be innocuous; however, high levels of *lacZ* expression seem to be poorly tolerated by some tissues and may lead to stunted growth (Lobe et al., 1999). More recently, the human placental alkaline phosphatase (hPLAP) gene has been used as a reporter gene in transgenic mice. The hPLAP reporter may be better tolerated than *lacZ* because it is of mammalian rather than bacterial origin, and alkaline phosphatases are commonly expressed in cells. hPLAP activity can be differentiated from endogenous alkaline phosphatase activity because of its resistance to heat inactivation. Both the *lacZ*-encoded β-galactosidase and the hPLAP enzyme are visualized by incubation with substrates that are converted to insoluble colored products.

GFP is a powerful new reporter that can be visualized in live tissue. However, fixation in glutaraldehyde causes autofluorescence and therefore high background, and must be avoided. However it is compatible with sorting of fluorescence-labeled cells (Novak et al., 2000), and thus it has great potential for expression analyses in hematopoietic lineages.

Critical Parameters

Cre activity may be assayed in embryos or in adult tissues. If embryos at E9 or earlier are being analyzed, the whole-mount staining procedure (see Basic Protocol 1) is generally used. The whole-mount procedure can also be used to get a general picture of Cre activity in small pieces of dissected adult tissues. For older embryos and to determine expression at the cell level, the protocol for tissue sections (see Basic Protocol 2) is followed.

During the staining step, the color development can be monitored by eye or under a dissecting microscope, however do not leave samples exposed to light more than 1 to 2 min or let slides dry out. For *lacZ* stain, look for a dark blue color and for AP stain look for dark purple. If a brown color starts to develop in the AP staining, stop the reaction because this is background not a hPLAP signal.

To test tissue specificity of Cre expression, the mouse breeding should be between a male

Table 15.4.1 Troubleshooting Guide for Cre Reporter Detection Methods

Problem	Cause/Solution
Poor *lacZ* signal	Cells fixed too long, particularly with paraformaldehyde.
High background hAP signal	Endogenous hAP activity was not completely inactivated.
	PBS should be preheated to 70°C and tissues incubated ≥30 min in PBS at 70°C.
	Stain allowed to proceed too long, allowing the background to become high.
GFP signal washes out of cells	If cells are treated with alcohol to fix or to dehydrate, the GFP leaches out of the cells.
	Some media for coverslip mounting leeches out the GFP.
	Minimal processing for the GFP reporter should be used.

Cre transgenic mouse and a female Cre reporter mouse. If, instead, the Cre-expressing mouse is the female, maternal expression of the Cre transgene can produce sporadic, nonspecific Cre excision in the embryos.

For timed matings, check females in the mornings for a vaginal plug and sacrifice the female and dissect the embryos at the required stage. For tissues, sacrifice the animal and dissect tissues into cold PBS. Signals will be best if initial tissue fixation and washing is done in ice-cold solutions on ice and with gentle shaking. Note that paraformaldehyde fixation will decrease *lacZ* activity, therefore it should be kept to a minimum and used at 4°C.

Troubleshooting

See Table 15.4.1 for potential problems related to reporter-gene staining and their solutions.

Anticipated Results

With Cre reporter mice, blue *lacZ* reporter gene activity typically shows up rapidly, and purple hPLAP staining occurs even more quickly. In double-reporter mice such as Z/AP, blue *lacZ*-positive tissues are negative for Cre excision and purple hPLAP-positive tissues have Cre activity. In most single-reporter mice, *lacZ* staining indicates Cre activity. However, negative tissues should be evaluated for their potential to express the reporter gene before assuming they lack Cre activity, because some Cre reporter mice have restricted expression of the reporter gene. This can be checked by crossing the Cre reporter mice to a Cre line that gives Cre excision in all tissues.

Many tissue-specific Cre lines have been found to have ectopic Cre activity. This is more significant in a Cre/*loxP* system than in an inducible promoter system because if Cre is expressed in a population of cells, a genomic alteration is made between the target *loxP* sites, and all descendants of those cells will also have the genomic alteration.

Different Cre reporters can have different sensitivities to Cre excision (Hebert and McConnell, 2000). This variability likely is due to different chromatin structure and probably reflects an equal variance in other *loxP* target sites used in experiments.

Time Considerations

Processing the tissues for whole-mount staining can be done in 1 day. After the initial fixation and washing steps, which take 1 to 2 hr, the *lacZ* stain usually goes for 2 to 4 hr. Subsequent preparation and staining for hPLAP takes an additional 2 hr, and slides can be dehydrated and coverslips mounted in another hour.

For tissue sections, samples are fixed and washed the first day and left in sucrose overnight. The second day they are equilibrated in OCT and can be frozen that day or the next (third) day. It normally takes ≥1 day (day three to day four) to section samples. Staining the slides requires one more day, making the process ~4 to 6 days.

Genotyping by PCR requires 1 hr on the first day, and ~30 min on the second day to start the PCR reaction. Gel analysis requires an additional 2 to 3 hr on the second or third day. Genotyping by *lacZ* expression requires 2 to 3 hr.

Literature Cited

Akagi, K., Sandig, V., Vooijs, M., Van Der Valk, M., Giovannini, M., Strauss, M., and Berns, A. 1997. Cre-mediated somatic site-specific recombination in mice. *Nucl. Acids Res.* 25:1766-1773.

Feil, R., Brocard, J., Mascrez, B., LeMeur, M., Metzger, D., and Chambon, P. 1996. Ligand-ac-

tivated site-specific recombination in mice. *Proc. Natl. Acad. Sci. U.S.A.* 93:10887-10890.

Furth, P.A., St. Onge, L., Boger, H., Gruss, P., Gossen, M., Kistner, A., Bujard, H., and Hennighausen, L. 1994. Temporal control of gene expression in transgenic mice by a tetracycline-responsive promoter. *Proc. Natl. Acad. Sci. U.S.A.* 91:9302-9306.

Hebert, J.M. and McConnell, S.K. 2000. Targeting of cre to the foxg1 (BF-1) locus mediates loxP recombination in the telencephalon and other developing head structures. *Dev. Biol.* 222:296-306.

Hoess, R.H., Wierzbicki, A., and Abremski, K. 1986. The role of the *loxP* spacer region in P1 site-specific recombination. *Nucl. Acids Res.* 14:2287-2300.

Kawamoto, S., Niwa, H., Tashiro, F., Sano, S., Kondoh, G., Takeda, J., Tabayashi, K., and Miyazaki, J. 2000. A novel reporter mouse strain that expresses enhanced green fluorescent protein upon Cre-mediated recombination. *FEBS Lett.* 470:263-268.

Kellendonk, C., Tronche, F., Monaghan, A.-P., Angrand, P.-O., Stewart, F., and Schutz, G. 1996. Regulation of Cre recombinase activity by the synthetic steroid RU 486. *Nucl. Acids Res.* 24:1404-1411.

Lobe, C.G. and Nagy, A. 1998. Conditional genome alteration in mice. *BioEssays* 20:200-208.

Lobe, C.G., Koop, K.E., Kreppner, W., Lomeli, H., Gertsenstein, M., and Nagy, A. 1999. Z/AP, a double reporter for cre-mediated recombination. *Dev. Biol.* 208:281-292.

Mao, X., Fujiwara, Y., and Orkin, S.H. 1999. Improved reporter strain for monitoring Cre recombinase-mediated DNA excisions in mice. *Proc. Natl. Acad. Sci. U.S.A.* 96:5037-5042.

Novak, A., Guo, C., Yang, W., Nagy, A., and Lobe, C.G. 2000. Z/EG, a double reporter transgenic mouse line that expresses enhanced Green Fluorescent Protein upon Cre-mediated recombination. *Genesis* 28:147-155.

Rivera, V.M., Clackson, T., Natesan, S., Pollock, R., Amara, J.F., Keenan, T., Magari, S.R., Phillips, T., Courage, N.L., Cerasoli, F., Holt, D.A., and Gilman, M. 1996. A humanized system for pharmacological control of gene-expression. *Nature Med.* 2:1028-1032.

Sauer, B. 1998. Inducible gene targeting in mice using the Cre/lox system. *Methods* 14:381-392.

Soriano, P. 1999. Generalized lacZ expression with the ROSA26 Cre reporter strain [letter]. *Nature Genet.* 21:70-71.

Southern, E.M. 1975. Detection of specific sequences among DNA fragments separated by gel electrophoresis. *J. Mol. Biol.* 98:503-517.

Sternberg, N. and Hamilton, D. 1981. Bacteriophage P1 site-specific recombination I. Recombination between *loxP* sites. *J. Mol. Biol.* 150:467-486.

Tsien, J., Chen, D., Gerber, D., Tom, C., Mercer, E., Anderson, D., Mayford, M., Kandel, E., and Tonegawa, S. 1996. Subregion- and cell type-restricted gene knockout in mouse brain. *Cell* 87:1317-1326.

Internet Resources

www.mshri.on.ca/develop/nagy/Cre.htm

This website lists Cre transgenic lines, available from laboratories, that have widespread tissue-specific or inducible Cre activity.

Contributed by Corrinne G. Lobe and Caiying Guo
Sunnybrook and Women's College Health Sciences Centre and University of Toronto
Toronto, Canada

CHAPTER 16
Male Reproductive Toxicology

INTRODUCTION

Over the past 20 to 25 years, male reproductive toxicology, like other specialties in toxicology, has evolved significantly. This maturation is evidenced by a broad acceptance and codification of what were previously research methods in detection and quantification, and by a generalized understanding of the relationships among the various endpoints. For example, the use of Bouin's as the fixative of choice for testes was a novel concept just 15 years ago, and is now recommended in the testing guidelines of multiple agencies. We recognize that sperm measures relate pretty directly to fertility, that Sertoli cell numbers underlie sperm count, and that Sertoli cell numbers can be manipulated during development with lasting effects into adulthood. Despite this progressive codification, there is still evolution of protocols, and refining of methods is a continual process.

The research forefront of many parts of male reproductive toxicology involves the elucidation of relationships among different interacting cell types, subcellular signaling systems that mediate these interactions, and the mechanisms by which toxicants perturb intracellular physiology. Progress in our understanding of mechanisms in reproductive toxicology is tightly linked with progress in reproductive biology and physiology. And these are truly exciting times, as our knowledge of reproductive biology and physiology is expanding at an exponential rate. Technical advances in the identification and quantification of expressed genes and their protein products are rapidly expanding both the sophistication of our insights and the inherent complexity of the processes we study.

In our initial organizational discussions, we—the editors of this chapter—started with the idea that we needed to provide non-expert readers with the tools to address apparently simple questions, such as "How do I determine the target cell of this novel male reproductive toxicant?" or "Why is my male transgenic mouse infertile?" Of course, given the complexity of male reproduction, these apparently simple questions can be difficult, and sometimes impossible, to answer. Nonetheless, the initial chapters in this unit are designed to present the conceptual framework and most up-to-date tools available to investigate targets of toxicants and mechanisms of male reproductive failure.

The units presented in this chapter were chosen to represent the continuing evolution of our field. Rochelle Tyl has done a superb job in capturing both the more standard methods of assessing fertility in toxicant-treated or gene-knockout animals (*UNIT 16.1*), and additionally provides a unit (*UNIT 16.2*) on measuring the more subtle endpoints of the development of the reproductive system, endpoints which have been shown to be sensitive to prenatal hormonal exposures. Dr. Tyls' references to the ways to integrate the various endpoints will be complemented by a group of units that provide details in quantifying spermatogenesis. Dianne Creasy provides two units on histopathology in the male reproductive system: how to prepare the tissues for analysis (*UNIT 16.3*), and how to evaluate them once you've got the sections (*UNIT 16.4*). This represents the very latest thinking in the most appropriate use of "staging", a concept that often strikes fear into the hearts of pathologists. Dr. Creasy explains why this fear is needless, what is really meant by the term "staging", and when stages of spermatogenesis should be counted versus when you simply need to examine the sections with a basic understanding of spermatogenesis. Rather than leaving you there, she then refers to sources that can provide this basic

Contributed by K. Boekelheide and R. Chapin
Current Protocols in Toxicology (2004) 16.0.1-16.0.2

understanding. Drs. Fail and Anderson (*UNIT 16.5*) provide a detailed explanation of alternative approaches that use in-dwelling catheters for repeated blood sampling in the rat. This valuable technique minimizes animal stress and handling while maximizing the quality of the hormonal data. In a new unit Dr. Wang (*UNIT 16.6*) succinctly describes a detailed procedure for determining epididymal sperm counts and sperm density in rodents. This is complemented by the method of Seung et al. who describe the quantitation of testicular homogenization resistant spermatid heads as a way of quantifying the latter parts of spermatogenesis (*UNIT 16.7*). Collectively these units provide good tools for describing spermatogenesis both qualitatively and quantitatively, and both approaches should be used whenever possible. In a new unit (*UNIT 16.8*), Drs. Ostby and Gray provide definitive information on how to evaluate a novel toxicant suspected of endocrine disrupting activity, a current "hot topic" in reproductive developmental toxicology.

Future units are envisioned which focus on advanced research techniques in reproductive toxicology, using methods for studying various cellular and subcellular processes in vivo and in vitro. Examples of such approaches include gene transfection, viral infection, and germ cell transplantation, all techniques which require sophisticated manipulations and offer the advantage of selective targeting. In addition, future units will focus on classes of toxicants with special properties. We hope you enjoy these units and derive as much benefit from reading and using them as we have.

K. Boekelheide and R. Chapin

In Vivo Models for Male Reproductive Toxicology

MALE REPRODUCTION

Male reproduction encompasses the production of viable sperm, their delivery into the female reproductive tract, fertilization of the female oocytes, and production of normal offspring. Successful male fertility requires an adequate sperm count, adequate sperm motility, the appropriate functioning of accessory sex organs (to produce and concentrate semen and to activate and capacitate sperm), and appropriate sexual behavior (i.e., mounting, intromission, ejaculation). The production of viable sperm (spermatogenesis) in the testes is under genetic control (a male-determining gene on the Y chromosome) and neuroendocrine regulation initiated in the brain by the hypothalamic-pituitary-gonadal (HPG) axis. There is also intratesticular endocrine, autocrine, and paracrine regulation. Once the sperm are produced and delivered to the epididymis, they are stored in the cauda epididymis and moved into the vas deferens. Epididymal maturation must occur; this includes acquisition of motility and the ability to penetrate and fertilize the oocytes, and acrosomal cap activation. Semen is produced from accessory sex organs—seminal vesicles, coagulating glands, the prostate, bulbourethral (Cowper's) glands, and preputial glands. The sperm in semen are moved through the blood-engorged erect penis and ejaculated into the female's vagina-cervix-uterus. Indirect influences also play a role, such as nutritional status, liver metabolism of xenobiotics and endogenous hormones, and vascularization. The testis is relatively anoxic, with low blood flow and low oxygen tension; insult can alter the permeability of the testicular vasculature and consequently affect blood flow (Miller, 1998).

Regulation of the neuroendocrine system begins with specialized cells in the hypothalamus in the brain that release gonadotropin-releasing hormone (GnRH) in a pulsatile pattern. GnRH travels via the hypothalamic-pituitary portal system directly to the anterior lobe of the pituitary. In a receptor-mediated process, GnRH stimulates cells of the anterior lobe of the pituitary to secrete the gonadotrophins, luteinizing hormone (LH), and follicle-stimulating hormone (FSH). LH and FSH travel via the systemic blood supply to the testes. LH binds to receptors on the interstitial cells of Leydig to stimulate steroidogenesis (i.e., synthesis of testosterone) in these cells. FSH binds to receptors on the intratubular Sertoli cells, which act as nurse cells for the developing germ cells and are necessary for spermatogenesis.

Inhibin, produced by the Sertoli cells, and testosterone (T) from the Leydig cells both exert negative feedback on the pituitary production of FSH and LH. T also exerts negative feedback on the hypothalamic production of GnRH (Russell et al., 1990; Miller, 1998). Sertoli cells have receptors for both FSH and T for additional coordination between the Sertoli and Leydig cell populations (Russell et al., 1990).

Male reproductive toxicants have been classified in a number of ways, based on direct or indirect action. Mattison (as described by Miller, 1998) proposed that direct-acting toxicants interacted with cellular components, based on inherent chemical reactivity or via specific receptor binding, whereas indirect-acting toxicants acted via disruption of endocrine homeostatis or by metabolic activation to a direct toxicant. Working (also described by Miller, 1998) used the direct-acting versus indirect-acting classification but proposed that a direct toxicant affects the testis without endocrine mediation, whereas an indirect toxicant acts at a non-germ-cell site (e.g., hypothalamic-pituitary axis or the Leydig cell; see discussion in Miller, 1998).

Miller (1998) also used the direct- versus indirect-acting classification but defined direct-acting toxicants as those that produced their primary effects on testicular cells, the duct system (e.g., the epididymis), or on mature spermatozoa. This definition would include effects on non-germ-cell testicular cell types such as the Leydig or Sertoli cells. Because the testis is subject to hormonal control and regulatory feedback loops, the action of direct toxicants on testicular cell types would result in secondary disruption of endocrine homeostasis. Indirect toxicants are defined as having a primary action on hypothalamic-pituitary neuroendocrine controls or on extragonadal systems. This last classification, which is based on the processes altered, does not consider whether the parent compound or a metabolite is eliciting the toxicity (Miller, 1998).

Other indirect effects that could affect male reproduction include anosmia (the absence or loss of the sense of smell), so that the male is

Contributed by Rochelle W. Tyl

Current Protocols in Toxicology (2002) 16.1.1-16.1.15

unable to detect pheromonal signals from receptive females. They also include peripheral neuropathy, so that the male cannot mount the female due to his hindlimb weakness or achieve appropriate intromission, ejaculation, and/or stimulation of the cervix. Inhibition of brain aromatase enzyme, which locally converts T to estrogen in the male rat brain, can also result in altered male reproduction. Local estrogen masculinizes the male rat brain, for example, the sexually dimorphic nucleus of the preoptic area (SDN-POA), and sexually dimorphic behaviors (e.g., play, mating, aggression) early in perinatal development. Either an absence of or reduction in brain-localized estrogen in the male rat will affect mating behavior, resulting in impaired reproductive performance. Alterations in neonatal thyroid hormone levels can also result in changes in testis size and sperm production. Goitrogen administration increases these parameters, presumably through a delay in differentiation of Sertoli cells, so that they continue to divide and, in the mature testis, can support more sperm per cell, resulting in larger testes and increased sperm production in the mouse (Joyce et al., 1993) and in rats and humans (Chowdury et al., 1984).

Steroidogenesis—the production of T and dihydrotestosterone (DHT) from cholesterol by a series of P450 enzymes in the Leydig cells of the testis—is necessary for both spermatogenesis and for development of secondary sex characteristics. In utero, T (produced locally by the interstitial cells of Leydig, which are regulated by LH) is responsible for the differentiation of the Wolffian ducts into the epididymides, vasa deferentia, seminal vesicles, and the growth of the levator ani-muscle and bulbocavernosus gland (the LABC complex). DHT (produced locally in the testis by the conversion of T using the enzyme 5-α-reductase) is responsible for the differentiation of the genital tubercle into the external genitalia and the urogenital sinus into the prostate and Cowper's glands, and for the regression of nipple anlagen in male fetuses. The Sertoli cells are also necessary for spermatogenesis. Inhibin (also called the Müllerian inhibiting substance) is produced locally by the fetal Sertoli cells and is regulated by FSH. It causes the Müllerian ducts (which are initially present in both sexes in utero and which form oviducts and the uterus in female fetuses) to regress, thereby suppressing female reproductive development. At puberty, there is another surge of FSH and LH and, therefore, T, which initiates preputial separation (PPS) in the rodent, development of tertiary sex characteristics, and spermatogene-

Figure 16.1.1 *(at right)* Detection of male reproductive toxicity when both sexes are exposed or transgenic. F1 through F6 indicate female reproductive effects and experimental strategies, as follows. F1: If there are fewer or no pups, and implantation sites are normal (with or without increased resorptions), the site of action is in utero development and/or altered corpus luteum function (so that postimplantation survival is compromised). F2: If there are fewer or no pups, implantation sites are reduced or absent, and corpora lutea counts are normal, then site of action is fertilization or implantation and/or maintenance of implantation. F3: If there are fewer or no pups, implantation sites are reduced or absent, and corpora lutea counts are reduced or absent, then site of action is ovarian (histopathology) or the hypothalamus-pituitary (gonadal) axis. F4: For exposed (or transgenic) females in vivo, measure plasma or serum for baseline follicle stimulating hormone (FSH), luteinizing hormone (LH), and prolactin (Prl) of pituitary origin, and 17β-estradiol (E_2) and progesterone (P) of ovarian origin. Challenge female in vivo with gonadotropin-releasing hormone (GnRH) of hypothalamic origin and sample plasma or serum for above hormones. If baseline and challenge levels are normal, the hypothalamic-pituitary-gonadal (HPG) axis is normal. If baseline and/or challenge levels are abnormal and the pituitary levels are abnormal, the pituitary is affected. The ovaries would be affected as well. If the pituitary levels are normal and ovarian hormones are abnormal, then the ovaries are affected. F5: For a specific evaluation, the in vitro assay involves control (untreated) minced ovaries exposed to test material in culture for E_2 and P release. Challenge would involve adding FSH or LH to culture medium and assaying for E_2 and P. If there is a response in baseline or challenge levels, the ovaries are affected. This assay does not evaluate hypothalamic or pituitary effects (Lasky et al., 1994). The ex vivo assay involves culturing ovaries from treated females and determining baseline and challenge ovarian hormone levels, as above. F6: Histopathologic evaluation of ovaries should include step sections with determination of profile of primordial, small antral, large antral, and mature Graafian follicles. If there is an effect, one can determine when in the cycle the effect may reside and in which cells derived from the follicle (e.g., granulosa or thecal) the insult occurred (Heindel et al., 1989). The double-headed arrow between female reproductive and nonreproductive effects indicates that each effect can, in turn, affect the other.

sis. Testis descent through the inguinal ring and into the scrotal sacs prior to puberty appears to be controlled by both T and DHT.

Male reproductive impairment can result from: (1) exposure to a xenobiotic during the perinatal (prenatal and early postnatal), peripubertal, or adult period of life; (2) a spontaneous mutation in regulatory and/or structural genes (or ligand receptors) involved in the development, structure, and/or function of the reproductive system; (3) construction of a transgenic animal (carrying an inserted gene or genes from another species) in order to evaluate the role of a particular gene or genes in the reproductive process, or in order to evaluate the role of the transgene in an entirely different process, organ, or developmental phase, with inadvertent effects on reproduction; or (4) construction of a so-called knockout animal, in which a particular gene (or genes) is deleted or otherwise prevented from producing its gene product. The deleted or blocked genes may be intentionally

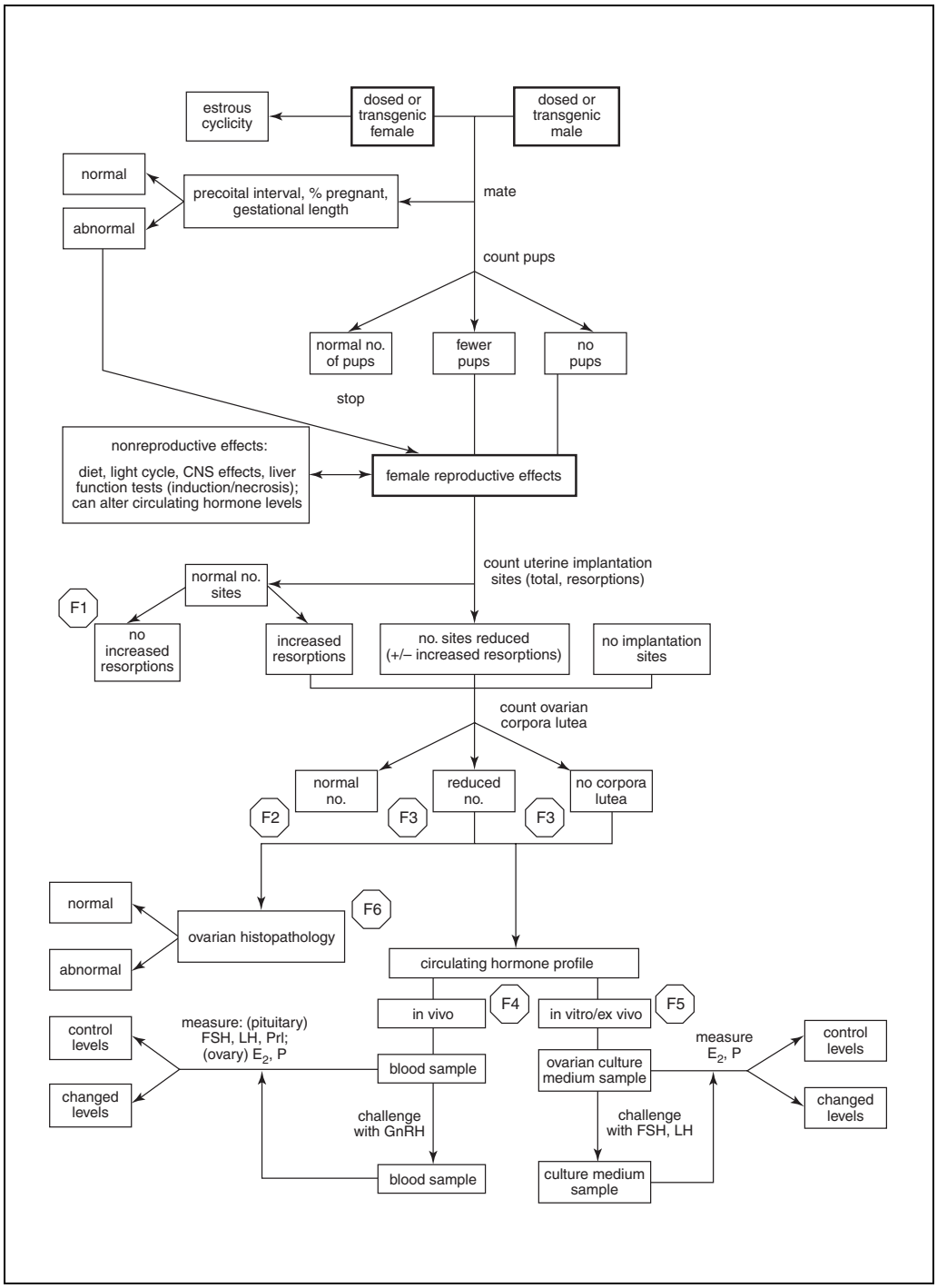

relevant to the reproductive process or may be directed to an entirely different system or function, with inadvertent effects on reproductive development and/or function.

This unit describes scenarios in which indications of possible male reproductive toxicity may be identified and the sequence to follow to determine the extent and nature of the toxicity. Useful in vivo models, methods, and endpoints are presented, as well as suggestions on how to interpret the results. *UNIT 16.2* presents guidelines for rodent mating.

Figure 16.1.1 is a flow chart illustrating how to detect male reproductive toxicity when both males and females are exposed to a xenobiotic (or are transgenic), with the focus on female assessment (the male assessment is presented in Fig. 16.1.2). Figure 16.1.2 is a similar flow chart showing how to detect male reproductive toxicity when the male is exposed or transgenic (regardless of the status of the female). Both flow charts begin with mating the male(s) of concern and assessing reproductive outcome. As the chart progresses, the type of potential adverse outcome is identified, with follow-up procedures to identify the site of the insult by in vivo, in vitro, or ex vivo evaluations, including options based on whether or not the male of concern can be necropsied. The specific endpoints are discussed in the figure legends.

IN VIVO MODELS

There are two general research or testing scenarios in which results may indicate or suggest possible direct or indirect male reproductive toxicity (Stoker et al., 2000 for males; Goldman et al., 2000 for females). In the first scenario, the study design is not oriented to reproductive evaluations. This would include acute studies, multiple-dose studies (such as 5 days, 14 days, or 28 days), subchronic studies (90 days), and/or chronic or carcinogenicity studies (e.g., 2-year studies in rats, 18-month studies in mice, 1-year studies in dogs). However, information collected may provide clues such as the following.

If exposure is during pre- or postnatal development, such as in the Food and Drug Administration (FDA) carcinogenicity study design where indirect exposure begins during gesta-

Figure 16.1.2 *(at right)* Detection of male reproductive toxicity when only the male is exposed or transgenic. M1 through M8 indicate male reproductive effects and experimental strategies, as follows. M1: Effects on pregnancy rate and precoital interval may be due to male reproductive dysfunction. M2: Although the assumption for an untreated (wild-type) female is that she is reproductively normal, she may not be. Evaluation of uterine implantation sites (total and resorptions) and ovarian corpora lutea (Fig. 16.1.1) may indicate that she is the cause of the reduced fertility or infertility, not the male. M3: Central nervous system (CNS) effects may be detected by use of a functional observational battery (FOB), which assesses home cage observations (e.g., convulsions, gait, tremors, abnormal motor movements), handling observations (e.g., muscle tone, ease of handling, signs of stress), open-field observations (e.g., posture, tremors, gait, convulsions, abnormal motor movements, rearing), and sensory and neuromuscular observations (e.g., approach, startle, tail pinch response, pupil size and response [Moser et al., 1991], forelimb and hindlimb grip strength, hindlimb foot splay [Meyer et al., 1979]). Effects on these parameters could interfere with mounting, intromission, and ejaculation. The double-headed arrow indicates that each effect can, in turn, affect the other. M4: Because release of male-specific hormones is pulsatile, serial blood samples will detect the normal (or abnormal) cyclical pattern. Serial samples can be obtained from multiple withdrawals from the lateral tail vein or from a cannulated animal. M5: Measure plasma or serum for follicle stimulating hormone (FSH) and luteinizing hormone (LH), originating in the pituitary in both sexes; testosterone (T) and dihydrotestosterone (DHT) from the testis; and gonadotropin-releasing hormone (GnRH), originating from the hypothalamus in both sexes. Challenge male in vivo with GnRH of hypothalamic origin and sample plasma or serum for above hormones (Fail et al. 1994). Results are interpreted as described (Fig. 16.1.1.1; F4). M6: Histopathologic evaluation of testis (and epididymis) should be performed after Bouin's or formalin fixation, embedding in glycol methacrylate (GMA) plastic or paraffin, sectioning at 2 to 4 μm, and staining with periodic acid Schiff's stain/hematoxylin (PAS-H). It should include integrity of cell types in seminiferous tubules (Sertoli, spermatogenic cells) and in the interstitium between the tubules (Leydig cells); spermatogenic staging may be necessary (Russell et al., 1990). M7: Ex vivo and in vitro evaluation of minced testes in culture performed like ex vivo and in vitro ovarian culture with challenge by FSH or LH (Payne and Sha, 1993; Fig. 16.1.1). Testicular hormonal output in culture is T, DHT, and inhibin. M8: Determination of homogenization-resistant spermatid head counts (SHCs) and calculation of daily sperm production (DSP) and efficiency of DSP (e.g., Sharpe et al., 1996).

tion and lactation and then direct exposure continues following weaning for 18 to 24 months, then anogenital distance (AGD) is a significant measure on postnatal day (P) 0 (at birth) and also on P21 (at weaning) and/or in adults; endocrine-mediated changes in AGD persist to adulthood. In the author's laboratory, based on six studies from 1996 to 2001, AGD on P0 is 0.73 to 0.96 mm in females and 1.97 to 2.25 mm in males for control CD (Sprague-Dawley; SD) rats.

The retention of areolae and/or nipples in preweanling (P11 to P13) males can be determined. In the author's laboratory, areolae are present in 0% to 3.5% of control CD (SD) male rats on P12 (out of over 500 control male pups examined to date). Dr. L. Earl Gray, Jr. of the U.S. Environmental Protection Agency (EPA) reports a 0% to 5% incidence in control prepubertal Long-Evans rats (L.E. Gray, Jr., unpub. observ.). The presence of retained nipples in males is usually detected on P11 to P13 before

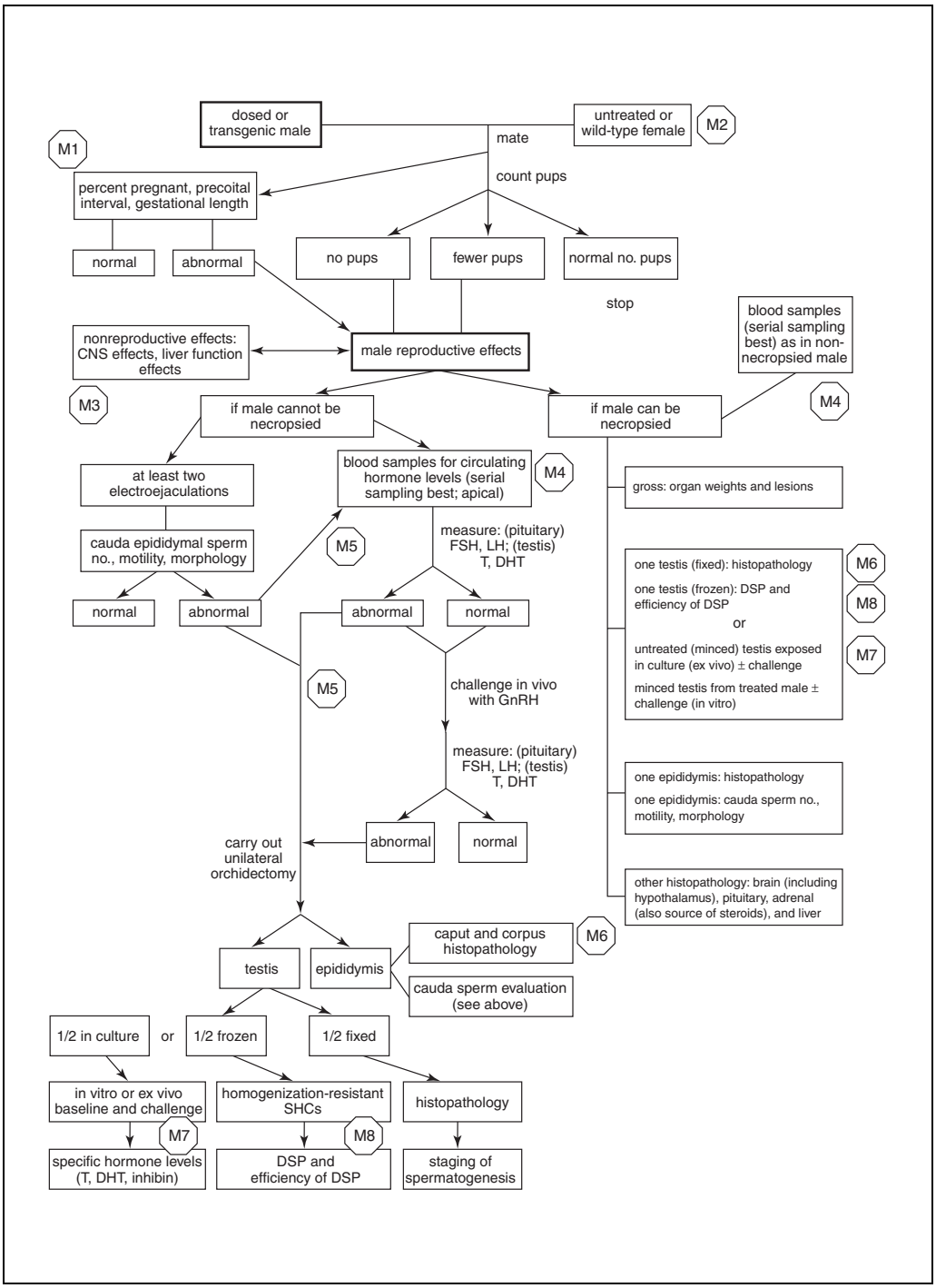

the hair grows in (but endocrine-mediated retained nipples persist through adulthood and can be detected on the shaved ventrum). In the author's laboratory, no retained nipples have been observed in control CD (SD) male rats on P11 to P13, based on over 500 control males examined (and over 3000 males examined in total).

Testis descent (into the scrotal sacs from the abdominal cavity through the inguinal canal and ring) is usually complete by P15 to P20 in male rats.

Acquisition of puberty, balanopreputial separation (or PPS) in male rodents, is defined as the age when the foreskin can be fully retracted from the penis. In the author's laboratory, the grand mean age at PPS for control CD (SD) rats is 41.9 days (based on fifteen studies from 1996 to 2001, with study means of 40.9 to 43.6 days).

Acquisition of puberty is defined as vaginal patency (VP) in female rodents. In the author's laboratory, the grand mean age at VP for CD (SD) rats is 31.1 days (based on fifteen studies from 1996 to 2001, with study means of 29.9 to 32.5 days).

Gross alterations in external genitalia (e.g., hypospadias, epispadias, and either unilateral or bilateral ectopic, small, or missing undescended testes) can also occur. Detection of these alterations is best done after puberty.

Postpubertal adult exposure to a xenobiotic obviously cannot interfere with normal reproductive system development perinatally or peripubertally. However, such exposure can result in toxicity to already formed organs. This toxicity may be expressed as reduced organ weights or evidence of impaired or lost function from histopathologic examination of target organs. The same consequences may occur in a transgenic male in which the apoptotic cascade is turned on inappropriately, with consequent cell death and damage to already formed organs. Damage to the adult testis from insult may be transient, with full or partial recovery, if the interstitial cells of Leydig (which produce T) are not completely lost, and if the intratubular Sertoli cells and spermatogonial cells (which divide mitotically to produce one daughter cell that goes through spermatogenesis and one daughter cell that remains a spermatogonial cell) are not completely lost.

The following endpoints are useful for monitoring effects of exposure to xenobiotics: (1) reproductive organ weights (absolute and relative to terminal body weight); (2) gross examination of reproductive organs; (3) histopathologic evaluations of reproductive organs; (4) andrologic assessments of epididymis and testis; and (5) circulating hormonal profiles for FSH, LH, prolactin (Prl), T, and DHT.

At necropsy, the following measures are suggested: (1) gross alterations in reproductive and associated organs; (2) organ weights for testes, epididymides, seminal vesicles, coagulating glands, prostate (whole and/or ventral and dorsolateral lobes), preputial glands, Cowper's glands, LABC complex, and glans penis (preferably absolute and relative weights, the better to correct for changes in body weights); and (3) histopathology of the above organs plus pituitary (especially anterior lobe), brain (especially hypothalamus and SDN-POA), adrenal gland (especially cortex), and liver (for possible effects on reproductive development, structure, and function).

In the second scenario, mating is part of the study design. This could include multigeneration studies (EPA, 1996, 1997, 1998a), the National Toxicology Program (NTP) reproductive assessment by continuous breeding (RACB; Reel et al., 1985; Chapin et al., 1997), the NTP 35-day assay (Kaiser et al., 1996, 1997, 1998; L.B. Kaiser, G.W. Wolfe, L. Lanning, R.E. Chapin, G. Klinefelter, and E.S. Hunt, unpub. observ.; and see Internet Resources), FDA Segment I and III studies (FDA, 1982, 1993, 2000), Organization for Economic and Cooperative Development 421 (OECD, 1995) and 422 (OECD, 1996) studies, and dominant lethal studies (Green et al., 1976, 1985; Ehling et al., 1978; EPA, 1998b). This scenario would also include transgenic males being bred to generate a colony of such animals. However, rodents are robust reproducers with excess sperm capacity and will reproduce normally when significant portions (up to ~80%) of the testes are damaged. Therefore, selection of in vivo parameters to be evaluated from animals in either scenario is critical to determine if there is potential reproductive toxicity. Obviously, histopathology and other postnecropsy assessments are definitive, but they require the demise of the study animals.

Assume in the breeding component of a rat study (the second scenario discussed above) that there is evidence of reduced fertility and/or fecundity (the former term relating to whether or not the female becomes pregnant, and the latter term relating to litter size and/or number of litters if there is continued or multiple periods of cohabitation, such as the NTP RACB protocol). If both sexes are exposed (Fig. 16.1.1), the effect from exposure could be in

either or both sexes. If only one sex is exposed (Fig. 16.1.2), the effect(s) from exposure must reside in the exposed sex.

If the female is expendable and was not exposed, we can assume (or evaluate) that she was cycling normally, had ovulated the appropriate number of eggs, and was appropriately receptive to the male. Female rats will continue to cycle in the absence of a male. Female mice will become anestrus in the absence of a male but can be induced to begin cycling if a male is maintained nearby or if the female is housed with dirty cage litter from a male. (Estrous cyclicity is obviously induced by a pheromone in the urine; Whitten, 1956.) Rabbit females do not ovulate until after copulation.

To assess reproductive toxicity, one must determine: (1) whether the male adequately stimulated the female and achieved intromission; (2) whether the male had motile, normal, capacitated sperm that reached the upper oviducts; (3) whether the sperm fertilized the ovulated eggs; (4) whether the zygote was able to implant in the uterine lining; and (5) whether the conceptus was able to develop normally to term (again, assume or confirm that the exposed female has a normal hormonal milieu and hospitable uterus). Male rats with very low epididymal sperm motility and progressive motility (defined as the percentage of motile sperm that move a predetermined linear distance over a predetermined time) and a high incidence of abnormal sperm can typically sire normal litters (Tyl et al., 1999, 2002; Table 16.2.3).

If the female was exposed, the same questions are relevant, in addition to the following questions: (1) was she cycling normally? (2) were her hormone levels normal? and (3) what was the incidence of preimplantation and/or postimplantation loss? These parameters should be normal in an unexposed female; historical control data are very important.

Evaluations of the female are listed below. They may be appropriate for both unexposed and exposed females.

1. Estrous cyclicity, its presence, duration, and normalcy, which requires examination for ≥14 days (21 days is best), should be analyzed.

2. Blood samples taken from the lateral tail vein should be analyzed for 17β-estradiol (E_2), progesterone (P), Prl, FSH, LH, and GnRH levels to assess the hormonal environment.

3. At necropsy the stage of estrus should be determined, as this information may be very useful to correlate with the appearance of the uterus.

4. If the necropsy occurs within 4 days of parturition (delivery of the litter), ovarian corpora lutea should be counted as a measure of the number of eggs ovulated in the cycle of interest. The corpora lutea involute after delivery. By P21 (when rat and mouse litters are usually weaned), the corpora lutea have fully involuted and regressed to corpora albicans, which are essentially indistinguishable from corpora albicans from previous estrous cycles.

5. Uterine nidation scars and sites of conceptual implantation and placental attachment can be counted at least out to 41 days postparturition and probably longer (R.W. Tyl, unpub. observ.). These scars are visible in the fresh tissue dissection if the conceptuses went to term.

6. If one or more conceptuses died in utero, then depending on the timing of demise, resorption sites (early, middle, or late) and dead fetuses should be visible in fresh uterine tissue. If the demise was early in gestation, the resorption site(s) may not be visible without staining. The fresh uterus (intact for rodents, longitudinally dissected for rabbits), when added to 10% ammonium or sodium sulfide, will exhibit blue-black deposits of elemental sulfur at the implantation and early resorption sites (within 10 to 15 min at room temperature for rodents; after overnight exposure at room temperature for rabbits). These can readily be counted and will remain visible for at least a week (Salewski, 1964). Incubation in the sulfide renders the tissue unsuitable for any subsequent biochemical or histological assessment. The formalin-fixed (buffered neutral 10% formalin) uterus, exposed to potassium ferricyanide (R.W. Tyl, unpub. observ. since 1988), will exhibit deposits of elemental iron at the implantation and early resorption sites. After staining and counting of the sites, the tissue preparation can be cleared (i.e., the stain washed out) with water rinses, and the tissue replaced in fixative. This staining procedure does not interfere with subsequent histologic assessments. Some laboratories compress the fresh uterine horns between glass or Plexiglas plates to discern early resorptions and total implantation sites. Dey (1989) reported in an abstract that he could intravenously inject maternal mice on gestational day (gd) 5 with a dye and visualize very early uterine implantation sites (the mouse conceptuses implant on gd 4 to 5; obviously, this method terminates the mouse as well as the pregnancy). These techniques can also be used when there is an apparent one-horn pregnancy or an apparent nonpregnant uterus.

The female maternal endpoints are as follows:

1. The number (or percent) of sperm-positive or copulation plug–positive females (based on the number paired).
2. The number (or percent) of pregnant females, based on the number paired and the number of sperm- or plug-positive females.
3. The number of ovarian corpora lutea per dam.
4. The number of total uterine implantations per dam.
5. The percent preimplantation loss (IL_{pre}) per litter:

$$IL_{pre} = (CL - I)/CL \times 100$$

where CL is the number of corpora lutea and *I* is the number of total implantations.

6. The number (or percent) of early (by staining or placenta only), middle (in the author's laboratory, placenta plus some fetal tissue), and late (in the author's laboratory, placenta plus fetus with limb buds) resorptions per litter.
7. The number (or percent) of dead fetuses (in the author's laboratory, above a certain fetal body weight with discernible digits) per litter.
8. The number (or percent) nonlive (resorptions plus dead fetuses) per litter.
9. The percent postimplantation loss (IL_{post}) per litter:

$$IL_{post} = (I - L)/I \times 100$$

where L is the number of live pups at term.

10. The percent prenatal loss (PL), which is the equivalent of IL_{pre} plus IL_{post}, or:

$$PL = (CL - L)/CL \times 100$$

11. The number of ovarian primordial follicles per female (which requires ovarian serial or step sections).
12. Organ weights: ovaries, uterus, pituitary, other (e.g., liver, adrenals, kidneys, spleen, brain).

INTERPRETATION OF RESULTS

In unexposed (or wild-type) females, the number of corpora lutea should be normal because ovulation is under the female rat's control. If preimplantation loss and/or postimplantation loss is increased or litter size is reduced (with or without increased prenatal loss), the male's sperm count, motility, and/or morphology may be affected (in such a way that fertility is impaired), and/or the sperm may bear induced mutation(s) that are incompatible with preimplantation or postimplantation survival (i.e., dominant lethal). Other direct or indirect toxicity to the male reproductive behavior, structures, and/or functions, including sperm, cannot be ruled out from this evaluation (see Male Endpoints).

In exposed (or transgenic) females, the number of ovarian corpora lutea may be affected if the test material affected the HPG axis, and the appropriate products from this neuroendocrine gland complex were not released, such as gonadotrophic releasing hormones (GnRH from the hypothalamus); FSH and LH from the anterior lobe of the pituitary; and E2, P, and Prl from the ovaries. Alternatively, there may be direct effects on the ovary.

If the number of corpora lutea is normal but fewer conceptuses implanted, preimplantation loss would be increased. This would also result in fewer total and live pups per litter. If preimplantation loss is increased, there may be something wrong with the eggs per se (if exposure to the test material occurred for this female while she was in utero and producing all the primary oocytes she will ever have or if the test material is toxic to the oocytes). Damage to the zygote (e.g., mutagenicity, clastogenicity or breakage in chromosomes) or to the male's sperm (that fertilized the egg) may also result in increased preimplantation loss.

Effects on the uterus or its hormonal controls, especially those that prepare the uterine lining for implantation, could also result in increased preimplantation loss. Partial litter losses (a reduced number of normal pups or fetuses in the absence of increased resorptions and/or dead fetuses) may be due to fewer eggs ovulated (and thus a reduced number of corpora lutea) and not intrauterine demise. If the study design precludes examining the dams for corpora lutea at parturition (i.e., a multigenerational reproductive toxicity study where the dams must maintain their litters until weaning on P21), and examination can only be done on P21, then the corpora lutea will have involuted into corpora albicans. These corpora albicans are indistinguishable from corpora albicans of previous estrous cycles, and one cannot ascertain whether there were any effects on the number of eggs ovulated and, therefore, on preimplantation loss.

If the corpora lutea count is normal and preimplantation loss is normal, but postimplantation loss is increased, then the interpretation depends on whether there was a full litter loss

or partial litter loss. Most researchers in this area interpret full litter losses as due to the compromised status of the dam (e.g., Narotsky et al., 1993; Bielmeier et al., 2001), such as hormonal imbalances (so that the uterine lining is not adequately maintained by the corpora lutea early in the pregnancy and/or by the placentas later) or an inhospitable uterus. The latter may result from an inappropriate release of oxytocin from the posterior pituitary or alterations in oxytocin receptors in the uterus, which would result in inappropriate contractions and would expel the conceptus. Incompetent cervix, in humans at least, also leads to premature delivery. Whereas the dogma is that rats do not abort, this author has observed multigestational abortions in rats twice in her 40 years in the laboratory. If there are normal corpora lutea and normal preimplantation loss but increased postimplantation loss, this could also lead to fewer live pups or fetuses (i.e., partial litter loss). This last observation could be due to an induction of malformations in the offspring or genetic alterations (mutagenesis, clastogenesis, altered genetic regulation) in the gametes or offspring that are incompatible with postimplantation prenatal survival. This is the outcome observed in a dominant lethal assay with a positive test material: increased postimplantation and possibly preimplantation loss.

The dominant lethal assay, as currently performed, is designed to evaluate germinal cell damage in male rodents (rats or mice), including effects on prenatal viability of offspring after exposure to a test agent (by the appropriate route of administration after one exposure or multiple or continuous exposures) by mating the exposed males to unexposed females. The males may be specifically obtained and exposed for this assay, or they may be part of a long-term study such as a 90-day or 2-year bioassay, or a multigeneration study. This dominant lethal breeding procedure may be done on a one male:one female or one male:two females (concurrently) basis until vaginal sperm are found or a predetermined period of time has elapsed, whichever comes first. Alternatively, the breeding may be done by pairing the male to one or more females consecutively for a number of weeks (usually the female or females are changed weekly). The females may be monitored for a period of time prior to breeding to ensure estrous cyclicity so that receptive females are provided to the males. Successfully bred females are sacrificed in midpregnancy (usually gd 13 to 15 in either rats or mice), and the following reproductive parameters are examined for each female: the number of ovarian corpora lutea (a measure of the number of eggs ovulated), the number of total uterine implantation sites (a measure of the number of fertilized eggs or zygotes implanted), and the number of live and nonlive conceptuses (a measure of postimplantation survival and loss). The extent of pre- and postimplantation loss can then be assessed.

The rationale for the assay is as follows: a dominant lethal mutation in a germ cell is one that does not cause dysfunction of the gamete (so that fertilization can occur) but that is lethal to the fertilized egg (prior to implantation) or developing embryo or fetus (after implantation). Dominant lethal mutations are generally accepted to be the result of chromosomal aberrations—structural breaks, rearrangements (clastogenic effects), and/or numerical changes (aneuploidy)—but gene mutations and toxic effects cannot be excluded. If a dominant lethal mutation is induced by treatment in the male and the male is mated to an unexposed female, the presence of the genetic lesion will be manifested as an increase in prenatal deaths. If the male is exposed acutely (for 1 to 5 days) and then mated consecutively to unexposed females for 8 to 10 weeks (rats) or 5 to 8 weeks (mice), and an effect is observed, then the stage of the spermatogenic cycle that was affected can be identified by determining what stage the sperm were in when the lesion was induced. For example, if the effect is observed in the first week of breeding, the target stage is epididymal sperm; if the effect is observed after the fifth week of breeding (in mice), then the target stage (the stage the sperm were in when the animal was last exposed) is spermatogonial cells.

The data reported may include the following:

1. The number of pregnant females per number of females mated (expressed as a ratio and/or percentage).
2. The number of fertile males per number of males mated (expressed as a ratio and/or percentage).
3. The number of ovarian corpora lutea per pregnant female.
4. Mean number of total uterine implantations (live plus dead or resorbed) per pregnant female.
5. Mean number of live implantations per pregnant female.
6. Mean number of dead implantations (early and late, includes resorptions and dead fetuses if applicable).

7. Dead implantations per total implantations (expressed as mean and total per group).

8. Percent preimplantation loss, calculated as described (see In Vivo Models) using totals per group.

9. Percent postimplantation loss, calculated as described (see In Vivo Models) using totals per group.

10. Frequency of dominant lethal factors, F_L, calculated as a percentage:

$$F_L = (I_T / I_C) \times 100$$

where I_T is the number of live implantations per female of the test group and I_C is the number of live implantations per female of the control group (Green et al., 1976, 1985; Ehling et al., 1978; EPA, 1998b).

Increased postimplantation loss may be due to a localized uterine problem, so that the losses are clustered at the ovarian and cervical ends of the uterine horns. This distribution of effects may be due to blood flow differences to specific conceptuses by uterine location, as spontaneous resorptions in rats and mice also occur preferentially at the ovarian and cervical ends of the horns.

Counting the follicles at the various stages of oogenesis in serial or step sections of the maternal ovaries will provide information on whether there is a full complement of primordial, primary, small preantral, large preantral, and antral (mature, Graafian) follicles in the ovary. One might see fewer primordial follicles if exposure occurred during the dam's own in utero development or if there was specific ovarian toxicity. Conversely, increased numbers of primordial follicles (and fewer later stage follicles) may be seen if the appropriate hormonal triggers are not functioning to cause normal cyclical waves of initiation of follicular development and atresia during her postpuberty estrous cycles.

MALE ENDPOINTS

A number of measures can be made on the living male animal, including: (1) an external examination of the urogenital region; (2) the number (or percent) of successful copulations (i.e., sperm-positive females); (3) the number (or percent) of successful breeders (the number of pregnant females, based on the number paired and the number of sperm- or plug-positive females); and (4) litter size (total, live, dead, and resorbed).

Sometimes the male is not expendable and is exposed. The male may be required for subsequent matings (e.g., he is an expensive, important, transgenic knockout animal; he carries an important mutation; it is important that his genotype continue). In this case, breeding data can be collected. Ejaculated sperm samples can also be obtained from these precious males by using an artificial vagina and a tubally-ligated teaser female in rabbits or electroejaculation (in rats it can be used only for a limited number of times, but it is very useful for repeated sperm sampling in rabbits, dogs, and other species). One could also surgically remove one testis and epididymis for the andrological assessments listed below during necropsy. The male will still be reproductively functional and fertile (if he was initially). One or more blood samples (e.g., from the lateral tail vein) could be taken for determination of circulating levels of GnRH, FSH, LH, T, DHT, and other hormones.

At necropsy, the following additional information is available.

Organ Weights and Histopathology

The sizes and weights of items one through eight, below, are T-dependent.

1. Testis (or testes).
2. Epididymis (or epididymides).
3. Seminal vesicles and their contents with coagulating glands and their contents (or separately).
4. Prostate (intact or separated into ventral and dorsolateral lobes).
5. Preputial glands.
6. Cowper's glands.
7. LABC complex
8. Glans penis.
9. Other organs, such as liver, kidneys, adrenals, spleen, brain.

Epididymal Andrology

1. Epididymal sperm (usually from the cauda epididymis) data: number (per cauda and per gram cauda); motility (the percentage of sperm that move relative to the total number of sperm present in the field), which is typically 85% to 95%; and progressive motility, which is typically 65% to 75% (Seed et al., 1996; ESHRE, 1998; Tyl et al., 2002).

2. Epididymal sperm morphology, which is currently almost always analyzed manually (Seed et al., 1996). Hamilton Thorne Biosciences, however, has developed a software module for sperm morphology in the rat using the angle of the arc between the tip of the acrosomal cap on the head to the mid-piece; thus historical control data on incidences of

abnormal sperm from manual examination, which ranges from ~1.5% to 3.5% in CD (SD) rats in the author's laboratory, will change if (or when) the automated module is used because the parameters evaluated are different.

3. Epididymal transit time (see below).

4. Blood sample(s) for GnRH, FSH, LH, circulating T, and other hormones.

Testicular Andrology

For these analyses, one testis is frozen and one is processed for histopathology (as discussed in the following section).

1. Intratesticular T levels.

2. Homogenization-resistant spermatid head counts (SHCs; see discussion of SHC below).

3. Daily sperm production per testis (DSP; see below).

4. Efficiency of DSP per gram testis (see below).

Current governmental test guidelines (EPA, 1996, 1997, 1998a) for assessment of reproductive toxicity in animal models require, among other parameters, the measurement of epididymal sperm numbers and testicular homogenization-resistant SHCs on parental males at necropsy. These parameters provide information on the integrity of the spermatogenesis process and, along with weights and histopathology of the testis, epididymis, and accessory sex organs (e.g., preputial glands, seminal vesicles, coagulating glands, prostate glands), provide a sensitive and relatively comprehensive assessment of the structural and functional state of the male reproductive system. Calculation of DSP (i.e., a measure of testicular output) and of efficiency of DSP (i.e., a measure of testicular output per gram of testis) can provide additional information to increase the sensitivity of reproductive assessment in laboratory models such as rats (Robb et al., 1978) and mice (Joyce et al., 1993), for extrapolation to human risk assessment, as well as to other mammals and non-mammalian populations (i.e., wildlife) potentially at risk from exposures to environmental contaminants.

Daily sperm production (DSP)

At necropsy, one testis from each male is weighed and frozen; the testis is subsequently thawed and homogenized. Certain specific stages (and steps) of spermatids formed during the process of spermatogenesis (from spermatogonia cells to spermatozoa) survive the homogenization step, and their nuclei are counted to provide the number of testicular homogenization-resistant spermatid heads (i.e., a SHC). The number of testicular homogenization-resistant spermatid heads in the testis is then divided by the duration (in days) during the spermatogenic cycle that the developing spermatids are in the homogenization-resistant stages, to obtain the DSP in millions of sperm produced per day.

For mice, the homogenization-resistant stages are II to VIII, steps 14 to 16, and the duration is 4.84 days (Joyce et al., 1993; vom Saal et al., 1998). For rats, the homogenization-resistant stages are VI to VIII, steps 18 and 19, and the duration is 4.61 days (Leblond and Clermont, 1952; Robb et al., 1978; Sharpe et al., 1996).

A sample calculation for a rat with a homogenization-resistant stage duration of 4.61 and a SHC per testis of 221.93×10^6 is as follows:

$$\text{DSP} = \frac{\text{SHC per testis}}{\text{homogenization-resistant duration}}$$

Therefore,

$$\text{DSP} = \frac{221.93 \times 10^6}{4.61 \text{ days}}$$

$$= 48.141 \times 10^6 \text{ sperm/testis/day}$$

Efficiency of DSP

Calculation of the efficiency of DSP requires the weight of the testis in grams as well as the calculation of the DSP. The DSP per testis is divided by the weight of the testis in grams to obtain the efficiency of DSP as millions of sperm per day per gram testis.

A sample calculation for a rat with a testis weight of 1.9293 g and a SHC per testis of 221.93×10^6 (i.e., the same DSP as calculated above) is as follows:

Efficiency of DSP = DSP/testis weight

Therefore,

$$\text{Efficiency of DSP} = \frac{48.141 \times 10^6 \text{ sperm/testis/day}}{1.9293 \text{ g}}$$

$$= 24.953 \times 10^6 \text{ sperm/g testis}$$

These calculations are made per animal and averaged within groups to obtain a mean ± SD or SE for each group. The means can then be statistically analyzed to evaluate whether there is a significant difference between groups. (Alternatively, these calculations can be made from group means for a relatively crude com-

parison.) Scientific judgment and the weight of the evidence (i.e., other information such as mating, fecundity, and fertility evaluations; histopathology of testes and other reproductive organs; and epididymal sperm number, motility, and morphology) will then be used to determine whether there is an effect of the test material on male reproductive function.

DSP may also be used to calculate epididymal transit time, the time it takes sperm to travel from the caput (head), through the corpus (body), and into the cauda (tail) of the epididymis. Sperm are modified during their transit through epididymis, becoming prepared for motility once ejaculated and mixed with accessory sex organ fluids and the fluids from the female reproductive tract; sperm sampled from the cauda epididymis are also motile. The typical epididymal transit time in rats is 1 to 2 weeks (Miller, 1998), but it can be accelerated (i.e., reduced) in response to estrogenic compounds or slowed (i.e., increased) in response to agents affecting smooth muscle motility in the absence (or presence) of any effects on DSP. The determination is as follows:

1. The testicular homogenization-resistant SHC is measured, and the DSP is calculated (see above).
2. The total number of epididymal sperm (from caput, corpus, and cauda) is determined. If cauda transit time is the parameter of interest, only the total number of cauda sperm is used.
3. The ratio of total epididymal sperm to testicular DSP will determine the number of days of sperm production in the testis that is required to result in the total epididymal sperm content and, therefore, the number of days it will take for the sperm to move through the epididymis (i.e., epididymal transit time). As an example, in the rat, DSP is typically 50×10^6 sperm/day, and the total number of epididymal sperm is typically (650×10^6 sperm). Therefore, transit time would be equal to (650×10^6 sperm)/(50×10^6 sperm/day) or 13.0 days.

Histopathology

The spermatogenic index, a semiquantitative estimate of the sperm-producing ability of the testes, is based on the types and percentage of germ cells in each stage present in the seminiferous epithelium. Testicular sections (preferably from fixed and glycol methacrylate-embedded tissue) are rated on a standardized scale (0 to 6), based upon the histologic appearance of the spermatogenic cells in the seminiferous tubules throughout one or more cross-sections of the rodent testis. Evaluation of the seminiferous tubules to assign the rating includes an assessment of the types of cells present (and the general impression that they are present in normal ratios) and quantitation of the number of late spermatids (steps 12 to 16 for mice and 15 to 19 for rats) present in the seminiferous tubules.

The numerical index and the criteria for rating are as follows: 0, no cells or only Sertoli cells present; 1, Sertoli and spermatogonia present; 2, spermatogonia and spermatocytes present; 3, spermatogonia, spermatocytes, and round early (i.e., steps 1 to 9 for mice and rats) spermatids present in normal numbers with fewer than 5 late spermatids per tubule; 4, spermatogonia, spermatocytes, and early spermatids with 5 to 25 late spermatids present per tubule; 5, all cell types present and 50 to 75 late spermatids present per tubule; or 6, all cell types present and more than 100 late spermatids present per tubule.

Several underlying assumptions are implicit when evaluating the testis using the spermatogenic index:

1. All stages of the seminiferous epithelium are affected in a similar manner by the parameter being studied.
2. Late spermatid counts are made in stage VII and VIII tubules where they are presented near the lumen.
3. Some stages of spermatogenesis normally have fewer cell types present, and ratios of cell types will vary.
4. Even normal testes may have some atrophied tubules.
5. At least 200 tubules are observed.
6. If the first assumption is violated (based on microscopic examination of testicular sections), a composite spermatogenic index must be estimated for each animal.

The spermatogenic index was first developed and used by Dr. Patricia A. Fail (née Noden) in the early 1980s (Whitsett et al., 1984, in deer mice; Fail et al., 1989, 1991, in Swiss mice; it has also been used in rats, P.A. Fail, unpub. observ.).

If spermatogenesis is evaluated in newly sexually mature males, the entire epididymis should be used for epididymal sperm parameters. Prior to P70 in rats (and P50 in mice), the cauda epididymis will contain little or no sperm from the first wave of spermatogenesis, which has just occurred in the testis, because the spermatozoa have not yet completed the transit from the testis through the epididymis to the cauda and have not yet accumulated in the cauda. Evaluation of sperm from the caput and

corpus of the epididymis (or the entire epididymis) is recommended in these young males. Also, if the male has been used for breeding, at least 4 to 7 days should transpire after cohabitation prior to necropsy and andrological assessment. If the assessment is performed too soon after copulation, the epididymal counts will be lower in males that were sexually active (and will skew the data).

LITERATURE CITED

Bielmeier, S.R., Best, D.S., Guidici, D.L., and Narotsky, M.G. 2001. Pregnancy loss in the rat caused by bromodichloromethane. *Toxicol. Sci.* 59:309-315.

Chapin, R.E., Sloane, R.A., and Haseman, J.K. 1997. The relationships among reproductive endpoints in Swiss mice using the reproductive assessment by continuous breeding database. *Fundam. Appl. Toxicol.* 38:129-142.

Chowdury, A., Gautam, A.K., and Chatterjee, B.B. 1984. Thyroid-testis interrelationship during development and sexual maturity. *Arch. Androl.* 13:233-239.

Dey, S.K. 1989. Embryo development and uterine interaction in the preimplantation period. Abstr. Society of Toxicology (SOT) Symposium on Early Embryo Loss as a Factor in Reproductive Failure. 28th Annual Meeting of the SOT, Atlanta, Ga.

Ehling, V.H., Machemer, L., Buselmaier, W., Dy'cka, J., Frohberg, H., Kratochvilova, J., Lang, R., Lorke, P., Muller, D., Peh, J., Rohrborn, G., Roll, R., Schulze-Schenlking, M., and Wiemann, H. 1978. Standard protocol for the dominant lethal test on male mice set up by the Work Group "Dominant Lethal Mutations of the Ad Hoc Committee Chemogenics." *Arch. Toxicol.* 39:173-185.

Environmental Protection Agency (EPA). 1996. Health Effects Test Guidelines, Report No. OPPTS 870.3800, Reproduction and Fertility Effects (Public Draft, February, 1996). Office of Prevention, Pesticides and Toxic Substances (OPPTS), U.S. EPA, Washington, D.C.

Environmental Protection Agency (EPA). 1997. 40CFR Part 799, Toxic Substances Control Act Test Guidelines; Final Rule. Section 799.9380, TSCA reproduction and fertility effects. *Fed. Regist.* 62:43834-43838.

Environmental Protection Agency (EPA). 1998a. Health Effects Testing Guidelines, Report No. OPPTS 870.3800, Reproduction and Fertility Effects (Final Guideline, August, 1998). Office of Prevention, Pesticides and Toxic Substances (OPPTS), U.S. EPA, Washington, D.C.

Environmental Protection Agency (EPA). 1998b. Rodent Dominant Lethal Assay, 870-5450. Office of Toxic Substances, U.S. EPA, Washington, D.C.

European Society for Human Reproduction and Embryology (ESHRE) Andrology Special Interest Group. 1998. Guidelines on the application of CASA technology in the analysis of spermatozoa. *Hum. Reprod.* 13:142-145.

Fail, P.A., George, J.D., Sauls, H.R., Dennis, S.W., and Seely, J.C. 1989. Effect of boric acid on reproduction and fertility of rodents. *Adv. Contra. Deliv. Syst.* 5:323-333.

Fail, P.A., George, J.D., Seely, J.C., Grizzle, T.B., and Heindel, J.J. 1991. Reproductive toxicity of boric acid in Swiss (CD-1) mice: Assessment using the continuous breeding protocol. *Fund. Appl. Toxicol.* 17:225-239.

Fail, P.A., Pearce, S.W., Anderson, S.A., and Gray, L.E. 1994. Methoxychlor alters testosterone and LH response to human chorionic gonadotropin or gonadotropin-releasing hormone in male Long-Evans hooded rats. *Biol. Reprod.* 50 (suppl. 1):102 (abstr. no. 206).

Food and Drug Administration (FDA). 1982. "Redbook I" Toxicological Principles for the Safety Assessment of Direct Food Additives and Color Additives Used in Food, pp. 119-122. Center for Food Safety and Applied Nutrition (CFSAN; Bureau of Foods), U.S. FDA, Washington, D.C.

Food and Drug Administration (FDA). 1993. Draft revised: Toxicological Principles for the Safety Assessment of Direct Food Additives and Color Additives used in Food. "Redbook II" Notice. Chapter IVc8, *In Utero* Exposure Phase for Addition to Carcinogenicity Studies with Rodents, in published draft. Center for Food Safety and Applied Nutrition (CFSAN), U.S. FDA, Washington, D.C.

Food and Drug Administration (FDA). 2000. "Redbook 2000" Toxicological Principles for the Safety of Food Ingredients. Center for Food Safety and Applied Nutrition, Office of Premarket Approval (CFSAN, OPA), U.S. FDA, Washington, D.C.

Goldman, J.M., Laws, S.C., Balchak, S.K., Cooper, R.L., and Kavlock, R.L. 2000. Endocrine-disrupting chemicals: Prepubertal exposures and effects on sexual maturation and thyroid activity in the female rat. A focus on the EDSTAC recommendations. *Crit. Rev. Toxicol.* 30:135-196.

Green, S., Zeiger, E., Palmer, K.A., Springer, J.A., and Legator, M.S. 1976. Protocols for the dominant lethal test, host-mediated assay, and *in vivo* cytogenetic test used in Food and Drug Administration's review of substances in the GRAS (Generally Regarded as Safe) list. *J. Toxicol. Environ. Health* 1:921-928.

Green, S., Auletta, A., Fabricant, J., Kapp, R., Manandhar, M., Shev, C.-J., Springer, J., and Whitfield, B. 1985. Current status of bioassays in genetic toxicology—the dominant lethal assay. A Report of the U.S. Environmental Protection Agency Gene-Tox Program. *Mutat. Res.* 154:49-67.

Heindel, J.J., Thomford, P.J., and Mattison, D.R. 1989. Histological assessment of ovarian follicle number in mice as a screen for ovarian toxicity. *In* Growth Factors and the Ovary (A.N. Hirshfield, ed.) pp. 421-426. Plenum, New York.

Joyce, K.L., Porcelli, J., and Cooke, P.S. 1993. Neonatal goitrogen treatment increases adult testis size and sperm production in the mouse. *J. Androl.* 14:448-455.

Kaiser, L.B., Wolfe, G.W., Lanning, L., Chapin, R.E., Klinefelter, G., and Hunter, E.S. 1996. Short-term reproductive and developmental effects of sodium bromate in S-D rats when administered in the drinking water. *Toxicologist* 30:121-122 (abstr. no. 620).

Kaiser, L.B., Wolfe, G.W., Lanning, L., Klinefelter, G., Hunter, E.S., and Chapin, R.E. 1997. Short-term reproductive and developmental effects of dibromoacetonitrile in the S-D rat when administered in the drinking water. *Toxicologist* 36:257 (abstr. no. 496).

Kaiser, L.B., Wolfe, G.W., Lanning, L., Klinefelter, G., Hunter, E.S., and Chapin, R.E. 1998. Short term reproductive and developmental effects of bromoacetonitrile and hexachloroacetone in the S-D rat when administered in the drinking water. *Toxicologist* 42(1-S):100-101 (abstr. no. 1306).

Laskey, J.W., Berman, E., and Ferrell, J.M. 1994. The use of cultured ovarian fragments to assess toxicant alterations in steroidogenesis in the Sprague-Dawley rat. *Reprod. Toxicol.* 9:131-140.

Leblond, C.P. and Clermont, Y. 1952. Definition of the stages of the cycle of the seminiferous epithelium in the rat. *Ann. N.Y. Acad. Sci.* 55:548-573.

Meyer, O.A., Tilson, H.A., Byrd, W.C., and Riley, M.T. 1979. A method for the routine assessment of fore- and hindlimb grip strength of rats and mice. *Neurobehav. Toxicol.* 1:233-236.

Miller, M.G. 1998. Reproductive system, male. *In* Encyclopedia of Toxicology, Vol. 3 (P. Wexler, ed.) pp. 38-49. Academic Press, New York.

Moser, V.C., McDaniel, K.M., and Phillips, P.M. 1991. Rat strain and stock comparisons using a functional observational battery: Baseline values and effects of Amitraz. *Toxicol. Appl. Pharmacol.* 1:233-236.

Narotsky, M.G., Hamby, B.T., Mitchell, D.S., and Kavlock, R.J. 1993. Evaluation of the critical period of bromodichloromethane-induced full-litter resorption in F-344 rats. *Teratology* 47:429 (abstr. no. P58).

Organization for Economic Cooperation and Development (OECD). 1995. Reproduction/developmental toxicity screening test, *In* Guideline for Testing of Chemicals, No. 421 (adopted July 27, 1995) pp. 1-10. OECD, Paris.

Organization for Economic Cooperation and Development (OECD). 1996. Combined repeated dose toxicity study with the reproductive/developmental toxicity screening test, *In* Guideline for Testing of Chemicals, No. 422 (adopted March 22, 1996) pp. 1-14. OECD, Paris.

Payne, A.H., and Sha, L. 1993. Purification and primary culture of Leydig cells. *In* Methods in Toxicology, Vol. 3, pt. B: Female reproductive toxicology (J.J. Heindel and R.E. Chapin, eds.) pp. 197-209. Academic Press, San Diego.

Reel, J.R., Lawton, A.D., Wolkowski-Tyl, R., Davis, G.W., and Lamb, J.C. IV. 1985. Evaluation of a new reproductive toxicology protocol using diethylstilbestrol (DES) as a positive control compound. *J. Am. College Toxicol.* 4:147-162.

Robb, G.W., Amann, R.P., and Killian, G.J. 1978. Daily sperm production and epididymal sperm reserves of pubertal and adult rats. *J. Reprod. Fertil.* 54:103-107.

Russell, L.D., Ettlin, R.A., Sinha Hakim, A.P., and Clegg, E.D. 1990. Histological and Histopathological Evaluation of the Testis. Cache River Press, Clearwater, Fla.

Salewski, E. 1964. Farbermethode zum makroskopischen nachweis von implantationsstellen am uterus der ratte. *Naunyn Schmiedebergs Arch. Exp. Pathol. Pharmakol.* 247:367.

Seed, J., Chapin, R.E., Clegg, E.D., Dostal, L.A., Foote, R.H., Hurtt, M.E., Klinefelter, G.R., Makris, S.L., Perreault, S.D., Schrader, S., Seyler, D., Sprando, R., Treinen, K.A., Veeramacheneni, D.N., and Wise, L.D. 1996. Methods for assessing sperm motility, morphology, and counts in the rat, rabbit, and dog: A consensus report. *Reprod. Toxicol.* 10:237-244.

Sharpe, R.M., Fisher, J.S., Millar, M.M., Jobling, S., and Sumpter, J.P. 1996. Gestational and lactational exposure of rats to xenoestrogens results in reduced testicular size and sperm production. *Environ. Health Perspect.* 103:1136-1143.

Stoker, T.E., Parks, L.G., Gray, L.E., and Cooper, R.L. 2000. Endocrine-disrupting chemicals: Prepubertal exposures and effects on sex maturation and thyroid function in the male rat. A focus on the EDSTAC recommendations. *Crit. Revs. Toxicol.* 30:197-252.

Tyl, R.W., Myers, C.B., Marr, M.C., Brine, D.R., Fail, P.A., Seely, J.C., and Van Miller, J.P. 1999. Two-generation reproduction study with para-tert octylphenol in rats. *Regul. Toxicol. Pharmacol.* 30:81-95.

Tyl, R.W., Myers, C.B., Marr, M.C., Thomas, B.F., Keimowitz, A.R., Brine, D.R., Veselica, M.M., Fail, P.A., Chang, T.Y., Seely, J.C., Joiner, R.L., Butala, J.H., Dimond, S.S., Shiotsuka, R.N., Stropp, G.D., and Waechter, J.M. 2002. Three-generation reproductive toxicity study of dietary Bisphenol A (BPA) in CD (Sprague-Dawley) Rats. *Toxicol. Sci.* In press.

vom Saal, F.S., Cooke, P.S., Buchanan, D.L., Palanza, P., Thayer, K.A., Nagel, S.C., Parmigiani, S., and Welshons, W.V. 1998. A physiologically based approach to the study of bisphenol a and other estrogenic chemicals on the size of reproductive organs, daily sperm production and behavior. *Toxicol. Ind. Health* 14:239-260.

Whitsett, J.M., Noden, P.F., Cherry, J., and Lawton, A.D. 1984. Effect of transitional photoperiods on testicular development and puberty in male deer mice (*Peromyscus maniculatus*). *J. Reprod. Fertil.* 72:277-286.

Whitten, W.K. 1956. Modification of the oestrus cycle of the mouse by external stimuli associated with the male. *J. Endocrinol.* 13:399-404.

INTERNET RESOURCES

ntp-server.niehs.nih.gov/

The National Toxicology Program (NTP) has carried out several relevant short-term developmental and reproductive toxicity studies (accessible from their search page), including: RDGT94003, RDGT94007, RDGT94009, RDGT94013, RDGT94014, RDGT94017, and RDGT96001.

Contributed by Rochelle W. Tyl
Center for Life Sciences and Toxicology
Research Triangle Institute
Research Triangle Park, North Carolina

Guidelines for Mating Rodents

Proper animal husbandry is essential for studies of male reproductive toxicology (*UNIT 16.1*), as it is for female toxicology and reproductive toxicology in general. This unit contains protocols for establishing estrous cyclicity (see Basic Protocol 1); mating (see Basic Protocol 2); and gestation, lactation, and postlactation (see Basic Protocol 3) in rats and mice. For the uninitiated, the following are recommendations gleaned from over 40 years of experience.

NOTE: All protocols using live animals must first be reviewed and approved by an Institutional Animal Care and Use Committee (IACUC) and must conform to governmental regulations regarding the care and use of animals.

DETERMINATION OF ESTROUS CYCLICITY IN RODENTS

BASIC PROTOCOL 1

It is necessary to establish that the female rat or mouse is cycling to accurately set up matings and to verify that the female is reproductively capable. The procedure is the same for both rat and mouse. This protocol is based on Haas (1981) as modified by Ms. T.-Y. Chang, HT-ASCP, histotechnologist in the author's research center.

Materials

Female rat or mouse
Saline: 0.9% (w/v) NaCl, sterile (*APPENDIX 2A*)
Spray-Cyte fixative (Clay Adam)
50%, 70%, 80%, 95%, and 100% (v/v) ethanol
1% (w/v) toluidine blue/1% (w/v) sodium borate
Xylene
Permount (Fisher)

Fire-polished eye dropper
Glass microscope slide prelabeled with a six-cell grid using a permanent marker (e.g., Securline Marker II/Superfrost; Precision Dynamics)
Coverslips

CAUTION: Xylene is toxic and should be used in a fume hood.

Collect cervical cells

1. At the same time each day (usually in the morning), for ≥14 consecutive days (a 21-day period is better), evaluate a female rat or mouse for the stage of sloughed cervical cells by gently inserting a fire-polished eyedropper containing 0.05 to 0.1 ml sterile saline into the vaginal tract.

   The eyedropper is fire-polished to ensure that the tip is absolutely smooth.

2. Instill (express) the saline into the tract and then draw it back up into the eyedropper.

3. Express the fluid in the eyedropper onto a prelabeled glass microscope slide and air dry. Use one slide per female per 6-day sampling period.

   The slide should be premarked with a numbered six-box grid using a permanent marker. Do not use a nonpermanent marker (e.g., Sharpie), as it will wash off during staining.

4. When the last vaginal smear for that female is placed on the slide, air dry for ≥1 day.

5. Spray the slide with Spray-Cyte fixative and air dry 1 additional day.

Contributed by Rochelle W. Tyl
Current Protocols in Toxicology (2002) 16.2.1-16.2.11

Stain and mount cells

6. Rehydrate the slide through an ethanol series consisting of 30-sec steps in 95%, 95%, 95%, 80%, 70%, and 50% ethanol.

   These instructions are for a Linistain GLX Stainer (Thermo Shandon). The staining can also be carried out manually.

7. Put the slide through running water twice, for 30 sec each.
8. Stain the slide with 1% toluidine blue/1% sodium borate for two 30-sec periods.
9. Rehydrate the slide with five 30-sec washes with running water.
10. Dry the slide for two 30-sec periods.

    If the staining procedure is done manually, drying (here and in step 12) is unnecessary.

11. Dehydrate the slide through an ethanol series consisting of 30-sec steps in 95%, 100%, and 100% ethanol.
12. Thoroughly dry slide with eight 30-sec drying periods.
13. Place slide in xylene (to clear the cells) until it is coverslipped.

    Slides should be coverslipped as soon as the batch of slides is processed; they should not sit in xylene.

14. Mount the slide with a coverslip using Permount.

Analyze cyclicity

15. Examine each slide under a microscope for the presence and duration of the stages of the cycle:

    a. Estrus: nucleated, cornified cells along with mostly nonnucleated squamous epithelial cells; duration ~12 hr in rodents.
    b. Metestrus: equal number of leukocytes and large, folded epithelial cells with translucent nuclei; duration ~21 hr.
    c. Diestrus: predominantly leukocytes and cell debris; duration ~57 hr.
    d. Proestrus: largely nucleated and some cornified epithelial cells; duration ~12 hr.

    The leukocyte cytoplasmic granules will stain red to purple, and the nuclei will stain blue.

    Some specialists do not identify metestrus at all, so only three stages are tracked.

16. Once the stages have been determined and recorded, examine the data to determine if the female is cycling. Consider the following questions:

    a. If she is not cycling, is she exhibiting persistent estrus or diestrus (most common)?
    b. If she is cycling, is it a normal cycle?
    c. If it is an abnormal cycle, which is defined as prolongation of specific stage or stages beyond normal as set by the laboratory, is estrus, metestrus, diestrus, or proestrus prolonged?

    Laboratory conventions should be set up and followed for such situations as mixed stages, the absence of any cells, or the inability to determine the stage.

17. Calculate the duration of the cycle using a stage that is easy to detect (e.g., estrus) and/or that is observed to periodically repeat.

    For example, the cycle length may be calculated from the sum of the duration of all cycles, beginning with the day after the sentinel stage to the first day of the next sentinel stage,

divided by the number of cycles, for each female. Although estrus is the most easily recognized, it is of very brief duration and may have occurred between the once-daily smears. It is safe to assume that it did occur if proestrus and metestrus are observed sequentially, or another sentinel stage can be selected to determine cycle length.

Charles River Laboratories will provide CD (Sprague-Dawley; SD) female rats with guaranteed 4- or 5-day cycles, but because shipment will most likely shift the cycle 1 day, it is strongly recommended to confirm cyclicity.

RODENT MATING

BASIC PROTOCOL 2

For studies of male or female reproductive toxicology, it is necessary to include mating of the male or female. The procedure is slightly different for rat and mouse.

Materials

Male and female mice or rats
Saline: 0.9% (w/v) NaCl, sterile (*APPENDIX 2A*), for rats only

Cages, for mating (with either a solid bottom and contact bedding or a wire bottom)
Plastic cages, for mated females (with a solid bottom and contact bedding)
Fire-polished eyedropper, for rats only
Glass microscope slides, for rats only
Microscope (with 10× and 40× eyepieces), for rats only

For mating mice:

1a. Pair one male mouse with two female mice, or preferably one male with one female. Place the female in the male's cage in the afternoon after he has been in that cage for at least a few hours.

If the male is paired with two females and inseminates both females on the same night, the second female may not be pregnant. Because a male mates numerous times with a receptive female, the successive ejaculations may exhaust the sperm reserves readily available for ejaculation, and one female may receive fewer sperm (or no sperm) relative to the other female and appear less fertile or nonpregnant.

The male should not be put in the female's cage. The animals should also not be placed in a clean cage at the same time. Placing the female in the male's cage allows him to mark his territory by appropriately placed urine deposits prior to the female's arrival.

The wire mesh bottom must be fine enough to allow the male to maintain his balance while mounting.

Female mice become acyclic (anestrus) without close proximity to a male (actually a pheromone in his urine). If necessary, estrous cyclicity can be reinstated in females by housing them near males or in cages with soiled bedding from the male cage (i.e., priming; Whitten, 1956).

Female mice exhibit 4- to 5-day estrous cycles, so one can determine the stage of the cycle for each female and only place females in proestrus or estrus with males, which should provide a high mating index. Alternatively, females can be paired with males (1:1) without checking the stage of the estrous cycle. From the latter random pairing, 20% to 25% of the females should be inseminated (based on the percentage of females in proestrus or estrus out of a 4- or 5-day cycle at any time).

2a. Check for insemination, as indicated by the presence of a copulation plug in the vaginal tract of the female, on the following morning.

Female rodents usually exhibit the luteinizing hormone (LH) surge prior to ovulation between 1300 and 1600 hr on the afternoon of proestrus and ovulate between 0100 and 0300 hr on the following morning.

Table 16.2.1 Historical Control Data on Selected Reproductive Parameters in CD-1 (Swiss) Mice[a]

Parameter	Segment I	Segment II	Segment III	
	F0	F0	F0	F1
Males:				
Mating index (%)[b]	100.0	NA	NA	100.0
Fertility index (%)[c]	96.0	NA	NA	100.0
Pregnancy index (%)[d]	100.0	NA	NA	100.0
Epididymal sperm count (10^6/g cauda)[e]	620.1	NA	NA	ND
Sperm motility (%)[e]	69.3	NA	NA	ND
Females:				
Estrous cycle length (days)	ND	NA	ND	4.29
Mating index (%)[f]	100.0	NA	100.0	100.0
Fertility index (%)[g]	96.0	NA	96.0	100.0
Gestational index (%)[h]	100.0	NA	100.0	100.0
Precoital interval (days)[i]	ND	NA	NA	2.2
Pregnancy index (%)[j]	100.0	NA	100.0	100.0
Corpora lutea/dam[e]	13.25	13.86, 13.80, 12.43	ND	ND
Total implantations/litter[e]	12.5	13.35, 12.88, 11.57	12.54	13.6
Preimplantation loss/litter (%)[e]	5.74	5.12, 8.70, 9.25	NA	NA
Postimplantation loss/litter (%)[e]	4.10	3.72, 10.88, 6.13	6.73	0.21
Live implantations or pups/litter	12.0	12.70, 12.38, 10.96	12.54	12.5
Gestational length (days)	NA	NA	18.8	19.0
Stillbirth index (%)[k]	NA	NA	0.26	0.50
Live birth index (%)[l]	NA	NA	99.74	99.50
Lactational survival index (%)[m]	NA	NA	97.75	NA
Acquisition of puberty:				
Female VP age (days)	NA	NA	NA	28.0
Body weight at VP (g)	NA	NA	NA	20.46
Male PPS age (days)	NA	NA	NA	30.4
Body weight at PPS (g)	NA	NA	NA	26.64

[a]Segment I (1 study; 25 animals of each sex), FDA study of fertility and early embryonic development; Segment II (3 studies; 25 to 30 females per group), FDA prenatal developmental toxicity study, previously termed a teratology study, essentially the same as OPPTS 870.3700 (EPA, 1998) and OECD 414 (OECD, 2001) testing guidelines; Segment III (1 study; 25 to 30 F0 females per group and 25 to 30 F1 males and females per group), FDA pre- and postnatal development study. Data are presented as control group means. Abbreviations: F0, parental generation (also termed P0); F1, first filial generation (offspring); NA, not appropriate (i.e., cannot be done given the study design); ND, not determined; PPS, preputial separation; VP, vaginal patency.

[b]Defined as (number of males impregnating females/number of males paired) × 100.

[c]Defined as (number of males siring litters/number of males impregnating females) × 100.

[d]Defined as (number of pregnant females/number of males impregnating females) × 100.

[e]As defined or discussed in *UNIT 16.1*.

[f]Defined as (number of sperm- or plug-positive females/number of females paired) × 100.

[g]Defined as (number of pregnant females/number of sperm- or plug-positive females) × 100.

[h]Defined as (number of females with live litters/number of pregnant females) × 100.

[i]Defined as the number of days from pairing to evidence of insemination.

[j]Defined as (number of pregnant females/number of inseminated females) × 100.

[k]Defined as (number of dead pups at birth/number of total pups delivered) per litter × 100.

[l]Defined as (number of live pups at birth/number of total pups delivered) per litter × 100.

[m]Defined as (number of pups alive at weaning/number of live pups on P4 postcull) per litter × 100.

Table 16.2.2 Historical Control Data on Selected Reproductive Parameters in CD (SD) Rats[a]

Parameter	Segment I (4 studies)	Segment II (28 studies)	Segment III (5 studies)	
	F0	F0	F0	F1
Males:				
Mating index (%)[b]	96.0-100.0	NA	NA	85.0-96.0
Fertility index (%)[c]	80.0-100.0	NA	NA	89.5-100.0
Pregnancy index (%)[d]	80.0-107.7	NA	NA	89.5-100.0
Epididymal sperm count (10^6/g cauda)[e]	807.7-1019.6	NA	NA	ND
Sperm motility (%)[e]	75.2-84.5	NA	NA	ND
Progressive sperm motility (%)[f]	46.7-61.7	NA	NA	ND
Abnormal sperm (%)[g]	1.8-2.0	NA	NA	ND
Females:				
Estrous cycle length (days)	4.09-4.64	NA	ND	ND
Mating index (%)[h]	96.0-100.0	NA	100.0	85.0-96.0
Fertility index (%)[i]	80.0-100.0	NA	88.0-100.0	89.5-100.0
Gestational index (%)[j]	95.0-100.0	NA	100.0	100.0
Precoital interval (days)[k]	2.0-2.9	NA	ND	2.5-3.7
Corpora lutea/dam[e]	15.2-16.3	14.91-18.74	NA	NA
Total implantations/litter[e]	14.7-15.8	13.71-16.75	14.4-15.4	14.8-16.9
Preimplantation loss/litter (%)[e]	4.5-11.5	0.55-14.76	NA	NA
Postimplantation loss/litter (%)[e]	2.08-12.51	1.18-6.82	3.2-9.4	4.8-9.6
Live implantations or pups/litter	14.14-15.43	13.30-16.24	13.2-15.1	13.8-16.1
Gestational length (days)	NA	NA	22.0-22.2	21.8-22.4
Stillbirth index (%)[l]	NA	NA	0.3-1.5	1.1-3.4
Live birth index (%)[m]	NA	NA	98.5-99.7	96.6-98.9
Lactational survival index (%)[n]	NA	NA	99.5-100.0	NA
Acquisition of puberty:				
Female VP age (days)	NA	NA	NA	29.9-31.6
Body weight at VP (g)	NA	NA	NA	103.12-110.28
Male PPS age (days)	NA	NA	NA	41.3-42.4
Body weight at PPS (g)	NA	NA	NA	223.65-235.49

[a]Segment I (4 studies; 25 to 30 animals of each sex per group), FDA study of fertility and early embryonic development; Segment II (28 studies; 25 to 30 females per group), FDA prenatal developmental toxicity study, previously termed a teratology study, essentially the same as OPPTS 870.3700 (EPA, 1998) and OECD 414 (OECD, 2001) testing guidelines; Segment III (1 study; 25 to 30 F0 females per group and 25 to 30 F1 males and females per group), FDA pre- and postnatal development study. Data are presented as control group means. Abbreviations: F0, parental generation (also termed P0); F1, first filial generation (offspring); NA, not appropriate (i.e., cannot be done given the study design); ND, not determined; PPS, preputial separation; VP, vaginal patency.

[b]Defined as (number of males impregnating females/number of males paired) × 100.

[c]Defined as (number of males siring litters/number of males impregnating females) × 100.

[d]Defined as (number of pregnant females/number of males impregnating females) × 100.

[e]As defined or discussed in *UNIT 16.1*.

[f]Defined as percentage of caudal epididymal motile sperm per male that moved a predetermined linear distance during a predetermined time; can be performed manually with a hemacytometer or by automated methods (Seed et al., 1996; ESHRE, 1998).

[g]Defined as percentage of fixed, Eosin Y–stained, and examined cauda epididymal sperm per male (if possible ≥200 sperm/male) that are abnormal by microscopic examination. Examples of abnormalities include abnormal head size and shape, tailless head (this author's laboratory does not count headless tails because they may be the other halves of the tailless heads), two-headed or two-tailed.

[h]Defined as (number of sperm- or plug-positive females/number of females paired) × 100.

[i]Defined as (number of pregnant females/number of sperm- or plug-positive females) × 100.

[j]Defined as (number of females with live litters/number of pregnant females) × 100.

[k]Defined as the number of days from pairing to evidence of insemination.

[l]Defined as (number of dead pups at birth/number of total pups delivered) per litter × 100.

[m]Defined as (number of live pups at birth/number of total pups delivered) per litter × 100.

Table 16.2.3 Historical Control Data on Selected Reproductive Parameters From Multigeneration Studies in CD (SD) Rats[a]

Parameter	F0	F1	F2	F3[b]
Males:				
Mating index (%)[c]	89.7-100.0	56.7-100.0	96.7	NA
Fertility index (%)[d]	75.9-100.0	76.2-96.6	96.6	NA
Pregnancy index (%)[d]	100.0-103.6	82.4-108.7	96.6	NA
Epididymal sperm count (10^6/g cauda)[e]	813.14-1153.51	504.54-1081.73	924.19	899.10
Sperm motility (%)	63.3-84.0	63.7[f]-79.4	79.0	72.4
Progressive sperm motility (%)	24.4-56.7	22.7[f]-66.5	65.8	63.9
Testicular SHC (10^6/g)[e]	84.26-127.70	65.12-124.85	91.86	88.34
DSP/testis[e]	31.65-52.91	38.44-54.63	37.15	34.84
Efficiency of DSP[e]	18.28-27.70	21.90-27.08	19.93	19.16
Abnormal sperm (%)	2.0-3.3	1.5-3.0 (6.1[f])	2.19	1.75
Females:				
Estrous cycle length (days)	4.11-4.69	4.22-5.12	4.54	4.32
Mating index (%)[g]	89.7-100.0	50.0-100.0	96.7	NA
Fertility index (%)[h]	76.7-100.0	70.8-96.6	96.6	NA
Gestational index (%)[i]	95.7-100.0	94.1-100.0	100.0	NA
Precoital interval (days)[j]	2.3	3.0	3.1	NA
Gestational length (days)	22.0-22.6	21.8-22.3	22.0	NA
Total implantations/dam[e]	11.8-16.9	14.1-16.5	15.25	NA
Postimplantation loss/litter (%)[e]	0.7-20.4	6.8-10.2	5.02	NA
Paired ovarian primordial follicle counts[k]	132.3-315.9	134.0-353.0	409.2	384.6
Offspring:				
Stillbirth index (%)	NA	0.2-10.2	0.0-6.3	0.7
Live birth index (%)	NA	89.8-99.8	93.7-100.0	99.3
Total pups/litter)[j]	NA	13.6-15.7	13.1-15.7	14.9
Live pups/litter[j]	NA	13.4-15.6	13.1-15.6	14.8
Four-day survival index (%)	NA	95.2-99.3	88.6-98.6	96.1
Lactational survival index (%)	NA	98.6-100.0	99.6-100.0	99.3
Sex ratio (% males)/litter	NA	43.8-54.7	43.2-56.9	44.8-46.3
Female AGD (mm/litter)[l]	NA	NA	0.73-0.95	0.92
Female body weight (g)[l]	NA	6.19[j]	5.93-6.17	5.98
Male AGD (mm/litter)[l]	NA	NA	1.96-2.25	1.97
Male body weight (g)[l]	NA	6.53[j]	6.27-6.52	6.36
Retained nipples/male (P11-P13)	NA	0	0	0

continued

To precisely identify the time of insemination, a 2-hr pairing can be set up in late afternoon, but the insemination rate (mating index) will be low.

The copulation plug is produced during ejaculation by the male, from protein secretions in the seminal fluid from the coagulating gland; the proteins form a yellow-white, waxy coagulum (presumably to retain the seminal fluid, including the sperm, in the female's reproductive tract). The plug can usually be detected by external examination (with the female also exhibiting swollen external genitalia), but a more definitive determination (especially if the plug is not visible upon inspection) is to place the female on the top of the cage, press down gently on her lower back, lift up her hind end by her tail, and place a blunt probe in her vaginal tract (making sure to avoid hitting the pelvic girdle). The presence of the copulation plug will prevent penetration of the probe. The copulation plug will ultimately drop, shrink, and fall out (although this takes a number of hours), so females

Table 16.2.3 Historical Control Data on Selected Reproductive Parameters From Multigeneration Studies in CD (SD) Rats[a], continued

Parameter	F0	F1	F2	F3[b]
Acquisition of puberty:				
Female VP age (days)	NA	30.5-32.1	31.0	31.3
Body weight at VP (g)	NA	99.52-102.52	105.0	105.6
Male: PPS age (days)	NA	41.9-43.6	42.1	42.1
Body weight at PPS (g)	NA	210.72-220.07	219.7	209.3

[a]Data are either from eight studies (F0, F1, F2) or one study (F3). Data are presented as group means with 25 to 30 animals of each sex per group. Data are presented as control group means. Abbreviations: AGD, anogenital distance; DSP, daily sperm production; F0, parental generation (also termed P0); F1, first filial generation (offspring); F2, second filial generation; F3, third filial generation; NA, not appropriate (i.e., cannot be done given the study design); PPS, preputial separation; SHC, spermatid head count; VP, vaginal patency.

[b]F3 offspring were not mated.

[c]Defined as (number of sperm- or plug-positive females/number of paired males) × 100.

[d]Defined as (number of pregnant females/number of mated males) × 100.

[e]As defined or discussed in *UNIT 16.1*.

[f]One control male exhibited low sperm motility and a high incidence of abnormal sperm; he sired a live litter.

[g]Defined as (number of sperm- or plug-positive females/number of paired females) × 100.

[h]Defined as (number of pregnant females/number of mated females) × 100.

[i]Defined as (number of females with live litters/number of pregnant females) × 100.

[j]Data were collected from only one study.

[k]Both ovaries per female (≥10/group) are embedded in paraffin, sectioned (10 ovarian sections taken ≥100 µm apart from the inner third of each ovary), stained, and then 20 section/female are examined for the number of primordial follicles.

[l]Measured at P0.

without plugs can be evaluated for sperm in the vaginal tract (see step 2b). If the mice are housed in wire bottom cages, the copulation plug (usually multiple plugs) can be identified on the paper below the cage.

3a. On the day of insemination, house the female singly in a plastic cage with a solid bottom and contact bedding.

The usual convention is to designate the date of copulation detection as gestational day (gd) 0, although some laboratories designate it as gd 0.5 or gd 1.

Alternatively, females with the same gd 0 date (and in the same dose group) can be housed together, up to four to five females per cage. Close to term, and especially if the dam will be allowed to litter, each female should be singly housed and provided with one or more cotton squares (e.g., Nestlets; Ancare) so she can build a nest.

Table 16.2.1 provides historical control data on reproductive parameters in CD-1 (Swiss) mice; these are a sturdy outbred strain with good fertility and fecundity. Based on five recent studies, the mean estrous cycle length is 4.3 days. The mating index, fertility or pregnancy index, and gestational index were all high.

For mating rats:

1b. Place a single female rat into a male rat's cage.

Rat females do not become acyclic in the absence of a male, so priming (Whitten, 1956) is unnecessary in rats.

Female rats are also 4- to 5-day cyclers; this should be taken into consideration when setting up mating pairs.

2b. Detect insemination in the female by the presence of sperm in the vaginal tract. On the morning after pairing (or each morning thereafter if the pair has previously been sperm negative), remove the female from the cage, restrain her, and gently insert a

fire-polished eyedropper containing 0.05 to 0.1 ml sterile saline into the vaginal tract. Instill (express) the saline into the tract and withdraw fluid from the tract.

Insemination can also be detected by dropped copulation plug(s) if the mating pair is housed in wire bottom cages. In the rat female, the copulation plug dries, shrinks, and falls out of the vaginal tract quickly, so it is rarely present in the vaginal tract. Therefore, vaginal smears for presence of sperm are the only reliable method to detect insemination if the mating pair is housed in solid-bottom cages and if there is no plug in the vaginal tract. For pairs housed in wire bottom cages, the plug drops through the bottom of the wire grid to the paper-covered shelf below. It is also suggested to confirm insemination in mating pairs housed in wire bottom cages with or without dropped plugs.

3b. Place the fluid on a glass microscope slide and examine it immediately under low and then high power on a microscope equipped with 10× and 40× eyepieces to detect sperm.

Sperm in the vaginal tract are usually accompanied by swollen, blood-engorged, external labia.

There may be one or more clumps of sperm (the earlier in the morning this is done, the better), or there may be only a few sperm in the entire smear.

4b. House the inseminated female singly in a plastic cage with a solid bottom and contact bedding.

The day insemination is confirmed is designated as gd 0.

Alternatively, one to three females with the same gd 0 date (and in the same dose group) can be housed together, but if they will litter, they must be singly housed by gd 18.

No Nestlets are needed, but the cage should have a solid bottom with contact bedding so the female can make a nest.

Tables 16.2.2 and 16.2.3 provide historical control data on reproductive parameters in CD (SD) rats from segment I, II, and III studies (Table 16.2.2) and from multigeneration reproductive toxicity studies (Table 16.2.3). The CD (SD) rat is a robust outbred strain with excellent fertility and fecundity. As with the CD-1 mouse, the CD (SD) rat mating, fertility, pregnancy, and gestational indices are all very high (slightly lower in multigenerational studies).

BASIC PROTOCOL 3

GESTATION AND LACTATION IN RATS AND MICE

For studies that include the analysis of reproductive outcomes, pregnant animals are allowed to complete gestation and may raise the pups to maturity. Mated females are housed appropriately, with a single animal per cage as they reach term. The author strongly suggests that dams with litters not be housed on metal floored caging (e.g., metal plates placed on cages with wire grid flooring), even with bedding, because dams will mound bedding around the pups to create a nest. The pups will therefore be lying directly on the metal floor (which acts as a heat sink) and become hypothermic. Pup mortality will increase, as will maternal infanticide and ingestion of offspring. Obviously, smaller, weaker pups will be at greater risk for morbidity or mortality. This may confound any treatment- or gene-related perinatal losses.

Neonatal and/or postnatal observations usually taken on litters include the following:

Parturition

Mice usually deliver on gd 19 ± 1, and rats usually deliver on gd 22 ± 1 (if date of copulation is designated gd 0). Unless there is a problem, the delivery usually takes a few hours. In the author's laboratory, pregnant females are examined at least twice daily,

starting 2 days before expected parturition. When the extra-pup membranes and placentas are eaten by the dam and the pups are licked clean and in a nesting pile, the litter is usually complete. Occasionally, it will appear that the litter is complete and an additional pup(s) will be present later (even the next day if the littering was completed late in the previous day). In the author's laboratory, if the litter is, in fact, complete on the following day, that day is designated postnatal day (P) 0. On the day of birth, pups are counted, sexed (by external qualitative examination of anogenital distance, unless anogenital distance is to be measured), weighed individually, and examined externally. By the following day (P1), a milk band (the visualization through the skin of the thin-walled stomach filled with milk) is present on the left-to-midline ventral abdominal area, if the dam has milk and the pup is nursing. The absence of a milk band should be noted, as well as pups cool to the touch, bluish in pallor (in which case it is likely that the ductus arteriosus, which is open between the pulmonary arch and aortic arch in utero to allow oxygenated blood from the dam to go from the heart to the systemic circulation, has not closed on schedule once the pup begins to breathe), or not in the nesting pile as evidence of impaired maternal care and/or problems with the pup(s). Typically, the greatest mortality is between P0 to P4. Count the litter daily to track any pup losses (the dam may fully or partially cannibalize dead or moribund pups, so there may be no dead pups in the cage but there may be missing pups). Pups can be identified at birth by tattooing the paws in a code within litters, but it takes a very light touch to subcutaneously inject enough dye on the dorsal surface of the foot to provide the tattoo, yet not so much that the paw swells (in which case the pup may be injured and/or the dam will chew off the paw).

Anogenital Distance

Anogenital distance (AGD) is the method to externally sex newborn rodents. It will also detect endocrine-mediated effects—the distance is under dihydroxytestosterone (DHT) control—although it is confounded by pup body weight. This measurement is from the cephalad (anterior) lip of the anus to the posterior base of the genital papilla (in the author's laboratory) for newborns, or to the base of the penis (for males) or to the caudal (posterior) lip of the open vagina (for females). The measurement on newborns can be done with an ocular reticle calibrated to a microscope stage micrometer (precision to 0.2 to 0.1 mm) or with a vernier or dial calipers (precision to 0.1 mm). For older animals, the vernier or dial calipers is strongly recommended. Newborn animals can be measured alive, but measurement of older animals (e.g., at wean or adulthood) is usually done at necropsy after terminal anesthesia. The intratechnician and intertechnician consistency of the extension of the animal on its back for measurement is critical because inconsistency will affect the distance measured. At weaning in CD (SD) rats, AGD is ~15 to 18 mm in males and 8 to 11 mm in females.

Standardization of Litters

Litters are usually standardized to eight or ten (with as equal a sex ratio as possible) on P4 by random selection procedures. The standardized litter removes the confounder of litter size (larger litters have lighter pups) and sex ratio (males are heavier than females). Pups can be individually identified within litters by tattooing the paw(s) (see discussion of parturition). The later this is done, the easier it is for the technician and the less stressful it is for the pups.

Nipple or Areolae Retention

In utero, both offspring sexes have nipple anlagen on the ventrum. In the presence of testosterone (T) or DHT in male fetuses, the anlagen regress. In the presence of an antiandrogen, the nipples and/or areolae in males are retained. In the author's laboratory,

preweanling male rats are examined on P11 to P13, when there is enough hair growth to detect areolae (roughly round areas of no hair), but not so much hair to obscure the nipples. Examination of older animals will require shaving the ventrum. Depending on the identity, potency, and dose of the antiandrogen (or in the presence of any one of a number of mutations in receptors such as androgen-insensitivity syndrome, or in enzymes such as 5-α-reductase), the male nipple count may approach or equal that of the normal female rats (usually 8 to 10).

Testis Descent

Testis descent, which occurs in the latter portion of lactation (typically P16 to P18 for rats), may be assessed in males. In the author's laboratory, males are placed in a transparent plastic cage and examined from below to detect the testes in the scrotal sacs. If the animal is held, he may retract the testis(es) into the abdominal cavity.

Weaning

CD (SD) rats are usually weaned on P21, as are CD-1 mice; Fischer 344 rats are usually weaned on P28. Weaning is accomplished by removing the dam (who is euthanized and necropsied, or mated again, depending on the researcher's intent) and counting, sexing, and individually weighing the pups. The pups are then selected for necropsy (if appropriate), for continuation to puberty or adulthood (to produce the next generation), or euthanized. Any nonselected pups are discarded (if appropriate). Selected rat pups should be individually and uniquely identified at weaning by eartag (e.g., Monel tag; National Band and Tag). Alternatively, rats may be tattooed with a unique number on the tail. For mice, in the author's laboratory, weanling mice to be eartagged may have the hole in the ear made a day or two before (because the ears are small and fragile) and the tag inserted into the prepared hole at weaning. Postweanling rats (and mice) may be housed individually or by sex by litter. If they are housed individually, the staff should check that they can reach the water and food sources. The pups can be placed against the sipper tube of the water bottle or the nipple of the automatic watering system to make sure they can find it and use it. If male rodents are housed together, especially mice, there is a dominance hierarchy established; the dominant male may barber the subservient males (i.e., remove the hair until the skin looks shaved). The dominant male may also exhibit heavier testes and sex accessory glands as an adult than the subservient males in the same cage.

Acquisition of Puberty

See *UNIT 16.1* for discussion. Vaginal patency (VP) in females and preputial separation (PPS) in males are the indicators of acquisition of puberty in rats. (VP and PPS are not so tightly correlated with onset of puberty in mice.) Starting on P25 in CD (SD) rats, on P35 in F344 rats, and on P20 in CD-1 mice (or earlier if a strong estrogen is involved or suspected), and continuing once daily until acquisition of VP, each offspring female is examined as follows. The pup's head and shoulders are restrained (with one hand), and the tail is raised with the other hand, exposing the urogenital area. The vaginal orifice is below the anal opening. Prior to VP, the membrane over the vagina thins and appears puckered; at VP, the opening appears as a pinhole. It may be necessary to gently spread the area with the fingers to see the vagina more clearly. Alternatively, the female may be held by the tail and allowed to grasp a wire cage lid. The tail is then lifted, as above, to expose the urogenital area. Starting on P35 in CD (SD) rats, on P40 in F344 rats, and on P25 in CD-1 mice, and continuing once daily until acquisition of PPS, each offspring male is examined as follows. The pup is restrained by one hand while the other hand gently attempts to retract the prepuce. PPS is acquired when the prepuce can be fully retracted to expose the glans penis, and the foreskin can be cuffed around the base of the

penis. The date, age in days, and body weight at acquisition are recorded for both sexes at acquisition. In females, age at first estrus or onset of estrous cyclicity is another commonly monitored parameter. This is done by commencing vaginal lavage, as described in Basic Protocol 1, as soon as the vagina is patent, and examining the slides for the first indication of estrus.

Other Endpoints

Other endpoints are also to be evaluated (e.g., body weights, developmental landmarks, neurotoxicity endpoints), the identity and timing of which would depend on the study design, objectives of the study, and/or the hypothesis being tested.

LITERATURE CITED

Environmental Protection Agency (EPA). 1998. Health Effects Test Guidelines, Report No. OPPTS 870.3700, Prenatal Developmental Toxicity Study. Office of Prevention, Pesticides and Toxic Substances (OPPTS), U.S. EPA, Washington, D.C.

European Society for Human Reproduction and Embryology (ESHRE) Andrology Special Interest Group. 1998. Guidelines on the application of CASA technology in the analysis of spermatozoa. *Hum. Reprod.* 13:142-145.

Haas, E. 1981. Fifty Diagnostic Special Stains for Surgical Pathology p.114. Lippincott, Philadelphia.

Organization for Economic Cooperation and Development (OECD). 2001. Proposal for Updating Guideline 414: Prenatal Developmental Toxicity Study, *In* Guideline for Testing of Chemicals (adopted January 22, 2001) pp. 1-11. OECD, Paris

Seed, J., Chapin, R.E., Clegg, E.D., Dostal, L.A., Foote, R.H., Hurtt, M.E., Klinefelter, G.R., Makris, S.L., Perreault, S.D., Schrader, S., Seyler, D., Sprando, R., Treinen, K.A., Veeramacheneni, D.N., and Wise, L.D. 1996. Methods for assessing sperm motility, morphology, and counts in the rat, rabbit, and dog: A consensus report. *Reprod. Toxicol.* 10:237-244.

Whitten, W.K. 1956. Modification of the oestrus cycle of the mouse by external stimuli associated with the male. *J. Endocrinol.* 13:399-404.

Contributed by Rochelle W. Tyl
Center for Life Sciences and Toxicology
Research Triangle Institute
Research Triangle Park, North Carolina

Histopathology of the Male Reproductive System I: Techniques

Effective evaluation of the male reproductive system relies on adequate sampling of the various parts of the reproductive tract as well as appropriate fixation, orientation, processing, embedding, and staining of the tissues. This unit describes protocols for these various aspects of tissue preparation.

The presence or absence, as well as the anatomical arrangement, of various components of the reproductive tract varies with species. These differences must be appreciated to ensure appropriate sampling. Basic Protocol 1 and Support Protocol 1 describe the identification and dissection procedures for the reproductive organs from the rodent, dog, and primate, which are the animals most frequently used in toxicological research. Basic Protocol 1 describes the routine immersion fixation of these tissues followed by processing and embedding in paraffin wax. For a variety of reasons, the testis presents a problem for good fixation. Conventional immersion fixation in formalin generally results in poor preservation of the seminiferous tubules, and the use of an alternative fixative, such as Bouin's, is recommended in most regulatory guidelines. Although Bouin's provides good morphology suitable for detecting subtle disturbances in spermatogenesis, it suffers from a number of increasingly important safety and disposal problems and also results in significant shrinkage of the tubules. This protocol recommends the use of a novel, alcohol-based fixative (modified Davidson's fixative), which provides comparable cellular and nuclear preservation to that achieved with Bouin's but with less tubular shrinkage and none of its safety and disposal hazards.

Once the tissues are fixed, sampling of specific structures and tissue orientation are very important to ensure that critical regions of the reproductive tract are presented for examination. Support Protocol 1 provides guidance on how to trim and sample tissues from rodents, dogs, and primates.

Basic Protocol 2 describes the methodology used to obtain excellent preservation of the rodent testis by whole-body perfusion via the heart. The testes of large animals can also be fixed by perfusion, but to reduce the volume of fixative required this is best carried out by introducing the fixative into the testicular artery. Support Protocols 2 and 3 describe the processing procedures required for embedding in epoxy and glycol methacrylate resin, respectively. Perfusion fixation followed by embedding in resin is essential for proper evaluation of the testis by electron microscopy. The use of epoxy resin is necessary to maintain stability of the section under the electron beam; however, epoxy-embedded tissue can only be stained with toluidine blue for light microscopic examination. Glycol methacrylate resin is a water-soluble resin that can be used to prepare semithin (2 μm) sections that can be stained with conventional histologic stains for high-resolution light microscopy. A compromise between the convenience of immersion fixation followed by paraffin embedding and the labor-intensive perfusion fixation followed by resin embedding can be achieved by immersion fixation followed by embedding in glycol methacrylate resin.

CAUTION: Many of the chemicals used in these protocols are hazardous, including formalin, glutaraldehyde, propylene oxide, epoxy and glycol methacrylate resins, sodium cacodylate, and osmium tetroxide. Refer to material safety data sheets for appropriate handling, storage, and disposal.

Contributed by Dianne M. Creasy

Current Protocols in Toxicology (2002) 16.3.1-16.3.18

NOTE: All protocols using live animals must first be reviewed and approved by an Institutional Animal Care and Use Committee (IACUC) and must conform to governmental regulations regarding the care and use of laboratory animals.

BASIC PROTOCOL 1

DISSECTION, IMMERSION FIXATION, AND PARAFFIN EMBEDDING OF MALE REPRODUCTIVE-TRACT TISSUES

This procedure is suitable for routine screening of tissues for toxicological changes. It involves dissection of the major reproductive tissues, measurement of organ weights, and immersion fixation of the testes using a special fixative (the remaining tissues can be fixed in the same fixative or in neutral buffered formalin). This is followed by careful trimming of the tissues to include specific structures and conventional processing through an ascending series of alcohols and clearing agents, followed by embedding in paraffin wax. Sections are then cut and stained with periodic acid Schiff's stain/hematoxylin (PAS-H; for testes and epididymides) and hematoxylin and eosin (for remaining tissues).

Materials

Male rodent, dog, or primate
Modified Davidson's fixative (see recipe)
10% neutral buffered formalin (~4% [w/v] formaldehyde; Sigma or standard recipe, see Bancroft et al., 1990)
Surgical instruments for dissection

Additional reagents and equipment for euthanization; dissecting the testes, epididymides, and accessory sex glands (see Support Protocol 1); dehydration, clearing, and infiltration with paraffin wax (Bancroft et al., 1990); and paraffin sectioning and staining (Bancroft et al., 1990)

1. Euthanize a male rodent, dog, or primate by an approved method.

   Some examples of euthanization methods include carbon dioxide (for rodents) and sodium pentobarbital (e.g., Sleepaway).

2. Depending on the species under investigation (Table 16.3.1), use surgical instruments to dissect out the testes, epididymides, and accessory sex glands (i.e., seminal vesicles with coagulating glands and prostate; see Support Protocol 1).

   Standard dissection guides, such as Feldman and Seeley (1988) and Evans (2000), contain detailed dissection procedures.

   It is important to minimize squeezing of the testes during handling to prevent artifactual sloughing of the germ cells from the seminiferous epithelium. When trimming the epididymis from the testes, take care not to cut the testicular capsule, which will cause extrusion of the seminiferous tubules through the cut and consequent disruption of tissue architecture.

3. Weigh each organ and record the weight to the nearest 1 mg (for rodents) or 100 mg (for dogs or primates).

   For paired organs, individual weights provide valuable information to support unilateral microscopic findings. Individual organ weights are also required where one testis and one epididymis are used for quantifying sperm parameters (Table 16.3.2).

   When weighing seminal vesicles and the prostate, it is important that the fluid be included in the weight because its volume reflects the functional activity of the glands. For some regulatory guidelines, the combined weight of seminal vesicles and prostate is recommended (Table 16.3.2). If separate weights are desired, dissect out the prostate and seminal vesicles as a unit, being careful to retain all fluids, and then separate the seminal vesicles and coagulating glands from the prostate over a weigh boat, so that any fluid leakage from the seminal vesicles is caught and included for weighing.

Table 16.3.1 Presence of Accessory Sex Glands in Common Laboratory Species

Species	Ampulla ductus deferens	Bulbourethral (Cowper's) glands	Coagulating glands	Preputial gland	Prostate	Seminal vesicles
Dog	+	–	–	–	+	–
Mouse	+	+	+	+	+	+
Primate	+	+	–	–	+[a]	+
Rabbit	+	+	–	+	+	+[b]
Rat	+	+	+	+	+	+

[a]No anterior lobe present.

[b]Present as rudimentary glandula vesicularis.

Table 16.3.2 Recommendations from Recently Revised Regulatory Guidelines for Reproductive Studies Relating to Sampling and Fixation of Male Reproductive Tissues

Guideline[a]	Tissues to be weighed	Tissues to be preserved	Tissues to be examined
OECD 416: Two-generation reproduction toxicity study (OECD, 2001)	Testes	One testis[b,c]	Testis
	Epididymides (total and cauda)	One epididymis[b]	Epididymis
	Seminal vesicles with coagulating glands and their fluids and prostate (as one unit)	Seminal vesicles	Seminal vesicles
		Coagulating glands	Coagulating glands
		Prostate	Prostate
OECD 421: Reproduction/developmental toxicity screening test (OECD, 1995)	Testes	Testes Testes[c]	
	Epididymides	Epididymides	Epididymides
		Seminal vesicles	
		Coagulating glands	
		Prostate	
OPPTS 870.3800: Reproduction and fertility effects (EPA, 1998)	Testes	Right testis[b,c]	Testis
	Epididymides (total and cauda)	Right epididymis[b]	Epididymis
	Seminal vesicles with coagulating glands and their fluids	Seminal vesicles	Seminal vesicles
		Coagulating glands	Coagulating glands
	Prostate	Prostate	Prostate
ICH S5A and S5B: Detection of toxicity to reproduction for medicinal products (ICH, 1994, 1996[d])	None	Testes[c] and epididymides	Testes and epididymides if indicated by altered fertility indices

[a]Abbreviations: ICH, International Conference on Harmonization of Technical Requirements of Registration of Pharmaceuticals for Human Use; OECD, Organization for Economic Cooperation and Development; OPPTS, Office of Prevention, Pesticides, and Toxic Substances.

[b]Remaining testis or epididymis is retained for assessment of sperm parameters (*UNITS 16.1 & 16.2*).

[c]Preserved in Bouin's or comparable fixative.

[d]An addendum on male fertility studies.

4. Place the testes into modified Davidson's fixative for ≥48 hr at room temperature and then transfer to 10% neutral buffered formalin for storage. Place the remaining tissues into 10% neutral buffered formalin for ≥48 hr at room temperature until required for processing.

   Speed of penetration of the fixative can be improved by pricking or nicking the capsule before immersion and also by slicing the testis following several hours in fixative (see Critical Parameters and Troubleshooting, discussion of choice of fixative).

   The tissues can be stored in 10% neutral buffered formalin for up to 10 years at room temperature.

   For convenience, the epididymides and secondary sex organs can also be fixed in Davidson's fixative, but the cytological and staining characteristics are slightly inferior to those of formalins.

5. Trim the tissues according to Support Protocol 1 and process through standard histology procedures for dehydration, clearing, and infiltration with paraffin wax. Embed in paraffin wax (Table 16.3.3).

   Standard histological processing methodology can be found in Bancroft et al. (1990).

   Alternatively, for high resolution light microscopy, the tissues can be embedded in glycol methacrylate resin following immersion fixation (see Support Protocol 3).

6. Prepare sections at 5 to 6 μm.

   Standard paraffin sectioning is described in Bancroft et al. (1990).

7. Stain testes and epididymides with PAS-H stain and the remaining tissues with hematoxylin and eosin.

   Standard histological staining methodology can be found in Bancroft et al. (1990).

   PAS-H staining in the testis will stain the glycoprotein component of the spermatid acrosomic granule or acrosome cap. These are very small structures, which can be difficult to visualize if the stain is not optimal. It is important that the periodic acid and the Schiff reagent are relatively fresh solutions. In dog testes, the acrosome does not stain with PAS and cannot be adequately distinguished in paraffin-embedded sections (see Anticipated Results).

Table 16.3.3 Schedule for Processing Fixed Tissues From Rodent, Dog, or Primate into Paraffin Wax

Solution[a]	Temperature (°C)	Time (hr)	
		Rodent	Dog/primate
Neutral buffered formalin	37	0.5	0.5
70% ethanol	37	1.0	1.0
80% ethanol	37	1.5	2.0
90% ethanol	37	1.0	1.5
100% ethanol	37	1.0	1.0
100% ethanol	37	1.5	1.5
100% ethanol	37	2.0	2.0
Xylene	37	0.5	0.5
Xylene	37	1.0	1.5
Xylene	37	1.5	2.0
Wax	60	1.0	1.0
Wax	60	1.0	1.5
Wax	60	2.0	2.0

[a]Tissues should be agitated in each solution.

PERFUSION FIXATION OF THE MALE RODENT REPRODUCTIVE TRACT BY CARDIAC PERFUSION AND RESIN EMBEDDING OF TISSUES

This method is used when high-resolution light microscopy or electron microscopy is required. The methodology is time consuming and labor intensive and is more suited to investigative studies than to large-scale screening studies. The procedure involves anesthetizing the animal, cannulating the thoracic aorta through the heart, and flushing out the systemic vasculature with Ringer's solution followed by systemic perfusion with a buffered paraformaldehyde and glutaraldehyde fixative. The method described is a whole-body perfusion using a peristaltic pump to maintain a constant pressure during perfusion. Following fixation, the tissue may be embedded in glycol methacrylate or epoxy resin for light microscopy. Electron microscopy requires the use of epoxy resin. Whole-body perfusion is not suitable for large animals such as primates and dogs because of the large volume of fixative required. An alternative technique introduces the fixative into the testicular artery (Frederick and Doorn, 1973; Russell et al., 1990).

Materials

Krebs Ringer's solution (see recipe)
Karnovsky's fixative (see recipe)
Male rodent
65 mg/ml sodium pentobarbital solution (e.g., Sleepaway; Fort Dodge Animal Health) or equivalent for anesthesia
0.1 M sodium cacodylate buffer (see recipe)
Osmium tetroxide/potassium ferrocyanide fixative (see recipe)

Perfusion setup (Fig. 16.3.1), including:
- Two 1-liter stoppered bottles, each connected to a length of silastic tubing (~3.0 mm internal diameter) and each vented to air
- Silastic tubing, ~3.0 mm internal diameter (e.g., Masterflex L/S 16 pump tubing; Cole-Parmer Instrument)
- Three-way stopcock
- Variable-speed peristaltic pump (e.g., Masterflex; Cole-Parmer Instrument)
- Manometer
- Dosing needle: stainless steel intubation needle with bulbous end, 16 to 18G (depending on size of animal), attached to a cut-off 1-ml tuberculin syringe
- Dissection board suspended in a tray
- Vacuum pump connected to 1-liter bottle trap

Rubber bands
Dissecting tools, including:
- Scalpel
- Hemostats
- Forceps

5-cm (2-in) Dieffenbach serrefine (bulldog) clamp
Single-edged blades

Additional reagents and equipment for dehydrating, infiltrating, and embedding in epoxy resin (see Support Protocol 2); sectioning and staining for electron microscopy *or* dehydrating, infiltrating, and embedding in glycol methacrylate (see Support Protocol 3); sectioning and staining for high-resolution light microscopy

Set up perfusion apparatus

1. Set up a perfusion apparatus as shown in Figure 16.3.1.

The perfusion needs to be carried out under a ventilation hood or on a ventilated table.

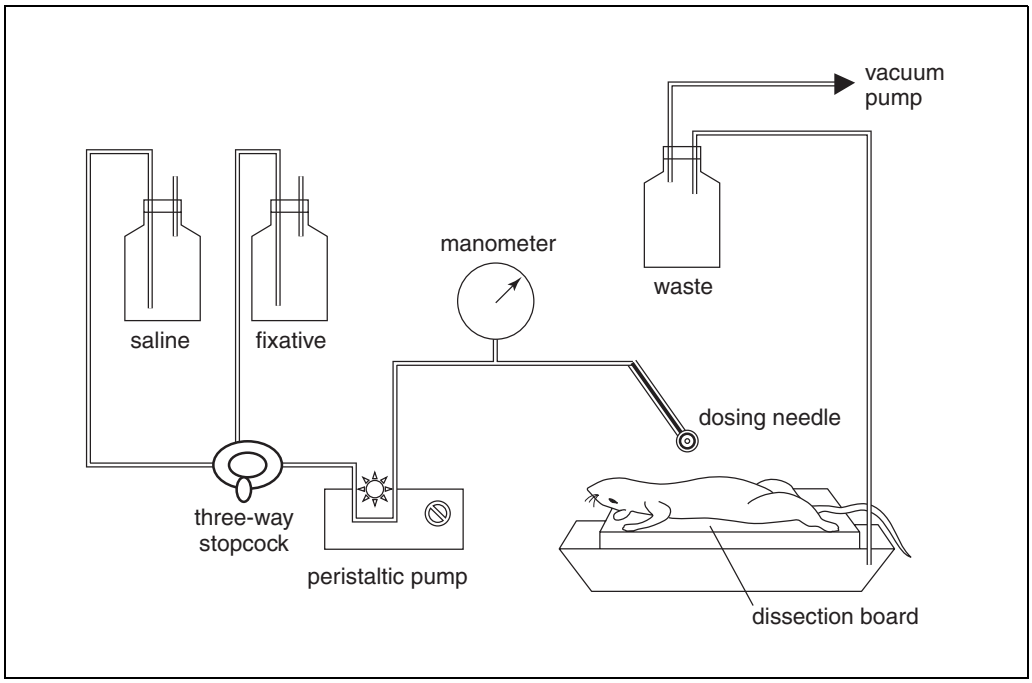

Figure 16.3.1 Apparatus for perfusion fixation of rodents. Two bottles, one containing Krebs Ringer's saline and the other containing fixative are connected via a three-way stopcock to tubing terminating in a blunt-ended gavage dosing needle. Perfusion pressure is generated using a peristaltic pump and monitored using an in-line manometer.

2. Fill one 1-liter bottle with Krebs Ringer's solution and a second one with Karnovsky's fixative. Connect these with silastic tubing and a three-way stopcock to a variable-speed peristaltic pump. Connect a manometer in-line and attach a dosing needle to the end of the tubing.
3. Open the stopcock and flush the tubing with Krebs Ringer's solution. Ensure that the tubing of the perfusion apparatus is filled with fluid and free of air bubbles.
4. Using the manometer, calibrate the speed of the peristaltic pump to a flow rate of 110 to 130 µl/min. This should be equivalent to a perfusion pressure of 100 to 120 mm Hg. During the perfusion the pressures should not be allowed to rise above 150 mm Hg.
5. Set up a dissection board suspended in a tray and a vacuum pump connected to a 1-liter bottle trap to drain used fluids.

Perfuse animal

6. Anesthetize a male rodent with 0.8 to 1.0 µl/Hg of 65 mg/ml sodium pentobarbital solution.

   It is important to achieve a level of anesthesia that results in maintenance of shallow breathing and adequate cardiac output and yet produces a sufficient level of surgical anesthesia.

   Speed is critical to the success of the technique. Once the animal is adequately anesthetized, dissection and introduction of the Krebs Ringer's solution must be accomplished as efficiently and quickly as possible.

7. Secure the animal on its back to the dissection board using rubber bands around its paws.

   The dissection board should be located over a draining vessel to catch the perfusion fluids.

8. Make a midline incision with a scalpel to open the abdomen and then cut through the rib cage in a V shape from the xiphoid process to the axilla. Avoid cutting any major blood vessels in the axilla or along the sternum.

9. Clamp the xiphoid process with a pair of hemostats and displace the flap of thoracic tissue cranially.

10. Cut through the pericardium and reflect it back from the heart and aorta.

11. Turn on perfusion pump and begin flow of Krebs Ringer's solution through the perfusion apparatus at 110 to 120 ml/min.

12. Grasping the ventricular apex with a pair of forceps, rapidly make an incision in the right ventricle to allow fluid efflux. Then make a small incision in the left ventricle and insert the dosing needle through the ventricle and into the aorta so that it is just visible through the vessel wall. Clamp it in place using a Dieffenbach serrefine clamp on the proximal portion of the aortic arch.

    Krebs Ringer's solution should be flowing through the apparatus when the dosing needle is inserted. The needle must not be pushed too far into the aorta, otherwise it will press against the aortic arch and block the flow. Once the perfusion is underway, the angle that the needle enters the heart and aorta needs to be maintained at a slight elevation so that the outflow of the fluid is not obstructed. This can be accomplished using clamps or supports.

13. Perfuse the animal at a flow rate of 110 to 120 ml/min until the blood has cleared from the testes (~1 to 2 min).

    The blood will gradually be replaced by the Krebs Ringer's solution.

14. During the perfusion, expose the testes by cutting through the scrotum. Leave the testes in situ and watch for the coiled, capsular testicular artery to clear of blood and for the testicular tissue to become uniformly pale.

Fix tissue

15. Once the testes have become pale and the effusate from the right ventricle is clear (~1 to 2 min), turn the stopcock to change over to fixative. Infuse the fixative for ≥30 min for electron microscopy and ≥20 min for light microscopy only. After the first 2 to 3 min, slow the rate of perfusion to ~10 ml/min.

    Duration of perfusion is more important than the volume of fluid perfused. The initial pressure and flow rate is important to introduce fixative rapidly while minimizing pressure artifacts. Once the vasculature and basic architecture have been stabilized, the perfusion pressure can be reduced to conserve fixative. A volume of ~300 ml is appropriate for a 300-g animal.

    As described, the technique will provide excellent fixation for ultrastructural studies with minimal fixation and handling artifacts. If the tissue is only intended for high-resolution light microscopy, then the perfusion time with fixative can be reduced. With this shorter time, the tissue may be subject to some minor handling artifacts.

16. Between perfusions, flush the perfusion line thoroughly with Krebs Ringer's solution to remove all traces of fixative.

Remove, trim, and process tissue

For electron microscopy:

17a. Remove the testes or tissue of interest and dice into cubes of ≤1 mm using a sharp single-edged blade. Place these into fresh fixative for ~1.5 hr at 4°C.

18a. Wash in three changes of 0.1 M sodium cacodylate buffer at 4°C, with one wash being overnight and other washes ≥15 min.

19a. Postfix 1 hr in osmium tetroxide/potassium ferrocyanide fixative at room temperature.

20a. Dehydrate, infiltrate, and embed tissues in epoxy resin as described (see Support Protocol 2).

21a. Section embedded tissue at 1 to 2 µm, float sections onto a hot water bath at ~60°C, and pick up onto grease-free glass microscope slides.

22a. Stain sections and examine with a light microscope.

A solution of 1% (w/v) toluidine blue at 60°C can be used for staining. Bancroft et al. (1990) describes resin sectioning and staining techniques.

23a. Section on an ultramicrotome (silver or gold interface colors), float sections onto water at room temperature, and pick up onto electron microscopy grids.

24a. Stain sections with uranyl acetate and lead citrate and examine under an electron microscope.

Preparation of tissues for examination by electron microscopy requires specialized techniques and equipment. Detailed instructions can be found in Hayat (1989).

For high-resolution light microscopy:

17b. Remove the testes or tissue of interest and trim with a single-edged blade to provide samples ~1 cm × 1 cm × 1 mm thick.

18b. Dehydrate, infiltrate, and embed samples in glycol methacrylate as described (see Support Protocol 3).

19b. Section at ~2 µm using a purpose-designed motorized, retracting microtome and a tungsten-carbide or large-area glass (Ralph) knife.

Examples of appropriate microtomes include the Reichert-Jung Supercut and LKB Historange.

When the resin blocks are trimmed to reach the tissue, the use of 70% (v/v) ethanol on the surface of the block will soften the resin and allow thicker sections to be taken without shattering the resin.

20b. Float the sections on a water bath at room temperature until the resin has expanded maximally (~1 to 2 min).

21b. Pick up sections on a grease-free glass slide and dry on a hot plate or in an oven at 60°C for ≥30 min before staining.

Flattening and picking up the section is aided if the water bath is previously wiped with 70% (v/v) ethanol to reduce surface tension.

22b. Stain with periodic acid Schiff's (PAS) stain with a light counterstain of hematoxylin (i.e., PAS-H) or with hematoxylin and eosin.

Staining times will depend on the solutions used. Bancroft et al. (1990) describe standard histological staining methodology.

PAS-H on the testis will stain the glycoprotein component of the spermatid acrosomic granule or acrosome cap. These are very small structures, which can be difficult to visualize if the stain is not optimal. It is important that the periodic acid and the Schiff reagent are relatively fresh solutions.

REMOVAL, TRIMMING, AND ORIENTATION OF MALE TESTES, EPIDIDYMIDES, AND ACCESSORY SEX GLANDS

This protocol describes the dissection of testes, epididymides, and accessory sex glands for male rodents, dogs, and primates that have been euthanized as described in Basic Protocol 1. Specific directions for fixing and sectioning the samples are described in Basic Protocol 1.

Rodent

For a male rodent, remove the testes and epididymides as a unit. Separate the epididymides from the testes and trim to remove the surrounding adipose tissue. Weigh the testes and epididymides separately. After fixation, take a 5-mm transverse section through the testis slightly cranial to the midline to include a small portion of the rete testis (which is subcapsular and originates at the point where the epididymis is attached and is where all the capsular blood vessels converge at the cranial pole). Alternatively, take a longitudinal section through the plane of the rete testis. (For a discussion of the advantages and disadvantages of the plane of section, see Critical Parameters and Troubleshooting, discussion of sampling and orientation of tissues). Take a longitudinal section through the epididymis to include the caput (head), corpus (body), and cauda (tail). To achieve this, trim a thin slice of tissue from the caput and the cauda so that the length of the epididymis can be embedded flat.

Remove the seminal vesicles, coagulating glands, prostate, and bladder as a unit (Fig. 16.3.2A). For detailed dissection guidance, see Feldman and Seeley (1988). Carefully remove the bladder and weigh and fix the seminal vesicles, coagulating glands, and prostate as a unit. If individual weights of seminal vesicles and prostate are required, carefully separate the glands, minimizing egress of fluid. Do this over a weigh boat to catch any fluid. After fixation, separate the seminal vesicles (with the coagulating glands) from the prostate. Take a transverse section through each seminal vesicle and its coagu-

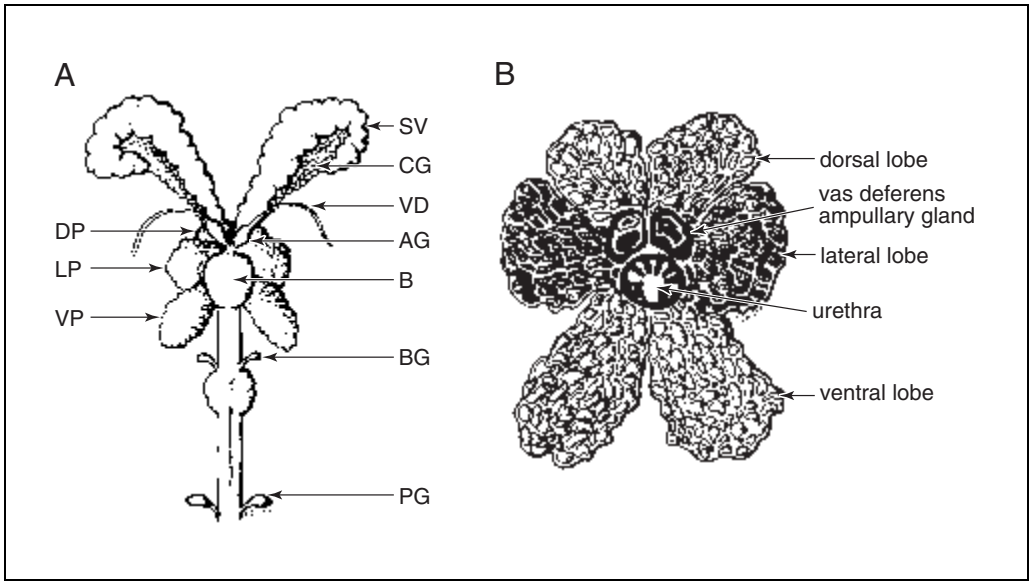

Figure 16.3.2 Accessory male reproductive organs in the rat. (**A**) Anatomic layout. (**B**) Histologic appearance of a longitudinal section of the prostate. In addition to the dorsal, lateral, and ventral lobes, sections through the urethra as well as the vas deferens (VD), with varying amounts of associated ampullary gland (AG), may be included. B, bladder; BG, bulbourethral gland; CG, coagulating gland; DP, dorsal prostrate; LP, lateral prostate; PG, preputial gland; SV, seminal vesicles; Ventral prostate. Figure drawn by Ann Hoffenberg.

lating gland. Take a midtransverse section through the prostate to include dorsal, lateral, and ventral lobes (Fig. 16.3.2B; Suwa et al., 2001).

Dog

For a male dog, remove each testis and epididymis as a unit. Carefully separate the epididymis from the testis and trim away any adipose tissue. Weigh the testes and epididymides separately. After fixation, take a 5-mm transverse slice through the midline of the testis. Depending on the size of the testis, it may be necessary to trim this further to fit into a standard histology processing cassette. If so, ensure that the rete testis (which is enclosed in the mediastinum and runs as a longitudinal central core through the middle of the testis) is included. Bisect the epididymis transversely through the corpus so that half remains with the caput and half with the cauda. Trim off a thin, longitudinal slice of tissue from the caput and the cauda to allow the tissue to be embedded flat. This will provide a longitudinal section through the caput, corpus, and cauda.

Remove the prostate and bladder as a unit (Fig. 16.3.3A). For detailed dissection guidance, see Evans (2000). Carefully remove the bladder. Weigh and fix the prostate. Take a transverse section through the prostate and the central urethra (Fig. 16.3.3B).

Primate

For a male primate, remove each testis and epididymis as a unit. Carefully separate the epididymis from the testis and trim away any adipose tissue. Weigh the testes and epididymides separately. After fixation, take a 5-mm transverse slice through the midline of the testis. Depending on the size of the testis, it may be necessary to trim this further to fit into a standard histology processing cassette. In primates, the rete testis lies in a subcapsular location along the epididymal edge. Ensure that this portion of the testis is sampled. Bisect the epididymis transversely through the corpus so that half remains with the caput and half with the cauda. Trim off a thin, longitudinal slice of tissue from the caput and the cauda to allow the tissue to be embedded flat. This will provide a longitudinal section through the caput, corpus, and cauda.

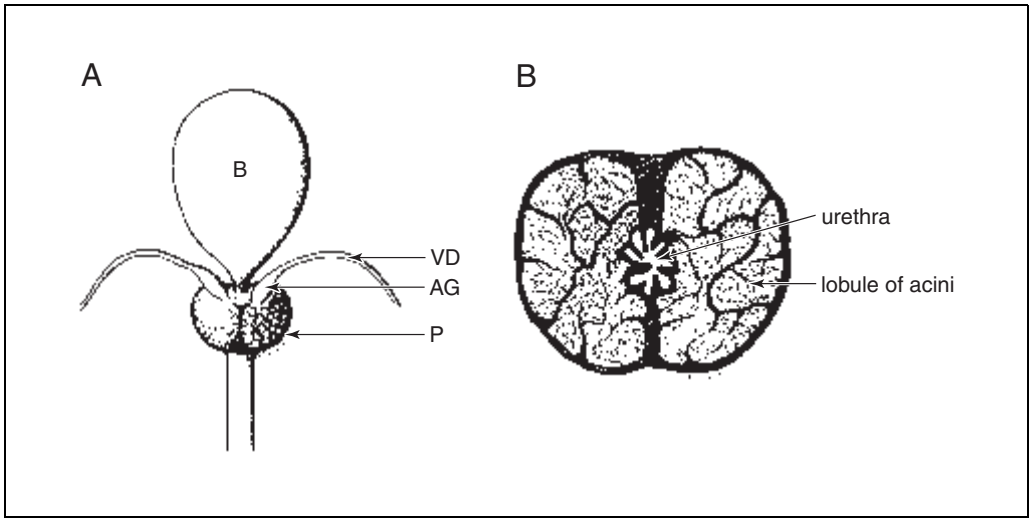

Figure 16.3.3 Accessory male reproductive organs in the dog. (**A**) Anatomic layout. (**B**) Transverse section through the prostate with lobules of acini separated by connective tissue trabeculae surrounding the central urethra. AG, ampullary gland; B, bladder; P, prostate; VD, vas deferens. Figure drawn by Ann Hoffenberg.

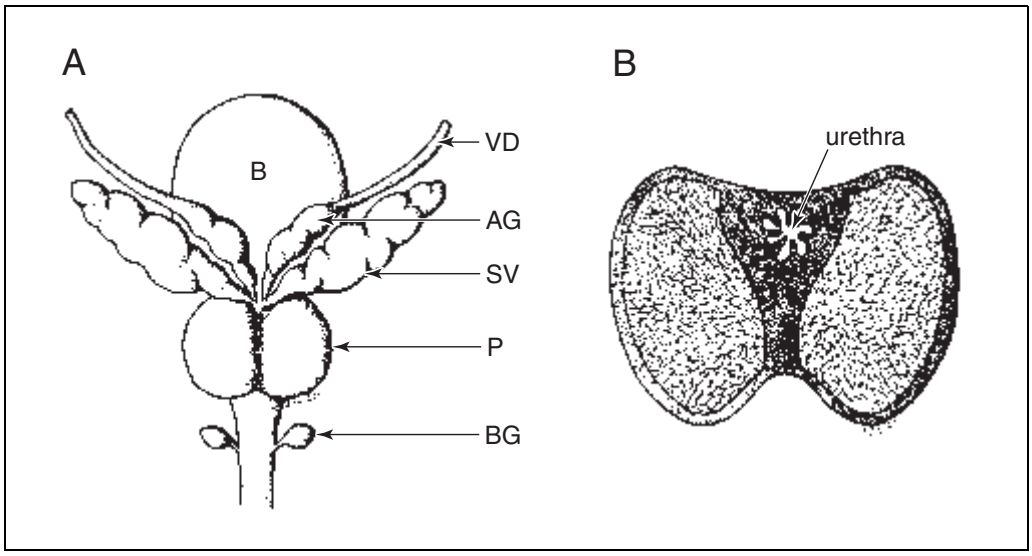

Figure 16.3.4 Accessory male reproductive organs in the primate. (**A**) Anatomic layout. (**B**) Transverse section through cynomologous monkey prostate, in which glandular acini are absent from the anterior aspect. AG, ampullary gland; B, bladder; BG, bulbourethral gland; P, prostate; SV, seminal vesicles; VD, vas deferens. Figure drawn by Ann Hoffenberg.

Remove the seminal vesicles, prostate, and bladder as a unit (Fig. 16.3.4A). Carefully remove the bladder. Weigh and fix the seminal vesicles and prostate as a unit. If individual weights of seminal vesicles and prostate are required, carefully separate the glands, minimizing egress of fluid. Do this over a weigh boat to catch any fluid. After fixation, separate the seminal vesicles from the prostate. Take a transverse section through each seminal vesicle and take a transverse section through the prostate and the prostatic urethra (Fig. 16.3.4B).

PROCESSING AND EMBEDDING OF TISSUES IN EPOXY RESIN

SUPPORT PROTOCOL 2

Epoxy resin embedding is used for fixed tissues to be examined by electron microscopy.

Materials

Fixed tissue sample postfixed in 1% osmium tetroxide/1.25% potassium ferrocyanide (see Basic Protocol 2)
30%, 50%, 70%, 85%, 95%, and 100% (v/v) ethanol
Propylene oxide (e.g., Electron Microscopy Sciences)
1:1 propylene oxide/epoxy resin
Epoxy resin (e.g., Araldite 502 or 506 lufts; Electron Microscopy Sciences)
Mold suitable for electron microscopy blocks (e.g., Electron Microscopy Sciences)

NOTE: During processing, all steps should be carried out with agitation.

1. Dehydrate a fixed tissue sample postfixed in 1% osmium tetroxide/1.25% potassium ferrocyanide using an alcohol series consisting of 15-min steps in 30%, 50%, 70%, 85%, 95%, and 100% ethanol.
2. Transfer sample to propylene oxide and incubate 5 min without agitation.
3. Incubate 1 hr in 1:1 propylene oxide/epoxy resin at room temperature.

   Incubation times here and in step 4 will vary. Refer to manufacturer's instructions for specific resin for details.
4. Incubate in epoxy resin, two changes, 1.5 hr each at room temperature.
5. Orient sample in a mold and embed in fresh resin. Polymerize ≥48 hr at 60°C.

SUPPORT PROTOCOL 3

PROCESSING AND EMBEDDING OF TISSUES IN GLYCOL METHACRYLATE

Fixed tissues are postfixed (optional) and embedded in glycol methacrylate for high-resolution light microscopy.

Materials

Fixed tissue sample, 3 to 5 mm thick (see Basic Protocol 2)
0.1 M sodium cacodylate buffer (Electron Microscopy Sciences or see recipe), optional
Osmium tetroxide/potassium ferrocyanide fixative (see recipe), optional
50%, 70%, 80%, 95%, and 100% (v/v) ethanol
JB4 glycol methacrylate embedding kit (e.g., Polysciences), including:
  Solution A (acrylic monomer)
  Catalyst (organic peroxide)
  Solution B (accelerator)
Ice bath
Glycol methocrylate embedding molds, available as block-mold system that allows polymerization directly onto a metal or plastic microtome chuck (Polysciences)

1. *Optional:* Wash the fixed tissue sample overnight in 0.1 M sodium cacodylate buffer and postfix 1 hr in 1% osmium tetroxide/1.25% potassium ferrocyanide at room temperature. Wash again in two changes, 15 min each, 0.1 M sodium cacodylate buffer.

   This step will provide improved fixation quality, but is optional.

2. Dehydrate tissue using an alcohol series consisting of 30-min steps in 50%, 70%, 80%, 95%, and 100% ethanol.

   NOTE*: Sample should be agitated slowly during all dehydration and infiltration steps.*

3. Prepare the glycol methacrylate infiltration solution according to the kit instructions by adding 100 ml solution A/1 g catalyst. Stir at room temperature to dissolve and store at 4°C for use in steps 4 to 7.

   Polymerization of the resin is an exothermic reaction, and the heat generated can cause artifacts in the tissue. A smaller proportion of catalyst can be used (0.7 g/100 ml solution A) to slow polymerization time and reduce heat artifacts. This is particularly important when larger blocks (e.g., 1.5 cm^2) are produced.

4. Infiltrate tissue sample with a 1:1 mixture of 100% ethanol/infiltration solution for 2 hr at 4°C.

5. Infiltrate overnight in full-strength infiltration solution at 4°C.

6. Infiltrate 2 hr in a second change of infiltration solution at 4°C.

7. Prepare the embedding solution by adding 1 ml solution B to 15 ml infiltration solution. Use immediately and keep solution in an ice bath while embedding.

8. Orient sample in a glycol methacrylate embedding mold and fill mold with embedding solution. Polymerize overnight at 4°C.

   Polymerization needs to be carried out in the absence of oxygen and in a dry atmosphere. The design of the molds largely excludes contact with air, but as an additional safety measure polymerization may be carried out in a vacuum desiccator or in a nitrogen-filled desiccator.

The use of glycol methacrylate resin as an embedding medium is technically demanding and potentially subject to numerous problems, including difficulties obtaining satisfactory polymerization (leading to sectioning difficulties) as well as morphological artifacts and difficulties with staining (Hess and Moore, 1993). It is advisable to experiment with the technique prior to its use in a study.

REAGENTS AND SOLUTIONS

Use Milli-Q-purified water or equivalent in all recipes and protocol steps. For common stock solutions, see ***APPENDIX 2A****; for suppliers, see* ***SUPPLIERS APPENDIX****.*

Karnovsky's fixative

10 ml 10% (w/v) paraformaldehyde (see recipe; 1% final)
35 ml 0.2 M sodium cacodylate (0.07 M final)
12 ml 25% (w/v) glutaraldehyde (e.g., Electron Microscopy Sciences; 3% final)
43 ml deionized H_2O
Adjust to pH 7.4 with 0.1 N hydrochloric acid
Store up to 1 week at 4°C.

Krebs Ringer's solution

Dissolve 6.6 g sodium chloride, 0.15 g potassium chloride, and 0.15 g calcium chloride in 1 liter deionized water. Adjust to pH 7.6 with 5% (w/v) sodium bicarbonate. Store up to 1 month at 4°C. Immediately before use add 5 g procaine hydrochloride and 1 ml heparin (10,000 IU).

Modified Davidson's fixative

140 ml ethanol
62.5 ml glacial acetic acid
375 ml 37% (w/v) formaldehyde
422.5 ml distilled H_2O
Store up to 3 months at room temperature.

Osmium tetroxide/potassium ferrocyanide fixative

Prepare a 2% (w/v) aqueous solution of osmium tetroxide and a 2.5% (w/v) aqueous solution of potassium ferrocyanide. Mix equal volumes together immediately before use (1% osmium tetroxide and 1.25% potassium ferrocyanide, final concentrations).

Paraformaldehyde, 10%

Dissolve 2 g paraformaldehyde in 20 ml deionized water. Stir 20 min at 60°C. Add a few drops of 1 M sodium hydroxide to clear the solution. Cool and filter through Whatman no. 5 filter paper. Store up to 1 month at 4°C.

Sodium cacodylate buffer, 0.1 M

Dissolve 10.7 g sodium cacodylate in 500 ml deionized water. Store up to 1 month at room temperature.

This buffer is also commercially available from Electron Microscopy Sciences.

COMMENTARY

Background Information

The procedures used for reproductive-tract histology will largely depend on the objectives of the study. For example, a regulatory screening study to detect toxicity will generally weigh and sample the tissues according to the appropriate regulatory guidelines (Table 16.3.2) and use routine immersion fixation followed by paraffin embedding. An investigative study to characterize toxicity may concentrate on target tissues of interest and use perfusion fixation followed by resin embedding. The latter procedure will provide enhanced resolution for light microscopy and, if epoxy resin is used, allow for ultrastructural examination with the electron microscope.

Critical Parameters and Troubleshooting

Sampling and orientation of tissues

Testes. There are a number of factors to consider when deciding how to trim the various tissues of the reproductive tract. In the case of the testes, a longitudinal or transverse section can be taken. The advantage of a longitudinal section is that it provides more tissue to examine and provides frequent longitudinal sections through seminiferous tubules, many of which will include consecutive stages of the spermatogenic cycle. The advantage of a transverse section is that it provides consistent cross-sections through all the seminiferous tubules. This makes staging of the tubule easier and allows quantitation of cell numbers and tubular measurements, if required. Most technicians sample the testis by taking a midline sample. However, the testis has asymmetric structures that may be missed by a midline section. For example, in the rodent, the rete testis (the network of canals into which the seminiferous tubules empty) is located at the cranial pole of the testis and spreads down directly beneath the capsule towards the midline. The rete can provide important information regarding fluid dynamics of the seminiferous tubule fluid. In cases of obstruction of the excurrent duct system or disturbances in fluid reabsorption, it will show dilation. It can also be the site of proliferative lesions and rete testis tumors. Both ends of the seminiferous tubules empty into the rete and this often appears to be a preferential site for germ cell degeneration and depletion for both spontaneous and chemically induced lesions. It is therefore an important site to sample, and routine sectioning should include at least part of the rete complex. In the dog the rete forms a central core that extends from the cranial surface to approximately two-thirds of the way towards the caudal tip and will be adequately sectioned with a midline transverse section. In the primate it is located in a peripheral position along the medial aspect for approximately half the medial border. Again it will be adequately sampled with a midline transverse section but a longitudinal sample needs to be specifically orientated to include it.

Efferent ducts. The efferent ducts link the rete testis with the ductus epididymis, which is a single, highly coiled duct, the convolutions of which form the caput, corpus, and cauda epididymis. The number and course of the efferent ducts vary with species. They are long and tortuous in rodents, extending up into the epididymal fat pad surrounding the caput epididymis; they are normally trimmed off and discarded when the epididymis is trimmed for weighing. In the dog and primate they are very short because the epididymis is more closely applied to the testis in these species; they are rarely sampled in routine studies but can be an important site for lesions. The efferent ducts in the dog are a frequent site for sperm granulomas because of the presence of numerous blind-ending tubules. Similarly in the rat, this may be the location of sperm granulomas that give rise to tubular dilation in the testes and absence or decreased sperm in the epididymis. More importantly, they have been shown to be a target site for a number of chemicals (Hess, 1998). Although it may not be practical to sample them in routine studies, their potential as a target site for toxicity or as a cause of secondary changes in the testes and epididymides should be appreciated.

Epididymides. The cellular composition and the function of the epididymis vary with region, and it is important that the different regions are sampled and examined. Routine sampling of the epididymis often only includes the cauda epididymis, but this precludes important information. There are a number of chemicals that have been shown to produce site-specific lesions to the epididymal epithelium, some in the caput, others in the cauda. An additional reason for sampling the entire epididymis is that the density of sperm and the presence of germ cells within the lumen of various segments of the epididymis reflect time-dependent events in the testis. For example, in the rodent, dog and primate sperm and cells present in the cauda epididymis were released from the testis ~2 weeks prior to their arrival there. The sperm in the caput epididymis reflect the release of sperm only days previously. Depending on the duration of the study, differential effects on the contents of the caput and cauda can provide important information on the timing of a toxic effect.

Prostate. The prostate of rodents is a heterogeneous gland with anatomically distinct ventral, dorsal, and lateral lobes (Fig. 16.3.2B). The histologic structure and the response to toxicants vary between lobes such that it is important to routinely sample as much as possible. A midtransverse section through the prostatic complex allows an adequate sample of all three lobes and often also includes the ampullary gland of the ductus deferens as it enters the prostatic urethra (Lee and Holland, 1987; Suwa et al., 2001). In the dog and the primate, the

glandular tissue is arranged circumferentially around the urethra, although in the primate it is only present on the posterior surface of the urogenital canal. In these species, a transverse section provides an appropriate sample for examination (Figs. 16.3.3B and 16.3.4B).

Seminal vesicles and coagulating gland. In rodents, a coagulating gland lies on the anterior aspect of each seminal vesicle. Both can be sampled by a cross-section. Similarly, a cross-section of the seminal vesicles in the primate provides adequate sampling. These organs are absent in the dog.

Choice of fixative

All of the recently revised regulatory guidelines for reproductive toxicity studies specifically recommend fixing the testes in Bouin's or a comparable fixative (Table 16.3.2). Implicit in this recommendation is that the use of formalin is avoided due to the excessive shrinkage of Sertoli cell and germ cell nuclei and cytoplasm, which occurs when formalin-fixed testes are embedded in paraffin. Although acceptable results can be obtained with formalin (Harleman and Nolte, 1997), Bouin's provides more reliable and consistent results. Testes fixed in Bouin's show greatly improved preservation of the nuclear and cytoplasmic features of Sertoli cells and germ cells, with very little shrinkage of the cells away from one another. However, due to its picric acid component, Bouin's has a number of drawbacks. It is potentially explosive, mutagenic, and possibly carcinogenic, presenting significant safety and disposal problems to laboratory personnel when used on a large scale. It also results in significant shrinkage of the tubules away from the interstitial tissue, especially in the center of the testis. Testes fixed with modified Davidson's fixative (see Basic Protocol 1) show comparable cellular and nuclear resolution with very little shrinkage of the germ cells and Sertoli cells. In addition, the tubules show significantly less shrinkage from the interstitial tissue than is seen with Bouin's. Interestingly, the problems with formalin fixation are associated with subsequent processing into paraffin wax, because formalin fixation of rodent testes followed by embedding in glycol methacrylate results in better preservation of structure than with Bouin's (Chapin et al., 1984). However, this does not hold true for all species and should be experimented with prior to use. For a detailed review of methods and the results that can be obtained using various combinations of fixatives, fixation methods, and embedding procedures for rodent testes, see Chapin et al. (1984), Russell et al. (1990), and Hess and Moore (1993).

Many of the difficulties associated with preserving the testes are due to the requirement to fix the tissue whole. This is necessary so that the architecture of the tubules and interstitial tissue is maintained and to prevent artifactual sloughing of germ cells. If the capsule is cut or removed, the tubules erupt and flow out of the holes. However, improved penetration of fixative can be achieved by pricking the capsule of rodent testes or making nicks in the capsule of dog or primate testes before immersing in fixative. (Large-animal testes have more fibrovascular stroma and are less likely to erupt than rodent testes.) If the pricks and cuts are made superficially and at a location distant from the area to be sampled, this will not disturb the architecture. Fixation quality can also be significantly improved if the testis is sliced after it has been partially fixed by immersion. Allow ≥4 to 5 hr (or overnight) before cutting the testis and then cut it in half or make 5-mm slices. Return to fixative to allow a total fixation time of 48 hr. Tissues should not be left in Bouin's or Davidson's for very much longer than 48 hr, otherwise they will harden and become difficult to section.

The Karnovsky's fixative recommended in Basic Protocol 2 and the subsequent postfixation in osmium tetroxide and potassium ferrocyanide are designed to give optimal fixation and staining of testicular structure for ultrastructural examination while minimizing osmotic artifacts. The high water content of testicular tissue and the distance of the seminiferous epithelium from the interstitial vasculature make fixation difficult and artifacts frequent. One of the most common artifacts seen is basal vacuolation of the seminiferous tubules. This is caused by the use of hyperosmotic fixative, which causes shrinkage of the cells in the basal compartment (below the level of the Sertoli cell tight junctions). Hyperosmotic fixatives will also cause artifactual condensation of Sertoli cell cytoplasm at the ultrastructural level. For ultrastructural studies it is therefore important to use approximately isotonic solutions and fixatives. The use of the osmium/ferrocyanide mixture as a postfixative is particularly good for membrane preservation, but it also has the advantage of improving the staining characteristics and resolution of Leydig cell structure at the ultrastructural level (Russell and Burguet, 1977). The choice of buffer for glutaraldehyde-based fixatives is a matter of personal prefer-

ence. Cacodylate buffer has been recommended in this protocol, but due to its toxicity and associated disposal problems, a phosphate buffer may be preferred as a substitute (Hess and Moore, 1993).

Perfusion

There are various techniques for perfusion fixation of tissues. The choice is largely a matter of personal preference and resource limitations. The procedure described in Basic Protocol 2 uses a peristaltic pump to perfuse the whole animal. This maintains a constant flow of fixative for a given speed of the pump, despite the increasing vascular resistance. A gravity-fed system can also be used, as described by Sprando (1990). This has the advantage of not requiring a peristaltic pump but has the disadvantage of requiring the fixative and saline bottles to be located some distance above the animal. With gravity-based perfusion, the flow rate also decreases as the vascular resistance increases.

Rather than perfuse the whole animal as described in this protocol, it is also possible to limit perfusion only to the abdominal tissues. Hess and Moore (1993) describe a method of cannulating the abdominal aorta via the left ventricle, which bypasses perfusion of the cranial and thoracic tissues. This conserves fixative, but the cannulation is slightly more technically demanding.

A critical step in the perfusion technique is the successful clearance of blood from the entire vascular bed. If vessels constrict or intravascular thrombi form, then the fixative will not be uniformly distributed. Clearance of the testicular vasculature appears to be particularly problematic. To overcome this problem, heparin and/or vasodilators have been employed. In this protocol the incorporation of both heparin and procaine in the flushing solution (Hess and Moore, 1993) has been recommended on the basis of a very good success rate combined with simplicity. However, Sprando (1990) suggests that the preinjection of animals with 130 to 150 IU heparin/kg body weight by intraperitoneal injection 15 min prior to perfusion improves the success rate without the need for additives to the perfusion fluids.

Anticipated Results

Using Basic Protocol 1, the quality of the paraffin sections of testes stained with periodic acid Schiff's stain/hematoxylin (PAS-H) will be suitable for detailed qualitative evaluation of spermatogenesis. Resolution and staining of the spermatid acrosome in rodent testes will be adequate to identify individual stages of the spermatogenic cycle. In dog and primate testes, the acrosome does not stain with PAS and cannot be adequately distinguished in paraffin-embedded sections. Therefore staging has to rely on the characteristics of the spermatocyte and round spermatid population in conjunction with the shape and position of the elongating spermatid population. Cytoplasmic and nuclear detail of the germ cells, Sertoli cells, and Leydig cells will be suitable for detecting early degenerative changes. Although quantitative procedures, such as cell counting and measuring tubular diameters is possible, it is better carried out on resin-embedded tissue where section thickness is more consistent and nuclear chromatin resolution is improved.

Longitudinal sections through the epididymis will provide information on the cellular morphology of the entire length of the coiled epididymal duct and of the relative sperm and cell content of the ductular lumen. In the dog and primate, the longitudinal section of the epididymis may also include some of the efferent ducts. The transverse section through the rodent prostate should provide comparative morphology of the dorsolateral lobes and ventral lobes of the tissue and may also include cross-sections of the vas deferens and of the associated ampullary gland of the vas. The secretory products of the various lobes and of the ampullary gland have different affinities for eosin. The differential staining pattern can be used to identify various regions (Lee and Holland, 1987; Yuan et al., 1987). In the dog and the primate, the prostatic acini should appear more or less homogeneous with no regional variation.

Using Basic Protocol 2, perfusion fixation should provide tissue with a minimum of artifacts. All interstitial capillaries should be open and empty of erythrocytes. There should be no shrinkage of tubules away from the interstitial tissue and no shrinkage of germ cells away from Sertoli cells. Vacuoles between adjacent Sertoli cells should be minimal or nonexistent and there should be no sloughing of germ cells into the tubular lumen. When viewed by electron microscopy, the morphology of the smooth endoplasmic reticulum and mitochondria in the basal Sertoli cell cytoplasm are good indicators of fixation quality. Toluidine blue–stained resin sections can be used to distinguish the spermatid acrosome in all species including the dog, although the thinness of the section results in many acrosomes being incompletely sectioned

or out of the plane of section. Glycol methacrylate–embedded, immersion-fixed tissue generally results in less tubular and cellular shrinkage than paraffin-embedded tissue and shows improved resolution of nuclear and cytoplasmic features. It too suffers from reduced numbers of complete acrosomes in the plane of section.

Time Considerations

Immersion fixation and embedding tissue in paraffin wax is the most economical methodology in terms of time and cost. Because all the procedures are more or less standard routine for a histology laboratory, the processing, embedding, and staining is largely automated. Overall time depends on the number of tissues sampled and weighed from each animal and the number of animals processed. For a routine study size (e.g., two to five treatment groups, each with five to ten animals), allowing 48 hr fixation time plus ~1 day processing and embedding into paraffin and 1 day sectioning and staining, sections could be ready for evaluation within a week.

Processing for glycol methacrylate can also be automated using routine, paraffin-embedding processors up to the point of resin infiltration. Processing for epoxy resin can be automated through to the point of embedding, but this requires a purpose-designed machine to handle the small tissue size and the viscuous resin mixtures. The alternative is to carry out the procedure in individual bottles, carefully draining and filling each with new solution. Embedding in resin requires special molds and special polymerization conditions and can take up to 48 hr for adequate polymerization. Sectioning of resin blocks requires the use of a special, automated microtome that uses prepared glass or tungsten carbide knives and is a technically demanding procedure requiring at least 1 to 2 days training and several days practice to become proficient. With glycol methacrylate, consistent polymerization of the resin and control of the relative hydration of the resin during sectioning can also add to the difficulty and the time taken to produce acceptable sections. Overall, the size of the tissue block and the proficiency and experience of the technician will determine the time taken to prepare adequate resin sections, but, as a guide, it probably takes at least twice to three times longer to prepare a 2- to 3-µm resin section than it does to prepare a paraffin section.

The duration of the perfusion means that this is also a time- and labor-intensive technique. If large numbers of animals are to be fixed by this method, multiple perfusion stations are required, and animals must be staggered through the various procedures. With three perfusion stations and two people carrying out the perfusions, it is feasible to complete 20 animals in a normal working day. (Sprando, 1990).

Literature Cited

Bancroft, J.D., Stevens, A., and Turner, D.R. 1990. Theory and Practice of Histological Techniques, 3rd ed. Churchill Livingston, New York.

Chapin, R.E., Ross, M.D., and Lamb, J.C. 1984. Immersion fixation methods for glycol methacrylate-embedded testes. *Toxicol. Pathol.* 12:221-227.

Environmental Protection Agency (EPA). 1998 Health Effects Test Guidelines, Report No. OPPTS 870.3800, Reproduction and Fertility Effects. pp. 1-12. EPA 712-C-98-208. Office of Prevention, Pesticides and Toxic Substances (OPPTS), U.S. EPA, Washington, D.C.

Evans, H.E. 2000. Guide to the Dissection of the Dog, 5th ed. W.B. Saunders, Philadelphia.

Feldman, D.B. and Seeley, J.C. 1988. Necropsy Guide: Rodents and the Rabbit. CRC Press, Boca Raton, Fla.

Frederick, P.M. and Doorn, L.G. 1973. A technique for perfusion of rat testis in situ through internal spermatic arteries. *J. Reprod. Fertil.* 35:117-121.

Harleman, J.H. and Nolte, T. 1997. Testicular toxicity: Regulatory guidelines—the end of formalin fixation? *Toxicol. Pathol.* 25:414-417.

Hayat, M.A. 1989. Principles and techniques of electron microscopy: Biological applications, 3rd ed. CRC Press, Boca Raton, Fla.

Hess, R.A. 1998. Effects of environmental toxicants on the efferent ducts, epididymis and fertility. *J. Reprod. Fertil. Suppl.* 53:247-259.

Hess, R.A. and Moore, B.J. 1993. Histological methods for evaluation of the testes. *In* Methods in Toxicology, Vol. 3, Part A. Male Reproductive Toxicology (R.E. Chapin and J.J. Heindel, eds.) pp. 86-94. Academic Press, San Diego.

International Conference on Harmonization of Technical Requirements for Registration of Pharmaceuticals for Human Use (ICH). 1994. Tripartite Harmonized ICH Guideline S5A: Reproductive Toxicology: Detection of toxicity to reproduction for medicinal products/CPMP/ICH/386/95. *Fed. Regist.* 59:48746-48752.

International Conference on Harmonization of Technical Requirements for Registration of Pharmaceuticals for Human Use (ICH). 1996. Tripartite Harmonized ICH Guideline S5B: Reproductive Toxicology: Male fertility studies/CPMP/ICH/136/95. *Fed. Regist.* 61:15360.

Lee, C. and Holland, J.M. 1987. Anatomy, histology and ultrastructure, prostate, rat. *In* Monographs on Pathology of Laboratory Animals: Genital System (T.C. Jones, U. Mohr, and R.D. Hint, eds.) pp. 239-251. Springer-Verlag, New York.

Organization for Economic Cooperation and Development (OECD). 1995. Reproduction/developmental toxicity screening test. *In* Guideline for Testing of Chemicals, No. 421 (adopted July 27, 1995) pp. 1-10. OECD, Paris.

Organization for Economic Cooperation and Development (OECD). 2001. Proposal for updating Guideline 416: Two generation reproduction toxicity study. *In* Guideline for Testing of Chemicals, No. 416 (adopted January 22, 2001) pp. 1-13. OECD, Paris

Russell, L. and Burguet, S. 1977. Ultrastructure of Leydig cells as revealed by secondary tissue treatment with a ferrocyanide-osmium mixture. *Tissue Cell* 9:751-766.

Russell, L.D., Ettlin, R., Sinha Hikim, A.P., and Clegg, E.D. 1990. Tissue Preparation for Evaluation of the Testis. *In* Histological and Histopathological Evaluation of the Testis (L.D. Russell, R. Ettlin, A.P. Sinha Hikim, and E.D. Clegg, eds.) pp. 195-209. Cache River Press, Clearwater, Fla.

Sprando, R.L. 1990. Perfusion of the rat testis through the heart using heparin. *In* Histological and Histopathological Evaluation of the Testis (L.D. Russell, R. Ettlin, A.P. Sinha Hikim, and E.D. Clegg, eds.) pp. 277-280. Cache River Press, Clearwater, Fla.

Suwa, R., Nyska, A., Peckham, J.C., Hanley, J.R., Mahler, J.F., Haseman, J.K., and Maronpot, R.R. 2001. A retrospective analysis of background lesions and tissue accountability for male accessory sex organs in Fisher-344 rats. *Toxicol. Pathol.* 29:467-478.

Yuan, Y.D., Ulrich, R.G., and Carlson, R.G. 1987. Histology and ultrastructure, glands of the ductus deferens (ampullary gland), rat. *In* Monographs on Pathology of Laboratory Animals: Genital System. (T.C. Jones, U. Mohr, and R.D. Hint, eds.) pp. 229-234. Springer-Verlag, New York.

Key References

Hess, R.A. and Moore, B.J. 1993. See above.

Provides a detailed comparison of the results achieved using different combinations of fixatives and embedding procedures to examine the testes. Also provides technical details for perfusion fixation and subsequent processing and embedding in resin for light and electron microscopy.

Russell et al., 1990. See above.

Provides various protocols for fixation, tissue processing, and staining of the testis and discusses the advantages and disadvantages of various methods.

Sprando, R.L. 1990. See above.

Provides detailed technical guidance on the art of perfusion fixation for the testes.

Contributed by Dianne M. Creasy
Huntingdon Life Sciences
East Millstone, New Jersey

Histopathology of the Male Reproductive System II: Interpretation

Toxicants can affect the male reproductive system at a broad range of target sites including the testis, epididymis, secondary sex organs, and the neuroendocrine/CNS regulatory system. No single endpoint can adequately reflect changes at such a diversity of sites, but it has been repeatedly demonstrated that histopathologic evaluation represents the most sensitive and reliable indicator of toxicologic disturbance in the tract as a whole (Linder et al., 1992; Ulbrich and Palmer, 1995). This is only true if the appropriate tissues have been taken and have been fixed and sampled in such a way that subtle or localized changes are adequately preserved and presented to the pathologist for examination. These preparative procedures are dealt with in *UNIT 16.3*. Even if material has been appropriately fixed and sampled, it is incumbent on the pathologist to have an adequate understanding of the organization and dynamics of spermatogenesis in the species under investigation. Without this, lesions will be missed or the significance of findings will be misinterpreted. Although it is beyond the scope of this unit to provide this knowledge, an attempt is made to illustrate why and when such knowledge is essential.

Once identified, interpretation of the significance of the findings to overall reproductive function and their implications for functional or morphological changes in the rest of the reproductive tract relies on a basic knowledge of reproductive physiology. Some examples of common chemically induced findings in the reproductive tract, their possible etiology, and their likely functional significance are provided. The pattern of morphological change as well as the specificity and severity of the findings are significantly influenced by the duration of dosing, such that the approach to examination is different in a short-term versus a long-term study. This unit includes a section providing practical guidance on how to evaluate testicular and epididymal sections for evidence of a chemically induced effect, including what to look for and how hard to look for it. This involves using knowledge of staging to identify when cells are missing or when cells are inappropriately present.

Terminology of findings and how to grade severity is a unique problem in the testis; whether to grade on the basis of number of germ cells affected, number of tubules affected, or both; whether to use broad terminology such as tubular atrophy and tubular degeneration, or to use specific terminology that differentiates between effects on specific types of germ cells and their stage localization. The decision is strongly influenced by the type of study and the specificity of the present findings.

As with the toxicological evaluation of any tissue, the species, age, and history of spontaneous pathology need to be taken into account. These factors are particularly important with respect to the testis because, in some species, such as dog, the relatively high incidence of spontaneous degenerative lesions, confounded by the small group size of animals used can provide difficult data for interpretation. In addition, the use of immature or borderline mature animals, which is the case for some regulatory studies, can mask or be mistaken for toxicologically induced lesions. It is important that these limitations are realized. Most of the discussion in this unit relates to the rat because this is the most commonly used species in toxicological research. It is also the species for which most information is available. Other species are specifically mentioned where appropriate.

ESSENTIAL KNOWLEDGE FOR EVALUATION AND INTERPRETATION OF TESTICULAR PATHOLOGY

Spermatogenesis and the Spermatogenic Cycle

The process and regulation of spermatogenesis is essentially similar in all mammalian species. Stem cell spermatogonia proliferate by mitosis and produce a population of differentiating or committed spermatogonia. These in turn divide and produce spermatocytes, which undergo DNA replication and divide by meiosis to produce haploid spermatids. A complex series of morphological transformations of the simple round spermatid finally produces a differentiated sperm, which is released into the tubule lumen and transported on into the epididymis. In the rat, the whole process takes ~56 days with spermatogonial divisions taking ~2 weeks, spermatocyte meiosis lasting >3 weeks, and spermatid development also requiring ~3 weeks. The arrangement of the different

Contributed by Dianne M. Creasy
Current Protocols in Toxicology (2002) 16.4.1-16.4.14

populations of germ cells within the seminiferous tubule is also similar between species, with Sertoli cells providing a supporting structural framework for discrete layers of the different germ cell types. Spermatogonia are always at the base of the tubule and progressively more mature germ cells are found in layers moving toward the lumen. In all species, 3 or 4 generations of germ cells are developing within a tubule at any given time. The development of each of these generations occurs in synchrony with each other, giving rise to specific and predictable cellular associations (Fig. 16.4.1). The complete sequence of cellular associations is referred to as the cycle of spermatogenesis while the individual cell associations form the stages of the cycle. Each stage is therefore defined by its germ cell complement and consequently, identifying the stage defines what cells should be in that tubule (and what cells are missing). In order for a pathologist to detect subtle changes in germ cell loss or, in the case of spermatid retention, the inappropriate presence of a population of germ cells, a thorough understanding of the cellular makeup of the spermatogenic cycle is essential.

Species-Specific Variations in the Organization of Spermatogenesis

Although the fundamentals of the spermatogenic cycle are similar between species, there are certain details that vary. These can have a significant impact on histopathologic evaluation.

Number of stages

The number of stages and their cellular makeup varies between species and depends on the morphological criteria used by the classification system. It is important that the pathologist is familiar with the germ cell development and the stage map of the species under investigation. A highly recommended text that explains in detail how to stage tubules in a number of common species and provides stage maps for each species is provided by Russell et al. (1990).

Duration

The duration of spermatogenesis (the time taken for a spermatogonium to develop into sperm) and the duration of the spermatogenic cycle (the time taken to complete a cycle of cell associations) varies between species. This information is important so that the pathologist can predict how long it should take for any particular cell to reach a later cell type (e.g., if a toxicant affects leptotene spermatocytes, how long will it take before the animal becomes infertile?). Alternatively, if a particular cell type is missing at some defined period after dosing, knowing the dynamics of the spermatogenic cycle will allow extrapolation as to what stage of development that cell was in when dosing began. Software programs have also been developed to calculate this type of information (Hess and Chen, 1992).

Cell associations

The organization of cell associations along the length of the tubule is linear for most mammalian species, including most species of monkey used in toxicological studies. This means that a tubular cross section normally contains only one cell association and that the adjoining length of tubule (which is often the adjacent tubule in a cross section of testis) will generally contain the consecutive stage. This is not the case in humans where cell associations are arranged in a helical pattern resulting in a mosaic of cell associations in a single cross section. In dogs, although only one stage is present in a cross section, adjoining lengths of tubule do not necessarily contain consecutive stages.

Disturbances in Spermatogenesis

Almost regardless of the cellular target of toxicity within the reproductive system, the most common morphological consequence of injury is a disturbance in spermatogenesis. This is because spermatogenesis is dependent on, or sensitive to, functional perturbations in most other parts of the reproductive tract. Spermatogenic disruption may reflect a direct effect on the seminiferous epithelium, affecting either the Sertoli cell or any one of the germ cell populations, or it may occur as a secondary response to altered hormone levels, altered vascular supply or altered fluid balance, either within the testis or within the epididymis. It is therefore extremely important that disturbances in spermatogenesis are detected. The pattern of disturbance can be very specific and diagnostic of the mechanism of toxicity, but generally, this is only seen during the early development of the lesion. With longer periods of dosing, the development of maturation depletion (whereby death of a specific precursor germ cell causes the progressive loss of its descendant generations), reduces the specificity of the pattern of spermatogenic disturbance as the tubules become depleted of more and more germ cells.

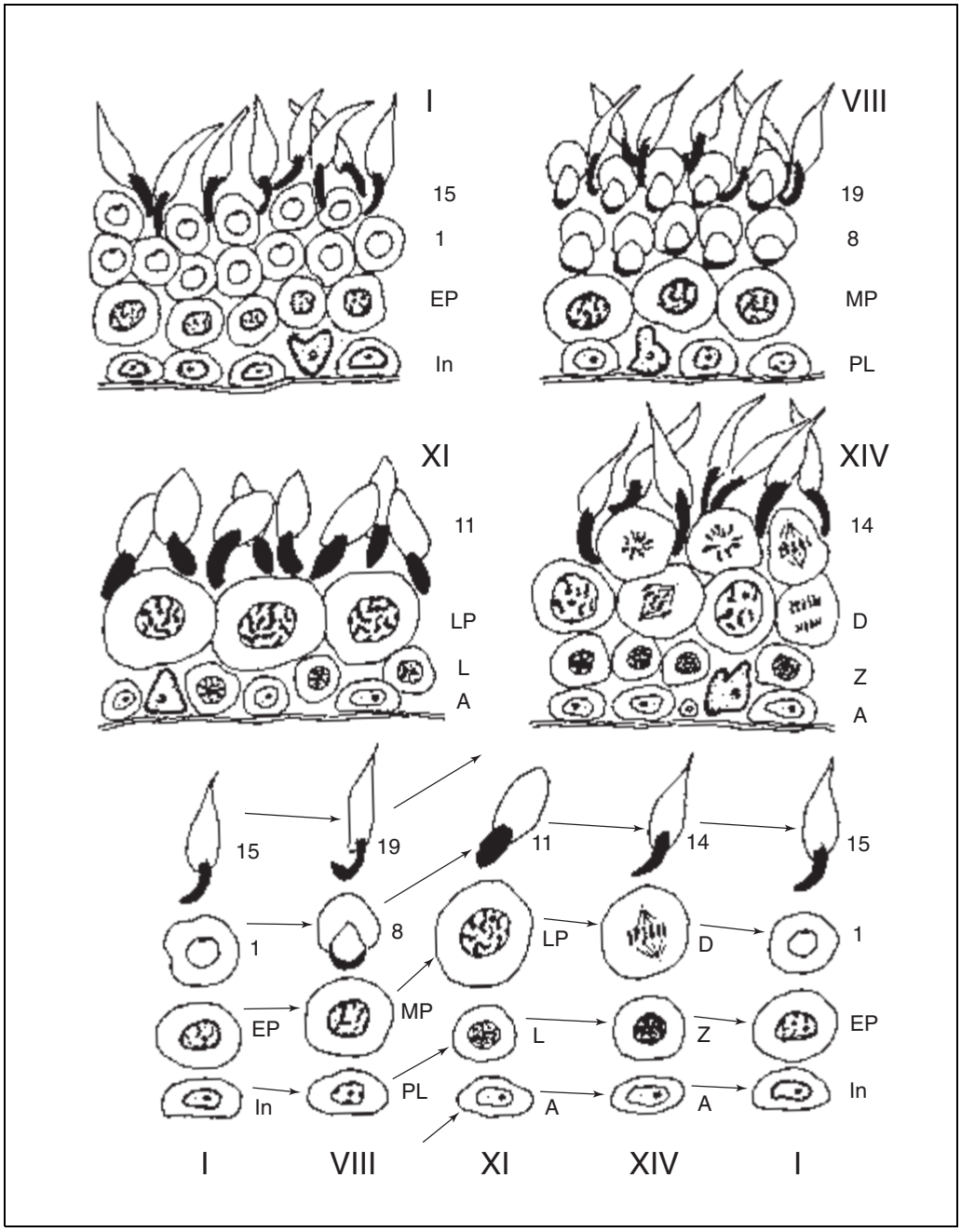

Figure 16.4.1 Stages of the spermatogenic cycle of the rat. Cell associations for 4 of the 14 stages of the spermatogenic cycle of the rat (stages I, VIII, XI, XIV). *Spermatogonia*: A, type A; In, intermediate; *Spermatocytes*: PL, preleptotene; L, leptotene; Z, zygotene; EP, early pachytene; MP, mid pachytene; LP, late pachytene; D, dividing. *Spermatids:* 1, 8, 11, 14, 15, and 19 indicates steps 1 to 19 of spermatid development. The tubular cross sections (stages I, VIII, XI, and XIV) show the arrangement of cells within the seminiferous epithelium. The columns of cells at the base of the figure show the maturation of the cells during one spermatogenic cycle. Each generation of cells develops sequentially. During stage VIII, the mature step 19 spermatids are shed into the lumen (arrows) while a new generation develops from stem cell spermatogonia. As spermatocytes undergo meiotic division (D) in stage XIV, they produce step 1 spermatids and the cell association returns to stage I to begin another cycle. (Reproduced from Creasy, 1997, with permission.)

Table 16.4.1 Specific EPA and OECD Recommendations for Histopathological Examination of the Testes and Epididymides in Studies to Detect Effects on Reproduction and Fertility

Testis	Epididymis
Detailed histopathological examination of testes should be conducted in order to identify treatment-related effects such as:	Examination of the intact epididymis should include the caput, corpus, and cauda. The epididymis should be evaluated for:
Retained spermatids	Leukocyte infiltration
Missing germ cell layers or types	Sperm granulomas
Multinucleate giant cells	Change in prevalence of cell types
Sloughing of spermatogenic cells into the lumen	Absence of clear cells in the cauda epithelium
	Aberrent cell types in the lumen
	Phagocytosis of sperm

Regulatory Guidelines and the Role of "Staging" in Histopathologic Examination of the Testis

Recently revised regulatory guidelines have placed increased emphasis on the importance of histopathology for detecting toxicological effects in the male reproductive system. Recommendations have been made, not only for fixation and staining procedures but also for the microscopic examination of tissues, providing examples of findings that should be recorded (Table 16.4.1). During the drafting of these guidelines, there was much discussion relating to the subject of "staging" of testes, and although there is no mention of staging in the final issued guidelines, the issue has become surrounded by confusion. The ability to recognize stages of the spermatogenic cycle is important in order for the pathologist to recognize when cells are missing or are inappropriately present. Due to the lack of understanding of this concept, there has been a move to expect the pathologist to produce a quantitative assessment of stages—e.g., a frequency distribution of tubules for individual stages of the spermatogenic cycle. While this may be useful information in an investigative study to determine whether the dynamics of the spermatogenic cycle have been disturbed (Hess, 1990), it is inappropriate to carry out in a regulatory study, which is designed as a screening study to detect effects on spermatogenesis. Knowledge of staging should be used in a qualitative way to evaluate the normality of the cellular makeup of the seminiferous tubules. In other words, the testis should be examined with an understanding of the normal progression of the stages of the spermatogenic cycle. This approach is explained below. For a more detailed discussion of this issue see Creasy (1997) and Chapin and Conner (1999).

COMMON TOXICOLOGICALLY INDUCED FINDINGS AND THEIR POSSIBLE SIGNIFICANCE

As with any tissue, the cellular response to injury is limited and at times, nonspecific. However, certain aspects of the early pathogenesis of toxicologically induced lesions in the testis and accessory tissues can provide important information on the mechanism of injury. Additional information can be found in Nolte et al. (1995), Creasy (2001), and Creasy and Foster (2001).

Testes

Germ cell degeneration/multinucleate aggregates

Whether spontaneous or induced, death of germ cells appears to occur predominantly through apoptosis, a process that is closely regulated by the Sertoli cell (Lee et al., 1997, 1999). This is particularly true for spermatogonia, which may be seen apoptosing in occasional stage XII tubules. However, many of the dying cells do not have the classic morphological appearance of apoptotic cells. Dying spermatocytes generally develop cytoplasmic eosinophilia and nuclear pyknosis while round spermatids show chromatin margination. If cell death progresses rapidly, then the apoptotic cell is rapidly phagocytized by the surrounding Sertoli cell cytoplasm and all evidence of cell death is rapidly removed. Cell death and phagocytosis of the remains can be complete within 24 hr, so if the process is not examined during this time span, the only evidence of cell death will be an absence of the cell (cell depletion). If the degenerative process is slow, then adjacent germ cells belonging to the same cohort, may form a multinucleate syncitium (symplast, multinucleate giant cells) probably due to the

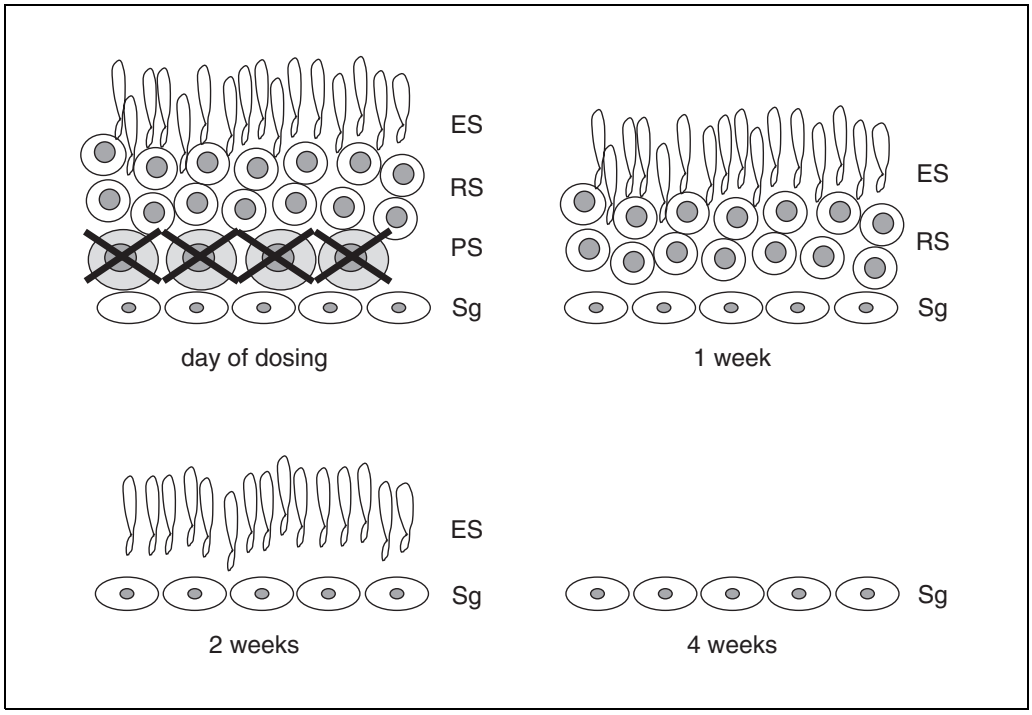

Figure 16.4.2 Development of maturation depletion following daily dosing with a spermatocyte toxicant. Time-dependent progression of maturation depletion following cell-specific damage to pachytene spermatocytes (PS). If the tubule is examined on the day of dosing, spermatocyte degeneration and necrosis will be seen (top left). Phagocytosis of the necrotic cells by Sertoli cells results in their rapid disappearance and because dosing continues, newly formed pachytene spermatocytes will also be killed. Examination of the same stage tubule after 1 week of dosing (top right) will reveal an absence of pachytene spermatocytes. After 2 weeks of dosing (one spermatogenic cycle duration) pachytene spermatocytes will still be missing but round spermatids will also be absent because their precursor cells were destroyed in the previous cycle (bottom left). Similarly, after 4 weeks of dosing (bottom right), pachytene spermatocytes, round spermatids, and elongated spermatids will be absent, leaving only spermatogonia. This progressive loss of subsequent germ cells following injury to a previous cell type is termed maturation depletion. ES, elongated spermatids; RS, round spermatids; PS, pachytene spermatocytes; Sg, spermatogonia. (Reproduced from Creasy, 1997, with permission.)

breakdown of the cytoskeletal fibers supporting the interconnecting cytoplasmic bridges. Multinucleate aggregates are less readily phagocytized by Sertoli cells and are present for longer periods and therefore more frequently seen. They are most often composed of round spermatids, but can also be formed by fusion of neighboring spermatocytes or elongating spermatids.

Germ cell depletion

This is the most common sequel to spermatogenic disturbance and is generally a consequence of germ cell death rather than exfoliation. It may be seen as a generalized or partial depletion of the germ cells or it may only affect a specific cell type (e.g., spermatogonia). Sometimes a specific cell type within specific stages may be affected (e.g., pachytene spermatocytes in stages XII and XIII). Once the cell has been phagocytized, the only way of recognizing the lesion is by the abnormal cellular association of individual stages of the spermatogenic cycle and the progressive development of maturation depletion with time (Fig. 16.4.2). The appearance of the testis, in terms of what cells are missing, will depend largely on how severe the initial effect was and how long after dosing the testis is examined.

Instead of a specific cell type being killed, a focal cohort of cells within a tubule may be affected and result in a focal "blow out" of the epithelium. This may be due to an effect on a few adjacent spermatogonia, which then fail to produce their cohort of spermatocytes and spermatids, or on one or two Sertoli cells, which are then unable to support spermatogenesis.

Partial or generalized germ cell depletion may affect only a small number of tubular profiles or a large proportion of the tubules. When only a few scattered tubules are affected, it is not possible to determine whether they

represent multiple convolutions of the same tubule or focal segments of multiple affected tubules. Prolonged dosing with a number of testicular toxicants may cause generalized germ cell depletion, affecting a large proportion of the tubules. It generally represents an advanced or end-stage lesion, and in order to elucidate the primary target cell, a time course study needs to be carried out.

It is not possible to say whether spermatogenic depletion is or is not reversible without carrying out an appropriate study. If spermatogonia are still present, then the lesion is potentially reversible but if the Sertoli cells are functionally compromised, spermatogenesis may not be supportable. The chronic effects of 2,5-hexanedione on the rat testis exemplify this. Although spermatogonia remain and are seen to divide, spermatogenesis does not recover. This is thought to be due to the inhibition of a critical Sertoli cell factor (Blanchard et al., 1998). Conversely, spermatogonia may be significantly depleted, but if the Sertoli cells are functionally intact and sufficient time is allowed for stem cell renewal and repopulation (and this may require several spermatogenic periods), substantial recovery may be seen (Meistrich, 1986).

Germ cell exfoliation

Loss of adhesion between Sertoli cell and germ cell, or shearing of Sertoli cell cytoplasm (as seen with cytoskeletal disrupting agents) will result in exfoliation of germ cells into the lumen of the seminiferous tubule and subsequent transport of the cells to the rete testis and the epididymis. The exfoliated cells may appear morphologically normal but are rapidly removed from the testis. Once the cells have been removed, cell depletion is the only recognizable finding. Lumenal germ cells may also be present as a result of handling trauma at necropsy. Care must be taken to distinguish between real and artifactual exfoliation (Foley, 2001). Abnormal residual bodies shed into the lumen can sometimes be mistaken for exfoliated germ cells. These generally occur as a result of disturbances in spermiation (see below).

Tubular vacuolation

Vacuolation within or between Sertoli cells is a common early sign of Sertoli cell damage. The vacuoles may be solitary and situated amongst the germ cells at varying depths throughout the epithelium. It is generally not possible by light microscopy to determine whether they are intra- or extra-cellular. In other cases, intracellular microvacuolation or swelling may be seen affecting the basal area of the Sertoli cell cytoplasm and causing germ cell displacement and disorganization. Such findings are suggestive of disturbances within the Sertoli cell and may represent alterations in the smooth endoplasmic reticulum or in fluid homeostasis. Vacuolation may also be seen in end-stage lesions, associated with extensive germ cell loss. In this situation, it should not be regarded as a primary effect on the Sertoli cell.

Occasional solitary vacuoles are sometimes seen in tubules from normal testes but these are generally few in number. Vacuoles in the basal compartment of the tubule, surrounding spermatogonia are generally fixation-induced artifacts due to osmotic shrinkage.

Tubular contraction

Reduction in the overall diameter of the seminiferous tubule will occur as a result of germ cell depletion and/or as a result of reduced secretion of seminiferous tubule fluid. Seminiferous tubule fluid is secreted by the Sertoli cell and maintains the lumenal size, which varies with the stage of spermatogenesis. This is an androgen-dependent function of the Sertoli cell and will be affected by altered testosterone secretion. Another major regulatory factor for fluid secretion is the presence of elongating and elongated spermatids. Therefore, if these cells are depleted, fluid production and consequently lumenal size are decreased. Germ cell loss and decreased fluid will have a significant effect on testis weight.

Tubular dilatation

Dilatation of the tubular lumen will occur as a result of increased lumenal fluid volume. This can occur through increased secretion by the Sertoli cell or decreased expulsion of fluid from the tubule, which is thought to be a function of the contractile peritubular cells. Also decreased resorption of fluid by the epithelial cells of the rete and efferent ducts or obstruction of the outflow (e.g., a sperm granuloma) can cause increased tubular fluid. The increased fluid volume will generally be reflected by an increased weight of the testis unless there is an accompanying significant cell loss. The pathological consequences of the finding depend on the severity and duration of the effect. Prolonged increased pressure on the seminiferous epithelium will generally result in pressure atrophy of varying degrees and may also lead to inspissated sperm and granulomatous inflammation.

Spermatid retention

This is a subtle but relatively common finding that may be caused by a number of chemicals as well as by hormonal disturbance. It is characterized by the retention of step 19 spermatids (which should be released during stage VIII) through stages VIII to XII. The position of the retained spermatids varies with different chemicals. In some cases, e.g., boric acid (Chapin and Ku, 1994), the retained spermatids remain in a predominantly lumenal position through stages VIII to XI and are then pulled down into the basal cytoplasm of stage XII tubules where they are phagocytized. With other chemicals the step 19 spermatids are rapidly pulled down into the basal cytoplasm and phagocytized during stages VIII to XI, leaving very few in a lumenal position. The formation and behavior of the residual bodies is often also disturbed with residual bodies of abnormal shape and size being seen in the tubular or epididymal lumen. Descent and phagocytosis of residual bodies normally occurs during stages IX to XI but in cases of spermatid retention this may be delayed into stage XII. The pathological significance of spermatid retention can be varied. It is often associated with abnormal sperm parameters (number, motility, or morphology) and it may be associated with alterations in fertility parameters. If homogenization resistant spermatids are measured, the retained spermatids should be reflected by an increase in this parameter. However, identification by histopathology is a much more sensitive endpoint since it can detect very small numbers of phagocytized spermatids.

Tubular necrosis

While germ-cell necrosis proceeds by apoptosis, tubular necrosis is characterized by coagulative (oncotic) necrosis of Sertoli and germ cells. Sertoli cells are normally highly resistant to cell death even though they may be very sensitive to functional perturbations. Consequently, they are often the only cell left lining severely damaged tubules (Sertoli cell–only tubules). Ischemia is one of the few situations where they are killed. The effects of this can be seen with cadmium toxicity, which damages the testicular capillary endothelium. It can also be seen following administration of vasoactive compounds such as serotonin. Necrosis and loss of the Sertoli cells from tubules is the major characteristic of the lesion, and this is associated with gross disorganization and necrosis of the germ cells as well as stasis of sperm in the tubular lumen. Due to the loss of the Sertoli cell blood-tubule barrier, the changes are also accompanied by an inflammatory infiltrate, which is an otherwise rare accompaniment to toxic injury. Tubular necrosis is a serious irreversible lesion because Sertoli cells are unable to proliferate and the affected tubules are likely to involute and be replaced by scar tissue.

Dilated rete

Both ends of the seminiferous tubules empty into the rete. Most of the tubule fluid is reabsorbed in the epithelium of the rete and efferent ducts. If there is an obstruction in the efferent ducts or in the epididymis, the fluid back-pressure will cause the rete to dilate and if the obstruction is severe, the back pressure will progressively dilate the seminiferous tubules. The tubules in the area of the rete also appear to be a preferential location for some testicular toxicants, but this should not be confused with the transitional tubuli rectii that join the seminiferous tubules to the rete and can be mistaken for depleted tubules.

Leydig cell atrophy/hypertrophy/ hyperplasia/adenoma

Testosterone secretion is the major function of the Leydig cell and the abundance of smooth endoplasmic reticulum in the cell reflects this activity. Increased stimulation by luteinizing hormone results in functional hypertrophy and hyperplasia. With prolonged gonadotropin stimulation in the rat, Leydig cell hyperplasia will usually progress to adenoma formation. Many classes of compounds with diverse chemical structures have been shown to produce this effect in the rat but the significance to man is considered limited (Clegg et al., 1997). Decreased secretion of testosterone, whether through inhibition of biosynthesis or decreased gonadotropin stimulation, will lead to atrophic changes in the Leydig cell.

Recognition of atrophy, hypertrophy, and hyperplasia on a qualitative basis is not easy unless the changes are marked. Contraction of tubules due to cell loss will result in an apparent increase in the volume of the interstitial space. This may or may not be contributed to by a real increase in size and number of Leydig cells, but quantitative analysis may be necessary to separate real from apparent effects.

Epididymis

Lumenal germ cells/debris

Cells and residual bodies exfoliated from the testis will be transported into the epididymis.

This can serve as useful confirmatory evidence for changes seen in the testis. It can also alert the pathologist to changes that may have been overlooked in the testis. Occasional exfoliated germ cells are sometimes seen in normal animals, and in immature and peripubertal animals this number is significantly increased. Abnormal residual bodies may also be detected in the epididymis as a consequence of disturbed spermiation in the testis. The presence or absence of germ cells in the luminal contents can also aid the pathologist in evaluating whether apparently exfoliated germ cells in the lumina of seminiferous tubules are real effects or artifacts of trimming; such artifacts will not be present in epididymal lumena.

Epithelial vacuolation

Microvacuolation of the epididymal epithelium can be seen as a specific chemically induced finding. Macrovacuolation and cribriform change (infolding of the epithelium within itself) is often seen accompanying contraction of the atrophic aspermic epididymis. This may represent a normal mechanism of surface area reduction but has also been reported as a toxicologic change (Foley, 2001). Epithelial vacuoles are also sometimes seen as a normal finding in some species at the junction of the corpus and cauda. Since fluid absorption and secretion are both major functions of the epididymal epithelium, vacuolation is a likely sequel to disturbance of either function.

Epithelial inflammation and sperm granuloma

The antigenically foreign sperm in the epididymal lumen and in the seminiferous tubule are in an immunologically protected environment. The protection is afforded by the lumenal tight junctions between epithelial cells in the excurrent ducts and by the basal occlusive junctions between Sertoli cells in the testis. If these barriers are damaged, then an inflammatory response against the sperm develops and generally progresses to form a sperm granuloma. This is a chronic, progressive lesion and in the coiled epididymal duct has the added complication of causing obstruction to the passage of sperm. Furthermore, the oxidative free radicals produced by inflammatory cells in contact with sperm can lead to genotoxic damage, which may have implications for male-mediated congenital defects and post-implantation losses (Chellman et al., 1986). The efferent ducts, which join the caput epididymis with the rete testis, are a particular site for damage. Certain chemicals, e.g., carbamates, cause sperm stasis and inflammation of these ducts resulting in partial or complete obstruction to sperm transit and secondary dilatation of seminiferous tubules. The mechanism may be through increased fluid absorption resulting in sperm stasis and inflammation (Hess, 1998). The efferent ducts are also a frequent site for the occurrence of spontaneous sperm granulomas. In species such as the dog, they often form blind ending tubules that contain inspissated sperm, which can develop inflammation and progress to sperm granulomas.

Ductular dilatation/interstitial edema

This can occur as a result of fluid imbalance mediated through the vasculature or inhibited fluid reabsorption by the epithelial cells. Inflammatory infiltrate and sperm granulomas are a frequent consequence.

Prostate/Seminal Vesicles

Acinar atrophy

Secretory activity by the prostate and seminal vesicles is a sensitive, androgen-dependent function. Decreased circulating testosterone levels, or interference with androgen receptors in these two tissues will result in reduced secretion leading to atrophic changes. These may be detected by organ weight changes as well as by microscopic changes

PRACTICAL APPROACH FOR EXAMINATION OF THE TESTIS AND EPIDIDYMIS FOR TOXICOLOGICAL EFFECTS

The approach used is influenced by the duration of the study. Cell- and stage-specific disturbances in spermatogenesis are usually only seen in short duration studies of <28 days. As discussed above, the kinetics of spermatogenesis combined with the process of maturation depletion, result in a progressive, germ cell loss, which becomes more generalized and affects more stages of spermatogenic cycle the longer dosing continues. Table 16.4.2 provides a rapid reference guide to common changes and their possible etiologic significance.

1. Review the testis and epididymis weights. Absolute weights are generally more useful than relative values because testis, like brain weight, is less influenced by body weight than most other tissues. A decrease in testis weight generally reflects germ cell loss and decreased tubule fluid production, while a decreased epididymal weight is likely to reflect

decreased sperm and fluid content. An increased weight in either tissue generally reflects increased fluid content, which is either interstitial or tubule fluid. Increased interstitial fluid will be seen as edema and suggests a vascular-mediated lesion while increased tubule fluid will be reflected by dilated tubular or ductal lumen size. There are various possible reasons for this (see Common Toxicologically Induced Findings and Their Possible Significance).

2. If testicular homogenization-resistant spermatids (HRS) and/or epididymal sperm have been counted, review these data. A decrease in HRS indicates a reduced number of elongated spermatids. This could be due to a direct effect on these cells or due to maturation depletion following effects on an earlier cell type (the answer should be apparent by histopathology). HRS data are particularly useful for confirming or alerting the pathologist to slight reductions in sperm production which may not be immediately obvious by qualitative histopathology. A reduction in HRS should be reflected by a decrease in epididymal sperm count, but only if sufficient time has elapsed between release of the reduced numbers of sperm from the testis and their arrival in the cauda epididymis or vas (~2 weeks). If caudal sperm are decreased in the absence of any effect on HRS, a direct effect on epididymal sperm or on sperm transit time is likely. An increase in HRS numbers suggests retention of elongated spermatids in the testis and should be confirmable by pathology.

3. Examine the testis at low power. Look for obvious depletion or disorganization of germ cells within the epithelium or exfoliation of germ cells into the lumen. Look for occasional atrophic tubules (shrunken tubules lined only by Sertoli cells) and determine whether the number is increased over control levels. Look for an increase in the number of vacuoles within the tubular epithelium. Look for tubular dilatation or tubular contraction.

4. At higher power, randomly scan tubules and check that the appropriate cell layers are present in their approximately normal numbers—i.e., that stages I to VIII contain a layer of spermatogonia, a layer of pachytene spermatocytes, and several layers of round spermatids interspersed with elongated spermatids. Stages IX to XIV should contain a layer of prepachytene spermatocytes, several layers of late pachytene or dividing (stage XIV) spermatocytes, and several layers of elongating spermatids. This does not require individual identification of stages, just a familiarization with the cellular make up of the two halves of the spermatogenic cycle. It will allow for the identification of when a cell population is missing. This is particularly important in studies of ≤28-days duration, where maturation depletion may not have progressed to produce an obvious lesion. If, for example, in a 28-day study in the rat, spermatogonia are killed, the most obvious finding in the terminal kill animals will be a loss of prepachytene spermatocytes in stages IX to XIV. Otherwise the testes may appear superficially normal. Check Leydig cells for relative number and evidence of hypertrophy, atrophy, or vacuolation. However, bear in mind that the morphological appearance of the Leydig cell is not a very sensitive indicator of function.

5. Identify a few tubules between stages IX to XI (there will be relatively few) and examine these at high power for evidence of sperm retention. There should be only one population of elongating spermatids at the lumen. Also examine a few stage XII tubules for evidence of sperm head phagocytosis in the basal Sertoli cell cytoplasm. These may occasionally be seen in normal stage XII tubules but rarely exceed more than ~2 to 3 per tubule cross section. Check a few stage VII tubules to ensure approximately normal numbers of step 19 (mature) sperm at the lumen and a normal appearing layer of residual bodies at the lumen. Also check stage VII tubules for any evidence of degenerate pachytene spermatocytes and round spermatids. Decreased testosterone levels will lead to an increased rate of degeneration in these cells in stages VII. The number of cells affected at any one time can be small (2 to 3 cells per tubule cross-section) but this stage-specific lesion is characteristic for and the most sensitive marker of decreased testosterone levels in the testis. Effects will become progressively more obvious with time, due to maturation depletion and direct effects on the elongating spermatids.

6. Examine the epididymis at low power for evidence of reduced sperm content, sperm granulomas, interstitial inflammation, or edema.

7. At higher power, examine ductal contents for evidence of testicular germ cells or residual bodies (increased above control levels). Examine epididymal epithelium for presence of vacuoles, inflammation, or altered cellular characteristics or complement compared with controls. If any alterations in sperm or cellular content of the epididymis is seen, go

Table 16.4.2 Rapid Reference Guide to Evaluation and Interpretation of Weight Changes and Histopathologic Findings in the Reproductive Tract

Finding/observation	What to look for	Possible causes
Increased testis weight	Seminiferous tubular lumen dilatation	Increased seminiferous tubule fluid that may be due to obstruction of outflow, decreased emptying of tubules, decreased resorption of fluid by rete/epididymis, increased production by Sertoli cell
	Increased interstitial fluid (interstitial edema)	Altered hemodynamics, injury to vascular endothelium, reduced lymphatic drainage
Decreased testis weight	Germ cell depletion	Disruption of spermatogenesis through effects on germ cells, Sertoli cells, hormonal disturbance, or blood supply
	Seminiferous tubule lumen contraction	Decreased production of seminiferous tubule fluid that may result from loss of elongating spermatids and/or decreased testosterone production
Increased epididymal weight	Increased interstitial fluid	Altered hemodynamics, injury to vascular endothelium, reduced lymphatic drainage
	Increased ductular fluid	Decreased resorption of fluid by rete, efferent ducts, and caput epithelium
	Sperm granulomas	May be spontaneous but may be induced by any agent causing inflammation or damage to the epididymal epithelial lining
Decreased epididymal weight	Reduced sperm content and contraction of ductular lumen size	Disruption of spermatogenesis resulting in reduced sperm production or release from the testis
Decreased weight of seminal vesicles and/or prostate	Atrophic changes in the secretory epithelium and decreased secretory product	Reduced levels of circulating testosterone, inhibition of 5-α reductase, or disruption of androgen receptor binding
Germ cell loss	Is a specific cell type(s) affected? Does the germ cell loss fit into a pattern of maturation depletion or is it nonspecific? Is it focal or diffuse, is it partial or generalized?	The pattern of the germ cell loss will provide valuable clues as to the likely mechanism of injury, but this will also be very much influenced by the duration of the study (see main text for detail). The pathogenesis of germ cell loss is best investigated in a short time-course study.
Loss of elongate and elongating spermatids	Degeneration of step 7 spermatids and pachytene spermatocytes in stage VII tubules	Disruption of testosterone secretion, which may be caused by direct effects on the Leydig cells or endocrine mediated effects. Alternatively, direct effects on elongating spermatids
Degeneration/apoptosis of germ cells	Is a specific cell type affected? Are the dying cells restricted to a specific tubular stage? Are the affected cells forming multinucleate aggregates?	The cause may be direct toxicity to the affected germ cell but it may also be mediated through a stage-specific disturbance to the Sertoli cell. Apoptotic cells are rapidly removed. Multinucleate aggregates suggest a slow, nonspecific degenerative process

continued

Table 16.4.2 Rapid Reference Guide to Evaluation and Interpretation of Weight Changes and Histopathologic Findings in the Reproductive Tract, continued

Finding/observation	What to look for	Possible causes
Germ cell exfoliation	Presence of exfoliated germ cells in the rete and epididymal lumens	Disruption of Sertoli/germ cell junctions leading to loss of adhesion; disruption of Sertoli cell cytoskeletal fibers leading to sloughing of apical Sertoli cell cytoplasm and attached germ cells
Macro/micro tubular vacuolation (in the absence of severe germ cell injury/loss)	Is this located in the basal Sertoli cell cytoplasm or scattered as large vacuoles throughout tubule? Look for accompanying or additional focal germ cell loss (suggesting focal Sertoli cell damage).	Disturbance of Sertoli cell function leading to vacuolation of organelles or disturbance of fluid balance. Do not confuse with osmotic-induced fixation artifact.
Necrosis and disorganization of tubular contents (including Sertoli cells)	Evidence of acute inflammatory infiltrate around affected tubules	Disturbance in hemodynamics or damage to the vascular endothelium leading to ischemic necrosis
Spermatid retention	Alteration in epididymal sperm parameters (morphology, motility, and count) and possible increase in HRS	Disturbance in testosterone secretion, in Sertoli cell function, or in spermatid development leading to failure in spermiation
Dilated seminiferous tubule lumens	Blockage of efferent ducts or epididymal duct; evidence of pressure-induced germ cell loss	Increased seminiferous tubule fluid that may be due to obstruction of outflow, decreased emptying of tubules, decreased resorption of fluid by rete/epididymis, increased production of fluid by Sertoli cell

back to the testis and examine carefully, since this probably reflects spermatogenic disturbance.

NOMENCLATURE AND SEVERITY GRADING OF SPERMATOGENIC DISTURBANCE (GERM CELL DEPLETION/GERM CELL DEGENERATION)

The nomenclature used to describe depletion and degeneration in the seminiferous epithelium will depend on the specificity of the findings seen, and this is most often related to the duration of the study. In a 1- or 2-year chronic study, any disturbance in spermatogenesis is likely to show as generalized germ cell depletion from some or all of the seminiferous tubules. Due to the duration of dosing and the effects of maturation depletion, there is unlikely to be any specificity in the germ cells lost or in the stages of tubules affected. The lesion seen is an end-stage lesion and therefore nonspecific terminology and simple severity grading based on proportion of tubules affected can be used (Table 16.4.3). Regulatory studies of ≤28 days duration or investigational time-course studies are much more likely to demonstrate specific patterns of germ cell loss and degeneration that may be restricted to specific stages of the spermatogenic cycle. The terminology used will depend on the specificity of such findings. Examples of general and specific findings are provided in Table 16.4.4.

The employment of a severity grading system will also depend on the nature of the findings. A general grading system based on the proportion of tubules affected by a given finding can be used for most nonspecific findings (Table 16.4.2). Grading becomes difficult for cell-specific and stage-specific findings. For example, if 50% of the pachytene spermatocytes in 100% of stage VII tubules are degenerate, how should this be graded? Although 100% of stage VII tubules are affected, this only constitutes ~20% of the total number of tubules in the testis cross section, and then only a proportion of the spermatocytes within the tubule are affected. Such situations have to be dealt with on a case-by-case basis and the terminology for each finding has to be made sufficiently detailed to impart the necessary information.

Table 16.4.3 Semiquantitative Grading System to Record the Severity of Germ Cell Degeneration or Depletion in Seminiferous Tubules

Severity grade	Approximate proportion of tubules affected
1 (minimal)	<5% of tubules affected
2 (slight)	5% to 25% tubules affected
3 (moderate)	25% to 50% tubules affected
4 (marked)	50% to 75% tubules affected
5 (severe)	>75% tubules affected

Table 16.4.4 Examples of NonSpecific and Specific Terminology to Categorize Germ Cell Loss and Degeneration in Seminiferous Tubules[a]

Nonspecific	Specific
Tubules with generalized germ cell depletion	Depletion/degeneration spermatogonia
Tubules with partial germ cell depletion	Depletion/degeneration prepachytene spermatocytes
Tubules with focal germ cell depletion	Depletion/degeneration pachytene spermatocytes
Occasional Sertoli cell–only (atrophic) tubules	Depletion/degeneration round spermatids
Germ cell degeneration/multinucleate aggregates	Depletion/degeneration elongating spermatids
	Depletion/degeneration elongated spermatids

[a]The choice of whether to use nonspecific or specific terminology depends on the cell specificity of the changes seen. In longer duration studies, germ cell loss is often patchy and nonspecific but shorter duration studies are more likely to show a cell-specific pattern of germ cell loss. If necessary, the cell-specific changes can be further specified in terms of the individual spermatogenic stage or range of stages affected. Each of the findings can then be graded using the approximate percentage of tubules affected (see Table 16.4.3).

ARTIFACTS, SPONTANEOUS PATHOLOGY, AND IMMATURITY

Preparative and Fixation Artifacts

As with any tissue, fixation and processing artifacts as well as spontaneous pathology need to be distinguished from toxicologic changes. Bouins fixation results in appreciable tubular shrinkage, which is more marked in the center than at the periphery of the testis. The enlarged interstitial area surrounding these shrunken tubules can be mistaken for edema. Formalin fixation, particularly in large animal testes can result in sufficiently severe cellular shrinkage that the cells appear pyknotic and the epithelium appears extensively vacuolated. Pressure from forceps during necropsy, or cutting into the testis before it is adequately fixed can result in displacement of germ cells into the tubular lumen that can be mistaken for exfoliation. For a review of some of the more common artifacts see Foley (2001).

Immaturity

In the testis, an additional factor that needs to be considered is the age and maturity of the animal. In the peripubertal animal, spermatogenesis is incomplete and inefficient. This is characterized by reduced numbers of elongating and elongated spermatids and a significantly increased population of degenerating germ cells of all types (spermatogonia, spermatocytes, and spermatids). Significant numbers of exfoliated germ cells and cell debris in the epididymal ducts and an absence or reduction of sperm usually accompany this. This appearance can be indistinguishable from chemically induced effects on spermatogenesis. In regulatory toxicity studies, this has proved a particular problem with respect to dogs since the regulatory guidelines recommend starting studies with dogs of an immature age (5 to 7 months). In studies of 13 weeks duration, the dogs are then on the borderline of maturity. Small group sizes and significant variations in the age that dogs attain full sexual maturity (8 to 12 months) can lead to difficulties in separating the appearance of varying levels of immaturity from chemically induced changes.

Primates used in toxicity testing are frequently immature and the variation between

age and maturity of individuals within a study can be marked. As a general guide, Cynomologous monkeys <4 years of age are likely to show varying levels of immaturity. An additional problem with primates is the effect of hierarchical status on testosterone levels and testicular development and regression.

In most routine regulatory studies using rodents, the guidelines recommend using animals of an age that are sexually mature by the termination of the study. In addition, there is much less variation in the age at which rodents attain sexual maturity. However, if a study design calls for the use of prepubertal animals, the increased rate of germ cell degeneration and the relative disorganization of the epithelium in this age of animal should be appreciated.

Spontaneous Pathology

Dog testes present a particular problem in terms of the level of spontaneous degenerative lesions and the prevalence of incomplete spermatogenesis in many tubules. Rehm (2001) has reported and quantified the incidence of various degenerative lesions in the testes of pure bred beagle dogs at various ages. Dogs 8 to 11 months of age showed a 27% incidence of testes with hypospermatogenesis (tubules with partial depletion of germ cells), a 100% incidence of testes with degenerating germ cells, and a 45% incidence of testes with segmental atrophy/hypoplasia. Since these changes are often indistinguishable from the nonspecific spermatogenic changes induced by chemical toxicants and because regulatory studies generally employ small group sizes, interpretation of slight increases in incidence can be a significant problem.

Rodent testes generally demonstrate a far lower incidence of spontaneous lesions. Unilateral or bilateral generalized tubular atrophy (Sertoli cell–only tubules) are not uncommon findings and occasional animals with partial or focal depletion of germ cells are also seen. However, in comparison with large animals, the use of larger group sizes generally allows ready distinction between spontaneous and treatment-related effects.

LITERATURE CITED

Blanchard, K.T., Lee, J., and Boekelheide, K. 1998. Leuprolide, a gonadotropin-releasing hormone agonist reestablishes spermatogenesis after 2,5-hexanedione-induced irreversible testicular injury in the rat resulting in normalized stem cell factor expression. *Endocrinology* 139:236-244.

Chapin, R.E. and Conner, M.W. 1999. Testicular histology and sperm parameters. *In* An Evaluation and Interpretation of Reproductive Endpoints for Human Health Risk Assessment. (G. Daston and C. Kimmel, eds). pp. 28-41. ILSI Press, Washington, D.C.

Chapin, R.E. and Ku, W.W. 1994. The reproductive toxicity of boric acid. *Environ. Health Persp.* 7:87-91.

Chellman, G.J., Bus, J.S., and Working, P.K. 1986. Role of epididymal inflammation in the induction of dominant lethal mutations in Fisher 344 rat sperm by methyl chloride. *Proc. Natl. Acad. Sci. U.S.A.* 83:8087-8091.

Clegg, E.D., Cook, J.C., Chapin, R.E., Foster, P.M.D., and Daston, G.P. 1997. Leydig cell hyperplasia and adenoma formation: Mechanisms and relevance to humans. *Reprod. Toxicol.* 11:107-121.

Creasy, D.M. 1997. Evaluation of testicular toxicity in safety evaluation studies: The appropriate use of spermatogenic staging. *Toxicol. Pathol.* 25:119-131.

Creasy, D.M. 2001. Pathogenesis of male reproductive toxicity. *Toxicol. Pathol.* 29:64-76.

Creasy, D.M. and Foster, P.M.D. 2001. Male reproductive system, Chapter 10. *In* Handbook of Toxicologic Pathology, 2nd Edition (W. Haschek, C. Rousseaux, and M. Wallig, eds.) Academic Press, San Diego.

Foley, G.M. 2001. Overview of male reproductive pathology *Toxicol. Pathol.* 29:49-63.

Hess, R.A. 1990. Quantitative and qualitative characteristics of the stages and transitions in the cycle of the rat seminiferous epithelium: Light microscopic observation of perfusion-fixed and plastic embedded testes. *Biol. Reprod.* 43:525-542.

Hess, R.A. 1998. Effects of environmental toxicants on the efferent ducts epididymis and fertility. *J. Reprod. Fertil. Suppl.* 53:247-259.

Hess, R.A. and Chen, P. 1992. Computer tracking of germ cells in the cycle of the seminiferous epithelium and prediction of changes in cycle duration in animals commonly used in reproductive biology and toxicology. *J. Androl.* 13:185-190.

Lee, J., Richburg, J.H., Younkin, S.C., and Boekelheide, K. 1997. The Fas system is a key regulator of germ cell apoptosis in the testis. *Endocrinology* 138:2081-2088.

Lee, J., Richburg, J.H., Shipp, E., Meistrich, M.L., and Boekelheide, K. 1999. The Fas system, a regulator of testicular germ cell apoptosis, is differentially up-regulated in Sertoli cell versus germ cell injury of the testis. *Endocrinology* 140:852-858.

Linder, R.E., Strader, L.F., Slott, V.L., and Suarez, J.D. 1992. Endpoints of spermatotoxicity in the rat after short duration exposures to 14 reproductive toxicants. *Reprod. Toxicol.* 6:491-505.

Meistrich, M.L. 1986. Critical components of testicular function and sensitivity to disruption. *Biol. Reprod.* 34:17-28.

Nolte, T., Harleman, J.H., and Jahn, W. 1995. Histopathology of chemically induced testicular atrophy in rats. *Exp. Toxicol. Pathol.* 47:267-286.

Rehm, S. 2001. Spontaneous testicular lesions in purpose bred beagle dogs. *Toxicol. Pathol.* 28:782-787.

Russell, L.D., Ettlin, R.A., Sinha-Hikim, A.P., and Clegg, E.D. 1990. Histological and histopathological evaluation of the testis. pp. 62-193. Cache River Press, Clearwater, Florida.

Ulbrich, B. and Palmer, A.K. 1995. Detection of effects on male reproduction—A literature survey. *J. Am. Coll. Toxicol.* 14:2293-3327.

KEY REFERENCES

Chapin and Conner, 1999. See above.

This chapter provides an overview on how to approach and carry out histopathological evaluation of the testis including the use of staging. It also reviews the inter-relationship of morphologic changes in the testis with functional outcome and discusses the utility of sperm parameters.

Creasy, 1997. See above.

This key reference provides more in-depth consideration of the proper use of an understanding of spermatogenesis in the histopathologic interpretation of testis lesions, and will help the pathologist understand the proper application of staging in the regulatory framework.

Creasy and Foster, 2001. See above.

This chapter provides a general overview of the structure, function and physiology of the male reproductive system as well as responses of the system to toxicologic disturbance.

Knobil, E., Neill, J., Greenwald, G., Markert, C., and Pfaff, D. 1994. The Physiology of Reproduction, 2nd Ed. Raven Press, New York.

This is an invaluable and comprehensive reference text dealing with all aspects of reproductive physiology.

Russell et al., 1990. See above.

This is an essential reference text for beginners as well as those experienced in testicular histopathology. It provides detailed instruction on how to identify stages of the spermatogenic cycle in the rat, mouse, and dog. It also provides a wealth of information on testicular biology, histopathological and toxicological evaluation, fixation, ultrastructure and much more.

Contributed by Dianne M. Creasy
Huntingdon Life Sciences
East Millstone, New Jersey

Monitoring Endocrine Function in Males: Using Intra-Atrial Cannulas to Monitor Plasma Hormonal Dynamics in Toxicology Experiments

The regulation of male reproductive function involves complicated, dynamic hormonal controls that include systemic (endocrine), local (paracrine), and intracellular (autocrine) components. As a result, concentrations of peripheral blood hormones are characterized by a great deal of inherent variation. Changes occur from point to point, minute to minute, hour to hour, and/or day to day. Given this situation, a single blood sample, for example at necropsy, is a poor representation of the dynamic health of any given hormone control system. A chronically cannulated animal provides a much better representation of endocrine homeostasis in animals being treated with potential toxicants. In a standard in vivo toxicology protocol, such as a multigeneration test or even a 30-day protocol, indirect evidence can suggest that an endocrine disruption has occurred (Tyl, 2002). Evidence of an endocrinopathy in endocrine organs (e.g., testes) or target organs of the hormones (e.g., prostate) includes increased or decreased organ size or altered histology. Significant differences in one or more organ parameters would suggest the presence of an endocrine anomaly and would provide additional information regarding the nature of that endocrinopathy. Finally, major changes in hormone secretion could be detected in a single sample of blood or urine.

Whereas some information can be obtained from a single blood sample or a cross-sectional experimental design (with different animals examined at each time point after treatment), longitudinal experimental designs optimize the data. With the cannulated rat model, one can assess (1) the point-to-point changes in a specific hormone (the pattern of release), (2) the relative changes in two or more hormones, and (3) the response (both acute and short term) to a hormonal or nonhormonal stimulus.

Other advantages of a cannula include (1) the elimination of multiple phlebotomies, (2) the ability to obtain longitudinal information (multiple samples) from a single animal, (3) a decrease in interanimal variability, and (4) a requirement for fewer animals (as compared with cross-sectional experiments). Cannulas can be used in combination with a tethering system to eliminate handling stressors and/or an automatic or manual infusion device for static treatment or rehydration.

When a toxicant affects the male reproductive organs, an endocrine disruption is very likely the cause. The cannulated rodent model can be used in one or more of these protocols to more clearly define endocrinopathies. This unit describes the authors' methods for surgical preparation for intra-atrial cannulation using a permanent tether apparatus (Basic Protocol 1) or a vascular access port (Basic Protocol 2) and blood sampling and collection (Support Protocol). The authors also present representative data obtained from two experimental designs that utilized these techniques.

NOTE: All protocols using live animals must first be reviewed and approved by an Institutional Animal Care and Use Committee (IACUC) and must conform to governmental regulations regarding the care and use of animals.

NOTE: Sterile technique should be used during all surgical procedures. Surgical instruments should be sterilized between animals. The surgeon should wear sterile gloves and use a sterile drape for each animal whenever possible.

Contributed by Patricia A. Fail and Stephanie A. Anderson
Current Protocols in Toxicology (2002) 16.5.1-16.5.17

BASIC PROTOCOL 1

INTRA-ATRIAL CANNULATION OF A MALE RAT WITH A PERMANENT TETHER APPARATUS

This method utilizes a permanently affixed tether system, sutured directly to the dorsal musculature between the scapulae. The rat has freedom of movement within its cage, and blood samples can be collected from outside the cage without disturbing the animal (Fig. 16.5.1). The animal cannot, however, be removed from its cage without the accompanying tether system. Maintenance of patency is more time consuming than with other techniques. This technique works best for studies of a shorter duration (7 to 10 days).

Materials

Silicone adhesive
Heparinized saline with gentamicin: 0.9% (w/v) NaCl (*APPENDIX 2A*)/20 IU/ml heparin/0.05 mg/ml gentamicin sulfate, sterile
Male rat
Anesthetic
Iodide scrub
70% (v/v) ethanol
Veterinary ophthalmic ointment (e.g., Paralube, Pharmaderm)
Microrenathane polyurethane tubing, 0.06-cm (0.025-in.) i.d., 0.1-cm (0.04-in.) o.d. and 0.1-cm (0.04-in.) i.d., 2-cm (0.8-in.) o.d. (Braintree Scientific)
Polysulfone anchor button with attached stainless steel spring tether (Instech Laboratories)
Swivel (Instech Laboratories)
Swivel-to-tether clamp (Instech Laboratories)
Ethylene oxide gas sterilizer
No. 22 scalpel blades, sterile
1-cc plastic tuberculin syringe with 23-G blunt-end needle, heparinized (i.e., coated with 1000 IU/ml liquid sodium heparin solution and allowed to dry)
Electric clipper
Toenail clipper or scissors
Hemostats and/or forceps, sterile
4-0 silk suture, sterile
20-G needles, sterile
Wound clips
Heating pad or heat lamp

Prepare cannula and tether system

1. Cut a 50.4-cm length of 0.06-cm i.d., 0.1-cm o.d. Microrenathane polyurethane tubing and a 3- to 4-mm piece of 0.1-cm i.d., 2-cm o.d. tubing to use as a collar.
2. Slide the short piece of tubing (collar) over the cannula tubing and place it ~5.0 cm from the end of the cannula.
3. Use a silicone adhesive to glue the collar in place at each end, forming a dumbbell-shaped anchor for sutures (Fig. 16.5.1A).

   The length of the cannula from the proximal end of the collar to the cannula tip will need to be modified at the time of surgery. This length is based on the weight of the rat (Table 16.5.1).

4. Thread the distal end of the cannula through a polysulfone anchor button and up through the attached spring tether. Attach the end of the tether to a swivel via a swivel-to-tether clamp.

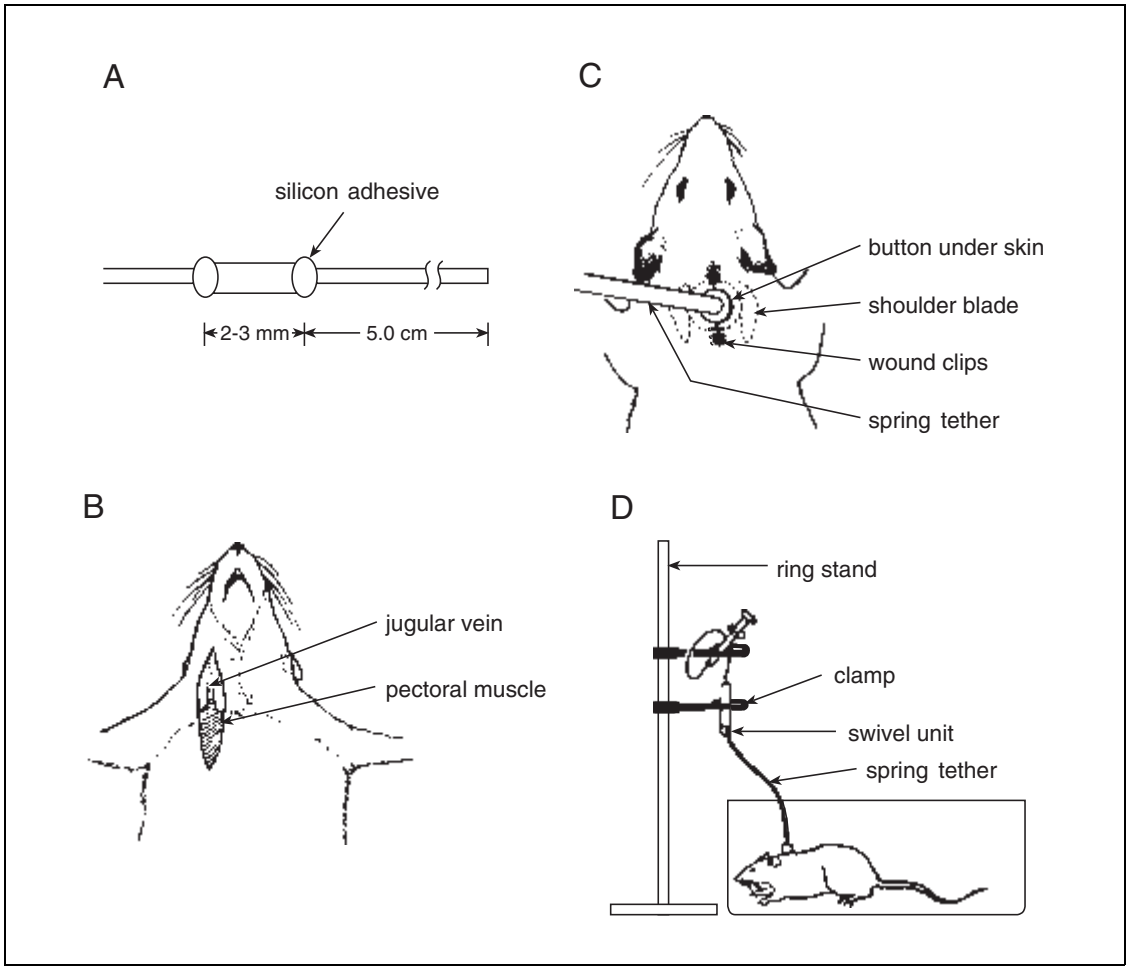

Figure 16.5.1 Cannulation procedure and permanently attached tether setup (see Basic Protocol 1). (**A**) The cannula with the attachment collar. (**B**) Surgical preparation of jugular vein. (**C**) Connection of permanent spring tether. (**D**) Relationship of animal to tether apparatus.

Table 16.5.1 Cannulation Surgery Information

Body weight range (g)	Cannula length (cm)[a]
210-245	2.5
246-60	2.6
261-320	2.8
321-350	3.2
351-375	3.4
376-400	3.6
401-450	3.8
451-475	4.0
476-525	4.2
525-550	4.3
>550	4.5

[a]The volume of the polyurethane cannula varies with its length and is ~0.15 ml; the volume of the Mini-Port is ~0.25 ml.

5. Sterilize the complete tether setup in an ethylene oxide gas sterilizer.

   Alternatively, complete sterile tether systems with custom-designed cannulas can be purchased (Strategic Applications) instead of being made in the lab.

Prepare for surgery

6. Place the sterilized tether system on a sterile surface. Use a sterile no. 22 scalpel blade to cut the cannula to the appropriate length based on the weight of the animal into which it will be inserted (Table 16.5.1). Cut the tip of the cannula at a 90° angle.

   A well-lit benchtop covered with an autoclaved drape is an appropriate sterile surface.

   The cannulation procedure can probably be carried out using smaller rats or even mice.

7. Fill a heparinized 1-cc plastic tuberculin syringe with a 23-G blunt-end needle with sterile heparinized saline with gentamicin and attach it to the distal end of the cannula. Fill the cannula with this flush solution, clearing all air from the cannula, and leave the syringe attached.

   The heparinized saline with gentamicin is used as the flush solution during surgery. It may be used with a computerized infusion pump for continuous infusion for maintenance of patency and hydration.

8. Clamp the cannula to a ring stand at the swivel for ease in handling during surgery.

9. Anesthetize a male rat using an appropriate anesthetic.

   Suggested choices are ketamine/xylazine/acepromazine (10:1:0.1 [w/w/w], 80 to 100 mg/kg intraperitoneally) or an inhalation anesthetic such as isoflurane. Injectable anesthesia can be supplemented with a methoxyflurane nose cone as needed.

10. Use an electric clipper to shave the fur from the ventral neck area and the dorsal surface over the scapulae. Clean both areas using an iodide scrub and 70% ethanol. Place a veterinary opthalmic ointment in each eye to protect them from drying during surgery.

11. Use a toenail clipper or a pair of scissors to trim the claws on all feet to reduce the chance of wound irritation by scratching.

12. Place the anesthetized rat and the prepared cannula and tether system on the surgical table.

Perform surgery

13. Use a sterile no. 22 scalpel blade to make an ~1-cm incision in the skin between the scapulae (midsagittal plane). Make a ventral incision (~2 cm) from below the point of the right lower jaw to just above the right clavicle (Fig. 16.5.1B).

14. Using sterile hemostats or forceps, bluntly tunnel subcutaneously from the ventral incision to the dorsal incision. Using the forceps, grasp the collar of the cannula and pull the cannula through the tunnel to the ventral incision.

15. Isolate the right jugular vein by bluntly dissecting away surrounding tissue. Elevate the vessel by placing forceps underneath it or by using a piece of sterile 4-0 silk suture held in one hand.

16. Using a sterile 20-G needle, make a hole in the jugular vein ~5 mm above the point where the vein widens to pass under the pectoral musculature (Fig. 16.5.1B).

    Pressure from the elevating forceps or suture should keep the vessel from bleeding.

17. Insert the cannula tip and advance it until the collar reaches the hole in the vein. Confirm correct placement of the cannula tip in the right atrium by drawing back on the syringe attached to the distal end of the cannula until blood appears in the proximal end. Flush blood back out of the cannula (into the animal) after confirming patency.

18. Pass one loop of 4-0 silk suture under the collar and vein and tie off between the ends of the collar to secure the cannula in place in the vein. Place a second suture under the vein and through surrounding muscle and fat and tie off between the collar ends to ensure that the cannula and vein are anchored to the surrounding tissue.

19. Close the ventral incision with wound clips.

20. Place the anchor button at the end of the spring tether under the skin and secure it by suturing it through at least two of the anchor holes to the underlying musculature. Close the incision over the anchor button with wound clips and/or suture (Fig. 16.5.1C).

21. Return the rat to its cage. Pass the tether and swivel through the wire cage top and secure the swivel to an appropriate anchor.

    A ring stand (Fig. 16.5.1D) or specially designed cages and/or cage racks can be used. Basic cage racks can be modified to accommodate ten cages with swivels clamped to permanent rack braces.

22. Disconnect the distal end of the cannula from the needle and syringe and connect it to the bottom of the swivel, leaving enough tubing to avoid tangling. Attach a second piece of 0.06-cm i.d., 0.1-cm o.d. tubing to the top of the swivel.

    This tubing may be connected to a blunt-end needle and syringe containing heparinized saline or may be connected to an infusion pump containing the same saline solution. Continuous infusion increases the length of time the cannula is patent for sampling and provides the needed postsurgical fluids (≤400 μl/hr may be infused). If the needle and syringe are used, ~0.3 to 0.5 ml solution should be flushed through the cannula at least three times per day.

23. Monitor animals following surgery for evidence of hemorrhage or other adverse clinical signs. If possible, use a heating pad under the cage or a heat lamp to keep the animal warm while it recovers from anesthesia. Provide a minimal 24-hr recovery period after surgery before proceeding with blood sampling experiments (see Support Protocol).

    In general, rats may be maintained with this tethering system for ≤10 days.

INTRA-ATRIAL CANNULATION OF A MALE RAT WITH A VASCULAR ACCESS PORT

BASIC PROTOCOL 2

This method utilizes the SIMS Deltec Preclinical Mini-Port. This is a totally implantable vascular access device that allows for repeated access for intravenous or intra-arterial injection or infusion (Fig. 16.5.2). The animal is not permanently attached to a tether and thus can move freely around the cage and can easily be removed from the cage. With proper cannula placement and postsurgical maintenance, the portal should remain patent (for infusion and blood sampling) for several months. The following surgical method that the authors use has been summarized from the *Preclinical Mini-Port Instructions for Use* pamphlet, which comes with the box of portals (see Key Reference).

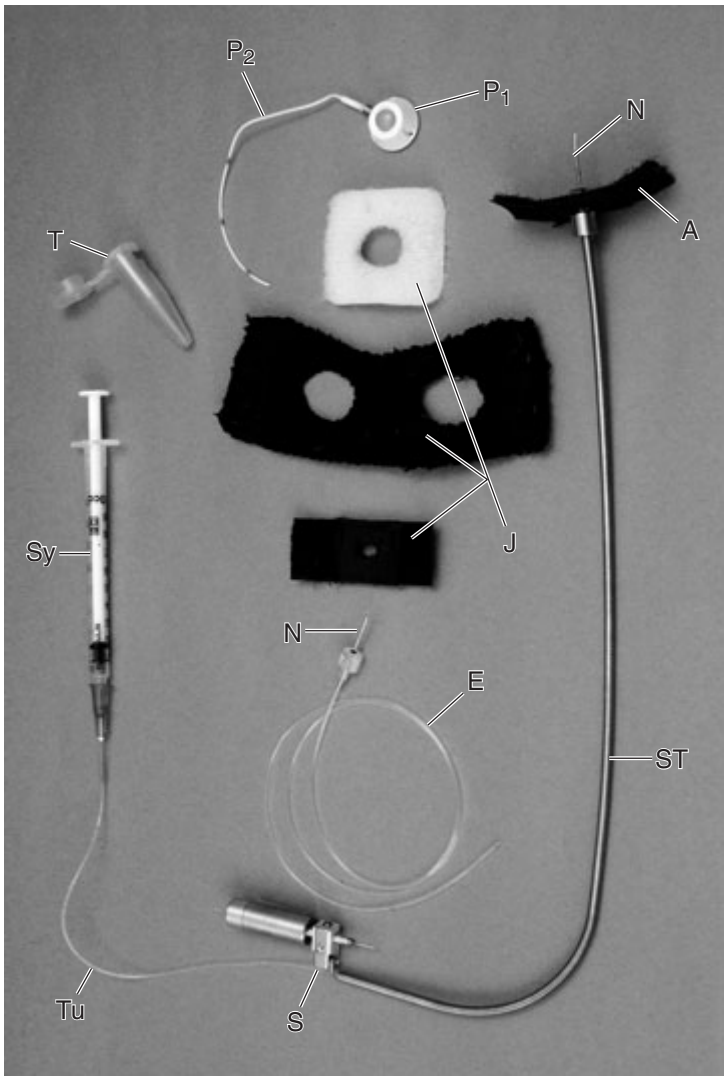

Figure 16.5.2 Mini-Port, tether apparatus, and jacket (see Basic Protocol 2). Shown are the vascular access port (P_1) with attached cannula (P_2); the jacket components (J); the external tubing (E) and noncoring needle (N); the assembled attachable tether (ST) with noncoring needle (N), jacket attachment (A), and spring (S) swivel, tubing (Tu), and sampling syringe (Sy); and polyethylene snap-cap blood sampling tube (T). Figure, without labels, used with permission from SIMS Deltec.

Materials

22-G noncoring Port-a-Cath needles (SIMS Deltec) attached to 5-ml syringes filled with sterile 0.9% (w/v) NaCl (saline; *APPENDIX 2A*)

Flush solution for ports: 0.9% (w/v) NaCl (*APPENDIX 2A*)/100 IU/ml heparin/0.05 mg/ml gentamicin sulfate, sterile

Surgical drape, sterile

Ruler with millimeter markings, sterile

Preclinical Mini-Port (SIMS Deltec)

Heating pad or heat lamp

Additional reagents and equipment for rat surgery (see Basic Protocol 1)

Prepare Mini-Port and catheter

1. Prepare a work area with good lighting, a sterile surgical drape, a sterilized ruler, and sterile no. 22 scalpel blades.
2. While wearing sterile gloves, place a sterile Preclinical Mini-Port on the sterile work area. Using a sterile 5-ml syringe and 22-G noncoring Port-a-Cath needle, flush the portal and catheter with sterile saline to remove all air from the reservoir. Hold the portal with the catheter attachment upward, and tap the portal gently while injecting the solution to remove air from the portal chamber.
3. Move the suture beads back toward the portal. To accomplish this, wet the catheter with sterile saline and then gently stretch a small section of the catheter at the bead site and begin moving the bead.
4. Cut off ~32 to 34 cm of excess tubing. Make the cut at a 90° angle to the catheter. Make sure the suture beads are still on the catheter tubing attached to the portal.

   The catheter has black marking at 2-cm increments to assist in measurement of the length to be removed.

5. Move the suture beads to the desired position.

   The distance from the tip of the catheter to the first suture bead will depend on the weight of the animal (Table 16.5.1). The second suture bead should be positioned ~3 to 5 mm from the first bead.

Perform surgery

6. Anesthetize a male rat and prepare the surgical sites as described (see Basic Protocol 1, steps 9 to 12).
7. Make a 3- to 4-cm dorsal incision just to the side of where the portal will be placed. Use blunt dissection to prepare a subcutaneous pocket that is just large enough to hold the portal. By trial insertion, check that the portal is the right size and that the portal does not lie directly under the incision.

   The portal should sit in the scapulae area.

8. Make a ventral incision (~2 cm) from below the point of the right lower jaw to just above the right clavicle. Make a small subcutaneous tunnel from the ventral incision to the portal pocket site. Grasp the catheter at the suture beads and gently pull it through the tunnel.

   Never use forceps with teeth to grasp the catheter. If the beads move as they are pulled through the subcutaneous tunnel, remeasure and reposition the beads before proceeding with jugular cannulation.

9. Isolate the right jugular vein by bluntly dissecting away surrounding tissue. Elevate the vessel by placing forceps underneath it or by using a piece of sterile 4-0 silk suture held in one hand.
10. Using a sterile 20-G needle, make a hole in the jugular vein ~5 mm above the point where the vein widens to pass under the pectoral musculature (Fig. 16.5.1B).

    Pressure from the elevating forceps or suture should keep the vessel from bleeding.

11. Insert the catheter into the vessel. Position the first suture bead inside the vessel if possible. Pass one loop of sterile 4-0 silk suture under the catheter and vein and tie off between the suture beads to secure the catheter in place in the vein. Place a second suture under the vein and through surrounding muscle and fat and tie off between the suture beads to ensure that the catheter and vein are anchored to the surrounding tissue. Place a tension loop (growth) at the site of insertion.

    The tension loop will provide extra catheter length to accommodate the growth of the animal.

12. Check for patency by flushing a small amount of saline through the portal and catheter using a 5-ml syringe and noncoring needle. Draw back on the syringe until blood is visible in the catheter. Flush the blood back into the animal with 0.4 to 0.6 ml sterile saline.

13. Lock the system by flushing through 0.3 ml flush solution for ports. Continue to inject the flushing solution while at the same time withdrawing the needle. Stabilize the portal using the thumb and finger.

    Injecting the flush solution while withdrawing the needle avoids the reflux of blood into the catheter.

14. Suture the portal to the underlying musculature using the portal suture holes. Close the incision with wound clips or suture, making sure the incision is not directly over the portal. Close the ventral incision with wound clips.

15. Return the animal to its home cage. If possible, use a heating pad under the cage or a heat lamp to keep the animal warm while it recovers from anesthesia. Observe the animal for any adverse clinical signs including wound hematoma, swelling, or any post-operative bleeding.

Perform postoperative maintenance

16. On the day after surgery, shave excess hair over the portal. Clean the area with an iodide scrub and 70% ethanol.

    Aseptic technique should be used when accessing the port whenever possible.

17. Palpate the area to locate the portal and stabilize it. Puncture the skin directly over and perpendicular to the plane of the septum using a 22-G noncoring Port-a-Cath needle attached to a 5-ml syringe filled with sterile saline.

18. Flush in ~0.2 ml saline, and then draw back on the plunger to confirm blood flow.

19. Flush blood out of the portal and catheter with 0.4 to 0.6 ml sterile saline.

20. Lock the system by flushing with 0.3 ml flush solution for ports. Continue injecting the flush solution while withdrawing the needle to avoid the reflux of blood into the catheter.

21. Repeat steps 16 to 20 on every other day following the surgery for the first week. Continue to flush the system twice a week for the next 4 weeks and weekly thereafter. Always flush the portal system well after injection or infusion or blood collection.

    As long as patency is maintained, this system can be used for ≤60 days.

SUPPORT PROTOCOL

COLLECTING AND PROCESSING BLOOD SAMPLES FROM A CANNULATED MALE RAT

Blood may be collected via the exteriorized cannula from outside the animal's cage with either of the cannulation techniques described above. When using the Preclinical Mini-Port, each rat must be fitted with a special jacket with attached tether, tubing, and specialized noncoring needle. The tether is then attached outside the cage to a swivel as in Basic Protocol 1. Blood samples are then collected in the same manner for either cannulation technique.

It is also possible to collect blood without using the jacket by removing the animal from the cage and accessing the port directly with a noncoring needle and syringe. The jacket system, however, avoids the effects of handling stress on parameters of interest.

Materials

Male rat with an intra-atrial cannulation with either a permanent tether apparatus (see Basic Protocol 1) or a vascular access port (see Basic Protocol 2)

Heparinized saline: 0.9% (w/v) NaCl (*APPENDIX 2A*)/20 IU/ml heparin, sterile

Rat jacket, steel spring tether, swivel, and polyurethane tubing with 1-cc syringe attached at distal end (complete setup may be purchased through Strategic Applications or jackets may be custom made; Fig. 16.5.2), for use with vascular access port only

Hand-held tubing clamp

1-cc syringes with 23-G (with 22-G i.d.) blunt-end needles, heparinized (i.e., coated with 1000 IU/ml liquid sodium heparin solution and allowed to dry)

1.5-ml heparinized blood collection tube

Prepare precollection setup

For vascular access port:

1a. Place a male rat with an intra-atrial cannulation with a vascular access port into a rat jacket.

The rat should be acclimated to the jacket for several days prior to blood collection. On the day of collection, acclimation of ≥30 min is suggested prior to blood sample collection.

2a. Before attaching the tethering system (which consists of a steel spring tether, swivel, and polyurethane tubing with a 1-cc syringe containing heparinized saline attached at the distal end) to the rat, fill the cannula with heparinized saline.

On the proximal end is the specialty noncoring needle attached to the tubing and the tether.

3a. Restrain the rat, insert the noncoring needle into the port, and secure the tethering system to the jacket.

4a. Return the rat to its cage. Attach the swivel to an appropriate anchor outside the cage (see Basic Protocol 1, step 21).

For permanent tether apparatus:

1b. Using a male rat with an intra-atrial cannulation with a permanent tether apparatus, proceed with blood collection as described in step 5.

Collect blood sample

5. Clamp the distal end of the cannula with a hand-held tubing clamp and disconnect the cannula from the swivel.

6. Attach a 1-cc syringe with a 23-G blunt-end needle to the end of the cannula, unclamp, and withdraw ~0.05 ml blood and heparinized saline into the syringe.

This is the presample consisting of the heparinized saline that was in the cannula and a small amount of blood. The presample syringe does not need to be heparinized, as this sample is discarded.

7. Clamp the cannula again and disconnect the presample syringe. Discard the presample and set needle and syringe aside for later use.

The presample needle and syringe can be used again for withdrawing heparinized saline from the cannulas of other animals.

8. Attach a second heparinized (clean) 1-cc syringe, unclamp the cannula, and withdraw the desired amount of blood. Place the blood in a labeled 1.5-ml heparinized blood collection tube.

Other appropriately sized containers can be used to hold blood sample.

9. Microcentrifuge the sample 2 min at 1200 × *g*. Using an appropriate pipet, remove the plasma, place in an appropriately labeled container, and freeze.

   Each blood sample should be immediately processed for plasma collection. Plasma storage conditions will depend on the requirements of the protocol.

Reinfuse red blood cells

10. Resuspend the remaining RBCs in a volume of heparinized saline (or other acceptable plasma substitute) equal to approximately one half of the total blood sample volume collected.

    These processing steps are generally done by personnel outside of the animal blood collection room.

    Because of the large blood volume collected for each blood sample, RBC reinfusion is necessary (blood sample size is usually 0.5 to 1.0 ml per sample as plasma is often analyzed for multiple hormones). If blood samples are being collected from some other indication (e.g., pharmacokinetics), then very small amounts of blood are collected at each time point (100 to 200 µl), and reinfusion is not done (no more than 15% of total blood volume should be removed in an 8-hr period). A different cannulation technique can be used. This approach, however, will not be discussed here.

11. Gently vortex (or invert) tube and draw the resuspended cells into a 1-cc syringe and attach a blunt-end needle, making sure there is no air in the syringe and needle.

12. Immediately after collecting a blood sample, attach the blood-filled syringe to the cannula, unclamp, and slowly reinfuse the resuspended sample.

    The resuspended RBCs from the previously collected blood sample should be reinfused (i.e., if this is the second blood sample collected, the RBCs from the first sample are reinfused).

13. Clamp the cannula, attach a clean blunt-end needle and syringe containing heparinized saline to the cannula, unclamp the tubing, and flush the cannula with ~0.3 to 0.5 ml heparinized saline to thoroughly clear it of blood.

    The volume of saline used will depend on the length of the cannula.

    If multiple samples are to be collected with short intervals between collection times (e.g., every 10 min for 2 hr), then the flush syringe may stay connected to the cannula until the next sample is collected. If the interval between samples is 20 to 30 min or more, the cannula should be reattached to the swivel apparatus.

14. Repeat this process for every blood sample collected. Make sure that the cannula is free of blood and filled with heparinized saline at the end of each collection.

COMMENTARY

Background Information

With the recent passage of the Clean Water Act and the Food and Water Safety Act, the effects of endocrine disruptors on human and animal health has national and international attention. Endocrine disruption may be the planned mechanism of action in the case of a pharmaceutical agent or an unplanned side effect of a drug, an agricultural product, or an industrial chemical exposure. Whereas the deliberate disruption of an endocrine system has therapeutic utility, endocrine disruption can also be the underlying basis for infertility, cancer, or other disease. Therefore, although endocrine testing is not a required portion of a preclinical testing battery, it can certainly be an important aspect of drug development and continued safety evaluation.

The cannulated rodent model has been used since 1964 (Weeks and Davis, 1964), and improvements have been made throughout the last 25 years (Harms and Ojeda, 1974; McKenna and Bier, 1984; Dons and Havlik, 1986; MacLeod and Shapiro, 1988). This approach

for endocrine studies in rodents as well as large animals contributed significantly to our understanding of endocrine controls (i.e., negative and positive feedback). The data obtained with this model very clearly illustrated the dynamic changes that occur in peripheral blood concentrations (Coquelin and Desjardins, 1982; Ellis and Desjardins, 1982; MacLeod and Shapiro, 1988).

The process of defining an endocrine perturbation involves a multifaceted, data-dependent approach. In animals, the first clue might be an enlarged endocrine gland or disrupted estrous cycles. For example, in males, hypertrophy of the Leydig cells may occur after exposure to an antiandrogen, such as occurs with flutamide (Viguier-Martinez et al., 1983a,b; Simard et al., 1986). In females, menstrual or estrous cycle may be disrupted after exposure to estrogenic compounds. In this case, the vaginal cytology should reveal increased cornification. These endocrine biomarkers can easily be included in standard protocols and are helpful clues upon which to base the design of additional testing.

Technical approaches for endocrine assessments are similar in any subspecialty of endocrinology (i.e., reproductive, thyroid, adrenal, or pancreatic studies). Sensitive quantification methods such as the radioimmunoassay are available to measure hormone content in blood, urine, feces, or cerebral spinal fluid. Receptor binding assays, bioassays, and molecular measures are also useful biomarkers of endocrine disruption(s), but they will not be discussed here. Nonetheless, it should be possible at selected times during a standard preclinical protocol to collect samples for one or more specific endocrine biomarkers. Radioimmunoassay of blood hormones has great utility and could be done on single samples collected periodically during the protocol or at necropsy.

Intra-atrial cannulation can be used to establish the functional status of endocrine organs, to administer chronic treatments, or for other situations when an undisturbed, unstressed animal is required. Blood hormone studies using the cannulated rat model can be designed as the situation warrants. Two special experimental designs are discussed below.

Functional evaluation approaches include (1) the longitudinal endocrine baseline assessment (LEBA) used to evaluate the secretion profiles of individual hormones or of two or more related hormones, (2) the endocrine challenge test (ECT), and (3) a combination of the two tests. Each of these tests must be specifically designed for the endocrine system that is being tested based on endocrine homeostatic relationships. ECTs have been used for many years in human medicine and to a lesser extent in veterinary medicine. For example, if the pituitary-testicular controls are of interest, an ECT design would be as follows: (1) to test testicular response, a challenge with human chorionic gonadotropin (hCG) is given to stimulate testosterone release; (2) to determine the pituitary's functional capacity to release luteinizing hormone (LH) and follicle stimulating hormone (FSH), a challenge with gonadotropin releasing hormone (GnRH) is appropriate; and (3) to determine whether the hypothalamic synthesis and release of GnRH is operational, stimulation or inhibition of GnRH using hypothalamic neuronal controls such as dopamine, norepinephrine, and/or melatonin may be appropriate.

In an experiment, one or more of these tests would be used in three types of test animals: controls, test-compound treated (at one or more doses), and pair-fed animals (if test article caused a decreased weight gain of ≥10% because of decreased feed consumption in preliminary studies). The authors have developed and defined ECTs in rodents based on the dose of a trophic hormone required to stimulate a 50% maximal response of the target organ hormone (effective dose 50; ED_{50}). Initially, GnRH and hCG ECTs were developed in rodent research to assess endocrinopathies of the reproductive system (Fail et al., 1992, 1998).

To accomplish these challenge tests in an in vivo study, intra-atrial cannulation would be used to facilitate frequent collection of blood samples. With respect to a GnRH challenge, samples would be collected at −30, 0, 2, 15, 30, 45, 60, 120, 240 and 1440 min (0 represents the time of GnRH treatment). LH and FSH concentrations would be determined in these samples, and the percent response, or the absolute response, at 2 and 15 min compared between groups. (For other ECTs, the time of maximal response should first be determined.) The area under the response curve might also be of interest. To prevent dehydration and anemia, red blood cells (RBCs) are reinfused after blood plasma has been harvested.

Each approach used to assess endocrine function has its strengths and weaknesses. The authors' initial approach was a permanent tethering system (see Basic Protocol 1). This system is very useful for studies of short duration

(2 to 10 days). But patency for sampling is limited, because a flap or clot forms on the end of the cannula and blood can no longer be obtained (O'Farrell et al., 1996). In another useful variation without restraint, if acute sampling is the objective (≤24 hr), the exteriorized cannula is cut short, plugged with a copper plug, and allowed to rest on the animal's back out of reach until use. When samples are to be collected for a short period (1 to 2 hr), the plug is removed, and a metal tube is inserted into the cannula (on one end) and connected to a longer tubing (on the other end). For this approach, the animals must be watched closely to prevent chewing on the sampling tubing.

The authors' second method, the use of an indwelling vascular access port (see Basic Protocol 2), is necessary when long-term patency for sampling is the desired objective (10 to 60 days). The titanium port (e.g., from Instech Laboratories, SIMS Deltec, or Strategic Applications) allows collection of a single sample (while another person holds the animal) or the temporary attachment of the tether (using a jacket) for serial sampling. The port is placed subcutaneously in the intrascapular region. The vascular access port is an improvement on the old system in that it is locked physiologically, preventing loss of heparinized saline out of the cannula or seepage of blood into the cannula between sampling. This approach also minimizes clotting at the cardiac end of the cannula.

The vascular access port not only increases the length of patency for both sampling and infusion but also avoids long-term tethering of animals. Animals can be tethered temporarily, samples collected, and then the jacket and tether are removed while the animals are treated for some period (5 to 30 days). Finally, the animals are reattached to the tether and a second series of samples is collected from each animal. In this design each animal serves as its own control, reducing variation between animals with associated endocrine data.

Critical Parameters and Troubleshooting

In order to increase the chances of long-term patency, sterile technique, if possible, should be used during the entire surgical procedure. This is especially important when using the vascular access port. Surgical instruments should be sterilized between animals. The surgeon should wear sterile gloves and use a sterile drape for each animal whenever possible. Surgical gloves should be used and changed between animals and after an animal has been handled during the surgical procedure. The prepared portal and catheter should be placed on a sterile towel or drape prior to insertion into the animal. The surgeon and other technicians should refrain from handling the portal and catheter without wearing sterile gloves. Use aseptic technique whenever accessing the port post-operatively. Prior to blood sampling, sterilize jackets, tethers, and additional tubing, and use only sterile needles and syringes. Otherwise, there is the possibility of bacteria-induced clots (white blood cells) forming in the cannula.

During a long-duration study, animal growth is a concern. Be sure to place growth or tension loops under the skin at the ventral incision site when using the Preclinical Mini-Port. Care in choosing the strain of rat and the age at which surgery will take place will help minimize this complication. If the animal grows rapidly, there is the possibility that the cannula will be pulled from its original placement and sampling patency will be lost (usually infusion patency remains).

Care should be taken not to give the animal too much heparin during surgery. Some strains of rats are more sensitive to heparin than others. It is often advisable to use unheparinized saline during surgery (when checking cannula placement), and then to use the heparin/gentamicin saline to flush the cannula once it is in place. An animal with too much heparin will often bleed around its incisions and will be more likely to form hematomas at the tether button or portal site.

During blood sampling, do not remove >1 ml blood at each time point. Remove the minimal volume required to complete the work, and reinfuse resuspended RBCs whenever possible. By reinfusing the RBCs resuspended in saline, the animal's blood volume and hematocrit remain somewhat constant even though large amounts of blood and plasma have been removed over the total sampling period. RBCs can be damaged, however, as a result of all the processing. Thus, it is advisable to check hematocrit levels of the animals periodically. Hematocrit levels will not change immediately following blood transfusions or blood loss. Thus checking the hematocrit at the beginning and end of a sampling period will yield little difference in levels. Check the hematocrit on the first blood sample collected and again 24 hr later. Rats rarely show adverse clinical signs until their hematocrits are quite low (40% to 50% of normal). It would, however, be advis-

able to make sure that the hematocrits are within 10% to 20% of the original values before initiating a second sampling period (e.g., 1 or 2 days later).

Additional do's and don'ts during blood sampling include (1) making sure there is no air in the cannula and/or syringe when reinfusing RBCs or flushing through heparinized saline, (2) flushing saline or reinfusing RBCs relatively slowly to avoid a vascular system overload with a large bolus of solution, (3) avoiding leaving blood in the cannula for more than a few seconds (clotting occurs rather rapidly), and (4) avoiding using infusion solutions colder than room temperature.

Whether the permanent tether system or the vascular access port is used, if the cannula is patent for infusion but blood cannot be withdrawn, then there is the possibility that a small clot or flap may have formed at the tip of the cannula. Filling the cannula with a fibrinolytic agent, such as streptokinase or trypsin, for 24 hr may dissolve the clot. Often a fibrous sheath will form around the cannula. This has been determined to be composed of vascularized fibrous connective tissue and not fibrin (O'Farrell et al., 1996). Thus, fibrinolytic agents have little to no effect on it. It is best to flush the cannula with heparinized saline (in the case of the tether system) as often as possible, or to use a continuous infusion pump, to keep clots from forming. With the vascular access port, flushing the port every other day for the first week postsurgery is recommended. Generally, it is not necessary to check patency and flush the port and cannula more than once or twice a week after that.

Depending upon study design, the blood sampling procedure can be very labor intensive. If blood samples (with RBC reinfusion) are to be collected every 10 min, one person should be able to sample up to three animals (if all goes well). If 30 animals are being sampled at one time, then blood sampling personnel will number at least 10. At least two additional persons will be needed to continually process the blood samples during the sampling period. One or two people may be used to transport blood samples and reinfusion samples back and forth between the animal room(s) and the processing room. Another individual can provide technical and troubleshooting support to all other staff (backup).

The use of cannulated animals is particularly important when (1) stress hormones are being studied, (2) the effects of anesthesia are undesirable, (3) only one person is available for sampling, or (4) infusions are administered via computerized or mechanical pumps. With either approach (permanent tether or vascular port), blood samples can be withdrawn and/or treatments administered without handling the animal. This minimizes the stress response of hormones such as prolactin, corticosterone, oxytocin, and/or epinephrine, which are released when animals are restrained, anesthetized, frightened, or in pain (Suzuki et al., 1997).

The collection of samples from cannulated animals minimizes the release of these stress hormones and their impact on the hormones being studied. For example, norepinephrine and epinephrine concentrations were 2- to 8-fold lower in blood samples collected from jugular cannulas than in those collected from decapitated animals (Paulose and Dakshinamurti, 1987). Corticosterone response due to handling or stress was minimized (MacLeod and Shapiro, 1988). Cardiac response to the cannulation is resolved within 24 hr (Paulose and Dakshinamurti, 1987), and LH response to GnRH is normal within 2 days (Fail et al., 1992, 1998). FSH response may not be normal until 5 to 7 days after cannulation (P. Fail, unpub. observ.). Replacement of RBCs is used to maintain hematocrit in the normal range (MacLeod and Shapiro, 1988) for single samples taken over several days or during intense sampling windows such as for the ECT or LEBA (Fail et al., 1992).

Anticipated Results

The use of intra-atrial cannulation for serial sampling of unrestrained, untreated animals to illustrate endocrine secretion patterns is well established in the reproductive endocrinology literature and has significantly contributed to our understanding of endocrine signaling. These LEBAs are designed based on knowledge of the endocrine system being evaluated. For example, samples collected every 10 to 15 min during a 2- to 4-hr period can be used to determine profiles of a single hormone such as LH or thyroid stimulating hormone (TSH) and/or the relationship of two or more hormones (such as LH and testosterone, or TSH and thyroxine).

The authors (Fail et al., 1992, 1995, 1998, 1999) have collected endocrine data using both of these designs. The relationship of secretory patterns of LH to those of testosterone for untreated male rats in a LEBA is shown (Fig.

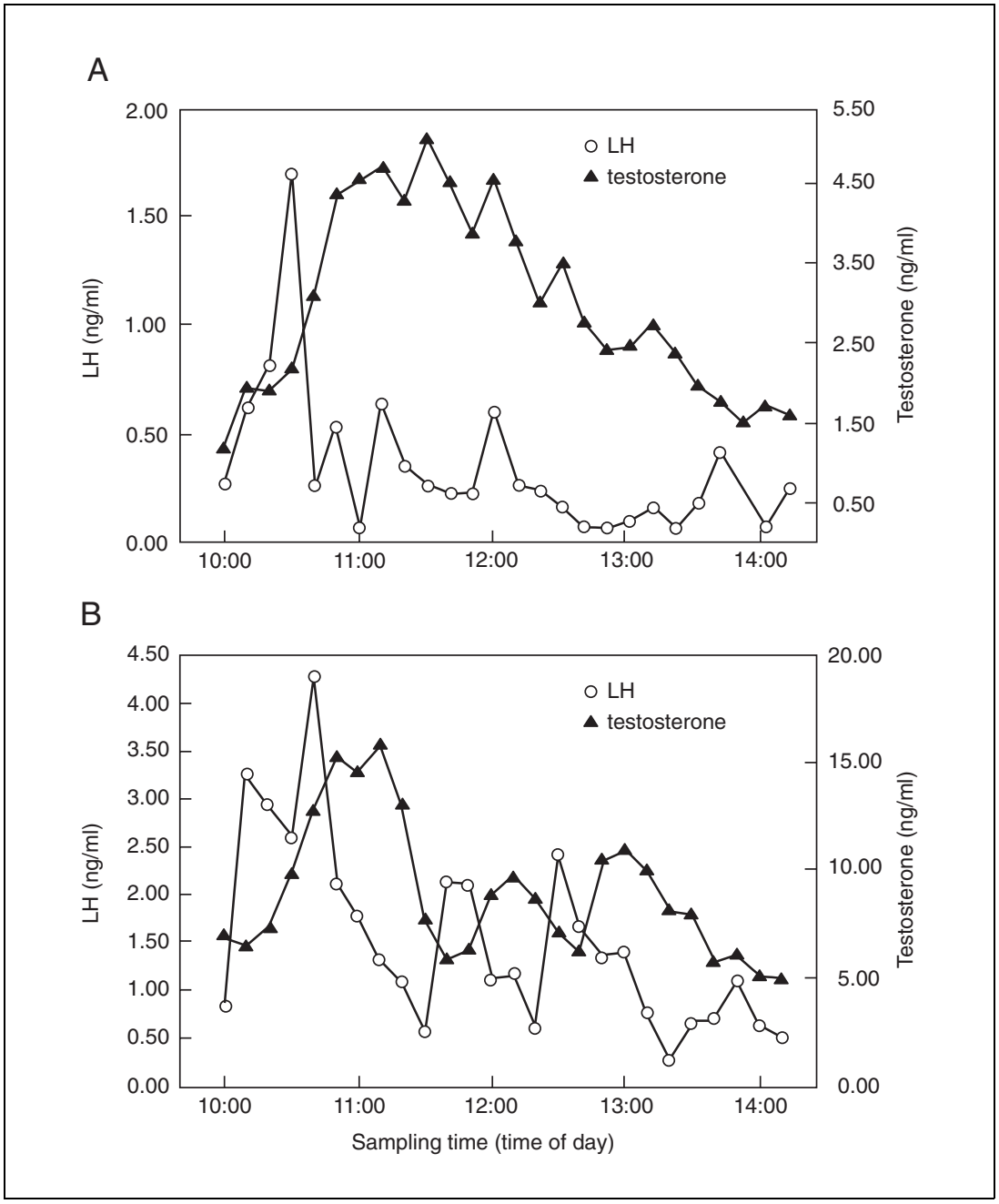

Figure 16.5.3 Longitudinal endocrine baseline assessment (LEBA) in two animals. Plasma luteinizing hormone (LH) and testosterone concentrations in a male Sprague Dawley rat were collected every 10 min during a 4-hr period. (**A**) Data are typical of a control (vehicle-treated) animal used for repeated sampling without endocrine challenge. The relationship of the two hormones within each time point and the prolonged response of testosterone to the LH spike is evident. In control animals, the LH spike lasted <30 min and evoked a broad plateau of testosterone release lasting >2 hr. (**B**) In animals treated with flutamide, LH concentrations were increased in amplitude and the spikes lasted longer than in controls. Testosterone response to LH, although it occurred, was of a shorter duration than for the control rat. Ten cannulated animals were prepared for each treatment group in this experiment, but the data were examined for individual animals, and typical curves are shown here. Data are from the authors' laboratory and are used with client's permission.

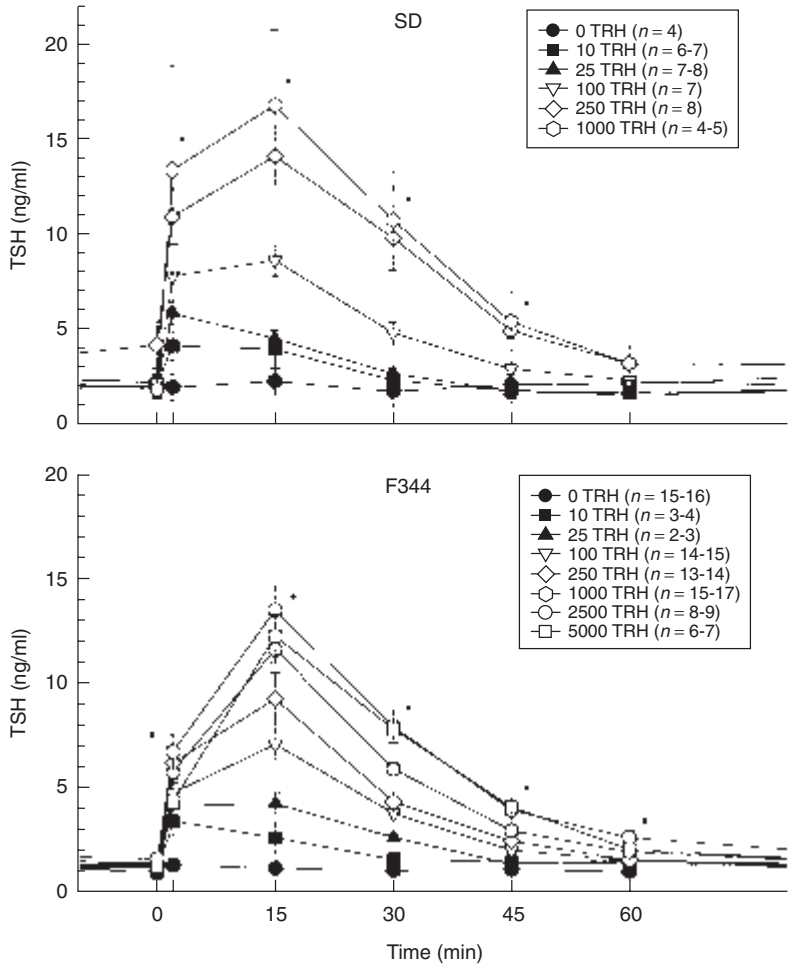

Figure 16.5.4 An endocrine challenge test (ECT) summarized for groups of animals. The response of thyroid stimulating hormone (TSH) to different concentrations of thyrotropin releasing hormone (TRH; dosage given in nanograms per 100 g) in male Sprague Dawley (SD) and Fisher 344 (F344) rats. In this ECT, an effective dose and duration of response was established. The difference in effective dose 50 (ED_{50}) for the two strains was established. Occasionally, samples could not be obtained from all animals for a specific time point. This is indicated by a range of *n* values. The lower number is the minimal number of animals represented in all points for that treatment. Asterisks indicate a statistically significant difference from controls within treatments ($p \leq 0.05$). Reprinted from Fail et al. (1999) with permission from Oxford University Press.

16.5.3A), and the data agree with those reported elsewhere (Ellis and Desjardins, 1982). The secretory patterns were changed for LH, FSH, and testosterone in males given flutamide (Fig. 16.5.3B). The authors also have ED_{50} data for LH, FSH, and testosterone after GnRH and hCG challenge in Sprague Dawley males, and for TSH, triodothyronine (T3), and thyroxine (T4) after thyrotropin releasing hormone (TRH) challenge (Fig. 16.5.4) in male Sprague Dawley and F344 rats.

Time Considerations

The total time for the cannulation protocol is short compared with that for the entire experiment. Planning should include the overall experimental plan. The total time will equal the sum of the following parts.

1. The development and design of the experiment requires 1 to 4 weeks depending on the available preliminary data and the knowledge of the endocrine system being evaluated. (An endocrine consultant should be used as needed.)

2. Animal Use Committee approval requires 1 to 4 weeks based on the frequency with which the committee meets. Also plan for Quality Assurance Unit approval of the experimental protocol if relevant.

3. Allow time for ordering supplies and materials; some materials are difficult to obtain or require assembly. The design will dictate whether vascular access ports are needed or if noncoring needles should be used for repeated access.

4. The surgery time per animal is based on the experience of the surgeon. Some animals will be more difficult to complete than others. If 30 animals are being used, allow 2 or 3 days. Sterilization of materials requires 1 to 7 days.

5. A recovery time of 7 days is recommended for indwelling (vascular access) ports. For an acute or short-term protocol, 2 days may be sufficient. The cannula should be flushed every other day during the recovery period.

6. The time required for sample collection depends on the experimental design. Allow 1 day for ECT and 1 day for LEBA studies. These times may be stretched out if all animals cannot be sampled during the same day (and same time regimen). Each technician can handle two to four animals simultaneously depending on the sampling regimen. The authors routinely handle 30 animals in a protocol using 10 to 14 technical staff. Allow 6 hr for a 4-hr LEBA.

7. Processing of the blood samples occurs simultaneously with sample collection. This includes the time needed to label and store the samples. Two technical staff are required.

Subsequent time considerations beyond the scope of these protocols include the sample radioimmunoassays (which require 2 days to 1 week per hormone and are hormone and sample number dependent), data management and statistical analysis (which require 2 to 4 weeks), and the generation of a study report (which requires 1 to 4 weeks, depending on the extent of the project and the use of good laboratory practices regulatory oversight).

Literature Cited

Coquelin, A. and Desjardins, C. 1982. Luteinizing hormone and testosterone secretion in young and old male mice. *Am. J. Physiol.* 243:E257-E263.

Dons, R.F. and Havlik, R. 1986. A multilayered cannula for long-term blood sampling of unrestrained rats. *Lab. Anim. Sci.* 36:544-547.

Ellis, G.B. and Desjardins, C. 1982. Male rats secrete luteinizing hormone and testosterone episodically. *Endocrinology* 110:1618-1627.

Fail, P.A., Sauls, H.R., Pearce, S.W., Anderson, S.A., and Izard, M.K. 1992. Measures of pituitary and testicular function evaluated with an endocrine challenge test (ECT) in cannulated male rats. *Toxicologist* 12:436 (abstr. 1725).

Fail, P.A., Pearce, S.W., Anderson, S.A., Tyl, R.W., and Gray, L.E. Jr. 1995. Endocrine and reproductive toxicity of vinclozolin (VIN) in male Long-Evans hooded rats. *Toxicologist* 15:293 (abstr. 1570).

Fail, P.A., Chapin, R.E., Price, C.J., and Heindel, J.J. 1998. General, reproductive, developmental, and endocrine toxicity of boric acid and inorganic boron-containing compounds: A review. *Reprod. Toxicol.* 12:1-18.

Fail, P.A., Anderson, S.A., and Friedman, M.A. 1999. Response of the pituitary and thyroid to tropic hormones in Sprague-Dawley versus Fischer 344 male rats. *Toxicol. Sci.* 52:107-121.

Harms, P.G. and Ojeda, S.R. 1974. A rapid and simple procedure for chronic cannulation of the rat jugular vein. *J. Appl. Physiol.* 36:391-392.

MacLeod, J.N. and Shapiro, B.H. 1988. Repetitive blood sampling in unrestrained and unstressed mice using a chronic indwelling right atrial catheterization apparatus. *Lab. Anim. Sci.* 38:603-608.

McKenna, M.L. and Bier, J.G. 1984. Multilayer cannula for long-term infusion of unrestrained rats. *Lab. Anim. Sci.* 34:308-310.

O'Farrell, L., Griffith, J.W., and Lang, C.M. 1996. Histological development of the sheath that forms around long-term implanted central venous catheters. *J. Parenter. Enteral Nutr.* 20:156-158.

Paulose, C.S. and Dakshinamurti, K. 1987. Chronic catheterization using vascular-access-port in rats: Blood sampling with minimal stress for plasma catecholamine determination. *J. Neurosci. Methods* 22:141-146.

Simard, J., Luthy, L., Guay, J., Belanger, A., and Labrie, F. 1986. Characteristics of interaction of the antiandrogen flutamide with the androgen receptor in various target tissues. *Mol. Cell. Endocrinol.* 44:261-270.

Suzuki, K., Koizumi, N., Hirose, H., Hokao, R., Takemura, N., and Motoyoshi, S. 1997. Blood sampling technique for measurement of plasma arginine vasopressin concentration in conscious and unrestrained rats. *Lab. Anim. Sci.* 47:190-193.

Tyl, R.W. 2002. In vivo models for male reproductive toxicity. *In* Current Protocols in Toxicology (M. Maines, L.G. Costa, E. Hodgson, and D.J. Reed, eds.) pp. 16.1.1-16.1.15. John Wiley & Sons, New York.

Viguier-Martinez, M.C., Hochereau de Reviers, M.T., Barenton, B., and Perreau, C. 1983a. Effect of a nonsteroidal antiandrogen, flutamide, on the hypothalamo-pituitary axis, genital tract and testis in immature rats: Endocrinological and histological data. *Acta Endocrinol.* 102:299-306.

Viguier-Martinez, M.C., Hochereau de Reviers, M.T., Barenton, B., and Perreau, C. 1983b. Endocrinological and histological changes induced by flutamide treatment on the hypothalamo-hy-

pophyseal testicular axis of the adult male rat and their incidences on fertility. *Acta Endocrinol.* 104:246-252.

Weeks, J.R. and Davis, J.D. 1964. Chronic intravenous cannulas for rats. *J. Appl. Physiol.* 19:540-541.

Key Reference

Anonymous, 1993. Preclinical Mini-Port Implantable Vascular Access Device, pamphlet 40-2931-01A. Pharmacia-Deltec (now SIMS Deltec), St. Paul, Minnesota.

This pamphlet is the basis for the surgical implantation and the use of the vascular access port.

Contributed by Patricia A. Fail and Stephanie A. Anderson
Research Triangle Institute
Research Triangle Park, North Carolina

Epididymal Sperm Count

Epididymal sperm count is a widely used, simple, and sensitive method for assessing the effects of male reproductive toxicants on the epididymis and/or testis. Usually the epididymis is divided into three parts: the caput, corpus, and cauda (Fig. 16.6.1). It is the epididymal cauda that is extensively used to perform epididymal sperm count. The method described in this unit is principally used for fresh tissue from rodents; however, the method can also be used for frozen epididymides with modifications.

Materials

PBS (*APPENDIX 2A*)
Necropsied male rats or mice, treated and control, euthanized
15 × 60–mm (rats) or 15 × 30–mm (mice) and 1.5 × 2.0–cm petri dishes
Slide warmer
13 × 100–mm test tubes and appropriate rack
Microscope: 10× and 40× objectives and 10× or 15× eyepieces
Necropsy board
0.1-mm-deep improved Neubauer hemacytometer and coverslips
No. 11 scalpel blades
60°C water bath
Gauze
Hand tally counter
Data collection system (i.e., hand-generated data form or computer-generated data collection system)

Additional reagents and equipment for using a hemacytometer (*APPENDIX 3B*)

NOTE: All protocols using live animals must first be reviewed and approved by an Institutional Animal Care and Use Committee (IACUC) and must follow officially approved procedures for the care and use of laboratory animals.

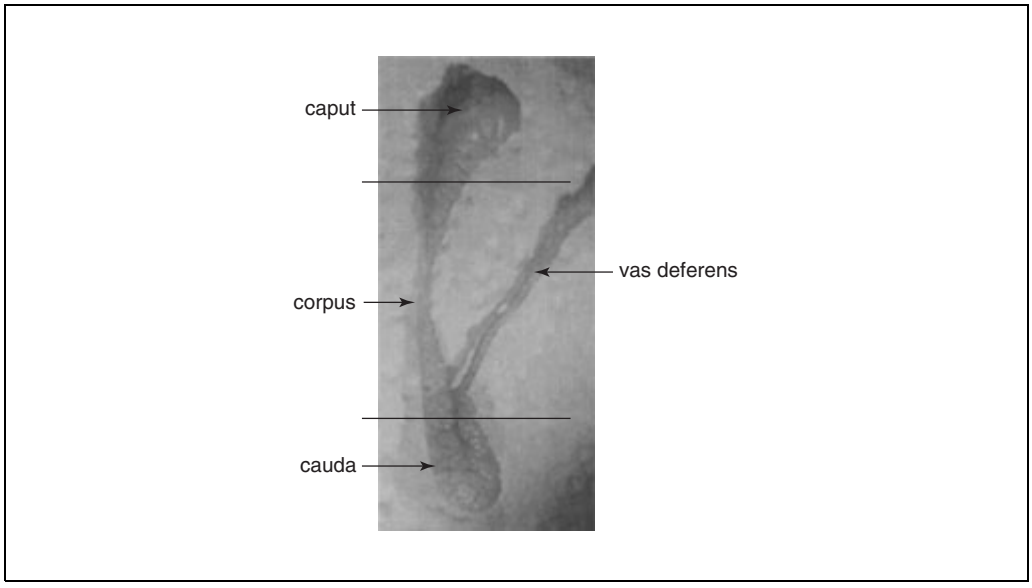

Figure 16.6.1 A rat epididymis and its three anatomic parts: caput, corpus, and cauda.

Contributed by Yefan Wang
Current Protocols in Toxicology (2002) 16.6.1-16.6.5

Prepare equipment

1. Label 15 × 60–mm (rats) or 15 × 30–mm (mice) petri dishes one for each animal, with the corresponding animal numbers. Fill with PBS (2 or 10 ml for mice or rats, respectively), and place on a slide warmer set at 35° to 37°C.
2. Equilibrate a water bath to ~60°C.

   If using a hot plate, use a glass beaker (100 ml) containing ~50 ml water.

   The purpose of the water bath is to kill motile sperm and allow an accurate count.
3. Label 13 × 100–mm test tubes, one for each animal, with the corresponding animal numbers. Add 2 ml PBS to each tube.
4. Turn the microscope on.
5. Clean a 0.1-mm-deep improved Neubauer hemocytometer and coverslips (both need to be cleaned between animals).

Prepare samples

6. Acquire the first necropsied male rats or mice, treated or control, euthanized by an approved method.
7. Place the animal on a necropsy board with the ventral side up. Open the abdominal cavity by making an ~5 cm incision in the lower right abdominal area. Pull out the right epididymis and testis by grasping the epididymal fat with a pair of forceps, leaving the vas deferens attached as a reference point (Fig. 16.6.1).
8. Isolate the epididymis from the testis and trim away fat. Place the entire epididymis on a flat surface. Procure the epididymal cauda by cutting ~1 mm down from the junction of the vas deferens and the epididymis cauda (see Fig. 16.6.1).
9. Measure and record the weight of the cauda in milligrams.
10. Place the cauda in a petri dish containing a known volume of PBS (2 or 10 ml for mice and rats, respectively) prewarmed to 35° to 37°C, and mince using two no. 11 scalpel blades to open the epididymal duct and release its contents. Swirl the petri dish several times to achieve a uniform sperm suspension.
11. After incubating at least 15 min at 35° to 37°C, mix the sperm suspension several times using a Pasteur pipet.
12. Using a 1-ml pipet, transfer 0.5 ml sperm suspension from the petri dish to a corresponding test tube containing 2 ml PBS, room temperature, avoiding transferring the epididymal tissue. Mix the tube by lightly tapping the bottom.
13. Place the test tube in a ~60°C water bath for ~1 min. Return the tube to the test tube rack and cool to room temperature.

Count sperm

14. Mix the diluted suspension, measure 10 µl with a micropipet, and load one side of the hemacytometer. Next, mix the suspension again by vortexing and load the other chamber. Place the loaded hemacytometer onto a clean 1.5 × 20–cm petri dish, bedded with a portion of moist gauze, for 2 min to allow the sperm to settle.
15. Place the hemacytometer on the microscope stage and focus on the top left secondary square (square no. 1; see Fig. A.3B.1 in *APPENDIX 3B*) of the tertiary square.
16. Count the number of sperm (entire structure) lying in the five secondary squares (nos. 1 to 5) and lying on or touching the top and left lines of the secondary squares (Fig.

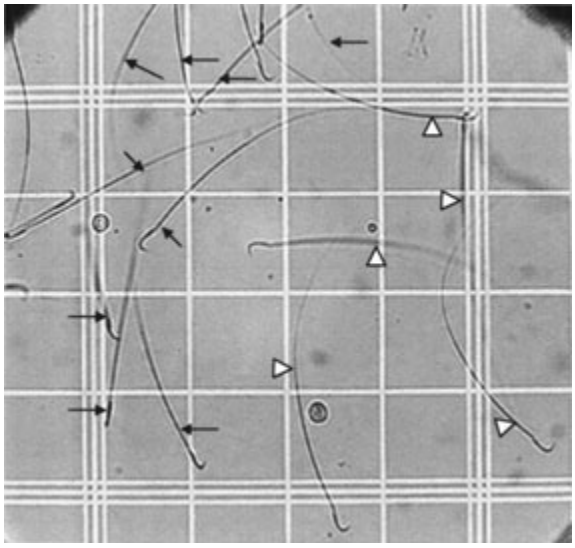

Figure 16.6.2 Actual microscopic photograph of the secondary square (area within the triple line border) of a hemacytometer (see Fig. A.3B.1 in *APPENDIX 3B*). The black arrows indicate the nine sperm that will be counted; five white arrows identify the sperm that will not be counted.

16.6.2). If there are less than 25 sperm in those five secondary squares, count the sperm in the entire tertiary square (all 25 secondary squares).

If any part of the sperm lies within or over the right and/or bottom lines, crossing right and bottom lines, it must be excluded from the count. If any part of the sperm lies within or over the left and/or top line, crossing either top or left line, that sperm must be counted.

There is one tertiary square on each side of the hemacytometer.

17. If clumped sperm are noted, reload and recount.
18. Record two counts for each animal on a hand tally counter and data collection system.
19. Calculate the total number of sperm per cauda epididymis based on the secondary count:

$$\text{Total sperm} = \text{mean count} \times \text{dilution factor}$$

where:

$$\text{Mean count} = (\text{count 1} + \text{count 2})/2$$

and

$$\text{dilution factor} = \frac{\text{total vol. PBS in dish}}{\text{transferred vol.}} \times \frac{\text{total vol. test tube}}{\text{vol. secondary square} \times \text{no. squares}}$$

For the protocol listed above, the transferred volume is 0.5 ml and the volume of a secondary square is 4×10^{-6} ml.

20. Calculate the epididymal sperm count per milligram cauda (sperm density):

Sperm density = (mean count × dilution factor)/cauda weight (mg) *or*

Sperm density = total number sperm per cauda/cauda weight (mg).

COMMENTARY

Background Information

The epididymis is a single, highly-coiled duct with functions that include reabsorption of the rete testis fluid, metabolism, epithelial cell secretions, sperm maturation, and sperm storage. The caput and the corpus play important roles in sperm maturation, with the cauda regarded as the site of sperm storage. The sperm require 1.8 to 4.9 days to move through the caput to the corpus epididymis and the travel time of sperm through the cauda ranges from 3.7 to 9.7 days among different species (Klassen, 1996). The first appearance of spermatozoa is detected in the caput at 45 days of age and in the cauda at 52 days of age, while the sperm population reaches the maximum in the caput at 72 days of age and in the cauda at 100 days of age. The sperm population is maintained beyond 450 days of age (Saksena et al., 1979). The number of sperm in the corpus and the caput epididymis is similar in sexually rested males and in males ejaculating daily. The number of sperm in the cauda epididymis may vary depending on the male's sexual activity (see Table 16.6.1).

Epididymal tissues are often obtained after a terminal sacrifice. This method can be modified and used on other species by adjusting the dilution. W.G. Kempinas (1988) recommends treating sperm suspensions with 0.05% collagenase for 20 to 60 min or 0.025% trypsin for 1 to 2 min at 34° to 37°C, which was found to result in a consistently homogeneous sperm sample. The Hamilton Thorne Biosciences Integrated Visual Optical System provides a fluorescent method of determining sperm concentration without the interference of detritus by

Table 16.6.1 Sperm Count in the Reproductive Track of Albino Rats[a]

	Number of animals	Number of Sperm in vas deferens[b]	Number of sperm in cauda[b]	Number of sperm in caput and corpus[b]
Sexually rested rats	13	28.2 ± 3.4	299.3 ± 19.7	153.9 ± 8.2
Mated rats	12	3.4 ± 1.6	110 ± 5.8	129.8 ± 11.1

[a]Rats are the Wistar strain of *Rattus norwegicus*. See Ratnasooiya and Wadsworth (1987) for details.

[b]Sperm count for the paired tract, given as mean ± s.e.m. All values are given in millions.

Table 16.6.2 Troubleshooting Guide for Sperm Count Errors

Problem	Possible cause	Solution
Count too low	Animals are too young (<60 days)	Use rats that are at least 60 days old
	Only a partial cauda was used	Refer to Fig. 16.6.1
	Settle time is too short (<2 min)	Use a timer (may help)
	Sharing cauda with sperm motility analysis	If possible, collect motility sample from vas deferens
	Incorrect dilution procedure	Review the dilution procedure
	Treatment effects reduced sperm output from the testis or speeds epididymal transit	Determine if a dose-related decrease is evident
Count too high	Cauda isolated with partial caput	Refer to Fig. 16.6.1
	Incorrect dilution procedure	Review the dilution procedure
	Clumping sample	Verify settle time and make dilution if necessary
Inconsistent count	Shorter settle time	Use a timer (may help)
	Clumping or nonhomogeneous sample	Mix well prior to sampling
	Inconsistent excision of the cauda	Refer to Fig. 16.6
	Underload or overload by using a Pasteur pipet	Switching to a micropipet might help

Table 16.6.3 Sperm Density and Total Number of Sperm per Cauda in Rodents[a]

Strain/species	Cauda sperm density (sperm/mg)[b]	Cauda sperm count[c]
CD-1 Mice	778.70 ± 331.718 (40)	16.35 ± 2.395 (40)
FVB Mice	470.90 ± 267.344 (53)	6.48 ± 3.726 (53)
C57BL/6 Mice	1376.49 ± 430.727 (19)	25.36 ± 5.728 (19)
Tg. AC Mice	437.44 ± 221.844 (42)	5.87 ± 3.268 (42)
CD-1 Rats	369.86 ± 114.480 (160)	145.06 ± 32.914 (160)
Fisher 344 Rat	702.00 ± 145.502 (30)	111.69 ± 26.251 (30)

[a]Values are given as mean ± std. dev. (sample size).

[b]Represents the sperm concentration (density) in cauda epididymis. Mean and std. dev. are given in thousands.

[c]Represents the total number of sperm stored in cauda epididymis. Mean and std. dev. are given in millions.

using IDENT STAIN, a DNA-specific fluorescent dye (Hamilton Thorne Research, 1989).

Another measurement that may be conducted with the remaining sperm suspension is preparing sperm suspension slides to perform sperm morphology evaluation.

Critical Parameters and Troubleshooting

As noted, this method is mainly a physical dilution process, so anything that affects the cauda weight and volume, and/or the homogeneity of suspension, consistency of sample collection, or counting will influence the results.

Table 16.6.2 presents some common problems encountered with these procedures, and their solutions.

Anticipated Results

The results, sperm density, and total number of sperm per cauda in a variety of strains of rodents, as determined in the author's laboratory, are listed in Table 16.6.3.

Time Considerations

The estimated processing time of epididymal sperm count samples is ~15 to 30 min per sample (necropsy time is not included).

Literature Cited

Hamilton Thorne Research 1989. HTM-IVOS Toxicology Application Version 10.8 Operation Manual. Hamilton Thorne Biosciences, Beverly, Mass.

Kempinas, W.G. and Lamano-Carvalho, T.L. 1988. A method for estimating the concentration of spermatozoa in the rat cauda epididymis. *Lab. Anim.* 22:154-156.

Klassen, C.D. 1996. Fifth Casarett & Doull's Toxicology: The Basic Science of Poisons, Fifth Edition. McGraw-Hill, New York.

Saksena, S.K., Lau, I-F. and Chang, M-C. 1979. Age dependent changes in the sperm population and fertility in the male rat. *Exp. Aging Res.* 5:373-381.

Ratnasooriya, W.D. and Wadsworth, R.M. 1987. Effect of mating on sperm distribution in the reproductive tract of the male rat. *Gamete Res.* 17:261-266.

Contributed by Yefan Wang
TherImmune Research Corporation
Gaithersburg, Maryland

Performing a Testicular Spermatid Head Count

The estimation of sperm production is an important parameter of male reproductive toxicology. One way to make the estimation is to count spermatid heads using a hemacytometer. The Basic Protocol describes this simple and reproducible method, which provides a good estimation of sperm production. The Support Protocol provides examples for calculating the testicular spermatid head concentration.

PERFORMING A TESTICULAR SPERMATID HEAD COUNT

BASIC PROTOCOL

This protocol describes procedures for preparing testes for homogenization, homogenizing a testis, loading the suspension onto a hemacytometer, and counting the spermatid heads using a compound microscope.

Materials

Frozen testes from mouse or rat (*UNIT 16.3*; Feldman and Seeley, 1988), frozen individually in scintillation vials on dry ice at −70°C or below
DMSO/saline solution (see recipe)
0.1% (w/v) trypan blue stain (see recipe)

125-ml Erlenmeyer flasks (for rats) or 12-ml test tubes (for mice)
Disposable weigh boats
Cyclone homogenizer with 20-mm (for rats) or 10-mm (for mice) rotor (VirTis)
Scalpel or razor blades
Microdissecting forceps (two pairs)
Homogenization vessels (50- to 100-ml for rats, 20-ml for mice; Jencons Scientific)
Lint-free wipes (e.g., Kimwipes)
10-, 50-, and 500-µl volumetric micropipettors
Hemacytometer with two chambers and coverslip
Compound microscope with 40× objective and 10× eyepiece
Cell counter

Prepare homogenizer

1. Label a 125-ml Erlenmeyer flask (for rats) or a 12-ml test tube (for mice) and a disposable weigh boat with identification corresponding to samples to be analyzed.
2. Turn on a cyclone homogenizer and set the homogenization duration to 1.0 min and rotor speed to 7500 rpm.
3. Secure a 20-mm (for rats) or a 10-mm (for mice) rotor in the homogenizer.

Prepare testis

4. Thaw a frozen testis for 2 to 3 min (for 1.5-g rat testis) or 1 min (for 0.1-g mice testis) in the labeled disposable weigh boat.
5. Make a shallow incision with a scalpel or razor blade in the tunica albuginea, the tough fibrous outer coat of the testis. Use a pair of microdissecting forceps to hold the testis.
6. Remove tunica and associated blood vessels from testis with a second pair of microdissecting forceps.

Contributed by Han Seung, Gary Wolfe, and Meredith Rocca
Current Protocols in Toxicology (2003) 16.7.1-16.7.6

7. Obtain the weight of the testis without tunica and associated blood vessels.

   A balance with three decimal places should be used for rats and one with four decimal places should be used for mice.

Homogenize testis

8. Transfer testis to an appropriate homogenization vessel.
9. Add 25 ml DMSO/saline solution for rat testis or add 5 ml DMSO/saline solution for mouse testis.
10. Drop rotor to 20 mm above the bottom of homogenization vessel for rat testis or to 10 mm above the bottom of homogenization vessel for mouse testis.
11. Homogenize testis 1 min at 7500 rpm.
12. Pour contents into the labeled 125-ml Erlenmeyer flask for rat testis or the 12-ml test tube for mouse testis.
13. Repeat steps 10 to 12 twice more for rat testis, first with another 25 ml and second with 50 ml DMSO/saline, adding both washes to labeled flask. Repeat only once more with 5 ml DMSO/saline for mouse testis.

    Alternatively, a smaller amount of DMSO/saline can be used, but further dilution will be necessary. For example, if only 25 ml DMSO/saline is used to make the homogenate, further dilution by a factor of 4 (i.e., adding 1 ml homogenate to 3 ml DMSO/saline) will be equivalent to a homogenate in a total volume of 100 ml DMSO/saline. When working with smaller volumes, however, any accidental losses in sample volume will have an even greater effect on the accuracy of the count; it is even more crucial that no spillage occurs.

14. Rinse homogenization vessel and rotor three times using deionized water.

    The inside of the rotor should be checked before rinsing. Occasionally the testis is stuck inside the rotor and does not get homogenized completely. In such an event, cut testis into two or three pieces with razor blade, and then rehomogenize with pooled 100 ml DMSO/saline (step 13), using 25 ml each for first and second washes and 50 ml for final wash. For mouse testis, use two 5-ml washes.

15. Dry homogenization vessel and rotor with lint-free wipes.

    The vessel and rotor are now ready for another sample.

Stain spermatid heads

16. Using an appropriate volumetric micropipettor, add 500 µl of 0.1% trypan blue into flask for a rat testis or add 50 µl of 0.1% trypan blue into test tube for a mouse testis.
17. Cover flask or test tube with Parafilm and vortex 5 sec at 2000 rpm. Stain ≥1 min.

    Although there is no upper time limit for staining, the homogenate will degrade after ~6 hr, making spermated counts unnecessarily harder.

Count spermatid heads

18. Vortex spermatid head suspension 10 sec and use a 10-µl micropipettor to load 10 µl suspension into a hemacytometer (Fig. A.3B.1) with coverslip already in place.
19. Let spermatid heads settle 5 min before counting.

    The suspension must not be allowed to evaporate. Placing the hemacytometer on moist gauze in a large petri dish will prevent evaporation of the suspension.

20. Place hemacytometer on the stage of a compound microscope so that both chambers can be viewed.

21. Set objective lens to 40× and focus on one of the counting chambers.

    Each hemacytometer contains two chambers. Each chamber has one tertiary square (Fig. A.3B.1).

22. Using a cell counter, count spermatid heads in first and last rows of secondary squares (a total of ten secondary squares) using a cell counter. Also count spermatid heads that are not touching any of the lines within secondary squares, as well as the spermatid heads touching bottom and right lines. Focus in and out of depth to count sperm not in focus. Record the number of spermatid heads.

    Trypan blue stains spermatid heads a light blue color.

23. Focus on the other counting chamber and repeat step 22.

24. Clean hemacytometer and its coverslip using wet lint-free wipes.

    Alternatively, the hemacytometer and the coverslip can be rinsed and then dried with a wipe.

    If the discrepancy between the two counts is >25% (i.e., the higher count is >125% of the lower count), the count should be repeated (steps 18 to 23). As an example, if the first count was 67 and the second count was 77, the second count is 15% higher than the first count: (77/67) × 100 = 1.149 or 15% higher. The count should also be repeated if any of the counts are <40 or >110. In the case of a repeated count only the two most recent counts are used to generate an average. Sperm samples with very high count (>150) can be diluted with DMSO/saline before recounting.

    Counts will generally range from 60 to 100 spermatids for a typical rat or mouse testis. Various factors such as low testis weight or incorrect homogenization volume can change the counts.

CALCULATING TESTICULAR SPERMATID HEAD CONCENTRATION

SUPPORT PROTOCOL

Each chamber of the hemacytometer is designed to hold 0.1 µl of solution in its tertiary square. The tertiary square is divided into 25 secondary squares, which are in turn divided into 16 primary squares. Thus each secondary square contains 0.004 µl. Because ten secondary squares are used for counting, 0.04 µl of suspension is used per chamber. The total volume of rat testis suspension is 100.5 ml, and mouse testis is 10.05 ml. Thus, the total number of spermatid heads in a rat testis is (mean count/0.00004 ml) × 100.5 ml. The total number of spermatid heads in a mouse testis is (mean count/0.00004 ml) × 10.05 ml.

Example 1: If counts for a rat were 75 and 79, or a mean count of (75 + 79)/2 = 77, then the total number of spermatid heads in the testis is (77/0.00004) × 100.5. This is equal to ~193 million spermatid heads. If the testis weighed 1.529 g, then there are 127 million spermatid heads per gram testis. The daily sperm production is then 20.7 million spermatids per gram testis per day or 31.7 million spermatids per testis per day, using 6.10 days as the time divisor (see Background Information; Oakberg, 1956).

Example 2: If the counts for a mouse testis were 69 and 76, or a mean count of (69 + 76)/2 = 72.5, then the total number of spermatid heads in the testes is (72.5/0.00004) × 10.05. This is equal to ~18.2 million spermatid heads. If the testis weighed 0.1016 g, then there are 179 million spermatid heads per gram testis. The daily sperm production is then 37.0 million spermatids per gram testis per day or 3.8 million spermatids per testis per day, using 4.84 days as the time divisor (see Background Information; Robb et al., 1978).

REAGENTS AND SOLUTIONS

Use Milli-Q-purified water or equivalent in all recipes and protocol steps. For common stock solutions, see ***APPENDIX 2A****; for suppliers, see* ***SUPPLIERS APPENDIX****.*

Dimethyl sulfoxide (DMSO)/saline solution

Place 18.00 g NaCl (0.9% final) in a 2-liter container. Add 1.60 liter water. Mix vigorously to dissolve NaCl. Add 200 ml DMSO (10% final). Bring to 2 liters with water. Store up to 30 days at room temperature.

This volume should be enough to suspend ~20 samples of rat testes or 200 samples of mice testes.

CAUTION: *DMSO can be very toxic because of its permeability.*

Trypan blue stain, 0.1% (w/v)

Mix together 10 mg trypan blue and 10 ml water. Stir until all crystals are dissolved. Store up to 1 year at room temperature.

The solution is a dark navy blue color. It may take a few minutes of stirring for all crystals to dissolve completely.

This volume should be enough for ~20 samples of rat testes or 200 samples of mice testes.

COMMENTARY

Background Information

The testis is a multicompartmental organ packed with highly convoluted tubules called seminiferous tubules. These tubules meet to form the rete testis. From the rete testis, ductuli efferentes connect to the epididymis where sperm mature and are stored. These tubules contain Leydig cells, Sertoli cells, spermatogonia, and other cells. Leydig cells secrete hormones such as testosterone. Sertoli cells secrete fluid into the lumen of the tubules. The testis is wrapped in a tough connective tissue called the tunica, which holds the seminiferous tubules together.

The seminiferous tubules are lined with spermatogonial stem cells known as A_0. A mitotic division of these cells gives rise to A_1 spermatogonial cells. These cells gradually displace toward the lumen by subsequent mitotic divisions. After six mitotic divisions, spermatogonial cells divide to produce primary spermatocytes. Further meiotic division produces secondary spermatocytes, and after another meiotic division, they form spermatids.

At the beginning, the heads of spermatids are round without remarkable morphology. However, they undergo a dramatic metamorphosis and become spermatozoa, which look like hooks. Toward the end of this metamorphosis, the nucleoprotein condenses and the cells become resistant to homogenization and detergent. The period during which cells are resistant to homogenization and detergent is referred to as the time divisor and is used to calculate the daily production of spermatids in a testis. The time divisor for rats is 6.10 and that of mice is 4.84 according to Oakberg (1956) and Robb et al. (1978), respectively. The overall duration of spermatogenesis within a testis is 52 days in rats and 36 days in mice.

An alternative method of estimating daily sperm production is by counting A_1 cells. A_1 cells are the spermatogonial cells derived from spermatogonial stem cells. By counting the A_1 cells, one can estimate the theoretical concentration of spermatids in a testis. Not all cells arising from A_1 cells, however, will become mature sperm. Also, this requires histological sampling. This method requires more time and materials and is more prone to error during preparation without better accuracy, as compared with the method of counting spermatid heads in testicular homogenates described here.

The epididymal sperm count (*UNIT 16.6*) provides quantitation of sperm that is stored and thus is available for ejaculation and fertility. Sperm is stored over a period of time, however, masking acute changes in the sperm production rate. Unlike epididymal sperm count, the testicular spermatid head count provides better quantitation of acute changes in sperm production, thus providing a better snapshot of changes in spermatogenesis within testes. This parameter can provide crucial information regarding reproductive toxicity of a test compound. Either an increase or decrease in the concentration of spermatid heads can indicate pathology. An increase in the spermatid head

concentration suggests that there is sperm retention (or inhibited sperm release; Ku et al., 1993; Linder et al., 1997). A decrease in the spermatid head concentration may be due to atrophy of the testis, changes in circulating hormones, loss of germ cell line, or physiological changes to Sertoli cells or Leydig cells. Histological examination may help clarify the underlying pathologic process (*UNITS 16.3 & 16.4*). Spermatid head count will not, however, provide any information about fertility without other parameters such as motility, morphology, and epididymal sperm counts.

There are two mixtures commonly used for homogenization. The authors prefer using DMSO/saline because of its shorter preparation time and longer expiration date. Another solution to suspend the spermatid heads is 0.9% (w/v) saline/0.1% (v/v) Triton X-100. This solution requires several hours to prepare and expires in weeks. Unlike saline/Triton X-100, DMSO/saline can be prepared within minutes, so as not to lose the capability of counting spermatid heads, and expires in 1 month.

The Basic Protocol describes a method that uses a hemacytometer to count testicular spermatid heads. An alternative method is to use a computer-assisted counting machine, such as the Hamilton Thorne 2030 (Hamilton Thorne Biosciences) or IVOS (Hamilton Thorne Biosciences). According to Centola (1996), the variability between samples is less when counts by the computer system are compared with manual ones, and counting error within a sample is comparable between the two methods.

Critical Parameters and Troubleshooting

Storage conditions

It is critical that the testes not be stored at −70°C for >6 months; for long-term storage (up to 12 months), they should be stored at −80°C or below. If the testes are not stored at −80°C or lower, they will be under risk of desiccation (freezer burn), a drying of the sample during storage in a freezer. Desiccation changes testicular weight, thus changing data for spermatids per gram testis.

Thawing

The purpose of thawing is to remove the parenchyma surrounding the testis. If the testis is not thawed sufficiently, it will make removal of the parenchyma difficult. If the testis is thawed too much, then there is a risk of removing a portion of the testis, decreasing the total number of spermatids per testis.

Homogenization

All the materials used during homogenization must be clean. Otherwise there will be cross-contamination between samples. Rinsing with deionized water three to four times will prevent cross-contamination between samples.

Consistency of counts

It is imperative for the person who counts the spermatids to be consistent. All the counts must be done in exactly the same manner. For example, if right and lower borders of secondary squares are included and not upper and left borders, then all the counts must include any spermatid heads touching lower and right borders, and they must exclude any spermatid heads touching upper and left borders of secondary squares.

Because only a small amount of the solution is used to count, the stained spermatids must be thoroughly suspended before loading the hemacytometer. Small deviations in the suspension will result in a great variability in the concentration of spermatids.

Also, it is important to focus in and out during counting. Because of the high magnification power of the microscope, the focal plane is rather shallow. Most of the spermatid heads will settle down on the hemacytometer, but some may stay suspended between the grids and the coverslip. Exclusion of these spermatid heads will underestimate the true concentration and renders the data inaccurate.

Data analysis

Repeating a spermatid head count if the higher count is >125% of the lower count is to prevent random abnormal sampling. Repeated counts ensure that an abnormally higher or lower count does not affect the mean of the group being analyzed. Counts of <40 spermatids are repeated to ascertain the values, because a change in a small number will make a more drastic change in the overall number. Counts of >110 spermatids are repeated to ensure accuracy of a dense field. It is harder to count when there are many overlapping spermatids in the field.

Anticipated Results

A typical count using the hemacytometer method described in this unit will yield between 60 to 100 testicular spermatid heads for rat or

mouse testis. According to a study conducted by Blazak et al. (1985) on the daily sperm production rate of Fischer 344 rats, a typical 20-week-old male rat has a testicular weight of 1.2 to 1.6 g/testis and produces 16 to 30 million sperm a day. With a time divisor of 6.10, a typical total spermatid head count for a rat testis will contain 185 million sperm.

In contrast, according to the same study, the daily sperm production rate of a typical 13-week-old male B6C3F1 mouse is 3.4 to 6.8 million per day, and its testis weighs 0.08 to 0.11 g. With a time divisor of 4.84 days, a typical total spermatid head count from a mouse testis is 24.1 million sperm.

Time Considerations

The whole procedure, including making solutions, will require 10 hr to perform spermatid head counts on 20 rat testes. The approximate time required for each step is as follows: solution preparation, 0.5 hr; setup and labeling flasks or tubes, 0.5 hr; sample preparation, 4 hr; spermatid head counts, 5 hr.

Literature Cited

Blazak, W.F., Ernst, T.L., and Stewart, B.E. 1985. Potential indicators of reproductive toxicity: Testicular sperm production and epididymal sperm number. Transit time, and motility in fischer 344 rats. *Fundam. Appl. Toxicol.* 5:1097-1103.

Centola, G.M. 1996. Comparison of manual microscopic and computer-assisted methods for analysis of sperm count and motility. *Arch. Androl.* 36:1-7.

Feldman, D.B. and Seeley, J.C. 1988. Necropsy Guide: Rodents and the Rabbit. CRC Press, Boca Raton, Fla.

Ku, W.W., Chapin, R.E., Wine, R.N., and Gladen, B.C. 1993. Testicular toxicity of boric acid (BA): Relationship of dose to lesion development and recovery in the F344 rat. *Reprod. Toxicol.* 7:305-319.

Linder, R.E., Klinefelter, G.R., Strader, L.F., Suarez, J.D., and Roberts, N.L. 1997. Spermatotoxicity of dichloroacetic acid. *Reprod. Toxicol.* 11:681-688.

Oakberg, E.F. 1956. Duration of spermatogenesis in the mouse and timing of stages of the cycle of the seminiferous epithelium. *Am. J. Anat.* 99:507-516.

Robb, G.W., Amann, R.P., and Killian, G.J. 1978. Daily sperm production and epididymal sperm reserves of pubertal and adult rats. *J. Reprod. Fertil.* 54:103-107.

Key Reference

Zenick, H., Clegg, E., Perreault, D., Klinefelter, G., and Gray, L. 1994. Assessment of male reproductive toxicity: A risk assessment approach. *In* Principles and Methods of Toxicology, 3rd ed. (A.W. Hayes, ed.) pp. 937-988. Raven Press, New York.

Useful and detailed background information.

Contributed by Han Seung, Gary Wolfe, and Meredith Rocca
TherImmune Research Corporation
Gaithersburg, Maryland

Transgenerational (In Utero/Lactational) Exposure to Investigate the Effects of Endocrine Disrupting Compounds (EDCs) in Rats

In this unit, timed-pregnant Sprague-Dawley rats are dosed daily during pregnancy and in some instances through lactation. At birth the number of pups/litter are counted and at 2 days of age, anogenital distance and body weight are recorded for all pups. When the pups are 13 days old, nipple and areolar retention are evaluated in females exposed to potential androgens or males exposed to potential antiandrogens. Pups are weaned at 21 to 28 days and housed in unisexual littermate groups of two to three pups/cage; the dams are sacrificed, and body weight and the number of implantation scars are recorded at this time. The onset of puberty is monitored by observing the age of vaginal opening in the females and the age of preputial separation in the males. Other endpoints that may be collected after puberty, if indicated, include estrous cyclicity and fertility in females after puberty, and ejaculated sperm counts, mating behavior, and fertility in males after sexual maturity (after 3 months). As soon as all necessary data have been collected, sexually mature rat offspring are necropsied and an extensive evaluation of the reproductive system is conducted.

The basic protocols recommended for transgenerational studies investigating the effects of EDCs on the reproductive system are: study design and exposure (see Basic Protocol 1); anogenital distance measurement (see Basic Protocol 2); assessment of areolae/nipple development (see Basic Protocol 3); detection of puberty (vaginal opening and preputial separation; see Basic Protocol 4); and necropsy, histology, and radioimmunoassays (see Basic Protocol 5).

NOTE: All protocols using live animals must first be reviewed and approved by an Institutional Animal Care and Use Committee (IACUC) and must conform to governmental regulations regarding the care and use of laboratory animals.

STUDY DESIGN

BASIC PROTOCOL 1

This protocol describes basic techniques for assigning timed-pregnant rats to treatment groups and administrating test compounds.

Materials

Individually housed timed-pregnant rats
Test compounds
Laboratory-grade corn oil (Sigma)

Balance, accurate to 0.1 g, that integrates the weight over several measurements (e.g., Sartorius IP65)
1-ml glass tuberculin syringe (BD)
1.5-in. × 18- or 20-G curved gavage needle (Popper and Sons)
25-G × 5/8-in. or 1/2-in. sterile needle (BD)
Saturated picric acid solution and envelope moistener or cotton swabs to apply picric acid to dams for treatment identification
Software such as Microsoft Excel or SAS (PC SAS or IBM Host on Demand) for calculating means and standard errors by treatment
FTP95 for transferring SAS output data sets to WordPerfect or Microsoft Word

Contributed by Joseph S. Ostby and L. Earl Gray Jr.
Current Protocols in Toxicology (2004) 16.8.1-16.8.16

Assign rats to treatment groups

1. On the morning when dosing is initiated, give a temporary cage number (cage cards numbered consecutively in pencil) to individually housed timed-pregnant rats and record their body weights.

2. After weighing, sort the rats by body weight from the lightest to the heaviest rat and assign treatment groups in the following manner:

   Randomly assign lightest rat to one treatment group
   Randomly assign next lightest rat to one of the remaining treatment groups
   Continue assigning rats in this manner until each treatment group contains one rat to form a block (block = a group of rats with similar body weights consisting of 1 rat/treatment group), which contains the lightest rats in the experiment.

3. Randomly assign a permanent cage number ranging from 1 through the total number of treatments to each rat in the first block. Assign the second block from the next lightest group of rats to treatment groups in a similar manner and give a permanent cage number ranging from the number equal to 1 plus the total number of treatment groups through the number equal to two times the total number of treatment groups in a random fashion. Thus, if the study has five treatment groups, the first block consists of the five lightest rats housed in cages 1 through 5 and the next block consists of the next five lightest rats housed in cages 6 through 10. Continue this procedure until all rats have been assigned to treatment groups and the number of blocks equals the number of rats/treatment group.

   This procedure minimizes potentially confounding experimental variables across treatment groups. The first block of rats (one rat/treatment group) representing the lightest rats in the experiment are placed on the first row(s) of the rack so that each rat is exposed to similar environmental conditions such as temperature, humidity, air flow, and light intensity. Likewise, the second block of rats will be placed on the next row(s) of the rack ensuring all rats in this block will also be exposed to similar environmental conditions.

4. After treatment assignment, calculate the mean body weights and standard errors for each treatment group to ensure that they are as similar as possible and not significantly different.

5. Once the rats have been assigned to treatment groups, give them an i.d. to identify their treatment group. Use picric acid to identify the treatment group.

   For example, rats could be marked as follows: left rear leg (LR), right rear leg (RR), left front leg (LF), right front leg (RF), back (B), both hind limbs (LRRR), both forelegs (LFRF), both left legs (LRLF), and both right legs (RRRF).

   Other means of marking the animals include ear tags, tail tattoos, or implantable transponders.

Prepare and administer dosing solutions

6. Prepare dosing formulations on the basis of microgram or milligram test compound/kilogram body weight/milliliter vehicle/day. Tare the dosing solution vial on a balance, add the calculated quantity of the test compound and record its weight, then add the necessary volume of the vehicle (laboratory-grade corn oil).

   After thorough mixing, further dilutions can be made from the original stock solution.

7. Weigh timed-pregnant rats and prepare the dose for gavage at 2.5 µl of the vehicle per gram body weight (2.5 ml corn oil/kg body weight; therefore, the volume administered to a 300- to 400-g pregnant rat would be 0.75 to 1 ml). Accurately measure this volume with a 1-ml glass tuberculin syringe.

A 1-ml dose is sufficient to allow most compounds to go into solution but does not exceed the stomach capacity of the rat.

Dose the timed-pregnant rats orally or inject subcutaneously (s.c.) with test compounds in a vehicle (e.g., laboratory-grade corn oil) depending on the chemical and its concentration (whether a solution or suspension).

Some compounds readily go into solution while others may require mixing for several days or even 1 week to form uniform suspensions. Suspensions must be stirred constantly while dosing and can be difficult to administer s.c. through small gauge needles. To avoid degradation of test compounds, avoid heating (to facilitate mixing) of dosing solutions unless chemical stability is assured. Depending upon solubility, a wide variety of other vehicles, other than corn oil, may be used.

8a. *For oral administration:* Dose orally by gently grasping the loose skin on the back and neck of the rat in such a manner that the head, neck, and back form a straight line. Gently insert a 1.5-in. × 18- or 20-G curved gavage needle into the left side of the oral cavity and down into the esophagus past the epiglottis (if any resistance is encountered, withdraw the needle and re-insert). To avoid discomfort and startling the rat, administer the dosing solution at a moderate rate and withdraw the needle along a path similar to the path used to insert the needle. Prior to oral dosing, the rats should be gently held in one hand and then held as described above to acclimate them to this type of restraint (since they are normally only picked up by their tails during cage changing).

Administration of compounds typically requires a health and safety research protocol. Prior to administration of these compounds the rats should be dosed for several days with water to acclimate them to this procedure and to reduce the possibility of the rat jumping while the compound is being administered. Rats undergoing rapid weight changes such as timed-pregnant rats should be weighed daily and the dose adjusted to body weight.

8b. *For subcutaneous administration:* Administer subcutaneous injections as microgram or milligram of the test compound/rat in a constant vehicle volume/day or microgram or milligram of the test compound/kilogram body weight/milliliter vehicle/day. Administer injections by placing the rat on a flat surface and gently grasping the loose skin on the back of the rat between the last three fingers and the heel of the hand and raise the skin on the neck with the thumb and index finger. Insert a 25-G × 5/8-in. needle into the raised skin on the neck below the thumb and index finger.

Once this is accomplished, the tip of the needle can be felt between the fingers, and injection can be confirmed by feeling the fluid flow into the injection site (the pressure produced even by microliter quantities can easily be detected in this manner). No more than ten rats should be injected with a single needle. Needles that are 25 or 27 G permit a moderate flow rate with corn oil (be aware that excessive plunger pressure may forcefully eject the needle and syringe contents) but are small enough to prevent excessive leakage at the injection site.

For example, potent steroidal androgens are administered at 0.1 to 10 mg per rat per day.

The optimum injection volume (~0.1 ml of the vehicle) can be accurately administered with a gas-tight microliter or a 1-ml tuberculin syringe, does not readily leak from the injection site due to excessive pressure, and is readily absorbed within 24 hours.

9. For the dosing described in steps 8a and 8b, use different dosing syringes and needles for each dose group to avoid contamination from residual material. Discard syringes on a daily basis, clean the gavage needles daily during the study and reuse but only for the same dosing solution.

10. Select exposure regime.

Exposure may be initiated on gestational day 8 (GD 8) prior to onset of fetal gonadal differentiation or on GD 14 near the onset of fetal testis steroid hormone synthesis (GD 1 = day of sperm positive smear). Exposure should continue through at least GD 18 to cover the primary period of reproductive tract development, but pups may also be exposed via the mother's milk through postnatal day (PND) 3 to encompass the period of sexual differentiation of the brain and central nervous system, or exposure may continue through the period of lactation. One final option would be to continue exposures to the pups after weaning using the same route and dosage levels given the dams.

BASIC PROTOCOL 2

MEASURING ANOGENITAL DISTANCE

The sexually dimorphic secondary sex characteristic in many mammalian species, anogenital distance (AGD; see Fig. 16.8.1), may be used to measure the degree of demasculinization of males as a consequence of developmental exposure to androgen receptor (AR) antagonists (e.g., vinclozolin, procymidone, flutamide, linuron, prochloraz, etc.), 5-alpha reductase inhibitors (finasteride), or compounds that inhibit steroidogenesis (some phthalates). Likewise, AGD is useful in measuring the degree of masculinization of females exposed during sexual differentiation to androgenic compounds such as testosterone or the anabolic growth stimulant trenbolone used in cattle.

AGD and body weight are normally measured in rats at birth or 2 days of age. As the animal grows, increased activity and variability in growth rates increase the variability of this measurement. However, decreased male AGD and increased female AGD observed in adult rats at necropsy demonstrates that endocrine disrupting compounds do permanently alter AGD.

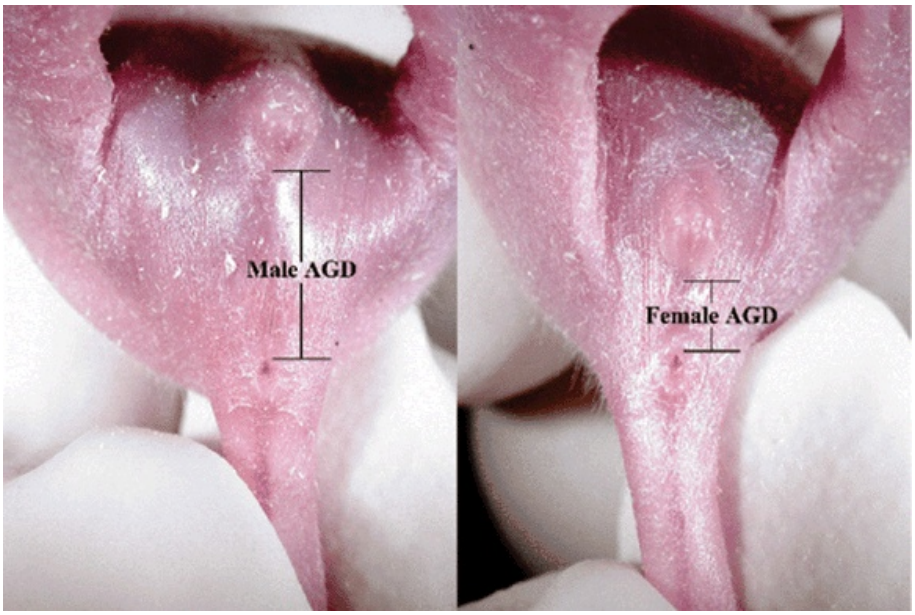

Figure 16.8.1 Anogenital distance in neonatal male and female SD rats. Photographs taken at the same magnification of perineal area of male and female siblings demonstrating the normal developmental effects of testicular androgens on AGD (the sexually dimorphic distance between the sex papilla and the anus). *This black and white facsimile is intended only as a placeholder; for full-color version of figure go to http://www.interscience.wiley.com/c_p/colorfigures.htm*

Studies conducted in the authors' laboratory that followed individual pups from birth to necropsy as adults have demonstrated there is a statistically significant correlation between AGD observed at birth and the presence of nipples in infant males, AGD at necropsy, as well as malformations observed when the rats were necropsied as adults. These results demonstrate that AGD is a reliable predictor of permanent alterations of the reproductive system that are not often apparent until the animal reaches sexual maturity. Similarly, increased AGD in female pups is associated with decreased numbers of nipples (as infants and adults) and malformations of the reproductive tract.

Materials

Sprague-Dawley or Long Evans pups at birth or on PND 2 and as adults
Dissecting microscope, 0.63× to 4× and 10-mm (0.1-mm divisions) ocular reticle (e.g., Leica MZ6)
1-mm stage micrometer (0.01-mm divisions)
Vernier caliper (0 to 150 mm with 0.1-mm divisions)
Two-place balance (e.g., Mettler PM2000)

1. Set a dissecting microscope fitted with a 10-mm ocular reticle (with graduated 0.1-mm divisions) at a magnification of ~1.5× and calibrate with a 1-mm stage micrometer (with graduated 0.01-mm divisions).

2. After the microscope has been set at ~1.5×, carefully adjust the magnification so that the 1-mm stage micrometer is exactly equal to 1.5 mm on the ocular reticle.

   A magnification of 1.5× has been determined to be the optimum magnification for obtaining the most accurate AGD measurement without being distracted by subtle pup movements.

3. After calibrating, raise the microscope ~4 to 6 in. using the coarse focus knob to allow the hands of the observer to rest comfortably on the stage while holding the pup. Position the perineal area of the pup in the focal plane and measure the distance between the posterior base of the sex papilla and the anterior anus using the ocular reticle. Record AGD along with the sex and body weight of the pup. Record the body weight to the nearest 0.01 g and record AGD to the nearest 0.1 scale on the micrometer (divide this measurement by 1.5, magnification = 1.5×, to obtain the actual AGD).

   At birth, AGD in male Sprague-Dawley or Long Evans rats is ~3 mm, while female AGD is ~50% smaller than the males or 1.5 mm.

4. At necropsy, measure AGD by placing the animal with the base of the tail on the edge of a table. Use the thumb to secure the tail to the side of the table and place the index finger above the phallus to maximally stretch the skin in the perineal area. Then, use a vernier caliper to measure the distance between the posterior base of the phallus and the anterior rim of the anus.

5. If pup body weight is significantly reduced by treatment, then adjust the AGD for body weight using body weight as a covariate in the statistical analysis.

   Since litter effects can occur particularly at this age, the data analyzed typically are litter means or n = number of litters/treatment unless it can be demonstrated that litter effects are not present in the data.

ASSESSING AREOLAE/NIPPLE DEVELOPMENT IN INFANT MALE AND FEMALE RATS

In the absence of testicular androgens, female rats develop areolae/nipples, while dihydrotestosterone induces regression or apoptosis of the nipple anlage. Thus, nipple development in male rats is a sensitive endpoint for evaluating the degree of demasculinization produced by in utero exposure to antiandrogenic compounds. Conversely, the partial or complete attenuation of areolae/nipples in female rats is useful in evaluating the masculinizing effects of androgenic compounds (see Fig. 16.8.2).

Although this endpoint is a sensitive indicator of endocrine disruptions, in 13-day-olds a small percent of the control males may have faint areolae. Therefore, it is recommended that prior to experimental data collection for this technique, and AGD as well, in experimental situations, researchers should practice collecting these data in pilot studies with both control and treated (testosterone propionate, TP, for females and vinclozolin for males) animals from several litters to establish a baseline for recording these data and to assure acceptable levels of reproducibility. If more than one observer is used in a study, then one must assure that there is a high degree of inter-observer reliability on these measures, and the study should be designed in a manner such that the treatment groups are split among different observers.

Due to the subjective nature of these endpoints, it is critical that the data are collected in a "blinded" manner, ensuring that the observer is not aware of the treatment group of each litter.

Because of the rapid development at this age, AGD and nipple data should be collected on all offspring at the same age in days over one 8-hr interval, by a single observer, if possible.

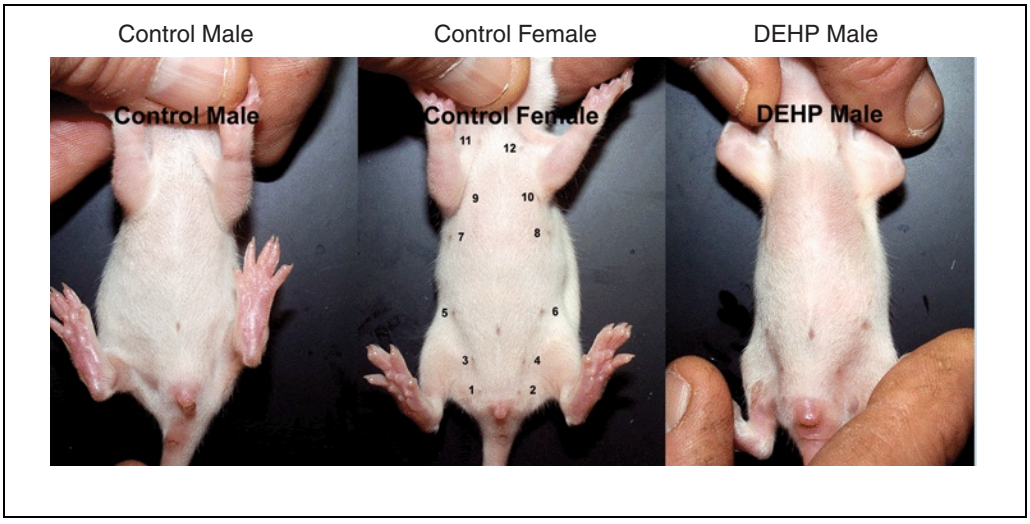

Figure 16.8.2 Areolas and nipples in infant male and female rats. Photographs taken when the pups were 14 days old showing a normal male without nipples, a normal female with twelve evenly spaced nipples (no. 9 not visible in photograph) and a male exposed to 750 mg of diethylhexyl phthalate from gestational 14 through postnatal 3. Some phthalate diesters such as diethylhexyl, benzylbutyl, and dibutyl phthalate inhibit fetal testosterone synthesis and thus prevent dihydrotestosterone from inhibiting development of the nipple anlage.
This black and white facsimile is intended only as a placeholder; for full-color version of figure go to http://www.interscience.wiley.com/c_p/colorfigures.htm

Materials

Infant male and female rats (e.g., Sprague-Dawley)
Bouins's fixative (see recipe)

Balance (e.g., Mettler PM2000)
Small animal clippers with size no. 40 clipper blade (Oster)

1. Collect areolae/nipple data shortly after control females develop prominent areolae/nipple buds but before the nipples are partially or completely hidden by rapid ventral hair growth (in Sprague-Dawley rats, this normally occurs when they are ~13 days old).

2. On PND 13, have an observer who is blind to treatment separate each litter by sex, determine the number of areolae/nipples, their position, and the body weight of the pup for each male or female in the litter, depending on the type of compound administered.

   If antiandrogens are administered, males exposed to antiandrogens are checked for nipple retention and females exposed to androgens are checked for nipple regression. The sex not checked for nipple development at 13 days can be counted and weighed together to determine average pup weight for that sex. Nipple data collection normally requires three technicians: an observer, a data recorder, and a technician responsible for removing and returning litters to their home cage.

3. Number the nipples to identify their location (female rats normally have twelve nipples, six symmetrical pairs, with the pairs distributed identically on all rats). For example, give nipples on the right side odd numbers (1, 3, 5, 7, 9, and 11) with no. 1 caudal and no. 11 cranial, and assign nipples on the left side even numbers (2, 4, 6, 8, 10, and 12), with no. 2 caudal and no. 12 cranial.

   Rats with nipple retention or regression can be given a unique picric acid i.d. when 13 days old and shaved and checked at necropsy to determine if abnormal nipple development observed persists into adulthood. Also, retained areolae/nipples in males may be scored as absent, faint, moderately developed, or prominent (female-like) and regressed areolae/nipples in females can be scored as normal, moderately faint, very faint, or absent.

4. At necropsy, shave the rats with small animal clippers and record the number of nipples/areolae. Fix retained or regressed nipples in Bouin's fixative and save for histological evaluation.

DETECTING PUBERTY—VAGINAL OPENING (VO) AND PREPUTIAL SEPARATION (PPS)

BASIC PROTOCOL 4

The onset of puberty in the rat can be evaluated by recording the body weight and age of the rat at vaginal opening (VO) or preputial separation (PPS). Although direct exposure from weaning through puberty may be the optimum period of time to alter this endpoint, in utero/lactational exposure can also impact puberty and consequently should be checked in transgenerational studies.

VO occurs when the rise in circulating ovarian hormones induces apoptosis of the vaginal membrane cells and development of the vaginal canal. The day of vaginal opening normally coincides with the day of first estrus and thus marks the initiation of the onset of estrous cyclicity in rats. The first few estrous cycles are typically longer and irregular after VO. VO is useful to identify/evaluate EDCs that accelerate (estrogen) or delay (antiestrogens, inhibitors of aromatase or inhibitors of hypothalamic-pituitary maturation) puberty in female rats. On occasion, females display a transient thread of tissue along the midline of the vaginal opening, which persists for several days or occasionally is

permanent. For this reason, the age and body weight at the onset of VO should be noted as well as the completion of VO, with dissolution of the thread, if present. The authors have found that female rats exposed in utero to Ah receptor agonists often display a permanent thread across the vaginal opening.

PPS in rats (complete manual retraction of the prepuce) occurs when increasing testicular androgen production produces cornification of the balano-preputial epithelial cells permitting the prepuce to retract along the length of the glans penis. The age at PPS is useful to identify antiandrogens which can delay puberty through altered development of the balano-preputial membrane (permanent incomplete PPS) or interfere with the normal rise in circulating androgens. Malformations such as incomplete PPS or hypospadias, which prevent accurate PPS data collection, are reported as a malformation when the adults are necropsied. Occasionally, males display a transient thread of tissue along the frenulum of the glans, which persists for several days or, on rare occasions, is permanent. For this reason, the age and weight at the onset of PPS should be noted as well as the completion of PPS, with the dissolution of the thread, if present. Also male rats with hypospadias may display a permanent thread on the glans or they are so malformed that PPS does not occur at all.

If time does not permit examining a large number of rats daily for VO or PPS, then the rats can be examined two or three times per week and the age of VO or PPS and body weight at puberty recorded. These data can then be analyzed and reported as the percentage of females or males which opened or separated on a given day for each treatment group.

Materials

Rats from litters of dams in treatment groups, approaching puberty
Balance for animal weight recorded to the nearest 0.01 g (e.g., Sartorius IP65) with integration capability to accurately weigh moving animals

Detect vaginal opening (VO)

1a. Check female rats daily for VO beginning at about PND 24, ~5 days prior to the onset of this landmark to ensure the day of VO is detected in all rats. Monitor each rat daily from then until the process is complete.

VO normally occurs in Sprague-Dawley and Long Evans rats between 29 and 35 days old (DOB = PND 1).

The index finger may be gently rubbed across the vaginal area to determine if the vaginal membrane is present or if the layer of dying cells are simply obscuring the vaginal opening.

2a. When VO is initiated and when complete, record the ages and body weights of each rat and calculate the mean ages and body weights for each treatment group, then check for statistical significance.

Detect preputial separation (PPS)

1b. Check male rats daily beginning at 35 to 37 days of age to ensure no rats have preputial separation. Apply gentle pressure to the prepuce to retract the prepuce and expose the glans penis.

PPS normally occurs in Sprague-Dawley and Long Evans rats between 39 and 45 days old (DOB = PND 1).

PPS is complete when the entire perimeter of the prepuce can be retracted evenly around the base of the glans penis.

2b. When PPS begins and when it is complete, record the ages and body weights of each rat and calculate the mean age, body weight, and standard errors by treatment group, and check for statistical significance.

NECROPSY

At 90 to 120 days of age, male and female Sprague-Dawley rats have reached sexual and physical maturity, therefore, this time frame represents the ideal time to evaluate their reproductive systems. Although the reproductive system of both males and females should be thoroughly evaluated when administering test compounds for the first time, the primary emphasis of each necropsy can be designed to focus on endpoints known or expected to be affected based upon previous in vitro/in vivo studies or on the results of data collected earlier in this study.

Materials

Male and female rats, 90 to 120 days old
CO_2

Bouin's fixative (see recipe)

Balance accurate to 0.1 g with integration capability for weighing rats (e.g., Sartorius IP65)
Rodent restraint cones (Harvard Apparatus)
Rodent guillotine
Vernier caliper (0 to 150 mm with 0.1-mm divisions)
Small animal clippers with size # 40 clipper blade (Oster) for shaving ventral surface to check areolae/nipples
Surgical instruments (Roboz): micro dissecting forceps (RS-5230 for grasping delicate tissues such as ventral prostate and RS-5236 for holding tougher tissue such as skin), micro dissecting scissors (RS-5852 for delicate dissections and RS-6814 for cutting tougher tissue such as skin) and hemostats (RS-7172 for clamping seminal vesicles)
Balance accurate to 0.0001 g for weighing tissues (e.g., Sartorius BP 121 S)

Perform male necropsy

The order of tissue dissection listed below is designed to minimize tissue dehydration and should facilitate accurate dissection in a timely manner.

1a. Weigh male rats, place in a restraint cone, and decapitate within 60 sec of removal from their cage. Collect the trunk blood for serum hormone analysis by radioimmunoassay.

2a. For external examination, shave the rat and examine for the presence of areolae/nipples and malformations of the external genitalia such as cleft prepuce, incomplete preputial separation, hypospadias (urethra opens along the underside of phallus rather than at the tip), or vaginal pouch. Measure anogenital distance at this time with a Vernier caliper, especially if it was affected at birth. Weigh the glans penis. Note if there are undescended, ectopic testes.

3a. Begin internal examination. Check for bladder stones (antiandrogens such as vinclozolin or procymidone increase the incidence of bladder stones), hydroureter, and obvious hydronephrosis resulting from back pressure on the kidneys. Check for undescended ectopic testes, which could be attached just below the kidneys to abdominal muscle wall by a cranial gonadal suspensory ligament or testes embedded in the abdominal muscle wall (ectopic). In the process of dissecting and weighing the tissues listed below, note any additional malformations.

4a. Dissect and weigh the ventral prostate; dissect (weighing is optional) the dorsolateral prostate from around the base of the seminal vesicles; and remove and weigh the seminal vesicles and coagulating glands after clamping the base of the seminal vesicles with hemostats to avoid leakage of seminal fluid. Note abnormalities such as infection, unusual coloration/texture, tissue adhesions, or missing or poorly

developed lobes of the seminal vesicles, coagulating glands, ventral or dorsolateral prostate and photograph if time permits.

The seminal vesicles can also be weighed dry after the seminal fluid is expressed and the tissue blotted dry.

5a. Withdraw the testes and epididymides from the scrotum and examine the gubernacular cords to ensure they are present and not elongated or filamentous (typically 4 to 8 mm in length), and dissect and weigh the testes and epididymides (see Fig. 16.8.3 and Fig. 16.8.4). Note any testicular/epididymal abnormalities such as undescended (also check for the presence of a cranial gonadal suspensory ligament) or ectopic testes (testis located in abdominal muscle wall), fluid-filled or hypoplastic or atrophic testes and epididymal hypoplasia or agenesis.

The testes can be saved for sonication resistant testicular sperm head counts or histology or both and the epididymides can be saved for whole, caudal, and caput plus corpus epididymal sperm counts or fixed for histology.

6a. Remove and weigh the Cowper's glands, and dissect and weigh the levator ani/bulbocavernosus (LABC), which loops around the colon and is attached at each end to the penile bulbs.

7a. Dissect and weigh nonreproductive tissues, which may be affected by EDCs. Include the pituitary, kidneys, adrenals, and liver. Weigh the brain and other tissues at this time.

It may also be helpful to slice the kidneys longitudinally to check for hydronephrosis and kidney stones.

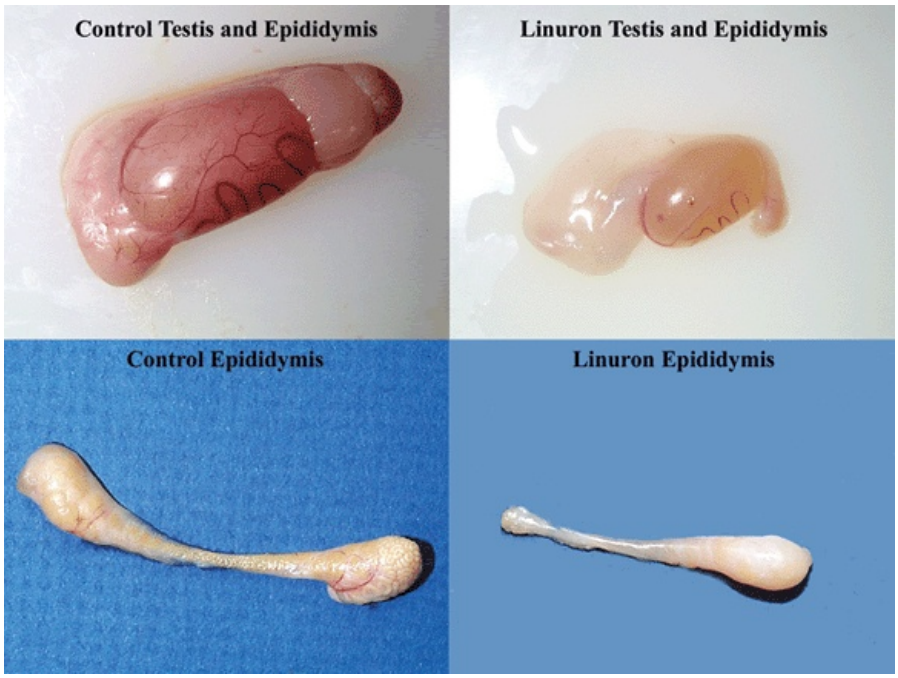

Figure 16.8.3 Testes and epididymides from control and in utero linuron-treated male rat offspring, necropsied as adults. Photographs in panels on the left show a control testis, epididymis and epididymal fat pad and the epididymis dissected from the testis with the fat removed. Panels on the right show a testis, epididymis and epididymal fat pad and the epididymis dissected from the testis with the fat removed, from a rat exposed in utero from gestational day 14 through 18 to 100 mg linuron/kg. Agenesis of the caput produces fluid pressure atrophy of the testis.
This black and white facsimile is intended only as a placeholder; for full-color version of figure go to http://www.interscience.wiley.com/c_p/colorfigures.htm

8a. Save all tissues weighed, especially tissues with gross malformations, and fix in Bouin's fixative for histological evaluation or process for other endpoints such as immunohistochemical staining.

Perform female necropsy

1b. Weigh females, anesthetize in CO_2, decapitate, and save the trunk blood for serum hormone analysis by radioimmunoassay.

2b. For external examination, shave the female rats and check for the absence/prominence of areolae/nipples (DHT inhibits development of nipples) and malformations of the external genitalia such as cleft phallus, vaginal threads, and absence of external vaginal opening (DHT inhibits development of lower vagina). Measure anogenital (AGD) and anovaginal distance (AVD) to calculate vaginal-genital distance (AGD-AVD), which decreases with exposure to androgens.

3b. Begin internal examination. Since androgens inhibit the development of the ovarian ligament, measure the kidney to ovary distance when females are exposed perinatally to suspected androgens. Androgens may also promote the development of male reproductive tissues such as prostatic tissue, seminal vesicles, penile bulbs with attached levator ani muscle, and Cowper's glands; note the presence of these tissues and photograph, if possible, and save for histological confirmation.

4b. Dissect and weigh the ovaries, and weigh the uterus with and without fluid (remove fluid by cutting each uterine horn open and blotting all fluid).

5b. Dissect and weigh the nonreproductive tissues—the pituitary, adrenals, kidneys (section each kidney to check for hydronephrosis), and liver.

6b. Save all tissues weighed, especially tissues with gross malformations, and fix in Bouin's fixative for histological evaluation or process for other endpoints such as immunohistochemical staining.

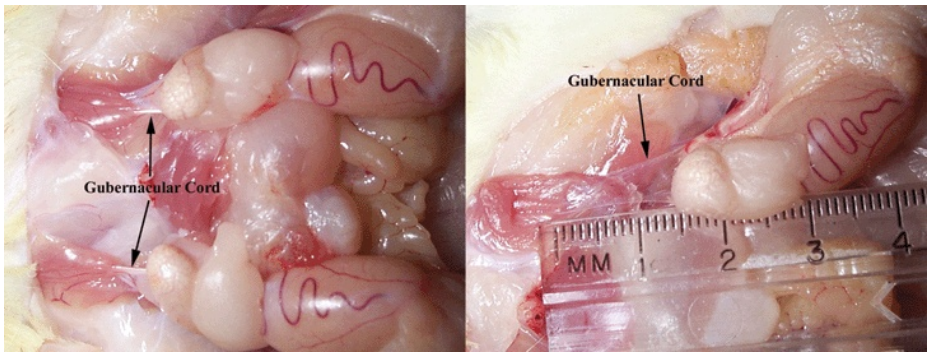

Figure 16.8.4 Gubernacular ligaments in control and phthalate ester–treated male rat offspring, necropsied as adults. Photographs showing a control rat with normal gubernacular cords (left panel) and a rat whose mother received received 750 mg diethylhexyl phthalate/kg from gestational day 14 through postnatal day 3 with a poorly developed gubernacular cord (right panel). Diethylhexyl, dibutyl, and benzylbutyl phthalate produced partial or complete agenesis of the gubernacular cord resulting in undescended testes in some rats, while other rats were observed with scrotal testes but absent or poorly developed, thin and elongated gubernacular cords.
This black and white facsimile is intended only as a placeholder; for full-color version of figure go to http://www.interscience.wiley.com/c_p/colorfigures.htm

DATA INTERPRETATION AND SUMMARY

Analyze AGD, areolar, nipple, pubertal landmark (VO or PPS), and organ weight data using litter means or a nested analysis that accounts for litter effects. If an overall ANOVA model analysis is significant, then use posthoc *t*-tests to compare dose groups to one another and the control group. Alternatively, use a one-tailed Dunnett's test to compare each treated group to the control group.

As these developmental reproductive toxicants (EDCs) produce characteristic syndromes, each containing a variety of effects, the data should be compiled in a manner that enables the investigator to determine what percentage of the offspring are normal and what percentage display any abnormality associated with the particular syndrome. For example, phthalate ester exposure in utero can induce any number of epididymal, testicular, gubernacular, internal sex organ, or external affects. Any animal displaying a morphological or histological alteration in any one of these tissues should be considered affected. If one of ten animals displayed epididymal agenesis, a second had a histological lesion of the epididymis, a third had testis agenesis, a fourth had seminiferous tubular agenesis, a fifth had agenesis of the gubernacular ligament, a sixth had agenesis of the ventral prostate, a seventh displayed hypoplasia of the right horn of the seminal vesicle, and an eighth had six permanent nipples, then it should be reported that 80% of the animals are adversely affected in this group. See Gray et al. 1994, 1997a or b, 2000; Lambright et al., 2000, and McIntyre et al. 2002 for examples of data presentation.

REAGENTS AND SOLUTIONS

Use Milli-Q-purified water or equivalent in all recipes and protocol steps. For common stock solutions, see ***APPENDIX 2A****; for suppliers, see* ***SUPPLIERS APPENDIX****.*

Bouin's fixative

3 liters saturated picric acid solution (Sigma)
1 liter 37% formaldehyde solution (Sigma)
200 ml glacial acetic acid (Sigma)
Store at room temperature in a fume hood; replace if a precipitate forms or at 4 months

CAUTION*: Upon drying, the picric acid solution will form a crystal residue that will ignite if sufficient heat or friction is applied. Any residue that forms on storage containers may be safely removed with a damp sponge.*

COMMENTARY

Background Information

Identification and comparison of the potency of endocrine disrupting compounds (EDCs) to natural ligands may be best accomplished using rapid in vitro screening assays such as receptor binding and transcriptional activation assays or short-term in vivo assays such as the Hershberger and uterotropic assay (Gray et al., 2002). In the authors' laboratory, the transgenerational protocol described has been used primarily to quantify and characterize the demasculinizing effects of antiandrogens in males or the masculinizing effects of androgens in females for compounds identified in these screening assays. Additionally, transgenerational exposure to EDCs such as androgen receptor (AR) antagonists or fetal testosterone synthesis inhibitors display unique profiles of malformations characteristic of their specific mechanism(s) of action (Gray et al., 1994, 1997a,b, 2000; Lambright et al. 2000; McIntyre et al., 2002).

Accurate oral or subcutaneous exposure is accomplished by administering the test compound on a milligram or microgram/kilogram body weight/milliliter vehicle/day basis and adjusting the dose daily according to body weight, which increases dramatically during the latter stages of gestation. Daily weighing also serves as a sensitive indicator of toxicity and consequently is monitored daily both on an individual basis and analyzed on a treatment group basis.

The sexually dimorphic androgen-sensitive perineal area between the anus and sex papilla (anogenital distance—AGD) provides a useful biomarker for quantitative evaluation of the fetal androgen status of a rat. Immunohistochemical staining demonstrates that androgen receptor expression in mesenchymal cells in the perineal and prepubic area first occurs on GD 19 (copulatory vaginal plug = GD 1) in male rats (Bentvelsen, 1995). AGD can be thought of as a phenotypic continuum between females (~1.5 mm) and males (~3 mm) in which developmental exposure of females to androgens masculinizes or increases female AGD, while developmental exposure of males to antiandrogens, feminizes or decreases male AGD. AGD at birth or PND 2 has been shown to correlate significantly with adult male urogenital malformations when the data analyzed are litter means. With the aid of a dissecting microscope fitted with an ocular reticle, neonatal AGD can be accurately measured to 0.1 mm and, if effected, this measurement should be repeated in the adult necropsy with the aid of vernier calipers.

Androgen receptor expression in mesenchymal cells of the nipple anlage is first demonstrated by immunohistochemical staining on GD 15 (vaginal plug = GD 1) in male rats and the presence of androgens (dihydrotestosterone) at this time promotes regression of the nipple anlage in both sexes (Bentvelsen, 1995). Consequently, recording the number of areolae/nipples at 13 days of age provides another sensitive endpoint for evaluating endocrine status of males potentially exposed to antiandrogens or females exposed to androgens during development. If the normal areolae/nipple phenotype is altered at this age, then at necropsy, the adults should be shaved, examined for the presence of areolae/nipples, and the tissues saved for histological evaluation.

Vaginal opening (VO) and preputial separation (PPS), which coincide with the rise in circulating estrogens or androgens, serve as indices of puberty in female and male rats, respectively. VO and PPS can be accelerated or delayed by hormonal manipulation and consequently provide useful endpoints for evaluating the hormonal status of animals exposed to potential EDCs (Korenbrot et al., 1977: Ojeda et al., 1976). For example, perinatal oral exposure to 200 mg of the AR antagonist, vinclozolin, from GD 14 through PND 3 (sperm + = GD 1) delayed preputial separation by 3 days (Gray et al., 1994), a single oral dose of 0.2 and 0.8 μg of 2,3,7,8-tetrachlorodibenzo-*p*-dioxin (TCDD) administered on GD 16 (sperm + = GD 1) delayed preputial separation by 1.5 and 3 days, respectively (Gray et al., 1997a), while 0.8 μg of 2,3,7,8 TCDD delayed vaginal opening by 1 day (Gray et al., 1997b).

At necropsy, sexually mature adult rats exposed perinatally to EDCs are examined externally to evaluate development of androgen-dependent tissues such as the perineal area and genital tubercle and tissues whose development are inhibited by androgens such as areolae/nipples. Permanent malformations of external tissues stimulated or inhibited developmentally by androgens in males include cleft prepuce/phallus, hypospadias, incomplete preputial separation, vaginal pouch, reduced glans penis weights, decreased anogenital distance, and nipples (Clark et al., 1990, 1993; Imperato-McGinley et al., 1992). Externally in females, androgens increase AGD, decrease the distance between the vagina and phallus, inhibit normal areolae/nipple development and prevent development of the lower vagina (Wolf et al., 2002). EDCs such as 2,3,7,8 TCDD decrease the distance between the urethral and vaginal openings, produce permanent vaginal threads (Gray et al., 1997b) and reduce glans penis weights (Gray et al., 1997a).

Internally, androgen-dependent tissues are examined for abnormal development, their weights are recorded and the tissues may be saved for histological evaluation. In male rats, these tissues should include the ventral prostate, seminal vesicles plus coagulating glands, testes, epididymides, and the levator ani/bulbocavernosus muscle complex. Other tissues that have been affected by EDCs in previous experiments and may be weighed, measured, or examined and saved for histology include the bulbourethral glands, gubernacular ligament, liver, kidneys, adrenals, dorsolateral prostate, bladder, and ureters (Gray et al., 1999; 2000). Additionally, malformations such as undescended or ectopic testis or the presence of cranial gonadal suspensory ligaments should be noted.

EDCs operating through different mechanisms of action produce different malformation profiles. AR antagonists such as vinclozolin target DHT-dependent tissue development including the ventral prostate and external genitalia and produce malformations such as permanent nipples, urinary bladder stones, ectopic testes, hypospadias, and vaginal pouches (Gray et al., 1994). In contrast, some EDCs, which inhibit fetal Leydig cell steroid and peptide hormone synthesis such as diethylhexyl phtha-

late (Parks et al., 2000), also induce malformations such as epididymal hypoplasia/agenesis and subsequent fluid pressure atrophy of the testes and undescended testes as a consequence of partial or complete agenesis of the gubernacular ligament (Gray et al., 2000; Kubota et al., 2001). Other EDCs such as linuron (Lambright et al., 2000) and prochloraz may alter reproductive development through several mechanisms of action (AR antagonism and steroid inhibition) and produce a profile of malformations intermediate between an AR antagonist and steroidogenesis inhibitor.

Critical Parameters and Troubleshooting

Ideally, test compound dosages should be selected to cover the full range of the dose-response curve with the lowest dose producing no or only minimal effects and the highest dose eliciting slightly less than maximal response without producing nonspecific, systemic maternal or neonatal toxicity. Generally, the highest dosage level should not induce a reduction in maternal weight >10%. Generally, litters are not culled and data collected on all offspring for each specific endpoint are used to provide the most accurate representation of the dose-response curve. If one is interested in subtle treatment-related changes in organ weights and somatic growth, the litters could be standardized to a litter size of 8 to 10 pups per litter. Because most data are analyzed as litter means (n = number of litters/treatment group), the number of litters/treatment group must be of sufficient size to ensure adequate statistical power. A typical study might consist of five treatment groups (a control and four different treatment groups) with eight dams/treatment group; this would potentially generate 500 offspring (100/treatment group).

Data for protocols in which data can be collected in 1 day, such as anogenital distance or nipple development at 13 days of age, should be collected one block at a time to minimize the effect of time on treatment and the data should be collected by only one observer who is blind to treatment. Likewise, data collection such as necropsy, which requires >1 day to complete, can be collected on one animal/litter for each treatment group in one block, again to minimize the effect of time/age on treatment and each technician should conduct the same tasks throughout the entire necropsy in order to reduce technician-to-technician variability for each specific endpoint.

Considerable attention should be given to assuring that the individuals involved are all adequately trained and follow similar procedures. If data on an endpoint like AGD or areolas must be collected by more than one technician, then the study director must ensure that the inter-observer reliability is high from training exercises; he also must avoid having one technician collect the data from the control group, while another collects the data from a treated group. All treatment/dose groups in a study should be run concurrently. If the whole experiment cannot be run at once, then it should be split into balanced complete block designs. While these comments might seem obvious, it has been known that investigators have had one technician collect the data on all the controls 1 month, while others collected the data on the treated groups at other times.

Anticipated Results

Perinatal exposure to EDCs such as antiandrogens or steroidogenic inhibitors may demasculinize males and reduce anogenital distance, induce female-like nipple development, delay preputial separation and inhibit normal development of the testes, epididymis, and sex accessory tissues such as the glans penis, ventral prostate, seminal vesicles/coagulating glands, bulbourethral glands, and levator ani/bulbocavernosus muscles in a dose-related fashion (Table 16.8.1).

In contrast, perinatal exposure to androgens can masculinize and defeminize the female offpsring resulting in increased anogenital distance, agenesis of areolae and nipples, agenesis of the lower vagina, absence of vaginal opening, hydrometrocolpus, and retained male tissues including the ventral prostate, seminal vesicles, and levator ani.

Time Considerations

Data collection for some endpoints such as anogenital distance at 2 days of age and areolae/nipple retention at 13 days of age, ideally, should be collected in 1 day by only one observer, while other protocols such as necropsy may be conducted over a considerably longer period such as 1 week or several weeks. Consequently the sample size (n = number of litters) should permit sufficient statistical power without jeopardizing data collection on all offspring at one time point. A study with five treatment groups and 8 to 10 dams/treatment or 100 to 120 offspring/treatment group should satisfy these criteria.

Table 16.8.1 Effects of Perinatal Vinclozolin on Male Offspring[a]

Observation	Percent affected[b]							
Dose (mg/kg/day)	0 (mean)	3	6.25	12.5	25	50	100	200
AGD reduction[c]	0 (3.43 mm)	7	4.2	9.1	14.7	24.9	35	50
Permanent nipples	0	1	2.6	3.6	5.4	50	100	100
Areolae/nipples in infants[d]	5	17	33	55	49	100	100	100
Ventral protstate gland size reduction[e]	0 (564 mg)	11	26	22	32	46	88	95
Hypospadiasis[e]	0	0	0	0	0	45	100	100
Vaginal pouch[e]	0	0	0	0	0	15	100	100
Ectopic testes[e]	0	0	0	0	0	0	20	50

[a]Combined data from Gray et al., 1994 and 1997.

[b]Perinatal oral maternal treatment with vinclozolin.

[c]Anogenital distance (AGD) was measured at PND 2.

[d]Areolae were observed at PND 13.

[e]Males were necropsied at full maturity as adults and organs were weighed and examined for structural malformations.

Disclaimer

The research described in this unit has been reviewed by the National Health and Ecological Effects Research Laboratory, U.S. Environmental Protection Agency, and approved for publication. Approval does not signify that the contents necessarily reflect the views and policies of the Agency nor does mention of trade names or commercial products constitute endorsement or recommendation for use.

Literature Cited

Bentvelsen, F.M., Brinkmann, A.O., van der Schoot, P., van der Linden, J.E., van der Kwast, T.H., Boersma, W.J., Schroder, F.H., and Nijman, J.M. 1995. Developmental pattern and regulation by androgens of androgen receptor expression in the urogential tract of the rat. *Mol. Cell Endocrinol.* 113:245-253

Clark, R.L., Antonello, J.M., Grossman, S.J., Wise, L.D., Anderson, C., Bagdon, W.J., Prahalada, S., MacDonald, J.S., and Robertson, R.T. 1990. External genitalia abnormalities in male rats exposed in utero to finasteride, a 5 alpha-reductase inhibitor. *Teratology* 42:91-100.

Clark, R.L., Anderson, C.A., Prahalada, S., Robertson, R.T., Lochry, E.A., Leonard, Y.M., Stevens, J.L., and Hoberman, A.M. 1993. Critical developmental periods for effects on male rat genitalia induced by finasteride, a 5 alpha–reductase inhibitor. *Toxicol. Appl. Pharmacol.* 119:34-40.

Gray, L.E. Jr., Ostby, J.S., and Kelce, W.R. 1994. Developmental effects of an environmental antiandrogen: The fungicide vinclozolin alters sex differentiation of the male rat. *Toxicol. Appl. Pharmacol.* 129:46-52.

Gray, L.E. Jr., Ostby, J.S., and Kelce, W.R. 1997a. A dose-response analysis of the reproductive effects of a single gestational dose of 2,3,7,8-tetreachlorodibenzo-*p*-dioxin in male Long Evans hooded rat offspring. *Toxicol. Appl. Pharmacol.* 146:11-20.

Gray, L.E. Jr., Ostby, J.S., and Kelce, W.R. 1997b. In utero exposure to low doses of 2,3,7,8-tetreachlorodibenzo-*p*-dioxin alters reproductive development of female Long Evans hooded rat offspring. *Toxicol. Appl. Pharmacol.* 146:237-244.

Gray, L.E. Jr., Wolf, C., Lambright, C., Mann, P., Price, M., Cooper, R.L., and Ostby, J. 1999. Administration of potentially antiandrogenic pesticides (procymidone, linuron, iprodione, chlozolinate, p,p′-DDE, and ketoconazole) and toxic substances (dibutyl- and diethylhexyl phthalate, PCB 169, and ethane dimethane sulphonate) during sexual differentiation produces diverse profiles of reproductive malformations in the male rat. *Toxicol. Ind. Health* 15:94-118.

Gray, L.E. Jr., Ostby, J., Furr, J., Price, M., Veeramachaneni, D.N., and Parks, L. 2000. Perinatal exposure to the phthalates DEHP, BBP, and DINP, but not DEP, DMP, or DOTP, alters sexual differentiation of the male rat. *Toxicol. Sci.* 58:350-365.

Gray, L.E. Jr., Ostby, J., Wilson, V., Lambright, C., Bobseine, K., Hartig, P., Hotchkiss, A., Wolf, C., Furr, J., Price, M., Parks, L., Cooper, R.L., Stoker, T.E., Laws, S.C., Degitz, S.J., Jensen, K.M., Kahl, M.D., Korte, J.J., Makynen, E.A., Tietge, J.E., and Ankley, G.T. 2002. Xenoendocrine disrupters_tiered screening and testing: Filling key data gaps. *Toxicology* 182:371-382.

Imperato-McGinley, J., Sanchez, R.S., Spencer, J.R., Yee, B., and Vaughan, E.D. 1992. Comparison of the effects of the 5 alpha-reductase inhibitor finasteride and the antiandrogen flutamide on prostate and genital differentiation: Dose-response studies. *Endocrinology* 131:1149-1156.

Korenbrot, C.C., Huhtaniemi, I.T., and Weiner, R.I. 1977. Preputial separation as an external sign of pubertal development in the male rat. *Biol. Reprod.* 17:298-303.

Kubota, Y., Nef, S., Farmer, P.J., Temelcos, C., Parada, L.F., and Hutson, J.M. 2001. Leydig insulin-like hormone, gubernacular development and testicular descent. *J. Urol.* 165:1673-1675.

Lambright, C., Ostby, J., Bobseine, K., Wilson, V., Hotchkiss, A.K., Mann, P.C., and Gray, L.E. Jr. 2000. Cellular and molecular mechanisms of action of linuron: An antiandrogenic herbicide that produces reproductive malformations in male rats. *Toxicol. Sci.* 56:389-399.

McIntyre, B.S., Barlow, N.J., and Foster, P.M. 2002. Male rats exposed to linuron in utero exhibit permanent changes in anogenital distance, nipple retention, and epididymal malformations that result in subsequent testicular atrophy. *Toxicol. Sci.* 65:62-70.

Ojeda, S.R., Wheaton, J.E., Jameson, H.E., and McCann, S.M. 1976. The onset of puberty in the female rat: Changes in plasma prolactin, gonadotropins, luteinizing hormone-releasing hormone (LHRH), and hypothalamic LHRH content. *Endocrinology* 98:630-638.

Parks, L.G., Ostby, J.S., Lambright, C.R., Abbott, B.D., Klinefelter, G.R., Barlow, N.J., and Gray, L.E. Jr. 2000. The plasticizer diethylhexyl phthalate induces malformations by decreasing fetal testosterone synthesis during sexual differentiation in the male rat. *Toxicol. Sci.* 58:339-349.

Wolf, C.J., Hotchkiss, A., Ostby, J.S., LeBlanc, G.A., and Gray, L.E. Jr. 2002. Effects of prenatal testosterone propionate on the sexual development of male and female rats: A dose-response study. *Toxicol. Sci.* 65:71-86.

Contributed by Joseph S. Ostby and L. Earl Gray Jr.
United States Environmental Protection Agency
Research Triangle Park, North Carolina

CHAPTER 17
Oxidative Stress

INTRODUCTION

Many chemical-induced toxic insults involve oxidative events as major components. Yet, we know that certain oxidative events are essential components of complex signaling processes in cell growth and regulation. Although natural antioxidants have essential roles in optima cellular functions and health, proper balance in both oxidative events and antioxidart functions remains to be fully elucidated. In this chapter, efforts are directed towards understanding and analyzing the oxidative events that appear crucial to toxicology. The formation and functions of protein sulfenic acids that are formed by oxidative processes are covered in an overview (*UNIT 17.1*). Sulfenic acids in proteins are formed upon reaction of cysteinyl thiols with oxidizing agents including mild oxidizing agents such as molecular oxygen and hydrogen peroxide. Topics covered in this overview include peroxide sensitivity, detection of nitrosative stress, participation of protein sulfenic acids in redox catalysis by antioxidant enzymes, in other catalytic functions and in transcriptional regulators. Examples of the role of protein sulfenic acids in catalysis and regulation are given including redox sensing mechanisms.

The measurement of protein sulfenic acid content is presented in *UNIT 17.2*. Notoriously difficult to identify due to their high reactivity, particularly outside the native protein environment, protein sulfenic acids are measured with techniques that are based upon this high degree of reactivity. Chemical modification methods are useful for sulfenic acid identification. Sulfenic acid can be trapped and detected using 7-chloro-4-nitrobenzo-2-oxa-1,3-diazole (NBD chloride), which reacts with both thiol groups and sulfenic acids in proteins but gives unique products that can be detected by their UV-visible spectra and mass spectrometry. An alternative utilizes a more reactive and less stable reagent 4-fluoro-7-nitrobenz-2-oxa-1,3-diazole (NBD fluoride). Another reagent, 2-nitro-5-thiobenzoic acid (TNB), reacts stoichiometrically with sulfenic acids for quantification. A fourth reagent, 5,5-dimethyl-1,3-cyclohexanedione (dimedone) reacts specifically with sulfenic acids but not thiol groups on proteins and relies on ESI-MS analysis for identification.

Oxidative stress and lipid peroxidation are implicated in chemical-induced cell injury/death. *UNIT 17.3* describes the adaptation of a fluorescence microplate reader for measuring tissue susceptibility to lipid peroxidation. Lipid peroxidation is initiated by Fe^{3+}-ADP in the presence ascorbate yielding oxidative products, including 4-hydroxy-2-nonenal, which form fluorescent products that are measured with a fluorescence microplate reader. Real-time measurement of a large number of samples for their susceptibility to lipid peroxidation is possible with this procedure.

Oxidative stress is a part of many disease states and may result from the accumulation of metals by tissues. Transition metals, including iron and copper, are widely studied for the many types of associated oxidative reactions. *UNIT 17.4* describes methods for in situ localization of nonenzymatic peroxidase-like activity of tissue-bound transition metals. A significant improvement over existing methods is an enhanced sensitivity based on the application of hydrogen peroxide and diaminobenzidine (DAB) for the detection of iron. An alternate protocol for the detection of redox-active transition metals is given

Contributed by Donald J. Reed
Current Protocols in Toxicology (2005) 17.0.1-17.0.2

as is a support procedure that utilizes selective chelating agents to evaluate the relative contributions of iron and copper to the redox activity.

An important measure of oxidant stress is the quantification of lipid peroxidation products. *UNIT 17.5* is an overview of the formation of lipid peroxidation products with emphasis on those products formed from the oxidation of ubiquitous arachidonic acid. This overview includes a discussion of the biochemistry of F2-isoprostanes as well as their utility as markers of oxidant stress. Mechanisms of formation of isoprostanes, their quantification in vitro, in vivo, and in animal models of oxidant stress are described. A major topic is the formation of F2-Isoprostanes in human diseases including atherosclerotic cardiovascular disease and Alzheimer's disease. The quantification of F2-isoprostanes in tissue lipids by gas chromatography/mass spectrometry as a measure of oxidant stress is the main protocol in *UNIT 17.6*. An alternative protocol is the extraction of lipids from phospholipid-containing biological fluids. The protocol for quantification F2-isoprostanes by GC/negative ionization MS is extremely sensitive with a lower limit of detection in the range of 1 to 5 picograms. An example is given for the analysis of F2-isoprostanes in plasma obtained from a rat 4 hour after treatment with carbon tetrachloride. A discussion of critical parameters and troubleshooting along with anticipated results are included in this protocol.

Oxidant stress leading to biological oxidative damage includes the formation of protein-centered radicals. *UNIT 17.7* describes a new technology that utilizes several protocols of immuno-spin trapping for the detection of protein-centered radicals. The spin trap being utilized is 5,5-dimethyl-1-pyrroline N-oxide (DMPO which, under proper conditions, can form stable DMPO-protein radical-derived nitrone adducts that are detected and identified by immuno-spin trapping with an antiserum against DMPO. A basic protocol describes the procedure for the production and detection of hemoprotein-centered radicals by immuno-spin trapping ELISA. A second basic describes the preparation and immunoblot analysis of DMPO-protein radical-derived nitrone adducts. Because *UNIT 17.7* focuses on a new technology, a detailed discussion of critical parameters and troubleshooting along with anticipated results are included in this protocol.

Donald J. Reed

Formation and Functions of Protein Sulfenic Acids

Sulfenic acids (R-SOH) are the simplest oxy-acids of organic sulfur and, unlike with higher sulfur oxidation states, sulfinic ($R-SO_2H$) and sulfonic ($R-SO_3H$) acids, they are inherently unstable and highly reactive (Hogg, 1990). Considerable insight has been gained through studies of small molecules wherein the sulfenic acid moieties have been stabilized by steric, hydrogen-bonding, and/or electronic factors. Recent progress in the identification and analysis of cysteine-sulfenic acids formed within proteins has also added to the understanding of the forces that contribute to their stabilization (Claiborne et al., 2001). Cysteine sulfenic acids, as reversibly oxidized products of peroxide, peroxynitrite, or NO-mediated oxidation of cysteinyl thiols, are outstanding candidates as players in redox regulation, an area of intense investigation in recent years (Poole et al., 2004). Indeed, protein sulfenic acids are involved in multiple ways in oxidative and nitrosative stress as (1) redox centers or catalytic intermediates in enzymes, (2) reversibly oxidized sensors of peroxide or NO levels in regulatory proteins, and (3) intermediates in the irreversible damage to cysteinyl residues caused by overoxidation of these amino acids.

Sulfenic acids in proteins have been notoriously difficult to identify due to their reactivity, particularly outside of their native protein environment. Early evidence supporting the formation and stabilization of sulfenic acids in two proteins, glyceraldehyde-3-phosphate dehydrogenase and papain, relied only on indirect methods for their identification (Allison, 1976). Over the last decade, the growing number of proteins known to form sulfenic acids of functional significance and the improvement in definitive identification via structural and chemical techniques have greatly enhanced recognition of their importance in biological systems. Hopefully, with the tools now available, the widespread biological significance of these cysteine modifications will be further clarified.

FORMATION, REACTIVITY, AND DETECTION OF CYSTEINE SULFENIC ACIDS IN PROTEINS

Sulfenic acids in proteins are formed upon reaction of cysteinyl thiols with mild oxidizing agents. Even molecular oxygen can act as an oxidant of protein thiols (termed autooxidation), although the rate of this reaction is insignificant in the absence of catalytic quantities of metals (particularly iron and copper; Torchinsky, 1981). Oxidizing agents of greatest biological significance are peroxides, including hydrogen peroxide, organic hydroperoxides, and peroxynitrite, and nitric oxide and/or its derivatives. All of these agents participate in cell signaling and have been shown to convert protein thiols to sulfenic acids. The reactivity of particular cysteinyl thiols toward these molecules is controlled by their respective protein environments. Important factors include accessibility of the thiol toward these agents and the proximity of other important amino acid side chains, which may interact with the thiol group or with the oxidant or its product. Most reactive are cysteine residues with relatively low pK_a values (below the typical value of ~8.5 for an unperturbed cysteine thiol), which are stabilized as the nucleophilic thiolate anion at neutral pH. Proximity to basic amino acids that stabilize the negative charge on the thiolate therefore promotes the oxidation of given cysteine residues.

Peroxide Sensitivity

Other factors are clearly involved, as well. Documented reactivities of thiolate anions with hydrogen peroxide, for example, range from ~20 M^{-1} sec^{-1} for protein tyrosine phosphatases to 10^5 to 10^6 M^{-1} sec^{-1} for cysteine-dependent peroxidases, such as peroxiredoxins and enterococcal NADH peroxidase (Poole et al., 2004). OxyR, a bacterial transcriptional regulator with exquisite sensitivity toward hydrogen peroxide, also exhibits peroxide reactivity within this range, at ~2×10^5 M^{-1} sec^{-1} (Åslund et al., 1999). A likely important active site feature in these peroxide-sensitive sites is the proximity of a general acid catalyst to protonate the poor RO^- leaving group of the hydroperoxides, although no such catalyst has as yet been identified in these proteins. Although some of these features in proteins are coming to light, understanding the molecular basis for redox sensitivity toward oxidants of given cysteinyl residues is still at an early stage.

Another mechanism for enhancement of cysteine reactivity toward peroxides, coordination of the cysteine sulfur to a metal, has re-

Contributed by Leslie B. Poole
Current Protocols in Toxicology (2003) 17.1.1-17.1.15

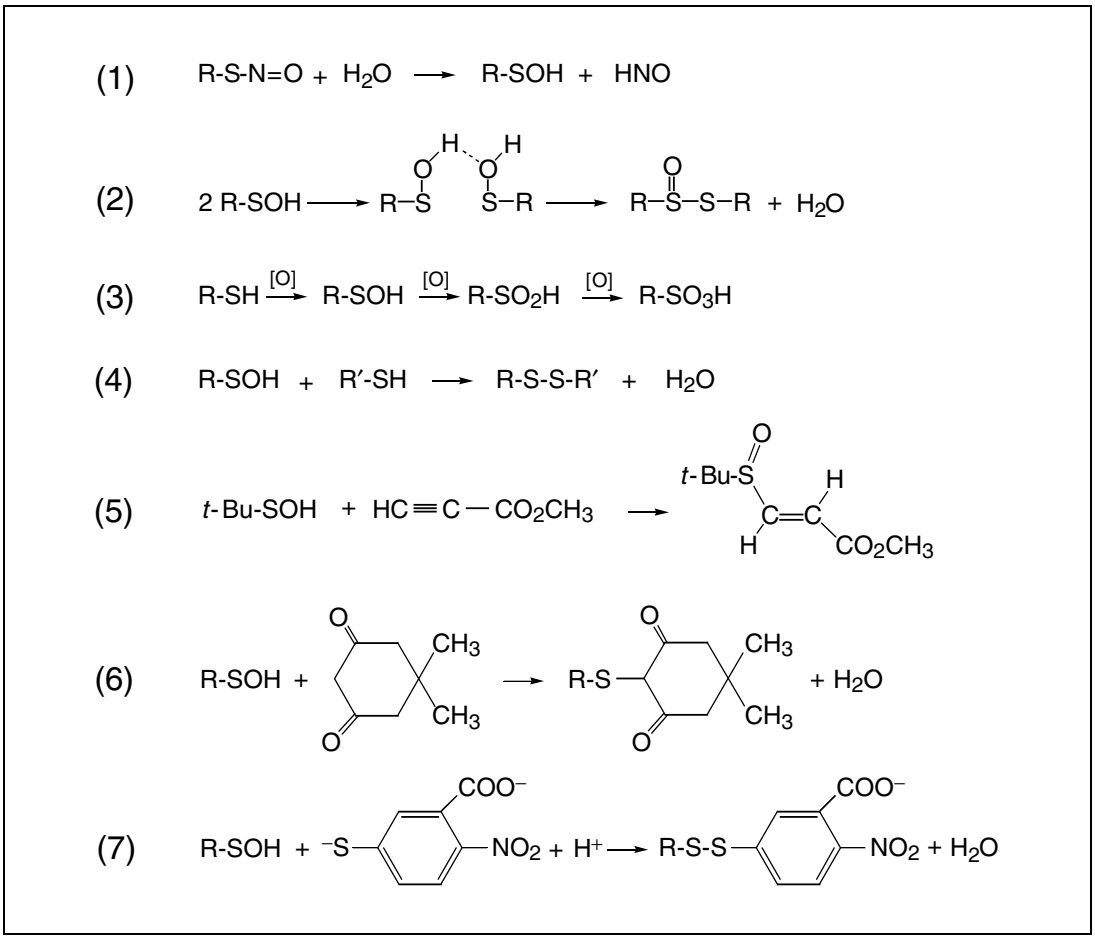

Figure 17.1.1 *(continues on right)* Chemical reactions relevant to the redox chemistry of sulfenic acids.

cently been characterized as well. In one heat shock protein from *Escherichia coli*, Hsp33 (Graumann et al., 2001), cysteinyl residues coordinated to zinc were shown to react with hydrogen peroxide, resulting in disulfide-bond formation. Furthermore, release of the bound metal concomitant with disulfide bond formation is an essential part of the activation of this protein. This mechanism likely also applies to the iron-coordinated cysteinyl residues within the peroxide-sensitive transcriptional repressor PerR from *Bacillus subtilis* (Mongkolsuk and Helmann, 2002). Although cysteine sulfenic acid formation was not demonstrated in these cases, its formation as an intermediate leading to disulfide bond formation is a plausible hypothesis. Such metal-enhanced reactivity of cysteine thiols may also be relevant to the sensitivity of Fe-S clusters toward oxidative damage (e.g., in aconitase and fumarase; Costa Seaver and Imlay, 2001). The release of the Fe(II) under conditions where H_2O_2 is already present undoubtedly exacerbates the deleterious effects of Fe-S center breakdown. Such cysteine-coordinated metal centers can thus serve as peroxide sensors, as well (Mongkolsuk and Helmann, 2002).

Nitrosative Stress and Sulfenic Acids

Several important players in nitrosative stress, including nitric oxide, S-nitrosoglutathione, and the product of nitric oxide and superoxide, peroxynitrite ($OONO^-$), deserve special attention as modifiers of cysteine thiols. Although the pathways through which nitric oxide modifies cysteinyl residues are complex, NO and its derivatives have been shown to modify free cysteine residues to give the S-nitrosothiol (R-SNO) and/or sulfenic acid (R-SOH) products or, in the presence of additional thiols, mixed disulfide bonds (Stamler and Hausladen, 1998; Marnett et al., 2003). Interestingly, when human glutathione reductase was inactivated with S-nitrosoglutathione (GSNO), the active-site cysteine residue proximal to the flavin (Cys63) was oxidized to a stable sulfenic acid and the interchange cysteine (Cys58) was linked through a mixed disulfide bond to glutathione (Becker et al., 1998). Oxidation of protein thiol groups to sulfenic,

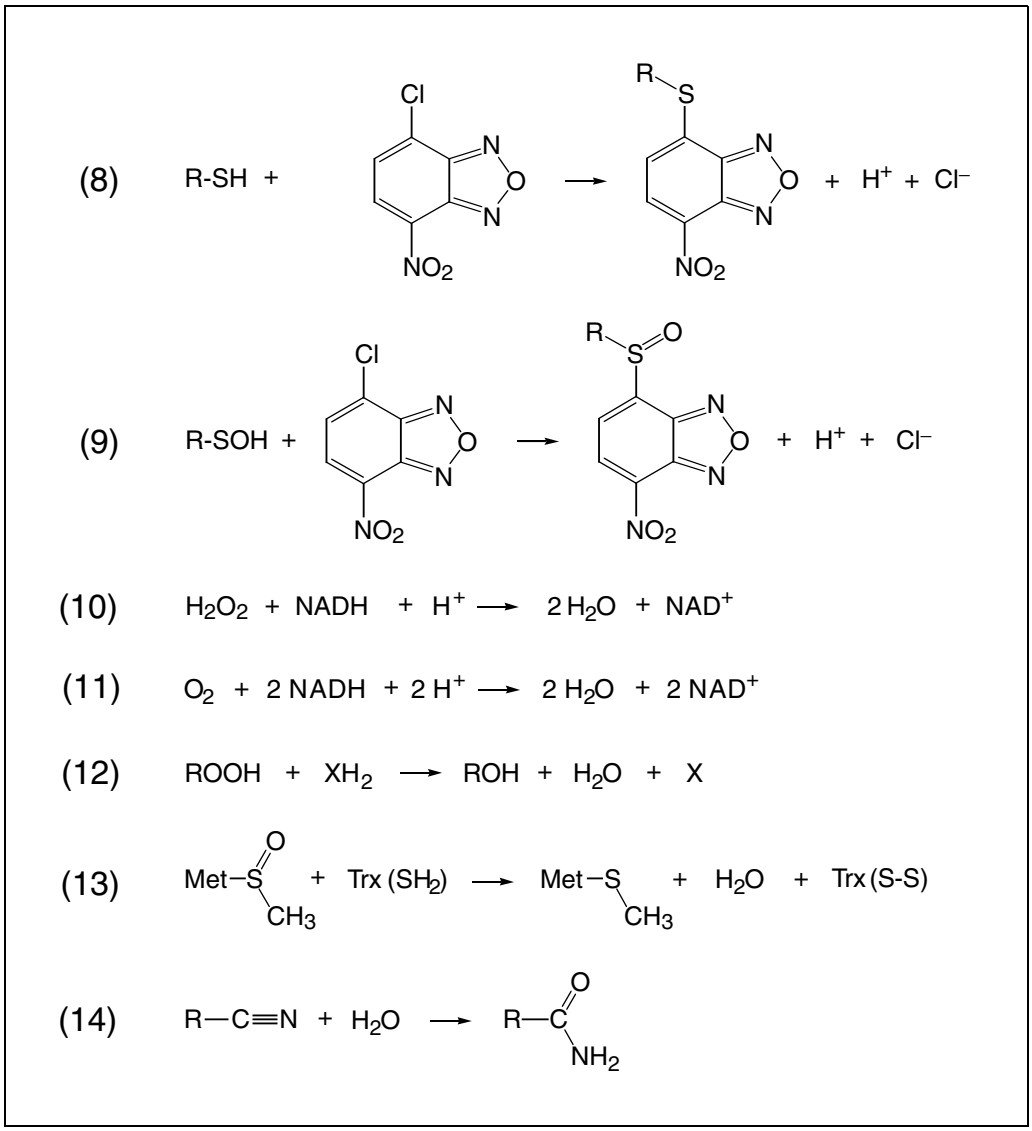

Figure 17.1.1 *(continued)*

sulfinic, and sulfonic acids has also been observed to occur subsequent to S-nitrosothiol generation, suggesting that these oxyacids are produced by initial hydrolysis of the nitrosothiol groups to generate the protein sulfenic acid and HNO, the one electron reduced form of NO (Fig. 17.1.1, reaction 1; Poole et al., 2004).

The sulfenic acid can then be further oxidized or condensed with reduced glutathione (GSH) or other thiol groups to form a mixed disulfide. Here again, factors stabilizing S-nitrosothiols, particularly those which preferentially yield either Cys–SNO or Cys–SOH products, are relatively poorly understood.

Chemistry of Sulfenic Acids

Once formed, sulfenic acids are intrinsically unstable due to their chemical reactivity but can be stabilized in the protein environment. The chemistry of sulfenic acids in small molecules and proteins, which has been reviewed elsewhere (Allison, 1976; Hogg, 1990; Claiborne et al., 2001), is summarized below in terms of the relevant reactions in which they participate and the forces which stabilize cysteine sulfenic acids in proteins.

Self condensation

Based on small molecules as model compounds, the greatest propensity of sulfenic acids is to undergo self-condensation via a hydrogen-bonded dimeric intermediate to yield a thiosulfinate linkage (Fig. 17.1.1, reaction 2).

This irreversible condensation reaction highlights a remarkable feature of sulfenic acids: the displacement of $^{-}$OH from one sulfur by the direct attack of the other demonstrates

their participation as both nucleophiles and electrophiles in chemical reactions. Given the intermediate which must be formed to promote this reaction, steric hindrance (preventing the close approach of two sulfenic acid moieties) and sulfenate anion stabilization (disfavoring generation of the hydrogen bonding network) are thus important factors in sulfenic acid stability in these molecules.

Oxidation, reduction, and trapping

Sulfenic acids have generally been considered transient intermediates in the oxidation of thiols to sulfinic ($R\text{-}SO_2H$) or sulfonic ($R\text{-}SO_3H$) acids (Fig. 17.1.1; reaction 3) and in the formation of disulfide bonds from free thiols (Fig. 17.1.1, reaction 4).

While sulfenic acids are readily reduced back to the thiol state with the chemical reductants dithiothreitol (DTT) or arsenite (which is reportedly unable to reduce disulfide bonds; Torchinsky, 1981), sulfinic acids are only reducible by such agents at very low pH (i.e., <4; Finlayson et al., 1979) and the oxidation to sulfonic acids is irreversible. The reactivity of sulfenic acids with both alkenes and alkynes (Allison, 1976; Hogg, 1990) has been used as the basis for the chemical trapping of unstable sulfenic acids formed, for example, upon thermolysis of sulfoxides. During thermolytic decomposition of di-*tert*-butyl sulfoxide, addition of methyl propiolate allowed for adduct formation with the *tert*-butyl-SOH product (Fig. 17.1.1, reaction 5), proving its formation (Shelton and Davis, 1973).

Reaction with nucleophiles

Sulfenic acids also react with nucleophiles such as benzylamine and cyanide. Adduct formation with 5,5-dimethyl-1,3-cyclohexanedione (dimedone) (Fig. 17.1.1, reaction 6) has been used as a diagnostic tool for demonstrating sulfenic acid formation in proteins (Allison, 1976).

Reaction with aromatic disulfides

The suggestion that sulfenic acids can react with aromatic disulfides (Torchinsky, 1981, p. 52) has been borne out by the demonstration of their reactivity with 5,5′-dithiobis(2-nitrobenzoic acid) (DTNB), a reagent typically considered to be thiol-specific (Poole and Ellis, 2002). Although the reaction of DTNB with sulfenic acids is complex and substoichiometric due to the additional reactivity of the 2-nitro-5-thiobenzoic acid (TNB) product with sulfenic acids (Fig. 17.1.1, reaction 7), this observation argues for caution in interpreting thiol contents as measured by DTNB reactivity in cases where sulfenic acids may also be present.

Identification of Sulfenic Acids in Proteins

For identification of sulfenic acids in proteins, recent developments in crystallographic and NMR approaches have led to important advances (Claiborne et al., 2001). In cases where these techniques have not been applicable, however, sulfenic acid identification has relied on several complementary protein chemical methods, as described in detail in the following unit (*UNIT 17.2*).

TNB and dimedone

Taking advantage of the unique reactivity of sulfenic acids toward the chromophoric thiol reagent TNB, quantitation of accessible sulfenic acids can be accomplished by monitoring the decrease in A_{412} as the mixed disulfide bond forms (Fig. 17.1.1, reaction 7).

As described above, dimedone reactivity also implies the presence of sulfenic acid (Fig. 17.1.1, reaction 6), although this product lacks any distinguishing spectral features and must be monitored either by incorporation of the radiolabeled reagent or by the mass increase imparted by adduct formation (Allison, 1976).

NBD chloride

Recent efforts taking advantage of the intrinsic nucleophilicity of sulfenic acids have led to the development of the thiol reagent 7-chloro-4-nitrobenzo-2-oxa-1,3-diazole (NBD chloride) as a diagnostic tool for sulfenic acid identification. Although NBD chloride reacts with both thiols (Fig. 17.1.1, reaction 8) and sulfenic acids (Fig. 17.1.1, reaction 9) at neutral pH, the adduct generated has distinct spectral features depending on the presence or absence of the sulfenate-derived oxygen.

The protein-S-NBD adduct has characteristic UV-visible (λ_{max} = 420 nm) and fluorescence (λ_{ex} = 422 nm, λ_{em} = 527 nm) properties which are readily distinguished from those of the nonfluorescent protein-S(O)-NBD adduct (λ_{max} = 347 nm; Fig. 17.1.2). The latter product is also larger by 16 amu as measured by electrospray ionization mass spectrometry (ESI-MS; Fig. 17.1.3). Whether the NBD adduct formed with the sulfenic acids is a sulfoxide or sulfenate ester was not established by these studies, although arguments supporting sulfoxide formation have been made based

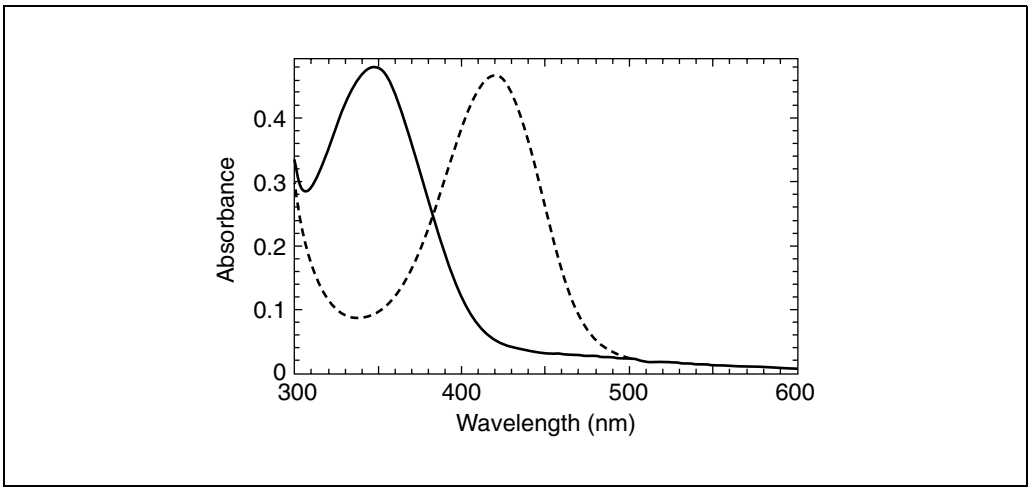

Figure 17.1.2 UV-visible spectra for NBD adducts of reduced and oxidized forms of C165S AhpC. Spectra correspond to the Cys46-S-NBD product (dotted line) and the Cys46-S(O)-NBD product (solid line). Reprinted with permission from Ellis, H. R., and Poole, L. B. *Biochemistry* 36:15013-15018. Copyright 1997 American Chemical Society.

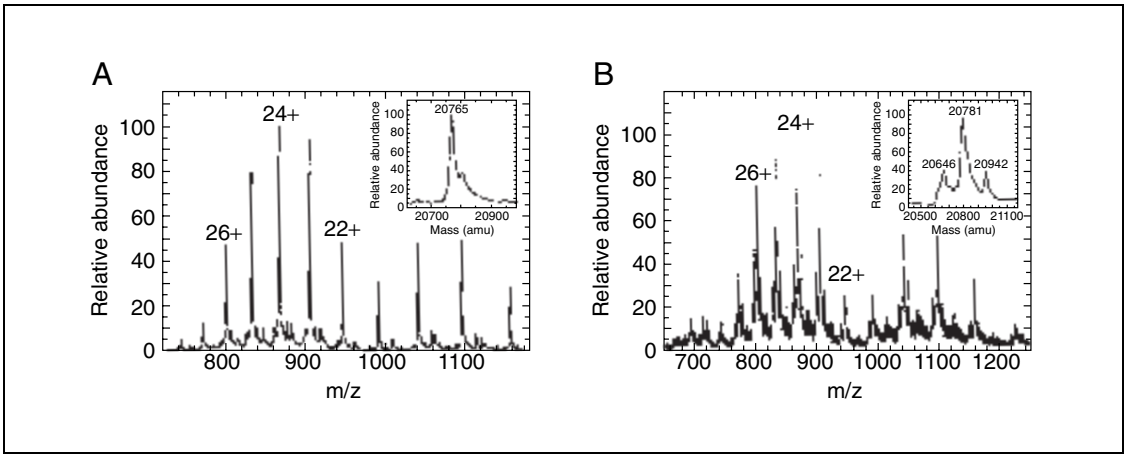

Figure 17.1.3 Electrospray ionization mass spectra of the Cys46-S-NBD (A) and Cys46-S(O)-NBD (B) adducts of C165S AhpC shown in Figure 17.1.2. Insets give the respective transformed spectra and mass values. Reprinted with permission from Ellis, H. R., and Poole, L. B. *Biochemistry* 36:15013-15018. Copyright 1997 American Chemical Society.

partly on the acid stability of the product (Claiborne et al., 2001).

Direct detection by ESI-MS

One final note on sulfenic acid detection in proteins should be made. Where protein subunit molecular weights are sufficiently small and relatively gentle nondenaturing conditions are employed (e.g., ammonium bicarbonate buffer), ESI-MS techniques may allow for direct detection of the sulfenic acid oxygen and resolution of this species from the thiol or further oxidized R-SO_2H- and R-SO_3H-containing species (Fuangthong and Helmann, 2002). Typically, however, adventitious overoxidation of the sulfenic acid to exclusively yield the sulfonic acid (R-SO_3H) product is observed, particularly where acetonitrile and formic acid must be added for detection of the ionized protein (Ellis and Poole, 1997b).

Stabilization

As alluded to above, protein sulfenic acids, once formed, can (1) be stabilized within the protein environment, (2) react with nearby protein thiols or exogenous thiol groups to form disulfide bonds, (3) be further oxidized to sulfinic and/or sulfonic acids by oxidants such as molecular oxygen, peroxides, or peroxynitrite, or (4) be directly reduced back to the thiol state. Critical factors in the stabilization of protein sulfenic acids have been described previously (Allison, 1976) and are continuing to be refined in light of recent structural data (Claiborne et

al., 2001). One important factor in sulfenic acid stabilization in proteins is the absence of proximal thiols. Other factors may include proximity of suitable hydrogen-bond acceptors to the sulfenic acid hydrogen or the stabilization of the deprotonated sulfenate base. An apolar and/or inaccessible microenvironment for sulfenic acids in proteins also provides a stabilizing environment. Where sufficiently accessible, sulfenic acids will likely react with the high concentrations of GSH within the cells of most organisms, a process known as glutathionylation or glutathiolation. Note that the thiol-disulfide interchange of a protein thiol with glutathione disulfide (GSSG) can also yield this product without the intermediacy of sulfenic acid. Susceptibility toward overoxidation involving reaction with excess peroxide is also controlled by structural and electronic factors, although again, few details of the molecular mechanisms involved are clear.

FUNCTIONS OF PROTEIN SULFENIC ACIDS

Because both sulfenic acids and the disulfide bonds that may ensue following SOH formation are reducible back to the thiol state, these species are highly suited as catalytic redox centers or as redox-sensitive regulatory components within enzymes and transcription factors. The phenomenon of redox regulation includes a wide variety of redox sensors which modulate protein function in response to changing environmental signals, intracellular signals, or both (Bauer et al., 1999; Marnett et al., 2003). Hydrogen peroxide and NO, as important cellular redox signals, have the propensity to generate stable cysteine sulfenic acids and disulfide bonds in proteins with redox-sensitive cysteinyl residues. With recently improved methodology for identifying sulfenic acid formation in proteins, the stage is set for the application of these approaches to the identification of protein sulfenic acids of functional significance. Based on current knowledge, the following represents a brief review of the catalytic and regulatory roles played by sulfenic acids in proteins.

Sulfenic Acid Participation in Redox Catalysis by Antioxidant Enzymes

NADH peroxidase

The first identified and best characterized naturally-occurring sulfenic acid in a protein is that of NADH peroxidase, a flavoprotein expressed in some lactic acid bacteria, which acts as a functional substitute for catalase in these heme-deficient organisms (Claiborne et al., 2001). In this protein, cysteine sulfenic acid represents the stable, oxidized form of the active site generated on reaction with its oxidizing substrate, hydrogen peroxide, during catalysis (Fig. 17.1.1, reaction 10 and Fig. 17.1.4, Scheme 1).

The cysteine sulfenic acid is then directly reduced back to its activated thiolate form (protein-S^-) via electrons from NADH provided via the proximal isoalloxazine of the tightly bound FAD.

Initial evidence supporting identification of this stable sulfenic acid came in part from the fact that only a single cysteine was present per subunit, and no intersubunit disulfide bond was formed on oxidation with peroxide (Poole and Claiborne, 1989). In the last decade, structural data obtained by cryocrystallography and ^{13}C-NMR have fully confirmed the presence of this unusual redox center (Claiborne et al., 2001). As observed in the X-ray crystal structure, the cysteine sulfenic acid (Cys42-SOH = Cyo42) is stabilized through H-bonding interactions of both S_γ and O_δ with the nearby FAD (3.3 – 3.6 Å) and a neutral histidine (~3.4 Å between Cyo42-O_δ and His10 $N_{\varepsilon 2}$), interactions which may serve to stabilize the sulfenate base. The relatively apolar microenvironment, its very limited solvent access, and the lack of any other cysteinyl residues in the protein all serve to stabilize this redox center in NADH peroxidase.

NADH oxidase

Another flavoprotein with homology to NADH peroxidase (44% identity between the two proteins from *Enterococcus faecalis*), NADH oxidase, has also been identified as a sulfenic acid–containing protein with mechanistic similarities to the NADH peroxidase (Claiborne et al., 2001). In this case, oxygen is fully reduced by four electrons to water (Fig. 17.1.1, reaction 11), and evidence strongly supports the generation of a flavin C(4a)-hydroperoxide intermediate (FADHOOH) formed on reaction of the reduced flavin with oxygen (Claiborne et al., 2001).

Although active site asymmetry in the dimeric enzyme has complicated the kinetic and structural analyses of NADH oxidase, it seems clear that the sulfenic acid of this protein is in quite a similar environment and playing an identical mechanistic role as that of the related NADH peroxidase (Claiborne et al., 2001). Thus, the Cys-SOH formed on oxidation of the active site cysteine by the peroxyflavin is rere-

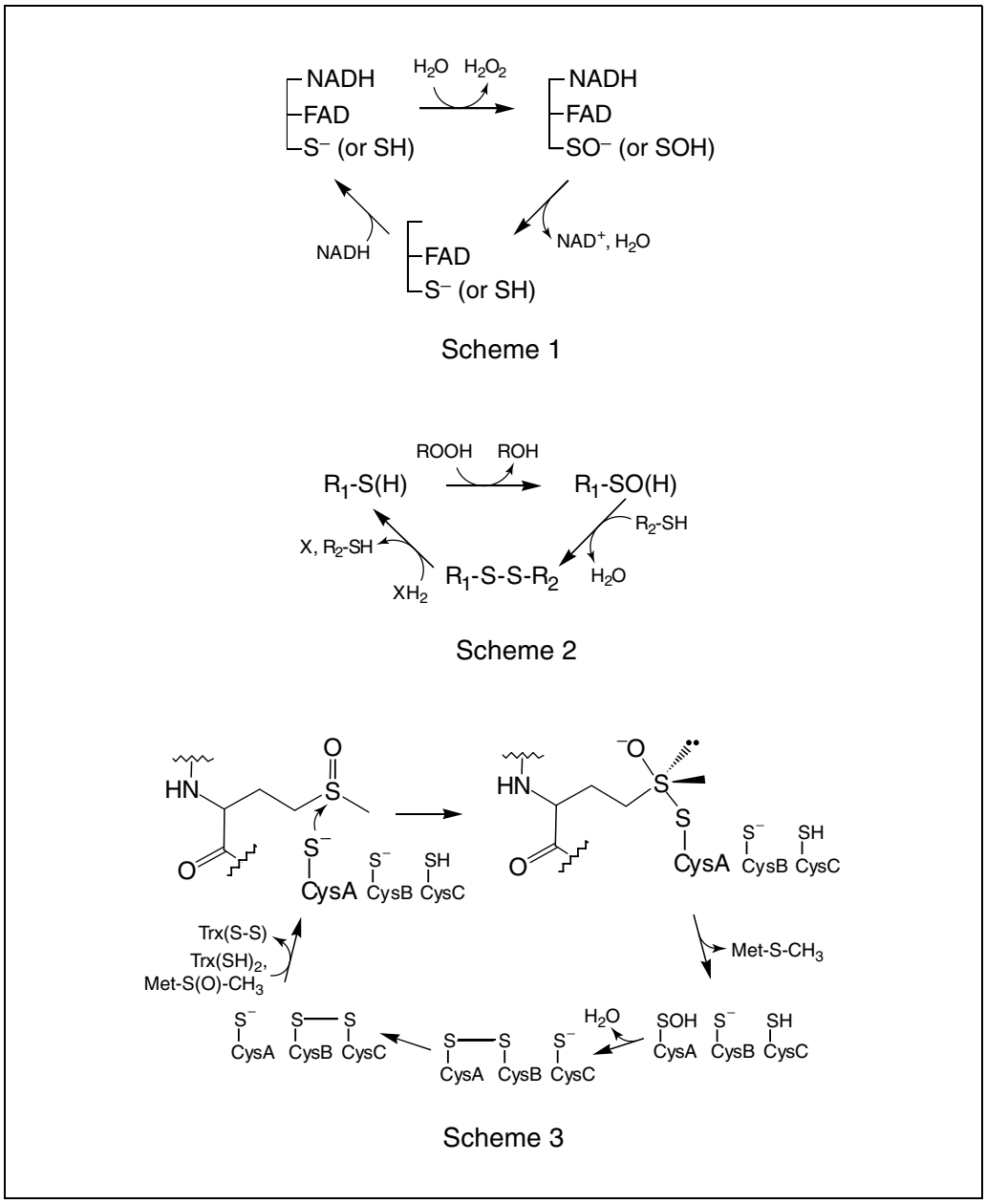

Figure 17.1.4 Reaction schemes involving protein sulfenic acids.

duced by NADH with the flavin playing an intermediary role in electron transfer between the two as in Scheme 1 (Fig. 17.1.4).

Peroxiredoxins

Over the last ~15 years, a ubiquitous family of peroxidases, named the peroxiredoxins (Prxs), has been identified which relies on a chemistry similar to that of the NADH peroxidase in catalyzing the cysteine-dependent reduction of peroxides (Fig. 17.1.1, reaction 12).

Prokaryotic and eukaryotic Prxs generally reduce a wide variety of peroxides, including hydrogen peroxide, organic hydroperoxides, and peroxynitrite, and are expressed at high levels in many cell types (Wood et al., 2003a). In bacteria, Prxs such as AhpC from *Escherichia coli* are essential for maintaining the low levels of hydrogen peroxide required for sustained growth (Costa Seaver and Imlay, 2001). The presence of up to six different subtypes of Prxs in mammalian cells also helps regulate levels of hydrogen peroxide, a mediator of cytokine-induced signal transduction (Hofmann et al., 2002). At least one Prx, PrxI, also known as heme-binding protein 23 (HBP23) and proliferation-associated gene (PAG), also interacts directly with and inhibits *c*-Abl, a nonreceptor tyrosine kinase. Thus, these proteins are important not only in protec-

tion against oxidative stress but also in regulation of cell signaling, with demonstrated roles in such processes as proliferation, differentiation, and apoptosis.

Prx classes

Prxs can be structurally and functionally divided into three classes known as the typical 2-Cys Prxs, the atypical 2-Cys Prxs and the 1-Cys Prxs (Wood et al., 2003a). Whereas Prxs in all three classes catalyze the reduction of hydroperoxides to yield a sulfenic acid at the conserved active site cysteine (Fig. 17.1.4, Scheme 2), the mechanism for recycling of the sulfenic acid to regenerate the activated thiolate differs among the three classes.

1-Cys Prxs: In 1-Cys Prxs, the sulfenic acid likely reacts with a small molecule thiol prior to reduction with a second molecule of the reductant, although the identity of the electron donor is as yet unclear (Fig. 17.1.4, Scheme 2; $XH_2 = R_2SH$ and the product is R_2-S-S-R_2 in this case).

2-Cys Prxs: In 2-Cys Prxs, the thiol which condenses with the nascent sulfenic acid comes from another cysteine group in the protein, either on the same subunit as the peroxidatic cysteine (atypical 2-Cys Prxs) or, more commonly, from an adjacent subunit of the head-to-tail homodimer (typical 2-Cys Prxs). The electron donor required for recycling of 2-Cys Prxs generally includes a reduced pyridine nucleotide (NADH or NADPH), a flavoprotein disulfide reductase (thioredoxin reductase, AhpF, trypanothione reductase, or lipoamide dehydrogenase) and an additional CXXC-containing protein or module (thioredoxin, the N-terminal domain of AhpF, tryparedoxin, or AhpD; Wood et al., 2003a).

2-Cys Prx to 1-Cys Prx: Prior to 1998, the strongest evidence for cysteine sulfenic acid involvement in Prx-catalyzed peroxide reduction came from the studies of a mutant of *Salmonella typhimurium* AhpC, C165S, in which the second cysteine had been removed by mutagenesis, leaving only the peroxidatic Cys46 (Ellis and Poole, 1997a,b). This enzyme exhibited full peroxidatic activity toward cumene hydroperoxide in the presence of excess NADH and AhpF, showing that it had effectively been converted to a 1-Cys Prx. Reactivity of the oxidized active site cysteinyl group toward TNB and dimedone was demonstrated as part of the proof of sulfenic acid production on peroxide treatment of this mutant. Reactivity of the thiol and sulfenic acid forms of this mutant toward NBD chloride was also studied, as described above, and it was this work that resulted in the development of a new protocol for the trapping and identification of cysteine sulfenic acids in proteins (Ellis and Poole, 1997b).

Prx structures

Structure of hORF6: In 1998, the 2.0 Å crystal structure of the C91S mutant of a human 1-Cys Prx, hORF6, demonstrated the sulfenic acid at the active site (Cys47-SOH = Cyo47) of this enzyme, as well (Choi et al., 1998). At least some of the environmental features known to stabilize protein sulfenic acids are also present in the hORF6 (PrxVI) structure. Solvent access to the Cyo47, which lies at the bottom of an active site pocket, is restricted. A nearby His (His39) is within H-bonding distance (3.0 Å) of the Cyo47-S_γ, and the only other cysteine in the protein (Cys91, mutated to Ser in the mutant studied by X-ray crystallography) is ~17 Å away.

Other Prx structures: Since the report of the hORF6 structure, six structures of reduced, oxidized, and overoxidized 2-Cys Prxs have been reported (Wood et al., 2003a,b). The most important findings are that the typical 2-Cys Prxs must undergo considerable structural rearrangements around the peroxidatic cysteine at the active site and the resolving cysteine in the C-terminal tail of the partner subunit in order to form the disulfide bond of the oxidized proteins. Typical 2-Cys Prxs also form strong decamers as pentameric arrangements of homodimers $[(\alpha_2)_5]$ in their reduced, but not oxidized (disulfide-bonded) forms.

Prx inactivation and signaling

As Prxs are intimately involved in the cellular control of H_2O_2 levels, they play an obvious role in modulating peroxide-linked redox signaling pathways. Thus, mechanisms by which Prx activities are regulated, reportedly including oligomerization, phosphorylation, proteolysis, and overoxidation of the active site cysteine, presumably dictate the ability of H_2O_2 to act as a second messenger (Poole et al., 2004). The phenomenon whereby Prxs are inactivated by their own substrate at the active site Cys-SOH is particularly striking; in fact, eukaryotic Prxs are significantly more sensitive (by ~110-fold) toward inactivation by H_2O_2 than are their bacterial counterparts (Wood et al., 2003b). The Cys-SOH, which persists longer in the eukaryotic versions of the 2-Cys Prxs prior to disulfide bond formation, therefore acts as a peroxide-sensitive switch in higher organisms.

Interestingly, the product of Cys-SOH oxidation in Prxs, the stabilized cysteine sulfinic acid, turns out not to be irreversibly oxidized in vivo. At least some eukaryotic cell types express a sulfinic acid reductase capable of reversing Cys-SO_2H formation in some Prxs (Poole et al., 2004).

Methionine sulfoxide reductases

Function: One hallmark of oxidative damage to proteins by reactive oxygen and nitrogen species is the oxidation of methionine residues to asymmetric methionine sulfoxides (epimeric R and S forms). Repair enzymes that can catalytically reduce these oxidized amino acids back to their original form using electrons from thioredoxins (Fig. 17.1.1, reaction 13) have been identified recently from bacterial and eukaryotic sources (Weissbach et al., 2002).

These peptide methionine sulfoxide reductases (Msrs) are therefore responsible for the reversal of such oxidative damage, suggesting that methionine oxidation, like reversible cysteine oxidation, may even be an important player in redox signaling. There is a growing list of proteins and peptides whose biological activities are affected by the oxidation of methionine residues (e.g., α-1-proteinase inhibitor, a voltage-gated K^+ channel, and calmodulin); the observation that Msrs can restore activity to at least some of these oxidized proteins supports a regulatory role for these enzymes (Weissbach et al., 2002).

Mechanism: Of interest in the context of this discussion is the intermediacy of a cysteine sulfenic acid (or, in some cases, the corresponding selenenic acid of selenocysteine-containing enzymes) in the catalytic cycle of Msrs (Boschi-Muller et al., 2000). During turnover, an essential, conserved cysteine at the active site (CysA) acts as the nucleophile and attacks the sulfur of the methionine sulfoxide, leading to the formation of a trigonal-bipyramidal intermediate (Fig. 17.1.4, Scheme 3; Boschi-Muller et al., 2000; Weissbach et al., 2002).

Collapse of the intermediate generates the restored methionine product and a sulfenic acid at the active site cysteine. Condensation with CysB to form a disulfide bond and a series of thiol-disulfide exchange reactions with CysA, B, and C in Msrs and the two cysteines of the thioredoxin electron donor results in reactivation of the enzyme for another turnover. The primary evidence for the intermediary cysteine sulfenic acid comes from the TNB and dimedone reactivity of the intermediate generated when only CysA is present (Boschi-Muller et al., 2000).

Other Catalytic Functions of Cysteine Sulfenic Acids in Proteins

Before leaving the topic of sulfenic acids important in catalysis, several systems distinct from the antioxidant enzymes presented above, yet depending on sulfenic acids for function, should also be noted. These proteins include nitrile hydratase, with a cysteine sulfenic acid at the active site, and human serum albumin, where sulfenic acid generation has been linked to the catalytic reduction of platinum drugs.

Nitrile hydratase

This enzyme from *Rhodococcus* sp. N-771 contains nonheme iron and catalyzes reaction 14 of Figure 17.1.1, a chemistry critical to the industrial production of acrylamide.

In the 1.7-Å X-ray crystal structure of the NO-inhibited enzyme published in 1998 (Nagashima et al., 1998), Cys112 was oxidized to a sulfinic acid (Cys112-SO_2H) and Cys114 to a sulfenic acid (Cys114-SOH). These two residues, along with Cys109-SH, act as ligands to the bound Fe(III). Oxygen atoms from each of the two oxidized cysteine residues also protrude above the equatorial plane of the Fe(III) ligand field and are within 2.8 to 3.0 Å of the NO nitrogen. Recent data has shown the essentiality of the oxidation of both cysteine residues in generating active enzyme (Murakami et al., 2000). Together, these data support catalytic roles for both Cys-SOH and Cys-SO_2H in this unusual active site, although the Cys-SOH is not undergoing changes in its redox state during the catalytic cycle.

Human serum albumin and activation of Pt(IV) drugs

Oxidation of Cys34 in human serum albumin (HSA) by the NO donor diethylamine nonoate was shown to result in the generation of the sulfenic acid form of this residue based on its reactivity with dimedone and GSH (DeMaster et al., 1995). This observation took on new significance with the more recent finding that Cys34-SH catalyzes the reduction of the iodide analogue of the anticancer drug cisplatin (*cis*-$[Pt(IV)Cl_2(NH_3)_2]$). During reaction of HSA with $[Pt(en)(OH)_2I_2]$, Cys34-SH was oxidized to the sulfenic acid and subsequently to higher oxidation states, likely through the intermediacy of the sulfenyl iodide at Cys34 (Cys34-SI; Kratochwil et al., 1999). The formation of the sulfenic acid at Cys34 was supported by NBD-modification and ESI-MS analyses. The importance of this observation lies in the fact that Pt(IV) anticancer drugs

undergo reductive activation in blood plasma, where HSA-Cys34 represents the major thiol (Claiborne et al., 2001). In vivo, the formation of the sulfenic acid at Cys-34 of HSA may be reversible, and its formation in the context of Pt(IV) drug activation may represent a sort of catalytic cycle for this abundant serum protein.

Redox Regulation Through Reversible Cysteine Sulfenic Acid Formation in Enzymes

An important role for sulfenic acids in proteins is in the regulation of activity in enzymes for which they are not part of the catalytic mechanisms. In particular, enzymes with an essential cysteinyl residue at their active site can be susceptible to this modification and inactivated by it. As long as the oxidation stops at the level of sulfenic acid or disulfide bond formation, enzymatic activity can be restored by a chemical reductant. Reduction in vivo will also occur as long as a pathway exists whereby a cellular reductant (typically reduced thioredoxin, GSH, or glutaredoxin) can carry out this reaction. Examples of enzymes shown to be inactivated by sulfenic acid formation and reactivated by chemical reduction include papain (Allison, 1976), glyceraldehyde-3-phosphate dehydrogenase (GAPDH; Allison, 1976; Ishii et al., 1999), and NO-inhibited GSSG reductase (Becker et al., 1998), as mentioned earlier. Given their importance in signal transduction pathways, two additional types of enzymes undergoing reversible peroxide- or NO-mediated inactivation through cysteine sulfenic acid formation, protein tyrosine phosphatases and cathepsin K, are discussed in more detail below. It should be noted again that enzymes that are glutathionylated as part of their reversible inactivation may also first be oxidized to sulfenic acids and then condense with GSH; this modification pathway has been observed, for example, for protein tyrosine phosphatases (Barrett et al., 1999). Indeed, reaction with one molecule of GSH can be viewed as the first step in reactivation which is followed by reaction with a second molecule of GSH, GSSG formation and regeneration of the active enzyme. This process is analogous to the reaction mechanism of glutathione peroxidases, where the chemical analog of cysteine sulfenic acid, the selenenic acid (Cys-SeOH), is regenerated with two molecules of GSH.

GAPDH

In the case of GAPDH, cysteine sulfenic acid formation inhibits one activity but also imparts a new enzymatic activity (Allison, 1976). As mentioned above, oxidation of GAPDH leads to stable sulfenic acid formation. In its thiol form, Cys149 of GAPDH from *Bacillus stearothermophilis* catalyzes the production of 1,3-bisphosphoglycerate. On oxidation to Cys149-SOH by hydrogen peroxide (Schmalhausen et al., 1999) or nitric oxide (Ishii et al., 1999), the modified enzyme does not catalyze the dehydrogenase reaction but instead participates directly in the hydrolytic decomposition of D-glyceraldehyde-3-phosphate through a new acyl phosphatase activity. Thus, this redox switch not only turns the activity of this glycolytic enzyme on and off, it also converts the enzyme to a form with a distinctly different catalytic activity.

hBCATm

It should also be noted that peroxide-sensing, regulatory dicysteinyl centers such as those within CXXC motifs are also likely to be converted to the disulfide form through intermediary sulfenic acid formation. For example, human mitochondrial branched-chain aminotransferase (hBCATm), a pyridoxal phosphate–dependent enzyme which does not require a cysteine residue in its catalytic mechanism, is completely inhibited by disulfide bond formation at a CXXC redox center proximal to the active site (Conway et al., 2002). Reaction of one of the cysteine residues, Cys315, with peroxide forms Cys315 sulfenic acid as the first step in the process, as established recently by combined mutagenesis and chemical modification studies (Conway, Poole, and Hutson, unpub. observ.). The proximity of the other cysteine thiol (Cys318) in the wild-type enzyme then leads to disulfide bond formation, and reversal of this oxidation by DTT reactivates the enzyme.

Protein tyrosine phosphatases

It is increasingly clear that cellular redox status has an important role to play in numerous signal transduction pathways, including those involving growth factors and tyrosine phosphorylation. For example, the src family protein tyrosine kinase Lck becomes highly phosphorylated on tyrosines when T lymphocytes are incubated with hydrogen peroxide, a phenomenon attributed to the oxidative inactivation of protein tyrosine phosphatases (PTPases; Nakamura et al., 1997). Several reports have confirmed the oxidation of the essential active site cysteine of PTPases such as VHR and PTP1B to a stable sulfenic acid by hydrogen peroxide

treatment, a reversible modification which inactivates these enzymes and can therefore lead to hyperphosphorylation of their target proteins (Denu and Tanner, 2002). The competitive inhibitor phosphate protected against peroxide-mediated inactivation, 2-mercaptoethanol reversed the effect of the hydrogen peroxide, and NBD chloride modification gave a clear indication of sulfenic acid formation, in spite of the contributions to the spectra of the NBD adducts of the other three cysteine residues (Denu and Tanner, 1998). Oxidation of the active site cysteine of PTP1B was also shown to occur in vivo on growth factor stimulation of cultured cells (Lee et al., 1998). In this study, reactivation of the peroxide-inhibited PTP1B ensued on treatment with either reduced thioredoxin or GSH. As noted above, glutathionylation is also observed for PTPases (Barrett et al., 1999), consistent with their oxidative conversion to sulfenic acid–containing proteins followed by condensation with and rereduction by GSH. Crystallographic studies of inactivated PTPases revealed a surprising new derivative of Cys-SOH; in these structures the main-chain nitrogen of an adjacent Ser residue is covalently linked to the sulfenyl sulfur, forming a stable, yet reducible, sulfenyl-amide at the active site (Salmeen et al., 2003). With PTPases as targets for reversible inactivation by hydrogen peroxide, sulfenic acid formation in one class of enzymes can have a big effect on signal transduction pathways involving a large number of other regulatory proteins.

Cathepsin K

Cathepsin K, a cysteine-dependent protease homologous with papain, is thought to play a key role in bone resorption as a result of its collagenolytic activity (Percival et al., 1999). It is expressed at high levels in bone-resorbing osteoclasts and may be responsible for the reduction in bone resorption which results from treatment with NO and NO donors. Indeed, cathepsin K activity of the purified protein or of the protein expressed in cultured cells was inhibited by treatment with GSNO or NOR-1, another NO donor; the activity of the GSNO-treated enzyme was largely regenerated by DTT treatment. Treatment with GSNO led to glutathionylation as shown by mass spectrometry; this technique also indicated the presence of sulfinic or sulfonic acid forms of the active site Cys25 following NOR-1 treatment. Cotreatment of cathepsin K with both NOR-1 and dimedone led to formation of the dimedone adduct, indicating that sulfenic acid was likely formed as an intermediate during the oxidation of Cys25 by one or both compounds. These findings compare nicely with earlier studies of sulfenic acid formation and stabilization in the closely related protease papain (Allison, 1976) and support an important role for sulfenic acid formation in cathepsin K as a mechanism by which NO exerts its inhibitory effect on bone resorption.

Redox Regulation Involving Cysteine Sulfenic Acid Formation in Transcription Factors

As for enzymes, a number of transcriptional regulators sense changes in redox status or peroxide levels specifically through oxidative modifications to Cys-SH. In many cases, the precise linkage between oxidation state of a critical thiol and transcriptional activity is as yet poorly characterized. For example, sulfenic acid generation at the conserved Cys-154 of Fos and the related Cys-278 of Jun, the two protein components of AP-1, was hypothesized more than a decade ago (Abate et al., 1990) but still has not been firmly established. Still, the location of these single cysteine residues within the long recognition helix and in very close proximity to the site of interaction with DNA (Chen et al., 1998a), and considerable data highlighting the importance of maintaining that cysteine in a reduced state for full transcriptional activation (Xanthoudakis and Curran, 1996), argue strongly for a role in regulation by sulfenic acid generation in these proteins. Furthermore, data were presented ruling out disulfide bond formation in oxidized AP-1 (Abate et al., 1990), and the naturally-occurring mutation of Cys278 to a Ser in *v*-Jun both removes its redox regulation and enhances its DNA binding and therefore cell transformation capability, leading to the designation of this mutation as a gain-of-function mutation (Abate et al., 1990; Xanthoudakis and Curran, 1996). A similar situation exists for the E2 protein of bovine papillomavirus-1. A conserved Cys (Cys340 in BPV-1 E2) also exhibits interaction with the DNA target as observed in the 1.7-Å X-ray crystal structure (Hegde et al., 1992). Through mutagenesis analyses of this and two other Cys residues in the recognition helix, it was shown that only Cys 340 is required for inactivation by diamide, a thiol-oxidizing agent (McBride et al., 1992). In this case, mutations of Cys340 to Ser and Ala also gave reduced DNA binding affinities (by ~50% and ≥90%, respectively),

arguing for the requirement of the free thiol at Cys340 for effective binding. Again, sulfenic acid formation has not been directly proven but has a high likelihood of playing an important role in redox regulation involved in the pathogenesis of these DNA tumor viruses.

The case for sulfenic acid–dependent redox regulation for several other transcriptional regulators, OxyR, OhrR, and NF-κB, is stronger, and each of these is covered in more detail below.

OxyR

The bacterial transcription factor OxyR was identified in 1985 and shown to act as a direct sensor of hydrogen peroxide, also transducing the signal to activate the transcription of a number of antioxidant proteins, including the peroxiredoxin system proteins AhpF and AhpC in *E. coli* and *S. typhimurium* (Storz and Imlay, 1999). Early investigations led to the suggestion that sulfenic acid formation might be involved in the activation of OxyR; subsequent mutagenesis studies have supported that notion, as primarily Cys199, but to some extent also Cys208, are required for peroxide activation (Kullik et al., 1995). In MALDI-TOF analyses of tryptic fragments, evidence was noted for thiosulfinate generation (ostensibly from condensation between sulfenic acids) in the oxidized form of a mutant lacking Cys208, supporting peroxide-mediated oxidation of Cys199 (Zheng et al., 1998). Disulfide bond formation between Cys199 and Cys208, as would be expected following Cys199-SOH formation if the two residues are close enough, was indeed observed after activation of OxyR with hydrogen peroxide (Zheng et al., 1998). Recent X-ray crystallographic data including 2.7- and 2.3-Å structures, respectively, for both reduced and oxidized forms of OxyR indicates a very large conformational change imparted to the protein upon disulfide bond formation (Choi et al., 2001). In fact, the two cysteine thiols are some 17 Å apart in the structure of the reduced protein, a situation similar to that observed for the Prxs wherein the two Cys sulfurs are brought together for disulfide bond formation through significant conformational changes (Wood et al., 2003a). A recent report has revisited cysteine modification in OxyR and concluded that Cys oxidation by hydrogen peroxide primarily results in sulfenic acid formation at Cys199 and not disulfide bond formation; other modifications such as nitrosation and glutathionylation of Cys199 were also observed in vivo and found to activate the protein in vitro, as well (Kim et al., 2002). Although the relative contributions of sulfenic acid and disulfide-bonded forms of OxyR in vivo are currently a matter of debate (Poole et al., 2004), rapid formation of sulfenic acid at Cys199 by hydrogen peroxide is clearly critical to the peroxide response.

OhrR

The best evidence for a functional cysteine sulfenic acid generated by peroxide modification of a transcriptional regulator has been reported for OhrR of *Bacillus subtilis*. OhrR in its reduced form represses transcription of the *ohrA* organic peroxide resistance gene and is representative of a family of peroxide sensors identified in both gram positive and negative organisms (Mongkolsuk and Helmann, 2002). The protein from *B. subtilis* has only one cysteine per subunit, which is conserved among other family members, and exposure to peroxides leads to the reversible oxidation of this residue (Cys15) to a sulfenic acid and derepression of *ohrA* transcription (Fuangthong and Helmann, 2002). Formation of the sulfenic acid was documented by spectral analysis of the NBD chloride–modified protein as well as direct observation of this and higher oxidized species ($-SO_2H$ and $-SO_3H$) by ESI-MS. DTT reversibility of the peroxide-mediated oxidation argues that this overoxidation is probably not of significance under most conditions, however. S-thiolation, in this case with cysteine or the thiol group of coenzyme A (*B. subtilis* does not contain glutathione), may also occur in vivo as part of the activation and/or rereduction process. Interestingly, other OhrR family members, including OhrR from *Xanthomonas campestris*, also likely sense peroxides through sulfenic acid formation at this conserved cysteine, although in at least some cases intramolecular disulfide bond formation may also ensue, much like the peroxide-sensing mechanism employed by OxyR (Panmanee et al., 2002).

NF-κB

Activity of the inducible transcription factor NF-κB is modulated, in part, by cellular redox status; oxidative and nitrosative stresses as well as treatment with thiol alkylating agents all lead to an inhibition of its DNA-binding activity (Marnett et al., 2003). These effects have been attributed to modification of a cysteine residue (Cys62) that lies within an electropositive en-

vironment, enhancing its susceptibility toward oxidation. The 2.9-Å crystal structure of the p65/p50 heterodimer in complex with the intronic enhancer DNA of the immunoglobulin light-chain gene also demonstrates the proximity of Cys62 to its target DNA (Chen et al., 1998b). Reported modifications to the cysteinyl residue on treatment with reactive oxygen or nitrogen species have included intra- or intermolecular disulfide bonds formation, nitrosation, and glutathionylation (Marnett et al., 2003). In a recent report, sulfenic acid formation was also detected in addition to glutathionylation at Cys62, even though the oxidizing conditions used were imparted by varying the ratio of GSH to GSSG incubated with the protein (Pineda-Molina et al., 2001). While the relative contributions of all of these modifications to the redox regulation of NF-kB in vivo will require further investigation, it is clear that sulfenic acid formation at Cys62 in NF-kB is a critical component of the redox sensitivity of its function.

SUMMARY

Sulfenic acid formation in enzymes and transcriptional regulators is now well documented and is clearly an important component of redox catalysis and signalling in many systems. While Cys-SOH can itself be a stabilized redox form in these proteins, it can also readily react with proximal thiol groups of other cysteines or external agents to form disulfide bonds. Both sulfenic acids and disulfide bonds are reducible by cellular thiols back to the thiol state and, as such, are appropriately suited for roles in both redox regulation and catalysis. On the other hand, cysteine sulfenic acids lie on the pathway toward oxidative inactivation through formation of cysteine sulfinic and sulfonic acids, forms which may themselves play functional roles in redox sensing. Given the increasing number of proteins shown to form sulfenic acids of functional significance, it seems likely that the application of chemical and structural methods to detect these species in other systems will continue to increase our appreciation for the diverse roles they play in biological phenomena.

LITERATURE CITED

Abate, C., Patel, L., Rauscher III, F.J., and Curran, T. 1990. Redox regulation of Fos and Jun DNA-binding activity *in vitro*. *Science* 249:1157-1161.

Allison, W.S. 1976. Formation and reactions of sulfenic acids in proteins. *Acc. Chem. Res.* 9:293-299.

Åslund, F., Zheng, M., Beckwith, J., and Storz, G. 1999. Regulation of the OxyR transcription factor by hydrogen peroxide and the cellular thiol-disulfide status. *Proc. Natl. Acad. Sci. U.S.A.* 96:6161-6165.

Barrett, W.C., DeGnore, J.P., Konig, S., Fales, H.M., Keng, Y.F., Zhang, Z.Y., Yim, M.B., and Chock, P.B. 1999. Regulation of PTP1B via glutathionylation of the active site cysteine 215. *Biochemistry* 38:6699-6705.

Bauer, C.E., Elsen, S., and Bird, T.H. 1999. Mechanisms for redox control of gene expression. *Annu. Rev. Microbiol.* 53:495-523.

Becker, K., Savvides, S.N., Keese, M., Schirmer, R.H., and Karplus, P.A. 1998. Enzyme inactivation through sulfhydryl oxidation by physiologic NO-carriers. *Nat. Struct. Biol.* 5:267-271.

Boschi-Muller, S., Assa, S., Sanglier-Cianferani, S., Talfournier, F., Van Dorsselear, A., and Branlant, G. 2000. A sulfenic acid enzyme intermediate is involved in the catalytic mechanism of peptide methionine sulfoxide reductase from *Escherichia coli*. *J. Biol. Chem.* 275:35908-35913.

Chen, L., Glover, J.N.M., Hogan, P.G., Rao, A., and Harrison, S.C. 1998a. Structure of the DNA-binding domains from NFAT, Fos and Jun bound specifically to DNA. *Nature* 392:42-48.

Chen, F., Huang, D.B., and Ghosh, G. 1998b. Crystal structure of p50/p65 heterodimer of transcription factor NF-kappaB bound to DNA. *Nature* 391:410-413.

Choi, H., Kim, S., Mukhopadhyay, P., Cho, S., Woo, J., Storz, G., and Ryu, S. 2001. Structural basis of the redox switch in the OxyR transcription factor. *Cell* 105:103-113.

Choi, H.-J., Kang, S.W., Yang, C.-H., Rhee, S.G., and Ryu, S.-E. 1998. Crystal structure of a novel human peroxidase enzyme at 2.0 Å resolution. *Nat. Struct. Biol.* 5:400-406.

Claiborne, A., Mallett, T.C., Yeh, J.I., Luba, J., and Parsonage, D. 2001. Structural, redox, and mechanistic parameters for cysteine-sulfenic acid function in catalysis and regulation. *Adv. Prot. Chem.* 58:215-276.

Conway, M., Poole, L.B., and Huston, S. 2002. Identification of a peroxide-sensitive redox switch at the CXXC motif in the human mitochondrial branched chain aminotransferase. *Biochemistry* 41:9070-9078.

Costa Seaver, L. and Imlay, J.A. 2001. Alkyl hydroperoxide reductase is the primary scavenger of endogenous hydrogen peroxide in *Escherichia coli*. *J. Bacteriol.* 183:7173-7181.

DeMaster, E.G., Quast, B.J., Redfern, B., and Nagasawa, H.T. 1995. Reaction of nitric oxide with the free sulfhydryl group of human serum albumin yields a sulfenic acid and nitrous oxide. *Biochemistry* 34:11494-11499.

Denu, J.M. and Tanner, K.G. 1998. Specific and reversible inactivation of protein tyrosine phosphatases by hydrogen peroxide: Evidence for a sulfenic acid intermediate and implications for redox regulation. *Biochemistry* 37:5633-5642.

Denu, J.M. and Tanner, K.G. 2002. Redox regulation of protein tyrosine phosphatases by hydrogen peroxide: Detecting sulfenic acid intermedi-

ates and examining reversible inactivation. *Methods Enzymol.* 348:297-305.

Ellis, H.R. and Poole, L.B. 1997a. Roles for the two cysteine residues of AhpC in catalysis of peroxide reduction by alkyl hydroperoxide reductase from *Salmonella typhimurium*. *Biochemistry* 36:13349-13356.

Ellis, H.R., and Poole, L.B. 1997b. Novel application of 7-chloro-4-nitrobenzo-2-oxa-1,3-diazole to identify cysteine sulfenic acid in the AhpC component of alkyl hydroperoxide reductase. *Biochemistry* 36:15013-15018.

Finlayson, A.J., MacKenzie, S.L., and Finley, F.W. 1979. Reaction of alanine-3-sulfinic acid with 2-mercaptoethanol. *Can. J. Chem.* 57:2073-2077.

Fuangthong, M., and Helmann, J.D. 2002. The OhrR repressor senses organic hydroperoxides by reversible formation of a cysteine-sulfenic acid derivative. *Proc. Natl. Acad. Sci. U.S.A.* 99:6690-6695.

Graumann, J., Lilie, H., Tang, X., Tucker, K.A., Hoffmann, J.H., Vijayalakshmi, J., Saper, M., Bardwell, J.C.A., and Jakob, U. 2001. Activation of the redox-regulated molecular chaperone Hsp33—A two-step mechanism. *Structure* 9:377-387.

Hegde, R.S., Grossman, S.R., Laimins, L.A., and Sigler, P.B. 1992. Crystal structure at 1.7 Å of the bovine papillomavirus-1 E2 DNA-binding domain bound to its DNA target. *Nature* 359:505-512.

Hofmann, B., Hecht, H.-J., and Flohe, L., 2002. Peroxiredoxins. *Biol. Chem.* 383:347-364.

Hogg, D.R. 1990. Chemistry of sulphenic acids and esters. *In* The Chemistry of Sulphenic Acids and Their Derivatives (S. Patai, ed.), pp. 361-402. John Wiley & Sons, New York.

Ishii, T., Sunami, O., Nakajima, H., Nishio, H., Takeuchi, T., and Hata, F. 1999. Critical role of sulfenic acid formation of thiols in the inactivation of glyceraldehyde-3-phosphate dehydrogenase by nitric oxide. *Biochem. Pharmacol.* 58:133-143.

Kim, S.O., Merchant, K., Nudelman, R., Beyer, W.F., Keng, T., DeAngelo, J., Hausladen, A., and Stamler, J.S. 2002. OxyR: A molecular code for redox-related signaling. *Cell* 109:383-396.

Kratochwil, N.A., Ivanov, A.I., Patriarca, M., Parkinson, J.A., Gouldsworthy, A.M., Murdoch, P.d.S., and Sadler, P.J. 1999. Surprising reactions of Iodo Pt(IV) and Pt(II) complexes with human albumin: Detection of Cys34 sulfenic acid. *J. Am. Chem. Soc.* 121:8193-8203.

Kullik, I., Toledano, M.B., Tartaglia, L.A., and Storz, G. 1995. Mutational analysis of the redox-sensitive transcriptional regulator OxyR: Regions important for oxidation and transcriptional activation. *J. Bacteriol.* 177:1275-1284.

Lee, S.-R., Kwon, K.-S., Kim, S.-R., and Rhee, S.G. 1998. Reversible inactivation of protein-tyrosine phosphatase 1B in A431 cells stimulated with epidermal growth factor. *J. Biol. Chem.* 273:15366-15372.

Marnett, L.J., Riggins, J.N., and West, J.D. 2003. Endogenous generation of reactive oxidants and electrophiles and their reactions with DNA and protein. *J. Clin. Invest.* 111:583-593.

McBride, A.A., Klausner, R.D., and Howley, P.M. 1992. Conserved cysteine residue in the DNA-binding domain of the bovine papillomavirus type 1 E2 protein confers redox regulation of the DNA-binding activity in vitro. *Proc. Natl. Acad. Sci. U.S.A.* 89:7531-7535.

Mongkolsuk, S., and Helmann, J.D. 2002. Regulation of inducible peroxide stress responses. *Mol. Microbiol.* 45:9-15.

Murakami, T., Nojiri, M., Nakayama, H., Odaka, M., Yohda, M., Dohmae, N., Takio, K., Nagamune, T., and Endo, L. 2000. Post-translational modification is essential for catalytic activity of nitrile hydratase. *Protein Sci.* 9:1024-1030.

Nagashima, S., Nakasako, M., Dohmae, N., Tsujimura, M., Takio, K., Odaka, M., Yohda, M., Kamiya, N., and Endo, I. 1998. Novel non-heme iron center of nitrile hydratase with a claw setting of oxygen atoms. *Nat. Struct. Biol.* 5:347-351.

Nakamura, H., Nakamura, K., and Yodoi, J. 1997. Redox regulation of cellular activation. *Annu. Rev. Immunol.* 15:351-369.

Panmanee, W., Vattanaviboon, P., Eiamphungporn, W., Whangsuk, W., Sallabhan, R., and Mongkolsuk, S. 2002. OhrR, a transcription repressor that senses and responds to changes in organic peroxide levels in *Xanthomonas campestris* pv. phaseoli. *Mol. Microbiol.* 45:1647-1654.

Percival, M.D., Ouellet, M., Campagnolo, C., Claveau, D., and Li, C. 1999. Inhibition of cathepsin K by nitric oxide donors: Evidence for the formation of mixed disulfides and a sulfenic acid. *Biochemistry* 38:13574-13583.

Pineda-Molina, E., Klatt, P., Vázquez, J., Marina, A., García de Lacoba, M., Pérez-Sala, D., and Lamas, S. 2001. Glutathionylation of the p50 subunit of NF-kappaB: A mechanism for redox-induced inhibition of DNA binding. *Biochemistry* 40:14134-14142.

Poole, L.B. and Claiborne, A. 1989. The non-flavin redox center of the streptococcal NADH peroxidase. II. Evidence for a stabilized cysteine-sulfenic acid. *J. Biol. Chem.* 264:12330-12338.

Poole, L.B. and Ellis, H.R. 2002. Identification of cysteine sulfenic acid in AhpC of alkyl hydroperoxide reductase. *Methods Enzymol.* 348:122-136.

Poole, L.B., Karplus, P.A., and Claiborne, A. 2004. Protein sulfenic acids in redox signaling. *Annu. Rev. Pharmacol. Toxicol.* 44:325-347.

Salmeen, A., Andersen, J.N., Myers, M.P., Meng, T.C., Hinks, J.A., Tonks, N.K., and Barford, D. 2003. Redox regulation of protein tyrosine phosphatase 1B involves a sulphenyl-amide intermediate. *Nature* 423:769-773.

Schmalhausen, E.V., Nagradova, N.K., Boschi-Muller, S., Branlant, G., and Muronetz, V.I. 1999. Mildly oxidized GAPDH: The coupling of the dehydrogenase and acyl phosphatase activities. *FEBS Lett.* 452:219-222.

Shelton, J.R. and Davis, K.E. 1973. Decomposition of sulfoxides. II. Formation of sulfenic acids. *Int. J. Sulfur Chem.* 8:205-216.

Stamler, J.S., and Hausladen, A. 1998. Oxidative modifications in nitrosative stress. *Nat. Struct. Biol.* 5:247-249.

Storz, G. and Imlay, J.A. 1999. Oxidative stress. *Curr. Opin. Microbiol.* 2:188-194.

Torchinsky, Y.M. 1981. Properties of SH groups. *In* Sulfur in Proteins (D. Metzler, ed.) pp. 52-53. Pergamon, Oxford.

Weissbach, H., Etienne, F., Hoshi, T., Heinemann, S.H., Lowther, W.T., Matthews, B., St. John, G., Nathan, C., and Brot, N. 2002. Peptide methionine sulfoxide reductase: Structure, mechanism of action, and biological function. *Arch. Biochem. Biophys.* 397:172-178.

Wood, Z.A., Schröder, E., Harris, J.R., and Poole, L.B. 2003a. Structure, mechanism and regulation of peroxiredoxins. *Trends Biochem. Sci.* 28: 32-40.

Wood, Z.A., Poole, L.B., and Karplus, P.A. 2003b. Preoxiredoxin evolution and the regulation of hydrogen peroxide signaling. *Science* 300:650-653.

Xanthoudakis, S. and Curran, T. 1996. Redox regulation of AP-1: Link between transcription factor signaling and DNA repair. *Adv. Exp. Med. Biol.* 387:69-75.

Zheng, M., Åslund, F., and Storz, G. 1998. Activation of the OxyR transcription factor by reversible disulfide bond formation. *Science* 279:1718-1721.

KEY REFERENCES

Claiborne, A., Yeh, J.I., Mallett, T.C., Luba, J., Crane, E.J., 3rd, Charrier, V., and Parsonage, D. 1999. Protein-sulfenic acids: Diverse roles for an unlikely player in enzyme catalysis and redox regulation. *Biochemistry* 38:15407-15416.

Review of the role of sulfenic acids in proteins.

Poole and Ellis, 2002. See above.

Gives practical details about the use of several protocols, including NBD chloride, TNB, and dimedone-based methods, for identification of sulfenic acids.

Poole et al., 2004. See above.

Review of the role of protein sulfenic acids in redox signaling.

Contributed by Leslie B. Poole
Wake Forest University School of Medicine
Winston-Salem, North Carolina

Measurement of Protein Sulfenic Acid Content

Cysteine sulfenic acids in proteins are of considerable biological interest as important players in redox catalysis and redox regulation, yet they have been notoriously difficult to identify due to their high reactivity, particularly outside their native protein environments. Where sulfenic acids are stabilized within proteins, factors contributing to their stability include the lack of proximal thiols, nearby hydrogen-bonding and/or basic side chains to stabilize the protonated or deprotonated sulfenic acid, and restricted access to solvent (see overview, *UNIT 17.1*). Direct observation of sulfenic acids within proteins has been possible only with crystallography, often requiring low-temperature cryotechniques to avoid overoxidation, and NMR using ^{13}C-cysteine-labeled protein (Claiborne et al., 1999). Electrospray ionization mass spectrometry (ESI-MS) can be successful for direct detection of the additional oxygen of the sulfenic acid (Fuangthong and Helmann, 2002), but more often it leads to detection only of the sulfonic acid form (Cys-SO_3H) generated through overoxidation of the sulfenic acid of interest (Ellis and Poole, 1997a).

The protocols outlined in this unit describe three chemical modification methods useful for sulfenic acid identification. The first reagent, 7-chloro-4-nitrobenzo-2-oxa-1,3-diazole (NBD chloride), reacts with both thiol groups and sulfenic acids in proteins at pH 7, but in each case the reactions give unique products that can be distinguished by their UV-visible spectra and by their masses (with the NBD-sulfenate adduct being 16 amu larger than the NBD-thiol adduct; see Basic Protocol 1). As an alternative, NBD chloride can be replaced by 4-fluoro-7-nitrobenz-2-oxa-1,3-diazole (NBD fluoride), a less stable reagent which reacts more quickly with thiols and sulfenic acids and gives the same products (see Alternate Protocol). The second reagent, 2-nitro-5-thiobenzoic acid (TNB), made from 5,5′-dithiobis(2-nitrobenzoic acid) (DTNB) and 1,4-dithio-DL-threitol (DTT), reacts stoichiometrically with sulfenic acids resulting in the loss of its bright yellow color, thereby allowing for accurate quantitation of R-SOH groups by spectroscopy as well as ESI-MS (see Basic Protocol 2). The third reagent, 5,5-dimethyl-1,3-cyclohexanedione (dimedone), reacts specifically with sulfenic acid, but not thiol, groups on proteins. Unfortunately, the product does not exhibit any distinguishing visible absorbance properties; therefore, proof of modification by dimedone generally relies on ESI-MS analysis, as the radiolabeled reagent is not commercially available (see Basic Protocol 3). Of the three, only the dimedone modification is not reversed by the reductant DTT, making the latter a particularly useful reagent for subsequent tryptic digestion and peptide analysis (see Support Protocol 3). If conversion of a given protein thiol group to a sulfenic acid (see Support Protocol 1) is accompanied by a spectral change, titration of the enzyme with buffers at different pH values may allow for the determination of the pK_a of that sulfenic acid (see Basic Protocol 4). Functional properties of a given protein may also be affected by sulfenic acid formation and/or modification and may be tested as well (see Support Protocol 2).

SULFENIC ACID TRAPPING AND DETECTION USING NBD CHLORIDE

BASIC PROTOCOL 1

This method is most useful in demonstrating sulfenic acid formation where this species is accessible to modification and is the only cysteine thiol or sulfenic acid present, accessible, or both. In cases where accessibility is the problem, denaturants can be used. If more than one accessible cysteine thiol and/or sulfenic acid is present per subunit, modification may still allow for the demonstration of sulfenic acid using difference spectra.

Contributed by Leslie B. Poole
Current Protocols in Toxicology (2003) 17.2.1-17.2.20

The sulfenic acid is generated by the method of choice, typically treatment with stoichiometric hydrogen peroxide, *t*-butyl hydroperoxide, or cumene hydroperoxide (see Support Protocol 1), then trapped by reaction with NBD chloride. Once the excess free reagent is removed from the modified protein by ultrafiltration, the presence of thiol- or sulfenate-adducts with NBD can be assessed by UV-visible spectroscopy and/or mass spectrometry.

Materials

Putative sulfenic acid–containing protein, purified and in neutral pH buffer
Neutral pH buffer: 25 mM potassium phosphate (pH 7.0)/1 mM EDTA, or equivalent pH ≤7 buffer
100 mM NBD chloride in DMSO (see recipe)
Acetonitrile
Formic acid

Ultrafiltration unit of appropriate MWCO (e.g., Millipore Centricon, Orbital Biosciences Apollo, Vivascience Vivaspin)
UV-visible scanning or diode-array spectrophotometer
Electrospray ionization mass spectrometer (ESI-MS) or access to a fee-for-service facility
Software for comparing observed and predicted mass (e.g., Calculate pI/MW tool; *http://www.expasy.ch*)

Additional reagents and equipment for preparing proteins containing sulfenic acid (see Support Protocol 1) and determination of protein concentration by a non-NBD affected assay

Prepare protein

1. Prepare at least 1 ml of a 15 μM (monomer or target thiol group concentration) solution of the putative sulfenic acid–containing protein in neutral pH buffer (i.e., pH ≤7) using the method described in this unit (see Support Protocol 1) or by other methods established by functional analyses.

   For example, in a typical reaction, add 3 μl of 8 mm hydrogen peroxide to 0.5 ml of 45 μM protein (see Support Protocol 1).

Modify with NBD chloride

2. To the protein of interest, with or without oxidant pretreatment, add a small volume of 100 mM NBD chloride, either directly or through the sidearm of the anaerobic cuvette. Incubate 10 to 30 min at room temperature.

   More reagent gives a faster reaction, allowing pseudo-first-order kinetics to be followed by any spectral changes observed; therefore, for most experiments, an excess of at least 10-fold NBD over protein-thiol and sulfenic-acid groups is desirable. Thus, continuing with the example in step 1, after oxidation, add 3 μl NBD chloride solution and incubate 10 to 30 min at room temperature. After modification, the protein in the cuvette can be exposed to air for the ultrafiltration step.

Analyze modified protein by spectroscopy

3. Transfer the protein-NBD solution to an ultrafiltration unit of appropriate molecular weight cutoff (MWCO). Remove the unreacted NBD chloride by washing with neutral pH buffer through repeated cycles of concentration and dilution (e.g., concentrate to 50 μl and redilute with 5 ml buffer two to three times) according to manufacturer's instructions.

   Attention must be made to the stated MWCO of the device so that the protein of interest will be retained. With each concentration cycle, the flow-through solution (filtrate) is removed and fresh neutral pH buffer is added to dilute the protein again, for a total of two to three concentration/redilution cycles.

Either Centricon ultrafiltration units, which allow 2 ml to be concentrated to 40 to 50 µl, or larger units offered by several other suppliers (e.g., Orbital Biosciences or Vivascience), which allow 6 to 7 ml to be concentrated to ~10 to 50 µl, can be used. In the case of the latter, the ability to concentrate more solution at once and to use swinging bucket rotors rather than fixed-angle rotors can speed up the washing process.

Alternatively, the modified protein without ultrafiltration can be isolated by HPLC in tandem with injection into a mass spectrometer.

4. Check for the presence of free NBD in the filtrate by determining the absorbance at 343 nm. Repeat steps 3 and 4 until no free reagent is detected (i.e., A_{343} is <0.02).

5. *Optional.* For best quantitation, assess the protein concentration using a protein assay that is not affected by the presence of the NBD—e.g., the Detergent-Compatible (DC) Protein Assay Kit from Bio-Rad.

   The A_{280} (APPENDIX 3G) now has a contribution from the presence of NBD and therefore cannot be used to determine the protein concentration. Colorimetric assays monitoring wavelengths beyond 500 nm may work (APPENDIX 3G).

6. Remove the concentrated protein from the ultrafiltration unit and bring to approximately the original concentration with neutral pH buffer, assuming there has been no loss of protein during the ultrafiltration step (protein recovery from the ultrafiltration devices can be tested independently with unmodified protein).

7. Perform a spectral scan from ~250 to 700 nm to allow for the assessment of the nature of the modification.

   Thiol adducts with NBD give a peak at 420 nm with an extinction coefficient of 13,000 M^{-1} cm^{-1} (Birkett et al., 1970). Sulfenic acid adducts with NBD give a peak at 347 nm with a similar extinction coefficient (Ellis and Poole, 1997a).

Prepare the modified protein for ESI-MS

8. Wash the modified protein sample at least three times (complete concentration and redilution) with water as described in step 3 to remove excess reagent and buffer components.

9. Prepare 1 nmol modified protein in 100 µl water. Add an equal volume of acetonitrile and 2 µl formic acid before injection. Analyze by ESI-MS.

   This amount of sample is far above that required for the analysis by most modern ESI-MS instruments. Optimization of sample analyses may involve changing the acetonitrile concentration and/or using a volatile buffer such as ammonium bicarbonate instead of water during the washing step (Fuangthong and Helmann, 2002).

   Alternatively, the modified protein without ultrafiltration can be isolated by HPLC in tandem with injection into the mass spectrometer. Once prepared for mass spectrometry, samples are generally stable at −20°C for weeks prior to analysis (at least in the absence of the acetonitrile and formic acid).

   Using this approach, the NBD adduct prepared from the thiol form of the protein will exhibit a mass 16 amu less than that prepared from the sulfenic acid form. NBD itself contributes 164 amu to the mass of the protein.

10. Compare the obtained mass with the predicted mass using a program that takes into account the natural abundance of all isotopes in the protein.

ALTERNATE PROTOCOL

SULFENIC ACID TRAPPING AND DETECTION USING NBD FLUORIDE

This method can be utilized to generate an NBD adduct with protein cysteine sulfenic acids which can then be followed by UV-visible spectroscopy and/or ESI-MS as described above (see Basic Protocol 1). The only difference between this and the Basic Protocol is that 100 mM NBD fluoride (see recipe) rather than NBD chloride is used as the chemical modification agent. The reactivity of NBD fluoride is approximately ten times greater than that of NBD chloride (as described in the handbook from Molecular Probes), allowing for more rapid modification. Note that NBD fluoride should be freshly made and used as soon as possible given its reactivity and instability. The incubation time with this reagent can be decreased relative to that needed for NBD chloride (step 2), and the ultrafiltration step should be performed very quickly after modification (steps 3 and 4).

BASIC PROTOCOL 2

QUANTITATION OF SULFENIC ACID FORMATION BY REACTION WITH TNB

In order to quantify cysteine sulfenic acids in proteins, this method takes advantage of the thiol reactivity of sulfenic acids and the resulting formation of mixed disulfide bonds with TNB, a chromophoric thiol-containing reagent generated by reduction of DTNB. The TNB reagent must be tested just before use to ensure that there is no excess of DTT or DTNB (see Reagents and Solutions). Assessment of the extent of reaction can be made immediately by monitoring the decrease in A_{412}. Further proof of disulfide bond formation is obtained by isolation of the TNB-labeled protein through ultrafiltration, analysis of spectral properties of the modified protein, and release of the protein-associated TNB by DTT treatment. TNB-labeled protein can also be digested by trypsin and peptides separated by HPLC and monitored for the presence of the TNB label.

Materials

Putative sulfenic acid–containing protein, purified and in neutral pH buffer (pH 7)
Neutral pH buffer: 25 mM potassium phosphate (pH 7.0)/1 mM EDTA, or other pH 7 to 7.5 buffer
4 mM TNB solution (see recipe)
100 mM DTT (see recipe)
Ultrafiltration unit of appropriate MWCO (e.g., Millipore Centricon, Orbital Biosciences Apollo, Vivascience Vivaspin)

Additional regents and materials for preparing proteins containing sulfenic acid (see Support Protocol 1), determining protein concentration, determining the identity of the labeled peptide (optional; see Support Protocol 3), and assay of protein function (optional; see Support Protocol 2)

Prepare protein

1. Prepare at least 1 ml of a 15 μM (monomer concentration) solution of the (putative) sulfenic acid–containing protein in neutral pH buffer (i.e., pH 7 to 7.5) using the method described in this unit (see Support Protocol 1) or by other methods established by functional analyses.

Modification with TNB

2. To the protein of interest, with or without oxidant pretreatment, add a small volume of 4 mM TNB either directly or through the sidearm of the anaerobic cuvette and incubate at room temperature. Monitor the decrease in A_{412} until the spectral changes are complete (usually within 2 to 5 min, if accessible).

At long incubation times (>20 to 30 min), TNB can air oxidize, a process that must be taken into account using appropriate control reactions.

A two- to three-fold excess of reagent can be used, keeping in mind that the quantitation of sulfenic acids will be most accurate where the total A_{412} of TNB added is 1.0 or slightly less (i.e., within the linear range of the spectrophotometer), and the absorbance change upon adding the reagent to the protein is >0.1.

3. Read the A_{412} of a blank consisting of neutral pH buffer containing the same concentration of TNB as the sample.
4. Calculate the sulfenic-acid content of the protein as follows.
   a. Subtract the final A_{412} value of the modified sample (step 2) from the A_{412} of the blank (step 3).
   b. Using the extinction coefficient 14,150 M^{-1} cm^{-1} (Riddles et al., 1979), convert this value to concentration of sulfenic acid–containing residues.
   c. Divide by the protein concentration to obtain the sulfenic acid content of the protein.

Excess peroxide and at least some other oxidants also react with TNB over time; if present, these oxidants should be added to control reactions without protein to assess the contribution of this reaction.

Isolate TNB-labeled protein

5. Transfer the reaction mixture to an ultrafiltration unit of appropriate molecular weight cutoff (MWCO). Remove unreacted TNB by washing with neutral pH buffer through repeated cycles of concentration and dilution (e.g., concentrate to 50 µl and redilute with 5 ml buffer two to three times) according to manufacturer's instructions.

Attention must be made to the stated MWCO of the device so that the protein of interest will be retained. With each concentration cycle, the flow-through solution (filtrate) is removed and fresh neutral pH buffer is added to dilute the protein again, for a total of two to three concentration/redilution cycles.

Either Centricon ultrafiltration units, which allow 2 ml to be concentrated to 40 to 50 µl, or larger units offered by several other suppliers (e.g., Orbital Biosciences or Vivascience) which allow 6 to 7 ml to be concentrated to ~10 to 50 µl, can be used. In the case of the latter, the ability to concentrate more solution at once and to use swinging bucket rotors rather than fixed-angle rotors can speed up the washing process.

6. Check for the presence of free TNB in the filtrate by determining the absorbance at 412 nm. Repeat steps 5 and 6 until no free reagent is detected (i.e., A_{412} is <0.02).
7. Remove the concentrated protein from the ultrafiltraton unit and bring to approximately the original concentration with neutral buffer. Transfer the solution to a quartz cuvette.
8. *Optional.* For best quantitation, assess the protein concentration using a protein assay that is not affected by the presence of the TNB—e.g., the Detergent-Compatible (DC) Protein Assay Kit from Bio-Rad.
9. *Optional.* If identification of the labeled peptide is important, perform a tryptic digest and analyze as described (see Support Protocol 3).

Release TNB from the modified protein

10. Add a 10- to 100-fold excess of 100 mM DTT, monitoring the spectral changes from 280 to 600 nm until complete (i.e., until no change is detected).

The increase in A_{412} is used to assess the amount of TNB released from the isolated, modified protein. The calculation is basically the same as in step 4 except that the A_{412} after DTT treatment is higher than before.

11. *Optional.* If regeneration of the thiol group(s) in the protein is expected to restore or alter the functional properties of the protein, perform an appropriate assay to determine this (see Support Protocol 2), with or without an additional ultrafiltration step (see step 5), depending mostly on the potential for the excess DTT to interfere with the assay.

BASIC PROTOCOL 3

MODIFICATION AND DETECTION OF PROTEIN SULFENIC ACIDS WITH DIMEDONE

Reactivity of proteins with dimedone is diagnostic for the presence of cysteine sulfenic acids. This reaction is not monitored by spectral changes but rather by the mass increase observed on modification of the sulfenic acid. Where localization of the incorporated dimedone is of interest, tryptic digests followed by HPLC and mass spectrometric analyses can be used to identify modified peptides and/or residues (see Support Protocol 3).

Materials

Putative sulfenic acid–containing protein sample, purified and in neutral pH buffer (pH 7)

Neutral pH buffer: 25 mM potassium phosphate (pH 7.0)/1 mM EDTA, or other buffer at pH 7

100 mM dimedone (see recipe)

Ultrafiltration unit of appropriate MWCO (e.g., Millipore Centricon, Orbital Biosciences Apollo, Vivascience Vivaspin)

Electrospray ionization mass spectrometer (ESI-MS) or access to a fee-for-service facility

Software for comparing observed and predicted mass (e.g., Calculate pI/MW tool; *http://www.expasy.ch)*

Additional reagents and materials for preparing proteins containing sulfenic acid (see Support Protocol 1) and determining the identity of the labeled peptide (optional; see Support Protocol 3)

Prepare protein

1. Prepare at least 200 µl of a 15 µM (monomer concentration) solution of the (putative) sulfenic acid–containing protein in neutral pH buffer (i.e., pH ≤7) using the method described in this unit (see Support Protocol 1) or by other methods established by functional analyses.

Modify with dimedone

2. To the protein of interest, with or without oxidant pretreatment, add a 100-fold excess of 100 mM dimedone either directly or through the sidearm of the anaerobic cuvette. Incubate 1 to 2 hr at 25°C.

Prepare modified protein for ESI-MS

3. Transfer the reaction mixture to an ultrafiltration unit of appropriate molecular weight cutoff (MWCO). Remove the unreacted dimedone and buffer components by washing thoroughly (at least three times) with water through repeated cycles of concentration and dilution (e.g., concentrate to 50 µl and redilute with 6 ml water three to four times) according to manufacturer's instructions.

Attention must be made to the stated MWCO of the device so that the protein of interest will be retained. With each concentration cycle, the flow-through solution (filtrate) is removed and deionized water is added to dilute the protein again, for a total of at least three concentration/redilution cycles.

Either Centricon ultrafiltration units, which allow 2 ml to be concentrated to 40 to 50 µl, or larger units offered by several other suppliers (e.g., Orbital Biosciences or Vivascience), which allow 6 to 7 ml to be concentrated to ~10 to 50 µl, can be used. In the case of the latter, the ability to concentrate more solution at once and to use swing-out bucket rotors rather than fixed-angle rotors can speed up the washing process.

Alternatively, the modified protein without ultrafiltration can be isolated by HPLC in tandem with injection into a mass spectrometer.

4. Prepare 1 nmol modified protein in 100 µl water. Add an equal volume of acetonitrile and 2 µl formic acid before injection. Analyze by ESI-MS.

   This amount of sample is far above that required for the analysis by most modern ESI-MS instruments. Optimization of sample analyses may involve changing the acetonitrile concentration and/or using a volatile buffer such as ammonium bicarbonate instead of water during the washing step (Fuangthong and Helmann, 2002).

   Alternatively, the modified protein without ultrafiltration can be isolated by HPLC in tandem with injection into the mass spectrometer. Once prepared for mass spectrometry, samples are generally stable at –20°C for weeks prior to analysis (at least in the absence of the acetonitrile and formic acid).

   Using this approach, only peptides containing a cysteine sulfenic acid will form adducts with dimedone. Dimedone itself contributes 140 amu to the mass of the protein.

5. *Optional.* If identification of the labeled peptide is important, perform a tryptic digest of the isolated modified protein and analyze as described (see Support Protocol 3).

DETERMINATION OF THE PROTEIN SULFENIC ACID DISSOCIATION CONSTANT (pK_a)

BASIC PROTOCOL 4

In some cases, proteins containing sulfenic acids may exhibit a low extinction absorbance band (ε_{max} of ~320 to 370 nm) due to the presence of the deprotonated sulfenate species (Poole and Ellis, 2002), as has been observed previously in small molecules (Tripolt et al., 1993). In these cases, lowering of the pH to protonate this group will result in the disappearance of this absorbance band. Titration of this absorbance can be used to determine the pK_a value of the cysteine sulfenic acid within the protein. Depending on the extinction coefficient for this absorbance and on the pH stability properties of the protein, large amounts of the protein containing the stable sulfenic acid and a stopped-flow spectrophotometer are optimal for this determination.

Materials

Citrate/phosphate buffer (pH from 3 through 7.6)/1 mM EDTA (see recipe)
Protein, purified and in 10 mM neutral pH buffer (e.g., potassium phosphate buffer diluted to 10 mM)

UV-visible spectrophotometer and/or stopped-flow spectrophotometer
3 to 5 ml syringes

Additional reagents and materials for preparing proteins containing sulfenic acid (see Support Protocol 1) and determining the identity of the labeled peptide (optional; see Support Protocol 3)

Prepare sample

1. Prepare at least a 150 µM (monomer concentration) solution of the (putative) sulfenic acid–containing protein in 10 mM neutral pH buffer (i.e., pH ~7) using the method described in this unit (see Support Protocol 1) or by other methods established by functional analyses.

2. To observe the expected absorbance change and determine the feasibility of this experiment, mix the protein with an equal volume of high and low pH citrate/phosphate buffers (e.g., pH 4 and 7.6) and record the UV-visible spectral change from 250 to 400 nm (should be immediate).

If the near UV absorbance band is lost at low pH, the following experiment is feasible.

In the case of the sulfenate anion of the C165S mutant of AhpC, maximal absorbance was at 367 nm (Poole and Ellis, 2002).

Conduct rapid mixing (pH jump) experiment

3. Set the monochromator wavelength of the spectrophotometer at the λ_{max} for the protein sulfenate peak (e.g., 367 nm in the case above).

4a. *For a stopped-flow spectrophotometer:* Load the sulfenic acid–containing protein into a 5-ml syringe and one of the buffers (i.e., high or low pH) into another. Rapidly mix the protein and buffer solutions and acquire data at the peak wavelength for 10 sec. Repeat each point ten times or more, controlling for instrument drift by frequently checking the absorbance of buffer alone.

Keep the sample volume as low as possible to minimize protein consumption (although protein may be recovered from this nondestructive procedure at pH values where the protein is stable). Any formation of precipitated protein or any conformational changes resulting from the pH change may, however, confound the results. The use of the stopped-flow spectrophotometer allows for the absorbance changes that ensue after the rapid pH change to be measured before any slower pH-dependent denaturation occurs. Data analysis to determine the pK_a is performed as described below.

4b. *For a standard spectrophotometer:* If a stopped-flow spectrophotometer is unavailable, hand mix the buffer and protein and measure the absorbance at the peak wavelength as rapidly as possible with a standard spectrophotometer.

For rapid mixing, the phosphate/citrate buffer can be added to the protein in the cuvette, a piece of Parafilm held tightly over the cuvette with the index finger, and the solution mixed rapidly (yet gently) as it is poured from top to bottom in the cuvette several times.

5. Plot absorbance versus pH, averaging all data which overlay at a given pH. If the expected sigmoidal curve is observed, fit data to the following equation:

$$y = \frac{\left(A \times 10^{x}\right) + \left(B \times 10^{\mathrm{pK_a}}\right)}{10^{x} + 10^{\mathrm{pK_a}}}$$

where A is the absorbance at high pH, B is the absorbance at low pH, and y is the absorbance at pH x.

SUPPORT PROTOCOL 1

PREPARATION OF SULFENIC ACID-CONTAINING PROTEIN

Susceptible protein thiol groups are oxidized to sulfenic acids by the addition of even mild oxidants including hydrogen peroxide, organic hydroperoxides, hypochlorous acid, peroxynitrite, S-nitrosoglutathione, and other NO-generating or NO-derived signaling molecules. This oxidation may be stoichiometric or may require an excess of the oxidant, and anaerobiosis may or may not be necessary. This protocol describes the use of peroxides as the oxidant but is generally applicable to use of the other oxidants, as well.

Materials

Protein solution
Argon or oxygen-free nitrogen (optional)
Neutral pH buffer: 25 mM potassium phosphate (pH 7.0)/1 mM EDTA, or other buffer at pH 7 or lower
Peroxide of choice—e.g., 8 mM H_2O_2 or cumene hydroperoxide (see recipes)
100 mM DTT (see recipe)
Anaerobic cuvette assembly (Williams et al., 1979) or small pear-shaped flask with stopcock

1. Determine if anaerobic conditions are necessary for the protein solution being used.

   Preparation of the sulfenic acid form of the target cysteinyl residue(s) on the protein may or may not require anaerobic conditions for stabilization. If the oxygen reactivity of this species is unknown, use anaerobic conditions.

   If the protein sulfenic acid can be detected by one of the Basic Protocols (1 to 3) when generated under anaerobic conditions, but the sulfenic acid content of the protein decreases quickly after shifting to aerobic conditions, then preparation and initial modification steps of the sulfenic acid–containing protein should be conducted anaerobically.

2. *Optional.* If anaerobic conditions are necessary, place the protein solution in an anaerobic cuvette assembly or small pear-shaped flask with stopcock, and, over a period of 20 to 30 min total and using approximately ten to twenty cycles with gentle rocking, flush with argon or nitrogen followed by gentle vacuum.

3. To the protein solution, add a stoichiometric amount of the peroxide of choice (e.g., 8 mM H_2O_2 or cumene hydroperoxide).

   Excess peroxide may also be added, although there is a risk of thiol overoxidation beyond the sulfenic acid oxidation state. For cysteine-based peroxidases (e.g., NADH peroxidase and peroxiredoxins) and at least one peroxide-sensitive transcriptional regulator (OxyR), this reaction is very fast ($\geq 10^5$ M^{-1} sec^{-1} second-order rate constant); however, it is generally much slower and varies greatly for other protein thiol or thiolate groups. As a result, no clear statement can be made as to the length of time required for the incubation of the protein with the peroxide (this should be treated as a variable). For example, continue treatment for 2 min to 24 hr at 4° or 25°C.

4. Perform a wavelength scan from 250 to 400 nm. Determine if any spectral changes due to addition of peroxide are present.

   Any spectral signature can provide both a way to monitor sulfenic acid formation and a way to discriminate between protonated and deprotonated forms of the sulfenic acid for pK_a determination (see Basic Protocol 4). However, for observations of such low-extinction coefficient spectral changes, the protein needs to be at very high concentration ($\geq$ 80 μm).

FUNCTIONAL ANALYSES OF THE MODIFIED PROTEIN

SUPPORT PROTOCOL 2

If a free thiol group is required for the functional activity of the protein under investigation, either modification of that group with NBD chloride or oxidation of the thiol group to sulfenic acid followed by NBD chloride or TNB modification should block its activity. Whether or not oxidation to the sulfenic acid itself alters the protein's activity depends on the function of this modification. In cysteine-based peroxidases, the sulfenic acid is a naturally occurring intermediate during turnover and is therefore catalytically active as long as the reductant being used will reduce this species and overoxidation to inactive sulfinic and sulfonic acids forms does not occur preferentially. In at least some peroxide-sensitive transcriptional regulators, the sulfenic acid form represents an important functional form, either activating or derepressing transcription from genes related to oxidative stress protection (see *UNIT 17.1*). In these cases an assay for transcriptional activation is appropriate. In protein tyrosine phosphatases, the active site cysteine is reversibly inhib-

ited by conversion to the sulfenic acid form. Therefore, an assay for phosphatase activity using a model phosphorylated peptide can be used for these proteins. It is of great interest to test the consequences of modification and/or oxidation of target cysteines in active sites of enzymes or binding sites of transcriptional regulators.

If the protein sulfenic acid is known to be stable toward air (or at least stable over the 10 to 30 min during which the functional analyses is performed; see Support Protocol 1), the assay of interest can be carried out aerobically. The air stability of the chemically-modified proteins is not a problem, although in these cases, an exogenous chemical has been added to the protein to give a non-native modification. For NBD- or TNB-modified protein, the thiol(ate) group is restored by DTT treatment (excess reagents may need to be removed by ultrafiltration prior to carrying out the functional assay). Dimedone modification of sulfenic acids is not reversed by DTT treatment.

SUPPORT PROTOCOL 3

TRYPTIC DIGESTION OF MODIFIED PROTEINS

To determine the peptide or even residue of the protein modified by one of the reagents described above, chemical modification of the protein can be followed by tryptic digestion and isolation and analysis of the peptides. The dimedone modification is best for this analysis due to its irreversibility, although its lack of distinguishing spectral features is a disadvantage.

Materials

Modified protein (see Basic Protocols 1, 2, or 3)
50 mM NEM (see recipe)
10 M urea or 8 M guanidine hydrochloride (see recipes)
100 mM Tris·Cl buffer, pH 8.0 (*APPENDIX 2A*) or 100 HEPES, pH 7.6 (see recipe)
100 mM calcium chloride (1.11 g anhydrous $CaCl_2$ in 100 ml water; store up to several weeks at room temperature)
TPCK-treated trypsin (see recipe)
10 mM EGTA
100 mM DTT

95° or 60°C waterbath
HPLC equipped with a C18 reversed-phase column, solvents for peptide isolation (e.g., 0.1% v/v trifluoroacetic acid, 70% v/v acetonitrile with 0.08% trifluoroacetic acid)
Electrospray ionization mass spectrometer (ESI-MS) or access to a fee-for-service facility

1. *Optional.* If the NBD-, TNB-, or dimedone-modified protein has additional cysteine thiol groups, use alkylation to block by adding 50 mM NEM to a 100-fold excess and incubating 1 hr at room temperature.

2. Prepare a small volume (≤200 µl) containing ~1 mg isolated, modified, blocked (if necessary) protein and 8 M urea or 6 M guanidinium hydrochloride. Optionally, incubate 15 to 20 min at 95°C or 45 to 60 min at 60°C to ensure denaturation.

3. Once the sample has cooled, add sufficient 100 mM Tris·Cl, pH 8.0, or, if the sample is NBD-labeled, 100 mM HEPES, pH 7.6, to lower the denaturant concentration to ≤1 M. Add 1/100 vol of 100 mM calcium chloride (1 mM final).

   If NBD- or TNB-labeled protein is used, the conditions for trypsin digestion can be pretested to ensure that the label remains covalently attached to the protein (reductants remove both labels and cannot be used, and amine groups can react with and remove the NBD moiety).

4. Add TPCK-treated trypsin to a protease/protein ratio of 1:100 to 1:40 (w/w). Incubate 12 hr at 37°C. Add a second aliquot of TPCK-treated trypsin and incubate another 12 hr.

   Shorter incubation times may also suffice.

5. *Optional.* To monitor the progress of the digestion, remove small aliquots of the reaction mixture and analyze using one of the following techniques: reversed-phased HPLC, MALDI-TOF mass spectrometry, SDS- or Tris-Tricine-PAGE.

6a. *For storage:* Freeze samples at −20°C and store up to 2 weeks.

6b. *For immediate use:* Inactivate the trypsin by adding sufficient acetic acid to lower the pH to <4, or by adding 10 mM EGTA to chelate calcium.

7a. *To analyze by absorbance (for NBD- and TND-labeled proteins only):* Analyze digested peptides by HPLC and absorbance using the following procedure:

   a. To an aliquot of digested peptide, add 1/10 vol of 100 mM DTT.

   b. Separate the digested peptides by HPLC, with and without DTT treatment, using an appropriate column and gradient.

      For example, use a C18 or C8 column and a linear gradient over 60 to 100 min from 0% to 60% solvent B (70% acetonitrile/0.08% trifluoracetic acid) with the balance being solvent A (0.1% trifluoracetic acid). Monitor the absorbance at 347 or 420 nm for NBD-treated samples, or 325 nm for TNB-treated samples. Peptide elution is typically monitored at 215 nm where the peptide bonds absorb strongly and the contributions of solvents A and B are appropriately balanced.

      For further analysis of these peptides, additional purification using a more shallow gradient should be carried out.

   c. For TNB- and NBD-labeled samples, identify labeled peptides by comparing HPLC chromatograms of the tryptic digest with the same digest sample treated with DTT (step a) before separation on HPLC. (DTT treatment will remove the chromophore and may shift the retention time of the peptide).

7b. *To analyze by ESI-MS:* Perform reversed-phase HPLC as described (step 7a, substep b) in tandem with ESI-MS on digests. Identify labeled residues by the added mass. Repeat steps 1 to 6 with unlabeled protein and analyze by HPLC in tandem with ESI-MS to verify labeling.

   Where only a single cysteine is encoded within that peptide, further localization is unnecessary. Additional analysis by MS-MS using collision-induced fragmentation can also be used to determine the sequence and location of the labeled cysteine. Alternatively, the peptide can be subjected to Edman degradation to determine the position of the blocked cysteine, although its identification may rely only on the absence of an identifiable peak at the position of the modified cysteine.

REAGENTS AND SOLUTIONS

Use Milli-Q-purified water or equivalent for all recipes and protocol steps. For common stock solutions, see ***APPENDIX 2A****; for suppliers, see* ***SUPPLIERS APPENDIX****.*

Citrate/phosphate buffer

To 245 ml water, add 9.61 g citric acid (~200 mM final), 7.10 g dibasic sodium phosphate (~200 mM Na_2HPO_4 final), and 93 mg disodium EDTA. Measure the pH, which should be ~3. Slowly drip in a solution of 1 M sodium hydroxide (4.0 g in 100 ml) to raise the pH, and remove ~10-ml aliquots at each desired pH value (about every 0.2 pH units). Store the aliquots up to 1 month at room temperature, but recheck pH of each before each use.

This allows for mixing of the sulfenic acid-containing protein with strong buffers at various pH values to determine the pK_a of the protein-associated sulfenic acid (Basic Protocol 4).

Cumene hydroperoxide, 8 mM

Prepare a stock solution containing 20 µl cumene hydroperoxide solution (80% stock from Sigma, aliquots stored at −20°C for up to one year) and 980 µl dimethyl sulfoxide (DMSO). Prepare a 15× dilution of the stock solution in water to give a final concentration of ~8 mM. Prepare fresh daily.

Dimedone, 100 mM

To 1 ml DMSO add 14 mg dimedone (Sigma-Aldrich). Aliquot and store up to several months at −20°C.

DTNB, 5 mM

Prepare a 100 mM stock solution by dissolving 0.198 g of 5,5′-dithiobis(2-nitrobenzoic acid) in 5 ml DMSO. Aliquot and store up to several months at −20°C. Before use, dilute the stock DTNB solution 20-fold into 25 mM phosphate buffer, pH 7 (*APPENDIX 2A*).

Standardize the working solution by diluting 3 µl in 0.5 ml 25 mM phosphate buffer. While monitoring the A_{412}, add 8-µl aliquots of 0.5 mM DTT, pausing between each addition until the spectral changes are complete. When the A_{412} no longer increases with additional DTT, use the maximal A_{412} to calculate the DTNB concentration using an ε_{412} value of 14,150 M^{-1} cm^{-1} for TNB (the solution resulting from the combination of DTNB and DTT), and the fact that 2 moles of TNB are released per mole DTNB (Riddles et al., 1979).

DTT, 100 mM

Dissolve 154 mg of 1,4-dithio-DL-threitol (DTT) in 10 ml water. Store in aliquots up to 2 weeks at −20°C.

Standardize the DTT by first performing the standardization of DTNB (see recipe). To calculate the DTT concentration, use the titration breakpoint from a plot of A_{412} versus volume of DTT added to determine the volume of DTT required to titrate the known amount of DTNB.

DTT has two thiols per molecule, therefore its concentration is equivalent to the concentration of DTNB with which it reacts.

Guanidine hydrochloride, 8 M

To ~4 ml water add 7.64 g guanidine hydrochloride (ultrapure; Sigma-Aldrich). Warm solution and add water to fully dissolve and bring volume to 10 ml total. Store up to several months in a tightly sealed bottle at room temperature.

HEPES, 100 mM (pH 7.6)

To 90 ml of water, add 2.38 g HEPES and dissolve. Add 1 M sodium hydroxide dropwise to bring the pH to 7.6, then add water to bring the final volume to 100 ml. Store up to several weeks at room temperature.

Hydrogen peroxide, 8 mM

Dilute ~182 µl of a 30% solution (stored at 4°C) into 250 ml water. Make fresh daily.

For standardization of hydrogen peroxide, prepare solutions of 10 mg/ml *o*-dianisidine in methanol and 1 mg/ml horseradish peroxidase (HRP) in an appropriate buffer—e.g., 25 mM potassium phosphate (pH 7.0)/1 mM EDTA or other buffer at pH 7; store these solutions up to 1 month or more at 4°C in the dark. Add 10 µl of the 10 mg/ml *o*-dianisidine solution and 2 to 10 µl of the 8 mM (putative) peroxide solution to 0.9 ml 25 mM phosphate buffer, pH 7 (*APPENDIX 2A*)/0.1% Triton X-100. Bring to 0.99 ml with deionized water. Use this solution to blank a spectrophotometer at 460 nm, then add 10 µl of the 1 mg/ml HRP solution to the cuvette. Monitor

continued

the A_{460} change which is complete within a few seconds. Use $\varepsilon_{460} = 11{,}300\ M^{-1}\ cm^{-1}$ for oxidized *o*-dianisidine and dilution factors to compute peroxide concentration. Use three to four different volumes of the hydrogen peroxide solution to be tested and added linear regression to determine the change in A_{460} per microliter (the slope of the line) to obtain an accurate concentration: slope/11,300 × cuvette path length in centimeters = millimolar concentration of hydrogen peroxide.

NBD chloride, 100 mM

To 1 ml DMSO, add 20 mg 7-chloro-4-nitrobenzo-2-oxa-1,3-diazole (NBD chloride). Store aliquots up to several weeks protected from light at −20°C.

Determine the concentration of the solution by first making a 20-fold dilution of the stock into 25 mM phosphate buffer, pH 7 (*APPENDIX 2A*), and then adding 16 µl of this diluted NBD chloride solution to 1.0 ml methanol. Use a glass pipet rather than micropipettor to measure out the methanol and avoid leakage. Measure the A_{336}. Use an ε_{336} of 9800 $M^{-1}\ cm^{-1}$ and the dilution factor to calculate the concentration of the stock.

NBD chloride is called 4-chloro-7-nitrobenz-2-oxa-1,3-diazole by Molecular Probes; this reagent is also available from other suppliers like Sigma-Aldrich. Another abbreviation for the compound is Nbf-Cl.

NBD fluoride, 100 mM

To 100 µl DMSO, add 1.8 mg of 4-fluoro-7-nitrobenz-2-oxa-1,3-diazole (NBD fluoride; Molecular Probes). Keep protected from light at room temperature, and use within several hours after it is prepared (do not store at −20°C as for NBD chloride).

Determine the concentration of the solution by first making a 20-fold dilution of the stock into 25 mM phosphate buffer, pH 7 (*APPENDIX 2A*), and then adding 16 µl of this diluted NBD fluoride solution to 1.0 ml methanol. Use a glass pipet rather than a micropipettor to measure the methanol and avoid leakage. Measure the A_{328}. Use an ε_{328} of 8000 $M^{-1}\ cm^{-1}$ and the dilution factor to calculate the concentration of the stock.

NEM, 50 mM

To 1 ml DMSO, add 6.3 mg *N*-ethylmaleimide (NEM). Aliquot and store up to a few weeks at −20°C.

If knowledge of the exact concentration of this solution is important, standardize by first preparing a 1:20 dilution of 100 mM DTT (see recipe) and then adding 6 µl of this dilution to 1 ml of 25 mM phosphate buffer, pH 7 (*APPENDIX 2A*). Add 14 µl of a 1:20 dilution of the NEM stock. Incubate 30 min at room temperature, then add 15 µl of 0.25 mM DTNB, diluted from the 5 mM working solution (see recipe). The loss of thiol groups corresponds to the amount of NEM added, allowing for calculation of the concentration of the stock solution. Therefore the concentration of NEM in the final test solution is equal to the A_{412} of the control (without NEM) minus the A_{412} in the presence of NEM divided by the ε_{412} value of 14,150 $M^{-1}\ sec^{-1}$ for TNB.

TNB solution, 4 mM

To a dark-colored microcentrifuge tube (or a tube wrapped with aluminum foil) containing 0.84 ml of 25 mM phosphate buffer, pH 7, add 80 µl of 100 mM stock DTNB (see recipe) and 80 µl of 100 mM DTT (see recipe). The solution will turn dark orange. Store up to 1 week at −20°C.

continued

Determine the concentration of TNB by adding 7.5 µl of the TNB solution to 0.5 ml phosphate buffer, measuring the A_{412}, and calculating the concentration using an ε_{412} of 14,150 M^{-1} cm^{-1} for TNB (Riddles et al., 1979). Add 1 µl of 100 mM or 2 µl of 5 mM DTNB (see recipe) and observe any increase in A_{412}. If there is an increase, calculate the amount of DTNB that should be added to the stock TNB solution to bring it to the maximum A_{412} but not beyond. This amount will be equal to 1/2 the concentration of TNB generated (according to the increased A_{412} divided by the ε_{412} of 14,150 M^{-1} sec^{-1}) taking into account the relevant dilutions factions and the volume of the TNB stock. Perform the same test using 100 mM DTT instead of DTNB, adding more DTT to the TNB stock solutions if necessary, as calculated for the needed addition above.

The reagent is properly prepared if addition of neither dithiothreitol nor DTNB leads to an increase in A_{412}. This reagent tends to air oxidize and should be tested every few hours for DTNB formation (readjust with additional DTT as needed).

TPCK-treated trypsin

Prepare a stock solution of 1 mg TPCK-treated trypsin (Worthington Biochemical) in 100 µl of 1 mM HCl (8.5 µl concentrated HCl in 100 ml water), or as indicated by the manufacturer. Aliquot and store up to several months at −70°C if necessary, but do not subject to multiple freeze/thaw cycles.

The best grades of trypsin available (e.g., sequencing-grade trypsin from Promega) include modified forms of trypsin that do not undergo self-digestion and are therefore active longer during the digestion (and don't generate contaminating peptides from the trypsin, itself). Immobilized trypsin (Pierce Biotechnology) can also be used so that the digestion can be stopped by centrifugation and removal of the supernatant to a separate tube.

Note that for digestion of 1 mg of the target protein using a protease/protein ratio of 1:50, 2 µl of the prepared trypsin solution is added.

Urea, 10 M

To ~4 ml of water add 6.01 g urea (ultrapure; Sigma-Aldrich). Warm the solution and add water to fully dissolve and bring to 10 ml final volume. Store 1 to 2 days at room temperature.

COMMENTARY

Background Information

The procedures described herein allow for the detection and measurement of sulfenic acids in proteins by chemical means and do not require the specialized approaches of crystallography or NMR. The intrinsic instability of sulfenic acids makes them inherently difficult to work with; mass spectrometry can theoretically be used to demonstrate the single oxygen added to the cysteine and/or protein, but without use of a trapping agent, only the further oxidized sulfinic (R-SO2H) and/or sulfonic (R-SO3H) acid species are typically observed. With NBD modification, the sulfenate oxygen is incorporated into the product, and subsequent mass spectrometry allows for its demonstration. The other two methods, TNB and dimedone modification, result in the loss of the oxygen but indicate the presence of the sulfenic acid in the protein simply by their ability to react with it.

Modification with NBD chloride

As described above, NBD modification may be the best way to trap and demonstrate sulfenic acids in proteins. In fact, access to a mass spectrometer is not required as the product of NBD reaction with sulfenic acids has a distinctive spectral signature with the peak shifted some 73 nm with respect to that generated on reaction with thiol groups. Because this peak is shifted only ~4 nm from that of the free reagent, however, the protein must be washed free of excess reagent before the spectral signature of the covalently-attached NBD can be discerned. This very slight spectral perturbation on modification of sulfenic acids by NBD limits the ability to follow the course of the reaction spectroscopically, although with sufficient protein and only a small excess of reagent, this may be possible. On the other hand, modification of thiols by NBD chloride is readily monitored

spectroscopically and can be used to determine the rate of modification and the extent of the reaction without subsequent washing steps. Note that rates of modification for thiol versus sulfenic acid groups by NBD chloride appear to be similar, as reported earlier by Ellis and Poole (1997a). NBD chloride may not be the reagent of choice if there are additional accessible thiol groups in the protein that may obscure the spectral signature of the R-S(O)-NBD adduct. Reactivity of NBD chloride toward other amino acid side chains can occasionally cause problems in these analyses, as well; however, the adducts with amino or tyrosyl groups are typically formed only at higher pH and have distinct spectral properties (i.e., λ_{max} of 382 and 480 nm for NBD adducts with tyrosines and amines, respectively; Ghosh and Whitehouse, 1968; Aboderin and Boedefeld, 1976; Miki, 1985). In some cases, NBD adducts with thiol groups have been shown to migrate to proximal amine groups of lysine (e.g., Senior et al., 1998), and this process may occur with the NBD adducts of sulfenic acids, as well.

Modification with NBD fluoride

The alternative protocol (see Alternate Protocol) describes the use of NBD fluoride as a replacement for NBD chloride. Since the product formed is identical, all the advantages and disadvantages described above for NBD chloride modification are relevant to this reagent as well. NBD fluoride has the advantage of reacting more quickly with thiol and sulfenic acid groups but has the related disadvantage of being rather unstable in solution and considerably more expensive than NBD chloride. Additionally, uncharacterized spectral changes also occur during the modification reaction, but the modified protein, once washed free of unbound reagent, still has the same appearance as that generated with NBD chloride.

Modification with TNB

Reactivity with TNB is very useful as the spectral changes that ensue allow for immediate quantitation of sulfenic acid content. Subsequent to this reaction, covalent modification of the protein with TNB can be confirmed upon washing, spectral analysis, and release of the bound TNB by DTT treatment. The major disadvantage of using this reagent is its tendency to air-oxidize, and any DTNB present in the solution can react with other thiol groups in the protein and cause an *increase* in the absorbance at 412 nm. TNB can also react with excess peroxides or other oxidants that may remain in the solution, and this reactivity may obscure the reaction of interest. This must therefore be accounted for by control reactions conducted in the absence of protein.

Modification with dimedone

Dimedone reacts only with sulfenic acids in proteins, a reaction considered diagnostic for these species. It is also not reversed by DTT treatment and is therefore particularly useful for peptide analysis following digestion of the modified protein by trypsin. Unfortunately, however, dimedone as a label has no distinguishing spectral features and thus requires the use of mass spectrometry to establish its incorporation. An advantage is that, because dimedone does not react with thiols, it can be added before or at the same time as the oxidant is added and may therefore allow for trapping of the sulfenic acid as it is formed and before it becomes further oxidized to the sulfinic and sulfonic acids. This could be particularly useful for systems where the sulfenic acid is formed rather slowly, and further oxidation of this species occurs readily.

Reversibility of modification

As noted above, NBD and TNB modifications of sulfenic acids are both reversible by addition of DTT, returning the target cysteine to the reduced (thiol) state. This can allow for restoration of function which may be shown in subsequent experiments. At the same time, the reversibility of these modifications may complicate the use of tryptic digests to verify the site of modification, although TNB- and NBD-modified peptides have in some cases been isolated successfully (Chae et al., 1994; Jeong et al., 2000).

Determination of pK_a

If spectral properties of the sulfenic acid–containing protein allow for the determination of the pK_a as described (see Basic Protocol 4), this relatively simple method of assessing this parameter can be a major advance, as only a few pK_a values for sulfenic acids, particularly within proteins, have been reported (Claiborne et al., 1999; Poole and Ellis, 2002). Unfortunately, such a spectral feature may not be observed, especially if other chromophores are present in the protein. The procedure requires large quantities of protein in which the sulfenic acid has been stably generated, but it is nondestructive as long as the protein is stable in the buffers at various pHs.

Critical Parameters

Before any of the spectral analyses can be performed, it must be clear that there is enough protein available to give absorbance changes that are sufficient for quantitative analysis (i.e., >0.1). In the case of the dimedone treatment, which doesn't rely on spectral analyses, the requirement for protein may be less, as the amount used must be sufficient for identification of the modification by ESI-MS.

The chemical modification reagents, if used in excess, do not necessarily have to be standardized by spectral titrations with model reagents unless there are problems with the modification or exact amounts are required. However, the oxidant levels used to generate the sulfenic acid in the first place may be quite critical. For addition of a stoichiometric amount of hydrogen peroxide, for example, exact quantitation of the hydrogen peroxide concentration by the HRP assay is an important first step. As has been mentioned above, the TNB reagent is particularly prone to air-oxidation and must be checked for the presence of excess DTNB or DTT every 2 hr or so. Loss of protein during ultrafiltration can be a major source of error, so it is advantageous to test in advance for the recovery of a given protein with the specific ultrafitration device to be used. Finally, it is helpful, particularly with the NBD modification methods, to know in advance how many accessible thiols are in the protein. This can be done by adding a 10-fold excess of DTNB and observing the rise in A_{412} over time, until completion of the reaction. The amount of TNB released is directly proportional to the number of reactive thiols present in the protein. However, reactivity and accessibility of given protein thiols to particular reagents can be different.

For pK_a determination, the pH values of all phosphate/citrate buffer solutions used should be measured on the day the analysis is performed.

Troubleshooting

Choice of modifying reagent

Where multiple thiol groups are present, only one of which is oxidant sensitive, the demonstration of sulfenic acid formation by NBD chloride modification may require the use of difference spectroscopy to clearly identify the 347 nm peak of the R-S(O)-NBD adduct. In these cases, quantitation will likely suffer as well. Other possibilities are to compare the modified spectra with those obtained when the cysteine of interest has been mutated to a serine. Alternatively, the cysteinyl thiols that obfuscate the analysis can themselves be removed by mutagenesis to serines (assuming that such changes do not affect the normal function of the protein). If there is a way to reversibly block only the cysteine of interest (e.g., by sulfenic-acid formation, then reaction with 1 mole reduced glutathione or TNB for each mole cysteine), this can be done initially, followed by alkylation of the remaining cysteine thiols by a reagent such as *N*-ethylmaleimide. If the rereduced enzyme is fully functional, then effects and detection of sulfenic acid formation at the target cysteine can be analyzed for the preblocked protein using the NBD chloride method without interference by the other cysteine thiols. Another approach could be to use the sulfenic acid–containing protein preblocked with dimedone, then reacted with NBD chloride to generate the control spectrum with only the interfering cysteine thiols modified for comparison with the spectrum of the modified protein containing the sulfenic acid as well as the additional thiols. If the problem is too great, then dimedone (and ESI-MS analysis) rather than NBD chloride should be used.

Use of denaturants

With all of the chemical modification methods for detecting sulfenic acids, the presumption is that the target sulfenic acids are accessible to reaction by these reagents. Where modification reactions are unsuccessful, lack of accessibility may be the problem (even if the corresponding thiol group is accessible toward DTNB and NBD chloride modification, the sulfenic acid moiety may not be accessible due to conformational changes or other differences). In these cases, addition of denaturants may be necessary for trapping of the sulfenic acid to take place (e.g., see modification of NADH peroxidase as reported in Ellis and Poole, 1997a). Denaturants can include guanidine hydrochloride (GuHCl), urea, or SDS, although urea may itself react with NBD chloride. Low amounts (0.5 to 2 M) of urea or GuHCl can be tried first, or, if necessary, higher amounts (4 to 6 M) can be used. In these cases, it is best if the modifying reagent is already present when the denaturant is added, since denaturation of the protein can also promote autoxidation of the sulfenic acid (the denaturant solution can also be bubbled with nitrogen or argon for 20 min before addition to remove oxygen). During ultrafiltration to remove excess reagent, the continued presence of some

amount of the denaturant (e.g., 2 M GuHCl), as is compatible with the ultrafiltration device being used, may be necessary to avoid protein precipitation. One adverse effect of denaturation could be to expose additional cysteinyl thiol groups if the protein has them; in this case, dimedone may be the reagent of choice. Proteins can be analyzed by spectroscopy in the presence of the denaturant but must be freed of denaturant for ESI-MS analysis and may be best analyzed using reversed-phase HPLC linked to ESI-MS analysis.

Interfering lysines

Where modification of the sulfenic acid by NBD chloride is successful, but the NBD group migrates to a proximal lysine side chain over time (as noted by the decrease in A_{347} and increase in A_{480}), one approach may be to preblock accessible amino groups of lysine using amine-specific reagents such as succinimidyl esters (see the handbook from Molecular Probes). Then, once the NBD modification of the sulfenic acid is complete, there should be no further migration of the NBD group and the full absorbance increase at 347 nm can be observed. Again, if the identity of the lysine group is known or suspected, mutagenesis can be used to change this lysine group to a different amino acid, provided this mutation does not also result in a change in the functional properties of the protein.

Poor ESI-MS resolution

The possibility also exists that, if there is insufficient resolution due to the large size of the target protein and/or the quality of data obtained from the mass spectrometer, a mass difference will be obtained for the NBD-modified sulfenic acid product that is less that the full 16 amu expected (relative to the NBD-thiol adduct). This may indicate only partial conversion of the protein to the sulfenic acid prior to modification and an inability to resolve the R-S-NBD and R-S(O)-NBD products by mass spectrometry. One solution is to allow the oxidation of the thiol group to proceed for a longer time or with more oxidant prior to NBD chloride modification. Alternatively, dimedone could be the preferred modification agent, as it gives a much greater mass shift on modification.

Anticipated Results

Modification with NBD

For modification reactions with NBD chloride (or NBD fluoride), the thiol form of the protein will generate a peak for the NBD adduct with a maximum at 420 nm, while the sulfenic acid form, once washed free of excess reagent, will exhibit a maximal absorbance at 347 nm, with the 347 nm peak rising concomitant with a decrease at 420 nm (Fig. 17.1.2). If multiple cysteine residues are present, demonstration of the 347 nm peak may be improved by using difference spectroscopy (Fig. 17.2.1), although quantitation will likely suffer under these conditions. ESI-MS analyses will indicate that the R-S(O)-NBD adduct is 16 amu larger than the R-S-NBD adduct (Fig. 17.1.3), and the R-S(O)-NBD adduct will be nonfluorescent, unlike the R-S-NBD adduct (λ^{ex}_{max} = 422 nm, λ^{em}_{max} = 527 nm). NBD itself accounts for an additional mass of 164 amu.

Modification with TNB

Modification of sulfenic acid–containing proteins with TNB will result in the stoichiometric incorporation of the TNB into the protein, as judged by the decrease in the A_{412} relative to that expected from the dilution of the TNB reagent into buffer lacking protein. Conversion of this A_{412} decrease to the concentration of TNB consumed using the extinction coefficient for TNB and dividing that result by the protein concentration will yield the sulfenic acid content of the protein. On isolation of the TNB-modified protein by ultrafiltration, the spectrum of the modified protein will have a peak at ~325 nm corresponding to the TNB-mixed disulfide bond formed at the cysteine of interest (Ellis and Poole, 1997b). Addition of DTT to this solution will then result in the isosbestic decrease in this peak and increase in the TNB peak with its absorbance maximum at 412 nm (Fig. 17.2.2). If no protein is lost during ultrafiltration, this is a second opportunity to quantitate the TNB modification of the protein. The quantitative decrease in A_{412} upon TNB modification can be used as an assay method for sulfenic acid generation during oxidant titration of the protein (e.g., as in Figure 4 of Poole and Ellis, 2002) or for sulfenic acid generation over time in the presence of excess oxidant, although reactivity of the TNB with the oxidant in the absence of protein must be considered in the latter case.

Modification with dimedone

Reaction of the sulfenic acid in the protein with dimedone will result in a 140-amu increase in mass. Dimedone modification should also eliminate the functionality of the cysteine residue and will block any additional attempts

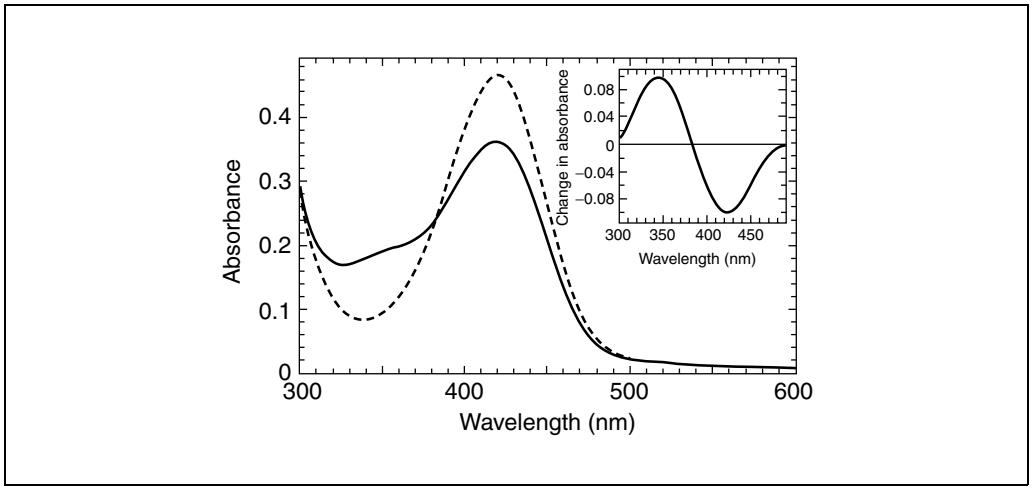

Figure 17.2.1 Hypothetical UV-visible spectra for NBD adducts of reduced and oxidized forms of a protein with three additional reactive cysteine thiol groups. As in Figure 17.1.1, spectra correspond to the R-S-NBD product (dotted line) and the products, including R-S(O)-NBD, after NBD chloride modification of the protein in which one of the four cysteine residues has been oxidized to a sulfenic acid (solid line). The inset represents the difference spectrum calculated by subtracting the spectrum of the fully reduced and modified form of the protein from that of the oxidized, modified form.

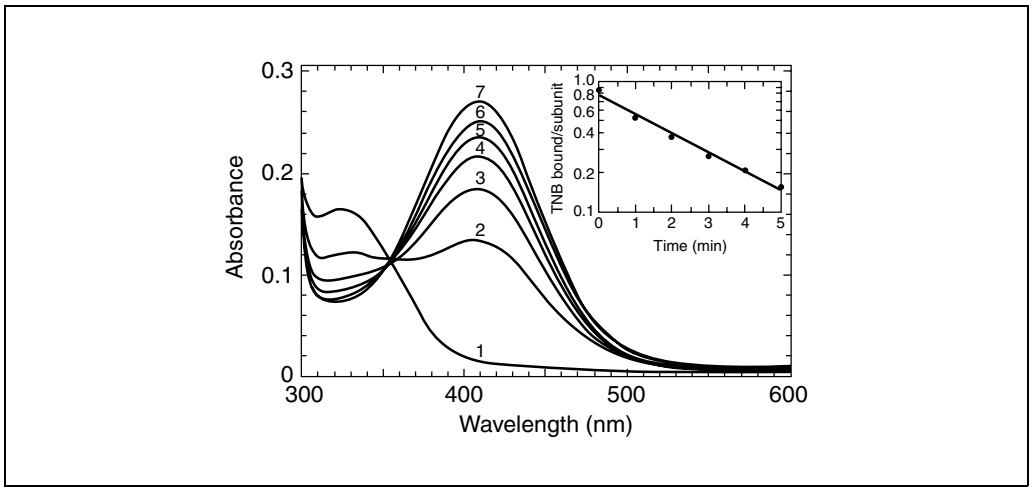

Figure 17.2.2 Reduction of TNB-labeled C165S AhpC by DTT. The TNB-labeled enzyme generated by TNB treatment of the protein oxidized by a stoichiometric amount of hydrogen peroxide was isolated by ultrafiltration with Centricon CM-30 concentrators, then treated with a 10-fold excess of DTT. Shown are spectra before (1), and after addition of DTT for 1, 2, 3, 4, 5 and 30 min (spectra 2 to 7, respectively). The inset represents a semilogarithmic plot of the change in absorbance, converted into units of TNB/subunit, versus time. Reprinted with permission from Ellis, H.R., and Poole, L.B., *Biochemistry* 36:13349-13356. Copyright 1997, American Chemical Society.

to modify this group with NBD chloride (as a cross-confirmation of the target of these reagents as the sulfenic acid).

Determination of pK$_a$

If there are observable differences between the absorbance of the deprotonated sulfenate base at higher pH values and the absorbance of the protonated sulfenic acid at lower pH values (Fig. 17.2.3), then a fit of the absorbance versus pH data to the equation given in Basic Protocol 4 will allow for the determination of the pK$_a$ of the sulfenic acid (Fig. 17.2.4). In several small molecules, pK$_a$ values for the stabilized sulfenic acids have ranged from 4.8 to 6.3 (Claiborne et al., 2001), while a pK$_a$ of ~6.1 has been determined for one protein sulfenic acid so far (Poole and Ellis, 2002).

Time Considerations

For most of the chemical modification procedures, once the reagents are prepared and the protein concentration is determined, the generation of the sulfenic acid and reaction with

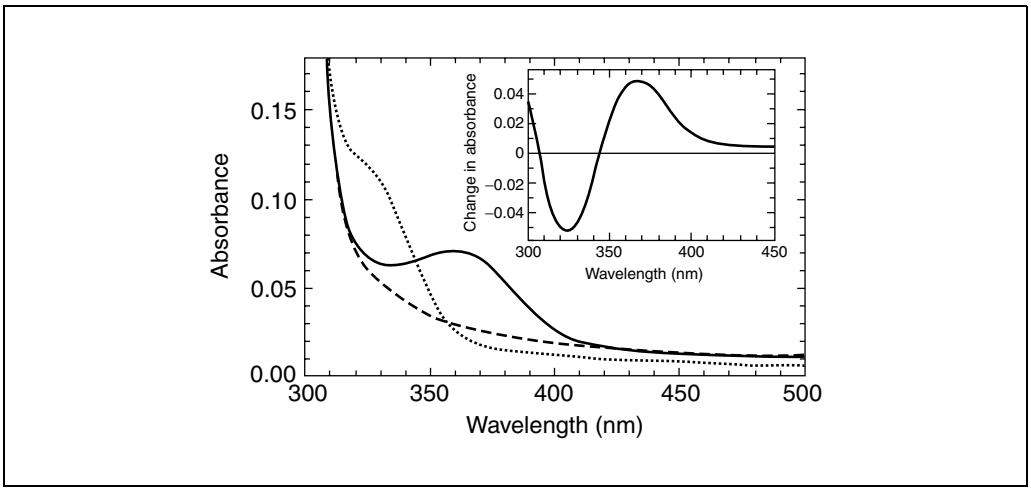

Figure 17.2.3 Spectral properties of thiol(ate) (Cys46-SH or Cys46-S^-), sulfenate (Cys46-SO^-), and sulfenic acid (Cys46-SOH) forms of C165S AhpC from *Salmonella typhimurium*. Spectra of the mutant enzyme (200 μM) at pH 7.0 in the absence (dotted line) or presence (solid line) of 1.1 equivalent of H_2O_2 are shown. The dashed spectrum represents the Cys46-SOH form of the enzyme at pH 4.6. The inset depicts the difference spectrum between the Cys46-S(H) and Cys46-SO^- forms of C165S AhpC. Reprinted with permission from Poole, L.B., and Ellis, H.R. 2002. *Methods Enzymol.* 348:122-136. Copyright 2002, Academic Press.

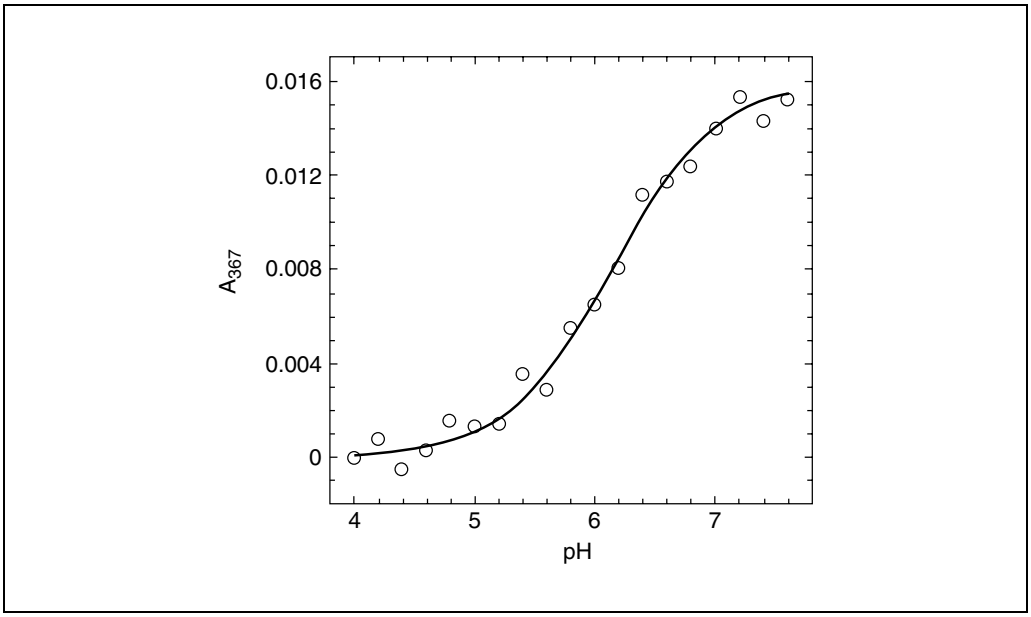

Figure 17.2.4 Hypothetical determination of pK_a value for a protein sulfenic acid given absorbance values determined in various pH buffers. Given an experiment similar to that described (see Basic Protocol 4), representative data are shown for absorbance values at 367 nm versus pH of a sulfenic acid–containing protein (~50 μM) with a pK_a of ~6.1. The fitted curve is obtained using the equation given in the protocol.

the modifying agent is complete within <1 to 2 hr. Ultrafiltration may take 20 min to 3 hr, depending on the particular device and the molecular weight cutoff (lower cutoff, slower filtration). The pK_a determination itself takes about 1 to 3 hr, with preparation and/or pH measurement of the citrate/phosphate buffers requiring 1 to 2 additional hr. Tryptic digests are carried out for 12 to 24 hr, and each HPLC run takes ~90 to 120 min.

Literature Cited

Aboderin, A.A. and Boedefeld, E. 1976. Reaction of chicken egg white lysozyme with 7-chloro-4-nitrobenz-2-oxa-1,3-diazole. II. Sites of modification. *Biochim. Biophys. Acta* 420:177-186.

Birkett, D.J., Price, N.C., Radda, G.K., and Salmon, A.G. 1970. The reactivity of SH groups with a fluorogenic reagent. *FEBS Lett.* 6:346-348.

Chae, H.Z., Uhm, T.B., and Rhee, S.G. 1994. Dimerization of thiol-specific antioxidant and the essential role of cysteine 47. *Proc. Natl. Acad. Sci. U.S.A.* 91:7022-7026.

Claiborne, A., Yeh, J.I., Mallett, T.C., Luba, J., Crane, E.J. III, Charrier, V., and Parsonage, D. 1999. Protein-sulfenic acids: Diverse roles for an unlikely player in enzyme catalysis and redox regulation. *Biochemistry* 38:15407-15416.

Claiborne, A., Mallett, T.C., Yeh, J.I., Luba, J., and Parsonage, D. 2001. Structural, redox, and mechanistic parameters for cysteine-sulfenic acid function in catalysis and regulation. *Adv. Prot. Chem.* 58:215-276.

Ellis, H.R. and Poole, L.B. 1997a. Novel application of 7-chloro-4-nitrobenzo-2-oxa-1,3-diazole to identify cysteine sulfenic acid in the AhpC component of alkyl hydroperoxide reductase. *Biochemistry* 36:15013-15018.

Ellis, H.R. and Poole, L.B. 1997b. Roles for the two cysteine residues of AhpC in catalysis of peroxide reduction by alkyl hydroperoxide reductase from *Salmonella typhimurium*. *Biochemistry* 36:13349-13356.

Fuangthong, M. and Helmann, J.D. 2002. The OhrR repressor senses organic hydroperoxides by reversible formation of a cysteine-sulfenic acid derivative. *Proc. Natl. Acad. Sci. U.S.A.* 99:6690-6695.

Ghosh, P.B. and Whitehouse, M.W. 1968. 7-chloro-4-nitrobenz-2-oxa-1,3-diazole: A new fluorigenic reagent for amino acids and other amines. *Biochem. J.* 108:155-156.

Jeong, W., Cha, M.K., and Kim, I.H. 2000. Thioredoxin-dependent hydroperoxide peroxidase activity of bacterioferritin comigratory protein (BCP) as a new member of the thiol-specific antioxidant protein (TSA)/alkyl hydroperoxide peroxidase C (AhpC) family. *J. Biol. Chem.* 275:2924-2930.

Miki, M. 1985. Chemical modification of tropomysosin with NBD-chloride. *J. Biochem.* (Tokyo) 97:1067-1072.

Poole, L.B. and Ellis, H.R. 2002. Identification of cysteine sulfenic acid in AhpC of alkyl hydroperoxide reductase. *Meth. Enzymol.* 348:122-136.

Riddles, P.W., Blakeley, R.L., and Zerner, B. 1979. Ellman's reagent: 5,5′-dithiobis(2-nitrobenzoic acid)—A reexamination. *Anal. Biochem.* 94:75-81.

Senior, A.E., Gros, P., and Urbatsch, I.L. 1998. Residues in P-glycoprotein catalytic sites that react with the inhibitor 7-chloro-4-nitrobenzo-2-oxa-1,3-diazole. *Arch. Biochem. Biophys.* 357:121-125.

Tripolt, R., Belaj, F., and Nachbaur, E. 1993. Unexpectedly stable sulfenic acid: 4,6-dimethoxy-1,3,5-triazine-2-sulfenic acid; synthesis, properties, molecular and crystal structure. *Z. Naturforsch.* 48b:1212-1222.

Williams, C.H., Jr., Arscott, L.D., Matthews, R.G., Thorpe, C., and Wilkinson, K.D. 1979. Methodology employed for anaerobic spectrophotometric titrations and for computer-assisted data analysis. *Meth. Enzymol.* 62:185-198.

Key References

Ellis and Poole, 1997a. See above.

Describes for the first time the use of the NBD chloride method for identification of the cysteine sulfenic acid of the C165S mutant of AhpC.

Poole and Ellis, 2002. See above.

Gives practical details about the use of several protocols, including NBD chloride, TNB, and dimedone-based methods, for identification of sulfenic acids.

Willett, W.S., and Copley, S.D. 1996. Identification and localization of a stable sulfenic acid in peroxide-treated tetrachlorohydroquinone dehalogenase using electrospray mass spectrometry. *Chem. Biol.* 3:851-857.

Describes the use of dimedone modification and LC/MS/MS to identify and localize sulfenic acids within proteins.

Contributed by Leslie B. Poole
Wake Forest University School of Medicine
Winston-Salem, North Carolina

Fluorescence Microplate Reader Measurement of Tissue Susceptibility to Lipid Peroxidation

BASIC PROTOCOL

Oxidative stress and lipid peroxidation have been implicated as important mechanisms for chemical-induced cell injury/death and the development of numerous disease states. The enrichment and maintenance of cellular antioxidant defense systems are potential strategies to prevent toxic oxidative damage. It is therefore important to estimate or monitor the susceptibility of biological samples to lipid peroxidation. Susceptibility to lipid peroxidation is determined by several factors, such as fatty acid composition and antioxidant levels present in membranes. As numerous antioxidants are present in cells, it is technically difficult to analyze biological specimens for each one. This unit describes a fluorescence microplate reader–based assay to measure the susceptibility of tissue samples by exposing them to an initiator and measuring the length of time to the start of lipid peroxidation. The lipid peroxidation reaction is initiated by addition of Fe^{3+}-ADP chelator in the presence of a low concentration of ascorbate. The by-products of lipid peroxidation, such as 4-hydroxy-2-nonenal, can subsequently react with amines of amino acids (e.g., glycine) to form fluorescent products that are measured with a fluorescence microplate reader. This assay allows the rapid monitoring of the susceptibility to lipid peroxidation in a large number of samples in real time.

Materials

Tissue, cells, or subcellular organelles
50 mM potassium phosphate buffer, pH 7.4 (see recipe)
Glycine/ascorbate solution (see recipe)
Initiator solution (see recipe), fresh

Sonicator
Flat-bottomed 96-well microplates (Rainin Instrument)
Cytofluor 4000 fluorescence multiwell microplate reader (PerSeptive Biosystems) with temperature control

Suspend samples

1. Sonicate biological samples (i.e., tissue, cells, or subcellular organelles) in 1 ml of 50 mM potassium phosphate buffer, pH 7.4, at a setting that evenly distributes the tissue into solution in ~5 to 15 sec. Keep all preparations on ice until use.

   The amount of sample used varies depending on the source of samples (see Table 17.3.1).

   Avoid buffers and reagents that may quench fluorescence (e.g., Triton, SDS) or that may chelate iron).

2. Add 90 µl of the sample to an allocated well on a flat-bottomed 96-well microplate. Add 100 µl glycine/ascorbate solution.

Measure fluorescence

3. Determine background fluorescence (one cycle) of each well using the following settings on a Cytofluor 4000 fluorescence multiwell microplate reader at 37°C:

Excitation:	360/40 nm
Emission:	460/40 nm
Gain:	90.

Contributed by Jin-Gang Zhang and Marc W. Fariss
Current Protocols in Toxicology (2003) 17.3.1-17.3.10

Table 17.3.1 Optimal Assay Conditions and Results for Different Biological Samples

Biological sample[a]	Sample amount (mg protein/well)	Initiator concentration (ADP mM/Fe^{3+} μM)	Lag time (min)[b]	Rate (AFU/min)[b]
Liver homogenate[c]	0.1	1/25	10 ± 3.0	10.1 ± 0.3
Liver mitochondria[c]	0.1	1/25	38 ± 10	14.1 ± 1.0
Liver inner mitochondrial membrane[c]	0.1	1/25	15 ± 3	21.4 ± 4.4
Brain	0.1	1/25	12 ± 1	18.8 ± 1.8
Kidney	0.1	1/25	12 ± 1	9.0 ± 1.7
Heart	0.4	4/100	10 ± 3	14.9 ± 2.2
Skeletal muscle	0.5	1/25	13 ± 8	25.0 ± 0.3

[a]All tissues were obtained from Sprague-Dawley rats. Ground tissue was suspended into 50 mM potassium phosphate buffer, pH 7.4, and sonicated for 5 sec. The tissue suspension was used for assay.

[b]Data are the mean ± standard error of three determinations.

[c]Liver homogenates, mitochondria, and inner mitochondrial membranes were isolated as described by Hovius et al. (1990) with modifications.

4. Add 10 μl fresh initiator solution to each well. Read immediately at 37°C and every 5 min for 60 cycles, for a total of 300 min.
5. Save the data and perform lag-time or maximal-rate analysis after completion of the reading.

Perform maximal-rate analysis

6. To determine rate of the propagation phase (Fig. 17.3.1), in the software that comes with the microplate-reader, open the kinetics option of Post Processing from the Cytofluor window.
7. Set the Window Size (i.e., range) for the rate to be calculated based on the second phase of the curve. Visually look at the kinetic curve and decide the number of points on the second phase of the curve that will be used for this calculation. Type the number into the Window Size. If necessary, modify the number of window-size points for the kinetic curve of other wells in the microplate to obtain an accurate rate for each sample.

   For example, thirteen window-size points were chosen in Fig. 17.3.1.

8. Click on the desired cell to cause the Maximal Rate measurement for the chosen number of observations in the range to be plotted and the equation for the line, max rate, correlation coefficient (r^2), and window size to appear (Fig. 17.3.1).

Obtain lag time

9. Calculate the lag time (x) from the rate equation (step 7) using the fluorescence value at the intersection of the rate line with the x axis as the Y value (for example, 1000 in Fig. 17.3.1).

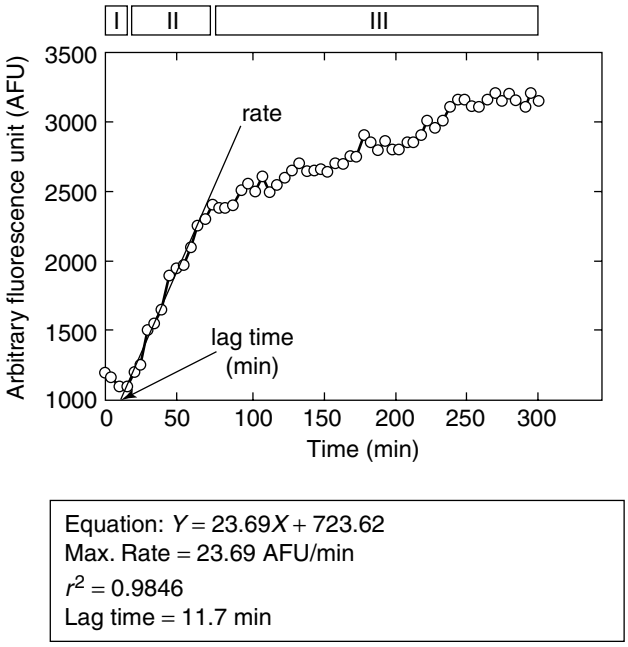

Figure 17.3.1 Kinetic profile of fluorescence during lipid peroxidation. The kinetic curve indicates three phases: (I) a latency phase, (II) a propagation phase, and (III) a termination phase. Lag time (i.e., time from commencement of the assay to the start of lipid peroxidation) can be determined by the latency phase or propagation phase via the equation shown. The maximal rate—i.e., slope expressed in arbitrary fluorescence units (AFU)/min—is also calculated via the equation.

REAGENTS AND SOLUTIONS

*Use Milli-Q-purified water or equivalent for all recipes and protocol steps. For common stock solutions, see **APPENDIX 2A**; for suppliers, see **SUPPLIERS APPENDIX**.*

Glycine/ascorbate solution

Prepare ascorbate stock solution by weighing 7.93 mg L-ascorbic acid and adding 1 ml of 200 mM glycine buffer (see recipe). Vortex to dissolve. Add 300 µl ascorbate stock solution to 14.7 ml of 200 mM glycine buffer (see recipe) and mix. Prepare fresh.

Glycine buffer, 200 mM

Dissolve 1.50 g glycine in 100 ml of 100 mM potassium phosphate buffer, pH 7.4 (see recipe). Store up to 6 months at 4°C.

Initiator solution

Weigh 2.7 mg ferric chloride hexahydrate ($FeCl_3 \cdot 6\ H_2O$) and add 1 ml water to dissolve. Weigh 17.5 mg of sodium adenosine 5′-diphosphate (ADP) from a bacterial source and dissolve in 1.9 ml of 50 mM potassium phosphate buffer, pH 7.4 (see recipe). Just prior to use, mix the ADP solution with 0.1 ml of the ferric chloride solution.

The concentration used depends on the source of biological samples being evaluated (see Table 17.3.1). For instance, higher concentrations of ADP and $FeCl_3 \cdot 6\ H_2O$ may be required for certain tissues. For most cases, the final concentrations are 1 mM ADP and 25 µM ferric chloride.

Potassium phosphate buffer (pH 7.4), 100 mM

Dissolve 13.6 g monobasic potassium phosphate (KH_2PO_4) in 1 liter water and 17.4 g dibasic potassium phosphate (K_2HPO_4) in 1 liter water. Mix 200 ml of the monobasic solution with 800 ml of the dibasic solution. Store up to 1 year at 4°C.

COMMENTARY

Background Information

Overwhelming evidence indicates that reactive oxygen species (ROS) and subsequent lipid peroxidation play critical roles in the pathogenesis of numerous clinical disease states, including drug/toxicant-induced cell injury/death. Unsaturated lipids in biological membranes are susceptible to peroxidation by ROS or free radicals. This lipid peroxidation may result in impairment of membrane properties and functions such as a decrease in membrane fluidity, inactivation or release of membrane-bound components (e.g., receptors and enzymes), and an increase in nonspecific permeability. To protect against the potentially damaging effects from ROS, cells are well equipped with a comprehensive set of antioxidant systems, which include enzymes such as superoxide dismutase, catalase, glutathione peroxidase, and glutathione reductase, macromolecules such as albumin, ceruloplasmin, ferritin, and thioredoxin, and a number of low-molecular-weight antioxidants including ascorbic acid, α-tocopherol, β-carotene, ubiquinol, glutathione, methionine, uric acid, and bilirubin. As oxidative stress is an imbalance between pro-oxidants and antioxidants, favoring oxidation, it is frequently important to determine the cellular antioxidant capacity or susceptibility of tissue to lipid peroxidation.

Since multiple antioxidants are normally present in cells, it is technically difficult to measure the level of each individual antioxidant in biological samples as well as to interpret the significance of these concentrations in terms of preventing oxidative damage. In vivo, antioxidants probably do not exert their effect alone, but rather act in combination with other antioxidants. Such interactions may lead to differences in total antioxidant capacity (Niki and Noguchi, 2000). For example, two antioxidants may interact with each other to produce a synergistic effect. It is known that vitamin E acts as a primary antioxidant, and resultant vitamin E radicals can regenerate vitamin E in the presence of vitamin C, ubiquinol, or glutathione. On the other hand, antioxidants may serve as pro-oxidants under certain conditions. Both vitamins C and E can reduce metal ions and have been shown to accelerate the oxidation of liposomes and low-density lipoprotein (LDL). In fact, β-carotene dietary supplementation at 20 mg per day increased the incidence of lung cancer in male smokers in one prospective trial (Woodford and Whitehead, 1998). Therefore, the assessment of total cellular membrane antioxidant status is important to estimate the tissue's capacity to resist oxidative stress in vivo and in vitro.

The antioxidant status of cellular membranes is also a valuable functional measure of experimental and clinical antioxidant supplementation. The addition of antioxidants to in vitro or in vivo systems does not guarantee that the administered antioxidant has been delivered in a functional form to a particular tissue, cell, or subcellular fraction of interest. This is especially true for lipophilic antioxidants such as vitamin E. For example, the authors have recently shown that the addition of D-α-tocopherol or D-α-tocopheryl acetate to hepatocyte suspensions results in high levels of these compounds in cells, mitochondria, and microsomes as determined by HPLC analyses (Fariss et al., 2001). However, functional antioxidant measurements of these tissues (using the fluorescence microplate reader assay) indicate that the vitamin E present was not functional and most likely represents clusters of lipophilic vitamin E adhered to cellular membranes (Fariss et al., 2001). In contrast, the same hepatocytes treated with D-α-tocopheryl succinate were protected against toxic oxidative stress, which appears to be related to the rapid uptake of tocopheryl succinate in cells and mitochondria followed by the rapid release of functional tochopherol (Fariss et al., 2001). This unique ability of tochopheryl succinate to serve as a rapid delivery system for functional tochopherol has also been observed following acute in vivo administration. As shown in Table 17.3.2, not all vitamin E derivatives are equal in terms of rapid delivery of functional tochopherol to tissue, mitochondria, and inner mitochondrial membranes. Based on these studies (using the microplate reader assay) and those demonstrating enhanced in vitro and in vivo cytoprotection with tocopheryl succinate treatment, the

Table 17.3.2 Effects of Single Administration of Tocopherol and Tocopheryl Esters on Liver Samples[a]

Tissue/treatment	Tocopherol (nmol/mg protein)	Tocopheryl ester (nmol/mg protein)	Lag time (min)	Rate (AFU/min)
Homogenate				
Vehicle	0.14 ± 0.01	—	8 ± 1	13.4 ± 1.4
α-Tocopherol	0.52 ± 0.18	—	>300	—
α-Tocopheryl acetate	0.20 ± 0.02	1.75 ± 0.65	14 ± 2	12.7 ± 0.3
α-Tocopheryl succinate	0.61 ± 0.07	1.60 ± 0.32	>300	—
Mitochondria				
Vehicle	0.07 ± 0.01	—	41 ± 8	15.0 ± 0.3
α-Tocopherol	0.08 ± 0.01	—	31 ± 7	15.1 ± 0.6
α-Tocopheryl acetate	0.08 ± 0.01	ND	49 ± 6	13.3 ± 0.1
α-Tocopheryl succinate	0.20 ± 0.01	1.81 ± 0.23	>300	—
Inner mitochondrial membrane				
Vehicle	0.06 ± 0.01	—	12 ± 2	23.3 ± 2.0
α-Tocopherol	0.06 ± 0.01	—	22 ± 3	20.5 ± 0.6
α-Tocopheryl acetate	0.06 ± 0.01	ND	18 ± 1	21.7 ± 1.2
α-Tocopheryl succinate	0.22 ± 0.05	3.86 ± 0.79	106 ± 49	15.3 ± 0.2

[a]Abbreviation: ND, not detectable.

[b]Rats were administered a single dose (i.p.) of vehicle (olive oil) or 0.19 mmol/kg of α-tocopherol, α-tocopheryl acetate, or α-tocopheryl succinate. After 18 hr, liver homogenates and subcellular fractions were isolated as described by Hovius et al. (1990) with modifications. Tocopherol and tocopheryl ester levels were then determined by HPLC assay (Fariss et al., 1989). Data are the mean ± std. error; the sample size is 3 to 5 rats.

authors conclude that the enrichment of mitochondrial and inner mitochondrial membrane with functional tochopherol is a critical event in tochopheryl succinate cytoprotection against toxic oxidative stress.

Antioxidant capacity can be estimated by direct measurement of the ability of biological samples to scavenge free radicals or by their susceptibility to lipid peroxidation. Several methods have been developed to assess the total antioxidant capacities of biological samples such as blood plasma, other body fluids, and plant extracts; the methods are mainly based on the ability of these biological samples to scavenge free radicals, or to chelate the transition metals (Ghiselli et al., 2000). These methods include the ferric reducing ability of plasma (FRAP; Benzie and Strain, 1996), total radical trapping parameter (TRAP; Wayner et al., 1985), trolox equivalent antioxidant capacity (TEAC; Re et al., 1999), oxygen radical absorbance capacity (ORAC), total oxyradical scavenging capacity (TOSC), and cycle voltammetry (CV) assays (Chevion et al., 2000). Although these methods can provide useful information, especially with the assessment of low-molecular-weight water-soluble antioxidants in particular, they may have some difficulties in assessing certain antioxidants. For example, protein antioxidants like superoxide dismutase were not suitable for the assessment with such assays (Yu and Ong, 1999). In addition, such assays may underestimate the antioxidant capability for antioxidants acting as iron chelators, such as albumin (Yu and Ong, 1999). Furthermore, most of these assays are limited to determining the total antioxidant capacity in plasma or serum, but not in tissue. In contrast, the fluorescence microplate reader assay reported here has the distinct advantage of assessing the antioxidant capacity of tissues, cells, and subcellular fractions. However, this fluorescence assay is not useful for serum or plasma, as the peroxidation of this tissue does not produce a strong fluorescent signal (apparently insufficient polyunsaturated fatty acids are present to produce reactive aldehydes and fluorescence). Another important advantage of this fluorescence microplate reader assay is in determining the functional antioxidant contributions of lipophilic antioxidants such as tocopherol. Unfortunately, this fluorescence assay's ability to assess the antioxidant contributions of water-soluble, non-enzymatic and enzymatic antioxidants has not been determined.

Other methods for evaluation of antioxidant capacity include the assessment of the susceptibility to lipid peroxidation (Tirmenstein et al., 1998; Cervato et al., 1999), which is the strength of the fluorescent assay reported here. Lipid peroxidation is probably the most extensively investigated process induced by free radicals. A number of assays exist for determining lipid peroxidation based on several different biochemical endpoints. One of the common methods is the thiobarbituric acid reactive substances (TBARS) assay, which is known to detect malondialdehyde (MDA) and other monofunctional aldehydes. However, most of these assays require considerable sample preparation and analysis time. Samples either need to be extracted with organic solvents or dissolved in SDS; furthermore, the assay is not in real-time.

The fluorescence microplate reader assay reported here has numerous advantages. First, assay procedures and sample preparations are rapid, inexpensive, and simple. Second, it allows the rapid monitoring of lipid peroxidation in real time using a large number of biological samples, including tissue, cells, and subcellular fractions. To clearly illustrate the advantages of this fluorescence microplate reader assay over the traditional TBARS assay, consider the time and expense required to analyze the samples in Table 17.3.2 for antioxidant capacity or susceptibility to lipid peroxidation. Using the microplate reader assay, these samples can be analyzed in a single 8-hr day by placing each sample (~5 samples per treatment and subcellular fraction for a total of 60 samples to be analyzed) in individual wells of the 96-well microplate, adding the appropriate buffer and initiator of lipid peroxidation, and reading each well for fluorescence in the plate reader for 300 min. (The microplate reader automatically reads the fluorescence of each well every 5 min.) In contrast, these same samples would take ~6 days to analyze for susceptibility to lipid peroxidation by the TBARS assay. Each sample (only 20 samples/day can be analyzed) is incubated in a glass scintillation vial with the appropriate buffer and initiators of lipid peroxidation, and an aliquot of this solution is collected every 15 min for 3 hr for TBARS analysis (12 aliquots for TBARS analysis per tissue sample). Accordingly, using the TBARS assay, it would take 3 full days to analyze all 60 tissue samples in this experiment (Table 17.3.2) and at least another 3 days to analyze the 720 aliquots for TBARS levels. Thus the advantages of this fluorescence microplate reader assay for determining a tissues' susceptibility to lipid peroxidation are substantial.

For the most part, the authors have found good agreement between the TBARS assay and the fluorescence microplate reader assay in assessing the susceptibility of biological samples to lipid peroxidation (Tirmenstein et al., 1998). However, the assay has disadvantages as well. For example, the microplate reader assay cannot be used for quantification of amounts of lipid peroxidation produced, since the identity of the fluorophore is not known. Regardless of the methods used for measuring lipid peroxidation, the susceptibility of biological samples to lipid peroxidation can be estimated by adding lipid peroxidation initiators in the assay system and measuring the commencement time of lipid peroxidation or maximal rate of second propagation phase.

To initiate the production of pro-oxidants in antioxidant capacity assays, numerous initiator systems have been used, such as hydrogen peroxide alone or coupled with horseradish peroxidase, 2,2′-azobis(2-amidinopropane)dihydrochloride (AAPH), 2,2′-azinobis(3-ethylbenzothiazoline 6-sulfonate) (ABTS), 2′-azobis(2,4-dimethylvaleronitrile) (AMVN), and inorganic iron or copper, given alone or in a chelated form. After examining several of these initiators, Fe^{3+}/ADP was selected for the susceptibility to lipid peroxidation assay. It is known that inorganic iron in certain chelated forms is capable of promoting free-radical-mediated peroxidation of membrane lipids. In addition, Fe^{2+}/ADP or Fe^{3+}/ADP-ascorbate has been extensively studied and used as an in vitro model. The mechanism of iron-induced lipid peroxidation is hydroxylradical–production related via the Fenton reaction. The transition metal iron reacts with oxygen to produce superoxides, which can be dismutased by superoxide dismutase to form hydrogen peroxides. Hydrogen peroxides undergo Fenton reaction in the presence of ferrous iron (Fe^{2+}) to form hydroxyl radicals ($OH^{\cdot}$; Fig. 17.3.2). Lipid peroxidation is initiated by this free radical and the chain reaction is promoted to the generation of lipid alkyl radicals (L·), followed by the formation of a lipid peroxyl radical (LOO·) due to the interaction with oxygen. LOO· eventually converts to LOOH via hydrogen abstraction from neighboring allylic bonds (Fig. 17.3.2). Lipid peroxides in the presence of ferrous iron are converted to lipid alkoxyl radicals (again by the Fenton reaction) which degrade and fragment (again with the help of iron) to form a wide variety of reactive aldehyde products, including

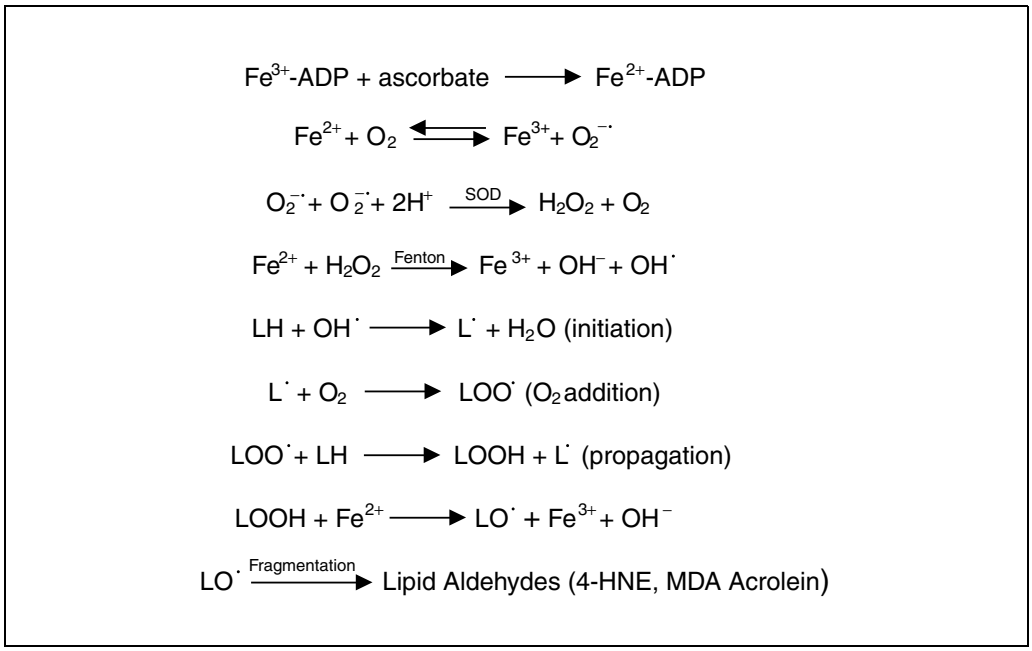

Figure 17.3.2 Fe^{2+}/Fe^{3+} initiation of generation of hydroxyl radicals and lipid peroxidation products.

4-hydroxy-2-nonenal, MDA, and acrolein. Amino acids, especially basic amino acids such as glycine, histidine, lysine, and arginine, can strongly react with the α, β-unsaturated carbonyl groups of these by-products to form fluorescence adducts. Such a process is believed to cause or at least be associated with numerous clinical conditions, including the formation of lipofuscin and ceroid pigments during aging, amyloid β-peptide plaques during Alzheimer's disease, Lewy bodies in Parkinson's disease, and the formation of advanced glycation end products (AGE)–associated protein adducts in diabetic complications such as nephropathy. The authors have experimented briefly with the use of other initiators in the assay, such as AAPH and Fe/H_2O_2, but found that the initiator Fe/ADP results in the greatest fluorescence signal and reproducibility in a wide variety of biological specimens (Tirmenstein, pers. comm.).

Critical Parameters and Troubleshooting

Both the lag time and maximal rate of propagation phase can be used for estimation of susceptibility to lipid peroxidation. Extended lag time or lowered maximal rate suggests increased tissue antioxidant capacity or decreased susceptibility to lipid peroxidation. Lag time is the most valuable parameter used in this assay. The area under the curve (AUC) may be an alternative way to describe the antioxidant capacity since both changes in lag time and maximal rate will significantly affect this parameter. All these values can be readily obtained from the array (Fig. 17.3.3).

This method was originally developed and used for the determination of the susceptibility of rat liver and its subcellular organelles to lipid peroxidation. In terms of use for other biological samples, a few factors should be considered. First, the quantity of antioxidants in plasma, brain, kidney, heart, lung, and liver, as well as their peroxidizable lipids are different. For example, the formation of MDA in rat liver mitochondria was 12-fold higher than those of cardiac mitochondria with the same iron/ascorbate system (Wiswedel et al., 1989). Therefore, selecting the correct amount of tissue and the concentrations of lipid peroxidation initiator are critical to ensure that the sample is peroxidized in the time frame of the assay. For example, with heart tissue, a greater amount of tissue and higher concentrations of lipid peroxidation initiator are required (see Table 17.3.1). The use of plasma or serum in this assay has not been successful, presumably due to the low level of unsaturated lipid in this biological specimen, thus limiting the ability to generate a detectable fluorescence signal.

Background fluorescence is increased slightly after 5 hr of incubation with the lipid peroxidation initiator as described (see Basic

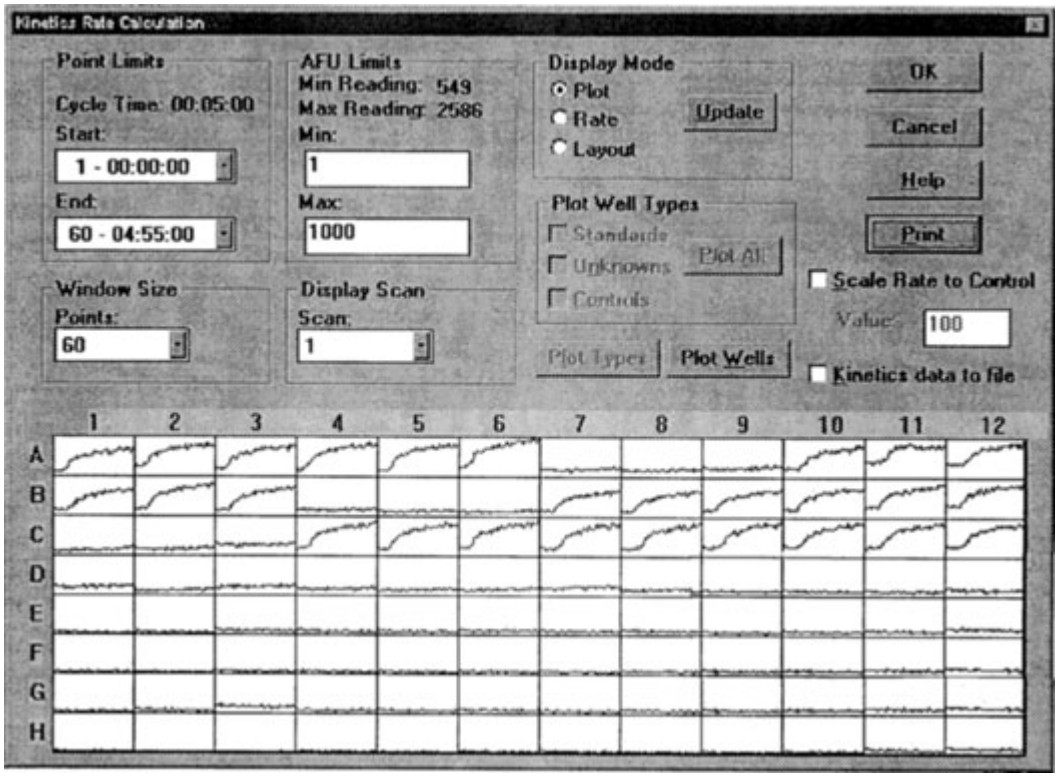

Figure 17.3.3 Kinetic traces of fluorescence for lipid peroxidation in isolated hepatic mitochondrial membrane induced by Fe^{3+}-ADP/ascorbate. The mitochondrial samples were isolated from rats administered (i.p.) either vehicle (traces A1-A3, A10-A12, B7-B9, C4-C6), tocopheryl acetate (A4-A6, B1-B3, B10-B12, C7-C12), or the Tris salt of tocopheryl succinate (A7-A9, B4-B6, C1-C3), 18 hr prior to isolation.

Protocol) but lacking biological samples. The results also indicate that the increase in fluorescence with incubation time only occurs in incubations containing ascorbate, ADP, ferric chloride, and glycine. If any one of these compounds is omitted from the incubation solution, no increase in fluorescence is detected. In general, the concentration of ascorbate is also important in determining whether it is pro-oxidant (reducing iron) or antioxidant. Ascorbate at higher concentrations acts as an antioxidant, but lipid peroxidation (MDA) production by Fe^{3+}/ADP was largely potentiated at lower concentrations of ascorbate. In the present assay, a final concentration of 450 mM ascorbate was used. The lag time can be shortened by increasing the concentration of ferric chloride/ADP, and thus varying the concentration of ferric chloride is an effective way of controlling lag time.

Metal chelators such as EDTA or EGTA are commonly used during sample preparation, such as fractionation of homogenates, mitochondria, and microsomes from tissue. These chelators can form complexes with iron and inhibit lipid peroxidation. Therefore, isolated fractions should be completely washed with non-EDTA or -EGTA buffer. Other considerations should also be taken into account during the studies of the antioxidant capacity of vitamin E esters, such as tocopheryl succinate. It has been shown that tocopheryl succinate can be taken up rapidly by the cells and incorporated into the membrane where it is hydrolyzed into tocopherol by membrane-bound esterase (Fariss et al., 2001). Thus, during the microplate reader assay, esterase inhibitors should be added in order to avoid any hydrolysis of tocopheryl succinate in the samples. A recent study by the authors showed that thenoyltrifluoroacetone is a potent inhibitor of esterase activity and it effectively inhibits the hydrolysis of tocopheryl succinate without affecting the measurement of susceptibility to lipid peroxidation (Zhang and Fariss, 2002). The addition of 25 μM thenoyltrifluoroacetone (final concentration) is recommended in these studies.

Anticipated Results

Figure 17.3.1 shows the kinetic profile of lipid peroxidation with a 5-hr incubation time. Typically, three phases are observed: (I) the initial latency phase, followed by (II) a second propagation phase, and finally (III) a termination phase. Lag time can vary depending on the source of tissues and concentration of lipid peroxidation initiator used. With the current assay method (see Basic Protocol), the lag time for different tissues ranged from 10 to 40 min and maximal rates from 10 to 25 AFU/min (Table 17.3.1).

As mentioned previously, the authors' laboratory has a long-term interest in the protective role of vitamin E derivatives, including tocopherol, tocopheryl acetate, and tocopheryl succinate. Tocopherol is a chain-breaking antioxidant and is known to react with a variety of free radicals, in particular peroxyl radicals Due to its lipophilic property, tocopherol does not rapidly accumulate in hepatic mitochondria. The authors and others have found that tocopheryl succinate is far more effective than tocopherol in protecting isolated hepatocytes against many different toxic oxidative changes, presumably via enriching mitochondria with tocopherol (Fariss et al., 2001). Recent in vivo studies by the authors showed that a single dose of 0.19 mmol/kg (~100 mg/kg) tocopheryl succinate i.p. can rapidly enrich not only rat hepatocytes, but most importantly, mitochondria and inner mitochondrial membranes, which consequently results in a decrease in their susceptibility to lipid peroxidation as compared with samples from vehicle control animals. The decrease in susceptibility to lipid peroxidation with this treatment provides important evidence that the measured enrichment of tocopherol in these mitochondrial fractions is functioning as an effective antioxidant. For example, as illustrated in Table 17.3.2 for mitochondria, the lag time (elapsed time between addition of initiator to the sample and the onset of lipid peroxidation, as measured by an increase in fluorescence in this assay) for samples isolated from vehicle control rats is very short, ~41 min. with a rate of 15.0 AFU/min. This rapid onset of lipid peroxidation (fluorescence) indicates that this sample is highly susceptible to lipid peroxidation. By contrast, hepatic mitochondria isolated from rats pretreated with tocopheryl succinate were completely resistant to the induction of lipid peroxidation, as indicated by a lag time of >300 min (maximum incubation time) and no measurable rate (an increase in fluorescence was not observed in this sample). Interestingly, pretreatment of rats with tocopherol or tocopheryl acetate did not significantly alter the susceptibility of their hepatic mitochondria to lipid peroxidation (with lag times and rates similar to those observed for vehicle control, Table 17.3.2). Decreased tissue susceptibility to lipid peroxidation in these studies correlated well with enhanced tocopherol levels in these samples. These results confirm that the assay is a reliable way to assess the total antioxidant status in tissue. It is interesting to note however, that unlike mitochondria, the inner mitochondrial membrane was not completely protected from the susceptibility to lipid peroxidation following tocopheryl succinate administration in vivo (Table 17.3.2), even though these two mitochondrial fractions were enriched with identical levels of tocopherol. These results can be explained by the greater cardiolipin content of inner mitochondrial membrane (as compared with mitochondria) and the well-known enhanced susceptibility of this inner mitochondrial membrane–specific phospholipid to lipid peroxidation (Lesnefsky et al., 2001).

Time Consideration

The total time required for this assay is ~6 hr. Sonication of samples and preparation of lipid peroxidation initiator can be finished within 1 hr.

Literature Cited

Benzie, I.F.F. and Strain, J.J. 1996. The ferric reducing ability of plasma (FRAP) as a measure of "antioxidant power": The FRAP assay. *Anal. Biochem.* 239:70-76.

Cervato, G., Viani, P., Cazzola, R., and Cestaro, B. 1999. A fluorescence method for the determination of plasma susceptibility to lipid peroxidation. *Clin. Biochem.* 32:171-177.

Chevion, S., Roberts, M.A., and Chevion, M. 2000. The use of cyclic voltammetry for the evaluation of antioxidant capacity. *Free Radic. Biol. Med.* 28:860-870.

Fariss, M.W., Merson, M.H., and O'Hara, T.M. 1989. Alpha tocopheryl succinate protects hepatocytes from chemical-induced toxicity under physiological calcium conditions. *Toxicol. Lett.* 47: 61-75.

Fariss, M.W., Nicholls-Grzemski, F.A., Tirmenstein, M.A., and Zhang, J-G. 2001. Enhanced antioxidant and cytoprotective abilities of vitamin E succinate is associated with a rapid uptake advantage in rat hepatocytes and mitochondria. *Free Rad. Biol. Med.* 31:530-541.

Ghiselli, A., Serafini, M., Natella, F., and Scaccini, C. 2000. Total antioxidant capacity as a tool to assess redox status: Critical view and experimental data. *Free Rad. Biol. Med.* 29:1106-1114.

Hovius, R., Lambrechts, H., Nicolay, K., and De Kruijff, B. 1990. Improved methods to isolate and subfractionate rat liver mitochondria. Lipid composition of the inner and outer membrane. *Biochim. Biophys. Acta.* 1021:217-226.

Lesnefsky, E.J., Slabe, T.J., Stoll, M.S.K., Minkler, P.E., and Hoppel, C.L., 2001. Myocardial ischemia selectively depletes cardiolipin in rabbit heart subsarcolemmal mitochondria. *Am. J. Physiol. Heart Circ. Physiol.* 280:H2770-H2778.

Niki, E. and Noguchi, N., 2000. Evaluation of antioxidant capacity. What capacity is being measured by which method? *IUBMB Life* 50:323-329.

Re, R., Pellegrini, N., Proteggente, A, Pannala, A., Yang, M., and Rice-Evans, C. 1999. Antioxidant activity applying an improved ABTS radical cation decolorization assay. *Free Rad. Biol. Med.* 26:1231-1237.

Tirmenstein, M.A., Pierce, C.A., Leraas, T.L., and Fariss, M.W. 1998. A fluorescence plate reader assay for monitoring the susceptibility of biological samples to lipid peroxidation. *Anal. Biochem.* 265:246-252.

Wayner, D.D.M., Burton, G.W., Ingold, K.U., and Locke, S. 1985. Quantitative measurement of the total, peroxyl radical-trapping antioxidant capacity of human blood plasma by controlled peroxidation. *FEBS Lett.* 187:33-37.

Wiswedel, I., Ulbricht, O., and Augustin, W. 1989. Studies of lipid peroxidation in isolated rat heart mitochondria. *Biomed. Biochim. Acta* 48:S73-S76.

Woodford, F.P. and Whitehead, T.P. 1998. Is measuring serum antioxidant capacity clinically useful? *Ann. Clin. Biochem.* 35:48-56.

Yu, T-W. and Ong, C.N. 1999. Lag-time measurement of antioxidant capacity using myoglobin and 2,2′-azino-bis(3-ethylbenzthiazoline-6-sulfonic acid): Rationale, application, and limitation. *Anal. Biochem.* 275:217-223.

Zhang, J.G. and Fariss, M.W. 2002. Thenoyltrifluoroacetone, a potent inhibitor of carboxylesterase activity. *Biochem. Pharmacol.* 63:753-757.

Contributed by Jin-Gang Zhang
BD Biosciences
Woburn, Massachusetts

Marc W. Fariss
University of Colorado Health Sciences Center
Denver, Colorado

In Situ Localization of Nonenzymatic Peroxidase-Like Activity of Tissue-Bound Transition Metals

The protocols described below pertain to detection of tissue iron using the DAB-enhanced Perls method (see Basic Protocol) as well as the general detection of redox-active transition metal ions without the introduction of any metal-containing reagents (see Alternate Protocol). In the latter case, use of the MBTH/*o*-phenylenediamine method in the absence of H_2O_2 pretreatment permits the selective visualization of endogenous enzymatic peroxidase-like activity, whereas use of DAB following the H_2O_2 pretreatment permits the visualization of endogenous nonenzymatic redox-active metals. Whether the staining reflects mainly iron or mainly copper can be ascertained by noting whether it is attenuated more by preincubation with increasing concentrations of the iron-selective chelator deferoxamine or by increasing concentrations of the copper-selective chelator diethylenetriaminepentaacetic acid (DTPA), as described in the Support Protocol. These methods do not permit one to distinguish other redox-active metals such as chromium, and possibly manganese, whose contributions cannot be excluded. Noting an inhibitory effect of prior incubation with chelating agents is further evidence that the DAB staining reflects adventitiously bound redox-active metals rather than enzymatic activity, because the latter is refractory to chelators.

A key advance represented by the protocols provided below is an enhanced sensitivity arising from the recognition that standard formalin fixation detracts from detection of metal-based redox activity, which is not the case with the fixative used in the protocols below (methacarn; 60:30:10 methanol/chloroform/acetic acid; see Reagents and Solutions), as verified by limited studies using nonfixed tissue.

DETECTION OF IRON

BASIC PROTOCOL

Iron can be detected in freshly isolated, paraffin-embedded tissue sections fixed in the absence of formalin, using potassium ferrocyanide and 3,3′-diaminobenzidine tetrahydrochloride (DAB).

Materials

Fresh tissue of interest
Fixative solution (see recipe)
30%, 50%, 70%, 80%, 95%, and 100% (v/v) ethanol
Xylene
Paraffin
50 mM Tris·Cl, pH 7.6 (*APPENDIX 2A*)
7% (w/v) potassium ferrocyanide solution (see recipe), freshly prepared
DAB/H_2O_2 solution (for Basic Protocol; see recipe), freshly prepared
Permount mounting medium (e.g., Fisher)

Tissue-embedding cassettes (Omnisette; Fisher)
Paraffin-embedding system or machine (e.g., TBS ATPI Automated Tissue Processor; Fisher)
Microtome
Superfrost Plus microscope slides (Fisher)
Coplin jars

Contributed by Lawrence M. Sayre, Peggy L.R. Harris, George Perry, and Mark A. Smith
Current Protocols in Toxicology (2004) 17.4.1-17.4.8

Humified chamber (storage container with sealable lid, lined with moistened paper towels and containing elevated surface on which to place slides) or container designed for immunohistochemical incubations
3-cc BD disposable syringes (Fisher)
0.22-μm Millex-GS syringe filters (Millipore)
Coverslips

Prepare tissue

1. Dissect the tissue sample.
2. Place an ~0.5-cm^3 sample of tissue in a tissue-embedding cassette and immerse in 50 ml of fixative solution. Incubate overnight at 4°C
3. Remove sample from fixative and place in 50% ethanol.
4. Using a histology paraffin-embedding system/machine, dehydrate sample through an ascending ethanol series and carry out paraffin embedding as follows:

   70% ethanol for 40 min at 40°C
   80% ethanol for 40 min at 40°C
   95% ethanol for 40 min at 40°C
   100% ethanol for 40 min at 40°C
   100% ethanol for 40 min at 40°C
   100% ethanol for 1 hr 10 min at 40°C
   xylene for 40 min at 40°C
   xylene for 40 min at 40°C
   paraffin for 40 min at 60°C
   paraffin for 1 hr at 60°C
   paraffin for 40 min at 60°C.

   Follow the manufacturer's suggested operating guidelines, but run the machine without formalin, thus avoiding the standard formalin fixative step at the beginning.
5. Once a paraffin block is obtained, cut 6-μm sections using a microtome and place the sections on Superfrost Plus microscope slides. Dry sections on the slide overnight at 37°C
6. Rehydrate sections by immersing in the following solutions in Coplin jars at room temperature for the indicated lengths of time.

   xylene for 10 min
   xylene (fresh) for 10 min
   100% ethanol for 10 min
   95% ethanol for 10 min
   70% ethanol for 10 min
   50% ethanol for 10 min
   30% ethanol for 10 min
   50 mM Tris·Cl, pH 7.6, for 10 min
   50 mM Tris·Cl, pH 7.6 (fresh) for 10 min.

Stain for iron

7. Apply enough freshly made 7% potassium ferrocyanide solution to cover the section. Place slide in humidified chamber and incubate 1.5 to 2 hr at 37°C or overnight at 4°C.
8. Rinse slide in 50 mM Tris·Cl, pH 7.6, for 10 min.

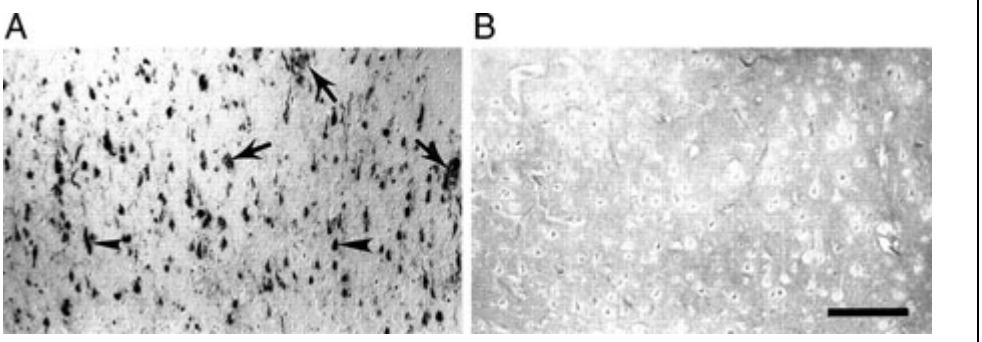

Figure 17.4.1 Histochemical detection of iron in Alzheimer's disease (**A**) compared with control case (**B**) shows striking association of iron with neurofibrillary tangles (arrowheads) and senile plaques (arrows) characteristic of the Alzheimer's disease brain. Scale bar = 200 μm.

9. Develop signal by covering the section with freshly prepared DAB/H_2O_2 solution (using a 3-cc syringe and 0.22-μm syringe filter to filter the DAB/H_2O_2) and leaving the solution on the section for 5 min.
10. Dehydrate sections by immersing in the following solutions (ascending ethanol series) in Coplin jars at room temperature for the indicated lengths of time:

    30% ethanol for 10 min
    50% ethanol for 10 min
    70% ethanol for 10 min
    95% ethanol for 10 min
    100% ethanol for 10 min
    xylene for 10 min.

11. Apply coverslip to slide using Permount.

    A dark brown precipitate, easily visualized by light microscopy, will form at sites containing iron (Fig. 17.4.1). Time consideration—approximately 4.5 to 18 hr.

DETECTION OF REDOX-ACTIVE TRANSITION METALS

ALTERNATE PROTOCOL

Redox activity, a key feature of non-sequestered transition metals (e.g., iron, copper) provides a key enhancement to metal localization studies.

Additional Materials *(also see Basic Protocol)*

Peroxide/methanol: add 4 ml of 30% hydrogen peroxide to 36 ml of 100% methanol; prepare fresh daily
DAB/H_2O_2 solution (for Alternate Protocol; see recipe), freshly prepared
MBTH/*o*-phenylenediamine/H_2O_2 solution (see recipe), freshly prepared

1. Dissect, fix, dehydrate, embed, and section sample; place sections on slides and dry overnight (see Basic Protocol, step 1 to 5).
2. Rehydrate sections (and optionally inactivate endogenous peroxidases) by immersing in the following solutions in Coplin jars at room temperature for the indicated lengths of time:

    xylene for 10 min
    xylene (fresh) for 10 min
    100% ethanol for 10 min

95% ethanol for 10 min
peroxide/methanol for 30 min (optional; to inactivate endogenous peroxidase activity)
70% ethanol for 10 min
50% ethanol for 10 min
30% ethanol for 10 min
50 mM Tris·Cl, pH 7.6, for 10 min
50 mM Tris·Cl, pH 7.6, for 10 min.

3. *Optional:* Perform chelation to titrate away endogenous metals to determine the source of activity (i.e., metal) and to verify the specificity of the finding (see Support Protocol).
4. Using a 3-cc syringe and 0.22-μm syringe, apply enough freshly made DAB/H_2O_2 solution to cover the section.
5. To an adjacent section on the same slide or a section on a second slide, using a 3-cc syringe and 0.22-μm syringe filter to filter the MBTH/*o*-phenylenediamine solution, apply MBTH/*o*-phenylenediamine solution for comparison purposes.
6. Place slides in a humidified chamber and incubate 1.5 to 2 hr at room temperature.
7. Rinse slides in 50 mM Tris·Cl, pH 7.6, for 10 min.
8. Dehydrate sections by immersing in the following solutions (ascending ethanol series) in Coplin jars at room temperature for the indicated lengths of time:

   30% ethanol for 10 min
   50% ethanol for 10 min
   70% ethanol for 10 min
   95% ethanol for 10 min
   100% ethanol for 10 min
   xylene for 10 min.

9. Apply coverslip to slide using Permount.

   A dark brown precipitate will form at sites containing redox activity.

SUPPORT PROTOCOL

CHELATION OF METALS FOR CONTROLS

After the tissue sections have been hydrated, a chelation step may be performed to selectively remove individual endogenous metals. A serial dilution of DEF (which selectively removes iron) and DTPA (which selectively removes copper) can be used, starting with a 0.1 M concentration and doing successive 1:10 dilutions with water (0.01 M and 0.001 M). Although higher concentrations of either chelator will remove all metals, a determination of the relative effectiveness of the chelators at lower concentration may permit an assessment of which metal ions are most responsible for the redox activity.

Additional Materials *(also see Basic Protocol and Alternate Protocol)*

0.1 M DEF stock: Weigh 65.68 mg deferoxamine (DEF; Sigma) and add 1 ml H_2O
0.1 M DTPA stock: Weigh 39.33 mg diethylenetriaminepentaacetic acid (DTPA; Sigma) and add 1 ml H_2O

1. After performing the rehydration series in step 2 of the Alternate Protocol, remove the slides from the Tris·Cl buffer, and apply either DEF or DTPA to appropriate sections at the desired concentration (e.g., serial dilutions of 0.1, 0.01, and 0.001 M).

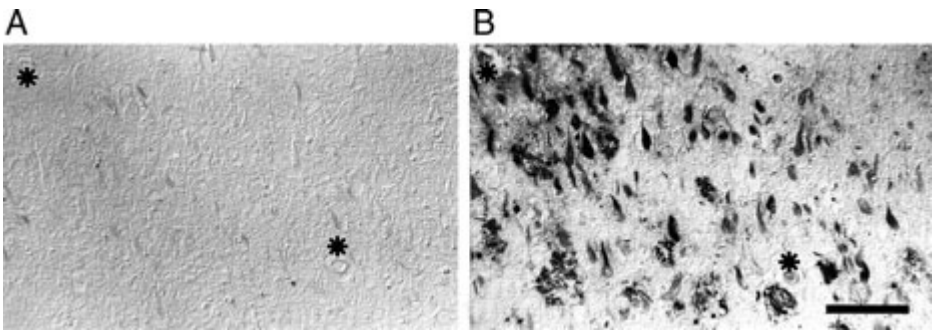

Figure 17.4.2 Lesion-associated iron (see Fig. 17.4.1) could be completely stripped with deferoxamine (**A**) but readily rebound to the same sites following incubation with iron(III) citrate and iron(II) chloride (**B**). Asterisks indicate landmark blood vessels in adjacent sections. Scale bar = 100 μm.

2. Incubate overnight at room temperature in humidified chamber.
3. Rinse extensively with 50 mM Tris·Cl, pH 7.6, prior to continuing the detection procedure (see Alternate Protocol, step 4).

Typical results are shown in Figure 17.4.2.

REAGENTS AND SOLUTIONS

Use Milli-Q-purified water or equivalent for the preparation of all solutions and in all protocol steps. For common stock solutions, see ***APPENDIX 2A****; for suppliers, see* ***SUPPLIERS APPENDIX****.*

DAB/H_2O_2 solution (for Alternate Protocol)

Weigh 5 mg of 3,3′-diaminobenzidine tetrahydrochloride (DAB). Add 6 ml 50 mM Tris·Cl, pH 7.6 (*APPENDIX 2A*), and 672 μl of 30% hydrogen peroxide, then mix. Prepare immediately before use.

Final concentrations: 0.75 mg/ml DAB/3% H_2O_2.

DAB/H_2O_2 solution (for Basic Protocol)

Weigh 5 mg of 3,3′-diaminobenzidine tetrahydrochloride (DAB). Add 6.67 ml 50 mM Tris·Cl, pH 7.6 (*APPENDIX 2A*), and 3.36 μl of 30% hydrogen peroxide, then mix. Prepare immediately before use.

Final concentrations: 0.75 mg/ml DAB/0.015% H_2O_2.

Fixative solution

Mix 300 ml methanol, 150 ml chloroform, and 50 ml glacial acetic acid to give a final volume of 500 ml. Store in a glass bottle at 4°C until needed.

Final concentrations: 60:30:10 (v/v/v) methanol/chloroform/acetic acid.

MBTH/o-phenylenediamine/H_2O_2 solution

Stock solutions:

3 *mg/ml MBTH:* Weigh 3 mg of 3-methyl-2-benzothiazolinone hydrazone (MBTH; Sigma) and add 1 ml of 50 mM Tris·Cl, pH 7.6 (*APPENDIX 2A*).

2 *mg/ml o-phenylenediamine:* Weigh 2 mg of *o*-phenylenediamine and add 1 ml of 50 mM Tris·Cl, pH 7.6 (*APPENDIX 2A*).

continued

Working solution:
Mix the following immediately before use:
125 µl of 3 mg/ml MBTH
125 µl of 2 mg/ml *o*-phenylenediamine
50 µl of 30% hydrogen peroxide
200 µl of 50 mM Tris·Cl, pH 7.6 (*APPENDIX 2A*)

Potassium ferrocyanide solution, 7%

Weigh 0.7 g $K_4Fe(CN)_6 \cdot 3H_2O$ into a graduated cylinder. Add 5 ml water and 300 µl concentrated hydrochloric acid. Mix, then bring to a final volume of 10 ml. Prepare immediately before use.

COMMENTARY

Background Information

Many disease states are associated with tissue accumulation of metals. This accumulation can reflect unusually high tissue levels of metal-storage proteins such as ferritin (iron) and ceruloplasmin (copper), or metal transporters such as transferrin (iron) and the copper-transporting ATPase implicated in Wilson's disease. When such proteins become saturated, free metal ions are released into plasma and, at least in the case of iron, may result in deposition of simple inorganic forms of the metal, such as Fe_2O_3. A number of techniques have been used for quantitation of tissue metals, including atomic absorption spectroscopy, magnetic resonance imaging, X-ray microanalysis, and laser microprobe mass analysis (LAMMA). For semiquantitative determination of tissue metals, however, various histochemical methods have always seen greater use on account of their convenience (Bancroft and Stevens, 1982; Pearse, 1985). Specificity of the latter methods for individual metals relies on the use of metal ion-specific chelating agents and often requires prior release of metals from their protein-binding sites by treatment with trichloroacetic acid or HCl.

The most popular method for histochemical detection of iron has been Perls' method (Perls, 1867; Thompson, 1966), which relies on the formation of the deep blue mixed-valent ($Fe^{2+}Fe^{3+}$) cyano complex known as Prussian blue. Usually, this technique localizes ferric iron that can be mobilized by treatment with ferrocyanide, though reaction of ferricyanide with Fe^{2+} gives the same complex (Parmley et al., 1978). A later development of this method was to take advantage of the fact that Prussian blue is especially active in catalyzing the H_2O_2-dependent oxidation of 3,3′-diaminobenzidine (DAB), the latter serving as the most commonly used chromogenic substrate for peroxidase. This so-called enhanced Perls' method (Nyguyen-Legros et al., 1980) has been widely applied to the histochemical localization of total iron (ferritin, transferrin, and free iron) in brain and other tissues as a function of aging and disease (Conner et al., 1990). The advantage of using DAB is that its oxidation yields an insoluble brown polymer deposited at the sites of enzyme localization and readily detected by microscopy.

Nonetheless, with application of H_2O_2 and DAB becoming the most generally used chromogenic method for immunohistochemical studies that involve the (horseradish) peroxidase-antiperoxidase (PAP) method or direct use of horseradish peroxidase–linked secondary antibodies, it has been important to eliminate any endogenous peroxidase activity in the tissue by prior treatment with H_2O_2 at a concentration (usually one part 3% H_2O_2 diluted with four parts methanol) that inactivates such enzymatic activity (Sternberger, 1986). Without the H_2O_2 pretreatment, any endogenous peroxidase-like activity would interfere. Indeed, the H_2O_2-dependent oxidation of peroxidase substrates such as DAB or 3,3′,5,5′-tetramethylbenzidine (TMB) has been directly used to localize endogenous peroxidase activity in neural tissue (Svensson et al., 1984). The key point here is that such activity can represent either authentic enzymatic (peroxidase or catalase) activity or nonenzymatic "pseudo"-peroxidase activity of adventitiously bound redox-active transition metal ions. A distinction between the two can be ascertained only by studies that probe the conditions under which the peroxidase-like activity persists. Thus, when the activity shows a pH dependence reminiscent of a particular heme enzyme, can be blocked by prior treatment with sodium azide (Schaermeyer, 1992) or 3-amino-1,2,4-triazole, or can be eliminated

by heating, such as occurs in the case of staining of peroxisomes (Schipper et al., 1990a), the interpretation has been in terms of endogenous enzyme activity. On the other hand, when staining is independent of pH, heat, or the presence of inhibitors (Schipper et al., 1990b), as has been found for astrocyte mitochondria in the aging brain (Schipper et al., 1998), the interpretation has been in terms of nonenzymatic redox activity. In the latter regard, concomitant use of X-ray microanalysis has provided evidence for localization of both iron (presumed to be nonenzymatic heme iron on the basis of lack of reaction with Prussian blue; Schipper et al., 1990a) and copper (Brawer et al., 1994).

The authors' studies revealed the presence of H_2O_2-dependent DAB oxidizing activity in the neurofibrillary pathology of Alzheimer disease (Sayre et al., 2000). Since this activity was not attenuated by prior exposure of the tissue sections to peroxidase-inactivating levels of H_2O_2, the interpretation was in terms of nonenzymatic redox-active transition metals. Nonetheless, to demonstrate that the level of H_2O_2 being used was sufficient to inactivate endogenous enzymatic peroxidase activity, a method was needed for detecting the latter which was independent of the use of DAB. A range of studies on the effect of added iron- and copper-selective chelating agents on the intrinsic ability of these metals to mediate H_2O_2-dependent DAB oxidation suggested, at least in the case of copper, that a key facet of this reaction was the ability of DAB to enter into bidendate coordination with Cu^{2+}. Thus, the authors found that simple transition metal complexes were incapable of mediating the H_2O_2-dependent oxidation of noncoordinating peroxidase substrates such as TMB. This would suggest that TMB is an ideal reagent for selective detection of enzymatic peroxidase activity in the face of redox-active free metal ions that are detected by DAB (Trojanowski et al., 1983). Indeed, the discrepancy between DAB staining and TMB staining observed by others (Svensson et al., 1984) most likely reflects the redox activity of nonenzymatic transition metals. The authors, however, were unable to observe a reproducible tissue staining using TMB. On the other hand, they found that a 1:1 mixture of 3-methyl-2-benzothiazolinone hydrazone (MBTH) and *o*-phenylenediamine, which, like TMB, gave a negative result with H_2O_2 in the presence of simple transition metal complexes, permitted the observation of endogenous enzymatic peroxidase activity. The reaction in this case involved an oxidative coupling (Ngo and Lenhoff, 1980) to generate an insoluble material similar to that seen using DAB. Staining using the MBTH/*o*-phenylenediamine reagent, albeit weak, was eliminated by the H_2O_2 pretreatment, unlike the DAB staining, confirming that the latter reflected nonenzymatic redox activity (Sayre et al., 2000).

Critical Parameters and Troubleshooting

The most important factor to ensure success is the fixative. The tissue should not be exposed to any aldehyde-containing fixative, e.g., formalin or formaldehyde. If this does occur, the methods will only show a limited stain or not work at all. Also, the potassium ferrocyanide, MBTH, and DTPA solutions should be made just prior to use so that they do not become oxidized and lose any of their strength. In any event, if the staining of the sample is weak, a longer incubation with the solutions may be needed. It is possible to incubate the samples overnight in the working solutions at 4°C to increase the stain intensity, or even at room temperature overnight, although this may increase the background of the stain. Occasionally, a precipitate forms when the DAB is applied to the samples. Once on the sections, it is difficult to remove; however, a more thorough filtering of freshly made DAB solution should correct this for future stains.

Anticipated Results

A brown precipitate, easily visualized by light microscopic techniques, will form at the sites containing iron (see Basic Protocol) or redox activity (see Alternate Protocol). Representative results are shown in Figures 17.4.1 and 17.4.2.

Time Considerations

After the tissue samples have been embedded in paraffin and sections cut (which will take 1 day), the procedure should take ~5 hr (or 48 hr if an overnight incubation is required).

Literature Cited

Bancroft, J.D. and Stevens, A. (eds.) 1982. Theory and Practice of Histological Techniques, 2nd ed. Churchill Livingstone, New York.

Brawer, J.R., Stein, R., Small, L., Cisse, S., and Schipper, H.M. 1994. Composition of Gomori-positive inclusions in astrocytes of the hypothalamic arcuate nucleus. *Anat. Record* 240:407-415.

Connor, J.R., Menzies, S.M., St. Martin, S.M., and Mufson, E.J. 1990. Cellular distribution of transferrin, ferritin, and iron in normal and aged human brains. *J. Neurosci. Res.* 27:595-611.

Ngo, T.T. and Lenhoff, H.M. 1980. A sensitive and versatile chromogenic assay for peroxidase and peroxidase-coupled reactions. *Anal. Biochem.* 105:389-397.

Nguyen-Legros, J., Bizot, J., Bolesse, M., and Pulicani, J.-P. 1980. Noir de diaminobenzidine: Une nouvelle methode histochimique de revelation du fer exogene. *Histochem.* 66:239-244.

Parmley, R.T., Spicer, S.S., and Alvarez, C.J. 1978. Ultrastructural localization of nonheme cellular iron with ferrocyanide. *J. Histochem. Cytochem.* 26:729-741.

Pearse, A.G.E. 1985. Histochemistry. Theoretical and Applied. Vol. 2. Analytical Technology, 4th ed., Churchill Livingstone, New York.

Perls, M. 1867. Nachweis von Eisenoxyd in gewissen Pigmenten. *Virchows Arch. Pathol. Anat.* 39:42-48.

Sayre, L.M., Perry, G., Harris, P.L.R., Liu, Y., Schubert, K., and Smith, M.A. 2000. In situ oxidative catalysis by neurofibrillary tangles and plaques in Alzheimer's disease: A central role for bound transition metals. *J. Neurochem.* 74:270-279.

Schaermeyer, U. 1992. Localization of peroxidase activity in the retina and the retinal pigment epithelium of the Syrian golden hamster (Mesocricetus auratus). *Comp. Biochem. Physiol.* 103:139-145.

Schipper, H.M., Scarborough, D.E., Lechan, R.M., and Reichlin, S., 1990a. Gomori-positive astrocytes in primary culture: Effects of in vitro age and cysteamine exposure. *Dev. Brain Res.* 54:71-79.

Schipper, H.M., Lechan, R.M., and Reichlin, S. 1990b. Glial peroxidase activity in the hypothalamic arcuate nucleus: Effects of estradiol valerate-induced persistent estrus. *Brain Res.* 507:200-207.

Schipper, H.M., Vininsky, R., Brull, R., Small, L., and Brawer, J.R. 1998. Astrocyte mitochondria: A substrate for iron deposition in the aging rat substantia nigra. *Exp. Neurol.* 152:188-196.

Sternberger, L.A. 1986. Immunocytochemistry, 3rd ed. John Wiley & Sons, New York.

Svensson, B.A., Rastad, J., and Westman, J. 1984. Endogenous peroxidase-like activity in the feline dorsal column nuclei and spinal cord. *Exp. Brain Res.* 55:325-332

Thompson, S.W. 1966. Histochemical and Histopathological Methods, pp. 592-594. Charles C. Thomas, Springfield, Ill.

Trojanowski, J.Q., Obrocka, M.A., and Lee, V.M.-Y. 1983. A comparison of eight different chromogen protocols for the demonstration of immunoreactive neurofilaments or glial filaments in rat cerebellum using the peroxidase-antiperoxidase method and monoclonal antibodies. *J. Histochem. Cytochem.* 31:1217-1223.

Contributed by Lawrence M. Sayre, Peggy L.R. Harris, George Perry, and Mark A. Smith
Case Western Reserve University
Cleveland, Ohio

F_2-Isoprostanes as Markers of Oxidant Stress: An Overview

Lipid peroxidation, the oxidation of cellular lipids, is a central feature of oxidant stress, a phenomenon that has been increasingly implicated as causative in numerous pathological conditions. Lipid peroxidation products are frequently used to quantify oxidative injury, and can be assessed by a number of methods that include the measurement of either primary or secondary peroxidation end products. The development of specific, reliable, and non-invasive methods for measuring oxidative stress in humans is of fundamental importance for establishing the role of free radicals in human diseases. Primary end products of lipid peroxidation include conjugated dienes and lipid hydroperoxides, while secondary end products include thiobarbituric reactive substances (TBARS), gaseous alkanes, and a group of prostaglandin (PG) F_2-like products termed F_2-isoprostanes (F_2-IsoPs; Halliwell and Grootveld, 1987; Morrow et al., 1990a). Quantification of these various compounds has proven highly useful for the study of free radical–mediated lipid peroxidation in in vitro model systems. However, the F_2-IsoPs appear to be a significantly more accurate marker of oxidative stress in vivo in humans and animals than other compounds (Liu et al., 1999; Morrow and Roberts, 1999; Fam and Morrow, 2003). The biochemistry of F_2-IsoPs, as well as considerations regarding their utility as markers of oxidative stress will be discussed herein.

MECHANISM OF FORMATION OF ISOPROSTANES

IsoPs are PG-like compounds formed from the peroxidation of arachidonic acid, a ubiquitous polyunsaturated fatty acid (Morrow et al., 1990a; Morrow and Roberts, 1999). Unlike PGs, which are formed via the action of the cyclooxygenase enzymes, F_2-IsoPs are formed non-enzymatically as a result of the free radical–mediated peroxidation of arachidonic acid. Figure 17.5.1 outlines the mechanism by which IsoPs are generated. Following abstraction of a bis-allylic hydrogen atom and the addition of a molecule of oxygen to arachidonic acid to form a peroxyl radical, endocyclization occurs and an additional molecule of oxygen is added to form PGG_2-like compounds. These unstable bicycloendoperoxide intermediates are then reduced to the F_2-IsoPs. Based on this mechanism of formation, four F_2-IsoP regioisomers are generated (see Fig. 17.5.1; Morrow et al., 1990a,b; Morrow and Roberts, 1999). Compounds are denoted as 5-, 12-, 8-, or 15-series regioisomers depending on the carbon atom to which the side chain hydroxyl is attached; the authors have proposed a nomenclature system based on this feature (Taber et al., 1997). An alternative system for the IsoPs has been proposed by FitzGerald and colleagues in which the abbreviation iP is used for isoprostane, and regioisomers are denoted as III to VI based upon their structure (Rokach et al., 1997). IsoPs that contain F-type prostane rings are isomeric to $PGF_{2\alpha}$ and are thus referred to as F_2-IsoPs. It should be noted that IsoPs containing alternative ring structures (such as those resembling PGD_2/E_2 and PGA_2/J_2) can also be formed by this mechanism (Chen et al., 1999; Reich et al., 2001a). F_2-IsoPs, however, have been the most studied class of IsoPs and, because of their stability, afford the most accurate measure of oxidative stress (Liu et al., 1999).

An important structural distinction between IsoPs and cyclooxygenase-derived PGs is that the former contain side chains that are predominantly oriented *cis* to the prostane ring while the latter possess exclusively *trans* side chains (Morrow et al., 1990a,b). A second important difference between IsoPs and PGs is that IsoPs are formed in situ esterified to phospholipids and are subsequently released by a phospholipase(s) (Liu et al., 1999; Morrow and Roberts, 1999), while PGs are generated only from free arachidonic acid.

QUANTIFICATION OF F_2-ISOPROSTANES

Over the past 12 years, several methods have been developed to quantify the F_2-IsoPs. The authors' laboratory uses a gas chromatographic/negative ion chemical ionization mass spectrometric (GC/NICI MS) approach employing stable isotope dilution (Morrow and Roberts, 1999). For quantification purposes, the F_2-IsoP, 15-F_{2t}-IsoP, and other F_2-IsoPs that co-elute with this compound are measured. Other investigators quantify different F_2-IsoP isomers, as discussed subsequently

Contributed by Erik S. Musiek and Jason D. Morrow
Current Protocols in Toxicology (2005) 17.5.1-17.5.10

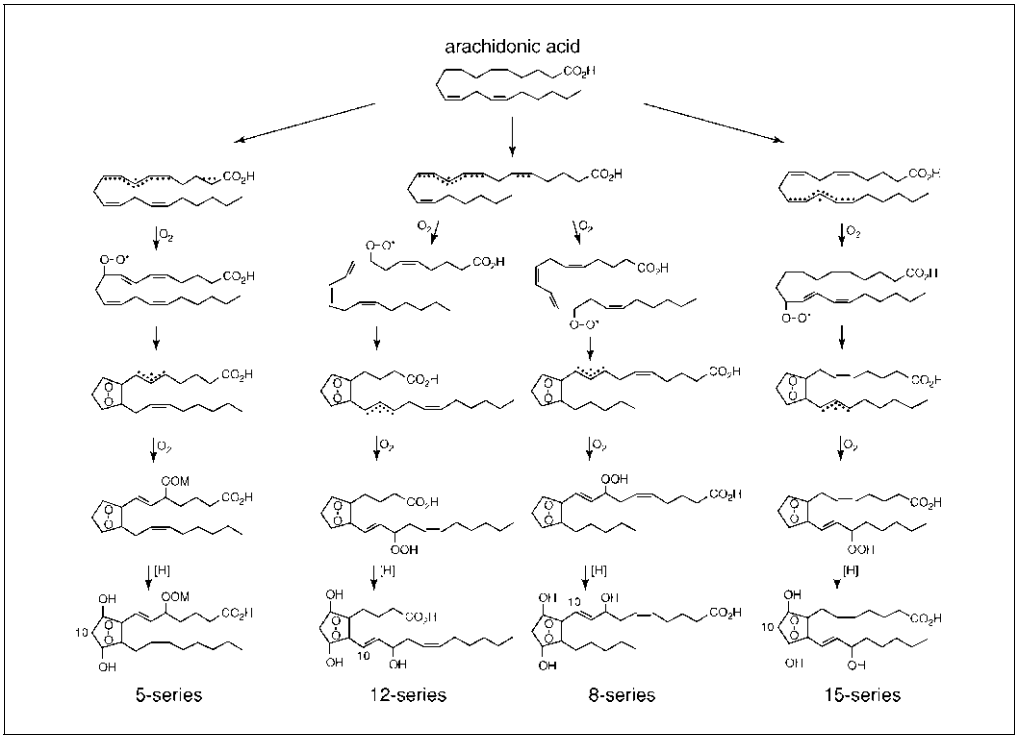

Figure 17.5.1 Mechanism of formation of the F_2-isoprostanes. Four regioisomers are formed, each consisting of eight racemic diastereomers. Stereochemistry is not indicated.

(Rokach et al., 1997). Several internal standards are available from commercial sources to quantify the IsoPs. These include [$^2H_4$]15-F_{2t}-IsoP ([$^2H_4$] 8-iso-$PGF_{2\alpha}$) and [$^2H_4$]-$PGF_{2\alpha}$. The advantages of mass spectrometry over other approaches include its high sensitivity and specificity, which yield quantitative results in the low picogram range. Its drawbacks are that it is labor intensive and requires considerable expenditures on equipment.

Several alternative mass spectrometric assays have been developed by different investigators including FitzGerald and colleagues (Rokach et al., 1997; Pratico et al. 1998a). As with the authors' assay, these methods require solid-phase extraction with a C18 column, TLC purification, and chemical derivatization. Furthermore, IsoPs are quantified using isotope dilution NICI GC/MS but the assay measures F_2-IsoP isomers other than 15-F_2-IsoP. These methods appear to be comparable to the authors' in terms of utility. In addition, a number of liquid chromatographic MS methods for F_2-IsoPs have been recently developed; these require less sample preparation (Liang et al., 2000; Bohnstedt et al., 2003), but the sensitivity and reliability of these for the analysis of IsoPs in complex biological samples is unknown.

Alternative methods have been developed to quantify IsoPs with immunological approaches (Morrow et al., 1999a). Antibodies have been generated against 15-F_{2t}-IsoP and at least three immunoassay kits are commercially available. A potential drawback of these methods is that limited information is currently available regarding their precision and accuracy. In addition, little data exist comparing IsoP levels determined by immunoassay to those determined by mass spectrometry. Analogous to immunological methods to quantify cyclooxygenase-derived PGs, it might be predicted that immunoassays for IsoPs will suffer from a lack of specificity (Roberts and Morrow, 2000). Furthermore, the sensitivity and/or specificity of these kits may vary substantially between manufacturers. However, while mass spectrometric methods of IsoP quantification are considered the "gold standard," immunoassays have expanded research in this area because of their low cost and relative ease of use.

F_2-ISOPROSTANES AS AN INDEX OF OXIDANT STRESS

Measurement of F_2-IsoPs In Vitro

To demonstrate the utility of quantifying F_2-IsoPs as an index of oxidant stress, it is necessary to compare the formation of these compounds with other known indices of oxidant stress using established in vitro models of oxidant stress. The formation of F_2-IsoPs has been compared to malondialdehyde (MDA), one of the most commonly used measures of lipid peroxidation that utilizes Fe/ADP/ascorbate-induced peroxidation of rat liver microsomes (Longmire et al., 1994). Both F_2-IsoP and MDA (measured as thiobarbituric acid reacting substances) formation increased in parallel in a time-dependent manner and correlated with the loss of arachidonic acid and with increasing oxygen concentrations up to 21%. Although the formation of F_2-IsoPs correlated with other measures of lipid peroxidation in this in vitro model, the authors have reported that quantification of F_2-IsoPs is far superior to measurements of MDA as an index of lipid peroxidation in vivo (Longmire et al., 1994).

It is hypothesized that the oxidation of low density lipoprotein (LDL) in vivo converts it to an atherogenic form, which is taken up by macrophages in the vessel wall. Subsequent activation of these cells likely plays an important role in the development and progression of atherosclerotic lesions in humans (Steinberg et al., 1989). Thus, the authors have performed studies examining the formation of F_2-IsoPs in LDL that is oxidized to determine whether measurement of F_2-IsoPs esterified to lipoproteins may provide an approach to assess lipoprotein oxidation in vivo (Lynch et al., 1994). In these studies, either plasma lipids or purified LDL from humans was peroxidized with Cu^{2+} or the water-soluble oxidizing agent 2,2-azo-bis(2-amidinopropane) (AAPH; Lynch et al., 1994), and the formation of F_2-IsoPs was compared to other markers of lipid peroxidation including formation of cholesterol ester hydroperoxides, phospholipid hydroperoxides, loss of antioxidants, and changes in the electrophoretic mobility of LDL. In plasma oxidized with AAPH, increases in the formation of F_2-IsoP paralleled increases in lipid hydroperoxide formation and occurred only after depletion of the antioxidants ascorbate and ubiquinol-10. In purified LDL that was oxidized, formation of F_2-IsoPs again correlated with increases in lipid hydroperoxides and increases in the electrophoretic mobility of LDL and occurred only after depletion of the antioxidants α-tocopherol and ubiquinol-10. Similar findings have been reported by others (Gopaul et al., 1994; Pratico and FitzGerald, 1996).

Taken together, these in vitro studies suggest that quantification of F_2-IsoP correlates with other established indices of oxidative stress, and serves as a useful marker of lipid peroxidation.

Measurement of F_2-IsoPs In Vivo

It has been previously recognized that one of the greatest needs in the field of free radical research is a reliable non-invasive method to assess lipid peroxidation in vivo in humans (Roberts and Morrow, 2000). In this respect, most methods available to assess oxidant stress, which are adequate for in vitro purposes, have suffered from a lack of sensitivity and/or specificity or are unreliable when applied to complex biological fluids and tissues. However, a substantial body of evidence indicates that measurement of F_2-IsoPs in body fluids such as plasma provides a reliable approach to assess lipid peroxidation in vivo and represents a major advance in the ability to assess oxidative stress status in animals and humans (Morrow and Roberts, 1997; Roberts and Morrow, 2000). Normal levels of F_2-IsoPs have been defined in human biological fluids such as plasma and urine. (Liu et al., 1999; Morrow et al., 1999a; Morrow and Roberts, 1999). It is important to note that quantities of these compounds exceed those of cyclooxygenase-derived PGs by at least an order of magnitude, suggesting that IsoPs are a major pathway of arachidonic acid disposition. Further, levels of F_2-IsoPs are sufficient to be detected in every normal biological fluid that has been assayed including plasma, urine, bronchoalveolar lavage fluid, cerebrospinal fluid, and bile (Morrow et al., 1999a).

The finding of significant levels of F_2-IsoPs in normal animal and human biological fluids and tissues indicates there is ongoing lipid peroxidation that is incompletely suppressed by antioxidant defenses, even in normal humans and animals, lending support to the hypothesis that the normal aging process is due to enhanced oxidant damage of relevant biological molecules over time. In this regard, previous studies have suggested that IsoP levels in normal mice and humans increase with age (Rokach et al. 1997; Roberts and Reckelhoff, 2001), although another report refutes this (Feillet-Coudray et al., 1999).

An attractive possibility suggested by these findings is the measurement of F_2-IsoPs in urine as an index of systemic or whole body oxidant stress integrated over time. However, the measurement of free F_2-IsoPs in urine can be confounded by the potential contribution of local IsoP production in the kidney, although the extent to which this occurs is unclear (Morrow and Roberts, 1997; Morrow et al., 1999a; Roberts and Morrow, 2000). In light of this issue, the primary urinary metabolite of 15-F_{2t}-IsoP has previously been identified to be 2,3-dinor-5,6-dihydro-15-F_{2t}-IsoP, and a highly sensitive and accurate mass spectrometric assay to quantify this molecule has been developed (Roberts et al. 1996; Morrow et al., 1999b; Morales et al., 2001). Thus, the quantification of 2,3-dinor-5,6-dihydro-15-F_{2t}-IsoP may represent a truly non-invasive, time-integrated measurement of systemic oxidation status that can be applied to living subjects.

Formation of Isoprostanes in Animal Models of Oxidant Stress

F_2-IsoPs have also proven highly valuable in studying oxidative injury in vivo in many animal models of disease. Administration of carbon tetrachloride ($CC1_4$) intragastrically to rats is a well-established model of oxidative injury, causing severe free radical–induced damage to the liver and other organs. Esterified levels of F_2-IsoPs in liver tissue increase by 200-fold within 1 hr of CCl_4 treatment and subsequently decline over 24 hr (Morrow et al., 1992), while plasma free and lipid-esterified IsoP concentrations increased after liver levels up to 50-fold in a dose-dependent manner. Administration of the antioxidant lazaroid U78517 to CCl_4-treated animals significantly blunted the enhanced formation of F_2-IsoPs in this model (Morrow and Roberts, 1997).

As a second example, F_2-IsoP formation has been employed to study the toxicity of diquat, a dipyridyl herbicide. Diaquat undergoes redox cycling in vivo, generating large amounts of the superoxide anion and causing hepatic and renal injury in rats. This effect is markedly augmented in animals deficient in selenium (Se), a trace element that is required for the enzymatic activities of glutathione peroxidase and other antioxidant proteins. To study whether lipid peroxidation occurs in this model, levels of F_2-IsoPs were quantified in plasma and tissues from Se-deficient rats following diquat administration. Se-deficient rats administered diquat showed 10- to 200-fold increases in plasma F_2-IsoPs, with the primary sites of IsoP generation being the kidney and liver (Awad et al., 1994). Further studies disclosed that the extent of tissue injury and IsoP formation directly correlated with the degree of Se depletion (Burk et al., 1995).

The measurement of F_2-IsoPs can also be employed to examine the oxidation status of transgenic animals. For instance, Pratico et al. (1998b) demonstrated that apolipoprotein E–deficient mice, which developed severe atherosclerotic disease, also showed marked increases in plasma F_2-IsoP levels. Dietary supplementation with the antioxidant α-tocopherol prevented the increase in plasma F_2-IsoP levels, and reduced atherosclerosis in these animals. Increases in F_2-IsoPs have been observed in animal models of disease in nearly every organ. Using the brain as an example, increased F_2-IsoP levels have been described in mice subjected to a vast array of neurological insults, including amyloid precursor protein overexpression (Pratico et al. 2001), intracerebroventricular lipopolysacharide injection (Montine et al., 2002a), kainate-induce seizures (Patel et al., 2001; Montine et al., 2002a), and cerebral ischemic injury (Marin et al., 2000). Taken together, these studies suggest that quantification of F_2-IsoPs in animal models of oxidant injury represents an accurate method to assess lipid peroxidation in vivo.

F_2-ISOPROSTANE FORMATION IN HUMAN DISEASES

From the above examples, measurement of IsoPs appears to be a reliable index of lipid peroxidation in vivo and thus potentially provides a tool to assess the role of oxidative stress in the pathophysiology of human disease. Elevations of IsoPs in human body fluids and tissues have been found in a diverse array of human disorders (Table 17.5.1). For purposes of this brief review, the authors have chosen to discuss IsoP formation in several human diseases in which their generation has been examined in some detail, namely atherosclerosis and Alzheimer's disease. For a more detailed discussion of these and other disorders, the reader is referred to the cited references in Table 17.5.1.

Atherosclerotic Cardiovascular Disease

The association between various risk factors for atherosclerosis and enhanced IsoP generation has been extensively explored, and it was found that IsoP formation is increased in humans with these risk factors. These data suggest that enhanced oxidant stress may play a role in the development of atherosclerosis, although the mechanisms involved have not been

Table 17.5.1 Disorders in Which F_2-IsoPs Have Implicated a Role for Free Radicals in Human Diseases

Disease	Reference
Acute chest syndrome of sickle cell disease	Klings et al., 2001
Acute cholestasis	Leo et al., 1997
Adult respiratory distress syndrome	Carpenter et al., 1998
Alcohol-induced liver injury	Aleynik et al., 1999
Allergic asthma	Dworski et al., 1999
Alzheimer's disease	Montine et al., 1999a
Chronic obstructive lung disease	Pratico et al., 1999
Crohn's disease	Wendland et al., 2001
Diabetes	Gopaul et al., 1995
Hemodialysis	Spittle et al., 2001
Hepatorenal syndrome	Morrow et al., 1993
Huntington's disease	Montine et al., 1999c
Hypercholesterolemia	Davi et al., 1997
Hyperhomocysteinemia	Voutilainen et al., 1999
Interstitial lung disease	Montuschi et al., 1998
Ischemia/reperfusion injury	Reilly et al., 1997
Muscular side effects of statins	Sinzinger et al., 2001
Pulmonary hypertension	Cracowski et al., 2001
Rhabdomyolysis renal injury	Holt et al., 1999
Rheumatic inflammatory response	Basu et al., 2001
Scleroderma	Stein et al., 1996
Sepsis	Ekmekcioglu et al., 2002
Smoking	Morrow et al., 1995

elucidated. Although trials with antioxidants have generally failed to show benefit in the prevention of heart disease in humans, there is still considerable evidence to support the hypothesis that oxidative stress is intimately involved in atherosclerosis.

A link between cigarette smoking and the risk of cardiovascular disease is well established (Kannel, 1981). However, the underlying mechanism(s) for this effect is not fully understood. The gaseous phase of cigarette smoke contains a number of oxidants and exposure of LDL to the gaseous phase of cigarette smoke in vitro induces oxidation of the LDL lipids (Frei et al., 1991). Thus, the hypothesis that smoking induces an oxidative stress by examining F_2-IsoP levels in plasma from smokers was explored. Ten individuals who smoked heavily (>30 cigarettes/day) and ten age and sex matched non-smoking normal volunteers were studied (Morrow et al., 1995). Plasma concentrations of free and esterified F_2-IsoPs were significantly elevated in the smokers compared to the non-smokers ($p = 0.02$ and $p = 0.03$, respectively). In all subjects, levels of F_2-IsoPs both free in the circulation and esterified to plasma lipoproteins were significantly reduced following 2 weeks of abstinence from smoking ($p = 0.03$ and $p = 0.02$, respectively). The occurrence of enhanced formation of IsoPs in smokers has also subsequently been confirmed in studies by other groups (Reilly et al., 1996). Collectively, these findings suggest strongly that smoking causes an oxidative stress and the observation that smokers have elevated levels of F_2-IsoPs esterified in plasma lipids also supports the hypothesis that the link between smoking and risk of cardiovascular disease may be attributed to enhanced oxidation of lipoproteins.

It has been well established that patients with hypercholesterolemia have an increased

risk for the development of atherosclerosis. Thus, it was of interest to determine whether levels of F_2-IsoPs are increased in patients with this condition.

Levels of F_2-IsoPs esterified in plasma lipids were determined in patients with polygenic hypercholesterolemia (Roberts and Morrow, 1999). Levels in patients with hypercholesterolemia were found to be significantly increased by a mean of 3.4-fold (range 1.7- to 7.5-fold) above levels measured in normal controls ($p < 0.001$). Interestingly, in these patients, there was no correlation between levels of F_2-IsoPs and serum cholesterol, triglycerides or LDL-cholesterol. In addition, plasma arachidonic acid content was measured in these patients and normal controls. Again, no correlation between IsoP and arachidonate levels was found. Thus, these data suggest that the finding of high levels of F_2-IsoPs in patients with hypercholesterolemia is not due simply to the presence of more lipid, i.e., arachidonic acid substrate. Rather, it is suggested that hypercholesterolemia is associated with enhanced oxidative stress. The underlying basis for this observation, however, remains unclear. Interestingly, a report also found that the urinary excretion of F_2-IsoPs was also increased in patients with Type II hypercholesterolemia by a mean of 2.5-fold, which was suppressed by ~60% with vitamin E treatment (600 mg/day; Davi et al., 1997).

Patients with diabetes are known to have an increased incidence of atherosclerotic vascular disease. Furthermore, the formation of F_2-IsoPs has been found to be induced in vascular smooth muscle cells by hyperglycemia (Natarajan et al., 1996). Thus, a link between enhanced oxidative stress in vivo and diabetes has been explored. Gopaul et al. (1995) reported a mean 3.3-fold increase in free F_2-IsoPs in plasma from diabetic patients compared to non-diabetic healthy control subjects. A later report demonstrated that plasma F_2-IsoP levels increased significantly within 90 min during acute hyperglycemia in type 2 diabetic patients (Sampson et al., 2002). In addition, Davi et al. (1999) reported that elevated urinary F_2-IsoP levels in diabetic patients could be suppressed by vitamin E supplementation or glycemic control.

High plasma levels of homocysteine are an independent risk factor for cardiovascular disease (Boushey et al., 1995). The mechanism by which hyperhomocysteinemia induces atherosclerosis is not fully understood but promotion of LDL oxidation has been suggested. The relationship between total plasma concentrations of homocysteine and F_2-IsoPs in 100 Finnish male participants in the Antioxidant Supplementation in Atherosclerosis Prevention study has been explored (Voutilainen et al., 1999). The mean plasma total homocysteine and F_2-IsoP concentrations were 11.1 μmol/liter and 29.6 ng/liter, respectively. The simple correlation coefficient for the association between plasma concentrations of homocysteine and F_2-IsoPs was 0.40 ($p < 0.0001$). Plasma concentrations of F_2-IsoPs increased linearly across quintiles of homocysteine levels. The finding of a positive correlation between plasma concentrations of F_2-IsoPs and homocysteine supports the suggestion that the mechanism underlying the link between high homocysteine levels and risk for cardiovascular disease may be attributed to enhanced lipid peroxidation.

In accordance with the LDL oxidation hypothesis of atherosclerosis, levels of F_2-IsoPs should be higher in atherosclerotic plaques than in normal vascular tissue. To address this issue, levels of F_2-IsoPs were measured in fresh advanced atherosclerotic plaque tissue removed during arterial thrombarterectomy ($n = 10$) and compared with levels measured in normal human umbilical veins removed from the placenta immediately after delivery ($n = 10$) (Gniwotta et al., 1997). Levels of F_2-IsoPs esterified in vascular tissue normalized to both wet weight and dry weight were significantly higher in atherosclerotic plaques compared to normal vascular tissue. When the data was normalized to arachidonic acid content, the F_2-IsoP/arachidonic acid ratio was about four-fold higher than the ratio in normal vascular tissue ($p = 0.009$). This finding indicates that unsaturated fatty acids in atherosclerotic plaques are more extensively oxidized than lipids in normal vascular tissue. These observations are also in accord with data from FitzGerald and colleagues who have shown increased amounts of F_2-IsoPs in human atherosclerotic lesions including the localization of F_2-IsoPs in atherosclerotic plaque tissue to foam cells and vascular smooth muscle cells (Pratico et al., 1997).

Alzheimer's Disease

Oxidative stress has been implicated in the pathogenesis of numerous neurodegenerative conditions, including Alzheimer's Disease (AD). Regional increases in oxidative damage and lipid peroxidation have been described in brain tissue obtained post mortem from patients with AD (Markesbery, 1997). Similarly,

F_2-IsoP levels are significantly elevated in affected regions of post-mortem brain samples from AD patients as compared to controls (Reich et al., 2001a). However, an objective index of oxidative damage associated with AD that can be assessed in living patients is lacking. Such a biomarker could be vital for understanding the role of oxidative damage in AD patients by permitting repeated evaluation of disease progression or responses to therapeutic interventions. Toward such a goal, the authors obtained post-mortem ventricular fluid from eleven patients with a pathological diagnosis of AD and eleven control patients, in order to evaluate F_2-IsoP levels in cerebrospinal fluid (CSF; Montine et al., 1998). All subjects participated in a rapid autopsy protocol such that fluid was collected within 3 hr of death. F_2-IsoP levels were significantly increased in ventricular fluid from AD patients (72 ± 7 pg /ml, mean $\pm$ S.E.M.) compared to CSF from control individuals (46 ± 4 pg/ml, $p < 0.01$), and correlations were identified between increases in IsoP levels and higher Braak stage and decreased brain weight, two indices of AD severity. In a larger study, the authors have shown that CSF F_2-IsoP level correlates with the extent of pathological neurodegeneration but not with density of neuritic plaques or neurofibrillary tangles (Montine et al., 1999a; Reich et al., 2001b).

Subsequently, the authors undertook a study to examine CSF F_2-IsoP levels in living patients with probable AD (Montine et al., 1999b). CSF was obtained from the lumbar cistern in 27 patients with AD and 25 controls without neurodegenerative disorders matched for age and gender. In keeping with post-mortem studies, lumbar CSF levels of F_2-IsoPs were significantly increased (31.0 ± 2.6 pg/ml) in AD patients compared to control subjects (22.9 ± 1.0 pg/ml, $p < 0.05$). Pratico et al. (2000) have also observed increased F_2-IsoPs in CSF of patients with probable AD, as well as in patients with mild cognitive impairment (MCI), a condition which precedes symptomatic dementia in AD (Pratico et al., 2002). However, this group also reports increased F_2-IsoPs in plasma and urine of both MCI and AD patients, though the authors' laboratory and others have not been able to detect these changes in peripheral F_2-IsoPs (Montine et al., 2002b; Bohnstedt et al., 2003). Taken together, these studies suggest that quantification of IsoPs in cerebrospinal fluid of patients with Alzheimer's disease may be of use as an intra vitum index of disease progression or as a tool to monitor response to therapy.

CONCLUSIONS

The discovery of IsoPs as products of non-enzymatic lipid peroxidation has been a major breakthrough regarding the quantification of oxidant stress in vivo. The quantification of these molecules has opened up new areas of investigation regarding the role of free radicals in human physiology and pathophysiology, and appears to be the most useful tool currently available to explore the role of free radicals in the pathogenesis of human disease. Although considerable information has been obtained since the initial discovery of IsoPs, much remains to be understood about the role of these molecules as markers of oxidant stress. It is anticipated that additional research in this area will continue to provide important insights into the role of oxidative stress in human disease.

LITERATURE CITED

Aleynik, S.I., Leo, M.A., Aleynik, M.K., and Lieber, C.S. 1999. Increased circulating products of lipid peroxidation in patients with alcoholic liver disease. *Alcohol Clin. Exp. Res.* 22:192-196.

Awad, J.A., Morrow, J.D., Hill, K.E., Roberts, L.J., and Burk, R.F. 1994. Detection and localization of lipid peroxidation in selenium- and vitamin-E deficient rats using F_2-isoprostanes, *J. Nutr.* 124:810-816.

Basu, S., Whiteman, M., Mattey, D.L., and Halliwell, B. 2001. Raised levels of F(2)-isoprostanes and prostaglandin F(2alpha) in different rheumatic diseases. *Ann. Rheum. Dis.* 60:627-631.

Bohnstedt, K.C., Karlberg, B., Wahlund, L.O., Jonhagen, M.E., Basun, H., and Schmidt, S. 2003. Determination of isoprostanes in urine samples from Alzheimer patients using porous graphitic carbon liquid chromatography-tandem mass spectrometry. *J. Chromatogr. B.* 796:11-19.

Boushey, C.J., Beresford, S.A., Omenn, G.S., and Motulsky, A.G. 1995. A quantitative assessment of plasma homocysteine as a risk factor for vascular disease. Probable benefits of increasing folic acid intakes. *J. Am. Med. Assoc.* 274:1049-1057.

Burk, R.F., Hill, K.E., Awad, J.A., Morrow, J.D., Kato, T., Cockell, K.A., and Lyons, P.R. 1995. Pathogenesis of diquat-induced liver necrosis in selenium-deficient rats: Assessment of the roles of lipid peroxidation and selenoprotein P. *Hepatology* 21:561-569.

Carpenter, C.T., Price, P.V., and Christman, B.W. 1998. Exhaled breath condensate isoprostanes are elevated in patients with acute lung injury or ARDS. *Chest* 114:1653-1659.

Chen, Y., Morrow, J.D., and Roberts, L.J. 2nd 1999. Formation of reactive cyclopentenone compounds in vivo as products of the isoprostane pathway. *J. Biol. Chem.* 274:10863-10868.

Cracowski, J.L., Cracowski, C., Bessard, G., Pepin, J.L., Bessard, J., Schwebel, C., Stanke-Labesque, F., and Pison, C. 2001. Increased lipid peroxidation in patients with pulmonary hypertension. *Am. J. Resp. Crit. Care Med.* 164:1038-1042.

Davi, G., Alessandrini, P, Mezzetti, A., Minotti, G., Bucciarelli, T., Costantini, F., Cipollone, F., Bon, G.B., Ciabattoni, G., and Patrono, C. 1997. In vivo formation of 8-Epi-prostaglandin F2 alpha is increased in hypercholesterolemia. *Atheroscler. Thromb. Vasc. Biol.* 117:3230-3235.

Davi, G., Ciabattoni, G., Consoli, A., Mezzetti, A., Falco, A., Santarone, S., Pennese, E., Vitacolonna, E., Bucciarelli, T., Costantini, F., Capani, F., and Patrono, C. 1999. In vivo formation of 8-iso-prostaglandin F2alpha and platelet activation in diabetes mellitus: Effects of improved metabolic control and vitamin E supplementation. *Circulation* 99:224-229.

Dworski, R., Murray, J.J., Roberts, L.J., Oates, J.A., Morrow, J.D., Fisher, L., and Sheller, J.R. 1999. Allergen-induced synthesis of F(2)-isoprostanes in atopic asthmatics. Evidence for oxidant stress. *Am. J. Respir. Crit. Care Med.* 160:1947-1951.

Ekmekcioglu, C., Schweiger, B., Strauss-Blasche, G., Mundigler, G., Siostrzonek, P., and Marktl, W. 2002. Urinary excretion of 8-iso-PGF(2 alpha) in three patients during sepsis, recovery and state of health. *Prostaglandins, Leukot. Essent. Fatty Acids* 66:441-442.

Fam, S.S. and Morrow, J.D. 2003. The isoprostanes: Unique products of arachidonic acid oxidation—A review. *Curr. Med. Chem.* 10:1723-1740.

Feillet-Coudray, C., Tourtauchaux, R., Niculescu, N., Rock, E., Tauveron, I., Alexandre-Gouabau, M., Rayssiguier, R., Jalenques, Y.I., and Mazur, A. 1999. Plasma levels of 8-epi-PGF2α, an in vivo marker of oxidative stress, are not affected by aging or Alzheimer's disease. *Free Rad. Biol. Med.* 27:463-469.

Frei, B., Forte, T.M., Ames, B.N., and Cross, C.E. 1991. Gas phase oxidants of cigarette smoke induce lipid peroxidation and changes in lipoprotein properties in human blood plasma. Protective effects of ascorbic acid. *Biochem. J.* 277:133-138.

Gniwotta, C., Morrow, J.D., Roberts, L.J., and Kuhn, H. 1997. Prostaglandin F2-like compounds, F2-isoprostanes, are present in increased amounts in human atherosclerotic lesions. *Arterioscler. Thromb. Vasc. Biol.* 17:3236-3241.

Gopaul, N.K., Nourooz-Zadeh, J., Malle, A.I., and Anggard, E.E. 1994. Formation of F_2-isoprostanes during aortic endothelial cell-mediated oxidation of low density lipoprotein. *FEBS Lett.* 348:297-300.

Gopaul, N.K., Anggard, E.E., Mallet, A.I., Beteridge, D.J., Wolff, S.P., and Nourooz-Zadey, J. 1995. Plasma 8-epi-PGF2 alpha levels are elevated in individuals with non-insulin dependent diabetes mellitus. *FEBS Lett.* 368:225-229.

Halliwell, B. and Grootveld, M. 1987. The measurement of free radical reactions in humans. *FEBS Lett.* 213:9-14.

Holt, S., Reeder, B., Wilson, M., Harvey, S., Morrow, J.D., Roberts, L.J. II, and Moore, K. 1999. Increased lipid peroxidation in patients with rhabdomyolysis. *Lancet* 353:1241.

Kannel, W.B. 1981. Update on the role of cigarette smoking in coronary artery disease. *Am. Heart J.* 101:319-328.

Klings, E.S., Christman, B.W., McClung, J., Stucchi, A.F., McMahon, L., Brauer, M., and Farber, H.W. 2001. Increased F2 isoprostanes in the acute chest syndrome of sickle cell disease as a marker of oxidative stress. *Am. J. Resp. Crit. Care Med.* 164:1248-1252.

Leo, M.A., Aleynik, S.I., Siegel, J.H., Kasmin, F.E., Aleynik, M.K., and Lieber, C.S. 1997. F2-isoprostane and 4-hydroxynonenal excretion in human bile of patients with biliary tract and pancreatic disorders. *Am. J. Gastroenterol.* 92:2069-2072.

Liang, Y., Wei, P., Duke, R.W., Reaven, P.D., Harman, S.M., Cutler, R.G., and Heward, C.B. 2000. Quantification of 8-iso-prostaglandin-F(2alpha) and 2,3-dinor-8-iso-prostaglandin-F(2alpha) in human urine using liquid chromatography-tandem mass spectrometry. *Free Radic. Biol. Med.* 34:409-418.

Liu, T., Stern, A., Roberts, L.J., and Morrow, J.D. 1999. The isoprostanes: Novel prostaglandin-like products of the free radical-catalyzed peroxidation of arachidonic acid. *J. Biomed. Sci.* 6:226-235.

Longmire, A.W., Swift, L.L., Roberts, L.J., Awad, J.A., Burk, R.F., and Morrow, J.D. 1994. Effect of oxygen tension on the generation of F_2-isoprostanes and malondialdehyde in peroxidizing rat liver microsomes. *Biochem. Pharm.* 47:1173-1177.

Lynch, S.M., Morrow, J.D., Roberts, L.J., and Frei, B. 1994. Formation of non-cyclooxygenase-derived prostanoids (F_2-isoprostanes) in plasma and low density lipoprotein exposed to oxidative stress in vitro. *J. Clin. Invest.* 93:998-1004.

Marin, J.G., Cornet, S., Spinnewyn, B., Demerle-Pallardy, C., Auguet, M., and Chabrier, P.E. 2000. BN 80933 inhibits F2-isoprostane elevation in focal cerebral ischaemia and hypoxic neuronal cultures. *Neuroreport.* 11:1357-1360.

Markesbery, W.R. 1997. Oxidative stress hypothesis in Alzheimer's disease. *Free Rad. Biol. Med.* 23:137-147.

Montine, T.J., Markesbery, W.R., Morrow, J.D., and Roberts, L.J. 1998. Cerebrospinal fluid F2-isoprostane levels are increased in Alzheimer's disease. *Ann. Neurol.* 44:410-413.

Montine, T.J., Markesbery, W.R., Zackert, W., Sanchez, S.C., Roberts, L.J. 2nd, and Morrow, J.D. 1999a. The magnitude of brain lipid peroxidation correlates with the extent of degeneration but not with density of neuritic plaques or neurofibrillary tangles or with APOE genotype

in Alzheimer's disease patients. *Am. J. Pathol.* 155:863-868.

Montine, T.J., Beal, M.F., Cudkowicz, M.E., O'Donnell, H., Margolin, R.A., McFarland, L., Bachrach, A.F., Zackert, W.E., Roberts, L.J., and Morrow, J.D. 1999b. Increased CSF F2-isoprostane concentration in probable AD. *Neurology.* 52:562.

Montine, T.J., Beal, M.F., Robertson, D., Cudkowicz, M.E., Biaggioni, I., Brown, R.H., O'Donnel, H., Zackert, W.E., Roberts, L.J., and Morrow, J.D. 1999c. Cerebrospinal fluid F2-isoprostanes are elevated in Huntington's disease. *Neurology* 52:1104-1105.

Montine, T.J., Milatovic, D., Gupta, R.C., Valyi-Nagy, T., Morrow, J.D., and Breyer, R.M. 2002a. Neuronal oxidative damage from activated innate immunity is EP2 receptor-dependent. *J. Neurochem.* 83:463-470.

Montine, T.J., Quinn, J.F., Milatovic, D., Silbert, L.C., Dang, T., Sanchez, S., Terry, E., Roberts, L.J. 2nd, Kaye, J.A., and Morrow, J.D. 2002b. Peripheral F2-isoprostanes and F4-neuroprostanes are not increased in Alzheimer's disease. *Ann. Neurol.* 52:175-179.

Montuschi, P., Ciabattoni, G., Paredi, P., Pantelidis, P., DuBois, R.M., Kharitoniv, S.A., and Barnes, P.J. 1998. 8-Isoprostane as a biomarker of oxidative stress in interstitial lung diseases. *Am. J. Resp. Crit. Care Med.* 158:1524-1527.

Morales, C.R., Terry, E.S., Zackert, W.E., Montine, T.J., and Morrow, J.D. 2001. Improved assay for the quantification of the isoprostane 15-F_{2t}-isoprostane (8-iso-$PGF_{2\alpha}$) by a stable isotope dilution mass spectrometric assay. *Clin. Chim. Acta* 314:93-99.

Morrow, J.D. and Roberts, L.J. 1997. The isoprostanes: Unique bioactive products of lipid peroxidation. *Prog. Lipid Res.* 36:1-21.

Morrow, J.D. and Roberts, L.J. 1999. Mass spectrometric quantification of F_2-isoprostanes in biological fluids and tissues as measure of oxidant stress. *Meth. Enzymol.* 300:3-12.

Morrow, J.D., Hill, K.E., Burk, R.F., Nammour, T.M., Badr, K.F., and Roberts, L.J. 1990a. A series of prostaglandin F_2-like compounds are produced in vivo in humans by a non-cyclooxygenase, free radical-catalyzed mechanism. *Proc. Natl. Acad. Sci. U.S.A.* 87:9383-9397.

Morrow, J.D., Harris, T.M., and Roberts, L.J. 1990b. Noncyclooxygenase oxidative formation of a series of novel prostaglandins: Analytical ramifications for measurement of eicosanoids. *Analyt. Biochem.* 184:1-10.

Morrow, J.D., Awad, J.A., Kato, T., Takahashi, K., Badr, K.F., Roberts, L.J., and Burk, R.F. 1992. Formation of novel non-cyclooxygenase-derived prostanoids (F_2-isoprostanes) in carbon tetrachloride hepatotoxicity. *J. Clin. Invest.* 90:2502-2507.

Morrow, J.D., Moore, K.P., Awad, J.A., Ravenscraft, M.D., Marini, G., Badr, K.F., Williams R., and Roberts, L.J. 1993. Marked overproduction of non-cyclooxygenase derived prostanoids (F2-isoprostanes) in the hepatorenal syndrome. *J. Lipid Mediators* 6:417-420.

Morrow, J.D, Frei, B., Longmire, A.W., Gaziano, M., Lynch, S.M., Shyr, Y., Strauss, W.E., Oates, J.A., and Roberts, L.J. 1995. Increase in circulating products of lipid peroxidation (F2-isoprostanes) in smokers. Smoking as a cause of oxidative damage. *N. Engl. J. Med.* 332:1198-1203.

Morrow, J.D., Chen, Y., Brame, C.J., Yang, J., Sanchez, S.C., Xu, J., Zackert, W.E., Awad, J.A., and Roberts, L.J. 1999a. The isoprostanes: Unique prostaglandin-like products of free radical-initiated lipid peroxidation. *Drug Metab. Rev.* 31:117-139.

Morrow, J.D., Zackert, W.E., Yang, J.P., Kurhts, E.H., Callawaert, D., Dworski, R., Kanai, K., Taber, D., Moore, K., Oates, J.A., and Roberts, L.J. 1999b. Quantification of the major urinary metabolite of 15-F_{2t}-isoprostane (8-iso-$PGF_{2\alpha}$) by a stable isotope dilution mass spectrometric assay. *Analyt. Biochem.* 269:326-331.

Natarajan, R., Lanting, L., Gonzales, N., and Nadler, J. 1996. Formation of an F2-isoprostane in vascular smooth muscle cells by elevated glucose and growth factors. *Am. J. Physiol.* 271:H159-165.

Patel, M., Liang, L.P., and Roberts, L.J. 2nd. 2001. Enhanced hippocampal F2-isoprostane formation following kainate-induced seizures. *J. Neurochem.* 79:1065-1069.

Pratico, D. and FitzGerald, G.A. 1996. Generation of 8-epi-prostaglandin $F_{2\alpha}$ by human monocytes. Discriminate production by reactive oxygen species and prostaglandin endoperoxide synthase-2. *J. Biol. Chem.* 271:8919-8924.

Pratico, D., Iuliano, L., Mauriello, A., Spagnoli, L., Lawson, J.A., Rokach, J., Maclouf, J., Violi, F., and FitzGerald, G.A. 1997. Localization of distinct F2-isoprostanes in human atherosclerotic lesions. *J. Clin. Invest.* 100:2028-2034.

Pratico, D., Barry, O.P., Lawson, J.A., Adiyaman, M., Hwang, S.W., Khanapure, S.P., Iuliano, L., Rokach, J., and FitzGerald, G.A. 1998a. IPF2alpha-I: An index of lipid peroxidation in humans. *Proc. Natl. Acad. Sci U.S.A.* 95:3449-3454.

Pratico, D., Tangirala, R.K., Rader, D.J., Rokach, J., and FitzGerald, G.A. 1998b. Vitamin E suppresses isoprostane generation in vivo and reduces atherosclerosis in ApoE-deficient mice. *Nat. Med.* 4:1189-1192.

Pratico, D., Basili, S., Vieri, M., Cordova, C., Violi, V., and FitzGerald, G.A. 1999. Chronic obstructive pulmonary disease is associated with an increase in urinary levels of isoprostane F2alpha-III, an index of oxidant stress. *Am. J. Resp. Crit. Care Med.* 158:1709-1714.

Pratico, D., Clark, C.M., Lee, V.M., Trojanowski, J.Q., Rokach, J., and FitzGerald, G.A. 2000. Increased 8,12-iso-iPF2alpha-VI in Alzheimer's disease: Correlation of a noninvasive index of

lipid peroxidation with disease severity. *Ann. Neurol.* 48:809-812.

Pratico, D., Uryu, K., Leight, S., Trojanoswki, J.Q., and Lee, V.M. 2001. Increased lipid peroxidation precedes amyloid plaque formation in an animal model of Alzheimer amyloidosis. *J. Neurosci.* 21:4183-4187.

Pratico, D., Clark, C.M., Liun, F., Rokach, J., Lee, V.Y., and Trojanowski, J.Q. 2002. Increase of brain oxidative stress in mild cognitive impairment: A possible predictor of Alzheimer disease. *Arch. Neurol.* 59:972-976.

Reich, E.E., Markesbery, W.R., Roberts, L.J. 2nd, Swift, L.L., Morrow, J.D., and Montine, T.J. 2001a. Brain regional quantification of F-ring and D-/E-ring isoprostanes and neuroprostanes in Alzheimer's disease. *Am. J. Pathol.* 158:293-297.

Reich, E.E., Markesbery, W.R., Roberts, L.J., Zackert, W.E., Swift, L.L., Morrow, J.D, and Montine, T.J. 2001b. Quantification of F-ring and D-/E-ring isoprostanes and neuroprostanes in Alzheimer's disease. *Adv. Exp. Med. Biol.* 500:253-256.

Reilly, M., Delanty, N., Lawson, J.A., and FitzGerald, G.A. 1996. Modulation of oxidant stress in vivo in chronic cigarette smokers. *Circulation* 94:19-25.

Reilly, M.P., Delanty, M., Roy, L., Rokach, J., Callaghan, P.O., Crean, P., Lawson, J.A., and FitzGerald, G.A. 1997. Increased formation of the isoprostanes IPF2alpha-I and 8-epi-prostaglandin F2alpha in acute coronary angioplasty: Evidence for oxidant stress during coronary reperfusion in humans. *Circulation* 96:3314-3320.

Roberts, L.J. and Morrow, J.D. 1999. Isoprostanes as markers of lipid peroxidation in atherosclerosis. *In* Molecular and Cellular Basis of Inflammation. (C.N. Serhan and P.A. Ward, eds.) pp. 141. Humana Press, Totowa, N.J.

Roberts, L.J. II and Morrow, J.D. 2000. Measurement of F2-Isoprostanes as an index of oxidative stress in vivo. *Free Radic. Biol. Med.* 28:505-513.

Roberts, L.J. and Reckelhoff, J.F. 2001. Measurement of F(2)-isoprostanes unveils profound oxidative stress in aged rats. *Biochem. Biophys. Res. Commun.* 287:254-256.

Roberts, L.J., Moore, K.P., Zackert, W.E., Oates, J.A., and Morrow, J.D. 1996. Identification of the major urinary metabolite of the F_2-isoprostane 8-iso-prostaglandin $F_{2\alpha}$ in humans. *J. Biol. Chem.* 271:20617-20620.

Rokach, J., Khanapure, S.P., Hwang, S.-W., Adiyaman, M., Lawson, J.A., and FitzGerald, G.A. 1997. The isoprostanes: A perspective. *Prostaglandins* 54:823-851.

Sampson, M.J., Gopaul, N., Davies, I.R., Hughes, D.A., and Carrier, M.J. 2002. Plasma F2 isoprostanes: Direct evidence of increased free radical damage during acute hyperglycemia in type 2 diabetes. *Diabetes Care* 25:537-541.

Sinzinger, H., Lupatelli, G., Chehne, F., Oguogho, A., and Furberg, C.D. 2001. Isoprostane 8-epi-PGF2alpha is frequently increased in patients with muscle pain and/or CK-elevation after HMG-Co-enzyme-A-reductase inhibitor therapy. *J. Clin. Pharm. Ther.* 26:303-310.

Spittle, M.A., Hoenich, N.A., Handelman, G.J., Adhikarla, R., Homel, P., and Levin, N.W. 2001. Oxidative stress and inflammation in hemodialysis patients. *Am. J. Kidney Dis.* 38:1408-1413.

Stein, C.M., Tanner, S.B., Awad, J.A., Roberts, L.J. II, and Morrow, J.D. 1996. Evidence of free radical-mediated injury (isoprostane overproduction) in scleroderma. *Arth. Rheum.* 39:1146-1150.

Steinberg, D., Parthasarathy, S., Carew, T.E., Khoo, J.C., and Witztum, J.L. 1989. Beyond cholesterol: Modifications of low density lipoprotein that increase its atherogenicity. *N. Engl. J. Med.* 86:915-924.

Taber, D.F., Morrow, J.D., and Roberts, L.J. 1997. A nomenclature system for the isoprostanes. *Prostaglandins* 53:63-67.

Voutilainen, S., Morrow, J.D., Roberts, L.J., Alfthan, G., Alho, H., Nyyssonen, K., and Salonen, J.T. 1999. Enhanced in vivo lipid peroxidation at elevated plasma total homocysteine levels. *Arterioscler. Thromb. Vasc. Biol.* 19:1263-1266.

Wendland, B.E., Aghdassi, E., Tam, C., Carrier, J., Steinhart, A.H., Wolman, S.L., Baron, D., and Allard, J.P. 2001. Lipid peroxidation and plasma antioxidant micronutrients in Crohn disease. *Am. J. Clin. Nutr.* 74:259-264.

Contributed by Erik S. Musiek and
Jason D. Morrow
Vanderbilt University School of Medicine
Nashville, Tennessee

Quantification of F_2-Isoprostanes by Gas Chromatography/Mass Spectrometry as a Measure of Oxidant Stress

This unit outlines methods to assess lipid peroxidation associated with oxidant injury in vivo by quantifying concentrations of either esterified or free F_2-isoprostanes (F_2-IsoPs). Quantification of these compounds overcomes many of the shortcomings associated with other assays of oxidant stress, especially in humans in vivo. Thus, measurement of F_2-IsoPs likely represents an important advancement in the ability to assess the role of oxidative stress in human disease (Fam and Morrow, 2003). The techniques employed for the analysis of F_2-IsoPs from biological sources that are detailed herein utilize mass spectrometric approaches. Procedures are outlined for the analysis of both F_2-IsoPs esterified to tissue phospholipids (see Basic Protocol 1) and free F_2-IsoPs (see Basic Protocol 2). In addition, quantification of F_2-IsoPs esterified in plasma lipids is also detailed (see Alternate Protocol).

NOTE: All inorganic solvents should be high purity HPLC or GC grade. All reagents/chemicals should be ACS certified or equivalent grade.

QUANTIFICATION OF F_2-ISOPROSTANES IN TISSUE LIPIDS

BASIC PROTOCOL 1

F_2-IsoPs from biological sources can only be quantified as free compounds using gas chromatography (GC)/mass spectrometry (MS) (Morrow and Roberts, 1999) Thus, to measure levels of these compounds esterified to phospholipids, the phospholipids are first extracted from the tissue sample and subjected to alkaline hydrolysis to release free F_2-IsoPs. Free F_2-IsoPs are then quantified using the same procedure for the measurement of free compounds in biological fluids (see Alternate Protocol). This protocol outlines the extraction and hydrolysis of F_2-IsoPs from tissue lipids.

The assay described herein is applicable to all animal and human tissues and cell samples. Preparation of phospholipid-containing biological fluids, such as plasma, differs slightly (see Alternate Protocol). To measure free F_2-IsoPs from low-protein fluids (such as urine or low-serum cell medium) that do not require lipid extraction, see Basic Protocol 2.

Materials

Fresh or frozen tissue
Folch solution (see recipe)
Butylated hydroxytoluene (BHT; Aldrich)
Nitrogen or argon source
0.9% (w/v) aqueous sodium chloride (NaCl; high purity; EMD Biosciences) prepared in ultrapure water
Methanol (high-quality; Burdick and Jackson or VWR Scientific) containing 0.005% (v/v) BHT
15% (w/v) aqueous potassium hydroxide (KOH pellets; high purity; EMD Biosciences) prepared in ultrapure water
1 N HCl (American Chemical Society certified or equivalent grade)
50-ml conical, polypropylene centrifuge tubes
Blade homogenizer (PTA 10S generator, Brinkman Instruments)
Table-top centrifuge
Analytical evaporation unit (Organomation Associates)
37°C water bath

Contributed by Erik S. Musiek and Jason D. Morrow
Current Protocols in Toxicology (2005) 17.6.1-17.6.9

1. Weigh out 0.05 to 1 g of either fresh tissue or tissue frozen at −70°C.

   If the sample weighs <0.15 g, the volume of Folch solution in step 2 and the volume of aqueous NaCl in step 5 can be reduced by half.

2. Add tissue to 20 ml of ice-cold Folch solution containing 0.005% (v/v) BHT in a 50-ml centrifuge tube with cap. Keep on ice.

   Polypropylene tubes are recommended, as polystyrene is not resistant to chloroform.

3. Homogenize tissue with blade homogenizer 30 sec at maximum speed or until fully homogenized. Keep on ice.

4. Purge airspace in centrifuge tube with nitrogen or argon, then cap. Let solution stand 1 hr at room temperature to allow maximal extraction of lipids from ground tissue. Shake tube occasionally for several seconds during this period of time.

5. Add 4 ml of 0.9% aqueous NaCl. Vortex or shake vigorously for 1 min at room temperature.

6. In a table-top centrifuge, centrifuge 10 min at 800 × *g*, room temperature, to separate aqueous and organic layers.

   Following centrifugation, a semi-solid protein layer should have formed between the upper (aqueous) and lower (organic) layers.

7. After centrifugation, carefully pipet off top aqueous layer and discard. Remove the lower organic layer carefully from under the intermediate semi-solid protein aqueous layer and transfer to a 50-ml conical centrifuge tube. Evaporate under nitrogen stream in an analytical evaporation unit to dryness.

8. Hydrolyze F_2-IsoPs from phospholipids by adding 4 ml methanol containing 0.005% BHT and vortex to resuspend lipids, then add 4 ml of 15% aqueous KOH. Purge tube with nitrogen and cap.

   If sample originally weighed <0.15 g, lipid extract can be resuspended in 1 ml methanol containing 0.005% BHT, to which 1 ml of 15% aqueous KOH is added.

9. Incubate mixture 20 min in a 37°C water bath.

10. After incubation, acidify the mixture to pH 3.0 with 1 N HCl. Then dilute the mixture to 80 ml with ultrapure water (pH 3.0) in preparation for extraction of free F_2-IsoPs (see Alternate Protocol).

    It is important to dilute the methanol in this solution to ≤5% to ensure proper column extraction of F_2-IsoPs in the subsequent purification procedure.

ALTERNATE PROTOCOL

EXTRACTION OF LIPIDS FROM PHOSPHOLIPID-CONTAINING BIOLOGICAL FLUIDS

The technique used to extract F_2-IsoP-containing phospholipids from biological fluids, e.g., plasma, differs somewhat from methods used for tissue. The authors have found that arachidonic acid in plasma is much more susceptible to autoxidation during lipid extraction than arachidonate in tissue samples. Thus, to suppress ex vivo oxidation of arachidonic acid in plasma, triphenylphosphine (TPP), in addition to BHT, is added to the Folch solution (Morrow and Roberts, 1999).

Additional Materials *(also see Basic Protocol 1)*

Biological fluid, e.g., plasma
Triphenylphosphine (TPP; Aldrich)
0.043% (w/v) magnesium chloride ($MgCl_2$; high purity; EMD Biosciences) in ultrapure water

1. Add 1 ml of biological fluid to 20 ml ice-cold Folch solution containing 0.005% BHT and 5 mg TPP in a 50-ml centrifuge tube. Shake vigorously for 2 min.
2. Add 10 ml of 0.043% $MgCl_2$ and shake vigorously for 1 min. Centrifuge 10 min at 800 × *g*, room temperature.
3. Separate lower organic layer from other layers and transfer to a new 50-ml centrifuge tube.
4. Dry organic layer at room temperature under nitrogen in an analytical evaporator unit.
5. Proceed immediately to hydrolysis procedure (see Basic Protocol 1, step 8).

QUANTIFICATION OF F_2-ISOPS

BASIC PROTOCOL 2

Quantification of F_2-IsoPs by GC/negative ion chemical ionization (NICI) MS is extremely sensitive with a lower limit of detection in the range of 1 to 5 pg using a deuterated internal standard with a [$^2H_0$] blank of <5 ppt (Morrow and Roberts, 1999) Thus, it is usually not necessary to assay >1 to 3 ml of a biological fluid or a lipid extract from >50 to 100 mg of tissue. Furthermore, because urinary levels of F_2-IsoPs are high (typically >1 ng/ml), 0.2 ml of urine was found to be more than adequate to quantify urinary F_2-IsoPs (Morrow et al., 2001). The following assay procedure that is described and summarized in Figure 17.6.1 is the method used for analysis of free F_2-IsoPs in plasma but is equally adaptable to other biological fluids and hydrolyzed lipid extracts of tissues (see Basic Protocol 1).

Materials

Fluid or tissue extract, hydrolyzed
1 N HCl
[$^2H_4$] 15-F_2-IsoP (8-iso-$PGF_{2\alpha}$) internal standard (Cayman Chemical)
C18 Sep-Pak column (Waters)
Methanol (high purity; Burdick and Jackson, VWR Scientific)
pH 3 water (ultrapure filtered, adjusted to pH 3 with ACS-grade HCl)
Heptane (high purity; Burdick and Jackson, VWR Scientific)
Ethyl acetate (high purity; Burdick and Jackson, VWR Scientific)

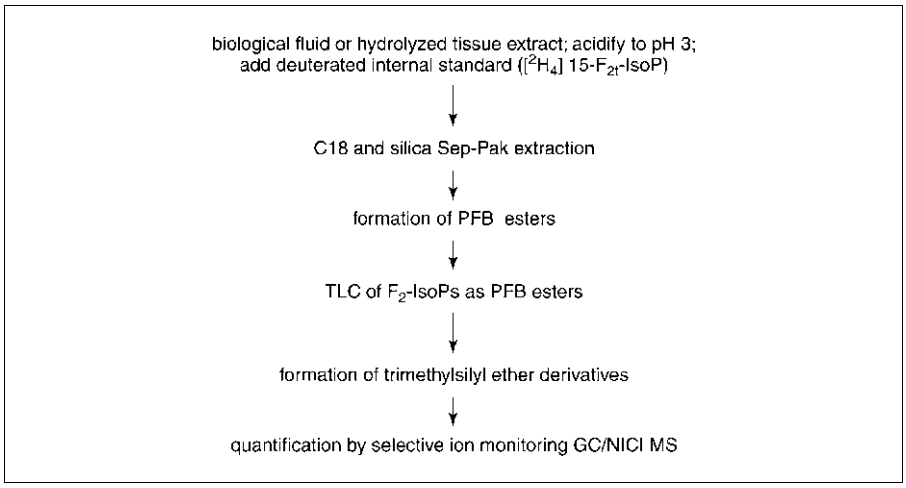

Figure 17.6.1 Outline of the procedures used for the extraction, purification, derivatization, and mass spectrometric analysis of F_2-IsoPs from biological sources.

Na_2SO_4 (anhydrous)
Silica Sep-Pak column (Waters)
10% (v/v) pentafluorobenzyl bromide (PFBB; Sigma-Aldrich) in acetonitrile
10% (v/v) *N*,*N*′-Diisopropylethylamine (DIPE; Sigma-Aldrich) in acetonitrile
Chloroform with ethanol (high purity; Burdick and Jackson, VWR Scientific)
Ethanol (high purity; Burdick and Jackson, VWR Scientific)
$PGF_{2\alpha}$ methyl ester (Cayman Chemical)
10% phosphomolybdic acid (Sigma) solution in ethanol
N,*O*-bis(trimethylsilyl)trifluoroacetamide (BSTFA; Supelco)
Dimethylformamide (DMF; Aldrich)
Undecane (Aldrich)

10-ml disposable plastic syringes
20-ml glass scintillation vials
5-ml Reacti-Vials (Pierce Scientific)
Analytical evaporation unit (Organomation Associates)
37°C water bath
Glass TLC tank and TLC paper
TLC plates (LK6B silica; Whatman)
90°C oven
Dessicator
1.5-ml microcentrifuge tubes
Gas chromatograph/mass spectrometer with capabilities for negative ion chemical ionization (NICI) mass spectrometry (model 6890N, Agilent Technologies or equivalent)
Capillary gas chromatography column (DB-1701, Fisons)

Prepare sample and apply on column

1. Acidify hydrolyzed extract to pH 3 with 1 N HCl.
2. Add 1 to 5 nmol of deuterated [$^2H_4$] 15-F_2-IsoP (8-iso-$PGF_{2\alpha}$) internal standard and vortex.
3. Precondition one C18 Sep-Pak column connected to a 10-ml disposable plastic syringe per sample with 5 ml methanol and then 7 ml pH 3 water.
4. Apply acidified sample mixture to the preconditioned Sep-Pak column.

   Care must be taken when applying the sample to the column to avoid loss of IsoPs. The sample should be pushed through the column at ∼1 to 2 ml/min, such that individual drops emerge from the Sep-Pak. Slightly more vigorous fluid flow is acceptable during the subsequent wash and elution steps, though a steady stream is not recommended.

Wash and elute column

5. Wash column first with 10 ml pH 3 water and then with 10 ml heptane.
6. Elute F_2-IsoPs from column with 10 ml of 50:50 (v/v) ethyl acetate/heptane into a 20-ml glass scintillation vial.
7. Add 5 g anhydrous Na_2SO_4 to the vial and swirl gently.

   This step removes residual water from the eluate.

8. Precondition silica Sep-Pak column with 5 ml ethyl acetate.
9. Apply eluate to silica Sep-Pak in the same manner as in step 3.
10. Wash cartridge with 5 ml ethyl acetate, then elute F_2-IsoPs from silica Sep-Pak with 5 ml of 1:1 (v/v) ethyl acetate/methanol into a 5-ml Reacti-Vial.

11. Evaporate eluate under nitrogen in an analytical evaporation unit.

Samples can be safely stored for up to 1 week at −20°C.

Prepare sample for TLC

12. Convert F_2-IsoPs to pentafluorobenzyl esters (which facilitates GC/MS analysis) by adding 40 µl of 10% PFBB in acetonitrile and 20 µl 10% DIPE in acetonitrile to the Reacti-Vial, vortex briefly, and incubate for 20 min in a 37°C water bath.

13. Prepare TLC tank by adding 97 ml chloroform, 3 ml ethanol, and TLC paper to saturate the tank, and allow to equilibrate for 30 min.

14. Dry sample thoroughly under nitrogen in an analytical evaporation unit in a fume hood and resuspend material in 50 µl methanol. Vortex briefly.

Perform TLC

15. Prewash a silica TLC plate with 90:10 (v/v) ethyl acetate/ethanol. Dry the plate 10 min in a 90°C oven then cool in a dessicator prior to sample application. Apply sample mixture to a lane on the prewashed silica TLC plate. For a TLC standard, apply ~2 to 5 µg of the methyl ester of $PGF_{2\alpha}$ to another TLC lane.

Avoid applying sample to the first 1 cm of the plate (preloading area).

16. Chromatograph to 13 cm. Visualize the TLC standard by spraying the lane with a 10% phosphomolybdic acid solution in ethanol and heating on a hot plate.

Only spray and heat the plate containing the $PGF_{2\alpha}$ standard, not the sample-containing plates. A single band will appear, which can be measured to determine the area to be scraped on the sample-containing plates.

17. Scrape silica from the TLC plate in the region of the methyl ester of $PGF_{2\alpha}$ (R_f = 0.18) and adjacent areas 1 cm above and below.

Extract isoprostanes

18. Place silica in a 1.5-ml microcentrifuge tube and add 1 ml ethyl acetate to extract isoprostanes. Vortex vigorously for 30 sec, then microcentrifuge 3 min at 13,000 rpm at room temperature.

19. Remove the ethyl acetate and place it in a new 1.5-ml microcentrifuge tube, taking care not to disrupt the silica pellet.

Samples can be safely stored for up to 1 week at −20°C.

20. Dry under nitrogen, then add 20 µl BSTFA and 7 µl DMF to residue to covert to trimethylsilyl ether derivatives for GC/MS analysis.

21. Vortex well and incubate sample 20 min at 37°C, then dry reagents under nitrogen.

22. Resuspend in 20 µl undecane and vortex briefly.

Undecane is stored over calcium hydride to prevent water accumulation.

Sample is now ready for mass spectrometric analysis and should be analyzed within 24 hr.

Perform mass spectrometry

23. For quantification of F_2-lsoPs by GC/NICI MS analysis, use an Agilent 6890N mass spectrometer with a computer interface. Chromatograph F_2-IsoPs on a 15-meter DB1701 fused silica capillary column. Program the column temperature from 190°C to 300°C at 20°C/mm. Use methane as the carrier gas for NICI at a flow rate of

1 μl/min. Set the ion source temperature to 250°C, the electron energy to 70 eV, and the filament current to 0.25 mA. Monitor for endogenous F_2-IsoPs using the carboxylate anion m/z 569 (M-181, loss of $CH_2C_6F_5$).

The corresponding carboxylate anion for the deuterated intemal standard is m/z 573.

In the authors' experience, the indicated column produces excellent separation of individual regioisomers compared to other columns.

REAGENTS AND SOLUTIONS

Use ultrapure (triply distilled) water or equivalent in all recipes and protocol steps. For common stock solutions, see ***APPENDIX 2A****; for suppliers, see* ***SUPPLIERS APPENDIX****.*

Folch solution

Combine 2 volumes of high-purity chloroform (containing ethanol as a preservative) with 1 volume of high-purity methanol, both available from Burdick and Jackson or VWR Scientific. Cool to 4°C. Store in dark in a brown bottle to prevent light degradation. Store up to 1 month at −20°C.

COMMENTARY

Background Information

Free radicals derived primarily from oxygen have been implicated in the pathophysiology of a wide variety of human diseases including atherosclerosis, cancer, neurodegenerative disorders, and even the normal aging process (Halliwell and Gutteridge, 1990). Much of the evidence for this, however, is indirect or circumstantial, largely because of limitations of methods that are available to quantify free radicals or the products they produce in biological systems. This is a particular problem when non-invasive approaches are used to assess oxidant injury in animals or humans (Halliwell and Grootveld, 1987; DeZwart et al., 1999).

Measures of lipid peroxidation are frequently utilized to implicate free radicals in pathophysiological processess. These measurements include quantification of short-chain alkanes, malondialdehyde, or conjugated dienes. Each of these, however, suffers from problems related to specificity and sensitivity, especially when utilized to quantify oxidant stress in vivo. Further, artifactual generation of these lipid peroxidation products can occur ex vivo, and factors such as endogenous metabolism can affect levels of compounds measured (DeZwart et al., 1999).

In 1990, the authors reported that a series of prostaglandin (PG)F_2-like compounds, termed F_2-isoprostanes (F_2-IsoPs), are produced in vivo in humans by a non-cyclooxygenase free radical–catalyzed mechanism involving the peroxidation of arachidonic acid (Morrow et al., 1990). Formation of these compounds initially involves the generation of four positional peroxyl radical isomers of arachidonic acid; these undergo endocyclization to PGG_2-like compounds that are subsequently reduced to PGF_2-like compounds. Four F_2-IsoP regioisomers are formed, each of which can theoretically be comprised of eight racemic diastereomers.

The authors have accumulated a large body of evidence that suggests that quantification of F_2-IsoPs represents a reliable and useful approach to assess lipid peroxidation and oxidant stress in vivo (see also *UNIT 17.5*). They readily increase in animal models of oxidant stress. Further, concentrations of F_2-IsoPs are present that are easily detected in normal human and animal biological fluids such as plasma and urine (Roberts and Morrow, 2000; Fam and Morrow, 2003). This allows the definition of a normal range, which permits an assessment of small increases in the formation of F_2-IsoPs in settings of mild oxidant stress. In addition, F_2-IsoPs can be detected in virtually every type of biological fluid analyzed thus far including plasma, urine, cerebrospinal fluid, bile, lymph, bronchoalveolar lavage fluid, and synovial fluid (Morrow et al., 2001). Levels of these compounds are also detectable in all types of tissues examined to date. These include liver, kidney, stomach, brain, lung, vascular tissue, muscle, and heart. Thus, the fact that F_2-IsoPs are detectable in various tissues and fluids provides the opportunity to assess the formation of these compounds at local sites of oxidant injury. Finally, F_2-IsoPs are increased in a number of human disorders associated with enhanced oxidant stress (Roberts and Morrow, 2000; Fam and Morrow, 2003).

The precursor of the F_2-IsoPs is arachidonic acid. The vast majority of arachidonic acid present in vivo exists esterified to phospholipids. Previously, the authors reported the novel finding that F_2-IsoPs are initially formed in situ from arachidonic acid esterified to phospholipids and then subsequently released in the free form by phospholipases (Morrow et al., 1992). This observation provides the basis for an important concept regarding the assessment of isoprostane formation in vivo in that when isoprostane generation is quantified, total production of F_2-IsoPs may be more accurately assessed by measuring levels of both free and esterified compounds. Furthermore, the fact that F_2-IsoPs are formed in situ in phospholipids can be utilized in an advantageous way to assess oxidant injury in specific animal or human organs by analyzing levels of these compounds esterified in phospholipids from tissue biopsy specimens obtained for diagnostic purposes.

Critical Parameters and Troubleshooting

Considerable care must be taken when harvesting and handling samples to prevent the artifactual ex vivo generation of F_2-IsoPs (Morrow and Roberts, 1997). F_2-IsoPs can be generated artifactually in arachidonate-containing biological fluids that remain >2 hr at room temperature, or stored at −20°C. However, storage of samples at −70°C prevents ex vivo oxidation and maintains sample integrity for at least 5 years. Ex vivo formation of F_2-IsoPs does not occur if samples are processed immediately after procurement or if BHT (and TPP in the case of arachidonate-rich fluids such as plasma) is added to the organic solvent during lipid extraction (Morrow and Roberts, 1997). Hydrolysis of lipids in tissues or biological fluids should be performed immediately after lipid extraction to avoid potential autoxidation of arachidonate contained in the phospholipids. In addition, artifactual generation of F_2-IsoP can also occur during sample preparation if reagents contain significant trace metal contamination. Thus, reagents should be of very high purity. The quality of water used during lipid extraction is extremely important. The authors routinely use triply distilled water or its equivalent. Finally, all glassware and plasticware should be rinsed with ultrapure (triply distilled) water prior to use (Morrow and Roberts, 2002).

During sample workup, there are several points in the assay during which tissue or fluid extracts can be safely stored overnight at −70°C. These include (1) following elution from the silica Sep-Pak in Basic Protocol 2, step 10, and (2) following extraction from silica after TLC purification in Basic Protocol 2, step 19.

A common problem encountered when performing this assay occurs after derivatization of F_2-IsoPs to trimethylsilyl ethers. These derivatives are readily hydrolyzed upon exposure to very small amounts of water. Loss of the trimethylsilyl ethers will result in a lack of detectable signal at the correct molecular weight when analyzed by MS. Should this occur, the sample should be dried under nitrogen and rederivatized and analyzed immediately.

Quantification by GC/negative ion chemical ionization (NICI) MS is an extremely sensitive method to quantify the F_2-IsoPs (Morrow and Roberts, 1999). The lower limits of detection of F_2-IsoPs is in the range of 1 to 5 pg using a deuterated standard with a blank of <5 ppt. Thus, it is not necessary to assay >1 to 3 ml of a fluid such as plasma, 0.2 ml urine, or 50 to 100 mg tissue.

It should be noted that the method outlined herein is one of several GC/MS techniques that have been developed by investigators to quantify F_2-IsoPs. The other assays utilize very similar purification and derivatization approaches although they quantify different F_2-IsoP regioisomers including $iPF_{2\alpha}$-I and $iPF_{2\alpha}$-VI (Lawson et al., 1998; Pratico et al., 1998). In addition, IsoPs can be quantified by liquid chromatography/MS and immunoassay although neither of these methods may be as sensitive or accurate as GC/MS (Fam and Morrow, 2003; Liang et al., 2003).

Anticipated Results

Figure 17.6.2 shows the selected ion current chromatogram obtained from the analysis of F_2-IsoPs in plasma from a rat after treatment with CCl_4 to induce an oxidant stress. The series of peaks in the upper m/z 569 selected ion current chromatogram represents different endogenous F_2-IsoPs. This pattern of peaks is virtually identical to that obtained from all other biological fluids and tissues that the authors have examined to date. In the lower m/z 573 chromatogram, the single peak represents the [$^2H_4$] 15-F_{2t}-IsoP internal standard that was added to the plasma sample. For quantification purposes, the peak denoted by an asterisk (*), which co-elutes with the 15-F_{2t}-IsoP internal standard, is routinely measured. Using the ratio of the intensity of this peak to that of the internal standard, the concentration of F_2-IsoPs was calculated to 742 pg/ml, ~36-fold above normal. The normal plasma

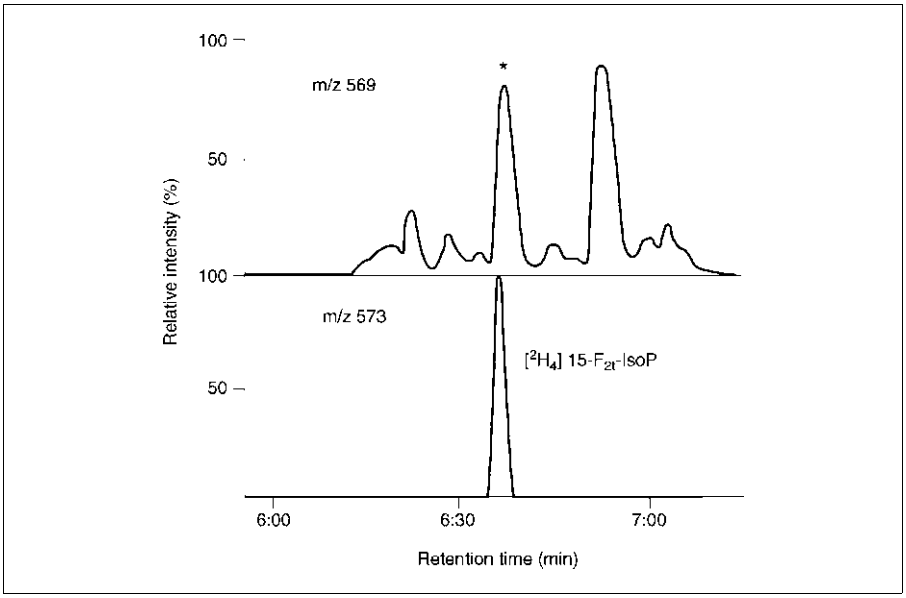

Figure 17.6.2 Analysis of F_2-IsoPs in plasma obtained from a rat 4 hr after treatment with CCl_4 (2 ml/kg orogastrically) to induce endogenous lipid peroxidation. The m/z 569 ion current chromatogram represents endogenous F_2-IsoPs. The m/z 573 ion current chromatogram represents the [$^2H_4$] 15-F_{2t}-IsoP internal standard. The peak in the upper chromatogram represented by the asterisk (*) is the one routinely used for quantification of the F_2-IsoPs. The concentration of F_2-IsoPs in the plasma using the asterisk (*) peak for quantification was calculated to be 742 pg/ml.

concentration of F_2-IsoPs in rats is 22 ± 4 pg/ml (mean ± 1 SD) and in normal human plasma is 35 ± 6 pg/ml (mean ± 1 SD) The reader is referred to previously published data for normal levels of F_2-IsoPs in other biological fluids and tissues (Morrow et al., 2001). Quantification of the F_2-IsoPs based on the intensity of the asterisk (*) peak shown in Figure 17.6.2 is highly precise and accurate. The precision is ± 6% and the accuracy is 96%.

Time Considerations

In general, 15 to 20 samples per day can be processed by an experienced investigator. Lipid extraction and hydrolysis of this number of samples requires ~3 hr, Sep-Pak purification requires ~1.5 hr, drying, derivatization, and TLC purification require ~2 hr, and extraction, drying, and silylation require 1 hr. Mass spectrometric analysis is automated and each sample requires ~15 min of machine time.

Literature Cited

DeZwart, L.L., Meerman, J.H.N., Commandeur, J.N.M., and Vermeulen, P.E. 1999. Biomarkers of free radical damage applications in experimental animals and in humans. *Free Rad. Biol. Med.* 26:202-226.

Fam, S.S. and Morrow, J.D. 2003. The isoprostanes: Unique products of arachidonic acid oxidation. *Curr. Med. Chem.* 10:1723-1740.

Halliwell, B. and Grootveld, M. 1987. The measurement of free radical reactions in humans. Some thoughts for future experimentation. *FEBS Lett.* 213:9-14.

Halliwell, B. and Gutteridge, J.M.C. 1990. Role of free radicals and catalytic metal ions in human disease: An overview. *Methods Enzymol.* 186: 1-85.

Lawson, J.A., Li, H., Rokach, J., Adiyaman, M., Hwang, S.W., Khanapure, S.P., and FitzGerald, G.A. 1998. Identification of two major F_2 isoprostanes, 8,12-iso- and 5-epi-8,12-iso-isoprostane $F_{2\alpha}$VI, in human urine. *J. Biol. Chem.* 293:29295-29301.

Liang, Y., Wei, P., Duke, R.W., Reaven, P.D., Harman, S.M., Cutler, R.G., and Heward, C.B. 2003. Quantification of 8-iso-prostaglandin $F_{2\alpha}$ and 2,3-dinor-8-iso-prostaglandin $F_{2\alpha}$ in human urine using liquid chromatography-tandem mass spectrometry. *Free Radic. Biol. Med.* 34:409-418.

Morrow, J.D. and Roberts, L.J. 1997. The isoprostanes: Unique bioactive products of lipid peroxidation. *Prog. Lipid Res.* 36:1-21.

Morrow, J.D. and Roberts, L.J. 1999. Mass spectrometric quantification of F_2-isoprostanes in biological fluids and tissues. *Meth. Enzymol.* 300:3-12.

Morrow, J.D. and Roberts, L.J. 2002. Mass spectrometric quantification of F_2-isoprostanes as indicators of oxidant stress. *Meth. Molec. Biol.* 186:57-66.

Morrow, J.D., Hill, K.E., Burk, R.F, Nammour, T.M., Badr, K.F, and Roberts, L.J. 1990. A series of prostaglandin F_2-like compounds are produced in vivo in humans by a non-cyclooxygenase, free radical catalyzed mechanism. *Proc. Natl. Acad. Sci. U.S.A.* 87:9383-9387.

Morrow, J.D., Awad, J.A., Boss, H.J., Blair, I.A., and Roberts, L.J. 1992. Non-cyclooxygenase-derived prostanoids (F_2-isoprostanes) are formed in situ on phospholipids. *Proc. Natl. Acad. Sci. U.S.A.* 89:10721-10725.

Morrow, J.D., Zackert, W.E., Van der Ende, D.S., Reich, E.E., Terry, E.S., Cox, B., Sanchez, S.C., Montine, T.J., and Roberts, L.J. 2001. Quantification of isoprostanes as indicators of oxidant stress in vivo. *In* Handbook of Antioxidants 2nd ed. (E. Cadenas and L. Packer, eds.) pp. 57-74. Marcel Dekker, New York.

Pratico, D., Barry, O.P., Lawson, J.A., Adiyaman, M., Hwang, S.W., Khanapure, S.P., Iuliano, L., Rokach, J., and FitzGerald, G.A. 1998. $IPF_{2\alpha}$-1: An index of lipid peroxidation in humans. *Proc. Natl. Acad. Sci. U.S.A.* 95:3449-3454.

Roberts, L.J. and Morrow, J.D. 2000. Measurement of F_2-isoprostanes as an index of oxidative stress in vivo. *Free Radic. Biol. Med.* 28:505-513.

Key References

Fam and Morrow, 2003. See above.

An up-to-date review of the isoprostane field.

Morrow et al., 1990. See above.

The initial report of isoprostane formation in vivo and the potential use of these compounds as an index of oxidant stress in vivo.

Contributed by Erik S. Musiek and Jason D. Morrow
Vanderbilt University School of Medicine
Nashville, Tennessee

Immuno-Spin Trapping: Detection of Protein-Centered Radicals

Protein-centered radicals are involved in biological oxidative damage induced by drugs, environmental hazards, and cellular reactive oxygen species. They can be generated by, among others, hydrogen peroxide (H_2O_2)-induced hemoprotein- or metal-catalyzed protein oxidations (Fig. 17.7.1). Because of their paramagnetic properties, these radicals can be detected and analyzed by direct electron spin resonance (ESR; also known as electron paramagnetic resonance, EPR). After a few microseconds or seconds, via mechanisms that are not completely understood, they decay to diamagnetic species (ESR-silent species).

In the presence of spin traps, such as 5,5-dimethyl-1-pyrroline *N*-oxide (DMPO), protein-centered radicals can be trapped to form DMPO-protein radical adducts in which the formation of a new covalent linkage between the spin trap and the protein-centered radical preserves their free radical character. These radical adducts have a longer half-life than their parent radicals, thus DMPO-protein nitroxide radical adducts can also be characterized and studied by ESR. However, after a few seconds or minutes these species also decay to ESR-silent species by reduction or oxidation reactions to hydroxylamine or nitrone adducts, respectively, with preservation of the covalent bridge but not their paramagnetic properties.

In an oxidizing environment, DMPO-protein nitroxide radical adducts decay to stable DMPO-protein radical–derived nitrone adducts, which can be detected and identified by immuno-spin trapping. This new technology combines the specificity and sensitivity of both spin trapping and antigen-antibody interaction and is based on the detection of the nitrone moiety in DMPO-protein radical–derived nitrone adducts by using an antiserum against DMPO (Fig. 17.7.1).

Some of the advantages of using immuno-spin trapping rather than ESR and ESR-spin trapping to detect protein-centered radicals are: (1) the feasibility of applying this technology in any research, clinic, or academic laboratory without needing complicated equipment or specialists in physical chemistry and quantum mechanics, (2) the small quantity of sample required (microgram), and (3) the possibility of detecting more than one protein-centered radical in the same system and determining their approximate molecular weights. Moreover, day-to-day immuno-spin trapping is proving to be a

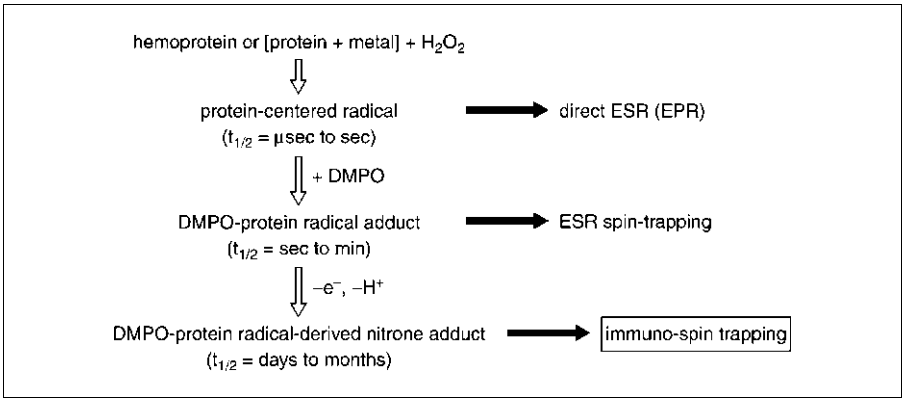

Figure 17.7.1 Detection of hydrogen peroxide (H_2O_2)-induced protein-centered radicals.

Contributed by Dario C. Ramirez and Ronald P. Mason
Current Protocols in Toxicology (2005) 17.7.1-17.7.18

simple, reliable, affordable, sensitive, and specific approach to detecting protein-centered radicals in situ and in real time in vitro, ex vivo, and in vivo, and it could be a powerful tool in toxicological research.

In this unit, protocols for the production and immuno-spin trapping detection of H_2O_2-induced horse heart metmyoglobin (metMb)- and human oxyhemoglobin (oxyHb)-DMPO radical–derived nitrone adducts are described (see Basic Protocols 1 and 2). Immuno-spin trapping assays include enzyme-linked immunosorbent assay (ELISA; *UNIT 18.7*) and immunoblotting to detect and characterize protein-centered radicals as their DMPO-protein radical–derived nitrone adducts.

BASIC PROTOCOL 1

PRODUCTION AND DETECTION OF HEMOPROTEIN-CENTERED RADICALS BY IMMUNO-SPIN TRAPPING ELISA

Enzyme-linked immunosorbent assay (ELISA; *UNIT 18.7*) is a heterogeneous—i.e., requires separation between bound and unbound material in some step(s)—immunochemical technique that allows simultaneous screening of many samples (Tijssen, 1985). In this technique, antigens (nitrone adducts) are bound under alkaline conditions at the bottom of a 96-well microtiter plate through hydrophobic interactions. After coating, unbound material is removed by a wash step with a buffer containing detergent and an inert protein to remove any nonspecific interactions. This step allows removal of any non-protein nitrone adducts that can interfere with the detection of protein nitrone adducts. This represents one of the most important advantages of heterogeneous assays like ELISA compared to homogeneous assays such as ESR-spin trapping.

After the wash step, the first antibody is added. After incubation, nonspecific bound and unbound antiserum is removed by two or three wash steps followed by addition of the secondary antibody labeled with an enzyme. Then, after further incubation, unbound and weak nonspecific interactions are removed by two or three wash steps. Finally, immuno-complexes are detected by adding enzyme substrates that produce luminescence or soluble-colored products that can be detected and measured.

Materials

Metmyoglobin (metMb; USB)
Oxyhemoglobin (oxyHb; Apex Biochemicals)
H_2O_2 (Alfa Aesar)
Chelex-treated sodium phosphate buffer, pH 7.7 (see recipe)
5,5-Dimethyl-1-pyrroline *N*-oxide (DMPO; Alexis Biochemicals)
Chelex-treated sodium phosphate buffer, pH 7.4, containing 1 mM diethylenetriaminepentaacetic acid (DTPA)
PD-10 desalting columns (Amersham Biosciences)
Catalase solution (100 or 500 IU, Roche Applied Bioscience)
Coating buffer (see recipe)
Wash buffer (see recipe)
Blocking buffer (see recipe)
Primary antibody solution (see recipe)
Secondary antibody solution (see recipe)
Chemiluminescence substrate for ELISA (see recipe)
37°C incubator with agitator
96-well white microtiter plates (e.g., Greiner Bio-One, PGC)
Automated microtiter plate washer (optional)
Multichannel pipettor
Luminescence reader for microtiter plates or strips (optional)

Table 17.7.1 Extinction Coefficients of Reagents

Reagent (abbreviation)	Supplier	Extinction coefficient
DMPO[a]	Alexis Biochemicals	$\varepsilon_{228} = 7800\ M^{-1}\ cm^{-1}$
H_2O_2	Alfa Aesar	$\varepsilon_{240} = 43.6\ M^{-1}\ cm^{-1}$
Metmyoglobin (metMb)	USB	$\varepsilon_{406} = 154\ mM^{-1}\ cm^{-1}$
Oxyhemoglobin (oxyHb)[b]	Apex Biochemicals	$\varepsilon_{541} = 13.8\ mM^{-1}\ cm^{-1}$

[a]Purified by vacuum sublimation at room temperature and stored under an argon atmosphere at −70°C.
[b]A gift from Apex Biochemicals.

Prepare DMPO-protein radical-derived nitrone adducts (i.e., sample to analyze)

1. Prepare hemoprotein [metmyoglobin (metMb) and oxyhemoglobin (oxyHb)] solutions by completely dissolving metMb or diluting oxyHb in 500 µl of Chelex-treated sodium phosphate buffer, pH 7.7, at room temperature. Pour solutions of metMb and oxyHb through PD-10 desalting columns to eliminate any preservatives and collect the colored eluate. Immediately before use, prepare 10× stock solutions of the reagents necessary to produce DMPO-protein radical-derived nitrone adducts (e.g., hemoprotein, H_2O_2, and DMPO) by using known extinction coefficients (see Table 17.7.1). Prepare all stock solutions in Chelex-treated sodium phosphate buffer and keep on ice until use.

   MetMb and oxyHb solutions are brown and red solutions, respectively. Hemoprotein stock solutions can be stored for 1 day at 4°C before use without significant variation in results.

   Typical reagent concentrations used in immuno-spin trapping experiments can be found in Figures 17.7.2 to 17.7.6 (also see Anticipated Results).

2. Prepare the reaction mixture by adding 30 µl of a 10× stock solution of hemoprotein (metMb or oxyHb) to 210 µl Chelex-treated sodium phosphate buffer containing 1 mM DTPA, at room temperature. Then, add 30 µl of 10× DMPO stock solution and start reaction by adding 30 µl of freshly prepared 10× H_2O_2 stock solution.

3. Incubate reaction mixture 1 hr at 37°C with agitation. Stop reaction by removing excess H_2O_2 with 10 µl of 100 IU/ml catalase solution.

   Under these conditions DMPO-protein radical-derived nitrone adducts are formed and are ready to be measured by ELISA.

   After the chemical reaction and before analysis, it is prudent, but not necessary, to eliminate excess reagent (e.g., DMPO and H_2O_2) by dialysis using a membrane with a cut-off appropriate for the molecular weight of the protein under analysis. Dialysis of the reaction mixture (300 µl) may be performed using a 0.1- to 0.5-ml Slide-A-Lyzer dialysis cassette (Pierce) against 2 liters of Chelex-treated sodium phosphate buffer, pH 7.4, containing 1 mM DTPA at 4°C with three changes of buffer.

   After stopping the reaction with catalase or elimination of reagent excess by dialysis, DMPO-protein radical-derived nitrone adducts can be stored up to 3 weeks at 4°C or up to 6 months at –20°C.

   Protein-centered radicals have been detected in many systems containing protein-redox active metals and peroxides. Consequently, careful selection of the conditions for preparing the nitrone adducts is a key factor for success.

Bind DMPO-protein radical-derived nitrone adducts to ELISA plates

4. Add 190 µl coating buffer and 10 µl (~0.5 to 3 µg proteins) experimental and control samples to each well of a 96-well white microtiter plate. Incubate plate 60 min at room temperature to allow samples to bind to the plate.

High protein binding microtiter plates are recommended. The authors use 96-well white microtiter plates.

Typically, 0.5 to 3 μg of protein are used for ELISA analysis of DMPO-protein radical–derived nitrone adducts.

5. Wash plate one time with 300 μl wash buffer in each well and incubate plate for 10 min at room temperature. Remove wash buffer.

   For more reproducible results, the authors recommend using multichannel pipettors and an automated microtiter plate washer. However, if an automated plate washer is not available, washing steps can be performed as follows without significant variations in the results: add 300 μl of wash buffer to each well and incubate the plate for 5 min in an orbital shaker. Remove the wash buffer by aspirating with a multichannel pipettor, being careful not to touch the bottom of the wells, or by inverting and shaking the plate. Repeat wash buffer addition, incubation, and evacuation two or three additional times. Remove the excess wash buffer from the last wash step by inverting the plate on paper towels. Do not let the plate dry.

6. Add 200 μl blocking buffer to each well and incubate the microtiter plate 60 min at room temperature.

7. Repeat step 5.

Detect antigen

8. Add 200 μl primary antibody solution to each well and incubate 60 min at 37°C to allow the antibodies to recognize and bind to the DMPO-protein radical–derived nitrone adducts.

9. Repeat step 5 three times.

   This step removes the unbound primary antibody.

10. Add 200 μl of the secondary antibody solution and incubate microtiter plate 60 min at 37°C to allow the secondary antibody to recognize and bind to the primary antibody.

11. Repeat step 5 three times.

Detect antigen-antibody complexes

12. Add 200 μl chemiluminescence substrate for ELISA and read immediately in a microtiter plate reader equipped with a luminometer.

    Alternatively, other chromogenic substrates for alkaline phosphatase can be used and the absorbance detected by studying the absorbance of its soluble product.

BASIC PROTOCOL 2

PREPARATION AND IMMUNOBLOT ANALYSIS OF DMPO-PROTEIN RADICAL–DERIVED NITRONE ADDUCTS

The authors use ELISA to quantify protein radical–derived nitrone adduct generation, but to study and identify any structural effect on the protein (e.g., aggregation or fragmentation), immunoblot analysis, which also provides an approximate molecular weight for the DMPO-protein radical–derived nitrone adduct(s), is used. Although less sensitive than ELISA, immunoblotting is the only immunochemical analysis that allows for the investigation of more than one protein-centered radical adduct in the same system (see Anticipated Results) or in complex mixtures such as cellular environments (Ramirez et al., 2003) or tissue homogenates (Detweiler et al., 2002). Once protein-centered radicals are detected, the corresponding band in gels stained by Coomassie blue can be cut, digested, and analyzed by mass spectrometry to identify the protein and even the residue where DMPO is bound, i.e., where the radical was produced (Deterding et al., 2004).

Materials

Metmyoglobin (metMb; USB)
H_2O_2 (Alfa Aesar)
Oxyhemoglobin (oxyHb; Apex Biochemicals)
5,5-Dimethyl-1-pyrroline *N*-oxide (DMPO; Alexis Biochemicals)
Chelex-treated sodium phosphate buffer, pH 7.4, containing 1 mM diethylenetriaminepentaacetic acid (DTPA)
PD-10 desalting columns (Amersham Biosciences)
Catalase solution (100 or 500 IU, Roche Applied Bioscience)
4× NuPage LDS sample buffer (Invitrogen)
10× NuPAGE sample reducing agent (Invitrogen)
4% to 12% NuPAGE Novex Bis-Tris gel (1.0-mm, 10-well; Invitrogen)
Running buffer (see recipe)
Nitrocellulose membranes (0.45-μm pore size, Invitrogen)
Transfer buffer (see recipe), cold
0.1% (w/v) Ponceau S red in 4% (v/v) acetic acid
Blocking buffer (see recipe)
Wash buffer (see recipe)
Primary antibody solution (see recipe)
Secondary antibody solution (see recipe)
TBS, pH 9.6 (see recipe)
Chemiluminescence substrate for westernblots (see recipe)
1-Step NBT/BCIP reagent (Pierce)

37°C incubator with agitator
70° to 80°C water bath
Mini electrophoresis system (e.g., XCell SureLock Mini-Cell system, Invitrogen)
Mini-gel blot module (e.g., XCell II Blot Module, Invitrogen)
X-ray film (e.g., CL-XPosure film, Pierce)

Prepare DMPO-protein radical-derived nitrone adducts (i.e., the sample to analyze)

1. Prepare 10× stock solutions of reagents [i.e., metmyoglobin (metMb), oxyhemoglobin (oxyHb), DMPO, and H_2O_2]. Completely dissolve metMb or dilute oxyHb solution in 500 μl of Chelex-treated sodium phosphate buffer, pH 7.4, at room temperature. Pour solutions of metMb and oxyHb through PD-10 desalting columns (equilibrated with distilled water) to eliminate any preservatives and collect the colored eluate. Immediately before use, prepare ten times concentrated stock reagent (hemoproteins, H_2O_2, and DMPO) solutions than the final concentrations required in the reaction mixture (see Fig. 17.7.4) in Chelex-treated sodium phosphate buffer by using known extinction coefficients (see Table 17.7.1) and keep on ice until used.

   MetMb and oxyHb solutions are brown and red, respectively. These hemoprotein solutions can be stored for 1 day at 4°C before use without significant variation in results.

2. Prepare the reaction mixture in disposable 1.5-ml microcentrifuge tubes. Add 30 μl of 10× stock solution of hemoprotein (metMb or oxyHb) to 210 μl Chelex-treated phosphate buffer containing 1 mM DTPA at room temperature. Then add 30 μl of 10× stock DMPO solution and start reaction by adding 30 μl of freshly prepared 10× H_2O_2 stock solution.

3. Incubate reaction mixture 1 hr at 37°C with agitation. Stop reaction by removing excess H_2O_2 with 10 μl of 500 IU/ml catalase solution.

   Under these conditions, DMPO-protein radical-derived nitrone adducts are formed and are ready to be resolved by SDS-PAGE.

It is recommended to eliminate excess reagent (i.e., DMPO and H_2O_2) by dialysis. Dialysis of the reaction mixture (300 μl) is performed using a 0.1- to 0.5-ml Slide-A-Lyzer dialysis cassette (Pierce) against 2 liters of Chelex-treated sodium phosphate buffer, pH 7.4, containing 1 mM DTPA at 4°C with three changes of buffer.

After stopping the reaction with catalase or eliminating reagent excess by dialysis, DMPO-protein radical-derived nitrone adducts can be stored for 3 weeks at 4°C or up to 6 months at –20°C.

Protein-centered radicals have been detected in many systems containing protein-redox active metals and peroxides. Consequently, careful selection of the conditions for preparing the nitrone adducts is a key factor for success.

Prepare sample to resolve by SDS-PAGE

4. Mix 30 μl of reaction mixture, 10 μl of 4× NuPage LDS sample buffer, and 4 μl of 10× NuPAGE sample reducing agent.

   In place of the NuPAGE sample reducing agent, 4 μl of fresh 0.5 M dithiotreitol (DTT) solution can be used with similar results.

5. Heat the sample 7 to 10 min in a 70° to 80°C water bath, and then let it cool to room temperature.

6. Load 10 μl sample per lane of a 4% to 12% NuPAGE Novex Bis-Tris gel.

   The ten-well, 1-mm, 4% to 12% NuPAGE Novex Bis-Tris gels are appropriate for separation of proteins between 3 and 100 kDa and resolve well for proteins used in this protocol. Careful selection of gels is a key factor in successful immuno-spin trapping.

   For better standard-molecular-weight band visualization, the authors add 1 to 3 μl of 1× SeeBlue Plus2 pre-stained standard (Invitrogen) to the first and middle lanes of the gel.

7. Perform protein separation using an electrophoresis system under continuous voltage conditions for 40 min at 200 V with running buffer. Remove the running buffer and add distilled water to cool the gel.

   This step in the procedure permits easier handling of the gel during the following steps.

8. Remove glass or plastic from the gel, cut a piece of nitrocellulose membrane for orientation, and place on top of the gel. Remove any bubbles between membrane and gel by submerging under cool (0° to 4°C) transfer buffer.

   CAUTION: *Acrylamide compounds are neurotoxic and carcinogenic for laboratory animals and humans; consequently, gloves and adequate safety practices must be followed to avoid exposure.*

9. Blot proteins onto nitrocellulose membrane by using a nitrocellulose membrane filter paper sandwich. Perform the transfer in a mini-gel blot module for 20 to 30 min at 40 V.

   Under the buffer conditions used in this process, proteins will migrate from the negative electrode to the positive electrode.

   Those who are unfamiliar with blotting may refer to the NuPAGE Bis-Tris gel instruction manual, where clear instructions on how to assemble the blotting sandwich are provided. This booklet is included in every box of NuPAGE gels and can also be found on the manufacturer's Web site (see Internet Resources).

Stain protein on membrane

10. Transfer the membrane to a clean tray or dish (e.g., weigh boats, pipet tip boxes, or other) and rinse with distilled water.

    To minimize the volume of stains, buffers, and antibody solutions, it is convenient that the tray or dish is only slightly larger than the membrane.

11. Incubate the membrane with 0.1% Ponceau S red in 4% acetic acid for 10 to 30 sec. Wash the membrane with distilled water until red bands (i.e., indication of proteins) appear on a white background, which can then be scanned or photographed.

    The red bands on the membrane will disappear during the blocking process.

    This staining allows for observation of any defects in the blotting process such as poor blotting or diffusion of proteins on the membrane. Usually, the latter is due to the poor quality of sponges used in the transfer sandwich. If this occurs, the authors recommend using new sponges. Sponges should not be used for >20 blotting processes.

    Before immunoblotting, membranes can be stored dry for weeks between pages of a book, or in water if the immunostaining is started the next morning. If stored dry, it is important to rehydrate the membrane for at least 30 min in distilled water at room temperature.

Detect DMPO-protein radical-derived nitrone adducts on membrane by immunoblotting

12. Incubate the membrane with enough volume of blocking buffer to cover the membrane 60 min at room temperature. Remove blocking buffer.

    Typically, the authors use 25 ml of reagents. In the following steps, use enough volume of buffers and solutions to cover the membrane.

13. Cover the membrane with wash buffer and incubate for 10 min at room temperature. Remove wash buffer.

14. Incubate the membrane with primary antibody solution 60 min at room temperature.

15. Repeat step 13 three times.

16. Incubate the membrane with secondary antibody solution 60 min at room temperature.

17. Repeat step 13 three times. After removal of the last wash buffer, cover the membrane with TBS, pH 9.6.

    Incubation of the membrane after the last wash with TBS, pH 9.6, will increase the activity of alkaline phosphatase with a consequent increase in detection sensitivity.

Develop antigen-antibody complexes by using ECL

18. Remove the membrane, place it face up onto a piece of plastic, add 5 ml chemiluminescence substrate for western blots, and incubate for 2 min in the dark.

19. Remove excess reagent by wicking with paper towels without touching the membrane and place the membrane between two pieces of plastic.

    The authors use office plastic folders.

20. Remove the bubbles remaining between the plastic and membrane by rolling with a pipet or pressing them onto a paper towel.

    This procedure also ensures the complete removal of excess liquid.

21. In a dark room, expose membrane to X-ray film.

    Exposure time may vary from a few seconds to a few minutes (or longer), depending upon the amount of antigen to be detected.

22. Develop the X-ray film.

    If desired, the same membrane can be used for colorimetric development of the antigen-antibody complexes (optional).

23. Scan or photograph the membrane to make a permanent record of the results.

Develop antigen-antibody complex by using one-step NBT/BCIP reagent (optional)

Sometimes unexpected problems can occur due to failure of the X-ray film, equipment, or developing reagents. NBT/BCIP development is also a way to keep a good record, but is not necessary.

24. (*Optional*) For membrane used for luminescent development, wash three times, 5 min each, in distilled water with agitation. Finally, wash with 25 ml TBS, pH 9.6, for 5 min.

25. (*Optional*) Add 10 ml 1-Step NBT/BCIP reagent, incubate 15 min or until purple bands are clearly visible, then stop the reaction by washing three times, 5 min each, with distilled water.

26. Scan or photograph the membrane to make a permanent record of the results.

CAUTION: *Use gloves and laboratory clothes when developing antigen-antibody complexes by either method as the reagents can be toxic and carcinogenic.*

REAGENTS AND SOLUTIONS

Use Milli-Q-purified water or equivalent in all recipes and protocol steps. For common stock solutions, see ***APPENDIX 2A****; for suppliers, see* ***SUPPLIERS APPENDIX****.*

Blocking buffer

100 ml coating buffer (see recipe)
2 ml gelatin from cold water fish skin (45% v/v, Sigma)
Mix until total dissolution.
Prepare 1 hr before use to ensure total solubilization

Alternatively, 2.5% (w/v) bovine serum albumin and 2.5% (w/v) casein in coating buffer or SeaBlock (Pierce) can be used without significant variation in results.

Chelex-treated sodium phosphate buffer, 0.1 M (pH 7.4)

Weigh 5 g of Chelex 100 resin (Bio-Rad) in a 1-liter beaker and add 1 liter of water with a magnetic stirrer, stir the resin at low speed (to avoid damaging the resin) for 2 hr at 4°C. Allow the resin to sediment and remove the water. Resuspend the resin in 1 liter of distilled water and allow the resin to wash overnight at 4°C. Repeat this procedure one more time for 2 hr. Then filter the suspension using a 0.45-μm filter and wash the resin with 1 liter of 0.1 M sodium phosphate buffer, pH 7.4, to adjust pH. Filter the excess buffer and add the washed resin to 1 liter phosphate buffer and stir with a magnetic stirrer at slow speed overnight at 4°C. On the next day, filter the treated phosphate buffer to eliminate the resin and add 1 ml of 100 mM DTPA solution (stock) to the filtrate to make 1 liter of Chelex-treated sodium phosphate buffer, pH 7.4, containing 1 mM DTPA.

Chemiluminescence substrate

For ELISA:
Add 50 μl CDP-star (Roche Applied Science) to 50 ml TBS, pH 9.6 (see recipe). Prepare immediately before use in buffer at room temperature and mix well.
For western blot:
Add 50 μl CDP-star to 50 ml TBS, pH 9.6 (see recipe) and 100 μl Nitro-Block II (Tropix). Prepare immediately before use in buffer at room temperature and mix well.

Coating buffer

1.59 g sodium carbonate (Na_2CO_3)
2.93 g sodium bicarbonate ($NaHCO_3$)

continued

0.20 g sodium azide (NaN_3)
Dissolve in 900 ml distilled water, adjust to pH 9.6 with NaOH or HCl and make up to 1 liter
Store up to 1 month at room temperature

In some cases, antigens bound under neutral conditions, such as distilled water or phosphate buffer, give lower backgrounds than bicarbonate buffer. The authors recommend that the coating buffer be optimized to produce the highest signal/background ratio.

Primary antibody solution

Dilute primary anti-DMPO (Alexis Biochemicals, Cayman Chemicals, and Oxford Biomedical Research) antibody 1:5000 in wash buffer (see recipe). Dilute the antiserum immediately before use.

Running buffer

50 ml 20× NuPAGE MES SDS running buffer (Invitrogen)
850 ml distilled water
Prepare immediately before use

Secondary antibody solution

Dilute secondary ImmunoPure goat anti-rabbit IgG (specific to Fc) antibody, alkaline phosphatase–conjugated (Pierce) 1:5000 in wash buffer. Dilute the antiserum immediately before use.

IMPORTANT NOTE: Hemoproteins and metal-protein complexes can catalyze the reduction of H_2O_2 and oxidation of peroxidase substrates with the production of nonspecific signals in ELISA and western blot analysis. Consequently, secondary antiserum conjugated to peroxidases will produce high unspecific signals that are not associated with antigen-antibody interaction, but related to the peroxidase activity of the hemoprotein or metal-protein under analysis.

Tris-buffered saline, 10× (pH 7.4)

30 g TRIZMA base
80 g NaCl
2 g KCl
800 ml distilled water
Adjust to pH 7.4 with concentrated HCl. Bring to 1 liter, and filter sterilize into 100-ml flasks
Store up to 1 month at room temperature

Tris-buffered saline, pH 9.6 (TBS, pH 9.6)

In 800 ml distilled H_2O, add the following:
32 g NaCl
0.8 g KCl
12 g Tris
Adjust to pH 9.6 with 1 M HCl
Bring up to 1 liter with H_2O
Sterilize by filtering through a 0.45-μm filter
Store up to 1 month at room temperature

Transfer buffer

800 ml distilled water
50 ml 20× NuPAGE transfer buffer (Invitrogen)
100 ml methanol
1 ml antioxidant
Add distilled water to make 1 liter
Prepare immediately before use

Wash buffer

100 ml 10× TBS (see recipe)
900 ml distilled water
2 ml cold-water fish gelatin
0.5 ml Tween 20 (USB)
Mix until total dissolution
Store at 4°C and let it reach room temperature before use

Alternatively, 0.25% (w/v) BSA plus 0.25% (w/v) casein acid hydrolyzate in 1× TBS and 0.05% (v/v) Tween 20 can be used in place of fish gelatin.

COMMENTARY

Background Information

A growing field of evidence suggests that free radicals and particularly protein-centered radicals are involved in aging, pathophysiology, and toxicological processes (Berlett and Stadtman, 1997; Dean et al., 1997; Mason, 2000; Hawkins and Davies, 2001). A free radical is an atom or group of atoms possessing one unpaired electron. The unpaired electron gives these species paramagnetic properties that make them suitable for detection by electron spin resonance (ESR). However, because of the high reactivity of protein-centered radicals, they are generally stable for only microseconds to seconds before they decay to ESR-silent species.

In the spin-trapping technique, a reactive radical ($R^{\bullet}$) adds across the double bond of a diamagnetic spin trap (S = T) to form a much more stable free radical, a radical adduct (R-S-$T^{\bullet}$), which can then be examined by electron spin resonance (ESR; Mason, 2000).

$$R^{\bullet} + S = T \rightarrow R\text{-}S\text{-}T^{\bullet}$$

The most popular of these spin traps is 5,5-dimethyl-1-pyrroline *N*-oxide (DMPO).

When DMPO traps a protein-centered radical, a nitroxide radical adduct is formed with a covalent bond between DMPO and the protein (Davies and Hawkins, 2004). This species conserves the unpaired electron of the parental protein-centered radical, resulting in another paramagnetic species that can be studied by ESR (Davies and Hawkins, 2004). The specificity of the reaction between a nitrone spin trap and protein-centered radicals has already made spin trapping with ESR detection the most universal, specific tool for the detection of free radicals (Mason, 2000) and protein-centered radicals (Clement et al., 2001; Davies and Hawkins, 2004) in biological systems. However, ESR and ESR-spin trapping require extensive knowledge of mathematics and physical chemistry and also require complicated equipment, which has limited their application in biomedical laboratories.

The radical adduct is a paramagnetic species that decays (seconds to minutes) by oxidation or reduction to ESR-silent species by mechanisms still not well understood. Although the oxidation of nitroxide radical adducts to the corresponding ESR-silent nitrone adduct has not been well studied (Mason, 2004), once the ESR signal has decayed, nitrone adducts are evidence of earlier radical reactions (Deterding et al., 2004).

Clearly, it would be advantageous to detect markers of protein radical formation without using ESR. A potential alternative to ESR was suggested by flow injection electrospray ionization mass spectrometry (ESI/MS) of the reaction products of myoglobin with H_2O_2 and DMPO. This analysis, performed after the ESR signal disappeared, demonstrated the presence of a myoglobin-derived product with a mass increase of 111 Da. This species corresponded to the addition of DMPO minus two hydrogen ions as expected for the formation of a covalent bond between Mb and DMPO (Detweiler et al., 2002). The persistence of the covalent bond after the radical character of the adduct was lost suggests that the oxidized form, the nitrone moiety, could form the basis of an antigen (Mason, 2004).

The nitrone group does not exist in nature, thus eliminating the possibility of a false-positive from endogenous cellular components. It should be highly antigenic, as is the related nitro group (Mason, 2004). Moreover, the site of DMPO attachment to the protein is a specific marker for where the radical resided. Consequently, an antiserum that recognizes DMPO was developed in the authors' laboratory (Detweiler et al., 2002). To facilitate antiserum production, a DMPO derivative containing an octanoic acid (OA) tail was synthesized, and this DMPO-OA was conjugated to a carrier protein chicken egg albumin for the immunization of rabbits. After the immunization

Table 17.7.2 Troubleshooting Guide to Immuno-Spin Trapping

Problem	Possible cause	Solution
No nitrone adducts are detected by ELISA in a solution of a hemoprotein with peroxidase activity, DMPO, and H_2O_2	No amino acid-centered radical was formed as is the case with horseradish peroxidase	Check if the protein radical has previously been detected by ESR and/or ESR-spin trapping with DMPO. Study a known system to obtain training.
High background/signal ratio in ELISA	Inappropriate blocking buffer	Probe with another blocking protein such as dry milk, casein/BSA, or SeaBlock solution (Pierce).
	DMPO was not purified	Use purified DMPO.
	High amount of protein added to well, producing high nonspecific antiserum binding.	Add a lower amount of protein to each well (typically 0.5 to 3 μg protein/well are enough).
	High nonspecific binding	Increase the number of washes or increase Tween-20 concentration in the washing buffer to 0.1%.
H_2O_2-concentration dependence in the nitrone adducts was observed by ELISA but not by immunoblot analysis	It is possible that DMPO binds nonspecifically to protein radicals formed at the high temperatures used to prepare samples for reducing blots	Dialyze samples before mixing with the sample buffer.
No protein-centered radicals are observed in immunoblot analysis but they were detected by ELISA	Nitrone epitope was modified by the reducing agent	Run the SDS-PAGE under non-reducing conditions or change the reducing agent. The use of 2-ME as a reducing agent (see Anticipated Results; Fig. 17.7.2B) is not recommended.
Diffuse band pattern was observed	If SDS-PAGE was well done, as confirmed by protein staining of the gel, it could be due to a low blot quality; this must be checked immediately after the transfer by using the temporary stain procedure described in the immunoblot protocol	Change sponges, check blotting apparatus in special electrodes.

regime, the rabbits were bled and the serum containing anti-DMPO polyclonal antibodies was collected (Detweiler et al., 2002). This antiserum has been used to develop immuno-spin trapping (Ramirez et al., 2003) and it is commercially available from Alexis Biochemicals, Cayman Chemicals, and Oxford Biomedical Research.

Initially, this antiserum was successfully used to detect myoglobin-centered radicals in supernatant obtained from rat heart homogenate (Detweiler et al., 2002). Later immuno-spin trapping was applied in the study of protein-centered radicals generated in hemoglobin treated with peroxynitrite (Romero et al., 2003), ketoprofen/UV-A irradiation (He et al., 2003), and H_2O_2 (Ramirez et al., 2003; Deterding et al., 2004). The H_2O_2-induced DMPO-hemoglobin adducts were detected by immuno-spin trapping (Ramirez et al., 2003), and then the exact localization of the radical sites where DMPO was bound to Hb was determined using LC/MS and MS/MS analysis of proteolytic fragments (Deterding et al., 2004). Recently, a lactoperoxidase-centered, thiol-dependent radical was also detected by immuno-spin trapping in incubations containing lactoperoxidase, thiols, and DMPO (Guo et al., 2004). Hypochlorite-induced DMPO-cytochrome *c* adducts have also been reported (Chen et al., 2004).

Critical Parameters and Troubleshooting

Mixing unpurified DMPO with oxyHb or metHb, in the absence of H_2O_2 produced protein aggregation detectable as dimers (~32 kDa) in reducing SDS-PAGE and high

background in ELISA and immunoblot experiments. These background and aggregation patterns were abolished when catalase was added before the addition of DMPO, suggesting that H_2O_2 is a contaminant present in commercial DMPO preparations (Ramirez and Mason, unpub. observ.). Before DMPO is used as a spin trap, it is appropriate to purify it by vacuum sublimation and store it in 50-µl aliquots under an argon atmosphere at −70°C. It is important that no protein radical–derived nitrone adducts or aggregation be observed when purified DMPO is incubated for 1 to 2 hr with hemoproteins.

On the other hand, when compounds such as reducing thiols are added to the analysis mixture, they have effects not associated with their metal-chelating abilities, and in these systems, they can modify nitrone adducts to immuno-spin trapping silent species (see the effect of 2-ME on DMPO-Hb radical–derived nitrone adducts) or even produce DMPO-trappable protein-centered radicals (Guo et al., 2004).

Because of the heating procedure required before SDS-PAGE separation, the nitrone adducts or the spin trap may react with the protein and thiols, i.e., under reducing

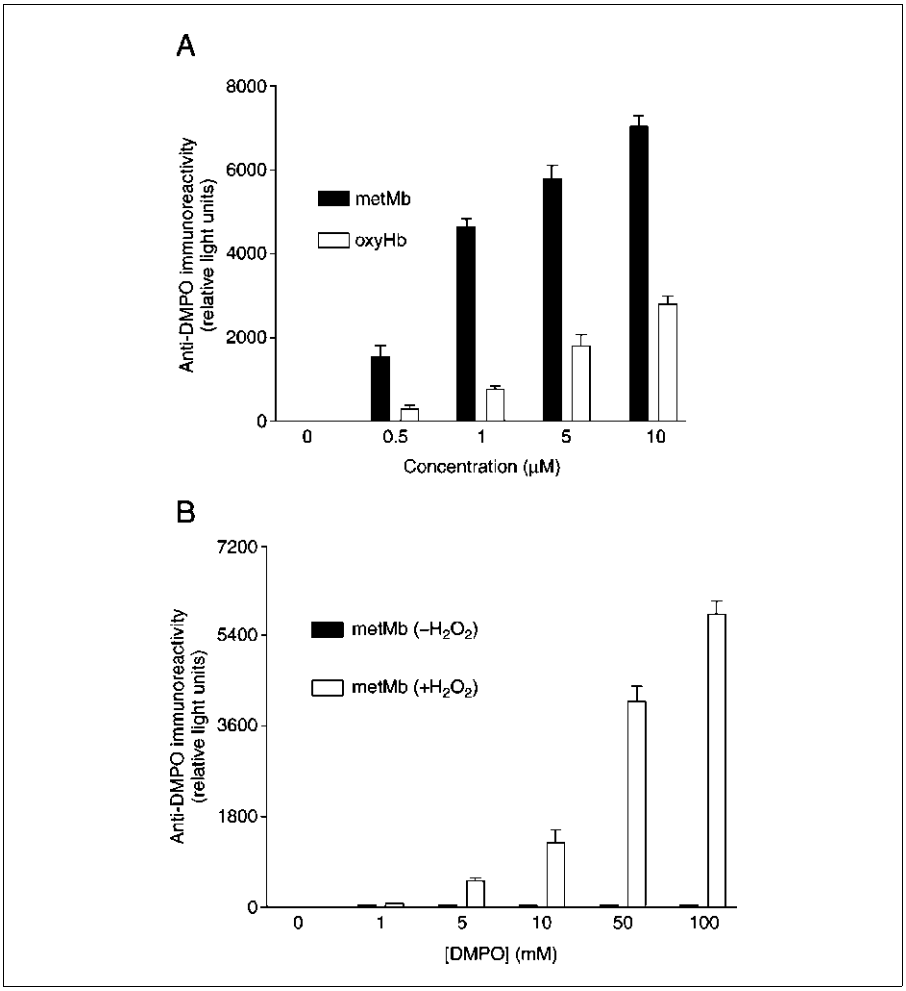

Figure 17.7.2 Detection of myoglobin (Mb) and hemoglobin (Hb) radical–derived nitrone adducts by immuno-spin trapping. (**A**) Reaction mixture contained 50 mM DMPO, 10 µM H_2O_2, and varying concentrations of metMb or oxyHb (as heme); (**B**) Reaction mixture contained 5 µM metMb (as heme), 5 µM H_2O_2, and varying concentrations of DMPO. Reactions were performed in 100 mM Chelex-treated sodium phosphate buffer, pH 7.4, containing 1 mM DTPA. After a 1-hr incubation at 37°C the excess H_2O_2 was removed by adding 50 IU catalase. Protein-radical–derived nitrone adducts were determined by ELISA (see Basic Protocol 1). Data show mean values ± S.E. from three experiments performed in triplicate.

conditions. In this case, sample dialysis prior to electrophoresis is sufficient to prevent false-positive results. Detailed analysis of parameters that can affect immunoassays can be found in immunoassay manuals (Tijssen, 1985).

See Table 17.7.2 for a guide on troubleshooting immuno-spin trapping.

Anticipated Results

The incubation of heme proteins with weak peroxidase activity such as hemoglobin (Hb), myoglobin (Mb), and cytochrome c with H_2O_2 produces protein-centered radicals that have been detected and characterized by direct ESR and ESR-spin trapping. With a very low concentration of H_2O_2, i.e., 10 μM, Hb- or Mb-centered radicals were produced and detected as DMPO-protein radical–derived nitrone adducts by ELISA (Fig. 17.7.2A). Even a low concentration of metMb (0.5 μM) produced significant amounts of DMPO-protein radical–derived nitrone adduct as detected by ELISA. As hemoprotein concentration

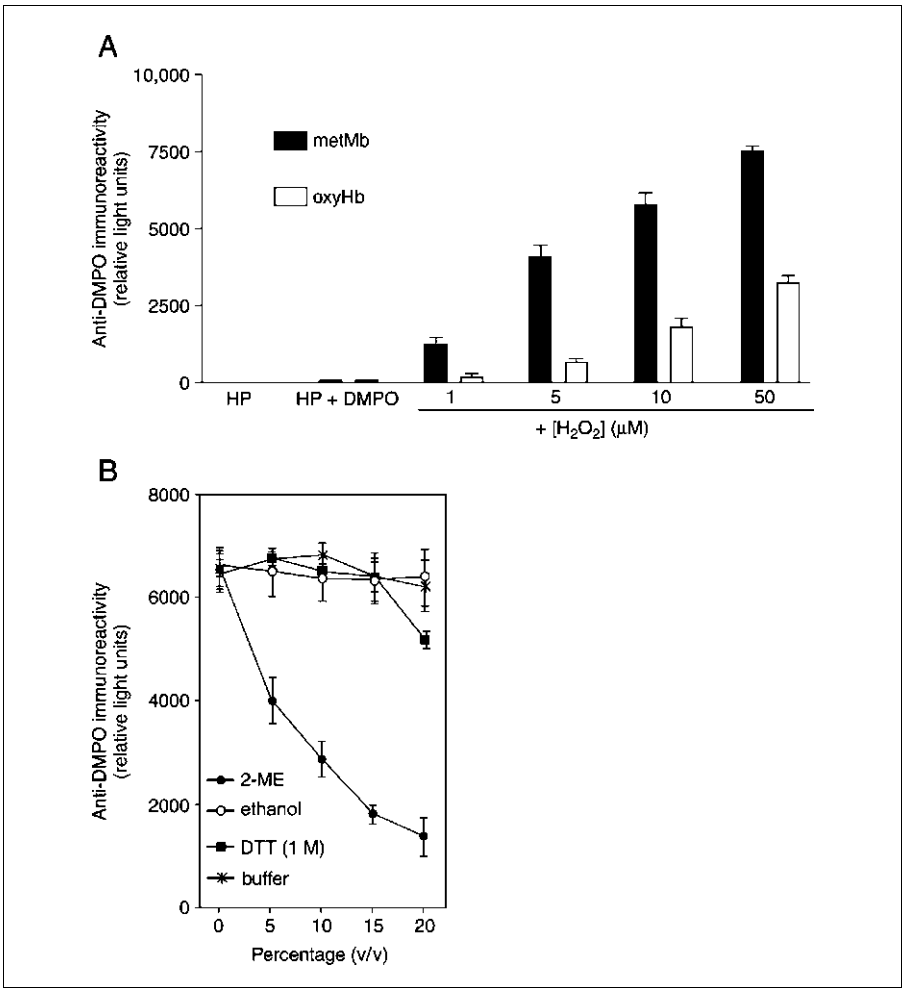

Figure 17.7.3 Detection of Hb- and Mb-centered radicals by immuno-spin trapping assays. (**A**) 5 μM hemoproteins (HP, as heme) were incubated with 50 mM DMPO and varying concentrations of H_2O_2 in 100 mM Chelex-treated sodium phosphate buffer, pH 7.4, containing 1 mM DTPA. (**B**) 10 μM oxyHb was reacted with 10 μM H_2O_2 and 50 mM DMPO in 100 mM Chelex-treated phosphate buffer containing 100 μM DTPA. Reaction was performed 1 hr at 37°C and stopped by adding 50 IU catalase. Then the reaction mixture was incubated 10 min at 37°C with different percentages of 2-mercaptoethanol (2-ME, stock 14 M), its chemical structural analog ethanol, DTT (1 M), or phosphate buffer to correct for changes in volume. Nitrone adducts were determined in 10 μl of the reaction mixture by ELISA (see Basic Protocol 1). Data show mean values ± S.E. from three experiments carried out in triplicate and in three separate experiments.

increases, generation of nitrone adducts rises steadily (Fig. 17.7.2A). Mb always produces more nitrone adducts than Hb or cytochrome *c* (data not shown), and metHb produces more adducts than oxyHb (Fig. 17.72A).

The amount of nitrone adducts detected by ELISA depends on the concentration of DMPO available to trap radical sites in the protein (Fig. 17.7.2B). The authors do not recommend the use of higher concentrations of DMPO because it may suppress hydrophobic binding of the protein to the ELISA microtiter plate or bind non-covalently to the protein during sample preparation for SDS-PAGE. If higher concentrations of DMPO must be used, try dialyzing the sample before processing by ELISA or immunoblotting. If purified DMPO is used, no hemoprotein radical–derived nitrone adducts should be detected when H_2O_2 is omitted (Fig. 17.7.2B, closed bars). It is also important to conduct control experiments in which one of the components is omitted.

Previously, hemoglobin-centered radicals were detected by direct ESR and ESR-spin trapping using millimolar concentrations of H_2O_2, which do not represent physiological conditions. With the immuno-spin trapping assay and ELISA, a significant amount of Mb radical–derived nitrone adduct can be detected with H_2O_2 concentrations as low as 1 μM. No DMPO-protein radical–derived nitrone adducts were detected when hemoprotein, DMPO, or H_2O_2 was omitted in the reaction mixture. In general, the production rate of DMPO-protein radical–derived nitrone adduct increases with hemoprotein (Fig. 17.7.2A), DMPO (Fig. 17.7.2B) and H_2O_2 (Fig. 17.7.3A) concentration.

Preliminary observations showed that immunoblot analysis of Hb radical–derived nitrone adducts obtained after protein separation under non-reducing conditions (i.e., without thiols) gave a higher signal/background ratio than those obtained after protein separation under reducing conditions (i.e., adding 10% v/v 2-mercaptoethanol during sample preparation). The authors hypothesized that this excessive background was due to the reaction

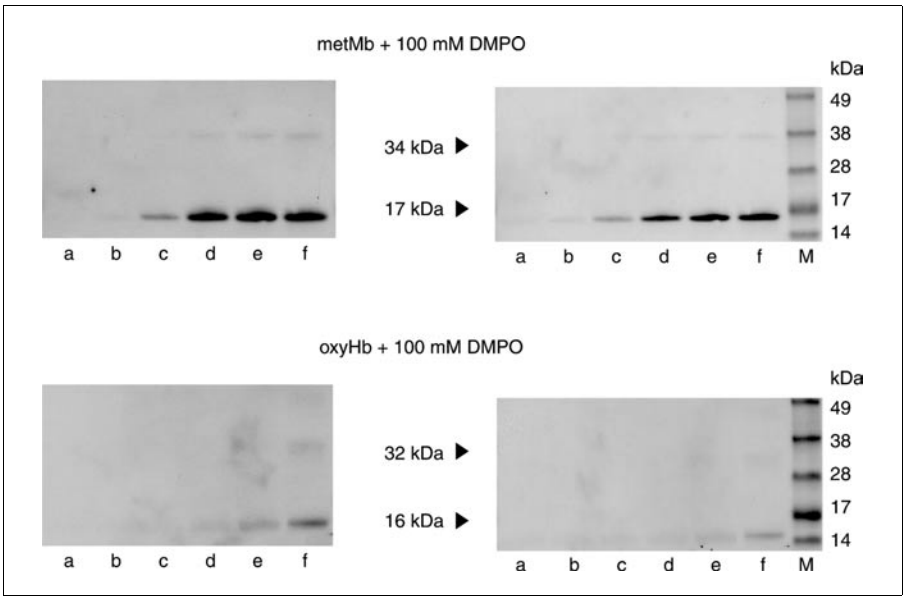

Figure 17.7.4 Immuno-spin trapping detection of hemoprotein radical–derived nitrone adducts by immunoblot analysis. The reaction contained 10 μM hemoprotein (metMb or oxyHb), with 0, 0.5, 1, 5, 10, and 50 μM H_2O_2 (lanes a through f, respectively) in the presence of 100 mM DMPO in 100 mM Chelex-treated sodium phosphate buffer, pH 7.4. Reactions were performed 1 hr at 37°C and stopped by adding 50 IU catalase. The reaction mixture was separated by SDS-PAGE and nitrone adducts were detected by immunoblotting and enhanced chemiluminescence (ECL) development (left membranes). The membranes were then washed with distilled water and incubated with 5 ml BCIP/NBT One-Step reagent until purple bands appeared on a white background (right membranes). The membranes were washed with distilled water and placed in a plastic office folder. X-ray films and membranes were scanned and acquired using an office scanner. M indicates molecular-weight marker.

of the nitrone adducts with the added thiols during the preparation for reducing gels. To investigate this, ELISA experiments, which do not require heating steps (Fig. 17.7.3B), were performed. Apparently, 2-ME changes the DMPO-Hb radical–derived nitrone adducts to an immuno-spin trapping silent species, and in this process, the thiol group of 2-ME affects the nitrone moiety of the adduct, the epitope recognized by the anti-DMPO antiserum. 2-ME did not affect the yield of DMPO-Mb or SOD1-radical derived nitrone adducts. Based on these results, the authors do not recommend the use of 2-ME as a reducing agent for reducing gels, especially when the system under study is unknown. The authors have also found that DTT can replace 2-ME without causing this effect (Fig. 17.7.3B).

Figure 17.7.4 shows typical immunoblot results obtained when metHb or oxyHb is incubated with H_2O_2 and DMPO; the blot is less sensitive than ELISA. The choice of enhanced

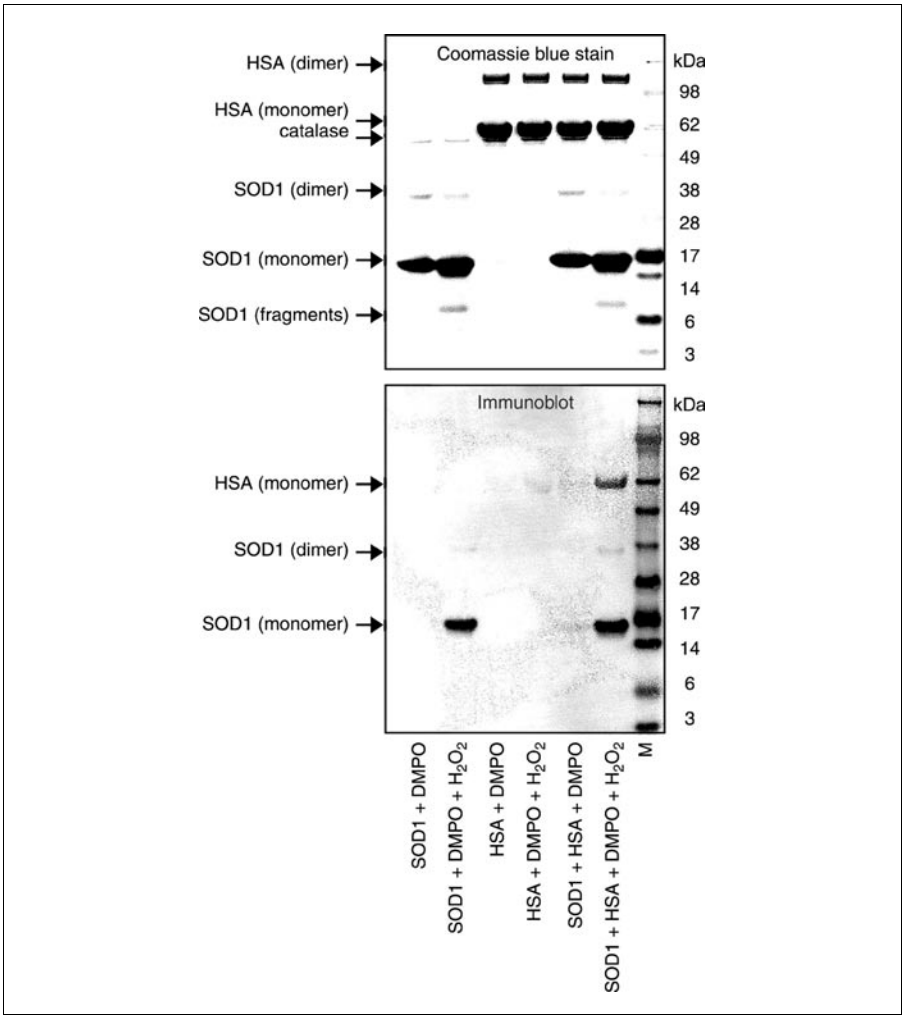

Figure 17.7.5 Simultaneous detection of two protein-centered radicals in the same system. Reaction mixtures contained 15 μM SOD1, 7.5 μM human serum albumin (HSA, $\varepsilon_{280\ nm} = 35{,}700\ M^{-1}\ cm^{-1}$), 100 mM DMPO and/or 1 mM H_2O_2 (as indicated in the figure) in 100 mM Chelex-treated (bi)carbonate buffer, pH 7.4, containing 1 mM DTPA. Reactions were incubated for 2 hr at 37°C and stopped by adding 10 IU catalase. Then 30 μl of the reaction mixtures were mixed with 10 μl sample buffer and 4 μl of 10× reducing agent. After heating 5 min at 70°C, the mixture was run on two 4% to 12% SDS-PAGE gels; one gel was stained with Coomassie blue (upper gel) and the other was blotted to a nitrocellulose membrane. Nitrone adducts were detected by immunoblotting (lower gel) as described in Basic Protocol 2. M indicates molecular-weight marker.

chemiluminescence (ECL) or colorimetric development (NBT/BCIP reagent, Pierce) depends on the sensitivity and amount of adducts to be detected and on the availability of the reagents and equipment. These results show that immuno-spin trapping is sufficiently flexible to fit academic, biomedical, or research laboratory needs in detecting protein-centered radicals.

Previously, the authors reported that DMPO-bovine Cu, Zn superoxide dismutase (SOD1) radical-derived nitrone adducts are induced by H_2O_2 only when (bi)carbonate, i.e., CO_2, HCO_3^-, or CO_3^{-2}, is present in the reaction medium (Ramirez et al., 2005). Under conditions described in that report, the generation of DMPO trappable radical sites in SOD1 was most probably due to oxidation promoted by the carbonate radical anion. When human serum albumin (HSA) is included in the SOD1/H_2O_2/DTPA/(bi)carbonate system, both SOD1- and HSA-centered radicals are produced and they can be simultaneously detected as DMPO-protein radical derived nitrone adducts by immunoblot analysis (Fig. 17.7.5). By comparison of the Coomassie blue stain (Fig. 17.7.5, upper gel) with the corresponding immunoblot (Fig. 17.7.5, lower gel), it is evident that only SOD1 monomer and dimer are detected as DMPO-protein radical derived nitrone adducts, even when fragments of SOD1 were also observed in the gel (compare lanes 2 and 6 in the upper and lower panels, Fig. 17.7.5). The origin of each one of these radicals is difficult, and sometimes impossible, to determine by direct ESR or ESR-spin trapping, due to the overlapping of ESR spectra of protein.

The application of ESR to detect protein radicals in vivo has been pursued for many years. The stability of the DMPO-protein radical–derived nitrone adducts made it possible to analyze them in red blood cells (RBC) of rats exposed to *tert*-buthyl hydroperoxide (Fig. 17.7.6). As little as 15 min after the administration of *tert*-butyl hydroperoxide and DMPO, the authors detected protein-centered radicals in RBC whose signal increased with time, demonstrating that the production of protein-centered radicals is related to the toxicokinetics of *tert*-butyl hydroperoxide. In toxicological studies, the amount and accessibility of the sample is very important. The authors used

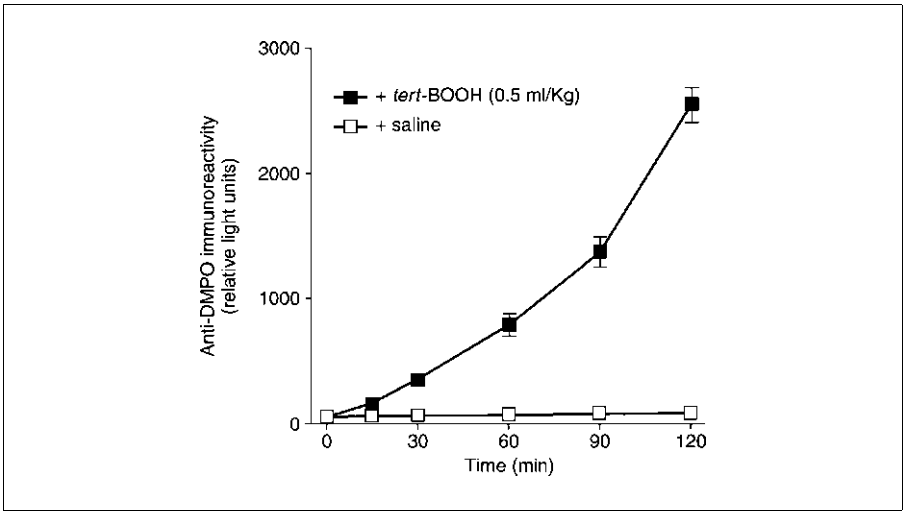

Figure 17.7.6 Detection of protein radical–derived nitrone adducts in blood of rats exposed to *tert*-buthyl hydroperoxide (*tert*-BOOH). Male Sprague Dawley rats (150 to 200 g) received 50 mg Nembutal/kg body weight (i.p.) and 50 μl blood was obtained by orbital bleeding. Then rats were injected with 1 g/kg DMPO (i.p.) and 0.5 ml/kg *tert*-BOOH or saline (8.5 g/liter NaCl) by intragastric intubation. Blood (10 to 50 μl) was obtained 15 min after the administration of *tert*-BOOH, from the orbital plexus, and red blood cells (RBC) were washed three times by centrifugation (5 min at 400 × *g*, each wash) and diluted to 10^8 cells/ml with 100 mM Chelex-treated sodium phosphate buffer, pH 7.4. Washed RBCs were broken by three freeze-thaw cycles and 15 μl (~1 μg proteins) was used to detect protein-centered radicals by ELISA as described in Basic Protocol 1. Animal studies mentioned in this protocol were performed according to an approved Animal Study Proposal, National Institute of Environmental Health Sciences.

10 to 50 μl of blood in these experiments, and this was adequate to run the sample in triplicate. In theory, any compound that can generate oxygen-active species in vivo, such as H_2O_2 or lipid peroxides, can induce protein-centered radicals that can be detected by immuno-spin trapping using very small amounts of sample.

Time Considerations

Depending on the equipment available (e.g., multichannel pipets, automated microtiter plate washer and reader), an ELISA experiment can take ~4 hr. Under the conditions described in this protocol, the authors did not find any difference between blocking overnight at 4°C and incubating for 40 to 90 min at 37°C with agitation. When an overnight experiment is required, it is important to let the plate and wash buffer stand at room temperature for at least 30 min to avoid gel formation, especially when gelatin is used as the blocking agent. Immunoblot analysis of DMPO-protein radical–derived nitrone adducts usually takes 5 to 7 hr including sample preparation if precast gels are available.

Literature Cited

Berlett, B.S. and Stadtman, E.R. 1997. Protein oxidation in aging, disease, and oxidative stress. *J. Biol. Chem.* 272:20313-20316.

Chen, Y.-R., Chen, C.-L., Liu, X., Li, H., Zweier, J.L., and Mason, R.P. 2004. Involvement of protein radical, protein aggregation, and effects on NO metabolism in the hypochlorite-mediated oxidation of mitochondrial cytochrome c. *Free Radic. Biol. Med.* 37:1591-1603.

Clement, J.-L., Gilbert, B.C., Rockenbauer, A., and Tordo, P. 2001. Radical damage to proteins studied by EPR spin trapping techniques. *J. Chem. Soc. Perkin Trans.* 9:1463-1470.

Davies, M.J. and Hawkins, C.L. 2004. EPR spin trapping of protein radicals. *Free Radic. Biol. Med.* 36:1072-1086.

Dean, R.T., Fu, S., Stocker, R., and Davies, M.J. 1997. Biochemistry and pathology of radical-mediated protein oxidation. *Biochem. J.* 324:1-18.

Deterding, L.J., Ramirez, D.C., Dubin, J.R., Mason, R.P., and Tomer, K.B. 2004. Identification of free radicals on hemoglobin from its self-peroxidation using mass spectrometry and immuno-spin trapping. *J. Biol. Chem.* 279:11600-11607.

Detweiler, C.D., Deterding, L.J., Tomer, K.B., Chignell, C.F., Germolec, D., and Mason, R.P. 2002. Immunological identification of the heart myoglobin radical formed by hydrogen peroxide. *Free Radic. Biol. Med.* 33:364-369.

Guo, Q., Detweiler, C.D., and Mason, R.P. 2004. Protein radical formation during lactoperoxidase-mediated oxidation of the suicide substrate glutathione. Immunochemical detection of a lactoperoxidase radical-derived 5,5-dimethyl-1-pyrroline *N*-oxide. *J. Biol. Chem.* 279:13272-13283.

Hawkins, C.L. and Davies, M.J. 2001. Generation and propagation of radical reactions on proteins. *Biochim. Biophys. Acta* 1504:196-219.

He, Y.Y., Ramirez, D.C., Detweiler, C.D., Mason, R.P., and Chignell, C.F. 2003. UVA-ketoprofen-induced hemoglobin radicals detected by immuno-spin trapping. *Photochem. Photobiol.* 77:585-591.

Mason, R.P. 2000. In vivo spin trapping-from chemistry to toxicology. *In* Toxicology of the Human Environment. The Critical Role of Free Radicals (C.J. Rhodes, ed.) pp. 49-70. Taylor and Francis, London.

Mason, R.P. 2004. Using anti-5,5-dimethyl-1-pyrroline *N*-oxide (anti-DMPO) to detect trapped protein radicals in time and space with immuno-spin trapping. *Free Radic. Biol. Med.* 36:1214-1223.

Ramirez, D.C., Chen, Y.R., and Mason, R.P. 2003. Immunochemical detection of hemoglobin-derived radicals formed by reaction with hydrogen peroxide: Involvement of a protein-tyrosyl radical. *Free Radic. Biol. Med.* 34:830-839.

Ramirez, D.C., Gomez-Mejiba, S.E., and Mason, R.P. 2005. Mechanism of hydrogen peroxide–induced Cu,Zn-superoxide dismutase-centered radical formation as explored by immuno-spin trapping. The role of copper- and carbonate radical anion-mediated oxidations. *Free Radic. Biol. Med.* 38:201-214.

Romero, N., Radi, R., Linares, E., Augusto, O., Detweiler, C.D., Mason, R.P., and Denicola, A. 2003. Reaction of human hemoglobin with peroxinitrite: Isomerization to nitrate and secondary formation of protein radicals. *J. Biol. Chem.* 278:44049-44057.

Tijssen, P. 1985. Practice and theory of enzyme immunoassays. *In* Laboratory Techniques in Biochemistry and Molecular Biology, Vol. 15 (R.H. Burdon and P.H. van Knippenberg, eds.). Elsevier, New York.

Key References

Detweiler et al., 2002. See above.

Describes the production and validation of the anti-DMPO antiserum and its application to the detection of DMPO-myoglobin radical-derived nitrone adducts.

Mason, 2004. See above.

Reviews all published literature relevant to immuno-spin trapping.

Ramirez et al., 2003. See above.

This report describes immuno-spin trapping and its validation for the detection of hemoglobin radical adducts in red blood cells.

Internet Resources

http://epr.niehs.nih.gov

Laboratory where the anti-DMPO antiserum was developed

https://catalog.invitrogen.com/

Commercial supplier of gels and electrophoresis equipment

http://www.piercenet.com

Commercial supplier for protein staining, dialysis cassettes, and anti-rabbit (IgG)–alkaline phosphatase conjugate

http://www.alexis-corp.com

http://www.oxfordbiomed.com

http://www.caymanchem.com

Commercial suppliers of the rabbit anti-DMPO antiserum

Contributed by Dario C. Ramirez and Ronald P. Mason
National Institute of Environmental Health Science, National Institutes of Health
Research Triangle Park, North Carolina

CHAPTER 18
Immunotoxicology

INTRODUCTION

As evolutionary principles would predict, the development of multicellular organisms with specialized cells has lead to highly complex, but efficient, compartmentalization (separate organ systems) for select processes. This expanded developmental organization has allowed specialized activities to increase, as is most evident with the nervous system. However, along with increased structural adaptation of an organ for a particular function, which improves upon an organism's adjustment to its environment, comes inter-organ dependency. The immune system also has been expanded in its specialization to assist with this interdependency. Immune cells and their factors (e.g., antibodies and cytokines) are critical for the homeostasis of each organ and maintenance of health.

The immune system has evolved to protect each organ against attack by pathogens and to accelerate the clearance of toxins and aberrant self cells, including those cells and cellular products altered by toxicants, drugs, carcinogenic transformations, and senescence. In performing the clearance of altered-self or non-self constituents, the immune system is unique, because somatic changes are constantly and consistently evolving to expand cellular clones to better recognize antigens. Furthermore, the antigen-specific cells (lymphocytes: B and T cells) and the innate, non-antigen-specific leukocytes (neutrophils, monocytes/macrophages, and NK cells) are continuously trafficking in search of altered-self and non-self antigens (immunosurveillance). Some immune cells also are relatively sessile cells in different organs: for example, the monocytic lineage includes the Langerhans cells of the skin, the Kupffer cells of the liver, the microglial cells of the brain, the mesangial cells of the kidney, and the osteoclasts of bones. Each of these cell types assist with normal organ functions as well as local defensive actions when necessary.

The importance of the immune system is obvious when an individual is born without a particular immune component. Lack of T cells because of a deficit in thymus development (the primary immune organ of T cells), as with DiGeorge Syndrome, causes loss of cell-mediated immunity, which manifests as the inability to eliminate numerous opportunistic infections, such as *Candida*, *Listeria*, and *Mycobacteria* infections. Lack of B cells because of a deficit in bone marrow development (the primary immune organ of B cells), as with Bruton's X-linked hypogammaglobulinemia, causes loss of humoral or antibody-mediated immunity, which manifests as the inability to clear exogenous pathogens, such as staphylococcal and streptococcal infections. Loss of both B and T cells (severe combined immunodeficiency disease, SCID) is a rapidly fatal disease unless major interventions are employed. Since the 1980's, the HIV epidemic has created public awareness of the consequences of HIV-mediated depletion of $CD4^+$ helper T cells (cells needed to promote both cell-mediated and humoral immunity), which can lead to acquired immunodeficiency syndrome (AIDS).

It is now apparent that environmental agents depleting or altering the function of just one type of immune cell can induce major illness. Although usually more subtle than HIV in their mechanisms of immunomodulation, many environmental agents can modify immune functions. Since the immune system is composed of multiple cell types, which localize

Contributed by David A. Lawrence
Current Protocols in Toxicology (2005) 18.0.1-18.0.3

in multiple organs and traffic throughout the organism, it is often arduous to delineate the cell type or cellular function being modulated, especially for clinical investigations when the only specimen usually available is blood. A further complication is age, in that early in life the immune system has not fully developed and late in life the immune system is intrinsically declining in function. Thus, the two most vulnerable times for the immunotoxic effects of environmental agents are during the neonatal and elderly stages. Additionally, immunomodulators are not restricted to pathogens and chemicals; physical and psychological stressors alone or combined with each other and/or chemical stressors can elicit changes of immune functions.

Unfortunately, immune responses, which develop to foreign antigens, can subsequently lead to pathologies, such as allergies/asthma. Additionally, immune responses can develop to self-antigens, giving rise to autoimmune responses with major immunopathologies and possibly fatal outcomes. Besides chemical, physical, and/or psychological stressors causing immunosuppression, they also may heighten immune reactivities, which could generate an overly zealous immune response that causes pathology, or induce a loss of tolerance to self. Cell-mediated and antibody-mediated immunities to self constituents are differentially involved in autoimmune diseases. Thus, both immunosuppression and immunoenhancement can lead to various diseases. This emphasizes the need to assess potential immunotoxicological outcomes for an imbalance in either direction. The units in this chapter describe in vitro and in vivo immunological assays to qualitatively and quantitatively determine various immune system changes that could accompany exposure to environmental agents or drugs.

UNIT 18.1 provides a commentary on the various types of immunotoxicological analyses necessary to fully understand the importance of immune components and immunoregulation in maintenance of a healthy state. As alluded to earlier, the immune system is a defense network sending its cellular components to multiple sites including the skin. *UNIT 18.2* describes the local lymph node assay. This is an assay to assess allergic contact dermatitis, which is a delayed-type hypersensitivity involving antigen-specific activation of T lymphocytes. Whereas the local lymph node assay evaluates allergic reactions originating in the skin, allergic hyperimmune reactions in the lungs can lead to airway hyperresponsiveness, which is referred to as asthma. *UNIT 18.3* provides an overview of the initiators of asthma, the resultant pathology, and the methods to evaluate sentization and elicitation of the asthmatic response. Respiratory distress occurs with asthma as well as with respiratory infections or septicemia. In experimental models, immune infiltrates into lung tissue can be evaluated to determine the extent of the pathology and the involved mechanisms. However, good estimates of ongoing reactions also can be achieved with investigation of the immune cells and their products in bronchoalveolar lavages. Although these lavages are invasive and can be dangerous under some circumstances, they are an efficient means to assess immune reactivities in animals as well as humans. *UNIT 18.4* describes how these lavages can be obtained and the methodologies utilized to assist in the determination of the associated lung injury.

The preceding units described more systemic approaches to evaluation of the immune system. *UNIT 18.5* delves into the molecular mechanisms by which immune cells are regulated for the proliferative and maturational changes signaled through their surface antigen-specific receptors and accessory molecules. The means to quantify the activators of transcription by enzyme-linked immunoadsorbent assays (ELISAs) are described. Although gel-shift assays have long been the standard for analysis of transcription factors, the ELISA method described outlines substantially more efficient process for screening of multiple specimens.

UNIT 18.6 provides the methodology to measure the cytolytic activity of natural killer (NK) cells and $CD8^+$ T cells. Although these cell types kill by similar mechanisms, they

represent the innate and adaptive arms of the immune system, respectively. The NK cells, often referred to as large granular lymphocytes, are not antigen-specific; whereas, $CD8^+$ T cells are activated through their antigen-specific receptor (TCR) by specific peptide presented by major histocompatability complex (MHC) class I molecules. Toxicant interference with either of these cytolytic lymphoid subsets can substantially lessen host defenses.

UNITS 18.7 & 18.8 provide protocols that are integral to most immunotoxicological investigations as well as evaluation of any antigenic or structural changes of non-immune cells and factors. *UNIT 18.7* deals with protocols that rely on antibody antigen interactions for quantification of either. The enzyme-linked immunoabsorbant assay (ELISA) has become a very standard method for multiple disciplines. For toxicological studies, however, it must be remembered that the assay relies on maintenance of the specificity of the antibody and conservation of the epitope of the antigen recognized by this specificity. A toxicant could potentially interfere with either compromising the quantitative nature of the assay. This possible complication exists for all assays that rely on complementary binding of proteins. The ELISPOT assay takes the ELISA to the level of the cells producing the antibody or antigen allowing quantification of the number of cells producing such factors. *UNIT 18.7* additionally presents a new methodology with substantial promise for future endeavors; grating-coupled surface plasmon resonance imaging (GCSPRI) takes the ELISA and transforms it into a rapid screening method. With GCSPRI, hundreds of antibodies or antigens can be simultaneously quantified with a minimum of specimen. *UNIT 18.8* describes the basics of flow cytometry procedures. Flow cytometry has become an important tool for biomedical and clinical studies. This unit provides critical methodologies that must be considered when using this method. Inaccurate results can be obtained if inappropriate gating or fluorescence compensation are not properly adjusted. Although the method can be useful for both quantification of the number of cells expressing a particular combination of markers and the quantification of these markers per cell, it must be realized that the instrument must be quality controlled for linearity and adjusted for optimal CV assessment of cell populations. This unit summarizes the important aspects that need to be considered when using flow cytometry for toxicological parameters.

UNIT 18.9 embarks on methodologies capable of assessing whether a toxicant can alter the development of an antigen-specific naive T cell and/or modify the activity of a select subclass of T cell. The approach to assay antigen-specific naive T cell utilizes transgenic T cells genetically engineered to express the α and β chains of an antigen-specific T cell receptor (TCR). Thus, most of the T cells in these transgenic mice will have many $CD4^+$ T cells or $CD8^+$ T cells dependent on whether the TCR is specific for antigenic peptide in association with major histocompatibility complex (MHC) class II or class I molecules, respectively. However, to ensure that the T cells are naive, the researcher must isolate resting, non-memory T cells ($CD62L^{hi}/CD44^{lo}/CD45RB^{hi}$ T cells). Alternatively, one can be assured of having naive T cells if the TCR transgenes are bred to Rag-deficient mice (mice with no antigen-specific lymphocytes except the TCR-transgene expressing T cells). In either case the mice need to be kept in specified pathogen free (SPF) conditions to maintain their health and lessen odds of activation by cross-reactive antigens. For analysis of differentiated T cells with specific effector functions, cloned T cells are utilized. Numerous Th1, Th2, Tc1 and Tc2 clones now exist, and can be obtained from various researchers. *UNIT 18.9* describes some of these clones and their use for toxicological assessments.

David A. Lawrence

Associating Changes in the Immune System with Clinical Diseases for Interpretation in Risk Assessment

While it is well established that immunosuppression (see Terminology) can lead to an increased incidence and/or severity of infectious and neoplastic diseases, interpreting immunosuppression data from experimental immunotoxicology studies, or even epidemiological studies, for use in quantitative risk assessment is problematic. This is mostly due to a paucity of information on the health consequence of minimal-to-moderate immunosuppression, as might be expected to occur from inadvertent exposure to immunotoxic agents in humans. It is important that a scientifically sound framework be established that allows for the accurate quantitative interpretation of such data for use in the risk assessment process. In immunotoxicology, this may require, for example, development of a model to equate moderate changes in leukocyte counts, CD4 cell numbers, and/or immunoglobulin levels, tests which can be readily performed in human populations, to potential changes in the incidence or severity of infectious diseases, as well as establishing the social and economic impact of the incidence change. Although experimental animal models usually provide an opportunity to establish more reliable exposure estimates and conduct more informative immune tests than those that can be conducted in humans, extrapolating these findings across species is always of concern.

The development of a framework to perform such extrapolations is currently being addressed by the authors' workgroup. As an integral process to this undertaking, a review of studies that address the qualitative and quantitative relationships between immune parameters and disease is contained herein. Initially, the most likely clinical consequences that may occur as a result of chronic mild-to-moderate immunosuppression are described, as well as nonimmune factors that may modify these disease outcomes. Clinical and experimental animal studies that have examined immunosuppression disease relationships are reviewed and quantitative relationships, when available, are delineated to help address gaps in human health risk assessment. To address the potential social and economic consequences that could result from immunotoxicity, a brief description of the general impact of infectious disease is provided on these parameters. The most comprehensive data bases that address immunodeficiency disease relationships, specifically primary (genetic) immunodeficiency and AIDS, are not discussed, as these represent extreme examples of immunosuppression and neither the specific clinical diseases that result nor the eventual outcomes have much in common to that which occurs in individuals with chronic mild-to-moderate immunosuppression.

TERMINOLOGY

Before continuing, it is useful to provide clarification of certain terminology. Immunosuppression, immunodeficiency, and immunocompromised are nonquantitative terms that reflect a reduced capacity of the immune system to respond to antigens, and the terms are often used interchangeably in immunotoxicology. For the purpose of risk assessment, *immunosuppression* can be defined as a loss in the ability of the immune system to respond to a challenge from a level considered normal, regardless of whether clinical disease ensues. *Immunodeficiency* often represents an alteration in the immune system that can potentially lead to clinical disease, whether primary (i.e., genetic etiology) or secondary (epigenetic) in nature. The term, *immunocompromised*, like immunosuppression, indicates a deficient immune response, independent of whether or not it is maladaptive. Immunotoxicity encompasses each of these terms, but it specifies that the effect on the immune system originates from xenobiotic exposure.

DISEASES ASSOCIATED WITH IMMUNOSUPPRESSION

As immunotoxicology testing is increasingly included in toxicological evaluations (House, 2003), there is added impetus to better associate detected changes with these tests to potential clinical outcomes. Although infectious disease is the most obvious, the consequences of maladaptive immunity can

Contributed by Michael I. Luster, Dori R. Germolec, Christine G. Parks, Laura Blanciforti, Michael Kashon, and Robert Luebke

Current Protocols in Toxicology (2004) 18.1.1-18.1.20

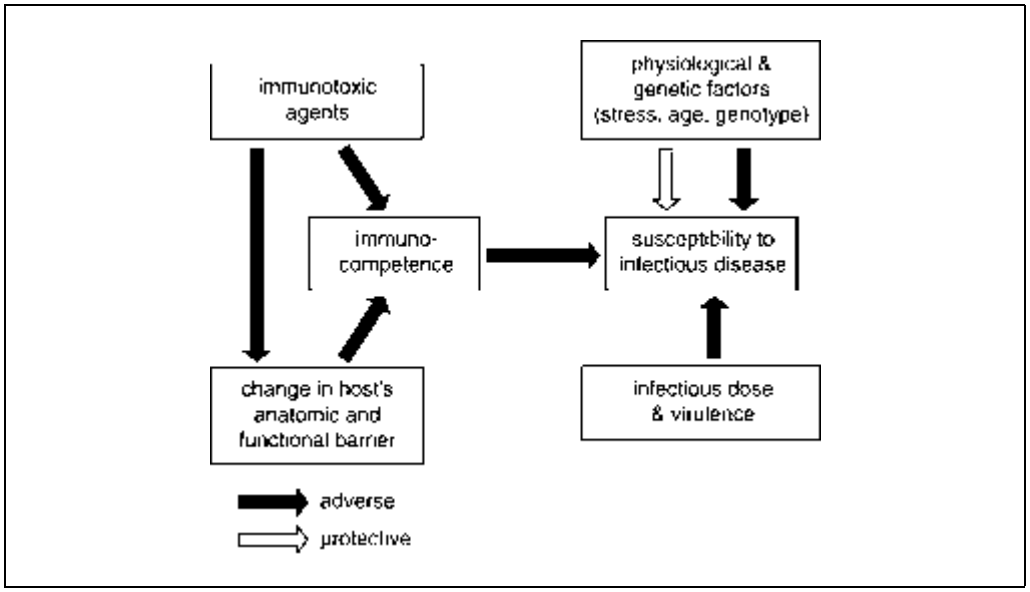

Figure 18.1.1 Changes in the onset, course, and outcome of infectious disease. Schematic shows factors which influence infectious disease susceptibility.

affect the etiology, progression, and/or severity of a much broader range of disorders, including certain cancers and autoimmune disease. Establishing the quantitative relationship between altered immune responses and frequency or severity of disease in human populations is challenging, as many factors may contribute (Morris and Potter, 1997). This is summarized schematically in Figure 18.1.1, where the appearance, progression, and outcome of infectious disease is viewed as an interrelationship between the virulence of the organism, infectious dose (number of organisms required to produce illness), integrity of the host's anatomical and functional barriers, and overall immunocompetence of the individual. The latter is affected by genetics as well as age, gender, use of certain medications, drug/alcohol use, smoking history, stress, and nutritional status. These factors probably account for most of the variability reported in mean immune values, which can exceed two standard deviations. Another challenge when establishing quantitative associations between immune function and disease is to account for the functional overlap (i.e., redundancy) that exists between the various immune responses and disease. As multiple effector mechanisms are evoked in response to a disease, redundancy is often misinterpreted as reserve; however, as with other organ-systems, such as the liver or central nervous system, the existence of an immune reserve in the general population, where disease can occur in uncompromised individuals, is unlikely. In contrast, immune redundancy, as discussed by Halloran (1996), is scientifically supported and can be empirically examined. The effect of redundancy on the interpretation of immunotoxicology studies was recently addressed by Keil et al. (2001) using factor analysis and multiple/logistic regression to quantitatively evaluate the contributions of different immune system parameters in host resistance.

Infectious Diseases

While both infectious and neoplastic diseases are associated with secondary immunodeficiency, infectious diseases are often the focus of epidemiological studies as neoplastic diseases usually have such a long latency period. The particular microorganism responsible for an infection may assist in identifying the qualitative and quantitative nature of the immunodeficiency. For example, extracellular pathogens such as *Streptococcus pneumoniae* and *Haemophilus influenza*, multiply only outside phagocytic cells and, thus, produce disease only when they can resist phagocytosis. Facultative intracellular pathogens, (e.g., *Mycobacterium tuberculosis*), are generally phagocytized but resist intracellular killing. Thus, infections with extracellular or facultative intracellular organisms are more frequent in individuals with impaired phagocytic mechanisms, (e.g., neutropenia), or when humoral immune deficiencies are present. Obligate intracellular pathogens, which include all viruses, cannot multiply unless they are within a host cell and are more commonly observed in individuals with defects in cellular immunity.

Microbial agents associated with immunodeficiency disorders can also be classified into common, opportunistic, or latent pathogens. Common pathogens occur in the general population at frequencies associated with their infectious nature (e.g., virulence, ease of transmission), as represented by viruses that cause influenza infection and severe acute respiratory syndrome (SARS). The respiratory system is the most vulnerable target for common pathogens, as it is directly exposed to the external environment and has a large surface area: four times the combined total surface area of the gastrointestinal tract and skin (Gardner, 2001). Upper-respiratory infections occur in all age groups but produce the most severe effects in the very young and very old due to their lesser immunocompetency. Although influenza is responsible for more morbidity and mortality than any other infectious agent in recorded history (Patriarca, 1994), the low individual rates of infections in the general population (only one or two episodes in an individual per year), combined with underreporting, make it difficult to detect changes in infection rates in most epidemiological studies.

While infections with common pathogens occur routinely in the healthy population, opportunistic infections are typically seen in individuals with severe immunosuppression, such as AIDS patients. Examples of microorganisms that can produce opportunistic infections are certain protozoans, including *Toxoplasma gondii*, which cause cerebral infections and intractable diarrhea, *Candida albicans*, *Mycobacterium avium* complex (MAC), and *Pneumocystis carinii*, a fungus causing severe lung diseases in AIDS patients (Morris and Potter, 1997). These organisms are commonly encountered in food, water, dust, or soil, but they cause disease in the general population at very low incidences.

Certain pathogenic microorganisms are responsible for latent infections. In the case of members of the herpes virus family, including cytomegalovirus (CMV), herpes simplex virus (HSV), and Epstein-Barr virus (EBV), the virus remains in the tissue in a latent form following primary infection for the duration of the host's life. In healthy individuals, the immune system maintains viral latency, with cellular immunity playing a major role. When the cellular immune response is compromised, viral replication can ensue and potentially cause severe complications or death. Preceding viral activation, a vigorous immune response to viral-specific antigens occurs in response to replication. As will be discussed later, changes in virus-specific immune response or activation of latent viruses has been observed in individuals with secondary immunodeficiency disorders where mild-to-moderate immunosuppression may exist.

Virally Induced Tumors

Immunodeficiency is also associated with an increased incidence of certain virally induced tumors, such as non-Hodgkin's lymphomas (NHLs) and tumors of the skin (Penn, 2000). In contrast to cancers of internal organs, in particular those in the lung and liver, which are often induced by chemical carcinogens, virus-induced cancers are more immunogenic and, thus, more likely influenced by immunological factors. Suppression of cell-mediated immunity has been associated with higher incidences of skin cancers, leukemias, and lymphoproliferative disorders in transplant patients, whereas Kaposi's sarcoma and EBV-associated B cell lymphomas are associated with severe immunosuppression as seen in patients with AIDS. Natural killer (NK) cells are more likely to play a role in resisting the progression and metastatic spread of tumors once they develop, rather than preventing initiation (Herberman, 2001). Unexpectedly, studies of individuals with NK cell deficiency states, most of which are associated with single gene mutations, have helped identify a role for NK cells in defense against human infectious disease. A resounding theme of NK cell deficiencies is susceptibility to herpes viruses, suggesting that unexplained severe herpes viral infection should raise the possibility of an NK cell deficit (Orange, 2002).

CONSIDERATIONS IN THE USE OF EPIDEMIOLOGICAL DATA IN IMMUNOTOXICOLOGY RISK ASSESSMENT

There are many advantages of using human data over experimental animal studies in quantitative risk assessment, especially as it avoids the difficulties in interspecies extrapolation and provides data on lower doses that are of interest to public health policy makers (Hertz-Picciotto, 1995). Human studies offer realistic exposure scenarios, including multiple routes of exposure, and include a much more diverse range of genetic backgrounds than experimental models, providing the potential to explore differences in susceptibility by genotype. The limitations and challenges of human studies, however, are considerable.

Here, a brief overview of issues surrounding the design and interpretation of human studies as it pertains to the assessment of risk due to immunotoxic exposures is provided.

Clinical Studies

The design of human studies can range from controlled clinical trials to large, population-based, observational studies. Clinical studies offer advantages in that exposure parameters of interest can often be controlled (e.g., chamber studies of inhaled toxicants, challenge studies of adenovirus infection), and outcomes can be prospectively monitored. There are also disadvantages, as ethical considerations provide little opportunity for exposure with toxic chemicals. Furthermore, studies with extensive biological monitoring and functional immune tests can be expensive, and exposures as well as outcomes of interest may be difficult to study in the available time frame as study participants are not typically available for long-term exposures or extended follow-up. For the purpose of obtaining data for immunotoxicological risk assessment, clinical studies are particularly useful as they can provide data on the frequency of infections or the level of immune response to vaccines. Variations on this type of study design might include follow-up of patient populations administered immunosuppressive therapy (i.e., transplant patients), that, as described below, may also have many of the characteristics of observational studies.

Epidemiological Studies

Other types of human studies that have been employed in immunotoxicology are typically classified as observational or epidemiological. Observational studies can be of varying size and they can be cross-sectional (one point in time), retrospective, or prospective in nature; each design has advantages and disadvantages. The initial means of control in observational studies is introduced through the study design and the quality and validity of results can be greatly affected by the methods used to select the study sample and the rigor with which exposures and outcomes are measured. In addition to high costs, observational studies are challenging for many reasons, including potential confounding by host (age, gender, and lifestyle) and environmental (frequency of exposure to chemicals and infectious agents) factors. A secondary measure of control in observational studies is through the use of multivariable analysis techniques (e.g., regression modeling), providing there is sufficient sample size and information on potential confounders. Overall, well-designed epidemiological studies (e.g., absence of selection bias, exposure or outcome misclassification, control of confounding factors) can contribute valuable information to the assessment of risk due to immunotoxic exposures.

Existing immunotoxicology studies in humans tend to be based upon either fairly small sample sizes, often in individuals with transient high-level occupational exposures, or large groups with chronic low-level exposures. Although in some instances body burdens of chemicals have been determined, drawing broadly applicable conclusions from some of these studies is difficult. This is because subjects may have been exposed to chemicals other than those specifically addressed by the study, and characterization of chemical exposure may rely on subject recall or rough estimates of the duration and intensity of exposure. Furthermore, in contrast to experimental animals, functional assessment is considerably more difficult in humans as it requires antigen challenge, which involves some risk to the individual. When such studies have been undertaken, subjects have been provided commercial vaccines, such as hepatitis antigen (Weisglas-Kuperus et al., 2000; van Loveren et al., 2001; Yucesoy et al., 2001; Sleijffers et al., 2003). The cellular and humoral immune response to vaccination is thought to be a sensitive indicator of immunosuppression (Glaser et al., 1993) and can reflect susceptibility to infectious disease (Deseda-Tous et al., 1978; van Loveren et al., 2001). In most epidemiological studies, testing in humans has been limited to blood collection where peripheral cell counts and differentials, immunoglobulin levels, or immunophenotyping are performed. While certainly of value, it is generally agreed these are not highly sensitive indicators of immunosuppression, making it difficult to detect low-to-moderate levels of immunosuppression (ITC, 1999).

IMMUNODEFICIENCY AND RELATIONSHIP TO INFECTIOUS DISEASE

Environmental Chemicals

*PCB*s

The need to extend data obtained in experimental studies to humans has been recently reviewed (Tryphonas, 2001); however, epidemiologic data on the effects of chemical exposures on immune parameters and

infectious outcomes in human populations are limited. Some of the more complete immunotoxicology studies have focused on persistent organochlorine compounds formerly found in pesticides and industrial chemicals—e.g., polychlorinated biphenyls (PCBs)—in children following prenatal or perinatal exposure via maternal diet and breast milk. Accidental exposures of populations in Japan (Yusho) and China (Yu-Cheng) suggest an association of PCBs, their thermal breakdown products (quaterphenyls), and polychlorinated dibenzofurans, found in contaminated rice oil, with immune abnormalities and increased infections. Children born to exposed mothers between 1978 and 1987 in the Yu-Cheng population had lower levels of serum IgA and IgM, and a higher frequency of respiratory infections and otitis media compared to matched unexposed controls (Lu and Wu, 1985; Nakanishi et al., 1985; Yu et al., 1998).

The association between PCBs and increased frequency of otitis media in children has also been described in other populations. A study of 343 children in the United States (Michigan) showed no general association between organochlorine levels and prevalence of infections, but there was a positive association between polychlorinated biphenyls (PCBs) and DDE (the primary metabolite of DDT), or PCBs and hexachlorobenzene with otitis media (Karmaus et al., 2001). In a study of Inuit infants in Arctic Quebec, Canada (Dewailly et al., 2000), the relative risk of recurrent episodes (at least three per year) of otitis media was higher in breast-fed infants in the second and third highest percentile of organochlorines exposure, compared to the lowest. At three months of age, breast-fed infants with higher exposure levels had lower numbers of white blood cells and lymphocytes, and lower serum IgA levels at ages 7 and 12 months, compared to bottle-fed infants. In Dutch preschool children (Weisglas-Kuperus et al., 2000), PCB levels in breast milk (nonortho and planar PCBs) were also associated with increased recurrent otitis media and other symptoms of respiratory infection. In this sample, the body burden of PCBs at age 42 months was associated with higher prevalence of recurrent otitis media and chicken pox. PCB body burden was not associated with differences in lymphocyte markers outside the normal range for age-matched children, although levels in breast milk and cord blood were positively correlated with lymphocyte counts and various T-cell subsets. While these findings linking otitis media with PCB exposure are consistent across three studies, it was not possible to determine whether the changes in immune parameters mediated this association or simply represented parallel findings.

Pesticides

The immunotoxicity of pesticides following human exposure has been reviewed by several authors (Thomas et al., 1995; Vial et al., 1996; Voccia et al., 1999; Luebke, 2002). Although some studies have described associations between pesticide exposure, altered immune function, and increased rates of infection, sample sizes were generally small and, in some cases, patients were self-selected based on symptoms rather than exposure. Furthermore, the frequency of infections was typically estimated by recall over several years and immune function data were scarce. Not all studies suffer from these shortcomings. For example, a relatively large ($n = 1600$) and well-defined population living in and around Aberdeen, North Carolina, near a pesticide dump site (a priority Superfund site containing organochlorine pesticides, volatile organic compounds, and metals), was evaluated for immune function and frequency of viral infections. Compared to a neighboring community, residents of Aberdeen, ages 18 to 40, were found to have higher incidence of herpes zoster (reactivated herpes infection causing shingles), but no difference in the frequency of other infectious diseases (Arndt et al., 1999). In a substudy of 302 individuals, those living in Aberdeen had significantly higher age-adjusted levels of plasma DDE than those living in neighboring communities. Furthermore, higher levels of plasma DDE were related to lower lymphocyte responses to mitogens but higher absolute lymphocyte counts and IgA levels (Vine et al., 2001). In a separate analysis, residents living nearer to the pesticide dump site had both a lower lymphocyte response to mitogen stimulation and a greater likelihood of having a lower percentage of $CD16^+$ (NK) cells, ($<8\%$, the lower limit of the normal reference range; Vine et al., 2000). The association seen with reactivated herpes infection is plausible in light of these changes, given that NK cells play an important role in the generation of cytotoxic T-cells required to help control viral infections. These studies illustrate several challenges in demonstrating the effects of chemical exposures in a population-based setting. Although an infectious outcome (zoster) was associated with residential history of chemical exposure in Aberdeen, suggesting immunosuppression related to proximity to the dump sites, the more

extensive and expensive immune markers and serum indicators of exposure were only examined in a small subset of the original sample. Thus, it was not possible to further examine potential pathways leading to the association with zoster.

Heavy metals and solvents

There are human data pertaining to the effects of heavy metals or solvents, such as lead and benzene, respectively, much of which comes from occupational exposures. Other metals (e.g., mercury and cadmium) have been shown to have immunotoxic effects, as have mixed exposures, such as those experienced by welders exposed to metal fumes and gases. As recently reviewed by Antonini et al. (2003), welders may experience increased susceptibility to pulmonary infection and recurrent respiratory infections (Tuschl et al., 1997), possibly due to decreased NK activity or cell-mediated immunity. Although a number of human studies have evaluated immune system endpoints in occupationally exposed cohorts, immune function and infectious outcomes generally have not been reported for the same cohort.

Chronic Stress

Effect on common infection

It is well established that chronic psychological factors (stressors), such as separation and divorce, caregiving for Alzheimer's patients, or bereavement, produce low-to-moderate degrees of immunosuppression and increase infectious disease incidences (Cohen, 1995; Biondi and Zannino, 1997; Yang and Glaser, 2000; Kiecolt-Glaser et al., 2002). For example, in a study that followed 100 members of 16 families for 1 year, infections were four times more likely to occur following a family-related stress event than if no stress event occurred (Meyer and Haggerty, 1962). In a prospective cohort study, 246 individuals from 58 families were followed for the effects of family functioning and stress on the incidence of influenza infection (Clover et al., 1989). Examinations ~2 weeks after an influenza epidemic ended showed that infection was negatively associated with both cohesion and adaptability. In a study where humans were challenged with an infectious agent, 394 healthy subjects were assessed for psychological stress and subsequently administered nasal droplets containing respiratory syncytial virus (RSV) or coronavirus (Cohen et al., 1991). The rate of respiratory infections ($p < 0.005$) and clinical colds ($p < 0.02$), as determined by virus-specific antibody levels and viral isolation, increased in a dose-responsive manner with increasing degrees of psychological stress (Fig. 18.1.2). Although usually conducted in small cohorts, immune testing in chronically stressed individuals has provided some insights into the relationship between mild-to-moderate immunosuppression and disease (Kiecolt-Glaser et al., 1986, 1987). In chronic stress groups showing an increased rate of infections, total circulating T cell numbers can be reduced to as much as 20%

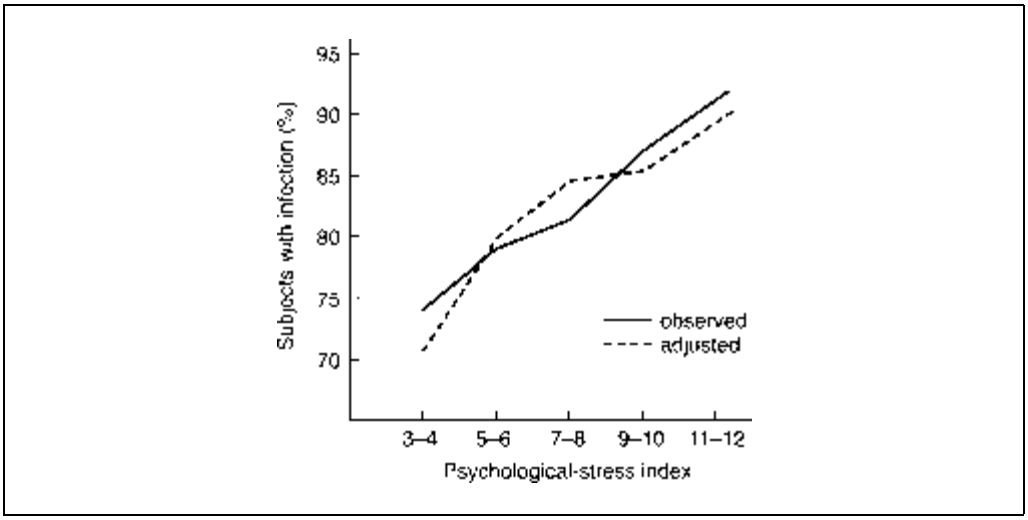

Figure 18.1.2 The rate of respiratory infections and clinical colds, as determined by virus-specific antibody levels and viral isolation, following challenge with nasal droplets containing respiratory syncytial virus or coronavirus, in individuals demonstrating increases in psychological-stress indices. Data are shown as observed association and association adjusted for standard control variables ($n = 397$). Adapted from Cohen et al. (1991).

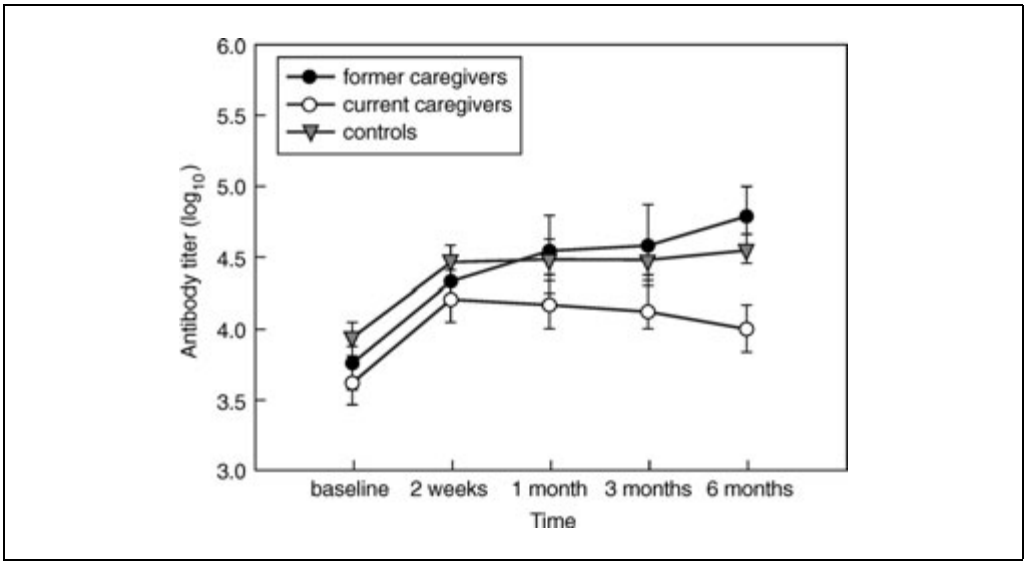

Figure 18.1.3 Pneumococcal vaccine responses in elderly caregivers, shown as antibody titer over the 6-month period following immunization. Controls are age-matched noncaregivers. Adapted from Glaser et al. (2000) with permission.

below control values, while the number of circulating B cells remain unaffected. Furthermore, CD4:CD8 ratios, while usually within normally reported ranges, can be reduced as much as 40% and NK cell activity by 10% to 25% below control values. Measurement of mitogen-stimulated T lymphocyte proliferation, although not generally considered a sensitive indicator for immune function, was reduced in the stressed population by ∼10% from control values. These changes are within the range of most reported normal values.

Effect on latent viruses

Associations between chronic stress and reactivation of latent viruses, such as CMV, HSV-1, or EBV, as measured either by clinical disease or elevations in specific antibody titers have also been observed (Kasl et al., 1979; Glaser et al., 1987, 1993; Esterling et al., 1993; Cohen, 1995; Biondi and Zannino, 1997; Yang and Glaser, 2000). An increase in specific antibody titers to latent viruses (i.e., seroconversion), which reflects viral activation and replication, precedes disease onset, although only ∼20% of seroconverters actually develop clinical manifestations. Studies have also been conducted to examine associations between psychological stress and the immune response following hepatitis B, influenza virus, or pneumococcal vaccination, (reviewed in Kiecolt-Glaser et al., 2002). In studies of students under defined academic stress, the ability to seroconvert following first and second immunizations with hepatitis B vaccine were highly associated with tests to measure stress levels. In studies involving influenza vaccinations, Alzheimer's disease caregivers responded less favorably to vaccination, with only 12 (38%) compared to 21 controls (66%) showing a 4-fold increase in antibody titer following immunization. A four-fold increase is considered an adequate response (Kiecolt-Glaser et al., 1996). As shown in Figure 18.1.3, even more striking were the effects on pneumococcal vaccine responses in caregivers, where a significant decrease in antibody titer occurred in current caregivers compared to controls over the 6-month period following immunization—$F(5.82,142.46) = 2.56$; $p < 0.03$; Glaser et al., 2000. Although acute stressors, like chronic stressors, also are moderately immunosuppressive, large interindividual differences exist due to the variability in stress-induced sympathetic nervous system activation, and most observed changes are short-lived (reviewed in Marsland et al., 2002).

Hematopoietic stem cell transplantation

Hematopoietic stem cell transplantation (HSCT), which came into general practice in the 1980s, is employed in the treatment of certain hematological malignancies, aplastic anemia, and inborn genetic errors originating in hematopoietic stem cells. Immunodeficiency can persist for well over a year following cell grafting due to pregrafting radiation treatment and is manifested as decreases in primary antibody responses and delayed hypersensitivity responses as well as lower $CD4^+$ cell

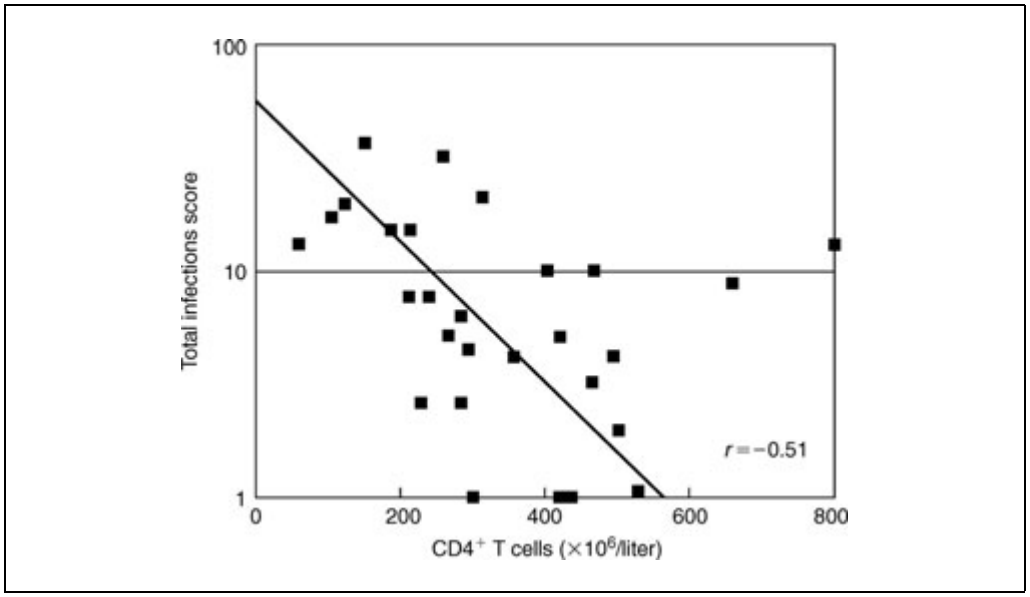

Figure 18.1.4 Twenty-nine patients were followed for 180 days preceding the one year post-transplant exam for $CD4^+$ T cell counts and total infection score, which includes frequency and severity. Reprinted with permission from Storek et al. (1997).

numbers and serum IgG2, IgG4, and IgA levels (Ochs et al., 1995). Thus, prospective studies provide an excellent model to help identify quantitative relationships between immune function and disease as the immune system undergoes recovery. Excluding upper-respiratory infections, which are seldom monitored in allogeneic bone marrow recipients, the incidence of infections exceeds 80% during the first 2 years post-engraftment, with 50% of the patients having three or more infections. Opportunistic infections predominate, with fungal infections being the most common followed by those of bacteria and viral origins (Ochs et al., 1995; Atkinson, 2000). Although infections that occur in the first month following transplant are most likely due to deficiencies in granulocytes, later infections appear to be due to deficiencies in $CD4^+$ T cells and B cells.

In a prospective study involving 108 transplant patients followed between days 100 and 365 post-engraftment, decreases in B, $CD4^+$, and $CD8^+$ lymphocytes, as well as total mononuclear cells, represented the strongest associations with infectious disease incidence ($P < 0.05$; Storek et al., 2000). A smaller but more detailed study by Storek et al. (1997), evaluating 29 patients for 180 days preceding the 1-year post-transplant exam, showed a highly significant inverse correlation ($P = 0.005$ in univariate analysis) between $CD4^+$ T cell counts and total infection score (i.e., frequency and severity) but not with $CD8^+$ T cell numbers, B cell numbers, serum immunoglobulin levels, or delayed hypersensitivity responses (Fig. 18.1.4). The significant association between disease and decreased $CD4^+$ T cell counts was primarily dependent upon activated cells, rather than memory T cell subpopulations. In comparing the efficacy of allogeneic marrow transplantation to blood stem cell transplantation, Storek et al. (2000) demonstrated that a 1.7-fold lower rate of infections in blood stem cell transplants corresponded to about a 4-fold higher $CD45RA^{high}$ (memory) $CD4^+$ T cells and about 2-fold higher count for $CD45RA^{low}$ (naive) $CD4^+$ T cells. In studies conducted by Small et al. (1999), which monitored immune cell recovery following bone marrow cell transplantation, the incidence of infections also correlated with $CD4^+$ cell counts. Only opportunistic infections were monitored, however, and they were almost exclusively present in patients considered severely immunosuppressed, with $CD4^+$ T cell counts of <200 cells/mm^3. The relationship between $CD4^+$ cell numbers and respiratory virus infections was examined over a 3- to 6-month period following transplantation in a small group of T-cell depleted (using anti-CD52 antibody treatment), stem cell recipients (Chakrabarti et al., 2001). The relationship between $CD4^+$ T cell numbers and the incidence of respiratory virus infection was relatively linear. The size of the population was small, however, and $CD4^+$ T cells in the experimental group did not progress

above 180 cells/mm^3, compared to 700 to 1100 cells/mm^3 found in the control group.

Although not well studied, HSCT patients also manifest deficiencies in humoral-mediated immunity, presumably due to insufficient T cell help, rather than direct B cell deficits. In this respect, Sheridan et al. (1990), in studying leukemia patients before and after allogeneic bone marrow transplantation, noted a high incidence of pneumococcal infections that were specifically associated with low-to-absent levels of detectable serum IgG2 and IgG4 levels.

Organ Transplants

Studies in organ transplant patients, particularly renal, have also provided insights into the long-term consequences of moderate immunosuppression. While immunosuppressive therapies have greatly improved over the past 40 years, transplant patients are still predisposed to high rates of malignancies and infections. Infection rates range between 65% and 70% during the first 6 months post-transplantation, with CMV representing 18% to 67% of the reported infections (Sia and Paya, 1998). With the advent of long-term monitoring, an increased incidence in cancer has also been noted in this population. For example, the risk of developing skin tumors following renal transplantation is 10% after 10 years and 40% after 20 years, while the incidence of squamous cell carcinoma is 250-fold higher and for basal cell carcinoma 10-fold higher than the general population (Hartevelt et al., 1990). The initial immunosuppressive therapy for renal transplant consists generally of a combination cyclosporin (CsA), azathioprine, and steroid cocktail. Therapies are subsequently reduced, but adjusted based upon the time following transplant, evidence of acute rejection, evidence of toxicity (usually serum creatinine levels), and white blood cell count, the latter of which is maintained above 4000 cells/mm^3. Jamil et al. (1999), examining 478 renal transplant patients, showed that the risk of lymphomas and infections during the first 6 months post-transplantation increased proportionally with the level of immunosuppressive therapy ranging from 1.5- to 3-fold. Urinary tract infections, which are associated with the transplant, were the most common type of infection in all groups, while severe bacterial infections (pneumonia and septicemia) and systemic/invasive fungal infections were almost exclusively associated with those on the most intensive immunosuppressive therapy. A high incidence of CMV antibodies occurred in all three groups with 9%, 29%, and 53% seroconverting, based upon the level of immunosuppressive therapy. In contrast to infectious diseases, there were fewer cases of squamous and basal cell carcinomas in the most aggressively treated group compared to the other groups, probably due to the anti-proliferative effects of some of the therapeutics. Wieneke et al. (1996), when also examining renal transplant patients, demonstrated that reduced IgG1 subclass levels and CD4 T cell counts were the best predictors for infections (relative risk increased from 9% in patients with normal values to 38% with lower values). Clark et al. (1993), following a small cohort of 27 patients, noted that by maintaining the level of CD3$^+$ lymphocytes to at least 500 cells/mm^3 a reduction in the number of serious viral infections occurred ($p < 0.04$).

IMMUNE SYSTEM, DISEASE, AND LIFE STAGE

The Neonate

Common infectious diseases occur more often and are usually more severe in the very young. In some cases, age-related physical or physiological differences in tissues or organs are responsible for the increased susceptibility to infections. However, in most cases, it is the relative immaturity of the immune system in the very young that prevents the host from making an adequate response to microorganisms. Neonates are particularly susceptible to infectious agents that require adult-like production of antibodies and complement to mediate phagocytosis and bacteria killing. This includes infections with encapsulated bacteria, (e.g., group B *Streptococcus* and *Haemophilus*), which, when combined with low expression levels of innate immune function, lead to inefficient bacterial killing and the subsequent development of infection.

Laboratory studies have provided qualitative and quantitative information on the differences in immune function that predispose neonates and young children to these infections. Bacteria that are commonly associated with neonatal sepsis and infections, such as gram negative *E. coli*, are initially controlled by polymorphonuclear leukocytes (PMNs), the first cells to arrive at sites of infection or tissue damage. PMNs in the newborn are not only produced at a lower rate than in adults (Wilson, 1986), but those produced have approximately half of the lysozyme and lactoferrin levels of adult cells (Ambruso et al., 1984) and only 30% of the adult content

Table 18.1.1 Distribution of Lymphocyte Subtypes in the Fetus, Newborn and Adult[a,b]

	Fetus				Neonate				Adult	
Marker	Percent	% of Adult	Absolute[c]	% of Adult	Percent	% of Adult	Absolute[c]	% of Adult	Percent	Absolute[c]
WBC	—	—	5154[e]	89.6	—	—	13,426[d]	234.1	—	5750
Lymphocytes	—	—	3700[d,e]	180.3	—	—	4263[d]	207.7	—	2052
$CD2^+$	57[d,e]	69.5	1936[e]	120.5	72[d]	87.8	2971[d]	185.0	82	1606
$CD3^+$	52[d]	67.5	1771[e]	127.3	61[d]	79.2	2579[d]	185.4	77	1391
$CD4^+$	39[d]	78.0	1321[e]	136.6	45[d]	90.0	1897[d]	196.2	50	967
$CD8^+$	15[d,e]	62.5	499[e]	107.3	18[d]	75.0	874[d]	188.0	24	465
CD4:CD8 ratio	—	—	2.9[d]	138.1	—	—	2.3	109.5	—	2.1
CD19 (B cells)	18[d,e]	138.5	547[d]	225.1	11	84.6	429[d]	176.5	13	243

[a]Adapted from Schultz et al. (2000).
[b]Dashes, Not applicable.
[c]Absolute values are given per cubic millimeter.
[d]Significantly different from adults.
[e]Significantly different from neonates.

of bactericidal/permeability-increasing protein that are important in destroying microorganisms (Levy et al., 1999).

Recovery from most infections involves opsonization of bacteria by antibody and complement. At birth, neonates have nearly 70% of their total adult immunoglobulin (Ig) levels, and ~90% of adult IgG levels, although a significant portion of this is maternally-derived. This form of passive protection wanes as the maternal antibody is catabolized, and by 1 to 3 months of age, infants have only 30% of adult Ig levels (Stiehm and Fudenberg, 1966). Antibody synthesis progresses slowly with age, and it is still only ~70% of adult levels at 12 to 16 years of age (Stiehm and Fudenberg, 1966). Wolach et al. (1994) reported that serum of preterm infants and newborns also have only ~80% of adult levels of complement activity, and only 60% of C3, the main opsonizing complement component.

Although neonates have a higher percentage of total lymphocytes in their circulation compared to adults, ~90% of their thymus-derived lymphocytes are immature, compared to 50% in adults (Ciccimarra, 1994). Immature cells are incapable of making cytokines that are critical to mounting effective immune responses and generating long-lived memory cells. Phenotypic analyses of cord, neonatal, and adult peripheral blood has also shown differences in T cell subpopulations (Table 18.1.1), as well as differences in the balance of Th1 and Th2 cytokine production. At birth, the response is skewed in favor of Th2 cell responses (Upham et al., 2002), presumably decreasing the efficiency of host-protective responses, particularly to intracellular bacteria, while increasing the risk of developing allergic asthma. Similar age-related defects in immune function may also be a predisposing factor in repeated inner ear infections in young children. Faden (2001) noted that 5% to 10% of children experience four or more inner ear infections within the first year of life, particularly with *H. influenzae*. IgG antibody responses to conserved bacterial capsular proteins did not increase after 2 years of age in the infection-prone group, and T cell responses to the same antigen were also reduced, suggesting that repeated infections may be caused by subtle immunologic abnormalities in susceptible children.

The Elderly

The immune system of the elderly is characterized by a gradual decline in function (immunosenescence) which, in addition to underlying chronic diseases such as diabetes or emphysema (Burns and Goodwin, 1997), results in an increased incidence and severity of infections with common pathogens. In adults over 75 years of age, pneumonia and influenza together are the fourth leading cause of death (Yoshikawa, 1983). Although immunization is effective on a population basis, the CDC estimates that 90% of the excess deaths each year from influenza occur in individuals over 65 years old, due in part to poor vaccination responses (Fukuda et al., 1999). While the neonatal immune system is characterized by

Associating Changes in the Immune System with Clinical Diseases

Table 18.1.2 Effects of Aging on the Distribution of Lymphocyte Subtypes[a]

Marker	Young elderly (65–85)		Old elderly (>90)		Young adults (25–35)
	Absolute[b]	% of young adult	Absolute	% of young adult	Absolute[b]
Lymphocytes	1980 ± 620	89.6	1830 ± 680[c]	82.8	2210 ± 470
$CD2^+$	1730 ± 410[c]	87.4	1605 ± 470[c]	81.1	1980 ± 310
$CD3^+$	1510 ± 320[c]	81.6	1360 ± 380[c,d]	73.5	1850 ± 280
$CD4^+$	1115 ± 260[c]	89.6	1084 ± 290[c]	87.1	1245 ± 190
$CD8^+$	460 ± 190[c]	68.7	405 ± 220[c]	60.5	670 ± 145
$CD4^+$:$CD8^+$ ratio	2.42	130.8	2.68	144.9	1.85
CD45RA (naive)	560 ± 180[c]	45.5	380 ± 200[c,d]	30.9	1230 ± 340
CD45RO (memory)	1090 ± 420[c]	143.4	1125 ± 470[c]	148.0	760 ± 235
CD57 (NK)	390 ± 180[c]	185.7	430 ± 205[c]	204.7	210 ± 135

[a]Adapted from Lesourd (1999).
[b]Absolute values are per cubic millimeter.
[c]Significantly different from young adults.
[d]Significantly different from young elderly.

immature cells, the immune system in the elderly is characterized by normal numbers of mature cells but a decline in their ability to respond to imunogen (Shou et al., 1976; Wayne et al., 1990). Increased rates and severity of infection that occur in the elderly is the product of these effects as well as other physiological changes associated with the aging process. Physical effects include inefficient bladder function, decreased clearance of lung secretions, and reduced gastric acidity (Gavazzi and Krause, 2002), culminating in reduced barrier or clearance functions that normally reduce bacterial load in these organs. Various degrees of malnutrition and micronutrient deficiencies are also more common in the elderly and can contribute to decreased resistance (Lesourd, 1997). Although the relative distribution of immune cells does not change dramatically in the elderly, changes in the relative abundance of certain cell subpopulations do occur. Loss of naïve cells, which is secondary to thymic involution, appears in the third decade of life. Naïve T cells predominate in the circulation of young adults, while the relative distribution in the elderly shifts towards an increased proportion of memory cells. For example, Lesourd (1999) reported a 55% decrease in $CD45RA^+$ T cell counts and a 43% increase in $CD45RO^+$ cells in a population with an average age of 78 years, compared to 30 year olds (Table 18.1.2). Despite increased populations of specifically educated memory cells, many of these cells respond poorly, presumably because they have reached their replicative limit (Effros and Pawelec, 1997). Patterns of cytokine production also change with aging. Although contradictory results have been obtained in human studies, Cakman et al. (1996) reported that IFN-γ production is reduced by 70% while IL-4 production is increased by 4-fold in the elderly compared to 20 to 35 year olds. This may in part explain reduced cell-mediated resistance to influenza infection in the elderly.

Although the total numbers of circulating B cells do not change with age, B cell responses are also compromised in the elderly (Weksler, 2000). Immunization with diphtheria toxin in younger subjects produces higher antibody titers that persist longer than titers in older subjects. When evaluated at the single cell level, plasma cells in younger subjects are more plentiful and produce more antibody, on a per cell basis, than those from the elderly (Burns et al., 1993). In addition to functional changes in cellular and humoral immunity, innate immunity is suppressed in the elderly, including PMN function, which results from reduced superoxide production and shorter half-lives (Lord et al., 2001).

EXPERIMENTAL ANIMAL MODELS

As it is relatively difficult to determine the contribution of chronic low-level immunosuppression or the cumulative effects

Table 18.1.3 Commonly Employed Experimental Disease Resistance Models[a,b]

Challenge agent	Endpoint measured
Listeria monocytogenes	Liver CFU, spleen CFU, morbidity
Streptococcus pneumoniae	Morbidity
Plasmodium yoelli	Parasitemia
Influenza virus	Morbidity, viral titer/tissue burden
Cytomegalovirus	Morbidity, viral titer/tissue burden
Trichinella spiralis	Muscle larvae, parasite numbers
PYB6 sarcoma	Tumor incidence (subcutaneous)
B16F10 melanoma	Tumor burden (lung nodules)

[a] Adapted from Selgrade et al. (1999), Burleson (2000), van Loveren (1995), and Bradley (1995a).
[b] Abbreviations: CFU, colony forming units.

of modest changes in immune function to the background incidence of disease in the human population, several efforts have been made to examine these relationships in experimental groups. In the field of immunotoxicology, a set of tests, usually referred to as host resistance assays, have evolved in which groups of experimental animals are challenged with either an infectious agent or transplantable tumor at a challenge level sufficient to produce either a low incidence or minimal infectivity in the control group (Table 18.1.3). As the endpoints in these tests have evolved from relatively nonspecific (e.g., animal morbidity and mortality) to continuous measures, such as tumor numbers, viral titers, or bacterial cell counts, the sensitivity of these models has increased, although they are still limited by the number of animals that can be realistically devoted to any laboratory study and interanimal variability.

While there have been considerable efforts to establish interlaboratory variability and the robustness of tests to measure specific endpoints, such as antibody responses (Temple et al., 1993), histopathology (ICICIS, 1998; Kuper et al., 2000), quantitation of cell surface markers by flow cytometry (Burchiel et al., 1997; Zenger et al., 1998), or cytokine production (Langezaal et al., 2002; Hermann et al., 2003), there have been only two efforts that have evaluated the sensitivity and predictive value of individual measures of immune outcomes with host resistance tests. In 1979, under the auspices of the U.S. National Toxicology Program (NTP), a panel of experts gathered to prioritize a list of immunological and host resistance assays that would be suitable for use in mouse studies and a formal validation was initiated (Luster et al., 1988). A smaller effort was undertaken at the National Institute of Public Health and the Environment (RIVM) which focused on the rat and was based on the OECD #407 guideline (Vos, 1977, 1980; van Loveren and Vos, 1989). In both programs, host resistance tests were usually considered in a second or third testing level (tiered) evaluation, and only performed when there were indications of alterations in immune function in the first or second tiers. Data subsequently obtained from these validation programs indicated that host resistance assays, while correlated with immune tests, were not as sensitive as many of the functional tests.

Single-Parameter Studies

Predictive values of individual immune tests for host resistance

As recently reviewed (Germolec, 2003), several studies have addressed individual relationships between changes in immune measurements and host resistance tests routinely used in rodent studies. While it is rare for a single component of the immune system to be solely responsible for resistance to a specific infectious agent or tumor type, certain immune measures show significant correlations with the outcomes of individual host resistance assays. For example, reduction in NK cell activity has been correlated with increased susceptibility to challenge with PYB6 sarcoma cells, B16F10 melanoma cells, and murine CMV (Luster et al., 1988; 1993; Selgrade et al., 1992). Suppression of cell-mediated immunity, complement deficiency, and depressed macrophage and neutrophil function has been associated with decreased resistance to *Listeria monocytogenes* (Petit, 1980; Luster et al., 1988; Bradley, 1995b). Clearance of parasitic infections, such as *Plasmodium yoelii* and *Trichinella spiralis*, have both a cellular and

humoral component and decreased resistance has been shown following depression of both arms of the immune system (Luebke, 1995; van Loveren et al., 1995). While the predictive values of individual immune tests for host resistance have been shown to range from relatively good (plaque forming cell assay, 73%; NK cell activity, 73%; delayed type hypersensitivity response, 82%) to poor (lymphoproliferative response to LPS <50%), combinations of several immune tests allow for very high concordance (Luster et al., 1993), indicating that only two or three specific tests are required to screen adequately for immunotoxicity.

Tests for contributions of specific molecules

Deletion or functional blocking of specific immune components in experimental animals has been used to elucidate the relative contributions of specific molecules, signaling pathways, and cells to disease resistance (Hickman-Davis, 2001). This can be achieved via targeted gene disruption resulting in animals deficient in specific cell populations or soluble mediators which contribute to host defense (e.g., CD4 T cell knockouts), treatment of normal animals with selective toxic agents (e.g., the use of gadolinium chloride to block macrophage function), or administration of neutralizing antibodies against critical cell-specific surface receptors. A study by Wilson et al. (2001) was specifically designed to determine the magnitude of NK cell suppression that would translate into altered resistance in three disease models. The studies were conducted by NK cell depletion with an antibody to the cell surface molecule, Asialo GM1, using a treatment regimen that did not alter other standard immune function tests used in the assessment of immunotoxicity in rodents. These authors demonstrated that at low levels of tumor challenge, an approximate reduction of 50% or more in NK cell activity, now thought to be involved primarily in metastatic processes, was required before significant effects on resistance to NK-sensitive tumors could be observed. These studies also demonstrated that the level of suppression needed to alter host resistance was related to the challenge level of the tumor. Conversely, studies that have used monoclonal antibodies to effectively deplete $CD4^+$ and $CD8^+$ T lymphocytes have found little evidence of altered resistance to challenge with PYB6 sarcoma cells, a model which was thought to be dependent on cell-mediated immunity (Weaver et al., 2002).

Multiparameter Studies

Studies designed to address the contribution of a single immune parameter in host resistance will have limitations. In studies designed to specifically address these limitations, Keil et al. (2001) demonstrated that monitoring several immunological parameters concurrently provides information that might not be evident from studies using single tests. Using the prototypical immunosuppressive agent dexamethasone, these authors demonstrated that contrary to what would be expected based on the compound's suppressive effects on cytokine production, T cell function, and NK cell activity, relatively high levels of dexamethasone were needed to decrease resistance to *Listeria monocytogenes*. At doses that suppressed many immune parameters, an increase in neutrophil numbers, and nitrite production by peritoneal macrophages was observed. It was suggested that at lower doses of dexamethasone, the significant increase in the concentration of neutrophils in the blood, in conjunction with increased production of nitric oxide, compensated for the decrements in other immune parameters so that overall resistance to the pathogen was not compromised (Keil et al., 2001). Heryzk et al. (1997) have developed a testing paradigm that evaluates immune function within the context of resistance to a specific infection. Following infection with *Candida albicans*, a four-parameter model is used that includes survival, spleen colony forming units (CFU), muscle CFU, and antibody titers, and which the authors suggest allows an inclusive evaluation of both nonspecific, cell-, and humoral-mediated immune responses. This approach has proved successful in identifying both immunosuppressive and immunostimulatory compounds and has the advantage of being able to evaluate multiple immune endpoints in an intact animal and directly relate them to a clinical endpoint. The utility of the method as a screening tool has yet to be evaluated using large numbers of test articles or environmental chemicals, and the procedure is not widely used outside of the pharmaceutical industry.

Control of Variables

Variables, such as virulence and dose of the infectious agent that impact the ability to clear an infection in humans, can be controlled in experimental animal models. Using groups of mice that had received increasing doses of an immunsuppressive agent, Luster et al. (1993) challenged these mice with increasing doses

of PYB6 tumor cells in order to help clarify the dose-response relationship. It was observed that even immunologically normal animals, provided a sufficient number of tumor cells, develop a high frequency of tumors and the number of tumor cells required to produce tumors decreased proportionally to the degree of immunosuppression. This was interpreted to indicate that immune function–disease response relationships tended to be linear in nature, rather than threshold. Although it is not possible to confirm these relationships in humans, it was suggested that similar response relationships would also be applicable to humans, albeit with different slopes, provided other modifiers were not present. Similar relationships were suggested in studies of mice treated with cyclosporin and challenged with group B streptococcus, although studies using *L. monocytogenes* challenge indicated that the dose-response curve would be affected by the composite effects on all immune parameters (Keil et al., 2001).

THE SOCIAL AND ECONOMIC IMPACT OF SOME COMMON PATHOGENS

Impact of Mortality

The major purpose for undertaking immuntoxicology studies, whether in animal models or clinical studies, is to identify potential hazards and ultimately to assist in the risk assessment/management process. This decision process should take into account the social and economic impact of the potential health effects that would ensue. In order to begin establishing a framework for incorporating immunotoxicology data in the risk assessment/management process, it is necessary to identify the social and economic impact of infectious diseases in the general population. While precise information is not readily available, several sources indicate these to be significant and that even small changes in infectious disease frequency has a major impact. The impacts associated with mortality, and to a lesser extent morbidity, from common pathogens such as influenza and pneumonia, have been determined and can serve as a basis in the risk management process. Deaths have the most costly impact on society. In 2000, the age-adjusted death rate for influenza and pneumonia was 23.0 and 0.6 per 100,000, respectively, based on the 10th Revision of the International Statistical Classification of Diseases and Related Health Problems, 10th Revision coding (ICD-10, 1992). Together these infections were ranked as the seventh leading cause of death in the U.S. for all ages (Anderson, 2002). In 2000, the mortality rates for all infants from influenza and pneumonia were 7.5 deaths per 100,000 live births, a decline from 8.4 in 1999 (Hoyert et al., 2001; Minino et al., 2002). In both years, this number was dominated by pneumonia. Other conditions secondarily related to these illnesses, such as disorders related to low birth weights, respiratory distress, or bacterial sepsis, accounted for higher infant deaths (Minino et al., 2002), including neonates (<28 days of age); however, influenza and pneumonia still ranked seventh for post neonates (Anderson, 2002). For the ≥65 years age group, chronic lower respiratory disease and influenza-pneumonia were the fourth and fifth ranked leading causes of death in 2000, respectively (Anderson, 2002); however, pneumonitis due to aspirating solids and liquids into the lung is becoming a more common cause of death among the elderly and is now ranked as the fifteenth leading cause of death (Minino et al., 2002).

Cost

Economic impacts resulting from infectious diseases are captured by determining the number of deaths, hospitalizations, and outpatient or emergency room visits for specific illnesses, usually collected in national surveys, and applying formulas to convert these to dollars. Cost of illness methodology can handle, with some degree of confidence, the valuing of medical costs and productivity losses in an attempt to capture the burden of infectious disease mortality and morbidity. It should be noted, however, that most estimates of this burden do not account for reduced functional abilities, losses from pain and suffering, or the cost to the individual, family member, or co-worker from psychological or emotional stress. There are many other fundamentally unobservable quantities, such as the value of output that is lost as a result of an employee having an infectious disease episode. Valuing lost work days does not explain entire productivity loss but provides a comparison indicator.

An NIH-sponsored effort used methods from previous disease-specific results to estimate costs and applied inflation factors for the time period under consideration to estimate the total cost of influenza and pneumonia (ICD-9-CM, 1991). This amount included $18.6 billion for medical costs and $7 billion for productivity losses. Leigh et al. (2003) focused on

fourteen occupational illnesses to determine annual medical costs of occupational illnesses in the U.S. Within this population, estimates for pneumonia, using ICD-9-CM codes 480 to 482 and 484, which included only the 25 to 64 age group, was $24.7 million, with males accounting for $19.9 of the total. Otitis media (ICD-9-CM, 1991), the most common cause of hearing loss in children, occurs in 80% of children under 3 years of age and is the major reason for doctor or emergency room visits in this age group. According to the Agency for Health Care Research and Quality, formerly the Agency for Health Care Policy and Research, the 1991 annual cost for treating 2-year olds for otitis media was $1 billion. Estimates for 2000 places the figure at $5 billion, with $2.9 billion in direct costs and $2.1 billion in indirect costs (Kirstein, 2000). Langley et al. (1997) have estimated the annual cost of RSV infection at $17 million using ICD-9-CM code 466.1 in children younger than 4 years of age. The largest cost was associated with hospital services for the ~0.7% of infected children requiring admission. The average medical care expenditure for all children 2 years of age or younger was $22 per child.

CONCLUSIONS

For most toxic agents, adequate clinical data (i.e., exposure levels, disease incidence) are rarely available to accurately determine safe exposure levels without the need to include observations from either experimental models or human biomarkers studies. Thus, it is important that a scientifically sound framework be established that allows for the accurate and quantitative interpretation of experimental or biomarker data in the risk assessment process. For immunotoxicology data, this may require, for example, development of models to equate changes in leukocyte counts, $CD4^+$ cell numbers and/or immunoglobulin levels, which can be readily performed in humans, to changes in the background incidence or severity of infectious diseases. Although experimental animal models provide an opportunity to perform more informative immune tests and establish reliable exposure estimates, extrapolating these findings across species also introduces considerable uncertainty. While this review does not provide a specific framework to perform these extrapolations, the authors have attempted to provide background information on qualitative and quantitative relationships between immune parameters and disease that would be integral to such an effort. The following general conclusions can be surmised:

1. The major clinical, or at least most readily discernible, consequence of mild-to-moderate chronic immunosuppression is an increase in the incidence of infectious diseases. Only a few studies have addressed infectious disease severity or neoplastic diseases.

2. In addition to immunosuppression, many nonimmune factors can affect infectious disease incidences and should be considered in data interpretation. This is particularly evident with infections from common pathogens, such as influenza and pneumonia in the very young and elderly.

3. The type of infectious disease observed is often dependent upon the specific arm of the immune system that is affected. Thus, increased infections with obligate intracellular pathogens, such as viral infections, will most likely occur following suppression of cell mediated immunity while defects in phagocytic activity, such as neutropenia, will more likely increase susceptibility to facultative intracellular microbes.

4. Increases in infectious disease incidence following chronic immunosuppression can be caused by common pathogens, opportunistic microbes, or activation of latent viruses (most often from the herpes family). The ability to detect changes in the frequency of infections from common pathogens in epidemiological studies, (e.g., increased respiratory infections from influenza) has proved difficult, most likely due to the required complexity in the study design. Increased incidences of infection with opportunistic microbes can be readily observed in individuals with severe immunodeficiency, such as AIDS when immunological parameters, especially $CD4^+$ cell numbers, are reduced by $>50\%$ from control values.

5. It is considerably more difficult to ascertain health consequences from low-to-moderate levels of immunosuppression, as would be most likely to occur from exposure to immunotoxic agents than from severe immunosuppression. There are a number of studies, however, that indicate that these populations are at an increased risk to infection with common pathogens and latent viruses, particularly those from the Herpes family, but not to opportunistic infections. There are insufficient clinical data to determine whether the relationship between a decrease in immune response and an increase in infectious disease follows a linear or threshold relationship in humans. Studies in experimental animal models, however, support a linear relationship when

multiple immune system parameters are affected. However, threshold relationships occur when single immune parameters (e.g., NK cell activity) are targeted. These differences may be associated with redundancy in the immune system.

6. The major gap in clarifying the shape of the dose-response curve between immune response changes and disease risk is a lack of large-scale epidemiological studies in populations with mild-to-moderate immunodeficiency that have been monitored simultaneously for immune system parameters and clinical disease. Large studies that have been previously undertaken are of limited value. For example, the assessment of immune relationships in patients with AIDS-defining illnesses, such as *Pnuemocyctis carinii* pneumonia (PCP), CMV, and *Mycobaterium avium* complex (MAC) by the Multicohort AIDS centers were limited to individuals with $CD4^+$ T cell counts of $<500 \times 10^6$/liter (Pauli and Kopferschmitt-Kubler, 1991; Margolick et al., 1998; Amornkul et al., 1999). Interestingly, the 5-year cumulative probabilities for AIDS and infectious disease deaths in the latter stages show a relatively linear response from 0% to 76% occurrence in patients with $CD4^+$ cell counts between 500×10^6/liter and 200×10^6/liter, respectively (Vlahov et al., 1998). Furthermore, in one study where 864 patients failed to meet the study criteria ($CD4^+$ cell counts $>500 \times 10^6$/liter), 50 developed PCP, four developed CMV, and three developed MAC, indicating that opportunistic infection can occur in less immunosuppressed individuals but at a lower incidence (Lyles et al., 1999).

Acknowledgment

This review was prepared in conjuction with the Immunotoxicology Workgroup sponsored by the U.S. Environmental Protection Agency (EPA) Office of Research and Development (National Center for Environmental Assessment), EPA Office of Children's Health Protection, National Institute of Environmental Health Sciences (National Toxicology Program), and National Institute for Occupational Safety and Health (Health Effects Laboratory Division). Members of the workgroup not included as authors are: Drs. David Chen (EPA/OCPH), Marquea King (EPA/ORD/NCEA) and Yung Yang (EPA, OPPTS). Special thanks to Dr. Bob Sonawane (EPA/ORD/NCEA) for helping to organize this effort.

Disclaimer

This report has been reviewed by the U.S. Environmental Protection Agency's Office of Research and Development and approved for publication. Approval does not signify that the contents reflect the views of the Agency.

Literature Cited

Ambruso, D.R., Bentwood, B., Henson, P.M. and Johnston, R.B. Jr. 1984. Oxidative metabolism of cord blood neutrophils: Relationship to content and degranulation of cytoplasmic granules. *Pediatr. Res.* 18:1148-1153.

Amornkul, P.N., Tansuphasawadikul, S., Limpakarnjanarat, K., Likanonsakul, S., Young, N., Eampokalap, B., Kaewkungwal, J., Naiwatanakul, T., Von Bargen, J., Hu, D.J. and Mastro, T.D. 1999. Clinical disease associated with HIV-1 subtype B′ and E infection among 2104 patients in Thailand. *AIDS* 13:1963-1969.

Anderson, R.N. 2002. Deaths: Leading causes for 2000. *Natl. Vital Stat. Rep.* 50:1-85.

Antonini, J.M. 2003. Health effects of welding. *Crit. Rev. Toxicol.* 33:61-103.

Arndt, V., Vine, M.F. and Weigle, K. 1999. Environmental chemical exposures and risk of herpes zoster. *Environ. Health Perspect.* 107:835-841.

Atkinson, K. 2000. Clinical Bone Marrow and Blood Stem Cell Transplantation, Cambridge University Press, Boston.

Biondi, M. and Zannino, L.G. 1997. Psychological stress, neuroimmunomodulation, and susceptibility to infectious diseases in animals and man: A review. *Psychother. Psychosom.* 66:3-26.

Bradley, S.G. 1995a. Introduction to animal models in immunotoxicology: Host resistance. *In* Methods in Immunotoxicology, (G.R. Burleson, J.H. Dean, and A.E. Munson, eds.) pp. 135-142. Wiley-Liss, New York.

Bradley, S.G. 1995b. Listeria host resistance model. *In* Methods in Immunotoxicology, (G.R. Burleson, J.H. Dean, and A.E. Munson, eds.) pp. 169-179. Wiley-Liss, New York.

Burchiel, S.W., Kerkvliet, N.L., Gerberick, G.F., Lawrence, D.A. and Ladics, G.S. 1997. Assessment of immunotoxicity by multiparameter flow cytometry. *Fundam. Appl. Toxicol.* 38:38-54.

Burleson, G.R. 2000. Models of respiratory immunotoxicology and host resistance. *Immunopharmacology* 48:315-318.

Burns, E.A. and Goodwin, J.S. 1997. Immunodeficiency of aging. *Drugs Aging* 11:374-397.

Burns, E.A., Lum, L.G., L'Hommedieu, G., and Goodwin, J.S. 1993. Specific humoral immunity in the elderly: In vivo and in vitro response to vaccination. *J. Gerontol.* 48:B231-236.

Cakman, I., Rohwer, J., Schutz, R.M., Kirchner, H. and Rink, L. 1996. Dysregulation between TH1 and TH2 T cell subpopulations in the elderly. *Mech. Aging Dev.* 87:197-209.

Chakrabarti, S., Collingham, K.E., Marshall, T., Holder, K., Gentle, T., Hale, G., Fegan, C.D., and Milligan, D.W. 2001. Respiratory virus infections in adult T cell-depleted transplant recipients: The role of cellular immunity. *Transplantation* 72:1460-1463.

Ciccimarra, F. 1994. Fetal and neonatal immunology. *J. Perinat. Med.* 22(Supp. 1):84-87.

Clark, K.R., Forsythe, J.L., Shenton, B.K., Lennard, T.W., Proud, G., and Taylor, R.M. 1993. Administration of ATG according to the absolute T lymphocyte count during therapy for steroid-resistant rejection. *Transpl. Int.* 6:18-21.

Clover, R.D., Abell, T., Becker, L.A., Crawford, S., and Ramsey, C.N. Jr. 1989. Family functioning and stress as predictors of influenza B infection. *J. Fam. Pract.* 28:535-539.

Cohen, S. 1995. Psychological stress and susceptibility to upper respiratory infections. *Am. J. Respir. Crit. Care Med.* 152:S53-58.

Cohen, S., Tyrrell, D.A., and Smith, A.P. 1991. Psychological stress and susceptibility to the common cold. *N. Engl. J. Med.* 325:606-612.

Deseda-Tous, J., Cherry, J.D., Spencer, M.J., Welliver, R.C., Boyer, K.M., Dudley, J.P., Zahradnik, J.M., Krause, P.J., and Walbergh, E.W. 1978. Measles revaccination. Persistence and degree of antibody titer by type of immune response. *Am. J. Dis. Child.* 132:287-290.

Dewailly, E., Ayotte, P., Bruneau, S., Gingras, S., Belles-Isles, M., and Roy, R. 2000. Susceptibility to infections and immune status in Inuit infants exposed to organochlorines. *Environ. Health Perspect.* 108:205-211.

Effros, R.B. and Pawelec, G. 1997. Replicative senescence of T cells: Does the Hayflick limit lead to immune exhaustion? *Immunol. Today* 18:450-454.

Esterling, B.A., Antoni, M.H., Kumar, M. and Schneiderman, N. 1993. Defensiveness, trait anxiety, and Epstein-Barr viral capsid antigen antibody titers in healthy college students. *Health Psychol.* 12:132-139.

Faden, H. 2001. The microbiologic and immunologic basis for recurrent otitis media in children. *Eur. J. Pediatr.* 160:407-413.

Fukuda, F., Bridges, C.B., Brammer, T.L., Izurieta, H.S., and Cox, N.J. 1999. Prevention and contol of influenza: Recommendations of the Advisory Committee on Immunization Practices. *Morbid. Mortal. Weekly Rep.* 48:1-28.

Gardner, D.E. 2001. Bioaerosols and disease. *In* Patty's Industrial Hygiene and Toxicology, (E. Bingham, B. Cohrssen, and C.H. Powell, eds.) pp. 679-711. Wiley Publishing, New York.

Gavazzi, G. and Krause, K.H. 2002. Aging and infection. *Lancet Infect. Dis.* 2:659-666.

Germolec, D.R. 2003. Selectivity and predictivity in immunotoxicity testing: Immune endpoints and disease resistance. Toxcol. Lett.: In press.

Glaser, R., Pearson, G.R., Bonneau, R.H., Esterling, B.A., Atkinson, C., and Kiecolt-Glaser, J.K. 1993. Stress and the memory T-cell response to the Epstein-Barr virus in healthy medical students. *Health Psychol.* 12:435-442.

Glaser, R., Rice, J., Sheridan, J., Fertel, R., Stout, J., Speicher, C., Pinsky, D., Kotur, M., Post, A., Beck, M., et al. 1987. Stress-related immune suppression: Health implications. *Brain. Behav. Immun.* 1:7-20.

Glaser, R., Sheridan, J., Malarkey, W.B., MacCallum, R.C., and Kiecolt-Glaser, J.K. 2000. Chronic stress modulates the immune response to a pneumococcal pneumonia vaccine. *Psychosom. Med.* 62:804-807.

Halloran, P.F. 1996. Rethinking immunosuppression in terms of the redundant and nonredundant steps in the immune response. *Transplant. Proc.* 28:11-18.

Hartevelt, M.M., Bavinck, J.N., Kootte, A.M., Vermeer, B.J., and Vandenbroucke, J.P. 1990. Incidence of skin cancer after renal transplantation in The Netherlands. *Transplantation* 49:506-509.

Herberman, R.B. 2001. Immunotherapy. *In* Clinical Oncology., (R.E. Jr. Lenhard, R.T. Osteen, and T. Gansler, eds.) pp. 215-223. American Cancer Society, Atlanta.

Hermann, C., von Aulock, S., Graf, K., and Hartung, T. 2003. A model of human whole blood lymphokine release for in vitro and ex vivo use. *J. Immunol. Methods* 275:69-79.

Hertz-Picciotto, I. 1995. Epidemiology and quantitative risk assessment: A bridge from science to policy. *Am. J. Public Health* 85:484-491.

Herzyk, D.J., Ruggieri, E.V., Cunningham, L., Polsky, R., Herold, C., Klinkner, A.M., Badger, A., Kerns, W.D., and Bugelski, P.J. 1997. Single-organism model of host defense against infection: A novel immunotoxicologic approach to evaluate immunomodulatory drugs. *Toxicol. Pathol.* 25:351-362.

Hickman-Davis, J.M. 2001. Implications of mouse genotype for phenotype. *News. Physiol. Sci.* 16:19-22.

House, R.V. 2003. A survey of immunotoxicology regulatory guidance. *In* Encyclpedia of Immunotoxicology, (H.-W. Vohr, ed.) In press. Springer Press, Heidelberg, Germany.

Hoyert, D.L., Arias, E., Smith, B.L., Murphy, S.L. and Kochanek, K.D. 2001. Deaths: Final data for 1999. *Natl. Vital Stat. Rep.* 49:1-113.

ICD-9-CM, International Classification of Diseases Clinical Modification. 1991. Vol. 1, 9th Rev., 4th Ed., Pub. No. PHS-91-1260. U.S. Dept. of Health & Human Services.

ICD-10, International Statistics Classification of Diseases and Related Health Problems. 1992. Vol. 1, 10th Rev. World Health Organization, Geneva.

ICICIS, 1998. Report of Validation Study of Assessment of Direct Immunotoxicity in the Rat. *Toxicology* 125:183-201.

ITC, Immunotoxicity Testing Committee. 1999. Application of Flow Cytometry to Immunotoxicity Testing: Summary of a Workshop Report. ILSI/HESI, Washington D.C.

Jamil, B., Nicholls, K., Becker, G.J., and Walker, R.G. 1999. Impact of acute rejection therapy on infections and malignancies in renal transplant recipients. *Transplantation* 68:1597-1603.

Karmaus, W., Kuehr, J., and Kruse, H. 2001. Infections and atopic disorders in childhood and organochlorine exposure. *Arch. Environ. Health* 56:485-492.

Kasl, S.V., Evans, A.S., and Niederman, J.C. 1979. Psychosocial risk factors in the development of infectious mononucleosis. *Psychosom. Med.* 41:445-466.

Keil, D., Luebke, R.W. and Pruett, S.B. 2001. Quantifying the relationship between multiple immunological parameters and host resistance: Probing the limits of reductionism. *J. Immunol.* 167:4543-4552.

Kiecolt-Glaser, J.K., Glaser, R., Strain, E.C., Stout, J.C., Tarr, K.L., Holliday, J.E. and Speicher, C.E. 1986. Modulation of cellular immunity in medical students. *J. Behav. Med.* 9:5-21.

Kiecolt-Glaser, J.K., Glaser, R., Shuttleworth, E.C., Dyer, C.S., Ogrocki, P., and Speicher, C.E. 1987. Chronic stress and immunity in family caregivers of Alzheimer's disease victims. *Psychosom. Med.* 49:523-535.

Kiecolt-Glaser, J.K., Glaser, R., Gravenstein, S., Malarkey, W.B., and Sheridan, J. 1996. Chronic stress alters the immune response to influenza virus vaccine in older adults. *Proc. Natl. Acad. Sci. U. S. A.* 93:3043-3047.

Kiecolt-Glaser, J.K., McGuire, L., Robles, T.F. and Glaser, R. 2002. Psychoneuroimmunology: Psychological influences on immune function and health. *J. Consult. Clin. Psychol.* 70:537-547.

Kirstein, R. 2000. Disease-Specific Estimates of Direct and Indirect Costs of Illness and NIH Support: Fiscal Year 2000 Update. Dept. Health and Human Services, Washington, D.C.

Kuper, C.F., Harleman, J.H., Richter-Reichelm, H.B. and Vos, J.G. 2000. Histopathologic approaches to detect changes indicative of immunotoxicity. *Toxicol. Pathol.* 28:454-466.

Langezaal, I., Hoffmann, S., Hartung, T. and Coecke, S. 2002. Evaluation and prevalidation of an immunotoxicity test based on human whole-blood cytokine release. *Altern. Lab. Anim.* 30:581-595.

Langley, J.M., Wang, E.E., Law, B.J., Stephens, D., Boucher, F.D., Dobson, S., McDonald, J., MacDonald, N.E., Mitchell, I. and Robinson, J.L. 1997. Economic evaluation of respiratory syncytial virus infection in Canadian children: A Pediatric Investigators Collaborative Network on Infections in Canada (PICNIC) study. *J. Pediatr.* 131:113-117.

Leigh, J.P., Yasmeen, S. and Miller, T.R. 2003. Medical costs of fourteen occupational illnesses in the United States in 1999. *Scand. J. Work. Environ. Health* 29:304-313.

Lesourd, B. 1999. Immune response during disease and recovery in the elderly. *Proc. Nutr. Soc.* 58:85-98.

Lesourd, B.M. 1997. Nutrition and immunity in the elderly: Modification of immune responses with nutritional treatments. *Am. J. Clin. Nutr.* 66:478S-484S.

Levy, O., Martin, S., Eichenwald, E., Ganz, T., Valore, E., Carroll, S.F., Lee, K., Goldmann, D., and Thorne, G.M. 1999. Impaired innate immunity in the newborn: Newborn neutrophils are deficient in bactericidal/permeability-increasing protein. *Pediatrics* 104:1327-1333.

Lord, J.M., Butcher, S., Killampali, V., Lascelles, D., and Salmon, M. 2001. Neutrophil ageing and immunesenescence. *Mech. Ageing Dev.* 122:1521-1535.

Lu, Y.C. and Wu, Y.C. 1985. Clinical findings and immunological abnormalities in Yu-Cheng patients. *Environ. Health Perspect.* 59:17-29.

Luebke, R.W. 1995. Assessment of host resistance to infection with rodent malaria. *In* Methods in Immunotoxicology (G.R. Burleson, J.H. Dean, and A.E. Munson, eds.) pp. 221-242. Wiley-Liss, New York.

Luebke, R.W. 2002. Pesticide-induced immunotoxicity: Are humans at risk? *Human Ecol. Risk Assess.* 8:293-303.

Luster, M.I., Munson, A.E., Thomas, P.T., Holsapple, M.P., Fenters, J.D., White, K.L. Jr., Lauer, L.D., Germolec, D.R., Rosenthal, G.J., and Dean, J.H. 1988. Development of a testing battery to assess chemical-induced immunotoxicity: National Toxicology Program's guidelines for immunotoxicity evaluation in mice. *Fundam. Appl. Toxicol.* 10:2-19.

Luster, M.I., Portier, C., Pait, D.G., Rosenthal, G.J., Germolec, D.R., Corsini, E., Blaylock, B.L., Pollock, P., Kouchi, Y., Craig, W., White, K.L., Munson, A.E., and Comment, C.E. 1993. Risk assessment in immunotoxicology. II. Relationships between immune and host resistance tests. *Fundam. Appl. Toxicol.* 21:71-82.

Lyles, R.H., Chu, C., Mellors, J.W., Margolick, J.B., Detels, R., Giorgi, J.V., Al-Shboul, Q., and Phair, J.P. 1999. Prognostic value of plasma HIV RNA in the natural history of *Pneumocystis carinii* pneumonia, cytomegalovirus and *Mycobacterium avium* complex. Multicenter AIDS Cohort Study. *AIDS* 13:341-349.

Margolick, J.B., Donnenberg, A.D., Chu, C., O'Gorman, M.R., Giorgi, J.V., and Munoz, A. 1998. Decline in total T cell count is associated with onset of AIDS, independent of CD4(+) lymphocyte count: Implications for AIDS pathogenesis. *Clin. Immunol. Immunopathol.* 88:256-263.

Marsland, A.L., Bachen, E.A., Cohen, S., Rabin, B., and Manuck, S.B. 2002. Stress, immune reactivity and susceptibility to infectious disease. *Physiol. Behav.* 77:711-716.

Meyer, R.J. and Haggerty, R.J. 1962. Streptococcal infections in families. Factors altering individual susceptibility. *Pediatrics* 29:539-549.

Minino, A.M., Arias, E., Kochanek, K.D., Murphy, S.L., and Smith, B.L. 2002. Deaths: Final data for 2000. *Natl. Vital Stat. Rep.* 50:1-119.

Morris, J.G. Jr. and Potter, M. 1997. Emergence of new pathogens as a function of changes in host susceptibility. *Emerg. Infect. Dis.* 3:435-441.

Nakanishi, Y., Shigematsu, N., Kurita, Y., Matsuba, K., Kanegae, H., Ishimaru, S., and Kawazoe, Y. 1985. Respiratory involvement and immune status in yusho patients. *Environ. Health Perspect.* 59:31-36.

Ochs, L., Shu, X.O., Miller, J., Enright, H., Wagner, J., Filipovich, A., Miller, W., and Weisdorf, D. 1995. Late infections after allogeneic bone marrow transplantations: Comparison of incidence in related and unrelated donor transplant recipients. *Blood* 86:3979-3986.

Orange, J.S. 2002. Human natural killer cell deficiencies and susceptibility to infection. *Microbes Infect.* 4:1545-1558.

Patriarca, P.A. 1994. A randomized controlled trial of influenza vaccine in the elderly. Scientific scrutiny and ethical responsibility. *JAMA* 272:1700-1701.

Pauli, G. and Kopferschmitt-Kubler, M.C. 1991. Isocyanates and asthma. Progress in allergy and clinical immunology. *In* Proceeding of the 14th International Congress of Allergology and Clinical Immunology, pp. 152-158. Sydney, Australia.

Penn, I. 2000. Post-transplant malignancy: The role of immunosuppression. *Drug Saf.* 23:101-113.

Petit, J.C. 1980. Resistance to listeriosis in mice that are deficient in the fifth component of complement. *Infect. Immun.* 27:61-67.

Schultz, C., Reiss, I., Bucsky, P., Gopel, W., Gembruch, U., Ziesenitz, S., and Gortner, L. 2000. Maturational changes of lymphocyte surface antigens in human blood: Comparison between fetuses, neonates and adults. *Biol. Neonate* 78:77-82.

Selgrade, M.K., Daniels, M.J., and Dean, J.H. 1992. Correlation between chemical suppression of natural killer cell activity in mice and susceptibility to cytomegalovirus: Rationale for applying murine cytomegalovirus as a host resistance model and for interpreting immunotoxicity testing in terms of risk of disease. *J. Toxicol. Environ. Health* 37:123-137.

Sheridan, J.F., Tutschka, P.J., Sedmak, D.D., and Copelan, E.A. 1990. Immunoglobulin G subclass deficiency and pneumococcal infection after allogeneic bone marrow transplantation. *Blood* 75:1583-1586.

Shou, L., Schwartz, S.A., and Good, R.A. 1976. Suppressor cell activity after concanavalin A treatment of lymphocytes from normal donors. *J. Exp. Med.* 143:1100-1110.

Sia, I.G. and Paya, C.V. 1998. Infectious complications following renal transplantation. *Surg. Clin. North Am.* 78:95-112.

Sleijffers, A., Yucesoy, B., Kashon, M., Garssen, J., De Gruijl, F.R., Boland, G.J., Van Hattum, J., Luster, M.I., and van Loveren, H. 2003. Cytokine polymorphisms play a role in susceptibility to ultraviolet B-induced modulation of immune responses after hepatitis B vaccination. *J. Immunol.* 170:3423-3428.

Small, T.N., Papadopoulos, E.B., Boulad, F., Black, P., Castro-Malaspina, H., Childs, B.H., Collins, N., Gillio, A., George, D., Jakubowski, A., Heller, G., Fazzari, M., Kernan, N., MacKinnon, S., Szabolcs, P., Young, J.W., and O'Reilly, R.J. 1999. Comparison of immune reconstitution after unrelated and related T-cell-depleted bone marrow transplantation: Effect of patient age and donor leukocyte infusions. *Blood* 93:467-480.

Stiehm, E.R. and Fudenberg, H.H. 1966. Serum levels of immune globulins in health and disease: A survey. *Pediatrics* 37:715-727.

Storek, J., Espino, G., Dawson, M.A., Storer, B., Flowers, M.E., and Maloney, D.G. 2000. Low B-cell and monocyte counts on day 80 are associated with high infection rates between days 100 and 365 after allogeneic marrow transplantation. *Blood* 96:3290-3293.

Storek, J., Gooley, T., Witherspoon, R.P., Sullivan, K.M., and Storb, R. 1997. Infectious morbidity in long-term survivors of allogeneic marrow transplantation is associated with low CD4 T cell counts. *Am. J. Hematol.* 54:131-138.

Temple, L., Kawabata, T.T., Munson, A.E., and White, K.L. Jr. 1993. Comparison of ELISA and plaque-forming cell assays for measuring the humoral immune response to SRBC in rats and mice treated with benzo[a]pyrene or cyclophosphamide. *Fundam. Appl. Toxicol.* 21:412-419.

Thomas, P.S., Yates, D.H., and Barnes, P.J. 1995. Tumor necrosis factor-α increases airway responsiveness and sputum neutrophilia in normal human subjects. *Am. J. Respir. Crit. Care Med.* 152:76-80.

Tryphonas, H. 2001. Approaches to detecting immunotoxic effects of environmental contaminants in humans. *Environ. Health Perspect.* 109(Suppl 6):877-884.

Tuschl, H., Weber, E., and Kovac, R. 1997. Investigations on immune parameters in welders. *J. Appl. Toxicol.* 17:377-383.

Upham, J.W., Lee, P.T., Holt, B.J., Heaton, T., Prescott, S.L., Sharp, M.J., Sly, P.D., and Holt, P.G. 2002. Development of interleukin-12-producing capacity throughout childhood. *Infect. Immun.* 70:6583-6588.

van Loveren, H. and Vos, J.G. 1989. Immunotoxicological considerations: A practical approach to immunotoxicity testing in the rat. *In* Advances in Applied Toxicology (A.D. Dayan and A.J. Paine, eds.) pp. 143-165. Taylor & Francis, London.

van Loveren, H., Luebke, R.W., and Vos, J.G. 1995. Assessment of immunotoxicity with the parasitic infection model *Trichinella spiralis*. *In* Methods in Immunotoxicology (G.R. Burleson, J.H. Dean, and A.E. Munson, eds.) pp. 243-271. Wiley-Liss, New York.

van Loveren, H., van Amsterdam, J.G., Vandebriel, R.J., Kimman, T.G., Rumke, H.C., Steerenberg, P.S., and Vos, J.G. 2001. Vaccine-induced antibody responses as parameters of the influence of endogenous and environmental factors. *Environ. Health Perspect.* 109:757-764.

Vial, T., Nicolas, B., and Descotes, J. 1996. Clinical immunotoxicity of pesticides. *J. Toxicol. Environ. Health* 48:215-229.

Vine, M.F., Stein, L., Weigle, K., Schroeder, J., Degnan, D., Tse, C.K., Hanchette, C., and Backer, L. 2000. Effects on the immune system associated with living near a pesticide dump site. *Environ. Health Perspect.* 108:1113-1124.

Vine, M.F., Stein, L., Weigle, K., Schroeder, J., Degnan, D., Tse, C.K., and Backer, L. 2001. Plasma 1,1-dichloro-2,2-bis(*p*-chlorophenyl) ethylene (DDE) levels and immune response. *Am. J. Epidemiol.* 153:53-63.

Vlahov, D., Graham, N., Hoover, D., Flynn, C., Bartlett, J.G., Margolick, J.B., Lyles, C.M., Nelson, K.E., Smith, D., Holmberg, S., and Farzadegan, H. 1998. Prognostic indicators for AIDS and infectious disease death in HIV-infected injection drug users: Plasma viral load and $CD4^+$ cell count. *JAMA* 279:35-40.

Voccia, I., Blakley, B., Brousseau, P., and Fournier, M. 1999. Immunotoxicity of pesticides: A review. *Toxicol. Ind. Health* 15:119-132.

Vos, J.G. 1977. Immune suppression as related to toxicology. *CRC Crit. Rev. Toxicol.* 5:67-101.

Vos, J.G. 1980. Immunotoxicity assessment: Screening and function studies. *Arch. Toxicol.* S4:95-108.

Wayne, S.J., Rhyne, R.L., Garry, P.J., and Goodwin, J.S. 1990. Cell-mediated immunity as a predictor of morbidity and mortality in subjects over 60. *J. Gerontol.* 45:M45-48.

Weaver, J.L., Broud, D.D., McKinnon, K., and Germolec, D.R. 2002. Serial phenotypic analysis of mouse peripheral blood leukocytes. *Toxicol. Mech. Methods* 12:95-118.

Weisglas-Kuperus, N., Patandin, S., Berbers, G.A., Sas, T.C., Mulder, P.G., Sauer, P.J., and Hooijkaas, H. 2000. Immunologic effects of background exposure to polychlorinated biphenyls and dioxins in Dutch preschool children. *Environ. Health Perspect.* 108:1203-1207.

Weksler, M.E. 2000. Changes in the B-cell repertoire with age. *Vaccine* 18:1624-1628.

Wieneke, H., Otte, B., Lang, D., and Heidenreich, S. 1996. Predictive value of IgG subclass levels for infectious complications in renal transplant recipients. *Clin. Nephrol.* 45:22-28.

Wilson, C.B. 1986. Immunologic basis for increased susceptibility of the neonate to infection. *J. Pediatr.* 108:1-12.

Wilson, S.D., McCay, J.A., Butterworth, L.F., Munson, A.E., and White, K.L. Jr., 2001. Correlation of suppressed natural killer cell activity with altered host resistance models in B6C3F1 mice. *Toxicol. Appl. Pharmacol.* 177:208-218.

Wolach, B., Carmi, D., Gilboa, S., Satar, M., Segal, S., Dolfin, T., and Schlesigner, M. 1994. Some aspects of the humoral immunity and the phagocytic function in newborn infants. *Israeli J. Med. Sci.* 30:331-335.

Yang, E.V. and Glaser, R. 2000. Stress-induced immunomodulation: Impact on immune defenses against infectious disease. *Biomed. Pharmacother.* 54:245-250.

Yoshikawa, T.T. 1983. Geriatric infectious diseases: An emerging issue. *J. Amer. Geriatr. Soc.* 31:34-39.

Yu, M.L., Hsin, J.W., Hsu, C.C., Chan, W.C., and Guo, Y.L. 1998. The immunologic evaluation of the Yucheng children. *Chemosphere* 37:1855-1865.

Yucesoy, B., Vallyathan, V., Landsittel, D.P., Sharp, D.S., Weston, A., Burleson, G.R., Simeonova, P., McKinstry, M., and Luster, M.I. 2001. Association of tumor necrosis factor-alpha and interleukin-1 gene polymorphisms with silicosis. *Toxicol. Appl. Pharmacol.* 172:75-82.

Zenger, V.E., Vogt, R., Mandy, F., Schwartz, A., and Marti, G.E. 1998. Quantitative flow cytometry: Inter-laboratory variation. *Cytometry* 33:138-145.

Contributed by Michael I. Luster, Laura Blanciforti, and Michael Kashon
National Institute for Occupational Safety and Health, Centers for Disease Control and Prevention
Morgantown, West Virginia

Dori R. Germolec and Christine G. Parks
National Institute of Environmental Health Sciences, National Institutes of Health
Research Triangle Park, North Carolina

Robert Luebke
U.S. Environmental Protection Agency
Research Triangle Park North, Carolina

Local Lymph Node Assays

Skin sensitization resulting in allergic contact dermatitis (ACD), a delayed-type hypersensitivity reaction in the skin characterized by a tissue-damaging inflammatory response, is an important occupational disease and certainly the most common manifestation of chemical allergy in humans. A wide variety of natural and synthetic chemicals has been shown to be capable of causing ACD (Cronin, 1980). In common with other forms of allergic disease, the development of ACD proceeds in two phases. During the first of these, the induction phase, an inherently susceptible subject is exposed to amounts of the inducing contact allergen sufficient to provoke an immune response of the vigor (and quality) necessary for the acquisition of skin sensitization. If the now sensitized individual is subsequently exposed to the same chemical allergen (or to an immunologically cross-reactive chemical allergen) at the same or a different skin site, an accelerated and more aggressive secondary immune response will be elicited at the site of contact. This, in turn, will initiate the cutaneous inflammatory reaction recognized clinically as ACD. This latter reaction is the elicitation, or challenge, phase.

A variety of techniques has been developed to identify the hazards and risks of ACD potentially associated with exposure to chemicals at work, at home, or in the environment. These include several guinea pig tests in which skin sensitizing potential is measured as a function of challenge-induced skin reactions in previously sensitized animals (Magnusson and Kligman, 1970; Buehler, 1985). This unit describes an alternative approach, the murine local lymph node assay (LLNA). In this method, and in contrast to guinea pig tests, skin sensitization potential is assessed as a function of events associated with the induction phase. Specifically, the LLNA measures proliferative responses in skin-draining lymph nodes following topical exposure to a chemical. This approach is based on an understanding that the acquisition of skin sensitization is characterized by (and dependent upon) the expansion within regional lymph nodes of allergen-responsive T lymphocytes. Lymph node cell (LNC) proliferation is assessed by the incorporation in situ of radiolabeled ^{3}H-thymidine. The protocol for the standard LLNA, in which lymph nodes are pooled on an experimental group basis, is provided (see Basic Protocol), as is a modified method in which lymph nodes are pooled on an individual animal basis, providing the opportunity to employ statistical analyses (see Alternate Protocol). These methods have been developed for contact sensitization hazard assessment. In addition, it is possible to use LLNA data for the measurement of relative potency in the context of risk assessment (see Support Protocol).

CAUTION: When working with radioactivity, take appropriate precautions to avoid contamination of the experimenter and the surroundings. Carry out the experiment and dispose of wastes in appropriately designated areas, following guidelines provided by the local radiation safety officer (see *APPENDIX 1A*).

NOTE: All protocols using live animals must first be reviewed and approved by an Institutional Animal Care and Use Committee (IACUC) and must follow officially approved procedures for the care and use of laboratory animals.

STANDARD LOCAL LYMPH NODE ASSAY

BASIC PROTOCOL

The standard LLNA identifies contact sensitization hazard potential as a function of radiolabeled thymidine incorporation into the lymph nodes draining the site of topical

Contributed by Rebecca J. Dearman and Ian Kimber
Current Protocols in Toxicology (2004) 18.2.1-18.2.12

exposure to chemical. Mice ($n = 4$ per group) are topically exposed to various concentrations of test chemical or to vehicle alone daily for 3 consecutive days on the dorsum of both ears. Five days after the initiation of exposure, animals receive an intravenous injection of radiolabeled thymidine. Five hours later, the draining auricular lymph nodes are excised and pooled on an experimental group basis, a single cell suspension of LNC is prepared, and thymidine incorporation is measured by β-scintillation counting.

Materials

Young adult (6- to 16-week-old) female CBA mice: maintain in semibarriered conditions
Chemicals to be tested
Vehicle—e.g., 4:1 (v/v) acetone olive oil (AOO), methylethyl ketone, dimethylformamide, or dimethyl sulfoxide (DMSO)
2 Ci/mmol [^{3}H]thymidine: pass through a 0.45-μm filter to sterilize
PBS, pH 7.2 to 7.4 (*APPENDIX 2A*)
5% (w/v) trichloroacetic acid (TCA)
Scintillation fluid (e.g., Hi-Safe Optiphase)
Temperature-controlled hot box (Harvard Apparatus)
Mouse restraining tube with outlet for tail
1-ml graduated syringes with 25-G, 1-in. needles, sterile
200-G stainless steel mesh: cut into ~3-cm squares, wash in 70% ethanol, autoclave, and turn edges up to form a box
600-mm plastic petri dish
5-ml syringe plungers, sterile
10-ml plastic centrifuge tubes

Topically expose mice to chemical

1. Acclimatize young adult female CBA mice in cages of four animals per group for at least 2 days after arrival.
2. Prepare dosing solutions of the chemical to be tested in an appropriate vehicle, generally selecting three consecutive concentrations from the following: 50, 25, 10, 5, 2.5, 1, 0.5, 0.25, and 0.1% (w/v). Also prepare vehicle solution alone.

   Solutions must be prepared fresh, within 1 hr of dosing. Although in the context of hazard identification it may be desirable to select the highest test concentrations possible, this is not always practical. Poor solubility and/or concerns regarding acute or systemic toxicity may dictate a more conservative approach. Many organic vehicles may be used; however, water is inappropriate as a result of its high surface tension. This property makes it impossible to apply evenly and does not allow solutions containing it to remain in contact with the surface of the skin for a sufficient period of time for absorption. Experience indicates that the vehicles of choice, in order of preference, are AOO, methylethyl ketone, dimethylformamide, and DMSO (also see Critical Parameters and Troubleshooting). Vehicle selection is dictated by the relative solubility of the test material. For most purposes, AOO is suitable.

3. Dispense 25 μl chemical or vehicle alone on the dorsum of both ears of each animal ($n = 4$ per group) using a micropipettor with disposable tip, ensuring an even distribution over the surface of the ear.
4. Perform identical treatment (steps 2 and 3) once daily for the next 2 consecutive days, if possible at a similar time of day.
5. Rest the animals 2 days.

Inject thymidine

6. Prepare an 80 μCi/ml solution of tritiated thymidine in PBS, pH 7.2 to 7.4.

   CAUTION: *Gloves must be worn and the area in which thymidine is used must be swabbed and monitored regularly for radioactive contamination (also see APPENDIX 1A)*

7. Place the animals in a temperature-controlled hot box, one experimental group at a time, for 5 min to allow the veins to dilate.

   The temperature must not exceed 37°C.

8. Restrain each mouse individually using a restraining tube with an outlet for the tail and inject 0.25 ml of 80 μCi/ml radiolabeled thymidine (step 6) into the tail vein using a 1-ml graduated syringe and 25-G $\frac{5}{8}$-in. needle.

   Care must be taken to ensure syringe is free of air bubbles.

9. Return animals to cages and allow to rest 5 hr.

   CAUTION: *Any bedding or tray papers must be disposed of as radiolabel-contaminated waste, and cages must be decontaminated with Decon or similar detergent (also see APPENDIX 1A).*

Process lymph nodes

10. Euthanize animals by anesthetic overdose (e.g., Fluothane, Concord Pharmaceuticals) followed by cervical dislocation. Excise draining (auricular) lymph nodes, and pool for each experimental group in a small volume (~2 ml) PBS.

11. Place a square of 200-G stainless steel mesh into a 60-mm plastic petri dish containing 2 ml fresh PBS. Using tweezers, place the nodes onto the mesh square.

12. Prepare a single-cell suspension of lymph node cells (LNC) by gently disrupting the lymph nodes and pushing them through the mesh using the sterile plunger of a 5-ml syringe (i.e., by mechanical disaggregation).

13. Transfer the LNC from the petri dish into a 10-ml plastic centrifuge tube, rinsing the gauze and the petri dish with 10 ml fresh PBS. Wash the LNC twice in 10 ml fresh PBS by centrifuging 10 min at 100 × *g*, room temperature.

14. After the final wash, resuspend the cell pellet in 3 ml of 5% (w/v) TCA and store overnight at 4°C.

    Avoid clumping of LNC by ensuring pellet is completely resuspended in small volume of liquid before making up to final volume.

Determine incorporation

15. Centrifuge 10 min at 100 × *g*, room temperature. Discard the supernatant and resuspend in 1 ml fresh TCA. Transfer to 10 ml scintillation fluid and measure thymidine incorporation by β-scintillation counting.

    Avoid clumping of LNC by ensuring pellet is completely resuspended in a small volume of liquid before making up to final volume.

16. Record results as total disintegrations per minute per node (dpm/node) for each experimental group. Use the vehicle control group as the comparator in order to derive a stimulation index (SI) according to the following equation:

$$\text{SI} = \frac{\text{test dpm/node}}{\text{vehicle dpm/node}}$$

17. If appropriate doses and number of groups (usually 5) are used, determine the EC3 value as described (see Support Protocol)

ALTERNATE PROTOCOL

LOCAL LYMPH NODE ASSAY: ASSESSMENT OF PROLIFERATION FOR INDIVIDUAL ANIMALS

This alternate LLNA protocol is also for the identification of contact sensitization hazard potential as a function of radiolabeled thymidine incorporation into the lymph nodes draining the site of topical chemical exposure. Mice ($n = 5$ per group) are exposed topically on the dorsum of both ears to various concentrations of test chemical or to vehicle alone daily for 3 consecutive days. Five days after the initiation of exposure, animals receive an intravenous injection of radiolabeled thymidine. Five hours later, the draining auricular lymph nodes are excised, pooled for each individual animal, a single-cell suspension of LNC is prepared, and thymidine incorporation is measured by β-scintillation counting. Processing of lymph nodes on an individual animal basis provides the opportunity to assess interanimal variation in thymidine incorporation and allows the application of statistical analyses. This protocol is identical to that presented above (see Basic Protocol 1) except for the following steps.

1a. Acclimatize young adult female CBA mice in cages of five animals per group for at least 2 days after arrival.

10a. Euthanize animals, excise draining (auricular) lymph nodes, and pool for each individual animal in a small volume (~2 ml) PBS. Process each pair of lymph nodes separately.

16a. Record results as total disintegrations per minute per node (dpm/node) for each individual animal.

17a. For each test and vehicle control experimental group, calculate the mean dpm/node. Use the vehicle control group as the comparator in order to derive a stimulation index (SI) according to the following equation:

$$\text{SI} = \frac{\text{mean test dpm/node}}{\text{mean vehicle dpm/node}}$$

For each experimental group, normalize the data by obtaining log values.

18. Depending on whether data are parametric or nonparametric, apply Dunnett's *t* test or Krushal-Wallis test followed by Dunn's multiple comparison procedure, respectively (Loveless et al., 1996), to determine statistical significance of differences between test and control.

19. If appropriate doses and number of groups (usually 5) are used, determine EC3 value as described (see Support Protocol).

SUPPORT PROTOCOL

LOCAL LYMPH NODE ASSAY: POTENCY ASSESSMENT

The purpose of this protocol is the application of LLNA data for the measurement of the relative sensitizing potency of contact allergens. It is recognized that contact allergens vary substantially (at least four orders of magnitude) with respect to the relative potency with which they are able to induce contact sensitization. An understanding of relative potency of contact allergens can provide useful information that can contribute to the risk assessment process. Data (i.e., SI) derived using lymph nodes pooled on a group basis (see Basic Protocol) or derived using lymph nodes pooled per individual animal (see Alternate Protocol) are suitable for this purpose. In order to obtain accurate potency data from the LLNA, however, it is necessary to have some prior information regarding the activity of the material in tests for skin sensitization hazard to inform dose setting. It is usually necessary to increase the number of groups to 5 for accurate determination of EC3 values. Once the SI has been derived, the EC3 value (i.e., the estimated concentration of chemical required

to induce an SI of 3 relative to concurrent vehicle treated controls) can be obtained by linear interpolation using the equation: $EC3 = c + [(3 - d)/(b - d)] \times (a - c)$, where the data points lying immediately above and below the SI value of three have the coordinates (a, b) and (c, d), respectively. Note that the vehicle-treated control (SI = 1) cannot be used for the (c, d) data point.

COMMENTARY

Background Information

Allergic contact dermatitis (ACD), or contact sensitization, is the most common manifestation of chemical hypersensitivity response, with a wide variety of synthetic and natural chemicals implicated as causative agents. The prospective identification of skin sensitization hazard is therefore an important step in the safety assessment of new ingredients or products.

Contact sensitization tests based on elicitation reactions

Since the 1940s, a number of guinea pig tests have been available for the evaluation of contact sensitizing potential. The occluded patch test of Buehler and the Magnusson and Kligman guinea pig maximization test currently have the widest application for predictive assessment of contact sensitizing activity (Magnusson and Kligman, 1970; Buehler, 1985). All such tests employ a biphasic protocol in which animals are sensitized (induction phase) and subsequently challenged (elicitation phase) with the test chemical. Sensitization potential is determined by the visual assessment of challenge-induced erythematous skin reactions. Such tests have important limitations, including the fact that the endpoint of assessment of erythema is subjective and may lead to interpretative difficulties when colored or irritant chemicals are examined. It is normal practice to challenge with the maximum subirritant concentration of chemical. Therefore, with highly irritant materials, the concentration selected for challenge may be too low to elicit a dermal hypersensitivity reaction. The assays are also relatively time consuming and can require substantial amounts of test material.

Other test methods have been developed in mice, including the mouse ear swelling test (MEST; Gad et al., 1986) and mouse ear sensitization assay (MESA; Descotes, 1988), in which elicitation reactions are measured as a function of challenge-induced increases in ear thickness. Of these methods, the MEST assay has been evaluated most thoroughly. The reliability and sensitivity of this assay have been improved by the introduction of a vitamin A–supplemented diet, which results in enhanced ear swelling responses; however this assay has not been adopted widely (Thorne et al., 1991).

Induction tests for ACD: the local lymph node assay: history and development

The approach adopted in the authors' laboratory has been to investigate whether an understanding of the events occurring in the induction rather than the elicitation phase of contact sensitization could be applied to the development of alternative methods for the prospective identification of contact allergens. The primary immunological response to epicutaneously applied skin-sensitizing agents is dependent upon the recognition of, and response to, chemical antigens by T lymphocytes and is characterized by hyperplasia in the draining lymph nodes (Parrott and De Sousa, 1966; De Sousa and Parrott, 1969). Lymph node activation is reflected by an increase in node weight, the appearance of large pyroninophilic cells, and the induction of lymphocyte proliferation. In the authors' preliminary studies, each of these parameters was examined following topical exposure to chemical (Kimber et al., 1986; Kimber and Weisenberger, 1989). It was concluded that lymphocyte proliferation, measured by the incorporation of ^{3}H-thymidine, provided the most sensitive and reliable correlate of skin sensitizing potential. This is a relevant read out for the evaluation of skin sensitizing potential, as confirmed by the demonstration that the vigor and duration of lymphocyte proliferation directly influences the extent to which contact sensitization occurs and consequently the severity of the dermatitic reaction that will develop following challenge (Kimber and Dearman, 1991).

These preliminary studies (Kimber et al., 1986; Kimber and Weisenberger, 1989) defined the optimum conditions required to provoke and measure LNC proliferation, including investigation of the kinetics of the response and strain comparisons. It was found that exposure of mice to skin allergens on the dorsum of both ears caused hyperplasia in draining auricular lymph nodes, peripheral lymph

nodes that can be readily identified and excised. Daily exposure for 3 consecutive days produced a more vigorous response than did a single application of the same total amount of chemical. In comparative investigations, mice of the CBA strain were found to exhibit greater responses than did other strains examined (Kimber and Weisenberger, 1989). In these early studies, proliferation was measured in vitro following culture of isolated draining LNC with [^{3}H]thymidine. In subsequent experiments an important modification was introduced that improved the sensitivity of the assay: the measurement of proliferative activity in situ by intravenous injection of [^{3}H]thymidine. It is this version of the assay that has been the subject of extensive evaluation in the context of national and international collaborative trials, and it has been the subject of detailed comparisons with guinea pig tests and human data (reviewed in Gerberick et al., 2000; Basketter et al. 2002; Kimber et al. 2002). After a thorough and independent evaluation, the method was validated in the U.S.A. (Interagency Coordinating Committee on the Validation of Alternative Methods, 1999) and subsequently in Europe by the European Centre for the Validation of Alternative Methods (ECVAM; Balls and Hellsten, 2000). The LLNA has now been incorporated into a new test guideline, *Skin Sensitization: Local Lymph Node Assay*, (No. 429) by the Organization for Economic Cooperation and Development and was adopted formally in 2002 (OECD, 2002).

LLNA: hazard identification and potency assessment

As described herein, the basic LLNA protocol, in which lymphocyte proliferation is measured as a function of thymidine incorporation in situ and lymph nodes are processed per experimental group, and the alternative in which lymph nodes are processed per experimental animal, provide data suitable for identification of contact sensitizing hazard. Skin sensitizing chemicals are defined as those that, at one or more test concentrations, provoke a threefold or greater increase in LNC proliferation compared with concurrent vehicle-treated controls. Conversely, chemicals that fail at all test concentrations to elicit a positive response in the LLNA should be classified as lacking significant skin-sensitizing potential and should be handled and labeled according. Initially, the threshold value of three was chosen empirically on the basis of previous experience with the LLNA, as it offered good discrimination between contact allergens and nonsensitizers. Subsequently, a retrospective statistical analysis was performed on data from 134 chemicals tested in the LLNA using receiver operating characteristic (ROC) curves (Basketter et al., 1999). These analyses confirmed that the empirically derived threefold threshold is an acceptable practical value for hazard identification. In addition, if LLNA potency assessment is used (see Support Protocol), an estimate of the relative skin sensitizing potency of the material can be derived. For this purpose, an EC3 value (i.e., the amount of chemical sensitizer required to elicit a three-fold increase in LNC proliferative activity) is calculated. EC3 values are derived by linear interpolation of values either side of the threefold SI on a LLNA dose-response curve, with values generally expressed as percentage concentrations. Experience has revealed that EC3 values determined in this way are robust determinants of relative skin sensitizing potential; equivalent results have been obtained in different laboratories, and over time within a single laboratory (Loveless et al., 1996; Dearman et al., 1998; 2001). The estimates of skin sensitizing potency measured as a function of derived EC3 values are relevant for the induction of skin sensitization in humans. Collaborative studies were conducted in the U.S. and U.K. in partnerships between experimental laboratories performing the LLNA and clinical dermatologists, with the latter providing a view of the relative induction potency of two series of known chemical allergens. A close correlation between clinical assessments of potency and LLNA EC3 values was reported (Basketter et al., 2000; Gerberick et al., 2001). Stronger sensitizers, such as 2,4-dinitrochlorobenzene (DNCB) have lower EC3 values than more moderate sensitizers, such as hexyl cinnamic aldehyde (HCA). The current recommendation for the categorization of contact allergens with respect to relative sensitizing activity based on LLNA EC3 values is divided into four categories as shown in Table 18.2.1.

LLNA: advantages and disadvantages

Compared with guinea pig test methods, the LLNA offers the advantages of (1) having an objective and quantitative endpoint that is unaffected by the color of the test material, (2) having animal welfare advantages with respect to both refinement (no use of adjuvants, shaving, depilation, or occlusive bandages or patches) and reduction in animal usage, and (3) requiring smaller amounts of chemical and less time for completion. Additionally, the

Table 18.2.1 Recommended Categorization of Contact Allergens[a]

Category	EC3
Extreme	<0.1%
Strong	>0.1% to <1%
Moderate	>1% to <10%
Weak	>10% to <100%

[a]Refer to Kimber et al. (2003) for details.

weight of evidence suggests that in most cases, irritant nonsensitizing chemicals fail to elicit positive responses. The limitations of the assay are that it does not evaluate the elicitation response and cannot be used to test the dose cross-challenge reactions.

Critical Parameters and Troubleshooting

Vehicle and dose selection

The selection of dose and vehicle are of critical importance for the conduct of the LLNA. The dose selection when using the standard LLNA (see Basic Protocol) or individual animal LLNA (see Alternate Protocol) for contact sensitization hazard identification is based on providing the highest possible test concentration to maximize the potential for hazard identification. Test concentration selection will be limited by compatibility with the vehicle chosen and the suitability of the resultant preparation for unoccluded dermal application and should preclude local (dermal) trauma or systemic toxicity. Selection of doses when using LLNA potency assessment (see Support Protocol) for relative potency assessment is usually based on prior information in order to obtain concentrations that provoke SIs above and below the threshold value of three. A variety of organic solvents are suitable for the performance of the LLNA. The following are recommended, in order of preference: AOO, acetone, dimethylformamide, methyl ethyl ketone and DMSO. Aqueous vehicles are not recommended, although aqueous and aqueous-organic mixtures such as 3:1 (v/v) acetone to water have been used successfully.

Positive controls

It is advisable for a laboratory to regularly demonstrate that competence has been achieved with the assay. This can be effected by the use of a positive control material such as HCA, which is currently recommended by the OECD as a positive control for tests for contact sensitization. This chemical has been evaluated thoroughly in the LLNA, both in the context of interlaboratory trials and with respect to the stability of responses with time; furthermore, the comparative data are available in the literature (Loveless et al., 1996; Dearman et al., 1998, 2001). These experiments have demonstrated that HCA is identified routinely as a contact sensitizer in the LLNA, with comparable EC3 values obtained between laboratories and for repeat assays within the same laboratory.

Interpretation of abnormal vehicle control data

The interpretation of LLNA data requires that the proliferation achieved in test groups be compared with the background activity in concurrent vehicle-treated controls so that the SI can be derived. Clearly, the use of the vehicle-treated control value as the denominator in the calculation for deriving the SI means that if this value is abnormally high or low, it will impact markedly on the calculated SI and hence on the EC3 calculation. An abnormal level of thymidine incorporation may be due to technical difficulties with the assay (such as failed intravenous injections) or may reflect the health status of the animals; for example, relatively high levels of basal proliferation accompanied by increased lymph node size can be indicative of a viral infection or a lymphoproliferative disorder. It is apparent that for experienced competent laboratories, control levels of proliferation in the LLNA are relatively consistent, although the absolute values vary according to the testing laboratory. For example, a recent series of experiments in which background levels using the preferred vehicle, AOO, were compared across laboratories revealed that control values accumulated from 44 independent LLNAs performed in one laboratory ranged from 97 to 662, with a mean of 321, whereas in another laboratory values ranged from 211 to 1000, with a mean of 410 (Basketter et al., 2003). Some biological variation and interlaboratory variation is to be expected in basal levels of thymidine incorporation. The important point, however, is that despite the interlaboratory and

interexperimental variation in absolute control values, in these studies, each laboratory observed very little interexperimental variation in derived SI values or EC3 values for a given chemical. Furthermore, there was very little interlaboratory variation in these parameters (Dearman et al., 2001). It is necessary therefore to establish a normal range of control values for a given vehicle and to monitor any excursions from this range in any laboratory conducting the LLNA.

Interpretation of dose response

In many experiments, a typical dose response curve will be observed for chemical allergen–induced proliferation, with dose-dependent increases in proliferation that may or may not reach a plateau. In some cases, a bell-shaped curve is recorded, with thymidine incorporation reaching maximal levels at intermediate doses, while at higher doses, less vigorous proliferation is observed. This effect may be due to systemic toxicity at high doses, which may be monitored by general health checks such as the daily recording of weight gain on an individual animal basis. The existence of a bell-shaped curve should not affect the interpretation of the LLNA with respect to hazard identification or relative potency assessment. In some cases, the proliferative response to chemical may show a dose-dependent increase in thymidine incorporation that does not attain an SI of three at the maximum dose tested. In this case, the most judicious interpretation is that the chemical has potential to cause contact allergy, and if possible, a repeat assay using higher concentrations

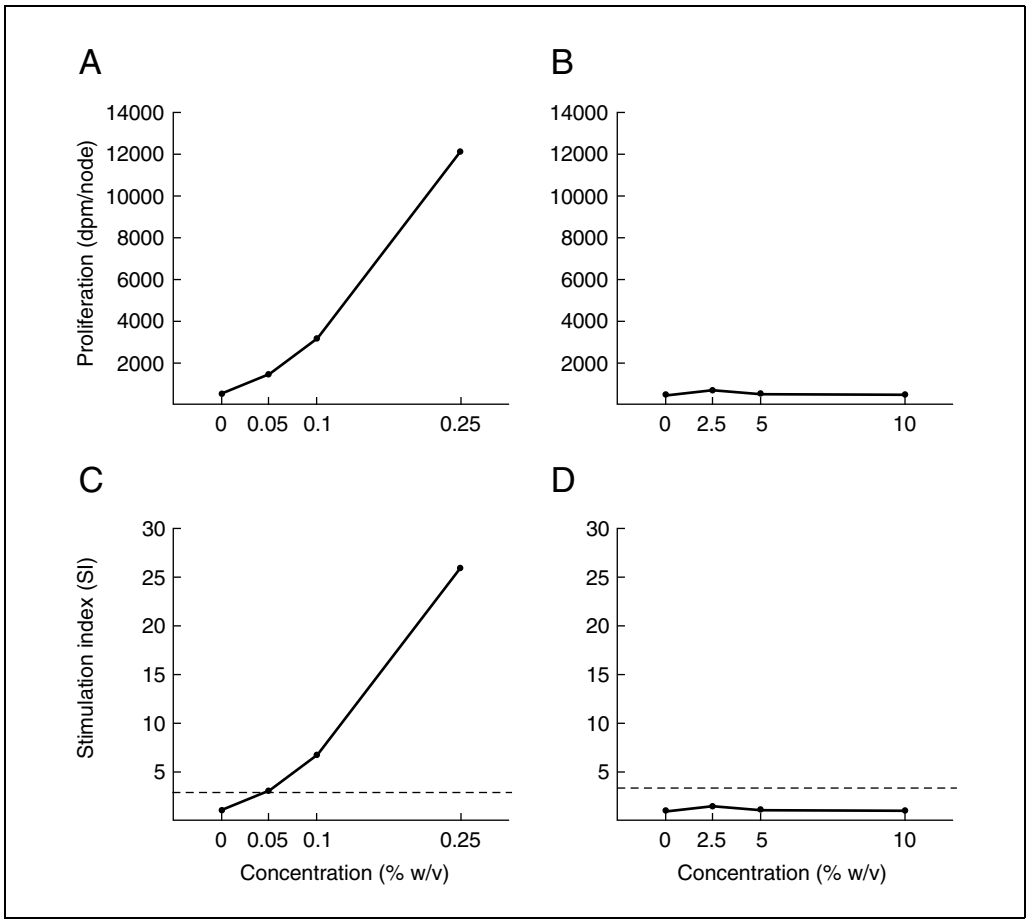

Figure 18.2.1 Typical results derived using standard LLNA (see Basic Protocol). CBA strain mice ($n = 4$) received 25 μl of various concentrations of (**A** and **C**) the potent contact allergen DNCB or (**B** and **D**) the nonsensitizing skin irritant *p*ABA, or vehicle (AOO) alone on the dorsum of both ears daily for 3 consecutive days. Five days after the initiation of exposure, all mice received an intravenous injection of radiolabeled thymidine. Five hours later, draining auricular lymph nodes were excised, pooled on a treatment group basis, and processed for β-scintillation counting. Results are expressed as group dpm/node in (A) and (B) or as a stimulation index (SI) relative to vehicle treated control groups in (C) and (D). An SI of 3 (current threshold value for a positive in the LLNA) is illustrated as a broken line in (C) and (D).

of material or an alternative vehicle should be performed.

Anticipated Results

Standard LLNA

Typical results derived using standard LLNA (see Basic Protocol), in which animals have been exposed to three concentrations of the potent contact allergen DNCB or to the nonsensitizing skin irritant *para*-aminobenzoic acid (*p*ABA), both formulated in AOO, are shown in Figure 18.2.1. Data are displayed as a function of dpm/node and as SI relative to concurrent vehicle-treated control values, the latter being the usual method for displaying results. Exposure to DNCB induced a marked dose-dependent increase in proliferation compared with vehicle-treated control mice, with all concentrations tested provoking an SI of greater than or equal to three. This material is therefore classified as a skin sensitizer. In contrast, the nonsensitizing skin irritant *p*ABA, despite testing at doses some 40-fold higher than those utilized for DNCB, failed to elicit increases in thymidine incorporation at any concentration examined. This material is therefore classified as lacking significant potential to cause skin sensitization.

Alternative LLNA

Typical results derived using the individual animal-based LLNA (see Alternate Protocol) are shown in Figure 18.2.2. Animals have been exposed to the same concentrations of DNCB or *p*ABA or to vehicle (AOO) alone

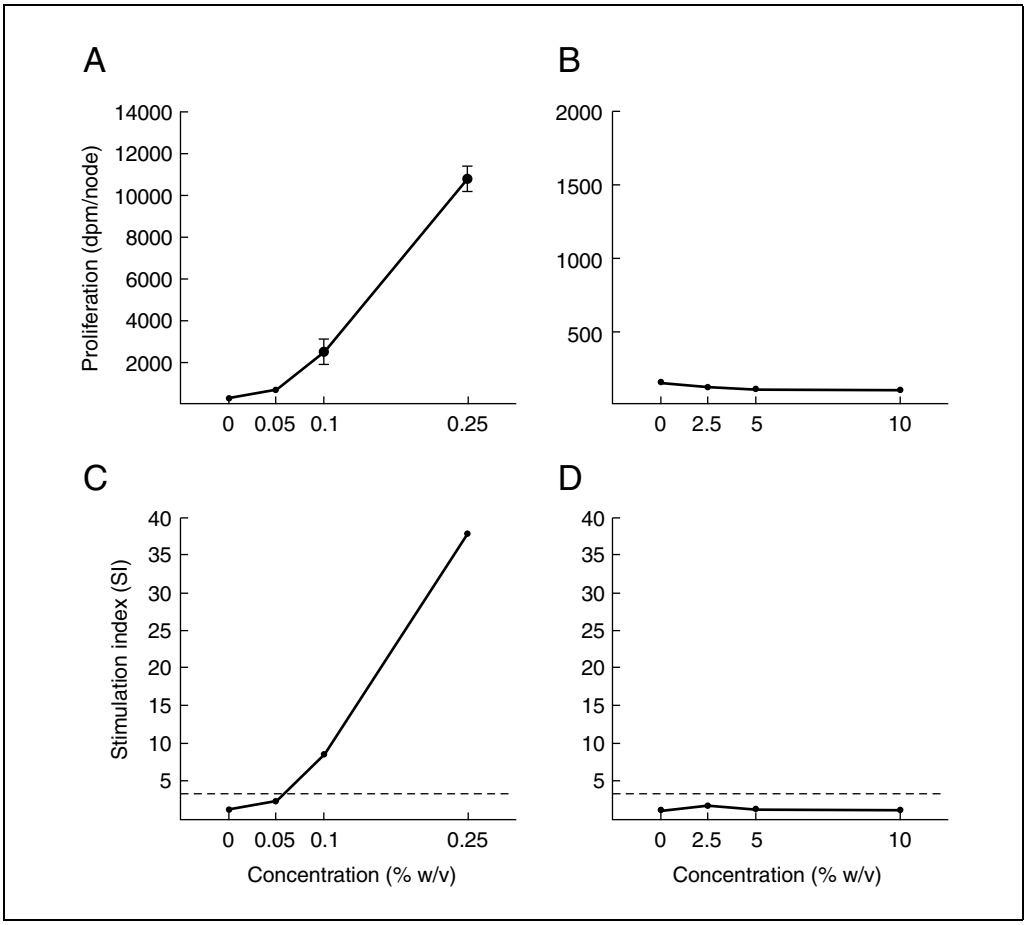

Figure 18.2.2 Typical results derived using the individual animal–based LLNA (see Alternate Protocol). CBA strain mice ($n = 5$) received 25 μl of various concentrations of (**A** and **C**) the potent contact allergen DNCB, (**B** and **D**) the nonsensitizing skin irritant *p*ABA, or vehicle (AOO) alone on the dorsum of both ears daily for 3 consecutive days. Five days after the initiation of exposure, all mice received an intravenous injection of radiolabeled thymidine. Five hours later, draining auricular lymph nodes were excised, pooled on an experimental animal basis, and processed for β-scintillation counting. Results are expressed as mean ± SE dpm/node per group in (A) and (B) or as a stimulation index (SI) relative to vehicle treated control groups in (C) and (D). An SI of 3 (current threshold value for a positive in the LLNA) is illustrated as a broken line.

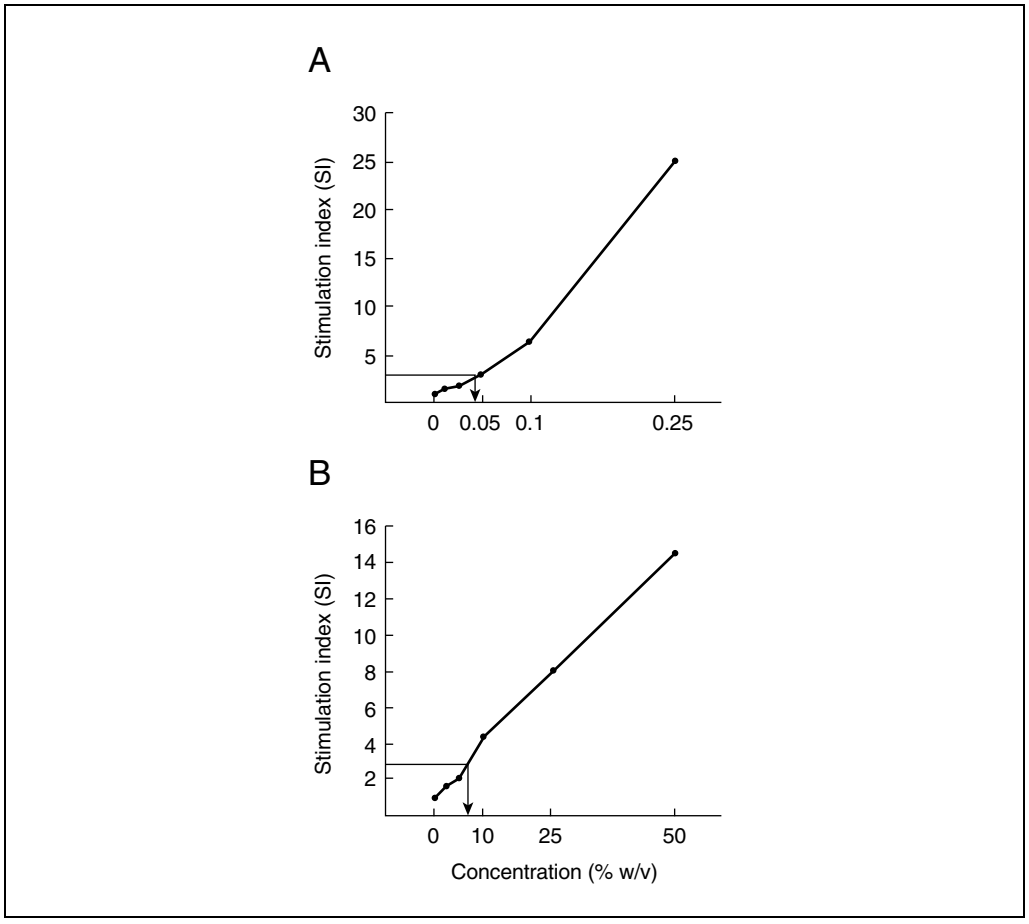

Figure 18.2.3 Typical results derived using LLNA for the assessment of relative skin sensitizing potency (see Support Protocol). CBA strain mice received 25 μl of various concentrations of (**A**) the potent contact allergen DNCB, (**B**) the more moderate allergen HCA, or vehicle (AOO) alone on the dorsum of both ears daily for 3 consecutive days. Five days after the initiation of exposure, all mice received an intravenous injection of radiolabeled thymidine. Five hours later, draining auricular lymph nodes were excised, pooled on a treatment group basis and processed for β-scintillation counting. Results are expressed as a stimulation index (SI) relative to vehicle treated control groups. The EC3 value (illustrated by an arrow) is calculated by linear interpolation.

as in the standard LLNA (see Basic Protocol) described above (Figure 18.2.1). In this experimental protocol, lymph nodes from individual animals were processed rather than lymph nodes pooled on an experimental group basis. Data are displayed as a function of mean ± SE dpm/node and as SI relative to concurrent vehicle-treated control values; the latter being the usual method of displaying the results. The modified protocol yields equivalent results to the standard LLNA, with DNCB identified as a skin sensitizer and *p*ABA classified as lacking significant potential to cause skin sensitization.

Skin sensitization potency

Typical results derived using LLNA for the assessment of relative skin sensitizing potency (see Support Protocol) are shown in Figure 18.2.3. Animals have been exposed to five concentrations of the potent contact allergen DNCB or to the more moderate skin sensitizer HCA, both formulated in the vehicle of choice for the LLNA, AOO. Data are displayed as SI relative to concurrent vehicle-treated control values. Both chemicals provoked marked dose-dependent increases in proliferation compared with vehicle-treated control mice. Both materials are therefore classified as skin sensitizers. In each case, concentrations of chemical have been selected that elicit SI values either side of an SI of 3. Thus the data are appropriate for the derivation of EC3 values: DNCB EC3 $= 0.025 + [(3 - 1.9)/(3.1 - 1.9)] \times (0.05 - 0.025) = 0.048\%$ and HCA EC3 $= 5 + [(3 - 2.12)/(4.35 - 2.12)] \times (10 - 5) = 7.0\%$. According to the recommendations of Kimber et al. (2003), DNCB is categorized as an extreme contact sensitizer, whereas HCA is classified as a moderate contact sensitizer.

Time Considerations

Topical exposure to chemical

For a LLNA assay with five concentrations of test chemical and vehicle control, it will take ~30 min to prepare the formulations. Topical application of test chemical/vehicle to six groups of mice will require ~30 min. This procedure will be repeated every day for 3 days.

Injection of thymidine and processing of lymph nodes

Preparation of dosing solution (thymidine) and loading syringes for a typical assay with six groups will take ~30 min. Intravenous injections for this number of groups will take 45 min to 1 hr. The mice are rested for 5 hr. Termination and excision of lymph nodes will require ~45 min to 1 hr. Processing of lymph nodes ready for overnight precipitation in 5% TCA will take ~2 hr. The following day, resuspension of lymph nodes in 5% TCA and addition of scintillation fluid will take ~30 min.

Literature Cited

Balls, M. and Hellsten, E. 2000. Statement on the validity of the local lymph node assay for skin sensitisation testing. *Altern. Lab. Anim.* 28:366-367.

Basketter, D.A., Lea, L.J., Cooper, K., Stocks, J., Dickens, A., Pate, I., Dearman, R.J., and Kimber, I. 1999. Threshold for classification as a skin sensitizer in the local lymph node assay: A statistical evaluation. *Food Chem. Toxicol.* 37:1167-1174.

Basketter, D.A., Blaikie, L., Dearman, R.J., Kimber, I., Ryan, C.A., Gerberick, G.F., Harvey, P., Evans, P., White, I.R., and Rycroft, R.J.G. 2000. Use of the local lymph node assay for estimation of relative contact allergenic potency. *Contact Dermatitis* 42:344-348.

Basketter, D.A., Evans, P., Fielder, R.J., Gerberick, G.F., Dearman, R.J., and Kimber, I. 2002. Local lymph node assay – validation and use in practice. *Food Chem. Toxicol.* 40:593-598.

Basketter, D.A., Glimour, N.J., Briggs, D., Ludwig, U., Gerberick, G.F., Ryan, C.A., Dearman, R.J., and Kimber, I. 2003. Utility of historical control data in the interpretation of the local lymph node assay. *Contact Dermatitis* 49:37-41.

Buehler, E.V. 1985. A rationale for the selection of occlusion to induce and elicit delayed contact hypersensitivity in the guinea pig. A prospective test. *In* Contact Allergy Predictive Tests in Guinea Pigs: Current Problems in Dermatology. (K.E. Andersen and H.I. Maibach, eds) pp. 39-58. S. Karger AG, Basel, Switzerland.

Cronin, E. 1980. Contact Dermatitis. Churchill Livingstone, London.

Dearman, R.J., Hilton, J., Evans, P., Harvey, P., Basketter, D.A., and Kimber, I. 1998. Temporal stability of local lymph node assay responses to hexyl cinnamic aldehyde. *J. Appl. Toxicol.* 18:281-284.

Dearman, R.J., Wright, Z.M., Basketter, D.A., Ryan, C.A., Gerberick, G.F., and Kimber, I. 2001. The suitability of hexyl cinnamic aldehyde as a calibrant for the local lymph node assay. *Contact Dermatitis* 44:357-361.

Descotes, J. 1988. Identification of contact allergens: The mouse ear sensitization assay. *J. Toxicol., Cutaneous and Ocular Toxicol.* 7:263-272.

De Sousa, M.A.B, and Parrott, D.M.V. 1969. Induction and recall in contact sensitivity, changes in skin and draining lymph nodes of intact and thymectomized mice. *J. Exp. Med.* 130:671-686.

Gad, S.C., Dunn, B.J., Dobbs, D.W., Reilly, C., and Walsh, R.D. 1986. Development and validation of an alternative dermal sensitization test: The mouse ear swelling test (MEST). *Toxicol. Appl. Pharmacol.* 8:93-114.

Gerberick, G.F., Ryan, C.A., Kimber, I., Dearman, R.J., Lea, L.J., and Basketter, D.A. 2000. Local lymph node assay: Validation assessment for regulatory purposes. *Am. J. Contact Dermatitis* 11:3-18.

Gerberick, G.F., Robinson, M.K., Ryan, C.A., Dearman, R.J., Kimber, I., Basketter, D.A., Wright, Z., and Marks, J.G. 2001. Contact allergenic potency: Correlation of human and local lymph node assay data. *Am. J. Contact Dermatitis* 12:156-161.

Interagency Coordinating Committee on the Validation of Alternative Methods 1999. The Murine Local Lymph Node Assay: A Test Method for Assessing the Allergic Dermatitis Potential of Chemicals/Compounds. NIH No. 99-4494.

Kimber, I., and Dearman, R.J. 1991. Investigation of lymph node cell proliferation as a possible immunological correlate of contact sensitizing potential. *Food Chem. Toxicol.* 29:125-129.

Kimber, I. and Weisenberger, C. 1989. A murine local lymph node assay for the identification of contact allergens. Assay development and results of an initial validation study. *Arch. Toxicol.* 63:274-282.

Kimber, I., Mitchell, J.A., and Griffin, A.C. 1986. Development of a murine local lymph node assay for the determination of sensitizing potential. *Food Chem. Toxicol.* 24:585-586.

Kimber, I., Dearman, R.J., Basketter, D.A., Ryan, C.A., and Gerberick, G.F. 2002. The local lymph node assay: Past, present and future. *Contact Dermatitis* 47:315-328.

Kimber, I., Basketter, D.A., Butler, M., Gamer, A., Garrigue, J.-L., Gerberick, G.F., Newsome, C., Steiling, W., and Vohr, H.-W. 2003. Classification of contact allergens according to potency: Proposals. *Food Chem. Toxicol.* 41:1799-1809.

Loveless, S.E., Ladics, G.L., Gerberick, G.F., Ryan, C.A., Basketter, D.A., Scholes, E.W., House, R.V., Hilton, J., Dearman, R.J., and Kimber, I., 1996. Further evaluation of the local lymph node assay in the final phase of an international collaborative trial. *Toxicology* 108:141-152.

Magnusson, B. and Kligman, A.M. 1970. Allergic Contact Dermatitis in the Guinea Pig. Charles C. Thomas, Springfield, Ill.

Organization for Economic Cooperation and Development 2002. Guidelines for testing of Chemicals. Guideline No. 429. Skin Sensitization: The Local Lymph Node Assay. OECD, Paris.

Parrott, D.M.V. and De Sousa, M.A.B. 1966. Changes in the thymus dependent areas of lymph nodes after immunological stimulation. *Nature* 212:1316-1317.

Thorne, P.S., Hawk, C., Kaliszewski, S.D., and Guiney, P.D. 1991. The noninvasive mouse ear swelling assay. I. Refinements for detecting weak contact sensitizers. *Fundam. Appl. Toxicol.* 17:790-806.

Contributed by Rebecca J. Dearman and Ian Kimber
Syngenta Central Toxicology Laboratory
Alderley Park, Macclesfield, Cheshire
United Kingdom

Murine Asthma Models

Immunotoxicity takes two general forms. One is an immunosuppression, resulting in an inability of the immune system to adequately defend against invaders such as cancer cells or pathogens. However, another type of immunotoxicity is an enhancement of the immune response or hyperreactivity of the immune system. In this situation, the offending substance or allergen is immunogenic and mobilizes the humoral and/or cellular arms of the immune system. Autoimmunity or hypersensitivity is the result. Asthma is one possible consequence of an increased immunoreactivity or an allergic response in the lung, either to environmental antigens or to antigens encountered in the workplace, i.e., occupational asthma.

The asthmatic response is divided into an induction phase (sensitization) and an effector (elicitation or challenge) phase. The induction phase involves the first exposure to a substance and a specific immune response is evoked. Re-exposure or challenge with the allergen then causes the effector phase—the asthmatic symptoms. Occupational asthma is categorized as immunological and non-immunological, depending on whether an induction phase or latent period is necessary to evoke the asthmatic symptoms. In addition, within the category of immunological occupational asthma, latitude is given for IgE, non-IgE, or unknown immune mechanisms that can lead to the asthma symptoms.

Regardless of cause, asthma is characterized by reversible airway obstruction, airway hyperresponsiveness to a variety of agonists including methacholine, mucus production, airway remodeling, and cell infiltration into the lung, particularly eosinophil infiltration. Various trigger factors for asthma, such as exercise, ozone, pollutants, viral infection, emotion, and passive smoke can have profound effects on the asthmatic response to allergens and exacerbate an ongoing inflammatory situation in the lung. In addition, high exposures to noxious substances have been reported to initiate asthmatic symptoms in the lung, without a latent period.

In toxicology, two primary areas of investigation prompt the measurement of the asthmatic response in an animal: (1) identification of chemicals or proteins that cause asthma, i.e., respiratory allergens, and (2) identification of exposures that will exacerbate existing asthma. Ovalbumin-induced asthma in the mouse is a model system that can readily be used to identify substances that could exacerbate existing asthma. The effect of exposure to a toxic substance on endpoints of the ovalbumin-induced asthmatic response is determined. With regard to identification of respiratory allergens, much effort has been expended to develop reliable methods. The LLNA (*UNIT 18.2*) can identify substances that have the potential to cause allergy after topical exposure, i.e., hazard identification. By determining if exposure to a substance results in proliferation of lymph node cells, the LLNA assay identifies substances that induce an immune response. Whether continued exposure to these substances, or exposure via the respiratory route, will result in asthma requires measurement of the asthma symptoms in an animal model after re-exposure or elicitation of the response.

With these potential uses in mind, the Basic Protocol describes a method to sensitize and challenge a mouse using the protein allergen ovalbumin to reliably elicit asthma symptoms. Ovalbumin is widely used in experimental systems in immunology and has been extensively used to explore the effector mechanisms in rodent models of asthma. In addition, ovalbumin is a known cause of occupational asthma in egg processing facilities. The assessment of characteristic asthma symptoms in the mouse are described by: airway

Contributed by Jean F. Regal
Current Protocols in Toxicology (2004) 18.3.1-18.3.21

hyperresponsiveness to the agonist methacholine in a conscious unrestrained mouse (see Support Protocol 1), cellular infiltration into the airspace (see Support Protocol 2), and cellular infiltration into the lung (see Support Protocol 3). As described here, the Support Protocols are used with mice sensitized and challenged with ovalbumin as in the Basic Protocol, however, they could also be used in non-sensitized animals to determine if inflammatory stimuli such as endotoxin, diesel exhaust, and other substances can cause airway hyperresponsiveness and cellular infiltration into the lung of the mouse.

BASIC PROTOCOL

MOUSE SENSITIZATION AND INTRANASAL CHALLENGE

Numerous methods are available for sensitization and challenge of a mouse using ovalbumin to elicit the symptoms of asthma. One such protocol that consistently results in an asthmatic response is described here using a Balb/c mouse. The mouse is injected by the intraperitoneal route with ovalbumin and alum as an adjuvant. After a selected waiting period for induction of the specific immune response, mice are then challenged intranasally on 3 successive days to elicit airway hyperresponsiveness and cellular infiltration into the lung. Depending on the purpose of the experiment, control mice are either sensitized with alum solution without ovalbumin, or challenged with water intranasally rather than ovalbumin. In some instances, both types of controls are indicated as well as animals sensitized with alum alone and challenged with water. After the time period of interest, the asthma symptoms are evaluated as outlined in Support Protocols 1, 2, and 3.

This protocol will be concerned with using ovalbumin as an antigen to sensitize and challenge the mouse. To determine if exposure to other chemicals or proteins results in asthma symptoms, the properties and normal exposure routes of the substance need to be taken into account. Convenient experimental systems are not always available, since many substances are not water soluble and the primary exposure is inhalation of dust. Some animal models of asthma caused by the occupational allergen trimellitic anhydride (TMA) have used sensitization of the mouse or guinea pig intradermally with TMA suspended in oil, followed by intratracheal challenge with TMA conjugated to albumin (Hayes et al., 1992b; Fraser et al., 1995; Regal et al., 2001). This method of sensitization and challenge with TMA resulted in eosinophil infiltration into the lung. Other methods of exposure to low-molecular-weight occupational allergens such as toluene diisocyanate and TMA have been tried, including inhalation of the dust (Hayes et al., 1992a), topical exposure to the dust (Zhang et al., 2002) and intratracheal exposure of oil suspensions of the molecule (Ebino et al., 2000). Various asthma endpoints have been examined after sensitization and challenge. In many of the studies, the primary concern was induction of the immune response as evidenced by IgE production or cytokine elaboration in local lymph nodes, i.e., hazard identification. Work still needs to be done to effectively and efficiently use rodent models of asthma to identify chemical or protein exposures that will cause asthma.

Materials

Ovalbumin for sensitization (see recipe)
Imject Alum aluminum hydroxide solution (Pierce Chemical)
Normal saline solution (endotoxin-free)
Mice of selected strain, age, and sex (e.g., Balb/c, 6 to 8 weeks old)
Ovalbumin for challenge (see recipe)
Ketamine/xylazine (see recipe)
Water (endotoxin-free)

2-ml polypropylene screw-cap vials
Micro stir bar
Animal balance (accurate to 0.1 g)
1-ml syringes and 27-G × 1/2-in. needles
100-μl pipet and tips

Sensitize with ovalbumin (day 1)

1. Thaw 1.2 ml ovalbumin for sensitization and begin stirring in a 2-ml screw-cap plastic vial with a micro stir bar. Add 0.4 ml Imject Alum dropwise to 1.2 ml solution of ovalbumin for sensitization or normal saline solution (endotoxin-free).

   This is enough ovalbumin for sensitization of 5 to 7 mice. Stir each vial continuously for 30 min at room temperature to allow adsorption of the antigen.

   Reagents and containers for sensitization and challenge should be endotoxin free. Use endotoxin-free reagents and sterile plastic ware. Alternatively, treat any glassware with E-Toxa clean concentrate (Sigma) or similar reagent to remove endotoxin contamination. Treating clean glassware at 175°C for a minimum of 3 hr will also destroy endotoxin. Ovalbumin can have endotoxin contamination. The amount of endotoxin contamination in a particular lot of ovalbumin can be determined using a Limulus Amebocyte Lysate assay supplied by Sigma (E-Toxate Kit) or BioWhittaker.

2. Weigh mouse and calculate volume for intraperitoneal injection at 0.2 ml/20 g mouse (0.5 mg ovalbumin/kg). Swirl the ovalbumin/aluminum hydroxide suspension prior to loading the calculated volume into a 1-ml syringe with attached 27-G × 1/2-in. needle.

3. Pick up mouse by the tail and allow the mouse to grab the cage top with its front paws. Pinch the skin at the nape of the neck firmly with thumb and forefinger of the other hand, holding the tail between the palm and other fingers.

4. Inject calculated volume intraperitoneally by tilting the animal slightly head down so the intestines fall forward, insert needle bevel up in the lower right quadrant of the abdomen, slightly off the midline, and then pull back slightly on the plunger before injecting to ensure that no fluid is withdrawn.

   The needle should be inserted high enough to avoid the bladder and the cecum and not deep enough to penetrate kidneys or spinal column.

   If yellow or greenish-brown fluid is withdrawn, the bladder or the cecum may have been penetrated. If this is the case, discard the syringe and its contents and start again.

5. Return the mouse to the cage. Repeat steps 2 through 5 if necessary, for other mice.

Intranasally challenge with ovalbumin (days 14 to 16)

6. Thaw ovalbumin solution for challenge and mix gently by inversion.

7. Weigh mouse and calculate volume of ketamine/xylazine solution for intramuscular injection (0.1 ml/20 g mouse). Load 1-ml syringe with 27-G × 1/2-in. needle with ketamine/xylazine.

   Ketamine is a Schedule III controlled substance and requires proper licensing and storage in an authorized locked cabinet.

8. Calculate volume of ovalbumin for challenge or water (endotoxin-free) for intranasal instillation (80 µl/20 g mouse; 5 mg/kg) and load 100-µl pipet with proper volume.

   Alternatively, a mouse serum albumin solution in water can be used as a control challenge.

9. Pick up mouse by the tail and allow it to grab the cage top with its front paws. Pinch the skin at the nape of the neck firmly with thumb and forefinger of the other hand, holding the tail and hind limb between the palm and other fingers.

10. Inject calculated volume of ketamine/xylazine (from step 7) into muscle of hind limb. Return mouse to cage until anesthesia takes effect in ~3 to 5 min.

11. Remove anesthetized mouse from cage and hold gently with nostrils pointing straight up. Using the 100-µl pipet, slowly drip calculated volume of ovalbumin for intranasal

instillation (from step 8) over nostrils, alternating nostrils until entire volume disappears from view. Return mouse to cage.

12. Repeat daily for 3 days at approximately the same time of day for each intranasal instillation.

A convenient challenge time is first thing in the morning so that the evaluation of airway hyperresponsiveness (see Support Protocol 1) and cellular infiltration (see Support Protocols 2 and 3) can be measured at 24 and/or 48 hr post-challenge.

SUPPORT PROTOCOL 1 MEASURING AIRWAY HYPERRESPONSIVENESS IN A CONSCIOUS UNRESTRAINED MOUSE

A hallmark of asthma in the human is increased reactivity of the airways to numerous different agonists, i.e., airway hyperresponsiveness. As the severity of the asthma increases, the reactivity of the airways to methacholine increases. A positive methacholine challenge test is used clinically in the differential diagnosis of asthma. In the mouse, various methods have been developed to measure pulmonary function. Whole-body plethysmography in conscious unrestrained animals (Hamelmann et al., 1997) uses changes in a plethysmograph box pressure to follow breathing patterns and calculate the dimensionless value-enhanced pause (PenH). The inspiratory time, the decay of the expiratory time, and the maximum changes in box pressure during inspiration and expiration are used to calculate PenH. Values of PenH have been shown to correlate with measures of pulmonary resistance and compliance obtained by invasive methods in anesthetized mice (Hamelmann et al., 1997). Various studies including a recent paper by Lundblad et al. (2002) have questioned the validity of PenH as a reliable indicator of bronchoconstriction in the mouse. Though the value of the method continues to be debated, it has the distinct advantage of being a high throughput, non-invasive method that allows measurement of individual animals over time, in the absence of confounding effects of anesthesia.

Materials

Methacholine (see recipe)
Mice sensitized and challenged with ovalbumin and appropriate control animals (see Basic Protocol)
Endotoxin-free saline

Buxco whole-body plethysmograph with Softmax XA software for whole-body flow-derived parameters (Buxco Electronics); four chambers monitored simultaneously
Balance (accurate to 0.1 g)

1. Remove methacholine stock solution from freezer.
2. Calibrate Buxco plethysmograph system per manufacturer's instructions.
3. Weigh mice.
4. For 4 animals, mix the following proportions of methacholine stock + endotoxin-free saline:

6 mg/ml	0.0625 ml + 3.9375 ml
12 mg/ml	0.125 ml + 3.875 ml
24 mg/ml	0.25 ml + 3.75 ml
48 mg/ml	0.5 ml + 3.5 ml
96 mg/ml	1 ml + 3 ml.

Place solutions on ice until loaded in the nebulizer cup.

5. Place mouse in whole-body plethysmograph box.

Depending on the available equipment, many mice can be monitored and exposed to methacholine simultaneously. Randomly assign treatments to each of the whole-body plethysmographs so as not to bias the results.

6. Place 4 ml endotoxin-free saline in the nebulizer cup. Nebulize for 2 min and then monitor respiratory variables for an additional 6 min during the drying phase.
7. Remove nebulizer cup and discard any remaining saline. Place 4 ml of 6 mg/ml methacholine in the nebulizer cup and repeat nebulization for 2 min plus a 6-min monitoring cycle.

   The changing of solutions in the nebulizer should be accomplished within 1 min or use a consistent time period between doses.
8. Repeat step 7 with 12, 24, 48 and 96 mg/ml methacholine, using the same 2-min nebulization period and 6-min monitoring cycle.
9. Remove the mice from the chambers and return them to their cages.
10. Export the data and save in Excel spreadsheet.
11. Refill nebulizer cup with 4 ml endotoxin-free saline and run another sequence to flush through the tubing.
12. Shut down the air flows, disassemble, and wipe clean all chambers before running a second set of animals.

    The system should also be recalibrated before running another set of animals.

MEASUREMENT OF CELLULAR INFILTRATION INTO THE AIRSPACE

SUPPORT PROTOCOL 2

A characteristic of the asthmatic response is eosinophil infiltration into the lung and airspace. Depending on the strain of mouse and the ovalbumin doses chosen for sensitization and challenge, cellular infiltration will be evident in the airspace and lung tissue of the animal anywhere from 6 hr after the last challenge to many days later. A common time point chosen is 48 hr after the last intranasal challenge, when both the measurement of airway hyperresponsiveness, as outlined in Support Protocol 1, and eosinophil infiltration are apparent. Cellular infiltration into the airspace is assessed using bronchoalveolar lavage (BAL). In this technique, the animal is euthanized, the trachea is cannulated, and PBS or other appropriate solution is introduced via the tracheal cannula to collect cells from the airway and alveolar space (also see *UNIT 18.4*). If airway hyperresponsiveness to methacholine is determined, wait at least 30 min before BAL to allow the methacholine-induced airway constriction to subside. This allows better recovery of BAL fluid and cells.

Materials

Mice sensitized and challenged with ovalbumin and appropriate control animals (see Basic Protocol)
Phosphate-buffered saline (PBS; *APPENDIX 2A*; or from GIBCO)
50 mg/ml pentobarbital sodium (Abbott)
Unopette Microcollection System solution (Becton Dickinson)
Normal guinea pig serum (Sigma)
Methanol
Modified Wrights' stain (Diff Quik, VWR)

Balance for weighing mice (accurate to 0.1 g)
10-ml beaker
3-ml syringes

Thread (4-0 silk)
Forceps (blunt, curved tip, serrated micro-dissecting forceps, Roboz Surgical Instruments)
Tracheal cannula (20-G needle, bevel filed off)
Dissecting scissors (5 1/2-in. blunt, Roboz Surgical Instruments)
Iris scissors (3-in., Roboz Surgical Instruments)
1.5-ml siliconized eppendorf tubes (low adhesion, Dot Scientific)
Refrigerated, low-speed centrifuge
Analytical balance (accurate to 0.001 g)
1.5-ml microcentrifuge tube
Neubauer hemacytometer (or automated cell counter such as a Coulter counter)
96-well U-bottomed microtiter plates (Sarstedt)
Shandon Cytospin 3 centrifuge (Shandon/Lipshaw)

Perform bronchoalveolar lavage (BAL)

1. Weigh the mouse sensitized and challenged with ovalbumin and appropriate control animals (see Basic Protocol).
2. Measure 1.8 ml endotoxin-free PBS for lavage into a 10-ml beaker. Prefill a 3-ml syringe with ~0.9 ml PBS and leave the syringe in the beaker.
3. Inject the mouse with 50 mg/ml pentobarbital (0.12 ml/20 g mouse) intraperitoneally.

   Once the animal does not respond to a toe pinch of the hind foot, it is ready for insertion of the tracheal cannula.

   If bleeding the mouse prior to BAL, be sure to monitor mouse continuously so that bleeding by retro-orbital or intracardiac method can be done before the heart stops beating or the blood pressure rapidly decreases. This dose of pentobarbital is intended to euthanize the animal.

   Pentobarbital is a Schedule II controlled substance and requires proper licensing and storage.
4. Immobilize the animal on its back. Make a midline incision over the trachea using dissecting scissors. Cut through muscle layers over the trachea and using the forceps, isolate the trachea and put two threads around it, each ~12 cm long. Make a loop in thread 1 over the trachea in preparation for tying a knot around the tracheal cannula (see Fig. 18.3.1). Tie a knot in thread 2, leaving a 4- to 5-cm diameter loop.

   When making an incision, stick to the midline so as to avoid severing arteries and veins. Be careful not to sever the trachea. When isolating the trachea, insert forceps with points together under the trachea and then spread the points apart underneath the trachea to spread the tissue. Grab both threads with the forceps and pull under the trachea to then form the loops of threads 1 and 2 as depicted in Figure 18.3.1.

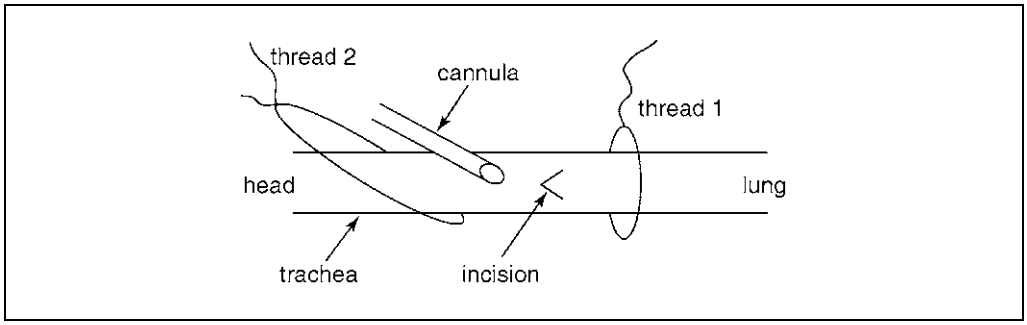

Figure 18.3.1 Schematic of tracheal cannulation of mouse.

5. Gently lift the loop of thread 1, nearest the lungs, to lift the trachea up. With iris scissors, make a V-shaped incision half way through the trachea. Insert the blunt needle cannula into the opening, advancing it ~3 to 5 mm into the trachea towards the lungs. Tie thread 1 securely with a single knot.

   Thread 2 can be used to put a small amount of tension on the trachea while making the incision and inserting the cannula.

6. Attach the 3-ml syringe containing room temperature PBS to the cannula. Gently deliver the volume of PBS into the lungs. Withdraw the fluid slowly until bubbles begin to appear, disengage the syringe from the cannula, and put the BAL fluid into a 1.5-ml siliconized eppendorf tube on ice. Repeat with the same volume of PBS and add to the BAL fluid already collected. Continue using the syringe to withdraw as much lavage fluid from the animal as possible.

   Throughout the procedure it is best to continue holding the hub of the cannula with one hand while manipulating the 3-ml syringe with the other hand until all of the lavage fluid is returned.

7. If the animal is to be used for assessment of cellular infiltration into the lung as well, proceed immediately to Support Protocol 3.

Count cells and determine differentials

8. Centrifuge the BAL fluid 12 min at ~600 × *g*, 4°C.

9. On an analytical balance, tare a 1.5-ml microcentrifuge tube. Using a 1-ml pipet, remove the supernatant from the cell pellet, being careful not to disturb the pellet. Add this BAL fluid to the tared 1.5-ml microcentrifuge tube. Record the weight of the BAL supernatant and freeze the supernatant (assume 1 g = 1 ml).

   Depending on the purpose of the experiment, antibodies, mediators, or other substances may be measured in the BAL supernatant.

10. Resuspend the cell pellet gently in 0.125 ml PBS and keep on ice.

11. Add 5 μl of cell suspension to 45 μl Unopette solution in a 1.5-ml microcentrifuge tube. Allow to sit for 10 min to ensure that any red blood cells are lysed.

    The Unopette Microcollection System solution is an ammonium oxalate diluent to lyse any red blood cells.

12. Load a standard Neubauer hemacytometer with the diluted cell suspension, in duplicate, and count the cells in each of the nine large squares, including those that lie on the top and left-hand perimeters. Do not count cells lying on the bottom and right-hand perimeters. Average the cell counts and calculate the number of white blood cells/ml of the original solution using the following formula:

    (Average no. of cells/9) × 10^5 = cells/ml in original cell suspension resuspended to 0.125 ml.

    Before loading the hemacytometer, make sure the cells are uniformly suspended in the liquid. In a control mouse, expect 1-10 × 10^4 cells total. In ovalbumin-sensitized and challenged animals, the number of white blood cells may be increased two to ten times.

13. Remove aliquots of 2 × 10^4 cells in 10- to 40-μl volume for cytospins. Dilute cells if necessary.

14. For cytospins, mix 2 × 10^4 cells, 130 μl PBS, 10 μl normal guinea pig serum, and 15 μl methanol in the well of a 96-well U-bottomed microtiter plate.

Table 18.3.1 Effect of Ovalbumin Challenge on Bronchoalveolar Lavage Cell Numbers[a]

Treatment	*N*	White blood cells ($\times 10^4$)	Macrophages ($\times 10^4$)	Eosinophils ($\times 10^4$)	Neutrophils ($\times 10^4$)
Water	5	6.5 ± 2.4	5.9 ± 2.3	0.04 ± 0.01	0.47 ± 0.20
Ovalbumin	8	7.8 ± 1.3	6.7 ± 1.1	0.29 ± 0.11[b]	0.79 ± 0.24

[a]Thirteen Balb/c mice were sensitized with ovalbumin and challenged with either ovalbumin or water as described in the Basic Protocol. At 48 hr after the last intranasal challenge, bronchoalveolar lavage was conducted as described in Support Protocol 2. Values represent mean ± SEM.
[b]$p<0.05$ compared to water treatment.

15. Add entire cell mixture to double cytospin funnel and cytospin 3 min at 1000 rpm with low acceleration, using double cytoslides for duplicate samples.
16. Air dry slides and stain with Diff Quik solution as recommended by the manufacturer.
17. Count 200 cells per spot (400 total), differentiating them as lymphocytes, macrophages, eosinophils, and neutrophils.
18. Express data as % cell type. Use total white blood cells from the mouse to calculate the total number of each cell type recovered from the mouse (typical results are seen in Table 18.3.1).

SUPPORT PROTOCOL 3

MEASURING CELLULAR INFILTRATION INTO THE LUNG

After sensitization and challenge of mice with ovalbumin (see Basic Protocol), depending on the experimental goals, a common scenario involves evaluation of airway hyperresponsiveness at 24 and/or 48 hr after the last intranasal challenge (see Support Protocol 1), followed by euthanasia of the mouse 30 to 60 min later for evaluation of cellular infiltration into the airspace and lung. The BAL as outlined in Support Protocol 2 is conducted, and then the lung lobes are removed as outlined in this protocol for the determination of eosinophil peroxidase (EPO) and myeloperoxidase (MPO) as indicators of the numbers of eosinophils and neutrophils, respectively, in the remaining lung tissue. Alternatively, the mouse can be euthanized and the lung lobes removed as outlined in this protocol without doing BAL.

Processing of lung lobes differs depending on whether EPO or MPO will be measured. For EPO, lung homogenates are centrifuged and the supernatant discarded. The resulting pellet is resuspended in the cetrimide buffer and sonicated prior to 2 cycles of freeze/thaw and sonication. EPO is tightly bound to membranes or contained within specific granules and is not liberated until the sonication and freeze/thaw cycles (Dimayuga et al., 1991). After freeze/thaw cycles and sonication, EPO activity is associated with both soluble and insoluble fractions, therefore, the assay of EPO uses both. For MPO, the enzyme is located within the primary granules of neutrophils. Extraction of MPO depends on disruption of the granules as well as the presence of cetrimide, which renders MPO soluble in aqueous solution (Bradley et al., 1982). The solubilized MPO is then separated from tissue debris by centrifugation. Aminotriazole is used in the MPO assay to inhibit any EPO contamination of the MPO sample.

Materials

Mice sensitized and challenged with ovalbumin and appropriate control animals (see Basic Protocol)
50 mg/ml pentobarbital sodium (Abbott)
Cetrimide (hexadecyltrimethylammonium bromide; see recipe)

Balance (accurate to 0.1 g)
2-ml glass vials (12 × 32–mm; Fisher)
Analytical balance (accurate to 0.0001 g)
Small hemostat (4 1/2-in.)
Dissecting scissors (5 1/2-in. blunt, Roboz Surgical Instruments)
Kimwipes in petri dish
Luxo magnifier (Daigger)
12 × 75–mm polystyrene round-bottomed tubes (Falcon)
Drying oven (Carbolite)
Homogenizer (Janke Kunkel Ultra-Turrax T-25, 24,000 rpm) with 8-mm generator probe for aqueous and organic solutions
250- and 50-ml beakers
Ear plugs
Forceps
1.0-ml pipet
Refrigerated, low-speed centrifuge
Sonicator (e.g., Daigger VC-130 ultrasonic processor) with microtip
Refrigerated, high-speed centrifuge and 12 × 75–mm high-speed centrifuge tubes
1.5-ml microcentrifuge tubes

Remove lung lobes

1. Weigh the mouse sensitized and challenged with ovalbumin and appropriate control animals (see Basic Protocol).
2. Preweigh a 2-ml glass vial on an analytical balance to 0.0001 g and record the weight.
3. Inject the mouse with 50 mg/ml pentobarbital (0.12 ml/20 g mouse) intraperitoneally.

   Once the animal does not respond to a toe pinch of the hind foot, it is ready for removal of the lungs.

   If bleeding the mouse prior to surgery, be sure to monitor mouse continuously so that bleeding by retro-orbital or intracardiac method can be done before the heart stops beating or the blood pressure rapidly decreases. This dose of pentobarbital is intended to euthanize the animal.

   Once the animal has been euthanized, the lung lobes should be removed as quickly as possible and placed on ice in cetrimide.

   Pentobarbital is a Schedule II controlled substance and requires proper licensing and storage.

4. Immobilize the animal on its back. Make a midline incision through the chest wall, being careful not to cut through the lungs. Clamp the trachea as high up as possible with a small hemostat, and use dissecting scissors to remove the heart and lungs intact, still attached to the trachea.
5. Invert the heart and lungs on a Kimwipe in a petri dish so the heart is underneath the lung lobes, as if observing by the dorsal view of the heart and lungs in situ.

   If the trachea is facing away, then the large left lobe is on the left side (see Fig. 18.3.2). Work quickly so tissue does not dry out.

6. Remove the inferior lobe of the right lung (see Fig. 18.3.2) for determination of MPO and the left lung lobe for determination of EPO. Be sure to trim pieces of the heart, esophagus, and fat tissue, using the Luxo magnifier for easy visualization.

   The remainder of the lung without the trachea is used to determine the wet/dry weight of the lung.

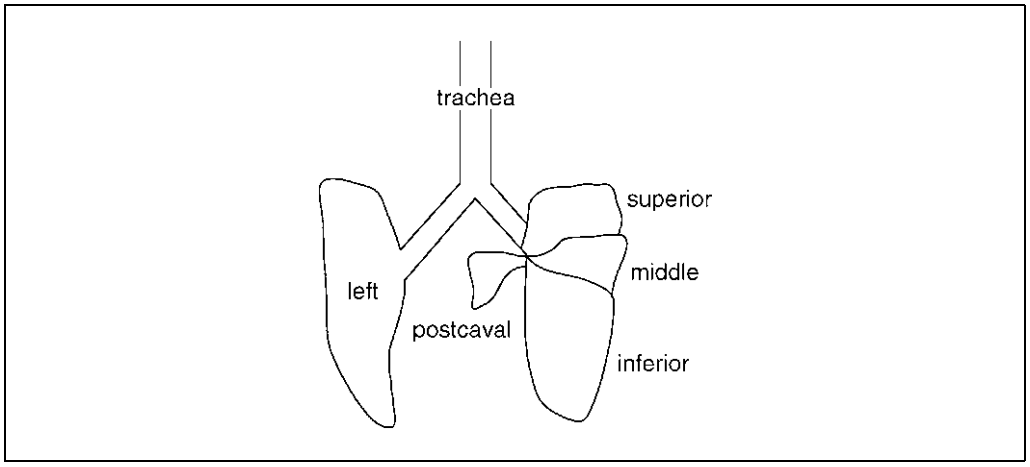

Figure 18.3.2 Schematic of dorsal view of mouse lung lobes. Lobes are named as described by Cook et al. (1983). The pattern of lobation may vary with the strain of mouse.

7. Tare a plastic 12 × 75–mm tube on the analytical balance and place the inferior lobe in the tube. Record the wet weight. Add 0.5 ml cetrimide to the tube and immediately place on ice.
8. Tare a second plastic 12 × 75–mm tube and place the left lobe in the tube. Record the wet weight. Add 0.5 ml cetrimide to the tube and immediately place on ice.
9. Place the wet/dry piece of lung in the preweighed 2-ml glass vial and record the weight of the vial plus the wet lung. Dry in a drying oven for 48 to 72 hr at 80°C to constant weight. Record weight of dried lung plus vial.

Homogenize left lung lobe and inferior lobe for enzyme assays

10. Rinse homogenizer by placing tip in 250-ml beaker of distilled water and turning it on for ∼15 sec.

    Use ear protection, e.g., ear plugs, when operating the homogenizer.

11. Wipe down tip thoroughly with Kimwipes and remove any debris remaining on tip with forceps.
12. Place the 12 × 75–mm tube containing lung lobe into a 50-ml beaker of wet ice.
13. Remove cap, and homogenize sample on ice ∼20 sec at 24,000 rpm.

    Take care to keep the sample on ice, and rotate the tube to homogenize the sample evenly.

14. Using a 1.0-ml pipet, rinse homogenizer with 0.5 ml of cetrimide, being sure to allow all liquid to drain into homogenized sample tube, giving a total volume of 1 ml plus the lung lobe.
15. Replace homogenized sample back on ice.

Prepare left lobe for eosinophil peroxidase (EPO) assay

16. Centrifuge the tube containing homogenized left lobe for 30 min at 400 × *g*, 4°C.
17. Discard supernatant and resuspend pellet in 0.5 ml cetrimide.
18. Sonicate for 15 sec, output 3, with tube on ice. Freeze sample at −20°C.

    Use ear protection when operating the homogenizer and sonicator.

19. Thaw, sonicate, and freeze (−20°C) the sample two additional times prior to determination of EPO (see Support Protocol 4). Store samples frozen at −20°C until assayed.

Place sample on ice immediately after thawing at room temperature. If samples are to be stored longer than 2 to 3 months, place at −70°C.

Prepare inferior lobe for MPO assay

20. Sonicate the sample containing the homogenized inferior lobe for 15 sec, output 3 with tube on ice. Freeze sample at −20°C.

    Use ear protection when operating the sonicator.

21. Thaw, sonicate, and freeze (−20°C) the sample two additional times prior to centrifugation.

    Place sample on ice immediately after thawing at room temperature.

22. Thaw sample, transfer to a 12 × 75–mm high-speed centrifuge tube, and centrifuge 30 min at 12,100 × *g*, 4°C.

23. Transfer supernatant to 1.5-ml microcentrifuge tube and store frozen at −20°C until assayed (see Support Protocol 5).

    If samples will be stored longer than 2 to 3 months, place at −70°C.

EOSINOPHIL PEROXIDASE (EPO) ASSAY

SUPPORT PROTOCOL 4

Eosinophils contain EPO and neutrophils contain MPO. Eosinophil peroxidase from tissues is measured as described by Strath et al. (1985) and Cheng et al. (1993). OD changes at 490 nm are monitored using the substrate solution *o*-phenylenediamine dihydrochloride (OPD) in a pH 8.0 buffer with 1 mM hydrogen peroxide. Assessment of EPO and MPO activity in a mixed cell population that contains both eosinophils and neutrophils is possible because of differences in the pH optimum for EPO and MPO (Worthington Enzyme Manual, 1972), as well as the ability of aminotriazole to inhibit EPO with minimal effects on MPO (Cramer et al., 1984). Thus, to achieve relative specificity for each enzyme, the EPO assay is conducted at pH 8.0, whereas the MPO assay is conducted at pH 6.0 in the presence of aminotriazole.

Materials

Homogenized left lung (see Support Protocol 3)
0.1% and 1% (v/v) Triton/Tris buffers (see recipes)
o-Phenylenediamine dihydrochloride (OPD; see recipe)
30% H_2O_2 (Sigma)

Spectrophotometer with visible light and kinetics software
Sonicator (Daigger) with microtip
Vortex
96-well U-bottomed microtiter plates (Sarstedt)
Glass cuvettes
Small squares of Parafilm (~2 × 2–cm)

CAUTION: Wear gloves throughout the procedure because OPD is a potential carcinogen. Hazardous waste containing OPD should be collected for proper disposal. Cover the work area with plastic-backed absorbent paper and wipe down all surfaces at the end with water.

1. Set up spectrophotometer for kinetic assays with a recommended starting point of determining OD every 5 sec for 2 min at a wavelength of 490 nm.

2. Thaw frozen homogenized left lung lobe sample (see Support Protocol 3, step 19). Keep tube on ice during assay.

    Place sample on ice immediately after thawing at room temperature.

3. Sonicate homogenized lung samples 15 sec on ice. Vortex before withdrawing 150 µl for dilution.
4. For a 1:2 dilution in a 96-well U-bottomed microtiter plate, mix 150 µl sample, 30 µl of 1% Triton/Tris buffer, and 120 µl of 0.1% Triton/Tris buffer. Serially dilute 70 µl of the 1:2 dilution back in 70 µl of 0.1% Triton/Tris buffer to a 1:4 dilution.
5. Place the following into cuvette, in order: 860 µl of 0.1% Triton/Tris buffer, 50 µl sample dilution, and 8.5 µl OPD. Top cuvette with Parafilm and invert to mix. Wipe sides of cuvette clean. Insert into the spectrophotometer and take a baseline reading at 490 nm. Remove cuvette from spectrophotometer.
6. Add 1 µl of 30% H_2O_2, place Parafilm on top, invert two times, and immediately place cuvette into spectrophotometer and begin to take kinetic readings.
7. When the reaction is complete, usually within 2 min, remove cuvette, pour contents into a hazardous waste container, rinse cuvette once with water, and pour into waste container. Finally, rinse cuvette eight to ten times with water and discard the waste down the drain.
8. If it is necessary to run an undiluted sample because the signal from the 1:2 dilution is very low, add 100 µl of 1:2 dilution to 810 µl of 0.1% Triton/Tris buffer, and 8.5 µl OPD. Take a baseline reading and then start the reaction as step 6 using 1 µl of 30% H_2O_2.

SUPPORT PROTOCOL 5

MYELOPEROXIDASE (MPO) ASSAY

Myeloperoxidase (MPO) is a constituent of neutrophil granules. For the assay of MPO, the hydrolysis of H_2O_2 is monitored by the change at 460 nm of *o*-dianisidine dihydrochloride (ODA) in a pH 6 phosphate buffer in the presence of the EPO inhibitor aminotriazole (AMT). Units of MPO activity are calculated as described in the Worthington Enzyme Manual (1972) and by Ormrod et al. (1987).

Materials

Frozen homogenized inferior lung lobe sample (see Support Protocol 3)
0.05 M potassium phosphate buffer, pH 6.0 (see recipe)
o-Dianisidine dihydrochloride (ODA; see recipe)
Aminotriazole (AMT; see recipe)
0.5 mM H_2O_2 (see recipe)

Spectrophotometer with visible light and kinetics software
Glass cuvettes
Small squares of parafilm (~2 × 2–cm)

CAUTION: Wear gloves throughout the procedure because ODA and AMT are potential carcinogens. Hazardous waste should be collected for proper disposal. Cover the work area with plastic-backed absorbent paper and wipe down all surfaces at the end with water.

1. Set up spectrophotometer for kinetic assays with a recommended starting point of determining OD every 5 sec for 3 min at a wavelength of 460 nm.
2. Thaw frozen homogenized inferior lung lobe sample (see Support Protocol 3, step 23). Keep sample tubes on ice during the assay.

Place sample on ice immediately after thawing at room temperature.

3. Place the following into cuvette, in order: 873 µl of 0.05 M potassium phosphate buffer, pH 6.0, 30 µl undiluted sample, 100 µl ODA, and 10 µl AMT. Top cuvette with Parafilm and invert two times to mix. Wipe sides of cuvette clean.

   If AMT solution yellows during the assay, discard aliquot and thaw a new one.

4. Insert cuvette into spectrophotometer. After 3 min, take baseline reading at a wavelength of 460 nm.

   This 3-min waiting period ensures that AMT has time to inhibit any EPO activity present.

5. Remove cuvette, add 10 µl of 0.5 mM H_2O_2, place Parafilm on top, invert two times, and immediately place cuvette into spectrophotometer and begin to take kinetic readings.

6. When the reaction is complete, usually within 3 min, remove cuvette, pour contents into hazardous waste container, rinse cuvette once with water, and pour into waste container. Finally, rinse cuvette eight to ten times with water and dispose of the waste down the drain.

7. If MPO activity is very low, double the sample size by adding 843 µl of 0.05 M potassium phosphate buffer, pH 6.0, 60 µl undiluted sample, 100 µl ODA, and 10 µl AMT. Wait 3 min, take a baseline reading, and then start the reaction as above using 10 µl of 0.5 mM H_2O_2.

   If ODA crystallizes in cuvette during the assay, discard the ODA aliquot and thaw a new one.

   The background reading is a good check to determine that the sample was added and that the ODA is not crystallizing (the background will be higher than normal).

REAGENTS AND SOLUTIONS

Use Milli-Q-purified water or equivalent for the preparation of all buffers. For common stock solutions, see ***APPENDIX 2A****; for suppliers, see* ***SUPPLIERS APPENDIX****.*

Aminotriazole (AMT)

3-Amino-1,2,4 triazole (Sigma)
Dissolve at 42 mg/ml water (final concentration of 0.5 M)
Store in 0.2-ml aliquots up to 1 year at −20°C

Aminotriazole is a potential carcinogen, care should be taken when handling.

Cetrimide

Add 0.5 g cetrimide (Hexadecyltrimethylammonium bromide; Sigma) to 100 ml of 0.05 M potassium phosphate buffer, pH 6.0 (see recipe). Store up to 4 weeks at 4°C. Warm to room temperature before use.

H_2O_2, 0.5 mM

Add 8.5 µl of 30% H_2O_2 (Sigma) to 4.99 ml 0.05 M potassium phosphate buffer, pH 6.0 (see recipe). Prepare on the day of the assay, keep on ice, and discard any remaining solution at the end of the assays.

Ketamine/xylazine

1 ml 100 mg/ml ketamine
1 ml 20 mg/ml xylazine
8 ml normal saline solution
Mix and store up to 1 month at room temperature

Ketamine is a controlled substance (Schedule III) and requires proper licensing and storage in an authorized locked cabinet.

Methacholine

To 19.2 g acetyl-β-methylcholine chloride (Sigma), add endotoxin-free saline up to 50 ml in a graduated cylinder. Dissolve at room temperature, transfer solution to ice bath, and dispense into 1-ml aliquots. Final solution concentration is 0.384 g/ml. Freeze 1-ml aliquots up to 6 months at −80°C.

ODA

Dissolve 1.67 mg/ml *o*-dianisidine dihydrochloride (Sigma) in water. Store in 1-ml aliquots up to 1 year at −20°C.

o-Dianisidine dihydrochloride is a potential carcinogen, care should be taken when handling.

OPD

Dissolve 90 mg/ml *o*-phenylenediamine dihydrochloride (Sigma) in water. Store 50-µl aliquots up to 1 year at −20°C.

Ovalbumin for challenge

Dissolve 1.25 mg/ml ovalbumin (Grade V; Sigma) in endotoxin-free water. Allow to dissolve for 2 to 3 hr or overnight at 4°C. Stir gently and dispense into convenient aliquots (1-ml) for freezing at −20° or −80°C up to 2 years.

Ovalbumin can have endotoxin contamination. The amount of endotoxin contamination in a particular lot of ovalbumin can be determined using a Limulus Amebocyte Lysate assay. Reagents and kits for this assay are commercially available from, e.g., Sigma (E-Toxate Kit) or BioWhittaker.

Be sure to use endotoxin-free water and sterile plastic ware. Alternatively, treat any glassware with E-Toxa clean concentrate (Sigma) to remove endotoxin contamination. Treating clean glassware at 175°C for a minimum of 3 hr will also destroy endotoxin.

Ovalbumin for sensitization

Dissolve 0.067 mg/ml ovalbumin (Grade V; Sigma) in endotoxin-free saline. Allow to dissolve for 2 to 3 hr or overnight at 4°C. Stir gently and dispense into 1.2-ml aliquots in 2-ml polypropylene screw-cap vials for freezing at −20° or −80°C up to 2 years.

Ovalbumin can have endotoxin contamination. The amount of endotoxin contamination in a particular lot of ovalbumin can be determined using a Limulus Amebocyte Lysate assay. Reagents and kits for this assay are commercially available from, e.g., Sigma (E-Toxate Kit) or BioWhittaker.

Be sure to use endotoxin-free saline and sterile plastic ware. Alternatively, treat any glassware with E-Toxa clean concentrate (Sigma) to remove endotoxin contamination. Treating clean glassware at 175°C for a minimum of 3 hr will also destroy endotoxin.

Potassium phosphate buffer, 0.05 M (pH 6.0)

1.361 g KH_2PO_4 dissolved in ~150 ml water
pH to 6.0 with 0.1 M K_2HPO_4
Add water to 200 ml
Store up to 6 months at 4°C
Warm to room temperature before use

Triton/Tris buffer, 0.1% (v/w)

0.657 g Tris (50 mM) dissolved in ~60 ml water
Add 100 µl of Triton X-100

continued

Mix well with stir bar
Adjust pH to 8.0 with 2 N HCl
Add water to 100 ml
Store up to 1 month at 4°C
Warm to room temperature before use

Triton/Tris buffer, 1% (v/w)

0.657 g Tris (50 mM) dissolved in ~60 ml water
Add 1 ml of Triton X-100
Mix well with stir bar
Adjust pH to 8.0 with 2 N HCl
Add water to 100 ml
Store up to 1 month at 4°C
Warm to room temperature before use

COMMENTARY

Background Information

Numerous studies have investigated the mechanism of ovalbumin-induced asthma in the mouse. Recent reviews summarize particular aspects of the mechanism in murine asthma models (Wills-Karp, 2000; Leong and Huston, 2001; Abraham, 2003). Bernstein et al. (1999) provides an overview of the studies done in occupational asthma in humans and in animal models. It is apparent that a wide variety of mouse model systems are used in investigating the asthmatic response. Asthma is a chronic inflammatory immune disease with a prominent role for CD4+ T cells producing a Th2 pattern of cytokines. When appropriately sensitized and challenged, the characteristic components of the asthmatic response can be demonstrated in murine asthma models: immediate bronchoconstriction to antigen, increased airway microvascular permeability, airway hyperresponsiveness to an agonist such as methacholine, and inflammatory cell infiltration into the lung, particularly eosinophils. Mice readily make IgE antibody to parallel the human situation. The mouse model of asthma has the advantage that extensive information is available regarding the mouse genome and numerous inbred strains and transgenic mice are available to examine specific hypotheses. A disadvantage of the mouse model is that extensive exposure to the antigen along with the use of an adjuvant may be required to reproducibly elicit the asthmatic response in a short period of time. This is in contrast to a species such as the guinea pig where the lung is the target organ and bronchoconstriction and eosinophil infiltration readily occur after antigen exposure.

In mouse models, the expression of different components of the effector phase of the asthmatic response, and the magnitude and time course of those responses, may differ depending on the routes of sensitization and challenge with the allergen, the dose of antigen, as well as the inbred strain of animal used. When examining 12 different strains of mice, Brewer et al. (1999) found a wide range of responses in both airway hyperresponsiveness to methacholine (zero- to three-fold change) and eosinophilia in the BAL (2% to 60%). Karp et al. (2000), using different strains of mice, found that complement component C5 is a susceptibility locus for airway hyperresponsiveness in ovalbumin-induced asthma. Thus, C5 deficient strains of mice such as A/J mice very readily develop airway hyperresponsiveness to ovalbumin sensitization and challenge.

Zhang et al. (1997) directly compared different routes of ovalbumin administration (intranasally versus intraperitoneally) in Balb/c mice and concluded that without local allergen exposure intranasally the mice did not develop airway hyperresponsiveness. The dose of allergen is also important in determining the asthmatic response. Mice sensitized with low doses of ovalbumin and alum intraperitoneally presented with both eosinophilia in the lung and airway hyperresponsiveness, whereas higher sensitizing doses by the same route resulted in a reduced eosinophilia and the absence of airway hyperresponsiveness (Sakai et al., 1999).

For sensitization, numerous studies have employed ovalbumin plus alum sensitization intraperitoneally. Alternatively, repeated aerosol administration of ovalbumin has also been used for sensitization. With regard to the ovalbumin challenge, repeated aerosol administration or multiple intranasal challenges help ensure a strong reproducible asthmatic response. Intratracheal challenge can also be

used to elicit the asthmatic symptoms and avoids exposure of the upper airways, but it is somewhat more invasive. Aerosolizing the ovalbumin requires a nebulizer and exposure chamber, as well as greater quantities of ovalbumin. The intranasal route has the advantage of simplicity, convenience, and a known dose of ovalbumin is delivered to the animal. Southam et al. (2002) systematically examined the effects of anesthesia, instillation volume, and position of the animal on the delivery of ovalbumin to the lung by intranasal instillation. The Basic Protocol utilizes three successive intranasal challenges to elicit the asthmatic response in the mouse. However, fewer challenges may also be sufficient. Tomkinson et al. (2001) successfully used a single intranasal challenge with ovalbumin to determine the time course of the airway hyperresponsiveness and eosinophil infiltration into the lung of the mouse.

In an asthmatic response, antigen challenge itself initiates an airway obstruction. After the response to antigen, the asthmatic airway becomes hyperresponsive to numerous agonists, including acetylcholine. The airways are more responsive to a lower dose of acetylcholine and the maximal response is also increased. Methacholine is a muscarinic agonist that is not as susceptible as acetylcholine to spontaneous hydrolysis and thus is useful in experimental situations to stimulate the muscarinic receptor. Many different methods are available to assess airway hyperresponsiveness. The one presented in this unit is the measurement of PenH using whole-body plethysmography in a conscious unrestrained mouse. Besides being minimally invasive, this technique allows high throughput and is not confounded by anesthesia. Airway reactivity can be assessed in a single animal at multiple time points to evaluate the time course of the event. Studies have been done to validate the technique as a measure of airway obstruction (Hamelmann et al., 1997). However, the method has been criticized as an indirect and imprecise measure of pulmonary function that is subject to changes in temperature and humidity (Lundblad et al., 2002). One experimental strategy is the use of PenH as an initial measure of airway hyperresponsiveness, followed by selected studies using more traditional measures of pulmonary mechanics in an anesthetized animal. Such methods in anesthetized ventilated mice may include measure of the airway pressure time index (Ewart et al., 1995), measurement of input impedance using the forced oscillation technique (Gomes et al., 2000), or a plethysmographic method of measuring pulmonary resistance and compliance (Martin et al., 1988). Isolated tracheal strips from ovalbumin-sensitized and -challenged mice have also been used to evaluate airway hyperresponsiveness, using either methacholine (De Bie et al., 1996) or electrical field stimulation (Hamelmann et al., 1999) as the constricting stimulus.

Many studies have utilized eosinophil peroxidase (EPO) and myeloperoxidase (MPO) as indicators of eosinophils and neutrophils, respectively, in lung tissue. The assays are quantitative and representative of the tissue as a whole. Measurements of EPO and MPO do not require histological interpretation and many measurements can be done in a short period of time. However, no information regarding the site of localization of the eosinophils and neutrophils—i.e., perivascular, interstitial, peribronchial, parenchymal—is obtained by measuring EPO and MPO in homogenized lung tissue.

The literature regarding the assay of EPO activity from cells and tissues is quite varied as to the tissue fractions analyzed. Some studies utilize the supernatant fraction after homogenization, freeze thawing and sonication in a Triton/Tris or cetrimide buffer (Collins et al., 1995; Hessel et al., 1997; Humbles et al., 1997). Other studies use both the soluble and insoluble fractions after a similar tissue preparation (Cheng et al., 1993; Dimayuga et al., 1991; Pettipher et al., 1994; Kung et al., 1995; Turner et al., 1996). Therefore, since methods vary considerably, especially homogenization and sonication techniques and buffers, it is very important in each laboratory to check soluble and insoluble fractions for EPO activity and confirm that the activity is inhibited by aminotriazole.

Besides measurement of cellular infiltration into the lung and airway hyperresponsiveness, mouse models of asthma lend themselves to the measurement of numerous other parameters not covered in this unit. Serum samples can be obtained and used for the measurement of antibodies. Antibody, protein, cytokines, and chemokines can be measured in the BAL fluid. Evidence of cell secretion (EPO) or cell injury (lactate dehydrogenase) may be evident in the BAL fluid. With proper precautions, the lung lobes can be used for isolation of RNA, cytokine measurements, histology, or immunocytochemistry. Collagenase digestion of lung lobes can be used to isolate lymphocyte populations for characterization.

Critical Parameters and Troubleshooting

As with any experiment, appropriate control groups of animals are essential and the protocol for sensitization and challenge will depend on the experimental question. Endotoxin contamination of solutions needs to be minimized because endotoxin will lead to neutrophilia itself, independent of an allergic reaction. Tissues should be removed from the animal as quickly as possible, keeping cells and tissues on ice in between manipulations. All samples should be frozen within 8 hr of removal from the animal.

Standard mouse feed is generally free of ovalbumin. However, if difficulties arise in seeing airway hyperresponsiveness or cellular infiltration, the possibility of ovalbumin exposure in the feed should be considered. Excessive exposure to ovalbumin could lead to tolerance and lack of reactivity to the allergen. As always, good animal husbandry is key to healthy animals and successful experiments.

When measuring EPO and MPO, it is important to use low amounts of enzyme so that the reaction rate is linear. If too much sample is used, the linear portion of the reaction will occur before the OD readings have begun. In the EPO assay, sonication prior to using the sample for assay is essential. Large pieces of tissue debris can interfere with the kinetic measurements. Low amounts of EPO in the sample will sometimes be difficult to distinguish from background. It may be useful to run EPO samples with and without the EPO inhibitor AMT so that noise can be distinguished from signal.

Anticipated Results

PenH for each mouse is averaged over the entire 8-min monitoring period to obtain an average PenH for each saline or methacholine dose. Data can then be expressed as the average for each dose, or as the ratio of the methacholine response over the control saline response for each animal. A change in control PenH values over time may indicate that environmental conditions are affecting baseline airway function. For example, excessive mold in the bedding or dust exposure may affect baseline PenH for the animals, and thus affect the airway responsiveness to methacholine after ovalbumin sensitization and challenge. Typical PenH results for the sensitization and challenge described in the Basic Protocol are shown in Figure 18.3.3. The concentration response curve to methacholine in the control animals tends to plateau. In contrast, PenH continues to increase over the methacholine concentration range in ovalbumin sensitized and challenged animals. Airway hyperresponsiveness is more apparent at 24 hr after the last intranasal challenge compared to the 48-hr time-point. The time course of the response

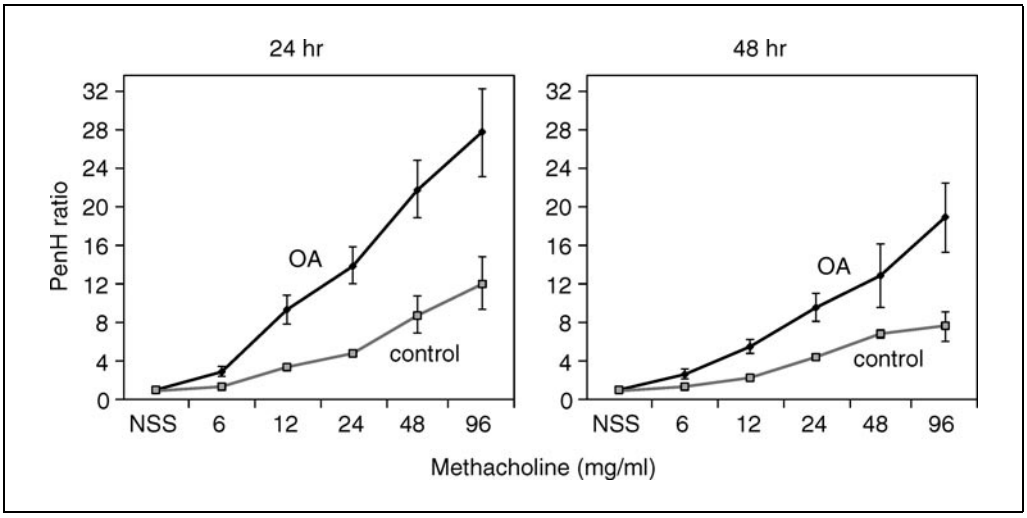

Figure 18.3.3 Six Balb/c mice were ovalbumin (OA)-sensitized and challenged as described in the Basic Protocol. At 24 and 48 hr after the last intranasal challenge, airway hyperresponsiveness to inhaled methacholine was determined as described in Support Protocol 1. PenH was determined and expressed as the PenH ratio (average PenH over the 8-min time interval with methacholine aerosol divided by the average PenH over the 8-min saline (NSS) aerosol exposure time). At 24 hr, the average PenH for NSS exposure was 0.58 $\pm$ 0.03 and 0.60 $\pm$ 0.09 for the control (water-challenged) and OA-challenged animals, respectively. At 48 hr, the average PenH for NSS exposure was 0.93 $\pm$ 0.06 and 0.80 $\pm$ 0.11 for the control (water-challenged) and OA-challenged animals, respectively. Values represent the mean $\pm$ SEM for 3 animals.

Table 18.3.2 Effect of Ovalbumin Challenge on EPO and MPO Measurements in the Lung[a]

Mouse	Challenge	Lobe for wet dry weight[b]		Left lobe[c]		EPO			Inferior lobe[d]		MPO			
		Wet weight (g)	Dry weight (g)	Wet weight (g)	Dry weight calculated (g)	OD/min[e]	Total OD/min[f]	EPO/g dry weight[g]	Wet weight (g)	Dry weight calculated (g)	OD/min[h]	Total OD/min[i]	Total units[j]	MPO/g dry weight[k]
1	OA	0.0118	0.0027	0.0486	0.0111	0.137	1.37	123.4	0.0412	0.0094	0.032	1.100	0.0974	10.362
2	OA	0.0130	0.0030	0.0525	0.0121	0.693	6.93	572.7	0.0325	0.0075	0.015	0.512	0.0454	6.047
3	OA	0.0143	0.0030	0.0556	0.0117	0.342	3.42	292.3	0.0427	0.0090	0.034	1.171	0.1037	11.519
4	Water	0.0106	0.0027	0.0404	0.0103	0.029	0.29	28.2	0.0275	0.0070	0.017	0.578	0.0512	7.311
5	Water	0.0109	0.0025	0.0473	0.0108	0.042	0.42	38.9	0.0312	0.0072	0.010	0.341	0.0302	4.195
6	Water	0.0123	0.0029	0.0417	0.0098	0.031	0.31	31.6	0.0288	0.0068	0.015	0.511	0.0452	6.650

[a] Six Balb/c mice were sensitized with ovalbumin (OA) and challenged 3 successive days with either ovalbumin or water as described in the Basic Protocol. The left lung lobe was removed for EPO measurements and the inferior lobe for MPO measurements as described in Support Protocol 3 at 48 hr after the last intranasal ovalbumin challenge. In this particular experiment, the postcaval lobe was used for wet/dry weight because the superior and middle lobes were used for RNA isolation. EPO, eosinophil peroxidase; MPO, myeloperoxidase.

[b] Lobe for wet/dry: Wet weight of postcaval lobe; Dry weight of postcaval lobe determined after 3 days at 80°C.

[c] Left lobe: Wet weight of left lobe; Dry weight calculated = (left lobe wet weight) × [(dry weight of lobe for wet dry)/(wet weight of lobe for wet dry)].

[d] Inferior lobe: Wet weight of inferior lobe; Dry weight calculated = (inferior lobe wet weight) × [(dry weight of lobe for wet dry)/(wet weight of lobe for wet dry)].

[e] EPO OD/min = OD/min in EPO assay for 50 µl undiluted sample.

[f] EPO total OD/min = EPO OD/min × 10. This is the total EPO for the 0.5-ml sample containing the whole left lobe.

[g] EPO/g dry weight = (EPO total OD/min)/(Left lobe dry weight calculated).

[h] MPO OD/min = OD/min in MPO assay for 30 µl undiluted sample.

[i] MPO total OD/min = (MPO OD/min) × (1 + Wet weight of inferior lobe − Dry weight calculated of inferior lobe)/0.030. This is the total MPO from the inferior lobe, accounting for the additional sample volume added by the water in the lung lobe.

[j] MPO total units = (MPO total OD/min)/11.3. MPO is expressed in units, where one unit is defined as that degrading 1 µmol of peroxide/min at 25°C, using the absorbancy index of H_2O_2 of 11.3 $(\mu mol/ml)^{-1}cm^{-1}$.

[k] MPO/g dry weight = (MPO total units)/(Inferior lobe dry weight calculated).

will differ depending on the sensitization and challenge regimen used.

Since Support Protocol 4 is a kinetic assay, the intent is to determine the initial reaction rate. Thus, the slope of the OD change over time is determined before it maximizes, and OD/min changes do not need to be large. The software for the kinetics program being used should be set to determine the OD/min from only the linear portion of the 2-min data-collection period. This is often no more than the first 30 to 60 sec. The number of sample dilutions assayed depends on the consistency of the OD/min readings obtained after they are corrected for the dilution. For ovalbumin-sensitized and -challenged mice, undiluted samples to 1:4 dilutions are usually within range. In samples with very few eosinophils, the kinetic readings show a great deal of noise due to the tissue debris. Background can be determined by conducting the assay in the presence of aminotriazole to inhibit EPO activity. Typical results are calculated as shown in Table 18.3.2 with OD/min values ranging from 0.031 to 0.693 for 50 μl of undiluted sample. In ovalbumin-challenged animals with higher EPO, the OD/min was determined on diluted samples and corrected for the dilution to arrive at the OD/min for a 50 μl undiluted sample. Final data is expressed as EPO/g dry weight lung, which is significantly greater for the ovalbumin-challenged animals compared to their water-challenged controls.

Since Support Protocol 5 is a kinetic assay, the intent is to determine the initial reaction rate. Thus, the slope of the OD change over time is determined before it maximizes, and OD/min changes do not need to be large. The software for the kinetics program being used should be set to determine the OD/min from only the linear portion of the 3-min data-collection period. This is often no more than the first 60 to 90 sec. The MPO activity should be completely inhibited by 0.1 mM sodium azide but not by 5 mM aminotriazole. In the absence of hydrogen peroxide, no change in OD should be evident. Typical results are shown in Table 18.3.2. OD/min for 30 μl undiluted sample range from 0.01 to 0.034. Final data is expressed as total MPO units/g dry weight of lung. As seen in Table 18.3.2, challenge with ovalbumin using the Basic Protocol does not result in a large increase in MPO in the lungs of sensitized mice as compared to water-challenged controls.

Time Considerations

The time from sensitization of the mouse to measurement of airway hyperresponsiveness and cellular infiltration is a 16-day period. Typically, 8 animals per day is a manageable number. This allows the intranasal challenge of 8 animals on 3 consecutive days first thing in the morning. Airway hyperresponsiveness measurements can then begin on the morning of the fourth or fifth day, depending on the experiment. Conducting methacholine dose response curves for the pulmonary function measurements requires ~2 hr for each group of mice. Thus, for 8 mice, measure airway hyperresponsiveness in 4 mice as Group 1 from 8 to 10 a.m. and 4 mice as Group 2 from 10 a.m. to 12 p.m. Then begin BAL and harvesting lung tissue in Group 1. For lavaging and removing lungs, allow ~10 to 15 min/mouse (2 hr total), with one person lavaging the lungs and another person removing the lung pieces. BAL cells can then be counted, cytospins made, lung tissue homogenized, and frozen by the end of the day. On the following day, further freeze/thaw and sonicate the lung homogenates, along with differential count of the cytospins can be completed. Later, EPO and MPO assays can be conducted. The wet/dry weight of the lung is available after 2 to 3 days of drying, and the final results may then be calculated.

Literature Cited

Abraham, W.M. 2003. Of mice and men. *Am. J. Resp. Cell Mol. Biol.* 28:1-4.

Bernstein, I.L., Bernstein, D.I., Chan-Yeung, M., and Malo, J.L. 1999. Definition and classification of asthma. *In* Asthma in the Workplace, 2nd ed. (I.L. Bernstein, M. Chan-Yeung, J.L. Malo, and D.I. Bernstein, eds.) pp. 1-3. Marcel Dekker, Inc., New York.

Bradley, P.P., Priebat, D.A., Christensen, R.D., and Rothstein, G. 1982. Measurement of cutaneous inflammation: Estimation of neutrophil content with an enzyme marker. *J. Invest. Dermatol.* 78:206-209.

Brewer, J.P., Kisselgof, A.B., and Martin, T.R. 1999. Genetic variability in pulmonary physiological, cellular, and antibody responses to antigen in mice. *Am. J. Respir. Crit. Care Med.* 160:1150-1156.

Cheng, J.B., Pillar, J.S., Shirley, J.T., Showell, H.J., Watson, J.W., and Cohan, V.L. 1993. Antigen-mediated pulmonary eosinophilia in immunoglobulin G1-sensitized guinea pigs: Eosinophil peroxidase as a simple specific marker for detecting eosinophils in bronchoalveolar lavage fluid. *J. Pharmacol. Exp. Therap.* 264:922-929.

Collins, P.D., Marleau, S., Griffiths-Johnson, D.A., Jose, P.J., and Williams, T.J. 1995. Cooperation between interleukin-5 and the chemokine eotaxin to induce eosinophil accumulation in vivo. *J. Exp. Med.* 182:1169-1174.

Cook, M.J. 1983. Anatomy. *In* The Mouse in Biomedical Research, Vol. III: Normative Biology, Immunology, and Husbandry (H.L. Foster, J.D. Small, and J.G. Fox, eds.) pp. 101-120. Academic Press, New York.

Cramer, R., Soranzo, M.R., Dri, P., Menegazzi, R., Pitotti, A., Zabucchi, G., and Patriarca, P. 1984. A simple reliable assay for myeloperoxidase activity in mixed neutrophil-eosinophil cell suspensions. Application to detection of myeloperoxidase deficiency. *J. Immunol. Methods* 70:119-125.

De Bie, J.J., Hessel, E.M., Van Ark, I., Van Esch, B., Hofman, G., Nijkamp, F.P., and Van Oosterhout, A.J.M. 1996. Effect of dexamethasone and endogenous corticosterone on airway hyperresponsiveness and eosinophilia in the mouse. *Br. J. Pharmacol.* 119:1484-1490.

Dimayuga, E., Stober, M., and Kayes, S.G. 1991. Eosinophil peroxidase levels in hearts and lungs of mice infected with Toxocara canis. *J. Parasitol.* 77:461-466.

Ebino, K., Ueda, H., Kawakatsu, H., Shutoh, Y., Kosaka, T., Nagayoshi, E., Lemus, R., and Karol, M.H. 2001. Isolated airway exposure to toluene diisocyanate results in skin sensitization. *Toxicology Letters* 121:79-85.

Ewart, S., Levitt, R., and Mitzner, W. 1995. Respiratory system mechanics in mice measured by end-inflation occlusion. *J. Appl. Physiol.* 79:560-566.

Fraser, D.G., Regal, J.F., and Arndt, M.L. 1995. Trimellitic anhydride-induced allergic response in the lung: Role of the complement system in cellular changes. *J. Pharmacol. Exp. Ther.* 273:793-801.

Gomes, R.F.M., Shen, X., Ramchandani, R., Tepper, R.S., and Bates, J.H.T. 2000. Comparative respiratory system mechanics in rodents. *J. Appl. Physiol.* 89:908-916.

Hamelmann, E., Schwarze, J., Takeda, K., Oshiba, A., Larsen, G.L., Irvin, C.G., and Gelfand, E.W. 1997. Noninvasive measurement of airway responsiveness in allergic mice using barometric plethysmography. *Am. J. Respir. Crit. Care Med.* 156:766-775.

Hamelmann, E., Takeda, K., Schwarze, J., Vella, A.T., and Irvin, C.G. 1999. Development of eosinophilic airway inflammation and airway hyperresponsiveness requires interleukin-5 but not immunoglobulin E or B lymphocytes. *Am. J. Respir. Cell Mol. Biol.* 21:480-489.

Hayes, J.P., Daniel, R., Tee, R.D., Barnes, P.J., Taylor, A.J.N., and Chung, K.F. 1992a. Bronchial hyperreactivity after inhalation of trimellitic anhydride dust in guinea pigs after intradermal sensitization to free hapten. *Am. Rev. Respir. Dis.* 146:1311-1314.

Hayes, J.P., Lotvall, J.O., Baraniuk, J., Daniel, R., Barnes, P.J., Newman Taylor, A.J., and Chung, K.F. 1992b. Bronchoconstriction and airway microvascular leakage in guinea pigs sensitized with trimellitic anhydride. *Am. Rev. Respir. Dis.* 146:1306-1310.

Hessel, E.M., Van Oosterhout, A.J.M., Van Ark, I., Van Esch, B., Gofman, G., Van Loveren, H., Savelkoul, H.F.J., and Nijkamp, F.P. 1997. Development of airway hyperresponsiveness is dependent on interferon-gamma and independent of eosinophil infiltration. *Am. J. Respir. Cell Mol. Biol.* 16:325-334.

Humbles, A.A., Conroy, D.M., Marleau, S., Rankin, S.M., Palframan, R.T., Proudfoot, A.E.I., Wells, T.N.C., Li, D., Jeffery, P.K., Griffiths-Johnson, D.A., Williams, T.J., and Jose, P.J. 1997. Kinetics of eotaxin generation and its relationship to eosinophil accumulation in allergic airways disease: Analysis in a guinea pig model in vivo. *J. Exp. Med.* 186:601-612.

Karp, C.L., Grupe, A., Schadt, E., Ewart, S.L., Keane-Moore, M., Cuomo, P.J., Kohl, J., Wahl, L., Kuperman, D., Germer, S., Aud, D., Peltz, G., and Wills-Karp, M. 2000. Identification of complement factor 5 as a susceptibility locus for experimental allergic asthma. *Nature Immunol.* 1:221-226.

Kung, T.T., Stelts, D., Zurcher, J.A., Jones, H., Umland, S.P., Kreutner, W., Egan, R.W., and Chapman, R.W. 1995. Mast cells modulate allergic pulmonary eosinophilia in mice. *Am. J. Respir. Cell Mol. Biol.* 12:404-409.

Leong, K.P., and Huston, D.P. 2001. Understanding the pathogenesis of allergic asthma using mouse models. *Ann. Allergy Asthma Immunol.* 87:96-110.

Lundblad, L.K.A., Irvin, C.G., Adler, A., and Bates, J.H.T. 2002. A reevaluation of the validity of unrestrained plethysmography in mice. *J. Appl. Physiol.* 93:1198-1207.

Martin, T.R., Gerard, N.P., Galli, S.J., and Drazen, J.M. 1988. Pulmonary responses to bronchoconstrictor agonists in the mouse. *J. Appl. Physiol.* 64:2318-2323.

Ormrod, D.J., Harrison, G.L., and Miller, T.E. 1987. Inhibition of neutrophil myeloperoxidase activity by selected tissues. *J. Pharmacol. Methods* 18:137-142.

Pettipher, E.R., Salter, E.D., and Showell, H.J. 1994. Effect of in vivo desensitization to leukotriene B_4 on eosinophil infiltration in response to C5a in guinea-pig skin. *Br. J. Pharmacol.* 113:117-120.

Regal, J.F., Mohrman, M.E., and Sailstad, D.M. 2001. Trimellitic anhydride-induced eosinophilia in a mouse model of occupational asthma. *Toxicol. Appl. Pharmacol.* 175:234-242.

Sakai, K., Yokoyama, A., Kohno, N., and Hiwada, K. 1999. Effect of different sensitizing doses of antigen in a murine model of atopic asthma. *Clin. Exp. Immunol.* 118:9-15.

Southam, D.S., Dolovich, M., O'Byrne, P.M., and Inman, M.D. 2002. Distribution of intranasal instillations in mice: Effects of volume, time, body position, and anesthesia. *Am. J. Physiol. Lung Cell. Mol. Physiol.* 282:L833-839.

Strath, M., Warren, D.J., and Sanderson, C.J. 1985. Detection of eosinophils using an eosinophil peroxidase assay. Its use as an assay for eosinophil differentiation factors. *J. Immunological Methods* 83:209-215.

Tomkinson, A., Cieslewicz, G., Duez, C., Larson, K.A., Lee, J.J., and Gelfand, E.W. 2001. Temporal association between airway hyperresponsiveness and airway eosinophilia in ovalbumin-sensitized mice. *Am. J Respir. Crit. Care Med.* 163:721-730.

Turner, C.R., Cohan, V.L., Cheng, J.B., Showell, H.J., Pazoles, C.J., and Watson, J.W. 1996. The in vivo pharmacology of CP-80,633, a selective inhibitor of phosphodiesterase 4. *J. Pharmacol. Exp. Ther.* 278:1349-1355.

Wills-Karp, M. 2000. Murine models of asthma in understanding immune dysregulation in human asthma. *Immunopharmacology* 48:263-268.

Worthington Enzyme Manual. 1972. pp. 43-45. Worthington Biochemical Corp., Freehold, NJ.

Zhang, X.D., Siegel, P., and Lewis, D.M. 2002. Immunotoxicology of organic acid anhydrides (OAAs). *International Immunopharmacol.* 2:239-248.

Zhang, Y., Lamm, W.J.E., Albert, R.K., Chi, E.Y., Henderson, W.R., and Lewis, D.B. 1997. Influence of the route of allergen administration and genetic background on the murine allergic pulmonary response. *Am. J. Respir. Crit. Care Med.* 155:661-669.

Contributed by Jean F. Regal
School of Medicine
University of Minnesota
Duluth, Minnesota

Use of Bronchoalveolar Lavage to Detect Lung Injury

The lung is the portal of entry into the body for inhaled pollutants. The interaction of the pollutant with the cells lining the respiratory tract can provide information on the toxicity of the pollutant and the level of pollutant required to induce an inflammatory response. The affected cells release mediators into the epithelial lining fluid (ELF), which can be sampled by isotonic washing (lavage) of the respiratory tract. The bronchoalveolar lavage fluid (BALF) will contain both biochemical and cytological indicators (biomarkers) of the tissue response to the inhaled pollutant. The fact that these indicators can be quantified provides a means of developing a dose-response curve for the inhalation toxicity of the agent of interest and may provide a "no-effect" level of exposure for regulatory purposes. For more mechanistic research, analysis of BALF can be used to test specific hypotheses. Finally, new proteomic techniques that determine changes in protein expression profiles in BALF can be used to stage disease processes and, in some cases, may be used to predict disease outcome.

This unit describes methods of performing bronchoalveolar lavage in laboratory animals and the choice of washing fluids that may be used. In addition, a discussion of the various types of biomarkers of lung injury or disease that may be measured is also provided. Three procedures are described: bronchoalveolar lavage performed in large animals in vivo (see Basic Protocol and Alternate Protocol 1), bronchoalveolar lavage performed in the excised lung (see Alternate Protocol 2), and processing BALF and analysis of lung damage indicators (see Support Protocol). Some discussion of proteomic analysis of lavage fluid is also made. The topic of how to perform bronchoalveolar lavage in humans is not discussed in this unit.

STRATEGIC PLANNING

The purpose of the lavage procedure is to obtain samples of the ELF and cells from the respiratory tract for analysis of biomarkers of respiratory tract disease. Below are listed major questions to be considered before performing the procedure.

Anesthesia

Studies have shown that various anesthetic agents can be used for the BAL procedure, including isoflurane, halothane, and sodium pentobarbital. However, CO_2 is not a suitable agent because of its profound effects on the epithelial lining fluid of the lung (Henderson and Lowry, 1983). For the selection, correct dose and use of preanesthetic agents and general anesthesia, the reader should consult with a laboratory animal veterinarian.

Wash Fluid

Wash fluid must be isotonic to avoid damage to cells and tissue. Physiological saline (0.15 M) is commonly used, but phosphate-buffered saline or various balanced salt solutions have been used as well. An important consideration is whether to have Ca^{2+} and Mg^{2+} in the fluid. These cations are necessary for the adherence of the macrophages to surfaces and fewer cells will be obtained if the wash fluid contains Ca^{2+} and Mg^{2+}; however, the decision to include these cations or not will depend on the objective of the study. If the objective is to obtain as many cells as possible for later assays to be performed in vitro, one should not include the cations. If, however, the objective is to obtain only

Contributed by Rogene F. Henderson and Bruce A. Muggenburg
Current Protocols in Toxicology (2004) 18.4.1-18.4.10

those cells that are free and unattached in the alveoli, it would be advisable to include Ca^{2+} and Mg^{2+}.

Wash Volume

For a total lung lavage, such as that normally performed in a small laboratory animal, a recommended volume is 80% of the volume required to raise intrapulmonary pressure to 30 cm water pressure (Mauderly, 1977). Extensive experience in measuring this volume in various species in the authors' laboratory has indicated that the following volumes may be used as standard procedure: 7 ml in a 300-g male rat, 5 ml in a 200-g female rat, 4 ml in a 120-g Syrian hamster, and 1 ml in a 35-g mouse. For segmental lavages in dogs or nonhuman primates, volumes of 10 and 7.5 ml, respectively, have been used successfully.

Number of Washes

For the purposes of many toxicology studies, it is advantageous to use the least number of washes necessary to obtain a sample of the epithelial lining fluid, as further washes will only serve to dilute the parameters one is trying to measure. In a study in which the recovery of one component of BALF, protein, was measured in each of six sequential washes of the right lung of a dog, 50% of what was recovered in all six washes was obtained in the first wash and another 25% was recovered in the second (Henderson, 1988, 1989; Henderson and Muggenburg, 1992). Thus, 75% of the total was recovered in two washes. For most purposes, in a total lung lavage procedure, two to four washes should be sufficient to give an adequate sample of the epithelial lining fluid without diluting the contents beyond what is convenient to measure. In segmental lavages, the recovery of the initial wash is usually low (see next section), and five or six washes may be needed.

An exception to these recommendations is if the objective of the study is to obtain as many pulmonary alveolar macrophages as possible for functional assays performed in vitro. In this case, one may want to use numerous washes and even massage the lung (in excised lung wash procedures; see Alternate Protocol 2) between the instillation of the wash fluid and its withdrawal. There are also reports that few functional macrophages are removed by the initial washes, while later washes contain the most active cells. As in all research, the study must be designed to meet the objectives. If one wishes to disturb the lung as little as possible to detect an inflammatory response, a gentle approach with few washes should be used. If the purpose is to obtain the most functionally active macrophages for further study, more drastic approaches with numerous washes may be required.

Recovery of Wash Fluid

In a total lung lavage, one normally recovers 75% of the initial wash fluid and 100% of the instilled fluid in subsequent washes. If one does two washes, this equals 88% recovery of the total fluid instilled. In a segmental lavage in a large animal, one normally recovers 40% of the first 10-ml wash and 100% of subsequent 10-ml washes. If one performs five washes, the total recovery is ~88%. If the lung being lavaged is severely injured, one may have problems recovering the lavage fluid. If the lung is severely edematous, one could possibly get back more fluid than was put in. This presents some problems for normalization of the data as will be discussed later (see Anticipated Results). In general, the lavage procedure works best in detecting early signs of lung injury before the lung has become so severely affected as to cause problems with recovery of the lavage fluid.

If BAL is performed in vivo in a small laboratory animal, it is usually done as a total lung lavage. There are species differences in how well the whole lung lavage is tolerated, and

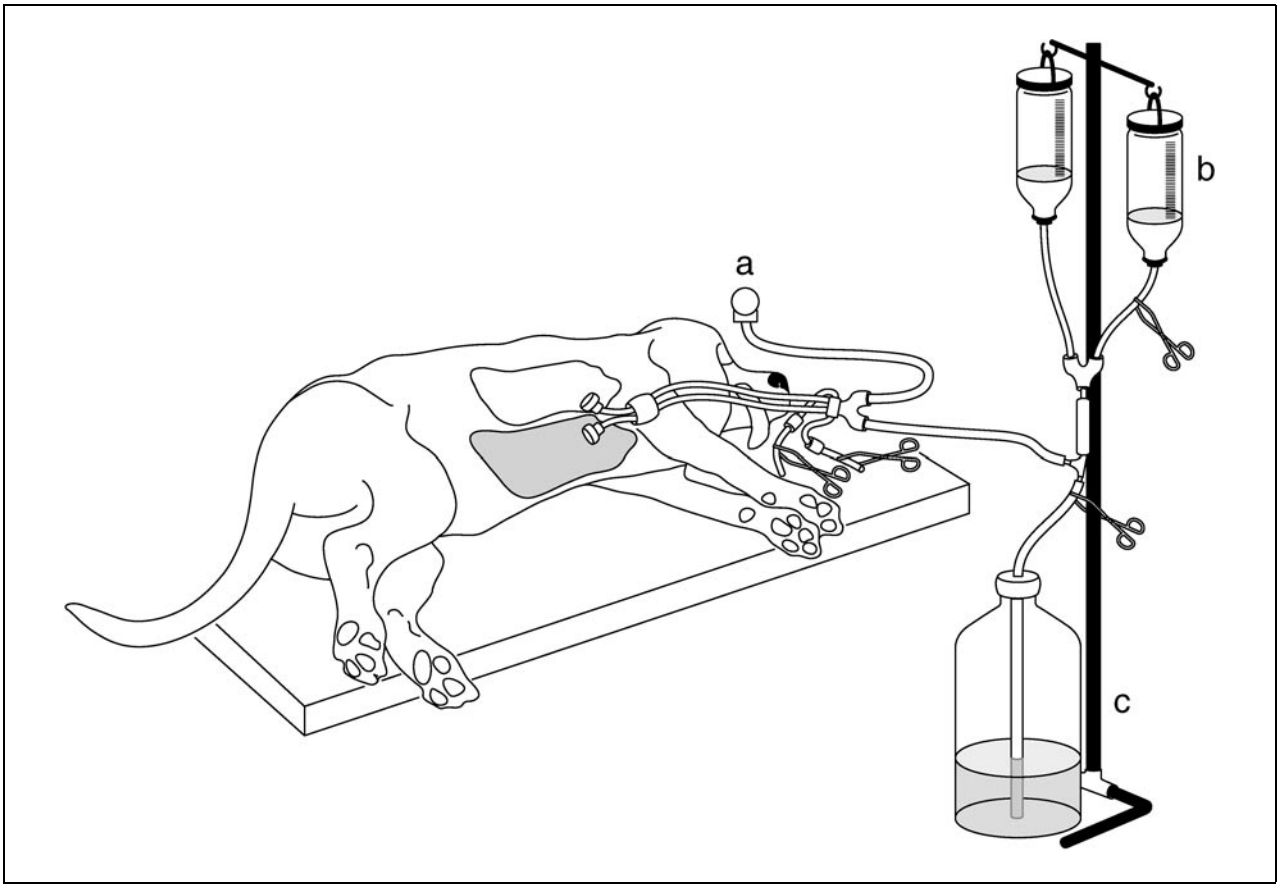

Figure 18.4.1 Schematic of bronchoalveolar lavage procedure in the beagle dog, including (a) anesthesia equipment, (b) wash fluid supply, and (c) receiving container. (From Boecker, B.B., Muggenburg, B.A., McClellan, R.O., et al.: *Health Phys* 1974; 26:505-517. Used by permission.)

the Syrian hamster, mouse, and rabbit appear to be more tolerant than the rat or guinea pig. Sequential lavages can be performed in this manner, if such a procedure is consistent with the experimental objectives of a study. However, for most purposes, the lavage of small laboratory animals is performed in the excised lung (see Alternate Protocol 2) because this involves less time and skill than the procedure performed in vivo.

Whole Lavage Apparatus

A lavage apparatus for use only in dogs or other large animals (Fig. 18.4.1) can be constructed from 3/8-in. internal diameter latex or polyethylene tubing, two 3/8-in. Y connectors, and one 3/8-in. T connector (Nalgene). The saline solution in 1-liter bottles can be 0.9% sodium chloride irrigation solution made by McGraw. Two containers are used so that it is unnecessary to change bottles during the procedure. The T connector is placed at the junction between the irrigation solution and the tube to the dog, and the anesthetic machine and the tube to the collection bottle on the floor. The second Y is used to divide the tubing to the dog and to the anesthetic machine. At the end of the tube to the dog, the connector from a plastic disposable endotracheal tube (Rusch) is attached to the tubing and this is the sized to make a quick disconnect to the Y connector. The other end of the tubing is slid over the end of the disposable endotracheal tube. For a 10-kg beagle, a 9-Fr. (from 8- to 9.5-Fr. for smaller or larger dogs, respectively) tube is generally of adequate size. A second endotracheal tube connector is placed at the end of the tubing to the anesthetic machine. Two large forceps or other clamps are needed to direct the flow of fluids to the dog, or to the collection container and to block off or open the line to the anesthetic machine.

BRONCHOALVEOLAR LAVAGE PERFORMED IN LARGE ANIMALS IN VIVO

In larger animals, BAL can be performed in the anesthetized subject by bronchoscopy as it is done in humans. A fiberoptic bronchoscope is wedged into an airway, and the broncholaveolar space distal to the tip of the bronchoscope is washed with wash fluid. There are several advantages to conducting segmental BAL in vivo. One can follow the progress of a tissue reaction or a disease state over time by repeated washing either of the same lobe or, if the reaction is fairly uniformly distributed throughout the lung, of different lobes. If one wants to test the pulmonary toxicity of a relatively insoluble substance, one can instill different amounts of the material in different lung lobes and subsequently wash the different lobes to conduct a type of dose-response study in one animal.

Depending on the question to be addressed, one may want to obtain ELF from only the bronchial region of the airways or from the deep lung (alveolar region). In small animals, one way to obtain lavage fluid from the two regions is to keep initial wash fluids separate from subsequent lavage fluids. The first wash is considered to have mainly bronchial material, and subsequent washes are considered to have mainly alveolar material. In large animals, another way to sample only the bronchial region is to place an inflatable balloon distal to the area to be washed (see Alternate Protocol 1). This will prevent lavage fluid from going beyond the bronchial region (as described for clinical procedures in Rennard et al., 1998). If a large BALF sample is desired, either the whole right or left lung can be lavaged.

Materials

Animal: dog or other large animal
Preanesthesia agents (e.g., acepromazine, ketamine, zylazine)
Atropine
General anesthetic: 5% (for induction) and 2% (for maintenance) isoflurane in O_2
Sterile wash fluid (see Strategic Planning)

Face mask
Endotracheal tube with balloon (Rusch)
Whole lavage apparatus (see Strategic Planning)

Additional reagents and equipment for storing and processing BALF fluid (see Support Protocol)

NOTE: Bronchoalveolar lavage of large animals in vivo should only be done under the supervision of a veterinarian or physician.

Prepare animal

1. Withhold food from the animal to be tested for 12 hr and water for 6 to 8 hr prior to the experiment.
2. Sedate the animal with preanesthetic agents.

   Phenothiazine-related agents, such as acepromazine can be used in dogs; ketamine or a ketamine-zylazine combination are the agents of choice for nonhuman primates.

3. Thirty minutes before anesthesia, administer atropine to control secretions.

Intubate

4. Induce general anesthesia via a face mask with an anesthetic gas such as isoflurane.
5. When a surgical plane of anesthesia has been achieved, insert endotracheal tube into tube a, shown in Fig. 18.4.1, and inflate balloon.

   At this point, a total lung lavage can be performed, or the fiberoptic bronchoscope can be inserted to perform a sublobar segmental lavage (see Alternate Protocol 1).

Position animal and induce apnea

6. Place the animal on its side, with the lung to be washed in the dependent (i.e., lower) position and connect the whole lavage apparatus (Fig. 18.4.1).

   If both lungs are to be washed in the same procedure, wash the right lung first, because it has the largest volume (Fig. 18.4.1).

7. Hyperventilate the animal for approximately 3 min to induce apnea (i.e., cessation of breathing by lowering the blood carbon dioxide levels).

Administer wash fluid

8. Close the clamp on the tube from the anesthesia machine and open the clamp on the tube from the sterile wash fluid reservoir.
9. Allow the wash fluid to fill the dependent lung to the predetermined volume.

   Use ~80% of functional residual capacity of the lung (equivalent to 80% of the volume required to raise intrapulmonary pressure to 30 cm H_2O) and consider the right lung to be 60% of the total lung (also see Strategic Planning)

Collect BALF

10. When the predetermined volume of wash fluid has entered the lung, immediately clamp off the tube from the wash fluid reservoir and open the clamp to the collection vessel on the floor to drain the fluid from the lung.
11. Before drainage is complete, open the clamp to the anesthetic machine to assist drainage.
12. Ventilate the animal several minutes to re-induce apnea and repeat the procedure (steps 9 to 11) as many times as required by the scientific question to be addressed (see Strategic Planning).
13. After the last wash, tilt the animal head-down to complete drainage from the lung. Store BALF as described (see Support Protocol).

Allow animal to recover

14. Ventilate the lung several times by hand to facilitate recovery. Remove the endotracheal tube when the cough reflex has returned.
15. Observe the animal carefully until it can maintain an upright posture.
16. Analyze and process BALF as described (see Support Protocol).

SEGMENTAL LAVAGE

ALTERNATE PROTOCOL 1

Segmental lavage or the lavage of a sublobar unit of the lung is performed with a fiberoptic bronchoscope. The scope is wedged into the region of the lung lobe of interest. Using isoflurane anesthesia, the animal breaths normally during the procedure and apnea is unnecessary. The airways in monkeys are generally more sensitive to minor submucosal hemorrhage and cough reflex than the dog. Thus, they require more care in manipulating the bronchoscope in the airways and careful attention to anesthesia.

Additional Materials *(also see Basic Protocol)*

Fiberoptic bronchoscope (e.g., Olympus, Pentex)
Syringes

1. Perform the same general anesthesia and intubation procedures as described for total lung lavage (see Basic Protocol, steps 1 to 5).

   The animal is usually placed in the prone position.

2. Insert a fiberoptic bronchoscope into the endotracheal tube and wedge the tip in the lobe of interest.

3. Use an appropriately sized syringe to instill wash fluid gently into the lobe.

   Recommended volumes are 10 ml for dogs weighing 5 to 15 kg, 10 ml for chimpanzees, and 7.5 ml for primates that weigh <10 kg.

4. Immediately suction the fluid out gently with an appropriately sized syringe. Transfer to an appropriate receiving container and store and process as described (see Support Protocol).

   The receiving container can be plastic.

5. Repeat the washing (steps 3 and 4) four to five times or as required by the scientific question being addressed.

6. After completion of the lavages, watch the animal carefully until it can maintain an upright posture.

7. Analyze and process BALF as described (see Support Protocol).

ALTERNATE PROTOCOL 2

BRONCHOALVEOLAR LAVAGE PERFORMED IN THE EXCISED LUNG

In this procedure, a catheter is tied into the trachea of the excised lung and a syringe is used to administer the lavage fluid (Fig. 18.4.2). The fluid is instilled slowly to prevent damage from the procedure itself, and the fluid is withdrawn as gently as possible. The advantage of doing lavage in excised lungs, besides the decreased time and skill requirements, is that it is easy to know what portion of the lung is being washed: it is easy to observe if a part of the lung is not expanded by the fluid. Also, in excised lungs, one normally washes the whole lung or a known portion of the lung. This makes normalization of the data more straightforward (see Anticipated Results). For these reasons, lavage of the excised lung from small laboratory animals has been the method of choice for use of BAL in screening tests for the pulmonary toxicity of inhaled or instilled materials. Studies have indicated little effect on the indicators of toxicity commonly measured in BALF whether the lavage is performed in vivo or in the excised lung.

Additional Materials *(also see Basic Protocol)*

Anesthetic for euthanasia (e.g., 5% halothane in O_2, sodium pentobarbital)
Dissection board and tools
Plastic tracheal catheter with Luer lock connector
Syringes

1. Weigh the animal and anesthetize.

   This can be achieved with 5% halothane in oxygen or sodium pentobarbital. Carbon dioxide should not be used because it increases the background level of some components of the epithelial lining fluid (see Strategic Planning).

2. Exsanguinate the animal via the carotid artery or by cardiac puncture.

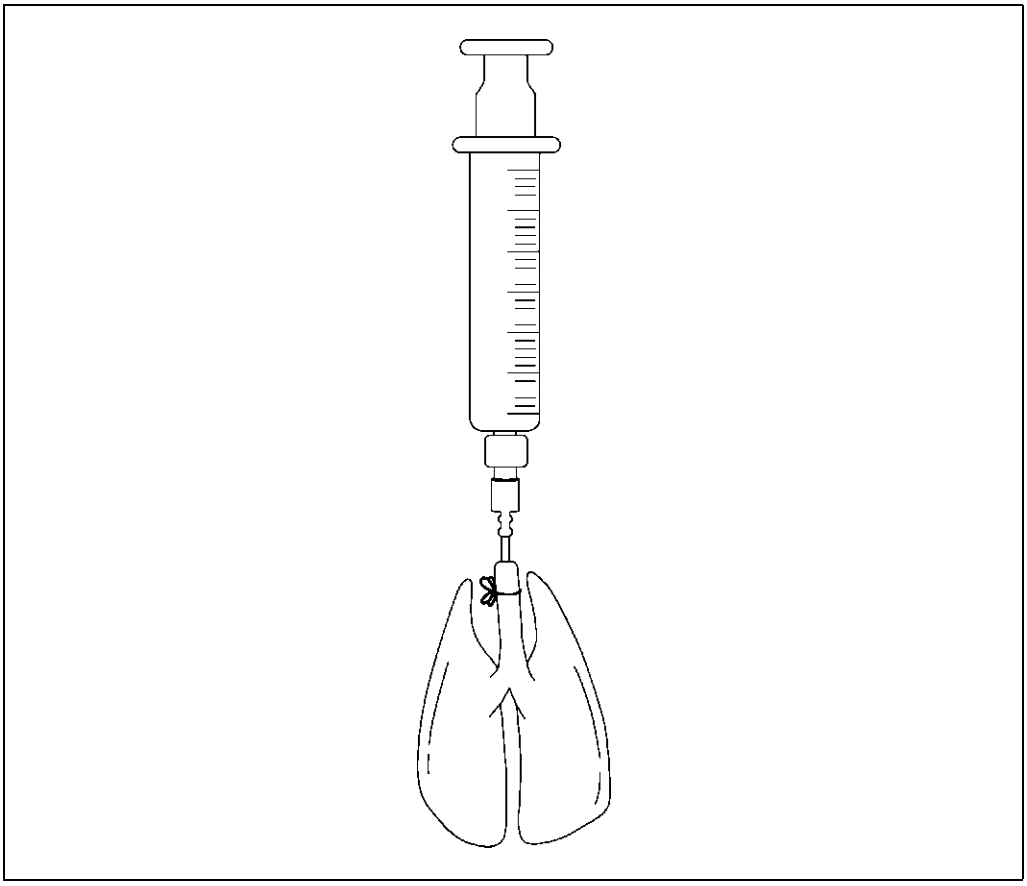

Figure 18.4.2 Total lung lavage in the excised lung.

3. Pin the animal to a dissection board, open the thoracic cavity, and remove the heart-lung block with trachea attached.
4. Place a plastic tracheal catheter with Luer lock connector into the trachea and tie in place. Attach an appropriately sized syringe containing the appropriate amount of wash fluid.
5. Use the syringe to slowly instill sterile wash fluid at a volume ~80% of the lung functional residual capacity into the lung until it appears to be fully extended. With gentle pressure, slowly withdraw the fluid.

   See the Strategic Planning for more information.
6. Repeat the procedure (step 5) as many times as required for the specific question being addressed.

   The first wash will contain more material from the upper respiratory tract than subsequent washes. In all cases, the components of the lavage fluid will be more dilute with each successive wash.
7. Measure the volume of lavage fluid recovered.

   In a healthy lung, one should achieve 75% recovery on the first wash and close to 100% recovery on subsequent washes. In a damaged lung, recovery may be less. In an edematous lung, recovery may appear greater, but this is rare.
8. Store and process BALF as described (see Support Protocol)

SUPPORT PROTOCOL

PROCESSING BRONCHOALVEOLAR LAVAGE FLUID (BALF) AND ANALYSIS OF LUNG DAMAGE INDICATORS

The lavage fluid obtained from the lung should be kept cold on ice, and the cells should be separated from the fluid as quickly as possible by centrifugation (10 min at 300 × *g* is adequate). The supernatant should be kept cold (0°C) and enzymatic activities should be measured as soon as possible (i.e., within the same day). Most enzymes are too dilute in the BALF to be stable to freezing. Three enzymes commonly analyzed are lactate dehydrogenase (indicator of cell death), β-glucuronidase (indicator of macrophage activation), and alkaline phosphatase (indicator of Type II cell secretions). Descriptions of these assays can be found in standard texts (see Bergmeyer, 1983). For other, more stable analytes, the supernatant may be stored for later analyses under conditions appropriate for the analyte. The samples may be concentrated using ultrafiltration through membranes of a small pore size to enhance analytical capabilities.

Additional Materials *(also see Basic Protocol)*

BALF (see Basic Protocol or Alternate Protocols 1 or 2)

Additional reagents and equipment for counting cells (*APPENDIX 3B*)

NOTE: Keep BALF on ice at all times.

1. Measure the volume of the BALF.
2. Centrifuge 10 min at 300 × g, room temperature, to remove the cells as soon as possible and thus avoid lysis.
3. Save the supernatant on ice for later analyses. Resuspend the cell pellet in 1 ml wash fluid and save for cell counting.
4. Conduct a total (*APPENDIX 3B*) and differential cell count.

   A Wright-Giemsa type stain is commonly used (Strober et al., 1997) to allow differential counting.

5. For the differential count, record both the absolute number of each cell type and the percentage of the total number of cells (see Background Information).
6. Analyze the supernatant for enzymatic, protein, and lipid factors that are indicative of a damaged lung or of a specific stage in lung disease (see Background Information).

   Enzymatic activity must be measured immediately, because most enzymes will not be stable in the diluted state of the BALF. Care must be taken to determine the conditions for stability of each factor to be measured and appropriate precautions taken to preserve the analyte.

7. If applicable, analyze the protein expression profile by proteomic techniques (see Background Information).

COMMENTARY

Background Information

Indicators of lung damage

In toxicology studies of inhaled or instilled agents, both the degree of an induced inflammatory response and the time course of recovery from or intensification of the process can be followed by analysis of BALF. The lavage fluid is analyzed for cellular and biochemical indicators or toxicity and inflammation.

Cell counts. The total and differential cell count in BALF is an informative measure of the inflammation in the respiratory tract. The major cell type (>90%) in BALF from a healthy animal is the pulmonary macrophage. Neutrophils are rare, and an influx of these cells is a sensitive indicator of an inflammatory response. Lymphocytes are not often seen in BALF from rats, mice, and hamsters, but

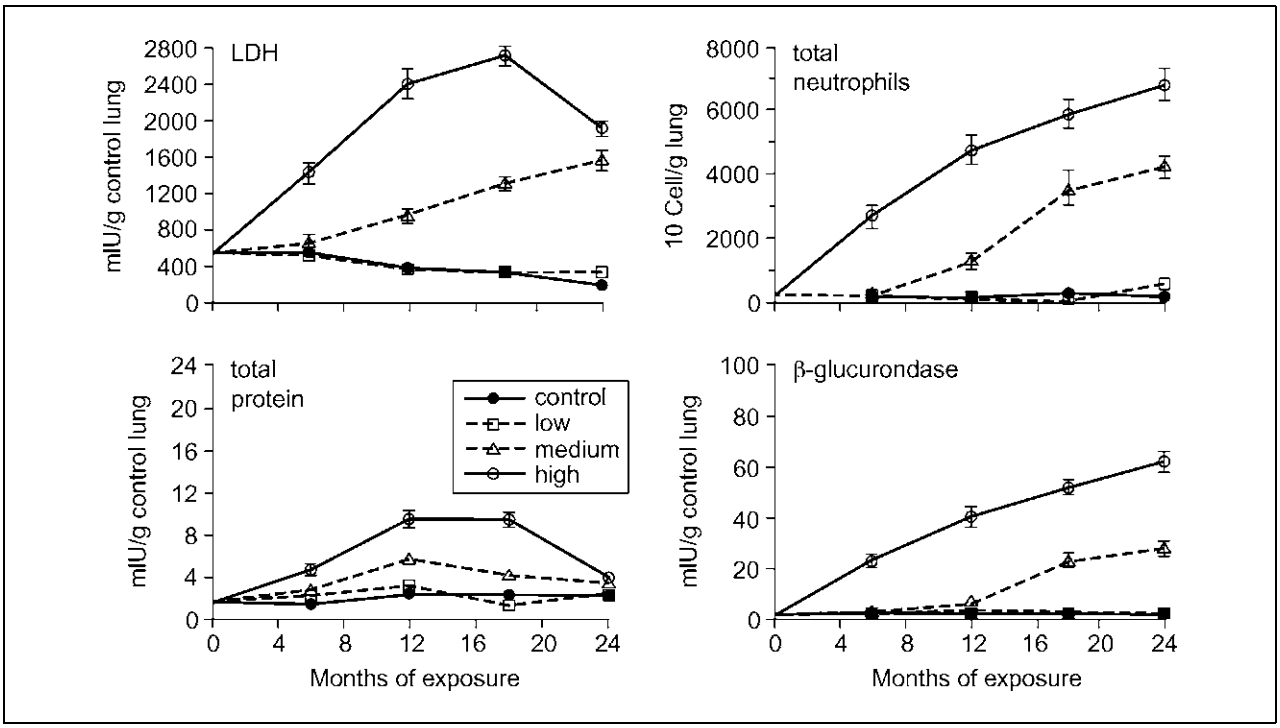

Figure 18.4.3 Bronchoalveolar lavage parameters in rats chronically exposed to diesel exhaust. Rats were exposed to diluted diesel exhaust at three levels (0.35 mg of particles/m^3, 3.5 mg/m^3, or 7.0 mg/m^3) for 24 months. Every 6 months a subset of animals was lavaged (excised lungs) and the BALF analyzed for indicators of lung damage or inflammation. The data were able to delineate a clear dose and time dependent response.

may represent up to 10% of BALF cells in larger animals such as sheep, horses, and monkeys. BALF from guinea pigs will contain eosinophils. An immune-based inflammatory response is indicated by an increase in lymphocytes or eosinophils in BALF.

Biochemical content. The biochemical content of BALF is also informative. Protein content in the lavage fluid can be used to monitor increased permeability of the alveolar-capillary barrier, which occurs in an inflammatory response. Lactate dehydrogenase is a cytoplasmic enzyme whose extracellular presence indicates cell death. β-glucuronidase activity in the extracellular fluid is a measure of activated macrophages, and alkaline phosphatase is an enzyme associated with Type II cell secretions. Proinflammatory cytokines can be measured in the lavage fluid or, as is frequently done, as secretions from cultured cells retrieved from the lavage fluid. Early biochemical mediators of pulmonary inflammation are tumor necrosis factor-α (TNF-α) and interleukin-1 (IL-1), which are cytokines released from the resident macrophages that promote the adherence of circulating inflammatory cells to the endothelium. These cytokines stimulate the release of chemoattractant factors such as IL-8 (a major chemoattractant for neutrophils in primates), macrophage inflammatory protein-2 (MIP-2, a neutrophilic chemoattractant in rodents), IL-6, and macrophage chemoattractant protein-1 (MCP-1, attracts inflammatory cells into the alveoli).

Proteomics. To measure the degree of inflammation, one need not go beyond the analysis of total and differential cell counts plus some of the biochemical parameters mentioned above; however, if mechanistic questions are to be addressed, the hypotheses to be tested will determine other pertinent analytes to be measured in BALF. A promising new approach called proteomics makes use of mass spectrometric techniques that allow analysis of the total protein expression profile (PEP) in body fluids such as BALF. Software packages allow comparison of PEP in BALF from healthy versus disease states. Such analyses may one day aid in the diagnosis and staging of disease processes in the respiratory tract, but they are not fully developed today.

Critical Parameters and Troubleshooting

Relatively few problems are encountered in this rather simple technique. If lavage of the excised lung is planned, one must be careful not to nick the lungs in removing them; lavage fluid will drain from any opening made

in the lung. One must remove the cells from the fluid as quickly and gently as possible to avoid leakage of enzymes from the lavaged cells into the supernatant. Enzymes must be assayed on the same day the fluid is collected unless prior studies have shown the enzymes to be stable under storage conditions. In studies on the response to inhaled or instilled material, it is possible that enough of the toxicant will be removed in the lavage fluid, especially if taken immediately after exposure, to inhibit assays for some of the parameters. This possibility should always be taken into consideration.

Anticipated Results

Because the volume of lavage fluid used is adjusted for the size of the lung being lavaged, if the technique used is consistent between animals, it is valid to normalize the data to the volume of recovered fluid—i.e., to use the concentration of the analyte in the BALF. If an edematous lung is lavaged, and the volume of fluid recovered is variable and greater than that instilled, one can calculate the total amount of analyte recovered (amount per volume times the volume) in order to make comparisons among the test animals. To compare data from different studies conducted in different species under different conditions, one can normalize the total amount of the analyte removed to the volume of lung washed (Henderson, 1989). An example of the type of data one might obtain with analysis of BALF in a toxicology study is shown in Fig. 18.4.3.

Time Considerations

Bronchoalveolar lavage studies involving up to 30 small animals can be completed in 1 day.

Literature Cited

Bergmeyer, H.U. (ed.) 1983. Methods of Enzymatic Analysis, 3rd edition, VCH Publishing, Weinheim, Germany.

Henderson, R.F. 1988. Use of bronchoalveolar lavage to detect lung damage. *In* Toxicology of the Lung (D.E. Gardner, J.D. Crapo, and E. J. Massaro, eds.) pp. 239-268. Raven Press, New York.

Henderson, R.F. 1989. Bronchoalveolar lavage: A tool for assessing the health status of the lung. *In* Concepts in Inhalation Toxicology (R.O. McClellan and R.F. Henderson, eds.) pp. 415-444. Hemisphere Publishing, New York.

Henderson, R.F. and Lowry, J.S. 1983. Effect of anesthetic agents on lavage fluid parameters used as indicators of pulmonary injury. *Lab. Anim. Sci.* 33:60-62.

Henderson, R.F. and Muggenburg, B.A. 1992. Bronchoalveolar lavage in animals. *In* Bronchoalveolar Lavage (R.P. Baughman, ed.) pp. 265-287. Mosby-Year Book, St. Louis.

Mauderly, J.L. 1977. Bronchopulmonary lavage of small laboratory animals. *Lab. Anim. Sci.* 27:255-261.

Rennard, S.I., Albers, R., Bleecker, E., Klech, H., Rosenwasser, L., Olivieri, D., and Sibelle, Y. 1998. Bronchoalveolar lavage: Performance, sampling procedure, processing and assessment. *Eur. Respir. J. Suppl.* 26:13S-15S.

Strober, W. 1997. Wright-Giemsa and nonspecific esterase staining of cells. *In* Current Protocols in Immunology (J.E. Coligan, A.M. Kruisbeek, D.H. Margulies, and W. Strober, eds.) pp. A.3C.1-A.3C.3. John Wiley & Sons, Hoboken, N.J.

Key References

Henderson, 1989. See above.

Reviews basic principles of the use of BALF analyses to quantitate lung responses in animals.

Rennard et al., 1998. See above.

Useful for comparing animal techniques with those used in human clinical studies.

Contributed by Rogene F. Henderson and Bruce A. Muggenburg

Lovelace Respiratory Research Institute

Albuquerque, New Mexico

Measuring Lymphocyte Transcription Factor Activity by ELISA

The primary function of the immune system is to provide host resistance to infectious microorganisms and malignant disease. This requires the complex interaction between cells via a series of biochemical and molecular events, culminating in altered gene expression. Initiation of transcription by sequence-specific DNA-binding proteins known as transcription factors (TFs) is the principle point at which the expression of most genes is regulated. Thus, an understanding of nuclear events affected by environmental toxicants and their mechanisms of action is critical to understanding toxic phenomena. For example, α,β-unsaturated aldehydes inhibit NFκB p50 DNA binding, while saturated aldehydes have no effect (Fig. 18.5.1). The level of p50 DNA binding correlates well with the level of IL-2 produced (Fig. 18.5.2).

Transcription factors affect fundamental biologic processes and have been implicated in numerous human diseases. Appropriate temporal and spatial activation of transcription factors is crucial for target cell function. It is not surprising that many new assays have been developed to improve the sensitivity and convenience of measuring transcription factor DNA-binding activity. Traditional methods utilize radiolabeled target DNA in gel-shift or electrophoretic mobility shift assays (EMSA). Even with the advancement of nonisotopic (chemiluminescent) detection, EMSA is cumbersome, not amenable to high-throughput applications, and has limited sensitivity. This unit will focus on colorimetric enzyme-linked immunosorbent assays (ELISA) to measure DNA-binding activity.

Colorimetric ELISA-based procedures have been developed to detect specific transcription factor activities in cell extracts (Shen et al., 2002). The sensitivity of ELISA can be up to ten-fold higher than electrophoretic mobility shift assays (Benotmane et al., 1997), and up to 96 reactions can be performed in 3 to 4 hr. Extracts are added to the

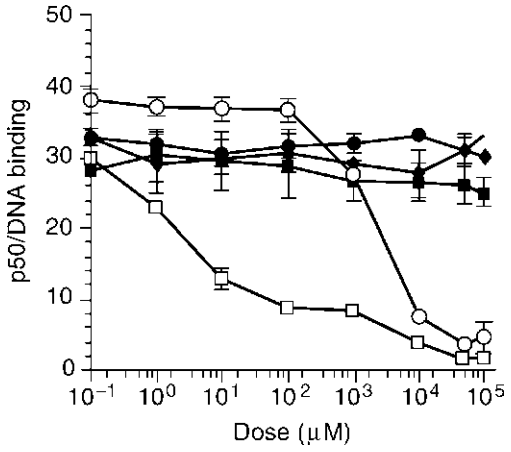

Figure 18.5.1 Inhibition of p50 DNA binding by cigarette smoke aldehydes. The ability of the various aldehydes to inhibit the interaction between recombinant p50 and the NF-κB promoter region was measured using a BD Mercury NF-κB/p50 TransFactor Kit. A saturating concentration of p50 (160 pmol) was treated with 0 to 100 mM acrolein (empty circles), crotonaldehyde (empty squares), acetaldehyde (colored squares), propionaldehyde (colored circles), or butyraldehyde (colored diamonds) and then added to wells coated with NF-κB consensus sequence (GGGGATCCC). The amount of p50 bound was measured using anti-p50, HRP-conjugated anti-rabbit IgG, and TMB and the results expressed as mOD/min. Results are the mean ±SE of two experiments.

Contributed by Jesica McCue and Brian Freed
Current Protocols in Toxicology (2004) 18.5.1-18.5.7

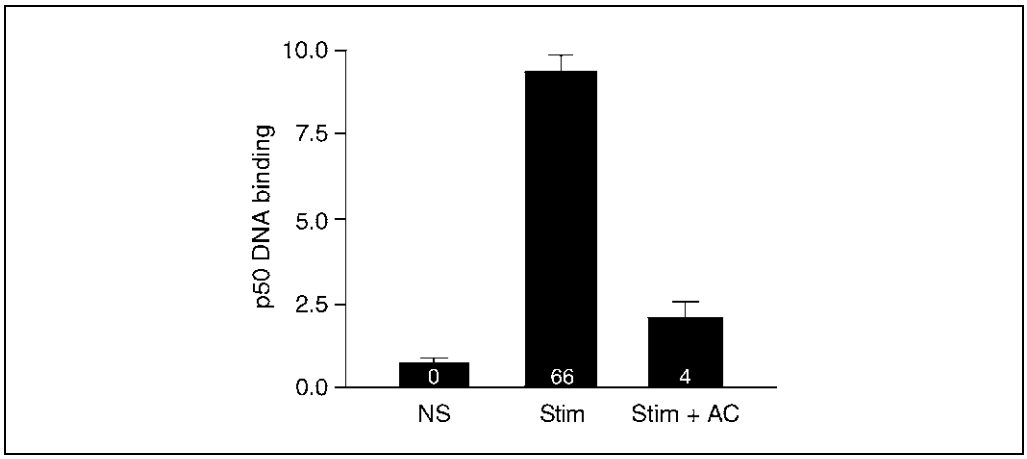

Figure 18.5.2 Acrolein blocks induction of p50 DNA activity. Jurkat T cells were treated with 10 μM acrolein (AC) for 3 hr and then stimulated with anti-CD3 plus PMA for 24 hr. Culture supernatants were analyzed for IL-2 levels, shown in white numbers as pg/ml. Nuclear extracts were prepared and assayed for p50 DNA binding using a 42-mer NF-κB consensus target sequence. NS, non-stimulated.

96-well plate precoated with a transcription factor DNA-binding consensus sequence and detected with an antibody specific to the transcription factor of interest. Thus, DNA ELISAs are easily adapted to study a large number of samples or parameters, as plates can be coated with the same DNA consensus sequence, or with DNA specific for different factors, to study multiple transcription factors in parallel. In short, ELISA provides increased speed and throughput, and allows improved sensitivity and convenience over the traditional methodologies. There are three protocols for this procedure: coat DNA to plates (see Support Protocol 1), prepare nuclear extracts (see Support Protocol 2), and perform DNA-binding ELISA (see Basic Protocol).

BASIC PROTOCOL

DNA-BINDING ELISA

To perform the ELISA, individual wells of a 96-well plate are precoated with oligonucleotides containing the DNA consensus binding sequence for a specific factor. Nuclear extracts are incubated in the wells to allow the transcription factor, if present, to bind its sequence. Unbound proteins are washed away, and primary antibody specific for that factor is added. Following incubation with horseradish peroxidase (HRP)-conjugated secondary antibody and substrate, color intensity is measured using a standard microtiter plate reader. The amount of signal detected correlates to the amount of transcription factor bound on the plate and is represented as the optical density (OD_{655}) for each sample. For quantitative results, a standard curve can be generated using purified transcription factor. As with EMSA, specificity of binding can be confirmed with mutant dsDNA (coated to wells) and competition assays (unbound wild-type dsDNA). Positive control reactions can be performed routinely to ensure reliability.

Materials

Blocking buffer (see recipe)
ELISA plate precoated with wild-type and mutant dsDNA (see Support Protocol 1)
Nuclear extract (see Support Protocol 2)
PBS (see recipe)
Wild-type competitor oligonucleotides
Wash buffer (see recipe)
Primary antibody
Secondary antibody e.g., anti-rabbit IgG-HRP or anti-mouse IgG-HRP (Clontech)

TMB substrate (Sigma)
Stop solution: 1 M H_2SO_4 (optional)
Microtiter plate reader

1. Incubate 150 µl blocking buffer per well of the precoated ELISA plate for 15 min at room temperature.
2. Prepare samples, in triplicate, by thawing nuclear extracts slowly on ice and diluting 6 µg extract to 50 µl with PBS. For background control, use 50 µl PBS alone. For competition assays, use 500 ng wild-type competitor oligonucleotide per sample.

   Extract and competitor oligonucleotide concentrations may need to be optimized (by measuring linearity of response) depending on the assay.
3. Remove blocking buffer and add 50 µl sample per well. Incubate 60 min at room temperature.
4. Wash wells three times with 150 µl wash buffer per well, incubating 4 min each wash. Decant final wash.
5. Dilute primary antibody (specific for transcription factor of interest) in blocking buffer (optimize by testing 1 to 500 ng/ml). Add 100 µl diluted primary antibody per well. Incubate 60 min at room temperature.
6. Wash wells three times with 150 µl wash buffer per well, incubating 4 min each wash. Decant final wash.
7. Dilute appropriate secondary antibody (1:1000 for anti-rabbit IgG-HRP or 1:200 for anti-mouse IgG-HRP) in blocking buffer. Incubate 100 µl secondary antibody per well for 30 min at room temperature.
8. Wash wells four times with 250 µl wash buffer per well, incubating 4 min each wash. Decant final wash.
9. Add 100 µl TMB substrate per well. Incubate 10 min at room temperature.

   Reading of plates without the addition of stop solutions allows the same wells to be read at various timepoints, which allows one to identify the optimal time for color development.
10. Measure absorbance of the plate wells at 655 nm with a microplate reader.

    If 1M H_2SO_4 is used as a stop solution (100 µl per well), read plates at 450 nm.

    The amount of signal detected correlates to the amount of transcription factor bound onto the plate and is represented as the optical density (OD_{655}) for each sample.
11. For quantitative results, generate a standard curve using purified transcription factor (1 to 100 ng).

COAT PLATES WITH DNA

SUPPORT PROTOCOL 1

DNA has a low binding affinity to unmodified microtiter plate surfaces, but immobilization of DNA onto plastic surfaces can be accomplished quickly and simply using Reacti-Bind DNA coating solution (Pierce). DNA diluted in Reacti-Bind is incubated in plates a minimum of 1 to 2 hr at room temperature. Unbound DNA is washed away using PBS and dry plates can be stored up to 1 month at 4°C. The use of ELISA plates that can be separated into eight 12-well strips (or even 96 individual wells) provides greater flexibility than standard microtiter plates.

Materials

ssDNA: consensus sequence of transcription factor of interest (e.g., BD Mercury TransFactor Kit, BD Biosciences)
TE buffer (see recipe)
Reacti-Bind DNA coating solution (Pierce)
PBS (see recipe)

ELISA plate precoated with wild-type and mutant dsDNA
13 × 100–mm glass test tube

1. Anneal ssDNA oligonucleotides (≥20 nucleotides in length) by mixing equal molar amounts of sense and anti-sense oligonucleotides and heating to 94°C. Slowly cool to room temperature and store at −20°C.
2. Incubate 1 vol (2.5 to 25 μg DNA/plate) DNA (diluted in water or TE buffer) with 1 vol Reacti-Bind DNA coating solution in a 13 × 100–mm glass test tube for 10 min at room temperature.

   The final DNA concentration should be between 0.5 and 5 μg/ml and must be empirically determined for each transcription factor.

   Reacti-Bind solution will immobilize DNA onto any plastic, including Eppendorf tubes.
3. Add 50 μl DNA per well of a 96-well, polystyrene plate. Incubate 2 hr to overnight at room temperature.
4. Wash unbound DNA with 100 μl PBS/well, remove liquid and store dry plates up to 1 month at 4°C.

SUPPORT PROTOCOL 2

PREPARE NUCLEAR EXTRACTS

To prepare nuclear extracts, washed cells are suspended in hypotonic buffer and allowed to swell (Dignam et al., 1983). Nuclei are pelleted and the cytosolic fraction is removed. Nuclei are resuspended in high-salt buffer to release soluble proteins from nuclei and then normalized with low-salt buffer. Following centrifugation, nuclear extracts are assayed for protein concentration and frozen in liquid nitrogen for storage.

Materials

Cells, e.g., PBMC (>10^6 cells)
PBS (see recipe), ice cold
Hypotonic buffer (see recipe), ice cold
High-salt buffer (see recipe), ice cold
Low-salt buffer (see recipe), ice cold
BCA or Bradford protein concentration kit (Sigma)
Liquid nitrogen
1.5-ml microcentrifuge tubes, prechilled

1. Harvest cells by Ficoll centrifugation (5 min at 500 × g, 4°C) and wash two times in ice-cold PBS. Remove and discard supernatant.
2. Add a volume of ice-cold hypotonic buffer equal to five times the cell pellet volume (e.g., 50 μl for 1 × 10^7 PBMC). Resuspend the cells gently, avoiding the production of foam. Incubate 10 min on ice. Mix gently by finger-flicking.
3. Pellet nuclei by centrifuging 10 min at 12,000 × *g*, 4°C. Carefully remove and discard supernatant (cytosolic fraction). Resuspend the nuclei pellet in a volume of ice-cold high-salt buffer equal to the original cell pellet volume (e.g., 40 μl for 1 × 10^7 PBMC). Incubate 15 min on ice.

4. Add an equal volume of ice-cold low-salt buffer (e.g., 40 μl for 1×10^7 PBMC).
5. Pellet cellular debris by centrifuging 10 min at 12,000 × *g*, 4°C.
6. Transfer supernanant (nuclear extract) to pre-chilled 1.5-ml microcentrifuge tube, discard pellet. Remove aliquot for determination of protein concentration (usually in the range of 0.25 to 1 μg/μl).

   This buffer is compatible with Bradford and BCA protein assays.
7. Snap-freeze nuclear extracts in 20- to 30-μl aliquots and store up to 6 months at −70°C. Avoid repeated freeze-thaws.

REAGENTS AND SOLUTIONS

Use Milli-Q-purified water or equivalent for the preparation of all buffers and in all protocol steps. For common stock solutions, see ***APPENDIX 2A****; for suppliers, see* ***SUPPLIERS APPENDIX****.*

Blocking buffer

1.6 g BSA (final 4%)
40 ml PBS
Store up to 6 months at −20°C

High-salt buffer

400 μl 500 mM HEPES, pH 7.9
15 μl 1 M $MgCl_2$
2.5 ml glycerol
10 μl 200 mM EDTA
840 μl 5 M NaCl
6.235 ml H_2O
Store up to 6 months at 4°C
Add fresh: 1 μl 0.5 M DTT and protease inhibitors (Sigma) per 500 μl buffer

Hypotonic buffer

400 μl 500 mM HEPES, pH 7.9
30 μl 1 M $MgCl_2$
66.7 μl 3M KCl
18.9 ml H_2O
Store up to 6 months at 4°C
Add fresh: 1 μl 0.5 M DTT, 2.5 μl NP-40, and protease inhibitors (Sigma) per 500 μl buffer

Low-salt buffer

400 μl 500 mM HEPES, pH 7.9
10 μl 200 mM EDTA
9.59 ml H_2O
Store up to 6 months at 4°C
Add fresh: 1 μl 0.5 M DTT and protease inhibitors (Sigma) per 500 μl buffer

PBS, 10 × (pH 7.2)

For 1 liter:
80 g NaCl
2 g KCl
11.5 g $Na_2HPO_4 \cdot 7H_2O$
2 g KH_2PO_4
Store up to 6 months at room temperature

TE buffer

10 mM Tris·Cl, pH 8.0
1 mM EDTA
Store up to 6 months at room temperature

Wash buffer

1 liter PBS (see recipe)
2 ml Tween-20 (final 0.2%)
Store up to 1 month at room temperature

COMMENTARY

Background Information

The regulation of gene expression in a coordinated manner and in response to various stimuli requires elaborate cellular machinery, focusing on sequence-specific DNA-binding proteins known as transcription factors (TFs). TFs control promoter activity through modification of basal transcription machinery and/or chromatin organization. The importance of these factors is demonstrated by their abundant representation in the human genome (>2000 genes code for TFs). A new classification system has been proposed grouping TFs according to their connections with signaling pathways, thereby providing a functional perspective to each TF (Brivanlou and Darnell, 2002).

Despite many similarities, each transcription factor possesses unique properties with regard to tissue expression patterns, response to receptor signals, and target gene specificity. Briefly, common factors such as NFκB, NFAT, and AP1 are known for regulating immune and inflammatory responses. Factors including LKLF, Tob, GILZ, and FOXO have been shown to participate in actively maintaining quiescence in lymphocytes, while Myc and E2F1 are the primary TFs involved in controlling cell growth, cell cycle progression, differentiation, and apoptosis. Fox3p is critical for generation of T regulatory cells. Finally, Th1:Th2 cytokine ratios are maintained by a balance of STAT4, Tbet, IRF1, IRF2,

Table 18.5.1 Troubleshooting Guidelines

Problem	Possible cause	Solution
Lack of signal or weak signal	Omission or improper preparation of reagent	Optimize dsDNA, primary antibody concentration
	Sample had less than optimal protein concentration or was mishandled	Test positive control
	Plate reader did not perform properly (i.e., UV light not warmed up)	Warm up UV light
High background	Inadequate washing	Wash four times
	Improper preparation of reagent (i.e., antibody concentrations too high)	Lower antibody concentration
	Overdeveloping	Decrease TMB incubation time and/or use stop solution
High background in sample wells	Sample concentration too high	Generate a dose response curve
	Improper dilution of antibody	Redilute antibody
Weak signal in sample wells	Sample concentration too low	Generate a dose response curve
	Improper dilution of antibody	Use more antibody

and STAT6, GATA3, respectively (for review, see Li-Weber and Krammer, 2003; Yusuf and Fruman, 2003).

Critical Parameters

This protocol uses dsDNA and antibody to detect TF activity and the results depend on the specificity of those reagents. Although TFs are sequence specific, many TFs within a family bind to the same DNA sequence. Similarly, many antibodies can cross-react with heterologous proteins. A number of controls should be performed to ensure specificity. Positive controls can include nuclear extracts or recombinant TF that have been tested and shown to have a standard amount of the desired TF DNA-binding activity. Note that a loss of DNA-binding activity can be seen with repeated freezing and thawing of these samples. Negative controls include buffer alone, nuclear extracts from cells lacking desired TF DNA-binding activity, and mutant DNA-coated wells. Samples lacking TF DNA binding activity address nonspecific antibody binding, and mutant consensus sequence wells account for nonspecific DNA binding from samples. Finally, the use of competitor DNA controls demonstrate the specificity of the DNA/protein interactions.

Troubleshooting

For troubleshooting guidelines, see Table 18.5.1.

Anticipated Results

Linearity. To ensure linearity, optimize ELISA for the specific samples by plotting a dose-response curve (0 to 30 μg nuclear extract).

Reproducibility. Due to the convenient and high-throughput nature of the ELISA, positive-control reactions (extract with known transcription factor activity or pure protein) can be performed routinely.

Specificity. As with EMSA, specificity of binding can be confirmed with mutant dsDNA (coated to wells) and competition assays (unbound wild-type dsDNA).

Sensitivity. The sensitivity of ELISA can be up to ten-fold higher than with EMSA. In some assays, as low as 1 nM pure transcription factor can be detected, but this can vary greatly. Individual results will depend upon abundance of transcription factor of interest in samples, its reactivity with target DNA coated on plate, and quality of primary antibody used.

Time Considerations

To coat plates, 2 to 24 hr is required. Plates can be prepared in advance. Store dry plates at 4°C. Preparing extracts requires 2 to 3 hr and can be prepared in advance. Store extracts at −70°C. To perform the assay, it takes 3 to 4 hr.

Literature Cited

Benotmane, A.M., Hoylaerts, M.F., Collen, D., and Belayew, A. 1997. Nonisotopic quantitative analysis of protein-DNA interactions at equilibrium. *Anal. Biochem.* 250:181-185.

Brivanlou, A.H. and Darnell, J.E. 2002. Signal transduction and the control of gene expression. *Science* 295:813-818.

Dignam, J.D., Lebovitz, R.M., and Roeder, R.G. 1983. Accurate transcription initiation by RNA polymerase II in a soluble extract from isolated mammalian nuclei. *Nucl. Acids Res.* 11:1475-1489.

Li-Weber, M. and Krammer, P.H. 2003. Regulation of IL4 gene expression by T cells and therapeutic perspectives. *Natu. Immun. Rev.* 3:534-543.

Shen, Z., Peedikayil, J., Olson, G.K., Siebert, P.D., and Fang, Y. 2002. Multiple transcription factor profiling by enzyme-linked immunoassay. *BioTechniques* 32:1168-1177.

Yusuf, I. and Fruman, D.A. 2003. Regulation of quiescence in lymphocytes. *Trends Immunol.* 24:380-386.

Contributed by Jesica McCue and Brian Freed
University of Colorado Health Sciences Center
Denver, Colorado

Measuring the Activity of Cytolytic Lymphocytes

There are two major sub-populations of lymphocytes with cytolytic activity: differentiated $CD8^+$ T cells (i.e., cytotoxic T lymphocytes or CTL) and natural killer (NK) cells. In some instances, $CD4^+$ T cells can acquire a cytolytic phenotype, but this occurs very rarely (Kagi et al., 1996). Cytolytic lymphocytes play an important role in resistance to intracellular pathogens. Specifically, CTL primarily kill host cells that are infected with viruses, whereas NK cells kill virally and bacterially infected host cells. Additionally, both CTL and NK cells recognize and kill certain types of tumor cells, and in some instances cells infected with bacteria are targets of CTL-mediated killing. This unit will focus on measuring CTL and NK cytolytic activity using an ex vivo chromium release assay.

The lysis of a target cell by NK cells and CTL requires cell-cell contact between the cytolytic lymphocyte (termed the effector cell) and the target cell. This interaction is directed by different molecules, which differ between CTL and NK cells (Russell and Ley, 2002). It is important to understand the distinctions between these two types of cells when one measures the activity of cytolytic lymphocytes. A brief overview of the mechanisms used by CTL and NK cells is provided in the following section.

CTL-mediated target cell lysis. The acquisition of killing ability by $CD8^+$ T cells requires the initial activation, clonal expansion, and differentiation of naïve $CD8^+$ T cells, which develop into CTL. In other words, naïve $CD8^+$ T cells do not have cytolytic capacity, whereas differentiated $CD8^+$ T cells (CTL) have acquired this ability. CTL recognize and react to a large variety of molecules, including major and minor histocompatibility molecules and peptides expressed in the context of syngeneic MHC class I molecules. These peptides are derived from proteins expressed within the cell, often from intracellular pathogens or tumors. CTL recognize these peptide/MHC class I complexes using T cell receptors (TCR). Each $CD8^+$ T cell expresses TCR that recognize a unique peptide/MHC class I complex, which confers the specificity of the response. While only $\sim 1{:}10^5$ CTL are specific for a given peptide/MHC class I complex, $\sim$10% of T cells in the body recognize allogeneic MHC molecules; therefore, in terms of measuring CTL activity, it is often useful to exploit the higher frequency of allo-reactive CTL.

NK cell-mediated target cell lysis. In contrast to $CD8^+$ T cells, NK cells do not require prior exposure to antigen in order to acquire cytolytic activity. NK cells also lack antigen-specific receptors. Instead, the cytolytic activity of NK cells is controlled by the expression of a large family of cell surface receptors referred to as the NK gene complex (Yokoyama and Plougastel, 2003). Members of this family act as either inhibitory or stimulatory receptors. Using these receptors, NK cells distinguish healthy syngeneic cells from infected cells and tumor cells.

While this aspect of NK cell function is well accepted, the overall mechanisms that control target cell recognition by NK cells remains an active area of study, and the ligands for many NK cell receptors have yet to be identified. One well-established pathway for NK cell recognition of target cells is often referred to as the "missing self hypothesis." This model is predicated on the idea that NK cells require a constant off signal, delivered through the interaction of cell surface inhibitory receptors with MHC class I molecules on host cells. In the absence of this signal, NK cells become activated and kill the cell in which they have come in contact. This inhibitory signal would be absent, for example,

Contributed by B. Paige Lawrence
Current Protocols in Toxicology (2004) 18.6.1-18.6.27

when aberrant MHC molecules are expressed or when a cell has down-modulated MHC class I expression due to viral infection. The NK-specific target cells used in the assays described here rely on this mechanism, as the target cells do not express MHC class I, making them susceptible to NK cell–mediated lysis and resistant to killing by CTL.

The basis for the protocol described here is measuring the killing of CTL-specific or NK cell–specific targets in an in vitro chromium release assay. Measurement of CTL activity requires priming of cells to obtain a clonally expanded and differentiated population of CTL. Three separate protocols for examining the activity of cytolytic T cells are provided in this unit. Methods for measuring CTL-specific cytolytic activity following in vitro (see Basic Protocol 1) and in vivo (see Alternate Protocols 1 and 2) priming are described. In contrast to CTL, the cytolytic activity of NK cells can be measured in the absence of antigen priming, and this method is described in Basic Protocol 2.

In all of these protocols, single-cell suspensions of effector and target cells are prepared separately. The target cells are labeled with ^{51}Cr, and then the effector and target cells are cultured together. The amount of target cell lysis is determined by measuring the amount of ^{51}Cr released into the culture medium after incubation for several hours. Separate controls are included to determine the maximum amount of ^{51}Cr released, as well as spontaneous or background release from the labeled target cells. Additional controls are suggested to validate the specificity of the assay system.

There is a large variation in possible effector and target cells that can be used to examine the activity of cytolytic lymphocytes. For the protocols described here, the effector cells are derived from mouse spleen. The target cells are either spleen cells from mice that express a different MHC haplotype, virus-infected cells, or cells derived from cultured cell lines. The reader should be aware that Basic Protocol 1 and underlying principles can be easily adapted. For example, one could use other antigens for in vivo priming, use effector cells derived from another organ, or even derive effector and target cells from another species (e.g., rat).

NOTE: All protocols using live animals must first be reviewed and approved by an Institutional Animal Care and Use Committee (IACUC) and must follow officially approved procedures for the care and use of laboratory animals.

NOTE: All solutions and equipment coming into contact with living cells must be sterile and aseptic technique should be used accordingly.

NOTE: All incubations are performed in a humidified 37°C, 5% CO_2 incubator unless otherwise specified.

BASIC PROTOCOL 1

CHROMIUM RELEASE ASSAY FOR MEASURING CTL ACTIVITY FOLLOWING IN VITRO SENSITIZATION OF MOUSE SPLEEN CELLS

This protocol consists of following four separate parts: (1) effector cell sensitization (in vitro); (2) target cell preparation and labeling with ^{51}Cr; (3) collection of effector cells; and (4) chromium release assay.

Each part is conducted separately; however, target cell preparation and labeling with ^{51}Cr (∼3 hr) and collection of effector cells need to be carried out such that the time between the completion of both does not exceed 30 min.

CAUTION: When working with radioactive materials, take appropriate precautions to avoid contamination of the experimenter and the surroundings. Carry out the experiment and dispose of wastes in an appropriately designated area, following guidelines provided by the local radiation safety officer.

Materials

Stimulator/target cells (e.g., spleen cells), single-cell suspension
Control target cells (to test specificity of cytolytic activity; e.g., syngeneic spleen cells), optional
Effector cells (e.g., alloantigen-sensitized spleen cells, also called responder cells)
Control effector cells (non-sensitized spleen cells or cells that were sensitized using an irrelevant antigen)
Complete RPMI (cRMPI, see recipe)
0.5 mg/ml mitomycin C in cRPMI
Lipopolysaccharide (LPS) or concanavalin A (Con A) (both available from Sigma)
Phosphate buffered saline (PBS), sterile and low-endotoxin (e.g., GIBCO, Invitrogen)
Serum-free RPMI (sfRPMI, see recipe)
≥5 mCi/ml $Na_2{}^{51}CrO_4$, sterile, aqueous solution (10 to 35 mCi/ml and 200 to 500 mCi/mg Cr; e.g., Amersham Biosciences)
0.5% SDS (see recipe)

Coulter counter or hemacytometer
24- or 96-well flat-bottom cell culture plates
25-cm^2 tissue culture flasks or 100-mm tissue culture dishes
15-ml and 50-ml conical centrifuge tubes with screw caps (sterile, polystyrene or polypropylene; e.g., Corning or Falcon)
96-well round-bottom microtiter plates
Multi-channel micropipettor (50- to 200-µl) with disposable tips
Reagent reservoirs, disposable
12 × 75–mm glass test tubes
Gamma counter

Additional reagents and equipment for counting cells and determining viability (*APPENDIX 3B*)

Sensitize CTL

1. In a 15-ml centrifuge tube, prepare separate, single cell suspensions of spleen cells from allogeneic strains of mice,—e.g., C57Bl/6 or 129 (H-2^b) and BALB/c or DBA (H-2^d)—see Support Protocol 1 for the preparation of spleen cells.

   Spleen cells from one strain will become the effector cells. In other words, these cells will recognize and respond to the different MHC class I haplotype of the spleen cells from the allogeneic mouse strain. In culture, these cells will clonally expand and differentiate into CTL. In the context of in vitro stimulation, these cells are also referred to as the responder cells.

   Splenocytes obtained from the other strain will serve as the stimulator cells in this portion of the assay. To measure the response of the effector cells, it is necessary to prevent the stimulator cells from dividing. This can be accomplished pharmacologically, as described here, or by irradiation (3000 rad) prior to co-culture.

2. Count the cells using a hemacytometer (*APPENDIX 3E*) or Coulter counter.

3. Resuspend the responder spleen cells in cRPMI at a final concentration of 5–10 × 10^6/ml.

4. Resuspend the stimulator cells at ~1 × 10^7 cells/ml in cRPMI. Add 0.5 mg/ml mitomycin C to the stimulator cells, such that the final concentration of mitomycin C is 25 µg/ml. Incubate the cells with mitomycin C 20 min at 37°C or in a 37°C water bath.

   Mitomycin C is light sensitive, therefore if a water bath is used, the cells should be protected from light.

If irradiation is used to block cell division, substitute steps 4 and 5 with cellular irradiation and proceed to step 7.

5. Fill 15- or 50-ml tube containing stimulator cells with ~10 ml cRMPI and centrifuge 5 min at 200 × *g*, room temperature.

6. Discard the supernatant. Wash the cells four more times with 15 ml cRPMI per wash. Centrifuge to pellet the cells between each wash (as in step 5). Pipet cells up and down in the medium to improve the efficiency of washing.

   It is imperative that all mitomycin C is removed from these cells prior to co-culture with the responder spleen cells.

   If irradiation was used instead of treatment with mitomycin C, then one wash is sufficient.

7. Resuspend the washed stimulator spleen cells in cRPMI at a final concentration of 2.5–5 × 10^6/ml.

   The optimal concentration of responder and stimulator cells will vary depending on the strains of mice used. Therefore, it is necessary to conduct a small pilot study to determine the optimal concentration for this assay. A suggested titration experiment is as follows: use three concentrations of responder cells (e.g., 10, 5, and 2.5 × 10^6 cells/ml) and three concentrations of stimulator cells (e.g., 5, 2.5, and 1.25 × 10^6 cells/ml). Set up the wells such that each concentration of responder cells is co-cultured with each concentration of stimulator cells. Perform the titration in duplicate.

8. Add 1 ml of the responder cells and 1 ml of the stimulator cells to the wells of a 24-well flat-bottom cell culture plate.

   The final number of cells should not exceed 12 × 10^6 cells in a volume of 2 ml.

   At the end of this in vitro co-culture, it is necessary to recover effector cells from the wells. Therefore, one must prepare culture wells that will generate the required number of effector cells. After a 5-day culture, cellular recovery is between 50% and 90% of the total number of responder cells initially added to the culture.

   Cultures can be scaled up or down as needed, but the ratio of responder to stimulator cells and the ratio of cells to culture volume and surface area needs to remain fixed.

   Recombinant IL-2 can be added to the cultures (10 to 50 U/ml) to improve CTL generation; however, the addition of IL-2 can bypass the function of other cells (e.g., $CD4^+$ T cells).

9. Incubate the cells for 5 days at 37°C.

   Although the cultures need to be covered to maintain asceptic conditions, do not seal the lids (i.e., allow air exchange).

Prepare target cells

10. Prepare a single cell suspension of spleen cells derived from the same strain of mouse used as the stimulator cells (see Support Protocol 1 for the preparation of spleen cells).

    These cells will be used as the target cells for the in vitro CTL assay.

    (Optional) For control target cells, obtain a single cell suspension of spleen cells from a naïve mouse that is the same strain used to generate the effector (responder) cells. Label the cells with ^{51}Cr.

11. Count the cells using a hemacytometer (*APPENDIX 3B*) or Coulter counter.

12. To activate the spleen cells (in vitro) using a mitogen, resuspend the cells at 5 × 10^6/ml in cRPMI containing either ~10 mg/ml LPS or ~2 μg/ml Con A.

Quiescent splenocytes from naïve mice do not take up ^{51}Cr well and are prone to spontaneous leakage of ^{51}Cr after labeling. To avoid low maximal release and high spontaneous release in the assay, it is necessary to activate the cells prior to labeling. Alternatives to using polyclonally activated spleen cells include cell lines and tumor cells. If these are used, it is generally not necessary to treat with a mitogen prior to labeling with chromium. If cultured cell lines or tumor cells are used, they must be of the same MHC haplotype as the stimulator splenocytes.

13. Transfer the cells to a 25-cm^2 tissue culture flask containing 10 to 12 ml cRPMI medium and stand flask upright in a 37°C incubator. Incubate 48 to 72 hr.

    Alternatively, the cells can be transferred to tissue culture dishes (e.g., 100-mm dishes) in a final volume of ~10-ml medium per dish (i.e., 50×10^6 cells/dish). Culture the cells in a 37°C, 5% CO_2 humidified incubator for 48 to 72 hr prior to labeling with ^{51}Cr.

Label target cells with ^{51}Cr

14. Collect the activated spleen cells (step 13), transfer to a 15-ml conical tube, and count the cells using a hemacytometer (*APPENDIX 3B*) or Coulter counter and determine % viable cells.

15. Wash the cells one time with 10 ml sterile PBS and then one time with 10 ml sfRPMI. Centrifuge 10 min at $200 \times g$, room temperature, to pellet the cells between washes. Discard the supernatant and resuspend the cells at 1×10^7 viable cells/ml in sfRPMI.

16. In a 15-ml conical tube, add 3–5 $\times$ 10^6 cells (150 to 250 µl) and 200 µCi ^{51}Cr (dilute stock $Na_2{}^{51}CrO_4$ in sfRPMI to 2 mCi/ml and add 100 µl).

    Scale up or down as needed but keep the proportion constant. It is very important to keep the volume to a minimum. Use of excess volume will lead to poor labeling efficiency.

17. Incubate the labeled cells at 37°C for 2 hr (do not exceed 2 hr because cells will start to die). After the first hour, gently mix the cells by swirling the tube (do not vortex or invert tube).

18. Wash cells three times with cRPMI using a minimum volume of 2 to 5 ml per wash. Centrifuge cells 10 min at $200 \times g$, room temperature, to pellet cells.

    Do not reduce the number of washes or a very high spontaneous release will occur.

    Do not use a vortex or other type of mechanical mixing device. Resuspend the cells by gently pipeting up and down.

19. Determine the number of viable cells (*APPENDIX 3B*).

    Do not skip this step. Even the most careful washing procedure results in the loss of some cells.

20. Resuspend the labeled cells at 1×10^6 cells/ml in cRPMI. Dilute an aliquot (or all cells, depending on the size of the assay) to 1×10^5 cells/ml in cRPMI.

    The concentration of diluted labeled cells (i.e., target cells) can be scaled up or down depending upon the number of effector cells used in the assay, but keep the ratio the same. For example, if the assay starts with an E:T ratio of 200:1 (2×10^6 effector cells:1 $\times 10^4$ target cells), then each assay well needs 1×10^4 cells in 100 µl. If the assay starts at the same E:T ratio, but only 2×10^5 effector cells are used, then the target cells need to be diluted such that each assay well contains 1×10^3 labeled cells.

    Labeled cells can remain up to 30 min at room temperature without compromising viability. Do not place the cells at 4°C.

Collect effector cells

21. Use a 1000-µl capacity micropipettor to harvest the effector cells. Remove the nonadherent cells by gentle aspiration. Transfer cells to a 15-ml conical tube and centrifuge 5 min at 200 × *g*, room temperature. Resuspend in cRPMI.

    To increase the number of cells recovered, wash wells with 1 ml of cRPMI, however, this step must be performed with the utmost care to avoid dislodging partially adherent stimulatory cells from the well.

22. Count the cells using a hemacytometer (*APPENDIX 3B*) or Coulter counter.

23. Resuspend the effector cells in cRPMI at a concentration such that 100 µl will contain the number of cells needed for the uppermost E:T ratio.

    The cells can be maintained up to 4 hr at room temperature with no appreciable loss of cytolytic activity. Gentle resuspension every 30 min is advised.

Carry out chromium release assay

24. Using round-bottom 96-well plates, plate a series of six 2-fold dilutions in the wells, starting with 200 µl of effector cells.

    a. Starting one column to the right of the first column in the 96-well plate, add 100 µl cRPMI (i.e., add medium to columns 2 to 6 and 8 to 12).
    b. With effector cells resuspended at 20×10^6 cells/ml, add 200 µl cells to the first well in each row (column 1 or column 7). These cells will serve as the 200:1 E:T ratio.
    c. With a micropipettor (single- or 8-channel), transfer 100 µl of the cells in column 1 to column 2. Genlty pipet up and down five times to mix cells with the medium. This will create a well for the 100:1 E:T ratio.
    d. Transfer 100 µl of the cells from column 2 to column 3. Mix by pipetting up and down, and continue down the dilution series. At the last well in the series (6 or 12), be certain to discard 100 µl after mixing (i.e., when finished, all wells should contain only 100 µl of effector cells).

    Each dilution series will use half of a row across the plate. Using this system, a dilution series of effector cells from 15 separate treatment groups can be assayed on one plate. (One set of eight wells should be reserved to assess maximal and spontaneous release, see step 25). For example, if the first E:T ratio is 200:1 with 2×10^6 effector cells, then the effector cells should be resuspended at a concentration of 20×10^6 cells/ml. The following description is for a series beginning at 200:1 and ending at 6.25:1, beginning with an E:T ratio of 2×10^6 effector cells:1×10^4 target cells.

    Generally, it is not necessary to extend the series below 6.25:1.

25. Set up maximum release (MR) and spontaneous release (SR) wells as follows:

    a. For MR wells, add 100 µl of 0.5% SDS to three wells.
    b. For SR wells, add 100 µl of cRPMI to three wells.

    For assays that will require more than one 96-well plate, each plate should have MR and SR wells to control for possible variation between plates.

26. Gently resuspend ^{51}Cr-labeled target cells. Add 100 µl ^{51}Cr-labeled target cells to each well, including the MR and SR wells. Carefully centrifuge plate 2 to 3 min at 200 × *g*, room temperature.

    This step is very important because cell-cell contact is necessary to initiate target cell recognition. Failure to centrifuge the cells will result in negligible specific ^{51}Cr release.

27. Incubate cells 5 hr in a 37°C, 5% CO_2 humidified incubator. Keep a cover or lid on the plate, but do not seal it.

28. Harvest 100 µl supernatant from each well and transfer to a 12 × 75–mm glass test tube. Be careful not to aspirate cells.

    Carefully remove the plates from the incubator in the order in which they were placed into the incubator without bumping or jostling them.

29. Count samples on a gamma counter (1-min counts are generally sufficient). Use the following formula to calculate the percent cytolytic activity:

$$\%\ \text{cytolytic activity} = \left(\frac{\text{sensitized effector cell CPM} - \text{control effector cell CPM}}{(\text{MR} - \text{SR})} \right) \times 100$$

    where CPM stands for counts per minute.

CHROMIUM RELEASE ASSAY FOR MEASURING CTL ACTIVITY FOLLOWING IN VIVO SENSITIZATION WITH ALLOGENEIC CELLS

ALTERNATE PROTOCOL 1

CTL can be generated in vivo using a large variety of antigens. Injection of allogeneic tumor cells and viral infection are the two most commonly used methods. This protocol is similar to Basic Protocol 1 and consists of four parts: (1) effector cell sensitization (in vivo: 9 to 10 days); (2) target cell preparation and labeling with ^{51}Cr; (3) collection of effector cells; and (4) chromium release assay.

Each of these parts is conducted separately; however, target cell preparation and collection of effector cells need to be carried out such that the time between the completion of these parts does not exceed 30 min. The chromium release assay is conducted as described in Basic Protocol 1. The steps described here pertain to the generation of CTL using P815 tumor cells. The sensitization of CTL using influenza virus is described in Alternate Protocol 2.

This procedure requires the propagation of P815 mastocytoma cells in DBA (H-2^d) mice. To generate CTL, P815 cells are injected into C57Bl/6 (H-2^b) mice. Spleen cells isolated from sensitized C57Bl/6 mice will have P815-specific CTL, with the maximum frequency of these CTL and peak cytolytic activity 9 to 10 days after sensitization.

CAUTION: When working with radioactive materials, take appropriate precautions to avoid contamination of the experimenter and the surroundings. Carry out the experiment and dispose of wastes in an appropriately designated area, following guidelines provided by the local radiation safety officer.

Materials

DBA mouse (see Support Protocol 2)
Target cells (e.g., a single-cell suspension of P815 mastocytoma cells; ATCC no. TIB-64)
Hank's balanced salt solution (HBSS, e.g., GIBCO, Invitrogen; see recipe)
C57Bl/6 mice
Phosphate buffered saline (PBS), sterile and low-endotoxin (e.g., GIBCO, Invitrogen)
Serum-free RPMI (sfRPMI, see recipe)
≥5 mCi/ml $Na_2{}^{51}CrO_4$ sterile, aqueous solution (10 to 35 mCi/ml and 200 to 500 mCi/mg Cr; e.g., Amersham Biosciences)
Control target cells (e.g., syngeneic spleen cells), optional
Complete RPMI (cRMPI, see recipe)
Effector cells (e.g., P815-sensitized spleen cells; see Support Protocol 1)

Control effector cells (non-sensitized spleen cells or cells that were sensitized using an irrelevant antigen)

15- and 50-ml conical centrifuge tubes with screw caps (sterile, polystyrene or polypropylene; e.g., Corning, Falcon)

26-G × 1/2-in. needle and 1-ml syringe

Additional reagents and equipment for counting cells (*APPENDIX 3B*), and chromium release assay (see Basic Protocol 1)

Sensitize CTL

1. Using a 50-ml centrifuge tube, collect ascites fluid from a DBA mouse (see Support Protocol 2 for the in vivo maintenance and passaging of P815 cells in the peritoneal cavity of DBA mice).
2. Centrifuge cells 10 min at 200 × *g*, room temperature, to remove ascites fluid.
3. Wash the P815 cells once by gently resuspending in 25 ml HBSS. Repeat step 2.
4. Resuspend cells in 25 ml HBSS. Remove an aliquot to determine cell count and viability (using trypan blue and hemacytometer; *APPENDIX 3B*). Adjust to a final concentration of 2×10^7 viable cells/ml in HBSS.
5. Inject C57Bl/6 mice (i.p.) with 0.5 ml of P815 tumor cells (i.e., 1×10^7 cells) using a 26-G × 1/2-in. needle attached to a 1-ml syringe.

   The maximum frequency of P815-specific CTL and peak cytolytic activity in the spleen of sensitized C57Bl/6 mice occurs 9 to 10 days after sensitization (i.e., 9 to 10 days after P815 cells are injected).

Prepare target cells

6. Acquire a single-cell suspension of P815 cells (as described in steps 1 through 4) and place into a 15-ml conical centrifuge tube.

   Steps 6 to 16 take ~3 hr. It is important to coordinate this procedure with the isolation of effector cells such that the time between labeling of the target cells and plating with effector cells does not exceed 30 min.

   It is advisable to start with at least two times the number of cells needed for the assay.

   Collecting P815 cells from a DBA host 7 to 8 days after the injection of cells generally results in the recovery of 5–7 × 10^8 viable P815 cells.

7. Wash cells one time with 10 ml sterile PBS and then one time with 10 ml sfRPMI. Centrifuge 10 min at 200 × *g*, room temperature, to pellet the cells between washes.
8. Resuspend cells at 2×10^7 viable cells/ml in sfRPMI.
9. In a 15-ml conical tube, add 3–5 × 10^6 P815 cells (150 to 250 µl) and 200 µCi ^{51}Cr (dilute ≥5 mCi/ml $Na_2{}^{51}CrO_4$ stock in sfRPMI to 2 mCi/ml, then add 100 µl).

   Scale up or down as needed but keep the proportion constant.

   It is very important to keep the volume to a minimum. Use of excess volume will lead to poor labeling efficiency.

   (Optional) For control target cells, one can use any type of cell or cell line that is not from an H-2^d mouse strain. The authors recommend to prepare a single-cell suspension of spleen cells from a naïve C57Bl/6 mouse and label with ^{51}Cr using this protocol.

10. Incubate labeled cells 2 hr at 37°C (do not exceed 2 hr because cells start to die). After the first hour, gently mix the cells by swirling the tube (do not vortex or invert tube).

11. Wash the cells three times with cRPMI using a minimum volume of 2 to 5 ml per wash. Centrifuge cells 10 min at 200 × *g*, room temperature, to pellet cells.

    Do not reduce the number of washes or a very high spontaneous release will occur.

    Do not use a vortexer or other type of mechanical mixing device. Resuspend the cells by gently pipeting up and down.

12. Determine the number of viable cells (*APPENDIX 3B*).

    Do not skip this step. Even the most careful washing procedure results in the loss of some cells.

13. Resuspend the labeled cells at 1×10^6 cells/ml in cRPMI.

14. Dilute an aliquot (or all cells, depending on the size of the assay) to 1×10^5 cells/ml in cRPMI.

    The concentration of diluted labeled cells (i.e., target cells) can be scaled up or down depending upon the number of effector cells used in the assay, but keep the ratio the same. For example, if the assay starts with an E:T ratio of 200:1 (2×10^6 effector cells:1 $\times 10^4$ target cells), then each assay needs 1×10^4 cells in 100 µl. If the assay starts at the same E:T ratio, but only 2×10^5 effector cells are used, then the target cells need to be diluted such that each assay well contains 1×10^3 labeled cells.

    Labeled cells can remain up to 30 min at room temperature without compromising viability. Do not place cells at 4°C.

Collect effector cells

15. Prepare a single-cell suspension of spleen cells from sensitized and naïve C57Bl/6 mice (see Support Protocol 1).

    The optimal time for measuring P815-specific cytolytic activity is 9 to 10 days after sensitization.

16. Count the cells using a hemacytometer (*APPENDIX 3B*) or Coulter counter.

17. Resuspend the spleen cells in cRPMI at a concentration such that 100 µl contains the number of cells needed for the uppermost E:T ratio.

    For the instructions provided below, the effector cells are resuspended at a final concentration of 2×10^7/ml.

Perform chromium release assay

18. Follow Basic Protocol 1, steps 24 to 29.

CHROMIUM RELEASE ASSAY FOR MEASURING CTL ACTIVITY FOLLOWING IN VIVO SENSITIZATION WITH INFLUENZA A VIRUS

ALTERNATE PROTOCOL 2

Virus-specific CTL are generated when mice are exposed to human influenza viruses. Generally, this experimental model system involves intranasal inoculation with murine-adapted strains of human influenza A virus, leading to a robust response in the lung and lymph nodes that drain the respiratory tract. This paradigm requires the use of live virus, which has many benefits as an experimental model, including relevance to human health, activation of multiple components of the immune system, and others. The primary disadvantage is that it requires the handling and use of an infectious human pathogen, which limits the ability of many laboratories to use this system.

As an alternative to using live virus, CTL can be induced by the i.p. injection of inactivated virus, which sensitizes virus-specific $CD8^+$ T cells in the spleen (Nonacs et al., 1992; Kos and Engleman, 1996; Cho et al., 2003). Thus, by injecting inactivated virus, one can sensitize animals to influenza virus and measure virus-specific CTL activity in a system in which an infectious agent and biological safety level (BSL)-2 laboratory are not needed.

Another advantage of administering the virus by i.p. injection is that the virus does not compromise the overall survival of the host.

The disadvantage of using inactivated virus instead of infectious virus is that some of the other immune pathways stimulated during infection are absent. Therefore, i.p. injection of virus should not be considered a model of infection, nor can it be used to correlate changes in the activity of CTL with host resistance. In fact, the i.p. injection of live influenza virus does not model infection because murine-adapted strains of human influenza A viruses cannot replicate in the peritoneal cavity. Thus, i.p. administration elicits an immune response but not the pathological sequelae that accompany infection of the respiratory tract with infectious virus. If an experimental system warrants testing the activity of cytotoxic lymphocytes in the context of host resistance, then infectious virus should be administered intranasally. This route leads to a robust CTL response in the lung and the lymph nodes that drain the pulmonary cavity, and CTL activity can be measured in lung, bronchoalveolar lavage cells, and peribronchiolar lymph nodes (Warren et al., 2000; Mitchell and Lawrence, 2003a,b). This approach requires the handling of infectious virus using BSL-2 facilities and laboratory safety practices appropriate to handling pathogens of this nature. Readers who are unfamiliar with growth, purification, and handling of influenza viruses and the requirements for a BSL-2 laboratory are referred to Barrett and Inglis (1985) and Biosafety in Microbiological and Biomedical Laboratories (see Internet Resources).

Stimulation of CTL by i.p. injection of influenza virus is described in this protocol. To measure the activity of virus-specific cytolytic activity in the spleen, it is necessary to first expose the mouse to influenza A virus and then culture isolated spleen cells for 5 days with virus-infected cells. The in vitro re-stimulation is necessary because it amplifies the size of the virus-specific CTL pool such that it can be measured by the chromium release assay. The overall protocol is similar to Alternate Protocol 1 and consists of the following four parts: (1) effector cell sensitization (in vivo 5 to 9 days; in vitro 5 days); (2) target cell preparation and labeling with ^{51}Cr; (3) collection of effector cells; and (4) chromium release assay.

Each of these parts is conducted separately; however, target cell preparation (~4 hr) and effector cell collection need to be carried out such that the time between the completion of target cell preparation and effector cell collection does not exceed 30 min. The chromium release assay is conducted as described in Basic Protocol 1.

CAUTION: When working with radioactive materials, take appropriate precautions to avoid contamination of the experimenter and the surroundings. Carry out the experiment and dispose of wastes in an appropriately designated area, following guidelines provided by the local radiation safety officer.

Materials

Influenza A virus stock (mouse-adapted, inactivated, e.g., SPAFAS/Charles River)
Phosphate buffered saline (PBS), sterile and low-endotoxin (e.g., GIBCO)
Mice
Effector cells (i.e., spleen cells from an infected mouse; see Support Protocol 1)
Control effector cells (non-sensitized spleen cells or cells from a mouse that was sensitized using an irrelevant antigen)
Complete RPMI (cRMPI, see recipe)
Serum-free RPMI (sfRPMI, see recipe)
0.5 mg/ml mitomycin C in cRPMI
Target cells (i.e., virus-infected or viral peptide–pulsed cells, e.g., MC57G cells, ATCC# CRL-2295; see Support Protocol 4)

Control target cells (e.g., ^{51}Cr-labeled MC57G cells that were not exposed to virus or viral peptide), optional

≥5 mCi/ml $Na_2{}^{51}CrO_4$ sterile, aqueous solution (10 to 35 mCi/ml and 200 to 500 mCi/mg Cr; e.g., Amersham Biosciences)

0.5% SDS (see recipe)

15- and 50-ml conical centrifuge tubes with screw caps (sterile, polystyrene or polypropylene; e.g., Corning or Falcon)

24-well tissue culture plates

Beckman Allegra GS-6 (or equivalent) refrigerated centrifuge with swinging bucket rotor

20-, 200-, and 1000-µl micropipettors with disposable tips

96-well U-bottom plates

12 × 75–mm glass test tubes

Gamma counter

Additional reagents and equipment for counting cells (*APPENDIX 3B*)

Sensitize effector cells

1. Inject (i.p.) mice (e.g., C57Bl/6, H-2^b) with 500 µl inactivated influenza A virus diluted in PBS.

   Spleen cells isolated from sensitized C57Bl6 mice will have virus-specific CTL, with the maximum frequency of these CTL and peak cytolytic activity 8 to 10 days after sensitization. These cells can be detected at the time of sacrifice using flow cytometry; however, to measure virus-specific cytolytic activity by chromium release assay, it is necessary to further expand this population of cells in vitro.

   The optimal concentration of virus used will vary depending on the strains of virus and mice used. It is therefore necessary to conduct a small pilot study to determine the optimal dose for this assay. A suggested titration experiment is as follows: use four inocula of virus (e.g., 250, 500, 1000, and 2000 HAU/mouse). Perform the titration in triplicate.

   Recommended strains of murine-adapted human influenza virus include the following: A/HKx31, A/NT60/68, A/WSN/33, and A/PR8/34. These strains are suggested because in immunocompetent mice, i.p. administration has been previously shown to induce a CTL response in the spleen (Nonacs et al., 1992; Kos and Engleman, 1996; Cho et al., 2003).

2. Eight to ten days after injection with virus, sacrifice the mice and prepare separate, single cell suspensions of spleen cells from each treated mouse (see Support Protocol 1 for the preparation of spleen cells). To obtain control effector cells, sacrifice a naïve mouse (or a mouse that was sensitized with an irrelevant antigen).

3. Count the cells using a hemacytometer (*APPENDIX 3B*) or Coulter counter.

4. Resuspend the spleen cells in cRPMI at a final concentration of 1–2 × 10^7/ml.

   The cells prepared in this portion of the assay will serve to stimulate the proliferation of the virus-specific CD8$^+$ T cells in vitro, permitting the expansion of this pool for use in a chromium release assay. It is necessary to prevent the stimulator cells from dividing in this co-culture. This can be accomplished pharmacologically, as described here, or by irradiation (3000 rad) prior to co-culture.

5. Prepare a single cell suspension of spleen cells from a naive syngeneic mouse.

   An alternative to using syngeneic spleen cells is to use a dendritic cell (DC) cell line (Warren et al., 2000; Mitchell and Lawrence, 2003a,b). The DC cell line must be derived from a mouse that expresses the same MHC haplotype as the mice that were sensitized with influenza virus.

6. Wash the cells two times with sfRPMI. Centrifuge cells 10 min at 200 × *g*, room temperature. Remove and discard the medium.

7. Resuspend the washed cells at 2×10^6/ml in sfRPMI.

   Usually 20–50 $\times$ 10^6/(10 to 25 ml) cells is necessary to set up cultures for the in vitro restimulation of spleen cells from virus-sensitized mice.

8. Add influenza virus stock such that the final concentration is 300 to 500 HAU/ml. Incubate cells with virus 3 hr in a 37°C incubator. Gently mix the cells at 60-min intervals.

   Do not use medium with serum during this step because FBS contains inhibitors of viral infection.

   Do not exceed 3 hr or the cells will start to die.

9. After exposure to virus, centrifuge (as in step 6) the infected stimulator cells. Discard the supernatant and resuspend the pelleted cells at $\sim 1 \times 10^7$ cells/ml in cRPMI. Add 0.5 mg/ml mitomycin C to the stimulator cells, such that the final concentration of mitomycin C is 25 μg/ml. Incubate the cells with mitomycin C for 20 min at 37°C in an incubator or water bath.

   Mitomycin C is light sensitive. If a water bath is used for this incubation, the cells should be protected from light.

   If irradiation is used to block cell division, substitute step 9 with cellular irradiation and proceed to step 11.

10. Fill the 15-ml tube containing stimulator cells with cRPMI and centrifuge 5 min at $200 \times g$, room temperature.

11. Discard the supernatant. Wash the cells four additional times with 15 ml of cRPMI per wash. Centrifuge (as in step 10) to pellet the cells between each wash. Pipet cells up and down in the medium to improve the efficiency of washing, as it is imperative that all mitomycin C is removed from these cells prior to co-culture with the responder spleen cells.

    If irradiation was used rather than treatment with mitomycin C, then one wash is sufficient.

12. Resuspend the washed stimulator spleen cells in cRPMI at a final concentration of $0.5–1 \times 10^7$ cells/ml.

13. Set up in vitro cultures in a 24-well tissue culture plate. Combine 2×10^6 infected, mitomycin C–treated spleen cells (or cultured DC) with 4×10^6 spleen cells from each animal in the experiment (6×10^6 cells in 2 ml final volume).

    At the end of this in vitro co-culture, it is necessary to recover effector cells from the wells. Therefore, one must prepare culture wells that will generate the required number of effector cells. After a 5-day culture, cellular recovery is between 50% and 90% of the total number of responder cells initially added to the culture.

    Cultures can be scaled up or down as needed, but the ratio of responder to stimulator cells and the ratio of cells to culture volume and surface area needs to remain fixed.

    Recombinant IL-2 can be added to the cultures (10 to 50 U/ml) to improve CTL generation, however, the addition of IL-2 can bypass the function of other cells (e.g., $CD4^+$ T cells).

14. Incubate the cells for 5 days at 37°C.

    Although the cultures need to be covered to maintain asceptic conditions, do not seal the lids (i.e., allow air exchange).

Prepare target cells and label with ^{51}Cr

15. Acquire a single cell suspension of MC57G cells (see Support Protocol 4 for the growth and maintenance of MC57G cells) and place into a 15-ml conical centrifuge tube.

    It is advisable to start with at least two times the number of cells needed for the assay.

    The best targets for H-2D^b-infected mice are MC57G fibroblasts, although EL-4 cells will also work. Syngeneic splenocytes should be avoided because they have been reported to give highly variable results.

16. Wash cells one time with sterile PBS and then one time with sfRPMI. Centrifuge 10 min at 200 × *g*, room temperature, to pellet the cells between washes.

17. Resuspend the MC57G cells at 1–2 × 10^7 viable cells/ml in sfRPMI.

    It is essential that the in vitro infection be conducted in the absence of serum in the medium because FBS contains enzymes that will inhibit the infection of the cells by influenza viruses.

18. Set up the infection and labeling in 15-ml polypropylene tubes by adding the following items to the tube:

    2 × 10^6 MC57G cells (in 200 µl)
    virus or peptide in 50 µl
    200 µCi ^{51}Cr in 100 µl (dilute ≥5 mCi/ml $Na_2{}^{51}CrO_4$ stock in sfRPMI to 2 mCi/ml).

    It is advisable to conduct a preliminary titration experiment to determine the dose of virus or viral peptide. Generally, 300 to 500 HAU/ml virus is used for in vitro infection or a final concentration of 1 µM nucleoprotein (NP) peptide.

    The final volume for this labeling is 350 µl for 2 × 10^6 cells. Scale up or down as needed but keep the proportion constant.

    It is very important to keep the volume to a minimum. Use of excess volume will lead to poor labeling efficiency.

    (Optional) For control target cells, add 50 µl sfRPMI in place of virus or viral peptide and label with ^{51}Cr using this protocol.

19. Incubate the labeled cells 2 hr at 37°C (do not exceed 2 hr because cells will start to die). After the first hour, gently mix the cells by swirling the tube (do not vortex or invert tube).

20. Wash cells five times with cRPMI using a minimum volume of 2 to 5 ml per wash. Centrifuge cells 10 min at 200 × *g*, room temperature, to pellet cells.

    Do not reduce the number of washes because a very high spontaneous release will occur.

    Do not use a vortexer or other type of mechanical mixing device. Resuspend the cells by gently pipeting up and down.

21. Determine the number of viable cells (*APPENDIX 3B*).

    Do not skip this step. Even the most careful washing procedure results in the loss of some cells.

22. Resuspend the labeled cells at 1 × 10^6 cells/ml in cRPMI.

23. Dilute an aliquot (or all cells, depending on the size of the assay) to 1 × 10^5 cells/ml in cRPMI.

The concentration of diluted labeled cells (i.e., target cells) can be scaled up or down depending upon the number of effector cells used in the assay, but keep the ratio the same. For example, if the assay starts with an E:T ratio of 200:1 (2×10^6 effector cells:1 $\times 10^4$ target cells), then each assay well will need 1×10^4 cells in 100 µl. If the assay starts at the same E:T ratio, but only 2×10^5 effector cells are used, then the target cells need to be diluted such that each assay well contains 1×10^3 labeled cells.

Labeled cells can remain up to 30 min at room temperature without compromising viability. Do not place cells at 4°C.

Collect effector cells

24. Use a 1000-µl capacity micropipettor to gently harvest the nonadherent effector cells by aspiration. Transfer cells to a 15-ml conical tube and centrifuge cells 5 min at 200 × *g*, room temperature. Resuspend in cRPMI.

    To increase the number of cells recovered, wells can be washed with 1 ml of medium, however, this step must be performed with the utmost care to avoid dislodging partially adherent cells from the well.

25. Count the cells using a hemacytometer (*APPENDIX 3B*) or Coulter counter.

26. Resuspend the effector cells in cRPMI at a concentration such that 100 µl will contain the number of cells needed for the uppermost E:T ratio.

    The cells can be maintained up to 4 hr at room temperature with no appreciable loss of cytolytic activity. Gentle resuspension every 30 min is advised.

Perform chromium release assay

27. Using 96-well U-bottom plates, plate a series of six two-fold dilutions in the wells, starting with 200 µl of effector cells. Each dilution series will use half of a row across the plate. Using this system, a dilution series of effector cells from 15 separate treatment groups can be assayed on one plate. (One set of eight wells should be reserved to assess maximal and spontaneous release, see step 28). For example, if the first E:T ratio is 200:1 with 2×10^6 effector cells, then the effector cells should be resuspended at a concentration of 20×10^6 cells/ml. The following description is for a series beginning at 200:1 and ending at 6.25:1, beginning with an E:T ratio of 2×10^6 effector cells:1×10^4 target cells.

    a. Starting one column to the right of the first column in the 96-well plate, add 100 µl cRPMI (i.e., add medium to columns 2 to 6 and 8 to 12).
    b. With effector cells resuspended at 20×10^6 cells/ml, add 200 µl cells to the first well in each row (column 1 or column 7) to serve as the 200:1 E:T ratio.
    c. With a micropipettor (single or 8-channel), transfer 100 µl of the cells in column 1 to column 2. Genlty pipet up and down five times to mix cells with the medium to create a well for the 100:1 E:T ratio.
    d. Transfer 100 µl of the cells from column 2 to column 3. Mix by pipetting up and down, and continue down the dilution series. At the last well in the series, be certain to discard 100 µl after mixing (i.e., when finished, all wells should contain only 100 µl of effector cells).

    Generally, it is not necessary to extend the series below 6.25:1.

28. Set up maximum release (MR) and spontaneous release (SR) wells as follows:

    a. For MR wells, add 100 µl of 0.5% SDS to three wells.
    b. For SR wells, add 100 µl of cRPMI to three wells.

    For assays that will require more than one 96-well plate, each plate should have MR and SR wells to control for possible variation between plates.

29. Gently resuspend ^{51}Cr-labeled target cells. Add 100 µl ^{51}Cr-labeled target cells to each well, including the MR and SR wells. Carefully centrifuge plate 2 to 3 min at 200 × *g*.

    This step is very important because cell-cell contact is necessary to initiate target cell recognition. Failure to centrifuge the cells will result in negligible specific ^{51}Cr release.

30. Incubate cells 5 hr at 37°C. Keep a cover or lid on the plate, but do not seal it.

31. Harvest 100 µl supernatant from each well and transfer to a 12 × 75–mm glass test tube. Be careful not to aspirate cells.

    Carefully remove the plates from the incubator in the order in which they were placed into the incubator without bumping or jostling them.

32. Count samples on a gamma counter (1-min counts are generally sufficient). Use the following formula to calculate the percent cytolytic activity:

$$\%\ \text{cytolytic activity} = \left(\frac{\text{sensitized effector cell CPM} - \text{control effector cell CPM}}{(\text{MR} - \text{SR})} \right) \times 100$$

    where CPM stands for counts per minute.

CHROMIUM RELEASE ASSAY FOR MEASURING NK CELL ACTIVITY

BASIC PROTOCOL 2

The cytolytic activity of NK cells is an innate function of these cells; however, cytolytic activity can be further boosted by the addition of NK cell stimulatory factors. A common reagent used to stimulate NK cell cytolytic activity is polyinosinic acid-polycytidylic acid (poly I:C). Poly I:C stimulates interferon production, which in turn stimulates NK cells. Thus, there are three ways to measure NK cell cytotoxic activity: (1) native activity, (2) in vitro–boosted activity, and (3) in vivo–boosted activity. All three of these options are described in this protocol. For any of these three options, the fundamental protocol consists of two separate components: (1) preparing target cell and labeling with ^{51}Cr, and (2) preparing effector cell and assay set-up.

Steps 1 through 7 take ~3 hr. It is important to coordinate this procedure with the isolation of effector cells such that the time between labeling of the target cells and plating with effector cells does not exceed 30 min. Yac-1 murine lymphoma cells are the prototype tumor target cells to test for murine NK cell cytolytic activity.

CAUTION: When working with radioactive materials, take appropriate precautions to avoid contamination of the experimenter and the surroundings. Carry out the experiment and dispose of wastes in an appropriately designated area, following guidelines provided by the local radiation safety officer.

Materials

Target cells (e.g., a single cell suspension of Yac-1 tumor cells, ATCC no. TIB-160; see Support Protocol 3)
Yac-1 growth medium (see recipe)
Control target cells (to test specificity of cytolytic activity; e.g., syngeneic spleen cells), optional
Phosphate buffered saline (PBS), sterile and low-endotoxin (e.g., GIBCO, Invitrogen)
Complete RPMI (cRMPI, see recipe)
Serum-free RPMI (sfRPMI, see recipe)
≥5 mCi/ml $Na_2{}^{51}CrO_4$ aqueous solution (10 to 35 mCi/ml and 200 to 500 mCi/mg Cr; Amersham Biosciences)

Effector cells (spleen cells; see Support Protocol 1)
Control effector cells (e.g., a single cell suspension of thymocytes from a syngenic mouse)
0.5% SDS (see recipe)
500 μg/ml polyinosinic acid-polycytidylic acid (poly I:C) in HBSS or PBS, optional
25-cm^2 culture flasks
15- and 50-ml conical centrifuge tubes with screw caps (sterile, polystyrene or polypropylene; e.g., Corning, Falcon)
96-well round-bottom microtiter plates
Beckman Allegra GS-6 (or equivalent) refrigerated centrifuge with swinging bucket rotor
12 × 75–mm glass test tubes
Gamma counter
Additional reagents and equipment for counting cells (*APPENDIX 3B*), and chromium release assay (see Basic Protocol 1)

Prepare target cells and label with ^{51}Cr

1. Twenty-four hours prior to the assay, passage cultured Yac-1 cells, and plate at 5 × 10^6 per 25-cm^2 flask in Yac-1 growth medium (see Support Protocol 3 for the growth and maintenance of Yac-1 cells).

   Use only Yac-1 cells that are in log phase growth, otherwise the cells may not label well with ^{51}Cr.

2. On the day of the assay, acquire a single-cell suspension of Yac-1 cells and place into a 15-ml conical centrifuge tube.

   It is advisable to start with at least two times the number of cells needed for the assay.

3. Wash cells one time with sterile PBS and then one time with cRPMI. Centrifuge 10 min at 200 × *g*, room temperature. to pellet the cells between washes. Discard supernatant.

4. Label the pelleted Yac-1 target cells using the following ratio: for 5 × 10^6 Yac-1 cells, add 200 μl sfRPMI and 200 μCi ^{51}Cr (dilute ≥5 mCi/ml $Na_2{}^{51}CrO_4$ stock in cRPMI to 2 mCi/ml, then add 100 μl). Incubate 60 min at 37°C.

   Scale up or down as needed but keep the proportion constant. It is very important to keep the volume to a minimum. Use of excess volume will lead to poor labeling efficiency.

5. Wash cells two times with Yac-1 growth medium by centrifuging 10 min at 200 × *g*, room temperature.

6. Resuspend cells with 10 ml Yac-1 growth medium and incubate 30 min at 37°C to allow nonspecific leakage of ^{51}Cr. Repeat wash as in step 5.

7. Resuspend cells in 5-ml cRPMI and determine cell concentration using a hemacytometer (*APPENDIX 3B*). Prepare a cell suspension of 1 × 10^5/ml in cRPMI.

Prepare effector cell and set up assay

For native NK cytotoxicity

8a. Prepare a single cell suspension of spleen cells from mice (see Support Protocol 1). Prepare a single-cell suspension of thymocytes similar to that of the splenocytes, without the lysis of red blood cells.

   The spleen cells will provide the NK cells and the thymocytes will serve as the control effector cells (i.e., there is no NK cell cytolytic activity in a population of thymocytes).

9a. Dilute the effector cells (i.e., spleen and thymus cells) and then plate into 96-well round-bottom well tissue culture plates in triplicate using the following steps:

a. Start with a cell suspension of 1.2×10^7 in 600 µl in a 12 × 100–mm culture tube,

b. In triplicate wells of a 96-well plate, add 100 µl of cells from step a,

These cells will serve as the effector cells for the 200:1 E:T ratio.

c. To the cells remaining in the culture tube(s), add 300 µl cRPMI, mix by gentle vortexing, and add 100 µl of these cells to three separate wells,

These cells will serve as the effector cells for the 100:1 E:T ratio.

d. Repeat step c two additional times, to generate samples at E:T ratios of 50:1 and 25:1, respectively.

10a. Set up the maximum release (MR) and spontaneous release (SR) wells as follows:

a. for MR wells, add 100 µl of 0.5% SDS to 3 wells,

b. for SR wells, add 100 µl of cRPMI to 3 wells.

For assays that will require more than one 96-well plate, each plate should have MR and SR wells to control for possible variation between plates.

11a. Gently resuspend the ^{51}Cr-labeled Yac-1 cells. Add 100 µl (1×10^4) ^{51}Cr-labeled target cells to every well, including MR and SR wells.

12a. Carefully centrifuge the plate 2 to 3 min at 200 × *g*, room temperature.

This step is very important because cell-cell contact is necessary to intitiate target cell recognition. Failure to centrifuge the cells will result in negligible specific ^{51}Cr release.

13a. Incubate cells 4 hr at 37°C. Keep a cover or lid on the plate, but do not seal it.

14a. Harvest 100 µl supernatant from each well and transfer to a 12 × 75–mm glass test tube. Be careful not to aspirate cells.

Remove the plates from the incubator in the order in which they were placed into the incubator without bumping or jostling them.

15a. Count samples on a gamma counter (1-min counts are generally sufficient). Use the following formula to calculate the percent cytolytic activity:

$$\% \text{ specific lysis} = \frac{\text{test sample} - \text{thymocyte}}{\text{MR} - \text{SR}} \times 100$$

For in vitro–boosted NK cytotoxicity

8b. Perform steps 8a and 9a.

9b. Add 25 µg poly I:C to each well in a volume of 50 µl.

10b. Incubate cultures 2 hr at 37°C.

11b. Proceed directly to step 10a and continue with the assay to step 15a.

For in vivo–boosted NK activity

8c. Prior to sacrifice (18 hr prior), administer 100 µg poly I:C to mice (i.p.) in a volume of 200 µl.

9c. Perform the assay as described for native NK cell activity (steps 8a through 15a, above).

SUPPORT PROTOCOL 1

PREPARATION OF A SINGLE -CELL SUSPENSION OF MURINE SPLEEN CELLS

This protocol describes the removal of a spleen from a mouse and the preparation of a single cell suspension of spleen cells. Careful preparation of splenocytes using this method should yield 80–120 $\times$ 10^6 viable nucleated cells, depending upon the age and strain of the mice used. All animals used should be housed in specific pathogen-free conditions and all media should be free from bacterial endotoxin and other immunostimulatory contaminants. Cells isolated from animals should be used as quickly as possible after animal sacrifice.

Materials

Mouse of appropriate strain
70% ethanol
sfRPMI (see recipe), ice cold
cRPMI (see recipe), ice cold
Sterile distilled water, endotoxin tested for cell culture (e.g., GIBCO, Invitrogen), ice cold
10× HBSS (e.g., GIBCO, Invitrogen; see recipe)

15-ml centrifuge tubes
4-in. dressing forceps
4 3/4-in. surgical scissors
60 × 15–mm cell culture dishes
Frosted microscope slides (25 × 75 × 1–mm)
Plastic transfer pipets (optional)
5- and 10-ml sterile serological pipets
Refrigerated centrifuge (e.g., Beckman GS-6 or equivalent)

Additional reagents and equipment for counting cells (*APPENDIX 3B*)

Remove spleen

1. For each animal, label two 15-ml centrifuge tubes (sterile if necessary) with a designation of treatment or animal number.
2. Euthanize mouse by asphyxiation using CO_2 or other approved method.
3. Thoroughly soak the abdominal hair using 70% ethanol.
4. Using 4-in. dressing forceps and 4 3/4-in. scissors, snip the skin on the lower abdominal area, and peel back the skin in both directions over the entire abdomen.
5. Using dressing forceps and scissors, open the peritoneal cavity and remove the spleen; trim free of connective tissue and fat as necessary.

   If sterile conditions are required, a second set of instruments that remain sterile will be needed for this step.

6. Place the spleen in the bottom half of a labeled 60 × 15–mm culture dish containing 5 ml ice-cold sfRPMI. Use a separate dish for the spleen from each animal.

Process into a single cell suspension

7. Press the spleen between the frosted ends of two microscope slides using a gentle circular motion until only the empty capsule remains.

   To ensure maximal cellular viability, it is important to avoid an up-and-down motion with the frosted ends of the two slides. The slides should remain in contact with each other as they are rubbed together in a circular pattern. Do not pull them apart until the empty capsule is all that remains.

8. Transfer the cell suspension using a plastic transfer pipet or sterile serological pipet to a labeled 15-ml conical centrifuge tube. Rinse the dish and capsule with an additional 3 ml sfRPMI and add to the cell suspension. Pipet the suspension up and down several times to disperse clumps.
9. Centrifuge samples 10 min at 200 × *g*, 4°C.
10. Resuspend cell pellet using a 5-ml serological pipet in 2 to 5 ml sfRPMI or cRPMI.
11. (Optional) Wash samples one additional time by repeating steps 9 and 10.
12. Remove red blood cells (RBC) by hypotonic lysis using the following steps:
    a. After centrifugation in step 9, aspirate the supernatant using a 5-ml pipet.
    b. Dislodge the cell pellet from the tube bottom by gently nudging with the tip of a 1000-µl micropipettor. Do not aspirate the dry pellet into the pipet tip.
    c. Add 4.5 ml cold distilled water and vortex the cells for 5 to 10 sec (do not exceed 10 sec). Quench hypotonic lysis by immediately adding 0.5 ml of 10× HBSS and vortex gently for 1 sec. Add 5 ml cRPMI and place the cells on ice. Proceed to the next tube of cells.
    d. Centrifuge samples as in step 9 and resuspend cells in 5 ml cRPMI.

    RBC removal using other methods, e.g., ammonium chloride or density gradient centrifugation, are viable alternatives.
13. Settle debris and clumps by letting the resuspended cells sit on ice for 8 to 10 min.
14. Transfer the clump-free supernatant using a transfer pipet (or sterile 5-ml pipet) to a new tube. Record the volume.
15. Determine cell concentrations using a Coulter counter or hemacytometer (*APPENDIX 3B*).
16. Determine viability of the spleen cell suspension using the trypan blue dye assay.

GROWTH AND MAINTENANCE OF P815 CELLS

SUPPORT PROTOCOL 2

Propagation of P815 mastocytoma cells in the peritoneal cavity of a DBA mouse is the recommended method for growing and maintaining these cells. Passaging this cell line in vivo results in tumor cells that elicit a robust CTL response when injected into allogeneic mice (e.g., C57Bl/6). This cell line can be propagated in vitro using standard tissue culture techniques, however this method is not recommended because it generally results in a reduced response.

Additional Materials *(also see Support Protocol 1)*

P815 cells (ATCC no. TIB-64)
DBA mice

Biological safety cabinet (level 2)
10-ml syringe
20- to 22-G × 1-in. needles
Small scissors
4-in. fine-tipped forceps
50-ml centrifuge tubes
Vortexer

Thaw stocks of P815 cells and inject into DBA mice

1. Place 10 ml warmed (37°C) HBSS in a 15-ml conical tube.
2. Using aseptic technique (i.e., standard cell culture methods), rapidly thaw the P815 cells and transfer the cell suspension to the 15-ml conical tube containing warmed HBSS.
3. Centrifuge the cells 10 min at 200 × *g*, room temperature. Remove and discard HBSS.
4. Resuspend P815 cells in 2 to 5 ml HBSS. Remove an aliquot of cells and determine the number of viable cells (*APPENDIX 3B*).
5. Resuspend the cells in HBSS at 1.2×10^6 viable cells/ml. Immediately inject 6×10^5 cells (0.5 ml) i.p. into each DBA recipient.

   For routine propagation of this cell line, it is advisable to inject two DBA hosts.

   Injection of 6×10^5 cells will yield 3–5 × 10^8 tumor cells 7 days later. The DBA mice will succumb to this tumor after ~9 days. Therefore, it is strongly advised to sacrifice the mice no later than 8 days after the injection of tumor cells.

Harvest P815 cells in ascites fluid

6. Working inside a biological safety cabinet, fill a 10-ml syringe with 10 ml cold HBSS and attach a 20- to 22-G needle.
7. Sacrifice a DBA mouse by asphyxiation with CO_2 or other approved method.
8. With the mouse lying on its back, thoroughly soak the fur with 70% ethanol.
9. Make a small incision in the skin and reveal peritoneum.

   It is important to not knick or puncture the peritoneal lining during this step.

10. With sterile forceps, carefully lift the peritoneal lining and insert the needle with the bevel facing down. Insert the needle only ~1 cm and do not puncture organs.
11. Inject HBSS rapidly to flush the peritoneal cavity. Using gloved fingertips, carefully massage peritoneal cavity and then withdraw as much fluid as possible (8 to 10 ml).
12. Remove and discard the needle and transfer the cells to a 50-ml centrifuge tube. Add 20 ml cold HBSS. Centrifuge 10 min at 200 × *g*, room temperature, to pellet cells.
13. Resuspend cells in 10 to 20 ml cold HBSS. Pipet cells up and down several times to disperse clumps.
14. Using a hemacytometer and trypan blue, determine the number of viable P815 cells (*APPENDIX 3B*).

    The cells are ready for injection into new DBA hosts (routine maintenance), injection into allogeneic mice (sensitization), or indefinite cryopreservation.

SUPPORT PROTOCOL 3

GROWTH AND MAINTENANCE OF YAC-1 TUMOR CELLS

Yac-1 cells are a murine lymphoma cell line that was derived from an A/Sn mouse. The cells are sensitive to killing by natural killer (NK) cells and are very useful measuring NK cell activity in an in vitro chromium release assay. These cells are not susceptible to the cytotoxic action of CTL. Yac-1 cells can be grown and maintained in vitro using standard tissue culture techniques. These are rapidly growing cells and require that the medium be replaced every 2 to 3 days. This is important to note because poorly cultured cells do not label well with ^{51}Cr.

Additional Materials *(see also Support Protocol 1)*

Yac-1 cells (ATCC no. TIB-160)
Yac-1 cell growth medium (see recipe)

Biological safety cabinet (level 2)
25- and 75-cm^2 tissue culture flasks

Additional reagents and equipment for counting cells and determining viability (*APPENDIX 3B*)

Prepare cultures of Yac-1 cells

1. Approximately 2 weeks prior to measuring NK cell activity using a chromium release assay, thaw the Yac-1 tumor cells using the following procedure:
   a. Warm Yac-1 cell medium in a 37°C water bath and place ~10 ml warmed medium into a 15-ml conical centrifuge tube.
   b. Obtain a vial of frozen Yac-1 cells. Thaw the cells rapidly. Working in a biological safety cabinet and using proper cell culture techniques, immediately transfer the cells into the 15-ml conical tube containing warmed Yac-1 medium.
2. Centrifuge cells 10 min at 200 × *g*, room temperature.
3. Remove and discard the Yac-1 medium which contains dead cells and DMSO.
4. Using a serological pipet, resuspend cells in 10 ml fresh Yac-1 cell medium. Pipet up and down several times to disperse cell clumps. Transfer cells to two 25-cm^2 tissue culture flasks (i.e., 5 ml medium/flask). Incubate cells at 37°C with the caps loosened to permit gas exchange.
5. Monitor cells daily, feed at 2- to 3-day intervals with fresh medium, and sub-culture when log-phase growth is observed.

Maintain and passage Yac-1 cells

6. To passage cells, withdraw Yac-1 medium from flask and transfer into a 15-ml conical centrifuge tube.

   There may be some cells that remain attached to the bottom of the flask. To remove these cells, rinse the flask with warm PBS and add the PBS to the tube containing the medium and cells.

7. Centrifuge cells 10 min at 200 × *g*, room temperature. Discard the supernatant.
8. Resuspend cells in Yac-1 cell medium. Remove an aliquot and determine the number of cells using a hemacytometer (*APPENDIX 3B*) or Coulter counter.
9. Seed new 25-cm^2 tissue culture flasks with 1×10^5 viable Yac-1 cells/flask (6 to 8 ml medium), or 75-cm^2 tissue culture flasks with 5×10^5 Yac-1 cells/flask (15 to 20 ml medium).

   These cells will double every 16 to 18 hr.

10. Sub-culture every 3 to 4 days.

GROWTH AND MAINTENANCE OF MC57G FIBROBLASTS

SUPPORT PROTOCOL 4

MC57G cells are a murine fibrosarcoma cell line derived from a C57Bl/6 mouse. These cells express both $H\text{-}2K^b$ and $H\text{-}2D^b$ and are susceptible to infection by many viruses, including influenza A viruses. MC57G cells can be grown and maintained in vitro using standard tissue culture techniques. These are rapidly growing cells and require that the

medium be replaced every 2 to 3 days. This is important to note because poorly cultured cells do not label well with ^{51}Cr.

Materials

MC57G (ATCC #CRL-2295)
MC57G growth medium (see recipe)
Cell culture–grade sterile PBS (e.g., from GIBCO, Invitrogen)
0.25% trypsin solution in PBS
15- and 50-ml conical centrifuge tubes
37°C water bath
75-cm^2 tissue culture flasks
37°C, 5% CO_2 humidified incubator

Prepare cultures of MC57G cells

1. Approximately 2 weeks prior to measuring virus-specific CTL activity using a chromium release assay, thaw the MC57G fibroblasts using the following procedure:
   a. Warm MC57G growth medium in a 37°C water bath. Place ~10 ml warmed medium into a 15-ml conical centrifuge tube.
   b. Thaw a vial of frozen MC57G cells rapidly. Working in a biological safety cabinet and using proper cell culture techniques, immediately transfer cells into the 15-ml conical tube containing warmed medium.
2. Centrifuge cells 10 min at 200 × *g*, room temperature.
3. Remove and discard the MC57G growth medium, which contains dead cells and DMSO.
4. Using a serological pipet, resuspend the cells in 10 ml fresh MC57G growth medium. Pipet the pellet up and down several times to disperse cell clumps. Transfer cells to two 75-cm^2 tissue culture flasks (15 to 20 ml medium/flask). Incubate cells at 37°C with the caps loosened to permit gas exchange.
5. Monitor cells daily, feed every 2 to 3 days, and sub-culture when log-phase growth is observed.

Maintain and passage MC57G cells

6. Sub-culture when the cell monolayer is ~90% confluent (every 3 to 4 days).

   At confluency, there should be ~30–40 × 10^6 viable cells/75-cm^2 tissue culture flask.

7. Aspirate medium and rinse the cell monolayer with 5 to 10 ml PBS.
8. Remove cells from the flask by adding 3 ml of 0.25% trypsin solution to each 75-cm^2 cell culture flask. Rock the flask back and forth to evenly distribute the trypsin solution.
9. At room temperature, continue to gently rock the flask(s) for 1 to 2 min. Watch the monolayer of cells carefully and when the monolayer sloughs off, immediately add 10 ml warm MC57G growth medium.

   Do not use PBS for this step. The serum in the medium contains trypsin inhibitors that will neutralize the trypsin solution.

10. Transfer the cells into a 15-ml conical tube and centrifuge 10 min at 200 × *g*, room temperature.

11. Decant the supernatant and resuspend cell pellet using 10 ml MC57G growth medium. Gently pipet cells up and down to disperse clumps.
12. Plate cells into 75-cm^2 tissue culture flasks in 15 to 20 ml warmed MC57G growth medium and incubate at 37°C.

    Plating 0.5–1 × 10^6 cells/ flask will typically yield a confluent flask in ∼5 days.

13. Exchange the medium after 48 to 72 hr of culture.

REAGENTS AND SOLUTIONS

Use Milli-Q-purified water or equivalent for the preparation of all recipes and in all protocol steps. For common stock solutions, see ***APPENDIX 2A****; for suppliers, see* ***SUPPLIERS APPENDIX****.*

Complete RPMI (cRPMI)

RPMI 1640 media, containing:
10% FBS
2 mM L-glutamine
1 mM sodium pyruvate
10 mM HEPES
100 U/ml penicillin
100 μg/ml streptomycin
50 μM 2-mercaptoethanol (optional, but be consistent)
Filter sterilize
Store up to 2 to 4 months at 4°C protected from light

HBSS

To make a 500-ml Hank's balanced salt solution (HBSS) with HEPES, for added buffering capacity, add:
50 ml 10× HBSS (e.g., GIBCO, Invitrogen)
445 ml H_2O, double-processed cell culture and endotoxin tested
5 ml 1 M HEPES, cell-culture tested
Adjust pH to 7.2 to 7.4, if necessary, with 1 N NaOH
Filter sterilize
Store up to 2 to 6 months at 4°C protected from light

MC57G growth medium

DMEM supplemented with:
10% (v/v) FBS
2 mM L-glutamine
1 mM sodium pyruvate
50 μg/ml gentamycin
Filter sterilize.
Store up to 2 to 4 months at 4°C protected from light

SDS, 0.5% (w/v)

Dissolve 0.5 g sodium dodecyl sulfate in 100 ml water. Store up to 1 year at room temperature.

Serum-free RPMI (sfRPMI)

RPMI 1640 medium containing 1% bovine serum albumin (BSA) and 10 mM HEPES, pH 7.4. Filter sterilize and store up to 2 to 4 months at 4°C protected from light.

Trypan blue, 0.4% (w/v)

Dissolve 0.4 g trypan blue in PBS or HBSS. Filter through Whatman no. 1 paper. Store >1 year at 4°C or up to 4 to 6 months at room temperature.

CAUTION: *Trypan blue is believed to be carcinogenic and teratogenic. Wear gloves and a particulate filter mask while working with it in powder form. Additionally, tubes containing trypan blue and cells need to be filled with dilute (~2%) bleach prior to being discarded.*

Yac-1 growth medium

RPMI 1640 media containing:
10% FBS
2 mM L-glutamine
1.5 g/liter sodium bicarbonate
4.5 g/liter glucose
10 mM HEPES
1 mM sodium pyruvate
100 U/ml penicillin
100 μg/ml streptomycin
Filter sterilize
Store up to 2 to 4 months at 4°C protected from light

COMMENTARY

Background Information

A major function of lymphocytes is the detection and destruction of infected cells and tumor cells. One mechanism by which lymphocytes carry out this function is by causing the death of antigen-bearing target cells. The two types of lymphocytes that have the capability to recognize and directly destroy target cells are CTL and NK cells. Although the mechanisms by which CTL and NK cells recognize their targets differ, the cytolytic machinery used by these two types of cells is very similar (Kagi et al., 1996; Russell and Ley, 2002). Moreover, given that the cytolytic function of lymphocytes constitutes a major component of host protection from pathogens and tumor cells, methods to measure this activity are well established and form a critical aspect of functional assessments of the immune system.

Since the molecular machinery that underlies the lysis of target cells is similar, the primary way in which one can distinguish killing by CTL from killing by NK cells is by understanding and exploiting the distinct constraints on target cell recognition by these two types of cells. CTL must recognize antigenic peptides in association with class I MHC molecules. Moreover, generating CTL requires sensitization of naïve T cells with antigen, followed by the clonal expansion and differentiation of naïve cells into CTL. Antigen recognition by NK cells is not MHC-restricted and sensitization with antigen is not required, because the cytolytic activity of NK cells is an innate feature of these cells. These distinctions can be used to separately quantify the activity of these two types of cytolytic lymphocytes. For example, Yac-1 tumor cells do not express class I MHC. This makes these cells highly sensitive to lysis by NK cells and resistant to recognition by CTL. In contrast, P815 tumor cells are sensitive to lysis by allo-reactive CTL, but because they express class I MHC molecules, they are resistant to killing by NK cells. In contrast to the effector cell selectivity of these two types of target cells, cells infected with influenza virus are susceptible to recognition and killing by CTL and NK cells.

A major consideration when using the protocols described in this unit is determining what specific aspect of immune function is to be tested and then selecting the most appropriate protocol(s) to accomplish this goal. For example, exogeneous agents that adversely affect cell proliferation would be expected to impair the generation of a CTL response, but not affect the native activity NK cells. Exogenous agents that interfere with cell-cell contact, exocytosis, or cellular trafficking would likely diminish CTL and NK cell cytolytic activity. Thus, these assays can be used in the following applications:

Table 18.6.1 Troubleshooting Guide for Assessing Cytolytic Activity of Lymphocytes

Problem	Possible cause	Solution
High (>5%) non-specific lysis, as indicated by high counts per minute in spontaneous release (SR) wells	Insufficient washing of target cells Poor target cell viability	Add more washes or increase the volume of medium used in each wash. Poor target cell viability after labeling.
Very low counts per minute in MR wells	Poor ^{51}Cr uptake by target cells Poor target cell viability	Use the freshest ^{51}Cr available, and do not use if decayed (even decaying by one half-life can adversely affect the sensitivity of these assays). Poor target cell viability after labeling.
Very low counts per minute in samples containing (or expected to contain) effector cells	Improper effector cell sensitization. Poor cellular viability.	Validate the efficacy of effector cell sensitizaiton using an alternate method (e.g., flow cytometry, cytokine production, or proliferation). Use cells isolated from animals as quickly as possible after the animal is sacrificed. Check the pH of solutions and wash the cells more gently.
Poor target cell viability after ^{51}Cr labeling	Poor cellular viability prior to labeling Cells were not used within 30 min of labeling	Use only viable cells. Wash cells more gently and very carefully maintain solution pH. Do not let the labeled target cells sit unused for >30 min.

1. To test whether in vitro exposure to a chemical affects the clonal expansion and differentiation of T cells (see Basic Protocol 1).

2. To test whether in vivo exposure to a chemical affects the clonal expansion and differentiation of T cells (see Alternate Protocols 1 and 2).

3. To determine whether exposure to a particular substance affects the inherent cytolytic function of NK cells (see Basic Protocol 2).

4. To determine whether exposure to a substance has differential effects on the native and boosted cytolytic activity of NK cells (see Basic Protocol 2).

5. To determine whether exposure to an agent exhibits differential or selective effects on CTL and NK cells (a combination of Basic Protocol 1 or Alternate Protocols 1 or 2 and Basic Protocol 2 in separate but simultaneous assays).

Critical Parameters

All animals used for these procedures should be housed in specific pathogen-free conditions and all media should be free from bacterial endotoxin and other immunostimulatory contaminants. Cells isolated from animals should be used as quickly as possible after animal sacrifice.

Troubleshooting

See Table 18.6.1 for troubleshooting tips.

Anticipated Results

If the effector cells recognize and kill the target cells, then the counts per minute and calculated percent specific cytolytic activity should increase with increasing E:T ratios, as depicted in Figure 18.6.1. On the other hand, the amount of cytolytic activity in wells set up using control effector cells should not change with increasing E:T ratios. In fact, the counts per minute in wells containing the negative control cells cultured with target cells ought to be about the same as the spontaneous release of the target cells.

The maximum achievable percent cytolytic activity will vary depending upon the type of

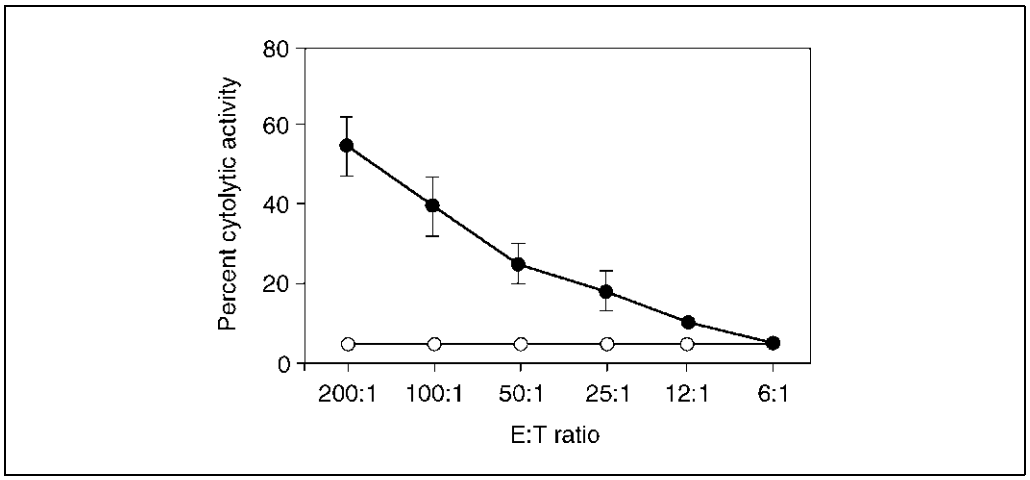

Figure 18.6.1 This graph depicts the average cytolytic activity of spleen cells in an in vitro chromium release assay. Spleen cells were isolated from a C57B1/6 mouse 9 days after i.p. injection with P815 mastocytoma cells (closed circles). As a control, spleen cells from a naïve mouse (open circles) were cultured with the labeled-P815 cells, which served as the target cells for this assay.

effector cells used and how they were sensitized. Lysis of 25% to 60% of the target cells at the highest E:T ratio is the typical range expected in chromium release assays for both NK cells and CTL. Lysis of 100% of the target cells by the effector cells should not be expected, and if observed, it likely indicates a technical problem with the assay. When measuring the activity of NK cells, treatment with poly I:C should lead to increased activity compared to native NK cell activity toward Yac-1 tumor cells, however, the magnitude of this change is not more than 2-fold (e.g., increasing the percent cytolytic activity from 35% to 50% at an E:T ratio of 100:1 is typical).

Time Considerations

A chromium release assay requires 1 full day. It takes ~3 hr to collect the effector cells and label the target cells, and these steps need to be performed simultaneously. The total time required to set up the assay (i.e., combine the effector and target cells) depends upon the size of the assay, but generally takes ~1 hr. The cells need to be incubated for 4 to 5 hr prior to harvesting supernatants. The duration of this step depends upon the size of the assay (number of 96-well plates), but generally takes ~1 hr.

While general steps and overall time commitment for the chromium release assays described here is similar among the protocols described, the total amount of time required to measure the cytolytic activity of CTL and NK cells is very different. $CD8^+$ T cells require sensitization with antigen to develop into CTL. Therefore, whether one uses an in vitro or in vivo approach, it takes 5 to 10 days to generate a population of CTL. The innate and in vitro–boosted cytolytic activity of NK cells can be measured in 1 day. However, if one wants to stimulate NK cells in vivo prior to measuring the cytolytic activity, then the assay will require 1 additional day for this step.

Literature Cited

Barrett, T. and Inglis, S.C. 1985. Growth, purification and titration of influenza viruses. *In* Virology: A Practical Approach (B.W. J. Mahy, ed.), pp. 119-150. IRL Press, Washington, D.C.

Cho, Y., Basta, S., Chen, W., Bennink, J.R., and Yewdell, W. 2003. Heat-aggregated noninfectious influenza virus induces a more balanced CD8+T lymphocyte immunodominance hierarchy than infectious virus. *J. Virol.* 77:4679-4684.

Kagi, D., Ledermann, B., Burki, K., Zinkernagel, R.M., and Hengartner, H. 1996 Molecular mechanisms of lymphocyte-mediated cytotoxicity and their role in immunological protection and pathogenesis in vivo. *Annu. Rev. Immunol.* 14:207-232.

Kos, F. and Engleman, E. 1996. Role of natural killer cells in the generation of influenza virus–specific cytotoxic T cells. *Cell Immunol.* 173:1-6.

Mitchell, K.A. and Lawrence, B.P. 2003a. Exposure to 2,3,7,8-tetrachlorodibenzo-*p*-dioxin (TCDD) renders influenza virus–specific $CD8^+$ T cells hyporesponsive to antigen. *Toxicol. Sci.* 74:74-84.

Mitchell, K.A. and Lawrence, B.P. 2003b. T cell receptor transgenic mice provide novel insights into understanding cellular targets of TCDD: Suppression of antibody production, but not the response of $CD8^+$ T cells, during infection with influenza virus. *Toxicol. Appl. Pharmacol.* 192:275-286.

Nonacs, R., Humborg, C., Tam, F., and Steinman, R. 1992. Mechanisms of mouse spleen dendritic cell function in the generation of influenza-specific cytolytic T lymphocytes. *J. Exp. Med.* 176:519-529.

Russell, J.H. and Ley, T.J. 2002. Lymphocyte-mediated cytotoxicity *Annu. Rev. Immunol.* 20:323-370.

Warren, T.K., Mitchell, K.A., and Lawrence, B.P. 2000. Exposure to 2,3,7,8-tetrachlorodibenzo-*p*-dioxin (TCDD) suppresses the humoral and cell-mediated immune responses to influenza A virus without affecting cytolytic activity in the lung. *Toxicol. Sci.* 56:114-123.

Yokoyama, W.M. and Plougastel, B.F.M. 2003. Immune functions encoded by the natural killer gene complex. *Nat. Rev. Immunol.* 3:304-316.

Internet Resources

http://www.cdc.gov/od/ohs/biosfty/bmbl4/bmbl4toc.htm

A pdf manual of Biosafety in Microbiological and Biomedical Laboratories, 4th Edition (1999), U.S. Department of Health and Human Services, Centers for Disease Control and Prevention, and National Institutes of Health. US Government Printing Office Washington, D.C.

Contributed by B. Paige Lawrence
Washington State University
Pullman, Washington

Solid-Phase Immunoassays

Solid-phase quantitative immunoassays can be configured in a multitude of ways to detect the presence and concentration of a specific antigen or an antibody of a particular isotype and specificity. These assays can provide a wealth of information about cellular and molecular events that are altered by toxicant exposure. For example, these assays can produce information related to antibody or antigen concentrations, the affinity and avidity of the interactions that produce immune complexes, and the organ, tissue, cellular, and subcellular distribution of target molecules (Probst et al., 1995). In the context of toxicological assessment, these assays provide a window on the effects that chemical and physical agents can have on developmental processes and effector mechanisms in the body. Since the immune system itself is often a target of toxin effects, evaluation of immune function can be extremely informative, but these same assay formats can be used to probe other biological systems with equal ease.

STRATEGIC PLANNING

The enzyme-linked immunosorbent assay (ELISA) is a multi-step process in which a target molecule (e.g., an antigen) is first immobilized onto an insoluble substrate—most often composed of polystyrene or another plastic in a 96-well microtiter plate configuration. Ordinarily, this immobilization is a non-specific binding event and must be followed with a blocking reagent to saturate any other non-specific binding sites on the substrate. A number of different kinds of reagents have been used to block subsequent non-specific binding, and examples of some of the common blocking agents are listed in Table 18.7.1. Bovine serum albumin (BSA) is most commonly used, but has some drawbacks under certain circumstances. BSA is a particularly sticky protein that can increase undesirable non-specific interactions. Moreover, polyvalent sera that have been raised against cultured cells may have secondary reactivity against BSA that was carried along with the immunizing cells from the fetal bovine serum that is often used to supplement culture media. Teleostean fish gelatin has the advantage of being antigenically distinct from the antigens present in samples associated with many common applications of the ELISA technology, and thus it will not often produce spurious cross-reactions. Since this protein derives from cold-water fish, it is soluble at room temperature, and will not gel in the microplate wells.

Table 18.7.1 Blocking Agents

Blocking agent	Suppliers	Commonly used concentration range
Bovine serum albumin (BSA)	Jackson ImmunoResearch Laboratories Sigma-Aldrich	1%–10%
Casein	Sigma-Aldrich	5%–10%
45% Teleostean fish gelatin in water	Sigma-Aldrich	1%–5% dilution of stock solution
Non-fat dried milk (NFDM)	Local grocery store, Sigma Chemical	2%–5%
Goat serum	Sigma-Aldrich	1%–10%

Contributed by Michael A. Lynes
Current Protocols in Toxicology (2005) 18.7.1-18.7.19

Table 18.7.2 Enzymes Used in Conjugates and Representative ELISA Substrates

Enzyme	Complementary substrates	Detection method for substrate	Enzyme limitations
Alkaline phosphatase (AP)	a. Para-nitrophenyl phosphate (PNPP) b. 4-Methyl-umbelliferyl phosphate (4-MUP)	a. Measure absorption at 405 nm b. Excitation at 360 nm and emission at 440 nm	Samples that contain a high level of endogenous phosphatase are not compatible with this enzyme conjugate
ß-galactosidase (ß-gal)	a. *o*-Nitrophenyl-ß-D-galactopyranosidase (ONPG) b. 4-Methyl-umbelliferyl-ß-D-galactopyranosidase (MUM-Gal)	a. Measure absorption at 405 nm b. Excitation at 360 nm and emission at 440 nm	This enzyme is not as active as the alternatives and produces a lower signal over time
Horseradish peroxidase (HRP)	a. 3,3′,5,5′-Tetramethylbenzidine (TMB) b. 2,2′-Azino-di-(3-ethylbenz-thiazoline sulfonic acid (ABTS)	a. Measure endpoint at 370 or 655 nm, or acidify and measure at 450 nm b. Measure at 416 nm 405 nm will also work	Do not use this enzyme conjugate if the sample contains oxidizing or reducing agents, or some preservatives

Once the surface has been blocked, the complementary molecular partner (e.g., a cognate antibody conjugated to an enzyme label) can be added to the surface and allowed to selectively interact with the target molecule. Following an appropriate period, the surface can be washed to remove any unbound antibody-enzyme conjugate. The next step is to add an appropriate substrate for that enzyme. The more enzyme that is present, the more substrate will be converted to a product that can be measured in a microtiter plate reader. Measurements of the amount of substrate conversion to product can be interpreted to indicate the degree of antibody-enzyme conjugate that has bound to the surface. A list of the most common enzyme labels and their substrates is provided in Table 18.7.2. Substrates must be stable until they interact with enzyme, must produce a soluble product, and should have a large extinction coefficient to maximize the signal-to-noise ratio. In some cases, fluorescent substrates can improve the sensitivity of an assay by 100- to 1000-fold over an absorbance assay, but these assays do require fluorescent microtiter plate readers that are more expensive and less commonplace than standard absorbance microtiter plate spectrophotometers. In addition to the listed substrates, there are also commercially available chemiluminescent substrates (often used with horseradish peroxidase–labeled antibody conjugates) that can further enhance the detection limits of ELISA. The disadvantage of chemiluminescent systems is that the signal persists for only a brief time (for 5 to 30 min) and then begins to degrade. Moreover, readings must be taken in a microtiter plate luminometer.

Another substrate alternative that can enhance the sensitivity of the ELISA is an enzymatic recycling system (e.g., commercially available from Invitrogen). In this type of substrate system, immobilized alkaline phosphatase catalyzes the conversion of the reduced form of nicotinamide adenine dinucleotide phosphate (NADPH) to reduced nicotinamide adenine dinucleotide (NADH). The NADH can then participate in a cyclic reaction in which diaphorase reduces a tetrazolium salt (iodonitrotetrazolium violet or INT-violet) to colored formazan and produces oxidized NAD^+. To continue the cycle, NAD^+ is then reduced back to NADH and ethanol is oxidized to acetaldehyde in the presence of alcohol dehydrogenase. The NADH can be recycled through this process and yields an approximately ten-fold signal amplification over that of standard ELISA protocols when absorption is read at 495 nm.

One of the initial issues to be considered for the design of an ELISA is the availability of antibodies specific for the target to be assessed. There are many sources of commercial antibodies that produce reagents of differing specificity, concentration, purity, quality, isotype, and species of origin. Identification of the appropriate reagent must take into account the singular or multiple applications for which the antibody will be used. For example, it may prove useful to employ a polyclonal antibody that cross-reacts with homologous antigens from different species to facilitate the assessment of cellular functions in cell cultures of different origins. Alternatively, a monoclonal antibody may enhance the specificity of the antibody/antigen interaction by minimizing the appearance of cross-reactions that decrease the signal-to-noise ratio of the assay. Equally important, it may prove useful to employ antibodies that are biotinylated to facilitate the use of a spectrum of different labeling reagents that have each been coupled to avidin. In this way, the same biotinylated antibody reagents incubated with an avidin-enzyme conjugate that could be used for an ELISA would also be useful in fluorescent assays when incubated with an avidin-fluorescent tag.

Once the appropriate antibodies have been identified, it is often useful to obtain a source of purified antigen for use as a standard in the reaction. While this is not always possible (or economical), it can serve to enrich the interpretations that are possible from data generated by the ELISA.

Having obtained the central reagents, the next step is to select the specific kind of ELISA that will be used. Figure 18.7.1 illustrates the most commonly used ELISA configurations.

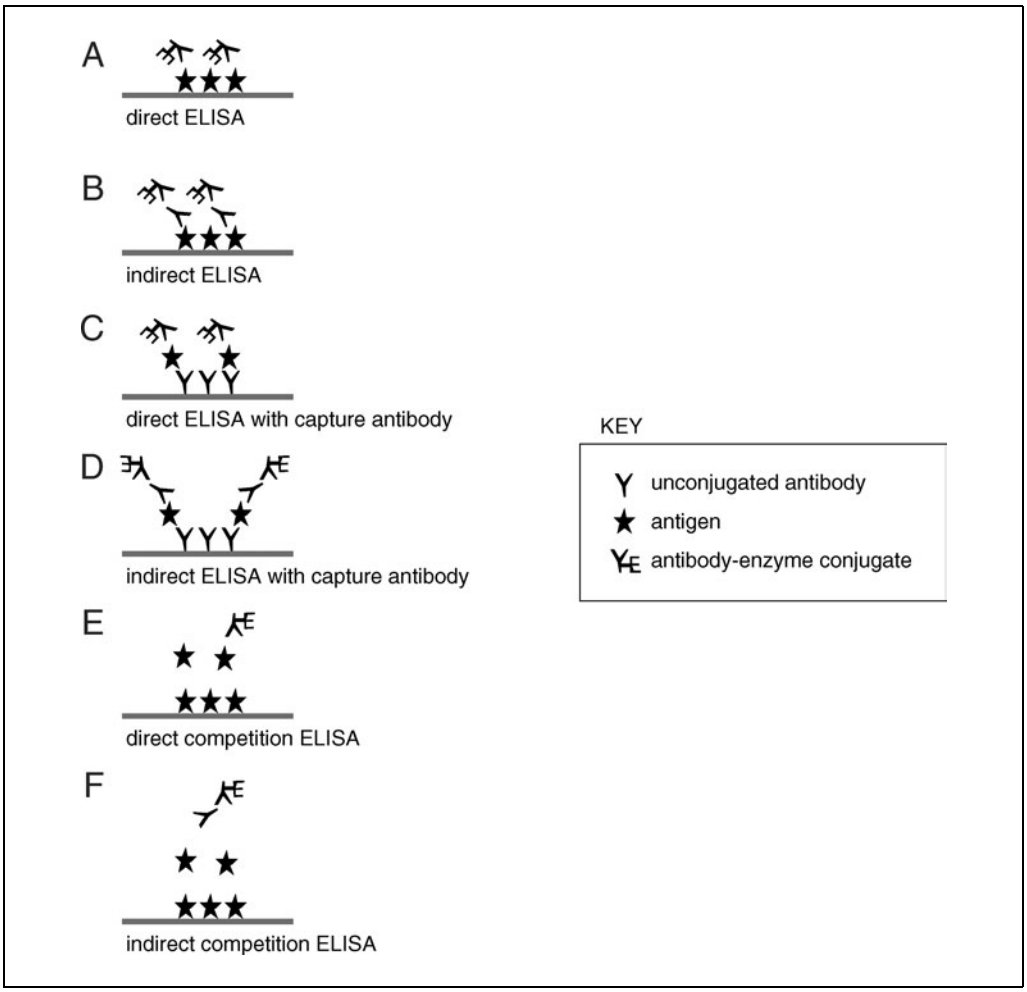

Figure 18.7.1 ELISA protocol formats.

The simplest of these assays is the direct ELISA (Fig. 18.7.1A). This assay is usually configured with non-specifically adsorbed target antigen on the surface of the microtiter plate well. The amount of adsorbed antigen is detected using a pre-established amount of cognate antibody coupled to an enzyme label. The more antigen that is immobilized on the surface, the more antibody-enzyme conjugate will subsequently bind. Ultimately, the larger the amount of enzyme that is immobilized after binding to the surface, the more detection reagent will be converted to a signal that can be measured by light absorption, fluorescence, or luminescence. A common variation of this assay is used to quantitate the amount of antibody specific for a particular antigen that is present in a sample. In this version of the ELISA (Fig. 18.7.1B), known amounts of antigen are immobilized on the surface of the microtiter plate well. After blocking the surface to prevent further non-specific binding, the surface is incubated with the sample that may contain antibody specific for the target antigen. If there is antibody present in the sample, it will be retained on the surface after washing, and will serve as a target for a secondary antibody that has been conjugated to enzyme. The anti-immunoglobulin-enzyme conjugate is added in a standardized amount (usually in excess), and thus the amount of signal that develops is directly proportional to the amount of primary antibody that has bound to the surface.

If the antigen to be detected is present in a heterogenous sample mixture that also contains other molecules, the actual detection of antigen will be subject to the influences of the competitive binding of those different molecules from the sample. For this reason, an ELISA that employs a capture antibody is more commonly used (Fig. 18.7.1C and D). Unconjugated antibodies against the target antigen are first immobilized on the substrate, and the surface is then blocked to prevent further irrelevant binding to the surface. At this point, antigen that is incubated on this surface will be captured by specific binding to the capture antibody. Irrelevant molecules will be left unbound. After washing away unbound molecules, antigen that remains bound to the surface can then be detected with antibody-enzyme conjugate in a direct ELISA with capture antibody, or in an indirect ELISA configuration.

Finally, the ELISA can be configured as a competition assay (Fig. 18.7.1E and F). In these assays, soluble antibodies will bind to immobilized antigen unless additional free antigen is added to the solution. As the amount of free antigen in solution increases, the amount of antibody that will bind to the immobilized substrate decreases. Antibody binding is again determined by the amount of directly conjugated enzyme that is present in a direct ELISA, or by subsequent measures of the amount of anti-immunoglobulin antibody-enzyme conjugate binding that can be made in an indirect ELISA. Competition ELISAs are particularly useful for measurements of antigen concentration in complex mixtures when the unknown samples that may contain antigen are compared to similar samples that contain known amounts of purified antigen.

The ELISPOT (enzyme-linked immunoSPOT) assay is a useful variation of the basic ELISA format. While ELISA measures the concentrations of analyte in solution, the ELISPOT enumerates cells that are actively secreting a specific protein (e.g., cytokine or immunoglobulin) in a heterogeneous population of cells. This assay differs from the basic ELISA protocol in both the configuration of the microtiter plate, and in the chemical characteristics of the enzyme substrate that is used. The microtiter plate wells that are used have filter bottoms. The filters are first coated with sterile capture antibody or antigen. Cells are then added to the wells of the plate and settle to the filter surface. Cells that secrete molecules that can be bound by the capture antibody, or cells secreting antibodies specific for immobilized antigen will secrete those molecules to a region immediately surrounding the cell. The analyte will bind to the filter-immobilized cognate molecule in highest concentrations nearby the cell source of the analyte. As analyte diffuses away from the cell, its concentration diminishes. Following an appropriate incubation period,

a secondary antibody-enzyme conjugate that is specific for the analyte is added and allowed to bind. Finally, enzyme substrate that produces a precipitating colored product is added. As the substrate is converted to this precipitating product, color will accumulate in specific regions of the filter that correspond to the original locations of the cells that secreted the analyte. These spots of accumulated color are proportional to the amount of analyte bound to the filter, and the precipitate spots can be counted microscopically and compared to the number of cells originally added to each individual well.

A new version of the solid-phase immunoassays is the grating-coupled surface plasmon resonance (GCSPR) assay. This assay has been used as a label-free variant of ELISA, and offers some interesting advantages over the more commonly used ELISA. GCSPR is based on the phenomenon of energy transfer that occurs at a metal-dielectric interface (e.g., the interface between gold and water) when light energy is coupled to the electrons within the metal. Under certain optical conditions, the energy of the light excites electron movement within the metal. This excitation reduces the intensity of the reflected light. SPR technologies match the wave vector of the illuminating beam of light with the plasmon wave vector using a prism (the Kretschman configuration) or with a grating embossed on the gold surface. There is a critical angle at which this vector matching is best, and at which the energy transfer into the metal is largest. The angle at which maximum energy transfer occurs is referred to as the SPR angle. Because the measurement of energy transfer is sensitive to the refractive index of the dielectric/metal interface, the addition of proteins to the surface (which have a higher index of refraction than water) will increase the angle at which coupling occurs. Antibodies or other capture molecules immobilized on the surface that subsequently capture analyte from the sample solution will cause an increase in the critical angle of reflection. GCSPR offers a significant advantage over the Kretschman configuration because the entire surface of the sensor chip can be illuminated, and images of the chip surface across a range of illuminating angles can be captured. Individual regions of interest (ROI) on the chip surface can be computationally assessed for protein capture by immobilized antibody according to the changes in SPR angle at each ROI. Thus, GCSPR offers a microarray format for the simultaneous analysis of multiple proteins in solution from a single small volume sample.

This unit describes several prototypical variations of these three types of solid-phase immunoassays and considers the use of these assays in the evaluation of toxic chemical effects on biological systems. Several different configurations of ELISA are described in Basic Protocol 1 (direct ELISA), Alternate Protocol 1 (indirect ELISA), and Alternate Protocol 2 (competitive ELISA). Basic Protocol 2 describes the ELISPOT assay, and Basic Protocol 3 describes the GCSPR protein microarray application.

DIRECT ENZYME-LINKED IMMUNOSORBENT ASSAYS

BASIC PROTOCOL 1

In this simplest of ELISA configurations (Fig. 18.7.2), known and potential sources of antigen are first incubated in wells of a microtiter plate. The known antigen solutions act as positive controls for those wells in which potential sources of antigen are added. It is advantageous to maximize antigen coupling to the surface, and so antigen is often diluted in a coupling buffer that will facilitate binding to the microtiter plate material. Incubation of the antigen solution in the well can be done for up to 1 hr at 37°C, or overnight at 4°C. Then the antigen is aspirated from the well, and the well is filled with a larger volume of blocking agent in phosphate-buffered saline. After blocking, the well is washed and then incubated with the antibody-enzyme conjugate, washed again, and then substrate is added. After incubating the substrate in the wells for a defined period, a single, endpoint reading can be taken to measure the amount of substrate conversion to product. Alternatively, a kinetic measurement can be made in which multiple sequential measurements of the optical density of the substrate are taken and then converted to a milli-optical density

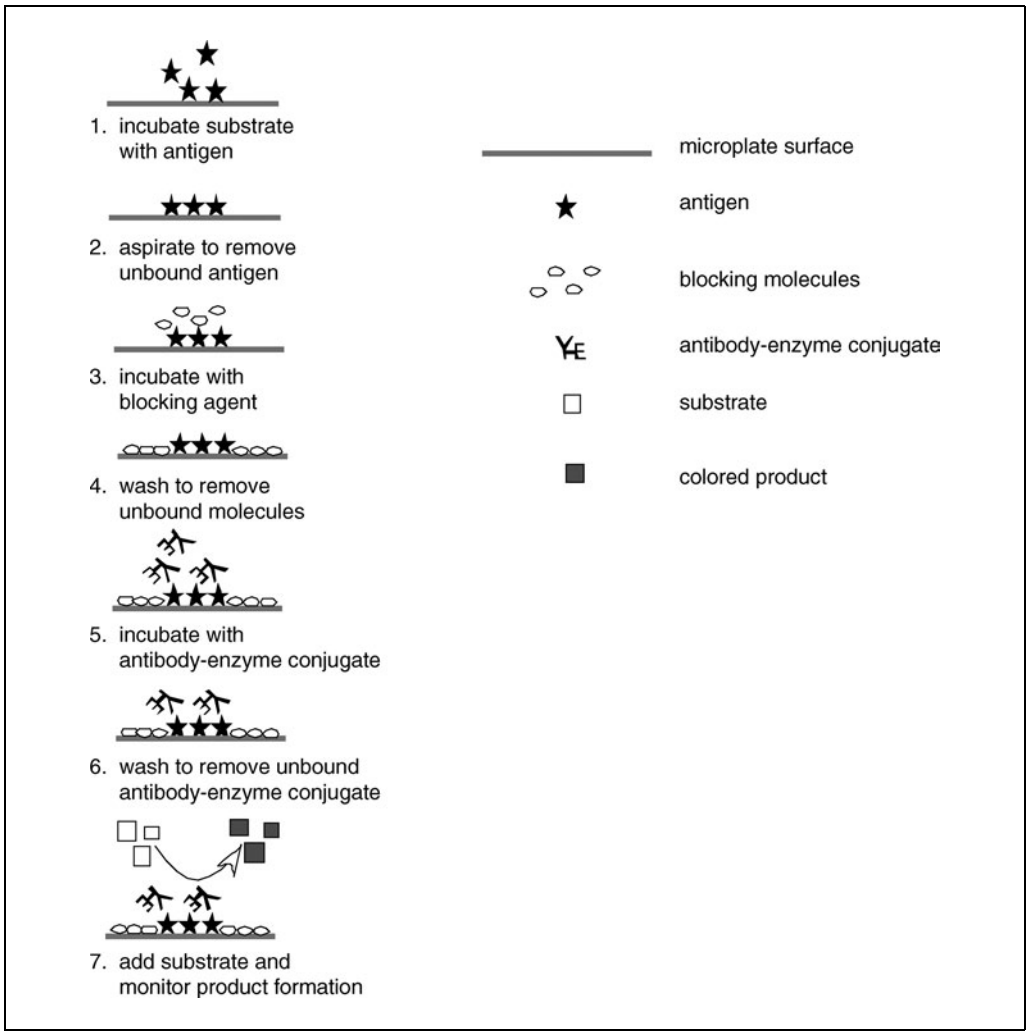

Figure 18.7.2 Sequential ELISA steps.

(mO.D.)/min reading, or a rate of substrate conversion. This second approach to quantifying the amount of enzyme in the well has the advantage of diminishing the differences that might result from the pipetting sequence. Wells initially loaded with substrate have more time to develop color than will wells loaded at a later time, but if the wells have equivalent amounts of enzyme, the rates of substrate conversion to colored product should be equal. Another advantage of the kinetic measurement of substrate conversion is that measurements can be started immediately after substrate addition. Usually 5 to 10 min of sequential measurements at 20- to 30-sec intervals from each well are sufficient to produce reliable estimates of substrate conversion rates. It is important to ensure that the conversion rate is linear and does not plateau, or the mathematical estimate of the absolute rate will be lower than the real rate. For that reason, the plate should be shaken in between readings to prevent substrate depletion at the surface of the microtiter plate well, and the assay should be set up to avoid approaching the maximum O.D. that the instrument can measure. For the same reason, substrate should be present in excess in each well. If the plate reader does not offer the capacity to do kinetic measurements, then the substrate should be incubated in each well for a fixed period of time (usually 30 min at 37°C), and the individual wells measured as an endpoint assay. If the rates of substrate conversion are rapid, the activity of the enzyme should be stopped before reading the plate. This is usually done by changing the pH of the substrate solution; for alkaline phosphatase conjugates conversion of *p*-nitrophenyl phosphate disodium hexahydrate (PNPP), the reaction can be stopped with the addition of 3 N NaOH.

Materials

Antigen diluted in ELISA coupling buffer (see recipe for ELISA coupling buffer)
Blocking reagent (Table 18.7.1)
ELISA wash buffer (see recipe)
Antibody-enzyme conjugate (e.g., Southern Biotech)
Substrate (Table 18.7.2) dissolved in the appropriate substrate buffer (e.g., for alkaline phosphatase-based assays, the most common substrate is *p*-nitrophenyl phosphate, PNPP, Sigma; see recipe)
96-well flat-bottom microtiter plates (plates specifically treated to enhance binding of hydrophobic or hydrophyllic proteins, or DNA molecules; e.g., Immulon 2 HB plates, Thermo Electron)
37°C incubator
Automated plate washer (optional)
Plate sealer (adhesive-backed mylar sheets, Fisher)
Microtiter plate reader with appropriate wavelength filters (e.g., Molecular Devices, Bio-Tek Instruments, Thermo Electron, and Tecan)
Plate shaker

Determine working dilutions of antigen and antibody-enzyme conjugate

1. Determine working dilutions of the antibody-enzyme conjugate and the immobilized target molecule in a 96-well microtiter plate. Set up the microtiter plate in a checkerboard fashion: with replicate wells containing 100 µl serial doubling dilutions of cognate antigen (approximate initial range: 10 µg/well to 0.01 µg/well) arranged across the plate from left to right. Use an underplate well indicator to guide the distribution of reagents. Incubate 60 min at 37°C.

   Include wells that lack one or both of the antigen and antibody-enzyme conjugate to determine the rate of spontaneous conversion of the chromogenic substrate to colored product. All measurements should be made in at least three replicate wells to allow the subsequent calculation of standard deviation, which should ideally be <5% of the average values for the triplicate wells. It is also useful to retain several microliters of the stock dilution of the antibody-enzyme conjugate to add to unused substrate in a separate tube to assure that the enzyme can produce color when the substrate is present.

   One of the commonplace errors in microtiter plate assays is the deposition of the wrong reagent to the wrong well. There are a number of ways to help avoid these mistakes, including plate holders that sequentially illuminate a light emitting diode beneath the wells in a specified pattern. For most uses, it is sufficient to place a photocopy of the plate underneath the plate with each well individually indicated.

   Eight- or twelve-channel pipettors can enable the transfer of replicate volumes to whole rows or columns of the plate at the same time. Since speed and consistency is critical to ensuring accurate results, these pipettors can prove quite useful. However, many of these pipettors can exhibit inconsistent volume transfer between channels, often owing to inconsistent seals of the disposable tips to the pipet shaft. Moreover, forcefully fitting the tip on the shaft to ensure a seal can slow the assay set up because of difficulty in removing the tips after use. If these pipettors are used, they should be pre-calibrated to ensure volume transfers are equivalent between channels.

   Microtiter plates can be irradiated with UV light in the laboratory to further enhance binding to the surface; this manipulation is detailed in the sample protocol for anti-double stranded DNA antibody ELISA (Amoura et al., 1994).

2. Wash the plate three times with at least three complete changes of 250 µl wash buffer/well.

   It is possible to wash the wells of the microtiter plate manually with a simple siphon system that drains wash buffer through tubing to a Pasteur pipet. Using a clamp to restrict the flow of wash buffer, liquid can be added to each well individually. The initial fluid is

removed from the wells by inverting the plate over the sink and sharply flicking the fluid out. After the wells have been emptied, the plate should be inverted and rapped against a few layers of paper towels to remove the last vestiges of remaining fluid and to blot the surface of the plate. Then, wash buffer is added to each well, and the wash cycle repeated two more times. The efficacy of each wash cycle can be increased by allowing the wash buffer to sit in each well (a soak step) for 2 to 5 min. Another inexpensive washing station can be made with a Bel-Art Vaccu-Pette/96 (http://www.bel-art.com/) and a 60-ml syringe, which can be configured to deliver wash buffer to all 96-wells in a microtiter plate simultaneously. There are a number of commercially available automated plate washers that can further improve the consistency and stringency of washing each well at each of the different wash steps, and which are invaluable when more than a couple of plates are used in a single assay. Automated microtiter plate washers have added features to further increase the success of the wash step, including shaking and soaking steps. Suppliers of this equipment include many of the manufacturers of microtiter plate readers.

3. Add 150 µl ELISA blocking buffer and incubate 60 min at 37°C.
4. Wash wells three times with ELISA wash buffer.
5. Add 100 µl serial doubling dilutions of antibody-enzyme conjugate (approximate range: 1:250 to 1:8000) arranged from the top row to the bottom row. Mix and incubate 1 hr at 37°C.

   Antibody-enzyme conjugates can be obtained commercially from a wide variety of sources. The most commonly available conjugates incorporate alkaline phosphatase, and can be used at dilutions from 1:250 to 1:8000 of the stock solutions that are provided by many commercial suppliers. It is important to store undiluted antibody-enzyme conjugates at 4°C to prevent aggregation and enzyme inactivation that can occur with repeated cycles of freeze-thawing.

   Mixing the contents of the microplate wells can be accomplished by the onboard shakers that many microplate readers now incorporate, or with freestanding shakers that are also commercially available. In its cheapest form, holding a microplate to the top of a vortex mixer will provide adequate mixing force, but other freestanding mixers designed for microtiter plates are also available. Whenever the microplates are shaken, a plate sealer should be used to prevent fluid transfer between wells, and care should be taken to preserve the optical clarity of the undersurface of all wells.

6. Wash plate three times with ELISA wash buffer.

   Incubations times, incubation temperatures, blocking conditions, washing conditions, and substrate concentrations should all be similar in the final assay to what is used to determine the working dilutions of antibody and antigen.

7. Add 100 µl substrate in appropriate substrate buffer, mix, and incubate 30 min at 37°C.
8. Measure substrate conversion to product using a microtiter plate reader at 405 nm, and use the patterns of enzyme activity to determine at what antibody-enzyme conjugate concentration the signal-to-noise ratio is most favorable and simultaneously economical.

   Endpoint reading of the microtiter plate is often done after a 30- or 60-min incubation at 37°C. Alternatively, reading can be done repeatedly immediately after substrate addition and a kinetic rate of substrate conversion determined (in mO.D./min). An example of data produced from a kinetic read is shown in Figure 18.7.3.

9. Set incubator to 37°C. Pre-run automated plate washer (if available) to replace distilled water in tubing with wash buffer.

   The incubator speeds the reaction and shortens the assay. It also ensures that the conditions of the assay do not vary over time as room air temperature might vary. A simple small

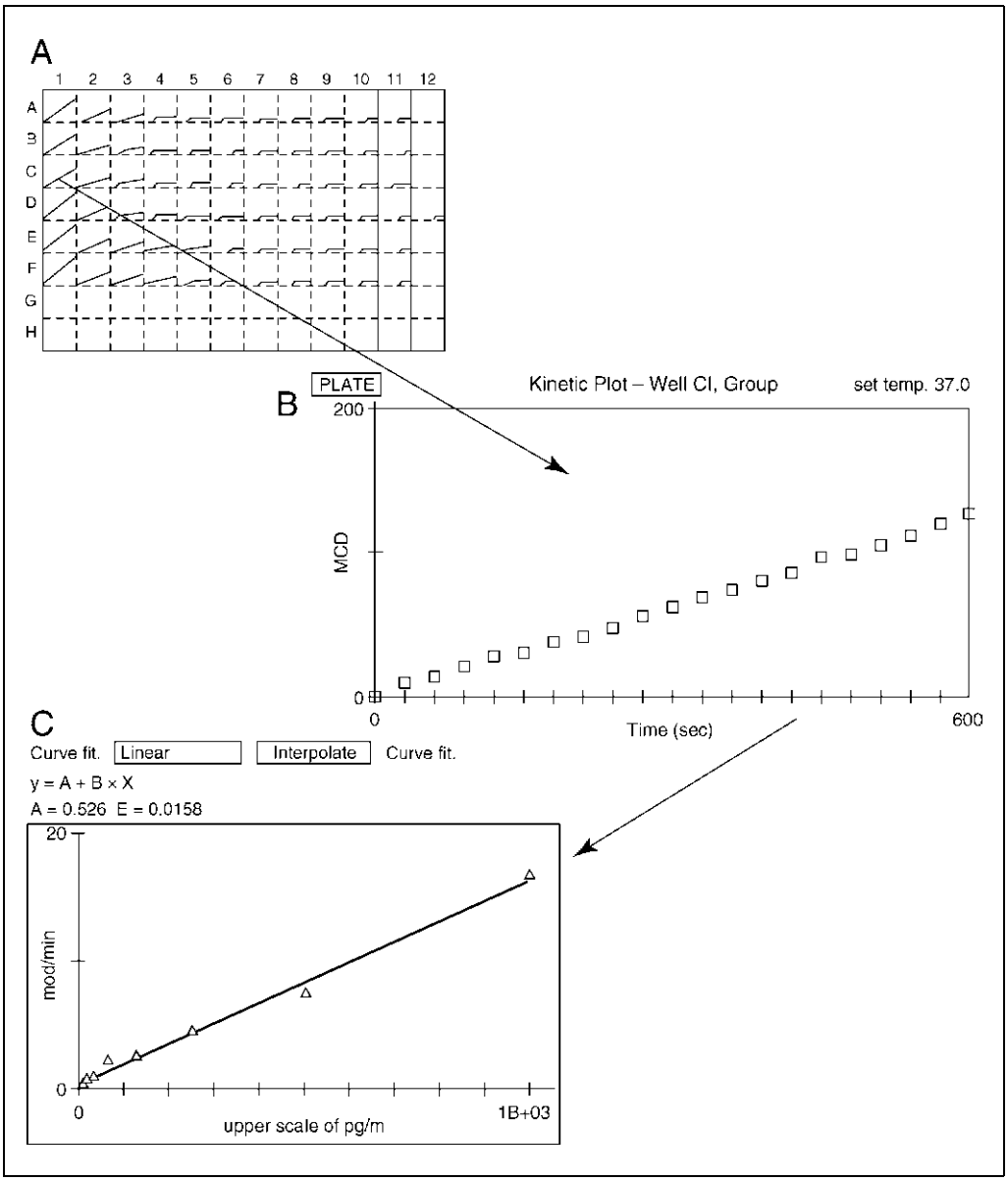

Figure 18.7.3 Each well of the microtiter plate is measured multiple times. (**A**) In this example, 20 measurements were done over a 6-min incubation. The individual kinetic plots can be examined individually (**B**), and the rates that are associated with each can be used to construct a standard curve (**C**).

incubator with ambient air is sufficient for this assay (some microplate readers have internal incubators that can be used for this purpose).

Prepare appropriate dilutions of antigen and antibody

10. Dilute samples that contain antigen in coupling buffer and pipet 100 µl of the antigen solution into the wells of a microtiter plate. Cover the filled wells with a plate sealer and incubate 60 min at 37°C.

    It is important to include wells for non-specific binding controls (often these are isotype-matched antibody-enzyme conjugates that are specific for an irrelevant antigen) and for positive- and negative-antigen control reactions (where known amounts of antigen are added to the well, or antigen is omitted from the coupling buffer that is placed in the wells).

    It is useful to hold the pipet tip at a consistent angle relative to the top surface of the plate, and to be consistent in the depth of pipet tip insertion into the well (ideally, the pipettor

should be held at ~45° and the tip inserted so that its end rests about half way down the well side). This ensures that the fluid is not adsorbed to the upper wall of the well, in an area that will later remain unblocked.

With additional experimentation, it may be possible to reduce incubation times to ≤30 min, although this abbreviation may come at the expense of sensitivity or with the use of higher concentrations of reagents. The plate sealer is removed at the end of each step by holding the plate firmly on a solid surface and slowly peeling the sealer off. It can be reused at each step if no liquid is transferred to the underside of the sealer.

Adhesive-backed mylar sheets prevent evaporation and inadvertent fluid transfer between wells that can alter the results and diminish the sensitivity of an ELISA. It is advantageous to seal the wells of the plate during each incubation, especially if the assay is done at 37°C to prevent changes in liquid volumes and salt concentrations due to evaporation.

Perform ELISA

11. Aspirate the antigen using a plate washer, or flick the antigen out over a sink by inverting the plate with a rapid downward motion. Blot the top of the plate with paper towels, and then add 150 µl of blocking solution. Incubate wells 60 min at 37°C.

    A larger volume of blocking solution (than the volumes used in other steps) is added to ensure that all possible non-specific binding sites near the meniscus of the antibody-enzyme conjugate solution will have been occupied before the conjugate is added to the well.

12. Empty the wells as in step 11, and wash manually or with an automated plate washer. If the plates are washed manually, add wash buffer to each well and immediately flick out wash buffer. Perform several more rapid washing steps, and then fill the wells with wash buffer and allow to soak 5 min before finally removing the wash buffer. If an automated washer is used, include a 5-min soak step after the first two of three cycles of washes to ensure non-adsorbed proteins are removed.

13. Immediately following removal of the wash buffer, add 100 µl antibody-enzyme conjugate at the optimal concentration to each well. Then re-seal wells with the plate sealer and incubate 60 min at 37°C.

    The dilution of antibody-enzyme conjugate is pre-determined during preliminary experiments (see steps 1 through 8).

14. Wash wells as described in step 12.

15. Finally, remove the final wash buffer, add 100 µl substrate in substrate buffer, and incubate plate 30 min at 37°C. Add an equal volume of 0.075 N NaOH to stop the reaction. Take an endpoint reading at 405 nm. Alternatively, for kinetic measurements, immediately place the plate, without stop solution, in a kinetic microtiter plate reader and measure at 20-sec intervals with shaking for 10 min.

    Standard microtiter plate spectrophotometers measure in the visible wavelengths, other reader formats can also measure fluorescence and/or luminescence.

ALTERNATE PROTOCOL 1

INDIRECT ELISA

An indirect ELISA (also called a sandwich assay) takes advantage of the commonly available antibody-enzyme conjugates that will bind to antibodies of specific isotypes, light chains, and from particular species. These reagents allow the experimental assessment of primary unlabeled antibodies from clinical samples, or from experimental culture or animal systems that would be impractical to prepare as individual conjugates to antibody. In essence, indirect ELISA is a modified direct ELISA where additional steps are added after the blocking step to allow initial binding of the primary, unconjugated test antibody, which is then indirectly measured as the target for binding by the secondary antibody-enzyme conjugate. Preliminary experiments to determine working dilutions are set up

essentially as described in Basic Protocol 1, steps 1 to 8. Several dilutions of antigen are each combined with several dilutions of unconjugated primary antibody and conjugated secondary antibody to establish optimum conditions for sensitivity.

Additional Materials *(also see Basic Protocol 1)*

Unconjugated primary antibody/antiserum reagent

1. Follow Basic Protocol 1, steps 10 through 12.
2. While the antigen solution is incubating in the wells, dilute the unconjugated primary antibody through a series of doubling dilutions from 1:10 to 1:10,240. Make at least 350 μl of each dilution to allow 100 μl to be added to each well in triplicate.
3. Add 100 μl of the diluted unconjugated primary antibody to the appropriate wells, seal, and incubate for 60 min at 37°C.
4. Wash the wells as described in Basic Protocol 1, step 12, and then add diluted antibody-enzyme conjugate to each well as described in Basic Protocol 1, step 13. Seal and incubate the wells for 60 min at 37°C.

   In many cases, this secondary antibody will be specific for the isotype of the primary antibody. Care should be taken to match the specificity of the secondary antibody based on species of animal from which the primary antibody was obtained. The secondary antibody can also be specific for both heavy and light chains of the primary antibody, or it can be a polyclonal antibody that is specific for a collection of immunoglobulin determinants of the different isotypes of antibody that might be in an antiserum that has been used as the primary antibody. It is also possible to use an antibody specific for a particular light chain of the primary antibody. For some species (e.g., mouse) one of the two light chain types is the predominant form, making an anti-light chain antibody a broad spectrum reagent for detection of many different primary antibodies.

5. Continue with Basic Protocol 1, steps 14 and 15.

COMPETITION ELISA

ALTERNATE PROTOCOL 2

A competition ELISA is essentially a direct or indirect ELISA in which the antigen-specific antibody is pre-incubated with soluble preparations of known solutions of antigen, or with unknown solutions that may include antigenic determinants. In this assay, antigen present in low concentrations in heterogenous mixtures of protein (e.g., secreted proteins in serum) can be quantified by comparison to a standard curve of purified protein.

Additional Materials *(also see Basic Protocol 1)*

Soluble antigen in purified form
Goat anti-mouse Ig-alkaline phosphatase conjugate that recognizes both heavy and light chains

Coat microtiter plate

1. Coat the 96-well flat-bottom microtiter plate (Immulon 2) with antigen diluted to 10 μg/ml in coating buffer by adding 100 μl to each well to immobilize 1 μg/well. Cover the wells with a plate sealer and incubate 1 hr at 37°C or overnight at 4°C.

Prepare samples and standards

2. While plate is incubating, prepare standards.

   a. Label 1.5-ml microcentrifuge tubes for each standard.
   b. For the first standard, add 160 μl of antigen from 1 mg/ml stock to the first tube and 240 μl of binding buffer (total volume is 400 μl).
   c. Add 200 μl of binding buffer to the remaining tubes.

d. Take 200 µl from the first tube and transfer into the second tube. Mix and transfer 200 µl to the next tube. Repeat this doubling serial dilution for the remaining tubes. Remove 200 µl from the last tube to ensure that all tubes have the same volume. Store all tubes on ice until use.

3. To prepare samples, add 200 µl of cell lysates, serum dilutions, or other unknown samples to 1.5-ml microcentrifuge tubes and keep all tubes on ice.

Preincubate antibody

4. Prepare pre-determined dilution of antibody specific for the target antigen in binding buffer, and add 200 µl of this diluted antibody to the tubes that already contain 200 µl of known antigen concentration standards or unknown samples.

   The final dilution of the antibody in each well will be two times the stock dilution, and the final concentrations of antigen will be half the dilution added. The antibody dilution to be used in this step is determined in a preliminary indirect ELISA where the titer of the antibody is determined. A dilution that is the penultimate dilution before the ELISA signal begins to significantly decline is the best to choose. This dilution will be halved by the addition to standards or sample. Any soluble antigen in the standards or the sample will reduce the amount that is available to bind the immobilized antigen on the microtiter plate surface. It is critical that all assay conditions (e.g., incubation times, antigen and antibody preparations, temperatures, and wash conditions) be identical between experiments that establish the dilution of primary antibody to be used.

5. Vortex all standard and sample tubes and incubate 1 hr at 37°C.

Perform competitive ELISA

6. After standards and samples have been added to the primary antibody, aspirate the antigen-coated plate, and block each well by adding 150 µl blocking buffer.

7. Microcentrifuge the tubes containing standard or sample for 10 min at 5000 rpm.

8. During the last 5 min of the microcentrifugation in step 8, take out the plate being blocked and wash three times with wash buffer using an automated plate washer.

9. Add 100 µl of standards and samples in triplicate to appropriate wells of a microtiter plate, seal with plate sealer, and incubate 1 hr at 37°C.

10. Wash plate three times with wash buffer using an automated plate washer.

11. Add 100 µl of a predetermined dilution of goat anti-mouse Ig-alkaline phosphatase conjugate (e.g., 1:500) to each well and incubate for 1 hr at 37°C.

    This dilution will have been predetermined at the same time that the primary antibody dilution was established.

12. Wash plate three times with wash buffer using an automated plate washer.

Detect binding

13. Add 100 µl of alkaline phosphatase substrate buffer to all wells.

14. Immediately read the plate at 405 nm for 10 min at 30-sec intervals in a kinetic plate reader, or as an endpoint read as described in Basic Protocol 1, step 8.

BASIC PROTOCOL 2

ELISPOT ASSAY

The ELISPOT assay, originally described >20 years ago (Czerkinsky et al., 1983; Sedgwick and Holt, 1983) can provide information about the number of cells in a population that are secreting a specific protein (usually a cytokine or immunoglobulin). Cytokine secretion can be interpreted to indicate pathways of immune activation such as T_h1- or T_h2-dependent pathways (Lalvani et al., 2001), and immunoglobulin secretion

can indicate either antigen-specific responses to antigen challenge, or total amounts of specific isotype production indicative of overall immune capacity. There are some suppliers of complete ELISPOT kits (e.g., Sanquin; Mabtech; and Diaclone), but it is often far more economical to develop the specific ELISPOT assay for an antigen of specific interest in the laboratory. In the prototype assay described below, antigen coupled to the membrane surface serves as a target for the quantification of cells secreting an antibody specific for that antigen.

Materials

Antigen
ELISPOT coating buffer (see recipe)
ELISPOT wash buffer (see recipe)
RPMI-1640 supplemented with 10% FBS or ELISPOT blocking buffer (see recipe)
Test cells
Capture and detection antibodies for the target molecule of interest
ELISPOT assay diluent
ELISPOT culture medium
ELISPOT substrate solution: BCIP (5-bromo,4-chloro,3-indolylphosphate)/NBT (Kirkegaard and Perry)

96-well filtration plates with sterile surfactant-free membrane (e.g., Millipore)
Automated plate washer (optional)
ELISPOT reader (ImmunoBiosys, Zeiss, Sanquin, or A. EL. VIS) *or* dissecting microscope and digital image analysis software (e.g., ImageJ available as freeware at *http://rsb.info.nih.gov/ij/*)

Add antigen to plates

1. Incubate ELISPOT plate with 100 µl/well of filter-sterilized (0.2-µm filter) antigen at 100 µg/ml in ELISPOT coating buffer. Incubate specificity control wells with 100 µl/well of an irrelevant antigen at 100 µg/ml in ELISPOT coating buffer. Incubate overnight at 4°C.

   These 96-well filtration plates with sterile surfactant-free membranes have filters on the bottom, which have a pore size of 0.45µm and are comprised of hydrophobic PVDF.

2. Wash three times with sterile ELISPOT wash buffer in an automated plate washer, or wash plates manually.

3. Block plate with 200 µl/well sterile RPMI-1640 supplemented with 10% FBS for 1.5 to 2 hr at room temperature, or with ELISPOT blocking buffer.

Add cells

4. Add 100 µl of the test cell populations in sterile RPMI-1640 supplemented with 10% FBS to each well at serially diluted cell suspensions of 10^6/well to 10^4/well in triplicate and incubate in a 37°C, 5% CO_2 humidified incubator for 24 hr.

5. Wash wells three times with ELISPOT wash buffer manually or in an automated plate washer.

Perform ELISPOT assay

6. Add 100 µl/well of ELISPOT detection antibody at 1 µg/ml in PBS (usually ~1:500 dilution of antibody) and incubate 2 hr at 37°C.

   It is important that the specificities of the capture and detection antibodies are compatible. The pair must be capable of binding to distinct epitopes on the same target molecule simultaneously.

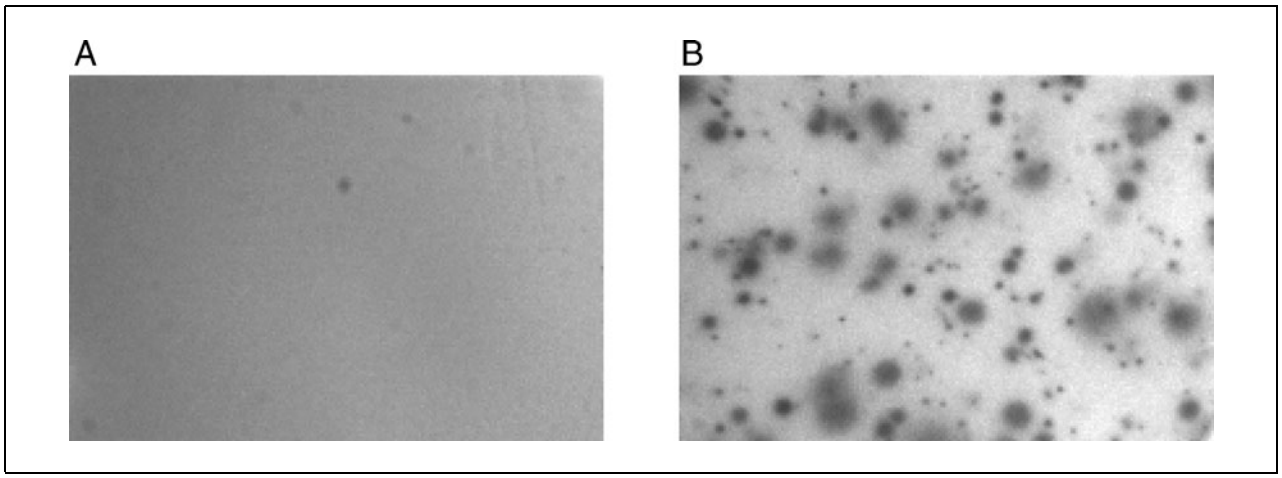

Figure 18.7.4 Examples of colored precipitate spots generated in the ELISPOT assay. (**A**) Control well containing unstimulated cells. (**B**) Well containing stimulated cells.

7. Wash three times with ELISPOT wash buffer manually or in an automated plate washer.
8. Add 100 µl/well of ELISPOT substrate solution and develop for 10 to 30 min at room temperature until spots appear.
9. Wash plate three times with 200 µl/well distilled water.
10. Air-dry the plate and count spots by using a dissecting microscope or ELISPOT reader.

Legitimate spots will be round and larger than a cell in size (usually 75 to 400 µm in diameter) when viewed with a dissecting microscope. An example of these spots can be seen in Figure 18.7.4. Artifacts will have eccentric shapes, and staining will not be uniform across the spot. It is often useful to look at a well that has not been seeded with cells before the staining protocol was done to identify known artifacts. While the trained eye is still best at identifying spots, it is advisable to have coded the wells so that enumeration can be done without bias.

BASIC PROTOCOL 3

GRATING-COUPLED SURFACE PLASMON RESONANCE IMMUNOASSAY

GCSPR is a new assay that offers the sensitivity of an ELISA in a microarray format (Fig. 18.7.5). This format enables the simultaneous evaluation of small volume samples to determine the presence of a large number of different antigenic determinants (Brockman and Fernández, 2001). Currently available chips have an active area that is ~1 cm^2, and can accommodate ~400 individual spots. With replicates, this allows for the assessment of >100 antibody/antigen interactions at the same time in a real-time assay that is label free. Currently, there is only one commercial supplier of GCSPR instrumentation (HTS Biosystems).

Materials

Ethanol
Capture antibody
Antigen
PBS (see recipe)
GCSPR blocking reagent
Analyte solution

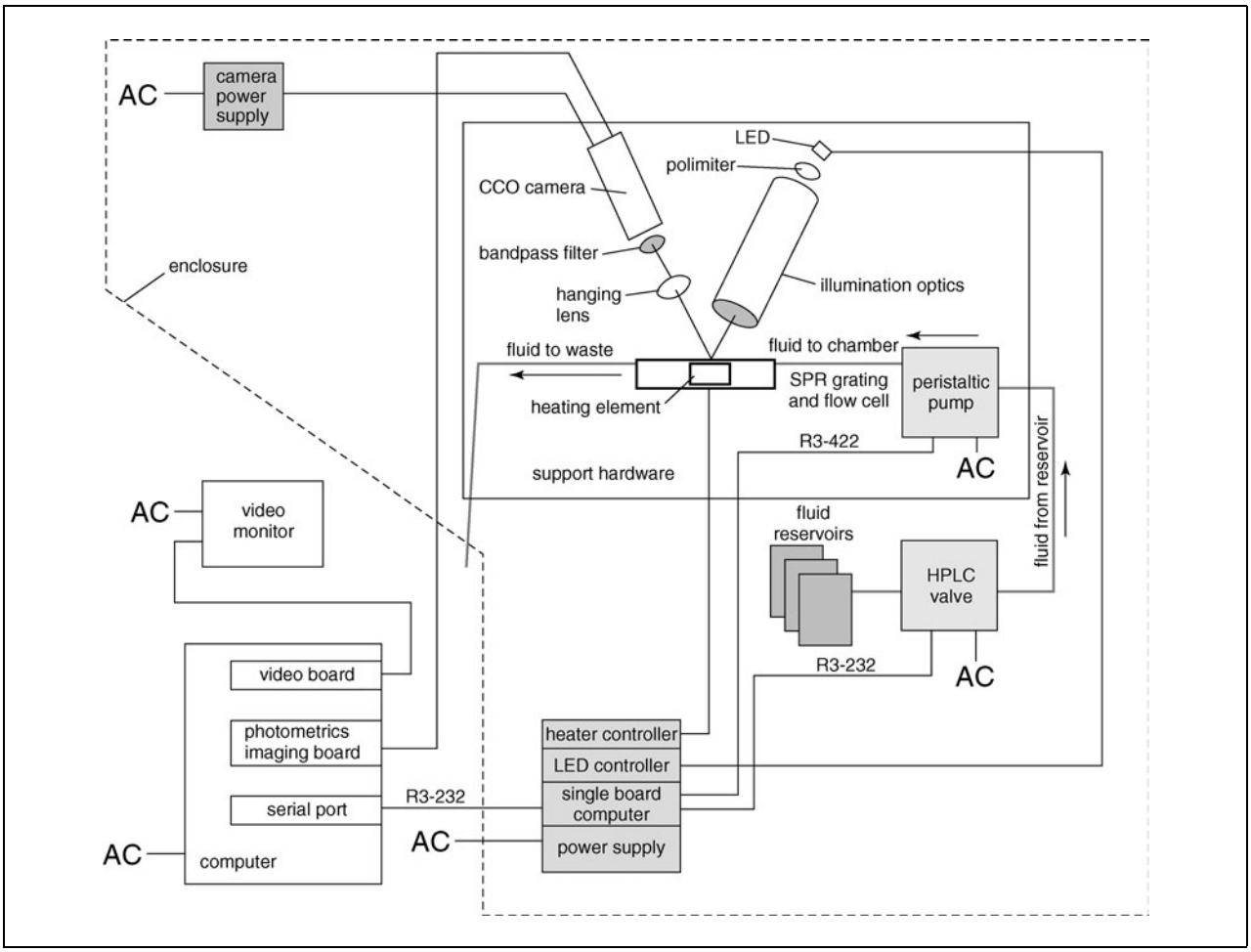

Figure 18.7.5 GCSPR optical diagram.

MicroCaster System, 8-pin manual arrayer (Schleicher and Schuell Bioscience), or another spotting system
GCSPR sensor chips (Applied Biosystems)
96-well microtiter plates
37°C incubator and humid box
Applied Biosystems 8500 affinity chip analyzer

1. Rinse pins of arrayer sequentially in ethanol and distilled water.
2. Rinse gold sensor chip surface sequentially in ethanol and distilled water. Allow to air dry.
3. Place chip in arrayer with the notch in the upper right hand corner. Determine which pins will spot inside the active area of the chip (the part of the chip that has the diffraction grating embossed on it).
4. Place captured antibodies in wells of a 96-well microtiter plate. Dip pins into antibody solutions.
5. Transfer samples to active area of chip on slide. Designate regions of interest (ROIs).
6. Move chip using MicroCaster indexing system and repeat for desired number of spots. Move chip in a horizontal direction.
7. Use a sharp needle to make a small scratch in the chip underneath the spots for orientation (make this mark at least 1 mm away from the ROIs).

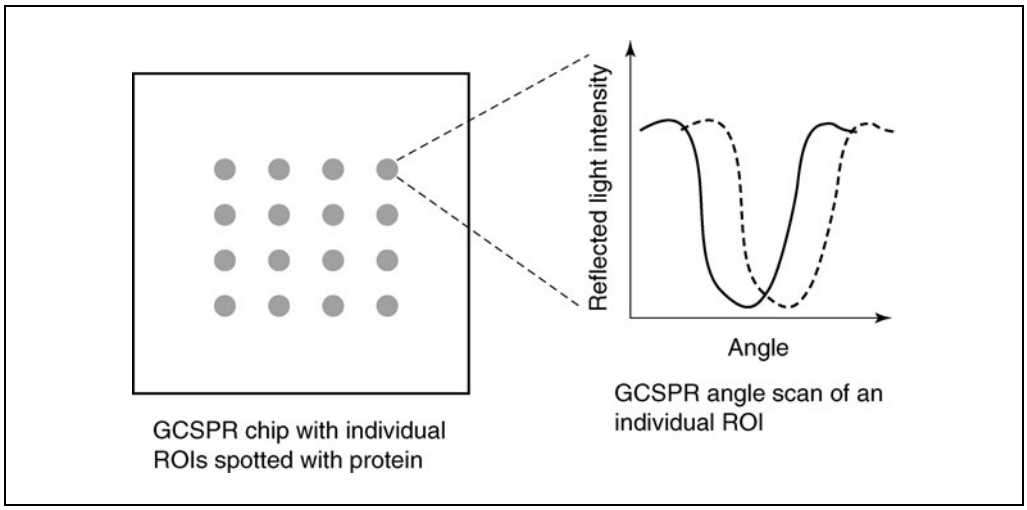

Figure 18.7.6 The GCSPR chip is illuminated following spotting of the chip surface with the capture antibody and reflected light intensity is measured at a range of angles (solid line). Following exposure of the chip to cognate antigen, the angle scan is repeated, and reflected light intensity is again measured (dashed line). The increase in the angle at which the maximum coupling occurs, which is the angle that has the least light reflected, is an indication of antigen binding to the capture antibody. The magnitude of this angle shift is a measure of the increase in molecular mass at the ROI.

8. Place spotted chips in 37°C incubator inside a humid box for 30 min to allow antibody to bind to the chip surface. Install chip in reader.
9. Initiate liquid flow at 200 µl/min and pass PBS over chip surface, take initial GCSPR data to assess the amount of protein that remains bound to the chip (compare to empty ROIs where no capture antibody has been placed)
10. Pass GCSPR blocking reagent over chip surface.
11. Pass analyte solution over surface and take GCSPR data to assess the change in the GCSPR angle (the illumination angle at which the greatest coupling and thus least reflection of light occurs).
12. Assess angle shift increases as an indicator of antigen capture (Fig. 18.7.6).

REAGENTS AND SOLUTIONS

Use Milli-Q-purified water or equivalent for all recipes and protocol steps. For common stock solutions, see ***APPENDIX 2A****; for suppliers, see* ***SUPPLIERS APPENDIX****.*

Alkaline phosphatase substrate buffer

9.7% (w/v) diethanolamine
0.02% (w/v) NaN_3
0.01% (w/v) $MgCl_2$, pH 9.8
Store buffer for several months at 4°C. Add *p*-nitrophenyl phosphate (1 mg/ml PNPP; Sigma) 10 min before use to allow the PNPP to dissolve.

Tablet or capsule forms of the substrate can simplify addition to the buffer.

ELISA blocking buffer (BSA-based)

PBS (see recipe)
0.2% (w/v) NaN_3
10% (w/v) BSA
Store up to 1 week at 4°C.

ELISA coupling buffer

15 mM $NaHCO_3$
35 mM Na_2CO_3
0.2% (w/v) NaN_3, pH 9.6
Store up to 6 months at 4°C

CAUTION: *NaN_3 is a toxic substance and should be handled with gloves and filter mask to avoid ingestion. Discarded solutions with azide should be substantially diluted with running water if poured down the drain to avoid the formation of lead azide in the pipes (a contact explosive).*

ELISA wash buffer

PBS
0.2% (w/v) NaN_3
0.05% (v/v) Tween 20, pH 7.2
Store up to 6 months at 4°C

ELISPOT blocking buffer

1% (w/v) Teleostean gelatin or 5% (w/v) nonfat dry milk in PBS (no azide). Store up to 1 week at 4°C.

ELISPOT coating buffer

1.57% (w/v) Na_2CO_3
2.93% (w/v) $NaHCO_3$
0.2% (w/v) NaN_3, pH 9.7
Store up to 6 months at 4°C

ELISPOT substrate solution

Prepare stock solutions of nitroblue tetrazolium (100 mg NBT/2 ml of 70% dimethylformamide in water) and bromo-4-chloro-3-indolyl phosphate (100 mg BCIP in 100% DMF). Add 33 µl NBT stock plus 17 µl BCIP stock to buffer comprised of 100 mM Tris·Cl, pH 9.5, 100 mM NaCl, and 5 mM $MgCl_2$. Use working substrate within 1 hr. Store NBT and BCIP stock solutions at −18°C.

ELISPOT wash buffer

PBS (see recipe)
0.05% (w/v) NaN_3
Store up to 6 months at 4°C

Phosphate buffered saline (PBS)

8 g/liter NaCl
0.2 g/liter KCl
1.15 g/liter Na_2HPO_4
0.2 g/liter KH_2PO_4
Store up to 6 months at 4°C

COMMENTARY

Background Information

ELISA has supplanted the radioimmunoassay (RIA) as the method of choice for measuring antibody/antigen interactions. Depending on the particular configuration used, a wealth of information can be obtained with ELISA. For the most part, this assay can enable the characterization of cellular antigens, soluble antigens, and the antibodies that detect these targets. It is important to design

Table 18.7.3 Troubleshooting Guide to ELISA/ELISPOT

Problem	Possible cause	Solution
No color development	Enzyme or substrate may be bad or left out of final step	Retain unused diluted antibody-enzyme conjugate and prepared substrate. Test for enzyme activity by mixing 10-µl aliquot of the diluted conjugate with 100 µl of substrate.
	Antibody-enzyme conjugate denatured or aggregated	Do not freeze-thaw conjugate, store at 4°C
Excess color development; non-linear changes in optical density with changes in antigen or antibody concentration	Some plate readers produce linear measurements up to an O.D. of 2.0. Others are linear to an O.D. of 3.0	Dilute the antigen or the antibody to reduce the amount of enzyme that is bound in the well
False positives in ELISA/ELISPOT	Antibody-enzyme conjugates will aggregate under some conditions and become quite sticky	To reduce non-specific binding, centrifuge conjugate in microcentrifuge at top speed, or ultrafilter diluted conjugate just before use.
		Inappropriate cross-reactivity may exist in the antigen-specific antibody preparation, or contaminating antigens may be present.

the ELISA with potential cross-reactions in mind, and to include both positive and negative controls in the assay for quality control. It is equally important, especially in the context of toxicological assessments, to ensure that the toxic agent does not have an undue influence over the performance of the assay. For example, toxins may diminish viability of input cell populations in the ELISPOT assay, which could alter the interpretation of results. Metals can alter structural features of target molecules, making their detection less certain. Lead has been shown to interact with IFN-γ in this way (David Lawrence, pers. comm.). Thus, it may be useful to run preliminary assays in the presence of the toxicant itself to assess the impact of this reagent on the ability of the antigen to adsorb to the microtiter plate surface, on the ability of the antibody to bind antigen, and on the enzymatic conversion of substrate to product.

Troubleshooting

See Table 18.7.3 for a list of possible problems, possible causes, and solutions.

Anticipated Results

Typically, ELISA can distinguish proteins in complex solutions at concentrations in the micro- to nanogram range, but specifically selected antibodies can be sufficiently sensitive to detect antigen in the picogram range. It is usually useful to test several dilutions of antigen or antibody to exclude artifactual results by showing that the reaction behaves as predicted (i.e., a ten-fold dilution will produce a ten-fold decrease in signal). For measurements of humoral immune responses, it is often of value to determine the titer of the solution—at what dilution the reactivity diminishes below a specific defined value. In assay configurations where the antigen must couple to a capture antibody and to an antibody-enzyme conjugate, care must be taken to match the antibody pairs; otherwise steric interference will impede the simultaneous binding of both antibodies to the antigen, thus making the assay unsuccessful.

The ELISPOT assay is an outgrowth of the plaque assay, where cells in soft agar were assayed for the secretion of antibody that could lyse erythrocytes in an overlying layer of agarose. As cells secret relevant antibodies, they diffuse into the overlying layer containing the erythrocytes, and will bind to the erythrocyte membranes. After this incubation is complete, a solution containing complement proteins (often a dilution of guinea pig serum) is added to the top of the agarose layers and allowed to saturate the agarose. Where antibody has bound to erythrocyte membranes, the complement cascade will be activated, and cells will lyse. This can be seen as a clearing of the granular erythrocyte suspension (visualized as a clear plaque) and can further be identified by

the lymophocyte that is located in the center of the plaque. The ELISPOT assay is a more universal assay because the antigens that can be assayed need not be naturally or artificially located on the erythrocyte membranes. An optimized ELISPOT can detect two to three secreting cells per 10^5 input cells.

The GCSPR protein microarray platform is a further improvement on the basic assessment of antigen-antibody interactions. Sensitivity of the GCSPR assay approximates that of an ELISA, and may be further improved as the sensing technology is improved, and as the chemistry of antigen immobilization is enhanced. Moreover, current investigations are underway to explore the application of the GCSPR to ELISPOT-type investigations.

Each of these assays can be used to assess the impact of toxins on the immune response by assessment of the degree of immunity that develops in the presence of different levels of toxin.

Time Considerations

ELISA usually takes about a half day to complete, but this can be accelerated by increasing the antigen and antibody concentrations as the time per step is shortened. Alternatively, the assay can incorporate an overnight step to prepare the initial antigen-bound plate, or can employ plates that have been commercially prepared to reduce the time before experimental sample is applied.

ELISPOT can take several hours to prepare, including the preparation of cells from harvested tissue or from cell culture. Once the cell culture incubation phase is complete (overnight incubation), the remainder of the assay can take an additional 1 to 2 hr to complete. Once stained, the spots can be enumerated under the microscope; this usually will take 1 or 2 hr to complete.

GCSPR assays can take 1 or 2 hr to complete; on a per antigen basis, this assay can be the fastest of those discussed here since several hundred spots can be assessed on a single chip.

Literature Cited

Amoura, Z., Chabre, H., Koutouzov, S., Lotton, C., Cabrespines, A., Bach, J.F., and Jacob, L. 1994. Nucleosome-restricted antibodies are detected before anti-dsDNA and/or antihistone antibodies in serum of MRL-Mp lpr/lpr and +/+ mice, and are present in kidney eluates of lupus mice with proteinuria. *Arthritis Rheum.* 37:1684-1688.

Brockman, J.M. and Fernández, S.M. 2001. Grating-coupled surface plasmon resonance for rapid, label-free, array-based sensing. *American Laboratory* 6:37-40.

Czerkinsky, C., Nilsson, Langstrom., Nygren, H., Ouchterlony, O., and Tarkowski, A. 1983. A solid-phase enzyme-linked immunospot (ELISPOT) assay for enumeration of specific antibody-secreting cells. *J. Immunol. Methods* 65:109-121.

Lalvani, A., Pathan, A.A., Durkan, H., Wilkinson, K.A., Whelan, A., Deeks, J.J., Reece, W.H., Latif, M., Pasvol, G., and Hill, A.V. 2001. Enhanced contact tracing and spatial tracking of Mycobacterium tuberculosis infection by enumeration of antigen-specific T cells. *Lancet.* 357:2017-2021.

Probst, P., Kuntzlin, D., and Fleischer, B. 1995. Th2-type infiltrating T cells in nickel-induced contact dermatitis. *Cell. Immunol.* 165:134-140.

Sedgwick, J.D. and Holt, P.G. 1983. A solid-phase immunoenzymatic technique for the enumeration of specific antibody-secreting cells. *J. Immunol. Methods* 57:301-309.

Internet Resources

http://www.probes.com

Molecular Probes is an excellent source for information and materials related to fluorescent immunoassays.

http://www.southernbiotech.com

http://www.rndsystems.com

These companies provide a wide range of antibody/enzyme conjugates.

http://www.abcam.com

http://biocompare.com

Online search engines for identifying sources of antibodies from a range of commercial vendors. Linscott's directory of immunological and biological reagents is available as a CD, or in print and is also available online at http://www.linscottsdirectory.com/directoryonline.htm.

http://www.piercenet.com

http://www.sigmaaldrich.com

Sources of antibodies, purified antigens, blocking reagents, and other useful reagents for these techniques.

http://www.elispotresource.com/

A Website supported by many of the vendors of ELISPOT materials and instrumentation.

http://www.htsbiosystems.com

Website for GCSPR Flexchip Analyzer.

Contributed by Michael A. Lynes
University of Connecticut
Storrs, Connecticut

Immune Cell Phenotyping Using Flow Cytometry

Immunophenotyping is a general term used to describe the use of fluorescently labeled antibodies to identify and quantify distinct subpopulations of cells within a heterogeneous population of cells. Frequently, the term is used more specifically to refer to the characterization of subsets of cells associated with the immune system (i.e., immune cell phenotyping). In either case, the antibodies used for immunophenotyping are usually specific for cell surface proteins that are known to be differentially expressed on discrete subsets of cells. Immunophenotyping can be carried out using either flow cytometry or immunohistochemical analysis. However, flow cytometry is often the method of choice, because it permits the acquisition of nonsubjective data on thousands of cells within seconds. Furthermore, each cell suspension can be labeled with several different antibodies simultaneously, and the fluorescence associated with each antibody can be collected on a per-cell basis as correlated data. Modern flow cytometers can routinely measure five or more different fluorescence emissions simultaneously, providing the means to easily detect unique subsets within a heterogeneous population of cells. More recently, cell surface phenotyping with immunofluorescent probes has been performed to ascertain the functional status (e.g., DNA or cytokine content, mitochondrial membrane integrity, glutathione status) of cells, making multiparameter flow cytometry a very powerful tool for characterizing the activation state of a cell. The only drawback of flow cytometry is that cells must be stained and analyzed in a single-cell suspension, which is easier to prepare from some tissues than from others. Because cells derived from blood and lymphoid tissues are readily maintained in suspension, flow cytometry has been widely used to phenotype these cells.

Immunophenotyping of lymphoid tissues, particularly spleen and thymus, has been used in the field of immunotoxicology for many years as part of a tiered screening approach for detecting immunotoxicity following chemical exposure. Since thymic involution frequently occurs after toxicant exposure, changes in thymocyte immunophenotypes are commonly evaluated. Similarly, just as white blood cell (WBC) counts and differentials have been used for many years to assess immune status in toxicant-exposed animals, newer screening approaches such as immunophenotyping of spleen and/or lymph nodes have been used to quantify frequencies of the major lymphocyte subtypes (B cells, T cells, and T cell subsets) following chemical exposure. In studies conducted by the National Toxicology Program, the utility of immune cell phenotyping has been validated using a large database of environmental toxins and certain pharmaceutical agents. In these studies, changes in lymphocyte phenotypes in the spleen or thymus following toxicant exposure was identified as one of the best single correlates with toxicant-induced changes in host resistance to pathogens or tumors (Luster et al., 1993). However, even though immunophenotyping of the spleen and thymus may correlate with toxic chemical exposure, it is not necessarily a robust predictor of immunotoxicity, particularly when naive animals are exposed to toxicants. Some highly immunotoxic chemicals, including cyclosporin A and 2,3,7,8-tetrachlorodibenzo-*p*-dioxin (TCDD), do not alter splenic immunophenotypes in the absence of antigen challenge (Kerkvliet and Brauner, 1990; Vandebriel et al., 1999). Likewise, changes in thymic phenotypes can occur indirectly, through stress-induced effects on the thymus that are independent of direct immunotoxicity. Thus, it is generally agreed that immunophenotypic analysis of B cells, T cells, and T cell subsets present in the thymus and/or spleen should be used in conjunction with conventional assessments of immune function when screening for the immunotoxic effects of drugs and chemicals (Immunotoxicology Technical Committee, 2001; Food and Drug Administration, 2002).

Contributed by Julie A. Oughton and Nancy I. Kerkvliet
Current Protocols in Toxicology (2005) 18.8.1-18.8.24

Although immunotoxicology studies have focused primarily on the phenotypic analysis of B cells and T cell subsets in spleen and/or thymus from naive mice, several extended applications of immunophenotyping are emerging in the immunotoxicological literature. One important extension is the analysis of peripheral blood cells from mice and rats (Oughton et al., 1995; Nygaard and Lovik, 2002; Funatake et al., 2004). The use of peripheral blood samples from rodents allows more direct comparisons to be made with toxicity data that may be available from human studies, which nearly always rely on peripheral blood samples. Analysis of blood also allows evaluation of systemic changes that may result from toxicant effects in lymphoid tissues, as well as the testing of multiple samples obtained from the same animal over an extended time.

Another important addition to standard immunophenotyping techniques is the analysis of activation markers. Most cells in the immune system respond to antigenic stimulation by altering their expression of a number of different proteins on the cell surface. Many of these proteins are known to be involved in the functional response of the cell (e.g., adhesion, migration, costimulation), while others may reflect the cell's antigenic history (as in memory cells). Evaluation of activation markers is likely to provide an enhanced ability to detect immunotoxic effects. For example, when mice were exposed to low doses of TCDD for more than a year, no changes in major T- and B cell subsets were observed. However, analysis of the naive/memory phenotypes of $CD4^+$ T cells revealed that TCDD exposure had significantly reduced the proportion of memory cells present (Oughton et al., 1995). Likewise, evaluation of activation markers in the context of an ongoing immune response may provide novel insight into the selective targets and mechanisms of action of immunotoxic chemicals. Several laboratories are now using immunophenotyping to track the effects of toxicants on the activation and fate of antigen-specific T cells following antigenic challenge, with very exciting results (Shepherd et al., 2000; Mitchell and Lawrence, 2003; Funatake et al., 2004).

Since the specific antibodies that one might use for immunophenotyping will vary depending on the species tested, the flow cytometer used, and the experimental questions being asked, the following protocol describes a generic approach to the staining of cells with fluorescently labeled monoclonal antibodies (MAbs) to assess cell surface protein expression. Work in the authors' laboratory has primarily involved mouse cells; however, all aspects of this unit easily apply to the analysis of cells from rats, dogs, and horses. The first protocol (Basic Protocol 1) describes the procedure by which cells obtained from lymphoid tissue are stained with fluorochrome-conjugated MAbs (direct staining method). A second protocol (Alternate Protocol) describes two indirect methods for the staining of cells with primary MAbs that are not conjugated to a fluorochrome. Finally, a third protocol (Basic Protocol 2) describes the staining of peripheral blood cells with MAbs.

Support protocols are presented for the preparation of lymphoid cells (Support Protocol 1), the fixation of cells (Support Protocol 2), and discrimination of dead cells (Support Protocol 3). When freshly stained cells cannot be analyzed immediately, samples must be fixed so that the cells are stable for storage (Support Protocol 2). Furthermore, because the inclusion of dead cells in flow cytometric analysis can lead to the misinterpretation of data and possibly to the rendering of erroneous conclusions, it is desirable to assess cell viability using DNA dyes (Support Protocol 3).

Finally, a procedure for the determination of optimal antibody concentrations is presented in Support Protocol 4.

NOTE: The investigator should consult the manufacturer's instruction manual for specific information regarding the operation of his or her flow cytometer.

DIRECT STAINING OF CELLS PREPARED FROM LYMPHOID TISSUES

BASIC PROTOCOL 1

This is the preferred method for staining cells obtained from lymphoid tissues (e.g., spleen, thymus, lymph nodes). Basic Protocol 1 is appropriate for immunophenotyping of cells from either rats or mice. Because this method uses MAbs that are directly conjugated to fluorochromes, staining is simple and quick and usually produces little background signal.

Toxicology studies usually involve the assessment of lymphoid tissues from several individual animals in a number of different treatment groups. For example, a 3-dose-plus-control experiment that examined spleen and thymus from 5 animals per treatment group would yield 40 individual cell samples that needed to be stained, usually in more than one staining configuration. Processing of large numbers of samples can be facilitated by staining cells in V-bottom 96-well microtiter plates, as opposed to 12 × 75–mm tubes. These plates can be centrifuged using a microtiter plate carrier, and the contents of the wells can be mixed easily using a vortex mixer (such as the Vortex-Genie 2, VWR Scientific Products) equipped with a platform head for a microtiter plate. Use of a multichannel pipettor (such as the 12-channel Pipet-Lite multichannel pipet from Rainin Instrument) facilitates rapid dispensing of media into the wells, as well as quick transfer of samples to Titertubes (Bio-Rad) for flow cytometric analysis. Titertubes are small tubes that can easily be inserted into 12 × 75–mm disposable tubes, which are commonly used to run samples on a flow cytometer. The abovementioned products greatly increase productivity and also simplify the processing of large numbers of samples. To help keep track of stained samples, a template of the microtiter plate can be prepared in which descriptions of the contents of each well (e.g., animal source, MAbs used) are recorded. In lieu of microtiter plates, cells can be stained in 12 × 75–mm plastic tubes or microcentrifuge tubes.

Materials

Tissue of interest (e.g., lymphoid cells, Support Protocol 1)
Fc receptor (FcR)-blocking immunoglobulin (Ig; e.g., normal rat IgG) solution, 200 μg/ml
MAbs *or* isotype Igs directly conjugated to fluorochromes
PBS supplemented with sodium azide and BSA (PAB; see recipe)
Micropipettor *or* multichannel pipettor with tips
96-well V-bottom microtiter plates, disposable 12 × 75–mm polystyrene tubes, or microcentrifuge tubes
Centrifuge, refrigerated and equipped with a microtiter plate carrier
Vortex mixer equipped with a platform head for a microtiter plate
Titertubes (Bio-Rad Laboratories; optional)
Additional reagents and equipment for preparation of lymphocyte suspension to be analyzed (Support Protocol 1)

NOTE: Several steps need to be performed to minimize antibody cross-linking and the subsequent internalization of cell surface receptors that may occur when these receptors are bound to MAbs. This process is often referred to as *capping* of the antigen-antibody complex. Some cell surface molecules are less likely to cap than others; however, surface immunoglobulin on B cells can cap almost instantaneously. The addition of sodium azide (final concentration, 0.1% w/v) to the staining medium will help to prevent capping. In addition, all cell preparations and staining procedures, including wash steps, should be performed at 4°C, a condition achieved by incubating the cells on ice. Staining samples on ice also reduces the off-rate constant associated with antibody binding by a factor of 10 compared with the off-rate constant at 25°C.

Prepare lymphocyte samples for staining

1. Prepare a single-cell suspension of lymphocytes in 5% HBSS. Lyse red blood cells (RBCs) if present in large numbers (Support Protocol 1).

2. Using a micropipettor or microchannel pipettor, dispense 1–4 × 10^6 cells into each well of a V-bottom 96-well microtiter plate.

   Alternatively, dispense cells into 12 × 75–mm tubes or microcentrifuge tubes.

3. Pellet cells by centrifugation for 3 min at 200 to 1500 × *g*, 4°C.

   The range of centrifugation speeds quoted in this step reflects the fact that no one speed is accepted by the entire flow cytometry community. Although 1500 × g may sound excessive, this is the speed most commonly used by Stewart and Stewart (2001a) in order to minimize the loss of cells during washing.

4. Remove supernatant by holding the plate over a sink and inverting with a flick of the wrist or by decanting liquid from tubes. Blot the plate or the lip of each plastic tube on an absorbent towel to remove excess supernatant.

5. Vortex plate or tubes lightly to resuspend cell pellet.

Label with fluorochrome-conjugated MAbs

6. Add 50 µl FcR-blocking Ig (10 µg) to each cell suspension. Vortex cells lightly and incubate on ice for 10 min.

   A number of cells (especially myeloid cells) have receptors for the Fc portion of an immunoglobulin and will bind to any MAb. In order to assess the antigen-specific binding of a MAb, FcR must be blocked using normal IgG from the same animal species as the selected MAb. For example, for cells stained with rat anti–mouse CD4 MAb, normal rat IgG should be used to block FcR-mediated binding. As an alternative, a MAb specific for mouse FcR (CD16/CD32) can be used, although this involves a substantially higher cost.

   FcR should not be blocked when assessing FcR expression.

7. Without removing the FcR-blocking reagent, add the appropriate fluorochrome-labeled MAbs (see Support Protocol 4 for determination of optimal antibody concentrations) or isotype Igs to each well or tube. Vortex plate or tubes and incubate cells on ice for 10 min, protected from light.

   Cells can be stained with a number of MAbs simultaneously as long as there are no interactions among these MAbs. For large studies, a cocktail of all the MAbs of interest can be used to stain each sample. For example, if cells are to be stained for CD3, CD4, and CD8, a single cocktail including all three MAbs can be prepared in a total volume of 10 µl. Cocktail staining greatly expedites sample preparation and ensures that all samples are stained uniformly.

   Over time, MAbs in solution tend to form aggregates. Cells that express Fc receptors can bind these antibody aggregates with far greater avidity than they can antibody monomers. Aggregates should be removed by microcentrifugation of the antibody solution for 5 min at 12,000 to 13,000 rpm, 4°C, prior to staining.

   Fluorochromes [especially the phycoerythrin (PE)–Cy5 and PE-Cy7 tandem conjugates] are particularly sensitive to photodegradation. Therefore, all staining procedures should be conducted in subdued light.

8. Add 150 µl PAB to each well or tube and centrifuge for 3 min at 200 to 1500 × *g*, 4°C. Remove supernatant as in step 4.

9. To remove unbound MAb, which can contribute to background fluorescence, wash cells once by adding PAB (total volume in microtiter plate not to exceed 200 μl) to each well or tube and centrifuging for 3 min at 200 to 1500 × *g*, 4°C. Remove supernatant as in step 4.

10. Resuspend cells in 500 μl PAB with gentle vortexing.

    For samples prepared in microtiter plates, resuspend each cell pellet in 200 μl PAB. Next, using a multichannel pipettor, transfer the contents of each well to a Titertube and add an additional 300 μl PAB, for a total volume of 500 μl. These Titertubes can then be inserted into 12 × 75–mm plastic tubes for flow cytometric analysis.

11. Keep samples on ice until analyzed using a flow cytometer.

    If stained cells cannot be analyzed on the day of preparation, they must be fixed for longer-term storage (Support Protocol 2).

INDIRECT STAINING OF CELLS PREPARED FROM LYMPHOID CELLS

ALTERNATE PROTOCOL

In general, it is best to stain lymphoid cells with a MAb that is directly conjugated to a fluorochrome (i.e., using the direct method). It is relatively easy to obtain MAbs specific for mouse or rat markers in a number of conjugated forms from commercial sources. However, there are very few mouse or rat MAbs that are conjugated to PE–Texas Red. This will impact studies requiring four or five colors for immunophenotypic analysis, since one MAb may require a second-step staining reagent. This concern is even more relevant when dealing with species other than mice, rats, or humans, as it is very difficult to find commercial sources of fluorochrome-conjugated MAbs for such species. In those situations, it may be necessary to resort to one of two indirect staining methods.

In one method, cells are incubated first with an unconjugated primary MAb and then with a fluorochrome-conjugated antibody that is specific for the primary antibody. For instance, if cells are stained with an unconjugated rat IgG_{2a} MAb that is specific for mouse CD4, the secondary antibody would be a fluorochrome-conjugated antibody that is specific for rat IgG. In most cases, the secondary antibody will be a polyclonal anti-Ig antibody, although Ig isotype–specific MAbs can sometimes be obtained from commercial sources. In this example, one can limit cross-reactivity of the secondary antibody with all other IgG isotypes by restricting the specificity of the secondary antibody to the rat IgG_{2a} isotype, if available. To minimize FcR-mediated binding of the secondary anti-Ig antibody, it is preferable to use the $F(ab')_2$ fragment rather than the whole immunoglobulin.

An alternative indirect staining method relies on the use of a biotin-conjugated primary antibody, which is then detected with fluorochrome-conjugated streptavidin (SA). This biotin-SA method is the preferred indirect staining approach, because reagent interactions, which are often associated with the use of anti-Ig antibodies, are less of a concern. In addition, there are commercially available SA conjugates to a variety of fluorochromes, making SA useful in multicolor staining protocols. However, as with directly conjugated MAbs, biotin-conjugated MAbs are not always available.

The use of secondary anti-Ig antibodies can be circumvented by labeling purified MAbs with specific fluorochromes in the laboratory. Detailed methods for MAb conjugation are available on the Internet (Roederer, 1997), and conjugation kits can be obtained from commercial vendors. The authors have had success using the Zenon Alexa Fluor 488 Mouse IgG Labeling Kit (Molecular Probes, 2004a) to label unconjugated MAbs. Using this antibody labeling kit, small quantities (≥0.4 μg) of primary MAbs can easily be conjugated to fluorescent labels. Currently, the Zenon system can only be used with mouse IgG_1, mouse IgG_{2a}, mouse IgG_{2b}, rabbit IgG, and human IgG antibodies.

Additional Materials *(see also Basic Protocol 1)*

Unconjugated primary MAb *or* biotin-labeled primary MAb
Fluorochrome-conjugated anti-Ig $F(ab')_2$ fragment (for use with unconjugated primary MAb) *or* fluorochrome-conjugated streptavidin (for use with biotin-labeled primary MAb)

1. Stain cells with primary MAbs according to steps 1 through 9 of Basic Protocol 1.

   If necessary, a combination of several fluorochrome-conjugated MAbs plus one non-fluorochrome-conjugated MAb (preferably a biotinylated MAb) can be used in a single MAb cocktail.

2. Resuspend cells in 50 µl PAB with gentle vortexing.
3. Add fluorochrome-labeled streptavidin or an appropriate secondary antibody. Vortex lightly and incubate on ice for 20 min.
4. Add 150 to 200 µl PAB and centrifuge cells for 3 min at 200 to 1500 × *g*, 4°C. Remove supernatant as in Basic Protocol 1, step 4.
5. Wash cells once in PAB as in Basic Protocol 1, step 9.
6. Resuspend cells in 500 µl PAB with gentle vortexing.

   Alternatively, for samples prepared in microtiter plates, resuspend each cell pellet in 200 µl PAB. Next, using a multichannel pipettor, transfer the contents of each well to a Titertube and add an additional 300 µl PAB, for a total volume of 500 µl. These Titertubes can then be inserted into 12 × 75–mm plastic tubes for flow cytometric analysis.

7. Keep samples on ice until analyzed using a flow cytometer.

   If stained cells cannot be analyzed on the day of preparation, they must be fixed for longer-term storage (Support Protocol 2).

SUPPORT PROTOCOL 1

PREPARATION OF CELLS FROM LYMPHOID ORGANS

The processing of mouse lymphoid organs into single-cell suspensions is a fairly simple procedure.

Materials

Lymphoid organ of interest
HBSS supplemented with 5% (v/v) FBS (5% HBSS; see recipe)
Endotoxin-screened distilled water for cell culture (Gibco)
10× HBSS (Sigma)
ACK lysis buffer (optional; see recipe)
60 × 15–mm untreated culture dish
25 × 75 × 1–mm frosted glass microscope slides
15-ml conical centrifuge tubes
12 × 75–mm disposable cell culture tubes
Coulter counter or hemacytometer

1. Transfer a freshly dissected lymphoid organ to a 60 × 15–mm culture dish containing 4 ml of 5% HBSS.
2. When ready for processing, place the lymphoid organ between the frosted ends of two glass microscope slides. Disrupt the organ by gently pressing the frosted ends in a circular motion until only the empty capsule remains.

3. Transfer the resulting cell suspension to a 15-ml conical centrifuge tube. Rinse the culture dish and capsule with a combined total of 3 ml of 5% HBSS and then add this liquid to the cell suspension.

4. Centrifuge the cell suspension for 10 min at 200 × *g*, 4°C. Discard supernatant.

For spleen cell preparations

5a. Lyse RBCs by adding 4.5 ml cold distilled water (for cell culture) to the cell pellet and resuspending with gentle vortexing for 10 sec. After vortexing, immediately add 0.5 ml of 10× HBSS to restore isotonicity, followed by an additional 5 ml of 5% HBSS. Centrifuge cells as in step 4, discard supernatant, and resuspend the cell pellet in 10 ml of 5% HBSS with gentle vortexing.

This procedure also lyses dead cells. If it is necessary to preserve dead cells (e.g., for apoptosis studies), RBCs can be removed by (1) resuspending the cell pellet in 5 ml of a standard ammonium chloride lysing solution (ACK lysing buffer; see recipe) and vortexing briefly; (2) incubating the resuspended pellet for 5 min at room temperature; (3) adding 5 ml of 5% HBSS (inverting the tube several times to mix); and then (4) centrifuging the cells for 10 min at 200 × g, 4°C, and discarding the supernatant.

In general, the viability of spleen cell suspensions will be substantially higher when the hypotonic lysis method (>95%), as opposed to the ammonium chloride lysis method (85%), is used.

6a. Let cell debris settle for 10 min on ice, and then remove the cell-rich supernatant and transfer to a clean tube.

For thymus and lymph node cell preparations

5b. Resuspend the cell pellet in 10 ml of 5% HBSS with gentle vortexing.

6b. Let cell debris and clumps settle for 8 to 10 min on ice, and then remove the cell-rich supernatant and transfer to a clean tube.

7. Determine cell concentration using a Coulter counter or hemacytometer (*APPENDIX 3B*). Use 5% HBSS to adjust the final concentration of the cell suspension to 10–40 × 10^6 cells/ml.

CELL FIXATION

SUPPORT PROTOCOL 2

If it is not possible to analyze freshly stained cells on the day of preparation, the cells must be fixed in electron microscopy (EM)–grade formaldehyde (such as Ultrapure formaldehyde, Polysciences) prior to storage at 4°C. Fixation not only cross-links proteins to make cells stable for storage but also inactivates the infectious activity of any viruses present. Hence, cell fixation is highly advisable when handling biological specimens capable of transmitting infection, and especially when handling human-derived cells.

Fixed samples should be analyzed within 5 days of fixation, since prolonged storage can result in increased autofluorescence. This is usually not a problem when antigens that are expressed at high levels are being analyzed. However, increased autofluorescence may make it more difficult to resolve negative cells from dimly stained cells. Cell fixation often leads to increased cell aggregation; therefore, it may be prudent to filter samples through a 40-μm nylon mesh prior to running them on the flow cytometer.

Additional Materials *(see also Basic Protocol 1)*

1% formaldehyde: 10% (v/v) Ultrapure EM-grade formaldehyde (Polysciences) diluted 1:10 in PAB (see recipe)
40-μm nylon mesh (Small Parts, Inc.; optional)

1. Stain cells with MAbs according to steps 1 through 9 of Basic Protocol 1 or steps 1 through 5 of the Alternate Protocol.
2. Resuspend cell pellet in residual supernatant by gently vortexing.

   Cells must be thoroughly resuspended prior to fixation. If gentle vortexing does not completely resuspend the cell pellets in the microtiter plate, use a multichannel pipettor (equipped with plastic tips) to break up the pellets.

3. Add 200 µl 1% formaldehyde to each well and store cells on ice, protected from light, for 30 min.

   If necessary, cells can be stored overnight in 1% (v/v) formaldehyde at 4°C.

4. Prior to flow cytometric analysis, centrifuge cells 3 min at 1500 × *g*, 4°C. Remove supernatant as in Basic Protocol 1, step 4, and resuspend the cell pellet in 500 µl PAB.

   After resuspension in PAB, it may be desirable to filter samples through a nylon mesh to remove cell aggregates, as this will prevent clogging of the flow cell nozzle.

BASIC PROTOCOL 2

STAINING OF PERIPHERAL BLOOD LEUKOCYTES

This protocol details the immunophenotyping of peripheral blood leukocytes, a process often referred to as a "whole-blood" technique, as RBC lysis takes place after the sample has been stained with specific MAbs. It is appropriate for the immunophenotyping of blood cells from a number of animal species, including mouse, rat, horse, and dog.

Materials

Animals of interest
Sodium heparin, 250 IU per ml in PBS (*APPENDIX 2A*)
PBS supplemented with sodium azide and BSA (PAB; see recipe)
FcR-blocking Ig solution, 2 mg/ml (note that concentration differs from that used in Basic Protocol 1)
Appropriate primary MAbs and (if necessary) secondary antibodies
FACS Lysing Solution (BD Biosciences), diluted 1:10 in distilled water according to the manufacturer's instructions
1-cc syringe equipped with 22-G needle
Coulter counter
Disposable 12 × 75–mm polystyrene tubes

NOTE: Staining conditions are similar to those noted in Basic Protocol 1. However, all staining procedures should be performed in 12 × 75–mm polystyrene tubes, not microtiter plates.

NOTE: Be sure to protect sample from light during incubation with fluorochrome-conjugated MAbs.

Prepare peripheral blood leukocytes for staining

1. Using aseptic technique (*APPENDIX 3B*), collect blood (by cardiac puncture for mice) in a 1-cc syringe containing sodium heparin.

   A sufficient amount of heparin can be drawn into the syringe barrel by simply pulling the plunger back to the 0.05-cc mark.

   In order to reduce animal-to-animal variation, the same volume of blood should be collected from each animal (for example, ~500 µl from each mouse).

2. Determine WBC concentration of blood sample using a Coulter counter.
3. Add 50 to 100 µl blood to a 12 × 75–mm polystyrene tube.

4. Wash cells twice by adding 2 to 3 ml PAB to tube, centrifuging for 5 min at 1500 × *g*, 4°C, and removing supernatant.

   This wash step minimizes artifactual staining of serum Igs with MAbs. Washing is performed by adding 2 ml PAB and centrifuging cells for 5 min at 1500 × g, 4°C. This centrifugation speed is required to produce a soft pellet of blood cells.

   The supernatant is removed by carefully decanting it and then touching the lip of the tube to an absorbent towel. Alternatively, the supernatant can be aspirated, taking care not to disturb the soft cell pellet.

5. Resuspend blood cells in residual medium (~100 µl) by gently vortexing.

Label with fluorochrome-conjugated MAbs

6. To block FcR-mediated binding of Igs, add 5 µl FcR-blocking Ig (10 µg) to the cell suspension. Vortex cells lightly and incubate on ice for 10 min (Basic Protocol 1, step 6).

7. Without removing the FcR-blocking reagent, add the appropriate MAbs (see Support Protocol 4 for determination of optimal antibody concentrations) to the cell suspension, vortex gently, and incubate on ice for 10 min.

   All MAbs can be added concurrently in this step (Basic Protocol 1, step 7). It is highly advisable to include a MAb to CD45 to help define the leukocyte gate during data acquisition and analysis.

8. If all MAbs are fluorochrome-conjugated, proceed to step 11.

9. Add 2 ml PAB to sample and centrifuge for 5 min at 1500 × *g*, 4°C. Remove supernatant and wash cells once with PAB as in step 4.

10. Add secondary antibodies to sample, vortex gently, and incubate on ice for 20 min.

11. Without removing or washing away the MAbs, add 2.0 ml FACS Lysing Solution, 1:10 dilution.

    FACS Lysing Solution does not lyse nucleated erythrocytes, which are present in certain animal species.

12. Vortex cells thoroughly and incubate for 10 min at room temperature.

13. Centrifuge sample for 5 min at 1500 × *g*, 4°C. Remove supernatant and wash cells once with PAB as in step 4.

14. Resuspend cells in 500 µl PAB with gentle vortexing.

15. Keep samples on ice until analyzed using a flow cytometer.

    The FACS Lysing Solution contains formaldehyde, so no further cell fixation is required for longer-term storage.

ASSESSMENT OF CELL VIABILITY

SUPPORT PROTOCOL 3

Cell viability should routinely be assessed in all flow cytometric analyses. Because the membrane integrity of dead cells has been compromised, most antibodies will freely pass through such membranes and stain dead cells nonspecifically. This nonspecific staining can make data difficult, if not impossible, to interpret and ultimately lead to erroneous conclusions.

In general, cell viability is high (>95%) when lymphoid cells are taken directly from animal tissues, unless the mechanical process used to create single-cell suspensions has resulted in large numbers of dead cells. In contrast, the viability of cultured cells can be quite low, especially when these cells are chemically treated. In either case, to minimize

cell death during sample processing, all cell preparations and staining procedures (including wash steps) should be performed at 4°C or on ice and in the presence of BSA or heat-inactivated FBS. The elimination of dead cells prior to staining is not recommended, since any manipulation of the cell sample could lead to the inadvertent loss of viable cells. Cells should be stained promptly after they are harvested and, if not fixed, analyzed in a flow cytometer as soon as possible.

To assess cell viability, a sample of unstained cells is incubated with a DNA dye, such as propidium iodide (PI) or 7-aminoactinomycin D (7-AAD); dead cells will stain positively for either of these two nuclear dyes. Next, a data acquisition region is placed around the positively stained cells. By color-eventing or backgating on the PI^+ or $7\text{-}AAD^+$ cells present, one can easily discern that most, *but not all*, dead cells exhibit lower forward scatter (FS) and higher side scatter (SS) than do viable cells. A gating region is then established around a cluster of viable cells (PI-negative) on the basis of their light scatter profile. This gating region can be used for all subsequent samples, even if these samples do not include a viability indicator. However, the best method for excluding dead cells from data analysis is to use a vital DNA dye in all samples. Some of the more common vital dyes used in multicolor analyses are PI, 7-AAD, TO-PRO-3 (Molecular Probes), and pyronin Y(G) [PY(G)].

Materials

Nuclear staining compound dissolved in PBS (*APPENDIX 2A*): 200 μg/ml PI, 250 μg/ml 7-AAD, 250 μg /ml TO-PRO-3 (Molecular Probes), or 200 μg/ml PY(G)

12 × 75–mm polystyrene tubes
Flow cytometer

1. Add 500 μl cells (1–2 × 10^6; unfixed and unstained) to a 12 × 75–mm polystyrene tube.
2. Add 5 μl PI to tube.

   Alternatively, add 4 μl 7-AAD, 4 μl TO-PRO-3, or 5 μl PY(G).

3. Incubate cells on ice for at least 5 min.
4. Analyze cells by flow cytometry.

SUPPORT PROTOCOL 4

TITRATION TO DETERMINE OPTIMUM ANTIBODY CONCENTRATION

The single most important factor in selecting an appropriate antibody is antibody quality. Good antibodies are characterized by their high specificities and high binding affinities, which allow specific staining to be distinguished from nonspecific staining. However, even with high-quality antibodies, it is important to determine the optimal staining concentration (or titer) for each MAb. This titer will ensure that cells are stained under saturating conditions. Under such conditions, specific fluorescence will not be readily influenced by cell number or incubation time (Kantor and Roederer, 1997). The method for titrating MAbs has previously been described by Stewart and Stewart (2001a).

Materials

Lymphoid cell suspension of interest (see Support Protocol 1)
Fc receptor (FcR)-blocking immunoglobulin (Ig) solution, 200 μg/ml
Fluorochrome-conjugated antibody solutions to be tested

Centrifuge fitted with a microtiter plate adapter
Vortex mixer fitted with a microtiter plate adapter
Flow cytometer

1. Add 2×10^6 lymphoid cells to each of five wells in a 96-well microtiter plate.
2. Centrifuge cells for 3 min at 200 to 1500 × *g*, 4°C, in a centrifuge fitted with a microtiter plate adapter.
3. Block FcR-mediated binding by adding 50 µl FcR-blocking Ig to each well, vortexing gently using a vortex mixer fitted with a microtiter plate adapter, and then incubating samples for 10 min on ice.
4. Without removing the FcR-blocking Ig added in step 3, add 0.125, 0.25, 0.5, 1.0, and 2.0 µg of MAb, respectively, to the five wells containing lymphoid cells. Vortex cells gently and incubate for 10 min on ice.
5. Acquire immunofluorescence data using a flow cytometer
6. Create a two-parameter histogram of forward scatter versus side scatter and establish an appropriate gating region that encompasses the majority of viable cells.
7. Display fluorescence data from viable cells in single-parameter histograms. Establish one region that encompasses the negative population and a second region that brackets the positive population. Determine the median channel of fluorescence (MCF) for each region.
8. Compute the signal-to-noise (S/N) ratio, treating the positive population as the signal (S) and the negative population as the noise (N). Plot the calculated S/N ratios as a function of MAb concentration.
9. Identify the optimal MAb titer (i.e., the titer that produces the highest S/N ratio).

Once the optimal titer is determined, it is not necessary to increase the amount of antibody used for staining unless the number of cells per sample exceeds 20 million. Even then, the amount of antibody needed for staining will only increase by a factor of two or three. However, it cannot be stressed enough that time and effort should be taken to optimize staining conditions (staining temperature, antibody concentration, staining time, and cell number) prior to any study. Doing so can also save money, as the manufacturer's recommended staining concentration is often higher than necessary.

REAGENTS AND SOLUTIONS

Use Milli-Q-purified water or equivalent for all recipes and protocol steps. For common stock solutions, see APPENDIX 2A; for suppliers, see SUPPLIERS APPENDIX.

ACK lysing buffer

0.15 M NH_4Cl
10 mM $KHCO_3$
0.1 mM disodium EDTA
Adjust pH to between 7.2 and 7.4 using 1 M HCl
Filter sterilize using a 0.2-µm filter
Store at room temperature
If the buffer is stored for an extended period, check its pH before use.

HBSS, pH 7.2, supplemented with 5% (v/v) FBS

1× Hanks' balanced salt solution (HBSS; Sigma) containing:
1 mM *N*-2-hydroxyethylpiperazine-*N*′-2-ethanesulfonic acid (HEPES)
5% (v/v) fetal bovine serum (FBS), low-endotoxin, characterized (HyClone)
1 mM sodium pyruvate
Adjust pH to 7.2 using 1 N NaOH
Store up to 1 month at 4°C

PBS, pH 7.2, supplemented with sodium azide and BSA

Dulbecco's PBS, calcium- and magnesium-free (e.g., Life Technologies), containing:
0.1% (w/v) sodium azide
1% (w/v) BSA
Adjust pH to 7.2 using 1 N NaOH or 1 N HCl
Filter solution through 0.22-μm filter paper
Store up to 1 month at 4°C

EDTA (1 mM) can be added to reduce cellular aggregation.

CAUTION: *Be extremely careful when handling sodium azide.*

COMMENTARY

Background Information

Secondary anti-Ig antibodies

Although indirect staining with secondary fluorochrome-conjugated anti-Ig antibodies is the least desirable staining method, due to problems with nonspecific staining, there are certain precautions that can be exercised to minimize these problems. The secondary anti-Ig antibody is usually a polyclonal anti-Ig antibody that is specific for a large number of epitopes on the primary antibody. Since polyclonal secondary antibodies will be directed against all the Ig isotypes (e.g., IgG, IgA, IgM) found in the serum of the animal from which they were derived, these antibodies should be purified by affinity chromatography so that their binding is restricted to the heavy chain of the appropriate Ig isotype. The binding of the secondary anti-Ig antibody can be further restricted by selecting a reagent with no light-chain activity (i.e., one that is Fc fragment–specific). This will further ensure that the anti-Ig antibody is highly specific for a particular class of Ig (e.g., IgG) and thus minimize cross-reactions with other Ig isotypes. In addition, it is essential to use the F(ab) or $F(ab')_2$ fragment of the affinity-purified secondary antibody to minimize FcR-mediated binding and, hence, reduce background staining. For example, a goat $F(ab')_2$ anti–mouse IgG antibody (heavy and light chain–specific, purified by affinity chromatography) is specific for the heavy chain of mouse IgG but will also bind to other Igs that have the same light chain as IgG (e.g., IgA, IgM). Therefore, this reagent is not specific for mouse IgG at all. The authors have had great success using polyclonal secondary antibodies purchased from Jackson ImmunoResearch Laboratories.

The binding of a secondary antibody can be further restricted to a specific Ig isotype and subclass. For example, if a rat IgG_1 MAb specific for CD4 were being used as the primary MAb, one could select a secondary MAb specific for rat IgG_1, if available.

In all cases, it is necessary to determine the optimum antibody titer as well as assess the binding specificity of the secondary anti-Ig antibody prior to a study. First, the secondary antibody should not react with any cellular epitope. This can be assessed by simply incubating the cells of interest with the secondary antibody alone. The signal produced by this staining should be nearly identical to the signal yielded by unstained cells. If not, the reagent is inappropriate and should be replaced. Second, if this secondary antibody is used in multicolor analyses, it should not cross-react with any other MAb used for staining. To test for potential reagent interactions, incubate two samples of cells with the fluorochrome-conjugated MAb, followed by washing. Next, add the secondary anti-Ig antibody to one sample and PAB to the other sample. The fluorescence pattern of the sample stained with the secondary anti-Ig reagent should be nearly identical to the pattern produced by the sample stained with PAB. If the fluorescence pattern is different, the secondary antibody in question should not be used in multicolor analyses.

Fluorochrome choice

Fluorochrome choice is highly contingent on the availability of the laser lines available on a particular flow cytometer. For instance, the Beckman Coulter XL flow cytometer is equipped with a single argon ion laser tuned to a wavelength of 488 nm, the most common wavelength used in flow cytometry. This instrument can handle up to four fluorescent emissions, all from dyes that can be excited by the 488-nm wavelength, but it cannot process the signal generated by a MAb conjugated to allophycocyanin (APC), which must be excited by a 633-nm laser line. However, APC signals can be processed on any benchtop analyzer, such as the FACScalibur

(BD Biosciences) or the FC500 (Beckman Coulter), that is equipped with a HeNe laser.

For multicolor analyses, there are a number of factors to be considered when selecting a MAb conjugated to a particular fluorochrome. This selection is particularly important when using antigens that are expressed at low density, as some fluorochromes have higher absorption coefficients and/or higher quantum yields than others, making them more suitable for detecting weakly expressed antigens. In order to achieve the highest possible staining intensity, select antibodies conjugated to the brightest possible fluorochromes, e.g., in order, from brightest to dullest—PE, PE-Cy5, PE–Texas Red, APC, and FITC. In general, the fluorescence emitted by MAbs conjugated to PE, PE-Cy5, and APC is 5 to 10 times brighter than the fluorescence emitted by FITC conjugates. PE is often the fluorochrome of choice when examining the expression of an antigen that is expressed at low levels (e.g., CD25, CD69) or detecting the presence of intracellular cytokines.

New fluorochromes are continually being developed, and they can be used in addition to or instead of the dyes mentioned above. Molecular Probes (2004b) has produced a new series of dyes, called the Alexa Fluor dyes, that exhibit more intense fluorescence than do other spectrally similar conjugates. For example, Alexa488, whose fluorescence spectrum is nearly identical to that of fluorescein isothiocyanate (FITC), is considered by many to be the best FITC-like reagent. A number of MAbs conjugated to Alexa488 can be obtained from commercial sources. If the experiment necessitates the use of a second-step reagent, the authors use fluorochrome-labeled SA, which is readily available from commercial sources, to stain biotin-labeled MAbs. For simple one- or two-color analyses, the second-step reagent of choice for the authors is PE-labeled SA, which will stain at the highest possible level. For multicolor studies, the authors routinely use a tandem conjugate PE–Texas Red–labeled SA. It is possible that PE-Alexa610-labeled SA, by virtue of its low background staining, may be a better option than the PE–Texas Red fluorochrome, which can exhibit the high background staining that is typical of Texas Red dyes. The authors rarely use FITC-labeled SA but have had great success with Alexa488-labeled SA, which is far superior to its FITC-labeled counterpart.

All MAbs should be stored in the dark, as most fluorochromes are photosensitive. PE-Cy5 and PE-Cy7 tandem conjugates are particularly sensitive to photodegradation. This phenomenon can easily be recognized by an increase in the PE signal and a concomitant decrease in the Cy5 or Cy7 signal. Use of cyanine tandem dyes can result in increased background staining, as these dyes can bind to monocytes and B cells. However, this binding is highly species-dependent; for instance, background binding can be high in mice with autoimmune disorders. Thus, again, it is prudent to assess the background staining of the reagents used prior to a large study.

Multicolor staining combinations for routine immunophenotyping of murine cells

Table 18.8.1 presents examples of possible staining strategies that can be used to phenotype various cell populations in the mouse. It is becoming increasingly clear that no single marker can be used to specifically identify a unique subset of cells. For instance, expression of CD4 and CD8a is not restricted to T cells, as these molecules are also expressed on subsets of dendritic cells ($CD11c^+$). In addition, CD4 is expressed on a subset of natural killer (NK) cells. Thus, in order to ensure that only T cells are analyzed, a MAb specific for CD3e, a marker that is expressed on thymocytes and mature T cells, can be included in the MAb cocktail. The authors have also found that the correlated expression of two markers, CD11b and Gr-1, is needed to phenotype either macrophages or granulocytes in mouse spleen. Both of these cell types express CD11b and Gr-1; however, the level of Gr-1 is lower on macrophages than on granulocytes. The two populations are more clearly resolved by including additional markers that are expressed on the macrophage, such as F4/80, CD86, or CD54 (Choi et al., 2003). It is essential to recognize that many markers can be expressed at varying levels on different cell types.

Critical Parameters

Autofluorescence

Cellular autofluorescence is most often associated with myeloid cells, due to the presence of intracellular flavins in such cells. These flavins are easily excited by the 488-nm laser line, with peak emission occurring around 525 nm. Therefore, any signal generated by autofluorescent cells will be processed by the same photomultiplier tube (PMT) that processes FITC fluorescence. It is obvious that the presence of highly autofluorescent cells can contribute an unwanted addition to the FITC signal. Autofluorescence can

Table 18.8.1 Examples of Possible Antibody Combinations for Staining Mouse Leukocytes Using Five Fluorochrome-Labeled Monoclonal Antibodies in a Staining Cocktail, with Analysis Performed on an FC500 Flow Cytometer (Beckman Coulter) with Dual Laser Excitation at 488 nm and 633 nm[a]

Cell type(s)	Possible combination of stains
T cells, NK cells	FITC-anti-CD4 PE-anti-CD3e Biotin-anti-NK1.1[b] PE-Cy5–anti-CD8[c] PE-Cy7–anti-CD45[d,e]
Viable T cells	FITC-anti-CD4 PE-anti-CD3e Biotin-anti-NK1.1[b] 7-AAD[f] PE-Cy7–anti-CD8
Granulocytes, dendritic cells, B cells, macrophages	FITC-anti-Gr-1 PE-anti-CD11c ECD-anti-B220[g] PE-Cy5–anti-CD11b PE-Cy7–anti-CD45
Activated T cells	FITC-anti-CD8 PE-anti-CD25 ECD-anti-CD4 PE-Cy5–anti-CD62L[h] PE-Cy7–anti-CD8

[a]Abbreviations: 7-AAD, 7-aminoactinomycin D; APC, allophycocyanin; FITC, fluorescein isothiocyanate; MAb, monoclonal antibody; NK, natural killer; PE, phycoerythrin.

[b]This biotinylated MAb necessitates the use of streptavidin labeled with PE–Texas Red or equivalent.

[c]PE-Cy5-labeled MAb could be replaced by a MAb conjugated to APC or equivalent.

[d]PE-Cy7-labeled MAb could be replaced by a MAb conjugated to APC-Cy7 or equivalent.

[e]CD45 is a pan-leukocyte marker that is very useful in discriminating leukocytes from contaminating red blood cells, especially in the phenotyping of peripheral blood cells. A gating region can be established on the $CD45^+$ leukocyte population as defined in a two-parameter histogram of side scatter versus CD45 expression.

[f]7-AAD is a DNA dye used as a viability indicator in unfixed cell samples. Its peak emission wavelength is 660 nm.

[g]ECD is the trade name for the PE–Texas Red tandem conjugate produced by Beckman Coulter. Very few mouse marker–specific MAbs that are directly conjugated to this fluorochrome are available.

[h]Because CD62L can easily be shed from the surface of cells, it is imperative to keep cells on ice throughout staining and data acquisition. The authors recommend that samples stained with anti-CD62L be kept on ice until loaded manually onto the flow cytometer for data collection. The use of a multisample carousel is not recommended when analyzing cells stained for CD62L, since cells cannot be kept cold while on such a device.

be particularly bothersome when measuring weak FITC fluorescence signals. If there are excessive numbers of myeloid cells in the experimental samples, the resulting high level of autofluorescence may make it difficult to interpret data. A sample of unstained cells can be used to determine the contribution of cellular autofluorescence to the background fluorescence signal as well as the minimum level of fluorescence exhibited by cells.

There are several approaches that can be used to circumvent the problems associated with cellular autofluorescence. When studying myeloid cells, it may be prudent to use MAbs that are conjugated to APC or APC-Cy7, as these dyes can be excited by a HeNe laser and emit at wavelengths greater than 600 nm, beyond the emission spectrum for cellular autofluorescence. When immunophenotyping lymphocytes in a sample containing elevated numbers of myeloid cells, one could include a MAb that specifically identifies the myeloid cells (such as one specific for Gr-1, a marker of myeloid/granulocyte lineage). The use of such an antibody allows one to gate out granulocytes and macrophages, thereby eliminating cellular autofluorescence from analysis.

Blocking FcR-mediated binding

There are two ways that an antibody can specifically bind to cells. Antibodies can bind to a specific antigen (epitope-specific binding) through their antigen-binding sites, the F(ab′) fragment, or they can bind to myeloid cells that express receptors for the Fc portion of the Ig. Even though FcR-mediated binding is not antigen-specific, it is highly specific and needs to be eliminated in order to assess antigen-specific staining.

FcR should be blocked with normal Ig prior to staining with epitope-specific MAbs. The authors typically incubate cells for 10 min at 4°C with purified normal Ig (Jackson ImmunoResearch Laboratories) taken from the same species that produced the antibodies used for staining. For instance, if a rat IgG_{2a} anti-CD4 MAb is used, FcR-mediated binding should be blocked with an excess of purified rat IgG. The use of 10 μg of normal IgG in a staining volume of 50 μl (final concentration, 200 μg/ml) should be sufficient to block FcR. After 10 min of blocking, the MAbs are added directly to the samples without removing the FcR block, so that epitope-specific staining can proceed in the presence of FcR-block. Another approach to blocking FcR is to incubate cells with an unconjugated MAb that is specific for the FcR (CD16/CD32). It should be noted that this approach is more expensive than the former approach. In any case, do not block FcR if there is interest in assessing FcR expression.

Isotype controls

Isotype controls are also used to determine the minimum level of cellular fluorescence following staining and to assess the effectiveness of FcR blocking. An isotype control must match the primary MAb in terms of isotype and subclass, as well as fluorochrome label and concentration. For example, the appropriate isotype control for cells incubated with 0.5 μg FITC-labeled rat IgG_{2a} MAb (specific for mouse CD4) is 0.5 μg FITC-labeled normal rat IgG_{2a}. The appropriate isotype control for cells stained with biotin-labeled rat IgG_1 MAb (specific for CD8) is treatment with biotin-labeled normal rat IgG_1, followed by incubation with fluorochrome-conjugated SA.

For multicolor analyses, one isotype control sample can be set up to assess all the MAb isotypes in a single tube. It is not necessary to analyze each isotype control separately. For example, a sample of cells can be incubated, in the presence of an FcR block, with a cocktail of isotype-matched Igs for each specific MAb used in the staining procedure. The fluorescence pattern of the isotype control should be nearly identical to that of the autofluorescence control. When this is not the case, it is indicative of an improperly titrated MAb, a poor-quality MAb, or both. This could have a profound effect on one's ability to interpret positive fluorescence, especially when studying antigens that are expressed either transiently or at very low levels.

In general, the authors have found that some isotype Igs (e.g., IgM, IgG_{2b}) exhibit more background staining than others, which can complicate the analysis of antigens expressed at very low levels. This is particularly relevant in analysis of intracellular antigens. In these cases, a cold block control is performed to verify antibody specificity. This can easily be accomplished by comparing the fluorescence of two cell samples, with one being pretreated with a cold blocking MAb (i.e., the same clone as the experimental MAb, but with no conjugate) for 15 min prior to the addition of the fluorochrome-conjugated MAb. The binding of the fluorochrome-conjugated MAb should be completely inhibited by the cold block. For example, to assess the expression of CD25, which can be present at low levels on activated T cells, cells are pretreated with unlabeled purified anti-CD25 MAb (at a 3-fold higher concentration compared with the conjugated MAb) for 15 min prior to the addition of the fluorochrome-conjugated anti-CD25 MAb. This sample should represent a true negative control for CD25 staining. Background staining for cell surface expression of CD69, another T cell marker that is transiently up-regulated upon activation, can be assessed similarly. Due to the complexities involved in multicolor analyses, it is prudent to invest a little time to test these conditions prior to a large study.

Background staining exhibited by cells stained with multiple reagents is very different from that seen in unstained cells or isotype controls, due to the broadening artifacts produced by compensation (see below) and/or reagent-reagent interactions. Therefore, the best negative control for any given marker in a multicolor stain is a sample of cells stained with all but one reagent (commonly referred to as "fluorescence minus one," or FMO). For example, when assessing CD25 expression on antigen-specific D011.10 T cells, the best negative control for CD25 expression is a cocktail containing MAbs to CD3, CD4, and KJ-126 (to identify the antigen-specific T cells in the D011.10 model) plus an isotype control for the CD25 MAb. In this way, the level of negative

staining for CD25 expression can be assessed by gating on the antigen-specific T cells.

Dead cells

Cell viability must be assessed in each experimental study. Since most MAbs freely pass through the cell membranes of dead and damaged cells, dead cells will stain positively even if there is no specificity for a particular MAb. This nonspecific fluorescence can interfere with data analysis, and if ignored, it can result in erroneous interpretation of the data.

For exclusion of dead cells, vital DNA dyes such as PI, 7-AAD, and TO-PRO-3 can be added to unfixed cell samples prior to analysis. These dyes cannot be used to assess the viability of cells that are permeabilized (as for intracellular staining) or fixed, since they will leak out of fixed cells. On the other hand, the vital dye ethidium monoazide (EMA; final concentration, 1 to 5 μg/ml) can be used to label dead cells prior to fixation (Reidy et al., 1991). Once inside a dead cell, EMA can be photochemically cross-linked to the DNA by exposure to visible light. This cross-linking allows EMA to be retained by fixed cells.

Compensation

One of the most critical issues in performing multicolor phenotyping is dealing with overlaps in the spectral emissions of different fluorochromes. Once excited by the laser, a fluorochrome will emit a broad band of light. Even though a band-pass filter is often placed in front of a PMT to restrict the wavelengths of light that are transmitted to the tube, it is nearly impossible to exclude all of the light emitted by the other fluorochromes used in multicolor staining. Because of these spectral overlaps, each fluorochrome will contribute an unwanted light signal to several PMTs that are not assigned to detect that fluorochrome. For example, there is significant overlap in the spectral emissions of FITC and PE, so much so that some of the FITC emission spills over into the PE PMT and it must be eliminated from this PMT before analyzing PE fluorescence. By the same accord, PE contributes an unwanted signal to the FITC PMT, albeit at much lower levels, and this signal must be eliminated from the FITC PMT. If not eliminated, these spillovers will make a "false" contribution to the data. The process by which these false contributions are eliminated electronically is called compensation.

Compensation is one of the least understood processes in multicolor analyses. It is important to consider compensation not only from the standpoint of applying it correctly but also from the perspective of designing and analyzing multicolor experiments. Investigators need to be able to recognize data that has resulted from improper compensation, as failure to do so can easily result in data misinterpretation. Any spillover signal not completely compensated (i.e., undercompensated) out of a PMT can result in an overestimation of the positive population. Proper compensation is always essential when measuring antigen density by MCF.

Compensation is often considered a process by which unwanted fluorescent signals are "subtracted" from the true fluorescent signal. However, compensation is not a subtraction process, but rather a straightforward application of linear algebra by which a proportion of the unwanted signal is eliminated from the true fluorescent signal. For some fluorochrome combinations, such as FITC and PE-Cy5 or APC, there is little, if any, overlap in spectral emissions; therefore, compensation is negligible. However, there is considerable overlap in the emission spectra of the PE, PE–Texas Red, and PE-Cy5 dyes, enough to make compensation quite challenging even for investigators who routinely perform multicolor analyses.

In order to set up compensation properly, a sample of cells must be stained with a representative reagent for each fluorochrome used in the experiment. The number of compensation controls will be equivalent to the number of fluorochromes used in staining. For example, five-color staining requires five compensation controls, one for each fluorochrome. It is not necessary to use the same MAbs in the experiment as in the compensation controls. This is especially true when a particular experimental reagent is expected to stain just a small subset of cells. For example, the frequency of antigen-specific T cells ($KJ1\text{-}26^+CD4^+$) adoptively transferred in the D011.10 model can be as low as 0.3% one day after injection with ovalbumin. Thus, it would be very difficult, if not impossible, to properly set compensation levels using the conjugated MAb that stains $KJ1\text{-}26^+$ cells. What is important is using the brightest possible reagents for compensation controls. Therefore, the authors routinely set up compensation controls using CD45, CD8a, CD19, or CD45R MAbs conjugated to the appropriate fluorochromes. These markers are expressed at high levels on most immune cells, making it much easier to properly set compensation levels. In order to set up compensation properly, the compensation control sample must contain at least two populations—specifically, one bright population and one

negative or not-so-bright population. When examining spleen cells, there will be two distinct populations that stain for MAbs to CD8a and CD45R; one is positive, and the other is negative. Because CD45 stains all leukocytes, it is necessary to add an aliquot of unstained cells to the CD45 compensation control after the staining process but just prior to flow analysis to artificially create a negative population.

There are two ways to perform compensation. Hardware compensation is performed during data acquisition, whereas software compensation is performed during data analysis. Because of the complexity of five-color analyses, the authors routinely collect flow cytometric data without performing hardware compensation in such analyses. Instead, prior to analyzing the experimental data using offline software, the data collected from compensation controls are used to perform software compensation using WinList software (Verity). The authors have found no disparity in the results obtained using software compensation as compared with hardware compensation.

Compensation controls must be evaluated in every possible pairwise combination using two-parameter histograms. For example, in studies using FITC, PE, and PE-Cy5 fluorochromes in a single sample, the FITC compensation control must be evaluated using the following two-parameter histograms: FITC versus PE and FITC versus PE-Cy5. Two-color samples require the assessment of just one pairwise combination, three-color samples require three combinations, four-color samples require six combinations; and five-color samples require ten combinations. Thus, it should be readily apparent that the complexity of compensation increases substantially with the addition of each fluorochrome. To properly set compensation levels, the center of the positive cell population (i.e., as determined by the median fluorescence intensity) is lined up with the center of the negative cell population. This is accomplished by adjusting compensation until the median channel for the positive population is equal to the median channel for the negative population. It is important to ensure that the fluorescence distribution for the negative population is not piled up on the baseline axis, as this will make it nearly impossible to determine the median channel and, thus, very difficult to set up compensation properly. An in-depth discussion on compensation can be found online (Roederer, 2000).

Not all flow cytometers can handle all the possible pairwise combinations that may be necessary for hardware compensation. For example, the Beckman Coulter FC500 and XL flow cytometers are capable of handling the pairwise compensation involving FITC and PE-Cy5, but the BD FACSCalibur is not. It can be argued that, in general, there is minimal, if any, FITC emission that spills over into the PE-Cy5 PMT. However, when using carboxyfluorescein diacetate succinimidyl ester (CFSE), a low but measurable signal from this dye can spill over into the PE-Cy5 PMT. Thus, when using the BD FACSCalibur, in lieu of hardware compensation, one must rely on software compensation to eliminate unwanted CFSE signal from the PE-Cy5 detector.

It is possible to minimize the need for compensation by carefully selecting reagents that are conjugated to fluorochromes whose emissions have little or no spectral overlap. For two-color analyses, the authors often select MAbs that are conjugated to FITC and either APC or PE-Cy5, since there is little, if any, overlap between the emission spectrum of FITC and the emission spectra of the latter two dyes. Beyond two-color analyses, fluorochrome choice gets more complicated with each additional fluorochrome. In general, PE–Texas Red–conjugated MAbs are used by the authors only when performing five-color immunophenotyping, as this fluorochrome has considerable spectral overlap with both PE and PE-Cy5 emissions, making compensation quite challenging. Of lesser importance, there are very few MAbs that are directly conjugated to PE–Texas Red, and two-step staining procedures are therefore often required. If a HeNe laser is available, the authors often select APC- or APC-Cy7-labeled reagents over PE-Cy5 conjugates.

Control samples

In order to ensure that data are collected and interpreted correctly, several control samples must be faithfully evaluated prior to running the experimental samples. These include controls to assess cellular autofluorescence, nonspecific binding, FcR-mediated binding, and compensation.

Sometimes, the number of essential control samples exceeds the number of experimental samples. However, it is only through the proper use of all appropriate control samples that data can be collected and interpreted correctly. Controls can be performed for each animal, but this can easily lead to excessive numbers of control samples. For large studies, a pool of cells is created for each treatment group, and this pool is used to test for autofluorescence and isotype staining. In this way, a pool will

contain representative cells from each animal in a given treatment group. For example, in an experimental study in which the effects of three different dose levels of a chemical are examined, there will be four pools of cells, each representing a particular treatment group (one for the vehicle control group and one for each of the three dose levels). Each treatment pool will have its own autofluorescence control and its own isotype control, resulting in a total of four autofluorescence controls and four isotype controls.

To assess autofluorescence, a sample of unstained cells (with no MAbs added) is processed in a similar fashion as for all experimental samples. This sample should always be analyzed first in an experiment. To begin, the voltages for the photodetectors collecting the light-scatter signals (both forward scatter and side scatter) are adjusted to define the cells of interest. Second, the voltage of each PMT is adjusted to place the negative cell population in the first log decade of the histogram. It is important to apply enough voltage to ensure that the majority of cells are off of the baseline; this assures that any positive staining will fall beyond the first log decade. In essence, this control sample provides the baseline representing the minimum (or negative) fluorescence exhibited by cells.

The next control to be analyzed is the isotype control. The fluorescence pattern of the isotype control should be similar to that of the unstained control if FcR-mediated binding has been blocked effectively. If not, one would need to evaluate the isotype controls used in the experiment. Like the autofluorescence control, the isotype control also determines the minimum level of fluorescence that is exhibited by cells.

For multicolor experiments, compensation controls must be analyzed in order to account for any spectral overlap not removed by filters. The number of compensation controls will be equivalent to the number of fluorochromes used in staining. Compensation is greatly simplified in four- or five-color analyses when the PMTs are balanced, with their voltages set at nearly identical levels. However, it is crucial to remember that once compensation is set, any change in the PMT voltages will necessitate repetition of the entire compensation process.

Standardization of flow cytometric data

There are three sources of error that can be introduced during immunophenotypic analysis: specifically, instrumental, technical, and biological. However, the amount of error introduced by the instrument can easily be minimized. The instrument's overall performance should be routinely evaluated prior to data acquisition using standardized beads, such as Beckman Coulter Flow-Check beads. These beads will assess the instrument's fluidics and optics to ensure proper alignment of the laser with the sample stream. Once the fluidics and optics have been checked, the authors routinely run a sample of Flow-Set beads (Beckman Coulter) to further standardize the instrument's settings. These beads mimic the immunofluorescence exhibited by human and mouse cells and can be used at the voltages required for immunophenotypic analyses. The voltages and gain settings for each photodetector are adjusted to position the fluorescence emitted by the beads within a prescribed region, a process commonly referred to as channel positioning. In this way, any apparent change in marker expression over time can be expected to be biologically relevant, and not a result of changes in the instrument.

Once it has been established that the instrument is performing under the expected experimental conditions, negative controls (autofluorescence and isotype) can be analyzed to ensure that the negative population falls within the first log decade for each channel being measured. Next, compensation controls should be performed to remove any unwanted fluorescence from the various PMTs due to overlaps in the spectral emissions of the fluorochromes used. It should be noted that improper compensation can result in false-positive or false-negative results, so great care should be exercised when performing these controls.

Once the instrument's settings have been established, the authors routinely run a control sample, referred to as the verification control, in order to determine whether the system will provide accurate information. This control sample is stained with a set of MAbs that are conjugated to the same fluorochromes used in the experimental study but are specific for well-recognized markers. For example, in a five-color staining experiment (using MAbs conjugated to FITC, PE, PE–Texas Red, APC, and APC-Cy7), the verification tube would contain MAbs specific for CD4, CD8, CD3, CD45R, and Gr-1, with each of these MAbs being conjugated to one of the fluorochromes used in the study. In general, spleen cells from a naive mouse are used in these controls. Not only are the authors familiar with the staining profiles of these markers, but they have established a historical record that they can use for comparison with the observed relative

frequencies. In short, this verification control is expected to yield easily recognizable data that enable the authors to make any necessary final changes to compensation values. Once the verification control has produced the expected results, one can be confident that the flow cytometer will provide accurate results for the experimental samples.

Data analysis

The authors routinely acquire listmode data on 10,000 cells of interest when performing multiparametric analysis. For example, when immunophenotyping spleen cells for lineage-specific markers (such as markers of B cell, T cell, macrophage, or granulocyte lineage), they typically collect flow cytometric data on 10,000 viable spleen cells. If the authors are interested in analyzing cell surface markers gated on a discrete subset, such as antigen-specific $CD4^+$ cells in the D011.1 model (which can represent as little as 0.5% to 4% of the total population), they collect data on 10,000 antigen-specific $CD4^+$ cells. Following data acquisition, flow cytometric data can be displayed in either single-parameter or two-parameter histograms to monitor the cells of interest. In this way, gating and analysis strategies can be fine-tuned.

Figure 18.8.1 illustrates one approach to the analysis of five-color flow cytometric data. The data represented in this figure are derived from studies monitoring the events of T cell activation in the graft-versus-host (GvH) response. T cells (both $CD4^+$ and $CD8^+$) were purified from the spleens of C57Bl/6 mice ($H\text{-}2^b$; referred to as donors) and injected into C57Bl/6 ($H\text{-}2^b$) $\times$ DBA/2 F_1 mice ($H\text{-}2^d$; referred to as hosts). The donor T cells recognize the $H\text{-}2^d$ antigens contributed by the DBA/2 strain in the F_1 host and become activated. Two days after the injection of these donor T cells, the F_1 mice were sacrificed, and their spleens were processed into single-cell suspensions. Spleen cells were then stained simultaneously with a cocktail of five MAbs specific for CD4, $H\text{-}2D^d$, CD28, CD25, and CD62L.

As shown in Figure 18.8.1A, a cluster of spleen cells was first identified by its light scatter profile (FS vs. SS), as is customary in flow cytometry. A rectilinear region was then established to exclude dead cells, debris, and cell aggregates from further analysis. This process is referred to as gating. The FS-versus-SS profile of dead cells, as determined by PI uptake, indicated that these cells were located below the gating region (data not shown). In general, the authors find that the viability of their splenic suspensions often exceeds 97%. When immunophenotyping blood cells, the authors routinely include a MAb to the pan-leukocyte marker CD45, which allows them to set a gate around all the leukocytes present, thereby eliminating, or gating out, residual RBCs and platelets; this is most often performed by setting a gate around the appropriate cell clusters as defined by their CD45-versus-SS profiles.

Two days after adoptive transfer into F_1 mice, one can easily identify a small but distinct cluster of cells that represent the donor $CD4^+$ cells (Fig. 18.8.1B). These cells are identified by their expression of CD4 and their lack of expression for $H2D^d$. As shown in this two-parameter histogram, the majority of cells, which are the host cells, express $H2D^d$. Only a small population of cells lacks $H2D^d$ expression, representing the donor T cells. An elliptical region has been set to establish a gate for these $CD4^+$ donor cells so that their expression of the T cell activation markers CD28, CD62L, and CD25 can be monitored throughout the course of the GvH response.

Gating on the donor $CD4^+$ cells (10,000) as shown in Figure 18.8.1B, one can generate single-parameter histograms that illustrate the expression of the T cell activation markers (Fig. 18.8.1C). The immunofluorescent profile for each marker is illustrated in the filled histograms, while the open histograms illustrate negative staining as determined by their appropriate isotype controls. Two populations can easily be distinguished on the basis of the differential expression of CD62L, $CD62L^{pos}$, and $CD62L^{neg}$. However, the staining profiles for CD25 or CD28, as seen in single-parameter histograms (Fig. 18.8.1C), are more homogeneous.

Figure 18.8.1D illustrates the power of multiparametric analysis. Multiple subpopulations can be resolved by displaying the correlated expression of two markers in two-parameter histograms. While there is a hint of two populations in each of the single-parameter histograms for CD25 and CD28 expression, one could easily identify two cell clusters by correlating the expression of these two markers in a two-parameter histogram. It is interesting to note that three distinct cell clusters can be distinguished on the basis of the correlated expression of CD62L and CD25 expression. One strategy is to "color-event" the events of interest. As shown in Figure 18.8.1D, two regions have been set around the cells that have down-regulated their expression of CD62L, one population expresses CD25 (color-evented red), and another does not express CD25

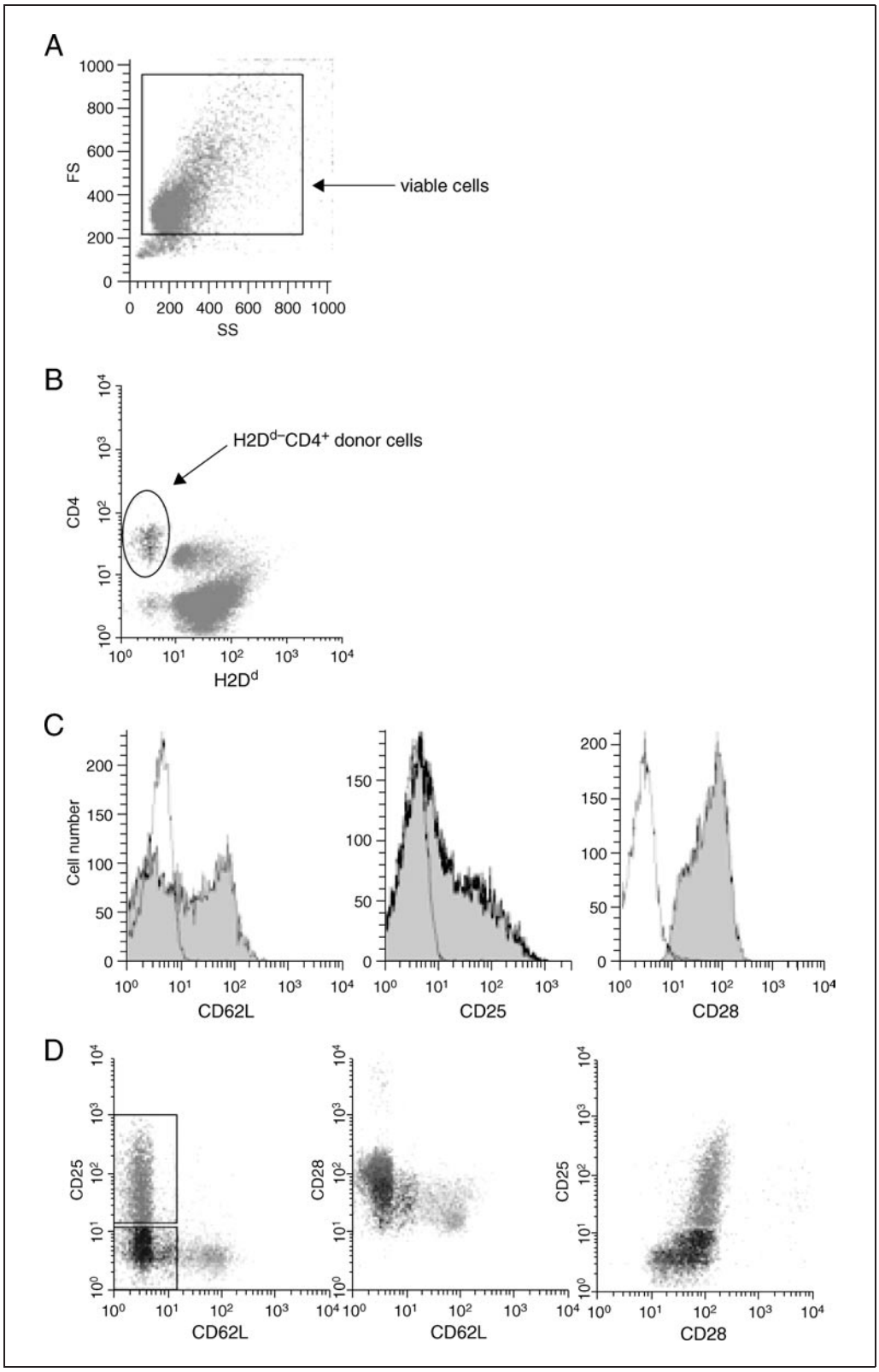

Figure 18.8.1 Legend at right.

(color-evented blue). The cells that have retained their CD62L expression have been color-evented gray. In this way, the expression of all their markers can be easily visualized for each population in all the histograms. For instance, the red population also expresses high levels of CD28 and elevated levels of CD4. In contrast, the blue population expresses intermediate levels of CD28 and CD4. By definition, both the red and blue cells are considered activated T cells since they have down-regulated their expression of CD62L; however, the red cells are further along in the activation pathway since they have also up-regulated their expression of CD25, which occurs only after several cell divisions. The gray population represents $CD4^+$ cells that have not become activated by day two of the GvH response.

There is a new approach in visualizing flow cytometric data, i.e., changing the traditional four-decade logarithmic scale for immunofluorescent data displayed in two-parameter histograms to a new Logicle axis (Tung et al., 2004). The plot axes have been redefined to allow the log-transformed scale to have a zero as well as a negative region. There are several advantages to this approach. Once data have been properly compensated, a large number of negative cells pile up in the first channel, against the axis, as these cells exhibit little to no fluorescence. Using the new Logicle scale, these negative cells can be visualized as distinct cell clusters. In addition, this new approach also makes it easier to assess compensation. Both FlowJo (Tree Star) and WinList (Verity Software House) offer the option to display flow cytometric data using the new Logicle axis.

Statistics

The data shown in Figure 18.8.1 represent the response of one individual animal. In most immunotoxicological studies, the authors use four to six animals per treatment group. In order to determine a treatment effect, data derived from the treatment group must be compared with data from the vehicle control group. The authors will often include a group of naive animals ($N = 2$ to 3) in order to monitor the antigen-induced response of the control animals.

In general, the authors prefer to present flow cytometric data in the form of histograms and use statistics to state the level of confidence in the accuracy of each result. Flow cytometric data are usually presented as the frequency of any given population that expresses a particular marker and/or as a measure of the intensity of the fluorescent or light scatter signals. There are three measures commonly used to describe the central tendency when assessing fluorescence intensity: mean, median, and mode. The mean fluorescence can be significantly skewed higher or lower by the presence of a few outliers. Therefore, when possible, one should use the median fluorescence of the positives, since

Figure 18.8.1 *(at left)* Five-color analysis of T cell activation in a graft versus host (GvH) model. T cells purified from the spleens of C57Bl/6 mice ($H\text{-}2^b$; referred to as donors) were injected into C57Bl/6 ($H\text{-}2^b$) x DBA/2 ($H\text{-}2^d$) F_1 mice. These donor T cells recognize the $H\text{-}2^d$ antigens contributed by the DBA/2 strain in the F_1 host and become activated. Two days after the injection of donor T cells, the F_1 mice were killed, and their spleens were processed into single-cell suspensions. The spleen cells were stained simultaneously with MAbs to CD4, $H\text{-}2D^d$, CD28, CD25, and CD62L. Cells were analyzed using an FC500 flow cytometer (Beckman Coulter). (**A**) Viable cells were identified on the basis of their forward scatter (FS)–versus–side scatter (SS) profiles. (**B**) $CD4^+$ donor cells (elliptical region) were identified by their expression of CD4 and their lack of expression of $H2D^d$. In this sample, the donor $CD4^+$ cells represent 1.9% of the total spleen cell population. (**C**) Expression of the T cell activation molecules CD28, CD25, and CD62L was assessed in single-parameter histograms by gating on 10,000 donor $CD4^+$ cells. Cells with positive staining for the specified MAbs are represented by the gray-filled histograms. Open histograms represent negative staining associated with the isotype control antibodies. (**D**) Correlated expression of activation molecules on donor $CD4^+$ cells as illustrated in two-parameter histograms. Donor $CD4^+$ cells that have up-regulated expression of CD25 are color-evented as red events. Using color-eventing, a distinct cluster of donor $CD4^+CD25^+$ cells that also express low levels of CD62L and high levels of CD28 is readily identifiable. When the data are displayed in a two-parameter histogram, the presence of at least three $CD4^+$ subpopulations distinguished by their differential expression of CD25 and CD62L is evident (far left histogram). It is interesting to note that not all cells with low CD62L expression exhibit high CD25 expression. Also of interest is that $CD4^+CD25^+$ cells have up-regulated expression of CD4, as shown in (B). This black and white facsimile of the figure is intended only as a placeholder; for full-color version of figure go to *http://www.interscience.wiley.com/c_p/colorfigures.htm*

the median is generally a more robust estimate of central tendency than the mean.

The precision in cell counting, or the extent to which replicate samples agree with each other, is highly dependent on the number of events sampled. The statistic which is most often used to measure precision is the coefficient of variation (CV), which can be determined using the following simple equation:

$$CV = [(\sqrt{N})/N] \times 100\%$$

where N is the number of events sampled and the square root of N represents the expected standard deviation. As the difference between two populations becomes smaller, better and better precision (i.e., a lower CV) is needed. For example, the CV for 25 cells is 20%; for 100 cells, 10%; and for 10,000 cells, 1%. In the authors' laboratory, in order to attain high precision, flow cytometric data are routinely collected on a minimum of 10,000 cells of interest, whether one is acquiring 10,000 viable cells or 10,000 antigen-specific T cells (such as the $CD4^+$ donor cells shown in Fig. 18.8.1B).

Anticipated Results

The objective in flow cytometric analyses is to resolve epitope-positive cells from epitope-negative cells with a high degree of precision and accuracy. Sometimes, it is necessary to select a MAb that is labeled with a fluorochrome such as PE in order to maximize the resolution of positive cells from negative cells, especially when assessing dim immunofluorescence. However, there are several procedures that can be employed to ensure the collection of accurate results.

Proper setup will help to eliminate instrumental error as a source of variation within an experiment. The systematic process by which an instrument's performance is validated is known as quality control, and this process should be conducted for every experiment. There are several sequential quality control steps that should be followed (as discussed in Critical Parameters): (1) the use of standardized beads, such as Flow-Check fluorospheres (Beckman Coulter), to check laser alignment as well as the fluidics and optics of the system; (2) the use of standardized beads, such as Flow-Set fluorospheres (Beckman Coulter), for channel positioning (to ensure that changes observed in time-course studies are the result of biological effects and not of changes in the instrument); (3) the use of compensation controls to remove unwanted fluorescence from fluorochromes with overlapping spectral emissions; and (4) the use of a verification control to establish the accuracy of the results yielded by the system. Once the instrument has been validated, there are several technical issues that must be addressed, such as cellular autofluorescence, FcR-mediated binding, and the presence of dead cells, which can result in the collection of inaccurate data and possibly lead to data misinterpretation or erroneous conclusions.

It is easy to obtain high precision in flow cytometric data; this can be done by simply collecting data on a minimum of 10,000 cells of interest. As an example, when assessing activation markers on $CD4^+$ T cells, data should be collected by gating on 10,000 of these cells. The precision of a given measurement is usually characterized by the statistic CV, and for 10,000 events, the expected CV would be 1%. Thus, the assessment of 10,000 cells of interest will help to ensure that small differences between two populations may still be biologically significant.

It is only through these steps that one can be confident that the results obtained are accurate, and this can ensure the validity of data interpretation. This is of utmost importance when assessing treatment effects in toxicological studies. Treatment effects can be discerned by changes in the relative frequency of a particular lineage-specific population (e.g., $CD4^+$ T cells, B cells, macrophages) or by changes in the relative frequency of a specific subset within these major leukocyte populations (e.g., activated $CD4^+$ T cells, cytolytic T effector cells). Sometimes it is necessary to report changes in the MCF for a particular marker, especially when all the cells of interest homogeneously express that marker (e.g., CD11a, CD54). However, the bottom line in flow cytometric analysis is that each result is expected to accurately reflect the cell population(s) being sampled. In this way, one can be assured that the data can be correctly interpreted and valid conclusions derived. In-depth discussions on the issues presented can be found in Stewart and Stewart (2001b) and Shapiro (2003).

Time Considerations

The time required to process, stain, and analyze samples is contingent on many factors, including the number of animals in the experiment and the number of staining combinations. The time needed to prepare single-cell suspensions from lymphoid tissues depends on the organ to be processed (spleen, thymus, and/or lymph nodes). Spleen cell suspensions will require an extra

step in sample processing to remove RBCs, whereas thymus and lymph node cell suspensions will not. The use of microtiter plates will greatly expedite the staining of large numbers of samples derived from lymphoid organs. Even though blood samples require no further processing once the blood is collected, the staining process requires the use of test tubes or microcentrifuge tubes, making sample manipulation more time-consuming. The time required for cell staining is dependent on the number of cell samples to be stained and the staining method employed (direct or indirect). In general, the direct staining method will take 10 min for FcR blocking and 10 min for incubation with fluorochrome-conjugated MAbs, followed by 10 to 20 min for wash steps. Indirect staining will require an additional 20 min to incubate cells with the second-step reagent, followed by 10 to 20 min for wash steps. The time necessary to acquire flow cytometric data will vary depending on cell concentration and on the total number of events to be collected. For example, it should take less than 1 min per sample to collect 10,000 to 20,000 events when determining the various lineage-specific populations in a sample of spleen cells. However, it will definitely take longer to collect 10,000 events when gating on a smaller population. Instrumental setup will take much longer for multicolor analyses as compared with one-color analyses, as proper compensation will need to be established in multicolor studies. The time involved in data analysis is contingent on the number of fluorochromes used in each MAb cocktail as well as the number of samples processed. Data analysis can take as little as just a few minutes per sample for samples stained with one fluorochrome-conjugated MAb and as many as several hours for samples stained with five different colors.

Acknowledgement

The authors would like to acknowledge Castle Funatake for her valuable editorial assistance. This unit was supported by the Cell and Tissue Analysis Facilities and Services Core of the Environmental Health Sciences Center, Oregon State University, grant number P30 ES00210, National Institute of Environmental Health Sciences, National Institutes of Health.

Literature Cited

Choi, J.-Y., Oughton, J.A., and Kerkvliet, N.I. 2003. Functional alterations in $CD11b^{+}Gr\text{-}1^{+}$ cells in mice injected with allogeneic tumor cells and treated with 2,3,7,8-tetrachlorodibenzo-p-dioxin. *Int. Immunopharmacol.* 3:553-570.

Food and Drug Administration. 2002. Guidance for Industry. Immunotoxicology Evaluation of Investigational New Drugs. *http://www.fda.gov/cder/guidance/4945fnl.doc*

Funatake, C.J., Dearstyne, E.A., Steppan, L.B., Shepherd, D.M., Spanjaard, E.S., Marshak-Rothstein, A., and Kerkvliet, N.I. 2004. Early consequences of 2,3,7,8-tetrachlorodibenzo-p-dioxin exposure on the activation and survival of antigen-specific T cells. *Toxicol. Sci.* 82:129-142.

Immunotoxicology Technical Committee, International Life Sciences Institute Health and Environmental Sciences Institute. 2001. Application of flow cytometry to immunotoxicity testing: Summary of a workshop. *Toxicology* 163:39-48.

Kantor, A. and Roederer, M. 1997. FACS analysis of lymphocytes. *In* Handbook of Experimental Immunology, 5th ed. (L.A. Herzenberg, D.M. Weir, L.A. Herzenberg, and C. Blackwell, eds.) pp. 49.1–49.13. Blackwell Science, Cambridge, UK.

Kerkvliet, N.I. and Brauner, J.A. 1990. Flow cytometric analysis of lymphocyte subpopulations in the spleen and thymus of mice exposed to an acute immunosuppressive dose of 2,3,7,8-tetrachlorodibenzo-p-dioxin (TCDD). *Environ. Res.* 52:146-154.

Luster, M.I., Portier, C., Pait, D.G., Rosenthal, G.J., Germolec, D.R., Corsini, E., Blaylock, B.L., Pollock, P., Kouchi, Y., Craig, W., White, D.L., Munson, A.E., and Comment, C.E. 1993. Risk assessment in immunotoxicology: II: Relationships between immune and host resistance tests. *Fundam. Appl. Toxicol.* 21:71-82.

Mitchell, K.A. and Lawrence, B.P. 2003. Exposure to 2,3,7,8-tetrachlorodibenzo-p-dioxin (TCDD) renders influenza virus-specific CD8+ T cells hyporesponsive to antigen. *Toxicol. Sci.* 74:74-84.

Molecular Probes. 2004a. Zenon technology: Versatile reagents for immunolabeling. *In* Handbook of Fluorescent Probes and Research Products, 9th ed. *http://www.probes.com/handbook/sections/0703.html*

Molecular Probes. 2004b. Alexa Fluor dyes: Simply the best. *In* Handbook of Fluorescent Probes and Research Products, 9th ed. *http://www.probes.com/handbook/sections/0103.html*

Nygaard, U.C. and Lovik, M. 2002. Blood and spleen lymphocytes as targets for immunotoxic effects in the rat: A comparison. *Toxicology* 174:153-161.

Oughton, J.A., Pereira, C.B., DeKrey, G.K., Collier, J.M., Frank, A.A., and Kerkvliet, N.I. 1995. Phenotypic analysis of spleen, thymus, and peripheral blood cells in aged C57Bl6 mice following long-term exposure to 2,3,7,8-tetrachlorodibenzo-p-dioxin. *Fundam. Appl. Toxicol.* 25:60-69.

Riedy, M.C., Muirhead, K.A., Jensen, C.P., and Stewart, C.C. 1991. Use of a photolabeling

technique to identify nonviable cells in fixed homologous or heterologous cell populations. *Cytometry* 12:133-139.

Roederer, M. 1997. Conjugation of Monoclonal Antibodies. *http://www.drmr.com/abcon/index.html*

Roederer, M. 2000. Compensation in Flow Cytometry: An Informal Perspective. *http://www.drmr.com/compensation/index.html*

Shapiro, H.M. 2003. Practical Flow Cytometry, 4th ed. John Wiley & Sons, Hoboken, N.J.

Shepherd, D.M., Dearstyne, E.A., and Kerkvliet, N.I. 2000. The effects of TCDD on the activation of ovalbumin (OVA)-specific DO11.10 transgenic CD4(+) T cells in adoptively transferred mice. *Toxicol. Sci.* 56:340-350.

Stewart, C.C. and Stewart, S.J. 2001a. Cell preparation for the identification of leukocytes. *In* Methods in Cell Biology, Vol. 63 (Z. Darzynkiewicz, H.A. Crissman, and J.P. Robinson, eds.) pp. 217-251. Academic Press, San Diego.

Stewart, C.C. and Stewart, S.J. 2001b. Multiparameter data acquisition and analysis of leukocytes by flow cytometry. *In* Methods in Cell Biology, Vol. 63 (Z. Darzynkiewicz, H.A. Crissman, and J.P. Robinson, eds.) pp. 289-312. Academic Press, San Diego.

Tung, J.W., Parks, D.R., Moore, W.A., and Herzenberg, L.A. 2004. New approaches to fluorescence compensation and visualization of FACS data. *Clin. Immunol.* 110:277-283.

Vandebriel, R.J., Spiekstra, S.W., Hudspith, B.N., Meredith, C., and Van Loveren, H. 1999. In vitro exposure effects of cyclosporin A and bis(tri-n-butyltin)oxide on lymphocyte proliferation, cytokine (receptor) mRNA expression, and cell surface marker expression in rat thymocytes and splenocytes. *Toxicology* 135:49-66.

Contributed by Julie A. Oughton and Nancy I. Kerkvliet
Oregon State University
Corvallis, Oregon

In Vitro Model for Modulation of Helper T Cell Differentiation and Activation

This unit provides an in vitro model for evaluating the effects of toxicants on murine helper T cell (T_H) reactivities. Protocols are included for studying the effects of such compounds on the development of precursor or naive $CD4^+$ T_H cells (T_{H0} cells) into type-1 (T_{H1}) or type-2 (T_{H2}) T helper effectors (see Basic Protocol 1) and on antigen-specific activation of cloned T_{H1} or T_{H2} cells (see Basic Protocol 2). The T_{H1} and T_{H2} subsets can be distinguished by patterns of cytokine secretion, and they exhibit different helper function for cell-mediated or humoral immunity (Mosmann and Coffman, 1989; Romagnani, 1996). In general, the T_H subsets are best differentiated by their quantitative expression of select cytokines (T_{H0}, low levels of IL-2, IL-4, and IFN-γ; T_{H1}, high levels of IL-2 and IFN-γ; T_{H2}, IL-4, IL-5, IL-6, IL-10, and IL-13). For analysis of T_{H0} differentiation, use of T cells from clonotypic transgenic mice—i.e., DO11.10 ovalbumin-specific transgenic (OV-tg) mice—is described. T_{H1} and T_{H2} reactivities are most readily assayed with use of cloned T cell lines (Sanderson et al., 1985; Fiorentino et al., 1989). A helper T cell clone, namely the egg white conalbumin–specific D10.G4.1 T_{H2} clone from ATCC, is the only commercially available clone at the moment; therefore it is recommended that readers contact authors cited in this unit who have worked with specific helper T cell lines.

An in vitro antigen-specific system is valuable for assessing the influence of toxins and toxicants on antigen-dependent interactions between antigen-presenting cells and T cells. The effect of a toxicant on T_H development can be investigated by evaluating its modulation of the acquisition of IL-4- or IFN-γ-producing ability in vitro with antigen-primed naive $CD4^+$ T cells. For example, spleens from DO11.10 OVA-tg mice suit the present investigation, because a large proportion (>50%) of the T cells are OVA-specific, naive (if raised in a pathogen-restricted environment), $CD4^+$ T cells. Cloned T cell lines are also available and useful for evaluating toxicant-mediated alteration of antigen-dependent helper T cell activation resulting in cytokine secretion. The cloned T_{H1} (D1.6) and T_{H2} (CDC35) lines can be activated in vitro with rabbit IgG (RGG), if presented properly by I-A^d (major histocompatibility complex class II antigen, MHC II) antigen-presenting cells (APC), which include macrophages, dendritic cells, and B cells in the spleen or lymph nodes of H-2^d mice (e.g., BALB/c mice).

NOTE: All protocols using live animals must first be reviewed and approved by an Institutional Animal Care and Use Committee (IACUC) and must follow officially approved procedures for the care and use of laboratory animals.

ANTIGEN-DEPENDENT DEVELOPMENT OF NAIVE HELPER T CELLS TO MEMORY T CELLS

BASIC PROTOCOL 1

In this procedure, splenocytes from unimmunized OVA-tg mice are stimulated with ovalbumin (OVA) in the presence or absence of a test toxicant. T cells are expanded at 72 hr under the same culture conditions as were used for the primary stimulation, and harvested on Day 7. The cells are then washed and restimulated with OVA and antigen-presenting cells (APC) in the absence of the test toxicant. Culture supernatants collected at 48 hr are used for IL-4 and IFN-γ quantification by ELISA (*UNIT 18.7*).

Contributed by Yong Heo
Current Protocols in Toxicology (2005) 18.9.1-18.9.10

Materials

OVA-tg mice (The Jackson Laboratory)
RPMI 1640 medium (e.g., Invitrogen), ice-cold
Red blood cell (RBC) lysing buffer (see recipe)
Phosphate-buffered saline (PBS), pH 7.2 to 7.4 (*APPENDIX 2A*)
Complete RPMI medium (see recipe)
OVA antigen solution (see recipe)
Recombinant human interleukin 2 (IL-2; e.g., Roche)
Experimental toxicant(s) (e.g., $PbCl_2$)
Physiological saline: 0.9% (w/v) NaCl
BALB/c mice (The Jackson Laboratory)
60 × 15–mm petri dishes
Frosted-end microscope slides, sterilized by autoclaving
6- and 15-ml conical polypropylene centrifuge tubes
Low-speed refrigerated centrifuge (e.g., Beckman GPKR or equivalent equipped with GH3.7 swinging-bucket rotor)
Hemacytometer or automatic cell counter (e.g., Beckman Coulter)
24- and 12-well culture plates
^{137}Cs γ irradiator
Sandwich ELISA kits for IL-4 and IFN-γ (e.g., BD Pharmingen; optional)
Additional reagents and equipment for counting cells (*APPENDIX 3B*) and sandwich ELISA (*UNIT 18.7*; also see Heo et al., 1996)

NOTE: All solutions and equipment coming into contact with living cells must be sterile and aseptic technique should be used accordingly.

NOTE: All incubations are performed in a humidified 37°C, 5% CO_2 incubator unless otherwise specified.

Prepare a single-cell suspension of spleen cells

1. Collect spleen from OVA-tg mouse and place it in a 60 × 15–mm petri dish containing 6 ml ice-cold RPMI.
2. Homogenize spleen as follows. Wet two frosted-end microscope slides with ice-cold RPMI. Place spleen between the frosted surfaces of the two slides and gently grind into small pieces to dissociate the spleen and free the cells. Rinse the slides with the medium to recover remaining cells.

   It is necessary to work under a laminar flow hood from this point on to maintain sterility.
3. Transfer the homogenate to a 15-ml centrifuge tube. Rinse the petri dish with 1 ml RPMI to collect remaining cells and transfer this to the tube containing the rest of the homogenate. Place tube on ice and allow cells to settle 3 min.

   This incubation on ice serves to remove dead cells and other tissue debris, which settle by gravity.
4. Collect supernatant from the settled homogenate and transfer to another 15-ml centrifuge tube. Centrifuge 10 min at 350 × *g*, 4°C. Aspirate and discard supernatant. Resuspend cell pellet in the residual liquid by tapping tube with fingers.
5. Add 2.5 ml RBC lysing buffer and incubate ~3 min at room temperature. Centrifuge 10 min at 350 × *g*, room temperature, and discard supernatant.

   It is recommended that RBC lysis not exceed 3 min, because viability of other spleen cells could be affected if the incubation lasts longer.

6. Wash cells by resuspending cell pellet in 10 ml cold PBS, centrifuging 10 min at 350 × *g*, 4°C, and discarding supernatant. Repeat the wash step. Resuspend the cell pellet in 2 ml ice-cold complete RPMI medium and count cells using a hemacytometer or automated cell counter (*APPENDIX 3B*).

   Anticipate 60 × 10^6 spleen cells from one 4- to 6-week old OVA-tg mouse.

Perform primary stimulation and expansion

7. Determine cell number required for the experiment and resuspend the appropriate number of cells in ice-cold complete RPMI. Adjust the final suspension to 2 × 10^6 cells/ml.

8. Place a 1-ml aliquot of cell suspension into each well of a 24-well culture plate (prepare sufficient wells to test each experimental condition in duplicate). To each of these cell-containing wells, add 0.5 mg OVA antigen and 10 to 12 U human recombinant IL-2. Immediately add experimental toxicant such as $PbCl_2$ to appropriate wells. Incubate 72 hr.

   It is advisable to include a control well with medium only (no OVA and experimental additives). The final culture volumes of all wells should be made equal by substituting an appropriate amount of vehicle solution, such as physiological saline, for antigen or additives. The appropriate final concentrations of toxicant should be determined with consideration of cytotoxicity, determined by propidium iodide uptake assayed by flow cytometry. It is generally appropriate to use a nanomolar to micromolar range of concentrations for heavy metals or organic compounds.

9. At 72 hr, resuspend cells by vigorous pipetting with Pasteur pipet and transfer cells from each well of the 24-well culture plate to an individual 6 ml-polypropylene tube. Centrifuge 10 min at 350 × *g*, 4°C, and discard supernatants. Resuspend each cell pellet in 2 ml ice-cold complete RPMI and transfer cell suspension from each 6-ml tube to an individual well of a 12-well culture plate.

10. To the wells of the 12-well plate, add the same reagents that were added in step 8, but at 2-fold doses (e.g., 1 mg OVA and 20 to 24 U recombinant IL-2 per well, plus twice the dose of experimental toxicant). Incubate plates an additional 72 hr.

11. At end of expansion period (day 7) harvest cells by vigorous pipetting with 10 ml-pipet and transfer to 15 ml-centrifuge tubes. Centrifuge 10 min at 350 × *g*, 4°C, and discard supernatants. Wash cells three times using the technique described in step 5. Resuspend each cell pellet in 1 ml ice-cold complete RPMI and count viable cells by trypan blue exclusion (*APPENDIX 3B*).

    Anticipate 12–18 × 10^6 cells from one well with OVA only, without experimental additives.

    In the author's experience, it is not a problem to keep the cells from this step, which have undergone primary stimulation, on ice during the preparation of the APCs in steps 12 and 13, which will take ∼1 hr. However, it is also possible to prepare the APCs just before harvesting the cells that have undergone primary stimulation.

Set up cultures of restimulating memory cells (antigen-presenting cells, APC)

12. Prepare a single-cell suspension from BALB/c mouse spleen as described in steps 1 to 6.

    Anticipate 6–10 × 10^7 spleen cells from one 2- to 3-month old BALB/c mouse.

13. Using a ^{137}Cs γ irradiator, deliver 20 Gy of irradiation to the BALB/c mouse spleen cell suspension.

    These cells will function as antigen-presenting cells in the following restimulation steps.

14. Prepare 24-well culture plates, adding to each well:

    2.5×10^6 irradiated BALB/c mouse spleen cells in complete RPMI
    0.5 mg OVA antigen
    10 to 12 U recombinant human IL-2.

15. To each well, add the 2×10^5 of the cells obtained in step 11 (i.e., those that have undergone the primary stimulation), adjusting the final volume of each well to 1.3 ml with complete RPMI. Incubate 48 hr.

    The restimulation is perfomed in the absence of experimental additives to evaluate whether experimental additives present during the primary stimulation of naive helper T cells could direct skewing of helper T cell development toward the type-1 or type-2 helper T cell phenotype.

16. At the end of restimulation, transfer the culture suspension from each well to an individual 6 ml-centrifuge tube. Centrifuge 10 min at $350 \times g$, 4°C, and collect each supernatant in an individual 1.7-ml microcentrifuge tube. Keep the supernatants in freezer below −20°C prior to cytokine ELISA.

Determine skewing of naive helper T cells differentiation

17. Determine level of IL-4 and IFN-γ for each individual culture supernatant by a sandwich ELISA (*UNIT 18.7*).

    IL-4 and IFN-γ in culture supernatants can be quantitated by a sandwich ELISA method described in the literature (Heo et al. 1996) or supplied commercially (e.g., BD PharMingen). Briefly 96-well Immulon 4 plates (Dynex) are coated by overnight incubation at 4°C with capture MAb (100 μl/well; 2 μg/ml). The plates are washed three times and, after a 2-hr incubation with 200 μl per well of PBS containing 10% heat-inactivated FBS at room temperature, the supernatants or the cytokine standards are added to appropriate wells in duplicate. After overnight incubation at 4°C, the plates are washed six times and 100 μl per well (1 μg/ml) of biotinylated detection MAb is added. Plates are then incubated at room temperature for 2 hr, washed six times, and further incubated with 100 μl per well (2.5 μg/ml) of avidin-peroxidase for ∼1 hr before detection using the substrate, 2,2′-azino-bis (3-ethylbenzthiazoline 6-sulfonic acid). Absorbance is measured at 405 nm. The amounts of cytokines are calculated from the linear portion of the standard curves. The capture/detection MAb pairs are as follows: IL-4, BVD4-1D11/BVD6-24G2; IFN-γ, R4-6A2/XMG1.2. It is necessary to dilute the supernatants ≥ 10-fold for IFN-γ, but supernatants are used undiluted for IL-4 measurement.

18. Calculate IL-4 versus IFN-γ ratio, and compare the ratio with that for the OVA antigen control (OVA supplementation in the absence of experimental additives at primary stimulation described in step 8).

    The IL-4:IFN-γ ratio is calculated by dividing the amount of IL-4 by the amount of IFN-γ in supernatants from each individual well.

BASIC PROTOCOL 2

ANTIGEN-DEPENDENT ACTIVATION OF CLONED T_H CELLS

In this procedure, resting D1.6 T_{H1} (Kurt-Jones et al., 1987) and CDC35 T_{H2} cells (Tony et al., 1985) are stimulated in the presence or absence of a test toxicant with irradiated BALB/c mouse splenocytes and antigen (RGG). Culture supernatants are collected at 48 hr and used for IL-4 and IFN-γ quantification by ELISA.

Materials

BALB/c mice (The Jackson Laboratory)
T_H cells: D1.6 T_{H1} clone and CDC35 T_{H2} clone (available from Dr. David Lawrence, New York State Department of Health; *david.lawrence@wadsworth.org*)
Recombinant human interleukin 2 (IL-2; e.g., Roche)

RGG antigen stock solution (see recipe)
Complete RPMI medium (see recipe)
RPMI 1640 medium (e.g., Invitrogen)
Ficoll-Paque (Amersham Biosciences)
Phosphate-buffered saline (PBS), pH 7.2 to 7.4 (*APPENDIX 2A*)
Experimental toxicant(s) (e.g., $PbCl_2$)
Physiological saline: 0.9% w/v NaCl
^{137}Cs γ irradiator
12- and 24-well culture plates
15- and 50-ml conical polypropylene centrifuge tubes
15-ml conical polystyrene centrifuge tubes
Low-speed refrigerated centrifuge (e.g., Beckman GPKR or equivalent equipped with GH3.7 swinging-bucket rotor)
Additional reagents and equipment for counting cells (*APPENDIX 3B*), preparing mouse spleen cells (see Basic Protocol 1, steps 1 to 6), and sandwich ELISA (*UNIT 18.7*; also see Heo et al., 1996)

NOTE: All solutions and equipment coming into contact with living cells must be sterile and aseptic technique should be used accordingly.

NOTE: All incubations are performed in a humidified 37°C, 5% CO_2 incubator unless otherwise specified.

Prepare irradiated spleen cells

1. Prepare a single-cell suspension from BALB/c mouse spleen (see Basic Protocol 1, steps 1 to 6).

   Anticipate 6–10 $\times$ 10^7 spleen cells from one 2- to 3-month old BALB/c mouse.

2. Using a ^{137}Cs γ irradiator, deliver 20 Gy of irradiation to the BALB/c mouse spleen cell suspension.

   These cells will function as antigen-presenting cells in the following steps.

Prepare lymphocytes

3. Prepare resting T_H cells by adding the following to each well of a 12-well culture plate:

   5×10^6 irradiated BALB/c mouse spleen cells in complete RPMI
   2×10^5 T_{H1} or T_{H2} cells
   20 to 24 U recombinant human IL-2
   0.2 mg RGG antigen
   Complete RPMI to 2 ml.

   Incubate plate 2 weeks.

4. Resuspend the resting T_H cells by vigorous pipetting with a Pasteur pipet and transfer the contents of all wells containing T_{H1} cells to one 50-ml conical polypropylene centrifuge tube and the contents of all wells containing T_{H2} cells to a second 50-ml polypropylene centrifuge tube. Rinse each well with 1 ml plain RPMI 1640 medium to collect remaining cells, and transfer to the corresponding 50-ml tube containing the rest of the cells. Centrifuge the tubes 10 min at 350 $\times$ *g*, 4°C, and discard the supernatants.

5. Resuspend each cell pellet in the residual liquid by tapping the tube with the fingers, and add 2 ml complete RPMI to each of the pellets.

6. For each tube prepared in steps 2 and 3, prepare a 15-ml conical polystyrene centrifuge tube containing 3 ml Ficoll-Paque. Carefully layer the 2-ml cell suspension (step 3) on top of the Ficoll-Paque.

   It is preferable to use polystyrene centrifuge tube for Ficoll-Paque density gradient isolation of viable cells because the tube is clear, making it easier to identify the lymphocyte layer.

7. Centrifuge the Ficoll-Paque gradients 15 min at 800 × *g*, room temperature. Using a sterile Pasteur pipet, transfer the lymphocyte layer to a clean 15-ml polypropylene centrifuge tube.

   The lymphocyte layer is generally found at the interface between the RPMI solution and the Ficoll-Paque.

8. Wash cells three times, each time by adding 10 ml ice-cold PBS, centrifuging 10 min at 350 × *g*, 4°C, and removing the supernatant. Resuspend cells in 1 to 2 ml complete RPMI. Take an aliquot and count viable cells (*APPENDIX 3B*).

Set up cultures for stimulation

9. Prepare irradiated BALB/c mouse spleen cells (in complete RPMI) as described in steps 1 and 2 of this protocol. Prepare 24-well culture plates, adding to each well:

   2.5×10^6 irradiated BALB/c mouse spleen cells in complete RPMI
   1×10^5 T_{H1} or T_{H2} cells (from step 8)
   10 to 12 U recombinant human IL-2.

   Adjust the volume of each well to 1 ml with complete RPMI.

10. Add 0.1 mg RGG antigen to each well. Add experimental toxicants, e.g., $PbCl_2$, to appropriate wells. For each individual experimental condition, set up duplicate wells.

    It is desirable to include a control well with cells only (no RGG or experimental additives). The final culture volumes of all wells should be made equal by substituting appropriate amount of vehicle solution, such as physiological saline, for the RGG antigen or experimental toxicants. In the author's experience, the final culture volume in each well will be equal to 1.3 ml.

11. Incubate plates 48 hr. Collect supernatant from each well in an individual 1.7-ml microcentrifuge tube. Keep the supernatants in freezer below −20°C prior to cytokine ELISA.

Evaluate cytokine expression

12. Determine level of IL-4 for T_{H2} supernatants or IFN-γ for T_{H1} supernatants by a sandwich ELISA (*UNIT 18.7*; also see Basic Protocol 1, step 17 annotation). Compare cytokine levels in experimental samples with those obtained for the RGG antigen control (RGG only without experimental additives; see step 10 annotation).

REAGENTS AND SOLUTIONS

Use Milli-Q-purified water or equivalent in all recipes and protocol steps. For common stock solutions, see ***APPENDIX 2A****; for suppliers, see* ***SUPPLIERS APPENDIX****.*

Complete RPMI medium

RPMI 1640 medium (e.g., Invitrogen) containing:
10% (v/v) fetal bovine serum (FBS), heat-inactivated 1 hr at 56°C
2 mM L-glutamine
50 μM 2-mercaptoethanol
1 mM sodium pyruvate
1× nonessential amino acids (Invitrogen)

continued

1× penicillin/streptomycin/neomycin (PSN) mixture (Invitrogen)
0.075% (w/v) $NaHCO_3$
Store up to 1 week at 4°C.

OVA antigen stock solution

Completely dissolve 2 g ovalbumin (OVA; Sigma, grade V; endotoxin < 10) in 100 ml physiological saline (0.9% w/v NaCl) and filter sterilize through a 0.45-μm low-protein-binding membrane filter (Corning). Determine OVA concentration by spectrophotometry at 280 nm, dividing the optical density value at that wavelength by 0.735 to obtain the concentration of OVA in mg/ml. Aliquot and store indefinitely in freezer below −20°C.

RBC lysing buffer

4.415 g NH_4Cl (0.15 M)
0.5 g $KHCO_3$ (10 mM)
18.6 mg Na_2EDTA (0.1 mM)
440 ml deionized, distilled H_2O
Adjust pH to 7.2 to 7.4 with 1 N HCl.
Add H_2O to 500 ml.
Filter sterilize through a 0.22-μm membrane filter.
Store indefinitely at room temperature.

RGG antigen stock solution

Completely dissolve 0.2 g rabbit IgG (RGG, Sigma cat. no. I-5006) in 100 ml physiological saline (0.9% w/v NaCl) and filter sterilize through a 0.45-μm low-protein-binding membrane filter. Determine RGG concentration by spectrophotometry at 280 nm, dividing the optical density value at that wavelength by 1.5 to obtain the concentration of RGG in mg/ml. Aliquot and store indefinitely in freezer below −20°C.

COMMENTARY

Background Information

Helper T cells have been subdivided into at least two distinct subsets based on the pattern of cytokine secretion; type-1 T cells produce IL-2 and IFN-γ (and other cytokines), but not IL-4, IL-5, or IL-10, while type-2 T cells produce IL-4, IL-5, and IL-10 (and other cytokines), but not IL-2 or IFN-γ (Cherwinski et al., 1987; Kurt-Jones et al., 1987). Among those cytokines, IL-4 and IFN-γ are known to be the cytokines most useful for defining the effector T_{H2} and T_{H1} phenotype subsets, respectively (Sedar and Paul, 1994). The production of distinct cytokines is believed to play a major role in the predominance of T_{H2} cells over T_{H1} cells or vice versa, which results in alteration of immune homeostasis between cell-mediated and humoral immunity, leading to various immunopathologic states such as lowered protection against microorganismal infection, allergic state, or autoimmune diseases. Concerning immune-modulatory ability of xenobiotics, differential influences of heavy metals (e.g., mercury and lead) or diesel exhaust particles on helper T cell activities have been demonstrated, which can cause aberrant cell-mediated immunity or humoral immunity (Prigent et al., 1995; Heo et al., 1996, 2001).

Murine T lymphocytes reactive with OVA have been primarily studied with the aim of obtaining specific T cell subsets in the presence of syngeneic BALB/c mouse spleen cells as a source of APC (Hsieh et al., 1992). When T cells from nonimmunized OVA-tg mice are stimulated in vitro with OVA and APC in the presence of immunotoxicant for 6 days, and subsequently restimulated in the absence of the immunotoxicant, these T cells acquire the capacity to produce substantial amounts of T_{H1} (e.g., IFN-γ) and T_{H2} (e.g., IL-4) cytokines, but they display an altered ratio of IL-4 versus IFN-γ compared with T cells primed with OVA only. The in vitro differentiation model described in Basic Protocol 1 might be close to the in vivo environmental conditions in which differentiation occurs. Basic Protocol 1 can be further extended using naive $CD4^+$ T cells from OVA-tg/RAG (recombinase activating gene)$2^{-/-}$ mice, in which endogenous T cell receptor TCR-α expression

is completely depleted and $CD44^+/LECAM^{low}$ memory T cells and B cells are not present (Rulifson et al., 1997). Owing to the complete lack of memory T cells and any TCR other than the DO11.10 clonotype in the OVA-tg/RAG $2^{-/-}$ mice, it is possible to exclude possible contamination with memory T cells in the in vitro differentiation model using OVA-tg mice. Mice bearing transgenic T cell receptor specific for hen egg lysozyme (Desbarats et al., 1999), pigeon cytochrome *c* (Vratsanos et al., 2001), or myelin basic protein (Olivares-Villagómez et al., 1998) could be used for antigen-dependent differentiation of naive helper T cells to memory T cells.

Cell lines expressing I-A^d (e.g., A20, K46R, 2PK3, BCL_1 B cell line, or PU5, WEHI-265 monocytic cell line) can be employed as antigen-presenting cells (APC) for activating the CDC35 or D1.6 T_H cells (Walker et al., 1982; Harris et al., 1984; Zuckerman et al., 1988; Spencer et al., 1993). Use of cell lines for the APC source provides two advantages: first, mice do not have to be sacrificed, and, second, homogeneous preparations of B cells versus monocytic lines can be compared. Furthermore, dendritic cells with high levels of MHC class II expression also can be used as APC; these are prepared by plastic adherence and rosetting with antibody-coated sheep erythrocytes following collagenase digestion of a BALB/c splenocyte suspension (Inaba et al., 1998).

Resting cloned CDC35 or D1.6 T_H cells can also be stimulated with polyclonal stimulators such as immobilized anti-mouse CD3 or phorbol 12-myristate 13-acetate (PMA) plus ionomycin (Basic Protocol 2). To investigate signaling pathways modulated by immunotoxicant, the author recommends parallel use of antigen/APC-dependent TCR-mediated stimulation with RGG and irradiated syngeneic APC, accessory cell–independent CD3/TCR complex–mediated stimulation with immobilized anti-CD3, and stimulation bypassing phospholipase C–initiated early signaling events with PMA for activation of protein kinase C, plus a calcium ionophore for upregulation of intracellular free calcium (Heo et al., 1997).

Critical Parameters and Troubleshooting

Experience has shown that cells should be completely harvested through vigorous pipetting at the time of expansion and restimulation of OVA-specific T cells (Basic Protocol 1). It will be necessary to rinse culture wells once with RPMI and collect the rinsed-out suspension as well.

It is recommended that exogenous recombinant IL-2 be added for in vitro differentiation of naive T_H cells and activation of T_H clones. Although cloned T_H cells can proliferate and be activated in culture when stimulated with antigen in the absence of exogenous IL-2, better growth of T_H cells is obtained when these are cultured with both IL-2 and antigen. IL-2 is known not to have direct effects on T_H subset differentiation (Duncan and Lawrence, 1995).

When an irradiation source is not available, treatment of APC with mitomycin C (a DNA cross-linking agent) can be used; like irradiation, this preserves the antigen-presenting function of syngeneic antigen-presenting cells. Mitomycin C should be completely washed out prior to mixing the APC with cloned T_H cells, because mitomycin C exerts its cytotoxicity by blocking cell division. Since activated lymphocytes will tend to enlarge, microscopic examination of the cultures for blasts will give an indication of successful activation. Meanwhile, to obtain T_H clonal cells at stationary phase, the cells should be passaged at least 14 days after initiating culture with soluble antigen (Kimoto and Fathman, 1982).

With all assays, it is critical that cultures in each well be adjusted to equal final volumes in order to correctly compare the resulting levels of cytokines. Experience has shown that recovery of live lymphocytes from spleen or culture wells is significantly enhanced if the resuspensions after each centrifugation are done by first discarding the supernatant, then resuspending the cells by tapping the tube with the fingers, and finally adding the solution for resuspension, in that order.

Anticipated Results

Using Basic Protocol 1, ~50 ng/ml of IFN-γ and 1 ng/ml of IL-4 will be detected in a well in which 2×10^5 OVA-specific T_H cells, differentiated in the absence of experimental additives, are stimulated with 2.5×10^6 APC. Skewing of T_H cell development toward the T_{H2} phenotype has been reported in the presence of heavy metal (25 μM Pb) during the primary stimulation of naive T_H cells with OVA. With this concentration of Pb, Heo et al. (1997) detected 1.2±0.2 ng/ml IL-4 and 32±7 ng/ml IFN-γ, while with no experimental additives, they detected 0.8±0.2 ng/ml IL-4 and 57±9 ng/ml IFN-γ. Using Basic Protocol 2, the levels of IL-4 and IFN-γ from CDC35 T_{H2} and D1.6 T_{H1} cells stimulated with RGG alone will be ~2 to 4 ng/ml and 4 to 8 ng/ml, respectively.

Pb-induced differential effects on activities of T_{H2} and T_{H1} cells has been demonstrated using CDC35 T_{H2} and D1.6 T_{H1} clones, in that the levels of IL-4 from CDC35 and IFN-γ from D1.6 clonal cells were 1.6±0.6 and 3.5±0.1 ng/ml, respectively. Addition of 25 μM Pb enhanced IL-4 production to 128% and inhibited IFN-γ production to 53% (Heo et al., 1997).

Time Considerations

In Basic Protocol 1, 2 to 3 hr of work are required for the steps from removal of spleens up to the point where the cells are ready for incubation on culture plates. Following an additional 6 days of primary stimulation and expansion, preparation of antigen-presenting cells and mixed culture with resting OVA-specific T_H cells takes ~4 hr. In Basic Protocol 2, preparing APCs and setting up the mixed culture with resting D1.6 or CDC35 T_H clonal cells takes ~4 hr. The exact length of time will depend on the size of the experiment and the skill of investigator.

Literature Cited

Cherwinski, H.M., Schumacher, J.H., Brown, K.D., and Mosmann, T.R. 1987. Two types of mouse helper T cell clone. III. Further differences in lymphokine synthesis between Th1 and Th2 clone revealed by RNA hybridization, functionally monospecific bioassays, and monoclonal antibodies. *J. Exp. Med.* 166:1229-1244.

Desbarats, J., Wade, T., Wade, W.F., and Newell, M.K. 1999. Dichotomy between naïve and memory $CD4^+$ T cell responses to Fas engagement. *Proc. Natl. Acad. Sci. U.S.A.* 96:8104-8109.

Duncan, D.D. and Lawrence, D.A. 1995. T cells and cloned and transformed T-cell lines to assess immune function. *In* Methods in Immunotoxicology Vol. 1 (G.R. Burleson, J.H. Dean, and A.E. Munson, eds.) pp. 483-505. Wiley-Liss, New York.

Fiorentino, D.F., Bond, M.W., and Mosmann, T.R., 1989. Two types of mouse T helper cell. IV. Th2 clones secret a factor that inhibits cytokine production by Th1 clones. *J. Exp. Med.* 170:2081-2095.

Harris, M.R., Kindle, C.S., Abruzzini, A.F., Pierce, C.W., and Cullen, S.E. 1984. Antigen presentation by the BCL_1 murine B cell line: In vitro stimulation by LPS. *J. Immunol.* 133:1202-1208.

Heo, Y., Parsons, P.J., and Lawrence, D.A. 1996. Lead differentially modifies cytokine production in vitro and in vivo. *Toxicol. Appl. Pharmacol.* 138:149-157.

Heo, Y., Lee, W.T., and Lawrence, D.A. 1997. Differential effects of lead and cAMP on development and activities of Th1- and Th2-lymphocytes. *Toxicol. Sci.* 43:172-185.

Heo, Y., Saxon, A., and Hankinson, O. 2001. Effect of diesel exhaust particles and their components on the allergen-specific IgE and IgG1 response in mice. *Toxicology* 159:3143-3158.

Hsieh, C.-S., Heimberger, A.B., Gold, J.S., O'Garra, A., and Murphy, K.M., 1992. Differential regulation of T helper phenotype development by interleukin 4 and 10 in an αβT-cell-receptor transgenic system. *Proc. Natl. Acad. Sci. U.S.A.* 89:6065-6069.

Inaba, K., Swiggard, W.J., Steinman, R.M., Romani, N., and Schuler, G. 1998. Isolation of dendritic cells. *In* Current Protocols in Immunology (J.E. Coligan, A.M. Kruisbeek, D.H. Margulies, E.M. Shevach, and W. Strober, eds.) pp. 3.7.1-3.7.15. John Wiley & Sons, Hoboken, N.J.

Kimoto, M. and Fathman, C.G., 1982. Immunization and long-term culture of murine immune lymph node cells. *In* Isolation, Characterization, and Utilization of T Lymphocyte Clones. (C.G. Fathman and F.W. Fitch, eds.) pp. 525-526. Academic Press, San Diego, Calif.

Kurt-Jones, E.A., Hamberg, S., Ohara, J., Paul, W.E., and Abbas, A.K. 1987. Heterogeneity of helper/inducer T lymphocytes I. Lymphokine production and lymphokine responsiveness. *J. Exp. Med.* 166:1774-1787.

Mosmann, T.R. and Coffman, R.L. 1989. T_{H1} and T_{H2} cells: Different patterns of lymphokine secretion lead to different functional properties. *Annu. Rev. Immunol.* 7:145-173.

Olivares-Villagómez, D., Wang, Y., and Lafaille, J.J. 1998. Regulatory $CD4^+$ T cells expressing endogenous T cell receptor chains protect myelin basic protein-specific transgenic mice from spontaneous autoimmune encephalomyelitis. *J. Exp. Med.* 188:1883-1894.

Prigent, P., Saoudi, A., Pannetier, C., Graber, P., Bonnefoy, J.Y., Druet, P., and Hirsch, F. 1995. Mercuric chloride, a chemical responsible for T helper cell (Th2)-mediated autoimmunity in Brown Norway rats, directly triggers T cells to produce interleukin-4. *J. Clin. Invest.* 96:1484-1489.

Romagnani, S. 1996. Th1 and Th2 Cells in Health and Disease, Karger, Basel, Switzerland.

Rulifson, I.C., Sperling, A.I., Field, P.E., Fitch, F.W., and Bluestone, J.A. 1997. CD28 costimulation promotes the production of Th2 cytokines. *J. Immunol.* 158:658-665.

Sanderson, C.J., Strath, M., Warren, D.J., O'Garra, A., and Kirkwood, T.B. 1985. The production of lymphokines by primary alloreactive T-cell clones: A co-ordinate analysis of 233 clones in seven lymphokine assays. *Immunology* 56:575-584.

Sedar, R.A. and Paul, W.E. 1994. Acquisition of lymphokine-producing phenotype by $CD4^+$ T cells. *Annu. Rev. Immunol.* 12:635-673.

Spencer, J.S., Freed, J.H., and Kubo, R.T. 1993. Expression and function of mixed iostype MHC class II molecules in normal mice. *J. Immunol.* 151:6822-6832.

Tony, H.P., Phillips, N.E., and Parker, D.C. 1985. Role of membrane immunoglobulin (Ig) crosslinking in membrane Ig-mediated, major histocompatibility complex-restricted T cell–B cell cooperations. *J. Exp. Med.* 162:1695-1708.

Vratsanos, G.S., Jung, S.-S., Park, Y.-M., and Craft, J. 2001. $CD4^+$ T cells from lupus-prone mice are hyperresponsive to T cell receptor engagement with low and high affinity peptide antigens: A model to explain spontaneous T cell activation in lupus. *J. Exp. Med.* 193:329-337.

Walker, E., Warner, N.L., Chestnut, R., Kappler, J., and Marrack, P. 1982. Antigen-specific, I-region-restricted interactions in vitro between tumor cell lines and T cell hybridomas. *J. Immunol.* 128:2164-2169.

Zuckerman, S.H., Schreiber, R.D., and Marder, P. 1988. Reactivation of class II antigen expression in murine macrophage hybrids. *J. Immunol.* 140:978-983.

Key References

Heo et al., 1996. See above.

Shows how metal toxicants differently modify helper T cell subset activation in vitro.

Heo et al., 1998. See above.

Contains the first description of lead(Pb)-mediated helper T cell development skewing toward type-2 effectors in vitro.

Contributed by Yong Heo
Catholic University of Daegu
Kyongbuk Province
Republic of Korea

USEFUL INFORMATION

Safe Use of Radioisotopes

The use of radioisotopes to label specific molecules in a defined way has greatly furthered the discovery and dissection of biochemical pathways. The development of methods to inexpensively synthesize such tagged biological compounds on an industrial scale has enabled them to be used routinely in laboratory protocols, including many detailed in this manual. Although most of these protocols involve the use of only microcurie (μCi) amounts of radioactivity, some (particularly those describing the metabolic labeling of proteins or nucleic acids within cells) require amounts on the order of millicuries (mCi). In all cases where radioisotopes are used, depending on the quantity and nature of the isotope, certain precautions must be taken to ensure the safety of the scientist. This appendix outlines a few such considerations relevant to the isotopes most frequently used in biological research.

In designing safe protocols for the use of radioactivity, the importance of common sense, based on an understanding of the general principles of isotopic decay and the importance of continuous monitoring with a hand-held radioactivity monitor (e.g., Geiger counter), cannot be overemphasized. In addition, it is also critical to take into account the rules, regulations, and limitations imposed by each specific institution. These are usually not optional considerations: an institution's license to use radioactivity normally depends on strict adherence to such rules.

Many of the protocols described have evolved (and are evolving still) over the years. The authors are indebted to those who have trained them in the safe use of radioactivity, in particular to the members of the Salk Institute Radiation Safety Department. Most of the designs for the shields and other safety equipment shown in Figures A.1A.2A, A.1A.3, and A.1A.4 were created at the Salk Institute in collaboration with Dave Clarkin and Mario Tengco. Safety equipment of similar design is available from several commercial vendors, including CBS Scientific and Research Products International.

BACKGROUND INFORMATION

The Decay Process

As anyone who has taken a basic chemistry course will remember, each element is characterized by its atomic number, defined as the number of orbital electrons or the number of protons in the nucleus of that atom. Isotopes of a given element exist because some atoms of each element, while by definition having the same number of protons, have a different number of neutrons and therefore a different nuclear weight. It should be noted that the number of electrons outside the nucleus remains the same for all isotopes of a given element, and so all isotopes of a given element are equivalent with respect to their chemical reactivity.

Radioactive decay occurs when subatomic particles are released from the nucleus of an atom of a heavy isotope. This often results in the conversion of an atom of one isotope to an isotope of a different element, because the original isotope's atomic number changes after decay. The subatomic particles released from naturally occurring radioisotopes are of three basic types: α and β particles and γ rays (see Table A.1A.1).

An α particle is essentially the nucleus of a helium atom, or two protons plus two neutrons. It is a relatively large, heavy particle that moves slowly and usually only across short distances before it encounters some other atom with which it interacts. These particles are released from isotopes with large nuclei (atomic number >82; e.g., plutonium or uranium); such isotopes are not commonly used in biological research.

In contrast to α particles, β particles are light, high-speed charged particles. Negatively charged β particles are essentially electrons of nuclear origin that are released when a neutron is converted to a proton. Release of a β particle thus changes the atomic number and elemental status of the isotope.

γ radiation has both particle and wave properties; its wavelength falls within the range of X-ray wavelengths. The distinction between γ rays and X rays was made when primitive X-ray machines produced X rays with a wavelength longer than those of the γ rays produced naturally by radioisotopes. Modern X-ray machines

Contributed by Jill Meisenhelder and Kentaro Semba
Current Protocols in Toxicology (1999) A.1A.1-A.1A.13

Table A.1A.1 Physical Characteristics of Commonly Used Radionuclides[a]

Nuclide	Half-life	Emission	Energy, max (MeV)	Range of emission, max	Approx. specific activity at 100% enrichment (Ci/mg)	Atom resulting from decay	Target organ
^{3}H	12.43 years	β	0.0186	0.42 cm (air)	9.6	$^{3}_{2}He$	Whole body
^{14}C	5370 years	β	0.156	21.8 cm (air)	4.4 mCi/mg	$^{14}_{7}N$	Bone, fat
^{32}P[b]	14.3 days	β	1.71	610 cm (air) 0.8 cm (water) 0.76 cm (Plexiglas)	285	$^{33}_{16}S$	Bone
^{33}P[b]	25.4 days	β	0.249	49 cm	156	$^{33}_{16}S$	Bone
^{35}S	87.4 days	β	0.167	24.4 cm (air)	43	$^{35}_{17}Cl$	Testes
^{125}I[c]	60 days	γ	0.27–0.035	0.2 mm (lead)	14.2	$^{125}_{52}Te$	Thyroid
^{131}I[c]	8.04 days	β	0.606	165 cm (air)	123	$^{130}_{54}Xe$	Thyroid
		γ	0.364	2.4 cm (lead)			

[a]Table compiled based on information in Lederer et al. (1967) and Shleien (1987).
[b]Recommended shielding is Plexiglas; half-value layer measurement is 1 cm.
[c]Recommended shielding is lead; half-value layer measurement is 0.02 mm.

produce a much broader spectrum of wavelengths, including γ radiation; currently this sort of X-ray radiation is termed γ when it is of nuclear origin. Unlike β-particle release, the release of γ radiation by itself produces an isotopic change rather than an elemental one; however, the resultant nuclei are unstable and often decay further, releasing β particles.

The energy of all α particles and γ rays (measured in electron volts) is fixed, because they are of specific composition or wavelength. The energy of β particles, however, varies depending on the atom they originate from (and with concomitant release of neutrinos or antineutrinos that serve to balance the conservation of energy aspect of the decay equation). Thus there are (relatively) high-energy β particles released during the decay of ^{32}P and low-energy β particles released when tritium (^{3}H) decays.

Isotopic decay usually involves a chain or sequence of events rather than a single loss of a particle, because the resultant, equally unstable atoms try to achieve equilibrium. During this course of decay, secondary forms of radiation can be generated that may also pose a hazard to workers. For example, when high-energy β particles released during the decay of ^{32}P encounter the nuclei of atoms with a large atomic number, a strong interaction occurs. The β particle loses some energy in the form of a photon. Such photons are called Bremsstrahlung radiation; they are detectable using a monitor suitable for the detection of γ or X rays.

Following their release, α, β, and γ emissions (as well as secondary forms of radiation) travel varying average distances at varying average speeds, depending on their energy and the density of the material through which they are moving. The distance they actually travel before encountering either the electrons or nucleus of another atom is termed their degree of penetrance. This value is expressed as an average for each type of particle. The energy of the particles released (and therefore their potential penetrance) thus dictates what type of shielding, if any, is necessary for protection against the radiation generated by the decay of a given isotope. α, β, and γ emissions all have the potential, upon encountering an atom, to knock out its electrons, thereby creating ions. Thus, these three types of emissions are called ionizing radiation. The formation of such ions may result in the perturbation of biological processes: therein lies the danger associated with radioactivity!

Measuring Radioactivity and Individual Exposure to It

The radioactivity of a given substance is measured in terms of its ionizing activity. A curie (Ci) by definition is the amount of radioactive material that will produce 3.7×10^{10} disintegrations per second (see Table A.1A.2). This, not coincidentally, happens to be the number of disintegrations that occur during the decay of one gram of radium and its decay products. Exposure to such radiation is measured as the amount of energy absorbed by the recipient, which, of course, is directly related to the potential damage such radiation may cause. One rad is the dose of radiation that will

Table A.1A.2 Conversion Factors for Radioactivity

Measurement of Radioactivity

The SI unit for measurement of radioactivity is the becquerel:

1 becquerel (Bq) = 1 disintegration per second

The more commonly encountered unit is the curie (Ci):

1 Ci = 3.7×10^{10} Bq
= 2.22×10^{12} disintegrations per minute (dpm)
1 millicurie (mCi) = 3.7×10^{7} Bq = 2.22×10^{9} dpm
1 microcurie (μCi) = 3.7×10^{4} Bq = 2.22×10^{6} dpm

Conversion factors:

1 day = 1.44×10^{3} min = 8.64×10^{4} sec
1 year = 5.26×10^{5} min = 3.16×10^{7}sec
counts per minute (cpm) = dpm × (counting efficiency)

Measurement of Dose

The SI unit for energy absorbed from radiation is the gray (Gy):

1 Gy = 1 joule/kg

Older units of absorbed energy are the rad (r) and roentgen (R):

1 r = 100 ergs/g = 10^{-2} Gy
1 R = 0.877 r in air = 0.93 – 0.98 r in water and tissue

The SI unit for radiation dosage is the sievert (Sv), which takes into account the empirically determined relative biological effectiveness (RBE) of a given form of radiation:

dosage [Sv] = RBE × dosage [Gy]

$$\text{RBE} = \frac{\text{(biological effect of a dose of standard radiation [Gy])}}{\text{(biological effect of a dose of other radiation [Gy])}}$$

RBE = 1 for commonly encountered radionuclides

The older unit for dosage is the rem (roentgen-equivalent-man):

1 rem = 0.01 Sv

cause 100 ergs of energy to be absorbed per gram of irradiated material. Another unit commonly used to measure radiation doses is the rem; this is related to the rad but takes into account a "quality factor" based on the type of ionizing radiation being received. For β particles and γ or X rays this factor is 1; therefore, rems β equal rads β. In contrast, the quality factor associated with α particles is 20, so an exposure of one rad due to α particles would be recorded as 20 rem.

The amount or dose of radiation received by materials (cells, scientists, etc.) near the source depends not only on the specific type and energy (penetrance) of the radiation being produced, but also on the subject's distance from the source, the existence of any intervening layers of attenuating material (shielding), and the length of time spent in the vicinity of the radiation source. To best measure such doses, every person working with or around radioactivity should wear an appropriate type of radiation detection badge (in addition to carrying a portable radiation monitor that can give an immediate, approximate reading). This is normally a requirement for compliance with an institution's license to use radioisotopes. Such badges are usually furnished by the safety department and collected at regular intervals for reading by a contracted company. At most institutions, the old-style film badges have been replaced with the more accurate TLDs (thermoluminescent dosimeters). These take advantage of chemicals such as calcium or lithium fluorides which, following exposure to ionizing radiation, will luminesce at temperatures below their normal thermal luminescence threshold. Different types of badges are sensitive to different types of radiation: always be sure to wear one that is appropriate for detecting exposure to the isotope being used! In most places pregnant women are asked to wear a more sensitive (and more expensive) dosimeter to better monitor their (and the developing fetus') exposure. Most often workers will be asked to wear a radiation detection badge on the labcoat lapel in order to measure whole-body radiation. When working with ^{32}P or ^{125}I it is also advisable to wear a ring badge to measure exposure to the unshielded extremities (fingers). The

limit set for "acceptable" exposure to whole-body radiation is several-fold less than the limit set for extremities. Nevertheless, the authors have found that the exposure recorded on ring badges is often significant with respect to the limit for extremities set by our institution.

What is known about the effects on humans of exposure to low levels of radiation (i.e., levels which would be received when briefly handling millicurie or microcurie amounts of radioactivity)? Not much, for the obvious reason that direct studies have not been undertaken. Accordingly, guidelines for exposure levels are set using extrapolations—either by extrapolating down from population statistics obtained following accidents or disasters (the Chernobyl meltdown, atomic bombings) or by extrapolating up from numbers obtained from animal experiments. Each form of extrapolation is subject to caveats, and given that predictions based on such extrapolations cannot be perfect, most health and safety personnel aim for radiation exposure levels said to be ALARA or "as low as reasonably achievable." Further discussion of exposure limits and the statistics on which they are based may be found in B. Shleien's health physics text (Shleien, 1987). Limiting exposure to radiation can be accomplished by adjusting several parameters of the exposure: the duration of exposure, distance from the source, and the density of the material (air, water, shielding) between the individual and the source.

Time is of the essence

When designing any experiment using radioactivity, every effort should be made to limit the time spent directly handling the vials or tubes containing the radioactive material. Speed should be encouraged in all manipulations, though not to the point of recklessness! Have everything needed for the experiment ready at hand before the radioactivity is introduced into the work area.

Distance helps to determine dose

When possible, experiments involving radioactivity should be performed in an area separate from the rest of the lab. Many institutions require that such work be performed in a designated "hot lab"; however, if many people in the laboratory routinely use radioisotopes, it is less than feasible to move them all into what is usually a smaller space. No matter where an individual is working, it is his or her responsibility to monitor the work area and ensure his or her own safety and the safety of those working nearby by using adequate shielding. Obviously, when handling the radioactive samples, it is necessary to work rapidly behind any required shielding. To protect bystanders, remember that the intensity of radiation from a source (moving through air) falls off in proportion to the square of the distance. Thus, if standing 1 foot away from a source for 5 min would result in an exposure of 45 units, standing 3 feet away for the same amount of time would result in an exposure $(1/3)^2$ of 45 units, or 5 units. This factor is also relevant when considering the storage of large amounts of radioactivity, particularly ^{125}I or ^{32}P, as no amount of shielding can completely eliminate radiation.

Shielding is the key to safety

As mentioned above, the energy of the particle(s) released during the decay of an isotope determines what, if any, type of shielding is appropriate (see Table A.1A.3). β particles released during the decay of ^{14}C and ^{35}S possess roughly ten times the energy of those released when ^{3}H decays. All three β particles are of relatively low energy, do not travel very far in air, and cannot penetrate solid surfaces. No barriers are necessary for shielding against this type of β radiation. The major health threat from these isotopes occurs through their accidental ingestion, inhalation, or injection.

β particles released during the decay of ^{32}P have 10-fold higher energy than those released from ^{14}C and pose a significant threat to workers. (One reported hazard is the potential for induction of cataracts in the unshielded eye.) The fact that these high-energy beta particles can potentially generate significant amounts of Bremsstrahlung radiation is the reason that low-density materials are used as the primary layer of shielding for ^{32}P β radiation. Water, glass, and plastic are suitable low-density materials (as opposed to lead). Obviously water is unsuitable as a shielding layer for work on the bench, although it does a reasonable job when samples are incubating in a water bath. Shields made from a thickness of glass sufficient to stop these particles would be extremely heavy and cumbersome (as well as dangerous if dropped). Fortunately, plastic or acrylic materials—variously called Plexiglas, Perspex, or Lucite—are available for shielding against ^{32}P β radiation. Shields as well as storage boxes constructed of various thicknesses of Plexiglas are necessary equipment in laboratories where ^{32}P is used. When millicurie amounts of ^{32}P are used at one time it is necessary to also block the Bremsstra-

Table A.1A.3 Shielding Radioactive Emission[a]

β emitters

Energy (MeV)	Mass (mg)/cm^2 to reduce intensity by 50%	Thickness (mm) to reduce intensity by 50%			
		Water	Glass	Lead	Plexiglas
0.1	1.3	0.013	0.005	0.0011	0.0125
1.0	48	0.48	0.192	0.042	0.38
2.0	130	1.3	0.52	0.115	1.1
5.0	400	4.0	1.6	0.35	4.2

γ emitters

Energy (MeV)	Thickness of material (cm) to attenuate a broad beam of γ-rays by a factor of 10			
	Water	Aluminum	Iron	Lead
0.5	54.6	20.3	6.1	1.8
1.0	70.0	24.4	8.2	3.8
2.0	76.0	32.0	11.0	5.9
3.0	89.0	37.0	12.0	6.4

[a]From Dawson et al. (1986). Reprinted with permission.

hlung radiation by adding a layer of high-density material (such as 4 to 6 mm lead) to the outside of the Plexiglas shield (covering the side farthest from the radioactive source).

γ rays released during the decay of ^{125}I have much higher penetrance than the β particles from ^{32}P decay; this radiation must be stopped by very-high-density material, such as lead. Lead foil of varying thicknesses (2 to 6 mm) can be purchased in rolls and can be cut and molded to cover any container, or taped to a Plexiglas shield (used in this instance for support). Obviously this latter arrangement has the disadvantage that it is impossible to see what one is doing through the shield. For routine shielding of manipulations involving ^{125}I, it is useful to purchase a lead-impregnated Plexiglas shield that is transparent, albeit inevitably very heavy (as well as relatively expensive).

Although it seems logical that the use of more radioactivity necessitates the use of thicker layers of shielding, it is also true that no shielding material is capable of completely stopping all radiation. When deciding how thick is "thick enough," consult the half-value layer measurement for each type of shielding material. This number gives the thickness of a given material necessary to stop half the radiation from a source; Table A.1A.3 lists half-value layer measurements for the β particles released from isotopes commonly used in the biology laboratory. In general, 1 to 2 cm of Plexiglas and/or 0.02 mm of lead are sufficient to shield the amounts of radioactivity used in most experiments.

GENERAL PRECAUTIONS

Before going on to a discussion of specific precautions to be taken with individual isotopes, a short list of general precautions to be taken with all isotopes seems pertinent:

1. Know the rules. Be sure that each individual is authorized to use each particular isotope and uses it in an authorized work area.

2. Don the appropriate apparel. Whenever working at the lab bench, it is good safety practice to wear a labcoat for protection. Disposable paper/synthetic coats of various styles are commercially available: at $4 each these may be conveniently thrown out if contaminated with radioactivity during an experiment, rather than held for decay as might be preferable with cloth coats costing about $30 each. As an alternative, disposable sleeves can be purchased and worn over those of the usual cloth coat. Other necessary accessories include radiation safety badges, gloves, and protective eyewear. It's handy to wear two pairs of gloves at once when using radioactivity; when the outer pair becomes contaminated, it is possible to strip it off and continue working without interruption.

3. Protect the work area as well as the workers. Lab benches and the bases of any shields used should be covered with some sort of disposable, preferably absorbent, paper sheet. Underpads or diapers (the kind normally used in hospitals) are convenient for this purpose.

4. Use appropriate designated equipment. It is very convenient, where use justifies

the expense, to have a few adjustable pipettors dedicated for use with each particular isotope. Likewise, it is good practice to use only certain labeled centrifuges and microcentrifuge rotors for radioactive samples so that all the lab's rotors do not become contaminated. Although such equipment should be cleaned after each use, complete decontamination is often not possible. A few pipettors or a single microcentrifuge can easily be stored (and used) behind appropriate shielding. Actually, contamination of the insides and tip ends of pipettors can be greatly reduced by using tips supplied with internal aerosol barriers; these have recently become very popular for setting up PCR reactions and are available to fit a variety of pipettors. To prevent contamination of the outside of the pipettor's barrel, simply wrap the hand-grip in Parafilm, which can be discarded later. Several manufacturers sell disposable paper inserts for their microcentrifuges that protect the wall of the rotor chamber from contamination that might spin off the outside of sample tubes. Trying to fashion homemade liners of this sort is not recommended, as we have had disastrous experiences using laminated adhesive paper that "unstuck" during microcentrifuge spins. These liners would get caught by the rotor, shattering sample tubes and creating an even bigger mess!

5. Know where to dispose of radioactive waste, both liquid and solid. Most institutions require that radioactive waste be segregated by isotope. This is done not only so that appropriate shielding can be placed around waste containers, but so that some waste can be allowed to decay prior to disposal through normal trash channels (see Table A.1A.4 and Fig. A.1A.1). With a decreasing number of radioactive waste disposal facilities able or willing to accept radioactive waste for burial (and a concomitant increase in dumping charges from those that still do), this practice of on-site decay can save an institution thousands of dollars a year in disposal charges.

6. Label your label! It is only common courtesy (as well as common sense) to alert coworkers to the existence of anything and everything radioactive that is left where they may come in contact with it! A simple piece of tape affixed to the sample box—with the investigator's name, the amount and type of isotope, and the date written on it—should do the trick. Yellow hazard tape printed with the international symbol for radioactivity is commercially available in a variety of widths.

7. Monitor radioactivity early and often. Portable radiation detection monitors are essential equipment for every laboratory using radioactivity. No matter how much or how little radioactivity is being used, the investigator should keep a hand-held monitor nearby—and it should be on! Turn it on before touching any radioactivity to avoid contaminating the monitor's switch. Use a monitor with the appropriate detection capacity (β for ^{35}S and ^{32}P; γ for ^{125}I) before, during, and after all procedures. The more frequently fingers and relevant equipment are monitored, the more quickly a spill or glove contamination will be detected. Such timely detection will keep both the potential mess and the cleanup time to a minimum. Because low-energy β emitters such as ^{3}H cannot be detected using such monitors, wipe tests of the bench and equipment used are necessary to ensure that contamination of the work area did not occur.

SPECIFIC PRECAUTIONS

The following sections describe precautions to be taken with individual isotopes in specific forms. Although the sections dealing with ^{35}S- or ^{32}P-labeling of proteins in intact cells are presented in terms of mammalian cells, most of the instructions are also pertinent (with minimal and obvious modifications) to the labeling of proteins in other cells (bacterial, insect, etc.).

Working with ^{35}S

Using ^{35}S to label cellular proteins and proteins translated in vitro

As discussed above, the β radiation generated during ^{35}S decay is not strong enough to make barrier forms of shielding necessary. The risk associated with ^{35}S comes primarily through its ingestion and subsequent concentration in various target organs, particularly the testes. Although willful ingestion of ^{35}S seems unlikely, accidental or unknowing ingestion may be more common. As reported several years ago (Meisenhelder and Hunter, 1988), ^{35}S-labeled methionine and cysteine, which are routinely used to label proteins in intact cells and by in vitro translation, break down chemically to generate a volatile radioactive component. The breakdown occurs independent of cellular metabolism. Thus the radioactive component is generated to the same extent in stock vials as in cell culture dishes. The process seems to be promoted by freezing and thawing ^{35}S-labeled materials. The exact identity of this component is not known, although it is probably SO_2 or CH_3SH. What is known is that it dissolves read-

Table A.1A.4 Decay factors for calculating the amount of radioactivity present at a given time after a reference date. For example, a vial containing 1.85 MBq (50 μCi) of a ^{35}S-labeled compound on the reference date will have the following activity 33 days later: 1.85 × 0.770 = 1.42 MBq; 50 × 0.770 = 38.5 μCi.

^{125}I Half-life: 60.0 days

Days	Days 0	2	4	6	8	10	12	14	16	18
0	1.000	0.977	0.955	0.933	0.912	0.891	0.871	0.851	0.831	0.812
20	0.794	0.776	0.758	0.741	0.724	0.707	0.691	0.675	0.660	0.645
40	0.630	0.616	0.602	0.588	0.574	0.561	0.548	0.536	0.524	0.512
60	0.500	0.489	0.477	0.467	0.456	0.445	0.435	0.425	0.416	0.406
80	0.397	0.388	0.379	0.370	0.362	0.354	0.345	0.338	0.330	0.322
100	0.315	0.308	0.301	0.294	0.287	0.281	0.274	0.268	0.262	0.256
120	0.250	0.244	0.239	0.233	0.228	0.223	0.218	0.213	0.208	0.203
140	0.198	0.194	0.189	0.185	0.181	0.177	0.173	0.169	0.165	0.161
160	0.157	0.154	0.150	0.147	0.144	0.140	0.137	0.134	0.131	0.128
180	0.125	0.122	0.119	0.117	0.114	0.111	0.109	0.106	0.104	0.102
200	0.099	0.097	0.095	0.093	0.090	0.088	0.086	0.084	0.082	0.081
220	0.079	0.077	0.075	0.073	0.072	0.070	0.069	0.067	0.065	0.064
240	0.063	0.061	0.060	0.058	0.057	0.056	0.054	0.053	0.052	0.051

^{32}P Half-life: 14.3 days

Days	Hours 0	12	24	36	48	60	72	84
0	1.000	0.976	0.953	0.930	0.908	0.886	0.865	0.844
4	0.824	0.804	0.785	0.766	0.748	0.730	0.712	0.695
8	0.679	0.662	0.646	0.631	0.616	0.601	0.587	0.573
12	0.559	0.546	0.533	0.520	0.507	0.495	0.483	0.472
16	0.460	0.449	0.439	0.428	0.418	0.408	0.398	0.389
20	0.379	0.370	0.361	0.353	0.344	0.336	0.328	0.320
24	0.312	0.305	0.298	0.291	0.284	0.277	0.270	0.264
28	0.257	0.251	0.245	0.239	0.234	0.228	0.223	0.217
32	0.212	0.207	0.202	0.197	0.192	0.188	0.183	0.179
36	0.175	0.170	0.166	0.162	0.159	0.155	0.151	0.147
40	0.144	0.140	0.137	0.134	0.131	0.127	0.124	0.121
44	0.119	0.116	0.113	0.110	0.108	0.105	0.102	0.100
48	0.098	0.095	0.093	0.091	0.089	0.086	0.084	0.082
52	0.080	0.078	0.077	0.075	0.073	0.071	0.070	0.068

^{131}I Half-life: 8.04 days

Days	Hours 0	6	12	18	24	30	36	42	48	54	60	66
0	1.000	0.979	0.958	0.937	0.917	0.898	0.879	0.860	0.842	0.824	0.806	0.789
3	0.772	0.756	0.740	0.724	0.708	0.693	0.678	0.664	0.650	0.636	0.622	0.609
6	0.596	0.583	0.571	0.559	0.547	0.533	0.524	0.513	0.502	0.491	0.481	0.470
9	0.460	0.450	0.441	0.431	0.422	0.413	0.405	0.396	0.387	0.379	0.371	0.363
12	0.355	0.348	0.340	0.333	0.326	0.319	0.312	0.306	0.299	0.293	0.286	0.280
15	0.274	0.269	0.263	0.257	0.252	0.246	0.241	0.236	0.231	0.226	0.221	0.216
18	0.212	0.207	0.203	0.199	0.194	0.190	0.186	0.182	0.178	0.175	0.171	0.167
21	0.164	0.160	0.157	0.153	0.150	0.147	0.144	0.141	0.138	0.135	0.132	0.129
24	0.126	0.124	0.121	0.118	0.116	0.113	0.111	0.109	0.106	0.104	0.102	0.100
27	0.098	0.095	0.093	0.091	0.089	0.088	0.086	0.084	0.082	0.080	0.079	0.077
30	0.075	0.074	0.072	0.071	0.069	0.068	0.066	0.065	0.064	0.063	0.061	0.059
33	0.058	0.057	0.056	0.054	0.053	0.052	0.051	0.050	0.049	0.048	0.047	0.046
36	0.045	0.044	0.043	0.042	0.041	0.040	0.039	0.039	0.038	0.037	0.036	0.035

^{35}S Half-life: 87.4 days

Weeks	Days 0	1	2	3	4	5	6
0	1.000	0.992	0.984	0.976	0.969	0.961	0.954
1	0.946	0.939	0.931	0.924	0.916	0.909	0.902
2	0.895	0.888	0.881	0.874	0.867	0.860	0.853
3	0.847	0.840	0.833	0.827	0.820	0.814	0.807
4	0.801	0.795	0.788	0.782	0.776	0.770	0.764
5	0.758	0.752	0.746	0.740	0.734	0.728	0.722
6	0.717	0.711	0.705	0.700	0.694	0.689	0.683
7	0.678	0.673	0.667	0.662	0.657	0.652	0.646
8	0.641	0.636	0.631	0.626	0.621	0.616	0.612
9	0.607	0.602	0.597	0.592	0.588	0.583	0.579
10	0.574	0.569	0.565	0.560	0.556	0.552	0.547
11	0.543	0.539	0.534	0.530	0.526	0.522	0.518
12	0.514	0.510	0.506	0.502	0.498	0.494	0.490

^{33}P Half-life: 25.4 days

Days	Days 0	1	2	3	4	5	6	7	8	9
0	1.000	0.973	0.947	0.921	0.897	0.872	0.849	0.826	0.804	0.782
10	0.761	0.741	0.721	0.701	0.683	0.664	0.646	0.629	0.612	0.595
20	0.579	0.564	0.549	0.534	0.520	0.506	0.492	0.479	0.466	0.453
30	0.441	0.429	0.418	0.406	0.395	0.385	0.374	0.364	0.355	0.345
40	0.336	0.327	0.318	0.309	0.301	0.293	0.285	0.277	0.270	0.263
50	0.256	0.249	0.242	0.236	0.229	0.223	0.217	0.211	0.205	0.200
60	0.195	0.189	0.184	0.179	0.174	0.170	0.165	0.161	0.156	0.152
70	0.148	0.144	0.140	0.136	0.133	0.129	0.126	0.122	0.119	0.116
80	0.113	0.110	0.107	0.104	0.101	0.098	0.096	0.093	0.091	0.088
90	0.086	0.084	0.081	0.079	0.077	0.075	0.073	0.071	0.069	0.067
100	0.065	0.064	0.062	0.060	0.059	0.057	0.055	0.054	0.053	0.051
110	0.050	0.048	0.047	0.046	0.045	0.043	0.042	0.041	0.040	0.039
120	0.038	0.037	0.036	0.035	0.034	0.033	0.032	0.031	0.030	0.030

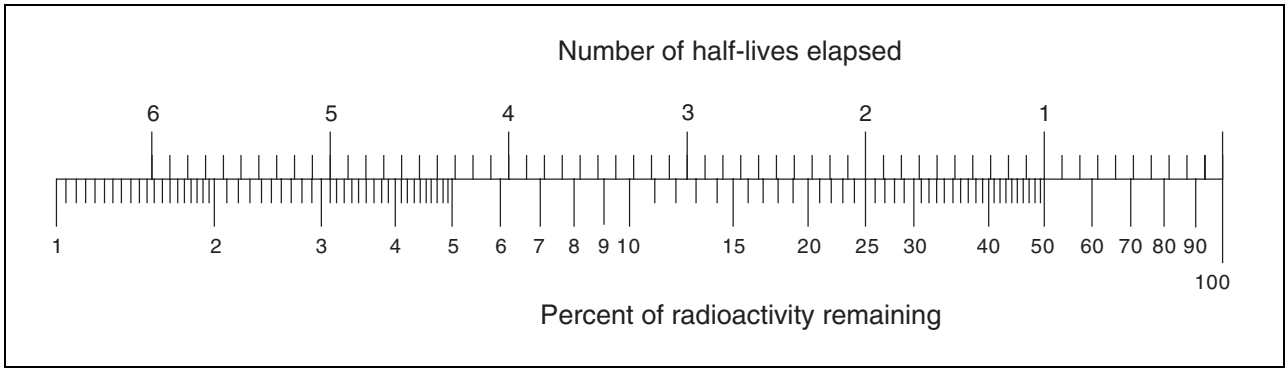

Figure A.1A.1 Correlation of loss of radioactivity with elapsing half-lives of an isotope.

ily in water and is absorbed by activated charcoal or copper.

The amount of this volatile radioactive component released, despite stabilizers added by the manufacturers, is about 1/8000 of the total radioactivity present. The amount of this radioactivity that a scientist is likely to inhale while using these compounds is presumably even smaller. Nevertheless, such a component can potentially contaminate a wide area because of its volatility, and also tends to concentrate in target organs. Thus, it is advisable to thaw vials of ^{35}S-labeled amino acids in a controlled area such as a hood equipped with a charcoal filter. This charcoal filter will become quite contaminated and should be changed every few months. If such an area is not available, the stock vial should be thawed using a needle attached to a charcoal-packed syringe to vent and trap the volatile compound.

Anyone who has ever added ^{35}S-labeled amino acids to dishes of cells for even short periods knows that the incubator(s) used for such labelings quickly becomes highly contaminated with ^{35}S. Such contamination is not limited to the dish itself, nor to the shelf on which the dish was placed. Rather, the radioactive component's solubility in water allows it to circulate throughout the moist atmosphere of the incubator and contaminate all the inside surfaces of the incubator. For this reason, in laboratories where such metabolic labelings are routine, it is highly convenient to designate one incubator to be used solely for working with ^{35}S-labeled samples. Such an incubator can be fitted with a large honeycomb-style filter, the size of an incubator shelf, made of pressed, activated charcoal. These filters are available from local air-quality-control companies. Such a filter will quickly become quite contaminated with radioactivity and should therefore be monitored and changed as necessary (usually about every three months if the incubator is used several times a week). The water used to humidify the incubator will also become quite "hot" (contaminated with radioactivity); keeping the water in a shallow glass pan on the bottom of the incubator makes it easy to change it after every use, thus preventing contamination from accumulating. Even with the charcoal filter and water as absorbents, the shelves, fan, and inner glass door of the incubator will become contaminated, as will the tray on which the cells are carried and incubated. Routine wipe tests and cleaning when necessary will help to minimize potential spread of this contamination.

If such labelings are done infrequently or there is no "spare" incubator, dishes of cells can be placed in a box during incubation. This box should be made of plastic, which is generally more easily decontaminated than metal. Along with the dishes of cells, a small sachet made of activated charcoal wrapped loosely in tissue (Kimwipes work well) should be placed in the box. If the box is sealed, it will obviously need to be gassed with the correct mixture of CO_2; otherwise small holes can be incorporated into the box design to allow equilibration with the incubator's atmosphere. In either case, the incubator used for the labeling should be carefully monitored for radioactivity after each experiment.

Working with ^{32}P

Microcurie amounts of ^{32}P

The amount of ^{32}P-labeled nucleotide used to label nucleic acid probes for northern or Southern blotting is typically under 250 µCi, and the amount of [γ-^{32}P]ATP used for in vitro phosphorylation of proteins does not usually exceed 50 µCi for a single kinase reaction (or several hundred microcuries per experiment). However, handling even these small amounts, given the time spent on such experiments, can result in an unacceptable level of exposure if proper shielding is not employed. With no intervening shielding, the dose rate 1 cm away from 1 mCi ^{32}P is 200,000 mrads/hr; the local dose rate to basal cells resulting from a skin contamination of 1 µCi/cm^2 is 9200 mrads/hr (Shleien, 1987). Such a skin contamination could be easily attained though careless pipetting and the resultant creation of an aerosol of radioactive microdroplets, because the concentration of a typical stock solution of labeled nucleotide may be 10 µCi/µl.

For proper protection during this sort of experiment, besides the usual personal attire (glasses, coat, safety badges, and gloves) it is necessary to use some form of Plexiglas screen between the body and the samples (see Fig. A.1A.2A). Check the level of radiation coming through the outside of the shield with a portable monitor to be sure the thickness of the Plexiglas is adequate. Hands can be shielded from some exposure by placing the sample tubes in a solid Plexiglas rack, which is also useful for transporting samples from the bench to a centrifuge or water bath (see Fig. A.1A.2B).

Experiments of these types often include an incubation step performed at a specific temperature, usually in a water bath. Although the water

surrounding the tubes or hybridization bags will effectively stop β radiation, shielding should be added over the top of the tubes (where there is no water)—e.g., a simple flat piece of Plexiglas. If the frequency of usage justifies the expense, an entire lid for the water bath can be constructed from Plexiglas. When hybridization reactions are performed in bags, care should be taken to monitor (and shield) the apparatus used to heat-seal the bags.

The waste generated during the experiments should also be shielded. It is convenient to have a temporary waste container right on the bench. Discard pipet tips and other solid waste into a beaker lined with a plastic bag and placed behind the shield. This bag can then be emptied into the appropriate shielded laboratory waste container when the experiment is done. Liquid waste can be pipetted into a disposable tube set in a stable rack behind the shield (see Fig. A.1A.2C).

When radiolabeled probes or proteins must be gel-purified, it may be necessary to shield the gel apparatus during electrophoresis if the samples are particularly hot. Be advised that the electrophoresis buffer is likely to become very radioactive if the unincorporated label is allowed to run off the bottom of the gel; check with a radiation safety officer for instructions on how to dispose of such buffer. It is also prudent to check the gel plates with a portable detection monitor after the electrophoresis is completed, because they sometimes become contaminated as well.

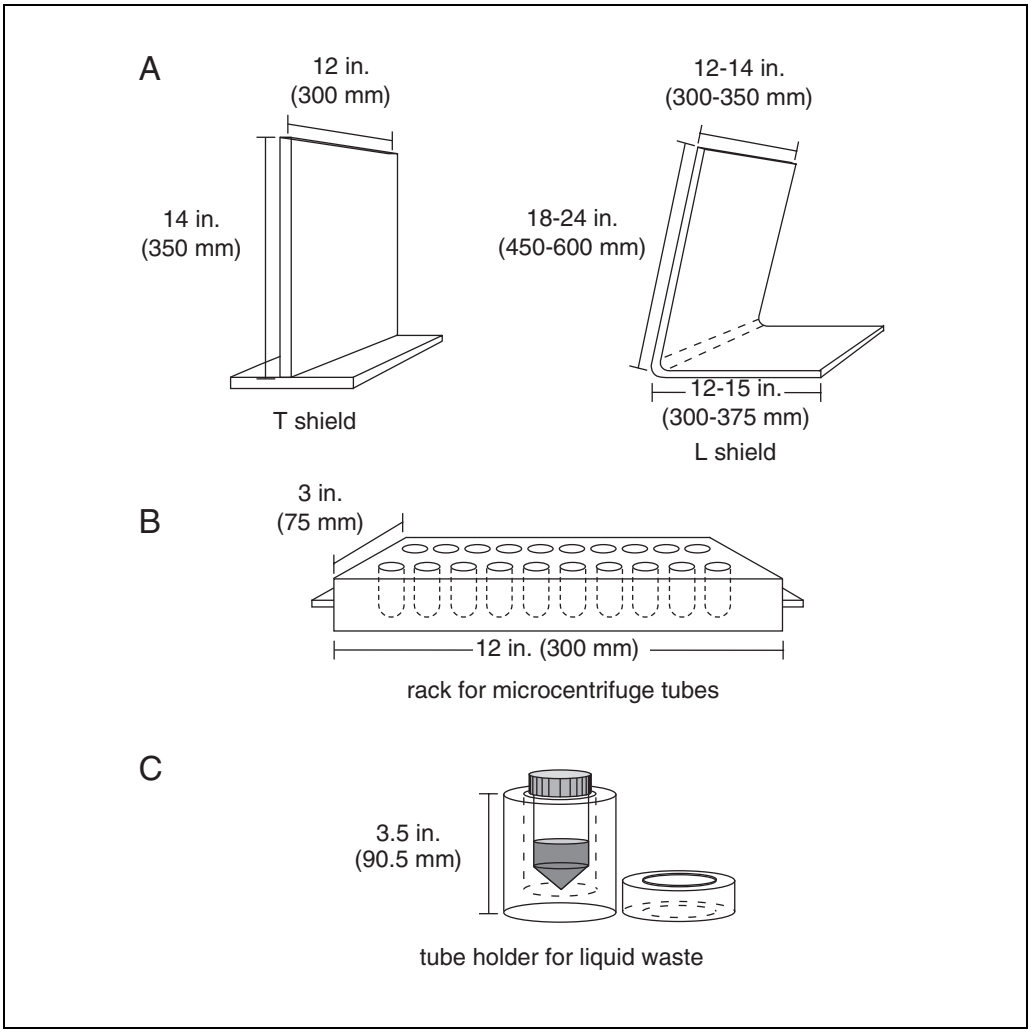

Figure A.1A.2 Plexiglas shielding for ^{32}P. (**A**) Two portable shields (L and T design) made of 0.5-in. Plexiglas. Either can be used to directly shield the scientist from the radioactivity he or she is using. Turned on its side, the L-shaped shield can be used to construct two sides of a cage around a temporary work area, providing shielding for other workers directly across or to the sides of the person working with ^{32}P. (**B**) Tube rack for samples in microcentrifuge tubes. (**C**) Tube holder for liquid waste collection.

Millicurie amounts of ^{32}P

In order to study protein phosphorylation in intact mammalian cells, cells in tissue culture dishes are incubated in phosphate-free medium with ^{32}P-labeled orthophosphate for a period of several hours or overnight to label the proteins. The amount of ^{32}P used in such labelings can be substantial. Cells are normally incubated in 1 to 2 mCi of ^{32}P/ml labeling medium; for each 6-cm dish of cells, 2.5 to 5 mCi ^{32}P may be used. When this figure is multiplied by the number of dishes necessary per sample, and the number of different samples in each experiment, it is clear that the amount of ^{32}P used in one experiment can easily reach 25 mCi or more. Because so much radioactivity is used in the initial labeling phase of such experiments, it is necessary for a researcher to take extra precautions in order to adequately shield him or herself and coworkers.

When adding label to dishes of cells, it is important to work as rapidly as possible. An important contribution to the speed of these manipulations is to have everything that will be needed at hand before even introducing the label into the work area. Prepare the work area, arranging shielding and covering the bench with diapers, in advance. Set out all necessary items, including any pipettors and tips needed, a portable detection monitor, extra gloves, and a cell house (see Fig. A.1A.3A).

Work involving this much radioactivity should be done behind a Plexiglas shield at least ¾ in. (2 cm) thick; the addition of a layer of lead to the outside lower section of this shield to stop Bremsstrahlung radiation is also needed. If one shield can be dedicated to this purpose at a specific location, a sheet of lead several centimeters thick can be permanently screwed to the

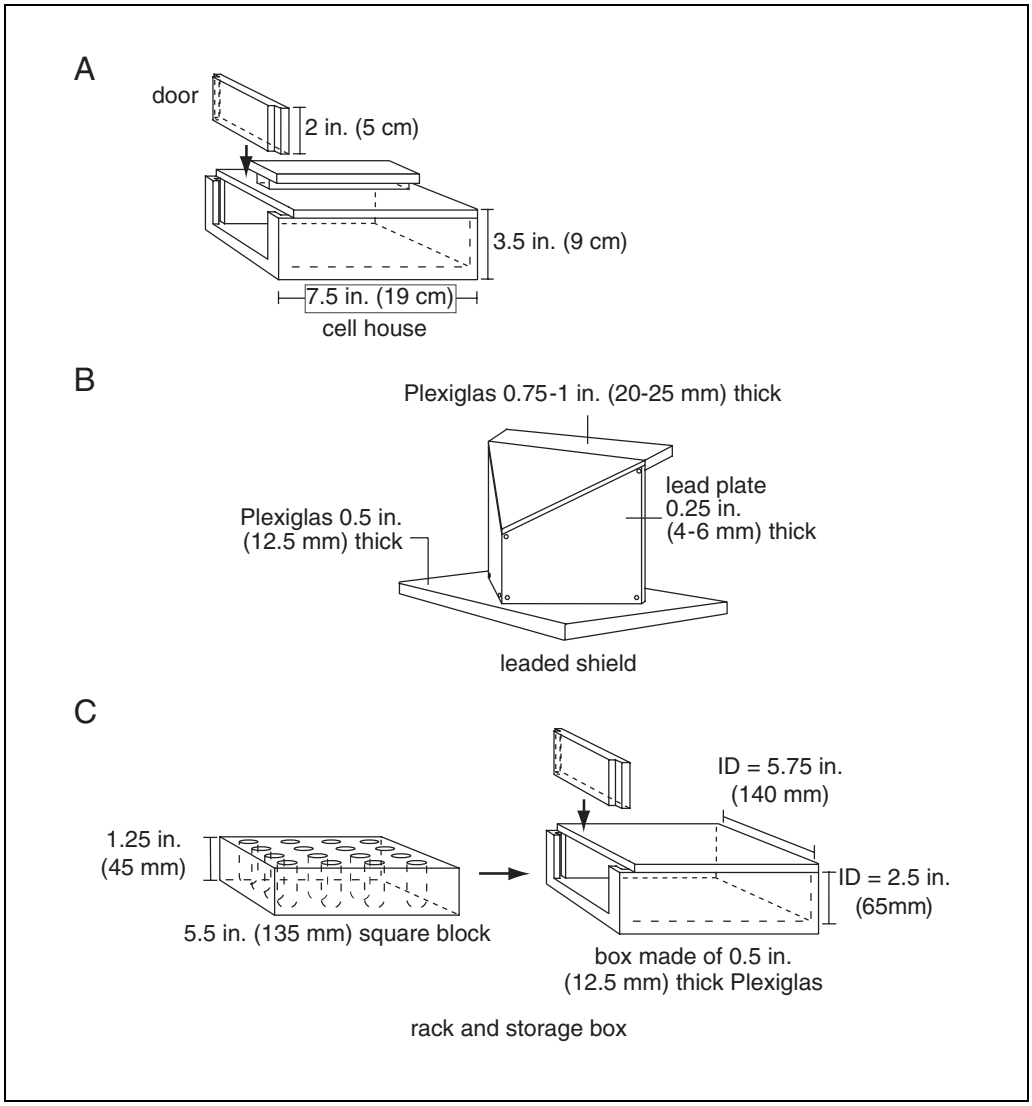

Figure A.1A.3 (**A**) Box for cell incubation (a "cell house"). (**B**) Stationary leaded shield. (**C**) Sample storage rack and box made of 0.5-in. Plexiglas. Abbreviations: ID, interior dimension.

Plexiglas (as shown in Fig. A.1A.3B); however, this lead makes the shield extremely heavy and therefore less than portable. If space constraints do not permit the existence of such a permanent labeling station, a layer or two of lead foil can be taped temporarily to the outside of the Plexiglas shield.

Again, each worker should take care to shield not only him or herself, but bystanders on all sides. Handling of label should be done away from the central laboratory if possible to take maximum advantage of distance as an additional form of shielding. It is also advisable not to perform such experiments in a tissue culture room or any other room that is designed for a purpose vital to the whole laboratory. An accident involving this much ^{32}P would seriously inconvenience future work in the area, if not make it altogether uninhabitable! If care is taken to minimize the amount of time the dish of cells is open when adding the label, use of a controlled air hood to prevent fungal or bacterial contamination of the cells should not be necessary.

Once the label has been added to the dishes of cells, they will also need to be shielded for transport to and from the incubator and other work areas. Plexiglas boxes that are open at one end (for insertion of the dishes) and have a handle on top (for safe carrying) make ideal "cell houses" (see Figure A.1A.3A). A Plexiglas door that slides into grooves at the open end is important to prevent dishes from sliding out if the box is tilted at all during transport. If this door is only two-thirds the height of the house wall, the open slot thus created will allow equilibration of the CO_2 level within the house with that in the incubator. Obviously, this slot will also allow a substantial stream of radiation to pass out of the cell house, so the house should be carried and placed in the incubator with its door facing away from the worker (and others)!

Following incubation with label and any treatments or other experimental manipulations, the cells are usually lysed in some type of detergent buffer. It is during this lysis procedure that a worker's hands receive their greatest exposure to radiation, because it is necessary to directly handle the dishes over a period of several minutes. It is therefore very important to streamline this procedure and use any shielding whenever possible. If the cell lysates must be made at 4°C, as required by most protocols, working on a bench in a cold room is preferable to placing the dishes on a slippery bed of ice. In either case, make the lysate using the same sort of shielding (with lead if necessary) that was used when initially adding the label. Pipet the labeling medium and any solution used to rinse unincorporated radioactivity from the cells into a small tube held in a solid Plexiglas holder (shown in Fig. A.1A.2C). The contents of this tube can later be poured into the appropriate liquid waste receptacle. If possible, it is a good practice to keep this high-specific-activity ^{32}P liquid waste separate from the lower-activity waste generated in other procedures so that it can be removed from the laboratory as soon as possible following the experiment. If it is necessary to store it in the laboratory for any time, the shielding for the waste container should also include a layer of lead.

The solid waste generated in the lysis part of these experiments (pipet tips, disposable pipets, cell scrapers, and dishes) is very hot and should be placed immediately into some sort of shielded container to avoid further exposure of

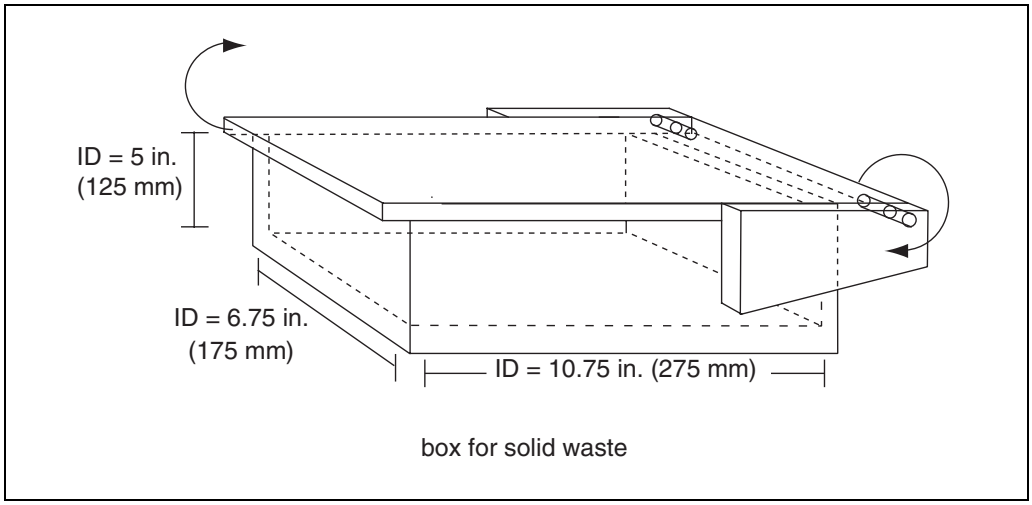

Figure A.1A.4 Box for solid waste collection made of 0.5-in. Plexiglas. Abbreviation: ID, interior dimension.

the hands. A Plexiglas box similar in design to that in Figure A.1A.4 is convenient; placed to the side of the shield and lined with a plastic bag, it will safely hold all radioactive waste during the experiment and is light enough to be easily carried to the main laboratory waste container where the plastic bag (and its contents) can be dumped after the experiment is done. If the lid of the box protrudes an inch or so over the front wall, it can be lifted using the back of a hand, thus decreasing the possibility of contaminating it with hot gloves.

When scraping the cell lysates from the dishes, it is good practice to add them to microcentrifuge tubes that are shielded in a solid Plexiglas rack; this will help to further reduce the exposure to which the hands are subjected. At this point, the lysates are usually centrifuged at high speed (>10,000 × *g*) to clear them of unsolubilized cell material. Use screw-cap tubes for this clarification step, as these will contain the labeled lysate more securely than flip-top tubes, which may open during centrifugation. No matter what type of tube is used, the rotor of the centrifuge often becomes contaminated, most probably due to tiny drops of lysate (aerosol) initially present on the rim of the tubes that are spun off during centrifugation. Monitor the rotor and wipe it out after each use.

The amount of ^{32}P taken up by cells during the incubation period varies considerably, depending on the growth state of the culture as well as on the cell type and its sensitivity to radiation. This makes it difficult to predict the percentage of the radioactivity initially added to the cells that is incorporated into the cell lysate; however, this figure probably does not exceed 10%. Thus, the amount of radioactivity being handled decreases dramatically after lysis, making effective shielding much simpler. However, at least ten times more radioactivity than is usual in other sorts of experiments is still involved! It is easy to determine if the shielding is adequate—just use both β and γ portable monitors to measure the radiation coming through it. Again, be sure to check that people working nearby (including those across the bench) are also adequately shielded. It is sometimes necessary to construct a sort of cage of Plexiglas shields around the ice bucket that contains the lysates.

At the end of the day or the experiment, it may be necessary to store radioactive samples; in some experiments, it may be desirable to save the cell lysates. These very hot samples are best stored in tubes placed in solid Plexiglas racks that can then be put into Plexiglas boxes (see Fig. A.1A.3C). Such boxes may be of similar construction to the cell houses described above; however, they should have a door that completely covers the opening. Be sure to check the γ radiation coming through these layers and add lead outside if necessary.

Working with ^{33}P

Using ^{33}P-labeled nucleotides to label nucleic acid probes or proteins

Several of the major companies that manufacture radiolabeled biological molecules have recently introduced nucleotides labeled with ^{33}P (both α- and γ-labeled forms). ^{33}P offers a clear advantage over ^{32}P with respect to ease of handling, because the energy of the β particles it releases lies between that of ^{35}S and ^{32}P and thus its use does not require as many layers of Plexiglas and lead shielding as for ^{32}P. In fact, the β radiation emitted can barely penetrate through gloves and the surface layer of skin, so the hazard associated with exposure to even millicurie amounts of ^{33}P is thought to be insignificant (as reported in the DuPont NEN product brochure). Gel bands visualized on autoradiographs of ^{33}P-labeled compounds are sharper than bands labeled with ^{32}P because the lower-energy β radiation does not have the scatter associated with that from ^{32}P. The half-life of ^{33}P is also longer (25 days compared to 14 days for ^{32}P). Despite its higher cost, these features have led many researchers to choose ^{33}P-labeled nucleotides for use in experiments such as band/gel shift assays where discrimination of closely-spaced gel bands is important.

The best way to determine what degree of shielding is needed when using ^{33}P is to monitor the source using a portable β monitor and add layers of Plexiglas as necessary.

Working with ^{125}I

Using ^{125}I to detect immune complexes (immunoblots)

^{125}I that is covalently attached to a molecule such as staphylococcal protein A is not volatile and therefore is much less hazardous than the unbound or free form. Most institutions do not insist that work with bound ^{125}I be performed in a hood, but shielding of the γ radiation is still necessary. Lead is a good high-density material for stopping these γ rays; its drawbacks are its weight and opacity. Commercially available shields for ^{125}I are made of lead-impregnated Plexiglas—though heavy, these are at least see-through. Alternatively, a piece of lead foil may be taped to a structural support, although this

arrangement does not provide shielding for the head as a worker peers over the lead!

Incubations of the membrane or blot with the [^{125}I] protein A solution and subsequent washes are usually done on a shaker. For shielding during these steps, a piece of lead foil may simply be wrapped around the container. Solutions of ^{125}I can be conveniently stored for repeated use in a rack placed in a lead box.

Using ^{125}I to label proteins or peptides in vitro

Any experiments that call for the use of free, unbound ^{125}I should be done behind a shield in a hood that contains a charcoal filter to absorb the volatile iodine. Most institutions require that such experiments be done in a special hot lab to which access is limited. Ingested or inhaled iodine is concentrated in the thyroid; a portable γ monitor should therefore be used to scan the neck and throat before beginning and after completing each experiment. Similar scans should routinely be performed on all members of any laboratory in which unbound iodine is used.

DEALING WITH ACCIDENTS

Despite the best intentions and utmost caution, accidents happen! Accidents involving spills of radioactivity are particularly insidious because they can be virtually undetectable yet pose a significant threat to laboratory workers. For this reason it is best to foster a community spirit in any laboratory where radioisotopes are routinely used—a sense of cooperativity that extends from shielding each other properly to helping each other clean up when such accidents occur.

The specific measures to be taken following an accident involving radioactivity naturally depend on the type and amount of the isotope involved, the chemical or biological hazards of the material it is associated with, and the physical parameters of the spill (i.e., where and onto what the isotope was "misplaced"). However, following any accident there are several immediate steps that should be taken:

1. Alert coworkers as well as Radiation Safety personnel to the fact that there has been an accident. This will give them the opportunity to shield themselves if necessary—and to help clean up as well!

2. Restrict access to and away from the site of the accident to ensure that any uncontained radioactive material is not spread around the laboratory. When leaving the site be sure to monitor the bottoms of the shoes as well as the rest of the body.

3. Take care of all contaminated personnel first, evacuating others if necessary. If anyone's skin is contaminated, first use a portable monitor to identify specific areas of contamination. Then wipe these areas with a damp tissue to remove as much surface radioactivity as possible. Try to scrub only small areas at a time to keep the contamination localized. If the contamination is not easily removed with paper tissues, try a sponge or an abrasive pad, but be careful not to break the skin! Sometimes soaking is required: do this only after all easily removed contamination is gone and keep the soaked area to a minimum. Contaminated strands of hair can be washed (or perhaps a new hairstyle may be in order).

4. When attempting to clean any contaminated equipment, floors, benches, etc., begin by soaking up any visible radioactive liquid with an absorbent material. Use a small amount of soap and water to clean the contaminated area, keeping the area wiped each time to a minimum to avoid smearing the contamination over an even greater surface. Many surfaces prove resistant to even Herculean cleaning efforts; in these instances the best that can be done is to remove all contamination possible and then shield whatever is left until the radioactivity decays sufficiently for safety.

LITERATURE CITED

Dawson, R.M.C., Elliot, D.C., Elliott, W.H., and Jones, K.M. (eds.) 1986. Data for Biochemical Research. Alden Press, London.

Lederer, C.M., Hollander, J.M., and Perlman, I. (eds.) 1967. Table of Radioisotopes, 6th edition. John Wiley and Sons, New York.

Meisenhelder, J. and Hunter, T. 1988. Radioactive protein-labelling techniques. *Nature* 335:120.

Shleien, B. (ed.) 1987. Radiation Safety Manual for Users of Radioisotopes in Research and Academic Institutions. Nucleon Lectern Associates, Olney, Md.

Contributed by Jill Meisenhelder and Kentaro Semba
The Salk Institute
La Jolla, California

Transgenic and Gene-Targeted Mouse Lines for Toxicology Studies

The isolation of mammalian genes is of utmost importance to toxicology because of the contributions these studies can make to the understanding of normal physiology and development as well as chemical-induced perturbations of normal biochemical processes. The development of methods that allow functional expression of specific genes, including human genes, in experimental animal models provides exciting and novel avenues for investigation into gene-environment interactions. Likewise, the ability to delete the function of a normal gene in living animals (e.g., "knockout" mice) also provides a unique approach to studying gene function. Methods for the direct microinjection of DNA into pronuclei of fertilized embryos are well established (see *UNIT 1.3*). Foreign genes can be incorporated into somatic germ-line tissues, with expression of these elements in the progeny of founder mice. An additional gene-transfer technology in mice involves the use of stem cells from the early embryo, so-called embryonic stem (ES) cells. The capacity of ES cells to undergo differentiation makes them useful for investigating the effects of genetic modifications of either gain or loss of function. These pluripotent genetically modified ES cells can then be targeted with specific genes and vectors aimed at creating point mutations or null mutations.

During the past several years, a large number of genetically engineered mouse models have been described and utilized for toxicology studies, including carcinogenicity testing, mutation analysis, chemical bioassays and risk assessment, gene action and the environment, and environmental stress response mechanisms. Table A.1B.1 briefly describes a selected number of transgenic and gene-targeted mouse models that have been used, or may be of interest, in investigations and testing relevant to the field of toxicology. The table is designed as an introductory guide and not an exhaustive and conclusive reference source. A number of the models are available from the Induced Mutant Mouse Resource at The Jackson Laboratory (*http://www.jax.org*), while others are available commercially from various animal vendors. Many, however, are only available from the individuals who originally described them. Attempts to increase the number and capacity of mutant mouse resource centers may provide the means of making more of these genetically altered mouse lines available to the toxicological community (Battey et al., 1999).

LITERATURE CITED

Battey, J., Jordon, E., Cox, D., and Dove, W. 1999. An action plan for mouse genomics. *Nature Genet.* 21:73-75.

Contributed by George Sanders, Carol Ware, and Warren Ladiges
University of Washington
Seattle, Washington

Table A.1B.1 Transgenic and Gene-Targeted Mice for Toxicology Studies

Gene symbol and name	Mutant type[a]	Description	Reference(s)	Available from[b]
AGT Angiotensinogen	Tg	Expression in liver, kidney, heart, adrenal gland, ovary, brain, and white and brown fat. Exogenous renin administration yields transient increase in blood pressure. Potential human hypertension model.	Yang et al., 1994. *JBC* 269:32497	JL
Ahr Aryl-hydrocarbon receptor				
AhR	Tm	Hepatic fibrosis and immune system impairment. Model for studying development of liver, immune system, and expression of dioxin-induced genes, as well as AhR activation in genital tubercle, palate, and other embryonic tissues. Model for evaluating endogenous role of AhR in proliferation or differentiation and developmental targets of dioxin-like compounds.	Fernandez-Salguero et al., 1995. *Science* 268:722; Schmidt et al., 1996. *PNAS* 93:6731; Willey et al., 1998. *Toxicol. Appl. Pharmacol.* 151:33	JL
Alox Arachidonate 5-lipoxygenase	Tm	Exhibits selective opposition to certain inflammatory insults. Model for studying importance of leukotrienes.	Chen et al., 1994. *Nature* 372:179	JL
Apc Adenoma polyposis coli	Chemical mutant	Causes multiple intestinal neoplasia. Model for studying carcinogen-induced neoplasia in transgenic mice.	Moser et al., 1990. *Science* 247:322; Su et al., 1992. *Science* 256:668 [Erratum, *Science* 256:1114]	JL
Apc716 Adenoma polyposis coli	Tm	More severe phenotype than apc or apc 1638. Multiple colonic polyps and gastrointestinal neoplasia. Model for evaluating the role of gene in intestinal tumorgenesis.	Oshima et al., 1996. *Cell* 87:803	—
Apc1638 Adenoma polyposis coli	Tm	Less severe phenotype than apc or apc716. Multiple colonic polyps and gastrointestinal neoplasia. Model for evaluating role of gene in intestinal tumorgenesis.	Fodde et al., 1994. *PNAS* 91:8969	—
Atase Alkylguanine-DNA alkyltransferase	Tg	Hepatic expression. Model for evaluating role of gene in adverse biological effects of alkylating agents.	Fan et al., 1990. *NAR* 18:5723	—
Atase Alkylguanine-DNA alkyltransferase CD2 promoter	Tg	Hepatic expression prevents *N*-methyl-*N*-nitrosourea–induced thymic lymphomas. Model for evaluating mechanisms involved in carcinogenesis.	Dumenco et al., 1993. *Science* 259:219	—

Atm Ataxia telangiectasia, mutated	Tm	Causes growth retardation, neurologic dysfunction, infertility, immunologic abnormalities, lymphoreticular malignancies, chromosomal instability, and extreme sensitivity to ionizing radiation. Model for evaluating role of gene in normal cellular function and as a model for ataxia-telangiectasia.	Barlow et al., 1996. *Cell* 86:159; Xu et al., 1996. *Genes Dev.* 10:2411	JL
bcl-2 2-bcl-2	Tg	Expression of high levels of protein in thymocytes and peripheral T cells. Model for evaluating variable resistance to chemotherapy regimens.	Siegel et al., 1992. *PNAS* 89:7003	—
bcl-2 B cell leukemia lymphoma bcl-2-Ig NL bcl-2-Ig SM	Tg	Extended B cell survival with follicular lymphoproliferation. Model for studying pathogenesis of B lymphoid neoplasms.	McDonnell et al., 1989. *Cell* 57:79	—
bcl-2 H2K-BCL-2	Tg	Overexpression in cells of hematolymphoid system. Model for increasing resistance of animals to apoptosis-inducing challenges like irradiation.	Domen et al., 1998. *Blood* 91:2272	—
bcl-2 NSE-Hu-BCL-2	Tg	Overexpression in cells of the nervous system, protects neuronal cells from ischemia-induced death and causes neuronal hypertrophy. Model for evaluating role of gene in developing nervous system and neurodegenerative disorders.	Martinou et al., 1994. *Neuron* 13:1017	—
bcl-2 HHK1 Human keratin 1 (Hk-1)	Tg	Epidermal expression yields multifocal hyperplasia with keratinocytes more resistant to cell death from radiation and chemical carcinogen exposure. Model for evaluating pathogenesis of nonmelanoma skin cancers.	Rodriguez-Villanueva et al., 1998. *Oncogene* 16:853	—
brca1 Breast cancer susceptibility gene 1	Tm	Embryonic lethality prior to gastrulation on day 7.5. Evaluation of role of gene in cellular proliferation during embryogenesis, cell cycle progression regulation, and function during oncogenesis.	Hakem et al., 1996. *Cell* 85:1009	—
brca2 Breast cancer susceptibility gene 2	Tm	Causes embryonic developmental arrest at day 6.5 and hypersensitivity to γ irradiation. Model for evaluation of role of gene in DNA repair and tumor suppression.	Sharan et al., 1997. *Nature* 386:804	—
cat Catalase	Tg	Increased catalase activity attenuates adriamycin-induced cardiotoxicity.	Kang et al., 1996. *JBC* 271:12610	—

continued

Table A.1B.1 Transgenic and Gene-Targeted Mice for Toxicology Studies, continued

Gene symbol and name	Mutant type[a]	Description	Reference(s)	Available from[b]
CEA Carcinoembryonic antigen gene cosCEA1	Tg	Epithelial spatiotemporal expression pattern similar to humans. Model for tumor immunotherapy.	Eades-Perner et al., 1994. *Cancer Res.* 54:4169	—
CEA TgN(CEAGe)18FJP	Tg	Overexpression in large intestine, cecum, and stomach. Model for antigen-specific vaccine studies, antibody-targeting studies, and other forms of immunotherapy.	Clarke et al., 1998. *Cancer Res.* 58:1469	—
COX-1 Cyclooxygenase-1 Ptgs1	Tm	Null mutation yields a decreased incidence of indomethacin-induced gastric ulceration, reduced platelet aggregation, and decreased response to arachidonic acid. Model for the evaluation of physiological roles of COX-1 and COX-2.	Langenbach et al., 1995. *Cell* 83:483	—
COX-2 Cyclooxygenase-2	Tm	Targeted disruption yields severe nephropathy and exhibits increased susceptibility to peritonitis. Models for COX isoform evaluation and improvement of NSAIDs, mitigation of endotoxin-induced hepatocellular cytotoxicity, and evaluation of COX-2 in early pregnancy.	Dinchuk et al., 1995. *Nature* 378:406; Lim et al., 1997. *Cell* 91:197	—
CRP C-reactive protein	Tg	Inflammation-induced liver-specific expression. Model to study liver development and regeneration.	Ciliberto et al., 1987. *EMBO J.* 6:4017	—
cyD1 Cyclin D1 EBVED-L2 cyD1	Tg	Epithelial dysplasia. Model for evaluating associated malignancies.	Mueller et al., 1997. *Cancer Res.* 57:5542	—
cyp Cytochrome P-450 1a-1 Cyp 1a-1-CAT	Tg	Exposure to an aromatic hydrocarbon increases hepatic expression of transgene, which may be gender-related. Model for evaluating the gender-related expression of the gene.	Jones et al., 1991. *NAR* 19:6547	—
Cyp Cytochrome P-450 1a-1, 1a-2	Tm	Neonatal lethality via respiratory distress. Potential neonatal respiratory distress syndrome models.	Pineau et al., 1995. *PNAS* 92:5134; Diliberto et al., 1997. *Biochem. Biophys. Res. Commun.* 236:431	JL
Cyp Cytochrome P-450 CYP2B2-19 CYP2B2-39	Tm	Negative and positive regulation of transgene by phenobarbital administration. Phenobarbital induction mechanism system model.	Ramsden et al., 1993. *JBC* 268:21722	—

Cyp Cytochrome P-450 Cyp2C2-luc	Tm	Modulation of tissue expression post male castration and post testosterone/rat growth hormone treatment in female. Model for evaluating transcriptional regulation of gene.	Li et al., 1996a. *Mol. Cell Endocrinol.* 120:77	—
Cyp Cytochrome P-450 MT-1-CYP3A7	Tm	Liver, kidney, lung, spleen, testis, small intestine, thymus, brain, skin, and heart expression. Model for studying the toxicological significance of P-450s during embryonic development.	Li et al., 1996b. *Arch. Biochem. Biophys.* 329:235	—
E2F1 K5-E2F1	Tg	Epidermal hyperplasia and decreased hair growth. Role in epithelial growth and tumorgenesis.	Pierce et al., 1998. *Oncogene* 16:1267	—
E2F1 Transcriptional activator gene	Tm	Model for evaluating role in apoptosis and cell proliferation suppression.	Field et al., 1996. *Cell* 85:549; Yamasaki et al., 1996. *Cell* 85:537	JL
fasL fas ligand fasL/TCR-β Fas ligand	Tg	Higher numbers of T cells in the thymus, lymph node, and spleen with increased numbers of T cells resistant to Fas-mediated apoptosis. Model for evaluating Fas-mediated apoptosis.	Cheng et al., 1997. *J. Immunol.* 159:674	—
fos MT-c-fos-209-4 MT-c-fos-211-5	Tg	Expression yields early abnormal bone development. Model for studying pathways responsible for specificity of induced tumorgenesis.	Ruther et al., 1987. *Nature* 325:412	—
$G\alpha_{I2}$ G-protein subunit that functions as tumor-suppressor gene	Tm	Gene deficiency yields growth retardation, lethal diffuse colitis, alteration in thymocyte maturation and function, plus colonic adenocarcinoma. Model for ulcerative colitis and colonic carcinogenesis.	Rudolph et al., 1995. *Nature Genet.* 10:143	—
GPx-1 Glutathione peroxidase	Tg	Increased activity confers increased tolerance to ischemia-reperfusion injury, H_2O_2-induced DNA-strand breakage in lens epithelial cells, and paraquat toxicity. Model for brain hydroperoxide metabolism and oxidative stress homeostasis. Model for evaluating thermoregulation and processes involving actions of hydroxy and lipid peroxidases.	Mirault et al., 1994. *Ann. N.Y. Acad. Sci.* 738:104; Mirochnitchenko et al., 1995. *PNAS* 92:8120; Yoshida et al., 1996. *J. Mol. Cell. Cardiol.* 28:1759; Reddy et al., 1997. *Ophthalmologica* 211:192; Cheng et al., 1998. *J. Nutr.* 128:1070	—
GPx-1 Glutathione peroxidase	Tm	Null mutant mice are more susceptible to acute paraquat toxicity and myocardial ischemia-reperfusion injury.	Cheng et al., 1998. *J. Nutr.* 128:1070	—
GST mu Mu-class glutathione transferase	Tg	Renal convoluted tubular epithelium expression. Model for in vivo study of GST modulation in carcinogenesis and drug toxicity.	Connelly et al., 1993. *Pathobiology* 61:7	—

continued

Table A.1B.1 Transgenic and Gene-Targeted Mice for Toxicology Studies, continued

Gene symbol and name	Mutant type[a]	Description	Reference(s)	Available from[b]
GST pi Pi-class glutathione transferase	Tm	Increased incidence of epithelial tumorgenesis after carcinogen exposure. Role as a determinant of carcinogen exposure and cancer susceptibility.	Henderson et al., 1998. *PNAS* 95:5275	—
HO-1 Heme oxygenase	Tg	Protein overexpression in neurons of various brain regions. Model for evaluating the function of carbon monoxide as a neuromodulator, iron as a gene regulator, and bile pigments as in vivo antioxidants.	Maines et al., 1998. *J. Neurochem.* 70:2057	—
HO-2 Heme oxygenase	Tm	Model for evaluation of role of carbon monoxide as retrograde neuronal messenger.	Poss et al., 1995. *Neuron* 15:867	—
hsp-70 Heat-shock protein	Tg	Increased myocardial expression demonstrates cardioprotective effect against ischemia. Model for evaluating cardiac post-ischemic recovery.	Marber et al., 1995. *J. Clin. Invest.* 95:1446; Radford et al., 1996. *PNAS* 93:2339	—
IL-6 Interleukin 6	Tm	Impairment of immune and acute-phase inflammatory responses. Model for studying response to injury or infection.	Kopf et al., 1994. *Nature* 368:339	—
IL-6 Interleukin 6 Eμ-IL-6	Tg	Polyclonal plasmacytosis of thymus, lymph node, spleen, lung, liver, and kidney. Useful in determining role of gene in polyclonal and monoclonal plasma cell abnormalities.	Suematsu et al., 1989. *PNAS* 86:7547	JL
L2hD	Tg	Tongue, esophagus, and forestomach epithelial dysplasia. Model of upper-digestive tract tumor initiation.	Nakagawa et al., 1997. *Oncogene* 14:1185	—
LacI β-galactosidase λ shuttle vector	Tm	Plasmid rescue from genome. Used in induced mutation assays.	Kohler et al., 1991. *PNAS* 88:7958	—
LacZ β-galactosidase λ shuttle vector	Tm	Plasmid rescue from genome. Used in induced mutation assays.	Gossen et al., 1989. *PNAS* 86:7971	JL
LCAT Lecithin cholesterol acyltransferase	Tg	Increased total cholesterol and HDL cholesterol levels. Model of hyperalphalipoprotenemia.	Vaisman et al., 1995. *JBC* 270:12269	—
lipox Lipoxygenase	Tm	Specific expression in endothelial cells of vessel walls and pulmonary epithelium. System for direct expression of molecules by vascular wall to evaluate select proteins.	Harats et al., 1995. *J. Clin. Invest.* 95:1335	—

MAO-A Monamine oxidase A Tg(H2-INF-β)8	Tm	Increased CNS serotonin and norepinephrine levels. Model for MAO-A deficiency.	Cases et al., 1995. *Science* 268:1763	—
MAO-B Monamine oxidase B pNSE	Tg	Neuronal-specific overexpression. Model for evaluating effects of high MAO-B levels on development and possible role in neurologic disease.	Andersen et al., 1992. *Ann. N.Y. Acad. Sci.* 648:241	—
Mdr-1a Multidrug resistance 1	Tm	Deficiency of the blood-brain barrier with subsequent sensitivity to drugs. Model for compartmental drug accumulation.	Schinkel et al., 1994. *Cell* 77:491	—
mdr-1a Multidrug resistance 1 β-actin/MDR1	Tg	Overexpression in bone marrow confers resistance to cytotoxic drug–induced leukopenia. Model for evaluating MDR1-dependent multidrug resistance and high- dose chemotherapy regimens.	Galski et al., 1989. *Mol. Cell Bio.* 9:4357	TF
mgmt Methylguanine-DNA methyltransferase DNA repair protein	Tg	Overexpressed in liver and brain. Possible use in evaluation of cellular resistance to DNA-alkylation toxicity and tumor induction.	Walter et al., 1993. *Carcinogenesis* 14:1537	—
Mgmt Methylguanine-DNA methyltransferase DNA repair protein	Tm	Significant reduction in skin tumor incidence post topical carcinogen application. Model for studying role in prevention of tumor initiation.	Becker et al., 1996. *Cancer Res.* 56:3244	JL
MS2 DNA mismatch repair gene	Tm	Null mutation yields microsatellite instability in several tissues, increased incidence of sarcomas and lymphomas, and male infertility. Model for evaluation of role in DNA repair, genetic recombination, and meiotic chromosome synapsis.	Baker et al., 1995. *Cell* 82:309	—
MSH2 DNA mismatch repair gene	Tm	Deficiency yields increased incidence of lymphoid tumors with microsatellite instabilities in 2-month-old mice. Model for evaluating progression of tumors and screening carcinogenic and anticancer agents.	Reitmair et al., 1995. *Nature Genet.* 11:64	—
myc (c-myc) Proto-oncogene B cell promoters	Tg	Overexpression yields B cell lymphomas or no increase in tumor incidence. Models for evaluating lymphoma development, B cell ontogeny, and immunoglobulin regulation.	Adams et al., 1985. *Nature* 318:533	JL, CR

continued

Table A.1B.1 Transgenic and Gene-Targeted Mice for Toxicology Studies, continued

Gene symbol and name	Mutant type[a]	Description	Reference(s)	Available from[b]
myc (c-myc) Proto-oncogene Pth-mycn	Tg	Neuroectodermal expression yields neuroblastoma development. Model for evaluating pathogenesis and therapy of neuroblastoma.	Weiss et al., 1997. *EMBO J.* 16:2985	—
myc (c-myc) Proto-oncogene T cell promoter	Tg	Increased incidence of spontaneous T cell tumors and inducible leukemia. System for screening novel *myc* genes involved in T cell lymphoma.	Stewart et al., 1993. *Int. J. Cancer* 53:1023	—
neu (c-neu) c-neu/erbB2 TG.NK	Tg	All mice fed a specifically formulated diet developed palpable mammary tumors by 28 weeks of age. Model for evaluation of dietary intervention strategies for breast cancer.	Rao et al., 1997. *Breast Cancer Res. Treat.* 45:149	—
neu (c-neu) Proto-oncogene MMTV-c-neu	Tg	One-step mammary tumor induction, used to study major determinants of malignant progression of tumors.	Muller et al., 1988. *Cell* 54:105	CR
NOS2 Nitric oxide synthase gene	Tg	Overexpression of NOS2 in pancreatic islets. Model for the evaluation of NOS2 in pancreatic β-cell degeneration.	Takamura et al., 1998. *JBC* 273:2493	—
NOS2 Nitric oxide synthase gene neuronal NOS	Tm	Neuronal NOS deficiency yields gastric distention, pyloric stenosis, and decreased NOS catalytic activity. Model of infantile pyloric stenosis.	Huang et al., 1993. *Cell* 75:1273	BK, JL
$p27^{Kip1}$ Cyclin-dependent kinase inhibitor	Tm	Targeted deletion results in multiorgan hyperplasia, gigantism, tumorgenesis, and female sterility. Model for the evaluation of $p27^{Kip1}$ function.	Fero et al., 1996. *Cell* 85:733	—
p53 Tumor suppressor gene	Tm	Development of spontaneous tumors by 6 months of age. Model for studying role in tumorigenesis and testing suspected carcinogens.	Donehower et al., 1992. *Nature* 356:215	JL, TF
p53 Tumor suppressor gene p53 172^{R-H}	Tg	Decrease in spontaneous tumors with concurrent acceleration of carcinogen and oncogene-mediated tumorgenesis. Model for evaluation of early events in mammary tumorgenesis. Preclinical model for new chemotherapeutic testing.	Li et al., 1998. *Oncogene* 16:997	—
paf Platelet activating factor PARF	Tg	Bronchial hyperreactivity, increased endotoxin lethality, and melanocytic tumorgenesis. Model for study of bronchial asthma and endotoxin-induced death.	Ishii et al., 1997. *EMBO J.* 16:133	—

pepck-ada Phosphoenolpyruvate carboxykinase Bacterial O^6 alkylguanine-DNA alkyltransferase	Tg	Expression in liver and kidney regulated by dietary manipulation. Model for evaluating role of DNA repair in protection from carcinogenesis induced by *N*-nitro compounds.	Lim et al., 1990. *Cancer Res.* 50:1701	—
pgis Prostacyclin synthase hSPC-rPGIS	Tg	Selective pulmonary prostacyclin expression. Lung displays less hypoxic vasoconstriction. Model for evaluation of role in vasoconstriction.	Geraci et al., 1998. *Chest* 114:99S	—
pim-1 *pim-1* proto-oncogene Eμ-pim-1	Tg	Overexpression promotes development of lymphomas before 7 months of age. Model for evaluating the cooperation between pim-1 and myc in lymphomagenesis.	van Lohuizen et al., 1989. *Cell* 56:673	TF
pim-2 *pim-2* proto-oncogene	Tg	Increased incidence of T cell lymphomas. Model for evaluating the tumorigenic properties of pim-2.	Allen et al., 1997. *Oncogene* 15:1133	—
PLA2 Phospholipase A2	Tm	Null mutation yielded reduced fertility and decreased the ischemic brain injury associated with cerebral arterial occlusion. Model for evaluation of regulation of eicosanoid and platelet activation factor in inflammation process.	Bonventre et al., 1997. *Nature* 390:622	—
RAR Retinoic acid receptor	Tg	Expression induces craniofacial abnormalities. Model for evaluating mechanism of gene regulation by retinoic acid.	Damm et al., 1993. *PNAS* 90:2989	—
RAR Retinoic acid receptor βRARE-LacZ	Tg	Specific epidermal expression. Model for determination of sites of transcriptional activation by retinoic acid.	Tsou et al., 1994. *Exp. Cell Res.* 214:27	—
RAR Retinoic acid receptor HK1-RARα403	Tm	Neonatal lethality due to loss of epidermal barrier function and transepidermal water. Model for evaluating lipid metabolism modulation in relation to epidermal formation and functional maintenance.	Imakado et al., 1995. *Genes Dev.* 9:317	—
ras Activated v-Ha-*ras* oncogene TG.AC	Tg	Multiple skin papilloma induction with further development to neoplasia. Model for screening tumor promoters and assessing antitumor and antiproliferative agents.	Leder et al., 1990. *PNAS* 87:9178	TF, CR
ras c-Ha-*ras* ras H2	Tg	Increased incidence of tumorgenesis in vascular endothelium, lymphocytes, skin, lung, and Harderian gland epithelium. Model for evaluation of somatic point mutations associated with transgene. Bioassay model for rapid carcinogenicity testing.	Saitoh et al.,1990. *Oncogene* 5:1195; Yamamoto et al., 1998. *Environ. Health Perspect.* 106(suppl. 1):57	—

continued

Table A.1B.1 Transgenic and Gene-Targeted Mice for Toxicology Studies, continued

Gene symbol and name	Mutant type[a]	Description	Reference(s)	Available from[b]
ras Ha-*ras* oncogene Whey acidic protein (wap)-ras	Tg	Increased incidence of mammary and salivary gland tumors. Model for in vivo evaluation of molecular mechanisms of proto-oncogene activation.	Andres et al., 1987. *PNAS* 84:1299	JL
Rb Retinoblastoma tumor-suppressor gene	Tm	Neuronal cell death and defective erythropoiesis in 14-15 day old homozygous pups and development of pituitary tumors in heterozygous adult mice. Model for evaluating normal function in cells and for human familial retinoblastoma. Heterozygous mice exhibit high incidence of spontaneous pituitary tumors between 2 and 11 months of age. Model for addressing tissue-specific tumor predisposition by inactivation of ubiquitously expressed tumor-suppressor gene.	Jacks et al., 1992. *Nature* 359:295; Hu et al., 1994. *Oncogene* 9:1021	JL
ret Proto-oncogene MMTV/ret	Tg	Increased incidence of mammary, salivary, and male reproductive tract tumors. Model for evaluating oncogenicity of activated *ret* gene.	Iwamoto et al., 1990. *Oncogene* 5:535	—
Ret Proto-oncogene MT/ret	Tg	Aberrant melanogenesis with melanocytic tumor development. Model for systematic development of melanocytic tumors.	Iwamoto et al., 1991. *EMBO J.* 10:3167	—
Ret Proto-oncogene ret/ptc1	Tm	Progressive thyroid tumors. Model for evaluating neoplastic progression of human thyroid carcinomas.	Santoro et al., 1996. *Oncogene* 12:1821	—
*SA*β*-gal, SA*β*-geo, and ROSA*β*-geo*	Tm	β-gal promoter trap selection for identification of active promoters/genes.	Friedrich and Soriano, 1991. *Genes Dev.* 5:1513	—
Smad3 Transforming growth factor β-receptor gene	Tm	Mouse model of colorectal adenocarcinoma with lymph node metastasis.	Zhu et al., 1998. *Cell* 94:703	—
SOD-1 Copper-zinc superoxide dismutase	Tg	Increased Cu-Zn SOD activity in CNS. Animal model of Down's syndrome. Increased Cu-Zn SOD expression in nervous tissue confers protection against various forms of brain trauma and focal cerebral ischemia. Model for evaluation of role of oxygen in ischemic and traumatic injury.	Epstein et al., 1987. *PNAS* 84:8044; Chan et al., 1994. *Ann. N.Y. Acad. Sci.* 738:93	JL
SOD-1 Copper-zinc superoxide dismutase	Tm	Null mutant mice show a pronounced sensitivity to paraquat and myocardial ischemia reperfusion injury.	Ho et al., 1998. *Environ. Health Perspect.* 106:1219	—

SOD-2 Manganese superoxide dismutase SP-C-Mn-SOD-hGH	Tg	Increased expression confers pulmonary epithelial cell protection against oxygen injury. Used to study the primary role of lung epithelial cell gene expression in oxygen-injury protection.	Wispe et al., 1992. *JBC* 267:23937	—
Tcr-α/β T cell receptor α/β chain genes	Tg	Expression of type II collagen–specific T cell receptor transgenes accelerates onset of arthritis in DBA/1 inbred mice.	Osman et al., 1998. *Int. Immunol.* 10:1613	—
TGF-α/c-myc Transforming growth factor α and the proto-oncogene c-myc	Tg double	Model of oxidation DNA damage and acceleration of hepatocarcinogenesis.	Factor et al., 1998. *JBC* 273:15846	JL
TNF-α Tumor necrosis factor	Tg	Development of chronic inflammatory polyarthritis with prevention possible by administration of anti-hTNF monoclonal antibody. Model for human arthritis.	Keffer et al., 1991. *EMBO J.* 10:4025	—
TNF-α Tumor necrosis factor CD2-TNF	Tm	Diffuse vascular thrombosis and tissue necrosis neutralizable by human TNF mAb administration. Model for evaluating the different contributions of the two TNF receptors in thymus development and signaling.	Probert et al., 1993. *J. Immunol.* 151:1894	JL, TF
tpl-2 Tumor progression loci 2, an oncogenic kinase	Tg	Expression of truncated protein in thymocytes predisposes to development of T cell lymphomas. Model for studying involvement in oncogenesis.	Ceci et al., 1997. *Genes Dev.* 11:688	—
trx Thioredoxin, a reduction/oxidation active protein Ins-TRX	Tm	Reduced incidence of diabetes. Used to assess oxidative stress in pancreatic β cell destruction in autoimmune diabetes.	Hotta et al., 1998. *J. Exp. Med.* 188:1445	—
XPA Xeroderma pigmentosum, group A	Tm	Deletion yields increased susceptibility to ultraviolet-B and carcinogen–induced skin and eye tumors and papillomas. Model for human XPA.	deVries et al., 1995. *Nature* 377:169; O'Neill, 1996. 24:642	—
XPC Xeroderma pigmentosum, group C	Tm	Gene deficiency yields increased susceptibility to ultraviolet-induced carcinogenesis. Animal model for human XPC.	Sands et al., 1995. *Nature* 377:162	TF

[a]Abbreviations: Tg, transgenic; Tm, targeted mutation.

[b]Abbreviations: BK, B & K Universal; JL, The Jackson Laboratory; CR, Charles River Labs; TF, Taconic Farms. See *SUPPLIERS APPENDIX* for contact information. If no commercial supplier is listed, consult the author of the cited paper.

LABORATORY STOCK SOLUTIONS AND EQUIPMENT

Common Stock Solutions and Buffers

This section describes the preparation of buffers and reagents used in this manual. When preparing solutions, use Milli-Q-purified water (or equivalent) and reagents of the highest available grade. Sterilization—by filtration through a 0.22-µm filter or by autoclaving—is recommended for most solutions stored at room temperature. Where storage conditions are not specified, store up to 6 months at room temperature. Discard any solution that shows evidence of contamination, precipitation, or discoloration.

Standardized and reference reagents are sometimes required—e.g., for quality control, positive and negative controls, equipment calibration, and assay validation. Environmental and chemical standards are available from a number of suppliers, including the National Institute of Standards and Technology (NIST), AccuStandard Inc., and Sigma Chemical Co. Consult the *LabGuide*, published annually by the American Chemical Society (ACS) for other suppliers (e.g., ACS, 1999).

Acid, concentrated stock solutions

See Table A.2A.1.

Ammonium acetate, 10 M

Dissolve 385.4 g ammonium acetate in 150 ml H_2O
Add H_2O to 500 ml

Ammonium hydroxide, concentrated stock solution

See Table A.2A.1.

Ammonium sulfate, saturated

76 g ammonium sulfate
100 ml H_2O
Heat with stirring to just below boiling point
Let stand overnight at room temperature

Table A.2A.1 Molarities and Specific Gravities of Concentrated Acids and Bases[a]

Acid/base	Molecular weight	% by weight	Molarity (approx.)	Specific gravity	1 M solution (ml/liter)
Acetic acid (glacial)	60.05	99.6	17.4	1.05	57.5
Ammonium hydroxide	35.0	28	14.8	0.90	67.6
Formic acid	46.03	90	23.6	1.205	42.4
		98	25.9	1.22	38.5
Hydrochloric acid	36.46	36	11.6	1.18	85.9
Nitric acid	63.01	70	15.7	1.42	63.7
Perchloric acid	100.46	60	9.2	1.54	108.8
		72	12.2	1.70	82.1
Phosphoric acid	98.00	85	14.7	1.70	67.8
Sulfuric acid	98.07	98	18.3	1.835	54.5

[a]*CAUTION:* Handle strong acids and bases carefully.

Current Protocols in Toxicology (1999) A.2A.1-A.2A.6

ATP, 100 mM

1 g ATP (adenosine triphosphate)
12 ml H_2O
Adjust pH to 7.0 with 4 M NaOH
Adjust volume to 16.7 ml with H_2O
Store in aliquots indefinitely at −20°C

Base, concentrated stock solutions

See Table A.2A.1.

$CaCl_2$, 1 M

147 g $CaCl_2 \cdot 2H_2O$
H_2O to 1 liter

Carbonate buffer

1.6 g Na_2CO_3 (15 mM final)
2.9 g $NaHCO_3$ (35 mM final)
0.2 g NaN_3 (3.1 mM final)
H_2O to 1 liter
Adjust to pH 9.5

CAUTION: *Sodium azide is poisonous; follow appropriate precautions for handling, storage, and disposal.*

CMF-DPBS (calcium- and magnesium-free Dulbecco's phosphate-buffered saline)

8.00 g NaCl (0.137 M)
0.20 g KCl (2.7 mM)
2.16 g $Na_2HPO_4 \cdot 7H_2O$ (8.1 mM)
0.20 g KH_2PO_4 (1.1 mM)
H_2O to 1 liter

DPBS (Dulbecco's phosphate-buffered saline)

8.00 g NaCl (0.137 M)
0.20 g KCl (2.7 mM)
0.20 g KH_2PO_4 (1.1 mM)
0.10 g $MgCl_2 \cdot 6H_2O$ (0.5 mM)
2.16 g $Na_2HPO_4 \cdot 7H_2O$ (8.1 mM)
0.10 g anhydrous $CaCl_2$ (0.9 mM)
H_2O to 1 liter

DTT (dithiothreitol), 1 M

Dissolve 1.55 g DTT in 10 ml water and filter sterilize. Store in aliquots at −20°C.

EDTA (ethylenediaminetetraacetic acid), 0.5 M (pH 8.0)

Dissolve 186.1 g disodium EDTA dihydrate in 700 ml water. Adjust pH to 8.0 with 10 M NaOH (~50 ml; add slowly). Add water to 1 liter and filter sterilize.

Begin titrating before the sample is completely dissolved. EDTA, even the disodium salt, is difficult to dissolve at this concentration unless the pH is increased to between 7 and 8.

HBSS (Hanks' balanced salt solution)

0.40 g KCl (5.4 mM final)
0.09 g $Na_2HPO_4 \cdot 7H_2O$ (0.3 mM final)
0.06 g KH_2PO_4 (0.4 mM final)
0.35 g $NaHCO_3$ (4.2 mM final)
0.14 g $CaCl_2$ (1.3 mM final)
0.10 g $MgCl_2 \cdot 6H_2O$ (0.5 mM final)

continued

0.10 g $MgSO_4 \cdot 7H_2O$ (0.6 mM final)
8.0 g NaCl (137 mM final)
1.0 g D-glucose (5.6 mM final)
0.2 g phenol red (0.02%; optional)
Add H_2O to l liter and adjust pH to 7.4 with 1 M HCl or 1 M NaOH
Filter sterilize and store up to 1 month at 4°C

HBSS may be made or purchased without Ca^{2+} and Mg^{2+} (CMF-HBSS). These components are optional and usually have no effect on an experiment; in a few cases, however, their presence may be detrimental. Consult individual protocols to see if the presence or absence of these components is recommended.

Bottles should be kept tightly closed to prevent CO_2 loss and subsequent alkalinization.

HCl, 1 M

Mix in the following order:
913.8 ml H_2O
86.2 ml concentrated HCl

KCl, 1 M

74.6 g KCl
H_2O to 1 liter

$MgCl_2$, 1 M

20.3 g $MgCl_2 \cdot 6H_2O$
H_2O to 100 ml

$MgSO_4$, 1 M

24.6 g $MgSO_4 \cdot 7H_2O$
H_2O to 100 ml

NaCl, 5 M

292 g NaCl
H_2O to 1 liter

NaCl (saline), 0.9% (w/v)

9 g NaCl (154 mM final)
H_2O to 1 liter

NaOH, 10 M

Dissolve 400 g NaOH in 450 ml H_2O
H_2O to 1 liter

PBS (phosphate-buffered saline)

8.00 g NaCl (0.137 M)
0.20 g KCl (2.7 mM)
0.24 g KH_2PO_4 (1.4 mM)
1.44 g Na_2HPO_4 (0.01 M)
H_2O to 1 liter

Potassium acetate buffer, 0.1 M

Solution A: 11.55 ml glacial acetic acid per liter (0.2 M) in water.

Solution B: 19.6 g potassium acetate ($KC_2H_3O_2$) per liter (0.2 M) in water.

Referring to Table A.2A.2 for desired pH, mix the indicated volumes of solutions A and B, then dilute with water to 100 ml. Filter sterilize if necessary. Store up to 3 months at room temperature.

continued

This may be made as a 5- or 10-fold concentrate by scaling up the amount of sodium acetate in the same volume. Acetate buffers show concentration-dependent pH changes, so check the pH by diluting an aliquot of concentrate to the final concentration.

To prepare buffers with pH intermediate between the points listed in Table A.2A.2, prepare closest higher pH, then titrate with solution A.

Potassium phosphate buffer, 0.1 M

Solution A: 27.2 g KH_2PO_4 per liter (0.2 M final) in water.

Solution B: 34.8 g K_2HPO_4 per liter (0.2 M final) in water.

Referring to Table A.2A.3 for desired pH, mix the indicated volumes of solutions A and B, then dilute with water to 200 ml. Filter sterilize if necessary. Store up to 3 months at room temperature.

This buffer may be made as a 5- or 10-fold concentrate simply by scaling up the amount of potassium phosphate in the same final volume. Phosphate buffers show concentration-dependent changes in pH, so check the pH of the concentrate by diluting an aliquot to the final concentration.

To prepare buffers with pH intermediate between the points listed in Table A.2A.3, prepare closest higher pH, then titrate with solution A.

Table A.2A.2 Preparation of 0.1 M Sodium and Potassium Acetate Buffers[a]

Desired pH	Solution A (ml)	Solution B (ml)
3.6	46.3	3.7
3.8	44.0	6.0
4.0	41.0	9.0
4.2	36.8	13.2
4.4	30.5	19.5
4.6	25.5	24.5
4.8	20.0	30.0
5.0	14.8	35.2
5.2	10.5	39.5
5.4	8.8	41.2
5.6	4.8	45.2

[a]Adapted by permission from CRC (1975).

Table A.2A.3 Preparation of 0.1 M Sodium and Potassium Phosphate Buffers[a]

Desired pH	Solution A (ml)	Solution B (ml)	Desired pH	Solution A (ml)	Solution B (ml)
5.7	93.5	6.5	6.9	45.0	55.0
5.8	92.0	8.0	7.0	39.0	61.0
5.9	90.0	10.0	7.1	33.0	67.0
6.0	87.7	12.3	7.2	28.0	72.0
6.1	85.0	15.0	7.3	23.0	77.0
6.2	81.5	18.5	7.4	19.0	81.0
6.3	77.5	22.5	7.5	16.0	84.0
6.4	73.5	26.5	7.6	13.0	87.0
6.5	68.5	31.5	7.7	10.5	90.5
6.6	62.5	37.5	7.8	8.5	91.5
6.7	56.5	43.5	7.9	7.0	93.0
6.8	51.0	49.0	8.0	5.3	94.7

[a]Adapted by permission from CRC (1975).

Table A.2A.4 Preparation of SDS Sample Buffer

Ingredient	2×	4×	Final conc. in 1× buffer
0.5 M Tris·Cl, pH 6.8[a]	2.5 ml	5.0 ml	62.5 mM
SDS	0.4 g	0.8 g	2% (w/v)
Glycerol	2.0 ml	4.0 ml	10% (v/v)
Bromphenol blue	20 mg	40 mg	0.1% (w/v)
2-Mercaptoethanol[b,c]	400 µl	800 µl	~300 mM
H_2O	to 10 ml	to 10 ml	—

[a]See recipe below.
[b]Alternatively, dithiothreitol (DTT), at a final concentration of 100 mM, can be substituted for 2-mercaptoethanol.
[c]Add just before use.

SDS, 20% (w/v)

Dissolve 20 g SDS (sodium dodecyl sulfate or sodium lauryl sulfate) in H_2O to 100 ml total volume with stirring. Filter sterilize using a 0.45-µm filter.

It may be necessary to heat the solution slightly to fully dissolve the powder.

SDS electrophoresis buffer, 5×

15.1 g Tris base
72.0 g glycine
5.0 g SDS
Distilled, deionized H_2O to 1 liter
Store up to 1 month at 0° to 4°C
Dilute to 1× before use

Do not adjust the pH of the stock solution; the pH is 8.3 when diluted to 1×.

Use purified SDS if appropriate.

SDS sample buffer

See Table A.2A.4.

Sodium acetate, 3 M

Dissolve 408 g sodium acetate trihydrate ($NaC_2H_3O_2{\cdot}3H_2O$) in 800 ml H_2O
Adjust pH to 4.8, 5.0, or 5.2 (as desired) with 3 M acetic acid (see Table A.2A.1)
Add H_2O to 1 liter
Filter sterilize

Sodium acetate buffer, 0.1 M

Solution A: 11.55 ml glacial acetic acid per liter (0.2 M) in water.

Solution B: 27.2 g sodium acetate ($NaC_2H_3O_2{\cdot}3H_2O$) per liter (0.2 M) in water.

Referring to Table A.2A.2 for desired pH, mix the indicated volumes of solutions A and B, then dilute with water to 100 ml. Filter sterilize if necessary. Store up to 3 months at room temperature.

This may be made as a 5- or 10-fold concentrate by scaling up the amount of sodium acetate in the same volume. Acetate buffers show concentration-dependent pH changes, so check the pH by diluting an aliquot of concentrate to the final concentration.

To prepare buffers with pH intermediate between the points listed in Table A.2A.2, prepare closest higher pH, then titrate with solution A.

Sodium phosphate buffer, 0.1 M

Solution A: 27.6 g $NaH_2PO_4 \cdot H_2O$ per liter (0.2 M final) in water.

Solution B: 53.65 g $Na_2HPO_4 \cdot 7H_2O$ per liter (0.2 M) in water.

Referring to Table A.2A.3 for desired pH, mix the indicated volumes of solutions A and B, then dilute with water to 200 ml. Filter sterilize if necessary. Store up to 3 months at room temperature.

This buffer may be made as a 5- or 10-fold concentrate by scaling up the amount of sodium phosphate in the same final volume. Phosphate buffers show concentration-dependent changes in pH, so check the pH by diluting an aliquot of the concentrate to the final concentration.

To prepare buffers with pH intermediate between the points listed in Table A.2A.3, prepare closest higher pH, then titrate with solution A.

TBS (Tris-buffered saline)

100 mM Tris·Cl, pH 7.5 (see recipe below)
0.9% (w/v) NaCl
Store up to several months at 4°C

Tris·Cl, 1 M

Dissolve 121 g Tris base in 800 ml H_2O
Adjust to desired pH with concentrated HCl
Adjust volume to 1 liter with H_2O
Filter sterilize if necessary
Store up to 6 months at 4°C or room temperature

Approximately 70 ml HCl is needed to achieve a pH 7.4 solution, and ~42 ml for a solution that is pH 8.0.

IMPORTANT NOTE: *The pH of Tris buffers changes significantly with temperature, decreasing approximately 0.028 pH units per 1°C. Tris-buffered solutions should be adjusted to the desired pH at the temperature at which they will be used. Because the pK_a of Tris is 8.08, Tris should not be used as a buffer below pH ~7.2 or above pH ~9.0.*

LITERATURE CITED

American Chemical Society (ACS). 1999. LabGuide 98-99. ACS, Washington, D.C. [also available online at *http://pubs.acs.org./labguide*].

Chemical Rubber Company (CRC). 1975. CRC Handbook of Biochemistry and Molecular Biology, Physical and Chemical Data, 3d ed., Vol. 1. CRC Press, Boca Raton, Fla.

Standard Laboratory Equipment

Listed below are pieces of equipment that are standard in the modern toxicology laboratory—i.e., items used extensively in this manual and thus not usually included in the individual materials lists. No attempt has been made to list all items required for each procedure in the Materials list of each protocol; rather, those lists note those items that might not be readily available in the laboratory or that require special preparation. See *SUPPLIERS APPENDIX* for contact information for commercial vendors of laboratory equipment.

Applicator, cotton-tipped and wooden

Autoclave

Bag sealer

Balances, analytical and preparative

Beakers

Bench protectors, plastic-backed (including "blue" pads)

Biohazard disposal containers and bags

Biosafety cabinet, tissue culture or laminar flow hood; filters air and maintains air flow pattern to protect cultured cells from investigator and vice versa

Bottles, glass, plastic, and squirt

Bunsen burners

Centrifuges, low-speed (to 20,000 rpm) refrigerated, ultracentrifuge (20,000 to 80,000 rpm), large-capacity low-speed, tabletop, with appropriate rotors and adapters

Centrifuge tubes and bottles, plastic and glass, various sizes

Clamps

Conical centrifuge tubes, plastic and glass

Containers, assortment of glass and plastic, for gel and membrane washes

Coplin jars, glass, for 25 × 75–mm slides

Cuvettes, glass and quartz

Desiccator and desiccant

Dry ice

Electrophoresis equipment, agarose and acrylamide, full-size and mini, with power supplies

Film developing system and darkroom

Filtration apparatus

Forceps

Freezers, –20°C, –70°C, and liquid nitrogen

Fume hood

Geiger counter

Gel dryer

Gloves, disposable plastic and heat-resistant

Graduated cylinders

Heating blocks, thermostatically controlled for test tubes and microcentrifuge tubes

Homogenizer

Humidified CO_2 incubator

Ice bucket

Ice maker

Immersion oil for microscopy

Lab coats

Laboratory glassware

Light box

Liquid nitrogen

Lyophilizer

Magnetic stirrer, with and without heater, and stir bars

Markers, including indelible markers, china-marking pens, and luminescent markers

Microcentrifuge, Eppendorf-type with 12,000 to 14,000 rpm maximum speed

Microcentrifuge tubes, 0.2-, 0.5-, 1.5-, 2-ml

Mortar and pestle

Ovens, drying and microwave

Paper cutter, large

Paper towels

Parafilm

Pasteur pipets and bulbs

pH meter

pH paper

Pipets, graduated

Pipettors, adjustable delivery, 0.5- to 10-µl, 10- to 200-µl, and 200- to 1000-µl

Plastic wrap (e.g., Saran Wrap)

Polaroid camera or video documentation system

Power supplies, 300-V for polyacrylamide gels, 2000- to 3000-V for other applications

Current Protocols in Toxicology (1999) A.2B.1-A.2B.2

Racks, test tube and microcentrifuge tubes

Radiation shield, Lucite or Plexiglas

Radioactive waste containers for liquid and solid wastes

Refrigerator, 4°C

Ring stand and rings

Rubber policemen or plastic scrapers

Rubber stoppers

Safety glasses

Scalpels and blades

Scintillation counter, β

Scissors

Shakers, orbital and platform, room temperature or 37°C

Spectrophotometer, visible and UV range

Speedvac evaporator

Syringes and needles

Tape, masking, electrician's black, autoclave, and Time tape

Test tubes, glass and plastic, various sizes, with and without caps

Timer

Toolbox with common tools

Trays, plastic and glass, various sizes

Tubing, rubber and Tygon

UV transparent plastic wrap (e.g., Saran Wrap)

Vacuum desiccator

Vacuum oven

Vacuum supply

Vortex mixers

Waring Blendor or equivalent blender

Water bath with adjustable temperature

Water purification system

X-ray film cassettes and intensifying screens

Molecular Biology Techniques

Protocols presented in *Current Protocols in Toxicology* (CPTX) may include molecular biological, biochemical, and other biological techniques that may not be fully described in this manual. Although it may be reasonable to assume that readers have at least a basic understanding of these techniques, there are times when a full step-by-step description of a procedure is helpful. For that reason we have included the following table (Table A.3A.1), which lists common molecular biology techniques, some of which are described in this manual and provides references to specific units in its sister publications *Current Protocols in Molecular Biology* (CPMB; Ausubel et al., 1999), *Current Protocols in Immunology* (CPI; Coligan et al., 1999), and *Current Protocols in Cell Biology* (CPCB; Bonifacino et al., 1999), which describe the methods in more detail. Protocols for some of these techniques will be added as units or as sections of this appendix in future supplements. Alternatively, the reader may wish to consult any of the many other texts and manuals specifically devoted to recombinant DNA technology and biochemical analysis.

Table A.3A.1 Molecular Biology Techniques

Technique	Unit(s)
Animal care and handling	*CPI* Chapter 1
Antibody	
affinity purification	*CPTX 2.3, CPI 2.7 & 2.9*
monoclonal	*CPMB 11.4-11.11, CPI 2.5*
polyclonal	*CPMB 11.12, CPI 2.4*
purification	*CPMB 11.11 & 11.13, CPI 2.7*
Antigen-hapten conjugation	*CPTX 2.3, CPI 9.4*
Autoradiography	*CPMB APPENDIX 3A, CPI APPENDIX 3J, CPCB 6.3*
Bacterial cell	
culture	*CPMB 1.2 & 1.3*
extracts	*CPTX 9.3*
Blotting	
northern	*CPMB 4.9, CPI 10.12*
Southern	*CPMB 2.9, CPI 10.6A*
Cells, preparation from tissues	*CPTX 6.3*
Chemiluminescent detection	*CPMB 10.8, CPI 8.10*
Chromatography	
cation-exchange	*CPTX 8.2*
gel-filtration	*CPTX 7.1, CPMB 10.9, CPI 9.2*
immunoaffinity	*CPTX 3.2, CPMB 10.11A, CPI 8.2*
ion-exchange	*CPTX 4.2, CPMB 10.10*
size-exclusion	*CPMB 10.9*, *CPI APPENDIX 3I*
Cloning	
PCR products	*CPMB 15.2*
subcloning DNA fragments	*CPMB 3.16*
Colorimetry, for protein quantitation	*CPMB 10.1A*

continued

Current Protocols in Toxicology (1999) A.3A.1-A.3A.3

Table A.3A.1 Molecular Biology Techniques, continued

Technique	Unit(s)
Dialysis	*CPMB APPENDIX 3C, CPI APPENDIX 3H*
DNA	*CPTX 2.2 & 3.2*
extraction from mammalian tissue	*CPMB 2.2, CPI 10.2*
ligation	*CPMB 3.14*
preparation, miniprep	*CPMB 1.6, CPI 10.3*
purification and concentration	*CPMB 2.14, CPI 10.1*
quantification, spectrophotometric	*CPMB APPENDIX 3D, CPI APPENDIX 3I*
recovery from agarose gels	*CPMB 2.6, CPI 10.1*
sequencing	*CPMB* Chapter 7, *CPI 10.25*
DNase I digestion	*CPTX 3.2*
E. coli	
growth in liquid medium	*CPMB 1.2, CPI 10.3*
growth on solid medium	*CPMB 1.3*
lysate preparation	*CPMB 1.7, CPI 10.3*
membrane preparation	*CPTX 8.5*
transformation	*CPMB 1.8*, *CPI APPENDIX 3N*
ELISA	*CPTX 2.3, CPMB 11.2, CPI 2.2*
Ethanol precipitation of DNA	*CPMB 2.1A, CPI 10.1*
Fixation, embedding, and sectioning	*CPMB 14.1, CPI 5.8*
Gel electrophoresis	
agarose, basic	*CPTX 2.2, CPMB 2.5A, CPI 10.4*
agarose, low gelling/melting temperature agarose	*CPMB 2.6, CPI 10.5*
agarose, minigels	*CPMB 2.5A, CPI 10.4*
denaturing polyacrylamide (oligonucletide)	*CPMB 2.12, CPI 10.4*
nondenaturing polyacrylamide (DNA)	*CPMB 2.7, CPI 10.7*
SDS-PAGE, basic	*CPMB 10.2, CPI 8.4*
SDS-PAGE, minigels	*CPTX 2.2*
SDS-PAGE, two-dimensional	*CPMB 10.3 & 10.4, CPI 8.5*
staining gels with Coomassie blue	*CPMB 10.6, CPI 10.9*
Genetic analysis of bacteria	*CPTX 3.1*
HPLC	
analytical	*CPTX 6.2 & 6.3*
purification	*CPTX 10.2*
Hybridization	
of Southern blots	*CPMB 2.10, CPI 10.6A*
in situ	*CPMB* Chapter 14, *CPI 12.8*
Immunoblotting	*CPTX 2.3, CPMB 10.8, CPI 8.10, CPCB 6.2, CPTX 2.3*
Immunohistochemistry	*CPMB 14.5, CPI 5.8, CPMB 4.6*
Immunoprecipitation	*CPTX 7.1, CPMB 10.16, CPI 8.3*
Interaction trap/two-hybrid system	*CPMB 20.1*
Isoelectric focusing	*CPTX 9.4*
Kinetic assay methods	*CPMB APPENDIX 3H*
Mammalian cell tissue culture	*CPMB APPENDIX 3F*
Mass spectrometry	*CPTX 3.2*
Media, preparation and use	
E. coli	*CPMB 1.1-1.3*
mammalian cell	*CPMB APPENDIX 3F, CPI APPENDIX 2, CPCB 1.2*
yeast	*CPMB 13.1 & 13.2*

continued

Table A.3A.1 Molecular Biology Techniques, continued

Technique	Unit(s)
Microsome preparation	*CPTX 4.1, 4.3 & 9.3*
Mitochondrial preparation	*CPTX 4.1 & 6.3*
PCR	
anchored	*CPMB 15.6, CPI 10.24*
end-labeling primers for	*CPMB 3.10, CPI 10.10*
general	*CPMB 15.1, CPI 10.20*
primer design	*CPMB 15.1, CPI 10.20*
primer synthesis	*CPMB 2.11*
using end-labeled primers	*CPMB 7.4*
Phenol/chloroform extraction	
DNA	*CPMB 2.1, CPI 10.4*
RNA	*CPMB 4.1, CPI 10.11*
Plasmid preparation	*CPMB 1.6, 1.7 & 2.1B, CPI 17.1*
Protein	
preparation from bacteria	*CPTX 9.4*
quantitation, spectrophotometric and colormetric	*CPMB 10.1A*
Pulsed-field gel electrophoresis	*CPTX 2.2*
Quantitation of DNA and RNA	*CPMB APPENDIX 3D, CPI APPENDIX 3L*
Radioimmunoassay	*CPTX 10.4, CPMB 9.7A, CPI 18.3*
Radiometric enzyme assay	*CPTX 8.2*
Random primer labeling	*CPMB 3.5, CPI 10.22*
Restriction endonuclease digestion	*CPMB 3.1-3.3, CPI 10.8*
RNA preparation and purification	
extraction with guanidinium isothiocyanate	*CPMB 4.2, CPI 10.11*
poly(A)$^+$	*CPMB 4.5, CPI 10.11*
total	*CPMB 4.1 & 4.2, CPI 10.11*
Silanization of glassware	*CPMB APPENDIX 3B, CPI APPENDIX 3K*
Spectrophotometry	
for quantitation of DNA and RNA	*CPMB APPENDIX 3D, CPI APPENDIX 3L*
for quantitation of protein	*CPMB APPENDIX 10.1A*
T4 DNA ligase	*CPMB 3.14*
Thin-layer chromatography	*CPTX 4.3, CPI 11.1*
Tissue fractionation	*CPTX 4.1*
Transfection	
calcium-mediated	*CPMB 9.1, CPI 10.13*
DEAE-dextran-mediated	*CPMB 9.2, CPI 10.14*
electroporation	*CPMB 1.8, CPI 10.15*
liposome-mediated	*CPMB 9.4, CPI 10.16*
TUNEL assay for DNA fragmentation	*CPTX 2.2, CPI 3.17*

LITERATURE CITED

Ausubel, F.A., Brent, R., Kingston, R.E., Moore, D.D., Seidman, J.G., Smith, J.A., and Struhl, K. (eds.). 1999. Current Protocols in Molecular Biology. John Wiley & Sons, New York.

Bonifacino, J.S., Dasso, M., Harford, J.B., Lippincott-Schwartz, J., and Yamada, K.M. (eds.). 1999. Current Protocols in Cell Biology. John Wiley & Sons, New York.

Coligan, J.E., Kruisbeek, A.M., Margulies, D.H., Shevach, E.M., and Strober, W. 1999. Current Protocols in Immunology. John Wiley & Sons, New York.

Techniques for Mammalian Cell Tissue Culture

Tissue culture technology has found wide application in biological research. Monolayer cell cultures and suspension are utilized in cytogenetic, biochemical, and molecular laboratories for diagnostic as well as research studies. In most cases, cells or tissues must be grown in culture for days or weeks to obtain sufficient numbers of cells for analysis. Maintenance of cells in long-term culture requires strict adherence to aseptic technique to avoid contamination and potential loss of valuable cell lines. The first section of this appendix discusses basic principles of aseptic technique.

An important factor influencing the growth of cells in culture is the choice of tissue culture medium. Many different recipes for tissue culture media are available and each laboratory must determine which medium best suits their needs. Individual laboratories may elect to use commercially prepared medium or prepare their own. Commercially available medium can be obtained as a sterile and ready-to-use liquid, in a concentrated liquid form, or in a powdered form. Besides providing nutrients for growing cells, medium is generally supplemented with antibiotics, fungicides, or both to inhibit contamination. The second section of this appendix discusses medium preparation.

As cells reach confluency, they must be subcultured or passaged. Failure to subculture confluent cells results in reduced mitotic index and eventually in cell death. The first step in subculturing monolayers is to detach cells from the surface of the primary culture vessel by trypsinization or mechanical means (see Basic Protocol). The resultant cell suspension is then subdivided, or reseeded, into fresh cultures. Suspension cells are more easily passaged (see Alternate Protocol). Secondary cultures are checked for growth, fed periodically, and may be subsequently subcultured to produce tertiary cultures, etc. The time between passaging cells varies with the cell line and depends on the growth rate.

Support protocols describe freezing of monolayer (see Support Protocol 1) and suspension cells (see Support Protocol 2), thawing and recovery of cells (see Support Protocol 3), cell counting using a hemacytometer (see Support Protocol 4), and preparation of cells for transport (see Support Protocol 5).

ASEPTIC TECHNIQUE

It is essential that aseptic technique be maintained when working with cell cultures. Aseptic technique involves a number of precautions to protect both the cultured cells and the laboratory worker from infection. Laboratory workers must realize that cells handled in the lab are potentially infectious and should be handled with caution. Protective apparel such as gloves, lab coats or aprons, and eyewear should be worn when appropriate (Knutsen, 1997). Care should be taken when handling sharp objects such as needles, scissors, scalpel blades, and glass that could puncture the skin. Sterile disposable plastic supplies may be used to avoid the risk of broken or splintered glass (Rooney and Czepulkowski, 1992).

Frequently, specimens received in the laboratory are not sterile, and cultures prepared from these specimens may become contaminated with bacteria, fungus, or yeast. The presence of microorganisms can inhibit growth, kill cell cultures, or lead to inconsistencies in test results. The contaminants deplete nutrients in the medium and may produce substances that are toxic to cells. Antibiotics (penicillin, streptomycin, kanamycin, or gentamycin) and fungicides (amphotericin B or mycostatin) may be added to tissue culture medium to combat potential contaminants (see Table A.3B.1). An antibiotic/an-

Contributed by Mary C. Phelan
Current Protocols in Toxicology (1999) A.3B.1-A.3B.15

timycotic solution or lyophilized powder that contains penicillin, streptomycin, and amphotericin B is available from Sigma. The solution can be used to wash specimens prior to culture and can be added to medium used for tissue culture. Similar preparations are available from other suppliers.

All materials that come into direct contact with cultures must be sterile. Sterile disposable dishes, flasks, pipets, etc., can be obtained directly from manufacturers. Reusable glassware must be washed, rinsed thoroughly, then sterilized by autoclaving or by dry heat before reusing. With dry heat, glassware should be heated 90 min to 2 hr at 160°C to ensure sterility. Materials that may be damaged by very high temperatures can be autoclaved 20 min at 120°C and 15 psi. All media, reagents, and other solutions that come into contact with the cultures must also be sterile; medium may be obtained as a sterile liquid from the manufacturer, autoclaved if not heat-sensitive, or filter sterilized. Supplements can be added to media prior to filtration, or they can be added aseptically after filtration. Filters with 0.20- to 0.22-μm pore size should be used to remove small gram-negative bacteria from culture media and solutions.

Contamination can occur at any step in handling cultured cells. Care should be taken when pipetting media or other solutions for tissue culture. The necks of bottles and flasks, as well as the tips of the pipets, should be flamed before the pipet is introduced into the bottle. If the pipet tip comes into contact with the benchtop or any other nonsterile surface, it should be discarded and a fresh pipet obtained. Forceps and scissors used in tissue culture can be rapidly sterilized by dipping in 70% alcohol and flaming.

Although tissue culture work can be done on an open bench if aseptic methods are strictly enforced, many labs prefer to perform tissue culture work in a room or low-traffic area reserved specifically for that purpose. At the very least, biological safety cabinets are recommended to protect the cultures as well as the laboratory worker. In a laminar-flow hood, the flow of air protects the work area from dust and contamination and acts as a barrier between the work surface and the worker. Many different styles of safety hoods are available and the laboratory should consider the types of samples being processed and the types of potential pathogenic exposure in making a selection. Manufacturer recommendations should be followed regarding routine maintenance checks on air flow and filters. For day-to-day use, the cabinet should be turned on for at least 5 min prior to beginning work. All work surfaces both inside and outside of the hood should be kept clean and disinfected daily and after each use.

Some safety cabinets are equipped with ultraviolet (UV) lights for decontamination of work surfaces. However, use of UV lamps is no longer recommended, as it is generally ineffective (Knutsen, 1997). UV lamps may actually produce a false sense of security as they maintain a visible blue glow long after their germicidal effectiveness is lost. Effectiveness diminishes over time as the glass tube gradually loses its ability to transmit short UV wavelengths, and it may also be reduced by dust on the glass tube, distance from the work surface, temperature, and air movement. Even when the UV output is adequate, the rays must directly strike a microorganism in order to kill it; bacteria or mold spores hidden below the surface of a material or outside the direct path of the rays will not be destroyed. Another rule of thumb is that anything that can be seen cannot be killed by UV. UV lamps will only destroy microorganisms such as bacteria, virus, and mold spores; they will not destroy insects or other large organisms (Westinghouse Electric Company, 1976). The current recommendation is that work surfaces be wiped down with ethanol instead of relying on UV lamps, although some labs use the lamps in addition to ethanol wipes to decontaminate work areas. A special metering device is available to measure the output of UV lamps, and the lamps should be replaced when they fall below the minimum requirements for protection (Westinghouse Electric Company, 1976).

Cultures should be checked routinely for contamination. Indicators in the tissue culture medium change color when contamination is present: for example, medium that contains phenol red changes to yellow because of increased acidity. Cloudiness and turbidity are also observed in contaminated cultures. Once contamination is confirmed with a microscope, infected cultures are generally discarded. Keeping contaminated cultures increases the risk of contaminating other cultures. Sometimes a contaminated cell line can be salvaged by treating it with various combinations of antibiotics and antimycotics in an attempt to eradicate the infection (e.g., see Fitch et al., 1997). However, such treatment may adversely affect cell growth and is often unsuccessful in any case. In addition to microscopically detectable bacteria and fungi, cultures can be contaminated by mycoplasma, which require more elaborate procedures to detect (Coté, 1999).

PREPARING CULTURE MEDIUM

Choice of tissue culture medium comes from experience. An individual laboratory must select the medium that best suits the type of cells being cultured. Chemically defined media are available in liquid or powdered form from a number of suppliers. Sterile, ready-to-use medium has the advantage of being convenient, although it is more costly than other forms. Powdered medium must be reconstituted with tissue culture–grade water according to manufacturer's directions. Distilled or deionized water is not of sufficiently high quality for medium preparation; double- or triple-distilled water or commercially available tissue culture water should be used. The medium should be filter sterilized and transferred to sterile bottles. Prepared medium can generally be stored ≤1 month in a 4°C refrigerator. Laboratories using large volumes of medium may choose to prepare their own medium from standard recipes. This is the most economical approach, but it is time-consuming.

Basic media such as Eagle's minimal essential medium (MEM), Dulbecco's modified Eagle medium (DMEM), Glasgow modified Eagle's medium (GMEM), and RPMI 1640 and Ham's F10 nutrient mixtures (e.g., Life Technologies) are composed of amino acids, glucose, salts, vitamins, and other nutrients. A basic medium is supplemented by addition of L-glutamine, antibiotics (typically penicillin and streptomycin sulfate), and usually serum to formulate a "complete medium." Where serum is added, the amount is indicated as a percentage of fetal bovine serum (FBS) or other serum. Some media are also supplemented with antimycotics, nonessential amino acids, various growth factors, and/or drugs that provide selective growth conditions. Supplements should be added to medium prior to sterilization or filtration, or added aseptically just before use.

The optimum pH for most mammalian cell cultures is 7.2 to 7.4. Adjust the medium's pH as necessary after all supplements are added. Buffers such as bicarbonate and HEPES are routinely used in tissue culture medium to prevent fluctuations in pH that might adversely affect cell growth. HEPES is especially useful in solutions used for procedures that do not take place in a controlled-CO_2 environment.

Most cultured cells will tolerate a wide range of osmotic pressure and an osmolarity between 260 and 320 mOsm/kg is acceptable for most cells. The osmolarity of human plasma is ~290 mOsm/kg, and this is probably the optimum for human cells in culture as well (Freshney, 1993).

Fetal bovine serum (FBS) is the most frequently used serum supplement. Calf serum, horse serum, and human serum are also used; some cell lines are maintained in serum-free medium (Freshney, 1993). Complete medium is supplemented with 5% to 30% (v/v) serum, depending on the requirements of the particular cell type being cultured. Serum

Table A.3B.1 Working Concentrations of Antibiotics and Fungicides for Mammalian Cell Culture

Additive	Final concentration
Penicillin	50–100 U/ml
Streptomycin sulfate	50–100 µg/ml
Kanamycin	100 µg/ml
Gentamycin	50 µg/ml
Mycostatin	20 µg/ml
Amphotericin B	0.25 µg/ml

that has been heat inactivated (30 min to 1 hr at 56°C; see recipe) is generally preferred, because this inactivates complement and is thought to reduce the number of contaminants. Serum is obtained frozen, then is thawed, divided into smaller portions, and refrozen until needed.

There is considerable lot-to-lot variation in FBS. Most suppliers will provide a sample of a specific lot and reserve a supply of that lot while the serum is tested for its suitability. The suitability of a serum lot depends upon the use. Frequently the ability of serum to promote cell growth equivalent to a laboratory standard is used to evaluate a serum lot. Once an acceptable lot is identified, enough of that lot should be purchased to meet the culture needs of the laboratory for an extended period of time.

Commercially prepared media containing L-glutamine are available, but many laboratories choose to obtain medium without L-glutamine and then add it to a final concentration of 2 mM just before use. L-glutamine is an unstable amino acid that, upon storage, converts to a form cells cannot use. Breakdown of L-glutamine is temperature and pH dependent. At 4°C, 80% of the L-glutamine remains after 3 weeks, but at incubator temperature (35°C) the amount diminishes more rapidly (Brown and Lawce, 1997). To prevent degradation, 100× L-glutamine (see recipe) should be stored frozen in aliquots until needed.

As well as practicing good aseptic technique, most laboratories add antimicrobial agents to medium to further reduce the risk of contamination. A combination of penicillin and streptomycin is the most commonly used antibiotic additive; kanamycin and gentamycin are used alone. Mycostatin and amphotericin B are the most commonly used fungicides (Rooney and Czepulkowski, 1992). Table A.3B.1 lists suggested working concentrations for the most commonly used antibiotics and antimycotics. Combining antibiotics in tissue culture medium can be tricky, as some antibiotics are not compatible, and one may inhibit the action of another. Furthermore, combined antibiotics may be cytotoxic at lower concentrations than is true for the individual antibiotics. In addition, prolonged use of antibiotics may cause cell lines to develop antibiotic resistance. For this reason, some laboratories add antibiotics and/or fungicides to medium when initially establishing a culture but eliminate them from medium used in later subcultures.

All tissue culture medium, whether prepared commercially or within the laboratory, should be tested for sterility prior to use. A small aliquot from each lot of medium is incubated 48 hr at 37°C and monitored for evidence of contamination such as turbidity (infected medium will be cloudy) and color change (if phenol red is the indicator, infected medium will turn yellow). Any contaminated medium should be discarded.

TRYPSINIZING AND SUBCULTURING CELLS FROM A MONOLAYER

BASIC PROTOCOL

A primary culture is grown to confluency in a 60-mm petri dish or 25-cm^2 tissue culture flask containing 5 ml tissue culture medium. Cells are dispersed by trypsin treatment and then reseeded into secondary cultures. The process of removing cells from the primary culture and transferring them to secondary cultures constitutes a passage or subculture.

Materials

Cells cultures
HBSS *without* Ca^{2+} and Mg^{2+} (*APPENDIX 2A*), 37°C
0.25% (w/v) trypsin/0.2% EDTA solution (see recipe), 37°C
Complete medium with serum: e.g., DMEM supplemented with 10% to 15% (v/v) FBS (complete DMEM-10; see recipe), 37°C

Sterile Pasteur pipets
37°C warming tray or incubator
Tissue culture plasticware or glassware including pipets and 25-cm^2 flasks or 60-mm petri dishes, sterile

NOTE: All incubations should be performed in a humidified 37°C, 5% CO_2 incubator unless otherwise specified.

1. Remove all medium from culture with a sterile Pasteur pipet. Wash adhering cell monolayer once or twice with a small volume of 37°C HBSS without Ca^{2+} and Mg^{2+} to remove any residual FBS, which may inhibit the action of trypsin.

   Use a buffered salt solution that is Ca^{2+}- and Mg^{2+}-free to wash cells. Ca^{2+} and Mg^{2+} in the salt solution can cause cells to stick together.

   If this is the first medium change from primary culture, rather than discarding medium that is removed from primary culture, transfer it to a fresh dish or flask. The medium contains unattached cells that may attach and grow, thereby providing a backup culture.

2. Add enough 37°C trypsin/EDTA solution to culture to cover adhering cell layer.
3. Place plate on a 37°C warming tray 1 to 2 min. Tap bottom of plate on the countertop to dislodge cells. Check culture with an inverted microscope to be sure that cells are rounded up and detached from the surface.

   If cells are not sufficiently detached, return plate to warming tray for an additional minute or two.

4. Add 2 ml of 37°C complete medium. Draw cell suspension into a Pasteur pipet and rinse cell layer two or three times to dissociate cells and to dislodge any remaining adherent cells. As soon as cells are detached, add serum or medium containing serum to inhibit further trypsin activity that might damage cells.

   If cultures are to be split 1/3 or 1/4 rather than 1/2, add sufficient medium such that 1 ml of cell suspension can be transferred into each fresh culture vessel.

5. Add an equal volume of cell suspension to fresh dishes or flasks that have been appropriately labeled.

   Alternatively, cells can be counted using a hemacytometer (see Support Protocol 4) or Coulter counter and diluted to the desired density so a specific number of cells can be added to each culture vessel. A final concentration of ~5×10^4 cells/ml is appropriate for most subcultures.

   For primary cultures and early subcultures, 60-mm petri dishes or 25-cm^2 flasks are generally used; larger petri dishes or flasks (e.g., 150-mm dishes or 75-cm^2 flasks) may be used for later subcultures.

   Cultures should be labeled with cell line identification, lab number, date of subculture, and passage number.

6. Add 4 ml fresh medium to each new culture. Incubate in a humidified 37°C, 5% CO_2 incubator.

   If using 75-cm^2 culture flasks, add 9 ml medium per flask.

   Some labs now use incubators with 5% CO_2 and 4% O_2. The low oxygen concentration is thought to simulate the in vivo environment of cells and to enhance cell growth. However, some media (e.g., DMEM) may require altered levels of CO_2 to maintain pH.

7. If necessary, feed subconfluent cultures after 3 or 4 days by removing old medium and adding fresh 37°C medium.

8. Passage secondary culture when it becomes confluent by repeating steps 1 to 7, and continue to passage as necessary.

ALTERNATE PROTOCOL

PASSAGING CELLS IN SUSPENSION CULTURE

A suspension culture is grown in culture flasks in a humidified 37°C, 5% CO_2 incubator. Passaging of suspension cultures is somewhat less complicated than passaging of monolayer cultures. Because the cells are suspended in medium rather than attached to a surface, it is not necessary to disperse them enzymatically before passaging. However, before passaging, cells must be maintained in culture by feeding every 2 to 3 days until they reach confluency (i.e., until the cells clump together in the suspension and the medium appears turbid when the flask is swirled).

NOTE: All culture incubations should be performed in a humidified 37°C, 5% CO_2 incubator unless otherwise specified.

1. Feed cells as follows every 2 to 3 days until the cultures are confluent:

   a. Remove flask of suspension cells from incubator, taking care not to disturb those that have settled to the flask bottom.

   b. Aseptically remove and discard about one-third of the medium from flask and replace with an equal volume of prewarmed (37°C) medium. If the cells are growing rapidly, add an additional 10% medium by volume in order to maintain optimum concentration of 1×10^6 cells/ml. Gently swirl flask to resuspend cells.

   c. Return flask to incubator. If there is <15 ml of medium in the flask, incubate flask in horizontal position to enhance cell/medium contact.

      At higher volumes of medium the flask can be incubated in the vertical position.

      If using a 25-cm^2 flask, there should be 20 to 30 ml of medium in the flask at confluency.

2. On the days cultures are not being fed, check them by swirling flask to resuspend cells and observing color changes in the medium that indicate good metabolic growth.

3. When cultures are confluent (~2.5×10^6 cells/ml), passage culture as follows:

   a. Remove flask from incubator and swirl flask so that cells are evenly distributed in the medium.

   b. Aseptically remove half of the volume of cell suspension and place into a fresh flask.

   c. Feed each flask with 7 to 10 ml prewarmed medium and return flask to incubator.

      Some labs prefer to split the cells 1:3 or 1:4, although increasing the split ratio will result in a longer interval before subcultures reach confluency.

FREEZING HUMAN CELLS GROWN IN MONOLAYER CULTURES

SUPPORT PROTOCOL 1

It is sometimes desirable to store cell lines for future study. To preserve cells, avoid senescence, reduce the risk of contamination, and minimize effects of genetic drift, cell lines may be frozen for long-term storage. Without the use of a cryoprotective agent freezing would be lethal to the cells in most cases. Generally, a cryoprotective agent such as dimethylsulfoxide (DMSO) is used in conjunction with complete medium for preserving cells at −70°C or lower. DMSO acts to reduce the freezing point and allows a slower cooling rate. Gradual freezing reduces the risk of ice crystal formation and cell damage.

Materials

Log-phase monolayer culture of cells in petri dish
Complete medium
Freezing medium: complete medium with 10% to 20% (v/v) FBS (e.g., complete DMEM-20 or complete RPMI-20; see recipe) supplemented with 5% to 10% (v/v) DMSO, 4°C
Benchtop clinical centrifuge (e.g., Fisher Centrific or Clay Adams Dynac) with 45° fixed-angle or swinging-bucket rotor

1. Trypsinize log-phase monolayer culture of cells from plate (see Basic Protocol, steps 1 to 4).

   It is best to use cells in log-phase growth for cryopreservation.

2. Transfer cell suspension to a sterile centrifuge tube and add 2 ml complete medium with serum. Centrifuge 5 min at 300 to 350 × *g* (~1500 rpm in Fisher Centrific rotor), room temperature.

   Cells from three or more dishes from the same subculture of the same patient can be combined in one tube.

3. Remove supernatant and add 1 ml of 4°C freezing medium. Resuspend pellet.

4. Add 4 ml of 4°C freezing medium, mix cells thoroughly, and place on wet ice.

5. Count cells using a hemacytometer (see Support Protocol 4). Dilute with more freezing medium as necessary to get a final cell concentration of 10^6 or 10^7 cells/ml.

   To freeze cells from a nearly confluent 25-cm^2 flask, resuspend in roughly 3 ml freezing medium.

6. Pipet 1-ml aliquots of cell suspension into labeled 2-ml cryovials. Tighten caps on vials.

7. Place vials 1 hr to overnight in a −70°C freezer, then transfer to liquid nitrogen storage freezer.

   Alternatively, freeze cells in a freezing chamber in the neck of a Dewar flask according to manufacturer's instructions. Some laboratories place vials directly into the liquid nitrogen freezer, omitting the gradual temperature drop. Although this is contrary to the general recommendation to gradually reduce the temperature, laboratories that routinely use a direct-freezing technique report no loss of cell viability on recovery.

   Liquid nitrogen is a potential source of contamination. It may seep into vials between the cap and tube. For this reason, some investigators prefer to freeze cells in flame-sealed glass vials.

   IMPORTANT NOTE: *Keep accurate records of the identity and location of cells stored in liquid nitrogen freezers. Cells may be stored for many years and proper information is imperative for locating a particular line for future use.*

SUPPORT PROTOCOL 2

FREEZING CELLS GROWN IN SUSPENSION CULTURE

Freezing cells from suspension culture is similar in principle to freezing cells from monolayer. The major difference is that suspension cultures need not be trypsinized.

1. Transfer cell suspension to a centrifuge tube and centrifuge 10 min at 300 to 350 × *g* (~1500 rpm in Fisher Centrific centrifuge), room temperature.
2. Remove supernatant and resuspend pellet in 4°C freezing medium at a density of 10^6 to 10^7 cells/ml.

   Some laboratories freeze lymphoblastoid lines at the higher cell density because they plan to recover them in a larger volume of medium and because there may be a greater loss of cell viability upon recovery as compared to other types of cells (e.g., fibroblasts).

3. Transfer 1-ml aliquots of cell suspension into labeled cryovials and freeze as for monolayer cultures.

   Liquid nitrogen is a potential source of contamination. It may seep into vials between the cap and tube. For this reason, some investigators prefer to freeze cells in flame-sealed glass vials.

SUPPORT PROTOCOL 3

THAWING AND RECOVERING FROZEN CELL CULTURES

When cryopreserved cells are needed for study, they should be thawed rapidly and plated at high density to optimize recovery.

CAUTION: Protective clothing, particularly insulated gloves and goggles, should be worn when removing frozen vials or ampules from the liquid nitrogen freezer. The room containing the liquid nitrogen freezer should be well-ventilated. Care should be taken not to spill liquid nitrogen on the skin.

Materials

Cryopreserved cells stored in liquid nitrogen freezer
70% (v/v) ethanol
Complete medium containing 20% FBS, 37°C: e.g., complete DMEM-20 or complete RPMI-20 (see recipes), 37°C
Tissue culture dish or flask

NOTE: All incubations are performed in a humidified 37°C, 5% CO_2 incubator unless otherwise specified.

1. Remove vial of cells from liquid nitrogen freezer and immediately place it into a 37°C water bath. Agitate vial continuously until medium is thawed.

   The medium usually thaws in <60 sec.

   Cells should be thawed as quickly as possible to prevent formation of ice crystals which can cause cell lysis. Try to avoid getting water around the cap of the vial.

2. Wipe top of vial with 70% ethanol before opening.

   Some labs prefer to submerge the vial in 70% ethanol and air dry before opening.

3. Transfer thawed cell suspension into a sterile centrifuge tube containing 2 ml warm complete medium containing 20% FBS. Centrifuge 10 min at 150 to 200 × *g* (~1000 rpm in Fisher Centrific), room temperature. Discard supernatant.

   Cells are washed with fresh medium to remove residual DMSO.

4. Gently resuspend cell pellet in small amount (~1 ml) of complete medium/20% FBS and transfer to properly labeled culture dish or flask containing the appropriate amount of medium.

   Cultures are reestablished at a higher cell density than that used for original cultures because there is some cell death associated with freezing. Generally, 1 ml cell suspension is reseeded in 5 to 20 ml medium.

5. Check cultures after ~24 hr to ensure that cells have attached to the plate.

6. Change medium after 5 to 7 days or when pH indicator (e.g., phenol red) in medium changes color. Keep cultures in medium with 20% FBS until cells are reestablished.

   If recovery rate is extremely low, only a subpopulation of the original culture may be growing; be extra careful of this when working with cell lines known to be mosaic.

DETERMINING CELL NUMBER AND VIABILITY WITH A HEMACYTOMETER AND TRYPAN BLUE STAINING

SUPPORT PROTOCOL 4

Determining the number of cells in culture is important in standardization of culture conditions and in performing accurate quantitation experiments. A hemacytometer is a thick glass slide with a central area designed as a counting chamber.

The exact design of the hemacytometer may vary; the one described here is the Improved Neubauer from Baxter Scientific (Fig. A.3B.1). The central portion of the slide is the counting platform, which is bordered by a 1-mm groove. The central platform is divided into two counting chambers by a transverse groove. Each counting chamber consists of a silver footplate on which is etched a 3 × 3–mm grid. This grid is divided into nine secondary squares, each 1 × 1 mm. The four corner squares and the central square are used for determining the cell count. The corner squares are further divided into 16 tertiary squares and the central square into 25 tertiary squares to aid in cell counting.

Accompanying the hemacytometer slide is a thick, even-surfaced coverslip. Ordinary coverslips may have uneven surfaces, which can introduce errors in cell counting; therefore, it is imperative that the coverslip provided with the hemacytometer be used in determining cell number.

Cell suspension is applied to a defined area and counted so cell density can be calculated.

Materials

70% (v/v) ethanol
Cell suspension
0.4% (w/v) trypan blue *or* 0.4% (w/v) nigrosin, prepared in HBSS (*APPENDIX 2A*)

Hemacytometer with coverslip (Improved Neubauer, Baxter Scientific)
Hand-held counter

Prepare hemacytometer

1. Clean surface of hemacytometer slide and coverslip with 70% alcohol.

   Coverslip and slide should be clean, dry, and free from lint, fingerprints, and watermarks.

2. Wet edge of coverslip slightly with tap water and press over grooves on hemacytometer. The coverslip should rest evenly over the silver counting area.

Prepare cell suspension

3. For cells grown in monolayer cultures, detach cells from surface of dish using trypsin (see Basic Protocol, steps 1 to 4).

4. Dilute cells as needed to obtain a uniform suspension. Disperse any clumps.

   When using the hemacytometer, a maximum cell count of 20 to 50 cells per 1-mm square is recommended.

Load hemacytometer

5. Use a sterile Pasteur pipet to transfer cell suspension to edge of hemacytometer counting chamber. Hold tip of pipet under the coverslip and dispense one drop of suspension.

   Suspension will be drawn under the coverslip by capillary action.

   The hemacytometer should be considered nonsterile. If cell suspension is to be used for cultures, do not reuse the pipet and do not return any excess cell suspension in the pipet to the original suspension.

6. Fill second counting chamber.

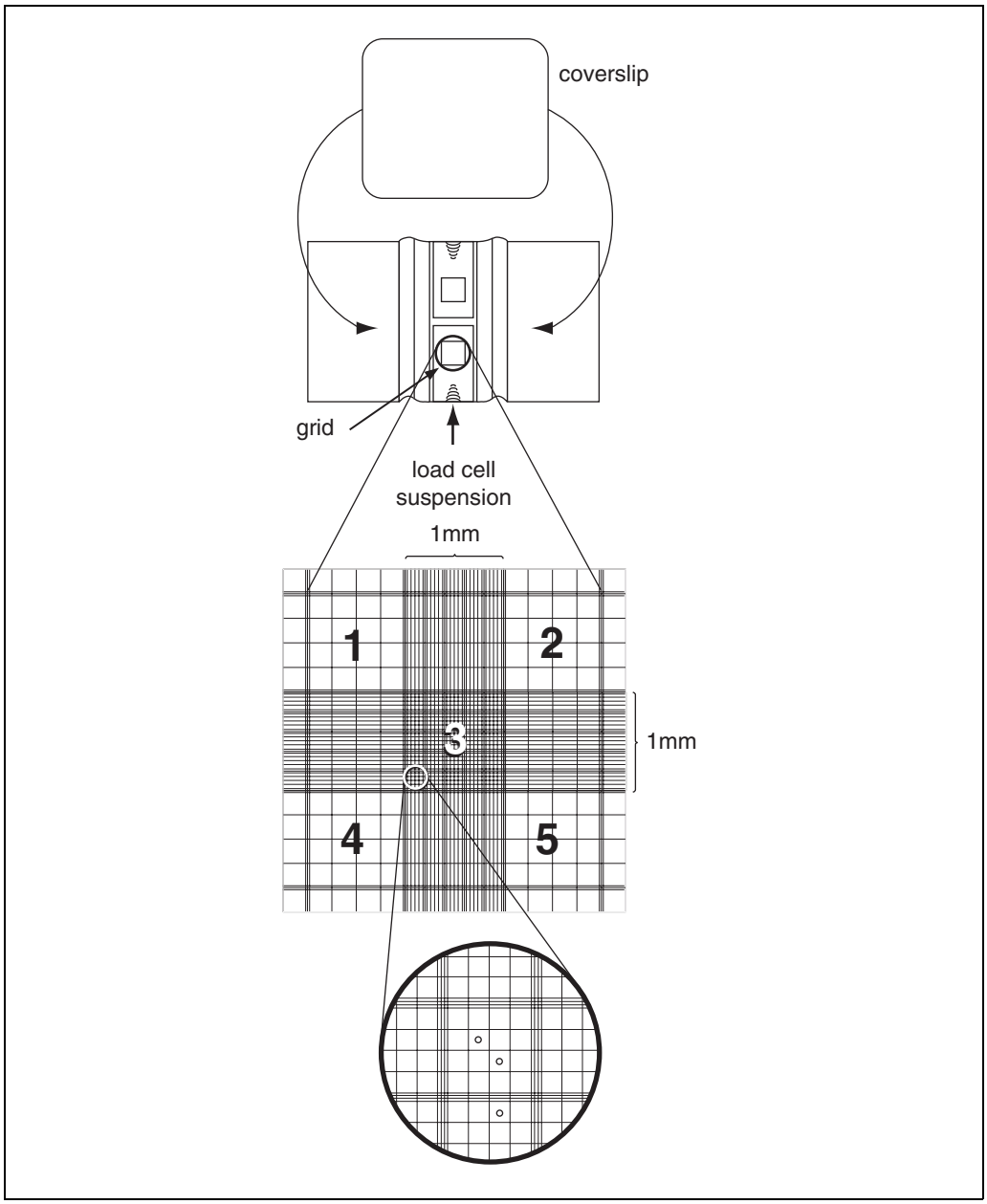

Figure A.3B.1 Hemacytometer slide (Improved Neubauer) and coverslip. Coverslip is applied to slide and cell suspension is added to counting chamber using a Pasteur pipet. Each counting chamber has a 3 × 3–mm grid (enlarged). The four corner squares (1, 2, 4, and 5) and the central square (3) are counted on each side of the hemacytometer (numbers added).

Count cells

7. Allow cells to settle for a few minutes before beginning to count. Blot off excess liquid.

8. View slide on microscope with 100× magnification.

   A 10× ocular with a 10× objective = 100× magnification.

   Position slide to view the large central area of the grid (section 3 in Fig. A.3B.1); this area is bordered by a set of three parallel lines. The central area of the grid should almost fill the microscope field. Subdivisions within the large central area are also bordered by three parallel lines and each subdivision is divided into sixteen smaller squares by single lines. Cells within this area should be evenly distributed without clumping. If cells are not evenly distributed, wash and reload hemacytometer.

9. Use a hand-held counter to count cells in each of the four corner and central squares (Fig. A.3B.1, squares numbered 1 to 5). Repeat counts for other counting chamber.

   Five squares (four corner and one center) are counted from each of the two counting chambers for a total of ten squares counted.

   Count cells touching the middle line of the triple line on the top and left of the squares. Do not count cells touching the middle line of the triple lines on the bottom or right side of the square.

Calculate cell number

10. Determine number of suspension cells per milliliter by the following calculations:

    cells/ml = average count per square × dilution factor × 10^4
    total cells = cells/ml × total original volume of cell suspension from which sample was taken.

    10^4 is the volume correction factor for the hemacytometer: each square is 1 × 1 mm and the depth is 0.1 mm.

Stain cells with trypan blue to determine cell viability

11. Determine number of viable cells by adding 0.5 ml of 0.4% trypan blue, 0.3 ml HBSS, and 0.1 ml cell suspension to a small tube. Mix thoroughly and let stand 5 min before loading hemacytometer.

    Either 0.4% trypan blue or 0.4% nigrosin can be used to determine the viable cell number. Nonviable cells will take up the dye, whereas live cells will be impermeable to it.

12. Count total number of cells and total number of viable (unstained) cells. Calculate percent viable cells as follows:

$$\%\ \text{viable cells} = \frac{\text{number of unstained cells}}{\text{total number of cells}} \times 100$$

13. Decontaminate coverslip and hemacytometer by rinsing with 70% ethanol and then deionized water. Air dry and store for future use.

PREPARING CELLS FOR TRANSPORT

SUPPORT PROTOCOL 5

Both monolayer and suspension cultures can easily be shipped in 25-cm^2 tissue culture flasks. Cells are grown to near confluency in a monolayer or to desired density in suspension. Medium is removed from monolayer cultures and the flask is filled with fresh medium. Fresh medium is added to suspension cultures to fill the flask. *It is essential that the flasks be completely filled with medium to protect cells from drying if flasks are*

inverted during transport. The cap is tightened and taped securely in place. The flask is sealed in a leak-proof plastic bag or other leak-proof container designed to prevent spillage in the event that the flask should become damaged. The primary container is then placed in a secondary insulated container to protect it from extreme temperatures during transport. A biohazard label is affixed to the outside of the package. Generally, cultures are transported by same-day or overnight courier.

Cells can also be shipped frozen. The vial containing frozen cells is removed from the liquid nitrogen freezer and placed immediately on dry ice in an insulated container to prevent thawing during transport.

REAGENTS AND SOLUTIONS

Use Milli-Q-purified water or equivalent in all recipes and protocol steps. For common stock solutions, see ***APPENDIX 2A****; for suppliers, see* ***SUPPLIERS APPENDIX****.*

Complete DMEM

Dulbecco's modified Eagle medium, high-glucose formulation (e.g., Life Technologies), containing:
5%, 10%, or 20% (v/v) FBS, heat inactivated (optional; see recipe below)
1% (v/v) nonessential amino acids
2 mM L-glutamine (see recipe below)
100 U/ml penicillin
100 µg/ml streptomycin sulfate
Filter sterilize if anything nonsterile has been added
Store up to 1 month at 4°C

DMEM containing this set of additives is sometimes called "complete DMEM." The percentage of serum used is indicated after the medium name—e.g., "DMEM/5% FBS." Absence of a number indicates no serum is used. DMEM is also known as Dulbecco's minimum essential medium.

Ham's F-12 nutrient mixture (e.g., Life Technologies) is sometimes added to DMEM; the resulting medium is known as DMEM/F-12.

Because of the higher bicarbonate content, DMEM requires ~10% CO_2 to maintain pH 7.4.

Culture media containing glutamine and penicillin should be warmed to 37°C as few times as possible since components, especially glutamine, degrade rapidly at 37°C.

Complete RPMI

RPMI 1640 medium (e.g., Life Technologies) containing:
2%, 5%, 10%, 15%, or 20% FBS, heat-inactivated (optional; *APPENDIX 2A*)
2 mM L-glutamine (see recipe)
100 U/ml penicillin
100 µg/ml streptomycin sulfate
Filter sterilize and store ≤1 month at 4°C

FBS (fetal bovine serum)

Thaw purchased fetal bovine serum (shipped on dry ice and kept frozen until needed). Store 3 to 4 weeks at 4°C. If FBS is not to be used within this time, aseptically divide into smaller aliquots and refreeze until used. Store ≤1 year at −20°C. To heat inactivate FBS, heat serum 30 min to 1 hr in a 56°C water bath with periodic gentle swirling during the first 10 to 15 min to ensure uniform heating.

Repeated thawing and refreezing should be avoided, as it may cause denaturation of the serum.

Heat-inactivated FBS (FBS that has been treated with heat to inactivate complement protein and thus prevent an immunological reaction against cultured cells) is useful for a variety of purposes. It can be purchased commercially or made in the lab as described above.

L-Glutamine, 0.2 M (100×)

Thaw commercially prepared frozen L-glutamine or prepare an 0.2 M solution in water, aliquot aseptically into usable portions, then refreeze. For convenience, L-glutamine can be stored in 1-ml aliquots if 100-ml bottles of medium are used and in 5-ml aliquots if 500-ml bottles are used. Store ≤1 year at −20°C.

Many laboratories supplement medium with 2 mM L-glutamine—1% (v/v) of 100× stock—just prior to use.

Trypsin/EDTA solution

Prepare in sterile HBSS (APPENDIX 2A) or 0.9% (w/v) NaCl:
0.25% (w/v) trypsin
0.2% (w/v) EDTA
Store ≤1 year (until needed) at −20°C

Specific applications may require different concentrations of trypsin.

Trypsin/EDTA solution is commercially available in various concentrations including 10×, 1×, and 0.25% (w/v). It is received frozen from the manufacturer and can be thawed and aseptically divided into smaller volumes. Preparing trypsin/EDTA from powdered stocks may reduce its cost; however, most laboratories prefer commercially prepared solutions for convenience.

EDTA (disodium ethylenediamine tetraacetic acid) is added as a chelating agent to bind Ca^{2+} and Mg^{2+} ions that can interfere with the action of trypsin.

COMMENTARY

Background Information

At its inception in the early twentieth century, tissue culture was applied to the study of tissue fragments in culture. New growth in culture was limited to cells that migrated out from the initial tissue fragment. Tissue culture techniques evolved rapidly, and since the 1950s culture methods have allowed the growth and study of dispersed cells in culture (Freshney, 1993). Cells dispersed from the original tissue can be grown in monolayers and passaged repeatedly to give rise to a relatively stable cell line.

Four distinct growth stages have been described for primary cells maintained in culture. First, cells adapt to the in vitro environment. Second, cells undergo an exponential growth phase lasting through ~30 passages. Third, the growth rate of cells slows, leading to a progressively longer generation time. Finally, after 40 or 50 passages, cells begin to senesce and die (Lee, 1991). It may be desirable to study a particular cell line over several months or years, so cultures can be preserved to retain the integrity of the cell line. Aliquots of early passage cell suspensions are frozen, then thawed, and cultures reestablished as needed. Freezing cultures prevents changes due to genetic drift and avoids loss of cultures due to senescence or accidental contamination (Freshney, 1993).

Cell lines are commercially available from a number of sources, including the American Type Culture Collection (ATCC) and the Human Genetic Mutant Cell Repository at the Coriell Cell Repository (CCR). These cell repositories are a valuable resource for researchers who do not have access to suitable patient populations.

Critical Parameters

Use of aseptic technique is essential for successful tissue culture. Cell cultures can be contaminated at any time during handling, so precautions must be taken to minimize the chance of contamination. All supplies and reagents that come into contact with cultures must be sterile and all work surfaces should be kept clean and free from clutter.

Cultures should be 75% to 100% confluent when selected for subculture. Growth in monolayer cultures will be adversely affected if cells are allowed to become overgrown. Passaging cells too early will result in a longer lag time before subcultures are established. Following dissociation of the monolayer by trypsinization, serum or medium containing serum should be added to the cell suspension to stop further action by trypsin that might be harmful to cells.

When subculturing cells, add a sufficient number of cells to give a final concentration of ~5×10^4 cells/ml in each new culture. Cells plated at too low a density may be inhibited or

delayed in entry into growth stage. Cells plated at too high a density may reach confluency before the next scheduled subculturing; this could lead to cell loss and/or cessation of proliferation. The growth characteristics for different cell lines vary. A lower cell concentration (10^4 cells/ml) may be used to initiate subcultures of rapidly growing cells, and a higher cell concentration (10^5 cells/ml) may be used to initiate subcultures of more slowly growing cells. Adjusting the initial cell concentration permits establishment of a regular, convenient schedule for subculturing—e.g., once or twice a week (Freshney, 1993).

Exposure of culture medium to light should be minimized to avoid photooxidation of tyrosine.

Cells in culture will undergo changes in growth, morphology, and genetic characteristics over time. Such changes can adversely affect reproducibility of laboratory results. Nontransformed cells will undergo senescence and eventual death if passaged indefinitely. The time of senescence will vary with cell line, but generally at between 40 and 50 population doublings fibroblast cell lines begin to senesce. Cryopreservation of cell lines will protect against these adverse changes and will avoid potential contamination.

Cultures selected for cryopreservation should be in log-phase growth and free from contamination. Cells should be frozen at a concentration of 10^6 to 10^7 cells/ml. Cells should be frozen gradually and thawed rapidly to prevent formation of ice crystals that may cause cells to lyse. Cell lines can be thawed and recovered after long-term storage in liquid nitrogen. The top of the freezing vial should be cleaned with 70% alcohol before opening to prevent introduction of contaminants. To aid in recovery of cultures, thawed cells should be reseeded at a higher concentration than that used for initiating primary cultures. Careful records regarding identity and characteristics of frozen cells as well as their location in the freezer should be maintained to allow for easy retrieval.

For accurate cell counting, the hemacytometer slide should be clean, dry, and free from lint, scratches, fingerprints, and watermarks. The coverslip supplied with the hemacytometer should always be used because it has an even surface and is specially designed for use with the counting chamber. Use of an ordinary coverslip may introduce errors in cell counting. If the cell suspension is too dense or the cells are clumped, inaccurate counts will be obtained. If the cell suspension is not evenly distributed over the counting chamber, the hemacytometer should be washed and reloaded.

Anticipated Results

Confluent cell lines can be successfully subcultured in the vast majority of cases. The yield of cells derived from monolayer culture is directly dependent on the available surface area of the culture vessel (Freshney, 1993). Overly confluent cultures or senescent cells may be difficult to trypsinize, but increasing the time of trypsin exposure will help dissociate resistant cells. Cell lines can be propagated to get sufficient cell populations for cytogenetic, biochemical, and molecular analyses.

It is well accepted that anyone can successfully freeze cultured cells; it is thawing and recovering the cultures that presents the challenge. Cultures that are healthy and free from contamination can be frozen and stored indefinitely. Cells stored in liquid nitrogen can be successfully thawed and recovered in over 95% of cases. Several aliquots of each cell line should be stored to increase the chance of recovery. Cells should be frozen gradually, with a temperature drop of ~1°C per minute, but thawed rapidly. Gradual freezing and rapid thawing prevents formation of ice crystals that might cause cell lysis.

Accurate cell counts can be obtained using the hemacytometer if cells are evenly dispersed in suspension and free from clumps. Determining the proportion of viable cells in a population will aid in standardization of experimental conditions.

Time Considerations

Establishment and maintenance of mammalian cell cultures require a regular routine for preparing media and feeding and passaging cells. Cultures should be inspected regularly for signs of contamination and to determine if the culture needs feeding or passaging.

Literature Cited

Brown, M.G., and Lawce, H.J. 1997. Peripheral blood cytogenetic methods. *In* The AGT Cytogenetics Laboratory Manual, 3rd ed. (M.J. Barch, T. Knutsen, and J.L. Spurbeck, eds.) pp. 77-87. Lippincott-Raven, New York.

Coté, R. 1999. Assessing and controlling microbial contamination in cell cultures. *In* Current Protocols in Cell Biology (J.S. Bonifacino, M. Dasso, J.B. Harford, J. Lippincott-Schwartz, and K.M. Yamada, eds.) pp. 1.5.1-1.5.18. John Wiley & Sons, New York.

Fitch, F.W., Gajewski, T.F., and Yokoyama, W.M. 1997. Diagnosis and treatment of mycoplasma-

contaminated cell cultures. *In* Current Protocols in Immunology (J.E. Coligan, A.M. Kruisbeek, D.H. Margulies, E.M. Shevach, and W. Strober, eds.) pp. A.3E.1-A.3E.4. John Wiley & Sons, New York.

Freshney, R.I. 1993. Culture of Animal Cells. A Manual of Basic Techniques, 3rd ed. Wiley-Liss, New York.

Knutsen, T. 1997. Laboratory safety, quality control, and regulations. *In* The AGT Cytogenetics Laboratory Manual, 3rd ed. (M.J. Barch, T. Knutsen, and J.L. Spurbeck, eds.) pp. 597-646. Lippincott-Raven, New York.

Lee, E.C. 1991. Cytogenetic Analysis of Continuous Cell Lines. *In* The ACT Cytogenetics Laboratory Manual, 2nd ed. (M.J. Barch, ed.) pp. 107-148. Raven Press, New York.

Rooney, D.E. and Czepulkowski, B.H. (eds.) 1992. Human Cytogenetics: A Practical Approach, Vol. I. Constitutional Analysis, 2nd ed. IRL Press, Washington, D.C.

Westinghouse Electric Company. 1976. Westinghouse sterilamp germicidal ultraviolet tubes. Westinghouse Electric Corp., Bloomfield, N.J.

Key Reference

Lee, E.C. 1991. See above.

Contains pertinent information on cell culture requirements including medium preparation and sterility. Also discusses trypsinization, freezing and thawing, and cell counting.

Contributed by Mary C. Phelan
T.C. Thompson Children's Hospital
Chattanooga, Tennessee

Enzymatic Amplification of DNA by PCR: Standard Procedures and Optimization

BASIC PROTOCOL

This unit describes a method for amplifying DNA enzymatically by the polymerase chain reaction (PCR), including procedures to quickly determine conditions for successful amplification of the sequence and primer sets of interest, and to optimize for specificity, sensitivity, and yield. The first step of PCR simply entails mixing template DNA, two appropriate oligonucleotide primers, *Taq* or other thermostable DNA polymerases, deoxyribonucleoside triphosphates (dNTPs), and a buffer. Once assembled, the mixture is cycled many times (usually 30) through temperatures that permit denaturation, annealing, and synthesis to exponentially amplify a product of specific size and sequence. The PCR products are then displayed on an appropriate gel and examined for yield and specificity.

Many important variables can influence the outcome of PCR. Careful titration of the $MgCl_2$ concentration is critical. Additives that promote polymerase stability and processivity or increase hybridization stringency, and strategies that reduce nonspecific primer-template interactions, especially prior to the critical first cycle, generally improve amplification efficiency. This protocol, using *Taq* DNA polymerase, is designed to optimize the reaction components and conditions in one or two stages. The first stage (steps 1 to 7) determines the optimal $MgCl_2$ concentration and screens several enhancing additives. Most suppliers of *Taq* and other thermostable DNA polymerases provide a unique optimized $MgCl_2$-free buffer with $MgCl_2$ in a separate vial for user titration. The second stage (steps 8 to 13) compares methods for preventing pre-PCR low-stringency primer extension, which can generate nonspecific products. This has come to be known as "hot start," whether one omits an essential reaction component prior to the first denaturing-temperature step or adds a reversible inhibitor of polymerase. Hot-start methods can greatly improve specificity, sensitivity, and yield. Use of any one of the hot-start approaches is strongly recommended if primer-dimers or other nonspecific products are generated or if relatively rare template DNA is contained in a complex mixture, such as viral nucleic acids in cell or tissue preparations. This protocol suggests some relatively inexpensive methods to achieve hot start, and lists several commercial hot-start options which may be more convenient, but of course more expensive.

Materials

Sterile H_2O
15 mM (L), 30 mM (M), and 45 mM (H) $MgCl_2$
10× $MgCl_2$-free PCR amplification buffer (see recipe)
25 mM 4dNTP mix (see recipe)
50 µM oligonucleotide primer 1: 50 pmol/µl in sterile H_2O (store at −20°C)
50 µM oligonucleotide primer 2: 50 pmol/µl in sterile H_2O (store at −20°C)
Template DNA: 1 µg mammalian genomic DNA or 1.0 to 100.0 pg plasmid DNA
5 U/µl *Taq* DNA polymerase (native or recombinant; many suppliers)
Enhancer agents (optional; see recipe)
TaqStart Antibody (Clontech)
Mineral oil
Ficoll 400 (optional)
Tartrazine dye (optional)

Thin-walled PCR tubes
Automated thermal cycler

Contributed by Martha F. Kramer and Donald M. Coen
Current Protocols in Toxicology (2000) A.3C.1-A.3C.14

Table A.3C.1 Master Mixes for Optimizing Reaction Components

Components	Final concentration	Per reaction	Master mix[a] (µl)			
			I	II	III	IV
10× PCR buffer	1×	10 µl	40.0	40.0	40.0	40.0
Primer 1	0.5 µM	1 µl	4.0	4.0	4.0	4.0
Primer 2	0.5 µM	1 µl	4.0	4.0	4.0	4.0
Template DNA	Undiluted	1 vol[b]	4 vol[b]	4 vol[b]	4 vol[b]	4 vol[b]
25 mM 4dNTP mix[c]	0.2 mM	0.8 µl	3.2	3.2	3.2	3.2
Taq polymerase	2.5 U	0.5 µl	2.0	2.0	2.0	2.0
DMSO[d] (20×)	5%	5 µl	—	20.0	—	—
Glycerol[d] (10×)	10%	10 µl	—	—	40.0	—
PMPE[d] (100×)	1%	1 µl	—	—	—	4.0
H_2O	—	To 90 µl	To 360	To 360	To 360	To 360

[a]Total volume = 360 µl (enough for $n + 1$ reactions).

[b]Template DNA volume ("vol") is generally 1 to 10 µl.

[c]If 2 mM 4dNTP mix is preferred, use 10 µl per reaction, or 40 µl for each master mix; adjust the volume of water accordingly.

[d]Substitute with other enhancer agents (see recipe in Reagents and Solutions) as available.

Additional reagents and equipment for DNA preparation, agarose gel electrophoresis, nondenaturing PAGE, or sieving agarose gel electrophoresis, restriction endonuclease digestion, and Southern blotting and hybridization (*APPENDIX 3*)

NOTE: Do not use DEPC to treat water, reagents, or glassware.

NOTE: Reagents should be prepared in sterile, disposable labware, taken directly from its packaging, or in glassware that has been soaked in 10% bleach, thoroughly rinsed in tap water followed by distilled water, and if available, exposed to UV irradiation for ~10 min. Multiple small volumes of each reagent should be stored in screw-cap tubes. This will then serve as the user's own optimization "kit." Thin-walled PCR tubes are recommended.

Optimize reaction components

1. Prepare four reaction master mixes according to the recipes given in Table A.3C.1.

   Enhancing agents probably work by different mechanisms, such as protecting enzyme activity and decreasing nonspecific primer binding. However, their effects cannot be readily predicted—what improves amplification efficiency for one primer pair may decrease the amplification efficiency for another. Thus it is best to check a panel of enhancers during development of a new assay.

2. Aliquot 90 µl master mix I into each of three 0.5-ml thin-walled PCR tubes labeled I-L, I-M, and I-H. Similarly, aliquot mixes II through IV into appropriately labeled tubes. Add 10 µl of 15 mM $MgCl_2$ into one tube of each master mix (labeled L; 1.5 mM final). Similarly, aliquot 10 µl of 30 mM and 45 mM $MgCl_2$ to separate tubes of each master mix (labeled M and H, respectively; 3.0 and 4.5 mM final concentrations respectively).

It is helpful to set the tubes up in a three-by-four array to simplify aliquotting. Each of the three Mg^{2+} concentrations is combined with each of the four master mixes.

3. Overlay the reaction mixture with 50 to 100 µl mineral oil (2 to 3 drops).

   To include hot start in the first step, overlay reaction mixes with oil before adding the $MgCl_2$, heat the samples to 95°C in the thermal cycler or other heating block, and add the $MgCl_2$ once the elevated temperature is reached. Once the $MgCl_2$ has been added, do not allow the samples to cool below the optimum annealing temperature prior to performing PCR.

Choose cycling parameters

4. Using the following guidelines, program the automated thermal cycler according to the manufacturers' instructions.

30 cycles:	30 sec	94°C	(denaturation)
	30 sec	55° (GC content ≤50%) *or* 60°C (GC content >50%)	(annealing)
	~60 sec/kb product sequence	72°C	(extension)

   Cycling parameters are dependent upon the sequence and length of the template DNA, the sequence and percent complementarity of the primers, and the ramp times of the thermal cycler used. Thoughtful primer design will reduce potential problems (see Commentary). Denaturation, annealing, and extension are each quite rapid at the optimal temperatures. The time it takes to achieve the desired temperature inside the reaction tube, i.e., the ramp time, is usually longer than either denaturation or primer annealing. Thus, ramp time is a crucial cycling parameter. Manufacturers of the various thermal cyclers on the market provide ramp time specifications for their instruments. Ramp times are lower with thin-walled reaction tubes. The optimal extension time also depends on the length of the target sequence. Allow ~1 min/kb for this step for target sequences >1 kb, and as little as a 2-sec pause for targets <100 bases in length.

   The number of cycles depends on both the efficiency of the reaction and the amount of template DNA in the reaction. Starting with as little as 100 ng of mammalian genomic DNA (~10^4 cell equivalents), after 30 cycles, 10% of the reaction should produce a band that is readily visible on an ethidium bromide–stained gel as a single predominant band. With more template, fewer cycles may suffice. With much less template, further optimization is recommended rather than increasing the cycle number. Greater cycle numbers (e.g., >40) can reduce the polymerase specific activity, increase nonspecific amplification, and deplete substrate (nucleotides). Many investigators lengthen the time for the last extension step—to 7 min, for example—to try to ensure that all the PCR products are full length.

   These guidelines are appropriate for most commercially available thermal cyclers. For rapid cyclers, consult the manufacturers' protocols.

Analyze the product

5. Electrophorese 10 µl from each reaction on an agarose, nondenaturing polyacrylamide, or sieving agarose gel appropriate for the PCR product size expected. Stain with ethidium bromide.

   For resolution of PCR products between 100 and 1000 bp, an alternative to nondenaturing polyacrylamide gels or sieving agarose is a composite 3% (w/v) NuSieve (FMC Bioproducts) agarose/1% (w/v) SeaKem (FMC Bioproducts) agarose gel. SeaKem increases the mechanical strength of the gel without decreasing resolution.

   An alternative to ethidium bromide, SYBR Gold Nucleic Acid Gel Stain (Molecular Probes), is 25 to 100 times more sensitive than ethidium bromide, is more convenient to use, and permits optimization of 10- to 100-fold lower starting template copy number.

6. Examine the stained gel to determine which condition resulted in the greatest amount of product.

   Minor, nonspecific products may be present even under optimal conditions.

Table A.3C.2 Master Mixes for Optimizing First-Cycle Reactions

Components	Final concentration	Master mix (µl)			
		A	B	C	D
10× PCR buffer	1×	10	10	10	10
$MgCl_2$ (L, M, or H)	Optimal	10	10	10	10
Primer 1	0.5 µM	1.0	1.0	1.0	1.0
Primer 2	0.5 µM	1.0	1.0	1.0	1.0
Additive	Optimal	V[a]	V[a]	V[a]	V[a]
Template DNA	—[b]	V[a]	V[a]	V[a]	V[a]
25 mM 4dNTP mix[b]	0.2 mM	0.8	0.8	0.8	0.8
Taq polymerase	2.5 U	0.5	0.5	—	—
Taq pol + TaqStart	2.5 U	—	—	—	1.0
H_2O	To 100 µl	V[a]	V[a]	V[a]	V[a]
Preparation temperature		Room temperature	Ice slurry	Room temperature	Room temperature

[a]V, variable amount (total volume should be 100 µl).

[b]Use undiluted or diluted template DNA based on results obtained in step 6.

7. To ensure that the major product is the correct one, digest an aliquot of the reaction with a restriction endonuclease known to cut within the PCR product. Check buffer compatibility for the restriction endonuclease of choice. If necessary, add Na^+ or precipitate in ethanol (*APPENDIX 3*), then resuspend in the appropriate buffer. Electrophorese the digestion product on a gel to verify that the resulting fragments have the expected sizes.

   Alternatively, transfer the PCR products to a nitrocellulose or nylon filter and hybridize with an oligonucleotide derived from the sequence internal to the primers. With appropriately stringent hybridization and washing conditions, only the correct product (and possibly some minor related products) should hybridize.

Optimize the first cycle

These optional steps optimize initial hybridization and may improve efficiency and yield. They are used when primer-dimers and other nonspecific products are detected, when there is only a very small amount of starting template, or when a rare sequence is to be amplified from a complex mixture. For an optimal reaction, polymerization during the initial denaturation and annealing steps should be prevented. *Taq* DNA polymerase activity can be inhibited by temperature (reaction B), physical separation (reaction C), or reversible antibody binding (reaction D). PCR without hot start is performed for comparison (reaction A).

8. Prepare four reaction mixtures using the optimal $MgCl_2$ concentration and additive requirement determined in step 6. Prepare the mixes according to the recipes in Table A.3C.2. Use the following variations for addition of *Taq* polymerase.

   a. Prepare reactions A and C at room temperature.

   b. Chill all components of reaction B in an ice slurry before they are combined.

   c. For reaction D, combine 1.0 µl TaqStart antibody with 4.0 µl of the dilution buffer provided with the antibody, add 1.0 µl *Taq* DNA polymerase (for 1:4:1 mixture of these components), mix, and incubate 5 to 10 min at room temperature before adding to reaction mixture D (glycerol and PMPE are compatible with TaqStart antibody but DMSO will interfere with antibody binding).

To ensure that the reaction does not plateau and thereby obfuscate the results, use the smallest amount of template DNA necessary for visualization of the PCR product by ethidium bromide staining. Use the results from step 6 to decide how much template to use. If the desired product stains intensely, dilute the starting material as much as 1/100. If only a faint signal is apparent, use undiluted sample.

9. Overlay each reaction mixture with 50 to 100 µl mineral oil.
10. Heat all reactions 5 min at 94°C.

    It is most convenient to use the automated thermal cycler for this step and then initiate the cycling program directly.

11. Cool the reactions to the appropriate annealing temperature as determined in step 4. Add 0.5 µl *Taq* DNA polymerase to reaction C, making sure the pipet tip is inserted through the layer of mineral oil into the reaction mix.

    Time is also an important factor in this step. If the temperature drops below the annealing temperature and is allowed to remain low, nonspecific annealing will occur. Taq DNA polymerase retains some activity even at room temperature.

12. Begin amplification of all four reactions at once, using the same cycling parameters as before.
13. Analyze the PCR products on an agarose gel and evaluate the results as in steps 5 and 6.
14. Prepare a batch of the optimized reaction mixture, but omit *Taq* DNA polymerase, TaqStart antibody, PMPE, and 4dNTP mix—these ingredients should be added fresh just prior to use. If desired, add Ficoll 400 to a final concentration of 0.5% to 1% (v/v) and tartrazine to a final concentration of 1 mM.

    Adding Ficoll 400 and tartrazine dye to the reaction mix precludes the need for a gel loading buffer and permits direct application of PCR products to agarose or acrylamide gels. At these concentrations, Ficoll 400 and tartrazine do not decrease PCR efficiency and do not interfere with PMPE or TaqStart antibodies. Other dyes, such as bromphenol blue and xylene cyanol, do inhibit PCR. Tartrazine is a yellow dye and is not as easily visualized as other dyes; this may make gel loading more difficult.

    Ficoll 400 and tartrazine dye may be prepared as 10× stocks and stored indefinitely at room temperature.

REAGENTS AND SOLUTIONS

Use deionized, distilled water in all recipes and protocol steps. For common stock solutions, see ***APPENDIX 2A****; for suppliers, see* ***SUPPLIERS APPENDIX****.*

Enhancer agents

For a discussion of how to select enhancer agents, see Commentary.

5× stocks:
25% acetamide (20 µl/reaction; 5% final)
5 M *N,N,N*-trimethylglycine (betaine; 20 µl/reaction; 1 M final)
40% polyethylene glycol (PEG) 8000 (20 µl/reaction; 8% final)

10× stocks:
Glycerol (concentrated; 10 µl/reaction; 10% final)

20× stocks:
Dimethylsulfoxide (DMSO; concentrated 5 µl/reaction; 5% final)
Formamide (concentrated; 5 µl/reaction; 5% final)

100× stocks:

1 U/µl Perfect Match Polymerase Enhancer [Strategene; 1 µl (1 U) per reaction, final]

10 mg/ml acetylated bovine serum albumin (BSA) or gelatin (1 µl/reaction; 10 µg/ml final)

1 to 5 U/µl thermostable pyrophosphatase [PPase; Boehringer Mannheim; 1 µl (1 to 5 U) per reaction, final]

5 M tetramethylammonium chloride (TMAC; betaine hydrochloride; 1 µl/reaction; 50 mM final)

0.5 mg/ml *E. coli* single-stranded DNA-binding protein (SSB; Sigma; 1 µl/reaction; 5 µg/ml final)

0.5 mg/ml Gene 32 protein (Amersham Pharmacia Biotech; 1 µl/reaction; 5 µg/ml final)

10% Tween 20, Triton X-100, or Nonidet P-40 (1 µl/reaction; 0.1% final)

1 M $(NH_4)_2SO_4$ (1 µl/reaction; 10 mM final; use with thermostable DNA polymerases other than *Taq*)

$MgCl_2$-free PCR amplification buffer, 10×

500 mM KCl
100 mM Tris·Cl, pH 9.0 (at 25°C)
0.1% Triton X-100
Store indefinitely at –20°C

This buffer can be obtained from Promega; it is supplied with Taq DNA polymerase.

4dNTP mix

For 2 mM 4dNTP mix: Prepare 2 mM each dNTP in TE buffer, pH 7.5 (see recipe). Store up to 1 year at –20°C in 1-ml aliquots.

For 25 mM 4dNTP mix: Combine equal volumes of 100 mM dNTPs (Promega). Store indefinitely at –20°C in 1-ml aliquots.

TE (Tris/EDTA) buffer, pH 7.5

10 mM Tris·Cl, pH 7.5 (*APPENDIX 2A*)
1 mM EDTA, pH 8.0 (*APPENDIX 2A*)
Store up to 6 months at room temperature

COMMENTARY

Background Information

The theoretical basis of the polymerase chain reaction (PCR) was probably first described in a paper by Kleppe et al. (1971). However, this technique did not excite general interest until the mid-1980s, when Kary Mullis and co-workers at Cetus developed PCR into a technique that could be used to generate large amounts of single-copy genes from genomic DNA (Saiki et al., 1985, 1986; Mullis et al., 1986; Embury et al., 1987).

The initial procedure entailed adding a fresh aliquot of the Klenow fragment of *E. coli* DNA polymerase I during each cycle because this enzyme was inactivated during the subsequent denaturation step. The introduction of thermostable *Taq* DNA polymerase from *Thermus aquaticus* (Saiki et al., 1988) alleviated this tedium and facilitated automation of the thermal cycling portion of the procedure. *Taq* DNA polymerase also permitted the use of higher temperatures for annealing and extension, which improved the stringency of primer–template hybridization and thus the specificity of the products. This also served to increase the yield of the desired product.

All applications for PCR depend upon an optimized PCR. The basic protocol in this unit optimizes PCR for several variables, including $MgCl_2$ concentration, enhancing additives—dimethyl sulfoxide (DMSO), glycerol, or Perfect Match Polymerase Enchancer (PMPE)—and prevention of pre-PCR mispriming. These and other parameters can be extremely important, as every element of PCR can affect the outcome; see Critical Parameters and Trou-

bleshooting for discussion of individual parameters.

There are several PCR optimization kits and proprietary enhancers on the market (Table A.3C.3). Optimization kits generally provide a panel of buffers in which the pH, buffer, nonionic detergents, and addition of $(NH_4)_2SO_4$ are varied, $MgCl_2$ may be added at several concentrations, and enhancers (e.g., DMSO, glycerol, formamide, betaine, and/or proprietary compounds) may be chosen. The protocol presented here is aimed at keeping the costs low and the options broad.

Critical Parameters and Troubleshooting

$MgCl_2$ concentration

Determining the optimum $MgCl_2$ concentration, which can vary even for different primers from the same region of a given template (Saiki, 1989), can have an enormous influence on PCR success. In this protocol three test concentrations are suggested—1.5 mM (L), 3.0 mM (M), and 4.5 mM (H). If further optimization is necessary, the $MgCl_2$ range can be extended or narrowed around the most successful concentration.

A 10× buffer optimized for a given enzyme and a separate vial of $MgCl_2$ are typically provided with the polymerase, so that the user may titrate the $MgCl_2$ concentration for their unique primer-template set. Note that some enhancers may broaden the $MgCl_2$ optimal range.

Reagent purity

For applications that amplify rare templates, reagent purity is the most important parameter, and avoiding contamination at every step is critical.

To maintain purity, store multiple small volumes of each reagent in screw-cap tubes.

For many applications, simply using high-quality reagents and avoiding nuclease contamination is sufficient. However, avoid one common reagent used to inactivate nucleases—diethylpyrocarbonate (DEPC). Even the tiny amounts of chemical left after treatment of water and autoclaving are enough to ruin a PCR.

Primer selection

This is the factor that is least predictable and most difficult to troubleshoot. Simply put, some primers just do not work. To maximize the probability that a given primer pair will work, pay attention to the following parameters.

General considerations. An optimal primer set should hybridize efficiently to the sequence of interest with negligible hybridization to other sequences present in the sample. If there are reasonable amounts of template available, hybridization specificity can be tested by performing oligonucleotide hybridization. The distance between the primers is rather flexible, ranging up to 10 kb. There is, however, a considerable drop-off in synthesis efficiency with distances >3 kb (Jeffreys et al., 1988). Small distances between primers, however, lessen the ability to obtain much sequence information or to reamplify with nested internal oligonucleotides, should that be necessary.

Design primers to allow demonstration of the specificity of the PCR product. Be sure that there are diagnostic restriction endonuclease sites between the primers or that an oligonucleotide can detect the PCR product specifically by hybridization.

Several computer programs can assist in primer design. These are most useful for avoiding primer sets with intra- and intermolecular complementarity, which can dramatically raise the effective melting temperature (T_m). Given the abundance of primers relative to template, this can preclude template priming. Computer primer design is not foolproof. If possible, start with a primer or primer set known to efficiently prime extensions. In addition, manufacturers' Web sites offer technical help with primer design.

Complementarity to template. For many applications, primers are designed to be exactly complementary to the template. For others, however, such as engineering of mutations or new restriction endonuclease sites (*UNIT 8.5*), or for efforts to clone or detect gene homologs where sequence information is lacking, base-pair mismatches will be intentionally or unavoidably created. It is best to have mismatches (e.g., in a restriction endonuclease linker) at the 5′ end of the primer. The closer a mismatch is to the 3′ end of the primer, the more likely it is to prevent extension. If cloned template is available, primers can be checked for suitability by using them in a sequencing reaction with *Taq* DNA polymerase.

The use of degenerate oligonucleotide primers to clone genes where only protein sequence is available, or to fish out gene homologs in other species, has sometimes been successful—but it has also failed an untold (and unpublished) number of times. When the reaction works it can be extremely valuable, but it can

Table A.3C.3 PCR Optimization Products

Optimization goal	Supplier	Product
Optimization support	PE Biosystems	Technical information in appendix to catalog
Optimization support	Promega	PCR troubleshooting program on the Internet: *http://www.promega.com/amplification/assistant*
Optimization kits	Boehringer Mannheim, Invitrogen, Stratagene, Sigma, Epicentre Technologies, Life Technologies	Several buffers, Mg^{2+}, and enhancers which may include DMSO, glycerol, formamide, $(NH_4)_2SO_4$, and other unspecified or proprietary agents
Quick startup	Amersham Pharmacia Biotech	Ready-To-Go Beads "optimized for standard PCR" and Ready-To-Go RAPD Analysis Beads (buffer, nucleotides, *Taq* DNA polymerase)
Quick startup	Fisher	EasyStart PCR Mix-in-a-Tube—tubes prepackaged with wax beads containing buffer, $MgCl_2$, nucleotides, *Taq* DNA polymerase
Quick startup	Life Technologies	PCR SuperMix—1.1× conc.—premix containing buffer, $MgCl_2$, nucleotides, *Taq* DNA polymerase
Quick startup	Marsh Biomedical	Advanced Biochemicals Red Hot DNA Polymerase—a new rival for *Taq* polymerase with convenience features
Hot-start/physical barrier	Fisher, Life Technologies	Molecular Bio-Products HotStart Storage and Reaction Tubes—preadhered wax bead in each tube; requires manual addition of one component at high temperature
Hot-start/separate $MgCl_2$	Invitrogen	HotWax Mg^{2+} beads—wax beads contain preformulated $MgCl_2$ which is released at first elevated-temperature step
Hot-start/separate $MgCl_2$	Stratagene	StrataSphere Magnesium Wax Beads—wax beads containing preformulated Mg^{2+}
Hot Start/separate polymerase	Promega	TaqBead Hot Start Polymerase—wax beads encapsulating *Taq* DNA polymerase which is released at first elevated-temperature step
Hot-start/reversible inactivation of polymerase by antibody binding	Clontech	TaqStart Antibody, TthStart Antibody—reversibly inactivate *Taq* and *Tth* DNA polymerases until first denaturation at 95°C
Hot-start/antibody binding	Life Technologies	PlatinumTaq—contains PlatinumTaq antibody
Hot-start/antibody binding	Sigma	JumpStart Taq—contains TaqStart antibody
Hot-start/reversible chemical modification	PE Biosystems	AmpliTaq Gold—activated at high temperature
Hot-start/reversible chemical modification	Qiagen	HotStarTaq DNA Polymerase—activated at high temperature
Enhancer	Boehringer Mannheim, New England Biolabs	*Tth* pyrophosphatase, thermostable
Enhancer	Clontech	GC-Melt (in Advantage-GC Kits)—proprietary
Enhancer	CPG	Taq-FORCE Amplification System and MIGHTY Buffer—proprietary
Enhancer	Fisher	Eppendorf MasterTaq Kit with TaqMaster Enhancer—proprietary
Enhancer	Life Technologies	PCRx Enhancer System—proprietary
Enhancer	Promega	*E.coli* Single Stranded Binding Protein (SSB)
Enhancer	Qiagen	Q-Solution—proprietary
Enhancer	Stratagene	Perfect Match Polymerase Enhancer—proprietary
Enhancer	Stratagene	TaqExtender PCR Additive—proprietary

also generate seemingly specific products that require much labor to identify and yield no useful information. The less degenerate the oligonucleotides, especially at the 3′ end, the better. Caveat emptor.

Primer length. A primer should be 20 to 30 bases in length. It is unlikely that longer primers will help increase specificity significantly.

Primer sequence. Design primers with a GC content similar to that of the template. Avoid primers with unusual sequence distributions, such as stretches of polypurines or polypyrimidines as their secondary structure can be disastrous. It is worthwhile to check for potential secondary structure using one of the appropriate computer programs that are available.

"Primer-dimers." Primer-dimers are a common artifact most frequently observed when small amounts of template are taken through many amplification cycles. They form when the 3′ end of one primer anneals to the 3′ end of the other primer, and polymerase then extends each primer to the end of the other. The ensuing product can compete very effectively against the PCR product of interest. Primer-dimers can best be avoided by using primers without complementarity, especially in their 3′ ends. Should they occur, optimizing the $MgCl_2$ concentration may minimize their abundance relative to that of the product of interest.

Template

Aside from standard methods for preparing DNA (*APPENDIX 3*), a number of simple and rapid procedures have been developed for particular tissues (Higuchi, 1989). Even relatively degraded DNA preparations can serve as useful templates for generation of moderate-sized PCR products. The two main concerns regarding template are purity and amount.

A number of contaminants found in DNA preparations can decrease the efficiency of PCR. These include urea, the detergent SDS (whose inhibitory action can be reversed by nonionic detergents), sodium acetate, and, sometimes, components carried over in purifying DNA from agarose gels (Gelfand, 1989; Gyllensten, 1989; K. Hicks and D. Coen, unpub. observ.). Additional organic extractions, ethanol precipitation from 2.5 M ammonium acetate, and/or gel purification on polyacrylamide rather than agarose, can all be beneficial in minimizing such contamination if the simplest method (precipitating the sample with ethanol and repeatedly washing the pellet with 70% ethanol) is not sufficient.

Clearly the amount of template must be sufficient to be able to visualize PCR products using ethidium bromide. Usually 100 ng of genomic DNA is sufficient to detect a PCR product from a single-copy mammalian gene. Using too much template is not advisable when optimizing for $MgCl_2$ or other parameters, as it may obscure differences in amplification efficiency. Moreover, too much template may decrease efficiency due to contaminants in the DNA preparation.

Amount of template, especially in terms of the amount of target sequence versus nonspecific sequences, can have a major effect on the yield of nonspecific products. With less target sequence, it is more likely that nonspecific products will be seen. For some applications, such as certain DNA sequencing protocols where it is important to have a single product, gel purification of the specific PCR product and reamplification are advisable.

Taq and other thermostable DNA polymerases

Among the advantages conferred by the thermostability of *Taq* DNA polymerase is its ability to withstand the repeated heating and cooling inherent in PCR and to synthesize DNA at high temperatures that melt out mismatched primers and regions of local secondary structure. The enzyme, however, is not infinitely resistant to heat, and for greatest efficiency it should not be put through unnecessary denaturation steps. Indeed, some protocols (e.g., the "hot start" method described here) recommend adding it after the first denaturation step.

Increasing the amount of *Taq* DNA polymerase beyond 2.5 U/reaction can sometimes increase PCR efficiency, but only up to a point. Adding more enzyme can sometimes increase the yield of nonspecific PCR products at the expense of the product of interest. Moreover, *Taq* DNA polymerase is not inexpensive.

A very important property of *Taq* DNA polymerase is its error rate, which was initially estimated at 2×10^{-4} nucleotides/cycle (Saiki et al., 1988). The purified enzyme supplied by manufacturers lacks a proofreading 3′→5′ exonuclease activity, which lowers error rates of other polymerases such as the Klenow fragment of *E. coli* DNA polymerase I. For many applications, this does not present any difficulties. However, for sequencing clones derived from PCR, or when starting with very few templates, this can lead to major problems. Direct sequencing of PCR products, sequencing numerous PCR-generated clones, and/or

the use of appropriate negative controls can help overcome these problems. Alternatively, changing reaction conditions (Eckert and Kunkel, 1990) or changing to a non–*Taq* DNA polymerase (with greater fidelity) may be useful.

Another important property of *Taq* DNA polymerase is its propensity for adding nontemplated nucleotides to the 3′ ends of DNA chains. This can be especially problematic in cloning PCR products. It is frequently necessary to "polish" PCR products with enzymes such as other DNA polymerases before adding linkers or proceeding to blunt-end cloning. Conversely, addition of a nontemplated A by *Taq* DNA polymerase can be advantageous in cloning.

Table A.3C.4 lists currently available thermostable DNA polymerases by generic and trade names, the original source of native and recombinant enzymes, the supplier, the end generated (3′A addition versus blunt), and associated exonuclease activities. A 3′ to 5′ exonuclease activity is proofreading. Removal of the 5′ to 3′ exonuclease activity of *Taq* DNA polymerase (N-terminal deletion) is reported to produce a higher yield. A 5′ to 3′ exonuclease activity may degrade the primers somewhat. Proofreading enzymes synthesize DNA with higher fidelity and can generate longer products than *Taq*, but tend to generate low yields. Enzyme blends (Table A.3C.5) have been optimized for increased fidelity and length along with sensitivity and yield.

Hot start

What happens prior to thermal cycling is critical to the success of PCR. *Taq* DNA polymerase retains some activity even at room temperature. Therefore, under nonstringent annealing conditions, such as at room temperature, products can be generated from annealing of primers to target DNA at locations of low complementarity or having complementarity of just a few nucleotides at the 3′ ends. The latter would in effect create new templates "tagged" with the primer sequences. Subsequent cycles amplify these tagged sequences in abundance, both generating nonspecific products and possibly reducing amplification efficiency of specific products by competition for substrates or polymerase. Thus conditions preventing polymerization prior to the first temperature-controlled steps are desirable. In this protocol, three methods of inhibiting polymerization prior to the temperature-controlled step are compared. These include physical separation of an essential reaction component prior to the first denaturation step, cooling reagents to 0°C, and reversibly blocking enzymatic activity with an antibody.

Denaturation of the template before *Taq* polymerase or $MgCl_2$ is added to the reaction provides a dramatic improvement in specificity and sensitivity in many cases (Chou et al., 1992). The main drawback of this method is that it requires opening the reaction tubes a second time to add the essential missing component. This creates both an inconvenience and an increase in the risk of contamination, an important consideration when testing for the presence of a given sequence in experimental or clinical samples.

Cooling all components of the reaction mixture to 0°C prior to mixing is more convenient and the least expensive method but is also the least reliable. Transferring the PCR reaction tubes from the ice slurry to a 95°C preheated thermocycler block may improve the chance of success.

Reversible inhibition of *Taq* DNA polymerase by TaqStart antibody (Clontech) is the most convenient and is very effective (Kellogg et al., 1994). Complete reactions can be set up, overlaid with oil, and stored at 4°C for up to several hours prior to thermal cycling with no loss of sensitivity or specificity compared to the other hot-start methods (M.F.K. and D.M.C., unpub. observ.). Cycling is initiated immediately following 5-min denaturation of the antibody at 94°C. DMSO inhibits antibody binding and should not be used with TaqStart.

Several hot-start products are now commercially available (Table A.3C.3). Success with each may depend on strict adherence to the manufacturer's protocols, even on a specific thermocycler. Wax barrier and reversible antibody binding methods are more forgiving, while chemical modifications have more stringent activation temperature requirements.

Deoxyribonucleoside triphosphates

In an effort to increase efficiency of PCR, it may be tempting to increase the concentration of dNTPs. Don't. When each dNTP is 200 μM, there is enough to synthesize 12.5 μg of DNA when half the dNTPs are incorporated. dNTPs chelate magnesium and thereby change the effective optimal magnesium concentration. Moreover, dNTP concentrations >200 μM each increase the error rate of the polymerase. Millimolar concentrations of dNTPs actually inhibit *Taq* DNA polymerase (Gelfand, 1989).

Table A.3C.4 Thermostable DNA Polymerases

DNA polymerase		Biological source	Supplier	Product ends	Exonuclease activity
Generic name	Trade name				
Pfu	—	*Pyrococcus furiosus*	Stratagene, Promega	Blunt	3′-5′ (proofreading)
Pfu (exo-)	—	*Pyrococcus furiosus*	Stratagene	Blunt	No
Psp	Deep Vent	*Pyrococcus* sp.GB-D	New England Biolabs	Blunt	3′-5′ (proofreading)
Psp (exo-)	Deep Vent (exo-)	*Pyrococcus* sp.GB-D	New England Biolabs	Blunt	No
Pwo		*Pyrococcus woesei*	Boehringer Mannheim	Blunt	3′-5′ (proofreading)
Taq (native and/or recombinant)	—	*Thermus aquaticus*	Ambion, Amersham Pharmacia Biotech, Boehringer Mannheim, Clontech, Fisher, Life Technologies, Marsh Biomedical, PE Biosystems, Promega, Qiagen, Sigma, Stratagene	3′A	5′-3′
Taq, N-terminal deletion	Stoffel fragment Klen-Taq	*Thermus aquaticus*	PE Biosystems, Sigma	3′A	No
Tbr	DyNAzyme	*Thermus brocianus*	MJ Research	—[a]	5′-3′
Tfl		*Thermus flavus*	Promega, Epicentre Technologies	Blunt	—[a]
Tli	Vent	*Thermococcus litoralis*	New England Biolabs (Vent), Promega	Blunt	3′-5′ (proofreading)
Tli (exo-)	Vent (exo-)	*Thermococcus litoralis*	New England Biolabs	Blunt	No
Tma	UlTma	*Thermotoga maritima*	PE Biosystems	Blunt	3′-5′ (proofreading)
Tth	—	*Thermus thermophilus*	Amersham Pharmacia Biotech, Boehringer Mannheim, Epicentre Technologies, PE Biosystems, Promega	3′ A	5′-3′

[a]No information at this time.

The protocol in this unit calls for preparing 4dNTPs in 10 mM Tris·Cl/1 mM EDTA (TE buffer), pH 7.4 to 7.5. This is easier and less prone to disaster than neutralization with sodium hydroxide. However, EDTA also chelates magnesium, and this should be taken into account if stocks of dNTPs are changed. Alternatively, to lower the risk of contamination, a 4dNTP mix can be made by combining equal volumes of commercially prepared stocks.

Enhancers

Enhancers are used to increase yield and specificity and to overcome difficulties encountered with high GC content or long templates. Nonionic detergents (Triton X-100, Tween 20, or Nonidet P-40) neutralize charges of ionic detergents often used in template preparation, and should be used in the basic reaction mixture, rather than as optional enhancers. Higher yields can be achieved by stabilizing/enhancing the polymerase activity with enzyme-stabilizing proteins (BSA or gelatin), enzyme-stabilizing solutes such as betaine or betaine·HCl (TMAC), enzyme-stabilizing solvents (glycerol), solubility-enhancing solvents (DMSO or acetamide), molecular crowding solvents (PEG), and polymerase salt preferences [$(NH_4)SO_4$ is recommended for polymerases other than *Taq*]. Greater specificity can be achieved by lowering the T_M of dsDNA (using formamide), destabilizing mismatched-primer annealing (using PMPE or hot-start strategies), and stabilizing ssDNA (using *E.*

Table A.3C.5 Thermostable DNA Polymerase Blends

Product (trade name)	Supplier	Thermostable DNA polymerases and other components
Expand High Fidelity, Expand Long Template, and Expand 20kb PCR Systems	Boehringer Mannheim	*Taq* + *Pwo*
KlenTaq LA Polymerase Mix	Clontech, Sigma	KlenTaq-1 (5′-exonuclease deficient *Taq*) + unspecified proofreading polymerase
Advantage-HF PCR Kit	Clontech	KlenTaq-1 + unspecified proofreading polymerase + TaqStart Antibody
Advantage-cDNA and Advantage-GC cDNA Polymerase Mixes and Kits	Clontech	KlenTaq-1 + unspecified proofreading polymerase + TaqStart Antibody; GC Kit contains GC Melt
Advantage Genomic and Advantage-GC Genomic Polymerase Mixes and Kits	Clontech	*Tth* + unspecified proofreading polymerase + TthStart Antibody; GC Kit contains GC Melt
eLONGase Enzyme Mix	Life Technologies	*Taq* + *Psp* + unspecified proofreading polymerase(s) + eLONGase Buffer
Platinum Taq DNA Polymerase	Life Technologies	*Taq* + *Psp* + Platinum *Taq* Antibody
Platinum High Fidelity DNA Polymerase	Life Technologies	*Taq* + *Psp* + *Taq* Antibody
DyNAzyme EXT Polymerase	MJ Research	*Tbr* with unspecified enhancer
GeneAmp XL PCR and XL RNA PCR Kits	PE Biosystems	*Tth* + *Tli*
OmniBase Sequencing Enzyme Mix	Promega	Unspecified proofreading polymerase(s) with thermostable pyrophosphatase
AccuTaq LA DNA Polymerase Mix	Sigma	*Taq* + unspecified proofreading polymerase
TaqPlus Long and TaqPlus Precision PCR Systems	Stratagene	*Pfu* + *Taq*; TaqPlus Precision Reaction Buffer (proprietary)
Accurase Fidelity PCR Enzyme Mix; Calypso High Fidelity Single Tube RT-PCR System	Tetralink	*Thermus sp*. + *Thermococcus sp*.; Calypso also contains AMV-RT

coli SSB or Gene 32 Protein). Amplification of high-GC-content templates can be improved by decreasing the base pair composition dependence of the T_M of dsDNA (with betaine; Rees et al., 1993). Betaine is an osmolyte widely distributed in plants and animals and is nontoxic, a feature that recommends it for convenience in handling, storage, and disposal. Betaine may be the proprietary ingredient in various commercial formulations. For long templates, a higher pH is recommended (pH 9.0). The pH of Tris buffer decreases at high temperatures, long-template PCR requires more time at high temperatures, and increased time at lower pH may cause some depurination of the template, resulting in reduced yield of specific product. Inorganic phosphate (PPi), a product of DNA synthesis, may accumulate with amplification of long products to levels that may favor reversal of polymerization. Accumulation of PPi may be prevented by addition of thermostable PPase. When large numbers of samples are being analyzed, the convenience of adding PCR products directly to a gel represents a significant time savings. Some companies combine their thermostable polymerase with a red dye and a high density component to facilitate loading of reaction products onto gels without further addition of loading buffer.

Thermal cycling parameters

Each step in the cycle requires a minimal amount of time to be effective, while too much time can be both wasteful and deleterious to the DNA polymerase. If the amount of time in each step can be reduced, so much the better.

Denaturation. It is critical that complete strand separation occur during the denaturation step. This is a unimolecular reaction which, in itself, is very fast. The suggested 30-sec denaturation used in the protocol ensures that the tube

contents reach 94°C. If PCR is not working, it is well worth checking the temperature inside a control tube containing 100 µl water. If GC content is extremely high, higher denaturation temperatures may be necessary; however, *Taq* DNA polymerase activity falls off quickly at higher temperatures (Gelfand, 1989). To amplify a long sequence (>3 kb), minimize the denaturation time to protect the target DNA from possible effects, such as depurination, of lowered pH of the Tris buffer at elevated temperatures.

Annealing. It is critical that the primers anneal stably to the template. Primers with relatively low GC content (<50%) may require temperatures lower than 55°C for full annealing. On the other hand, this may also increase the quantity of nonspecific products. For primers with high GC content, higher annealing temperatures may be necessary. It can be worthwhile, although time-consuming, to experiment with this parameter. Two manufacturers have thermal cyclers on the market which are capable of forming a temperature gradient across the heating units, thus permitting annealing temperature optimization in one run. These are Stratagene's Robocyclers, and Eppendorf's Master Cycler. As with denaturation, the time for this step is based mainly on the time it takes to reach the proper temperature, because the primers are in such excess that the annealing reaction occurs very quickly.

Extension. The extension temperature of 72°C is close to the optimal temperature for *Taq* DNA polymerase (~75°C), yet prevents the primers from falling off. Indeed, primer extension begins during annealing, because *Taq* DNA polymerase is partially active at 55°C and even lower temperatures (Gelfand, 1989).

The duration of extension depends mainly on the length of the sequence to be amplified. A duration of 1 min per kb product length is usually sufficient.

Certain protocols end the PCR with a long final extension time in an attempt to try to make products as complete as possible.

Ramp time. Ramp time refers to the time it takes to change from one temperature to another. Using water baths and moving samples manually from temperature to temperature probably gives the shortest ramp times, which are mainly the time required for the tube's contents to change temperature. Different thermal cyclers have different ramp times; basically, the shorter the better.

The Stratagene Robocycler uses a robotic arm to move samples from one constant-temperature block to another, virtually eliminating ramp time. Rapid cyclers utilize positive-displacement pipet tips or capillary tubes for the PCR reactions, dramatically reducing the ramp times.

Generally, the more "high-performance" thermal cyclers with short ramp times are proportionally more costly. There are many new thermal cyclers on the market priced below $5000, which perform quite well (Beck, 1998).

Anticipated Results

Starting with ≥100 ng mammalian DNA (≥10^4 molecules), the basic protocol can be used to determine which $MgCl_2$ concentration, enhancing additive, and initial conditions will yield a predominant PCR product from a single-copy sequence that is readily visible on an ethidium bromide–stained gel. It is possible that other minor products will also be visible.

Time Considerations

The basic protocol can be completed in a single day. Assembly of the reaction mixtures should take ~1 hr. Cycling should take less than 3 hr. Preparing, running, and staining the gel should take another few hours. Further checks on specificity of the product such as restriction endonuclease digestion or Southern blot hybridization will take another few hours or days, respectively.

Literature Cited

Beck, S. 1998. How low can you go? Nineteen thermal cyclers priced under $5000. *The Scientist* 12:19-20.

Chou, Q., Russell, M., Birch, D.E., Raymond, J., and Bloch, W. 1992. Prevention of pre-PCR mispriming and primer dimerization improves low-copy-number amplifications. *Nucl. Acids Res.* 20:1717-1723.

Eckert, K.A. and Kunkel, T.A. 1990. High fidelity DNA synthesis by the *Thermus aquaticus* DNA polymerase. *Nucl. Acids Res.* 18:3739-3752.

Embury, S.H., Scharf, S.J., Saiki, R.K., Gholson, M.A., Golbus, M., Arnheim, N., and Erlich, H.A. 1987. Rapid prenatal diagnosis of sickle cell anemia by a new method of DNA analysis. *N. Engl. J. Med.* 316:656-661.

Gelfand, D.H. 1989. *Taq* DNA polymerase. *In* PCR Technology: Principles and Applications for DNA Amplification (H.A. Erlich, ed.) pp. 17-22. Stockton Press, New York.

Gyllensten, U. 1989. Direct sequencing of in vitro amplified DNA. *In* PCR Technology: Principles and Applications for DNA Amplification (H.A. Erlich, ed.) pp. 45-60. Stockton Press, New York.

Higuchi, R. 1989. Simple and rapid preparation of samples for PCR. *In* PCR Technology: Princi-

ples and Applications for DNA Amplification (H.A. Erlich, ed.) pp. 31-38. Stockton Press, New York.

Jeffreys, A.J., Wilson, V., Neumann, R., and Keyte, J. 1988. Amplification of human minisatellites by the polymerase chain reaction: Towards DNA fingerprinting of single cells. *Nucl. Acids Res.* 16:10,953-10,971.

Kellogg, D.E., Rybalkin, I., Chen, S., Mukhamedova, N., Vlasik, T., Siebert, P.D., and Chencik, A. 1994. TaqStart antibody: "Hot start" PCR facilitated by a neutralizing monoclonal antibody directed against *Taq* DNA polymerase. *BioTechniques* 16:1134-1137.

Kleppe, K., Ohtsuka, E., Kleppe, R., Molineux, I., and Khorana, H.G. 1971. Studies on polynucleotides. XCVI. Repair replication of short synthetic DNA's as catalyzed by DNA polymerases. *J. Mol. Biol.* 56:341-361.

Mullis, K.B., Faloona, F., Scharf, S.J., Saiki, R.K., Horn, G.T., and Erlich, H.A. 1986. Specific enzymatic amplification of DNA in vitro: The polymerase chain reaction. *Cold Spring Harbor Symp. Quant. Biol.* 51:263-273.

Rees, W.A., Yager, T.D., Korte, J., and von Hippel, P.H. 1993. Betaine can eliminate the base pair composition dependence of DNA melting. *Biochemistry* 32:137-144.

Saiki, R.K. 1989. The design and optimization of the PCR. *In* PCR Technology: Principles and Applications for DNA Amplification (H.A. Erlich, ed.) pp. 7-16. Stockton Press, New York.

Saiki, R.K., Scharf, S., Faloona, F., Mullis, K., Horn, G., Erlich, H.A., and Arnheim, N. 1985. Enzymatic amplification of β-globin genomic sequences and restriction site analysis for diagnosis of sickle cell anemia. *Science* 230:1350-1354.

Saiki, R.K., Bugawan, T.L., Horn, G.T., Mullis, K.B., and Erlich, H.A. 1986. Analysis of enzymatically amplified β-globin and HLA-DQα DNA with allele-specific oligonucleotide probes. *Nature* 324:163-166.

Saiki, R.K., Gelfand, D.H., Stoffel, S., Scharf, S.J., Higuchi, R., Horn, G.T., Mullis, K.B., and Erlich, H.A. 1988. Primer-directed enzymatic amplification of DNA with a thermostable DNA polymerase. *Science* 239:487-491.

Key Reference

Saiki et al., 1988. See above.

Demonstrates the ease and power of PCR using Taq DNA polymerase.

Internet Resources

http://www.pebio.com

http://www.promega.com

http://www.stratagene.com

Most companies can be accessed at "http://company-name.com". Many such company Web sites provide protocols, information on primer design, and other PCR assistance.

Contributed by Martha F. Kramer and Donald M. Coen
Harvard Medical School
Boston, Massachusetts

Detection and Quantitation of Radiolabeled Proteins in Gels and Blots

This unit presents procedures for visualizing and quantitating radiolabeled proteins separated by sodium dodecyl sulfate–polyacrylamide gel electrophoresis or affixed to filter membranes. Autoradiography (see Basic Protocol) is the most common method by which this is accomplished, and X-ray film is the traditional recording medium. The use of autoradiography with gels requires that the gel be dried prior to being placed in contact with the film (see Support Protocol 1). The decay of radioactive materials within the dried gel or filter leaves an image on the film that reflects its distribution in the sample. Film images can be quantified by densitometry (see Support Protocol 4) to obtain a relative measure of the amount of radioactivity in the sample.

The use of X-ray films for autoradiography, however, suffers from two drawbacks: lack of sensitivity and a limited linear range over which the image density reflects the amount of radioactivity. Lack of sensitivity can be overcome by fluorography (see Alternate Protocol 1) or by the use of intensifying screens (see Support Protocol 2), both of which enhance the radioactive signal. Ensuring that the exposure is within a linear range requires careful controls; film is often preflashed (see Support Protocol 3) to increase the linear measurement range for weakly radioactive samples, and it is important to ensure that the film not be saturated to attain strong radioactive signals. Sensitivity and linear ranges of measurement can be greatly extended by using a phosphor imaging system (see Alternate Protocol 2). Phosphor imaging also makes it much faster and easier to quantify radioactive samples.

To enhance radioactive signals, solid-state scintillation is frequently employed to convert the energy released by radioactive molecules to visible light. This is accomplished in several different ways. In fluorography (see Alternate Protocol 1) organic scintillants are incorporated into the sample to increase the proportion of emitted energy detected from low-energy β particles (e.g., from ^{3}H, ^{14}C, and ^{35}S). Another method uses high-density, fluorescent "intensifying screens" (see Support Protocol 2), which are placed next to the sample and used to capture the excess energy of γ rays (e.g., those produced by ^{125}I) and high-energy β particles (e.g., from ^{32}P).

CAUTION: When working with radioactivity, take appropriate precautions to avoid contamination of the experimenter and the surroundings. Carry out the experiment and dispose of wastes in appropriately designated areas, following the guidelines provided by your local radiation safety officer (also see *APPENDIX 1A*).

AUTORADIOGRAPHY

BASIC PROTOCOL

Autoradiography uses X-ray film to visualize and quantitate radioactive molecules that have been electrophoresed through agarose or polyacrylamide gels, hybridized to filters, or chromatographed through paper or thin-layer plates. A photon of light or the β particles and γ rays released from radioactive molecules "activate" silver bromide crystals on the film emulsion. This renders them capable of being reduced through the developing process to form silver metal (a "grain"). The silver grains on the film form the image.

The choice of film is critical for autoradiography. Double-coated films (e.g., Kodak X-Omat AR and Fuji RX) contain two emulsion layers on either side of a polyester support and are most commonly used for autoradiography (Laskey and Mills, 1977). Double-coated films are ideal for detecting the high-energy β particles emitted by ^{32}P and ^{125}I, since they can penetrate the polyester support and expose both emulsion layers. These

Contributed by Daniel Voytas and Ning Ke
Current Protocols in Toxicology (2001) A.3D.1-A.3D.10

films are normally used with calcium tungstate ($CaWO_4$) intensifying screens at reduced temperature (−70°C); they are highly sensitive to the blue light emitted by these screens. The green-light-sensitive BioMax MS film (Kodak) is a double-coated film spectrally matched to the blue- and green-light-emitting BioMax MS intensifying screen. The BioMax MS film/BioMax MS intensifying screen system normally gives greatest sensitivity to ^{32}P (four times greater than that of X-Omat AR film with $CaWO_4$ screens).

Single-coated films, containing one emulsion layer (e.g., Kodak BioMax MR), are optimized for direct-exposure techniques with medium-energy radioisotopes (e.g., ^{14}C, ^{35}S, and ^{33}P, but not ^{3}H). The majority of the β particles emitted by these isotopes cannot pass through the polyester support of double-coated films, and therefore the emulsion layer on the other side of the film is useless. Even though direct exposure with single-coated films gives better clarity for medium-energy isotopes, single-coated films often require longer exposure times. Fluorography, therefore, is often used to enhance sensitivity. The blue-light-sensitive double-coated X-Omat AR film is generally used for fluorography with 2,5-diphenyloxazole (PPO; which emits at 388 nm), sodium salicylate (which emits at 420 nm), and commercial fluorographic solutions and sprays (e.g., from Amersham and DuPont NEN; which emit light in the blue end of the spectrum).

Materials

Fixed and dried gel (see Support Protocol 1) or filter
Developer: Kodak developer and replenisher, prepared according to the manufacturer's instructions, 18° to 20°C
Fixer: Kodak fixer and replenisher, prepared according to the manufacturer's instructions, 18° to 20°C

Metal film cassette or paper film cassette with particle-board supports and metal binder clips
Plastic wrap (e.g., Saran Wrap)
X-ray film
Trays to hold film processing solutions
Clips for hanging film

1. In a darkroom illuminated with a safelight, place the sample (e.g., dried gel or filter) in the film cassette. Cover the sample with plastic wrap to prevent it from sticking to the film and contaminating the cassette with radioactivity.

   The safelight should be a bulb of <15 W that is equipped with a Kodak GBX-2 red filter (or equivalent).

   Fluorescent glow-in-the-dark ink (available at craft stores) is a convenient way to mark samples exposed to film. The ink can be spread on adhesive labels, which in turn are placed on the plastic wrap around the edge of the sample. If exposed to light prior to autoradiography, the ink will fluoresce and expose the film, making it possible to orient the film image on the dried gel after developing.

2. Place a sheet of X-ray film on top of the sample, then close and secure the film cassette (see Fig. A.3D.1).

   If preflashed film is used for direct exposure (see Support Protocol 3), the exposed side should face the sample. Preflashed film should be used if sample is weakly radioactive or if quantitation of the radioactivity is desired. For single-coated film, the emulsion layer should face the sample.

   If a paper cassette is used, particle-board supports the same size as the cassette should be placed on either side and secured with the metal binder clips. This will ensure that the sample and film are held in contact and do not shift during exposure.

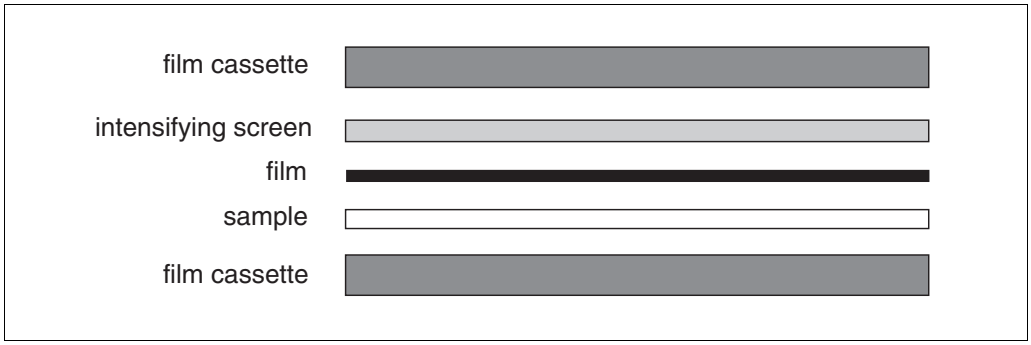

Figure A.3D.1 Autoradiography setup: intensifying screen, film, and sample in film cassette.

3. Expose the film for the desired length of time and at the appropriate temperature.

   Time of exposure will depend on the strength of the radioactivity in the sample and, in most cases, will have to be determined empirically by making multiple exposures for different lengths of time. To help estimate exposure time, a Geiger counter can often be used to detect the relative amount of radioactivity in the sample. With experience, this can help alleviate the trial and error often associated with obtaining the optimum exposure. Time of exposure and use of internal controls are particularly important if quantitative comparisons between experiments are desired.

4. After exposure, return cassette to the darkroom and remove film for developing.

   If the film was exposed at −70°C, allow the cassette to come to room temperature before developing. This will avoid static discharge, which can cause black dots or stripes on the autoradiogram.

   Automated film developers are also available and can be used to develop the film.

5. Immerse the film for 5 min in 18° to 20°C developer, then wash 1 min in running water at room temperature.

   Shorter periods of time in developer will yield a lighter image. The amount of time in developer, therefore, can be used to roughly control intensity of the image.

6. Immerse the film for 5 min in 18° to 20°C fixer, then wash for 15 min in running water.

7. Hang the film to dry.

   The orientation of the film with respect to the gel can be determined by the images of the fluorescent markers.

FIXING AND DRYING GELS FOR AUTORADIOGRAPHY

SUPPORT PROTOCOL 1

SDS-PAGE gels containing radiolabeled proteins should be fixed and dried before exposure to film. This will prevent the gel from sticking to the film, improve the sharpness of the image, and increase sensitivity slightly. However, if the specific activity of the sample is high or the detection method is sensitive (e.g., where a phosphor imager is used; see Alternate Protocol 2), then fixing and drying the gel may not be necessary. Gel dryers are available from a number of manufacturers (e.g., Bio-Rad), most of which use heat and a vacuum to accelerate the drying process.

Materials

Gel from SDS-PAGE
Fixing solution: 10% (v/v) glacial acetic acid/20% (v/v) methanol in H_2O
Alternative fixing solution (for gels with ≥15% acrylamide or thicker than 1.5 mm): 3% (v/v) glycerol/10% (v/v) glacial acetic acid/20% (v/v) methanol in H_2O

Glass dish
Rotary shaker
Filter paper (Whatman 3MM) in sheets at least 1 to 2 cm larger than gel
Plastic wrap (e.g., Saran Wrap)
Gel dryer with vacuum pump

1. After electrophoresis, remove the gel and the supporting glass plates from the electrophoresis apparatus and place in a glass dish. Carefully remove the upper glass plate by gently prying apart the corners with a metal spatula. Make a notch in the upper right hand corner of the gel for orientation.

   Since the gel contains radiolabeled proteins, be sure to follow the necessary guidelines for handling radioactivity. Everything that comes in contact with the gel is potentially radioactive.

2a. *For gels with <15% acrylamide and <1.5 mm thick:* Place the glass dish in a fume hood and pour enough fixing solution into the dish to cover the gel. Place the dish on a rotary shaker and gently rotate until 5 min after all of the blue color from the bromphenol blue in the sample buffer (if used) has disappeared (~30 min total).

   The bromphenol blue typically used in SDS-PAGE sample buffer will turn yellow as the acidic fixing solution diffuses into the gel.

   During fixing, the gel will typically slide off the lower glass plate, which can be removed.

2b. *For gels with ≥15% acrylamide or >1.5 mm thick:* Fix gel as in step 2a, but soak 1 hr in alternative fixing solution.

   The glycerol in the alternative fixing solution should help prevent cracking during drying.

3. Pour off the fixing solution and rinse the gel for a few minutes with deionized water.

   CAUTION: *Remember that solutions that come in contact with the gel are potentially radioactive.*

4. Carefully pour off the water and position the gel in the center of the glass dish. Be sure that any excess water is drained. Place a sheet of Whatman 3MM filter paper, at least 1 to 2 cm larger than the gel, over the gel.

   The gel will stick to the filter paper, which will allow it to be lifted and turned over with the gel side facing up.

5. Cover gel with plastic wrap. Smooth the wrap with a piece of tissue paper to remove any air bubbles or wrinkles.

6. Place a piece of filter paper on the gel support of the gel dryer to prevent contamination of the dryer by radioactivity.

7. Place the filter paper/gel/plastic wrap sandwich on the filter paper in the gel dryer with the plastic sheet facing up.

8. Position the rubber sealing gasket of the gel dryer over the gel. Set the appropriate heat setting on the gel dryer (normally 80°C; 60°C if the gel contains a fluor). Apply the vacuum and allow the gel to dry (typically 2 hr for a gel of 1 mm thickness).

   Removing the gel before it is completely dry can lead to cracking; it is therefore not a good idea to rush the drying process. A rough indication of whether the gel is dry can be obtained by feeling the gel under the sealing gasket. If the gel is dry, it should be warm over the entire surface.

9. Remove gel from dryer and proceed with autoradiography (see Basic Protocol).

USE OF INTENSIFYING SCREENS

SUPPORT PROTOCOL 2

Intensifying screens are used to enhance the film image generated by radioactive molecules (Laskey and Mills, 1977; Laskey, 1980). They are used strictly in conjunction with strong β-emitting isotopes such as ^{32}P or γ-emitting isotopes such as ^{125}I. Emissions from these forms of radiation will frequently pass completely through a film, but they can be absorbed by an intensifying screen which fluoresces and exposes the film with multiple photons of light. While an intensifying screen will substantially enhance the film image as compared with direct exposure (Table A.3D.1), some loss of image resolution will occur due to light scatter. Intensifying screens are distributed by most laboratory supply companies (e.g., Fisher, Sigma, and Kodak).

As shown in Figure A.3D.1, the film should be placed between the sample and the intensifying screen. Preflashed film (see Support Protocol 3) should be used if the sample is weakly radioactive or if quantitation of the radioactivity is desired. The preflashed side of the film should be placed adjacent to the intensifying screen. For very weakly radioactive samples, a second screen can be placed on the other side of the radioactive sample (i.e., screen, then sample, then film, then screen), but this causes further loss in resolution due to light scatter. Also, the sample and sample support must be sufficiently transparent to allow light from the second screen to reach the film. The film should be exposed at −70°C to stabilize the silver bromide crystals activated by the radioactivity or the light emitted from the screen.

Table A.3D.1 Different Methods for Isotope Detection and Their Sensitivities[a]

Isotope	Method[b]	Sensitivity[c]	Enhancement over direct autoradiography[d]
^{125}I	S	100	16
^{32}P	S	50	10.5
^{14}C	F	400	15
^{35}S	F	400	15
^{3}H	F	8000	>100

[a]Exposures conducted at −70°C using preexposed film.

[b]S, intensifying screen; F, fluorography using PPO.

[c]Defined as dpm/cm^2 required for detectable image (A_{540} = 0.02) in 24 hr.

[d]Direct autoradiography for comparison was performed on Kodirex film (Laskey, 1980).

PREFLASHING (PRE-EXPOSING) FILM

SUPPORT PROTOCOL 3

Silver bromide crystals that are activated by light, β particles, or γ rays are highly unstable and quickly revert back to their stable form. The absorption of several photons increases their stability but does not ensure development; approximately five photons of light are required to obtain a 50% probability that any single silver bromide crystal will be developed during film processing. This inefficiency means that film images produced by very low levels of exposure will be disproportionately faint. However, two measures can be taken to maximize efficiency and linearity of exposure at the low levels commonly encountered in ordinary use. First, the film should be pre-exposed to a hypersensitizing flash of light, which provides several photons per silver bromide crystal and stably activates them without providing enough exposure to cause them to become developed. This allows a linear relationship to be drawn between the film image and the amount of radioactivity in the sample. Second, film exposure should be conducted at low tempera-

tures (−70°C) to slow the reversal of activated silver bromide crystals to their stable form (Laskey and Mills, 1975).

Film can be hypersensitized by exposure to a flash of light (<1 msec) provided by a photographic flash unit or a stroboscope before being placed onto the radioactive sample for exposure of the autoradiogram (Laskey and Mills, 1975, 1977). As the optimal light intensity required for pre-exposure varies with the type of film and the flash unit being used, the ideal exposure is best determined empirically as described below.

Materials

Stroboscope or flash unit (e.g., Auto 22 Electronic Flash from Vivitar or Sensitize Pre-Flash from Amersham Pharmacia Biotech)
Neutral-density filter (Kodak)
Orange filter (Wratten 22; Kodak)
X-ray film
Spectrophotometer

1. Cover the stroboscope or flash unit with the neutral-density and orange filters.

   This serves to decrease the intensity of emitted light, particularly the blue wavelengths to which X-ray films are most sensitive. Filters are not required for the Amersham flash unit.

2. Place the film perpendicular to the light source at a distance of ≥50 cm to ensure uniform illumination.

3. Expose a series of test films for different flash lengths, then develop them (see Basic Protocol).

   An uneven fog level on film can be remedied by placing a porous paper diffuser, such as Whatman no. 1 filter paper, between the film and the light source.

4. Cut the films into pieces that fit into a cuvette holder of a spectrophotometer and measure the absorbance at 540 nm.

   Choose an exposure time that causes the absorbance of the pre-exposed film to increase by 0.15 with respect to film that was not pre-exposed.

ALTERNATE PROTOCOL 1

FLUOROGRAPHY

Organic scintillants can be included in radioactive samples to obtain autoradiograms of weak β-emitting isotopes such as ^{3}H, ^{14}C, and ^{35}S. The scintillant fluoresces upon absorption of β particles from these isotopes, facilitating film exposure. Fluorographs of radioactive molecules in polyacrylamide gels have traditionally used the scintillant PPO (2,5-diphenyloxazole; Laskey and Mills, 1975). PPO, however, has largely been replaced with commercial scintillation formulations that reduce the amount of preparation time and are considerably safer to use. These scintillants (e.g., Enhance from NEN Life Science) come with complete instructions for their use. In addition, spray applicators are also available that can be used on filters or thin-layer plates. The expected levels of image enhancement obtained through fluorography are listed in Table A.3D.1. Sodium salicylate can also be used for fluorography as described below (Chamberlain, 1979). It yields levels of image enhancement comparable to organic scintillants, although it sometimes causes a more diffuse film image. The conditions should work for most standard sizes and thicknesses of gels.

CAUTION: Gloves should be worn at all times; sodium salicylate can elicit allergic reactions and is readily absorbed through the skin.

Materials

Polyacrylamide gel
1 M sodium salicylate, pH 5 to 7, freshly prepared

Additional reagents and equipment for fixing and drying gels (see Support Protocol 1)

1. If gel is acid-fixed, soak for 1 to 5 hr in ~20 vol water to prevent precipitation of salicylic acid from the sodium salicylate.
2. Soak gel 30 min in 10 vol of 1 M sodium salicylate, pH 5 to 7.

   To prevent cracking of gels with >15% acrylamide or thicker than 1.5 mm, 2% (v/v) glycerol can be added to the 1 M sodium salicylate.
3. Dry the gel (see Support Protocol 1) and proceed with autoradiography (see Basic Protocol).

DENSITOMETRY

SUPPORT PROTOCOL 4

Film images obtained by autoradiographic methods can be quantified by densitometry. Densitometers work by comparing the intensity of light transmitted through a sample with the intensity of the incident light. The amount of light transmitted will be proportional to the amount of radioactivity in the gel, provided that the film has been properly pre-exposed (see Support Protocol 3). The linear range of correctly pre-exposed film is 0.1 to 1.0 absorbance units. However, if the pre-exposure is excessive—i.e., an increase of >0.2 absorbance units (A_{540}) treated film/untreated film—smaller amounts of radioactivity will produce disproportionately dense images. Autoradiograms that exceed an absorbance of 1.4 absorbance units (A_{540}) have saturated all available silver bromide crystals and also cannot be evaluated quantitatively.

Densitometers are available from several manufacturers (e.g., Molecular Dynamics, Bio-Rad, and UVP). Most models come with software that facilitates calculations and allows the user to define the region of the film to be measured. Procedures for the use of these machines vary and instructions are provided by the manufacturer. Densitometers are also available that measure light reflected from a sample. Reflectance densitometers are useful in instances where the sample medium is completely opaque—e.g., filters that have been probed using nonradioactive colorimetric detection assays.

PHOSPHOR IMAGING

ALTERNATE PROTOCOL 2

Phosphor imaging screens can be used as an alternative to film for recording and quantifying autoradiographic images (Johnston et al., 1990). They can detect radioisotopes such as ^{32}P, ^{125}I, ^{14}C, ^{35}S, and ^{3}H. There are several advantages of phosphor imaging over film: (1) linear dynamic ranges are 5 orders of magnitude, compared to ~1.5 orders of magnitude for film (Fig. A.3D.2); (2) exposure times are 10 to 250 times faster than with film; (3) quantification is much easier and faster, and most imagers come with software to directly analyze data; (4) fluorography and gel drying are often unnecessary because of the sensitivity of phosphor imaging; and (5) phosphor screens can be reused indefinitely if handled carefully.

Phosphor imaging screens are composed of crystals of $BaFBr:Eu^{+2}$. When the screen is exposed to ionizing radiation such as α, β, or γ radiation, or wavelengths of light shorter than 380 nm, the electrons from Eu^{+2} are excited and then trapped in an "F-center" of the $BaFBr^{-}$ complex; this results in the oxidation of Eu^{+2} to Eu^{+3}, which forms the latent image on the screen. After exposure, the latent image is released by scanning the screen with a

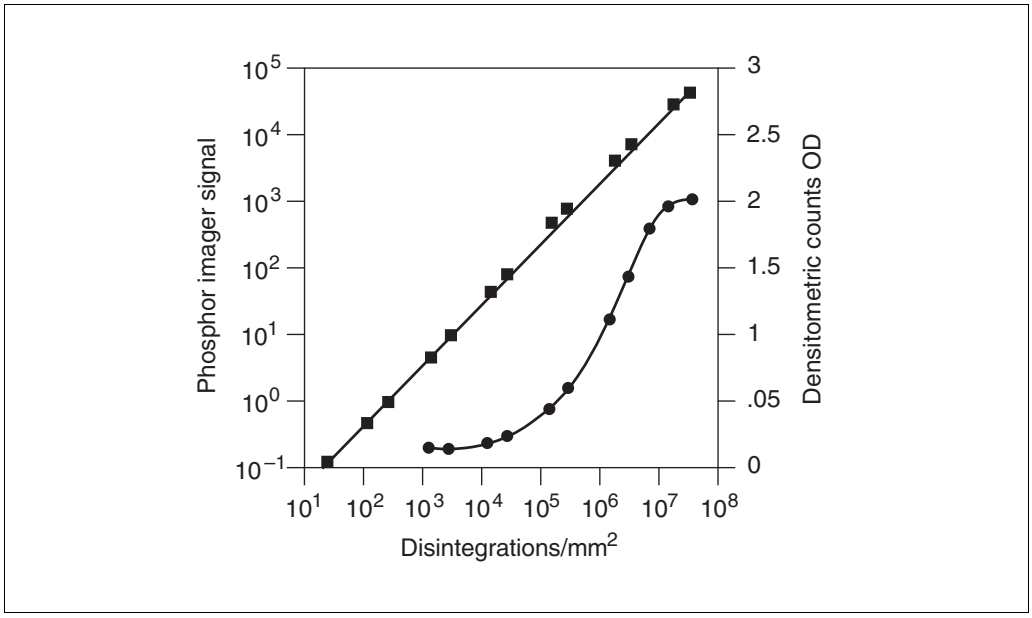

Figure A.3D.2 ^{32}P dilution series quantified on Model GS-525 phosphor imager (squares), compared to film (circles). Image courtesy of Bio-Rad, Hercules, Calif.

laser (633 nm). During scanning, Eu^{3+} reverts back to Eu^{+2}, releasing a photon at 390 nm. The luminescence can then be collected and measured in relation to the position of the scanning laser beam. The result is a representation of the latent image on the storage phosphor imaging plates. The image can then be viewed on a video monitor and analyzed with the aid of appropriate software.

Some companies (e.g., Bio-Rad) offer different screens for use with different isotopes. They vary principally in the protective coating on the screen, which is optimized for low- or high-energy β particles or γ rays. No coating is typically used for weak β emitters such as tritium. More recently, screens have also been developed that measure chemiluminescence. Such screens are particularly valuable for use with many nonradioactive labeling protocols.

The protocol below is for the PhosphorImager system from Molecular Dynamics; other phosphor imaging systems are available from Bio-Rad, Imaging Research, and National Diagnostics.

Materials

Gel or filter
PhosphorImager system (Molecular Dynamics) including:
ImageEraser light box
Exposure cassette with phosphor screen
Scanning software

1. Erase any latent image on the phosphor screen left by a previous user, or caused by background radiation, by exposure to visible light.

   The PhosphorImager system comes with an extra-bright light box (ImageEraser) for this purpose. Standard laboratory light boxes may also be used.

2. Cover gel or filter with plastic wrap to protect the exposure cassette. Place wrapped gel or filter in the PhosphorImager cassette and close to begin exposure.

   The gel does not have to be dried for this procedure. The phosphor screen is affixed to the lid of the cassette. Exposure times are typically one-tenth of the time required for film exposure.

3. After exposure, slide the screen face down into the PhosphorImager system.
4. Select the scanning area using the software supplied with the PhosphorImager and start scanning.

   The blue light emitted during scanning is collected to produce the latent image.

5. Analyze and quantitate the image using the software provided.
6. Erase the phosphor screen by exposing it to visible light as in step 1.

COMMENTARY

Background Information

The ability to detect radiolabeled proteins is critical to many studies in biology. A variety of labeling methods are described throughout this manual. More often than not, detection of radiolabeled proteins is coupled with the resolving power of SDS polyacrylamide gel electrophoresis (SDS-PAGE). Radiolabeled proteins separated on gels can be used directly to obtain an autoradiographic image. Alternatively, proteins separated by SDS-PAGE are frequently transferred to membranes and detected using radiolabeled probes such as antibodies and ^{125}I-labeled protein A. The autoradiographic image, whether generated on film or a phosphor screen, reflects the distribution of the radioactive proteins on the two-dimensional surface of the gel or filter. Molecular sizes of radiolabeled proteins, therefore, can be determined by correlating their positions with molecular markers. Also, the density of the band images can be used to determine the relative quantities of the radiolabeled proteins in the sample.

Critical Parameters

The sensitivity of the detection device and the strength of the radioactive signal are the two most important parameters for autoradiography. Sensitivity can be enhanced by treating samples with fluors or by using intensifying screens (Table A.3D.2). Because phosphor imaging is 10 to 250 times more sensitive than film (Johnston et al., 1990), this technology makes it possible to monitor radioactive samples that would previously have gone undetected with film.

A second important parameter is the range over which the measurement device is linear. Film requires preflashing in order for the intensity of the image to be linear with respect to the amount of radioactivity, particularly for weakly radioactive samples (Laskey and Mills, 1975, 1977). Phosphor imaging offers a much wider linear range of measurement (5 orders of magnitude compared to 1.5 for film; Johnston et al., 1990). This makes it possible to accurately quantitate very weak or very strong radioactive samples.

Troubleshooting

Cracking is one of the most common problems encountered when drying gels. This often occurs if the gel is removed from the dryer before it has adequately dried or if drying temperatures are too high. To overcome this problem, drying times should be extended and the performance of the vacuum pump and heater unit should be checked. For many gels, particularly for those with high percentages of polyacrylamide or >1.5 mm thick, cracking can be reduced by using an alternative fixing solution containing glycerol (3% glycerol/10% glacial acetic acid/20% methanol; see Support Protocol 1).

Among the biggest problems encountered in autoradiography are images that are either too weak or too intense. Such problems can be solved by varying the exposure time. Estimating initial exposure time is difficult, since the

Table A.3D.2 Film Choice and Exposure Temperature for Autoradiography

Isotope	Enhancement method	Film	Exposure temperature
^{3}H	Fluorography	Double-coated	–70°C
^{35}S, ^{14}C, ^{32}P	None	Single-coated	Room temperature
^{35}S, ^{14}C, ^{32}P	Fluorography	Double-coated	–70°C
^{32}P, ^{125}I	$CaWO_4$ intensifying screens	Double-coated	–70°C

amount of radioactivity in the sample is often unknown. A Geiger counter can offer some guidance with certain isotopes. For highly exposed film, the length of time in developer can be reduced to produce a lighter image. It is particularly important to remember that if accurate quantification of the film image is desired, film must be preflashed so that there is a linear relationship between the amount of radioactivity in the sample and the image intensity.

Artifacts, such as black spots and stripes, can be avoided during developing by making sure that no moisture comes in contact with the film and that films exposed at −70°C are brought to room temperature before developing. Also, it must be noted that β particles from weak isotopes such as ^{3}H cannot penetrate plastic wrap, and plastic wraps can attenuate signals from ^{35}S and ^{14}C up to two-fold.

Anticipated Results

The protocols described here should yield a film image of a gel that can be quantified, stored, and photographed for publication.

Time Considerations

Fixing a gel will require ~45 min. Drying will take an additional 2 hr for a gel 1 mm in thickness. Incorporation of a fluor will add ~45 min to the processing time.

For gels >1.5 mm thick or with >15% acrylamide, an additional 30 min will be required for fixing and ~30 additional minutes will be required for drying.

The length of exposure for films in autoradiography can range from a few minutes to a few weeks, depending on the strength of the radioactivity in the sample. Most exposures last from several hours to a few days. Exposure time can be reduced more than 10-fold with a phosphor imager.

Literature Cited

Chamberlain, J.P. 1979. Fluorographic detection of radioactivity in polyacrylamide gels with the water-soluble fluor, sodium salicylate. *Anal. Biochem.* 98:132-135.

Johnston, R.F., Pickett, S.C., and Barker, D.L. 1990. Autoradiography using storage phosphor technology. *Electrophoresis* 11:355-360.

Laskey, R.A. 1980. The use of intensifying screens or organic scintillators for visualizing radioactive molecules resolved by gel electrophoresis. *Methods Enzymol.* 65:363-371.

Laskey, R.A. and Mills, A.D. 1975. Quantitative film detection of ^{3}H and ^{14}C in polyacrylamide gels by fluorography. *Eur. J. Biochem.* 56:335-341.

Laskey, R.A. and Mills, A.D. 1977. Enhanced autoradiographic detection of ^{32}P and ^{125}I using intensifying screens and hypersensitized film. *FEBS Lett.* 82:314-316.

Contributed by Daniel Voytas and Ning Ke
Iowa State University
Ames, Iowa

Northern Blot Analysis of RNA

Northern blot hybridization is used to determine quantitatively the presence of specific mRNA transcripts in cell or tissue lysates and to evaluate the specificity of a select oligonucleotide probe. First the RNA is extracted from a tissue or cell culture (see Support Protocol 1). Following agarose gel separation, the RNA is transferred by capillary action to a nylon membrane (see Basic Protocol). The RNA is then UV-crosslinked to the membrane and stained with methylene blue to verify RNA integrity and equal RNA loading and transfer and then used for hybridization. After prehybridization, which blocks the nonspecific binding sites, the membrane is probed with a specific cDNA oligonucleotide, which is labeled with ^{32}P using terminal deoxynucleotidyl transferase (TdT; see Support Protocol 2). Following successive washes of increasing stringency, the membrane is exposed to an autoradiographic film. The presence of a band on the film emulsion indicates RNA hybridization with the radioactive probe. The probe can then be removed from the membrane, and subsequent probes rehybridized for further analysis (see Support Protocol 3).

In general, it is preferable to isolate mRNA instead of total RNA, as mRNA represents only 1% to 5% of the total cellular RNA; therefore, mRNA samples give a substantially higher signal than total RNA. For mRNA isolation, use commercially available kits (e.g., Invitrogen's Fastrack 2), which allow mRNA isolation directly from tissues or cells without prior total RNA extraction. Although extraction of total RNA is simpler and faster, and verification of RNA integrity is easier (the prominent bands corresponding to the 18 S and 28 S ribosomal subunits, which are 1.8 to 2 kb and 4 to 5 kb, respectively, can be used as an indication that the RNA has not been degraded during the extraction protocol), total RNA should be used for northern blots only if there is preliminary information of abundant expression of the transcript. If total RNA has to be used because of a limited amount of cells or tissues and no signal can be detected by northern blot analysis, reverse transcriptase amplification (RT-PCR) may be used.

The major problem in the analysis of RNA is contamination with ribonucleases (RNase), which are very stable enzymes that do not require any cofactors for activity. Avoid RNase contamination by wearing clean powder-free gloves for all procedures and by using RNase-free reagents, plasticware, and glassware. Autoclaving solutions, glassware, and plasticware is usually not enough to inactivate all RNases. Instead, all heat-resistant glassware and plasticware should be baked at 140° to 150°C overnight. Equipment such as the electrophoresis tank should be rinsed in RNase-free water for 30 min prior to use. All solutions (except Tris-containing solutions) can be made from water treated with the RNase inhibitor diethylpyrocarbonate (DEPC; see *UNIT 2.9*). The use of RNase-free solutions (made up with DEPC-treated water, unless otherwise stated) is recommended for the preparation of all solutions before and during the hybridization steps. Because DEPC-treated water from commercial sources is quite expensive, the use of low-cost, DEPC-treated water made in the lab is recommended. The use of RNase-free solutions is not required in post-hybridization procedures because of the resistance of RNA:RNA hybrids to RNase degradation. Because even the smallest contaminants of DEPC may affect many subsequent enzymatic steps such as labeling or amplification, purified RNA should be solubilized in water from a known RNase/DNase-free source (not DEPC-treated and pyrogen-free). RNA samples should be kept on ice when they are not protected by RNase inhibitors.

NOTE: For commentary concerning northern blot analysis, see *UNIT 2.9*.

Contributed by Marcelle Bergeron, Jari Honkaniemi, and Frank R. Sharp
Current Protocols in Toxicology (2001) A.3E.1-A.3E.13

BASIC PROTOCOL

NORTHERN BLOT HYBRIDIZATION

Isolated RNA (see Support Protocol 1) is size fractionated by gel electrophoresis using a 1% (w/v) agarose gel to separate RNA in the 1- to 10-kb range prior to transfer. If ethidium bromide is incorporated into the gel, bands can be visualized using a transilluminator.

After size fractionation, the RNA is transferred to a membrane. Capillary flow is the most common and inexpensive method to transfer nucleic acids (RNA and DNA) from an agarose gel to a membrane. The nucleic acid is washed out of the gel onto the membrane using a stack of dry paper towels, which draws the transfer solution from the reservoir through a wick of Whatman 3 MM blotting paper, then through the gel, the membrane, and into the dry paper towels. Two variants of the capillary flow transfer method currently exist: upward and downward transfer (Figs. A.3E.1A and A.3E.1B, respectively). In both systems, the gel is closest to the reservoir. The membrane is in direct contact with the surface of the gel followed by some blotter paper and a stack of dry paper towels. Although both setups work very well, downward transfer (e.g., using the TurboBlotter, Schleicher and Shuell) is recommended since it results in somewhat sharper bands as no extra weight is applied on the gel.

Once the materials are prepared, the nylon membrane bearing size-fractionated RNA is incubated with the radiolabeled oligonucleotide probe to allow hybridization between the single-stranded DNA and the single-stranded RNA. After hybridization the membrane is washed with a series of solutions of increasing stringency and then exposed to autoradiographic film to visualize the hybridized bands. This protocol is adapted for the use of short oligonucleotides (30- to 45-mer) in northern blot hybridization. Any variations in temperature, salts or denaturing conditions may greatly affect the probe hybridization.

Materials

Ultrapure agarose, low-melting temperature (e.g., Life Technologies, Bio-Rad, Sigma, or Fisher)
DEPC-treated H_2O (*UNIT 2.9*)
10× and 1× MOPS (see recipe)
37% formaldehyde (Sigma)
Purified RNA (20 to 40 µg total or 4 to 10 µg mRNA; see Support Protocol 1)
≥99.5% formamide, deionized (Sigma)
RNA loading dye (see recipe)
10 mg/ml ethidium bromide (optional; see recipe)
Nylon membrane, positively charged (Hybond from Amersham Pharmacia Biotech or Nytran SuPerCharge from Schleicher & Schuell)

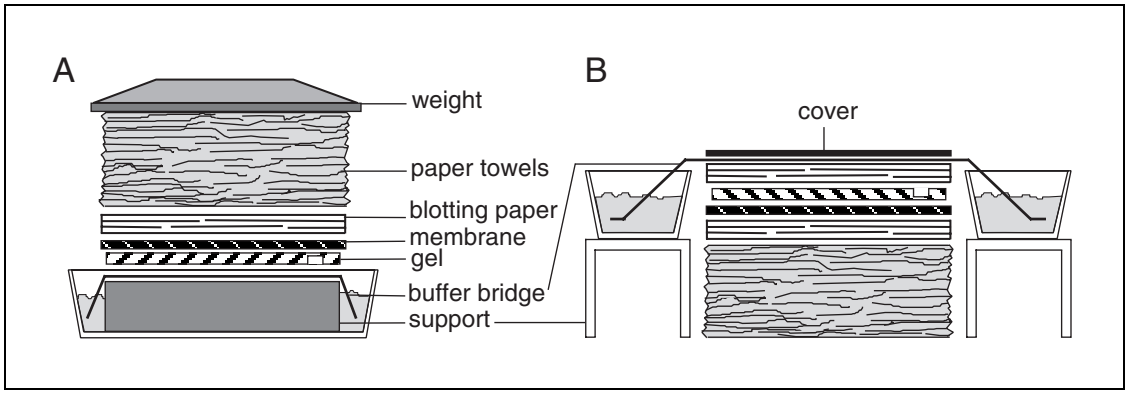

Figure A.3E.1 Capillary flow transfer of RNA from agarose gels to a membrane. (**A**) Upward capillary transfer. (**B**) Downward capillary transfer.

20× and 2× SSC (*UNIT 2.9*)
0.02% (w/v) methylene blue RNA staining solution (*UNIT 2.9*)
20× SSPE (*UNIT 2.9*)
20% (w/v) SDS (*APPENDIX 2A*)
100× Denhardt's solution (*UNIT 2.9*)
10 mg/ml heat-denatured salmon sperm DNA (Life Technologies)
50% (w/v) dextran sulfate (*UNIT 2.9*)
100 cpm/μg [α-^{32}P]dATP-labeled oligonucleotide probe (see Support Protocol 2)
1× and 2× SSPE/0.1% SDS
1× STE buffer (see recipe)

Horizontal gel electrophoresis system with casting box and Teflon combs with 3- to 4-mm teeth (e.g., Bio-Rad, Amersham Pharmacia Biotech, Owl, Shadel) and appropriate power supply
Microcentrifuge tubes, RNase-free
UV transilluminator, ruler, and camera (optional)
Elevated support (e.g., empty pipet tip box)
Whatman 3 MM papers
10- to 15-cm stack of paper towels
Small weight (~500 g) or light-weight cover
UV Cross-linker (Stratagene)
Pencil or fluorescent pen (optional)
Hybridization oven with glass hybridization bottle (Hybaid) or
42°C water bath and sealable bag
Geiger counter
Autoradiographic cassette, light-tight with intensifying screen
X-ray film (e.g., X-Omat AR5 or BioMax MS from Kodak)

CAUTION: When working with radioactivity, take appropriate precautions to avoid contamination of the experimenter and the surroundings. Carry out the experiment and dispose of wastes in an appropriately designated area, following the guidelines provided by the local radiation safety officer (also see *APPENDIX 1A*).

CAUTION: Radiolabeled probes are hazardous; see *APPENDIX 1A* for guidelines on handling, storage, and disposal. To protect from radioactivity and RNase contamination as well as finger smudges, always wear clean, powder-free gloves when working with RNA and radioactive substances. Do not reuse gloves.

Prepare agarose gel

1. Set up the casting box (mold) following the manufacturer's instructions.
2. In a flask, mix 1.0 g ultrapure low-melting-temperature agarose with 85 ml DEPC-treated water. Heat on a heating/stirring plate (or in a microwave oven) until all crystals are dissolved.

   NOTE: *Do not boil the agarose solution.*

   The volume of agarose solution needed depends on the size of the electrophoresis chamber used. Keep the gel thickness between 4 and 6 mm to obtain sharper bands and to allow efficient RNA transfer.

   Transcripts of 1 to 10 kb are easily separated by 1% agarose gels, whereas transcripts shorter than 0.5 to 4 kb are better separated by 1.6% to 1.8% agarose gels. Gels with <1% agarose are extremely fragile and hard to handle, while gels with ≥2% agarose do not transfer RNA well.

3. Let the solution cool to ~60°C to avoid excess evaporation of the formaldehyde to be added. Add 10 ml 10× MOPS and 5 ml 37% formaldehyde in a fume hood. Swirl gently without creating air bubbles.

   CAUTION: *Formaldehyde is a denaturing agent that protects RNA from degradation. It is toxic if inhaled or absorbed through the skin. All procedures involving formaldehyde should be carried out in a fume hood. Wear gloves at all times.*

4. Place the gel casting apparatus on a leveled surface, pour the molten agarose gel mixture into the mold, and insert the Teflon comb immediately.

   To obtain sharp bands, use a gel thickness of no more than 3 to 4 mm and a comb tooth width of 6 to 8 mm. Narrower teeth or wells may result in smeared bands.

5. When the gel has set (15 to 20 min), remove the comb gently. Place the gel in the horizontal electrophoresis tank with the wells towards the anode (RNA migrates towards the cathode) and add enough 1× MOPS solution to cover up to 1 mm over the gel surface.

Prepare RNA

6. Prepare the RNA sample by combining the following in an RNase-free microcentrifuge tube:

   6 µl purified RNA (20 to 40 µg total RNA or 4 to 10 µg mRNA)
   12.5 µl ≥99.5% deionized formamide
   2.5 µl 10× MOPS
   4.0 µl 37% formaldehyde

   Mix and incubate 10 min at 65°C.

   If RNA size markers are used, treat in the same fashion as the RNA samples.

7. Place the denatured samples on ice and add 2.5 µl RNA loading dye. If desired, add 1 µl 10 mg/ml ethidium bromide. Vortex briefly and microcentrifuge for 5 sec.

   The use of ethidium bromide to stain the RNA in gels is not recommended since it is highly toxic and can interfere with RNA transfer. If necessary, the gel can be stained after the transfer to verify that all the RNA was transferred from the gel. Staining the membrane instead is generally enough to verify that the electrophoresis was successful.

Run the gel

8. Load the RNA samples into each well. Run the gel at 5 to 8 V/cm until the bromophenol blue dye has migrated two-thirds the length of the gel.

   CAUTION: *To avoid electrocution, connect the electrode leads one at a time with one hand only and then turn on the power supply.*

   The amount of RNA needed for each lane depends on the abundance of the transcript of interest and the type of RNA used. For mRNA, 4 µg is usually enough, but up to 10 µg can be loaded on the gel. For total RNA, 20 µg is typically used, but up to 40 µg can be loaded on a gel.

9. Turn off the power supply and remove the connections with one hand.

10. Remove the gel from the mold and rinse briefly in deionized water.

    If ethidium bromide is used in the samples, place the gel on a UV-transilluminator to visualize the RNA and photograph the gel along with a ruler on its side so that band positions can be transposed to the membrane after transfer.

Prepare gel for transfer

11. To save solutions and materials, cut off excess agarose from the gel (e.g., the empty lanes on the sides).

12. Cut the positively charged nylon membrane slightly larger than the gel.

    NOTE: *Keep the protective paper on both side of the membrane while cutting and handling to prevent fingerprints and high background signal.*

13. Prewet the membrane in DEPC-treated water and then soak in 20× SSC (transfer buffer) for 1 min each at room temperature.

Translocate RNA to membrane by upward transfer

NOTE: The following steps describe how to assemble the upward transfer apparatus depicted in Figure A.3E.1A.

14a. Using a clean flat dish as a reservoir, place an elevated support (island) in the middle of the dish.

    Use a support slightly larger than the gel (an empty plastic pipet tip box works well).

15a. Pour 20× SSC in the reservoir to a depth of ~2 to 3 cm.

16a. Construct a buffer bridge with a clean piece of Whatman 3 MM paper (see Fig. A.3E.1A). Wet the bridge with 20× SSC and place on top of the elevated support with the ends of the bridge hanging in the transfer solution.

17a. Place the gel (face down) directly on top of the elevated support and cover the exposed blotter paper (from the bridge) around the edge of the gel with strips of parafilm or cellophane to prevent wicking of buffer through the paper rather than the gel.

18a. Place the wet membrane (step 13) directly on top of the gel, making sure to eliminate all air bubbles between the membrane and the gel.

    To minimize the distance the nucleic acid has to migrate out from the gel to the membrane, it is important to place the side of the gel corresponding to the bottom of the wells directly against the membrane.

19a. Presoak 2 to 3 Whatman 3 MM papers cut the same size as the gel (or slightly bigger) in 20× SSC and apply to the membrane.

20a. Top with a 10- to 15-cm stack of dry paper towels cut the same size as the gel. Put a small weight (~500 g) on top of the system and transfer overnight at room temperature.

Translocate RNA to membrane by downward transfer

NOTE: The following steps describe how to assemble the downward transfer apparatus depicted in Figure A.3E.1B, which is inverted compared with the upward system.

14b. Form the island with a ~5- to 8-cm stack of dry towels or blotter paper. Place two clean buffer reservoirs (e.g., two clean pipet tip box lids, slightly wider than the height of the gel) on both sides of the blotter stack. Pour 65 ml (for gels up to 11 × 14 cm) or 100 ml (for gels up to 20 × 25 cm) of 20× SSC in each reservoirs.

    Blotter papers, paper towels, and the membrane are all cut the size of the gel (or slightly bigger).

15b. Add 4 or 5 dry Whatman 3 MM papers on top of the island.

16b. Add 2 to 3 Whatman 3 MM papers presoaked in 20× SSC.

17b. Add the wet membrane (step 13).

18b. Place the gel face up on top of the membrane, making sure to eliminate all air bubbles between the membrane and the gel..

See step 18a for specific instructions on gel placement.

19b. Place 3 sheets of Whatman 3MM blotter paper, presoaked in 20× SSC on top of the gel. Construct a transfer buffer bridge with a clean piece of Whatman 3MM paper (see Figure A.3E.1B). Presoak the bridge in 20× SSC and carefully apply on top of the blotter stack so that the short dimension of the wick completely covers the blotting stack, leaving the ends of the bridge hanging at the bottom of the transfer reservoirs. Place a light wick-cover on top to prevent evaporation.

20b. Transfer overnight at room temperature.

A TurboBlotter System (Schleicher and Shuell) can also be used according to the manufacturer's instructions. Depending on the thickness of the gel and the size of the RNA of interest, transfer time with this system can be as short as 4 hr.

Crosslink RNA

21. After transfer is complete, remove the membrane from the transfer system. Place it face up on a wet Whatman 3MM paper and crosslink the RNA using a UV-crosslinker (Stratagene) according to the manufacturer's instructions.

At this point, the wet membrane can be stored sealed in a plastic wrap at 4°C for up to 2 weeks before analysis.

Stain the membrane

22. Stain the membrane with 0.02% (w/v) methylene blue RNA staining solution until the lanes become visible (~15 min). Delineate the RNA marker bands on the side of the membrane with a pencil, fluorescent pen, or dye.

Methylene blue RNA staining solution is 0.02% methylene blue in 0.3 M sodium acetate solution, pH 5.5 (see UNIT 2.9).

23. Destain with 2× SSC. Cut one corner away to establish the orientation of the lanes.

Prehybridize membrane

24. Transfer the UV-crosslinked membrane with RNA to a sealable bag or a glass hybridization bottle.

25. Prepare the prehybridization solution by mixing the following in order, in a sterile tube (8 ml total volume):

4.4 ml DEPC-treated H_2O
2.5 ml 20× SSPE
0.5 ml 20% SDS
0.5 ml 100× Denhardt's solution
0.1 ml 10 mg/ml heat-denatured salmon sperm DNA.

When made at room temperature, the solution may cloud up after addition of SDS. This can be corrected by heating the water and the 20× SSPE mixture to 42°C before adding the other ingredients to the solution.

Use ~8 to 10 ml solution per 10 cm^2 of membrane.

26. Add the prehybridization solution to the membrane and prehybridize at least 2 hr at 42°C using either a hybridization oven or a sealed bag submerged in a shaker water bath.

Add label

27. Add 2 ml 50% dextran sulfate to the prehybridization solution and mix well.

    The total hybridization volume is 10 ml.

28. Add 10^6 to 10^7 cpm labeled probe for each 1 ml prehybridization solution. Mix well.

29. Hybridize overnight at 42°C as described above (step 26).

Wash the hybridized membrane

30. The next day, wash the membrane twice with 2× SSPE/0.1% SDS, 42°C for 15 min each and once with 1× SSPE/0.1% SDS, 42°C for 15 min. Check the activity of the membrane after each wash by holding a Geiger counter 2 to 3 cm above the membrane surface. At the first sign of significantly decreased signal intensity, stop the washing procedures.

    The signal should be very intense after the first washes. With increasing wash stringency, the signal should decrease.

    Dilutions of SSPE from the 20× SSPE stock should preferably be made with DEPC-treated water but high-quality deionized sterile water can also be used.

31. *Optional:* If necessary (i.e., too much noise), wash four times with 1× SSPE/0.1% SDS, increasing the temperature by 5°C each time from 45° to 60°C.

    If the membrane is still too radioactive after washing at 60°C, decrease the SSPE concentration to 0.5×, 0.2× and then 0.1× SSPE/0.1% SDS.

    Increasing the temperature and decreasing the SSC concentration provide more stringent conditions that facilitate the elimination of mismatched probe, thus decreasing nonspecific background.

Perform autoradiography

32. Drain the excess solution from the membrane and seal it in plastic wrap.

    Do not allow the membrane to dry between washes or during autoradiographic exposure.

33. Tape the membrane against the lid (inner surface) of a light-tight autoradiography cassette. Place an intensifying screen in the bottom of the cassette. In a dark room, place an X-ray film directly on top of the screen and then close the lid.

    The membrane attached to the inside of the lid should be in direct contact with the film emulsion.

34. Place the autoradiography cassette at −70°C for the appropriate length of time, depending on the specific activity of each sample and the abundance of mRNA.

    To save time in trying to determine which exposure time is adequate, three films can be exposed at the same time. The film closest to the intensifying screen usually gives the strongest signal whereas the one closest to the membrane (farthest from the screen) gives the lowest signal.

35. Develop the film according to the manufacturer's instructions.

TOTAL RNA EXTRACTION

SUPPORT PROTOCOL 1

This protocol describes a method to isolate undegraded, DNA-free, total RNA using Trizol Reagent (Life Technologies) followed by extractions with acidic phenol/chloroform (Ambion). This method uses a mixture of guanidine isothiocyanate and phenol, which inactivates the RNases and yields excellent quality RNA for all downstream experiments.

Additional Materials *(also see Basic Protocol)*

Tissue
Trizol Reagent (Life Technologies) or TriReagent (Sigma) or RNA STAT-60 (Tel-Test) or Ultraspec (Biotech Labs)
Chloroform
5:1 (v/v) acid phenol/chloroform, pH 4.7 (Ambion)
Isopropyl alcohol
75% and 100% ethanol
dH_2O, sterile, non-DEPC treated, RNase/DNase- and pyrogen-free (Ambion or Life Technologies)
40 U/µl RNasin (Promega)
1 M Tris·Cl, pH 7.5, RNase-free (Sigma, Ambion, Life Technologies)
50 mM $MgCl_2$, RNase-free (Sigma, Ambion, Life Technologies)
10 U/µl DNase, RNase free (Life Technologies, Roche Molecular Biochemical, Ambion)
3 M sodium acetate solution, pH 5.2, RNase-free (Sigma, Ambion)
Phosphate-buffered saline (PBS; *APPENDIX 2A*)

Polytron or Dounce homogenizer
Pipet tips, RNase-free (Fischer, Ambion, Promega)

NOTE: Because Tris·Cl, $MgCl_2$, and sodium acetate solution listed here are added directly to the RNA preparation, we recommend that they be absolutely RNase-free. Because of the small volumes used in this protocol, we recommend a commercial supplier as the source for these solutions.

CAUTION: Guanidine isothiocyanate and phenol are highly toxic. The use of gloves, adequate ventilation, and special disposal methods are required.

Collect tissue

1. Excise the tissue and freeze immediately in sterile tubes on powdered dry ice. Store at −70°C until analysis.
2. Take the tissue sample out of the freezer and place in an RNase-free microcentrifuge tube. Do not thaw.

Extract RNA

3. Immediately add 1 ml Trizol Reagent per 100 mg tissue and homogenize with a Polytron (for larger tissue samples) or Dounce homogenizer (for small tissue samples). Transfer to an RNase-free microcentrifuge tube.

   For monolayer cell culture, first rinse quickly with ice-cold sterile PBS and then add 1 ml Trizol Reagent directly to the 150-mm dish (10^2 to 10^6 cells). Scrape cells from the dish with a sterile cell scraper and transfer the lysate to an RNase-free microcentrifuge tube. Homogenize up and down through a 1000-µl pipet tip.

   Trizol reagent is equivalent to TriReagent from Sigma, RNA STAT-60 from Tel-Test, or Ultraspec from Biotech Labs.

4. Incubate 5 min at room temperature.
5. Add 0.2 ml chloroform per 1 ml Trizol Reagent and vortex the tubes vigorously for 15 sec.
6. Incubate at room temperature for 2 to 3 min.
7. Microcentrifuge 15 min at 14,000 rpm, 4°C.

8. Carefully remove the upper aqueous phase (which contains the RNA) with a pipet and transfer to an RNase-free microcentrifuge tube. Do not pipet the white protein interphase, which will result in contamination of the RNA.

Extract and precipitate RNA

9. *Optional*: Mix the supernatant with an equal amount of 5:1 acid phenol/chloroform, vortex, and microcentrifuge 15 min at 14,000 rpm, 4°C.

10. *Optional*: Transfer the upper aqueous phase to an RNase-free microcentrifuge tube. Repeat step 9 until no white interphase is visible.

    NOTE: *Steps 9 and 10 will yield higher quality RNA, free of protein contamination. This is no absolutely required for northern blot analysis but can be advantageous in RT-PCR reactions and other reactions requiring high-quality RNA.*

11. Mix the resulting upper phase with 0.5 ml isopropyl alcohol per 1 ml Trizol Reagent used. Incubate for 30 min at −20°C or overnight in order to precipitate the RNA.

12. Microcentrifuge 30 min at 14,000 rpm, 4°C.

13. Carefully remove the supernatant and keep the RNA pellet. Keep the tubes on ice after this step.

    The RNA pellet is transparent and easy to lose.

Wash RNA pellet

14. Wash pellet with 1 ml 75% ethanol.

    The pellet will turn white and will be easier to see.

15. Microcentrifuge 15 min at 14,000 rpm, 4°C and then carefully remove the supernatant.

16. Wash the pellet with 1 ml 100% ethanol.

17. Microcentrifuge 15 min at 12,000 × *g*, 4°C and then carefully remove the supernatant.

18. Dry the RNA pellet at room temperature.

    The RNA pellet becomes whiter as it dries.

    It is essential to remove all ethanol since trace contamination may affect all subsequent enzymatic reactions; however, do not overdry and absolutely never vacuum dry (SpeedVac), since this procedure will make the RNA pellet almost impossible to resolubilize.

19. Resuspend the pellet in 35 µl deionized, sterile, non-DEPC treated, RNase/DNase- and pyrogen-free water.

    NOTE: *At this stage, the pellet can also be resuspended in 10 to 25 µl of water (step 26), quantitated (step 27), and then used directly in northern blot analysis.*

    Do not use DEPC-treated H_2O since it may interfere with subsequent enzymatic reactions.

Remove DNA

20. *Optional*: To the 35 µl RNA sample, add in the following order (50 ml final volume):

    0.5 µl 40 U/µl RNasin
    2.5 µl 1 M Tris·Cl, pH 7.5
    10 µl 50 mM RNase-free $MgCl_2$
    2 µl 10 U/µl DNase (RNase-free).

    Incubate 30 min at 37°C.

21. *Optional*: Add 200 µl 5:1 acid phenol/chloroform and mix vigorously.

22. *Optional*: Centrifuge 15 min at 14,000 rpm, then transfer the upper phase to an RNase-free microcentrifuge tube. Repeat extraction (steps 21 and 22) until no white interphase can be seen.

23. *Optional*: Estimate the volume of the resulting RNA solution and add 2.5 vol 100% ethanol and 1/20 vol 3 M sodium acetate, pH 5.2.

24. *Optional*: Precipitate RNA at −20°C for 30 to 60 min or overnight.

25. *Optional*: Repeat steps 12 to 18.

26. *Optional*: Dissolve the RNA pellet in 10 to 25 µl sterile RNase/DNase- and pyrogen-free water.

    Do not use DEPC-treated water.

27. Determine the concentrations by measuring the absorbance at 260 and 280 nm. Dilute to the desired concentration (e.g., 1 µg/µl) and store in small aliquots of about 10 to 20 µg in each tube.

    The A_{260}/A_{280} ratio should be 1.8 to 2.1. Note that an A_{260} of 1 AU for single-stranded RNA = 40 µg/ml.

    If the RNA is to be used within 3 or 4 months, and the tubes are not frozen and thawed more than about 5 times, storing the RNA in sterile RNase/DNase-and pyrogen free water at −70°C is acceptable. For long-term storage, add 1/10 vol of 3 M sodium acetate, pH 5.2, and 2.5 vol of 100% ethanol to the RNA solution and freeze at −70°C. Before analysis, microcentrifuge and wash as described above (steps 25 to 26) and determine the RNA concentration in the final solution.

SUPPORT PROTOCOL 2

RADIOLABELING AN OLIGONUCLEOTIDE PROBE

The oligonucleotide probe for northern blot hybridization is labeled at the 3′ end using [α-^{32}P]dATP and terminal deoxynucleotidyl transferase (TdT).

Additional Materials *(also see Support Protocol 1)*

25 to 30 U/µl terminal deoxynucleotidyl transferase (TdT) and 5× TdT buffer (e.g., Life Technologies, Roche Molecular Biochemicals)
100 ng/µl antisense single-stranded oligonucleotide probe in H_2O
6000 Ci/mmol [α-^{32}P]dATP (20 mCi/ml; 3.33 nmol/ml)
Scintillant solution for aqueous samples (ReadySafe from Beckman or Aquasol from Packard)
1× STE (see recipe), sterile

37°C heating block
Sephadex columns: DNase/RNase-free STE Mirco Select-D G-25 Spin Column (5 Prime → 3 Prime) or NucTrap Push Column (Stratagene)
Scintillation counter and appropriate vials
β-shield column holder (Stratogene)
10- to 20-ml syringes

CAUTION: When working with radioactivity, take appropriate precautions to avoid contamination of the experimenter and the surroundings. Carry out the experiment and dispose of wastes in an appropriately designated area, following the guidelines provided by the local radiation safety officer (also see *APPENDIX 1A*).

CAUTION: When working with a radioactive isotope such as ^{32}P, strict radiation safety precautions should be taken to avoid exposure to harmful radioactivity and to prevent contamination of nonradioactive instruments and laboratory areas (also see *APPENDIX 1A*). Always wear powder-free gloves when working with RNA and radioactivity. Do not reuse gloves.

Prepare labeling-reaction mixture

1. Label the oligonucleotide by mixing the following reagents in an RNase-free sterile microcentrifuge tube in order (20 µl total volume):

   1.5 µl sterile RNase/DNase- and pyrogen-free H_2O (no DEPC)
   4 µl 5× TdT buffer
   2.5 µl 100 ng/µl antisense single-stranded oligonucleotide probe in H_2O
   10 µl [α-^{32}P]dATP (200 µCi)
   2 µl terminal deoxynucleotidyl transferase (TdT)

   Mix gently and incubate 1 to 1.5 hr in a heating block at 37°C.

   TdT labels the oligonucleotide by adding a radioactive poly(A) tail to the 3′ end.

Purify the probe by spin column

2a. At the end of the labeling incubation, elute the buffer from a DNase/RNase-free STE Micro-Select-D G-25 Spin Column by microcentrifuging 90 sec at 14,000 rpm. Transfer the spin column to a new RNase-free sterile microcentrifuge tube and set aside.

3a. Remove 1 µl (5% of total volume) from the labeling reaction mixture (step 1) and add to a scintillation vial containing 5 to 10 ml scintillant solution. Keep the vial for determination of percentage incorporation (step 6).

4a. Apply the rest of labeling reaction mixture from step 1 (now 19 µl) to the top of the column and let stand 2 to 3 min at room temperature. Microcentrifuge 60 sec at 14,000 rpm.

The resulting solution in the tube contains the purified oligonucleotide probe.

5a. Measure the volume of the eluate by drawing into a 20-µl pipetman. Remove an aliquot equivalent to 5% of the measured volume and add to a scintillation vial containing 5 to 10 ml scintillant solution to determine the counts after purification (see step 6).

CAUTION: *The column, which contains the unincorporated radioactive nucleotides, should be discarded strictly according to the institution's radiation safety guidelines.*

Purify the probe by Nuc Trap Push columns

2b. Put one column in the β-shield column holder and prime by adding 70 µl sterile 1× STE on top of the resin. Using a 10- to 20-ml syringe, push the buffer down the column slowly until the first drop appears at the tip end.

3b. Stop the labeling reaction (step 1) by adding 50 µl sterile 1× STE buffer to the microcentrifuge tube (total volume 70 µl). Take 2.8 µl (4% of total volume) from the final reaction mixture and add to a scintillation vial containing 5 to 10 ml scintillant solution. Keep the vial for determination of percent incorporation (step 6).

4b. Apply the rest of the final reaction mixture (now 67.3 µl) to the top of the primed Nuc Trap column and slowly push the sample down the column, using a 10- to 20-ml syringe, until most of the original volume has been eluted.

To avoid cross-contamination, use a different syringe for each sample.

5b. Measure the volume of the eluate by drawing into a 200-µl pipetman. Take out an aliquot equivalent to 4% of the measured volume and add to a scintillation vial containing 5 to 10 ml of scintillant solution to determine the counts after purification (see step 6).

CAUTION: *The column, which contains the unincorporated radioactive nucleotides, should be discarded strictly according to the radiation safety guidelines of the institution.*

In general, the total volume recovered is ~90 to 120 µl. The resulting solution contains the purified oligonucleotide probe.

6. Count the aliquots taken before and after column purification of the probe in a scintillation counter.

The first aliquot taken right before column purification gives the total counts (100%). The second aliquot taken after column purification gives the amount incorporated in the probe (final counts). Thus % incorporation = (final counts/total counts) × 100. The percent incorporation should be 20% to 60%. If the incorporation <10%, do not use the probe. The specific activity should be at least 100 cpm/µg [i.e., total final counts in cpm (after purification)/total amount of oligonucleotide probe labeled (assuming 100% recovery = 250 ng)].

SUPPORT PROTOCOL 3

STRIPPING AND REPROBING THE MEMBRANE

Bound radioactive oligonucleotides are stripped from a membrane before probing with another labeled oligonucleotide. This procedure saves considerable time by avoiding the RNA extraction and agarose gel separation steps for individual probes. Depending on the quality of the initial RNA and the type of probe used, membranes can be probed several times. By hybridizing with a probe detecting one of several housekeeping genes (e.g., cyclophilin, actin, ribosomal RNA subunit 18 S), which are known to be unaffected by stressful stimuli, the level of stress gene mRNA can be quantitatively normalized.

Additional Materials *(see Basic Protocol)*

Radioactive membrane to be stripped (see Basic Protocol)
0.01× SSPE (*UNIT 2.9*) containing 0.1% (w/v) SDS (*APPENDIX 2A*)
Formamide, deionized, minimum 99.5% (Sigma)
Secondary radioactive probe (see Support Protocol 2)

CAUTION: When working with radioactivity, take appropriate precautions to avoid contamination of the experimenter and the surroundings. Carry out the experiment and dispose of wastes in an appropriately designated area, following the guidelines provided by the local radiation safety officer (also see *APPENDIX 1A*).

CAUTION: To protect from radioactivity and RNase contamination as well as fingerprint smudges, always wear clean, powder-free gloves when working with RNA and radioisotopes. Do not reuse gloves.

1. After autoradiographic exposure (Basic Protocol, steps 34 and 35), incubate the radioactive membrane in 0.01× SSPE/0.1% SDS/50% formamide (final concentration), at 65°C for 0.5 to 1 min.
2. At the end of the incubation, check the activity of the membrane by holding a Geiger counter 2 to 3 cm above its surface.

After the stripping treatment, there should be no or a very minimal signal.

3. *Optional:* Expose the membrane to an X-ray film in an autoradiography cassette for 4 to 8 hr to determine the magnitude of the residual radioactive signal.

4. Hybridize with another radioactive probe or store membrane wrapped in plastic up to 2 to 3 weeks at 4°C.

REAGENTS AND SOLUTIONS

Use Milli-Q-purified water or equivalent in all recipes and protocol steps. For common solutions, see ***APPENDIX 2A****; for suppliers, see* ***SUPPLIERS APPENDIX****.*

Ethidium bromide, 10 mg/ml

0.01 g ethidium bromide
1 ml DEPC-treated H_2O (*UNIT 2.9*)
Mix well and store several months at 4°C in the dark (i.e., wrap with foil)

CAUTION: *Ethidium bromide is a mutagen. Wear gloves and make only a small volume at a time as needed.*

MOPS, 10×, 1×

Combine 400 ml DEPC-treated water and 20.9 g MOPS. Adjust pH to 7.0 with 10 M NaOH (*APPENDIX 2A*). Add 8.3 ml 3 M sodium acetate, pH 6.0 (*APPENDIX 2A*) and 10 ml 0.5 M EDTA, pH 8.0 (*APPENDIX 2A*). Adjust volume to 500 ml with water. Filter sterilize. Store in the dark at room temperature. Discard if it turns yellow. Dilute to 1× with DEPC-treated water.

RNA loading dye

0.5 ml glycerol
2 ml 0.5 M EDTA, pH 8.0 (*APPENDIX 2A*)
2.5 mg bromophenol blue
2.5 mg xylene cyanol FF
DEPC-treated H_2O (*UNIT 2.9*) to 1 ml
Store several months at 4°C

STE, 1×

2 ml 1 M Tris·Cl, pH 7.5 (20 mM final; *APPENDIX 2A*)
0.4 g $Na_4EDTA{\cdot}4\ H_2O$ (10 mM final)
0.6 g NaCl (100 mM final)
H_2O to 100 ml
Store up to 1 month above 4°C

Contributed by Marcelle Bergeron
Lilly Research Laboratories
Indianapolis, Indiana

Jari Honkaniemi
Tampere University Hospital
Tampere, Finland

Frank R. Sharp
University of Cincinnati
Cincinnati, Ohio

One-Dimensional SDS Gel Electrophoresis of Proteins

Electrophoresis is used to separate complex mixtures of proteins, (e.g., from cells, subcellular fractions, column fractions, or immunoprecipitates) to investigate subunit compositions, and to verify homogeneity of protein samples. It can also serve to purify proteins for use in further applications. In polyacrylamide gel electrophoresis, proteins migrate in response to an electrical field through pores in the gel matrix; pore size decreases with higher acrylamide concentrations. The combination of gel pore size and protein charge, size, and shape determines the migration rate of the protein.

The standard Laemmli method (see Basic Protocol 1) is used for discontinuous gel electrophoresis under denaturing conditions, that is, in the presence of sodium dodecyl sulfate (SDS). The standard method for full-size gels (e.g., 14 × 14 cm) can be adapted for the minigel format (e.g., 7.3 × 8.3 cm; see Basic Protocol 2). Minigels provide rapid separation but give lower resolution.

Several alternate protocols are provided for specific applications. The first two alternate protocols cover electrophoresis of peptides and small proteins, separations that require modification of standard buffers: either a Tris-tricine buffer system (see Alternate Protocol 1), or modified Tris buffer in the absence of urea (see Alternate Protocol 2). Continuous SDS-PAGE is a simplified method in which the same buffer is used for both gel and electrode solutions and the stacking gel is omitted (see Alternate Protocol 3). Other protocols cover the preparation and electrophoresis of various types of gels: ultrathin gels (see Alternate Protocol 4), multiple single-concentration gels (see Support Protocol 1), gradient gels (see Alternate Protocol 5), multiple gradient gels (see Support Protocol 2), and multiple gradient minigels (see Support Protocol 3). Proteins separated on gels can be subsequently analyzed by immunoblotting, autoradiography, or phosphor imaging (*APPENDIX 3D*), or staining with protein dyes.

CAUTION: Before any protocols are used, it is extremely important to read the following section about electricity and electrophoresis.

ELECTRICITY AND ELECTROPHORESIS

Many researchers are poorly informed concerning the electrical parameters of running a gel. It is important to note that the voltages and currents used during electrophoresis are dangerous and potentially lethal. Thus, safety should be an overriding concern. A working knowledge of electricity is an asset in determining what conditions to use and in troubleshooting the electrophoretic separation, if necessary. For example, an unusually high or low voltage for a given current (milliampere) might indicate an improperly made buffer or an electrical leak in the chamber.

Safety Considerations

1. Never remove or insert high-voltage leads unless the power supply voltage is turned down to zero and the power supply is turned off. Always grasp high-voltage leads one at a time with one hand only. Never insert or remove high-voltage leads with both hands. This can shunt potentially lethal electricity through the chest and heart should electrical contact be made between a hand and a bare wire. On older or homemade instruments, the banana plugs may not be shielded and can still be connected to the

Contributed by Sean R. Gallagher
Current Protocols in Toxicology (2001) A.3F.1-A.3F.34

power supply at the same time they make contact with a hand. Carefully inspect all cables and connections and replace frayed or exposed wires immediately.

2. Always start with the power supply turned off. Have the power supply controls turned all the way down to zero. Then hook up the gel apparatus: generally, connect the red high-voltage lead to the red outlet and the black high-voltage lead to the black outlet. Turn the power supply on with the controls set at zero and the high-voltage leads connected. Then, turn up the voltage, current, or power to the desired level. Reverse the process when the power supply is turned off: i.e., to disconnect the gel, turn the power supply down to zero, wait for the meters to read zero, turn off the power supply, and then disconnect the gel apparatus one lead at a time.

   CAUTION: *If the gel is first disconnected and then the power supply turned off, a considerable amount of electrical charge is stored internally. The charge will stay in the power supply over a long time. This will discharge through the outlets even though the power supply is turned off and can deliver an electrical shock.*

Ohm's Law and Electrophoresis

Understanding how a gel apparatus is connected to the power supply requires a basic understanding of Ohm's law: voltage = current × resistance, or $V = IR$. A gel can be viewed as a resistor and the power supply as the voltage and current source. Most power supplies deliver constant current or constant voltage. Some will also deliver constant power: power = voltage × current, or $VI = I^2R$. The discussion below focuses on constant current because this is the most common mode in vertical SDS-PAGE.

Most modern commercial equipment is color-coded so that the red or positive terminal of the power supply can simply be connected to the red lead of the gel apparatus, which goes to the lower buffer chamber. The black lead is connected to the black or negative terminal and goes to the upper buffer chamber. This configuration is designed to work with vertical slab gel electrophoreses in which negatively charged proteins or nucleic acids move to the positive electrode in the lower buffer chamber (an anionic system).

When a single gel is attached to a power supply, the negative charges flow from the negative cathode (black) terminal into the upper buffer chamber, through the gel, and into the lower buffer chamber. The lower buffer chamber is connected to the positive anode (red) terminal to complete the circuit. Thus, negatively charged molecules, such as SDS-coated proteins and nucleic acids, move from the negative cathode attached to the upper buffer chamber toward the positive anode attached to the lower chamber. SDS-PAGE is an anionic system because of the negatively charged SDS.

Occasionally, proteins are separated in cationic systems. In these gels, the proteins are positively charged because of the very low pH of the gel buffers (e.g., acetic acid/urea gels for histone separations) or the presence of a cationic detergent (e.g., cetyltrimethyl-ammonium bromide, CTAB). Proteins move toward the negative electrode (cathode) in cationic gel systems, and the polarity is reversed compared to SDS-PAGE: the red lead from the lower buffer chamber is attached to the black outlet of the power supply, and the black lead from the upper buffer chamber is attached to the red outlet of the power supply.

Most SDS-PAGE separations are performed under constant current (consult instructions from the manufacturer to set the power supply for constant current operation). The resistance of the gel will increase during SDS-PAGE in the standard Laemmli system. If the current is constant, then the voltage will increase during the run as the resistance goes up.

Power supplies usually have more than one pair of outlets. The pairs are connected in parallel with one another internally. If more than one gel is connected directly to the outlets

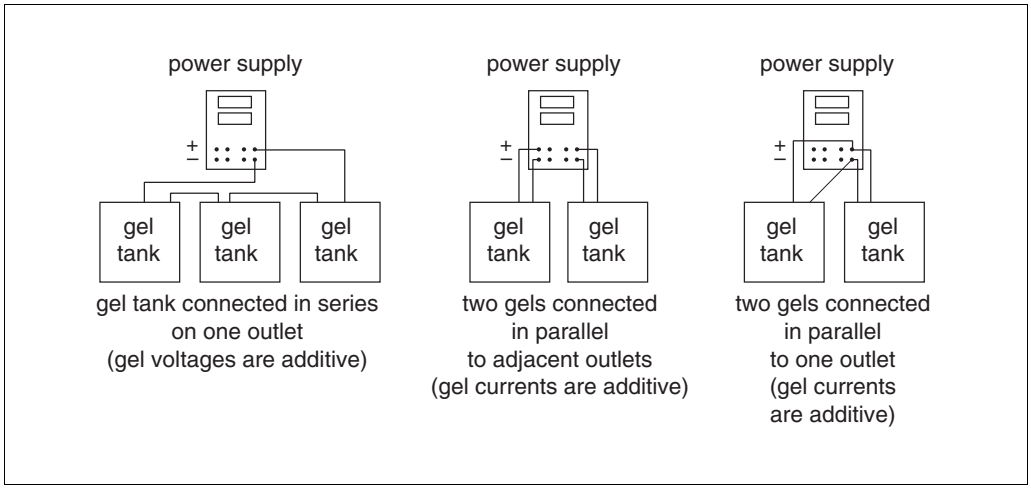

Figure A.3F.1 Series and parallel connections of gel tanks to power supply.

of a power supply, then these gels are connected in parallel. In a parallel circuit, the voltage is the same across each gel. In other words, if the power supply reads 100 V, then each gel has 100 V across its electrodes. The total current, however, is the sum of the individual currents going through each gel. Therefore, under constant current it is necessary to increase the current for each additional gel that is connected to the power supply. Two identical gels require double the current to achieve the same starting voltages and electrophoresis separation times.

Multiple gel apparatuses can also be connected to one pair of outlets on a power supply. This is useful with older power supplies that have a limited number of outlets. When connecting several gel units to one outlet, make certain the connections between the units are shielded and protected from moisture. The gels can be connected in parallel or in series (Fig. A.3F.1). In the case of two or more gels running off the same outlet in series, the current is the same for every gel. If 10 mA is displayed by the power supply meter, for example, each gel in series will experience 10 mA. The voltage, however, is additive for each gel. If one gel at a constant 10 mA produces 100 V, then two identical gels in series will produce 200 V (100 V each) and so on. Thus, the voltage can limit the number of units connected in series on low-voltage power supplies.

Gel thickness affects the above relationships. A 1.5-mm gel can be thought of as consisting of two 0.75-mm-thick gels run in parallel. Because currents are additive in parallel circuits, a 0.75-mm gel will require half the current of the 1.5-mm gel to achieve the same starting voltage and separation time. If a gel thickness is doubled, then the current must also be doubled. There are limits to the amount of current that can be applied. Thicker gels require more current, generating more heat that must be dissipated. Unless temperature control is available in the gel unit, a thick gel should be run more slowly than a thin gel.

NOTE: Milli-Q-purified water or equivalent should be used throughout the protocols.

BASIC PROTOCOL 1

DENATURING (SDS) DISCONTINUOUS GEL ELECTROPHORESIS: LAEMMLI GEL METHOD

One-dimensional gel electrophoresis under denaturing conditions (i.e., in the presence of 0.1% SDS) separates proteins based on molecular size as they move through a polyacrylamide gel matrix toward the anode. The polyacrylamide gel is cast as a separating gel (sometimes called resolving or running gel) topped by a stacking gel and secured in an electrophoresis apparatus. After sample proteins are solubilized by boiling in the presence of SDS, an aliquot of the protein solution is applied to a gel lane, and the individual proteins are separated electrophoretically. 2-Mercaptoethanol (2-ME) or dithiothreitol (DTT) is added during solubilization to reduce disulfide bonds.

This protocol is designed for a vertical slab gel with a maximum size of 0.75 mm × 14 cm × 14 cm. For thicker gels, or minigels (see Basic Protocol 2 and Support Protocol 3), the volumes of stacking and separating gels and the operating current must be adjusted. Additional protocols describe the preparation of ultrathin gels (see Alternate Protocol 4) and gradient gels (see Alternate Protocol 5), as well as the use of gel casters to make multiple gels, both single-concentration gels (see Support Protocol 1) and gradient gels (see Support Protocol 2).

Materials

Separating and stacking gel solutions (Table A.3F.1)
H_2O-saturated isobutyl alcohol
1× Tris·Cl/SDS, pH 8.8 (dilute 4× Tris·Cl/SDS, pH 8.8; Table A.3F.1)
Protein sample to be analyzed
2× and 1× SDS sample buffer (see recipe for 2×)
Protein molecular-weight-standards mixture (Table A.3F.2)
6× SDS sample buffer (see recipe; optional)
1× SDS electrophoresis buffer (see recipe for 5×)

Electrophoresis apparatus: Protean II 16-cm cell (Bio-Rad) or SE 600/400 16-cm unit (Amersham Pharmacia Biotech) with clamps, glass plates, casting stand, and buffer chambers
0.75-mm spacers
0.45-µm filters (used in stock solution preparation)
25-ml Erlenmeyer side-arm flask
Vacuum pump with cold trap
0.75-mm Teflon comb with 1, 3, 5, 10, 15, or 20 teeth
25- or 100-µl syringe with flat-tipped needle
Constant-current power supply (see introduction)

Pour the separating gel

1. Assemble the glass-plate sandwich of the electrophoresis apparatus according to manufacturer's instructions using two clean glass plates and two 0.75-mm spacers.

   If needed, clean the glass plates in liquid Alconox or RBS-35 (Pierce). These aqueous-based solutions are compatible with silver and Coomassie blue staining procedures.

2. Lock the sandwich to the casting stand.

3. Prepare the separating gel solution as directed in Table A.3F.1, degassing using a rubber-stoppered 25-ml Erlenmeyer side-arm flask connected with vacuum tubing to a vacuum pump with a cold trap. After adding the specified amount of 10% ammonium persulfate and TEMED to the degassed solution, stir gently to mix.

   Table A.3F.1 was prepared as a convenient summary to aid in the preparation of separating and stacking gels. The stacking gel is the same regardless of the separating gel used.

The desired percentage of acrylamide in the separating gel depends on the molecular size of the protein being separated. Generally, use 5% gels for SDS-denatured proteins of 60 to 200 kDa, 10% gels for SDS-denatured proteins of 16 to 70 kDa, and 15% gels for SDS-denatured proteins of 12 to 45 kDa (Table A.3F.1).

4. Using a Pasteur pipet, apply the separating gel solution to the sandwich along an edge of one of the spacers until the height of the solution between the glass plates is ~11 cm.

   Use the solution immediately; otherwise it will polymerize in the flask.

   Sample volumes <10 µl do not require a stacking gel. In this case, cast the resolving gel as you normally would, but extend the resolving gel into the comb to form the well. The proteins are then separated under the same conditions as used when a stacking gel is present. Although this protocol works well with single-concentration gels, a gradient gel is recommended for maximum resolution (see Alternate Protocol 5).

5. Using another Pasteur pipet, slowly cover the top of the gel with a layer (~1 cm thick) of H_2O-saturated isobutyl alcohol, by gently layering the isobutyl alcohol against the edge of one and then the other of the spacers.

   Be careful not to disturb the gel surface. The overlay provides a barrier to oxygen, which inhibits polymerization, and allows a flat interface to form during gel formation.

   The H_2O-saturated isobutyl alcohol is prepared by shaking isobutyl alcohol and H_2O in a separatory funnel. The aqueous (lower) phase is removed. This procedure is repeated several times. The final upper phase is H_2O-saturated isobutyl alcohol.

6. Allow the gel to polymerize 30 to 60 min at room temperature.

   A sharp optical discontinuity at the overlay/gel interface will be visible on polymerization. Failure to form a firm gel usually indicates a problem with the ammonium persulfate, TEMED (N, N, N′, N′-tetramethylethylenediamine), or both. Ammonium persulfate solution should be made fresh before use. Ammonium persulfate should "crackle" when added to the water. If not, fresh ammonium persulfate should be purchased. Purchase TEMED in small bottles so, if necessary, a new previously unopened source can be tried.

Pour the stacking gel

7. Pour off the layer of H_2O-saturated isobutyl alcohol and rinse with 1× Tris·Cl/SDS, pH 8.8.

   Residual isobutyl alcohol can reduce resolution of the protein bands; therefore, it must be completely removed. The isobutyl alcohol overlay should not be left on the gel longer than 2 hr.

8. Prepare the stacking gel solution as directed in Table A.3F.1.

   Use the solution immediately to keep it from polymerizing in the flask.

9. Using a Pasteur pipet, slowly allow the stacking gel solution to trickle into the center of the sandwich along an edge of one of the spacers until the height of the solution in the sandwich is ~1 cm from the top of the plates.

   Be careful not to introduce air bubbles into the stacking gel.

10. Insert a 0.75-mm Teflon comb into the layer of stacking gel solution. If necessary, add additional stacking gel to fill the spaces in the comb completely.

    Again, be careful not to trap air bubbles in the tooth edges of the comb; they will cause small circular depressions in the well after polymerization that will lead to distortion in the protein bands during separation.

11. Allow the stacking gel solution to polymerize 30 to 45 min at room temperature.

    A sharp optical discontinuity will be visible around wells on polymerization.

Table A.3F.1 Recipes for Polyacrylamide Separating and Stacking Gels[a]

SEPARATING GEL

Stock solution[b]	Final acrylamide concentration in separating gel (%)[c]									
	5	6	7	7.5	8	9	10	12	13	15
30% acrylamide/ 0.8% bisacrylamide	2.50	3.00	3.50	3.75	4.00	4.50	5.00	6.00	6.50	7.50
4× Tris·Cl/SDS, pH 8.8	3.75	3.75	3.75	3.75	3.75	3.75	3.75	3.75	3.75	3.75
H_2O	8.75	8.25	7.75	7.50	7.25	6.75	6.25	5.25	4.75	3.75
10% (w/v) ammonium persulfate[d]	0.05	0.05	0.05	0.05	0.05	0.05	0.05	0.05	0.05	0.05
TEMED	0.01	0.01	0.01	0.01	0.01	0.01	0.01	0.01	0.01	0.01

[a]The recipes produce 15 ml of separating gel and 5 ml of stacking gel, which are adequate for a gel of dimensions 0.75 mm × 14 cm × 14 cm. The recipes are based on the SDS (denaturing) discontinuous buffer system of Laemmli (1970).
[b]All reagents and solutions used in the protocol must be prepared with Milli-Q-purified water or equivalent.
[c]Units of numbers in table body are milliliters. The desired percentage of acrylamide in the separating gel depends on the molecular size of the protein being separated. See annotation to step 3, Basic Protocol 1.
[d]Best to prepare fresh.

Preparation of separating gel

In a 25-ml side-arm flask, mix 30% acrylamide/0.8% bisacrylamide solution, 4× Tris·Cl/SDS, pH 8.8 (see reagents, below), and H_2O. Degas under vacuum ~5 min. Add 10% ammonium persulfate and TEMED. Swirl gently to mix. Use immediately.

STACKING GEL (*3.9% acrylamide*)

In a 25-ml side-arm flask, mix 0.65 ml of 30% acrylamide/0.8% bisacrylamide, 1.25 ml of 4× Tris·Cl/SDS, pH 6.8 (see reagents, below), and 3.05 ml H_2O. Degas under vacuum 10 to 15 min. Add 25 µl of 10% ammonium persulfate and 5 µl TEMED. Swirl gently to mix. Use immediately. Failure to form a firm gel usually indicates a problem with the persulfate, TEMED, or both.

REAGENTS USED IN GELS

30% acrylamide/0.8% bisacrylamide

Mix 30.0 g acrylamide and 0.8 g *N,N′*-methylenebisacrylamide with H_2O in a total volume of 100 ml. Filter the solution through a 0.45-µm filter and store at 4°C in the dark. The 2× crystallized grades of acrylamide and bisacrylamide are recommended. Discard after 30 days, as acrylamide gradually hydrolyzes to acrylic acid and ammonia.

CAUTION: *Acrylamide monomer is neurotoxic. A mask should be worn when weighing acrylamide powder. Gloves should be worn while handling the solution, and the solution should not be pipetted by mouth.*

4× Tris·Cl/SDS, pH 6.8 *(0.5 M Tris·Cl containing 0.4% SDS)*

Dissolve 6.05 g Tris base in 40 ml H_2O. Adjust to pH 6.8 with 1 N HCl. Add H_2O to 100 ml total volume. Filter the solution through a 0.45-µm filter, add 0.4 g SDS, and store at 4°C up to 1 month.

4× Tris·Cl/SDS, pH 8.8 *(1.5 M Tris·Cl containing 0.4% SDS)*

Dissolve 91 g Tris base in 300 ml H_2O. Adjust to pH 8.8 with 1 N HCl. Add H_2O to 500 ml total volume. Filter the solution through a 0.45-µm filter, add 2 g SDS, and store at 4°C up to 1 month.

Prepare the sample and load the gel

12. Dilute a portion of the protein sample to be analyzed 1:1 (v/v) with 2× SDS sample buffer and heat 3 to 5 min at 100°C in a sealed screw-cap microcentrifuge tube. If the sample is a precipitated protein pellet, dissolve the protein in 50 to 100 µl of 1× SDS sample buffer and boil 3 to 5 min at 100°C. Dissolve protein-molecular-weight standards mixture in 1× SDS sample buffer according to supplier's instructions; use these standards as a control (Table A.3F.2).

For dilute protein solutions, consider adding 5:1 protein solution/6× SDS sample buffer to increase the amount of protein loaded. Proteins can also be concentrated by precipitation in acetone, ethanol, or trichloroacetic acid (TCA), but losses will occur.

For a 0.8-cm-wide well, 25 to 50 µg total protein in <20 µl is recommended for a complex mixture when staining with Coomassie blue, and 1 to 10 µg total protein is needed for samples containing one or a few proteins. If silver staining is used, 10- to 100-fold less protein can be applied (0.01 to 5 µg in <20 µl depending on sample complexity).

To achieve the highest resolution possible, the following precautions are recommended. Prior to adding the sample buffer, keep samples at 0°C. Add the SDS sample buffer (room temperature) directly to the 0°C sample (still on ice) in a screw-top microcentrifuge tube. Cap the tube to prevent evaporation, vortex, and transfer directly to a 100°C water bath for 3 to 5 min. Let immunoprecipitates dissolve for 1 hr at 56°C in 1× SDS sample buffer prior to boiling. DO NOT leave the sample in SDS sample buffer at room temperature without first heating to 100°C to inactivate proteases (see Critical Parameters and Troubleshooting). Endogenous proteases are very active in SDS sample buffer and will cause severe degradation of the sample proteins after even a few minutes at room temperature. To test for possible proteases, mix the sample with SDS sample buffer without heating and leave at room temperature for 1 to 3 hr. A loss of high-molecular-weight bands

Table A.3F.2 Molecular Weights of Protein Standards for Polyacrylamide Gel Electrophoresis[a]

Protein	Molecular weight
Cytochrome *c*	11,700
α-Lactalbumin	14,200
Lysozyme (hen egg white)	14,300
Myoglobin (sperm whale)	16,800
β-Lactoglobulin	18,400
Trypsin inhibitor (soybean)	20,100
Trypsinogen, PMSF treated	24,000
Carbonic anhydrase (bovine erythrocytes)	29,000
Glyceraldehyde-3-phosphate dehydrogenase (rabbit muscle)	36,000
Lactate dehydrogenase (porcine heart)	36,000
Aldolase	40,000
Ovalbumin	45,000
Catalase	57,000
Bovine serum albumin	66,000
Phosphorylase *b* (rabbit muscle)	97,400
β-Galactosidase	116,000
RNA polymerase, *E. coli*	160,000
Myosin, heavy chain (rabbit muscle)	205,000

[a]Protein standards are commercially available in kits (e.g., Amersham Pharmacia Biotech, Life Technologies, Bio-Rad, or Sigma).

and a general smearing of the banding pattern indicate a protease problem. Once heated, the samples can sit at room temperature for the time it takes to load samples.

13. Carefully remove the Teflon comb without tearing the edges of the polyacrylamide wells. After the comb is removed, rinse wells with 1× SDS electrophoresis buffer.

    The rinse removes unpolymerized monomer; otherwise, the monomer will continue to polymerize after the comb is removed, creating uneven wells that will interfere with sample loading and subsequent separation.

14. Using a Pasteur pipet, fill the wells with 1× SDS electrophoresis buffer.

    If well walls are not upright, they can be manipulated with a flat-tipped needle attached to a syringe.

15. Attach gel sandwich to upper buffer chamber following manufacturer's instructions.

16. Fill lower buffer chamber with the recommended amount of 1× SDS electrophoresis buffer.

17. Place sandwich attached to upper buffer chamber into lower buffer chamber.

18. Partially fill the upper buffer chamber with 1× SDS electrophoresis buffer so that the sample wells of the stacking gel are filled with buffer.

    Monitor the upper buffer chamber for leaks and if necessary, reassemble the unit. A slow leak in the upper buffer chamber may cause arcing around the upper electrode and damage the upper buffer chamber.

19. Using a 25- or 100-µl syringe with a flat-tipped needle, load the protein sample(s) into one or more wells by carefully applying the sample as a thin layer at the bottom of the wells. Load control wells with molecular weight standards. Add an equal volume of 1× SDS sample buffer to any empty wells to prevent spreading of adjoining lanes.

    Preparing the samples at approximately the same concentration and loading an equal volume to each well will ensure that all lanes are the same width and that the proteins run evenly. If unequal volumes of sample buffer are added to wells, the lane with the larger volume will spread during electrophoresis and constrict the adjacent lanes, causing distortions.

    The samples will layer on the bottom of the wells because the glycerol added to the sample buffer gives the solution a greater density than the electrophoresis buffer. The bromphenol blue in the sample buffer makes sample application easy to follow visually.

20. Fill the remainder of the upper buffer chamber with additional 1× SDS electrophoresis buffer so that the upper platinum electrode is completely covered. Do this slowly so that samples are not swept into adjacent wells.

Run the gel

21. Connect the power supply to the cell and run at 10 mA of constant current for a slab gel 0.75 mm thick, until the bromphenol blue tracking dye enters the separating gel. Then increase the current to 15 mA.

    For a standard 16-cm gel sandwich, 4 mA per 0.75-mm-thick gel will run ~15 hr (i.e., overnight); 15 mA per 0.75-mm gel will take 4 to 5 hr. To run two gels or a 1.5-mm-thick gel, simply double the current. When running a 1.5-mm gel at 30 mA, the temperature must be controlled (10° to 20°C) with a circulating constant-temperature water bath to prevent "smiling" (curvature in the migratory band). Temperatures <5°C should not be used because SDS in the running buffer will precipitate. If the level of buffer in the upper chamber decreases, a leak has occurred.

22. After the bromphenol blue tracking dye has reached the bottom of the separating gel, disconnect the power supply.

    Refer to Safety Considerations under Electricity and Electrophoresis.

Disassemble the gel

23. Discard electrode buffer and remove the upper buffer chamber with the attached gel sandwich.

24. Orient the gel so that the order of the sample wells is known, remove the sandwich from the upper buffer chamber, and lay the sandwich on a sheet of absorbent paper or paper towels.

25. Carefully slide one of the spacers halfway from the edge of the sandwich along its entire length. Use the exposed spacer as a lever to pry open the glass plate, exposing the gel.

26. Carefully remove the gel from the lower plate. Cut a small triangle off one corner of the gel so the lane orientation is not lost during staining and drying. Proceed with protein detection.

    The gel can be stained with Coomassie blue or silver (APPENDIX 3), or proteins can be electroeluted, electroblotted onto a polyvinylidene difluoride (PVDF) membrane for subsequent staining or sequence analysis, or transferred to a membrane for immunoblotting. If the proteins are radiolabeled, they can be detected by autoradiography (APPENDIX 3D).

ELECTROPHORESIS IN TRIS-TRICINE BUFFER SYSTEMS

ALTERNATE PROTOCOL 1

Separation of peptides and proteins under 10 to 15 kDa is not possible in the traditional Laemmli discontinuous gel system (see Basic Protocol 1). This is due to the comigration of SDS and smaller proteins, obscuring the resolution. Two approaches to obtain the separation of small proteins and peptides in the range of 5 to 20 kDa are presented: the following Tris-tricine method and a system using increased buffer concentrations (see Alternate Protocol 2). The Tris-tricine system uses a modified buffer to separate the SDS and peptides, thus improving resolution. Several precast gels are available for use with the tricine formulations (Table A.3F.3).

Table A.3F.3 Vertical Format Precast Gel Compatibility

Gel type and compatibility	Gel supplier			
	Bio-Rad	ISS/Daiichi	Jule	Novex
SDS-PAGE gel type offered				
Peptide (tricine)	×	×	×	×
Single concentration	×	×	×	×
Gradient	×	×	×	×
Minigel size	×	×	×	×
Standard gel size		×	×	
Compatibility of gel with equipment manufactured by				
Amersham Pharmacia Biotech		×	×	×
Bio-Rad	×	×	×	
Life Technologies	×	×	×	×
Novex		×		×
ISS/Daiichi		×	×	

Additional Materials *(also see Basic Protocol 1)*

Separating and stacking gel solutions (Table A.3F.4)
2× tricine sample buffer (see recipe)
Peptide molecular-weight-standards mixture (Table A.3F.5)
Cathode buffer (see recipe)
Anode buffer (see recipe)
Coomassie blue G-250 staining solution (see recipe)
10% (v/v) acetic acid

1. Prepare and pour the separating and stacking gels (see Basic Protocol 1, steps 1 to 11), using Table A.3F.4 in place of Table A.3F.1.
2. Prepare the sample (see Basic Protocol 1, step 12), but make the following changes for tricine gels. Substitute 2× tricine sample buffer for the 2× SDS sample buffer. Dilute an aliquot of the protein or peptide sample to be analyzed 1:1 (v/v) with 2× tricine sample buffer. Treat the sample at 40°C for 30 to 60 min prior to loading.

   If proteolytic activity is a problem, heating samples to 100°C for 3 to 5 min before loading the wells may be required (see Basic Protocol 1, annotation to step 12). Use the peptide molecular-weight-standards mixture for peptide separations (Table A.3F.5).

3. Load the gel and set up the electrophoresis apparatus (see Basic Protocol 1, steps 13 to 20) with the following alterations. Remove comb and, using the tricine-containing

Table A.3F.4 Recipes for Tricine Peptide Separating and Stacking Gels[a]

SEPARATING AND STACKING GELS

Stock solution[b]	Separating gel	Stacking gel
30% acrylamide/0.8% bisacrylamide	9.80 ml	1.62 ml
Tris·Cl/SDS, pH 8.45	10.00 ml	3.10 ml
H_2O	7.03 ml	7.78 ml
Glycerol	4.00 g (3.17 ml)	—
10% (w/v) ammonium persulfate[c]	50 µl	25 µl
TEMED	10 µl	5 µl

[a]The recipes produce 30 ml of separating gel and 12.5 ml of stacking gel, which are adequate for two gels of dimensions 0.75 mm × 14 cm × 14 cm. The recipes are based on the Tris-tricine buffer system of Schagger and von Jagow (1987).
[b]All reagents and solutions used in the protocol must be prepared with Milli-Q-purified water or equivalent.
[c]Best to prepare fresh.

Prepare separating and stacking gel solutions separately.

In a 50-ml side-arm flask, mix 30% acrylamide/0.8% bisacrylamide solution (Table A.3F.1), Tris·Cl/SDS, pH 8.45 (see reagents, below), and H_2O. Add glycerol to separating gel only. Degas under vacuum 10 to 15 min. Add 10% ammonium persulfate and TEMED. Swirl gently to mix, use immediately. Failure to form a firm gel usually indicates a problem with the persulfate, TEMED, or both.

ADDITIONAL REAGENTS USED IN GELS

Tris·Cl/SDS, pH 8.45 (3.0 M Tris·Cl containing 0.3% SDS)

Dissolve 182 g Tris base in 300 ml H_2O. Adjust to pH 8.45 with 1 N HCl. Add H_2O to 500 ml total volume. Filter the solution through a 0.45-µm filter, add 1.5 g SDS, and store at 4°C up to 1 month.

Table A.3F.5 Molecular Weights of Peptide Standards for Polyacrylamide Gel Electrophoresis[a]

Peptide	Molecular weight (Da)
Myoglobin (polypeptide backbone)	16,950
Myoglobin 1-131	14,440
Myoglobin 56-153	10,600
Myoglobin 56-131	8,160
Myoglobin 1-55	6,210
Glucagon	3,480
Myoglobin 132-153	2,510

[a]Peptide standards are commercially available from Sigma.

cathode buffer, or water, rinse once and fill wells. Fill the lower buffer chamber with anode buffer, assemble the unit, and attach the upper buffer chamber. Fill the upper buffer chamber with cathode buffer and load the samples.

4. Connect the power supply to the cell and run 1 hr at 30 V (constant voltage) followed by 4 to 5 hr at 150 V (constant voltage). Use heat exchanger to keep the electrophoresis chamber at room temperature.

5. After the tracking dye has reached the bottom of the separating gel, disconnect the power supply.

   Refer to Safety Considerations in the introduction.

   Coomassie blue G-250 is used as a tracking dye instead of bromphenol blue because it moves ahead of the smallest peptides.

6. Disassemble the gel (see Basic Protocol 1, steps 23 to 26). Stain proteins in the gel for 1 to 2 hr in Coomassie blue G-250 staining solution. Follow by destaining with 10% acetic acid, changing the solution every 30 min until background is clear (3 to 5 changes). For higher sensitivity, use silver staining as a recommended alternative.

   Prolonged staining and destaining will result in the loss of resolution of the smaller proteins (<10 kDa). Proteins diffuse within the gel and out of the gel, resulting in a loss of staining intensity and resolution.

NONUREA PEPTIDE SEPARATIONS WITH TRIS BUFFERS

ALTERNATE PROTOCOL 2

A simple modification of the traditional Laemmli buffer system presented in Basic Protocol 1, in which the increased concentration of buffers provides better separation between the stacked peptides and the SDS micelles, permits reasonable separation of peptides as small as 5 kDa.

Additional Materials *(also see Basic Protocol 1)*

Separating and stacking gel solutions (Table A.3F.6)
2× SDS electrophoresis buffer (see recipe)
2× Tris·Cl/SDS, pH 8.8 (dilute 4× Tris·Cl/SDS, pH 8.8; Table A.3F.1)

1. Prepare and pour the separating gel (see Basic Protocol 1, steps 1 to 6) using Table A.3F.6 in place of Table A.3F.1.

2. Prepare and pour the stacking gel (see Basic Protocol 1, steps 7 to 11), using 2× Tris·Cl/SDS, pH 8.8, rather than 1× Tris·Cl/SDS buffer, for rinsing the gel after removing the isobutyl alcohol overlay.

3. Prepare the sample and load the gel (see Basic Protocol 1, steps 12 to 20) and substitute 2× SDS electrophoresis buffer for the 1× SDS electrophoresis buffer.

   Table A.3F.5 lists the standards for small protein separations.

4. Run the gel (see Basic Protocol 1, steps 21 and 22).

   Note that the separations will take ~25% longer than those using Basic Protocol 1. The increased buffer concentrations lead to faster transit through the stacking gel but lower mobility in the resolving gel.

5. Disassemble the gel (see Basic Protocol 1, steps 23 to 26).

   Proteins in the gel may now be stained.

Table A.3F.6 Recipes for Modified Laemmli Peptide Separating and Stacking Gels[a]

SEPARATING AND STACKING GELS

Stock solution[b]	Separating gel	Stacking gel
30% acrylamide/0.8% bisacrylamide	10.00 ml	0.65 ml
8× Tris·Cl, pH 8.8	3.75 ml	—
4× Tris·Cl, pH 6.8	—	1.25 ml
10% (w/v) SDS	0.15 ml	50 µl
H_2O	1.00 ml	3.00 ml
10% (w/v) ammonium persulfate[c]	50 µl	25 µl
TEMED	10 µl	5 µl

[a]The recipes produce 15 ml of separating gel and 5 ml of stacking gel, which are adequate for one gel of dimensions 0.75 mm × 14 cm × 14 cm. The recipes are based on the modified Laemmli peptide separation system of Okajima et al. (1993).

[b]All reagents and solutions used in the protocol must be prepared with Milli-Q-purified water or equivalent.

[c]Best to prepare fresh.

Prepare separating and stacking gel solutions separately

In a 25-ml side-arm flask, mix 30% acrylamide/0.8% bisacrylamide solution (see Table A.3F.1), 8× Tris·Cl, pH 8.8 (separating gel) or 4× Tris·Cl, pH 6.8 (stacking gel), 10% SDS (see reagents, below), and H_2O. Degas under vacuum 10 to 15 min. Add 10% ammonium persulfate and TEMED. Swirl gently to mix; use immediately. Failure to form a firm gel usually indicates a problem with the persulfate, TEMED, or both.

ADDITIONAL REAGENTS USED IN GELS

4× Tris·Cl, pH 6.8 *(0.5 M Tris·Cl)*

Dissolve 6.05 g Tris base in 40 ml H_2O. Adjust to pH 6.8 with 1 N HCl. Add H_2O to 100 ml total volume. Filter the solution through a 0.45-µm filter and store up to 1 month at 4°C.

8× Tris·Cl, pH 8.8 *(3.0 M Tris·Cl)*

Dissolve 182 g Tris base in 300 ml H_2O. Adjust to pH 8.8 with 1 N HCl. Add H_2O to 500 ml total volume. Filter the solution through a 0.45-µm filter and store up to 1 month at 4°C.

10% (w/v) SDS

Mix 1 g SDS in 10 ml of H_2O. Use immediately.

CONTINUOUS SDS-PAGE

With continuous SDS-PAGE, the same buffer is used for both the gel and electrode solutions. Although continuous gels lack the resolution of the discontinuous systems, they are extremely versatile, less prone to mobility artifacts, and much easier to prepare. The stacking gel is omitted.

Additional Materials *(also see Basic Protocol 1)*

Separating gel solution (Table A.3F.7)
2× and 1× phosphate/SDS sample buffer (see recipe)
1× phosphate/SDS electrophoresis buffer (see recipe)

1. Prepare and pour a single separating gel (see Basic Protocol 1, steps 1 to 4), except use solutions in Table A.3F.7 in place of those in Table A.3F.1 and fill the gel sandwich to the top. Omit the stacking gel. Insert the comb (see Basic Protocol 1, step 10) and allow the gel to polymerize 30 to 60 min at room temperature.
2. Mix the protein sample 1:1 with 2× phosphate/SDS sample buffer and heat to 100°C for 2 min.

   For large sample volumes or samples suspended in high ionic strength buffers (>50 mM), dialyze against 1× sample buffer prior to electrophoresis. Note that the precautions about proteases (see Basic Protocol 1, step 12) apply here.

Table A.3F.7 Recipes for Separating Gels for Continuous SDS-PAGE[a]

SEPARATING GEL

Stock solution[b]	Final acrylamide concentration in separating gel (%)[c]										
	5	6	7	8	9	10	11	12	13	14	15
30% acrylamide/ 0.8% bisacrylamide	2.5	3.00	3.50	4.00	4.50	5.00	5.50	6.00	6.50	7.00	7.50
4× phosphate/SDS, pH 7.2	3.75	3.75	3.75	3.75	3.75	3.75	3.75	3.75	3.75	3.75	3.75
H_2O	8.75	8.25	7.75	7.25	6.75	6.25	5.75	5.25	4.75	4.25	3.75
10% (w/v) ammonium persulfate[d]	0.05	0.05	0.05	0.05	0.05	0.05	0.05	0.05	0.05	0.05	0.05
TEMED	0.01	0.01	0.01	0.01	0.01	0.01	0.01	0.01	0.01	0.01	0.01

[a]The recipes produce 15 ml of separating gel, which is adequate for one gel of dimensions 0.75 mm × 14 cm × 14 cm. The recipes are based on the original continuous phosphate buffer system of Weber et al. (1972). The stacking gel is omitted.
[b]All reagents and solutions used in the protocol must be prepared with Milli-Q-purified water or equivalent.
[c]Units of numbers in table body are milliliters. The desired percentage of acrylamide in the separating gel depends on the molecular size of the protein being separated. See Basic Protocol 1, annotation to step 3.
[d]Best to prepare fresh.

Preparation of separating gel

In a 25-ml side-arm flask, mix 30% acrylamide/0.8% bisacrylamide solution (see Table A.3F.1), 4× phosphate/SDS, pH 7.2, and H_2O. Degas under vacuum about 5 min. Add 10% ammonium persulfate and TEMED. Swirl gently to mix. Use immediately.

ADDITIONAL REAGENTS USED IN GELS

4× phosphate/SDS, pH 7.2 *(0.4 M sodium phosphate/0.4% SDS)*

Mix 46.8 g $NaH_2PO_4 \cdot H_2O$, 231.6 g $Na_2HPO_4 \cdot 7\ H_2O$, and 12 g SDS in 3 liters H_2O.

Store at 4°C for up to 3 months.

3. Assemble the electrophoresis apparatus and load the sample (see Basic Protocol 1, steps 13 to 20), using the phosphate/SDS electrophoresis buffer and loading empty wells with 1× phosphate/SDS sample buffer.

4. Connect the power supply and start the run with 15 mA per 0.75-mm-thick gel until the tracking dye has entered the gel. Continue electrophoresis at 30 mA for 3 hr (5% gel), 5 hr (10% gel), 8 hr (15% gel), or until the dye reaches the bottom of the gel.

   Use temperature control if available to maintain the gel at 15° to 20°C. SDS will precipitate below 15°C in this system.

5. Disassemble the gel (see Basic Protocol 1, steps 23 to 26).

   Refer to Safety Considerations in introduction. Proteins in the gel may now be stained.

ALTERNATE PROTOCOL 4

CASTING AND RUNNING ULTRATHIN GELS

Ultrathin gels provide superb resolution but are difficult to handle. In this application, gels are cast on Gel Bond, a Mylar support material. Silver staining is recommended for the best resolution. Combs and spacers for gels <0.5 mm thick are not readily available for most protein electrophoresis units. However, by adapting combs and spacers used for DNA sequencing, casting gels from 0.2 to 0.5 mm thick is straightforward.

Additional Materials *(also see Basic Protocol 1)*

95% (v/v) ethanol
Gel Bond (FMC BioProducts) cut to a size slightly smaller than the gel plate dimensions
Glue stick
Ink roller (available from art supply stores)
Combs and spacers (0.19 to 0.5 mm; sequencing gel spacers and combs can be cut to fit)

1. Wash gel plates with water-based laboratory detergent followed by successive rinses with hot tap water, deionized water, and finally 95% ethanol. Allow to air dry.

   Gel plates must be extremely clean for casting thin gels.

   Gloves are needed throughout these procedures to prevent contamination by proteins on the surface of skin.

2. Apply a streak of adhesive from a glue stick to the bottom edge of the glass plate. Quickly position the Gel Bond with the hydrophobic side down (a drop of water will bead up on the hydrophobic surface). Apply pressure with Kimwipe tissue to attach the Gel Bond firmly to the plate. Finally, pull the top portion of the Gel Bond back, place a few drops of water underneath, and roll flat with an ink roller.

   Make sure the Gel Bond does not extend beyond the edges of the upper and lower sealing surface of the plate. This will cause it to buckle on sealing. Reposition the Gel Bond if needed to prevent it from extending beyond the glass plate. Material may also be trimmed to fit flush with the plate edge.

3. Assemble the gel cassette according to the manufacturer's instructions (also see Basic Protocol 1, steps 1 and 2). Just prior to assembly, blow air over the surface of both the Gel Bond and the opposing glass surface to remove any particulate material (e.g., dust).

   Sequencing gel spacers can be easily adapted. First, cut the spacers slightly longer than the length of the gel plate. Position a spacer along each edge of the glass plate and assemble the gel sandwich, clamping in place. With a razor blade, trim the excess spacer at top and bottom to get a reusable spacer exactly the size of the plate.

4. Prepare and pour the separating and stacking gels (see Basic Protocol 1, steps 3 to 9). In place of the Teflon comb, insert a square well sequencing comb cut to fit within the gel sandwich. Allow the stacking gel to polymerize 30 to 45 min at room temperature.

   Less solution is needed for ultrathin gels. For example, a 0.5-mm-thick gel requires 33% less gel solution than a 0.75-mm gel.

5. Prepare the sample and load the gel (see Basic Protocol 1, steps 12 to 20).

   When preparing protein samples for ultrathin gels, 3 to 4 µl at 5 µg protein/µl is required for Coomassie blue R-250 staining, whereas 10-fold less is needed for silver staining.

6. Run the gel (see Basic Protocol 1, steps 21 and 22), except conduct the electrophoresis at 7 mA/gel (0.25-mm-thick gels) or 14 mA/gel (0.5-mm-thick gels) for 4 to 5 hr.

7. When the separation is complete, disassemble the unit and remove the gel (see Basic Protocol 1, steps 23 to 26) with the Gel Bond still attached. With a gloved hand, wash away the adhesive material from the back of the Gel Bond under a stream of water before proceeding to protein detection.

   Either Coomassie blue or silver staining may be used, but silver staining produces particularly fine resolution with thin Gel Bond–backed gels. Compared to staining thicker (>0.75 mm) gels, thin (<0.75 mm) gels stain and destain more quickly. Although the optimum staining times must be empirically determined, all steps in Coomassie blue and silver staining procedures are generally reduced by half.

CASTING MULTIPLE SINGLE-CONCENTRATION GELS

SUPPORT PROTOCOL 1

Casting multiple gels at one time has several advantages. All the gels are identical, so sample separation is not affected by gel-to-gel variation. Furthermore, casting ten gels is only slightly more difficult than casting two gels. Once cast, gels can be stored for several days in a refrigerator.

Additional Materials *(also see Basic Protocol 1)*

Separating and stacking gels for single-concentration gels (Table A.3F.8)
H_2O-saturated isobutyl alcohol

Multiple gel caster (Bio-Rad, Amersham Pharmacia Biotech)
100-ml disposable syringe and flat-tipped needle
Extra plates and spacers
14 × 14–cm acrylic blocks or polycarbonate sheets
250- and 500-ml side-arm flasks (used in gel preparation)
Long razor blade *or* plastic wedge (Wonder Wedge, Amersham Pharmacia Biotech)
Resealable plastic bags

Pour the separating gel

1. Assemble the multiple gel caster according to the manufacturer's instructions.

   With the Amersham Pharmacia Biotech unit make sure to insert the large triangular space filler plug in the base of the caster. The plug is removed when casting gradient gels (see Support Protocol 2).

2. Assemble glass sandwiches and stack them in the casting chamber. Stack up to ten 1.5-mm gels and fill in extra space with acrylic blocks or polycarbonate sheets to hold the sandwiches tightly in place. Make sure the spacers are straight along the top, right, and left edges of the glass plates and that all edges of the stack are flush.

   The presence of loosely fitting sandwiches in the caster will lead to unevenly cast gels, creating distortions during electrophoresis. Polycarbonate inhibits gel polymerization.

Table A.3F.8 Recipes for Multiple Single-Concentration Polyacrylamide Gels[a]

SEPARATING GEL

Stock solution[b]	Final acrylamide concentration in separating gel (%)[c]										
	5	6	7	8	9	10	11	12	13	14	15
30% acrylamide/0.8% bisacrylamide	52	62	72	83	93	103	114	124	134	145	155
4× Tris·Cl/SDS, pH 8.8	78	78	78	78	78	78	78	78	78	78	78
H_2O	181	171	160	150	140	129	119	109	98	88	78
10% (w/v) ammonium persulfate[d]	1.0	1.0	1.0	1.0	1.0	1.0	1.0	1.0	1.0	1.0	1.0
TEMED	0.21	0.21	0.21	0.21	0.21	0.21	0.21	0.21	0.21	0.21	0.21

[a]The recipes produce about 300 ml of separating gel and 100 ml of stacking gel, which are adequate for ten gels of dimensions 1.5 mm × 14 cm × 14 cm. Volumes were measured using 1.5-mm spacers. For thinner spacers or fewer gels, calculate volumes using the equation in the annotation to step 4. The recipes are based on the SDS (denaturing) discontinuous buffer system of Laemmli (1970).

[b]All reagents and solutions used in the protocol must be prepared with Milli-Q-purified water or equivalent.

[c]Units of numbers in table body are milliliters. The desired percentage of acrylamide in separating gel depends on the molecular size of the protein being separated. See Basic Protocol 1, annotation to step 3.

[d]Best to prepare fresh.

Preparation of separating gel

In a 500-ml side-arm flask, mix 30% acrylamide/0.8% bisacrylamide solution (see Table A.3F.1), 4× Tris·Cl/SDS, pH 8.8 (Table A.3F.1), and H_2O. Degas under vacuum ~5 min. Add 10% ammonium persulfate and TEMED. Swirl gently to mix; use immediately.

STACKING GEL

In a 250-ml side-arm flask, mix 13.0 ml 30% acrylamide/0.8% bisacrylamide solution, 25 ml 4× Tris·Cl/SDS, pH 6.8 (Table A.3F.1), and 61 ml H_2O. Degas under vacuum ~5 min. Add 0.25 ml 10% ammonium persulfate and 50 µl TEMED. Swirl gently to mix. Use immediately. Failure to form a firm gel usually indicates a problem with the persulfate, TEMED, or both.

Therefore, if polycarbonate sheets are placed in the caster before and after the set of glass sandwiches, the entire set will slide out as one block after polymerization. Placing polycarbonate sheets between each gel sandwich makes them easier to separate from one another after polymerization.

3. Place the front sealing plate on the casting chamber, making sure the stack fits snugly. Secure the plate with four spring clamps and tighten the bottom thumb screws.

4. Prepare the separating (resolving) gel solution (Table A.3F.8).

   A 12-cm separating gel with a 4-cm stacking gel is recommended.

   If fewer than ten gels are prepared (Table A.3F.8), use the following formula to estimate the amount of separating gel volume needed:

   Volume = gel number × height (cm) × width (cm) × thickness (cm) + 4 × gel number + 10 ml.

5. Using a 100-ml disposable syringe with flat-tipped needle, inject the resolving gel solution down the side of one spacer into the multiple caster. A channel in the silicone plug distributes the solution throughout the whole caster. Avoid introducing bubbles by giving the caster a quick tap on the benchtop once the caster is filled.

6. Overlay the center of each gel with 100 µl H_2O-saturated isobutyl alcohol and let polymerize for 1 to 2 hr.
7. Drain off the overlay and rinse the surface with 1× Tris·Cl/SDS, pH 8.8. If the gels will not be used immediately, skip to step 12.

Pour the stacking gel

8. Prepare the stacking gel solution either singly (see Basic Protocol 1, step 8) or for all the gels at once (Table A.3F.8).

   The stacking gel solution should be prepared just before pouring the gel.

9. Fill each sandwich in the caster with stacking gel solution.
10. Insert a comb into each sandwich and let the gel polymerize for 2 hr.

    Insert the combs at a 45° angle to avoid trapping air underneath the comb teeth. Air bubbles will inhibit polymerization and cause dents in the wells and a distorted pattern of protein bands.

11. Remove the combs and rinse wells with 1× SDS electrophoresis buffer.

Remove the gels from the caster

12. Remove the gels from the caster and separate by carefully inserting a long razor blade or knife between each gel sandwich.

    A plastic wedge (Amersham Pharmacia Biotech's Wonder Wedge) also works well.

13. Clean the outside of each gel plate with running water to remove the residual polymerized and unpolymerized acrylamide.
14. Overlay gels to be stored with 1× Tris·Cl/SDS, pH 8.8, place in a resealable plastic bag, and store at 4°C until needed (up to 1 week).

SEPARATION OF PROTEINS ON GRADIENT GELS

ALTERNATE PROTOCOL 5

Gels that consist of a gradient of increasing polyacrylamide concentration resolve a much wider size range of proteins than standard uniform-concentration gels (see Critical Parameters and Troubleshooting). The protein bands, particularly in the low-molecular-weight range, are also much sharper. Unlike single-concentration gels, gradient gels separate proteins in a way that can be represented easily to give a linear plot from 10 to 200 kDa. This facilitates molecular weight estimations.

The quantities given below provide separating gel solution sufficient for two 0.75-mm gels (~7 ml of each concentration) or one 1.5-mm gel (~14 ml of each concentration). Volumes can be adjusted to accommodate gel sandwiches of different dimensions.

Additional Materials *(also see Basic Protocol 1)*

Light and heavy acrylamide gel solutions (Table A.3F.9 and Table A.3F.10)
Bromphenol blue (optional; for checking practice gradient)
TEMED

Gradient maker (30 to 50 ml, Amersham Pharmacia Biotech SG30 or SG50; *or* 30 to 100 ml, Bio-Rad 385)
Tygon tubing with micropipet tip
Peristaltic pump (optional; e.g., Markson A-13002, A-34040, or A-34105 minipump)
Whatman 3MM filter paper

Set up the gradient maker and prepare the gel solutions

1. Assemble the magnetic stirrer and gradient maker on a ring stand as shown in Figure A.3F.2. Connect the outlet valve of the gradient maker to Tygon tubing attached to a micropipet tip that is placed over the vertical gel sandwich. If desired, place a peristaltic pump in line between the gradient maker and the gel sandwich.

   A peristaltic pump will simplify casting by providing a smooth flow rate.

2. Place a small stir-bar into the mixing chamber of the gradient maker (i.e., the chamber connected to the outlet).

3. Using the recipes in Table A.3F.9 and Table A.3F.10, prepare light and heavy acrylamide gel solutions. Do not add ammonium persulfate until just before use (step 7).

4. With the outlet port and interconnecting valve between the two chambers closed, pipet 7 ml of light (low-concentration) acrylamide gel solution into the reservoir chamber for one 0.75-mm-thick gradient gel.

   Recommended gradient ranges are 5% to 20% for most applications (to separate proteins of 10 to several hundred kilodaltons).

   A practice run with heavy and light solutions is recommended. Bromphenol blue should be added to the heavy solution to demonstrate linearity of the practice gradient.

5. Open the interconnecting valve briefly to allow a small amount (~200 µl) of light solution to flow through the valve and into the mixing chamber.

   The presence of air bubbles in the interconnecting valve may obstruct the flow between chambers during casting.

   Deaeration is not recommended for either the light or heavy solution. Omitting the deaeration will allow polymerization to proceed more slowly, letting the gradient establish itself in the gel sandwich before polymerization takes place.

6. Add 7 ml of heavy (high-concentration) acrylamide gel solution to the mixing chamber.

   Keep the heavy solution on ice until use. Once the ammonium persulfate is added to the heavy solution, it will polymerize without TEMED, albeit more slowly; keeping the solution on ice prevents this. The gel solution will come to room temperature during casting. The higher the percentage of acrylamide, the more severe the problem of premature polymerization is.

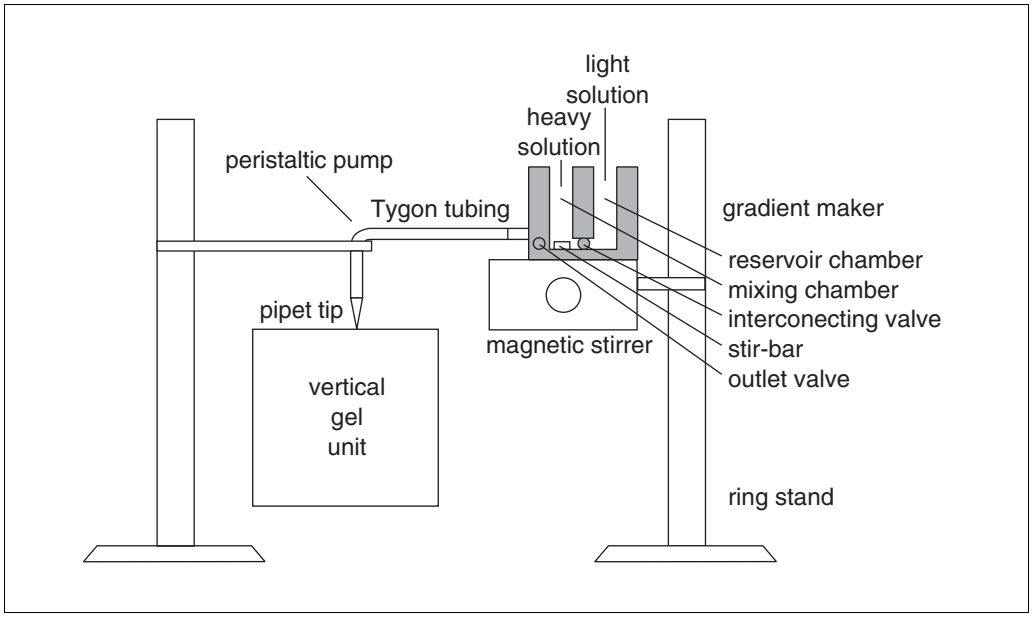

Figure A.3F.2 Gradient gel setup. A peristaltic pump, though not required, will provide better control.

Table A.3F.9 Light Acrylamide Gel Solutions for Gradient Gels[a]

Stock solution	Acrylamide concentration of light gel solution (%)[b]									
	5	6	7	8	9	10	11	12	13	14
30% acrylamide/ 0.8% bisacrylamide[c]	2.5	3.0	3.5	4.0	4.5	5.0	5.5	6.0	6.5	7.0
4× Tris·Cl/SDS, pH 8.8[c]	3.75	3.75	3.75	3.75	3.75	3.75	3.75	3.75	3.75	3.75
H_2O	8.75	8.25	7.75	7.25	6.75	6.25	5.75	5.25	4.75	4.25
10% (w/v) ammonium persulfate[d]	0.05	0.05	0.05	0.05	0.05	0.05	0.05	0.05	0.05	0.05

[a]To survey proteins ≥10 kDa, 5%-20% gradient gels are recommended. To expand the range between 10 and 200 kD, a 10%-20% gel is recommended.

[b]Numbers in body of table are milliliters of stock solution. Deaeration is not required. Keep solution at room temperature prior to adding TEMED no longer than 1 hr.

[c]See Table A.3F.1 for preparation.

[d]Best to prepare fresh.

Table A.3F.10 Heavy Acrylamide Gel Solutions for Gradient Gels[a]

Stock solution	Acrylamide concentration of heavy gel solution (%)[b]										
	10	11	12	13	14	15	16	17	18	19	20
30% acrylamide/ 0.8% bisacrylamide[c]	5.0	5.5	6.0	6.5	7.0	7.5	8.0	8.5	9.0	9.5	10.0
4× Tris·Cl/SDS, pH 8.8[c]	3.75	3.75	3.75	3.75	3.75	3.75	3.75	3.75	3.75	3.75	3.75
H_2O	5.0	4.5	4.0	3.5	3.0	2.5	2.0	1.5	1.0	0.5	0
Sucrose (g)	2.25	2.25	2.25	2.25	2.25	2.25	2.25	2.25	2.25	2.25	2.25
10% (w/v) ammonium persulfate[d]	0.05	0.05	0.05	0.05	0.05	0.05	0.05	0.05	0.05	0.05	0.05

[a]Deaeration is not recommended for gradient gels.

[b]Numbers in body of table are milliliters of stock solution (except sucrose). Do not add the ammonium persulfate until just before use. The heavy acrylamide will polymerize, albeit more slowly, without the addition of TEMED. Keep the heavy solution on ice after adding ammonium persulfate.

[c]See Table A.3F.1 for preparation.

[d]Best to prepare fresh.

7. Add the specified amount of 10% ammonium persulfate and ~2.3 µl TEMED per 7 ml acrylamide solution to each chamber. Mix the solutions in each chamber with a disposable pipet.

Form the gradient and cast the gel

8. Open the interconnecting valve completely.

   Some of the heavy solution will flow back into the reservoir chamber containing light solution as the two chambers equilibrate. This will not affect the formation of the gradient.

9. Turn on the magnetic stirrer and adjust the rate to produce a slight vortex in the mixing chamber.

10. Open the outlet of the gradient maker slowly. Adjust the outlet valve to a flow rate of 2 ml/min. If using a peristaltic pump, calibrate the flow rate with a graduated cylinder prior to casting the gel.

    Some adjustment of the flow rate may be necessary during casting. If the light solution is not flowing into the mixing chamber, a bubble may be caught in the interconnecting valve.

Quickly close the outlet and cover the top of the reservoir chamber with a gloved thumb. Push down with the thumb to increase the pressure in the chamber and force the air bubble out of the center valve.

11. Fill the gel sandwich from the top. Place the pipet tip against one side of the sandwich so the solution flows down one plate only. The heavy solution will flow into the sandwich first, followed by progressively lighter solution.

12. Watch as the last of the light solution drains into the outlet tube and adjust the flow rate to ensure that the last few milliliters of solution do not flow quickly into the gel sandwich and disturb the gradient.

13. Overlay the gradient gel with H_2O-saturated isobutyl alcohol. Allow the gel to polymerize ~1 hr.

    In this gel system, the gel will polymerize from the bottom (i.e., heavy solution) up. Because polymerization is an exothermic reaction, heat can be felt evolving from the bottom of the gel sandwich during polymerization. A sharp optical discontinuity at the gel-overlay interface indicates that polymerization has occurred. In general, 1 hr is adequate for polymerization.

14. Remove the H_2O-saturated isobutyl alcohol and rinse with 1× Tris·Cl/SDS, pH 8.8. Cast the stacking gel (see Basic Protocol 1, steps 8 to 11).

    The gel can be covered with 1× Tris·Cl/SDS, pH 8.8, sealed in a plastic bag, and stored for up to 1 week.

Load and run the gel

15. Prepare the protein sample and protein molecular-weight-standards mixture. Load and run the gel (see Basic Protocol 1, steps 13 to 26).

    The gel can be stained with Coomassie blue or silver (APPENDIX 3).

16. After staining, dry the gels onto Whatman 3MM or equivalent filter paper.

    Gradient gels >0.75 mm thick require special handling during drying to prevent cracking. The simplest approach to drying gradient gels is to use thin gels; ≤0.75-mm gradient gels with ≤20% acrylamide solutions will dry without cracking as long as the vacuum pump is working properly and the cold trap is dry at the onset of drying. For gradient gels >0.75 mm thick, add 3% (w/v) glycerol to the final destaining solution to help prevent cracking. Another method is to dehydrate and shrink the gel in 30% methanol for up to 3 hr prior to drying. Then place the gel in distilled water for 5 min before drying.

SUPPORT PROTOCOL 2

CASTING MULTIPLE GRADIENT GELS

Casting gradient gels in a multiple gel caster has several advantages. In addition to the time savings, batch casting gives gels that are essentially identical. This is particularly important for gradient gels, where slight variations in casting technique can cause variations in protein mobility. The gels may be stored for up to 1 week after casting to ensure internal consistency from run to run during the week. Furthermore, gels with several ranges of concentrations (e.g., 5% to 20% and 10% to 20% acrylamide) can be cast and stored, giving much more flexibility to optimize separations.

Additional Materials *(also see Alternate Protocol 5)*

Plug solution (see recipe)
Light and heavy acrylamide gel solutions for multiple gradient gels (Table A.3F.11 and Table A.3F.12)
TEMED
H_2O-saturated isobutyl alcohol

Multiple gel caster (Bio-Rad, Amersham Pharmacia Biotech)
Peristaltic pump (25 ml/min)
500- or 1000-ml gradient maker (Bio-Rad, Amersham Pharmacia Biotech)
Tygon tubing

Set up system and pour separating gel

1. Assemble the multiple caster as in casting multiple single-concentration gels (see Support Protocol 1, steps 1 to 3), making sure to remove the triangular space filler plugs in the bottom of the caster.

   The plug is used only when casting single-concentration gels.

2. Set up the peristaltic pump (Fig. A.3F.3). Using a graduated cylinder and water, adjust the flow rate so that the volume of the gradient solution plus volume of plug solution is poured in ~15 to 18 min (~25 ml/min).

3. Set up the gradient maker. Close all valves and place a stir-bar in the mixing chamber, which is the one with the outlet port. Attach one end of a piece of Tygon tubing to the outlet of the gradient maker. Run the other end of the tubing through the peristaltic pump and attach it to the red inlet port at the bottom of the caster.

   Choose a gradient maker that holds no more than four times the total volume of the gradient solution to be poured (i.e., a 1000- or 500-ml gradient maker).

4. Prepare solutions for the gradient maker (Table A.3F.11 and Table A.3F.12).

5. Add the TEMED to both heavy and light solutions (54 µl/165 ml) and immediately pour the light (low-concentration) solution into the mixing chamber (the one with the port). Open the mixing valve slightly to allow the tunnel to fill and to avoid air bubbles. Close the valve again and pour the heavy (high-concentration) acrylamide solution into the reservoir chamber.

6. Start the magnetic stirrer and open the outlet valve; then start the pump and open the mixing valve.

   In units for casting multiple gels, acrylamide solution flows in from the bottom. To use a multiple casting unit, the light solution is placed in the mixing chamber and the heavy solution in the reservoir. This is the reverse of casting a single gel (see Alternate Protocol 5).

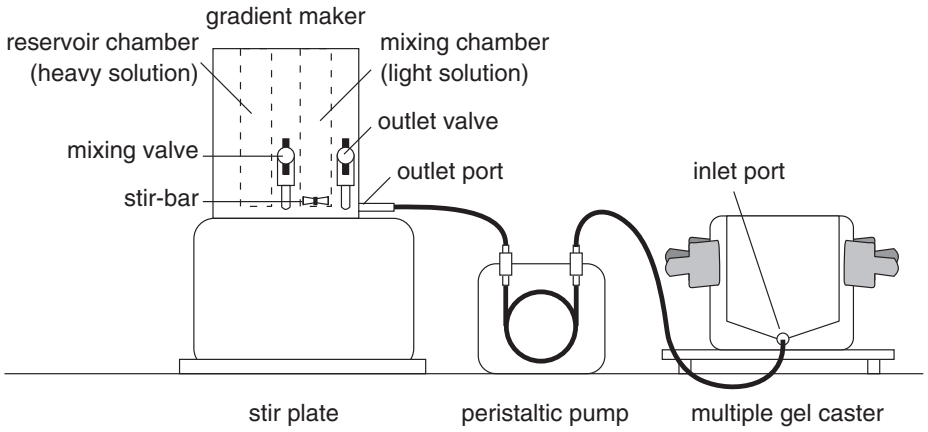

Figure A.3F.3 Setup for casting multiple gradient gels. Casting multiple gradient gels requires a peristaltic pump and a multiple gel caster. Gel solution is introduced through the bottom of the multiple caster.

Table A.3F.11 Light Acrylamide Gel Solutions for Multiple Gradient Gels[a,b]

Stock solution	Acrylamide concentration of light separating gel solution (%)[c]									
	5	6	7	8	9	10	11	12	13	14
30% acrylamide/ 0.8% bisacrylamide[d]	28	33	39	44	50	55	61	66	72	77
4× Tris·Cl/SDS, pH 8.8[d]	41	41	41	41	41	41	41	41	41	41
H_2O	96	91	85	80	74	69	63	58	52	47
10% (w/v) ammonium persulfate[e]	0.55	0.55	0.55	0.55	0.55	0.55	0.55	0.55	0.55	0.55

[a]To survey proteins ≥10 kDa, 5%-20% gradient gels are recommended. To expand the range between 10 and 200 kDa, a 10%-20% gel is recommended.

[b]Recipes produce ten 1.5-mm-thick gradient gels with 10 ml extra solution to account for losses in tubing.

[c]Numbers in body of table are milliliters of stock solution. Deaeration is not required. Keep solution at room temperature prior to adding TEMED no longer than 1 hr.

[d]See Table A.3F.1 for preparation.

[e]Best to prepare fresh.

Table A.3F.12 Heavy Acrylamide Gel Solutions for Multiple Gradient Gels[a,b]

Stock solution	Acrylamide concentration of heavy gel solution (%)[c]										
	10	11	12	13	14	15	16	17	18	19	20
30% acrylamide/ 0.8% bisacrylamide[d]	55	61	66	72	77	83	88	94	99	105	110
4× Tris·Cl/SDS, pH 8.8[d]	41	41	41	41	41	41	41	41	41	41	41
H_2O	55	50	44	39	33	28	22	17	11	5.5	0
Sucrose (g)	25	25	25	25	25	25	25	25	25	25	25
10% (w/v) ammonium persulfate[e]	0.55	0.55	0.55	0.55	0.55	0.55	0.55	0.55	0.55	0.55	0.55

[a]Deaeration is not recommended for gradient gels.

[b]Recipes produce 10 ml extra solution to account for losses in tubing.

[c]Numbers in body of table are milliliters of stock solution (except sucrose). Do not add the ammonium persulfate until just before use. The heavy acrylamide will polymerize, albeit more slowly, without the addition of TEMED. Keep the heavy solution on ice after adding ammonium persulfate.

[d]See Table A.3F.1 for preparation.

[e]Best to prepare fresh.

Thus, light solution enters the multiple caster first, followed by progressively heavier solution. Finally, the acrylamide solution is stabilized in the multiple caster with a heavy plug solution and allowed to polymerize (see step 8 and manufacturer's instructions).

7. When almost all the acrylamide solution is gone from the gradient maker, stop the pump and close the mixing valve. Tilt the gradient maker toward the outlet side and remove the last milliliters of the mix. Do not allow air bubbles to enter the tubing.
8. Add the plug solution to the mixing chamber and start the pump. Make sure that no bubbles are introduced. Continue pumping until the bottom of the caster is filled with plug solution to just below the glass plates; then turn off the pump. Clamp the tubing close to the red port of the casting chamber.
9. Quickly overlay each separate gel sandwich with 100 µl H_2O-saturated isobutyl alcohol. Use the same amount on each sandwich.

Failure to use the same amount of overlay solution will cause the gel sandwiches to polymerize at different heights.

10. Drain off the overlay and rinse the surface of the gels with 1× Tris·Cl/SDS, pH 8.8.

Pour stacking gel and remove gels from caster

11. Prepare and cast the stacking gel as in casting multiple single-concentration gels (see Support Protocol 1, steps 8 to 11).

12. Remove gels from the caster and clean the gel sandwiches (see Support Protocol 1, steps 12 and 13). Store gels, if necessary, according to the instructions for multiple single-concentration gels (see Support Protocol 1, step 14).

ELECTROPHORESIS IN SINGLE-CONCENTRATION MINIGELS

BASIC PROTOCOL 2

Separation of proteins in a small-gel format is becoming increasingly popular for applications that range from isolating material for peptide sequencing to performing routine protein separations. The unique combination of speed and high resolution is the foremost advantage of small gels. Additionally, small gels are easily adapted to single-concentration, gradient, and two-dimensional SDS-PAGE procedures. The minigel procedures described are adaptations of larger gel systems.

This protocol describes the use of a multiple gel caster. The caster is simple to use, and up to five gels can be prepared at one time with this procedure. Single gels can be prepared using adaptations in the manufacturer's instructions. A multiple gel caster is the only practical way to produce small linear polyacrylamide gradient gels (see Support Protocol 3).

Materials

Minigel vertical gel unit (Amersham Pharmacia Biotech Mighty Small SE 250/280 *or* Bio-Rad Mini-Protean II) with glass plates, clamps, and buffer chambers
0.75-mm spacers
Multiple gel caster (Amersham Pharmacia Biotech SE-275/295 *or* Bio-Rad Mini-Protean II multicasting chamber)
Acrylic plate (Amersham Pharmacia Biotech SE-217 *or* Bio-Rad 165-1957) or polycarbonate separation sheet (Amersham Pharmacia Biotech SE-213 *or* Bio-Rad 165-1958)
10- and 50-ml syringes
Combs (Teflon, Amersham Pharmacia Biotech SE-211A series or Bio-Rad Mini-Protean II)
Long razor blade
Micropipet

Additional reagents and equipment for standard denaturing SDS-PAGE (see Basic Protocol 1)

Pour the separating gel

1. Assemble each gel sandwich by stacking, in order, the notched (Amersham Pharmacia Biotech) or small rectangular (Bio-Rad) plate, 0.75-mm spacers, and the larger rectangular plate. Be sure to align the spacers properly, with the ends flush with the top and bottom edge of the two plates, when positioning the sandwiches in the multiple gel caster (Fig. A.3F.4).

   The protocol described is basically for the Amersham Pharmacia Biotech system. For other systems, make adjustments according to the manufacturer's instructions. Alternatively, precast minigels can be purchased from a number of suppliers (see Table A.3F.3).

   The multiple casters from Amersham Pharmacia Biotech have a notch in the base designed for casting gradient gels. A silicone rubber insert fills up this space when casting

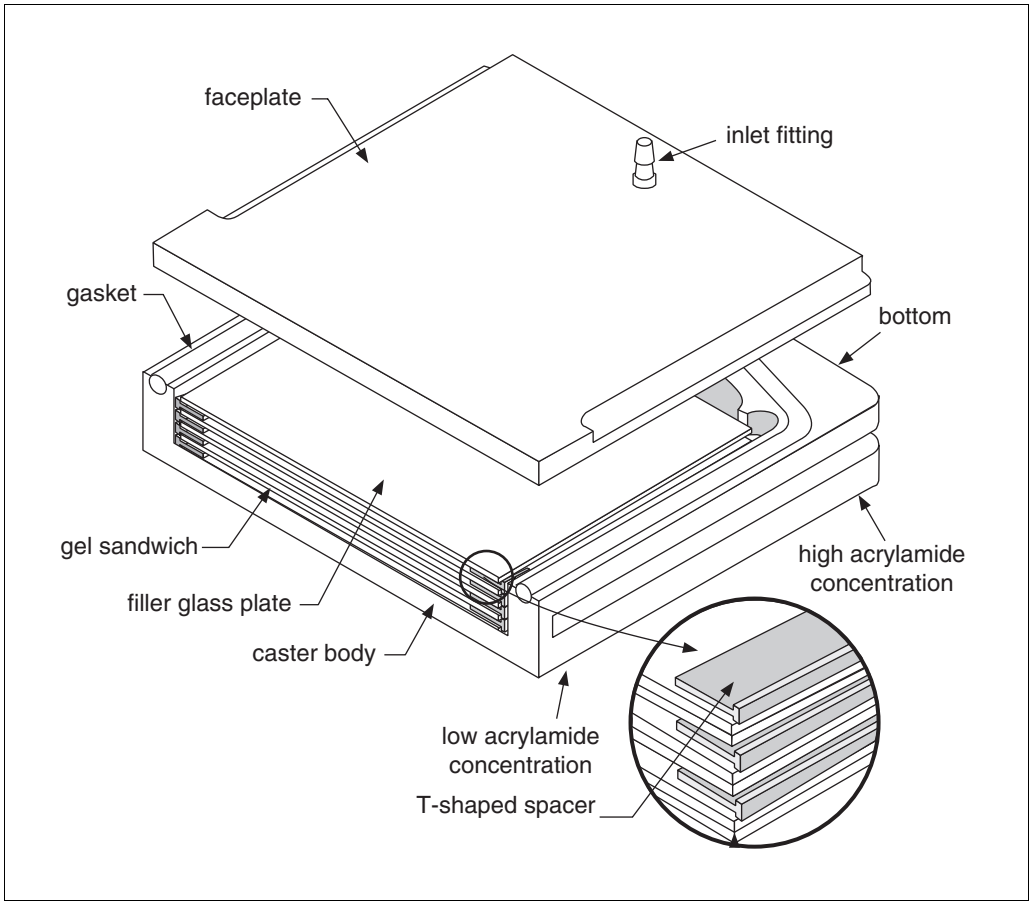

Figure A.3F.4 Minigel sandwiches positioned in the multiple gel caster. Extra glass or acrylic plates or polycarbonate sheets are used to fill any free space in the caster and to ensure that the gel sandwiches are held firmly in place.

single-concentration gels. The Amersham Pharmacia Biotech spacers are T-shaped to prevent slipping. The flanged edge of the spacer must be positioned against the outside edge of the glass plate. Placing a sheet of wax paper between the gel sandwiches will help separate the sandwiches after polymerization.

2. Fit the gel sandwiches tightly in the multiple gel caster. Use an acrylic plate or polycarbonate separation sheet to eliminate any slack in the chamber.

   Loosely fitting sandwiches in the caster will lead to unevenly cast gels, creating distortions during electrophoresis.

3. Place the front faceplate on the caster, clamp it in place against the silicone gasket, and verify alignment of the glass plates and spacers.

4. Prepare the separating gel solution as directed in Table A.3F.1. For five 0.75-mm-thick gels, prepare ~30 ml solution (i.e., double the volumes listed).

   To compute the total gel volume needed, multiply the area of the gel (e.g., 7.3 × 8.3 cm) by the thickness of the gel (e.g., 0.75 mm) and then by the number of gels in the caster. If needed, add ~4 to 5 ml of extra gel solution to account for the space around the outside of the gel sandwiches.

   Do not add TEMED and ammonium persulfate until just before use.

5. Fill a 50-ml syringe with the separating gel solution and slowly inject it into the caster until the gels are 6 cm high, allowing 1.5 cm for the stacking gel.

6. Overlay each gel with 100 µl H_2O-saturated isobutyl alcohol. Allow the gels to polymerize for ~1 hr.

Pour the stacking gel

7. Remove the isobutyl alcohol and rinse with 1× Tris·Cl/SDS, pH 8.8.

   Stacking gels can be cast one at a time with the gel mounted on the electrophoresis unit, or all at once in the multiple caster.

8. Practice placing a comb in the gel sandwiches before preparing the stacking gel solution. Press the comb against the rectangular or taller plate so that all teeth of the comb are aligned with the opening in the gel sandwich, then insert into the sandwich. Remove combs after practicing.

9. Prepare the stacking gel solution (2 ml per gel) as directed in Table A.3F.1. Fill a 10-ml syringe with stacking gel solution and inject the solution into each gel sandwich.

10. Insert combs, taking care not to trap bubbles. Allow gels to polymerize 1 hr.

11. Remove the front faceplate. Carefully pull the gels out of the caster, using a long razor blade to separate the sandwiches.

    If the gels are left to polymerize for prolonged periods, they will be difficult to remove from the caster.

    The gels can be stored tightly wrapped in plastic wrap with the combs left in place inside a sealable bag to prevent drying for ~1 week. Without the stacking gel, the separating gel can be stored for 2 to 3 weeks. Keep gels moist with 1× Tris·Cl/SDS, pH 8.8, at 4°C. Do not store gels in the multiple caster.

Prepare the sample, load the gel, and conduct electrophoresis

12. Remove the combs and rinse the sample wells with 1× SDS electrophoresis buffer. Place a line indicating the bottom of each well on the front glass plate with a marker.

13. Fill the upper and lower buffer chambers with 1× SDS electrophoresis buffer. The upper chamber should be filled to 1 to 2 cm over the notched plate.

14. Prepare the protein sample and protein-standards mixture (see Basic Protocol 1, step 12).

15. Load the sample using a micropipet. Insert the pipet tip through the upper buffer and into the well. The mark on the glass plate will act as a guide. Dispense the sample into the well.

    For a complex mixture, 20 to 25 µg protein in 10 µl SDS sample buffer will give a strongly stained Coomassie blue pattern. Much smaller amounts (1 to 5 µg) are required for highly purified proteins, and a 10- to 100-fold smaller amount of protein in the same volume (e.g., 10 µl) is required for silver staining.

16. Electrophorese samples at 10 to 15 mA per 0.75-mm gel until the dye front reaches the bottom of the gel (~1 to 1.5 hr).

17. Disassemble the gel (see Basic Protocol 1, steps 23 to 26). Proceed with detection of proteins.

SUPPORT PROTOCOL 3

PREPARING MULTIPLE GRADIENT MINIGELS

Polyacrylamide gradients not only enhance the resolution of larger-format gels but also greatly improve protein separation in the small format. Casting gradient minigels one at a time is not generally feasible because of the small volumes used, but multiple gel casters make it easy to cast several small gradient gels at one time. The gels are cast from the bottom in multiple casters, with the light acrylamide solution entering first. This is the opposite of casting one gel at a time, in which the heavy solution enters from the top of the gel sandwich and flows down to the bottom.

Additional Materials *(also see Basic Protocol 2)*

Plug solution (see recipe)

Additional reagents and equipment for preparing gradient gels (see Alternate Protocol 5)

Set up the system and prepare the gel solutions

1. Assemble minigel sandwiches in the multiple gel caster as described for single-concentration minigels (see Basic Protocol 2, steps 1 to 3).
2. Set up the 30-ml gradient maker, magnetic stirrer, peristaltic pump (optional), and Tygon tubing as in Figure A.3F.3. Connect the outlet of the 30-ml gradient maker to the inlet at the base of the front faceplate of the caster.

   The monomer solution will be introduced through the inlet at the bottom of the front faceplate of the caster first, followed by progressively heavier solution.
3. Prepare light (Table A.3F.9) and heavy (Table A.3F.10) acrylamide gel solutions. Use ~12 ml of each solution for five 0.75-mm-thick minigels.

   Adjust volumes if a different thickness or number of gels is needed. Do not add ammonium persulfate until just before use. Deaeration is not recommended for gradient gels.
4. With the outlet and interconnecting valve closed, add the heavy solution to the reservoir chamber. Briefly open the interconnecting valve to let a small amount of heavy solution through to the mixing chamber, clearing the valve of air.
5. Fill the mixing chamber with light solution. Add 4 µl TEMED per 12 ml acrylamide solution to each chamber and mix with a disposable pipet.

Form the gradient and cast the gels

6. Turn on the magnetic stirrer. Open the interconnecting valve and allow the chambers to equilibrate. Then slowly open the outlet port to allow the solution to flow from the gradient maker to the multiple caster by gravity (a peristaltic pump may be used for better control). Adjust the flow rate to 3 to 4 ml/min.

   Faster flow rates are possible and will also produce good gradients. However, a fast flow increases the potential for introduction of bubbles into the caster.
7. Close the outlet port as the last of the gradient solution leaves the mixing chamber, just before air enters the outlet tube. Fill the two chambers with plug solution and slowly open the outlet once again.
8. Allow the plug solution to push the acrylamide in the caster up into the plates. Close the outlet when the plug solution reaches the bottom of the plates.

   A discontinuity between the bottom of the gels and the plug solution will be obvious.
9. Quickly add 100 µl H_2O-saturated isobutyl alcohol to each gel sandwich. Let the gels polymerize undisturbed for ~1 hr.
10. Prepare and pour the stacking gel (see Basic Protocol 2, steps 9 and 10).

Disassemble the system

11. Disconnect the gradient maker, place the caster in a sink, and remove the front faceplate. The plug solution will drain out from the bottom of the caster.

12. Remove the gels (see Basic Protocol 2, step 11).

Gradient minigels can be stored as described for single-concentration minigels (see Basic Protocol 2, step 11 annotation). For instructions on preparing, loading, and running the gels, see Basic Protocol 2, steps 12 to 17.

REAGENTS AND SOLUTIONS

Use Milli-Q purified water in all recipes and protocol steps. For common stock solutions, see ***APPENDIX 2A****; for suppliers, see* ***SUPPLIERS APPENDIX****.*

Anode buffer

121.1 g Tris base (0.2 M final)
500 ml H_2O
Adjust to pH 8.9 with concentrated HCl
Dilute to 5 liters with H_2O
Store at 4°C up to 1 month

Final concentration is 0.2 M Tris·Cl, pH 8.9.

Cathode buffer

12.11 g Tris base (0.1 M final)
17.92 g tricine (0.1 M final)
1 g SDS (0.1% final)
Dilute to 1 liter with H_2O
Do not adjust pH
Store at 4°C up to 1 month

Coomassie blue G-250 staining solution

200 ml acetic acid (20% final)
1800 ml H_2O
0.5 g Coomassie blue G-250 (0.025% final)
Mix 1 hr and filter (Whatman no. 1 paper)
Store at room temperature indefinitely

Phosphate/SDS electrophoresis buffer

Dilute 500 ml of 4× phosphate/SDS, pH 7.2 (Table A.3F.7) with H_2O to 2 liters.
Store at 4°C up to 1 month.

Final concentrations are 0.1 M sodium phosphate (pH 7.2)/0.1% (w/v) SDS.

Phosphate/SDS sample buffer, 2*× (for continuous systems)*

0.5 ml 4× phosphate/SDS, pH 7.2 (Table A.3F.7; 20 mM sodium phosphate final)
0.2 g SDS (2% final)
0.1 mg bromphenol blue (0.001% final)
0.31 g DTT (0.2 M final)
2.0 ml glycerol (2% final)
Add H_2O to 10 ml and mix

Plug solution

0.125 M Tris·Cl, pH 8.8 (*APPENDIX 2A*)
50% (w/v) sucrose
0.001% (w/v) bromphenol blue
Store at 4°C up to 1 month

Recrystallized SDS *(optional)*

High-purity SDS is available from several suppliers, but for some sensitive applications (e.g., protein sequencing) recrystallization is useful. Commercially available electrophoresis-grade SDS is usually of sufficient purity for most applications.

Add 100 g SDS to 450 ml ethanol and heat to 55°C. While stirring, gradually add 50 to 75 ml hot H_2O until all SDS dissolves. Add 10 g activated charcoal (Norit 1, Sigma) to solution. After 10 min, filter solution through Whatman no. 5 paper on a Buchner funnel to remove charcoal. Chill filtrate 24 hr at 4°C and 24 hr at −20°C. Collect crystalline SDS on a coarse-frit (porosity A) sintered-glass funnel and wash with 800 ml −20°C ethanol (reagent grade). Repeat crystallization without adding activated charcoal. Dry recrystallized SDS under vacuum overnight at room temperature. Store in a desiccator over phosphorous pentoxide (P_2O_5) in a dark bottle.

If proteins will be electroeluted or electroblotted for protein sequence analysis, it may be desirable to crystallize the SDS twice from ethanol/H_2O (Hunkapiller et al., 1983).

SDS electrophoresis buffer, 5×

15.1 g Tris base (0.125 M final)
72.0 g glycine (0.96 M final)
5.0 g SDS (0.5% final)
H_2O to 1000 ml
Dilute to 1× or 2× for working solution, as appropriate

Do not adjust the pH of the stock solution, as the solution is pH 8.3 when diluted. Store at 0° to 4°C until use (up to 1 month).

SDS sample buffer, 2× *(for discontinuous systems)*

25 ml 4× Tris·Cl/SDS, pH 6.8 (Table A.3F.1)
20 ml glycerol (20% final)
4 g SDS (4% final)
2 ml 2-ME *or* 3.1 g DTT (0.2% 2-ME or 0.2 M DTT final)
1 mg bromphenol blue (0.001% final)
Add H_2O to 100 ml and mix
Store in 1-ml aliquots at −70°C

To avoid reducing proteins to subunits (if desired), omit 2-ME or DTT (reducing agent) and add 10 mM iodoacetamide to prevent disulfide interchange.

SDS sample buffer, 6× *(for discontinuous systems)*

7 ml 4× Tris·Cl/SDS, pH 6.8 (Table A.3F.1)
3.0 ml glycerol (30% final)
1 g SDS (10% final)
0.93 g DTT (0.6 M final)
1.2 mg bromphenol blue (0.012% final)
Add H_2O to 10 ml (if needed)
Store in 0.5-ml aliquots at −70°C

Tricine sample buffer, 2×

2 ml 4× Tris·Cl/SDS, pH 6.8 (Table A.3F.1; 0.1 M)
2.4 ml (3.0 g) glycerol (24% final)
0.8 g SDS (8% final)
0.31 g DTT (0.2 M final)
2 mg Coomassie blue G-250 (0.02% final)
Add H_2O to 10 ml and mix

COMMENTARY

Background Information

Polyacrylamide gels form after polymerization of monomeric acrylamide into polymeric polyacrylamide chains and cross-linking of the chains by *N,N′*-methylenebisacrylamide. The polymerization reaction is initiated by the addition of ammonium persulfate, and the reaction is accelerated by TEMED, which catalyzes the formation of free radicals from ammonium persulfate. Because oxygen inhibits the polymerization process, deaerating the gel solution before the polymerization catalysts are added will speed up polymerization; deaeration is not recommended for the gradient gel protocols because slower polymerization facilitates casting of gradient gels.

Precast gels for commonly used vertical minigel and standard-sized SDS-PAGE apparatuses are available from several manufacturers (Table A.3F.3). Flatbed (horizontal) isoelectric focusing (IEF) and SDS-PAGE gels are not listed. Amersham Pharmacia Biotech supplies a range of horizontal gels for a variety of applications and should be consulted for further information. When using precast gels, pay strict attention to shelf life. In general, manufacturers overrate the shelf life, and the sooner the gels are used, the better. When reasonably fresh, precast gels provide excellent resolution that is as good or better than a typical gel cast in the laboratory.

The most widely used method for discontinuous gel electrophoresis is the system described by Laemmli (1970). This is the denaturing (SDS) discontinuous method used in Basic Protocol 1. A discontinuous buffer system uses buffers of different pH and composition to generate a discontinuous pH and voltage gradient in the gel. Because the discontinuous gel system concentrates the proteins in each sample into narrow bands, the applied sample may be more dilute than that used for continuous electrophoresis.

In the discontinuous system the sample first passes through a stacking gel, which has large pores. The stacking gel buffer contains chloride ions (called the leading ions) whose electrophoretic mobility is greater than the mobility of the proteins in the sample. The electrophoresis buffer contains glycine ions (called the trailing ions) whose electrophoretic mobility is less than the mobility of the proteins in the sample. The net result is that the faster migrating ions leave a zone of lower conductivity between themselves and the migrating protein. The higher voltage gradient in this zone allows the proteins to move faster and to "stack" in the zone between the leading and trailing ions. After leaving the stacking gel, the protein enters the separating gel. The separating gel has a smaller pore size, a higher salt concentration, and higher pH compared to the stacking gel. In the separating gel, the glycine ions migrate past the proteins, and the proteins are separated according to either molecular size in a denaturing gel (containing SDS) or molecular shape, size, and charge in a nondenaturing gel.

Proteins are denatured by heating in the presence of a low-molecular-weight thiol (2-ME or DTT) and SDS. Most proteins bind SDS in a constant-weight ratio, leading to identical charge densities for the denatured proteins. Thus, the SDS-protein complexes migrate in the polyacrylamide gel according to size, not charge. Most proteins are resolved on polyacrylamide gels containing from 5% to 15% acrylamide and 0.2% to 0.5% bisacrylamide (see Table A.3F.1). The relationship between the relative mobility and log molecular weight is linear over these ranges (Fig. A.3F.5). With the use of plots like those shown in Figure A.3F.5, the molecular weight of an unknown protein (or its subunits) may be determined by comparison with known protein standards (Table A.3F.2). In general, all of the procedures in this unit are suitable for radiolabeled and biotinylated proteins without modification.

Basic Protocol 1 relies on denaturing proteins in the presence of SDS and 2-ME or DTT. Under these conditions, the subunits of proteins are dissociated and their biological activities are lost. A true estimate of a protein's molecular size can be made by comparing the relative mobility of the unknown protein to proteins in a calibration mixture (Fig. A.3F.5). Gradient gels (see Alternate Protocol 5) simplify molecular-weight determinations by producing a linear relationship between log molecular weight of the protein and log % T over a much wider size range than single-concentration gels. Although percent acrylamide monomer is a more common measure of gel concentration, % T, the percentage of total monomer (acrylamide plus bisacrylamide) in the solution or gel, is used for molecular weight calculations in gradient gels. The % T of a stained protein is estimated assuming the acrylamide gradient is linear. For example, proteins in the gel shown in Figure A.3F.6 were separated in a 5.1% to 20.5% T acrylamide gradient. The % T of the

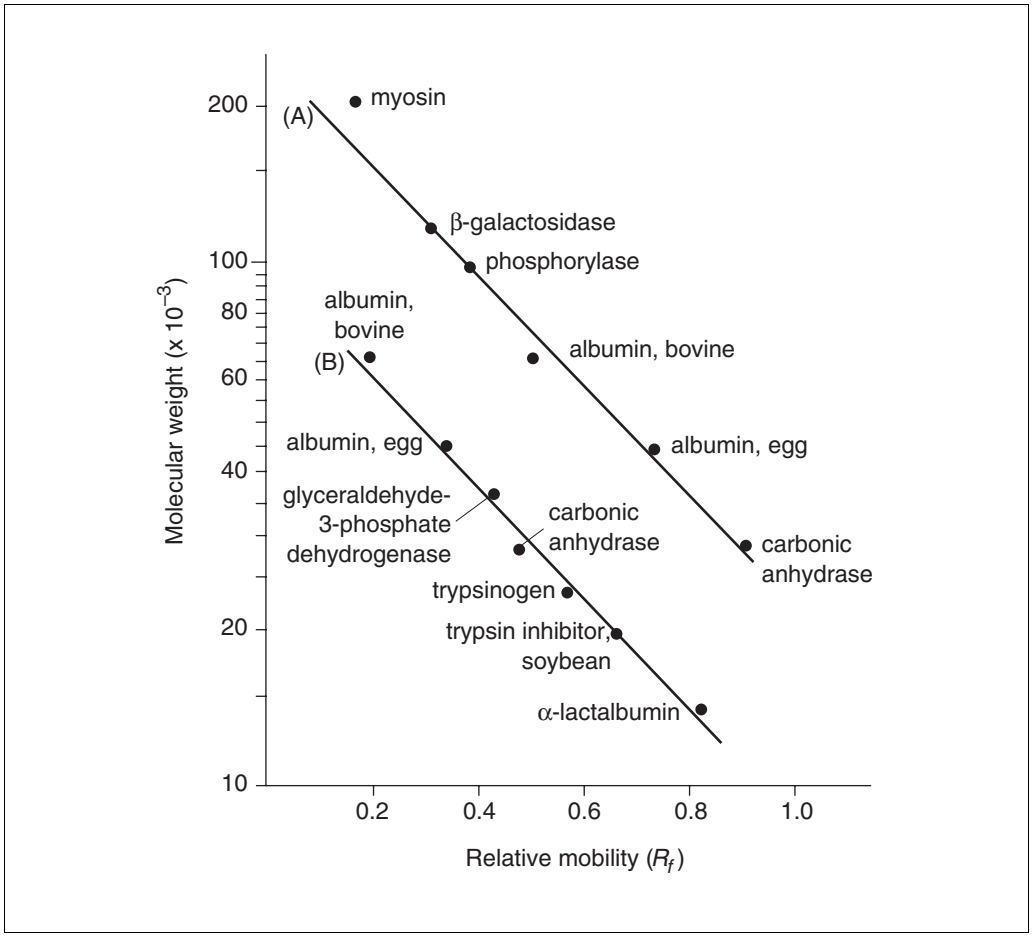

Figure A.3F.5 Typical calibration curves obtained with standard proteins separated by nongradient denaturing (SDS) discontinuous gel electrophoresis based on the method of Laemmli (1970). (**A**) Gel with 7% polyacrylamide. (**B**) Gel with 11% polyacrylamide. (Redrawn with permission from Sigma.)

point halfway through the resolving gel is 12.5% T. Simply plotting log molecular mass versus distance moved into the gel (or R_f) also produces a relatively linear standard curve over a fairly wide size range.

If two proteins have identical molecular sizes, they more than likely will not be resolved with one-dimensional SDS-PAGE, and two-dimensional SDS-PAGE should be considered. Unusual protein compositions can cause anomalous mobilities during electrophoresis (see Critical Parameters and Troubleshooting), but similar-sized proteins of widely different amino acid composition or structure may still be resolved from one another using one-dimensional SDS-PAGE. Purified protein complexes or multimeric proteins consisting of subunits of different molecular size will be resolved into constituent polypeptides. Comparison of the protein bands obtained under nonreducing and reducing conditions provides information about the molecular size of disulfide cross-linked component subunits. The individual polypeptides can be isolated by electroelution or electroblotting, and the amino acid sequences can be determined.

Both the tricine (Schagger and von Jagow, 1987) and the modified Laemmli (Okajima et al., 1993) peptide separation procedures presented here (see Alternate Protocols 1 and 2) are simple to set up and provide resolution down to 5 kDa. To separate peptides below 5 kDa, the tricine procedure must be modified by preparing a 16.5% T, 2.7% C resolving gel that uses a 10% T spacer gel between the stacking and resolving gel (Schagger and von Jagow, 1987). % C is the percentage of cross-linker (bisacrylamide) in the total monomer (acrylamide plus bisacrylamide).

Continuous electrophoresis, where the same buffer is used throughout the tank and gel, is popular because of its versatility and simplicity. The phosphate system described in Alternate Protocol 3 is based on that of Weber et al.

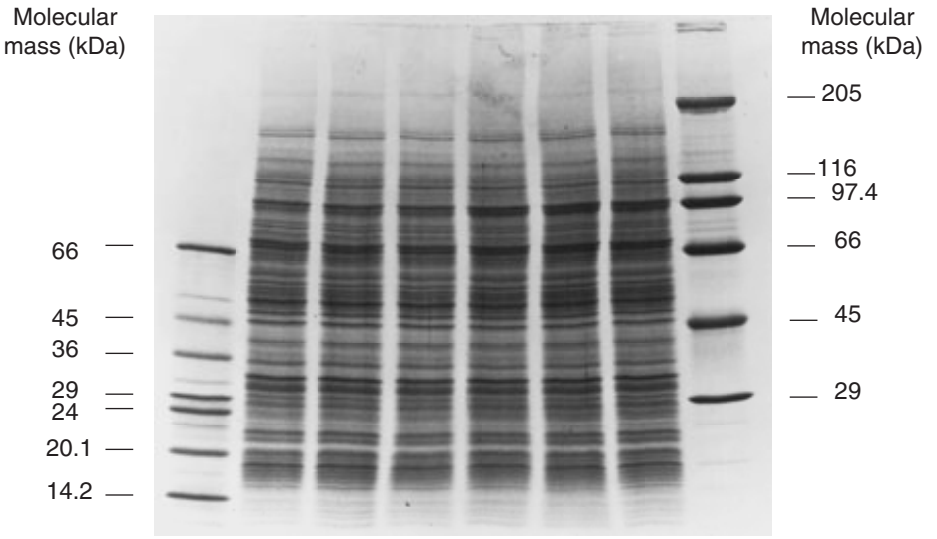

Figure A.3F.6 Separation of membrane proteins by 5.1% to 20.5% T polyacrylamide gradient SDS-PAGE. Approximately 30 μl of 1× SDS sample buffer containing 30 μg of Alaskan pea (*Pisum sativum*) membrane proteins was loaded in wells of a 14 × 14–cm, 0.75-mm-thick gel. Standard proteins were included in the outside lanes. The gel was run at 4 mA for ~15 hr.

(1972). Although unable to produce the high-resolution separations of the discontinuous SDS-PAGE procedures, continuous SDS-PAGE uses fewer solutions with one basic buffer and no stacking gel. Artifacts are also less likely to occur in continuous systems. Pepsin, for example, migrates anomalously on Laemmli-based discontinuous SDS-PAGE but has the expected mobility after electrophoresis in the phosphate-based continuous system described here. This is also true of cross-linked proteins.

Multiple gel casting (see Support Protocols 1 to 3) is appropriate when gel-to-gel consistency is paramount or when the number of gels processed exceeds five a week. The variety of multiple gel casters, gradient makers, and inexpensive pumps available from major suppliers simplifies the process of casting gels in the laboratory. Alternatively, precast gradient gels are available for most major brands of gel apparatuses (Table A.3F.3).

Minigels (see Basic Protocol 2) are generally considered to be in the 8 × 10–cm size range, although there is considerable variation in exact size. Every technique that is used on larger systems can be translated with little difficulty into the minigel format. This includes standard and gradient SDS-PAGE and separations for immunoblotting and peptide sequencing. Two-dimensional SDS-PAGE electrophoresis also adapts well, but here the limitation of separation area becomes apparent; for high-resolution separations, large-format gels are required. Gradient minigels (see Support Protocol 3) are popular due to the combination of separation range and resolution (Matsudaira and Burgess, 1978). They are particularly useful for separation of proteins prior to peptide sequencing.

Mylar support (Gel Bond) provides a practical way of casting, running, and, staining extremely thin gels. When gels <0.75 mm thick are used, reagents have much better access both into and out of the gel, reducing staining time in both Coomassie blue and silver staining. Double and broadened images caused by differential migration of the protein across the thickness of the gel are minimized, improving resolution.

Critical Parameters and Troubleshooting

If an electrophoretically separated protein will be electroeluted or electroblotted for sequence analysis, the highest-purity reagents available should be used. If necessary, SDS can be purified by recrystallization following the procedure given in Reagents and Solutions.

If the gels polymerize too fast, the amount of ammonium persulfate should be reduced by

one-third to one-half. If the gels polymerize too slowly or fail to polymerize all the way to the top, use fresh ammonium persulfate or increase the amount of ammonium persulfate by one-third to one-half. The overlay should be added slowly down the spacer edge to prevent the overlay solution from crashing down and disturbing the gel interface.

After a separating gel is poured, it may be stored with an overlay of the same buffer used in the gel. Immediately prior to use, the stacking gel should be poured; otherwise, there will be a gradual diffusion-driven mixing of buffers between the two gels, which will cause a loss of resolution.

The protein of interest should be present in 0.2- to 1-μg amounts in a complex mixture of proteins if the gel will be stained by Coomassie blue. Typically, 30 to 50 μg of a complex protein mixture in a total volume of <20 μl is loaded on a 0.75-mm-thick slab gel (16 cm, 10 wells).

When casting multiple gradient gels, eliminate all bubbles in the outlet tubing of the gradient maker. If air bubbles get into the outlet tube, they may flow into the caster and then up through the gradient being poured, causing an area of distortion in the polymerized gel. Air bubbles are not so great a problem when casting single gradient gels from the top. As the gels are cast, the stirrer must be slowed so that the vortex in the mixing chamber does not allow air to enter the outlet.

Uneven heating of the gel causes differential migration of proteins, with the outer lanes moving more slowly than the center lanes (called smiling). Increased heat transfer eliminates smiling and can be achieved by filling the lower buffer chamber with buffer all the way to the level of the sample wells, by maintaining a constant temperature between 10° to 20°C, and by stirring the lower buffer with a magnetic stirrer. Alternatively, decrease the heat load by running at a lower current.

If the tracking dye band is diffuse, prepare fresh buffer and acrylamide monomer stocks. If the protein bands are diffuse, increase the current by 25% to 50% to complete the run more quickly and minimize band diffusion, use a higher percentage of acrylamide, or try a gradient gel. Lengthy separations using gradient gels generally produce good results (Fig. A.3F.6). Check for possible proteolytic degradation that may cause loss of high-molecular-weight bands and create a smeared banding pattern.

If there is vertical streaking of protein bands, decrease the amount of sample loaded on the gel, further purify the protein of interest to reduce the amount of contaminating protein applied to the gel, or reduce the current by 25%. Another cause of vertical streaking of protein bands is precipitation, which can sometimes be eliminated by centrifuging the sample or by reducing the percentage of acrylamide in the gel.

Proteins can migrate faster or slower than their actual molecular weight would indicate. Abnormal migration is usually associated with a high proportion of basic or charged amino acids (Takano et al., 1988). Other problems can occur during isolation and preparation of the protein sample for electrophoresis. Proteolysis of proteins during cell fractionation by endogenous proteases can cause subtle band splitting and smearing in the resulting electrophoretogram (electrophoresis pattern). Many endogenous proteases are very active in SDS sample buffers and will rapidly degrade the sample; thus, first heating the samples to 70° to 100°C for 3 min is recommended.

In some cases, heating to 100°C in sample buffer will cause selective aggregation of proteins, creating a smeared layer of Coomassie blue–stained material at the top of the gel (Gallagher and Leonard, 1987). To avoid heating artifacts and also prevent proteolysis, the use of specific protease inhibitors during protein isolation and/or lower heating temperatures (70° to 80°C) have been effective (Dhugga et al., 1988).

Although continuous gels suffer from poor band sharpness, they are less prone to artifacts caused by aggregation and protein cross-linking. If streaking or aggregation appear to be a problem with the Laemmli system, then the same sample should be subjected to continuous SDS-PAGE to see if the problem is intrinsic to the Laemmli gel or the sample.

If the protein bands spread laterally from gel lanes, the time between applying the sample and running the gel should be reduced in order to decrease the diffusion of sample out of the wells. Alternatively, the acrylamide percentage should be increased in the stacking gels from 4% to 4.5% or 5% acrylamide, or the operating current should be increased by 25% to decrease diffusion in the stacking gel. Use caution when adding 1× SDS electrophoresis buffer to the upper buffer chamber. Samples can get swept into adjacent wells and onto the top of the well arm.

If the protein bands are uneven, the stacking gel may not have been adequately polymerized. This can be corrected by deaerating the stacking

gel solution thoroughly or by increasing the ammonium persulfate and TEMED concentrations by one-third to one-half. Another cause of distorted bands is salt in the protein sample, which can be removed by dialysis, gel filtration, or precipitation. Skewed protein bands can be caused by an uneven interface between the stacking and separating gels, which can be corrected by starting over and being careful not to disturb the separating gel while overlaying with isobutyl alcohol.

If a run takes too long, the buffers may be too concentrated or the operating current too low. If the run is too short, the buffers may be too dilute or the operating current too high.

If double bands are observed, the protein may be partially oxidized or partially degraded. Oxidation can be minimized by increasing the 2-ME concentration in the sample buffer or by preparing a fresh protein sample. If fewer bands than expected are observed and there is a heavy protein band at the dye front, increase the acrylamide percentage in the gel.

Anticipated Results

Polyacrylamide gel electrophoresis done under denaturing and reducing conditions should resolve any two proteins, except two of identical size. Resolution of proteins in the presence of SDS is a function of gel concentration and the size of the proteins being separated. Under nondenaturing conditions, the biological activity of a protein will be maintained.

Comparison of reducing and nonreducing denaturing gels can also provide valuable information about the number of disulfide cross-linked subunits in a protein complex. If the subunits are held together by disulfide linkages, the protein will separate in denaturing gels as a complex or as smaller-sized subunits under nonreducing or reducing conditions, respectively. However, proteins separated on nonreducing denaturing gels appear more diffuse and exhibit less overall resolution than those separated on reducing gels.

Gradient gels provide superior protein-band sharpness and resolve a larger size range of proteins, making them ideal for most types of experiments in spite of being more difficult to prepare. Molecular-weight calculations are simplified because of the extended linear relationship between size and protein position in the gel. Increased band sharpness of both high- and low-molecular-weight proteins on the same gel greatly simplifies survey experiments, such as gene expression studies where the characteristics of the responsive protein are not known. Furthermore, the increased resolution dramatically improves autoradiographic analysis. Preparation of gradient gels is straightforward, although practice with gradient solutions containing dye is recommended. The gradient gels can be stored for several days at 0° to 4°C before casting the stacking gel.

Time Considerations

Preparation of separating and stacking gels requires 2 to 3 hr. Gradient gels generally take 5 min to cast singly. Casting multiple single-concentration gels requires an additional 10 min for assembly. Casting multiple gradient gels takes 15 to 20 min plus assembly time. It takes 4 to 5 hr to run a 14 × 14–cm, 0.75-mm gel at 15 mA (70 to 150 V), and 3 to 4 hr to run a 0.75-mm gel at 20 mA (80 to 200 V). Overnight separations of ~12 hr require 4 mA per 0.75-mm gel. It takes 4 to 5 hr to run a 1.5-mm gel at 30 mA. Electrophoresis is normally performed at 15° to 20°C, with the temperature held constant using a circulating water bath. For air-cooled electrophoresis units, lower currents and thus longer run times are recommended.

It takes ~1 hr to run a 0.75-mm minigel at 20 mA (100 to 120 V). Separation times are not significantly different for gradient minigels.

Literature Cited

Dhugga, K.S., Waines, J.G., and Leonard, R.T. 1988. Correlated induction of nitrate uptake and membrane polypeptides in corn roots. *Plant Physiol.* 87:120-125.

Gallagher, S.R. and Leonard, R.T. 1987. Electrophoretic characterization of a detergent-treated plasma membrane fraction from corn roots. *Plant Physiol.* 83:265-271.

Hunkapiller, M.W., Lujan, E., Ostrander, F., and Hood, L.E. 1983. Isolation of microgram quantities of proteins from polyacrylamide gels for amino acid sequence analysis. *Methods Enzymol.* 91:227-236.

Laemmli, U.K. 1970. Cleavage of structural proteins during the assembly of the head of bacteriophage T4. *Nature* 227:680-685.

Matsudaira, P.T. and Burgess, D.R. 1978. SDS microslab linear gradient polyacrylamide gel electrophoresis. *Anal. Biochem.* 87:386-396.

Okajima, T., Tanabe, T., and Yasuda, T. 1993. Nonurea sodium dodecyl sulfate-polyacrylamide gel electrophoresis with high-molarity buffers for the separation of proteins and peptides. *Anal. Biochem.* 211:293-300.

Schagger, H. and von Jagow, G. 1987. Tricine-sodium dodecyl sulfate-polyacrylamide gel electrophoresis for the separation of proteins in the range from 1 to 100 kDa. *Anal. Biochem.* 166:368-379.

Sigma. Molecular weight markers for proteins kit (Technical Bulletin MWS-877L). Sigma Chemical Company, St. Louis, Mo.

Takano, E., Maki, M., Mori, H., Hatanaka, N., Marti, T., Titani, K., Kannagi, R., Ooi, T., and Murachi, T. 1988. Pig heart calpastatin: Identification of repetitive domain structures and anomalous behavior in polyacrylamide gel electrophoresis. *Biochemistry* 27:1964-1972.

Weber, K., Pringle, J.R., and Osborn, M. 1972. Measurement of molecular weights by electrophoresis on SDS-acrylamide gel. *Methods Enzymol.* 26:3-27.

Key Reference

Hames, B.D. and Rickwood, D. (eds.) 1990. Gel Electrophoresis of Proteins: A Practical Approach, 2nd ed. Oxford University Press, New York.

An excellent book describing gel electrophoresis of proteins.

Contributed by Sean R. Gallagher
Motorola Corporation
Tempe, Arizona

Spectrophotometric Determination of Protein Concentration

This unit describes spectrophotometric methods for measuring the concentration of a sample protein in solution. In Basic Protocol 1, absorbance measured at 280 nm (A_{280}) is used to calculate protein concentration by comparison with a standard curve or published absorptivity values for that protein (a_{280}). In the Alternate Protocol, absorbance measured at 205 nm (A_{205}) is used to calculate the protein concentration. The A_{280} and A_{205} methods can be used to quantitate total protein in crude lysates and purified or partially purified protein. Both of these methods are simple and can be completed quickly. The A_{280} method is the most commonly used. The A_{205} method can detect lower concentrations of protein and is useful for dilute protein samples, but it is more susceptible to interference by reagents in the protein sample than the A_{280} method. Basic Protocol 2 uses a spectrofluorometer or a filter fluorometer to measure the intrinsic fluorescence emission of a sample solution; this value is compared with the emissions from standard solutions to determine the sample concentration. The fluorescence emission method is used to quantitate purified protein. This simple method is useful for dilute protein samples and can be completed in a short amount of time.

USING A_{280} TO DETERMINE PROTEIN CONCENTRATION

BASIC PROTOCOL 1

Determination of protein concentration by measuring absorbance at 280 nm (A_{280}) is based on the absorbance of UV light by the aromatic amino acids, tryptophan and tyrosine, and by cystine, disulfide-bonded cysteine residues, in protein solutions. The measured absorbance of a protein sample solution is used to calculate the concentration either from its published absorptivity at 280 nm (a_{280}) or by comparison with a calibration curve prepared from measurements with standard protein solutions. This assay can be used to quantitate solutions with protein concentrations of 20 to 3000 μg/ml.

Materials

3 mg/ml standard protein solution (see recipe; optional)
Sample protein
Spectrophotometer with UV lamp

1. For calibrating with standards, use the 3 mg/ml standard protein solution to prepare dilutions of 20, 50, 100, 250, 500, 1000, 2000, and 3000 μg/ml in the same solvent as used to prepare the sample protein. Prepare a blank consisting of solvent alone.

   Ideally, for purified or partially purified protein, the protein standard should have an aromatic amino acid content similar to that of the sample protein. For the total protein of a crude lysate, bovine serum albumin (BSA) is a commonly used standard for spectrophotometric quantitation of protein concentration. A 3 mg/ml solution of BSA should have an A_{280} of 1.98, based on an A_{280} of 6.61 for a 1% (w/v) solution.

2. Turn on the UV lamp of the spectrophotometer and set the wavelength to 280 nm. Allow the instrument to warm up 30 min before taking measurements.

3. Zero the spectrophotometer with the solvent blank.

4. Measure the absorbance of the protein standard and unknown solutions.

   If the A_{280} of the sample protein is >2.0, dilute the sample further in the same solvent and measure the A_{280} again.

Contributed by Michael H. Simonian
Current Protocols in Toxicology (2004) A.3G.1-A.3G.7

5a. *If the a_{280} of the protein is known:* Calculate the unknown sample concentration from its absorbance value using Equation A.3G.1.

In this equation a_{280} has units of ml/mg cm and b is the path length in cm.

$$\text{concentration (mg/ml)} = \frac{A_{280}}{a_{280} \times b}$$

Equation A.3G.1

5b. *If standard solutions are used for quantitation:* Create a calibration curve by either plotting or performing regression analysis of the A_{280} versus concentration of the standards. Use the absorbance of the sample protein to determine the concentration from the calibration curve.

ALTERNATE PROTOCOL

USING A_{205} TO DETERMINE PROTEIN CONCENTRATION

Determination of protein concentration by measurement of absorbance at 205 nm (A_{205}) is based on absorbance by the peptide bond. The concentration of a protein sample is determined from the measured absorbance and the absorptivity at 205 nm (a_{205}). This assay can be used to quantitate protein solutions with concentrations of 1 to 100 μg/ml protein.

Additional Materials *(also see Basic Protocol 1)*

Brij 35 solution: 0.01% (v/v) Brij 35 (Sigma) in an aqueous solution appropriate for dissolving or diluting the sample protein

1. Dissolve or dilute the protein sample in Brij 35 solution.
2. Turn on the UV lamp of the spectrophotometer and set the wavelength to 205 nm. Allow the instrument to warm up 30 min before taking measurements.
3. Zero the spectrophotometer with the Brij 35 solution alone.
4. Measure the absorbance of the sample protein.

5a. *If the a_{205} of the protein is known:* Use Equation A.3G.1 to calculate the concentration of the sample protein *except* substitute the appropriate values for A_{205} and a_{205}.

5b. *If the a_{205} is not known:* Estimate the concentration of the sample protein from its measured absorbance using Equation A.3G.2.

$$\text{concentration (mg/ml)} = \frac{A_{205}}{31 \times b}$$

Equation A.3G.2

In this equation, the absorptivity value, 31, has units of ml/mg cm and b is the path length in cm.

USING FLUORESCENCE EMISSION TO DETERMINE PROTEIN CONCENTRATION

Protein concentration can also be determined by measuring the intrinsic fluorescence based on fluorescence emission by the aromatic amino acids tryptophan, tyrosine, and/or phenylalanine. Usually tryptophan fluorescence is measured. The fluorescence intensity of the protein sample solution is measured and the concentration calculated from a calibration curve based on the fluorescence emission of standard solutions prepared from the purified protein. This assay can be used to quantitate protein solutions with concentrations of 5 to 50 μg/ml.

Materials

Standard protein solution prepared using the purified protein (see recipe)
Sample protein
Spectrofluorometer *or* filter fluorometer with an excitation cutoff filter ≤285 nm and an emission filter >320 nm

1. Prepare dilutions of the purified protein at 5, 7.5, 10, 25, and 50 μg/ml in the same solvent as the sample protein. Prepare a blank consisting of solvent alone.
2. Turn on the lamp of the instrument and allow it to warm up 30 min before taking measurements.

   If a spectrofluorometer is used, set the excitation wavelength to 280 nm and the emission wavelength to between 320 and 350 nm. If the exact emission wavelength is not known, determine it empirically by scanning the standard solution with the excitation wavelength set to 280 nm. If the instrument is a filter fluorometer, use an excitation cutoff filter ≤285 nm and an emission filter >320 nm.
3. Zero the instrument with the solvent blank.
4. Measure the fluorescence of the protein standard and sample protein solutions.
5. Create a calibration curve by either plotting or performing regression analysis of the fluorescence intensity versus concentration of the standards. Using the fluorescence intensity of the sample protein, determine the concentration from the calibration curve.

   Fluorescence emission is a linear function of concentration only over a limited range.

REAGENTS AND SOLUTIONS

Use Milli-Q purified water or equivalent for the preparation of all recipes and in all steps. For common stock solutions, see ***APPENDIX 2A****; for suppliers, see* ***SUPPLIERS APPENDIX****.*

Standard protein solution, 3 mg/ml

Weigh out dry protein and prepare a stock solution at a concentration of 3 mg/ml in the same solvent as used for the sample protein. Store up to 3 months at −20°C.
To prepare calibration standard solutions, dilute the stock solution in solvent to give the desired final concentrations for the standard curve.

Bovine serum albumin (BSA, fraction V; Sigma) is frequently used for a protein standard solution. A 3 mg/ml solution of BSA should have an A_{280} of 1.98, based on an A_{280} of 6.61 for a 1% (w/v) solution.

For quantitation of a purified or partially purified protein, if possible, the protein standard should have an aromatic amino acid content similar to that of the sample protein.

COMMENTARY

Background Information

Measuring absorbance at 280 nm (A_{280}) is one of the oldest methods for determining protein concentration (Warburg and Christian, 1942; Layne, 1957). This method is still widely used because it is simple and does not require incubating the sample with exogenous chromophores. However, the detection limit is higher than colorimetric methods and therefore higher concentrations of protein are necessary. The A_{280} method requires that the protein being quantitated have aromatic amino acids, primarily tryptophan. Because of the variability in aromatic amino acid content among different proteins, their absorptivity at 280 nm (a_{280}) also varies. Therefore, if calibration standards are used for quantitation, the aromatic amino acid content of the standard must be similar to that of the sample protein for accurate results. For many previously studied proteins, the a_{280} is known and can be obtained from the literature (Fasman, 1989).

If the absorptivity is not known but the amino acid composition is known, the molar absorptivity at 280 nm (ε_{280}) can be predicted from Equation A.3G.3 (Pace et al., 1995):

$$\varepsilon_{280} = (\text{no. of Trp})(5500) + (\text{no. of Tyr})(1490) + (\text{no. of cystine})(125)$$

Equation A.3G.3

In this equation, the number of tryptophan (Trp), tyrosine (Tyr), and cystine residues are each multiplied by an estimated ε_{280} value for each residue. This equation was derived for folded proteins in water. With the DNA sequence for many proteins now available, the predicted ε_{280} can be derived for newer proteins where this value is not published. However, there are caveats that should be considered if the predicted ε_{280} in Equation A.3G.3 is used. First, the predicted ε_{280} is most reliable if the protein contains tryptophan residues and less so if there are no tryptophan residues. Second, the number of cystine residues must be accurately known and one cannot presume that all cysteine residues, to an even number, are involved in disulfide bonds. Alternatively, there are methods for measuring the ε_{280} value that are reliable (Pace et al., 1995).

Accordingly, the quantitation of proteins by peptide bond absorption at 205 nm (A_{205}) is more universally applicable among proteins. Furthermore, the absorptivity for a given protein at 205 nm is several-fold greater than that at 280 nm (Scopes, 1974; Stoscheck, 1990). Thus lower concentrations of protein can be quantitated with the A_{205} method. The disadvantage of this method is that some buffers and other components absorb at 205 nm (Stoscheck, 1990).

In addition to the aromatic amino acids, several others have absorption maxima in the UV range. Table A.3G.1 shows the wavelengths of absorption maxima and corresponding molar absorptivity (ε) for the amino acids with appreciable absorbance in the UV range. Only

Table A.3G.1 Absorption Maxima and Molar Absorptivity (ε) of Amino Acids[a]

Amino acid	Wavelength maxima (nm)	$\varepsilon \times 10^{-3}$ (l/mol cm)
Cysteine	250	0.3
Histidine	211	5.9
Phenylalanine	188	60.0
	206	9.3
	257	0.2
Tryptophan	219	47.0
	279	5.6
Tyrosine	193	48.0
	222	8.0
	275	1.4

[a]Values are for aqueous solutions at pH 7.1 (Freifelder, 1982; Fasman, 1989).

Table A.3G.2 Molar Absorptivity (ε) of Amino Acids at 280 nm[a]

Amino acid	$\varepsilon \times 10^{-3}$ (l/mol cm)
Cystine	0.110
Phenylalanine	0.0007
Tryptophan	5.559
Tyrosine	1.197

[a]Values are for aqueous solutions at pH 7.1 except for cystine, which is for water (Fasman, 1989).

Table A.3G.3 Fluorescence Properties of Aromatic Amino Acids[a]

Amino acid	Excitation wavelength	Emission wavelength	Quantum yield
Phenylalanine	260 nm	283 nm	0.04
Tryptophan	285 nm	360 nm	0.20
Tyrosine	275 nm	310 nm	0.21

[a]Values are for aqueous solutions at pH 7 and 25°C (Hawkins and Honigs, 1987; Fasman, 1989).

tryptophan has an absorption maximum at 280 nm, although, tyrosine and cystine will also slightly absorb. The ε_{280} for tryptophan is nearly five-fold greater than that for tyrosine and 50-fold greater than that for cystine (Table A.3G.2). The contribution to the absorbance at 280 nm of the third aromatic amino acid, phenylalanine, and cysteine are negligible. Several amino acids other than those in Table A.3G.1 absorb light below 205 nm (Fasman, 1989), but either the molar absorptivities are too low to be significant or the wavelengths are too short for practical absorbance measurements.

The aromatic amino acids also have fluorescence emissions when excited by light in the UV range. Table A.3G.3 gives the excitation wavelength, fluorescence emission wavelength, and quantum yield (Q) for tryptophan, tyrosine, and phenylalanine. The quantum yield is the ratio of photons emitted to photons absorbed. Typically, phenylalanine fluorescence is not detected in the presence of tyrosine and tryptophan due to low Q. Furthermore, tyrosine fluorescence is nearly completely quenched if the tyrosine residue is ionized or near an amino group, a carboxyl group, or a tryptophan residue (Teale, 1960; Freifelder, 1982). Therefore, tryptophan fluorescence is what is customarily measured.

Measurement of intrinsic fluorescence by aromatic amino acids is primarily used to obtain qualitative information (Freifelder, 1982). However, with a protein standard whose aromatic amino acid content is similar to that of the sample, intrinsic fluorescence can be used for quantitation (Hawkins and Honigs, 1987). An additional consideration is that the tertiary structure of a protein will influence the fluorescence, e.g., adjacent protonated acidic groups in a protein molecule will quench tryptophan fluorescence (Freifelder, 1982).

Critical Parameters and Troubleshooting

A 1-cm path length quartz cuvette is most often used to make absorbance measurements. However, quartz cuvettes with shorter path lengths, 0.01 to 0.5 cm, are available (e.g., from Hellma Cells or Beckman); these shorter path length cuvettes allow higher concentrations of protein solutions to be measured. Equation A.3G.1 and Equation A.3G.2 assume the cuvette has a path length of 1 cm; when cuvettes of shorter path length are used, the correct value for b must be substituted in the equation.

The solvent pH and polarity will affect the absorbance and fluorescence properties of a protein. A notable example of pH effects on absorbance is seen with tyrosine residues, where a change in pH from neutral to alkaline results in a shift of the absorbance maximum to a longer wavelength and an increase in absorptivity due to dissociation of the tyrosine phenolic hydroxyl group (Freifelder, 1982; Fasman, 1989). An example of solvent polarity effects on fluorescence is observed with tryptophan,

Table A.3G.4 Concentration Limits of Interfering Reagents for A_{205} and A_{280} Protein Assays[a]

Reagent[b]	A_{205}	A_{280}
Ammonium sulfate	9% (w/v)	>50% (w/v)
Brij 35	1% (v/v)	1% (v/v)
DTT	0.1 mM	3 mM
EDTA	0.2 mM	30 mM
Glycerol	5% (v/v)	40% (v/v)
KCl	50 mM	100 mM
2-ME	<10 mM	10 mM
NaCl	0.6 M	>1 M
NaOH	25 mM	>1 M
Phosphate buffer	50 mM	1 M
SDS	0.10% (w/v)	0.10% (w/v)
Sucrose	0.5 M	2 M
Tris buffer	40 mM	0.5 M
Triton X-100	<0.01% (v/v)	0.02% (v/v)
TCA	<1% (w/v)	10% (w/v)
Urea	<0.1 M	>1 M

[a]Values from Stoscheck (1990).
[b]Abbreviations: DTT, dithiothreitol; EDTA, ethylenediaminetetraacetic acid; 2-ME, 2-mercaptoethanol; SDS, sodium dodecyl sulfate; TCA, trichloroacetic acid.

where a decrease in solvent polarity results in a shift in fluorescence emission to shorter wavelengths and an increase in intensity (Freifelder, 1982). Because of these effects, the following precautions should be taken for accurate results: (1) when calibration curves are used for quantitation by absorbance or fluorescence, standards must be in the same solvent as the samples; and (2) when a published absorptivity at a given wavelength is used for quantitation, the solvent composition of the sample must be the same as that used in obtaining the published data.

Many buffers and other reagents can interfere with A_{280} and A_{205} spectrophotometric measurements. Stoscheck (1990) lists the concentration limits for many such reagents used in these spectrophotometric methods. The more commonly used reagents that absorb at 280 and 205 nm are listed in Table A.3G.4. In addition, reagents that contain carbon-carbon or carbon-oxygen double bonds can interfere with the A_{205} method.

Because stray light can affect the linearity of absorbance versus concentration, absorbance values >2.0 should not be used for sample proteins measured by the A_{280} or A_{205} method. Samples with absorbance >2.0 should be diluted further in the appropriate buffer to obtain absorbances <2.0.

Nucleic acids have substantial absorbance at 280 nm and can interfere with A_{280} quantitation of protein in crude samples. To resolve the protein concentration in such samples, measure the absorbance at 260 nm and 280 nm and calculate the protein concentration as follows (Warburg and Christian, 1942; Layne, 1957): protein concentration (mg/ml) = $1.55 \times A_{280} - 0.76 \times A_{260}$.

This estimation of protein concentration is valid up to 20% (w/v) nucleic acid or an A_{280}/A_{260} ratio <0.6.

Anticipated Results

Depending on the protein, the concentration range for the A_{280} method is 20 to 3000 μg/ml, for the A_{205} method is 1 to 100 μg/ml, and for the fluorescence emission method is 5 to 50 μg/ml.

Published absorptivities of proteins at 280 nm are usually given as the absorbance for a 1% (w/v) protein solution per cm, $A^{1\%}$, or as the molar absorptivity, ε, which has units of l/mol cm. To convert these published

coefficients to units of mg/ml, use either Equation A.3G.4 or Equation A.3G.5.

$$\text{concentration (mg/ml)} = \frac{A_{280} \times 10}{A^{1\%} \times b}$$

Equation A.3G.4

Molecular weight in Equation A.3G.5 is the molecular weight of the protein.

$$\text{concentration (mg/ml)} = \frac{A_{280} \times \text{molecular weight}}{\varepsilon_{280} \times b}$$

Equation A.3G.5

Time Considerations

When the absorptivity for a protein is known, the A_{280} and A_{205} measurements require <30 min depending on the number of samples. When standards are used for quantitation with these assays or for intrinsic fluorescence quantitation, 1 hr is required.

Literature Cited

Fasman, G.D. 1989. Practical Handbook of Biochemistry and Molecular Biology. CRC Press, Boca Raton, Fla.

Freifelder, D. 1982. Physical Biochemistry: Applications to Biochemistry and Molecular Biology 2nd ed.W.H. Freeman, New York.

Hawkins, B.K. and Honigs, D.E. 1987. A comparison of spectroscopic techniques for protein quantification in aqueous solutions. *Am. Biotechnol. Lab.* 5:26-37.

Layne, E. 1957. Spectrophotometric and turbidimetric methods for measuring proteins. *Methods Enzymol.* 3:447-454.

Pace, C.N., Vajdos, F., Fee, L., Grimsley, G., and Gray, T. 1995. How to measure and predict the molar absorption coefficient of a protein. *Protein Sci.* 4:2411-2423.

Scopes, R.K. 1974. Measurement of protein by spectrophotometry at 205 nm. *Anal. Biochem.* 59:277-282.

Stoscheck, C.M. 1990. Quantitation of protein. *Methods Enzymol.* 182:50-68.

Teale, F.W.J. 1960. The ultraviolet fluorescence of proteins in neutral solutions. *Biochem. J.* 76:381-388.

Warburg, O. and Christian, W. 1942. Isolierung und Kristallisation des Garungsferments Enolase. *Biochem. Z.* 310:384-421.

Key References

Chen, R.F. 1990. Fluorescence of proteins and peptides. *In* Practical Fluorescence, 2nd ed. (G.G. Guilbault, ed.) pp. 575-682. Marcel Dekker, Inc., New York.

Detailed discussion of intrinsic fluorescence of proteins and what factors affect fluorescence emission by the aromatic amino acids (see pp. 618-663).

Fasman, 1989. See above.

Contains tables with absorptivities for UV spectrophotometric detection and tables with data on excitation and emission wavelengths for fluorescence detection of many proteins. Also includes a table with molecular weights for many characterized proteins.

Stoscheck, 1990. See above.

Contains list of substances that can interfere with 205- and 280-nm spectrophotometric measurements of proteins and of concentration limits for these substances.

Contributed by Michael H. Simonian
Beckman Coulter Inc.
Fullerton, California

Dialysis and Concentration of Protein Solutions

DIALYSIS

Conventional dialysis separates small molecules from large molecules by allowing diffusion of only the small molecules through selectively permeable membranes. Dialysis is usually used to change the salt (small-molecule) composition of a macromolecule-containing solution. The solution to be dialyzed is placed in a sealed dialysis membrane and immersed in a selected buffer; small solute molecules then equilibrate between the sample and the dialysate. Concomitant with the movement of small solutes across the membrane, however, is the movement of solvent in the opposite direction. This can result in some sample dilution (usually <50%).

This unit describes dialysis of large- and small-volume samples using cellulose membranes with pore sizes designed to exclude molecules above a selected molecular weight (see Basic Protocol 1 and Alternate Protocol). The Support Protocol describes preparation of membranes for dialysis and discusses issues related to the selection of membranes including commercial kits. Solutions of proteins or peptides can be concentrated using commercially available reagents (see Basic Protocol 2).

Large-Volume Dialysis

BASIC PROTOCOL 1

This protocol describes the use of membranes, prepared using the Support Protocol, for dialysis of samples in large, easily handled volumes, typically 0.1 to 500 ml.

Materials

Dialysis membrane (see Support Protocol)
Clamps (Spectra/Por Closures, Spectrum, or equivalent)
Macromolecule-containing sample to be dialyzed
Appropriate dialysis buffer

1. Remove dialysis membrane from ethanol storage solution and rinse with distilled water. Secure clamp to one end of the membrane or knot one end with double-knots.

   Always use gloves to handle the dialysis membrane because the membrane is susceptible to cellulolytic microorganisms.

   See Support Protocol for a discussion of commercially available membranes and preparation and storage procedures.

   Clamps are less likely to leak than knots, but either type of closure should be carefully tested as described in steps 2 and 3.

2. Fill membrane with water or buffer, hold the unclamped end closed, and squeeze membrane. A fine spray of liquid indicates a pinhole in the membrane; discard and try a new membrane.

   Pinholes are rare but cause traumatic sample loss. Hard squeezing will cause some liquid to seep from the bag; this is normal.

3. Replace the water or buffer in dialysis membrane with the macromolecule-containing sample and clamp the open end. Again, squeeze to check the integrity of the membrane and clamps.

   If dialyzing a concentrated or high-salt sample, leave some space in the clamped membrane; there will be a net flow of water into the sample, and if sufficient pressure builds up the membrane can burst.

Contributed by Sarah M. Andrew, Julie A. Titus, and Louis Zumstein
Current Protocols in Toxicology (2001) A.3H.1-A.3H.5

4. Immerse dialysis membrane in a beaker or flask containing a large volume (relative to the sample) of the desired buffer. Dialyze at least 3 hr at the desired temperature with gentle stirring of the buffer.

   Dialysis rates are dependent on membrane pore size, sample viscosity, and ratio of membrane surface to sample volume. Temperature has little effect on dialysis rate, but low temperatures (i.e., 4°C) are usually chosen to enhance macromolecule stability. Common salts will equilibrate across a 15,000-MWCO membrane (see Support Protocol) in ~3 hr with stirring.

   Some compounds, especially detergents above their critical micelle concentration (CMC), dialyze very slowly.

5. Change dialysis buffer as necessary.

   Usually two to three dialysis buffer changes are sufficient. For example, when 100 mM Tris·Cl is removed from a protein for sequence analysis or other amino-reactive chemistry, two equilibrations against a 1000-fold volume excess of buffer will decrease the Tris concentration 10^6-fold, to 100 nM; three dialyses will decrease the concentration to 100 pM.

6. Remove dialysis membrane from the buffer. Hold the membrane vertically and remove excess buffer trapped in end of membrane outside upper clamp. Release upper clamp and remove the sample with a Pasteur pipet.

ALTERNATE PROTOCOL

Small-Volume Dialysis

For solution volumes less than ~100 µl, the use of dialysis membrane as described above can result in unacceptable sample loss. The method described below can easily dialyze volumes as small as 10 µl. The sample is held in a 0.5-ml microcentrifuge tube, with dialysis membrane covering the open end of the tube.

Additional Materials *(also see Basic Protocol 1)*

0.5-ml microcentrifuge tube
Pasteur pipet
Cork borer

1. Puncture the lid of each microcentrifuge tube using a heated glass Pasteur pipet (wide end heated) or cork borer to completely remove the center part of the lid (see Fig. A.3H.1). Open lid and place a single layer of dialysis tubing over top of tube, then close lid to hold dialysis tubing in place.

   The success of this protocol is dependent on a tight-fitting cap, so make sure the cap is well-seated. On the other hand, an excessively tight-fitting cap can rip the membrane when it is inserted.

   Alternatively, some researchers use a microcentrifuge tube without a cap. The sample is placed in the microcentrifuge tube, a dialysis membrane is placed over the top of the tube, and the membrane is secured with a rubber band. With this method, however, there is a risk that a small sample—e.g., 10 to 20 µl—may be lost around the edge of the tube.

2. Turn tube upside down and shake reaction mixture onto the membrane surface. Tape each tube, dialysis surface down, to the side of a beaker, then fill the beaker with PBS or buffer of choice. Dialyze 2 hr at 4°C with stirring.

   Alternatively, place the tube in a styrofoam or foam sheet (e.g., foam microcentrifuge rack, Fisher) then place, with the tube inverted, on the surface of the dialysis buffer.

   Make sure the dialysis surface is in contact with the buffer and that no bubbles exist. This can be accomplished by gently centrifuging the tube in an inverted position in a tabletop centrifuge.

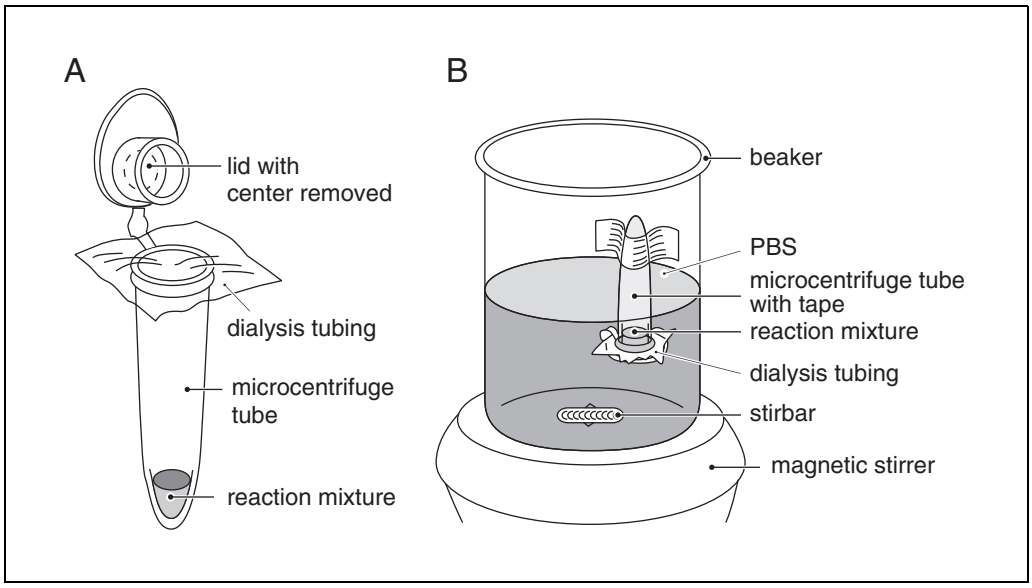

Figure A.3H.1 Making a microdialysis chamber. (**A**) Remove the center of the cap of a microcentrifuge tube with a heated Pasteur pipet (wide end). Place reaction mixture to be dialyzed into the tube. Place a piece of softened dialysis membrane loosely over top of tube. (**B**) Invert tube, shake sample down onto dialysis membrane (or centrifuge the tube inverted, if the sample is small), and tape tube into a beaker of buffer. Check that no bubbles are caught under the membrane.

The microdialysis method can be used for volumes of 50 to 500 µl (larger volumes can be dialyzed using a 1.5-ml microcentrifuge tube). The protein concentration is not important but should be 0.1 to 10 mg/ml. Most dialysis is complete after 2 hr but because proteins have a high buffering capacity, use 4 hr for a high protein concentration.

3. To recover the sample, remove microcentrifuge tube from the buffer and centrifuge briefly right-side-up.

Commercially available alternatives to this method include use of individual hollow-fiber filters from Spectrum (with sample capacities of 1 to 140 µl), and many different microdialysis machines, both single-sample and multisample (Spectrum, Cole-Parmer, Amersham Pharmacia Biotech, and others).

Selection and Preparation of Dialysis Membrane

SUPPORT PROTOCOL

Dialysis membranes are available in a number of thicknesses and pore sizes. Thicker membranes are tougher, but restrict solute flow; thus equilibrium is reached more slowly. Pore size is defined by "molecular weight cutoff" (MWCO)—i.e., the size of the smallest particle that cannot penetrate the membrane. The MWCO designation should be used only as a very rough guide; if accurate MWCO information is required, it should be determined empirically (see Craig, 1967, for a discussion of parameters affecting MWCO). Knowledge of the precise MWCO is usually not required; it is necessary only to use a membrane with a pore size that is much smaller than the macromolecule of interest. For most plasmid and protein dialyses, a MWCO of 12,000 to 14,000 is appropriate, whereas a MWCO of 3500, 2000, or even 1000 is appropriate for peptides.

Most dialysis membranes are made of derivatives of cellulose. They come in a wide variety of MWCO values, ranging from 500 to 500,000, and also vary in cleanliness, sterility, and cost. Spectrum has the most impressive inventory. The least expensive membranes come dry on rolls; these contain glycerol to keep them flexible as well as residual sulfides and traces of heavy metals from their manufacture. If glycerol, sulfur compounds, or small amounts of heavy metals are problematic, cleaner membranes should be purchased or

membranes should be prepared as described below. Protein dialysis should only be done with clean membranes.

It should be noted that several commercial kits for performing either large-scale or microdialysis are also available. For example, use of microdialysis cassettes (Slide-A-Lyzer, Pierce; or Dispo-Dialyzer, Spectrum) eliminates the need for boiling or presoaking dialysis tubing as well as the cumbersome task of clamping the dialysis tubing. Other vendors provide vessels for dialyzing multiple samples simultaneously. Selection of the best dialysis approach to be used will depend on a number of factors including the volumes to be dialyzed, the MWCO appropriate for the sample, and, of course, costs when considering the use of kits.

Materials

Dialysis membrane
10 mM sodium bicarbonate
10 mM Na_2EDTA, pH 8.0
20% to 50% (v/v) ethanol

1. Remove membrane from the roll and cut into usable lengths (usually 8 to 12 in.).

   Always use gloves to handle dialysis membrane as it is susceptible to a number of cellulolytic microorganisms. Membrane is available as sheets or preformed tubing.

2. Wet membrane and boil it for several minutes in a large excess of 10 mM sodium bicarbonate.
3. Boil several minutes in 10 mM Na_2EDTA. Repeat.

   Boiling speeds up the treatment process but is not necessary. A 30-min soak with some agitation can substitute for the boiling step.

4. Wash several times in distilled water.
5. Store at 4°C in 20% to 50% ethanol to prevent growth of cellulolytic microorganisms.

   Alternatively, bacteriostatic agents (e.g., sodium azide or sodium cacodylate) may be used for storage; however, ethanol is preferred for ease and convenience.

BASIC PROTOCOL 2

CONCENTRATION

Because it is usually more convenient to store antibodies or other proteins at >1 mg/ml, it may be necessary to concentrate the solution. In addition, concentration of protein solutions is often necessary to decrease the volume of a sample; e.g., to load onto a size-exclusion column when the volume must be ≤5 ml.

There are several simple and relatively inexpensive methods for concentrating protein solutions. Dialysis against Aquacide 11A (Calbiochem), which removes water through the dialysis tubing, may be used. After concentration, the solution must be redialyzed into the appropriate buffer. Another method is to use Immersible-CX Ultrafilters (Millipore) which, when connected to a vacuum, remove everything below their molecular weight cutoff (MWCO).

Alternatively, centrifugal concentrators which are operated with the aid of ordinary laboratory centrifuges may be used. Centricon microconcentrators (Amicon), which are available in different MWCO sizes, are very useful for concentrating small amounts of material in small volumes. Follow the instructions from the manufacturer when using these devices. Centriprep Centrifugal Filter Devices (Millipore) are disposable ultrafiltration devices used for purifying, concentrating, and desalting biological samples in the 2 to 15 ml volume range and are designed for use with most centrifuges that can accommodate 50-ml centrifuge tubes. Further description of these devices and instructions for their use are available at *http://www.millipore.com*.

LITERATURE CITED

Craig, L.C. 1967. Techniques for the study of peptides and proteins by dialysis and diffusion. *Methods Enzymol.* 11:870-905.

KEY REFERENCES

Craig. 1967. See above.

McPhie, P. 1971. Dialysis. *Methods Enzymol.* 22:23-32.

Describes the theory and practice of dialysis and diffusion.

Contributed by Sarah M. Andrew
Chester College
Chester, United Kingdom

Julie A. Titus
National Cancer Institute
Bethesda, Maryland

Louis Zumstein
Introgen Therapeutics, Inc.
Houston, Texas

The Colorimetric Detection and Quantitation of Total Protein

Protein quantification is an important step for handling protein samples for isolation and characterization, and is a prerequisite step before submitting proteins for chromatographic, electrophoretic, or immunochemical analysis and separation. The methods included in this appendix are colorimetric measurements, whose procedures are fast and simple.

This appendix describes four of the most commonly used total protein assay methods. Three of the four are copper-based assays to quantitate total protein: the Lowry method (see Basic Protocol 1 and Alternate Protocols 1 and 2), the bicinchoninic acid assay (BCA; see Basic Protocol 2 and Alternate Protocols 3 and 4), and the biuret method (see Basic Protocol 3 and Alternate Protocol 5). The fourth is the Coomassie dye binding or Bradford assay (see Basic Protocol 4 and Alternate Prortocols 6 and 7), which is included as a simple and sensitive assay, although it sometimes gives a variable response depending on how well or how poorly the protein binds the dye in acidic pH. A protein assay method should be chosen based on the sensitivity and accuracy of method as well as the condition of the sample to be analyzed.

STRATEGIC PLANNING

Colorimetric Protein Assays

The four colorimetric methods for the detection and quantitation presented in this appendix have withstood the test of time. They are all well-characterized robust assays that consistently work well. The methods were introduced over the past 15 to 50 years. They collectively represent the state of the art for colorimetric detection and quantitation of total proteins in the microgram to milligram range.

When confronted with the need to determine the total protein concentration of a sample, one of the first issues to consider is selection of a protein assay method. The choice among the available protein assays usually is made based upon consideration of the compatibility of the method with the samples to be assayed. The objective is to select a method that requires the least manipulation or pretreatment of the samples due to the presence of substances that may interfere. If the total protein concentration in the samples is high (i.e., in the range of 5 to 160 mg/ml), the biuret total protein reagent is the best choice. If the total protein concentration in the samples is low (i.e., in the range of 1 to 2000 μg/ml), then any one of the other three (i.e., the Lowry, the Coomassie Plus, or the BCA method) would be suitable. If the sample contains reducing agents or copper-chelating reagents, the Coomassie Plus Protein Assay Reagent (Pierce) would be the best choice. If the sample contains one or more detergents (at concentrations up to 5%), the BCA Protein Assay Reagent is the best choice.

Sometimes the sample contains substances that make it incompatible with any of the protein assay methods. In those cases, some pretreatment of the sample is necessary.

Each method has its advantages and disadvantages. No one method can be considered to be the ideal or best protein assay method. Because of this, most researchers keep more than one type of protein assay reagent available in their laboratory.

Contributed by Randall I. Krohn
Current Protocols in Toxicology (2005) A.3I.1-A.3I.28

Selection of the Protein Standard

The selection of a protein standard is potentially *the* greatest source of error in any protein assay. Of course, the best choice for a standard is a highly purified version of the predominant protein found in the samples. This is not always possible nor always necessary. In some cases, all that is needed is a rough estimate of the total protein concentration in the sample. For example, in the early stages of purifying a protein, identifying which fractions contain the most protein may be all that is required. If a highly purified version of the protein of interest is not available or it is too expensive to use as the standard, the alternative is to choose a protein that will produce a very similar color response curve with the selected protein assay method.

For general protein assay work, bovine serum albumin (BSA) works well as the choice for a protein standard, because it is widely available in high purity and relatively inexpensive. Although it is a mixture containing several immunoglobulins, bovine gamma globulin (BGG) is also a good choice for a standard when determining the concentration of antibodies, since BGG produces a color response curve that is very similar to that of immunoglobulin G (IgG).

For greatest accuracy of the estimates of the total protein concentration in unknown samples, it is essential to include a standard curve in each run. This is particularly true for the protein assay methods that produce nonlinear standard curves (e.g., Lowry method, Coomassie dye–binding method). The decision about the number of standards used to define the standard curve and the number of replicates to be done on each standard depends upon the degree of nonlinearity in the standard curve and the degree of accuracy required of the results. In general, fewer points are needed to construct a standard curve if the color response curve is linear. For assays done in test tubes, duplicates are sufficient; however, triplicates are recommended for assays performed in microtiter plates due to the increased error associated with microtiter plates and microtiter plate readers.

Preparation of the Samples

Before a sample can be analyzed for total protein content, it must be solubilized, usually in a buffered aqueous solution. The entire process is usually done in the cold, with additional precautions taken to inhibit microbial growth or to avoid casual contamination of the sample by foreign debris such as hair, skin, or body oils. When working with tissues, cells, or solids, the first step of the solubilization process is usually disruption of the sample's cellular structure by grinding and/or sonication, or by the use of specially designed reagents containing surfactants to lyse the cells (i.e., the POPPERS line of products, available from Pierce). This is done in a cold aqueous buffer containing one or more surfactants (to aid the solubilization of the membrane-bound proteins), one or more biocides (to prevent microbial growth), and protease inhibitors (to minimize or prevent digestion of the proteins into peptide fragments by endogenous proteases). After filtration or centrifugation (to remove the cellular debris), additional steps such as sterile filtration, removal of lipids, or further purification of the protein of interest from the other sample components may be necessary.

Calculation of the Results

If calculating the protein concentrations manually, it is best to use point-to-point interpolation. This is especially true if the standard curve is nonlinear. Point-to-point interpolation refers to a method of calculating the results for each sample using the equation for a linear regression line obtained from just two points on the standard curve. The first point is the standard that has an absorbance just below that of the sample and the second point is the standard that has an absorbance just above that of the sample. In this way, the

concentration of each sample is calculated from the most appropriate section of the whole standard curve. The average total protein concentration for each sample is determined from the average of its replicates. If multiple dilutions of each sample have been run, the results for the dilutions that fall within the most linear portion of the working range are averaged.

If using a computer program, use a quadratic curve fit for the nonlinear standard curve to calculate the protein concentration of the samples. If the standard curve is linear or if the absorbance readings for the samples fall within the linear portion of the standard curve, the total protein concentrations of the samples can be estimated using the linear regression equation.

Most software programs will allow the experimenter to construct and print a graph of the standard curve as well as calculate the protein concentration for each sample and display statistics for the replicates. Typically, the statistics displayed will include the average of the absorbance readings (or the average of the calculated protein concentrations), the standard deviation (SD), and the coefficient of variation (CV) for each standard or sample. If multiple dilutions of each sample have been run, average the results for the dilutions that fall in the most linear portion of the working range.

THE LOWRY PROTEIN ASSAY FOR DETERMINATION OF TOTAL PROTEINS

BASIC PROTOCOL 1

In 1951, Oliver H. Lowry introduced this colorimetric total protein assay method. It offered a significant improvement over previous protein assays, and his paper became one of the most cited references in the life-science literature (Lowry et al., 1951). The Lowry assay is easy to perform since the incubations are done at room temperature and the assay is sensitive enough to allow the detection of total protein in the low microgram per milliliter range. It is one of three copper chelation chemistry–based methods presented in this appendix. Essentially, the Lowry protein assay is an enhanced biuret assay (see Basic Protocol 3). After a short incubation, Lowry's reagent C (Folin phenol) is added for enhanced color development (Fig. A.3I.1). The Lowry assay requires fresh (daily) preparation of two reagents and a meticulously timed incubation step. The two reagents are combined just before use to make a buffered alkaline cupric sulfate working solution. The addition of sodium dodecyl sulfate (SDS) to Lowry's reagent D (i.e., Lowry's reagent D′) allows the method to be used with samples that contain detergents.

Materials

Standard protein: 2 mg/ml BSA (see recipe)
Sample buffer or solvent
Protein sample(s)
Lowry's Reagents C and D or D′ (see recipes)

1. Dispense 0 to 100 µl standard protein to appropriately labeled tubes and bring the total volume to 100 µl with sample buffer or solvent to prepare a dilution series from 10 to 100 µg.

   These concentrations of albumin should produce A_{750} readings from ~0.10 to 1.0 AU in 1-cm cuvettes.

2. Dispense ≤100 µl protein sample(s) to separate labeled tubes and adjust the final volume to 100 µl using the same buffer or solvent used to prepare the sample.

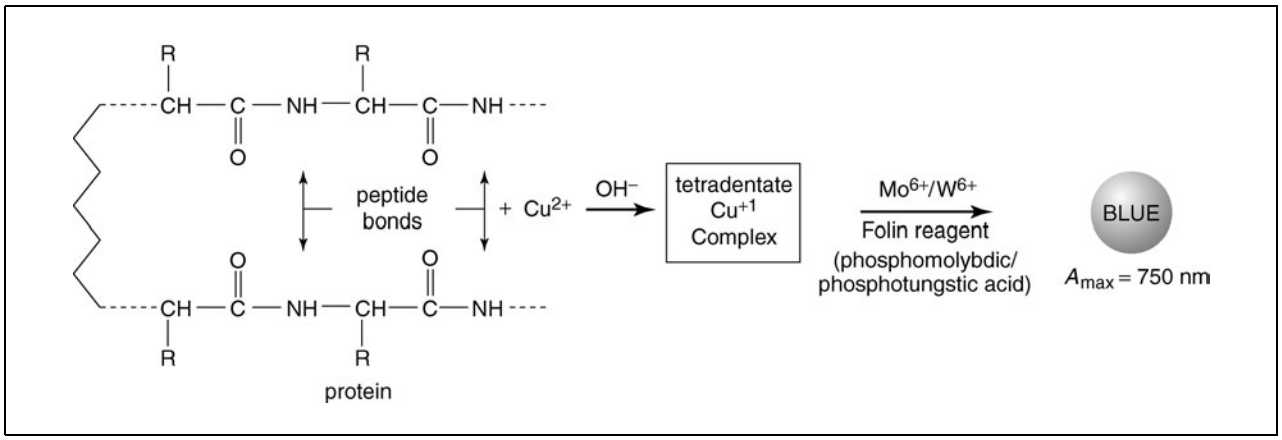

Figure A.3I.1 The reaction schematic for the Lowry Protein Assay.

3. Add 1 ml reagent D (or reagent D′) to each of the standards and unknown samples. Vortex the tubes immediately to develop optimum color. Incubate for precisely 10 min at room temperature.

   If samples contain detergent, use reagent D′ to eliminate the interference associated with up to 1% of various detergents. If a precipitate forms in reagent D′, warm the reagent and vortex before addition.

4. While mixing, add 0.1 ml reagent C. Vortex the tubes immediately. Incubate for 30 min at room temperature.

5. Measure the color at 750 nm (A_{750}) on a spectrophotometer zeroed with deionized water.

   Read samples within 10 min, as samples continue to develop color. Samples incubated >60 min should be discarded.

   If the absorbance reading of the sample is higher than that of the highest concentration of standard, dilute the sample with buffer and repeat the procedure on the diluted sample.

6. Plot a standard curve by graphing the average net or blank-corrected A_{750} values for each standard versus its protein concentration in milligrams per milliliter.

7. Determine sample protein concentration by interpolating from the standard curve (see Strategic Planning).

ALTERNATE PROTOCOL 1

MODIFIED LOWRY PROTEIN ASSAY FOR DETERMINATION OF TOTAL PROTEINS

Preformulated, stabilized, modified versions of the Lowry reagent are now commercially available from Pierce (the Modified Lowry Protein Assay Reagent) or from Bio-Rad (the DC Protein Assay). The assay can be performed in test tubes or a microtiter plate (see Alternate Protocol 2). The working range of this assay is 1 to 1500 μg/ml if the Pierce reagent is used, or 200 to 1400 μg/ml if the Bio-Rad reagent is used. Table A.3I.1 is a brief troubleshooting guide for this technique.

Additional Materials *(also see Basic Protocol 1)*

Modified Lowry Protein Assay Kit (Pierce) containing:
2 mg/ml BSA in 0.9% (w/v) NaCl/0.05% (w/v) sodium azide
2 N Folin-Ciocalteu reagent: dilute fresh to 1 N
Modified Lowry's Reagent

Table A.3I.1 Troubleshooting Guide for the Modified Lowry Protein Assay

Problem	Possible cause	Solution
No color in any tubes	Sample contains a chelating agent (e.g., EDTA, EGTA)	Dialyze or dilute the sample
		Precipitate the protein with TCA and dissolve the pellet in modified Lowry reagent
Blank A_{750} is normal, but standards show less color than expected	Sample changed the pH of the reagent	Dialyze or dilute the sample
	Color measured at the wrong wavelength	Measure the color at 750 nm
Precipitate forms in all tubes	Sample contains a surfactant (detergent)	Dialyze or dilute the sample
	Sample contains potassium ions	Precipitate the protein with TCA, dissolve the pellet in Modified Lowry Reagent
All tubes (including the blank) are dark purple	Sample contains a reducing agent	Dialyze or dilute the sample
	Sample contains a thiol	Precipitate the protein with TCA, dissolve pellet in Modified Lowry Reagent
Need to read color at a different wavelength	Colorimeter does not have 750-nm filter	Color may be read at any wavelength between 650 nm and 750 nm

1. Prepare a dilution series of 2 mg/ml BSA (e.g., the standard provided in the Modified Lowry Protein Assay Kit) in buffer to cover the range 2.0 to 1500 μg/ml.

   If possible, use the same diluent or buffer cocktail for the blanks and for diluting the stock BSA standard that was used with the samples.

2. In duplicate, add 200 μl diluted standard, sample, or buffer (blank) into appropriately labeled test tubes.

   If possible, use the same diluent or buffer cocktail for the blanks and for diluting the stock BSA standard that was used with the samples.

3. At 15-sec intervals, add 1.0 ml Modified Lowry Protein Assay Reagent to each of the tubes. Vortex 2 to 3 sec to mix the contents of the tube and incubate at room temperature for *exactly* 10 min.

4. At the end of the first tube's 10-min incubation, add 100 μl freshly diluted 1 N Folin-Ciocalteu reagent (freshly diluted from a 2 N stock). Immediately vortex the tube for 2 to 3 sec. Continue to maintain the 15-sec intervals from step 3 for addition of the reagent to the remaining tubes.

5. Allow each of the tubes to incubate for 30 min at room temperature.

6. Measure the color at 750 nm (A_{750}) on a spectrophotometer zeroed with deionized water.

7. Plot a standard curve by graphing the average net or blank-corrected A_{750} values for each BSA standard versus its concentration in micrograms per milliliter.

   Example color response curves for BSA and BGG are shown in Figure A.3I.2.

8. Determine the sample concentration by interpolating from the plot (see Strategic Planning). Determine the average total protein concentration for each sample from the average of its replicates.

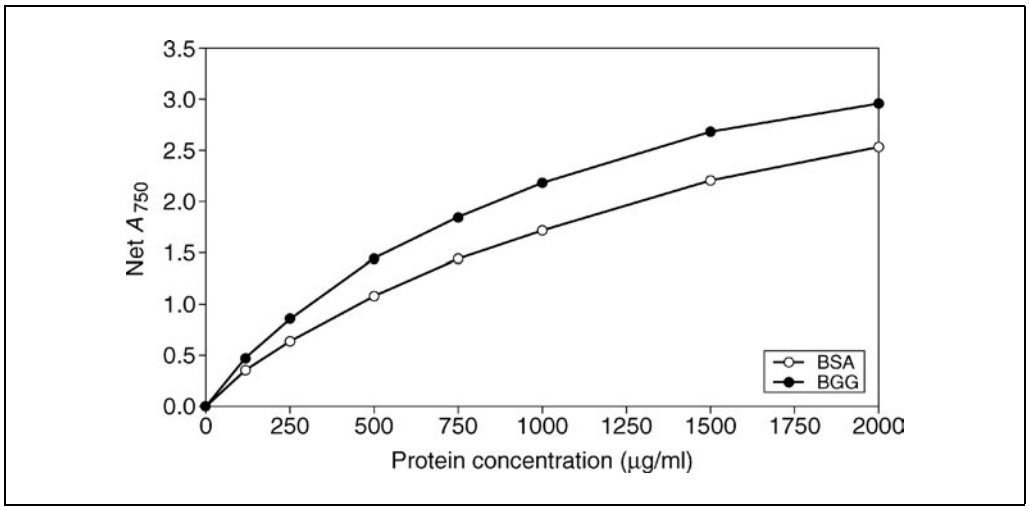

Figure A.3I.2 Graph of the color response curves obtained with Pierce's Modified Lowry Protein Assay Reagent using bovine serum albumin (BSA) and bovine gamma globulin (BGG). The standard tube protocol was performed and the color was measured at 750 nm in a Hitachi U-2000 spectrophotometer.

ALTERNATE PROTOCOL 2

MICROTITER PLATE MODIFIED LOWRY ASSAY FOR TOTAL PROTEIN

The modified Lowry assay can also be done in a 96-well microtiter plate format. The assay has a working range of 1 to 1500 µg/ml.

Additional Materials *(also see Alternate Protocol 1)*

Microtiter plate and cover or tape seals
200-µl multichannel pipettor
Microtiter plate reader for 750 nm

1. Draw a template for placement of samples and standards on the microtiter plate.

   Blanks, standards, and samples should be prepared in triplicate.

2. Add 40 µl of each diluted BSA standard (see Alternate Protocol 1, step 1), sample, or diluent (blank) to the appropriate wells of a 96-well plate.

   If possible, use the same diluent or buffer cocktail for the blanks and for diluting the stock BSA standard that was used with the samples.

3. Using a multichannel pipettor, quickly add 200 µl Modified Lowry Protein Assay Reagent to each of the wells. Mix immediately on a plate mixer for 30 sec.

4. Allow the plate to incubate at room temperature for *exactly* 10 min.

5. Using a multichannel pipettor, quickly add 20 µl freshly diluted 1 N Folin-Ciocalteu reagent to each well. Immediately mix on a plate mixer for 30 sec.

6. Cover the plate (to prevent evaporation) and incubate 30 min at room temperature.

7. Mix the plate again and measure the color (absorbance) of each well in a microtiter plate reader at 750 nm.

8. Plot a standard curve by graphing the average net or blank-corrected A_{750} values for each standard versus its protein concentration in micrograms per milliliter.

9. Determine the sample concentration by interpolating from the plot (see Strategic Planning). Calculate the average total protein concentration for each sample from the average of its replicates.

THE BICINCHONINIC ACID (BCA) ASSAY FOR DETERMINATION OF TOTAL PROTEIN

BASIC PROTOCOL 2

Smith et al. (1985) introduced the bicinchoninic acid (BCA) protein assay reagent. In one sense, it is a modification of the Lowry protein assay reagent. The mechanism of color formation with protein for the BCA protein assay reagent is similar to that of the Lowry reagent, but there are several significant differences. The BCA protein assay reagent combines the reduction of Cu^{2+} to Cu^{+} by protein in an alkaline medium (i.e., the biuret reaction; see Basic Protocol 3) with the highly sensitive and selective colorimetric detection of the cuprous cation (Cu^{+}) by bicinchoninic acid.The purple-colored reaction product of this method is formed by the chelation of two molecules of BCA with one cuprous ion (Fig. A.3I.3). The BCA/copper complex is water-soluble and exhibits a strong linear absorbance at 562 nm with increasing protein concentrations. The primary advantage of the BCA protein assay reagent is that most surfactants, even if present in the sample at concentrations up to 5% (v/v), are compatible with this method. Table A.3I.2 is a brief troubleshooting guide for this technique.

Materials

Protein standard: 2 mg/ml BSA (see recipe)
Sample buffer or solvent
Protein sample
BCA working reagent: mix 100 parts BCA reagent A with 2 parts reagent B (see recipes for each reagent)

1. Prepare a dilution series of 2 mg/ml BSA in sample buffer or diluent to cover a range from 125 to 2000 μg/ml.
2. Add 100 μl sample, diluted standard, or buffer (blank) into appropriately labeled tubes.
3. Add 2 ml BCA working reagent mix to each tube. Vortex immediately.

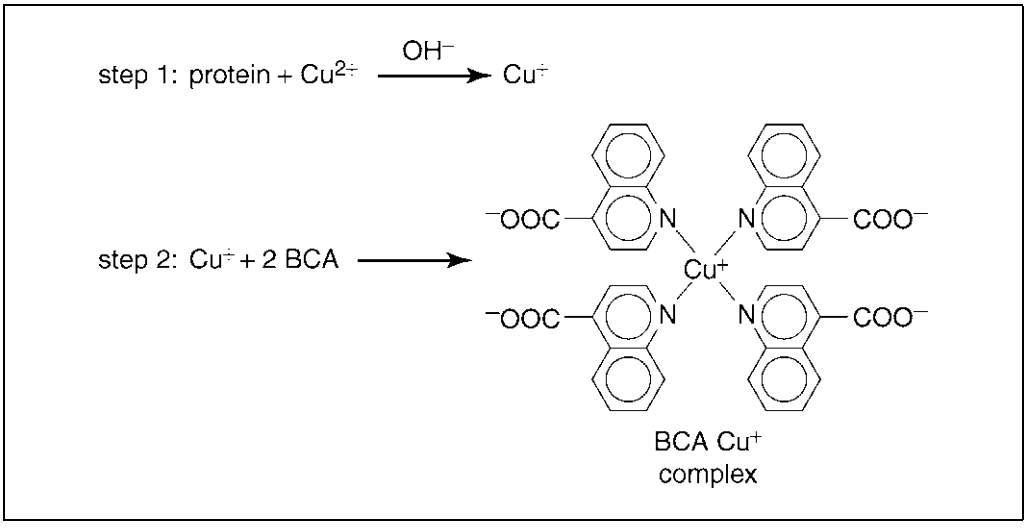

Figure A.3I.3 The reaction schematic for the BCA Protein Assay.

Table A.3I.2 Troubleshooting Guide for BCA Protein Assay

Problem	Possible cause	Solution
No color in any tubes	Sample contains a copper chelating agent	Dialyze or dilute the sample
		Increase the copper concentration in the working reagent (use 48 parts reagent A and 2 parts reagent B)
Blank A_{562} is normal, but standards and samples show less color than expected	Strong acid or alkaline buffer, alters working reagent pH	Dialyze or dilute the sample
	Color measured at the wrong wavelength	Measure the color at 562 nm
Color of samples appear darker than expected	Protein concentration is too high	Dilute the sample
	Sample contains lipids or lipoproteins	Add 2% (w/v) SDS to the sample to eliminate interference from lipids
All tubes (including the blank) are dark purple	Sample contains a reducing agent	Dialyze or dilute the sample
	Sample contains a thiol	Precipitate the protein with trichloroacetic acid (TCA) and deoxycholate (DOC), dissolve pellet in BCA working reagent
	Sample contains biogenic amines (catecholamines)	Treat the sample with iodoacetamide (for thiols)
Need to read color at a different wavelength	Colorimeter does not have 562-nm filter	Color may be read at any wavelength between 550 nm and 570 nm

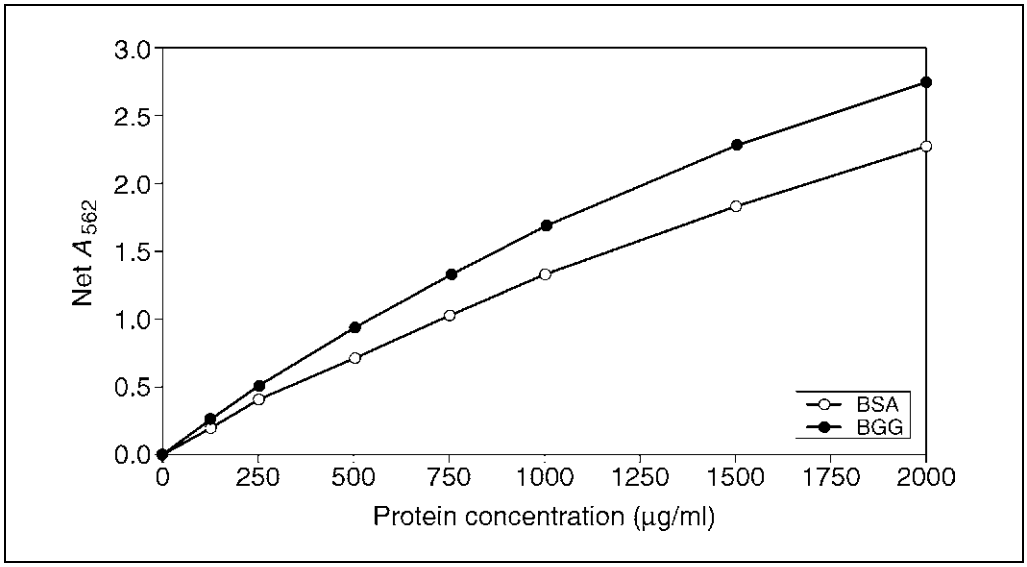

Figure A.3I.4 Graph of the color response curves obtained with Pierce's BCA Protein Assay Reagent using bovine serum albumin (BSA) and bovine gamma globulin (BGG). The standard tube protocol was performed and the color was measured at 562 nm in a Hitachi U-2000 spectrophotometer.

4. Incubate samples and standards for 30 min at 37°C, then cool to room temperature.
5. Measure the color at 562 nm (A_{562}) on a spectrophotometer zeroed with deionized water.
6. Plot a standard curve by graphing the average net or blank-corrected A_{562} values for the standards versus protein concentration in micrograms per milliliter.

   Example color response curves for BSA and BGG are shown in Fig. A.3I.4.

7. Determine the protein concentration of the sample by interpolation from the plot (see Strategic Planning).

USING KITS FOR BCA MEASUREMENTS OF TOTAL PROTEIN

ALTERNATE PROTOCOL 3

Preformulated versions of the BCA reagent are now commercially available from Pierce (BCA Protein Assay Reagent) or Sigma (Bicinchoninic Acid Kit for Protein Determination). This assay can be performed in test tubes or microtiter plates (see Alternate Protocol 4), and has a working range of 20 to 2000 μg/ml.

Additional Materials

BCA Protein Assay Reagent Kit (Pierce) or Bicinchoninic Acid Kit (Sigma) containing:
2 mg/ml BSA in 0.9% NaCl/0.05% sodium azide (also see recipe)
BCA reagent A (also see recipe)
BCA reagent B (also see recipe)
37°C water bath

1. Prepare a dilution series of BSA standard in buffer to cover the range 125 to 2000 μg/ml.

   If possible, use the same diluent or buffer cocktail for the blanks and for diluting the stock BSA standard that was used with the samples.

2. Prepare sufficient BCA working reagent (a minimum of 2 ml/tube or 20 ml/96-well microtiter plate) by adding 2 parts BCA reagent B to 100 parts of BCA reagent A.

   After mixing, the BCA working reagent is clear and apple green in color.

3. In duplicate, add 100 μl standard, sample, or buffer (blank) into appropriately labeled test tubes.
4. Add 2.0 ml BCA working reagent to each tube. Mix well by vortexing each tube 2 to 3 sec.

5a. *Standard tube protocol:* Incubate all tubes in a 37°C water bath for 30 min.

5b. *Enhanced assay protocol:* Alternatively, incubate all tubes in a 60°C water bath for 30 min.

   Increasing the incubation temperature to 60°C lowers the minimum detection level to 5 μg/ml and narrows the working range of the assay to a maximum of 250 μg/ml. This is known as the enhanced BCA assay.

6. After incubation, cool all tubes to room temperature.

   Since the BCA reagent does not reach a true end point, color development will continue even after cooling to room temperature; however, the rate of color development is very slow after cooling to room temperature, so no significant error is introduced if the A_{562} readings of all the tubes can be read within ~10 min.

7. Before reading, mix each tube again and measure the amount of color produced in each tube with a spectrophotometer at 562 nm (A_{562}) versus deionized water.
8. Plot a standard curve by graphing the average net or blank-corrected A_{562} values for the standards versus protein concentration in micrograms per milliliter.
9. Determine the sample concentration by interpolating from the plot (see Strategic Planning). Calculate the average sample concentration from its replicates.

ALTERNATE PROTOCOL 4

MICROTITER PLATE ASSAY FOR BCA MEASUREMENT OF TOTAL PROTEIN

BCA assays can be run in 96-well microtiter plates. The assay has a working range of 125 to 2000 μg/ml.

Additional Materials *(also see Alternate Protocol 3)*

96-well microtiter plate with cover or tape seal
200-μl multichannel pipettor
Microtiter plate shaker
37°C dry-heat incubator
Microtiter plate reader

1. Draw a template for the placement of samples and standards on a microtiter plate.

   Blanks, standards, and samples should be prepared in triplicate.

2. Add 10 μl of each diluted BSA standard (see Alternate Protocol 3, step 1), sample, or diluent (blank) to the appropriate wells.
3. Using a multichannel pipettor, add 200 μl BCA working reagent (see Alternate Protocol 3, step 2) to each well. Mix well on a microtiter plate shaker for 30 sec.
4. Cover the plate and incubate in a 37°C dry-heat incubator for 30 min.
5. After incubation, allow the plate to cool to room temperature.
6. Mix the plate again, remove the plate cover and measure the color in each well of the plate at 562 nm (A_{562}) in a microtiter plate reader.
7. Plot a standard curve by graphing the average net or blank-corrected A_{562} values for each BSA standard versus its concentration in micrograms per milliliter.
8. Determine the sample concentration by interpolating from the plot (see Strategic Planning). Calculate the average total protein concentration for each sample from the average of its replicates.

BASIC PROTOCOL 3

THE BIURET ASSAY FOR DETERMINING TOTAL PROTEIN

All proteins are composed of amino acids joined by peptide bonds in a linear sequence. There are ~20 naturally occurring amino acids found in proteins. The amino acids are joined to each other by peptide bonds formed by a condensation reaction that occurs between the terminal amine of one amino acid and the carboxyl end of the next. Peptides containing three or more amino acid residues will form a colored chelate complex with cupric ions in an alkaline environment containing sodium potassium tartrate. A similar colored chelate complex forms with the organic compound biuret (NH_2–CO–NH–CO–NH_2) and the cupric ion. The reaction in which a colored chelation complex is formed with peptide bonds in the presence of an alkaline cupric sulfate solution became known as the biuret reaction (Fig. A.3I.5). Thus, the biuret protein assay reagent gets its name

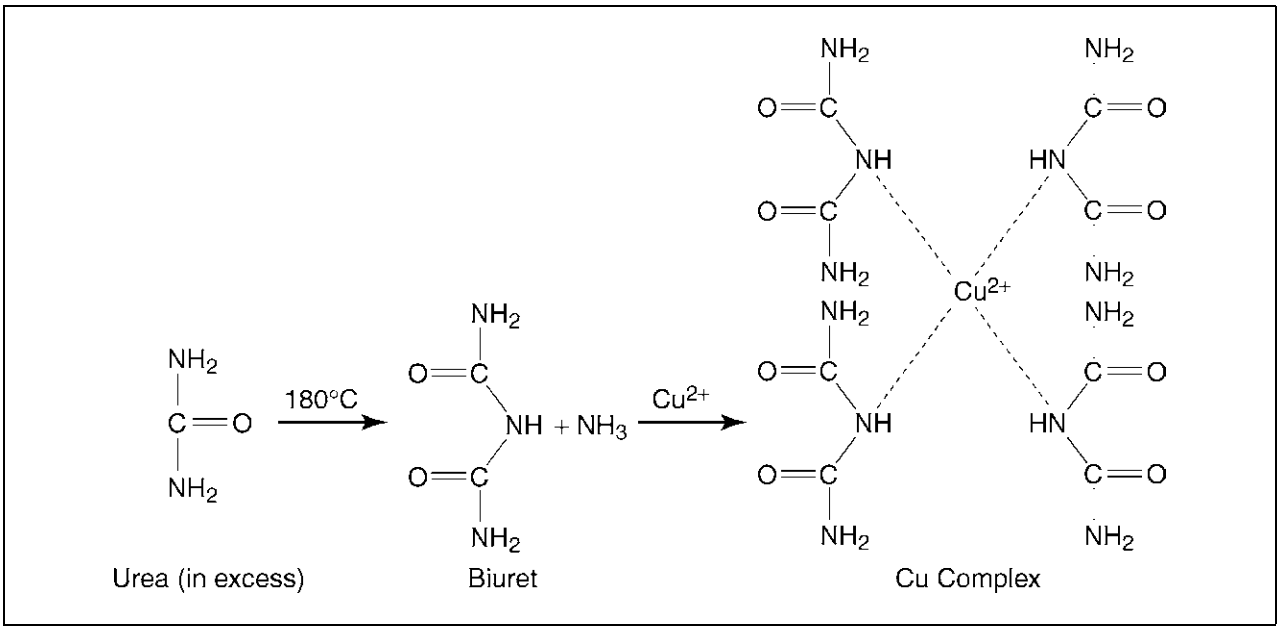

Figure A.3I.5 The schematic of the biuret reaction.

Table A.3I.3 Troubleshooting Guide for Biuret Protein Assay

Problem	Possible cause	Solution
No color in any tubes	Sample contains copper chelating agent	Dialyze or dilute the sample
Blank A_{540} is normal, but standards show less color than expected	Color measured at the wrong wavelength	Measure the color at 540 nm
All tubes (including the blank) are dark purple	Sample contains a reducing agent	Dialyze or dilute the sample

from the above reaction even though it does not actually contain the organic compound biuret. Single amino acids or dipeptides do not give the biuret reaction, but tripeptides and larger polypeptides or proteins will react to produce the light-blue to violet complex that absorbs light at 540 nm. One cupric ion forms the colored coordinate complex with 4 to 6 nearby peptides bonds. The intensity of the color produced is proportional to the number of peptide bonds participating in the reaction. Thus, the biuret reaction is the basis for a simple and rapid colorimetric method of quantitatively determining total protein concentration.

Because the working range for the biuret assay is from 5 to 160 mg/ml, the biuret reagent has found utility in the clinical laboratories for the quantitation of total protein in serum. The formulation employed in the biuret total protein reagent (Sigma Diagnostics) was developed by Doumas et al. (1981) as a candidate reference method for the determination of serum total protein in the clinical lab. Using Sigma's biuret reagent, the expected range for total protein in serum is from 63 to 83 mg/ml. Bilirubin, lipids, hemoglobin, and dextran are known to interfere in the biuret assay for total serum protein. Outside of this application, other copper chelating agents such as EDTA, EGTA, citrate,

Tris, iminodiacetic acid, and nitrilotriacetic acid will interfere. The working range of this assay is 5 to 160 mg/ml. Table A.3I.3 is a brief troubleshooting guide for this technique.

Materials

Standard protein (also see Commentary)
Sample (unknown) protein
Biuret total protein reagent (Sigma Diagnostics; also see recipe)

1. Select a protein to use as the standard (see Strategic Planning) and prepare a dilution series with buffer to cover the range 10 to 160 mg/ml.

   If possible, use the same diluent or buffer cocktail for the blanks and for diluting the standard that was used with the samples.

2. In duplicate, add 20 µl standard, sample, or diluent (blank) to appropriately labeled test tubes.
3. Add 1.0 ml biuret reagent to each tube. Mix well by vortexing 2 to 3 sec.
4. Incubate tubes at ambient room temperature (18° to 26°C) for 10 min.
5. Measure the color of each tube with a spectrophotometer at 540 nm (A_{540}). Compare to the blank.
6. Plot a standard curve by graphing the blank-corrected A_{540} values for the standards versus protein concentration in milligrams per milliliter.

   Example color response curves for BSA and BGG are shown in Figure A.3I.6.

7. Determine the sample concentration by interpolation from the standard curve (see Strategic Planning).

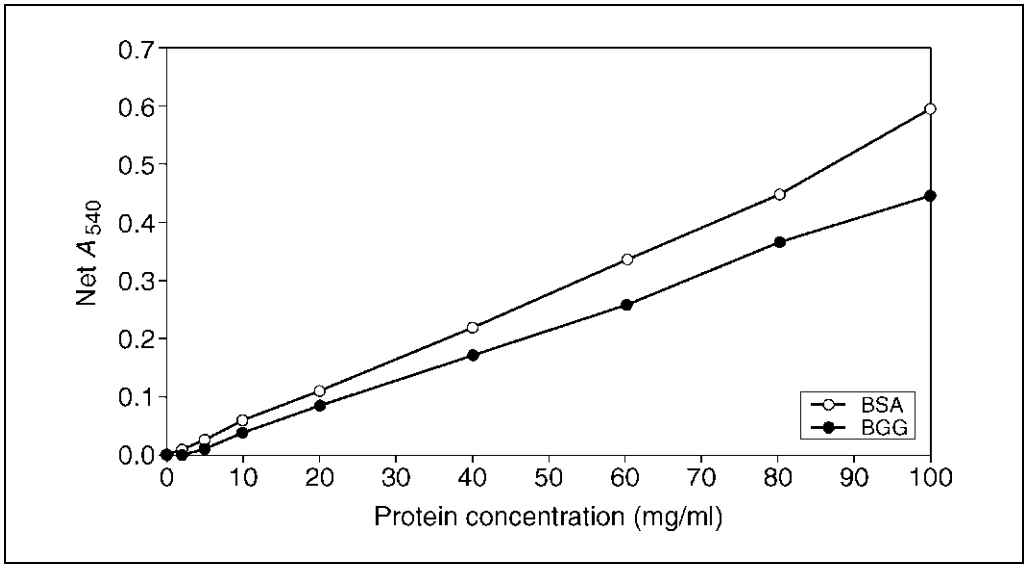

Figure A.3I.6 Graph of the color response curves obtained with Sigma's biuret Total Protein Reagent using bovine serum albumin (BSA) and bovine gamma globulin (BGG). The standard tube protocol was performed and the color was measured at 540 nm in a Hitachi U-2000 spectrophotometer.

MICROTITER PLATE BIURET ASSAY FOR TOTAL PROTEIN

ALTERNATE PROTOCOL 5

The biuret assay can be performed in a 96-well microtiter plate and has a working concentration of 10 to 160 mg/ml.

Additional Materials *(also see Basic Protocol 3)*

96-well microtiter plate and cover or tape sealer
250-µl multichannel pipettor and appropriate tips
Microtiter plate mixer
Microtiter plate reader

1. Draw a template for placement of samples and standards on the microtiter plate.
2. Select a protein to use as the standard (see Strategic Planning). Prepare a dilution series with the same buffer used to dilute the samples to cover the range of 10 to 160 mg/ml.
3. In triplicate, add 5.0 µl of each diluted standard or sample into the appropriate microtiter plate wells. Use the buffer or diluent that was used to dilute the standard and samples for the blank wells.
4. Using a multichannel pipettor, add 250 µl biuret reagent to each well. Mix well on a plate shaker for 30 sec.
5. Cover the plate and incubate at room temperature for 10 min.
6. Mix again. Remove the plate cover and measure the color in each well of the plate at 540 nm (A_{540}) in a microtiter plate reader.
7. Prepare a standard curve by graphing the average net or blank-corrected A_{540} values for each standard versus its concentration in milligrams per milliliter.
8. Determine the sample concentration by interpolating from the plot (see Strategic Planning).

THE COOMASSIE DYE–BINDING (BRADFORD) ASSAY FOR DETERMINING TOTAL PROTEIN

BASIC PROTOCOL 4

The Coomassie dye–based protein-binding assays have the advantage of being the fastest and the easiest to perform (Fig. A.3I.7). In addition, the assay is performed at room temperature and no special equipment, other than a spectrophotometer, is required. Briefly, the sample is added to the ready-to-use reagent and, following a short incubation, the resultant blue color is measured at 595 nm versus deionized water.

In 1976, Marion Bradford introduced the first Coomassie dye–based reagent for the rapid colorimetric detection and quantitation of total protein. The Coomassie dye (Bradford) protein assay reagents have the advantage of being compatible with most salts, solvents, buffers, thiols, reducing substances, and metal chelating agents encountered in protein samples.

Materials

Sample buffer or solvent
Protein standard (e.g., 2 mg/ml BSA; see recipe)
Protein sample
Coomassie dye reagent (Pierce or Bio-Rad; also see recipe)

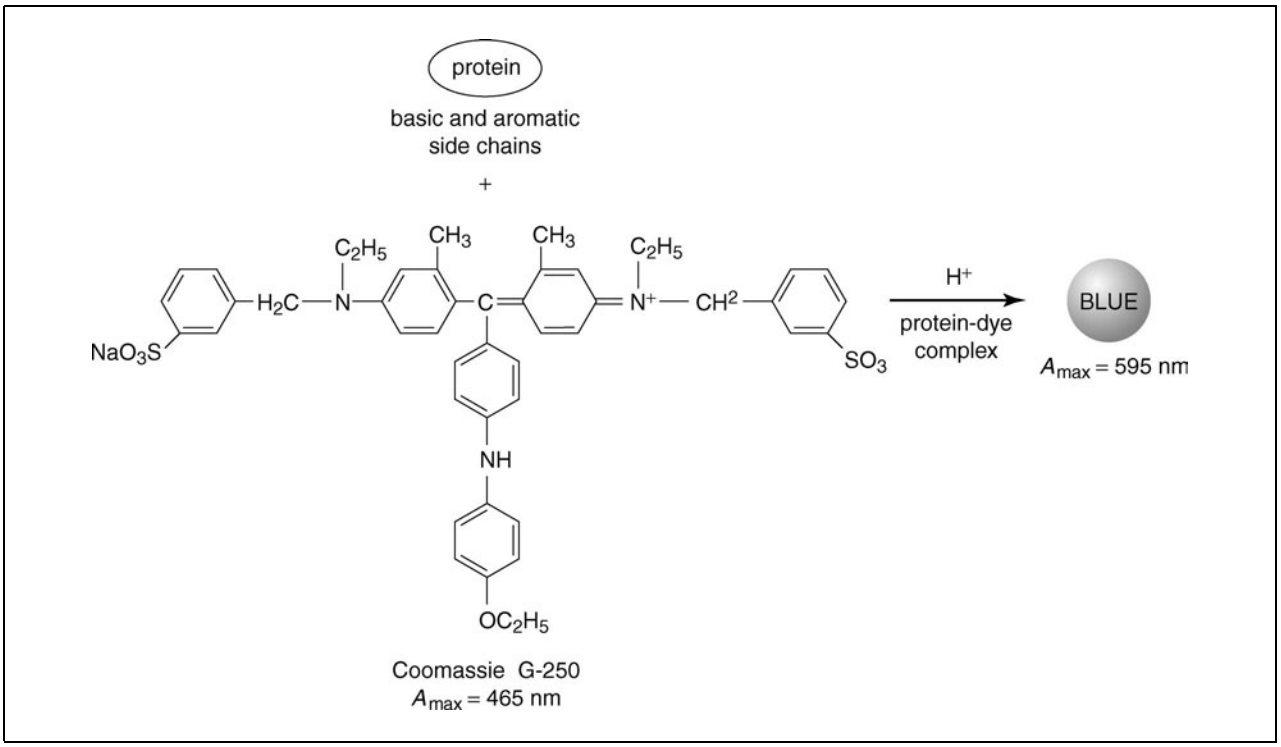

Figure A.3I.7 The reaction schematic for the Coomassie Protein Assay.

1. Prepare a dilution series from protein standard (e.g., 2 mg/ml BSA) and sample buffer to cover the range 100 to 1000 μg/ml.

   Bovine serum albumin (BSA) is often used as a calibration standard, but it has greater general dye-binding capacity than most proteins (Bradford, 1976).

2. Dispense 0.1 ml standard, sample, or buffer to appropriately labeled tubes.

   If commercially prepared Coomassie reagent is used, follow the manufacturer's instructions. Commercial reagents tend to produce less turbidity and more consistent results.

3. Add 5 ml Coomassie dye reagent. Vortex immediately.
4. Incubate 10 min at room temperature.
5. Vortex each tube just before measuring the absorbance at 595 nm (A_{595}).
6. Plot a standard curve by graphing the average net or blank-corrected A_{595} values for the standard versus its protein concentration in micrograms per milliliter.
7. Determine the sample concentration by interpolation from the standard curve (see Strategic Planning).

ALTERNATE PROTOCOL 6

THE COOMASSIE PLUS PROTEIN ASSAY FOR DETERMINATION OF TOTAL PROTEIN

Several companies offer modified Bradford Coomassie dye–based protein assay reagents. Perhaps the most popular such reagent is the Protein Assay Reagent available from Bio-Rad. The Coomassie Plus Protein Assay Reagent available from Pierce is another modification of the Bradford formulation. In addition to the attributes cited above, the Coomassie Plus Protein Assay Reagent has the unique advantage of producing a linear response curve within a portion of its working range. For BSA, the response curve is linear from 125 to 1000 μg/ml and for bovine gamma globulin (BGG), the response curve is linear from 125 to 1500 μg/ml. The complete working range of the assay covers

Table A.3I.4 Troubleshooting Guide for Coomassie Plus Protein Assay

Problem	Possible cause	Solution
Blank A_{595} is normal, but standards show less color than expected	Improper reagent storage	Store reagent refrigerated
	Reagent still cold	Warm to room temperature before use
	Color measured at the wrong wavelength	Measure the color at 595 nm
Blank and standards are normal, but samples show little color	Low molecular weight of sample protein (<3000 kDa)	Use the BCA (see Basic Protocol 2) or Lowry protein assay (see Basic Protocol 1)
A precipitate forms in all tubes	Sample contains a surfactant (detergent)	Dialyze or dilute the sample
		Precipitate the protein with TCA, dissolve pellet in 50 mM NaOH
All tubes (including the blank) are dark blue	Strong alkaline buffer or reagent raises reagent's pH	Dialyze or dilute the sample
	Sample volume too large, reagent pH raised	Maximum of 1 part sample and 1 part reagent
Need to read color at a different wavelength	Colorimeter does not have 595 nm filter	Color may be read at any wavelength between 575 nm and 615 nm

the concentration range from 100 to 2000 μg/ml for the tube protocol and from 1 to 25 μg/ml for the microtiter protocol (see Alternate Protocol 7).

The main disadvantage of all Bradford-type protein assay reagents is that they are not compatible with surfactants at concentrations routinely used to solubilize membrane proteins. With some exceptions, the presence of a surfactant in the sample, even at low concentrations, causes precipitation of the reagent. Table A.3I.4 is a brief troubleshooting guide for this technique.

Additional Materials *(also see Basic Protocol 4)*

Coomassie Plus Protein Assay Reagent Kit (Pierce) containing Coomassie Plus Protein Assay Reagent

1. Prepare a dilution series with 2 mg/ml BSA and buffer to cover a range from 100 to 2000 μg/ml.

   If possible, use the same diluent or buffer cocktail for the blanks and for diluting the stock BSA standard that was used with the samples.

2. Allow the Coomassie Plus Protein Assay Reagent to come to room temperature. Mix the assay reagent well by gentle inversion before use.

3. In duplicate, dispense 50 μl standard, sample, or diluent (blank) into appropriately labeled test tubes.

4. Add 1.5 ml Coomassie Plus Protein Assay Reagent to each tube. Mix each tube well by vortexing 2 to 3 sec.

5. Let the tubes stand 10 min at room temperature.

6. Mix each tube again just before measuring the absorbance at 595 nm (A_{595}).

   Disposable polystyrene cuvettes eliminate the job of cleaning dye-stained quartz or glass cuvettes.

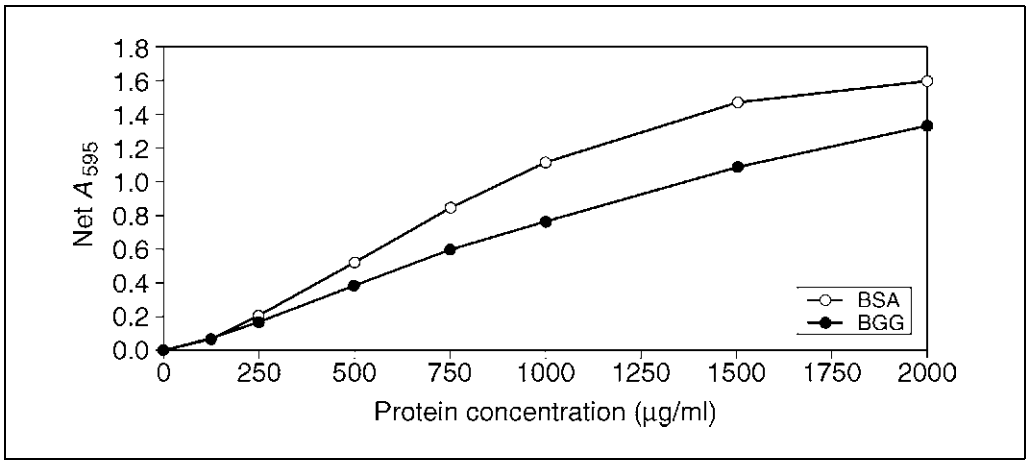

Figure A.3I.8 Graph of the color response curves obtained with Pierce's Coomassie Plus Protein Assay Reagent using bovine serum albumin (BSA) and bovine gamma globulin (BGG). The standard tube protocol was performed and the color was measured at 595 nm in a Hitachi U-2000 spectrophotometer.

7. Plot a standard curve by graphing the average net or blank-corrected A_{595} reading for each standard versus its concentration in micrograms per milliliter.

   Example color response curves for BSA and BGG are shown in Figure A.3I.8.

8. Determine the protein concentration for each sample by interpolating from the standard curve (see Strategic Planning). Calculate the average total protein concentration for each sample from the replicates.

ALTERNATE PROTOCOL 7

MICROTITER PLATE COOMASSIE ASSAY FOR TOTAL PROTEIN

This microtiter plate assay has a working range of 1 to 25 μg/ml.

Additional Materials *(see Basic Protocol 4)*

Coomassie Plus Protein Assay Reagent Kit (Pierce) containing Coomassie Plus Protein Assay reagent
96-well microtiter plate
300-μl multichannel pipettor
Microtiter plate mixer
Microtiter plate reader

1. Allow the Coomassie Plus Protein Assay Reagent to come to room temperature. Once the reagent is at room temperature, mix the reagent well by gentle inversion of the bottle.
2. Draw a template for placement of samples and standards on a 96-well microtiter plate.
3. In triplicate, dispense 10 μl of each diluted BSA standard, sample, or diluent (blank) into the appropriate wells of a 96-well microtiter plate.

   If possible, use the same diluent or buffer cocktail for the blanks and for diluting the stock standard that was used with the samples.

4. Dispense 300 μl Coomassie Plus Protein Assay reagent into each well with a multichannel pipettor. Mix the plate well on a plate shaker for 30 sec.
5. Let the plate incubate 10 min at room temperature.
6. Just before reading, mix the plate again, then measure the absorbance at 595 nm (A_{595}) on a plate reader.

7. Prepare a standard curve by graphing the average net or blank-corrected A_{595} values for each standard versus its concentration in micrograms per milliliter.

8. Determine the sample concentration by interpolating from the standard curve (see Strategic Planning). Calculate the average total protein concentration for each sample from the replicates.

REAGENTS AND SOLUTIONS

Use Milli-Q purified water or equivalent in all recipes and protocol steps. For common stock solutions, see ***APPENDIX 2A****; for suppliers, see* ***SUPPLIERS APPENDIX****.*

BCA reagent A

1 g 4,4′-dicarboxy-2,2′-biquinoline, disodium salt (Na_2BCA; Pierce or Sigma; 1% w/v final)
2 g $Na_2CO_3 \cdot H_2O$ (2% w/v final)
160 mg sodium tartrate dihydrate (0.16% w/v final)
0.4 g NaOH (0.4% w/v final)
0.95 g $NaHCO_3$ (0.95% w/v final)
Dissolve all of the above chemicals except the sodium bicarbonate in water and adjust the final volume to 100 ml. Adjust the pH to 11.25 by adding the sodium bicarbonate a little at a time. Store this alkaline reagent in a plastic container 1 to 3 weeks at room temperature, longer at 4°C.

Only the disodium salt of BCA is soluble at neutral pH; the free acid is not readily soluble.

BCA reagent B

4 g $CuSO_4 \cdot 5H_2O$ (4% w/v final)
100 ml H_2O
Store up to 6 months at room temperature

Biuret total protein reagent

0.6 mol/liter sodium hydroxide
12.0 mmol/liter copper sulfate
31.9 mmol/liter sodium potassium tartrate
30.1 mmol/liter potassium iodide
Store up to 6 months at room temperature

This reagent is based upon the candidate reference method for the determination of total protein in serum developed by Doumas et al. (1981). It is available from Sigma Diagnostics.

BSA, 2 mg/ml (w/v)

200 mg BSA (crystallized or lyophilized or one of the Cohn Fraction V preparations which are 96% to 98% protein and 3% to 4% water) in 100 ml of 0.9% (w/v) saline containing 0.05% (w/v) sodium azide. Store up to 6 months at 4°C.

Coomassie dye reagent

100 mg Coomassie Brilliant Blue G-250 (0.01% w/v final)
50 ml 95% ethanol (4.7% w/v final)
100 ml 85% (w/v) phosphoric acid (8.5% w/v final)

In a small container, dissolve the dye in ~25 ml ethanol, add the dye/ethanol solution to 800 ml water. Use the remaining ethanol to rinse the dye/ethanol container and add the rinses to the formulation. While mixing, slowly add the acid to the formulation and adjust the final volume to 1000 ml with water. Filter the reagent through a single pad of Whatman no. 2 filter paper. Store up to 1 month at room temperature in a glass container.

continued

Coomassie Brilliant Blue G-250 (color index 42655) is available from a number of different suppliers (e.g., ACROS, Aldrich, AMRESCO, Bio-Rad, Fisher Biotech, Fluka, ICN Biomedicals, J.T. Baker, Research Organics, Serva, Sigma, or USB).

Lowry's reagent A

21.2 g sodium carbonate (2% w/v)
40 ml 1 N NaOH (or 4.0 g NaOH; 0.1 N final)
Add water to 1 liter
Make fresh daily

Lowry's reagent B

0.5 g $CuSO_4 \cdot 5H_2O$ (0.5% w/v final)
1 g sodium tartrate (1% w/v final)
Make fresh daily
H_2O to 100 ml

Sodium tartrate may be replaced with disodium tartrate, potassium sodium tartrate, or sodium citrate for better solubility.

Lowry's reagent C (1 N Folin phenol reagent)

Dilute 2 N Folin phenol (Sigma, Fisher, or VWR) with an equal volume water. Prepare immediately before use.

Lowry's reagent D (reagent A and B mix)

Mix 1 vol Lowry's reagent B and 50 vol Lowry's reagent A (see recipes). Prepare immediately before use.

Lowry's reagent D′

Add 2 ml of 10% (w/v) sodium dodecyl sulfate (SDS; *APPENDIX 2A* for 20% solution) in water to each 100 ml Lowry's reagent D (see recipe). Prepare immediately before use.

COMMENTARY

Background Information

The modified Lowry protein assay

Although the exact mechanism of color formation reaction in the Lowry protein assay remains poorly understood, it is known that the color producing reaction with protein occurs in two distinct steps. As seen in Figure A.3I.1, protein is first reacted with alkaline cupric sulfate in the presence of tartrate during a 10-min incubation at room temperature. During this incubation, a tetradentate copper complex forms from four peptide bonds and one atom of copper. The tetradentate copper complex is light blue in color (this is the "biuret reaction"). Following the 10-min incubation, Folin phenol reagent is added. It is believed that color enhancement occurs when the tetradentate copper complex transfers electrons to the phospho-molybdic/phosphotungstic acid complex (i.e., the Folin phenol reagent).

The reduced phosphomolybdic/phosphotungstic acid complex produced by this reaction is intensely blue in color. The Folin phenol reagent loses its reactivity almost immediately upon addition to the alkaline working reagent/sample solution. The blue color continues to intensify during a 30-min room temperature incubation. It has been suggested by Lowry et al. (1951) and by Legler et al. (1985) that during the 30-min incubation, a rearrangement of the initial unstable blue complex leads to the stable final blue colored complex, which has higher absorbance.

For small peptides, the amount of color increases with the size of the peptide. The presence of any of five amino acid residues (tyrosine, tryptophan, cysteine, histidine, and asparagine) in the peptide or protein backbone further enhances the amount of color produced, because they contribute additional reducing equivalents for further reduction of the phosphomolybdic/phosphotungstic acid complex. With the exception of tyrosine and tryptophan, free amino acids will not produce a

colored product with the Lowry reagent; however, most dipeptides can be detected. In the absence of any of the five amino acids listed above, proteins containing proline residues have a lower color response with the Lowry reagent because it interferes with complex formation.

The final blue color is optimally measured at 750 nm, but it can be measured at any wavelength between 650 nm and 750 nm with little loss of color intensity. Lowry (1951) recommended reading the color at 750 nm because few other substances absorb light at that wavelength. The amount of light absorbed at 750 nm is directly proportional to the amount of protein in the sample, but the color response curve produced is nonlinear.

The sensitivity of the Modified Lowry Protein Assay Reagent is greatly enhanced over that of the biuret total protein reagent. The working range of the method covers the total protein range from 1 to 1500 μg/ml. In comparison, the working range for the biuret assay is from 5 to 160 mg/ml.

The Modified Lowry Protein Assay Reagent will form precipitates in the presence of surfactants or potassium ions. The problem of precipitation that is caused by the presence of potassium ions in the sample can sometimes be overcome by centrifuging the tube and reading the color in the supernatant. Most surfactants will cause precipitation of the reagent even at very low concentrations. One exception is sodium dodecyl sulfate (SDS), which is compatible with the reagent at concentrations up to 1% (w/v) in the sample. Chelating agents interfere because they bind copper and thus prevent formation of the copper-peptide bond complex. Reducing agents and free thiols interfere, as they reduce the phosphotungstate-phosphomolybdate complex, immediately forming an intensely blue colored product upon their addition to the Modified Lowry Protein Assay Reagent.

The Coomassie Plus protein assay

The primary advantage of the Coomassie Plus Protein Assay is that it is generally compatible with most of the buffers and reagents found in samples and is unaffected by the presence of chelating agents, reducing agents, or free sulfhydryls in the sample.

The development of color in the Coomassie dye–binding methods has been associated with the presence of certain basic amino acids (primarily arginine, lysine, and histidine) in the protein. Van der Waals forces and hydrophobic interactions also participate in the binding of the dye by protein. The number of Coomassie dye ligands bound to each protein molecule is approximately proportional to the number of positive charges found on the protein. In the acidic environment of the Coomassie Plus Protein Assay Reagent, protein binds to the Coomassie dye. This results in a spectral shift of the reagent from the reddish/brown form of the dye, with an absorbance maximum at 465 nm, to the blue form of the dye, with an absorbance maximum at 610 nm (see Fig. A.3I.7).

The difference between the two forms is greatest at 595 nm; therefore, this is the optimal wavelength to measure the blue color from the Coomassie dye–protein complex. If desired, the blue color can be read at any wavelength between 575 and 615 nm. At the two extremes (575 and 615 nm) there is a loss of ~10% in the measured amount of color (absorbance) compared to the value obtained at 595 nm.

Free amino acids, peptides, and low-molecular-weight proteins do not produce color with the Coomassie Plus Protein Assay Reagent. In general the molecular weight of the peptide or protein must be at least 3000 Da to be assayed with this reagent. In some applications this can be an advantage. The reagent has been used to measure "high-molecular-weight proteins" during fermentation in the beer brewing industry.

One disadvantage of any Coomassie dye–based protein assay is that surfactants in the sample will cause precipitation of the reagent. Another disadvantage is that the Coomassie Plus Protein Assay Reagent shows almost twice as much protein-to-protein variation as that obtained with the protein-copper chelation–based assay reagents (the Lowry Protein Assay Reagent or the BCA Protein Assay Reagent). While this is true, the reagent exhibits the least protein-to-protein variation of all Coomassie dye–based (Bradford) reagents. Since the Coomassie dye reagent is highly acidic, a small number of proteins cannot be assayed with this reagent due to poor solubility. In addition, the glass or quartz cuvettes routinely used to hold the solution in the spectrophotometer while the color intensity is being measured are stained by Coomassie dye–based reagents.

The BCA protein assay

The BCA Protein Assay is a modification of the Lowry protein assay in which enhanced color production is due to the reaction of reduced copper with bicinchoninic acid (BCA). This reagent has a unique advantage

over the Lowry Protein Assay Reagent and the Coomassie Plus Protein Assay Reagent because it is compatible with samples that contain up to 5% (v/v) surfactants (detergents). Unlike the Lowry protein assay, all reactants needed are present in the BCA working reagent. Large numbers of tubes can be run without regard to the limits imposed in the Lowry assay by the need to add a second reagent at a precise time interval.

The working range of the BCA Protein Assay Reagent is from 20 to 2000 μg/ml for both the standard tube and the standard microtiter plate protocols. Since the color reaction is not a true end-point reaction, this allows more protocol flexibility. By increasing the incubation temperature, the sensitivity of the reagent can be increased. When using the enhanced tube protocol (incubating at 60°C for 30 min), the working range for the assay shifts to 5 to 250 μg/ml and the minimum detection level becomes 5 μg/ml.

Although the mechanism of color formation with protein for the BCA Protein Assay Reagent is similar to that of the Lowry reagent, there are several significant differences. The BCA Protein Assay combines the well-known reduction of Cu^{2+} to Cu^{+} by protein in an alkaline medium (the so-called biuret reaction) with the highly sensitive and selective colorimetric detection of the cuprous cation (Cu^{+}) by bicinchoninic acid.The purple-colored reaction product of this assay is formed by the chelation of two molecules of BCA with one cuprous ion (see Fig. A.3I.3). The resultant BCA/Cu^{+} complex is water-soluble and exhibits a strong linear absorbance maximum at 562 nm with increasing protein concentrations. If desired, the purple color may be measured at any wavelength between 550 nm and 570 nm with minimum (<10%) loss of signal.

The reaction that leads to BCA color formation as a result of the reduction of Cu^{2+} is also strongly influenced by the presence of any of four amino acid residues (tyrosine, tryptophan, cysteine, or cystine) in the amino acid sequence of the protein. Unlike the Coomassie dye–binding (Bradford) methods, which require a minimum mass of protein to be present for the dye to bind, the presence of only a single amino acid residue in the sample may result in the formation of a colored BCA-Cu^{+} chelate. This is true for any of the four amino acids cited above. Studies done with di- and tripeptides indicate that the total amount of color produced is greater than can be accounted for by the simple addition of the color produced with each BCA-reactive amino acid, so the peptide backbone must contribute to the reduction of copper as well.

The rate of color formation is dependent on the incubation temperature, the types of protein present in the sample, and the relative amounts of reactive amino acids contained in the proteins. The recommended protocols do not result in end-point determinations, so the incubation periods were chosen to yield maximal color response in a reasonable time frame.

The protein-to-protein variation in the amount of color produced with the BCA Protein Assay Reagent (CV = 15% for the group of 14 proteins at 1000 μg/ml in the standard tube protocol) is similar to that observed for the Modified Lowry Protein Assay Reagent.

The biuret total protein assay

Riegler (1914) introduced the biuret reaction as a method for the estimation of albumin in urine in 1914. Modifications and improvements to the biuret method were made by Autenrieth and Mink (1915), Hiller (1926), and Fine (1935). All of these early methods required the separate addition of a sodium hydroxide solution and the separate addition of a copper sulfate solution to the sample. The methods suffered from poor precision due to ineffective mixing and variation in reaction time during mixing. The first "one solution" biuret reagent was introduced by Kingsley (1942) for use in measuring total protein, albumin, and globulin in human serum. Weichselbaum (1946) and Gornall et al. (1949) modified Kingsley's biuret reagent by decreasing the sodium hydroxide concentration to prevent the formation of precipitates and by adding sodium potassium tartrate to stabilize the reagent. Potassium iodide was added to prevent the autoreduction of Cu^{2+}. Goa (1953) published on the use of the biuret reagent for determining total protein in human cerebrospinal fluid.

Sigma Diagnostic's biuret total protein reagent is based upon the candidate reference method formulation used for the determination of total protein in serum developed by Doumas et al. (1981). Because the primary application for this reagent is the determination of total protein in serum, most of the studies regarding assay precision, assay linearity, and interfering substances have been done on clinical samples. On samples with total protein concentrations in the range of 26 to 121 mg/ml, within-run and between-run precision was found to be excellent (CV's ranged from 4.2% to 1.4%). Lipids, bilirubin, hemoglobin, dextran, and certain drugs have been shown to interfere with

the total protein results obtained with the biuret Total Protein Reagent. Interference caused by the presence of lipid in the sample is due to turbidity. Interference caused by the presence of bilirubin or hemoglobin is small, almost negligible. Dextran causes precipitation in the reaction mixture during color development; however, centrifuging the reaction mixture before reading the color can minimize this. The biuret Total Protein Reagent contains 0.6 mol/liter sodium hydroxide, 12.0 mmol/liter copper sulfate, 31.9 mmol/liter sodium potassium tartrate, and 30.1 mmol/liter potassium iodide. It should be stored at ambient room temperature until the expiration date shown on the label. Certain drugs and other substances are known to influence circulating levels of total protein (Young, 1990).

Critical Parameters

The modified Lowry protein assay reagent

The Modified Lowry Protein Assay Reagent must be refrigerated for long-term storage. If the entire bottle of reagent will be used within a reasonable time, the reagent may be stored at ambient room temperature (18° to 26°C) for up to 1 month. Reagent that has been left at room temperature for more than a month may show lower color response with protein, especially at the higher end of the working range. If the reagent has been stored refrigerated, it must be warmed to room temperature before use. The use of cold Modified Lowry Protein Assay Reagent will result in low A_{750} values.

The protocol requires that the Folin phenol reagent be added to each tube precisely at the end of the 10-min incubation. At the alkaline pH of the Lowry reagent, the Folin phenol reagent is almost immediately inactivated; therefore, it is best to add the Folin phenol reagent at the precise time while simultaneously mixing each tube. Because it is somewhat cumbersome, it requires some practice to do the assay well. From a practical point of view, it also limits the total number of tubes that can be done in a single run. If a 10-sec interval between tubes is used, the maximum number of tubes that can be done within 10 min is 60 (10 sec/tube × 60 tubes = 600 sec or 10 min).

The Coomassie Plus protein assay reagent

The Coomassie Plus Protein Assay Reagent must be refrigerated for long-term storage. If the entire bottle of reagent will be used within a reasonable time, the reagent may be stored at ambient room temperature (18° to 26°C) for up to 1 month. Reagent that has been left at room temperature for more than a month may show lower color response with protein, especially at the higher end of the working range. If the reagent has been stored refrigerated, it must be warmed to room temperature before use. The use of cold Coomassie Plus Protein Assay Reagent will result in low A_{595} values.

The Coomassie Plus Protein Assay Reagent must be mixed gently by inversion just before use. The Coomassie dye in the reagent spontaneously forms loosely associated dye-dye aggregates upon standing. These aggregates may become visible after the reagent has been standing for as little as 60 min. Gentle mixing of the reagent by inversion of the bottle will uniformly disperse the dye-dye aggregates. After binding to protein, the dye also forms protein-dye-protein-dye aggregates. Fortunately, these aggregates can be dispersed easily by mixing the reaction tube. This is common to all Coomassie dye–based (Bradford) protein assay reagents. Since these aggregates form relatively quickly, it is a good idea to routinely mix (vortex for 2 to 3 sec) each sample just before measuring the color.

Bradford-type reagents containing Coomassie dye will leave a blue stain on glass or quartz cuvettes. The stain can be removed by washing the cuvettes in a dilute detergent solution in hot tap water, rinsing with water, then washing with methanol or ethanol, and finally rinsing with deionized water. Disposable plastic (polystyrene) cuvettes are strongly recommended because they eliminate the need to clean; however, these cuvettes are not compatible with samples containing organic solvents (e.g., acetone, DMF, acetonitrile).

The BCA protein assay reagent

Since the BCA Protein Assay is not a true end-point assay, the amount of color produced varies with the incubation time and the incubation temperature. While this allows considerable flexibility in optimizing the BCA assay for each application, it also requires that the optimized procedure be followed exactly every time the assay is done.

At room temperature, following an initial lag phase, the rate of color formation remains relatively constant for hours. If the incubation time alone is increased, the total amount of color produced by a given mass of protein increases.

If the incubation temperature is increased, the rate of color formation increases and the

total amount of color produced by a given mass of protein increases. After cooling the reaction mixture back to room temperature, the rate of color development slows from its initial rate. As both time and temperature are increased, the total amount of color produced by a given mass of protein approaches a maximum. This is apparent from the dramatic decrease in the rate of color formation upon cooling to room temperature following incubation at 60°C for 30 min.

Above 75°C, a black precipitate forms in the BCA reaction mixture and the absorbance at 562 nm of the blank increases dramatically. This appears to be caused by the formation of copper oxide at high temperature.

For greatest accuracy and precision when comparing sets of data from multiple runs, a set of standards must be included with each run, and the standards and the samples must be treated exactly the same.

The biuret total protein reagent

The biuret total protein reagent is considerably less sensitive to total protein than the other three protein assay reagents discussed in this appendix. This limits the applications in which the biuret reagent can be used. Since the primary use of the biuret reagent has been for serum total protein in the clinical laboratory, there is little published information about its compatibility with substances and reagents common to nonclinical samples.

Anticipated Results

Standard curves

Typical standard curves are shown in Figures A.3I.2, A.3I.4, A.3I.6, and A.3I.8 for each of the four assay methods. In each case, the tube protocols were performed in duplicate on diluted BSA or BGG standard. The color in each tube was measured at the appropriate wavelength in a dual-beam spectrophotometer. The net absorbance for each sample was plotted versus its protein concentration.

Figure A.3I.2 shows the color response curves obtained with the Modified Lowry Protein Assay Reagent using BSA and BGG. The graph shows the net absorbance at 750 nm versus the protein concentration at seven concentrations from 125 to 2000 μg/ml for each protein. Note that the response curve for BGG is higher than the response curve for BSA.

Figure A.3I.4 shows the color response curves obtained with the BCA Protein Assay Reagent using BSA and BGG. The graph shows the net absorbance at 562 nm versus the protein concentration at seven concentrations from 125 to 2000 μg/ml for each protein. Note that the response curve for BGG is higher than the response curve for BSA.

Figure A.3I.6 shows the color response curves obtained with the biuret total protein reagent using BSA and BGG. The graph shows the net absorbance at 540 nm versus the protein at eight concentrations from 5 to 100 mg/ml.

Figure A.3I.8 shows the color response curves obtained with the Coomassie Plus Protein Assay Reagent using BSA and BGG. The graph shows the net absorbance at 595 nm versus the protein concentration at seven concentrations from 125 to 2000 μg/ml for each protein. Note that the color response curve for BGG is lower than the response curve for BSA.

Protein-to-protein variation

Each protein in a sample is unique and can demonstrate that individuality in protein assays as variation in the color response. Such protein-to-protein variation refers to differences in the amount of color (absorbance) that are obtained when the same mass (microgram or milligram) of various proteins are assayed concurrently (i.e., in the same run) by the same method. These differences in color response relate to differences among proteins due to amino acid sequence, isoelectric point (pI), secondary structure, and the presence of certain side chains or prosthetic groups.

To analyze protein-to-protein variation for each method, a group of fourteen proteins was assayed in duplicate using the standard tube protocol in a single run. The net (blank-corrected) average absorbance for each protein was calculated. To make it easier to interpret, the net absorbance for each protein was expressed as a ratio to the net absorbance for BSA. If a protein has a ratio of 0.80, it means that the protein produces ~80% of the color that is obtained for an equivalent mass of BSA.

Table A.3I.5 demonstrates the relative degree of protein-to-protein variation that can be expected with the different protein assay methods. This differential may be a consideration in selecting a protein assay method, especially if the relative color response ratio of the protein in the samples is unknown. As expected, the protein assay methods that share the same basic chemistry show similar protein-to-protein variation.

The protein-to-protein variation observed with the various protein assay methods makes it obvious why the largest source of error for protein assays is the choice of protein for the standard curve. If the sample contained IgG

Table A.3I.5 Protein-to-Protein Variation[a]

Protein tested	Ratios obtained with the BCA method	Ratios obtained with the Coomassie plus method	Ratios obtained with the modified Lowry method
Albumin, bovine (BSA)	1.00	1.00	1.00
Aldolase, rabbit	0.85	0.74	0.94
α-Chymotrypsinogen, bovine	1.14	0.52	1.17
Cytochrome C, horse	0.83	1.03	0.94
Gamma globulin, bovine	1.11	0.58	1.14
IgG, bovine	1.21	0.63	1.29
IgG, human	1.09	0.66	1.13
IgG, mouse	1.18	0.62	1.20
IgG, rabbit	1.12	0.43	1.19
IgG, sheep	1.17	0.57	1.28
Insulin, bovine pancreas	1.08	0.67	1.12
Myoglobin	0.74	1.15	0.90
Ovalbumin	0.93	0.68	1.02
Transferrin, human	0.89	0.90	0.92
Average ratio	1.02	0.73	1.09
Standard Deviation (SD)	0.15	0.12	0.13
Coefficient of Variation	0.15	0.29	0.12

[a]The protein-to-protein variation in color response was measured at 1000 μg/ml for each protein in duplicate using the standard tube protocol. Within each assay, the average net or blank-corrected absorbance was determined for each protein. The average net absorbance for each protein was divided by the average net absorbance obtained with BSA and expressed as a ratio. The standard deviation (SD) and the coefficient of variation (CV) is presented for the fourteen proteins assayed on the three methods. By comparing the CV's, the relative degree of protein-to-protein variation to be expected with the three methods can be assessed.

as the major protein and BSA was used for the standard curve, the estimated total protein concentration of the sample will be inaccurate. Whether the concentration was underestimated or overestimated depends upon which total protein assay method was used. If the Coomassie Plus Protein Assay Reagent was used, the total protein (IgG) concentration in the sample would be underestimated by ~40%. (From Table A.3I.5, the response ratio for IgG is ~0.58 for IgG compared to 1.00 for BSA.) If the BCA Protein Assay Reagent was used, the total protein (IgG) concentration in the sample would be overestimated by ~15%. (From Table A.3I.5, the response ratio for IgG is ~1.15 for IgG compared to 1.00 for BSA.) On the other hand, if BGG had been used for both standard curves, the total protein estimates for the sample would have been in much greater agreement between the two methods.

While Table A.3I.5 is useful because it provides an estimate of the protein-to-protein variation in color response that can be expected with each method, it does not tell the whole story. Because the comparisons were done at a single protein concentration, it is not apparent that the color response ratio also varies with changes in protein concentration.

Compatible and incompatible substances

An extensive list of substances that have been found to be compatible with each of the reagents is shown in Table A.3I.6 Each substance was assayed in duplicate using the standard tube protocol for each reagent. In addition to adding the substance to a sample containing 1000 μg/ml BSA, a blank sample containing only the substance was tested. When added to the sample, a substance was deemed to be compatible with a reagent if the blank-corrected absorbance for the sample containing the substance was within 10% of the blank-corrected absorbance for the sample containing only BSA (also at 1000 μg/ml).

Time Considerations

The amount of time required to complete a total protein assay will vary for the four colorimetric total protein assay methods described. For the purpose of providing an estimate of the amount of time required to perform a run by each method, it was assumed that the run

Table A.3I.6 Maximum Compatible Sample Concentration of 92 Substances[a]

Substance tested	BCA method	Coomassie plus method	Modified Lowry method
Detergents			
Brij 35	5.0%	0.062%	0.031%
Brij 56	1.0%	0.031%	0.062%
Brij 58	1.0%	0.016%	0.062%
CHAPS	5.0%	5.0%	0.062%
CHAPSO	5.0%	5.0%	0.031%
Deoxycholic acid	5.0%	0.04%	Not tested
Lubrol PX	1.0%	0.031%	0.031%
Nonidet P-40	5.0%	0.5%	0.016%
Octyl glucoside	5.0%	0.5%	0.031%
Octyl β-thioglucoside	5.0%	3.0%	Not tested
SDS (lauryl)	5.0%	0.016%	1.0%
SPAN 20	1.0%	0.5%	0.25%
Triton X-100	5.0%	0.062%	0.031%
Triton X-114	1.0%	0.062%	0.031%
Triton X-305	1.0%	0.125%	0.031%
Triton X-405	1.0%	0.25%	0.031%
Tween 20	5.0%	0.031%	0.062%
Tween 60	5.0%	0.025%	Not tested
Tween 80	5.0%	0.016%	0.031%
Zwittergent 3-14	1.0%	0.025%	Not tested
Salts and buffers			
ACES, pH 7.8	25 mM	100 mM	Not tested
Ammonium sulfate	1.5 M	1 M	Not compatible
Asparagine	1 mM	10 mM	5 mM
Bicine, pH 8.4	20 mM	100 mM	Not tested
Bis-Tris, pH 6.5	33 mM	100 mM	Not tested
Borate (50 mM), pH 8.5 (BupH pack)	Undiluted	Undiluted	Not tested
B-PER cell lysis reagent	Undiluted	Diluted 1:2	Not tested
Calcium chloride in TBS	10 mM	10 mM	Not tested
Carbonate/bicarbonate, Na (0.2 M), pH 9.4	Undiluted	Undiluted	Not tested
Cesium bicarbonate	100 mM	100 mM	50 mM
CHES, pH 9.0	100 mM	100 mM	Not tested
Cobalt chloride in TBS	0.8 mM	10 mM	Not tested
EPPS, pH 8.0	100 mM	100 mM	Not tested
Ferric chloride in TBS	10 mM	10 mM	Not tested
Glycine	1 mM	100 mM	100 mM
HEPES	100 mM	100 mM	1 mM
Imidazole, pH 10.2	50 mM	200 mM	25 mM
MES, pH 6.1	100 mM	100 mM	100 mM

continued

Table A.3I.6 Maximum Compatible Sample Concentration of 92 Substances[a], *continued*

Substance tested	BCA method	Coomassie plus method	Modified Lowry method
Salts and buffers (continued)			
0.1 M MES/0.9% NaCl, pH 4.7	Undiluted	Undiluted	Not tested
MOPS, pH 7.2	100 mM	100 mM	Not tested
Modified Dulbecco's PBS	Undiluted	Undiluted	Not tested
Nickel chloride in TBS	10 mM	10 mM	Not tested
Phosphate buffered saline (PBS), pH 7.2	Undiluted	Undiluted	Not tested
PIPES, pH 6.8	100 mM	100 mM	Not tested
RIPA lysis buffer, pH 8.0	Undiluted	Diluted 1:40	Not tested
Sodium acetate	200 mM	180 mM	200 mM
Sodium azide	0.2%	0.5%	0.2%
Sodium bicarbonate	100 mM	100 mM	100 mM
Sodium chloride	1.0 M	1 M	1 M
Sodium citrate, pH 4.8	200 mM	200 mM	Not tested
Sodium phosphate	100 mM	100 mM	100 mM
Tricine, pH 8.0	25 mM	100 mM	Not tested
Triethanolamine, pH 7.8	25 mM	100 mM	Not tested
Tris	250 mM	2 M	10 mM
TBS, pH 7.6	Undiluted	Undiluted	Not tested
25 mM Tris/192 mM glycine, pH 8.0	Diluted 1:3	Undiluted	Not tested
25 mM Tris/192 mM glycine/0.1% SDS, pH 8.0	Undiluted	Diluted 1:4	Not tested
Zinc chloride in TBS	10 mM	10 mM	Not tested
Reducing agents			
N-acetylglucosamine in PBS	10 mM	100 mM	Not tested
Ascorbic acid	Not compatible	50 mM	1 mM
Catecholamines	Not compatible	Not tested	Not tested
Creatinine	Not compatible	Not tested	Not tested
Glucose	10 mM	1 M	0.1 mM
Melibiose	Not compatible		
Potassium thiocyanate	3 M		
Thiol-containing agents			
Cysteine	Not compatible	10 mM	1 mM
Dithioerythritol (DTE)	1 mM	1 mM	Not compatible
Dithiothreitol (DTT)	1 mM	5 mM	Not compatible
2-Mercaptoethanol	0.01%	1 M	1 mM
Thimerosal	0.01%	0.01%	0.01%
Chelating agents			
EDTA	10 mM	100 mM	1 mM
EGTA	Not compatible	2 mM	1 mM
Sodium citrate, pH 4.8	200 mM	200 mM	0.1 mM

continued

Table A.3I.6 Maximum Compatible Sample Concentration of 92 Substances[a], *continued*

Substance tested	BCA method	Coomassie plus method	Modified Lowry method
Solvents/miscellaneous			
Acetone	10%	10%	10%
Acetonitrile	10%	10%	10%
Aprotinin	10 mg/liter	10 mg/liter	10 mg/liter
DMF	10%	10%	10%
DMSO	10%	10%	10%
Ethanol	10%	10%	10%
Glycerol (fresh)	10%	10%	10%
Guanidine·HCl	4 M	3.5 M	100 mM
Hydrochloric acid	100 mM	100 mM	100 mM
Leupeptin	10 mg/liter	10 mg/liter	10 mg/liter
Methanol	10%	10%	10%
Phenol Red	Not compatible	0.5 mg/liter	0.1 mg/liter
PMSF	1 mM	1 mM	1 mM
Sodium hydroxide	100 mM	100 mM	100 mM
Sucrose	40%	10%	7.5%
TLCK	0.1 mg/liter	0.1 mg/liter	0.01 mg/liter
TPCK	0.1 mg/liter	0.1 mg/liter	0.1 mg/liter
Urea	3 M	3 M	3 M
o-vanadate in PBS	1 mM	1 mM	Not tested

[a]Taken from the Protein Assay Technical Handbook, Pierce Chemical, 1999.

Table A.3I.7 Estimated Time Requirements

Method	Incubation time(s)	Estimated total assay time
Modified Lowry Reagent	10 and 30 min	110 min (1 hr, 50 min)
Coomassie Plus Reagent	10 min	80 min (1 hr, 20 min)
BCA Reagent	30 min	100 min (1 hr, 40 min)
Biuret Reagent	10 min	80 min (1 hr, 20 min)

included twenty samples and eight standards (including the blank) and that each sample or standard was assayed in duplicate using the standard tube protocol. The estimates do not include the time spent obtaining the samples or the time it takes to prepare the samples for analysis, but they do include the incubation time(s) plus an estimate of the time it takes to do the following:

1. Prepare (dilute) the standard protein in the diluent buffer (10 min).
2. Organize the run and label the tubes (5 min).
3. Pipet the samples and reagents into the tubes (10 min).
4. Mix or incubate the tubes or plates (varies).
5. Measure the color produced in the tubes (15 min).
6. Graph the standard curve, calculate, record, and report the results (30 min).

For each of the four methods, a run of 20 samples (unknowns) and the standard curve (each done in duplicate) can be completed in the time estimated in Table A.3I.7

Acknowledgments

The author is indebted to Bob Vigna, Greg Hermanson, and Patti Domen for their assistance in reviewing this unit.

Literature Cited

Autenrieth, W. and Mink, F. 1915. Über kolorimetrische Bestimmungsmethoden: Die quantitative Bestimmung von Harneiweiss. *München Med. Wochenschr.* 62:1417.

Bradford, M.M. 1976. A rapid and sensitive method for the quantitation of microgram quantities of protein utilizing the principle of protein-dye binding. *Anal. Biochem.* 72:248-254.

Doumas, B.T., Bayse, D.D., and Carter, R.J. 1981. A candidate reference method for determination of total protein in serum. *Clin. Chem.* 27:1642.

Fine, J. 1935. Biuret method of estimating albumin and globulin in serum and urine. *Biochem. J.* 29:799.

Goa, J. 1953. A microbiuret method for protein determination. *Scand. J. Clin. Lab. Invest.* 5:218-222.

Gornall, A.G., Baardawill, C.J., and David, M.M. 1949. Determination of serum proteins by means of the biuret reagent. *J. Biol. Chem.* 177:751-766.

Hiller, A. 1926. Determination of albumin and globulin in urine. *Proc. Soc. Exp. Biol. Med.* 24:385.

Kingsley, G.R. 1942. The direct biuret method for the determination of serum proteins as applied to photoelectric and visual colorimetry. *J. Lab. Clin. Med.* 27:840-845.

Legler, G., Muller-Platz, C.M., Mentges-Hettkamp, M., Pflieger, G., and Julich, E. 1985. On the chemical basis of the Lowry protein determination. *Anal. Biochem.* 150:278-287.

Lowry, O.H., Nira, J., Rosenbrough, A., Farr, L., and Randall, R.J. 1951. Protein measurement with the Folin phenol reagent. *J. Biol. Chem.* 193:265-275.

Riegler, E. 1914. Eine kolorimetrische Bestimmungsmethode des Eiweisses. *Z. Anal. Chem.* 53:242-254.

Smith, P.K., Krohn, R.I., Hermanson, G.H., Mallia, A.K., Gartner, F.H., Provenzano, M.D., Fujimoto, E.K., Goike, N.M., Olson, B.J., and Klenk, D.K. 1985. Measurement of protein using bicinchoninic acid. *Anal. Biochem.* 150:76-85.

Weichselbaum, T.E. 1946. An accurate and rapid method for the determination of proteins in small amounts of blood serum and plasma. *Am. J. Clin. Pathol.* 16:40.

Young, D.S. 1990. Effects of Drugs on Clinical Tests. (Suppl. 1 ,1991). AACC Press. Washington, D.C.

Key References

Akins, R.E. and Tuan, R.S. 1992. Measurement of protein in 20 seconds using a microwave BCA assay. *Biotechniques* 12:496-499.

Use of the BCA protein assay in a microtiter-plate format which utilizes a microwave oven as the heat source to shorten the color development time to 20 sec.

Beyer, R.E. 1983. A rapid biuret assay for protein of whole fatty tissues. *Anal. Biochem.* 129:483-485.

Accurate total protein quantitation of fatty tissues was achieved by adding 0.1 ml 10% sodium deoxycholate, pH 8.0 and 2.9 ml biuret reagent to each protein pellet following an acetone/ether wash step. After sonication, each sample was heated for 30 sec in a boiling water bath to develop full color.

Brown, A.J., Jarvis, K., and Hyland, K. 1989. Protein measurement using bicinchoninic acid: Elimination of interfering substances. *Anal. Biochem.* 180:136-139.

Describes a procedure using trichloroacetic acid and sodium deoxycholate to precipitate protein and thus remove soluble substances in the sample that would otherwise interfere in the BCA protein assay.

Compton, S.J. and Jones, C.G. 1985. Mechanism of dye response and interference in the Bradford protein assay. *Anal. Biochem.* 151:369-374.

Found that the anionic form of the Coomassie dye reacts primarily with arginine residues within the macromolecular protein. Coomassie dye reacts to a lesser extent with other basic amino acid residues (His, Lys) and aromatic residues (Trp, Tyr, Phe) present in macromolecular proteins but not with the free amino acids. Dye binding is attributed to van der Waals forces and hydrophobic interactions. The interference seen with bases, detergents, and other compounds can be explained by their effects upon the equilibrium between the three dye forms (cationic, neutral, anionic).

Crowley, L.V. 1969. Interference with certain chemical analyses caused by dextran. *Am. J. Clin. Pathol.* 51:425.

Dextran at high concentrations causes a slight overestimation of the total protein concentration with the biuret reagent.

Peterson, G.L. 1977. A simplification of the protein assay method of Lowry, et al. Which is more generally applicable? *Anal. Biochem.* 83:346-356.

A deoxycholate-trichloroacetic acid protein precipitation technique that provides for rapid recovery of soluble and membrane-bound proteins from interfering substances. Interference by lipids and nonionic or cationic detergents is alleviated by adding SDS.

Peterson, G.L. 1979. Review of the Folin phenol protein quantitation method of Lowry, Rosebrough, Farr and Randall. *Anal. Biochem.* 100:201-220.

A thorough review article that examines the reaction mechanism involved when protein reacts with the Lowry reagent. An extensive list of possibly interfering substances is presented along with methods of coping with those interfering substances. Finally, the method of Lowry is compared to other methods. There is an extensive list of references.

Sorenson, K. and Brodbeck, U. 1986. A sensitive protein assay method using micro-titer plates. *Experientia* 42:161-162.

A direct scale-down of the BCA method for test tubes that is suitable for microtiter plates.

Tal, M., Silberstein, A., and Nusser, D. 1980. Why does Coomassie Brilliant Blue interact differently with different proteins? *J. Biol. Chem.* 260:9976-9980.

Analysis of Scatchard plots showed that the number of Coomassie dye ligands bound to each protein is approximately proportional to the number of positive charges on the protein. About 1.5 to 3 dye molecules are bound to each positive charge on the protein.

Watters, C. 1978. A one-step biuret assay for protein in the presence of detergent. *Anal. Biochem.* 88:695-698.

A modified biuret reagent was formulated (sodium tartrate replaces sodium potassium tartrate, the sodium hydroxide concentration is reduced, and potassium iodide was deleted). When the modified biuret reagent was mixed with samples containing 2% detergent (SDS or sodium cholate or Triton X-100), it resulted in less protein-to-protein variation among six proteins.

Weichselbaum, 1946. See above.

Used sodium potassium tartrate as a stabilizer and added potassium iodide to prevent autoreduction of the biuret reagent; however, this reagent was found to be unstable after long storage.

Wiechelman, K., Braun, R., and Fitzpatrick, J. 1988. Investigation of the bicinchoninic acid protein assay: Identification of the groups responsible for color formation. *Anal. Biochem.* 175:231-237.

Cysteine, cystine, tryptophan, tyrosine, and the peptide bond are capable of reducing Cu^{2+} to Cu^{+}, but the extent of color formation is not simply the sum of the contributions from the various color producing functional groups. At 60°C, tryptophan, tyrosine, and the peptide bond are more completely oxidized than they are at 37°C, which is observed by the much greater extent of color developed at the higher temperature.

Internet Resources

http://www.piercenet.com

This site allows access to Pierce's on-line product catalog and special notice of all new products and other Pierce publications. If specific information on a product is needed, the instruction booklet can be downloaded. If additional help is needed, the technical assistance department can be reached by e-mail.

http://www.sigma-aldrich.com

This site allows access to the Sigma Diagnostics product line and applications or other technical information on their products. Questions can be sent by e-mail to the technical assistance department.

Contributed by Randall I. Krohn
Pierce Biotechnology, Inc.
Rockford, Illinois

SELECTED SUPPLIERS OF REAGENTS AND EQUIPMENT

Listed below are addresses and phone numbers of commercial suppliers who have been recommended for particular items used in our manuals because: (1) the particular brand has actually been found to be of superior quality, or (2) the item is difficult to find in the marketplace. Consequently, this compilation may not include some important vendors of biological supplies. For comprehensive listings, see *Linscott's Directory of Immunological and Biological Reagents* (Santa Rosa, CA), *The Biotechnology Directory* (Stockton Press, New York), the annual Buyers' Guide supplement to the journal *Bio/Technology*, as well as various sites on the Internet.

A.C. Daniels
72-80 Akeman Street
Tring, Hertfordshire, HP23 6AJ, UK
(44) 1442 826881
FAX: (44) 1442 826880

A. EL. VIS GmbH
Asternstrasse 47
30167 Hanover, Germany
(49) 511-6963-100
FAX: (49) 511-6063-101
http://www.aelvis.net

A.D. Instruments
5111 Nations Crossing Road #8
Suite 2
Charlotte, NC 28217
(704) 522-8415 FAX: (704) 527-5005
http://www.us.endress.com

A.J. Buck
11407 Cronhill Drive
Owings Mill, MD 21117
(800) 638-8673 FAX: (410) 581-1809
(410) 581-1800
http://www.ajbuck.com

A.M. Systems
131 Business Park Loop
P.O. Box 850
Carlsborg, WA 98324
(800) 426-1306 FAX: (360) 683-3525
(360) 683-8300
http://www.a-msystems.com

Aaron Medical Industries
7100 30th Avenue North
St. Petersburg, FL 33710
(727) 384-2323 FAX: (727) 347-9144
http://www.aaronmed.com

Abbott Laboratories
100 Abbott Park Road
Abbott Park, IL 60064
(800) 323-9100 FAX: (847) 938-7424
http://www.abbott.com

ABCO Dealers
55 Church Street Central Plaza
Lowell, MA 01852
(800) 462-3326 (978) 459-6101
http://www.lomedco.com/abco.htm

Aber Instruments
5 Science Park
Aberystwyth, Wales SY23 3AH, UK
(44) 1970 636300
FAX: (44) 1970 615455
http://www.aber-instruments.co.uk

ABI Biotechnologies
See Perkin-Elmer

ABI Biotechnology
See Apotex

Access Technologies
Subsidiary of Norfolk Medical
7350 N. Ridgeway
Skokie, IL 60076
(877) 674-7131 FAX: (847) 674-7066
(847) 674-7131
http://www.norfolkaccess.com

Accurate Chemical and Scientific
300 Shames Drive
Westbury, NY 11590
(800) 645-6264 FAX: (516) 997-4948
(516) 333-2221
http://www.accuratechemical.com

AccuScan Instruments
5090 Trabue Road
Columbus, OH 43228
(800) 822-1344 FAX: (614) 878-3560
(614) 878-6644
http://www.accuscan-usa.com

AccuStandard
125 Market Street
New Haven, CT 06513
(800) 442-5290 FAX: (877) 786-5287
http://www.accustandard.com

Ace Glass
1430 NW Boulevard
Vineland, NJ 08360
(800) 223-4524 FAX: (800) 543-6752
(609) 692-3333

ACO Pacific
2604 Read Avenue
Belmont, CA 94002
(650) 595-8588 FAX: (650) 591-2891
http://www.acopacific.com

Acros Organic
See Fisher Scientific

Action Scientific
P.O. Box 1369
Carolina Beach, NC 28428
(910) 458-0401 FAX: (910) 458-0407

AD Instruments
1949 Landings Drive
Mountain View, CA 94043
(888) 965-6040 FAX: (650) 965-9293
(650) 965-9292
http://www.adinstruments.com

Adaptive Biosystems
15 Ribocon Way
Progress Park
Luton, Bedsfordshire LU4 9UR, UK
(44)1 582-597676
FAX: (44)1 582-581495
http://www.adaptive.co.uk

Adobe Systems
1585 Charleston Road
P.O. Box 7900
Mountain View, CA 94039
(800) 833-6687 FAX: (415) 961-3769
(415) 961-4400
http://www.adobe.com

Advanced Bioscience Resources
1516 Oak Street, Suite 303
Alameda, CA 94501
(510) 865-5872 FAX: (510) 865-4090

Advanced Biotechnologies
9108 Guilford Road
Columbia, MD 21046
(800) 426-0764 FAX: (301) 497-9773
(301) 470-3220
http://www.abionline.com

Advanced ChemTech
5609 Fern Valley Road
Louisville, KY 40228
(502) 969-0000
http://www.peptide.com

Advanced Machining and Tooling
9850 Businesspark Avenue
San Diego, CA 92131
(858) 530-0751 FAX: (858) 530-0611
http://www.amtmfg.com

Advanced Magnetics
See PerSeptive Biosystems

Advanced Process Supply
See Naz-Dar-KC Chicago

Advanced Separation Technologies
37 Leslie Court
P.O. Box 297
Whippany, NJ 07981
(973) 428-9080 FAX: (973) 428-0152
http://www.astecusa.com

Advanced Targeting Systems
11175-A Flintkote Avenue
San Diego, CA 92121
(877) 889-2288 FAX: (858) 642-1989
(858) 642-1988
http://www.ATSbio.com

Advent Research Materials
Eynsham, Oxford OX29 4JA, UK
(44) 1865-884440
FAX: (44) 1865-84460
http://www.advent-rm.com

Advet
Industrivagen 24
S-972 54 Lulea, Sweden
(46) 0920-211887
FAX: (46) 0920-13773

Aesculap
1000 Gateway Boulevard
South San Francisco, CA 94080
(800) 282-9000
http://www.aesculap.com

Affinity Chromatography
307 Huntingdon Road
Girton, Cambridge CB3 OJX, UK
(44) 1223 277192
FAX: (44) 1223 277502
http://www.affinity-chrom.com

Affinity Sensors
See Labsystems Affinity Sensors

Affymetrix
3380 Central Expressway
Santa Clara, CA 95051
(408) 731-5000 FAX: (408) 481-0422
(800) 362-2447
http://www.affymetrix.com

Agar Scientific
66a Cambridge Road
Stansted CM24 8DA, UK
(44) 1279-813-519
FAX: (44) 1279-815-106
http://www.agarscientific.com

A/G Technology
101 Hampton Avenue
Needham, MA 02494
(800) AGT-2535 FAX: (781) 449-5786
(781) 449-5774
http://www.agtech.com

Agen Biomedical Limited
11 Durbell Street
P.O. Box 391
Acacia Ridge 4110
Brisbane, Australia
61-7-3370-6300
FAX: 61-7-3370-6370
http://www.agen.com

Agilent Technologies
395 Page Mill Road
P.O. Box 10395
Palo Alto, CA 94306
(650) 752-5000
http://www.agilent.com/chem

Agouron Pharmaceuticals
10350 N. Torrey Pines Road
La Jolla, CA 92037
(858) 622-3000 FAX: (858) 622-3298
http://www.agouron.com

Agracetus
8520 University Green
Middleton, WI 53562
(608) 836-7300 FAX: (608) 836-9710
http://www.monsanto.com

AIDS Research and Reference
Reagent Program
U.S. Department of Health and Human Services
625 Lofstrand Lane
Rockville, MD 20850
(301) 340-0245 FAX: (301) 340-9245
http://www.aidsreagent.org

AIN Plastics
249 East Sanford Boulevard
P.O. Box 151
Mt. Vernon, NY 10550
(914) 668-6800 FAX: (914) 668-8820
http://www.tincna.com

Air Products and Chemicals
7201 Hamilton Boulevard
Allentown, PA 18195
(800) 345-3148 FAX: (610) 481-4381
(610) 481-6799
http://www.airproducts.com

ALA Scientific Instruments
1100 Shames Drive
Westbury, NY 11590
(516) 997-5780 FAX: (516) 997-0528
http://www.alascience.com

Aladin Enterprises
1255 23rd Avenue
San Francisco, CA 94122
(415) 468-0433 FAX: (415) 468-5607

Aladdin Systems
165 Westridge Drive
Watsonville, CA 95076
(831) 761-6200 FAX: (831) 761-6206
http://www.aladdinsys.com

Alcide
8561 154th Avenue NE
Redmond, WA 98052
(800) 543-2133 FAX: (425) 861-0173
(425) 882-2555
http://www.alcide.com

Aldrich Chemical
P.O. Box 2060
Milwaukee, WI 53201
(800) 558-9160 FAX: (800) 962-9591
(414) 273-3850 FAX: (414) 273-4979
http://www.aldrich.sial.com

Alexis Biochemicals
6181 Cornerstone Court East,
Suite 103
San Diego, CA 92121
(800) 900-0065 FAX: (858) 658-9224
(858) 658-0065
http://www.alexis-corp.com

Alfa Aesar
30 Bond Street
Ward Hill, MA 10835
(800) 343-0660 FAX: (800) 322-4757
(978) 521-6300 FAX: (978) 521-6350
http://www.alfa.com

Alfa Laval
Avenue de Ble 5 -Bazellaan 5
BE-1140 Brussels, Belgium
32(2) 728 3811
FAX: 32(2) 728 3917 or 32(2) 728 3985
http://www.alfalaval.com

Alice King Chatham Medical Arts
11915-17 Inglewood Avenue
Hawthorne, CA 90250
(310) 970-1834 FAX: (310) 970-0121
(310) 970-1063

Allegiance Healthcare
800-964-5227
http://www.allegiance.net

Allelix Biopharmaceuticals
6850 Gorway Drive
Mississauga, Ontario
L4V 1V7 Canada
(905) 677-0831 FAX: (905) 677-9595
http://www.allelix.com

Allentown Caging Equipment
Route 526, P.O. Box 698
Allentown, NJ 08501
(800) 762-CAGE FAX: (609)
259-0449
(609) 259-7951
http://www.acecaging.com

Alltech Associates
Applied Science Labs
2051 Waukegan Road
P.O. Box 23
Deerfield, IL 60015
(800) 255-8324 FAX: (847) 948-1078
(847) 948-8600
http://www.alltechweb.com

Alomone Labs
HaMarpeh 5
P.O. Box 4287
Jerusalem 91042, Israel
972-2-587-2202 FAX:
972-2-587-1101
US: (800) 791-3904
FAX: (800) 791-3912
http://www.alomone.com

Alpha Innotech
14743 Catalina Street
San Leandro, CA 94577
(800) 795-5556 FAX: (510) 483-3227
(510) 483-9620
http://www.alphainnotech.com

Altec Plastics
116 B Street
Boston, MA 02127
(800) 477-8196 FAX: (617) 269-8484
(617) 269-1400

Alza
1900 Charleston Road P.O. Box 7210
Mountain View, CA 94043
(800) 692-2990 FAX: (650) 564-7070
(650) 564-5000
http://www.alza.com

Alzet
c/o Durect Corporation
P.O. Box 530
10240 Bubb Road
Cupertion, CA 95015
(800) 692-2990 FAX: (408) 865-1406
(408) 367-4036
http://www.alzet.com

Amac
160B Larrabee Road
Westbrook, ME 04092
(800) 458-5060 FAX: (207) 854-0116
(207) 854-0426

Amaresco
30175 Solon Industrial Parkway
Solon, Ohio 44139
(800) 366-1313 FAX: (440) 349-1182
(440) 349-1313

Ambion
2130 Woodward Street, Suite 200
Austin, TX 78744
(800) 888-8804 FAX: (512) 651-0190
(512) 651-0200
http://www.ambion.com

American Association of Blood Banks College of American Pathologists
325 Waukegan Road
Northfield, IL 60093
(800) 323-4040 FAX: (847) 8166
(847) 832-7000
http://www.cap.org

American Bio-Technologies
See Intracel Corporation

American Bioanalytical
15 Erie Drive
Natick, MA 01760
(800) 443-0600 FAX: (508) 655-2754
(508) 655-4336
http://www.americanbio.com

American Cyanamid
P.O. Box 400
Princeton, NJ 08543
(609) 799-0400 FAX: (609) 275-3502
http://www.cyanamid.com

American HistoLabs
7605-F Airpark Road
Gaithersburg, MD 20879
(301) 330-1200 FAX: (301) 330-6059

American International Chemical
17 Strathmore Road
Natick, MA 01760
(800) 238-0001 (508) 655-5805
http://www.aicma.com

American Laboratory Supply
See American Bioanalytical

American Medical Systems
10700 Bren Road West
Minnetonka, MN 55343
(800) 328-3881 FAX: (612) 930-6654
(612) 933-4666
http://www.visitams.com

American Qualex
920-A Calle Negocio
San Clemente, CA 92673
(949) 492-8298 FAX: (949) 492-6790
http://www.americanqualex.com

American Radiolabeled Chemicals
11624 Bowling Green
St. Louis, MO 63146
(800) 331-6661 FAX: (800) 999-9925
(314) 991-4545 FAX: (314) 991-4692
http://www.arc-inc.com

American Scientific Products
See VWR Scientific Products

American Society for Histocompatibility and Immunogenetics
P.O. Box 15804
Lenexa, KS 66285
(913) 541-0009 FAX: (913) 541-0156
http://www.swmed.edu/home_pages/ASHI/ashi.htm

American Type Culture Collection (ATCC)
10801 University Boulevard
Manassas, VA 20110
(800) 638-6597 FAX: (703) 365-2750
(703) 365-2700
http://www.atcc.org

Amersham
See Amersham Pharmacia Biotech

Amersham International
Amersham Place
Little Chalfont, Buckinghamshire
HP7 9NA, UK
(44) 1494-544100
FAX: (44) 1494-544350
http://www.apbiotech.com

Amersham Medi-Physics
Also see Nycomed Amersham
3350 North Ridge Avenue
Arlington Heights, IL 60004
(800) 292-8514 FAX: (800) 807-2382
http://www.nycomed-amersham.com

Amersham Pharmacia Biotech
800 Centennial Avenue
P.O. Box 1327
Piscataway, NJ 08855
(800) 526-3593 FAX: (877) 295-8102
(732) 457-8000
http://www.apbiotech.com

Amgen
1 Amgen Center Drive
Thousand Oaks, CA 91320
(800) 926-4369 FAX: (805) 498-9377
(805) 447-5725
http://www.amgen.com

Amicon
Scientific Systems Division
72 Cherry Hill Drive
Beverly, MA 01915
(800) 426-4266 FAX: (978) 777-6204
(978) 777-3622
http://www.amicon.com

Amika
8980F Route 108
Oakland Center
Columbia, MD 21045
(800) 547-6766 FAX: (410) 997-7104
(410) 997-0100
http://www.amika.com

Amoco Performance Products
See BPAmoco

AMPI
See Pacer Scientific

Amrad
576 Swan Street
Richmond, Victoria 3121, Australia
613-9208-4000
FAX: 613-9208-4350
http://www.amrad.com.au

Amresco
30175 Solon Industrial Parkway
Solon, OH 44139
(800) 829-2805 FAX: (440) 349-1182
(440) 349-1199

Anachemia Chemicals
3 Lincoln Boulevard
Rouses Point, NY 12979
(800) 323-1414 FAX: (518) 462-1952
(518) 462-1066
http://www.anachemia.com

Ana-Gen Technologies
4015 Fabian Way
Palo Alto, CA 94303
(800) 654-4671 FAX: (650) 494-3893
(650) 494-3894
http://www.ana-gen.com

Analox Instruments USA
P.O. Box 208
Lunenburg, MA 01462
(978) 582-9368 FAX: (978) 582-9588
http://www.analox.com

Analytical Biological Services
Cornell Business Park 701-4
Wilmington, DE 19801
(800) 391-2391 FAX: (302) 654-8046
(302) 654-4492
http://www.ABSbioreagents.com

Analytical Genetics Testing Center
7808 Cherry Creek S. Drive, Suite 201
Denver, CO 80231
(800) 204-4721 FAX: (303) 750-2171
(303) 750-2023
http://www.geneticid.com

AnaSpec
2149 O'Toole Avenue, Suite F
San Jose, CA 95131
(800) 452-5530 FAX: (408) 452-5059
(408) 452-5055
http://www.anaspec.com

Ancare
2647 Grand Avenue
P.O. Box 814
Bellmore, NY 11710
(800) 645-6379 FAX: (516) 781-4937
(516) 781-0755
http://www.ancare.com

Ancell
243 Third Street North
P.O. Box 87
Bayport, MN 55033
(800) 374-9523 FAX: (651) 439-1940
(651) 439-0835
http://www.ancell.com

Anderson Instruments
500 Technology Court
Smyrna, GA 30082
(800) 241-6898 FAX: (770) 319-5306
(770) 319-9999
http://www.graseby.com

Andreas Hettich
Gartenstrasse 100
Postfach 260
D-78732 Tuttlingen, Germany
(49) 7461 705 0
FAX: (49) 7461 705-122
http://www.hettich-centrifugen.de

Anesthetic Vaporizer Services
10185 Main Street
Clarence, NY 14031
(719) 759-8490
http://www.avapor.com

Animal Identification and
Marking Systems (AIMS)
13 Winchester Avenue
Budd Lake, NJ 07828
(908) 684-9105 FAX: (908) 684-9106
http://www.animalid.com

Annovis
34 Mount Pleasant Drive
Aston, PA 19014
(800) EASY-DNA
FAX: (610) 361-8255
(610) 361-9224
http://www.annovis.com

Apotex
150 Signet Drive
Weston, Ontario M9L 1T9, Canada
(416) 749-9300 FAX: (416) 749-2646
http://www.apotex.com

Apple Scientific
11711 Chillicothe Road, Unit 2
P.O. Box 778
Chesterland, OH 44026
(440) 729-3056 FAX: (440) 729-0928
http://www.applesci.com

Applied Biosystems
See PE Biosystems

Applied Imaging
2380 Walsh Avenue, Bldg. B
Santa Clara, CA 95051
(800) 634-3622 FAX: (408) 562-0264
(408) 562-0250
http://www.aicorp.com

Applied Photophysics
203-205 Kingston Road
Leatherhead, Surrey, KT22 7PB
UK
(44) 1372-386537

Applied Precision
1040 12th Avenue Northwest
Issaquah, Washington 98027
(425) 557-1000
FAX: (425) 557-1055
http://www.api.com/index.html

Appligene Oncor
Parc d'Innovation
Rue Geiler de Kaysersberg, BP 72
67402 Illkirch Cedex, France
(33) 88 67 22 67
FAX: (33) 88 67 19 45
http://www.oncor.com/prod-app.htm

Applikon
1165 Chess Drive, Suite G
Foster City, CA 94404
(650) 578-1396 FAX: (650) 578-8836
http://www.applikon.com

Appropriate Technical Resources
9157 Whiskey Bottom Road
Laurel, MD 20723
(800) 827-5931 FAX: (410) 792-2837
http://www.atrbiotech.com

APV Gaulin
100 S. CP Avenue
Lake Mills, WI 53551
(888) 278-4321 FAX: (888) 278-5329
http://www.apv.com

Aqualon
See Hercules Aqualon

Aquarium Systems
8141 Tyler Boulevard
Mentor, OH 44060
(800) 822-1100 FAX: (440) 255-8994
(440) 255-1997
http://www.aquariumsystems.com

Aquebogue Machine
and Repair Shop
Box 2055
Main Road
Aquebogue, NY 11931
(631) 722-3635 FAX: (631) 722-3106

Archer Daniels Midland
4666 Faries Parkway
Decatur, IL 62525
(217) 424-5200
http://www.admworld.com

Archimica Florida
P.O. Box 1466
Gainesville, FL 32602
(800) 331-6313 FAX: (352) 371-6246
(352) 376-8246
http://www.archimica.com

Arcor Electronics
1845 Oak Street #15
Northfield, IL 60093
(847) 501-4848

Arcturus Engineering
400 Logue Avenue
Mountain View, CA 94043
(888) 446 7911 FAX: (650) 962 3039
(650) 962 3020
http://www.arctur.com

Argonaut Technologies
887 Industrial Road, Suite G
San Carlos, CA 94070
(650) 998-1350 FAX: (650) 598-1359
http://www.argotech.com

Ariad Pharmaceuticals
26 Landsdowne Street
Cambridge, MA 02139
(617) 494-0400 FAX: (617) 494-8144
http://www.ariad.com

Armour Pharmaceuticals
See Rhone-Poulenc Rorer

Aronex Pharmaceuticals
8707 Technology Forest Place
The Woodlands, TX 77381
(281) 367-1666 FAX: (281) 367-1676
http://www.aronex.com

Artisan Industries
73 Pond Street
Waltham, MA 02254
(617) 893-6800
http://www.artisanind.com

ASCO (Apothecaries Sundries
Manufacturing Company)
P.O. Box No. 1
New Delhi, 110 001, India
http://www.ascoindia.com/

ASI Instruments
12900 Ten Mile Road
Warren, MI 48089
(800) 531-1105 FAX: (810) 756-9737
(810) 756-1222
http://www.asi-instruments.com

Aspen Research Laboratories
1700 Buerkle Road
White Bear Lake, MN 55140
(651) 264-6000 FAX: (651) 264-6270
http://www.aspenresearch.com

Associates of Cape Cod
704 Main Street
Falmouth, MA 02540
(800) LAL-TEST
FAX: (508) 540-8680
(508) 540-3444
http://www.acciusa.com

Astra Pharmaceuticals
See AstraZeneca

AstraZeneca
1800 Concord Pike
Wilmington, DE 19850
(302) 886-3000 FAX: (302) 886-2972
http://www.astrazeneca.com

AT Biochem
30 Spring Mill Drive
Malvern, PA 19355
(610) 889-9300 FAX: (610) 889-9304

ATC Diagnostics
See Vysis

ATCC
See American Type Culture Collection

Athens Research and Technology
P.O. Box 5494
Athens, GA 30604
(706) 546-0207 FAX: (706) 546-7395

Atlanta Biologicals
1425-400 Oakbrook Drive
Norcross, GA 30093
(800) 780-7788 or (770) 446-1404
FAX: (800) 780-7374 or
(770) 446-1404
http://www.atlantabio.com

Atomergic Chemical
71 Carolyn Boulevard
Farmingdale, NY 11735
(631) 694-9000 FAX: (631) 694-9177
http://www.atomergic.com

Atomic Energy of Canada
2251 Speakman Drive
Mississauga, Ontario
L5K 1B2 Canada
(905) 823-9040 FAX: (905) 823-1290
http://www.aecl.ca

ATR
P.O. Box 460
Laurel, MD 20725
(800) 827-5931 FAX: (410) 792-2837
(301) 470-2799
http://www.atrbiotech.com

Aurora Biosciences
11010 Torreyana Road
San Diego, CA 92121
(858) 404-6600 FAX: (858) 404-6714
http://www.aurorabio.com

Automatic Switch Company
A Division of Emerson Electric
50 Hanover Road
Florham Park, NJ 07932
(800) 937-2726 FAX: (973) 966-2628
(973) 966-2000
http://www.asco.com

Avanti Polar Lipids
700 Industrial Park Drive
Alabaster, AL 35007
(800) 227-0651 FAX: (800) 229-1004
(205) 663-2494 FAX: (205) 663-0756
http://www.avantilipids.com

Aventis
BP 67917
67917 Strasbourg Cedex 9, France
33 (0) 388 99 11 00
FAX: 33 (0) 388 99 11 01
http://www.aventis.com

Aventis Pasteur
1 Discovery Drive
Swiftwater, PA 18370
(800) 822-2463 FAX: (570) 839-0955
(570) 839-7187
http://www.aventispasteur.com/usa

Avery Dennison
150 North Orange Grove Boulevard
Pasadena, CA 91103
(800) 462-8379 FAX: (626) 792-7312
(626) 304-2000
http://www.averydennison.com

Avestin
2450 Don Reid Drive
Ottawa, Ontario K1H 1E1, Canada
(888) AVESTIN FAX: (613) 736-8086
(613) 736-0019
http://www.avestin.com

AVIV Instruments
750 Vassar Avenue
Lakewood, NJ 08701
(732) 367-1663 FAX: (732) 370-0032
http://www.avivinst.com

Axon Instruments
1101 Chess Drive
Foster City, CA 94404
(650) 571-9400 FAX: (650) 571-9500
http://www.axon.com

Azon
720 Azon Road
Johnson City, NY 13790
(800) 847-9374 FAX: (800) 635-6042
(607) 797-2368
http://www.azon.com

BAbCO
1223 South 47th Street
Richmond, CA 94804
(800) 92-BABCO
FAX: (510) 412-8940
(510) 412-8930
http://www.babco.com

Bacharach
625 Alpha Drive
Pittsburgh, PA 15238
(800) 736-4666 FAX: (412) 963-2091
(412) 963-2000
http://www.bacharach-inc.com

Bachem Bioscience
3700 Horizon Drive
King of Prussia, PA 19406
(800) 634-3183 FAX: (610) 239-0800
(610) 239-0300
http://www.bachem.com

Bachem California
3132 Kashiwa Street
P.O. Box 3426
Torrance, CA 90510
(800) 422-2436 FAX: (310) 530-1571
(310) 539-4171
http://www.bachem.com

Baekon
18866 Allendale Avenue
Saratoga, CA 95070
(408) 972-8779 FAX: (408) 741-0944

Baker Chemical
See J.T. Baker

Bangs Laboratories
9025 Technology Drive
Fishers, IN 46038
(317) 570-7020 FAX: (317) 570-7034
http://www.bangslabs.com

Bard Parker
See Becton Dickinson

Barnstead/Thermolyne
P.O. Box 797
2555 Kerper Boulevard
Dubuque, IA 52004
(800) 446-6060 FAX: (319) 589-0516
http://www.barnstead.com

Barrskogen
4612 Laverock Place N
Washington, DC 20007
(800) 237-9192 FAX: (301) 464-7347

BAS
See Bioanalytical Systems

BASF
Specialty Products
3000 Continental Drive North
Mt. Olive, NJ 07828
(800) 669-2273 FAX: (973) 426-2610
http://www.basf.com

Baum, W.A.
620 Oak Street
Copiague, NY 11726
(631) 226-3940 FAX: (631) 226-3969
http://www.wabaum.com

Bausch & Lomb
One Bausch & Lomb Place
Rochester, NY 14604
(800) 344-8815 FAX: (716) 338-6007
(716) 338-6000
http://www.bausch.com

Baxter
Fenwal Division
1627 Lake Cook Road
Deerfield, IL 60015
(800) 766-1077 FAX: (800) 395-3291
(847) 940-6599 FAX: (847) 940-5766
http://www.powerfulmedicine.com

Baxter Healthcare
One Baxter Parkway
Deerfield, IL 60015
(800) 777-2298 FAX: (847) 948-3948
(847) 948-2000
http://www.baxter.com

Baxter Scientific Products
See VWR Scientific

Bayer
Agricultural Division
Animal Health Products
12707 Shawnee Mission Pkwy.
Shawnee Mission, KS 66201
(800) 255-6517 FAX: (913) 268-2803
(913) 268-2000
http://www.bayerus.com

Bayer
Diagnostics Division (Order Services)
P.O. Box 2009
Mishiwaka, IN 46546
(800) 248-2637 FAX: (800) 863-6882
(219) 256-3390
http://www.bayer.com

Bayer Diagnostics
511 Benedict Avenue
Tarrytown, NY 10591
(800) 255-3232 FAX: (914) 524-2132
(914) 631-8000
http://www.bayerdiag.com

Bayer Plc
Diagnostics Division
Bayer House, Strawberry Hill
Newbury, Berkshire RG14 1JA, UK
(44) 1635-563000
FAX: (44) 1635-563393
http://www.bayer.co.uk

BD Immunocytometry Systems
2350 Qume Drive
San Jose, CA 95131
(800) 223-8226 FAX: (408) 954-BDIS
http://www.bdfacs.com

BD Labware
Two Oak Park
Bedford, MA 01730
(800) 343-2035 FAX: (800) 743-6200
http://www.bd.com/labware

BD PharMingen
10975 Torreyana Road
San Diego, CA 92121
(800) 848-6227 FAX: (858) 812-8888
(858) 812-8800
http://www.pharmingen.com

BD Transduction Laboratories
133 Venture Court
Lexington, KY 40511
(800) 227-4063 FAX: (606) 259-1413
(606) 259-1550
http://www.translab.com

BDH Chemicals
Broom Road
Poole, Dorset BH12 4NN, UK
(44) 1202-745520
FAX: (44) 1202-2413720

BDH Chemicals
See Hoefer Scientific Instruments

BDIS
See BD Immunocytometry Systems

Beckman Coulter
4300 North Harbor Boulevard
Fullerton, CA 92834
(800) 233-4685 FAX: (800) 643-4366
(714) 871-4848
http://www.beckman-coulter.com

Beckman Instruments
Spinco Division/Bioproducts Operation
1050 Page Mill Road
Palo Alto, CA 94304
(800) 742-2345 FAX: (415) 859-1550
(415) 857-1150
http://www.beckman-coulter.com

Becton Dickinson Immunocytometry & Cellular Imaging
2350 Qume Drive
San Jose, CA 95131
(800) 223-8226 FAX: (408) 954-2007
(408) 432-9475
http://www.bdfacs.com

Becton Dickinson Labware
1 Becton Drive
Franklin Lakes, NJ 07417
(888) 237-2762 FAX: (800) 847-2220
(201) 847-4222
http://www.bdfacs.com

Becton Dickinson Labware
2 Bridgewater Lane
Lincoln Park, NJ 07035
(800) 235-5953 FAX: (800) 847-2220
(201) 847-4222
http://www.bdfacs.com

Becton Dickinson Primary
Care Diagnostics
7 Loveton Circle
Sparks, MD 21152
(800) 675-0908 FAX: (410) 316-4723
(410) 316-4000
http://www.bdfacs.com

Behringwerke Diagnostika
Hoechster Strasse 70
P-65835 Liederback, Germany
(49) 69-30511 FAX: (49) 69-303-834

Bellco Glass
340 Edrudo Road
Vineland, NJ 08360
(800) 257-7043 FAX: (856) 691-3247
(856) 691-1075
http://www.bellcoglass.com

Bender Biosystems
See Serva

Beral Enterprises
See Garren Scientific

Berkeley Antibody
See BAbCO

Bernsco Surgical Supply
25 Plant Avenue
Hauppague, NY 11788
(800) TIEMANN FAX: (516) 273-6199
(516) 273-0005
http://www.bernsco.com

Beta Medical and Scientific (Datesand Ltd.)
2 Ferndale Road
Sale, Manchester M33 3GP, UK
(44) 1612 317676
FAX: (44) 1612 313656

Bethesda Research Laboratories (BRL)
See Life Technologies

Biacore
200 Centennial Avenue, Suite 100
Piscataway, NJ 08854
(800) 242-2599 FAX: (732) 885-5669
(732) 885-5618
http://www.biacore.com

Bilaney Consultants
St. Julian's
Sevenoaks, Kent TN15 0RX, UK
(44) 1732 450002
FAX: (44) 1732 450003
http://www.bilaney.com

Binding Site
5889 Oberlin Drive, Suite 101
San Diego, CA 92121
(800) 633-4484 FAX: (619) 453-9189
(619) 453-9177
http://www.bindingsite.co.uk

BIO 101
See Qbiogene

Bio Image
See Genomic Solutions

Bioanalytical Systems
2701 Kent Avenue
West Lafayette, IN 47906
(800) 845-4246 FAX: (765) 497-1102
(765) 463-4527
http://www.bioanalytical.com

Biocell
2001 University Drive
Rancho Dominguez, CA 90220
(800) 222-8382 FAX: (310) 637-3927
(310) 537-3300
http://www.biocell.com

Biocoat
See BD Labware

BioComp Instruments
650 Churchill Road
Fredericton, New Brunswick
E3B 1P6 Canada
(800) 561-4221 FAX: (506) 453-3583
(506) 453-4812
http://131.202.97.21

BioDesign
P.O. Box 1050
Carmel, NY 10512
(914) 454-6610 FAX: (914) 454-6077
http://www.biodesignofny.com

BioDiscovery
4640 Admiralty Way, Suite 710
Marina Del Rey, CA 90292
(310) 306-9310 FAX: (310) 306-9109
http://www.biodiscovery.com

Bioengineering AG
Sagenrainstrasse 7
CH8636 Wald, Switzerland
(41) 55-256-8-111
FAX: (41) 55-256-8-256

Biofluids
Division of Biosource International
1114 Taft Street
Rockville, MD 20850
(800) 972-5200 FAX: (301) 424-3619
(301) 424-4140
http://www.biosource.com

BioFX Laboratories
9633 Liberty Road, Suite S
Randallstown, MD 21133
(800) 445-6447 FAX: (410) 498-6008
(410) 496-6006
http://www.biofx.com

BioGenex Laboratories
4600 Norris Canyon Road
San Ramon, CA 94583
(800) 421-4149 FAX: (925) 275-0580
(925) 275-0550
http://www.biogenex.com

Bioline
2470 Wrondel Way
Reno, NV 89502
(888) 257-5155 FAX: (775) 828-7676
(775) 828-0202
http://www.bioline.com

Bio-Logic Research & Development
1, rue de l-Europe
A.Z. de Font-Ratel
38640 CLAIX, France
(33) 76-98-68-31
FAX: (33) 76-98-69-09

Biological Detection Systems
See Cellomics or Amersham

Biomeda
1166 Triton Drive, Suite E
P.O. Box 8045
Foster City, CA 94404
(800) 341-8787 FAX: (650) 341-2299
(650) 341-8787
http://www.biomeda.com

BioMedic Data Systems
1 Silas Road
Seaford, DE 19973
(800) 526-2637 FAX: (302) 628-4110
(302) 628-4100
http://www.bmds.com

Biomedical Engineering
P.O. Box 980694
Virginia Commonwealth University
Richmond, VA 23298
(804) 828-9829 FAX: (804) 828-1008

Biomedical Research Instruments
12264 Wilkins Avenue
Rockville, MD 20852
(800) 327-9498
(301) 881-7911
http://www.biomedinstr.com

Bio/medical Specialties
P.O. Box 1687
Santa Monica, CA 90406
(800) 269-1158 FAX: (800) 269-1158
(323) 938-7515

BioMerieux
100 Rodolphe Street
Durham, North Carolina 27712
(919) 620-2000
http://www.biomerieux.com

BioMetallics
P.O. Box 2251
Princeton, NJ 08543
(800) 999-1961 FAX: (609) 275-9485
(609) 275-0133
http://www.microplate.com

Biomol Research Laboratories
5100 Campus Drive
Plymouth Meeting, PA 19462
(800) 942-0430 FAX: (610) 941-9252
(610) 941-0430
http://www.biomol.com

Bionique Testing Labs
Fay Brook Drive
RR 1, Box 196
Saranac Lake, NY 12983
(518) 891-2356 FAX: (518) 891-5753
http://www.bionique.com

Biopac Systems
42 Aero Camino
Santa Barbara, CA 93117
(805) 685-0066 FAX: (805) 685-0067
http://www.biopac.com

Bioproducts for Science
See Harlan Bioproducts for Science

Bioptechs
3560 Beck Road Butler, PA 16002
(877) 548-3235 FAX: (724) 282-0745
(724) 282-7145
http://www.bioptechs.com

BIOQUANT-R&M Biometrics
5611 Ohio Ave
Nashville, TN 37209
(800) 221-0549 (615) 350-7866
FAX: (615) 350-7282
http://www.bioquant.com

Bio-Rad Laboratories
2000 Alfred Nobel Drive
Hercules, CA 94547
(800) 424-6723 FAX: (800) 879-2289
(510) 741-1000 FAX: (510) 741-5800
http://www.bio-rad.com

Bio-Rad Laboratories
Maylands Avenue
Hemel Hempstead, Herts HP2 7TD, UK
http://www.bio-rad.com

BioRobotics
3-4 Bennell Court
Comberton, Cambridge CB3 7DS, UK
(44) 1223-264345
FAX: (44) 1223-263933
http://www.biorobotics.co.uk

BIOS Laboratories
See Genaissance Pharmaceuticals

Biosearch Technologies
81 Digital Drive
Novato, CA 94949
(800) GENOME1
FAX: (415) 883-8488
(415) 883-8400
http://www.biosearchtech.com

BioSepra
111 Locke Drive
Marlborough, MA 01752
(800) 752-5277 FAX: (508) 357-7595
(508) 357-7500
http://www.biosepra.com

Bio-Serv
1 8th Street, Suite 1
Frenchtown, NJ 08825
(908) 996-2155 FAX: (908) 996-4123
http://www.bio-serv.com

BioSignal
1744 William Street, Suite 600
Montreal, Quebec H3J 1R4, Canada
(800) 293-4501 FAX: (514) 937-0777
(514) 937-1010
http://www.biosignal.com

Biosoft
P.O. Box 10938
Ferguson, MO 63135
(314) 524-8029 FAX: (314) 524-8129
http://www.biosoft.com

Biosource International
820 Flynn Road
Camarillo, CA 93012
(800) 242-0607 FAX: (805) 987-3385
(805) 987-0086
http://www.biosource.com

BioSpec Products
P.O. Box 788
Bartlesville, OK 74005
(800) 617-3363 FAX: (918) 336-3363
(918) 336-3363
http://www.biospec.com

Biosure
See Riese Enterprises

Biosym Technologies
See Molecular Simulations

Biosys
21 quai du Clos des Roses
602000 Compiegne, France
(33) 03 4486 2275
FAX: (33) 03 4484 2297

Bio-Tech Research Laboratories
NIAID Repository
Rockville, MD 20850
http://www.niaid.nih.gov/ncn/repos.htm

Biotech Instruments
Biotech House
75A High Street
Kimpton, Hertfordshire SG4 8PU, UK
(44) 1438 832555
FAX: (44) 1438 833040
http://www.biotinst.demon.co.uk

Biotech International
11 Durbell Street
Acacia Ridge, Queensland 4110
Australia
61-7-3370-6396
FAX: 61-7-3370-6370
http://www.avianbiotech.com

Biotech Source
Inland Farm Drive
South Windham, ME 04062
(207) 892-3266 FAX: (207) 892-6774

Bio-Tek Instruments
Highland Industrial Park
P.O. Box 998
Winooski, VT 05404
(800) 451-5172 FAX: (802) 655-7941
(802) 655-4040
http://www.biotek.com

Biotecx Laboratories
6023 South Loop East
Houston, TX 77033
(800) 535-6286 FAX: (713) 643-3143
(713) 643-0606
http://www.biotecx.com

BioTherm
3260 Wilson Boulevard
Arlington, VA 22201
(703) 522-1705 FAX: (703) 522-2606

Bioventures
P.O. Box 2561
848 Scott Street
Murfreesboro, TN 37133
(800) 235-8938 FAX: (615) 896-4837
http://www.bioventures.com

BioWhittaker
8830 Biggs Ford Road
P.O. Box 127
Walkersville, MD 21793
(800) 638-8174 FAX: (301) 845-8338
(301) 898-7025
http://www.biowhittaker.com

Biozyme Laboratories
9939 Hibert Street, Suite 101
San Diego, CA 92131
(800) 423-8199 FAX: (858) 549-0138
(858) 549-4484
http://www.biozyme.com

Bird Products
1100 Bird Center Drive
Palm Springs, CA 92262
(800) 328-4139 FAX: (760) 778-7274
(760) 778-7200
http://www.birdprod.com/bird

B & K Universal
2403 Yale Way
Fremont, CA 94538
(800) USA-MICE
FAX: (510) 490-3036

BLS Ltd.
Zselyi Aladar u. 31
1165 Budapest, Hungary
(36) 1-407-2602
FAX: (36) 1-407-2896
http://www.bls-ltd.com

Blue Sky Research
3047 Orchard Parkway
San Jose, CA 95134
(408) 474-0988 FAX: (408) 474-0989
http://www.blueskyresearch.com

Blumenthal Industries
7 West 36th Street, 13th floor
New York, NY 10018
(212) 719-1251 FAX: (212) 594-8828

BOC Edwards
One Edwards Park
301 Ballardvale Street
Wilmington, MA 01887
(800) 848-9800 FAX: (978) 658-7969
(978) 658-5410
http://www.bocedwards.com

Boehringer Ingelheim
900 Ridgebury Road
P.O. Box 368
Ridgefield, CT 06877
(800) 243-0127 FAX: (203) 798-6234
(203) 798-9988
http://www.boehringer-ingelheim.com

Boehringer Mannheim
Biochemicals Division
See Roche Diagnostics

Boekel Scientific
855 Pennsylvania Boulevard
Feasterville, PA 19053
(800) 336-6929 FAX: (215) 396-8264
(215) 396-8200
http://www.boekelsci.com

Bohdan Automation
1500 McCormack Boulevard
Mundelein, IL 60060
(708) 680-3939 FAX: (708) 680-1199

BPAmoco
4500 McGinnis Ferry Road
Alpharetta, GA 30005
(800) 328-4537 FAX: (770) 772-8213
(770) 772-8200
http://www.bpamoco.com

Brain Research Laboratories
Waban P.O. Box 88
Newton, MA 02468
(888) BRL-5544 FAX: (617) 965-6220
(617) 965-5544
http://www.brainresearchlab.com

Braintree Scientific
P.O. Box 850929
Braintree, MA 02185
(781) 843-1644 FAX: (781) 982-3160
http://www.braintreesci.com

Brandel
8561 Atlas Drive
Gaithersburg, MD 20877
(800) 948-6506 FAX: (301) 869-5570
(301) 948-6506
http://www.brandel.com

Branson Ultrasonics
41 Eagle Road
Danbury, CT 06813
(203) 796-0400 FAX: (203) 796-9838
http://www.plasticsnet.com/branson

B. Braun Biotech
999 Postal Road
Allentown, PA 18103
(800) 258-9000 FAX: (610) 266-9319
(610) 266-6262
http://www.bbraunbiotech.com

B. Braun Biotech International
Schwarzenberg Weg 73-79
P.O. Box 1120
D-34209 Melsungen, Germany
(49) 5661-71-3400
FAX: (49) 5661-71-3702
http://www.bbraunbiotech.com

B. Braun-McGaw
2525 McGaw Avenue
Irvine, CA 92614
(800) BBRAUN-2 (800) 624-2963
http://www.bbraunusa.com

B. Braun Medical
Thorncliffe Park
Sheffield S35 2PW, UK
(44) 114-225-9000
FAX: (44) 114-225-9111
http://www.bbmuk.demon.co.uk

Brenntag
P.O. Box 13788
Reading, PA 19612-3788
(610) 926-4151 FAX: (610) 926-4160
http://www.brenntagnortheast.com

Bresatec
See GeneWorks

Bright/Hacker Instruments
17 Sherwood Lane
Fairfield, NJ 07004
(973) 226-8450 FAX: (973) 808-8281
http://www.hackerinstruments.com

Brinkmann Instruments
Subsidiary of Sybron
1 Cantiague Road
P.O. Box 1019
Westbury, NY 11590
(800) 645-3050 FAX: (516) 334-7521
(516) 334-7500
http://www.brinkmann.com

Bristol-Meyers Squibb
P.O. Box 4500
Princeton, NJ 08543
(800) 631-5244 FAX: (800) 523-2965
http://www.bms.com

Broadley James
19 Thomas
Irvine, CA 92618
(800) 288-2833 FAX: (949) 829-5560
(949) 829-5555
http://www.broadleyjames.com

Brookhaven Instruments
750 Blue Point Road
Holtsville, NY 11742
(631) 758-3200 FAX: (631) 758-3255
http://www.bic.com

Brownlee Labs
See Applied Biosystems
Distributed by Pacer Scientific

Bruel & Kjaer
Division of Spectris Technologies
2815 Colonnades Court
Norcross, GA 30071
(800) 332-2040 FAX: (770) 847-8440
(770) 209-6907
http://www.bkhome.com

Bruker Analytical X-Ray Systems
5465 East Cheryl Parkway
Madison, WI 53711
(800) 234-XRAY
FAX: (608) 276-3006
(608) 276-3000
http://www.bruker-axs.com

Bruker Instruments
19 Fortune Drive
Billerica, MA 01821
(978) 667-9580 FAX: (978) 667-0985
http://www.bruker.com

BS Pyromatic India
27/1, XII Avenue
Ashok Nagar, Chennai, 600083, India
http://www.bspyromatic.com/

BTX
Division of Genetronics
11199 Sorrento Valley Road
San Diego, CA 92121
(800) 289-2465 FAX: (858) 597-9594
(858) 597-6006
http://www.genetronics.com/btx

Buchler Instruments
See Baxter Scientific Products

Buckshire
2025 Ridge Road
Perkasie, PA 18944
(215) 257-0116

Burdick and Jackson
Division of Baxter Scientific Products
1953 S. Harvey Street
Muskegon, MI 49442
(800) 368-0050 FAX: (231) 728-8226
(231) 726-3171
http://www.bandj.com/mainframe.htm

Burleigh Instruments
P.O. Box E
Fishers, NY 14453
(716) 924-9355 FAX: (716) 924-9072
http://www.burleigh.com

Burns Veterinary Supply
1900 Diplomat Drive
Farmer's Branch, TX 75234
(800) 92-BURNS
FAX: (972) 243-6841
http://www.burnsvet.com

Burroughs Wellcome
See Glaxo Wellcome

The Butler Company
5600 Blazer Parkway
Dublin, OH 43017
(800) 551-3861 FAX: (614) 761-9096
(614) 761-9095
http://www.wabutler.com

Butterworth Laboratories
54-56 Waldegrave Road
Teddington, Middlesex
TW11 8LG, UK
(44)(0)20-8977-0750
FAX: (44)(0)28-8943-2624
http://www.butterworth-labs.co.uk

Buxco Electronics
95 West Wood Road #2
Sharon, CT 06069
(860) 364-5558 FAX: (860) 364-5116
http://www.buxco.com

C/D/N Isotopes
88 Leacock Street Pointe-Claire,
Quebec
H9R 1H1 Canada
(800) 697-6254 FAX: (514) 697-6148

C.M.A./Microdialysis AB
73 Princeton Street
North Chelmsford, MA 01863
(800) 440-4980 FAX: (978) 251-1950
(978) 251-1940
http://www.microdialysis.com

Calbiochem-Novabiochem
P.O. Box 12087-2087
La Jolla, CA 92039
(800) 854-3417 FAX: (800) 776-0999
(858) 450-9600
http://www.calbiochem.com

California Fine Wire
338 South Fourth Street
Grover Beach, CA 93433
(805) 489-5144 FAX: (805) 489-5352
http://www.calfinewire.com

Calorimetry Sciences
155 West 2050 North
Spanish Fork, UT 84660
(801) 794-2600 FAX: (801) 794-2700
http://www.calscorp.com

Caltag Laboratories
1849 Bayshore Highway, Suite 200
Burlingame, CA 94010
(800) 874-4007 FAX: (650) 652-9030
(650) 652-0468
http://www.caltag.com

Cambridge Electronic Design
Science Park, Milton Road
Cambridge CB4 0FE, UK
44 (0) 1223-420-186
FAX: 44 (0) 1223-420-488
http://www.ced.co.uk

Cambridge Isotope Laboratories
50 Frontage Road
Andover, MA 01810
(800) 322-1174 FAX: (978) 749-2768
(978) 749-8000
http://www.isotope.com

Cambridge Research Biochemicals
See Zeneca/CRB

Cambridge Technology
109 Smith Place
Cambridge, MA 02138
(6l7) 441-0600 FAX: (617) 497-8800
http://www.camtech.com

Camlab
Nuffield Road
Cambridge CB4 1TH, UK
(44) 122-3424222
FAX: (44) 122-3420856
http://www.camlab.co.uk/home.htm

Campden Instruments
Park Road
Sileby Loughborough
Leicestershire LE12 7TU, UK
(44) 1509-814790
FAX: (44) 1509-816097
http://www.campden-inst.com/home.htm

Cappel Laboratories
See Organon Teknika Cappel

Carl Roth GmgH & Company
Schoemperlenstrasse 1-5
76185 Karlsrube
Germany
(49) 72-156-06164
FAX: (49) 72-156-06264
http://www.carl-roth.de

Carl Zeiss
One Zeiss Drive
Thornwood, NY 10594
(800) 233-2343 FAX: (914) 681-7446
(914) 747-1800
http://www.zeiss.com

Carlo Erba Reagenti
Via Winckelmann 1
20148 Milano
Lombardia, Italy
(39) 0-29-5231
FAX: (39) 0-29-5235-904
http://www.carloerbareagenti.com

Carolina Biological Supply
2700 York Road
Burlington, NC 27215
(800) 334-5551
FAX: (336) 584-76869
(336) 584-0381
http://www.carolina.com

Carolina Fluid Components
9309 Stockport Place
Charlotte, NC 28273
(704) 588-6101 FAX: (704) 588-6115
http://www.cfcsite.com

Cartesian Technologies
17851 Skypark Circle, Suite C
Irvine, CA 92614
(800) 935-8007
http://cartesiantech.com

Cayman Chemical
1180 East Ellsworth Road
Ann Arbor, MI 48108
(800) 364-9897 FAX: (734) 971-3640
(734) 971-3335
http://www.caymanchem.com

CB Sciences
One Washington Street, Suite 404
Dover, NH 03820
(800) 234-1757 FAX: (603) 742-2455
http://www.cbsci.com

CBS Scientific
P.O. Box 856
Del Mar, CA 92014
(800) 243-4959 FAX: (858) 755-0733
(858) 755-4959
http://www.cbssci.com

CCR (Coriell Cell Repository)
See Coriell Institute for Medical Research

CE Instruments
Grand Avenue Parkway
Austin, TX 78728
(800) 876-6711 FAX: (512) 251-1597
http://www.ceinstruments.com

Cedarlane Laboratories
5516 8th Line, R.R. #2
Hornby, Ontario L0P 1E0, Canada
(905) 878-8891 FAX: (905) 878-7800
http://www.cedarlanelabs.com

CEL Associates
P.O. Box 721854
Houston, TX 77272
(800) 537-9339 FAX: (281) 933-0922
(281) 933-9339
http://www.cel-1.com

Cel-Line Associates
See Erie Scientific

Celite World Minerals
130 Castilian Drive
Santa Barbara, CA 93117
(805) 562-0200 FAX: (805) 562-0299
http://www.worldminerals.com/celite

Cell Genesys
342 Lakeside Drive
Foster City, CA 94404
(650) 425-4400 FAX: (650) 425-4457
http://www.cellgenesys.com

Cell Systems
12815 NE 124th Street, Suite A
Kirkland, WA 98034
(800) 697-1211 FAX: (425) 820-6762
(425) 823-1010

Cellmark Diagnostics
20271 Goldenrod Lane
Germantown, MD 20876
(800) 872-5227 FAX: (301) 428-4877
(301) 428-4980
http://www.cellmark-labs.com

Cellomics
635 William Pitt Way
Pittsburgh, PA 15238
(888) 826-3857 FAX: (412) 826-3850
(412) 826-3600
http://www.cellomics.com

Celltech
216 Bath Road
Slough, Berkshire SL1 4EN, UK
(44) 1753 534655
FAX: (44) 1753 536632
http://www.celltech.co.uk

Cellular Products
872 Main Street
Buffalo, NY 14202
(800) CPI-KITS FAX: (716) 882-0959
(716) 882-0920
http://www.zeptometrix.com

CEM
P.O. Box 200
Matthews, NC 28106
(800) 726-3331

Centers for Disease Control
1600 Clifton Road NE
Atlanta, GA 30333
(800) 311-3435 FAX: (888) 232-3228
(404) 639-3311
http://www.cdc.gov

CERJ
Centre d'Elevage Roger Janvier
53940 Le Genest Saint Isle
France

Cetus
See Chiron

Chance Propper
Warly, West Midlands B66 1NZ, UK
(44)(0)121-553-5551
FAX: (44)(0)121-525-0139

Charles River Laboratories
251 Ballardvale Street
Wilmington, MA 01887
(800) 522-7287 FAX: (978) 658-7132
(978) 658-6000
http://www.criver.com

Charm Sciences
36 Franklin Street
Malden, MA 02148
(800) 343-2170 FAX: (781) 322-3141
(781) 322-1523
http://www.charm.com

Chase-Walton Elastomers
29 Apsley Street
Hudson, MA 01749
(800) 448-6289 FAX: (978) 562-5178
(978) 568-0202
http://www.chase-walton.com

ChemGenes
Ashland Technology Center
200 Homer Avenue
Ashland, MA 01721
(800) 762-9323 FAX: (508) 881-3443
(508) 881-5200
http://www.chemgenes.com

Chemglass
3861 North Mill Road
Vineland, NJ 08360
(800) 843-1794 FAX: (856) 696-9102
(800) 696-0014
http://www.chemglass.com

Chemicon International
28835 Single Oak Drive
Temecula, CA 92590
(800) 437-7500 FAX: (909) 676-9209
(909) 676-8080
http://www.chemicon.com

Chem-Impex International
935 Dillon Drive
Wood Dale, IL 60191
(800) 869-9290 FAX: (630) 766-2218
(630) 766-2112
http://www.chemimpex.com

Chem Service
P.O. Box 599
West Chester, PA 19381-0599
(610) 692-3026 FAX: (610) 692-8729
http://www.chemservice.com

Chemsyn Laboratories
13605 West 96th Terrace
Lenexa, KS 66215
(913) 541-0525 FAX: (913) 888-3582
http://www.tech.epcorp.com/ChemSyn/chemsyn.htm

Chemunex USA
1 Deer Park Drive, Suite H-2
Monmouth Junction, NJ 08852
(800) 411-6734
http://www.chemunex.com

Cherwell Scientific Publishing
The Magdalen Centre
Oxford Science Park
Oxford OX44GA, UK
(44)(1) 865-784-800
FAX: (44)(1) 865-784-801
http://www.cherwell.com

ChiRex Cauldron
383 Phoenixville Pike
Malvern, PA 19355
(610) 727-2215 FAX: (610) 727-5762
http://www.chirex.com

Chiron Diagnostics
See Bayer Diagnostics

Chiron Mimotopes Peptide Systems
See Multiple Peptide Systems

Chiron
4560 Horton Street
Emeryville, CA 94608
(800) 244-7668 FAX: (510) 655-9910
(510) 655-8730
http://www.chiron.com

Chrom Tech
P.O. Box 24248
Apple Valley, MN 55124
(800) 822-5242 FAX: (952) 431-6345
http://www.chromtech.com

Chroma Technology
72 Cotton Mill Hill, Unit A-9
Brattleboro, VT 05301
(800) 824-7662 FAX: (802) 257-9400
(802) 257-1800
http://www.chroma.com

Chromatographie
ZAC de Moulin No. 2
91160 Saulx les Chartreux
France
(33) 01-64-54-8969
FAX: (33) 01-69-0988091
http://www.chromatographie.com

Chromogenix
Taljegardsgatan 3
431-53 MIndal, Sweden
(46) 31-706-20-70
FAX: (46) 31-706-20-80
http://www.chromogenix.com

Chrompack USA
c/o Varian USA
2700 Mitchell Drive
Walnut Creek, CA 94598
(800) 526-3687 FAX: (925) 945-2102
(925) 939-2400
http://www.chrompack.com

Chugai Biopharmaceuticals
6275 Nancy Ridge Drive
San Diego, CA 92121
(858) 535-5900 FAX: (858) 546-5973
http://www.chugaibio.com

Ciba-Corning Diagnostics
See Bayer Diagnostics

Ciba-Geigy
See Ciba Specialty Chemicals or Novartis Biotechnology

Ciba Specialty Chemicals
540 White Plains Road
Tarrytown, NY 10591
(800) 431-1900 FAX: (914) 785-2183
(914) 785-2000
http://www.cibasc.com

Ciba Vision
Division of Novartis AG
11460 Johns Creek Parkway
Duluth, GA 30097
(770) 476-3937
http://www.cvworld.com

Cidex
Advanced Sterilization Products
33 Technology Drive
Irvine, CA 92618
(800) 595-0200 (949) 581-5799
http://www.cidex.com/ASPnew.htm

Cinna Scientific
Subsidiary of Molecular Research Center
5645 Montgomery Road
Cincinnati, OH 45212
(800) 462-9868 FAX: (513) 841-0080
(513) 841-0900
http://www.mrcgene.com

Cistron Biotechnology
10 Bloomfield Avenue
Pine Brook, NJ 07058
(800) 642-0167 FAX: (973) 575-4854
(973) 575-1700
http://www.cistronbio.com

Clark Electromedical Instruments
See Harvard Apparatus

Clay Adam
See Becton Dickinson Primary Care Diagnostics

CLB (Central Laboratory
of the Netherlands)
Blood Transfusion Service
P.O. Box 9190
1006 AD Amsterdam, The Netherlands
(31) 20-512-9222
FAX: (31) 20-512-3332

Cleveland Scientific
P.O. Box 300
Bath, OH 44210
(800) 952-7315 FAX: (330) 666-2240
http:://www.clevelandscientific.com

Clonetics
Division of BioWhittaker
http://www.clonetics.com
Also see BioWhittaker

Clontech Laboratories
1020 East Meadow Circle
Palo Alto, CA 94303
(800) 662-2566 FAX: (800) 424-1350
(650) 424-8222 FAX: (650) 424-1088
http://www.clontech.com

Closure Medical Corporation
5250 Greens Dairy Road
Raleigh, NC 27616
(919) 876-7800 FAX: (919) 790-1041
http://www.closuremed.com

CMA Microdialysis AB
73 Princeton Street
North Chelmsford, MA 01863
(800) 440-4980 FAX: (978) 251-1950
(978) 251 1940
http://www.microdialysis.com

Cocalico Biologicals
449 Stevens Road
P.O. Box 265
Reamstown, PA 17567
(717) 336-1990 FAX: (717) 336-1993

Coherent Laser
5100 Patrick Henry Drive
Santa Clara, CA 95056
(800) 227-1955 FAX: (408) 764-4800
(408) 764-4000
http://www.cohr.com

Cohu
P.O. Box 85623
San Diego, CA 92186
(858) 277-6700 FAX: (858) 277-0221
http://www.COHU.com/cctv

Cole-Parmer Instrument
625 East Bunker Court
Vernon Hills, IL 60061
(800) 323-4340 FAX: (847) 247-2929
(847) 549-7600
http://www.coleparmer.com

Collaborative Biomedical Products and Collaborative Research
See Becton Dickinson Labware

Collagen Aesthetics
1850 Embarcadero Road
Palo Alto, CA 94303
(650) 856-0200 FAX: (650) 856-0533
http://www.collagen.com

Collagen Corporation
See Collagen Aesthetics

College of American Pathologists
325 Waukegan Road
Northfield, IL 60093
(800) 323-4040 FAX: (847) 832-8000
(847) 446-8800
http://www.cap.org/index.cfm

Colonial Medical Supply
504 Wells Road
Franconia, NH 03580
(603) 823-9911 FAX: (603) 823-8799
http://www.colmedsupply.com

Colorado Serum
4950 York Street
Denver, CO 80216
(800) 525-2065 FAX: (303) 295-1923
http://www.colorado-serum.com

Columbia Diagnostics
8001 Research Way
Springfield, VA 22153
(800) 336-3081 FAX: (703) 569-2353
(703) 569-7511
http://www.columbiadiagnostics.com

Columbus Instruments
950 North Hague Avenue
Columbus, OH 43204
(800) 669-5011 FAX: (614) 276-0529
(614) 276-0861
http://www.columbusinstruments.com

Computer Associates International
One Computer Associates Plaza
Islandia, NY 11749
(631) 342-6000 FAX: (631) 342-6800
http://www.cai.com

Connaught Laboratories
See Aventis Pasteur

Connectix
2955 Campus Drive, Suite 100
San Mateo, CA 94403
(800) 950-5880 FAX: (650) 571-0850
(650) 571-5100
http://www.connectix.com

Contech
99 Hartford Avenue
Providence, RI 02909
(401) 351-4890 FAX: (401) 421-5072
http://www.iol.ie/~burke/contech.html

Continental Laboratory Products
5648 Copley Drive
San Diego, CA 92111
(800) 456-7741 FAX: (858) 279-5465
(858) 279-5000
http://www.conlab.com

ConvaTec
Professional Services
P.O. Box 5254
Princeton, NJ 08543
(800) 422-8811
http://www.convatec.com

Cooper Instruments & Systems
P.O. Box 3048
Warrenton, VA 20188
(800) 344-3921 FAX: (540) 347-4755
(540) 349-4746
http://www.cooperinstruments.com

Cora Styles Needles 'N Blocks
56 Milton Street
Arlington, MA 02474
(781) 648-6289 FAX: (781) 641-7917

Coriell Cell Repository (CCR)
See Coriell Institute for Medical Research

Coriell Institute for Medical Research
Human Genetic Mutant Repository
401 Haddon Avenue
Camden, NJ 08103
(856) 966-7377 FAX: (856) 964-0254
http://arginine.umdnj.edu

Corion
8 East Forge Parkway
Franklin, MA 02038
(508) 528-4411 FAX: (508) 520-7583
(800) 598-6783
http://www.corion.com

Corning and Corning Science Products
P.O. Box 5000
Corning, NY 14831
(800) 222-7740 FAX: (607) 974-0345
(607) 974-9000
http://www.corning.com

Costar
See Corning

Coulbourn Instruments
7462 Penn Drive
Allentown, PA 18106
(800) 424-3771 FAX: (610) 391-1333
(610) 395-3771
http://www.coulbourninst.com

Coulter Cytometry
See Beckman Coulter

Covance Research Products
465 Swampbridge Road
Denver, PA 17517
(800) 345-4114 FAX: (717) 336-5344
(717) 336-4921
http://www.covance.com

Coy Laboratory Products
14500 Coy Drive
Grass Lake, MI 49240
(734) 475-2200 FAX: (734) 475-1846
http://www.coylab.com

CPG
3 Borinski Road
Lincoln Park, NJ 07035
(800) 362-2740 FAX: (973) 305-0884
(973) 305-8181
http://www.cpg-biotech.com

CPL Scientific
43 Kingfisher Court
Hambridge Road
Newbury RG14 5SJ, UK
(44) 1635-574902
FAX: (44) 1635-529322
http://www.cplscientific.co.uk

CraMar Technologies
8670 Wolff Court, #160
Westminster, CO 80030
(800) 4-TOMTEC
http://www.cramar.com

Crescent Chemical
1324 Motor Parkway Hauppauge, NY 11788
(800) 877-3225 FAX: (631) 348-0913
(631) 348-0333
http://www.creschem.com

Crist Instrument
P.O. Box 128
10200 Moxley Road
Damascus, MD 20872
(301) 253-2184 FAX: (301) 253-0069
http://www.cristinstrument.com

Cruachem
See Annovis
http://www.cruachem.com

CS Bio
1300 Industrial Road
San Carlos, CA 94070
(800) 627-2461 FAX: (415) 802-0944
(415) 802-0880
http://www.csbio.com

CS-Chromatographie Service
Am Parir 27
D-52379 Langerwehe, Germany
(49) 2423-40493-0
FAX: (49) 2423-40493-49
http://www.cs-chromatographie.de

Cuno
400 Research Parkway
Meriden, CT 06450
(800) 231-2259 FAX: (203) 238-8716
(203) 237-5541
http://www.cuno.com

Curtin Matheson Scientific
9999 Veterans Memorial Drive
Houston, TX 77038
(800) 392-3353 FAX: (713) 878-3598
(713) 878-3500

CWE
124 Sibley Avenue
Ardmore, PA 19003
(610) 642-7719 FAX: (610) 642-1532
http://www.cwe-inc.com

Cybex Computer Products
4991 Corporate Drive
Huntsville, AL 35805
(800) 932-9239 FAX: (800) 462-9239
http://www.cybex.com

Cygnus Technology
P.O. Box 219
Delaware Water Gap, PA 18327
(570) 424-5701 FAX: (570) 424-5630
http://www.cygnustech.com

Cymbus Biotechnology
Eagle Class, Chandler's Ford
Hampshire SO53 4NF, UK
(44) 1-703-267-676
FAX: (44) 1-703-267-677
http://www.biotech.cymbus.com

Cytogen
600 College Road East
Princeton, NJ 08540
(609) 987-8200 FAX: (609) 987-6450
http://www.cytogen.com

Cytogen Research and Development
89 Bellevue Hill Road
Boston, MA 02132
(617) 325-7774 FAX: (617) 327-2405

CytRx
154 Technology Parkway
Norcross, GA 30092
(800) 345-2987 FAX: (770) 368-0622
(770) 368-9500
http://www.cytrx.com

Dade Behring
Corporate Headquarters
1717 Deerfield Road
Deerfield, IL 60015
(847) 267-5300 FAX: (847) 267-1066
http://www.dadebehring.com

Dagan
2855 Park Avenue
Minneapolis, MN 55407
(612) 827-5959 FAX: (612) 827-6535
http://www.dagan.com

Dako
6392 Via Real
Carpinteria, CA 93013
(800) 235-5763 FAX: (805) 566-6688
(805) 566-6655
http://www.dakousa.com

Dako A/S
42 Produktionsvej
P.O. Box 1359
DK-2600 Glostrup, Denmark
(45) 4492-0044 FAX: (45) 4284-1822

Dakopatts
See Dako A/S

Dalton Chemical Laboratoris
349 Wildcat Road
Toronto, Ontario
M3J 253 Canada
(416) 661-2102 FAX: (416) 661-2108
(800) 567-5060 (in Canada only)
http://www.dalton.com

Damon, IEC
See Thermoquest

Dan Kar Scientific
150 West Street
Wilmington, MA 01887
(800) 942-5542 FAX: (978) 658-0380
(978) 988-9696
http://www.dan-kar.com

DataCell
Falcon Business Park
40 Ivanhoe Road
Finchampstead, Berkshire
RG40 4QQ, UK
(44) 1189 324324
FAX: (44) 1189 324325
http://www.datacell.co.uk
In the US:
(408) 446-3575 FAX: (408) 446-3589
http://www.datacell.com

DataWave Technologies
380 Main Street, Suite 209
Longmont, CO 80501
(800) 736-9283 FAX: (303) 776-8531
(303) 776-8214

Datex-Ohmeda
3030 Ohmeda Drive
Madison, WI 53718
(800) 345-2700 FAX: (608) 222-9147
(608) 221-1551
http://www.us.datex-ohmeda.com

DATU
82 State Street
Geneva, NY 14456
(315) 787-2240 FAX: (315) 787-2397
http://www.nysaes.cornell.edu/datu

David Kopf Instruments
7324 Elmo Street
P.O. Box 636
Tujunga, CA 91043
(818) 352-3274 FAX: (818) 352-3139

Decagon Devices
P.O. Box 835
950 NE Nelson Court
Pullman, WA 99163
(800) 755-2751 FAX: (509) 332-5158
(509) 332-2756
http://www.decagon.com

Decon Labs
890 Country Line Road
Bryn Mawr, PA 19010
(800) 332-6647 FAX: (610) 964-0650
(610) 520-0610
http://www.deconlabs.com

Decon Laboratories
Conway Street
Hove, Sussex BN3 3LY, UK
(44) 1273 739241
FAX: (44) 1273 722088

Degussa
Precious Metals Division
3900 South Clinton Avenue
South Plainfield, NJ 07080
(800) DEGUSSA
FAX: (908) 756-7176
(908) 561-1100
http://www.degussa-huls.com

Deneba Software
1150 NW 72nd Avenue
Miami, FL 33126
(305) 596-5644 FAX: (305) 273-9069
http://www.deneba.com

Deseret Medical
524 West 3615 South
Salt Lake City, UT 84115
(801) 270-8440 FAX: (801) 293-9000

Devcon Plexus
30 Endicott Street
Danvers, MA 01923
(800) 626-7226 FAX: (978) 774-0516
(978) 777-1100
http://www.devcon.com

Developmental Studies Hybridoma Bank
University of Iowa
436 Biology Building
Iowa City, IA 52242
(319) 335-3826 FAX: (319) 335-2077
http://www.uiowa.edu/~dshbwww

DeVilbiss
Division of Sunrise Medical Respiratory
100 DeVilbiss Drive
P.O. Box 635 Somerset, PA 15501
(800) 338-1988 FAX: (814) 443-7572
(814) 443-4881
http://www.sunrisemedical.com

Dharmacon Research
1376 Miners Drive #101
Lafayette, CO 80026
(303) 604-9499 FAX: (303) 604-9680
http://www.dharmacon.com

DiaCheM
Triangle Biomedical
Gardiners Place
West Gillibrands, Lancashire WN8
9SP, UK
(44) 1695-555581
FAX: (44) 1695-555518
http://www.diachem.co.uk

Diaclone
Tepnel Lifecodes Corp.
550 West Ave.
Stamford, CT 06902
(888) 329-0255 FAX: (203) 328-9599
http://www.diaclone.com

Diagen
Max-Volmer Strasse 4
D-40724 Hilden, Germany
(49) 2103-892-230
FAX: (49) 2103-892-222

Diagnostic Concepts
6104 Madison Court
Morton Grove, IL 60053
(847) 604-0957

Diagnostic Developments
See DiaCheM

Diagnostic Instruments
6540 Burroughs
Sterling Heights, MI 48314
(810) 731-6000 FAX: (810) 731-6469
http://www.diaginc.com

Diamedix
2140 North Miami Avenue
Miami, FL 33127
(800) 327-4565 FAX: (305) 324-2395
(305) 324-2300

DiaSorin
1990 Industrial Boulevard
Stillwater, MN 55082
(800) 328-1482 FAX: (651) 779-7847
(651) 439-9719
http://www.diasorin.com

Diatome US
321 Morris Road
Fort Washington, PA 19034
(800) 523-5874 FAX: (215) 646-8931
(215) 646-1478
http://www.emsdiasum.com

Difco Laboratories
See Becton Dickinson

Digene
1201 Clopper Road
Gaithersburg, MD 20878
(301) 944-7000 (800) 344-3631
FAX: (301) 944-7121
http://www.digene.com

Digi-Key
701 Brooks Avenue South
Thief River Falls, MN 56701
(800) 344-4539 FAX: (218) 681-3380
(218) 681-6674
http://www.digi-key.com

Digitimer
37 Hydeway
Welwyn Garden City, Hertfordshire
AL7 3BE, UK
(44) 1707-328347
FAX: (44) 1707-373153
http://www.digitimer.com

Dimco-Gray
8200 South Suburban Road
Dayton, OH 45458
(800) 876-8353 FAX: (937) 433-0520
(937) 433-7600
http://www.dimco-gray.com

Dionex
1228 Titan Way
P.O. Box 3603
Sunnyvale, CA 94088
(408) 737-0700 FAX: (408) 730-9403
http://dionex2.promptu.com

Display Systems Biotech
1260 Liberty Way, Suite B
Vista, CA 92083
(800) 697-1111 FAX: (760) 599-9930
(760) 599-0598
http://www.displaysystems.com

Diversified Biotech
1208 VFW Parkway
Boston, MA 02132
(617) 965-8557 FAX: (617) 323-5641
(800) 796-9199
http://www.divbio.com

DNA ProScan
P.O. Box 121585
Nashville, TN 37212
(800) 841-4362 FAX: (615) 292-1436
(615) 298-3524
http://www.dnapro.com

DNAStar
1228 South Park Street
Madison, WI 53715
(608) 258-7420 FAX: (608) 258-7439
http://www.dnastar.com

DNAVIEW
Attn: Charles Brenner
http://www.wco.com
~cbrenner/dnaview.htm

Doall NYC
36-06 48th Avenue
Long Island City, NY 11101
(718) 392-4595 FAX: (718) 392-6115
http://www.doall.com

Dojindo Molecular Technologies
211 Perry Street Parkway, Suite 5
Gaitherbusburg, MD 20877
(877) 987-2667
http://www.dojindo.com

Dolla Eastern
See Doall NYC

Dolan Jenner Industries
678 Andover Street
Lawrence, MA 08143
(978) 681-8000 (978) 682-2500
http://www.dolan-jenner.com

Dow Chemical
Customer Service Center
2040 Willard H. Dow Center
Midland, MI 48674
(800) 232-2436 FAX: (517) 832-1190
(409) 238-9321
http://www.dow.com

Dow Corning
Northern Europe
Meriden Business Park
Copse Drive
Allesley, Coventry CV5 9RG, UK
(44) 1676 528 000
FAX: (44) 1676 528 001

Dow Corning
P.O. Box 994
Midland, MI 48686
(517) 496-4000
http://www.dowcorning.com

Dow Corning (Lubricants)
2200 West Salzburg Road
Auburn, MI 48611
(800) 248-2481 FAX: (517) 496-6974
(517) 496-6000

Dremel
4915 21st Street
Racine, WI 53406
(414) 554-1390
http://www.dremel.com

Drummond Scientific
500 Parkway
P.O. Box 700
Broomall, PA 19008
(800) 523-7480 FAX: (610) 353-6204
(610) 353-0200
http://www.drummondsci.com

Duchefa Biochemie BV
P.O. Box 2281
2002 CG Haarlem, The Netherlands
31-0-23-5319093
FAX: 31-0-23-5318027
http://www.duchefa.com

Duke Scientific
2463 Faber Place
Palo Alto, CA 94303
(800) 334-3883 FAX: (650) 424-1158
(650) 424-1177
http://www.dukescientific.com

Duke University Marine Laboratory
135 Duke Marine Lab Road
Beaufort, NC 28516-9721
(252) 504-7503 FAX: (252) 504-7648
http://www.env.duke.edu/marinelab

DuPont Biotechnology Systems
See NEN Life Science Products

DuPont Medical Products
See NEN Life Science Products

DuPont Merck Pharmaceuticals
331 Treble Cove Road
Billerica, MA 01862
(800) 225-1572 FAX: (508) 436-7501
http://www.dupontmerck.com

DuPont NEN Products
See NEN Life Science Products

Dynal
5 Delaware Drive
Lake Success, NY 11042
(800) 638-9416 FAX: (516) 326-3298
(516) 326-3270
http://www.dynal.net

Dynal AS
Ullernchausen 52,
0379 Oslo, Norway
47-22-06-10-00 FAX: 47-22-50-70-15
http://www.dynal.no

Dynalab
P.O. Box 112
Rochester, NY 14692
(800) 828-6595 FAX: (716) 334-9496
(716) 334-2060
http://www.dynalab.com

Dynarex
1 International Boulevard
Brewster, NY 10509
(888) DYNAREX
FAX: (914) 279-9601
(914) 279-9600
http://www.dynarex.com

Dynatech
See Dynex Technologies

Dynex Technologies
14340 Sullyfield Circle
Chantilly, VA 22021
(800) 336-4543 FAX: (703) 631-7816
(703) 631-7800
http://www.dynextechnologies.com

Dyno Mill
See Willy A. Bachofen

E.S.A.
22 Alpha Road
Chelmsford, MA 01824
(508) 250-7000 FAX: (508) 250-7090

E.W. Wright
760 Durham Road
Guilford, CT 06437
(203) 453-6410 FAX: (203) 458-6901
http://www.ewwright.com

E-Y Laboratories
107 N. Amphlett Boulevard
San Mateo, CA 94401
(800) 821-0044 FAX: (650) 342-2648
(650) 342-3296
http://www.eylabs.com

Eastman Kodak
1001 Lee Road
Rochester, NY 14650
(800) 225-5352 FAX: (800) 879-4979
(716) 722-5780 FAX: (716) 477-8040
http://www.kodak.com

ECACC
See European Collection of Animal Cell Cultures

EC Apparatus
See Savant/EC Apparatus

Ecogen, SRL
Gensura Laboratories
Ptge. Dos de Maig
9(08041) Barcelona, Spain
(34) 3-450-2601
FAX: (34) 3-456-0607
http://www.ecogen.com

Ecolab
370 North Wabasha Street
St. Paul, MN 55102
(800) 35-CLEAN
FAX: (651) 225-3098
(651) 352-5326
http://www.ecolab.com

ECO PHYSICS
3915 Research Park Drive, Suite A-3
Ann Arbor, MI 48108
(734) 998-1600 FAX: (734) 998-1180
http://www.ecophysics.com

Edge Biosystems
19208 Orbit Drive
Gaithersburg, MD 20879-4149
(800) 326-2685 FAX: (301) 990-0881
(301) 990-2685
http://www.edgebio.com

Edmund Scientific
101 E. Gloucester Pike
Barrington, NJ 08007
(800) 728-6999 FAX: (856) 573-6263
(856) 573-6250
http://www.edsci.com

EG&G
See Perkin-Elmer

Ekagen
969 C Industry Road
San Carlos, CA 94070
(650) 592-4500 FAX: (650) 592-4500

Elcatech
P.O. Box 10935
Winston-Salem, NC 27108
(336) 544-8613 FAX: (336) 777-3623
(910) 777-3624
http://www.elcatech.com

Electron Microscopy Sciences
321 Morris Road
Fort Washington, PA 19034
(800) 523-5874 FAX: (215) 646-8931
(215) 646-1566
http://www.emsdiasum.com

Electron Tubes
100 Forge Way, Unit F
Rockaway, NJ 07866
(800) 521-8382 FAX: (973) 586-9771
(973) 586-9594
http://www.electrontubes.com

Elicay Laboratory Products, (UK) Ltd.
4 Manborough Mews
Crockford Lane
Basingstoke, Hampshire
RG 248NA, England
(256) 811-118 FAX: (256) 811-116
http://www.elkay-uk.co.uk

Eli Lilly
Lilly Corporate Center
Indianapolis, IN 46285
(800) 545-5979 FAX: (317) 276-2095
(317) 276-2000
http://www.lilly.com

ELISA Technologies
See Neogen

Elkins-Sinn
See Wyeth-Ayerst

EMBI
See European Bioinformatics Institute

EM Science
480 Democrat Road
Gibbstown, NJ 08027
(800) 222-0342 FAX: (856) 423-4389
(856) 423-6300
http://www.emscience.com

EM Separations Technology
See R & S Technology

Endogen
30 Commerce Way
Woburn, MA 01801
(800) 487-4885 FAX: (617) 439-0355
(781) 937-0890
http://www.endogen.com

ENGEL-Loter
HSGM Heatcutting Equipment
& Machines
1865 E. Main Street, No. 5
Duncan, SC 29334
(888) 854-HSGM FAX: (864)
486-8383
(864) 486-8300
http://www.engelgmbh.com

Enzo Diagnostics
60 Executive Boulevard
Farmingdale, NY 11735
(800) 221-7705 FAX: (516) 694-7501
(516) 694-7070
http://www.enzo.com

Enzogenetics
4197 NW Douglas Avenue
Corvallis, OR 97330
(541) 757-0288

The Enzyme Center
See Charm Sciences

Enzyme Systems Products
486 Lindbergh Avenue
Livermore, CA 94550
(888) 449-2664 FAX: (925) 449-1866
(925) 449-2664
http://www.enzymesys.com

Epicentre Technologies
1402 Emil Street
Madison, WI 53713
(800) 284-8474 FAX: (608) 258-3088
(608) 258-3080
http://www.epicentre.com

Erie Scientific
20 Post Road
Portsmouth, NH 03801
(888) ERIE-SCI FAX: (603) 431-8996
(603) 431-8410
http://www.eriesci.com

ES Industries
701 South Route 73
West Berlin, NJ 08091
(800) 356-6140 FAX: (856) 753-8484
(856) 753-8400
http://www.esind.com

ESA
22 Alpha Road
Chelmsford, MA 01824
(800) 959-5095 FAX: (978) 250-7090
(978) 250-7000
http://www.esainc.com

Ethicon
Route 22, P.O. Box 151
Somerville, NJ 08876
(908) 218-0707
http://www.ethiconinc.com

Ethicon Endo-Surgery
4545 Creek Road
Cincinnati, OH 45242
(800) 766-9534 FAX: (513) 786-7080

Eurogentec
Parc Scientifique du Sart Tilman
4102 Seraing, Belgium
32-4-240-76-76 FAX: 32-4-264-07-88
http://www.eurogentec.com

European Bioinformatics Institute
Wellcome Trust Genomes Campus
Hinxton, Cambridge CB10 1SD, UK
(44) 1223-49444
FAX: (44) 1223-494468

European Collection of Animal
Cell Cultures (ECACC)
Centre for Applied Microbiology &
Research
Salisbury, Wiltshire SP4 0JG, UK
(44) 1980-612 512
FAX: (44) 1980-611 315
http://www.camr.org.uk

Evergreen Scientific
2254 E. 49th Street
P.O. Box 58248
Los Angeles, CA 90058
(800) 421-6261 FAX: (323) 581-2503
(323) 583-1331
http://www.evergreensci.com

Exalpha Biologicals
20 Hampden Street
Boston, MA 02205
(800) 395-1137 FAX: (617) 969-3872
(617) 558-3625
http://www.exalpha.com

Exciton
P.O. Box 31126
Dayton, OH 45437
(937) 252-2989 FAX: (937) 258-3937
http://www.exciton.com

Extrasynthese
ZI Lyon Nord
SA-BP62
69730 Genay, France
(33) 78-98-20-34
FAX: (33) 78-98-19-45

Factor II
1972 Forest Avenue
P.O. Box 1339
Lakeside, AZ 85929
(800) 332-8688 FAX: (520) 537-8066
(520) 537-8387
http://www.factor2.com

Falcon
See Becton Dickinson Labware

Fenwal
See Baxter Healthcare

Filemaker
5201 Patrick Henry Drive
Santa Clara, CA 95054
(800) 325-2747
(408) 987-7000

Fine Science Tools
202-277 Mountain Highway
North Vancouver, British Columbia
V7J 3P2 Canada
(800) 665-5355 FAX: (800) 665 4544
(604) 980-2481 FAX: (604) 987-3299

Fine Science Tools
373-G Vintage Park Drive
Foster City, CA 94404
(800) 521-2109 FAX: (800) 523-2109
(650) 349-1636 FAX: (630) 349-3729

Fine Science Tools
Fahrtgasse 7-13
D-69117 Heidelberg, Germany
(49) 6221 905050
FAX: (49) 6221 600001
http://www.finescience.com

Finn Aqua
AMSCO Finn Aqua Oy
Teollisuustiez, FIN-04300
Tuusula, Finland
358 025851 FAX: 358 0276019

Finnigan
355 River Oaks Parkway
San Jose, CA 95134
(408) 433-4800 FAX: (408) 433-4821
http://www.finnigan.com

Dr. L. Fisher
Lutherstrasse 25A
D-69120 Heidelberg
Germany
(49) 6221-16-0368
http://home.eplus-
online.de/electroporation

Fisher Chemical Company
Fisher Scientific Limited
112 Colonnade Road Nepean
Ontario K2E 7L6, Canada
(800) 234-7437 FAX: (800) 463-2996
http://www.fisherscientific.com

Fisher Scientific
2000 Park Lane
Pittsburgh, PA 15275
(800) 766-7000 FAX: (800) 926-1166
(412) 562-8300
http://www3.fishersci.com

W.F. Fisher & Son
220 Evans Way, Suite #1
Somerville, NJ 08876
(908) 707-4050 FAX: (908) 707-4099

Fitzco
5600 Pioneer Creek Drive
Maple Plain, MN 55359
(800) 367-8760 FAX: (612) 479-2880
(612) 479-3489
http://www.fitzco.com

5 Prime → 3 Prime
See 2000 Eppendorf-5 Prime
http://www.5prime.com

Flambeau
15981 Valplast Road
Middlefield, Ohio 44062
(800) 232-3474 FAX: (440) 632-1581
(440) 632-1631
http://www.flambeau.com

Fleisch (Rusch)
2450 Meadowbrook Parkway
Duluth, GA 30096
(770) 623-0816 FAX: (770) 623-1829
http://ruschinc.com

Flow Cytometry Standards
P.O. Box 194344
San Juan, PR 00919
(800) 227-8143 FAX: (787) 758-3267
(787) 753-9341
http://www.fcstd.com

Flow Labs
See ICN Biomedicals

Flow-Tech Supply
P.O. Box 1388
Orange, TX 77631
(409) 882-0306 FAX: (409) 882-0254
http://www.flow-tech.com

Fluid Marketing
See Fluid Metering

Fluid Metering
5 Aerial Way, Suite 500
Sayosett, NY 11791
(516) 922-6050 FAX: (516) 624-8261
http://www.fmipump.com

Fluorochrome
1801 Williams, Suite 300
Denver, CO 80264
(303) 394-1000 FAX: (303) 321-1119

Fluka Chemical
See Sigma-Aldrich

FMC BioPolymer
1735 Market Street
Philadelphia, PA 19103
(215) 299-6000 FAX: (215) 299-5809
http://www.fmc.com

FMC BioProducts
191 Thomaston Street
Rockland, ME 04841
(800) 521-0390 FAX: (800) 362-1133
(207) 594-3400 FAX: (207) 594-3426
http://www.bioproducts.com

Forma Scientific
Milcreek Road
P.O. Box 649
Marietta, OH 45750
(800) 848-3080 FAX: (740) 372-6770
(740) 373-4765
http://www.forma.com

Fort Dodge Animal Health
800 5th Street NW
Fort Dodge, IA 50501
(800) 685-5656 FAX: (515) 955-9193
(515) 955-4600
http://www.ahp.com

Fotodyne
950 Walnut Ridge Drive
Hartland, WI 53029
(800) 362-3686 FAX: (800) 362-3642
(262) 369-7000 FAX: (262) 369-7013
http://www.fotodyne.com

Fresenius HemoCare
6675 185th Avenue NE, Suite 100
Redwood, WA 98052
(800) 909-3872
(425) 497-1197
http://www.freseniusht.com

Fresenius Hemotechnology
See Fresenius HemoCare

Fuji Medical Systems
419 West Avenue
P.O. Box 120035
Stamford, CT 06902
(800) 431-1850 FAX: (203) 353-0926
(203) 324-2000
http://www.fujimed.com

Fujisawa USA
Parkway Center North
Deerfield, IL 60015-2548
(847) 317-1088 FAX: (847) 317-7298

Ernest F. Fullam
900 Albany Shaker Road
Latham, NY 12110
(800) 833-4024 FAX: (518) 785-8647
(518) 785-5533
http://www.fullam.com

Gallard-Schlesinger Industries
777 Zechendorf Boulevard Garden
City, NY 11530
(516) 229-4000 FAX: (516) 229-4015
http://www.gallard-schlessinger.com

Gambro
Box 7373
SE 103 91 Stockholm, Sweden
(46) 8 613 65 00
FAX: (46) 8 611 37 31
In the US: COBE Laboratories
225 Union Boulevard
Lakewood, CO 80215
(303) 232-6800 FAX: (303) 231-4915
http://www.gambro.com

Garner Glass
177 Indian Hill Boulevard
Claremont, CA 91711
(909) 624-5071 FAX: (909) 625-0173
http://www.garnerglass.com

Garon Plastics
16 Byre Avenue
Somerton Park, South Australia 5044
(08) 8294-5126 FAX: (08) 8376-1487
http://www.apache.airnet.com.au/
~garon

Garren Scientific
9400 Lurline Avenue, Unit E
Chatsworth, CA 91311
(800) 342-3725 FAX: (818) 882-3229
(818) 882-6544
http://www.garren-scientific.com

GATC Biotech AG
Jakob-Stadler-Platz 7
D-78467 Constance, Germany
(49) 07531-8160-0
FAX: (49) 07531-8160-81
http://www.gatc-biotech.com

Gaussian
Carnegie Office Park
Building 6, Suite 230
Carnegie, PA 15106
(412) 279-6700 FAX: (412) 279-2118
http://www.gaussian.com

G.C. Electronics/A.R.C. Electronics
431 Second Street
Henderson, KY 42420
(270) 827-8981 FAX: (270) 827-8256
http://www.arcelectronics.com

GDB (Genome Data Base, Curation)
2024 East Monument Street,
Suite 1200
Baltimore, MD 21205
(410) 955-9705 FAX: (410) 614-0434
http://www.gdb.org

GDB (Genome Data Base, Home)
Hospital for Sick Children
555 University Avenue
Toronto, Ontario
M5G 1X8 Canada
(416) 813-8744 FAX: (416) 813-8755
http://www.gdb.org

Gelman Sciences
See Pall-Gelman

Gemini BioProducts
5115-M Douglas Fir Road
Calabasas, CA 90403
(818) 591-3530 FAX: (818) 591-7084

Gen Trak
5100 Campus Drive
Plymouth Meeting, PA 19462
(800) 221-7407 FAX: (215) 941-9498
(215) 825-5115
http://www.informagen.com

Genaissance Pharmaceuticals
5 Science Park
New Haven, CT 06511
(800) 678-9487 FAX: (203) 562-9377
(203) 773-1450
http://www.genaissance.com

GENAXIS Biotechnology
Parc Technologique
10 Avenue Ampère
Montigny le Bretoneux
78180 France
(33) 01-30-14-00-20
FAX: (33) 01-30-14-00-15
http://www.genaxis.com

GenBank
National Center for Biotechnology
Information
National Library of Medicine/NIH
Building 38A, Room 8N805
8600 Rockville Pike
Bethesda, MD 20894
(301) 496-2475 FAX: (301) 480-9241
http://www.ncbi.nlm.nih.gov

Gene Codes
640 Avis Drive
Ann Arbor, MI 48108
(800) 497-4939 FAX: (734) 930-0145
(734) 769-7249
http://www.genecodes.com

Genemachines
935 Washington Street
San Carlos, CA 94070
(650) 508-1634 FAX: (650) 508-1644
(877) 855-4363
http://www.genemachines.com

Genentech
1 DNA Way
South San Francisco, CA 94080
(800) 551-2231 FAX: (650) 225-1600
(650) 225-1000
http://www.gene.com

General Scanning/GSI Luminomics
500 Arsenal Street
Watertown, MA 02172
(617) 924-1010 FAX: (617) 924-7327
http://www.genescan.com

General Valve
Division of Parker Hannifin Pneutronics
19 Gloria Lane
Fairfield, NJ 07004
(800) GVC-VALV
FAX: (800) GVC-1-FAX
http://www.pneutronics.com

Genespan
19310 North Creek Parkway, Suite 100
Bothell, WA 98011
(800) 231-2215 FAX: (425) 482-3005
(425) 482-3003
http://www.genespan.com

Gene Therapy Systems
10190 Telesis Court
San Diego, CA 92122
(858) 457-1919 FAX: (858) 623-9494
http://www.genetherapysystems.com

Généthon Human Genome
Research Center
1 bis rue de l'Internationale
91000 Evry, France
(33) 169-472828
FAX: (33) 607-78698
http://www.genethon.fr

Genetic Microsystems
34 Commerce Way
Wobum, MA 01801
(781) 932-9333 FAX: (781) 932-9433
http://www.genticmicro.com

Genetic Mutant Repository
See Coriell Institute for Medical
Research

Genetic Research Instrumentation
Gene House
Queenborough Lane
Rayne, Braintree, Essex CM7 8TF, UK
(44) 1376 332900
FAX: (44) 1376 344724
http://www.gri.co.uk

Genetics Computer Group
575 Science Drive
Madison, WI 53711
(608) 231-5200 FAX: (608) 231-5202
http://www.gcg.com

Genetics Institute/American Home Products
87 Cambridge Park Drive
Cambridge, MA 02140
(617) 876-1170 FAX: (617) 876-0388
http://www.genetics.com

Genetix
63-69 Somerford Road
Christchurch, Dorset BH23 3QA, UK
(44) (0) 1202 483900
FAX: (44)(0) 1202 480289
In the US: (877) 436 3849
US FAX: (888) 522 7499
http://www.genetix.co.uk

Gene Tools
One Summerton Way
Philomath, OR 97370
(541) 9292-7840
FAX: (541) 9292-7841
http://www.gene-tools.com

GeneWorks
P.O. Box 11, Rundle Mall
Adelaide, South Australia 5000,
Australia
1800 882 555 FAX: (08) 8234 2699
(08) 8234 2644
http://www.geneworks.com

Genome Systems (INCYTE)
4633 World Parkway Circle
St. Louis, MO 63134
(800) 430-0030 FAX: (314) 427-3324
(314) 427-3222
http://www.genomesystems.com

Genomic Solutions
4355 Varsity Drive, Suite E
Ann Arbor, MI 48108
(877) GENOMIC
FAX: (734) 975-4808
(734) 975-4800
http://www.genomicsolutions.com

Genomyx
See Beckman Coulter

Genosys Biotechnologies
1442 Lake Front Circle, Suite 185
The Woodlands, TX 77380
(281) 363-3693 FAX: (281) 363-2212
http://www.genosys.com

Genotech
92 Weldon Parkway
St. Louis, MO 63043
(800) 628-7730 FAX: (314) 991-1504
(314) 991-6034

GENSET
876 Prospect Street, Suite 206
La Jolla, CA 92037
(800) 551-5291 FAX: (619) 551-2041
(619) 515-3061
http://www.genset.fr

Gensia Laboratories Ltd.
19 Hughes
Irvine, CA 92718
(714) 455-4700 FAX: (714) 855-8210

Genta
99 Hayden Avenue, Suite 200
Lexington, MA 02421
(781) 860-5150 FAX: (781) 860-5137
http://www.genta.com

GENTEST
6 Henshaw Street
Woburn, MA 01801
(800) 334-5229 FAX: (888) 242-2226
(781) 935-5115 FAX: (781) 932-6855
http://www.gentest.com

Gentra Systems
15200 25th Avenue N., Suite 104
Minneapolis, MN 55447
(800) 866-3039 FAX: (612) 476-5850
(612) 476-5858
http://www.gentra.com

Genzyme
1 Kendall Square
Cambridge, MA 02139
(617) 252-7500 FAX: (617) 252-7600
http://www.genzyme.com
See also R&D Systems

Genzyme Genetics
One Mountain Road
Framingham, MA 01701
(800) 255-7357 FAX: (508) 872-9080
(508) 872-8400
http://www.genzyme.com

George Tiemann & Co.
25 Plant Avenue
Hauppauge, NY 11788
(516) 273-0005 FAX: (516) 273-6199

GIBCO/BRL
A Division of Life Technologies
1 Kendall Square
Grand Island, NY 14072
(800) 874-4226 FAX: (800) 352-1968
(716) 774-6700
http://www.lifetech.com

Gilmont Instruments
A Division of Barnant Company
28N092 Commercial Avenue
Barrington, IL 60010
(800) 637-3739 FAX: (708) 381-7053
http://barnant.com

Gilson
3000 West Beltline Highway
P.O. Box 620027
Middletown, WI 53562
(800) 445-7661
(608) 836-1551
http://www.gilson.com

Glas-Col Apparatus
P.O. Box 2128
Terre Haute, IN 47802
(800) Glas-Col FAX: (812) 234-6975
(812) 235-6167
http://www.glascol.com

Glaxo Wellcome
Five Moore Drive
Research Triangle Park, NC 27709
(800) SGL-AXO5 FAX: (919)
248-2386
(919) 248-2100
http://www.glaxowellcome.com

Glen Mills
395 Allwood Road
Clifton, NJ 07012
(973) 777-0777 FAX: (973) 777-0070
http://www.glenmills.com

Glen Research
22825 Davis Drive
Sterling, VA 20166
(800) 327-4536 FAX: (800) 934-2490
(703) 437-6191 FAX: (703) 435-9774
http://www.glenresearch.com

Glo Germ
P.O. Box 189
Moab, UT 84532
(800) 842-6622 FAX: (435) 259-5930
http://www.glogerm.com

Glyco
11 Pimentel Court
Novato, CA 94949
(800) 722-2597 FAX: (415) 382-3511
(415) 884-6799
http://www.glyco.com

Gould Instrument Systems
8333 Rockside Road
Valley View, OH 44125
(216) 328-7000 FAX: (216) 328-7400
http://www.gould13.com

Gralab Instruments
See Dimco-Gray

GraphPad Software
5755 Oberlin Drive #110
San Diego, CA 92121
(800) 388-4723 FAX: (558) 457-8141
(558) 457-3909
http://www.graphpad.com

Graseby Anderson
See Andersen Instruments
http://www.graseby.com

Grass Instrument
A Division of Astro-Med
600 East Greenwich Avenue
W. Warwick, RI 02893
(800) 225-5167 FAX: (877) 472-7749
http://www.grassinstruments.com

Greenacre and Misac Instruments
Misac Systems
27 Port Wood Road
Ware, Hertfordshire SF12 9NJ, UK
(44) 1920 463017
FAX: (44) 1920 465136

Greer Labs
639 Nuway Circle
Lenois, NC 28645
(704) 754-5237
http://greerlabs.com

Greiner
Maybachestrasse 2
Postfach 1162
D-7443 Frickenhausen, Germany
(49) 0 91 31/80 79 0
FAX: (49) 0 91 31/80 79 30
http://www.erlangen.com/greiner

GSI Lumonics
130 Lombard Street Oxnard, CA 93030
(805) 485-5559 FAX: (805) 485-3310
http://www.gsilumonics.com

GTE Internetworking
150 Cambridge Park Drive
Cambridge, MA 02140
(800) 472-4565 FAX: (508) 694-4861
http://www.bbn.com

GW Instruments
35 Medford Street
Somerville, MA 02143
(617) 625-4096 FAX: (617) 625-1322
http://www.gwinst.com

H & H Woodworking
1002 Garfield Street
Denver, CO 80206
(303) 394-3764

Hacker Instruments
17 Sherwood Lane
P.O. Box 10033
Fairfield , NJ 07004
800-442-2537 FAX: (973) 808-8281
(973) 226-8450
http://www.hackerinstruments.com

Haemenetics
400 Wood Road
Braintree, MA 02184
(800) 225-5297 FAX: (781) 848-7921
(781) 848-7100
http://www.haemenetics.com

Halocarbon Products
P.O. Box 661
River Edge, NJ 07661
(201) 242-8899 FAX: (201) 262-0019
http://halocarbon.com

Hamamatsu Photonic Systems
A Division of Hamamatsu
360 Foothill Road
P.O. Box 6910
Bridgewater, NJ 08807
(908) 231-1116 FAX: (908) 231-0852
http://www.photonicsonline.com

Hamilton Company
4970 Energy Way
P.O. Box 10030
Reno, NV 89520
(800) 648-5950 FAX: (775) 856-7259
(775) 858-3000
http://www.hamiltoncompany.com

Hamilton Thorne Biosciences
100 Cummings Center, Suite 102C
Beverly, MA 01915
http://www.hamiltonthorne.com

Hampton Research
27631 El Lazo Road
Laguna Niguel, CA 92677
(800) 452-3899 FAX: (949) 425-1611
(949) 425-6321
http://www.hamptonresearch.com

Harlan Bioproducts for Science
P.O. Box 29176
Indianapolis, IN 46229
(317) 894-7521 FAX: (317) 894-1840
http://www.hbps.com

Harlan Sera-Lab
Hillcrest, Dodgeford Lane
Belton, Loughborough
Leicester LE12 9TE, UK
(44) 1530 222123
FAX: (44) 1530 224970
http://www.harlan.com

Harlan Teklad
P.O. Box 44220
Madison, WI 53744
(608) 277-2070 FAX: (608) 277-2066
http://www.harlan.com

Harrick Scientific Corporation
88 Broadway
Ossining, NY 10562
(914) 762-0020 FAX: (914) 762-0914
http://www.harricksci.com

Harrison Research
840 Moana Court
Palo Alto, CA 94306
(650) 949-1565 FAX: (650) 948-0493

Harvard Apparatus
84 October Hill Road
Holliston, MA 01746
(800) 272-2775 FAX: (508) 429-5732
(508) 893-8999
http://harvardapparatus.com

Harvard Bioscience
See Harvard Apparatus

Haselton Biologics
See JRH Biosciences

Hazelton Research Products
See Covance Research Products

Health Products
See Pierce Chemical

Heat Systems-Ultrasonics
1938 New Highway
Farmingdale, NY 11735
(800) 645-9846 FAX: (516) 694-9412
(516) 694-9555

Heidenhain Corp
333 East State Parkway
Schaumberg, IL 60173
(847) 490-1191 FAX: (847) 490-3931
http://www.heidenhain.com

Hellma Cells
11831 Queens Boulevard
Forest Hills, NY 11375
(718) 544-9166 FAX: (718) 263-6910
http://www.helmaUSA.com

Hellma
Postfach 1163
D-79371 Müllheim/Baden, Germany
(49) 7631-1820
FAX: (49) 7631-13546
http://www.hellma-worldwide.de

Henry Schein
135 Duryea Road, Mail Room 150
Melville, NY 11747
(800) 472-4346 FAX: (516) 843-5652
http://www.henryschein.com

Heraeus Kulzer
4315 South Lafayette Boulevard
South Bend, IN 46614
(800) 343-5336
(219) 291-0661
http://www.kulzer.com

Heraeus Sepatech
See Kendro Laboratory Products

Hercules Aqualon
Aqualon Division
Hercules Research Center, Bldg. 8145
500 Hercules Road
Wilmington, DE 19899
(800) 345-0447 FAX: (302) 995-4787
http://www.herc.com/aqualon/pharma

Heto-Holten A/S
Gydevang 17-19
DK-3450 Allerod, Denmark
(45) 48-16-62-00
FAX: (45) 48-16-62-97
Distributed by ATR

Hettich-Zentrifugen
See Andreas Hettich

Hewlett-Packard
3000 Hanover Street
Mailstop 20B3
Palo Alto, CA 94304
(650) 857-1501 FAX: (650) 857-5518
http://www.hp.com

HGS Hinimoto Plastics
1-10-24 Meguro-Honcho
Megurouko
Tokyo 152, Japan
3-3714-7226 FAX: 3-3714-4657

Hitachi Scientific Instruments
Nissei Sangyo America
8100 N. First Street
San Elsa, CA 95314
(800) 548-9001 FAX: (408) 432-0704
(408) 432-0520
http://www.hii.hitachi.com

Hi-Tech Scientific
Brunel Road
Salisbury, Wiltshire, SP2 7PU
UK
(44) 1722-432320
(800) 344-0724 (US only)
http://www.hi-techsci.co.uk

Hoechst AG
See Aventis Pharmaceutical

Hoefer Scientific Instruments
Division of Amersham-Pharmacia
Biotech
800 Centennial Avenue
Piscataway, NJ 08855
(800) 227-4750 FAX: (877) 295-8102
http://www.apbiotech.com

Hoffman-LaRoche
340 Kingsland Street
Nutley, NJ 07110
(800) 526-0189 FAX: (973) 235-9605
(973) 235-5000
http://www.rocheUSA.com

Holborn Surgical and Medical
Instruments
Westwood Industrial Estate
Ramsgate Road Margate, Kent CT9
4JZ UK
(44) 1843 296666
FAX: (44) 1843 295446

Honeywell
101 Columbia Road
Morristown, NJ 07962
(973) 455-2000 FAX: (973) 455-4807
http://www.honeywell.com

Honeywell Specialty Films
P.O. Box 1039
101 Columbia Road
Morristown, NJ 07962
(800) 934-5679 FAX: (973) 455-6045
http://www.honeywell-
specialtyfilms.com

Hood Thermo-Pad Canada
Comp. 20, Site 61A, RR2
Summerland, British Columbia
V0H 1Z0 Canada
(800) 665-9555 FAX: (250) 494-5003
(250) 494-5002
http://www.thermopad.com

Horiba Instruments
17671 Armstrong Avenue
Irvine, CA 92714
(949) 250-4811 FAX: (949) 250-0924
http://www.horiba.com

Hoskins Manufacturing
10776 Hall Road
P.O. Box 218
Hamburg, MI 48139
(810) 231-1900 FAX: (810) 231-4311
http://www.hoskinsmfgco.com

Hosokawa Micron Powder Systems
10 Chatham Road
Summit, NJ 07901
(800) 526-4491 FAX: (908) 273-7432
(908) 273-6360
http://www.hosokawamicron.com

HT Biotechnology
Unit 4
61 Ditton Walk
Cambridge CB5 8QD, UK
(44) 1223-412583

Hugo Sachs Electronik
Postfach 138
7806 March-Hugstetten, Germany
D-79229(49) 7665-92000
FAX: (49) 7665-920090

Human Biologics International
7150 East Camelback Road, Suite 245
Scottsdale, AZ 85251
(480) 990-2005 FAX: (480)-990-2155
http://www.humanbiological.com

Human Genetic Mutant Cell
Repository
See Coriell Institute for Medical
Research

HVS Image
P.O. Box 100
Hampton, Middlesex TW12 2YD, UK
FAX: (44) 208 783 1223
In the US: (800) 225-9261
FAX: (888) 483-8033
http://www.hvsimage.com

Hybaid
111-113 Waldegrave Road
Teddington, Middlesex TW11 8LL, UK
(44) 0 1784 42500
FAX: (44) 0 1784 248085
http://www.hybaid.co.uk

Hybaid Instruments
8 East Forge Parkway
Franklin, MA 02028
(888)4-HYBAID FAX: (508) 541-3041
(508) 541-6918
http://www.hybaid.com

Hybridon
155 Fortune Boulevard
Milford, MA 01757
(508) 482-7500 FAX: (508) 482-7510
http://www.hybridon.com

HyClone Laboratories
1725 South HyClone Road
Logan, UT 84321
(800) HYCLONE
FAX: (800) 533-9450
(801) 753-4584 FAX: (801) 750-0809
http://www.hyclone.com

Hyseq
670 Almanor Avenue
Sunnyvale, CA 94086
(408) 524-8100 FAX: (408) 524-8141
http://www.hyseq.com

IBA GmbH
1508 South Grand Blvd.
St. Louis, MO 63104
(877) 422-4624 FAX: (888) 531-6813
http://www.iba-go.com

IBF Biotechnics
See Sepracor

IBI (International Biotechnologies)
See Eastman Kodak
For technical service (800) 243-2555
(203) 786-5600

ICN Biochemicals
See ICN Biomedicals

ICN Biomedicals
3300 Hyland Avenue
Costa Mesa, CA 92626
(800) 854-0530 FAX: (800) 334-6999
(714) 545-0100 FAX: (714) 641-7275
http://www.icnbiomed.com

ICN Flow and Pharmaceuticals
See ICN Biomedicals

ICN Immunobiochemicals
See ICN Biomedicals

ICN Radiochemicals
See ICN Biomedicals

ICONIX
100 King Street West, Suite 3825
Toronto, Ontario
M5X 1E3 Canada
(416) 410-2411 FAX: (416) 368-3089
http://www.iconix.com

ICRT (Imperial Cancer Research Technology)
Sardinia House
Sardinia Street
London WC2A 3NL, UK
(44) 1712-421136
FAX: (44) 1718-314991

Idea Scientific Company
P.O. Box 13210
Minneapolis, MN 55414
(800) 433-2535 FAX: (612) 331-4217
http://www.ideascientific.com

IEC
See International Equipment Co.

IITC
23924 Victory Boulevard
Woodland Hills, CA 91367
(888) 414-4482 (818) 710-1556
FAX: (818) 992-5185
http://www.iitcinc.com

IKA Works
2635 N. Chase Parkway, SE
Wilmington, NC 28405
(910) 452-7059 FAX: (910) 452-7693
http://www.ika.net

Ikegami Electronics
37 Brook Avenue
Maywood, NJ 07607
(201) 368-9171 FAX: (201) 569-1626

Ikemoto Scientific Technology
25-11 Hongo
3-chome, Bunkyo-ku
Tokyo 101-0025, Japan
(81) 3-3811-4181
FAX: (81) 3-3811-1960

Imagenetics
See ATC Diagnostics

Imaging Research
c/o Brock University
500 Glenridge Avenue
St. Catharines, Ontario
L2S 3A1 Canada
(905) 688-2040 FAX: (905) 685-5861
http://www.imaging.brocku.ca

Imclone Systems
180 Varick Street
New York, NY 10014
(212) 645-1405 FAX: (212) 645-2054
http://www.imclone.com

IMCO Corporation LTD., AB
P.O. Box 21195
SE-100 31
Stockholm, Sweden
46-8-33-53-09 FAX: 46-8-728-47-76
http://www.imcocorp.se

Imgenex Corporation
11175 Flintkote Avenue
Suite E
San Diego, CA 92121
(888) 723-4363 FAX: (858) 642-0937
(858) 642.0978
http://www.imgenex.com

IMICO
Calle Vivero, No. 5-4a Planta
E-28040, Madrid, Spain
(34) 1-535-3960
FAX: (34) 1-535-2780

Immunex
51 University Street
Seattle, WA 98101
(206) 587-0430 FAX: (206) 587-0606
http://www.immunex.com

Immunocorp
1582 W. Deere Avenue
Suite C
Irvine, CA 92606
(800) 446-3063
http://www.immunocorp.com

Immunotech
130, av. Delattre de Tassigny
B.P. 177
13276 Marseilles Cedex 9
France
(33) 491-17-27-00
FAX: (33) 491-41-43-58
http://www.immunotech.fr

Imperial Chemical Industries
Imperial Chemical House
Millbank, London SW1P 3JF, UK
(44) 171-834-4444
FAX: (44)171-834-2042
http://www.ici.com

Inceltech
See New Brunswick Scientific

Incstar
See DiaSorin

Incyte
6519 Dumbarton Circle
Fremont, CA 94555
(510) 739-2100 FAX: (510) 739-2200
http://www.incyte.com

Incyte Pharmaceuticals
3160 Porter Drive
Palo Alto, CA 94304
(877) 746-2983 FAX: (650) 855-0572
(650) 855-0555
http://www.incyte.com

Individual Monitoring Systems
6310 Harford Road
Baltimore, MD 21214

Indo Fine Chemical
P.O. Box 473
Somerville, NJ 08876
(888) 463-6346 FAX: (908) 359-1179
(908) 359-6778
http://www.indofinechemical.com

Industrial Acoustics
1160 Commerce Avenue
Bronx, NY 10462
(718) 931-8000 FAX: (718) 863-1138
http://www.industrialacoustics.com

Inex Pharmaceuticals
100-8900 Glenlyon Parkway
Glenlyon Business Park
Burnaby, British Columbia
V5J 5J8 Canada
(604) 419-3200 FAX: (604) 419-3201
http://www.inexpharm.com

Ingold, Mettler, Toledo
261 Ballardvale Street
Wilmington, MA 01887
(800) 352-8763 FAX: (978) 658-0020
(978) 658-7615
http://www.mt.com

Innogenetics N.V.
Technologie Park 6
B-9052 Zwijnaarde
Belgium
(32) 9-329-1329
FAX: (32) 9-245-7623
http://www.innogenetics.com

Innovative Medical Services
1725 Gillespie Way
El Cajon, CA 92020
(619) 596-8600 FAX: (619) 596-8700
http://www.imspure.com

Innovative Research
3025 Harbor Lane N, Suite 300
Plymouth, MN 55447
(612) 519-0105 FAX: (612) 519-0239
http://www.inres.com

Innovative Research of America
2 N. Tamiami Trail, Suite 404
Sarasota, FL 34236
(800) 421-8171 FAX: (800) 643-4345
(941) 365-1406 FAX: (941) 365-1703
http://www.innovrsrch.com

Inotech Biosystems
15713 Crabbs Branch Way, #110
Rockville, MD 20855
(800) 635-4070 FAX: (301) 670-2859
(301) 670-2850
http://www.inotechintl.com

INOVISION
22699 Old Canal Road
Yorba Linda, CA 92887
(714) 998-9600 FAX: (714) 998-9666
http://www.inovision.com

Instech Laboratories
5209 Militia Hill Road
Plymouth Meeting, PA 19462
(800) 443-4227 FAX: (610) 941-0134
(610) 941-0132
http://www.instechlabs.com

Instron
100 Royall Street
Canton, MA 02021
(800) 564-8378 FAX: (781) 575-5725
(781) 575-5000
http://www.instron.com

Instrumentarium
P.O. Box 300
00031 Instrumentarium
Helsinki, Finland
(10) 394-5566
http://www.instrumentarium.fi

Instruments SA
Division Jobin Yvon
16-18 Rue du Canal
91165 Longjumeau, Cedex, France
(33)1 6454-1300
FAX: (33)1 6909-9319
http://www.isainc.com

Instrutech
20 Vanderventer Avenue, Suite 101E
Port Washington, NY 11050
(516) 883-1300 FAX: (516) 883-1558
http://www.instrutech.com

Integrated DNA Technologies
1710 Commercial Park
Coralville, IA 52241
(800) 328-2661 FAX: (319) 626-8444
http://www.idtdna.com

Integrated Genetics
See Genzyme Genetics

Integrated Scientific Imaging Systems
3463 State Street, Suite 431
Santa Barbara, CA 93105
(805) 692-2390 FAX: (805) 692-2391
http://www.imagingsystems.com

Integrated Separation Systems (ISS)
See OWL Separation Systems

IntelliGenetics
See Oxford Molecular Group

Interactiva BioTechnologie
Sedanstrasse 10
D-89077 Ulm, Germany
(49) 731-93579-290
FAX: (49) 731-93579-291
http://www.interactiva.de

Interchim
213 J.F. Kennedy Avenue
B.P. 1140
Montlucon
03103 France
(33) 04-70-03-83-55
FAX: (33) 04-70-03-93-60

Interfocus
14/15 Spring Rise
Falcover Road
Haverhill, Suffolk CB9 7XU, UK
(44) 1440 703460
FAX: (44) 1440 704397
http://www.interfocus.ltd.uk

Intergen
2 Manhattanville Road
Purchase, NY 10577
(800) 431-4505 FAX: (800) 468-7436
(914) 694-1700 FAX: (914) 694-1429
http://www.intergenco.com

Intermountain Scientific
420 N. Keys Drive
Kaysville, UT 84037
(800) 999-2901 FAX: (800) 574-7892
(801) 547-5047 FAX: (801) 547-5051
http://www.bioexpress.com

International Biotechnologies (IBI)
See Eastman Kodak

International Equipment Co. (IEC)
See Thermoquest

International Institute for the
Advancement of Medicine
1232 Mid-Valley Drive
Jessup, PA 18434
(800) 486-IIAM FAX: (570) 343-6993
(570) 496-3400
http://www.iiam.org

International Light
17 Graf Road
Newburyport, MA 01950
(978) 465-5923 FAX: (978) 462-0759

International Market Supply (I.M.S.)
Dane Mill
Broadhurst Lane
Congleton, Cheshire CW12 1LA, UK
(44) 1260 275469
FAX: (44) 1260 276007

International Marketing Services
See International Marketing Ventures

International Marketing Ventures
6301 Ivy Lane, Suite 408
Greenbelt, MD 20770
(800) 373-0096 FAX: (301) 345-0631
(301) 345-2866
http://www.imvlimited.com

International Products
201 Connecticut Drive
Burlington, NJ 08016
(609) 386-8770 FAX: (609) 386-8438
http://www.mkt.ipcol.com

Intracel Corporation
Bartels Division
2005 Sammamish Road, Suite 107
Issaquah, WA 98027
(800) 542-2281 FAX: (425) 557-1894
(425) 392-2992
http://www.intracel.com

Invitrogen
1600 Faraday Avenue
Carlsbad, CA 92008
(800) 955-6288 FAX: (760) 603-7201
(760) 603-7200
http://www.invitrogen.com

In Vitro Technologies
1450 South Rolling Road
Baltimore, Maryland 21227
(888) 488-3232 FAX: (443) 836-0340
(410) 455-1242
http://www.invitrotech.com/index.cfm

In Vivo Metric
P.O. Box 249
Healdsburg, CA 95448
(707) 433-4819 FAX: (707) 433-2407

IRORI
9640 Towne Center Drive
San Diego, CA 92121
(858) 546-1300 FAX: (858) 546-3083
http://www.irori.com

Irvine Scientific
2511 Daimler Street
Santa Ana, CA 92705
(800) 577-6097 FAX: (949) 261-6522
(949) 261-7800
http://www.irvinesci.com

ISC BioExpress
420 North Kays Drive
Kaysville, UT 84037
(800) 999-2901 FAX: (800) 574-7892
(801) 547-5047
http://www.bioexpress.com

ISCO
P.O. Box 5347
4700 Superior
Lincoln, NE 68505
(800) 228-4373 FAX: (402) 464-0318
(402) 464-0231
http://www.isco.com

Isis Pharmaceuticals
Carlsbad Research Center
2292 Faraday Avenue
Carlsbad, CA 92008
(760) 931-9200
http://www.isip.com

Isolabs
See Wallac

ISS
See Integrated Separation Systems

J & W Scientific
See Agilent Technologies

J.A. Webster
86 Leominster Road
Sterling , MA 01564
(800) 225-7911 FAX: (978) 422-8959
http://www.jawebster.com

J.T. Baker
See Mallinckrodt Baker
222 Red School Lane
Phillipsburg, NJ 08865
(800) JTBAKER FAX: (908) 859-6974
http://www.jtbaker.com

Jackson ImmunoResearch
Laboratories
P.O. Box 9
872 W. Baltimore Pike
West Grove, PA 19390
(800) 367-5296 FAX: (610) 869-0171
(610) 869-4024
http://www.jacksonimmuno.com

The Jackson Laboratory
600 Maine Street
Bar Harbor, ME 04059
(800) 422-6423 FAX: (207) 288-5079
(207) 288-6000
http://www.jax.org

Jaece Industries
908 Niagara Falls Boulevard
North Tonawanda, NY 14120
(716) 694-2811 FAX: (716) 694-2811
http://www.jaece.com

Jandel Scientific
See SPSS

Janke & Kunkel
See Ika Works

Janssen Life Sciences Products
See Amersham

Janssen Pharmaceutica
1125 Trenton-Harbourton Road
Titusville, NJ 09560
(609) 730-2577 FAX: (609) 730-2116
http://us.janssen.com

Jasco
8649 Commerce Drive
Easton, MD 21601
(800) 333-5272 FAX: (410) 822-7526
(410) 822-1220
http://www.jascoinc.com

Jena Bioscience
Loebstedter Str. 78
07749 Jena, Germany
(49) 3641-464920
FAX: (49) 3641-464991
http://www.jenabioscience.com

Jencons Scientific
800 Bursca Drive, Suite 801
Bridgeville, PA 15017
(800) 846-9959 FAX: (412) 257-8809
(412) 257-8861
http://www.jencons.co.uk

JEOL Instruments
11 Dearborn Road
Peabody, MA 01960
(978) 535-5900 FAX: (978) 536-2205
http://www.jeol.com/index.html

Jewett
750 Grant Street
Buffalo, NY 14213
(800) 879-7767 FAX: (716) 881-6092
(716) 881-0030
http://www.JewettInc.com

John's Scientific
See VWR Scientific

John Weiss and Sons
95 Alston Drive
Bradwell Abbey
Milton Keynes, Buckinghamshire
MK1 4HF UK
(44) 1908-318017
FAX: (44) 1908-318708

Johnson & Johnson Medical
2500 Arbrook Boulevard East
Arlington, TX 76004
(800) 423-4018
http://www.jnjmedical.com

Johnston Matthey Chemicals
Orchard Road
Royston, Hertfordshire SG8 5HE, UK
(44) 1763-253000
FAX: (44) 1763-253466
http://www.chemicals.matthey.com

Jolley Consulting and Research
683 E. Center Street, Unit H
Grayslake, IL 60030
(847) 548-2330 FAX: (847) 548-2984
http://www.jolley.com

Jordan Scientific
See Shelton Scientific

Jorgensen Laboratories
1450 N. Van Buren Avenue
Loveland, CO 80538
(800) 525-5614 FAX: (970) 663-5042
(970) 669-2500
http://www.jorvet.com

JRH Biosciences and
JR Scientific
13804 W. 107th Street
Lenexa, KS 66215
(800) 231-3735 FAX: (913) 469-5584
(913) 469-5580

Jule Bio Technologies
25 Science Park, #14, Suite 695
New Haven, CT 06511
(800) 648-1772 FAX: (203) 786-5489
(203) 786-5490
http://hometown.aol.com/precastgel/index.htm

K.R. Anderson
2800 Bowers Avenue
Santa Clara, CA 95051
(800) 538-8712 FAX: (408) 727-2959
(408) 727-2800
http://www.kranderson.com

Kabi Pharmacia Diagnostics
See Pharmacia Diagnostics

Kanthal H.P. Reid
1 Commerce Boulevard
P.O. Box 352440
Palm Coast, FL 32135
(904) 445-2000 FAX: (904) 446-2244
http://www.kanthal.com

Kapak
5305 Parkdale Drive
St. Louis Park, MN 55416
(800) KAPAK-57
FAX: (612) 541-0735
(612) 541-0730
http://www.kapak.com

Karl Hecht
Stettener Str. 22-24
D-97647 Sondheim
Rhön, Germany
(49) 9779-8080
FAX: (49) 9779-80888

Karl Storz
Köningin-Elisabeth Str. 60
D-14059 Berlin, Germany
(49) 30-30 69 09-0
FAX: (49) 30-30 19 452
http://www.karlstorz.de

KaVo EWL
P.O. Box 1320
D-88293 Leutkirch im Allgäu, Germany
(49) 7561-86-0
FAX: (49) 7561-86-371
http://www.kavo.com/english/startseite.htm

Keithley Instruments
28775 Aurora Road
Cleveland, OH 44139
(800) 552-1115 FAX: (440) 248-6168
(440) 248-0400
http://www.keithley.com

Kemin
2100 Maury Street, Box 70
Des Moines, IA 50301
(515) 266-2111 FAX: (515) 266-8354
http://www.kemin.com

Kemo
3 Brook Court, Blakeney Road
Beckenham, Kent BR3 1HG, UK
(44) 0181 658 3838
FAX: (44) 0181 658 4084
http://www.kemo.com

Kendall
15 Hampshire Street
Mansfield, MA 02048
(800) 962-9888 FAX: (800) 724-1324
http://www.kendallhq.com

Kendro Laboratory Products
31 Pecks Lane
Newtown, CT 06470
(800) 522-SPIN FAX: (203) 270-2166
(203) 270-2080
http://www.kendro.com

Kendro Laboratory Products
P.O. Box 1220
Am Kalkberg
D-3360 Osterod, Germany
(55) 22-316-213
FAX: (55) 22-316-202
http://www.heraeus-instruments.de

Kent Laboratories
23404 NE 8th Street
Redmond, WA 98053
(425) 868-6200 FAX: (425) 868-6335
http://www.kentlabs.com

Kent Scientific
457 Bantam Road, #16
Litchfield, CT 06759
(888) 572-8887 FAX: (860) 567-4201
(860) 567-5496
http://www.kentscientific.com

Keuffel & Esser
See Azon

Keystone Scientific
Penn Eagle Industrial Park 320 Rolling Ridge Drive
Bellefonte, PA 16823
(800) 437-2999 FAX: (814) 353-2305
(814) 353-2300 Ext 1
http://www.keystonescientific.com

Kimble/Kontes Biotechnology
1022 Spruce Street
P.O. Box 729
Vineland, NJ 08360
(888) 546-2531 FAX: (856) 794-9762
(856) 692-3600
http://www.kimble-kontes.com

Kinematica AG
Luzernerstrasse 147a
CH-6014 Littau-Luzern, Switzerland
(41) 41 2501257
FAX: (41) 41 2501460
http://www.kinematica.ch

Kin-Tek
504 Laurel Street
LaMarque, TX 77568
(800) 326-3627
FAX: (409) 938-3710
http://www.kin-tek.com

Kipp & Zonen
125 Wilbur Place
Bohemia, NY 11716
(800) 645-2065 FAX: (516) 589-2068
(516) 589-2885
http://www.kippzonen.thomasregister.com/olc/kippzonen

Kirkegaard & Perry Laboratories
2 Cessna Court
Gaithersburg, MD 20879
(800) 638-3167 FAX: (301) 948-0169
(301) 948-7755
http://www.kpl.com

Kodak
See Eastman Kodak

Kontes Glass
See Kimble/Kontes Biotechnology

Kontron Instruments AG
Postfach CH-8010
Zurich, Switzerland
41-1-733-5733 FAX: 41-1-733-5734

David Kopf Instruments
P.O. Box 636
Tujunga, CA 91043
(818) 352-3274 FAX: (818) 352-3139

Kraft Apparatus
See Glas-Col Apparatus

Kramer Scientific Corporation
711 Executive Boulevard
Valley Cottage, NY 10989
(845) 267-5050 FAX: (845) 267-5550

Kulite Semiconductor Products
1 Willow Tree Road
Leonia, NJ 07605
(201) 461-0900 FAX: (201) 461-0990
http://www.kulite.com

Lab-Line Instruments
15th & Bloomingdale Avenues
Melrose Park, IL 60160
(800) LAB-LINE FAX: (708) 450-5830
FAX: (800) 450-4LAB
http://www.labline.com

Lab Products
742 Sussex Avenue
P.O. Box 639
Seaford, DE 19973
(800) 526-0469 FAX: (302) 628-4309
(302) 628-4300
http://www.labproductsinc.com

LabRepco
101 Witmer Road, Suite 700
Horsham, PA 19044
(800) 521-0754 FAX: (215) 442-9202
http://www.labrepco.com

Lab Safety Supply
P.O. Box 1368
Janesville, WI 53547
(800) 356-0783 FAX: (800) 543-9910
(608) 754-7160 FAX: (608) 754-1806
http://www.labsafety.com

Lab-Tek Products
See Nalge Nunc International

Labconco
8811 Prospect Avenue
Kansas City, MO 64132
(800) 821-5525 FAX: (816) 363-0130
(816) 333-8811
http://www.labconco.com

Labindustries
See Barnstead/Thermolyne

Labnet International
P.O. Box 841
Woodbridge, NJ 07095
(888) LAB-NET1
FAX: (732) 417-1750
(732) 417-0700
http://www.nationallabnet.com

LABO-MODERNE
37 rue Dombasle
Paris
75015 France
(33) 01-45-32-62-54
FAX: (33) 01-45-32-01-09
http://www.labomoderne.com/fr

Laboratory of Immunoregulation
National Institute of Allergy and Infectious Diseases/NIH
9000 Rockville Pike
Building 10, Room 11B13
Bethesda, MD 20892
(301) 496-1124

Laboratory Supplies
29 Jefry Lane
Hicksville, NY 11801
(516) 681-7711

Labscan Limited
Stillorgan Industrial Park
Stillorgan
Dublin, Ireland
(353) 1-295-2684
FAX: (353) 1-295-2685
http://www.labscan.ie

Labsystems
See Thermo Labsystems

Labsystems Affinity Sensors
Saxon Way, Bar Hill
Cambridge CB3 8SL, UK
44 (0) 1954 789976
FAX: 44 (0) 1954 789417
http://www.affinity-sensors.com

Labtronics
546 Governors Road
Guelph, Ontario
N1K 1E3, Canada
(519) 763-4930 FAX: (519) 836-4431
http://www.labtronics.com

Labtronix Manufacturing
3200 Investment Boulevard
Hayward, CA 94545
(510) 786-3200 FAX: (510) 786-3268
http://www.labtronix.com

Lafayette Instrument
3700 Sagamore Parkway North
P.O. Box 5729
Lafayette, IN 47903
(800) 428-7545 FAX: (765) 423-4111
(765) 423-1505
http://www.lafayetteinstrument.com

Lambert Instruments
Turfweg 4
9313 TH Leutingewolde
The Netherlands
(31) 50-5018461
FAX: (31) 50-5010034
http://www.lambert-instruments.com

Lancaster Synthesis
P.O. Box 1000
Windham, NH 03087
(800) 238-2324 FAX: (603) 889-3326
(603) 889-3306
http://www.lancastersynthesis-us.com

Lancer
140 State Road 419
Winter Springs, FL 32708
(800) 332-1855 FAX: (407) 327-1229
(407) 327-8488
http://www.lancer.com

LaVision GmbH
Gerhard-Gerdes-Str. 3
D-37079
Goettingen, Germany
(49) 551-50549-0
FAX: (49) 551-50549-11
http://www.lavision.de

Lawshe
See Advanced Process Supply

Laxotan
20, rue Leon Blum
26000 Valence, France
(33) 4-75-41-91-91
FAX: (33) 4-75-41-91-99
http://www.latoxan.com

LC Laboratories
165 New Boston Street
Woburn, MA 01801
(781) 937-0777 FAX: (781) 938-5420
http://www.lclaboratories.com

LC Packings
80 Carolina Street
San Francisco, CA 94103
(415) 552-1855 FAX: (415) 552-1859
http://www.lcpackings.com

LC Services
See LC Laboratories

LECO
3000 Lakeview Avenue
St. Joseph, MI 49085
(800) 292-6141 FAX: (616) 982-8977
(616) 985-5496
http://www.leco.com

Lederle Laboratories
See Wyeth-Ayerst

Lee Biomolecular Research
Laboratories
11211 Sorrento Valley Road, Suite M
San Diego, CA 92121
(858) 452-7700

The Lee Company
2 Pettipaug Road
P.O. Box 424
Westbrook, CT 06498
(800) LEE-PLUG
FAX: (860) 399-7058
(860) 399-6281
http://www.theleeco.com

Lee Laboratories
1475 Athens Highway
Grayson, GA 30017
(800) 732-9150 FAX: (770) 979-9570
(770) 972-4450
http://www.leelabs.com

Leica
111 Deer Lake Road
Deerfield, IL 60015
(800) 248-0123 FAX: (847) 405-0147
(847) 405-0123
http://www.leica.com

Leica Microsystems
Imneuenheimer Feld 518
D-69120
Heidelberg, Germany
(49) 6221-41480
FAX: (49) 6221-414833
http://www.leica-microsystems.com

Leinco Technologies
359 Consort Drive
St. Louis, MO 63011
(314) 230-9477 FAX: (314) 527-5545
http://www.leinco.com

Leitz U.S.A.
See Leica

LenderKing Metal Products
8370 Jumpers Hole Road
Millersville, MD 21108
(410) 544-8795 FAX: (410) 544-5069
http://www.lenderking.com

Letica Scientific Instruments
Panlab s.i., c/Loreto 50
08029 Barcelona, Spain
(34) 93-419-0709
FAX: (34) 93-419-7145
http://www.panlab-sl.com

Leybold-Heraeus Trivac DZA
5700 Mellon Road
Export, PA 15632
(412) 327-5700

LI-COR
Biotechnology Division
4308 Progressive Avenue
Lincoln, NE 68504
(800) 645-4267 FAX: (402) 467-0819
(402) 467-0700
http://www.licor.com

Life Science Laboratories
See Adaptive Biosystems

Life Science Resources
Two Corporate Center Drive
Melville, NY 11747
(800) 747-9530 FAX: (516) 844-5114
(516) 844-5085
http://www.astrocam.com

Life Sciences
2900 72nd Street North
St. Petersburg, FL 33710
(800) 237-4323 FAX: (727) 347-2957
(727) 345-9371
http://www.lifesci.com

Life Technologies
9800 Medical Center Drive
P.O. Box 6482
Rockville, MD 20849
(800) 828-6686 FAX: (800) 331-2286
http://www.lifetech.com

Lifecodes
550 West Avenue
Stamford, CT 06902
(800) 543-3263 FAX: (203) 328-9599
(203) 328-9500
http://www.lifecodes.com

Lightnin
135 Mt. Read Boulevard
Rochester, NY 14611
(888) MIX-BEST
FAX: (716) 527-1742
(716) 436-5550
http://www.lightnin-mixers.com

Linear Drives
Luckyn Lane, Pipps Hill
Basildon, Essex SS14 3BW, UK
(44) 1268-287070
FAX: (44) 1268-293344
http://www.lineardrives.com

Linscott's Directory
4877 Grange Road
Santa Rosa, CA 95404
(707) 544-9555 FAX: (415) 389-6025
http://www.linscottsdirectory.co.uk

Linton Instrumentation
Unit 11, Forge Business Center
Upper Rose Lane
Palgrave, Diss, Norfolk IP22 1AP, UK
(44) 1-379-651-344
FAX: (44) 1-379-650-970
http://www.lintoninst.co.uk

List Biological Laboratories
501-B Vandell Way
Campbell, CA 95008
(800) 726-3213 FAX: (408) 866-6364
(408) 866-6363
http://www.listlabs.com

LKB Instruments
See Amersham Pharmacia Biotech

Lloyd Laboratories
604 West Thomas Avenue
Shenandoah, IA 51601
(800) 831-0004 FAX: (712) 246-5245
(712) 246-4000
http://www.lloydinc.com

Loctite
1001 Trout Brook Crossing
Rocky Hill, CT 06067
(860) 571-5100 FAX: (860) 571-5465
http://www.loctite.com

Lofstrand Labs
7961 Cessna Avenue
Gaithersburg, MD 20879
(800) 541-0362 FAX: (301) 948-9214
(301) 330-0111
http://www.lofstrand.com

Lomir Biochemical
99 East Main Street
Malone, NY 12953
(877) 425-3604 FAX: (518) 483-8195
(518) 483-7697
http://www.lomir.com

LSL Biolafitte
10 rue de Temara
7810C St.-Germain-en-Laye, France
(33) 1-3061-5260
FAX: (33) 1-3061-5234

Ludl Electronic Products
171 Brady Avenue
Hawthorne, NY 10532
(888) 769-6111 FAX: (914) 769-4759
(914) 769-6111
http://www.ludl.com

Lumigen
24485 W. Ten Mile Road
Southfield, MI 48034
(248) 351-5600 FAX: (248) 351-0518
http://www.lumigen.com

Luminex
12212 Technology Boulevard
Austin, TX 78727
(888) 219-8020 FAX: (512) 258-4173
(512) 219-8020
http://www.luminexcorp.com

LYNX Therapeutics
25861 Industrial Boulevard
Hayward, CA 94545
(510) 670-9300 FAX: (510) 670-9302
http://www.lynxgen.com

Lyphomed
3 Parkway North
Deerfield, IL 60015
(847) 317-8100 FAX: (847) 317-8600

M.E.D. Associates
See Med Associates

Mabtech
Mariemont Executive Building
Suite 112
3814 West Street
Mariemont, Ohio 45227
(866) ELISPOT FAX: (513) 821-7353
(513) 821-4500
http://www.mabtech.com

Macherey-Nagel
6 South Third Street, #402
Easton, PA 18042
(610) 559-9848 FAX: (610) 559-9878
http://www.macherey-nagel.com

Macherey-Nagel
Valencienner Strasse 11
P.O. Box 101352
D-52313 Dueren, Germany
(49) 2421-969141
FAX: (49) 2421-969199
http://www.macherey-nagel.ch

Mac-Mod Analytical
127 Commons Court
Chadds Ford, PA 19317
800-441-7508 FAX: (610) 358-5993
(610) 358-9696
http://www.mac-mod.com

Mallinckrodt Baker
222 Red School Lane
Phillipsburg, NJ 08865
(800) 582-2537 FAX: (908) 859-6974
(908) 859-2151
http://www.mallbaker.com

Mallinckrodt Chemicals
16305 Swingley Ridge Drive
Chesterfield, MD 63017
(314) 530-2172 FAX: (314) 530-2563
http://www.mallchem.com

Malven Instruments
Enigma Business Park
Grovewood Road
Malven, Worchestershire
WR 141 XZ, United Kingdom

Marinus
1500 Pier C Street
Long Beach, CA 90813
(562) 435-6522 FAX: (562) 495-3120

Markson Science
c/o Whatman Labs Sales
P.O. Box 1359
Hillsboro, OR 97123
(800) 942-8626 FAX: (503) 640-9716
(503) 648-0762

Marsh Biomedical Products
565 Blossom Road
Rochester, NY 14610
(800) 445-2812 FAX: (716) 654-4810
(716) 654-4800
http://www.biomar.com

Marshall Farms USA
5800 Lake Bluff Road
North Rose, NY 14516
(315) 587-2295
e-mail:info@marfarms.com

Martek
6480 Dobbin Road
Columbia, MD 21045
(410) 740-0081 FAX: (410) 740-2985
http://www.martekbio.com

Martin Supply
Distributor of Gerber Scientific
2740 Loch Raven Road
Baltimore, MD 21218
(800) 282-5440 FAX: (410) 366-0134
(410) 366-1696

Mast Immunosystems
630 Clyde Court
Mountain View, CA 94043
(800) 233-MAST
FAX: (650) 969-2745
(650) 961-5501
http://www.mastallergy.com

Matheson Gas Products
P.O. Box 624
959 Route 46 East
Parsippany, NJ 07054
(800) 416-2505 FAX: (973) 257-9393
(973) 257-1100
http://www.mathesongas.com

Mathsoft
1700 Westlake Avenue N., Suite 500
Seattle, WA 98109
(800) 569-0123 FAX: (206) 283-8691
(206) 283-8802
http://www.mathsoft.com

Matreya
500 Tressler Street
Pleasant Gap, PA 16823
(814) 359-5060 FAX: (814) 359-5062
http://www.matreya.com

Matrigel
See Becton Dickinson Labware

Matrix Technologies
22 Friars Drive
Hudson, NH 03051
(800) 345-0206 FAX: (603) 595-0106
(603) 595-0505
http://www.matrixtechcorp.com

MatTek Corp.
200 Homer Avenue
Ashland, Massachusetts 01721
(508) 881-6771 FAX: (508) 879-1532
http://www.mattek.com

Maxim Medical
89 Oxford Road
Oxford OX2 9PD
United Kingdom
44 (0)1865-865943
FAX: 44 (0)1865-865291
http://www.maximmed.com

Mayo Clinic
Section on Engineering
Project #ALA-1, 1982
200 1st Street SW
Rochester, MN 55905
(507) 284-2511 FAX: (507) 284-5988

McGaw
See B. Braun-McGaw

McMaster-Carr
600 County Line Road
Elmhurst, IL 60126
(630) 833-0300 FAX: (630) 834-9427
http://www.mcmaster.com

McNeil Pharmaceutical
See Ortho McNeil Pharmaceutical

MCNC
3021 Cornwallis Road
P.O. Box 12889
Research Triangle Park, NC 27709
(919) 248-1800 FAX: (919) 248-1455
http://www.mcnc.org

MD Industries
5 Revere Drive, Suite 415
Northbrook, IL 60062
(800) 421-8370 FAX: (847) 498-2627
(708) 339-6000
http://www.mdindustries.com

MDS Nordion
447 March Road
P.O. Box 13500
Kanata, Ontario
K2K 1X8, Canada
(800) 465-3666 FAX: (613) 592-6937
(613) 592-2790
http://www.mds.nordion.com

MDS Sciex
71 Four Valley Drive
Concord, Ontario
Canada L4K 4V8
(905) 660-9005 FAX: (905) 660-2600
http://www.sciex.com

Mead Johnson
See Bristol-Meyers Squibb

Med Associates
P.O. Box 319
St. Albans, VT 05478
(802) 527-2343 FAX: (802) 527-5095
http://www.med-associates.com

Medecell
239 Liverpool Road
London N1 1LX, UK
(44) 20-7607-2295
FAX: (44) 20-7700-4156
http://www.medicell.co.uk

Media Cybernetics
8484 Georgia Avenue, Suite 200
Silver Spring, MD 20910
(301) 495-3305 FAX: (301) 495-5964
http://www.mediacy.com

Mediatech
13884 Park Center Road
Herndon, VA 20171
(800) cellgro
(703) 471-5955
http://www.cellgro.com

Medical Systems
See Harvard Apparatus

Medifor
647 Washington Street
Port Townsend, WA 98368
(800) 366-3710 FAX: (360) 385-4402
(360) 385-0722
http://www.medifor.com

MedImmune
35 W. Watkins Mill Road
Gaithersburg, MD 20878
(301) 417-0770 FAX: (301) 527-4207
http://www.medimmune.com

MedProbe AS
P.O. Box 2640
St. Hanshaugen
N-0131 Oslo, Norway
(47) 222 00137 FAX: (47) 222 00189
http://www.medprobe.com

Megazyme
Bray Business Park
Bray, County Wicklow
Ireland
(353) 1-286-1220
FAX: (353) 1-286-1264
http://www.megazyme.com

Melles Griot
4601 Nautilus Court South
Boulder, CO 80301
(800) 326-4363 FAX: (303) 581-0960
(303) 581-0337
http://www.mellesgriot.com

Menzel-Glaser
Postfach 3157
D-38021 Braunschweig, Germany
(49) 531 590080
FAX: (49) 531 509799

E. Merck
Frankfurterstrasse 250
D-64293 Darmstadt 1, Germany
(49) 6151-720

Merck
See EM Science

Merck & Company
Merck National Service Center
P.O. Box 4
West Point, PA 19486
(800) NSC-MERCK
(215) 652-5000
http://www.merck.com

Merck Research Laboratories
See Merck & Company

Merck Sharpe Human Health Division
300 Franklin Square Drive
Somerset, NJ 08873
(800) 637-2579 FAX: (732) 805-3960
(732) 805-0300

Merial Limited
115 Transtech Drive
Athens, GA 30601
(800) MERIAL-1 FAX: (706) 548-0608
(706) 548-9292
http://www.merial.com

Meridian Instruments
P.O. Box 1204
Kent, WA 98035
(253) 854-9914 FAX: (253) 854-9902
http://www.minstrument.com

Meta Systems Group
32 Hammond Road
Belmont, MA 02178
(617) 489-9950 FAX: (617) 489-9952

Metachem Technologies
3547 Voyager Street, Bldg. 102
Torrance, CA 90503
(310) 793-2300 FAX: (310) 793-2304
http://www.metachem.com

Metallhantering
Box 47172
100-74 Stockholm, Sweden
(46) 8-726-9696

MethylGene
7220 Frederick-Banting, Suite 200
Montreal, Quebec
H4S 2A1, Canada
http://www.methylgene.com

Metro Scientific
475 Main Street, Suite 2A
Farmingdale, NY 11735
(800) 788-6247 FAX: (516) 293-8549
(516) 293-9656

Metrowerks
980 Metric Boulevard
Austin, TX 78758
(800) 377-5416
(512) 997-4700
http://www.metrowerks.com

Mettler Instruments
Mettler-Toledo
1900 Polaris Parkway
Columbus, OH 43240
(800) METTLER
FAX: (614) 438-4900
http://www.mt.com

Miami Serpentarium Labs
34879 Washington Loop Road
Punta Gorda, FL 33982
(800) 248-5050 FAX: (813) 639-1811
(813) 639-8888
http://www.miamiserpentarium.com

Michrom BioResources
1945 Industrial Drive
Auburn, CA 95603
(530) 888-6498 FAX: (530) 888-8295
http://www.michrom.com

Mickle Laboratory Engineering
Gomshall, Surrey, UK
(44) 1483-202178

Micra Scientific
A division of Eichrom Industries
8205 S. Cass Ave, Suite 111
Darien, IL 60561
(800) 283-4752 FAX: (630) 963-1928
(630) 963-0320
http://www.micrasci.com

MicroBrightField
74 Hegman Avenue
Colchester, VT 05446
(802) 655-9360 FAX: (802) 655-5245
http://www.microbrightfield.com

Micro Essential Laboratory
4224 Avenue H
Brooklyn, NY 11210
(718) 338-3618 FAX: (718) 692-4491

Micro Filtration Systems
7-3-Chome, Honcho
Nihonbashi, Tokyo, Japan
(81) 3-270-3141

Micro-Metrics
P.O. Box 13804
Atlanta, GA 30324
(770) 986-6015 FAX: (770) 986-9510
http://www.micro-metrics.com

Micro-Tech Scientific
140 South Wolfe Road
Sunnyvale, CA 94086
(408) 730-8324 FAX: (408) 730-3566
http://www.microlc.com

Microbix Biosystems
341 Bering Avenue
Toronto, Ontario
M8Z 3A8 Canada
(800)-794-6694 FAX: (416)-234-1626
(416)-234-1624
http://www.microbix.com

MicroCal
22 Industrial Drive East
Northampton, MA 01060
(800) 633-3115 FAX: (413) 586-0149
(413) 586-7720
http://www.microcalorimetry.com

Microfluidics
30 Ossipee Road
P.O. Box 9101
Newton, MA 02164
(800) 370-5452 FAX: (617) 965-1213
(617) 969-5452
http://www.microfluidicscorp.com

Microgon
See Spectrum Laboratories

Microlase Optical Systems
West of Scotland Science Park
Kelvin Campus, Maryhill Road
Glasgow G20 0SP, UK
(44) 141-948-1000
FAX: (44) 141-946-6311
http://www.microlase.co.uk

Micron Instruments
4509 Runway Street
Simi Valley, CA 93063
(800) 638-3770 FAX: (805) 522-4982
(805) 552-4676
http://www.microninstruments.com

Micron Separations
See MSI

Micro Photonics
4949 Liberty Lane, Suite 170
P.O. Box 3129
Allentown, PA 18106
(610) 366-7103 FAX: (610) 366-7105
http://www.microphotonics.com

MicroTech
1420 Conchester Highway
Boothwyn, PA 19061
(610) 459-3514

Midland Certified Reagent Company
3112-A West Cuthbert Avenue
Midland, TX 79701
(800) 247-8766 FAX: (800) 359-5789
(915) 694-7950 FAX: (915) 694-2387
http://www.mcrc.com

Midwest Research Institute
425 Volker Boulevard
Kansas City, Missouri 64110
(816) 753-7600
www.mriresearch.org

Midwest Scientific
280 Vance Road
Valley Park, MO 63088
(800) 227-9997 FAX: (636) 225-9998
(636) 225-9997
http://www.midsci.com

Miles
See Bayer

Miles Laboratories
See Serological

Miles Scientific
See Nunc

Millar Instruments
P.O. Box 230227
6001-A Gulf Freeway
Houston, TX 77023
(713) 923-9171 FAX: (713) 923-7757
http://www.millarinstruments.com

MilliGen/Biosearch
See Millipore

Millipore
80 Ashbury Road
P.O. Box 9125
Bedford, MA 01730
(800) 645-5476 FAX: (781) 533-3110
(781) 533-6000
http://www.millipore.com

Miltenyi Biotec
251 Auburn Ravine Road, Suite 208
Auburn, CA 95603
(800) 367-6227 FAX: (530) 888-8925
(530) 888-8871
http://www.miltenyibiotec.com

Miltex
6 Ohio Drive
Lake Success, NY 11042
(800) 645-8000 FAX: (516) 775-7185
(516) 349-0001

Milton Roy
See Spectronic Instruments

Mini-Instruments
15 Burnham Business Park
Springfield Road
Burnham-on-Crouch, Essex CM0 8TE, UK
(44) 1621-783282
FAX: (44) 1621-783132
http://www.mini-instruments.co.uk

Mini Mitter
P.O. Box 3386
Sunriver, OR 97707
(800) 685-2999 FAX: (541) 593-5604
(541) 593-8639
http://www.minimitter.com

Mirus Corporation
505 S. Rosa Road
Suite 104
Madison, WI 53719
(608) 441-2852 FAX: (608) 441-2849
http://www.genetransfer.com

Misonix
1938 New Highway
Farmingdale, NY 11735
(800) 645-9846 FAX: (516) 694-9412
http://www.misonix.com

Mitutoyo (MTI)
See Dolla Eastern

MJ Research
Waltham, MA 02451
(800) PELTIER FAX: (617) 923-8080
(617) 923-8000
http://www.mjr.com

Modular Instruments
228 West Gay Street
Westchester, PA 19380
(610) 738-1420 FAX: (610) 738-1421
http://www.mi2.com

Molecular Biology Insights
8685 US Highway 24
Cascade, CO 80809-1333
(800) 747-4362 FAX: (719) 684-7989
(719) 684-7988
http://www.oligo.net

Molecular Biosystems
10030 Barnes Canyon Road
San Diego, CA 92121
(858) 452-0681 FAX: (858) 452-6187
http://www.mobi.com

Molecular Devices
1312 Crossman Avenue
Sunnyvale, CA 94089
(800) 635-5577 FAX: (408) 747-3602
(408) 747-1700
http://www.moldev.com

Molecular Designs
1400 Catalina Street
San Leandro, CA 94577
(510) 895-1313 FAX: (510) 614-3608

Molecular Dynamics
928 East Arques Avenue
Sunnyvale, CA 94086
(800) 333-5703 FAX: (408) 773-1493
(408) 773-1222
http://www.apbiotech.com

Molecular Probes
4849 Pitchford Avenue
Eugene, OR 97402
(800) 438-2209 FAX: (800) 438-0228
(541) 465-8300 FAX: (541) 344-6504
http://www.probes.com

Molecular Research Center
5645 Montgomery Road
Cincinnati, OH 45212
(800) 462-9868 FAX: (513) 841-0080
(513) 841-0900
http://www.mrcgene.com

Molecular Simulations
9685 Scranton Road
San Diego, CA 92121
(800) 756-4674 FAX: (858) 458-0136
(858) 458-9990
http://www.msi.com

Monoject Disposable Syringes & Needles/Syrvet
16200 Walnut Street
Waukee, IA 50263
(800) 727-5203 FAX: (515) 987-5553
(515) 987-5554
http://www.syrvet.com

Monsanto Chemical
800 North Lindbergh Boulevard
St. Louis, MO 63167
(314) 694-1000 FAX: (314) 694-7625
http://www.monsanto.com

Moravek Biochemicals
577 Mercury Lane
Brea, CA 92821
(800) 447-0100 FAX: (714) 990-1824
(714) 990-2018
http://www.moravek.com

Moss
P.O. Box 189
Pasadena, MD 21122
(800) 932-6677 FAX: (410) 768-3971
(410) 768-3442
http://www.mosssubstrates.com

Motion Analysis
3617 Westwind Boulevard
Santa Rosa, CA 95403
(707) 579-6500 FAX: (707) 526-0629
http://www.motionanalysis.com

Mott
Farmington Industrial Park
84 Spring Lane
Farmington, CT 06032
(860) 747-6333 FAX: (860) 747-6739
http://www.mottcorp.com

MSI (Micron Separations)
See Osmonics

Multi Channel Systems
Markwiesenstrasse 55
72770 Reutlingen, Germany
(49) 7121-503010
FAX: (49) 7121-503011
http://www.multichannelsystems.com

Multiple Peptide Systems
3550 General Atomics Court
San Diego, CA 92121
(800) 338-4965 FAX: (800) 654-5592
(858) 455-3710 FAX: (858) 455-3713
http://www.mps-sd.com

Murex Diagnostics
3075 Northwoods Circle
Norcross, GA 30071
(707) 662-0660 FAX: (770) 447-4989

MWG-Biotech
Anzinger Str. 7
D-85560 Ebersberg, Germany
(49) 8092-82890
FAX: (49) 8092-21084
http://www.mwg_biotech.com

Myriad Industries
3454 E Street
San Diego, CA 92102
(800) 999-6777 FAX: (619) 232-4819
(619) 232-6700
http://www.myriadindustries.com

Nacalai Tesque
Nijo Karasuma, Nakagyo-ku
Kyoto 604, Japan
81-75-251-1723
FAX: 81-75-251-1762
http://www.nacalai.co.jp

Nalge Nunc International
Subsidiary of Sybron International
75 Panorama Creek Drive
P.O. Box 20365
Rochester, NY 14602
(800) 625-4327 FAX: (716) 586-8987
(716) 264-9346
http://www.nalgenunc.com

Nanogen
10398 Pacific Center Court
San Diego, CA 92121
(858) 410-4600 FAX: (858) 410-4848
http://www.nanogen.com

Nanoprobes
95 Horse Block Road
Yaphank, NY 11980
(877) 447-6266 FAX: (631) 205-9493
(631) 205-9490
http://www.nanoprobes.com

Narishige USA
1710 Hempstead Turnpike
East Meadow, NY 11554
(800) 445-7914 FAX: (516) 794-0066
(516) 794-8000
http://www.narishige.co.jp

National Bag Company
2233 Old Mill Road
Hudson, OH 44236
(800) 247-6000 FAX: (330) 425-9800
(330) 425-2600
http://www.nationalbag.com

National Band and Tag
Department X 35, Box 72430
Newport, KY 41032
(606) 261-2035 FAX: (800) 261-8247
https://www.nationalband.com

National Biosciences
See Molecular Biology Insights

National Diagnostics
305 Patton Drive
Atlanta, GA 30336
(800) 526-3867 FAX: (404) 699-2077
(404) 699-2121
http://www.nationaldiagnostics.com

National Institute of Standards and Technology
100 Bureau Drive
Gaithersburg, MD 20899
(301) 975-NIST FAX: (301) 926-1630
http://www.nist.gov

National Instruments
11500 North Mopac Expressway
Austin, TX 78759
(512) 794-0100 FAX: (512) 683-8411
http://www.ni.com

National Labnet
See Labnet International

National Scientific Instruments
975 Progress Circle
Lawrenceville, GA 300243
(800) 332-3331 FAX: (404) 339-7173
http://www.nationalscientific.com

National Scientific Supply
1111 Francisco Bouldvard East
San Rafael, CA 94901
(800) 525-1779 FAX: (415) 459-2954
(415) 459-6070
http://www.nat-sci.com

Naz-Dar-KC Chicago
Nazdar
1087 N. North Branch Street
Chicago, IL 60622
(800) 736-7636 FAX: (312) 943-8215
(312) 943-8338
http://www.nazdar.com

NB Labs
1918 Avenue A
Denison, TX 75021
(903) 465-2694 FAX: (903) 463-5905
http://www.nblabslarry.com

NEB
See New England Biolabs

NEN Life Science Products
549 Albany Street
Boston, MA 02118
(800) 551-2121 FAX: (617) 451-8185
(617) 350-9075
http://www.nen.com

NEN Research Products, Dupont (UK)
Diagnostics and Biotechnology Systems
Wedgewood Way
Stevenage, Hertfordshire SG1 4QN, UK
44-1438-734831
44-1438-734000
FAX: 44-1438-734836
http://www.dupont.com

Neogen
628 Winchester Road
Lexington, KY 40505
(800) 477-8201 FAX: (606) 255-5532
(606) 254-1221
http://www.neogen.com

Neosystems
380, 11012 Macleod Trail South
Calgary, Alberta
T2J 6A5 Canada
(403) 225-9022 FAX: (403) 225-9025
http://www.neosystems.com

Neuralynx
2434 North Pantano Road
Tucson, AZ 85715
(520) 722-8144 FAX: (520) 722-8163
http://www.neuralynx.com

Neuro Probe
16008 Industrial Drive
Gaithersburg, MD 20877
(301) 417-0014 FAX: (301) 977-5711
http://www.neuroprobe.com

Neurocrine Biosciences
10555 Science Center Drive
San Diego, CA 92121
(619) 658-7600 FAX: (619) 658-7602
http://www.neurocrine.com

Nevtek
HCR03, Box 99
Burnsville, VA 24487
(540) 925-2322 FAX: (540) 925-2323
http://www.nevtek.com

New Brunswick Scientific
44 Talmadge Road
Edison, NJ 08818
(800) 631-5417 FAX: (732) 287-4222
(732) 287-1200
http://www.nbsc.com

New England Biolabs (NEB)
32 Tozer Road
Beverly, MA 01915
(800) 632-5227 FAX: (800) 632-7440
http://www.neb.com

New England Nuclear (NEN)
See NEN Life Science Products

New MBR
Gubelstrasse 48
CH8050 Zurich, Switzerland
(41) 1-313-0703

Newark Electronics
4801 N. Ravenswood Avenue
Chicago, IL 60640
(800) 4-NEWARK
FAX: (773) 907-5339
(773) 784-5100
http://www.newark.com

Newell Rubbermaid
29 E. Stephenson Street
Freeport, IL 61032
(815) 235-4171 FAX: (815) 233-8060
http://www.newellco.com

Newport Biosystems
1860 Trainor Street
Red Bluff, CA 96080
(530) 529-2448 FAX: (530) 529-2648

Newport
1791 Deere Avenue
Irvine, CA 92606
(800) 222-6440 FAX: (949) 253-1800
(949) 253-1462
http://www.newport.com

Nexin Research B.V.
P.O. Box 16
4740 AA Hoeven, The Netherlands
(31) 165-503172
FAX: (31) 165-502291

NIAID
See Bio-Tech Research Laboratories

Nichiryo
230 Route 206
Building 2-2C
Flanders, NJ 07836
(877) 548-6667 FAX: (973) 927-0099
(973) 927-4001
http://www.nichiryo.com

Nichols Institute Diagnostics
33051 Calle Aviador
San Juan Capistrano, CA 92675
(800) 286-4NID FAX: (949) 240-5273
(949) 728-4610
http://www.nicholsdiag.com

Nichols Scientific Instruments
3334 Brown Station Road
Columbia, MO 65202
(573) 474-5522 FAX: (603) 215-7274
http://home.beseen.com
technology/nsi_technology

Nicolet Biomedical Instruments
5225 Verona Road, Building 2
Madison, WI 53711
(800) 356-0007 FAX: (608) 441-2002
(608) 273-5000
http://nicoletbiomedical.com

N.I.G.M.S. (National Institute of
General Medical Sciences)
See Coriell Institute for Medical Research

Nikon
Science and Technologies Group
1300 Walt Whitman Road
Melville, NY 11747
(516) 547-8500 FAX: (516) 547-4045
http://www.nikonusa.com

Nippon Gene
1-29, Ton-ya-machi
Toyama 930, Japan
(81) 764-51-6548
FAX: (81) 764-51-6547

Noldus Information Technology
751 Miller Drive
Suite E-5
Leesburg, VA 20175
(800) 355-9541 FAX: (703) 771-0441
(703) 771-0440
http://www.noldus.com

Nordion International
See MDS Nordion

North American Biologicals (NABI)
16500 NW 15th Avenue
Miami, FL 33169
(800) 327-7106 (305) 625-5305
http://www.nabi.com

North American Reiss
See Reiss

Northwestern Bottle
24 Walpole Park South
Walpole, MA 02081
(508) 668-8600 FAX: (508) 668-7790

NOVA Biomedical
Nova Biomedical 200
Prospect Street Waltham, MA 02454
(800) 822-0911 FAX: (781) 894-5915
http://www.novabiomedical.com

Novagen
601 Science Drive
Madison, WI 53711
(800) 526-7319 FAX: (608) 238-1388
(608) 238-6110
http://www.novagen.com

Novartis
59 Route 10
East Hanover, NJ 07936
(800)526-0175 FAX: (973) 781-6356
http://www.novartis.com

Novartis Biotechnology
3054 Cornwallis Road
Research Triangle Park, NC 27709
(888) 462-7288 FAX: (919) 541-8585
http://www.novartis.com

Nova Sina AG
Subsidiary of Airflow Lufttechnik GmbH
Kleine Heeg 21
52259 Rheinbach, Germany
(49) 02226 920-0
FAX: (49) 02226 9205-11

Novex/Invitrogen
1600 Faraday
Carlsbad, CA 92008
(800) 955-6288 FAX: (760) 603-7201
http://www.novex.com

Novo Nordisk Biochem
77 Perry Chapel Church Road
Franklington, NC 27525
(800) 879-6686 FAX: (919) 494-3450
(919) 494-3000
http://www.novo.dk

Novo Nordisk BioLabs
See Novo Nordisk Biochem

Novocastra Labs
Balliol Business Park West
Benton Lane
Newcastle-upon-Tyne
Tyne and Wear NE12 8EW, UK
(44) 191-215-0567
FAX: (44) 191-215-1152
http://www.novocastra.co.uk

Novus Biologicals
P.O. Box 802
Littleton, CO 80160
(888) 506-6887 FAX: (303) 730-1966
http://www.novus-biologicals.com/
main.html

NPI Electronic
Hauptstrasse 96
D-71732 Tamm, Germany
(49) 7141-601534
FAX: (49) 7141-601266
http://www.npielectronic.com

NSG Precision Cells
195G Central Avenue
Farmingdale, NY 11735
(516) 249-7474 FAX: (516) 249-8575
http://www.nsgpci.com

Nu Chek Prep
109 West Main
P.O. Box 295
Elysian, MN 56028
(800) 521-7728 FAX: (507) 267-4790
(507) 267-4689

Nuclepore
See Costar

Numonics
101 Commerce Drive
Montgomeryville, PA 18936
(800) 523-6716 FAX: (215) 361-0167
(215) 362-2766
http://www.interactivewhiteboards.com

NYCOMED AS Pharma
c/o Accurate Chemical & Scientific
300 Shames Drive
Westbury, NY 11590
(800) 645-6524 FAX: (516) 997-4948
(516) 333-2221
http://www.accuratechemical.com

Nycomed Amersham
Health Care Division
101 Carnegie Center
Princeton, NJ 08540
(800) 832-4633 FAX: (800) 807-2382
(609) 514-6000
http://www.nycomed-amersham.com

Nyegaard
Herserudsvagen 5254
S-122 06 Lidingo, Sweden
(46) 8-765-2930

Ohmeda Catheter Products
See Datex-Ohmeda

Ohwa Tsusbo
Hiby Dai Building
1-2-2 Uchi Saiwai-cho
Chiyoda-ku
Tokyo 100, Japan
03-3591-7348 FAX: 03-3501-9001

Oligos Etc.
9775 S.W. Commerce Circle, C-6
Wilsonville, OR 97070
(800) 888-2358
FAX: (503) 6822D1635
(503) 6822D1814
http://www.oligoetc.com

Olis Instruments
130 Conway Drive
Bogart, GA 30622
(706) 353-6547 (800) 852-3504
http://www.olisweb.com

Olympus America
2 Corporate Center Drive
Melville, NY 11747
(800) 645-8160 FAX: (516) 844-5959
(516) 844-5000
http://www.olympusamerica.com

Omega Engineering
One Omega Drive
P.O. Box 4047
Stamford, CT 06907
(800) 848-4286 FAX: (203) 359-7700
(203) 359-1660
http://www.omega.com

Omega Optical
3 Grove Street
P.O. Box 573
Brattleboro, VT 05302
(802) 254-2690 FAX: (802) 254-3937
http://www.omegafilters.com

Omnetics Connector Corporation
7260 Commerce Circle
East Minneapolis, MN 55432
(800) 343-0025 (763) 572-0656
FAX: (763) 572-3925
http://www.omnetics.com/main.htm

Omni International
6530 Commerce Court
Warrenton, VA 20187
(800) 776-4431 FAX: (540) 347-5352
(540) 347-5331
http://www.omni-inc.com

Omnion
2010 Energy Drive
P.O. Box 879
East Troy, WI 53120
(262) 642-7200 FAX: (262) 642-7760
http://www.omnion.com

Omnitech Electronics
See AccuScan Instruments

Oncogene Research Products
P.O. Box Box 12087
La Jolla, CA 92039-2087
(800) 662-2616 FAX: (800) 766-0999
http://www.apoptosis.com

Oncogene Science
See OSI Pharmaceuticals

Oncor
See Intergen

Online Instruments
130 Conway Drive, Suites A & B
Bogart, GA 30622
(800) 852-3504 (706) 353-1972
(706) 353-6547
http://www.olisweb.com

Operon Technologies
1000 Atlantic Avenue
Alameda, CA 94501
(800) 688-2248 FAX: (510) 865-5225
(510) 865-8644
http://www.operon.com

Optiscan
P.O. Box 1066
Mount Waverly MDC, Victoria
Australia 3149
61-3-9538 3333 FAX: 61-3-9562
7742
http://www.optiscan.com.au

Optomax
9 Ash Street
P.O. Box 840
Hollis, NH 03049
(603) 465-3385 FAX: (603) 465-2291

Opto-Line Associates
265 Ballardvale Street
Wilmington, MA 01887
(978) 658-7255 FAX: (978) 658-7299
http://www.optoline.com

Orbigen
6827 Nancy Ridge Drive
San Diego, CA 92121
(866) 672-4436 FAX: (858) 362-2030
(858) 362-2026
http://www.orbigen.com

Oread BioSaftey
1501 Wakarusa Drive
Lawrence, KS 66047
(800) 447-6501 FAX: (785) 749-1882
(785) 749-0034
http://www.oread.com

Organomation Associates
266 River Road West
Berlin, MA 01503
(888) 978-7300 FAX: (978) 838-2786
(978) 838-7300
http://www.organomation.com

Organon
375 Mount Pleasant Avenue
West Orange, NJ 07052
(800) 241-8812 FAX: (973) 325-4589
(973) 325-4500
http://www.organon.com

Organon Teknika (Canada)
30 North Wind Place
Scarborough, Ontario
M1S 3R5 Canada
(416) 754-4344 FAX: (416) 754-4488
http://www.organonteknika.com

Organon Teknika Cappel
100 Akzo Avenue
Durham, NC 27712
(800) 682-2666 FAX: (800) 432-9682
(919) 620-2000 FAX: (919) 620-2107
http://www.organonteknika.com

Oriel Corporation of America
150 Long Beach Boulevard
Stratford, CT 06615
(203) 377-8282 FAX: (203) 378-2457
http://www.oriel.com

OriGene Technologies
6 Taft Court, Suite 300
Rockville, MD 20850
(888) 267-4436 FAX: (301) 340-9254
(301) 340-3188
http://www.origene.com

OriginLab
One Roundhouse Plaza
Northhampton, MA 01060
(800) 969-7720 FAX: (413) 585-0126
http://www.originlab.com

Orion Research
500 Cummings Center
Beverly, MA 01915
(800) 225-1480 FAX: (978) 232-6015
(978) 232-6000
http://www.orionres.com

Ortho Diagnostic Systems
Subsidiary of Johnson & Johnson
1001 U.S. Highway 202
P.O. Box 350
Raritan, NJ 08869
(800) 322-6374 FAX: (908) 218-8582
(908) 218-1300

Ortho McNeil Pharmaceutical
Welsh & McKean Road
Spring House, PA 19477
(800) 682-6532
(215) 628-5000
http://www.orthomcneil.com

Oryza
200 Turnpike Road, Unit 5
Chelmsford, MA 01824
(978) 256-8183 FAX: (978) 256-7434
http://www.oryzalabs.com

OSI Pharmaceuticals
106 Charles Lindbergh Boulevard
Uniondale, NY 11553
(800) 662-2616 FAX: (516) 222-0114
(516) 222-0023
http://www.osip.com

Osmonics
135 Flanders Road
P.O. Box 1046
Westborough, MA 01581
(800) 444-8212 FAX: (508) 366-5840
(508) 366-8212
http://www.osmolabstore.com

Oster Professional Products
150 Cadillac Lane
McMinnville, TN 37110
(931) 668-4121 FAX: (931) 668-4125
http://www.sunbeam.com

Out Patient Services
1260 Holm Road
Petaluma, CA 94954
(800) 648-1666 FAX: (707) 762-7198
(707) 763-1581

OWL Scientific Plastics
See OWL Separation Systems

OWL Separation Systems
55 Heritage Avenue
Portsmouth, NH 03801
(800) 242-5560 FAX: (603) 559-9258
(603) 559-9297
http://www.owlsci.com

Oxford Biochemical Research
P.O. Box 522
Oxford, MI 48371
(800) 692-4633 FAX: (248) 852-4466
http://www.oxfordbiomed.com

Oxford GlycoSystems
See Glyco

Oxford Instruments
Old Station Way
Eynsham
Witney, Oxfordshire OX8 1TL, UK
(44) 1865-881437
FAX: (44) 1865-881944
http://www.oxinst.com

Oxford Labware
See Kendall

Oxford Molecular Group
Oxford Science Park
The Medawar Centre
Oxford OX4 4GA, UK
(44) 1865-784600
FAX: (44) 1865-784601
http://www.oxmol.co.uk

Oxford Molecular Group
2105 South Bascom Avenue, Suite 200
Campbell, CA 95008
(800) 876-9994 FAX: (408) 879-6302
(408) 879-6300
http://www.oxmol.com

OXIS International
6040 North Cutter Circle
Suite 317
Portland, OR 97217
(800) 547-3686 FAX: (503) 283-4058
(503) 283-3911
http://www.oxis.com

Oxoid
800 Proctor Avenue
Ogdensburg, NY 13669
(800) 567-8378 FAX: (613) 226-3728
http://www.oxoid.ca

Oxoid
Wade Road
Basingstoke, Hampshire RG24 8PW,
UK
(44) 1256-841144
FAX: (4) 1256-814626
http://www.oxoid.ca

Oxyrase
P.O. Box 1345
Mansfield, OH 44901
(419) 589-8800 FAX: (419) 589-9919
http://www.oxyrase.com

Ozyme
10 Avenue Ampère
Montigny de Bretoneux
78180 France
(33) 13-46-02-424
FAX: (33) 13-46-09-212
http://www.ozyme.fr

PAA Laboratories
2570 Route 724
P.O. Box 435
Parker Ford, PA 19457
(610) 495-9400 FAX: (610) 495-9410
http://www.paa-labs.com

Pacer Scientific
5649 Valley Oak Drive
Los Angeles, CA 90068
(323) 462-0636 FAX: (323) 462-1430
http://www.pacersci.com

Pacific Bio-Marine Labs
P.O. Box 1348
Venice, CA 90294
(310) 677-1056 FAX: (310) 677-1207

Packard Instrument
800 Research Parkway
Meriden, CT 06450
(800) 323-1891 FAX: (203) 639-2172
(203) 238-2351
http://www.packardinst.com

Padgett Instrument
1730 Walnut Street
Kansas City, MO 64108
(816) 842-1029

Pall Filtron
50 Bearfoot Road
Northborough, MA 01532
(800) FILTRON FAX: (508) 393-1874
(508) 393-1800

Pall-Gelman
25 Harbor Park Drive
Port Washington, NY 11050
(800) 289-6255 FAX: (516) 484-2651
(516) 484-3600
http://www.pall.com

PanVera
545 Science Drive
Madison, WI 53711
(800) 791-1400 FAX: (608) 233-3007
(608) 233-9450
http://www.panvera.com

Parke-Davis
See Warner-Lambert

Parr Instrument
211 53rd Street
Moline, IL 61265
(800) 872-7720 FAX: (309) 762-9453
(309) 762-7716
http://www.parrinst.com

Partec
Otto Hahn Strasse 32
D-48161 Munster, Germany
(49) 2534-8008-0
FAX: (49) 2535-8008-90

PCR
See Archimica Florida

PE Biosystems
850 Lincoln Centre Drive
Foster City, CA 94404
(800) 345-5224 FAX: (650) 638-5884
(650) 638-5800
http://www.pebio.com

Pel-Freez Biologicals
219 N. Arkansas
P.O. Box 68
Rogers, AR 72757
(800) 643-3426 FAX: (501) 636-3562
(501) 636-4361
http://www.pelfreez-bio.com

Pel-Freez Clinical Systems
Subsidiary of Pel-Freez Biologicals
9099 N. Deerbrook Trail
Brown Deer, WI 53223
(800) 558-4511 FAX: (414) 357-4518
(414) 357-4500
http://www.pelfreez-bio.com

Peninsula Laboratories
601 Taylor Way
San Carlos, CA 94070
(800) 650-4442 FAX: (650) 595-4071
(650) 592-5392
http://www.penlabs.com

Pentex
24562 Mando Drive
Laguna Niguel, CA 92677
(800) 382-4667 FAX: (714) 643-2363
http://www.pentex.com

PeproTech
5 Crescent Avenue
P.O. Box 275 Rocky Hill, NJ 08553
(800) 436-9910 FAX: (609) 497-0321
(609) 497-0253
http://www.peprotech.com

Peptide Institute
4-1-2 Ina, Minoh-shi Osaka 562-8686, Japan
81-727-29-4121 FAX:
81-727-29-4124
http://www.peptide.co.jp

Peptide Laboratory
4175 Lakeside Drive
Richmond, CA 94806
(800) 858-7322 FAX: (510) 262-9127
(510) 262-0800
http://www.peptidelab.com

Peptides International
11621 Electron Drive
Louisville, KY 40299
(800) 777-4779 FAX: (502) 267-1329
(502) 266-8787
http://www.pepnet.com

Perceptive Science Instruments
2525 South Shore Boulevard,
Suite 100
League City, TX 77573
(281) 334-3027 FAX: (281) 538-2222
http://www.persci.com

Perimed
4873 Princeton Drive
North Royalton, OH 44133
(440) 877-0537 FAX: (440) 877-0534
http://www.perimed.se

Perkin-Elmer
761 Main Avenue
Norwalk, CT 06859
(800) 762-4002 FAX: (203) 762-6000
(203) 762-1000
http://www.perkin-elmer.com
See also PE Biosystems

PerSeptive Bioresearch Products
See PerSeptive BioSystems

PerSeptive BioSystems
500 Old Connecticut Path
Framingham, MA 01701
(800) 899-5858 FAX: (508) 383-7885
(508) 383-7700
http://www.pbio.com

PerSeptive Diagnostic
See PE Biosystems
(800) 343-1346

Pettersson Elektronik AB
Tallbacksvagen 51
S-756 45 Uppsala, Sweden
(46) 1830-3880 FAX: (46) 1830-3840
http://www.bahnhof.se/∼pettersson

Pfanstiehl Laboratories, Inc.
1219 Glen Rock Avenue
Waukegan, IL 60085
(800) 383-0126 FAX: (847) 623-9173
http://www.pfanstiehl.com

PGC Scientifics
7311 Governors Way
Frederick, MD 21704
(800) 424-3300 FAX: (800) 662-1112
(301) 620-7777 FAX: (301) 620-7497
http://www.pgcscientifics.com

Pharmacia Biotech
See Amersham Pharmacia Biotech

Pharmacia Diagnostics
See Wallac

Pharmacia LKB Biotech
See Amersham Pharmacia Biotech

Pharmacia LKB Biotechnology
See Amersham Pharmacia Biotech

Pharmacia LKB Nuclear
See Wallac

Pharmaderm Veterinary Products
60 Baylis Road
Melville, NY 11747
(800) 432-6673
http://www.pharmaderm.com

Pharmed (Norton)
Norton Performance Plastics
See Saint-Gobain Performance Plastics

PharMingen
See BD PharMingen

Phenomex
2320 W. 205th Street
Torrance, CA 90501
(310) 212-0555 FAX: (310) 328-7768
http://www.phenomex.com

PHLS Centre for Applied
Microbiology and Research
See European Collection of Animal Cell Cultures (ECACC)

Phoenix Flow Systems
11575 Sorrento Valley Road, Suite 208
San Diego, CA 92121
(800) 886-3569 FAX: (619) 259-5268
(619) 453-5095
http://www.phnxflow.com

Phoenix Pharmaceutical
4261 Easton Road, P.O. Box 6457
St. Joseph, MO 64506
(800) 759-3644 FAX: (816) 364-4969
(816) 364-5777
http://www.phoenixpharmaceutical.com

Photometrics
See Roper Scientific

Photon Technology International
1 Deerpark Drive, Suite F
Monmouth Junction, NJ 08852
(732) 329-0910 FAX: (732) 329-9069
http://www.pti-nj.com

Physik Instrumente
Polytec PI
23 Midstate Drive, Suite 212
Auburn, MA 01501
(508) 832-3456 FAX: (508) 832-0506
http://www.polytecpi.com

Physitemp Instruments
154 Huron Avenue
Clifton, NJ 07013
(800) 452-8510 FAX: (973) 779-5954
(973) 779-5577
http://www.physitemp.com

Pico Technology
The Mill House, Cambridge Street
St. Neots, Cambridgeshire
PE19 1QB, UK
(44) 1480-396-395
FAX: (44) 1480-396-296
http://www.picotech.com

Pierce Chemical
P.O. Box 117
3747 Meridian Road
Rockford, IL 61105
(800) 874-3723 FAX: (800) 842-5007
FAX: (815) 968-7316
http://www.piercenet.com

Pierce & Warriner
44, Upper Northgate Street
Chester, Cheshire CH1 4EF, UK
(44) 1244 382 525
FAX: (44) 1244 373 212
http://www.piercenet.com

Pilling Weck Surgical
420 Delaware Drive
Fort Washington, PA 19034
(800) 523-2579 FAX: (800) 332-2308
http://www.pilling-weck.com

PixelVision
A division of Cybex Computer Products
14964 NW Greenbrier Parkway
Beaverton, OR 97006
(503) 629-3210 FAX: (503) 629-3211
http://www.pixelvision.com

P.J. Noyes
P.O. Box 381
89 Bridge Street
Lancaster, NH 03584
(800) 522-2469 FAX: (603) 788-3873
(603) 788-4952
http://www.pjnoyes.com

Plas-Labs
917 E. Chilson Street
Lansing, MI 48906
(800) 866-7527 FAX: (517) 372-2857
(517) 372-7177
http://www.plas-labs.com

Plastics One
6591 Merriman Road, Southwest
P.O. Box 12004
Roanoke, VA 24018
(540) 772-7950 FAX: (540) 989-7519
http://www.plastics1.com

Platt Electric Supply
2757 6th Avenue South
Seattle, WA 98134
(206) 624-4083 FAX: (206) 343-6342
http://www.platt.com

Plexon
6500 Greenville Avenue
Suite 730
Dallas, TX 75206
(214) 369-4957 FAX: (214) 369-1775
http://www.plexoninc.com

Polaroid
784 Memorial Drive
Cambridge, MA 01239
(800) 225-1618 FAX: (800) 832-9003
(781) 386-2000
http://www.polaroid.com

Polyfiltronics
136 Weymouth St.
Rockland, MA 02370
(800) 434-7659 FAX: (781) 878-0822
(781) 878-1133
http://www.polyfiltronics.com

Polylabo Paul Block
Parc Tertiare de la Meinau
10, rue de la Durance
B.P. 36
67023 Strasbourg Cedex 1
Strasbourg, France
33-3-8865-8020
FAX: 33-3-8865-8039

PolyLC
9151 Rumsey Road, Suite 180
Columbia, MD 21045
(410) 992-5400 FAX: (410) 730-8340

Polymer Laboratories
Amherst Research Park
160 Old Farm Road
Amherst, MA 01002
(800) 767-3963 FAX: (413) 253-2476
http://www.polymerlabs.com

Polymicro Technologies
18019 North 25th Avenue
Phoenix, AZ 85023
(602) 375-4100 FAX: (602) 375-4110
http://www.polymicro.com

Polyphenols AS
Hanabryggene Technology Centre
Hanaveien 4-6
4327 Sandnes, Norway
(47) 51-62-0990
FAX: (47) 51-62-51-82
http://www.polyphenols.com

Polysciences
400 Valley Road
Warrington, PA 18976
(800) 523-2575 FAX: (800) 343-3291
http://www.polysciences.com

Polyscientific
70 Cleveland Avenue
Bayshore, NY 11706
(516) 586-0400 FAX: (516) 254-0618

Polytech Products
285 Washington Street
Somerville, MA 02143
(617) 666-5064 FAX: (617) 625-0975

Polytron
8585 Grovemont Circle
Gaithersburg, MD 20877
(301) 208-6597 FAX: (301) 208-8691
http://www.polytron.com

Popper and Sons
300 Denton Avenue
P.O. Box 128
New Hyde Park, NY 11040
(888) 717-7677 FAX: (800) 557-6773
(516) 248-0300 FAX: (516) 747-1188
http://www.popperandsons.com

Porphyrin Products
P.O. Box 31
Logan, UT 84323
(435) 753-1901 FAX: (435) 753-6731
http://www.porphyrin.com

Portex
See SIMS Portex Limited

Powderject Vaccines
585 Science Drive
Madison, WI 53711
(608) 231-3150 FAX: (608) 231-6990
http://www.powderject.com

Praxair
810 Jorie Boulevard
Oak Brook, IL 60521
(800) 621-7100
http://www.praxair.com

Precision Dynamics
13880 Del Sur Street
San Fernando, CA 91340
(800) 847-0670 FAX: (818) 899-4-45
http://www.pdcorp.com

Precision Scientific Laboratory Equipment
Division of Jouan
170 Marcel Drive
Winchester, VA 22602
(800) 621-8820 FAX: (540) 869-0130
(540) 869-9892
http://www.precisionsci.com

Primary Care Diagnostics
See Becton Dickinson Primary Care Diagnostics

Primate Products
1755 East Bayshore Road, Suite 28A
Redwood City, CA 94063
(650) 368-0663 FAX: (650) 368-0665
http://www.primateproducts.com

5 Prime → 3 Prime
See 2000 Eppendorf-5 Prime
http://www.5prime.com

Princeton Applied Research
PerkinElmer Instr.: Electrochemistry
801 S. Illinois
Oak Ridge, TN 37830
(800) 366-2741 FAX: (423) 425-1334
(423) 481-2442
http://www.eggpar.com

Princeton Instruments
A division of Roper Scientific
3660 Quakerbridge Road
Trenton, NJ 08619
(609) 587-9797 FAX: (609) 587-1970
http://www.prinst.com

Princeton Separations
P.O. Box 300
Aldephia, NJ 07710
(800) 223-0902 FAX: (732) 431-3768
(732) 431-3338

Prior Scientific
80 Reservoir Park Drive
Rockland, MA 02370
(781) 878-8442 FAX: (781) 878-8736
http://www.prior.com

PRO Scientific
P.O. Box 448
Monroe, CT 06468
(203) 452-9431 FAX: (203) 452-9753
http://www.proscientific.com

Professional Compounding Centers of America
9901 South Wilcrest Drive
Houston, TX 77099
(800) 331-2498 FAX: (281) 933-6227
(281) 933-6948
http://www.pccarx.com

Progen Biotechnik
Maass-Str. 30
69123 Heidelberg, Germany
(49) 6221-8278-0
FAX: (49) 6221-8278-23
http://www.progen.de

Prolabo
A division of Merck Eurolab
54 rue Roger Salengro
94126 Fontenay Sous Bois Cedex
France
33-1-4514-8500
FAX: 33-1-4514-8616
http://www.prolabo.fr

Proligo
2995 Wilderness Place Boulder, CO
80301
(888) 80-OLIGO
FAX: (303) 801-1134
http://www.proligo.com

Promega
2800 Woods Hollow Road
Madison, WI 53711
(800) 356-9526 FAX: (800) 356-1970
(608) 274-4330 FAX: (608) 277-2516
http://www.promega.com

Protein Databases (PDI)
405 Oakwood Road
Huntington Station, NY 11746
(800) 777-6834 FAX: (516) 673-4502
(516) 673-3939

Protein Polymer Technologies
10655 Sorrento Valley Road
San Diego, CA 92121
(619) 558-6064 FAX: (619) 558-6477
http://www.ppti.com

Protein Solutions
391 G Chipeta Way
Salt Lake City, UT 84108
(801) 583-9301 FAX: (801) 583-4463
http://www.proteinsolutions.com

Prozyme
1933 Davis Street, Suite 207
San Leandro, CA 94577
(800) 457-9444 FAX: (510) 638-6919
(510) 638-6900
http://www.prozyme.com

PSI
See Perceptive Science Instruments

Pulmetrics Group
82 Beacon Street
Chestnut Hill, MA 02167
(617) 353-3833 FAX: (617) 353-6766

Purdue Frederick
100 Connecticut Avenue
Norwalk, CT 06850
(800) 633-4741 FAX: (203) 838-1576
(203) 853-0123
http://www.pharma.com

Purina Mills
LabDiet
P. O. Box 66812
St. Louis, MO 63166
(800) 227-8941 FAX: (314) 768-4894
http://www.purina-mills.com

Qbiogene
2251 Rutherford Road
Carlsbad, CA 92008
(800) 424-6101 FAX: (760) 918-9313
http://www.qbiogene.com

Qiagen
28159 Avenue Stanford
Valencia, CA 91355
(800) 426-8157 FAX: (800) 718-2056
http://www.qiagen.com

Quality Biological
7581 Lindbergh Drive
Gaithersburg, MD 20879
(800) 443-9331 FAX: (301) 840-5450
(301) 840-9331
http://www.qualitybiological.com

Quantitative Technologies
P.O. Box 470
Salem Industrial Park, Bldg. 5
Whitehouse, NJ 08888
(908) 534-4445 FAX: (908) 534-1054
http://www.qtionline.com

Quantum Appligene
Parc d'Innovation
Rue Geller de Kayserberg
67402 Illkirch, Cedex, France
(33) 3-8867-5425
FAX: (33) 3-8867-1945
http://www.quantum-appligene.com

Quantum Biotechnologies
See Qbiogene

Quantum Soft
Postfach 6613
CH-8023
Zürich, Switzerland
FAX: 41-1-481-69-51
profit@quansoft.com

Questcor Pharmaceuticals
26118 Research Road
Hayward, CA 94545
(510) 732-5551 FAX: (510) 732-7741
http://www.questcor.com

Quidel
10165 McKellar Court
San Diego, CA 92121
(800) 874-1517 FAX: (858) 546-8955
(858) 552-1100
http://www.quidel.com

R-Biopharm
7950 Old US 27 South
Marshall, MI 49068
(616) 789-3033 FAX: (616) 789-3070
http://www.r-biopharm.com

R. C. Electronics
6464 Hollister Avenue
Santa Barbara, CA 93117
(805) 685-7770 FAX: (805) 685-5853
http://www.rcelectronics.com

R & D Systems
614 McKinley Place NE
Minneapolis, MN 55413
(800) 343-7475 FAX: (612) 379-6580
(612) 379-2956
http://www.rndsystems.com

R & S Technology
350 Columbia Street
Peacedale, RI 02880
(401) 789-5660 FAX: (401) 792-3890
http://www.septech.com

RACAL Health and Safety
See 3M
7305 Executive Way
Frederick, MD 21704
(800) 692-9500 FAX: (301) 695-8200

Radiometer America
811 Sharon Drive
Westlake, OH 44145
(800) 736-0600 FAX: (440) 871-2633
(440) 871-8900
http://www.rameusa.com

Radiometer A/S
The Chemical Reference Laboratory
kandevej 21
DK-2700 Brnshj, Denmark
45-3827-3827 FAX: 45-3827-2727

Radionics
22 Terry Avenue
Burlington, MA 01803
(781) 272-1233 FAX: (781) 272-2428
http://www.radionics.com

Radnoti Glass Technology
227 W. Maple Avenue
Monrovia, CA 91016
(800) 428-l4l6 FAX: (626) 303-2998
(626) 357-8827
http://www.radnoti.com

Rainin Instrument
Rainin Road
P.O. Box 4026
Woburn, MA 01888
(800)-4-RAININ FAX: (781) 938-1152
(781) 935-3050
http://www.rainin.com

Raj Scientific Industries
601-A Wing
Hemavathi Co-op. HSG.
Society, Plot No. 9, Sector No. 7
Charkop, Kandivali (W)
Mumbai, 400 067, India
http://www.rajscientificind.com/

Rank Brothers
56 High Street
Bottisham, Cambridge
CB5 9DA UK
(44) 1223 811369
FAX: (44) 1223 811441
http://www.rankbrothers.com

Rapp Polymere
Ernst-Simon Strasse 9
D 72072 Tübingen, Germany
(49) 7071-763157
FAX: (49) 7071-763158
http://www.rapp-polymere.com

Raven Biological Laboratories
8607 Park Drive
P.O. Box 27261
Omaha, NE 68127
(800) 728-5702 FAX: (402) 593-0995
(402) 593-0781
http://www.ravenlabs.com

Razel Scientific Instruments
100 Research Drive
Stamford, CT 06906
(203) 324-9914 FAX: (203) 324-5568

Reagents International
See Biotech Source

Receptor Biology
10000 Virginia Manor Road, Suite 360
Beltsville, MD 20705
(888) 707-4200 FAX: (301) 210-6266
(301) 210-4700
http://www.receptorbiology.com

Regis Technologies
8210 N. Austin Avenue
Morton Grove, IL 60053
(800) 323-8144 FAX: (847) 967-1214
(847) 967-6000
http://www.registech.com

Reichert Ophthalmic Instruments
P.O. Box 123
Buffalo, NY 14240
(716) 686-4500 FAX: (716) 686-4545
http://www.reichert.com

Reiss
1 Polymer Place
P.O. Box 60 Blackstone, VA 23824
(800) 356-2829 FAX: (804) 292-1757
(804) 292-1600
http://www.reissmfg.com

Remel
12076 Santa Fe Trail Drive
P.O. Box 14428
Shawnee Mission, KS 66215
(800) 255-6730 FAX: (800) 621-8251
(913) 888-0939 FAX: (913) 888-5884
http://www.remelinc.com

Reming Bioinstruments
6680 County Route 17
Redfield, NY 13437
(315) 387-3414 FAX: (315) 387-3415

RepliGen
117 Fourth Avenue
Needham, MA 02494
(800) 622-2259 FAX: (781) 453-0048
(781) 449-9560
http://www.repligen.com

Research Biochemicals
1 Strathmore Road
Natick, MA 01760
(800) 736-3690 FAX: (800) 736-2480
(508) 651-8151 FAX: (508) 655-1359
http://www.resbio.com

Research Corporation Technologies
101 N. Wilmot Road, Suite 600
Tucson, AZ 85711
(520) 748-4400 FAX: (520) 748-0025
http://www.rctech.com

Research Diagnostics
Pleasant Hill Road
Flanders, NJ 07836
(800) 631-9384 FAX: (973) 584-0210
(973) 584-7093
http://www.researchd.com

Research Diets
121 Jersey Avenue
New Brunswick, NJ 08901
(877) 486-2486 FAX: (732) 247-2340
(732) 247-2390
http://www.researchdiets.com

Research Genetics
2130 South Memorial Parkway
Huntsville, AL 35801
(800) 533-4363 FAX: (256) 536-9016
(256) 533-4363
http://www.resgen.com

Research Instruments
Kernick Road Pernryn
Cornwall TR10 9DQ, UK
(44) 1326-372-753
FAX: (44) 1326-378-783
http://www.research-instruments.com

Research Organics
4353 E. 49th Street
Cleveland, OH 44125
(800) 321-0570 FAX: (216) 883-1576
(216) 883-8025
http://www.resorg.com

Research Plus
P.O. Box 324
Bayonne, NJ 07002
(800) 341-2296 FAX: (201) 823-9590
(201) 823-3592
http://www.researchplus.com

Research Products International
410 N. Business Center Drive
Mount Prospect, IL 60056
(800) 323-9814 FAX: (847) 635-1177
(847) 635-7330
http://www.rpicorp.com

Research Triangle Institute
P.O. Box 12194
Research Triangle Park, NC 27709
(919) 541-6000 FAX: (919) 541-6515
http://www.rti.org

Restek
110 Benner Circle
Bellefonte, PA 16823
(800) 356-1688 FAX: (814) 353-1309
(814) 353-1300
http://www.restekcorp.com

Rheodyne
P.O. Box 1909
Rohnert Park, CA 94927
(707) 588-2000 FAX: (707) 588-2020
http://www.rheodyne.com

Rhone Merieux
See Merial Limited

Rhone-Poulenc
2 T W Alexander Drive
P.O. Box 12014
Research Triangle Park, NC 08512
(919) 549-2000 FAX: (919) 549-2839
http://www.Rhone-Poulenc.com
Also see Aventis

Rhone-Poulenc Rorer
500 Arcola Road
Collegeville, PA 19426
(800) 727-6737 FAX: (610) 454-8940
(610) 454-8975
http://www.rp-rorer.com

Rhone-Poulenc Rorer
Centre de Recherche de
Vitry-Alfortville
13 Quai Jules Guesde, BP14 94403
Vitry Sur Seine, Cedex, France
(33) 145-73-85-11
FAX: (33) 145-73-81-29
http://www.rp-rorer.com

Ribi ImmunoChem Research
563 Old Corvallis Road
Hamilton, MT 59840
(800) 548-7424 FAX: (406) 363-6129
(406) 363-3131
http://www.ribi.com

RiboGene
See Questcor Pharmaceuticals

Ricca Chemical
448 West Fork Drive
Arlington, TX 76012
(888) GO-RICCA FAX: (800)
RICCA-93
(817) 461-5601
http://www.riccachemical.com

Richard-Allan Scientific
225 Parsons Street
Kalamazoo, MI 49007
(800) 522-7270 FAX: (616) 345-3577
(616) 344-2400
http://www.rallansci.com

Richelieu Biotechnologies
11 177 Hamon
Montral, Quebec
H3M 3E4 Canada
(802) 863-2567 FAX: (802) 862-2909
http://www.richelieubio.com

Richter Enterprises
20 Lake Shore Drive
Wayland, MA 01778
(508) 655-7632 FAX: (508) 652-7264
http://www.richter-enterprises.com

Riese Enterprises
BioSure Division
12301 G Loma Rica Drive
Grass Valley, CA 95945
(800) 345-2267 FAX: (916) 273-5097
(916) 273-5095
http://www.biosure.com

Robbins Scientific
1250 Elko Drive
Sunnyvale, CA 94086
(800) 752-8585 FAX: (408) 734-0300
(408) 734-8500
http://www.robsci.com

Roboz Surgical Instruments
9210 Corporate Boulevard, Suite 220
Rockville, MD 20850
(800) 424-2984 FAX: (301) 590-1290
(301) 590-0055

Roche Applied Science
See Roche Diagnostics

Roche Diagnostics
9115 Hague Road
P.O. Box 50457
Indianapolis, IN 46256
(800) 262-1640 FAX: (317) 845-7120
(317) 845-2000
http://www.roche.com

Roche Molecular Systems
See Roche Diagnostics

Rocklabs
P.O. Box 18-142
Auckland 6, New Zealand
(64) 9-634-7696
FAX: (64) 9-634-7696
http://www.rocklabs.com

Rockland
P.O. Box 316
Gilbertsville, PA 19525
(800) 656-ROCK
FAX: (610) 367-7825
(610) 369-1008
http://www.rockland-inc.com

Rohm
Chemische Fabrik
Kirschenallee
D-64293 Darmstadt, Germany
(49) 6151-1801 FAX: (49) 6151-1802
http://www.roehm.com

Roper Scientific
3440 East Brittania Drive, Suite 100
Tucson, AZ 85706
(520) 889-9933 FAX: (520) 573-1944
http://www.roperscientific.com

Rosetta Inpharmatics
12040 115th Avenue NE
Kirkland, WA 98034
(425) 820-8900 FAX: (425) 820-5757
http://www.rii.com

ROTH-SOCHIEL
3 rue de la Chapelle
Lauterbourg
67630 France
(33) 03-88-94-82-42
FAX: (33) 03-88-54-63-93

Rotronic Instrument
160 E. Main Street
Huntington, NY 11743
(631) 427-3898 FAX: (631) 427-3902
http://www.rotronic-usa.com

Roundy's
23000 Roundy Drive
Pewaukee, WI 53072
(262) 953-7999 FAX: (262) 953-7989
http://www.roundys.com

RS Components
Birchington Road
Weldon Industrial Estate
Corby, Northants NN17 9RS, UK
(44) 1536 201234
FAX: (44) 1536 405678
http://www.rs-components.com

Rubbermaid
See Newell Rubbermaid

SA Instrumentation
1437 Tzena Way
Encinitas, CA 92024
(858) 453-1776
FAX: (800) 266-1776
http://www.sainst.com

Safe Cells
See Bionique Testing Labs

Sage Instruments
240 Airport Boulevard
Freedom, CA 95076
831-761-1000 FAX: 831-761-1008
http://www.sageinst.com

Sage Laboratories
11 Huron Drive
Natick, MA 01760
(508) 653-0844 FAX: 508-653-5671
http://www.sagelabs.com

Saint-Gobain Performance Plastics
P.O. Box 3660
Akron, OH 44309
(330) 798-9240 FAX: (330) 798-6968
http://www.nortonplastics.com

San Diego Instruments
7758 Arjons Drive
San Diego, CA 92126
(858) 530-2600 FAX: (858) 530-2646
http://www.sd-inst.com

Sandown Scientific
Beards Lodge
25 Oldfield Road
Hampden, Middlesex TW12 2AJ, UK
(44) 2089 793300
FAX: (44) 2089 793311
http://www.sandownsci.com

Sandoz Pharmaceuticals
See Novartis

Sanofi Recherche
Centre de Montpellier
371 Rue du Professor Blayac
34184 Montpellier, Cedex 04
France
(33) 67-10-67-10
FAX: (33) 67-10-67-67

Sanofi Winthrop Pharmaceuticals
90 Park Avenue
New York, NY 10016
(800) 223-5511 FAX: (800) 933-3243
(212) 551-4000
http://www.sanofi-synthelabo.com/us

Sanquin
Postbus 9892
1006 AN
Amsterdam, The Netherlands
(20) 512-3000 FAX: (20) 512-3303
http://www.sanquin.nl
http://www.sanquinreagents.com

Santa Cruz Biotechnology
2161 Delaware Avenue
Santa Cruz, CA 95060
(800) 457-3801 FAX: (831) 457-3801
(831) 457-3800
http://www.scbt.com

Sarasep
(800) 605-0267 FAX: (408) 432-3231
(408) 432-3230
http://www.transgenomic.com

Sarstedt
P.O. Box 468
Newton, NC 28658
(800) 257-5101 FAX: (828) 465-4003
(828) 465-4000
http://www.sarstedt.com

Sartorius
131 Heartsland Boulevard
Edgewood, NY 11717
(800) 368-7178 FAX: (516) 254-4253
http://www.sartorius.com

SAS Institute
Pacific Telesis Center
One Montgomery Street
San Francisco, CA 94104
(415) 421-2227 FAX: (415) 421-1213
http://www.sas.com

Savant/EC Apparatus
A ThermoQuest company
100 Colin Drive
Holbrook, NY 11741
(800) 634-8886 FAX: (516) 244-0606
(516) 244-2929
http://www.savec.com

Savillex
6133 Baker Road
Minnetonka, MN 55345
(612) 935-5427

Scanalytics
Division of CSP
8550 Lee Highway, Suite 400
Fairfax, VA 22031
(800) 325-3110 FAX: (703) 208-1960
(703) 208-2230
http://www.scanalytics.com

Schering Laboratories
See Schering-Plough

Schering-Plough
1 Giralda Farms
Madison, NJ 07940
(800) 222-7579 FAX: (973) 822-7048
(973) 822-7000
http://www.schering-plough.com

Schleicher & Schuell
10 Optical Avenue
Keene, NH 03431
(800) 245-4024 FAX: (603) 357-3627
(603) 352-3810
http://www.s-und-s.de/english-index.html

Science Technology Centre
1250 Herzberg Laboratories
Carleton University
1125 Colonel Bay Drive
Ottawa, Ontario
K1S 5B6 Canada
(613) 520-4442 FAX: (613) 520-4445
http://www.carleton.ca/universities/stc

Scientific Instruments
200 Saw Mill River Road
Hawthorne, NY 10532
(800) 431-1956 FAX: (914) 769-5473
(914) 769-5700
http://www.scientificinstruments.com

Scientific Solutions
9323 Hamilton
Mentor, OH 44060
(440) 357-1400 FAX: (440) 357-1416
http://www.labmaster.com

Scion
82 Worman's Mill Court, Suite H
Frederick, MD 21701
(301) 695-7870 FAX: (301) 695-0035
http://www.scioncorp.com

Scott Specialty Gases
6141 Easton Road
P.O. Box 310
Plumsteadville, PA 18949
(800) 21-SCOTT
FAX: (215) 766-2476
(215) 766-8861
http://www.scottgas.com

Scripps Clinic and Research
Foundation
Instrumentation and Design Lab
10666 N. Torrey Pines Road
La Jolla, CA 92037
(800) 992-9962 FAX: (858) 554-8986
(858) 455-9100
http://www.scrippsclinic.com

SDI Sensor Devices
407 Pilot Court, 400A
Waukesha, WI 53188
(414) 524-1000 FAX: (414) 524-1009

Sefar America
111 Calumet Street
Depew, NY 14043
(716) 683-4050 FAX: (716) 683-4053
http://www.sefaramerica.com

Seikagaku America
Division of Associates of Cape Cod
704 Main Street
Falmouth, MA 02540
(800) 237-4512 FAX: (508) 540-8680
(508) 540-3444
http://www.seikagaku.com

Sellas Medizinische Gerate
Hagener Str. 393
Gevelsberg-Vogelsang, 58285
Germany
(49) 23-326-1225

Sensor Medics
22705 Savi Ranch Parkway
Yorba Linda, CA 92887
(800) 231-2466 FAX: (714) 283-8439
(714) 283-2228
http://www.sensormedics.com

Sensor Systems LLC
2800 Anvil Street, North
Saint Petersburg, FL 33710
(800) 688-2181 FAX: (727) 347-3881
(727) 347-2181
http://www.vsensors.com

SenSym/Foxboro ICT
1804 McCarthy Boulevard
Milpitas, CA 95035
(800) 392-9934 FAX: (408) 954-9458
(408) 954-6700
http://www.sensym.com

Separations Group
See Vydac

Sepracor
111 Locke Drive
Marlboro, MA 01752
(877)-SEPRACOR (508) 357-7300
http://www.sepracor.com

Sera-Lab
See Harlan Sera-Lab

Sermeter
925 Seton Court, #7
Wheeling, IL 60090
(847) 537-4747

Serological
195 W. Birch Street
Kankakee, IL 60901
(800) 227-9412 FAX: (815) 937-8285
(815) 937-8270

Seromed Biochrom
Leonorenstrasse 2-6
D-12247 Berlin, Germany
(49) 030-779-9060

Serotec
22 Bankside
Station Approach
Kidlington, Oxford OX5 1JE, UK
(44) 1865-852722
FAX: (44) 1865-373899
In the US: (800) 265-7376
http://www.serotec.co.uk

Serva Biochemicals
Distributed by Crescent Chemical

S.F. Medical Pharmlast
See Chase-Walton Elastomers

SGE
2007 Kramer Lane
Austin, TX 78758
(800) 945-6154 FAX: (512) 836-9159
(512) 837-7190
http://www.sge.com

Shandon/Lipshaw
171 Industry Drive
Pittsburgh, PA 15275
(800) 245-6212 FAX: (412) 788-1138
(412) 788-1133
http://www.shandon.com

Sharpoint
P.O. Box 2212
Taichung, Taiwan
Republic of China
(886) 4-3206320
FAX: (886) 4-3289879
http://www.sharpoint.com.tw

Shelton Scientific
230 Longhill Crossroads
Shelton, CT 06484
(800) 222-2092 FAX: (203) 929-2175
(203) 929-8999
http://www.sheltonscientific.com

Sherwood-Davis & Geck
See Kendall

Sherwood Medical
See Kendall

Shimadzu Scientific Instruments
7102 Riverwood Drive
Columbia, MD 21046
(800) 477-1227 FAX: (410) 381-1222
(410) 381-1227
http://www.ssi.shimadzu.com

Sialomed
See Amika

Siemens Analytical X-Ray Systems
See Bruker Analytical X-Ray Systems

Sievers Instruments
Subsidiary of Ionics
6060 Spine Road
Boulder, CO 80301
(800) 255-6964 FAX: (303) 444-6272
(303) 444-2009
http://www.sieversinst.com

SIFCO
970 East 46th Street
Cleveland, OH 44103
(216) 881-8600 FAX: (216) 432-6281
http://www.sifco.com

Sigma-Aldrich
3050 Spruce Street
St. Louis, MO 63103
(800) 358-5287 FAX: (800) 962-9591
(800) 325-3101 FAX: (800) 325-5052
http://www.sigma-aldrich.com

Sigma-Aldrich Canada
2149 Winston Park Drive
Oakville, Ontario
L6H 6J8 Canada
(800) 5652-1400
FAX: (800) 2652-3858
http://www.sigma-aldrich.com

Silenus/Amrad
34 Wadhurst Drive
Boronia, Victoria 3155 Australia
(613) 9887-3909
FAX: (613) 9887-3912
http://www.amrad.com.au

Silicon Genetics
2601 Spring Street
Redwood City, CA 94063
(866) SIG SOFT FAX: (650) 365 1735
(650) 367 9600
http://www.sigenetics.com

SIMS Deltec
1265 Grey Fox Road
St. Paul, Minnesota 55112
(800) 426-2448 FAX: (615) 628-7459
http://www.deltec.com

SIMS Portex
10 Bowman Drive
Keene, NH 03431
(800) 258-5361 FAX: (603) 352-3703
(603) 352-3812
http://www.simsmed.com

SIMS Portex Limited
Hythe, Kent CT21 6JL, UK
(44)1303-260551
FAX: (44)1303-266761
http://www.portex.com

Siris Laboratories
See Biosearch Technologies

Skatron Instruments
See Molecular Devices

SLM Instruments
See Spectronic Instruments

SLM-AMINCO Instruments
See Spectronic Instruments

Small Parts
13980 NW 58th Court
P.O. Box 4650
Miami Lakes, FL 33014
(800) 220-4242 FAX: (800) 423-9009
(305) 558-1038 FAX: (305) 558-0509
http://www.smallparts.com

Smith & Nephew
11775 Starkey Road
P.O. Box 1970
Largo, FL 33779
(800) 876-1261
http://www.smith-nephew.com

SmithKline Beecham
1 Franklin Plaza, #1800
Philadelphia, PA 19102
(215) 751-4000 FAX: (215) 751-4992
http://www.sb.com

Solid Phase Sciences
See Biosearch Technologies

SOMA Scientific Instruments
5319 University Drive, PMB #366
Irvine, CA 92612
(949) 854-0220 FAX: (949) 854-0223
http://somascientific.com

Somatix Therapy
See Cell Genesys

Sonics & Materials
53 Church Hill Road
Newtown, CT 06470
(800) 745-1105 FAX: (203) 270-4610
(203) 270-4600
http://www.sonicsandmaterials.com

Sonosep Biotech
See Triton Environmental Consultants

Sorvall
See Kendro Laboratory Products

Southern Biotechnology Associates
P.O. Box 26221
Birmingham, AL 35260
(800) 722-2255 FAX: (205) 945-8768
(205) 945-1774
http://SouthernBiotech.com

SPAFAS
190 Route 165
Preston, CT 06365
(800) SPAFAS-1
FAX: (860) 889-1991
(860) 889-1389
http://www.spafas.com

Specialty Media
Division of Cell & Molecular Technologies
580 Marshall Street
Phillipsburg, NJ 08865
(800) 543-6029 FAX: (908) 387-1670
(908) 454-7774
http://www.specialtymedia.com

Spectra Physics
See Thermo Separation Products

Spectramed
See BOC Edwards

SpectraSource Instruments
31324 Via Colinas, Suite 114
Westlake Village, CA 91362
(818) 707-2655 FAX: (818) 707-9035
http://www.spectrasource.com

Spectronic Instruments
820 Linden Avenue
Rochester, NY 14625
(800) 654-9955 FAX: (716) 248-4014
(716) 248-4000
http://www.spectronic.com

Spectrum Medical Industries
See Spectrum Laboratories

Spectrum Laboratories
18617 Broadwick Street
Rancho Dominguez, CA 90220
(800) 634-3300 FAX: (800) 445-7330
(310) 885-4601 FAX: (310) 885-4666
http://www.spectrumlabs.com

Spherotech
1840 Industrial Drive, Suite 270
Libertyville, IL 60048
(800) 368-0822 FAX: (847) 680-8927
(847) 680-8922
http://www.spherotech.com

SPSS
233 S. Wacker Drive, 11th floor
Chicago, IL 60606
(800) 521-1337 FAX: (800) 841-0064
http://www.spss.com

SS White Burs
1145 Towbin Avenue
Lakewood, NJ 08701
(732) 905-1100 FAX: (732) 905-0987
http://www.sswhiteburs.com

Stag Instruments
16 Monument Industrial Park
Chalgrove, Oxon OX44 7RW, UK
(44) 1865-891116
FAX: (44) 1865-890562

Standard Reference Materials
Program
National Institute of Standards and Technology
Building 202, Room 204
Gaithersburg, MD 20899
(301) 975-6776 FAX: (301) 948-3730

Starna Cells
P.O. Box 1919
Atascandero, CA 93423
(800) 228-4482 FAX: (805) 461-1575
(805) 466-8855
http://www.starnacells.com

Starplex Scientific
50 Steinway
Etobieoke, Ontario
M9W 6Y3 Canada
(800) 665-0954 FAX: (416) 674-6067
(416) 674-7474
http://www.starplexscientific.com

State Laboratory Institute of Massachusetts
305 South Street
Jamaica Plain, MA 02130
(617) 522-3700 FAX: (617) 522-8735
http://www.state.ma.us/dph

Stedim Labs
1910 Mark Court, Suite 110
Concord, CA 94520
(800) 914-6644 FAX: (925) 689-6988
(925) 689-6650
http://www.stedim.com

Steinel America
9051 Lyndale Avenue
Bloomington, MN 55420
(800) 852 4343 FAX: (952) 888-5132
http://www.steinelamerica.com

Stem Cell Technologies
777 West Broadway, Suite 808
Vancouver, British Columbia
V5Z 4J7 Canada
(800) 667-0322 FAX: (800) 567-2899
(604) 877-0713 FAX: (604) 877-0704
http://www.stemcell.com

Stephens Scientific
107 Riverdale Road
Riverdale, NJ 07457
(800) 831-8099 FAX: (201) 831-8009
(201) 831-9800

Steraloids
P.O. Box 689
Newport, RI 02840
(401) 848-5422 FAX: (401) 848-5638
http://www.steraloids.com

Sterling Medical
2091 Springdale Road, Ste. 2
Cherry Hill, NJ 08003
(800) 229-0900 FAX: (800) 229-7854
http://www.sterlingmedical.com

Sterling Winthrop
90 Park Avenue
New York, NY 10016
(212) 907-2000 FAX: (212) 907-3626

Sternberger Monoclonals
10 Burwood Court
Lutherville, MD 21093
(410) 821-8505 FAX: (410) 821-8506
http://www.sternbergermonoclonals.com

Stoelting
502 Highway 67
Kiel, WI 53042
(920) 894-2293 FAX: (920) 894-7029
http://www.stoelting.com

Stovall Lifescience
206-G South Westgate Drive
Greensboro, NC 27407
(800) 852-0102 FAX: (336) 852-3507
http://www.slscience.com

Stratagene
11011 N. Torrey Pines Road
La Jolla, CA 92037
(800) 424-5444 FAX: (888) 267-4010
(858) 535-5400
http://www.stratagene.com

Strategic Applications
530A N. Milwaukee Avenue
Libertyville, IL 60048
(847) 680-9385 FAX: (847) 680-9837

Strem Chemicals
7 Mulliken Way
Newburyport, MA 01950
(800) 647-8736 FAX: (800) 517-8736
(978) 462-3191 FAX: (978) 465-3104
http://www.strem.com

StressGen Biotechnologies
Biochemicals Division
120-4243 Glanford Avenue
Victoria, British Columbia
V8Z 4B9 Canada
(800) 661-4978 FAX: (250) 744-2877
(250) 744-2811
http://www.stressgen.com

Structure Probe/SPI Supplies
(Epon-Araldite)
P.O. Box 656
West Chester, PA 19381
(800) 242-4774 FAX: (610) 436-5755
http://www.2spi.com

Süd-Chemie Performance Packaging
101 Christine Drive
Belen, NM 87002
(800) 989-3374 FAX: (505) 864-9296
http://www.uniteddesiccants.com

Sumitomo Chemical
Sumitomo Building
5-33, Kitahama 4-chome
Chuo-ku, Osaka 541-8550, Japan
(81) 6-6220-3891
FAX: (81)-6-6220-3345
http://www.sumitomo-chem.co.jp

Sun Box
19217 Orbit Drive
Gaithersburg, MD 20879
(800) 548-3968 FAX: (301) 977-2281
(301) 869-5980
http://www.sunboxco.com

Sunbrokers
See Sun International

Sun International
3700 Highway 421 North
Wilmington, NC 28401
(800) LAB-VIAL FAX: (800) 231-7861
http://www.autosamplervial.com

Sunox
1111 Franklin Boulevard, Unit 6
Cambridge, Ontario
N1R 8B5 Canada
(519) 624-4413 FAX: (519) 624-8378
http://www.sunox.ca

Supelco
See Sigma-Aldrich

SuperArray
P.O. Box 34494
Bethesda, MD 20827
(888) 503-3187 FAX: (301) 765-9859
(301) 765-9888
http://www.superarray.com

Surface Measurement Systems
3 Warple Mews, Warple Way
London W3 ORF, UK
(44) 20-8749-4900
FAX: (44) 20-8749-6749
http://www.smsuk.co.uk/index.htm

SurgiVet
N7 W22025 Johnson Road, Suite A
Waukesha, WI 53186
(262) 513-8500 (888) 745-6562
FAX: (262) 513-9069
http://www.surgivet.com

Sutter Instruments
51 Digital Drive
Novato, CA 94949
(415) 883-0128 FAX: (415) 883-0572
http://www.sutter.com

Swiss Precision Instruments
1555 Mittel Boulevard, Suite F
Wooddale, IL 60191
(800) 221-0198 FAX: (800) 842-5164

Synaptosoft
3098 Anderson Place
Decatur, GA 30033
(770) 939-4366 FAX: 770-939-9478
http://www.synaptosoft.com

SynChrom
See Micra Scientific

Synergy Software
2457 Perkiomen Avenue
Reading, PA 19606
(800) 876-8376 FAX: (610) 370-0548
(610) 779-0522
http://www.synergy.com

Synteni
See Incyte

Synthetics Industry
Lumite Division
2100A Atlantic Highway
Gainesville, GA 30501
(404) 532-9756 FAX: (404) 531-1347

Systat
See SPSS

Systems Planning and Analysis (SPA)
2000 N. Beauregard Street
Suite 400
Alexandria, VA 22311
(703) 931-3500
http://www.spa-inc.net

3M Bioapplications
3M Center
Building 270-15-01
St. Paul, MN 55144
(800) 257-7459 FAX: (651) 737-5645
(651) 736-4946

T Cell Diagnostics and T Cell Sciences
38 Sidney Street
Cambridge, MA 02139
(617) 621-1400

TAAB Laboratory Equipment
3 Minerva House
Calleva Park
Aldermaston, Berkshire RG7 8NA, UK
(44) 118 9817775
FAX: (44) 118 9817881

Taconic
273 Hover Avenue
Germantown, NY 12526
(800) TAC-ONIC FAX: (518)
537-7287
(518) 537-6208
http://www.taconic.com

Tago
See Biosource International

TaKaRa Biochemical
719 Alliston Way
Berkeley, CA 94710
(800) 544-9899 FAX: (510) 649-8933
(510) 649-9895
http://www.takara.co.jp/english

Takara Shuzo
Biomedical Group Division
Seta 3-4-1
Otsu Shiga 520-21, Japan
(81) 75-241-5100
FAX: (81) 77-543-9254
http://www.Takara.co.jp/english

Takeda Chemical Products
101 Takeda Drive
Wilmington, NC 28401
(800) 825-3328 FAX: (800) 825-0333
(910) 762-8666 FAX: (910) 762-6846
http://takeda-usa.com

TAO Biomedical
73 Manassas Court
Laurel Springs, NJ 08021
(609) 782-8622 FAX: (609) 782-8622

Tecan US
P.O. Box 13953
Research Triangle Park, NC 27709
(800) 33-TECAN
FAX: (919) 361-5201
(919) 361-5208
http://www.tecan-us.com

Techne
University Park Plaza
743 Alexander Road
Princeton, NJ 08540
(800) 225-9243 FAX: (609) 987-8177
(609) 452-9275
http://www.techneusa.com

Technical Manufacturing
15 Centennial Drive
Peabody, MA 01960
(978) 532-6330 FAX: (978) 531-8682
http://www.techmfg.com

Technical Products International
5918 Evergreen
St. Louis, MO 63134
(800) 729-4451 FAX: (314) 522-6360
(314) 522-8671
http://www.vibratome.com

Technicon
See Organon Teknika Cappel

Techno-Aide
P.O. Box 90763
Nashville, TN 37209
(800) 251-2629 FAX: (800) 554-6275
(615) 350-7030
http://www.techno-aid.com

Ted Pella
4595 Mountain Lakes Boulevard
P.O. Box 492477
Redding, CA 96049
(800) 237-3526 FAX: (530) 243-3761
(530) 243-2200
http://www.tedpella.com

TEGAM
10 TEGAM Way
Geneva, OH 44041
(800) 666-1010 FAX: (440) 466-6110
(440) 466-6100
http://www.tegam.com/

Tekmar-Dohrmann
P.O. Box 429576 Cincinnati, OH 45242
(800) 543-4461 FAX: (800) 841-5262
(513) 247-7000 FAX: (513) 247-7050

Tektronix
142000 S.W. Karl Braun Drive
Beaverton, OR 97077
(800) 621-1966 FAX: (503) 627-7995
(503) 627-7999
http://www.tek.com

Tel-Test
P.O. Box 1421
Friendswood, TX 77546
(800) 631-0600 FAX: (281) 482-1070
(281) 482-2672
http://www.isotex-diag.com

TeleChem International
524 East Weddell Drive, Suite 3
Sunnyvale, CA 94089
(408) 744-1331 FAX: (408) 744-1711
http://www.gst.net/~telechem

Terrachem
Mallaustrasse 57
D-68219 Mannheim, Germany
0621-876797-0
FAX: 0621-876797-19
http://www.terrachem.de

Terumo Medical
2101 Cottontail Lane
Somerset, NJ 08873
(800) 283-7866 FAX: (732) 302-3083
(732) 302-4900
http://www.terumomedical.com

Tetko
333 South Highland Manor
Briarcliff, NY 10510
(800) 289-8385 FAX: (914) 941-1017
(914) 941-7767
http://www.tetko.com

TetraLink
4240 Ridge Lea Road
Suite 29
Amherst, NY 14226
(800) 747-5170 FAX: (800) 747-5171
http://www.tetra-link.com

TEVA Pharmaceuticals USA
1090 Horsham Road
P.O. Box 1090
North Wales, PA 19454
(215) 591-3000 FAX: (215) 721-9669
http://www.tevapharmusa.com

Texas Fluorescence Labs
9503 Capitol View Drive
Austin, TX 78747
(512) 280-5223 FAX: (512) 280-4997
http://www.teflabs.com

The Nest Group
45 Valley Road
Southborough, MA 01772
(800) 347-6378 FAX: (508) 485-5736
(508) 481-6223
http://world.std.com/~nestgrp

ThermoCare
P.O. Box 6069
Incline Village, NV 89450
(800) 262-4020
(775) 831-1201

Thermo Labsystems
8 East Forge Parkway
Franklin, MA 02038
(800) 522-7763 FAX: (508) 520-2229
(508) 520-0009
http://www.finnpipette.com

Thermometric
Spjutvagen 5A
S-175 61 Jarfalla, Sweden
(46) 8-564-72-200

Thermoquest
IEC Division
300 Second Avenue
Needham Heights, MA 02194
(800) 843-1113 FAX: (781) 444-6743
(781) 449-0800
http://www.thermoquest.com

Thermo Separation Products
Thermoquest
355 River Oaks Parkway
San Jose, CA 95134
(800) 538-7067 FAX: (408) 526-9810
(408) 526-1100
http://www.thermoquest.com

Thermo Shandon
171 Industry Drive
Pittsburgh, PA 15275
(800) 547-7429 FAX: (412) 899-4045
http://www.thermoshandon.com

Thermo Spectronic
820 Linden Avenue
Rochester, NY 14625
(585) 248-4000 FAX: (585) 248-4200
http://www.thermo.com

Thomas Scientific
99 High Hill Road at I-295
Swedesboro, NJ 08085
(800) 345-2100 FAX: (800) 345-5232
(856) 467-2000 FAX: (856) 467-3087
http://www.wheatonsci.com/html/nt/Thomas.html

Thomson Instrument
354 Tyler Road
Clearbrook, VA 22624
(800) 842-4752 FAX: (540) 667-6878
(800) 541-4792 FAX: (760) 757-9367
http://www.hplc.com

Thorn EMI
See Electron Tubes

Thorlabs
435 Route 206
Newton, NJ 07860
(973) 579-7227 FAX: (973) 383-8406
http://www.thorlabs.com

Tiemann
See Bernsco Surgical Supply

Timberline Instruments
1880 South Flatiron Court, H-2
P.O. Box 20356
Boulder, CO 80308
(800) 777-5996 FAX: (303) 440-8786
(303) 440-8779
http://www.timberlineinstruments.com

Tissue-Tek
A Division of Sakura Finetek USA
1750 West 214th Street
Torrance, CA 90501
(800) 725-8723 FAX: (310) 972-7888
(310) 972-7800
http://www.sakuraus.com

Tocris Cookson
114 Holloway Road, Suite 200
Ballwin, MO 63011
(800) 421-3701 FAX: (800) 483-1993
(636) 207-7651 FAX: (636) 207-7683
http://www.tocris.com

Tocris Cookson
Northpoint, Fourth Way
Avonmouth, Bristol BS11 8TA, UK
(44) 117-982-6551
FAX: (44) 117-982-6552
http://www.tocris.com

Tomtec
See CraMar Technologies

TopoGen
P.O. Box 20607
Columbus, OH 43220
(800) TOPOGEN
FAX: (800) ADD-TOPO
(614) 451-5810 FAX: (614) 451-5811
http://www.topogen.com

Toray Industries, Japan
Toray Building 2-1
Nihonbash-Muromach
2-Chome, Chuo-Ku
Tokyo, Japan 103-8666
(03) 3245-5115 FAX: (03) 3245-5555
http://www.toray.co.jp

Toray Industries, U.S.A.
600 Third Avenue
New York, NY 10016
(212) 697-8150 FAX: (212) 972-4279
http://www.toray.com

Toronto Research Chemicals
2 Brisbane Road
North York, Ontario
M3J 2J8, Canada
(416) 665-9696 FAX: (416) 665-4439
http://www.trc-canada.com

TosoHaas
156 Keystone Drive
Montgomeryville, PA 18036
(800) 366-4875 FAX: (215) 283-5035
(215) 283-5000
http://www.tosohaas.com

Towhill
647 Summer Street
Boston, MA 02210
(617) 542-6636 FAX: (617) 464-0804

Toxin Technology
7165 Curtiss Avenue
Sarasota, FL 34231
(941) 925-2032
FAX: (9413) 925-2130
http://www.toxintechnology.com

Toyo Soda
See TosoHaas

Trace Analytical
3517-A Edison Way
Menlo Park, CA 94025
(650) 364-6895 FAX: (650) 364-6897
http://www.traceanalytical.com

Transduction Laboratories
See BD Transduction Laboratories

Transgenomic
2032 Concourse Drive
San Jose, CA 95131
(408) 432-3230 FAX: (408) 432-3231
http://www.transgenomic.com

Transonic Systems
34 Dutch Mill Road
Ithaca, NY 14850
(800) 353-3569 FAX: (607) 257-7256
http://www.transonic.com

Travenol Lab
See Baxter Healthcare

Tree Star Software
20 Winding Way
San Carlos, CA 94070
800-366-6045
http://www.treestar.com

Trevigen
8405 Helgerman Court
Gaithersburg, MD 20877
(800) TREVIGEN
FAX: (301) 216-2801
(301) 216-2800
http://www.trevigen.com

Trilink Biotechnologies
6310 Nancy Ridge Drive
San Diego, CA 92121
(800) 863-6801 FAX: (858) 546-0020
http://www.trilink.biotech.com

Tripos Associates
1699 South Hanley Road, Suite 303
St. Louis, MO 63144
(800) 323-2960 FAX: (314) 647-9241
(314) 647-1099
http://www.tripos.com

Triton Environmental Consultants
120-13511 Commerce Parkway
Richmond, British Columbia
V6V 2L1 Canada
(604) 279-2093 FAX: (604) 279-2047
http://www.triton-env.com

Tropix
47 Wiggins Avenue
Bedford, MA 01730
(800) 542-2369 FAX: (617) 275-8581
(617) 271-0045
http://www.tropix.com

TSI Center for Diagnostic Products
See Intergen

2000 Eppendorf-5 Prime
5603 Arapahoe Avenue
Boulder, CO 80303
(800) 533-5703 FAX: (303) 440-0835
(303) 440-3705

Tyler Research
10328 73rd Avenue
Edmonton, Alberta
T6E 6N5 Canada
(403) 448-1249 FAX: (403) 433-0479

UBI
See Upstate Biotechnology

Ugo Basile Biological Research Apparatus
Via G. Borghi 43
21025 Comerio, Varese, Italy
(39) 332 744 574
FAX: (39) 332 745 488
http://www.ugobasile.com

UltraPIX
See Life Science Resources

Ultrasonic Power
239 East Stephenson Street
Freeport, IL 61032
(815) 235-6020 FAX: (815) 232-2150
http://www.upcorp.com

Ultrasound Advice
23 Aberdeen Road
London N52UG, UK
(44) 020-7359-1718
FAX: (44) 020-7359-3650
http://www.ultrasoundadvice.co.uk

UNELKO
14641 N. 74th Street
Scottsdale, AZ 85260
(480) 991-7272 FAX: (480) 483-7674
http://www.unelko.com

Unifab Corp.
5260 Lovers Lane
Kalamazoo, MI 49002
(800) 648-9569 FAX: (616) 382-2825
(616) 382-2803

Union Carbide
10235 West Little York Road, Suite 300
Houston, TX 77040
(800) 568-4000 FAX: (713) 849-7021
(713) 849-7000
http://www.unioncarbide.com

United Desiccants
See Süd-Chemie Performance Packaging

United States Biochemical
See USB

United States Biological (US Biological)
P.O. Box 261
Swampscott, MA 01907
(800) 520-3011 FAX: (781) 639-1768
http://www.usbio.net

Universal Imaging
502 Brandywine Parkway
West Chester, PA 19380
(610) 344-9410 FAX: (610) 344-6515
http://www.image1.com

Upchurch Scientific
619 West Oak Street
P.O. Box 1529
Oak Harbor, WA 98277
(800) 426-0191 FAX: (800) 359-3460
(360) 679-2528 FAX: (360) 679-3830
http://www.upchurch.com

Upjohn
Pharmacia & Upjohn
http://www.pnu.com

Upstate Biotechnology (UBI)
1100 Winter Street, Suite 2300
Waltham, MA 02451
(800) 233-3991 FAX: (781) 890-7738
(781) 890-8845
http://www.upstatebiotech.com

USA/Scientific
346 SW 57th Avenue
P.O. Box 3565
Ocala, FL 34478
(800) LAB-TIPS FAX: (352) 351-2057
(3524) 237-6288
http://www.usascientific.com

USB
26111 Miles Road
P.O. Box 22400
Cleveland, OH 44122
(800) 321-9322 FAX: (800) 535-0898
FAX: (216) 464-5075
http://www.usbweb.com

USCI Bard
Bard Interventional Products
129 Concord Road
Billerica, MA 01821
(800) 225-1332 FAX: (978) 262-4805
http://www.bardinterventional.com

UVP (Ultraviolet Products)
2066 W. 11th Street
Upland, CA 91786
(800) 452-6788 FAX: (909) 946-3597
(909) 946-3197
http://www.uvp.com

V & P Scientific
9823 Pacific Heights Boulevard,
Suite T
San Diego, CA 92121
(800) 455-0644 FAX: (858) 455-0703
(858) 455-0643
http://www.vp-scientific.com

Valco Instruments
P.O. Box 55603
Houston, TX 77255
(800) FOR-VICI FAX: (713) 688-8106
(713) 688-9345
http://www.vici.com

Valpey Fisher
75 South Street
Hopkin, MA 01748
(508) 435-6831 FAX: (508) 435-5289
http://www.valpeyfisher.com

Value Plastics
3325 Timberline Road
Fort Collins, CO 80525
(800) 404-LUER
FAX: (970) 223-0953
(970) 223-8306
http://www.valueplastics.com

Vangard International
P.O. Box 308
3535 Rt. 66, Bldg. #4
Neptune, NJ 07754
(800) 922-0784 FAX: (732) 922-0557
(732) 922-4900
http://www.vangard1.com

Varian Analytical Instruments
2700 Mitchell Drive
Walnut Creek, CA 94598
(800) 926-3000 FAX: (925) 945-2102
(925) 939-2400
http://www.varianinc.com

Varian Associates
3050 Hansen Way
Palo Alto, CA 94304
(800) 544-4636 FAX: (650) 424-5358
(650) 493-4000
http://www.varian.com

Vector Core Laboratory/
National Gene Vector Labs
University of Michigan
3560 E MSRB II
1150 West Medical Center Drive
Ann Arbor, MI 48109
(734) 936-5843 FAX: (734) 764-3596

Vector Laboratories
30 Ingold Road
Burlingame, CA 94010
(800) 227-6666 FAX: (650) 697-0339
(650) 697-3600
http://www.vectorlabs.com

Vedco
2121 S.E. Bush Road
St. Joseph, MO 64504
(888) 708-3326 FAX: (816) 238-1837
(816) 238-8840
http://database.vedco.com

Ventana Medical Systems
3865 North Business Center Drive
Tucson, AZ 85705
(800) 227-2155 FAX: (520) 887-2558
(520) 887-2155
http://www.ventanamed.com

Verity Software House
P.O. Box 247
45A Augusta Road
Topsham, ME 04086
(207) 729-6767 FAX: (207) 729-5443
http://www.vsh.com

Vernitron
See Sensor Systems LLC

Vertex Pharmaceuticals
130 Waverly Street
Cambridge, MA 02139
(617) 577-6000 FAX: (617) 577-6680
http://www.vpharm.com

Vetamac
Route 7, Box 208
Frankfort, IN 46041
(317) 379-3621

Vet Drug
Unit 8
Lakeside Industrial Estate
Colnbrook, Slough SL3 0ED, UK

Vetus Animal Health
See Burns Veterinary Supply

Viamed
15 Station Road
Cross Hills, Keighley
W. Yorkshire BD20 7DT, UK
(44) 1-535-634-542
FAX: (44) 1-535-635-582
http://www.viamed.co.uk

Vical
9373 Town Center Drive, Suite 100
San Diego, CA 92121
(858) 646-1100 FAX: (858) 646-1150
http://www.vical.com

Victor Medical
2349 North Watney Way, Suite D
Fairfield, CA 94533
(800) 888-8908 FAX: (707) 425-6459
(707) 425-0294

Virion Systems
9610 Medical Center Drive, Suite 100
Rockville, MD 20850
(301) 309-1844 FAX: (301) 309-0471
http://www.radix.net/~virion

VirTis Company
815 Route 208
Gardiner, NY 12525
(800) 765-6198 FAX: (914) 255-5338
(914) 255-5000
http://www.virtis.com

Visible Genetics
700 Bay Street, Suite 1000
Toronto, Ontario
M5G 1Z6 Canada
(888) 463-6844 (416) 813-3272
http://www.visgen.com

Vitrocom
8 Morris Avenue
Mountain Lakes, NJ 07046
(973) 402-1443 FAX: (973) 402-1445

VTI
7650 W. 26th Avenue
Hialeah, FL 33106
(305) 828-4700 FAX: (305) 828-0299
http://www.vticorp.com

VWR Scientific Products
200 Center Square Road
Bridgeport, NJ 08014
(800) 932-5000 FAX: (609) 467-5499
(609) 467-2600
http://www.vwrsp.com

Vydac
17434 Mojave Street
P.O. Box 867 Hesperia, CA 92345
(800) 247-0924 FAX: (760) 244-1984
(760) 244-6107
http://www.vydac.com

Vysis
3100 Woodcreek Drive
Downers Grove, IL 60515
(800) 553-7042 FAX: (630) 271-7138
(630) 271-7000
http://www.vysis.com

W&H Dentalwerk Bürmoos
P.O. Box 1
A-5111 Bürmoos, Austria
(43) 6274-6236-0
FAX: (43) 6274-6236-55
http://www.wnhdent.com

Wako BioProducts
See Wako Chemicals USA

Wako Chemicals USA
1600 Bellwood Road
Richmond, VA 23237
(800) 992-9256 FAX: (804) 271-7791
(804) 271-7677
http://www.wakousa.com

Wako Pure Chemicals
1-2, Doshomachi 3-chome
Chuo-ku, Osaka 540-8605, Japan
81-6-6203-3741 FAX:
81-6-6222-1203
http://www.wako-chem.co.jp/egaiyo/index.htm

Wallac
See Perkin-Elmer

Wallac
A Division of Perkin-Elmer
3985 Eastern Road
Norton, OH 44203
(800) 321-9632 FAX: (330) 825-8520
(330) 825-4525
http://www.wallac.com

Waring Products
283 Main Street
New Hartford, CT 06057
(800) 348-7195 FAX: (860) 738-9203
(860) 379-0731
http://www.waringproducts.com

Warner Instrument
1141 Dixwell Avenue
Hamden, CT 06514
(800) 599-4203 FAX: (203) 776-1278
(203) 776-0664
http://www.warnerinstrument.com

Warner-Lambert
Parke-Davis
201 Tabor Road
Morris Plains, NJ 07950
(973) 540-2000 FAX: (973) 540-3761
http://www.warner-lambert.com

Washington University Machine Shop
615 South Taylor
St. Louis, MO 63310
(314) 362-6186 FAX: (314) 362-6184

Waters Chromatography
34 Maple Street
Milford, MA 01757
(800) 252-HPLC
FAX: (508) 478-1990
(508) 478-2000
http://www.waters.com

Watlow
12001 Lackland Road
St. Louis, MO 63146
(314) 426-7431 FAX: (314) 447-8770
http://www.watlow.com

Watson-Marlow
220 Ballardvale Street
Wilmington, MA 01887
(978) 658-6168 FAX: (978) 988 0828
http://www.watson-marlow.co.uk

Waukesha Fluid Handling
611 Sugar Creek Road
Delavan, WI 53115
(800) 252-5200 FAX: (800) 252-5012
(414) 728-1900 FAX: (414) 728-4608
http://www.waukesha-cb.com

WaveMetrics
P.O. Box 2088
Lake Oswego, OR 97035
(503) 620-3001 FAX: (503) 620-6754
http://www.wavemetrics.com

Weather Measure
P.O. Box 41257
Sacramento, CA 95641
(916) 481-7565

Weber Scientific
2732 Kuser Road
Hamilton, NJ 08691
(800) FAT-TEST FAX: (609) 584-8388
(609) 584-7677
http://www.weberscientific.com

Weck, Edward & Company
1 Weck Drive
Research Triangle Park, NC 27709
(919) 544-8000

Wellcome Diagnostics
See Burroughs Wellcome

Wellington Laboratories
398 Laird Road
Guelph Ontario
N1G 3X7 Canada
(800) 578-6985 FAX: (519) 822-2849
http://www.well-labs.com

Wesbart Engineering
Daux Road
Billingshurst, West Sussex
RH14 9EZ, UK
(44) 1-403-782738
FAX: (44) 1-403-784180
http://www.wesbart.co.uk

Whatman
9 Bridewell Place
Clifton, NJ 07014
(800) 631-7290 FAX: (973) 773-3991
(973) 773-5800
http://www.whatman.com

Wheaton Science Products
1501 North 10th Street
Millville, NJ 08332
(800) 225-1437 FAX: (800) 368-3108
(856) 825-1100 FAX: (856) 825-1368
http://www.algroupwheaton.com

Whittaker Bioproducts
See BioWhittaker

Wild Heerbrugg
Juerg Dedual Gaebrisstrasse 8 CH
9056 Gais, Switzerland
(41) 71-793-2723
FAX: (41) 71-726-5957
http://www.homepage.swissonline.net/dedual/wild_heerbrugg

Willy A. Bachofen AG Maschinenfabrik
Utengasse 15/17
CH4005 Basel, Switzerland
(41) 61-681-5151
FAX: (41) 61-681-5058
http://www.wab.ch

Winthrop
See Sterling Winthrop

Wolfram Research
100 Trade Center Drive
Champaign, IL 61820
(800) 965-3726 FAX: (217) 398-0747
(217) 398-0700
http://www.wolfram.com

World Health Organization
Microbiology and Immunology Support
20 Avenue Appia
1211 Geneva 27, Switzerland
(41-22) 791-2602
FAX: (41-22) 791-0746
http://www.who.org

World Precision Instruments
175 Sarasota Center Boulevard
International Trade Center
Sarasota, FL 34240
(941) 371-1003 FAX: (941) 377-5428
http://www.wpiinc.com

Worthington Biochemical
Halls Mill Road
Freehold, NJ 07728
(800) 445-9603 FAX: (800) 368-3108
(732) 462-3838 FAX: (732) 308-4453
http://www.worthington-biochem.com

WPI
See World Precision Instruments

Wyeth-Ayerst
2 Esterbrook Lane
Cherry Hill, NJ 08003
(800) 568-9938 FAX: (858) 424-8747
(858) 424-3700

Wyeth-Ayerst Laboratories
P.O. Box 1773
Paoli, PA 19301
(800) 666-7248 FAX: (610) 889-9669
(610) 644-8000
http://www.ahp.com

Xenotech
3800 Cambridge Street
Kansas City, KS 66103
(913) 588-7930 FAX: (913) 588-7572
http://www.xenotechllc.com

Xeragon
19300 Germantown Road
Germantown, MD 20874
(240) 686-7860 FAX: (240) 686-7861
http://www.xeragon.com

Xillix Technologies
300-13775 Commerce Parkway
Richmond, British Columbia
V6V 2V4 Canada
(800) 665-2236 FAX: (604) 278-3356
(604) 278-5000
http://www.xillix.com

Xomed Surgical Products
6743 Southpoint Drive N
Jacksonville, FL 32216
(800) 874-5797 FAX: (800) 678-3995
(904) 296-9600 FAX: (904) 296-9666
http://www.xomed.com

Yakult Honsha
1-19, Higashi-Shinbashi 1-chome
Minato-ku Tokyo 105-8660, Japan
81-3-3574-8960

Yamasa Shoyu
23-8 Nihonbashi Kakigaracho
1-chome, Chuoku
Tokyo, 103 Japan
(81) 3-479 22 0095
FAX: (81) 3-479 22 3435

Yeast Genetic Stock Center
See ATCC

Yellow Spring Instruments
See YSI

YMC
YMC Karasuma-Gojo Building
284 Daigo-Cho, Karasuma Nisihiirr
Gojo-dori Shimogyo-ku
Kyoto, 600-8106, Japan
(81) 75-342-4567
FAX: (81) 75-342-4568
http://www.ymc.co.jp

YSI
1725-1700 Brannum Lane
Yellow Springs, OH 45387
(800) 765-9744 FAX: (937) 767-9353
(937) 767-7241
http://www.ysi.com

Zeneca/CRB
See AstraZeneca
(800) 327-0125 FAX: (800) 321-4745

Zivic-Miller Laboratories
178 Toll Gate Road
Zelienople, PA 16063
(800) 422-LABS FAX: (724) 452-4506
(800) MBM-RATS
FAX: (724) 452-5200
http://zivicmiller.com

ZYF Pharm Chemical Shanghi
Lansheng Corp. China
Shanghai, China
(86) 21 65365517
FAX: (86) 21-65612897
www.pharmchemical.com

Zymark
Zymark Center
Hopkinton, MA 01748
(508) 435-9500 FAX: (508) 435-3439
http://www.zymark.com

Zymed Laboratories
458 Carlton Court
South San Francisco, CA 94080
(800) 874-4494 FAX: (650) 871-4499
(650) 871-4494
http://www.zymed.com

Zymo Research
625 W. Katella Avenue, Suite 30
Orange, CA 92867
(888) 882-9682 FAX: (714) 288-9643
(714) 288-9682
http://www.zymor.com

Zynaxis Cell Science
See ChiRex Cauldron